

# REVIEW OF PARTICLE PHYSICS\*

Particle Data Group

## *Abstract*

This biennial *Review* summarizes much of particle physics. Using data from previous editions, plus 2658 new measurements from 644 papers, we list, evaluate, and average measured properties of gauge bosons, leptons, quarks, mesons, and baryons. We summarize searches for hypothetical particles such as Higgs bosons, heavy neutrinos, and supersymmetric particles. All the particle properties and search limits are listed in Summary Tables. We also give numerous tables, figures, formulae, and reviews of topics such as the Standard Model, particle detectors, probability, and statistics. Among the 112 reviews are many that are new or heavily revised including those on Heavy-Quark and Soft-Collinear Effective Theory, Neutrino Cross Section Measurements, Monte Carlo Event Generators, Lattice QCD, Heavy Quarkonium Spectroscopy, Top Quark, Dark Matter,  $V_{cb}$  &  $V_{ub}$ , Quantum Chromodynamics, High-Energy Collider Parameters, Astrophysical Constants, Cosmological Parameters, and Dark Matter.

A booklet is available containing the Summary Tables and abbreviated versions of some of the other sections of this full *Review*. All tables, listings, and reviews (and errata) are also available on the Particle Data Group website: <http://pdg.lbl.gov>.

DOI: 10.1103/PhysRevD.86.010001

The 2012 edition of *Review of Particle Physics* is published for the Particle Data Group as article 010001 in volume 86 of *Physical Review D*.

This edition should be cited as: J. Beringer et al. (Particle Data Group), Phys. Rev. D **86**, 010001 (2012).

©2012 Regents of the University of California

\*The publication of the *Review of Particle Physics* is supported by the Director, Office of Science, Office of High Energy and Nuclear Physics, the Division of High Energy Physics of the U.S. Department of Energy under Contract No. DE-AC02-05CH11231; by the U.S. National Science Foundation under Agreement No. PHY-0652989; by the European Laboratory for Particle Physics (CERN); by an implementing arrangement between the governments of Japan (MEXT: Ministry of Education, Culture, Sports, Science and Technology) and the United States (DOE) on cooperative research and development; and by the Italian National Institute of Nuclear Physics (INFN).

## Particle Data Group

J. Beringer,<sup>1</sup> J.-F. Arguin,<sup>1,2</sup> R.M. Barnett,<sup>1</sup> K. Copic,<sup>1</sup> O. Dahl,<sup>1</sup> D.E. Groom,<sup>1</sup> C.-J. Lin,<sup>1</sup> J. Lys,<sup>1</sup> H. Murayama,<sup>3,4,1</sup> C.G. Wohl,<sup>1</sup> W.-M. Yao,<sup>1</sup> P.A. Zyla,<sup>1</sup> C. Amsler,<sup>5,6</sup> M. Antonelli,<sup>7</sup> D.M. Asner,<sup>8</sup> H. Baer,<sup>9</sup> H.R. Band,<sup>10</sup> T. Basaglia,<sup>11</sup> C.W. Bauer,<sup>1</sup> J.J. Beatty,<sup>12</sup> V.I. Belousov,<sup>13</sup> E. Bergren,<sup>14</sup> G. Bernardi,<sup>14</sup> W. Bertl,<sup>15</sup> S. Bethke,<sup>16</sup> H. Bichsel,<sup>17</sup> O. Biebel,<sup>18</sup> E. Blucher,<sup>19</sup> S. Blusk,<sup>20</sup> G. Brooijmans,<sup>21</sup> O. Buchmueller,<sup>22</sup> R.N. Cahn,<sup>1</sup> M. Carena,<sup>23,19,24</sup> A. Ceccucci,<sup>11</sup> D. Chakraborty,<sup>25</sup> M.-C. Chen,<sup>26</sup> R.S. Chivukula,<sup>27</sup> G. Cowan,<sup>28</sup> G. D'Ambrosio,<sup>29</sup> T. Damour,<sup>30</sup> D. de Florian,<sup>31</sup> A. de Gouvêa,<sup>32</sup> T. DeGrand,<sup>33</sup> P. de Jong,<sup>34</sup> G. Dissertori,<sup>35</sup> B. Dobrescu,<sup>23</sup> M. Doser,<sup>11</sup> M. Drees,<sup>36</sup> D.A. Edwards,<sup>37</sup> S. Eidelman,<sup>38</sup> J. Erler,<sup>39</sup> V.V. Ezhela,<sup>13</sup> W. Fetscher,<sup>35</sup> B.D. Fields,<sup>40</sup> B. Foster,<sup>41,37,42</sup> T.K. Gaiser,<sup>43</sup> L. Garren,<sup>23</sup> H.-J. Gerber,<sup>35</sup> G. Gerbier,<sup>44</sup> T. Gherghetta,<sup>45</sup> S. Golwala,<sup>46</sup> M. Goodman,<sup>47</sup> C. Grab,<sup>35</sup> A.V. Gritsan,<sup>48</sup> J.-F. Grivaz,<sup>49</sup> M. Grünewald,<sup>50</sup> A. Gurtu,<sup>51,11</sup> T. Gutsche,<sup>52</sup> H.E. Haber,<sup>53</sup> K. Hagiwara,<sup>54</sup> C. Hagmann,<sup>55</sup> C. Hanhart,<sup>56</sup> S. Hashimoto,<sup>54</sup> K.G. Hayes,<sup>57</sup> M. Heffner,<sup>55</sup> B. Heltsley,<sup>58</sup> J.J. Hernández-Rey,<sup>59†</sup> K. Hikasa,<sup>60</sup> A. Höcker,<sup>11</sup> J. Holder,<sup>61,43</sup> A. Holtkamp,<sup>11</sup> J. Huston,<sup>27</sup> J.D. Jackson,<sup>1</sup> K.F. Johnson,<sup>62</sup> T. Junk,<sup>23</sup> D. Karlen,<sup>63</sup> D. Kirkby,<sup>26</sup> S.R. Klein,<sup>64</sup> E. Klempt,<sup>65</sup> R.V. Kowalewski,<sup>63</sup> F. Krauss,<sup>66</sup> M. Kreps,<sup>67</sup> B. Krusche,<sup>68</sup> Yu.V. Kuyanov,<sup>13</sup> Y. Kwon,<sup>69</sup> O. Lahav,<sup>70</sup> J. Laiho,<sup>71</sup> P. Langacker,<sup>72</sup> A. Liddle,<sup>73</sup> Z. Ligeti,<sup>1</sup> T.M. Liss,<sup>74</sup> L. Littenberg,<sup>75</sup> K.S. Lugovsky,<sup>13</sup> S.B. Lugovsky,<sup>13</sup> T. Mannel,<sup>76</sup> A.V. Manohar,<sup>77</sup> W.J. Marciano,<sup>75</sup> A.D. Martin,<sup>66</sup> A. Masoni,<sup>78</sup> J. Matthews,<sup>79</sup> D. Milstead,<sup>80</sup> R. Miquel,<sup>81</sup> K. Mönig,<sup>82</sup> F. Moortgat,<sup>35</sup> K. Nakamura,<sup>3,54</sup> M. Narain,<sup>83</sup> P. Nason,<sup>84</sup> S. Navas,<sup>85†</sup> M. Neubert,<sup>86</sup> P. Nevski,<sup>75</sup> Y. Nir,<sup>87</sup> K.A. Olive,<sup>88</sup> L. Pape,<sup>35</sup> J. Parsons,<sup>21</sup> C. Patrignani,<sup>89</sup> J.A. Peacock,<sup>90</sup> S.T. Petcov,<sup>91,3,92</sup> A. Piepke,<sup>93</sup> A. Pomarol,<sup>94</sup> G. Punzi,<sup>95</sup> A. Quadt,<sup>96</sup> S. Raby,<sup>12</sup> G. Raffelt,<sup>97</sup> B.N. Ratcliff,<sup>98</sup> P. Richardson,<sup>66</sup> S. Roesler,<sup>11</sup> S. Rolli,<sup>99</sup> A. Romaniouk,<sup>100</sup> L.J. Rosenberg,<sup>17</sup> J.L. Rosner,<sup>19</sup> C.T. Sachrajda,<sup>101</sup> Y. Sakai,<sup>54</sup> G.P. Salam,<sup>11,102,103</sup> S. Sarkar,<sup>104</sup> F. Sauli,<sup>11</sup> O. Schneider,<sup>105</sup> K. Scholberg,<sup>106</sup> D. Scott,<sup>107</sup> W.G. Seligman,<sup>108</sup> M.H. Shaevitz,<sup>21</sup> S.R. Sharpe,<sup>17</sup> M. Silari,<sup>11</sup> T. Sjöstrand,<sup>109</sup> P. Skands,<sup>11</sup> J.G. Smith,<sup>33</sup> G.F. Smoot,<sup>1</sup> S. Spanier,<sup>110</sup> H. Spieler,<sup>1</sup> A. Stahl,<sup>111</sup> T. Stanev,<sup>43</sup> S.L. Stone,<sup>20</sup> T. Sumiyoshi,<sup>112</sup> M.J. Syphers,<sup>113</sup> F. Takahashi,<sup>60</sup> M. Tanabashi,<sup>114</sup> J. Terning,<sup>115</sup> M. Titov,<sup>116</sup> N.P. Tkachenko,<sup>13</sup> N.A. Törnqvist,<sup>117</sup> D. Tovey,<sup>118</sup> G. Valencia,<sup>119</sup> K. van Bibber,<sup>55</sup> G. Venanzoni,<sup>7</sup> M.G. Vincter,<sup>120</sup> P. Vogel,<sup>121</sup> A. Vogt,<sup>122</sup> W. Walkowiak,<sup>76</sup> C.W. Walter,<sup>106</sup> D.R. Ward,<sup>123</sup> T. Watari,<sup>3</sup> G. Weiglein,<sup>37</sup> E.J. Weinberg,<sup>21</sup> L.R. Wiencke,<sup>124</sup> L. Wolfenstein,<sup>125</sup> J. Womersley,<sup>126</sup> C.L. Woody,<sup>75</sup> R.L. Workman,<sup>127</sup> A. Yamamoto,<sup>54</sup> G.P. Zeller,<sup>23</sup> O.V. Zenin,<sup>13</sup> J. Zhang,<sup>128</sup> R.-Y. Zhu<sup>129</sup>

Technical Associates: G. Harper,<sup>1</sup> V.S. Lugovsky,<sup>13</sup> P. Schaffner<sup>1</sup>

1. *Physics Division, Lawrence Berkeley National Laboratory, 1 Cyclotron Road, Berkeley, CA 94720, USA*
2. *Département de physique, Université de Montréal, C.P. 6128, succ. centre-ville, Montréal (Québec) H3C 3J7, Canada*
3. *Kavli IPMU (WPI), Todai Institutes for Advanced Study, University of Tokyo, Kashiwa, Chiba 277-8583, Japan*
4. *Department of Physics, University of California, Berkeley, CA 94720, USA*
5. *Physik-Institut, Universität Zürich, CH-8057 Zürich, Switzerland*
6. *Albert Einstein Center for Fundamental Physics, Universität Bern, CH-3012 Bern, Switzerland*
7. *Lab. Nazionali di Frascati dell'INFN, CP 13, via E. Fermi, 40, I-00044 Frascati (Roma), Italy*
8. *Pacific Northwest National Laboratory, 902 Battelle Boulevard, Richland, WA 99352, USA*
9. *Department of Physics, Florida State University, Tallahassee, FL 32306, USA*
10. *Department of Physics, University of Wisconsin, Madison, WI 53706, USA*
11. *CERN, European Organization for Nuclear Research, CH-1211 Genève 23, Switzerland*
12. *Department of Physics, The Ohio State University, 191 W. Woodruff Ave., Columbus, OH 43210*
13. *COMPAS Group, Institute for High Energy Physics, RU-142284, Protvino, Russia*
14. *LPNHE, IN2P3-CNRS et Universités de Paris 6 et 7, F-75252 Paris, France*
15. *Paul Scherrer Institut, CH-5232 Villigen PSI, Switzerland*
16. *Max-Planck-Institute of Physics, 80805 Munich, Germany*
17. *Department of Physics, University of Washington, Seattle, WA 98195, USA*
18. *Ludwig-Maximilians-Universität, Fakultät für Physik, Schellingstr. 4, D-80799 München, Germany*
19. *Enrico Fermi Institute and Department of Physics, University of Chicago, Chicago, IL 60637-1433, USA*
20. *Department of Physics, Syracuse University, Syracuse, NY, 13244-1130, USA*
21. *Department of Physics, Columbia University, 538 W. 120th Street, New York, NY, 10027 USA*
22. *High Energy Physics Group, Blackett Laboratory, Imperial College, Prince Consort Road, London SW7 2AZ, UK*
23. *Fermi National Accelerator Laboratory, P.O. Box 500, Batavia, IL 60510, USA*
24. *Kavli Institute for Cosmological Physics, University of Chicago, Chicago, IL 60637-1433, USA*
25. *Department of Physics, Northern Illinois University, DeKalb, IL 60115, USA*
26. *Department of Physics and Astronomy, University of California, Irvine, CA 92697-4576, USA*
27. *Michigan State University, Dept. of Physics and Astronomy, East Lansing, MI 48824-2320, USA*

† J.J. Hernández-Rey and S. Navas acknowledge support from MICINN, Spain (FPA2009-07264-E)



28. *Department of Physics, Royal Holloway, University of London, Egham, Surrey TW20 0EX, UK*
29. *INFN - Sezione di Napoli Complesso Universitario Monte Sant'Angelo, Via Cintia, 80126 Napoli, Italy*
30. *Institut des Hautes Etudes Scientifiques, F-91440 Bures-sur-Yvette, France*
31. *Departamento de Física, FCEyN, Universidad de Buenos Aires, Pab.1, Ciudad Universitaria, (1428) Capital Federal, Argentina*
32. *Department of Physics and Astronomy, Northwestern University, Evanston, IL 60208, USA*
33. *Department of Physics, University of Colorado at Boulder, Boulder, CO 80309, USA*
34. *Nikhef, P.O. Box 41882, 1009 DB Amsterdam, the Netherlands*
35. *Institute for Particle Physics, ETH Zurich, 8093 Zurich, Switzerland*
36. *Universität Bonn, Physikalisches Institut, Nussallee 12, D-53115 Bonn, Germany*
37. *Deutsches Elektronen-Synchrotron DESY, Notkestraße 85, D-22603 Hamburg, Germany*
38. *Budker Institute of Nuclear Physics SB RAS and Novosibirsk State University, Novosibirsk 630090, Russia*
39. *Departamento de Física Teórica, Instituto de Física, Universidad Nacional Autónoma de México, México D.F. 04510, México*
40. *Department of Astronomy, University of Illinois, 1002 W. Green St., Urbana, IL 61801, USA*
41. *University of Hamburg, Notkestrasse 85, D-22603 Hamburg, Germany*
42. *Denys Wilkinson Building, Department of Physics, University of Oxford, Oxford, OX1 3RH, UK*
43. *Bartol Research Institute, University of Delaware, Newark, DE 19716, USA*
44. *CEA/Saclay, DSM/IRFU, BP 2, F-91191 Gif-sur-Yvette, France*
45. *School of Physics, University of Melbourne, Victoria, 3010 Australia*
46. *California Institute of Technology, Division of Physics, Mathematics, and Astronomy, Mail Code 367-17, Pasadena, CA 91125, USA*
47. *Argonne National Laboratory, 9700 S. Cass Ave., Argonne, IL 60439-4815, USA*
48. *Johns Hopkins University, Baltimore, Maryland 21218, USA*
49. *LAL, IN2P3-CNRS et Univ. de Paris 11, F-91898 Orsay CEDEX, France*
50. *Dept. of Physics and Astronomy, University of Ghent, Proeftuinstraat 86, B-9000 Ghent, Belgium*
51. *King Abdulaziz University, Jeddah, Saudi Arabia*
52. *Institut für Theoretische Physik, Universität Tübingen, Auf der Morgenstelle 14, D-72076 Tübingen, Germany*
53. *Santa Cruz Institute for Particle Physics, University of California, Santa Cruz, CA 95064, USA*
54. *KEK, High Energy Accelerator Research Organization, Oho, Tsukuba-shi, Ibaraki-ken 305-0801, Japan*
55. *Lawrence Livermore National Laboratory, 7000 East Ave., Livermore, CA 94550, USA*
56. *Institut für Kernphysik and Institute for Advanced Simulation, Forschungszentrum Jülich, Jülich, Germany*
57. *Department of Physics, Hillsdale College, Hillsdale, MI 49242, USA*
58. *Laboratory of Elementary-Particle Physics, Cornell University, Ithaca, NY 14853, USA*
59. *IFIC — Instituto de Física Corpuscular, Universitat de València — C.S.I.C., E-46071 València, Spain*
60. *Department of Physics, Tohoku University, Aoba-ku, Sendai 980-8578, Japan*
61. *Department of Physics and Astronomy, University of Delaware, Newark, DE 19716, USA*
62. *Los Alamos National Laboratory, Los Alamos, NM 87545, USA*
63. *University of Victoria, Victoria, BC V8W 3P6, Canada*
64. *Nuclear Science Division, Lawrence Berkeley National Laboratory, 1 Cyclotron Road, Berkeley, CA 94720, USA*
65. *Helmholtz-Institut für Strahlen- und Kernphysik, Universität Bonn, Bonn, Germany*
66. *Institute for Particle Physics Phenomenology, Department of Physics, University of Durham, Durham DH1 3LE, UK*
67. *Department of Physics, University of Warwick, Coventry, CV4 7AL, UK*
68. *Institute of Physics, University of Basel, CH-4056 Basel, Switzerland*
69. *Yonsei University, Department of Physics, 134 Sinchon-dong, Sudaemoon-gu, Seoul 120-749, South Korea*
70. *Department of Physics and Astronomy, University College London, Gower Street, London WC1E 6BT, UK*
71. *University of Glasgow, School of Physics and Astronomy, Glasgow G12 8QQ, Scotland, UK*
72. *School of Natural Science, Institute for Advanced Study, Princeton, NJ 08540, USA*
73. *Astronomy Centre, University of Sussex, Falmer, Brighton BN1 9QH, UK*
74. *Department of Physics, University of Illinois, 1110 W. Green Street, Urbana, IL 61801, USA*
75. *Physics Department, Brookhaven National Laboratory, Upton, NY 11973, USA*
76. *Department Physik, Universität Siegen, Walter-Flex-Str. 3, 57068 Siegen, Germany*
77. *Department of Physics, University of California at San Diego, La Jolla, CA 92093, USA*
78. *INFN Sezione di Cagliari, Cittadella Universitaria de Monserrato, Casella postale 170, I-09042 Monserrato (CA), Italy*
79. *Department of Physics and Astronomy, Louisiana State University, Baton Rouge, LA 70803*
80. *Fysikum, Stockholms Universitet, AlbaNova University Centre, SE-106 91 Stockholm, Sweden*

81. *Institució Catalana de Recerca i Estudis Avancats, Institut de Física d'Altes Energies, E-08193 Bellaterra (Barcelona), Spain*
82. *DESY-Zeuthen, D-15735 Zeuthen, Germany*
83. *Brown University, Department of Physics, 182 Hope Street, Providence, RI 02912, USA*
84. *INFN, Sez. di Milano-Bicocca, Piazza della Scienza, 3, I-20126 Milano, Italy*
85. *Dpto. de Física Teórica y del Cosmos & C.A.F.P.E., Universidad de Granada, 18071 Granada, Spain*
86. *Institut für Physik, Johannes-Gutenberg Universität Mainz, D-55099 Mainz, Germany*
87. *Weizmann Institute of Science, Department of Particle Physics and Astrophysics, P.O. Box 26 Rehovot 76100, Israel*
88. *University of Minnesota, School of Physics and Astronomy, 116 Church St. S.E., Minneapolis, MN 55455, USA*
89. *Dipartimento di Fisica e INFN, Università di Genova, I-16146 Genova, Italy*
90. *Institute for Astronomy, University of Edinburgh, Royal Observatory, Blackford Hill, Edinburgh, EH9 3JZ, Scotland, UK*
91. *SISSA/INFN, via Bonomea, 265, 34136 Trieste TS, Italy*
92. *INRNE, Bulgarian Academy of Sciences, 1784 Sofia, Bulgaria*
93. *Department of Physics and Astronomy University of Alabama, 206 Gallalee Hall, Box 870324, Tuscaloosa, AL 35487-0324, USA*
94. *Departament de Física, Universitat Autònoma de Barcelona, 08193 Bellaterra, Barcelona, Spain*
95. *INFN and Dipartimento di Fisica, Università di Pisa, I-56127 Pisa, Italy*
96. *Georg-August-Universität Göttingen, II. Physikalisches Institut, Friedrich-Hund-Platz 1, D-37077 Göttingen, Germany*
97. *Max-Planck-Institut für Physik (Werner-Heisenberg-Institut), Föhringer Ring 6, D-80805 München, Germany*
98. *SLAC National Accelerator Laboratory, 2575 Sand Hill Road, Menlo Park, CA 94025, USA*
99. *DOE, 1000 Independence Ave, SW, SC-25 Germantown Bldg, Washington, DC 20585, USA*
100. *Moscow Engineering and Physics Institute, 31, Kashirskoye shosse, 115409 Moscow, Russia*
101. *School of Physics and Astronomy, University of Southampton, Highfield, Southampton SO17 1BJ, UK*
102. *Department of Physics, Princeton University, Princeton, NJ 08544, USA*
103. *LPTHE, UPMC Université de Paris 6, CNRS UMR 7589, 4 place Jussieu, Paris, France*
104. *Rudolf Peierls Centre for Theoretical Physics, University of Oxford, 1 Keble Road, Oxford OX1 3NP, UK*
105. *Ecole Polytechnique Fédérale de Lausanne (EPFL), CH-1015 Lausanne, Switzerland*
106. *Physics Department, Duke University, Durham, NC 27708, USA*
107. *Department of Physics and Astronomy, University of British Columbia, Vancouver, BC V6T 1Z1, Canada*
108. *Columbia University, Nevis Labs, PO Box 137, Irvington, NY 10533, USA*
109. *Department of Theoretical Physics, Lund University, S-223 62 Lund, Sweden*
110. *Department of Physics and Astronomy, University of Tennessee, Knoxville, TN 37996, USA*
111. *III. Physikalisches Institut, Physikzentrum, RWTH Aachen University, 52056 Aachen, Germany*
112. *High Energy Physics Laboratory, Tokyo Metropolitan University, Tokyo, 192-0397, Japan*
113. *Michigan State University, National Superconducting Cyclotron Laboratory, East Lansing, MI 48824, USA*
114. *Kobayashi-Maskawa Institute, Nagoya University, Chikusa-ku, Nagoya 464-0028, Japan*
115. *Department of Physics, University of California, Davis, CA 95616, USA*
116. *CEA/Saclay, B.P.2, Orme des Merisiers, F-91191 Gif-sur-Yvette Cedex, France*
117. *Department of Physics, POB 64 FIN-00014 University of Helsinki, Finland*
118. *Department of Physics and Astronomy, University of Sheffield, Sheffield S3 7RH, UK*
119. *Department of Physics, Iowa State University, Ames, IA 50011, USA*
120. *Department of Physics, Carleton University, 1125 Colonel By Drive, Ottawa, ON K1S 5B6, Canada*
121. *California Institute of Technology, Kellogg Radiation Laboratory 106-38, Pasadena, CA 91125, USA*
122. *Division of Theoretical Physics, Department of Mathematical Sciences, The University of Liverpool, Liverpool, L69 3BX, UK*
123. *Cavendish Laboratory, J.J. Thomson Avenue, Cambridge CB3 0HE, UK*
124. *Dept. of Physics, Colorado School of Mines, Golden Colorado, 80401 USA*
125. *Department of Physics, Carnegie Mellon University, Pittsburgh, PA 15213, USA*
126. *STFC Rutherford Appleton Laboratory, Didcot, OX11 0QX, UK*
127. *Department of Physics, George Washington University Virginia Campus, Ashburn, VA 20147-2604, USA*
128. *IHEP, Chinese Academy of Sciences, Beijing 100049, P.R. China*
129. *California Institute of Technology, High Energy Physics, MC 256-48, Pasadena, CA 91125, USA*

## HIGHLIGHTS OF THE 2012 EDITION OF THE REVIEW OF PARTICLE PHYSICS

644 new papers with 2658 new measurements

- Over 100 papers from **LHC** experiments (ATLAS, CMS, and LHCb).
- Major exclusions in **SUSY** results from the LHC.
- Latest from **B-meson** physics: 120 papers with 555 measurements, including first LHCb results. Stringent limits on  $B_s \rightarrow \mu^+ \mu^-$  from LHCb and CMS approaching the SM expectation.
- Updated and new results in **neutrino mixing**, including observation of mixing angle  $\theta_{13}$  from reactor experiments.
- 63 new **top** results since 2010, many from LHC experiments.
- New CDF/D0 value of **W-mass** with very small error, impact on prediction of Higgs mass.
- New  $\eta_c(1S)$  branching ratio fit removing circular dependencies.
- First observations of  $h_b(1P)$ ,  $h_b(2P)$ , and the  $\chi_b(3P)$  triplet, as well as two exotic charged states with bottomonium content (unconfirmed).

112 reviews (most are revised or new)

- **New reviews on:**
  - Heavy-Quark and Soft-Collinear Effective Theory
  - Neutrino Cross Section Measurements
  - Neutrino Beam Lines at High-Energy Proton Synchrotrons
  - Monte Carlo Event Generators
  - Lattice QCD
  - Scalar Meson and  $\sigma(500)$  Parameters
  - Heavy Quarkonium Spectroscopy
- **Significant update/revision** to reviews on:
  - **Higgs Boson** (with addendum on new **July 2012 results**)
  - **Astrophysical Constants** (extended to include more cosmological parameters from the **7-year WMAP** analysis)
  - **Dark Matter**
  - **Top Quark** with detailed coverage of LHC results
  - $V_{cb}$  and  $V_{ub}$  **CKM elements**
  - **Quantum Chromodynamics**
  - **High-Energy Collider Parameters** (includes CLIC and latest LHC parameters)
  - Particle Detectors for Non-Accel. Physics (addition of **Coherent Radio Cherenkov Detectors**)

See [pdgLive.lbl.gov](http://pdgLive.lbl.gov) for online access to PDG database.

See [pdg.lbl.gov/AtomicNuclearProperties](http://pdg.lbl.gov/AtomicNuclearProperties) for Atomic Properties of Materials.

---

**TABLE OF CONTENTS**

<b>HIGHLIGHTS</b>	5		
<b>INTRODUCTION</b>		<b>Astrophysics and Cosmology</b>	
1. Overview	11	20. Experimental tests of gravitational theory (rev.)	259
2. Particle Listings responsibilities	11	21. Big-Bang cosmology (rev.)	264
3. Consultants	12	22. Big-Bang nucleosynthesis (rev.)	275
4. Naming scheme for hadrons	13	23. The cosmological parameters (rev.)	280
5. Procedures	13	24. Dark matter (rev.)	289
5.1 Selection and treatment of data	13	25. Cosmic microwave background (rev.)	297
5.2 Averages and fits	14	26. Cosmic rays (rev.)	305
5.2.1 Treatment of errors	14	<b>Experimental Methods and Colliders</b>	
5.2.2 Unconstrained averaging	14	27. Accelerator physics of colliders (rev.)	313
5.2.3 Constrained fits	15	28. High-energy collider parameters (rev.)	317
5.3 Rounding	16	29. Neutrino Beam Lines at High-Energy Proton Synchrotrons (new)	322
5.4 Discussion	16	30. Passage of particles through matter (rev.)	323
History plots (rev.)	17	31. Particle detectors at accelerators (rev.)	339
Online particle physics information (rev.)	18	32. Particle detectors for non-accelerator phys. (rev.)	368
		33. Radioactivity and radiation protection (rev.)	381
<b>PARTICLE PHYSICS SUMMARY TABLES</b>		34. Commonly used radioactive sources	385
Gauge and Higgs bosons	27	<b>Mathematical Tools or Statistics, Monte Carlo, Group Theory</b>	
Leptons	30	35. Probability (rev.)	386
Quarks	33	36. Statistics (rev.)	390
Mesons	34	37. Monte Carlo techniques (rev.)	402
Baryons	78	38. Monte Carlo Generators (new)	405
Searches (Supersymmetry, Compositeness, <i>etc.</i> )	93	39. Monte Carlo particle numbering scheme (rev.)	415
Tests of conservation laws	95	40. Clebsch-Gordan coefficients, spherical harmonics, and <i>d</i> functions	419
<b>REVIEWS, TABLES, AND PLOTS</b>		41. SU(3) isoscalar factors and representation matrices	420
<b>Constants, Units, Atomic and Nuclear Properties</b>		42. SU( <i>n</i> ) multiplets and Young diagrams	421
1. Physical constants (rev.)	107	<b>Kinematics, Cross-Section Formulae, and Plots</b>	
2. Astrophysical constants (rev.)	108	43. Kinematics (rev.)	422
3. International System of Units (SI)	110	44. Cross-section formulae for specific processes (rev.)	427
4. Periodic table of the elements (rev.)	111	45. Neutrino Cross Section Measurements (new)	436
5. Electronic structure of the elements	112	46. Plots of cross sections and related quantities (rev.)	439
6. Atomic and nuclear properties of materials	114		
7. Electromagnetic relations	116		
8. Naming scheme for hadrons	118		
<b>Standard Model and Related Topics</b>			
9. Quantum chromodynamics (rev.)	120		
10. Electroweak model and constraints on new physics (rev.)	136		
11. The Cabibbo-Kobayashi-Maskawa quark-mixing matrix (rev.)	157		
12. <i>CP</i> violation (rev.)	166		
13. Neutrino Mass, Mixing, and Oscillations (rev.)	177		
14. Quark model (rev.)	199		
15. Grand Unified Theories (rev.)	209		
16. Heavy-Quark & Soft-Collinear Effective Theory (new)	218		
17. Lattice Quantum Chromodynamics (new)	225		
18. Structure functions (rev.)	234		
19. Fragmentation functions in $e^+e^-$ , $ep$ and $pp$ collisions (rev.)	249		

(Continued on next page.)

## PARTICLE LISTINGS\*

<b>Illustrative key and abbreviations</b>	457
<b>Gauge and Higgs bosons</b>	
( $\gamma$ , gluon, graviton, $W$ , $Z$ , Higgs, Axions)	469
<b>Leptons</b>	
( $e$ , $\mu$ , $\tau$ , Heavy-charged lepton searches,	581
Neutrino properties, Number of neutrino types	
Double- $\beta$ decay, Neutrino mixing,	
Heavy-neutral lepton searches)	
<b>Quarks</b>	
( $u$ , $d$ , $s$ , $c$ , $b$ , $t$ , $b'$ , $t'$ ( $4^{th}$ generation), Free quarks)	655
<b>Mesons</b>	
Light unflavored ( $\pi$ , $\rho$ , $a$ , $b$ ) ( $\eta$ , $\omega$ , $f$ , $\phi$ , $h$ )	695
Other light unflavored	815
Strange ( $K$ , $K^*$ )	820
Charmed ( $D$ , $D^*$ )	885
Charmed, strange ( $D_s$ , $D_s^*$ , $D_{sJ}$ )	941
Bottom ( $B$ , $V_{cb}/V_{ub}$ , $B^*$ , $B_J^*$ )	963
Bottom, strange ( $B_s$ , $B_s^*$ , $B_{sJ}^*$ )	1128
Bottom, charmed ( $B_c$ )	1139
$c\bar{c}$ ( $\eta_c$ , $J/\psi(1S)$ , $\chi_c$ , $h_c$ , $\psi$ )	1146
$b\bar{b}$ ( $\eta_b$ , $\Upsilon$ , $\chi_b$ , $h_b$ )	1223
<b>Baryons</b>	
$N$	1253
$\Delta$	1305
$\Lambda$	1327
$\Sigma$	1343
$\Xi$	1367
$\Omega$	1380
Charmed ( $\Lambda_c$ , $\Sigma_c$ , $\Xi_c$ , $\Omega_c$ )	1383
Doubly charmed ( $\Xi_{cc}$ )	1404
Bottom ( $\Lambda_b$ , $\Sigma_b$ , $\Sigma_b^*$ , $\Xi_b$ , $\Omega_b$ , $b$ -baryon admixture)	1405
<b>Miscellaneous searches</b>	
Monopoles	1413
Supersymmetry	1420
Technicolor	1475
Compositeness	1484
Extra Dimensions	1489
Searches for WIMPs and Other Particles	1500

<b>INDEX</b>	1511
--------------	------

## MAJOR REVIEWS IN THE PARTICLE LISTINGS

<b>Gauge and Higgs bosons</b>	
The Mass of the $W$ Boson (rev.)	470
Triple Gauge Couplings (rev.)	474
Anomalous $W/Z$ Quartic Couplings (rev.)	477
The $Z$ Boson	478
Anomalous $ZZ\gamma$ , $Z\gamma\gamma$ , and $ZZV$ Couplings (rev.)	498
Searches for Higgs Bosons (rev.)	501
The $W'$ Searches (rev.)	543
The $Z'$ Searches (rev.)	547
Leptoquarks (rev.)	555
Axions and Other Very Light Bosons (rev.)	562
<b>Leptons</b>	
Muon Anomalous Magnetic Moment (rev.)	587
Muon Decay Parameters (rev.)	587
$\tau$ Branching Fractions (rev.)	596
$\tau$ -Lepton Decay Parameters	617
Number of Light Neutrino Types	629
Neutrinoless Double- $\beta$ Decay (rev.)	631
<b>Quarks</b>	
Quark Masses (rev.)	655
The Top Quark (rev.)	668
Free Quark Searches	688
<b>Mesons</b>	
Form Factors for Rad. Pion & Kaon Decays	696
Note on Scalar Mesons (rev.)	706
The $\eta(1405)$ , $\eta(1475)$ , $f_1(1420)$ , and $f_1(1510)$ (rev.)	759
Rare Kaon Decays (rev.)	822
$K_{\ell 3}^{\pm}$ and $K_{\ell 3}^0$ Form Factors (rev.)	833
$CPT$ Invariance Tests in Neutral Kaon Decay (rev.)	839
$CP$ Violation in $K_S \rightarrow 3\pi$	845
$V_{ud}$ , $V_{us}$ , Cabibbo Angle, and CKM Unitarity (rev.)	852
$CP$ -Violation in $K_L$ Decays (rev.)	859
Dalitz-Plot Analysis Formalism (rev.)	889
Review of Charm Dalitz-Plot Analyses	893
$D^0-\bar{D}^0$ Mixing (rev.)	903
$D_s^+$ Branching Fractions	943
Decay Cons. of Charged Pseudoscalar Mesons (rev.)	946
Production and Decay of $b$ -flavored Hadrons (rev.)	963
Polarization in $B$ Decays (rev.)	1060
$B^0-\bar{B}^0$ Mixing (rev.)	1066
Determination of $V_{cb}$ and $V_{ub}$ (rev.)	1111
Heavy Quarkonium Spectroscopy (new)	1139
Branching Ratios of $\psi(2S)$ and $\chi_{c0,1,2}$ (rev.)	1168
<b>Baryons</b>	
Baryon Decay Parameters	1264
$N$ and $\Delta$ Resonances (rev.)	1268
Radiative Hyperon Decays	1368
Charmed Baryons (rev.)	1383
$\Lambda_c^+$ Branching Fractions	1386
<b>Miscellaneous searches</b>	
Magnetic Monopoles (rev.)	1413
Supersymmetry (rev.)	1420
Dynamical Electroweak Symmetry Breaking (rev.)	1475
Searches for Quark & Lepton Compositeness	1484
Extra Dimensions (rev.)	1489

\*The divider sheets give more detailed indices for each main section of the Particle Listings.



## INTRODUCTION

1. Overview	11
2. Particle Listings responsibilities	11
3. Consultants	12
4. Naming scheme for hadrons	13
5. Procedures	13
5.1 Selection and treatment of data	13
5.2 Averages and fits	14
5.2.1 Treatment of errors	14
5.2.2 Unconstrained averaging	14
5.2.3 Constrained fits	15
5.3 Rounding	16
5.4 Discussion	16
History plots	17

## ONLINE PARTICLE PHYSICS INFORMATION

1. Introduction	18
2. Particle Data Group (PDG) Resources	18
3. Particle Physics Information Platforms	18
4. Literature Databases	18
5. Particle Physics Journals and Conference Proceedings Series	19
6. Conference Databases	19
7. Research Institutions	19
8. People	19
9. Experiments	19
10. Jobs	20
11. Software Repositories	20
12. Data Repositories	21
13. Data preservation	21
14. Particle Physics Education and Outreach Sites	21





## INTRODUCTION

### 1. Overview

The *Review of Particle Physics* and the abbreviated version, the *Particle Physics Booklet*, are reviews of the field of Particle Physics. This complete *Review* includes a compilation/evaluation of data on particle properties, called the “Particle Listings.” These Listings include 2,658 new measurements from 644 papers, in addition to the 29,495 measurements from 8,300 papers that first appeared in previous editions [1].

Both books include Summary Tables with our best values and limits for particle properties such as masses, widths or lifetimes, and branching fractions, as well as an extensive summary of searches for hypothetical particles. In addition, we give a long section of “Reviews, Tables, and Plots” on a wide variety of theoretical and experimental topics, a quick reference for the practicing particle physicist.

The *Review* and the *Booklet* are published in even-numbered years. This edition is an updating through January 2012 (and, in some areas, well into 2012). As described in the section “Online Particle Physics Information” following this introduction, the content of this *Review* is available on the World-Wide Web, and is updated between printed editions (<http://pdg.lbl.gov/>).

The Summary Tables give our best values of the properties of the particles we consider to be well established, a summary of search limits for hypothetical particles, and a summary of experimental tests of conservation laws.

The Particle Listings contain all the data used to get the values given in the Summary Tables. Other measurements considered recent enough or important enough to mention, but which for one reason or another are not used to get the best values, appear separately just beneath the data we do use for the Summary Tables. The Particle Listings also give information on unconfirmed particles and on particle searches, as well as short “reviews” on subjects of particular interest or controversy.

The Particle Listings were once an archive of all published data on particle properties. This is no longer possible because of the large quantity of data. We refer interested readers to earlier editions for data now considered to be obsolete.

We organize the particles into six categories:

- Gauge and Higgs bosons
- Leptons
- Quarks
- Mesons
- Baryons
- Searches for monopoles, supersymmetry, compositeness, extra dimensions, *etc.*

The last category only includes searches for particles that do not belong to the previous groups; searches for heavy charged leptons and massive neutrinos, by contrast, are with the leptons.

In Sec. 2 of this Introduction, we list the main areas of responsibility of the authors, and also list our large number of consultants, without whom we would not have been able to produce this *Review*. In Sec. 4, we mention briefly the naming scheme for hadrons. In Sec. 5, we discuss our procedures for choosing among measurements of particle properties and for obtaining best values of the properties

from the measurements.

The accuracy and usefulness of this *Review* depend in large part on interaction between its users and the authors. We appreciate comments, criticisms, and suggestions for improvements of any kind. Please send them to the appropriate author, according to the list of responsibilities in Sec. 2 below, or to the LBNL addresses below.

To order a copy of the *Review* or the *Particle Physics Booklet* from North and South America, Australia, and the Far East, send email to [PDG@LBL.GOV](mailto:PDG@LBL.GOV)

or via the web at:

<http://pdg.lbl.gov/pdgmail>

or write to:

Particle Data Group, MS 50R6008  
Lawrence Berkeley National Laboratory  
Berkeley, CA 94720-8166, USA

From all other areas email [library.desk@cern.ch](mailto:library.desk@cern.ch), see <http://library.web.cern.ch/library/Library/request.html>

or write to

CERN Scientific Information Service  
CH-1211 Geneva 23, Switzerland

### 2. Particle Listings responsibilities

\* Asterisk indicates the people to contact with questions or comments about Particle Listings sections.

#### Gauge and Higgs bosons

$\gamma$	C. Grab, D.E. Groom*
Gluons	R.M. Barnett,* A.V. Manohar
Graviton	D.E. Groom*
$W, Z$	A. Gurtu,* M. Grünewald*
Higgs bosons	K. Hikasa, G. Weiglein*
Heavy bosons	K. Copic,* M. Tanabashi
Axions	K.A. Olive, F. Takahashi, G. Raffelt*

#### Leptons

Neutrinos	M. Goodman, C.-J. Lin,* K. Nakamura, K.A. Olive, A. Piepke, P. Vogel
$e, \mu$	J.-F. Arguin,* C. Grab
$\tau$	K.G. Hayes, K. Mönig*

#### Quarks

Quarks	R.M. Barnett,* A.V. Manohar
Top quark	J.-F. Arguin,* K. Hagiwara
$b', t'$	K. Hagiwara, W.-M. Yao*
Free quark	J. Beringer*

#### Mesons

$\pi, \eta$	J.-F. Arguin,* C. Grab
Unstable mesons	C. Amsler, M. Doser,* S. Eidelman,* T. Gutsche, C. Hanhart, B. Heltsley, J.J. Hernández-Rey, A. Masoni, S. Navas, C. Patrignani, S. Spanier, N.A. Törnqvist, G. Venanzoni
$K$ (stable)	G. D’Ambrosio, C.-J. Lin*
$D$ (stable)	D.M. Asner, S. Blusk, C.G. Wohl*
$B$ (stable)	J.-F. Arguin*, M. Kreps, Y. Kwon, J.G. Smith, W.-M. Yao*

Baryons

Stable baryons C. Grab, C.G. Wohl\*  
 Unstable baryons E. Klempt, C.G. Wohl,\* R.L. Workman  
 Charmed baryons S. Blusk, C.G. Wohl\*  
 Bottom baryons M. Kreps, Y. Kwon, J.G. Smith, W.-M. Yao\*

Miscellaneous searches

Monopole D. Milstead\*  
 Supersymmetry A. de Gouvêa, F. Moortgat,  
 K.A. Olive, L. Pape, G. Weiglein\*  
 Technicolor M. Tanabashi, J. Terning\*  
 Compositeness M. Tanabashi, J. Terning\*  
 Extra Dimensions J.-F. Arguin\*, T. Gherghetta  
 WIMPs and Other K. Hikasa,\*

**3. Consultants**

The Particle Data Group benefits greatly from the assistance of some 700 physicists who are asked to verify every piece of data entered into this *Review*. Of special value is the advice of the PDG Advisory Committee which meets biennially and thoroughly reviews all aspects of our operation. The members of the 2012 committee are:

D. Harris (FNAL)  
 P. Janot (CERN)  
 J. Olson (Princeton)  
 G. Perez (Weizmann)  
 J. Tanaka (Tokyo)

We have especially relied on the expertise of the following people for advice on particular topics:

- M. Achasov (BINP, Novosibirsk)
- K.S. Agashe (Maryland)
- H. Aihara (Tokyo)
- S.I. Alekhin (COMPAS Group, IHEP, Protvino)
- F. Anulli (INFN, Rome)
- M. Artuso (Syracuse University)
- H. Bachacou (CEA Saclay)
- S. Banerjee (Victoria U, BC)
- R. Barlow (Manchester U.)
- V. B. Bezerra (UFPb)
- M. Beneke (Aachen, Germany)
- A.M. Bernstein (MIT)
- M. Billing (Cornell University)
- P. B. Mackenzie (FNAL)
- C. Bozzi (INFN, Ferrara)
- T. Brooks (SLAC)
- T. Browder (University of Hawaii)
- O. Bruening (CERN)
- A. Buras (Munich Tech. U.)
- V.D. Burkert (Thomas Jefferson Lab)
- J. Butterworth (UCL)
- A. Chao (SLAC)
- C. Davies (U of Glasgow)
- F. Deliot (CEA, Saclay)
- L. Demortier (Rockefeller University)
- D. Denisov (FNAL)
- J. Dingfelder (Bonn, Germany)
- R. Dixon (FNAL)
- A. Donnachie (University of Manchester)
- A.T. Doyle (Glasgow Univ.)
- W. Fischer (BNL)
- M. Furman (LBNL)

- H. Gallagher (Tufts U.)
- P. Gambino (Univ. degli Studi di Torino)
- R. Garisto (PRL)
- A. Gasparian (NC A&T)
- T. Gershon (U. of Warwick, UK)
- E.W.N. Glover (Durham U)
- B. Golob (U. Ljubljana, Slovenia)
- O. Gonzalez Lopez (CIEMAT, Spain)
- M. Grazzini (U of Zurich)
- E. Gschwendtner (U. of Geneva)
- F. Harris (University of Hawaii)
- R. Harr (Wayne State University)
- R. Hawkings (CERN) - verifier with useful comments
- Y. Hayato (ICRR, U. of Tokyo)
- J. Heinrich (University of Pennsylvania)
- C. Hill (Ohio State)
- G. Isidori (INFN, Frascati)
- R. Itoh (KEK)
- J. Jowett (CERN)
- S.G. Karshenboim (VNIIM, St-Petersburg)
- B. Kayser (FNAL)
- Yu. Khokhlov (IHEP, Protvino)
- S.F. King (Southampton U.)
- T. Kobayashi (KEK)
- S.E. Kopp (U. Texas, Austin)
- T. Koseki (KEK)
- K. Kousouris (FNAL)
- W. Kozanecki (Saclay)
- A. Kronfeld (FNAL)
- S.-I. Kurokawa (KEK)
- L. Lellouch (CNRS Marseilles)
- O. Leroy (CPPM, Marseille)
- E.B. Levichev (BINP, Novosibirsk)
- E. Linder (LBNL)
- R. Louvot (EPFL, Switzerland)
- V. Lubicz (U of Roma 3)
- V. Luth (SLAC)
- L. Lyons (Oxford U.)
- M.L. Mangano (CERN)
- S. Manly (U. of Rochester)
- F. Margaroli (INFN Roma)
- G. Marshall (TRIUMF)
- K. McFarland (U. of Rochester)
- B. Meadows (U. of Cincinnati)
- U.-G. Meißner (U. Bonn & Jülich)
- C. Milardi (INFN, Frascati)
- P.J. Mohr (NIST)
- R. Moore (FNAL)
- U. Mosel (U. Giessen)
- F. Muheim (Edinburgh, England)
- Y. Nakajima (LBNL)
- H. O'Connell (FNAL)
- Y. Ohnishi (KEK, Japan)
- K. Oide (KEK, Japan)
- J.R. Pelaez (UCM, Madrid)
- F. Petriello (Northwestern U.)
- S. Rahatlou (U. of Rome, INFN)
- H. Robertson (U. of Washington)
- N. Roe (LBNL)
- M. Roney (University of Victoria)
- G. Ross (Oxford)

- M. Ross (FNAL)
- M. Rotondo (Padova, INFN)
- K. Sachs (DESY)
- J.E. Sansonetti (NIST)
- D. Schulte (CERN)
- C. Schwanda (HEPHY, Vienna)
- A.J. Schwartz (University of Cincinnati)
- T. Schwetz-Mangold (MPI)
- J.T. Seeman (SLAC)
- G. Senjanovic (ICTP, Trieste)
- M. Seymour (Manchester)
- Yu.M. Shatunov (BINP, Novosibirsk)
- A. Soffer (Tel Aviv, Israel)
- M. Sorel (U. of Valencia)
- S. Stapnes (CERN)
- I. Stewart (MIT)
- S.I. Striganov (COMPAS Group, IHEP, Protvino)
- A. Švarc (Rudjer Bošković Inst., Croatia)
- T. Tait (UC Irvine)
- H. Tanaka (U. of British Columbia)
- R. Tenchini (INFN Pisa)
- R. Tesarek (FNAL)
- J. Thaler (MIT)
- L. Tiator (U. Mainz)
- D. Tonelli (CERN)
- P. Uwer (Humbolt U)
- J. Valle (U. of Valencia)
- R. Van de Water (BNL)
- R. Van Kooten (Indiana University)
- G. Velev (Fermilab)
- M. Verzocchi (FNAL)
- S. Warner (Cornell U.)
- G. Wilkinson (Oxford U.)
- M. Wise (Caltech)
- M. Yokoyama (U. of Tokyo)
- C.Z. Yuan (IHEP, Beijing)
- C. Zhang (IHEP, Beijing)
- B. Zwaska (FNAL)

#### 4. Naming scheme for hadrons

We introduced in the 1986 edition [2] a new naming scheme for the hadrons. Changes from older terminology affected mainly the heavier mesons made of  $u$ ,  $d$ , and  $s$  quarks. Otherwise, the only important change to known hadrons was that the  $F^\pm$  became the  $D_s^\pm$ . None of the lightest pseudoscalar or vector mesons changed names, nor did the  $c\bar{c}$  or  $b\bar{b}$  mesons (we do, however, now use  $\chi_c$  for the  $c\bar{c}$   $\chi$  states), nor did any of the established baryons. The Summary Tables give both the new and old names whenever a change has occurred.

The scheme is described in “Naming Scheme for Hadrons” (p. 118) of this *Review*.

We give here our conventions on type-setting style. Particle symbols are italic (or slanted) characters:  $e^-$ ,  $p$ ,  $\Lambda$ ,  $\pi^0$ ,  $K_L$ ,  $D_s^+$ ,  $b$ . Charge is indicated by a superscript:  $B^-$ ,  $\Delta^{++}$ . Charge is not normally indicated for  $p$ ,  $n$ , or the quarks, and is optional for neutral isosinglets:  $\eta$  or  $\eta^0$ . Antiparticles and particles are distinguished by charge for charged leptons and mesons:  $\tau^+$ ,  $K^-$ . Otherwise, distinct antiparticles are indicated by a bar (overline):  $\bar{\nu}_\mu$ ,  $\bar{t}$ ,  $\bar{p}$ ,  $\bar{K}^0$ , and  $\bar{\Sigma}^+$  (the antiparticle of the  $\Sigma^-$ ).

#### 5. Procedures

**5.1. Selection and treatment of data :** The Particle Listings contain all relevant data known to us that are published in journals. With very few exceptions, we do not include results from preprints or conference reports. Nor do we include data that are of historical importance only (the Listings are not an archival record). We search every volume of 20 journals through our cutoff date for relevant data. We also include later published papers that are sent to us by the authors (or others).

In the Particle Listings, we clearly separate measurements that are used to calculate or estimate values given in the Summary Tables from measurements that are not used. We give explanatory comments in many such cases. Among the reasons a measurement might be excluded are the following:

- It is superseded by or included in later results.
- No error is given.
- It involves assumptions we question.
- It has a poor signal-to-noise ratio, low statistical significance, or is otherwise of poorer quality than other data available.
- It is clearly inconsistent with other results that appear to be more reliable. Usually we then state the criterion, which sometimes is quite subjective, for selecting “more reliable” data for averaging. See Sec. 5.4.
- It is not independent of other results.
- It is not the best limit (see below).
- It is quoted from a preprint or a conference report.

In some cases, *none* of the measurements is entirely reliable and no average is calculated. For example, the masses of many of the baryon resonances, obtained from partial-wave analyses, are quoted as estimated ranges thought to probably include the true values, rather than as averages with errors. This is discussed in the Baryon Particle Listings.

For upper limits, we normally quote in the Summary Tables the strongest limit. We do not average or combine upper limits except in a very few cases where they may be re-expressed as measured numbers with Gaussian errors.

As is customary, we assume that particle and antiparticle share the same spin, mass, and mean life. The Tests of Conservation Laws table, following the Summary Tables, lists tests of  $CPT$  as well as other conservation laws.

We use the following indicators in the Particle Listings to tell how we get values from the tabulated measurements:

- OUR AVERAGE—From a weighted average of selected data.
- OUR FIT—From a constrained or overdetermined multi-parameter fit of selected data.
- OUR EVALUATION—Not from a direct measurement, but evaluated from measurements of related quantities.
- OUR ESTIMATE—Based on the observed range of the data. Not from a formal statistical procedure.
- OUR LIMIT—For special cases where the limit is evaluated by us from measured ratios or other data. Not from a direct measurement.

An experimentalist who sees indications of a particle will of course want to know what has been seen in that region in the past. Hence we include in the Particle Listings all

reported states that, in our opinion, have sufficient statistical merit and that have not been disproved by more reliable data. However, we promote to the Summary Tables only those states that we feel are well established. This judgment is, of course, somewhat subjective and no precise criteria can be given. For more detailed discussions, see the minireviews in the Particle Listings.

**5.2. Averages and fits:** We divide this discussion on obtaining averages and errors into three sections: (1) treatment of errors; (2) unconstrained averaging; (3) constrained fits.

**5.2.1. Treatment of errors:** In what follows, the “error”  $\delta x$  means that the range  $x \pm \delta x$  is intended to be a 68.3% confidence interval about the central value  $x$ . We treat this error as if it were Gaussian. Thus when the error is Gaussian,  $\delta x$  is the usual one standard deviation ( $1\sigma$ ). Many experimenters now give statistical and systematic errors separately, in which case we usually quote both errors, with the statistical error first. For averages and fits, we then add the two errors in quadrature and use this combined error for  $\delta x$ .

When experimenters quote asymmetric errors  $(\delta x)^+$  and  $(\delta x)^-$  for a measurement  $x$ , the error that we use for that measurement in making an average or a fit with other measurements is a continuous function of these three quantities. When the resultant average or fit  $\bar{x}$  is less than  $x - (\delta x)^-$ , we use  $(\delta x)^-$ ; when it is greater than  $x + (\delta x)^+$ , we use  $(\delta x)^+$ . In between, the error we use is a linear function of  $x$ . Since the errors we use are functions of the result, we iterate to get the final result. Asymmetric output errors are determined from the input errors assuming a linear relation between the input and output quantities.

In fitting or averaging, we usually do not include correlations between different measurements, but we try to select data in such a way as to reduce correlations. Correlated errors are, however, treated explicitly when there are a number of results of the form  $A_i \pm \sigma_i \pm \Delta$  that have identical systematic errors  $\Delta$ . In this case, one can first average the  $A_i \pm \sigma_i$  and then combine the resulting statistical error with  $\Delta$ . One obtains, however, the same result by averaging  $A_i \pm (\sigma_i^2 + \Delta_i^2)^{1/2}$ , where  $\Delta_i = \sigma_i \Delta [\sum (1/\sigma_j^2)]^{1/2}$ . This procedure has the advantage that, with the modified systematic errors  $\Delta_i$ , each measurement may be treated as independent and averaged in the usual way with other data. Therefore, when appropriate, we adopt this procedure. We tabulate  $\Delta$  and invoke an automated procedure that computes  $\Delta_i$  before averaging and we include a note saying that there are common systematic errors.

Another common case of correlated errors occurs when experimenters measure two quantities and then quote the two and their difference, e.g.,  $m_1$ ,  $m_2$ , and  $\Delta = m_2 - m_1$ . We cannot enter all of  $m_1$ ,  $m_2$  and  $\Delta$  into a constrained fit because they are not independent. In some cases, it is a good approximation to ignore the quantity with the largest error and put the other two into the fit. However, in some cases correlations are such that the errors on  $m_1$ ,  $m_2$  and  $\Delta$  are comparable and none of the three values can be ignored. In this case, we put all three values into the fit and invoke an automated procedure to increase the errors prior to fitting such that the three quantities can be treated as independent measurements in the constrained fit. We include a note saying that this has been done.

**5.2.2. Unconstrained averaging:** To average data, we use a standard weighted least-squares procedure and in some cases, discussed below, increase the errors with a “scale factor.” We begin by assuming that measurements of a given quantity are uncorrelated, and calculate a weighted average and error as

$$\bar{x} \pm \delta\bar{x} = \frac{\sum_i w_i x_i}{\sum_i w_i} \pm (\sum_i w_i)^{-1/2}, \quad (1)$$

where

$$w_i = 1/(\delta x_i)^2.$$

Here  $x_i$  and  $\delta x_i$  are the value and error reported by the  $i$ th experiment, and the sums run over the  $N$  experiments. We then calculate  $\chi^2 = \sum w_i (\bar{x} - x_i)^2$  and compare it with  $N - 1$ , which is the expectation value of  $\chi^2$  if the measurements are from a Gaussian distribution.

If  $\chi^2/(N - 1)$  is less than or equal to 1, and there are no known problems with the data, we accept the results.

If  $\chi^2/(N - 1)$  is very large, we may choose not to use the average at all. Alternatively, we may quote the calculated average, but then make an educated guess of the error, a conservative estimate designed to take into account known problems with the data.

Finally, if  $\chi^2/(N - 1)$  is greater than 1, but not greatly so, we still average the data, but then also do the following:

(a) We increase our quoted error,  $\delta\bar{x}$  in Eq. (1), by a scale factor  $S$  defined as

$$S = [\chi^2/(N - 1)]^{1/2}. \quad (2)$$

Our reasoning is as follows. The large value of the  $\chi^2$  is likely to be due to underestimation of errors in at least one of the experiments. Not knowing which of the errors are underestimated, we assume they are all underestimated by the same factor  $S$ . If we scale up all the input errors by this factor, the  $\chi^2$  becomes  $N - 1$ , and of course the output error  $\delta\bar{x}$  scales up by the same factor. See Ref. 3.

When combining data with widely varying errors, we modify this procedure slightly. We evaluate  $S$  using only the experiments with smaller errors. Our cutoff or ceiling on  $\delta x_i$  is arbitrarily chosen to be

$$\delta_0 = 3N^{1/2} \delta\bar{x},$$

where  $\delta\bar{x}$  is the unscaled error of the mean of all the experiments. Our reasoning is that although the low-precision experiments have little influence on the values  $\bar{x}$  and  $\delta\bar{x}$ , they can make significant contributions to the  $\chi^2$ , and the contribution of the high-precision experiments thus tends to be obscured. Note that if each experiment has the same error  $\delta x_i$ , then  $\delta\bar{x}$  is  $\delta x_i/N^{1/2}$ , so each  $\delta x_i$  is well below the cutoff. (More often, however, we simply exclude measurements with relatively large errors from averages and fits: new, precise data chase out old, imprecise data.)

Our scaling procedure has the property that if there are two values with comparable errors separated by much more than their stated errors (with or without a number of other values of lower accuracy), the scaled-up error  $\delta\bar{x}$  is approximately half the interval between the two discrepant values.

We emphasize that our scaling procedure for *errors* in no way affects central values. And if you wish to recover the unscaled error  $\delta\bar{x}$ , simply divide the quoted error by  $S$ .

(b) If the number  $M$  of experiments with an error smaller than  $\delta_0$  is at least three, and if  $\chi^2/(M-1)$  is greater than 1.25, we show in the Particle Listings an ideogram of the data. Figure 1 is an example. Sometimes one or two data points lie apart from the main body; other times the data split into two or more groups. We extract no numbers from these ideograms; they are simply visual aids, which the reader may use as he or she sees fit.

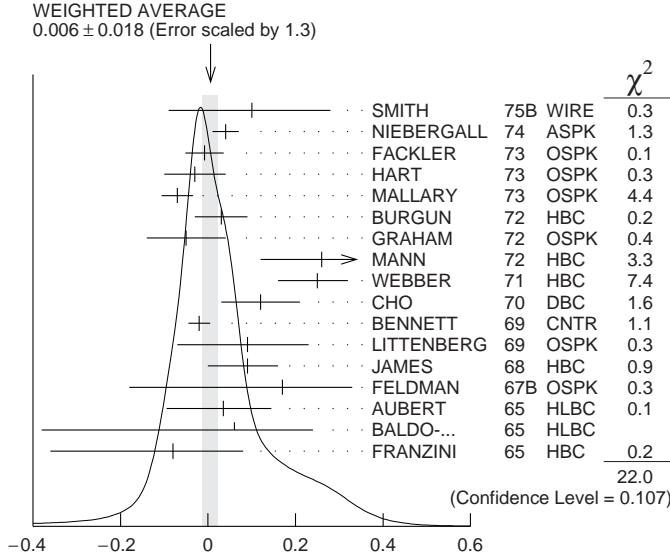


**Figure 1:** A typical ideogram. The arrow at the top shows the position of the weighted average, while the width of the shaded pattern shows the error in the average after scaling by the factor  $S$ . The column on the right gives the  $\chi^2$  contribution of each of the experiments. Note that the next-to-last experiment, denoted by the incomplete error flag ( $\perp$ ), is not used in the calculation of  $S$  (see the text).

Each measurement in an ideogram is represented by a Gaussian with a central value  $x_i$ , error  $\delta x_i$ , and area proportional to  $1/\delta x_i$ . The choice of  $1/\delta x_i$  for the area is somewhat arbitrary. With this choice, the center of gravity of the ideogram corresponds to an average that uses weights  $1/\delta x_i$  rather than the  $(1/\delta x_i)^2$  actually used in the averages. This may be appropriate when some of the experiments have seriously underestimated systematic errors. However, since for this choice of area the height of the Gaussian for each measurement is proportional to  $(1/\delta x_i)^2$ , the peak position of the ideogram will often favor the high-precision measurements at least as much as does the least-squares average. See our 1986 edition [2] for a detailed discussion of the use of ideograms.

**5.2.3. Constrained fits:** In some cases, such as branching ratios or masses and mass differences, a constrained fit may be needed to obtain the best values of a set of parameters. For example, most branching ratios and rate measurements are analyzed by making a simultaneous least-squares fit to all the data and extracting the partial decay fractions  $P_i$ , the partial widths  $\Gamma_i$ , the full width  $\Gamma$  (or mean life), and the associated error matrix.

Assume, for example, that a state has  $m$  partial decay fractions  $P_i$ , where  $\sum P_i = 1$ . These have been measured in  $N_r$  different ratios  $R_r$ , where, e.g.,  $R_1 = P_1/P_2$ ,  $R_2$

$= P_1/P_3$ , etc. [We can handle any ratio  $R$  of the form  $\sum \alpha_i P_i / \sum \beta_i P_i$ , where  $\alpha_i$  and  $\beta_i$  are constants, usually 1 or 0. The forms  $R = P_i P_j$  and  $R = (P_i P_j)^{1/2}$  are also allowed.] Further assume that each ratio  $R$  has been measured by  $N_k$  experiments (we designate each experiment with a subscript  $k$ , e.g.,  $R_{1k}$ ). We then find the best values of the fractions  $P_i$  by minimizing the  $\chi^2$  as a function of the  $m-1$  independent parameters:

$$\chi^2 = \sum_{r=1}^{N_r} \sum_{k=1}^{N_k} \left( \frac{R_{rk} - R_r}{\delta R_{rk}} \right)^2, \quad (3)$$

where the  $R_{rk}$  are the measured values and  $R_r$  are the fitted values of the branching ratios.

In addition to the fitted values  $\bar{P}_i$ , we calculate an error matrix  $\langle \delta \bar{P}_i \delta \bar{P}_j \rangle$ . We tabulate the diagonal elements of  $\delta \bar{P}_i = \langle \delta \bar{P}_i \delta \bar{P}_i \rangle^{1/2}$  (except that some errors are scaled as discussed below). In the Particle Listings, we give the complete correlation matrix; we also calculate the fitted value of each ratio, for comparison with the input data, and list it above the relevant input, along with a simple unconstrained average of the same input.

Three comments on the example above:

(1) There was no connection assumed between measurements of the full width and the branching ratios. But often we also have information on partial widths  $\Gamma_i$  as well as the total width  $\Gamma$ . In this case we must introduce  $\Gamma$  as a parameter in the fit, along with the  $P_i$ , and we give correlation matrices for the widths in the Particle Listings.

(2) We try to pick those ratios and widths that are as independent and as close to the original data as possible. When one experiment measures all the branching fractions and constrains their sum to be one, we leave one of them (usually the least well-determined one) out of the fit to make the set of input data more nearly independent. We now do allow for correlations between input data.

(3) We calculate scale factors for both the  $R_r$  and  $P_i$  when the measurements for any  $R$  give a larger-than-expected contribution to the  $\chi^2$ . According to Eq. (3), the double sum for  $\chi^2$  is first summed over experiments  $k = 1$  to  $N_k$ , leaving a single sum over ratios  $\chi^2 = \sum \chi_r^2$ . One is tempted to define a scale factor for the ratio  $r$  as  $S_r = \chi_r^2 / \langle \chi_r^2 \rangle$ . However, since  $\langle \chi_r^2 \rangle$  is not a fixed quantity (it is somewhere between  $N_k$  and  $N_{k-1}$ ), we do not know how to evaluate this expression. Instead we define

$$S_r^2 = \frac{1}{N_k} \sum_{k=1}^{N_k} \frac{(R_{rk} - \bar{R}_r)^2}{\langle (R_{rk} - \bar{R}_r)^2 \rangle}. \quad (4)$$

With this definition the expected value of  $S_r^2$  is one. We can show that

$$\langle (R_{rk} - \bar{R}_r)^2 \rangle = \langle (\delta R_{rk})^2 \rangle - (\delta \bar{R}_r)^2, \quad (5)$$

where  $\delta \bar{R}_r$  is the fitted error for ratio  $r$ .

The fit is redone using errors for the branching ratios that are scaled by the larger of  $S_r$  and unity, from which new and often larger errors  $\delta \bar{P}_i'$  are obtained. The scale factors we finally list in such cases are defined by  $S_i = \delta \bar{P}_i' / \delta \bar{P}_i$ . However, in line with our policy of not letting  $S$  affect the central values, we give the values of  $\bar{P}_i$  obtained from the original (unscaled) fit.

There is one special case in which the errors that are obtained by the preceding procedure may be changed. When a fitted branching ratio (or rate)  $\overline{P}_i$  turns out to be less than three standard deviations ( $\delta\overline{P}_i'$ ) from zero, a new smaller error ( $\delta\overline{P}_i''$ )<sup>-</sup> is calculated on the low side by requiring the area under the Gaussian between  $\overline{P}_i - (\delta\overline{P}_i'')^-$  and  $\overline{P}_i$  to be 68.3% of the area between zero and  $\overline{P}_i$ . A similar correction is made for branching fractions that are within three standard deviations of one. This keeps the quoted errors from overlapping the boundary of the physical region.

**5.3. Rounding:** While the results shown in the Particle Listings are usually exactly those published by the experiments, the numbers that appear in the Summary Tables (means, averages and limits) are subject to a set of rounding rules.

The basic rule states that if the three highest order digits of the error lie between 100 and 354, we round to two significant digits. If they lie between 355 and 949, we round to one significant digit. Finally, if they lie between 950 and 999, we round up to 1000 and keep two significant digits. In all cases, the central value is given with a precision that matches that of the error. So, for example, the result (coming from an average)  $0.827 \pm 0.119$  would appear as  $0.83 \pm 0.12$ , while  $0.827 \pm 0.367$  would turn into  $0.8 \pm 0.4$ .

Rounding is not performed if a result in a Summary Table comes from a single measurement, without any averaging. In that case, the number of digits published in the original paper is kept, unless we feel it inappropriate. Note that, even for a single measurement, when we combine statistical and systematic errors in quadrature, rounding rules apply to the result of the combination. It should be noted also that most of the limits in the Summary Tables come from a single source (the best limit) and, therefore, are not subject to rounding.

Finally, we should point out that in several instances, when a group of results come from a single fit to a set of data, we have chosen to keep two significant digits for all the results. This happens, for instance, for several properties of the  $W$  and  $Z$  bosons and the  $\tau$  lepton.

**5.4. Discussion:** The problem of averaging data containing discrepant values is nicely discussed by Taylor in Ref. 4. He considers a number of algorithms that attempt to incorporate inconsistent data into a meaningful average. However, it is difficult to develop a procedure that handles simultaneously in a reasonable way two basic types of situations: (a) data that lie apart from the main body of the data are incorrect (contain unreported errors); and (b) the opposite—it is the main body of data that is incorrect. Unfortunately, as Taylor shows, case (b) is not infrequent. He concludes that the choice of procedure is less significant than the initial choice of data to include or exclude.

We place much emphasis on this choice of data. Often we solicit the help of outside experts (consultants). Sometimes, however, it is simply impossible to determine which of a set of discrepant measurements are correct. Our scale-factor technique is an attempt to address this ignorance by increasing the error. In effect, we are saying that present experiments do not allow a precise determination of this quantity because of unresolvable discrepancies, and one must await further measurements. The reader is warned of this situation by the size of the scale factor, and if he or she desires can go back to the literature (via the Particle

Listings) and redo the average with a different choice of data.

Our situation is less severe than most of the cases Taylor considers, such as estimates of the fundamental constants like  $\hbar$ , *etc.* Most of the errors in his case are dominated by systematic effects. For our data, statistical errors are often at least as large as systematic errors, and statistical errors are usually easier to estimate. A notable exception occurs in partial-wave analyses, where different techniques applied to the same data yield different results. In this case, as stated earlier, we often do not make an average but just quote a range of values.

A brief history of early Particle Data Group averages is given in Ref. 3. Figure 2 shows some histories of our values of a few particle properties. Sometimes large changes occur. These usually reflect the introduction of significant new data or the discarding of older data. Older data are discarded in favor of newer data when it is felt that the newer data have smaller systematic errors, or have more checks on systematic errors, or have made corrections unknown at the time of the older experiments, or simply have much smaller errors. Sometimes, the scale factor becomes large near the time at which a large jump takes place, reflecting the uncertainty introduced by the new and inconsistent data. By and large, however, a full scan of our history plots shows a dull progression toward greater precision at central values quite consistent with the first data points shown.

We conclude that the reliability of the combination of experimental data and our averaging procedures is usually good, but it is important to be aware that fluctuations outside of the quoted errors can and do occur.

## ACKNOWLEDGMENTS

The publication of the *Review of Particle Physics* is supported by the Director, Office of Science, Office of High Energy and Nuclear Physics, the Division of High Energy Physics of the U.S. Department of Energy under Contract No. DE-AC02-05CH11231; by the U.S. National Science Foundation under Agreement No. PHY-0652989; by the European Laboratory for Particle Physics (CERN); by an implementing arrangement between the governments of Japan (Monbusho) and the United States (DOE) on cooperative research and development.

We thank all those who have assisted in the many phases of preparing this *Review*. We particularly thank the many who have responded to our requests for verification of data entered in the Listings, and those who have made suggestions or pointed out errors.

## REFERENCES

1. The previous edition was Particle Data Group: K. Nakamura *et al.*, *J. Phys.* **G37**, 075021 (2010).
2. Particle Data Group: M. Aguilar-Benitez *et al.*, *Phys. Lett.* **170B** (1986).
3. A.H. Rosenfeld, *Ann. Rev. Nucl. Sci.* **25**, 555 (1975).
4. B.N. Taylor, "Numerical Comparisons of Several Algorithms for Treating Inconsistent Data in a Least-Squares Adjustment of the Fundamental Constants," U.S. National Bureau of Standards NBSIR 81-2426 (1982).

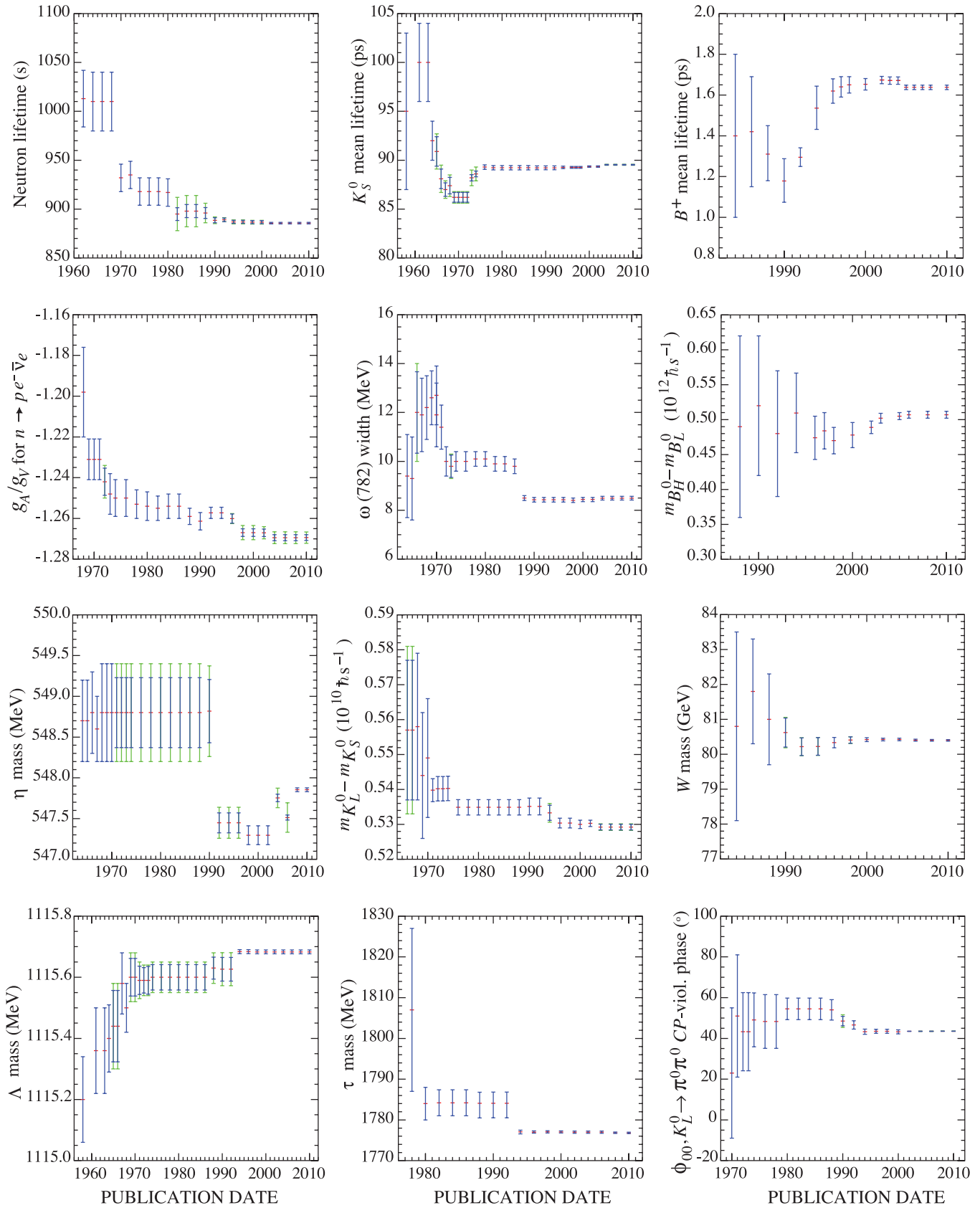


**Figure 2:** A historical perspective of values of a few particle properties tabulated in this *Review* as a function of date of publication of the *Review*. A full error bar indicates the quoted error; a dark portion indicates the same but without the “scale factor.”

## ONLINE PARTICLE PHYSICS INFORMATION

Updated Jan. 2012 by T. Basaglia (CERN), A. Holtkamp (CERN).<sup>†</sup>

1. Introduction . . . . .	18
2. Particle Data Group (PDG) resources . . . . .	18
3. Particle Physics Information Platforms . . . . .	18
4. Literature Databases . . . . .	18
5. Particle Physics Journals and Conference Proceedings Series . . . . .	19
6. Conference Databases . . . . .	19
7. Research Institutions . . . . .	19
8. People . . . . .	19
9. Experiments . . . . .	19
10. Jobs . . . . .	20
11. Software Repositories . . . . .	20
12. Data repositories . . . . .	21
13. Data preservation . . . . .	21
14. Particle Physics Education and Outreach Sites . . . . .	21

### 1. Introduction

The collection of online information resources in particle physics and related areas presented in this chapter is of necessity incomplete. An expanded and regularly updated online version can be found at

<http://library.web.cern.ch/library/rpp>.

Suggestions for additions and updates are very welcome.

### 2. Particle Data Group (PDG) resources

- **REVIEW OF PARTICLE PHYSICS (RPP):** A comprehensive report on the fields of particle physics and cosmology, including both review articles and a compilation/evaluation of data on particle properties. The review section includes articles, tables and plots on a wide variety of theoretical and experimental topics of interest to particle physicists and astrophysicists. The particle properties section provides tables of published measurements as well as the Particle Data Group's best values and limits for particle properties such as masses, widths, lifetimes, and branching fractions, and an extensive summary of searches for hypothetical particles. RPP is published as a 1400-page book every two years, with partial updates made available once each year on the web. All the contents of the 1400-page book version of RPP are available online at:

<http://pdg.lbl.gov>

- **PARTICLE PHYSICS BOOKLET:** An abridged version of the Review of Particle Physics available as a pocket-sized 300-page booklet. Although produced in print and available online only as a PDF file, the booklet is included in this guide because it is one of the most useful summaries of physics data. The booklet contains an abbreviated set of reviews and the summary tables from the most recent edition of the Review of Particle Physics.

The PDF file of the booklet can be downloaded:

<http://pdg.lbl.gov/current/booklet.pdf>.

The printed booklet can be ordered:

[http://pdg.lbl.gov/current/html/receive\\_our\\_products.html](http://pdg.lbl.gov/current/html/receive_our_products.html).

<sup>†</sup> Please send comments and corrections to [Annette.Holtkamp@cern.ch](mailto:Annette.Holtkamp@cern.ch) or [tullio.basaglia@cern.ch](mailto:tullio.basaglia@cern.ch).

- **PDGLive:** A web application for browsing the contents of the PDG database that contains the information published in the Review of Particle Physics. It allows one to navigate to a particle of interest, see a summary of the information available, and then proceed to the detailed information published in the Review of Particle Physics. Data entries are directly linked to the corresponding bibliographic information in INSPIRE. pdgLive can be accessed at:

<http://pdglive.lbl.gov>

- **COMPUTER-READABLE FILES:** Data files that can be downloaded from PDG include tables of particle masses and widths, PDG Monte Carlo particle numbers, and cross-section data. The files are updated with each new edition of the Review of Particle Physics and are available at:

[http://pdg.lbl.gov/current/html/computer\\_read.html](http://pdg.lbl.gov/current/html/computer_read.html)

Of historical interest is the complete RPP collection which, apart from the very first version from the year 1957, can be found online at

[http://tiny.cc/RPP\\_historical](http://tiny.cc/RPP_historical)

### 3. Particle Physics Information Platforms

- **SPIRES:** This indispensable information tool for high energy physicists worldwide was replaced by INSPIRE in November 2011. SPIRES started as a bibliographic database SPIRES-HEP in 1974 hosted at SLAC in collaboration with DESY and became remotely accessible in the mid 80's. Several databases - CONF, EXP, INST, HEPNames and JOBS - followed and FermiLab joined the team. In December 1991 SPIRES became the first web server outside Europe, from the start closely related to the arXiv repository. For High Energy Physics SPIRES-HEP was the reference for publications, covering not only journal articles and preprints but also conference proceedings, technical reports, theses and other 'gray' literature, the value of the information enhanced by thorough proof-reading, keywords and links to the sister SPIRES databases and other information services. Content and service are now taken over by INSPIRE.

- **INSPIRE:** The time-honored SPIRES database suite has now been replaced by INSPIRE which combines the most successful aspects of SPIRES like comprehensive content and high-quality metadata - with the modern technology of Invenio, the CERN open-source digital-library software, offering major improvements like increased speed and Google-like free-text search syntax. INSPIRE serves as one-stop information platform for the particle physics community, comprising 6 interlinked databases on literature, conferences, institutions, researchers, experiments, jobs. INSPIRE is jointly developed and maintained by the three laboratories that have been running SPIRES (DESY, Fermilab and SLAC) and CERN. Close interaction with the user community and with arXiv, ADS, HepData, PDG and publishers is the backbone of INSPIRE's evolution.

<http://inspirehep.net/>

More information on this project at

<http://www.projecthepinpire.net/>

### 4. Literature Databases

- **ADS:** The SAO/NASA Astrophysics Data System is a Digital Library portal for researchers in Astronomy and Physics, operated by the Smithsonian Astrophysical Observatory (SAO) under a NASA grant. The ADS maintains three bibliographic databases containing more than 9.3 million records: Astronomy and Astrophysics, Physics, and arXiv e-prints. The main body of data in the ADS consists of bibliographic records, which are searchable through highly customizable query forms, and full-text scans of much of the astronomical literature which can be browsed or searched via a full-text search interface. Integrated in its databases, the ADS provides access and pointers to a wealth of external resources, including electronic articles, data catalogues and archives. In addition, ADS provides the myADS Update Service, a free custom



notification service promoting current awareness of the recent literature in astronomy and physics based on each individual subscriber's queries.

<http://adswww.harvard.edu/>

- arXiv.org: A repository of full text papers in physics, mathematics, computer science, statistics, nonlinear sciences, quantitative finance and quantitative biology interlinked with ADS and INSPIRE. Papers are usually sent by their authors to arXiv in advance of submission to a journal for publication. Primarily covers 1991 to the present but authors are encouraged to post older papers retroactively. Permits searching by author, title, and words in abstract and experimentally also in the fulltext. Allows limiting by subfield archive or by date.  
<http://arXiv.org>
- CDS: The CERN Document Server contains records of more than 1,000,000 CERN and non-CERN articles, preprints, theses. It includes records for internal and technical notes, official CERN committee documents, and multimedia objects. CDS is going to focus on its role as institutional repository covering all CERN material from the early 50s and reflecting the holdings of the CERN library. Non-CERN particle and accelerator physics content is in the process of being exported to INSPIRE.  
<http://cdsweb.cern.ch>
- INSPIRE HEP: The HEP database serves almost 1 Mio bibliographic records covering particle physics and related topics with a growing number of fulltexts attached and metadata including author affiliations, abstracts, references, keywords as well as links to arXiv, PDG, HepData and publisher platforms. It provides fast metadata and fulltext searches, plots extracted from fulltext, author disambiguation, author profile pages and citation analysis and is expanding its content to e.g. experimental notes.  
<http://inspirehep.net>
- JACoW: The Joint Accelerator Conference Website publishes the proceedings of APAC, EPAC, PAC, ABDW, BIW, COOL, CYCLOTRONS, DIPAC, ECR, FEL, ICALEPCS, ICAP, LINAC, North American PAC, PCaPAC, RuPAC, SRF. A custom interface allows searching on keywords, titles, authors, and in the fulltext.  
<http://www.JACoW.org/>
- KISS (KEK INFORMATION SERVICE SYSTEM) FOR PREPRINTS: The KEK Library preprint and technical report database contains bibliographic records of preprints and technical reports held in the KEK library with links to the full text images of more than 100,000 papers scanned from their worldwide collection of preprints. Particularly useful for older scanned preprints:  
[http://www-lib.kek.jp/KISS/kiss\\_preprint.html](http://www-lib.kek.jp/KISS/kiss_preprint.html)
- OSTI: The Office of Scientific and Technical Information databases search collections of research results, including those produced throughout the DOE National Laboratory complex and by Departmental grantees. You can find current and legacy research results, search ongoing research and development project descriptions, browse scientific subject portals of interest, access and search scientific e-prints, sign up for alerts, search science conference papers and proceedings. Among the key resources are the Energy Citations Database, providing free access to over 2,450,000 science research citations and 292,000 electronic documents, primarily from 1943 forward, and Information Bridge, covering DOE R&D reports with searchable full-text and bibliographic citations.  
<http://www.osti.gov/>

## 5. Particle Physics Journals and Conference Proceedings Series

A list of journals and conference series publishing particle physics content can be found at:

<http://library.web.cern.ch/library/journals.html>

For each journal or conference series, information is given on Open Access and copyright policies and terms of use.

## 6. Conference Databases

- INSPIRE CONFERENCES: The database of more than 18,400 past, present and future conferences, schools, and meetings of interest to high-energy physics and related fields is searchable by title, acronym, series, date, location. Included are information about published proceedings, links to conference contributions in the INSPIRE HEP database, and links to the conference Web site when available. New conferences can be submitted from the entry page.

<http://inspirehep.net/Conferences>

## 7. Research Institutions

- INSPIRE INSTITUTIONS: The database of over 9,800 institutes, laboratories, and university departments in which research on particle physics and astrophysics is performed covers six continents and over a hundred countries. Included are address, e-mail address, and Web links where available as well as links to the papers from each institution in the HEP database. Searches can be performed by name, acronym, location, etc. The site offers an alphabetical list by country as well as a list of the top 500 HEP and astrophysics institutions sorted by country.

<http://inspirehep.net/Institutions>

## 8. People

- INSPIRE HEPNames: Searchable worldwide database of over 97,000 people associated with particle physics and related fields. The affiliation history of these researchers, their e-mail addresses, web pages, experiments they participated in, PhD advisor, information on their graduate students and links to their papers in the INSPIRE HEP, arXiv and ADS databases are provided as well as a user interface to update these information.

<http://inspirehep.net/HepNames>

## 9. Experiments

- SPIRES/INSPIRE EXPERIMENTS: Contains more than 2,400 past, present, and future experiments in particle physics. Lists both accelerator and non-accelerator experiments. Includes official experiment name and number, location, and collaboration lists. Simple searches by participant, title, experiment number, institution, date approved, accelerator, or detector, return a description of the experiment, including a complete list of authors, title, overview of the experiment's goals and methods, and a link to the experiment's Web page if available. Publication lists distinguish articles in refereed journals, theses, technical or instrumentation papers and those which rank among Topcite at 50 or more citations.

<http://www.slac.stanford.edu/spires/experiments/>

soon to be replaced by

<http://inspirehep.net/Experiments>

- COSMIC RAY/GAMMA RAY/NEUTRINO AND SIMILAR EXPERIMENTS: This extensive collection of experimental Web sites is organized by focus of study and also by location. Additional sections link to educational materials, organizations, related Web sites, etc. The site is maintained at the Max Planck Institute for Nuclear Physics, Heidelberg:

<http://www.mpi-hd.mpg.de/hfm/CosmicRay/CosmicRaySites.html>

## 10. Jobs

- APS Careers: gateway for physicists, students, and physics enthusiasts to information about physics jobs and careers. Physics job listings, career advice, upcoming workshops and meetings, and career and job related resources provided by the American Physical Society:  
<http://www.aps.org/jobs/>
- BRIGHTRECRUITS.COM: A recruitment service run by IOP Publishing that connects employers from different industry sectors with jobseekers who have a background in physics and engineering  
<http://brightrecruits.com/>
- IOP CAREERS: careers information and resources primarily aimed at university students provided by the UK Institute of Physics:  
<http://www.iop.org/careers/>
- INSPIRE HEPJobs: lists academic and research jobs in high energy physics, nuclear physics, accelerator physics and astrophysics with the option to post a job or to receive email notices of new job listings. About 1300 jobs are currently listed.  
<http://inspirehep.net/Jobs>
- PHYSICSTODAY JOBS: online recruitment advertising website for Physics Today magazine, published by the American Institute of Physics. Physics TodayJobs is the managing partner of the AIP Career Network, an online job board network for the physical science, engineering, and computing disciplines. Over 8,500 resumes are currently available, and almost 3,000 jobs were posted in 2011.  
<http://www.physicstoday.org/jobs>

## 11. Software Repositories

### Particle Physics

- BSM Generators: a repository of codes relevant to Beyond-the-Standard-Model (BSM) physics  
<http://www.ipp.pdur.ac.uk/montecarlo/BSM>
- CERNLIB: The CERN PROGRAM LIBRARY contains a large collection of general purpose libraries and modules offered in both source code and object code forms. It provides programs applicable to a wide range of physics research problems such as general mathematics, data analysis, detectors simulation, data-handling, etc. It also includes links to commercial, free, and other software. Development of this site has been discontinued.  
<http://wwwasd.web.cern.ch/wwwasd/index.html>
- FERMITOOLS: Fermilab's software tools program provides a repository of Fermilab-developed software packages of value to the HEP community. Permits searching for packages by title or subject category:  
<http://www.fnal.gov/fermitools/>
- FREEHEP: A collection of software and information about software useful in high-energy physics and adjacent disciplines, focusing on open-source software for data analysis and visualization. Searching can be done by title, subject, date acquired, date updated, or by browsing an alphabetical list of all packages. The site does not seem to be updated any longer but still provides useful information.  
<http://www.freehep.org/>
- GEANT4: Toolkit for the simulation of the passage of particles through matter, maintained by a world-wide collaboration of scientists and software engineers. Its areas of application include high energy, nuclear and accelerator physics, as well as studies in medical and space science.  
<http://geant4.cern.ch/>
- GENSER: The Generator Services project collaborates with Monte Carlo (MC) generators authors and with LHC experiments in order to prepare validated LCG compliant code for both the theoretical and experimental communities at the LHC, sharing the user support duties, providing assistance for the development of the

new object-oriented generators and guaranteeing the maintenance of the older packages on the LCG supported platforms. The project consists of the generators repository, validation, HepMC record and MCDB event databases.

<http://sftweb.cern.ch/generators/>

- HEPFORGE: A development environment for high-energy physics software development projects, in particular housing many event-generator related projects, that offers a ready-made, easy-to-use set of Web based tools, including shell account with up to date development tools, web page hosting, subversion and CVS code management systems, mailing lists, bug tracker and wiki system.  
<http://www.hepforge.org/>
  - PYTHIA: A program for the generation of high-energy physics events, i.e. for the description of collisions at high energies between elementary particles such as  $e^+$ ,  $e^-$ ,  $p$  and  $p$ -bar in various combinations. It contains theory and models for a number of physics aspects, including hard and soft interactions, parton distributions, initial- and final-state parton showers, multiple interactions, fragmentation and decay.  
<http://home.thep.lu.se/torbjorn/Pythia.html>
  - QUDA: library for performing calculations in lattice QCD on GPUs using NVIDIA's "C for CUDA" API. The current release includes optimized solvers for Wilson, Clover-improved Wilson, Twisted mass, Improved staggered (asqtad or HISQ) and Domain wall fermion actions  
<http://lattice.github.com/quda/>
  - ROOT: This framework for data processing in high-energy physics, born at CERN, offers applications to store, access, process, analyze and represent data or perform simulations.  
<http://root.cern.ch/drupal>
  - tmLQCD: This freely available software suite provides a set of tools to be used in lattice QCD simulations, mainly a (P)HMC implementation for Wilson and Wilson twisted mass fermions and inverter for different versions of the Dirac operator.  
<https://github.com/etmc/tmLQCD>
  - USQCD: The software suite enables lattice QCD computations to be performed with high performance across a variety of architectures. The page contains links to the project web pages of the individual software modules, as well as to complete lattice QCD application packages which use them.  
<http://usqcd.jlab.org/usqcd-software/>
- A list of Monte Carlo generators may be found at  
<http://cmsdoc.cern.ch/cms/PRS/gentools/www/geners/collection/collection.html>
- The homepage of the SUSY Les Houches Accord contains links to codes relevant for supersymmetry calculations and phenomenology  
<http://home.fnal.gov/skands/slha/>
- A variety of codes and algorithmic tools for analysing supersymmetric phenomenology is described in [arXiv:0805.2088](https://arxiv.org/abs/0805.2088)  
<http://arxiv.org/abs/0805.2088>
- ### Astrophysics
- IRAF: The Image Reduction and Analysis Facility is a general purpose software system for the reduction and analysis of astronomical data. IRAF is written and supported by the IRAF programming group at the National Optical Astronomy Observatories (NOAO) in Tucson, Arizona.  
<http://iraf.noao.edu/>
  - STARLINK: Starlink was a UK Project supporting astronomical data processing. It was shut down in 2005 but its open-source software continues to be developed at the Joint Astronomy Centre. The software products are a collection of applications and libraries, usually focused on a specific aspect of data reduction or analysis.  
<http://starlink.jach.hawaii.edu/starlink>

Links to a large number of astronomy software archives are listed at

<http://heasarc.nasa.gov/docs/heasarc/astro-update/>

## 12. Data repositories

### Particle Physics

- HEPDATA: The HepData Project, funded by the STFC(UK) and based at the IPPP at Durham University, has for more than 30 years compiled a Reaction Data database, comprising total and differential cross sections, structure functions, fragmentation functions, distributions of jet measures, polarisations, etc from a wide range of particle physics scattering experiments worldwide. It is regularly updated to cover the latest data including those from the LHC. In addition, it provides a series of on-line data reviews on a wide variety of topics with links to the data in the Reaction Database. It also hosts a Parton Distribution Function server with an on-line PDF calculator and plotter.

<http://durpdg.dur.ac.uk/>

- ILDG: The International Lattice Data Grid is an international organization which provides standards, services, methods and tools that facilitates the sharing and interchange of lattice QCD gauge configurations among scientific collaborations, by uniting their regional data grids. It offers semantic access with local tools to worldwide distributed data. See e.g.

<http://www.usqcd.org/ildg/>

- MCPLOTS: mcplots is a repository of Monte Carlo plots comparing High Energy Physics event generators to a wide variety of available experimental data. The site is supported by the LHC Physics Centre at CERN.

<http://mcplots.cern.ch/>

### Astrophysics

- SIMBAD: archives data in the form of object catalogues from many heterogeneous sources

<http://simbad.u-strasbg.fr/simbad/>

- NED: NASA/IPAC extragalactic database, operated by the Jet Propulsion Laboratory, California Institute of Technology

<http://ned.ipac.caltech.edu/>

- The NASA archives provide access to raw and processed datasets from numerous NASA missions.

Hubble telescope, other missions (UV, optical):

<http://archive.stsci.edu/>

Spitzer telescope, other missions (Infrared):

<http://irsa.ipac.caltech.edu/>

Chandra, Fermi telescopes, other missions:

<http://heasarc.gsfc.nasa.gov/>

- The Virtual Observatory provides a suite of resources to query for original data from a large number of archives. Two main tools are provided. One runs queries across multiple databases (such as the SDSS database) and combines the results. The other queries hundreds of archives for all datasets that fall on a particular piece of sky.

<http://www.us-vo.org/>

### General Physics

- NIST PHYSICAL MEASUREMENT LABORATORY: The National Institute of Standards and Technology provides access to physical reference data (physical constants, atomic spectroscopy data, x-ray and gamma-ray data, radiation dosimetry data, nuclear physics data and more) and measurements and calibrations data (dimensional measurements, electromagnetic measurements). The site points to a general interest page, linking to exhibits of the Physical Measurement Laboratory in the NIST Virtual Museum.

<http://physics.nist.gov/>

- SPRINGER MATERIALS - THE LANDOLT-BÖRNSTEIN DATABASE: Landolt-Börnstein is a high-quality data collection in all areas of physical sciences and engineering, among others particle physics, electronic structure and transport, magnetism, superconductivity. International experts scan the primary literature in more than 8,000 peer-reviewed journals and evaluate and select the most valid information to be included in the database. It includes more than 100,000 online documents, 1.2 million references, and covers 250,000 chemical substances. The search functionality is freely accessible and the search results are displayed in their context, whereas the full text is secured to subscribers:

<http://www.springermaterials.com/>

## 13. Data preservation

### Particle Physics

- DPHEP: The efforts to define and coordinate Data Preservation and Long Term Analysis in HEP are coordinated by a study group formed to investigate the issues associated with these activities. The group, DPHEP, was initiated during 2008-2009 and includes all HEP major experiments and laboratories. It is endorsed by the International Committee for Future Accelerators (ICFA). Details of the organizational structure, the objectives, workshops and publications can be found at

<http://dphep.org>

The experiments at colliders: BaBar, Belle, BES-III, Cleo, CDF, D0, H1 and ZEUS and the associated computing centres at SLAC (USA), KEK (Japan), IHEP (China), Jlab (USA), BNL (USA), Fermilab (USA), DESY (Germany), and CERN are all represented in the group. The LHC collaborations have also joined the initiative in 2011. The participating experiments are in various stages of studying, preparing, or operating long-term data preservation and analysis systems. Technological methods, such as virtualization, and information management tools such as INSPIRE are also helpful in this area of research. Data access policies and outreach in HEP using real data are among the investigative areas of the DPHEP Study Group.

### Astrophysics

More formal and advanced data preservation activity is ongoing in the field of Experimental Astrophysics, including

- SDSS

<http://sdss.org>

- Fermi

<http://fermi.gsfc.nasa.gov/ssc/data>

- IVOA

<http://www.ivoa.net/>

## 14. Particle Physics Education and Outreach Sites

### Science Educators' Networks:

- IPPOG: The International Particle Physics Outreach Group is a network of particle physicists, researchers, informal science educators and science explainers aiming to raise awareness, understanding and standards of global outreach efforts in particle physics and general science by providing discussion forums and regular information exchange for science institutions, proposing and implementing strategies to share lessons learned and best practices and promoting current outreach efforts of network members:

<http://ippog.web.cern.ch/ippog/>

- Interactions.org: designed to serve as a central resource for communicators of particle physics. The daily updated site provides links to current particle physics news from the world's press, high-resolution photos and graphics from the particle physics laboratories of the world; links to education and outreach programs; information about science policy and funding; links to universities; a glossary; a conference calendar; and links to many educational sites

<http://www.interactions.org>

**Physics Courses**

- MIT OPENCOURSEWARE - PHYSICS: These MIT course materials reflect almost all the undergraduate and graduate subjects taught at MIT. In addition to physics courses, supplementary educational resources are also available.

<http://ocw.mit.edu/courses/physics/>

**Master Classes**

- INTERNATIONAL MASTERCLASSES: Each year about 6000 high school students in 28 countries come to one of about 130 nearby universities or research centres for one day in order to unravel the mysteries of particle physics. Lectures from active scientists give insight in topics and methods of basic research at the fundamentals of matter and forces, enabling the students to perform measurements on real data from particle physics experiments themselves. At the end of each day, like in an international research collaboration, the participants join in a video conference for discussion and combination of their results.

<http://physicsmasterclasses.org/>

**General Sites**

- CONTEMPORARY PHYSICS EDUCATION PROJECT (CPEP): Provides charts, brochures, Web links, and classroom activities. Online interactive courses include: Fundamental Particles and Interactions; Plasma Physics and Fusion; History and Fate of the Universe; and Nuclear Science.

<http://www.cpepweb.org/>

- PHYSICSCENTRAL: This site maintained by the American Physical Society provides information about current research and people in physics, experiments that can be performed at home or at school and the possibility to get physics questions answered by physicists.

<http://www.physicscentral.com>

**General Physics Lessons & Activities**

- HYPERPHYSICS: An exploration environment for concepts in physics employing concept maps and other linking strategies and providing opportunities for numerical exploration.
- PHYSICS2000: An interactive journey through modern physics. Have fun learning visually and conceptually about 20th century science and high-tech devices. Supported by the Colorado Commission on Higher Education and the National Science Foundation

<http://www.colorado.edu/physics/2000>

**Particle Physics Lessons & Activities**

- Angels and Demons: With the aim of looking at the myth versus the reality of science at CERN this site offers teacher resources, slide shows and videos of talks given to teachers visiting CERN
- ANTIMATTER: MIRROR OF THE UNIVERSE: Find out what antimatter is, where it is made, the history behind its discovery, and how it is a part of our lives. Features colorful photos, illustrations, webcasts, a Kids Corner, and CERN physicists answering your questions on antimatter:

<http://livefromcern.web.cern.ch/livefromcern/antimatter/>

- BIG BANG: An exhibition of the UK Science Museum with an interactive game about the hunt for the Higgs

<http://www.sciencemuseum.org.uk/antenna/bigbang/>

- BIG BANG SCIENCE: EXPLORING THE ORIGINS OF MATTER: This Web site, produced by the Particle Physics and Astronomy Research Council of the UK (PPARC), explains what physicists are looking for with their giant instruments. Big Bang Science focuses on CERN particle detectors and on United Kingdom scientists' contribution to the search for the fundamental building blocks of matter.

<http://hepwww.rl.ac.uk/pub/bigbang/part1.html>

- CERNland: With a range of games, multimedia applications and films CERNland is the virtual theme park developed to bring the excitement of CERN's research to a young audience aged between 7 and 12. CERNland is designed to show children what is being done at CERN and inspire them with some physics at the same time.

<http://www.cernland.net/>

- Collidingparticles: a series of films following a team of physicists involved in research at the LHC

<http://www.collidingparticles.com/>

- Lancaster Particle Physics: This site, suitable for 16+ students, offers a number of simulations and explanations of particle physics, including a section on the LHC.

<http://www.lppp.lancs.ac.uk/>

- PARTICLE ADVENTURE: One of the most popular Web sites for learning the fundamentals of matter and force. An award-winning interactive tour of quarks, neutrinos, antimatter, extra dimensions, dark matter, accelerators and particle detectors from the Particle Data Group of Lawrence Berkeley National Laboratory. Simple elegant graphics and translations into 15 languages:

<http://ParticleAdventure.org>

- PARTICLE DETECTIVES: This website, maintained by the Science and Technology Facilities Council (STFC), is for inquisitive 14-19 year olds, their teachers and for researchers who want to find out and talk about the world's biggest scientific adventure, the Large Hadron Collider, featuring e.g. An LHC experiment simulator.

<http://www.lhc.ac.uk/The+Particle+Detectives/15273.aspx>

- Quarked! - Adventures in the Subatomic Universe: This project, targeted to kids aged 7-12 (and their families), brings subatomic physics to life through a multimedia project including an interactive website, a facilitated program for museums and schools, and an educational outreach program

<http://www.quarked.org/>

- QUARKNET: QuarkNet brings the excitement of particle physics research to high school teachers and their students. Teachers join research groups at about 50 universities and labs across the country. These research groups are part of particle physics experiments at CERN or Fermilab. About 100,000 students from 500+ US high schools learn fundamental physics as they participate in inquiry-oriented investigations and analyze real data online. QuarkNet is supported in part by the National Science Foundation and the U.S. Department of Energy:

<http://QuarkNet.fnal.gov>

- Rewarding Learning videos about CERN: The three videos based on interviews with scientists and engineers at CERN introduce pupils to CERN and the type of research and work undertaken there and are accompanied by teachers' notes.

<http://www.rewardinglearning.org.uk/STEM/cern/>

**Lab Education Offices**

- Brookhaven National Laboratory (BNL) Educational Programs: The Office of Educational Programs mission is to design, develop, implement, and facilitate workforce development and education initiatives that support the scientific mission at Brookhaven National Laboratory and the Department of Energy.

<http://www.bnl.gov/education/>

- CERN: The CERN education website offers information about teacher programmes and educational resources for schools

<http://education.web.cern.ch/education/>

- DESY: offers courses for pupils and teachers as well as information for the general public, mostly in German.

[http://www.desy.de/information\\_services/education/](http://www.desy.de/information_services/education/)

- FERMILAB EDUCATION OFFICE: provides education resources and information about activities for educators, physicists, students

and visitors to the Lab. In addition to information on 25 programs, the site provides online data-based investigations for high school students, online versions of exhibits in the Lederman Science Center, links to particle physics discovery resources, web-based instructional resources, what works for education and outreach, and links to the Lederman Science Center and the Teacher Resource Center.

<http://ed.fnal.gov/>

- LBL: Berkeley Lab's Center for Science & Engineering Education (CSEE) carries out the Department of Energy's education mission to train the next generation of scientists, as well as helping them to gain an understanding of the relationships among frontier science, technology, and society.  
<http://www.lbl.gov/Education/>
- EXPLORING SLAC SCIENCE: This Stanford Linear Accelerator Center Web site explains physics concepts related to experiments conducted at SLAC.  
<http://www6.slac.stanford.edu/ExploringSLACScience.aspx>
- Symmetry: This magazine about particle physics and its connections to other aspects of life and science, from interdisciplinary collaborations to policy to culture is published 6 times per year by Fermilab and SLAC.  
<http://www.symmetrymagazine.org>

#### Educational Programs of Experiments

- ATLAS DISCOVERY QUEST: One of several access points to ATLAS education and outreach pages. This page gives access to explanations of physical concepts, blogs, ATLAS facts, news, and information for students and teachers.  
<http://www.atlas.ch/physics.html>
- ATLAS eTours: give a description of the Large Hadron Collider, explain how the ATLAS detector at the LHC works and give an overview over the experiments and their physics goals.  
<http://www.atlas.ch/etours.html>
- CMS EDUCATION: Provides access to educational resources (Story of the Universe, The Size of Things, What is a Particle), and to multimedia material, such as interviews, movies and photos.  
<http://cms.web.cern.ch/content/cms-education>
- EDUCATION AND OUTREACH @ ICECUBE: Educational pages of the IceCube (South Pole Neutrino Detector)  
<http://icecube.wisc.edu/outreach>
- LIGO SCIENCE EDUCATION CENTER: The LIGO (Laser Interferometer Gravitational-wave Observatory) Science Education Center has over 40 interactive, hands-on exhibits that relate to the science of LIGO. The site hosts field trips for students, teacher training programs, and tours for the general public. Visitors can explore science concepts such as light, gravity, waves, and interference; learn about LIGO's search for gravitational waves; and interact with scientists and engineers.  
<http://www.ligo-la.caltech.edu/SEC.html>
- PIERRE AUGER OBSERVATORY'S EDUCATIONAL PAGES: The site offers information about cosmic rays and their detection, and provides material for students and teachers.  
[http://www.auger.org/cosmic\\_rays/](http://www.auger.org/cosmic_rays/)

#### Art in Physics

- Arts@CERN: a 3-year artist's residency programme in Digital Arts and Dance/Performance  
<http://arts.web.cern.ch/collide/>
- Art of Physics Competition: The Canadian Association of Physicists organizes this competition, the first was launched in 1992, with the aim of stimulating interest, especially among non-scientists, in some of the captivating imagery associated with physics. The challenge is to capture photographically a beautiful or unusual physics phenomenon and explain it in less than 200 words in terms that everyone can understand.  
<http://www.cap.ca/aop/art.html>
- Photowalk: More than 200 amateur photographers from around the world had the opportunity to experience state-of-the-art accelerators and detectors. Five of the world's leading particle physics laboratories in Asia, Europe and North America offered special behind-the-scenes access to their scientific facilities. The winning photos can be viewed.  
<http://www.interactions.org/cms/?pid=1029664>

#### Blogs

This is a very incomplete collection of particle physics related blogs:

- ATLAS blog  
<http://www.atlas.ch/blog>
- U.S. LHC blog: The blog give a vivid account of the daily activity of US LHC researchers.  
<http://www.quantumdiaries.org/lab-81/>
- Physics arXiv blog: Technology Review blog on new ideas at arXiv.org  
<http://www.technologyreview.com/blog/arxiv/>
- CERN Love:  
<http://www.cernlove.org/blog/>
- Not Even Wrong: Peter Woit's blog on topics in physics and mathematics  
<http://www.math.columbia.edu/woit/wordpress/>
- Quantum diaries: Thoughts on work and life from particle physicists from around the world.  
<http://www.quantumdiaries.org/>
- Science blogs: Launched in January 2006, ScienceBlogs features bloggers from a wide array of scientific disciplines, including physics:  
<http://scienceblogs.com/channel/physical-science/>
- Life and Physics: Jon Butterworth's blog in the Guardian  
<http://www.guardian.co.uk/science/life-and-physics>



## SUMMARY TABLES OF PARTICLE PHYSICS

Gauge and Higgs Bosons . . . . .	27
Leptons . . . . .	30
Quarks . . . . .	33
Mesons . . . . .	34
Baryons . . . . .	79
Miscellaneous searches* . . . . .	93
Tests of conservation laws . . . . .	95
Meson Quick Reference Table . . . . .	77
Baryon Quick Reference Table . . . . .	78

\* There are also search limits in the Summary Tables for the Gauge and Higgs Bosons, the Leptons, the Quarks, and the Mesons.





## Gauge &amp; Higgs Boson Summary Table

## SUMMARY TABLES OF PARTICLE PROPERTIES

Extracted from the Particle Listings of the  
*Review of Particle Physics*

J. Beringer *et al.* (PDG), PR **D86**, 010001 (2012)  
Available at <http://pdg.lbl.gov>

## Particle Data Group

J. Beringer, J.-F. Arguin, R.M. Barnett, K. Copic, O. Dahl, D.E. Groom, C.-J. Lin, J. Lys, H. Murayama, C.G. Wohl, W.-M. Yao, P.A. Zyla, C. Amsler, M. Antonelli, D.M. Asner, H. Baer, H.R. Band, T. Basaglia, C.W. Bauer, J.J. Beatty, V.I. Belousov, E. Bergren, G. Bernardi, W. Bertl, S. Bethke, H. Bichsel, O. Biebel, E. Blucher, S. Blusk, G. Brooijmans, O. Buchmueller, R.N. Cahn, M. Carena, A. Ceccucci, D. Chakraborty, M.-C. Chen, R.S. Chivukula, G. Cowan, G. D'Ambrosio, T. Damour, D. de Florian, A. de Gouvêa, T. DeGrand, P. DeJong, G. Dissertori, B. Dobrescu, M. Doser, M. Drees, D.A. Edwards, S. Eidelman, J. Erler, V.V. Ezhela, W. Fetscher, B.D. Fields, B. Foster, T.K. Gaisser, L. Garren, H.-J. Gerber, G. Gerbier, T. Gherghetta, S. Golwala, M. Goodman, C. Grab, A.V. Gritsan, J.-F. Grivaz, M. Grünewald, A. Gurtu, T. Gutsche, H.E. Haber, K. Hagiwara, C. Hagmann, C. Hanhart, S. Hashimoto, K.G. Hayes, M. Hefner, B. Heltsley, J.J. Hernández-Rey, K. Hikasa, A. Höcker, J. Holder, A. Holtkamp, J. Huston, J.D. Jackson, K.F. Johnson, T. Junk, D. Karlen, D. Kirkby, S.R. Klein, E. Klempt, R.V. Kowalewski, F. Krauss, M. Kreps, B. Krusche, Yu.V. Kuyanov, Y. Kwon, O. Lahav, J. Laiho, P. Langacker, A. Liddle, Z. Ligeti, T.M. Liss, L. Littenberg, K.S. Lugovsky, S.B. Lugovsky, T. Mannel, A.V. Manohar, W.J. Marciano, A.D. Martin, A. Masoni, J. Matthews, D. Milstead, R. Miquel, K. Mönig, F. Moortgat, K. Nakamura, M. Narain, P. Nason, S. Navas, M. Neubert, P. Nevski, Y. Nir, K.A. Olive, L. Pape, J. Parsons, C. Patrignani, J.A. Peacock, S.T. Petcov, A. Piepke, A. Pomarol, G. Punzi, A. Quadt, S. Raby, G. Raffelt, B.N. Ratcliff, P. Richardson, S. Roesler, S. Rolli, A. Romaniouk, L.J. Rosenberg, J.L. Rosner, C.T. Sachrajda, Y. Sakai, G.P. Salam, S. Sarkar, F. Sauli, O. Schneider, K. Scholberg, D. Scott, W.G. Seligman, M.H. Shaevitz, S.R. Sharpe, M. Silari, T. Sjöstrand, P. Skands, J.G. Smith, G.F. Smoot, S. Spanier, H. Spieler, A. Stahl, T. Stanev, S.L. Stone, T. Sumiyoshi, M.J. Syphers, F. Takahashi, M. Tanabashi, J. Terning, M. Titov, N.P. Tkachenko, N.A. Törnqvist, D. Tovey, G. Valencia, K. van Bibber, G. Venanzoni, M.G. Vincter, P. Vogel, A. Vogt, W. Walkowiak, C.W. Walter, D.R. Ward, T. Watari, G. Weiglein, E.J. Weinberg, L.R. Wiencke, L. Wolfenstein, J. Womersley, C.L. Woody, R.L. Workman, A. Yamamoto, G.P. Zeller, O.V. Zenin, J. Zhang, R.-Y. Zhu

## Technical Associates:

G. Harper, V.S. Lugovsky, P. Schaffner

©2012 Regents of the University of California  
(Approximate closing date for data: January 15, 2012)

## GAUGE AND HIGGS BOSONS

**γ**

$$I(J^{PC}) = 0,1(1^{--})$$

Mass  $m < 1 \times 10^{-18}$  eV  
Charge  $q < 1 \times 10^{-35}$  e  
Mean life  $\tau$  = Stable

**g**  
or gluon

$$I(J^P) = 0(1^-)$$

Mass  $m = 0$  [a]  
SU(3) color octet

**graviton**

$$J = 2$$

Mass  $m < 7 \times 10^{-32}$  eV

**W**

$$J = 1$$

Charge =  $\pm 1$  e  
Mass  $m = 80.385 \pm 0.015$  GeV  
 $m_Z - m_W = 10.4 \pm 1.6$  GeV  
 $m_{W^+} - m_{W^-} = -0.2 \pm 0.6$  GeV  
Full width  $\Gamma = 2.085 \pm 0.042$  GeV  
 $\langle N_{\pi^\pm} \rangle = 15.70 \pm 0.35$   
 $\langle N_{K^\pm} \rangle = 2.20 \pm 0.19$   
 $\langle N_p \rangle = 0.92 \pm 0.14$   
 $\langle N_{\text{charged}} \rangle = 19.39 \pm 0.08$

$W^-$  modes are charge conjugates of the modes below.

<b>W<sup>+</sup> DECAY MODES</b>	Fraction ( $\Gamma_i/\Gamma$ )	Confidence level	$\rho$ (MeV/c)
$\ell^+ \nu$	[b] (10.80 $\pm$ 0.09) %		–
$e^+ \nu$	(10.75 $\pm$ 0.13) %		40192
$\mu^+ \nu$	(10.57 $\pm$ 0.15) %		40192
$\tau^+ \nu$	(11.25 $\pm$ 0.20) %		40173
hadrons	(67.60 $\pm$ 0.27) %		–
$\pi^+ \gamma$	< 8	$\times 10^{-5}$	95% 40192
$D_s^+ \gamma$	< 1.3	$\times 10^{-3}$	95% 40168
$cX$	(33.4 $\pm$ 2.6) %		–
$c\bar{s}$	(31 $^{+13}_{-11}$ ) %		–
invisible	[c] (1.4 $\pm$ 2.9) %		–

**Z**

$$J = 1$$

Charge = 0  
Mass  $m = 91.1876 \pm 0.0021$  GeV [d]  
Full width  $\Gamma = 2.4952 \pm 0.0023$  GeV  
 $\Gamma(\ell^+ \ell^-) = 83.984 \pm 0.086$  MeV [d]  
 $\Gamma(\text{invisible}) = 499.0 \pm 1.5$  MeV [e]  
 $\Gamma(\text{hadrons}) = 1744.4 \pm 2.0$  MeV  
 $\Gamma(\mu^+ \mu^-)/\Gamma(e^+ e^-) = 1.0009 \pm 0.0028$   
 $\Gamma(\tau^+ \tau^-)/\Gamma(e^+ e^-) = 1.0019 \pm 0.0032$  [f]

## Average charged multiplicity

$$\langle N_{\text{charged}} \rangle = 20.76 \pm 0.16 \quad (S = 2.1)$$

## Couplings to leptons

$$g_V^\ell = -0.03783 \pm 0.00041$$

$$g_V^u = 0.25^{+0.07}_{-0.06}$$

$$g_V^d = -0.33^{+0.05}_{-0.06}$$

$$g_A^\ell = -0.50123 \pm 0.00026$$

$$g_A^u = 0.50^{+0.04}_{-0.06}$$

$$g_A^d = -0.523^{+0.050}_{-0.029}$$

$$g^{V\ell} = 0.5008 \pm 0.0008$$

$$g^{Ve} = 0.53 \pm 0.09$$

$$g^{V\mu} = 0.502 \pm 0.017$$

## Asymmetry parameters [g]

$$A_e = 0.1515 \pm 0.0019$$

$$A_\mu = 0.142 \pm 0.015$$

$$A_\tau = 0.143 \pm 0.004$$

$$A_S = 0.90 \pm 0.09$$

$$A_C = 0.670 \pm 0.027$$

$$A_b = 0.923 \pm 0.020$$

## Charge asymmetry (%) at Z pole

$$A_{FB}^{(0\ell)} = 1.71 \pm 0.10$$

$$A_{FB}^{(0u)} = 4 \pm 7$$

$$A_{FB}^{(0s)} = 9.8 \pm 1.1$$

$$A_{FB}^{(0c)} = 7.07 \pm 0.35$$

$$A_{FB}^{(0b)} = 9.92 \pm 0.16$$

## Gauge &amp; Higgs Boson Summary Table

Z DECAY MODES	Fraction ( $\Gamma_i/\Gamma$ )	Scale factor/ Confidence level	$p$ (MeV/c)
$e^+e^-$	( 3.363 ± 0.004 ) %		45594
$\mu^+\mu^-$	( 3.366 ± 0.007 ) %		45594
$\tau^+\tau^-$	( 3.370 ± 0.008 ) %		45559
$\ell^+\ell^-$	[b] ( 3.3658 ± 0.0023 ) %		—
invisible	(20.00 ± 0.06 ) %		—
hadrons	(69.91 ± 0.06 ) %		—
$(u\bar{u}+c\bar{c})/2$	(11.6 ± 0.6 ) %		—
$(d\bar{d}+s\bar{s}+b\bar{b})/3$	(15.6 ± 0.4 ) %		—
$c\bar{c}$	(12.03 ± 0.21 ) %		—
$b\bar{b}$	(15.12 ± 0.05 ) %		—
$b\bar{b}b\bar{b}$	( 3.6 ± 1.3 ) × 10 <sup>-4</sup>		—
$g\bar{g}$	< 1.1	% CL=95%	—
$\pi^0\gamma$	< 5.2	× 10 <sup>-5</sup> CL=95%	45594
$\eta\gamma$	< 5.1	× 10 <sup>-5</sup> CL=95%	45592
$\omega\gamma$	< 6.5	× 10 <sup>-4</sup> CL=95%	45590
$\eta'(958)\gamma$	< 4.2	× 10 <sup>-5</sup> CL=95%	45589
$\gamma\gamma$	< 5.2	× 10 <sup>-5</sup> CL=95%	45594
$\gamma\gamma\gamma$	< 1.0	× 10 <sup>-5</sup> CL=95%	45594
$\pi^\pm W^\mp$	[h] < 7	× 10 <sup>-5</sup> CL=95%	10162
$\rho^\pm W^\mp$	[h] < 8.3	× 10 <sup>-5</sup> CL=95%	10136
$J/\psi(1S)X$	( 3.51 $\begin{smallmatrix} +0.23 \\ -0.25 \end{smallmatrix}$ ) × 10 <sup>-3</sup>	S=1.1	—
$\psi(2S)X$	( 1.60 ± 0.29 ) × 10 <sup>-3</sup>		—
$\chi_{c1}(1P)X$	( 2.9 ± 0.7 ) × 10 <sup>-3</sup>		—
$\chi_{c2}(1P)X$	< 3.2	× 10 <sup>-3</sup> CL=90%	—
$T(1S)X + T(2S)X$ + $T(3S)X$	( 1.0 ± 0.5 ) × 10 <sup>-4</sup>		—
$T(1S)X$	< 4.4	× 10 <sup>-5</sup> CL=95%	—
$T(2S)X$	< 1.39	× 10 <sup>-4</sup> CL=95%	—
$T(3S)X$	< 9.4	× 10 <sup>-5</sup> CL=95%	—
$(D^0/\bar{D}^0)X$	(20.7 ± 2.0 ) %		—
$D^\pm X$	(12.2 ± 1.7 ) %		—
$D^*(2010)^\pm X$	[h] (11.4 ± 1.3 ) %		—
$D_{s1}(2536)^\pm X$	( 3.6 ± 0.8 ) × 10 <sup>-3</sup>		—
$D_{sJ}(2573)^\pm X$	( 5.8 ± 2.2 ) × 10 <sup>-3</sup>		—
$D^*(2629)^\pm X$	searched for		—
$B^+X$	[i] ( 6.08 ± 0.13 ) %		—
$B_s^0X$	[i] ( 1.59 ± 0.13 ) %		—
$B_c^+X$	searched for		—
$\Lambda_c^+X$	( 1.54 ± 0.33 ) %		—
$\Xi_c^0X$	seen		—
$\Xi_c^-X$	seen		—
b-baryon X	[i] ( 1.38 ± 0.22 ) %		—
anomalous $\gamma$ + hadrons	[j] < 3.2	× 10 <sup>-3</sup> CL=95%	—
$e^+e^-\gamma$	[j] < 5.2	× 10 <sup>-4</sup> CL=95%	45594
$\mu^+\mu^-\gamma$	[j] < 5.6	× 10 <sup>-4</sup> CL=95%	45594
$\tau^+\tau^-\gamma$	[j] < 7.3	× 10 <sup>-4</sup> CL=95%	45559
$\ell^+\ell^-\gamma\gamma$	[k] < 6.8	× 10 <sup>-6</sup> CL=95%	—
$q\bar{q}\gamma\gamma$	[k] < 5.5	× 10 <sup>-6</sup> CL=95%	—
$\nu\bar{\nu}\gamma\gamma$	[k] < 3.1	× 10 <sup>-6</sup> CL=95%	45594
$e^\pm\mu^\mp$	LF [h] < 1.7	× 10 <sup>-6</sup> CL=95%	45594
$e^\pm\tau^\mp$	LF [h] < 9.8	× 10 <sup>-6</sup> CL=95%	45576
$\mu^\pm\tau^\mp$	LF [h] < 1.2	× 10 <sup>-5</sup> CL=95%	45576
$\rho e$	L,B < 1.8	× 10 <sup>-6</sup> CL=95%	45589
$\rho\mu$	L,B < 1.8	× 10 <sup>-6</sup> CL=95%	45589

Higgs Bosons —  $H^0$  and  $H^\pm$ , Searches for

The July 2012 news about Higgs searches is described in the addendum to the Higgs review in the data listings, but is not reflected here.

The limits for  $H_1^0$  and  $A^0$  refer to the  $m_h^{max}$  benchmark scenario for the supersymmetric parameters.

$H^0$  Mass  $m > 115.5$  and none 127–600 GeV, CL = 95%

$H_1^0$  in Supersymmetric Models ( $m_{H_1^0} < m_{H_2^0}$ )

Mass  $m > 92.8$  GeV, CL = 95%

$A^0$  Pseudoscalar Higgs Boson in Supersymmetric Models [1]

Mass  $m > 93.4$  GeV, CL = 95%  $\tan\beta > 0.4$

$H^\pm$  Mass  $m > 79.3$  GeV, CL = 95%

See the Particle Listings for a Note giving details of Higgs Bosons.

## Heavy Bosons Other Than Higgs Bosons, Searches for

## Additional W Bosons

$W'$  with standard couplings

Mass  $m > 2.150 \times 10^3$  GeV, CL = 95%

## Additional Z Bosons

$Z'_{SM}$  with standard couplings

Mass  $m > 1.830 \times 10^3$  GeV, CL = 95% ( $p\bar{p}$  direct search)

Mass  $m > 1.500 \times 10^3$  GeV, CL = 95% (electroweak fit)

$Z_{LR}$  of  $SU(2)_L \times SU(2)_R \times U(1)$  (with  $g_L = g_R$ )

Mass  $m > 630$  GeV, CL = 95% ( $p\bar{p}$  direct search)

Mass  $m > 1162$  GeV, CL = 95% (electroweak fit)

$Z_\chi$  of  $SO(10) \rightarrow SU(5) \times U(1)_\chi$  (with  $g_\chi = e/\cos\theta_W$ )

Mass  $m > 1.640 \times 10^3$  GeV, CL = 95% ( $p\bar{p}$  direct search)

Mass  $m > 1.141 \times 10^3$  GeV, CL = 95% (electroweak fit)

$Z_\psi$  of  $E_6 \rightarrow SO(10) \times U(1)_\psi$  (with  $g_\psi = e/\cos\theta_W$ )

Mass  $m > 1.490 \times 10^3$  GeV, CL = 95% ( $p\bar{p}$  direct search)

Mass  $m > 476$  GeV, CL = 95% (electroweak fit)

$Z_\eta$  of  $E_6 \rightarrow SU(3) \times SU(2) \times U(1) \times U(1)_\eta$  (with  $g_\eta = e/\cos\theta_W$ )

Mass  $m > 1.540 \times 10^3$  GeV, CL = 95% ( $p\bar{p}$  direct search)

Mass  $m > 619$  GeV, CL = 95% (electroweak fit)

## Scalar Leptoquarks

Mass  $m > 660$  GeV, CL = 95% (1st generation, pair prod.)

Mass  $m > 298$  GeV, CL = 95% (1st gener., single prod.)

Mass  $m > 422$  GeV, CL = 95% (2nd gener., pair prod.)

Mass  $m > 73$  GeV, CL = 95% (2nd gener., single prod.)

Mass  $m > 247$  GeV, CL = 95% (3rd gener., pair prod.)

(See the Particle Listings for assumptions on leptoquark quantum numbers and branching fractions.)

Axions ( $A^0$ ) and Other Very Light Bosons, Searches for

The standard Peccei-Quinn axion is ruled out. Variants with reduced couplings or much smaller masses are constrained by various data.

The Particle Listings in the full Review contain a Note discussing axion searches.

The best limit for the half-life of neutrinoless double beta decay with Majoron emission is  $> 7.2 \times 10^{24}$  years (CL = 90%).

## Gauge &amp; Higgs Boson Summary Table

## NOTES

In this Summary Table:

When a quantity has "(S = ...)" to its right, the error on the quantity has been enlarged by the "scale factor"  $S$ , defined as  $S = \sqrt{\chi^2/(N-1)}$ , where  $N$  is the number of measurements used in calculating the quantity. We do this when  $S > 1$ , which often indicates that the measurements are inconsistent. When  $S > 1.25$ , we also show in the Particle Listings an ideogram of the measurements. For more about  $S$ , see the Introduction.

A decay momentum  $p$  is given for each decay mode. For a 2-body decay,  $p$  is the momentum of each decay product in the rest frame of the decaying particle. For a 3-or-more-body decay,  $p$  is the largest momentum any of the products can have in this frame.

- [a] Theoretical value. A mass as large as a few MeV may not be precluded.
- [b]  $\ell$  indicates each type of lepton ( $e$ ,  $\mu$ , and  $\tau$ ), not sum over them.
- [c] This represents the width for the decay of the  $W$  boson into a charged particle with momentum below detectability,  $p < 200$  MeV.

[d] The  $Z$ -boson mass listed here corresponds to a Breit-Wigner resonance parameter. It lies approximately 34 MeV above the real part of the position of the pole (in the energy-squared plane) in the  $Z$ -boson propagator.

[e] This partial width takes into account  $Z$  decays into  $\nu\bar{\nu}$  and any other possible undetected modes.

[f] This ratio has not been corrected for the  $\tau$  mass.

[g] Here  $A \equiv 2g_V g_A / (g_V^2 + g_A^2)$ .

[h] The value is for the sum of the charge states or particle/antiparticle states indicated.

[i] This value is updated using the product of (i) the  $Z \rightarrow b\bar{b}$  fraction from this listing and (ii) the  $b$ -hadron fraction in an unbiased sample of weakly decaying  $b$ -hadrons produced in  $Z$ -decays provided by the Heavy Flavor Averaging Group (HFAG, [http://www.slac.stanford.edu/xorg/hfag/osc/PDG\\_2009/#FRACZ](http://www.slac.stanford.edu/xorg/hfag/osc/PDG_2009/#FRACZ)).

[j] See the  $Z$  Particle Listings for the  $\gamma$  energy range used in this measurement.

[k] For  $m_{\gamma\gamma} = (60 \pm 5)$  GeV.

[l] The limits assume no invisible decays.

## Lepton Summary Table

## LEPTONS

e

$$J = \frac{1}{2}$$

Mass  $m = (548.57990946 \pm 0.00000022) \times 10^{-6}$  u  
 Mass  $m = 0.510998928 \pm 0.00000011$  MeV  
 $|m_{e^+} - m_{e^-}|/m < 8 \times 10^{-9}$ , CL = 90%  
 $|q_{e^+} + q_{e^-}|/e < 4 \times 10^{-8}$   
 Magnetic moment anomaly  
 $(g-2)/2 = (1159.65218076 \pm 0.00000027) \times 10^{-6}$   
 $(g_{e^+} - g_{e^-}) / g_{\text{average}} = (-0.5 \pm 2.1) \times 10^{-12}$   
 Electric dipole moment  $d < 10.5 \times 10^{-28}$  ecm, CL = 90%  
 Mean life  $\tau > 4.6 \times 10^{26}$  yr, CL = 90% [a]

 $\mu$ 

$$J = \frac{1}{2}$$

Mass  $m = 0.1134289267 \pm 0.0000000029$  u  
 Mass  $m = 105.6583715 \pm 0.00000035$  MeV  
 Mean life  $\tau = (2.1969811 \pm 0.0000022) \times 10^{-6}$  s  
 $\tau_{\mu^+}/\tau_{\mu^-} = 1.00002 \pm 0.00008$   
 $c\tau = 658.6384$  m  
 Magnetic moment anomaly  $(g-2)/2 = (11659209 \pm 6) \times 10^{-10}$   
 $(g_{\mu^+} - g_{\mu^-}) / g_{\text{average}} = (-0.11 \pm 0.12) \times 10^{-8}$   
 Electric dipole moment  $d = (-0.1 \pm 0.9) \times 10^{-19}$  ecm

## Decay parameters [b]

$\rho = 0.74979 \pm 0.00026$   
 $\eta = 0.057 \pm 0.034$   
 $\delta = 0.75047 \pm 0.00034$   
 $\xi P_{\mu} = 1.0009^{+0.0016}_{-0.0007}$  [c]  
 $\xi P_{\mu} \delta / \rho = 1.0018^{+0.0016}_{-0.0007}$  [c]  
 $\xi' = 1.00 \pm 0.04$   
 $\xi'' = 0.7 \pm 0.4$   
 $\alpha/A = (0 \pm 4) \times 10^{-3}$   
 $\alpha'/A = (-10 \pm 20) \times 10^{-3}$   
 $\beta/A = (4 \pm 6) \times 10^{-3}$   
 $\beta'/A = (2 \pm 7) \times 10^{-3}$   
 $\overline{\eta} = 0.02 \pm 0.08$

$\mu^+$  modes are charge conjugates of the modes below.

$\mu^-$ DECAY MODES	Fraction ( $\Gamma_i/\Gamma$ )	Confidence level	$P$ (MeV/c)
$e^- \overline{\nu}_e \nu_{\mu}$	$\approx 100\%$		53
$e^- \overline{\nu}_e \nu_{\mu} \gamma$	[d] (1.4±0.4) %		53
$e^- \overline{\nu}_e \nu_{\mu} e^+ e^-$	[e] (3.4±0.4) × 10 <sup>-5</sup>		53
Lepton Family number (LF) violating modes			
$e^- \nu_e \overline{\nu}_{\mu}$	LF [f] < 1.2 %	90%	53
$e^- \gamma$	LF < 2.4 × 10 <sup>-12</sup>	90%	53
$e^- e^+ e^-$	LF < 1.0 × 10 <sup>-12</sup>	90%	53
$e^- 2\gamma$	LF < 7.2 × 10 <sup>-11</sup>	90%	53

 $\tau$ 

$$J = \frac{1}{2}$$

Mass  $m = 1776.82 \pm 0.16$  MeV  
 $(m_{\tau^+} - m_{\tau^-})/m_{\text{average}} < 2.8 \times 10^{-4}$ , CL = 90%  
 Mean life  $\tau = (290.6 \pm 1.0) \times 10^{-15}$  s  
 $c\tau = 87.11$   $\mu\text{m}$   
 Magnetic moment anomaly  $> -0.052$  and  $< 0.013$ , CL = 95%  
 $\text{Re}(d_{\tau}) = -0.220$  to  $0.45 \times 10^{-16}$  ecm, CL = 95%  
 $\text{Im}(d_{\tau}) = -0.250$  to  $0.0080 \times 10^{-16}$  ecm, CL = 95%

## Weak dipole moment

$\text{Re}(d_{\tau}^W) < 0.50 \times 10^{-17}$  ecm, CL = 95%  
 $\text{Im}(d_{\tau}^W) < 1.1 \times 10^{-17}$  ecm, CL = 95%

## Weak anomalous magnetic dipole moment

$\text{Re}(\alpha_{\tau}^W) < 1.1 \times 10^{-3}$ , CL = 95%  
 $\text{Im}(\alpha_{\tau}^W) < 2.7 \times 10^{-3}$ , CL = 95%

## Decay parameters

See the  $\tau$  Particle Listings for a note concerning  $\tau$ -decay parameters.

$\rho(e \text{ or } \mu) = 0.745 \pm 0.008$   
 $\rho(e) = 0.747 \pm 0.010$   
 $\rho(\mu) = 0.763 \pm 0.020$   
 $\xi(e \text{ or } \mu) = 0.985 \pm 0.030$   
 $\xi(e) = 0.994 \pm 0.040$   
 $\xi(\mu) = 1.030 \pm 0.059$   
 $\eta(e \text{ or } \mu) = 0.013 \pm 0.020$   
 $\eta(\mu) = 0.094 \pm 0.073$   
 $(\delta\xi)(e \text{ or } \mu) = 0.746 \pm 0.021$   
 $(\delta\xi)(e) = 0.734 \pm 0.028$   
 $(\delta\xi)(\mu) = 0.778 \pm 0.037$   
 $\xi(\pi) = 0.993 \pm 0.022$   
 $\xi(\rho) = 0.994 \pm 0.008$   
 $\xi(a_1) = 1.001 \pm 0.027$   
 $\xi(\text{all hadronic modes}) = 0.995 \pm 0.007$

$\tau^+$  modes are charge conjugates of the modes below. " $h^{\pm}$ " stands for  $\pi^{\pm}$  or  $K^{\pm}$ . " $e$ " stands for  $e$  or  $\mu$ . "Neutrals" stands for  $\gamma$ 's and/or  $\pi^0$ 's.

$\tau^-$ DECAY MODES	Fraction ( $\Gamma_i/\Gamma$ )	Scale factor/ Confidence level	$P$ (MeV/c)
Modes with one charged particle			
particle <sup>-</sup> ≥ 0 neutrals ≥ 0 $K^0 \nu_{\tau}$	(85.35 ± 0.07) %	S=1.3	-
("1-prong")			
particle <sup>-</sup> ≥ 0 neutrals ≥ 0 $K_L^0 \nu_{\tau}$	(84.71 ± 0.08) %	S=1.3	-
$\mu^- \overline{\nu}_{\mu} \nu_{\tau}$	[g] (17.41 ± 0.04) %	S=1.1	885
$\mu^- \overline{\nu}_{\mu} \nu_{\tau} \gamma$	[e] (3.6 ± 0.4) × 10 <sup>-3</sup>		885
$e^- \overline{\nu}_e \nu_{\tau}$	[g] (17.83 ± 0.04) %		888
$e^- \overline{\nu}_e \nu_{\tau} \gamma$	[e] (1.75 ± 0.18) %		888
$h^- \geq 0 K_L^0 \nu_{\tau}$	(12.06 ± 0.06) %	S=1.2	883
$h^- \nu_{\tau}$	(11.53 ± 0.06) %	S=1.2	883
$\pi^- \nu_{\tau}$	[g] (10.83 ± 0.06) %	S=1.2	883
$K^- \nu_{\tau}$	[g] (7.00 ± 0.10) × 10 <sup>-3</sup>	S=1.1	820
$h^- \geq 1$ neutrals $\nu_{\tau}$	(37.10 ± 0.10) %	S=1.2	-
$h^- \geq 1\pi^0 \nu_{\tau}$ (ex. $K^0$ )	(36.57 ± 0.10) %	S=1.2	-
$h^- \pi^0 \nu_{\tau}$	(25.95 ± 0.09) %	S=1.1	878
$\pi^- \pi^0 \nu_{\tau}$	[g] (25.52 ± 0.09) %	S=1.1	878
$\pi^- \pi^0$ non- $\rho(770) \nu_{\tau}$	(3.0 ± 3.2) × 10 <sup>-3</sup>		878
$K^- \pi^0 \nu_{\tau}$	[g] (4.29 ± 0.15) × 10 <sup>-3</sup>		814
$h^- \geq 2\pi^0 \nu_{\tau}$	(10.87 ± 0.11) %	S=1.2	-
$h^- 2\pi^0 \nu_{\tau}$	(9.52 ± 0.11) %	S=1.1	862
$h^- 2\pi^0 \nu_{\tau}$ (ex. $K^0$ )	(9.36 ± 0.11) %	S=1.2	862
$\pi^- 2\pi^0 \nu_{\tau}$ (ex. $K^0$ )	[g] (9.30 ± 0.11) %	S=1.2	862
$\pi^- 2\pi^0 \nu_{\tau}$ (ex. $K^0$ ),	< 9 × 10 <sup>-3</sup>	CL=95%	862
$\pi^- 2\pi^0 \nu_{\tau}$ (ex. $K^0$ ),	< 7 × 10 <sup>-3</sup>	CL=95%	862
vector			
$K^- 2\pi^0 \nu_{\tau}$ (ex. $K^0$ )	[g] (6.5 ± 2.3) × 10 <sup>-4</sup>		796
$h^- \geq 3\pi^0 \nu_{\tau}$	(1.35 ± 0.07) %	S=1.1	-
$h^- \geq 3\pi^0 \nu_{\tau}$ (ex. $K^0$ )	(1.26 ± 0.07) %	S=1.1	-
$h^- 3\pi^0 \nu_{\tau}$	(1.19 ± 0.07) %		836
$\pi^- 3\pi^0 \nu_{\tau}$ (ex. $K^0$ )	[g] (1.05 ± 0.07) %		836
$K^- 3\pi^0 \nu_{\tau}$ (ex. $K^0$ ),	[g] (4.8 ± 2.2) × 10 <sup>-4</sup>		765
$\eta$			
$h^- 4\pi^0 \nu_{\tau}$ (ex. $K^0$ )	(1.6 ± 0.4) × 10 <sup>-3</sup>		800
$h^- 4\pi^0 \nu_{\tau}$ (ex. $K^0, \eta$ )	[g] (1.1 ± 0.4) × 10 <sup>-3</sup>		800
$K^- \geq 0\pi^0 \geq 0K^0 \geq 0\gamma \nu_{\tau}$	(1.572 ± 0.033) %	S=1.1	820
$K^- \geq 1(\pi^0 \text{ or } K^0 \text{ or } \gamma) \nu_{\tau}$	(8.72 ± 0.32) × 10 <sup>-3</sup>	S=1.1	-
Modes with $K^0$ 's			
$K_S^0$ (particles) <sup>-</sup> $\nu_{\tau}$	(9.2 ± 0.4) × 10 <sup>-3</sup>	S=1.5	-
$h^- \overline{K}^0 \nu_{\tau}$	(1.00 ± 0.05) %	S=1.8	812
$\pi^- \overline{K}^0 \nu_{\tau}$	[g] (8.4 ± 0.4) × 10 <sup>-3</sup>	S=2.1	812
$\pi^- \overline{K}^0$	(5.4 ± 2.1) × 10 <sup>-4</sup>		812
(non- $K^*(892)^-$ ) $\nu_{\tau}$			
$K^- K^0 \nu_{\tau}$	[g] (1.59 ± 0.16) × 10 <sup>-3</sup>		737
$K^- K^0 \geq 0\pi^0 \nu_{\tau}$	(3.18 ± 0.23) × 10 <sup>-3</sup>		737
$h^- \overline{K}^0 \pi^0 \nu_{\tau}$	(5.5 ± 0.4) × 10 <sup>-3</sup>		794
$\pi^- \overline{K}^0 \pi^0 \nu_{\tau}$	[g] (4.0 ± 0.4) × 10 <sup>-3</sup>		794
$\overline{K}^0 \rho^- \nu_{\tau}$	(2.2 ± 0.5) × 10 <sup>-3</sup>		612
$K^- K^0 \pi^0 \nu_{\tau}$	[g] (1.59 ± 0.20) × 10 <sup>-3</sup>		685



## Lepton Summary Table

$\mu^- \phi$	LF	< 8.4	$\times 10^{-8}$	CL=90%	590
$e^- e^+ e^-$	LF	< 2.7	$\times 10^{-8}$	CL=90%	888
$e^- \mu^+ \mu^-$	LF	< 2.7	$\times 10^{-8}$	CL=90%	882
$e^+ \mu^- \mu^-$	LF	< 1.7	$\times 10^{-8}$	CL=90%	882
$\mu^- e^+ e^-$	LF	< 1.8	$\times 10^{-8}$	CL=90%	885
$\mu^+ e^- e^-$	LF	< 1.5	$\times 10^{-8}$	CL=90%	885
$\mu^- \mu^+ \mu^-$	LF	< 2.1	$\times 10^{-8}$	CL=90%	873
$e^- \pi^+ \pi^-$	LF	< 4.4	$\times 10^{-8}$	CL=90%	877
$e^+ \pi^- \pi^-$	L	< 8.8	$\times 10^{-8}$	CL=90%	877
$\mu^- \pi^+ \pi^-$	LF	< 3.3	$\times 10^{-8}$	CL=90%	866
$\mu^+ \pi^- \pi^-$	L	< 3.7	$\times 10^{-8}$	CL=90%	866
$e^- \pi^+ K^-$	LF	< 5.8	$\times 10^{-8}$	CL=90%	813
$e^- \pi^- K^+$	LF	< 5.2	$\times 10^{-8}$	CL=90%	813
$e^+ \pi^- K^-$	L	< 6.7	$\times 10^{-8}$	CL=90%	813
$e^- K_S^0 K_S^0$	LF	< 7.1	$\times 10^{-8}$	CL=90%	736
$e^- K^+ K^-$	LF	< 5.4	$\times 10^{-8}$	CL=90%	738
$e^+ K^- K^-$	L	< 6.0	$\times 10^{-8}$	CL=90%	738
$\mu^- \pi^+ K^-$	LF	< 1.6	$\times 10^{-7}$	CL=90%	800
$\mu^- \pi^- K^+$	LF	< 1.0	$\times 10^{-7}$	CL=90%	800
$\mu^+ \pi^- K^-$	L	< 9.4	$\times 10^{-8}$	CL=90%	800
$\mu^- K_S^0 K_S^0$	LF	< 8.0	$\times 10^{-8}$	CL=90%	696
$\mu^- K^+ K^-$	LF	< 6.8	$\times 10^{-8}$	CL=90%	699
$\mu^+ K^- K^-$	L	< 9.6	$\times 10^{-8}$	CL=90%	699
$e^- \pi^0 \pi^0$	LF	< 6.5	$\times 10^{-6}$	CL=90%	878
$\mu^- \pi^0 \pi^0$	LF	< 1.4	$\times 10^{-5}$	CL=90%	867
$e^- \eta \eta$	LF	< 3.5	$\times 10^{-5}$	CL=90%	699
$\mu^- \eta \eta$	LF	< 6.0	$\times 10^{-5}$	CL=90%	653
$e^- \pi^0 \eta$	LF	< 2.4	$\times 10^{-5}$	CL=90%	798
$\mu^- \pi^0 \eta$	LF	< 2.2	$\times 10^{-5}$	CL=90%	784
$\bar{p} \gamma$	L,B	< 3.5	$\times 10^{-6}$	CL=90%	641
$\bar{p} \pi^0$	L,B	< 1.5	$\times 10^{-5}$	CL=90%	632
$\bar{p} 2\pi^0$	L,B	< 3.3	$\times 10^{-5}$	CL=90%	604
$\bar{p} \eta$	L,B	< 8.9	$\times 10^{-6}$	CL=90%	475
$\bar{p} \pi^0 \eta$	L,B	< 2.7	$\times 10^{-5}$	CL=90%	360
$\Lambda \pi^-$	L,B	< 7.2	$\times 10^{-8}$	CL=90%	525
$\bar{\Lambda} \pi^-$	L,B	< 1.4	$\times 10^{-7}$	CL=90%	525
$e^-$ light boson	LF	< 2.7	$\times 10^{-3}$	CL=95%	-
$\mu^-$ light boson	LF	< 5	$\times 10^{-3}$	CL=95%	-

## Heavy Charged Lepton Searches

 $L^\pm$  – charged lepton

Mass  $m > 100.8$  GeV, CL = 95% <sup>[h]</sup> Decay to  $\nu W$ .

 $L^\pm$  – stable charged heavy lepton

Mass  $m > 102.6$  GeV, CL = 95%

## Neutrino Properties

See the note on “Neutrino properties listings” in the Particle Listings.

Mass  $m < 2$  eV (tritium decay)

Mean life/mass,  $\tau/m > 300$  s/eV, CL = 90% (reactor)

Mean life/mass,  $\tau/m > 7 \times 10^9$  s/eV (solar)

Mean life/mass,  $\tau/m > 15.4$  s/eV, CL = 90% (accelerator)

Magnetic moment  $\mu < 0.32 \times 10^{-10} \mu_B$ , CL = 90% (solar)

## Number of Neutrino Types

Number  $N = 2.984 \pm 0.008$  (Standard Model fits to LEP data)

Number  $N = 2.92 \pm 0.05$  ( $S = 1.2$ ) (Direct measurement of invisible  $Z$  width)

## Neutrino Mixing

The following values are obtained through data analyses based on the 3-neutrino mixing scheme described in the review “Neutrino Mass, Mixing, and Oscillations” by K. Nakamura and S.T. Petcov in this Review.

$$\sin^2(2\theta_{12}) = 0.857 \pm 0.024$$

$$\Delta m_{21}^2 = (7.50 \pm 0.20) \times 10^{-5} \text{ eV}^2$$

$$\sin^2(2\theta_{23}) > 0.95 \text{ [i]}$$

$$\Delta m_{32}^2 = (2.32^{+0.12}_{-0.08}) \times 10^{-3} \text{ eV}^2 \text{ [j]}$$

$$\sin^2(2\theta_{13}) = 0.098 \pm 0.013$$

## Heavy Neutral Leptons, Searches for

For excited leptons, see Compositeness Limits below.

## Stable Neutral Heavy Lepton Mass Limits

Mass  $m > 45.0$  GeV, CL = 95% (Dirac)

Mass  $m > 39.5$  GeV, CL = 95% (Majorana)

## Neutral Heavy Lepton Mass Limits

Mass  $m > 90.3$  GeV, CL = 95%

(Dirac  $\nu_L$  coupling to  $e, \mu, \tau$ ; conservative case( $\tau$ ))

Mass  $m > 80.5$  GeV, CL = 95%

(Majorana  $\nu_L$  coupling to  $e, \mu, \tau$ ; conservative case( $\tau$ ))

## NOTES

In this Summary Table:

When a quantity has “(S = ...)” to its right, the error on the quantity has been enlarged by the “scale factor” S, defined as  $S = \sqrt{N^2/(N-1)}$ , where  $N$  is the number of measurements used in calculating the quantity. We do this when  $S > 1$ , which often indicates that the measurements are inconsistent. When  $S > 1.25$ , we also show in the Particle Listings an ideogram of the measurements. For more about S, see the Introduction.

A decay momentum  $p$  is given for each decay mode. For a 2-body decay,  $p$  is the momentum of each decay product in the rest frame of the decaying particle. For a 3-or-more-body decay,  $p$  is the largest momentum any of the products can have in this frame.

[a] This is the best limit for the mode  $e^- \rightarrow \nu \gamma$ . The best limit for “electron disappearance” is  $6.4 \times 10^{24}$  yr.

[b] See the “Note on Muon Decay Parameters” in the  $\mu$  Particle Listings for definitions and details.

[c]  $P_\mu$  is the longitudinal polarization of the muon from pion decay. In standard  $V-A$  theory,  $P_\mu = 1$  and  $\rho = \delta = 3/4$ .

[d] This only includes events with the  $\gamma$  energy  $> 10$  MeV. Since the  $e^- \bar{\nu}_e \nu_\mu$  and  $e^- \bar{\nu}_e \nu_\mu \gamma$  modes cannot be clearly separated, we regard the latter mode as a subset of the former.

[e] See the relevant Particle Listings for the energy limits used in this measurement.

[f] A test of additive vs. multiplicative lepton family number conservation.

[g] Basis mode for the  $\tau$ .

[h]  $L^\pm$  mass limit depends on decay assumptions; see the Full Listings.

[i] The limit quoted corresponds to the projection onto the  $\sin^2(2\theta_{23})$  axis of the 90% CL contour in the  $\sin^2(2\theta_{23}) - \Delta m_{32}^2$  plane.

[j] The sign of  $\Delta m_{32}^2$  is not known at this time. The range quoted is for the absolute value.

## Quark Summary Table

## QUARKS

The  $u$ -,  $d$ -, and  $s$ -quark masses are estimates of so-called “current-quark masses,” in a mass-independent subtraction scheme such as  $\overline{MS}$  at a scale  $\mu \approx 2$  GeV. The  $c$ - and  $b$ -quark masses are the “running” masses in the  $\overline{MS}$  scheme. For the  $b$ -quark we also quote the 1S mass. These can be different from the heavy quark masses obtained in potential models.

**u**

$$I(J^P) = \frac{1}{2}(\frac{1}{2}^+)$$

$$m_u = 2.3_{-0.5}^{+0.7} \text{ MeV} \quad \text{Charge} = \frac{2}{3} e \quad I_z = +\frac{1}{2}$$

$$m_u/m_d = 0.38\text{--}0.58$$

**d**

$$I(J^P) = \frac{1}{2}(\frac{1}{2}^+)$$

$$m_d = 4.8_{-0.3}^{+0.7} \text{ MeV} \quad \text{Charge} = -\frac{1}{3} e \quad I_z = -\frac{1}{2}$$

$$m_s/m_d = 17\text{--}22$$

$$\overline{m} = (m_u + m_d)/2 = 3.2\text{--}4.4 \text{ MeV}$$

**s**

$$I(J^P) = 0(\frac{1}{2}^+)$$

$$m_s = 95 \pm 5 \text{ MeV} \quad \text{Charge} = -\frac{1}{3} e \quad \text{Strangeness} = -1$$

$$m_s / ((m_u + m_d)/2) = 27 \pm 1$$

**c**

$$I(J^P) = 0(\frac{1}{2}^+)$$

$$m_c = 1.275 \pm 0.025 \text{ GeV} \quad \text{Charge} = \frac{2}{3} e \quad \text{Charm} = +1$$

**b**

$$I(J^P) = 0(\frac{1}{2}^+)$$

$$\text{Charge} = -\frac{1}{3} e \quad \text{Bottom} = -1$$

$$m_b(\overline{MS}) = 4.18 \pm 0.03 \text{ GeV}$$

$$m_b(1S) = 4.65 \pm 0.03 \text{ GeV}$$

**t**

$$I(J^P) = 0(\frac{1}{2}^+)$$

$$\text{Charge} = \frac{2}{3} e \quad \text{Top} = +1$$

$$\text{Mass (direct measurements)} \quad m = 173.5 \pm 0.6 \pm 0.8 \text{ GeV} \quad [a,b]$$

$$\text{Mass } (\overline{MS}) \text{ from cross-section measurements} \quad m = 160_{-4}^{+5} \text{ GeV} \quad [a]$$

$$m_t - m_{\bar{t}} = -1.4 \pm 2.0 \text{ GeV} \quad (S = 1.6)$$

$$\text{Full width } \Gamma = 2.0_{-0.6}^{+0.7} \text{ GeV}$$

$$\Gamma(Wb)/\Gamma(Wq(q = b, s, d)) = 0.91 \pm 0.04$$

<b>DECAY MODES</b>	Fraction ( $\Gamma_i/\Gamma$ )	Confidence level	$P$ (MeV/c)
$Wq(q = b, s, d)$			—
$Wb$			—
$\ell\nu_\ell$ anything	[c,d] (9.4±2.4) %		—
$\gamma q(q=u,c)$	[e] < 5.9	$\times 10^{-3}$	95%
<b><math>\Delta T = 1</math> weak neutral current (T1) modes</b>			
$Zq(q=u,c)$	T1 [f] < 3.2	%	95%

### $b'$ (4<sup>th</sup> Generation) Quark, Searches for

$$\text{Mass } m > 190 \text{ GeV, CL} = 95\% \quad (p\bar{p}, \text{ quasi-stable } b')$$

$$\text{Mass } m > 199 \text{ GeV, CL} = 95\% \quad (p\bar{p}, \text{ neutral-current decays})$$

$$\text{Mass } m > 128 \text{ GeV, CL} = 95\% \quad (p\bar{p}, \text{ charged-current decays})$$

$$\text{Mass } m > 46.0 \text{ GeV, CL} = 95\% \quad (e^+e^-, \text{ all decays})$$

### $t'$ (4<sup>th</sup> Generation) Quark, Searches for

$$\text{Mass } m \quad (p\bar{p}, t'\bar{t}' \text{ prod.}, t' \rightarrow Wq)$$

$$\text{Mass } m$$

### Free Quark Searches

All searches since 1977 have had negative results.

#### NOTES

- [a] A discussion of the definition of the top quark mass in these measurements can be found in the review “The Top Quark.”
- [b] Based on published top mass measurements using data from Tevatron Run-I and Run-II and LHC at  $\sqrt{s} = 7$  TeV. Including the most recent unpublished results from Tevatron Run-II, the Tevatron Electroweak Working Group reports a top mass of  $173.2 \pm 0.9$  GeV. See the note “The Top Quark” in the Quark Particle Listings of this Review.
- [c]  $\ell$  means  $e$  or  $\mu$  decay mode, not the sum over them.
- [d] Assumes lepton universality and  $W$ -decay acceptance.
- [e] This limit is for  $\Gamma(t \rightarrow \gamma q)/\Gamma(t \rightarrow Wb)$ .
- [f] This limit is for  $\Gamma(t \rightarrow Zq)/\Gamma(t \rightarrow Wb)$ .

## Meson Summary Table

## LIGHT UNFLAVORED MESONS ( $S = C = B = 0$ )

For  $I = 1$  ( $\pi, b, \rho, a$ ):  $u\bar{d}, (u\bar{u}-d\bar{d})/\sqrt{2}, d\bar{u}$ ;  
for  $I = 0$  ( $\eta, \eta', h, h', \omega, \phi, f, f'$ ):  $c_1(u\bar{u} + d\bar{d}) + c_2(s\bar{s})$

 $\pi^\pm$ 

$$J^{PC} = 1^-(0^-)$$

Mass  $m = 139.57018 \pm 0.00035$  MeV ( $S = 1.2$ )  
Mean life  $\tau = (2.6033 \pm 0.0005) \times 10^{-8}$  s ( $S = 1.2$ )  
 $c\tau = 7.8045$  m

$\pi^\pm \rightarrow \ell^\pm \nu \gamma$  form factors [a]

$F_V = 0.0254 \pm 0.0017$   
 $F_A = 0.0119 \pm 0.0001$   
 $F_V$  slope parameter  $a = 0.10 \pm 0.06$   
 $R = 0.059^{+0.009}_{-0.008}$

$\pi^-$  modes are charge conjugates of the modes below.

For decay limits to particles which are not established, see the section on Searches for Axions and Other Very Light Bosons.

$\pi^\pm$ DECAY MODES	Fraction ( $\Gamma_i/\Gamma$ )	Confidence level	$p$ (MeV/c)
$\mu^+ \nu_\mu$	[b] (99.98770 $\pm$ 0.00004) %		30
$\mu^+ \nu_\mu \gamma$	[c] (2.00 $\pm$ 0.25) $\times 10^{-4}$		30
$e^+ \nu_e$	[b] (1.230 $\pm$ 0.004) $\times 10^{-4}$		70
$e^+ \nu_e \gamma$	[c] (7.39 $\pm$ 0.05) $\times 10^{-7}$		70
$e^+ \nu_e \pi^0$	(1.036 $\pm$ 0.006) $\times 10^{-8}$		4
$e^+ \nu_e e^+ e^-$	(3.2 $\pm$ 0.5) $\times 10^{-9}$		70
$e^+ \nu_e \nu \bar{\nu}$	< 5 $\times 10^{-6}$	90%	70
<b>Lepton Family number (LF) or Lepton number (L) violating modes</b>			
$\mu^+ \bar{\nu}_e$	L [d] < 1.5	$\times 10^{-3}$ 90%	30
$\mu^+ \nu_e$	LF [d] < 8.0	$\times 10^{-3}$ 90%	30
$\mu^- e^+ e^+ \nu$	LF < 1.6	$\times 10^{-6}$ 90%	30

 $\pi^0$ 

$$J^{PC} = 1^-(0^{++})$$

Mass  $m = 134.9766 \pm 0.0006$  MeV ( $S = 1.1$ )  
 $m_{\pi^\pm} - m_{\pi^0} = 4.5936 \pm 0.0005$  MeV  
Mean life  $\tau = (8.52 \pm 0.18) \times 10^{-17}$  s ( $S = 1.2$ )  
 $c\tau = 25.5$  nm

For decay limits to particles which are not established, see the appropriate Search sections ( $A^0$  (axion) and Other Light Boson ( $X^0$ ) Searches, etc.).

$\pi^0$ DECAY MODES	Fraction ( $\Gamma_i/\Gamma$ )	Scale factor/ Confidence level	$p$ (MeV/c)
$2\gamma$	(98.823 $\pm$ 0.034) %	S=1.5	67
$e^+ e^- \gamma$	(1.174 $\pm$ 0.035) %	S=1.5	67
$\gamma$ positronium	(1.82 $\pm$ 0.29) $\times 10^{-9}$		67
$e^+ e^+ e^- e^-$	(3.34 $\pm$ 0.16) $\times 10^{-5}$		67
$e^+ e^-$	(6.46 $\pm$ 0.33) $\times 10^{-8}$		67
$4\gamma$	< 2 $\times 10^{-8}$	CL=90%	67
$\nu \bar{\nu}$	[e] < 2.7 $\times 10^{-7}$	CL=90%	67
$\nu_e \bar{\nu}_e$	< 1.7 $\times 10^{-6}$	CL=90%	67
$\nu_\mu \bar{\nu}_\mu$	< 1.6 $\times 10^{-6}$	CL=90%	67
$\nu_\tau \bar{\nu}_\tau$	< 2.1 $\times 10^{-6}$	CL=90%	67
$\gamma \nu \bar{\nu}$	< 6 $\times 10^{-4}$	CL=90%	67
<b>Charge conjugation (C) or Lepton Family number (LF) violating modes</b>			
$3\gamma$	C < 3.1 $\times 10^{-8}$	CL=90%	67
$\mu^+ e^-$	LF < 3.8 $\times 10^{-10}$	CL=90%	26
$\mu^- e^+$	LF < 3.4 $\times 10^{-9}$	CL=90%	26
$\mu^+ e^- + \mu^- e^+$	LF < 3.6 $\times 10^{-10}$	CL=90%	26

 $\eta$ 

$$J^{PC} = 0^+(0^{-+})$$

Mass  $m = 547.853 \pm 0.024$  MeV  
Full width  $\Gamma = 1.30 \pm 0.07$  keV

### C-nonconserving decay parameters

$\pi^+ \pi^- \pi^0$  left-right asymmetry =  $(0.09^{+0.11}_{-0.12}) \times 10^{-2}$   
 $\pi^+ \pi^- \pi^0$  sextant asymmetry =  $(0.12^{+0.10}_{-0.11}) \times 10^{-2}$   
 $\pi^+ \pi^- \pi^0$  quadrant asymmetry =  $(-0.09 \pm 0.09) \times 10^{-2}$   
 $\pi^+ \pi^- \gamma$  left-right asymmetry =  $(0.9 \pm 0.4) \times 10^{-2}$   
 $\pi^+ \pi^- \gamma$   $\beta$  (D-wave) =  $-0.02 \pm 0.07$  ( $S = 1.3$ )

### CP-nonconserving decay parameters

$\pi^+ \pi^- e^+ e^-$  decay-plane asymmetry  $A_\phi = (-0.6 \pm 3.1) \times 10^{-2}$

### Dalitz plot parameter

$\pi^0 \pi^0 \pi^0$   $\alpha = -0.0315 \pm 0.0015$

$\eta$ DECAY MODES	Fraction ( $\Gamma_i/\Gamma$ )	Scale factor/ Confidence level	$p$ (MeV/c)
<b>Neutral modes</b>			
neutral modes	(71.91 $\pm$ 0.34) %	S=1.2	-
$2\gamma$	(39.31 $\pm$ 0.20) %	S=1.1	274
$3\pi^0$	(32.57 $\pm$ 0.23) %	S=1.1	179
$\pi^0 2\gamma$	(2.7 $\pm$ 0.5) $\times 10^{-4}$	S=1.1	257
$2\pi^0 2\gamma$	< 1.2 $\times 10^{-3}$	CL=90%	238
$4\gamma$	< 2.8 $\times 10^{-4}$	CL=90%	274
invisible	< 6 $\times 10^{-4}$	CL=90%	-
<b>Charged modes</b>			
charged modes	(28.10 $\pm$ 0.34) %	S=1.2	-
$\pi^+ \pi^- \pi^0$	(22.74 $\pm$ 0.28) %	S=1.2	174
$\pi^+ \pi^- \gamma$	(4.60 $\pm$ 0.16) %	S=2.0	236
$e^+ e^- \gamma$	(6.9 $\pm$ 0.4) $\times 10^{-3}$	S=1.2	274
$\mu^+ \mu^- \gamma$	(3.1 $\pm$ 0.4) $\times 10^{-4}$		253
$e^+ e^-$	< 5.6 $\times 10^{-6}$	CL=90%	274
$\mu^+ \mu^-$	(5.8 $\pm$ 0.8) $\times 10^{-6}$		253
$2e^+ 2e^-$	(2.40 $\pm$ 0.22) $\times 10^{-5}$		274
$\pi^+ \pi^- e^+ e^- (\gamma)$	(2.68 $\pm$ 0.11) $\times 10^{-4}$		235
$e^+ e^- \mu^+ \mu^-$	< 1.6 $\times 10^{-4}$	CL=90%	253
$2\mu^+ 2\mu^-$	< 3.6 $\times 10^{-4}$	CL=90%	161
$\mu^+ \mu^- \pi^+ \pi^-$	< 3.6 $\times 10^{-4}$	CL=90%	113
$\pi^+ \pi^- 2\gamma$	< 2.0 $\times 10^{-3}$		236
$\pi^+ \pi^- \pi^0 \gamma$	< 5 $\times 10^{-4}$	CL=90%	174
$\pi^0 \mu^+ \mu^- \gamma$	< 3 $\times 10^{-6}$	CL=90%	210

### Charge conjugation (C), Parity (P), Charge conjugation $\times$ Parity (CP), or Lepton Family number (LF) violating modes

$\pi^0 \gamma$	C	< 9 $\times 10^{-5}$	CL=90%	257
$\pi^+ \pi^-$	P, CP	< 1.3 $\times 10^{-5}$	CL=90%	236
$2\pi^0$	P, CP	< 3.5 $\times 10^{-4}$	CL=90%	238
$2\pi^0 \gamma$	C	< 5 $\times 10^{-4}$	CL=90%	238
$3\pi^0 \gamma$	C	< 6 $\times 10^{-5}$	CL=90%	179
$3\gamma$	C	< 1.6 $\times 10^{-5}$	CL=90%	274
$4\pi^0$	P, CP	< 6.9 $\times 10^{-7}$	CL=90%	40
$\pi^0 e^+ e^-$	C	[f] < 4 $\times 10^{-5}$	CL=90%	257
$\pi^0 \mu^+ \mu^-$	C	[f] < 5 $\times 10^{-6}$	CL=90%	210
$\mu^+ e^- + \mu^- e^+$	LF	< 6 $\times 10^{-6}$	CL=90%	264

$f_0(500)$  or  $\sigma$  [g]  
was  $f_0(600)$

$$J^{PC} = 0^+(0^{++})$$

Mass  $m = (400-550)$  MeV  
Full width  $\Gamma = (400-700)$  MeV

$f_0(500)$ DECAY MODES	Fraction ( $\Gamma_i/\Gamma$ )	$p$ (MeV/c)
$\pi \pi$	dominant	-
$\gamma \gamma$	seen	-

 $\rho(770)$  [h]

$$J^{PC} = 1^+(1^{--})$$

Mass  $m = 775.49 \pm 0.34$  MeV  
Full width  $\Gamma = 149.1 \pm 0.8$  MeV  
 $\Gamma_{ee} = 7.04 \pm 0.06$  keV



## Meson Summary Table

$\rho(770)$ DECAY MODES	Fraction ( $\Gamma_i/\Gamma$ )	Scale factor/ Confidence level	$\rho$ (MeV/c)
$\pi^+\pi^-$	$\sim 100$	%	363
<b><math>\rho(770)^\pm</math> decays</b>			
$\pi^\pm\gamma$	( 4.5 $\pm$ 0.5 ) $\times 10^{-4}$	S=2.2	375
$\pi^\pm\eta$	< 6 $\times 10^{-3}$	CL=84%	153
$\pi^\pm\pi^+\pi^-\pi^0$	< 2.0 $\times 10^{-3}$	CL=84%	254
<b><math>\rho(770)^0</math> decays</b>			
$\pi^+\pi^-\gamma$	( 9.9 $\pm$ 1.6 ) $\times 10^{-3}$		362
$\pi^0\gamma$	( 6.0 $\pm$ 0.8 ) $\times 10^{-4}$		376
$\eta\gamma$	( 3.00 $\pm$ 0.20 ) $\times 10^{-4}$		194
$\pi^0\pi^0\gamma$	( 4.5 $\pm$ 0.8 ) $\times 10^{-5}$		363
$\mu^+\mu^-$	[i] ( 4.55 $\pm$ 0.28 ) $\times 10^{-5}$		373
$e^+e^-$	[i] ( 4.72 $\pm$ 0.05 ) $\times 10^{-5}$		388
$\pi^+\pi^-\pi^0$	( 1.01 $\pm$ 0.54 $\pm$ 0.34 ) $\times 10^{-4}$		323
$\pi^+\pi^-\pi^+\pi^-$	( 1.8 $\pm$ 0.9 ) $\times 10^{-5}$		251
$\pi^+\pi^-\pi^0\pi^0$	( 1.6 $\pm$ 0.8 ) $\times 10^{-5}$		257
$\pi^0e^+e^-$	< 1.2 $\times 10^{-5}$	CL=90%	376

 **$\omega(782)$** 

$$J^{PC} = 0^-(1^--)$$

Mass  $m = 782.65 \pm 0.12$  MeV (S = 1.9)  
 Full width  $\Gamma = 8.49 \pm 0.08$  MeV  
 $\Gamma_{ee} = 0.60 \pm 0.02$  MeV

$\omega(782)$ DECAY MODES	Fraction ( $\Gamma_i/\Gamma$ )	Scale factor/ Confidence level	$\rho$ (MeV/c)
$\pi^+\pi^-\pi^0$	(89.2 $\pm$ 0.7) %		327
$\pi^0\gamma$	( 8.28 $\pm$ 0.28 ) %	S=2.1	380
$\pi^+\pi^-$	( 1.53 $\pm$ 0.11 $\pm$ 0.13 ) %	S=1.2	366
neutrals (excluding $\pi^0\gamma$ )	( 8 $\pm$ 5 ) $\times 10^{-3}$	S=1.1	-
$\eta\gamma$	( 4.6 $\pm$ 0.4 ) $\times 10^{-4}$	S=1.1	200
$\pi^0e^+e^-$	( 7.7 $\pm$ 0.6 ) $\times 10^{-4}$		380
$\pi^0\mu^+\mu^-$	( 1.3 $\pm$ 0.4 ) $\times 10^{-4}$	S=2.1	349
$e^+e^-$	( 7.28 $\pm$ 0.14 ) $\times 10^{-5}$	S=1.3	391
$\pi^+\pi^-\pi^0\pi^0$	< 2 $\times 10^{-4}$	CL=90%	262
$\pi^+\pi^-\gamma$	< 3.6 $\times 10^{-3}$	CL=95%	366
$\pi^+\pi^-\pi^+\pi^-$	< 1 $\times 10^{-3}$	CL=90%	256
$\pi^0\pi^0\gamma$	( 6.6 $\pm$ 1.1 ) $\times 10^{-5}$		367
$\eta\pi^0\gamma$	< 3.3 $\times 10^{-5}$	CL=90%	162
$\mu^+\mu^-$	( 9.0 $\pm$ 3.1 ) $\times 10^{-5}$		377
$3\gamma$	< 1.9 $\times 10^{-4}$	CL=95%	391

**Charge conjugation (C) violating modes**

$\eta\pi^0$	C	< 2.1 $\times 10^{-4}$	CL=90%	162
$2\pi^0$	C	< 2.1 $\times 10^{-4}$	CL=90%	367
$3\pi^0$	C	< 2.3 $\times 10^{-4}$	CL=90%	330

 **$\eta'(958)$** 

$$J^{PC} = 0^+(0^{+-})$$

Mass  $m = 957.78 \pm 0.06$  MeV  
 Full width  $\Gamma = 0.199 \pm 0.009$  MeV

$\eta'(958)$ DECAY MODES	Fraction ( $\Gamma_i/\Gamma$ )	Confidence level	$\rho$ (MeV/c)
$\pi^+\pi^-\eta$	(43.4 $\pm$ 0.7) %		232
$\rho^0\gamma$ (including non-resonant $\pi^+\pi^-\gamma$ )	(29.3 $\pm$ 0.6) %		165
$\pi^0\pi^0\eta$	(21.6 $\pm$ 0.8) %		239
$\omega\gamma$	( 2.75 $\pm$ 0.22 ) %		159
$\gamma\gamma$	( 2.18 $\pm$ 0.08 ) %		479
$3\pi^0$	( 1.68 $\pm$ 0.22 ) $\times 10^{-3}$		430
$\mu^+\mu^-\gamma$	( 1.07 $\pm$ 0.26 ) $\times 10^{-4}$		467
$\pi^+\pi^-\mu^+\mu^-$	< 2.2 $\times 10^{-4}$	90%	401
$\pi^+\pi^-\pi^0$	( 3.6 $\pm$ 1.1 $\pm$ 0.9 ) $\times 10^{-3}$		428
$\pi^0\rho^0$	< 4 %	90%	111
$2(\pi^+\pi^-)$	< 2.4 $\times 10^{-4}$	90%	372
$\pi^+\pi^-2\pi^0$	< 2.6 $\times 10^{-3}$	90%	376
$2(\pi^+\pi^-)$ neutrals	< 1 %	95%	-
$2(\pi^+\pi^-)\pi^0$	< 1.9 $\times 10^{-3}$	90%	298
$2(\pi^+\pi^-)2\pi^0$	< 1 %	95%	197

$3(\pi^+\pi^-)$	< 5 $\times 10^{-4}$	90%	189
$\pi^+\pi^-e^+e^-$	( 2.4 $\pm$ 1.3 $\pm$ 1.0 ) $\times 10^{-3}$		458
$\gamma e^+e^-$	< 9 $\times 10^{-4}$	90%	479
$\pi^0\gamma\gamma$	< 8 $\times 10^{-4}$	90%	469
$4\pi^0$	< 5 $\times 10^{-4}$	90%	380
$e^+e^-$	< 2.1 $\times 10^{-7}$	90%	479
invisible	< 9 $\times 10^{-4}$	90%	-

**Charge conjugation (C), Parity (P),  
Lepton family number (LF) violating modes**

$\pi^+\pi^-$	$P, CP$	< 6 $\times 10^{-5}$	90%	458
$\pi^0\pi^0$	$P, CP$	< 4 $\times 10^{-4}$	90%	459
$\pi^0e^+e^-$	C	[f] < 1.4 $\times 10^{-3}$	90%	469
$\eta e^+e^-$	C	[f] < 2.4 $\times 10^{-3}$	90%	322
$3\gamma$	C	< 1.0 $\times 10^{-4}$	90%	479
$\mu^+\mu^-\pi^0$	C	[f] < 6.0 $\times 10^{-5}$	90%	445
$\mu^+\mu^-\eta$	C	[f] < 1.5 $\times 10^{-5}$	90%	273
$e\mu$	LF	< 4.7 $\times 10^{-4}$	90%	473

 **$f_0(980)$  [i]**

$$J^{PC} = 0^+(0^{++})$$

Mass  $m = 990 \pm 20$  MeV  
 Full width  $\Gamma = 40$  to 100 MeV

$f_0(980)$ DECAY MODES	Fraction ( $\Gamma_i/\Gamma$ )	$\rho$ (MeV/c)
$\pi\pi$	dominant	476
$K\bar{K}$	seen	36
$\gamma\gamma$	seen	495

 **$a_0(980)$  [i]**

$$J^{PC} = 1^-(0^{++})$$

Mass  $m = 980 \pm 20$  MeV  
 Full width  $\Gamma = 50$  to 100 MeV

$a_0(980)$ DECAY MODES	Fraction ( $\Gamma_i/\Gamma$ )	$\rho$ (MeV/c)
$\eta\pi$	dominant	319
$K\bar{K}$	seen	†
$\gamma\gamma$	seen	490

 **$\phi(1020)$** 

$$J^{PC} = 0^-(1^{--})$$

Mass  $m = 1019.455 \pm 0.020$  MeV (S = 1.1)  
 Full width  $\Gamma = 4.26 \pm 0.04$  MeV (S = 1.4)

$\phi(1020)$ DECAY MODES	Fraction ( $\Gamma_i/\Gamma$ )	Scale factor/ Confidence level	$\rho$ (MeV/c)
$K^+K^-$	(48.9 $\pm$ 0.5) %	S=1.1	127
$K_L^0K_S^0$	(34.2 $\pm$ 0.4) %	S=1.1	110
$\rho\pi + \pi^+\pi^-\pi^0$	(15.32 $\pm$ 0.32) %	S=1.1	-
$\eta\gamma$	( 1.309 $\pm$ 0.024 ) %	S=1.2	363
$\pi^0\gamma$	( 1.27 $\pm$ 0.06 ) $\times 10^{-3}$		501
$\ell^+\ell^-$	-		510
$e^+e^-$	( 2.954 $\pm$ 0.030 ) $\times 10^{-4}$	S=1.1	510
$\mu^+\mu^-$	( 2.87 $\pm$ 0.19 ) $\times 10^{-4}$		499
$\eta e^+e^-$	( 1.15 $\pm$ 0.10 ) $\times 10^{-4}$		363
$\pi^+\pi^-$	( 7.4 $\pm$ 1.3 ) $\times 10^{-5}$		490
$\omega\pi^0$	( 4.7 $\pm$ 0.5 ) $\times 10^{-5}$		171
$\omega\gamma$	< 5 %	CL=84%	209
$\rho\gamma$	< 1.2 $\times 10^{-5}$	CL=90%	215
$\pi^+\pi^-\gamma$	( 4.1 $\pm$ 1.3 ) $\times 10^{-5}$		490
$f_0(980)\gamma$	( 3.22 $\pm$ 0.19 ) $\times 10^{-4}$	S=1.1	29
$\pi^0\pi^0\gamma$	( 1.13 $\pm$ 0.06 ) $\times 10^{-4}$		492
$\pi^+\pi^-\pi^+\pi^-$	( 4.0 $\pm$ 2.8 $\pm$ 2.2 ) $\times 10^{-6}$		410
$\pi^+\pi^+\pi^-\pi^-\pi^0$	< 4.6 $\times 10^{-6}$	CL=90%	342
$\pi^0e^+e^-$	( 1.12 $\pm$ 0.28 ) $\times 10^{-5}$		501
$\pi^0\eta\gamma$	( 7.27 $\pm$ 0.30 ) $\times 10^{-5}$	S=1.5	346
$a_0(980)\gamma$	( 7.6 $\pm$ 0.6 ) $\times 10^{-5}$		39
$K^0\bar{K}^0\gamma$	< 1.9 $\times 10^{-8}$	CL=90%	110
$\eta'(958)\gamma$	( 6.25 $\pm$ 0.21 ) $\times 10^{-5}$		60
$\eta\pi^0\pi^0\gamma$	< 2 $\times 10^{-5}$	CL=90%	293
$\mu^+\mu^-\gamma$	( 1.4 $\pm$ 0.5 ) $\times 10^{-5}$		499
$\rho\gamma\gamma$	< 1.2 $\times 10^{-4}$	CL=90%	215
$\eta\pi^+\pi^-$	< 1.8 $\times 10^{-5}$	CL=90%	288
$\eta\mu^+\mu^-$	< 9.4 $\times 10^{-6}$	CL=90%	321

## Meson Summary Table

**Lepton Family number (LF) violating modes**  
 $e^\pm \mu^\mp$   $LF < 2 \times 10^{-6}$  CL=90% 504

**$h_1(1170)$**   $I^G(J^{PC}) = 0^-(1^+ -)$

Mass  $m = 1170 \pm 20$  MeV  
 Full width  $\Gamma = 360 \pm 40$  MeV

$h_1(1170)$ DECAY MODES	Fraction ( $\Gamma_i/\Gamma$ )	$\rho$ (MeV/c)
$\rho\pi$	seen	307

**$b_1(1235)$**   $I^G(J^{PC}) = 1^+(1^+ -)$

Mass  $m = 1229.5 \pm 3.2$  MeV ( $S = 1.6$ )  
 Full width  $\Gamma = 142 \pm 9$  MeV ( $S = 1.2$ )

$b_1(1235)$ DECAY MODES	Fraction ( $\Gamma_i/\Gamma$ )	Confidence level	$\rho$ (MeV/c)
$\omega\pi$	dominant		348
$\pi^\pm\gamma$	$[D/S \text{ amplitude ratio} = 0.277 \pm 0.027]$		
$\eta\rho$	$(1.6 \pm 0.4) \times 10^{-3}$		607
$\pi^+\pi^+\pi^-\pi^0$	seen	†	
$K^*(892)^\pm K^\mp$	$< 50$ %	84%	535
$(K\bar{K})^\pm\pi^0$	seen	†	
$K_S^0 K_L^0 \pi^\pm$	$< 8$ %	90%	248
$K_S^0 K_S^0 \pi^\pm$	$< 6$ %	90%	235
$K_S^0 K_S^0 \pi^\pm$	$< 2$ %	90%	235
$\phi\pi$	$< 1.5$ %	84%	147

**$a_1(1260)$  [k]**  $I^G(J^{PC}) = 1^-(1^+ +)$

Mass  $m = 1230 \pm 40$  MeV [l]  
 Full width  $\Gamma = 250$  to  $600$  MeV

$a_1(1260)$ DECAY MODES	Fraction ( $\Gamma_i/\Gamma$ )	$\rho$ (MeV/c)
$(\rho\pi)_{S\text{-wave}}$	seen	353
$(\rho\pi)_{D\text{-wave}}$	seen	353
$(\rho(1450)\pi)_{S\text{-wave}}$	seen	†
$(\rho(1450)\pi)_{D\text{-wave}}$	seen	†
$\sigma\pi$	seen	-
$f_0(980)\pi$	not seen	179
$f_0(1370)\pi$	seen	†
$f_2(1270)\pi$	seen	†
$K\bar{K}^*(892) + \text{c.c.}$	seen	†
$\pi\gamma$	seen	608

**$f_2(1270)$**   $I^G(J^{PC}) = 0^+(2^+ +)$

Mass  $m = 1275.1 \pm 1.2$  MeV ( $S = 1.1$ )  
 Full width  $\Gamma = 185.1^{+2.9}_{-2.4}$  MeV ( $S = 1.5$ )

$f_2(1270)$ DECAY MODES	Fraction ( $\Gamma_i/\Gamma$ )	Scale factor/ Confidence level	$\rho$ (MeV/c)
$\pi\pi$	$(84.8 \pm 2.4) \%$	$S=1.2$	623
$\pi^+\pi^-2\pi^0$	$(7.1 \pm 1.4) \%$	$S=1.3$	562
$K\bar{K}$	$(4.6 \pm 0.4) \%$	$S=2.8$	403
$2\pi^+2\pi^-$	$(2.8 \pm 0.4) \%$	$S=1.2$	559
$\eta\eta$	$(4.0 \pm 0.8) \times 10^{-3}$	$S=2.1$	326
$4\pi^0$	$(3.0 \pm 1.0) \times 10^{-3}$		564
$\gamma\gamma$	$(1.64 \pm 0.19) \times 10^{-5}$	$S=1.9$	638
$\eta\pi\pi$	$< 8 \times 10^{-3}$	CL=95%	477
$K^0 K^- \pi^+ + \text{c.c.}$	$< 3.4 \times 10^{-3}$	CL=95%	293
$e^+e^-$	$< 6 \times 10^{-10}$	CL=90%	638

**$f_1(1285)$**

$I^G(J^{PC}) = 0^+(1^+ +)$

Mass  $m = 1282.1 \pm 0.6$  MeV ( $S = 1.7$ )  
 Full width  $\Gamma = 24.2 \pm 1.1$  MeV ( $S = 1.3$ )

$f_1(1285)$ DECAY MODES	Fraction ( $\Gamma_i/\Gamma$ )	Scale factor/ Confidence level	$\rho$ (MeV/c)
$4\pi$	$(33.1 \pm 2.1) \%$	$S=1.3$	568
$\pi^0\pi^0\pi^+\pi^-$	$(22.0 \pm 1.4) \%$	$S=1.3$	566
$2\pi^+2\pi^-$	$(11.0 \pm 0.7) \%$	$S=1.3$	563
$\rho^0\pi^+\pi^-$	$(11.0 \pm 0.7) \%$	$S=1.3$	336
$4\pi^0$	seen		†
$\eta\pi^+\pi^-$	$< 7 \times 10^{-4}$	CL=90%	568
$\eta\pi\pi$	$(35 \pm 15) \%$		479
$a_0(980)\pi$ [ignoring $a_0(980) \rightarrow K\bar{K}$ ]	$(52.4 \pm 1.9) \%$	$S=1.2$	482
$\eta\pi\pi$ [excluding $a_0(980)\pi$ ]	$(36 \pm 7) \%$		238
$K\bar{K}\pi$	$(16 \pm 7) \%$		482
$K\bar{K}^*(892)$	$(9.0 \pm 0.4) \%$	$S=1.1$	308
$\pi^+\pi^-\pi^0$	not seen	†	
$\rho^\pm\pi^\mp$	$(3.0 \pm 0.9) \times 10^{-3}$		603
$\gamma\rho^0$	$< 3.1 \times 10^{-3}$	CL=95%	390
$\phi\gamma$	$(5.5 \pm 1.3) \%$	$S=2.8$	407
	$(7.4 \pm 2.6) \times 10^{-4}$		236

**$\eta(1295)$**

$I^G(J^{PC}) = 0^+(0^- +)$

Mass  $m = 1294 \pm 4$  MeV ( $S = 1.6$ )  
 Full width  $\Gamma = 55 \pm 5$  MeV

$\eta(1295)$ DECAY MODES	Fraction ( $\Gamma_i/\Gamma$ )	$\rho$ (MeV/c)
$\eta\pi^+\pi^-$	seen	487
$a_0(980)\pi$	seen	248
$\eta\pi^0\pi^0$	seen	490
$\eta(\pi\pi)_{S\text{-wave}}$	seen	-

**$\pi(1300)$**

$I^G(J^{PC}) = 1^-(0^- +)$

Mass  $m = 1300 \pm 100$  MeV [l]  
 Full width  $\Gamma = 200$  to  $600$  MeV

$\pi(1300)$ DECAY MODES	Fraction ( $\Gamma_i/\Gamma$ )	$\rho$ (MeV/c)
$\rho\pi$	seen	404
$\pi(\pi\pi)_{S\text{-wave}}$	seen	-

**$a_2(1320)$**

$I^G(J^{PC}) = 1^-(2^+ +)$

Mass  $m = 1318.3^{+0.5}_{-0.6}$  MeV ( $S = 1.2$ )  
 Full width  $\Gamma = 107 \pm 5$  MeV [l]

$a_2(1320)$ DECAY MODES	Fraction ( $\Gamma_i/\Gamma$ )	Scale factor/ Confidence level	$\rho$ (MeV/c)
$3\pi$	$(70.1 \pm 2.7) \%$	$S=1.2$	624
$\eta\pi$	$(14.5 \pm 1.2) \%$		535
$\omega\pi\pi$	$(10.6 \pm 3.2) \%$	$S=1.3$	366
$K\bar{K}$	$(4.9 \pm 0.8) \%$		437
$\eta'(958)\pi$	$(5.3 \pm 0.9) \times 10^{-3}$		288
$\pi^\pm\gamma$	$(2.68 \pm 0.31) \times 10^{-3}$		652
$\gamma\gamma$	$(9.4 \pm 0.7) \times 10^{-6}$		659
$e^+e^-$	$< 5 \times 10^{-9}$	CL=90%	659

## Meson Summary Table

 **$f_0(1370)$**  [l]

$$J^G(J^{PC}) = 0^+(0^{++})$$

Mass  $m = 1200$  to  $1500$  MeV  
 Full width  $\Gamma = 200$  to  $500$  MeV

$f_0(1370)$ DECAY MODES	Fraction ( $\Gamma_i/\Gamma$ )	$\rho$ (MeV/c)
$\pi\pi$	seen	672
$4\pi$	seen	617
$4\pi^0$	seen	617
$2\pi^+2\pi^-$	seen	612
$\pi^+\pi^-2\pi^0$	seen	615
$\rho\rho$	dominant	†
$2(\pi\pi)$ s-wave	seen	–
$\pi(1300)\pi$	seen	†
$a_1(1260)\pi$	seen	35
$\eta\eta$	seen	411
$K\bar{K}$	seen	475
$K\bar{K}n\pi$	not seen	†
$6\pi$	not seen	508
$\omega\omega$	not seen	†
$\gamma\gamma$	seen	685
$e^+e^-$	not seen	685

 **$\pi_1(1400)$**  [m]

$$J^G(J^{PC}) = 1^-(1^{-+})$$

Mass  $m = 1354 \pm 25$  MeV ( $S = 1.8$ )  
 Full width  $\Gamma = 330 \pm 35$  MeV

$\pi_1(1400)$ DECAY MODES	Fraction ( $\Gamma_i/\Gamma$ )	$\rho$ (MeV/c)
$\eta\pi^0$	seen	557
$\eta\pi^-$	seen	556

 **$\eta(1405)$**  [n]

$$J^G(J^{PC}) = 0^+(0^{-+})$$

Mass  $m = 1408.9 \pm 2.4$  MeV [l] ( $S = 2.3$ )  
 Full width  $\Gamma = 51.1 \pm 3.2$  MeV [l] ( $S = 2.0$ )

$\eta(1405)$ DECAY MODES	Fraction ( $\Gamma_i/\Gamma$ )	Confidence level	$\rho$ (MeV/c)
$K\bar{K}\pi$	seen		424
$\eta\pi\pi$	seen		562
$a_0(980)\pi$	seen		345
$\eta(\pi\pi)$ s-wave	seen		–
$f_0(980)\eta$	seen		†
$4\pi$	seen		639
$\rho\rho$	<58 %	99.85%	†
$\rho^0\gamma$	seen		491
$K^*(892)K$	seen		123

 **$f_1(1420)$**  [o]

$$J^G(J^{PC}) = 0^+(1^{++})$$

Mass  $m = 1426.4 \pm 0.9$  MeV ( $S = 1.1$ )  
 Full width  $\Gamma = 54.9 \pm 2.6$  MeV

$f_1(1420)$ DECAY MODES	Fraction ( $\Gamma_i/\Gamma$ )	$\rho$ (MeV/c)
$K\bar{K}\pi$	dominant	438
$K\bar{K}^*(892) + c.c.$	dominant	163
$\eta\pi\pi$	possibly seen	573
$\phi\gamma$	seen	349

 **$\omega(1420)$**  [p]

$$J^G(J^{PC}) = 0^-(1^{--})$$

Mass  $m$  (1400–1450) MeV  
 Full width  $\Gamma$  (180–250) MeV

$\omega(1420)$ DECAY MODES	Fraction ( $\Gamma_i/\Gamma$ )	$\rho$ (MeV/c)
$\rho\pi$	dominant	486
$\omega\pi\pi$	seen	444
$b_1(1235)\pi$	seen	125
$e^+e^-$	seen	710

 **$a_0(1450)$**  [l]

$$J^G(J^{PC}) = 1^-(0^{++})$$

Mass  $m = 1474 \pm 19$  MeV  
 Full width  $\Gamma = 265 \pm 13$  MeV

$a_0(1450)$ DECAY MODES	Fraction ( $\Gamma_i/\Gamma$ )	$\rho$ (MeV/c)
$\pi\eta$	seen	627
$\pi\eta'(958)$	seen	410
$K\bar{K}$	seen	547
$\omega\pi\pi$	seen	484
$a_0(980)\pi\pi$	seen	342
$\gamma\gamma$	seen	737

 **$\rho(1450)$**  [q]

$$J^G(J^{PC}) = 1^+(1^{--})$$

Mass  $m = 1465 \pm 25$  MeV [l]  
 Full width  $\Gamma = 400 \pm 60$  MeV [l]

$\rho(1450)$ DECAY MODES	Fraction ( $\Gamma_i/\Gamma$ )	$\rho$ (MeV/c)
$\pi\pi$	seen	720
$4\pi$	seen	669
$e^+e^-$	seen	732
$\eta\rho$	possibly seen	310
$a_2(1320)\pi$	not seen	54
$K\bar{K}$	not seen	541
$K\bar{K}^*(892) + c.c.$	possibly seen	229
$\eta\gamma$	possibly seen	630
$f_0(500)\gamma$	not seen	–
$f_0(980)\gamma$	not seen	398
$f_0(1370)\gamma$	not seen	92
$f_2(1270)\gamma$	not seen	178

 **$\eta(1475)$**  [n]

$$J^G(J^{PC}) = 0^+(0^{-+})$$

Mass  $m = 1476 \pm 4$  MeV ( $S = 1.3$ )  
 Full width  $\Gamma = 85 \pm 9$  MeV ( $S = 1.5$ )

$\eta(1475)$ DECAY MODES	Fraction ( $\Gamma_i/\Gamma$ )	$\rho$ (MeV/c)
$K\bar{K}\pi$	dominant	477
$K\bar{K}^*(892) + c.c.$	seen	245
$a_0(980)\pi$	seen	396
$\gamma\gamma$	seen	738

 **$f_0(1500)$**  [m]

$$J^G(J^{PC}) = 0^+(0^{++})$$

Mass  $m = 1505 \pm 6$  MeV ( $S = 1.3$ )  
 Full width  $\Gamma = 109 \pm 7$  MeV

$f_0(1500)$ DECAY MODES	Fraction ( $\Gamma_i/\Gamma$ )	Scale factor	$\rho$ (MeV/c)
$\pi\pi$	(34.9±2.3) %	1.2	741
$\pi^+\pi^-$	seen		740
$2\pi^0$	seen		741
$4\pi$	(49.5±3.3) %	1.2	691
$4\pi^0$	seen		691
$2\pi^+2\pi^-$	seen		687
$2(\pi\pi)$ s-wave	seen		–
$\rho\rho$	seen		†
$\pi(1300)\pi$	seen		144
$a_1(1260)\pi$	seen		218
$\eta\eta$	( 5.1±0.9) %	1.4	516
$\eta\eta'(958)$	( 1.9±0.8) %	1.7	†
$K\bar{K}$	( 8.6±1.0) %	1.1	568
$\gamma\gamma$	not seen		753

 **$f_2'(1525)$** 

$$J^G(J^{PC}) = 0^+(2^{++})$$

Mass  $m = 1525 \pm 5$  MeV [l]  
 Full width  $\Gamma = 73 \pm 6$  MeV [l]

## Meson Summary Table

$f_2'(1525)$ DECAY MODES	Fraction ( $\Gamma_i/\Gamma$ )	$\rho$ (MeV/c)
$K\bar{K}$	(88.7 $\pm$ 2.2 ) %	581
$\eta\eta$	(10.4 $\pm$ 2.2 ) %	530
$\pi\pi$	( 8.2 $\pm$ 1.5 ) $\times 10^{-3}$	750
$\gamma\gamma$	( 1.11 $\pm$ 0.14 ) $\times 10^{-6}$	763

$$\pi_1(1600) [m] \quad I^G(J^{PC}) = 1^-(1^+ +)$$

Mass  $m = 1662 \pm 8$  MeV  
Full width  $\Gamma = 241 \pm 40$  MeV ( $S = 1.4$ )

$\pi_1(1600)$ DECAY MODES	Fraction ( $\Gamma_i/\Gamma$ )	$\rho$ (MeV/c)
$\pi\pi\pi$	not seen	803
$\rho^0\pi^-$	not seen	641
$f_2(1270)\pi^-$	not seen	318
$b_1(1235)\pi$	seen	357
$\eta'(958)\pi^-$	seen	543
$f_1(1285)\pi$	seen	314

$$\eta_2(1645) \quad I^G(J^{PC}) = 0^+(2^- +)$$

Mass  $m = 1617 \pm 5$  MeV  
Full width  $\Gamma = 181 \pm 11$  MeV

$\eta_2(1645)$ DECAY MODES	Fraction ( $\Gamma_i/\Gamma$ )	$\rho$ (MeV/c)
$a_2(1320)\pi$	seen	242
$K\bar{K}\pi$	seen	580
$K^+\bar{K}$	seen	404
$\eta\pi^+\pi^-$	seen	685
$a_0(980)\pi$	seen	499
$f_2(1270)\eta$	not seen	†

$$\omega(1650) [r] \quad I^G(J^{PC}) = 0^-(1^- -)$$

Mass  $m = 1670 \pm 30$  MeV  
Full width  $\Gamma = 315 \pm 35$  MeV

$\omega(1650)$ DECAY MODES	Fraction ( $\Gamma_i/\Gamma$ )	$\rho$ (MeV/c)
$\rho\pi$	seen	646
$\omega\pi\pi$	seen	617
$\omega\eta$	seen	500
$e^+e^-$	seen	835

$$\omega_3(1670) \quad I^G(J^{PC}) = 0^-(3^- -)$$

Mass  $m = 1667 \pm 4$  MeV  
Full width  $\Gamma = 168 \pm 10$  MeV [l]

$\omega_3(1670)$ DECAY MODES	Fraction ( $\Gamma_i/\Gamma$ )	$\rho$ (MeV/c)
$\rho\pi$	seen	645
$\omega\pi\pi$	seen	615
$b_1(1235)\pi$	possibly seen	361

$$\pi_2(1670) \quad I^G(J^{PC}) = 1^-(2^- +)$$

Mass  $m = 1672.2 \pm 3.0$  MeV [l] ( $S = 1.4$ )  
Full width  $\Gamma = 260 \pm 9$  MeV [l] ( $S = 1.2$ )

$\pi_2(1670)$ DECAY MODES	Fraction ( $\Gamma_i/\Gamma$ )	Confidence level	$\rho$ (MeV/c)
$3\pi$	(95.8 $\pm$ 1.4) %		809
$f_2(1270)\pi$	(56.3 $\pm$ 3.2) %		329
$\rho\pi$	(31 $\pm$ 4 ) %		648
$\sigma\pi$	(10.9 $\pm$ 3.4) %		-
$(\pi\pi)$ s-wave	( 8.7 $\pm$ 3.4) %		-
$K\bar{K}^*(892) + \text{c.c.}$	( 4.2 $\pm$ 1.4) %		455
$\omega\rho$	( 2.7 $\pm$ 1.1) %		304
$\gamma\gamma$	< 2.8 $\times 10^{-7}$	90%	836
$\rho(1450)\pi$	< 3.6 $\times 10^{-3}$	97.7%	147
$b_1(1235)\pi$	< 1.9 $\times 10^{-3}$	97.7%	365
$f_1(1285)\pi$	possibly seen		323
$a_2(1320)\pi$	not seen		292

$$\phi(1680)$$

$$I^G(J^{PC}) = 0^-(1^- -)$$

Mass  $m = 1680 \pm 20$  MeV [l]  
Full width  $\Gamma = 150 \pm 50$  MeV [l]

$\phi(1680)$ DECAY MODES	Fraction ( $\Gamma_i/\Gamma$ )	$\rho$ (MeV/c)
$K\bar{K}^*(892) + \text{c.c.}$	dominant	462
$K_S^0 K\pi$	seen	621
$K\bar{K}$	seen	680
$e^+e^-$	seen	840
$\omega\pi\pi$	not seen	623
$K^+K^-\pi^+\pi^-$	seen	544

$$\rho_3(1690)$$

$$I^G(J^{PC}) = 1^+(3^- -)$$

Mass  $m = 1688.8 \pm 2.1$  MeV [l]  
Full width  $\Gamma = 161 \pm 10$  MeV [l] ( $S = 1.5$ )

$\rho_3(1690)$ DECAY MODES	Fraction ( $\Gamma_i/\Gamma$ )	Scale factor	$\rho$ (MeV/c)
$4\pi$	(71.1 $\pm$ 1.9 ) %		790
$\pi^\pm\pi^+\pi^-\pi^0$	(67 $\pm$ 22 ) %		787
$\omega\pi$	(16 $\pm$ 6 ) %		655
$\pi\pi$	(23.6 $\pm$ 1.3 ) %		834
$K\bar{K}\pi$	( 3.8 $\pm$ 1.2 ) %		629
$K\bar{K}$	( 1.58 $\pm$ 0.26) %	1.2	685
$\eta\pi^+\pi^-$	seen		727
$\rho(770)\eta$	seen		520
$\pi\pi\rho$	seen		633
Excluding $2\rho$ and $a_2(1320)\pi$ .			
$a_2(1320)\pi$	seen		307
$\rho\rho$	seen		334

$$\rho(1700) [q]$$

$$I^G(J^{PC}) = 1^+(1^- -)$$

Mass  $m = 1720 \pm 20$  MeV [l] ( $\eta\rho^0$  and  $\pi^+\pi^-$  modes)  
Full width  $\Gamma = 250 \pm 100$  MeV [l] ( $\eta\rho^0$  and  $\pi^+\pi^-$  modes)

$\rho(1700)$ DECAY MODES	Fraction ( $\Gamma_i/\Gamma$ )	$\rho$ (MeV/c)
$2(\pi^+\pi^-)$	large	803
$\rho\pi\pi$	dominant	653
$\rho^0\pi^+\pi^-$	large	650
$\rho^\pm\pi^\mp\pi^0$	large	652
$a_1(1260)\pi$	seen	404
$h_1(1170)\pi$	seen	447
$\pi(1300)\pi$	seen	349
$\rho\rho$	seen	372
$\pi^+\pi^-$	seen	849
$\pi\pi$	seen	849
$K\bar{K}^*(892) + \text{c.c.}$	seen	496
$\eta\rho$	seen	545
$a_2(1320)\pi$	not seen	334
$K\bar{K}$	seen	704
$e^+e^-$	seen	860
$\pi^0\omega$	seen	674

$$f_0(1710) [s]$$

$$I^G(J^{PC}) = 0^+(0^+ +)$$

Mass  $m = 1720 \pm 6$  MeV ( $S = 1.6$ )  
Full width  $\Gamma = 135 \pm 8$  MeV ( $S = 1.1$ )

$f_0(1710)$ DECAY MODES	Fraction ( $\Gamma_i/\Gamma$ )	$\rho$ (MeV/c)
$K\bar{K}$	seen	704
$\eta\eta$	seen	663
$\pi\pi$	seen	849
$\omega\omega$	seen	357

$$\pi(1800)$$

$$I^G(J^{PC}) = 1^-(0^- +)$$

Mass  $m = 1812 \pm 12$  MeV ( $S = 2.3$ )  
Full width  $\Gamma = 208 \pm 12$  MeV

## Meson Summary Table

$\pi(1800)$ DECAY MODES	Fraction ( $\Gamma_i/\Gamma$ )	$\rho$ (MeV/c)
$\pi^+ \pi^- \pi^-$	seen	879
$f_0(500) \pi^-$	seen	-
$f_0(980) \pi^-$	seen	625
$f_0(1370) \pi^-$	seen	368
$f_0(1500) \pi^-$	not seen	250
$\rho \pi^-$	not seen	732
$\eta \eta \pi^-$	seen	661
$a_0(980) \eta$	seen	473
$a_2(1320) \eta$	not seen	†
$f_2(1270) \pi$	not seen	442
$f_0(1370) \pi^-$	not seen	368
$f_0(1500) \pi^-$	seen	250
$\eta \eta' (958) \pi^-$	seen	375
$K_0^*(1430) K^-$	seen	†
$K^*(892) K^-$	not seen	570

 **$\phi_3(1850)$** 

$$I^G(J^{PC}) = 0^-(3^{--})$$

Mass  $m = 1854 \pm 7$  MeV  
 Full width  $\Gamma = 87^{+28}_{-23}$  MeV ( $S = 1.2$ )

$\phi_3(1850)$ DECAY MODES	Fraction ( $\Gamma_i/\Gamma$ )	$\rho$ (MeV/c)
$K \bar{K}$	seen	785
$K \bar{K}^*(892) + c.c.$	seen	602

 **$\pi_2(1880)$** 

$$I^G(J^{PC}) = 1^-(2^{-+})$$

Mass  $m = 1895 \pm 16$  MeV  
 Full width  $\Gamma = 235 \pm 34$  MeV

 **$f_2(1950)$** 

$$I^G(J^{PC}) = 0^+(2^{++})$$

Mass  $m = 1944 \pm 12$  MeV ( $S = 1.5$ )  
 Full width  $\Gamma = 472 \pm 18$  MeV

$f_2(1950)$ DECAY MODES	Fraction ( $\Gamma_i/\Gamma$ )	$\rho$ (MeV/c)
$K^*(892) \bar{K}^*(892)$	seen	387
$\pi^+ \pi^-$	seen	962
$\pi^0 \pi^0$	seen	963
$4\pi$	seen	925
$\eta \eta$	seen	803
$K \bar{K}$	seen	837
$\gamma \gamma$	seen	972
$\rho \bar{\rho}$	seen	254

 **$f_2(2010)$** 

$$I^G(J^{PC}) = 0^+(2^{++})$$

Mass  $m = 2011^{+60}_{-80}$  MeV  
 Full width  $\Gamma = 202 \pm 60$  MeV

$f_2(2010)$ DECAY MODES	Fraction ( $\Gamma_i/\Gamma$ )	$\rho$ (MeV/c)
$\phi \phi$	seen	†
$K \bar{K}$	seen	876

 **$a_4(2040)$** 

$$I^G(J^{PC}) = 1^-(4^{++})$$

Mass  $m = 1996^{+10}_{-9}$  MeV ( $S = 1.1$ )  
 Full width  $\Gamma = 255^{+28}_{-24}$  MeV ( $S = 1.3$ )

$a_4(2040)$ DECAY MODES	Fraction ( $\Gamma_i/\Gamma$ )	$\rho$ (MeV/c)
$K \bar{K}$	seen	868
$\pi^+ \pi^- \pi^0$	seen	974
$\rho \pi$	seen	841
$f_2(1270) \pi$	seen	580
$\omega \pi^- \pi^0$	seen	819
$\omega \rho$	seen	624
$\eta \pi^0$	seen	918
$\eta'(958) \pi$	seen	761

 **$f_4(2050)$** 

$$I^G(J^{PC}) = 0^+(4^{++})$$

Mass  $m = 2018 \pm 11$  MeV ( $S = 2.1$ )  
 Full width  $\Gamma = 237 \pm 18$  MeV ( $S = 1.9$ )

$f_4(2050)$ DECAY MODES	Fraction ( $\Gamma_i/\Gamma$ )	$\rho$ (MeV/c)
$\omega \omega$	seen	637
$\pi \pi$	(17.0 ± 1.5) %	1000
$K \bar{K}$	(6.8 ± 3.4 / -1.8) × 10 <sup>-3</sup>	880
$\eta \eta$	(2.1 ± 0.8) × 10 <sup>-3</sup>	848
$4\pi^0$	< 1.2 %	964
$a_2(1320) \pi$	seen	567

 **$\phi(2170)$** 

$$I^G(J^{PC}) = 0^-(1^{--})$$

Mass  $m = 2175 \pm 15$  MeV ( $S = 1.6$ )  
 Full width  $\Gamma = 61 \pm 18$  MeV

$\phi(2170)$ DECAY MODES	Fraction ( $\Gamma_i/\Gamma$ )	$\rho$ (MeV/c)
$e^+ e^-$	seen	1087
$\phi f_0(980)$	seen	416
$K^+ K^- f_0(980) \rightarrow$ $K^+ K^- \pi^+ \pi^-$	seen	-
$K^+ K^- f_0(980) \rightarrow K^+ K^- \pi^0 \pi^0$	seen	-
$K^{*0} K^\pm \pi^\mp$	not seen	770
$K^*(892)^0 \bar{K}^*(892)^0$	not seen	622

 **$f_2(2300)$** 

$$I^G(J^{PC}) = 0^+(2^{++})$$

Mass  $m = 2297 \pm 28$  MeV  
 Full width  $\Gamma = 149 \pm 40$  MeV

$f_2(2300)$ DECAY MODES	Fraction ( $\Gamma_i/\Gamma$ )	$\rho$ (MeV/c)
$\phi \phi$	seen	529
$K \bar{K}$	seen	1037
$\gamma \gamma$	seen	1149

 **$f_2(2340)$** 

$$I^G(J^{PC}) = 0^+(2^{++})$$

Mass  $m = 2339 \pm 60$  MeV  
 Full width  $\Gamma = 319^{+80}_{-70}$  MeV

$f_2(2340)$ DECAY MODES	Fraction ( $\Gamma_i/\Gamma$ )	$\rho$ (MeV/c)
$\phi \phi$	seen	573
$\eta \eta$	seen	1033

## STRANGE MESONS ( $S = \pm 1, C = B = 0$ )

$$K^+ = u\bar{s}, K^0 = d\bar{s}, \bar{K}^0 = \bar{d}s, K^- = \bar{u}s, \text{ similarly for } K^{*s}$$

 **$K^\pm$** 

$$I(J^P) = \frac{1}{2}(0^-)$$

Mass  $m = 493.677 \pm 0.016$  MeV [1] ( $S = 2.8$ )  
 Mean life  $\tau = (1.2380 \pm 0.0021) \times 10^{-8}$  s ( $S = 1.9$ )  
 $c\tau = 3.712$  m

**Slope parameter  $g^{[u]}$** 

(See Particle Listings for quadratic coefficients and alternative parametrization related to  $\pi\pi$  scattering)

$$K^\pm \rightarrow \pi^\pm \pi^+ \pi^- \quad g = -0.21134 \pm 0.00017$$

$$(g_+ - g_-) / (g_+ + g_-) = (-1.5 \pm 2.2) \times 10^{-4}$$

$$K^\pm \rightarrow \pi^\pm \pi^0 \pi^0 \quad g = 0.626 \pm 0.007$$

$$(g_+ - g_-) / (g_+ + g_-) = (1.8 \pm 1.8) \times 10^{-4}$$

 **$K^\pm$  decay form factors  $[a, v]$** 

Assuming  $\mu$ - $e$  universality

$$\lambda_+(K_{\mu 3}^+) = \lambda_+(K_{e 3}^+) = (2.97 \pm 0.05) \times 10^{-2}$$

$$\lambda_0(K_{\mu 3}^+) = (1.95 \pm 0.12) \times 10^{-2}$$

# Meson Summary Table

Not assuming  $\mu$ - $e$  universality

$$\lambda_+(K_{e3}^+) = (2.98 \pm 0.05) \times 10^{-2}$$

$$\lambda_+(K_{\mu 3}^+) = (2.96 \pm 0.17) \times 10^{-2}$$

$$\lambda_0(K_{\mu 3}^+) = (1.96 \pm 0.13) \times 10^{-2}$$

$K_{e3}$  form factor quadratic fit

$$\lambda'_+(K_{e3}^+) \text{ linear coeff.} = (2.49 \pm 0.17) \times 10^{-2}$$

$$\lambda''_+(K_{e3}^+) \text{ quadratic coeff.} = (0.19 \pm 0.09) \times 10^{-2}$$

$$K_{e3}^+ |f_S/f_+| = (-0.3^{+0.8}_{-0.7}) \times 10^{-2}$$

$$K_{e3}^+ |f_T/f_+| = (-1.2 \pm 2.3) \times 10^{-2}$$

$$K_{\mu 3}^+ |f_S/f_+| = (0.2 \pm 0.6) \times 10^{-2}$$

$$K_{\mu 3}^+ |f_T/f_+| = (-0.1 \pm 0.7) \times 10^{-2}$$

$$K^+ \rightarrow e^+ \nu_e \gamma \quad |F_A + F_V| = 0.133 \pm 0.008 \quad (S = 1.3)$$

$$K^+ \rightarrow \mu^+ \nu_\mu \gamma \quad |F_A + F_V| = 0.165 \pm 0.013$$

$$K^+ \rightarrow e^+ \nu_e \gamma \quad |F_A - F_V| < 0.49$$

$$K^+ \rightarrow \mu^+ \nu_\mu \gamma \quad |F_A - F_V| = -0.24 \text{ to } 0.04, \text{ CL} = 90\%$$

## Charge Radius

$$\langle r \rangle = 0.560 \pm 0.031 \text{ fm}$$

## CP violation parameters

$$\Delta(K_{\pi e e}^\pm) = (-2.2 \pm 1.6) \times 10^{-2}$$

$$\Delta(K_{\pi \mu \mu}^\pm) = 0.010 \pm 0.023$$

$$\Delta(K_{\pi \pi \gamma}^\pm) = (0.0 \pm 1.2) \times 10^{-3}$$

$$A_{FB}(K_{\pi \mu \mu}^\pm) = \frac{\Gamma(\cos(\theta_{K\mu}) > 0) - \Gamma(\cos(\theta_{K\mu}) < 0)}{\Gamma(\cos(\theta_{K\mu}) > 0) + \Gamma(\cos(\theta_{K\mu}) < 0)} < 2.3 \times 10^{-2}, \text{ CL} = 90\%$$

## T violation parameters

$$K^+ \rightarrow \pi^0 \mu^+ \nu_\mu \quad P_T = (-1.7 \pm 2.5) \times 10^{-3}$$

$$K^+ \rightarrow \mu^+ \nu_\mu \gamma \quad P_T = (-0.6 \pm 1.9) \times 10^{-2}$$

$$K^+ \rightarrow \pi^0 \mu^+ \nu_\mu \quad \text{Im}(\xi) = -0.006 \pm 0.008$$

$K^-$  modes are charge conjugates of the modes below.

$K^+$ DECAY MODES	Fraction ( $\Gamma_i/\Gamma$ )	Scale factor/ Confidence level (MeV/c)	$p$
<b>Leptonic and semileptonic modes</b>			
$e^+ \nu_e$	$(1.581 \pm 0.008) \times 10^{-5}$		247
$\mu^+ \nu_\mu$	$(63.55 \pm 0.11) \%$	S=1.2	236
$\pi^0 e^+ \nu_e$	$(5.07 \pm 0.04) \%$	S=2.1	228
Called $K_{e3}^+$ .			
$\pi^0 \mu^+ \nu_\mu$	$(3.353 \pm 0.034) \%$	S=1.8	215
Called $K_{\mu 3}^+$ .			
$\pi^0 \pi^0 e^+ \nu_e$	$(2.2 \pm 0.4) \times 10^{-5}$		206
$\pi^+ \pi^- e^+ \nu_e$	$(4.09 \pm 0.10) \times 10^{-5}$		203
$\pi^+ \pi^- \mu^+ \nu_\mu$	$(1.4 \pm 0.9) \times 10^{-5}$		151
$\pi^0 \pi^0 \pi^0 e^+ \nu_e$	$< 3.5 \times 10^{-6}$	CL=90%	135
<b>Hadronic modes</b>			
$\pi^+ \pi^0$	$(20.66 \pm 0.08) \%$	S=1.2	205
$\pi^+ \pi^0 \pi^0$	$(1.761 \pm 0.022) \%$	S=1.1	133
$\pi^+ \pi^+ \pi^-$	$(5.59 \pm 0.04) \%$	S=1.3	125
<b>Leptonic and semileptonic modes with photons</b>			
$\mu^+ \nu_\mu \gamma$	[w,x] $(6.2 \pm 0.8) \times 10^{-3}$		236
$\mu^+ \nu_\mu \gamma$ (SD <sup>+</sup> )	[a,y] $(1.33 \pm 0.22) \times 10^{-5}$		-
$\mu^+ \nu_\mu \gamma$ (SD <sup>+</sup> INT)	[a,y] $< 2.7 \times 10^{-5}$	CL=90%	-
$\mu^+ \nu_\mu \gamma$ (SD <sup>-</sup> + SD <sup>-</sup> INT)	[a,y] $< 2.6 \times 10^{-4}$	CL=90%	-
$e^+ \nu_e \gamma$	$(9.4 \pm 0.4) \times 10^{-6}$		247
$\pi^0 e^+ \nu_e \gamma$	[w,x] $(2.56 \pm 0.16) \times 10^{-4}$		228
$\pi^0 e^+ \nu_e \gamma$ (SD)	[a,y] $< 5.3 \times 10^{-5}$	CL=90%	228
$\pi^0 \mu^+ \nu_\mu \gamma$	[w,x] $(1.25 \pm 0.25) \times 10^{-5}$		215
$\pi^0 \pi^0 e^+ \nu_e \gamma$	$< 5 \times 10^{-6}$	CL=90%	206
<b>Hadronic modes with photons or <math>\ell\ell</math> pairs</b>			
$\pi^+ \pi^0 \gamma$ (INT)	$(-4.2 \pm 0.9) \times 10^{-6}$		-
$\pi^+ \pi^0 \gamma$ (DE)	[w,z] $(6.0 \pm 0.4) \times 10^{-6}$		205
$\pi^+ \pi^0 \pi^0 \gamma$	[w,x] $(7.6 \pm 6.0_{-3.0}) \times 10^{-6}$		133
$\pi^+ \pi^+ \pi^- \gamma$	[w,x] $(1.04 \pm 0.31) \times 10^{-4}$		125
$\pi^+ \gamma \gamma$	[w] $(1.10 \pm 0.32) \times 10^{-6}$		227
$\pi^+ 3\gamma$	[w] $< 1.0 \times 10^{-4}$	CL=90%	227
$\pi^+ e^+ e^- \gamma$	$(1.19 \pm 0.13) \times 10^{-8}$		227

## Leptonic modes with $\ell\ell$ pairs

$e^+ \nu_e \nu \bar{\nu}$	$< 6 \times 10^{-5}$	CL=90%	247
$\mu^+ \nu_\mu \nu \bar{\nu}$	$< 6.0 \times 10^{-6}$	CL=90%	236
$e^+ \nu_e e^+ e^-$	$(2.48 \pm 0.20) \times 10^{-8}$		247
$\mu^+ \nu_\mu e^+ e^-$	$(7.06 \pm 0.31) \times 10^{-8}$		236
$e^+ \nu_e \mu^+ \mu^-$	$(1.7 \pm 0.5) \times 10^{-8}$		223
$\mu^+ \nu_\mu \mu^+ \mu^-$	$< 4.1 \times 10^{-7}$	CL=90%	185

## Lepton Family number (LF), Lepton number (L), $\Delta S = \Delta Q$ (SQ)

violating modes, or  $\Delta S = 1$  weak neutral current (S1) modes

$\pi^+ \pi^+ e^- \bar{\nu}_e$	SQ	$< 1.2 \times 10^{-8}$	CL=90%	203
$\pi^+ \pi^+ \mu^- \bar{\nu}_\mu$	SQ	$< 3.0 \times 10^{-6}$	CL=95%	151
$\pi^+ e^+ e^-$	S1	$(3.00 \pm 0.09) \times 10^{-7}$		227
$\pi^+ \mu^+ \mu^-$	S1	$(9.4 \pm 0.6) \times 10^{-8}$	S=2.6	172
$\pi^+ \nu \bar{\nu}$	S1	$(1.7 \pm 1.1) \times 10^{-10}$		227
$\pi^+ \pi^0 \nu \bar{\nu}$	S1	$< 4.3 \times 10^{-5}$	CL=90%	205
$\mu^- \nu e^+ e^+$	LF	$< 2.0 \times 10^{-8}$	CL=90%	236
$\mu^+ \nu_e$	LF	[d] $< 4 \times 10^{-3}$	CL=90%	236
$\pi^+ \mu^+ e^-$	LF	$< 1.3 \times 10^{-11}$	CL=90%	214
$\pi^+ \mu^- e^+$	LF	$< 5.2 \times 10^{-10}$	CL=90%	214
$\pi^- \mu^+ e^+$	L	$< 5.0 \times 10^{-10}$	CL=90%	214
$\pi^- e^+ e^+$	L	$< 6.4 \times 10^{-10}$	CL=90%	227
$\pi^- \mu^+ \mu^+$	L	[d] $< 1.1 \times 10^{-9}$	CL=90%	172
$\mu^+ \bar{\nu}_e$	L	[d] $< 3.3 \times 10^{-3}$	CL=90%	236
$\pi^0 e^+ \bar{\nu}_e$	L	$< 3 \times 10^{-3}$	CL=90%	228
$\pi^+ \gamma$	[a $\bar{a}$ ] $< 2.3 \times 10^{-9}$	CL=90%	227	

$K^0$

$$I(J^P) = \frac{1}{2}(0^-)$$

50%  $K_S$ , 50%  $K_L$

$$\text{Mass } m = 497.614 \pm 0.024 \text{ MeV} \quad (S = 1.6)$$

$$m_{K^0} - m_{K^\pm} = 3.937 \pm 0.028 \text{ MeV} \quad (S = 1.8)$$

## Mean Square Charge Radius

$$\langle r^2 \rangle = -0.077 \pm 0.010 \text{ fm}^2$$

## T-violation parameters in $K^0$ - $\bar{K}^0$ mixing [v]

$$\text{Asymmetry } A_T \text{ in } K^0\text{-}\bar{K}^0 \text{ mixing} = (6.6 \pm 1.6) \times 10^{-3}$$

## CPT-violation parameters [v]

$$\text{Re } \delta = (2.5 \pm 2.3) \times 10^{-4}$$

$$\text{Im } \delta = (-1.5 \pm 1.6) \times 10^{-5}$$

$$\text{Re}(y), K_{e3} \text{ parameter} = (0.4 \pm 2.5) \times 10^{-3}$$

$$\text{Re}(x_-), K_{e3} \text{ parameter} = (-2.9 \pm 2.0) \times 10^{-3}$$

$$|m_{K^0} - m_{\bar{K}^0}| / m_{\text{average}} < 6 \times 10^{-19}, \text{ CL} = 90\% \text{ [bb]}$$

$$(\Gamma_{K^0} - \Gamma_{\bar{K}^0}) / m_{\text{average}} = (8 \pm 8) \times 10^{-18}$$

## Tests of $\Delta S = \Delta Q$

$$\text{Re}(x_+), K_{e3} \text{ parameter} = (-0.9 \pm 3.0) \times 10^{-3}$$

$K_S^0$

$$I(J^P) = \frac{1}{2}(0^-)$$

$$\text{Mean life } \tau = (0.8954 \pm 0.0004) \times 10^{-10} \text{ s} \quad (S = 1.1) \quad \text{Assuming CPT}$$

$$\text{Mean life } \tau = (0.89564 \pm 0.00033) \times 10^{-10} \text{ s} \quad \text{Not assuming CPT}$$

$$c\tau = 2.6844 \text{ cm} \quad \text{Assuming CPT}$$

## CP-violation parameters [c $\bar{c}$ ]

$$\text{Im}(\eta_{+-0}) = -0.002 \pm 0.009$$

$$\text{Im}(\eta_{000}) = (-0.1 \pm 1.6) \times 10^{-2}$$

$$|\eta_{000}| = |A(K_S^0 \rightarrow 3\pi^0)/A(K_L^0 \rightarrow 3\pi^0)| < 0.018, \text{ CL} = 90\%$$

$$\text{CP asymmetry } A \text{ in } \pi^+ \pi^- e^+ e^- = (-0.4 \pm 0.8) \%$$

## Meson Summary Table

$K_S^0$ DECAY MODES	Fraction ( $\Gamma_i/\Gamma$ )	Scale factor/ Confidence level	$p$ (MeV/c)
<b>Hadronic modes</b>			
$\pi^0 \pi^0$	$(30.69 \pm 0.05) \%$		209
$\pi^+ \pi^-$	$(69.20 \pm 0.05) \%$		206
$\pi^+ \pi^- \pi^0$	$(3.5 \pm_{-0.9}^{+1.1}) \times 10^{-7}$		133
<b>Modes with photons or <math>\ell\bar{\ell}</math> pairs</b>			
$\pi^+ \pi^- \gamma$	[x, dd] $(1.79 \pm 0.05) \times 10^{-3}$		206
$\pi^+ \pi^- e^+ e^-$	$(4.79 \pm 0.15) \times 10^{-5}$		206
$\pi^0 \gamma \gamma$	[dd] $(4.9 \pm 1.8) \times 10^{-8}$		231
$\gamma \gamma$	$(2.63 \pm 0.17) \times 10^{-6}$	S=3.0	249
<b>Semileptonic modes</b>			
$\pi^\pm e^\mp \nu_e$	[ee] $(7.04 \pm 0.08) \times 10^{-4}$		229
<b>CP violating (CP) and <math>\Delta S = 1</math> weak neutral current (S1) modes</b>			
$3\pi^0$	CP $< 1.2 \times 10^{-7}$	CL=90%	139
$\mu^+ \mu^-$	S1 $< 3.2 \times 10^{-7}$	CL=90%	225
$e^+ e^-$	S1 $< 9 \times 10^{-9}$	CL=90%	249
$\pi^0 e^+ e^-$	S1 [dd] $(3.0 \pm_{-1.2}^{+1.5}) \times 10^{-9}$		230
$\pi^0 \mu^+ \mu^-$	S1 $(2.9 \pm_{-1.2}^{+1.5}) \times 10^{-9}$		177

 $K_L^0$ 

$$I(J^P) = \frac{1}{2}(0^-)$$

$$m_{K_L} - m_{K_S}$$

$$= (0.5293 \pm 0.0009) \times 10^{10} \text{ h s}^{-1} \quad (S = 1.3) \quad \text{Assuming } CPT$$

$$= (3.484 \pm 0.006) \times 10^{-12} \text{ MeV} \quad \text{Assuming } CPT$$

$$= (0.5289 \pm 0.0010) \times 10^{10} \text{ h s}^{-1} \quad \text{Not assuming } CPT$$

$$\text{Mean life } \tau = (5.116 \pm 0.021) \times 10^{-8} \text{ s} \quad (S = 1.1)$$

$$c\tau = 15.34 \text{ m}$$

**Slope parameter  $g$  [u]**

(See Particle Listings for quadratic coefficients)

$$K_L^0 \rightarrow \pi^+ \pi^- \pi^0: g = 0.678 \pm 0.008 \quad (S = 1.5)$$

 **$K_L$  decay form factors [v]**Linear parametrization assuming  $\mu$ -e universality

$$\lambda_+(K_{\mu 3}^0) = \lambda_+(K_{e 3}^0) = (2.82 \pm 0.04) \times 10^{-2} \quad (S = 1.1)$$

$$\lambda_0(K_{\mu 3}^0) = (1.38 \pm 0.18) \times 10^{-2} \quad (S = 2.2)$$

Quadratic parametrization assuming  $\mu$ -e universality

$$\lambda'_+(K_{\mu 3}^0) = \lambda'_+(K_{e 3}^0) = (2.40 \pm 0.12) \times 10^{-2} \quad (S = 1.2)$$

$$\lambda''_+(K_{\mu 3}^0) = \lambda''_+(K_{e 3}^0) = (0.20 \pm 0.05) \times 10^{-2} \quad (S = 1.2)$$

$$\lambda_0(K_{\mu 3}^0) = (1.16 \pm 0.09) \times 10^{-2} \quad (S = 1.2)$$

Pole parametrization assuming  $\mu$ -e universality

$$M_V^\mu(K_{\mu 3}^0) = M_V^e(K_{e 3}^0) = 878 \pm 6 \text{ MeV} \quad (S = 1.1)$$

$$M_S^\mu(K_{\mu 3}^0) = 1252 \pm 90 \text{ MeV} \quad (S = 2.6)$$

$$K_{e 3}^0 \quad |f_S/f_+| = (1.5 \pm_{-1.6}^{+1.4}) \times 10^{-2}$$

$$K_{e 3}^0 \quad |f_T/f_+| = (5 \pm_{-6}^{+4}) \times 10^{-2}$$

$$K_{\mu 3}^0 \quad |f_T/f_+| = (12 \pm 12) \times 10^{-2}$$

$$K_L \rightarrow \ell^+ \ell^- \gamma, K_L \rightarrow \ell^+ \ell^- \ell'^+ \ell'^-: \alpha_{K^*} = -0.205 \pm 0.022 \quad (S = 1.8)$$

$$K_L^0 \rightarrow \ell^+ \ell^- \gamma, K_L^0 \rightarrow \ell^+ \ell^- \ell'^+ \ell'^-: \alpha_{DIP} = -1.69 \pm 0.08 \quad (S = 1.7)$$

$$K_L \rightarrow \pi^+ \pi^- e^+ e^-: a_1/a_2 = -0.737 \pm 0.014 \text{ GeV}^2$$

$$K_L \rightarrow \pi^0 2\gamma: a_V = -0.43 \pm 0.06 \quad (S = 1.5)$$

**CP-violation parameters [cc]**

$$A_L = (0.332 \pm 0.006) \%$$

$$|\eta_{00}| = (2.220 \pm 0.011) \times 10^{-3} \quad (S = 1.8)$$

$$|\eta_{+-}| = (2.232 \pm 0.011) \times 10^{-3} \quad (S = 1.8)$$

$$|\epsilon| = (2.228 \pm 0.011) \times 10^{-3} \quad (S = 1.8)$$

$$|\eta_{00}/\eta_{+-}| = 0.9950 \pm 0.0007 [^m] \quad (S = 1.6)$$

$$\text{Re}(\epsilon'/\epsilon) = (1.66 \pm 0.23) \times 10^{-3} [^m] \quad (S = 1.6)$$

Assuming  $CPT$ 

$$\phi_{+-} = (43.51 \pm 0.05)^\circ \quad (S = 1.2)$$

$$\phi_{00} = (43.52 \pm 0.05)^\circ \quad (S = 1.3)$$

$$\phi_\epsilon = \phi_{\text{sw}} = (43.52 \pm 0.05)^\circ \quad (S = 1.2)$$

$$\text{Im}(\epsilon'/\epsilon) = -(\phi_{00} - \phi_{+-})/3 = (-0.002 \pm 0.005)^\circ \quad (S = 1.7)$$

Not assuming  $CPT$ 

$$\phi_{+-} = (43.4 \pm 0.5)^\circ \quad (S = 1.2)$$

$$\phi_{00} = (43.7 \pm 0.6)^\circ \quad (S = 1.2)$$

$$\phi_\epsilon = (43.5 \pm 0.5)^\circ \quad (S = 1.3)$$

CP asymmetry  $A$  in  $K_L^0 \rightarrow \pi^+ \pi^- e^+ e^- = (13.7 \pm 1.5) \%$  $\beta_{CP}$  from  $K_L^0 \rightarrow e^+ e^- e^+ e^- = -0.19 \pm 0.07$  $\gamma_{CP}$  from  $K_L^0 \rightarrow e^+ e^- e^+ e^- = 0.01 \pm 0.11 \quad (S = 1.6)$  $j$  for  $K_L^0 \rightarrow \pi^+ \pi^- \pi^0 = 0.0012 \pm 0.0008$  $f$  for  $K_L^0 \rightarrow \pi^+ \pi^- \pi^0 = 0.004 \pm 0.006$ 

$$|\eta_{+-\gamma}| = (2.35 \pm 0.07) \times 10^{-3}$$

$$\phi_{+-\gamma} = (44 \pm 4)^\circ$$

$$|\epsilon'_{+-\gamma}|/\epsilon < 0.3, \text{ CL} = 90\%$$

$$|g_{E1}| \text{ for } K_L^0 \rightarrow \pi^+ \pi^- \gamma < 0.21, \text{ CL} = 90\%$$

**T-violation parameters**

$$\text{Im}(\xi) \text{ in } K_{\mu 3}^0 = -0.007 \pm 0.026$$

**CPT invariance tests**

$$\phi_{00} - \phi_{+-} = (0.34 \pm 0.32)^\circ$$

$$\text{Re}(\frac{2}{3}\eta_{+-} + \frac{1}{3}\eta_{00}) - \frac{A_L}{2} = (-3 \pm 35) \times 10^{-6}$$

 **$\Delta S = -\Delta Q$  in  $K_{e 3}^0$  decay**

$$\text{Re } x = -0.002 \pm 0.006$$

$$\text{Im } x = 0.0012 \pm 0.0021$$

$K_L^0$ DECAY MODES	Fraction ( $\Gamma_i/\Gamma$ )	Scale factor/ Confidence level (MeV/c)	$p$
<b>Semileptonic modes</b>			
$\pi^\pm e^\mp \nu_e$	[ee] $(40.55 \pm 0.11) \%$	S=1.7	229
Called $K_{e 3}^0$ .			
$\pi^\pm \mu^\mp \nu_\mu$	[ee] $(27.04 \pm 0.07) \%$	S=1.1	216
Called $K_{\mu 3}^0$ .			
$(\pi \mu \text{atom}) \nu$	$(1.05 \pm 0.11) \times 10^{-7}$		188
$\pi^0 \pi^\pm e^\mp \nu$	[ee] $(5.20 \pm 0.11) \times 10^{-5}$		207
$\pi^\pm e^\mp \nu e^+ e^-$	[ee] $(1.26 \pm 0.04) \times 10^{-5}$		229
<b>Hadronic modes, including Charge conjugation <math>\times</math> Parity Violating (CPV) modes</b>			
$3\pi^0$	$(19.52 \pm 0.12) \%$	S=1.6	139
$\pi^+ \pi^- \pi^0$	$(12.54 \pm 0.05) \%$		133
$\pi^+ \pi^-$	CPV [gg] $(1.967 \pm 0.010) \times 10^{-3}$	S=1.5	206
$\pi^0 \pi^0$	CPV $(8.64 \pm 0.06) \times 10^{-4}$	S=1.8	209
<b>Semileptonic modes with photons</b>			
$\pi^\pm e^\mp \nu_e \gamma$	[x, ee, hh] $(3.79 \pm 0.06) \times 10^{-3}$		229
$\pi^\pm \mu^\mp \nu_\mu \gamma$	$(5.65 \pm 0.23) \times 10^{-4}$		216
<b>Hadronic modes with photons or <math>\ell\bar{\ell}</math> pairs</b>			
$\pi^0 \pi^0 \gamma$	$< 2.43 \times 10^{-7}$	CL=90%	209
$\pi^+ \pi^- \gamma$	[x, hh] $(4.15 \pm 0.15) \times 10^{-5}$	S=2.8	206
$\pi^+ \pi^- \gamma (\text{DE})$	$(2.84 \pm 0.11) \times 10^{-5}$	S=2.0	206
$\pi^0 2\gamma$	[hh] $(1.273 \pm 0.033) \times 10^{-6}$		231
$\pi^0 \gamma e^+ e^-$	$(1.62 \pm 0.17) \times 10^{-8}$		230
<b>Other modes with photons or <math>\ell\bar{\ell}</math> pairs</b>			
$2\gamma$	$(5.47 \pm 0.04) \times 10^{-4}$	S=1.1	249
$3\gamma$	$< 7.4 \times 10^{-8}$	CL=90%	249
$e^+ e^- \gamma$	$(9.4 \pm 0.4) \times 10^{-6}$	S=2.0	249
$\mu^+ \mu^- \gamma$	$(3.59 \pm 0.11) \times 10^{-7}$	S=1.3	225
$e^+ e^- \gamma \gamma$	[hh] $(5.95 \pm 0.33) \times 10^{-7}$		249
$\mu^+ \mu^- \gamma \gamma$	[hh] $(1.0 \pm_{-0.6}^{+0.8}) \times 10^{-8}$		225

## Meson Summary Table

Charge conjugation $\times$ Parity ( $CP$ ) or Lepton Family number ( $LF$ ) violating modes, or $\Delta S = 1$ weak neutral current ( $SI$ ) modes			
$\mu^+ \mu^-$	$SI$	$(6.84 \pm 0.11) \times 10^{-9}$	225
$e^+ e^-$	$SI$	$(9 \pm \frac{6}{4}) \times 10^{-12}$	249
$\pi^+ \pi^- e^+ e^-$	$SI$ [hh]	$(3.11 \pm 0.19) \times 10^{-7}$	206
$\pi^0 \pi^0 e^+ e^-$	$SI$	$< 6.6 \times 10^{-9}$	CL=90% 209
$\pi^0 \pi^0 \mu^+ \mu^-$	$SI$	$< 9.2 \times 10^{-11}$	CL=90% 57
$\mu^+ \mu^- e^+ e^-$	$SI$	$(2.69 \pm 0.27) \times 10^{-9}$	225
$e^+ e^- e^+ e^-$	$SI$	$(3.56 \pm 0.21) \times 10^{-8}$	249
$\pi^0 \mu^+ \mu^-$	$CP, SI$ [ii]	$< 3.8 \times 10^{-10}$	CL=90% 177
$\pi^0 e^+ e^-$	$CP, SI$ [ii]	$< 2.8 \times 10^{-10}$	CL=90% 230
$\pi^0 \nu \bar{\nu}$	$CP, SI$ [jj]	$< 2.6 \times 10^{-8}$	CL=90% 231
$\pi^0 \pi^0 \nu \bar{\nu}$	$SI$	$< 8.1 \times 10^{-7}$	CL=90% 209
$e^\pm \mu^\mp$	$LF$ [ee]	$< 4.7 \times 10^{-12}$	CL=90% 238
$e^\pm e^\pm \mu^\mp \mu^\mp$	$LF$ [ee]	$< 4.12 \times 10^{-11}$	CL=90% 225
$\pi^0 \mu^\pm e^\mp$	$LF$ [ee]	$< 7.6 \times 10^{-11}$	CL=90% 217
$\pi^0 \pi^0 \mu^\pm e^\mp$	$LF$	$< 1.7 \times 10^{-10}$	CL=90% 159

 **$K^*(892)$** 

$$I(J^P) = \frac{1}{2}(1^-)$$

$K^*(892)^\pm$  mass  $m = 891.66 \pm 0.26$  MeV  
 Mass  $m = 895.5 \pm 0.8$  MeV  
 $K^*(892)^0$  mass  $m = 895.94 \pm 0.22$  MeV ( $S = 1.4$ )  
 $K^*(892)^\pm$  full width  $\Gamma = 50.8 \pm 0.9$  MeV  
 Full width  $\Gamma = 46.2 \pm 1.3$  MeV  
 $K^*(892)^0$  full width  $\Gamma = 48.7 \pm 0.8$  MeV ( $S = 1.7$ )

$K^*(892)$ DECAY MODES	Fraction ( $\Gamma_i/\Gamma$ )	Confidence level	$\rho$ (MeV/c)
$K\pi$	$\sim 100$ %		289
$K^0 \gamma$	$(2.39 \pm 0.21) \times 10^{-3}$		307
$K^\pm \gamma$	$(9.9 \pm 0.9) \times 10^{-4}$		309
$K\pi\pi$	$< 7 \times 10^{-4}$	95%	223

 **$K_1(1270)$** 

$$I(J^P) = \frac{1}{2}(1^+)$$

Mass  $m = 1272 \pm 7$  MeV [I]  
 Full width  $\Gamma = 90 \pm 20$  MeV [I]

$K_1(1270)$ DECAY MODES	Fraction ( $\Gamma_i/\Gamma$ )	$\rho$ (MeV/c)
$K\rho$	$(42 \pm 6)$ %	45
$K_0^*(1430)\pi$	$(28 \pm 4)$ %	†
$K^*(892)\pi$	$(16 \pm 5)$ %	302
$K\omega$	$(11.0 \pm 2.0)$ %	†
$K f_0(1370)$	$(3.0 \pm 2.0)$ %	†
$\gamma K^0$	seen	539

 **$K_1(1400)$** 

$$I(J^P) = \frac{1}{2}(1^+)$$

Mass  $m = 1403 \pm 7$  MeV  
 Full width  $\Gamma = 174 \pm 13$  MeV ( $S = 1.6$ )

$K_1(1400)$ DECAY MODES	Fraction ( $\Gamma_i/\Gamma$ )	$\rho$ (MeV/c)
$K^*(892)\pi$	$(94 \pm 6)$ %	402
$K\rho$	$(3.0 \pm 3.0)$ %	292
$K f_0(1370)$	$(2.0 \pm 2.0)$ %	†
$K\omega$	$(1.0 \pm 1.0)$ %	284
$K_0^*(1430)\pi$	not seen	†
$\gamma K^0$	seen	613

 **$K^*(1410)$** 

$$I(J^P) = \frac{1}{2}(1^-)$$

Mass  $m = 1414 \pm 15$  MeV ( $S = 1.3$ )  
 Full width  $\Gamma = 232 \pm 21$  MeV ( $S = 1.1$ )

 **$K^*(1410)$  DECAY MODES**

	Fraction ( $\Gamma_i/\Gamma$ )	Confidence level	$\rho$ (MeV/c)
$K^*(892)\pi$	$> 40$ %	95%	410
$K\pi$	$(6.6 \pm 1.3)$ %		612
$K\rho$	$< 7$ %	95%	305
$\gamma K^0$	seen		619

 **$K_0^*(1430)$  [kk]**

$$I(J^P) = \frac{1}{2}(0^+)$$

Mass  $m = 1425 \pm 50$  MeV  
 Full width  $\Gamma = 270 \pm 80$  MeV

 **$K_0^*(1430)$  DECAY MODES**

	Fraction ( $\Gamma_i/\Gamma$ )	$\rho$ (MeV/c)
$K\pi$	$(93 \pm 10)$ %	619

 **$K_2^*(1430)$** 

$$I(J^P) = \frac{1}{2}(2^+)$$

$K_2^*(1430)^\pm$  mass  $m = 1425.6 \pm 1.5$  MeV ( $S = 1.1$ )  
 $K_2^*(1430)^0$  mass  $m = 1432.4 \pm 1.3$  MeV  
 $K_2^*(1430)^\pm$  full width  $\Gamma = 98.5 \pm 2.7$  MeV ( $S = 1.1$ )  
 $K_2^*(1430)^0$  full width  $\Gamma = 109 \pm 5$  MeV ( $S = 1.9$ )

$K_2^*(1430)$ DECAY MODES	Fraction ( $\Gamma_i/\Gamma$ )	Scale factor / Confidence level	$\rho$ (MeV/c)
$K\pi$	$(49.9 \pm 1.2)$ %		619
$K^*(892)\pi$	$(24.7 \pm 1.5)$ %		419
$K^*(892)\pi\pi$	$(13.4 \pm 2.2)$ %		372
$K\rho$	$(8.7 \pm 0.8)$ %	$S=1.2$	318
$K\omega$	$(2.9 \pm 0.8)$ %		311
$K^+ \gamma$	$(2.4 \pm 0.5) \times 10^{-3}$	$S=1.1$	627
$K\eta$	$(1.5 \pm \frac{3.4}{1.0}) \times 10^{-3}$	$S=1.3$	486
$K\omega\pi$	$< 7.2 \times 10^{-4}$	CL=95%	100
$K^0 \gamma$	$< 9 \times 10^{-4}$	CL=90%	626

 **$K^*(1680)$** 

$$I(J^P) = \frac{1}{2}(1^-)$$

Mass  $m = 1717 \pm 27$  MeV ( $S = 1.4$ )  
 Full width  $\Gamma = 322 \pm 110$  MeV ( $S = 4.2$ )

 **$K^*(1680)$  DECAY MODES**

	Fraction ( $\Gamma_i/\Gamma$ )	$\rho$ (MeV/c)
$K\pi$	$(38.7 \pm 2.5)$ %	781
$K\rho$	$(31.4 \pm \frac{5.0}{2.1})$ %	570
$K^*(892)\pi$	$(29.9 \pm \frac{2.2}{5.0})$ %	618

 **$K_2(1770)$  [ll]**

$$I(J^P) = \frac{1}{2}(2^-)$$

Mass  $m = 1773 \pm 8$  MeV  
 Full width  $\Gamma = 186 \pm 14$  MeV

 **$K_2(1770)$  DECAY MODES**

	Fraction ( $\Gamma_i/\Gamma$ )	$\rho$ (MeV/c)
$K\pi\pi$		794
$K_2^*(1430)\pi$	dominant	288
$K^*(892)\pi$	seen	654
$K f_2(1270)$	seen	55
$K\phi$	seen	441
$K\omega$	seen	607

 **$K_3^*(1780)$** 

$$I(J^P) = \frac{1}{2}(3^-)$$

Mass  $m = 1776 \pm 7$  MeV ( $S = 1.1$ )  
 Full width  $\Gamma = 159 \pm 21$  MeV ( $S = 1.3$ )



## Meson Summary Table

$K_3^*(1780)$ DECAY MODES	Fraction ( $\Gamma_i/\Gamma$ )	Confidence level	$\rho$ (MeV/c)
$K\rho$	(31 $\pm$ 9 ) %		613
$K^*(892)\pi$	(20 $\pm$ 5 ) %		656
$K\pi$	(18.8 $\pm$ 1.0) %		813
$K\eta$	(30 $\pm$ 13 ) %		719
$K_2^*(1430)\pi$	< 16 %	95%	291

 **$K_2(1820)$  [mm]**

$$I(J^P) = \frac{1}{2}(2^-)$$

Mass  $m = 1816 \pm 13$  MeV  
Full width  $\Gamma = 276 \pm 35$  MeV

$K_2(1820)$ DECAY MODES	Fraction ( $\Gamma_i/\Gamma$ )	$\rho$ (MeV/c)
$K_2^*(1430)\pi$	seen	327
$K^*(892)\pi$	seen	681
$K f_2(1270)$	seen	186
$K\omega$	seen	638

 **$K_4^*(2045)$** 

$$I(J^P) = \frac{1}{2}(4^+)$$

Mass  $m = 2045 \pm 9$  MeV ( $S = 1.1$ )  
Full width  $\Gamma = 198 \pm 30$  MeV

$K_4^*(2045)$ DECAY MODES	Fraction ( $\Gamma_i/\Gamma$ )	$\rho$ (MeV/c)
$K\pi$	(9.9 $\pm$ 1.2) %	958
$K^*(892)\pi\pi$	(9 $\pm$ 5 ) %	802
$K^*(892)\pi\pi\pi$	(7 $\pm$ 5 ) %	768
$\rho K\pi$	(5.7 $\pm$ 3.2) %	741
$\omega K\pi$	(5.0 $\pm$ 3.0) %	738
$\phi K\pi$	(2.8 $\pm$ 1.4) %	594
$\phi K^*(892)$	(1.4 $\pm$ 0.7) %	363

## CHARMED MESONS ( $C = \pm 1$ )

$D^+ = c\bar{d}, D^0 = c\bar{u}, \bar{D}^0 = \bar{c}u, D^- = \bar{c}d$ , similarly for  $D^{* \pm}$

 **$D^{\pm}$** 

$$I(J^P) = \frac{1}{2}(0^-)$$

Mass  $m = 1869.62 \pm 0.15$  MeV ( $S = 1.1$ )  
Mean life  $\tau = (1040 \pm 7) \times 10^{-15}$  s  
 $c\tau = 311.8$   $\mu\text{m}$

**c-quark decays**

$\Gamma(c \rightarrow \ell^+ \text{anything})/\Gamma(c \rightarrow \text{anything}) = 0.096 \pm 0.004$  [mm]  
 $\Gamma(c \rightarrow D^*(2010)^+ \text{anything})/\Gamma(c \rightarrow \text{anything}) = 0.255 \pm 0.017$

**CP-violation decay-rate asymmetries**

$A_{CP}(\mu^\pm \nu) = (8 \pm 8)\%$   
 $A_{CP}(K_S^0 \pi^\pm) = (-0.54 \pm 0.14)\%$   
 $A_{CP}(K^\pm 2\pi^\pm) = (-0.1 \pm 1.0)\%$   
 $A_{CP}(K^\mp \pi^\pm \pi^\pm \pi^0) = (1.0 \pm 1.3)\%$   
 $A_{CP}(K_S^0 \pi^\pm \pi^0) = (0.3 \pm 0.9)\%$   
 $A_{CP}(K_S^0 \pi^\pm \pi^+ \pi^-) = (0.1 \pm 1.3)\%$   
 $A_{CP}(\pi^\pm \pi^0) = (2.9 \pm 2.9)\%$   
 $A_{CP}(\pi^\pm \eta) = (1.0 \pm 1.5)\%$  ( $S = 1.4$ )  
 $A_{CP}(\pi^\pm \eta'(958)) = (-0.5 \pm 1.2)\%$  ( $S = 1.1$ )  
 $A_{CP}(K_S^0 K^\pm) = (-0.1 \pm 0.6)\%$   
 $A_{CP}(K^+ K^- \pi^\pm) = (0.3 \pm 0.6)\%$   
 $A_{CP}(K^\pm K^*0) = (0.1 \pm 1.3)\%$   
 $A_{CP}(\phi \pi^\pm) = (0.42 \pm 0.28)\%$   
 $A_{CP}(K^\pm K_0^*(1430)^0) = (8 \pm 7)\%$   
 $A_{CP}(K^\pm K_2^*(1430)^0) = (43 \pm 20)\%$   
 $A_{CP}(K^\pm K_0^*(800)) = (-12 \pm 13)\%$   
 $A_{CP}(a_0(1450)^0 \pi^\pm) = (-19 \pm 14)\%$   
 $A_{CP}(\phi(1680) \pi^\pm) = (-9 \pm 26)\%$   
 $A_{CP}(\pi^+ \pi^- \pi^\pm) = (-2 \pm 4)\%$   
 $A_{CP}(K_S^0 K^\pm \pi^+ \pi^-) = (-4 \pm 7)\%$   
 $A_{CP}(K^\pm \pi^0) = (-4 \pm 11)\%$

**T-violation decay-rate asymmetry**

$$A_T(K_S^0 K^\pm \pi^+ \pi^-) = (-12 \pm 11) \times 10^{-3}$$
 [oo]

 **$D^+$  form factors**

$f_+(0)|V_{cs}|$  in  $\bar{K}^0 \ell^+ \nu_\ell = 0.707 \pm 0.013$   
 $r_1 \equiv a_1/a_0$  in  $\bar{K}^0 \ell^+ \nu_\ell = -1.7 \pm 0.5$   
 $r_2 \equiv a_2/a_0$  in  $\bar{K}^0 \ell^+ \nu_\ell = -14 \pm 11$   
 $f_+(0)|V_{cd}|$  in  $\pi^0 \ell^+ \nu_\ell = 0.146 \pm 0.007$   
 $r_1 \equiv a_1/a_0$  in  $\pi^0 \ell^+ \nu_\ell = -1.4 \pm 0.9$   
 $r_2 \equiv a_2/a_0$  in  $\pi^0 \ell^+ \nu_\ell = -4 \pm 5$   
 $f_+(0)|V_{cd}|$  in  $D^+ \rightarrow \eta e^+ \nu_e = 0.086 \pm 0.006$   
 $r_1 \equiv a_1/a_0$  in  $D^+ \rightarrow \eta e^+ \nu_e = -1.8 \pm 2.2$   
 $r_V \equiv V(0)/A_1(0)$  in  $\bar{K}^*(892)^0 \ell^+ \nu_\ell = 1.51 \pm 0.07$  ( $S = 2.2$ )  
 $r_2 \equiv A_2(0)/A_1(0)$  in  $\bar{K}^*(892)^0 \ell^+ \nu_\ell = 0.807 \pm 0.025$   
 $r_3 \equiv A_3(0)/A_1(0)$  in  $\bar{K}^*(892)^0 \ell^+ \nu_\ell = 0.0 \pm 0.4$   
 $\Gamma_L/\Gamma_T$  in  $\bar{K}^*(892)^0 \ell^+ \nu_\ell = 1.13 \pm 0.08$   
 $\Gamma_+/ \Gamma_-$  in  $\bar{K}^*(892)^0 \ell^+ \nu_\ell = 0.22 \pm 0.06$  ( $S = 1.6$ )

Most decay modes (other than the semileptonic modes) that involve a neutral  $K$  meson are now given as  $K_S^0$  modes, not as  $\bar{K}^0$  modes. Nearly always it is a  $K_S^0$  that is measured, and interference between Cabibbo-allowed and doubly Cabibbo-suppressed modes can invalidate the assumption that  $2\Gamma(K_S^0) = \Gamma(\bar{K}^0)$ .

$D^+$ DECAY MODES	Fraction ( $\Gamma_i/\Gamma$ )	Scale factor/ Confidence level	$\rho$ (MeV/c)
-------------------	--------------------------------	-----------------------------------	----------------

**Inclusive modes**

$e^+$ semileptonic	(16.07 $\pm$ 0.30) %		—
$\mu^+$ anything	(17.6 $\pm$ 3.2) %		—
$K^-$ anything	(25.7 $\pm$ 1.4) %		—
$\bar{K}^0$ anything + $K^0$ anything	(61 $\pm$ 5) %		—
$K^+$ anything	(5.9 $\pm$ 0.8) %		—
$K^*(892)^-$ anything	(6 $\pm$ 5) %		—
$\bar{K}^*(892)^0$ anything	(23 $\pm$ 5) %		—
$K^*(892)^0$ anything	< 6.6 %	CL=90%	—
$\eta$ anything	(6.3 $\pm$ 0.7) %		—
$\eta'$ anything	(1.04 $\pm$ 0.18) %		—
$\phi$ anything	(1.03 $\pm$ 0.12) %		—

**Leptonic and semileptonic modes**

$e^+ \nu_e$	< 8.8	$\times 10^{-6}$	CL=90%	935
$\mu^+ \nu_\mu$	(3.82 $\pm$ 0.33)	$\times 10^{-4}$		932
$\tau^+ \nu_\tau$	< 1.2	$\times 10^{-3}$	CL=90%	91
$\bar{K}^0 e^+ \nu_e$	(8.83 $\pm$ 0.22) %			869
$\bar{K}^0 \mu^+ \nu_\mu$	(9.2 $\pm$ 0.6) %			865
$K^- \pi^+ e^+ \nu_e$	(4.00 $\pm$ 0.10) %			864
$\bar{K}^*(892)^0 e^+ \nu_e, \bar{K}^*(892)^0 \rightarrow$	(3.68 $\pm$ 0.10) %			722
$K^- \pi^+$				
$(K^- \pi^+)_{S\text{-wave}} e^+ \nu_e$	(2.32 $\pm$ 0.10)	$\times 10^{-3}$		—
$\bar{K}^*(1410)^0 e^+ \nu_e,$	< 6	$\times 10^{-3}$	CL=90%	—
$\bar{K}^*(1410)^0 \rightarrow K^- \pi^+$				
$\bar{K}_2^*(1430)^0 e^+ \nu_e,$	< 5	$\times 10^{-4}$	CL=90%	—
$\bar{K}_2^*(1430)^0 \rightarrow K^- \pi^+$				
$K^- \pi^+ e^+ \nu_e$ nonresonant	< 7	$\times 10^{-3}$	CL=90%	864
$K^- \pi^+ \mu^+ \nu_\mu$	(3.8 $\pm$ 0.4) %			851
$\bar{K}^*(892)^0 \mu^+ \nu_\mu,$	(3.52 $\pm$ 0.10) %			717
$\bar{K}^*(892)^0 \rightarrow K^- \pi^+$				
$K^- \pi^+ \mu^+ \nu_\mu$ nonresonant	(2.0 $\pm$ 0.5)	$\times 10^{-3}$		851
$K^- \pi^+ \pi^0 \mu^+ \nu_\mu$	< 1.6	$\times 10^{-3}$	CL=90%	825
$\pi^0 e^+ \nu_e$	(4.05 $\pm$ 0.18)	$\times 10^{-3}$		930
$\eta e^+ \nu_e$	(1.14 $\pm$ 0.10)	$\times 10^{-3}$		855
$\rho^0 e^+ \nu_e$	(2.2 $\pm$ 0.4)	$\times 10^{-3}$		774
$\rho^0 \mu^+ \nu_\mu$	(2.4 $\pm$ 0.4)	$\times 10^{-3}$		770
$\omega e^+ \nu_e$	(1.6 $\pm$ 0.7)	$\times 10^{-3}$		771
$\eta'(958) e^+ \nu_e$	(2.2 $\pm$ 0.5)	$\times 10^{-4}$		689
$\phi e^+ \nu_e$	< 9	$\times 10^{-5}$	CL=90%	657

Fractions of some of the following modes with resonances have already appeared above as submodes of particular charged-particle modes.

$\bar{K}^*(892)^0 e^+ \nu_e$	(5.52 $\pm$ 0.15) %		722
$\bar{K}^*(892)^0 \mu^+ \nu_\mu$	(5.28 $\pm$ 0.15) %		717
$\bar{K}_0^*(1430)^0 \mu^+ \nu_\mu$	< 2.4	$\times 10^{-4}$	380
$\bar{K}^*(1680)^0 \mu^+ \nu_\mu$	< 1.5	$\times 10^{-3}$	105

## Meson Summary Table

Hadronic modes with a $\bar{K}$ or $\bar{K}K\bar{K}$			
$K_S^0 \pi^+$	(1.47 ± 0.07) %	S=2.0	863
$K_L^0 \pi^+$	(1.46 ± 0.05) %		863
$K^- 2\pi^+$	[pp] (9.13 ± 0.19) %		846
$(K^- \pi^+)_{S\text{-wave}} \pi^+$	(7.32 ± 0.19) %		846
$\bar{K}_0^*(1430)^0 \pi^+$	[qq] (1.21 ± 0.06) %		382
$\bar{K}_0^*(1430)^0 \rightarrow K^- \pi^+$			
$\bar{K}^*(892)^0 \pi^+$	(1.01 ± 0.11) %		714
$\bar{K}^*(892)^0 \rightarrow K^- \pi^+$			
$\bar{K}^*(1410)^0 \pi^+, \bar{K}^{*0} \rightarrow$	not seen		381
$\bar{K}_2^*(1430)^0 \pi^+$	[qq] (2.2 ± 0.7) × 10 <sup>-4</sup>		371
$\bar{K}_2^*(1430)^0 \rightarrow K^- \pi^+$			
$\bar{K}^*(1680)^0 \pi^+$	[qq] (2.1 ± 1.1) × 10 <sup>-4</sup>		58
$\bar{K}^*(1680)^0 \rightarrow K^- \pi^+$			
$K^-(2\pi^+)_{I=2}$	(1.41 ± 0.26) %		-
$K_S^0 \pi^+ \pi^0$	[pp] (6.99 ± 0.27) %		845
$K_S^0 \rho^+$	(4.8 ± 1.0) %		677
$\bar{K}^*(892)^0 \pi^+, \bar{K}^*(892)^0 \rightarrow K_S^0 \pi^0$	(1.3 ± 0.6) %		714
$K_S^0 \pi^+ \pi^0$ nonresonant	(9 ± 7) × 10 <sup>-3</sup>		845
$K^- 2\pi^+ \pi^0$	[rr] (5.99 ± 0.18) %		816
$K_S^0 2\pi^+ \pi^-$	[rr] (3.12 ± 0.11) %		814
$K^- 3\pi^+ \pi^-$	[pp] (5.6 ± 0.5) × 10 <sup>-3</sup>	S=1.1	772
$\bar{K}^*(892)^0 2\pi^+ \pi^-, \bar{K}^*(892)^0 \rightarrow K^- \pi^+$	(1.2 ± 0.4) × 10 <sup>-3</sup>		645
$\bar{K}^*(892)^0 \rho^0 \pi^+, \bar{K}^*(892)^0 \rightarrow K^- \pi^+$	(2.2 ± 0.4) × 10 <sup>-3</sup>		239
$\bar{K}^*(892)^0 a_1(1260)^+$	[ss] (9.0 ± 1.8) × 10 <sup>-3</sup>		†
$K^- \rho^0 2\pi^+$	(1.68 ± 0.27) × 10 <sup>-3</sup>		524
$K^- 3\pi^+ \pi^-$ nonresonant	(3.9 ± 2.9) × 10 <sup>-4</sup>		772
$K^+ 2K_S^0$	(4.5 ± 2.0) × 10 <sup>-3</sup>		545
$K^+ K^- K_S^0 \pi^+$	(2.4 ± 0.6) × 10 <sup>-4</sup>		436
Pionic modes			
$\pi^+ \pi^0$	(1.19 ± 0.06) × 10 <sup>-3</sup>		925
$2\pi^+ \pi^-$	(3.18 ± 0.18) × 10 <sup>-3</sup>		909
$\rho^0 \pi^+$	(8.1 ± 1.5) × 10 <sup>-4</sup>		767
$\pi^+(\pi^+ \pi^-)_{S\text{-wave}}$	(1.78 ± 0.16) × 10 <sup>-3</sup>		909
$\sigma \pi^+, \sigma \rightarrow \pi^+ \pi^-$	(1.34 ± 0.12) × 10 <sup>-3</sup>		-
$f_0(980) \pi^+, f_0(980) \rightarrow \pi^+ \pi^-$	(1.52 ± 0.33) × 10 <sup>-4</sup>		669
$f_0(1370) \pi^+, f_0(1370) \rightarrow \pi^+ \pi^-$	(8 ± 4) × 10 <sup>-5</sup>		-
$f_2(1270) \pi^+, f_2(1270) \rightarrow \pi^+ \pi^-$	(4.9 ± 0.9) × 10 <sup>-4</sup>		485
$\rho(1450)^0 \pi^+, \rho(1450)^0 \rightarrow \pi^+ \pi^-$	< 8 × 10 <sup>-5</sup>	CL=95%	338
$f_0(1500) \pi^+, f_0(1500) \rightarrow \pi^+ \pi^-$	(1.1 ± 0.4) × 10 <sup>-4</sup>		-
$f_0(1710) \pi^+, f_0(1710) \rightarrow \pi^+ \pi^-$	< 5 × 10 <sup>-5</sup>	CL=95%	-
$f_0(1790) \pi^+, f_0(1790) \rightarrow \pi^+ \pi^-$	< 6 × 10 <sup>-5</sup>	CL=95%	-
$(\pi^+ \pi^+)_{S\text{-wave}} \pi^-$	< 1.2 × 10 <sup>-4</sup>	CL=95%	909
$2\pi^+ \pi^-$ nonresonant	< 1.1 × 10 <sup>-4</sup>	CL=95%	909
$\pi^+ 2\pi^0$	(4.6 ± 0.4) × 10 <sup>-3</sup>		910
$2\pi^+ \pi^- \pi^0$	(1.13 ± 0.08) %		883
$\eta \pi^+, \eta \rightarrow \pi^+ \pi^- \pi^0$	(8.0 ± 0.5) × 10 <sup>-4</sup>		848
$\omega \pi^+, \omega \rightarrow \pi^+ \pi^- \pi^0$	< 3 × 10 <sup>-4</sup>	CL=90%	763
$3\pi^+ 2\pi^-$	(1.61 ± 0.16) × 10 <sup>-3</sup>		845
Fractions of some of the following modes with resonances have already appeared above as submodes of particular charged-particle modes.			
$\eta \pi^+$	(3.53 ± 0.21) × 10 <sup>-3</sup>		848
$\eta \pi^+ \pi^0$	(1.38 ± 0.35) × 10 <sup>-3</sup>		830
$\omega \pi^+$	< 3.4 × 10 <sup>-4</sup>	CL=90%	764
$\eta'(958) \pi^+$	(4.67 ± 0.29) × 10 <sup>-3</sup>		681
$\eta'(958) \pi^+ \pi^0$	(1.6 ± 0.5) × 10 <sup>-3</sup>		654
Hadronic modes with a $K\bar{K}$ pair			
$K^+ K_S^0$	(2.83 ± 0.16) × 10 <sup>-3</sup>	S=2.2	793
$K^+ K^- \pi^+$	[pp] (9.54 ± 0.26) × 10 <sup>-3</sup>	S=1.1	744
$\phi \pi^+, \phi \rightarrow K^+ K^-$	(2.65 ± 0.08) × 10 <sup>-3</sup>		647
$K^+ \bar{K}^*(892)^0, \bar{K}^*(892)^0 \rightarrow K^- \pi^+$	(2.45 ± 0.09) × 10 <sup>-3</sup>		613
$K^+ \bar{K}_0^*(1430)^0, \bar{K}_0^*(1430)^0 \rightarrow K^- \pi^+$	(1.79 ± 0.34) × 10 <sup>-3</sup>		-
$K^+ \bar{K}_2^*(1430)^0, \bar{K}_2^* \rightarrow K^- \pi^+$	(1.6 ± 1.2) × 10 <sup>-4</sup>		-
$K^+ \bar{K}_0^*(800), \bar{K}_0^* \rightarrow K^- \pi^+$	(6.7 ± 3.4) × 10 <sup>-4</sup>		-
$a_0(1450)^0 \pi^+, a_0^0 \rightarrow K^+ K^-$	(4.4 ± 7.0) × 10 <sup>-4</sup>		-
$\phi(1680) \pi^+, \phi \rightarrow K^+ K^-$	(4.9 ± 4.0) × 10 <sup>-5</sup>		-
$K^+ K^- \pi^+$ nonresonant	not seen		744
$K^+ K_S^0 \pi^+ \pi^-$	(1.75 ± 0.18) × 10 <sup>-3</sup>		678
$K_S^0 K^- 2\pi^+$	(2.40 ± 0.18) × 10 <sup>-3</sup>		678
$K^+ K^- 2\pi^+ \pi^-$	(2.2 ± 1.2) × 10 <sup>-4</sup>		600
A few poorly measured branching fractions:			
$\phi \pi^+ \pi^0$	(2.3 ± 1.0) %		619
$\phi \rho^+$	< 1.5 %	CL=90%	259
$K^+ K^- \pi^+ \pi^0$ non- $\phi$	(1.5 ± 0.7) %		682
$K^*(892)^+ K_S^0$	(1.6 ± 0.7) %		612
Doubly Cabibbo-suppressed modes			
$K^+ \pi^0$	(1.83 ± 0.26) × 10 <sup>-4</sup>	S=1.4	864
$K^+ \eta$	(1.08 ± 0.17) × 10 <sup>-4</sup>		776
$K^+ \eta'(958)$	(1.76 ± 0.22) × 10 <sup>-4</sup>		571
$K^+ \pi^+ \pi^-$	(5.27 ± 0.23) × 10 <sup>-4</sup>		846
$K^+ \rho^0$	(2.0 ± 0.5) × 10 <sup>-4</sup>		679
$K^*(892)^0 \pi^+, K^*(892)^0 \rightarrow K^+ \pi^-$	(2.5 ± 0.4) × 10 <sup>-4</sup>		714
$K^+ f_0(980), f_0(980) \rightarrow \pi^+ \pi^-$	(4.7 ± 2.8) × 10 <sup>-5</sup>		-
$K_2^*(1430)^0 \pi^+, K_2^*(1430)^0 \rightarrow K^+ \pi^-$	(4.2 ± 2.9) × 10 <sup>-5</sup>		-
$K^+ \pi^+ \pi^-$ nonresonant	not seen		846
$2K^+ K^-$	(8.7 ± 2.0) × 10 <sup>-5</sup>		550
$\Delta C = 1$ weak neutral current (C1) modes, or Lepton Family number (LF) or Lepton number (L) violating modes			
$\pi^+ e^+ e^-$	C1 < 1.1 × 10 <sup>-6</sup>	CL=90%	930
$\pi^+ \phi, \phi \rightarrow e^+ e^-$	[tt] (1.7 ± 1.4) × 10 <sup>-6</sup>		-
$\pi^+ \mu^+ \mu^-$	C1 < 3.9 × 10 <sup>-6</sup>	CL=90%	918
$\pi^+ \phi, \phi \rightarrow \mu^+ \mu^-$	[tt] (1.8 ± 0.8) × 10 <sup>-6</sup>		-
$\rho^+ \mu^+ \mu^-$	C1 < 5.6 × 10 <sup>-4</sup>	CL=90%	757
$K^+ e^+ e^-$	[uu] < 1.0 × 10 <sup>-6</sup>	CL=90%	870
$K^+ \mu^+ \mu^-$	[uu] < 4.3 × 10 <sup>-6</sup>	CL=90%	856
$\pi^+ e^+ \mu^-$	LF < 2.9 × 10 <sup>-6</sup>	CL=90%	927
$\pi^+ e^- \mu^+$	LF < 3.6 × 10 <sup>-6</sup>	CL=90%	927
$K^+ e^+ \mu^-$	LF < 1.2 × 10 <sup>-6</sup>	CL=90%	866
$K^+ e^- \mu^+$	LF < 2.8 × 10 <sup>-6</sup>	CL=90%	866
$\pi^- 2e^+$	L < 1.1 × 10 <sup>-6</sup>	CL=90%	930
$\pi^- 2\mu^+$	L < 2.0 × 10 <sup>-6</sup>	CL=90%	918
$\pi^- e^+ \mu^+$	L < 2.0 × 10 <sup>-6</sup>	CL=90%	927
$\rho^- 2\mu^+$	L < 5.6 × 10 <sup>-4</sup>	CL=90%	757
$K^- 2e^+$	L < 9 × 10 <sup>-7</sup>	CL=90%	870
$K^- 2\mu^+$	L < 1.0 × 10 <sup>-5</sup>	CL=90%	856
$K^- e^+ \mu^+$	L < 1.9 × 10 <sup>-6</sup>	CL=90%	866
$K^*(892)^- 2\mu^+$	L < 8.5 × 10 <sup>-4</sup>	CL=90%	703

 $D^0$ 

$$I(J^P) = \frac{1}{2}(0^-)$$

Mass  $m = 1864.86 \pm 0.13$  MeV $m_{D^\pm} - m_{D^0} = 4.76 \pm 0.10$  MeV (S = 1.1)Mean life  $\tau = (410.1 \pm 1.5) \times 10^{-15}$  s $c\tau = 122.9$   $\mu\text{m}$  $|m_{D_1^0} - m_{D_2^0}| = (1.44_{-0.50}^{+0.48}) \times 10^{10} \hbar \text{ s}^{-1}$  $(\Gamma_{D_1^0} - \Gamma_{D_2^0})/\Gamma = 2\gamma = (1.60_{-0.26}^{+0.25}) \times 10^{-2}$  $|q/p| = 0.88_{-0.15}^{+0.16}$  $A_\Gamma = (0.26 \pm 2.31) \times 10^{-3}$  $K^+ \pi^-$  relative strong phase:  $\cos \delta = 1.03_{-0.18}^{+0.32}$  $K^- \pi^+ \pi^0$  coherence factor  $R_{K\pi\pi^0} = 0.78_{-0.25}^{+0.11}$  $K^- \pi^+ \pi^0$  average relative strong phase  $\delta^{K\pi\pi^0} = (239 \pm 32)^\circ$  $K^- \pi^- 2\pi^+$  coherence factor  $R_{K3\pi} = 0.36_{-0.30}^{+0.24}$  $K^- \pi^- 2\pi^+$  average relative strong phase  $\delta^{K3\pi} = (118 \pm 60)^\circ$

## Meson Summary Table

CP-violation decay-rate asymmetries (labeled by the  $D^0$  decay)
$$A_{CP}(K^+K^-) = (-0.21 \pm 0.17)\%$$

$$A_{CP}(2K_S^0) = (-23 \pm 19)\%$$

$$A_{CP}(\pi^+\pi^-) = (0.22 \pm 0.21)\%$$

$$A_{CP}(2\pi^0) = (0 \pm 5)\%$$

$$A_{CP}(\pi^+\pi^-\pi^0) = (0.3 \pm 0.4)\%$$

$$A_{CP}(\rho(770)^+\pi^- \rightarrow \pi^+\pi^-\pi^0) = (1.2 \pm 0.9)\% \text{ [vv]}$$

$$A_{CP}(\rho(770)^0\pi^0 \rightarrow \pi^+\pi^-\pi^0) = (-3.1 \pm 3.0)\% \text{ [vv]}$$

$$A_{CP}(\rho(770)^-\pi^+ \rightarrow \pi^+\pi^-\pi^0) = (-1.0 \pm 1.7)\% \text{ [vw]}$$

$$A_{CP}(\rho(1450)^+\pi^- \rightarrow \pi^+\pi^-\pi^0) = (0 \pm 70)\% \text{ [vw]}$$

$$A_{CP}(\rho(1450)^0\pi^0 \rightarrow \pi^+\pi^-\pi^0) = (-20 \pm 40)\% \text{ [vv]}$$

$$A_{CP}(\rho(1450)^-\pi^+ \rightarrow \pi^+\pi^-\pi^0) = (6 \pm 9)\% \text{ [vw]}$$

$$A_{CP}(\rho(1700)^+\pi^- \rightarrow \pi^+\pi^-\pi^0) = (-5 \pm 14)\% \text{ [vw]}$$

$$A_{CP}(\rho(1700)^0\pi^0 \rightarrow \pi^+\pi^-\pi^0) = (13 \pm 9)\% \text{ [vv]}$$

$$A_{CP}(\rho(1700)^-\pi^+ \rightarrow \pi^+\pi^-\pi^0) = (8 \pm 11)\% \text{ [vw]}$$

$$A_{CP}(f_0(980)\pi^0 \rightarrow \pi^+\pi^-\pi^0) = (0 \pm 35)\% \text{ [vw]}$$

$$A_{CP}(f_0(1370)\pi^0 \rightarrow \pi^+\pi^-\pi^0) = (25 \pm 18)\% \text{ [vw]}$$

$$A_{CP}(f_0(1500)\pi^0 \rightarrow \pi^+\pi^-\pi^0) = (0 \pm 18)\% \text{ [vw]}$$

$$A_{CP}(f_0(1710)\pi^0 \rightarrow \pi^+\pi^-\pi^0) = (0 \pm 24)\% \text{ [vw]}$$

$$A_{CP}(f_2(1270)\pi^0 \rightarrow \pi^+\pi^-\pi^0) = (-4 \pm 6)\% \text{ [vw]}$$

$$A_{CP}(\sigma(400)\pi^0 \rightarrow \pi^+\pi^-\pi^0) = (6 \pm 8)\% \text{ [vw]}$$

$$A_{CP}(\text{nonresonant } \pi^+\pi^-\pi^0) = (-13 \pm 23)\% \text{ [vw]}$$

$$A_{CP}(K^+K^-\pi^0) = (-1.0 \pm 1.7)\%$$

$$A_{CP}(K^*(892)^+K^- \rightarrow K^+K^-\pi^0) = (-0.9 \pm 1.3)\% \text{ [vw]}$$

$$A_{CP}(K^*(1410)^+K^- \rightarrow K^+K^-\pi^0) = (-21 \pm 24)\% \text{ [vw]}$$

$$A_{CP}((K^+\pi^0)_S K^- \rightarrow K^+K^-\pi^0) = (7 \pm 15)\% \text{ [vw]}$$

$$A_{CP}(\phi(1020)\pi^0 \rightarrow K^+K^-\pi^0) = (1.1 \pm 2.2)\% \text{ [vw]}$$

$$A_{CP}(f_0(980)\pi^0 \rightarrow K^+K^-\pi^0) = (-3 \pm 19)\% \text{ [vw]}$$

$$A_{CP}(a_0(980)^0\pi^0 \rightarrow K^+K^-\pi^0) = (-5 \pm 16)\% \text{ [vw]}$$

$$A_{CP}(f_2(1525)\pi^0 \rightarrow K^+K^-\pi^0) = (0 \pm 160)\% \text{ [vw]}$$

$$A_{CP}(K^*(892)^-K^+ \rightarrow K^+K^-\pi^0) = (-5 \pm 4)\% \text{ [vw]}$$

$$A_{CP}(K^*(1410)^-K^+ \rightarrow K^+K^-\pi^0) = (-17 \pm 29)\% \text{ [vw]}$$

$$A_{CP}((K^-\pi^0)_{S-wave} K^+ \rightarrow K^+K^-\pi^0) = (-10 \pm 40)\% \text{ [vw]}$$

$$A_{CP}(K_S^0\pi^0) = (-0.27 \pm 0.21)\%$$

$$A_{CP}(K_S^0\eta) = (0.5 \pm 0.5)\%$$

$$A_{CP}(K_S^0\eta') = (1.0 \pm 0.7)\%$$

$$A_{CP}(K_S^0\phi) = (-3 \pm 9)\%$$

$$A_{CP}(K^-\pi^+) = (0.1 \pm 0.7)\%$$

$$A_{CP}(K^+\pi^-) = (2.2 \pm 3.2)\%$$

$$A_{CP}(K^-\pi^+\pi^0) = (0.2 \pm 0.9)\%$$

$$A_{CP}(K^+\pi^-\pi^0) = (0 \pm 5)\%$$

$$A_{CP}(K_S^0\pi^+\pi^-) = (-0.9 \pm 2.6)\%$$

$$A_{CP}(K^*(892)^-\pi^+ \rightarrow K_S^0\pi^+\pi^-) < 3.5 \times 10^{-4}, \text{ CL} = 95\%$$

$$A_{CP}(K^*(892)^+\pi^- \rightarrow K_S^0\pi^+\pi^-) < 7.8 \times 10^{-4}, \text{ CL} = 95\%$$

$$A_{CP}(\overline{K}^0\rho^0 \rightarrow K_S^0\pi^+\pi^-) < 4.8 \times 10^{-4}, \text{ CL} = 95\%$$

$$A_{CP}(\overline{K}^0\omega \rightarrow K_S^0\pi^+\pi^-) < 9.2 \times 10^{-4}, \text{ CL} = 95\%$$

$$A_{CP}(\overline{K}^0 f_0(980) \rightarrow K_S^0\pi^+\pi^-) < 6.8 \times 10^{-4}, \text{ CL} = 95\%$$

$$A_{CP}(\overline{K}^0 f_2(1270) \rightarrow K_S^0\pi^+\pi^-) < 13.5 \times 10^{-4}, \text{ CL} = 95\%$$

$$A_{CP}(\overline{K}^0 f_0(1370) \rightarrow K_S^0\pi^+\pi^-) < 25.5 \times 10^{-4}, \text{ CL} = 95\%$$

$$A_{CP}(K_0^*(1430)^-\pi^+ \rightarrow K_S^0\pi^+\pi^-) < 9.0 \times 10^{-4}, \text{ CL} = 95\%$$

$$A_{CP}(K_2^*(1430)^-\pi^+ \rightarrow K_S^0\pi^+\pi^-) < 6.5 \times 10^{-4}, \text{ CL} = 95\%$$

$$A_{CP}(K^*(1680)^-\pi^+ \rightarrow K_S^0\pi^+\pi^-) < 28.4 \times 10^{-4}, \text{ CL} = 95\%$$

$$A_{CP}(K^-\pi^+\pi^+\pi^-) = (0.7 \pm 1.0)\%$$

$$A_{CP}(K^+\pi^-\pi^+\pi^-) = (-2 \pm 4)\%$$

$$A_{CP}(K^+K^-\pi^+\pi^-) = (-8 \pm 7)\%$$

$$\Delta A_{CP} = A_{CP}(K^+K^-) - A_{CP}(\pi^+\pi^-) = (-0.65 \pm 0.18)\%$$

## T-violation decay-rate asymmetry

$$A_T(K^+K^-\pi^+\pi^-) = (1 \pm 7) \times 10^{-3} \text{ [oo]}$$

## CPT-violation decay-rate asymmetry

$$A_{CPT}(K^\mp\pi^\pm) = 0.008 \pm 0.008$$

## Form factors

$$r_V \equiv V(0)/A_1(0) \text{ in } D^0 \rightarrow K^*(892)^-\ell^+\nu_\ell = 1.7 \pm 0.8$$

$$r_2 \equiv A_2(0)/A_1(0) \text{ in } D^0 \rightarrow K^*(892)^-\ell^+\nu_\ell = 0.9 \pm 0.4$$

$$f_+(0) \text{ in } D^0 \rightarrow K^-\ell^+\nu_\ell = 0.727 \pm 0.011$$

$$f_+(0)|V_{cs}| \text{ in } D^0 \rightarrow K^-\ell^+\nu_\ell = 0.726 \pm 0.009$$

$$\eta_1 \equiv a_1/a_0 \text{ in } D^0 \rightarrow K^-\ell^+\nu_\ell = -2.65 \pm 0.35$$

$$r_2 \equiv a_1/a_0 \text{ in } D^0 \rightarrow K^-\ell^+\nu_\ell = 13 \pm 9$$

$$f_+(0)|V_{cd}| \text{ in } D^0 \rightarrow \pi^-\ell^+\nu_\ell = 0.152 \pm 0.005$$

$$\eta_1 \equiv a_1/a_0 \text{ in } D^0 \rightarrow \pi^-\ell^+\nu_\ell = -2.8 \pm 0.5$$

$$r_2 \equiv a_1/a_0 \text{ in } D^0 \rightarrow \pi^-\ell^+\nu_\ell = 6 \pm 3.0$$

Most decay modes (other than the semileptonic modes) that involve a neutral  $K$  meson are now given as  $K_S^0$  modes, not as  $\overline{K}^0$  modes. Nearly always it is a  $K_S^0$  that is measured, and interference between Cabibbo-allowed and doubly Cabibbo-suppressed modes can invalidate the assumption that  $2\Gamma(K_S^0) = \Gamma(\overline{K}^0)$ .

$D^0$ DECAY MODES	Fraction ( $\Gamma_i/\Gamma$ )	Scale factor/ Confidence level (MeV/c)	$p$
<b>Topological modes</b>			
0-prongs	[vv] (15 ± 6 ) %		–
2-prongs	(70 ± 6 ) %		–
4-prongs	[xx] (14.5 ± 0.5 ) %		–
6-prongs	[yy] ( 6.4 ± 1.3 ) × 10 <sup>-4</sup>		–
<b>Inclusive modes</b>			
$e^+$ anything	[zz] ( 6.49 ± 0.11 ) %		–
$\mu^+$ anything	( 6.7 ± 0.6 ) %		–
$K^-$ anything	(54.7 ± 2.8 ) %	S=1.3	–
$\overline{K}^0$ anything + $K^0$ anything	(47 ± 4 ) %		–
$K^+$ anything	( 3.4 ± 0.4 ) %		–
$K^*(892)^-$ anything	(15 ± 9 ) %		–
$\overline{K}^*(892)^0$ anything	( 9 ± 4 ) %		–
$K^*(892)^+$ anything	< 3.6 %	CL=90%	–
$K^*(892)^0$ anything	( 2.8 ± 1.3 ) %		–
$\eta$ anything	( 9.5 ± 0.9 ) %		–
$\eta'$ anything	( 2.48 ± 0.27 ) %		–
$\phi$ anything	( 1.05 ± 0.11 ) %		–
<b>Semileptonic modes</b>			
$K^- e^+ \nu_e$	( 3.55 ± 0.04 ) %	S=1.2	867
$K^- \mu^+ \nu_\mu$	( 3.30 ± 0.13 ) %		864
$K^*(892)^- e^+ \nu_e$	( 2.16 ± 0.16 ) %		719
$K^*(892)^- \mu^+ \nu_\mu$	( 1.90 ± 0.24 ) %		714
$K^- \pi^0 e^+ \nu_e$	( 1.6 ± 1.3 / 0.5 ) %		861
$\overline{K}^0 \pi^- e^+ \nu_e$	( 2.7 ± 0.9 / 0.7 ) %		860
$K^- \pi^+ \pi^- e^+ \nu_e$	( 2.8 ± 1.4 / -1.1 ) × 10 <sup>-4</sup>		843
$K_1(1270)^- e^+ \nu_e$	( 7.6 ± 4.0 / -3.1 ) × 10 <sup>-4</sup>		498
$K^- \pi^+ \pi^- \mu^+ \nu_\mu$	< 1.2 × 10 <sup>-3</sup>	CL=90%	821
$(\overline{K}^*(892)\pi)^- \mu^+ \nu_\mu$	< 1.4 × 10 <sup>-3</sup>	CL=90%	692
$\pi^- e^+ \nu_e$	( 2.89 ± 0.08 ) × 10 <sup>-3</sup>	S=1.1	927
$\pi^- \mu^+ \nu_\mu$	( 2.37 ± 0.24 ) × 10 <sup>-3</sup>		924
$\rho^- e^+ \nu_e$	( 1.9 ± 0.4 ) × 10 <sup>-3</sup>		771
<b>Hadronic modes with one <math>\overline{K}</math></b>			
$K^-\pi^+$	( 3.88 ± 0.05 ) %	S=1.2	861
$K_S^0\pi^0$	( 1.19 ± 0.04 ) %		860
$K_0^0\pi^0$	(10.0 ± 0.7 ) × 10 <sup>-3</sup>		860
$K_S^0\pi^+\pi^-$	[pp] ( 2.82 ± 0.19 ) %	S=1.1	842
$K_S^0\rho^0$	( 6.3 ± 0.7 / -0.8 ) × 10 <sup>-3</sup>		674
$K_S^0\omega, \omega \rightarrow \pi^+\pi^-$	( 2.0 ± 0.6 ) × 10 <sup>-4</sup>		670
$K_S^0(\pi^+\pi^-)_{S-wave}$	( 3.4 ± 0.8 ) × 10 <sup>-3</sup>		842
$K_S^0 f_0(980),$ $f_0(980) \rightarrow \pi^+\pi^-$	( 1.21 ± 0.40 / 0.24 ) × 10 <sup>-3</sup>		549
$K_S^0 f_0(1370),$ $f_0(1370) \rightarrow \pi^+\pi^-$	( 2.8 ± 0.9 / -1.3 ) × 10 <sup>-3</sup>		†
$K_S^0 f_2(1270),$ $f_2(1270) \rightarrow \pi^+\pi^-$	( 9 ± 10 / -6 ) × 10 <sup>-5</sup>		262
$K^*(892)^-\pi^+,$ $K^*(892)^- \rightarrow K_S^0\pi^-$	( 1.66 ± 0.15 / 0.17 ) %		711
$K_0^*(1430)^-\pi^+,$ $K_0^*(1430)^- \rightarrow K_S^0\pi^-$	( 2.69 ± 0.40 / 0.33 ) × 10 <sup>-3</sup>		378
$K_2^*(1430)^-\pi^+,$ $K_2^*(1430)^- \rightarrow K_S^0\pi^-$	( 3.4 ± 1.9 / 1.0 ) × 10 <sup>-4</sup>		367
$K^*(1680)^-\pi^+,$ $K^*(1680)^- \rightarrow K_S^0\pi^-$	( 4 ± 4 ) × 10 <sup>-4</sup>		46
$K^*(892)^+\pi^-,$ $K^*(892)^+ \rightarrow K_S^0\pi^+$	[aaa] ( 1.13 ± 0.60 / 0.34 ) × 10 <sup>-4</sup>		711
$K_0^*(1430)^+\pi^-,$ $K_0^*(1430)^+ \rightarrow K_S^0\pi^+$	[aaa] < 1.4 × 10 <sup>-5</sup>	CL=95%	–
$K_2^*(1430)^+\pi^-,$ $K_2^*(1430)^+ \rightarrow K_S^0\pi^+$	[aaa] < 3.4 × 10 <sup>-5</sup>	CL=95%	–

## Meson Summary Table

$K_S^0 \pi^+ \pi^-$ nonresonant	( 2.5 $\pm$ 6.0 $\pm$ 1.6 ) $\times 10^{-4}$	842	$\bar{K}^*(892)^0 \pi^+ \pi^-$ total	( 2.4 $\pm$ 0.5 ) %	685
$K^- \pi^+ \pi^0$	[ $\rho\rho$ ] (13.9 $\pm$ 0.5 ) %	S=1.7 844	$\bar{K}^*(892)^0 \pi^+ \pi^-$ 3-body	( 1.48 $\pm$ 0.34 ) %	685
$K^- \rho^+$	(10.8 $\pm$ 0.7 ) %	675	$\bar{K}^*(892)^0 \rho^0$	( 1.57 $\pm$ 0.34 ) %	417
$K^- \rho(1700)^+$ ,	( 7.9 $\pm$ 1.7 ) $\times 10^{-3}$	†	$\bar{K}^*(892)^0 \rho^0$ transverse	( 1.7 $\pm$ 0.6 ) %	417
$\rho(1700)^+ \rightarrow \pi^+ \pi^0$			$\bar{K}^*(892)^0 \rho^0$ S-wave	( 3.0 $\pm$ 0.6 ) %	417
$K^*(892)^- \pi^+$ ,	( 2.22 $\pm$ 0.40 $\pm$ 0.19 ) %	711	$\bar{K}^*(892)^0 \rho^0$ S-wave long.	< 3 $\times 10^{-3}$	CL=90% 417
$K^*(892)^- \rightarrow K^- \pi^0$			$\bar{K}^*(892)^0 \rho^0$ P-wave	< 3 $\times 10^{-3}$	CL=90% 417
$\bar{K}^*(892)^0 \pi^0$ ,	( 1.88 $\pm$ 0.23 ) %	711	$\bar{K}^*(892)^0 \rho^0$ D-wave	( 2.1 $\pm$ 0.6 ) %	417
$\bar{K}^*(892)^0 \rightarrow K^- \pi^+$			$K_1(1270)^- \pi^+$	[ $bbb$ ] ( 1.6 $\pm$ 0.8 ) %	484
$K_0^*(1430)^- \pi^+$ ,	( 4.6 $\pm$ 2.1 ) $\times 10^{-3}$	378	$K_1(1400)^- \pi^+$	< 1.2	CL=90% 386
$K_0^*(1430)^- \rightarrow K^- \pi^0$			$\bar{K}^*(892)^0 \pi^+ \pi^- \pi^0$	( 1.9 $\pm$ 0.9 ) %	644
$\bar{K}_0^*(1430)^0 \pi^0$ ,	( 5.7 $\pm$ 5.0 $\pm$ 1.5 ) $\times 10^{-3}$	379	$K^- \pi^+ \omega$	( 3.0 $\pm$ 0.6 ) %	605
$\bar{K}_0^*(1430)^0 \rightarrow K^- \pi^+$			$\bar{K}^*(892)^0 \omega$	( 1.1 $\pm$ 0.5 ) %	410
$K^*(1680)^- \pi^+$ ,	( 1.8 $\pm$ 0.7 ) $\times 10^{-3}$	46	$K^- \pi^+ \eta'(958)$	( 7.5 $\pm$ 1.9 ) $\times 10^{-3}$	479
$K^*(1680)^- \rightarrow K^- \pi^0$			$\bar{K}^*(892)^0 \eta'(958)$	< 1.1 $\times 10^{-3}$	CL=90% 120
$K^- \pi^+ \pi^0$ nonresonant	( 1.11 $\pm$ 0.50 $\pm$ 0.19 ) %	844	<b>Hadronic modes with three K's</b>		
$K_S^0 2\pi^0$	( 9.1 $\pm$ 1.1 ) $\times 10^{-3}$	S=2.2 843	$K_S^0 K^+ K^-$	( 4.45 $\pm$ 0.34 ) $\times 10^{-3}$	544
$K_S^0(2\pi^0)$ -S-wave	( 2.6 $\pm$ 0.7 ) $\times 10^{-3}$	-	$K_S^0 a_0(980)^0, a_0^0 \rightarrow K^+ K^-$	( 3.0 $\pm$ 0.4 ) $\times 10^{-3}$	-
$\bar{K}^*(892)^0 \pi^0$ ,	( 7.8 $\pm$ 0.7 ) $\times 10^{-3}$	711	$K^- a_0(980)^+, a_0^+ \rightarrow K^+ K_S^0$	( 6.0 $\pm$ 1.8 ) $\times 10^{-4}$	-
$\bar{K}^*(892)^0 \rightarrow K_S^0 \pi^0$			$K^+ a_0(980)^-, a_0^- \rightarrow K^- K_S^0$	< 1.1 $\times 10^{-4}$	CL=95% -
$\bar{K}^*(1430)^0 \pi^0, \bar{K}^{*0} \rightarrow$	( 4 $\pm$ 23 ) $\times 10^{-5}$	-	$K_S^0 f_0(980), f_0 \rightarrow K^+ K^-$	< 9 $\times 10^{-5}$	CL=95% -
$K_S^0 \pi^0$			$K_S^0 \phi, \phi \rightarrow K^+ K^-$	( 2.04 $\pm$ 0.16 ) $\times 10^{-3}$	520
$\bar{K}^*(1680)^0 \pi^0, \bar{K}^{*0} \rightarrow$	( 1.0 $\pm$ 0.4 ) $\times 10^{-3}$	-	$K_S^0 f_0(1370), f_0 \rightarrow K^+ K^-$	( 1.7 $\pm$ 1.1 ) $\times 10^{-4}$	-
$K_S^0 \pi^0$			$3K_S^0$	( 9.1 $\pm$ 1.3 ) $\times 10^{-4}$	539
$K_0^*(1270), f_2 \rightarrow 2\pi^0$	( 2.3 $\pm$ 1.1 ) $\times 10^{-4}$	-	$K^+ 2K^- \pi^+$	( 2.21 $\pm$ 0.31 ) $\times 10^{-4}$	434
$2K_S^0$ , one $K_S^0 \rightarrow 2\pi^0$	( 3.2 $\pm$ 1.1 ) $\times 10^{-4}$	-	$K^+ K^- \bar{K}^*(892)^0$ ,	( 4.4 $\pm$ 1.7 ) $\times 10^{-5}$	†
$K^- 2\pi^+ \pi^-$	[ $\rho\rho$ ] ( 8.07 $\pm$ 0.21 $\pm$ 0.19 ) %	S=1.3 813	$\bar{K}^*(892)^0 \rightarrow K^- \pi^+$		
$K^- \pi^+ \rho^0$ total	( 6.74 $\pm$ 0.33 ) %	609	$K^- \pi^+ \phi, \phi \rightarrow K^+ K^-$	( 4.0 $\pm$ 1.7 ) $\times 10^{-5}$	422
$K^- \pi^+ \rho^0$ 3-body	( 5.1 $\pm$ 2.3 ) $\times 10^{-3}$	609	$\phi \bar{K}^*(892)^0$ ,	( 1.06 $\pm$ 0.20 ) $\times 10^{-4}$	†
$\bar{K}^*(892)^0 \rho^0$ ,	( 1.05 $\pm$ 0.23 ) %	416	$\phi \rightarrow K^+ K^-$ ,		
$\bar{K}^*(892)^0 \rightarrow K^- \pi^+$			$\bar{K}^*(892)^0 \rightarrow K^- \pi^+$		
$K^- a_1(1260)^+$ ,	( 3.6 $\pm$ 0.6 ) %	327	$K^+ 2K^- \pi^+$ nonresonant	( 3.3 $\pm$ 1.5 ) $\times 10^{-5}$	434
$a_1(1260)^+ \rightarrow 2\pi^+ \pi^-$			$2K_S^0 K^\pm \pi^\mp$	( 6.0 $\pm$ 1.3 ) $\times 10^{-4}$	427
$\bar{K}^*(892)^0 \pi^+ \pi^-$ total,	( 1.6 $\pm$ 0.4 ) %	685	<b>Pionic modes</b>		
$\bar{K}^*(892)^0 \rightarrow K^- \pi^+$			$\pi^+ \pi^-$	( 1.401 $\pm$ 0.027 ) $\times 10^{-3}$	S=1.1 922
$\bar{K}^*(892)^0 \pi^+ \pi^-$ 3-body,	( 9.9 $\pm$ 2.3 ) $\times 10^{-3}$	685	$2\pi^0$	( 8.0 $\pm$ 0.5 ) $\times 10^{-4}$	923
$\bar{K}^*(892)^0 \rightarrow K^- \pi^+$			$\pi^+ \pi^- \pi^0$	( 1.43 $\pm$ 0.06 ) %	S=1.9 907
$K_1(1270)^- \pi^+$ ,	[ $bbb$ ] ( 2.9 $\pm$ 0.3 ) $\times 10^{-3}$	484	$\rho^+ \pi^-$	( 9.8 $\pm$ 0.4 ) $\times 10^{-3}$	764
$K_1(1270)^- \rightarrow K^- \pi^+ \pi^-$			$\rho^0 \pi^0$	( 3.72 $\pm$ 0.22 ) $\times 10^{-3}$	764
$K^- 2\pi^+ \pi^-$ nonresonant	( 1.88 $\pm$ 0.26 ) %	813	$\rho^- \pi^+$	( 4.96 $\pm$ 0.24 ) $\times 10^{-3}$	764
$K_S^0 \pi^+ \pi^- \pi^0$	[ $ccc$ ] ( 5.2 $\pm$ 0.6 ) %	813	$\rho(1450)^+ \pi^-, \rho(1450)^+ \rightarrow$	( 1.6 $\pm$ 2.0 ) $\times 10^{-5}$	-
$K_S^0 \eta, \eta \rightarrow \pi^+ \pi^- \pi^0$	( 1.02 $\pm$ 0.09 ) $\times 10^{-3}$	772	$\pi^+ \pi^0$		
$K_S^0 \omega, \omega \rightarrow \pi^+ \pi^- \pi^0$	( 9.9 $\pm$ 0.5 ) $\times 10^{-3}$	670	$\rho(1450)^0 \pi^0, \rho(1450)^0 \rightarrow$	( 4.3 $\pm$ 1.9 ) $\times 10^{-5}$	-
$K^- 2\pi^+ \pi^- \pi^0$	( 4.2 $\pm$ 0.4 ) %	771	$\pi^+ \pi^-$		
$\bar{K}^*(892)^0 \pi^+ \pi^- \pi^0$ ,	( 1.3 $\pm$ 0.6 ) %	643	$\rho(1450)^- \pi^+, \rho(1450)^- \rightarrow$	( 2.6 $\pm$ 0.4 ) $\times 10^{-4}$	-
$\bar{K}^*(892)^0 \rightarrow K^- \pi^+$			$\pi^- \pi^0$		
$K^- \pi^+ \omega, \omega \rightarrow \pi^+ \pi^- \pi^0$	( 2.7 $\pm$ 0.5 ) %	605	$\rho(1700)^+ \pi^-, \rho(1700)^+ \rightarrow$	( 5.9 $\pm$ 1.4 ) $\times 10^{-4}$	-
$\bar{K}^*(892)^0 \omega$ ,	( 6.5 $\pm$ 3.0 ) $\times 10^{-3}$	410	$\pi^+ \pi^0$		
$\bar{K}^*(892)^0 \rightarrow K^- \pi^+$ ,			$\rho(1700)^0 \pi^0, \rho(1700)^0 \rightarrow$	( 7.2 $\pm$ 1.7 ) $\times 10^{-4}$	-
$\omega \rightarrow \pi^+ \pi^- \pi^0$			$\pi^+ \pi^-$		
$K_S^0 \eta \pi^0$	( 5.5 $\pm$ 1.1 ) $\times 10^{-3}$	721	$\rho(1700)^- \pi^+, \rho(1700)^- \rightarrow$	( 4.6 $\pm$ 1.1 ) $\times 10^{-4}$	-
$K_S^0 a_0(980), a_0(980) \rightarrow \eta \pi^0$	( 6.5 $\pm$ 2.0 ) $\times 10^{-3}$	-	$\pi^- \pi^0$		
$\bar{K}^*(892)^0 \eta$ ,	( 1.6 $\pm$ 0.5 ) $\times 10^{-3}$	-	$f_0(980) \pi^0, f_0(980) \rightarrow$	( 3.6 $\pm$ 0.8 ) $\times 10^{-5}$	-
$\bar{K}^*(892)^0 \rightarrow K_S^0 \pi^0$			$\pi^+ \pi^-$		
$K_S^0 2\pi^+ 2\pi^-$	( 2.68 $\pm$ 0.30 ) $\times 10^{-3}$	768	$f_0(500) \pi^0, f_0(500) \rightarrow$	( 1.18 $\pm$ 0.21 ) $\times 10^{-4}$	-
$K_S^0 \rho^0 \pi^+ \pi^-$ , no $K^*(892)^-$	( 1.1 $\pm$ 0.7 ) $\times 10^{-3}$	-	$\pi^+ \pi^-$		
$K^*(892)^- 2\pi^+ \pi^-$ ,	( 5 $\pm$ 8 ) $\times 10^{-4}$	642	$f_0(1370) \pi^0, f_0(1370) \rightarrow$	( 5.3 $\pm$ 2.0 ) $\times 10^{-5}$	-
$K^*(892)^- \rightarrow K_S^0 \pi^-$ ,			$\pi^+ \pi^-$		
no $\rho^0$			$f_0(1500) \pi^0, f_0(1500) \rightarrow$	( 5.6 $\pm$ 1.5 ) $\times 10^{-5}$	-
$K^*(892)^- \rho^0 \pi^+$ ,	( 1.6 $\pm$ 0.6 ) $\times 10^{-3}$	230	$\pi^+ \pi^-$		
$K^*(892)^- \rightarrow K_S^0 \pi^-$			$f_0(1710) \pi^0, f_0(1710) \rightarrow$	( 4.4 $\pm$ 1.5 ) $\times 10^{-5}$	-
$K_S^0 2\pi^+ 2\pi^-$ nonresonant	< 1.2 $\times 10^{-3}$	CL=90% 768	$\pi^+ \pi^-$		
$K^- 3\pi^+ 2\pi^-$	( 2.2 $\pm$ 0.6 ) $\times 10^{-4}$	713	$f_2(1270) \pi^0, f_2(1270) \rightarrow$	( 1.89 $\pm$ 0.20 ) $\times 10^{-4}$	-
Fractions of many of the following modes with resonances have already appeared above as submodes of particular charged-particle modes. (Modes for which there are only upper limits and $\bar{K}^*(892)\rho$ submodes only appear below.)			$\pi^+ \pi^- \pi^0$ nonresonant	( 1.20 $\pm$ 0.35 ) $\times 10^{-4}$	907
$K_S^0 \eta$	( 4.78 $\pm$ 0.30 ) $\times 10^{-3}$	772	$3\pi^0$	< 3.5 $\times 10^{-4}$	CL=90% 908
$K_S^0 \omega$	( 1.11 $\pm$ 0.06 ) %	670	$2\pi^+ 2\pi^-$	( 7.42 $\pm$ 0.21 ) $\times 10^{-3}$	S=1.1 880
$K_S^0 \eta'(958)$	( 9.4 $\pm$ 0.5 ) $\times 10^{-3}$	565	$a_1(1260)^+ \pi^-, a_1^+ \rightarrow$	( 4.45 $\pm$ 0.31 ) $\times 10^{-3}$	-
$K^- a_1(1260)^+$	( 7.8 $\pm$ 1.1 ) %	327	$2\pi^+ \pi^-$ total		
$K^- a_2(1320)^+$	< 2 $\times 10^{-3}$	CL=90% 198	$a_1(1260)^+ \pi^-, a_1^+ \rightarrow$	( 3.21 $\pm$ 0.25 ) $\times 10^{-3}$	-
			$\rho^0 \pi^+$ S-wave		
			$a_1(1260)^+ \pi^-, a_1^+ \rightarrow$	( 1.9 $\pm$ 0.5 ) $\times 10^{-4}$	-
			$\rho^0 \pi^+$ D-wave		
			$a_1(1260)^+ \pi^-, a_1^+ \rightarrow$	( 6.2 $\pm$ 0.7 ) $\times 10^{-4}$	-
			$\sigma \pi^+$		
			$2\rho^0$ total	( 1.82 $\pm$ 0.13 ) $\times 10^{-3}$	518
			$2\rho^0$ , parallel helicities	( 8.2 $\pm$ 3.2 ) $\times 10^{-5}$	-

## Meson Summary Table

$2\rho^0$ , perpendicular helicities	$(4.7 \pm 0.6) \times 10^{-4}$	-	$K^*(892)^+\pi^-$ , $DC$	$(1.13 \pm_{-0.34}^{+0.60}) \times 10^{-4}$	711	
$2\rho^0$ , longitudinal helicities	$(1.25 \pm 0.10) \times 10^{-3}$	-	$K^*(892)^+ \rightarrow K_S^0 \pi^+$			
Resonant $(\pi^+\pi^-)\pi^+\pi^-$	$(1.48 \pm 0.12) \times 10^{-3}$	-	$K_0^*(1430)^+\pi^-$ , $DC$	$< 1.4 \times 10^{-5}$	-	
3-body total			$K_0^*(1430)^+ \rightarrow K_S^0 \pi^+$			
$\sigma\pi^+\pi^-$	$(6.1 \pm 0.9) \times 10^{-4}$	-	$K_2^*(1430)^+\pi^-$ , $DC$	$< 3.4 \times 10^{-5}$	-	
$f_0(980)\pi^+\pi^-$ , $f_0 \rightarrow \pi^+\pi^-$	$(1.8 \pm 0.5) \times 10^{-4}$	-	$K_2^*(1430)^+ \rightarrow K_S^0 \pi^+$			
$f_2(1270)\pi^+\pi^-$ , $f_2 \rightarrow \pi^+\pi^-$	$(3.6 \pm 0.6) \times 10^{-4}$	-	$K^+\pi^-\pi^0$ , $DC$	$(3.04 \pm 0.17) \times 10^{-4}$	844	
$\pi^+\pi^-2\pi^0$	$(10.0 \pm 0.9) \times 10^{-3}$	882	$K^+\pi^-\pi^0$ via $\bar{D}^0$	$(7.3 \pm 0.5) \times 10^{-4}$	-	
$\eta\pi^0$	$(6.8 \pm 0.7) \times 10^{-4}$	846	$K^+\pi^+2\pi^-$ , $DC$	$(2.61 \pm_{-0.19}^{+0.21}) \times 10^{-4}$	813	
$\omega\pi^0$	$< 2.6 \times 10^{-4}$	CL=90%	$K^+\pi^+2\pi^-$ via $\bar{D}^0$	$< 4 \times 10^{-4}$	CL=90%	
$2\pi^+2\pi^-\pi^0$	$(4.1 \pm 0.5) \times 10^{-3}$	844	$\mu^-$ anything via $\bar{D}^0$	$< 4 \times 10^{-4}$	CL=90%	
$\eta\pi^+\pi^-$	$(1.09 \pm 0.16) \times 10^{-3}$	827	<b><math>\Delta C = 1</math> weak neutral current (CI) modes, Lepton Family number (LF) violating modes, Lepton (L) or Baryon (B) number violating modes</b>			
$\omega\pi^+\pi^-$	$(1.6 \pm 0.5) \times 10^{-3}$	738	$\gamma\gamma$	CI	$< 2.6 \times 10^{-5}$	
$3\pi^+3\pi^-$	$(4.2 \pm 1.2) \times 10^{-4}$	795	$e^+e^-$	CI	$< 7.9 \times 10^{-8}$	
$\eta'(958)\pi^0$	$(8.9 \pm 1.4) \times 10^{-4}$	678	$\mu^+\mu^-$	CI	$< 1.4 \times 10^{-7}$	
$\eta'(958)\pi^+\pi^-$	$(4.5 \pm 1.7) \times 10^{-4}$	650	$\pi^0 e^+e^-$	CI	$< 4.5 \times 10^{-5}$	
$2\eta$	$(1.67 \pm 0.20) \times 10^{-3}$	755	$\pi^0 \mu^+\mu^-$	CI	$< 1.8 \times 10^{-4}$	
$\eta\eta'(958)$	$(1.05 \pm 0.26) \times 10^{-3}$	537	$\eta e^+e^-$	CI	$< 1.1 \times 10^{-4}$	
<b>Hadronic modes with a <math>K\bar{K}</math> pair</b>			$\eta\mu^+\mu^-$	CI	$< 5.3 \times 10^{-4}$	
$K^+K^-$	$(3.96 \pm 0.08) \times 10^{-3}$	S=1.4 791	$\pi^+\pi^-e^+e^-$	CI	$< 3.73 \times 10^{-4}$	
$2K_S^0$	$(1.7 \pm 0.4) \times 10^{-4}$	S=2.5 789	$\rho^0 e^+e^-$	CI	$< 1.0 \times 10^{-4}$	
$K_S^0 K^- \pi^+$	$(3.3 \pm 0.5) \times 10^{-3}$	S=1.1 739	$\pi^+\pi^-\mu^+\mu^-$	CI	$< 3.0 \times 10^{-5}$	
$\bar{K}^*(892)^0 K_S^0$	$< 5 \times 10^{-4}$	CL=90%	$\rho^0 \mu^+\mu^-$	CI	$< 2.2 \times 10^{-5}$	
$\bar{K}^*(892)^0 \rightarrow K^-\pi^+$			$\omega e^+e^-$	CI	$< 1.8 \times 10^{-4}$	
$K_S^0 K^+\pi^-$	$(2.6 \pm 0.5) \times 10^{-3}$	739	$\omega \mu^+\mu^-$	CI	$< 8.3 \times 10^{-4}$	
$K^*(892)^0 K_S^0$	$< 2.8 \times 10^{-4}$	CL=90%	$K^-K^+e^+e^-$	CI	$< 3.15 \times 10^{-4}$	
$K^*(892)^0 \rightarrow K^+\pi^-$			$\phi e^+e^-$	CI	$< 5.2 \times 10^{-5}$	
$K^+K^-\pi^0$	$(3.28 \pm 0.14) \times 10^{-3}$	743	$K^-K^+\mu^+\mu^-$	CI	$< 3.3 \times 10^{-5}$	
$K^*(892)^+K^-$	$(1.46 \pm 0.07) \times 10^{-3}$	-	$\phi\mu^+\mu^-$	CI	$< 3.1 \times 10^{-5}$	
$K^*(892)^+ \rightarrow K^+\pi^0$			$\bar{K}^0 e^+e^-$	[uu]	$< 1.1 \times 10^{-4}$	
$K^*(892)^-K^+$	$(5.2 \pm 0.4) \times 10^{-4}$	-	$\bar{K}^0 \mu^+\mu^-$	[uu]	$< 2.6 \times 10^{-4}$	
$K^*(892)^- \rightarrow K^-\pi^0$			$K^-\pi^+e^+e^-$	CI	$< 3.85 \times 10^{-4}$	
$(K^+\pi^0)_{S\text{-wave}} K^-$	$(2.34 \pm 0.17) \times 10^{-3}$	743	$\bar{K}^*(892)^0 e^+e^-$	[uu]	$< 4.7 \times 10^{-5}$	
$(K^-\pi^0)_{S\text{-wave}} K^+$	$(1.3 \pm 0.4) \times 10^{-4}$	743	$K^-\pi^+\mu^+\mu^-$	CI	$< 3.59 \times 10^{-4}$	
$f_0(980)\pi^+\pi^-$ , $f_0 \rightarrow K^+K^-$	$(3.4 \pm 0.6) \times 10^{-4}$	-	$\bar{K}^*(892)^0 \mu^+\mu^-$	[uu]	$< 2.4 \times 10^{-5}$	
$\phi\pi^0$ , $\phi \rightarrow K^+K^-$	$(6.4 \pm 0.4) \times 10^{-4}$	-	$\pi^+\pi^-\pi^0\mu^+\mu^-$	CI	$< 8.1 \times 10^{-4}$	
$2K_S^0\pi^0$	$< 5.9 \times 10^{-4}$	740	$\mu^\pm e^\mp$	LF	$[ee] < 2.6 \times 10^{-7}$	
$K^+K^-\pi^+\pi^-$	$(2.43 \pm 0.12) \times 10^{-3}$	677	$\pi^0 e^\pm \mu^\mp$	LF	$[ee] < 8.6 \times 10^{-5}$	
$\phi\pi^+\pi^-$ 3-body, $\phi \rightarrow K^+K^-$	$(2.4 \pm 2.4) \times 10^{-5}$	614	$\eta e^\pm \mu^\mp$	LF	$[ee] < 1.0 \times 10^{-4}$	
$\phi\rho^0$ , $\phi \rightarrow K^+K^-$	$(7.0 \pm 0.6) \times 10^{-4}$	250	$\pi^+\pi^-e^\pm\mu^\mp$	LF	$[ee] < 1.5 \times 10^{-5}$	
$K^+K^-\rho^0$ 3-body	$(5 \pm 7) \times 10^{-5}$	302	$\rho^0 e^\pm \mu^\mp$	LF	$[ee] < 4.9 \times 10^{-5}$	
$f_0(980)\pi^+\pi^-$ , $f_0 \rightarrow K^+K^-$	$(3.6 \pm 0.9) \times 10^{-4}$	-	$\omega e^\pm \mu^\mp$	LF	$[ee] < 1.2 \times 10^{-4}$	
$K^*(892)^0 K^\pm \pi^\pm$ 3-body, $K^{*0} \rightarrow K^\pm \pi^\mp$	$(2.7 \pm 0.6) \times 10^{-4}$	531	$K^-K^+e^\pm\mu^\mp$	LF	$[ee] < 1.8 \times 10^{-4}$	
$K^*(892)^0 \bar{K}^*(892)^0$ , $K^{*0} \rightarrow K^\pm \pi^\mp$	$(7 \pm 5) \times 10^{-5}$	272	$\phi e^\pm \mu^\mp$	LF	$[ee] < 3.4 \times 10^{-5}$	
$K_1(1270)^\pm K^\mp$	$(8.0 \pm 1.8) \times 10^{-4}$	-	$\bar{K}^0 e^\pm \mu^\mp$	LF	$[ee] < 1.0 \times 10^{-4}$	
$K_1(1270)^\pm \rightarrow K^\pm \pi^+ \pi^-$			$K^-\pi^+e^\pm\mu^\mp$	LF	$[ee] < 5.53 \times 10^{-4}$	
$K_1(1400)^\pm K^\mp$	$(5.3 \pm 1.2) \times 10^{-4}$	-	$\bar{K}^*(892)^0 e^\pm\mu^\mp$	LF	$[ee] < 8.3 \times 10^{-5}$	
$K_1(1400)^\pm \rightarrow K^\pm \pi^+ \pi^-$			$2\pi^-2e^+ + c.c.$	L	$< 1.12 \times 10^{-4}$	
$2K_S^0\pi^+\pi^-$	$(1.23 \pm 0.23) \times 10^{-3}$	673	$2\pi^-2\mu^+ + c.c.$	L	$< 2.9 \times 10^{-5}$	
$K_S^0 K^-2\pi^+\pi^-$	$< 1.4 \times 10^{-4}$	CL=90%	$K^-\pi^-2e^+ + c.c.$	L	$< 2.06 \times 10^{-4}$	
$K^+K^-\pi^+\pi^-\pi^0$	$(3.1 \pm 2.0) \times 10^{-3}$	600	$K^-\pi^-2\mu^+ + c.c.$	L	$< 3.9 \times 10^{-4}$	
Other $K\bar{K}X$ modes. They include all decay modes of the $\phi$ , $\eta$ , and $\omega$ .			$2K^-2e^+ + c.c.$	L	$< 1.52 \times 10^{-4}$	
$\phi\eta$	$(1.4 \pm 0.5) \times 10^{-4}$	489	$2K^-2\mu^+ + c.c.$	L	$< 9.4 \times 10^{-5}$	
$\phi\omega$	$< 2.1 \times 10^{-3}$	CL=90%	$\pi^-\pi^-e^+\mu^+ + c.c.$	L	$< 7.9 \times 10^{-5}$	
<b>Radiative modes</b>			$K^-\pi^-e^+\mu^+ + c.c.$	L	$< 2.18 \times 10^{-4}$	
$\rho^0\gamma$	$< 2.4 \times 10^{-4}$	CL=90%	771	$2K^-e^+\mu^+ + c.c.$	L	$< 5.7 \times 10^{-5}$
$\omega\gamma$	$< 2.4 \times 10^{-4}$	CL=90%	768	$p e^-$	L,B [ggg]	$< 1.0 \times 10^{-5}$
$\phi\gamma$	$(2.70 \pm 0.35) \times 10^{-5}$	654	696	$\bar{p} e^+$	L,B [hhh]	$< 1.1 \times 10^{-5}$
$\bar{K}^*(892)^0\gamma$	$(3.27 \pm 0.34) \times 10^{-4}$	719				
<b>Doubly Cabibbo suppressed (DC) modes or <math>\Delta C = 2</math> forbidden via mixing (C2M) modes</b>			<b><math>D^*(2007)^0</math></b>			
$K^+ \ell^- \bar{\nu}_\ell$ via $\bar{D}^0$	$< 2.2 \times 10^{-5}$	CL=90%	-	$I(J^P) = \frac{1}{2}(1^-)$		
$K^+$ or $K^*(892)^+ e^- \bar{\nu}_e$ via $\bar{D}^0$	$< 6 \times 10^{-5}$	CL=90%	-	$I, J, P$ need confirmation.		
$K^+\pi^-$	$(1.47 \pm 0.07) \times 10^{-4}$	S=2.8 861	Mass $m = 2006.98 \pm 0.15$ MeV			
$K^+\pi^-$ via DCS	$(1.31 \pm 0.08) \times 10^{-4}$	-	$m_{D^{*0}} - m_{D^0} = 142.12 \pm 0.07$ MeV			
$K^+\pi^-$ via $\bar{D}^0$	$< 1.6 \times 10^{-5}$	CL=95%	Full width $\Gamma < 2.1$ MeV, CL = 90%			
$K_S^0\pi^+\pi^-$ in $D^0 \rightarrow \bar{D}^0$	$< 1.8 \times 10^{-4}$	CL=95%	$\bar{D}^*(2007)^0$ modes are charge conjugates of modes below.			
<b><math>D^*(2007)^0</math> DECAY MODES</b>			Fraction ( $\Gamma_i/\Gamma$ )			
$D^0\pi^0$			(61.9 $\pm$ 2.9) %		43	
$D^0\gamma$			(38.1 $\pm$ 2.9) %		137	

## Meson Summary Table

<b><math>D^*(2010)^\pm</math></b>	$I(J^P) = \frac{1}{2}(1^-)$ <i>I, J, P need confirmation.</i>
Mass $m = 2010.28 \pm 0.13$ MeV	
$m_{D^*(2010)^+} - m_{D^+} = 140.66 \pm 0.10$ MeV ( $S = 1.1$ )	
$m_{D^*(2010)^+} - m_{D^0} = 145.421 \pm 0.010$ MeV ( $S = 1.1$ )	
Full width $\Gamma = 96 \pm 22$ keV	
$D^*(2010)^-$ modes are charge conjugates of the modes below.	

<b><math>D^*(2010)^\pm</math> DECAY MODES</b>	Fraction ( $\Gamma_i/\Gamma$ )	$\rho$ (MeV/c)
$D^0 \pi^+$	(67.7±0.5) %	39
$D^+ \pi^0$	(30.7±0.5) %	38
$D^+ \gamma$	(1.6±0.4) %	136

<b><math>D_0^*(2400)^0</math></b>	$I(J^P) = \frac{1}{2}(0^+)$
Mass $m = 2318 \pm 29$ MeV ( $S = 1.7$ )	
Full width $\Gamma = 267 \pm 40$ MeV	

<b><math>D_0^*(2400)^0</math> DECAY MODES</b>	Fraction ( $\Gamma_i/\Gamma$ )	$\rho$ (MeV/c)
$D^+ \pi^-$	seen	385

<b><math>D_1(2420)^0</math></b>	$I(J^P) = \frac{1}{2}(1^+)$ <i>I needs confirmation.</i>
Mass $m = 2421.3 \pm 0.6$ MeV ( $S = 1.2$ )	
$m_{D_1^0} - m_{D^{*+}} = 411.0 \pm 0.6$ ( $S = 1.2$ )	
Full width $\Gamma = 27.1 \pm 2.7$ MeV ( $S = 2.4$ )	
$\bar{D}_1(2420)^0$ modes are charge conjugates of modes below.	

<b><math>D_1(2420)^0</math> DECAY MODES</b>	Fraction ( $\Gamma_i/\Gamma$ )	$\rho$ (MeV/c)
$D^*(2010)^+ \pi^-$	seen	354
$D^0 \pi^+ \pi^-$	seen	425
$D^+ \pi^-$	not seen	473
$D^{*0} \pi^+ \pi^-$	not seen	279

<b><math>D_2^*(2460)^0</math></b>	$I(J^P) = \frac{1}{2}(2^+)$
$J^P = 2^+$ assignment strongly favored.	
Mass $m = 2462.6 \pm 0.7$ MeV ( $S = 1.3$ )	
$m_{D_2^{*0}} - m_{D^+} = 593.0 \pm 0.7$ MeV ( $S = 1.3$ )	
$m_{D_2^{*0}} - m_{D^{*+}} = 452.3 \pm 0.7$ MeV ( $S = 1.3$ )	
Full width $\Gamma = 49.0 \pm 1.4$ MeV ( $S = 1.7$ )	
$\bar{D}_2^*(2460)^0$ modes are charge conjugates of modes below.	

<b><math>D_2^*(2460)^0</math> DECAY MODES</b>	Fraction ( $\Gamma_i/\Gamma$ )	$\rho$ (MeV/c)
$D^+ \pi^-$	seen	507
$D^*(2010)^+ \pi^-$	seen	391
$D^0 \pi^+ \pi^-$	not seen	463
$D^{*0} \pi^+ \pi^-$	not seen	326

<b><math>D_2^*(2460)^\pm</math></b>	$I(J^P) = \frac{1}{2}(2^+)$
$J^P = 2^+$ assignment strongly favored.	
Mass $m = 2464.4 \pm 1.9$ MeV ( $S = 1.9$ )	
$m_{D_2^*(2460)^\pm} - m_{D_2^*(2460)^0} = 2.4 \pm 1.7$ MeV	
Full width $\Gamma = 37 \pm 6$ MeV ( $S = 1.4$ )	
$D_2^*(2460)^-$ modes are charge conjugates of modes below.	

<b><math>D_2^*(2460)^\pm</math> DECAY MODES</b>	Fraction ( $\Gamma_i/\Gamma$ )	$\rho$ (MeV/c)
$D^0 \pi^+$	seen	512
$D^{*0} \pi^+$	seen	395
$D^+ \pi^+ \pi^-$	not seen	461
$D^{*+} \pi^+ \pi^-$	not seen	325

## CHARMED, STRANGE MESONS ( $C = S = \pm 1$ )

$$D_s^+ = c\bar{s}, D_s^- = \bar{c}s, \text{ similarly for } D_s^{* \pm}$$

**$D_s^\pm$**

$$I(J^P) = 0(0^-)$$

Mass $m = 1968.49 \pm 0.32$ MeV ( $S = 1.3$ )
$m_{D_s^\pm} - m_{D^\pm} = 98.87 \pm 0.29$ MeV ( $S = 1.4$ )
Mean life $\tau = (500 \pm 7) \times 10^{-15}$ s ( $S = 1.3$ )
$c\tau = 149.9$ $\mu\text{m}$

### CP-violating decay-rate asymmetries

$A_{CP}(\mu^\pm \nu)$	$= (5 \pm 6)\%$
$A_{CP}(K^\pm K_S^0)$	$= (0.3 \pm 0.4)\%$
$A_{CP}(K^+ K^- \pi^\pm)$	$= (0.3 \pm 1.4)\%$
$A_{CP}(K^+ K^- \pi^\pm \pi^0)$	$= (-6 \pm 4)\%$
$A_{CP}(K_S^0 K^\mp 2\pi^\pm)$	$= (-1 \pm 4)\%$
$A_{CP}(\pi^+ \pi^- \pi^\pm)$	$= (2 \pm 5)\%$
$A_{CP}(\pi^\pm \eta)$	$= (-4.6 \pm 2.9)\%$
$A_{CP}(\pi^\pm \eta')$	$= (-6.1 \pm 3.0)\%$
$A_{CP}(K^\pm \pi^0)$	$= (-27 \pm 24)\%$
$A_{CP}(K_S^0 \pi^\pm)$	$= (6.6 \pm 3.3)\%$ ( $S = 1.4$ )
$A_{CP}(K^\pm \pi^+ \pi^-)$	$= (11 \pm 7)\%$
$A_{CP}(K^\pm \eta)$	$= (9 \pm 15)\%$
$A_{CP}(K^\pm \eta'(958))$	$= (6 \pm 19)\%$

### T-violating decay-rate asymmetry

$$A_T(K_S^0 K^\pm \pi^+ \pi^-) = (-14 \pm 8) \times 10^{-3} [00]$$

### $D_s^+ \rightarrow \phi \ell^+ \nu_\ell$ form factors

$r_2 = 0.84 \pm 0.11$ ( $S = 2.4$ )
$r_V = 1.80 \pm 0.08$
$\Gamma_L/\Gamma_T = 0.72 \pm 0.18$

Unless otherwise noted, the branching fractions for modes with a resonance in the final state include all the decay modes of the resonance.  $D_s^-$  modes are charge conjugates of the modes below.

<b><math>D_s^\pm</math> DECAY MODES</b>	Fraction ( $\Gamma_i/\Gamma$ )	Scale factor / $\rho$	
		Confidence level	(MeV/c)
<b>Inclusive modes</b>			
$e^+$ semileptonic	[iii] (6.5±0.4) %		—
$\pi^+$ anything	(119.3±1.4) %		—
$\pi^-$ anything	(43.2±0.9) %		—
$\pi^0$ anything	(123±7) %		—
$K^-$ anything	(18.7±0.5) %		—
$K^+$ anything	(28.9±0.7) %		—
$K_S^0$ anything	(19.0±1.1) %		—
$\eta$ anything	[jjj] (29.9±2.8) %		—
$\omega$ anything	(6.1±1.4) %		—
$\eta'$ anything	[kkk] (11.7±1.8) %		—
$f_0(980)$ anything, $f_0 \rightarrow \pi^+ \pi^-$	< 1.3 %	CL=90%	—
$\phi$ anything	(15.7±1.0) %		—
$K^+ K^-$ anything	(15.8±0.7) %		—
$K_S^0 K^+$ anything	(5.8±0.5) %		—
$K_S^0 K^-$ anything	(1.9±0.4) %		—
$2K_S^0$ anything	(1.70±0.32) %		—
$2K^+$ anything	< 2.6 $\times 10^{-3}$	CL=90%	—
$2K^-$ anything	< 6 $\times 10^{-4}$	CL=90%	—
<b>Leptonic and semileptonic modes</b>			
$e^+ \nu_e$	< 1.2 $\times 10^{-4}$	CL=90%	984
$\mu^+ \nu_\mu$	(5.90±0.33) $\times 10^{-3}$		981
$\tau^+ \nu_\tau$	(5.43±0.31) %		182
$K^+ K^- e^+ \nu_e$	—		851
$\phi e^+ \nu_e$	[lll] (2.49±0.14) %		720
$\eta e^+ \nu_e + \eta'(958) e^+ \nu_e$	[lll] (3.66±0.37) %		—
$\eta e^+ \nu_e$	[lll] (2.67±0.29) %	$S=1.1$	908
$\eta'(958) e^+ \nu_e$	[lll] (9.9±2.3) $\times 10^{-3}$		751
$\omega e^+ \nu_e$	[mmm] < 2.0 $\times 10^{-3}$	CL=90%	829
$K^0 e^+ \nu_e$	(3.7±1.0) $\times 10^{-3}$		921
$K^*(892)^0 e^+ \nu_e$	(1.8±0.7) $\times 10^{-3}$		782
$f_0(980) e^+ \nu_e, f_0 \rightarrow \pi^+ \pi^-$	(2.00±0.32) $\times 10^{-3}$		—

## Meson Summary Table

Hadronic modes with a $K\bar{K}$ pair			
$K^+ K_S^0$		( 1.48±0.08 ) %	850
$K^+ K^- \pi^+$	[pp]	( 5.49±0.27 ) %	805
$\phi \pi^+$	[ll,nnn]	( 4.5 ±0.4 ) %	712
$\phi \pi^+, \phi \rightarrow K^+ K^-$	[nnn]	( 2.28±0.12 ) %	712
$K^+ \bar{K}_0^*(892)^0, \bar{K}_0^{*0} \rightarrow$		( 2.63±0.13 ) %	416
$K^- \pi^+$			
$f_0(980) \pi^+, f_0 \rightarrow K^+ K^-$		( 1.16±0.32 ) %	732
$f_0(1370) \pi^+, f_0 \rightarrow K^+ K^-$		( 7 ±5 ) × 10 <sup>-4</sup>	-
$f_0(1710) \pi^+, f_0 \rightarrow K^+ K^-$		( 6.7 ±2.9 ) × 10 <sup>-4</sup>	198
$K^+ \bar{K}_0^*(1430)^0, \bar{K}_0^{*0} \rightarrow$		( 1.9 ±0.4 ) × 10 <sup>-3</sup>	218
$K^0 \bar{K}_0^0 \pi^+$		-	802
$K^*(892)^+ \bar{K}_0^0$	[lll]	( 5.4 ±1.2 ) %	683
$K^+ K^- \pi^+ \pi^0$		( 5.6 ±0.5 ) %	748
$\phi \rho^+$	[lll]	( 8.4 <sup>+1.9</sup> <sub>-2.3</sub> ) %	401
$K_S^0 K^- 2\pi^+$		( 1.64±0.12 ) %	744
$K^*(892)^+ \bar{K}^*(892)^0$	[lll]	( 7.2 ±2.6 ) %	417
$K^+ K_S^0 \pi^+ \pi^-$		( 9.6 ±1.3 ) × 10 <sup>-3</sup>	744
$K^+ K^- 2\pi^+ \pi^-$		( 8.8 ±1.6 ) × 10 <sup>-3</sup>	673
$\phi 2\pi^+ \pi^-$	[lll]	( 1.21±0.16 ) %	640
$K^+ K^- \rho^0 \pi^+$ non- $\phi$		< 2.6 × 10 <sup>-4</sup>	CL=90% 249
$\phi \rho^0 \pi^+, \phi \rightarrow K^+ K^-$		( 6.6 ±1.3 ) × 10 <sup>-3</sup>	181
$\phi a_1(1260)^+, \phi \rightarrow$		( 7.5 ±1.3 ) × 10 <sup>-3</sup>	†
$K^+ K^-, a_1^+ \rightarrow \rho^0 \pi^+$			
$K^+ K^- 2\pi^+ \pi^-$ nonresonant		( 9 ±7 ) × 10 <sup>-4</sup>	673
$2K_S^0 2\pi^+ \pi^-$		( 8.3 ±3.5 ) × 10 <sup>-4</sup>	669
Hadronic modes without $K$ 's			
$\pi^+ \pi^0$		< 3.4 × 10 <sup>-4</sup>	CL=90% 975
$2\pi^+ \pi^-$		( 1.10±0.06 ) %	959
$\rho^0 \pi^+$		( 2.0 ±1.2 ) × 10 <sup>-4</sup>	825
$\pi^+ (\pi^+ \pi^-)_{S\text{-wave}}$	[ooo]	( 9.2 ±0.6 ) × 10 <sup>-3</sup>	959
$f_2(1270) \pi^+, f_2 \rightarrow \pi^+ \pi^-$		( 1.11±0.20 ) × 10 <sup>-3</sup>	559
$\rho(1450)^0 \pi^+, \rho^0 \rightarrow \pi^+ \pi^-$		( 3.0 ±2.0 ) × 10 <sup>-4</sup>	421
$\pi^+ 2\pi^0$		( 6.5 ±1.3 ) × 10 <sup>-3</sup>	961
$2\pi^+ \pi^- \pi^0$		-	935
$\eta \pi^+$	[lll]	( 1.83±0.15 ) %	902
$\omega \pi^+$	[lll]	( 2.5 ±0.7 ) × 10 <sup>-3</sup>	822
$3\pi^+ 2\pi^-$		( 8.0 ±0.9 ) × 10 <sup>-3</sup>	899
$2\pi^+ \pi^- 2\pi^0$		-	902
$\eta \rho^+$	[lll]	( 8.9 ±0.8 ) %	724
$\eta \pi^+ \pi^0$ 3-body	[lll]	< 5 %	CL=90% 886
$\omega \pi^+ \pi^0$	[lll]	( 2.8 ±0.7 ) %	802
$3\pi^+ 2\pi^- \pi^0$		( 4.9 ±3.2 ) %	856
$\omega 2\pi^+ \pi^-$	[lll]	( 1.6 ±0.5 ) %	766
$\eta'(958) \pi^+$	[kkk,lll]	( 3.94±0.33 ) %	743
$3\pi^+ 2\pi^- 2\pi^0$		-	803
$\omega \eta \pi^+$	[lll]	< 2.13 %	CL=90% 654
$\eta'(958) \rho^+$	[kkk,lll]	( 12.5 ±2.2 ) %	465
$\eta'(958) \pi^+ \pi^0$ 3-body	[lll]	< 1.8 %	CL=90% 720
Modes with one or three $K$ 's			
$K^+ \pi^0$		( 6.2 ±2.1 ) × 10 <sup>-4</sup>	917
$K_S^0 \pi^+$		( 1.21±0.08 ) × 10 <sup>-3</sup>	916
$K^+ \eta$	[lll]	( 1.75±0.35 ) × 10 <sup>-3</sup>	835
$K^+ \omega$	[lll]	< 2.4 × 10 <sup>-3</sup>	CL=90% 741
$K^+ \eta'(958)$	[lll]	( 1.8 ±0.6 ) × 10 <sup>-3</sup>	646
$K^+ \pi^+ \pi^-$		( 6.9 ±0.5 ) × 10 <sup>-3</sup>	900
$K^+ \rho^0$		( 2.7 ±0.5 ) × 10 <sup>-3</sup>	745
$K^+ \rho(1450)^0, \rho^0 \rightarrow \pi^+ \pi^-$		( 7.3 ±2.6 ) × 10 <sup>-4</sup>	-
$K^*(892)^0 \pi^+, K^{*0} \rightarrow$		( 1.50±0.26 ) × 10 <sup>-3</sup>	775
$K^+ \pi^-$			
$K^*(1410)^0 \pi^+, K^{*0} \rightarrow$		( 1.30±0.31 ) × 10 <sup>-3</sup>	-
$K^+ \pi^-$			
$K^*(1430)^0 \pi^+, K^{*0} \rightarrow$		( 5 ±4 ) × 10 <sup>-4</sup>	-
$K^+ \pi^-$			
$K^+ \pi^+ \pi^-$ nonresonant		( 1.1 ±0.4 ) × 10 <sup>-3</sup>	900
$K^0 \pi^+ \pi^0$		( 1.00±0.18 ) %	900
$K_S^0 2\pi^+ \pi^-$		( 2.9 ±1.1 ) × 10 <sup>-3</sup>	870
$K^+ \omega \pi^0$	[lll]	< 8.2 × 10 <sup>-3</sup>	CL=90% 684
$K^+ \omega \pi^+ \pi^-$	[lll]	< 5.4 × 10 <sup>-3</sup>	CL=90% 603
$K^+ \omega \eta$	[lll]	< 7.9 × 10 <sup>-3</sup>	CL=90% 367
$2K^+ K^-$		( 2.20±0.23 ) × 10 <sup>-4</sup>	628
$\phi K^+, \phi \rightarrow K^+ K^-$		( 9.0 ±2.1 ) × 10 <sup>-5</sup>	-

Doubly Cabibbo-suppressed modes			
$2K^+ \pi^-$		( 1.28±0.14 ) × 10 <sup>-4</sup>	805
$K^+ K^*(892)^0, K^{*0} \rightarrow$		( 6.0 ±3.5 ) × 10 <sup>-5</sup>	-
$K^+ \pi^-$			
Baryon-antibaryon mode			
$p\bar{p}$		( 1.3 ±0.4 ) × 10 <sup>-3</sup>	295
$\Delta C = 1$ weak neutral current (C1) modes, Lepton family number (LF), or Lepton number (L) violating modes			
$\pi^+ e^+ e^-$	[uu]	< 1.3 × 10 <sup>-5</sup>	CL=90% 979
$\pi^+ \phi, \phi \rightarrow e^+ e^-$	[tt]	( 6 <sup>+8</sup> <sub>-4</sub> ) × 10 <sup>-6</sup>	-
$\pi^+ \mu^+ \mu^-$	[uu]	< 2.6 × 10 <sup>-5</sup>	CL=90% 968
$K^+ e^+ e^-$	C1	< 3.7 × 10 <sup>-6</sup>	CL=90% 922
$K^+ \mu^+ \mu^-$	C1	< 2.1 × 10 <sup>-5</sup>	CL=90% 909
$K^*(892)^+ \mu^+ \mu^-$	C1	< 1.4 × 10 <sup>-3</sup>	CL=90% 765
$\pi^+ e^+ \mu^-$	LF	< 1.2 × 10 <sup>-5</sup>	CL=90% 976
$\pi^+ e^- \mu^+$	LF	< 2.0 × 10 <sup>-5</sup>	CL=90% 976
$K^+ e^+ \mu^-$	LF	< 1.4 × 10 <sup>-5</sup>	CL=90% 919
$K^+ e^- \mu^+$	LF	< 9.7 × 10 <sup>-6</sup>	CL=90% 919
$\pi^- 2e^+$	L	< 4.1 × 10 <sup>-6</sup>	CL=90% 979
$\pi^- 2\mu^+$	L	< 1.4 × 10 <sup>-5</sup>	CL=90% 968
$\pi^- e^+ \mu^+$	L	< 8.4 × 10 <sup>-6</sup>	CL=90% 976
$K^- 2e^+$	L	< 5.2 × 10 <sup>-6</sup>	CL=90% 922
$K^- 2\mu^+$	L	< 1.3 × 10 <sup>-5</sup>	CL=90% 909
$K^- e^+ \mu^+$	L	< 6.1 × 10 <sup>-6</sup>	CL=90% 919
$K^*(892)^- 2\mu^+$	L	< 1.4 × 10 <sup>-3</sup>	CL=90% 765

 **$D_s^{\pm}$** 

$$I(J^P) = 0(2^-)$$

 $J^P$  is natural, width and decay modes consistent with  $1^-$ .

Mass  $m = 2112.3 \pm 0.5$  MeV ( $S = 1.1$ )

$m_{D_s^{\pm}} - m_{D_s^{\pm}} = 143.8 \pm 0.4$  MeV

Full width  $\Gamma < 1.9$  MeV, CL = 90%

 $D_s^{\pm}$  modes are charge conjugates of the modes below.

$D_s^{\pm}$ DECAY MODES	Fraction ( $\Gamma_i/\Gamma$ )	$\rho$ (MeV/c)
$D_s^+ \gamma$	(94.2±0.7) %	139
$D_s^+ \pi^0$	( 5.8±0.7 ) %	48

 **$D_{s0}^*(2317)^{\pm}$** 

$$I(J^P) = 0(0^+)$$

$J, P$  need confirmation.

 $J^P$  is natural, low mass consistent with  $0^+$ .

Mass  $m = 2317.8 \pm 0.6$  MeV ( $S = 1.1$ )

$m_{D_{s0}^*(2317)^{\pm}} - m_{D_s^{\pm}} = 349.3 \pm 0.6$  MeV ( $S = 1.1$ )

Full width  $\Gamma < 3.8$  MeV, CL = 95%

 $D_{s0}^*(2317)^{\pm}$  modes are charge conjugates of modes below.

$D_{s0}^*(2317)^{\pm}$ DECAY MODES	Fraction ( $\Gamma_i/\Gamma$ )	$\rho$ (MeV/c)
$D_{s0}^+ \pi^0$	seen	298
$D_{s0}^+ \pi^0 \pi^0$	not seen	205

 **$D_{s1}(2460)^{\pm}$** 

$$I(J^P) = 0(1^+)$$

Mass  $m = 2459.6 \pm 0.6$  MeV ( $S = 1.1$ )

$m_{D_{s1}(2460)^{\pm}} - m_{D_s^{\pm}} = 347.2 \pm 0.7$  MeV ( $S = 1.2$ )

$m_{D_{s1}(2460)^{\pm}} - m_{D_s^{\pm}} = 491.1 \pm 0.7$  MeV ( $S = 1.1$ )

Full width  $\Gamma < 3.5$  MeV, CL = 95%

 $D_{s1}(2460)^{\pm}$  modes are charge conjugates of the modes below.

$D_{s1}(2460)^{\pm}$ DECAY MODES	Fraction ( $\Gamma_i/\Gamma$ )	Scale factor/ Confidence level	$\rho$ (MeV/c)
$D_{s1}^+ \pi^0$	(48 ±11) %		297
$D_{s1}^+ \gamma$	(18 ±4) %		442
$D_{s1}^+ \pi^+ \pi^-$	( 4.3±1.3 ) %	$S=1.1$	363
$D_{s1}^+ \gamma$	< 8 %	CL=90%	323
$D_{s0}^*(2317)^+ \gamma$	( 3.7 <sup>+5.0</sup> <sub>-2.4</sub> ) %		138

# Meson Summary Table

## $D_{s1}(2536)^\pm$

$I(J^P) = 0(1^+)$   
 $J, P$  need confirmation.

Mass  $m = 2535.12 \pm 0.13$  MeV  
 Full width  $\Gamma = 0.92 \pm 0.05$  MeV

$D_{s1}(2536)^-$  modes are charge conjugates of the modes below.

$D_{s1}(2536)^+$ DECAY MODES	Fraction ( $\Gamma_i/\Gamma$ )	$\rho$ (MeV/c)
$D^*(2010)^+ K^0$	seen	149
$D^*(2007)^0 K^+$	seen	167
$D^+ K^0$	not seen	381
$D^0 K^+$	not seen	391
$D_s^{*+} \gamma$	possibly seen	388
$D_s^+ \pi^+ \pi^-$	seen	437

## $D_{s2}^*(2573)$

$I(J^P) = 0(?^?)$

$J^P$  is natural, width and decay modes consistent with  $2^+$ .

Mass  $m = 2571.9 \pm 0.8$  MeV  
 Full width  $\Gamma = 17 \pm 4$  MeV ( $S = 1.3$ )

$D_{s2}^*(2573)^-$  modes are charge conjugates of the modes below.

$D_{s2}^*(2573)^+$ DECAY MODES	Fraction ( $\Gamma_i/\Gamma$ )	$\rho$ (MeV/c)
$D^0 K^+$	seen	434
$D^*(2007)^0 K^+$	not seen	243

## BOTTOM MESONS

$(B = \pm 1)$

$B^+ = u\bar{b}, B^0 = d\bar{b}, \bar{B}^0 = \bar{d}b, B^- = \bar{u}b$ , similarly for  $B^{*+}$ s

### B-particle organization

Many measurements of  $B$  decays involve admixtures of  $B$  hadrons. Previously we arbitrarily included such admixtures in the  $B^\pm$  section, but because of their importance we have created two new sections: " $B^\pm/B^0$  Admixture" for  $\Upsilon(4S)$  results and " $B^\pm/B^0/B_s^0/b$ -baryon Admixture" for results at higher energies. Most inclusive decay branching fractions and  $\chi_b$  at high energy are found in the Admixture sections.  $B^0-\bar{B}^0$  mixing data are found in the  $B^0$  section, while  $B_s^0-\bar{B}_s^0$  mixing data and  $B-\bar{B}$  mixing data for a  $B^0/B_s^0$  admixture are found in the  $B_s^0$  section.  $CP$ -violation data are found in the  $B^\pm, B^0$ , and  $B^\pm/B_s^0$  Admixture sections.  $b$ -baryons are found near the end of the Baryon section.

The organization of the  $B$  sections is now as follows, where bullets indicate particle sections and brackets indicate reviews.

- $B^\pm$   
mass, mean life,  $CP$  violation, branching fractions
- $B^0$   
mass, mean life,  $B^0-\bar{B}^0$  mixing,  $CP$  violation, branching fractions
- $B^\pm/B^0$  Admixtures  
 $CP$  violation, branching fractions
- $B^\pm/B^0/B_s^0/b$ -baryon Admixtures  
mean life, production fractions, branching fractions
- $B^*$   
mass
- $B_1(5721)^0$   
mass
- $B_2^*(5747)^0$   
mass
- $B_s^0$

mass, mean life,  $B_s^0-\bar{B}_s^0$  mixing,  $CP$  violation, branching fractions

- $B_s^*$   
mass
- $B_{s1}(5830)^0$   
mass
- $B_{s2}^*(5840)^0$   
mass
- $B_c^\pm$   
mass, mean life, branching fractions

At the end of Baryon Listings:

- $\Lambda_b$   
mass, mean life, branching fractions
- $\Sigma_b$   
mass
- $\Sigma_b^*$   
mass
- $\Xi_b^0, \Xi_b^-$   
mass, mean life, branching fractions
- $\Omega_b^-$   
mass, branching fractions
- $b$ -baryon Admixture  
mean life, branching fractions

## $B^\pm$

$I(J^P) = \frac{1}{2}(0^-)$

$I, J, P$  need confirmation. Quantum numbers shown are quark-model predictions.

Mass  $m_{B^\pm} = 5279.25 \pm 0.17$  MeV  
 Mean life  $\tau_{B^\pm} = (1.641 \pm 0.008) \times 10^{-12}$  s  
 $c\tau = 492.0$   $\mu\text{m}$

### $CP$ violation

- $A_{CP}(B^+ \rightarrow J/\psi(1S)K^+) = (1 \pm 7) \times 10^{-3}$  ( $S = 1.8$ )  
 $A_{CP}(B^+ \rightarrow J/\psi(1S)\pi^+) = 0.01 \pm 0.07$  ( $S = 1.3$ )  
 $A_{CP}(B^+ \rightarrow J/\psi\rho^+) = -0.11 \pm 0.14$   
 $A_{CP}(B^+ \rightarrow J/\psi K^*(892)^+) = -0.048 \pm 0.033$   
 $A_{CP}(B^+ \rightarrow \eta_c K^+) = -0.16 \pm 0.08$   
 $A_{CP}(B^+ \rightarrow \psi(2S)\pi^+) = 0.02 \pm 0.09$   
 $A_{CP}(B^+ \rightarrow \psi(2S)K^+) = -0.025 \pm 0.024$   
 $A_{CP}(B^+ \rightarrow \psi(2S)K^*(892)^+) = 0.08 \pm 0.21$   
 $A_{CP}(B^+ \rightarrow \chi_{c1}(1P)\pi^+) = 0.07 \pm 0.18$   
 $A_{CP}(B^+ \rightarrow \chi_{c0}K^+) = -0.20 \pm 0.18$  ( $S = 1.5$ )  
 $A_{CP}(B^+ \rightarrow \chi_{c1}K^+) = -0.009 \pm 0.033$   
 $A_{CP}(B^+ \rightarrow \chi_{c1}K^*(892)^+) = 0.5 \pm 0.5$   
 $A_{CP}(B^+ \rightarrow \bar{D}^0\pi^+) = -0.008 \pm 0.008$   
 $A_{CP}(B^+ \rightarrow D_{CP(+1)}\pi^+) = 0.035 \pm 0.024$   
 $A_{CP}(B^+ \rightarrow D_{CP(-1)}\pi^+) = 0.017 \pm 0.026$   
 $A_{CP}(B^+ \rightarrow \bar{D}^0K^+) = 0.07 \pm 0.04$   
 $r_B(B^+ \rightarrow D^0K^+) = 0.113^{+0.024}_{-0.021}$   
 $\delta_B(B^+ \rightarrow D^0K^+) = (125 \pm 16)^\circ$   
 $r_B(B^+ \rightarrow DK^{*+}) = 0.34 \pm 0.09$  ( $S = 1.3$ )  
 $\delta_B(B^+ \rightarrow DK^{*+}) = (157 \pm 70)^\circ$  ( $S = 2.0$ )  
 $A_{CP}(B^+ \rightarrow [K^-\pi^+]_D K^+) = -0.58 \pm 0.21$   
 $A_{CP}(B^+ \rightarrow [K^-\pi^+]_{\bar{D}} K^*(892)^+) = -0.3 \pm 0.5$   
 $A_{CP}(B^+ \rightarrow [K^-\pi^+]_D \pi^+) = 0.00 \pm 0.09$   
 $A_{CP}(B^+ \rightarrow [K^-\pi^+]_{(D\pi)} \pi^+) = -0.09 \pm 0.27$   
 $A_{CP}(B^+ \rightarrow [K^-\pi^+]_{(D\gamma)} \pi^+) = -0.7 \pm 0.6$   
 $A_{CP}(B^+ \rightarrow [K^-\pi^+]_{(D\pi)} K^+) = 0.8 \pm 0.4$   
 $A_{CP}(B^+ \rightarrow [K^-\pi^+]_{(D\gamma)} K^+) = 0.4 \pm 1.0$   
 $A_{CP}(B^+ \rightarrow [\pi^+\pi^-\pi^0]_D K^+) = -0.02 \pm 0.15$   
 $A_{CP}(B^+ \rightarrow D_{CP(+1)}K^+) = 0.24 \pm 0.06$  ( $S = 1.1$ )  
 $A_{CP}(B^+ \rightarrow D_{CP(-1)}K^+) = -0.10 \pm 0.07$   
 $A_{CP}(B^+ \rightarrow \bar{D}^{*0}\pi^+) = -0.014 \pm 0.015$   
 $A_{CP}(B^+ \rightarrow (D_{CP(+1)}^*)^0\pi^+) = -0.02 \pm 0.05$   
 $A_{CP}(B^+ \rightarrow (D_{CP(-1)}^*)^0\pi^+) = -0.09 \pm 0.05$



## Meson Summary Table

$$\begin{aligned}
A_{CP}(B^+ \rightarrow D^{*0} K^+) &= -0.07 \pm 0.04 \\
r_B^*(B^+ \rightarrow D^{*0} K^+) &= 0.123^{+0.026}_{-0.029} \\
\delta_B^*(B^+ \rightarrow D^{*0} K^+) &= (300 \pm 30)^\circ \quad (S = 1.7) \\
A_{CP}(B^+ \rightarrow D_{CP(+1)}^{*0} K^+) &= -0.12 \pm 0.08 \\
A_{CP}(B^+ \rightarrow D_{CP(-1)}^{*0} K^+) &= 0.07 \pm 0.10 \\
A_{CP}(B^+ \rightarrow D_{CP(+1)} K^*(892)^+) &= 0.09 \pm 0.14 \\
A_{CP}(B^+ \rightarrow D_{CP(-1)} K^*(892)^+) &= -0.23 \pm 0.22 \\
A_{CP}(B^+ \rightarrow D^{*+} \bar{D}^{*0}) &= -0.15 \pm 0.11 \\
A_{CP}(B^+ \rightarrow D^{*+} \bar{D}^0) &= -0.06 \pm 0.13 \\
A_{CP}(B^+ \rightarrow D^+ \bar{D}^{*0}) &= 0.13 \pm 0.18 \\
A_{CP}(B^+ \rightarrow D^+ \bar{D}^0) &= -0.03 \pm 0.07 \\
A_{CP}(B^+ \rightarrow K_S^0 \pi^+) &= 0.009 \pm 0.029 \quad (S = 1.2) \\
A_{CP}(B^+ \rightarrow K^+ \pi^0) &= 0.051 \pm 0.025 \\
A_{CP}(B^+ \rightarrow \eta' K^+) &= 0.013 \pm 0.017 \\
A_{CP}(B^+ \rightarrow \eta' K^*(892)^+) &= -0.26 \pm 0.27 \\
A_{CP}(B^+ \rightarrow \eta' K_S^0(1430)^+) &= 0.06 \pm 0.20 \\
A_{CP}(B^+ \rightarrow \eta' K_2^*(1430)^+) &= 0.15 \pm 0.13 \\
\mathbf{A_{CP}(B^+ \rightarrow \eta K^+)} &= -0.37 \pm 0.08 \\
A_{CP}(B^+ \rightarrow \eta K^*(892)^+) &= 0.02 \pm 0.06 \\
A_{CP}(B^+ \rightarrow \eta K_0^*(1430)^+) &= 0.05 \pm 0.13 \\
A_{CP}(B^+ \rightarrow \eta K_2^*(1430)^+) &= -0.45 \pm 0.30 \\
A_{CP}(B^+ \rightarrow \omega K^+) &= 0.02 \pm 0.05 \\
A_{CP}(B^+ \rightarrow \omega K^{*+}) &= 0.29 \pm 0.35 \\
A_{CP}(B^+ \rightarrow \omega(K\pi)_0^{*+}) &= -0.10 \pm 0.09 \\
A_{CP}(B^+ \rightarrow \omega K_2^*(1430)^+) &= 0.14 \pm 0.15 \\
A_{CP}(B^+ \rightarrow K^{*0} \pi^+) &= -0.04 \pm 0.09 \quad (S = 2.1) \\
A_{CP}(B^+ \rightarrow K^*(892)^+ \pi^0) &= -0.06 \pm 0.24 \\
A_{CP}(B^+ \rightarrow K^+ \pi^- \pi^+) &= 0.038 \pm 0.022 \\
A_{CP}(B^+ \rightarrow f_0(980) K^+) &= -0.09^{+0.05}_{-0.04} \quad (S = 1.1) \\
\mathbf{A_{CP}(B^+ \rightarrow f_2(1270) K^+)} &= -0.68^{+0.19}_{-0.17} \\
A_{CP}(B^+ \rightarrow f_0(1500) K^+) &= 0.28 \pm 0.30 \\
\mathbf{A_{CP}(B^+ \rightarrow \rho^0 K^+)} &= 0.37 \pm 0.10 \\
A_{CP}(B^+ \rightarrow K_S^0(1430)^0 \pi^+) &= 0.055 \pm 0.033 \\
A_{CP}(B^+ \rightarrow K_2^*(1430)^0 \pi^+) &= 0.05^{+0.29}_{-0.24} \\
A_{CP}(B^+ \rightarrow K^+ \pi^0 \pi^0) &= -0.06 \pm 0.07 \\
A_{CP}(B^+ \rightarrow K^0 \rho^+) &= -0.12 \pm 0.17 \\
A_{CP}(B^+ \rightarrow K^{*+} \pi^+ \pi^-) &= 0.07 \pm 0.08 \\
A_{CP}(B^+ \rightarrow \rho^0 K^*(892)^+) &= 0.31 \pm 0.13 \\
A_{CP}(B^+ \rightarrow K^*(892)^+ f_0(980)) &= -0.15 \pm 0.12 \\
A_{CP}(B^+ \rightarrow a_1^+ K^0) &= 0.12 \pm 0.11 \\
A_{CP}(B^+ \rightarrow b_1^+ K^0) &= -0.03 \pm 0.15 \\
A_{CP}(B^+ \rightarrow K^*(892)^0 \rho^+) &= -0.01 \pm 0.16 \\
A_{CP}(B^+ \rightarrow b_1^0 K^+) &= -0.46 \pm 0.20 \\
A_{CP}(B^+ \rightarrow K^0 K^+) &= 0.12 \pm 0.18 \\
A_{CP}(B^+ \rightarrow K^+ K_S^0 K_S^0) &= -0.04 \pm 0.11 \\
A_{CP}(B^+ \rightarrow K^+ K^- \pi^+) &= 0.00 \pm 0.10 \\
A_{CP}(B^+ \rightarrow K^+ K^- K^+) &= -0.017 \pm 0.030 \\
A_{CP}(B^+ \rightarrow \phi K^+) &= -0.01 \pm 0.06 \\
A_{CP}(B^+ \rightarrow X_0(1550) K^+) &= -0.04 \pm 0.07 \\
A_{CP}(B^+ \rightarrow K^{*+} K^+ K^-) &= 0.11 \pm 0.09 \\
A_{CP}(B^+ \rightarrow \phi K^*(892)^+) &= -0.01 \pm 0.08 \\
A_{CP}(B^+ \rightarrow \phi(K\pi)_0^{*+}) &= 0.04 \pm 0.16 \\
A_{CP}(B^+ \rightarrow \phi K_1(1270)^+) &= 0.15 \pm 0.20 \\
A_{CP}(B^+ \rightarrow \phi K_2^*(1430)^+) &= -0.23 \pm 0.20 \\
A_{CP}(B^+ \rightarrow K^+ \phi) &= -0.10 \pm 0.08 \\
A_{CP}(B^+ \rightarrow K^+ [\phi\phi]_{\eta_c}) &= 0.09 \pm 0.10 \\
A_{CP}(B^+ \rightarrow K^*(892)^+ \gamma) &= 0.018 \pm 0.029 \\
A_{CP}(B^+ \rightarrow \eta K^+ \gamma) &= -0.12 \pm 0.07 \\
A_{CP}(B^+ \rightarrow \phi K^+ \gamma) &= -0.13 \pm 0.11 \quad (S = 1.1) \\
A_{CP}(B^+ \rightarrow \rho^+ \gamma) &= -0.11 \pm 0.33 \\
A_{CP}(B^+ \rightarrow \pi^+ \pi^0) &= 0.06 \pm 0.05 \\
A_{CP}(B^+ \rightarrow \pi^+ \pi^- \pi^+) &= 0.03 \pm 0.06 \\
A_{CP}(B^+ \rightarrow \rho^0 \pi^+) &= 0.18^{+0.09}_{-0.17} \\
A_{CP}(B^+ \rightarrow f_2(1270) \pi^+) &= 0.41 \pm 0.30 \\
A_{CP}(B^+ \rightarrow \rho^0(1450) \pi^+) &= -0.1^{+0.4}_{-0.5} \\
\mathbf{A_{CP}(B^+ \rightarrow f_0(1370) \pi^+)} &= 0.72 \pm 0.22 \\
A_{CP}(B^+ \rightarrow \pi^+ \pi^- \pi^+ \text{ nonresonant}) &= -0.14^{+0.23}_{-0.16} \\
A_{CP}(B^+ \rightarrow \rho^+ \pi^0) &= 0.02 \pm 0.11 \\
A_{CP}(B^+ \rightarrow \rho^+ \rho^0) &= -0.05 \pm 0.05 \\
A_{CP}(B^+ \rightarrow \omega \pi^+) &= -0.04 \pm 0.06 \\
A_{CP}(B^+ \rightarrow \omega \rho^+) &= -0.20 \pm 0.09
\end{aligned}$$

$$\begin{aligned}
A_{CP}(B^+ \rightarrow \eta \pi^+) &= -0.14 \pm 0.07 \quad (S = 1.4) \\
A_{CP}(B^+ \rightarrow \eta \rho^+) &= 0.11 \pm 0.11 \\
A_{CP}(B^+ \rightarrow \eta' \pi^+) &= 0.06 \pm 0.16 \\
A_{CP}(B^+ \rightarrow \eta' \rho^+) &= 0.26 \pm 0.17 \\
A_{CP}(B^+ \rightarrow b_1^0 \pi^+) &= 0.05 \pm 0.16 \\
A_{CP}(B^+ \rightarrow \rho \bar{\rho} \pi^+) &= 0.00 \pm 0.04 \\
A_{CP}(B^+ \rightarrow \rho \bar{\rho} K^+) &= -0.16 \pm 0.07 \\
A_{CP}(B^+ \rightarrow \rho \bar{\rho} K^*(892)^+) &= 0.21 \pm 0.16 \quad (S = 1.4) \\
A_{CP}(B^+ \rightarrow \rho \bar{\rho} \gamma) &= 0.17 \pm 0.17 \\
A_{CP}(B^+ \rightarrow \rho \bar{\rho} \pi^0) &= 0.01 \pm 0.17 \\
A_{CP}(B^+ \rightarrow K^+ \ell^+ \ell^-) &= -0.01 \pm 0.09 \quad (S = 1.1) \\
A_{CP}(B^+ \rightarrow K^+ e^+ e^-) &= 0.14 \pm 0.14 \\
A_{CP}(B^+ \rightarrow K^+ \mu^+ \mu^-) &= -0.05 \pm 0.13 \\
A_{CP}(B^+ \rightarrow K^{*+} \ell^+ \ell^-) &= -0.09 \pm 0.14 \\
A_{CP}(B^+ \rightarrow K^* e^+ e^-) &= -0.14 \pm 0.23 \\
A_{CP}(B^+ \rightarrow K^* \mu^+ \mu^-) &= -0.12 \pm 0.24 \\
\mathbf{\gamma(B^+ \rightarrow D^{*+} K^{(*)+})} &= (73 \pm 10)^\circ
\end{aligned}$$

$B^-$  modes are charge conjugates of the modes below. Modes which do not identify the charge state of the  $B$  are listed in the  $B^\pm/B^0$  ADMIXTURE section.

The branching fractions listed below assume 50%  $B^0 \bar{B}^0$  and 50%  $B^+ B^-$  production at the  $\Upsilon(4S)$ . We have attempted to bring older measurements up to date by rescaling their assumed  $\Upsilon(4S)$  production ratio to 50:50 and their assumed  $D, D_s, D^*$ , and  $\psi$  branching ratios to current values whenever this would affect our averages and best limits significantly.

Indentation is used to indicate a subchannel of a previous reaction. All resonant subchannels have been corrected for resonance branching fractions to the final state so the sum of the subchannel branching fractions can exceed that of the final state.

For inclusive branching fractions, e.g.,  $B \rightarrow D^\pm$  anything, the values usually are multiplicities, not branching fractions. They can be greater than one.

$B^+$ DECAY MODES	Fraction ( $\Gamma_i/\Gamma$ )	Scale factor / Confidence level (MeV/c)	$p$
<b>Semileptonic and leptonic modes</b>			
$\ell^+ \nu_\ell$ anything	[ppp] ( 10.99 $\pm$ 0.28 ) %		–
$e^+ \nu_e X_c$	( 10.8 $\pm$ 0.4 ) %		–
$D \ell^+ \nu_\ell$ anything	( 9.8 $\pm$ 0.7 ) %		–
$\bar{D}^0 \ell^+ \nu_\ell$	[ppp] ( 2.26 $\pm$ 0.11 ) %		2310
$\bar{D}^0 \tau^+ \nu_\tau$	( 7.7 $\pm$ 2.5 ) $\times 10^{-3}$		1911
$\bar{D}^*(2007)^0 \ell^+ \nu_\ell$	[ppp] ( 5.70 $\pm$ 0.19 ) %		2258
$\bar{D}^*(2007)^0 \tau^+ \nu_\tau$	( 2.04 $\pm$ 0.30 ) %		1839
$D^- \pi^+ \ell^+ \nu_\ell$	( 4.2 $\pm$ 0.5 ) $\times 10^{-3}$		2306
$\bar{D}_0^*(2420)^0 \ell^+ \nu_\ell \times$ $B(\bar{D}_0^* \rightarrow D^- \pi^+)$	( 2.5 $\pm$ 0.5 ) $\times 10^{-3}$		–
$\bar{D}_2^*(2460)^0 \ell^+ \nu_\ell \times$ $B(\bar{D}_2^* \rightarrow D^- \pi^+)$	( 1.53 $\pm$ 0.16 ) $\times 10^{-3}$		2065
$D^{(*)} n \pi \ell^+ \nu_\ell (n \geq 1)$	( 1.87 $\pm$ 0.26 ) %		–
$D^{*-} \pi^+ \ell^+ \nu_\ell$	( 6.1 $\pm$ 0.6 ) $\times 10^{-3}$		2254
$D_s^{*-} K^+ \ell^+ \nu_\ell$	( 6.1 $\pm$ 1.2 ) $\times 10^{-4}$		2185
$\bar{D}_1(2420)^0 \ell^+ \nu_\ell \times B(\bar{D}_1^0 \rightarrow$ $D^{*-} \pi^+)$	( 3.03 $\pm$ 0.20 ) $\times 10^{-3}$		2084
$\bar{D}_1'(2430)^0 \ell^+ \nu_\ell \times$ $B(\bar{D}_1'^0 \rightarrow D^{*-} \pi^+)$	( 2.7 $\pm$ 0.6 ) $\times 10^{-3}$		–
$\bar{D}_2^*(2460)^0 \ell^+ \nu_\ell \times$ $B(\bar{D}_2^* \rightarrow D^{*-} \pi^+)$	( 1.01 $\pm$ 0.24 ) $\times 10^{-3}$	S=2.0	2065
$\pi^0 \ell^+ \nu_\ell$	( 7.78 $\pm$ 0.28 ) $\times 10^{-5}$		2638
$\eta \ell^+ \nu_\ell$	( 3.9 $\pm$ 0.8 ) $\times 10^{-5}$	S=1.3	2611
$\eta' \ell^+ \nu_\ell$	( 2.3 $\pm$ 0.8 ) $\times 10^{-5}$		2553
$\omega \ell^+ \nu_\ell$	[ppp] ( 1.15 $\pm$ 0.17 ) $\times 10^{-4}$		2582
$\rho^0 \ell^+ \nu_\ell$	[ppp] ( 1.07 $\pm$ 0.13 ) $\times 10^{-4}$		2583
$\rho \bar{\rho} e^+ \nu_e$	< 5.2 $\times 10^{-3}$	CL=90%	2467
$e^+ \nu_e$	< 9.8 $\times 10^{-7}$	CL=90%	2640
$\mu^+ \nu_\mu$	< 1.0 $\times 10^{-6}$	CL=90%	2639
$\tau^+ \nu_\tau$	( 1.65 $\pm$ 0.34 ) $\times 10^{-4}$		2341
$\ell^+ \nu_\ell \gamma$	< 1.56 $\times 10^{-5}$	CL=90%	2640
$e^+ \nu_e \gamma$	< 1.7 $\times 10^{-5}$	CL=90%	2640
$\mu^+ \nu_\mu \gamma$	< 2.4 $\times 10^{-5}$	CL=90%	2639

## Meson Summary Table

Inclusive modes				$\bar{D}_2^*(2462)^0 \pi^+ \times B(\bar{D}_2^{*0} \rightarrow \bar{D}^0 \pi^- \pi^+)$ (nonresonant)				
$D^0 X$	( 8.6 ± 0.7 ) %	-		$\bar{D}_2^*(2462)^0 \pi^+ \times B(\bar{D}_2^{*0} \rightarrow D^* \pi^+)$	< 1.7	$\times 10^{-4}$	CL=90%	-
$\bar{D}^0 X$	( 79 ± 4 ) %	-		$\bar{D}_2^*(2462)^0 \pi^+ \times B(\bar{D}_2^{*0} \rightarrow D^*(2010)^- \pi^+)$	( 2.2 ± 1.1 )	$\times 10^{-4}$		-
$D^+ X$	( 2.5 ± 0.5 ) %	-		$\bar{D}_0^*(2400)^0 \pi^+$	( 6.4 ± 1.4 )	$\times 10^{-4}$		2128
$D^- X$	( 9.9 ± 1.2 ) %	-		$\times B(\bar{D}_0^*(2400)^0 \rightarrow D^- \pi^+)$				
$D_s^+ X$	( 7.9 $\begin{smallmatrix} +1.4 \\ -1.3 \end{smallmatrix}$ ) %	-		$\bar{D}_1(2421)^0 \pi^+$	( 6.8 ± 1.5 )	$\times 10^{-4}$		-
$D_s^- X$	( 1.10 $\begin{smallmatrix} +0.40 \\ -0.32 \end{smallmatrix}$ ) %	-		$\times B(\bar{D}_1(2421)^0 \rightarrow D^{*-} \pi^+)$				
$A_c^+ X$	( 2.1 $\begin{smallmatrix} +0.9 \\ -0.6 \end{smallmatrix}$ ) %	-		$\bar{D}_2^*(2462)^0 \pi^+$	( 1.8 ± 0.5 )	$\times 10^{-4}$		-
$\bar{A}_c^- X$	( 2.8 $\begin{smallmatrix} +1.1 \\ -0.9 \end{smallmatrix}$ ) %	-		$\times B(\bar{D}_2^*(2462)^0 \rightarrow D^{*-} \pi^+)$				
$\bar{c} X$	( 97 ± 4 ) %	-		$\bar{D}_1(2427)^0 \pi^+$	( 5.0 ± 1.2 )	$\times 10^{-4}$		-
$c X$	( 23.4 $\begin{smallmatrix} +2.2 \\ -1.8 \end{smallmatrix}$ ) %	-		$\times B(\bar{D}_1(2427)^0 \rightarrow D^{*-} \pi^+)$				
$\bar{c} c X$	( 120 ± 6 ) %	-		$\bar{D}_1(2420)^0 \pi^+ \times B(\bar{D}_1^0 \rightarrow \bar{D}^{*0} \pi^+ \pi^-)$	< 6	$\times 10^{-6}$	CL=90%	2082
D, D*, or D <sub>s</sub> modes				$\bar{D}_1^*(2420)^0 \rho^+$ <td>&lt; 1.4</td> <td><math>\times 10^{-3}</math></td> <td>CL=90%</td> <td>1996</td>	< 1.4	$\times 10^{-3}$	CL=90%	1996
$\bar{D}^0 \pi^+$	( 4.81 ± 0.15 ) $\times 10^{-3}$	2308		$\bar{D}_2^*(2460)^0 \rho^+$	< 1.3	$\times 10^{-3}$	CL=90%	2062
$D_{CP(+1)} \pi^+$	[qqq] ( 2.5 ± 0.4 ) $\times 10^{-3}$	-		$\bar{D}_2^*(2460)^0 \pi^+ \times B(\bar{D}_2^{*0} \rightarrow \bar{D}^{*0} \pi^+ \pi^-)$	< 2.2	$\times 10^{-5}$	CL=90%	2062
$D_{CP(-1)} \pi^+$	[qqq] ( 2.0 ± 0.4 ) $\times 10^{-3}$	-		$\bar{D}_2^*(2460)^0 \rho^+$	< 4.7	$\times 10^{-3}$	CL=90%	1975
$\bar{D}^0 \rho^+$	( 1.34 ± 0.18 ) %	2237		$\bar{D}^0 D_s^+$	( 10.0 ± 1.7 )	$\times 10^{-3}$		1815
$\bar{D}^0 K^+$	( 3.65 ± 0.33 ) $\times 10^{-4}$	2281		$D_{s0}(2317)^+ \bar{D}^0 \times B(D_{s0}(2317)^+ \rightarrow D_s^+ \pi^0)$	( 7.3 $\begin{smallmatrix} +2.2 \\ -1.7 \end{smallmatrix}$ )	$\times 10^{-4}$		1605
$D_{CP(+1)} K^+$	[qqq] ( 2.18 ± 0.26 ) $\times 10^{-4}$	-		$D_{s0}(2317)^+ \bar{D}^0 \times B(D_{s0}(2317)^+ \rightarrow D_s^{*+} \gamma)$	< 7.6	$\times 10^{-4}$	CL=90%	1605
$D_{CP(-1)} K^+$	[qqq] ( 1.97 ± 0.24 ) $\times 10^{-4}$	-		$D_{s0}(2317)^+ \bar{D}^0 \times B(D_{s0}(2317)^+ \rightarrow D_s^+ \pi^0)$	( 9 ± 7 )	$\times 10^{-4}$		1511
$[K^- \pi^+]_D K^+$	[rrr] < 2.8 $\times 10^{-7}$	CL=90%		$D_{sJ}(2457)^+ \bar{D}^0$	( 3.1 $\begin{smallmatrix} +1.0 \\ -0.9 \end{smallmatrix}$ )	$\times 10^{-3}$		-
$[K^+ \pi^-]_D K^+$	[rrr] < 1.8 $\times 10^{-5}$	CL=90%		$D_{sJ}(2457)^+ \bar{D}^0 \times B(D_{sJ}(2457)^+ \rightarrow D_s^+ \gamma)$	( 4.6 $\begin{smallmatrix} +1.3 \\ -1.1 \end{smallmatrix}$ )	$\times 10^{-4}$		-
$[K^- \pi^+]_D \pi^+$	[rrr] ( 6.3 ± 1.1 ) $\times 10^{-7}$	-		$D_{sJ}(2457)^+ \bar{D}^0 \times B(D_{sJ}(2457)^+ \rightarrow D_s^+ \pi^0)$	< 2.2	$\times 10^{-4}$	CL=90%	-
$[K^+ \pi^-]_D \pi^+$	( 2.0 ± 0.4 ) $\times 10^{-4}$	-		$D_{sJ}(2457)^+ \bar{D}^0 \times B(D_{sJ}(2457)^+ \rightarrow D_s^{*+} \gamma)$	< 9.8	$\times 10^{-4}$	CL=90%	-
$[\pi^+ \pi^- \pi^0]_D K^-$	( 4.6 ± 0.9 ) $\times 10^{-6}$	-		$D_{sJ}(2457)^+ \bar{D}^0 \times B(D_{sJ}(2457)^+ \rightarrow D_s^+ \gamma)$	( 1.20 ± 0.30 ) %			-
$\bar{D}^0 K^*(892)^+$	( 5.3 ± 0.4 ) $\times 10^{-4}$	2213		$D_{sJ}(2457)^+ \bar{D}^0 \times B(D_{sJ}(2457)^+ \rightarrow D_s^+ \gamma)$	( 1.4 $\begin{smallmatrix} +0.7 \\ -0.6 \end{smallmatrix}$ )	$\times 10^{-3}$		-
$D_{CP(-1)} K^*(892)^+$	[qqq] ( 2.7 ± 0.8 ) $\times 10^{-4}$	-		$\bar{D}^0 D_{s1}(2536)^+ \times B(D_{s1}(2536)^+ \rightarrow D^*(2007)^0 K^+)$	( 2.2 ± 0.7 )	$\times 10^{-4}$		1447
$D_{CP(+1)} K^*(892)^+$	[qqq] ( 5.8 ± 1.1 ) $\times 10^{-4}$	-		$\bar{D}^0 D_{s1}(2536)^+ \times B(D_{s1}(2536)^+ \rightarrow D^*(2007)^0 K^+)$	( 2.2 ± 0.7 )	$\times 10^{-4}$		1447
$\bar{D}^0 K^+ \bar{K}^0$	( 5.5 ± 1.6 ) $\times 10^{-4}$	2189		$\bar{D}^0 D_{s1}(2536)^+ \times B(D_{s1}(2536)^+ \rightarrow D^*(2007)^0 K^+)$	( 5.5 ± 1.6 )	$\times 10^{-4}$		1339
$\bar{D}^0 K^+ \bar{K}^*(892)^0$	( 7.5 ± 1.7 ) $\times 10^{-4}$	2071		$\bar{D}^0 D_{s1}(2536)^+ \times B(D_{s1}(2536)^+ \rightarrow D^*(2007)^0 K^+)$	( 2.3 ± 1.1 )	$\times 10^{-4}$		1447
$\bar{D}^0 \pi^+ \pi^+ \pi^-$	( 5.7 ± 2.2 ) $\times 10^{-3}$	S=3.6		$\bar{D}^0 D_{s1}(2536)^+ \times B(D_{s1}(2536)^+ \rightarrow D^*(2007)^0 K^+)$	( 1.13 $\begin{smallmatrix} +0.26 \\ -0.40 \end{smallmatrix}$ )	$\times 10^{-3}$		-
$\bar{D}^0 \pi^+ \pi^+ \pi^-$ nonresonant	( 5 ± 4 ) $\times 10^{-3}$	2289		$\bar{D}^0 D_{s1}(2536)^+ \times B(D_{s1}(2536)^+ \rightarrow D^*(2007)^0 K^+)$	( 3.9 ± 2.6 )	$\times 10^{-4}$		1339
$\bar{D}^0 \pi^+ \rho^0$	( 4.2 ± 3.0 ) $\times 10^{-3}$	2207		$\bar{D}^0 D_{s1}(2536)^+ \times B(D_{s1}(2536)^+ \rightarrow D^*(2007)^0 K^+)$	< 2	$\times 10^{-4}$	CL=90%	1306
$\bar{D}^0 a_1(1260)^+$	( 4 ± 4 ) $\times 10^{-3}$	2123		$\bar{D}^0 D_{s1}(2536)^+ \times B(D_{s1}(2536)^+ \rightarrow D^*(2007)^0 K^+)$	< 5	$\times 10^{-4}$	CL=90%	1306
$\bar{D}^0 \omega \pi^+$	( 4.1 ± 0.9 ) $\times 10^{-3}$	2206		$\bar{D}^0 D_s^{*+}$	( 7.6 ± 1.6 )	$\times 10^{-3}$		1734
$D^*(2010)^- \pi^+ \pi^+$	( 1.35 ± 0.22 ) $\times 10^{-3}$	2247		$\bar{D}^*(2007)^0 D^+$	( 8.2 ± 1.7 )	$\times 10^{-3}$		1737
$\bar{D}_1(2420)^0 \pi^+ \times B(\bar{D}_1^0 \rightarrow D^*(2010)^- \pi^+)$	( 5.3 ± 2.3 ) $\times 10^{-4}$	2082		$\bar{D}^*(2007)^0 D_s^{*+}$	( 1.71 ± 0.24 ) %			1651
$D^- \pi^+ \pi^+$	( 1.07 ± 0.05 ) $\times 10^{-3}$	2299		$D^{(*)+} \bar{D}^{*0}$	( 2.7 ± 1.2 ) %			-
$D^+ K^0$	< 2.9 $\times 10^{-6}$	CL=90%	2278	$\bar{D}^*(2007)^0 D^*(2010)^+$	( 8.1 ± 1.7 )	$\times 10^{-4}$		1713
$D^+ K^{*0}$	< 3.0 $\times 10^{-6}$	CL=90%	2211	$\bar{D}^0 D^*(2010)^+ + \bar{D}^0 D^*(2007)^0 D^+$	< 1.30	%	CL=90%	1792
$\bar{D}^*(2007)^0 \pi^+$	( 5.18 ± 0.26 ) $\times 10^{-3}$	2256		$\bar{D}^0 D^*(2010)^+$	( 3.9 ± 0.5 )	$\times 10^{-4}$		1792
$\bar{D}_{CP(+1)}^0 \pi^+$	[sss] ( 2.9 ± 0.7 ) $\times 10^{-3}$	-		$\bar{D}^0 D^+$	( 3.8 ± 0.4 )	$\times 10^{-4}$		1866
$D_{CP(-1)}^0 \pi^+$	[sss] ( 2.6 ± 1.0 ) $\times 10^{-3}$	-		$\bar{D}^0 D^+ K^0$	( 1.55 ± 0.21 )	$\times 10^{-3}$		1571
$\bar{D}^*(2007)^0 \omega \pi^+$	( 4.5 ± 1.2 ) $\times 10^{-3}$	2149		$D^+ \bar{D}^*(2007)^0$	( 6.3 ± 1.7 )	$\times 10^{-4}$		1791
$\bar{D}^*(2007)^0 \rho^+$	( 9.8 ± 1.7 ) $\times 10^{-3}$	2181		$D^*(2007)^0 D^+ K^0$	( 2.1 ± 0.5 )	$\times 10^{-3}$		1474
$\bar{D}^*(2007)^0 K^+$	( 4.20 ± 0.34 ) $\times 10^{-4}$	2227		$\bar{D}^0 \bar{D}^*(2010)^+ K^0$	( 3.8 ± 0.4 )	$\times 10^{-3}$		1476
$\bar{D}_{CP(+1)}^{*0} K^+$	[sss] ( 2.8 ± 0.4 ) $\times 10^{-4}$	-						
$\bar{D}_{CP(-1)}^{*0} K^+$	[sss] ( 2.31 ± 0.33 ) $\times 10^{-4}$	-						
$\bar{D}^*(2007)^0 K^*(892)^+$	( 8.1 ± 1.4 ) $\times 10^{-4}$	2156						
$\bar{D}^*(2007)^0 K^+ \bar{K}^0$	< 1.06 $\times 10^{-3}$	CL=90%	2132					
$\bar{D}^*(2007)^0 K^+ K^*(892)^0$	( 1.5 ± 0.4 ) $\times 10^{-3}$	2008						
$\bar{D}^*(2007)^0 \pi^+ \pi^+ \pi^-$	( 1.03 ± 0.12 ) %	2236						
$\bar{D}^*(2007)^0 a_1(1260)^+$	( 1.9 ± 0.5 ) %	2063						
$\bar{D}^*(2007)^0 \pi^- \pi^+ \pi^+ \pi^0$	( 1.8 ± 0.4 ) %	2219						
$\bar{D}^{*0} 3\pi^+ 2\pi^-$	( 5.7 ± 1.2 ) $\times 10^{-3}$	2196						
$D^*(2010)^+ \pi^0$	< 3.6 $\times 10^{-6}$	2255						
$D^*(2010)^+ K^0$	< 9.0 $\times 10^{-6}$	CL=90%	2225					
$D^*(2010)^- \pi^+ \pi^+ \pi^0$	( 1.5 ± 0.7 ) %	2235						
$D^*(2010)^- \pi^+ \pi^+ \pi^+ \pi^-$	( 2.6 ± 0.4 ) $\times 10^{-3}$	2217						
$\bar{D}^{*0} \pi^+$	[ttt] ( 5.9 ± 1.3 ) $\times 10^{-3}$	-						
$\bar{D}_1^*(2420)^0 \pi^+$	( 1.5 ± 0.6 ) $\times 10^{-3}$	S=1.3	2082					
$\bar{D}_1(2420)^0 \pi^+ \times B(\bar{D}_1^0 \rightarrow \bar{D}^0 \pi^+ \pi^-)$	( 2.5 $\begin{smallmatrix} +1.7 \\ -1.4 \end{smallmatrix}$ ) $\times 10^{-4}$	S=4.0	2082					
$\bar{D}_1(2420)^0 \pi^+ \times B(\bar{D}_1^0 \rightarrow \bar{D}^0 \pi^+ \pi^-)$ (nonresonant)	( 2.3 ± 1.0 ) $\times 10^{-4}$	2082						
$\bar{D}_2^*(2462)^0 \pi^+$	( 3.5 ± 0.4 ) $\times 10^{-4}$	-						
$\times B(\bar{D}_2^*(2462)^0 \rightarrow D^- \pi^+)$								
$\bar{D}_2^*(2462)^0 \pi^+ \times B(\bar{D}_2^{*0} \rightarrow \bar{D}^0 \pi^- \pi^+)$	( 2.3 ± 1.1 ) $\times 10^{-4}$	-						

## Meson Summary Table

$\bar{D}^*(2007)^0 D^*(2010)^+ K^0$	( 9.2 ±1.2 ) × 10 <sup>-3</sup>	1362	$J/\psi(1S) K^*(892)^+$	( 1.43 ±0.08 ) × 10 <sup>-3</sup>	1571
$\bar{D}^0 D^0 K^+$	( 1.45 ±0.33 ) × 10 <sup>-3</sup>	S=2.6 1577	$J/\psi(1S) K(1270)^+$	( 1.8 ±0.5 ) × 10 <sup>-3</sup>	1390
$\bar{D}^*(2007)^0 D^0 K^+$	( 2.26 ±0.23 ) × 10 <sup>-3</sup>	1481	$J/\psi(1S) K(1400)^+$	< 5 × 10 <sup>-4</sup>	CL=90% 1308
$\bar{D}^0 D^*(2007)^0 K^+$	( 6.3 ±0.5 ) × 10 <sup>-3</sup>	1481	$J/\psi(1S) \eta K^+$	( 1.08 ±0.33 ) × 10 <sup>-4</sup>	1510
$\bar{D}^*(2007)^0 D^*(2007)^0 K^+$	( 1.12 ±0.13 ) %	1368	$J/\psi(1S) \eta' K^+$	< 8.8 × 10 <sup>-5</sup>	CL=90% 1273
$D^- D^+ K^+$	( 2.2 ±0.7 ) × 10 <sup>-4</sup>	1570	$J/\psi(1S) \phi K^+$	( 5.2 ±1.7 ) × 10 <sup>-5</sup>	S=1.2 1227
$D^- D^*(2010)^+ K^+$	( 6.3 ±1.1 ) × 10 <sup>-4</sup>	1475	$J/\psi(1S) \omega K^+$	( 3.20 <sup>+0.60</sup> <sub>-0.32</sub> ) × 10 <sup>-4</sup>	1388
$D^*(2010)^- D^+ K^+$	( 6.0 ±1.3 ) × 10 <sup>-4</sup>	1475	$X(3872) K^+ \times B(X \rightarrow J/\psi \omega)$	( 6.0 ±2.2 ) × 10 <sup>-6</sup>	1141
$D^*(2010)^- D^*(2010)^+ K^+$	( 1.32 ±0.18 ) × 10 <sup>-3</sup>	1363	$X(3915) K^+ \times B(X \rightarrow J/\psi \omega)$	( 3.0 <sup>+0.9</sup> <sub>-0.7</sub> ) × 10 <sup>-5</sup>	1104
$(\bar{D}^+ \bar{D}^*)(D^+ D^*) K$	( 4.05 ±0.30 ) %	-	$J/\psi(1S) \pi^+$	( 4.9 ±0.4 ) × 10 <sup>-5</sup>	S=1.2 1727
$D_s^+ \pi^0$	( 1.6 ±0.5 ) × 10 <sup>-5</sup>	2270	$J/\psi(1S) \rho^+$	( 5.0 ±0.8 ) × 10 <sup>-5</sup>	1611
$D_s^{*+} \pi^0$	< 2.6 × 10 <sup>-4</sup>	CL=90% 2215	$J/\psi(1S) \pi^+ \pi^0$ nonresonant	< 7.3 × 10 <sup>-6</sup>	CL=90% 1717
$D_s^+ \eta$	< 4 × 10 <sup>-4</sup>	CL=90% 2235	$J/\psi(1S) a_1(1260)^+$	< 1.2 × 10 <sup>-3</sup>	CL=90% 1415
$D_s^{*+} \eta$	< 6 × 10 <sup>-4</sup>	CL=90% 2178	$J/\psi(1S) p \bar{p}$	( 1.18 ±0.31 ) × 10 <sup>-5</sup>	567
$D_s^+ \rho^0$	< 3.0 × 10 <sup>-4</sup>	CL=90% 2197	$J/\psi(1S) \bar{\Sigma}^0 p$	< 1.1 × 10 <sup>-5</sup>	CL=90% -
$D_s^{*+} \rho^0$	< 4 × 10 <sup>-4</sup>	CL=90% 2138	$J/\psi(1S) D^+$	< 1.2 × 10 <sup>-4</sup>	CL=90% 870
$D_s^+ \omega$	< 4 × 10 <sup>-4</sup>	CL=90% 2195	$J/\psi(1S) \bar{D}^0 \pi^+$	< 2.5 × 10 <sup>-5</sup>	CL=90% 665
$D_s^{*+} \omega$	< 6 × 10 <sup>-4</sup>	CL=90% 2136	$\psi(2S) \pi^+$	( 2.44 ±0.30 ) × 10 <sup>-5</sup>	1347
$D_s^+ a_1(1260)^0$	< 1.8 × 10 <sup>-3</sup>	CL=90% 2079	$\psi(2S) K^+$	( 6.39 ±0.33 ) × 10 <sup>-4</sup>	1284
$D_s^{*+} a_1(1260)^0$	< 1.3 × 10 <sup>-3</sup>	CL=90% 2015	$\psi(2S) K^*(892)^+$	( 6.7 ±1.4 ) × 10 <sup>-4</sup>	S=1.3 1115
$D_s^+ \phi$	< 1.9 × 10 <sup>-6</sup>	CL=90% 2141	$\psi(2S) K^+ \pi^+ \pi^-$	( 4.3 ±0.5 ) × 10 <sup>-4</sup>	1179
$D_s^{*+} \phi$	< 1.2 × 10 <sup>-5</sup>	CL=90% 2079	$\psi(3770) K^+$	( 4.9 ±1.3 ) × 10 <sup>-4</sup>	1218
$D_s^+ \bar{K}^0$	< 8 × 10 <sup>-4</sup>	CL=90% 2242	$\psi(3770) K^+ \times B(\psi \rightarrow D^0 \bar{D}^0)$	( 1.6 ±0.4 ) × 10 <sup>-4</sup>	S=1.1 1218
$D_s^{*+} \bar{K}^0$	< 9 × 10 <sup>-4</sup>	CL=90% 2185	$\psi(3770) K^+ \times B(\psi \rightarrow D^+ D^-)$	( 9.4 ±3.5 ) × 10 <sup>-5</sup>	1218
$D_s^+ \bar{K}^*(892)^0$	< 4 × 10 <sup>-4</sup>	CL=90% 2172	$\chi_{c0} \pi^+ \times B(\chi_{c0} \rightarrow \pi^+ \pi^-)$	< 1 × 10 <sup>-7</sup>	CL=90% 1531
$D_s^{*+} \bar{K}^*(892)^0$	< 3.5 × 10 <sup>-4</sup>	CL=90% 2112	$\chi_{c0}(1P) K^+$	( 1.34 <sup>+0.19</sup> <sub>-0.16</sub> ) × 10 <sup>-4</sup>	1478
$D_s^- \pi^+ K^+$	( 1.80 ±0.22 ) × 10 <sup>-4</sup>	2222	$\chi_{c0} K^*(892)^+$	< 2.1 × 10 <sup>-4</sup>	CL=90% 1341
$D_s^{*-} \pi^+ K^+$	( 1.45 ±0.24 ) × 10 <sup>-4</sup>	2164	$\chi_{c2} \pi^+ \times B(\chi_{c2} \rightarrow \pi^+ \pi^-)$	< 1 × 10 <sup>-7</sup>	CL=90% 1437
$D_s^- \pi^+ K^*(892)^+$	< 5 × 10 <sup>-3</sup>	CL=90% 2138	$\chi_{c2} K^+$	( 1.1 ±0.4 ) × 10 <sup>-5</sup>	1379
$D_s^{*-} \pi^+ K^*(892)^+$	< 7 × 10 <sup>-3</sup>	CL=90% 2076	$\chi_{c2} K^*(892)^+$	< 1.2 × 10 <sup>-4</sup>	CL=90% 1227
$D_s^- K^+ K^+$	( 1.1 ±0.4 ) × 10 <sup>-5</sup>	2149	$\chi_{c1}(1P) \pi^+$	( 2.2 ±0.5 ) × 10 <sup>-5</sup>	1468
$D_s^{*-} K^+ K^+$	< 1.5 × 10 <sup>-5</sup>	CL=90% 2088	$\chi_{c1}(1P) K^+$	( 4.79 ±0.23 ) × 10 <sup>-4</sup>	1412
			$\chi_{c1}(1P) K^*(892)^+$	( 3.0 ±0.6 ) × 10 <sup>-4</sup>	S=1.1 1265
			$h_c(1P) K^+$	< 3.8 × 10 <sup>-5</sup>	1401
$\eta_c K^+$	( 9.6 ±1.2 ) × 10 <sup>-4</sup>	1753	<b>K or K* modes</b>		
$\eta_c K^+, \eta_c \rightarrow K_S^0 K^\mp \pi^\pm$	( 2.7 ±0.6 ) × 10 <sup>-5</sup>	-	$K^0 \pi^+$	( 2.31 ±0.10 ) × 10 <sup>-5</sup>	2614
$\eta_c K^*(892)^+$	( 1.1 <sup>+0.5</sup> <sub>-0.4</sub> ) × 10 <sup>-3</sup>	1648	$K^+ \pi^0$	( 1.29 ±0.06 ) × 10 <sup>-5</sup>	2615
$\eta_c(2S) K^+$	( 3.4 ±1.8 ) × 10 <sup>-4</sup>	1319	$\eta' K^+$	( 7.06 ±0.25 ) × 10 <sup>-5</sup>	2528
$\eta_c(2S) K^+, \eta_c(2S) \rightarrow K_S^0 K^\mp \pi^\pm$	( 3.4 <sup>+2.3</sup> <sub>-1.6</sub> ) × 10 <sup>-6</sup>	-	$\eta' K^*(892)^+$	( 4.8 <sup>+1.8</sup> <sub>-1.6</sub> ) × 10 <sup>-6</sup>	2472
$J/\psi(1S) K^+$	( 1.016±0.033 ) × 10 <sup>-3</sup>	1683	$\eta' K_0^*(1430)^+$	( 5.2 ±2.1 ) × 10 <sup>-6</sup>	-
$J/\psi(1S) K^+ \pi^+ \pi^-$	( 8.1 ±1.3 ) × 10 <sup>-4</sup>	S=2.5 1612	$\eta' K_2^*(1430)^+$	( 2.8 ±0.5 ) × 10 <sup>-5</sup>	2346
$h_c(1P) K^+ \times B(h_c(1P) \rightarrow J/\psi \pi^+ \pi^-)$	< 3.4 × 10 <sup>-6</sup>	CL=90% 1401	$\eta K^+$	( 2.4 ±0.4 ) × 10 <sup>-6</sup>	S=1.7 2588
$X(3872) K^+$	< 3.2 × 10 <sup>-4</sup>	CL=90% 1141	$\eta K^*(892)^+$	( 1.93 ±0.16 ) × 10 <sup>-5</sup>	2534
$X(3872) K^+ \times B(X \rightarrow J/\psi \pi^+ \pi^-)$	( 8.6 ±0.8 ) × 10 <sup>-6</sup>	1141	$\eta K_0^*(1430)^+$	( 1.8 ±0.4 ) × 10 <sup>-5</sup>	-
$X(3872) K^+ \times B(X \rightarrow J/\psi \gamma)$	( 2.1 ±0.4 ) × 10 <sup>-6</sup>	S=1.1 1141	$\eta K_2^*(1430)^+$	( 9.1 ±3.0 ) × 10 <sup>-6</sup>	2414
$X(3872) K^*(892)^+ \times B(X \rightarrow J/\psi \gamma)$	< 4.8 × 10 <sup>-6</sup>	CL=90% 939	$\eta(1295) K^+ \times B(\eta(1295) \rightarrow \eta \pi \pi)$	( 2.9 <sup>+0.8</sup> <sub>-0.7</sub> ) × 10 <sup>-6</sup>	2455
$X(3872) K^+ \times B(X \rightarrow \psi(2S) \gamma)$	( 4 ±4 ) × 10 <sup>-6</sup>	S=2.5 1141	$\eta(1405) K^+ \times B(\eta(1405) \rightarrow \eta \pi \pi)$	< 1.3 × 10 <sup>-6</sup>	CL=90% 2425
$X(3872) K^*(892)^+ \times B(X \rightarrow \psi(2S) \gamma)$	< 2.8 × 10 <sup>-5</sup>	CL=90% 939	$\eta(1405) K^+ \times B(\eta(1405) \rightarrow K^* K)$	< 1.2 × 10 <sup>-6</sup>	CL=90% 2425
$X(3872) K^+ \times B(X \rightarrow D^0 \bar{D}^0)$	< 6.0 × 10 <sup>-5</sup>	CL=90% 1141	$\eta(1475) K^+ \times B(\eta(1475) \rightarrow K^* K)$	( 1.38 <sup>+0.21</sup> <sub>-0.18</sub> ) × 10 <sup>-5</sup>	2406
$X(3872) K^+ \times B(X \rightarrow D^+ D^-)$	< 4.0 × 10 <sup>-5</sup>	CL=90% 1141	$f_1(1285) K^+$	< 2.0 × 10 <sup>-6</sup>	CL=90% 2458
$X(3872) K^+ \times B(X \rightarrow D^0 \bar{D}^0 \pi^0)$	( 1.0 ±0.4 ) × 10 <sup>-4</sup>	1141	$f_1(1420) K^+ \times B(f_1(1420) \rightarrow \eta \pi \pi)$	< 2.9 × 10 <sup>-6</sup>	CL=90% 2420
$X(3872) K^+ \times B(X \rightarrow \bar{D}^0 D^0)$	( 8.5 ±2.6 ) × 10 <sup>-5</sup>	S=1.4 1141	$f_1(1420) K^+ \times B(f_1(1420) \rightarrow K^* K)$	< 4.1 × 10 <sup>-6</sup>	CL=90% 2420
$X(3872) K^+ \times B(X(3872) \rightarrow J/\psi(1S) \eta)$	< 7.7 × 10 <sup>-6</sup>	CL=90% 1141	$\phi(1680) K^+ \times B(\phi(1680) \rightarrow K^* K)$	< 3.4 × 10 <sup>-6</sup>	CL=90% 2344
$X(3872)^+ K^0 \times B(X(3872)^+ \rightarrow [uuu])$	< 6.1 × 10 <sup>-6</sup>	CL=90% -	$\omega K^+$	( 6.7 ±0.8 ) × 10 <sup>-6</sup>	S=1.8 2557
$X(4430)^+ K^0 \times B(X^+ \rightarrow J/\psi \pi^+)$	< 1.5 × 10 <sup>-5</sup>	CL=95% -	$\omega K^*(892)^+$	< 7.4 × 10 <sup>-6</sup>	CL=90% 2503
$X(4430)^+ K^0 \times B(X^+ \rightarrow \psi(2S) \pi^+)$	< 4.7 × 10 <sup>-5</sup>	CL=95% -	$\omega(K\pi)_0^{*+}$	( 2.8 ±0.4 ) × 10 <sup>-5</sup>	-
$X(4260)^0 K^+ \times B(X^0 \rightarrow J/\psi \pi^+ \pi^-)$	< 2.9 × 10 <sup>-5</sup>	CL=95% -	$\omega K_0^*(1430)^+$	( 2.4 ±0.5 ) × 10 <sup>-5</sup>	-
$X(3915)^0 K^+ \times B(X^0 \rightarrow J/\psi \gamma)$	< 1.4 × 10 <sup>-5</sup>	CL=90% -	$\omega K_2^*(1430)^+$	( 2.1 ±0.4 ) × 10 <sup>-5</sup>	2380
$Z(3930)^0 K^+ \times B(Z^0 \rightarrow J/\psi \gamma)$	< 2.5 × 10 <sup>-6</sup>	CL=90% -	$a_0(980)^+ K^0 \times B(a_0(980)^+ \rightarrow \eta \pi^+)$	< 3.9 × 10 <sup>-6</sup>	CL=90% -
			$a_0(980)^0 K^+ \times B(a_0(980)^0 \rightarrow \eta \pi^0)$	< 2.5 × 10 <sup>-6</sup>	CL=90% -
			$K^*(892)^0 \pi^+$	( 1.01 ±0.09 ) × 10 <sup>-5</sup>	2562
			$K^*(892)^+ \pi^0$	( 8.2 ±1.9 ) × 10 <sup>-6</sup>	2562
			$K^+ \pi^- \pi^+$	( 5.10 ±0.29 ) × 10 <sup>-5</sup>	2609

## Meson Summary Table

$K^+ \pi^- \pi^+$ nonresonant	$(1.63^{+0.21}_{-0.15}) \times 10^{-5}$	2609	$\phi K_2^*(1770)^+$	$< 1.50 \times 10^{-5}$	CL=90%	-
$\omega(782) K^+$	$(6 \pm 9) \times 10^{-6}$	2557	$\phi K_2^*(1820)^+$	$< 1.63 \times 10^{-5}$	CL=90%	-
$K^+ f_0(980) \times B(f_0(980) \rightarrow \pi^+ \pi^-)$	$(9.4^{+1.0}_{-1.2}) \times 10^{-6}$	2522	$a_1^+ K^*0$	$< 3.6 \times 10^{-6}$	CL=90%	-
$f_2(1270)^0 K^+$	$(1.07 \pm 0.27) \times 10^{-6}$	-	$K^+ \phi$	$(5.0 \pm 1.2) \times 10^{-6}$	S=2.3	2306
$f_0(1370)^0 K^+ \times B(f_0(1370)^0 \rightarrow \pi^+ \pi^-)$	$< 1.07 \times 10^{-5}$	CL=90%	$\eta'/\eta' K^+$	$< 2.5 \times 10^{-5}$	CL=90%	2338
$\rho^0(1450) K^+ \times B(\rho^0(1450) \rightarrow \pi^+ \pi^-)$	$< 1.17 \times 10^{-5}$	CL=90%	$\omega \phi K^+$	$< 1.9 \times 10^{-6}$	CL=90%	2374
$f_0(1500) K^+ \times B(f_0(1500) \rightarrow \pi^+ \pi^-)$	$(7 \pm 5) \times 10^{-7}$	2398	$X(1812) K^+ \times B(X \rightarrow \omega \phi)$	$< 3.2 \times 10^{-7}$	CL=90%	-
$f_2'(1525) K^+ \times B(f_2'(1525) \rightarrow \pi^+ \pi^-)$	$< 3.4 \times 10^{-6}$	CL=90%	$K^*(892)^+ \gamma$	$(4.21 \pm 0.18) \times 10^{-5}$		2564
$K^+ \rho^0$	$(3.7 \pm 0.5) \times 10^{-6}$	2559	$K_1(1270)^+ \gamma$	$(4.3 \pm 1.3) \times 10^{-5}$		2486
$K_2^*(1430)^0 \pi^+$	$(4.5^{+0.9}_{-0.7}) \times 10^{-5}$	S=1.5	$\eta' K^+ \gamma$	$(7.9 \pm 0.9) \times 10^{-6}$		2588
$K_2^*(1430)^0 \pi^+$	$(5.6^{+2.2}_{-1.5}) \times 10^{-6}$	2445	$\eta' K^+ \gamma$	$(2.9^{+1.0}_{-0.9}) \times 10^{-6}$		2528
$K^*(1410)^0 \pi^+$	$< 4.5 \times 10^{-5}$	CL=90%	$\phi K^+ \gamma$	$(2.7 \pm 0.4) \times 10^{-6}$	S=1.2	2516
$K^*(1680)^0 \pi^+$	$< 1.2 \times 10^{-5}$	CL=90%	$K^+ \pi^- \pi^+ \gamma$	$(2.76 \pm 0.22) \times 10^{-5}$	S=1.2	2609
$K^+(980) K^+ \times B(f_0 \rightarrow \pi^0 \pi^0)$	$(1.62 \pm 0.19) \times 10^{-5}$	2610	$K^*(892)^0 \pi^+ \gamma$	$(2.0^{+0.7}_{-0.6}) \times 10^{-5}$		2562
$K^- \pi^+ \pi^+$ nonresonant	$< 9.5 \times 10^{-7}$	CL=90%	$K^+ \rho^0 \gamma$	$< 2.0 \times 10^{-5}$	CL=90%	2559
$K_1(1270)^0 \pi^+$	$< 5.6 \times 10^{-5}$	CL=90%	$K^+ \pi^- \pi^+ \gamma$ nonresonant	$< 9.2 \times 10^{-6}$	CL=90%	2609
$K_1(1400)^0 \pi^+$	$< 3.9 \times 10^{-5}$	CL=90%	$K^0 \pi^+ \pi^0 \gamma$	$(4.6 \pm 0.5) \times 10^{-5}$		2609
$K^0 \pi^+ \pi^0$	$< 6.6 \times 10^{-5}$	CL=90%	$K_1(1400)^+ \gamma$	$< 1.5 \times 10^{-5}$	CL=90%	2453
$K^0 \rho^+$	$(8.0 \pm 1.5) \times 10^{-6}$	2558	$K_2^*(1430)^+ \gamma$	$(1.4 \pm 0.4) \times 10^{-5}$		2447
$K^*(892)^+ \pi^+ \pi^-$	$(7.5 \pm 1.0) \times 10^{-5}$	2557	$K^*(1680)^+ \gamma$	$< 1.9 \times 10^{-3}$	CL=90%	2360
$K^*(892)^+ \rho^0$	$(4.6 \pm 1.1) \times 10^{-6}$	2504	$K_3^*(1780)^+ \gamma$	$< 3.9 \times 10^{-5}$	CL=90%	2341
$K^*(892)^+ f_0(980)$	$(4.2 \pm 0.7) \times 10^{-6}$	2466	$K_4^*(2045)^+ \gamma$	$< 9.9 \times 10^{-3}$	CL=90%	2244
$a_1^+ K^0$	$(3.5 \pm 0.7) \times 10^{-5}$	-	<b>Light unflavored meson modes</b>			
$b_1^+ K^0 \times B(b_1^+ \rightarrow \omega \pi^+)$	$(9.6 \pm 1.9) \times 10^{-6}$	-	$\rho^+ \gamma$	$(9.8 \pm 2.5) \times 10^{-7}$		2583
$K^*(892)^0 \rho^+$	$(9.2 \pm 1.5) \times 10^{-6}$	2504	$\pi^+ \pi^0$	$(5.7 \pm 0.5) \times 10^{-6}$	S=1.4	2636
$K_1(1400)^+ \rho^0$	$< 7.8 \times 10^{-4}$	CL=90%	$\pi^+ \pi^+ \pi^-$	$(1.52 \pm 0.14) \times 10^{-5}$		2630
$K_2^*(1430)^+ \rho^0$	$< 1.5 \times 10^{-3}$	CL=90%	$\rho^0 \pi^+$	$(8.3 \pm 1.2) \times 10^{-6}$		2581
$b_1^0 K^+ \times B(b_1^0 \rightarrow \omega \pi^0)$	$(9.1 \pm 2.0) \times 10^{-6}$	-	$\pi^+ f_0(980) \times B(f_0(980) \rightarrow \pi^+ \pi^-)$	$< 1.5 \times 10^{-6}$	CL=90%	2545
$b_1^+ K^*0 \times B(b_1^+ \rightarrow \omega \pi^+)$	$< 5.9 \times 10^{-6}$	CL=90%	$\pi^+ f_2(1270)$	$(1.6^{+0.7}_{-0.4}) \times 10^{-6}$		2484
$b_1^0 K^*+ \times B(b_1^0 \rightarrow \omega \pi^0)$	$< 6.7 \times 10^{-6}$	CL=90%	$\rho(1450)^0 \pi^+ \times B(\rho^0 \rightarrow \pi^+ \pi^-)$	$(1.4^{+0.6}_{-0.9}) \times 10^{-6}$		2434
$K^+ \bar{K}^0$	$(1.36 \pm 0.27) \times 10^{-6}$	2593	$f_0(1370) \pi^+ \times B(f_0(1370) \rightarrow \pi^+ \pi^-)$	$< 4.0 \times 10^{-6}$	CL=90%	2460
$\bar{K}^0 K^+ \pi^0$	$< 2.4 \times 10^{-5}$	CL=90%	$f_0(500) \pi^+ \times B(f_0(500) \rightarrow \pi^+ \pi^-)$	$< 4.1 \times 10^{-6}$	CL=90%	-
$K^+ K_S^0 K_S^0$	$(1.15 \pm 0.13) \times 10^{-5}$	2521	$\pi^+ \pi^- \pi^+ \pi^+$ nonresonant	$(5.3^{+1.5}_{-1.1}) \times 10^{-6}$		2630
$K_S^0 K_S^0 \pi^+$	$< 5.1 \times 10^{-7}$	CL=90%	$\pi^+ \pi^0 \pi^0$	$< 8.9 \times 10^{-4}$	CL=90%	2631
$K^+ K^- \pi^+$	$(5.0 \pm 0.7) \times 10^{-6}$	2578	$\rho^+ \pi^0$	$(1.09 \pm 0.14) \times 10^{-5}$		2581
$K^+ K^- \pi^+$ nonresonant	$< 7.5 \times 10^{-5}$	CL=90%	$\pi^+ \pi^- \pi^+ \pi^0$	$< 4.0 \times 10^{-3}$	CL=90%	2622
$K^+ \bar{K}^*(892)^0$	$< 1.1 \times 10^{-6}$	CL=90%	$\rho^+ \rho^0$	$(2.40 \pm 0.19) \times 10^{-5}$		2523
$K^+ \bar{K}_0^*(1430)^0$	$< 2.2 \times 10^{-6}$	CL=90%	$\rho^+ f_0(980) \times B(f_0(980) \rightarrow \pi^+ \pi^-)$	$< 2.0 \times 10^{-6}$	CL=90%	2486
$K^+ K^+ \pi^-$	$< 1.6 \times 10^{-7}$	CL=90%	$a_1(1260)^+ \pi^0$	$(2.6 \pm 0.7) \times 10^{-5}$		2494
$K^+ K^+ \pi^-$ nonresonant	$< 8.79 \times 10^{-5}$	CL=90%	$a_1(1260)^0 \pi^+$	$(2.0 \pm 0.6) \times 10^{-5}$		2494
$K^*+ \pi^+ K^-$	$< 1.18 \times 10^{-5}$	CL=90%	$\omega \pi^+$	$(6.9 \pm 0.5) \times 10^{-6}$		2580
$K^*(892)^+ K^*(892)^0$	$(1.2 \pm 0.5) \times 10^{-6}$	2484	$\omega \rho^+$	$(1.59 \pm 0.21) \times 10^{-5}$		2522
$K^*+ K^+ \pi^-$	$< 6.1 \times 10^{-6}$	CL=90%	$\eta \pi^+$	$(4.02 \pm 0.27) \times 10^{-6}$		2609
$K^+ K^- K^+$	$(3.37 \pm 0.22) \times 10^{-5}$	S=1.4	$\eta \rho^+$	$(7.0 \pm 2.9) \times 10^{-6}$	S=2.8	2553
$K^+ \phi$	$(8.3 \pm 0.7) \times 10^{-6}$	2516	$\eta' \pi^+$	$(2.7 \pm 0.9) \times 10^{-6}$	S=1.9	2551
$f_0(980) K^+ \times B(f_0(980) \rightarrow K^+ K^-)$	$< 2.9 \times 10^{-6}$	CL=90%	$\eta' \rho^+$	$(9.7 \pm 2.2) \times 10^{-6}$		2492
$a_2(1320) K^+ \times B(a_2(1320) \rightarrow K^+ K^-)$	$< 1.1 \times 10^{-6}$	CL=90%	$\phi \pi^+$	$< 2.4 \times 10^{-7}$	CL=90%	2539
$f_2'(1525) K^+ \times B(f_2'(1525) \rightarrow K^+ K^-)$	$< 4.9 \times 10^{-6}$	CL=90%	$\phi \rho^+$	$< 3.0 \times 10^{-6}$	CL=90%	2480
$X_0(1550) K^+ \times B(X_0(1550) \rightarrow K^+ K^-)$	$(4.3 \pm 0.7) \times 10^{-6}$	-	$a_0(980)^0 \pi^+ \times B(a_0(980)^0 \rightarrow \eta \pi^0)$	$< 5.8 \times 10^{-6}$	CL=90%	-
$\phi(1680) K^+ \times B(\phi(1680) \rightarrow K^+ K^-)$	$< 8 \times 10^{-7}$	CL=90%	$a_0(980)^+ \pi^0 \times B(a_0^+ \rightarrow \eta \pi^+)$	$< 1.4 \times 10^{-6}$	CL=90%	-
$f_0(1710) K^+ \times B(f_0(1710) \rightarrow K^+ K^-)$	$(1.7 \pm 1.0) \times 10^{-6}$	2331	$\pi^+ \pi^+ \pi^+ \pi^- \pi^-$	$< 8.6 \times 10^{-4}$	CL=90%	2608
$K^+ K^- K^+$ nonresonant	$(2.8^{+0.9}_{-1.6}) \times 10^{-5}$	S=3.3	$\rho^0 a_1(1260)^+$	$< 6.2 \times 10^{-4}$	CL=90%	2433
$K^*(892)^+ K^+ K^-$	$(3.6 \pm 0.5) \times 10^{-5}$	2466	$\rho^0 a_2(1320)^+$	$< 7.2 \times 10^{-4}$	CL=90%	2410
$K^*(892)^+ \phi$	$(10.0 \pm 2.0) \times 10^{-6}$	S=1.7	$b_1^0 \pi^+ \times B(b_1^0 \rightarrow \omega \pi^0)$	$(6.7 \pm 2.0) \times 10^{-6}$		-
$\phi(K \pi)_0^+*$	$(8.3 \pm 1.6) \times 10^{-6}$	-	$b_1^+ \pi^0 \times B(b_1^+ \rightarrow \omega \pi^+)$	$< 3.3 \times 10^{-6}$	CL=90%	-
$\phi K_1(1270)^+$	$(6.1 \pm 1.9) \times 10^{-6}$	2375	$\pi^+ \pi^+ \pi^+ \pi^- \pi^- \pi^0$	$< 6.3 \times 10^{-3}$	CL=90%	2592
$\phi K_1(1400)^+$	$< 3.2 \times 10^{-6}$	CL=90%	$b_1^+ \rho^0 \times B(b_1^+ \rightarrow \omega \pi^+)$	$< 5.2 \times 10^{-6}$	CL=90%	-
$\phi K^*(1410)^+$	$< 4.3 \times 10^{-6}$	CL=90%	$a_1(1260)^+ a_1(1260)^0$	$< 1.3 \%$	CL=90%	2336
$\phi K_0^*(1430)^+$	$(7.0 \pm 1.6) \times 10^{-6}$	-	$b_1^0 \rho^+ \times B(b_1^0 \rightarrow \omega \pi^0)$	$< 3.3 \times 10^{-6}$	CL=90%	-
$\phi K_2^*(1430)^+$	$(8.4 \pm 2.1) \times 10^{-6}$	2333	<b>Charged particle (<math>h^\pm</math>) modes</b>			
			$h^\pm = K^\pm \text{ or } \pi^\pm$			
			$h^+ \pi^0$	$(1.6^{+0.7}_{-0.6}) \times 10^{-5}$		2636
			$\omega h^+$	$(1.38^{+0.27}_{-0.24}) \times 10^{-5}$		2580
			$h^+ X^0$ (Familon)	$< 4.9 \times 10^{-5}$	CL=90%	-

## Meson Summary Table

Baryon modes			
$p\bar{p}\pi^+$	( 1.62 $\pm$ 0.20 ) $\times 10^{-6}$		2439
$p\bar{p}\pi^+$ nonresonant	< 5.3 $\times 10^{-5}$	CL=90%	2439
$p\bar{p}K^+$	( 5.9 $\pm$ 0.5 ) $\times 10^{-6}$	S=1.5	2348
$\Theta(1710)^{++}\bar{p} \times$ $B(\Theta(1710)^{++} \rightarrow pK^+)$	[vvi] < 9.1 $\times 10^{-8}$	CL=90%	-
$f_J(2220)K^+ \times B(f_J(2220) \rightarrow \{vv\})$	< 4.1 $\times 10^{-7}$	CL=90%	2135
$\rho\bar{\Lambda}(1520)$	< 1.5 $\times 10^{-6}$	CL=90%	2322
$\rho\bar{p}K^+$ nonresonant	< 8.9 $\times 10^{-5}$	CL=90%	2348
$p\bar{p}K^*(892)^+$	( 3.6 $\begin{smallmatrix} +0.8 \\ -0.7 \end{smallmatrix}$ ) $\times 10^{-6}$		2215
$f_J(2220)K^+ \times B(f_J(2220) \rightarrow$ $\rho\bar{p})$	< 7.7 $\times 10^{-7}$	CL=90%	2059
$\rho\bar{\Lambda}$	< 3.2 $\times 10^{-7}$	CL=90%	2430
$\rho\bar{\Lambda}\gamma$	( 2.4 $\begin{smallmatrix} +0.5 \\ -0.4 \end{smallmatrix}$ ) $\times 10^{-6}$		2430
$\rho\bar{\Lambda}\pi^0$	( 3.0 $\begin{smallmatrix} +0.7 \\ -0.6 \end{smallmatrix}$ ) $\times 10^{-6}$		2402
$\rho\bar{\Sigma}^+(1385)^0$	< 4.7 $\times 10^{-7}$	CL=90%	2362
$\Delta^+\bar{\Lambda}$	< 8.2 $\times 10^{-7}$	CL=90%	-
$\rho\bar{\Sigma}\gamma$	< 4.6 $\times 10^{-6}$	CL=90%	2413
$\rho\bar{\Lambda}\pi^+\pi^-$	( 5.9 $\pm$ 1.1 ) $\times 10^{-6}$		2367
$\rho\bar{\Lambda}\rho^0$	( 4.8 $\pm$ 0.9 ) $\times 10^{-6}$		2214
$\rho\bar{\Lambda}f_2(1270)$	( 2.0 $\pm$ 0.8 ) $\times 10^{-6}$		2026
$\Lambda\bar{\Lambda}\pi^+$	< 9.4 $\times 10^{-7}$	CL=90%	2358
$\Lambda\bar{\Lambda}K^+$	( 3.4 $\pm$ 0.6 ) $\times 10^{-6}$		2251
$\Lambda\bar{\Lambda}K^{*+}$	( 2.2 $\begin{smallmatrix} +1.2 \\ -0.9 \end{smallmatrix}$ ) $\times 10^{-6}$		2098
$\Delta^0\rho$	< 1.38 $\times 10^{-6}$	CL=90%	2403
$\Delta^{++}\bar{p}$	< 1.4 $\times 10^{-7}$	CL=90%	2403
$D^+\rho\bar{p}$	< 1.5 $\times 10^{-5}$	CL=90%	1860
$D^*(2010)^+ + \rho\bar{p}$	< 1.5 $\times 10^{-5}$	CL=90%	1786
$\rho\bar{\Lambda}^0\bar{D}^0$	( 1.43 $\pm$ 0.32 ) $\times 10^{-5}$		-
$\rho\bar{\Lambda}^0\bar{D}^*(2007)^0$	< 5 $\times 10^{-5}$	CL=90%	-
$\bar{\Lambda}_c^- \rho\pi^+$	( 2.8 $\pm$ 0.8 ) $\times 10^{-4}$		1980
$\bar{\Lambda}_c^- \Delta(1232)^{++}$	< 1.9 $\times 10^{-5}$	CL=90%	1928
$\bar{\Lambda}_c^- \Delta_X(1600)^{++}$	( 5.9 $\pm$ 1.9 ) $\times 10^{-5}$		-
$\bar{\Lambda}_c^- \Delta_X(2420)^{++}$	( 4.7 $\pm$ 1.6 ) $\times 10^{-5}$		-
$(\bar{\Lambda}_c^- \rho)_s \pi^+$	[www] ( 3.9 $\pm$ 1.3 ) $\times 10^{-5}$		-
$\bar{\Sigma}_c(2520)^0 \rho$	< 3 $\times 10^{-6}$	CL=90%	1904
$\bar{\Sigma}_c(2800)^0 \rho$	( 3.3 $\pm$ 1.3 ) $\times 10^{-5}$		-
$\bar{\Lambda}_c^- \rho\pi^+\pi^0$	( 1.8 $\pm$ 0.6 ) $\times 10^{-3}$		1935
$\bar{\Lambda}_c^- \rho\pi^+\pi^+\pi^-$	( 2.2 $\pm$ 0.7 ) $\times 10^{-3}$		1880
$\bar{\Lambda}_c^- \rho\pi^+\pi^+\pi^-\pi^0$	< 1.34 %	CL=90%	1823
$\Lambda_c^+ \Lambda_c^- K^+$	( 8.7 $\pm$ 3.5 ) $\times 10^{-4}$		-
$\bar{\Sigma}_c(2455)^0 \rho$	( 3.7 $\pm$ 1.3 ) $\times 10^{-5}$		1938
$\bar{\Sigma}_c(2455)^0 \rho\pi^0$	( 4.4 $\pm$ 1.8 ) $\times 10^{-4}$		1896
$\bar{\Sigma}_c(2455)^0 \rho\pi^+\pi^-$	( 4.4 $\pm$ 1.7 ) $\times 10^{-4}$		1845
$\bar{\Sigma}_c(2455)^- \rho\pi^+\pi^+$	( 2.8 $\pm$ 1.2 ) $\times 10^{-4}$		1845
$\bar{\Lambda}_c(2593)^- / \bar{\Lambda}_c(2625)^- \rho\pi^+$	< 1.9 $\times 10^{-4}$	CL=90%	-
$\bar{\Xi}_c^0 \Lambda_c^+ \times B(\bar{\Xi}_c^0 \rightarrow \Xi^+ \pi^-)$	( 3.0 $\pm$ 1.1 ) $\times 10^{-5}$		1144
$\bar{\Xi}_c^0 \Lambda_c^+ \times B(\bar{\Xi}_c^0 \rightarrow \Lambda K^+ \pi^-)$	( 2.6 $\pm$ 1.1 ) $\times 10^{-5}$	S=1.1	1144

Lepton Family number (LF) or Lepton number (L) or Baryon number (B) violating modes, or/and  $\Delta B = 1$  weak neutral current (BI) modes

$\pi^+ \ell^+ \ell^-$	B1	< 4.9 $\times 10^{-8}$	CL=90%	2638
$\pi^+ e^+ e^-$	B1	< 8.0 $\times 10^{-8}$	CL=90%	2638
$\pi^+ \mu^+ \mu^-$	B1	< 6.9 $\times 10^{-8}$	CL=90%	2634
$\pi^+ \nu\bar{\nu}$	B1	< 1.0 $\times 10^{-4}$	CL=90%	2638
$K^+ \ell^+ \ell^-$	B1	[ppp] ( 5.1 $\pm$ 0.5 ) $\times 10^{-7}$		2617
$K^+ e^+ e^-$	B1	( 5.5 $\pm$ 0.7 ) $\times 10^{-7}$		2617
$K^+ \mu^+ \mu^-$	B1	( 4.8 $\pm$ 0.4 ) $\times 10^{-7}$		2612
$K^+ \bar{\nu}\nu$	B1	< 1.3 $\times 10^{-5}$	CL=90%	2617
$\rho^+ \nu\bar{\nu}$	B1	< 1.5 $\times 10^{-4}$	CL=90%	2583
$K^*(892)^+ \ell^+ \ell^-$	B1	[ppp] ( 1.29 $\pm$ 0.21 ) $\times 10^{-6}$		2564
$K^*(892)^+ e^+ e^-$	B1	( 1.55 $\begin{smallmatrix} +0.40 \\ -0.31 \end{smallmatrix}$ ) $\times 10^{-6}$		2564
$K^*(892)^+ \mu^+ \mu^-$	B1	( 1.07 $\pm$ 0.22 ) $\times 10^{-6}$		2560
$K^*(892)^+ \nu\bar{\nu}$	B1	< 8 $\times 10^{-5}$	CL=90%	2564
$\pi^+ e^+ \mu^-$	LF	< 6.4 $\times 10^{-3}$	CL=90%	2637
$\pi^+ e^- \mu^+$	LF	< 6.4 $\times 10^{-3}$	CL=90%	2637
$\pi^+ e^\pm \mu^\mp$	LF	< 1.7 $\times 10^{-7}$	CL=90%	2637
$K^+ e^+ \mu^-$	LF	< 9.1 $\times 10^{-8}$	CL=90%	2615
$K^+ e^- \mu^+$	LF	< 1.3 $\times 10^{-7}$	CL=90%	2615
$K^+ e^\pm \mu^\mp$	LF	< 9.1 $\times 10^{-8}$	CL=90%	2615
$K^+ \mu^\pm \tau^\mp$	LF	< 7.7 $\times 10^{-5}$	CL=90%	2298
$K^*(892)^+ e^+ \mu^-$	LF	< 1.3 $\times 10^{-6}$	CL=90%	2563

$K^*(892)^+ e^- \mu^+$	LF	< 9.9 $\times 10^{-7}$	CL=90%	2563
$K^*(892)^+ e^\pm \mu^\mp$	LF	< 1.4 $\times 10^{-6}$	CL=90%	2563
$\pi^- e^+ e^+$	L	< 1.6 $\times 10^{-6}$	CL=90%	2638
$\pi^- \mu^+ \mu^+$	L	< 4.4 $\times 10^{-8}$	CL=90%	2634
$\pi^- e^+ \mu^+$	L	< 1.3 $\times 10^{-6}$	CL=90%	2637
$\rho^- e^+ e^+$	L	< 2.6 $\times 10^{-6}$	CL=90%	2583
$\rho^- \mu^+ \mu^+$	L	< 5.0 $\times 10^{-6}$	CL=90%	2578
$\rho^- e^+ \mu^+$	L	< 3.3 $\times 10^{-6}$	CL=90%	2582
$K^- e^+ e^+$	L	< 1.0 $\times 10^{-6}$	CL=90%	2617
$K^- \mu^+ \mu^+$	L	< 4.1 $\times 10^{-8}$	CL=90%	2612
$K^- e^+ \mu^+$	L	< 2.0 $\times 10^{-6}$	CL=90%	2615
$K^*(892)^- e^+ e^+$	L	< 2.8 $\times 10^{-6}$	CL=90%	2564
$K^*(892)^- \mu^+ \mu^+$	L	< 8.3 $\times 10^{-6}$	CL=90%	2560
$K^*(892)^- e^+ \mu^+$	L	< 4.4 $\times 10^{-6}$	CL=90%	2563
$D^- e^+ e^+$	L	< 2.6 $\times 10^{-6}$	CL=90%	2309
$D^- e^+ \mu^+$	L	< 1.8 $\times 10^{-6}$	CL=90%	2307
$D^- \mu^+ \mu^+$	L	< 1.1 $\times 10^{-6}$	CL=90%	2303
$\Lambda^0 \mu^+$	L,B	< 6 $\times 10^{-8}$	CL=90%	-
$\Lambda^0 e^+$	L,B	< 3.2 $\times 10^{-8}$	CL=90%	-
$\bar{\Lambda}^0 \mu^+$	L,B	< 6 $\times 10^{-8}$	CL=90%	-
$\bar{\Lambda}^0 e^+$	L,B	< 8 $\times 10^{-8}$	CL=90%	-

$B^0$

$$I(J^P) = \frac{1}{2}(0^-)$$

$I, J, P$  need confirmation. Quantum numbers shown are quark-model predictions.

Mass  $m_{B^0} = 5279.58 \pm 0.17$  MeV  
 $m_{B^0} - m_{B^\pm} = 0.32 \pm 0.06$  MeV  
 Mean life  $\tau_{B^0} = (1.519 \pm 0.007) \times 10^{-12}$  s  
 $c\tau = 455.4$   $\mu$ m  
 $\tau_{B^+}/\tau_{B^0} = 1.079 \pm 0.007$  (direct measurements)

$B^0\text{-}\bar{B}^0$  mixing parameters

$\chi_d = 0.1862 \pm 0.0023$   
 $\Delta m_{B^0} = m_{B_H^0} - m_{B_L^0} = (0.507 \pm 0.004) \times 10^{12} \hbar s^{-1}$   
 $= (3.337 \pm 0.033) \times 10^{-10}$  MeV  
 $x_d = \Delta m_{B^0}/\Gamma_{B^0} = 0.770 \pm 0.008$   
 $\text{Re}(\lambda_{CP} / |\lambda_{CP}|) \text{Re}(z) = 0.01 \pm 0.05$   
 $\Delta\Gamma \text{Re}(z) = -0.007 \pm 0.004$   
 $\text{Re}(z) = (2 \pm 5) \times 10^{-2}$   
 $\text{Im}(z) = (-0.8 \pm 0.4) \times 10^{-2}$

CP violation parameters

$\text{Re}(\epsilon_{B^0}) / (1 + |\epsilon_{B^0}|^2) = (-0.8 \pm 0.8) \times 10^{-3}$   
 $A_{T/CP} = 0.005 \pm 0.018$   
 $A_{CP}(B^0 \rightarrow D^*(2010)^+ D^-) = 0.02 \pm 0.04$   
 $A_{CP}(B^0 \rightarrow K^+ \pi^-) = -0.097 \pm 0.012$   
 $A_{CP}(B^0 \rightarrow \eta' K^*(892)^0) = 0.02 \pm 0.23$   
 $A_{CP}(B^0 \rightarrow \eta' K_0^*(1430)^0) = -0.19 \pm 0.17$   
 $A_{CP}(B^0 \rightarrow \eta' K_2^*(1430)^0) = 0.14 \pm 0.18$   
 $A_{CP}(B^0 \rightarrow \eta K^*(892)^0) = 0.19 \pm 0.05$   
 $A_{CP}(B^0 \rightarrow \eta K_0^*(1430)^0) = 0.06 \pm 0.13$   
 $A_{CP}(B^0 \rightarrow \eta K_2^*(1430)^0) = -0.07 \pm 0.19$   
 $A_{CP}(B^0 \rightarrow b_1 K^+) = -0.07 \pm 0.12$   
 $A_{CP}(B^0 \rightarrow \omega K^*0) = 0.45 \pm 0.25$   
 $A_{CP}(B^0 \rightarrow \omega (K\pi)_0^0) = -0.07 \pm 0.09$   
 $A_{CP}(B^0 \rightarrow \omega K_2^*(1430)^0) = -0.37 \pm 0.17$   
 $A_{CP}(B^0 \rightarrow K^+ \pi^- \pi^0) = (0 \pm 6) \times 10^{-2}$   
 $A_{CP}(B^0 \rightarrow \rho^- K^+) = 0.20 \pm 0.11$   
 $A_{CP}(B^0 \rightarrow \rho(1450)^- K^+) = -0.10 \pm 0.33$   
 $A_{CP}(B^0 \rightarrow \rho(1700)^- K^+) = -0.4 \pm 0.6$   
 $A_{CP}(B^0 \rightarrow K^+ \pi^- \pi^0 \text{ nonresonant}) = 0.10 \pm 0.18$   
 $A_{CP}(B^0 \rightarrow K^0 \pi^+ \pi^-) = -0.01 \pm 0.05$   
 $A_{CP}(B^0 \rightarrow K^*(892)^+ \pi^-) = -0.22 \pm 0.06$   
 $A_{CP}(B^0 \rightarrow (K\pi)_0^+ \pi^-) = 0.09 \pm 0.07$   
 $A_{CP}(B^0 \rightarrow (K\pi)_0^0 \pi^0) = -0.15 \pm 0.11$   
 $A_{CP}(B^0 \rightarrow K^*0 \pi^0) = -0.15 \pm 0.13$   
 $A_{CP}(B^0 \rightarrow K^*(892)^0 \pi^+ \pi^-) = 0.07 \pm 0.05$   
 $A_{CP}(B^0 \rightarrow K^*(892)^0 \rho^0) = 0.09 \pm 0.19$   
 $A_{CP}(B^0 \rightarrow K^*0 f_0(980)) = -0.17 \pm 0.28$   
 $A_{CP}(B^0 \rightarrow K^*(892)^0 K^+ K^-) = 0.01 \pm 0.05$   
 $A_{CP}(B^0 \rightarrow a_1^- K^+) = -0.16 \pm 0.12$   
 $A_{CP}(B^0 \rightarrow K^0 K^0) = -0.6 \pm 0.7$   
 $A_{CP}(B^0 \rightarrow K^*(892)^0 \phi) = 0.01 \pm 0.05$

## Meson Summary Table

$A_{CP}(B^0 \rightarrow K^*(892)^0 K^- \pi^+) = 0.2 \pm 0.4$	$C_{K_S^0 \pi^0 \gamma}(B^0 \rightarrow K_S^0 \pi^0 \gamma) = 0.36 \pm 0.33$
$A_{CP}(B^0 \rightarrow \phi(K \pi)_0^0) = 0.20 \pm 0.15$	$S_{K_S^0 \pi^0 \gamma}(B^0 \rightarrow K_S^0 \pi^0 \gamma) = -0.8 \pm 0.6$
$A_{CP}(B^0 \rightarrow \phi K_2^*(1430)^0) = -0.08 \pm 0.13$	$C_{K^{*0} \gamma}(B^0 \rightarrow K^*(892)^0 \gamma) = -0.04 \pm 0.16 \quad (S = 1.2)$
$A_{CP}(B^0 \rightarrow K^*(892)^0 \gamma) = -0.016 \pm 0.023$	$S_{K^{*0} \gamma}(B^0 \rightarrow K^*(892)^0 \gamma) = -0.15 \pm 0.22$
$A_{CP}(B^0 \rightarrow K_2^*(1430)^0 \gamma) = -0.08 \pm 0.15$	$C_{\eta K^0 \gamma}(B^0 \rightarrow \eta K^0 \gamma) = -0.3 \pm 0.4$
$A_{CP}(B^0 \rightarrow \rho^+ \pi^-) = 0.08 \pm 0.12 \quad (S = 2.0)$	$S_{\eta K^0 \gamma}(B^0 \rightarrow \eta K^0 \gamma) = -0.2 \pm 0.5$
$A_{CP}(B^0 \rightarrow \rho^- \pi^+) = -0.16 \pm 0.23 \quad (S = 1.7)$	$C_{K^0 \phi \gamma}(B^0 \rightarrow K^0 \phi \gamma) = -0.3 \pm 0.6$
$A_{CP}(B^0 \rightarrow a_1(1260)^\pm \pi^\mp) = -0.07 \pm 0.07$	$S_{K^0 \phi \gamma}(B^0 \rightarrow K^0 \phi \gamma) = 0.7^{+0.7}_{-1.1}$
$A_{CP}(B^0 \rightarrow b_1 \pi^+) = -0.05 \pm 0.10$	$C(B^0 \rightarrow K_S^0 \rho^0 \gamma) = -0.05 \pm 0.19$
$A_{CP}(B^0 \rightarrow \rho \bar{\rho} K^*(892)^0) = 0.05 \pm 0.12$	$S(B^0 \rightarrow K_S^0 \rho^0 \gamma) = 0.11 \pm 0.34$
$A_{CP}(B^0 \rightarrow \rho \bar{\Lambda} \pi^-) = 0.04 \pm 0.07$	$C(B^0 \rightarrow \rho^0 \gamma) = 0.4 \pm 0.5$
$A_{CP}(B^0 \rightarrow K^{*0} \ell^+ \ell^-) = -0.05 \pm 0.10$	$S(B^0 \rightarrow \rho^0 \gamma) = -0.8 \pm 0.7$
$A_{CP}(B^0 \rightarrow K^{*0} e^+ e^-) = -0.21 \pm 0.19$	$C_{\pi \pi}(B^0 \rightarrow \pi^+ \pi^-) = -0.38 \pm 0.17 \quad (S = 2.6)$
$A_{CP}(B^0 \rightarrow K^{*0} \mu^+ \mu^-) = 0.00 \pm 0.15$	<b><math>S_{\pi \pi}(B^0 \rightarrow \pi^+ \pi^-) = -0.61 \pm 0.08</math></b>
$C_{D^{*+} D^+}(B^0 \rightarrow D^*(2010)^- D^+) = 0.07 \pm 0.14$	$C_{\pi^0 \pi^0}(B^0 \rightarrow \pi^0 \pi^0) = -0.48 \pm 0.30$
<b><math>S_{D^{*+} D^+}(B^0 \rightarrow D^*(2010)^- D^+) = -0.78 \pm 0.21</math></b>	$C_{\rho \pi}(B^0 \rightarrow \rho^+ \pi^-) = 0.01 \pm 0.14 \quad (S = 1.9)$
$C_{D^{*+} D^-}(B^0 \rightarrow D^*(2010)^+ D^-) = -0.09 \pm 0.22 \quad (S = 1.6)$	$S_{\rho \pi}(B^0 \rightarrow \rho^+ \pi^-) = 0.01 \pm 0.09$
<b><math>S_{D^{*+} D^-}(B^0 \rightarrow D^*(2010)^+ D^-) = -0.61 \pm 0.19</math></b>	<b><math>\Delta C_{\rho \pi}(B^0 \rightarrow \rho^+ \pi^-) = 0.37 \pm 0.08</math></b>
$C_{D^{*+} D^{*-}}(B^0 \rightarrow D^{*+} D^{*-}) = -0.01 \pm 0.09 \quad (S = 1.2)$	$\Delta S_{\rho \pi}(B^0 \rightarrow \rho^+ \pi^-) = -0.05 \pm 0.10$
<b><math>S_{D^{*+} D^{*-}}(B^0 \rightarrow D^{*+} D^{*-}) = -0.76 \pm 0.14</math></b>	$C_{\rho^0 \pi^0}(B^0 \rightarrow \rho^0 \pi^0) = 0.3 \pm 0.4$
$C_+(B^0 \rightarrow D^{*+} D^{*-}) = 0.00 \pm 0.12$	$S_{\rho^0 \pi^0}(B^0 \rightarrow \rho^0 \pi^0) = 0.1 \pm 0.4$
<b><math>S_+(B^0 \rightarrow D^{*+} D^{*-}) = -0.76 \pm 0.16</math></b>	$C_{a_1 \pi}(B^0 \rightarrow a_1(1260)^+ \pi^-) = -0.10 \pm 0.17$
$C_-(B^0 \rightarrow D^{*+} D^{*-}) = 0.4 \pm 0.5$	$S_{a_1 \pi}(B^0 \rightarrow a_1(1260)^+ \pi^-) = 0.37 \pm 0.22$
$S_-(B^0 \rightarrow D^{*+} D^{*-}) = -1.8 \pm 0.7$	$\Delta C_{a_1 \pi}(B^0 \rightarrow a_1(1260)^+ \pi^-) = 0.26 \pm 0.17$
$C(B^0 \rightarrow D^*(2010)^+ D^*(2010)^- K_S^0) = 0.01 \pm 0.29$	$\Delta S_{a_1 \pi}(B^0 \rightarrow a_1(1260)^+ \pi^-) = -0.14 \pm 0.22$
$S(B^0 \rightarrow D^*(2010)^+ D^*(2010)^- K_S^0) = 0.1 \pm 0.4$	$C(B^0 \rightarrow b_1^- K^+) = -0.22 \pm 0.24$
$C_{D^+ D^-}(B^0 \rightarrow D^+ D^-) = -0.5 \pm 0.4 \quad (S = 2.5)$	$\Delta C(B^0 \rightarrow b_1^- \pi^+) = -1.04 \pm 0.24$
<b><math>S_{D^+ D^-}(B^0 \rightarrow D^+ D^-) = -0.87 \pm 0.26</math></b>	$C_{\rho^0 \rho^0}(B^0 \rightarrow \rho^0 \rho^0) = 0.2 \pm 0.9$
$C_{J/\psi(1S) \pi^0}(B^0 \rightarrow J/\psi(1S) \pi^0) = -0.13 \pm 0.13$	$S_{\rho^0 \rho^0}(B^0 \rightarrow \rho^0 \rho^0) = 0.3 \pm 0.7$
<b><math>S_{J/\psi(1S) \pi^0}(B^0 \rightarrow J/\psi(1S) \pi^0) = -0.94 \pm 0.29 \quad (S = 1.9)</math></b>	$C_{\rho \rho}(B^0 \rightarrow \rho^+ \rho^-) = -0.05 \pm 0.13$
$C_{D_{CP}^*(*) h^0}(B^0 \rightarrow D_{CP}^*(*) h^0) = -0.23 \pm 0.16$	$S_{\rho \rho}(B^0 \rightarrow \rho^+ \rho^-) = -0.06 \pm 0.17$
$S_{D_{CP}^*(*) h^0}(B^0 \rightarrow D_{CP}^*(*) h^0) = -0.56 \pm 0.24$	$ \lambda (B^0 \rightarrow J/\psi K^*(892)^0) < 0.25, \text{CL} = 95\%$
$C_{K^0 \pi^0}(B^0 \rightarrow K^0 \pi^0) = 0.00 \pm 0.13 \quad (S = 1.4)$	$\cos 2\beta(B^0 \rightarrow J/\psi K^*(892)^0) = 1.7^{+0.7}_{-0.9} \quad (S = 1.6)$
<b><math>S_{K^0 \pi^0}(B^0 \rightarrow K^0 \pi^0) = 0.58 \pm 0.17</math></b>	$\cos 2\beta(B^0 \rightarrow [K_S^0 \pi^+ \pi^-]_{D^{(*)} h^0}) = 1.0^{+0.6}_{-0.7} \quad (S = 1.8)$
$C_{\eta'(958) K_S^0}(B^0 \rightarrow \eta'(958) K_S^0) = -0.04 \pm 0.20 \quad (S = 2.5)$	$(S_+ + S_-)/2(B^0 \rightarrow D^* \pi^+) = -0.039 \pm 0.011$
$S_{\eta'(958) K_S^0}(B^0 \rightarrow \eta'(958) K_S^0) = 0.43 \pm 0.17 \quad (S = 1.5)$	$(S_- - S_+)/2(B^0 \rightarrow D^* \pi^+) = -0.009 \pm 0.015$
$C_{\eta' K^0}(B^0 \rightarrow \eta' K^0) = -0.05 \pm 0.05$	$(S_+ + S_-)/2(B^0 \rightarrow D^- \pi^+) = -0.046 \pm 0.023$
<b><math>S_{\eta' K^0}(B^0 \rightarrow \eta' K^0) = 0.60 \pm 0.07</math></b>	$(S_- - S_+)/2(B^0 \rightarrow D^- \pi^+) = -0.022 \pm 0.021$
$C_{\omega K_S^0}(B^0 \rightarrow \omega K_S^0) = -0.30 \pm 0.28 \quad (S = 1.6)$	$(S_+ + S_-)/2(B^0 \rightarrow D^- \rho^+) = -0.024 \pm 0.032$
$S_{\omega K_S^0}(B^0 \rightarrow \omega K_S^0) = 0.43 \pm 0.24$	$(S_- - S_+)/2(B^0 \rightarrow D^- \rho^+) = -0.10 \pm 0.06$
$C(B^0 \rightarrow K_S^0 \pi^0 \pi^0) = 0.2 \pm 0.5$	$C_{\eta_c K_S^0}(B^0 \rightarrow \eta_c K_S^0) = 0.08 \pm 0.13$
$S(B^0 \rightarrow K_S^0 \pi^0 \pi^0) = 0.7 \pm 0.7$	<b><math>S_{\eta_c K_S^0}(B^0 \rightarrow \eta_c K_S^0) = 0.93 \pm 0.17</math></b>
$C_{\rho^0 K_S^0}(B^0 \rightarrow \rho^0 K_S^0) = -0.04 \pm 0.20$	$C_{c \bar{c} K^{(*)0}}(B^0 \rightarrow c \bar{c} K^{(*)0}) = (0.5 \pm 1.7) \times 10^{-2}$
$S_{\rho^0 K_S^0}(B^0 \rightarrow \rho^0 K_S^0) = 0.50^{+0.17}_{-0.21}$	$\sin(2\beta) = 0.679 \pm 0.020$
$C_{f_0 K_S^0}(B^0 \rightarrow f_0(980) K_S^0) = 0.14 \pm 0.17$	$C_{J/\psi(nS) K^0}(B^0 \rightarrow J/\psi(nS) K^0) = (0.5 \pm 2.0) \times 10^{-2}$
$S_{f_0 K_S^0}(B^0 \rightarrow f_0(980) K_S^0) = -0.73^{+0.27}_{-0.09} \quad (S = 1.6)$	<b><math>S_{J/\psi(nS) K^0}(B^0 \rightarrow J/\psi(nS) K^0) = 0.676 \pm 0.021</math></b>
$S_{f_2 K_S^0}(B^0 \rightarrow f_2(1270) K_S^0) = -0.5 \pm 0.5$	$C_{J/\psi K^{*0}}(B^0 \rightarrow J/\psi K^{*0}) = 0.03 \pm 0.10$
$C_{f_2 K_S^0}(B^0 \rightarrow f_2(1270) K_S^0) = 0.3 \pm 0.4$	$S_{J/\psi K^{*0}}(B^0 \rightarrow J/\psi K^{*0}) = 0.60 \pm 0.25$
$S_{f_x K_S^0}(B^0 \rightarrow f_x(1300) K_S^0) = -0.2 \pm 0.5$	$C_{\chi_{c0} K_S^0}(B^0 \rightarrow \chi_{c0} K_S^0) = -0.3^{+0.5}_{-0.4}$
$C_{f_x K_S^0}(B^0 \rightarrow f_x(1300) K_S^0) = 0.13 \pm 0.35$	$S_{\chi_{c0} K_S^0}(B^0 \rightarrow \chi_{c0} K_S^0) = -0.7 \pm 0.5$
$S_{K^0 \pi^+ \pi^-}(B^0 \rightarrow K^0 \pi^+ \pi^- \text{ nonresonant}) = -0.01 \pm 0.33$	$C_{\chi_{c1} K_S^0}(B^0 \rightarrow \chi_{c1} K_S^0) = 0.13 \pm 0.11$
$C_{K^0 \pi^+ \pi^-}(B^0 \rightarrow K^0 \pi^+ \pi^- \text{ nonresonant}) = 0.01 \pm 0.26$	<b><math>S_{\chi_{c1} K_S^0}(B^0 \rightarrow \chi_{c1} K_S^0) = 0.61 \pm 0.16</math></b>
$C_{K_S^0 K_S^0}(B^0 \rightarrow K_S^0 K_S^0) = 0.0 \pm 0.4 \quad (S = 1.4)$	$\sin(2\beta_{\text{eff}})(B^0 \rightarrow \phi K^0) = 0.22 \pm 0.30$
$S_{K_S^0 K_S^0}(B^0 \rightarrow K_S^0 K_S^0) = -0.8 \pm 0.5$	$\sin(2\beta_{\text{eff}})(B^0 \rightarrow \phi K_S^0(1430)^0) = 0.97^{+0.03}_{-0.52}$
$C_{K^+ K^- K_S^0}(B^0 \rightarrow K^+ K^- K_S^0 \text{ nonresonant}) = 0.09 \pm 0.09$	<b><math>\sin(2\beta_{\text{eff}})(B^0 \rightarrow K^+ K^- K_S^0) = 0.77^{+0.13}_{-0.12}</math></b>
<b><math>S_{K^+ K^- K_S^0}(B^0 \rightarrow K^+ K^- K_S^0 \text{ nonresonant}) = -0.74^{+0.12}_{-0.10}</math></b>	$\sin(2\beta_{\text{eff}})(B^0 \rightarrow [K_S^0 \pi^+ \pi^-]_{D^{(*)} h^0}) = 0.45 \pm 0.28$
$C_{K^+ K^- K_S^0}(B^0 \rightarrow K^+ K^- K_S^0 \text{ inclusive}) = 0.01 \pm 0.09$	$ \lambda (B^0 \rightarrow [K_S^0 \pi^+ \pi^-]_{D^{(*)} h^0}) = 1.01 \pm 0.08$
<b><math>S_{K^+ K^- K_S^0}(B^0 \rightarrow K^+ K^- K_S^0 \text{ inclusive}) = -0.65 \pm 0.12</math></b>	$ \sin(2\beta + \gamma)  > 0.40, \text{CL} = 90\%$
$C_{\phi K_S^0}(B^0 \rightarrow \phi K_S^0) = 0.03 \pm 0.14$	$2\beta + \gamma = (83 \pm 60)^\circ$
$S_{\phi K_S^0}(B^0 \rightarrow \phi K_S^0) = 0.39 \pm 0.17$	$\gamma(B^0 \rightarrow D^0 K^{*0}) = (162 \pm 60)^\circ$
$C_{K_S K_S K_S}(B^0 \rightarrow K_S K_S K_S) = -0.15 \pm 0.16 \quad (S = 1.1)$	$\alpha = (90 \pm 5)^\circ$
$S_{K_S K_S K_S}(B^0 \rightarrow K_S K_S K_S) = -0.4 \pm 0.5 \quad (S = 2.5)$	

## Meson Summary Table

$\bar{B}^0$  modes are charge conjugates of the modes below. Reactions indicate the weak decay vertex and do not include mixing. Modes which do not identify the charge state of the  $B$  are listed in the  $B^\pm/B^0$  ADMIXTURE section.

The branching fractions listed below assume 50%  $B^0\bar{B}^0$  and 50%  $B^+B^-$  production at the  $\Upsilon(4S)$ . We have attempted to bring older measurements up to date by rescaling their assumed  $\Upsilon(4S)$  production ratio to 50:50 and their assumed  $D, D_s, D^*$ , and  $\psi$  branching ratios to current values whenever this would affect our averages and best limits significantly.

Indentation is used to indicate a subchannel of a previous reaction. All resonant subchannels have been corrected for resonance branching fractions to the final state so the sum of the subchannel branching fractions can exceed that of the final state.

For inclusive branching fractions, e.g.,  $B \rightarrow D^\pm$  anything, the values usually are multiplicities, not branching fractions. They can be greater than one.

$B^0$ DECAY MODES	Fraction ( $\Gamma_i/\Gamma$ )	Scale factor / Confidence level	$p$ (MeV/c)
$\ell^+ \nu_\ell$ anything	[ppp] ( 10.33 ± 0.28 ) %	–	–
$e^+ \nu_e X_c$	( 10.1 ± 0.4 ) %	–	–
$D \ell^+ \nu_\ell$ anything	( 9.2 ± 0.8 ) %	–	–
$D^- \ell^+ \nu_\ell$	[ppp] ( 2.18 ± 0.12 ) %	2309	–
$D^- \tau^+ \nu_\tau$	( 1.1 ± 0.4 ) %	1909	–
$D^*(2010)^- \ell^+ \nu_\ell$	[ppp] ( 4.95 ± 0.11 ) %	2257	–
$D^*(2010)^- \tau^+ \nu_\tau$	( 1.5 ± 0.5 ) %	S=1.4 1837	–
$\bar{D}^0 \pi^- \ell^+ \nu_\ell$	( 4.3 ± 0.6 ) × 10 <sup>-3</sup>	2308	–
$D_0^*(2400)^- \ell^+ \nu_\ell \times$ B( $D_0^{*-} \rightarrow \bar{D}^0 \pi^-$ )	( 3.0 ± 1.2 ) × 10 <sup>-3</sup>	S=1.8	–
$D_2^*(2460)^- \ell^+ \nu_\ell \times$ B( $D_2^{*-} \rightarrow \bar{D}^0 \pi^-$ )	( 1.21 ± 0.33 ) × 10 <sup>-3</sup>	S=1.8	2065
$\bar{D}^{(*)0} n \pi \ell^+ \nu_\ell$ ( $n \geq 1$ )	( 2.3 ± 0.5 ) %	–	–
$\bar{D}^{*0} \pi^- \ell^+ \nu_\ell$	( 4.9 ± 0.8 ) × 10 <sup>-3</sup>	2256	–
$D_1(2420)^- \ell^+ \nu_\ell \times$ B( $D_1^- \rightarrow \bar{D}^{*0} \pi^-$ )	( 2.80 ± 0.28 ) × 10 <sup>-3</sup>	–	–
$D_1'(2430)^- \ell^+ \nu_\ell \times$ B( $D_1'^- \rightarrow \bar{D}^{*0} \pi^-$ )	( 3.1 ± 0.9 ) × 10 <sup>-3</sup>	–	–
$D_2^*(2460)^- \ell^+ \nu_\ell \times$ B( $D_2^{*-} \rightarrow \bar{D}^{*0} \pi^-$ )	( 6.8 ± 1.2 ) × 10 <sup>-4</sup>	2065	–
$\rho^- \ell^+ \nu_\ell$	[ppp] ( 2.34 ± 0.28 ) × 10 <sup>-4</sup>	2583	–
$\pi^- \ell^+ \nu_\ell$	[ppp] ( 1.44 ± 0.05 ) × 10 <sup>-4</sup>	2638	–
<b>Inclusive modes</b>			
$K^\pm$ anything	( 78 ± 8 ) %	–	–
$D^0 X$	( 8.1 ± 1.5 ) %	–	–
$\bar{D}^0 X$	( 47.4 ± 2.8 ) %	–	–
$D^+ X$	< 3.9 %	CL=90%	–
$D^- X$	( 36.9 ± 3.3 ) %	–	–
$D_s^+ X$	( 10.3 ± 2.1 ) %	–	–
$D_s^- X$	< 2.6 %	CL=90%	–
$A_c^+ X$	< 3.1 %	CL=90%	–
$\bar{A}_c^- X$	( 5.0 ± 2.1 ) %	–	–
$\bar{c} X$	( 95 ± 5 ) %	–	–
$c X$	( 24.6 ± 3.1 ) %	–	–
$\bar{c} c X$	( 119 ± 6 ) %	–	–
<b>D, D*, or D<sub>s</sub> modes</b>			
$D^- \pi^+$	( 2.68 ± 0.13 ) × 10 <sup>-3</sup>	2306	–
$D^- \rho^+$	( 7.8 ± 1.3 ) × 10 <sup>-3</sup>	2235	–
$D^- K^0 \pi^+$	( 4.9 ± 0.9 ) × 10 <sup>-4</sup>	2259	–
$D^- K^*(892)^+$	( 4.5 ± 0.7 ) × 10 <sup>-4</sup>	2211	–
$D^- \omega \pi^+$	( 2.8 ± 0.6 ) × 10 <sup>-3</sup>	2204	–
$D^- K^+$	( 1.97 ± 0.21 ) × 10 <sup>-4</sup>	2279	–
$D^- K^+ \bar{K}^0$	< 3.1 × 10 <sup>-4</sup>	CL=90%	2188
$D^- K^+ \bar{K}^*(892)^0$	( 8.8 ± 1.9 ) × 10 <sup>-4</sup>	2070	–
$\bar{D}^0 \pi^+ \pi^-$	( 8.4 ± 0.9 ) × 10 <sup>-4</sup>	2301	–
$D^*(2010)^- \pi^+$	( 2.76 ± 0.13 ) × 10 <sup>-3</sup>	2255	–
$D^- \pi^+ \pi^+ \pi^-$	( 6.4 ± 0.7 ) × 10 <sup>-3</sup>	2287	–
( $D^- \pi^+ \pi^+ \pi^-$ ) nonresonant	( 3.9 ± 1.9 ) × 10 <sup>-3</sup>	2287	–
$D^- \pi^+ \rho^0$	( 1.1 ± 1.0 ) × 10 <sup>-3</sup>	2206	–
$D^- a_1(1260)^+$	( 6.0 ± 3.3 ) × 10 <sup>-3</sup>	2121	–
$D^*(2010)^- \pi^+ \pi^0$	( 1.5 ± 0.5 ) %	2247	–
$D^*(2010)^- \rho^+$	( 6.8 ± 0.9 ) × 10 <sup>-3</sup>	2180	–
$D^*(2010)^- K^+$	( 2.14 ± 0.16 ) × 10 <sup>-4</sup>	2226	–
$D^*(2010)^- K^0 \pi^+$	( 3.0 ± 0.8 ) × 10 <sup>-4</sup>	2205	–
$D^*(2010)^- K^*(892)^+$	( 3.3 ± 0.6 ) × 10 <sup>-4</sup>	2155	–

$D^*(2010)^- K^+ \bar{K}^0$	< 4.7 × 10 <sup>-4</sup>	CL=90%	2131
$D^*(2010)^- K^+ \bar{K}^*(892)^0$	( 1.29 ± 0.33 ) × 10 <sup>-3</sup>	–	2007
$D^*(2010)^- \pi^+ \pi^+ \pi^-$	( 7.0 ± 0.8 ) × 10 <sup>-3</sup>	S=1.3	2235
( $D^*(2010)^- \pi^+ \pi^+ \pi^-$ ) non-resonant	( 0.0 ± 2.5 ) × 10 <sup>-3</sup>	–	2235
$D^*(2010)^- \pi^+ \rho^0$	( 5.7 ± 3.2 ) × 10 <sup>-3</sup>	–	2150
$D^*(2010)^- a_1(1260)^+$	( 1.30 ± 0.27 ) %	–	2061
$D^*(2010)^- \pi^+ \pi^+ \pi^- \pi^0$	( 1.76 ± 0.27 ) %	–	2218
$D^*- 3\pi^+ 2\pi^-$	( 4.7 ± 0.9 ) × 10 <sup>-3</sup>	–	2195
$\bar{D}^*(2010)^- \omega \pi^+$	( 2.89 ± 0.30 ) × 10 <sup>-3</sup>	–	2148
$D_1(2430)^0 \omega \times$ B( $D_1(2430)^0 \rightarrow$ $D^{*-} \pi^+$ )	( 4.1 ± 1.6 ) × 10 <sup>-4</sup>	–	1992
$\bar{D}^{*-} \pi^+$	[ttt] ( 2.1 ± 1.0 ) × 10 <sup>-3</sup>	–	–
$D_1(2420)^- \pi^+ \times$ B( $D_1^- \rightarrow$ $D^- \pi^+ \pi^-$ )	( 1.00 ± 0.21 ) × 10 <sup>-4</sup>	–	–
$D_1(2420)^- \pi^+ \times$ B( $D_1^- \rightarrow$ $D^* \pi^+ \pi^-$ )	< 3.3 × 10 <sup>-5</sup>	CL=90%	–
$\bar{D}_2^*(2460)^- \pi^+ \times$ B( $D_2^*(2460)^- \rightarrow D^0 \pi^-$ )	( 2.15 ± 0.35 ) × 10 <sup>-4</sup>	–	2062
$\bar{D}_0^*(2400)^- \pi^+ \times$ B( $D_0^*(2400)^- \rightarrow D^0 \pi^-$ )	( 6.0 ± 3.0 ) × 10 <sup>-5</sup>	–	2090
$D_2^*(2460)^- \pi^+ \times$ B( $(D_2^*)^- \rightarrow$ $D^* \pi^+ \pi^-$ )	< 2.4 × 10 <sup>-5</sup>	CL=90%	–
$\bar{D}_2^*(2460)^- \rho^+$	< 4.9 × 10 <sup>-3</sup>	CL=90%	1975
$D^0 \bar{D}^0$	< 4.3 × 10 <sup>-5</sup>	CL=90%	1868
$D^{*0} \bar{D}^0$	< 2.9 × 10 <sup>-4</sup>	CL=90%	1794
$D^- D^+$	( 2.11 ± 0.31 ) × 10 <sup>-4</sup>	S=1.2	1864
$D^- D_s^+$	( 7.2 ± 0.8 ) × 10 <sup>-3</sup>	–	1812
$D^*(2010)^- D_s^+$	( 8.0 ± 1.1 ) × 10 <sup>-3</sup>	–	1735
$D^- D_s^{*+}$	( 7.4 ± 1.6 ) × 10 <sup>-3</sup>	–	1732
$D^*(2010)^- D_s^{*+}$	( 1.77 ± 0.14 ) %	–	1649
$D_{s0}(2317)^- K^+ \times$ B( $D_{s0}(2317)^- \rightarrow D_s^- \pi^0$ )	( 4.2 ± 1.4 ) × 10 <sup>-5</sup>	–	2097
$D_{s0}(2317)^- \pi^+ \times$ B( $D_{s0}(2317)^- \rightarrow D_s^- \pi^0$ )	< 2.5 × 10 <sup>-5</sup>	CL=90%	2128
$D_{sJ}(2457)^- K^+ \times$ B( $D_{sJ}(2457)^- \rightarrow D_s^- \pi^0$ )	< 9.4 × 10 <sup>-6</sup>	CL=90%	–
$D_{sJ}(2457)^- \pi^+ \times$ B( $D_{sJ}(2457)^- \rightarrow D_s^- \pi^0$ )	< 4.0 × 10 <sup>-6</sup>	CL=90%	–
$D_s^- D_s^+$	< 3.6 × 10 <sup>-5</sup>	CL=90%	1759
$D_s^{*-} D_s^+$	< 1.3 × 10 <sup>-4</sup>	CL=90%	1674
$D_s^{*0} D_s^+$	< 2.4 × 10 <sup>-4</sup>	CL=90%	1583
$D_{s0}(2317)^+ D^- \times$ B( $D_{s0}(2317)^+ \rightarrow D_s^+ \pi^0$ )	( 9.7 ± 4.0 ) × 10 <sup>-4</sup>	S=1.5	1602
$D_{s0}(2317)^+ D^- \times$ B( $D_{s0}(2317)^+ \rightarrow D_s^{*+} \gamma$ )	< 9.5 × 10 <sup>-4</sup>	CL=90%	–
$D_{s0}(2317)^+ D^*(2010)^- \times$ B( $D_{s0}(2317)^+ \rightarrow D_s^+ \pi^0$ )	( 1.5 ± 0.6 ) × 10 <sup>-3</sup>	–	1509
$D_{sJ}(2457)^+ D^-$	( 3.5 ± 1.1 ) × 10 <sup>-3</sup>	–	–
$D_{sJ}(2457)^+ D^- \times$ B( $D_{sJ}(2457)^+ \rightarrow D_s^+ \gamma$ )	( 6.5 ± 1.7 ) × 10 <sup>-4</sup>	–	–
$D_{sJ}(2457)^+ D^- \times$ B( $D_{sJ}(2457)^+ \rightarrow D_s^{*+} \gamma$ )	< 6.0 × 10 <sup>-4</sup>	CL=90%	–
$D_{sJ}(2457)^+ D^- \times$ B( $D_{sJ}(2457)^+ \rightarrow D_s^{*+} \gamma$ )	< 2.0 × 10 <sup>-4</sup>	CL=90%	–
$D_{sJ}(2457)^+ D^- \times$ B( $D_{sJ}(2457)^+ \rightarrow D_s^+ \pi^0$ )	< 3.6 × 10 <sup>-4</sup>	CL=90%	–
$D^*(2010)^- D_{sJ}(2457)^+$	( 9.3 ± 2.2 ) × 10 <sup>-3</sup>	–	–
$D_{sJ}(2457)^+ D^*(2010)^- \times$ B( $D_{sJ}(2457)^+ \rightarrow D_s^+ \gamma$ )	( 2.3 ± 0.9 ) × 10 <sup>-3</sup>	–	–
$D^- D_{s1}(2536)^+ \times$ B( $D_{s1}(2536)^+ \rightarrow D^{*0} K^+$ + $D^{*+} K^0$ )	( 2.8 ± 0.7 ) × 10 <sup>-4</sup>	–	1444
$D^- D_{s1}(2536)^+ \times$ B( $D_{s1}(2536)^+ \rightarrow$ $D^{*0} K^+$ )	( 1.7 ± 0.6 ) × 10 <sup>-4</sup>	–	1444
$D^- D_{s1}(2536)^+ \times$ B( $D_{s1}(2536)^+ \rightarrow$ $D^{*+} K^0$ )	( 2.6 ± 1.1 ) × 10 <sup>-4</sup>	–	1444

## Meson Summary Table

$D^*(2010)^- D_{s1}(2536)^+ \times$ $B(D_{s1}(2536)^+ \rightarrow D^0 K^+ + D^{*+} K^0)$	$(5.0 \pm 1.4) \times 10^{-4}$	1336	$\bar{D}^0 D^*(2007)^0 K^0 + \bar{D}^*(2007)^0 D^0 K^0$	$(1.1 \pm 0.5) \times 10^{-3}$	1478
$D^*(2010)^- D_{s1}(2536)^+ \times$ $B(D_{s1}(2536)^+ \rightarrow D^{*0} K^+)$	$(3.3 \pm 1.1) \times 10^{-4}$	1336	$\bar{D}^*(2007)^0 D^*(2007)^0 K^0$ $(\bar{D} + \bar{D}^*)(D + D^*) K$	$(2.4 \pm 0.9) \times 10^{-3}$ $(3.68 \pm 0.26) \%$	1365 -
$D^* D_{s1}(2536)^+ \times$ $B(D_{s1}(2536)^+ \rightarrow D^{*+} K^0)$	$(5.0 \pm 1.7) \times 10^{-4}$	1336	<b>Charmonium modes</b>		
$D^- D_{sJ}(2573)^+ \times$ $B(D_{sJ}(2573)^+ \rightarrow D^0 K^+)$	$< 1 \times 10^{-4}$	CL=90% 1414	$\eta_c K^0$	$(8.3 \pm 1.2) \times 10^{-4}$	1752
$D^*(2010)^- D_{sJ}(2573)^+ \times$ $B(D_{sJ}(2573)^+ \rightarrow D^0 K^+)$	$< 2 \times 10^{-4}$	CL=90% 1304	$\eta_c K^*(892)^0$	$(6.4 \pm 0.9) \times 10^{-4}$	1648
$D^+ \pi^-$	$(7.8 \pm 1.4) \times 10^{-7}$	2306	$\eta_c(2S) K^{*0}$	$< 3.9 \times 10^{-4}$	CL=90% 1157
$D_s^+ \pi^-$	$(2.16 \pm 0.26) \times 10^{-5}$	2270	$h_c(1P) K^{*0}$	$< 4 \times 10^{-4}$	CL=90% 1253
$D_s^{*+} \pi^-$	$(2.1 \pm 0.4) \times 10^{-5}$	S=1.4 2215	$J/\psi(1S) K^0$	$(8.74 \pm 0.32) \times 10^{-4}$	1683
$D_s^+ \rho^-$	$< 2.4 \times 10^{-5}$	CL=90% 2197	$J/\psi(1S) K^+ \pi^-$	$(1.2 \pm 0.6) \times 10^{-3}$	1652
$D_s^{*+} \rho^-$	$(4.1 \pm 1.3) \times 10^{-5}$	2138	$J/\psi(1S) K^*(892)^0$	$(1.34 \pm 0.06) \times 10^{-3}$	1571
$D_s^+ a_0^-$	$< 1.9 \times 10^{-5}$	CL=90% -	$J/\psi(1S) \eta K_S^0$	$(8 \pm 4) \times 10^{-5}$	1508
$D_s^{*+} a_0^-$	$< 3.6 \times 10^{-5}$	CL=90% -	$J/\psi(1S) \eta' K_S^0$	$< 2.5 \times 10^{-5}$	CL=90% 1271
$D_s^+ a_1(1260)^-$	$< 2.1 \times 10^{-3}$	CL=90% 2080	$J/\psi(1S) \phi K^0$	$(9.4 \pm 2.6) \times 10^{-5}$	1224
$D_s^{*+} a_1(1260)^-$	$< 1.7 \times 10^{-3}$	CL=90% 2015	$J/\psi(1S) \omega K^0$	$(2.3 \pm 0.4) \times 10^{-4}$	1386
$D_s^+ a_2^-$	$< 1.9 \times 10^{-4}$	CL=90% -	$X(3872) K^0 \times B(X \rightarrow J/\psi \omega)$	$(6.0 \pm 3.2) \times 10^{-6}$	1140
$D_s^{*+} a_2^-$	$< 2.0 \times 10^{-4}$	CL=90% -	$X(3915) K^0 \times B(X \rightarrow J/\psi \omega)$	$(2.1 \pm 0.9) \times 10^{-5}$	1103
$D_s^- K^+$	$(2.2 \pm 0.5) \times 10^{-5}$	S=1.8 2242	$J/\psi(1S) K(1270)^0$	$(1.3 \pm 0.5) \times 10^{-3}$	1390
$D_s^- K^+$	$(2.19 \pm 0.30) \times 10^{-5}$	2185	$J/\psi(1S) \pi^0$	$(1.76 \pm 0.16) \times 10^{-5}$	S=1.1 1728
$D_s^- K^*(892)^+$	$(3.5 \pm 1.0) \times 10^{-5}$	2172	$J/\psi(1S) \eta$	$(9.5 \pm 1.9) \times 10^{-6}$	1672
$D_s^{*-} K^*(892)^+$	$(3.2 \pm 1.5) \times 10^{-5}$	2112	$J/\psi(1S) \pi^+ \pi^-$	$(4.6 \pm 0.9) \times 10^{-5}$	1716
$D_s^- \pi^+ K^0$	$(1.10 \pm 0.33) \times 10^{-4}$	2222	$J/\psi(1S) \pi^+ \pi^-$ nonresonant	$< 1.2 \times 10^{-5}$	CL=90% 1716
$D_s^{*-} \pi^+ K^0$	$< 1.10 \times 10^{-4}$	CL=90% 2164	$J/\psi(1S) f_2$	$< 4.6 \times 10^{-6}$	CL=90% -
$D_s^- \pi^+ K^*(892)^0$	$< 3.0 \times 10^{-3}$	CL=90% 2138	$J/\psi(1S) \rho^0$	$(2.7 \pm 0.4) \times 10^{-5}$	1612
$D_s^{*-} \pi^+ K^*(892)^0$	$< 1.6 \times 10^{-3}$	CL=90% 2076	$J/\psi(1S) \omega$	$< 2.7 \times 10^{-4}$	CL=90% 1609
$\bar{D}^0 K^0$	$(5.2 \pm 0.7) \times 10^{-5}$	2280	$J/\psi(1S) \phi$	$< 9.4 \times 10^{-7}$	CL=90% 1520
$\bar{D}^0 K^+ \pi^-$	$(8.8 \pm 1.7) \times 10^{-5}$	2261	$J/\psi(1S) \eta'(958)$	$< 6.3 \times 10^{-5}$	CL=90% 1546
$\bar{D}^0 K^*(892)^0$	$(4.2 \pm 0.6) \times 10^{-5}$	2213	$J/\psi(1S) K^0 \pi^+ \pi^-$	$(1.0 \pm 0.4) \times 10^{-3}$	1611
$D_2^*(2460)^- K^+ \times$ $B(D_2^*(2460)^- \rightarrow \bar{D}^0 \pi^-)$	$(1.8 \pm 0.5) \times 10^{-5}$	2028	$J/\psi(1S) K^0 \rho^0$	$(5.4 \pm 3.0) \times 10^{-4}$	1390
$\bar{D}^0 K^+ \pi^-$ non-resonant	$< 3.7 \times 10^{-5}$	CL=90% -	$J/\psi(1S) K^*(892)^+ \pi^-$	$(8 \pm 4) \times 10^{-4}$	1514
$\bar{D}^0 \pi^0$	$(2.63 \pm 0.14) \times 10^{-4}$	2308	$J/\psi(1S) K^*(892)^0 \pi^+ \pi^-$	$(6.6 \pm 2.2) \times 10^{-4}$	1447
$\bar{D}^0 \rho^0$	$(3.2 \pm 0.5) \times 10^{-4}$	2237	$X(3872)^- K^+ \times$ $B(X(3872)^- \rightarrow J/\psi(1S) \pi^- \pi^0)$	$< 5 \times 10^{-4}$	CL=90% -
$\bar{D}^0 f_2$	$(1.2 \pm 0.4) \times 10^{-4}$	-	$X(3872)^- K^+ \times$ $B(X(3872)^- \rightarrow J/\psi(1S) \pi^- \pi^0)$	$< 4.2 \times 10^{-6}$	CL=90% -
$\bar{D}^0 \eta$	$(2.36 \pm 0.32) \times 10^{-4}$	S=2.5 2274	$X(3872)^- K^+ \times$ $B(X(3872)^- \rightarrow J/\psi \pi^+ \pi^-)$	$(4.3 \pm 1.3) \times 10^{-6}$	1140
$\bar{D}^0 \eta'$	$(1.38 \pm 0.16) \times 10^{-4}$	S=1.3 2198	$X(3872) K^0 \times B(X \rightarrow J/\psi \gamma)$	$< 2.4 \times 10^{-6}$	CL=90% 1140
$\bar{D}^0 \omega$	$(2.53 \pm 0.16) \times 10^{-4}$	2235	$X(3872) K^*(892)^0 \times B(X \rightarrow J/\psi \gamma)$	$< 2.8 \times 10^{-6}$	CL=90% 940
$D^0 \phi$	$< 1.16 \times 10^{-5}$	CL=90% 2183	$X(3872) K^0 \times B(X \rightarrow \psi(2S) \gamma)$	$< 6.62 \times 10^{-6}$	CL=90% 1140
$D^0 K^+ \pi^-$	$(6 \pm 4) \times 10^{-6}$	2261	$X(3872) K^*(892)^0 \times B(X \rightarrow \psi(2S) \gamma)$	$< 4.4 \times 10^{-6}$	CL=90% 940
$D^0 K^*(892)^0$	$< 1.1 \times 10^{-5}$	CL=90% 2213	$X(3872) K^0 \times B(X \rightarrow D^0 \bar{D}^0 \pi^0)$	$(1.7 \pm 0.8) \times 10^{-4}$	1140
$\bar{D}^{*0} \gamma$	$< 2.5 \times 10^{-5}$	CL=90% 2258	$X(4430)^\pm K^\mp \times B(X^\pm \rightarrow \psi(2S) \pi^\pm)$	$(1.2 \pm 0.4) \times 10^{-4}$	1140
$\bar{D}^*(2007)^0 \pi^0$	$(2.2 \pm 0.6) \times 10^{-4}$	S=2.6 2256	$X(4430)^\pm K^\mp \times B(X^\pm \rightarrow J/\psi \pi^\pm)$	$(3.2 \pm 1.8) \times 10^{-5}$	621
$\bar{D}^*(2007)^0 \rho^0$	$< 5.1 \times 10^{-4}$	CL=90% 2182	$J/\psi(1S) p \bar{p}$	$< 8.3 \times 10^{-7}$	CL=90% 862
$\bar{D}^*(2007)^0 \eta$	$(2.3 \pm 0.6) \times 10^{-4}$	S=2.8 2220	$J/\psi(1S) \gamma$	$< 1.6 \times 10^{-6}$	CL=90% 1731
$\bar{D}^*(2007)^0 \eta'$	$(1.40 \pm 0.22) \times 10^{-4}$	2141	$J/\psi(1S) \bar{D}^0$	$< 1.3 \times 10^{-5}$	CL=90% 877
$\bar{D}^*(2007)^0 \pi^+ \pi^-$	$(6.2 \pm 2.2) \times 10^{-4}$	2248	$\psi(2S) K^0$	$(6.2 \pm 0.5) \times 10^{-4}$	1283
$\bar{D}^*(2007)^0 K^0$	$(3.6 \pm 1.2) \times 10^{-5}$	2227	$\psi(3770) K^0 \times B(\psi \rightarrow \bar{D}^0 D^0)$	$< 1.23 \times 10^{-4}$	CL=90% 1217
$\bar{D}^*(2007)^0 K^*(892)^0$	$< 6.9 \times 10^{-5}$	CL=90% 2157	$\psi(3770) K^0 \times B(\psi \rightarrow D^- D^+)$	$< 1.88 \times 10^{-4}$	CL=90% 1217
$\bar{D}^*(2007)^0 K^*(892)^0$	$< 4.0 \times 10^{-5}$	CL=90% 2157	$\psi(2S) K^+ \pi^-$	$(5.7 \pm 0.4) \times 10^{-4}$	1238
$D^*(2007)^0 \pi^+ \pi^+ \pi^- \pi^-$	$(2.7 \pm 0.5) \times 10^{-3}$	2219	$\psi(2S) K^*(892)^0$	$(6.1 \pm 0.5) \times 10^{-4}$	S=1.1 1116
$D^*(2010)^+ D^*(2010)^-$	$(8.2 \pm 0.9) \times 10^{-4}$	1711	$\chi_{c0}(1P) K^0$	$(1.4 \pm 0.6) \times 10^{-4}$	1477
$\bar{D}^*(2007)^0 \omega$	$(3.6 \pm 1.1) \times 10^{-4}$	S=3.1 2180	$\chi_{c0} K^*(892)^0$	$(1.7 \pm 0.4) \times 10^{-4}$	1341
$D^*(2010)^+ D^-$	$(6.1 \pm 1.5) \times 10^{-4}$	S=1.6 1790	$\chi_{c2} K^0$	$< 1.5 \times 10^{-5}$	CL=90% 1378
$D^*(2007)^0 \bar{D}^*(2007)^0$	$< 9 \times 10^{-5}$	CL=90% 1715	$\chi_{c2} K^*(892)^0$	$(6.6 \pm 1.9) \times 10^{-5}$	1228
$D^- D^0 K^+$	$(1.07 \pm 0.11) \times 10^{-3}$	1574	$\chi_{c1}(1P) \pi^0$	$(1.12 \pm 0.28) \times 10^{-5}$	1468
$D^- D^*(2007)^0 K^+$	$(3.5 \pm 0.4) \times 10^{-3}$	1478	$\chi_{c1}(1P) K^0$	$(3.93 \pm 0.27) \times 10^{-4}$	1411
$D^*(2010)^- D^0 K^+$	$(2.47 \pm 0.21) \times 10^{-3}$	1479	$\chi_{c1}(1P) K^- \pi^+$	$(3.8 \pm 0.4) \times 10^{-4}$	1371
$D^*(2010)^- D^*(2007)^0 K^+$	$(1.06 \pm 0.09) \%$	1366	$\chi_{c1}(1P) K^*(892)^0$	$(2.22 \pm 0.40) \times 10^{-4}$	S=1.6 1265
$D^- D^+ K^0$	$(7.5 \pm 1.7) \times 10^{-4}$	1568	$X(4051)^+ K^- \times B(X^+ \rightarrow \chi_{c1} \pi^+)$	$(3.0 \pm 1.8) \times 10^{-5}$	-
$D^*(2010)^- D^+ K^0 +$ $D^- D^*(2010)^+ K^0$	$(6.4 \pm 0.5) \times 10^{-3}$	1473	$X(4248)^+ K^- \times B(X^+ \rightarrow \chi_{c1} \pi^+)$	$(4.0 \pm 2.0) \times 10^{-5}$	-
$D^*(2010)^- D^*(2010)^+ K^0$	$(8.1 \pm 0.7) \times 10^{-3}$	1360			
$D^* D_{s1}(2536)^+ \times$ $B(D_{s1}(2536)^+ \rightarrow D^{*+} K^0)$	$(8.0 \pm 2.4) \times 10^{-4}$	1336			
$\bar{D}^0 D^0 K^0$	$(2.7 \pm 1.1) \times 10^{-4}$	1574			



## Meson Summary Table

K or K* modes		K <sup>+</sup> K <sup>-</sup> π <sup>0</sup>		Light unflavored meson modes	
K <sup>+</sup> π <sup>-</sup>	( 1.94 ± 0.06 ) × 10 <sup>-5</sup>	2615	< 1.9	× 10 <sup>-5</sup>	CL=90% 2579
K <sup>0</sup> π <sup>0</sup>	( 9.5 ± 0.8 ) × 10 <sup>-6</sup>	S=1.3 2615	< 9	× 10 <sup>-7</sup>	CL=90% 2578
η' K <sup>0</sup>	( 6.6 ± 0.4 ) × 10 <sup>-5</sup>	S=1.4 2528	< 1.0	× 10 <sup>-6</sup>	CL=90% 2515
η' K <sup>*</sup> (892) <sup>0</sup>	( 3.1 ± 0.9 ) × 10 <sup>-6</sup>	2472	< 2.0	× 10 <sup>-6</sup>	CL=90% 2452
η' K <sub>0</sub> <sup>*</sup> (1430) <sup>0</sup>	( 6.3 ± 1.6 ) × 10 <sup>-6</sup>	2346	( 2.47 ± 0.23 ) × 10 <sup>-5</sup>		2522
η' K <sub>2</sub> <sup>*</sup> (1430) <sup>0</sup>	( 1.37 ± 0.32 ) × 10 <sup>-5</sup>	2346	( 8.6 ± 1.3 ) × 10 <sup>-6</sup>		2516
η K <sup>0</sup>	( 1.23 ± 0.27 ) × 10 <sup>-6</sup>	2587	( 6.2 ± 1.2 ) × 10 <sup>-6</sup>	S=1.3	2521
η K <sup>*</sup> (892) <sup>0</sup>	( 1.59 ± 0.10 ) × 10 <sup>-5</sup>	2534	( 1.6 ± 1.1 ) × 10 <sup>-5</sup>	CL=90%	2521
η K <sub>0</sub> <sup>*</sup> (1430) <sup>0</sup>	( 1.10 ± 0.22 ) × 10 <sup>-5</sup>	2415	( 2.75 ± 0.26 ) × 10 <sup>-5</sup>		2467
η K <sub>2</sub> <sup>*</sup> (1430) <sup>0</sup>	( 9.6 ± 2.1 ) × 10 <sup>-6</sup>	2414	( 9.8 ± 0.6 ) × 10 <sup>-6</sup>		2460
ω K <sup>0</sup>	( 5.0 ± 0.6 ) × 10 <sup>-6</sup>	2557	< 7.17	× 10 <sup>-5</sup>	CL=90% 2559
a <sub>0</sub> (980) <sup>0</sup> K <sup>0</sup> × B(a <sub>0</sub> (980) <sup>0</sup> → ηπ <sup>0</sup> )	< 7.8	× 10 <sup>-6</sup>	( 4.5 ± 1.3 ) × 10 <sup>-6</sup>		2524
b <sub>1</sub> <sup>0</sup> K <sup>0</sup> × B(b <sub>1</sub> <sup>0</sup> → ωπ <sup>0</sup> )	< 7.8	× 10 <sup>-6</sup>	( 8 ± 5 ) × 10 <sup>-7</sup>	S=2.2	2485
a <sub>0</sub> (980) <sup>±</sup> K <sup>∓</sup> × B(a <sub>0</sub> (980) <sup>±</sup> → ηπ <sup>±</sup> )	< 1.9	× 10 <sup>-6</sup>	< 6.0	× 10 <sup>-6</sup>	CL=90% 2559
b <sub>1</sub> <sup>-</sup> K <sup>+</sup> × B(b <sub>1</sub> <sup>-</sup> → ωπ <sup>-</sup> )	( 7.4 ± 1.4 ) × 10 <sup>-6</sup>	-	< 2.2	× 10 <sup>-6</sup>	CL=90% 2524
b <sub>1</sub> <sup>0</sup> K <sup>0</sup> × B(b <sub>1</sub> <sup>0</sup> → ωπ <sup>0</sup> )	< 8.0	× 10 <sup>-6</sup>	< 2	× 10 <sup>-7</sup>	CL=90% 2485
b <sub>1</sub> <sup>-</sup> K <sup>+</sup> × B(b <sub>1</sub> <sup>-</sup> → ωπ <sup>-</sup> )	< 5.0	× 10 <sup>-6</sup>	< 2.0	× 10 <sup>-6</sup>	CL=90% 2485
a <sub>0</sub> (1450) <sup>±</sup> K <sup>∓</sup> × B(a <sub>0</sub> (1450) <sup>±</sup> → ηπ <sup>±</sup> )	< 3.1	× 10 <sup>-6</sup>	< 5.0	× 10 <sup>-3</sup>	CL=90% 2339
K <sub>S</sub> <sup>0</sup> X <sup>0</sup> (Familon)	< 5.3	× 10 <sup>-5</sup>	φ(Kπ) <sup>0</sup>	( 4.3 ± 0.7 ) × 10 <sup>-6</sup>	-
ω K <sup>*</sup> (892) <sup>0</sup>	( 2.0 ± 0.5 ) × 10 <sup>-6</sup>	2503	φ(Kπ) <sup>0</sup>	φ(Kπ) <sup>0</sup> (1.60 < m <sub>Kπ</sub> < 2.15) [zzzz]	< 1.7
ω(Kπ) <sup>0</sup>	( 1.84 ± 0.25 ) × 10 <sup>-5</sup>	-	K <sub>0</sub> <sup>*</sup> (1430) <sup>0</sup> K <sup>-</sup> π <sup>+</sup>	< 3.18	× 10 <sup>-5</sup>
ω K <sub>0</sub> <sup>*</sup> (1430) <sup>0</sup>	( 1.60 ± 0.34 ) × 10 <sup>-5</sup>	2380	K <sub>0</sub> <sup>*</sup> (1430) <sup>0</sup> K <sup>+</sup> π <sup>-</sup>	< 3.3	× 10 <sup>-6</sup>
ω K <sub>2</sub> <sup>*</sup> (1430) <sup>0</sup>	( 1.01 ± 0.23 ) × 10 <sup>-5</sup>	2380	K <sub>0</sub> <sup>*</sup> (1430) <sup>0</sup> K <sup>*</sup> (892) <sup>0</sup>	< 8.4	× 10 <sup>-6</sup>
ω K <sup>+</sup> π <sup>-</sup> nonresonant	( 5.1 ± 1.0 ) × 10 <sup>-6</sup>	2542	K <sub>0</sub> <sup>*</sup> (1430) <sup>0</sup> K <sub>0</sub> <sup>*</sup> (1430) <sup>0</sup>	( 3.9 ± 0.8 ) × 10 <sup>-6</sup>	2333
K <sup>+</sup> π <sup>-</sup> π <sup>0</sup>	( 3.78 ± 0.32 ) × 10 <sup>-5</sup>	2609	K <sub>0</sub> <sup>*</sup> (1430) <sup>0</sup> K <sup>*</sup> (892) <sup>0</sup>	< 1.7	× 10 <sup>-6</sup>
K <sup>+</sup> ρ <sup>-</sup>	( 7.0 ± 0.9 ) × 10 <sup>-6</sup>	2559	K <sub>0</sub> <sup>*</sup> (1430) <sup>0</sup> K <sub>0</sub> <sup>*</sup> (1430) <sup>0</sup>	< 4.7	× 10 <sup>-6</sup>
K <sup>+</sup> ρ(1450) <sup>-</sup>	( 2.4 ± 1.2 ) × 10 <sup>-6</sup>	-	K <sup>*</sup> (1680) <sup>0</sup> φ	< 3.5	× 10 <sup>-6</sup>
K <sup>+</sup> ρ(1700) <sup>-</sup>	( 6 ± 7 ) × 10 <sup>-7</sup>	-	K <sup>*</sup> (1780) <sup>0</sup> φ	< 2.7	× 10 <sup>-6</sup>
(K <sup>+</sup> π <sup>-</sup> π <sup>0</sup> ) non-resonant	( 2.8 ± 0.6 ) × 10 <sup>-6</sup>	-	K <sup>*</sup> (2045) <sup>0</sup> φ	< 1.53	× 10 <sup>-5</sup>
(Kπ) <sup>0</sup> π <sup>+</sup> × B((Kπ) <sup>0</sup> π <sup>+</sup> → K <sup>+</sup> π <sup>0</sup> )	( 3.4 ± 0.5 ) × 10 <sup>-5</sup>	-	K <sub>2</sub> <sup>*</sup> (1430) <sup>0</sup> ρ <sup>0</sup>	< 1.1	× 10 <sup>-3</sup>
(Kπ) <sup>0</sup> π <sup>0</sup> × B((Kπ) <sup>0</sup> π <sup>0</sup> → K <sup>+</sup> π <sup>-</sup> )	( 8.6 ± 1.7 ) × 10 <sup>-6</sup>	-	K <sub>2</sub> <sup>*</sup> (1430) <sup>0</sup> φ	( 7.5 ± 1.0 ) × 10 <sup>-6</sup>	2333
K <sub>2</sub> <sup>*</sup> (1430) <sup>0</sup> π <sup>0</sup>	< 4.0	× 10 <sup>-6</sup>	K <sup>0</sup> φ φ	( 4.5 ± 0.9 ) × 10 <sup>-6</sup>	2305
K <sup>*</sup> (1680) <sup>0</sup> π <sup>0</sup>	< 7.5	× 10 <sup>-6</sup>	η' η' K <sup>0</sup>	< 3.1	× 10 <sup>-5</sup>
K <sub>x</sub> <sup>0</sup> π <sup>0</sup> [xxx]	( 6.1 ± 1.6 ) × 10 <sup>-6</sup>	-	η' K <sup>0</sup> γ	( 7.6 ± 1.8 ) × 10 <sup>-6</sup>	2587
K <sup>0</sup> π <sup>+</sup> π <sup>-</sup> charmless	( 4.96 ± 0.20 ) × 10 <sup>-5</sup>	2609	η' K <sup>0</sup> γ	< 6.4	× 10 <sup>-6</sup>
K <sup>0</sup> π <sup>+</sup> π <sup>-</sup> non-resonant	( 1.47 ± 0.40 ) × 10 <sup>-5</sup>	S=2.1	K <sup>0</sup> φ γ	( 2.7 ± 0.7 ) × 10 <sup>-6</sup>	2516
K <sup>0</sup> ρ <sup>0</sup>	( 4.7 ± 0.6 ) × 10 <sup>-6</sup>	2558	K <sup>+</sup> π <sup>-</sup> γ	( 4.6 ± 1.4 ) × 10 <sup>-6</sup>	2615
K <sup>*</sup> (892) <sup>+</sup> π <sup>-</sup>	( 8.4 ± 0.8 ) × 10 <sup>-6</sup>	2563	K <sup>*</sup> (892) <sup>0</sup> γ	( 4.33 ± 0.15 ) × 10 <sup>-5</sup>	2564
K <sub>0</sub> <sup>*</sup> (1430) <sup>+</sup> π <sup>-</sup>	( 3.3 ± 0.7 ) × 10 <sup>-5</sup>	S=2.0	K <sup>*</sup> (1410) γ	< 1.3	× 10 <sup>-4</sup>
K <sub>x</sub> <sup>+</sup> π <sup>-</sup> [xxx]	( 5.1 ± 1.6 ) × 10 <sup>-6</sup>	-	K <sup>+</sup> π <sup>-</sup> γ nonresonant	< 2.6	× 10 <sup>-6</sup>
K <sup>*</sup> (1410) <sup>+</sup> π <sup>-</sup> × B(K <sup>*</sup> (1410) <sup>+</sup> → K <sup>0</sup> π <sup>+</sup> )	< 3.8	× 10 <sup>-6</sup>	K <sup>*</sup> (892) <sup>0</sup> X(214) × B(X → μ <sup>+</sup> μ <sup>-</sup> )	< 2.26	× 10 <sup>-8</sup>
f <sub>0</sub> (980) K <sup>0</sup> × B(f <sub>0</sub> (980) → π <sup>+</sup> π <sup>-</sup> )	( 7.0 ± 0.9 ) × 10 <sup>-6</sup>	2522	K <sup>0</sup> π <sup>+</sup> π <sup>-</sup> γ	( 1.95 ± 0.22 ) × 10 <sup>-5</sup>	2609
f <sub>2</sub> (1270) K <sup>0</sup>	( 2.7 ± 1.3 ) × 10 <sup>-6</sup>	2459	K <sup>+</sup> π <sup>-</sup> π <sup>0</sup> γ	( 4.1 ± 0.4 ) × 10 <sup>-5</sup>	2609
f <sub>x</sub> (1300) K <sup>0</sup> × B(f <sub>x</sub> → π <sup>+</sup> π <sup>-</sup> )	( 1.8 ± 0.7 ) × 10 <sup>-6</sup>	-	K <sub>1</sub> (1270) <sup>0</sup> γ	< 5.8	× 10 <sup>-5</sup>
K <sup>*</sup> (892) <sup>0</sup> π <sup>0</sup>	( 3.3 ± 0.6 ) × 10 <sup>-6</sup>	2563	K <sub>1</sub> (1400) <sup>0</sup> γ	< 1.2	× 10 <sup>-5</sup>
K <sub>2</sub> <sup>*</sup> (1430) <sup>+</sup> π <sup>-</sup>	< 6	× 10 <sup>-6</sup>	K <sub>2</sub> <sup>*</sup> (1430) <sup>0</sup> γ	( 1.24 ± 0.24 ) × 10 <sup>-5</sup>	2447
K <sup>*</sup> (1680) <sup>+</sup> π <sup>-</sup>	< 1.0	× 10 <sup>-5</sup>	K <sup>*</sup> (1680) <sup>0</sup> γ	< 2.0	× 10 <sup>-3</sup>
K <sup>+</sup> π <sup>-</sup> π <sup>+</sup> π <sup>-</sup> [γγγ]	< 2.3	× 10 <sup>-4</sup>	K <sub>3</sub> <sup>*</sup> (1780) <sup>0</sup> γ	< 8.3	× 10 <sup>-5</sup>
ρ <sup>0</sup> K <sup>+</sup> π <sup>-</sup>	( 2.8 ± 0.7 ) × 10 <sup>-6</sup>	2543	K <sub>4</sub> <sup>*</sup> (2045) <sup>0</sup> γ	< 4.3	× 10 <sup>-3</sup>
f <sub>0</sub> (980) K <sup>+</sup> π <sup>-</sup>	( 1.4 ± 0.5 ) × 10 <sup>-6</sup>	2506	ρ <sup>0</sup> γ	( 8.6 ± 1.5 ) × 10 <sup>-7</sup>	2583
K <sup>+</sup> π <sup>-</sup> π <sup>+</sup> π <sup>-</sup> nonresonant	< 2.1	× 10 <sup>-6</sup>	ρ <sup>0</sup> X(214) × B(X → μ <sup>+</sup> μ <sup>-</sup> ) [aaaa]	< 1.73	× 10 <sup>-8</sup>
K <sup>*</sup> (892) <sup>0</sup> π <sup>+</sup> π <sup>-</sup>	( 5.5 ± 0.5 ) × 10 <sup>-5</sup>	2557	ω γ	( 4.4 ± 1.8 ) × 10 <sup>-7</sup>	2582
K <sup>*</sup> (892) <sup>0</sup> ρ <sup>0</sup>	( 3.4 ± 1.7 ) × 10 <sup>-6</sup>	S=1.8 2504	φ γ	< 8.5	× 10 <sup>-7</sup>
K <sup>*</sup> (892) <sup>0</sup> f <sub>0</sub> (980)	< 2.2	× 10 <sup>-6</sup>	π <sup>+</sup> π <sup>-</sup>	( 5.15 ± 0.22 ) × 10 <sup>-6</sup>	2636
K <sub>1</sub> (1270) <sup>+</sup> π <sup>-</sup>	< 3.0	× 10 <sup>-5</sup>	π <sup>0</sup> π <sup>0</sup>	( 1.62 ± 0.31 ) × 10 <sup>-6</sup>	S=1.3 2636
K <sub>1</sub> (1400) <sup>+</sup> π <sup>-</sup>	< 2.7	× 10 <sup>-5</sup>	η π <sup>0</sup>	< 1.5	× 10 <sup>-6</sup>
a <sub>1</sub> (1260) <sup>-</sup> K <sup>+</sup> [γγγ]	( 1.6 ± 0.4 ) × 10 <sup>-5</sup>	2471	η η	< 1.0	× 10 <sup>-6</sup>
K <sup>*</sup> (892) <sup>+</sup> ρ <sup>-</sup>	< 1.20	× 10 <sup>-5</sup>	η' π <sup>0</sup>	( 1.2 ± 0.6 ) × 10 <sup>-6</sup>	S=1.7 2551
K <sub>1</sub> (1400) <sup>0</sup> ρ <sup>0</sup>	< 3.0	× 10 <sup>-3</sup>	η' η'	< 1.7	× 10 <sup>-6</sup>
K <sup>+</sup> K <sup>-</sup>	< 4.1	× 10 <sup>-7</sup>	η' η	< 1.2	× 10 <sup>-6</sup>
K <sup>0</sup> K <sup>0</sup>	( 9.6 ± 2.0 ) × 10 <sup>-7</sup>	2592	η' ρ <sup>0</sup>	< 1.3	× 10 <sup>-6</sup>
K <sup>0</sup> K <sup>-</sup> π <sup>+</sup>	( 6.4 ± 1.2 ) × 10 <sup>-6</sup>	2578	η' f <sub>0</sub> (980) × B(f <sub>0</sub> (980) → π <sup>+</sup> π <sup>-</sup> )	< 9	× 10 <sup>-7</sup>
K <sup>*</sup> 0 K <sup>0</sup> + K <sup>*</sup> 0 K <sup>0</sup>	< 1.9	× 10 <sup>-6</sup>	η ρ <sup>0</sup>	< 1.5	× 10 <sup>-6</sup>
			η f <sub>0</sub> (980) × B(f <sub>0</sub> (980) → π <sup>+</sup> π <sup>-</sup> )	< 4	× 10 <sup>-7</sup>
			ω η	( 9.4 ± 4.0 ) × 10 <sup>-7</sup>	2552
			ω η'	( 1.0 ± 0.5 ) × 10 <sup>-6</sup>	2491
			ω ρ <sup>0</sup>	< 1.6	× 10 <sup>-6</sup>
			ω f <sub>0</sub> (980) × B(f <sub>0</sub> (980) → π <sup>+</sup> π <sup>-</sup> )	< 1.5	× 10 <sup>-6</sup>

## Meson Summary Table

$\omega\omega$	< 4.0	$\times 10^{-6}$	CL=90%	2521
$\phi\pi^0$	< 2.8	$\times 10^{-7}$	CL=90%	2540
$\phi\eta$	< 5	$\times 10^{-7}$	CL=90%	2511
$\phi\eta'$	< 5	$\times 10^{-7}$	CL=90%	2448
$\phi\rho^0$	< 3.3	$\times 10^{-7}$	CL=90%	2480
$\phi f_0(980) \times B(f_0 \rightarrow \pi^+\pi^-)$	< 3.8	$\times 10^{-7}$	CL=90%	2441
$\phi\omega$	< 1.2	$\times 10^{-6}$	CL=90%	2479
$\phi\phi$	< 2	$\times 10^{-7}$	CL=90%	2435
$a_0(980)^\pm \pi^\mp \times B(a_0(980)^\pm \rightarrow \eta\pi^\pm)$	< 3.1	$\times 10^{-6}$	CL=90%	-
$a_0(1450)^\pm \pi^\mp \times B(a_0(1450)^\pm \rightarrow \eta\pi^\pm)$	< 2.3	$\times 10^{-6}$	CL=90%	-
$\pi^+\pi^-\pi^0$	< 7.2	$\times 10^{-4}$	CL=90%	2631
$\rho^0\pi^0$	( 2.0 $\pm$ 0.5 )	$\times 10^{-6}$		2581
$\rho^\mp\pi^\pm$	[ee] ( 2.30 $\pm$ 0.23 )	$\times 10^{-5}$		2581
$\pi^+\pi^-\pi^+\pi^-$	< 1.93	$\times 10^{-5}$	CL=90%	2621
$\rho^0\pi^+\pi^-$	< 8.8	$\times 10^{-6}$	CL=90%	2575
$\rho^0\rho^0$	( 7.3 $\pm$ 2.8 )	$\times 10^{-7}$		2523
$f_0(980)\pi^+\pi^-$	< 3.8	$\times 10^{-6}$	CL=90%	2539
$\rho^0 f_0(980) \times B(f_0(980) \rightarrow \pi^+\pi^-)$	< 3	$\times 10^{-7}$	CL=90%	2486
$f_0(980) f_0(980) \times B^2(f_0(980) \rightarrow \pi^+\pi^-)$	< 1	$\times 10^{-7}$	CL=90%	2447
$f_0(980) f_0(980) \times B(f_0 \rightarrow \pi^+\pi^-) \times B(f_0 \rightarrow K^+K^-)$	< 2.3	$\times 10^{-7}$	CL=90%	2447
$a_1(1260)^\mp\pi^\pm$	[ee] ( 3.3 $\pm$ 0.5 )	$\times 10^{-5}$		2494
$a_2(1320)^\mp\pi^\pm$	[ee] < 3.0	$\times 10^{-4}$	CL=90%	2473
$\pi^+\pi^-\pi^0\pi^0$	< 3.1	$\times 10^{-3}$	CL=90%	2622
$\rho^+\rho^-$	( 2.42 $\pm$ 0.31 )	$\times 10^{-5}$		2523
$a_1(1260)^0\pi^0$	< 1.1	$\times 10^{-3}$	CL=90%	2495
$\omega\pi^0$	< 5	$\times 10^{-7}$	CL=90%	2580
$\pi^+\pi^+\pi^-\pi^-\pi^0$	< 9.0	$\times 10^{-3}$	CL=90%	2609
$a_1(1260)^+\rho^-$	< 6.1	$\times 10^{-5}$	CL=90%	2433
$a_1(1260)^0\rho^0$	< 2.4	$\times 10^{-3}$	CL=90%	2433
$b_1^\mp\pi^\pm \times B(b_1^\mp \rightarrow \omega\pi^\mp)$	( 1.09 $\pm$ 0.15 )	$\times 10^{-5}$		-
$b_1^0\pi^0 \times B(b_1^0 \rightarrow \omega\pi^0)$	< 1.9	$\times 10^{-6}$	CL=90%	-
$b_1^-\rho^+ \times B(b_1^- \rightarrow \omega\pi^-)$	< 1.4	$\times 10^{-6}$	CL=90%	-
$b_1^0\rho^0 \times B(b_1^0 \rightarrow \omega\pi^0)$	< 3.4	$\times 10^{-6}$	CL=90%	-
$\pi^+\pi^+\pi^+\pi^-\pi^-\pi^-$	< 3.0	$\times 10^{-3}$	CL=90%	2592
$a_1(1260)^+ a_1(1260)^- \times B^2(a_1^+ \rightarrow 2\pi^+\pi^-)$	( 1.18 $\pm$ 0.31 )	$\times 10^{-5}$		2336
$\pi^+\pi^+\pi^+\pi^-\pi^-\pi^-\pi^0$	< 1.1	%	CL=90%	2572
<b>Barion modes</b>				
$p\bar{p}$	< 1.1	$\times 10^{-7}$	CL=90%	2467
$p\bar{p}\pi^+\pi^-$	< 2.5	$\times 10^{-4}$	CL=90%	2406
$p\bar{p}K^0$	( 2.66 $\pm$ 0.32 )	$\times 10^{-6}$		2347
$\Theta(1540)^+\bar{p} \times B(\Theta(1540)^+ \rightarrow pK_S^0)$	[bbbb] < 5	$\times 10^{-8}$	CL=90%	2318
$f_J(2220)K^0 \times B(f_J(2220) \rightarrow p\bar{p})$	< 4.5	$\times 10^{-7}$	CL=90%	2135
$p\bar{p}K^*(892)^0$	( 1.24 $\pm$ 0.28 )	$\times 10^{-6}$		2216
$f_J(2220)K_S^0 \times B(f_J(2220) \rightarrow p\bar{p})$	< 1.5	$\times 10^{-7}$	CL=90%	-
$p\bar{p}\pi^-$	( 3.14 $\pm$ 0.29 )	$\times 10^{-6}$		2401
$p\bar{p}\Sigma(1385)^-$	< 2.6	$\times 10^{-7}$	CL=90%	2363
$\Delta^0\bar{\Lambda}$	< 9.3	$\times 10^{-7}$	CL=90%	2364
$p\bar{p}\Lambda K^-$	< 8.2	$\times 10^{-7}$	CL=90%	2308
$p\bar{p}\Sigma^0\pi^-$	< 3.8	$\times 10^{-6}$	CL=90%	2383
$\bar{\Lambda}\Lambda$	< 3.2	$\times 10^{-7}$	CL=90%	2392
$\bar{\Lambda}\Lambda K^0$	( 4.8 $\pm$ 1.0 )	$\times 10^{-6}$		2250
$\bar{\Lambda}\Lambda K^{*0}$	( 2.5 $\pm$ 0.9 )	$\times 10^{-6}$		2098
$\bar{\Lambda}\Lambda D^0$	( 1.1 $\pm$ 0.6 )	$\times 10^{-5}$		1661
$\Delta^0\bar{\Delta}^0$	< 1.5	$\times 10^{-3}$	CL=90%	2335
$\Delta^{++}\bar{\Delta}^{--}$	< 1.1	$\times 10^{-4}$	CL=90%	2335
$\bar{D}^0 p\bar{p}$	( 1.14 $\pm$ 0.09 )	$\times 10^{-4}$		1863
$D_s^- \bar{\Lambda} p$	( 2.8 $\pm$ 0.9 )	$\times 10^{-5}$		1710
$\bar{D}^*(2007)^0 p\bar{p}$	( 1.03 $\pm$ 0.13 )	$\times 10^{-4}$		1788
$D^*(2010)^- p\bar{n}$	( 1.4 $\pm$ 0.4 )	$\times 10^{-3}$		1785
$D^- p\bar{p}\pi^+$	( 3.38 $\pm$ 0.32 )	$\times 10^{-4}$		1786
$D^*(2010)^- p\bar{p}\pi^+$	( 5.0 $\pm$ 0.5 )	$\times 10^{-4}$		1707
$\Theta_c \bar{p}\pi^+ \times B(\Theta_c \rightarrow D^- p)$	< 9	$\times 10^{-6}$	CL=90%	-
$\Theta_c \bar{p}\pi^+ \times B(\Theta_c \rightarrow D^{*-} p)$	< 1.4	$\times 10^{-5}$	CL=90%	-
$\Sigma_c^{--} \Delta^{++}$	< 1.0	$\times 10^{-3}$	CL=90%	1839

$\bar{\Lambda}_c^- p\pi^+\pi^-$	( 1.3 $\pm$ 0.4 )	$\times 10^{-3}$		1934
$\bar{\Lambda}_c^- p$	( 2.0 $\pm$ 0.4 )	$\times 10^{-5}$		2021
$\bar{\Lambda}_c^- p\pi^0$	( 1.9 $\pm$ 0.5 )	$\times 10^{-4}$		1982
$\Sigma_c(2455)^- p$	< 3.0	$\times 10^{-5}$		-
$\bar{\Lambda}_c^- p\pi^+\pi^-\pi^0$	< 5.07	$\times 10^{-3}$	CL=90%	1882
$\bar{\Lambda}_c^- p\pi^+\pi^-\pi^+\pi^-$	< 2.74	$\times 10^{-3}$	CL=90%	1821
$\bar{\Lambda}_c^- p\pi^+\pi^-$	( 1.12 $\pm$ 0.32 )	$\times 10^{-3}$		1934
$\bar{\Lambda}_c^- p\pi^+\pi^-$ (nonresonant)	( 6.4 $\pm$ 1.9 )	$\times 10^{-4}$		1934
$\Sigma_c(2520)^{--} p\pi^+$	( 1.2 $\pm$ 0.4 )	$\times 10^{-4}$		1860
$\Sigma_c(2520)^0 p\pi^-$	< 3.8	$\times 10^{-5}$	CL=90%	1860
$\Sigma_c(2455)^0 p\pi^-$	( 1.5 $\pm$ 0.5 )	$\times 10^{-4}$		1895
$\Sigma_c(2455)^0 N^0 \times B(N^0 \rightarrow p\pi^-)$	( 8.0 $\pm$ 2.9 )	$\times 10^{-5}$		-
$\Sigma_c(2455)^{--} p\pi^+$	( 2.2 $\pm$ 0.7 )	$\times 10^{-4}$		1895
$\bar{\Lambda}_c^- pK^+\pi^-$	( 4.3 $\pm$ 1.4 )	$\times 10^{-5}$		-
$\Sigma_c(2455)^{--} pK^+ \times B(\Sigma_c^{--} \rightarrow \bar{\Lambda}_c^- \pi^-)$	( 1.1 $\pm$ 0.4 )	$\times 10^{-5}$		1754
$\bar{\Lambda}_c^- pK^*(892)^0$	< 2.42	$\times 10^{-5}$	CL=90%	-
$\bar{\Lambda}_c^- \Lambda K^+$	( 3.8 $\pm$ 1.3 )	$\times 10^{-5}$		1767
$\bar{\Lambda}_c^- \Lambda_c^+$	< 6.2	$\times 10^{-5}$	CL=90%	1319
$\bar{\Lambda}_c^-(2593)^- / \bar{\Lambda}_c^-(2625)^- p$	< 1.1	$\times 10^{-4}$	CL=90%	-
$\Xi_c^- \Lambda_c^+ \times B(\Xi_c^- \rightarrow \Xi^+ \pi^- \pi^-)$	( 2.2 $\pm$ 2.3 )	$\times 10^{-5}$	S=1.9	1147
$\Lambda_c^+ K^0$	( 5.4 $\pm$ 3.2 )	$\times 10^{-4}$		-

Lepton Family number (LF) or Lepton number (L) or Baryon number (B) violating modes, or/and  $\Delta B = 1$  weak neutral current (BI) modes

$\gamma\gamma$	BI	< 3.2	$\times 10^{-7}$	CL=90%	2640
$e^+e^-$	BI	< 8.3	$\times 10^{-8}$	CL=90%	2640
$e^+e^-\gamma$	BI	< 1.2	$\times 10^{-7}$	CL=90%	2640
$\mu^+\mu^-$	BI	< 1.4	$\times 10^{-9}$	CL=90%	2638
$\mu^+\mu^-\gamma$	BI	< 1.6	$\times 10^{-7}$	CL=90%	2638
$\tau^+\tau^-$	BI	< 4.1	$\times 10^{-3}$	CL=90%	1952
$\pi^0 \ell^+ \ell^-$	BI	< 1.2	$\times 10^{-7}$	CL=90%	2638
$\pi^0 e^+ e^-$	BI	< 1.4	$\times 10^{-7}$	CL=90%	2638
$\pi^0 \mu^+ \mu^-$	BI	< 1.8	$\times 10^{-7}$	CL=90%	2634
$\pi^0 \nu\bar{\nu}$	BI	< 2.2	$\times 10^{-4}$	CL=90%	2638
$K^0 \ell^+ \ell^-$	BI [ppp]	( 3.1 $\pm$ 0.8 )	$\times 10^{-7}$		2616
$K^0 e^+ e^-$	BI	( 1.6 $\pm$ 1.0 )	$\times 10^{-7}$		2616
$K^0 \mu^+ \mu^-$	BI	( 3.8 $\pm$ 0.8 )	$\times 10^{-7}$		2612
$K^0 \nu\bar{\nu}$	BI	< 5.6	$\times 10^{-5}$	CL=90%	2616
$\rho^0 \nu\bar{\nu}$	BI	< 4.4	$\times 10^{-4}$	CL=90%	2583
$K^*(892)^0 \ell^+ \ell^-$	BI [ppp]	( 9.9 $\pm$ 1.2 )	$\times 10^{-7}$		2564
$K^*(892)^0 e^+ e^-$	BI	( 1.03 $\pm$ 0.19 )	$\times 10^{-6}$		2564
$K^*(892)^0 \mu^+ \mu^-$	BI	( 1.06 $\pm$ 0.17 )	$\times 10^{-6}$		2560
$K^*(892)^0 \nu\bar{\nu}$	BI	< 1.2	$\times 10^{-4}$	CL=90%	2564
$\phi \nu\bar{\nu}$	BI	< 5.8	$\times 10^{-5}$	CL=90%	2541
$e^\pm \mu^\mp$	LF [ee]	< 6.4	$\times 10^{-8}$	CL=90%	2639
$\pi^0 e^\pm \mu^\mp$	LF	< 1.4	$\times 10^{-7}$	CL=90%	2637
$K^0 e^\pm \mu^\mp$	LF	< 2.7	$\times 10^{-7}$	CL=90%	2615
$K^*(892)^0 e^+ \mu^-$	LF	< 5.3	$\times 10^{-7}$	CL=90%	2563
$K^*(892)^0 e^- \mu^+$	LF	< 3.4	$\times 10^{-7}$	CL=90%	2563
$K^*(892)^0 e^\pm \mu^\mp$	LF	< 5.8	$\times 10^{-7}$	CL=90%	2563
$e^\pm \tau^\mp$	LF [ee]	< 2.8	$\times 10^{-5}$	CL=90%	2341
$\mu^\pm \tau^\mp$	LF [ee]	< 2.2	$\times 10^{-5}$	CL=90%	2339
invisible	BI	< 2.2	$\times 10^{-4}$	CL=90%	-
$\nu\bar{\nu}\gamma$	BI	< 4.7	$\times 10^{-5}$	CL=90%	2640
$\Lambda_c^+ \mu^-$	L,B	< 1.8	$\times 10^{-6}$	CL=90%	2143
$\Lambda_c^+ e^-$	L,B	< 5	$\times 10^{-6}$	CL=90%	2145

 **$B^\pm/B^0$  ADMIXTURE**

## CP violation

$$\begin{aligned}
A_{CP}(B \rightarrow K^*(892)\gamma) &= -0.003 \pm 0.017 \\
A_{CP}(b \rightarrow s\gamma) &= -0.008 \pm 0.029 \\
A_{CP}(b \rightarrow (s+d)\gamma) &= -0.09 \pm 0.07 \\
A_{CP}(B \rightarrow X_s \ell^+ \ell^-) &= -0.22 \pm 0.26 \\
A_{CP}(B \rightarrow K^* e^+ e^-) &= -0.18 \pm 0.15 \\
A_{CP}(B \rightarrow K^* \mu^+ \mu^-) &= -0.03 \pm 0.13 \\
A_{CP}(B \rightarrow K^* \ell^+ \ell^-) &= -0.07 \pm 0.08 \\
A_{CP}(B \rightarrow \eta \text{anything}) &= -0.13 \pm_{-0.05}^{0.04}
\end{aligned}$$

## Meson Summary Table

The branching fraction measurements are for an admixture of  $B$  mesons at the  $\Upsilon(4S)$ . The values quoted assume that  $B(\Upsilon(4S) \rightarrow B\bar{B}) = 100\%$ .

For inclusive branching fractions, e.g.,  $B \rightarrow D^\pm$  anything, the treatment of multiple  $D$ 's in the final state must be defined. One possibility would be to count the number of events with one-or-more  $D$ 's and divide by the total number of  $B$ 's. Another possibility would be to count the total number of  $D$ 's and divide by the total number of  $B$ 's, which is the definition of average multiplicity. The two definitions are identical if only one  $D$  is allowed in the final state. Even though the "one-or-more" definition seems sensible, for practical reasons inclusive branching fractions are almost always measured using the multiplicity definition. For heavy final state particles, authors call their results inclusive branching fractions while for light particles some authors call their results multiplicities. In the  $B$  sections, we list all results as inclusive branching fractions, adopting a multiplicity definition. This means that inclusive branching fractions can exceed 100% and that inclusive partial widths can exceed total widths, just as inclusive cross sections can exceed total cross section.

$\bar{B}$  modes are charge conjugates of the modes below. Reactions indicate the weak decay vertex and do not include mixing.

<b>B DECAY MODES</b>	Fraction ( $\Gamma_j/\Gamma$ )	Scale factor/ Confidence level (MeV/c)	$p$
<b>Semileptonic and leptonic modes</b>			
$e^+ \nu_e$ anything	[cccc] ( 10.72 ± 0.13 ) %		—
$\bar{p} e^+ \nu_e$ anything	< 5.9 × 10 <sup>-4</sup>	CL=90%	—
$\mu^+ \nu_\mu$ anything	[cccc] ( 10.72 ± 0.13 ) %		—
$\ell^+ \nu_\ell$ anything	[ppp,cccc] ( 10.72 ± 0.13 ) %		—
$D^- \ell^+ \nu_\ell$ anything	[ppp] ( 2.8 ± 0.9 ) %		—
$\bar{D}^0 \ell^+ \nu_\ell$ anything	[ppp] ( 7.2 ± 1.4 ) %		—
$\bar{D} \ell \nu_\ell$	( 2.39 ± 0.12 ) %		2310
$D \tau^+ \nu_\tau$	( 8.6 ± 2.7 ) × 10 <sup>-3</sup>		1911
$D^{*-} \ell^+ \nu_\ell$ anything	[dddd] ( 6.7 ± 1.3 ) × 10 <sup>-3</sup>		—
$D^* \tau^+ \nu_\tau$	( 1.62 ± 0.33 ) %		1837
$\bar{D}^{*+} \ell^+ \nu_\ell$	[ppp,eeee] ( 2.7 ± 0.7 ) %		—
$\bar{D}_1(2420) \ell^+ \nu_\ell$ anything	( 3.8 ± 1.3 ) × 10 <sup>-3</sup>	S=2.4	—
$D \pi \ell^+ \nu_\ell$ anything + $D^* \pi \ell^+ \nu_\ell$ anything	( 2.6 ± 0.5 ) %	S=1.5	—
$D \pi \ell^+ \nu_\ell$ anything	( 1.5 ± 0.6 ) %		—
$D^* \pi \ell^+ \nu_\ell$ anything	( 1.9 ± 0.4 ) %		—
$\bar{D}_2^*(2460) \ell^+ \nu_\ell$ anything	( 4.4 ± 1.6 ) × 10 <sup>-3</sup>		—
$D^{*-} \pi^+ \ell^+ \nu_\ell$ anything	( 1.00 ± 0.34 ) %		—
$D_s^- \ell^+ \nu_\ell$ anything	[ppp] < 7 × 10 <sup>-3</sup>	CL=90%	—
$D_s^- \ell^+ \nu_\ell K^+$ anything	[ppp] < 5 × 10 <sup>-3</sup>	CL=90%	—
$D_s^- \ell^+ \nu_\ell K^0$ anything	[ppp] < 7 × 10 <sup>-3</sup>	CL=90%	—
$\ell^+ \nu_\ell$ charm	( 10.51 ± 0.13 ) %		—
$X_H \ell^+ \nu_\ell$	( 2.08 ± 0.30 ) × 10 <sup>-3</sup>		—
$K^+ \ell^+ \nu_\ell$ anything	[ppp] ( 6.2 ± 0.5 ) %		—
$K^- \ell^+ \nu_\ell$ anything	[ppp] ( 10 ± 4 ) × 10 <sup>-3</sup>		—
$K^0/\bar{K}^0 \ell^+ \nu_\ell$ anything	[ppp] ( 4.5 ± 0.5 ) %		—
<b>D, D*, or D<sub>s</sub> modes</b>			
$D^\pm$ anything	( 23.7 ± 1.3 ) %		—
$D^0/\bar{D}^0$ anything	( 62.7 ± 2.9 ) %	S=1.3	—
$D^*(2010)^\pm$ anything	( 22.5 ± 1.5 ) %		—
$D^*(2007)^0$ anything	( 26.0 ± 2.7 ) %		—
$D_s^\pm$ anything	[ee] ( 8.3 ± 0.8 ) %		—
$D_s^{*\pm}$ anything	( 6.3 ± 1.0 ) %		—
$D_s^\pm \bar{D}^*(*)$	( 3.4 ± 0.6 ) %		—
$D^{(*)} \bar{D}^{(*)} K^0 +$ $D^{(*)} \bar{D}^{(*)} K^\pm$	[ee,ffff] ( 7.1 ± 2.7 / 1.7 ) %		—
$b \rightarrow c \bar{c} s$	( 22 ± 4 ) %		—
$D_s^{(*)} \bar{D}^{(*)}$	[ee,ffff] ( 3.9 ± 0.4 ) %		—
$D^* D^*(2010)^\pm$	[ee] < 5.9 × 10 <sup>-3</sup>	CL=90%	1711
$D^* D^*(2010)^\pm + D^* D^\pm$	[ee] < 5.5 × 10 <sup>-3</sup>	CL=90%	—
$DD^\pm$	[ee] < 3.1 × 10 <sup>-3</sup>	CL=90%	1866
$D_s^{(*)} \pm \bar{D}^{(*)} X(n\pi^\pm)$	[ee,ffff] ( 9 ± 5 / 4 ) %		—
$D^*(2010)\gamma$	< 1.1 × 10 <sup>-3</sup>	CL=90%	2257
$D_s^+ \pi^-, D_s^{*+} \pi^-, D_s^+ \rho^-,$ $D_s^{*+} \rho^-, D_s^+ \pi^0, D_s^{*+} \pi^0,$ $D_s^+ \eta, D_s^{*+} \eta, D_s^+ \rho^0,$ $D_s^{*+} \rho^0, D_s^+ \omega, D_s^{*+} \omega$	[ee] < 4 × 10 <sup>-4</sup>	CL=90%	—
$D_{S1}(2536)^+$ anything	< 9.5 × 10 <sup>-3</sup>	CL=90%	—

## Charmonium modes

$J/\psi(1S)$ anything	( 1.094 ± 0.032 ) %	S=1.1	—
$J/\psi(1S)$ (direct) anything	( 7.8 ± 0.4 ) × 10 <sup>-3</sup>	S=1.1	—
$\psi(2S)$ anything	( 3.07 ± 0.21 ) × 10 <sup>-3</sup>		—
$\chi_{c1}(1P)$ anything	( 3.86 ± 0.27 ) × 10 <sup>-3</sup>		—
$\chi_{c1}(1P)$ anything	( 3.22 ± 0.25 ) × 10 <sup>-3</sup>		—
$\chi_{c2}(1P)$ anything	( 1.3 ± 0.4 ) × 10 <sup>-3</sup>	S=1.9	—
$\chi_{c2}(1P)$ (direct) anything	( 1.65 ± 0.31 ) × 10 <sup>-3</sup>		—
$\eta_c(1S)$ anything	< 9 × 10 <sup>-3</sup>	CL=90%	—
$KX(3872) \times B(X \rightarrow$ $D^0 \bar{D}^0 \pi^0)$	( 1.2 ± 0.4 ) × 10 <sup>-4</sup>		1141
$KX(3872) \times B(X \rightarrow$ $D^{*0} D^0)$	( 8.0 ± 2.2 ) × 10 <sup>-5</sup>		1141
$KX(3940) \times B(X \rightarrow$ $D^{*0} D^0)$	< 6.7 × 10 <sup>-5</sup>	CL=90%	1084
$KX(3915) \times B(X \rightarrow \omega J/\psi)gggg$	( 7.1 ± 3.4 ) × 10 <sup>-5</sup>		1104

## K or K\* modes

$K^\pm$ anything	[ee] ( 78.9 ± 2.5 ) %		—
$K^+$ anything	( 66 ± 5 ) %		—
$K^-$ anything	( 13 ± 4 ) %		—
$K^0/\bar{K}^0$ anything	[ee] ( 64 ± 4 ) %		—
$K^*(892)^\pm$ anything	( 18 ± 6 ) %		—
$K^*(892)^0/\bar{K}^*(892)^0$ anything	[ee] ( 14.6 ± 2.6 ) %		—
$K^*(892)\gamma$	( 4.2 ± 0.6 ) × 10 <sup>-5</sup>		2564
$\eta K \gamma$	( 8.5 ± 1.8 / 1.6 ) × 10 <sup>-6</sup>		2588
$K_1(1400)\gamma$	< 1.27 × 10 <sup>-4</sup>	CL=90%	2453
$K_2^*(1430)\gamma$	( 1.7 ± 0.6 / 0.5 ) × 10 <sup>-5</sup>		2447
$K_2(1770)\gamma$	< 1.2 × 10 <sup>-3</sup>	CL=90%	2342
$K_3^*(1780)\gamma$	< 3.7 × 10 <sup>-5</sup>	CL=90%	2341
$K_4^*(2045)\gamma$	< 1.0 × 10 <sup>-3</sup>	CL=90%	2244
$K\eta'(958)$	( 8.3 ± 1.1 ) × 10 <sup>-5</sup>		2528
$K^*(892)\eta'(958)$	( 4.1 ± 1.1 ) × 10 <sup>-6</sup>		2472
$K\eta$	< 5.2 × 10 <sup>-6</sup>	CL=90%	2588
$K^*(892)\eta$	( 1.8 ± 0.5 ) × 10 <sup>-5</sup>		2534
$K\phi\phi$	( 2.3 ± 0.9 ) × 10 <sup>-6</sup>		2306
$\bar{b} \rightarrow \bar{s} \gamma$	( 3.53 ± 0.24 ) × 10 <sup>-4</sup>		—
$\bar{b} \rightarrow \bar{d} \gamma$	( 9.2 ± 3.0 ) × 10 <sup>-6</sup>		—
$\bar{b} \rightarrow \bar{s} \text{gluon}$	< 6.8 %	CL=90%	—
$\eta$ anything	( 2.6 ± 0.5 / 0.8 ) × 10 <sup>-4</sup>		—
$\eta'$ anything	( 4.2 ± 0.9 ) × 10 <sup>-4</sup>		—
$K^+$ gluon (charmless)	< 1.87 × 10 <sup>-4</sup>	CL=90%	—
$K^0$ gluon (charmless)	( 1.9 ± 0.7 ) × 10 <sup>-4</sup>		—

## Light unflavored meson modes

$\rho\gamma$	( 1.39 ± 0.25 ) × 10 <sup>-6</sup>	S=1.2	2583
$\rho/\omega\gamma$	( 1.30 ± 0.23 ) × 10 <sup>-6</sup>	S=1.2	—
$\pi^\pm$ anything	[ee,hhhh] ( 35.8 ± 7 ) %		—
$\pi^0$ anything	( 235 ± 11 ) %		—
$\eta$ anything	( 17.6 ± 1.6 ) %		—
$\rho^0$ anything	( 21 ± 5 ) %		—
$\omega$ anything	< 81 %	CL=90%	—
$\phi$ anything	( 3.43 ± 0.12 ) %		—
$\phi K^*(892)$	< 2.2 × 10 <sup>-5</sup>	CL=90%	2460
$\pi^+$ gluon (charmless)	( 3.7 ± 0.8 ) × 10 <sup>-4</sup>		—

## Baryon modes

$\Lambda_c^+/\bar{\Lambda}_c^-$ anything	( 4.5 ± 1.2 ) %		—
$\bar{\Lambda}_c^- e^+$ anything	< 1.1 × 10 <sup>-3</sup>	CL=90%	—
$\bar{\Lambda}_c^- p$ anything	( 2.6 ± 0.8 ) %		—
$\bar{\Lambda}_c^- p e^+ \nu_e$	< 1.0 × 10 <sup>-3</sup>	CL=90%	2021
$\Sigma_c^-$ anything	( 4.2 ± 2.4 ) × 10 <sup>-3</sup>		—
$\Sigma_c^-$ anything	< 9.6 × 10 <sup>-3</sup>	CL=90%	—
$\Sigma_c^0$ anything	( 4.6 ± 2.4 ) × 10 <sup>-3</sup>		—
$\Sigma_c^0 N(N = p \text{ or } n)$	< 1.5 × 10 <sup>-3</sup>	CL=90%	1938
$\Xi_c^-$ anything	( 1.93 ± 0.30 ) × 10 <sup>-4</sup>	S=1.1	—
$\Xi_c^0$ anything	( 4.5 ± 1.3 / 1.2 ) × 10 <sup>-4</sup>		—
$\Xi_c^+/\bar{\Xi}_c^-$ anything			—
$\rho/\bar{p}$ anything	[ee] ( 8.0 ± 0.4 ) %		—
$p/\bar{p}$ (direct) anything	[ee] ( 5.5 ± 0.5 ) %		—
$\Lambda/\bar{\Lambda}$ anything	[ee] ( 4.0 ± 0.5 ) %		—
$\Xi^-/\bar{\Xi}^+$ anything	[ee] ( 2.7 ± 0.6 ) × 10 <sup>-3</sup>		—
baryons anything	( 6.8 ± 0.6 ) %		—

## Meson Summary Table

$p\bar{p}$ anything		( 2.47 ± 0.23 ) %	–
$\Lambda\bar{\Lambda}/\bar{\Lambda}p$ anything	[ee]	( 2.5 ± 0.4 ) %	–
$\Lambda\bar{\Lambda}$ anything		< 5 × 10 <sup>-3</sup>	CL=90%
<b>Lepton Family number (LF) violating modes or <math>\Delta B = 1</math> weak neutral current (BI) modes</b>			
$s e^+ e^-$	BI	( 4.7 ± 1.3 ) × 10 <sup>-6</sup>	–
$s \mu^+ \mu^-$	BI	( 4.3 ± 1.2 ) × 10 <sup>-6</sup>	–
$s \ell^+ \ell^-$	BI [ppp]	( 4.5 ± 1.0 ) × 10 <sup>-6</sup>	–
$\pi \ell^+ \ell^-$	BI	< 6.2 × 10 <sup>-8</sup>	CL=90% 2638
$K e^+ e^-$	BI	( 4.4 ± 0.6 ) × 10 <sup>-7</sup>	2617
$K^*(892) e^+ e^-$	BI	( 1.19 ± 0.20 ) × 10 <sup>-6</sup>	S=1.2 2564
$K \mu^+ \mu^-$	BI	( 4.4 ± 0.4 ) × 10 <sup>-7</sup>	2612
$K^*(892) \mu^+ \mu^-$	BI	( 1.06 ± 0.09 ) × 10 <sup>-6</sup>	2560
$K \ell^+ \ell^-$	BI	( 4.5 ± 0.4 ) × 10 <sup>-7</sup>	2617
$K^*(892) \ell^+ \ell^-$	BI	( 1.08 ± 0.11 ) × 10 <sup>-6</sup>	2564
$K \nu \bar{\nu}$	BI	< 1.4 × 10 <sup>-5</sup>	CL=90% 2617
$K^* \nu \bar{\nu}$	BI	< 8 × 10 <sup>-5</sup>	CL=90% –
$s e^\pm \mu^\mp$	LF [ee]	< 2.2 × 10 <sup>-5</sup>	CL=90% –
$\pi e^\pm \mu^\mp$	LF	< 9.2 × 10 <sup>-8</sup>	CL=90% 2637
$\rho e^\pm \mu^\mp$	LF	< 3.2 × 10 <sup>-6</sup>	CL=90% 2582
$K e^\pm \mu^\mp$	LF	< 3.8 × 10 <sup>-8</sup>	CL=90% 2616
$K^*(892) e^\pm \mu^\mp$	LF	< 5.1 × 10 <sup>-7</sup>	CL=90% 2563

 **$B^\pm/B^0/B_s^0/b$ -baryon ADMIXTURE**

These measurements are for an admixture of bottom particles at high energy (LHC, LEP, Tevatron,  $Sp\bar{p}S$ ).

$$\text{Mean life } \tau = (1.568 \pm 0.009) \times 10^{-12} \text{ s}$$

$$\text{Mean life } \tau = (1.72 \pm 0.10) \times 10^{-12} \text{ s} \quad \text{Charged } b\text{-hadron admixture}$$

$$\text{Mean life } \tau = (1.58 \pm 0.14) \times 10^{-12} \text{ s} \quad \text{Neutral } b\text{-hadron admixture}$$

$$\tau_{\text{charged } b\text{-hadron}}/\tau_{\text{neutral } b\text{-hadron}} = 1.09 \pm 0.13$$

$$|\Delta\tau_b|/\tau_{b,\bar{b}} = -0.001 \pm 0.014$$

$$\text{Re}(\epsilon_b) / (1 + |\epsilon_b|^2) = (-2.0 \pm 0.5) \times 10^{-3}$$

The branching fraction measurements are for an admixture of  $B$  mesons and baryons at energies above the  $\Upsilon(4S)$ . Only the highest energy results (LHC, LEP, Tevatron,  $Sp\bar{p}S$ ) are used in the branching fraction averages. In the following, we assume that the production fractions are the same at the LHC, LEP, and at the Tevatron.

For inclusive branching fractions, e.g.,  $B \rightarrow D^\pm$  anything, the values usually are multiplicities, not branching fractions. They can be greater than one.

The modes below are listed for a  $\bar{b}$  initial state.  $b$  modes are their charge conjugates. Reactions indicate the weak decay vertex and do not include mixing.

$\bar{b}$ DECAY MODES	Fraction ( $\Gamma_i/\Gamma$ )	Scale factor/ Confidence level	$p$ (MeV/c)
-----------------------	--------------------------------	-----------------------------------	----------------

**PRODUCTION FRACTIONS**

The production fractions for weakly decaying  $b$ -hadrons at high energy have been calculated from the best values of mean lives, mixing parameters, and branching fractions in this edition by the Heavy Flavor Averaging Group (HFAG) as described in the note “ $B^0$ - $\bar{B}^0$  Mixing” in the  $B^0$  Particle Listings. The production fractions in  $b$ -hadronic  $Z$  decay or  $p\bar{p}$  collisions at the Tevatron are also listed at the end of the section. Values assume

$$B(\bar{b} \rightarrow B^+) = B(\bar{b} \rightarrow B^0)$$

$$B(\bar{b} \rightarrow B^+) + B(\bar{b} \rightarrow B^0) + B(\bar{b} \rightarrow B_s^0) + B(b \rightarrow b\text{-baryon}) = 100 \text{ \%}$$

The correlation coefficients between production fractions are also reported:

$$\text{cor}(B_s^0, b\text{-baryon}) = -0.277$$

$$\text{cor}(B_s^0, B^\pm=B^0) = -0.119$$

$$\text{cor}(b\text{-baryon}, B^\pm=B^0) = -0.921.$$

The notation for production fractions varies in the literature ( $f_d, d_{B^0}, f(b \rightarrow \bar{B}^0), B_f(b \rightarrow \bar{B}^0)$ ). We use our own branching fraction notation here,  $B(\bar{b} \rightarrow B^0)$ .

Note these production fractions are  $b$ -hadronization fractions, not the conventional branching fractions of  $b$ -quark to a  $B$ -hadron, which may have considerable dependence on the initial and final state kinematic and production environment.

$B^+$	( 40.1 ± 0.8 ) %	–
$B^0$	( 40.1 ± 0.8 ) %	–
$B_s^0$	( 10.5 ± 0.6 ) %	–
$b$ -baryon	( 9.3 ± 1.6 ) %	–

**DECAY MODES****Semileptonic and leptonic modes**

$\nu$ anything	( 23.1 ± 1.5 ) %	–
$\ell^+ \nu_\ell$ anything	[ppp] ( 10.69 ± 0.22 ) %	–
$e^+ \nu_e$ anything	( 10.86 ± 0.35 ) %	–
$\mu^+ \nu_\mu$ anything	( 10.95 ± 0.29 ) %	–
$D^- \ell^+ \nu_\ell$ anything	[ppp] ( 2.27 ± 0.35 ) %	S=1.7 –
$D^- \pi^+ \ell^+ \nu_\ell$ anything	( 4.9 ± 1.9 ) × 10 <sup>-3</sup>	–
$D^- \pi^- \ell^+ \nu_\ell$ anything	( 2.6 ± 1.6 ) × 10 <sup>-3</sup>	–
$\bar{D}^0 \ell^+ \nu_\ell$ anything	[ppp] ( 6.84 ± 0.35 ) %	–
$\bar{D}^0 \pi^- \ell^+ \nu_\ell$ anything	( 1.07 ± 0.27 ) %	–
$\bar{D}^0 \pi^+ \ell^+ \nu_\ell$ anything	( 2.3 ± 1.6 ) × 10 <sup>-3</sup>	–
$D^{*-} \ell^+ \nu_\ell$ anything	[ppp] ( 2.75 ± 0.19 ) %	–
$D^{*-} \pi^- \ell^+ \nu_\ell$ anything	( 6 ± 7 ) × 10 <sup>-4</sup>	–
$D^{*-} \pi^+ \ell^+ \nu_\ell$ anything	( 4.8 ± 1.0 ) × 10 <sup>-3</sup>	–
$\bar{D}_j^0 \ell^+ \nu_\ell$ anything × $B(\bar{D}_j^0 \rightarrow D^{*+} \pi^-)$	[ppp,iiii] ( 2.6 ± 0.9 ) × 10 <sup>-3</sup>	–
$D_j^- \ell^+ \nu_\ell$ anything × $B(D_j^- \rightarrow D^0 \pi^-)$	[ppp,iiii] ( 7.0 ± 2.3 ) × 10 <sup>-3</sup>	–
$\bar{D}_2^*(2460)^0 \ell^+ \nu_\ell$ anything × $B(\bar{D}_2^*(2460)^0 \rightarrow D^{*-} \pi^+)$	< 1.4 × 10 <sup>-3</sup>	CL=90% –
$D_2^*(2460)^- \ell^+ \nu_\ell$ anything × $B(D_2^*(2460)^- \rightarrow D^0 \pi^-)$	( 4.2 ± 1.5 ) × 10 <sup>-3</sup>	–
$\bar{D}_2^*(2460)^0 \ell^+ \nu_\ell$ anything × $B(\bar{D}_2^*(2460)^0 \rightarrow D^- \pi^+)$	( 1.6 ± 0.8 ) × 10 <sup>-3</sup>	–
charmless $\ell \bar{\nu}_\ell$	[ppp] ( 1.7 ± 0.5 ) × 10 <sup>-3</sup>	–
$\tau^+ \nu_\tau$ anything	( 2.41 ± 0.23 ) %	–
$D^{*-} \tau \nu_\tau$ anything	( 9 ± 4 ) × 10 <sup>-3</sup>	–
$\bar{c} \rightarrow \ell^- \bar{\nu}_\ell$ anything	[ppp] ( 8.02 ± 0.19 ) %	–
$c \rightarrow \ell^+ \nu$ anything	( 1.6 ± 0.4 ) %	–

**Charmed meson and baryon modes**

$\bar{D}^0$ anything	( 59.8 ± 2.9 ) %	–
$D^0 D_s^\pm$ anything	[ee] ( 9.1 ± 4.0 ) %	–
$D^\mp D_s^\pm$ anything	[ee] ( 4.0 ± 2.3 ) %	–
$\bar{D}^0 D^0$ anything	[ee] ( 5.1 ± 2.0 ) %	–
$D^0 D^\pm$ anything	[ee] ( 2.7 ± 1.8 ) %	–
$D^\pm D^\mp$ anything	[ee] < 9 × 10 <sup>-3</sup>	CL=90% –
$D^-$ anything	( 23.3 ± 1.7 ) %	–
$D^*(2010)^+$ anything	( 17.3 ± 2.0 ) %	–
$D_1(2420)^0$ anything	( 5.0 ± 1.5 ) %	–
$D^*(2010)^\mp D_s^\pm$ anything	[ee] ( 3.3 ± 1.6 ) %	–
$D^0 D^*(2010)^\pm$ anything	[ee] ( 3.0 ± 1.1 ) %	–
$D^*(2010)^\pm D^\mp$ anything	[ee] ( 2.5 ± 1.2 ) %	–
$D^*(2010)^\pm D^*(2010)^\mp$ anything	[ee] ( 1.2 ± 0.4 ) %	–
$\bar{D} D$ anything	( 10 ± 11 ) %	–
$D_2^*(2460)^0$ anything	( 4.7 ± 2.7 ) %	–
$D_s^-$ anything	( 14.7 ± 2.1 ) %	–
$D_s^+$ anything	( 10.1 ± 3.1 ) %	–
$\Lambda_c^+$ anything	( 9.7 ± 2.9 ) %	–
$\bar{c}/c$ anything	[hhhh] (116.2 ± 3.2) %	–

**Charmonium modes**

$J/\psi(1S)$ anything	( 1.16 ± 0.10 ) %	–
$\psi(2S)$ anything	( 4.8 ± 2.4 ) × 10 <sup>-3</sup>	–
$\chi_{c1}(1P)$ anything	( 1.4 ± 0.4 ) %	–

**K or K\* modes**

$\bar{3}\gamma$	( 3.1 ± 1.1 ) × 10 <sup>-4</sup>	–
$\bar{3}P\nu$	< 6.4 × 10 <sup>-4</sup>	CL=90% –
$K^\pm$ anything	( 74 ± 6 ) %	–
$K_S^0$ anything	( 29.0 ± 2.9 ) %	–

**Pion modes**

$\pi^\pm$ anything	( 397 ± 21 ) %	–
$\pi^0$ anything	[hhhh] (278 ± 60) %	–
$\phi$ anything	( 2.82 ± 0.23 ) %	–

## Meson Summary Table

Baryon modes		
$p/\bar{p}$ anything	$(13.1 \pm 1.1) \%$	-
Other modes		
charged anything	$[hhhh] (497 \pm 7) \%$	-
hadron <sup>+</sup> hadron <sup>-</sup>	$(1.7 \pm_{0.7}^{1.0}) \times 10^{-5}$	-
charmless	$(7 \pm_{21}) \times 10^{-3}$	-
Baryon modes		
$\Lambda/\bar{\Lambda}$ anything	$(5.9 \pm 0.6) \%$	-
b-baryon anything	$(10.2 \pm 2.8) \%$	-
$\Delta B = 1$ weak neutral current ( $B1$ ) modes		
$\mu^+ \mu^-$ anything	$B1 < 3.2 \times 10^{-4}$	CL=90%

 **$B^*$** 

$$I(J^P) = \frac{1}{2}(1^-)$$

$I, J, P$  need confirmation. Quantum numbers shown are quark-model predictions.

$$\text{Mass } m_{B^*} = 5325.2 \pm 0.4 \text{ MeV}$$

$$m_{B^*} - m_B = 45.78 \pm 0.35 \text{ MeV}$$

$B^*$ DECAY MODES	Fraction ( $\Gamma_i/\Gamma$ )	$\rho$ (MeV/c)
$B^* \gamma$	dominant	45

 **$B_1(5721)^0$** 

$$I(J^P) = \frac{1}{2}(1^+)$$

$I, J, P$  need confirmation.

$$B_1(5721)^0 \text{ MASS} = 5723.5 \pm 2.0 \text{ MeV} \quad (S = 1.1)$$

$$m_{B_1^0} - m_{B^+} = 444.3 \pm 2.0 \text{ MeV} \quad (S = 1.1)$$

$B_1(5721)^0$ DECAY MODES	Fraction ( $\Gamma_i/\Gamma$ )	$\rho$ (MeV/c)
$B^{*+} \pi^-$	dominant	-

 **$B_2^*(5747)^0$** 

$$I(J^P) = \frac{1}{2}(2^+)$$

$I, J, P$  need confirmation.

$$B_2^*(5747)^0 \text{ MASS} = 5743 \pm 5 \text{ MeV} \quad (S = 2.9)$$

$$\text{Full width } \Gamma = 23 \pm_{11}^5 \text{ MeV}$$

$$m_{B_2^{*0}} - m_{B_1^0} = 19 \pm 6 \text{ MeV} \quad (S = 3.0)$$

$B_2^*(5747)^0$ DECAY MODES	Fraction ( $\Gamma_i/\Gamma$ )	$\rho$ (MeV/c)
$B^+ \pi^-$	dominant	424
$B^{*+} \pi^-$	dominant	-

## BOTTOM, STRANGE MESONS ( $B = \pm 1, S = \mp 1$ )

$$B_s^0 = s\bar{b}, \bar{B}_s^0 = \bar{s}b, \text{ similarly for } B_s^{*+}s$$

 **$B_s^0$** 

$$I(J^P) = 0(0^-)$$

$I, J, P$  need confirmation. Quantum numbers shown are quark-model predictions.

$$\text{Mass } m_{B_s^0} = 5366.77 \pm 0.24 \text{ MeV}$$

$$m_{B_s^0} - m_B = 87.35 \pm 0.23 \text{ MeV}$$

$$\text{Mean life } \tau = (1.497 \pm 0.015) \times 10^{-12} \text{ s}$$

$$c\tau = 449 \mu\text{m}$$

$$\Delta\Gamma_{B_s^0} = \Gamma_{B_{sL}^0} - \Gamma_{B_{sH}^0} = (0.100 \pm 0.013) \times 10^{12} \text{ s}^{-1}$$

 **$B_s^0$ - $\bar{B}_s^0$  mixing parameters**

$$\Delta m_{B_s^0} = m_{B_{sH}^0} - m_{B_{sL}^0} = (17.69 \pm 0.08) \times 10^{12} \text{ } \hbar \text{ s}^{-1}$$

$$= (116.4 \pm 0.5) \times 10^{-10} \text{ MeV}$$

$$x_s = \Delta m_{B_s^0} / \Gamma_{B_s^0} = 26.49 \pm 0.29$$

$$\chi_s = 0.499292 \pm 0.000016$$

**CP violation parameters in  $B_s^0$** 

$$\text{Re}(\epsilon_{B_s^0}) / (1 + |\epsilon_{B_s^0}|^2) = (-2.6 \pm 1.6) \times 10^{-3}$$

$$\text{CP Violation phase } \beta_s = 0.08 \pm_{0.07}^{0.05}$$

$$A_{CP}(B_s \rightarrow \pi^+ K^-) = 0.39 \pm 0.17$$

These branching fractions all scale with  $B(\bar{b} \rightarrow B_s^0)$ .

The branching fraction  $B(B_s^0 \rightarrow D_s^- \ell^+ \nu_\ell \text{ anything})$  is not a pure measurement since the measured product branching fraction  $B(\bar{b} \rightarrow B_s^0) \times B(B_s^0 \rightarrow D_s^- \ell^+ \nu_\ell \text{ anything})$  was used to determine  $B(\bar{b} \rightarrow B_s^0)$ , as described in the note on " $B^0$ - $\bar{B}^0$  Mixing"

For inclusive branching fractions, e.g.,  $B \rightarrow D^\pm \text{ anything}$ , the values usually are multiplicities, not branching fractions. They can be greater than one.

$B_s^0$ DECAY MODES	Fraction ( $\Gamma_i/\Gamma$ )	Confidence level	$\rho$ (MeV/c)
$D_s^-$ anything	$(93 \pm_{25}) \%$	-	-
$\ell \nu_\ell X$	$(9.5 \pm_{2.7}) \%$	-	-
$D_s^- \ell^+ \nu_\ell \text{ anything}$	$[jjjj] (7.9 \pm_{2.4}) \%$	-	-
$D_{s1}(2536)^- \mu^+ \nu_\mu$	$(2.5 \pm_{0.7}) \times 10^{-3}$	-	-
$D_{s1}^- \rightarrow D^{*-} K_S^0$			
$D_{s1}(2536)^- X \mu^+ \nu$	$(4.3 \pm_{1.7}) \times 10^{-3}$	-	-
$D_{s1}^- \rightarrow \bar{D}^0 K^+$			
$D_{s2}(2573)^- X \mu^+ \nu$	$(2.6 \pm_{1.2}) \times 10^{-3}$	-	-
$D_{s2}^- \rightarrow \bar{D}^0 K^+$			
$D_s^- \pi^+$	$(3.2 \pm_{0.4}) \times 10^{-3}$	2320	
$D_s^- \rho^+$	$(7.4 \pm_{1.7}) \times 10^{-3}$	2248	
$D_s^- \pi^+ \pi^+ \pi^-$	$(6.5 \pm_{1.2}) \times 10^{-3}$	2301	
$D_s^- K^\pm$	$(2.9 \pm_{0.6}) \times 10^{-4}$	2293	
$D_s^+ D_s^-$	$(5.3 \pm_{0.9}) \times 10^{-3}$	1824	
$D_s^- \pi^+$	$(2.1 \pm_{0.6}) \times 10^{-3}$	2265	
$D_s^- \rho^+$	$(1.03 \pm_{0.26}) \%$	2190	
$D_s^{*+} D_s^- + D_s^{*-} D_s^+$	$(1.24 \pm_{0.21}) \%$	1742	
$D_s^+ D_s^{*-}$	$(1.88 \pm_{0.34}) \%$	1655	
$D_s^{(*)+} D_s^{(*)-}$	$(4.5 \pm_{1.4}) \%$	-	
$\bar{D}^0 \bar{K}^*(892)^0$	$(4.7 \pm_{1.4}) \times 10^{-4}$	2264	
$J/\psi(1S) \phi$	$(1.09 \pm_{0.23}^{0.28}) \times 10^{-3}$	1588	
$J/\psi(1S) \pi^0$	$< 1.2 \times 10^{-3}$	90%	1786
$J/\psi(1S) \eta$	$(5.1 \pm_{1.0}^{1.3}) \times 10^{-4}$		1733
$J/\psi(1S) K^0$	$(3.6 \pm_{0.8}) \times 10^{-5}$		1743
$J/\psi(1S) K^{*0}$	$(9 \pm_4) \times 10^{-5}$		-
$J/\psi(1S) \eta'$	$(3.7 \pm_{0.9}^{1.0}) \times 10^{-4}$		1612
$J/\psi(1S) f_0(980), f_0 \rightarrow \pi^+ \pi^-$	$(1.36 \pm_{0.28}^{0.35}) \times 10^{-4}$		-
$J/\psi(1S) f_0(1370), f_0 \rightarrow \pi^+ \pi^-$	$(3.4 \pm_{1.4}) \times 10^{-5}$		-
$\psi(2S) \phi$	$(5.7 \pm_{1.6}^{1.8}) \times 10^{-4}$	1120	
$\pi^+ \pi^-$	$< 1.2 \times 10^{-6}$	90%	2680
$\pi^0 \pi^0$	$< 2.1 \times 10^{-4}$	90%	2680
$\eta \pi^0$	$< 1.0 \times 10^{-3}$	90%	2654
$\eta \eta$	$< 1.5 \times 10^{-3}$	90%	2627
$\rho^0 \rho^0$	$< 3.20 \times 10^{-4}$	90%	2569
$\phi \rho^0$	$< 6.17 \times 10^{-4}$	90%	2526
$\phi \phi$	$(1.9 \pm_{0.5}^{0.6}) \times 10^{-5}$		2482
$\pi^+ K^-$	$(5.3 \pm_{1.0}) \times 10^{-6}$		2659
$K^+ K^-$	$(2.64 \pm_{0.28}) \times 10^{-5}$		2638
$K^0 \bar{K}^0$	$< 6.6 \times 10^{-5}$	90%	2637
$\bar{K}^*(892)^0 \rho^0$	$< 7.67 \times 10^{-4}$	90%	2550
$\bar{K}^*(892)^0 K^*(892)^0$	$(2.8 \pm_{0.7}) \times 10^{-5}$		2531
$\phi K^*(892)^0$	$< 1.013 \times 10^{-3}$	90%	2507
$\rho \bar{\rho}$	$< 5.9 \times 10^{-5}$	90%	2514
$\gamma \gamma$	$< 8.7 \times 10^{-6}$	90%	2683
$\phi \gamma$	$(5.7 \pm_{1.9}^{2.2}) \times 10^{-5}$		2587

## Meson Summary Table

Lepton Family number (LF) violating modes or $\Delta B = 1$ weak neutral current (BI) modes						
$\mu^+ \mu^-$	BI	< 6.4	$\times 10^{-9}$	90%	2681	
$e^+ e^-$	BI	< 2.8	$\times 10^{-7}$	90%	2683	
$e^\pm \mu^\mp$	LF	[ee]	< 2.0	$\times 10^{-7}$	90%	2682
$\phi(1020) \mu^+ \mu^-$	BI	$(1.23 \pm_{-0.34}^{+0.40})$	$\times 10^{-6}$		2582	
$\phi \nu \bar{\nu}$	BI	< 5.4	$\times 10^{-3}$	90%	2587	

 **$B_s^*$** 

$$I(J^P) = 0(1^-)$$

$I, J, P$  need confirmation. Quantum numbers shown are quark-model predictions.

$$\text{Mass } m = 5415.4 \pm_{-2.1}^{+2.4} \text{ MeV} \quad (S = 3.0)$$

$$m_{B_s^*} - m_{B_s} = 48.7 \pm_{-2.1}^{+2.3} \text{ MeV} \quad (S = 2.8)$$

$B_s^*$ DECAY MODES	Fraction ( $\Gamma_i/\Gamma$ )	$\rho$ (MeV/c)
$B_s \gamma$	dominant	-

 **$B_{s1}(5830)^0$** 

$$I(J^P) = 0(1^+)$$

$I, J, P$  need confirmation.

$$\text{Mass } m = 5829.4 \pm 0.7 \text{ MeV}$$

$$m_{B_{s1}^0} - m_{B^{*+}} = 504.41 \pm 0.25 \text{ MeV}$$

$B_{s1}(5830)^0$ DECAY MODES	Fraction ( $\Gamma_i/\Gamma$ )	$\rho$ (MeV/c)
$B^{*+} K^-$	dominant	-

 **$B_{s2}^*(5840)^0$** 

$$I(J^P) = 0(2^+)$$

$I, J, P$  need confirmation.

$$\text{Mass } m = 5839.7 \pm 0.6 \text{ MeV}$$

$$m_{B_{s2}^0} - m_{B_{s1}^0} = 10.5 \pm 0.6 \text{ MeV}$$

$B_{s2}^*(5840)^0$ DECAY MODES	Fraction ( $\Gamma_i/\Gamma$ )	$\rho$ (MeV/c)
$B^+ K^-$	dominant	25.2

## BOTTOM, CHARMED MESONS ( $B = C = \pm 1$ )

$$B_c^+ = c\bar{b}, B_c^- = \bar{c}b, \text{ similarly for } B_c^{* \prime s}$$

 **$B_c^\pm$** 

$$I(J^P) = 0(0^-)$$

$I, J, P$  need confirmation.

Quantum numbers shown are quark-model predictions.

$$\text{Mass } m = 6.277 \pm 0.006 \text{ GeV} \quad (S = 1.6)$$

$$\text{Mean life } \tau = (0.453 \pm 0.041) \times 10^{-12} \text{ s}$$

$B_c^-$  modes are charge conjugates of the modes below.

$B_c^\pm$ DECAY MODES $\times B(\bar{b} \rightarrow B_c)$	Fraction ( $\Gamma_i/\Gamma$ )	Confidence level	$\rho$ (MeV/c)
---	--------------------------------	------------------	----------------

The following quantities are not pure branching ratios; rather the fraction  $\Gamma_i/\Gamma \times B(\bar{b} \rightarrow B_c)$ .

$J/\psi(1S) \ell^+ \nu_\ell \text{ anything}$	$(5.2 \pm_{-2.1}^{+2.4}) \times 10^{-5}$	-	
$J/\psi(1S) \pi^+$	< 8.2	$\times 10^{-5}$	90%
$J/\psi(1S) \pi^+ \pi^+ \pi^-$	< 5.7	$\times 10^{-4}$	90%
$J/\psi(1S) a_1(1260)$	< 1.2	$\times 10^{-3}$	90%
$D^*(2010) \rightarrow \bar{D}^0$	< 6.2	$\times 10^{-3}$	90%

## $c\bar{c}$ MESONS

 **$\eta_c(1S)$** 

$$I^G(J^{PC}) = 0^+(0^{-+})$$

$$\text{Mass } m = 2981.0 \pm 1.1 \text{ MeV} \quad (S = 1.7)$$

$$\text{Full width } \Gamma = 29.7 \pm 1.0 \text{ MeV}$$

 **$\eta_c(1S)$  DECAY MODES**Fraction ( $\Gamma_i/\Gamma$ )

Confidence level

 $\rho$  (MeV/c)

Decays involving hadronic resonances			
$\eta'(958) \pi \pi$	(4.1 $\pm$ 1.7) %		1322
$\rho \rho$	(1.8 $\pm$ 0.5) %		1273
$K^*(892)^0 K^- \pi^+ + \text{c.c.}$	(2.0 $\pm$ 0.7) %		1276
$K^*(892) \bar{K}^*(892)$	(6.8 $\pm$ 1.3) $\times 10^{-3}$		1194
$K^* \bar{K}^* \pi^+ \pi^-$	(1.1 $\pm$ 0.5) %		1071
$\phi K^+ K^-$	(2.9 $\pm$ 1.4) $\times 10^{-3}$		1102
$\phi \phi$	(1.94 $\pm$ 0.30) $\times 10^{-3}$		1087
$\phi 2(\pi^+ \pi^-)$	< 3.5	$\times 10^{-3}$	90%
$a_0(980) \pi$	< 2	%	90%
$a_2(1320) \pi$	< 2	%	90%
$K^*(892) \bar{K} + \text{c.c.}$	< 1.28	%	90%
$f_2(1270) \eta$	< 1.1	%	90%
$\omega \omega$	< 3.1	$\times 10^{-3}$	90%
$\omega \phi$	< 1.7	$\times 10^{-3}$	90%
$f_2(1270) f_2(1270)$	(9.7 $\pm$ 2.5) $\times 10^{-3}$		772
$f_2(1270) f_2'(1525)$	(9.3 $\pm$ 3.1) $\times 10^{-3}$		509

## Decays into stable hadrons

$K \bar{K} \pi$	(7.2 $\pm$ 0.6) %		1379
$\eta \pi^+ \pi^-$	(4.9 $\pm$ 1.8) %		1426
$K^+ K^- \pi^+ \pi^-$	(6.1 $\pm$ 1.2) $\times 10^{-3}$		1343
$K^+ K^- \pi^+ \pi^- \pi^0$	(3.4 $\pm$ 0.6) %		1303
$K^+ K^- 2(\pi^+ \pi^-)$	(7.1 $\pm$ 2.9) $\times 10^{-3}$		1252
$2(K^+ K^-)$	(1.34 $\pm$ 0.32) $\times 10^{-3}$		1054
$2(\pi^+ \pi^-)$	(8.6 $\pm$ 1.3) $\times 10^{-3}$		1458
$3(\pi^+ \pi^-)$	(1.5 $\pm$ 0.5) %		1405
$\rho \bar{\rho}$	(1.41 $\pm$ 0.17) $\times 10^{-3}$		1158
$\Lambda \bar{\Lambda}$	(9.4 $\pm$ 3.2) $\times 10^{-4}$		988
$K \bar{K} \eta$	< 3.1	%	90%
$\pi^+ \pi^- \rho \bar{\rho}$	< 1.2	%	90%

## Radiative decays

$\gamma \gamma$	(1.78 $\pm$ 0.16) $\times 10^{-4}$		1490
-----------------	------------------------------------	--	------

### Charge conjugation (C), Parity (P), Lepton family number (LF) violating modes

$\pi^+ \pi^-$	$P, CP$	< 1.1	$\times 10^{-4}$	90%	1484
$\pi^0 \pi^0$	$P, CP$	< 3.5	$\times 10^{-5}$	90%	1484
$K^+ K^-$	$P, CP$	< 6	$\times 10^{-4}$	90%	1406
$K_S^0 K_S^0$	$P, CP$	< 3.1	$\times 10^{-4}$	90%	1405

 **$J/\psi(1S)$** 

$$I^G(J^{PC}) = 0^-(1^{--})$$

$$\text{Mass } m = 3096.916 \pm 0.011 \text{ MeV}$$

$$\text{Full width } \Gamma = 92.9 \pm 2.8 \text{ keV} \quad (S = 1.1)$$

$$\Gamma_{ee} = 5.55 \pm 0.14 \pm 0.02 \text{ keV}$$

 **$J/\psi(1S)$  DECAY MODES**Fraction ( $\Gamma_i/\Gamma$ )Scale factor/  
Confidence level (MeV/c)

hadrons	(87.7 $\pm$ 0.5) %		-
virtual $\gamma \rightarrow$ hadrons	(13.50 $\pm$ 0.30) %		-
$g g g$	(64.1 $\pm$ 1.0) %		-
$\gamma g g$	(8.8 $\pm$ 1.1) %		-
$e^+ e^-$	(5.94 $\pm$ 0.06) %		1548
$e^+ e^- \gamma$	[kkkk] (8.8 $\pm$ 1.4) $\times 10^{-3}$		1548
$\mu^+ \mu^-$	(5.93 $\pm$ 0.06) %		1545

## Decays involving hadronic resonances

$\rho \pi$	(1.69 $\pm$ 0.15) %	S=2.4	1448
$\rho^0 \pi^0$	(5.6 $\pm$ 0.7) $\times 10^{-3}$		1448
$a_2(1320) \rho$	(1.09 $\pm$ 0.22) %		1123
$\omega \pi^+ \pi^+ \pi^- \pi^-$	(8.5 $\pm$ 3.4) $\times 10^{-3}$		1392
$\omega \pi^+ \pi^- \pi^0$	(4.0 $\pm$ 0.7) $\times 10^{-3}$		1418
$\omega \pi^+ \pi^-$	(8.6 $\pm$ 0.7) $\times 10^{-3}$	S=1.1	1435
$\omega f_2(1270)$	(4.3 $\pm$ 0.6) $\times 10^{-3}$		1142
$K^*(892)^0 \bar{K}^*(892)^0$	(2.3 $\pm$ 0.7) $\times 10^{-4}$		1266
$K^*(892)^\pm \bar{K}^*(892)^\mp$	(1.00 $\pm_{-0.40}^{+0.22}$ ) $\times 10^{-3}$		1266
$K^*(892)^\pm \bar{K}^*(800)^\mp$	(1.1 $\pm_{-0.6}^{+1.0}$ ) $\times 10^{-3}$		-
$\eta K^*(892)^0 \bar{K}^*(892)^0$	(1.15 $\pm$ 0.26) $\times 10^{-3}$		1003
$K^*(892)^0 \bar{K}_2^*(1430)^0 + \text{c.c.}$	(6.0 $\pm$ 0.6) $\times 10^{-3}$		1012
$K^*(892)^0 \bar{K}_2^*(1770)^0 + \text{c.c.} \rightarrow$	(6.9 $\pm$ 0.9) $\times 10^{-4}$		-
$K^*(892)^0 K^- \pi^+ + \text{c.c.}$			
$\omega K^*(892) \bar{K} + \text{c.c.}$	(6.1 $\pm$ 0.9) $\times 10^{-3}$		1097
$K^+ \bar{K}^*(892)^- + \text{c.c.}$	(5.12 $\pm$ 0.30) $\times 10^{-3}$		1373

## Meson Summary Table

$K^+ \bar{K}^*(892)^- + \text{c.c.} \rightarrow$	$(1.97 \pm 0.20) \times 10^{-3}$	-	$K \bar{K} \pi$	$(6.1 \pm 1.0) \times 10^{-3}$	1442
$K^+ \bar{K}^*(892)^0 + \text{c.c.} \rightarrow$	$(3.0 \pm 0.4) \times 10^{-3}$	-	$2(\pi^+ \pi^-)$	$(3.55 \pm 0.23) \times 10^{-3}$	1517
$K^0 \bar{K}^*(892)^0 + \text{c.c.} \rightarrow$	$(4.39 \pm 0.31) \times 10^{-3}$	1373	$3(\pi^+ \pi^-)$	$(4.3 \pm 0.4) \times 10^{-3}$	1466
$K^0 \bar{K}^*(892)^0 + \text{c.c.} \rightarrow$	$(3.2 \pm 0.4) \times 10^{-3}$	-	$2(\pi^+ \pi^- \pi^0)$	$(1.62 \pm 0.21) \%$	1468
$K_1(1400)^\pm K^\mp$	$(3.8 \pm 1.4) \times 10^{-3}$	1170	$2(\pi^+ \pi^-) \eta$	$(2.29 \pm 0.24) \times 10^{-3}$	1446
$\bar{K}^*(892)^0 K^+ \pi^- + \text{c.c.}$	seen	1343	$3(\pi^+ \pi^-) \eta$	$(7.2 \pm 1.5) \times 10^{-4}$	1379
$\omega \pi^0 \pi^0$	$(3.4 \pm 0.8) \times 10^{-3}$	1436	$\rho \bar{\rho}$	$(2.17 \pm 0.07) \times 10^{-3}$	1232
$b_1(1235)^\pm \pi^\mp$	[ee] $(3.0 \pm 0.5) \times 10^{-3}$	1300	$\rho \bar{\rho} \pi^0$	$(1.19 \pm 0.08) \times 10^{-3}$	S=1.1 1176
$\omega K^\pm K_S^0 \pi^\mp$	[ee] $(3.4 \pm 0.5) \times 10^{-3}$	1210	$\rho \bar{\rho} \pi^+ \pi^-$	$(6.0 \pm 0.5) \times 10^{-3}$	S=1.3 1107
$b_1(1235)^0 \pi^0$	$(2.3 \pm 0.6) \times 10^{-3}$	1300	$\rho \bar{\rho} \pi^+ \pi^- \pi^0$	[    ] $(2.3 \pm 0.9) \times 10^{-3}$	S=1.9 1033
$\eta K^\pm K_S^0 \pi^\mp$	[ee] $(2.2 \pm 0.4) \times 10^{-3}$	1278	$\rho \bar{\rho} \eta$	$(2.00 \pm 0.12) \times 10^{-3}$	948
$\phi K^*(892) \bar{K} + \text{c.c.}$	$(2.18 \pm 0.23) \times 10^{-3}$	969	$\rho \bar{\rho} \rho$	$< 3.1 \times 10^{-4}$	CL=90% 774
$\omega K \bar{K}$	$(1.70 \pm 0.32) \times 10^{-3}$	1268	$\rho \bar{\rho} \omega$	$(1.10 \pm 0.15) \times 10^{-3}$	S=1.3 768
$\omega f_0(1710) \rightarrow \omega K \bar{K}$	$(4.8 \pm 1.1) \times 10^{-4}$	878	$\rho \bar{\rho} \eta'(958)$	$(2.1 \pm 0.4) \times 10^{-4}$	596
$\phi 2(\pi^+ \pi^-)$	$(1.66 \pm 0.23) \times 10^{-3}$	1318	$\rho \bar{\rho} \phi$	$(4.5 \pm 1.5) \times 10^{-5}$	527
$\Delta(1232)^{++} \bar{p} \pi^-$	$(1.6 \pm 0.5) \times 10^{-3}$	1030	$n \bar{n}$	$(2.2 \pm 0.4) \times 10^{-3}$	1231
$\omega \eta$	$(1.74 \pm 0.20) \times 10^{-3}$	S=1.6 1394	$n \bar{n} \pi^+ \pi^-$	$(4 \pm 4) \times 10^{-3}$	1106
$\phi K \bar{K}$	$(1.83 \pm 0.24) \times 10^{-3}$	S=1.5 1179	$\Sigma^+ \bar{\Sigma}^-$	$(1.50 \pm 0.24) \times 10^{-3}$	992
$\phi f_0(1710) \rightarrow \phi K \bar{K}$	$(3.6 \pm 0.6) \times 10^{-4}$	875	$\Sigma^0 \bar{\Sigma}^0$	$(1.29 \pm 0.09) \times 10^{-3}$	988
$\phi f_2(1270)$	$(7.2 \pm 1.3) \times 10^{-4}$	1036	$2(\pi^+ \pi^-) K^+ K^-$	$(4.7 \pm 0.7) \times 10^{-3}$	S=1.3 1320
$\Delta(1232)^{++} \bar{\Delta}(1232)^{--}$	$(1.10 \pm 0.29) \times 10^{-3}$	938	$\rho \bar{\rho} \pi^-$	$(2.12 \pm 0.09) \times 10^{-3}$	1174
$\Sigma(1385)^- \bar{\Sigma}(1385)^+ (\text{or c.c.})$	[ee] $(1.03 \pm 0.13) \times 10^{-3}$	697	$n N(1440)$	seen	978
$\phi f_2'(1525)$	$(8 \pm 4) \times 10^{-4}$	S=2.7 871	$n N(1520)$	seen	924
$\phi \pi^+ \pi^-$	$(9.4 \pm 0.9) \times 10^{-4}$	S=1.2 1365	$n N(1535)$	seen	914
$\phi \pi^0 \pi^0$	$(5.6 \pm 1.6) \times 10^{-4}$	1366	$\Xi^- \bar{\Xi}^+$	$(8.5 \pm 1.6) \times 10^{-4}$	S=1.5 807
$\phi K^\pm K_S^0 \pi^\mp$	[ee] $(7.2 \pm 0.8) \times 10^{-4}$	1114	$\Lambda \bar{\Lambda}$	$(1.61 \pm 0.15) \times 10^{-3}$	S=1.9 1074
$\omega f_1(1420)$	$(6.8 \pm 2.4) \times 10^{-4}$	1062	$\Lambda \bar{\Sigma}^- \pi^+ (\text{or c.c.})$	[ee] $(8.3 \pm 0.7) \times 10^{-4}$	S=1.2 950
$\phi \eta$	$(7.5 \pm 0.8) \times 10^{-4}$	S=1.5 1320	$\rho K^- \bar{\Lambda}$	$(8.9 \pm 1.6) \times 10^{-4}$	876
$\Xi(1530)^0 \Xi^0$	$(1.20 \pm 0.24) \times 10^{-3}$	818	$2(K^+ K^-)$	$(7.6 \pm 0.9) \times 10^{-4}$	1131
$\Xi(1530)^- \Xi^+$	$(5.9 \pm 1.5) \times 10^{-4}$	600	$\rho K^- \bar{\Sigma}^0$	$(2.9 \pm 0.8) \times 10^{-4}$	819
$\rho K^- \bar{\Sigma}(1385)^0$	$(5.1 \pm 3.2) \times 10^{-4}$	646	$K^+ K^-$	$(2.37 \pm 0.31) \times 10^{-4}$	1468
$\omega \pi^0$	$(4.5 \pm 0.5) \times 10^{-4}$	S=1.4 1446	$K_S^0 K_L^0$	$(1.46 \pm 0.26) \times 10^{-4}$	S=2.7 1466
$\phi \eta'(958)$	$(4.0 \pm 0.7) \times 10^{-4}$	S=2.1 1192	$\Lambda \bar{\Lambda} \eta$	$(2.6 \pm 0.7) \times 10^{-4}$	672
$\phi f_0(980)$	$(3.2 \pm 0.9) \times 10^{-4}$	S=1.9 1178	$\Lambda \bar{\Lambda} \pi^0$	$< 6.4 \times 10^{-5}$	CL=90% 998
$\phi f_0(980) \rightarrow \phi \pi^+ \pi^-$	$(1.8 \pm 0.4) \times 10^{-4}$	-	$\bar{\Lambda} n K_S^0 + \text{c.c.}$	$(6.5 \pm 1.1) \times 10^{-4}$	872
$\phi f_0(980) \rightarrow \phi \pi^0 \pi^0$	$(1.7 \pm 0.7) \times 10^{-4}$	-	$\pi^+ \pi^-$	$(1.47 \pm 0.23) \times 10^{-4}$	1542
$\eta \phi f_0(980) \rightarrow \eta \phi \pi^+ \pi^-$	$(3.2 \pm 1.0) \times 10^{-4}$	-	$\Lambda \bar{\Sigma} + \text{c.c.}$	$< 1.5 \times 10^{-4}$	CL=90% 1034
$\phi a_0(980)^0 \rightarrow \phi \eta \pi^0$	$(5 \pm 4) \times 10^{-6}$	-	$K_S^0 K_S^0$	$< 1 \times 10^{-6}$	CL=95% 1466
$\Xi(1530)^0 \Xi^0$	$(3.2 \pm 1.4) \times 10^{-4}$	608			
$\Sigma(1385)^- \bar{\Sigma}^+ (\text{or c.c.})$	[ee] $(3.1 \pm 0.5) \times 10^{-4}$	855	<b>Radiative decays</b>		
$\phi f_1(1285)$	$(2.6 \pm 0.5) \times 10^{-4}$	S=1.1 1032	$3\gamma$	$(1.2 \pm 0.4) \times 10^{-5}$	1548
$\eta \pi^+ \pi^-$	$(4.0 \pm 1.7) \times 10^{-4}$	1487	$4\gamma$	$< 9 \times 10^{-6}$	CL=90% 1548
$\rho \eta$	$(1.93 \pm 0.23) \times 10^{-4}$	1396	$5\gamma$	$< 1.5 \times 10^{-5}$	CL=90% 1548
$\omega \eta'(958)$	$(1.82 \pm 0.21) \times 10^{-4}$	1279	$\gamma \eta_c(1S)$	$(1.7 \pm 0.4) \%$	S=1.6 114
$\omega f_0(980)$	$(1.4 \pm 0.5) \times 10^{-4}$	1267	$\gamma \eta_c(1S) \rightarrow 3\gamma$	$(1.2 \pm 2.7_{-1.1}) \times 10^{-6}$	-
$\rho \eta'(958)$	$(1.05 \pm 0.18) \times 10^{-4}$	1281	$\gamma \pi^+ \pi^- 2\pi^0$	$(8.3 \pm 3.1) \times 10^{-3}$	1518
$a_2(1320)^\pm \pi^\mp$	[ee] $< 4.3 \times 10^{-3}$	CL=90% 1263	$\gamma \eta \pi \pi$	$(6.1 \pm 1.0) \times 10^{-3}$	1487
$K \bar{K}_2^*(1430) + \text{c.c.}$	$< 4.0 \times 10^{-3}$	CL=90% 1159	$\gamma \eta_2(1870) \rightarrow \gamma \eta \pi^+ \pi^-$	$(6.2 \pm 2.4) \times 10^{-4}$	-
$K_1(1270)^\pm K^\mp$	$< 3.0 \times 10^{-3}$	CL=90% 1231	$\gamma \eta(1405/1475) \rightarrow \gamma K \bar{K} \pi$	[η] $(2.8 \pm 0.6) \times 10^{-3}$	S=1.6 1223
$K_2^*(1430)^0 \bar{K}_2^*(1430)^0$	$< 2.9 \times 10^{-3}$	CL=90% 604	$\gamma \eta(1405/1475) \rightarrow \gamma \gamma \rho^0$	$(7.8 \pm 2.0) \times 10^{-5}$	S=1.8 1223
$\phi \pi^0$	$< 6.4 \times 10^{-6}$	CL=90% 1377	$\gamma \eta(1405/1475) \rightarrow \gamma \eta \pi^+ \pi^-$	$(3.0 \pm 0.5) \times 10^{-4}$	-
$\phi \eta(1405) \rightarrow \phi \eta \pi \pi$	$< 2.5 \times 10^{-4}$	CL=90% 946	$\gamma \eta(1405/1475) \rightarrow \gamma \gamma \phi$	$< 8.2 \times 10^{-5}$	CL=95% -
$\omega f_2'(1525)$	$< 2.2 \times 10^{-4}$	CL=90% 1003	$\gamma \rho \rho$	$(4.5 \pm 0.8) \times 10^{-3}$	1340
$\eta \phi(2170) \rightarrow$	$< 2.52 \times 10^{-4}$	CL=90% -	$\gamma \rho \omega$	$< 5.4 \times 10^{-4}$	CL=90% 1338
$\eta K^*(892)^0 \bar{K}^*(892)^0$			$\gamma \rho \phi$	$< 8.8 \times 10^{-5}$	CL=90% 1258
$\Sigma(1385)^0 \bar{\Lambda}$	$< 2 \times 10^{-4}$	CL=90% 912	$\gamma \eta'(958)$	$(5.16 \pm 0.15) \times 10^{-3}$	S=1.1 1400
$\Delta(1232)^+ \bar{p}$	$< 1 \times 10^{-4}$	CL=90% 1100	$\gamma 2\pi^+ 2\pi^-$	$(2.8 \pm 0.5) \times 10^{-3}$	S=1.9 1517
$\Theta(1540) \bar{\Theta}(1540) \rightarrow$	$< 1.1 \times 10^{-5}$	CL=90% -	$\gamma f_2(1270) f_2(1270)$	$(9.5 \pm 1.7) \times 10^{-4}$	879
$K_S^0 p K^- \bar{p} + \text{c.c.}$			$\gamma f_2(1270) f_2(1270) (\text{non reso-})$	$(8.2 \pm 1.9) \times 10^{-4}$	-
$\Theta(1540) K^- \bar{p} \rightarrow K_S^0 p K^- \bar{p}$	$< 2.1 \times 10^{-5}$	CL=90% -	$\gamma K^+ K^- \pi^+ \pi^-$	$(2.1 \pm 0.6) \times 10^{-3}$	1407
$\Theta(1540) K_S^0 \bar{p} \rightarrow K_S^0 \bar{p} K^+ n$	$< 1.6 \times 10^{-5}$	CL=90% -	$\gamma f_4(2050)$	$(2.7 \pm 0.7) \times 10^{-3}$	891
$\bar{\Theta}(1540) K^+ n \rightarrow K_S^0 \bar{p} K^+ n$	$< 5.6 \times 10^{-5}$	CL=90% -	$\gamma \omega \omega$	$(1.61 \pm 0.33) \times 10^{-3}$	1336
$\bar{\Theta}(1540) K_S^0 p \rightarrow K_S^0 p K^- \bar{p}$	$< 1.1 \times 10^{-5}$	CL=90% -	$\gamma \eta(1405/1475) \rightarrow \gamma \rho^0 \rho^0$	$(1.7 \pm 0.4) \times 10^{-3}$	S=1.3 1223
$\Sigma^0 \bar{\Lambda}$	$< 9 \times 10^{-5}$	CL=90% 1032	$\gamma f_2(1270)$	$(1.43 \pm 0.11) \times 10^{-3}$	1286
			$\gamma f_0(1710) \rightarrow \gamma K \bar{K}$	$(8.5 \pm 1.2_{-0.9}) \times 10^{-4}$	S=1.2 1075
			$\gamma f_0(1710) \rightarrow \gamma \pi \pi$	$(4.0 \pm 1.0) \times 10^{-4}$	-
			$\gamma f_0(1710) \rightarrow \gamma \omega \omega$	$(3.1 \pm 1.0) \times 10^{-4}$	-
<b>Decays into stable hadrons</b>			$\gamma \eta$	$(1.104 \pm 0.034) \times 10^{-3}$	1500
$2(\pi^+ \pi^-) \pi^0$	$(4.1 \pm 0.5) \%$	S=2.4 1496	$\gamma f_1(1420) \rightarrow \gamma K \bar{K} \pi$	$(7.9 \pm 1.3) \times 10^{-4}$	1220
$3(\pi^+ \pi^-) \pi^0$	$(2.9 \pm 0.6) \%$	1433	$\gamma f_1(1285)$	$(6.1 \pm 0.8) \times 10^{-4}$	1283
$\pi^+ \pi^- \pi^0$	$(2.07 \pm 0.12) \%$	S=1.6 1533	$\gamma f_1(1510) \rightarrow \gamma \eta \pi^+ \pi^-$	$(4.5 \pm 1.2) \times 10^{-4}$	-
$\pi^+ \pi^- \pi^0 K^+ K^-$	$(1.79 \pm 0.29) \%$	S=2.2 1368	$\gamma f_2'(1525)$	$(4.5 \pm 0.7_{-0.4}) \times 10^{-4}$	1173
$4(\pi^+ \pi^-) \pi^0$	$(9.0 \pm 3.0) \times 10^{-3}$	1345	$\gamma f_2(1640) \rightarrow \gamma \omega \omega$	$(2.8 \pm 1.8) \times 10^{-4}$	-
$\pi^+ \pi^- K^+ K^-$	$(6.6 \pm 0.5) \times 10^{-3}$	1407	$\gamma f_2(1910) \rightarrow \gamma \omega \omega$	$(2.0 \pm 1.4) \times 10^{-4}$	-
$\pi^+ \pi^- K^+ K^- \eta$	$(1.84 \pm 0.28) \times 10^{-3}$	1221			
$\pi^0 \pi^0 K^+ K^-$	$(2.45 \pm 0.31) \times 10^{-3}$	1410			

## Meson Summary Table

$\gamma f_2(1950) \rightarrow \gamma K^*(892) \bar{K}^*(892)$	$(7.0 \pm 2.2) \times 10^{-4}$	-	-
$\gamma K^*(892) \bar{K}^*(892)$	$(4.0 \pm 1.3) \times 10^{-3}$	1266	-
$\gamma \phi \phi$	$(4.0 \pm 1.2) \times 10^{-4}$	S=2.1	1166
$\gamma \rho \bar{\rho}$	$(3.8 \pm 1.0) \times 10^{-4}$		1232
$\gamma \eta(2225)$	$(3.3 \pm 0.5) \times 10^{-4}$		749
$\gamma \eta(1760) \rightarrow \gamma \rho^0 \rho^0$	$(1.3 \pm 0.9) \times 10^{-4}$		1048
$\gamma \eta(1760) \rightarrow \gamma \omega \omega$	$(1.98 \pm 0.33) \times 10^{-3}$		-
$\gamma X(1835) \rightarrow \gamma \pi^+ \pi^- \eta'$	$(2.6 \pm 0.4) \times 10^{-4}$		1006
$\gamma X(1835) \rightarrow \gamma \rho \bar{\rho}$	$(7.5 \pm 1.9) \times 10^{-5}$		-
$\gamma (K \bar{K} \pi) [J^{PC} = 0^{-+}]$	$(7 \pm 4) \times 10^{-4}$	S=2.1	1442
$\gamma \pi^0$	$(3.49 \pm 0.33) \times 10^{-5}$		1546
$\gamma \rho \bar{\rho} \pi^+ \pi^-$	$< 7.9 \times 10^{-4}$	CL=90%	1107
$\gamma \Lambda \bar{\Lambda}$	$< 1.3 \times 10^{-4}$	CL=90%	1074
$\gamma f_J(2220)$	$> 2.50 \times 10^{-3}$	CL=99.9%	745
$\gamma f_J(2220) \rightarrow \gamma \pi \pi$	$(8 \pm 4) \times 10^{-5}$		-
$\gamma f_J(2220) \rightarrow \gamma K \bar{K}$	$< 3.6 \times 10^{-5}$		-
$\gamma f_J(2220) \rightarrow \gamma \rho \bar{\rho}$	$(1.5 \pm 0.8) \times 10^{-5}$		-
$\gamma f_0(1500)$	$(1.01 \pm 0.32) \times 10^{-4}$		1183
$\gamma A \rightarrow \gamma$ invisible	$[mmmm] < 6.3 \times 10^{-6}$	CL=90%	-

## Weak decays

$D^- e^+ \nu_e + c.c.$	$< 1.2 \times 10^{-5}$	CL=90%	984
$\bar{D}^0 e^+ e^- + c.c.$	$< 1.1 \times 10^{-5}$	CL=90%	987
$D_s^- e^+ \nu_e + c.c.$	$< 3.6 \times 10^{-5}$	CL=90%	923
$D^- \pi^+ + c.c.$	$< 7.5 \times 10^{-5}$	CL=90%	977
$\bar{D}^0 K^0 + c.c.$	$< 1.7 \times 10^{-4}$	CL=90%	898
$D_s^- \pi^+ + c.c.$	$< 1.3 \times 10^{-4}$	CL=90%	915

Charge conjugation (C), Parity (P),  
Lepton Family number (LF) violating modes

$\gamma \gamma$	C	$< 5 \times 10^{-6}$	CL=90%	1548
$e^\pm \mu^\mp$	LF	$< 1.1 \times 10^{-6}$	CL=90%	1547
$e^\pm \tau^\mp$	LF	$< 8.3 \times 10^{-6}$	CL=90%	1039
$\mu^\pm \tau^\mp$	LF	$< 2.0 \times 10^{-6}$	CL=90%	1035

## Other decays

invisible	$< 7 \times 10^{-4}$	CL=90%	-
-----------	----------------------	--------	---

 **$\chi_{c0}(1P)$** 

$$I^G(J^{PC}) = 0^+(0^{++})$$

Mass  $m = 3414.75 \pm 0.31$  MeV

Full width  $\Gamma = 10.4 \pm 0.6$  MeV

$\chi_{c0}(1P)$ DECAY MODES	Fraction ( $\Gamma_i/\Gamma$ )	Scale factor/ Confidence level	$p$ (MeV/c)
-----------------------------	--------------------------------	-----------------------------------	----------------

## Hadronic decays

$2(\pi^+ \pi^-)$	$(2.26 \pm 0.19) \%$		1679
$\rho^0 \pi^+ \pi^-$	$(8.8 \pm 2.8) \times 10^{-3}$		1607
$f_0(980) f_0(980)$	$(6.7 \pm 2.1) \times 10^{-4}$		1391
$\pi^+ \pi^- \pi^0 \pi^0$	$(3.4 \pm 0.4) \%$		1680
$\rho^+ \pi^- \pi^0 + c.c.$	$(2.9 \pm 0.4) \%$		1607
$4\pi^0$	$(3.3 \pm 0.4) \times 10^{-3}$		1681
$\pi^+ \pi^- K^+ K^-$	$(1.79 \pm 0.15) \%$		1580
$K_0^*(1430)^0 \bar{K}_0^*(1430)^0 \rightarrow \pi^+ \pi^- K^+ K^-$	$(9.9 \pm 2.9) \times 10^{-4}$		-
$K_0^*(1430)^0 \bar{K}_2^*(1430)^0 + c.c. \rightarrow \pi^+ \pi^- K^+ K^-$	$(8.1 \pm 2.0) \times 10^{-4}$		-
$K_1(1270)^+ K^- + c.c. \rightarrow \pi^+ \pi^- K^+ K^-$	$(6.3 \pm 1.9) \times 10^{-3}$		-
$K_1(1400)^+ K^- + c.c. \rightarrow \pi^+ \pi^- K^+ K^-$	$< 2.7 \times 10^{-3}$	CL=90%	-
$f_0(980) f_0(980)$	$(1.6 \pm 1.1) \times 10^{-4}$		1391
$f_0(980) f_0(2200)$	$(8.0 \pm 2.0) \times 10^{-4}$		584
$f_0(1370) f_0(1370)$	$< 2.8 \times 10^{-4}$	CL=90%	1019
$f_0(1370) f_0(1500)$	$< 1.7 \times 10^{-4}$	CL=90%	920
$f_0(1370) f_0(1710)$	$(6.8 \pm 4.0) \times 10^{-4}$		723
$f_0(1500) f_0(1370)$	$< 1.3 \times 10^{-4}$	CL=90%	920
$f_0(1500) f_0(1500)$	$< 5 \times 10^{-5}$	CL=90%	805
$f_0(1500) f_0(1710)$	$< 7 \times 10^{-5}$	CL=90%	559
$K^+ K^- \pi^+ \pi^- \pi^0$	$(1.13 \pm 0.27) \%$		1545
$K^+ K^- \pi^0 \pi^0$	$(5.6 \pm 0.9) \times 10^{-3}$		1582
$K^+ \pi^- K^0 \pi^0 + c.c.$	$(2.52 \pm 0.34) \%$		1581
$\rho^+ K^- K^0 + c.c.$	$(1.22 \pm 0.21) \%$		1458

$K^*(892)^- K^+ \pi^0 \rightarrow K^+ \pi^- K^0 \pi^0 + c.c.$	$(4.7 \pm 1.2) \times 10^{-3}$	-	-
$K_S^0 K_S^0 \pi^+ \pi^-$	$(5.8 \pm 1.1) \times 10^{-3}$		1579
$K^+ K^- \eta \pi^0$	$(3.0 \pm 0.7) \times 10^{-3}$		1468
$3(\pi^+ \pi^-)$	$(1.20 \pm 0.18) \%$		1633
$K^+ \bar{K}^*(892)^0 \pi^- + c.c.$	$(7.3 \pm 1.6) \times 10^{-3}$		1523
$K^*(892)^0 \bar{K}^*(892)^0$	$(1.7 \pm 0.6) \times 10^{-3}$		1456
$\pi \pi$	$(8.5 \pm 0.4) \times 10^{-3}$		1702
$\pi^0 \eta$	$< 1.8 \times 10^{-4}$		1661
$\pi^0 \eta'$	$< 1.1 \times 10^{-3}$		1570
$\eta \eta$	$(3.03 \pm 0.21) \times 10^{-3}$		1617
$\eta \eta'$	$< 2.4 \times 10^{-4}$	CL=90%	1521
$\eta' \eta'$	$(2.02 \pm 0.22) \times 10^{-3}$		1413
$\omega \omega$	$(9.8 \pm 1.1) \times 10^{-4}$		1517
$\omega \phi$	$(1.19 \pm 0.22) \times 10^{-4}$		1447
$K^+ K^-$	$(6.06 \pm 0.35) \times 10^{-3}$		1634
$K_S^0 K_S^0$	$(3.14 \pm 0.18) \times 10^{-3}$		1633
$\pi^+ \pi^- \eta$	$< 2.0 \times 10^{-4}$	CL=90%	1651
$\pi^+ \pi^- \eta'$	$< 4 \times 10^{-4}$	CL=90%	1560
$\bar{K}^0 K^+ \pi^- + c.c.$	$< 1.0 \times 10^{-4}$	CL=90%	1610
$K^+ K^- \pi^0$	$< 6 \times 10^{-5}$	CL=90%	1611
$K^+ K^- \eta$	$< 2.3 \times 10^{-4}$	CL=90%	1512
$K^+ K^- K_S^0 K_S^0$	$(1.4 \pm 0.5) \times 10^{-3}$		1331
$K^+ K^- K^+ K^-$	$(2.79 \pm 0.29) \times 10^{-3}$		1333
$K^+ K^- \phi$	$(9.8 \pm 2.5) \times 10^{-4}$		1381
$\phi \phi$	$(8.2 \pm 0.8) \times 10^{-4}$		1370
$\rho \bar{\rho}$	$(2.23 \pm 0.13) \times 10^{-4}$		1426
$\rho \bar{\rho} \pi^0$	$(7.0 \pm 0.7) \times 10^{-4}$	S=1.2	1379
$\rho \bar{\rho} \eta$	$(3.6 \pm 0.4) \times 10^{-4}$		1187
$\rho \bar{\rho} \omega$	$(5.3 \pm 0.6) \times 10^{-4}$		1043
$\rho \bar{\rho} \phi$	$(6.1 \pm 1.5) \times 10^{-5}$		876
$\rho \bar{\rho} \pi^+ \pi^-$	$(2.1 \pm 0.7) \times 10^{-3}$	S=1.4	1320
$\rho \bar{\rho} \pi^0 \pi^0$	$(1.05 \pm 0.28) \times 10^{-3}$		1324
$\rho \bar{\rho} K^+ K^-$ (non-resonant)	$(1.23 \pm 0.27) \times 10^{-4}$		890
$\rho \bar{\rho} K_S^0 K_S^0$	$< 8.8 \times 10^{-4}$	CL=90%	884
$\rho \bar{\rho} \pi^-$	$(1.14 \pm 0.31) \times 10^{-3}$		1376
$\Lambda \bar{\Lambda}$	$(3.3 \pm 0.4) \times 10^{-4}$		1292
$\Lambda \bar{\Lambda} \pi^+ \pi^-$	$< 4.0 \times 10^{-3}$	CL=90%	1153
$K^+ \bar{p} \Lambda + c.c.$	$(1.02 \pm 0.19) \times 10^{-3}$		1132
$K^+ p \Lambda(1520) + c.c.$	$(3.0 \pm 0.8) \times 10^{-4}$		858
$\Lambda(1520) \bar{\Lambda}(1520)$	$(3.2 \pm 1.2) \times 10^{-4}$		779
$\Sigma^0 \bar{\Sigma}^0$	$(4.2 \pm 0.7) \times 10^{-4}$		1222
$\Sigma^+ \bar{\Sigma}^-$	$(3.1 \pm 0.7) \times 10^{-4}$		1225
$\Xi^0 \bar{\Xi}^0$	$(3.2 \pm 0.8) \times 10^{-4}$		1089
$\Xi^- \bar{\Xi}^+$	$(4.9 \pm 0.7) \times 10^{-4}$		1081

## Radiative decays

$\gamma J/\psi(1S)$	$(1.17 \pm 0.08) \%$		303
$\gamma \rho^0$	$< 9 \times 10^{-6}$	CL=90%	1619
$\gamma \omega$	$< 8 \times 10^{-6}$	CL=90%	1618
$\gamma \phi$	$< 6 \times 10^{-6}$	CL=90%	1555
$\gamma \gamma$	$(2.23 \pm 0.17) \times 10^{-4}$		1707

 **$\chi_{c1}(1P)$** 

$$I^G(J^{PC}) = 0^+(1^{++})$$

Mass  $m = 3510.66 \pm 0.07$  MeV ( $S = 1.5$ )

Full width  $\Gamma = 0.86 \pm 0.05$  MeV

$\chi_{c1}(1P)$ DECAY MODES	Fraction ( $\Gamma_i/\Gamma$ )	Scale factor/ Confidence level	$p$ (MeV/c)
-----------------------------	--------------------------------	-----------------------------------	----------------

## Hadronic decays

$3(\pi^+ \pi^-)$	$(5.8 \pm 1.4) \times 10^{-3}$	S=1.2	1683
$2(\pi^+ \pi^-)$	$(7.6 \pm 2.6) \times 10^{-3}$		1728
$\pi^+ \pi^- \pi^0 \pi^0$	$(1.26 \pm 0.17) \%$		1729
$\rho^+ \pi^- \pi^0 + c.c.$	$(1.53 \pm 0.26) \%$		1658
$\rho^0 \pi^+ \pi^-$	$(3.9 \pm 3.5) \times 10^{-3}$		1657
$4\pi^0$	$(5.7 \pm 0.8) \times 10^{-4}$		1729
$\pi^+ \pi^- K^+ K^-$	$(4.5 \pm 1.0) \times 10^{-3}$		1632
$K^+ K^- \pi^0 \pi^0$	$(1.18 \pm 0.29) \times 10^{-3}$		1634
$K^+ \pi^- K^0 \pi^0 + c.c.$	$(9.0 \pm 1.5) \times 10^{-3}$		1632
$\rho^+ K^- K^0 + c.c.$	$(5.3 \pm 1.3) \times 10^{-3}$		1514
$K^*(892)^0 K^0 \pi^0 \rightarrow K^+ \pi^- K^0 \pi^0 + c.c.$	$(2.5 \pm 0.7) \times 10^{-3}$		-
$K^+ K^- \eta \pi^0$	$(1.2 \pm 0.4) \times 10^{-3}$		1523
$\pi^+ \pi^- K_S^0 K_S^0$	$(7.2 \pm 3.1) \times 10^{-4}$		1630
$K^+ K^- \eta$	$(3.3 \pm 1.0) \times 10^{-4}$		1566
$K^0 K^+ \pi^- + c.c.$	$(7.3 \pm 0.6) \times 10^{-3}$		1661



## Meson Summary Table

$K^*(892)^0 \bar{K}^0 + c.c.$	$(1.0 \pm 0.4) \times 10^{-3}$	1602
$K^*(892)^+ K^- + c.c.$	$(1.5 \pm 0.7) \times 10^{-3}$	1602
$K^*_j(1430)^0 \bar{K}^0 + c.c. \rightarrow$	$< 8 \times 10^{-4}$	CL=90% -
$K^*_S K^+ \pi^- + c.c.$		
$K^*_j(1430)^+ K^- + c.c. \rightarrow$	$< 2.3 \times 10^{-3}$	CL=90% -
$K^*_S K^+ \pi^- + c.c.$		
$K^+ K^- \pi^0$	$(1.91 \pm 0.26) \times 10^{-3}$	1662
$\eta \pi^+ \pi^-$	$(5.0 \pm 0.5) \times 10^{-3}$	1701
$a_0(980)^+ \pi^- + c.c. \rightarrow \eta \pi^+ \pi^-$	$(1.9 \pm 0.7) \times 10^{-3}$	-
$f_2(1270) \eta$	$(2.8 \pm 0.8) \times 10^{-3}$	1468
$\pi^+ \pi^- \eta'$	$(2.4 \pm 0.5) \times 10^{-3}$	1612
$\pi^0 f_0(980) \rightarrow \pi^0 \pi^+ \pi^-$	$< 6 \times 10^{-6}$	CL=90% -
$K^+ \bar{K}^*(892)^0 \pi^- + c.c.$	$(3.2 \pm 2.1) \times 10^{-3}$	1577
$K^*(892)^0 \bar{K}^*(892)^0$	$(1.5 \pm 0.4) \times 10^{-3}$	1512
$K^+ K^- K^*_S K^*_S$	$< 5 \times 10^{-4}$	CL=90% 1390
$K^+ K^- K^+ K^-$	$(5.6 \pm 1.2) \times 10^{-4}$	1393
$K^+ K^- \phi$	$(4.3 \pm 1.6) \times 10^{-4}$	1440
$\omega \omega$	$(6.0 \pm 0.7) \times 10^{-4}$	1571
$\omega \phi$	$(2.2 \pm 0.6) \times 10^{-5}$	1503
$\phi \phi$	$(4.4 \pm 0.6) \times 10^{-4}$	1429
$\rho \bar{\rho}$	$(7.3 \pm 0.4) \times 10^{-5}$	1484
$\rho \bar{\rho} \pi^0$	$(1.64 \pm 0.20) \times 10^{-4}$	1438
$\rho \bar{\rho} \eta$	$(1.53 \pm 0.26) \times 10^{-4}$	1254
$\rho \bar{\rho} \omega$	$(2.24 \pm 0.33) \times 10^{-4}$	1117
$\rho \bar{\rho} \phi$	$< 1.8 \times 10^{-5}$	CL=90% 962
$\rho \bar{\rho} \pi^+ \pi^-$	$(5.0 \pm 1.9) \times 10^{-4}$	1381
$\rho \bar{\rho} K^+ K^-$ (non-resonant)	$(1.34 \pm 0.24) \times 10^{-4}$	974
$\rho \bar{\rho} K^*_S K^*_S$	$< 4.5 \times 10^{-4}$	CL=90% 968
$\Lambda \bar{\Lambda}$	$(1.18 \pm 0.19) \times 10^{-4}$	1355
$\Lambda \bar{\Lambda} \pi^+ \pi^-$	$< 1.5 \times 10^{-3}$	CL=90% 1223
$K^+ \bar{p} \Lambda$	$(3.2 \pm 1.0) \times 10^{-4}$	1203
$K^+ p \Lambda(1520) + c.c.$	$(1.8 \pm 0.5) \times 10^{-4}$	950
$\Lambda(1520) \bar{\Lambda}(1520)$	$< 1.0 \times 10^{-4}$	CL=90% 879
$\Sigma^0 \bar{\Sigma}^0$	$< 4 \times 10^{-5}$	CL=90% 1288
$\Sigma^+ \bar{\Sigma}^-$	$< 6 \times 10^{-5}$	CL=90% 1291
$\Xi^0 \bar{\Xi}^0$	$< 6 \times 10^{-5}$	CL=90% 1163
$\Xi^- \bar{\Xi}^+$	$(8.4 \pm 2.3) \times 10^{-5}$	1155
$\pi^+ \pi^- + K^+ K^-$	$< 2.1 \times 10^{-3}$	-
$K^*_S K^*_S$	$< 6 \times 10^{-5}$	CL=90% 1683
<b>Radiative decays</b>		
$\gamma J/\psi(1S)$	$(34.4 \pm 1.5) \%$	389
$\gamma \rho^0$	$(2.28 \pm 0.19) \times 10^{-4}$	1670
$\gamma \omega$	$(7.1 \pm 0.9) \times 10^{-5}$	1668
$\gamma \phi$	$(2.6 \pm 0.6) \times 10^{-5}$	1607

 **$h_c(1P)$** 

$$I^G(J^{PC}) = ?^?(1^{+-})$$

Mass  $m = 3525.41 \pm 0.16$  MeV ( $S = 1.2$ )  
 Full width  $\Gamma < 1$  MeV

$h_c(1P)$ DECAY MODES	Fraction ( $\Gamma_i/\Gamma$ )	$\rho$ (MeV/c)
$J/\psi(1S) \pi \pi$	not seen	312
$\eta_c(1S) \gamma$	$(51 \pm 6) \%$	502
$\pi^+ \pi^- \pi^0$	$< 2.2 \times 10^{-3}$	1749
$2\pi^+ 2\pi^- \pi^0$	$(2.2^{+0.8}_{-0.7}) \%$	1716
$3\pi^+ 3\pi^- \pi^0$	$< 2.9 \%$	1661

 **$\chi_{c2}(1P)$** 

$$I^G(J^{PC}) = 0^+(2^{++})$$

Mass  $m = 3556.20 \pm 0.09$  MeV  
 Full width  $\Gamma = 1.98 \pm 0.11$  MeV

 **$\chi_{c2}(1P)$  DECAY MODES**Fraction ( $\Gamma_i/\Gamma$ )

Confidence level

 $\rho$   
(MeV/c)

<b>Hadronic decays</b>		
$2(\pi^+ \pi^-)$	$(1.10 \pm 0.11) \%$	1751
$\pi^+ \pi^- \pi^0 \pi^0$	$(2.00 \pm 0.26) \%$	1752
$\rho^+ \pi^- \pi^0 + c.c.$	$(2.4 \pm 0.4) \%$	1682
$4\pi^0$	$(1.21 \pm 0.17) \times 10^{-3}$	1752
$K^+ K^- \pi^0 \pi^0$	$(2.2 \pm 0.5) \times 10^{-3}$	1658
$K^+ \pi^- K^0 \pi^0 + c.c.$	$(1.51 \pm 0.22) \%$	1657
$\rho^+ K^- K^0 + c.c.$	$(4.5 \pm 1.4) \times 10^{-3}$	1540
$K^*(892)^0 K^+ \pi^- \rightarrow$	$(3.2 \pm 0.9) \times 10^{-3}$	-
$K^+ \pi^- K^0 \pi^0 + c.c.$		
$K^*(892)^0 K^0 \pi^0 \rightarrow$	$(4.2 \pm 0.9) \times 10^{-3}$	-
$K^+ \pi^- K^0 \pi^0 + c.c.$		
$K^*(892)^- K^0 \pi^0 \rightarrow$	$(4.1 \pm 0.9) \times 10^{-3}$	-
$K^+ \pi^- K^0 \pi^0 + c.c.$		
$K^*(892)^+ K^0 \pi^- \rightarrow$	$(3.2 \pm 0.9) \times 10^{-3}$	-
$K^+ \pi^- K^0 \pi^0 + c.c.$		
$K^+ K^- \eta \pi^0$	$(1.4 \pm 0.5) \times 10^{-3}$	1549
$K^+ K^- \pi^+ \pi^-$	$(9.1 \pm 1.1) \times 10^{-3}$	1656
$K^+ K^- \pi^+ \pi^- \pi^0$	$(1.3 \pm 0.4) \%$	1623
$K^+ \bar{K}^*(892)^0 \pi^- + c.c.$	$(2.3 \pm 1.2) \times 10^{-3}$	1602
$K^*(892)^0 \bar{K}^*(892)^0$	$(2.5 \pm 0.5) \times 10^{-3}$	1538
$3(\pi^+ \pi^-)$	$(8.6 \pm 1.8) \times 10^{-3}$	1707
$\phi \phi$	$(1.14 \pm 0.12) \times 10^{-3}$	1457
$\omega \omega$	$(9.2 \pm 1.1) \times 10^{-4}$	1597
$\pi \pi$	$(2.43 \pm 0.13) \times 10^{-3}$	1773
$\rho^0 \pi^+ \pi^-$	$(4.0 \pm 1.7) \times 10^{-3}$	1681
$\pi^+ \pi^- \eta$	$(5.2 \pm 1.4) \times 10^{-4}$	1724
$\pi^+ \pi^- \eta'$	$(5.5 \pm 2.0) \times 10^{-4}$	1636
$\eta \eta$	$(5.9 \pm 0.5) \times 10^{-4}$	1692
$K^+ K^-$	$(1.09 \pm 0.08) \times 10^{-3}$	1708
$K^*_S K^*_S$	$(5.8 \pm 0.5) \times 10^{-4}$	1707
$\bar{K}^0 K^+ \pi^- + c.c.$	$(1.40 \pm 0.20) \times 10^{-3}$	1685
$K^+ K^- \pi^0$	$(3.3 \pm 0.8) \times 10^{-4}$	1686
$K^+ K^- \eta$	$< 3.5 \times 10^{-4}$	90% 1592
$\eta \eta'$	$< 6 \times 10^{-5}$	90% 1600
$\eta' \eta'$	$< 1.1 \times 10^{-4}$	90% 1498
$\pi^+ \pi^- K^*_S K^*_S$	$(2.4 \pm 0.6) \times 10^{-3}$	1655
$K^+ K^- K^*_S K^*_S$	$< 4 \times 10^{-4}$	90% 1418
$K^+ K^- K^+ K^-$	$(1.78 \pm 0.22) \times 10^{-3}$	1421
$K^+ K^- \phi$	$(1.55 \pm 0.33) \times 10^{-3}$	1468
$\rho \bar{\rho}$	$(7.2 \pm 0.4) \times 10^{-5}$	1510
$\rho \bar{\rho} \pi^0$	$(5.1 \pm 0.5) \times 10^{-4}$	1465
$\rho \bar{\rho} \eta$	$(1.90 \pm 0.28) \times 10^{-4}$	1285
$\rho \bar{\rho} \omega$	$(3.9 \pm 0.5) \times 10^{-4}$	1152
$\rho \bar{\rho} \phi$	$(3.0 \pm 1.0) \times 10^{-5}$	1002
$\rho \bar{\rho} \pi^+ \pi^-$	$(1.32 \pm 0.34) \times 10^{-3}$	1410
$\rho \bar{\rho} \pi^0 \pi^0$	$(8.6 \pm 2.6) \times 10^{-4}$	1414
$\rho \bar{\rho} K^+ K^-$ (non-resonant)	$(2.1 \pm 0.4) \times 10^{-4}$	1013
$\rho \bar{\rho} K^*_S K^*_S$	$< 7.9 \times 10^{-4}$	90% 1007
$\rho \bar{\rho} \pi^-$	$(1.1 \pm 0.4) \times 10^{-3}$	1463
$\Lambda \bar{\Lambda}$	$(1.86 \pm 0.27) \times 10^{-4}$	1385
$\Lambda \bar{\Lambda} \pi^+ \pi^-$	$< 3.5 \times 10^{-3}$	90% 1255
$K^+ \bar{p} \Lambda + c.c.$	$(9.1 \pm 1.8) \times 10^{-4}$	1236
$K^+ p \Lambda(1520) + c.c.$	$(3.1 \pm 0.7) \times 10^{-4}$	992
$\Lambda(1520) \bar{\Lambda}(1520)$	$(5.1 \pm 1.6) \times 10^{-4}$	923
$\Sigma^0 \bar{\Sigma}^0$	$< 8 \times 10^{-5}$	90% 1319
$\Sigma^+ \bar{\Sigma}^-$	$< 7 \times 10^{-5}$	90% 1322
$\Xi^0 \bar{\Xi}^0$	$< 1.1 \times 10^{-4}$	90% 1197
$\Xi^- \bar{\Xi}^+$	$(1.55 \pm 0.35) \times 10^{-4}$	1189
$J/\psi(1S) \pi^+ \pi^- \pi^0$	$< 1.5 \%$	90% 185
<b>Radiative decays</b>		
$\gamma J/\psi(1S)$	$(19.5 \pm 0.8) \%$	430
$\gamma \rho^0$	$< 2.1 \times 10^{-5}$	90% 1694
$\gamma \omega$	$< 6 \times 10^{-6}$	90% 1692
$\gamma \phi$	$< 8 \times 10^{-6}$	90% 1632
$\gamma \gamma$	$(2.59 \pm 0.16) \times 10^{-4}$	1778

## Meson Summary Table

 **$\eta_c(2S)$** 

$$J^G(J^{PC}) = 0^+(0^-)$$

Quantum numbers are quark model predictions.

Mass  $m = 3638.9 \pm 1.3$  MeV  
Full width  $\Gamma = 10 \pm 4$  MeV

$\eta_c(2S)$ DECAY MODES	Fraction ( $\Gamma_i/\Gamma$ )	Confidence level	$\rho$ (MeV/c)
hadrons	not seen	–	–
$K\bar{K}\pi$	$(1.9 \pm 1.2)\%$	–	1730
$2\pi^+2\pi^-$	not seen	–	1793
$\rho^0\rho^0$	not seen	–	1646
$3\pi^+3\pi^-$	not seen	–	1750
$K^+K^-\pi^+\pi^-$	not seen	–	1701
$K^*0\bar{K}^*0$	not seen	–	1586
$K^+K^-\pi^+\pi^-\pi^0$	$(1.4 \pm 1.0)\%$	–	1668
$K^+K^-2\pi^+2\pi^-$	not seen	–	1628
$K_S^0K_S^02\pi^+\pi^- + c.c.$	not seen	–	1666
$2K^+2K^-$	not seen	–	1471
$\phi\phi$	not seen	–	1507
$\gamma\gamma$	$< 5 \times 10^{-4}$	90%	1819
$\pi^+\pi^-\eta$	not seen	–	1767
$\pi^+\pi^-\eta'$	not seen	–	1681
$K^+K^-\eta$	not seen	–	1638
$\pi^+\pi^-\eta_c(1S)$	not seen	–	541

 **$\psi(2S)$** 

$$J^G(J^{PC}) = 0^-(1^{--})$$

Mass  $m = 3686.109^{+0.012}_{-0.014}$  MeV  
Full width  $\Gamma = 304 \pm 9$  keV  
 $\Gamma_{ee} = 2.35 \pm 0.04$  keV

$\psi(2S)$ DECAY MODES	Fraction ( $\Gamma_i/\Gamma$ )	Scale factor/ Confidence level	$\rho$ (MeV/c)
hadrons	$(97.85 \pm 0.13)\%$	–	–
virtual $\gamma \rightarrow$ hadrons	$(1.73 \pm 0.14)\%$	S=1.5	–
$ggg$	$(10.6 \pm 1.6)\%$	–	–
$\gamma g g$	$(1.03 \pm 0.29)\%$	–	–
light hadrons	$(15.4 \pm 1.5)\%$	–	–
$e^+e^-$	$(7.73 \pm 0.17) \times 10^{-3}$	–	1843
$\mu^+\mu^-$	$(7.7 \pm 0.8) \times 10^{-3}$	–	1840
$\tau^+\tau^-$	$(3.0 \pm 0.4) \times 10^{-3}$	–	490

Decays into  $J/\psi(1S)$  and anything

$J/\psi(1S)$ anything	$(59.5 \pm 0.8)\%$	–	–
$J/\psi(1S)$ neutrals	$(24.6 \pm 0.4)\%$	–	–
$J/\psi(1S)\pi^+\pi^-$	$(33.6 \pm 0.4)\%$	–	477
$J/\psi(1S)\pi^0\pi^0$	$(17.75 \pm 0.34)\%$	–	481
$J/\psi(1S)\eta$	$(3.28 \pm 0.07)\%$	–	199
$J/\psi(1S)\pi^0$	$(1.30 \pm 0.10) \times 10^{-3}$	S=1.4	528

## Hadronic decays

$\pi^0 h_c(1P)$	$(8.6 \pm 1.3) \times 10^{-4}$	–	85
$3(\pi^+\pi^-\pi^0)$	$(3.5 \pm 1.6) \times 10^{-3}$	–	1746
$2(\pi^+\pi^-\pi^0)$	$(2.9 \pm 1.0) \times 10^{-3}$	S=4.6	1799
$\rho a_2(1320)$	$(2.6 \pm 0.9) \times 10^{-4}$	–	1500
$\rho\bar{\rho}$	$(2.76 \pm 0.12) \times 10^{-4}$	–	1586
$\Delta^{++}\bar{\Delta}^{--}$	$(1.28 \pm 0.35) \times 10^{-4}$	–	1371
$\Lambda\bar{\Lambda}\pi^0$	$< 1.2 \times 10^{-4}$	CL=90%	1412
$\Lambda\bar{\Lambda}\eta$	$< 4.9 \times 10^{-5}$	CL=90%	1197
$\Lambda\bar{p}K^+$	$(1.00 \pm 0.14) \times 10^{-4}$	–	1327
$\Lambda\bar{p}K^+\pi^+\pi^-$	$(1.8 \pm 0.4) \times 10^{-4}$	–	1167
$\Lambda\bar{\Lambda}\pi^+\pi^-$	$(2.8 \pm 0.6) \times 10^{-4}$	–	1346
$\Lambda\bar{\Lambda}$	$(2.8 \pm 0.5) \times 10^{-4}$	S=2.6	1467
$\Sigma^+\bar{\Sigma}^-$	$(2.6 \pm 0.8) \times 10^{-4}$	–	1408
$\Sigma^0\bar{\Sigma}^0$	$(2.2 \pm 0.4) \times 10^{-4}$	S=1.5	1405
$\Sigma^-(1385)^+\bar{\Sigma}^-(1385)^-$	$(1.1 \pm 0.4) \times 10^{-4}$	–	1218
$\Xi^-\bar{\Xi}^+$	$(1.8 \pm 0.6) \times 10^{-4}$	S=2.8	1284
$\Xi^0\bar{\Xi}^0$	$(2.8 \pm 0.9) \times 10^{-4}$	–	1292
$\Xi^-(1530)^0\bar{\Xi}^-(1530)^0$	$< 8.1 \times 10^{-5}$	CL=90%	1025
$\Omega^-\bar{\Omega}^+$	$< 7.3 \times 10^{-5}$	CL=90%	774
$\pi^0\rho\bar{\rho}$	$(1.50 \pm 0.08) \times 10^{-4}$	S=1.1	1543
$N_s^*(1440)\bar{p} \rightarrow \pi^0\rho\bar{\rho}$	$(8.1 \pm 0.8) \times 10^{-5}$	–	–
$\pi^0 f_0(2100) \rightarrow \pi^0\rho\bar{\rho}$	$(1.1 \pm 0.4) \times 10^{-5}$	–	–
$\eta\rho\bar{\rho}$	$(5.7 \pm 0.6) \times 10^{-5}$	–	1373
$\eta f_0(2100) \rightarrow \eta\rho\bar{\rho}$	$(1.2 \pm 0.4) \times 10^{-5}$	–	–
$N^*(1535)\bar{p} \rightarrow \eta\rho\bar{\rho}$	$(4.4 \pm 0.7) \times 10^{-5}$	–	–

$\omega\rho\bar{\rho}$	$(6.9 \pm 2.1) \times 10^{-5}$	–	1247
$\phi\rho\bar{\rho}$	$< 2.4 \times 10^{-5}$	CL=90%	1109
$\pi^+\pi^-\rho\bar{\rho}$	$(6.0 \pm 0.4) \times 10^{-4}$	–	1491
$\rho\bar{\rho}\pi^-\pi^0$ or c.c.	$(2.48 \pm 0.17) \times 10^{-4}$	–	–
$\rho\bar{\rho}\pi^-\pi^0$	$(3.2 \pm 0.7) \times 10^{-4}$	–	1492
$2(\pi^+\pi^-\pi^0)$	$(4.8 \pm 1.5) \times 10^{-3}$	–	1776
$\eta\pi^+\pi^-$	$< 1.6 \times 10^{-4}$	CL=90%	1791
$\eta\pi^+\pi^-\pi^0$	$(9.5 \pm 1.7) \times 10^{-4}$	–	1778
$2(\pi^+\pi^-\eta)$	$(1.2 \pm 0.6) \times 10^{-3}$	–	1758
$\eta'\pi^+\pi^-\pi^0$	$(4.5 \pm 2.1) \times 10^{-4}$	–	1692
$\omega\pi^+\pi^-$	$(7.3 \pm 1.2) \times 10^{-4}$	S=2.1	1748
$b_{\pm}^{\pm}\pi^{\mp}$	$(4.0 \pm 0.6) \times 10^{-4}$	S=1.1	1635
$b_1^0\pi^0$	$(2.4 \pm 0.6) \times 10^{-4}$	–	–
$\omega f_2(1270)$	$(2.2 \pm 0.4) \times 10^{-4}$	–	1515
$\pi^+\pi^-\pi^+K^-$	$(7.5 \pm 0.9) \times 10^{-4}$	S=1.9	1726
$\rho^0 K^+K^-$	$(2.2 \pm 0.4) \times 10^{-4}$	–	1616
$K^*(892)^0\bar{K}_S^0(1430)^0$	$(1.9 \pm 0.5) \times 10^{-4}$	–	1418
$K^+K^-\pi^+\pi^-\eta$	$(1.3 \pm 0.7) \times 10^{-3}$	–	1574
$K^+K^-2(\pi^+\pi^-\pi^0)$	$(1.00 \pm 0.31) \times 10^{-3}$	–	1611
$K^+K^-2(\pi^+\pi^-)$	$(1.9 \pm 0.9) \times 10^{-3}$	–	1654
$K_1(1270)^{\pm}K^{\mp}$	$(1.00 \pm 0.28) \times 10^{-3}$	–	1581
$K_S^0 K_S^0 \pi^+ \pi^-$	$(2.2 \pm 0.4) \times 10^{-4}$	–	1724
$\rho^0\rho\bar{\rho}$	$(5.0 \pm 2.2) \times 10^{-5}$	–	1251
$K^+\bar{K}^*(892)^0\pi^- + c.c.$	$(6.7 \pm 2.5) \times 10^{-4}$	–	1674
$2(\pi^+\pi^-)$	$(2.4 \pm 0.6) \times 10^{-4}$	S=2.2	1817
$\rho^0\pi^+\pi^-$	$(2.2 \pm 0.6) \times 10^{-4}$	S=1.4	1750
$K^+K^-\pi^+\pi^-\pi^0$	$(1.26 \pm 0.09) \times 10^{-3}$	–	1694
$\omega f_0(1710) \rightarrow \omega K^+K^-$	$(5.9 \pm 2.2) \times 10^{-5}$	–	–
$K^*(892)^0 K^-\pi^+\pi^0 + c.c.$	$(8.6 \pm 2.2) \times 10^{-4}$	–	–
$K^*(892)^+ K^-\pi^+\pi^- + c.c.$	$(9.6 \pm 2.8) \times 10^{-4}$	–	–
$K^*(892)^+ K^-\rho^0 + c.c.$	$(7.3 \pm 2.6) \times 10^{-4}$	–	–
$K^*(892)^0 K^-\rho^+ + c.c.$	$(6.1 \pm 1.8) \times 10^{-4}$	–	–
$\eta K^+K^-$	$< 1.3 \times 10^{-4}$	CL=90%	1664
$\omega K^+K^-$	$(1.85 \pm 0.25) \times 10^{-4}$	S=1.1	1614
$3(\pi^+\pi^-)$	$(3.5 \pm 2.0) \times 10^{-4}$	S=2.8	1774
$\rho\bar{\rho}\pi^+\pi^-\pi^0$	$(7.3 \pm 0.7) \times 10^{-4}$	–	1435
$K^+K^-$	$(6.3 \pm 0.7) \times 10^{-5}$	–	1776
$K_S^0 K_L^0$	$(5.4 \pm 0.5) \times 10^{-5}$	–	1775
$\pi^+\pi^-\pi^0$	$(1.68 \pm 0.26) \times 10^{-4}$	S=1.4	1830
$\rho(2150)\pi \rightarrow \pi^+\pi^-\pi^0$	$(1.9 \pm 1.2) \times 10^{-4}$	–	–
$\rho(770)\pi \rightarrow \pi^+\pi^-\pi^0$	$(3.2 \pm 1.2) \times 10^{-5}$	S=1.8	–
$\pi^+\pi^-$	$(8 \pm 5) \times 10^{-5}$	–	1838
$K_1(1400)^{\pm}K^{\mp}$	$< 3.1 \times 10^{-4}$	CL=90%	1532
$K^+K^-\pi^0$	$< 2.96 \times 10^{-5}$	CL=90%	1754
$K^+\bar{K}^*(892)^- + c.c.$	$(1.7 \pm 0.8) \times 10^{-5}$	–	1698
$K^*(892)^0\bar{K}^0 + c.c.$	$(1.09 \pm 0.20) \times 10^{-4}$	–	1697
$\phi\pi^+\pi^-$	$(1.17 \pm 0.29) \times 10^{-4}$	S=1.7	1690
$\phi f_0(980) \rightarrow \pi^+\pi^-$	$(6.8 \pm 2.5) \times 10^{-5}$	S=1.1	–
$2(K^+K^-)$	$(6.0 \pm 1.4) \times 10^{-5}$	–	1499
$\phi K^+K^-$	$(7.0 \pm 1.6) \times 10^{-5}$	–	1546
$2(K^+K^-)\pi^0$	$(1.10 \pm 0.28) \times 10^{-4}$	–	1440
$\phi\eta$	$(2.8 \pm 1.0) \times 10^{-5}$	–	1654
$\phi\eta'$	$(3.1 \pm 1.6) \times 10^{-5}$	–	1555
$\omega\eta'$	$(3.2 \pm 2.5) \times 10^{-5}$	–	1623
$\omega\pi^0$	$(2.1 \pm 0.6) \times 10^{-5}$	–	1757
$\rho\eta'$	$(1.9 \pm 1.7) \times 10^{-5}$	–	1625
$\rho\eta$	$(2.2 \pm 0.6) \times 10^{-5}$	S=1.1	1717
$\omega\eta$	$< 1.1 \times 10^{-5}$	CL=90%	1715
$\phi\pi^0$	$< 4 \times 10^{-6}$	CL=90%	1699
$\eta_c\pi^+\pi^-\pi^0$	$< 1.0 \times 10^{-3}$	CL=90%	–
$\bar{p}\bar{p}K^+K^-$	$(2.7 \pm 0.7) \times 10^{-5}$	–	1118
$\bar{\Lambda}n K_S^0 + c.c.$	$(8.1 \pm 1.8) \times 10^{-5}$	–	1324
$\phi f_2'(1525)$	$(4.4 \pm 1.6) \times 10^{-5}$	–	1321
$\Theta(1540)\bar{\Theta}(1540) \rightarrow$ $K_S^0 p K^-\bar{n} + c.c.$	$< 8.8 \times 10^{-6}$	CL=90%	–
$\Theta(1540)K^-\bar{n} \rightarrow K_S^0 p K^-\bar{n}$	$< 1.0 \times 10^{-5}$	CL=90%	–
$\Theta(1540)K_S^0\bar{p} \rightarrow K_S^0\bar{p}K^+n$	$< 7.0 \times 10^{-6}$	CL=90%	–
$\bar{\Theta}(1540)K^+n \rightarrow K_S^0\bar{p}K^+n$	$< 2.6 \times 10^{-5}$	CL=90%	–
$\bar{\Theta}(1540)K_S^0 p \rightarrow K_S^0 p K^-\bar{n}$	$< 6.0 \times 10^{-6}$	CL=90%	–
$K_S^0 K_S^0$	$< 4.6 \times 10^{-6}$	–	1775

## Meson Summary Table

Radiative decays			
$\gamma\chi_{c0}(1P)$	( 9.68±0.31 ) %		261
$\gamma\chi_{c1}(1P)$	( 9.2 ±0.4 ) %		171
$\gamma\chi_{c2}(1P)$	( 8.72±0.34 ) %		128
$\gamma\eta_c(1S)$	( 3.4 ±0.5 ) × 10 <sup>-3</sup>	S=1.3	638
$\gamma\eta_c(2S)$	< 8 × 10 <sup>-4</sup>	CL=90%	47
$\gamma\pi^0$	( 1.6 ±0.4 ) × 10 <sup>-6</sup>		1841
$\gamma\eta'(958)$	( 1.23±0.06 ) × 10 <sup>-4</sup>		1719
$\gamma f_2(1270)$	( 2.1 ±0.4 ) × 10 <sup>-4</sup>		1623
$\gamma f_0(1710) \rightarrow \gamma\pi\pi$	( 3.0 ±1.3 ) × 10 <sup>-5</sup>		-
$\gamma f_0(1710) \rightarrow \gamma K\bar{K}$	( 6.0 ±1.6 ) × 10 <sup>-5</sup>		-
$\gamma\gamma$	< 1.4 × 10 <sup>-4</sup>	CL=90%	1843
$\gamma\eta$	( 1.4 ±0.5 ) × 10 <sup>-6</sup>		1802
$\gamma\eta\pi^+\pi^-$	( 8.7 ±2.1 ) × 10 <sup>-4</sup>		1791
$\gamma\eta(1405) \rightarrow \gamma K\bar{K}\pi$	< 9 × 10 <sup>-5</sup>	CL=90%	1569
$\gamma\eta(1405) \rightarrow \eta\pi^+\pi^-$	( 3.6 ±2.5 ) × 10 <sup>-5</sup>		-
$\gamma\eta(1475) \rightarrow K\bar{K}\pi$	< 1.4 × 10 <sup>-4</sup>	CL=90%	-
$\gamma\eta(1475) \rightarrow \eta\pi^+\pi^-$	< 8.8 × 10 <sup>-5</sup>	CL=90%	-
$\gamma 2(\pi^+\pi^-)$	( 4.0 ±0.6 ) × 10 <sup>-4</sup>		1817
$\gamma K^{*0}K^+\pi^- + c.c.$	( 3.7 ±0.9 ) × 10 <sup>-4</sup>		1674
$\gamma K^{*0}\bar{K}^{*0}$	( 2.4 ±0.7 ) × 10 <sup>-4</sup>		1613
$\gamma K_S^0K^+\pi^- + c.c.$	( 2.6 ±0.5 ) × 10 <sup>-4</sup>		1753
$\gamma K^+K^-\pi^+\pi^-$	( 1.9 ±0.5 ) × 10 <sup>-4</sup>		1726
$\gamma\rho\bar{\rho}$	( 3.9 ±0.5 ) × 10 <sup>-5</sup>	S=2.0	1586
$\gamma f_2(1950) \rightarrow \gamma\rho\bar{\rho}$	( 1.20±0.22 ) × 10 <sup>-5</sup>		-
$\gamma f_2(2150) \rightarrow \gamma\rho\bar{\rho}$	( 7.2 ±1.8 ) × 10 <sup>-6</sup>		-
$\gamma X(1835) \rightarrow \gamma\rho\bar{\rho}$	< 1.6 × 10 <sup>-6</sup>	CL=90%	-
$\gamma X \rightarrow \gamma\rho\bar{\rho}$	[nnnn] < 2 × 10 <sup>-6</sup>	CL=90%	-
$\gamma\pi^+\pi^-\rho\bar{\rho}$	( 2.8 ±1.4 ) × 10 <sup>-5</sup>		1491
$\gamma 2(\pi^+\pi^-)K^+K^-$	< 2.2 × 10 <sup>-4</sup>	CL=90%	1654
$\gamma 3(\pi^+\pi^-)$	< 1.7 × 10 <sup>-4</sup>	CL=90%	1774
$\gamma K^+K^-K^+K^-$	< 4 × 10 <sup>-5</sup>	CL=90%	1499

 **$\psi(3770)$** 

$$J^{PC} = 0^-(1^{--})$$

Mass  $m = 3773.15 \pm 0.33$  MeVFull width  $\Gamma = 27.2 \pm 1.0$  MeV $\Gamma_{ee} = 0.262 \pm 0.018$  keV (S = 1.4)

In addition to the dominant decay mode to  $D\bar{D}$ ,  $\psi(3770)$  was found to decay into the final states containing the  $J/\psi$  (BAI 05, ADAM 06), ADAMS 06 and HUANG 06A searched for various decay modes with light hadrons and found a statistically significant signal for the decay to  $\phi\eta$  only (ADAMS 06).

$\psi(3770)$ DECAY MODES	Fraction ( $\Gamma_i/\Gamma$ )	Scale factor/ Confidence level	$\rho$ (MeV/c)
$D\bar{D}$	(93 $\pm$ 8 / $\pm$ 9 ) %	S=2.0	285
$D^0\bar{D}^0$	(52 $\pm$ 5 ) %	S=2.0	285
$D^+D^-$	(41 $\pm$ 4 ) %	S=2.0	252
$J/\psi\pi^+\pi^-$	( 1.93±0.28 ) × 10 <sup>-3</sup>		560
$J/\psi\pi^0\pi^0$	( 8.0 ±3.0 ) × 10 <sup>-4</sup>		564
$J/\psi\eta$	( 9 ±4 ) × 10 <sup>-4</sup>		360
$J/\psi\pi^0$	< 2.8 × 10 <sup>-4</sup>	CL=90%	603
$e^+e^-$	( 9.6 ±0.7 ) × 10 <sup>-6</sup>	S=1.3	1887
Decays to light hadrons			
$b_1(1235)\pi$	< 1.4 × 10 <sup>-5</sup>	CL=90%	1683
$\phi\eta'$	< 7 × 10 <sup>-4</sup>	CL=90%	1607
$\omega\eta'$	< 4 × 10 <sup>-4</sup>	CL=90%	1672
$\rho^0\eta'$	< 6 × 10 <sup>-4</sup>	CL=90%	1674
$\phi\eta$	( 3.1 ±0.7 ) × 10 <sup>-4</sup>		1703
$\omega\eta$	< 1.4 × 10 <sup>-5</sup>	CL=90%	1762
$\rho^0\eta$	< 5 × 10 <sup>-4</sup>	CL=90%	1764
$\phi\pi^0$	< 3 × 10 <sup>-5</sup>	CL=90%	1746
$\omega\pi^0$	< 6 × 10 <sup>-4</sup>	CL=90%	1803
$\pi^+\pi^-\pi^0$	< 5 × 10 <sup>-6</sup>	CL=90%	1874
$\rho\pi$	< 5 × 10 <sup>-6</sup>	CL=90%	1804
$K^*(892)^+K^- + c.c.$	< 1.4 × 10 <sup>-5</sup>	CL=90%	1745
$K^*(892)^0\bar{K}^0 + c.c.$	< 1.2 × 10 <sup>-3</sup>	CL=90%	1744
$K_S^0K_L^0$	< 1.2 × 10 <sup>-5</sup>	CL=90%	1820
$2(\pi^+\pi^-)$	< 1.12 × 10 <sup>-3</sup>	CL=90%	1861
$2(\pi^+\pi^-)\pi^0$	< 1.06 × 10 <sup>-3</sup>	CL=90%	1843
$2(\pi^+\pi^-\pi^0)$	< 5.85 %	CL=90%	1821
$\omega\pi^+\pi^-$	< 6.0 × 10 <sup>-4</sup>	CL=90%	1794
$3(\pi^+\pi^-)$	< 9.1 × 10 <sup>-3</sup>		1819
$3(\pi^+\pi^-\pi^0)$	< 1.37 %		1792
$3(\pi^+\pi^-)2\pi^0$	< 11.74 %	CL=90%	1760

$\eta\pi^+\pi^-$	< 1.24 × 10 <sup>-3</sup>	CL=90%	1836
$\pi^+\pi^-2\pi^0$	< 8.9 × 10 <sup>-3</sup>	CL=90%	1862
$\rho^0\pi^+\pi^-$	< 6.9 × 10 <sup>-3</sup>	CL=90%	1796
$\eta 3\pi$	< 1.34 × 10 <sup>-3</sup>	CL=90%	1824
$\eta 2(\pi^+\pi^-)$	< 2.43 %		1804
$\eta\rho^0\pi^+\pi^-$	< 1.45 %	CL=90%	1708
$\eta' 3\pi$	< 2.44 × 10 <sup>-3</sup>	CL=90%	1740
$K^+K^-\pi^+\pi^-$	< 9.0 × 10 <sup>-4</sup>	CL=90%	1772
$\phi\pi^+\pi^-$	< 4.1 × 10 <sup>-4</sup>	CL=90%	1737
$K^+K^-2\pi^0$	< 4.2 × 10 <sup>-3</sup>	CL=90%	1774
$4(\pi^+\pi^-)$	< 1.67 %	CL=90%	1757
$4(\pi^+\pi^-\pi^0)$	< 3.06 %	CL=90%	1720
$\phi f_0(980)$	< 4.5 × 10 <sup>-4</sup>	CL=90%	1597
$K^+K^-\pi^+\pi^- \pi^0$	< 2.36 × 10 <sup>-3</sup>	CL=90%	1741
$K^+K^-\rho^0\pi^0$	< 8 × 10 <sup>-4</sup>	CL=90%	1624
$K^+K^-\rho^+\pi^-$	< 1.46 %	CL=90%	1622
$\omega K^+K^-$	< 3.4 × 10 <sup>-4</sup>	CL=90%	1664
$\phi\pi^+\pi^-\pi^0$	< 3.8 × 10 <sup>-3</sup>	CL=90%	1722
$K^{*0}K^-\pi^+\pi^0 + c.c.$	< 1.62 %	CL=90%	1693
$K^{*+}K^-\pi^+\pi^- + c.c.$	< 3.23 %	CL=90%	1692
$K^+K^-\pi^+\pi^-2\pi^0$	< 2.67 %	CL=90%	1705
$K^+K^-2(\pi^+\pi^-)$	< 1.03 %	CL=90%	1702
$K^+K^-2(\pi^+\pi^-\pi^0)$	< 3.60 %	CL=90%	1660
$\eta K^+K^-$	< 4.1 × 10 <sup>-4</sup>	CL=90%	1712
$\eta K^+K^-\pi^+\pi^-$	< 1.24 %	CL=90%	1624
$\rho^0 K^+K^-$	< 5.0 × 10 <sup>-3</sup>	CL=90%	1665
$2(K^+K^-)$	< 6.0 × 10 <sup>-4</sup>	CL=90%	1552
$\phi K^+K^-$	< 7.5 × 10 <sup>-4</sup>	CL=90%	1598
$2(K^+K^-)\pi^0$	< 2.9 × 10 <sup>-4</sup>	CL=90%	1493
$2(K^+K^-)\pi^+\pi^-$	< 3.2 × 10 <sup>-3</sup>	CL=90%	1425
$K_S^0K^-\pi^+$	< 3.2 × 10 <sup>-3</sup>	CL=90%	1799
$K_S^0K^-\pi^+\pi^0$	< 1.33 %	CL=90%	1773
$K_S^0K^-\rho^+$	< 6.6 × 10 <sup>-3</sup>	CL=90%	1664
$K_S^0K^-\pi^+\pi^-$	< 8.7 × 10 <sup>-3</sup>	CL=90%	1739
$K_S^0K^-\pi^+\rho^0$	< 1.6 %	CL=90%	1621
$K_S^0K^-\pi^+\eta$	< 1.3 %	CL=90%	1669
$K_S^0K^-\pi^+\pi^-\pi^0$	< 4.18 %	CL=90%	1703
$K_S^0K^-\pi^+\pi^-\eta$	< 4.8 %	CL=90%	1570
$K_S^0K^-\pi^+2(\pi^+\pi^-)$	< 1.22 %	CL=90%	1658
$K_S^0K^-\pi^+2\pi^0$	< 2.65 %	CL=90%	1742
$K_S^0K^-\pi^+K^-\pi^+$	< 4.9 × 10 <sup>-3</sup>	CL=90%	1490
$K_S^0K^-\pi^+K^-\pi^+\pi^0$	< 3.0 %	CL=90%	1427
$K_S^0K^-\pi^+K^-\pi^+\eta$	< 2.2 %	CL=90%	1214
$K^{*0}K^-\pi^+ + c.c.$	< 9.7 × 10 <sup>-3</sup>	CL=90%	1722
$\rho\bar{\rho}\pi^0$	< 1.2 × 10 <sup>-3</sup>		1595
$\rho\bar{\rho}\pi^+\pi^-$	< 5.8 × 10 <sup>-4</sup>	CL=90%	1544
$\Lambda\bar{\Lambda}$	< 1.2 × 10 <sup>-4</sup>	CL=90%	1521
$\rho\bar{\rho}\pi^+\pi^-\pi^0$	< 1.85 × 10 <sup>-3</sup>	CL=90%	1490
$\omega\rho\bar{\rho}$	< 2.9 × 10 <sup>-4</sup>	CL=90%	1309
$\Lambda\bar{\Lambda}\pi^0$	< 1.2 × 10 <sup>-3</sup>	CL=90%	1469
$\rho\bar{\rho}2(\pi^+\pi^-)$	< 2.6 × 10 <sup>-3</sup>	CL=90%	1425
$\eta\rho\bar{\rho}$	< 5.4 × 10 <sup>-4</sup>	CL=90%	1430
$\eta\rho\bar{\rho}\pi^+\pi^-$	< 3.3 × 10 <sup>-3</sup>	CL=90%	1284
$\rho^0\rho\bar{\rho}$	< 1.7 × 10 <sup>-3</sup>	CL=90%	1313
$\rho\bar{\rho}K^+K^-$	< 3.2 × 10 <sup>-4</sup>	CL=90%	1185
$\eta\rho\bar{\rho}K^+K^-$	< 6.9 × 10 <sup>-3</sup>	CL=90%	736
$\pi^0\rho\bar{\rho}K^+K^-$	< 1.2 × 10 <sup>-3</sup>	CL=90%	1093
$\phi\rho\bar{\rho}$	< 1.3 × 10 <sup>-4</sup>	CL=90%	1178
$\Lambda\bar{\Lambda}\pi^+\pi^-$	< 2.5 × 10 <sup>-4</sup>	CL=90%	1405
$\Lambda\bar{\Lambda}K^+$	< 2.8 × 10 <sup>-4</sup>	CL=90%	1387
$\Lambda\bar{\Lambda}K^+\pi^+\pi^-$	< 6.3 × 10 <sup>-4</sup>	CL=90%	1234
Radiative decays			
$\gamma\chi_{c2}$	< 9 × 10 <sup>-4</sup>	CL=90%	211
$\gamma\chi_{c1}$	( 2.9 ±0.6 ) × 10 <sup>-3</sup>		253
$\gamma\chi_{c0}$	( 7.3 ±0.9 ) × 10 <sup>-3</sup>		341
$\gamma\eta'$	< 1.8 × 10 <sup>-4</sup>	CL=90%	1765
$\gamma\eta$	< 1.5 × 10 <sup>-4</sup>	CL=90%	1847
$\gamma\pi^0$	< 2 × 10 <sup>-4</sup>	CL=90%	1884

## Meson Summary Table

**X(3872)**  $I^G(J^{PC}) = 0^?(?^{?+})$ 

Quantum numbers not established.

Mass  $m = 3871.68 \pm 0.17$  MeV $m_{X(3872)} - m_{J/\psi} = 775 \pm 4$  MeV $m_{X(3872)} - m_{\psi(2S)}$ Full width  $\Gamma < 1.2$  MeV, CL = 90%

<b>X(3872) DECAY MODES</b>	Fraction ( $\Gamma_i/\Gamma$ )	$\rho$ (MeV/c)
$\pi^+ \pi^- J/\psi(1S)$	>2.6 %	650
$\omega J/\psi(1S)$	>1.9 %	†
$D^0 \bar{D}^0 \pi^0$	>3.2 × 10 <sup>-3</sup>	116
$\bar{D}^{*0} D^0$	>5 × 10 <sup>-3</sup>	†
$\gamma J/\psi$	>6 × 10 <sup>-3</sup>	697
$\gamma \psi(2S)$	[oooo] >3.0 %	181

**X(3915)**  $I^G(J^{PC}) = 0^+(?^{?+})$ Observed in  $\omega J/\psi$ , thus  $C = +$ Mass  $m = 3917.5 \pm 2.7$  MeVFull width  $\Gamma = 27 \pm 10$  MeV ( $S = 1.4$ )

<b>X(3915) DECAY MODES</b>	Fraction ( $\Gamma_i/\Gamma$ )	$\rho$ (MeV/c)
$\omega J/\psi$	seen	219
$\gamma \gamma$	seen	1959

**Xc2(2P)**  $I^G(J^{PC}) = 0^+(2^{++})$ Mass  $m = 3927.2 \pm 2.6$  MeVFull width  $\Gamma = 24 \pm 6$  MeV

<b>Xc2(2P) DECAY MODES</b>	Fraction ( $\Gamma_i/\Gamma$ )	$\rho$ (MeV/c)
$\gamma \gamma$	seen	1964
$D \bar{D}$	seen	615
$D^+ D^-$	seen	600
$D^0 \bar{D}^0$	seen	615

 **$\psi(4040)$  [pppp]**  $I^G(J^{PC}) = 0^-(1^{--})$ Mass  $m = 4039 \pm 1$  MeVFull width  $\Gamma = 80 \pm 10$  MeV $\Gamma_{ee} = 0.86 \pm 0.07$  keV

Due to the complexity of the  $c\bar{c}$  threshold region, in this listing, "seen" ("not seen") means that a cross section for the mode in question has been measured at effective  $\sqrt{s}$  near this particle's central mass value, more (less) than  $2\sigma$  above zero, without regard to any peaking behavior in  $\sqrt{s}$  or absence thereof. See mode listing(s) for details and references.

<b><math>\psi(4040)</math> DECAY MODES</b>	Fraction ( $\Gamma_i/\Gamma$ )	Confidence level	$\rho$ (MeV/c)
$e^+ e^-$	$(1.07 \pm 0.16) \times 10^{-5}$		2019
$D \bar{D}$	seen		775
$D^0 \bar{D}^0$	seen		775
$D^+ D^-$	seen		763
$D^* \bar{D}^+ + c.c.$	seen		569
$D^*(2007)^0 \bar{D}^0 + c.c.$	seen		575
$D^*(2010)^+ D^- + c.c.$	seen		561
$D^* \bar{D}^*$	seen		193
$D^*(2007)^0 \bar{D}^*(2007)^0$	seen		224
$D^*(2010)^+ D^*(2010)^-$	seen		193
$D^0 D^- \pi^+ + c.c.$ (excl.)	not seen		-
$D^*(2007)^0 \bar{D}^0 + c.c.,$ $D^*(2010)^+ D^- + c.c.)$			
$D \bar{D}^* \pi$ (excl. $D^* \bar{D}^*$ )	not seen		-
$D^0 \bar{D}^{*-} \pi^+ + c.c.$ (excl.)	seen		-
$D^*(2010)^+ D^*(2010)^-$			
$D_s^+ D_s^-$	seen		451
$J/\psi \pi^+ \pi^-$	< 4 × 10 <sup>-3</sup>	90%	794
$J/\psi \pi^0 \pi^0$	< 2 × 10 <sup>-3</sup>	90%	797
$J/\psi \eta$	< 7 × 10 <sup>-3</sup>	90%	675
$J/\psi \pi^0$	< 2 × 10 <sup>-3</sup>	90%	823

$J/\psi \pi^+ \pi^- \pi^0$	< 2	× 10 <sup>-3</sup>	90%	746
$\chi_{c1} \gamma$	< 1.1	%	90%	494
$\chi_{c2} \gamma$	< 1.7	%	90%	454
$\chi_{c1} \pi^+ \pi^- \pi^0$	< 1.1	%	90%	306
$\chi_{c2} \pi^+ \pi^- \pi^0$	< 3.2	%	90%	233
$h_c(1P) \pi^+ \pi^-$	< 3	× 10 <sup>-3</sup>	90%	403
$\phi \pi^+ \pi^-$	< 3	× 10 <sup>-3</sup>	90%	1880

 **$\psi(4160)$  [pppp]**  $I^G(J^{PC}) = 0^-(1^{--})$ Mass  $m = 4153 \pm 3$  MeVFull width  $\Gamma = 103 \pm 8$  MeV $\Gamma_{ee} = 0.83 \pm 0.07$  keV

Due to the complexity of the  $c\bar{c}$  threshold region, in this listing, "seen" ("not seen") means that a cross section for the mode in question has been measured at effective  $\sqrt{s}$  near this particle's central mass value, more (less) than  $2\sigma$  above zero, without regard to any peaking behavior in  $\sqrt{s}$  or absence thereof. See mode listing(s) for details and references.

<b><math>\psi(4160)</math> DECAY MODES</b>	Fraction ( $\Gamma_i/\Gamma$ )	Confidence level	$\rho$ (MeV/c)
$e^+ e^-$	$(8.1 \pm 0.9) \times 10^{-6}$		2076
$D \bar{D}$	seen		913
$D^0 \bar{D}^0$	seen		913
$D^+ D^-$	seen		904
$D^* \bar{D}^+ + c.c.$	seen		746
$D^*(2007)^0 \bar{D}^0 + c.c.$	seen		751
$D^*(2010)^+ D^- + c.c.$	seen		740
$D^* \bar{D}^*$	seen		520
$D^*(2007)^0 \bar{D}^*(2007)^0$	seen		533
$D^*(2010)^+ D^*(2010)^-$	seen		520
$D^0 D^- \pi^+ + c.c.$ (excl.)	not seen		-
$D^*(2007)^0 \bar{D}^0 + c.c.,$ $D^*(2010)^+ D^- + c.c.)$			
$D \bar{D}^* \pi + c.c.$ (excl. $D^* \bar{D}^*$ )	seen		-
$D^0 D^{*-} \pi^+ + c.c.$ (excl.)	not seen		-
$D^*(2010)^+ D^*(2010)^-$			
$D_s^+ D_s^-$	not seen		661
$D_s^{*+} D_s^{*-} + c.c.$	seen		385
$J/\psi \pi^+ \pi^-$	< 3 × 10 <sup>-3</sup>	90%	888
$J/\psi \pi^0 \pi^0$	< 3 × 10 <sup>-3</sup>	90%	891
$J/\psi K^+ K^-$	< 2 × 10 <sup>-3</sup>	90%	324
$J/\psi \eta$	< 8 × 10 <sup>-3</sup>	90%	786
$J/\psi \pi^0$	< 1 × 10 <sup>-3</sup>	90%	914
$J/\psi \eta'$	< 5 × 10 <sup>-3</sup>	90%	385
$J/\psi \pi^+ \pi^- \pi^0$	< 1 × 10 <sup>-3</sup>	90%	847
$\psi(2S) \pi^+ \pi^-$	< 4 × 10 <sup>-3</sup>	90%	353
$\chi_{c1} \gamma$	< 7 × 10 <sup>-3</sup>	90%	593
$\chi_{c2} \gamma$	< 1.3 %	90%	554
$\chi_{c1} \pi^+ \pi^- \pi^0$	< 2 × 10 <sup>-3</sup>	90%	452
$\chi_{c2} \pi^+ \pi^- \pi^0$	< 8 × 10 <sup>-3</sup>	90%	398
$h_c(1P) \pi^+ \pi^-$	< 5 × 10 <sup>-3</sup>	90%	519
$h_c(1P) \pi^0 \pi^0$	< 2 × 10 <sup>-3</sup>	90%	523
$h_c(1P) \eta$	< 2 × 10 <sup>-3</sup>	90%	282
$h_c(1P) \pi^0$	< 4 × 10 <sup>-4</sup>	90%	567
$\phi \pi^+ \pi^-$	< 2 × 10 <sup>-3</sup>	90%	1941

**X(4260)**  $I^G(J^{PC}) = ?^?(1^{--})$ Mass  $m = 4263^{+8}_{-9}$  MeV ( $S = 1.1$ )Full width  $\Gamma = 95 \pm 14$  MeV

<b>X(4260) DECAY MODES</b>	Fraction ( $\Gamma_i/\Gamma$ )	$\rho$ (MeV/c)
$J/\psi \pi^+ \pi^-$	seen	976
$J/\psi \pi^0 \pi^0$	seen	978
$J/\psi K^+ K^-$	seen	530
$J/\psi \eta$	not seen	886
$J/\psi \pi^0$	not seen	999
$J/\psi \eta'$	not seen	569
$J/\psi \pi^+ \pi^- \pi^0$	not seen	939
$J/\psi \eta \eta$	not seen	339
$\psi(2S) \pi^+ \pi^-$	not seen	470
$\psi(2S) \eta$	not seen	167
$\chi_{c0} \omega$	not seen	292
$\chi_{c1} \gamma$	not seen	686
$\chi_{c2} \gamma$	not seen	648

## Meson Summary Table

$\chi_{c1} \pi^+ \pi^- \pi^0$	not seen	571
$\chi_{c2} \pi^+ \pi^- \pi^0$	not seen	524
$h_c(1P) \pi^+ \pi^-$	not seen	623
$\phi \pi^+ \pi^-$	not seen	1999
$\phi f_0(980) \rightarrow \phi \pi^+ \pi^-$	not seen	-
$D \bar{D}$	not seen	1032
$D^0 \bar{D}^0$	not seen	1032
$D^+ D^-$	not seen	1023
$D^* \bar{D}^* + c.c.$	not seen	887
$D^*(2007)^0 \bar{D}^0 + c.c.$	not seen	-
$D^*(2010)^+ D^- + c.c.$	not seen	-
$D^* \bar{D}^*$	not seen	708
$D^*(2007)^0 \bar{D}^*(2007)^0$	not seen	717
$D^*(2010)^+ D^*(2010)^-$	not seen	708
$D^0 D^- \pi^+ + c.c. (excl. D^*(2007)^0 \bar{D}^{*0} + c.c., D^*(2010)^+ D^- + c.c.)$	not seen	-
$D \bar{D}^* \pi + c.c. (excl. D^* \bar{D}^*)$	not seen	723
$D^0 D^{*-} \pi^+ + c.c. (excl. D^*(2010)^+ D^*(2010)^-)$	not seen	-
$D^0 D^*(2010)^- \pi^+ + c.c.$	not seen	716
$D^* \bar{D}^* \pi$	not seen	474
$D_s^+ D_s^-$	not seen	817
$D_s^{*+} D_s^- + c.c.$	not seen	615
$D_s^{*+} D_s^{*-}$	not seen	284
$\rho \bar{\rho}$	not seen	1914
$K_s^0 K^\pm \pi^\mp$	not seen	2054
$K^+ K^- \pi^0$	not seen	2055

**X(4360)**

$$I^G(J^{PC}) = ??(1^{--})$$

X(4360) MASS =  $4361 \pm 13$  MeV  
X(4360) WIDTH =  $74 \pm 18$  MeV

<b>X(4360) DECAY MODES</b>	Fraction ( $\Gamma_i/\Gamma$ )	$\rho$ (MeV/c)
$\psi(2S) \pi^+ \pi^-$	seen	567

 **$\psi(4415)$  [pppp]**

$$I^G(J^{PC}) = 0^-(1^{--})$$

Mass  $m = 4421 \pm 4$  MeV  
Full width  $\Gamma = 62 \pm 20$  MeV  
 $\Gamma_{ee} = 0.58 \pm 0.07$  keV

Due to the complexity of the  $c\bar{c}$  threshold region, in this listing, "seen" ("not seen") means that a cross section for the mode in question has been measured at effective  $\sqrt{s}$  near this particle's central mass value, more (less) than  $2\sigma$  above zero, without regard to any peaking behavior in  $\sqrt{s}$  or absence thereof. See mode listing(s) for details and references.

<b><math>\psi(4415)</math> DECAY MODES</b>	Fraction ( $\Gamma_i/\Gamma$ )	Confidence level	$\rho$ (MeV/c)
$D \bar{D}$	not seen		1187
$D^0 \bar{D}^0$	seen		1187
$D^+ D^-$	seen		1179
$D^* \bar{D}^* + c.c.$	not seen		1063
$D^*(2007)^0 \bar{D}^0 + c.c.$	seen		1066
$D^*(2010)^+ D^- + c.c.$	seen		1059
$D^* \bar{D}^*$	not seen		919
$D^*(2007)^0 \bar{D}^*(2007)^0 + c.c.$	seen		926
$D^*(2010)^+ D^*(2010)^- + c.c.$	seen		919
$D^0 D^- \pi^+ (excl. D^*(2007)^0 \bar{D}^0 + c.c., D^*(2010)^+ D^- + c.c.)$	$< 2.3$ %	90%	-
$D \bar{D}_2^*(2460) \rightarrow D^0 D^- \pi^+ + c.c.$	$(10 \pm 4)$ %		-
$D^0 D^{*-} \pi^+ + c.c.$	$< 11$ %	90%	926
$D_s^+ D_s^-$	not seen		1006
$D_s^{*+} D_s^- + c.c.$	seen		-
$D_s^{*+} D_s^{*-}$	not seen		651
$e^+ e^-$	$(9.4 \pm 3.2) \times 10^{-6}$		2210

**X(4660)**

$$I^G(J^{PC}) = ??(1^{--})$$

X(4660) MASS =  $4664 \pm 12$  MeV  
X(4660) WIDTH =  $48 \pm 15$  MeV

<b>X(4660) DECAY MODES</b>	Fraction ( $\Gamma_i/\Gamma$ )	$\rho$ (MeV/c)
$\psi(2S) \pi^+ \pi^-$	seen	838

 **$b\bar{b}$  MESONS** **$\Upsilon(1S)$** 

$$I^G(J^{PC}) = 0^-(1^{--})$$

Mass  $m = 9460.30 \pm 0.26$  MeV ( $S = 3.3$ )  
Full width  $\Gamma = 54.02 \pm 1.25$  keV  
 $\Gamma_{ee} = 1.340 \pm 0.018$  keV

<b><math>\Upsilon(1S)</math> DECAY MODES</b>	Fraction ( $\Gamma_i/\Gamma$ )	Confidence level	$\rho$ (MeV/c)
$\tau^+ \tau^-$	$(2.60 \pm 0.10)$ %		4384
$e^+ e^-$	$(2.38 \pm 0.11)$ %		4730
$\mu^+ \mu^-$	$(2.48 \pm 0.05)$ %		4729

**Hadronic decays**

$ggg$	$(81.7 \pm 0.7)$ %		-
$\gamma g g$	$(2.2 \pm 0.6)$ %		-
$\eta'(958)$ anything	$(2.94 \pm 0.24)$ %		-
$J/\psi(1S)$ anything	$(6.5 \pm 0.7) \times 10^{-4}$		4223
$\chi_{c0}$ anything	$< 5 \times 10^{-3}$	90%	-
$\chi_{c1}$ anything	$(2.3 \pm 0.7) \times 10^{-4}$		-
$\chi_{c2}$ anything	$(3.4 \pm 1.0) \times 10^{-4}$		-
$\psi(2S)$ anything	$(2.7 \pm 0.9) \times 10^{-4}$		-
$\rho\pi$	$< 2 \times 10^{-4}$	90%	4697
$\pi^+ \pi^-$	$< 5 \times 10^{-4}$	90%	4728
$K^+ K^-$	$< 5 \times 10^{-4}$	90%	4704
$\rho \bar{\rho}$	$< 5 \times 10^{-4}$	90%	4636
$\pi^0 \pi^+ \pi^-$	$< 1.84 \times 10^{-5}$	90%	4725
$D^*(2010)^\pm$ anything	$(2.52 \pm 0.20)$ %		-
$\bar{d}$ anything	$(2.86 \pm 0.28) \times 10^{-5}$		-

**Radiative decays**

$\gamma \pi^+ \pi^-$	$(6.3 \pm 1.8) \times 10^{-5}$		4728
$\gamma \pi^0 \pi^0$	$(1.7 \pm 0.7) \times 10^{-5}$		4728
$\gamma \pi^0 \eta$	$< 2.4 \times 10^{-6}$	90%	4713
$\gamma K^+ K^-$	$(1.14 \pm 0.13) \times 10^{-5}$		4704
$\gamma \rho \bar{\rho}$	$[qqqq] [rrrr] < 6 \times 10^{-6}$	90%	4636
$\gamma 2h^+ 2h^-$	$(7.0 \pm 1.5) \times 10^{-4}$		4720
$\gamma 3h^+ 3h^-$	$(5.4 \pm 2.0) \times 10^{-4}$		4703
$\gamma 4h^+ 4h^-$	$(7.4 \pm 3.5) \times 10^{-4}$		4679
$\gamma \pi^+ \pi^- K^+ K^-$	$(2.9 \pm 0.9) \times 10^{-4}$		4686
$\gamma 2\pi^+ 2\pi^-$	$(2.5 \pm 0.9) \times 10^{-4}$		4720
$\gamma 3\pi^+ 3\pi^-$	$(2.5 \pm 1.2) \times 10^{-4}$		4703
$\gamma 2\pi^+ 2\pi^- K^+ K^-$	$(2.4 \pm 1.2) \times 10^{-4}$		4658
$\gamma \pi^+ \pi^- \rho \bar{\rho}$	$(1.5 \pm 0.6) \times 10^{-4}$		4604
$\gamma 2\pi^+ 2\pi^- \rho \bar{\rho}$	$(4 \pm 6) \times 10^{-5}$		4563
$\gamma 2K^+ 2K^-$	$(2.0 \pm 2.0) \times 10^{-5}$		4601
$\gamma \eta'(958)$	$< 1.9 \times 10^{-6}$	90%	4682
$\gamma \eta$	$< 1.0 \times 10^{-6}$	90%	4714
$\gamma f_0(980)$	$< 3 \times 10^{-5}$	90%	4678
$\gamma f_2'(1525)$	$(3.8 \pm 0.9) \times 10^{-5}$		4607
$\gamma f_2(1270)$	$(1.01 \pm 0.09) \times 10^{-4}$		4644
$\gamma \eta(1405)$	$< 8.2 \times 10^{-5}$	90%	4625
$\gamma f_0(1500)$	$< 1.5 \times 10^{-5}$	90%	4610
$\gamma f_0(1710)$	$< 2.6 \times 10^{-4}$	90%	4574
$\gamma f_0(1710) \rightarrow \gamma K^+ K^-$	$< 7 \times 10^{-6}$	90%	-
$\gamma f_0(1710) \rightarrow \gamma \pi^0 \pi^0$	$< 1.4 \times 10^{-6}$	90%	-
$\gamma f_0(1710) \rightarrow \gamma \eta \eta$	$< 1.8 \times 10^{-6}$	90%	-
$\gamma f_4(2050)$	$< 5.3 \times 10^{-5}$	90%	4515
$\gamma f_0(2200) \rightarrow \gamma K^+ K^-$	$< 2 \times 10^{-4}$	90%	4475
$\gamma f_J(2220) \rightarrow \gamma K^+ K^-$	$< 8 \times 10^{-7}$	90%	4469
$\gamma f_J(2220) \rightarrow \gamma \pi^+ \pi^-$	$< 6 \times 10^{-7}$	90%	-
$\gamma f_J(2220) \rightarrow \gamma \rho \bar{\rho}$	$< 1.1 \times 10^{-6}$	90%	-
$\gamma \eta(2225) \rightarrow \gamma \phi \phi$	$< 3 \times 10^{-3}$	90%	4469
$\gamma \eta_c(1S)$	$< 5.7 \times 10^{-5}$	90%	4260
$\gamma \chi_{c0}$	$< 6.5 \times 10^{-4}$	90%	4114
$\gamma \chi_{c1}$	$< 2.3 \times 10^{-5}$	90%	4079
$\gamma \chi_{c2}$	$< 7.6 \times 10^{-6}$	90%	4062
$\gamma X(3872) \rightarrow \pi^+ \pi^- J/\psi$	$< 1.6 \times 10^{-6}$	90%	-
$\gamma X(3872) \rightarrow \pi^+ \pi^- \pi^0 J/\psi$	$< 2.8 \times 10^{-6}$	90%	-
$\gamma X(3915) \rightarrow \omega J/\psi$	$< 3.0 \times 10^{-6}$	90%	-

## Meson Summary Table

$\gamma X(4140) \rightarrow \phi J/\psi$	$< 2.2$	$\times 10^{-6}$	90%	-
$\gamma X$	[ssss] $< 4.5$	$\times 10^{-6}$	90%	-
$\gamma X \bar{X} (m_X < 3.1 \text{ GeV})$	[tttt] $< 1$	$\times 10^{-3}$	90%	-
$\gamma X \bar{X} (m_X < 4.5 \text{ GeV})$	[uuuu] $< 2.4$	$\times 10^{-4}$	90%	-
$\gamma X \rightarrow \gamma + \geq 4 \text{ prongs}$	[vvvv] $< 1.78$	$\times 10^{-4}$	95%	-
$\gamma a_1^0 \rightarrow \gamma \mu^+ \mu^-$	[wwww] $< 9$	$\times 10^{-6}$	90%	-
$\gamma a_1^0 \rightarrow \gamma \tau^+ \tau^-$	[qqqq] $< 5.0$	$\times 10^{-5}$	90%	-

## Lepton Family number (LF) violating modes

$\mu^\pm \tau^\mp$	LF	$< 6.0$	$\times 10^{-6}$	95%	4563
--------------------	----	---------	------------------	-----	------

## Other decays

invisible	$< 3.0$	$\times 10^{-4}$	90%	-
-----------	---------	------------------	-----	---

 **$\chi_{b0}(1P)$  [xxxx]**

$$J^G(J^{PC}) = 0^+(0^{++})$$

$J$  needs confirmation.

$$\text{Mass } m = 9859.44 \pm 0.42 \pm 0.31 \text{ MeV}$$

$\chi_{b0}(1P)$ DECAY MODES	Fraction ( $\Gamma_i/\Gamma$ )	Confidence level	$p$ (MeV/c)
$\gamma \mathcal{T}(1S)$	$(1.76 \pm 0.35) \%$		391
$D^0 X$	$< 10.4$	%	90%
$\pi^+ \pi^- K^+ K^- \pi^0$	$< 1.6$	$\times 10^{-4}$	90%
$2\pi^+ 2\pi^- K^- K_S^0$	$< 5$	$\times 10^{-5}$	90%
$2\pi^+ 2\pi^- K^- K_S^0 2\pi^0$	$< 5$	$\times 10^{-4}$	90%
$2\pi^+ 2\pi^- 2\pi^0$	$< 2.1$	$\times 10^{-4}$	90%
$2\pi^+ 2\pi^- K^+ K^-$	$(1.1 \pm 0.6) \times 10^{-4}$		4861
$2\pi^+ 2\pi^- K^+ K^- \pi^0$	$< 2.7$	$\times 10^{-4}$	90%
$2\pi^+ 2\pi^- K^+ K^- 2\pi^0$	$< 5$	$\times 10^{-4}$	90%
$3\pi^+ 2\pi^- K^- K_S^0 \pi^0$	$< 1.6$	$\times 10^{-4}$	90%
$3\pi^+ 3\pi^-$	$< 8$	$\times 10^{-5}$	90%
$3\pi^+ 3\pi^- 2\pi^0$	$< 6$	$\times 10^{-4}$	90%
$3\pi^+ 3\pi^- K^+ K^-$	$(2.4 \pm 1.2) \times 10^{-4}$		4827
$3\pi^+ 3\pi^- K^+ K^- \pi^0$	$< 1.0$	$\times 10^{-3}$	90%
$4\pi^+ 4\pi^-$	$< 8$	$\times 10^{-5}$	90%
$4\pi^+ 4\pi^- 2\pi^0$	$< 2.1$	$\times 10^{-3}$	90%

 **$\chi_{b1}(1P)$  [xxxx]**

$$J^G(J^{PC}) = 0^+(1^{++})$$

$J$  needs confirmation.

$$\text{Mass } m = 9892.78 \pm 0.26 \pm 0.31 \text{ MeV}$$

$\chi_{b1}(1P)$ DECAY MODES	Fraction ( $\Gamma_i/\Gamma$ )	Confidence level	$p$ (MeV/c)
$\gamma \mathcal{T}(1S)$	$(33.9 \pm 2.2) \%$		423
$D^0 X$	$(12.6 \pm 2.2) \%$		-
$\pi^+ \pi^- K^+ K^- \pi^0$	$(2.0 \pm 0.6) \times 10^{-4}$		4892
$2\pi^+ 2\pi^- K^- K_S^0$	$(1.3 \pm 0.5) \times 10^{-4}$		4892
$2\pi^+ 2\pi^- K^- K_S^0 2\pi^0$	$< 6$	$\times 10^{-4}$	90%
$2\pi^+ 2\pi^- 2\pi^0$	$(8.0 \pm 2.5) \times 10^{-4}$		4921
$2\pi^+ 2\pi^- K^+ K^-$	$(1.5 \pm 0.5) \times 10^{-4}$		4878
$2\pi^+ 2\pi^- K^+ K^- \pi^0$	$(3.5 \pm 1.2) \times 10^{-4}$		4863
$2\pi^+ 2\pi^- K^+ K^- 2\pi^0$	$(8.6 \pm 3.2) \times 10^{-4}$		4845
$3\pi^+ 2\pi^- K^- K_S^0 \pi^0$	$(9.3 \pm 3.3) \times 10^{-4}$		4844
$3\pi^+ 3\pi^-$	$(1.9 \pm 0.6) \times 10^{-4}$		4921
$3\pi^+ 3\pi^- 2\pi^0$	$(1.7 \pm 0.5) \times 10^{-3}$		4898
$3\pi^+ 3\pi^- K^+ K^-$	$(2.6 \pm 0.8) \times 10^{-4}$		4844
$3\pi^+ 3\pi^- K^+ K^- \pi^0$	$(7.5 \pm 2.6) \times 10^{-4}$		4825
$4\pi^+ 4\pi^-$	$(2.6 \pm 0.9) \times 10^{-4}$		4897
$4\pi^+ 4\pi^- 2\pi^0$	$(1.4 \pm 0.6) \times 10^{-3}$		4867

 **$h_b(1P)$** 

$$J^G(J^{PC}) = ?^?(1^{+-})$$

$$\text{Mass } m = 9898.6 \pm 1.4 \text{ MeV}$$

$h_b(1P)$ DECAY MODES	Fraction ( $\Gamma_i/\Gamma$ )	$p$ (MeV/c)
$\eta_b(1S) \gamma$	seen	495

 **$\chi_{b2}(1P)$  [xxxx]**

$$J^G(J^{PC}) = 0^+(2^{++})$$

$J$  needs confirmation.

$$\text{Mass } m = 9912.21 \pm 0.26 \pm 0.31 \text{ MeV}$$

 **$\chi_{b2}(1P)$  DECAY MODES**

DECAY MODES	Fraction ( $\Gamma_i/\Gamma$ )	Confidence level	$p$ (MeV/c)
$\gamma \mathcal{T}(1S)$	$(19.1 \pm 1.2) \%$		442
$D^0 X$	$< 7.9$	%	90%
$\pi^+ \pi^- K^+ K^- \pi^0$	$(8 \pm 5) \times 10^{-5}$		4902
$2\pi^+ 2\pi^- K^- K_S^0$	$< 1.0$	$\times 10^{-4}$	90%
$2\pi^+ 2\pi^- K^- K_S^0 2\pi^0$	$(5.3 \pm 2.4) \times 10^{-4}$		4873
$2\pi^+ 2\pi^- 2\pi^0$	$(3.5 \pm 1.4) \times 10^{-4}$		4931
$2\pi^+ 2\pi^- K^+ K^-$	$(1.1 \pm 0.4) \times 10^{-4}$		4888
$2\pi^+ 2\pi^- K^+ K^- \pi^0$	$(2.1 \pm 0.9) \times 10^{-4}$		4872
$2\pi^+ 2\pi^- K^+ K^- 2\pi^0$	$(3.9 \pm 1.8) \times 10^{-4}$		4855
$3\pi^+ 2\pi^- K^- K_S^0 \pi^0$	$< 5$	$\times 10^{-4}$	90%
$3\pi^+ 3\pi^-$	$(7.0 \pm 3.1) \times 10^{-5}$		4931
$3\pi^+ 3\pi^- 2\pi^0$	$(1.0 \pm 0.4) \times 10^{-3}$		4908
$3\pi^+ 3\pi^- K^+ K^-$	$< 8$	$\times 10^{-5}$	90%
$3\pi^+ 3\pi^- K^+ K^- \pi^0$	$(3.6 \pm 1.5) \times 10^{-4}$		4835
$4\pi^+ 4\pi^-$	$(8 \pm 4) \times 10^{-5}$		4907
$4\pi^+ 4\pi^- 2\pi^0$	$(1.8 \pm 0.7) \times 10^{-3}$		4877

 **$\mathcal{T}(2S)$** 

$$J^G(J^{PC}) = 0^-(1^{--})$$

$$\text{Mass } m = 10.02326 \pm 0.00031 \text{ GeV}$$

$$m_{\mathcal{T}(3S)} - m_{\mathcal{T}(2S)} = 331.50 \pm 0.13 \text{ MeV}$$

$$\text{Full width } \Gamma = 31.98 \pm 2.63 \text{ keV}$$

$$\Gamma_{ee} = 0.612 \pm 0.011 \text{ keV}$$

 **$\mathcal{T}(2S)$  DECAY MODES**

DECAY MODES	Fraction ( $\Gamma_i/\Gamma$ )	Confidence level	Scale factor/ $p$ (MeV/c)
$\mathcal{T}(1S) \pi^+ \pi^-$	$(17.92 \pm 0.26) \%$		475
$\mathcal{T}(1S) \pi^0 \pi^0$	$(8.6 \pm 0.4) \%$		480
$\tau^+ \tau^-$	$(2.00 \pm 0.21) \%$		4686
$\mu^+ \mu^-$	$(1.93 \pm 0.17) \%$	S=2.2	5011
$e^+ e^-$	$(1.91 \pm 0.16) \%$		5012
$\mathcal{T}(1S) \pi^0$	$< 1.8$	$\times 10^{-4}$	CL=90%
$\mathcal{T}(1S) \eta$	$(2.34 \pm 0.31) \times 10^{-4}$		126
$J/\psi(1S)$ anything	$< 6$	$\times 10^{-3}$	CL=90%
$d$ anything	$(3.4 \pm 0.6) \times 10^{-5}$		-
hadrons	$(94 \pm 11) \%$		-
$ggg$	$(58.8 \pm 1.2) \%$		-
$\gamma gg$	$(8.8 \pm 1.1) \%$		-

## Radiative decays

$\gamma \chi_{b1}(1P)$	$(6.9 \pm 0.4) \%$		130
$\gamma \chi_{b2}(1P)$	$(7.15 \pm 0.35) \%$		110
$\gamma \chi_{b0}(1P)$	$(3.8 \pm 0.4) \%$		162
$\gamma f_0(1710)$	$< 5.9$	$\times 10^{-4}$	CL=90%
$\gamma f_2'(1525)$	$< 5.3$	$\times 10^{-4}$	CL=90%
$\gamma f_2(1270)$	$< 2.41$	$\times 10^{-4}$	CL=90%
$\gamma \eta_c(1S)$	$< 2.7$	$\times 10^{-5}$	CL=90%
$\gamma \chi_{c0}$	$< 1.0$	$\times 10^{-4}$	CL=90%
$\gamma \chi_{c1}$	$< 3.6$	$\times 10^{-6}$	CL=90%
$\gamma \chi_{c2}$	$< 1.5$	$\times 10^{-5}$	CL=90%
$\gamma X(3872) \rightarrow \pi^+ \pi^- J/\psi$	$< 8$	$\times 10^{-7}$	CL=90%
$\gamma X(3872) \rightarrow \pi^+ \pi^- \pi^0 J/\psi$	$< 2.4$	$\times 10^{-6}$	CL=90%
$\gamma X(3915) \rightarrow \omega J/\psi$	$< 2.8$	$\times 10^{-6}$	CL=90%
$\gamma X(4140) \rightarrow \phi J/\psi$	$< 1.2$	$\times 10^{-6}$	CL=90%
$\gamma X(4350) \rightarrow \phi J/\psi$	$< 1.3$	$\times 10^{-6}$	CL=90%
$\gamma \eta_b(1S)$	$(3.9 \pm 1.5) \times 10^{-4}$		612
$\gamma X \rightarrow \gamma + \geq 4 \text{ prongs}$	[yyyy] $< 1.95$	$\times 10^{-4}$	CL=95%
$\gamma A^0 \rightarrow \gamma \text{hadrons}$	$< 8$	$\times 10^{-5}$	CL=90%

## Lepton Family number (LF) violating modes

$e^\pm \tau^\mp$	LF	$< 3.2$	$\times 10^{-6}$	CL=90%	4854
$\mu^\pm \tau^\mp$	LF	$< 3.3$	$\times 10^{-6}$	CL=90%	4854

 **$\mathcal{T}(1D)$** 

$$J^G(J^{PC}) = 0^-(2^{--})$$

$$\text{Mass } m = 10163.7 \pm 1.4 \text{ MeV} \quad (S = 1.7)$$

 **$\mathcal{T}(1D)$  DECAY MODES**

DECAY MODES	Fraction ( $\Gamma_i/\Gamma$ )	$p$ (MeV/c)
$\gamma \gamma \mathcal{T}(1S)$	seen	679
$\gamma \chi_{bJ}(1P)$	seen	300
$\eta \mathcal{T}(1S)$	not seen	426
$\pi^+ \pi^- \mathcal{T}(1S)$	$(6.6 \pm 1.6) \times 10^{-3}$	623

## Meson Summary Table

 **$\chi_{b0}(2P)$**  [xxxx]

$$J^G(J^{PC}) = 0^+(0^{++})$$

$J$  needs confirmation.

Mass  $m = 10.2325 \pm 0.0004 \pm 0.0005$  GeV

$\chi_{b0}(2P)$ DECAY MODES	Fraction ( $\Gamma_i/\Gamma$ )	Confidence level	$p$ (MeV/c)
$\gamma T(2S)$	$(4.6 \pm 2.1)\%$		207
$\gamma T(1S)$	$(9 \pm 6) \times 10^{-3}$		743
$D^0 X$	$< 8.2\%$	90%	—
$\pi^+ \pi^- K^+ K^- \pi^0$	$< 3.4 \times 10^{-5}$	90%	5064
$2\pi^+ \pi^- K^- K^0_S$	$< 5 \times 10^{-5}$	90%	5063
$2\pi^+ \pi^- K^- K^0_S 2\pi^0$	$< 2.2 \times 10^{-4}$	90%	5036
$2\pi^+ 2\pi^- 2\pi^0$	$< 2.4 \times 10^{-4}$	90%	5092
$2\pi^+ 2\pi^- K^+ K^-$	$< 1.5 \times 10^{-4}$	90%	5050
$2\pi^+ 2\pi^- K^+ K^- \pi^0$	$< 2.2 \times 10^{-4}$	90%	5035
$2\pi^+ 2\pi^- K^+ K^- 2\pi^0$	$< 1.1 \times 10^{-3}$	90%	5019
$3\pi^+ 2\pi^- K^- K^0_S \pi^0$	$< 7 \times 10^{-4}$	90%	5018
$3\pi^+ 3\pi^-$	$< 7 \times 10^{-5}$	90%	5091
$3\pi^+ 3\pi^- 2\pi^0$	$< 1.2 \times 10^{-3}$	90%	5070
$3\pi^+ 3\pi^- K^+ K^-$	$< 1.5 \times 10^{-4}$	90%	5017
$3\pi^+ 3\pi^- K^+ K^- \pi^0$	$< 7 \times 10^{-4}$	90%	4999
$4\pi^+ 4\pi^-$	$< 1.7 \times 10^{-4}$	90%	5069
$4\pi^+ 4\pi^- 2\pi^0$	$< 6 \times 10^{-4}$	90%	5039

 **$\chi_{b1}(2P)$**  [xxxx]

$$J^G(J^{PC}) = 0^+(1^{++})$$

$J$  needs confirmation.

Mass  $m = 10.25546 \pm 0.00022 \pm 0.00050$  GeV $m_{\chi_{b1}(2P)} - m_{\chi_{b0}(2P)} = 23.5 \pm 1.0$  MeV

$\chi_{b1}(2P)$ DECAY MODES	Fraction ( $\Gamma_i/\Gamma$ )	Scale factor/ Confidence level	$p$ (MeV/c)
$\omega T(1S)$	$(1.63^{+0.40}_{-0.34})\%$		135
$\gamma T(2S)$	$(19.9 \pm 1.9)\%$		230
$\gamma T(1S)$	$(9.2 \pm 0.8)\%$	1.1	764
$\pi\pi\chi_{b1}(1P)$	$(9.1 \pm 1.3) \times 10^{-3}$		238
$D^0 X$	$(8.8 \pm 1.7)\%$		—
$\pi^+ \pi^- K^+ K^- \pi^0$	$(3.1 \pm 1.0) \times 10^{-4}$		5075
$2\pi^+ \pi^- K^- K^0_S$	$(1.1 \pm 0.5) \times 10^{-4}$		5075
$2\pi^+ \pi^- K^- K^0_S 2\pi^0$	$(7.7 \pm 3.2) \times 10^{-4}$		5047
$2\pi^+ 2\pi^- 2\pi^0$	$(5.9 \pm 2.0) \times 10^{-4}$		5104
$2\pi^+ 2\pi^- K^+ K^-$	$(10 \pm 4) \times 10^{-5}$		5062
$2\pi^+ 2\pi^- K^+ K^- \pi^0$	$(5.5 \pm 1.8) \times 10^{-4}$		5047
$2\pi^+ 2\pi^- K^+ K^- 2\pi^0$	$(10 \pm 4) \times 10^{-4}$		5030
$3\pi^+ 2\pi^- K^- K^0_S \pi^0$	$(6.7 \pm 2.6) \times 10^{-4}$		5029
$3\pi^+ 3\pi^-$	$(1.2 \pm 0.4) \times 10^{-4}$		5103
$3\pi^+ 3\pi^- 2\pi^0$	$(1.2 \pm 0.4) \times 10^{-3}$		5081
$3\pi^+ 3\pi^- K^+ K^-$	$(2.0 \pm 0.8) \times 10^{-4}$		5029
$3\pi^+ 3\pi^- K^+ K^- \pi^0$	$(6.1 \pm 2.2) \times 10^{-4}$		5011
$4\pi^+ 4\pi^-$	$(1.7 \pm 0.6) \times 10^{-4}$		5080
$4\pi^+ 4\pi^- 2\pi^0$	$(1.9 \pm 0.7) \times 10^{-3}$		5051

 **$\chi_{b2}(2P)$**  [xxxx]

$$J^G(J^{PC}) = 0^+(2^{++})$$

$J$  needs confirmation.

Mass  $m = 10.26865 \pm 0.00022 \pm 0.00050$  GeV $m_{\chi_{b2}(2P)} - m_{\chi_{b1}(2P)} = 13.5 \pm 0.6$  MeV

$\chi_{b2}(2P)$ DECAY MODES	Fraction ( $\Gamma_i/\Gamma$ )	Scale factor/ Confidence level	$p$ (MeV/c)
$\omega T(1S)$	$(1.10^{+0.34}_{-0.30})\%$		194
$\gamma T(2S)$	$(10.6 \pm 2.6)\%$	S=2.0	242
$\gamma T(1S)$	$(7.0 \pm 0.7)\%$		777
$\pi\pi\chi_{b2}(1P)$	$(5.1 \pm 0.9) \times 10^{-3}$		229
$D^0 X$	$< 2.4\%$	CL=90%	—
$\pi^+ \pi^- K^+ K^- \pi^0$	$< 1.1 \times 10^{-4}$	CL=90%	5082
$2\pi^+ \pi^- K^- K^0_S$	$< 9 \times 10^{-5}$	CL=90%	5082
$2\pi^+ \pi^- K^- K^0_S 2\pi^0$	$< 7 \times 10^{-4}$	CL=90%	5054
$2\pi^+ 2\pi^- 2\pi^0$	$(3.9 \pm 1.6) \times 10^{-4}$		5110
$2\pi^+ 2\pi^- K^+ K^-$	$(9 \pm 4) \times 10^{-5}$		5068
$2\pi^+ 2\pi^- K^+ K^- \pi^0$	$(2.4 \pm 1.1) \times 10^{-4}$		5054
$2\pi^+ 2\pi^- K^+ K^- 2\pi^0$	$(4.7 \pm 2.3) \times 10^{-4}$		5037
$3\pi^+ 2\pi^- K^- K^0_S \pi^0$	$< 4 \times 10^{-4}$	CL=90%	5036
$3\pi^+ 3\pi^-$	$(9 \pm 4) \times 10^{-5}$		5110

$3\pi^+ 3\pi^- 2\pi^0$	$(1.2 \pm 0.4) \times 10^{-3}$	5088
$3\pi^+ 3\pi^- K^+ K^-$	$(1.4 \pm 0.7) \times 10^{-4}$	5036
$3\pi^+ 3\pi^- K^+ K^- \pi^0$	$(4.2 \pm 1.7) \times 10^{-4}$	5017
$4\pi^+ 4\pi^-$	$(9 \pm 5) \times 10^{-5}$	5087
$4\pi^+ 4\pi^- 2\pi^0$	$(1.3 \pm 0.5) \times 10^{-3}$	5058

 **$T(3S)$** 

$$J^G(J^{PC}) = 0^-(1^{--})$$

Mass  $m = 10.3552 \pm 0.0005$  GeV $m_{T(3S)} - m_{T(2S)} = 331.50 \pm 0.13$  MeVFull width  $\Gamma = 20.32 \pm 1.85$  keV $\Gamma_{ee} = 0.443 \pm 0.008$  keV

$T(3S)$ DECAY MODES	Fraction ( $\Gamma_i/\Gamma$ )	Scale factor/ Confidence level	$p$ (MeV/c)
$T(2S)$ anything	$(10.6 \pm 0.8)\%$		296
$T(2S) \pi^+ \pi^-$	$(2.82 \pm 0.18)\%$	S=1.6	177
$T(2S) \pi^0 \pi^0$	$(1.85 \pm 0.14)\%$		190
$T(2S) \gamma \gamma$	$(5.0 \pm 0.7)\%$		327
$T(2S) \pi^0 \eta$	$< 5.1 \times 10^{-4}$	CL=90%	298
$T(1S) \pi^+ \pi^-$	$(4.37 \pm 0.08)\%$		813
$T(1S) \pi^0 \pi^0$	$(2.20 \pm 0.13)\%$		816
$T(1S) \eta$	$< 1 \times 10^{-4}$	CL=90%	677
$T(1S) \pi^0$	$< 7 \times 10^{-5}$	CL=90%	846
$h_b(1P) \pi^0$	$< 1.2 \times 10^{-3}$	CL=90%	427
$h_b(1P) \pi^0 \rightarrow \gamma \eta_b(1S) \pi^0$	$(4.3 \pm 1.4) \times 10^{-4}$		—
$h_b(1P) \pi^+ \pi^-$	$< 1.2 \times 10^{-4}$	CL=90%	353
$\tau^+ \tau^-$	$(2.29 \pm 0.30)\%$		4863
$\mu^+ \mu^-$	$(2.18 \pm 0.21)\%$	S=2.1	5177
$e^+ e^-$	seen		5178
$ggg$	$(35.7 \pm 2.6)\%$		—
$\gamma gg$	$(9.7 \pm 1.8) \times 10^{-3}$		—

## Radiative decays

$\gamma \chi_{b2}(2P)$	$(13.1 \pm 1.6)\%$	S=3.4	86
$\gamma \chi_{b1}(2P)$	$(12.6 \pm 1.2)\%$	S=2.4	99
$\gamma \chi_{b0}(2P)$	$(5.9 \pm 0.6)\%$	S=1.4	122
$\gamma \chi_{b2}(1P)$	$(9.9 \pm 1.3) \times 10^{-3}$	S=2.0	434
$\gamma A^0 \rightarrow \gamma$ hadrons	$< 8 \times 10^{-5}$	CL=90%	—
$\gamma \chi_{b1}(1P)$	$(9 \pm 5) \times 10^{-4}$	S=1.9	452
$\gamma \chi_{b0}(1P)$	$(2.7 \pm 0.4) \times 10^{-3}$		484
$\gamma \eta_b(2S)$	$< 6.2 \times 10^{-4}$	CL=90%	—
$\gamma \eta_b(1S)$	$(5.1 \pm 0.7) \times 10^{-4}$		919
$\gamma X \rightarrow \gamma + \geq 4$ prongs	[zzzz] $< 2.2 \times 10^{-4}$	CL=95%	—
$\gamma a_1^0 \rightarrow \gamma \tau^+ \tau^-$	[aaaa] $< 1.6 \times 10^{-4}$	CL=90%	—

## Lepton Family number (LF) violating modes

$e^\pm \tau^\mp$	LF	$< 4.2 \times 10^{-6}$	CL=90%	5025
$\mu^\pm \tau^\mp$	LF	$< 3.1 \times 10^{-6}$	CL=90%	5025

 **$T(4S)$** or  **$T(10580)$** 

$$J^G(J^{PC}) = 0^-(1^{--})$$

Mass  $m = 10.5794 \pm 0.0012$  GeVFull width  $\Gamma = 20.5 \pm 2.5$  MeV $\Gamma_{ee} = 0.272 \pm 0.029$  keV (S = 1.5)

$T(4S)$ DECAY MODES	Fraction ( $\Gamma_i/\Gamma$ )	Confidence level	$p$ (MeV/c)
$B\bar{B}$	$> 96\%$	95%	327
$B^+ B^-$	$(51.3 \pm 0.6)\%$		332
$D^+$ anything + c.c.	$(17.8 \pm 2.6)\%$		—
$B^0 \bar{B}^0$	$(48.7 \pm 0.6)\%$		327
$J/\psi K_S^0 (J/\psi, \eta_c) K_S^0$	$< 4 \times 10^{-7}$	90%	—
non- $B\bar{B}$	$< 4\%$	95%	—
$e^+ e^-$	$(1.57 \pm 0.08) \times 10^{-5}$		5290
$\rho^+ \rho^-$	$< 5.7 \times 10^{-6}$	90%	5233
$J/\psi(1S)$ anything	$< 1.9 \times 10^{-4}$	95%	—
$D^{*+}$ anything + c.c.	$< 7.4\%$	90%	5099
$\phi$ anything	$(7.1 \pm 0.6)\%$		5240
$\phi \eta$	$< 1.8 \times 10^{-6}$	90%	5226
$\phi \eta'$	$< 4.3 \times 10^{-6}$	90%	5196
$\rho \eta$	$< 1.3 \times 10^{-6}$	90%	5247
$\rho \eta'$	$< 2.5 \times 10^{-6}$	90%	5217
$T(1S)$ anything	$< 4 \times 10^{-3}$	90%	1053
$T(1S) \pi^+ \pi^-$	$(8.1 \pm 0.6) \times 10^{-5}$		1026

## Meson Summary Table

$\Upsilon(1S)\eta$	$(1.96 \pm 0.11) \times 10^{-4}$	924
$\Upsilon(2S)\pi^+\pi^-$	$(8.6 \pm 1.3) \times 10^{-5}$	468
$h_b(1P)\pi^+\pi^-$	not seen	601
$\bar{d}$ anything	$< 1.3 \times 10^{-5}$	90% -

NOTES

In this Summary Table:

When a quantity has “(S = . . .)” to its right, the error on the quantity has been enlarged by the “scale factor” S, defined as  $S = \sqrt{\chi^2/(N-1)}$ , where N is the number of measurements used in calculating the quantity. We do this when  $S > 1$ , which often indicates that the measurements are inconsistent. When  $S > 1.25$ , we also show in the Particle Listings an ideogram of the measurements. For more about S, see the Introduction.

A decay momentum  $p$  is given for each decay mode. For a 2-body decay,  $p$  is the momentum of each decay product in the rest frame of the decaying particle. For a 3-or-more-body decay,  $p$  is the largest momentum any of the products can have in this frame.

### $\Upsilon(10860)$ $J^G(J^{PC}) = 0^-(1^{--})$

Mass  $m = 10876 \pm 11$  MeV  
 Full width  $\Gamma = 55 \pm 28$  MeV  
 $\Gamma_{ee} = 0.31 \pm 0.07$  keV (S = 1.3)

$\Upsilon(10860)$ DECAY MODES	Fraction ( $\Gamma_i/\Gamma$ )	Confidence level	$p$ (MeV/c)
$B\bar{B}X$	$(75.9^{+2.7}_{-4.0})\%$		-
$B\bar{B}$	$(5.5 \pm 1.0)\%$		1303
$B\bar{B}^* + \text{c.c.}$	$(13.7 \pm 1.6)\%$		-
$B^*\bar{B}^*$	$(38.1 \pm 3.4)\%$		1102
$B\bar{B}^*(*)\pi$	$< 19.7\%$	90%	990
$B\bar{B}\pi$	$(0.0 \pm 1.2)\%$		990
$B^*\bar{B}^*\pi + B\bar{B}^*\pi$	$(7.3 \pm 2.3)\%$		-
$B^*\bar{B}^*\pi$	$(1.0 \pm 1.4)\%$		701
$B\bar{B}\pi\pi$	$< 8.9\%$	90%	504
$B_s^{(*)}\bar{B}_s^{(*)}$	$(19.9 \pm 3.0)\%$		877
$B_s\bar{B}_s$	$(5 \pm 5) \times 10^{-3}$		877
$B_s\bar{B}_s^* + \text{c.c.}$	$(1.5 \pm 0.7)\%$		-
$B_s^*\bar{B}_s^*$	$(17.9 \pm 2.8)\%$		495
no open-bottom	$(4.2^{+5.0}_{-0.6})\%$		-
$e^+e^-$	$(5.6 \pm 3.1) \times 10^{-6}$		5438
$\Upsilon(1S)\pi^+\pi^-$	$(5.3 \pm 0.6) \times 10^{-3}$		1297
$\Upsilon(2S)\pi^+\pi^-$	$(7.8 \pm 1.3) \times 10^{-3}$		774
$\Upsilon(3S)\pi^+\pi^-$	$(4.8^{+1.9}_{-1.7}) \times 10^{-3}$		429
$\Upsilon(1S)K^+K^-$	$(6.1 \pm 1.8) \times 10^{-4}$		947
$h_b(1P)\pi^+\pi^-$	$(3.5^{+1.0}_{-1.3}) \times 10^{-3}$		895
$h_b(2P)\pi^+\pi^-$	$(6.0^{+2.1}_{-1.8}) \times 10^{-3}$		534

## Inclusive Decays.

These decay modes are submodes of one or more of the decay modes above.

$\phi$ anything	$(13.8^{+2.4}_{-1.7})\%$	-
$D^0$ anything + c.c.	$(108 \pm 8)\%$	-
$D_s$ anything + c.c.	$(46 \pm 6)\%$	-
$J/\psi$ anything	$(2.06 \pm 0.21)\%$	-
$B^0$ anything + c.c.	$(77 \pm 8)\%$	-
$B^+$ anything + c.c.	$(72 \pm 6)\%$	-

### $\Upsilon(11020)$ $J^G(J^{PC}) = 0^-(1^{--})$

Mass  $m = 11.019 \pm 0.008$  GeV  
 Full width  $\Gamma = 79 \pm 16$  MeV  
 $\Gamma_{ee} = 0.130 \pm 0.030$  keV

$\Upsilon(11020)$ DECAY MODES	Fraction ( $\Gamma_i/\Gamma$ )	$p$ (MeV/c)
$e^+e^-$	$(1.6 \pm 0.5) \times 10^{-6}$	5510

[a] See the “Note on  $\pi^\pm \rightarrow \ell^\pm \nu \gamma$  and  $K^\pm \rightarrow \ell^\pm \nu \gamma$  Form Factors” in the  $\pi^\pm$  Particle Listings for definitions and details.

[b] Measurements of  $\Gamma(e^+ \nu_e)/\Gamma(\mu^+ \nu_\mu)$  always include decays with  $\gamma$ 's, and measurements of  $\Gamma(e^+ \nu_e \gamma)$  and  $\Gamma(\mu^+ \nu_\mu \gamma)$  never include low-energy  $\gamma$ 's. Therefore, since no clean separation is possible, we consider the modes with  $\gamma$ 's to be subreactions of the modes without them, and let  $[\Gamma(e^+ \nu_e) + \Gamma(\mu^+ \nu_\mu)]/\Gamma_{\text{total}} = 100\%$ .

[c] See the  $\pi^\pm$  Particle Listings for the energy limits used in this measurement; low-energy  $\gamma$ 's are not included.

[d] Derived from an analysis of neutrino-oscillation experiments.

[e] Astrophysical and cosmological arguments give limits of order  $10^{-13}$ ; see the  $\pi^0$  Particle Listings.

[f] C parity forbids this to occur as a single-photon process.

[g] See the “Note on scalar mesons” in the  $f_0(500)$  Particle Listings. The interpretation of this entry as a particle is controversial.

[h] See the “Note on  $\rho(770)$ ” in the  $\rho(770)$  Particle Listings.

[i] The  $\omega\rho$  interference is then due to  $\omega\rho$  mixing only, and is expected to be small. If  $e\mu$  universality holds,  $\Gamma(\rho^0 \rightarrow \mu^+\mu^-) = \Gamma(\rho^0 \rightarrow e^+e^-) \times 0.99785$ .

[j] See the “Note on scalar mesons” in the  $f_0(500)$  Particle Listings.

[k] See the “Note on  $a_1(1260)$ ” in the  $a_1(1260)$  Particle Listings in PDG 06, Journal of Physics, G **33** 1 (2006).

[l] This is only an educated guess; the error given is larger than the error on the average of the published values. See the Particle Listings for details.

[m] See the “Note on non- $q\bar{q}$  mesons” in the Particle Listings in PDG 06, Journal of Physics, G **33** 1 (2006).

[n] See the “Note on the  $\eta(1405)$ ” in the  $\eta(1405)$  Particle Listings.

[o] See the “Note on the  $f_1(1420)$ ” in the  $\eta(1405)$  Particle Listings.

[p] See also the  $\omega(1650)$  Particle Listings.

[q] See the “Note on the  $\rho(1450)$  and the  $\rho(1700)$ ” in the  $\rho(1700)$  Particle Listings.

[r] See also the  $\omega(1420)$  Particle Listings.

[s] See the “Note on  $f_0(1710)$ ” in the  $f_0(1710)$  Particle Listings in 2004 edition of *Review of Particle Physics*.

[t] See the note in the  $K^\pm$  Particle Listings.

[u] The definition of the slope parameter  $g$  of the  $K \rightarrow 3\pi$  Dalitz plot is as follows (see also “Note on Dalitz Plot Parameters for  $K \rightarrow 3\pi$  Decays” in the  $K^\pm$  Particle Listings):

$$|M|^2 = 1 + g(s_3 - s_0)/m_{\pi^+}^2 + \dots$$

[v] For more details and definitions of parameters see the Particle Listings.

[w] See the  $K^\pm$  Particle Listings for the energy limits used in this measurement.

[x] Most of this radiative mode, the low-momentum  $\gamma$  part, is also included in the parent mode listed without  $\gamma$ 's.

[y] Structure-dependent part.

[z] Direct-emission branching fraction.

[aa] Violates angular-momentum conservation.

[bb] Derived from measured values of  $\phi_{+-}$ ,  $\phi_{00}$ ,  $|\eta|$ ,  $|m_{K_L^0} - m_{K_S^0}|$ , and  $\tau_{K_S^0}$ , as described in the introduction to “Tests of Conservation Laws.”

[cc] The  $CP$ -violation parameters are defined as follows (see also “Note on  $CP$  Violation in  $K_S \rightarrow 3\pi$ ” and “Note on  $CP$  Violation in  $K_L^0$  Decay” in the Particle Listings):

$$\eta_{+-} = |\eta_{+-}|e^{i\phi_{+-}} = \frac{A(K_L^0 \rightarrow \pi^+\pi^-)}{A(K_S^0 \rightarrow \pi^+\pi^-)} = \epsilon + \epsilon'$$



## Meson Summary Table

$$\eta_{00} = |\eta_{00}| e^{i\phi_{00}} = \frac{A(K_L^0 \rightarrow \pi^0 \pi^0)}{A(K_S^0 \rightarrow \pi^0 \pi^0)} = \epsilon - 2\epsilon'$$

$$\delta = \frac{\Gamma(K_L^0 \rightarrow \pi^- \ell^+ \nu) - \Gamma(K_L^0 \rightarrow \pi^+ \ell^- \nu)}{\Gamma(K_L^0 \rightarrow \pi^- \ell^+ \nu) + \Gamma(K_L^0 \rightarrow \pi^+ \ell^- \nu)},$$

$$\text{Im}(\eta_{+-0})^2 = \frac{\Gamma(K_S^0 \rightarrow \pi^+ \pi^- \pi^0)_{CP \text{ viol.}}}{\Gamma(K_L^0 \rightarrow \pi^+ \pi^- \pi^0)},$$

$$\text{Im}(\eta_{000})^2 = \frac{\Gamma(K_S^0 \rightarrow \pi^0 \pi^0 \pi^0)}{\Gamma(K_L^0 \rightarrow \pi^0 \pi^0 \pi^0)}.$$

where for the last two relations  $CPT$  is assumed valid, *i.e.*,  $\text{Re}(\eta_{+-0}) \simeq 0$  and  $\text{Re}(\eta_{000}) \simeq 0$ .

- [*dd*] See the  $K_S^0$  Particle Listings for the energy limits used in this measurement.
- [*ee*] The value is for the sum of the charge states or particle/antiparticle states indicated.
- [*ff*]  $\text{Re}(\epsilon'/\epsilon) = \epsilon'/\epsilon$  to a very good approximation provided the phases satisfy  $CPT$  invariance.
- [*gg*] This mode includes gammas from inner bremsstrahlung but not the direct emission mode  $K_L^0 \rightarrow \pi^+ \pi^- \gamma$  (DE).
- [*hh*] See the  $K_L^0$  Particle Listings for the energy limits used in this measurement.
- [*ij*] Allowed by higher-order electroweak interactions.
- [*jj*] Violates  $CP$  in leading order. Test of direct  $CP$  violation since the indirect  $CP$ -violating and  $CP$ -conserving contributions are expected to be suppressed.
- [*kk*] See the "Note on  $f_0(1370)$ " in the  $f_0(1370)$  Particle Listings and in the 1994 edition.
- [*ll*] See the note in the  $L(1770)$  Particle Listings in Reviews of Modern Physics **56** S1 (1984), p. S200. See also the "Note on  $K_2(1770)$  and the  $K_2(1820)$ " in the  $K_2(1770)$  Particle Listings.
- [*mm*] See the "Note on  $K_2(1770)$  and the  $K_2(1820)$ " in the  $K_2(1770)$  Particle Listings.
- [*nn*] This result applies to  $Z^0 \rightarrow c\bar{c}$  decays only. Here  $\ell^+$  is an average (not a sum) of  $e^+$  and  $\mu^+$  decays.
- [*oo*] See the Particle Listings for the (complicated) definition of this quantity.
- [*pp*] The branching fraction for this mode may differ from the sum of the submodes that contribute to it, due to interference effects. See the relevant papers in the Particle Listings.
- [*qq*] These subfractions of the  $K^- 2\pi^+$  mode are uncertain: see the Particle Listings.
- [*rr*] Submodes of the  $D^+ \rightarrow K^- 2\pi^+ \pi^0$  and  $K_S^0 2\pi^+ \pi^-$  modes were studied by ANJOS 92C and COFFMAN 92B, but with at most 142 events for the first mode and 229 for the second – not enough for precise results. With nothing new for 18 years, we refer to our 2008 edition, Physics Letters **B667** 1 (2008), for those results.
- [*ss*] The natural decay modes of the resonances are included.
- [*tt*] This is *not* a test for the  $\Delta C=1$  weak neutral current, but leads to the  $\pi^+ \ell^+ \ell^-$  final state.
- [*uu*] This mode is not a useful test for a  $\Delta C=1$  weak neutral current because both quarks must change flavor in this decay.
- [*vv*] In the 2010 *Review*, the values for these quantities were given using a measure of the asymmetry that was inconsistent with the usual definition.
- [*ww*] This value is obtained by subtracting the branching fractions for 2-, 4- and 6-prongs from unity.
- [*xx*] This is the sum of our  $K^- 2\pi^+ \pi^-$ ,  $K^- 2\pi^+ \pi^- \pi^0$ ,  $\bar{K}^0 2\pi^+ 2\pi^-$ ,  $K^+ 2K^- \pi^+$ ,  $2\pi^+ 2\pi^-$ ,  $2\pi^+ 2\pi^- \pi^0$ ,  $K^+ K^- \pi^+ \pi^-$ , and  $K^+ K^- \pi^+ \pi^- \pi^0$ , branching fractions.
- [*yy*] This is the sum of our  $K^- 3\pi^+ 2\pi^-$  and  $3\pi^+ 3\pi^-$  branching fractions.
- [*zz*] The branching fractions for the  $K^- e^+ \nu_e$ ,  $K^*(892)^- e^+ \nu_e$ ,  $\pi^- e^+ \nu_e$ , and  $\rho^- e^+ \nu_e$  modes add up to  $6.19 \pm 0.17\%$ .
- [*aaa*] This is a doubly Cabibbo-suppressed mode.
- [*bbb*] The two experiments measuring this fraction are in serious disagreement. See the Particle Listings.
- [*ccc*] Submodes of the  $D^0 \rightarrow K_S^0 \pi^+ \pi^- \pi^0$  mode with a  $K^*$  and/or  $\rho$  were studied by COFFMAN 92B, but with only 140 events. With nothing new for 18 years, we refer to our 2008 edition, Physics Letters **B667** 1 (2008), for those results.
- [*ddd*] This branching fraction includes all the decay modes of the resonance in the final state.
- [*eee*] The experiments on the division of this charge mode amongst its submodes disagree, and the submode branching fractions here add up to considerably more than the charged-mode fraction.
- [*fff*] However, these upper limits are in serious disagreement with values obtained in another experiment.
- [*ggg*] This limit is for either  $D^0$  or  $\bar{D}^0$  to  $p e^-$ .
- [*hhh*] This limit is for either  $D^0$  or  $\bar{D}^0$  to  $\bar{p} e^+$ .
- [*iii*] This is the purely  $e^+$  semileptonic branching fraction: the  $e^+$  fraction from  $\tau^+$  decays has been subtracted off. The sum of our (non- $\tau$ )  $e^+$  exclusive fractions — an  $e^+ \nu_e$  with an  $\eta$ ,  $\eta'$ ,  $\phi$ ,  $K^0$ ,  $K^*$ , or  $f_0(980)$  — is  $7.0 \pm 0.4\%$ .
- [*jjj*] This fraction includes  $\eta$  from  $\eta'$  decays.
- [*kkk*] Two times (to include  $\mu$  decays) the  $\eta' e^+ \nu_e$  branching fraction, plus the  $\eta' \pi^+$ ,  $\eta' \rho^+$ , and  $\eta' K^+$  fractions, is  $(18.6 \pm 2.3)\%$ , which considerably exceeds the inclusive  $\eta'$  fraction of  $(11.7 \pm 1.8)\%$ . Our best guess is that the  $\eta' \rho^+$  fraction,  $(12.5 \pm 2.2)\%$ , is too large.
- [*lll*] This branching fraction includes all the decay modes of the final-state resonance.
- [*mmm*] A test for  $u\bar{u}$  or  $d\bar{d}$  content in the  $D_s^+$ . Neither Cabibbo-favored nor Cabibbo-suppressed decays can contribute, and  $\omega - \phi$  mixing is an unlikely explanation for any fraction above about  $2 \times 10^{-4}$ .
- [*nnn*] We decouple the  $D_s^+ \rightarrow \phi \pi^+$  branching fraction obtained from mass projections (and used to get some of the other branching fractions) from the  $D_s^+ \rightarrow \phi \pi^+$ ,  $\phi \rightarrow K^+ K^-$  branching fraction obtained from the Dalitz-plot analysis of  $D_s^+ \rightarrow K^+ K^- \pi^+$ . That is, the ratio of these two branching fractions is not exactly the  $\phi \rightarrow K^+ K^-$  branching fraction 0.491.
- [*ooo*] This is the average of a model-independent and a  $K$ -matrix parametrization of the  $\pi^+ \pi^-$   $S$ -wave and is a sum over several  $f_0$  mesons.
- [*ppp*] An  $\ell$  indicates an  $e$  or a  $\mu$  mode, not a sum over these modes.
- [*qqq*] An  $CP(\pm 1)$  indicates the  $CP=+1$  and  $CP=-1$  eigenstates of the  $D^0$ - $\bar{D}^0$  system.
- [*rrr*]  $D$  denotes  $D^0$  or  $\bar{D}^0$ .
- [*sss*]  $D_{CP\pm}^0$  decays into  $D^0 \pi^0$  with the  $D^0$  reconstructed in  $CP$ -even eigenstates  $K^+ K^-$  and  $\pi^+ \pi^-$ .
- [*ttt*]  $\bar{D}^{*}$  represents an excited state with mass  $2.2 < M < 2.8$  GeV/ $c^2$ .
- [*uuu*]  $X(3872)^+$  is a hypothetical charged partner of the  $X(3872)$ .
- [*vvv*]  $\Theta(1710)^{++}$  is a possible narrow pentaquark state and  $G(2220)$  is a possible glueball resonance.
- [*www*]  $(\bar{A}_c^- \rho)_s$  denotes a low-mass enhancement near 3.35 GeV/ $c^2$ .
- [*xxx*] Stands for the possible candidates of  $K^*(1410)$ ,  $K_0^*(1430)$  and  $K_2^*(1430)$ .
- [*yyy*]  $B^0$  and  $B_s^0$  contributions not separated. Limit is on weighted average of the two decay rates.
- [*zzz*] This decay refers to the coherent sum of resonant and nonresonant  $J^P = 0^+ K \pi$  components with  $1.60 < m_{K\pi} < 2.15$  GeV/ $c^2$ .
- [*aaaa*]  $X(214)$  is a hypothetical particle of mass 214 MeV/ $c^2$  reported by the HyperCP experiment, Physical Review Letters **94** 021801 (2005)
- [*bbbb*]  $\Theta(1540)^+$  denotes a possible narrow pentaquark state.
- [*cccc*] These values are model dependent.
- [*dddd*] Here "anything" means at least one particle observed.
- [*eeee*]  $D^{**}$  stands for the sum of the  $D(1^1 P_1)$ ,  $D(1^3 P_0)$ ,  $D(1^3 P_1)$ ,  $D(1^3 P_2)$ ,  $D(2^1 S_0)$ , and  $D(2^1 S_1)$  resonances.
- [*ffff*]  $D^{(*)} \bar{D}^{(*)}$  stands for the sum of  $D^* \bar{D}^*$ ,  $D^* \bar{D}$ ,  $D \bar{D}^*$ , and  $D \bar{D}$ .
- [*gggg*]  $X(3915)$  denotes a near-threshold enhancement in the  $\omega J/\psi$  mass spectrum.
- [*hhhh*] Inclusive branching fractions have a multiplicity definition and can be greater than 100%.
- [*iii*]  $D_j$  represents an unresolved mixture of pseudoscalar and tensor  $D^{**}$  ( $P$ -wave) states.
- [*jjjj*] Not a pure measurement. See note at head of  $B_S^0$  Decay Modes.
- [*kkkk*] For  $E_\gamma > 100$  MeV.
- [*llll*] Includes  $p\bar{p}\pi^+ \pi^- \gamma$  and excludes  $p\bar{p}\eta$ ,  $p\bar{p}\omega$ ,  $p\bar{p}\eta'$ .
- [*mmmm*] For a narrow state  $A$  with mass less than 960 MeV.
- [*nnnn*] For a narrow resonance in the range  $2.2 < M(X) < 2.8$  GeV.

## Meson Summary Table

---

[oooo] BHARDWAJ 11 does not observe this decay and presents a stronger 90% CL limit than this value. See measurements listings for details.

[pppp]  $J^{PC}$  known by production in  $e^+e^-$  via single photon annihilation.  $I^G$  is not known; interpretation of this state as a single resonance is unclear because of the expectation of substantial threshold effects in this energy region.

[qqqq]  $2m_\tau < M(\tau^+\tau^-) < 7500$  MeV

[rrrr]  $2 < m_{K^+K^-} < 3$  GeV

[ssss]  $X = \text{scalar with } m < 8.0$  GeV

[tttt]  $X\bar{X} = \text{vectors with } m < 3.1$  GeV

[uuuu]  $X$  and  $\bar{X} = \text{zero spin with } m < 4.5$  GeV

[vvvv]  $1.5 \text{ GeV} < m_X < 5.0$  GeV

[wwww]  $201 < M(\mu^+\mu^-) < 3565$  MeV

[xxxx] Spectroscopic labeling for these states is theoretical, pending experimental information.

[yyyy]  $1.5 \text{ GeV} < m_X < 5.0$  GeV

[zzzz]  $1.5 \text{ GeV} < m_X < 5.0$  GeV

[aaaa] For  $m_{\tau^+\tau^-}$  in the ranges 4.03–9.52 and 9.61–10.10 GeV.

## Meson Summary Table

See also the table of suggested  $q\bar{q}$  quark-model assignments in the Quark Model section.

• Indicates particles that appear in the preceding Meson Summary Table. We do not regard the other entries as being established.

LIGHT UNFLAVORED ( $S = C = B = 0$ )		STRANGE ( $S = \pm 1, C = B = 0$ )		CHARMED, STRANGE ( $C = S = \pm 1$ )		$c\bar{c}$ $I^G(J^{PC})$	
$I^G(J^{PC})$	$I^G(J^{PC})$	$I(J^P)$	$I(J^P)$	$I(J^P)$	$I(J^P)$		
• $\pi^\pm$ 1 <sup>-</sup> (0 <sup>-</sup> )	• $\pi_2(1670)$ 1 <sup>-</sup> (2 <sup>-+</sup> )	• $K^\pm$ 1/2(0 <sup>-</sup> )	• $K^\pm$ 1/2(0 <sup>-</sup> )	• $D_s^\pm$ 0(0 <sup>-</sup> )	• $\eta_c(1S)$ 0 <sup>+</sup> (0 <sup>-+</sup> )		
• $\pi^0$ 1 <sup>-</sup> (0 <sup>-+</sup> )	• $\phi(1680)$ 0 <sup>-</sup> (1 <sup>-</sup> -)	• $K^0$ 1/2(0 <sup>-</sup> )	• $K^0$ 1/2(0 <sup>-</sup> )	• $D_s^{*\pm}$ 0(? <sup>?</sup> )	• $J/\psi(1S)$ 0 <sup>-</sup> (1 <sup>-</sup> -)		
• $\eta$ 0 <sup>+</sup> (0 <sup>-+</sup> )	• $\rho_3(1690)$ 1 <sup>+</sup> (3 <sup>-</sup> -)	• $K_S^0$ 1/2(0 <sup>-</sup> )	• $K_S^0$ 1/2(0 <sup>-</sup> )	• $D_{s0}^*(2317)^\pm$ 0(0 <sup>+</sup> )	• $\chi_{c0}(1P)$ 0 <sup>+</sup> (0 <sup>++</sup> )		
• $f_0(500)$ 0 <sup>+</sup> (0 <sup>++</sup> )	• $\rho(1700)$ 1 <sup>+</sup> (1 <sup>-</sup> -)	• $K_L^0$ 1/2(0 <sup>-</sup> )	• $K_L^0$ 1/2(0 <sup>-</sup> )	• $D_{s1}^*(2460)^\pm$ 0(1 <sup>+</sup> )	• $\chi_{c1}(1P)$ 0 <sup>+</sup> (1 <sup>++</sup> )		
• $\rho(770)$ 1 <sup>+</sup> (1 <sup>-</sup> -)	$a_2(1700)$ 1 <sup>-</sup> (2 <sup>++</sup> )	$K_0^*(800)$ 1/2(0 <sup>+</sup> )	$K_0^*(800)$ 1/2(0 <sup>+</sup> )	• $D_{s1}(2536)^\pm$ 0(1 <sup>+</sup> )	• $h_c(1P)$ ? <sup>?</sup> (1 <sup>-+</sup> )		
• $\omega(782)$ 0 <sup>-</sup> (1 <sup>-</sup> -)	• $f_0(1710)$ 0 <sup>+</sup> (0 <sup>++</sup> )	• $K^*(892)$ 1/2(1 <sup>-</sup> )	• $K^*(892)$ 1/2(1 <sup>-</sup> )	• $D_{s2}^*(2573)$ 0(? <sup>?</sup> )	• $\chi_{c2}(1P)$ 0 <sup>+</sup> (2 <sup>++</sup> )		
• $\eta'(958)$ 0 <sup>+</sup> (0 <sup>-+</sup> )	$\eta(1760)$ 0 <sup>+</sup> (0 <sup>-+</sup> )	• $K_1(1270)$ 1/2(1 <sup>+</sup> )	• $K_1(1270)$ 1/2(1 <sup>+</sup> )	$D_{s1}^*(2700)^\pm$ 0(1 <sup>-</sup> )	• $\eta_c(2S)$ 0 <sup>+</sup> (0 <sup>-+</sup> )		
• $f_0(980)$ 0 <sup>+</sup> (0 <sup>++</sup> )	• $\pi(1800)$ 1 <sup>-</sup> (0 <sup>-+</sup> )	• $K_1(1400)$ 1/2(1 <sup>+</sup> )	• $K_1(1400)$ 1/2(1 <sup>+</sup> )	$D_{sJ}^*(2860)^\pm$ 0(? <sup>?</sup> )	• $\psi(2S)$ 0 <sup>-</sup> (1 <sup>-</sup> -)		
• $a_0(980)$ 1 <sup>-</sup> (0 <sup>++</sup> )	$f_2(1810)$ 0 <sup>+</sup> (2 <sup>++</sup> )	• $K^*(1410)$ 1/2(1 <sup>-</sup> )	• $K^*(1410)$ 1/2(1 <sup>-</sup> )	$D_{sJ}^*(3040)^\pm$ 0(? <sup>?</sup> )	• $\psi(3770)$ 0 <sup>-</sup> (1 <sup>-</sup> -)		
• $\phi(1020)$ 0 <sup>-</sup> (1 <sup>-</sup> -)	$X(1835)$ ? <sup>?</sup> (? <sup>-+</sup> )	• $K_0^*(1430)$ 1/2(0 <sup>+</sup> )	• $K_0^*(1430)$ 1/2(0 <sup>+</sup> )		• $X(3872)$ 0 <sup>?</sup> (? <sup>?</sup> ?)		
• $h_1(1170)$ 0 <sup>-</sup> (1 <sup>+-</sup> )	• $\phi_3(1850)$ 0 <sup>-</sup> (3 <sup>-</sup> -)	• $K_2^*(1430)$ 1/2(2 <sup>+</sup> )	• $K_2^*(1430)$ 1/2(2 <sup>+</sup> )	BOTTOM ( $B = \pm 1$ )		• $X(3915)$ 0 <sup>+</sup> (? <sup>?</sup> ?)	
• $b_1(1235)$ 1 <sup>+</sup> (1 <sup>+-</sup> )	$\eta_2(1870)$ 0 <sup>+</sup> (2 <sup>-+</sup> )	$K(1460)$ 1/2(0 <sup>-</sup> )	$K(1460)$ 1/2(0 <sup>-</sup> )	• $B^\pm$ 1/2(0 <sup>-</sup> )	• $\chi_{c2}(2P)$ 0 <sup>+</sup> (2 <sup>++</sup> )		
• $a_1(1260)$ 1 <sup>-</sup> (1 <sup>++</sup> )	• $\pi_2(1880)$ 1 <sup>-</sup> (2 <sup>-+</sup> )	$K_2(1580)$ 1/2(2 <sup>-</sup> )	$K_2(1580)$ 1/2(2 <sup>-</sup> )	• $B^0$ 1/2(0 <sup>-</sup> )	$X(3940)$ ? <sup>?</sup> (? <sup>?</sup> ?)		
• $f_2(1270)$ 0 <sup>+</sup> (2 <sup>++</sup> )	$\rho(1900)$ 1 <sup>+</sup> (1 <sup>-</sup> -)	$K(1630)$ 1/2(? <sup>?</sup> )	$K(1630)$ 1/2(? <sup>?</sup> )	• $B^\pm/B^0$ ADMIXTURE	• $\psi(4040)$ 0 <sup>-</sup> (1 <sup>-</sup> -)		
• $f_1(1285)$ 0 <sup>+</sup> (1 <sup>++</sup> )	$f_2(1910)$ 0 <sup>+</sup> (2 <sup>++</sup> )	$K_1(1650)$ 1/2(1 <sup>+</sup> )	$K_1(1650)$ 1/2(1 <sup>+</sup> )	• $B^\pm/B^0/B_s^0/b$ -baryon ADMIXTURE	$X(4050)^\pm$ ?(? <sup>?</sup> )		
• $\eta(1295)$ 0 <sup>+</sup> (0 <sup>-+</sup> )	• $f_2(1950)$ 0 <sup>+</sup> (2 <sup>++</sup> )	• $K^*(1680)$ 1/2(1 <sup>-</sup> )	• $K^*(1680)$ 1/2(1 <sup>-</sup> )	$V_{cb}$ and $V_{ub}$ CKM Ma- trix Elements	$X(4140)$ 0 <sup>+</sup> (? <sup>?</sup> ?)		
• $\pi(1300)$ 1 <sup>-</sup> (0 <sup>-+</sup> )	$\rho_3(1990)$ 1 <sup>+</sup> (3 <sup>-</sup> -)	• $K_2(1770)$ 1/2(2 <sup>-</sup> )	• $K_2(1770)$ 1/2(2 <sup>-</sup> )	• $B^*$ 1/2(1 <sup>-</sup> )	• $\psi(4160)$ 0 <sup>-</sup> (1 <sup>-</sup> -)		
• $a_2(1320)$ 1 <sup>-</sup> (2 <sup>++</sup> )	• $f_2(2010)$ 0 <sup>+</sup> (2 <sup>++</sup> )	• $K_3^*(1780)$ 1/2(3 <sup>-</sup> )	• $K_3^*(1780)$ 1/2(3 <sup>-</sup> )	$B_s^*(5732)$ ?(? <sup>?</sup> )	$X(4160)$ ? <sup>?</sup> (? <sup>?</sup> ?)		
• $f_0(1370)$ 0 <sup>+</sup> (0 <sup>++</sup> )	$f_0(2020)$ 0 <sup>+</sup> (0 <sup>++</sup> )	• $K_2(1820)$ 1/2(2 <sup>-</sup> )	• $K_2(1820)$ 1/2(2 <sup>-</sup> )	• $B_1(5721)^0$ 1/2(1 <sup>+</sup> )	$X(4250)^\pm$ ?(? <sup>?</sup> )		
$h_1(1380)$ ? <sup>-</sup> (1 <sup>+-</sup> )	• $a_4(2040)$ 1 <sup>-</sup> (4 <sup>++</sup> )	$K(1830)$ 1/2(0 <sup>-</sup> )	$K(1830)$ 1/2(0 <sup>-</sup> )	• $B_2^*(5747)^0$ 1/2(2 <sup>+</sup> )	• $X(4260)$ ? <sup>?</sup> (1 <sup>-</sup> -)		
• $\pi_1(1400)$ 1 <sup>-</sup> (1 <sup>-+</sup> )	• $f_4(2050)$ 0 <sup>+</sup> (4 <sup>++</sup> )	$K_0^*(1950)$ 1/2(0 <sup>+</sup> )	$K_0^*(1950)$ 1/2(0 <sup>+</sup> )		$X(4350)$ 0 <sup>+</sup> (? <sup>?</sup> ?)		
• $\eta(1405)$ 0 <sup>+</sup> (0 <sup>-+</sup> )	$\pi_2(2100)$ 1 <sup>-</sup> (2 <sup>-+</sup> )	$K_2^*(1980)$ 1/2(2 <sup>+</sup> )	$K_2^*(1980)$ 1/2(2 <sup>+</sup> )	BOTTOM, STRANGE ( $B = \pm 1, S = \mp 1$ )		• $\psi(4415)$ 0 <sup>-</sup> (1 <sup>-</sup> -)	
• $f_1(1420)$ 0 <sup>+</sup> (1 <sup>++</sup> )	$f_0(2100)$ 0 <sup>+</sup> (0 <sup>++</sup> )	• $K_4^*(2045)$ 1/2(4 <sup>+</sup> )	• $K_4^*(2045)$ 1/2(4 <sup>+</sup> )	• $B_s^0$ 0(0 <sup>-</sup> )	$X(4360)$ ? <sup>?</sup> (1 <sup>-</sup> -)		
• $\omega(1420)$ 0 <sup>-</sup> (1 <sup>-</sup> -)	$f_2(2150)$ 0 <sup>+</sup> (2 <sup>++</sup> )	$K_2(2250)$ 1/2(2 <sup>-</sup> )	$K_2(2250)$ 1/2(2 <sup>-</sup> )	• $B_s^*$ 0(1 <sup>-</sup> )	$X(4430)^\pm$ ?(? <sup>?</sup> )		
$f_2(1430)$ 0 <sup>+</sup> (2 <sup>++</sup> )	$\rho(2150)$ 1 <sup>+</sup> (1 <sup>-</sup> -)	$K_3(2320)$ 1/2(3 <sup>+</sup> )	$K_3(2320)$ 1/2(3 <sup>+</sup> )	• $B_{s1}(5830)^0$ 0(1 <sup>+</sup> )	$X(4660)$ ? <sup>?</sup> (1 <sup>-</sup> -)		
• $a_0(1450)$ 1 <sup>-</sup> (0 <sup>++</sup> )	• $\phi(2170)$ 0 <sup>-</sup> (1 <sup>-</sup> -)	$K_5(2380)$ 1/2(5 <sup>-</sup> )	$K_5(2380)$ 1/2(5 <sup>-</sup> )	• $B_{s2}^*(5840)^0$ 0(2 <sup>+</sup> )			
• $\rho(1450)$ 1 <sup>+</sup> (1 <sup>-</sup> -)	$f_0(2200)$ 0 <sup>+</sup> (0 <sup>++</sup> )	$K_4(2500)$ 1/2(4 <sup>-</sup> )	$K_4(2500)$ 1/2(4 <sup>-</sup> )	$B_{sJ}^*(5850)$ ?(? <sup>?</sup> )			
• $\eta(1475)$ 0 <sup>+</sup> (0 <sup>-+</sup> )	$f_J(2220)$ 0 <sup>+</sup> (2 <sup>++</sup> or 4 <sup>++</sup> )	$K(3100)$ ? <sup>?</sup> (? <sup>?</sup> ?)	$K(3100)$ ? <sup>?</sup> (? <sup>?</sup> ?)	BOTTOM, CHARMED ( $B = C = \pm 1$ )			
• $f_0(1500)$ 0 <sup>+</sup> (0 <sup>++</sup> )	$\eta(2225)$ 0 <sup>+</sup> (0 <sup>-+</sup> )	CHARMED ( $C = \pm 1$ )		• $B_c^\pm$ 0(0 <sup>-</sup> )			
$f_1(1510)$ 0 <sup>+</sup> (1 <sup>++</sup> )	$\rho_3(2250)$ 1 <sup>+</sup> (3 <sup>-</sup> -)	• $D^\pm$ 1/2(0 <sup>-</sup> )	• $D^\pm$ 1/2(0 <sup>-</sup> )				
• $f_2'(1525)$ 0 <sup>+</sup> (2 <sup>++</sup> )	• $f_2(2300)$ 0 <sup>+</sup> (2 <sup>++</sup> )	• $D^0$ 1/2(0 <sup>-</sup> )	• $D^0$ 1/2(0 <sup>-</sup> )				
$f_2(1565)$ 0 <sup>+</sup> (2 <sup>++</sup> )	$f_4(2300)$ 0 <sup>+</sup> (4 <sup>++</sup> )	• $D^*(2007)^0$ 1/2(1 <sup>-</sup> )	• $D^*(2007)^0$ 1/2(1 <sup>-</sup> )				
$\rho(1570)$ 1 <sup>+</sup> (1 <sup>-</sup> -)	$f_0(2330)$ 0 <sup>+</sup> (0 <sup>++</sup> )	• $D^*(2010)^\pm$ 1/2(1 <sup>-</sup> )	• $D^*(2010)^\pm$ 1/2(1 <sup>-</sup> )				
$h_1(1595)$ 0 <sup>-</sup> (1 <sup>+-</sup> )	• $f_2(2340)$ 0 <sup>+</sup> (2 <sup>++</sup> )	• $D_0^*(2400)^0$ 1/2(0 <sup>+</sup> )	• $D_0^*(2400)^0$ 1/2(0 <sup>+</sup> )				
• $\pi_1(1600)$ 1 <sup>-</sup> (1 <sup>-+</sup> )	$\rho_5(2350)$ 1 <sup>+</sup> (5 <sup>-</sup> -)	• $D_0^*(2400)^\pm$ 1/2(0 <sup>+</sup> )	• $D_0^*(2400)^\pm$ 1/2(0 <sup>+</sup> )				
$a_1(1640)$ 1 <sup>-</sup> (1 <sup>++</sup> )	$a_6(2450)$ 1 <sup>-</sup> (6 <sup>++</sup> )	• $D_1(2420)^0$ 1/2(1 <sup>+</sup> )	• $D_1(2420)^0$ 1/2(1 <sup>+</sup> )				
$f_2(1640)$ 0 <sup>+</sup> (2 <sup>++</sup> )	$f_6(2510)$ 0 <sup>+</sup> (6 <sup>++</sup> )	• $D_1(2420)^\pm$ 1/2(? <sup>?</sup> )	• $D_1(2420)^\pm$ 1/2(? <sup>?</sup> )				
• $\eta_2(1645)$ 0 <sup>+</sup> (2 <sup>-+</sup> )	OTHER LIGHT						
• $\omega(1650)$ 0 <sup>-</sup> (1 <sup>-</sup> -)	Further States		• $D_1(2430)^0$ 1/2(1 <sup>+</sup> )				
• $\omega_3(1670)$ 0 <sup>-</sup> (3 <sup>-</sup> -)			• $D_1(2430)^0$ 1/2(1 <sup>+</sup> )				
			• $D_2^*(2460)^0$ 1/2(2 <sup>+</sup> )				
			• $D_2^*(2460)^\pm$ 1/2(2 <sup>+</sup> )				
			$D(2550)^0$ 1/2(0 <sup>-</sup> )				
			$D(2600)$ 1/2(? <sup>?</sup> )				
			$D^*(2640)^\pm$ 1/2(? <sup>?</sup> )				
			$D(2750)$ 1/2(? <sup>?</sup> )				

## Baryon Summary Table

This short table gives the name, the quantum numbers (where known), and the status of baryons in the Review. Only the baryons with 3- or 4-star status are included in the Baryon Summary Table. Due to insufficient data or uncertain interpretation, the other entries in the table are not established baryons. The names with masses are of baryons that decay strongly. The spin-parity  $J^P$  (when known) is given with each particle. For the strongly decaying particles, the  $J^P$  values are considered to be part of the names.

$p$	$1/2^+$	****	$\Delta(1232)$	$3/2^+$	****	$\Sigma^+$	$1/2^+$	****	$\Xi^0$	$1/2^+$	****	$\Lambda_c^+$	$1/2^+$	****
$n$	$1/2^+$	****	$\Delta(1600)$	$3/2^+$	***	$\Sigma^0$	$1/2^+$	****	$\Xi^-$	$1/2^+$	****	$\Lambda_c(2595)^+$	$1/2^-$	***
$N(1440)$	$1/2^+$	****	$\Delta(1620)$	$1/2^-$	****	$\Sigma^-$	$1/2^+$	****	$\Xi(1530)$	$3/2^+$	****	$\Lambda_c(2625)^+$	$3/2^-$	***
$N(1520)$	$3/2^-$	****	$\Delta(1700)$	$3/2^-$	****	$\Sigma(1385)$	$3/2^+$	****	$\Xi(1620)$	*		$\Lambda_c(2765)^+$	*	
$N(1535)$	$1/2^-$	****	$\Delta(1750)$	$1/2^+$	*	$\Sigma(1480)$	*		$\Xi(1690)$	***		$\Lambda_c(2880)^+$	$5/2^+$	***
$N(1650)$	$1/2^-$	****	$\Delta(1900)$	$1/2^-$	**	$\Sigma(1560)$	**		$\Xi(1820)$	$3/2^-$	***	$\Lambda_c(2940)^+$	*	
$N(1675)$	$5/2^-$	****	$\Delta(1905)$	$5/2^+$	****	$\Sigma(1580)$	$3/2^-$	*	$\Xi(1950)$	***		$\Sigma_c(2455)$	$1/2^+$	****
$N(1680)$	$5/2^+$	****	$\Delta(1910)$	$1/2^+$	****	$\Sigma(1620)$	$1/2^-$	**	$\Xi(2030)$	$\geq \frac{5}{2}^?$	***	$\Sigma_c(2520)$	$3/2^+$	***
$N(1685)$	*		$\Delta(1920)$	$3/2^+$	***	$\Sigma(1660)$	$1/2^+$	***	$\Xi(2120)$	*		$\Sigma_c(2800)$	***	
$N(1700)$	$3/2^-$	***	$\Delta(1930)$	$5/2^-$	***	$\Sigma(1670)$	$3/2^-$	****	$\Xi(2250)$	**		$\Xi_c^+$	$1/2^+$	***
$N(1710)$	$1/2^+$	***	$\Delta(1940)$	$3/2^-$	**	$\Sigma(1690)$	**		$\Xi(2370)$	**		$\Xi_c^0$	$1/2^+$	***
$N(1720)$	$3/2^+$	****	$\Delta(1950)$	$7/2^+$	****	$\Sigma(1750)$	$1/2^-$	***	$\Xi(2500)$	*		$\Xi_c^+$	$1/2^+$	***
$N(1860)$	$5/2^+$	**	$\Delta(2000)$	$5/2^+$	**	$\Sigma(1770)$	$1/2^+$	*	$\Xi(2500)$	*		$\Xi_c^0$	$1/2^+$	***
$N(1875)$	$3/2^-$	***	$\Delta(2150)$	$1/2^-$	*	$\Sigma(1775)$	$5/2^-$	****	$\Omega^-$	$3/2^+$	****	$\Xi_c(2645)$	$3/2^+$	***
$N(1880)$	$1/2^+$	**	$\Delta(2200)$	$7/2^-$	*	$\Sigma(1840)$	$3/2^+$	*	$\Omega(2250)^-$	***		$\Xi_c(2790)$	$1/2^-$	***
$N(1895)$	$1/2^-$	**	$\Delta(2300)$	$9/2^+$	**	$\Sigma(1880)$	$1/2^+$	**	$\Omega(2380)^-$	**		$\Xi_c(2815)$	$3/2^-$	***
$N(1900)$	$3/2^+$	***	$\Delta(2350)$	$5/2^-$	*	$\Sigma(1915)$	$5/2^+$	****	$\Omega(2470)^-$	**		$\Xi_c(2930)$	*	
$N(1990)$	$7/2^+$	**	$\Delta(2390)$	$7/2^+$	*	$\Sigma(1940)$	$3/2^-$	***				$\Xi_c(2980)$	***	
$N(2000)$	$5/2^+$	**	$\Delta(2400)$	$9/2^-$	**	$\Sigma(2000)$	$1/2^-$	*				$\Xi_c(3055)$	**	
$N(2040)$	$3/2^+$	*	$\Delta(2420)$	$11/2^+$	****	$\Sigma(2030)$	$7/2^+$	****				$\Xi_c(3080)$	***	
$N(2060)$	$5/2^-$	**	$\Delta(2750)$	$13/2^-$	**	$\Sigma(2070)$	$5/2^+$	*				$\Xi_c(3123)$	*	
$N(2100)$	$1/2^+$	*	$\Delta(2950)$	$15/2^+$	**	$\Sigma(2080)$	$3/2^+$	**				$\Omega_c^0$	$1/2^+$	***
$N(2120)$	$3/2^-$	**				$\Sigma(2100)$	$7/2^-$	*				$\Omega_c(2770)^0$	$3/2^+$	***
$N(2190)$	$7/2^-$	****	$\Lambda$	$1/2^+$	****	$\Sigma(2250)$	***					$\Xi_{cc}^+$	*	
$N(2220)$	$9/2^+$	****	$\Lambda(1405)$	$1/2^-$	****	$\Sigma(2455)$	**							
$N(2250)$	$9/2^-$	****	$\Lambda(1520)$	$3/2^-$	****	$\Sigma(2620)$	**							
$N(2600)$	$11/2^-$	***	$\Lambda(1600)$	$1/2^+$	***	$\Sigma(3000)$	*					$\Lambda_b^0$	$1/2^+$	***
$N(2700)$	$13/2^+$	**	$\Lambda(1670)$	$1/2^-$	****	$\Sigma(3170)$	*					$\Sigma_b$	$1/2^+$	***
			$\Lambda(1690)$	$3/2^-$	****							$\Sigma_b^*$	$3/2^+$	***
			$\Lambda(1800)$	$1/2^-$	***							$\Xi_b^0, \Xi_b^-$	$1/2^+$	***
			$\Lambda(1810)$	$1/2^+$	***							$\Omega_b^-$	$1/2^+$	***
			$\Lambda(1820)$	$5/2^+$	****									
			$\Lambda(1830)$	$5/2^-$	****									
			$\Lambda(1890)$	$3/2^+$	****									
			$\Lambda(2000)$	*										
			$\Lambda(2020)$	$7/2^+$	*									
			$\Lambda(2100)$	$7/2^-$	****									
			$\Lambda(2110)$	$5/2^+$	***									
			$\Lambda(2325)$	$3/2^-$	*									
			$\Lambda(2350)$	$9/2^+$	***									
			$\Lambda(2585)$	**										

\*\*\*\* Existence is certain, and properties are at least fairly well explored.

\*\*\* Existence ranges from very likely to certain, but further confirmation is desirable and/or quantum numbers, branching fractions, etc. are not well determined.

\*\* Evidence of existence is only fair.

\* Evidence of existence is poor.

## Baryon Summary Table

## N BARYONS ( $S = 0, I = 1/2$ )

$$p, N^+ = uud; \quad n, N^0 = udd$$

**p**

$$I(J^P) = \frac{1}{2}(\frac{1}{2}^+)$$

Mass  $m = 1.00727646681 \pm 0.00000000009$  u  
 Mass  $m = 938.272046 \pm 0.000021$  MeV [a]  
 $|m_p - m_{\bar{p}}|/m_p < 2 \times 10^{-9}$ , CL = 90% [b]  
 $|\frac{q_p}{m_p} - \frac{q_{\bar{p}}}{m_{\bar{p}}}|/(\frac{q_p}{m_p}) = 0.99999999991 \pm 0.00000000009$   
 $|q_p + q_{\bar{p}}|/e < 2 \times 10^{-9}$ , CL = 90% [b]  
 $|q_p + q_e|/e < 1 \times 10^{-21}$  [c]  
 Magnetic moment  $\mu = 2.792847356 \pm 0.000000023 \mu_N$   
 $(\mu_p + \mu_{\bar{p}}) / \mu_p = (-0.1 \pm 2.1) \times 10^{-3}$   
 Electric dipole moment  $d < 0.54 \times 10^{-23}$  ecm  
 Electric polarizability  $\alpha = (12.0 \pm 0.6) \times 10^{-4}$  fm<sup>3</sup>  
 Magnetic polarizability  $\beta = (1.9 \pm 0.5) \times 10^{-4}$  fm<sup>3</sup>  
 Charge radius =  $0.877 \pm 0.005$  fm  
 Magnetic radius =  $0.777 \pm 0.016$  fm  
 Mean life  $\tau > 2.1 \times 10^{29}$  years, CL = 90% [d] ( $p \rightarrow$  invisible mode)  
 Mean life  $\tau > 10^{31}$  to  $10^{33}$  years [d] (mode dependent)

See the "Note on Nucleon Decay" in our 1994 edition (Phys. Rev. **D50**, 1173) for a short review.

The "partial mean life" limits tabulated here are the limits on  $\tau/B_j$ , where  $\tau$  is the total mean life and  $B_j$  is the branching fraction for the mode in question. For  $N$  decays,  $p$  and  $n$  indicate proton and neutron partial lifetimes.

<b>p</b> DECAY MODES	Partial mean life ( $10^{30}$ years)	Confidence level	$p$ (MeV/c)
<b>Antilepton + meson</b>			
$N \rightarrow e^+ \pi$	> 158 (n), > 8200 (p)	90%	459
$N \rightarrow \mu^+ \pi$	> 100 (n), > 6600 (p)	90%	453
$N \rightarrow \nu \pi$	> 112 (n), > 25 (p)	90%	459
$p \rightarrow e^+ \eta$	> 313	90%	309
$p \rightarrow \mu^+ \eta$	> 126	90%	297
$n \rightarrow \nu \eta$	> 158	90%	310
$N \rightarrow e^+ \rho$	> 217 (n), > 75 (p)	90%	149
$N \rightarrow \mu^+ \rho$	> 228 (n), > 110 (p)	90%	113
$N \rightarrow \nu \rho$	> 19 (n), > 162 (p)	90%	149
$p \rightarrow e^+ \omega$	> 107	90%	143
$p \rightarrow \mu^+ \omega$	> 117	90%	105
$n \rightarrow \nu \omega$	> 108	90%	144
$N \rightarrow e^+ K$	> 17 (n), > 150 (p)	90%	339
$p \rightarrow e^+ K_S^0$	> 120	90%	337
$p \rightarrow e^+ K_L^0$	> 51	90%	337
$N \rightarrow \mu^+ K$	> 26 (n), > 120 (p)	90%	329
$p \rightarrow \mu^+ K_S^0$	> 150	90%	326
$p \rightarrow \mu^+ K_L^0$	> 83	90%	326
$N \rightarrow \nu K$	> 86 (n), > 670 (p)	90%	339
$n \rightarrow \nu K_S^0$	> 51	90%	338
$p \rightarrow e^+ K^*(892)^0$	> 84	90%	45
$N \rightarrow \nu K^*(892)$	> 78 (n), > 51 (p)	90%	45
<b>Antilepton + mesons</b>			
$p \rightarrow e^+ \pi^+ \pi^-$	> 82	90%	448
$p \rightarrow e^+ \pi^0 \pi^0$	> 147	90%	449
$n \rightarrow e^+ \pi^- \pi^0$	> 52	90%	449
$p \rightarrow \mu^+ \pi^+ \pi^-$	> 133	90%	425
$p \rightarrow \mu^+ \pi^0 \pi^0$	> 101	90%	427
$n \rightarrow \mu^+ \pi^- \pi^0$	> 74	90%	427
$n \rightarrow e^+ K^0 \pi^-$	> 18	90%	319
<b>Lepton + meson</b>			
$n \rightarrow e^- \pi^+$	> 65	90%	459
$n \rightarrow \mu^- \pi^+$	> 49	90%	453
$n \rightarrow e^- \rho^+$	> 62	90%	150
$n \rightarrow \mu^- \rho^+$	> 7	90%	114
$n \rightarrow e^- K^+$	> 32	90%	340
$n \rightarrow \mu^- K^+$	> 57	90%	330

**Lepton + mesons**

$p \rightarrow e^- \pi^+ \pi^+$	> 30	90%	448
$n \rightarrow e^- \pi^+ \pi^0$	> 29	90%	449
$p \rightarrow \mu^- \pi^+ \pi^+$	> 17	90%	425
$n \rightarrow \mu^- \pi^+ \pi^0$	> 34	90%	427
$p \rightarrow e^- \pi^+ K^+$	> 75	90%	320
$p \rightarrow \mu^- \pi^+ K^+$	> 245	90%	279

**Antilepton + photon(s)**

$p \rightarrow e^+ \gamma$	> 670	90%	469
$p \rightarrow \mu^+ \gamma$	> 478	90%	463
$n \rightarrow \nu \gamma$	> 28	90%	470
$p \rightarrow e^+ \gamma \gamma$	> 100	90%	469
$n \rightarrow \nu \gamma \gamma$	> 219	90%	470

**Three (or more) leptons**

$p \rightarrow e^+ e^+ e^-$	> 793	90%	469
$p \rightarrow e^+ \mu^+ \mu^-$	> 359	90%	457
$p \rightarrow e^+ \nu \nu$	> 17	90%	469
$n \rightarrow e^+ e^- \nu$	> 257	90%	470
$n \rightarrow \mu^+ e^- \nu$	> 83	90%	464
$n \rightarrow \mu^+ \mu^- \nu$	> 79	90%	458
$p \rightarrow \mu^+ e^+ e^-$	> 529	90%	463
$p \rightarrow \mu^+ \mu^+ \mu^-$	> 675	90%	439
$p \rightarrow \mu^+ \nu \nu$	> 21	90%	463
$p \rightarrow e^- \mu^+ \mu^+$	> 6	90%	457
$n \rightarrow 3\nu$	> 0.0005	90%	470

**Inclusive modes**

$N \rightarrow e^+$ anything	> 0.6 (n, p)	90%	—
$N \rightarrow \mu^+$ anything	> 12 (n, p)	90%	—
$N \rightarrow e^+ \pi^0$ anything	> 0.6 (n, p)	90%	—

 **$\Delta B = 2$  dinucleon modes**

The following are lifetime limits per iron nucleus.

$pp \rightarrow \pi^+ \pi^+$	> 0.7	90%	—
$pn \rightarrow \pi^+ \pi^0$	> 2	90%	—
$nn \rightarrow \pi^+ \pi^-$	> 0.7	90%	—
$nn \rightarrow \pi^0 \pi^0$	> 3.4	90%	—
$pp \rightarrow e^+ e^+$	> 5.8	90%	—
$pp \rightarrow e^+ \mu^+$	> 3.6	90%	—
$pp \rightarrow \mu^+ \mu^+$	> 1.7	90%	—
$pn \rightarrow e^+ \bar{\nu}$	> 2.8	90%	—
$pn \rightarrow \mu^+ \bar{\nu}$	> 1.6	90%	—
$nn \rightarrow \nu_e \bar{\nu}_e$	> 0.000049	90%	—
$pn \rightarrow$ invisible	> $2.10 \times 10^{25}$	90%	—
$pp \rightarrow$ invisible	> 0.00005	90%	—

 **$\bar{p}$  DECAY MODES**

$\bar{p}$ DECAY MODES	Partial mean life (years)	Confidence level	$p$ (MeV/c)
$\bar{p} \rightarrow e^- \gamma$	> $7 \times 10^5$	90%	469
$\bar{p} \rightarrow \mu^- \gamma$	> $5 \times 10^4$	90%	463
$\bar{p} \rightarrow e^- \pi^0$	> $4 \times 10^5$	90%	459
$\bar{p} \rightarrow \mu^- \pi^0$	> $5 \times 10^4$	90%	453
$\bar{p} \rightarrow e^- \eta$	> $2 \times 10^4$	90%	309
$\bar{p} \rightarrow \mu^- \eta$	> $8 \times 10^3$	90%	297
$\bar{p} \rightarrow e^- K_S^0$	> 900	90%	337
$\bar{p} \rightarrow \mu^- K_S^0$	> $4 \times 10^3$	90%	326
$\bar{p} \rightarrow e^- K_L^0$	> $9 \times 10^3$	90%	337
$\bar{p} \rightarrow \mu^- K_L^0$	> $7 \times 10^3$	90%	326
$\bar{p} \rightarrow e^- \gamma \gamma$	> $2 \times 10^4$	90%	469
$\bar{p} \rightarrow \mu^- \gamma \gamma$	> $2 \times 10^4$	90%	463
$\bar{p} \rightarrow e^- \omega$	> 200	90%	143

**n**

$$I(J^P) = \frac{1}{2}(\frac{1}{2}^+)$$

Mass  $m = 1.0086649160 \pm 0.00000000004$  u  
 Mass  $m = 939.565379 \pm 0.000021$  MeV [a]  
 $(m_n - m_{\bar{n}}) / m_n = (9 \pm 6) \times 10^{-5}$   
 $m_n - m_p = 1.2933322 \pm 0.0000004$  MeV  
 $= 0.00138844920(46)$  u  
 Mean life  $\tau = 880.1 \pm 1.1$  s ( $S = 1.8$ )  
 $c\tau = 2.6383 \times 10^8$  km  
 Magnetic moment  $\mu = -1.9130427 \pm 0.0000005 \mu_N$   
 Electric dipole moment  $d < 0.29 \times 10^{-25}$  ecm, CL = 90%

## Baryon Summary Table

Mean-square charge radius  $\langle r_n^2 \rangle = -0.1161 \pm 0.0022$   
 $\text{fm}^2$  ( $S = 1.3$ )  
 Magnetic radius  $\sqrt{\langle r_M^2 \rangle} = 0.862_{-0.008}^{+0.009}$  fm  
 Electric polarizability  $\alpha = (11.6 \pm 1.5) \times 10^{-4}$  fm<sup>3</sup>  
 Magnetic polarizability  $\beta = (3.7 \pm 2.0) \times 10^{-4}$  fm<sup>3</sup>  
 Charge  $q = (-0.2 \pm 0.8) \times 10^{-21}$  e  
 Mean  $n\bar{n}$ -oscillation time  $> 8.6 \times 10^7$  s, CL = 90% (free  $n$ )  
 Mean  $n\bar{n}$ -oscillation time  $> 1.3 \times 10^8$  s, CL = 90% [e] (bound  $n$ )  
 Mean  $n\bar{n}'$ -oscillation time  $> 414$  s, CL = 90% [f]

 **$p e^- \nu_e$  decay parameters [g]**

$\lambda \equiv g_A / g_V = -1.2701 \pm 0.0025$  ( $S = 1.9$ )  
 $A = -0.1176 \pm 0.0011$  ( $S = 2.1$ )  
 $B = 0.9807 \pm 0.0030$   
 $C = -0.2377 \pm 0.0026$   
 $a = -0.103 \pm 0.004$   
 $\phi_{AV} = (180.018 \pm 0.026)^\circ$  [h]  
 $D = (-1.2 \pm 2.0) \times 10^{-4}$  [i]  
 $R = 0.008 \pm 0.016$  [j]

$n$ DECAY MODES	Fraction ( $\Gamma_i/\Gamma$ )	Confidence level	$\rho$ (MeV/c)
$p e^- \bar{\nu}_e$	100	%	1
$p e^- \bar{\nu}_e \gamma$	[j] ( $3.09 \pm 0.32$ ) $\times 10^{-3}$		1
<b>Charge conservation (Q) violating mode</b>			
$p \nu_e \bar{\nu}_e$	Q < 8	$\times 10^{-27}$	68% 1

 **$N(1440) 1/2^+$** 

$$I(J^P) = \frac{1}{2}(\frac{1}{2}^+)$$

Breit-Wigner mass = 1420 to 1470 ( $\approx 1440$ ) MeV  
 Breit-Wigner full width = 200 to 450 ( $\approx 300$ ) MeV  
 $p_{\text{beam}} = 0.61$  GeV/c  $4\pi\lambda^2 = 31.0$  mb  
 Re(pole position) = 1350 to 1380 ( $\approx 1365$ ) MeV  
 $-2\text{Im}(\text{pole position}) = 160$  to 220 ( $\approx 190$ ) MeV

$N(1440)$ DECAY MODES	Fraction ( $\Gamma_i/\Gamma$ )	$\rho$ (MeV/c)
$N\pi$	55–75 %	398
$N\eta$	( $0.0 \pm 1.0$ ) %	†
$N\pi\pi$	30–40 %	347
$\Delta\pi$	20–30 %	147
$\Delta(1232)\pi$ , <i>P</i> -wave	15–30 %	147
$N\rho$	< 8 %	†
$N\rho$ , $S=1/2$ , <i>P</i> -wave	( $0.0 \pm 1.0$ ) %	†
$N(\pi\pi)_{S\text{-wave}}^{J=0}$	10–20 %	–
$p\gamma$	0.035–0.048 %	414
$p\gamma$ , helicity=1/2	0.035–0.048 %	414
$n\gamma$	0.02–0.04 %	413
$n\gamma$ , helicity=1/2	0.02–0.04 %	413

 **$N(1520) 3/2^-$** 

$$I(J^P) = \frac{1}{2}(\frac{3}{2}^-)$$

Breit-Wigner mass = 1515 to 1525 ( $\approx 1520$ ) MeV  
 Breit-Wigner full width = 100 to 125 ( $\approx 115$ ) MeV  
 $p_{\text{beam}} = 0.74$  GeV/c  $4\pi\lambda^2 = 23.5$  mb  
 Re(pole position) = 1505 to 1515 ( $\approx 1510$ ) MeV  
 $-2\text{Im}(\text{pole position}) = 105$  to 120 ( $\approx 110$ ) MeV

$N(1520)$ DECAY MODES	Fraction ( $\Gamma_i/\Gamma$ )	$\rho$ (MeV/c)
$N\pi$	55–65 %	457
$N\eta$	( $2.3 \pm 0.4$ ) $\times 10^{-3}$	154
$N\pi\pi$	20–30 %	414
$\Delta\pi$	15–25 %	230
$\Delta(1232)\pi$ , <i>S</i> -wave	10–20 %	230
$\Delta(1232)\pi$ , <i>D</i> -wave	10–15 %	230
$N\rho$	15–25 %	†
$N\rho$ , $S=3/2$ , <i>S</i> -wave	( $9.0 \pm 1.0$ ) %	†
$N(\pi\pi)_{S\text{-wave}}^{J=0}$	< 8 %	–
$p\gamma$	0.31–0.52 %	470
$p\gamma$ , helicity=1/2	0.01–0.02 %	470
$p\gamma$ , helicity=3/2	0.30–0.50 %	470
$n\gamma$	0.30–0.53 %	470
$n\gamma$ , helicity=1/2	0.04–0.10 %	470
$n\gamma$ , helicity=3/2	0.25–0.45 %	470

 **$N(1535) 1/2^-$** 

$$I(J^P) = \frac{1}{2}(\frac{1}{2}^-)$$

Breit-Wigner mass = 1525 to 1545 ( $\approx 1535$ ) MeV  
 Breit-Wigner full width = 125 to 175 ( $\approx 150$ ) MeV  
 $p_{\text{beam}} = 0.76$  GeV/c  $4\pi\lambda^2 = 22.5$  mb  
 Re(pole position) = 1490 to 1530 ( $\approx 1510$ ) MeV  
 $-2\text{Im}(\text{pole position}) = 90$  to 250 ( $\approx 170$ ) MeV

$N(1535)$ DECAY MODES	Fraction ( $\Gamma_i/\Gamma$ )	$\rho$ (MeV/c)
$N\pi$	35–55 %	468
$N\eta$	( $42 \pm 10$ ) %	186
$N\pi\pi$	1–10 %	426
$\Delta\pi$	< 1 %	244
$\Delta(1232)\pi$ , <i>D</i> -wave	0–4 %	244
$N\rho$	< 4 %	†
$N\rho$ , $S=1/2$ , <i>S</i> -wave	( $2.0 \pm 1.0$ ) %	†
$N\rho$ , $S=3/2$ , <i>D</i> -wave	( $0.0 \pm 1.0$ ) %	†
$N(\pi\pi)_{S\text{-wave}}^{J=0}$	( $2 \pm 1$ ) %	–
$N(1440)\pi$	( $8 \pm 3$ ) %	†
$p\gamma$	0.15–0.30 %	481
$p\gamma$ , helicity=1/2	0.15–0.30 %	481
$n\gamma$	0.01–0.25 %	480
$n\gamma$ , helicity=1/2	0.01–0.25 %	480

 **$N(1650) 1/2^-$** 

$$I(J^P) = \frac{1}{2}(\frac{1}{2}^-)$$

Breit-Wigner mass = 1645 to 1670 ( $\approx 1655$ ) MeV  
 Breit-Wigner full width = 120 to 180 ( $\approx 150$ ) MeV  
 $p_{\text{beam}} = 0.97$  GeV/c  $4\pi\lambda^2 = 16.2$  mb  
 Re(pole position) = 1640 to 1670 ( $\approx 1655$ ) MeV  
 $-2\text{Im}(\text{pole position}) = 100$  to 170 ( $\approx 135$ ) MeV

$N(1650)$ DECAY MODES	Fraction ( $\Gamma_i/\Gamma$ )	$\rho$ (MeV/c)
$N\pi$	50–90 %	551
$N\eta$	5–15 %	354
$\Lambda K$	3–11 %	179
$N\pi\pi$	10–20 %	517
$\Delta\pi$	0–25 %	349
$\Delta(1232)\pi$ , <i>D</i> -wave	0–25 %	349
$N\rho$	4–12 %	†
$N\rho$ , $S=1/2$ , <i>S</i> -wave	( $1.0 \pm 1.0$ ) %	†
$N\rho$ , $S=3/2$ , <i>D</i> -wave	( $13.0 \pm 3.0$ ) %	†
$N(\pi\pi)_{S\text{-wave}}^{J=0}$	< 4 %	–
$N(1440)\pi$	< 5 %	156
$p\gamma$	0.04–0.20 %	562
$p\gamma$ , helicity=1/2	0.04–0.20 %	562
$n\gamma$	0.003–0.17 %	561
$n\gamma$ , helicity=1/2	0.003–0.17 %	561

 **$N(1675) 5/2^-$** 

$$I(J^P) = \frac{1}{2}(\frac{5}{2}^-)$$

Breit-Wigner mass = 1670 to 1680 ( $\approx 1675$ ) MeV  
 Breit-Wigner full width = 130 to 165 ( $\approx 150$ ) MeV  
 $p_{\text{beam}} = 1.01$  GeV/c  $4\pi\lambda^2 = 15.4$  mb  
 Re(pole position) = 1655 to 1665 ( $\approx 1660$ ) MeV  
 $-2\text{Im}(\text{pole position}) = 125$  to 150 ( $\approx 135$ ) MeV

$N(1675)$ DECAY MODES	Fraction ( $\Gamma_i/\Gamma$ )	$\rho$ (MeV/c)
$N\pi$	35–45 %	564
$N\eta$	( $0.0 \pm 1.0$ ) %	376
$\Lambda K$	< 1 %	216
$N\pi\pi$	50–60 %	532
$\Delta\pi$	50–60 %	366
$\Delta(1232)\pi$ , <i>D</i> -wave	( $50 \pm 15$ ) %	366
$N\rho$	< 1–3 %	†
$N\rho$ , $S=1/2$ , <i>D</i> -wave	( $0.0 \pm 1.0$ ) %	†
$N\rho$ , $S=3/2$ , <i>D</i> -wave	( $1.0 \pm 1.0$ ) %	†
$N(\pi\pi)_{S\text{-wave}}^{J=0}$	( $7.0 \pm 3.0$ ) %	–
$p\gamma$	0–0.02 %	575
$p\gamma$ , helicity=1/2	0–0.01 %	575
$p\gamma$ , helicity=3/2	0–0.01 %	575
$n\gamma$	0–0.15 %	574
$n\gamma$ , helicity=1/2	0–0.05 %	574
$n\gamma$ , helicity=3/2	0–0.10 %	574

## Baryon Summary Table

 **$N(1680) 5/2^+$** 

$$I(J^P) = \frac{1}{2}(\frac{5}{2}^+)$$

Breit-Wigner mass = 1680 to 1690 ( $\approx 1685$ ) MeV  
 Breit-Wigner full width = 120 to 140 ( $\approx 130$ ) MeV  
 $p_{\text{beam}} = 1.02 \text{ GeV}/c$   $4\pi\lambda^2 = 15.0 \text{ mb}$   
 Re(pole position) = 1665 to 1680 ( $\approx 1675$ ) MeV  
 $-2\text{Im}(\text{pole position}) = 110 \text{ to } 135$  ( $\approx 120$ ) MeV

<b><math>N(1680)</math> DECAY MODES</b>	Fraction ( $\Gamma_i/\Gamma$ )	$\rho$ (MeV/c)
$N\pi$	65–70 %	571
$N\eta$	( 0.0 $\pm$ 1.0) %	386
$N\pi\pi$	30–40 %	539
$\Delta\pi$	5–15 %	374
$\Delta(1232)\pi$ , $P$ -wave	(10 $\pm 5$ ) %	374
$\Delta(1232)\pi$ , $F$ -wave	0–12 %	374
$N\rho$	3–15 %	†
$N\rho$ , $S=3/2$ , $P$ -wave	<12%	†
$N\rho$ , $S=3/2$ , $F$ -wave	1–5 %	†
$N(\pi\pi)_{S\text{-wave}}^{J=0}$	(11 $\pm 5$ ) %	–
$p\gamma$	0.21–0.32 %	581
$p\gamma$ , helicity=1/2	0.001–0.011 %	581
$p\gamma$ , helicity=3/2	0.20–0.32 %	581
$n\gamma$	0.021–0.046 %	581
$n\gamma$ , helicity=1/2	0.004–0.029 %	581
$n\gamma$ , helicity=3/2	0.01–0.024 %	581

 **$N(1700) 3/2^-$** 

$$I(J^P) = \frac{1}{2}(\frac{3}{2}^-)$$

Breit-Wigner mass = 1650 to 1750 ( $\approx 1700$ ) MeV  
 Breit-Wigner full width = 100 to 250 ( $\approx 150$ ) MeV  
 $p_{\text{beam}} = 1.05 \text{ GeV}/c$   $4\pi\lambda^2 = 14.5 \text{ mb}$   
 Re(pole position) = 1650 to 1750 ( $\approx 1700$ ) MeV  
 $-2\text{Im}(\text{pole position}) = 100 \text{ to } 300$  MeV

<b><math>N(1700)</math> DECAY MODES</b>	Fraction ( $\Gamma_i/\Gamma$ )	$\rho$ (MeV/c)
$N\pi$	(12 $\pm 5$ ) %	581
$N\eta$	( 0.0 $\pm$ 1.0) %	402
$\Lambda K$	< 3 %	255
$N\pi\pi$	85–95 %	550
$\Delta(1232)\pi$ , $S$ -wave	10–90 %	386
$\Delta(1232)\pi$ , $D$ -wave	< 20 %	386
$N\rho$	< 35 %	†
$N\rho$ , $S=3/2$ , $S$ -wave	( 7.0 $\pm$ 1.0) %	†
$p\gamma$	0.01–0.05 %	591
$p\gamma$ , helicity=1/2	0.0–0.024 %	591
$p\gamma$ , helicity=3/2	0.002–0.026 %	591
$n\gamma$	0.01–0.13 %	590
$n\gamma$ , helicity=1/2	0.0–0.09 %	590
$n\gamma$ , helicity=3/2	0.01–0.05 %	590

 **$N(1710) 1/2^+$** 

$$I(J^P) = \frac{1}{2}(\frac{1}{2}^+)$$

Breit-Wigner mass = 1680 to 1740 ( $\approx 1710$ ) MeV  
 Breit-Wigner full width = 50 to 250 ( $\approx 100$ ) MeV  
 $p_{\text{beam}} = 1.07 \text{ GeV}/c$   $4\pi\lambda^2 = 14.2 \text{ mb}$   
 Re(pole position) = 1670 to 1770 ( $\approx 1720$ ) MeV  
 $-2\text{Im}(\text{pole position}) = 80 \text{ to } 380$  ( $\approx 230$ ) MeV

<b><math>N(1710)</math> DECAY MODES</b>	Fraction ( $\Gamma_i/\Gamma$ )	$\rho$ (MeV/c)
$N\pi$	5–20 %	588
$N\eta$	10–30 %	412
$N\omega$	(13.0 $\pm$ 2.0) %	†
$\Lambda K$	5–25 %	269
$N\pi\pi$	40–90 %	557
$\Delta\pi$	15–40 %	394
$N\rho$	5–25 %	†
$N(\pi\pi)_{S\text{-wave}}^{J=0}$	10–40 %	–
$p\gamma$	0.002–0.08 %	598
$p\gamma$ , helicity=1/2	0.002–0.08 %	598
$n\gamma$	0.0–0.02%	597
$n\gamma$ , helicity=1/2	0.0–0.02%	597

 **$N(1720) 3/2^+$** 

$$I(J^P) = \frac{1}{2}(\frac{3}{2}^+)$$

Breit-Wigner mass = 1700 to 1750 ( $\approx 1720$ ) MeV  
 Breit-Wigner full width = 150 to 400 ( $\approx 250$ ) MeV  
 $p_{\text{beam}} = 1.09 \text{ GeV}/c$   $4\pi\lambda^2 = 13.9 \text{ mb}$   
 Re(pole position) = 1660 to 1690 ( $\approx 1675$ ) MeV  
 $-2\text{Im}(\text{pole position}) = 150 \text{ to } 400$  ( $\approx 250$ ) MeV

<b><math>N(1720)</math> DECAY MODES</b>	Fraction ( $\Gamma_i/\Gamma$ )	$\rho$ (MeV/c)
$N\pi$	(11 $\pm 3$ ) %	594
$N\eta$	( 4 $\pm 1$ ) %	422
$\Lambda K$	1–15 %	283
$N\pi\pi$	>70 %	564
$\Delta(1232)\pi$ , $P$ -wave	(75 $\pm$ 15) %	402
$N\rho$	70–85 %	73
$N\rho$ , $S=1/2$ , $P$ -wave	large	73
$p\gamma$	0.05–0.25 %	604
$p\gamma$ , helicity=1/2	0.05–0.15 %	604
$p\gamma$ , helicity=3/2	0.002–0.16 %	604
$n\gamma$	0.0–0.016 %	603
$n\gamma$ , helicity=1/2	0.0–0.01 %	603
$n\gamma$ , helicity=3/2	0.0–0.015 %	603

 **$N(1875) 3/2^-$** 

$$I(J^P) = \frac{1}{2}(\frac{3}{2}^-)$$

Breit-Wigner mass = 1820 to 1920 ( $\approx 1875$ ) MeV  
 Breit-Wigner full width = 160 to 320 ( $\approx 220$ ) MeV  
 Re(pole position) = 1800 to 1950 MeV  
 $-2\text{Im}(\text{pole position}) = 150 \text{ to } 250$  MeV

<b><math>N(1875)</math> DECAY MODES</b>	Fraction ( $\Gamma_i/\Gamma$ )	Scale factor	$\rho$ (MeV/c)
$N\pi$	(12 $\pm 10$ ) %		695
$N\eta$	( 3.5 $\pm 3.5$ ) %	2.5	559
$N\omega$	(21 $\pm 7$ ) %		371
$\Sigma K$	( 7 $\pm 4$ ) $\times 10^{-3}$		384
$\Delta(1232)\pi$ , $S$ -wave	(40 $\pm 10$ ) %		520
$\Delta(1232)\pi$ , $D$ -wave	(17 $\pm 10$ ) %		520
$N\rho$ , $S=3/2$ , $S$ -wave	( 6 $\pm 6$ ) %		379
$N(\pi\pi)_{S\text{-wave}}^{J=0}$	(24 $\pm 24$ ) %		–
$p\gamma$	0.008–0.016 %		703
$p\gamma$ , helicity=1/2	0.006–0.010 %		703
$p\gamma$ , helicity=3/2	0.002–0.006 %		703

 **$N(1900) 3/2^+$** 

$$I(J^P) = \frac{1}{2}(\frac{3}{2}^+)$$

Breit-Wigner mass  $\approx 1900$  MeV  
 Breit-Wigner full width  $\sim 250$  MeV  
 Re(pole position) = 1900  $\pm 30$  MeV  
 $-2\text{Im}(\text{pole position}) = 200 \pm \frac{100}{60}$  MeV

<b><math>N(1900)</math> DECAY MODES</b>	Fraction ( $\Gamma_i/\Gamma$ )	$\rho$ (MeV/c)
$N\pi$	$\sim 10$ %	710
$N\eta$	$\sim 12$ %	579
$N\omega$	(39 $\pm 9$ ) %	401
$\Lambda K$	0–10 %	477
$\Sigma K$	( 5.0 $\pm$ 2.0) %	410

 **$N(2190) 7/2^-$** 

$$I(J^P) = \frac{1}{2}(\frac{7}{2}^-)$$

Breit-Wigner mass = 2100 to 2200 ( $\approx 2190$ ) MeV  
 Breit-Wigner full width = 300 to 700 ( $\approx 500$ ) MeV  
 $p_{\text{beam}} = 2.07 \text{ GeV}/c$   $4\pi\lambda^2 = 6.21 \text{ mb}$   
 Re(pole position) = 2050 to 2100 ( $\approx 2075$ ) MeV  
 $-2\text{Im}(\text{pole position}) = 400 \text{ to } 520$  ( $\approx 450$ ) MeV

## Baryon Summary Table

<b>N(2190) DECAY MODES</b>	Fraction ( $\Gamma_i/\Gamma$ )	$\rho$ (MeV/c)
$N\pi$	10–20 %	888
$N\eta$	(0.0±1.0) %	791
$N\omega$	seen	676
$\Lambda K$	seen	712
$N\pi\pi$	seen	870
$N\rho$	seen	680
$p\gamma$	0.02–0.06 %	894
$\rho\gamma$ , helicity=1/2	0.02–0.04 %	894
$\rho\gamma$ , helicity=3/2	0.002–0.02 %	894

**N(2220) 9/2<sup>+</sup>**

$$I(J^P) = \frac{1}{2}(\frac{9}{2}^+)$$

Breit-Wigner mass = 2200 to 2300 ( $\approx$  2250) MeV  
 Breit-Wigner full width = 350 to 500 ( $\approx$  400) MeV  
 $p_{\text{beam}} = 2.21 \text{ GeV}/c$      $4\pi\lambda^2 = 5.74 \text{ mb}$   
 Re(pole position) = 2130 to 2200 ( $\approx$  2170) MeV  
 $-2\text{Im}(\text{pole position}) = 400 \text{ to } 560$  ( $\approx$  480) MeV

<b>N(2220) DECAY MODES</b>	Fraction ( $\Gamma_i/\Gamma$ )	$\rho$ (MeV/c)
$N\pi$	15–25 %	924

**N(2250) 9/2<sup>-</sup>**

$$I(J^P) = \frac{1}{2}(\frac{9}{2}^-)$$

Breit-Wigner mass = 2200 to 2350 ( $\approx$  2275) MeV  
 Breit-Wigner full width = 230 to 800 ( $\approx$  500) MeV  
 $p_{\text{beam}} = 2.27 \text{ GeV}/c$      $4\pi\lambda^2 = 5.56 \text{ mb}$   
 Re(pole position) = 2150 to 2250 ( $\approx$  2200) MeV  
 $-2\text{Im}(\text{pole position}) = 350 \text{ to } 550$  ( $\approx$  450) MeV

<b>N(2250) DECAY MODES</b>	Fraction ( $\Gamma_i/\Gamma$ )	$\rho$ (MeV/c)
$N\pi$	5–15 %	938

**N(2600) 11/2<sup>-</sup>**

$$I(J^P) = \frac{1}{2}(\frac{11}{2}^-)$$

Breit-Wigner mass = 2550 to 2750 ( $\approx$  2600) MeV  
 Breit-Wigner full width = 500 to 800 ( $\approx$  650) MeV  
 $p_{\text{beam}} = 3.12 \text{ GeV}/c$      $4\pi\lambda^2 = 3.86 \text{ mb}$

<b>N(2600) DECAY MODES</b>	Fraction ( $\Gamma_i/\Gamma$ )	$\rho$ (MeV/c)
$N\pi$	5–10 %	1126

## Δ BARYONS ( $S = 0, I = 3/2$ )

$$\Delta^{++} = uuu, \quad \Delta^+ = uud, \quad \Delta^0 = udd, \quad \Delta^- = ddd$$

**Δ(1232) 3/2<sup>+</sup>**

$$I(J^P) = \frac{3}{2}(\frac{3}{2}^+)$$

Breit-Wigner mass (mixed charges) = 1230 to 1234 ( $\approx$  1232) MeV  
 Breit-Wigner full width (mixed charges) = 114 to 120 ( $\approx$  117) MeV  
 $p_{\text{beam}} = 0.30 \text{ GeV}/c$      $4\pi\lambda^2 = 94.8 \text{ mb}$   
 Re(pole position) = 1209 to 1211 ( $\approx$  1210) MeV  
 $-2\text{Im}(\text{pole position}) = 98 \text{ to } 102$  ( $\approx$  100) MeV

<b>Δ(1232) DECAY MODES</b>	Fraction ( $\Gamma_i/\Gamma$ )	$\rho$ (MeV/c)
$N\pi$	100 %	229
$N\gamma$	0.55–0.65 %	259
$N\gamma$ , helicity=1/2	0.11–0.13 %	259
$N\gamma$ , helicity=3/2	0.44–0.52 %	259

**Δ(1600) 3/2<sup>+</sup>**

$$I(J^P) = \frac{3}{2}(\frac{3}{2}^+)$$

Breit-Wigner mass = 1500 to 1700 ( $\approx$  1600) MeV  
 Breit-Wigner full width = 220 to 420 ( $\approx$  320) MeV  
 $p_{\text{beam}} = 0.87 \text{ GeV}/c$      $4\pi\lambda^2 = 18.6 \text{ mb}$   
 Re(pole position) = 1460 to 1560 ( $\approx$  1510) MeV  
 $-2\text{Im}(\text{pole position}) = 200 \text{ to } 350$  ( $\approx$  275) MeV

<b>Δ(1600) DECAY MODES</b>	Fraction ( $\Gamma_i/\Gamma$ )	$\rho$ (MeV/c)
$N\pi$	10–25 %	513
$N\pi\pi$	75–90 %	477
$\Delta\pi$	40–70 %	303
$N\rho$	<25 %	†
$N(1440)\pi$	10–35 %	82
$N\gamma$	0.001–0.035 %	525
$N\gamma$ , helicity=1/2	0.0–0.02 %	525
$N\gamma$ , helicity=3/2	0.001–0.015 %	525

**Δ(1620) 1/2<sup>-</sup>**

$$I(J^P) = \frac{3}{2}(\frac{1}{2}^-)$$

Breit-Wigner mass = 1600 to 1660 ( $\approx$  1630) MeV  
 Breit-Wigner full width = 130 to 150 ( $\approx$  140) MeV  
 $p_{\text{beam}} = 0.93 \text{ GeV}/c$      $4\pi\lambda^2 = 17.2 \text{ mb}$   
 Re(pole position) = 1590 to 1610 ( $\approx$  1600) MeV  
 $-2\text{Im}(\text{pole position}) = 120 \text{ to } 140$  ( $\approx$  130) MeV

<b>Δ(1620) DECAY MODES</b>	Fraction ( $\Gamma_i/\Gamma$ )	$\rho$ (MeV/c)
$N\pi$	20–30 %	534
$N\pi\pi$	70–80 %	499
$\Delta\pi$	30–60 %	328
$N\rho$	7–25 %	†
$N\gamma$	0.03–0.10 %	545
$N\gamma$ , helicity=1/2	0.03–0.10 %	545

**Δ(1700) 3/2<sup>-</sup>**

$$I(J^P) = \frac{3}{2}(\frac{3}{2}^-)$$

Breit-Wigner mass = 1670 to 1750 ( $\approx$  1700) MeV  
 Breit-Wigner full width = 200 to 400 ( $\approx$  300) MeV  
 $p_{\text{beam}} = 1.05 \text{ GeV}/c$      $4\pi\lambda^2 = 14.5 \text{ mb}$   
 Re(pole position) = 1620 to 1680 ( $\approx$  1650) MeV  
 $-2\text{Im}(\text{pole position}) = 160 \text{ to } 300$  ( $\approx$  230) MeV

<b>Δ(1700) DECAY MODES</b>	Fraction ( $\Gamma_i/\Gamma$ )	$\rho$ (MeV/c)
$N\pi$	10–20 %	581
$N\pi\pi$	80–90 %	550
$\Delta\pi$	30–60 %	386
$\Delta(1232)\pi$ , S-wave	25–50 %	386
$\Delta(1232)\pi$ , D-wave	5–15 %	386
$N\rho$	30–55 %	†
$N\rho$ , S=3/2, S-wave	5–20 %	†
$\Delta(1232)\eta$	(5.0±2.0) %	†
$N\gamma$	0.22–0.60 %	591
$N\gamma$ , helicity=1/2	0.12–0.30 %	591
$N\gamma$ , helicity=3/2	0.10–0.30 %	591

**Δ(1905) 5/2<sup>+</sup>**

$$I(J^P) = \frac{3}{2}(\frac{5}{2}^+)$$

Breit-Wigner mass = 1855 to 1910 ( $\approx$  1880) MeV  
 Breit-Wigner full width = 270 to 400 ( $\approx$  330) MeV  
 $p_{\text{beam}} = 1.40 \text{ GeV}/c$      $4\pi\lambda^2 = 10.1 \text{ mb}$   
 Re(pole position) = 1805 to 1835 ( $\approx$  1820) MeV  
 $-2\text{Im}(\text{pole position}) = 265 \text{ to } 300$  ( $\approx$  280) MeV

<b>Δ(1905) DECAY MODES</b>	Fraction ( $\Gamma_i/\Gamma$ )	$\rho$ (MeV/c)
$N\pi$	9–15 %	698
$N\pi\pi$	85–95 %	673
$\Delta\pi$	<25 %	524
$N\rho$	>60 %	385
$N\gamma$	0.012–0.036 %	706
$N\gamma$ , helicity=1/2	0.002–0.006 %	706
$N\gamma$ , helicity=3/2	0.01–0.03 %	706

**Δ(1910) 1/2<sup>+</sup>**

$$I(J^P) = \frac{3}{2}(\frac{1}{2}^+)$$

Breit-Wigner mass = 1860 to 1910 ( $\approx$  1890) MeV  
 Breit-Wigner full width = 220 to 340 ( $\approx$  280) MeV  
 $p_{\text{beam}} = 1.42 \text{ GeV}/c$      $4\pi\lambda^2 = 9.89 \text{ mb}$   
 Re(pole position) = 1830 to 1880 ( $\approx$  1855) MeV  
 $-2\text{Im}(\text{pole position}) = 200 \text{ to } 500$  ( $\approx$  350) MeV



## Baryon Summary Table

$\Delta(1910)$ DECAY MODES	Fraction ( $\Gamma_i/\Gamma$ )	$\rho$ (MeV/c)
$N\pi$	15-30 %	704
$\Sigma K$	( 9 $\pm$ 5 ) %	400
$\Delta\pi$	(60 $\pm$ 28) %	531
$N\gamma$	0.0-0.02 %	712
$N\gamma$ , helicity=1/2	0.0-0.02 %	712

 $\Delta(1920) 3/2^+$ 

$$I(J^P) = \frac{3}{2}(\frac{3}{2}^+)$$

Breit-Wigner mass = 1900 to 1970 ( $\approx$  1920) MeV  
 Breit-Wigner full width = 180 to 300 ( $\approx$  260) MeV  
 $p_{\text{beam}} = 1.48 \text{ GeV}/c$   $4\pi\lambda^2 = 9.37 \text{ mb}$   
 Re(pole position) = 1850 to 1950 ( $\approx$  1900) MeV  
 $-2\text{Im}(\text{pole position}) = 200 \text{ to } 400$  ( $\approx$  300) MeV

$\Delta(1920)$ DECAY MODES	Fraction ( $\Gamma_i/\Gamma$ )	$\rho$ (MeV/c)
$N\pi$	5-20 %	723
$\Sigma K$	( 2.14 $\pm$ 0.30 ) %	431
$\Delta(1232)\eta$	(15 $\pm$ 8 ) %	336
$N\gamma$	0.0-0.4 %	731
$N\gamma$ , helicity=1/2	0.0-0.2 %	731
$N\gamma$ , helicity=3/2	0.0-0.2 %	731

 $\Delta(1930) 5/2^-$ 

$$I(J^P) = \frac{3}{2}(\frac{5}{2}^-)$$

Breit-Wigner mass = 1900 to 2000 ( $\approx$  1950) MeV  
 Breit-Wigner full width = 220 to 500 ( $\approx$  360) MeV  
 $p_{\text{beam}} = 1.54 \text{ GeV}/c$   $4\pi\lambda^2 = 8.91 \text{ mb}$   
 Re(pole position) = 1840 to 1960 ( $\approx$  1900) MeV  
 $-2\text{Im}(\text{pole position}) = 175 \text{ to } 360$  ( $\approx$  270) MeV

$\Delta(1930)$ DECAY MODES	Fraction ( $\Gamma_i/\Gamma$ )	$\rho$ (MeV/c)
$N\pi$	5-15 %	742
$N\gamma$	0.0-0.02 %	749
$N\gamma$ , helicity=1/2	0.0-0.01 %	749
$N\gamma$ , helicity=3/2	0.0-0.01 %	749

 $\Delta(1950) 7/2^+$ 

$$I(J^P) = \frac{3}{2}(\frac{7}{2}^+)$$

Breit-Wigner mass = 1915 to 1950 ( $\approx$  1930) MeV  
 Breit-Wigner full width = 235 to 335 ( $\approx$  285) MeV  
 $p_{\text{beam}} = 1.50 \text{ GeV}/c$   $4\pi\lambda^2 = 9.21 \text{ mb}$   
 Re(pole position) = 1870 to 1890 ( $\approx$  1880) MeV  
 $-2\text{Im}(\text{pole position}) = 220 \text{ to } 260$  ( $\approx$  240) MeV

$\Delta(1950)$ DECAY MODES	Fraction ( $\Gamma_i/\Gamma$ )	$\rho$ (MeV/c)
$N\pi$	35-45 %	729
$N\pi\pi$		706
$\Delta\pi$	20-30 %	560
$N\rho$	<10 %	442
$N\gamma$	0.08-0.13 %	737
$N\gamma$ , helicity=1/2	0.03-0.055 %	737
$N\gamma$ , helicity=3/2	0.05-0.075 %	737

 $\Delta(2420) 11/2^+$ 

$$I(J^P) = \frac{3}{2}(\frac{11}{2}^+)$$

Breit-Wigner mass = 2300 to 2500 ( $\approx$  2420) MeV  
 Breit-Wigner full width = 300 to 500 ( $\approx$  400) MeV  
 $p_{\text{beam}} = 2.64 \text{ GeV}/c$   $4\pi\lambda^2 = 4.68 \text{ mb}$   
 Re(pole position) = 2260 to 2400 ( $\approx$  2330) MeV  
 $-2\text{Im}(\text{pole position}) = 350 \text{ to } 750$  ( $\approx$  550) MeV

$\Delta(2420)$ DECAY MODES	Fraction ( $\Gamma_i/\Gamma$ )	$\rho$ (MeV/c)
$N\pi$	5-15 %	1023

## $\Lambda$ BARYONS

### ( $S = -1, I = 0$ )

$$\Lambda^0 = uds$$

 $\Lambda$ 

$$I(J^P) = 0(\frac{1}{2}^+)$$

Mass  $m = 1115.683 \pm 0.006 \text{ MeV}$   
 $(m_\Lambda - m_\pi) / m_\Lambda = (-0.1 \pm 1.1) \times 10^{-5}$  ( $S = 1.6$ )  
 Mean life  $\tau = (2.632 \pm 0.020) \times 10^{-10} \text{ s}$  ( $S = 1.6$ )  
 $(\tau_\Lambda - \tau_{\bar{\Lambda}}) / \tau_\Lambda = -0.001 \pm 0.009$   
 $c\tau = 7.89 \text{ cm}$   
 Magnetic moment  $\mu = -0.613 \pm 0.004 \mu_N$   
 Electric dipole moment  $d < 1.5 \times 10^{-16} \text{ e cm}$ , CL = 95%

## Decay parameters

$p\pi^-$   $\alpha_- = 0.642 \pm 0.013$   
 $\bar{p}\pi^+$   $\alpha_+ = -0.71 \pm 0.08$   
 $p\pi^-$   $\phi_- = (-6.5 \pm 3.5)^\circ$   
 "  $\gamma_- = 0.76 \text{ [k]}$   
 "  $\Delta_- = (8 \pm 4)^\circ \text{ [k]}$   
 $n\pi^0$   $\alpha_0 = 0.65 \pm 0.04$   
 $p e^- \bar{\nu}_e$   $g_A/g_V = -0.718 \pm 0.015 \text{ [g]}$

$\Lambda$ DECAY MODES	Fraction ( $\Gamma_i/\Gamma$ )	$\rho$ (MeV/c)
$p\pi^-$	(63.9 $\pm$ 0.5 ) %	101
$n\pi^0$	(35.8 $\pm$ 0.5 ) %	104
$n\gamma$	( 1.75 $\pm$ 0.15 ) $\times 10^{-3}$	162
$p\pi^- \gamma$	[ ] ( 8.4 $\pm$ 1.4 ) $\times 10^{-4}$	101
$p e^- \bar{\nu}_e$	( 8.32 $\pm$ 0.14 ) $\times 10^{-4}$	163
$p\mu^- \bar{\nu}_\mu$	( 1.57 $\pm$ 0.35 ) $\times 10^{-4}$	131

 $\Lambda(1405) 1/2^-$ 

$$I(J^P) = 0(\frac{1}{2}^-)$$

Mass  $m = 1405.1^{+1.3}_{-1.0} \text{ MeV}$   
 Full width  $\Gamma = 50 \pm 2 \text{ MeV}$   
 Below  $\bar{K}N$  threshold

$\Lambda(1405)$ DECAY MODES	Fraction ( $\Gamma_i/\Gamma$ )	$\rho$ (MeV/c)
$\Sigma\pi$	100 %	155

 $\Lambda(1520) 3/2^-$ 

$$I(J^P) = 0(\frac{3}{2}^-)$$

Mass  $m = 1519.5 \pm 1.0 \text{ MeV [m]}$   
 Full width  $\Gamma = 15.6 \pm 1.0 \text{ MeV [m]}$   
 $p_{\text{beam}} = 0.39 \text{ GeV}/c$   $4\pi\lambda^2 = 82.8 \text{ mb}$

$\Lambda(1520)$ DECAY MODES	Fraction ( $\Gamma_i/\Gamma$ )	$\rho$ (MeV/c)
$N\bar{K}$	45 $\pm$ 1%	243
$\Sigma\pi$	42 $\pm$ 1%	268
$\Lambda\pi\pi$	10 $\pm$ 1%	259
$\Sigma\pi\pi$	0.9 $\pm$ 0.1%	169
$\Lambda\gamma$	0.85 $\pm$ 0.15%	350

 $\Lambda(1600) 1/2^+$ 

$$I(J^P) = 0(\frac{1}{2}^+)$$

Mass  $m = 1560 \text{ to } 1700$  ( $\approx$  1600) MeV  
 Full width  $\Gamma = 50 \text{ to } 250$  ( $\approx$  150) MeV  
 $p_{\text{beam}} = 0.58 \text{ GeV}/c$   $4\pi\lambda^2 = 41.6 \text{ mb}$

$\Lambda(1600)$ DECAY MODES	Fraction ( $\Gamma_i/\Gamma$ )	$\rho$ (MeV/c)
$N\bar{K}$	15-30 %	343
$\Sigma\pi$	10-60 %	338

## Baryon Summary Table

 **$\Lambda(1670) 1/2^-$**   $I(J^P) = 0(\frac{1}{2}^-)$ 

Mass  $m = 1660$  to  $1680$  ( $\approx 1670$ ) MeV  
 Full width  $\Gamma = 25$  to  $50$  ( $\approx 35$ ) MeV  
 $p_{\text{beam}} = 0.74$  GeV/ $c$   $4\pi\lambda^2 = 28.5$  mb

$\Lambda(1670)$ DECAY MODES	Fraction ( $\Gamma_i/\Gamma$ )	$\rho$ (MeV/ $c$ )
$N\bar{K}$	20–30 %	414
$\Sigma\pi$	25–55 %	394
$\Lambda\eta$	10–25 %	69

 **$\Lambda(1690) 3/2^-$**   $I(J^P) = 0(\frac{3}{2}^-)$ 

Mass  $m = 1685$  to  $1695$  ( $\approx 1690$ ) MeV  
 Full width  $\Gamma = 50$  to  $70$  ( $\approx 60$ ) MeV  
 $p_{\text{beam}} = 0.78$  GeV/ $c$   $4\pi\lambda^2 = 26.1$  mb

$\Lambda(1690)$ DECAY MODES	Fraction ( $\Gamma_i/\Gamma$ )	$\rho$ (MeV/ $c$ )
$N\bar{K}$	20–30 %	433
$\Sigma\pi$	20–40 %	410
$\Lambda\pi\pi$	$\sim 25$ %	419
$\Sigma\pi\pi$	$\sim 20$ %	358

 **$\Lambda(1800) 1/2^-$**   $I(J^P) = 0(\frac{1}{2}^-)$ 

Mass  $m = 1720$  to  $1850$  ( $\approx 1800$ ) MeV  
 Full width  $\Gamma = 200$  to  $400$  ( $\approx 300$ ) MeV  
 $p_{\text{beam}} = 1.01$  GeV/ $c$   $4\pi\lambda^2 = 17.5$  mb

$\Lambda(1800)$ DECAY MODES	Fraction ( $\Gamma_i/\Gamma$ )	$\rho$ (MeV/ $c$ )
$N\bar{K}$	25–40 %	528
$\Sigma\pi$	seen	494
$\Sigma(1385)\pi$	seen	349
$N\bar{K}^*(892)$	seen	†

 **$\Lambda(1810) 1/2^+$**   $I(J^P) = 0(\frac{1}{2}^+)$ 

Mass  $m = 1750$  to  $1850$  ( $\approx 1810$ ) MeV  
 Full width  $\Gamma = 50$  to  $250$  ( $\approx 150$ ) MeV  
 $p_{\text{beam}} = 1.04$  GeV/ $c$   $4\pi\lambda^2 = 17.0$  mb

$\Lambda(1810)$ DECAY MODES	Fraction ( $\Gamma_i/\Gamma$ )	$\rho$ (MeV/ $c$ )
$N\bar{K}$	20–50 %	537
$\Sigma\pi$	10–40 %	501
$\Sigma(1385)\pi$	seen	357
$N\bar{K}^*(892)$	30–60 %	†

 **$\Lambda(1820) 5/2^+$**   $I(J^P) = 0(\frac{5}{2}^+)$ 

Mass  $m = 1815$  to  $1825$  ( $\approx 1820$ ) MeV  
 Full width  $\Gamma = 70$  to  $90$  ( $\approx 80$ ) MeV  
 $p_{\text{beam}} = 1.06$  GeV/ $c$   $4\pi\lambda^2 = 16.5$  mb

$\Lambda(1820)$ DECAY MODES	Fraction ( $\Gamma_i/\Gamma$ )	$\rho$ (MeV/ $c$ )
$N\bar{K}$	55–65 %	545
$\Sigma\pi$	8–14 %	509
$\Sigma(1385)\pi$	5–10 %	366

 **$\Lambda(1830) 5/2^-$**   $I(J^P) = 0(\frac{5}{2}^-)$ 

Mass  $m = 1810$  to  $1830$  ( $\approx 1830$ ) MeV  
 Full width  $\Gamma = 60$  to  $110$  ( $\approx 95$ ) MeV  
 $p_{\text{beam}} = 1.08$  GeV/ $c$   $4\pi\lambda^2 = 16.0$  mb

$\Lambda(1830)$ DECAY MODES	Fraction ( $\Gamma_i/\Gamma$ )	$\rho$ (MeV/ $c$ )
$N\bar{K}$	3–10 %	553
$\Sigma\pi$	35–75 %	516
$\Sigma(1385)\pi$	>15 %	374

 **$\Lambda(1890) 3/2^+$**   $I(J^P) = 0(\frac{3}{2}^+)$ 

Mass  $m = 1850$  to  $1910$  ( $\approx 1890$ ) MeV  
 Full width  $\Gamma = 60$  to  $200$  ( $\approx 100$ ) MeV  
 $p_{\text{beam}} = 1.21$  GeV/ $c$   $4\pi\lambda^2 = 13.6$  mb

$\Lambda(1890)$ DECAY MODES	Fraction ( $\Gamma_i/\Gamma$ )	$\rho$ (MeV/ $c$ )
$N\bar{K}$	20–35 %	599
$\Sigma\pi$	3–10 %	560
$\Sigma(1385)\pi$	seen	423
$N\bar{K}^*(892)$	seen	236

 **$\Lambda(2100) 7/2^-$**   $I(J^P) = 0(\frac{7}{2}^-)$ 

Mass  $m = 2090$  to  $2110$  ( $\approx 2100$ ) MeV  
 Full width  $\Gamma = 100$  to  $250$  ( $\approx 200$ ) MeV  
 $p_{\text{beam}} = 1.68$  GeV/ $c$   $4\pi\lambda^2 = 8.68$  mb

$\Lambda(2100)$ DECAY MODES	Fraction ( $\Gamma_i/\Gamma$ )	$\rho$ (MeV/ $c$ )
$N\bar{K}$	25–35 %	751
$\Sigma\pi$	$\sim 5$ %	705
$\Lambda\eta$	<3 %	617
$\Xi K$	<3 %	491
$\Lambda\omega$	<8 %	443
$N\bar{K}^*(892)$	10–20 %	515

 **$\Lambda(2110) 5/2^+$**   $I(J^P) = 0(\frac{5}{2}^+)$ 

Mass  $m = 2090$  to  $2140$  ( $\approx 2110$ ) MeV  
 Full width  $\Gamma = 150$  to  $250$  ( $\approx 200$ ) MeV  
 $p_{\text{beam}} = 1.70$  GeV/ $c$   $4\pi\lambda^2 = 8.53$  mb

$\Lambda(2110)$ DECAY MODES	Fraction ( $\Gamma_i/\Gamma$ )	$\rho$ (MeV/ $c$ )
$N\bar{K}$	5–25 %	757
$\Sigma\pi$	10–40 %	711
$\Lambda\omega$	seen	455
$\Sigma(1385)\pi$	seen	591
$N\bar{K}^*(892)$	10–60 %	525

 **$\Lambda(2350) 9/2^+$**   $I(J^P) = 0(\frac{9}{2}^+)$ 

Mass  $m = 2340$  to  $2370$  ( $\approx 2350$ ) MeV  
 Full width  $\Gamma = 100$  to  $250$  ( $\approx 150$ ) MeV  
 $p_{\text{beam}} = 2.29$  GeV/ $c$   $4\pi\lambda^2 = 5.85$  mb

$\Lambda(2350)$ DECAY MODES	Fraction ( $\Gamma_i/\Gamma$ )	$\rho$ (MeV/ $c$ )
$N\bar{K}$	$\sim 12$ %	915
$\Sigma\pi$	$\sim 10$ %	867

## Σ BARYONS

### ( $S = -1, I = 1$ )

$$\Sigma^+ = uus, \quad \Sigma^0 = uds, \quad \Sigma^- = dds$$

 **$\Sigma^+$**   $I(J^P) = 1(\frac{1}{2}^+)$ 

Mass  $m = 1189.37 \pm 0.07$  MeV ( $S = 2.2$ )  
 Mean life  $\tau = (0.8018 \pm 0.0026) \times 10^{-10}$  s  
 $c\tau = 2.404$  cm  
 $(\tau_{\Sigma^+} - \tau_{\Sigma^-}) / \tau_{\Sigma^+} = (-0.6 \pm 1.2) \times 10^{-3}$   
 Magnetic moment  $\mu = 2.458 \pm 0.010 \mu_N$  ( $S = 2.1$ )  
 $(\mu_{\Sigma^+} + \mu_{\Sigma^-}) / \mu_{\Sigma^+} = 0.014 \pm 0.015$   
 $\Gamma(\Sigma^+ \rightarrow n\ell^+\nu) / \Gamma(\Sigma^- \rightarrow n\ell^-\bar{\nu}) < 0.043$

## Baryon Summary Table

## Decay parameters

$p\pi^0$	$\alpha_0 = -0.980^{+0.017}_{-0.015}$
"	$\phi_0 = (36 \pm 34)^\circ$
"	$\gamma_0 = 0.16 [k]$
"	$\Delta_0 = (187 \pm 6)^\circ [k]$
$n\pi^+$	$\alpha_+ = 0.068 \pm 0.013$
"	$\phi_+ = (167 \pm 20)^\circ (S = 1.1)$
"	$\gamma_+ = -0.97 [k]$
"	$\Delta_+ = (-73^{+133}_{-10})^\circ [k]$
$p\gamma$	$\alpha_\gamma = -0.76 \pm 0.08$

$\Sigma^+$ DECAY MODES	Fraction ( $\Gamma_i/\Gamma$ )	Confidence level	$\rho$ (MeV/c)
$p\pi^0$	$(51.57 \pm 0.30) \%$		189
$n\pi^+$	$(48.31 \pm 0.30) \%$		185
$p\gamma$	$(1.23 \pm 0.05) \times 10^{-3}$		225
$n\pi^+\gamma$	[ $\eta$ ] $(4.5 \pm 0.5) \times 10^{-4}$		185
$\Lambda e^+ \nu_e$	$(2.0 \pm 0.5) \times 10^{-5}$		71

 $\Delta S = \Delta Q$  (SQ) violating modes or  $\Delta S = 1$  weak neutral current (SI) modes

$n e^+ \nu_e$	SQ	$< 5 \times 10^{-6}$	90%	224
$n \mu^+ \nu_\mu$	SQ	$< 3.0 \times 10^{-5}$	90%	202
$p e^+ e^-$	SI	$< 7 \times 10^{-6}$		225
$p \mu^+ \mu^-$	SI	$(9^{+9}_{-8}) \times 10^{-8}$		121

$$\boxed{\Sigma^0} \quad I(J^P) = 1(\frac{1}{2}^+)$$

Mass  $m = 1192.642 \pm 0.024$  MeV  
 $m_{\Sigma^-} - m_{\Sigma^0} = 4.807 \pm 0.035$  MeV ( $S = 1.1$ )  
 $m_{\Sigma^0} - m_\Lambda = 76.959 \pm 0.023$  MeV  
Mean life  $\tau = (7.4 \pm 0.7) \times 10^{-20}$  s  
 $c\tau = 2.22 \times 10^{-11}$  m  
Transition magnetic moment  $|\mu_{\Sigma\Lambda}| = 1.61 \pm 0.08 \mu_N$

$\Sigma^0$ DECAY MODES	Fraction ( $\Gamma_i/\Gamma$ )	Confidence level	$\rho$ (MeV/c)
$\Lambda\gamma$	100 %		74
$\Lambda\gamma\gamma$	$< 3 \%$	90%	74
$\Lambda e^+ e^-$	[ $\eta$ ] $5 \times 10^{-3}$		74

$$\boxed{\Sigma^-} \quad I(J^P) = 1(\frac{1}{2}^+)$$

Mass  $m = 1197.449 \pm 0.030$  MeV ( $S = 1.2$ )  
 $m_{\Sigma^-} - m_{\Sigma^+} = 8.08 \pm 0.08$  MeV ( $S = 1.9$ )  
 $m_{\Sigma^-} - m_\Lambda = 81.766 \pm 0.030$  MeV ( $S = 1.2$ )  
Mean life  $\tau = (1.479 \pm 0.011) \times 10^{-10}$  s ( $S = 1.3$ )  
 $c\tau = 4.434$  cm  
Magnetic moment  $\mu = -1.160 \pm 0.025 \mu_N$  ( $S = 1.7$ )  
 $\Sigma^-$  charge radius =  $0.78 \pm 0.10$  fm

## Decay parameters

$n\pi^-$	$\alpha_- = -0.068 \pm 0.008$
"	$\phi_- = (10 \pm 15)^\circ$
"	$\gamma_- = 0.98 [k]$
"	$\Delta_- = (249^{+12}_{-120})^\circ [k]$
$n e^- \bar{\nu}_e$	$g_A/g_V = 0.340 \pm 0.017 [g]$
"	$f_2(0)/f_1(0) = 0.97 \pm 0.14$
"	$D = 0.11 \pm 0.10$
$\Lambda e^- \bar{\nu}_e$	$g_V/g_A = 0.01 \pm 0.10 [g]$ ( $S = 1.5$ )
"	$g_{WM}/g_A = 2.4 \pm 1.7 [g]$

 $\Sigma^-$  DECAY MODES

Fraction ( $\Gamma_i/\Gamma$ )	$\rho$ (MeV/c)
$n\pi^-$	$(99.848 \pm 0.005) \%$
$n\pi^-\gamma$	[ $\eta$ ] $(4.6 \pm 0.6) \times 10^{-4}$
$n e^- \bar{\nu}_e$	$(1.017 \pm 0.034) \times 10^{-3}$
$n \mu^- \bar{\nu}_\mu$	$(4.5 \pm 0.4) \times 10^{-4}$
$\Lambda e^- \bar{\nu}_e$	$(5.73 \pm 0.27) \times 10^{-5}$

$$\boxed{\Sigma(1385) 3/2^+} \quad I(J^P) = 1(\frac{3}{2}^+)$$

$\Sigma(1385)^+$  mass  $m = 1382.80 \pm 0.35$  MeV ( $S = 1.9$ )  
 $\Sigma(1385)^0$  mass  $m = 1383.7 \pm 1.0$  MeV ( $S = 1.4$ )  
 $\Sigma(1385)^-$  mass  $m = 1387.2 \pm 0.5$  MeV ( $S = 2.2$ )  
 $\Sigma(1385)^+$  full width  $\Gamma = 36.0 \pm 0.7$  MeV  
 $\Sigma(1385)^0$  full width  $\Gamma = 36 \pm 5$  MeV  
 $\Sigma(1385)^-$  full width  $\Gamma = 39.4 \pm 2.1$  MeV ( $S = 1.7$ )  
Below  $\bar{K}N$  threshold

$\Sigma(1385)$ DECAY MODES	Fraction ( $\Gamma_i/\Gamma$ )	Confidence level	$\rho$ (MeV/c)
$\Lambda\pi$	$(87.0 \pm 1.5) \%$		208
$\Sigma\pi$	$(11.7 \pm 1.5) \%$		129
$\Lambda\gamma$	$(1.25^{+0.13}_{-0.12}) \%$		241
$\Sigma^-\gamma$	$< 2.4 \times 10^{-4}$	90%	173

$$\boxed{\Sigma(1660) 1/2^+} \quad I(J^P) = 1(\frac{1}{2}^+)$$

Mass  $m = 1630$  to  $1690$  ( $\approx 1660$ ) MeV  
Full width  $\Gamma = 40$  to  $200$  ( $\approx 100$ ) MeV  
 $\rho_{\text{beam}} = 0.72$  GeV/c  $4\pi\lambda^2 = 29.9$  mb

$\Sigma(1660)$ DECAY MODES	Fraction ( $\Gamma_i/\Gamma$ )	$\rho$ (MeV/c)
$N\bar{K}$	10–30 %	405
$\Lambda\pi$	seen	440
$\Sigma\pi$	seen	387

$$\boxed{\Sigma(1670) 3/2^-} \quad I(J^P) = 1(\frac{3}{2}^-)$$

Mass  $m = 1665$  to  $1685$  ( $\approx 1670$ ) MeV  
Full width  $\Gamma = 40$  to  $80$  ( $\approx 60$ ) MeV  
 $\rho_{\text{beam}} = 0.74$  GeV/c  $4\pi\lambda^2 = 28.5$  mb

$\Sigma(1670)$ DECAY MODES	Fraction ( $\Gamma_i/\Gamma$ )	$\rho$ (MeV/c)
$N\bar{K}$	7–13 %	414
$\Lambda\pi$	5–15 %	448
$\Sigma\pi$	30–60 %	394

$$\boxed{\Sigma(1750) 1/2^-} \quad I(J^P) = 1(\frac{1}{2}^-)$$

Mass  $m = 1730$  to  $1800$  ( $\approx 1750$ ) MeV  
Full width  $\Gamma = 60$  to  $160$  ( $\approx 90$ ) MeV  
 $\rho_{\text{beam}} = 0.91$  GeV/c  $4\pi\lambda^2 = 20.7$  mb

$\Sigma(1750)$ DECAY MODES	Fraction ( $\Gamma_i/\Gamma$ )	$\rho$ (MeV/c)
$N\bar{K}$	10–40 %	486
$\Lambda\pi$	seen	507
$\Sigma\pi$	$< 8 \%$	456
$\Sigma\eta$	15–55 %	98

$$\boxed{\Sigma(1775) 5/2^-} \quad I(J^P) = 1(\frac{5}{2}^-)$$

Mass  $m = 1770$  to  $1780$  ( $\approx 1775$ ) MeV  
Full width  $\Gamma = 105$  to  $135$  ( $\approx 120$ ) MeV  
 $\rho_{\text{beam}} = 0.96$  GeV/c  $4\pi\lambda^2 = 19.0$  mb

## Baryon Summary Table

$\Sigma(1775)$ DECAY MODES	Fraction ( $\Gamma_i/\Gamma$ )	$\rho$ (MeV/c)
$N\bar{K}$	37–43%	508
$\Lambda\pi$	14–20%	525
$\Sigma\pi$	2–5%	475
$\Sigma(1385)\pi$	8–12%	327
$\Lambda(1520)\pi$	17–23%	201

 **$\Sigma(1915) 5/2^+$** 

$$I(J^P) = 1(\frac{5}{2}^+)$$

Mass  $m = 1900$  to  $1935$  ( $\approx 1915$ ) MeV  
 Full width  $\Gamma = 80$  to  $160$  ( $\approx 120$ ) MeV  
 $\rho_{\text{beam}} = 1.26$  GeV/c  $4\pi\lambda^2 = 12.8$  mb

$\Sigma(1915)$ DECAY MODES	Fraction ( $\Gamma_i/\Gamma$ )	$\rho$ (MeV/c)
$N\bar{K}$	5–15 %	618
$\Lambda\pi$	seen	623
$\Sigma\pi$	seen	577
$\Sigma(1385)\pi$	<5 %	443

 **$\Sigma(1940) 3/2^-$** 

$$I(J^P) = 1(\frac{3}{2}^-)$$

Mass  $m = 1900$  to  $1950$  ( $\approx 1940$ ) MeV  
 Full width  $\Gamma = 150$  to  $300$  ( $\approx 220$ ) MeV  
 $\rho_{\text{beam}} = 1.32$  GeV/c  $4\pi\lambda^2 = 12.1$  mb

$\Sigma(1940)$ DECAY MODES	Fraction ( $\Gamma_i/\Gamma$ )	$\rho$ (MeV/c)
$N\bar{K}$	<20 %	637
$\Lambda\pi$	seen	640
$\Sigma\pi$	seen	595
$\Sigma(1385)\pi$	seen	463
$\Lambda(1520)\pi$	seen	355
$\Delta(1232)\bar{K}$	seen	410
$N\bar{K}^*(892)$	seen	322

 **$\Sigma(2030) 7/2^+$** 

$$I(J^P) = 1(\frac{7}{2}^+)$$

Mass  $m = 2025$  to  $2040$  ( $\approx 2030$ ) MeV  
 Full width  $\Gamma = 150$  to  $200$  ( $\approx 180$ ) MeV  
 $\rho_{\text{beam}} = 1.52$  GeV/c  $4\pi\lambda^2 = 9.93$  mb

$\Sigma(2030)$ DECAY MODES	Fraction ( $\Gamma_i/\Gamma$ )	$\rho$ (MeV/c)
$N\bar{K}$	17–23 %	702
$\Lambda\pi$	17–23 %	700
$\Sigma\pi$	5–10 %	657
$\Xi K$	<2 %	422
$\Sigma(1385)\pi$	5–15 %	532
$\Lambda(1520)\pi$	10–20 %	430
$\Delta(1232)\bar{K}$	10–20 %	498
$N\bar{K}^*(892)$	<5 %	439

 **$\Sigma(2250)$** 

$$I(J^P) = 1(?^?)$$

Mass  $m = 2210$  to  $2280$  ( $\approx 2250$ ) MeV  
 Full width  $\Gamma = 60$  to  $150$  ( $\approx 100$ ) MeV  
 $\rho_{\text{beam}} = 2.04$  GeV/c  $4\pi\lambda^2 = 6.76$  mb

$\Sigma(2250)$ DECAY MODES	Fraction ( $\Gamma_i/\Gamma$ )	$\rho$ (MeV/c)
$N\bar{K}$	<10 %	851
$\Lambda\pi$	seen	842
$\Sigma\pi$	seen	803

 **$\Xi$  BARYONS**  
**( $S = -2, I = 1/2$ )**

$$\Xi^0 = uss, \Xi^- = dss$$

 **$\Xi^0$** 

$$I(J^P) = \frac{1}{2}(\frac{1}{2}^+)$$

$P$  is not yet measured; + is the quark model prediction.

Mass  $m = 1314.86 \pm 0.20$  MeV  
 $m_{\Xi^-} - m_{\Xi^0} = 6.85 \pm 0.21$  MeV  
 Mean life  $\tau = (2.90 \pm 0.09) \times 10^{-10}$  s  
 $c\tau = 8.71$  cm

Magnetic moment  $\mu = -1.250 \pm 0.014 \mu_N$

**Decay parameters**

$\Lambda\pi^0$	$\alpha = -0.406 \pm 0.013$
"	$\phi = (21 \pm 12)^\circ$
"	$\gamma = 0.85$ [k]
"	$\Delta = (218^{+12}_{-19})^\circ$ [k]
$\Lambda\gamma$	$\alpha = -0.70 \pm 0.07$
$\Lambda e^+ e^-$	$\alpha = -0.8 \pm 0.2$
$\Sigma^0 \gamma$	$\alpha = -0.69 \pm 0.06$
$\Sigma^+ e^- \bar{\nu}_e$	$g_1(0)/f_1(0) = 1.21 \pm 0.05$
$\Sigma^+ e^- \bar{\nu}_e$	$f_2(0)/f_1(0) = 2.0 \pm 1.3$

 **$\Xi^0$  DECAY MODES**

DECAY MODES	Fraction ( $\Gamma_i/\Gamma$ )	Confidence level	$\rho$ (MeV/c)
$\Lambda\pi^0$	$(99.525 \pm 0.012) \%$		135
$\Lambda\gamma$	$(1.17 \pm 0.07) \times 10^{-3}$		184
$\Lambda e^+ e^-$	$(7.6 \pm 0.6) \times 10^{-6}$		184
$\Sigma^0 \gamma$	$(3.33 \pm 0.10) \times 10^{-3}$		117
$\Sigma^+ e^- \bar{\nu}_e$	$(2.53 \pm 0.08) \times 10^{-4}$		120
$\Sigma^+ \mu^- \bar{\nu}_\mu$	$(4.6^{+1.8}_{-1.4}) \times 10^{-6}$		64

 **$\Delta S = \Delta Q$  (SQ) violating modes or  
 $\Delta S = 2$  forbidden (S2) modes**

$\Sigma^- e^+ \nu_e$	SQ < 9	$\times 10^{-4}$	90%	112
$\Sigma^- \mu^+ \nu_\mu$	SQ < 9	$\times 10^{-4}$	90%	49
$\rho\pi^-$	S2 < 8	$\times 10^{-6}$	90%	299
$\rho e^- \bar{\nu}_e$	S2 < 1.3	$\times 10^{-3}$		323
$\rho\mu^- \bar{\nu}_\mu$	S2 < 1.3	$\times 10^{-3}$		309

 **$\Xi^-$** 

$$I(J^P) = \frac{1}{2}(\frac{1}{2}^+)$$

$P$  is not yet measured; + is the quark model prediction.

Mass  $m = 1321.71 \pm 0.07$  MeV  
 $(m_{\Xi^-} - m_{\Xi^+}) / m_{\Xi^-} = (-3 \pm 9) \times 10^{-5}$   
 Mean life  $\tau = (1.639 \pm 0.015) \times 10^{-10}$  s  
 $c\tau = 4.91$  cm

$(\tau_{\Xi^-} - \tau_{\Xi^+}) / \tau_{\Xi^-} = -0.01 \pm 0.07$   
 Magnetic moment  $\mu = -0.6507 \pm 0.0025 \mu_N$   
 $(\mu_{\Xi^-} + \mu_{\Xi^+}) / |\mu_{\Xi^-}| = +0.01 \pm 0.05$

**Decay parameters**

$\Lambda\pi^-$	$\alpha = -0.458 \pm 0.012$ ( $S = 1.8$ )
$[\alpha(\Xi^-)\alpha_-(\Lambda) - \alpha(\Xi^+)\alpha_+(\bar{\Lambda})] / [\text{sum}] = (0 \pm 7) \times 10^{-4}$	
"	$\phi = (-2.1 \pm 0.8)^\circ$
"	$\gamma = 0.89$ [k]
"	$\Delta = (175.9 \pm 1.5)^\circ$ [k]
$\Lambda e^- \bar{\nu}_e$	$g_A/g_V = -0.25 \pm 0.05$ [g]

## Baryon Summary Table

$\Xi^-$ DECAY MODES	Fraction ( $\Gamma_i/\Gamma$ )	Confidence level	$\rho$ (MeV/c)
$\Lambda\pi^-$	(99.887 ± 0.035) %		140
$\Sigma^- \gamma$	(1.27 ± 0.23) × 10 <sup>-4</sup>		118
$\Lambda e^- \bar{\nu}_e$	(5.63 ± 0.31) × 10 <sup>-4</sup>		190
$\Lambda \mu^- \bar{\nu}_\mu$	(3.5 <sup>+3.5</sup> / <sub>-2.2</sub> ) × 10 <sup>-4</sup>		163
$\Sigma^0 e^- \bar{\nu}_e$	(8.7 ± 1.7) × 10 <sup>-5</sup>		123
$\Sigma^0 \mu^- \bar{\nu}_\mu$	< 8 × 10 <sup>-4</sup>	90%	70
$\Xi^0 e^- \bar{\nu}_e$	< 2.3 × 10 <sup>-3</sup>	90%	7
<b><math>\Delta S = 2</math> forbidden (<math>S_2</math>) modes</b>			
$n\pi^-$	$S_2$ < 1.9 × 10 <sup>-5</sup>	90%	304
$n e^- \bar{\nu}_e$	$S_2$ < 3.2 × 10 <sup>-3</sup>	90%	327
$n \mu^- \bar{\nu}_\mu$	$S_2$ < 1.5 %	90%	314
$p\pi^- \pi^-$	$S_2$ < 4 × 10 <sup>-4</sup>	90%	223
$p\pi^- e^- \bar{\nu}_e$	$S_2$ < 4 × 10 <sup>-4</sup>	90%	305
$p\pi^- \mu^- \bar{\nu}_\mu$	$S_2$ < 4 × 10 <sup>-4</sup>	90%	251
$p\mu^- \mu^-$	$L$ < 4 × 10 <sup>-8</sup>	90%	272

 **$\Xi(1530) 3/2^+$** 

$$I(J^P) = \frac{1}{2}(\frac{3}{2}^+)$$

$\Xi(1530)^0$  mass  $m = 1531.80 \pm 0.32$  MeV ( $S = 1.3$ )  
 $\Xi(1530)^-$  mass  $m = 1535.0 \pm 0.6$  MeV  
 $\Xi(1530)^0$  full width  $\Gamma = 9.1 \pm 0.5$  MeV  
 $\Xi(1530)^-$  full width  $\Gamma = 9.9^{+1.7}_{-1.9}$  MeV

$\Xi(1530)$ DECAY MODES	Fraction ( $\Gamma_i/\Gamma$ )	Confidence level	$\rho$ (MeV/c)
$\Xi\pi$	100 %		158
$\Xi\gamma$	< 4 %	90%	202

 **$\Xi(1690)$** 

$$I(J^P) = \frac{1}{2}(?^?)$$

Mass  $m = 1690 \pm 10$  MeV [ $m$ ]  
 Full width  $\Gamma < 30$  MeV

$\Xi(1690)$ DECAY MODES	Fraction ( $\Gamma_i/\Gamma$ )	$\rho$ (MeV/c)
$\Lambda\bar{K}$	seen	240
$\Sigma\bar{K}$	seen	70
$\Xi\pi$	seen	311
$\Xi^- \pi^+ \pi^-$	possibly seen	213

 **$\Xi(1820) 3/2^-$** 

$$I(J^P) = \frac{1}{2}(\frac{3}{2}^-)$$

Mass  $m = 1823 \pm 5$  MeV [ $m$ ]  
 Full width  $\Gamma = 24^{+15}_{-10}$  MeV [ $m$ ]

$\Xi(1820)$ DECAY MODES	Fraction ( $\Gamma_i/\Gamma$ )	$\rho$ (MeV/c)
$\Lambda\bar{K}$	large	402
$\Sigma\bar{K}$	small	324
$\Xi\pi$	small	421
$\Xi(1530)\pi$	small	237

 **$\Xi(1950)$** 

$$I(J^P) = \frac{1}{2}(?^?)$$

Mass  $m = 1950 \pm 15$  MeV [ $m$ ]  
 Full width  $\Gamma = 60 \pm 20$  MeV [ $m$ ]

$\Xi(1950)$ DECAY MODES	Fraction ( $\Gamma_i/\Gamma$ )	$\rho$ (MeV/c)
$\Lambda\bar{K}$	seen	522
$\Sigma\bar{K}$	possibly seen	460
$\Xi\pi$	seen	519

 **$\Xi(2030)$** 

$$I(J^P) = \frac{1}{2}(\geq \frac{5}{2}^?)$$

Mass  $m = 2025 \pm 5$  MeV [ $m$ ]  
 Full width  $\Gamma = 20^{+15}_{-5}$  MeV [ $m$ ]

$\Xi(2030)$ DECAY MODES	Fraction ( $\Gamma_i/\Gamma$ )	$\rho$ (MeV/c)
$\Lambda\bar{K}$	~ 20 %	585
$\Sigma\bar{K}$	~ 80 %	529
$\Xi\pi$	small	574
$\Xi(1530)\pi$	small	416
$\Lambda\bar{K}\pi$	small	499
$\Sigma\bar{K}\pi$	small	428

 **$\Omega$  BARYONS**  
**( $S = -3, I = 0$ )**

$$\Omega^- = sss$$

 **$\Omega^-$** 

$$I(J^P) = 0(\frac{3}{2}^+)$$

$J^P = \frac{3}{2}^+$  is the quark-model prediction; and  $J = 3/2$  is fairly well established.

Mass  $m = 1672.45 \pm 0.29$  MeV  
 $(m_{\Omega^-} - m_{\bar{\Omega}^+}) / m_{\Omega^-} = (-1 \pm 8) \times 10^{-5}$   
 Mean life  $\tau = (0.821 \pm 0.011) \times 10^{-10}$  s  
 $c\tau = 2.461$  cm  
 $(\tau_{\Omega^-} - \tau_{\bar{\Omega}^+}) / \tau_{\Omega^-} = 0.00 \pm 0.05$   
 Magnetic moment  $\mu = -2.02 \pm 0.05 \mu_N$

**Decay parameters**

$\Lambda K^-$   $\alpha = 0.0180 \pm 0.0024$   
 $\Lambda K^-, \bar{\Lambda} K^+$   $(\alpha + \bar{\alpha}) / (\alpha - \bar{\alpha}) = -0.02 \pm 0.13$   
 $\Xi^0 \pi^-$   $\alpha = 0.09 \pm 0.14$   
 $\Xi^- \pi^0$   $\alpha = 0.05 \pm 0.21$

$\Omega^-$ DECAY MODES	Fraction ( $\Gamma_i/\Gamma$ )	Confidence level	$\rho$ (MeV/c)
$\Lambda K^-$	(67.8 ± 0.7) %		211
$\Xi^0 \pi^-$	(23.6 ± 0.7) %		294
$\Xi^- \pi^0$	(8.6 ± 0.4) %		289
$\Xi^- \pi^+ \pi^-$	(3.7 <sup>+0.7</sup> / <sub>-0.6</sub> ) × 10 <sup>-4</sup>		189
$\Xi(1530)^0 \pi^-$	< 7 × 10 <sup>-5</sup>	90%	17
$\Xi^0 e^- \bar{\nu}_e$	(5.6 ± 2.8) × 10 <sup>-3</sup>		319
$\Xi^- \gamma$	< 4.6 × 10 <sup>-4</sup>	90%	314
<b><math>\Delta S = 2</math> forbidden (<math>S_2</math>) modes</b>			
$\Lambda\pi^-$	$S_2$ < 2.9 × 10 <sup>-6</sup>	90%	449

 **$\Omega(2250)^-$** 

$$I(J^P) = 0(?^?)$$

Mass  $m = 2252 \pm 9$  MeV  
 Full width  $\Gamma = 55 \pm 18$  MeV

$\Omega(2250)^-$ DECAY MODES	Fraction ( $\Gamma_i/\Gamma$ )	$\rho$ (MeV/c)
$\Xi^- \pi^+ K^-$	seen	532
$\Xi(1530)^0 K^-$	seen	437

**CHARMED BARYONS**  
**( $C = +1$ )**

$$\Lambda_c^+ = udc, \quad \Sigma_c^{++} = uuc, \quad \Sigma_c^+ = udc, \quad \Sigma_c^0 = ddc,$$

$$\Xi_c^+ = usc, \quad \Xi_c^0 = dsc, \quad \Omega_c^0 = ssc$$

 **$\Lambda_c^+$** 

$$I(J^P) = 0(\frac{1}{2}^+)$$

$J$  is not well measured;  $\frac{1}{2}$  is the quark-model prediction.

Mass  $m = 2286.46 \pm 0.14$  MeV  
 Mean life  $\tau = (200 \pm 6) \times 10^{-15}$  s ( $S = 1.6$ )  
 $c\tau = 59.9 \mu\text{m}$

## Baryon Summary Table

## Decay asymmetry parameters

$$\begin{aligned} \Lambda\pi^+ & \alpha = -0.91 \pm 0.15 \\ \Sigma^+\pi^0 & \alpha = -0.45 \pm 0.32 \\ \Lambda\ell^+\nu_\ell & \alpha = -0.86 \pm 0.04 \\ (\alpha + \bar{\alpha})/(\alpha - \bar{\alpha}) \text{ in } \Lambda_C^+ \rightarrow \Lambda\pi^+, \bar{\Lambda}_C^- \rightarrow \bar{\Lambda}\pi^- & = -0.07 \pm 0.31 \\ (\alpha + \bar{\alpha})/(\alpha - \bar{\alpha}) \text{ in } \Lambda_C^+ \rightarrow \Lambda e^+\nu_e, \bar{\Lambda}_C^- \rightarrow \bar{\Lambda}e^-\bar{\nu}_e & = 0.00 \pm 0.04 \end{aligned}$$

Nearly all branching fractions of the  $\Lambda_C^+$  are measured relative to the  $pK^-\pi^+$  mode, but there are no model-independent measurements of this branching fraction. We explain how we arrive at our value of  $B(\Lambda_C^+ \rightarrow pK^-\pi^+)$  in a Note at the beginning of the branching-ratio measurements in the Listings. When this branching fraction is eventually well determined, all the other branching fractions will slide up or down proportionally as the true value differs from the value we use here.

$\Lambda_C^+$ DECAY MODES	Fraction ( $\Gamma_i/\Gamma$ )	Scale factor/ Confidence level	$\rho$ (MeV/c)
<b>Hadronic modes with a <math>p</math>: <math>S = -1</math> final states</b>			
$p\bar{K}^0$	( 2.3 $\pm$ 0.6 ) %		873
$pK^-\pi^+$	[ $\rho$ ] ( 5.0 $\pm$ 1.3 ) %		823
$p\bar{K}^*(892)^0$	[ $\rho$ ] ( 1.6 $\pm$ 0.5 ) %		685
$\Delta(1232)^{++}K^-$	( 8.6 $\pm$ 3.0 ) $\times 10^{-3}$		710
$\Lambda(1520)\pi^+$	[ $\rho$ ] ( 1.8 $\pm$ 0.6 ) %		627
$pK^-\pi^+$ nonresonant	( 2.8 $\pm$ 0.8 ) %		823
$p\bar{K}^0\pi^0$	( 3.3 $\pm$ 1.0 ) %		823
$p\bar{K}^0\eta$	( 1.2 $\pm$ 0.4 ) %		568
$p\bar{K}^0\pi^+\pi^-$	( 2.6 $\pm$ 0.7 ) %		754
$pK^-\pi^+\pi^0$	( 3.4 $\pm$ 1.0 ) %		759
$pK^*(892)^-\pi^+$	[ $\rho$ ] ( 1.1 $\pm$ 0.5 ) %		580
$p(K^-\pi^+)_{\text{nonresonant}}\pi^0$	( 3.6 $\pm$ 1.2 ) %		759
$\Delta(1232)\bar{K}^*(892)$	seen		419
$pK^-\pi^+\pi^+\pi^-$	( 1.1 $\pm$ 0.8 ) $\times 10^{-3}$		671
$pK^-\pi^+\pi^0\pi^0$	( 8 $\pm$ 4 ) $\times 10^{-3}$		678
<b>Hadronic modes with a <math>p</math>: <math>S = 0</math> final states</b>			
$p\pi^+\pi^-$	( 3.5 $\pm$ 2.0 ) $\times 10^{-3}$		927
$p f_0(980)$	[ $\rho$ ] ( 2.8 $\pm$ 1.9 ) $\times 10^{-3}$		614
$p\pi^+\pi^+\pi^-\pi^-$	( 1.8 $\pm$ 1.2 ) $\times 10^{-3}$		852
$pK^+K^-$	( 7.7 $\pm$ 3.5 ) $\times 10^{-4}$		616
$p\phi$	[ $\rho$ ] ( 8.2 $\pm$ 2.7 ) $\times 10^{-4}$		590
$pK^+K^-$ non- $\phi$	( 3.5 $\pm$ 1.7 ) $\times 10^{-4}$		616
<b>Hadronic modes with a hyperon: <math>S = -1</math> final states</b>			
$\Lambda\pi^+$	( 1.07 $\pm$ 0.28 ) %		864
$\Lambda\pi^+\pi^0$	( 3.6 $\pm$ 1.3 ) %		844
$\Lambda\rho^+$	< 5 %	CL=95%	635
$\Lambda\pi^+\pi^+\pi^-$	( 2.6 $\pm$ 0.7 ) %		807
$\Sigma(1385)^+\pi^+\pi^-, \Sigma^{*+} \rightarrow$	( 7 $\pm$ 4 ) $\times 10^{-3}$		688
$\Lambda\pi^+$			
$\Sigma(1385)^-\pi^+\pi^+, \Sigma^{*-} \rightarrow$	( 5.5 $\pm$ 1.7 ) $\times 10^{-3}$		688
$\Lambda\pi^0$			
$\Lambda\pi^+\rho^0$	( 1.1 $\pm$ 0.5 ) %		523
$\Sigma(1385)^+\rho^0, \Sigma^{*+} \rightarrow \Lambda\pi^+$	( 3.7 $\pm$ 3.1 ) $\times 10^{-3}$		363
$\Lambda\pi^+\pi^+\pi^-$ nonresonant	< 8 %	CL=90%	807
$\Lambda\pi^+\pi^+\pi^-\pi^0$ total	( 1.8 $\pm$ 0.8 ) %		757
$\Lambda\pi^+\eta$	[ $\rho$ ] ( 1.8 $\pm$ 0.6 ) %		691
$\Sigma(1385)^+\eta$	[ $\rho$ ] ( 8.5 $\pm$ 3.3 ) $\times 10^{-3}$		570
$\Lambda\pi^+\omega$	[ $\rho$ ] ( 1.2 $\pm$ 0.5 ) %		517
$\Lambda\pi^+\pi^+\pi^-\pi^0$ , no $\eta$ or $\omega$	< 7 %	CL=90%	757
$\Lambda K^+\bar{K}^0$	( 4.7 $\pm$ 1.5 ) $\times 10^{-3}$	S=1.2	443
$\Xi(1690)^0 K^+, \Xi^{*0} \rightarrow \Lambda\bar{K}^0$	( 1.3 $\pm$ 0.5 ) $\times 10^{-3}$		286
$\Sigma^0\pi^+$	( 1.05 $\pm$ 0.28 ) %		825
$\Sigma^+\pi^0$	( 1.00 $\pm$ 0.34 ) %		827
$\Sigma^+\eta$	( 5.5 $\pm$ 2.3 ) $\times 10^{-3}$		713
$\Sigma^+\pi^+\pi^-$	( 3.6 $\pm$ 1.0 ) %		804
$\Sigma^+\rho^0$	< 1.4 %	CL=95%	575
$\Sigma^-\pi^+\pi^+$	( 1.7 $\pm$ 0.5 ) %		799
$\Sigma^0\pi^+\pi^0$	( 1.8 $\pm$ 0.8 ) %		803
$\Sigma^0\pi^+\pi^+\pi^-$	( 8.3 $\pm$ 3.1 ) $\times 10^{-3}$		763
$\Sigma^+\pi^+\pi^-\pi^0$	—		767
$\Sigma^+\omega$	[ $\rho$ ] ( 2.7 $\pm$ 1.0 ) %		569
$\Sigma^+K^+K^-$	( 2.8 $\pm$ 0.8 ) $\times 10^{-3}$		349
$\Sigma^+\phi$	[ $\rho$ ] ( 3.1 $\pm$ 0.9 ) $\times 10^{-3}$		295
$\Xi(1690)^0 K^+, \Xi^{*0} \rightarrow$	( 8.1 $\pm$ 3.0 ) $\times 10^{-4}$		286
$\Sigma^+K^-$			
$\Sigma^+K^+K^-$ nonresonant	< 6 %	CL=90%	349
$\Xi^0 K^+$	( 3.9 $\pm$ 1.4 ) $\times 10^{-3}$		653
$\Xi^- K^+\pi^+$	( 5.1 $\pm$ 1.4 ) $\times 10^{-3}$		565
$\Xi(1530)^0 K^+$	[ $\rho$ ] ( 2.6 $\pm$ 1.0 ) $\times 10^{-3}$		473

Hadronic modes with a hyperon:  $S = 0$  final states

$\Lambda K^+$	( 5.0 $\pm$ 1.6 ) $\times 10^{-4}$		781
$\Lambda K^+\pi^+\pi^-$	< 4 %	CL=90%	637
$\Sigma^0 K^+$	( 4.2 $\pm$ 1.3 ) $\times 10^{-4}$		735
$\Sigma^0 K^+\pi^+\pi^-$	< 2.1 %	CL=90%	574
$\Sigma^+ K^+\pi^-$	( 1.7 $\pm$ 0.7 ) $\times 10^{-3}$		670
$\Sigma^+ K^*(892)^0$	[ $\rho$ ] ( 2.8 $\pm$ 1.1 ) $\times 10^{-3}$		470
$\Sigma^- K^+\pi^+$	< 1.0 %	CL=90%	664

## Doubly Cabibbo-suppressed modes

$pK^+\pi^-$	< 2.3 %	CL=90%	823
-------------	---------	--------	-----

## Semileptonic modes

$\Lambda\ell^+\nu_\ell$	[ $q$ ] ( 2.0 $\pm$ 0.6 ) %		871
$\Lambda e^+\nu_e$	( 2.1 $\pm$ 0.6 ) %		871
$\Lambda\mu^+\nu_\mu$	( 2.0 $\pm$ 0.7 ) %		867

## Inclusive modes

$e^+$ anything	( 4.5 $\pm$ 1.7 ) %		—
$p e^+$ anything	( 1.8 $\pm$ 0.9 ) %		—
$p$ anything	( 50 $\pm$ 16 ) %		—
$p$ anything (no $\Lambda$ )	( 12 $\pm$ 19 ) %		—
$n$ anything	( 50 $\pm$ 16 ) %		—
$n$ anything (no $\Lambda$ )	( 29 $\pm$ 17 ) %		—
$\Lambda$ anything	( 35 $\pm$ 11 ) %	S=1.4	—
$\Sigma^\pm$ anything	[ $r$ ] ( 10 $\pm$ 5 ) %		—
3prongs	( 24 $\pm$ 8 ) %		—

 $\Delta C = 1$  weak neutral current ( $CI$ ) modes, or Lepton Family number ( $LF$ ), or Lepton number ( $L$ ), or Baryon number ( $B$ ) violating modes

$p e^+ e^-$	$CI$	< 5.5 %	$\times 10^{-6}$	CL=90%	951
$p\mu^+\mu^-$	$CI$	< 4.4 %	$\times 10^{-5}$	CL=90%	937
$p e^+\mu^-$	$LF$	< 9.9 %	$\times 10^{-6}$	CL=90%	947
$p e^-\mu^+$	$LF$	< 1.9 %	$\times 10^{-5}$	CL=90%	947
$\bar{p}2e^+$	$L, B$	< 2.7 %	$\times 10^{-6}$	CL=90%	951
$\bar{p}2\mu^+$	$L, B$	< 9.4 %	$\times 10^{-6}$	CL=90%	937
$\bar{p}e^+\mu^+$	$L, B$	< 1.6 %	$\times 10^{-5}$	CL=90%	947
$\Sigma^-\mu^+\mu^+$	$L$	< 7.0 %	$\times 10^{-4}$	CL=90%	812

 $\Lambda_C(2595)^+$ 

$$J^P = 0(\frac{1}{2}^-)$$

The spin-parity follows from the fact that  $\Sigma_c(2455)\pi$  decays, with little available phase space, are dominant. This assumes that  $J^P = 1/2^+$  for the  $\Sigma_c(2455)$ .

$$\text{Mass } m = 2592.25 \pm 0.28 \text{ MeV}$$

$$m - m_{\Lambda_C^+} = 305.79 \pm 0.24 \text{ MeV}$$

$$\text{Full width } \Gamma = 2.6 \pm 0.6 \text{ MeV}$$

$\Lambda_C^+\pi\pi$  and its submode  $\Sigma_c(2455)\pi$  — the latter just barely — are the only strong decays allowed to an excited  $\Lambda_C^+$  having this mass; and the submode seems to dominate.

 $\Lambda_C(2595)^+$  DECAY MODES

$\Lambda_C(2595)^+$ DECAY MODES	Fraction ( $\Gamma_i/\Gamma$ )	$\rho$ (MeV/c)
$\Lambda_C^+\pi^+\pi^-$	[ $s$ ] $\approx$ 67 %	117
$\Sigma_c(2455)^{++}\pi^-$	24 $\pm$ 7 %	†
$\Sigma_c(2455)^0\pi^+$	24 $\pm$ 7 %	†
$\Lambda_C^+\pi^+\pi^-\pi^0$ 3-body	18 $\pm$ 10 %	117
$\Lambda_C^+\pi^0$	[ $t$ ] not seen	258
$\Lambda_C^+\gamma$	not seen	288

 $\Lambda_C(2625)^+$ 

$$J^P = 0(\frac{3}{2}^-)$$

$J^P$  has not been measured;  $\frac{3}{2}^-$  is the quark-model prediction.

$$\text{Mass } m = 2628.11 \pm 0.19 \text{ MeV} \quad (S = 1.1)$$

$$m - m_{\Lambda_C^+} = 341.65 \pm 0.13 \text{ MeV} \quad (S = 1.1)$$

$$\text{Full width } \Gamma < 0.97 \text{ MeV, CL} = 90\%$$

## Baryon Summary Table

$\Lambda_c^+ \pi \pi$  and its submode  $\Sigma(2455) \pi$  are the only strong decays allowed to an excited  $\Lambda_c^+$  having this mass.

$\Lambda_c^+ \pi$  is the only strong decay allowed to a  $\Sigma_c$  having this mass.

$\Lambda_c(2625)^+$ DECAY MODES	Fraction ( $\Gamma_i/\Gamma$ )	Confidence level	$\rho$ (MeV/c)
$\Lambda_c^+ \pi^+ \pi^-$	[s] $\approx 67\%$		184
$\Sigma_c(2455)^{++} \pi^-$	$<5$	90%	102
$\Sigma_c(2455)^0 \pi^+$	$<5$	90%	102
$\Lambda_c^+ \pi^+ \pi^-$ 3-body	large		184
$\Lambda_c^+ \pi^0$	[t] not seen		293
$\Lambda_c^+ \gamma$	not seen		319

 **$\Lambda_c(2880)^+$** 

$$I(J^P) = 0(\frac{5}{2}^+)$$

There is some good evidence that indeed  $J^P = 5/2^+$

Mass  $m = 2881.53 \pm 0.35$  MeV  
 $m - m_{\Lambda_c^+} = 595.1 \pm 0.4$  MeV  
 Full width  $\Gamma = 5.8 \pm 1.1$  MeV

$\Lambda_c(2880)^+$ DECAY MODES	Fraction ( $\Gamma_i/\Gamma$ )	$\rho$ (MeV/c)
$\Lambda_c^+ \pi^+ \pi^-$	seen	471
$\Sigma_c(2455)^0, ++ \pi^\pm$	seen	376
$\Sigma_c(2520)^0, ++ \pi^\pm$	seen	317
$\rho D^0$	seen	316

 **$\Lambda_c(2940)^+$** 

$$I(J^P) = 0(?^?)$$

Mass  $m = 2939.3^{+1.4}_{-1.5}$  MeV  
 Full width  $\Gamma = 17^{+8}_{-6}$  MeV

$\Lambda_c(2940)^+$ DECAY MODES	Fraction ( $\Gamma_i/\Gamma$ )	$\rho$ (MeV/c)
$\rho D^0$	seen	420
$\Sigma_c(2455)^0, ++ \pi^\pm$	seen	-

 **$\Sigma_c(2455)$** 

$$I(J^P) = 1(\frac{1}{2}^+)$$

$\Sigma_c(2455)^{++}$  mass  $m = 2453.98 \pm 0.16$  MeV  
 $\Sigma_c(2455)^+$  mass  $m = 2452.9 \pm 0.4$  MeV  
 $\Sigma_c(2455)^0$  mass  $m = 2453.74 \pm 0.16$  MeV  
 $m_{\Sigma_c^{++}} - m_{\Lambda_c^+} = 167.52 \pm 0.08$  MeV  
 $m_{\Sigma_c^+} - m_{\Lambda_c^+} = 166.4 \pm 0.4$  MeV  
 $m_{\Sigma_c^0} - m_{\Lambda_c^+} = 167.27 \pm 0.08$  MeV  
 $m_{\Sigma_c^{++}} - m_{\Sigma_c^0} = 0.24 \pm 0.09$  MeV ( $S = 1.1$ )  
 $m_{\Sigma_c^+} - m_{\Sigma_c^0} = -0.9 \pm 0.4$  MeV  
 $\Sigma_c(2455)^{++}$  full width  $\Gamma = 2.26 \pm 0.25$  MeV  
 $\Sigma_c(2455)^+$  full width  $\Gamma < 4.6$  MeV, CL = 90%  
 $\Sigma_c(2455)^0$  full width  $\Gamma = 2.16 \pm 0.26$  MeV ( $S = 1.1$ )

$\Lambda_c^+ \pi$  is the only strong decay allowed to a  $\Sigma_c$  having this mass.

$\Sigma_c(2455)$ DECAY MODES	Fraction ( $\Gamma_i/\Gamma$ )	$\rho$ (MeV/c)
$\Lambda_c^+ \pi$	$\approx 100\%$	94

 **$\Sigma_c(2520)$** 

$$I(J^P) = 1(\frac{3}{2}^+)$$

$J^P$  has not been measured;  $\frac{3}{2}^+$  is the quark-model prediction.

$\Sigma_c(2520)^{++}$  mass  $m = 2517.9 \pm 0.6$  MeV ( $S = 1.6$ )  
 $\Sigma_c(2520)^+$  mass  $m = 2517.5 \pm 2.3$  MeV  
 $\Sigma_c(2520)^0$  mass  $m = 2518.8 \pm 0.6$  MeV ( $S = 1.5$ )  
 $m_{\Sigma_c(2520)^{++}} - m_{\Lambda_c^+} = 231.4 \pm 0.6$  MeV ( $S = 1.6$ )  
 $m_{\Sigma_c(2520)^+} - m_{\Lambda_c^+} = 231.0 \pm 2.3$  MeV  
 $m_{\Sigma_c(2520)^0} - m_{\Lambda_c^+} = 232.3 \pm 0.5$  MeV ( $S = 1.6$ )  
 $m_{\Sigma_c(2520)^{++}} - m_{\Sigma_c(2520)^0}$   
 $\Sigma_c(2520)^{++}$  full width  $\Gamma = 14.9 \pm 1.5$  MeV  
 $\Sigma_c(2520)^+$  full width  $\Gamma < 17$  MeV, CL = 90%  
 $\Sigma_c(2520)^0$  full width  $\Gamma = 14.5 \pm 1.5$  MeV

$\Sigma_c(2520)$ DECAY MODES	Fraction ( $\Gamma_i/\Gamma$ )	$\rho$ (MeV/c)
$\Lambda_c^+ \pi$	$\approx 100\%$	179

 **$\Sigma_c(2800)$** 

$$I(J^P) = 1(?^?)$$

$\Sigma_c(2800)^{++}$  mass  $m = 2801^{+4}_{-6}$  MeV  
 $\Sigma_c(2800)^+$  mass  $m = 2792^{+14}_{-5}$  MeV  
 $\Sigma_c(2800)^0$  mass  $m = 2806^{+5}_{-7}$  MeV ( $S = 1.3$ )  
 $m_{\Sigma_c(2800)^{++}} - m_{\Lambda_c^+} = 514^{+4}_{-6}$  MeV  
 $m_{\Sigma_c(2800)^+} - m_{\Lambda_c^+} = 505^{+14}_{-5}$  MeV  
 $m_{\Sigma_c(2800)^0} - m_{\Lambda_c^+} = 519^{+5}_{-7}$  MeV ( $S = 1.3$ )  
 $\Sigma_c(2800)^{++}$  full width  $\Gamma = 75^{+22}_{-17}$  MeV  
 $\Sigma_c(2800)^+$  full width  $\Gamma = 62^{+60}_{-40}$  MeV  
 $\Sigma_c(2800)^0$  full width  $\Gamma = 72^{+22}_{-15}$  MeV

$\Sigma_c(2800)$ DECAY MODES	Fraction ( $\Gamma_i/\Gamma$ )	$\rho$ (MeV/c)
$\Lambda_c^+ \pi$	seen	443

 **$\Xi_c^+$** 

$$I(J^P) = \frac{1}{2}(\frac{1}{2}^+)$$

$J^P$  has not been measured;  $\frac{1}{2}^+$  is the quark-model prediction.

Mass  $m = 2467.8^{+0.4}_{-0.6}$  MeV  
 Mean life  $\tau = (442 \pm 26) \times 10^{-15}$  s ( $S = 1.3$ )  
 $c\tau = 132 \mu\text{m}$

$\Xi_c^+$ DECAY MODES	Fraction ( $\Gamma_i/\Gamma$ )	Confidence level	$\rho$ (MeV/c)
-----------------------	--------------------------------	------------------	----------------

No absolute branching fractions have been measured.  
 The following are branching ratios relative to  $\Xi^- 2\pi^+$ .

**Cabibbo-favored ( $S = -2$ ) decays**

$p 2K_S^0$	[u]	0.087 $\pm$ 0.022	767
$\Lambda \bar{K}^0 \pi^+$		—	852
$\Sigma(1385)^+ \bar{K}^0$	[p, u]	1.0 $\pm$ 0.5	746
$\Lambda K^- 2\pi^+$	[u]	0.323 $\pm$ 0.033	787
$\Lambda \bar{K}^*(892)^0 \pi^+$	[p, u]	$<0.2$	90% 608
$\Sigma(1385)^+ K^- \pi^+$	[p, u]	$<0.3$	90% 678
$\Sigma^+ K^- \pi^+$	[u]	0.94 $\pm$ 0.11	810
$\Sigma^+ \bar{K}^*(892)^0$	[p, u]	0.81 $\pm$ 0.15	658
$\Sigma^0 K^- 2\pi^+$	[u]	0.29 $\pm$ 0.16	735
$\Xi^0 \pi^+$	[u]	0.55 $\pm$ 0.16	877
$\Xi^- 2\pi^+$	[u]	DEFINED AS 1	851
$\Xi(1530)^0 \pi^+$	[p, u]	$<0.1$	90% 750
$\Xi^0 \pi^+ \pi^0$	[u]	2.34 $\pm$ 0.68	856
$\Xi^0 \pi^- 2\pi^+$	[u]	1.74 $\pm$ 0.50	818
$\Xi^0 e^+ \nu_e$	[u]	2.3 $\pm$ 0.7 0.9	884
$\Omega^- K^+ \pi^+$	[u]	0.07 $\pm$ 0.04	399

**Cabibbo-suppressed decays**

$p K^- \pi^+$	[u]	0.21 $\pm$ 0.03	944
$\rho \bar{K}^*(892)^0$	[p, u]	0.12 $\pm$ 0.02	828
$\Sigma^+ \pi^+ \pi^-$	[u]	0.48 $\pm$ 0.20	922
$\Sigma^- 2\pi^+$	[u]	0.18 $\pm$ 0.09	918
$\Sigma^+ K^+ K^-$	[u]	0.15 $\pm$ 0.07	579
$\Sigma^+ \phi$	[p, u]	$<0.11$	90% 549
$\Xi(1690)^0 K^+, \Xi(1690)^0 \rightarrow \Sigma^+ K^-$	[u]	$<0.05$	90% 501

 **$\Xi_c^0$** 

$$I(J^P) = \frac{1}{2}(\frac{1}{2}^+)$$

$J^P$  has not been measured;  $\frac{1}{2}^+$  is the quark-model prediction.

Mass  $m = 2470.88^{+0.34}_{-0.80}$  MeV ( $S = 1.1$ )  
 $m_{\Xi_c^0} - m_{\Xi^+} = 3.1^{+0.4}_{-0.5}$  MeV  
 Mean life  $\tau = (112^{+13}_{-10}) \times 10^{-15}$  s  
 $c\tau = 33.6 \mu\text{m}$

## Baryon Summary Table

## Decay asymmetry parameters

$$\Xi^- \pi^+ \quad \alpha = -0.6 \pm 0.4$$

No absolute branching fractions have been measured. Several measurements of ratios of fractions may be found in the Listings that follow.

$\Xi_c^0$ DECAY MODES	Fraction ( $\Gamma_i/\Gamma$ )	$\rho$ (MeV/c)
$\rho K^- K^- \pi^+$	seen	676
$\rho K^- \bar{K}^*(892)^0$	seen	413
$\rho K^- K^- \pi^+$ no $\bar{K}^*(892)^0$	seen	676
$\Lambda K_S^0$	seen	906
$\Lambda \bar{K}^0 \pi^+ \pi^-$	seen	787
$\Lambda K^- \pi^+ \pi^+ \pi^-$	seen	703
$\Xi^- \pi^+$	seen	875
$\Xi^- \pi^+ \pi^+ \pi^-$	seen	816
$\Omega^- K^+$	seen	522
$\Xi^- e^+ \nu_e$	seen	882
$\Xi^- \ell^+$ anything	seen	-

 $\Xi_c^{'+}$ 

$$I(J^P) = \frac{1}{2}(\frac{1}{2}^+)$$

$J^P$  has not been measured;  $\frac{1}{2}^+$  is the quark-model prediction.

Mass  $m = 2575.6 \pm 3.1$  MeV

$$m_{\Xi_c^{'+}} - m_{\Xi_c^+} = 107.8 \pm 3.0 \text{ MeV}$$

The  $\Xi_c^{'+} - \Xi_c^+$  mass difference is too small for any strong decay to occur.

$\Xi_c^{'+}$ DECAY MODES	Fraction ( $\Gamma_i/\Gamma$ )	$\rho$ (MeV/c)
$\Xi_c^{'+} \gamma$	seen	106

 $\Xi_c^{'0}$ 

$$I(J^P) = \frac{1}{2}(\frac{1}{2}^+)$$

$J^P$  has not been measured;  $\frac{1}{2}^+$  is the quark-model prediction.

Mass  $m = 2577.9 \pm 2.9$  MeV

$$m_{\Xi_c^{'0}} - m_{\Xi_c^0} = 107.0 \pm 2.9 \text{ MeV}$$

The  $\Xi_c^{'0} - \Xi_c^0$  mass difference is too small for any strong decay to occur.

$\Xi_c^{'0}$ DECAY MODES	Fraction ( $\Gamma_i/\Gamma$ )	$\rho$ (MeV/c)
$\Xi_c^{'0} \gamma$	seen	105

 $\Xi_c(2645)$ 

$$I(J^P) = \frac{1}{2}(\frac{3}{2}^+)$$

$J^P$  has not been measured;  $\frac{3}{2}^+$  is the quark-model prediction.

$$\Xi_c(2645)^+ \text{ mass } m = 2645.9^{+0.5}_{-0.6} \text{ MeV} \quad (S = 1.1)$$

$$\Xi_c(2645)^0 \text{ mass } m = 2645.9 \pm 0.5 \text{ MeV}$$

$$m_{\Xi_c(2645)^+} - m_{\Xi_c^0} = 175.0^{+0.8}_{-0.6} \text{ MeV} \quad (S = 1.2)$$

$$m_{\Xi_c(2645)^0} - m_{\Xi_c^+} = 178.1 \pm 0.6 \text{ MeV}$$

$$m_{\Xi_c(2645)^+} - m_{\Xi_c(2645)^0} = 0.0 \pm 0.5 \text{ MeV}$$

$$\Xi_c(2645)^+ \text{ full width } \Gamma < 3.1 \text{ MeV, CL} = 90\%$$

$$\Xi_c(2645)^0 \text{ full width } \Gamma < 5.5 \text{ MeV, CL} = 90\%$$

$\Xi_c \pi$  is the only strong decay allowed to a  $\Xi_c$  resonance having this mass.

$\Xi_c(2645)$ DECAY MODES	Fraction ( $\Gamma_i/\Gamma$ )	$\rho$ (MeV/c)
$\Xi_c^0 \pi^+$	seen	102
$\Xi_c^+ \pi^-$	seen	107

 $\Xi_c(2790)$ 

$$I(J^P) = \frac{1}{2}(\frac{1}{2}^-)$$

$J^P$  has not been measured;  $\frac{1}{2}^-$  is the quark-model prediction.

$$\Xi_c(2790)^+ \text{ mass} = 2789.1 \pm 3.2 \text{ MeV}$$

$$\Xi_c(2790)^0 \text{ mass} = 2791.8 \pm 3.3 \text{ MeV}$$

$$m_{\Xi_c(2790)^+} - m_{\Xi_c^0} = 318.2 \pm 3.2 \text{ MeV}$$

$$m_{\Xi_c(2790)^0} - m_{\Xi_c^+} = 324.0 \pm 3.3 \text{ MeV}$$

$$\Xi_c(2790)^+ \text{ width} < 15 \text{ MeV, CL} = 90\%$$

$$\Xi_c(2790)^0 \text{ width} < 12 \text{ MeV, CL} = 90\%$$

 $\Xi_c(2790)$  DECAY MODESFraction ( $\Gamma_i/\Gamma$ ) $\rho$  (MeV/c)

$\Xi_c^+ \pi^-$	seen	159
-----------------	------	-----

 $\Xi_c(2815)$ 

$$I(J^P) = \frac{1}{2}(\frac{3}{2}^-)$$

$J^P$  has not been measured;  $\frac{3}{2}^-$  is the quark-model prediction.

$$\Xi_c(2815)^+ \text{ mass } m = 2816.6 \pm 0.9 \text{ MeV}$$

$$\Xi_c(2815)^0 \text{ mass } m = 2819.6 \pm 1.2 \text{ MeV}$$

$$m_{\Xi_c(2815)^+} - m_{\Xi_c^+} = 348.8 \pm 0.9 \text{ MeV}$$

$$m_{\Xi_c(2815)^0} - m_{\Xi_c^0} = 348.7 \pm 1.2 \text{ MeV}$$

$$m_{\Xi_c(2815)^+} - m_{\Xi_c(2815)^0} = -3.1 \pm 1.3 \text{ MeV}$$

$$\Xi_c(2815)^+ \text{ full width } \Gamma < 3.5 \text{ MeV, CL} = 90\%$$

$$\Xi_c(2815)^0 \text{ full width } \Gamma < 6.5 \text{ MeV, CL} = 90\%$$

The  $\Xi_c \pi \pi$  modes are consistent with being entirely via  $\Xi_c(2645) \pi$ .

 $\Xi_c(2815)$  DECAY MODESFraction ( $\Gamma_i/\Gamma$ ) $\rho$  (MeV/c)

$\Xi_c^+ \pi^+ \pi^-$	seen	196
$\Xi_c^0 \pi^+ \pi^-$	seen	191

 $\Xi_c(2980)$ 

$$I(J^P) = \frac{1}{2}(?)$$

$$\Xi_c(2980)^+ \text{ } m = 2971.4 \pm 3.3 \text{ MeV} \quad (S = 2.1)$$

$$\Xi_c(2980)^0 \text{ } m = 2968.0 \pm 2.6 \text{ MeV} \quad (S = 1.2)$$

$$\Xi_c(2980)^+ \text{ width } \Gamma = 26 \pm 7 \text{ MeV} \quad (S = 1.5)$$

$$\Xi_c(2980)^0 \text{ width } \Gamma = 20 \pm 7 \text{ MeV} \quad (S = 1.3)$$

 $\Xi_c(2980)$  DECAY MODESFraction ( $\Gamma_i/\Gamma$ ) $\rho$  (MeV/c)

$\Lambda_c^+ \bar{K} \pi$	seen	231
$\Sigma_c(2455) \bar{K}$	seen	134
$\Lambda_c^+ \bar{K}$	not seen	414
$\Xi_c 2\pi$	seen	-
$\Xi_c(2645) \pi$	seen	277

 $\Xi_c(3080)$ 

$$I(J^P) = \frac{1}{2}(?)$$

$$\Xi_c(3080)^+ \text{ } m = 3077.0 \pm 0.4 \text{ MeV}$$

$$\Xi_c(3080)^0 \text{ } m = 3079.9 \pm 1.4 \text{ MeV} \quad (S = 1.3)$$

$$\Xi_c(3080)^+ \text{ width } \Gamma = 5.8 \pm 1.0 \text{ MeV}$$

$$\Xi_c(3080)^0 \text{ width } \Gamma = 5.6 \pm 2.2 \text{ MeV}$$

 $\Xi_c(3080)$  DECAY MODESFraction ( $\Gamma_i/\Gamma$ ) $\rho$  (MeV/c)

$\Lambda_c^+ \bar{K} \pi$	seen	415
$\Sigma_c(2455) \bar{K}$	seen	342
$\Sigma_c(2455) \bar{K} + \Sigma_c(2520) \bar{K}$	seen	-
$\Lambda_c^+ \bar{K}$	not seen	536
$\Lambda_c^+ \bar{K} \pi^+ \pi^-$	not seen	143

 $\Omega_c^0$ 

$$I(J^P) = 0(\frac{1}{2}^+)$$

$J^P$  has not been measured;  $\frac{1}{2}^+$  is the quark-model prediction.

$$\text{Mass } m = 2695.2 \pm 1.7 \text{ MeV} \quad (S = 1.3)$$

$$\text{Mean life } \tau = (69 \pm 12) \times 10^{-15} \text{ s}$$

$$c\tau = 21 \mu\text{m}$$

5 No absolute branching fractions have been measured.

 $\Omega_c^0$  DECAY MODESFraction ( $\Gamma_i/\Gamma$ ) $\rho$  (MeV/c)

$\Sigma^+ K^- K^- \pi^+$	seen	689
$\Xi^0 K^- \pi^+$	seen	901
$\Xi^- K^- \pi^+ \pi^+$	seen	830
$\Omega^- e^+ \nu_e$	seen	829
$\Omega^- \pi^+$	seen	821
$\Omega^- \pi^+ \pi^0$	seen	797
$\Omega^- \pi^- \pi^+ \pi^+$	seen	753



## Baryon Summary Table

 **$\Omega_c(2770)^0$** 

$$I(J^P) = 0(\frac{3}{2}^+)$$

 $J^P$  has not been measured;  $\frac{3}{2}^+$  is the quark-model prediction.

Mass  $m = 2765.9 \pm 2.0$  MeV ( $S = 1.2$ )

$$m_{\Omega_c(2770)^0} - m_{\Omega_c^0} = 70.7_{-0.9}^{+0.8}$$
 MeV

The  $\Omega_c(2770)^0 - \Omega_c^0$  mass difference is too small for any strong decay to occur.

$\Omega_c(2770)^0$ DECAY MODES	Fraction ( $\Gamma_i/\Gamma$ )	$\rho$ (MeV/c)
$\Omega_c^0 \gamma$	presumably 100%	70

**BOTTOM BARYONS**  
**( $B = -1$ )**

$$\Lambda_b^0 = udb, \Xi_b^0 = usb, \Xi_b^- = dsb, \Omega_b^- = ssb$$

 **$\Lambda_b^0$** 

$$I(J^P) = 0(\frac{1}{2}^+)$$

 $I(J^P)$  not yet measured;  $0(\frac{1}{2}^+)$  is the quark model prediction.

Mass  $m = 5619.4 \pm 0.7$  MeV

$$m_{\Lambda_b^0} - m_{B^0} = 339.2 \pm 1.4$$
 MeV

$$m_{\Lambda_b^0} - m_{B^+} = 339.7 \pm 0.7$$
 MeV

Mean life  $\tau = (1.425 \pm 0.032) \times 10^{-12}$  s

$$c\tau = 427 \mu\text{m}$$

$$A_{CP}(\Lambda_b \rightarrow p\pi^-) = 0.03 \pm 0.18$$

$$A_{CP}(\Lambda_b \rightarrow pK^-) = 0.37 \pm 0.17$$

The branching fractions  $B(b\text{-baryon} \rightarrow \Lambda \ell^- \bar{\nu}_\ell \text{anything})$  and  $B(\Lambda_b^0 \rightarrow \Lambda_c^+ \ell^- \bar{\nu}_\ell \text{anything})$  are not pure measurements because the underlying measured products of these with  $B(b \rightarrow b\text{-baryon})$  were used to determine  $B(b \rightarrow b\text{-baryon})$ , as described in the note "Production and Decay of  $b$ -Flavored Hadrons."For inclusive branching fractions, e.g.,  $\Lambda_b \rightarrow \bar{\Lambda}_c \text{anything}$ , the values usually are multiplicities, not branching fractions. They can be greater than one.

$\Lambda_b^0$ DECAY MODES	Fraction ( $\Gamma_i/\Gamma$ )	Scale factor/ Confidence level	$\rho$ (MeV/c)
$J/\psi(1S) \Lambda \times B(b \rightarrow \Lambda_b^0)$	$(5.8 \pm 0.8) \times 10^{-5}$		1740
$\Lambda_c^+ \pi^-$	$(5.7_{-2.6}^{+4.0}) \times 10^{-3}$	$S=1.6$	2342
$\Lambda_c^+ a_1(1260)^-$	seen		2152
$\Lambda_c^+ \pi^+ \pi^- \pi^-$	$(8_{-4}^{+5}) \times 10^{-3}$	$S=1.6$	2323
$\Lambda_c(2595)^+ \pi^-$ , $\Lambda_c(2595)^+ \rightarrow \Lambda_c^+ \pi^+ \pi^-$	$(3.7_{-2.3}^{+2.8}) \times 10^{-4}$		2210
$\Lambda_c(2625)^+ \pi^-$ , $\Lambda_c(2625)^+ \rightarrow \Lambda_c^+ \pi^+ \pi^-$	$(3.6_{-2.1}^{+2.7}) \times 10^{-4}$		2193
$\Sigma_c(2455)^0 \pi^+ \pi^-$ , $\Sigma_c^0 \rightarrow \Lambda_c^+ \pi^-$	$(6_{-4}^{+5}) \times 10^{-4}$		2265
$\Sigma_c(2455)^{++} \pi^- \pi^-$ , $\Sigma_c^{++} \rightarrow \Lambda_c^+ \pi^+$	$(3.5_{-2.3}^{+2.8}) \times 10^{-4}$		2265
$\Lambda_c^+ \ell^- \bar{\nu}_\ell \text{anything}$	[v] $(9.8 \pm 2.3) \%$		-
$\Lambda_c^+ \ell^- \bar{\nu}_\ell$	$(6.5_{-2.5}^{+3.2}) \%$	$S=1.8$	2345
$\Lambda_c^+ \pi^+ \pi^- \ell^- \bar{\nu}_\ell$	$(5.6 \pm 3.1) \%$		2335
$\Lambda_c(2595)^+ \ell^- \bar{\nu}_\ell$	$(8 \pm 5) \times 10^{-3}$		2212
$\Lambda_c(2625)^+ \ell^- \bar{\nu}_\ell$	$(1.4_{-0.7}^{+0.9}) \%$		2195
$p h^-$	[w] $< 2.3 \times 10^{-5}$	CL=90%	2730
$p \pi^-$	$(3.5 \pm 1.0) \times 10^{-6}$		2730
$p K^-$	$(5.5 \pm 1.4) \times 10^{-6}$		2708
$\Lambda \mu^+ \mu^-$	$(1.7 \pm 0.7) \times 10^{-6}$		2695
$\Lambda \gamma$	$< 1.3 \times 10^{-3}$	CL=90%	2699

 **$\Sigma_b$** 

$$I(J^P) = 1(\frac{1}{2}^+)$$

 $I, J, P$  need confirmation.

Mass  $m(\Sigma_b^+) = 5811.3 \pm 1.9$  MeV

Mass  $m(\Sigma_b^-) = 5815.5 \pm 1.8$  MeV

$$m_{\Sigma_b^+} - m_{\Sigma_b^-} = -4.2 \pm 1.1$$
 MeV

$$\Gamma(\Sigma_b^+) = 9.7_{-3.0}^{+4.0}$$
 MeV

$$\Gamma(\Sigma_b^-) = 4.9_{-2.4}^{+3.3}$$
 MeV

$\Sigma_b$ DECAY MODES	Fraction ( $\Gamma_i/\Gamma$ )	$\rho$ (MeV/c)
$\Lambda_b^0 \pi$	dominant	134

 **$\Sigma_b^*$** 

$$I(J^P) = 1(\frac{3}{2}^+)$$

 $I, J, P$  need confirmation.

Mass  $m(\Sigma_b^{*+}) = 5832.1 \pm 1.9$  MeV

Mass  $m(\Sigma_b^{*-}) = 5835.1 \pm 1.9$  MeV

$$m_{\Sigma_b^{*+}} - m_{\Sigma_b^{*-}} = -3.0_{-0.9}^{+1.0}$$
 MeV

$$\Gamma(\Sigma_b^{*+}) = 11.5 \pm 2.8$$
 MeV

$$\Gamma(\Sigma_b^{*-}) = 7.5 \pm 2.3$$
 MeV

$$m_{\Sigma_b^*} - m_{\Sigma_b} = 21.2 \pm 2.0$$
 MeV

$\Sigma_b^*$ DECAY MODES	Fraction ( $\Gamma_i/\Gamma$ )	$\rho$ (MeV/c)
$\Lambda_b^0 \pi$	dominant	161

 **$\Xi_b^0, \Xi_b^-$** 

$$I(J^P) = \frac{1}{2}(\frac{1}{2}^+)$$

 $I, J, P$  need confirmation.

$$m(\Xi_b^-) = 5791.1 \pm 2.2$$
 MeV

$$m(\Xi_b^0) = 5788 \pm 5$$
 MeV

$$m_{\Xi_b^-} - m_{\Xi_b^0} = 3 \pm 6$$
 MeV

Mean life  $\tau_{\Xi_b^-} = (1.56 \pm 0.26) \times 10^{-12}$  s

Mean life  $\tau_{\Xi_b^0} = (1.49_{-0.18}^{+0.19}) \times 10^{-12}$  s

$\Xi_b$ DECAY MODES	Fraction ( $\Gamma_i/\Gamma$ )	Scale factor	$\rho$ (MeV/c)
$\Xi_b^- \rightarrow \Xi^- \ell^- \bar{\nu}_\ell X \times B(\bar{b} \rightarrow \Xi_b^-)$	$(3.9 \pm 1.2) \times 10^{-4}$	1.4	-
$\Xi_b^- \rightarrow J/\psi \Xi^- \times B(b \rightarrow \Xi_b^-)$	$(1.02_{-0.21}^{+0.26}) \times 10^{-5}$		-

 **$\Omega_b^-$** 

$$I(J^P) = 0(\frac{1}{2}^+)$$

 $I, J, P$  need confirmation.

Mass  $m = 6071 \pm 40$  MeV ( $S = 6.2$ )

Mean life  $\tau = (1.1_{-0.4}^{+0.5}) \times 10^{-12}$  s

$\Omega_b^-$ DECAY MODES	Fraction ( $\Gamma_i/\Gamma$ )	$\rho$ (MeV/c)
$J/\psi \Omega^- \times B(b \rightarrow \Omega_b^-)$	$(2.9_{-0.8}^{+1.1}) \times 10^{-6}$	1826

 **$b$ -baryon ADMIXTURE ( $\Lambda_b, \Xi_b, \Sigma_b, \Omega_b$ )**

Mean life  $\tau = (1.382 \pm 0.029) \times 10^{-12}$  s

These branching fractions are actually an average over weakly decaying  $b$ -baryons weighted by their production rates at the LHC, LEP, and Tevatron, branching ratios, and detection efficiencies. They scale with the  $b$ -baryon production fraction  $B(b \rightarrow b\text{-baryon})$ .The branching fractions  $B(b\text{-baryon} \rightarrow \Lambda \ell^- \bar{\nu}_\ell \text{anything})$  and  $B(\Lambda_b^0 \rightarrow \Lambda_c^+ \ell^- \bar{\nu}_\ell \text{anything})$  are not pure measurements because the underlying measured products of these with  $B(b \rightarrow b\text{-baryon})$  were used to determine  $B(b \rightarrow b\text{-baryon})$ , as described in the note "Production and Decay of  $b$ -Flavored Hadrons."For inclusive branching fractions, e.g.,  $B \rightarrow D^\pm \text{anything}$ , the values usually are multiplicities, not branching fractions. They can be greater than one.

# Baryon Summary Table

## b-baryon ADMIXTURE DECAY MODES

$(\Lambda_b, \Xi_b, \Sigma_b, \Omega_b)$	Fraction ( $\Gamma_i/\Gamma$ )	$p$ (MeV/c)
$p\mu^- \bar{\nu}$ anything	$(5.3 \pm 2.2) \%$ $(1.9)$	—
$p\ell \bar{\nu}_\ell$ anything	$(5.1 \pm 1.2) \%$	—
$p$ anything	$(63 \pm 21) \%$	—
$\Lambda \ell^- \bar{\nu}_\ell$ anything	$(3.4 \pm 0.6) \%$	—
$\Lambda/\bar{\Lambda}$ anything	$(35 \pm 8) \%$	—
$\Xi^- \ell^- \bar{\nu}_\ell$ anything	$(5.9 \pm 1.6) \times 10^{-3}$	—

### NOTES

This Summary Table only includes established baryons. The Particle Listings include evidence for other baryons. The masses, widths, and branching fractions for the resonances in this Table are Breit-Wigner parameters, but pole positions are also given for most of the  $N$  and  $\Delta$  resonances.

For most of the resonances, the parameters come from various partial-wave analyses of more or less the same sets of data, and it is not appropriate to treat the results of the analyses as independent or to average them together. Furthermore, the systematic errors on the results are not well understood. Thus, we usually only give ranges for the parameters. We then also give a best guess for the mass (as part of the name of the resonance) and for the width. The *Note on  $N$  and  $\Delta$  Resonances* and the *Note on  $\Lambda$  and  $\Sigma$  Resonances* in the Particle Listings review the partial-wave analyses.

When a quantity has “(S = ...)” to its right, the error on the quantity has been enlarged by the “scale factor” S, defined as  $S = \sqrt{\chi^2/(N-1)}$ , where  $N$  is the number of measurements used in calculating the quantity. We do this when  $S > 1$ , which often indicates that the measurements are inconsistent. When  $S > 1.25$ , we also show in the Particle Listings an ideogram of the measurements. For more about S, see the Introduction.

A decay momentum  $p$  is given for each decay mode. For a 2-body decay,  $p$  is the momentum of each decay product in the rest frame of the decaying particle. For a 3-or-more-body decay,  $p$  is the largest momentum any of the products can have in this frame. For any resonance, the *nominal* mass is used in calculating  $p$ . A dagger (“†”) in this column indicates that the mode is forbidden when the nominal masses of resonances are used, but is in fact allowed due to the nonzero widths of the resonances.

- [a] The masses of the  $p$  and  $n$  are most precisely known in  $u$  (unified atomic mass units). The conversion factor to MeV,  $1 u = 931.494028(23)$  MeV, is less well known than are the masses in  $u$ .
- [b] The  $|m_p - m_{\bar{p}}|/m_p$  and  $|q_p + q_{\bar{p}}|/e$  are not independent, and both use the more precise measurement of  $|q_{\bar{p}}/m_{\bar{p}}|/(q_p/m_p)$ .
- [c] The limit is from neutrality-of-matter experiments; it assumes  $q_n = q_p + q_e$ . See also the charge of the neutron.

[d] The first limit is for  $p \rightarrow$  anything or “disappearance” modes of a bound proton. The second entry, a rough range of limits, assumes the dominant decay modes are among those investigated. For antiprotons the best limit, inferred from the observation of cosmic ray  $\bar{p}$ 's is  $\tau_{\bar{p}} > 10^7$  yr, the cosmic-ray storage time, but this limit depends on a number of assumptions. The best direct observation of stored antiprotons gives  $\tau_{\bar{p}}/B(\bar{p} \rightarrow e^- \gamma) > 7 \times 10^9$  yr.

[e] There is some controversy about whether nuclear physics and model dependence complicate the analysis for bound neutrons (from which the best limit comes). The first limit here is from reactor experiments with free neutrons.

[f] Lee and Yang in 1956 proposed the existence of a mirror world in an attempt to restore global parity symmetry—thus a search for oscillations between the two worlds. Oscillations between the worlds would be maximal when the magnetic fields  $B$  and  $B'$  were equal. The limit for any  $B'$  in the range 0 to  $12.5 \mu\text{T}$  is  $>12$  s (95% CL).

[g] The parameters  $g_A$ ,  $g_V$ , and  $g_{WM}$  for semileptonic modes are defined by  $\bar{B}_f[\gamma_\lambda(g_V + g_A\gamma_5) + i(g_{WM}/m_{B_i})\sigma_{\lambda\nu}q^\nu]B_i$ , and  $\phi_{AV}$  is defined by  $g_A/g_V = |g_A/g_V|e^{i\phi_{AV}}$ . See the “Note on Baryon Decay Parameters” in the neutron Particle Listings.

[h] Time-reversal invariance requires this to be  $0^\circ$  or  $180^\circ$ .

[i] This coefficient is zero if time invariance is not violated.

[j] This limit is for  $\gamma$  energies between 15 and 340 keV.

[k] The decay parameters  $\gamma$  and  $\Delta$  are calculated from  $\alpha$  and  $\phi$  using

$$\gamma = \sqrt{1-\alpha^2} \cos\phi, \quad \tan\Delta = -\frac{1}{\alpha} \sqrt{1-\alpha^2} \sin\phi.$$

See the “Note on Baryon Decay Parameters” in the neutron Particle Listings.

[l] See the Listings for the pion momentum range used in this measurement.

[m] The error given here is only an educated guess. It is larger than the error on the weighted average of the published values.

[n] A theoretical value using QED.

[o] See the note on “ $\Lambda_c^+$  Branching Fractions” in the  $\Lambda_c^+$  Particle Listings.

[p] This branching fraction includes all the decay modes of the final-state resonance.

[q] An  $\ell$  indicates an  $e$  or a  $\mu$  mode, not a sum over these modes.

[r] The value is for the sum of the charge states or particle/antiparticle states indicated.

[s] Assuming isospin conservation, so that the other third is  $\Lambda_c^+ \pi^0 \pi^0$ .

[t] A test that the isospin is indeed 0, so that the particle is indeed a  $\Lambda_c^+$ .

[u] No absolute branching fractions have been measured. The value here is the branching *ratio* relative to  $\Xi^- 2\pi^+$ .

[v] Not a pure measurement. See note at head of  $\Lambda_b^0$  Decay Modes.

[w] Here  $h^-$  means  $\pi^-$  or  $K^-$ .

## SEARCHES FOR MONOPOLES, SUPERSYMMETRY, TECHNICOLOR, COMPOSITENESS, EXTRA DIMENSIONS, etc.

### Magnetic Monopole Searches

Isolated supermassive monopole candidate events have not been confirmed. The most sensitive experiments obtain negative results.

Best cosmic-ray supermassive monopole flux limit:

$$< 1.0 \times 10^{-15} \text{ cm}^{-2}\text{sr}^{-1}\text{s}^{-1} \quad \text{for } 1.1 \times 10^{-4} < \beta < 0.1$$

### Supersymmetric Particle Searches

Limits are based on the Minimal Supersymmetric Standard Model.

Assumptions include: 1)  $\tilde{\chi}_1^0$  (or  $\tilde{\gamma}$ ) is lightest supersymmetric particle; 2)  $R$ -parity is conserved; 3) With the exception of  $\tilde{t}$  and  $\tilde{b}$ , all scalar quarks are assumed to be degenerate in mass and  $m_{\tilde{q}_R} = m_{\tilde{q}_L}$ . 4) Limits for sleptons refer to the  $\tilde{\ell}_R$  states. 5) Gaugino mass unification at the GUT scale.

See the Particle Listings for a Note giving details of supersymmetry.

$\tilde{\chi}_i^0$  — neutralinos (mixtures of  $\tilde{\gamma}$ ,  $\tilde{Z}^0$ , and  $\tilde{H}_i^0$ )

Mass  $m_{\tilde{\chi}_1^0} > 46 \text{ GeV}$ , CL = 95%

[all  $\tan\beta$ , all  $m_0$ , all  $m_{\tilde{\chi}_2^0} - m_{\tilde{\chi}_1^0}$ ]

Mass  $m_{\tilde{\chi}_2^0} > 62.4 \text{ GeV}$ , CL = 95%

[ $1 < \tan\beta < 40$ , all  $m_0$ , all  $m_{\tilde{\chi}_2^0} - m_{\tilde{\chi}_1^0}$ ]

Mass  $m_{\tilde{\chi}_3^0} > 99.9 \text{ GeV}$ , CL = 95%

[ $1 < \tan\beta < 40$ , all  $m_0$ , all  $m_{\tilde{\chi}_3^0} - m_{\tilde{\chi}_1^0}$ ]

Mass  $m_{\tilde{\chi}_4^0} > 116 \text{ GeV}$ , CL = 95%

[ $1 < \tan\beta < 40$ , all  $m_0$ , all  $m_{\tilde{\chi}_4^0} - m_{\tilde{\chi}_1^0}$ ]

$\tilde{\chi}_i^\pm$  — charginos (mixtures of  $\tilde{W}^\pm$  and  $\tilde{H}_i^\pm$ )

Mass  $m_{\tilde{\chi}_1^\pm} > 94 \text{ GeV}$ , CL = 95%

[ $\tan\beta < 40$ ,  $m_{\tilde{\chi}_1^\pm} - m_{\tilde{\chi}_1^0} > 3 \text{ GeV}$ , all  $m_0$ ]

$\tilde{e}$  — scalar electron (selectron)

Mass  $m > 107 \text{ GeV}$ , CL = 95% [all  $m_{\tilde{e}_R} - m_{\tilde{\chi}_1^0}$ ]

$\tilde{\mu}$  — scalar muon (smuon)

Mass  $m > 94 \text{ GeV}$ , CL = 95%

[ $1 \leq \tan\beta \leq 40$ ,  $m_{\tilde{\mu}_R} - m_{\tilde{\chi}_1^0} > 10 \text{ GeV}$ ]

$\tilde{\tau}$  — scalar tau (stau)

Mass  $m > 81.9 \text{ GeV}$ , CL = 95%

[ $m_{\tilde{\tau}_R} - m_{\tilde{\chi}_1^0} > 15 \text{ GeV}$ , all  $\theta_\tau$ ]

$\tilde{q}$  — scalar quark (squark)

These limits include the effects of cascade decays, evaluated assuming a fixed value of the parameters  $\mu$  and  $\tan\beta$ . The limits are weakly sensitive to these parameters over much of parameter space. Limits assume GUT relations between gaugino masses and the gauge coupling.

Mass  $m > 1.100 \times 10^3 \text{ GeV}$ , CL = 95% [ $\tan\beta=10$ ,  $\mu > 0$ ,  $A_0=0$ ]

$\tilde{b}$  — scalar bottom (sbottom)

Mass  $m > 89 \text{ GeV}$ , CL = 95% [ $m_{\tilde{b}_1} - m_{\tilde{\chi}_1^0} > 8 \text{ GeV}$ , all  $\theta_b$ ]

$\tilde{t}$  — scalar top (stop)

Mass  $m > 95.7 \text{ GeV}$ , CL = 95%

[ $\tilde{t} \rightarrow c\tilde{\chi}_1^0$ , all  $\theta_t$ ,  $m_{\tilde{t}} - m_{\tilde{\chi}_1^0} > 10 \text{ GeV}$ ]

$\tilde{g}$  — gluino

The limits summarised here refer to the high-mass region ( $m_{\tilde{g}} \gtrsim 5 \text{ GeV}$ ), and include the effects of cascade decays, evaluated assuming a fixed value of the parameters  $\mu$  and  $\tan\beta$ .

The limits are weakly sensitive to these parameters over much of parameter space. Limits assume GUT relations between gaugino masses and the gauge coupling,

Mass  $m > 500 \text{ GeV}$ , CL = 95% [any  $m_{\tilde{q}}$ ]

### Technicolor

Searches for a color-octet techni- $\rho$  constrain its mass to be greater than 260 to 480 GeV, depending on allowed decay channels. Similar bounds exist on the color-octet techni- $\omega$ .

### Quark and Lepton Compositeness, Searches for

#### Scale Limits $\Lambda$ for Contact Interactions (the lowest dimensional interactions with four fermions)

If the Lagrangian has the form

$$\pm \frac{g^2}{2\Lambda^2} \bar{\psi}_L \gamma_\mu \psi_L \bar{\psi}_L \gamma^\mu \psi_L$$

(with  $g^2/4\pi$  set equal to 1), then we define  $\Lambda \equiv \Lambda_{LL}^\pm$ . For the full definitions and for other forms, see the Note in the Listings on Searches for Quark and Lepton Compositeness in the full Review and the original literature.

$$\Lambda_{LL}^+(eeee) > 8.3 \text{ TeV, CL} = 95\%$$

$$\Lambda_{LL}^-(eeee) > 10.3 \text{ TeV, CL} = 95\%$$

$$\Lambda_{LL}^+(e\mu\mu\mu) > 8.5 \text{ TeV, CL} = 95\%$$

$$\Lambda_{LL}^-(e\mu\mu\mu) > 9.5 \text{ TeV, CL} = 95\%$$

$$\Lambda_{LL}^+(e\tau\tau\tau) > 7.9 \text{ TeV, CL} = 95\%$$

$$\Lambda_{LL}^-(e\tau\tau\tau) > 7.2 \text{ TeV, CL} = 95\%$$

$$\Lambda_{LL}^+(\ell\ell\ell\ell) > 9.1 \text{ TeV, CL} = 95\%$$

$$\Lambda_{LL}^-(\ell\ell\ell\ell) > 10.3 \text{ TeV, CL} = 95\%$$

$$\Lambda_{LL}^+(eeuu) > 23.3 \text{ TeV, CL} = 95\%$$

$$\Lambda_{LL}^-(eeuu) > 12.5 \text{ TeV, CL} = 95\%$$

$$\Lambda_{LL}^+(eedd) > 11.1 \text{ TeV, CL} = 95\%$$

$$\Lambda_{LL}^-(eedd) > 26.4 \text{ TeV, CL} = 95\%$$

$$\Lambda_{LL}^+(eccc) > 9.4 \text{ TeV, CL} = 95\%$$

$$\Lambda_{LL}^-(eccc) > 5.6 \text{ TeV, CL} = 95\%$$

$$\Lambda_{LL}^+(ebbb) > 9.4 \text{ TeV, CL} = 95\%$$

$$\Lambda_{LL}^-(ebbb) > 10.2 \text{ TeV, CL} = 95\%$$

$$\Lambda_{LL}^+(\mu\mu qq) > 4.5 \text{ TeV, CL} = 95\%$$

$$\Lambda_{LL}^-(\mu\mu qq) > 4.9 \text{ TeV, CL} = 95\%$$

$$\Lambda(\ell\nu\ell\nu) > 3.10 \text{ TeV, CL} = 90\%$$

$$\Lambda(e\nu qq) > 2.81 \text{ TeV, CL} = 95\%$$

$$\Lambda_{LL}^+(qqqq) > 5.6 \text{ TeV, CL} = 95\%$$

$$\Lambda_{LL}^-(qqqq) > 6.7 \text{ TeV, CL} = 95\%$$

$$\Lambda_{LL}^+(\nu\nu qq) > 5.0 \text{ TeV, CL} = 95\%$$

$$\Lambda_{LL}^-(\nu\nu qq) > 5.4 \text{ TeV, CL} = 95\%$$

#### Excited Leptons

The limits from  $\ell^{*+}\ell^{*-}$  do not depend on  $\lambda$  (where  $\lambda$  is the  $\ell\ell^*$  transition coupling). The  $\lambda$ -dependent limits assume chiral coupling.

$e^{*\pm}$  — excited electron

Mass  $m > 103.2 \text{ GeV}$ , CL = 95% (from  $e^*e^*$ )

Mass  $m > 1.070 \times 10^3 \text{ GeV}$ , CL = 95% (from  $ee^*$ )

Mass  $m > 356 \text{ GeV}$ , CL = 95% (if  $\lambda_\gamma = 1$ )

## Searches Summary Table

$\mu^{*\pm}$  — excited muon

Mass  $m > 103.2$  GeV, CL = 95% (from  $\mu^* \mu^*$ )

Mass  $m > 1.090 \times 10^3$  GeV, CL = 95% (from  $\mu \mu^*$ )

$\tau^{*\pm}$  — excited tau

Mass  $m > 103.2$  GeV, CL = 95% (from  $\tau^* \tau^*$ )

Mass  $m > 185$  GeV, CL = 95% (from  $\tau \tau^*$ )

$\nu^*$  — excited neutrino

Mass  $m > 102.6$  GeV, CL = 95% (from  $\nu^* \nu^*$ )

Mass  $m > 213$  GeV, CL = 95% (from  $\nu \nu^*$ )

$q^*$  — excited quark

Mass  $m > 338$  GeV, CL = 95% (from  $q^* q^*$ )

Mass  $m > 2.490 \times 10^3$  GeV, CL = 95% (from  $q^* X$ )

### Color Sextet and Octet Particles

Color Sextet Quarks ( $q_6$ )

Mass  $m > 84$  GeV, CL = 95% (Stable  $q_6$ )

Color Octet Charged Leptons ( $\ell_8$ )

Mass  $m > 86$  GeV, CL = 95% (Stable  $\ell_8$ )

Color Octet Neutrinos ( $\nu_8$ )

Mass  $m > 110$  GeV, CL = 90% ( $\nu_8 \rightarrow \nu g$ )

### Extra Dimensions

Please refer to the Extra Dimensions section of the full *Review* for a discussion of the model-dependence of these bounds, and further constraints.

#### Constraints on the fundamental gravity scale

$M_{TT} > 1.74$  TeV, CL = 95% (dim-8 ops;  $\Lambda = +1$ ;  $pp \rightarrow \gamma\gamma$ )

$M_C > 1.59$  TeV, CL = 95% (compactification scale with TeV extra dimensions;  $p\bar{p} \rightarrow$  dijet, angular distrib.)

$M_D > 1.63$  TeV, CL = 95% ( $pp \rightarrow G \rightarrow \ell\bar{\ell}$ )

#### Constraints on the radius of the extra dimensions, for the case of two-flat dimensions of equal radii

$R < 30 \mu\text{m}$ , CL = 95% (direct tests of Newton's law)

$R < 72 \mu\text{m}$ , CL = 95% ( $pp \rightarrow jG$ )

$R < 0.16\text{--}916$  nm (astrophysics; limits depend on technique and assumptions)

## TESTS OF CONSERVATION LAWS

Updated May 2012 by L. Wolfenstein (Carnegie-Mellon University) and C.-J. Lin (LBNL) .

In keeping with the current interest in tests of conservation laws, we collect together a Table of experimental limits on all weak and electromagnetic decays, mass differences, and moments, and on a few reactions, whose observation would violate conservation laws. The Table is given only in the full *Review of Particle Physics*, not in the Particle Physics Booklet. For the benefit of Booklet readers, we include the best limits from the Table in the following text. Limits in this text are for CL=90% unless otherwise specified. The Table is in two parts: “Discrete Space-Time Symmetries,” *i.e.*,  $C$ ,  $P$ ,  $T$ ,  $CP$ , and  $CPT$ ; and “Number Conservation Laws,” *i.e.*, lepton, baryon, hadronic flavor, and charge conservation. The references for these data can be found in the the Particle Listings in the *Review*. A discussion of these tests follows.

### $CPT$ INVARIANCE

General principles of relativistic field theory require invariance under the combined transformation  $CPT$ . The simplest tests of  $CPT$  invariance are the equality of the masses and lifetimes of a particle and its antiparticle. The best test comes from the limit on the mass difference between  $K^0$  and  $\bar{K}^0$ . Any such difference contributes to the  $CP$ -violating parameter  $\epsilon$ . Assuming  $CPT$  invariance,  $\phi_\epsilon$ , the phase of  $\epsilon$  should be very close to  $44^\circ$ . (See the review “ $CP$  Violation in  $K_L$  decay” in this edition.) In contrast, if the entire source of  $CP$  violation in  $K^0$  decays were a  $K^0 - \bar{K}^0$  mass difference,  $\phi_\epsilon$  would be  $44^\circ + 90^\circ$ .

Assuming that there is no other source of  $CPT$  violation than this mass difference, it is possible to deduce that[1]

$$m_{\bar{K}^0} - m_{K^0} \approx \frac{2(m_{K_L^0} - m_{K_S^0}) |\eta| (\frac{2}{3}\phi_{+-} + \frac{1}{3}\phi_{00} - \phi_{SW})}{\sin \phi_{SW}},$$

where  $\phi_{SW} = (43.51 \pm 0.05)^\circ$ , the superweak angle. Using our best values of the  $CP$ -violation parameters, we get  $|(m_{\bar{K}^0} - m_{K^0})/m_{K^0}| \leq 0.6 \times 10^{-18}$  at CL=90%. Limits can also be placed on specific  $CPT$ -violating decay amplitudes. Given the small value of  $(1 - |\eta_{00}/\eta_{+-}|)$ , the value of  $\phi_{00} - \phi_{+-}$  provides a measure of  $CPT$  violation in  $K_L^0 \rightarrow 2\pi$  decay. Results from CERN [1] and Fermilab [2] indicate no  $CPT$ -violating effect.

### $CP$ AND $T$ INVARIANCE

Given  $CPT$  invariance,  $CP$  violation and  $T$  violation are equivalent. The original evidence for  $CP$  violation came from the measurement of  $|\eta_{+-}| = |A(K_L^0 \rightarrow \pi^+\pi^-)/A(K_S^0 \rightarrow \pi^+\pi^-)| = (2.232 \pm 0.011) \times 10^{-3}$ . This could be explained in terms of  $K^0 - \bar{K}^0$  mixing, which also leads to the asymmetry  $[\Gamma(K_L^0 \rightarrow \pi^- e^+ \nu) - \Gamma(K_L^0 \rightarrow \pi^+ e^- \bar{\nu})]/[\text{sum}] = (0.334 \pm 0.007)\%$ . Evidence for  $CP$  violation in the kaon decay amplitude comes from the measurement of  $(1 - |\eta_{00}/\eta_{+-}|)/3 = \text{Re}(\epsilon'/\epsilon) = (1.66 \pm 0.23) \times 10^{-3}$ . In the Standard Model much larger  $CP$ -violating effects are expected. The first of these, which is associated with  $B - \bar{B}$  mixing, is the parameter  $\sin(2\beta)$  now measured

quite accurately to be  $0.679 \pm 0.020$ . A number of other  $CP$ -violating observables are being measured in  $B$  decays; direct evidence for  $CP$  violation in the  $B$  decay amplitude comes from the asymmetry  $[\Gamma(\bar{B}^0 \rightarrow K^- \pi^+) - \Gamma(B^0 \rightarrow K^+ \pi^-)]/[\text{sum}] = -0.097 \pm 0.012$ . Direct tests of  $T$  violation are much more difficult; a measurement by CPLEAR of the difference between the oscillation probabilities of  $K^0$  to  $\bar{K}^0$  and  $\bar{K}^0$  to  $K^0$  is related to  $T$  violation [3]. Other searches for  $CP$  or  $T$  violation involve effects that are expected to be unobservable in the Standard Model. The most sensitive are probably the searches for an electric dipole moment of the neutron, measured to be  $< 2.9 \times 10^{-26}$  e cm, and the electron  $(10.5 \pm 0.07) \times 10^{-28}$  e cm. A nonzero value requires both  $P$  and  $T$  violation.

### CONSERVATION OF LEPTON NUMBERS

Present experimental evidence and the standard electroweak theory are consistent with the absolute conservation of three separate lepton numbers: electron number  $L_e$ , muon number  $L_\mu$ , and tau number  $L_\tau$ , except for the effect of neutrino mixing associated with neutrino masses. Searches for violations are of the following types:

**a)  $\Delta L = 2$  for one type of charged lepton.** The best limit comes from the search for neutrinoless double beta decay  $(Z, A) \rightarrow (Z + 2, A) + e^- + e^-$ . The best laboratory limit is  $t_{1/2} > 1.9 \times 10^{25}$  yr (CL=90%) for  $^{76}\text{Ge}$ .

**b) Conversion of one charged-lepton type to another.** For purely leptonic processes, the best limits are on  $\mu \rightarrow e\gamma$  and  $\mu \rightarrow 3e$ , measured as  $\Gamma(\mu \rightarrow e\gamma)/\Gamma(\mu \rightarrow \text{all}) < 2.4 \times 10^{-12}$  and  $\Gamma(\mu \rightarrow 3e)/\Gamma(\mu \rightarrow \text{all}) < 1.0 \times 10^{-12}$ . For semileptonic processes, the best limit comes from the coherent conversion process in a muonic atom,  $\mu^- + (Z, A) \rightarrow e^- + (Z, A)$ , measured as  $\Gamma(\mu^- \text{Ti} \rightarrow e^- \text{Ti})/\Gamma(\mu^- \text{Ti} \rightarrow \text{all}) < 4.3 \times 10^{-12}$ . Of special interest is the case in which the hadronic flavor also changes, as in  $K_L \rightarrow e\mu$  and  $K^+ \rightarrow \pi^+ e^- \mu^+$ , measured as  $\Gamma(K_L \rightarrow e\mu)/\Gamma(K_L \rightarrow \text{all}) < 4.7 \times 10^{-12}$  and  $\Gamma(K^+ \rightarrow \pi^+ e^- \mu^+)/\Gamma(K^+ \rightarrow \text{all}) < 1.3 \times 10^{-11}$ . Limits on the conversion of  $\tau$  into  $e$  or  $\mu$  are found in  $\tau$  decay and are much less stringent than those for  $\mu \rightarrow e$  conversion, *e.g.*,  $\Gamma(\tau \rightarrow \mu\gamma)/\Gamma(\tau \rightarrow \text{all}) < 4.4 \times 10^{-8}$  and  $\Gamma(\tau \rightarrow e\gamma)/\Gamma(\tau \rightarrow \text{all}) < 3.3 \times 10^{-8}$ .

**c) Conversion of one type of charged lepton into another type of charged antilepton.** The case most studied is  $\mu^- + (Z, A) \rightarrow e^+ + (Z - 2, A)$ , the strongest limit being  $\Gamma(\mu^- \text{Ti} \rightarrow e^+ \text{Ca})/\Gamma(\mu^- \text{Ti} \rightarrow \text{all}) < 3.6 \times 10^{-11}$ .

**d) Neutrino oscillations.** It is expected even in the standard electroweak theory that the lepton numbers are not separately conserved, as a consequence of lepton mixing analogous to Cabibbo-Kobayashi-Maskawa quark mixing. However, if the only source of lepton-number violation is the mixing of low-mass neutrinos then processes such as  $\mu \rightarrow e\gamma$  are expected to have extremely small unobservable probabilities. For small neutrino masses, the lepton-number violation would be observed first in neutrino oscillations, which have been the subject of extensive experimental studies. Compelling evidence for neutrino mixing has come from atmospheric, solar, accelerator, and

## Tests of Conservation Laws

reactor neutrinos. Recently, the reactor neutrino experiments have measured the last neutrino mixing angle  $\theta_{13}$  and found it to be relatively large. For a comprehensive review on neutrino mixing, including the latest results on  $\theta_{13}$ , see the review “*Neutrino Mass, Mixing, and Oscillations*” by K. Nakamura and S.T. Petcov in this edition of RPP.

### CONSERVATION OF HADRONIC FLAVORS

In strong and electromagnetic interactions, hadronic flavor is conserved, *i.e.* the conversion of a quark of one flavor ( $d, u, s, c, b, t$ ) into a quark of another flavor is forbidden. In the Standard Model, the weak interactions violate these conservation laws in a manner described by the Cabibbo-Kobayashi-Maskawa mixing (see the section “Cabibbo-Kobayashi-Maskawa Mixing Matrix”). The way in which these conservation laws are violated is tested as follows:

(a)  $\Delta S = \Delta Q$  rule. In the strangeness-changing semileptonic decay of strange particles, the strangeness change equals the change in charge of the hadrons. Tests come from limits on decay rates such as  $\Gamma(\Sigma^+ \rightarrow ne^+\nu)/\Gamma(\Sigma^+ \rightarrow \text{all}) < 5 \times 10^{-6}$ , and from a detailed analysis of  $K_L \rightarrow \pi e \nu$ , which yields the parameter  $x$ , measured to be  $(\text{Re } x, \text{Im } x) = (-0.002 \pm 0.006, 0.0012 \pm 0.0021)$ . Corresponding rules are  $\Delta C = \Delta Q$  and  $\Delta B = \Delta Q$ .

(b) **Change of flavor by two units.** In the Standard Model this occurs only in second-order weak interactions. The classic example is  $\Delta S = 2$  via  $K^0 - \bar{K}^0$  mixing, which is directly measured by  $m(K_L) - m(K_S) = (0.5293 \pm 0.0009) \times 10^{10} \hbar s^{-1}$ . The  $\Delta B = 2$  transitions in the  $B^0$  and  $B_s^0$  systems via mixing are also well established. The measured mass differences between the eigenstates are  $(m_{B_H^0} - m_{B_L^0}) = (0.507 \pm 0.004) \times 10^{12} \hbar s^{-1}$  and  $(m_{B_{sH}^0} - m_{B_{sL}^0}) = (17.69 \pm 0.08) \times 10^{12} \hbar s^{-1}$ . There is now strong evidence of  $\Delta C = 2$  transition in the charm sector with the mass difference  $m_{D_H^0} - m_{D_L^0} = (1.44^{+0.48}_{-0.50}) \times 10^{10} \hbar s^{-1}$ . All results are consistent with the second-order calculations in the Standard Model.

(c) **Flavor-changing neutral currents.** In the Standard Model the neutral-current interactions do not change flavor. The low rate  $\Gamma(K_L \rightarrow \mu^+\mu^-)/\Gamma(K_L \rightarrow \text{all}) = (6.84 \pm 0.11) \times 10^{-9}$  puts limits on such interactions; the nonzero value for this rate is attributed to a combination of the weak and electromagnetic interactions. The best test should come from  $K^+ \rightarrow \pi^+\nu\bar{\nu}$ , which occurs in the Standard Model only as a second-order weak process with a branching fraction of  $(0.4 \text{ to } 1.2) \times 10^{-10}$ . Combining results from BNL-E787 and BNL-E949 experiments yield  $\Gamma(K^+ \rightarrow \pi^+\nu\bar{\nu})/\Gamma(K^+ \rightarrow \text{all}) = (1.7 \pm 1.1) \times 10^{-10}$ [4]. Limits for charm-changing or bottom-changing neutral currents are less stringent:  $\Gamma(D^0 \rightarrow \mu^+\mu^-)/\Gamma(D^0 \rightarrow \text{all}) < 1.4 \times 10^{-7}$  and  $\Gamma(B^0 \rightarrow \mu^+\mu^-)/\Gamma(B^0 \rightarrow \text{all}) < 1.4 \times 10^{-9}$ . One cannot isolate flavor-changing neutral current (FCNC) effects in non leptonic

decays. For example, the FCNC transition  $s \rightarrow d + (\bar{u} + u)$  is equivalent to the charged-current transition  $s \rightarrow u + (\bar{u} + d)$ . Tests for FCNC are therefore limited to hadron decays into lepton pairs. Such decays are expected only in second-order in the electroweak coupling in the Standard Model.

### References

1. R. Carosi *et al.*, Phys. Lett. **B237**, 303 (1990).
2. E. Abouzaid *et al.*, Phys. Rev. **D83**, 092001 (2011); B. Schwingerheuer *et al.*, Phys. Rev. Lett. **74**, 4376 (1995).
3. A. Angelopoulos *et al.*, Phys. Lett. **B444**, 43 (1998); L. Wolfenstein, Phys. Rev. Lett. **83**, 911 (1999).
4. A.V. Artamonov *et al.*, Phys. Rev. Lett. **101**, 191802 (2008).

## TESTS OF DISCRETE SPACE-TIME SYMMETRIES

### CHARGE CONJUGATION (C) INVARIANCE

$\Gamma(\pi^0 \rightarrow 3\gamma)/\Gamma_{\text{total}}$	$< 3.1 \times 10^{-8}$ , CL = 90%
$\eta$ C-nonconserving decay parameters	
$\pi^+\pi^-\pi^0$ left-right asymmetry	$(0.09^{+0.11}_{-0.12}) \times 10^{-2}$
$\pi^+\pi^-\pi^0$ sextant asymmetry	$(0.12^{+0.10}_{-0.11}) \times 10^{-2}$
$\pi^+\pi^-\pi^0$ quadrant asymmetry	$(-0.09 \pm 0.09) \times 10^{-2}$
$\pi^+\pi^-\gamma$ left-right asymmetry	$(0.9 \pm 0.4) \times 10^{-2}$
$\pi^+\pi^-\gamma$ parameter $\beta$ (D-wave)	$-0.02 \pm 0.07$ ( $S = 1.3$ )
$\Gamma(\eta \rightarrow \pi^0\gamma)/\Gamma_{\text{total}}$	$< 9 \times 10^{-5}$ , CL = 90%
$\Gamma(\eta \rightarrow 2\pi^0\gamma)/\Gamma_{\text{total}}$	$< 5 \times 10^{-4}$ , CL = 90%
$\Gamma(\eta \rightarrow 3\pi^0\gamma)/\Gamma_{\text{total}}$	$< 6 \times 10^{-5}$ , CL = 90%
$\Gamma(\eta \rightarrow 3\gamma)/\Gamma_{\text{total}}$	$< 1.6 \times 10^{-5}$ , CL = 90%
$\Gamma(\eta \rightarrow \pi^0 e^+ e^-)/\Gamma_{\text{total}}$	[a] $< 4 \times 10^{-5}$ , CL = 90%
$\Gamma(\eta \rightarrow \pi^0 \mu^+ \mu^-)/\Gamma_{\text{total}}$	[a] $< 5 \times 10^{-6}$ , CL = 90%
$\Gamma(\omega(782) \rightarrow \eta\pi^0)/\Gamma_{\text{total}}$	$< 2.1 \times 10^{-4}$ , CL = 90%
$\Gamma(\omega(782) \rightarrow 2\pi^0)/\Gamma_{\text{total}}$	$< 2.1 \times 10^{-4}$ , CL = 90%
$\Gamma(\omega(782) \rightarrow 3\pi^0)/\Gamma_{\text{total}}$	$< 2.3 \times 10^{-4}$ , CL = 90%
asymmetry parameter for $\eta'(958) \rightarrow \pi^+\pi^-\gamma$ decay	$-0.03 \pm 0.04$
$\Gamma(\eta'(958) \rightarrow \pi^0 e^+ e^-)/\Gamma_{\text{total}}$	[a] $< 1.4 \times 10^{-3}$ , CL = 90%
$\Gamma(\eta'(958) \rightarrow \eta e^+ e^-)/\Gamma_{\text{total}}$	[a] $< 2.4 \times 10^{-3}$ , CL = 90%
$\Gamma(\eta'(958) \rightarrow 3\gamma)/\Gamma_{\text{total}}$	$< 1.0 \times 10^{-4}$ , CL = 90%
$\Gamma(\eta'(958) \rightarrow \mu^+ \mu^- \pi^0)/\Gamma_{\text{total}}$	[a] $< 6.0 \times 10^{-5}$ , CL = 90%
$\Gamma(\eta'(958) \rightarrow \mu^+ \mu^- \eta)/\Gamma_{\text{total}}$	[a] $< 1.5 \times 10^{-5}$ , CL = 90%
$\Gamma(J/\psi(1S) \rightarrow \gamma\gamma)/\Gamma_{\text{total}}$	$< 5 \times 10^{-6}$ , CL = 90%

### PARITY (P) INVARIANCE

$e$ electric dipole moment	$< 10.5 \times 10^{-28}$ e cm, CL = 90%
$\mu$ electric dipole moment	$(-0.1 \pm 0.9) \times 10^{-19}$ e cm
$\text{Re}(d_\tau = \tau \text{ electric dipole moment})$	$-0.220 \text{ to } 0.45 \times 10^{-16}$ e cm, CL = 95%
$\Gamma(\eta \rightarrow \pi^+\pi^-)/\Gamma_{\text{total}}$	$< 1.3 \times 10^{-5}$ , CL = 90%
$\Gamma(\eta \rightarrow 2\pi^0)/\Gamma_{\text{total}}$	$< 3.5 \times 10^{-4}$ , CL = 90%
$\Gamma(\eta \rightarrow 4\pi^0)/\Gamma_{\text{total}}$	$< 6.9 \times 10^{-7}$ , CL = 90%
$\Gamma(\eta'(958) \rightarrow \pi^+\pi^-)/\Gamma_{\text{total}}$	$< 6 \times 10^{-5}$ , CL = 90%
$\Gamma(\eta'(958) \rightarrow \pi^0\pi^0)/\Gamma_{\text{total}}$	$< 4 \times 10^{-4}$ , CL = 90%
$\Gamma(\eta_C(1S) \rightarrow \pi^+\pi^-)/\Gamma_{\text{total}}$	$< 1.1 \times 10^{-4}$ , CL = 90%
$\Gamma(\eta_C(1S) \rightarrow \pi^0\pi^0)/\Gamma_{\text{total}}$	$< 3.5 \times 10^{-5}$ , CL = 90%
$\Gamma(\eta_C(1S) \rightarrow K^+K^-)/\Gamma_{\text{total}}$	$< 6 \times 10^{-4}$ , CL = 90%
$\Gamma(\eta_C(1S) \rightarrow K_S^0 K_S^0)/\Gamma_{\text{total}}$	$< 3.1 \times 10^{-4}$ , CL = 90%
$p$ electric dipole moment	$< 0.54 \times 10^{-23}$ e cm
$n$ electric dipole moment	$< 0.29 \times 10^{-25}$ e cm, CL = 90%
$\Lambda$ electric dipole moment	$< 1.5 \times 10^{-16}$ e cm, CL = 95%

Unless otherwise stated, limits are given at the 90% confidence level, while errors are given as  $\pm 1$  standard deviation.

## TIME REVERSAL (T) INVARIANCE

$e$ electric dipole moment	$<10.5 \times 10^{-28}$ e cm, CL = 90%
$\mu$ electric dipole moment	$(-0.1 \pm 0.9) \times 10^{-19}$ e cm
$\mu$ decay parameters	
transverse $e^+$ polarization normal to plane of $\mu$ spin, $e^+$ momentum	$(-2 \pm 8) \times 10^{-3}$
$\alpha'/A$	$(-10 \pm 20) \times 10^{-3}$
$\beta'/A$	$(2 \pm 7) \times 10^{-3}$
$\text{Re}(d_\tau = \tau$ electric dipole moment)	$-0.220$ to $0.45 \times 10^{-16}$ e cm, CL = 95%
$P_T$ in $K^+ \rightarrow \pi^0 \mu^+ \nu_\mu$	$(-1.7 \pm 2.5) \times 10^{-3}$
$P_T$ in $K^+ \rightarrow \mu^+ \nu_\mu \gamma$	$(-0.6 \pm 1.9) \times 10^{-2}$
$\text{Im}(\xi)$ in $K^+ \rightarrow \pi^0 \mu^+ \nu_\mu$ decay (from transverse $\mu$ pol.)	$-0.006 \pm 0.008$
asymmetry $A_T$ in $K^0$ - $\bar{K}^0$ mixing	$(6.6 \pm 1.6) \times 10^{-3}$
$\text{Im}(\xi)$ in $K_{\mu 3}^0$ decay (from transverse $\mu$ pol.)	$-0.007 \pm 0.026$
$A_T(D^\pm \rightarrow K_S^0 K^\pm \pi^+ \pi^-)$	[b] $(-12 \pm 11) \times 10^{-3}$
$A_T(D^0 \rightarrow K^+ K^- \pi^+ \pi^-)$	[b] $(1 \pm 7) \times 10^{-3}$
$A_T(D_S^\pm \rightarrow K_S^0 K^\pm \pi^+ \pi^-)$	[b] $(-14 \pm 8) \times 10^{-3}$
$p$ electric dipole moment	$<0.54 \times 10^{-23}$ e cm
$n$ electric dipole moment	$<0.29 \times 10^{-25}$ e cm, CL = 90%
$n \rightarrow p e^- \bar{\nu}_e$ decay parameters	
$\phi_{AV}$ , phase of $g_A$ relative to $g_V$	[c] $(180.018 \pm 0.026)^\circ$
triple correlation coefficient $D$	[d] $(-1.2 \pm 2.0) \times 10^{-4}$
triple correlation coefficient $R$	[d] $0.008 \pm 0.016$
$\Lambda$ electric dipole moment	$<1.5 \times 10^{-16}$ e cm, CL = 95%
triple correlation coefficient $D$ for $\Sigma^- \rightarrow n e^- \bar{\nu}_e$	$0.11 \pm 0.10$

## CP INVARIANCE

$\text{Re}(d_\tau^W)$	$<0.50 \times 10^{-17}$ e cm, CL = 95%
$\text{Im}(d_\tau^W)$	$<1.1 \times 10^{-17}$ e cm, CL = 95%
$\eta \rightarrow \pi^+ \pi^- e^+ e^-$ decay-plane asymmetry	$(-0.6 \pm 3.1) \times 10^{-2}$
$\Gamma(\eta \rightarrow \pi^+ \pi^-) / \Gamma_{\text{total}}$	$<1.3 \times 10^{-5}$ , CL = 90%
$\Gamma(\eta \rightarrow 2\pi^0) / \Gamma_{\text{total}}$	$<3.5 \times 10^{-4}$ , CL = 90%
$\Gamma(\eta \rightarrow 4\pi^0) / \Gamma_{\text{total}}$	$<6.9 \times 10^{-7}$ , CL = 90%
$\Gamma(\eta'(958) \rightarrow \pi^+ \pi^-) / \Gamma_{\text{total}}$	$<6 \times 10^{-5}$ , CL = 90%
$\Gamma(\eta'(958) \rightarrow \pi^0 \pi^0) / \Gamma_{\text{total}}$	$<4 \times 10^{-4}$ , CL = 90%
$K^\pm \rightarrow \pi^\pm \pi^+ \pi^-$ rate difference/average	$(0.08 \pm 0.12)\%$
$K^\pm \rightarrow \pi^\pm \pi^0 \pi^0$ rate difference/average	$(0.0 \pm 0.6)\%$
$K^\pm \rightarrow \pi^\pm \pi^0 \gamma$ rate difference/average	$(0.9 \pm 3.3)\%$
$K^\pm \rightarrow \pi^\pm \pi^+ \pi^- (g_+ - g_-) / (g_+ + g_-)$	$(-1.5 \pm 2.2) \times 10^{-4}$
$K^\pm \rightarrow \pi^\pm \pi^0 \pi^0 (g_+ - g_-) / (g_+ + g_-)$	$(1.8 \pm 1.8) \times 10^{-4}$
$\Delta(K_{\pi e e}^\pm) = \frac{\Gamma(K_{\pi e e}^+) - \Gamma(K_{\pi e e}^-)}{\Gamma(K_{\pi e e}^+) + \Gamma(K_{\pi e e}^-)}$	$(-2.2 \pm 1.6) \times 10^{-2}$
$\Delta(K_{\pi \mu \mu}^\pm) = \frac{\Gamma(K_{\pi \mu \mu}^+) - \Gamma(K_{\pi \mu \mu}^-)}{\Gamma(K_{\pi \mu \mu}^+) + \Gamma(K_{\pi \mu \mu}^-)}$	$0.010 \pm 0.023$
$\Delta(K_{\pi \pi \gamma}^\pm) = \frac{\Gamma(K_{\pi \pi \gamma}^+) - \Gamma(K_{\pi \pi \gamma}^-)}{\Gamma(K_{\pi \pi \gamma}^+) + \Gamma(K_{\pi \pi \gamma}^-)}$	$(0.0 \pm 1.2) \times 10^{-3}$
$A_S = [\Gamma(K_S^0 \rightarrow \pi^- e^+ \nu_e) - \Gamma(K_S^0 \rightarrow \pi^+ e^- \bar{\nu}_e)] / \text{SUM}$	$(2 \pm 10) \times 10^{-3}$
$\text{Im}(\eta_{+-0}) = \text{Im}(A(K_S^0 \rightarrow \pi^+ \pi^- \pi^0, \text{CP-violating}) / A(K_L^0 \rightarrow \pi^+ \pi^- \pi^0))$	$-0.002 \pm 0.009$
$\text{Im}(\eta_{000}) = \text{Im}(A(K_S^0 \rightarrow \pi^0 \pi^0 \pi^0) / A(K_L^0 \rightarrow \pi^0 \pi^0 \pi^0))$	$(-0.1 \pm 1.6) \times 10^{-2}$
$ \eta_{000}  =  A(K_S^0 \rightarrow \pi^0 \pi^0 \pi^0) / A(K_L^0 \rightarrow \pi^0 \pi^0 \pi^0) $	$<0.018$ , CL = 90%
CP asymmetry $A$ in $K_S^0 \rightarrow \pi^+ \pi^- e^+ e^-$	$(-0.4 \pm 0.8)\%$
$\Gamma(K_S^0 \rightarrow 3\pi^0) / \Gamma_{\text{total}}$	$<1.2 \times 10^{-7}$ , CL = 90%
linear coefficient $j$ for $K_L^0 \rightarrow \pi^+ \pi^- \pi^0$	$0.0012 \pm 0.0008$
quadratic coefficient $f$ for $K_L^0 \rightarrow \pi^+ \pi^- \pi^0$	$0.004 \pm 0.006$
$ \epsilon'_{+-\gamma}  / \epsilon$ for $K_L^0 \rightarrow \pi^+ \pi^- \gamma$	$<0.3$ , CL = 90%
$ \epsilon_{E1} $ for $K_L^0 \rightarrow \pi^+ \pi^- \gamma$	$<0.21$ , CL = 90%
$\Gamma(K_L^0 \rightarrow \pi^0 \mu^+ \mu^-) / \Gamma_{\text{total}}$	[e] $<3.8 \times 10^{-10}$ , CL = 90%
$\Gamma(K_L^0 \rightarrow \pi^0 e^+ e^-) / \Gamma_{\text{total}}$	[e] $<2.8 \times 10^{-10}$ , CL = 90%
$\Gamma(K_L^0 \rightarrow \pi^0 \nu \bar{\nu}) / \Gamma_{\text{total}}$	[f] $<2.6 \times 10^{-8}$ , CL = 90%
$A_{CP}(D^\pm \rightarrow \mu^\pm \nu)$	$(8 \pm 8)\%$
$A_{CP}(D^\pm \rightarrow K_S^0 \pi^\pm)$	$(-0.54 \pm 0.14)\%$

$A_{CP}(D^\pm \rightarrow K^{\mp} 2\pi^\pm)$	$(-0.1 \pm 1.0)\%$
$A_{CP}(D^\pm \rightarrow K^{\mp} \pi^\pm \pi^\pm \pi^0)$	$(1.0 \pm 1.3)\%$
$A_{CP}(D^\pm \rightarrow K_S^0 \pi^\pm \pi^0)$	$(0.3 \pm 0.9)\%$
$A_{CP}(D^\pm \rightarrow K_S^0 \pi^\pm \pi^+ \pi^-)$	$(0.1 \pm 1.3)\%$
$A_{CP}(D^\pm \rightarrow \pi^\pm \pi^0)$	$(2.9 \pm 2.9)\%$
$A_{CP}(D^\pm \rightarrow \pi^\pm \eta)$	$(1.0 \pm 1.5)\%$ ( $S = 1.4$ )
$A_{CP}(D^\pm \rightarrow \pi^\pm \eta'(958))$	$(-0.5 \pm 1.2)\%$ ( $S = 1.1$ )
$A_{CP}(D^\pm \rightarrow K_S^0 K^\pm)$	$(-0.1 \pm 0.6)\%$
$A_{CP}(D^\pm \rightarrow K^+ K^- \pi^\pm)$	$(0.3 \pm 0.6)\%$
$A_{CP}(D^\pm \rightarrow K^\pm K^* 0)$	$(0.1 \pm 1.3)\%$
$A_{CP}(D^\pm \rightarrow \phi \pi^\pm)$	$(0.42 \pm 0.28)\%$
$A_{CP}(D^\pm \rightarrow K^\pm K_S^*(1430)^0)$	$(8 \pm 7)\%$
$A_{CP}(D^\pm \rightarrow K^\pm K_2^*(1430)^0)$	$(43 \pm 20)\%$
$A_{CP}(D^\pm \rightarrow K^\pm K_0^*(800))$	$(-12 \pm 18)\%$
$A_{CP}(D^\pm \rightarrow a_0(1450)^0 \pi^\pm)$	$(-19 \pm 14)\%$
$A_{CP}(D^\pm \rightarrow \phi(1680) \pi^\pm)$	$(-9 \pm 26)\%$
$A_{CP}(D^\pm \rightarrow \pi^+ \pi^- \pi^\pm)$	$(-2 \pm 4)\%$
$A_{CP}(D^\pm \rightarrow K_S^0 K^\pm \pi^+ \pi^-)$	$(-4 \pm 7)\%$
$A_{CP}(D^\pm \rightarrow K^\pm \pi^0)$	$(-4 \pm 11)\%$
$ q/p $ of $D^0$ - $\bar{D}^0$ mixing	$0.88 \pm 0.16$ $-0.15$
$A_\Gamma$ of $D^0$ - $\bar{D}^0$ mixing	$(0.26 \pm 2.31) \times 10^{-3}$
Where there is ambiguity, the CP test is labelled by the $D^0$ decay mode.	
$A_{CP}(D^0 \rightarrow K^+ K^-)$	$(-0.21 \pm 0.17)\%$
$A_{CP}(D^0 \rightarrow K_S^0 K_S^0)$	$(-23 \pm 19)\%$
$A_{CP}(D^0 \rightarrow \pi^+ \pi^-)$	$(0.22 \pm 0.21)\%$
$A_{CP}(D^0 \rightarrow \pi^0 \pi^0)$	$(0 \pm 5)\%$
$A_{CP}(D^0 \rightarrow \pi^+ \pi^- \pi^0)$	$(0.3 \pm 0.4)\%$
$A_{CP}(D^0 \rightarrow \rho(770)^+ \pi^- \rightarrow \pi^+ \pi^- \pi^0)$	[g] $(1.2 \pm 0.9)\%$
$A_{CP}(D^0 \rightarrow \rho(770)^0 \pi^0 \rightarrow \pi^+ \pi^- \pi^0)$	[g] $(-3.1 \pm 3.0)\%$
$A_{CP}(D^0 \rightarrow \rho(770)^- \pi^+ \rightarrow \pi^+ \pi^- \pi^0)$	[g] $(-1.0 \pm 1.7)\%$
$A_{CP}(D^0 \rightarrow \rho(1450)^+ \pi^- \rightarrow \pi^+ \pi^- \pi^0)$	[g] $(0 \pm 70)\%$
$A_{CP}(D^0 \rightarrow \rho(1450)^0 \pi^0 \rightarrow \pi^+ \pi^- \pi^0)$	[g] $(-20 \pm 40)\%$
$A_{CP}(D^0 \rightarrow \rho(1450)^- \pi^+ \rightarrow \pi^+ \pi^- \pi^0)$	[g] $(6 \pm 9)\%$
$A_{CP}(D^0 \rightarrow \rho(1700)^+ \pi^- \rightarrow \pi^+ \pi^- \pi^0)$	[g] $(-5 \pm 14)\%$
$A_{CP}(D^0 \rightarrow \rho(1700)^0 \pi^0 \rightarrow \pi^+ \pi^- \pi^0)$	[g] $(13 \pm 9)\%$
$A_{CP}(D^0 \rightarrow \rho(1700)^- \pi^+ \rightarrow \pi^+ \pi^- \pi^0)$	[g] $(8 \pm 11)\%$
$A_{CP}(D^0 \rightarrow f_0(980) \pi^0 \rightarrow \pi^+ \pi^- \pi^0)$	[g] $(0 \pm 35)\%$
$A_{CP}(D^0 \rightarrow f_0(1370) \pi^0 \rightarrow \pi^+ \pi^- \pi^0)$	[g] $(25 \pm 18)\%$
$A_{CP}(D^0 \rightarrow f_0(1500) \pi^0 \rightarrow \pi^+ \pi^- \pi^0)$	[g] $(0 \pm 18)\%$
$A_{CP}(D^0 \rightarrow f_0(1710) \pi^0 \rightarrow \pi^+ \pi^- \pi^0)$	[g] $(0 \pm 24)\%$
$A_{CP}(D^0 \rightarrow f_2(1270) \pi^0 \rightarrow \pi^+ \pi^- \pi^0)$	[g] $(-4 \pm 6)\%$
$A_{CP}(D^0 \rightarrow \sigma(400) \pi^0 \rightarrow \pi^+ \pi^- \pi^0)$	[g] $(6 \pm 8)\%$
$A_{CP}(\text{nonresonant } D^0 \rightarrow \pi^+ \pi^- \pi^0)$	[g] $(-13 \pm 23)\%$
$A_{CP}(D^0 \rightarrow K^+ K^- \pi^0)$	$(-1.0 \pm 1.7)\%$
$A_{CP}(D^0 \rightarrow K^*(892)^+ K^- \rightarrow K^+ K^- \pi^0)$	[g] $(-0.9 \pm 1.3)\%$
$A_{CP}(D^0 \rightarrow K^*(1410)^+ K^- \rightarrow K^+ K^- \pi^0)$	[g] $(-21 \pm 24)\%$
$A_{CP}(D^0 \rightarrow (K^+ \pi^0)_S K^- \rightarrow K^+ K^- \pi^0)$	[g] $(7 \pm 15)\%$
$A_{CP}(D^0 \rightarrow \phi(1020) \pi^0 \rightarrow K^+ K^- \pi^0)$	[g] $(1.1 \pm 2.2)\%$
$A_{CP}(D^0 \rightarrow f_0(980) \pi^0 \rightarrow K^+ K^- \pi^0)$	[g] $(-3 \pm 19)\%$
$A_{CP}(D^0 \rightarrow a_0(980)^0 \pi^0 \rightarrow K^+ K^- \pi^0)$	[g] $(-5 \pm 16)\%$
$A_{CP}(D^0 \rightarrow f'_2(1525) \pi^0 \rightarrow K^+ K^- \pi^0)$	[g] $(0 \pm 160)\%$
$A_{CP}(D^0 \rightarrow K^*(892)^- K^+ \rightarrow K^+ K^- \pi^0)$	[g] $(-5 \pm 4)\%$
$A_{CP}(D^0 \rightarrow K^*(1410)^- K^+ \rightarrow K^+ K^- \pi^0)$	[g] $(-17 \pm 29)\%$
$A_{CP}(D^0 \rightarrow (K^- \pi^0)_S \text{-wave } K^+ \rightarrow K^+ K^- \pi^0)$	[g] $(-10 \pm 40)\%$
$A_{CP}(D^0 \rightarrow K_S^0 \pi^0)$	$(-0.27 \pm 0.21)\%$
$A_{CP}(D^0 \rightarrow K_S^0 \eta)$	$(0.5 \pm 0.5)\%$
$A_{CP}(D^0 \rightarrow K_S^0 \eta')$	$(1.0 \pm 0.7)\%$
$A_{CP}(D^0 \rightarrow K_S^0 \phi)$	$(-3 \pm 9)\%$
$A_{CP}(D^0 \rightarrow K^- \pi^+)$	$(0.1 \pm 0.7)\%$
$A_{CP}(D^0 \rightarrow K^+ \pi^-)$	$(2.2 \pm 3.2)\%$
$A_{CP}(D^0 \rightarrow K^- \pi^+ \pi^0)$	$(0.2 \pm 0.9)\%$
$A_{CP}(D^0 \rightarrow K^+ \pi^- \pi^0)$	$(0 \pm 5)\%$
$A_{CP}(D^0 \rightarrow K_S^0 \pi^+ \pi^-)$	$(-0.9 \pm 2.6)\%$ $-6.0$
$A_{CP}(D^0 \rightarrow K^*(892)^- \pi^+ \rightarrow K_S^0 \pi^+ \pi^-)$	$<3.5 \times 10^{-4}$ , CL = 95%
$A_{CP}(D^0 \rightarrow K^*(892)^+ \pi^- \rightarrow K_S^0 \pi^+ \pi^-)$	$<7.8 \times 10^{-4}$ , CL = 95%
$A_{CP}(D^0 \rightarrow K_S^0 \rho^0 \rightarrow K_S^0 \pi^+ \pi^-)$	$<4.8 \times 10^{-4}$ , CL = 95%

# Tests of Conservation Laws

$A_{CP}(D^0 \rightarrow K_S^0 \omega \rightarrow K_S^0 \pi^+ \pi^-)$	$<9.2 \times 10^{-4}$ , CL = 95%	$A_{CP}(B^+ \rightarrow D_{CP(-1)} K^*(892)^+)$	$-0.23 \pm 0.22$
$A_{CP}(D^0 \rightarrow K_S^0 f_0(980) \rightarrow K_S^0 \pi^+ \pi^-)$	$<6.8 \times 10^{-4}$ , CL = 95%	$A_{CP}(B^+ \rightarrow D^{*+} \bar{D}^{*0})$	$-0.15 \pm 0.11$
$A_{CP}(D^0 \rightarrow K_S^0 f_2(1270) \rightarrow K_S^0 \pi^+ \pi^-)$	$<13.5 \times 10^{-4}$ , CL = 95%	$A_{CP}(B^+ \rightarrow D^{*+} \bar{D}^0)$	$-0.06 \pm 0.13$
$A_{CP}(D^0 \rightarrow K_S^0 f_0(1370) \rightarrow K_S^0 \pi^+ \pi^-)$	$<25.5 \times 10^{-4}$ , CL = 95%	$A_{CP}(B^+ \rightarrow D^+ \bar{D}^{*0})$	$0.13 \pm 0.18$
$A_{CP}(D^0 \rightarrow K_S^0(1430)^- \pi^+ \rightarrow K_S^0 \pi^+ \pi^-)$	$<9.0 \times 10^{-4}$ , CL = 95%	$A_{CP}(B^+ \rightarrow D^+ \bar{D}^0)$	$-0.03 \pm 0.07$
$A_{CP}(D^0 \rightarrow K_S^0(1430)^- \pi^+ \rightarrow K_S^0 \pi^+ \pi^-)$	$<6.5 \times 10^{-4}$ , CL = 95%	$A_{CP}(B^+ \rightarrow K_S^0 \pi^+)$	$0.009 \pm 0.029$ (S = 1.2)
$A_{CP}(D^0 \rightarrow K_S^0(1680)^- \pi^+ \rightarrow K_S^0 \pi^+ \pi^-)$	$<28.4 \times 10^{-4}$ , CL = 95%	$A_{CP}(B^+ \rightarrow K^+ \pi^0)$	$0.051 \pm 0.025$
$A_{CP}(D^0 \rightarrow K^- \pi^+ \pi^+ \pi^-)$	$(0.7 \pm 1.0)\%$	$A_{CP}(B^+ \rightarrow \eta' K^+)$	$0.013 \pm 0.017$
$A_{CP}(D^0 \rightarrow K^+ \pi^- \pi^+ \pi^-)$	$(-2 \pm 4)\%$	$A_{CP}(B^+ \rightarrow \eta' K^*(892)^+)$	$-0.26 \pm 0.27$
$A_{CP}(D^0 \rightarrow K^+ K^- \pi^+ \pi^-)$	$(-8 \pm 7)\%$	$A_{CP}(B^+ \rightarrow \eta' K_S^0(1430)^+)$	$0.06 \pm 0.20$
$\Delta A_{CP}^D = A_{CP}(K^+ K^-) - A_{CP}(\pi^+ \pi^-)$	$(-0.65 \pm 0.18)\%$	$A_{CP}(B^+ \rightarrow \eta' K_S^0(1430)^+)$	$0.15 \pm 0.13$
$A_{CP}(D_S^{\pm} \rightarrow \mu^{\pm} \nu)$	$(5 \pm 6)\%$	$A_{CP}(B^+ \rightarrow \eta K^+)$	$-0.37 \pm 0.08$
$A_{CP}(D_S^{\pm} \rightarrow K^{\pm} K_S^0)$	$(0.3 \pm 0.4)\%$	$A_{CP}(B^+ \rightarrow \eta K^*(892)^+)$	$0.02 \pm 0.06$
$A_{CP}(D_S^{\pm} \rightarrow K^+ K^- \pi^{\pm})$	$(0.3 \pm 1.4)\%$	$A_{CP}(B^+ \rightarrow \eta K_S^0(1430)^+)$	$0.05 \pm 0.13$
$A_{CP}(D_S^{\pm} \rightarrow K^+ K^- \pi^{\pm} \pi^0)$	$(-6 \pm 4)\%$	$A_{CP}(B^+ \rightarrow \eta K_S^0(1430)^+)$	$-0.45 \pm 0.30$
$A_{CP}(D_S^{\pm} \rightarrow K_S^0 K^{\mp} 2\pi^{\pm})$	$(-1 \pm 4)\%$	$A_{CP}(B^+ \rightarrow \omega K^+)$	$0.02 \pm 0.05$
$A_{CP}(D_S^{\pm} \rightarrow \pi^+ \pi^- \pi^{\pm})$	$(2 \pm 5)\%$	$A_{CP}(B^+ \rightarrow \omega K^{*+})$	$0.29 \pm 0.35$
$A_{CP}(D_S^{\pm} \rightarrow \pi^{\pm} \eta)$	$(-4.6 \pm 2.9)\%$	$A_{CP}(B^+ \rightarrow \omega(K\pi)_0^{*+})$	$-0.10 \pm 0.09$
$A_{CP}(D_S^{\pm} \rightarrow \pi^{\pm} \eta')$	$(-6.1 \pm 3.0)\%$	$A_{CP}(B^+ \rightarrow \omega K_S^0(1430)^+)$	$0.14 \pm 0.15$
$A_{CP}(D_S^{\pm} \rightarrow K^{\pm} \pi^0)$	$(-27 \pm 24)\%$	$A_{CP}(B^+ \rightarrow K^{*0} \pi^+)$	$-0.04 \pm 0.09$ (S = 2.1)
$A_{CP}(D_S^{\pm} \rightarrow K_S^0 \pi^{\pm})$	$(6.6 \pm 3.3)\%$ (S = 1.4)	$A_{CP}(B^+ \rightarrow K^*(892)^+ \pi^0)$	$-0.06 \pm 0.24$
$A_{CP}(D_S^{\pm} \rightarrow K^{\pm} \pi^+ \pi^-)$	$(11 \pm 7)\%$	$A_{CP}(B^+ \rightarrow K^+ \pi^- \pi^+)$	$0.038 \pm 0.022$
$A_{CP}(D_S^{\pm} \rightarrow K^{\pm} \eta)$	$(9 \pm 15)\%$	$A_{CP}(B^+ \rightarrow f_0(980) K^+)$	$-0.09^{+0.05}_{-0.04}$ (S = 1.1)
$A_{CP}(D_S^{\pm} \rightarrow K^{\pm} \eta'(958))$	$(6 \pm 19)\%$	$A_{CP}(B^+ \rightarrow f_2(1270) K^+)$	$-0.68^{+0.19}_{-0.17}$
$A_{CP}(B^+ \rightarrow J/\psi(1S) K^+)$	$(1 \pm 7) \times 10^{-3}$ (S = 1.8)	$A_{CP}(B^+ \rightarrow f_0(1500) K^+)$	$0.28 \pm 0.30$
$A_{CP}(B^+ \rightarrow J/\psi(1S) \pi^+)$	$0.01 \pm 0.07$ (S = 1.3)	$A_{CP}(B^+ \rightarrow \rho^0 K^+)$	$0.37 \pm 0.10$
$A_{CP}(B^+ \rightarrow J/\psi \rho^+)$	$-0.11 \pm 0.14$	$A_{CP}(B^+ \rightarrow K_S^0(1430)^0 \pi^+)$	$0.055 \pm 0.033$
$A_{CP}(B^+ \rightarrow J/\psi K^*(892)^+)$	$-0.048 \pm 0.033$	$A_{CP}(B^+ \rightarrow K_S^0(1430)^0 \pi^+)$	$0.05^{+0.29}_{-0.24}$
$A_{CP}(B^+ \rightarrow \eta_c K^+)$	$-0.16 \pm 0.08$	$A_{CP}(B^+ \rightarrow K^+ \pi^0 \pi^0)$	$-0.06 \pm 0.07$
$A_{CP}(B^+ \rightarrow \psi(2S) \pi^+)$	$0.02 \pm 0.09$	$A_{CP}(B^+ \rightarrow K^0 \rho^+)$	$-0.12 \pm 0.17$
$A_{CP}(B^+ \rightarrow \psi(2S) K^+)$	$-0.025 \pm 0.024$	$A_{CP}(B^+ \rightarrow K^{*+} \pi^+ \pi^-)$	$0.07 \pm 0.08$
$A_{CP}(B^+ \rightarrow \psi(2S) K^*(892)^+)$	$0.08 \pm 0.21$	$A_{CP}(B^+ \rightarrow \rho^0 K^*(892)^+)$	$0.31 \pm 0.13$
$A_{CP}(B^+ \rightarrow \chi_{c1}(1P) \pi^+)$	$0.07 \pm 0.18$	$A_{CP}(B^+ \rightarrow K^*(892)^+ f_0(980))$	$-0.15 \pm 0.12$
$A_{CP}(B^+ \rightarrow \chi_{c0} K^+)$	$-0.20 \pm 0.18$ (S = 1.5)	$A_{CP}(B^+ \rightarrow \chi_1^+ K^0)$	$0.12 \pm 0.11$
$A_{CP}(B^+ \rightarrow \chi_{c1} K^+)$	$-0.009 \pm 0.033$	$A_{CP}(B^+ \rightarrow b_1^+ K^0)$	$-0.03 \pm 0.15$
$A_{CP}(B^+ \rightarrow \chi_{c1} K^*(892)^+)$	$0.5 \pm 0.5$	$A_{CP}(B^+ \rightarrow K^*(892)^0 \rho^+)$	$-0.01 \pm 0.16$
$A_{CP}(B^+ \rightarrow \bar{D}^0 \pi^+)$	$-0.008 \pm 0.008$	$A_{CP}(B^+ \rightarrow b_1^0 K^+)$	$-0.46 \pm 0.20$
$A_{CP}(B^+ \rightarrow D_{CP(+1)} \pi^+)$	$0.035 \pm 0.024$	$A_{CP}(B^+ \rightarrow K^0 K^+)$	$0.12 \pm 0.18$
$A_{CP}(B^+ \rightarrow D_{CP(-1)} \pi^+)$	$0.017 \pm 0.026$	$A_{CP}(B^+ \rightarrow K^+ K_S^0 K_S^0)$	$-0.04 \pm 0.11$
$A_{CP}(B^+ \rightarrow \bar{D}^0 K^+)$	$0.07 \pm 0.04$	$A_{CP}(B^+ \rightarrow K^+ K^- \pi^+)$	$0.00 \pm 0.10$
$r_B(B^+ \rightarrow D^0 K^+)$	$0.113^{+0.024}_{-0.021}$	$A_{CP}(B^+ \rightarrow K^+ K^- K^+)$	$-0.017 \pm 0.030$
$\delta_B(B^+ \rightarrow D^0 K^+)$	$(125 \pm 16)^\circ$	$A_{CP}(B^+ \rightarrow \phi K^+)$	$-0.01 \pm 0.06$
$r_B(B^+ \rightarrow D K^*)$	$0.34 \pm 0.09$ (S = 1.3)	$A_{CP}(B^+ \rightarrow X_0(1550) K^+)$	$-0.04 \pm 0.07$
$\delta_B(B^+ \rightarrow D K^*)$	$(157 \pm 70)^\circ$ (S = 2.0)	$A_{CP}(B^+ \rightarrow K^+ + K + K^-)$	$0.11 \pm 0.09$
$A_{CP}(B^+ \rightarrow [K^- \pi^+]_D K^+)$	$-0.58 \pm 0.21$	$A_{CP}(B^+ \rightarrow \phi K^*(892)^+)$	$-0.01 \pm 0.08$
$A_{CP}(B^+ \rightarrow [K^- \pi^+]_{\bar{D}} K^*(892)^+)$	$-0.3 \pm 0.5$	$A_{CP}(B^+ \rightarrow \phi(K\pi)_0^+)$	$0.04 \pm 0.16$
$A_{CP}(B^+ \rightarrow [K^- \pi^+]_D \pi^+)$	$0.00 \pm 0.09$	$A_{CP}(B^+ \rightarrow \phi K_1(1270)^+)$	$0.15 \pm 0.20$
$A_{CP}(B^+ \rightarrow [K^- \pi^+]_{(D\pi)} \pi^+)$	$-0.09 \pm 0.27$	$A_{CP}(B^+ \rightarrow \phi K_S^0(1430)^+)$	$-0.23 \pm 0.20$
$A_{CP}(B^+ \rightarrow [K^- \pi^+]_{(D\gamma)} \pi^+)$	$-0.7 \pm 0.6$	$A_{CP}(B^+ \rightarrow K^+ \phi \phi)$	$-0.10 \pm 0.08$
$A_{CP}(B^+ \rightarrow [K^- \pi^+]_{(D\pi)} K^+)$	$0.8 \pm 0.4$	$A_{CP}(B^+ \rightarrow K^+[\phi\phi]_{\eta_c})$	$0.09 \pm 0.10$
$A_{CP}(B^+ \rightarrow [K^- \pi^+]_{(D\gamma)} K^+)$	$0.4 \pm 1.0$	$A_{CP}(B^+ \rightarrow K^*(892)^+ \gamma)$	$0.018 \pm 0.029$
$A_{CP}(B^+ \rightarrow [\pi^+ \pi^- \pi^0]_D K^+)$	$-0.02 \pm 0.15$	$A_{CP}(B^+ \rightarrow \eta K^+ \gamma)$	$-0.12 \pm 0.07$
$A_{CP}(B^+ \rightarrow D_{CP(+1)} K^+)$	$0.24 \pm 0.06$ (S = 1.1)	$A_{CP}(B^+ \rightarrow \phi K^+ \gamma)$	$-0.13 \pm 0.11$ (S = 1.1)
$A_{CP}(B^+ \rightarrow D_{CP(-1)} K^+)$	$-0.10 \pm 0.07$	$A_{CP}(B^+ \rightarrow \rho^+ \gamma)$	$-0.11 \pm 0.33$
$A_{CP}(B^+ \rightarrow \bar{D}^{*0} \pi^+)$	$-0.014 \pm 0.015$	$A_{CP}(B^+ \rightarrow \pi^+ \pi^0)$	$0.06 \pm 0.05$
$A_{CP}(B^+ \rightarrow (D_{CP(+1)}^*)^0 \pi^+)$	$-0.02 \pm 0.05$	$A_{CP}(B^+ \rightarrow \pi^+ \pi^- \pi^+)$	$0.03 \pm 0.06$
$A_{CP}(B^+ \rightarrow (D_{CP(-1)}^*)^0 \pi^+)$	$-0.09 \pm 0.05$	$A_{CP}(B^+ \rightarrow \rho^0 \pi^+)$	$0.18^{+0.09}_{-0.17}$
$A_{CP}(B^+ \rightarrow D^{*0} K^+)$	$-0.07 \pm 0.04$	$A_{CP}(B^+ \rightarrow f_2(1270) \pi^+)$	$0.41 \pm 0.30$
$r_B^*(B^+ \rightarrow D^{*0} K^+)$	$0.123^{+0.026}_{-0.029}$	$A_{CP}(B^+ \rightarrow \rho^0(1450) \pi^+)$	$-0.1^{+0.4}_{-0.5}$
$\delta_B^*(B^+ \rightarrow D^{*0} K^+)$	$(300 \pm 30)^\circ$ (S = 1.7)	$A_{CP}(B^+ \rightarrow \pi^+ \pi^- \pi^+ \text{ nonresonant})$	$-0.14^{+0.23}_{-0.16}$
$A_{CP}(B^+ \rightarrow D_{CP(+1)}^{*0} K^+)$	$-0.12 \pm 0.08$	$A_{CP}(B^+ \rightarrow \rho^+ \pi^0)$	$0.02 \pm 0.11$
$A_{CP}(B^+ \rightarrow D_{CP(-1)}^{*0} K^+)$	$0.07 \pm 0.10$	$A_{CP}(B^+ \rightarrow \rho^+ \rho^0)$	$-0.05 \pm 0.05$
$A_{CP}(B^+ \rightarrow D_{CP(+1)} K^*(892)^+)$	$0.09 \pm 0.14$	$A_{CP}(B^+ \rightarrow \omega \pi^+)$	$-0.04 \pm 0.06$
		$A_{CP}(B^+ \rightarrow \omega \rho^+)$	$-0.20 \pm 0.09$
		$A_{CP}(B^+ \rightarrow \eta \pi^+)$	$-0.14 \pm 0.07$ (S = 1.4)
		$A_{CP}(B^+ \rightarrow \eta \rho^+)$	$0.11 \pm 0.11$
		$A_{CP}(B^+ \rightarrow \eta' \pi^+)$	$0.06 \pm 0.16$
		$A_{CP}(B^+ \rightarrow \eta' \rho^+)$	$0.26 \pm 0.17$
		$A_{CP}(B^+ \rightarrow b_1^0 \pi^+)$	$0.05 \pm 0.16$

Unless otherwise stated, limits are given at the 90% confidence level, while errors are given as  $\pm 1$  standard deviation.



## Tests of Conservation Laws

$A_{CP}(B^+ \rightarrow p\bar{p}\pi^+)$	$0.00 \pm 0.04$	$C_{\eta'(958)K_S^0}(B^0 \rightarrow \eta'(958)K_S^0)$	$-0.04 \pm 0.20$ (S = 2.5)
$A_{CP}(B^+ \rightarrow p\bar{p}K^+)$	$-0.16 \pm 0.07$	$S_{\eta'(958)K_S^0}(B^0 \rightarrow \eta'(958)K_S^0)$	$0.43 \pm 0.17$ (S = 1.5)
$A_{CP}(B^+ \rightarrow p\bar{p}K^*(892)^+)$	$0.21 \pm 0.16$ (S = 1.4)	$C_{\eta'K^0}(B^0 \rightarrow \eta'K^0)$	$-0.05 \pm 0.05$
$A_{CP}(B^+ \rightarrow p\bar{p}\gamma)$	$0.17 \pm 0.17$	$C_{\omega K_S^0}(B^0 \rightarrow \omega K_S^0)$	$-0.30 \pm 0.28$ (S = 1.6)
$A_{CP}(B^+ \rightarrow p\bar{p}\pi^0)$	$0.01 \pm 0.17$	$S_{\omega K_S^0}(B^0 \rightarrow \omega K_S^0)$	$0.43 \pm 0.24$
$A_{CP}(B^+ \rightarrow K^+\ell^+\ell^-)$	$-0.01 \pm 0.09$ (S = 1.1)	$C(B^0 \rightarrow K_S^0\pi^0\pi^0)$	$0.2 \pm 0.5$
$A_{CP}(B^+ \rightarrow K^+e^+e^-)$	$0.14 \pm 0.14$	$S(B^0 \rightarrow K_S^0\pi^0\pi^0)$	$0.7 \pm 0.7$
$A_{CP}(B^+ \rightarrow K^+\mu^+\mu^-)$	$-0.05 \pm 0.13$	$C_{\rho^0 K_S^0}(B^0 \rightarrow \rho^0 K_S^0)$	$-0.04 \pm 0.20$
$A_{CP}(B^+ \rightarrow K^{*+}\ell^+\ell^-)$	$-0.09 \pm 0.14$	$S_{\rho^0 K_S^0}(B^0 \rightarrow \rho^0 K_S^0)$	$0.50^{+0.17}_{-0.21}$
$A_{CP}(B^+ \rightarrow K^{*+}e^+e^-)$	$-0.14 \pm 0.23$	$C_{f_0(980)K_S^0}(B^0 \rightarrow f_0(980)K_S^0)$	$0.14 \pm 0.17$
$A_{CP}(B^+ \rightarrow K^{*+}\mu^+\mu^-)$	$-0.12 \pm 0.24$	$S_{f_0(980)K_S^0}(B^0 \rightarrow f_0(980)K_S^0)$	$-0.73^{+0.27}_{-0.09}$ (S = 1.6)
$\text{Re}(\epsilon_{B^0})/(1+ \epsilon_{B^0} ^2)$	$(-0.8 \pm 0.8) \times 10^{-3}$	$S_{f_2(1270)K_S^0}(B^0 \rightarrow f_2(1270)K_S^0)$	$-0.5 \pm 0.5$
$A_{T/CP}$	$0.005 \pm 0.018$	$C_{f_2(1270)K_S^0}(B^0 \rightarrow f_2(1270)K_S^0)$	$0.3 \pm 0.4$
$A_{CP}(B^0 \rightarrow D^*(2010)^+D^-)$	$0.02 \pm 0.04$	$S_{f_x(1300)K_S^0}(B^0 \rightarrow f_x(1300)K_S^0)$	$-0.2 \pm 0.5$
$A_{CP}(B^0 \rightarrow \eta'K^*(892)^0)$	$0.02 \pm 0.23$	$C_{f_x(1300)K_S^0}(B^0 \rightarrow f_x(1300)K_S^0)$	$0.13 \pm 0.35$
$A_{CP}(B^0 \rightarrow \eta'K_0^*(1430)^0)$	$-0.19 \pm 0.17$	$S_{K^0\pi^+\pi^-}(B^0 \rightarrow K^0\pi^+\pi^- \text{ nonresonant})$	$-0.01 \pm 0.33$
$A_{CP}(B^0 \rightarrow \eta'K_2^*(1430)^0)$	$0.14 \pm 0.18$	$C_{K^0\pi^+\pi^-}(B^0 \rightarrow K^0\pi^+\pi^- \text{ nonresonant})$	$0.01 \pm 0.26$
$A_{CP}(B^0 \rightarrow \eta K_0^*(1430)^0)$	$0.06 \pm 0.13$	$C_{K_S^0 K_S^0}(B^0 \rightarrow K_S^0 K_S^0)$	$0.0 \pm 0.4$ (S = 1.4)
$A_{CP}(B^0 \rightarrow \eta K_2^*(1430)^0)$	$-0.07 \pm 0.19$	$S_{K_S^0 K_S^0}(B^0 \rightarrow K_S^0 K_S^0)$	$-0.8 \pm 0.5$
$A_{CP}(B^0 \rightarrow b_1 K^+)$	$-0.07 \pm 0.12$	$C_{K^+K^-K_S^0}(B^0 \rightarrow K^+K^-K_S^0)$	$0.09 \pm 0.09$
$A_{CP}(B^0 \rightarrow \omega K^{*0})$	$0.45 \pm 0.25$	$C_{K^+K^-K_S^0}(B^0 \rightarrow K^+K^-K_S^0 \text{ nonresonant})$	$0.01 \pm 0.09$
$A_{CP}(B^0 \rightarrow \omega(K\pi)_0^0)$	$-0.07 \pm 0.09$	$C_{K^+K^-K_S^0}(B^0 \rightarrow K^+K^-K_S^0 \text{ inclusive})$	$0.01 \pm 0.09$
$A_{CP}(B^0 \rightarrow \omega K_2^*(1430)^0)$	$-0.37 \pm 0.17$	$C_{\phi K_S^0}(B^0 \rightarrow \phi K_S^0)$	$0.03 \pm 0.14$
$A_{CP}(B^0 \rightarrow K^+\pi^-\pi^0)$	$(0 \pm 6) \times 10^{-2}$	$S_{\phi K_S^0}(B^0 \rightarrow \phi K_S^0)$	$0.39 \pm 0.17$
$A_{CP}(B^0 \rightarrow \rho^- K^+)$	$0.20 \pm 0.11$	$C_{K_S K_S K_S}(B^0 \rightarrow K_S K_S K_S)$	$-0.15 \pm 0.16$ (S = 1.1)
$A_{CP}(B^0 \rightarrow \rho(1450)^- K^+)$	$-0.10 \pm 0.33$	$S_{K_S K_S K_S}(B^0 \rightarrow K_S K_S K_S)$	$-0.4 \pm 0.5$ (S = 2.5)
$A_{CP}(B^0 \rightarrow \rho(1700)^- K^+)$	$-0.4 \pm 0.6$	$C_{K_S^0\pi^0\gamma}(B^0 \rightarrow K_S^0\pi^0\gamma)$	$0.36 \pm 0.33$
$A_{CP}(B^0 \rightarrow K^+\pi^-\pi^0 \text{ nonresonant})$	$0.10 \pm 0.18$	$S_{K_S^0\pi^0\gamma}(B^0 \rightarrow K_S^0\pi^0\gamma)$	$-0.8 \pm 0.6$
$A_{CP}(B^0 \rightarrow K^0\pi^+\pi^-)$	$-0.01 \pm 0.05$	$C_{K^*(892)^0\gamma}(B^0 \rightarrow K^*(892)^0\gamma)$	$-0.04 \pm 0.16$ (S = 1.2)
$A_{CP}(B^0 \rightarrow K^*(892)^+\pi^-)$	$-0.22 \pm 0.06$	$S_{K^*(892)^0\gamma}(B^0 \rightarrow K^*(892)^0\gamma)$	$-0.15 \pm 0.22$
$A_{CP}(B^0 \rightarrow (K\pi)_0^{*+}\pi^-)$	$0.09 \pm 0.07$	$C_{\eta K^0\gamma}(B^0 \rightarrow \eta K^0\gamma)$	$-0.3 \pm 0.4$
$A_{CP}(B^0 \rightarrow (K\pi)_0^0\pi^0)$	$-0.15 \pm 0.11$	$S_{\eta K^0\gamma}(B^0 \rightarrow \eta K^0\gamma)$	$-0.2 \pm 0.5$
$A_{CP}(B^0 \rightarrow K^{*0}\pi^0)$	$-0.15 \pm 0.13$	$C_{K^0\phi\gamma}(B^0 \rightarrow K^0\phi\gamma)$	$-0.3 \pm 0.6$
$A_{CP}(B^0 \rightarrow K^*(892)^0\pi^+\pi^-)$	$0.07 \pm 0.05$	$S_{K^0\phi\gamma}(B^0 \rightarrow K^0\phi\gamma)$	$0.7^{+0.7}_{-1.1}$
$A_{CP}(B^0 \rightarrow K^*(892)^0\rho^0)$	$0.09 \pm 0.19$	$C(B^0 \rightarrow K_S^0\rho^0\gamma)$	$-0.05 \pm 0.19$
$A_{CP}(B^0 \rightarrow K^{*0}f_0(980))$	$-0.17 \pm 0.28$	$S(B^0 \rightarrow K_S^0\rho^0\gamma)$	$0.11 \pm 0.34$
$A_{CP}(B^0 \rightarrow K^*(892)^0 K^+ K^-)$	$0.01 \pm 0.05$	$C(B^0 \rightarrow \rho^0\gamma)$	$0.4 \pm 0.5$
$A_{CP}(B^0 \rightarrow a_1^- K^+)$	$-0.16 \pm 0.12$	$S(B^0 \rightarrow \rho^0\gamma)$	$-0.8 \pm 0.7$
$A_{CP}(B^0 \rightarrow K^0 K^0)$	$-0.6 \pm 0.7$	$C_{\pi^-\pi}(B^0 \rightarrow \pi^+\pi^-)$	$-0.38 \pm 0.17$ (S = 2.6)
$A_{CP}(B^0 \rightarrow K^*(892)^0\phi)$	$0.01 \pm 0.05$	$C_{\pi^0\pi^0}(B^0 \rightarrow \pi^0\pi^0)$	$-0.48 \pm 0.30$
$A_{CP}(B^0 \rightarrow K^*(892)^0 K^- \pi^+)$	$0.2 \pm 0.4$	$C_{\rho^0\pi}(B^0 \rightarrow \rho^+\pi^-)$	$0.01 \pm 0.14$ (S = 1.9)
$A_{CP}(B^0 \rightarrow \phi(K\pi)_0^0)$	$0.20 \pm 0.15$	$S_{\rho^0\pi}(B^0 \rightarrow \rho^+\pi^-)$	$0.01 \pm 0.09$
$A_{CP}(B^0 \rightarrow \phi K_2^*(1430)^0)$	$-0.08 \pm 0.13$	$\Delta S_{\rho\pi}(B^0 \rightarrow \rho^+\pi^-)$	$-0.05 \pm 0.10$
$A_{CP}(B^0 \rightarrow K^*(892)^0\gamma)$	$-0.016 \pm 0.023$	$C_{\rho^0\pi^0}(B^0 \rightarrow \rho^0\pi^0)$	$0.3 \pm 0.4$
$A_{CP}(B^0 \rightarrow K_2^*(1430)^0\gamma)$	$-0.08 \pm 0.15$	$S_{\rho^0\pi^0}(B^0 \rightarrow \rho^0\pi^0)$	$0.1 \pm 0.4$
$A_{CP}(B^0 \rightarrow \rho^+\pi^-)$	$0.08 \pm 0.12$ (S = 2.0)	$C_{a_1\pi}(B^0 \rightarrow a_1(1260)^+\pi^-)$	$-0.10 \pm 0.17$
$A_{CP}(B^0 \rightarrow \rho^-\pi^+)$	$-0.16 \pm 0.23$ (S = 1.7)	$S_{a_1\pi}(B^0 \rightarrow a_1(1260)^+\pi^-)$	$0.37 \pm 0.22$
$A_{CP}(B^0 \rightarrow a_1(1260)^{\pm}\pi^{\mp})$	$-0.07 \pm 0.07$	$\Delta C_{a_1\pi}(B^0 \rightarrow a_1(1260)^+\pi^-)$	$0.26 \pm 0.17$
$A_{CP}(B^0 \rightarrow b_1\pi^+)$	$-0.05 \pm 0.10$	$\Delta S_{a_1\pi}(B^0 \rightarrow a_1(1260)^+\pi^-)$	$-0.14 \pm 0.22$
$A_{CP}(B^0 \rightarrow p\bar{p}K^*(892)^0)$	$0.05 \pm 0.12$	$C(B^0 \rightarrow b_1^- K^+)$	$-0.22 \pm 0.24$
$A_{CP}(B^0 \rightarrow p\bar{p}\pi^-)$	$0.04 \pm 0.07$	$\Delta C(B^0 \rightarrow b_1^- \pi^+)$	$-1.04 \pm 0.24$
$A_{CP}(B^0 \rightarrow K^{*0}\ell^+\ell^-)$	$-0.05 \pm 0.10$	$C_{\rho^0\rho^0}(B^0 \rightarrow \rho^0\rho^0)$	$0.2 \pm 0.9$
$A_{CP}(B^0 \rightarrow K^{*0}e^+e^-)$	$-0.21 \pm 0.19$	$S_{\rho^0\rho^0}(B^0 \rightarrow \rho^0\rho^0)$	$0.3 \pm 0.7$
$A_{CP}(B^0 \rightarrow K^{*0}\mu^+\mu^-)$	$0.00 \pm 0.15$	$C_{\rho\rho}(B^0 \rightarrow \rho^+\rho^-)$	$-0.05 \pm 0.13$
$C_{D^*(2010)^-D^+}(B^0 \rightarrow D^*(2010)^-D^+)$	$0.07 \pm 0.14$	$S_{\rho\rho}(B^0 \rightarrow \rho^+\rho^-)$	$-0.06 \pm 0.17$
$C_{D^*(2010)^+D^-}(B^0 \rightarrow D^*(2010)^+D^-)$	$-0.09 \pm 0.22$ (S = 1.6)	$ \lambda (B^0 \rightarrow J/\psi K^*(892)^0)$	$<0.25$ , CL = 95%
$C_{D^+D^+}(B^0 \rightarrow D^{*+}D^{*-})$	$-0.01 \pm 0.09$ (S = 1.2)	$\cos 2\beta(B^0 \rightarrow J/\psi K^*(892)^0)$	$1.7^{+0.7}_{-0.9}$ (S = 1.6)
$C_+(B^0 \rightarrow D^{*+}D^{*-})$	$0.00 \pm 0.12$	$\cos 2\beta(B^0 \rightarrow [K_S^0\pi^+\pi^-]_{D^{(*)}} h^0)$	$1.0^{+0.6}_{-0.7}$ (S = 1.8)
$C_-(B^0 \rightarrow D^{*+}D^{*-})$	$0.4 \pm 0.5$		
$S_-(B^0 \rightarrow D^{*+}D^{*-})$	$-1.8 \pm 0.7$		
$C(B^0 \rightarrow D^*(2010)^+D^*(2010)^-K_S^0)$	$0.01 \pm 0.29$		
$S(B^0 \rightarrow D^*(2010)^+D^*(2010)^-K_S^0)$	$0.1 \pm 0.4$		
$C_{D^+D^-}(B^0 \rightarrow D^+D^-)$	$-0.5 \pm 0.4$ (S = 2.5)		
$C_{J/\psi(1S)\pi^0}(B^0 \rightarrow J/\psi(1S)\pi^0)$	$-0.13 \pm 0.13$		
$C_{D^{(*)}h^0}(B^0 \rightarrow D_{CP}^{(*)}h^0)$	$-0.23 \pm 0.16$		
$S_{D^{(*)}h^0}(B^0 \rightarrow D_{CP}^{(*)}h^0)$	$-0.56 \pm 0.24$		
$C_{K^0\pi^0}(B^0 \rightarrow K^0\pi^0)$	$0.00 \pm 0.13$ (S = 1.4)		

Unless otherwise stated, limits are given at the 90% confidence level, while errors are given as  $\pm 1$  standard deviation.

# Tests of Conservation Laws

$(S_+ + S_-)/2 (B^0 \rightarrow D^{*-}\pi^+)$	$-0.039 \pm 0.011$	$\phi_{+-}, \text{ phase of } \eta_{+-}$	$(43.51 \pm 0.05)^\circ (S = 1.2)$
$(S_- - S_+)/2 (B^0 \rightarrow D^{*-}\pi^+)$	$-0.009 \pm 0.015$	$\phi_{00}, \text{ phase of } \eta_{00}$	$(43.52 \pm 0.05)^\circ (S = 1.3)$
$(S_+ + S_-)/2 (B^0 \rightarrow D^-\pi^+)$	$-0.046 \pm 0.023$	$\phi_\epsilon = (2\phi_{+-} + \phi_{00})/3$	$(43.52 \pm 0.05)^\circ (S = 1.2)$
$(S_- - S_+)/2 (B^0 \rightarrow D^-\pi^+)$	$-0.022 \pm 0.021$	Not assuming <i>CPT</i>	
$(S_+ + S_-)/2 (B^0 \rightarrow D^-\rho^+)$	$-0.024 \pm 0.032$	$\phi_{+-}, \text{ phase of } \eta_{+-}$	$(43.4 \pm 0.5)^\circ (S = 1.2)$
$(S_- - S_+)/2 (B^0 \rightarrow D^-\rho^+)$	$-0.10 \pm 0.06$	$\phi_{00}, \text{ phase of } \eta_{00}$	$(43.7 \pm 0.6)^\circ (S = 1.2)$
$C_{\eta_c K_S^0} (B^0 \rightarrow \eta_c K_S^0)$	$0.08 \pm 0.13$	$\phi_\epsilon = (2\phi_{+-} + \phi_{00})/3$	$(43.5 \pm 0.5)^\circ (S = 1.3)$
$C_{c\bar{c}K^{(*)0}} (B^0 \rightarrow c\bar{c}K^{(*)0})$	$(0.5 \pm 1.7) \times 10^{-2}$	<i>CP</i> asymmetry <i>A</i> in $K_L^0 \rightarrow \pi^+\pi^-e^+e^-$	$(13.7 \pm 1.5)\%$
$C_{J/\psi(nS)K^0} (B^0 \rightarrow J/\psi(nS)K^0)$	$(0.5 \pm 2.0) \times 10^{-2}$	$\beta_{CP}$ from $K_L^0 \rightarrow e^+e^-e^+e^-$	$-0.19 \pm 0.07$
$C_{J/\psi K^{*0}} (B^0 \rightarrow J/\psi K^{*0})$	$0.03 \pm 0.10$	$\gamma_{CP}$ from $K_L^0 \rightarrow e^+e^-e^+e^-$	$0.01 \pm 0.11 (S = 1.6)$
$S_{J/\psi K^{*0}} (B^0 \rightarrow J/\psi K^{*0})$	$0.60 \pm 0.25$	parameters for $K_L^0 \rightarrow \pi^+\pi^-\gamma$ decay	
$C_{\chi_{c0} K_S^0} (B^0 \rightarrow \chi_{c0} K_S^0)$	$-0.3^{+0.5}_{-0.4}$	$ \eta_{+-\gamma}  =  A(K_L^0 \rightarrow \pi^+\pi^-\gamma, CP \text{ violating})/A(K_S^0 \rightarrow \pi^+\pi^-\gamma) $	$(2.35 \pm 0.07) \times 10^{-3}$
$S_{\chi_{c0} K_S^0} (B^0 \rightarrow \chi_{c0} K_S^0)$	$-0.7 \pm 0.5$	$\phi_{+-\gamma} = \text{phase of } \eta_{+-\gamma}$	$(44 \pm 4)^\circ$
$C_{\chi_{c1} K_S^0} (B^0 \rightarrow \chi_{c1} K_S^0)$	$0.13 \pm 0.11$	$\Gamma(K_L^0 \rightarrow \pi^+\pi^-)/\Gamma_{\text{total}}$	[i] $(1.967 \pm 0.010) \times 10^{-3} (S = 1.5)$
$\sin(2\beta_{\text{eff}})(B^0 \rightarrow \phi K^0)$	$0.22 \pm 0.30$	$\Gamma(K_L^0 \rightarrow \pi^0\pi^0)/\Gamma_{\text{total}}$	$(8.64 \pm 0.06) \times 10^{-4} (S = 1.8)$
$\sin(2\beta_{\text{eff}})(B^0 \rightarrow \phi K_0^{*0}(1430)^0)$	$0.97^{+0.03}_{-0.52}$	$A_{CP}(B^+ \rightarrow f_0(1370)\pi^+)$	$0.72 \pm 0.22$
$\sin(2\beta_{\text{eff}})(B^0 \rightarrow [K_S^0\pi^+\pi^-]_{D^{(*)}} h^0)$	$0.45 \pm 0.28$	$\gamma(B^+ \rightarrow D^{(*)}K^{(*)+})$	$(73 \pm 10)^\circ$
$ \lambda  (B^0 \rightarrow [K_S^0\pi^+\pi^-]_{D^{(*)}} h^0)$	$1.01 \pm 0.08$	$A_{CP}(B^0 \rightarrow K^+\pi^-)$	$-0.097 \pm 0.012$
$ \sin(2\beta + \gamma) $	$>0.40, \text{ CL} = 90\%$	$A_{CP}(B^0 \rightarrow \eta K^*(892)^0)$	$0.19 \pm 0.05$
$2\beta + \gamma$	$(83 \pm 60)^\circ$	$S_{D^*(2010)-D^+} (B^0 \rightarrow D^*(2010)^-D^+)$	$-0.78 \pm 0.21$
$\gamma(B^0 \rightarrow D^0 K^{*0})$	$(162 \pm 60)^\circ$	$S_{D^*(2010)+D^-} (B^0 \rightarrow D^*(2010)^+D^-)$	$-0.61 \pm 0.19$
$A_{CP}(B \rightarrow K^*(892)\gamma)$	$-0.003 \pm 0.017$	$S_{D^{*+}D^{*-}} (B^0 \rightarrow D^{*+}D^{*-})$	$-0.76 \pm 0.14$
$A_{CP}(b \rightarrow s\gamma)$	$-0.008 \pm 0.029$	$S_+ (B^0 \rightarrow D^{*+}D^{*-})$	$-0.76 \pm 0.16$
$A_{CP}(b \rightarrow (s+d)\gamma)$	$-0.09 \pm 0.07$	$S_{D^+D^-} (B^0 \rightarrow D^+D^-)$	$-0.87 \pm 0.26$
$A_{CP}(B \rightarrow X_S \ell^+ \ell^-)$	$-0.22 \pm 0.26$	$S_{J/\psi(1S)\pi^0} (B^0 \rightarrow J/\psi(1S)\pi^0)$	$-0.94 \pm 0.29 (S = 1.9)$
$A_{CP}(B \rightarrow K^*e^+e^-)$	$-0.18 \pm 0.15$	$S_{K^0\pi^0} (B^0 \rightarrow K^0\pi^0)$	$0.58 \pm 0.17$
$A_{CP}(B \rightarrow K^*\mu^+\mu^-)$	$-0.03 \pm 0.13$	$S_{\eta'K^0} (B^0 \rightarrow \eta'K^0)$	$0.60 \pm 0.07$
$A_{CP}(B \rightarrow K^*\ell^+\ell^-)$	$-0.07 \pm 0.08$	$S_{K^+K^-K_S^0} (B^0 \rightarrow K^+K^-K_S^0)$	$-0.74^{+0.12}_{-0.10}$
$A_{CP}(B \rightarrow \eta \text{ anything})$	$-0.13^{+0.04}_{-0.05}$	nonresonant)	
$\text{Re}(\epsilon_{B_S}) / (1 +  \epsilon_{B_S} ^2)$	$(-2.6 \pm 1.6) \times 10^{-3}$	$S_{K^+K^-K_S^0} (B^0 \rightarrow K^+K^-K_S^0 \text{ inclusive})$	$-0.65 \pm 0.12$
<i>CP</i> Violation phase $\beta_S$	$0.08^{+0.05}_{-0.07}$	$S_{\pi\pi} (B^0 \rightarrow \pi^+\pi^-)$	$-0.61 \pm 0.08$
$A_{CP}(B_S \rightarrow \pi^+K^-)$	$0.39 \pm 0.17$	$\Delta C_{\rho\pi} (B^0 \rightarrow \rho^+\pi^-)$	$0.37 \pm 0.08$
$\Gamma(\eta_c(1S) \rightarrow \pi^+\pi^-)/\Gamma_{\text{total}}$	$<1.1 \times 10^{-4}, \text{ CL} = 90\%$	$S_{\eta_c K_S^0} (B^0 \rightarrow \eta_c K_S^0)$	$0.93 \pm 0.17$
$\Gamma(\eta_c(1S) \rightarrow \pi^0\pi^0)/\Gamma_{\text{total}}$	$<3.5 \times 10^{-5}, \text{ CL} = 90\%$	$\sin(2\beta) (B^0 \rightarrow J/\psi K_S^0)$	$0.679 \pm 0.020$
$\Gamma(\eta_c(1S) \rightarrow K^+K^-)/\Gamma_{\text{total}}$	$<6 \times 10^{-4}, \text{ CL} = 90\%$	$S_{J/\psi(nS)K^0} (B^0 \rightarrow J/\psi(nS)K^0)$	$0.676 \pm 0.021$
$\Gamma(\eta_c(1S) \rightarrow K_S^0 K_S^0)/\Gamma_{\text{total}}$	$<3.1 \times 10^{-4}, \text{ CL} = 90\%$	$S_{\chi_{c1} K_S^0} (B^0 \rightarrow \chi_{c1} K_S^0)$	$0.61 \pm 0.16$
$(\alpha + \bar{\alpha})/(\alpha - \bar{\alpha})$ in $\Lambda \rightarrow p\pi^-, \bar{\Lambda} \rightarrow \bar{p}\pi^+$	$0.006 \pm 0.021$	$\sin(2\beta_{\text{eff}})(B^0 \rightarrow K^+K^-K_S^0)$	$0.77^{+0.13}_{-0.12}$
$[\alpha(\Xi^-)\alpha_-(\Lambda) - \alpha(\Xi^+)\alpha_+(\Lambda)]$	$(0 \pm 7) \times 10^{-4}$	$\alpha$	$(90 \pm 5)^\circ$
$[\alpha(\Xi^-)\alpha_-(\Lambda) + \alpha(\Xi^+)\alpha_+(\Lambda)]$		$\text{Re}(\epsilon_b) / (1 +  \epsilon_b ^2)$	$(-2.0 \pm 0.5) \times 10^{-3}$
$(\alpha + \bar{\alpha})/(\alpha - \bar{\alpha})$ in $\Omega^- \rightarrow \Lambda K^-, \bar{\Omega}^+ \rightarrow \bar{\Lambda} K^+$	$-0.02 \pm 0.13$		
$(\alpha + \bar{\alpha})/(\alpha - \bar{\alpha})$ in $\Lambda_C^+ \rightarrow \Lambda\pi^+, \bar{\Lambda}_C^- \rightarrow \bar{\Lambda}\pi^-$	$-0.07 \pm 0.31$		
$(\alpha + \bar{\alpha})/(\alpha - \bar{\alpha})$ in $\Lambda_C^+ \rightarrow \Lambda e^+\nu_e, \bar{\Lambda}_C^- \rightarrow \bar{\Lambda} e^-\bar{\nu}_e$	$0.00 \pm 0.04$		
$A_{CP}(\Lambda_b \rightarrow p\pi^-)$	$0.03 \pm 0.18$		
$A_{CP}(\Lambda_b \rightarrow pK^-)$	$0.37 \pm 0.17$		
<b>CP VIOLATION OBSERVED</b>			
$\text{Re}(\epsilon)$	$(1.596 \pm 0.013) \times 10^{-3}$		
charge asymmetry in $K_{L3}^0$ decays			
$A_L = \text{weighted average of } A_L(\mu) \text{ and } A_L(e)$	$(0.332 \pm 0.006)\%$		
$A_L(\mu) = [\Gamma(\pi^-\mu^+\nu_\mu) - \Gamma(\pi^+\mu^-\nu_\mu)]/\text{sum}$	$(0.304 \pm 0.025)\%$		
$A_L(e) = [\Gamma(\pi^-e^+\nu_e) - \Gamma(\pi^+e^-\nu_e)]/\text{sum}$	$(0.334 \pm 0.007)\%$		
parameters for $K_L^0 \rightarrow 2\pi$ decay			
$ \eta_{00}  =  A(K_L^0 \rightarrow 2\pi^0) / A(K_S^0 \rightarrow 2\pi^0) $	$(2.220 \pm 0.011) \times 10^{-3} (S = 1.8)$		
$ \eta_{+-}  =  A(K_L^0 \rightarrow \pi^+\pi^-) / A(K_S^0 \rightarrow \pi^+\pi^-) $	$(2.232 \pm 0.011) \times 10^{-3} (S = 1.8)$		
$ \epsilon  = (2 \eta_{+-}  +  \eta_{00} )/3$	$(2.228 \pm 0.011) \times 10^{-3} (S = 1.8)$		
$ \eta_{00}/\eta_{+-} $	[h] $0.9950 \pm 0.0007 (S = 1.6)$		
$\text{Re}(\epsilon'/\epsilon) = (1 -  \eta_{00}/\eta_{+-} )/3$	[h] $(1.66 \pm 0.23) \times 10^{-3} (S = 1.6)$		
Assuming <i>CPT</i>			
		$(m_{W^+} - m_{W^-}) / m_{\text{average}}$	$-0.002 \pm 0.007$
		$(m_{e^+} - m_{e^-}) / m_{\text{average}}$	$<8 \times 10^{-9}, \text{ CL} = 90\%$
		$ q_{e^+} + q_{e^-} /e$	$<4 \times 10^{-8}$
		$(g_{e^+} - g_{e^-}) / g_{\text{average}}$	$(-0.5 \pm 2.1) \times 10^{-12}$
		$(\tau_{\mu^+} - \tau_{\mu^-}) / \tau_{\text{average}}$	$(2 \pm 8) \times 10^{-5}$
		$(g_{\mu^+} - g_{\mu^-}) / g_{\text{average}}$	$(-0.11 \pm 0.12) \times 10^{-8}$
		$(m_{\tau^+} - m_{\tau^-})/m_{\text{average}}$	$<2.8 \times 10^{-4}, \text{ CL} = 90\%$
		$m_t - m_{\bar{t}}$	$-1.4 \pm 2.0 \text{ GeV} (S = 1.6)$
		$(m_{\pi^+} - m_{\pi^-}) / m_{\text{average}}$	$(2 \pm 5) \times 10^{-4}$
		$(\tau_{\pi^+} - \tau_{\pi^-}) / \tau_{\text{average}}$	$(6 \pm 7) \times 10^{-4}$
		$(m_{K^+} - m_{K^-}) / m_{\text{average}}$	$(-0.6 \pm 1.8) \times 10^{-4}$
		$(\tau_{K^+} - \tau_{K^-}) / \tau_{\text{average}}$	$(0.10 \pm 0.09)\% (S = 1.2)$
		$K^\pm \rightarrow \mu^\pm \nu_\mu$ rate difference/average	$(-0.5 \pm 0.4)\%$
		$K^\pm \rightarrow \pi^\pm \pi^0$ rate difference/average	[j] $(0.8 \pm 1.2)\%$
		$\delta$ in $K^0 - \bar{K}^0$ mixing	
		real part of $\delta$	$(2.5 \pm 2.3) \times 10^{-4}$
		imaginary part of $\delta$	$(-1.5 \pm 1.6) \times 10^{-5}$
		$\text{Re}(y), K_{e3}$ parameter	$(0.4 \pm 2.5) \times 10^{-3}$
		$\text{Re}(x_-), K_{e3}$ parameter	$(-2.9 \pm 2.0) \times 10^{-3}$
		$ m_{K^0} - m_{\bar{K}^0}  / m_{\text{average}}$	[k] $<6 \times 10^{-19}, \text{ CL} = 90\%$
		$(\Gamma_{K^0} - \Gamma_{\bar{K}^0})/m_{\text{average}}$	$(8 \pm 8) \times 10^{-18}$

## Tests of Conservation Laws

phase difference $\phi_{00} - \phi_{+-}$	$(0.34 \pm 0.32)^\circ$
$\text{Re}(\frac{2}{3}\eta_{+-} + \frac{1}{3}\eta_{00}) - \frac{A_{\pi^0}}{A_{\pi^+}}$	$(-3 \pm 35) \times 10^{-6}$
$A_{CP\bar{T}}(D^0 \rightarrow K^- \pi^+)$	$0.008 \pm 0.008$
$ \frac{m_{D^0} - m_{\bar{D}^0}}{m_{D^0}}  / \frac{q_p}{m_p}$	[f] $< 2 \times 10^{-9}$ , CL = 90%
$(\frac{q_p}{m_p} - \frac{q_{\bar{p}}}{m_{\bar{p}}}) / \frac{q_p}{m_p}$	$(-9 \pm 9) \times 10^{-11}$
$ q_p + q_{\bar{p}} /e$	[f] $< 2 \times 10^{-9}$ , CL = 90%
$(\mu_p + \mu_{\bar{p}}) / \mu_p$	$(-0.1 \pm 2.1) \times 10^{-3}$
$(m_n - m_{\bar{n}}) / m_n$	$(9 \pm 6) \times 10^{-5}$
$(m_\Lambda - m_{\bar{\Lambda}}) / m_\Lambda$	$(-0.1 \pm 1.1) \times 10^{-5}$ (S = 1.6)
$(\tau_\Lambda - \tau_{\bar{\Lambda}}) / \tau_\Lambda$	$-0.001 \pm 0.009$
$(\tau_{\Sigma^+} - \tau_{\bar{\Sigma}^-}) / \tau_{\Sigma^+}$	$(-0.6 \pm 1.2) \times 10^{-3}$
$(\mu_{\Sigma^+} + \mu_{\bar{\Sigma}^-}) / \mu_{\Sigma^+}$	$0.014 \pm 0.015$
$(m_{\Xi^-} - m_{\bar{\Xi}^+}) / m_{\Xi^-}$	$(-3 \pm 9) \times 10^{-5}$
$(\tau_{\Xi^-} - \tau_{\bar{\Xi}^+}) / \tau_{\Xi^-}$	$-0.01 \pm 0.07$
$(\mu_{\Xi^-} + \mu_{\bar{\Xi}^+}) /  \mu_{\Xi^-} $	$+0.01 \pm 0.05$
$(m_{\Omega^-} - m_{\bar{\Omega}^+}) / m_{\Omega^-}$	$(-1 \pm 8) \times 10^{-5}$
$(\tau_{\Omega^-} - \tau_{\bar{\Omega}^+}) / \tau_{\Omega^-}$	$0.00 \pm 0.05$
$m_{\Sigma_b^+} - m_{\Sigma_b^-}$	$-4.2 \pm 1.1$ MeV
$m_{\Sigma_b^{*+}} - m_{\Sigma_b^{*-}}$	$-3.0_{-0.9}^{+1.0}$ MeV

## TESTS OF NUMBER CONSERVATION LAWS

## LEPTON FAMILY NUMBER

Lepton family number conservation means separate conservation of each of  $L_e, L_\mu, L_\tau$ .

$\Gamma(Z \rightarrow e^\pm \mu^\mp) / \Gamma_{\text{total}}$	[m] $< 1.7 \times 10^{-6}$ , CL = 95%
$\Gamma(Z \rightarrow e^\pm \tau^\mp) / \Gamma_{\text{total}}$	[m] $< 9.8 \times 10^{-6}$ , CL = 95%
$\Gamma(Z \rightarrow \mu^\pm \tau^\mp) / \Gamma_{\text{total}}$	[m] $< 1.2 \times 10^{-5}$ , CL = 95%
$\sigma(e^+ e^- \rightarrow e^\pm \tau^\mp) / \sigma(e^+ e^- \rightarrow \mu^+ \mu^-)$	$< 8.9 \times 10^{-6}$ , CL = 95%
$\sigma(e^+ e^- \rightarrow \mu^\pm \tau^\mp) / \sigma(e^+ e^- \rightarrow \mu^+ \mu^-)$	$< 4.0 \times 10^{-6}$ , CL = 95%
limit on $\mu^- \rightarrow e^-$ conversion $\sigma(\mu^- 32\text{S} \rightarrow e^- 32\text{S}) / \sigma(\mu^- 32\text{S} \rightarrow \nu_\mu 32\text{P}^*)$	$< 7 \times 10^{-11}$ , CL = 90%
$\sigma(\mu^- \text{Ti} \rightarrow e^- \text{Ti}) / \sigma(\mu^- \text{Ti} \rightarrow \text{capture})$	$< 4.3 \times 10^{-12}$ , CL = 90%
$\sigma(\mu^- \text{Pb} \rightarrow e^- \text{Pb}) / \sigma(\mu^- \text{Pb} \rightarrow \text{capture})$	$< 4.6 \times 10^{-11}$ , CL = 90%
limit on muonium $\rightarrow$ antimuonium conversion $R_g = G_C / G_F$	$< 0.0030$ , CL = 90%
$\Gamma(\mu^- \rightarrow e^- \nu_e \bar{\nu}_\mu) / \Gamma_{\text{total}}$	[n] $< 1.2 \times 10^{-2}$ , CL = 90%
$\Gamma(\mu^- \rightarrow e^- \gamma) / \Gamma_{\text{total}}$	$< 2.4 \times 10^{-12}$ , CL = 90%
$\Gamma(\mu^- \rightarrow e^- e^+ e^-) / \Gamma_{\text{total}}$	$< 1.0 \times 10^{-12}$ , CL = 90%
$\Gamma(\mu^- \rightarrow e^- 2\gamma) / \Gamma_{\text{total}}$	$< 7.2 \times 10^{-11}$ , CL = 90%
$\Gamma(\tau^- \rightarrow e^- \gamma) / \Gamma_{\text{total}}$	$< 3.3 \times 10^{-8}$ , CL = 90%
$\Gamma(\tau^- \rightarrow \mu^- \gamma) / \Gamma_{\text{total}}$	$< 4.4 \times 10^{-8}$ , CL = 90%
$\Gamma(\tau^- \rightarrow e^- \pi^0) / \Gamma_{\text{total}}$	$< 8.0 \times 10^{-8}$ , CL = 90%
$\Gamma(\tau^- \rightarrow \mu^- \pi^0) / \Gamma_{\text{total}}$	$< 1.1 \times 10^{-7}$ , CL = 90%
$\Gamma(\tau^- \rightarrow e^- K_S^0) / \Gamma_{\text{total}}$	$< 2.6 \times 10^{-8}$ , CL = 90%
$\Gamma(\tau^- \rightarrow \mu^- K_S^0) / \Gamma_{\text{total}}$	$< 2.3 \times 10^{-8}$ , CL = 90%
$\Gamma(\tau^- \rightarrow e^- \eta) / \Gamma_{\text{total}}$	$< 9.2 \times 10^{-8}$ , CL = 90%
$\Gamma(\tau^- \rightarrow \mu^- \eta) / \Gamma_{\text{total}}$	$< 6.5 \times 10^{-8}$ , CL = 90%
$\Gamma(\tau^- \rightarrow e^- \rho^0) / \Gamma_{\text{total}}$	$< 1.8 \times 10^{-8}$ , CL = 90%
$\Gamma(\tau^- \rightarrow \mu^- \rho^0) / \Gamma_{\text{total}}$	$< 1.2 \times 10^{-8}$ , CL = 90%
$\Gamma(\tau^- \rightarrow e^- \omega) / \Gamma_{\text{total}}$	$< 4.8 \times 10^{-8}$ , CL = 90%
$\Gamma(\tau^- \rightarrow \mu^- \omega) / \Gamma_{\text{total}}$	$< 4.7 \times 10^{-8}$ , CL = 90%
$\Gamma(\tau^- \rightarrow e^- K^*(892)^0) / \Gamma_{\text{total}}$	$< 3.2 \times 10^{-8}$ , CL = 90%
$\Gamma(\tau^- \rightarrow \mu^- K^*(892)^0) / \Gamma_{\text{total}}$	$< 5.9 \times 10^{-8}$ , CL = 90%
$\Gamma(\tau^- \rightarrow e^- \bar{K}^*(892)^0) / \Gamma_{\text{total}}$	$< 3.4 \times 10^{-8}$ , CL = 90%
$\Gamma(\tau^- \rightarrow \mu^- \bar{K}^*(892)^0) / \Gamma_{\text{total}}$	$< 7.0 \times 10^{-8}$ , CL = 90%
$\Gamma(\tau^- \rightarrow e^- \eta'(958)) / \Gamma_{\text{total}}$	$< 1.6 \times 10^{-7}$ , CL = 90%
$\Gamma(\tau^- \rightarrow \mu^- \eta'(958)) / \Gamma_{\text{total}}$	$< 1.3 \times 10^{-7}$ , CL = 90%
$\Gamma(\tau^- \rightarrow e^- f_0(980) \rightarrow e^- \pi^+ \pi^-) / \Gamma_{\text{total}}$	$< 3.2 \times 10^{-8}$ , CL = 90%

$\Gamma(\tau^- \rightarrow \mu^- f_0(980) \rightarrow \mu^- \pi^+ \pi^-) / \Gamma_{\text{total}}$	$< 3.4 \times 10^{-8}$ , CL = 90%
$\Gamma(\tau^- \rightarrow e^- \phi) / \Gamma_{\text{total}}$	$< 3.1 \times 10^{-8}$ , CL = 90%
$\Gamma(\tau^- \rightarrow \mu^- \phi) / \Gamma_{\text{total}}$	$< 8.4 \times 10^{-8}$ , CL = 90%
$\Gamma(\tau^- \rightarrow e^- e^+ e^-) / \Gamma_{\text{total}}$	$< 2.7 \times 10^{-8}$ , CL = 90%
$\Gamma(\tau^- \rightarrow e^- \mu^+ \mu^-) / \Gamma_{\text{total}}$	$< 2.7 \times 10^{-8}$ , CL = 90%
$\Gamma(\tau^- \rightarrow e^+ \mu^- \mu^-) / \Gamma_{\text{total}}$	$< 1.7 \times 10^{-8}$ , CL = 90%
$\Gamma(\tau^- \rightarrow \mu^+ e^+ e^-) / \Gamma_{\text{total}}$	$< 1.8 \times 10^{-8}$ , CL = 90%
$\Gamma(\tau^- \rightarrow \mu^+ e^- e^-) / \Gamma_{\text{total}}$	$< 1.5 \times 10^{-8}$ , CL = 90%
$\Gamma(\tau^- \rightarrow \mu^- \mu^+ \mu^-) / \Gamma_{\text{total}}$	$< 2.1 \times 10^{-8}$ , CL = 90%
$\Gamma(\tau^- \rightarrow e^- \pi^+ \pi^-) / \Gamma_{\text{total}}$	$< 4.4 \times 10^{-8}$ , CL = 90%
$\Gamma(\tau^- \rightarrow \mu^- \pi^+ \pi^-) / \Gamma_{\text{total}}$	$< 3.3 \times 10^{-8}$ , CL = 90%
$\Gamma(\tau^- \rightarrow e^- \pi^+ K^-) / \Gamma_{\text{total}}$	$< 5.8 \times 10^{-8}$ , CL = 90%
$\Gamma(\tau^- \rightarrow e^- \pi^- K^+) / \Gamma_{\text{total}}$	$< 5.2 \times 10^{-8}$ , CL = 90%
$\Gamma(\tau^- \rightarrow e^- K_S^0 K_S^0) / \Gamma_{\text{total}}$	$< 7.1 \times 10^{-8}$ , CL = 90%
$\Gamma(\tau^- \rightarrow e^- K^+ K^-) / \Gamma_{\text{total}}$	$< 5.4 \times 10^{-8}$ , CL = 90%
$\Gamma(\tau^- \rightarrow \mu^- \pi^+ K^-) / \Gamma_{\text{total}}$	$< 1.6 \times 10^{-7}$ , CL = 90%
$\Gamma(\tau^- \rightarrow \mu^- \pi^- K^+) / \Gamma_{\text{total}}$	$< 1.0 \times 10^{-7}$ , CL = 90%
$\Gamma(\tau^- \rightarrow \mu^- K_S^0 K_S^0) / \Gamma_{\text{total}}$	$< 8.0 \times 10^{-8}$ , CL = 90%
$\Gamma(\tau^- \rightarrow \mu^- K^+ K^-) / \Gamma_{\text{total}}$	$< 6.8 \times 10^{-8}$ , CL = 90%
$\Gamma(\tau^- \rightarrow e^- \pi^0 \pi^0) / \Gamma_{\text{total}}$	$< 6.5 \times 10^{-6}$ , CL = 90%
$\Gamma(\tau^- \rightarrow \mu^- \pi^0 \pi^0) / \Gamma_{\text{total}}$	$< 1.4 \times 10^{-5}$ , CL = 90%
$\Gamma(\tau^- \rightarrow e^- \eta \eta) / \Gamma_{\text{total}}$	$< 3.5 \times 10^{-5}$ , CL = 90%
$\Gamma(\tau^- \rightarrow \mu^- \eta \eta) / \Gamma_{\text{total}}$	$< 6.0 \times 10^{-5}$ , CL = 90%
$\Gamma(\tau^- \rightarrow e^- \pi^0 \eta) / \Gamma_{\text{total}}$	$< 2.4 \times 10^{-5}$ , CL = 90%
$\Gamma(\tau^- \rightarrow \mu^- \pi^0 \eta) / \Gamma_{\text{total}}$	$< 2.2 \times 10^{-5}$ , CL = 90%
$\Gamma(\tau^- \rightarrow e^- \text{light boson}) / \Gamma_{\text{total}}$	$< 2.7 \times 10^{-3}$ , CL = 95%
$\Gamma(\tau^- \rightarrow \mu^- \text{light boson}) / \Gamma_{\text{total}}$	$< 5 \times 10^{-3}$ , CL = 95%

## LEPTON FAMILY NUMBER VIOLATION IN NEUTRINOS

Solar Neutrinos $\sin^2(2\theta_{12})$	$0.857 \pm 0.024$
$\Delta m_{21}^2$	$(7.50 \pm 0.20) \times 10^{-5} \text{ eV}^2$
Atmospheric Neutrinos $\sin^2(2\theta_{23})$	[o] $> 0.95$
$\Delta m_{32}^2$	[p] $(2.32_{-0.08}^{+0.12}) \times 10^{-3} \text{ eV}^2$
Reactor Neutrinos $\sin^2(2\theta_{13})$	$0.098 \pm 0.013$
$\Gamma(\pi^+ \rightarrow \mu^+ \nu_e) / \Gamma_{\text{total}}$	[q] $< 8.0 \times 10^{-3}$ , CL = 90%
$\Gamma(\pi^+ \rightarrow \mu^- e^+ e^+) / \Gamma_{\text{total}}$	$< 1.6 \times 10^{-6}$ , CL = 90%
$\Gamma(\pi^0 \rightarrow \mu^+ e^-) / \Gamma_{\text{total}}$	$< 3.8 \times 10^{-10}$ , CL = 90%
$\Gamma(\pi^0 \rightarrow \mu^- e^+) / \Gamma_{\text{total}}$	$< 3.4 \times 10^{-9}$ , CL = 90%
$\Gamma(\pi^0 \rightarrow \mu^+ e^- + \mu^- e^+) / \Gamma_{\text{total}}$	$< 3.6 \times 10^{-10}$ , CL = 90%
$\Gamma(\eta \rightarrow \mu^+ e^- + \mu^- e^+) / \Gamma_{\text{total}}$	$< 6 \times 10^{-6}$ , CL = 90%
$\Gamma(\eta'(958) \rightarrow e \mu) / \Gamma_{\text{total}}$	$< 4.7 \times 10^{-4}$ , CL = 90%
$\Gamma(\phi(1020) \rightarrow e^\pm \mu^\mp) / \Gamma_{\text{total}}$	$< 2 \times 10^{-6}$ , CL = 90%
$\Gamma(K^+ \rightarrow \mu^- \nu e^+) / \Gamma_{\text{total}}$	$< 2.0 \times 10^{-8}$ , CL = 90%
$\Gamma(K^+ \rightarrow \mu^+ \nu_e) / \Gamma_{\text{total}}$	[q] $< 4 \times 10^{-3}$ , CL = 90%
$\Gamma(K^+ \rightarrow \pi^+ \mu^+ e^-) / \Gamma_{\text{total}}$	$< 1.3 \times 10^{-11}$ , CL = 90%
$\Gamma(K^+ \rightarrow \pi^+ \mu^- e^+) / \Gamma_{\text{total}}$	$< 5.2 \times 10^{-10}$ , CL = 90%
$\Gamma(K_L^0 \rightarrow e^\pm \mu^\mp) / \Gamma_{\text{total}}$	[m] $< 4.7 \times 10^{-12}$ , CL = 90%
$\Gamma(K_L^0 \rightarrow e^\pm e^\pm \mu^\mp \mu^\mp) / \Gamma_{\text{total}}$	[m] $< 4.12 \times 10^{-11}$ , CL = 90%
$\Gamma(K_L^0 \rightarrow \pi^0 \mu^\pm e^\mp) / \Gamma_{\text{total}}$	[m] $< 7.6 \times 10^{-11}$ , CL = 90%
$\Gamma(K_L^0 \rightarrow \pi^0 \pi^0 \mu^\pm e^\mp) / \Gamma_{\text{total}}$	$< 1.7 \times 10^{-10}$ , CL = 90%
$\Gamma(D^+ \rightarrow \pi^+ e^+ \mu^-) / \Gamma_{\text{total}}$	$< 2.9 \times 10^{-6}$ , CL = 90%
$\Gamma(D^+ \rightarrow \pi^+ e^- \mu^+) / \Gamma_{\text{total}}$	$< 3.6 \times 10^{-6}$ , CL = 90%
$\Gamma(D^+ \rightarrow K^+ e^+ \mu^-) / \Gamma_{\text{total}}$	$< 1.2 \times 10^{-6}$ , CL = 90%
$\Gamma(D^+ \rightarrow K^+ e^- \mu^+) / \Gamma_{\text{total}}$	$< 2.8 \times 10^{-6}$ , CL = 90%
$\Gamma(D^0 \rightarrow \mu^\pm e^\mp) / \Gamma_{\text{total}}$	[m] $< 2.6 \times 10^{-7}$ , CL = 90%
$\Gamma(D^0 \rightarrow \pi^0 e^\pm \mu^\mp) / \Gamma_{\text{total}}$	[m] $< 8.6 \times 10^{-5}$ , CL = 90%
$\Gamma(D^0 \rightarrow \eta e^\pm \mu^\mp) / \Gamma_{\text{total}}$	[m] $< 1.0 \times 10^{-4}$ , CL = 90%
$\Gamma(D^0 \rightarrow \pi^+ \pi^- e^\pm \mu^\mp) / \Gamma_{\text{total}}$	[m] $< 1.5 \times 10^{-5}$ , CL = 90%
$\Gamma(D^0 \rightarrow \rho^0 e^\pm \mu^\mp) / \Gamma_{\text{total}}$	[m] $< 4.9 \times 10^{-5}$ , CL = 90%
$\Gamma(D^0 \rightarrow \omega e^\pm \mu^\mp) / \Gamma_{\text{total}}$	[m] $< 1.2 \times 10^{-4}$ , CL = 90%
$\Gamma(D^0 \rightarrow K^- K^+ e^\pm \mu^\mp) / \Gamma_{\text{total}}$	[m] $< 1.8 \times 10^{-4}$ , CL = 90%
$\Gamma(D^0 \rightarrow \phi e^\pm \mu^\mp) / \Gamma_{\text{total}}$	[m] $< 3.4 \times 10^{-5}$ , CL = 90%
$\Gamma(D^0 \rightarrow \bar{K}^0 e^\pm \mu^\mp) / \Gamma_{\text{total}}$	[m] $< 1.0 \times 10^{-4}$ , CL = 90%
$\Gamma(D^0 \rightarrow K^- \pi^+ e^\pm \mu^\mp) / \Gamma_{\text{total}}$	[m] $< 5.53 \times 10^{-4}$ , CL = 90%
$\Gamma(D^0 \rightarrow \bar{K}^*(892)^0 e^\pm \mu^\mp) / \Gamma_{\text{total}}$	[m] $< 8.3 \times 10^{-5}$ , CL = 90%
$\Gamma(D_S^+ \rightarrow \pi^+ e^+ \mu^-) / \Gamma_{\text{total}}$	$< 1.2 \times 10^{-5}$ , CL = 90%
$\Gamma(D_S^+ \rightarrow \pi^+ e^- \mu^+) / \Gamma_{\text{total}}$	$< 2.0 \times 10^{-5}$ , CL = 90%
$\Gamma(D_S^+ \rightarrow K^+ e^+ \mu^-) / \Gamma_{\text{total}}$	$< 1.4 \times 10^{-5}$ , CL = 90%
$\Gamma(D_S^+ \rightarrow K^+ e^- \mu^+) / \Gamma_{\text{total}}$	$< 9.7 \times 10^{-6}$ , CL = 90%

# Tests of Conservation Laws

$\Gamma(B^+ \rightarrow \pi^+ e^+ \mu^-)/\Gamma_{\text{total}}$	$<6.4 \times 10^{-3}$ , CL = 90%	$\Gamma(D^+ \rightarrow \pi^- e^+ \mu^+)/\Gamma_{\text{total}}$	$<2.0 \times 10^{-6}$ , CL = 90%
$\Gamma(B^+ \rightarrow \pi^+ e^- \mu^+)/\Gamma_{\text{total}}$	$<6.4 \times 10^{-3}$ , CL = 90%	$\Gamma(D^+ \rightarrow \rho^- 2\mu^+)/\Gamma_{\text{total}}$	$<5.6 \times 10^{-4}$ , CL = 90%
$\Gamma(B^+ \rightarrow \pi^+ e^\pm \mu^\mp)/\Gamma_{\text{total}}$	$<1.7 \times 10^{-7}$ , CL = 90%	$\Gamma(D^+ \rightarrow K^- 2e^+)/\Gamma_{\text{total}}$	$<9 \times 10^{-7}$ , CL = 90%
$\Gamma(B^+ \rightarrow K^+ e^+ \mu^-)/\Gamma_{\text{total}}$	$<9.1 \times 10^{-8}$ , CL = 90%	$\Gamma(D^+ \rightarrow K^- 2\mu^+)/\Gamma_{\text{total}}$	$<1.0 \times 10^{-5}$ , CL = 90%
$\Gamma(B^+ \rightarrow K^+ e^- \mu^+)/\Gamma_{\text{total}}$	$<1.3 \times 10^{-7}$ , CL = 90%	$\Gamma(D^+ \rightarrow K^- e^+ \mu^+)/\Gamma_{\text{total}}$	$<1.9 \times 10^{-6}$ , CL = 90%
$\Gamma(B^+ \rightarrow K^+ e^\pm \mu^\mp)/\Gamma_{\text{total}}$	$<9.1 \times 10^{-8}$ , CL = 90%	$\Gamma(D^+ \rightarrow K^*(892)^- 2\mu^+)/\Gamma_{\text{total}}$	$<8.5 \times 10^{-4}$ , CL = 90%
$\Gamma(B^+ \rightarrow K^+ \mu^\pm \tau^\mp)/\Gamma_{\text{total}}$	$<7.7 \times 10^{-5}$ , CL = 90%	$\Gamma(D^0 \rightarrow 2\pi^- 2e^+ + \text{c.c.})/\Gamma_{\text{total}}$	$<1.12 \times 10^{-4}$ , CL = 90%
$\Gamma(B^+ \rightarrow K^*(892)^+ e^+ \mu^-)/\Gamma_{\text{total}}$	$<1.3 \times 10^{-6}$ , CL = 90%	$\Gamma(D^0 \rightarrow 2\pi^- 2\mu^+ + \text{c.c.})/\Gamma_{\text{total}}$	$<2.9 \times 10^{-5}$ , CL = 90%
$\Gamma(B^+ \rightarrow K^*(892)^+ e^- \mu^+)/\Gamma_{\text{total}}$	$<9.9 \times 10^{-7}$ , CL = 90%	$\Gamma(D^0 \rightarrow K^- \pi^- 2e^+ + \text{c.c.})/\Gamma_{\text{total}}$	$<2.06 \times 10^{-4}$ , CL = 90%
$\Gamma(B^+ \rightarrow K^*(892)^+ e^\pm \mu^\mp)/\Gamma_{\text{total}}$	$<1.4 \times 10^{-6}$ , CL = 90%	$\Gamma(D^0 \rightarrow K^- \pi^- 2\mu^+ + \text{c.c.})/\Gamma_{\text{total}}$	$<3.9 \times 10^{-4}$ , CL = 90%
$\Gamma(B^0 \rightarrow e^\pm \mu^\mp)/\Gamma_{\text{total}}$	[m] $<6.4 \times 10^{-8}$ , CL = 90%	$\Gamma(D^0 \rightarrow 2K^- 2e^+ + \text{c.c.})/\Gamma_{\text{total}}$	$<1.52 \times 10^{-4}$ , CL = 90%
$\Gamma(B^0 \rightarrow \pi^0 e^\pm \mu^\mp)/\Gamma_{\text{total}}$	$<1.4 \times 10^{-7}$ , CL = 90%	$\Gamma(D^0 \rightarrow 2K^- 2\mu^+ + \text{c.c.})/\Gamma_{\text{total}}$	$<9.4 \times 10^{-5}$ , CL = 90%
$\Gamma(B^0 \rightarrow K^0 e^\pm \mu^\mp)/\Gamma_{\text{total}}$	$<2.7 \times 10^{-7}$ , CL = 90%	$\Gamma(D^0 \rightarrow \pi^- \pi^- e^+ \mu^+ + \text{c.c.})/\Gamma_{\text{total}}$	$<7.9 \times 10^{-5}$ , CL = 90%
$\Gamma(B^0 \rightarrow K^*(892)^0 e^+ \mu^-)/\Gamma_{\text{total}}$	$<5.3 \times 10^{-7}$ , CL = 90%	$\Gamma(D^0 \rightarrow K^- \pi^- e^+ \mu^+ + \text{c.c.})/\Gamma_{\text{total}}$	$<2.18 \times 10^{-4}$ , CL = 90%
$\Gamma(B^0 \rightarrow K^*(892)^0 e^- \mu^+)/\Gamma_{\text{total}}$	$<3.4 \times 10^{-7}$ , CL = 90%	$\Gamma(D^0 \rightarrow 2K^- e^+ \mu^+ + \text{c.c.})/\Gamma_{\text{total}}$	$<5.7 \times 10^{-5}$ , CL = 90%
$\Gamma(B^0 \rightarrow K^*(892)^0 e^\pm \mu^\mp)/\Gamma_{\text{total}}$	$<5.8 \times 10^{-7}$ , CL = 90%	$\Gamma(D^0 \rightarrow p e^-)/\Gamma_{\text{total}}$	[r] $<1.0 \times 10^{-5}$ , CL = 90%
$\Gamma(B^0 \rightarrow e^\pm \tau^\mp)/\Gamma_{\text{total}}$	[m] $<2.8 \times 10^{-5}$ , CL = 90%	$\Gamma(D^0 \rightarrow \bar{p} e^+)/\Gamma_{\text{total}}$	[s] $<1.1 \times 10^{-5}$ , CL = 90%
$\Gamma(B^0 \rightarrow \mu^\pm \tau^\mp)/\Gamma_{\text{total}}$	[m] $<2.2 \times 10^{-5}$ , CL = 90%	$\Gamma(D_S^+ \rightarrow \pi^- 2e^+)/\Gamma_{\text{total}}$	$<4.1 \times 10^{-6}$ , CL = 90%
$\Gamma(B \rightarrow s e^\pm \mu^\mp)/\Gamma_{\text{total}}$	[m] $<2.2 \times 10^{-5}$ , CL = 90%	$\Gamma(D_S^+ \rightarrow \pi^- 2\mu^+)/\Gamma_{\text{total}}$	$<1.4 \times 10^{-5}$ , CL = 90%
$\Gamma(B \rightarrow \pi e^\pm \mu^\mp)/\Gamma_{\text{total}}$	$<9.2 \times 10^{-8}$ , CL = 90%	$\Gamma(D_S^+ \rightarrow \pi^- e^+ \mu^+)/\Gamma_{\text{total}}$	$<8.4 \times 10^{-6}$ , CL = 90%
$\Gamma(B \rightarrow \rho e^\pm \mu^\mp)/\Gamma_{\text{total}}$	$<3.2 \times 10^{-6}$ , CL = 90%	$\Gamma(D_S^+ \rightarrow K^- 2e^+)/\Gamma_{\text{total}}$	$<5.2 \times 10^{-6}$ , CL = 90%
$\Gamma(B \rightarrow K e^\pm \mu^\mp)/\Gamma_{\text{total}}$	$<3.8 \times 10^{-8}$ , CL = 90%	$\Gamma(D_S^+ \rightarrow K^- 2\mu^+)/\Gamma_{\text{total}}$	$<1.3 \times 10^{-5}$ , CL = 90%
$\Gamma(B \rightarrow K^*(892) e^\pm \mu^\mp)/\Gamma_{\text{total}}$	$<5.1 \times 10^{-7}$ , CL = 90%	$\Gamma(D_S^+ \rightarrow K^- e^+ \mu^+)/\Gamma_{\text{total}}$	$<6.1 \times 10^{-6}$ , CL = 90%
$\Gamma(B_S^0 \rightarrow e^\pm \mu^\mp)/\Gamma_{\text{total}}$	[m] $<2.0 \times 10^{-7}$ , CL = 90%	$\Gamma(D_S^+ \rightarrow K^*(892)^- 2\mu^+)/\Gamma_{\text{total}}$	$<1.4 \times 10^{-3}$ , CL = 90%
$\Gamma(J/\psi(1S) \rightarrow e^\pm \mu^\mp)/\Gamma_{\text{total}}$	$<1.1 \times 10^{-6}$ , CL = 90%	$\Gamma(B^+ \rightarrow \pi^- e^+ e^+)/\Gamma_{\text{total}}$	$<1.6 \times 10^{-6}$ , CL = 90%
$\Gamma(J/\psi(1S) \rightarrow e^\pm \tau^\mp)/\Gamma_{\text{total}}$	$<8.3 \times 10^{-6}$ , CL = 90%	$\Gamma(B^+ \rightarrow \pi^- \mu^+ \mu^+)/\Gamma_{\text{total}}$	$<4.4 \times 10^{-8}$ , CL = 90%
$\Gamma(J/\psi(1S) \rightarrow \mu^\pm \tau^\mp)/\Gamma_{\text{total}}$	$<2.0 \times 10^{-6}$ , CL = 90%	$\Gamma(B^+ \rightarrow \pi^- e^+ \mu^+)/\Gamma_{\text{total}}$	$<1.3 \times 10^{-6}$ , CL = 90%
$\Gamma(\Upsilon(1S) \rightarrow \mu^\pm \tau^\mp)/\Gamma_{\text{total}}$	$<6.0 \times 10^{-6}$ , CL = 95%	$\Gamma(B^+ \rightarrow \rho^- e^+ e^+)/\Gamma_{\text{total}}$	$<2.6 \times 10^{-6}$ , CL = 90%
$\Gamma(\Upsilon(2S) \rightarrow e^\pm \tau^\mp)/\Gamma_{\text{total}}$	$<3.2 \times 10^{-6}$ , CL = 90%	$\Gamma(B^+ \rightarrow \rho^- \mu^+ \mu^+)/\Gamma_{\text{total}}$	$<5.0 \times 10^{-6}$ , CL = 90%
$\Gamma(\Upsilon(2S) \rightarrow \mu^\pm \tau^\mp)/\Gamma_{\text{total}}$	$<3.3 \times 10^{-6}$ , CL = 90%	$\Gamma(B^+ \rightarrow \rho^- e^+ \mu^+)/\Gamma_{\text{total}}$	$<3.3 \times 10^{-6}$ , CL = 90%
$\Gamma(\Upsilon(3S) \rightarrow e^\pm \tau^\mp)/\Gamma_{\text{total}}$	$<4.2 \times 10^{-6}$ , CL = 90%	$\Gamma(B^+ \rightarrow K^- e^+ e^+)/\Gamma_{\text{total}}$	$<1.0 \times 10^{-6}$ , CL = 90%
$\Gamma(\Upsilon(3S) \rightarrow \mu^\pm \tau^\mp)/\Gamma_{\text{total}}$	$<3.1 \times 10^{-6}$ , CL = 90%	$\Gamma(B^+ \rightarrow K^- \mu^+ \mu^+)/\Gamma_{\text{total}}$	$<4.1 \times 10^{-8}$ , CL = 90%
$\Gamma(\Lambda_C^+ \rightarrow p e^+ \mu^-)/\Gamma_{\text{total}}$	$<9.9 \times 10^{-6}$ , CL = 90%	$\Gamma(B^+ \rightarrow K^- e^+ \mu^+)/\Gamma_{\text{total}}$	$<2.0 \times 10^{-6}$ , CL = 90%
$\Gamma(\Lambda_C^+ \rightarrow p e^- \mu^+)/\Gamma_{\text{total}}$	$<1.9 \times 10^{-5}$ , CL = 90%	$\Gamma(B^+ \rightarrow K^*(892)^- e^+ e^+)/\Gamma_{\text{total}}$	$<2.8 \times 10^{-6}$ , CL = 90%
<b>TOTAL LEPTON NUMBER</b>			
Violation of total lepton number conservation also implies violation of lepton family number conservation.			
$\Gamma(Z \rightarrow p e)/\Gamma_{\text{total}}$	$<1.8 \times 10^{-6}$ , CL = 95%	$\Gamma(B^+ \rightarrow K^*(892)^- \mu^+ \mu^+)/\Gamma_{\text{total}}$	$<8.3 \times 10^{-6}$ , CL = 90%
$\Gamma(Z \rightarrow p \mu)/\Gamma_{\text{total}}$	$<1.8 \times 10^{-6}$ , CL = 95%	$\Gamma(B^+ \rightarrow K^*(892)^- e^+ \mu^+)/\Gamma_{\text{total}}$	$<4.4 \times 10^{-6}$ , CL = 90%
limit on $\mu^- \rightarrow e^+$ conversion		$\Gamma(B^+ \rightarrow D^- e^+ e^+)/\Gamma_{\text{total}}$	$<2.6 \times 10^{-6}$ , CL = 90%
$\sigma(\mu^- 32S \rightarrow e^+ 32Si^*) / \sigma(\mu^- 32S \rightarrow \nu_\mu 32P^*)$	$<9 \times 10^{-10}$ , CL = 90%	$\Gamma(B^+ \rightarrow D^- e^+ \mu^+)/\Gamma_{\text{total}}$	$<1.8 \times 10^{-6}$ , CL = 90%
$\sigma(\mu^- 127I \rightarrow e^+ 127Sb^*) / \sigma(\mu^- 127I \rightarrow \text{anything})$	$<3 \times 10^{-10}$ , CL = 90%	$\Gamma(B^+ \rightarrow D^- \mu^+ \mu^+)/\Gamma_{\text{total}}$	$<1.1 \times 10^{-6}$ , CL = 90%
$\sigma(\mu^- Ti \rightarrow e^+ Ca) / \sigma(\mu^- Ti \rightarrow \text{capture})$	$<3.6 \times 10^{-11}$ , CL = 90%	$\Gamma(B^+ \rightarrow \Lambda^0 \mu^+)/\Gamma_{\text{total}}$	$<6 \times 10^{-8}$ , CL = 90%
$\Gamma(\tau^- \rightarrow e^+ \pi^- \pi^-)/\Gamma_{\text{total}}$	$<8.8 \times 10^{-8}$ , CL = 90%	$\Gamma(B^+ \rightarrow \Lambda^0 e^+)/\Gamma_{\text{total}}$	$<3.2 \times 10^{-8}$ , CL = 90%
$\Gamma(\tau^- \rightarrow \mu^+ \pi^- \pi^-)/\Gamma_{\text{total}}$	$<3.7 \times 10^{-8}$ , CL = 90%	$\Gamma(B^+ \rightarrow \bar{\Lambda}^0 \mu^+)/\Gamma_{\text{total}}$	$<6 \times 10^{-8}$ , CL = 90%
$\Gamma(\tau^- \rightarrow e^+ K^- K^-)/\Gamma_{\text{total}}$	$<6.7 \times 10^{-8}$ , CL = 90%	$\Gamma(B^+ \rightarrow \bar{\Lambda}^0 e^+)/\Gamma_{\text{total}}$	$<8 \times 10^{-8}$ , CL = 90%
$\Gamma(\tau^- \rightarrow e^+ K^- K^-)/\Gamma_{\text{total}}$	$<6.0 \times 10^{-8}$ , CL = 90%	$\Gamma(B^0 \rightarrow \Lambda_C^+ \mu^-)/\Gamma_{\text{total}}$	$<1.8 \times 10^{-6}$ , CL = 90%
$\Gamma(\tau^- \rightarrow \mu^+ \pi^- K^-)/\Gamma_{\text{total}}$	$<9.4 \times 10^{-8}$ , CL = 90%	$\Gamma(B^0 \rightarrow \Lambda_C^+ e^-)/\Gamma_{\text{total}}$	$<5 \times 10^{-6}$ , CL = 90%
$\Gamma(\tau^- \rightarrow \mu^+ K^- K^-)/\Gamma_{\text{total}}$	$<9.6 \times 10^{-8}$ , CL = 90%	$\Gamma(\Xi^- \rightarrow p \mu^- \mu^-)/\Gamma_{\text{total}}$	$<4 \times 10^{-8}$ , CL = 90%
$\Gamma(\tau^- \rightarrow \bar{p} \gamma)/\Gamma_{\text{total}}$	$<3.5 \times 10^{-6}$ , CL = 90%	$\Gamma(\Lambda_C^+ \rightarrow \bar{p} 2e^+)/\Gamma_{\text{total}}$	$<2.7 \times 10^{-6}$ , CL = 90%
$\Gamma(\tau^- \rightarrow \bar{p} \pi^0)/\Gamma_{\text{total}}$	$<1.5 \times 10^{-5}$ , CL = 90%	$\Gamma(\Lambda_C^+ \rightarrow \bar{p} 2\mu^+)/\Gamma_{\text{total}}$	$<9.4 \times 10^{-6}$ , CL = 90%
$\Gamma(\tau^- \rightarrow \bar{p} 2\pi^0)/\Gamma_{\text{total}}$	$<3.3 \times 10^{-5}$ , CL = 90%	$\Gamma(\Lambda_C^+ \rightarrow \bar{p} e^+ \mu^+)/\Gamma_{\text{total}}$	$<1.6 \times 10^{-5}$ , CL = 90%
$\Gamma(\tau^- \rightarrow \bar{p} \eta)/\Gamma_{\text{total}}$	$<8.9 \times 10^{-6}$ , CL = 90%	$\Gamma(\Lambda_C^+ \rightarrow \Sigma^- \mu^+ \mu^+)/\Gamma_{\text{total}}$	$<7.0 \times 10^{-4}$ , CL = 90%
$\Gamma(\tau^- \rightarrow \bar{p} \pi^0 \eta)/\Gamma_{\text{total}}$	$<2.7 \times 10^{-5}$ , CL = 90%		
$\Gamma(\tau^- \rightarrow \Lambda \pi^-)/\Gamma_{\text{total}}$	$<7.2 \times 10^{-8}$ , CL = 90%	<b>BARYON NUMBER</b>	
$\Gamma(\tau^- \rightarrow \bar{\Lambda} \pi^-)/\Gamma_{\text{total}}$	$<1.4 \times 10^{-7}$ , CL = 90%	$\Gamma(Z \rightarrow p e)/\Gamma_{\text{total}}$	$<1.8 \times 10^{-6}$ , CL = 95%
$t_{1/2}(^{76}\text{Ge} \rightarrow ^{76}\text{Se} + 2 e^-)$	$>1.9 \times 10^{25}$ yr, CL = 90%	$\Gamma(Z \rightarrow p \mu)/\Gamma_{\text{total}}$	$<1.8 \times 10^{-6}$ , CL = 95%
$\Gamma(\pi^+ \rightarrow \mu^+ \bar{\nu}_e)/\Gamma_{\text{total}}$	[q] $<1.5 \times 10^{-3}$ , CL = 90%	$\Gamma(\tau^- \rightarrow \bar{p} \gamma)/\Gamma_{\text{total}}$	$<3.5 \times 10^{-6}$ , CL = 90%
$\Gamma(K^+ \rightarrow \pi^- \mu^+ e^+)/\Gamma_{\text{total}}$	$<5.0 \times 10^{-10}$ , CL = 90%	$\Gamma(\tau^- \rightarrow \bar{p} \pi^0)/\Gamma_{\text{total}}$	$<1.5 \times 10^{-5}$ , CL = 90%
$\Gamma(K^+ \rightarrow \pi^- e^+ e^+)/\Gamma_{\text{total}}$	$<6.4 \times 10^{-10}$ , CL = 90%	$\Gamma(\tau^- \rightarrow \bar{p} 2\pi^0)/\Gamma_{\text{total}}$	$<3.3 \times 10^{-5}$ , CL = 90%
$\Gamma(K^+ \rightarrow \pi^- \mu^+ \mu^+)/\Gamma_{\text{total}}$	[q] $<1.1 \times 10^{-9}$ , CL = 90%	$\Gamma(\tau^- \rightarrow \bar{p} \eta)/\Gamma_{\text{total}}$	$<8.9 \times 10^{-6}$ , CL = 90%
$\Gamma(K^+ \rightarrow \mu^+ \bar{\nu}_e)/\Gamma_{\text{total}}$	[q] $<3.3 \times 10^{-3}$ , CL = 90%	$\Gamma(\tau^- \rightarrow \bar{p} \pi^0 \eta)/\Gamma_{\text{total}}$	$<2.7 \times 10^{-5}$ , CL = 90%
$\Gamma(K^+ \rightarrow \pi^0 e^+ \bar{\nu}_e)/\Gamma_{\text{total}}$	$<3 \times 10^{-3}$ , CL = 90%	$\Gamma(\tau^- \rightarrow \Lambda \pi^-)/\Gamma_{\text{total}}$	$<7.2 \times 10^{-8}$ , CL = 90%
$\Gamma(D^+ \rightarrow \pi^- 2e^+)/\Gamma_{\text{total}}$	$<1.1 \times 10^{-6}$ , CL = 90%	$\Gamma(\tau^- \rightarrow \bar{\Lambda} \pi^-)/\Gamma_{\text{total}}$	$<1.4 \times 10^{-7}$ , CL = 90%
$\Gamma(D^+ \rightarrow \pi^- 2\mu^+)/\Gamma_{\text{total}}$	$<2.0 \times 10^{-6}$ , CL = 90%	$\Gamma(D^0 \rightarrow p e^-)/\Gamma_{\text{total}}$	[r] $<1.0 \times 10^{-5}$ , CL = 90%
		$\Gamma(D^0 \rightarrow \bar{p} e^+)/\Gamma_{\text{total}}$	[s] $<1.1 \times 10^{-5}$ , CL = 90%
		$\Gamma(B^+ \rightarrow \Lambda^0 \mu^+)/\Gamma_{\text{total}}$	$<6 \times 10^{-8}$ , CL = 90%
		$\Gamma(B^+ \rightarrow \Lambda^0 e^+)/\Gamma_{\text{total}}$	$<3.2 \times 10^{-8}$ , CL = 90%
		$\Gamma(B^+ \rightarrow \bar{\Lambda}^0 \mu^+)/\Gamma_{\text{total}}$	$<6 \times 10^{-8}$ , CL = 90%
		$\Gamma(B^+ \rightarrow \bar{\Lambda}^0 e^+)/\Gamma_{\text{total}}$	$<8 \times 10^{-8}$ , CL = 90%
		$\Gamma(B^0 \rightarrow \Lambda_C^+ \mu^-)/\Gamma_{\text{total}}$	$<1.8 \times 10^{-6}$ , CL = 90%

## Tests of Conservation Laws

$\Gamma(B^0 \rightarrow \Lambda_C^+ e^-)/\Gamma_{\text{total}}$	$< 5 \times 10^{-6}$ , CL = 90%
$p$ mean life	[t] $> 2.1 \times 10^{29}$ years, CL = 90%
A few examples of proton or bound neutron decay follow. For limits on many other nucleon decay channels, see the Baryon Summary Table.	
$\tau(N \rightarrow e^+ \pi)$	$> 158 (n), > 8200 (p) \times 10^{30}$ years, CL = 90%
$\tau(N \rightarrow \mu^+ \pi)$	$> 100 (n), > 6600 (p) \times 10^{30}$ years, CL = 90%
$\tau(N \rightarrow e^+ K)$	$> 17 (n), > 150 (p) \times 10^{30}$ years, CL = 90%
$\tau(N \rightarrow \mu^+ K)$	$> 26 (n), > 120 (p) \times 10^{30}$ years, CL = 90%
limit on $n\bar{n}$ oscillations (free $n$ )	$> 0.86 \times 10^8$ s, CL = 90%
limit on $n\bar{n}$ oscillations (bound $n$ )	[u] $> 1.3 \times 10^8$ s, CL = 90%
$\Gamma(\Lambda_C^+ \rightarrow \bar{p} 2e^+)/\Gamma_{\text{total}}$	$< 2.7 \times 10^{-6}$ , CL = 90%
$\Gamma(\Lambda_C^+ \rightarrow \bar{p} 2\mu^+)/\Gamma_{\text{total}}$	$< 9.4 \times 10^{-6}$ , CL = 90%
$\Gamma(\Lambda_C^+ \rightarrow \bar{p} e^+ \mu^+)/\Gamma_{\text{total}}$	$< 1.6 \times 10^{-5}$ , CL = 90%

## ELECTRIC CHARGE (Q)

$e \rightarrow \nu_e \gamma$ and astrophysical limits	[v] $> 4.6 \times 10^{26}$ yr, CL = 90%
$\Gamma(n \rightarrow p \nu_e \bar{\nu}_e)/\Gamma_{\text{total}}$	$< 8 \times 10^{-27}$ , CL = 68%

 $\Delta S = \Delta Q$  RULE

Violations allowed in second-order weak interactions.

$\Gamma(K^+ \rightarrow \pi^+ \pi^+ e^- \bar{\nu}_e)/\Gamma_{\text{total}}$	$< 1.2 \times 10^{-8}$ , CL = 90%
$\Gamma(K^+ \rightarrow \pi^+ \pi^+ \mu^- \bar{\nu}_\mu)/\Gamma_{\text{total}}$	$< 3.0 \times 10^{-6}$ , CL = 95%
Re( $x_+$ ), $K_{e3}$ parameter	$(-0.9 \pm 3.0) \times 10^{-3}$
$x = A(\bar{K}^0 \rightarrow \pi^- \ell^+ \nu)/A(K^0 \rightarrow \pi^- \ell^+ \nu) = A(\Delta S = -\Delta Q)/A(\Delta S = \Delta Q)$	
real part of $x$	$-0.002 \pm 0.006$
imaginary part of $x$	$0.0012 \pm 0.0021$
$\Gamma(\Sigma^+ \rightarrow n \ell^+ \nu)/\Gamma(\Sigma^- \rightarrow n \ell^- \bar{\nu})$	$< 0.043$
$\Gamma(\Sigma^+ \rightarrow n e^+ \nu_e)/\Gamma_{\text{total}}$	$< 5 \times 10^{-6}$ , CL = 90%
$\Gamma(\Sigma^+ \rightarrow n \mu^+ \nu_\mu)/\Gamma_{\text{total}}$	$< 3.0 \times 10^{-5}$ , CL = 90%
$\Gamma(\Xi^0 \rightarrow \Sigma^- e^+ \nu_e)/\Gamma_{\text{total}}$	$< 9 \times 10^{-4}$ , CL = 90%
$\Gamma(\Xi^0 \rightarrow \Sigma^- \mu^+ \nu_\mu)/\Gamma_{\text{total}}$	$< 9 \times 10^{-4}$ , CL = 90%

 $\Delta S = 2$  FORBIDDEN

Allowed in second-order weak interactions.

$\Gamma(\Xi^0 \rightarrow p \pi^-)/\Gamma_{\text{total}}$	$< 8 \times 10^{-6}$ , CL = 90%
$\Gamma(\Xi^0 \rightarrow p e^- \bar{\nu}_e)/\Gamma_{\text{total}}$	$< 1.3 \times 10^{-3}$
$\Gamma(\Xi^0 \rightarrow p \mu^- \bar{\nu}_\mu)/\Gamma_{\text{total}}$	$< 1.3 \times 10^{-3}$
$\Gamma(\Xi^- \rightarrow n \pi^-)/\Gamma_{\text{total}}$	$< 1.9 \times 10^{-5}$ , CL = 90%
$\Gamma(\Xi^- \rightarrow n e^- \bar{\nu}_e)/\Gamma_{\text{total}}$	$< 3.2 \times 10^{-3}$ , CL = 90%
$\Gamma(\Xi^- \rightarrow n \mu^- \bar{\nu}_\mu)/\Gamma_{\text{total}}$	$< 1.5 \times 10^{-2}$ , CL = 90%
$\Gamma(\Xi^- \rightarrow p \pi^- \pi^-)/\Gamma_{\text{total}}$	$< 4 \times 10^{-4}$ , CL = 90%
$\Gamma(\Xi^- \rightarrow p \pi^- e^- \bar{\nu}_e)/\Gamma_{\text{total}}$	$< 4 \times 10^{-4}$ , CL = 90%
$\Gamma(\Xi^- \rightarrow p \pi^- \mu^- \bar{\nu}_\mu)/\Gamma_{\text{total}}$	$< 4 \times 10^{-4}$ , CL = 90%
$\Gamma(\Omega^- \rightarrow \Lambda \pi^-)/\Gamma_{\text{total}}$	$< 2.9 \times 10^{-6}$ , CL = 90%

 $\Delta S = 2$  VIA MIXING

Allowed in second-order weak interactions, e.g. mixing.

$m_{K_L^0} - m_{K_S^0}$	$(0.5293 \pm 0.0009) \times 10^{10} \hbar s^{-1}$ (S = 1.3)
$m_{K_L^0} - m_{K_S^0}$	$(3.484 \pm 0.006) \times 10^{-12}$ MeV

 $\Delta C = 2$  VIA MIXING

Allowed in second-order weak interactions, e.g. mixing.

$ m_{D_1^0} - m_{D_2^0}  = x\Gamma$	$(1.44_{-0.50}^{+0.48}) \times 10^{10} \hbar s^{-1}$
$(\Gamma_{D_1^0} - \Gamma_{D_2^0})/\Gamma = 2y$	$(1.60_{-0.26}^{+0.25}) \times 10^{-2}$

 $\Delta B = 2$  VIA MIXING

Allowed in second-order weak interactions, e.g. mixing.

$x_d$	$0.1862 \pm 0.0023$
$\Delta m_{B^0} = m_{B_H^0} - m_{B_L^0}$	$(0.507 \pm 0.004) \times 10^{12} \hbar s^{-1}$
$x_d = \Delta m_{B^0}/\Gamma_{B^0}$	$0.770 \pm 0.008$
$\Delta m_{B_s^0} = m_{B_s^0} - m_{B_s^0}$	$(17.69 \pm 0.08) \times 10^{12} \hbar s^{-1}$
$x_s = \Delta m_{B_s^0}/\Gamma_{B_s^0}$	$26.49 \pm 0.29$
$x_s$	$0.499292 \pm 0.000016$

 $\Delta S = 1$  WEAK NEUTRAL CURRENT FORBIDDEN

Allowed by higher-order electroweak interactions.

$\Gamma(K^+ \rightarrow \pi^+ e^+ e^-)/\Gamma_{\text{total}}$	$(3.00 \pm 0.09) \times 10^{-7}$
$\Gamma(K^+ \rightarrow \pi^+ \mu^+ \mu^-)/\Gamma_{\text{total}}$	$(9.4 \pm 0.6) \times 10^{-8}$ (S = 2.6)
$\Gamma(K^+ \rightarrow \pi^+ \nu \bar{\nu})/\Gamma_{\text{total}}$	$(1.7 \pm 1.1) \times 10^{-10}$
$\Gamma(K^+ \rightarrow \pi^+ \pi^0 \nu \bar{\nu})/\Gamma_{\text{total}}$	$< 4.3 \times 10^{-5}$ , CL = 90%
$\Gamma(K_S^0 \rightarrow \mu^+ \mu^-)/\Gamma_{\text{total}}$	$< 3.2 \times 10^{-7}$ , CL = 90%
$\Gamma(K_S^0 \rightarrow e^+ e^-)/\Gamma_{\text{total}}$	$< 9 \times 10^{-9}$ , CL = 90%
$\Gamma(K_S^0 \rightarrow \pi^0 e^+ e^-)/\Gamma_{\text{total}}$	[w] $(3.0_{-1.2}^{+1.5}) \times 10^{-9}$
$\Gamma(K_S^0 \rightarrow \pi^0 \mu^+ \mu^-)/\Gamma_{\text{total}}$	$(2.9_{-1.2}^{+1.5}) \times 10^{-9}$
$\Gamma(K_L^0 \rightarrow \mu^+ \mu^-)/\Gamma_{\text{total}}$	$(6.84 \pm 0.11) \times 10^{-9}$
$\Gamma(K_L^0 \rightarrow e^+ e^-)/\Gamma_{\text{total}}$	$(9_{-4}^{+6}) \times 10^{-12}$
$\Gamma(K_L^0 \rightarrow \pi^+ \pi^- e^+ e^-)/\Gamma_{\text{total}}$	[x] $(3.11 \pm 0.19) \times 10^{-7}$
$\Gamma(K_L^0 \rightarrow \pi^0 \pi^0 e^+ e^-)/\Gamma_{\text{total}}$	$< 6.6 \times 10^{-9}$ , CL = 90%
$\Gamma(K_L^0 \rightarrow \pi^0 \pi^0 \mu^+ \mu^-)/\Gamma_{\text{total}}$	$< 9.2 \times 10^{-11}$ , CL = 90%
$\Gamma(K_L^0 \rightarrow \mu^+ \mu^- e^+ e^-)/\Gamma_{\text{total}}$	$(2.69 \pm 0.27) \times 10^{-9}$
$\Gamma(K_L^0 \rightarrow e^+ e^- e^+ e^-)/\Gamma_{\text{total}}$	$(3.56 \pm 0.21) \times 10^{-8}$
$\Gamma(K_L^0 \rightarrow \pi^0 \mu^+ \mu^-)/\Gamma_{\text{total}}$	$< 3.8 \times 10^{-10}$ , CL = 90%
$\Gamma(K_L^0 \rightarrow \pi^0 e^+ e^-)/\Gamma_{\text{total}}$	$< 2.8 \times 10^{-10}$ , CL = 90%
$\Gamma(K_L^0 \rightarrow \pi^0 \nu \bar{\nu})/\Gamma_{\text{total}}$	$< 2.6 \times 10^{-8}$ , CL = 90%
$\Gamma(K_L^0 \rightarrow \pi^0 \pi^0 \nu \bar{\nu})/\Gamma_{\text{total}}$	$< 8.1 \times 10^{-7}$ , CL = 90%
$\Gamma(\Sigma^+ \rightarrow p e^+ e^-)/\Gamma_{\text{total}}$	$< 7 \times 10^{-6}$
$\Gamma(\Sigma^+ \rightarrow p \mu^+ \mu^-)/\Gamma_{\text{total}}$	$(9_{-8}^{+9}) \times 10^{-8}$

 $\Delta C = 1$  WEAK NEUTRAL CURRENT FORBIDDEN

Allowed by higher-order electroweak interactions.

$\Gamma(D^+ \rightarrow \pi^+ e^+ e^-)/\Gamma_{\text{total}}$	$< 1.1 \times 10^{-6}$ , CL = 90%
$\Gamma(D^+ \rightarrow \pi^+ \mu^+ \mu^-)/\Gamma_{\text{total}}$	$< 3.9 \times 10^{-6}$ , CL = 90%
$\Gamma(D^+ \rightarrow \rho^+ \mu^+ \mu^-)/\Gamma_{\text{total}}$	$< 5.6 \times 10^{-4}$ , CL = 90%
$\Gamma(D^0 \rightarrow \gamma \gamma)/\Gamma_{\text{total}}$	$< 2.6 \times 10^{-5}$ , CL = 90%
$\Gamma(D^0 \rightarrow e^+ e^-)/\Gamma_{\text{total}}$	$< 7.9 \times 10^{-8}$ , CL = 90%
$\Gamma(D^0 \rightarrow \mu^+ \mu^-)/\Gamma_{\text{total}}$	$< 1.4 \times 10^{-7}$ , CL = 90%
$\Gamma(D^0 \rightarrow \pi^0 e^+ e^-)/\Gamma_{\text{total}}$	$< 4.5 \times 10^{-5}$ , CL = 90%
$\Gamma(D^0 \rightarrow \pi^0 \mu^+ \mu^-)/\Gamma_{\text{total}}$	$< 1.8 \times 10^{-4}$ , CL = 90%
$\Gamma(D^0 \rightarrow \eta e^+ e^-)/\Gamma_{\text{total}}$	$< 1.1 \times 10^{-4}$ , CL = 90%
$\Gamma(D^0 \rightarrow \eta \mu^+ \mu^-)/\Gamma_{\text{total}}$	$< 5.3 \times 10^{-4}$ , CL = 90%
$\Gamma(D^0 \rightarrow \pi^+ \pi^- e^+ e^-)/\Gamma_{\text{total}}$	$< 3.73 \times 10^{-4}$ , CL = 90%
$\Gamma(D^0 \rightarrow \rho^0 e^+ e^-)/\Gamma_{\text{total}}$	$< 1.0 \times 10^{-4}$ , CL = 90%
$\Gamma(D^0 \rightarrow \pi^+ \pi^- \mu^+ \mu^-)/\Gamma_{\text{total}}$	$< 3.0 \times 10^{-5}$ , CL = 90%
$\Gamma(D^0 \rightarrow \rho^0 \mu^+ \mu^-)/\Gamma_{\text{total}}$	$< 2.2 \times 10^{-5}$ , CL = 90%
$\Gamma(D^0 \rightarrow \omega e^+ e^-)/\Gamma_{\text{total}}$	$< 1.8 \times 10^{-4}$ , CL = 90%
$\Gamma(D^0 \rightarrow \omega \mu^+ \mu^-)/\Gamma_{\text{total}}$	$< 8.3 \times 10^{-4}$ , CL = 90%
$\Gamma(D^0 \rightarrow K^- K^+ e^+ e^-)/\Gamma_{\text{total}}$	$< 3.15 \times 10^{-4}$ , CL = 90%
$\Gamma(D^0 \rightarrow \phi e^+ e^-)/\Gamma_{\text{total}}$	$< 5.2 \times 10^{-5}$ , CL = 90%
$\Gamma(D^0 \rightarrow K^- K^+ \mu^+ \mu^-)/\Gamma_{\text{total}}$	$< 3.3 \times 10^{-5}$ , CL = 90%
$\Gamma(D^0 \rightarrow \phi \mu^+ \mu^-)/\Gamma_{\text{total}}$	$< 3.1 \times 10^{-5}$ , CL = 90%
$\Gamma(D^0 \rightarrow K^- \pi^+ e^+ e^-)/\Gamma_{\text{total}}$	$< 3.85 \times 10^{-4}$ , CL = 90%
$\Gamma(D^0 \rightarrow K^- \pi^+ \mu^+ \mu^-)/\Gamma_{\text{total}}$	$< 3.59 \times 10^{-4}$ , CL = 90%
$\Gamma(D^0 \rightarrow \pi^+ \pi^- \pi^0 \mu^+ \mu^-)/\Gamma_{\text{total}}$	$< 8.1 \times 10^{-4}$ , CL = 90%
$\Gamma(D_s^+ \rightarrow K^+ e^+ e^-)/\Gamma_{\text{total}}$	$< 3.7 \times 10^{-6}$ , CL = 90%
$\Gamma(D_s^+ \rightarrow K^+ \mu^+ \mu^-)/\Gamma_{\text{total}}$	$< 2.1 \times 10^{-5}$ , CL = 90%
$\Gamma(D_s^+ \rightarrow K^*(892)^+ \mu^+ \mu^-)/\Gamma_{\text{total}}$	$< 1.4 \times 10^{-3}$ , CL = 90%

# Tests of Conservation Laws

$\Gamma(\Lambda_C^+ \rightarrow p e^+ e^-)/\Gamma_{\text{total}}$	$<5.5 \times 10^{-6}$ , CL = 90%
$\Gamma(\Lambda_C^+ \rightarrow p \mu^+ \mu^-)/\Gamma_{\text{total}}$	$<4.4 \times 10^{-5}$ , CL = 90%

NOTES

## $\Delta B = 1$ WEAK NEUTRAL CURRENT FORBIDDEN

Allowed by higher-order electroweak interactions.

$\Gamma(B^+ \rightarrow \pi^+ \ell^+ \ell^-)/\Gamma_{\text{total}}$	$<4.9 \times 10^{-8}$ , CL = 90%
$\Gamma(B^+ \rightarrow \pi^+ e^+ e^-)/\Gamma_{\text{total}}$	$<8.0 \times 10^{-8}$ , CL = 90%
$\Gamma(B^+ \rightarrow \pi^+ \mu^+ \mu^-)/\Gamma_{\text{total}}$	$<6.9 \times 10^{-8}$ , CL = 90%
$\Gamma(B^+ \rightarrow \pi^+ \nu \bar{\nu})/\Gamma_{\text{total}}$	$<1.0 \times 10^{-4}$ , CL = 90%
$\Gamma(B^+ \rightarrow K^+ \ell^+ \ell^-)/\Gamma_{\text{total}}$	[y] $(5.1 \pm 0.5) \times 10^{-7}$
$\Gamma(B^+ \rightarrow K^+ e^+ e^-)/\Gamma_{\text{total}}$	$(5.5 \pm 0.7) \times 10^{-7}$
$\Gamma(B^+ \rightarrow K^+ \mu^+ \mu^-)/\Gamma_{\text{total}}$	$(4.8 \pm 0.4) \times 10^{-7}$
$\Gamma(B^+ \rightarrow K^+ \nu \bar{\nu})/\Gamma_{\text{total}}$	$<1.3 \times 10^{-5}$ , CL = 90%
$\Gamma(B^+ \rightarrow \rho^+ \nu \bar{\nu})/\Gamma_{\text{total}}$	$<1.5 \times 10^{-4}$ , CL = 90%
$\Gamma(B^+ \rightarrow K^*(892)^+ \ell^+ \ell^-)/\Gamma_{\text{total}}$	[y] $(1.29 \pm 0.21) \times 10^{-6}$
$\Gamma(B^+ \rightarrow K^*(892)^+ e^+ e^-)/\Gamma_{\text{total}}$	$(1.55^{+0.40}_{-0.31}) \times 10^{-6}$
$\Gamma(B^+ \rightarrow K^*(892)^+ \mu^+ \mu^-)/\Gamma_{\text{total}}$	$(1.07 \pm 0.22) \times 10^{-6}$
$\Gamma(B^+ \rightarrow K^*(892)^+ \nu \bar{\nu})/\Gamma_{\text{total}}$	$<8 \times 10^{-5}$ , CL = 90%
$\Gamma(B^0 \rightarrow \gamma \gamma)/\Gamma_{\text{total}}$	$<3.2 \times 10^{-7}$ , CL = 90%
$\Gamma(B^0 \rightarrow e^+ e^-)/\Gamma_{\text{total}}$	$<8.3 \times 10^{-8}$ , CL = 90%
$\Gamma(B^0 \rightarrow e^+ e^- \gamma)/\Gamma_{\text{total}}$	$<1.2 \times 10^{-7}$ , CL = 90%
$\Gamma(B^0 \rightarrow \mu^+ \mu^-)/\Gamma_{\text{total}}$	$<1.4 \times 10^{-9}$ , CL = 90%
$\Gamma(B^0 \rightarrow \mu^+ \mu^- \gamma)/\Gamma_{\text{total}}$	$<1.6 \times 10^{-7}$ , CL = 90%
$\Gamma(B^0 \rightarrow \tau^+ \tau^-)/\Gamma_{\text{total}}$	$<4.1 \times 10^{-3}$ , CL = 90%
$\Gamma(B^0 \rightarrow \pi^0 \ell^+ \ell^-)/\Gamma_{\text{total}}$	$<1.2 \times 10^{-7}$ , CL = 90%
$\Gamma(B^0 \rightarrow \pi^0 e^+ e^-)/\Gamma_{\text{total}}$	$<1.4 \times 10^{-7}$ , CL = 90%
$\Gamma(B^0 \rightarrow \pi^0 \mu^+ \mu^-)/\Gamma_{\text{total}}$	$<1.8 \times 10^{-7}$ , CL = 90%
$\Gamma(B^0 \rightarrow \pi^0 \nu \bar{\nu})/\Gamma_{\text{total}}$	$<2.2 \times 10^{-4}$ , CL = 90%
$\Gamma(B^0 \rightarrow K^0 \ell^+ \ell^-)/\Gamma_{\text{total}}$	[y] $(3.1^{+0.8}_{-0.7}) \times 10^{-7}$
$\Gamma(B^0 \rightarrow K^0 e^+ e^-)/\Gamma_{\text{total}}$	$(1.6^{+1.0}_{-0.8}) \times 10^{-7}$
$\Gamma(B^0 \rightarrow K^0 \mu^+ \mu^-)/\Gamma_{\text{total}}$	$(3.8 \pm 0.8) \times 10^{-7}$
$\Gamma(B^0 \rightarrow K^0 \nu \bar{\nu})/\Gamma_{\text{total}}$	$<5.6 \times 10^{-5}$ , CL = 90%
$\Gamma(B^0 \rightarrow \rho^0 \nu \bar{\nu})/\Gamma_{\text{total}}$	$<4.4 \times 10^{-4}$ , CL = 90%
$\Gamma(B^0 \rightarrow K^*(892)^0 \ell^+ \ell^-)/\Gamma_{\text{total}}$	[y] $(9.9^{+1.2}_{-1.1}) \times 10^{-7}$
$\Gamma(B^0 \rightarrow K^*(892)^0 e^+ e^-)/\Gamma_{\text{total}}$	$(1.03^{+0.19}_{-0.17}) \times 10^{-6}$
$\Gamma(B^0 \rightarrow K^*(892)^0 \mu^+ \mu^-)/\Gamma_{\text{total}}$	$(1.06 \pm 0.10) \times 10^{-6}$
$\Gamma(B^0 \rightarrow K^*(892)^0 \nu \bar{\nu})/\Gamma_{\text{total}}$	$<1.2 \times 10^{-4}$ , CL = 90%
$\Gamma(B^0 \rightarrow \phi \nu \bar{\nu})/\Gamma_{\text{total}}$	$<5.8 \times 10^{-5}$ , CL = 90%
$\Gamma(B^0 \rightarrow \text{invisible})/\Gamma_{\text{total}}$	$<2.2 \times 10^{-4}$ , CL = 90%
$\Gamma(B^0 \rightarrow \nu \bar{\nu} \gamma)/\Gamma_{\text{total}}$	$<4.7 \times 10^{-5}$ , CL = 90%
$\Gamma(B \rightarrow s e^+ e^-)/\Gamma_{\text{total}}$	$(4.7 \pm 1.3) \times 10^{-6}$
$\Gamma(B \rightarrow s \mu^+ \mu^-)/\Gamma_{\text{total}}$	$(4.3 \pm 1.2) \times 10^{-6}$
$\Gamma(B \rightarrow s \ell^+ \ell^-)/\Gamma_{\text{total}}$	[y] $(4.5 \pm 1.0) \times 10^{-6}$
$\Gamma(B \rightarrow \pi \ell^+ \ell^-)/\Gamma_{\text{total}}$	$<6.2 \times 10^{-8}$ , CL = 90%
$\Gamma(B \rightarrow K e^+ e^-)/\Gamma_{\text{total}}$	$(4.4 \pm 0.6) \times 10^{-7}$
$\Gamma(B \rightarrow K^*(892) e^+ e^-)/\Gamma_{\text{total}}$	$(1.19 \pm 0.20) \times 10^{-6}$ (S = 1.2)
$\Gamma(B \rightarrow K \mu^+ \mu^-)/\Gamma_{\text{total}}$	$(4.4 \pm 0.4) \times 10^{-7}$
$\Gamma(B \rightarrow K^*(892) \mu^+ \mu^-)/\Gamma_{\text{total}}$	$(1.06 \pm 0.09) \times 10^{-6}$
$\Gamma(B \rightarrow K \ell^+ \ell^-)/\Gamma_{\text{total}}$	$(4.5 \pm 0.4) \times 10^{-7}$
$\Gamma(B \rightarrow K^*(892) \ell^+ \ell^-)/\Gamma_{\text{total}}$	$(1.08 \pm 0.11) \times 10^{-6}$
$\Gamma(B \rightarrow K \nu \bar{\nu})/\Gamma_{\text{total}}$	$<1.4 \times 10^{-5}$ , CL = 90%
$\Gamma(B \rightarrow K^* \nu \bar{\nu})/\Gamma_{\text{total}}$	$<8 \times 10^{-5}$ , CL = 90%
$\Gamma(\bar{B} \rightarrow e^+ e^- \text{ anything})/\Gamma_{\text{total}}$	—
$\Gamma(\bar{B} \rightarrow \mu^+ \mu^- \text{ anything})/\Gamma_{\text{total}}$	$<3.2 \times 10^{-4}$ , CL = 90%
$\Gamma(\bar{B} \rightarrow \nu \bar{\nu} \text{ anything})/\Gamma_{\text{total}}$	—
$\Gamma(B_S^0 \rightarrow \gamma \gamma)/\Gamma_{\text{total}}$	$<8.7 \times 10^{-6}$ , CL = 90%
$\Gamma(B_S^0 \rightarrow \mu^+ \mu^-)/\Gamma_{\text{total}}$	$<6.4 \times 10^{-9}$ , CL = 90%
$\Gamma(B_S^0 \rightarrow e^+ e^-)/\Gamma_{\text{total}}$	$<2.8 \times 10^{-7}$ , CL = 90%
$\Gamma(B_S^0 \rightarrow \phi(1020) \mu^+ \mu^-)/\Gamma_{\text{total}}$	$(1.23^{+0.40}_{-0.34}) \times 10^{-6}$
$\Gamma(B_S^0 \rightarrow \phi \nu \bar{\nu})/\Gamma_{\text{total}}$	$<5.4 \times 10^{-3}$ , CL = 90%

## $\Delta T = 1$ WEAK NEUTRAL CURRENT FORBIDDEN

Allowed by higher-order electroweak interactions.

$\Gamma(t \rightarrow Z q(q=u,c))/\Gamma_{\text{total}}$	[z] $<3.2 \times 10^{-2}$ , CL = 95%
--	--------------------------------------

In this Summary Table:

When a quantity has “(S = ...)” to its right, the error on the quantity has been enlarged by the “scale factor” S, defined as  $S = \sqrt{\chi^2/(N-1)}$ , where N is the number of measurements used in calculating the quantity. We do this when  $S > 1$ , which often indicates that the measurements are inconsistent. When  $S > 1.25$ , we also show in the Particle Listings an ideogram of the measurements. For more about S, see the Introduction.

- [a] C parity forbids this to occur as a single-photon process.
- [b] See the Particle Listings for the (complicated) definition of this quantity.
- [c] Time-reversal invariance requires this to be  $0^\circ$  or  $180^\circ$ .
- [d] This coefficient is zero if time invariance is not violated.
- [e] Allowed by higher-order electroweak interactions.
- [f] Violates CP in leading order. Test of direct CP violation since the indirect CP-violating and CP-conserving contributions are expected to be suppressed.
- [g] In the 2010 Review, the values for these quantities were given using a measure of the asymmetry that was inconsistent with the usual definition.
- [h]  $\text{Re}(\ell'/\epsilon) = \ell'/\epsilon$  to a very good approximation provided the phases satisfy CPT invariance.
- [i] This mode includes gammas from inner bremsstrahlung but not the direct emission mode  $K_L^0 \rightarrow \pi^+ \pi^- \gamma$  (DE).
- [j] Neglecting photon channels. See, e.g., A. Pais and S.B. Treiman, Phys. Rev. **D12**, 2744 (1975).
- [k] Derived from measured values of  $\phi_{+-}$ ,  $\phi_{00}$ ,  $|\eta|$ ,  $|m_{K_L^0} - m_{K_S^0}|$ , and  $\tau_{K_S^0}$ , as described in the introduction to “Tests of Conservation Laws.”
- [l] The  $|m_p - m_{\bar{p}}|/m_p$  and  $|q_p + q_{\bar{p}}|/e$  are not independent, and both use the more precise measurement of  $|q_{\bar{p}}/m_{\bar{p}}|/(q_p/m_p)$ .
- [m] The value is for the sum of the charge states or particle/antiparticle states indicated.
- [n] A test of additive vs. multiplicative lepton family number conservation.
- [o] The limit quoted corresponds to the projection onto the  $\sin^2(2\theta_{23})$  axis of the 90% CL contour in the  $\sin^2(2\theta_{23}) - \Delta m_{32}^2$  plane.
- [p] The sign of  $\Delta m_{32}^2$  is not known at this time. The range quoted is for the absolute value.
- [q] Derived from an analysis of neutrino-oscillation experiments.
- [r] This limit is for either  $D^0$  or  $\bar{D}^0$  to  $p e^-$ .
- [s] This limit is for either  $D^0$  or  $\bar{D}^0$  to  $\bar{p} e^+$ .
- [t] The first limit is for  $p \rightarrow$  anything or “disappearance” modes of a bound proton. The second entry, a rough range of limits, assumes the dominant decay modes are among those investigated. For antiprotons the best limit, inferred from the observation of cosmic ray  $\bar{p}$ 's is  $\tau_{\bar{p}} > 10^7$  yr, the cosmic-ray storage time, but this limit depends on a number of assumptions. The best direct observation of stored antiprotons gives  $\tau_{\bar{p}}/B(\bar{p} \rightarrow e^- \gamma) > 7 \times 10^5$  yr.
- [u] There is some controversy about whether nuclear physics and model dependence complicate the analysis for bound neutrons (from which the best limit comes). The first limit here is from reactor experiments with free neutrons.
- [v] This is the best limit for the mode  $e^- \rightarrow \nu \gamma$ . The best limit for “electron disappearance” is  $6.4 \times 10^{24}$  yr.
- [w] See the  $K_S^0$  Particle Listings for the energy limits used in this measurement.
- [x] See the  $K_L^0$  Particle Listings for the energy limits used in this measurement.
- [y] An  $\ell$  indicates an e or a  $\mu$  mode, not a sum over these modes.
- [z] This limit is for  $\Gamma(t \rightarrow Z q)/\Gamma(t \rightarrow W b)$ .

## REVIEWS, TABLES, AND PLOTS

### Constants, Units, Atomic and Nuclear Properties

1. Physical constants (rev.)	107
2. Astrophysical constants (rev.)	108
3. International System of Units (SI)	110
4. Periodic table of the elements (rev.)	111
5. Electronic structure of the elements	112
6. Atomic and nuclear properties of materials	114
7. Electromagnetic relations	116
8. Naming scheme for hadrons	118

### Standard Model and Related Topics

9. Quantum chromodynamics (rev.)	120
10. Electroweak model & constraints on new phys.	136
11. The CKM quark-mixing matrix (rev.)	157
12. $CP$ violation (rev.)	166
13. Neutrino Mass, Mixing, & Oscillations (rev.)	177
14. Quark model (rev.)	199
15. Grand Unified Theories (rev.)	209
16. Heavy-Quark & Soft-Collinear Eff. Theory(new)	218
17. Lattice Quantum Chromodynamics (new)	225
18. Structure functions (rev.)	234
19. Fragmentation functions in $e^+e^-$ , $ep$ & $pp$ (rev.)	249

### Astrophysics and cosmology

20. Experimental tests of gravitational theory (rev.)	259
21. Big-Bang cosmology (rev.)	264
22. Big-Bang nucleosynthesis (rev.)	275
23. The cosmological parameters (rev.)	280
24. Dark matter (rev.)	289
25. Cosmic microwave background (rev.)	297
26. Cosmic rays (rev.)	305

### Experimental Methods and Colliders

27. Accelerator physics of colliders (rev.)	313
28. High-energy collider parameters (rev.)	317
29. Neutrino Beam Lines at Proton Synchro. (new)	322
30. Passage of particles through matter (rev.)	323
31. Particle detectors at accelerators (rev.)	339
32. Particle detectors for non-accelerators (rev.)	368
33. Radioactivity and radiation protection (rev.)	381
34. Commonly used radioactive sources	385

### Mathematical Tools or Statistics, Monte Carlo,

<b>Group Theory</b>	
35. Probability (rev.)	386
36. Statistics (rev.)	390
37. Monte Carlo techniques (rev.)	402
38. Monte Carlo Generators (new)	405
39. Monte Carlo particle numbering scheme (rev.)	415
40. Clebsch-Gordan coefficients, etc.	419
41. $SU(3)$ isoscalar factors & represent. matrices	420
42. $SU(n)$ multiplets and Young diagrams	421

### Kinematics, Cross-Section Formulae, and Plots

43. Kinematics (rev.)	422
44. Cross-section formulae for specific proc. (rev.)	427
45. Neutrino Cross Section Measurements (new)	436
46. Plots of cross secs. and related quant. (rev.)	439

## MAJOR REVIEWS IN THE PARTICLE LISTINGS

### Gauge and Higgs bosons

The Mass of the $W$ Boson (rev.)	470
Triple Gauge Couplings (rev.)	474
Anomalous $W/Z$ Quartic Couplings (rev.)	477
The $Z$ Boson	478
Anomalous $ZZ\gamma$ , $Z\gamma\gamma$ , and $ZZV$ Couplings (rev.)	498
Searches for Higgs Bosons (rev.)	501
The $W'$ Searches (rev.)	543
The $Z'$ Searches (rev.)	547
Leptoquarks (rev.)	555
Axions and Other Very Light Bosons (rev.)	562

### Leptons

Muon Anomalous Magnetic Moment (rev.)	587
Muon Decay Parameters (rev.)	587
$\tau$ Branching Fractions (rev.)	596
$\tau$ -Lepton Decay Parameters	617
Neutrinoless Double- $\beta$ Decay (rev.)	631

### Quarks

Quark Masses (rev.)	655
The Top Quark (rev.)	668
Free Quark Searches	688

### Mesons

Form Factors for Rad. Pion & Kaon Decays	696
Note on Scalar Mesons (rev.)	706
The $\eta(1405)$ , $\eta(1475)$ , $f_1(1420)$ , and $f_1(1510)$ (rev.)	759
Rare Kaon Decays (rev.)	822
$K_{\ell 3}^{\pm}$ and $K_{\ell 3}^0$ Form Factors (rev.)	833
$CPT$ Invariance Tests in Neutral Kaon Decay (rev.)	839
$CP$ Violation in $K_S \rightarrow 3\pi$	845
$V_{ud}$ , $V_{us}$ , Cabibbo Angle, and CKM Unitarity (new)	852
$CP$ -Violation in $K_L$ Decays (rev.)	859
Dalitz-Plot Analysis Formalism (rev.)	889
Review of Charm Dalitz-Plot Analyses	893
$D^0-\bar{D}^0$ Mixing (rev.)	903
$D_s^+$ Branching Fractions	943
Decay Cons. of Charged Pseudoscalar Mesons (rev.)	946
Production and Decay of $b$ -flavored Hadrons (rev.)	963
Polarization in $B$ Decays (rev.)	1060
$B^0-\bar{B}^0$ Mixing (rev.)	1066
Determination of $V_{cb}$ and $V_{ub}$ (rev.)	1111
Heavy Quarkonium Spectroscopy (new)	1139
Branching Ratios of $\psi(2S)$ and $\chi_{c0,1,2}$ (rev.)	1168

### Baryons

Baryon Decay Parameters	1264
$N$ and $\Delta$ Resonances (rev.)	1268
Radiative Hyperon Decays	1368
Charmed Baryons (rev.)	1383
$\Lambda_c^+$ Branching Fractions	1386

### Miscellaneous searches

Magnetic Monopoles (rev.)	1413
Supersymmetry (rev.)	1420
Dynamical Electroweak Symmetry Breaking (rev.)	1475
Searches for Quark & Lepton Compositeness	1484
Extra Dimensions (rev.)	1489

Additional Reviews and Notes related to specific particles are located in the Particle Listings.





## 1. PHYSICAL CONSTANTS

**Table 1.1.** Reviewed 2011 by P.J. Mohr (NIST). Mainly from the “CODATA Recommended Values of the Fundamental Physical Constants: 2010” by P.J. Mohr, B.N. Taylor, and D.B. Newell in arXiv:1203.5425 and Rev. Mod. Phys. (to be published). The last group of constants (beginning with the Fermi coupling constant) comes from the Particle Data Group. The figures in parentheses after the values give the 1-standard-deviation uncertainties in the last digits; the corresponding fractional uncertainties in parts per 10<sup>9</sup> (ppb) are given in the last column. This set of constants (aside from the last group) is recommended for international use by CODATA (the Committee on Data for Science and Technology). The full 2010 CODATA set of constants may be found at <http://physics.nist.gov/constants>. See also P.J. Mohr and D.B. Newell, “Resource Letter FC-1: The Physics of Fundamental Constants,” Am. J. Phys., **78** (2010) 338.

Quantity	Symbol, equation	Value	Uncertainty (ppb)
speed of light in vacuum	$c$	299 792 458 m s <sup>-1</sup>	exact*
Planck constant	$h$	6.626 069 57(29)×10 <sup>-34</sup> J s	44
Planck constant, reduced	$\hbar \equiv h/2\pi$	1.054 571 726(47)×10 <sup>-34</sup> J s = 6.582 119 28(15)×10 <sup>-22</sup> MeV s	44 22
electron charge magnitude	$e$	1.602 176 565(35)×10 <sup>-19</sup> C = 4.803 204 50(11)×10 <sup>-10</sup> esu	22, 22
conversion constant	$\hbar c$	197.326 9718(44) MeV fm	22
conversion constant	$(\hbar c)^2$	0.389 379 338(17) GeV <sup>2</sup> mbarn	44
electron mass	$m_e$	0.510 998 928(11) MeV/c <sup>2</sup> = 9.109 382 91(40)×10 <sup>-31</sup> kg	22, 44
proton mass	$m_p$	938.272 046(21) MeV/c <sup>2</sup> = 1.672 621 777(74)×10 <sup>-27</sup> kg = 1.007 276 466 812(90) u = 1836.152 672 45(75) $m_e$	22, 44 0.089, 0.41
deuteron mass	$m_d$	1875.612 859(41) MeV/c <sup>2</sup>	22
unified atomic mass unit (u)	(mass <sup>12</sup> C atom)/12 = (1 g)/(N <sub>A</sub> mol)	931.494 061(21) MeV/c <sup>2</sup> = 1.660 538 921(73)×10 <sup>-27</sup> kg	22, 44
permittivity of free space	$\epsilon_0 = 1/\mu_0 c^2$	8.854 187 817 ... ×10 <sup>-12</sup> F m <sup>-1</sup>	exact
permeability of free space	$\mu_0$	4π × 10 <sup>-7</sup> N A <sup>-2</sup> = 12.566 370 614 ... ×10 <sup>-7</sup> N A <sup>-2</sup>	exact
fine-structure constant	$\alpha = e^2/4\pi\epsilon_0\hbar c$	7.297 352 5698(24)×10 <sup>-3</sup> = 1/137.035 999 074(44) <sup>†</sup>	0.32, 0.32
classical electron radius	$r_e = e^2/4\pi\epsilon_0 m_e c^2$	2.817 940 3267(27)×10 <sup>-15</sup> m	0.97
(e <sup>-</sup> Compton wavelength)/2π	$\lambda_e = \hbar/m_e c = r_e \alpha^{-1}$	3.861 592 6800(25)×10 <sup>-13</sup> m	0.65
Bohr radius ( $m_{\text{nucleus}} = \infty$ )	$a_\infty = 4\pi\epsilon_0\hbar^2/m_e e^2 = r_e \alpha^{-2}$	0.529 177 210 92(17)×10 <sup>-10</sup> m	0.32
wavelength of 1 eV/c particle	$\hbar c/(1 \text{ eV})$	1.239 841 930(27)×10 <sup>-6</sup> m	22
Rydberg energy	$\hbar c R_\infty = m_e c^4/2(4\pi\epsilon_0)^2 \hbar^2 = m_e c^2 \alpha^2/2$	13.605 692 53(30) eV	22
Thomson cross section	$\sigma_T = 8\pi r_e^2/3$	0.665 245 8734(13) barn	1.9
Bohr magneton	$\mu_B = e\hbar/2m_e$	5.788 381 8066(38)×10 <sup>-11</sup> MeV T <sup>-1</sup>	0.65
nuclear magneton	$\mu_N = e\hbar/2m_p$	3.152 451 2605(22)×10 <sup>-14</sup> MeV T <sup>-1</sup>	0.71
electron cyclotron freq./field	$\omega_{\text{cycl}}^e/B = e/m_e$	1.758 820 088(39)×10 <sup>11</sup> rad s <sup>-1</sup> T <sup>-1</sup>	22
proton cyclotron freq./field	$\omega_{\text{cycl}}^p/B = e/m_p$	9.578 833 58(21)×10 <sup>7</sup> rad s <sup>-1</sup> T <sup>-1</sup>	22
gravitational constant <sup>‡</sup>	$G_N$	6.673 84(80)×10 <sup>-11</sup> m <sup>3</sup> kg <sup>-1</sup> s <sup>-2</sup> = 6.708 37(80)×10 <sup>-39</sup> $\hbar c$ (GeV/c <sup>2</sup> ) <sup>-2</sup>	1.2 × 10 <sup>5</sup> 1.2 × 10 <sup>5</sup>
standard gravitational accel.	$g_N$	9.806 65 m s <sup>-2</sup>	exact
Avogadro constant	$N_A$	6.022 141 29(27)×10 <sup>23</sup> mol <sup>-1</sup>	44
Boltzmann constant	$k$	1.380 6488(13)×10 <sup>-23</sup> J K <sup>-1</sup> = 8.617 3324(78)×10 <sup>-5</sup> eV K <sup>-1</sup>	910 910
molar volume, ideal gas at STP	$N_A k(273.15 \text{ K})/(101 325 \text{ Pa})$	22.413 968(20)×10 <sup>-3</sup> m <sup>3</sup> mol <sup>-1</sup>	910
Wien displacement law constant	$b = \lambda_{\text{max}} T$	2.897 7721(26)×10 <sup>-3</sup> m K	910
Stefan-Boltzmann constant	$\sigma = \pi^2 k^4/60\hbar^3 c^2$	5.670 373(21)×10 <sup>-8</sup> W m <sup>-2</sup> K <sup>-4</sup>	3600
Fermi coupling constant**	$G_F/(\hbar c)^3$	1.166 378 7(6)×10 <sup>-5</sup> GeV <sup>-2</sup>	500
weak-mixing angle	$\sin^2 \hat{\theta}(M_Z)$ ( $\overline{\text{MS}}$ )	0.231 16(12) <sup>††</sup>	5.2 × 10 <sup>5</sup>
W <sup>±</sup> boson mass	$m_W$	80.385(15) GeV/c <sup>2</sup>	1.9 × 10 <sup>5</sup>
Z <sup>0</sup> boson mass	$m_Z$	91.1876(21) GeV/c <sup>2</sup>	2.3 × 10 <sup>4</sup>
strong coupling constant	$\alpha_s(m_Z)$	0.1184(7)	5.9 × 10 <sup>6</sup>
$\pi = 3.141 592 653 589 793 238$		$e = 2.718 281 828 459 045 235$	$\gamma = 0.577 215 664 901 532 861$
1 in ≡ 0.0254 m	1 G ≡ 10 <sup>-4</sup> T	1 eV = 1.602 176 565(35) × 10 <sup>-19</sup> J	$kT$ at 300 K = [38.681 731(35)] <sup>-1</sup> eV
1 Å ≡ 0.1 nm	1 dyne ≡ 10 <sup>-5</sup> N	1 eV/c <sup>2</sup> = 1.782 661 845(39) × 10 <sup>-36</sup> kg	0 °C ≡ 273.15 K
1 barn ≡ 10 <sup>-28</sup> m <sup>2</sup>	1 erg ≡ 10 <sup>-7</sup> J	2.997 924 58 × 10 <sup>9</sup> esu = 1 C	1 atmosphere ≡ 760 Torr ≡ 101 325 Pa

\* The meter is the length of the path traveled by light in vacuum during a time interval of 1/299 792 458 of a second.

† At  $Q^2 = 0$ . At  $Q^2 \approx m_W^2$  the value is  $\sim 1/128$ .

‡ Absolute lab measurements of  $G_N$  have been made only on scales of about 1 cm to 1 m.

\*\* See the discussion in Sec. 10, “Electroweak model and constraints on new physics.”

†† The corresponding  $\sin^2 \theta$  for the effective angle is 0.23146(12).

## 2. ASTROPHYSICAL CONSTANTS AND PARAMETERS

**Table 2.1.** Revised February 2012 by E. Bergren and D.E. Groom (LBNL). The figures in parentheses after some values give the 1- $\sigma$  uncertainties in the last digit(s). Physical constants are from Ref. 1. While every effort has been made to obtain the most accurate current values of the listed quantities, the table does not represent a critical review or adjustment of the constants, and is not intended as a primary reference.

The values and uncertainties for the cosmological parameters depend on the exact data sets, priors, and basis parameters used in the fit. Many of the derived parameters reported in this table have non-Gaussian likelihoods. Parameters may be highly correlated, so care must be taken in propagating errors. Unless otherwise specified, cosmological parameters are from six-parameter fits to a flat  $\Lambda$ CDM cosmology using 7-year WMAP data alone [2]. For more information see Ref. 3 and the original papers.

Quantity	Symbol, equation	Value	Reference, footnote
speed of light	$c$	299 792 458 m s <sup>-1</sup>	exact[4]
Newtonian gravitational constant	$G_N$	6.673 8(8) $\times 10^{-11}$ m <sup>3</sup> kg <sup>-1</sup> s <sup>-2</sup>	[1]
Planck mass	$\sqrt{\hbar c/G_N}$	1.220 93(7) $\times 10^{19}$ GeV/ $c^2$ = 2.176 51(13) $\times 10^{-8}$ kg	[1]
Planck length	$\sqrt{\hbar G_N/c^3}$	1.616 20(10) $\times 10^{-35}$ m	[1]
standard gravitational acceleration	$g_N$	9.806 65 m s <sup>-2</sup> $\approx \pi^2$	exact[1]
jansky (flux density)	Jy	10 <sup>-26</sup> W m <sup>-2</sup> Hz <sup>-1</sup>	definition
tropical year (equinox to equinox) (2011)	yr	31 556 925.2 s $\approx \pi \times 10^7$ s	[5]
sidereal year (fixed star to fixed star) (2011)		31 558 149.8 s $\approx \pi \times 10^7$ s	[5]
mean sidereal day (2011) (time between vernal equinox transits)		23 <sup>h</sup> 56 <sup>m</sup> 04 <sup>s</sup> .9090 53	[5]
astronomical unit	$au, A$	149 597 870 700(3) m	[6]
parsec (1 $au/1$ arc sec)	pc	3.085 677 6 $\times 10^{16}$ m = 3.262 ... ly	[7]
light year (deprecated unit)	ly	0.306 6 ... pc = 0.946 053 ... $\times 10^{16}$ m	
Schwarzschild radius of the Sun	$2G_N M_\odot/c^2$	2.953 250 077 0(2) km	[8]
Solar mass	$M_\odot$	1.988 5(2) $\times 10^{30}$ kg	[9]
Solar equatorial radius	$R_\odot$	6.9551(4) $\times 10^8$ m	[10]
Solar luminosity	$L_\odot$	3.828 $\times 10^{26}$ W	[11]
Schwarzschild radius of the Earth	$2G_N M_\oplus/c^2$	8.870 055 94(2) mm	[12]
Earth mass	$M_\oplus$	5.972 6(7) $\times 10^{24}$ kg	[13]
Earth mean equatorial radius	$R_\oplus$	6.378 137 $\times 10^6$ m	[5]
luminosity conversion (deprecated)	$L$	3.02 $\times 10^{28} \times 10^{-0.4 M_{\text{bol}}}$ W ( $M_{\text{bol}}$ = absolute bolometric magnitude = bolometric magnitude at 10 pc)	[14]
flux conversion (deprecated)	$\mathcal{F}$	2.52 $\times 10^{-8} \times 10^{-0.4 m_{\text{bol}}}$ W m <sup>-2</sup> ( $m_{\text{bol}}$ = apparent bolometric magnitude)	from above
ABsolute monochromatic magnitude	AB	-2.5 log <sub>10</sub> $f_\nu$ - 56.10 (for $f_\nu$ in W m <sup>-2</sup> Hz <sup>-1</sup> ) = -2.5 log <sub>10</sub> $f_\nu$ + 8.90 (for $f_\nu$ in Jy)	[15]
Solar circular velocity $v_0$ at $R_0$ from Galactic center	$v_0/R_0$	30.2 $\pm$ 0.2 km s <sup>-1</sup> kpc <sup>-1</sup>	[16]
Solar distance from Galactic center	$R_0$	8.4(4) kpc	[17]
circular velocity at $R_0$	$v_0$ or $\Theta_0$	240(10) km s <sup>-1</sup>	[18]
local disk density	$\rho_{\text{disk}}$	3-12 $\times 10^{-24}$ g cm <sup>-3</sup> $\approx$ 2-7 GeV/ $c^2$ cm <sup>-3</sup>	[19]
local dark matter density	$\rho_\chi$	canonical value 0.3 GeV/ $c^2$ cm <sup>-3</sup> within factor 2-3	[20]
escape velocity from Galaxy	$v_{\text{esc}}$	498 km/s $< v_{\text{esc}} < 608$ km/s	[21]
present day CMB temperature	$T_0$	2.7255(6) K	[22]
present day CMB dipole amplitude		3.355(8) mK	[2]
Solar velocity with respect to CMB		369(1) km/s towards $(\ell, b) = (263.99(14)^\circ, 48.26(3)^\circ)$	[2]
Local Group velocity with respect to CMB	$v_{\text{LG}}$	627(22) km/s towards $(\ell, b) = (276(3)^\circ, 30(3)^\circ)$	[23]
entropy density/Boltzmann constant	$s/k$	2 889.2 $(T/2.725)^3$ cm <sup>-3</sup>	[14]
number density of CMB photons	$n_\gamma$	410.5 $(T/2.725)^3$ cm <sup>-3</sup>	[24]
baryon-to-photon ratio	$\eta = n_b/n_\gamma$	6.19(15) $\times 10^{-10}$ 5.1 $\times 10^{-10} \leq \eta \leq 6.5 \times 10^{-10}$ (95% CL)	[2]
number density of baryons	$n_b$	(2.54 $\pm$ 0.06) $\times 10^{-7}$ cm <sup>-3</sup> (2.1 $\times 10^{-7} < n_b < 2.7 \times 10^{-7}$ ) cm <sup>-3</sup> (95% CL)	from $\eta$ in [2] from $\eta$ in [25]
present day Hubble expansion rate	$H_0$	100 $h$ km s <sup>-1</sup> Mpc <sup>-1</sup> = $h \times (9.777 752 \text{ Gyr})^{-1}$	[26]
scale factor for Hubble expansion rate	$h$	0.710(25) WMAP7; WMAP7 $\oplus$ Cepheids=0.721(17)	[2,27]
Hubble length	$c/H_0$	0.925 063 $\times 10^{26} h^{-1}$ m = 1.28(5) $\times 10^{26}$ m	
scale factor for cosmological constant	$c^2/3H_0^2$	2.852 $\times 10^{51} h^{-2}$ m <sup>2</sup> = 5.5(5) $\times 10^{51}$ m <sup>2</sup>	
critical density of the Universe	$\rho_c = 3H_0^2/8\pi G_N$	2.775 366 27 $\times 10^{11} h^2 M_\odot \text{Mpc}^{-3}$ = 1.878 47(23) $\times 10^{-29} h^2$ g cm <sup>-3</sup> = 1.053 75(13) $\times 10^{-5} h^2$ (GeV/ $c^2$ ) cm <sup>-3</sup>	
baryon density of the Universe	$\Omega_b = \rho_b/\rho_c$	$\dagger$ 0.0226(6) $h^{-2} = \dagger$ 0.045(3)	[2,3]
cold dark matter density of the universe	$\Omega_{\text{cdm}} = \rho_{\text{cdm}}/\rho_c$	$\dagger$ 0.111(6) $h^{-2} = \dagger$ 0.22(3)	[2,3]
dark energy density of the $\Lambda$ CDM Universe	$\Omega_\Lambda$	$\dagger$ 0.73(3)	[2,3]
pressureless matter density of the Universe	$\Omega_m = \Omega_{\text{cdm}} + \Omega_b$	0.27 $\pm$ 0.03 (From $\Omega_\Lambda$ and flatness constraint)	[2,3]
dark energy equation of state parameter	$w$	$\#$ -0.98 $\pm$ 0.05 (WMAP7+BAO+ $H_0$ )	[28]
CMB radiation density of the Universe	$\Omega_\gamma = \rho_\gamma/\rho_c$	2.471 $\times 10^{-5} (T/2.725)^4 h^{-2} = 4.75(23) \times 10^{-5}$	[24]
neutrino density of the Universe	$\Omega_\nu$	0.0005 $< \Omega_\nu h^2 < 0.025 \Rightarrow 0.0009 < \Omega_\nu < 0.048$	[29]
total energy density of the Universe (curvature)	$\Omega_{\text{tot}} = \Omega_m + \dots + \Omega_\Lambda$	$\#$ 1.002 $\pm$ 0.011 (WMAP7+BAO+ $H_0$ )	[2,3]

Quantity	Symbol, equation	Value	Reference, footnote
fluctuation amplitude at $8h^{-1}$ Mpc scale	$\sigma_8$	$\dagger 0.80(3)$	[2,3]
curvature fluct. amplitude at $k_0 = 0.002$ Mpc $^{-1}$	$\Delta_{\mathcal{R}}^2$	$\ddagger 2.43(11) \times 10^{-9}$	[2,3]
scalar spectral index	$n_s$	$\ddagger 0.963(14)$	[2,3]
running spectral index slope, $k_0 = 0.002$ Mpc $^{-1}$	$dn_s/d \ln k$	$\# -0.03(3)$	[2]
tensor-to-scalar field perturbations ratio, $k_0 = 0.002$ Mpc $^{-1}$	$r = T/S$	$\# < 0.36$ at 95% CL	[2,3]
redshift at decoupling	$z_{\text{dec}}$	$\dagger 1091(1)$	[2]
age at decoupling	$t_*$	$\dagger 3.79(5) \times 10^5$ yr	[2]
sound horizon at decoupling	$r_s(z_*)$	$\dagger 147(2)$ Mpc	[2]
redshift of matter-radiation equality	$z_{\text{eq}}$	$\dagger 3200 \pm 130$	[2]
redshift of reionization	$z_{\text{reion}}$	$\dagger 10.5 \pm 1.2$	[2]
age at reionization	$t_{\text{reion}}$	$430^{+90}_{-70}$ Myr	[2,30]
reionization optical depth	$\tau$	$\ddagger 0.088(15)$	[2,3]
age of the Universe	$t_0$	$\dagger 13.75 \pm 0.13$ Gyr	[2]

$\ddagger$  Parameter in six-parameter  $\Lambda$ CDM fit [2].

$\dagger$  Derived parameter in six-parameter  $\Lambda$ CDM fit [2].

$\#$  Extended model parameter [2].

## References:

- P.J. Mohr, B.N. Taylor, & D.B. Newell, *CODATA Recommended Values of the Fundamental Constants: 2010*, (to be published); [physics.nist.gov/constants](http://physics.nist.gov/constants).
- N. Jarosik *et al.*, *Astrophys. J. Supp.* **192**, 14 (2011); D. Larson *et al.*, *Astrophys. J. Supp.* **192**, 16 (2011); E. Komatsu *et al.*, *Astrophys. J. Supp.* **192**, 18 (2011).
- O. Lahav & A.R. Liddle, “The Cosmological Parameters,” in this *Review*.
- B.W. Petley, *Nature* **303**, 373 (1983).
- The Astronomical Almanac for the year 2011*, U.S. Government Printing Office, Washington, and The U.K. Hydrographic Office (2010).
- While  $A$  is approximately equal to the semi-major axis of the Earth’s orbit, it is not exactly so. Nor is it exactly the mean Earth-Sun distance. There are a number of reasons: a) the Earth’s orbit is not exactly Keplerian due to relativity and to perturbations from other planets; b) the adopted value for the Gaussian gravitational constant  $k$  is not exactly equal to the Earth’s mean motion; and c) the mean distance in a Keplerian orbit is not equal to the semi-major axis  $a$ :  $\langle r \rangle = a(1 + e^2/2)$ , where  $e$  is the eccentricity. (Discussion courtesy of Myles Standish, JPL).
- The distance at which 1  $A$  subtends 1 arc sec: 1  $A$  divided by  $\pi/648000$ .
- Product of  $2/c^2$  and the heliocentric gravitational constant  $G_N M_\odot = A^3 k^2 / 86400^2$ , where  $k$  is the Gaussian gravitational constant, 0.017 202 098 95 (exact) [5]. The value and error for  $A$  given in this table are used.
- Obtained from the  $G_N M_\odot$  product [5] and  $G_N$  [1].
- T. M. Brown & J. Christensen-Dalsgaard, *Astrophys. J.* **500**, L195 (1998) Many values for the Solar radius have been published, most of which are consistent with this result.
- $4\pi A^2 \times (1361 \text{ W m}^{-2})$  [31]. Assumes isotropic irradiance.
- Schwarzschild radius of the Sun (above) scaled by the Earth/Sun mass ratio given in Ref. 5.
- Obtained from the  $G_N M_\oplus$  product [5] and  $G_N$  [1].
- E.W. Kolb & M.S. Turner, *The Early Universe*, Addison-Wesley (1990);  
The IAU (Commission 36) has recommended  $3.055 \times 10^{28}$  W for the zero point. Based on newer Solar measurements, the value and significance given in the table seems more appropriate.
- J. B. Oke & J. E. Gunn, *Astrophys. J.* **266**, 713 (1983). Note that in the definition of AB the sign of the constant is wrong.
- M.J. Reid & A. Brunthaler, *Astrophys. J.* **616**, 872 (2004) as corrected using new value for Solar proper motion in Ref. 18. Note that  $v_\odot/R_0$  is better determined than either  $\Theta_0$  or  $R_0$ .
- A. M. Ghez *et al.*, *Astrophys. J.* **689**, 1044 (2008); S. Gillessen *et al.*, *Astrophys. J.* **692**, 1075 (2009); M. Shen & Z. Zhu, *Chin. Astron. Astrophys.* **7**, 120 (2007). In their Fig. 2 Zhu & Chin present a summary of a dozen values published 1984–2007. Most are closer to  $R_0 = 8.0(5)$  kpc than those cited above.
- C. McCabe, *Phys. Rev.* **D82**, 023530 (2010) Other papers report values closer to 220(20) km s $^{-1}$ ; S.E. Koposov, H.-W. Rix, & D.W. Hogg, *Astrophys. J.* **712**, 260 (2010); P.J. McMillan & J.J. Binney, (2009) [arXiv:0907.4685](http://arxiv.org/abs/0907.4685).
- G. Gilmore, R.F.G. Wyse, & K. Kuijken, *Ann. Rev. Astron. Astrophys.* **27**, 555 (1989).
- Sampling of many references:  
M. Mori *et al.*, *Phys. Lett.* **B289**, 463 (1992); E.I. Gates *et al.*, *Astrophys. J.* **449**, L133 (1995); M. Kamionkowski, A. Kinkhabwala, *Phys. Rev.* **D57**, 325 (1998); M. Weber, W. de Boer, *Astron. & Astrophys.* **509**, A25 (2010); P. Salucci *et al.*, *Astron. & Astrophys.* **523**, A83 (2010).
- M. C. Smith *et al.*, *Mon. Not. R. Astr. Soc.* **379**, 755 (2007) ([astro-ph/0611671](http://arxiv.org/abs/astro-ph/0611671)).
- D. Fixsen, *Astrophys. J.* **707**, 916 (2009).
- D. Scott & G.F. Smoot, “Cosmic Microwave Background,” in this *Review*.
- $n_\gamma = \frac{2\zeta(3)}{\pi^2} \left(\frac{kT}{hc}\right)^3$  and  $\rho_\gamma = \frac{\pi^2}{15} \frac{(kT)^4}{(hc)^3 c^2}$ ;  $\frac{kT_0}{hc} = 11.900(4)/\text{cm}$ .
- B.D. Fields, S. Sarkar, “Big-Bang Nucleosynthesis,” this *Review*.
- Conversion using length of sidereal year.
- Average of WMAP7 [2] and independent Cepheid-based measurement by A.G. Reiss *et al.*, *Astrophys. J.* **730**, 119 (2011). Other high-quality measurements could have been included.
- R. Amanullah *et al.*, *Astrophys. J.* **716**, 712 (2010). Fit with curvature unconstrained. For a flat Universe,  $w = -1.00 \pm 0.08$ .
- $\Omega_\nu h^2 = \sum m_{\nu_j} / 93 \text{ eV}$ , where the sum is over all neutrino mass eigenstates. The lower limit follows from neutrino mixing results reported in this *Review* combined with the assumptions that there are three light neutrinos ( $m_\nu < 45 \text{ GeV}/c^2$ ) and that the lightest neutrino is substantially less massive than the others:  $\Delta m_{32}^2 = (2.43 \pm 0.13) \times 10^{-3} \text{ eV}^2$ , so  $\sum m_{\nu_j} \geq m_{\nu_3} \approx \sqrt{\Delta m_{32}^2} = 0.05 \text{ eV}$ . (This becomes 0.10 eV if the mass hierarchy is inverted, with  $m_{\nu_1} \approx m_{\nu_2} \gg m_{\nu_3}$ .) Astrophysical determinations of  $\sum m_{\nu_j}$ , reported in the Full Listings of this *Review* under “Sum of the neutrino masses,” range from  $< 0.17 \text{ eV}$  to  $< 2.3 \text{ eV}$  in papers published since 2003. Alternatively, if the limit obtained from tritium decay experiments ( $m_\nu < 2 \text{ eV}$ ) is used for the upper limit, then  $\Omega_\nu < 0.04$ .
- If the Universe were reionized instantaneously at  $z_{\text{reion}}$ .
- G. Kopp & J.L. Lean, *Geophys. Res. Lett.* **38**, L01706 (2011). Kopp & Lean give  $1360.8 \pm 0.6 \text{ W m}^{-2}$ , but given the scatter in the data we use the rounded value without quoting an error.

### 3. INTERNATIONAL SYSTEM OF UNITS (SI)

See “The International System of Units (SI),” NIST Special Publication **330**, B.N. Taylor, ed. (USGPO, Washington, DC, 1991); and “Guide for the Use of the International System of Units (SI),” NIST Special Publication **811**, 1995 edition, B.N. Taylor (USGPO, Washington, DC, 1995).

Physical quantity	Name of unit	Symbol
<i>Base units</i>		
length	meter	m
mass	kilogram	kg
time	second	s
electric current	ampere	A
thermodynamic temperature	kelvin	K
amount of substance	mole	mol
luminous intensity	candela	cd
<i>Derived units with special names</i>		
plane angle	radian	rad
solid angle	steradian	sr
frequency	hertz	Hz
energy	joule	J
force	newton	N
pressure	pascal	Pa
power	watt	W
electric charge	coulomb	C
electric potential	volt	V
electric resistance	ohm	$\Omega$
electric conductance	siemens	S
electric capacitance	farad	F
magnetic flux	weber	Wb
inductance	henry	H
magnetic flux density	tesla	T
luminous flux	lumen	lm
illuminance	lux	lx
celsius temperature	degree celsius	$^{\circ}\text{C}$
activity (of a radioactive source)*	becquerel	Bq
absorbed dose (of ionizing radiation)*	gray	Gy
dose equivalent*	sievert	Sv

#### SI prefixes

$10^{24}$	yotta	(Y)
$10^{21}$	zetta	(Z)
$10^{18}$	exa	(E)
$10^{15}$	peta	(P)
$10^{12}$	tera	(T)
$10^9$	giga	(G)
$10^6$	mega	(M)
$10^3$	kilo	(k)
$10^2$	hecto	(h)
10	deca	(da)
$10^{-1}$	deci	(d)
$10^{-2}$	centi	(c)
$10^{-3}$	milli	(m)
$10^{-6}$	micro	( $\mu$ )
$10^{-9}$	nano	(n)
$10^{-12}$	pico	(p)
$10^{-15}$	femto	(f)
$10^{-18}$	atto	(a)
$10^{-21}$	zepto	(z)
$10^{-24}$	yocto	(y)

\*See our section 33, on “Radioactivity and radiation protection,” p. 381.

**Table 4.1.** Revised 2011 by D.E. Groom (LBNL), and E. Bergren. Atomic weights of stable elements are adapted from the Commission on Isotopic Abundances and Atomic Weights, "Atomic Weights of the Elements 2007," <http://www.chem.qmul.ac.uk/iupac/AtWt/>. The atomic number (top left) is the number of protons in the nucleus. The atomic mass (bottom) of a stable elements is weighted by isotopic abundances in the Earth's surface. If the element has no stable isotope, the atomic mass (in parentheses) of the most stable isotope currently known is given. In this case the mass is from <http://www.nndc.bnl.gov/amdc/masstable/Ame2003/mass.mas03> and the longest-lived isotope is from [www.nndc.bnl.gov/ensdf/za.form.jsp](http://www.nndc.bnl.gov/ensdf/za.form.jsp). The exceptions are Th, Pa, and U, which do have characteristic terrestrial compositions. Atomic masses are relative to the mass of  $^{12}\text{C}$ , defined to be exactly 12 unified atomic mass units (u) (approx. g/mole). Relative isotopic abundances often vary considerably, both in natural and commercial samples; this is reflected in the number of significant figures given for the atomic mass. IUPAC does not accept the claims for elements 113, 115, 117, and 118 as conclusive at this time.

1 IA																											18 VIIIA
1 H Hydrogen 1.00794																	2 He Helium 4.002602										
3 Li Lithium 6.941		4 Be Beryllium 9.012182		<b>PERIODIC TABLE OF THE ELEMENTS</b>																5 B Boron 10.811	6 C Carbon 12.0107	7 N Nitrogen 14.0067	8 O Oxygen 15.9994	9 F Fluorine 18.9984032	10 Ne Neon 20.1797		
11 Na Sodium 22.98976928		12 Mg Magnesium 24.3050		3 IIIB	4 IVB	5 VB	6 VIB	7 VIIB	8 VIII		9 VIIIB	10	11 IB	12 IIB	13 Al Aluminum 26.9815386	14 Si Silicon 28.0855	15 P Phosph. 30.973762	16 S Sulfur 32.065	17 Cl Chlorine 35.453	18 Ar Argon 39.948							
19 K Potassium 39.0983	20 Ca Calcium 40.078	21 Sc Scandium 44.955912	22 Ti Titanium 47.867	23 V Vanadium 50.9415	24 Cr Chromium 51.9961	25 Mn Manganese 54.938045	26 Fe Iron 55.845	27 Co Cobalt 58.933195	28 Ni Nickel 58.6934	29 Cu Copper 63.546	30 Zn Zinc 65.38	31 Ga Gallium 69.723	32 Ge German. 72.64	33 As Arsenic 74.92160	34 Se Selenium 78.96	35 Br Bromine 79.904	36 Kr Krypton 83.798										
37 Rb Rubidium 85.4678	38 Sr Strontium 87.62	39 Y Yttrium 88.90585	40 Zr Zirconium 91.224	41 Nb Niobium 92.90638	42 Mo Molybd. 95.96	43 Tc Technet. (97.90722)	44 Ru Ruthen. 101.07	45 Rh Rhodium 102.90550	46 Pd Palladium 106.42	47 Ag Silver 107.8682	48 Cd Cadmium 112.411	49 In Indium 114.818	50 Sn Tin 118.710	51 Sb Antimony 121.760	52 Te Tellurium 127.60	53 I Iodine 126.90447	54 Xe Xenon 131.293										
55 Cs Cesium 132.9054519	56 Ba Barium 137.327	57–71 Lanthanides	72 Hf Hafnium 178.49	73 Ta Tantalum 180.94788	74 W Tungsten 183.84	75 Re Rhenium 186.207	76 Os Osmium 190.23	77 Ir Iridium 192.217	78 Pt Platinum 195.084	79 Au Gold 196.966569	80 Hg Mercury 200.59	81 Tl Thallium 204.3833	82 Pb Lead 207.2	83 Bi Bismuth 208.98040	84 Po Polonium (208.98243)	85 At Astatine (209.98715)	86 Rn Radon (222.01758)										
87 Fr Francium (223.01974)	88 Ra Radium (226.02541)	89–103 Actinides	104 Rf Rutherford. (267.122)	105 Db Dubnium (268.125)	106 Sg Seaborg. (271.133)	107 Bh Bohrium (270.134)	108 Hs Hassium (269.134)	109 Mt Meitner. (276.151)	110 Ds Darmstadt. (281.162)	111 Rg Roentgen. (280.164)	112 Cn Copernicium (277)	114 Fl Flerovium (289)	116 Lv Livermorium (288)														

Lanthanide series	57 La Lanthan. 138.90547	58 Ce Cerium 140.116	59 Pr Praseodym. 140.90765	60 Nd Neodym. 144.242	61 Pm Prometh. (144.91275)	62 Sm Samarium 150.36	63 Eu Europium 151.964	64 Gd Gadolin. 157.25	65 Tb Terbium 158.92535	66 Dy Dyspros. 162.500	67 Ho Holmium 164.93032	68 Er Erbium 167.259	69 Tm Thulium 168.93421	70 Yb Ytterbium 173.054	71 Lu Lutetium 174.9668
Actinide series	89 Ac Actinium (227.02775)	90 Th Thorium 232.03806	91 Pa Protactin. 231.03588	92 U Uranium 238.02891	93 Np Neptunium (237.04817)	94 Pu Plutonium (244.06420)	95 Am Americ. (243.06138)	96 Cm Curium (247.07035)	97 Bk Berkelium (247.07031)	98 Cf Californ. (251.07959)	99 Es Einstein. (252.0830)	100 Fm Fermium (257.09510)	101 Md Mendelev. (258.09843)	102 No Nobelium (259.1010)	103 Lr Lawrenc. (262.110)

## 5. ELECTRONIC STRUCTURE OF THE ELEMENTS

**Table 5.1.** Reviewed 2011 by J.E. Sansonetti (NIST). The electronic configurations and the ionization energies are from the NIST database, “Ground Levels and Ionization Energies for the Neutral Atoms,” W.C. Martin, A. Musgrove, S. Kotochigova, and J.E. Sansonetti, [http://www.nist.gov/pml/data/ion\\_energy.cfm](http://www.nist.gov/pml/data/ion_energy.cfm). The electron configuration for, say, iron indicates an argon electronic core (see argon) plus six  $3d$  electrons and two  $4s$  electrons.

	Element	Electron configuration ( $3d^5 =$ five $3d$ electrons, <i>etc.</i> )	Ground state $2S+1L_J$	Ionization energy (eV)
1	H Hydrogen	$1s$	$^2S_{1/2}$	13.5984
2	He Helium	$1s^2$	$^1S_0$	24.5874
3	Li Lithium	(He) $2s$	$^2S_{1/2}$	5.3917
4	Be Beryllium	(He) $2s^2$	$^1S_0$	9.3227
5	B Boron	(He) $2s^2 2p$	$^2P_{1/2}$	8.2980
6	C Carbon	(He) $2s^2 2p^2$	$^3P_0$	11.2603
7	N Nitrogen	(He) $2s^2 2p^3$	$^4S_{3/2}$	14.5341
8	O Oxygen	(He) $2s^2 2p^4$	$^3P_2$	13.6181
9	F Fluorine	(He) $2s^2 2p^5$	$^2P_{3/2}$	17.4228
10	Ne Neon	(He) $2s^2 2p^6$	$^1S_0$	21.5645
11	Na Sodium	(Ne) $3s$	$^2S_{1/2}$	5.1391
12	Mg Magnesium	(Ne) $3s^2$	$^1S_0$	7.6462
13	Al Aluminum	(Ne) $3s^2 3p$	$^2P_{1/2}$	5.9858
14	Si Silicon	(Ne) $3s^2 3p^2$	$^3P_0$	8.1517
15	P Phosphorus	(Ne) $3s^2 3p^3$	$^4S_{3/2}$	10.4867
16	S Sulfur	(Ne) $3s^2 3p^4$	$^3P_2$	10.3600
17	Cl Chlorine	(Ne) $3s^2 3p^5$	$^2P_{3/2}$	12.9676
18	Ar Argon	(Ne) $3s^2 3p^6$	$^1S_0$	15.7596
19	K Potassium	(Ar) $4s$	$^2S_{1/2}$	4.3407
20	Ca Calcium	(Ar) $4s^2$	$^1S_0$	6.1132
21	Sc Scandium	(Ar) $3d 4s^2$	$^2D_{3/2}$	6.5615
22	Ti Titanium	(Ar) $3d^2 4s^2$	$^3F_2$	6.8281
23	V Vanadium	(Ar) $3d^3 4s^2$	$^4F_{3/2}$	6.7462
24	Cr Chromium	(Ar) $3d^5 4s$	$^7S_3$	6.7665
25	Mn Manganese	(Ar) $3d^5 4s^2$	$^6S_{5/2}$	7.4340
26	Fe Iron	(Ar) $3d^6 4s^2$	$^5D_4$	7.9024
27	Co Cobalt	(Ar) $3d^7 4s^2$	$^4F_{9/2}$	7.8810
28	Ni Nickel	(Ar) $3d^8 4s^2$	$^3F_4$	7.6399
29	Cu Copper	(Ar) $3d^{10} 4s$	$^2S_{1/2}$	7.7264
30	Zn Zinc	(Ar) $3d^{10} 4s^2$	$^1S_0$	9.3942
31	Ga Gallium	(Ar) $3d^{10} 4s^2 4p$	$^2P_{1/2}$	5.9993
32	Ge Germanium	(Ar) $3d^{10} 4s^2 4p^2$	$^3P_0$	7.8994
33	As Arsenic	(Ar) $3d^{10} 4s^2 4p^3$	$^4S_{3/2}$	9.7886
34	Se Selenium	(Ar) $3d^{10} 4s^2 4p^4$	$^3P_2$	9.7524
35	Br Bromine	(Ar) $3d^{10} 4s^2 4p^5$	$^2P_{3/2}$	11.8138
36	Kr Krypton	(Ar) $3d^{10} 4s^2 4p^6$	$^1S_0$	13.9996
37	Rb Rubidium	(Kr) $5s$	$^2S_{1/2}$	4.1771
38	Sr Strontium	(Kr) $5s^2$	$^1S_0$	5.6949
39	Y Yttrium	(Kr) $4d 5s^2$	$^2D_{3/2}$	6.2173
40	Zr Zirconium	(Kr) $4d^2 5s^2$	$^3F_2$	6.6339
41	Nb Niobium	(Kr) $4d^4 5s$	$^6D_{1/2}$	6.7589
42	Mo Molybdenum	(Kr) $4d^5 5s$	$^7S_3$	7.0924
43	Tc Technetium	(Kr) $4d^5 5s^2$	$^6S_{5/2}$	7.28
44	Ru Ruthenium	(Kr) $4d^7 5s$	$^5F_5$	7.3605
45	Rh Rhodium	(Kr) $4d^8 5s$	$^4F_{9/2}$	7.4589
46	Pd Palladium	(Kr) $4d^{10}$	$^1S_0$	8.3369
47	Ag Silver	(Kr) $4d^{10} 5s$	$^2S_{1/2}$	7.5762
48	Cd Cadmium	(Kr) $4d^{10} 5s^2$	$^1S_0$	8.9938

49	In	Indium	(Kr)4d <sup>10</sup> 5s <sup>2</sup> 5p			<sup>2</sup> P <sub>1/2</sub>	5.7864
50	Sn	Tin	(Kr)4d <sup>10</sup> 5s <sup>2</sup> 5p <sup>2</sup>			<sup>3</sup> P <sub>0</sub>	7.3439
51	Sb	Antimony	(Kr)4d <sup>10</sup> 5s <sup>2</sup> 5p <sup>3</sup>			<sup>4</sup> S <sub>3/2</sub>	8.6084
52	Te	Tellurium	(Kr)4d <sup>10</sup> 5s <sup>2</sup> 5p <sup>4</sup>			<sup>3</sup> P <sub>2</sub>	9.0096
53	I	Iodine	(Kr)4d <sup>10</sup> 5s <sup>2</sup> 5p <sup>5</sup>			<sup>2</sup> P <sub>3/2</sub>	10.4513
54	Xe	Xenon	(Kr)4d <sup>10</sup> 5s <sup>2</sup> 5p <sup>6</sup>			<sup>1</sup> S <sub>0</sub>	12.1298
55	Cs	Cesium	(Xe) 6s			<sup>2</sup> S <sub>1/2</sub>	3.8939
56	Ba	Barium	(Xe) 6s <sup>2</sup>			<sup>1</sup> S <sub>0</sub>	5.2117
57	La	Lanthanum	(Xe) 5d 6s <sup>2</sup>			<sup>2</sup> D <sub>3/2</sub>	5.5769
58	Ce	Cerium	(Xe)4f 5d 6s <sup>2</sup>			<sup>1</sup> G <sub>4</sub>	5.5387
59	Pr	Praseodymium	(Xe)4f <sup>3</sup> 6s <sup>2</sup>	L		<sup>4</sup> I <sub>9/2</sub>	5.473
60	Nd	Neodymium	(Xe)4f <sup>4</sup> 6s <sup>2</sup>	a		<sup>5</sup> I <sub>4</sub>	5.5250
61	Pm	Promethium	(Xe)4f <sup>5</sup> 6s <sup>2</sup>	n		<sup>6</sup> H <sub>5/2</sub>	5.582
62	Sm	Samarium	(Xe)4f <sup>6</sup> 6s <sup>2</sup>	t		<sup>7</sup> F <sub>0</sub>	5.6437
63	Eu	Europium	(Xe)4f <sup>7</sup> 6s <sup>2</sup>	h		<sup>8</sup> S <sub>7/2</sub>	5.6704
64	Gd	Gadolinium	(Xe)4f <sup>7</sup> 5d 6s <sup>2</sup>	a		<sup>9</sup> D <sub>2</sub>	6.1498
65	Tb	Terbium	(Xe)4f <sup>9</sup> 6s <sup>2</sup>	n		<sup>6</sup> H <sub>15/2</sub>	5.8638
66	Dy	Dysprosium	(Xe)4f <sup>10</sup> 6s <sup>2</sup>	i		<sup>5</sup> I <sub>8</sub>	5.9389
67	Ho	Holmium	(Xe)4f <sup>11</sup> 6s <sup>2</sup>	d		<sup>4</sup> I <sub>15/2</sub>	6.0215
68	Er	Erbium	(Xe)4f <sup>12</sup> 6s <sup>2</sup>	e		<sup>3</sup> H <sub>6</sub>	6.1077
69	Tm	Thulium	(Xe)4f <sup>13</sup> 6s <sup>2</sup>	s		<sup>2</sup> F <sub>7/2</sub>	6.1843
70	Yb	Ytterbium	(Xe)4f <sup>14</sup> 6s <sup>2</sup>			<sup>1</sup> S <sub>0</sub>	6.2542
71	Lu	Lutetium	(Xe)4f <sup>14</sup> 5d 6s <sup>2</sup>			<sup>2</sup> D <sub>3/2</sub>	5.4259
72	Hf	Hafnium	(Xe)4f <sup>14</sup> 5d <sup>2</sup> 6s <sup>2</sup>	T		<sup>3</sup> F <sub>2</sub>	6.8251
73	Ta	Tantalum	(Xe)4f <sup>14</sup> 5d <sup>3</sup> 6s <sup>2</sup>	r		<sup>4</sup> F <sub>3/2</sub>	7.5496
74	W	Tungsten	(Xe)4f <sup>14</sup> 5d <sup>4</sup> 6s <sup>2</sup>	a		<sup>5</sup> D <sub>0</sub>	7.8640
75	Re	Rhenium	(Xe)4f <sup>14</sup> 5d <sup>5</sup> 6s <sup>2</sup>	n		<sup>6</sup> S <sub>5/2</sub>	7.8335
76	Os	Osmium	(Xe)4f <sup>14</sup> 5d <sup>6</sup> 6s <sup>2</sup>	s		<sup>5</sup> D <sub>4</sub>	8.4382
77	Ir	Iridium	(Xe)4f <sup>14</sup> 5d <sup>7</sup> 6s <sup>2</sup>	i		<sup>4</sup> F <sub>9/2</sub>	8.9670
78	Pt	Platinum	(Xe)4f <sup>14</sup> 5d <sup>9</sup> 6s	t		<sup>3</sup> D <sub>3</sub>	8.9588
79	Au	Gold	(Xe)4f <sup>14</sup> 5d <sup>10</sup> 6s	i		<sup>2</sup> S <sub>1/2</sub>	9.2255
80	Hg	Mercury	(Xe)4f <sup>14</sup> 5d <sup>10</sup> 6s <sup>2</sup>	o		<sup>1</sup> S <sub>0</sub>	10.4375
81	Tl	Thallium	(Xe)4f <sup>14</sup> 5d <sup>10</sup> 6s <sup>2</sup> 6p	n		<sup>2</sup> P <sub>1/2</sub>	6.1082
82	Pb	Lead	(Xe)4f <sup>14</sup> 5d <sup>10</sup> 6s <sup>2</sup> 6p <sup>2</sup>			<sup>3</sup> P <sub>0</sub>	7.4167
83	Bi	Bismuth	(Xe)4f <sup>14</sup> 5d <sup>10</sup> 6s <sup>2</sup> 6p <sup>3</sup>			<sup>4</sup> S <sub>3/2</sub>	7.2855
84	Po	Polonium	(Xe)4f <sup>14</sup> 5d <sup>10</sup> 6s <sup>2</sup> 6p <sup>4</sup>			<sup>3</sup> P <sub>2</sub>	8.414
85	At	Astatine	(Xe)4f <sup>14</sup> 5d <sup>10</sup> 6s <sup>2</sup> 6p <sup>5</sup>			<sup>2</sup> P <sub>3/2</sub>	
86	Rn	Radon	(Xe)4f <sup>14</sup> 5d <sup>10</sup> 6s <sup>2</sup> 6p <sup>6</sup>			<sup>1</sup> S <sub>0</sub>	10.7485
87	Fr	Francium	(Rn) 7s			<sup>2</sup> S <sub>1/2</sub>	4.0727
88	Ra	Radium	(Rn) 7s <sup>2</sup>			<sup>1</sup> S <sub>0</sub>	5.2784
89	Ac	Actinium	(Rn) 6d 7s <sup>2</sup>			<sup>2</sup> D <sub>3/2</sub>	5.3807
90	Th	Thorium	(Rn) 6d <sup>2</sup> 7s <sup>2</sup>			<sup>3</sup> F <sub>2</sub>	6.3067
91	Pa	Protactinium	(Rn)5f <sup>2</sup> 6d 7s <sup>2</sup>	A		<sup>4</sup> K <sub>11/2</sub> *	5.89
92	U	Uranium	(Rn)5f <sup>3</sup> 6d 7s <sup>2</sup>	c		<sup>5</sup> L <sub>6</sub> *	6.1939
93	Np	Neptunium	(Rn)5f <sup>4</sup> 6d 7s <sup>2</sup>	t		<sup>6</sup> L <sub>11/2</sub> *	6.2657
94	Pu	Plutonium	(Rn)5f <sup>6</sup> 7s <sup>2</sup>	i		<sup>7</sup> F <sub>0</sub>	6.0260
95	Am	Americium	(Rn)5f <sup>7</sup> 7s <sup>2</sup>	n		<sup>8</sup> S <sub>7/2</sub>	5.9738
96	Cm	Curium	(Rn)5f <sup>7</sup> 6d 7s <sup>2</sup>	d		<sup>9</sup> D <sub>2</sub>	5.9914
97	Bk	Berkelium	(Rn)5f <sup>9</sup> 7s <sup>2</sup>	e		<sup>6</sup> H <sub>15/2</sub>	6.1979
98	Cf	Californium	(Rn)5f <sup>10</sup> 7s <sup>2</sup>	s		<sup>5</sup> I <sub>8</sub>	6.2817
99	Es	Einsteinium	(Rn)5f <sup>11</sup> 7s <sup>2</sup>			<sup>4</sup> I <sub>15/2</sub>	6.3676
100	Fm	Fermium	(Rn)5f <sup>12</sup> 7s <sup>2</sup>			<sup>3</sup> H <sub>6</sub>	6.50
101	Md	Mendelevium	(Rn)5f <sup>13</sup> 7s <sup>2</sup>			<sup>2</sup> F <sub>7/2</sub>	6.58
102	No	Nobelium	(Rn)5f <sup>14</sup> 7s <sup>2</sup>			<sup>1</sup> S <sub>0</sub>	6.65
103	Lr	Lawrencium	(Rn)5f <sup>14</sup> 7s <sup>2</sup> 7p?			<sup>2</sup> P <sub>1/2</sub> ?	4.9?
104	Rf	Rutherfordium	(Rn)5f <sup>14</sup> 6d <sup>2</sup> 7s <sup>2</sup> ?			<sup>3</sup> F <sub>2</sub> ?	6.0?

\* The usual *LS* coupling scheme does not apply for these three elements. See the introductory note to the NIST table from which this table is taken.

## 6. ATOMIC AND NUCLEAR PROPERTIES OF MATERIALS

**Table 6.1** Abridged from [pdg.lbl.gov/AtomicNuclearProperties](http://pdg.lbl.gov/AtomicNuclearProperties) by D. E. Groom (2007). See web pages for more detail about entries in this table including chemical formulae, and for several hundred other entries. Quantities in parentheses are for NTP (20° C and 1 atm), and square brackets indicate quantities evaluated at STP. Boiling points are at 1 atm. Refractive indices  $n$  are evaluated at the sodium D line blend (589.2 nm); values  $\gg 1$  in brackets are for  $(n - 1) \times 10^6$  (gases).

Material	$Z$	$A$	$\langle Z/A \rangle$	Nucl.coll. length $\lambda_T$ {g cm <sup>-2</sup> }	Nucl.inter. length $\lambda_I$ {g cm <sup>-2</sup> }	Rad.len. $X_0$ {g cm <sup>-2</sup> }	$dE/dx _{\min}$ { MeV g <sup>-1</sup> cm <sup>2</sup> }	Density {g cm <sup>-3</sup> } {(gℓ <sup>-1</sup> )}	Melting point (K)	Boiling point (K)	Refract. index (@ Na D)
H <sub>2</sub>	1	1.00794(7)	0.99212	42.8	52.0	63.04	(4.103)	0.071(0.084)	13.81	20.28	1.11[132.]
D <sub>2</sub>	1	2.01410177803(8)	0.49650	51.3	71.8	125.97	(2.053)	0.169(0.168)	18.7	23.65	1.11[138.]
He	2	4.002602(2)	0.49967	51.8	71.0	94.32	(1.937)	0.125(0.166)		4.220	1.02[35.0]
Li	3	6.941(2)	0.43221	52.2	71.3	82.78	1.639	0.534	453.6	1615.	
Be	4	9.012182(3)	0.44384	55.3	77.8	65.19	1.595	1.848	1560.	2744.	
C diamond	6	12.0107(8)	0.49955	59.2	85.8	42.70	1.725	3.520			2.42
C graphite	6	12.0107(8)	0.49955	59.2	85.8	42.70	1.742	2.210			
N <sub>2</sub>	7	14.0067(2)	0.49976	61.1	89.7	37.99	(1.825)	0.807(1.165)	63.15	77.29	1.20[298.]
O <sub>2</sub>	8	15.9994(3)	0.50002	61.3	90.2	34.24	(1.801)	1.141(1.332)	54.36	90.20	1.22[271.]
F <sub>2</sub>	9	18.9984032(5)	0.47372	65.0	97.4	32.93	(1.676)	1.507(1.580)	53.53	85.03	[195.]
Ne	10	20.1797(6)	0.49555	65.7	99.0	28.93	(1.724)	1.204(0.839)	24.56	27.07	1.09[67.1]
Al	13	26.9815386(8)	0.48181	69.7	107.2	24.01	1.615	2.699	933.5	2792.	
Si	14	28.0855(3)	0.49848	70.2	108.4	21.82	1.664	2.329	1687.	3538.	3.95
Cl <sub>2</sub>	17	35.453(2)	0.47951	73.8	115.7	19.28	(1.630)	1.574(2.980)	171.6	239.1	[773.]
Ar	18	39.948(1)	0.45059	75.7	119.7	19.55	(1.519)	1.396(1.662)	83.81	87.26	1.23[281.]
Ti	22	47.867(1)	0.45961	78.8	126.2	16.16	1.477	4.540	1941.	3560.	
Fe	26	55.845(2)	0.46557	81.7	132.1	13.84	1.451	7.874	1811.	3134.	
Cu	29	63.546(3)	0.45636	84.2	137.3	12.86	1.403	8.960	1358.	2835.	
Ge	32	72.64(1)	0.44053	86.9	143.0	12.25	1.370	5.323	1211.	3106.	
Sn	50	118.710(7)	0.42119	98.2	166.7	8.82	1.263	7.310	505.1	2875.	
Xe	54	131.293(6)	0.41129	100.8	172.1	8.48	(1.255)	2.953(5.483)	161.4	165.1	1.39[701.]
W	74	183.84(1)	0.40252	110.4	191.9	6.76	1.145	19.300	3695.	5828.	
Pt	78	195.084(9)	0.39983	112.2	195.7	6.54	1.128	21.450	2042.	4098.	
Au	79	196.966569(4)	0.40108	112.5	196.3	6.46	1.134	19.320	1337.	3129.	
Pb	82	207.2(1)	0.39575	114.1	199.6	6.37	1.122	11.350	600.6	2022.	
U	92	[238.02891(3)]	0.38651	118.6	209.0	6.00	1.081	18.950	1408.	4404.	
Air (dry, 1 atm)			0.49919	61.3	90.1	36.62	(1.815)	(1.205)		78.80	
Shielding concrete			0.50274	65.1	97.5	26.57	1.711	2.300			
Borosilicate glass (Pyrex)			0.49707	64.6	96.5	28.17	1.696	2.230			
Lead glass			0.42101	95.9	158.0	7.87	1.255	6.220			
Standard rock			0.50000	66.8	101.3	26.54	1.688	2.650			
Methane (CH <sub>4</sub> )			0.62334	54.0	73.8	46.47	(2.417)	(0.667)	90.68	111.7	[444.]
Ethane (C <sub>2</sub> H <sub>6</sub> )			0.59861	55.0	75.9	45.66	(2.304)	(1.263)	90.36	184.5	
Propane (C <sub>3</sub> H <sub>8</sub> )			0.58962	55.3	76.7	45.37	(2.262)	0.493(1.868)	85.52	231.0	
Butane (C <sub>4</sub> H <sub>10</sub> )			0.59497	55.5	77.1	45.23	(2.278)	(2.489)	134.9	272.6	
Octane (C <sub>8</sub> H <sub>18</sub> )			0.57778	55.8	77.8	45.00	2.123	0.703	214.4	398.8	
Paraffin (CH <sub>3</sub> (CH <sub>2</sub> ) <sub>n</sub> ≈23CH <sub>3</sub> )			0.57275	56.0	78.3	44.85	2.088	0.930			
Nylon (type 6, 6/6)			0.54790	57.5	81.6	41.92	1.973	1.18			
Polycarbonate (Lexan)			0.52697	58.3	83.6	41.50	1.886	1.20			
Polyethylene ([CH <sub>2</sub> CH <sub>2</sub> ] <sub>n</sub> )			0.57034	56.1	78.5	44.77	2.079	0.89			
Polyethylene terephthalate (Mylar)			0.52037	58.9	84.9	39.95	1.848	1.40			
Polyimide film (Kapton)			0.51264	59.2	85.5	40.58	1.820	1.42			
Polymethylmethacrylate (acrylic)			0.53937	58.1	82.8	40.55	1.929	1.19			1.49
Polypropylene			0.55998	56.1	78.5	44.77	2.041	0.90			
Polystyrene ([C <sub>6</sub> H <sub>5</sub> CHCH <sub>2</sub> ] <sub>n</sub> )			0.53768	57.5	81.7	43.79	1.936	1.06			1.59
Polytetrafluoroethylene (Teflon)			0.47992	63.5	94.4	34.84	1.671	2.20			
Polyvinyltoluene			0.54141	57.3	81.3	43.90	1.956	1.03			1.58
Aluminum oxide (sapphire)			0.49038	65.5	98.4	27.94	1.647	3.970	2327.	3273.	1.77
Barium fluoride (BaF <sub>2</sub> )			0.42207	90.8	149.0	9.91	1.303	4.893	1641.	2533.	1.47
Bismuth germanate (BGO)			0.42065	96.2	159.1	7.97	1.251	7.130	1317.		2.15
Carbon dioxide gas (CO <sub>2</sub> )			0.49989	60.7	88.9	36.20	1.819	(1.842)			[449.]
Solid carbon dioxide (dry ice)			0.49989	60.7	88.9	36.20	1.787	1.563		Sublimes at 194.7 K	
Cesium iodide (CsI)			0.41569	100.6	171.5	8.39	1.243	4.510	894.2	1553.	1.79
Lithium fluoride (LiF)			0.46262	61.0	88.7	39.26	1.614	2.635	1121.	1946.	1.39
Lithium hydride (LiH)			0.50321	50.8	68.1	79.62	1.897	0.820	965.		
Lead tungstate (PbWO <sub>4</sub> )			0.41315	100.6	168.3	7.39	1.229	8.300	1403.		2.20
Silicon dioxide (SiO <sub>2</sub> , fused quartz)			0.49930	65.2	97.8	27.05	1.699	2.200	1986.	3223.	1.46
Sodium chloride (NaCl)			0.55509	71.2	110.1	21.91	1.847	2.170	1075.	1738.	1.54
Sodium iodide (NaI)			0.42697	93.1	154.6	9.49	1.305	3.667	933.2	1577.	1.77
Water (H <sub>2</sub> O)			0.55509	58.5	83.3	36.08	1.992	1.000(0.756)	273.1	373.1	1.33
Silica aerogel			0.50093	65.0	97.3	27.25	1.740	0.200		(0.03 H <sub>2</sub> O, 0.97 SiO <sub>2</sub> )	



Material	Dielectric constant ( $\kappa = \epsilon/\epsilon_0$ ) ( ) is $(\kappa-1)\times 10^6$ for gas	Young's modulus [ $10^6$ psi]	Coeff. of thermal expansion [ $10^{-6}$ cm/cm- $^{\circ}$ C]	Specific heat [cal/g- $^{\circ}$ C]	Electrical resistivity [ $\mu\Omega$ cm(@ $^{\circ}$ C)]	Thermal conductivity [cal/cm- $^{\circ}$ C-sec]
H <sub>2</sub>	(253.9)	—	—	—	—	—
He	(64)	—	—	—	—	—
Li	—	—	56	0.86	8.55(0 $^{\circ}$ )	0.17
Be	—	37	12.4	0.436	5.885(0 $^{\circ}$ )	0.38
C	—	0.7	0.6–4.3	0.165	1375(0 $^{\circ}$ )	0.057
N <sub>2</sub>	(548.5)	—	—	—	—	—
O <sub>2</sub>	(495)	—	—	—	—	—
Ne	(127)	—	—	—	—	—
Al	—	10	23.9	0.215	2.65(20 $^{\circ}$ )	0.53
Si	11.9	16	2.8–7.3	0.162	—	0.20
Ar	(517)	—	—	—	—	—
Ti	—	16.8	8.5	0.126	50(0 $^{\circ}$ )	—
Fe	—	28.5	11.7	0.11	9.71(20 $^{\circ}$ )	0.18
Cu	—	16	16.5	0.092	1.67(20 $^{\circ}$ )	0.94
Ge	16.0	—	5.75	0.073	—	0.14
Sn	—	6	20	0.052	11.5(20 $^{\circ}$ )	0.16
Xe	—	—	—	—	—	—
W	—	50	4.4	0.032	5.5(20 $^{\circ}$ )	0.48
Pt	—	21	8.9	0.032	9.83(0 $^{\circ}$ )	0.17
Pb	—	2.6	29.3	0.038	20.65(20 $^{\circ}$ )	0.083
U	—	—	36.1	0.028	29(20 $^{\circ}$ )	0.064

## 7. ELECTROMAGNETIC RELATIONS

Revised September 2005 by H.G. Spieler (LBNL).

Quantity	Gaussian CGS	SI
Conversion factors:		
Charge:	$2.997\,924\,58 \times 10^9$ esu	$= 1\text{ C} = 1\text{ A s}$
Potential:	$(1/299.792\,458)$ statvolt (ergs/esu)	$= 1\text{ V} = 1\text{ J C}^{-1}$
Magnetic field:	$10^4$ gauss $= 10^4$ dyne/esu	$= 1\text{ T} = 1\text{ N A}^{-1}\text{m}^{-1}$
	$\mathbf{F} = q(\mathbf{E} + \frac{\mathbf{v}}{c} \times \mathbf{B})$	$\mathbf{F} = q(\mathbf{E} + \mathbf{v} \times \mathbf{B})$
	$\nabla \cdot \mathbf{D} = 4\pi\rho$ $\nabla \times \mathbf{H} - \frac{1}{c} \frac{\partial \mathbf{D}}{\partial t} = \frac{4\pi}{c} \mathbf{J}$ $\nabla \cdot \mathbf{B} = 0$ $\nabla \times \mathbf{E} + \frac{1}{c} \frac{\partial \mathbf{B}}{\partial t} = 0$	$\nabla \cdot \mathbf{D} = \rho$ $\nabla \times \mathbf{H} - \frac{\partial \mathbf{D}}{\partial t} = \mathbf{J}$ $\nabla \cdot \mathbf{B} = 0$ $\nabla \times \mathbf{E} + \frac{\partial \mathbf{B}}{\partial t} = 0$
Constitutive relations:	$\mathbf{D} = \mathbf{E} + 4\pi\mathbf{P}$ , $\mathbf{H} = \mathbf{B} - 4\pi\mathbf{M}$	$\mathbf{D} = \epsilon_0\mathbf{E} + \mathbf{P}$ , $\mathbf{H} = \mathbf{B}/\mu_0 - \mathbf{M}$
Linear media:	$\mathbf{D} = \epsilon\mathbf{E}$ , $\mathbf{H} = \mathbf{B}/\mu$ 1 1	$\mathbf{D} = \epsilon\mathbf{E}$ , $\mathbf{H} = \mathbf{B}/\mu$ $\epsilon_0 = 8.854\,187 \dots \times 10^{-12}$ F m <sup>-1</sup> $\mu_0 = 4\pi \times 10^{-7}$ N A <sup>-2</sup>
	$\mathbf{E} = -\nabla V - \frac{1}{c} \frac{\partial \mathbf{A}}{\partial t}$ $\mathbf{B} = \nabla \times \mathbf{A}$	$\mathbf{E} = -\nabla V - \frac{\partial \mathbf{A}}{\partial t}$ $\mathbf{B} = \nabla \times \mathbf{A}$
	$V = \sum_{\text{charges}} \frac{q_i}{r_i} = \int \frac{\rho(\mathbf{r}')}{ \mathbf{r} - \mathbf{r}' } d^3x'$ $\mathbf{A} = \frac{1}{c} \oint \frac{I d\boldsymbol{\ell}}{ \mathbf{r} - \mathbf{r}' } = \frac{1}{c} \int \frac{\mathbf{J}(\mathbf{r}')}{ \mathbf{r} - \mathbf{r}' } d^3x'$	$V = \frac{1}{4\pi\epsilon_0} \sum_{\text{charges}} \frac{q_i}{r_i} = \frac{1}{4\pi\epsilon_0} \int \frac{\rho(\mathbf{r}')}{ \mathbf{r} - \mathbf{r}' } d^3x'$ $\mathbf{A} = \frac{\mu_0}{4\pi} \oint \frac{I d\boldsymbol{\ell}}{ \mathbf{r} - \mathbf{r}' } = \frac{\mu_0}{4\pi} \int \frac{\mathbf{J}(\mathbf{r}')}{ \mathbf{r} - \mathbf{r}' } d^3x'$
	$\mathbf{E}'_{\parallel} = \mathbf{E}_{\parallel}$ $\mathbf{E}'_{\perp} = \gamma(\mathbf{E}_{\perp} + \frac{1}{c} \mathbf{v} \times \mathbf{B})$ $\mathbf{B}'_{\parallel} = \mathbf{B}_{\parallel}$ $\mathbf{B}'_{\perp} = \gamma(\mathbf{B}_{\perp} - \frac{1}{c} \mathbf{v} \times \mathbf{E})$	$\mathbf{E}'_{\parallel} = \mathbf{E}_{\parallel}$ $\mathbf{E}'_{\perp} = \gamma(\mathbf{E}_{\perp} + \mathbf{v} \times \mathbf{B})$ $\mathbf{B}'_{\parallel} = \mathbf{B}_{\parallel}$ $\mathbf{B}'_{\perp} = \gamma(\mathbf{B}_{\perp} - \frac{1}{c^2} \mathbf{v} \times \mathbf{E})$
	$\frac{1}{4\pi\epsilon_0} = c^2 \times 10^{-7} \text{ N A}^{-2} = 8.987\,55 \dots \times 10^9 \text{ m F}^{-1}$ ; $\frac{\mu_0}{4\pi} = 10^{-7} \text{ N A}^{-2}$ ; $c = \frac{1}{\sqrt{\mu_0\epsilon_0}} = 2.997\,924\,58 \times 10^8 \text{ m s}^{-1}$	

### 7.1. Impedances (SI units)

$\rho$  = resistivity at room temperature in  $10^{-8} \Omega \text{ m}$ :  
 $\sim 1.7$  for Cu  $\sim 5.5$  for W  
 $\sim 2.4$  for Au  $\sim 73$  for SS 304  
 $\sim 2.8$  for Al  $\sim 100$  for Nichrome  
 (Al alloys may have double the Al value.)

For alternating currents, instantaneous current  $I$ , voltage  $V$ , angular frequency  $\omega$ :

$$V = V_0 e^{j\omega t} = ZI. \quad (7.1)$$

Impedance of self-inductance  $L$ :  $Z = j\omega L$ .

Impedance of capacitance  $C$ :  $Z = 1/j\omega C$ .

Impedance of free space:  $Z = \sqrt{\mu_0/\epsilon_0} = 376.7 \Omega$ .

High-frequency surface impedance of a good conductor:

$$Z = \frac{(1+j)\rho}{\delta}, \quad \text{where } \delta = \text{skin depth}; \quad (7.2)$$

$$\delta = \sqrt{\frac{\rho}{\pi\nu\mu}} \approx \frac{6.6 \text{ cm}}{\sqrt{\nu \text{ (Hz)}}} \quad \text{for Cu}. \quad (7.3)$$

### 7.2. Capacitors, inductors, and transmission Lines

The capacitance between two parallel plates of area  $A$  spaced by the distance  $d$  and enclosing a medium with the dielectric constant  $\epsilon$  is

$$C = K\epsilon A/d, \quad (7.4)$$

where the correction factor  $K$  depends on the extent of the fringing field. If the dielectric fills the capacitor volume without extending beyond the electrodes, the correction factor  $K \approx 0.8$  for capacitors of typical geometry.

The inductance at high frequencies of a straight wire whose length  $\ell$  is much greater than the wire diameter  $d$  is

$$L \approx 2.0 \left[ \frac{\text{nH}}{\text{cm}} \right] \cdot \ell \left( \ln \left( \frac{4\ell}{d} \right) - 1 \right). \quad (7.5)$$

For very short wires, representative of vias in a printed circuit board, the inductance is

$$L(\text{in nH}) \approx \ell/d. \quad (7.6)$$

A transmission line is a pair of conductors with inductance  $L$  and capacitance  $C$ . The characteristic impedance  $Z = \sqrt{L/C}$  and the phase velocity  $v_p = 1/\sqrt{LC} = 1/\sqrt{\mu\epsilon}$ , which decreases with the inverse square root of the dielectric constant of the medium. Typical coaxial and ribbon cables have a propagation delay of about 5 ns/cm. The impedance of a coaxial cable with outer diameter  $D$  and inner diameter  $d$  is

$$Z = 60 \Omega \cdot \frac{1}{\sqrt{\epsilon_r}} \ln \frac{D}{d}, \quad (7.7)$$

where the relative dielectric constant  $\epsilon_r = \epsilon/\epsilon_0$ . A pair of parallel wires of diameter  $d$  and spacing  $a > 2.5d$  has the impedance

$$Z = 120 \Omega \cdot \frac{1}{\sqrt{\epsilon_r}} \ln \frac{2a}{d}. \quad (7.8)$$

This yields the impedance of a wire at a spacing  $h$  above a ground plane,

$$Z = 60 \Omega \cdot \frac{1}{\sqrt{\epsilon_r}} \ln \frac{4h}{d}. \quad (7.9)$$

A common configuration utilizes a thin rectangular conductor above a ground plane with an intermediate dielectric (microstrip). Detailed calculations for this and other transmission line configurations are given by Gunston.\*

### 7.3. Synchrotron radiation (CGS units)

For a particle of charge  $e$ , velocity  $v = \beta c$ , and energy  $E = \gamma mc^2$ , traveling in a circular orbit of radius  $R$ , the classical energy loss per revolution  $\delta E$  is

$$\delta E = \frac{4\pi}{3} \frac{e^2}{R} \beta^3 \gamma^4. \quad (7.10)$$

For high-energy electrons or positrons ( $\beta \approx 1$ ), this becomes

$$\delta E \text{ (in MeV)} \approx 0.0885 [E(\text{in GeV})]^4 / R(\text{in m}). \quad (7.11)$$

For  $\gamma \gg 1$ , the energy radiated per revolution into the photon energy interval  $d(\hbar\omega)$  is

$$dI = \frac{8\pi}{9} \alpha \gamma F(\omega/\omega_c) d(\hbar\omega), \quad (7.12)$$

where  $\alpha = e^2/\hbar c$  is the fine-structure constant and

$$\omega_c = \frac{3\gamma^3 c}{2R} \quad (7.13)$$

is the critical frequency. The normalized function  $F(y)$  is

$$F(y) = \frac{9}{8\pi} \sqrt{3} y \int_y^\infty K_{5/3}(x) dx, \quad (7.14)$$

where  $K_{5/3}(x)$  is a modified Bessel function of the third kind. For electrons or positrons,

$$\hbar\omega_c \text{ (in keV)} \approx 2.22 [E(\text{in GeV})]^3 / R(\text{in m}). \quad (7.15)$$

Fig. 7.1 shows  $F(y)$  over the important range of  $y$ .

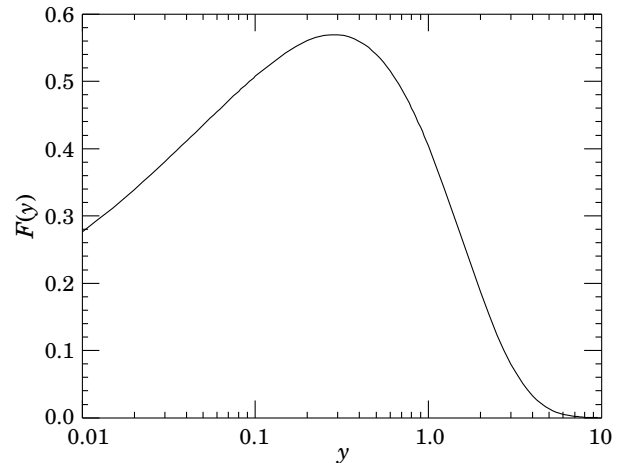


Figure 7.1: The normalized synchrotron radiation spectrum  $F(y)$ .

For  $\gamma \gg 1$  and  $\omega \ll \omega_c$ ,

$$\frac{dI}{d(\hbar\omega)} \approx 3.3\alpha (\omega R/c)^{1/3}, \quad (7.16)$$

whereas for

$$\gamma \gg 1 \text{ and } \omega \gtrsim 3\omega_c,$$

$$\frac{dI}{d(\hbar\omega)} \approx \sqrt{\frac{3\pi}{2}} \alpha \gamma \left( \frac{\omega}{\omega_c} \right)^{1/2} e^{-\omega/\omega_c} \left[ 1 + \frac{55}{72} \frac{\omega_c}{\omega} + \dots \right]. \quad (7.17)$$

The radiation is confined to angles  $\lesssim 1/\gamma$  relative to the instantaneous direction of motion. For  $\gamma \gg 1$ , where Eq. (7.12) applies, the mean number of photons emitted per revolution is

$$N_\gamma = \frac{5\pi}{\sqrt{3}} \alpha \gamma, \quad (7.18)$$

and the mean energy per photon is

$$\langle \hbar\omega \rangle = \frac{8}{15\sqrt{3}} \hbar\omega_c. \quad (7.19)$$

When  $\langle \hbar\omega \rangle \gtrsim O(E)$ , quantum corrections are important.

\* M.A.R. Gunston. Microwave Transmission Line Data, Noble Publishing Corp., Atlanta (1997) ISBN 1-884932-57-6, TK6565.T73G85.

See J.D. Jackson, *Classical Electrodynamics*, 3rd edition (John Wiley & Sons, New York, 1998) for more formulae and details. (Note that earlier editions had  $\omega_c$  twice as large as Eq. (7.13).

## 8. NAMING SCHEME FOR HADRONS

Revised 2008 by M. Roos (University of Finland) and C.G. Wohl (LBNL).

## 8.1. Introduction

We introduced in the 1986 edition [1] a new naming scheme for the hadrons. Changes from older terminology affected mainly the heavier mesons made of the light ( $u$ ,  $d$ , and  $s$ ) quarks. Old and new names were listed alongside until 1994. Names also change from edition to edition because some characteristic like mass or spin changes. The Summary Tables give both the new and old names whenever a change occurred.

8.2. “Neutral-flavor” mesons ( $S=C=B=T=0$ )

Table 8.1 shows the names for mesons having the strangeness and all heavy-flavor quantum numbers equal to zero. The scheme is designed for all ordinary non-exotic mesons, but it will work for many exotic types too, if needed.

**Table 8.1:** Symbols for mesons with the strangeness and all heavy-flavor quantum numbers equal to zero.

$J^{PC}$	$\begin{cases} 0^{-+} \\ 2^{-+} \\ \vdots \end{cases}$	$\begin{cases} 1^{+-} \\ 3^{+-} \\ \vdots \end{cases}$	$\begin{cases} 1^{--} \\ 2^{--} \\ \vdots \end{cases}$	$\begin{cases} 0^{++} \\ 1^{++} \\ \vdots \end{cases}$	
$q\bar{q}$ content	$2^{S+1}L_J$	${}^1(L\text{ even})_J$	${}^1(L\text{ odd})_J$	${}^3(L\text{ even})_J$	${}^3(L\text{ odd})_J$
$u\bar{d}, u\bar{u} - d\bar{d}, d\bar{u}$ ( $I=1$ )	$\pi$	$b$	$\rho$	$a$	
$d\bar{d} + u\bar{u}$ and/or $s\bar{s}$ } ( $I=0$ )	$\eta, \eta'$	$h, h'$	$\omega, \phi$	$f, f'$	
$c\bar{c}$	$\eta_c$	$h_c$	$\psi^\dagger$	$\chi_c$	
$b\bar{b}$	$\eta_b$	$h_b$	$\Upsilon$	$\chi_b$	
$t\bar{t}$	$\eta_t$	$h_t$	$\theta$	$\chi_t$	

<sup>†</sup>The  $J/\psi$  remains the  $J/\psi$ .

First, we assign names to those states with quantum numbers compatible with being  $q\bar{q}$  states. The rows of the Table give the possible  $q\bar{q}$  content. The columns give the possible parity/charge-conjugation states,

$$PC = -+, ++, --, \text{ and } ++;$$

these combinations correspond one-to-one with the angular-momentum state  $2^{S+1}L_J$  of the  $q\bar{q}$  system being

$${}^1(L\text{ even})_J, {}^1(L\text{ odd})_J, {}^3(L\text{ even})_J, \text{ or } {}^3(L\text{ odd})_J.$$

Here  $S$ ,  $L$ , and  $J$  are the spin, orbital, and total angular momenta of the  $q\bar{q}$  system. The quantum numbers are related by  $P = (-1)^{L+1}$ ,  $C = (-1)^{L+S}$ , and  $G$  parity  $= (-1)^{L+S+I}$ , where of course the  $C$  quantum number is only relevant to neutral mesons.

The entries in the Table give the meson names. The spin  $J$  is added as a subscript except for pseudoscalar and vector mesons, and the mass is added in parentheses for mesons that decay strongly. However, for the lightest meson resonances, we omit the mass.

Measurements of the mass, quark content (where relevant), and quantum numbers  $I$ ,  $J$ ,  $P$ , and  $C$  (or  $G$ ) of a meson thus fix its symbol. Conversely, these properties may be inferred unambiguously from the symbol.

If the main symbol cannot be assigned because the quantum numbers are unknown,  $X$  is used. Sometimes it is not known whether a meson is mainly the isospin-0 mix of  $u\bar{u}$  and  $d\bar{d}$  or is mainly  $s\bar{s}$ . A prime (or pair  $\omega$ ,  $\phi$ ) may be used to distinguish two such mixing states.

We follow custom and use spectroscopic names such as  $\Upsilon(1S)$  as the primary name for most of those  $\psi$ ,  $\Upsilon$ , and  $\chi$  states whose spectroscopic identity is known. We use the form  $\Upsilon(9460)$  as an alternative, and as the primary name when the spectroscopic identity is not known.

Names are assigned for  $t\bar{t}$  mesons, although the top quark is evidently so heavy that it is expected to decay too rapidly for bound states to form.

Gluonium states or other mesons that are not  $q\bar{q}$  states are, if the quantum numbers are *not* exotic, to be named just as are the  $q\bar{q}$  mesons. Such states will probably be difficult to distinguish from  $q\bar{q}$  states and will likely mix with them, and we make no attempt to distinguish those “mostly gluonium” from those “mostly  $q\bar{q}$ .”

An “exotic” meson with  $J^{PC}$  quantum numbers that a  $q\bar{q}$  system cannot have, namely  $J^{PC} = 0^{--}, 0^{+-}, 1^{-+}, 2^{+-}, 3^{-+}, \dots$ , would use the same symbol as does an ordinary meson with all the same quantum numbers as the exotic meson except for the  $C$  parity. But then the  $J$  subscript may still distinguish it; for example, an isospin-0  $1^{-+}$  meson could be denoted  $\omega_1$ .

8.3. Mesons with nonzero  $S$ ,  $C$ ,  $B$ , and/or  $T$ 

Since the strangeness or a heavy flavor of these mesons is nonzero, none of them are eigenstates of charge conjugation, and in each of them one of the quarks is heavier than the other. The rules are:

1. The main symbol is an upper-case italic letter indicating the heavier quark as follows:

$$s \rightarrow \bar{K} \quad c \rightarrow D \quad b \rightarrow \bar{B} \quad t \rightarrow T.$$

We use the convention that *the flavor and the charge of a quark have the same sign*. Thus the strangeness of the  $s$  quark is negative, the charm of the  $c$  quark is positive, and the bottom of the  $b$  quark is negative. In addition,  $I_3$  of the  $u$  and  $d$  quarks are positive and negative, respectively. The effect of this convention is as follows: *Any flavor carried by a charged meson has the same sign as its charge*. Thus the  $K^+$ ,  $D^+$ , and  $B^+$  have positive strangeness, charm, and bottom, respectively, and all have positive  $I_3$ . The  $D_s^+$  has positive charm *and* strangeness. Furthermore, the  $\Delta(\text{flavor}) = \Delta Q$  rule, best known for the kaons, applies to every flavor.

2. If the lighter quark is not a  $u$  or a  $d$  quark, its identity is given by a subscript. The  $D_s^+$  is an example.
3. If the spin-parity is in the “normal” series,  $J^P = 0^+, 1^-, 2^+, \dots$ , a superscript “\*” is added.
4. The spin is added as a subscript except for pseudoscalar or vector mesons.

## 8.4. Ordinary (3-quark) baryons

The symbols  $N$ ,  $\Delta$ ,  $\Lambda$ ,  $\Sigma$ ,  $\Xi$ , and  $\Omega$  used for more than 30 years for the baryons made of light quarks ( $u$ ,  $d$ , and  $s$  quarks) tell the isospin and quark content, and the same information is conveyed by the symbols used for the baryons containing one or more heavy quarks ( $c$  and  $b$  quarks). The rules are:

1. Baryons with *three*  $u$  and/or  $d$  quarks are  $N$ 's (isospin 1/2) or  $\Delta$ 's (isospin 3/2).
2. Baryons with *two*  $u$  and/or  $d$  quarks are  $\Lambda$ 's (isospin 0) or  $\Sigma$ 's (isospin 1). If the third quark is a  $c$ ,  $b$ , or  $t$  quark, its identity is given by a subscript.
3. Baryons with *one*  $u$  or  $d$  quark are  $\Xi$ 's (isospin 1/2). One or two subscripts are used if one or both of the remaining quarks are heavy: thus  $\Xi_c$ ,  $\Xi_{cc}$ ,  $\Xi_b$ , *etc.*\*
4. Baryons with *no*  $u$  or  $d$  quarks are  $\Omega$ 's (isospin 0), and subscripts indicate any heavy-quark content.
5. A baryon that decays strongly has its mass as part of its name. Thus  $p$ ,  $\Sigma^-, \Omega^-, \Lambda_c^+$ , *etc.*, but  $\Delta(1232)^0$ ,  $\Sigma(1385)^-$ ,  $\Xi_c(2645)^+$ , *etc.*

In short, the number of  $u$  plus  $d$  quarks together with the isospin determine the main symbol, and subscripts indicate any content of heavy quarks. A  $\Sigma$  always has isospin 1, an  $\Omega$  always has isospin 0, *etc.*

### 8.5. Exotic baryons

In 2003, several experiments reported finding a strangeness  $S = +1$ , charge  $Q = +1$  baryon, and one experiment reported finding an  $S = -2$ ,  $Q = -2$  baryon. Baryons with such quantum numbers cannot be made from three quarks, and thus they are exotic. The  $S = +1$  baryon, which once would have been called a  $Z$ , was quickly dubbed the  $\Theta(1540)^+$ , and we proposed to name the  $S = -2$  baryon the  $\Phi(1860)$ . However, these “discoveries” were then completely ruled out by many experiments with far larger statistics: See our 2008 *Review* [2].

#### Footnote and Reference:

- \* Sometimes a prime is necessary to distinguish two  $\Xi_c$ 's in the same  $SU(n)$  multiplet. See the “Note on Charmed Baryons” in the Charmed Baryon Listings.
1. Particle Data Group: M. Aguilar-Benitez *et al.*, Phys. Lett. **170B** (1986).
  2. Particle Data Group: C. Amsler *et al.*, Phys. Lett. **B667**, 1 (2008).

## 9. QUANTUM CHROMODYNAMICS

Revised April 2012 by S. Bethke (MPP, Munich), G. Dissertori (ETH, Zurich) and G.P. Salam (CERN, Princeton University and LPTHE, Paris).

### 9.1. Basics

Quantum Chromodynamics (QCD), the gauge field theory that describes the strong interactions of colored quarks and gluons, is the SU(3) component of the SU(3)×SU(2)×U(1) Standard Model of Particle Physics.

The Lagrangian of QCD is given by

$$\mathcal{L} = \sum_q \bar{\psi}_{q,a} (i\gamma^\mu \partial_\mu \delta_{ab} - g_s \gamma^\mu t_{ab}^C \mathcal{A}_\mu^C - m_q \delta_{ab}) \psi_{q,b} - \frac{1}{4} F_{\mu\nu}^A F^{A\mu\nu}, \quad (9.1)$$

where repeated indices are summed over. The  $\gamma^\mu$  are the Dirac  $\gamma$ -matrices. The  $\psi_{q,a}$  are quark-field spinors for a quark of flavor  $q$  and mass  $m_q$ , with a color-index  $a$  that runs from  $a = 1$  to  $N_c = 3$ , *i.e.* quarks come in three “colors.” Quarks are said to be in the fundamental representation of the SU(3) color group.

The  $\mathcal{A}_\mu^C$  correspond to the gluon fields, with  $C$  running from 1 to  $N_c^2 - 1 = 8$ , *i.e.* there are eight kinds of gluon. Gluons are said to be in the adjoint representation of the SU(3) color group. The  $t_{ab}^C$  correspond to eight  $3 \times 3$  matrices and are the generators of the SU(3) group (cf. the section on “SU(3) isoscalar factors and representation matrices” in this *Review* with  $t_{ab}^C \equiv \lambda_{ab}^C/2$ ). They encode the fact that a gluon’s interaction with a quark rotates the quark’s color in SU(3) space. The quantity  $g_s$  is the QCD coupling constant. Finally, the field tensor  $F_{\mu\nu}^A$  is given by

$$F_{\mu\nu}^A = \partial_\mu \mathcal{A}_\nu^A - \partial_\nu \mathcal{A}_\mu^A - g_s f_{ABC} \mathcal{A}_\mu^B \mathcal{A}_\nu^C \quad [t^A, t^B] = i f_{ABC} t^C, \quad (9.2)$$

where the  $f_{ABC}$  are the structure constants of the SU(3) group.

Neither quarks nor gluons are observed as free particles. Hadrons are color-singlet (*i.e.* color-neutral) combinations of quarks, anti-quarks, and gluons.

Ab-initio predictive methods for QCD include lattice gauge theory and perturbative expansions in the coupling. The Feynman rules of QCD involve a quark-antiquark-gluon ( $q\bar{q}g$ ) vertex, a 3-gluon vertex (both proportional to  $g_s$ ), and a 4-gluon vertex (proportional to  $g_s^2$ ). A full set of Feynman rules is to be found for example in Ref. 3.

Useful color-algebra relations include:  $t_{ab}^A t_{bc}^A = C_F \delta_{ac}$ , where  $C_F \equiv (N_c^2 - 1)/(2N_c) = 4/3$  is the color-factor (“Casimir”) associated with gluon emission from a quark;  $f^{ACD} f^{BCD} = C_A \delta_{AB}$  where  $C_A \equiv N_c = 3$  is the color-factor associated with gluon emission from a gluon;  $t_{ab}^A t_{ab}^B = T_R \delta_{AB}$ , where  $T_R = 1/2$  is the color-factor for a gluon to split to a  $q\bar{q}$  pair.

The fundamental parameters of QCD are the coupling  $g_s$  (or  $\alpha_s = \frac{g_s^2}{4\pi}$ ) and the quark masses  $m_q$ .

There is freedom for an additional CP-violating term to be present in the QCD Lagrangian,  $\frac{\theta}{8\pi} F_{\mu\nu}^A \tilde{F}^{A\mu\nu}$ , where  $F_{\mu\nu}^A \tilde{F}^{A\mu\nu}$  is the dual of the gluon field tensor,  $\frac{1}{2} \epsilon_{\mu\nu\rho\sigma} F^{A\sigma\rho}$ . Experimental limits on the neutron electric dipole moment [1] constrain the coefficient of this contribution to satisfy  $|\theta| \lesssim 10^{-10}$ . Further discussion is to be found in Ref. 2 and Axions section in the Listings of this *Review*.

This section will concentrate mainly on perturbative aspects of QCD as they relate to collider physics. Related textbooks and reviews include Refs. 3–6. Aspects specific to Monte Carlo event generators are reviewed in a dedicated section Chap. 38. Lattice QCD is also reviewed in a section of its own Chap. 17, with additional discussion of non-perturbative aspects to be found in the sections on “Quark Masses”, “The CKM quark-mixing matrix”, “Structure Functions” and event generators in this *Review*. For an overview of some of the QCD issues and recent results in heavy-ion physics, see for example Refs. 7, 8.

#### 9.1.1. Running coupling :

In the framework of perturbative QCD (pQCD), predictions for observables are expressed in terms of the renormalized coupling  $\alpha_s(\mu_R^2)$ , a function of an (unphysical) renormalization scale  $\mu_R$ . When one takes  $\mu_R$  close to the scale of the momentum transfer  $Q$  in a given process, then  $\alpha_s(\mu_R^2 \simeq Q^2)$  is indicative of the effective strength of the strong interaction in that process.

The coupling satisfies the following renormalization group equation (RGE):

$$\mu_R^2 \frac{d\alpha_s}{d\mu_R^2} = \beta(\alpha_s) = -(b_0 \alpha_s^2 + b_1 \alpha_s^3 + b_2 \alpha_s^4 + \dots) \quad (9.3)$$

where  $b_0 = (11C_A - 4n_f T_R)/(12\pi) = (33 - 2n_f)/(12\pi)$  is referred to as the 1-loop beta-function coefficient, the 2-loop coefficient is  $b_1 = (17C_A^2 - n_f T_R(10C_A + 6C_F))/(24\pi^2) = (153 - 19n_f)/(24\pi^2)$ , and the 3-loop coefficient is  $b_2 = (2857 - \frac{5033}{9}n_f + \frac{325}{27}n_f^2)/(128\pi^3)$ . The 4-loop coefficient,  $b_3$ , is to be found in Refs. 9, 10<sup>†</sup>. The minus sign in Eq. (9.3) is the origin of Asymptotic Freedom, *i.e.* the fact that the strong coupling becomes weak for processes involving large momentum transfers (“hard processes”),  $\alpha_s \sim 0.1$  for momentum transfers in the 100 GeV – TeV range.

The  $\beta$ -function coefficients, the  $b_i$ , are given for the coupling of an *effective theory* in which  $n_f$  of the quark flavors are considered light ( $m_q \ll \mu_R$ ), and in which the remaining heavier quark flavors decouple from the theory. One may relate the coupling for the theory with  $n_f + 1$  light flavors to that with  $n_f$  flavors through an equation of the form

$$\alpha_s^{(n_f+1)}(\mu_R^2) = \alpha_s^{(n_f)}(\mu_R^2) \left( 1 + \sum_{n=1}^{\infty} \sum_{\ell=0}^n c_{n\ell} [\alpha_s^{(n_f)}(\mu_R^2)]^n \ln^\ell \frac{\mu_R^2}{m_h^2} \right), \quad (9.4)$$

where  $m_h$  is the mass of the  $(n_f + 1)$ <sup>th</sup> flavor, and the first few  $c_{n\ell}$  coefficients are  $c_{11} = \frac{1}{6\pi}$ ,  $c_{10} = 0$ ,  $c_{22} = c_{11}^2$ ,  $c_{21} = \frac{19}{24\pi^2}$ , and  $c_{20} = -\frac{11}{72\pi^2}$  when  $m_h$  is the  $\overline{\text{MS}}$  mass at scale  $m_h$  ( $c_{20} = \frac{7}{24\pi^2}$  when  $m_h$  is the pole mass — mass definitions are discussed below and in the review on “Quark Masses”). Terms up to  $c_{4\ell}$  are to be found in Refs. 11, 12. Numerically, when one chooses  $\mu_R = m_h$ , the matching is a modest effect, owing to the zero value for the  $c_{10}$  coefficient. Relations between  $n_f$  and  $(n_f + 2)$  flavors where the two heavy flavors are close in mass are given to three loops in Ref. 13.

Working in an energy range where the number of flavors is taken constant, a simple exact analytic solution exists for Eq. (9.3) only if one neglects all but the  $b_0$  term, giving  $\alpha_s(\mu_R^2) = (b_0 \ln(\mu_R^2/\Lambda^2))^{-1}$ . Here  $\Lambda$  is a constant of integration, which corresponds to the scale where the perturbatively-defined coupling would diverge, *i.e.* it is the non-perturbative scale of QCD. A convenient approximate analytic solution to the RGE that includes also the  $b_1$ ,  $b_2$ , and  $b_3$  terms is given by (see for example Ref. 14),

$$\alpha_s(\mu_R^2) \simeq \frac{1}{b_0 t} \left( 1 - \frac{b_1 \ln t}{b_0^2 t} + \frac{b_1^2 (\ln^2 t - \ln t - 1) + b_0 b_2}{b_0^4 t^2} - \frac{b_1^3 (\ln^3 t - \frac{5}{2} \ln^2 t - 2 \ln t + \frac{1}{2}) + 3b_0 b_1 b_2 \ln t - \frac{1}{2} b_0^2 b_3}{b_0^6 t^3} \right), \quad t \equiv \ln \frac{\mu_R^2}{\Lambda^2}, \quad (9.5)$$

again parametrized in terms of a constant  $\Lambda$ . Note that Eq. (9.5) is one of several possible approximate 4-loop solutions for  $\alpha_s(\mu_R^2)$ , and that a value for  $\Lambda$  only defines  $\alpha_s(\mu_R^2)$  once one knows which particular approximation is being used. An alternative to the use of formulas such as Eq. (9.5) is to solve the RGE exactly, numerically (including the discontinuities, Eq. (9.4), at flavor thresholds). In such cases the quantity  $\Lambda$  is not defined at all. For these reasons, in determinations

<sup>†</sup> One should be aware that the  $b_2$  and  $b_3$  coefficients are renormalization-scheme-dependent, and given here in the  $\overline{\text{MS}}$  scheme, as discussed below.

of the coupling, it has become standard practice to quote the value of  $\alpha_s$  at a given scale (typically  $M_Z$ ) rather than to quote a value for  $\Lambda$ .

The value of the coupling, as well as the exact forms of the  $b_2, c_{10}$  (and higher order) coefficients, depend on the renormalization scheme in which the coupling is defined, *i.e.* the convention used to subtract infinities in the context of renormalization. The coefficients given above hold for a coupling defined in the modified minimal subtraction ( $\overline{\text{MS}}$ ) scheme [15], by far the most widely used scheme.

A discussion of determinations of the coupling and a graph illustrating its scale dependence (“running”) are to be found in Section 9.3.4.

### 9.1.2. Quark masses :

Free quarks are never observed, *i.e.* a quark never exists on its own for a time longer than  $\sim 1/\Lambda$ : up, down, strange, charm, and bottom quarks all *hadronize*, *i.e.* become part of a meson or baryon, on a timescale  $\sim 1/\Lambda$ ; the top quark instead decays before it has time to hadronize. This means that the question of what one means by the quark mass is a complex one, which requires that one adopts a specific prescription. A perturbatively defined prescription is the pole mass,  $m_q$ , which corresponds to the position of the divergence of the propagator. This is close to one’s physical picture of mass. However, when relating it to observable quantities, it suffers from substantial non-perturbative ambiguities (see *e.g.* Ref. 16). An alternative is the  $\overline{\text{MS}}$  mass,  $\overline{m}_q(\mu_R^2)$ , which depends on the renormalization scale  $\mu_R$ .

Results for the masses of heavier quarks are often quoted either as the pole mass or as the  $\overline{\text{MS}}$  mass evaluated at a scale equal to the mass,  $\overline{m}_q(\overline{m}_q^2)$ ; light quark masses are generally quoted in the  $\overline{\text{MS}}$  scheme at a scale  $\mu_R \sim 2 \text{ GeV}$ . The pole and  $\overline{\text{MS}}$  masses are related by a slowly converging series that starts  $m_q = \overline{m}_q(\overline{m}_q^2)(1 + \frac{4\alpha_s(\overline{m}_q^2)}{3\pi} + \mathcal{O}(\alpha_s^2))$ , while the scale-dependence of  $\overline{\text{MS}}$  masses is given by

$$\mu_R^2 \frac{d\overline{m}_q(\mu_R^2)}{d\mu_R^2} = \left[ -\frac{\alpha_s(\mu_R^2)}{\pi} + \mathcal{O}(\alpha_s^2) \right] \overline{m}_q(\mu_R^2). \quad (9.6)$$

More detailed discussion is to be found in a dedicated section of the *Review*, “Quark Masses.”

## 9.2. Structure of QCD predictions

### 9.2.1. Fully inclusive cross sections :

The simplest observables in QCD are those that do not involve initial-state hadrons and that are fully inclusive with respect to details of the final state. One example is the total cross section for  $e^+e^- \rightarrow \text{hadrons}$  at center-of-mass energy  $Q$ , for which one can write

$$\frac{\sigma(e^+e^- \rightarrow \text{hadrons}, Q)}{\sigma(e^+e^- \rightarrow \mu^+\mu^-, Q)} \equiv R(Q) = R_{\text{EW}}(Q)(1 + \delta_{\text{QCD}}(Q)), \quad (9.7)$$

where  $R_{\text{EW}}(Q)$  is the purely electroweak prediction for the ratio and  $\delta_{\text{QCD}}(Q)$  is the correction due to QCD effects. To keep the discussion simple, we can restrict our attention to energies  $Q \ll M_Z$ , where the process is dominated by photon exchange ( $R_{\text{EW}} = 3 \sum_q e_q^2$ , neglecting finite-quark-mass corrections),

$$\delta_{\text{QCD}}(Q) = \sum_{n=1}^{\infty} c_n \cdot \left( \frac{\alpha_s(Q^2)}{\pi} \right)^n + \mathcal{O}\left(\frac{\Lambda^4}{Q^4}\right). \quad (9.8)$$

The first four terms in the  $\alpha_s$  series expansion are then to be found in Refs. 17, 18

$$c_1 = 1, \quad c_2 = 1.9857 - 0.1152n_f, \quad (9.9a)$$

$$c_3 = -6.63694 - 1.20013n_f - 0.00518n_f^2 - 1.240\eta \quad (9.9b)$$

$$c_4 = -156.61 + 18.77n_f - 0.7974n_f^2 + 0.0215n_f^3 + C\eta, \quad (9.9c)$$

with  $\eta = (\sum e_q^2)/(3 \sum e_q^2)$  and where the coefficient  $C$  of the  $\eta$ -dependent piece in the  $\alpha_s^4$  term has yet to be determined. For

corresponding expressions including also  $Z$  exchange and finite-quark-mass effects, see Refs. 19, 20.

A related series holds also for the QCD corrections to the hadronic decay width of the  $\tau$  lepton, which essentially involves an integral of  $R(Q)$  over the allowed range of invariant masses of the hadronic part of the  $\tau$  decay (see *e.g.* Ref. 17). The series expansions for QCD corrections to Higgs-boson (partial) decay widths are summarized in Refs. 21, 22.

One characteristic feature of Eqs. (9.8) and (9.9) is that the coefficients of  $\alpha_s^n$  increase rapidly order by order: calculations in perturbative QCD tend to converge more slowly than would be expected based just on the size of  $\alpha_s^{\dagger\dagger}$ . Another feature is the existence of an extra “power-correction” term  $\mathcal{O}(\Lambda^4/Q^4)$  in Eq. (9.8), which accounts for contributions that are fundamentally non-perturbative. All high-energy QCD predictions involve such corrections, though the exact power of  $\Lambda/Q$  depends on the observable.

**Scale dependence.** In Eq. (9.8) the renormalization scale for  $\alpha_s$  has been chosen equal to  $Q$ . The result can also be expressed in terms of the coupling at an arbitrary renormalization scale  $\mu_R$ ,

$$\delta_{\text{QCD}}(Q) = \sum_{n=1}^{\infty} \overline{c}_n \left( \frac{\mu_R^2}{Q^2} \right) \cdot \left( \frac{\alpha_s(\mu_R^2)}{\pi} \right)^n + \mathcal{O}\left(\frac{\Lambda^4}{Q^4}\right), \quad (9.10)$$

where  $\overline{c}_1(\mu_R^2/Q^2) \equiv c_1$ ,  $\overline{c}_2(\mu_R^2/Q^2) = c_2 + \pi b_0 c_1 \ln(\mu_R^2/Q^2)$ ,  $\overline{c}_3(\mu_R^2/Q^2) = c_3 + (2b_0 c_2 \pi + b_1 c_1 \pi^2) \ln(\mu_R^2/Q^2) + b_0^2 c_1 \pi^2 \ln^2(\mu_R^2/Q^2)$ , *etc.*. Given an infinite number of terms in the  $\alpha_s$  expansion, the  $\mu_R$  dependence of the  $\overline{c}_n(\mu_R^2/Q^2)$  coefficients will exactly cancel that of  $\alpha_s(\mu_R^2)$ , and the final result will be independent of the choice of  $\mu_R$ : physical observables do not depend on unphysical scales.

With just terms up to  $n = N$ , a residual  $\mu_R$  dependence will remain, which implies an uncertainty on the prediction of  $R(Q)$  due to the arbitrariness of the scale choice. This uncertainty will be  $\mathcal{O}(\alpha_s^{N+1})$ , *i.e.* of the same order as the neglected terms. For this reason it is standard to use QCD predictions’ scale dependence as an estimate of the uncertainties due to neglected terms. One usually takes a central value for  $\mu_R \sim Q$ , in order to avoid the poor convergence of the perturbative series that results from the large  $\ln^{n-1}(\mu_R^2/Q^2)$  terms in the  $\overline{c}_n$  coefficients when  $\mu_R \ll Q$  or  $\mu_R \gg Q$ .

#### 9.2.1.1. Processes with initial-state hadrons:

**Deep Inelastic Scattering.** To illustrate the key features of QCD cross sections in processes with initial-state hadrons, let us consider deep-inelastic scattering (DIS),  $ep \rightarrow e + X$ , where an electron  $e$  with four-momentum  $k$  emits a highly off-shell photon (momentum  $q$ ) that interacts with the proton (momentum  $p$ ). For photon virtualities  $Q^2 \equiv -q^2$  far above the squared proton mass (but far below the  $Z$  mass), the differential cross section in terms of the kinematic variables  $Q^2$ ,  $x = Q^2/(2p \cdot q)$  and  $y = (q \cdot p)/(k \cdot p)$  is

$$\frac{d^2\sigma}{dx dQ^2} = \frac{4\pi\alpha}{2xQ^4} \left[ (1 + (1-y)^2)F_2(x, Q^2) - y^2 F_L(x, Q^2) \right], \quad (9.11)$$

where  $\alpha$  is the electromagnetic coupling and  $F_2(x, Q^2)$  and  $F_L(x, Q^2)$  are proton structure functions, which encode the interaction between the photon (in given polarization states) and the proton. In the presence of parity-violating interactions (*e.g.*  $\nu p$  scattering) an additional  $F_3$  structure function is present. For an extended review, including equations for the full electroweak and polarized cases, see Sec. 18 of this *Review*.

Structure functions are not calculable in perturbative QCD, nor is any other cross section that involves initial-state hadrons. To zeroth order in  $\alpha_s$ , the structure functions are given directly in terms of non-perturbative parton (quark or gluon) distribution functions (PDFs),

$$F_2(x, Q^2) = x \sum_q e_q^2 f_{q/p}(x), \quad F_L(x, Q^2) = 0, \quad (9.12)$$

<sup>††</sup> The situation is significantly worse near thresholds, *e.g.* the  $\bar{t}\bar{t}$  production threshold. An overview of some of the effective field theory techniques used in such cases is to be found for example in Ref. 23.

where  $f_{q/p}(x)$  is the PDF for quarks of type  $q$  inside the proton, *i.e.* the number density of quarks of type  $q$  inside a fast-moving proton that carry a fraction  $x$  of its longitudinal momentum (the quark flavor index  $q$ , here, is not to be confused with the photon momentum  $q$  in the lines preceding Eq. (9.11)). Since PDFs are non-perturbative, and difficult to calculate in lattice QCD [24], they must be extracted from data.

The above result, with PDFs  $f_{q/p}(x)$  that are independent of the scale  $Q$ , corresponds to the “quark-parton model” picture in which the photon interacts with point-like free quarks, or equivalently, one has incoherent elastic scattering between the electron and individual constituents of the proton. As a consequence, in this picture also  $F_2$  and  $F_L$  are independent of  $Q$ . When including higher orders in pQCD, Eq. (9.12) becomes

$$F_2(x, Q^2) = x \sum_{n=0}^{\infty} \frac{\alpha_s^n(\mu_R^2)}{(2\pi)^n} \sum_{i=q,g} \int_x^1 \frac{dz}{z} C_{2,i}^{(n)}(z, Q^2, \mu_R^2, \mu_F^2) f_{i/p}\left(\frac{x}{z}, \mu_F^2\right) + \mathcal{O}\left(\frac{\Lambda^2}{Q^2}\right). \quad (9.13)$$

Just as in Eq. (9.10), we have a series in powers  $\alpha_s(\mu_R^2)$ , each term involving a coefficient  $C_{2,i}^{(n)}$  that can be calculated using Feynman graphs. An important difference relative to Eq. (9.10) stems from the fact that the quark’s momentum, when it interacts with the photon, can differ from its momentum when it was extracted from the proton, because it may have radiated gluons in between. As a result, the  $C_{2,i}^{(n)}$  coefficients are functions that depend on the ratio,  $z$ , of these two momenta, and one must integrate over  $z$ . At zeroth order,  $C_{2,q}^{(0)} = e_q^2 \delta(1-z)$  and  $C_{2,g}^{(0)} = 0$ .

The majority of the emissions that modify a parton’s momentum are collinear (parallel) to that parton, and don’t depend on the fact that the parton is destined to interact with a photon. It is natural to view these emissions as modifying the proton’s structure rather than being part of the coefficient function for the parton’s interaction with the photon. Technically, one uses a procedure known as *collinear factorization* to give a well-defined meaning to this distinction, most commonly through the  $\overline{\text{MS}}$  factorization scheme, defined in the context of dimensional regularization. The  $\overline{\text{MS}}$  factorization scheme involves an arbitrary choice of *factorization scale*,  $\mu_F$ , whose meaning can be understood roughly as follows: emissions with transverse momenta above  $\mu_F$  are included in the  $C_{2,q}^{(n)}(z, Q^2, \mu_R^2, \mu_F^2)$ ; emissions with transverse momenta below  $\mu_F$  are accounted for within the PDFs,  $f_{i/p}(x, \mu_F^2)$ . While collinear factorization is generally believed to be valid for suitable (sufficiently inclusive) observables in processes with hard scales, Ref. 35, which reviews the factorization proofs in detail, is cautious in the statements it makes about their exhaustivity, notably for the hadron-collider processes that we shall discuss below. Further discussion is to be found in Refs. 36,37.

The PDFs’ resulting dependence on  $\mu_F$  is described by the Dokshitzer-Gribov-Lipatov-Altarelli-Parisi (DGLAP) equations [25], which to leading order (LO) read\*

$$\mu^2 \frac{\partial f_{i/p}(x, \mu_F^2)}{\partial \mu_F^2} = \sum_j \frac{\alpha_s(\mu_F^2)}{2\pi} \int_x^1 \frac{dz}{z} P_{i \leftarrow j}^{(1)}(z) f_{j/p}\left(\frac{x}{z}, \mu_F^2\right), \quad (9.14)$$

with, for example,  $P_{q \leftarrow g}^{(1)}(z) = T_R(z^2 + (1-z)^2)$ . The other LO splitting functions are listed in Sec. 18 of this *Review*, while results up

\* LO is generally taken to mean the lowest order at which a quantity is non-zero. This definition is nearly always unambiguous, the one major exception being for the case of the hadronic branching ratio of virtual photons,  $Z$ ,  $\tau$ , etc., for which two conventions exist: LO can either mean the lowest order that contributes to the hadronic branching fraction, *i.e.* the term “1” in Eq. (9.7); or it can mean the lowest order at which the hadronic branching ratio becomes sensitive to the coupling,  $n = 1$  in Eq. (9.8), as is relevant when extracting the value of the coupling from a measurement of the branching ratio. Because of this ambiguity, we avoided use of the term “LO” in that context.

to next-to-leading order (NLO),  $\alpha_s^2$ , and next-to-next-to-leading order (NNLO),  $\alpha_s^3$ , are given in Refs. 26 and 27 respectively. The coefficient functions are also  $\mu_F$  dependent, for example  $C_{2,i}^{(1)}(x, Q^2, \mu_R^2, \mu_F^2) = C_{2,i}^{(1)}(x, Q^2, \mu_R^2, Q^2) - \ln\left(\frac{\mu_F^2}{Q^2}\right) \sum_j \int_x^1 \frac{dz}{z} C_{2,j}^{(0)}\left(\frac{x}{z}\right) P_{j \leftarrow i}^{(1)}(z)$ . For the electromagnetic component of DIS with light quarks and gluons they are known to  $\mathcal{O}(\alpha_s^3)$  (N<sup>3</sup>LO) [28]. For weak currents they are known fully to  $\alpha_s^2$  (NNLO) [29] with substantial results known also at N<sup>3</sup>LO [30]. For heavy quark production they are known to  $\mathcal{O}(\alpha_s^2)$  [31] (NLO insofar as the series starts at  $\mathcal{O}(\alpha_s)$ ), with work ongoing towards NNLO [32,33].

As with the renormalization scale, the choice of factorization scale is arbitrary, but if one has an infinite number of terms in the perturbative series, the  $\mu_F$ -dependences of the coefficient functions and PDFs will compensate each other fully. Given only  $N$  terms of the series, a residual  $\mathcal{O}(\alpha_s^{N+1})$  uncertainty is associated with the ambiguity in the choice of  $\mu_F$ . As with  $\mu_R$ , varying  $\mu_F$  provides an input in estimating uncertainties on predictions. In inclusive DIS predictions, the default choice for the scales is usually  $\mu_R = \mu_F = Q$ .

**Hadron-hadron collisions.** The extension to processes with two initial-state hadrons is straightforward, and for example the total (inclusive) cross section for  $W$  boson production in collisions of hadrons  $h_1$  and  $h_2$  can be written as

$$\sigma(h_1 h_2 \rightarrow W + X) = \sum_{n=0}^{\infty} \alpha_s^n(\mu_R^2) \sum_{i,j} \int dx_1 dx_2 f_{i/h_1}(x_1, \mu_F^2) f_{j/h_2}(x_2, \mu_F^2) \times \hat{\sigma}_{ij \rightarrow W+X}^{(n)}(x_1 x_2 s, \mu_R^2, \mu_F^2), \quad (9.15)$$

where  $s$  is the squared center-of-mass energy of the collision. At LO,  $n = 0$ , the hard (partonic) cross section  $\hat{\sigma}_{ij \rightarrow W+X}^{(0)}(x_1 x_2 s, \mu_R^2, \mu_F^2)$  is simply proportional to  $\delta(x_1 x_2 s - M_W^2)$ , in the narrow  $W$ -boson width approximation (see Sec. 44 of this *Review* for detailed expressions for this and other hard scattering cross sections). It is non-zero only for choices of  $i, j$  that can directly give a  $W$ , such as  $i = u, j = \bar{d}$ . At higher orders,  $n \geq 1$ , new partonic channels contribute, such as  $gq$ , and there is no restriction  $x_1 x_2 s = M_W^2$ .

Equation 9.15 involves a collinear factorization between hard cross section and PDFs, just like Eq. (9.13). As long as the same factorization scheme is used in DIS and  $pp$  or  $p\bar{p}$  (usually the  $\overline{\text{MS}}$  scheme), then PDFs extracted in DIS can be directly used in  $pp$  and  $p\bar{p}$  predictions [34,35] (with the anti-quark distributions in an anti-proton being the same as the quark distributions in a proton). Note that Eq. (9.15) only holds to within contributions that are suppressed by powers of  $m_p^2/m_W^2$ .

Fully inclusive hard cross sections are known to NNLO, *i.e.* corrections up to relative order  $\alpha_s^2$ , for Drell-Yan (DY) lepton-pair and vector-boson production [38,39], Higgs-boson production via gluon fusion [39–41], Higgs-boson production in association with a vector boson [42] and Higgs-boson production via vector-boson fusion [43] (in an approximation that factorizes the production of the two vector bosons). A review of fully inclusive Higgs-related results is to be found in Ref. 44.

**Photoproduction.**  $\gamma p$  (and  $\gamma\gamma$ ) collisions are similar to  $pp$  collisions, with the subtlety that the photon can behave in two ways: there is “direct” photoproduction, in which the photon behaves as a point-like particle and takes part directly in the hard collision, with hard subprocesses such as  $\gamma g \rightarrow q\bar{q}$ ; there is also resolved photoproduction, in which the photon behaves like a hadron, with non-perturbative partonic substructure and a corresponding PDF for its quark and gluon content,  $f_{i/\gamma}(x, Q^2)$ .

While useful to understand the general structure of  $\gamma p$  collisions, the distinction between direct and resolved photoproduction is not well defined beyond leading order, as discussed for example in Ref. 45.

**The high-energy limit.** In situations in which the total center-of-mass energy  $\sqrt{s}$  is much larger than other scales in the problem (*e.g.*  $Q$  in DIS,  $m_b$  for  $b\bar{b}$  production in  $pp$  collisions, etc.), each power of  $\alpha_s$  beyond LO can be accompanied by a power of  $\ln(s/Q^2)$  (or  $\ln(s/m_b^2)$ , etc.). This is known as the high-energy or Balitsky-Fadin-Kuraev-Lipatov (BFKL) limit [46–48]. Currently it is possible to account



for the dominant and first subdominant [49,50] power of  $\ln s$  at each order of  $\alpha_s$ , and also to estimate further subdominant contributions that are numerically large (see Refs. 51–53 and references therein).

Physically, the summation of all orders in  $\alpha_s$  can be understood as leading to a growth with  $s$  of the gluon density in the proton. At sufficiently high energies this implies non-linear effects, whose treatment has been the subject of intense study (see for example Refs. 54, 55 and references thereto). Note that it is not straightforward to relate these results to the genuinely non-perturbative total, elastic and diffractive cross sections for hadron-hadron scattering (experimental results for which are summarized in section Chap. 46 of this *Review*).

### 9.2.2. Non fully inclusive cross-sections :

QCD final states always consist of hadrons, while perturbative QCD calculations deal with partons. Physically, an energetic parton fragments (“showers”) into many further partons, which then, on later timescales, undergo a transition to hadrons (“hadronization”). Fixed-order perturbation theory captures only a small part of these dynamics.

This does not matter for the fully inclusive cross sections discussed above: the showering and hadronization stages are “unitary”, *i.e.* they do not change the overall probability of hard scattering, because they occur long after it has taken place.

Less inclusive measurements, in contrast, may be affected by the extra dynamics. For those sensitive just to the main directions of energy flow (jet rates, event shapes, cf. Sec. 9.3.1) fixed order perturbation theory is often still adequate, because showering and hadronization don’t substantially change the overall energy flow. This means that one can make a prediction using just a small number of partons, which should correspond well to a measurement of the same observable carried out on hadrons. For observables that instead depend on distributions of individual hadrons (which, *e.g.*, are the inputs to detector simulations), it is mandatory to account for showering and hadronization. The range of predictive techniques available for QCD final states reflects this diversity of needs of different measurements.

While illustrating the different methods, we shall for simplicity mainly use expressions that hold for  $e^+e^-$  scattering. The extension to cases with initial-state partons will be mostly straightforward (space constraints unfortunately prevent us from addressing diffraction and exclusive hadron-production processes; extensive discussion is to be found in Refs. 56, 57).

#### 9.2.2.1. Preliminaries: Soft and collinear limits:

Before examining specific predictive methods, it is useful to be aware of a general property of QCD matrix elements in the soft and collinear limits. Consider a squared tree-level matrix element  $|M_n^2(p_1, \dots, p_n)|$  for the process  $e^+e^- \rightarrow n$  partons with momenta  $p_1, \dots, p_n$ , and a corresponding phase-space integration measure  $d\Phi_n$ . If particle  $n$  is a gluon, and additionally it becomes collinear (parallel) to another particle  $i$  and its momentum tends to zero (it becomes “soft”), the matrix element simplifies as follows,

$$\lim_{\theta_{in} \rightarrow 0, E_n \rightarrow 0} d\Phi_n |M_n^2(p_1, \dots, p_n)| = d\Phi_{n-1} |M_{n-1}^2(p_1, \dots, p_{n-1})| \frac{\alpha_s C_i}{\pi} \frac{d\theta_{in}^2}{\theta_{in}^2} \frac{dE_n}{E_n}, \quad (9.16)$$

where  $C_i = C_F$  ( $C_A$ ) if  $i$  is a quark (gluon). This formula has non-integrable divergences both for the inter-parton angle  $\theta_{in} \rightarrow 0$  and for the gluon energy  $E_n \rightarrow 0$ , which are mirrored also in the structure of divergences in loop diagrams. These divergences are important for at least two reasons: firstly, they govern the typical structure of events (inducing many emissions either with low energy or at small angle with respect to hard partons); secondly, they will determine which observables can be calculated within perturbative QCD.

#### 9.2.2.2. Fixed-order predictions:

Let us consider an observable  $\mathcal{O}$  that is a function  $\mathcal{O}_n(p_1, \dots, p_n)$  of the four-momenta of the  $n$  particles in an event (whether partons or hadrons). In what follows, we shall consider the cross section for events weighted with the value of the observable,  $\sigma_{\mathcal{O}}$ . As examples, if  $\mathcal{O}_n \equiv 1$  for all  $n$ , then  $\sigma_{\mathcal{O}}$  is just the total cross section; if  $\mathcal{O}_n \equiv \hat{\tau}(p_1, \dots, p_n)$  where  $\hat{\tau}$  is the value of the Thrust for that event (see Sec. 9.3.1.2), then the average value of the Thrust is  $\langle \tau \rangle = \sigma_{\mathcal{O}}/\sigma_{\text{tot}}$ ; if  $\mathcal{O}_n \equiv \delta(\tau - \hat{\tau}(p_1, \dots, p_n))$  then one gets the differential cross section as a function of the Thrust,  $\sigma_{\mathcal{O}} \equiv d\sigma/d\tau$ .

In the expressions below, we shall omit to write the non-perturbative power correction term, which for most common observables is proportional to a single power of  $\Lambda/Q$ .

**LO.** If the observable  $\mathcal{O}$  is non-zero only for events with at least  $n$  particles, then the LO QCD prediction for the weighted cross section in  $e^+e^-$  annihilation is

$$\sigma_{\mathcal{O},LO} = \alpha_s^{n-2} (\mu_R^2)^2 \int d\Phi_n |M_n^2(p_1, \dots, p_n)| \mathcal{O}_n(p_1, \dots, p_n), \quad (9.17)$$

where the squared tree-level matrix element,  $|M_n^2(p_1, \dots, p_n)|$ , includes relevant symmetry factors, has been summed over all subprocesses (*e.g.*  $e^+e^- \rightarrow q\bar{q}q\bar{q}$ ,  $e^+e^- \rightarrow q\bar{q}gg$ ) and has had all factors of  $\alpha_s$  extracted in front. In processes other than  $e^+e^-$  collisions, the powers of the coupling are often brought inside the integrals, with the scale  $\mu_R$  chosen event by event, as a function of the event kinematics.

Other than in the simplest cases (see the review on Cross Sections in this *Review*), the matrix elements in Eq. (9.17) are usually calculated automatically with programs such as CompHEP [58], MadGraph [59], Alpgen [60], Comix/Sherpa [61], and Helac/Phegas [62]. Some of these (CompHEP, MadGraph) use formulas obtained from direct evaluations of Feynman diagrams. Others (Alpgen, Helac/Phegas and Comix/Sherpa) use methods designed to be particularly efficient at high multiplicities, such as Berends-Giele recursion [63] (see also the reviews [64,65]), which builds up amplitudes for complex processes from simpler ones.

The phase-space integration is usually carried out by Monte Carlo sampling, in order to deal with the sometimes complicated cuts that are used in corresponding experimental measurements. Because of the divergences in the matrix element, Eq. (9.16), the integral converges only if the observable vanishes for kinematic configurations in which one of the  $n$  particles is arbitrarily soft or it is collinear to another particle. As an example, the cross section for producing any configuration of  $n$  partons will lead to an infinite integral, whereas a finite result will be obtained for the cross section for producing  $n$  deposits of energy (or jets, see Sec. 9.3.1.1), each above some energy threshold and well separated from each other in angle.

LO calculations can be carried out for  $2 \rightarrow n$  processes with  $n \lesssim 6-10$ . The exact upper limit depends on the process, the method used to evaluate the matrix elements (recursive methods are more efficient), and the extent to which the phase-space integration can be optimized to work around the large variations in the values of the matrix elements.

**NLO.** Given an observable that is non-zero starting from  $n$  particles, its prediction at NLO involves supplementing the LO result with the  $(n+1)$ -particle tree-level matrix element ( $|M_{n+1}^2|$ ), and the interference of a  $n$ -particle tree-level and  $n$ -particle 1-loop amplitude ( $2\text{Re}(M_n M_{n,1\text{-loop}}^*)$ ),

$$\begin{aligned} \sigma_{\mathcal{O}}^{NLO} &= \sigma_{\mathcal{O}}^{LO} + \alpha_s^{n-1} (\mu_R^2)^2 \int d\Phi_{n+1} \\ &|M_{n+1}^2(p_1, \dots, p_{n+1})| \mathcal{O}_{n+1}(p_1, \dots, p_{n+1}) \\ &+ \alpha_s^{n-1} (\mu_R^2)^2 \int d\Phi_n 2\text{Re}[M_n(p_1, \dots, p_n) \\ &M_{n,1\text{-loop}}^*(p_1, \dots, p_n)] \mathcal{O}_n(p_1, \dots, p_n). \end{aligned} \quad (9.18)$$

Relative to LO calculations, two important issues appear in the NLO calculations. Firstly, the extra complexity of loop-calculations relative to tree-level calculations means that their automation is at a comparatively early stage (see below). Secondly, loop amplitudes

are infinite in 4 dimensions, while tree-level amplitudes are finite, but their *integrals* are infinite, due to the divergences of Eq. (9.16). These two sources of infinities have the same soft and collinear origins and cancel after the integration only if the observable  $\mathcal{O}$  satisfies the property of infrared and collinear safety,

$$\begin{aligned} \mathcal{O}_{n+1}(p_1, \dots, p_s, \dots, p_n) &\rightarrow \mathcal{O}_n(p_1, \dots, p_n) && \text{if } p_s \rightarrow 0 \\ \mathcal{O}_{n+1}(p_1, \dots, p_a, p_b, \dots, p_n) &\rightarrow \mathcal{O}_n(p_1, \dots, p_a + p_b, \dots, p_n) \\ &&& \text{if } p_a \parallel p_b. \end{aligned} \quad (9.19)$$

Examples of infrared safe quantities include event-shape distributions and jet cross sections (with appropriate jet algorithms, see below). Unsafe quantities include the distribution of the momentum of the hardest QCD particle (which is not conserved under collinear splitting), observables that require the complete absence of radiation in some region of phase-space (e.g. rapidity gaps or 100% isolation cuts, which are affected by soft emissions), or the particle multiplicity (affected by both soft and collinear emissions). The non-cancellation of divergences at NLO due to infrared or collinear unsafety compromises the usefulness not only of the NLO calculation, but also that of a LO calculation, since LO is only an acceptable approximation if one can prove that higher order terms are smaller. Infrared and collinear unsafety usually also imply large non-perturbative effects.

As with LO calculations, the phase-space integrals in Eq. (9.18) are usually carried out by Monte Carlo integration, so as to facilitate the study of arbitrary observables. Various methods exist to obtain numerically efficient cancellation among the different infinities. These include notably dipole [66], FKS [67] and antenna [68] subtraction.

NLO calculations have existed for a while for a wide range of  $2 \rightarrow n$  processes with  $n \leq 3$ , as reviewed in Ref. 69. Some of the corresponding codes are public, and those that provide access to multiple processes include NLOJet++ [70] for  $e^+e^-$ , DIS, and hadron-hadron processes involving just light partons in the final state, MCFM [71] for hadron-hadron processes with vector bosons and/or heavy quarks in the final state, VBFNLO for vector-boson fusion, di- and tri-boson processes [72], and the Phox family [73] for processes with photons in the final state. One forefront of NLO calculations is  $2 \rightarrow 4$  and  $2 \rightarrow 5$  processes in  $pp$  scattering (and for  $1 \rightarrow 5$  in  $e^+e^- \rightarrow \gamma/Z \rightarrow \text{hadrons}$  [74]), where recent results include  $t\bar{t}b\bar{b}$  [80,81],  $t\bar{t}+2\text{jets}$  [82] and  $b\bar{b}b\bar{b}$  [83],  $pp \rightarrow W/Z+3\text{jets}$  [75,76,77] and  $pp \rightarrow W/Z+4\text{jets}$  [78,79] as well as  $W^+W^-b\bar{b}$  [84] and  $W^+W^\pm+2\text{jets}$  [85]. A related forefront is automation: a number of the above results have been obtained with partially automated approaches. A first example of full automation applied to a large number of processes has been presented recently in Ref. 86, and a public automated code is described in Ref. 87. A number of the above calculations have made use of unitarity-type techniques [88] and powerful integrand reduction methods (notably Ref. 89), which have seen significant development over the past few years, as reviewed in Refs. 65,90.

**NNLO.** Conceptually, NNLO and NLO calculations are similar, except that one must add a further order in  $\alpha_s$ , consisting of: the squared  $(n+2)$ -parton tree-level amplitude, the interference of the  $(n+1)$ -parton tree-level and 1-loop amplitudes, the interference of the  $n$ -parton tree-level and 2-loop amplitudes, and the squared  $n$ -parton 1-loop amplitude.

Each of these elements involves large numbers of soft and collinear divergences, satisfying relations analogous to Eq. (9.16) that now involve multiple collinear or soft particles and higher loop orders (see e.g. Refs. 88,91,92). Arranging for the cancellation of the divergences after numerical Monte Carlo integration is one of the significant challenges of NNLO calculations, as is the determination of the relevant 2-loop amplitudes. At the time of writing, the processes for which fully exclusive NNLO calculations exist include the 3-jet cross section in  $e^+e^-$  collisions [93,94] (for which NNLO means  $\alpha_s^3$ ), as well as vector-boson [95,96], Higgs-boson [97,98], WH [99] and di-photon [100] production in  $pp$  and  $p\bar{p}$  collisions.

### 9.2.2.3. Resummation:

Many experimental measurements place tight constraints on emissions in the final state, for example, in  $e^+e^-$  events, that one minus the Thrust should be less than some value  $\tau \ll 1$ , or in  $pp \rightarrow Z$  events that the  $Z$ -boson transverse momentum should be much smaller than its mass,  $p_{t,Z} \ll M_Z$ . A further example is the production of heavy particles or jets near threshold (so that little energy is left over for real emissions) in DIS and  $pp$  collisions.

In such cases, the constraint vetoes a significant part of the integral over the soft and collinear divergence of Eq. (9.16). As a result, there is only a partial cancellation between real emission terms (subject to the constraint) and loop (virtual) contributions (not subject to the constraint), causing each order of  $\alpha_s$  to be accompanied by a large coefficient  $\sim L^2$ , where e.g.  $L = \ln \tau$  or  $L = \ln(M_Z/p_{t,Z})$ . One ends up with a perturbative series whose terms go as  $\sim (\alpha_s L^2)^n$ . It is not uncommon that  $\alpha_s L^2 \gg 1$ , so that the perturbative series converges very poorly if at all.\*\* In such cases one may carry out a “resummation,” which accounts for the dominant logarithmically enhanced terms to all orders in  $\alpha_s$ , by making use of known properties of matrix elements for multiple soft and collinear emissions, and of the all-orders properties of the divergent parts of virtual corrections, following original works such as Refs. 101–110 and also through soft-collinear effective theory [111,112] (cf. also the review in Ref. 113).

For cases with double logarithmic enhancements (two powers of logarithm per power of  $\alpha_s$ ), there are two classification schemes for resummation accuracy. Writing the cross section including the constraint as  $\sigma(L)$  and the unconstrained (total) cross section as  $\sigma_{\text{tot}}$ , the series expansion takes the form

$$\sigma(L) \simeq \sigma_{\text{tot}} \sum_{n=0}^{\infty} \sum_{k=0}^{2n} R_{nk} \alpha_s^n (\mu_R^2) L^k, \quad L \gg 1 \quad (9.20)$$

and leading log (LL) resummation means that one accounts for all terms with  $k = 2n$ , next-to-leading-log (NLL) includes additionally all terms with  $k = 2n - 1$ , etc. Often  $\sigma(L)$  (or its Fourier or Mellin transform) *exponentiates* †,

$$\sigma(L) \simeq \sigma_{\text{tot}} \exp \left[ \sum_{n=1}^{\infty} \sum_{k=0}^{n+1} G_{nk} \alpha_s^n (\mu_R^2) L^k \right], \quad L \gg 1, \quad (9.21)$$

where one notes the different upper limit on  $k$  ( $\leq n+1$ ) compared to Eq. (9.20). This is a more powerful form of resummation: the  $G_{12}$  term alone reproduces the full LL series in Eq. (9.20). With the form Eq. (9.21) one still uses the nomenclature LL, but this now means that all terms with  $k = n+1$  are included, and NLL implies all terms with  $k = n$ , etc.

For a large number of observables, NLL resummations are available in the sense of Eq. (9.21) (see Refs. 117–119 and references therein). NNLL has been achieved for the DY and Higgs-boson  $p_t$  distributions [120,121,122,123] (in addition the NLL ResBos program [124] is still widely used), the back-to-back energy-energy correlation in  $e^+e^-$  [125], the production of top anti-top pairs near threshold [126–128] (and references therein), high- $p_t$   $W$  and  $Z$  production [129], and an event-shape type observable known as the beam Thrust [130]. Finally, the parts believed to be dominant in the N<sup>3</sup>LL resummation are available for the Thrust variable and

\*\* To be precise one should distinguish two causes of the divergence of perturbative series. That which interests us here is associated with the presence of a new large parameter (e.g. ratio of scales). Nearly all perturbative series also suffer from “renormalon” divergences  $\alpha_s^n n!$  (reviewed in Ref. 16), which however have an impact only at very high perturbative orders and have a deep connection with non-perturbative uncertainties.

† Whether or not this happens depends on the quantity being resummed. A classic example involves jet rates in  $e^+e^-$  collisions as a function of a jet-resolution parameter  $y_{\text{cut}}$ . The logarithms of  $1/y_{\text{cut}}$  exponentiate for the  $k_t$  (Durham) jet algorithm [114], but not [115] for the JADE algorithm [116] (both are discussed below in Sec. 9.3.1.1).

heavy-jet mass in  $e^+e^-$  annihilations [131,132] (confirmed for Thrust at NNLL in Ref. 133), and for Higgs- and vector-boson production near threshold [134,135] in hadron collisions (NNLL in Refs. 136,137). The inputs and methods involved in these various calculations are somewhat too diverse to discuss in detail here, so we recommend that the interested reader consult the original references for further details.

#### 9.2.2.4. Fragmentation functions:

Since the parton-hadron transition is non-perturbative, it is not possible to perturbatively calculate quantities such as the energy-spectra of specific hadrons in high-energy collisions. However, one can factorize perturbative and non-perturbative contributions via the concept of fragmentation functions. These are the final-state analogue of the parton distribution functions that are used for initial-state hadrons.

It should be added that if one ignores the non-perturbative difficulties and just calculates the energy and angular spectrum of partons in perturbative QCD with some low cutoff scale  $\sim \Lambda$  (using resummation to sum large logarithms of  $\sqrt{s}/\Lambda$ ), then this reproduces many features of the corresponding hadron spectra. This is often taken to suggest that hadronization is “local” in momentum space.

Sec. 19 of this *Review* provides further information (and references) on these topics, including also the question of heavy-quark fragmentation.

#### 9.2.2.5. Parton-shower Monte Carlo generators:

Parton-shower Monte Carlo (MC) event generators like PYTHIA [138–140], HERWIG [141–143], SHERPA [144], and ARIADNE [145] provide fully exclusive simulations of QCD events. Because they provide access to “hadron-level” events they are a crucial tool for all applications that involve simulating the response of detectors to QCD events. Here we give only a brief outline of how they work and refer the reader to Chap. 38 and Ref. 146 for a full overview.

The MC generation of an event involves several stages. It starts with the random generation of the kinematics and partonic channels of whatever *hard scattering process* the user has requested at some high scale  $Q_0$ . This is followed by a *parton shower*, usually based on the successive random generation of gluon emissions (or  $g \rightarrow q\bar{q}$  splittings). Each is generated at a scale lower than the previous emission, following a (soft and collinear resummed) perturbative QCD distribution that depends on the momenta of all previous emissions. Common choices of scale for the ordering of emissions are virtuality, transverse momentum or angle. Parton showering stops at a scale of order 1 GeV, at which point a *hadronization model* is used to convert the resulting partons into hadrons. One widely-used model involves stretching a color “string” across quarks and gluons, and breaking it up into hadrons [147,148]. Another breaks each gluon into a  $q\bar{q}$  pair and then groups quarks and anti-quarks into colorless “clusters”, which then give the hadrons [141]. For  $pp$  and  $\gamma p$  processes, modeling is also needed to treat the collision between the two hadron remnants, which generates an *underlying event* (UE), usually implemented via additional  $2 \rightarrow 2$  scatterings (“multiple parton interactions”) at a scale of a few GeV, following Ref. 149.

A deficiency of the soft and collinear approximations that underlie parton showers is that they may fail to reproduce the full pattern of hard wide-angle emissions, important, for example, in many new physics searches. It is therefore common to use LO multi-parton matrix elements to generate hard high-multiplicity partonic configurations as additional starting points for the showering, supplemented with some prescription (CKKW [150], MLM [151]) for consistently merging samples with different initial multiplicities.

MCs, as described above, generate cross sections for the requested hard process that are correct at LO. For a number of processes there also exist MC implementations that are correct to NLO, using the MC@NLO [152] or POWHEG [153] prescriptions. Techniques also exist to combine NLO accuracy for a low order process, with LO accuracy for higher multiplicity processes [154,155].

#### 9.2.3. Accuracy of predictions :

Estimating the accuracy of perturbative QCD predictions is not an exact science. It is often said that LO calculations are accurate to within a factor of two. This is based on experience with NLO corrections in the cases where these are available. In processes involving new partonic scattering channels at NLO and/or large ratios of scales (such as the production of high- $p_t$  jets containing  $B$ -hadrons), the NLO to LO  $K$ -factors can be substantially larger than 2.

For calculations beyond LO, a conservative approach to estimate the perturbative uncertainty is to take it to be the last known perturbative order; a more widely used method is to estimate it from the change in the prediction when varying the renormalization and factorization scales around a central value  $Q$  that is taken close to the physical scale of the process. A conventional range of variation is  $Q/2 < \mu_R, \mu_F < 2Q$ , however this should not be assumed to give uncertainty estimates of guaranteed reliability.††

There does not seem to be a broad consensus on whether  $\mu_R$  and  $\mu_F$  should be kept identical or varied independently. One option is to vary them independently with the restriction  $\frac{1}{2}\mu_R < \mu_F < 2\mu_R$  [160]. This limits the risk of misleadingly small uncertainties due to fortuitous cancellations between the  $\mu_F$  and  $\mu_R$  dependence when both are varied together, while avoiding the appearance of large logarithms of  $\mu_R^2/\mu_F^2$  when both are varied completely independently.

Calculations that involve resummations usually have an additional source of uncertainty associated with the choice of argument of the logarithms being resummed, e.g.  $\ln(2\frac{p_t Z}{M_Z})$  as opposed to  $\ln(\frac{1}{2}\frac{p_t Z}{M_Z})$ . In addition to varying renormalization and factorization scales, it is therefore also advisable to vary the argument of the logarithm by a factor of two in either direction with respect to the “natural” argument.

The accuracy of QCD predictions is limited also by non-perturbative corrections, which typically scale as a power of  $\Lambda/Q$ . For measurements that are directly sensitive to the structure of the hadronic final state the corrections are usually linear in  $\Lambda/Q$ . The non-perturbative corrections are further enhanced in processes with a significant underlying event (*i.e.* in  $pp$  and  $p\bar{p}$  collisions) and in cases where the perturbative cross sections fall steeply as a function of  $p_t$  or some other kinematic variable.

Non-perturbative corrections are commonly estimated from the difference between Monte Carlo events at the parton level and after hadronization. An issue to be aware of with this procedure is that “parton level” is not a uniquely defined concept. For example, in an event generator it depends on a (somewhat arbitrary and tunable) internal cutoff scale that separates the parton showering from the hadronization. In contrast no such cutoff scale exists in a NLO or NNLO partonic calculation. For this reason there are widespread reservations as to the appropriateness of deriving hadronization corrections from a Monte Carlo program and then applying them to NLO or NNLO prediction. There exist alternative methods for estimating hadronization corrections, which attempt to analytically deduce non-perturbative effects in one observable based on measurements of other observables (see the reviews [16,161]). While they directly address the problem of different possible definitions of parton level, it should also be said that they are far less flexible than Monte Carlo programs and not always able to provide equally good descriptions of the data.

### 9.3. Experimental QCD

Since we are not able to directly measure partons (quarks or gluons), but only hadrons and their decay products, a central issue for every experimental test of QCD is establishing a correspondence between observables obtained at the partonic and the hadronic level. The only theoretically sound correspondence is achieved by means of *infrared and collinear safe* quantities, which allow one to obtain finite predictions at any order of perturbative QCD.

†† A number of prescriptions also exist for setting the scale automatically, e.g. Refs. 156–159, eliminating uncertainties from scale variation, though not from the truncation of the perturbative series itself.

As stated above, the simplest case of infrared and collinear safe observables are total cross sections. More generally, when measuring fully inclusive observables, the final state is not analyzed at all regarding its (topological, kinematical) structure or its composition. Basically the relevant information consists in the rate of a process ending up in a partonic or hadronic final state. In  $e^+e^-$  annihilation, widely used examples are the ratios of partial widths or branching ratios for the electroweak decay of particles into hadrons or leptons, such as  $Z$  or  $\tau$  decays, (cf. Sec. 9.2.1). Such ratios are often favored over absolute cross sections or partial widths because of large cancellations of experimental and theoretical systematic uncertainties. The strong suppression of non-perturbative effects,  $\mathcal{O}(\Lambda^4/Q^4)$ , is one of the attractive features of such observables, however, at the same time the sensitivity to radiative QCD corrections is small, which for example affects the statistical uncertainty when using them for the determination of the strong coupling constant. In the case of  $\tau$  decays not only the hadronic branching ratio is of interest, but also moments of the spectral functions of hadronic tau decays, which sample different parts of the decay spectrum and thus provide additional information. Other examples of fully inclusive observables are structure functions (and related sum rules) in DIS. These are extensively discussed in Sec. 18 of this *Review*.

On the other hand, often the structure or composition of the final state are analyzed and cross sections differential in one or more variables characterizing this structure are of interest. Examples are jet rates, jet substructure, event shapes or transverse momentum distributions of jets or vector bosons in hadron collisions. The case of fragmentation functions, *i.e.* the measurement of hadron production as a function of the hadron momentum relative to some hard scattering scale, is discussed in Sec. 19 of this *Review*.

It is worth mentioning that, besides the correspondence between the parton and hadron level, also a correspondence between the hadron level and the actually measured quantities in the detector has to be established. The simplest examples are corrections for finite experimental acceptance and efficiencies. Whereas acceptance corrections essentially are of theoretical nature, since they involve extrapolations from the measurable (partial) to the full phase space, other corrections such as for efficiency, resolution and response, are of experimental nature. For example, measurements of differential cross sections such as jet rates require corrections in order to relate, *e.g.* the energy deposits in a calorimeter to the jets at the hadron level. Typically detector simulations and/or data driven methods are used in order to obtain these corrections. Care should be taken here in order to have a clear separation between the parton-to-hadron level and hadron-to-detector level corrections. Finally, for the sake of an easy comparison to the results of other experiments and/or theoretical calculations, it is suggested to provide, whenever possible, measurements corrected for detector effects and/or all necessary information related to the detector response (*e.g.* the detector response matrix).

### 9.3.1. Hadronic final-state observables :

#### 9.3.1.1. Jets:

In hard interactions, final-state partons and hadrons appear predominantly in collimated bunches. These bunches are generically called *jets*. To a first approximation, a jet can be thought of as a hard parton that has undergone soft and collinear showering and then hadronization. Jets are used both for testing our understanding and predictions of high-energy QCD processes, and also for identifying the hard partonic structure of decays of massive particles like top quarks.

In order to map observed hadrons onto a set of jets, one uses a *jet definition*. The mapping involves explicit choices: for example when a gluon is radiated from a quark, for what range of kinematics should the gluon be part of the quark jet, or instead form a separate jet? Good jet definitions are infrared and collinear safe, simple to use in theoretical and experimental contexts, applicable to any type of inputs (parton or hadron momenta, charged particle tracks, and/or energy deposits in the detectors) and lead to jets that are not too sensitive to non-perturbative effects. An extensive treatment of the topic of jet definitions is given in Ref. 162 (for  $e^+e^-$  collisions) and Refs. 163, 164 (for  $pp$  or  $p\bar{p}$  collisions). Here we briefly review the two main

classes: cone algorithms, extensively used at older hadron colliders, and sequential recombination algorithms, more widespread in  $e^+e^-$  and  $ep$  colliders and at the LHC.

Very generically, most (iterative) cone algorithms start with some seed particle  $i$ , sum the momenta of all particles  $j$  within a cone of opening-angle  $R$ , typically defined in terms of (pseudo-)rapidity and azimuthal angle. They then take the direction of this sum as a new seed and repeat until the cone is stable, and call the contents of the resulting stable cone a jet if its transverse momentum is above some threshold  $p_{t,\min}$ . The parameters  $R$  and  $p_{t,\min}$  should be chosen according to the needs of a given analysis.

There are many variants of cone algorithm, and they differ in the set of seeds they use and the manner in which they ensure a one-to-one mapping of particles to jets, given that two stable cones may share particles (“overlap”). The use of seed particles is a problem w.r.t. infrared and collinear safety, and seeded algorithms are generally not compatible with higher-order (or sometimes even leading-order) QCD calculations, especially in multi-jet contexts, as well as potentially subject to large non-perturbative corrections and instabilities. Seeded algorithms (JetCLU, MidPoint, and various other experiment-specific iterative cone algorithms) are therefore to be deprecated. A modern alternative is to use a seedless variant, SIScone [165].

Sequential recombination algorithms at hadron colliders (and in DIS) are characterized by a distance  $d_{ij} = \min(k_{t,i}^{2p}, k_{t,j}^{2p}) \Delta_{ij}^2 / R^2$  between all pairs of particles  $i, j$ , where  $\Delta_{ij}$  is their distance in the rapidity-azimuthal plane,  $k_{t,i}$  is the transverse momentum w.r.t. the incoming beams, and  $R$  is a free parameter. They also involve a “beam” distance  $d_{iB} = k_{t,i}^{2p}$ . One identifies the smallest of all the  $d_{ij}$  and  $d_{iB}$ , and if it is a  $d_{ij}$ , then  $i$  and  $j$  are merged into a new pseudo-particle (with some prescription, a recombination scheme, for the definition of the merged four-momentum). If the smallest distance is a  $d_{iB}$ , then  $i$  is removed from the list of particles and called a jet. As with cone algorithms, one usually considers only jets above some transverse-momentum threshold  $p_{t,\min}$ . The parameter  $p$  determines the kind of algorithm:  $p = 1$  corresponds to the (*inclusive*-) $k_t$  algorithm [114,166,167],  $p = 0$  defines the *Cambridge-Aachen* algorithm [168,169], while for  $p = -1$  we have the *anti- $k_t$*  algorithm [170]. All these variants are infrared and collinear safe to all orders of perturbation theory. Whereas the former two lead to irregularly shaped jet boundaries, the latter results in cone-like boundaries. The *anti- $k_t$*  algorithm has become the de-facto standard for the LHC experiments.

In  $e^+e^-$  annihilations the  $k_t$  algorithm [114] uses  $y_{ij} = 2 \min(E_i^2, E_j^2) (1 - \cos \theta_{ij}) / Q^2$  as distance measure and repeatedly merges the pair with smallest  $y_{ij}$ , until all  $y_{ij}$  distances are above some threshold  $y_{\text{cut}}$ , the jet resolution parameter. The (pseudo)-particles that remain at this point are called the jets. Here it is  $y_{\text{cut}}$  (rather than  $R$  and  $p_{t,\min}$ ) that should be chosen according to the needs of the analysis. As mentioned above, the  $k_t$  algorithm has the property that logarithms  $\ln(1/y_{\text{cut}})$  exponentiate in resummation calculations. This is one reason why it is preferred over the earlier JADE algorithm [116], which uses the distance measure  $y_{ij} = 2 E_i E_j (1 - \cos \theta_{ij}) / Q^2$ .

Efficient implementations of the above algorithms are available through the *FastJet* package [171], which is also packaged within *SpartyJet* [172].

#### 9.3.1.2. Event Shapes:

Event-shape variables are functions of the four momenta in the hadronic final state that characterize the topology of an event’s energy flow. They are sensitive to QCD radiation (and correspondingly to the strong coupling) insofar as gluon emission changes the shape of the energy flow.

The classic example of an event shape is the *Thrust* [173,174] in  $e^+e^-$  annihilations, defined as

$$\hat{\tau} = \max_{\vec{n}_\tau} \frac{\sum_i |\vec{p}_i \cdot \vec{n}_\tau|}{\sum_i |\vec{p}_i|}, \quad (9.22)$$

where  $\vec{p}_i$  are the momenta of the particles or the jets in the final-state and the maximum is obtained for the Thrust axis  $\vec{n}_\tau$ . In the Born

limit of the production of a perfect back-to-back  $q\bar{q}$  pair the limit  $\hat{\tau} \rightarrow 1$  is obtained, whereas a perfectly symmetric many-particle configuration leads to  $\hat{\tau} \rightarrow 1/2$ . Further event shapes of similar nature have been defined and extensively measured at LEP and at HERA, and for their definitions and reviews we refer to Refs. 3,4,161,175,176. Phenomenological discussions of event shapes at hadron colliders can be found in Refs. 177–179. Very recently, measurements of hadronic event-shape distributions have been published by CDF [180] and CMS [181].

Event shapes are used for many purposes. These include measuring the strong coupling, tuning the parameters of Monte Carlo programs, investigating analytical models of hadronization and distinguishing QCD events from events that might involve decays of new particles (giving event-shape values closer to the spherical limit).

### 9.3.1.3. Jet substructure, quark vs. gluon jets:

Jet substructure, which can be resolved by finding subjets or by measuring jet shapes, is sensitive to the details of QCD radiation in the shower development inside a jet and has been extensively used to study differences in the properties of quark and gluon induced jets, strongly related to their different color charges. In general there is clear experimental evidence that gluon jets are “broader” and have a softer particle spectrum than (light-) quark jets, whereas b-quark jets are similar to gluon jets. As an example of an observable, the jet shape  $\Psi(r/R)$  is the fractional transverse momentum contained within a sub-cone of cone-size  $r$  for jets of cone-size  $R$ . It is sensitive to the relative fractions of quark and gluon jets in an inclusive jet sample and receives contributions from soft-gluon initial-state radiation and beam remnant-remnant interactions. Therefore, it has been widely employed for validation and tuning of Monte Carlo models. CDF has measured the jet shape  $\Psi(r/R)$  for an inclusive jet sample [182] as well as for b-jets [183]. Similar measurements in photo-production and DIS at HERA have been reported in Refs. 184–186. First measurements at the LHC have been presented by ATLAS [187]. Further discussions, references and recent summaries can be found in Refs. 176, 188 and Sec. 4 of Ref. 189.

The use of jet substructure has also been suggested in order to distinguish QCD jets from jets that originate from hadronic decays of boosted massive particles (high- $p_t$  electroweak bosons, top quarks and hypothesized new particles). For reviews and detailed references, see Ref. 189 and sec. 5.3 of Ref. 163.

### 9.3.2. State of the art QCD measurements at colliders :

There exists an enormous wealth of data on QCD-related measurements in  $e^+e^-$ ,  $ep$ ,  $pp$ , and  $p\bar{p}$  collisions, to which a short overview like this would not be able to do any justice. Extensive reviews of the subject have been published in Refs. 175, 176 for  $e^+e^-$  colliders, whereas for hadron colliders comprehensive overviews are given in Refs. 164, 190, and recent summaries can be found in, *e.g.* Refs. 191–194. Below we concentrate our discussion on measurements that are most sensitive to hard QCD processes, in particular jet production.

**9.3.2.1.  $e^+e^-$  colliders:** Analyses of jet production in  $e^+e^-$  collisions are mostly based on JADE data at center-of-mass energies between 14 and 44 GeV, as well as on LEP data at the  $Z$  resonance and up to 209 GeV. They cover the measurements of (differential or exclusive) jet rates (with multiplicities typically up to 4, 5 or 6 jets), the study of 3-jet events and particle production between the jets as a tool for testing hadronization models, as well as 4-jet production and angular correlations in 4-jet events. The latter are useful for measurements of the strong coupling constant and putting constraints on the QCD color factors, thus probing the non-abelian nature of QCD. There have also been extensive measurements of event shapes. The tuning of parton shower MC models, typically matched to matrix elements for 3-jet production, has led to good descriptions of the available, highly precise data. Especially for the large LEP data sample at the  $Z$  peak, the statistical errors are mostly negligible and the experimental systematic uncertainties are at the per-cent level or even below. These are usually dominated by the uncertainties related to the MC model dependence of the efficiency and acceptance corrections (often referred to as “detector corrections”).

**9.3.2.2. DIS and photoproduction:** Multi-jet production in  $ep$  collisions at HERA, both in the DIS and photoproduction regime, allows for tests of QCD factorization (one initial-state proton and its associated PDF versus the hard scattering which leads to high- $p_t$  jets) and NLO calculations which exist for 2- and 3-jet final states. Sensitivity is also obtained to the product of the coupling constant and the gluon PDF. By now experimental uncertainties of the order of 5–10% have been achieved, mostly dominated by jet energy scale uncertainties, whereas statistical errors are negligible to a large extent. For comparison to theoretical predictions, at large jet  $p_t$  the PDF uncertainty dominates the theoretical error (typically of order 5–10%, in some regions of phase-space up to 20%), therefore jet observables become useful inputs for PDF fits. In general, for  $Q^2$  above  $\sim 100 \text{ GeV}^2$  the data are well described by NLO matrix element calculations, combined with DGLAP evolution equations. Results at lower values ( $Q^2 < 100 \text{ GeV}^2$ ) point to the necessity of including NNLO effects. Also, at low values of  $Q^2$  and  $x$ , in particular for large jet pseudo-rapidities, there are indications for the need of BFKL-type evolution, though the predictions for such schemes are still limited. In the case of photoproduction, the data-theory comparisons are hampered by the uncertainties related to the photon PDF.

A few examples of recent measurements can be found in Refs. 195–200 for DIS and in Refs. 201–205 for photoproduction.

**9.3.2.3. Hadron colliders:** Jet measurements at the TEVATRON have been published for data samples up to  $\sim 2 \text{ fb}^{-1}$ . Also, first results from the LHC have become available, for a center-of-mass energy of 7 TeV and sample sizes of up to  $\sim 36 \text{ pb}^{-1}$ . Among the most important cross sections measured is the inclusive jet production as a function of the jet transverse energy ( $E_t$ ) or the jet transverse momentum ( $p_t$ ), for several rapidity regions and for  $p_t$  up to 700 GeV at the TEVATRON and  $\sim 1 \text{ TeV}$  at the LHC. The TEVATRON experiments have measurements based on the infrared- and collinear-safe  $k_t$  algorithm in addition to the more widely used Midpoint and JetCLU algorithms of the past, whereas the LHC experiments focus on the *anti- $k_t$*  algorithm. Results by the CDF and D0 collaborations can be found in Refs. 206–208, whereas first measurements of ATLAS and CMS have been published in Refs. 209 and 210, respectively. In general we observe a good description of the data by the NLO QCD predictions. The experimental systematic uncertainties are dominated by the jet energy scale error, by now quoted to be in the range of 1 to 3% and thus leading to uncertainties of 10 to 60% on the cross section, increasing with  $p_t$ . The PDF uncertainties dominate the theoretical error. In fact, inclusive jet data are important inputs to global PDF fits, in particular for constraining the high- $x$  gluon PDF.

A rather comprehensive summary, comparing NLO QCD predictions to data for inclusive jet production in DIS,  $pp$ , and  $p\bar{p}$  collisions, is given in Ref. 211 and reproduced here in Fig. 9.1.

Dijet events are analyzed in terms of their invariant mass and angular distributions, which allow one to put stringent limits on deviations from the Standard Model, such as quark compositeness (some recent examples can be found in Refs. 212–217). Furthermore, dijet azimuthal correlations between the two leading jets, normalized to the total dijet cross section, are an extremely valuable tool for studying the spectrum of gluon radiation in the event. For example, results from the TEVATRON [218] and the LHC [219,220] show that the LO (non-trivial) prediction for this observable, with at most three partons in the final state, is not able to describe the data for an azimuthal separation below  $2\pi/3$ , where NLO contributions (with 4 partons) restore the agreement with data. In addition, this observable can be employed to tune Monte Carlo predictions of soft gluon radiation. Beyond dijet final states, recently measurements of the production of three or more jets have been performed [221–223], as a means of testing perturbative QCD predictions, tuning MC models, constraining PDFs or determining the strong coupling constant.

Similarly important tests of QCD arise from measurements of vector boson (photon,  $W$ ,  $Z$ ) production together with jets. A recent analysis of photon+jet production by D0 [224] indicates that NLO calculations, combined with modern PDF sets, are unable to describe the shape of the photon  $p_t$  across the entire measured range, showing the need for an improved and consistent theoretical description of this

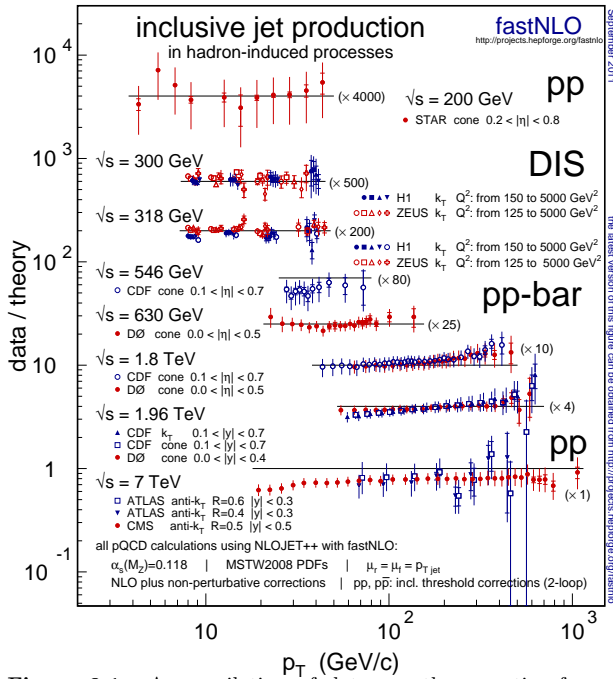


**Figure 9.1:** A compilation of data-over-theory ratios for inclusive jet cross sections as a function of jet transverse momentum ( $p_T$ ), measured in different hadron-induced processes at different center-of-mass energies; from Ref. 211. The various ratios are scaled by arbitrary numbers (indicated between parentheses) for better readability of the plot. The theoretical predictions have been obtained at NLO accuracy, for parameter choices (coupling constant, PDFs, renormalization, and factorization scales) as indicated at the bottom of the figure.

process.

In the case of  $Z$ +jets, the  $Z$  momentum can be precisely reconstructed using the leptons, allowing for a precise determination of the  $Z$   $p_T$  distribution, which is sensitive to QCD radiation both at high and low scales and thus probes perturbative as well as non-perturbative effects. For example, a recent D0 result [225] quotes experimental statistical and systematic uncertainties of the order of 10%, increasing up to 20% in the lowest momentum range. The data are compared to predictions from NLO QCD and from different Monte Carlo models, where, for example, LO matrix elements for up to three partons are matched to a parton shower. Whereas the total cross section is underestimated, the shape is well reproduced over a large phase-space region. Similar conclusions are drawn from further results on  $Z$  (or  $W$ ) plus jets production, both from the TEVATRON [226–231] and the LHC [232,233]. A very important recent development is the completion of NLO calculations for vector boson plus 3jet [75–77] and 4jet production [78,79], which is relevant also for background estimations in the searches for new physics. This type of process is an example where jets need to be found with an infrared and collinear safe jet algorithm in order to obtain finite NLO predictions. This would not be possible with algorithms such as Midpoint or JetCLU, used in analyses at the TEVATRON [228,231]. There the measurements are compared to the NLO QCD prediction obtained with SIScone as jet algorithm. Besides this inconsistency, the agreement appears to be reasonably good.

Finally, examples of recent TEVATRON measurements of heavy quark ( $b$ ,  $c$ ) jet production, inclusive or in association with vector bosons, can be found in Refs. 234–240. Also, first results for vector boson production in association with  $b$ -jets have been obtained at the LHC [241,242]. It is worth noting that for  $W$ + $b$  production there is some tension between the measurements and the NLO predictions, in particular in the case of the CDF result [239].

### 9.3.3. Tests of the non-abelian nature of QCD :

QCD is a gauge theory with  $SU(3)$  as underlying gauge group. For a general gauge theory with a simple Lie group, the couplings of the fermion fields to the gauge fields and the self-interactions in the non-abelian case are determined by the coupling constant and Casimir operators of the gauge group, as introduced in Sec. 9.1. Measuring the eigenvalues of these operators, called color factors, probes the underlying structure of the theory in a gauge invariant way and provides evidence of the gluon self-interactions. Typically, cross sections can be expressed as functions of the color factors, for example  $\sigma = f(\alpha_s C_F, C_A/C_F, n_f T_R/C_F)$ . Sensitivity at leading order in perturbation theory can be achieved by measuring angular correlations in 4-jet events in  $e^+e^-$  annihilation or 3-jet events in DIS. Some sensitivity, although only at NLO, is also obtained from event-shape distributions. Scaling violations of fragmentation functions and the different subjet structure in quark and gluon induced jets also give access to these color factors. In order to extract absolute values, *e.g.* for  $C_F$  and  $C_A$ , certain assumptions have to be made for other parameters, such as  $T_R$ ,  $n_f$  or  $\alpha_s$ , since typically only combinations (ratios, products) of all the relevant parameters appear in the perturbative prediction. A recent compilation of results [176] quotes world average values of  $C_A = 2.89 \pm 0.03(\text{stat}) \pm 0.21(\text{syst})$  and  $C_F = 1.30 \pm 0.01(\text{stat}) \pm 0.09(\text{syst})$ , with a correlation coefficient of 82%. These results are in perfect agreement with the expectations from  $SU(3)$  of  $C_A = 3$  and  $C_F = 4/3$ . An overview of the history and the current status of tests of Asymptotic Freedom, closely related to the non-abelian nature of QCD, can be found in Ref. 243.

### 9.3.4. Measurements of the strong coupling constant :

If the quark masses are fixed, there is only one free parameter in the QCD Lagrangian, the strong coupling constant  $\alpha_s$ . The coupling constant in itself is not a physical observable, but rather a quantity defined in the context of perturbation theory, which enters predictions for experimentally measurable observables, such as  $R$  in Eq. (9.7).

Many experimental observables are used to determine  $\alpha_s$ . Considerations in such determinations include:

- The observable's sensitivity to  $\alpha_s$  as compared to the experimental precision. For example, for the  $e^+e^-$  cross section to hadrons (cf.  $R$  in Sec. 9.2.1), QCD effects are only a small correction, since the perturbative series starts at order  $\alpha_s^0$ ; 3-jet production or event shapes in  $e^+e^-$  annihilations are directly sensitive to  $\alpha_s$  since they start at order  $\alpha_s$ ; the hadronic decay width of heavy quarkonia,  $\Gamma(\Upsilon \rightarrow \text{hadrons})$ , is very sensitive to  $\alpha_s$  since its leading order term is  $\propto \alpha_s^3$ .
- The accuracy of the perturbative prediction, or equivalently of the relation between  $\alpha_s$  and the value of the observable. The minimal requirement is generally considered to be an NLO prediction. Some observables are predicted to NNLO (many inclusive observables, 3-jet rates and event shapes in  $e^+e^-$  collisions) or even N<sup>3</sup>LO ( $e^+e^-$  hadronic cross section and  $\tau$  branching fraction to hadrons). In certain cases, fixed-order predictions are supplemented with resummation. The precise magnitude of theory uncertainties is usually estimated as discussed in Sec. 9.2.3.
- The size of uncontrolled non-perturbative effects (except for lattice-based determinations of  $\alpha_s$ ). Sufficiently inclusive quantities, like the  $e^+e^-$  cross section to hadrons, have small non-perturbative uncertainties  $\sim \Lambda^4/Q^4$ . Others, such as event-shape distributions, have uncertainties  $\sim \Lambda/Q$ .
- The scale at which the measurement is performed. An uncertainty  $\delta$  on a measurement of  $\alpha_s(Q^2)$ , at a scale  $Q$ , translates to an uncertainty  $\delta' = (\alpha_s^2(M_Z^2)/\alpha_s^2(Q^2)) \cdot \delta$  on  $\alpha_s(M_Z^2)$ . For example, this enhances the already important impact of precise low- $Q$  measurements, such as from  $\tau$  decays, in combinations performed at the  $M_Z$  scale.

In this review, we update the measurements of  $\alpha_s$  summarized in the 2009 review, which was based on an analysis by Bethke [244], and we extract a new world average value of  $\alpha_s(M_Z^2)$  from the most significant and complete results available today<sup>#</sup>.

<sup>#</sup> The time evolution of  $\alpha_s$  combinations can be followed by consult-

While in general we follow the same selection strategy and summary procedure as applied in the 2009 review, here we restrict the selection of results from which to calculate the world average value of  $\alpha_s(M_Z^2)$  to those which are

- published in a peer-reviewed journal
- based on the most complete perturbative QCD predictions, i.e. to those using NNLO or higher order expansions.

While this excludes e.g. results from jet production in DIS at HERA and at the Tevatron, as well as those from heavy quarkonia decays for which calculations are available in NLO only, these NLO results will nevertheless be listed and cited in this review as they are important ingredients for the experimental evidence of the energy dependence of  $\alpha_s$ , i.e. for Asymptotic Freedom, one of the key features of QCD.

In addition, here we add an intermediate step of pre-averaging results within certain sub-fields like  $e^+e^-$ -annihilation, DIS and hadronic  $\tau$ -decays, and calculate the overall world average from those pre-averages rather than from individual measurements. This is done because in a number of sub-fields one observes that different determinations of the strong coupling from substantially similar datasets lead to values of  $\alpha_s$  that are only marginally compatible with each other, or with the final world average value, which presumably is a reflection of the challenges of evaluating systematic uncertainties. In such cases, a pre-average value will be determined, with a symmetric, overall error that encompasses the central values of all individual determinations.

#### Hadronic $\tau$ decays

Several re-analyses of the hadronic  $\tau$  decay width [17,246–250], based on the new N<sup>3</sup>LO predictions [17], have been performed, with different approaches towards the detailed treatment of the perturbative (fixed-order or contour-improved perturbative expansions) and non-perturbative contributions. We also include the result from  $\tau$  decay and lifetime measurements, obtained in Sec. *Electroweak Model and constraints on New Physics* of this Review, which amounts, if converted to the  $\tau$ -mass scale and for  $n_f = 3$  quark flavours, to  $\alpha_s(M_\tau) = 0.327^{+0.019}_{-0.016}$ . This result and the one from Baikov et al. [17] include both fixed-order and contour-improved perturbation, while the others adhere to either one or the other of the two. All these results are summarized in Fig. 9.2(a). We note that there are more studies of  $\alpha_s$  from  $\tau$ -decays, [251–254], which are not yet available as peer-reviewed publications but which are compatible with the overall picture. Another recent study [255] argues that an improved treatment of non-perturbative effects results in values of  $\alpha_s$  which are systematically lower than those discussed above. Results using the same analysis framework, but employing an updated version of the OPAL tau spectral function data are reported in Ref. 256, which at the time of writing was as yet unpublished.

We determine the pre-average result from  $\tau$ -decays, to be used for calculating the final world average of  $\alpha_s(M_Z^2)$ , using the simple method defined above, as  $\alpha_s(M_\tau^2) = 0.330 \pm 0.014$ , which spans the range of central values obtained by the different groups. This value of  $\alpha_s(M_\tau^2)$  corresponds, when evolved to the scale of the  $Z$ -boson, using the QCD 4-loop beta-function plus 3-loop matching at the charm- and the bottom-quark masses (see Sec. *Quark Masses* in this Review), to  $\alpha_s(M_Z^2) = 0.1197 \pm 0.0016$ , unchanged from its value in the 2009 review.

#### Lattice QCD

There are several recent results on  $\alpha_s$  from lattice QCD, see also Sec. *Lattice QCD* in this Review. The HPQCD collaboration [257] computes Wilson loops and similar short-distance quantities with lattice QCD and analyzes them with NNLO perturbative QCD. This yields a value for  $\alpha_s$ , but the lattice scale must be related to a physical energy/momentum scale. This is achieved with the  $\Upsilon^{\prime}\Upsilon$  mass difference, however, many other quantities could be used as well [258]. HPQCD obtains  $\alpha_s(M_Z^2) = 0.1184 \pm 0.0006$ , where the uncertainty includes effects from truncating perturbation theory, finite lattice spacing and extrapolation of lattice data. An

independent perturbative analysis of a subset of the same lattice-QCD data yields  $\alpha_s(M_Z^2) = 0.1192 \pm 0.0011$  [259]. Using another, independent methodology, the current-current correlator method, HPQCD obtains  $\alpha_s(M_Z^2) = 0.1183 \pm 0.0007$  [257]. The analysis of Ref. 89, which avoids the staggered fermion treatment of Ref. 257, finds  $\alpha_s(M_Z^2) = 0.1205 \pm 0.0008 \pm 0.0005^{+0.0000}_{-0.0017}$ , where the first uncertainty is statistical and the others are from systematics. Since this approach uses a different discretization of lattice fermions and a different general methodology, it provides an independent cross check of other lattice extractions of  $\alpha_s$ . Finally, the JLQCD collaboration - in an analysis of Adler functions - obtains  $\alpha_s(M_Z^2) = 0.1181 \pm 0.0003^{+0.0014}_{-0.0012}$  [261]. A very recent but unpublished study of the ETM collaboration [262] used lattice data with u, d, s and c quarks in the sea, obtaining results which are compatible with those quoted above.

The published lattice results are summarized in Fig. 9.2(b). Since they are compatible with each other, we calculate a pre-average of lattice results using the same method as applied to determine the final world average value of the strong coupling, i.e. calculate a weighted average and a (correlated) error such that the overall  $\chi^2$  equals unity per degree of freedom - rather than using the simple method as applied in the case of  $\tau$  decays. This gives  $\alpha_s(M_Z^2) = 0.1185 \pm 0.0007$  which we take as result from the sub-field of lattice determinations.

#### Deep inelastic lepton-nucleon scattering (DIS)

Studies of DIS final states have led to a number of precise determinations of  $\alpha_s$ : A combination [263] of precision measurements at HERA, based on NLO fits to inclusive jet cross sections in neutral current DIS at high  $Q^2$ , quotes a combined result of  $\alpha_s(M_Z^2) = 0.1198 \pm 0.0032$ , which includes a theoretical uncertainty of  $\pm 0.0026$ . A combined analysis of non-singlet structure functions from DIS [264], based on QCD predictions up to N<sup>3</sup>LO in some of its parts, gave  $\alpha_s(M_Z^2) = 0.1142 \pm 0.0023$ , including a theoretical error of  $\pm 0.0008$  (BBG). Further studies of singlet and non-singlet structure functions, based on NNLO predictions, resulted in  $\alpha_s(M_Z^2) = 0.1129 \pm 0.0014$  [265] (ABKM; updated in a recent unpublished note [266]) and in  $\alpha_s(M_Z^2) = 0.1158 \pm 0.0035$  [267] (JR). The MSTW group [268], also including data on jet production at the Tevatron, obtains, at NNLO<sup>#</sup>,  $\alpha_s(M_Z^2) = 0.1171 \pm 0.0024$ . Most recently, the NNPDF group [269] has presented a result,  $\alpha_s(M_Z^2) = 0.1173 \pm 0.0011$ , which is in line with the one from the MSTW group.

Summarizing these results from world data on structure functions, applying the same method as in the case of summarizing results from  $\tau$  decays, leads to a pre-average value of  $\alpha_s(M_Z^2) = 0.1151 \pm 0.0022$  (see Fig. 9.2(c)).

We note that criticism has been expressed on some of the above extractions. Among the issues raised, we mention the neglect of singlet contributions at  $x \geq 0.3$  in pure non-singlet fits [270], the impact and detailed treatment of particular classes of data in the fits [270,271] and possible biases due to insufficiently flexible parametrizations of the PDFs [272].

#### Heavy quarkonia decays

The most recent extraction of the strong coupling constant from an analysis of radiative  $\Upsilon$  decays [273] resulted in  $\alpha_s(M_Z) = 0.119^{+0.006}_{-0.005}$ . This determination is based on QCD in NLO only, so it will not be considered for the final extraction of the world average value of  $\alpha_s$ ; it is, however, an important ingredient for the demonstration of Asymptotic Freedom as given in Fig. 9.4.

#### Hadronic final states of $e^+e^-$ annihilations

Re-analyses of event shapes in  $e^+e^-$ -annihilation, measured at the  $Z$  peak and LEP2 energies up to 209 GeV, using NNLO predictions matched to NLL resummation, resulted in  $\alpha_s(M_Z^2) = 0.1224 \pm 0.0039$  [274], with a dominant theoretical uncertainty of 0.0035, and in  $\alpha_s(M_Z^2) = 0.1189 \pm 0.0043$  [275]. Similarly, an analysis of JADE data [276] at center-of-mass energies between 14 and 46 GeV gives  $\alpha_s(M_Z^2) = 0.1172 \pm 0.0051$ , with contributions from hadronization model (perturbative QCD) uncertainties of 0.0035 (0.0030). A precise determination of  $\alpha_s$  from 3-jet production alone, in NNLO, resulted in

<sup>#</sup> Note that for jet production at the hadron collider, only NLO predictions are available, while for the structure functions full NNLO was utilized.



$\alpha_s(M_Z^2) = 0.1175 \pm 0.0025$  [277]. Computation of the NLO corrections to 5-jet production and comparison to the measured 5-jet rates at LEP [74] gave  $\alpha_s(M_Z^2) = 0.1156^{+0.0041}_{-0.0034}$ . More recently, a study using the world data of Thrust distributions and soft-collinear effective theory, including fixed order NNLO, gave  $\alpha_s(M_Z^2) = 0.1135 \pm 0.0010$  [278]. We note that there is criticism on both classes of  $\alpha_s$  extractions just described: those based on corrections of non-perturbative hadronisation effects using QCD-inspired Monte Carlo generators (since the parton level of a Monte Carlo is not defined in a manner equivalent to that of a fixed-order calculation), as well as the studies based on effective field theory, as their systematics have not yet been verified e.g. by using observables other than Thrust.

A summary of the  $e^+e^-$  results based on NNLO predictions is shown in Fig. 9.2(d). They average, according to the simple procedure defined above, to  $\alpha_s(M_Z^2) = 0.1172 \pm 0.0037$ .

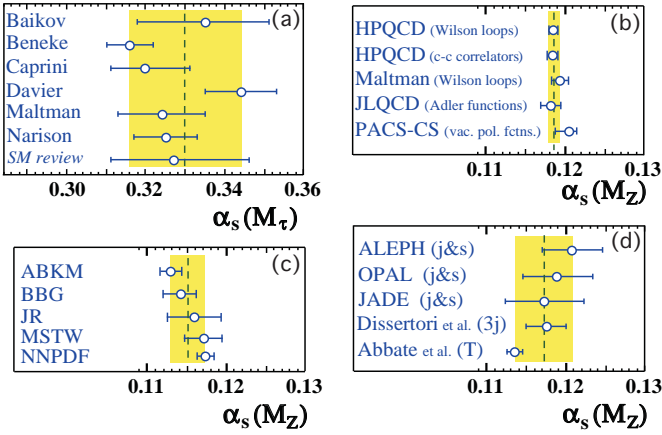


**Figure 9.2:** Summary of determinations of  $\alpha_s$  from hadronic  $\tau$ -decays (a), from lattice calculations (b), from DIS structure functions (c) and from event shapes and jet production in  $e^+e^-$ -annihilation (d). The shaded bands indicate the average values chosen to be included in the determination of the new world average of  $\alpha_s$ .

#### Hadron collider jets

A determination of  $\alpha_s$  from the  $p_T$  dependence of the inclusive jet cross section in  $p\bar{p}$  collisions at  $\sqrt{s} = 1.96$  TeV, in the transverse momentum range of  $50 < p_T < 145$  GeV, based on NLO ( $\mathcal{O}(\alpha_s^3)$ ) QCD, led to  $\alpha_s(M_Z^2) = 0.1161^{+0.0041}_{-0.0048}$  [279], which is the most precise  $\alpha_s$  result obtained at a hadron collider. Experimental uncertainties from the jet energy calibration, the  $p_T$  resolution and the integrated luminosity dominate the overall error.

#### Electroweak precision fits

The  $N^3$ LO calculation of the hadronic  $Z$  decay width was used in a revision of the global fit to electroweak precision data [280], resulting in  $\alpha_s(M_Z^2) = 0.1193 \pm 0.0028$ , claiming a negligible theoretical uncertainty. For this *Review* the value obtained in Sec. *Electroweak model and constraints on new physics* from data at the  $Z$ -pole,  $\alpha_s(M_Z^2) = 0.1197 \pm 0.0028$  will be used instead, as it is based on a more constrained data set where QCD corrections directly enter through the hadronic decay width of the  $Z$ . We note that all these results from electroweak precision data, however, strongly depend on the strict validity of Standard Model predictions and the existence of the minimal Higgs mechanism to implement electroweak symmetry breaking. Any - even small - deviation of nature from this model could strongly influence this extraction of  $\alpha_s$ .

#### Determination of the world average value of $\alpha_s(M_Z^2)$

A non-trivial exercise consists in the evaluation of a world-average value for  $\alpha_s(M_Z^2)$ . A certain arbitrariness and subjective component is inevitable because of the choice of measurements to be included in the average, the treatment of (non-Gaussian) systematic uncertainties of mostly theoretical nature, as well as the treatment of correlations among the various inputs, of theoretical as well as experimental origin.

In earlier reviews [243–245] an attempt was made to take account of such correlations, using methods as proposed, e.g., in Ref. 281, and - likewise - to treat cases of apparent incompatibilities or possibly underestimated systematic uncertainties in a meaningful and well defined manner:

The central value is determined as the weighted average of the different input values. An initial error of the central value is determined treating the uncertainties of all individual measurements as being uncorrelated and being of Gaussian nature, and the overall  $\chi^2$  to the central value is determined. If this initial  $\chi^2$  is larger than the number of degrees of freedom, i.e. larger than the number of individual inputs minus one, then all individual errors are enlarged by a common factor such that  $\chi^2/\text{d.o.f.}$  equals unity. If the initial value of  $\chi^2$  is smaller than the number of degrees of freedom, an overall, a-priori unknown correlation coefficient is introduced and determined by requiring that the total  $\chi^2/\text{d.o.f.}$  of the combination equals unity. In both cases, the resulting final overall uncertainty of the central value of  $\alpha_s$  is larger than the initial estimate of a Gaussian error.

This procedure is only meaningful if the individual measurements are known not to be correlated to large degrees, i.e. if they are not - for instance - based on the same input data, and if the input values are largely compatible with each other and with the resulting central value, within their assigned uncertainties. The list of selected individual measurements discussed above, however, violates both these requirements: there are several measurements based on (partly or fully) identical data sets, and there are results which apparently do not agree with others and/or with the resulting central value, within their assigned uncertainty. Examples for the first case are results from the hadronic width of the  $\tau$  lepton, from DIS processes and from jets and event shapes in  $e^+e^-$  final states. An example of the second case is the apparent disagreement between results from the  $\tau$  width and those from DIS [264] or from Thrust distributions in  $e^+e^-$  annihilation [278].

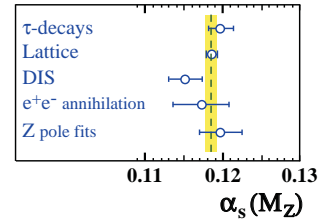


**Figure 9.3:** Summary of values of  $\alpha_s(M_Z^2)$  obtained for various sub-classes of measurements (see Fig. 9.2 (a) to (d)). The new world average value of  $\alpha_s(M_Z^2) = 0.1184 \pm 0.0007$  is indicated by the dashed line and the shaded band.

Due to these obstacles, we have chosen to determine pre-averages for each class of measurements, and then to combine those to the final world average value of  $\alpha_s(M_Z^2)$ , using the methods of error treatment as just described. The five pre-averages are summarized in Fig. 9.3; we recall that these are exclusively obtained from extractions which are based on (at least) full NNLO QCD predictions, and are published in peer-reviewed journals at the time of completing this *Review*. From these, we determine the new world average value of

$$\alpha_s(M_Z^2) = 0.1184 \pm 0.0007, \quad (9.23)$$

with an uncertainty of well below 1 %.<sup>\*\*\*</sup> This world average value is - in spite of several new contributions to this determination - identical to and thus, in excellent agreement with the 2009 result [244]. For

<sup>\*\*\*</sup> The weighted average, treating all inputs as uncorrelated measurements with Gaussian errors, results in  $\alpha_s(M_Z^2) = 0.11844 \pm 0.00059$  with  $\chi^2/\text{d.o.f.} = 3.2/4$ . Requiring  $\chi^2/\text{d.o.f.}$  to reach unity leads to a common correlation factor of 0.19 which increases the overall error to 0.00072.



convenience, we also provide corresponding values for  $\Lambda_{\overline{MS}}$  suitable for use with Eq. (9.5):

$$\Lambda_{\overline{MS}}^{(5)} = (213 \pm 8) \text{ MeV} , \quad (9.24a)$$

$$\Lambda_{\overline{MS}}^{(4)} = (296 \pm 10) \text{ MeV} , \quad (9.24b)$$

$$\Lambda_{\overline{MS}}^{(3)} = (339 \pm 10) \text{ MeV} , \quad (9.24c)$$

for  $n_f = 5, 4$  and  $3$  quark flavors, respectively.

In order to further test and verify the sensitivity of the new average value of  $\alpha_s(M_Z^2)$  to the different pre-averages and classes of  $\alpha_s$  determinations, we give each of the averages obtained when leaving out one of the five input values:

$$\alpha_s(M_Z^2) = 0.1182 \pm 0.0007 \quad (\text{w/o } \tau \text{ results}), \quad (9.25a)$$

$$\alpha_s(M_Z^2) = 0.1183 \pm 0.0012 \quad (\text{w/o lattice results}), \quad (9.25b)$$

$$\alpha_s(M_Z^2) = 0.1187 \pm 0.0009 \quad (\text{w/o DIS results}), \quad (9.25c)$$

$$\alpha_s(M_Z^2) = 0.1185 \pm 0.0006 \quad (\text{w/o } e^+e^- \text{ results}), \text{ and} \quad (9.25d)$$

$$\alpha_s(M_Z^2) = 0.1184 \pm 0.0006 \quad (\text{w/o res. from e.w. prec. fit}), \quad (9.25e)$$

They are well within the error of the overall world average quoted above. Most notably, the result from lattice calculations, which has the smallest assigned error, agrees well with the exclusive average of the other results. However, it largely determines the size of the (small) overall uncertainty.

There are apparent systematic differences between the various structure function results, and also between the new result from Thrust in  $e^+e^-$  annihilation and the other determinations. Expressing this in terms of a  $\chi^2$  between a given measurement and the world average as obtained when *excluding* that particular measurement, the largest values are  $\chi^2 = 12.6$  and  $\chi^2 = 16.1$ , corresponding to 3.5 and 4.0 standard deviations, for the measurements of [265] and [278], respectively. We note that such and other differences between some of the measurements have been extensively discussed at a specific workshop on measurements of  $\alpha_s$ , however none of the explanations proposed so far have obtained enough of a consensus to definitely resolve the tensions between different extractions [282].

Notwithstanding these open issues, a rather stable and well defined world average value emerges from the compilation of current determinations of  $\alpha_s$ :

$$\alpha_s(M_Z^2) = 0.1184 \pm 0.0007 .$$

The results also provide a clear signature and proof of the energy dependence of  $\alpha_s$ , in full agreement with the QCD prediction of Asymptotic Freedom. This is demonstrated in Fig. 9.4, where results of  $\alpha_s(Q^2)$  obtained at discrete energy scales  $Q$ , now also including those based just on NLO QCD, are summarized and plotted.

#### 9.4. Acknowledgments

We are grateful to J.-F. Arguin, G. Altarelli, J. Butterworth, M. Cacciari, L. del Debbio, P. Gambino, N. Glover, M. Grazzini, A. Kronfeld, K. Kousouris, M. d'Onofrio, S. Sharpe, G. Sterman, D. Treille, N. Varelas, M. Wobisch, W.M. Yao, C.P. Yuan, and G. Zanderighi for their suggestions and comments on this and earlier versions of this review.

#### References:

1. C.A. Baker *et al.*, Phys. Rev. Lett. **97** 131801 (2006) [hep-ex/0602020].
2. H.-Y. Cheng, Phys. Rept. **158** 1(1988).
3. R.K. Ellis, W.J. Stirling, and B.R. Webber, "QCD and collider physics," *Camb. Monogr. Part. Phys. Nucl. Phys. Cosmol.* **81** (1996).
4. G. Dissertori, I.G. Knowles, and M. Schmelling, "High energy experiments and theory," Oxford, UK: Clarendon (2003).
5. R. Brock *et al.*, [CTEQ Collab.], Rev. Mod. Phys. **67**, 157 (1995), see also <http://www.phys.psu.edu/~cteq/handbook/v1.1/handbook.pdf>.

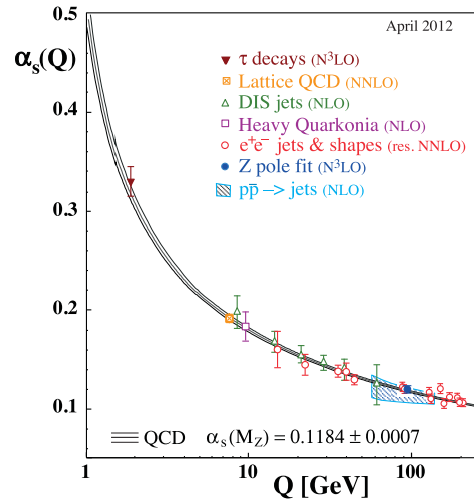


**Figure 9.4:** Summary of measurements of  $\alpha_s$  as a function of the respective energy scale  $Q$ . The respective degree of QCD perturbation theory used in the extraction of  $\alpha_s$  is indicated in brackets (NLO: next-to-leading order; NNLO: next-to-next-to-leading order; res. NNLO: NNLO matched with resummed next-to-leading logs; N<sup>3</sup>LO: next-to-NNLO).

6. A.S. Kronfeld and C. Quigg, Am. J. Phys. **78**, 1081 (2010). [arXiv:1002.5032 [hep-ph]].
7. R. Stock (Ed.), *Relativistic Heavy Ion Physics*, Springer-Verlag Berlin, Heidelberg, 2010.
8. *Proceedings of the Quark Matter 2011 Conference*, to appear J. Phys. G.
9. T. van Ritbergen, J.A.M. Vermaseren, and S.A. Larin, Phys. Lett. **B400**, 379 (1997) [arXiv:hep-ph/9701390].
10. M. Czakon, Nucl. Phys. **B710**, 485 (2005) [arXiv:hep-ph/0411261].
11. Y. Schroder and M. Steinhauser, JHEP **0601**, 051 (2006) [arXiv:hep-ph/0512058].
12. K.G. Chetyrkin, J.H. Kuhn, and C. Sturm, Nucl. Phys. **B744**, 121 (2006) [arXiv:hep-ph/0512060].
13. A.G. Grozin *et al.*, arXiv:1107.5970 [hep-ph].
14. K.G. Chetyrkin, B.A. Kniehl, and M. Steinhauser, Nucl. Phys. **B510**, 61 (1998) [arXiv:hep-ph/9708255].
15. See for example section 11.4 of M.E. Peskin and D.V. Schroeder, "An Introduction To Quantum Field Theory," Reading, USA: Addison-Wesley (1995).
16. M. Beneke, Phys. Reports **317**, 1 (1999) [arXiv:hep-ph/9807443].
17. P.A. Baikov, K.G. Chetyrkin, and J.H. Kuhn, Phys. Rev. Lett. **101**, 012002 (2008) [arXiv:0801.1821 [hep-ph]].
18. P.A. Baikov, K.G. Chetyrkin, and J.H. Kuhn, Nucl. Phys. (Proc. Supp.) **189**, 49 (2009) arXiv:0906.2987 [hep-ph].
19. K.G. Chetyrkin, J.H. Kuhn, and A. Kwiatkowski, Phys. Reports **277**, 189 (1996).
20. Y. Kiyo *et al.*, Nucl. Phys. **B823**, 269 (2009) [arXiv:0907.2120 [hep-ph]].
21. A. Djouadi, Phys. Reports **457**, 1 (2008) [arXiv:hep-ph/0503172].
22. P.A. Baikov, K.G. Chetyrkin, J.H. Kuhn, Phys. Rev. Lett. **96**, 012003 (2006). [hep-ph/0511063].
23. A.H. Hoang, PoS **TOP2006** 032, (2006) [arXiv:hep-ph/0604185].
24. D.B. Renner, arXiv:1103.3655 [hep-lat].
25. V.N. Gribov and L.N. Lipatov, Sov. J. Nucl. Phys. **15**, 438 (1972); G. Altarelli and G. Parisi, Nucl. Phys. **B126**, 298 (1977); Yu.L. Dokshitzer, Sov. Phys. JETP **46**, 641 (1977).

26. G. Curci, W. Furmanski, and R. Petronzio, Nucl. Phys. **B175** 27 (1980);  
W. Furmanski and R. Petronzio, Phys. Lett. **B97** 437 (1980).
27. A. Vogt, S. Moch, and J.A.M. Vermaseren, Nucl. Phys. **B691**, 129 (2004) [arXiv:hep-ph/0404111];  
S. Moch, J.A.M. Vermaseren, and A. Vogt, Nucl. Phys. **B688**, 101 (2004) [arXiv:hep-ph/0403192].
28. J.A.M. Vermaseren, A. Vogt, and S. Moch, Nucl. Phys. **B724**, 3 (2005) [arXiv:hep-ph/0504242].
29. E.B. Zijlstra and W.L. van Neerven, Phys. Lett. **B297**, 377 (1992).
30. S. Moch, J.A.M. Vermaseren, and A. Vogt, Nucl. Phys. **B813**, 220 (2009) [arXiv:0812.4168 [hep-ph]].
31. E. Laenen *et al.*, Nucl. Phys. **B392**, 162 (1993);  
S. Riemersma, J. Smith, and W.L. van Neerven, Phys. Lett. **B347**, 143 (1995) [arXiv:hep-ph/9411431].
32. I. Bierenbaum, J. Blumlein, and S. Klein, Nucl. Phys. **B820**, 417 (2009) [arXiv:0904.3563 [hep-ph]].
33. J. Ablinger *et al.*, Nucl. Phys. **B844**, 26 (2011) [arXiv:1008.3347 [hep-ph]].
34. J.C. Collins, D.E. Soper, and G. Sterman, Nucl. Phys. **B261**, 104 (1985).
35. J.C. Collins, D.E. Soper, and G.F. Sterman, Adv. Ser. Direct. High Energy Phys. **5**, 1 (1988) [hep-ph/0409313].
36. J. C. Collins, *Foundations of Perturbative QCD*, Cambridge University Press, 2011.
37. G. C. Nayak, J. -W. Qiu, G. F. Sterman, Phys. Rev. **D72**, 114012 (2005) [hep-ph/0509021].
38. R. Hamberg, W.L. van Neerven, and T. Matsuura, Nucl. Phys. **B359**, 343 (1991); Erratum *ibid.*, **B 644**, 403 (2002).
39. R.V. Harlander and W.B. Kilgore, Phys. Rev. Lett. **88**, 201801 (2002) [arXiv:hep-ph/0201206].
40. C. Anastasiou and K. Melnikov, Nucl. Phys. **B646**, 220 (2002) [arXiv:hep-ph/0207004].
41. V. Ravindran, J. Smith, and W.L. van Neerven, Nucl. Phys. **B665**, 325 (2003) [arXiv:hep-ph/0302135].
42. O. Brein, A. Djouadi, and R. Harlander, Phys. Lett. **B579**, 149 (2004) [hep-ph/0307206].
43. P. Bolzoni *et al.*, Phys. Rev. Lett. **105**, 011801 (2010) [arXiv:1003.4451 [hep-ph]].
44. S. Dittmaier *et al.* [LHC Higgs Cross Section Working Group Collab.], arXiv:1101.0593 [hep-ph].
45. M. Greco and A. Vicini, Nucl. Phys. **B415**, 386 (1994).
46. L.N. Lipatov, Sov. J. Nucl. Phys. **23**, 338 (1976) [Yad. Fiz. **23**, 642 (1976)].
47. E.A. Kuraev, L.N. Lipatov, and V.S. Fadin, Sov. Phys. JETP **45**, 199 (1977) [Zh. Eksp. Teor. Fiz. **72**, 377 (1977)].
48. I.I. Balitsky and L.N. Lipatov, Sov. J. Nucl. Phys. **28**, 822 (1978) [Yad. Fiz. **28**, 1597 (1978)].
49. V.S. Fadin and L.N. Lipatov, Phys. Lett. **B429**, 127 (1998) [arXiv:hep-ph/9802290].
50. M. Ciafaloni and G. Camici, Phys. Lett. **B430**, 329 (1998) [arXiv:hep-ph/9803389].
51. G. Altarelli, R. D. Ball, and S. Forte, Nucl. Phys. **B799**, 199 (2008) [arXiv:0802.0032 [hep-ph]].
52. M. Ciafaloni *et al.*, JHEP **0708**, 046 (2007) [arXiv:0707.1453 [hep-ph]].
53. C.D. White and R.S. Thorne, Phys. Rev. **D75**, 034005 (2007) [arXiv:hep-ph/0611204].
54. I. Balitsky, Nucl. Phys. **B463**, 99 (1996) [arXiv:hep-ph/9509348].
55. Y.V. Kovchegov, Phys. Rev. **D60**, 034008 (1999) [arXiv:hep-ph/9901281].
56. A. Hebecker, Phys. Reports **331**, 1 (2000) [arXiv:hep-ph/9905226].
57. A.V. Belitsky and A.V. Radyushkin, Phys. Reports **418**, 1 (2005) [arXiv:hep-ph/0504030].
58. E. Boos *et al.*, [CompHEP Collab.], Nucl. Instrum. Methods **A534**, 250 (2004) [arXiv:hep-ph/0403113];  
<http://comphep.sinp.msu.ru/>.
59. J. Alwall *et al.*, JHEP **1106**, 128 (2011) [arXiv:1106.0522 [hep-ph]]; <http://madgraph.hep.uiuc.edu/>.
60. M.L. Mangano *et al.*, JHEP **0307**, 001 (2003) [arXiv:hep-ph/0206293]; <http://cern.ch/mlm/alpgen/>.
61. T. Gleisberg and S. Hoche, JHEP **0812**, 039 (2008) [arXiv:0808.3674 [hep-ph]].
62. A. Cafarella, C.G. Papadopoulos, and M. Worek, Comp. Phys. Comm. **180**, 1941 (2009) [arXiv:0710.2427 [hep-ph]]; <http://cern.ch/helac-phegas/>.
63. F.A. Berends and W.T. Giele, Nucl. Phys. **B306**, 759 (1988).
64. L.J. Dixon, arXiv:hep-ph/9601359.
65. Z. Bern, L.J. Dixon, and D. A. Kosower, Annals Phys. **322**, 1587 (2007) [arXiv:0704.2798 [hep-ph]].
66. S. Catani and M.H. Seymour, Nucl. Phys. **B485**, 291 (1997) [Erratum-*ibid.* **B510** 503 (1998)] [arXiv:hep-ph/9605323].
67. S. Frixione, Z. Kunszt, and A. Signer, Nucl. Phys. **B467**, 399 (1996) [arXiv:hep-ph/9512328].
68. D.A. Kosower, Phys. Rev. **D57**, 5410 (1998) [arXiv:hep-ph/9710213];  
J.M. Campbell, M.A. Cullen, and E.W.N. Glover, Eur. Phys. J. **C9**, 245 (1999) [arXiv:hep-ph/9809429];  
D.A. Kosower, Phys. Rev. **D71**, 045016 (2005) [arXiv:hep-ph/0311272].
69. Z. Bern *et al.*, [NLO Multileg Working Group], arXiv:0803.0494 [hep-ph].
70. Z. Nagy, Phys. Rev. **D68**, 094002 (2003) [arXiv:hep-ph/0307268];  
<http://www.desy.de/~znagy/Site/NLOJet++.html>.
71. J.M. Campbell and R.K. Ellis, Phys. Rev. **D62**, 114012 (2000) [arXiv:hep-ph/0006304]; <http://mcfm.fnal.gov/>.
72. K. Arnold *et al.*, [arXiv:1107.4038 [hep-ph]]; <http://www-itp.particle.uni-karlsruhe.de/~vbfnlweb/>.
73. T. Binoth *et al.*, Eur. Phys. J. **C16**, 311 (2000) [arXiv:hep-ph/9911340]; [http://laph.in2p3.fr/PHOX\\_FAMILY/](http://laph.in2p3.fr/PHOX_FAMILY/).
74. R. Frederix *et al.*, JHEP **1011**, 050 (2010) [arXiv:1008.5313 [hep-ph]].
75. C.F. Berger *et al.*, Phys. Rev. **D80**, 074036 (2009) [arXiv:0907.1984 [hep-ph]].
76. R. Keith Ellis, K. Melnikov, and G. Zanderighi, Phys. Rev. **D80**, 094002 (2009) [arXiv:0906.1445 [hep-ph]].
77. C.F. Berger *et al.*, Phys. Rev. **D82**, 074002 (2010) [arXiv:1004.1659 [hep-ph]].
78. C.F. Berger *et al.*, Phys. Rev. Lett. **106**, 092001 (2011) [arXiv:1009.2338 [hep-ph]].
79. H. Ita *et al.*, [arXiv:1108.2229 [hep-ph]].
80. G. Bevilacqua *et al.*, JHEP **0909**, 109 (2009) [arXiv:0907.4723 [hep-ph]].
81. A. Bredenstein *et al.*, Phys. Rev. Lett. **103**, 012002 (2009) [arXiv:0905.0110 [hep-ph]].
82. G. Bevilacqua *et al.*, [arXiv:1108.2851 [hep-ph]].
83. N. Greiner *et al.*, [arXiv:1105.3624 [hep-ph]].
84. A. Denner *et al.*, Phys. Rev. Lett. **106**, 052001 (2011). [arXiv:1012.3975 [hep-ph]].
85. T. Melia *et al.*, JHEP **1012**, 053 (2010). [arXiv:1007.5313 [hep-ph]]; *idem.* Phys. Rev. **D83**, 114043 (2011) [arXiv:1104.2327 [hep-ph]].
86. V. Hirschi *et al.*, JHEP **1105**, 044 (2011). [arXiv:1103.0621 [hep-ph]].
87. G. Bevilacqua *et al.*, arXiv:1110.1499 [hep-ph].
88. Z. Bern *et al.*, Nucl. Phys. **B425**, 217 (1994) [hep-ph/9403226].
89. G. Ossola, C. G. Papadopoulos, and R. Pittau, Nucl. Phys. **B763**, 147 (2007) [hep-ph/0609007].
90. R.K. Ellis *et al.*, [arXiv:1105.4319 [hep-ph]].
91. J.M. Campbell and E.W.N. Glover, Nucl. Phys. **B527**, 264 (1998) [hep-ph/9710255].
92. S. Catani and M. Grazzini, Phys. Lett. **B446** 143 (1999) [hep-ph/9810389].
93. A. Gehrmann-De Ridder *et al.*, Phys. Rev. Lett. **99** 132002 (2007) [arXiv:0707.1285 [hep-ph]];

- JHEP **0712**, 094 (2007) [arXiv:0711.4711 [hep-ph]]; Phys. Rev. Lett. **100**, 172001 (2008) [arXiv:0802.0813 [hep-ph]].
94. S. Weinzierl, Phys. Rev. Lett. **101**, 162001 (2008) [arXiv:0807.3241 [hep-ph]]; JHEP **0906**, 041 (2009) [arXiv:0904.1077 [hep-ph]].
95. K. Melnikov and F. Petriello, Phys. Rev. **D74**, 114017 (2006) [arXiv:hep-ph/0609070]; <http://gate.hep.anl.gov/fpetriello/FEWZ.html>.
96. S. Catani *et al.*, Phys. Rev. Lett. **103**, 082001 (2009). arXiv:0903.2120 [hep-ph]; <http://theory.fi.infn.it/grazzini/dy.html>.
97. C. Anastasiou, K. Melnikov, and F. Petriello, Nucl. Phys. **B724**, 197 (2005) [arXiv:hep-ph/0501130]; <http://www.phys.ethz.ch/~pheno/fehipro/>.
98. S. Catani and M. Grazzini, Phys. Rev. Lett. **98**, 222002 (2007) [arXiv:hep-ph/0703012]; <http://theory.fi.infn.it/grazzini/codes.html>.
99. G. Ferrera, M. Grazzini, and F. Tramontano, [arXiv:1107.1164 [hep-ph]].
100. S. Catani *et al.*, arXiv:1110.2375 [hep-ph].
101. Y.L. Dokshitzer, D.Diakonov, and S.I. Troian, Phys. Reports **58**, 269 (1980).
102. G. Parisi and R. Petronzio, Nucl. Phys. **B154**, 427 (1979).
103. G. Curci, M. Greco, and Y. Srivastava, Nucl. Phys. **B159**, 451 (1979).
104. A. Bassetto, M. Ciafaloni, and G. Marchesini, Nucl. Phys. **B163**, 477 (1980).
105. J.C. Collins and D.E. Soper, Nucl. Phys. **B193**, 381 (1981) [Erratum-*ibid.* **B213**, 545 (1983)].
106. J.C. Collins and D.E. Soper, Nucl. Phys. **B197**, 446 (1982).
107. J. Kodaira and L. Trentadue, Phys. Lett. **B112**, 66 (1982).
108. J. Kodaira and L. Trentadue, Phys. Lett. **B123**, 335 (1983).
109. J.C. Collins, D.E. Soper, and G. Sterman, Nucl. Phys. **B250**, 199 (1985).
110. S. Catani, *et al.*, Nucl. Phys. **B407**, 3 (1993).
111. C.W. Bauer *et al.*, Phys. Rev. **D63**, 114020 (2001) [hep-ph/0011336].
112. C.W. Bauer, D. Pirjol, and I.W. Stewart, Phys. Rev. **D65**, 054022 (2002) [hep-ph/0109045].
113. S. Fleming, PoS **EFT09**, 002 (2009) arXiv:0907.3897 [hep-ph].
114. S. Catani, *et al.*, Phys. Lett. **B269**, 432 (1991).
115. N. Brown and W.J. Stirling, Phys. Lett. **B252**, 657 (1990).
116. W. Bartel, *et al.*, [JADE Collab.], Z. Phys. **C33**, 23 (1986).
117. N. Kidonakis, G. Ordera, and G. Sterman, Nucl. Phys. **B531**, 365 (1998) [arXiv:hep-ph/9803241].
118. R. Bonciani *et al.*, Phys. Lett. **B575**, 268 (2003) [arXiv:hep-ph/0307035].
119. A. Banfi, G.P. Salam, and G. Zanderighi, JHEP **0503**, 073 (2005) [arXiv:hep-ph/0407286].
120. D. de Florian and M. Grazzini, Phys. Rev. Lett. **85**, 4678 (2000) [arXiv:hep-ph/0008152].
121. G. Bozzi *et al.*, Nucl. Phys. **B737**, 73 (2006) [hep-ph/0508068]; <http://theory.fi.infn.it/grazzini/codes.html>.
122. G. Bozzi *et al.*, Phys. Lett. **B696**, 2-7 (2011) [arXiv:1007.2351 [hep-ph]].
123. T. Becher and M. Neubert, Eur. Phys. J. **C71**, 1665 (2011) [arXiv:1007.4005 [hep-ph]].
124. C. Balazs and C.P. Yuan, Phys. Rev. **D56**, 5558 (1997) [arXiv:hep-ph/9704258].
125. D. de Florian and M. Grazzini, Nucl. Phys. **B704**, 387 (2005) [arXiv:hep-ph/0407241].
126. V. Ahrens *et al.*, JHEP **1009**, 097 (2010) [arXiv:1003.5827 [hep-ph]].
127. M. Aliev *et al.*, Comp. Phys. Comm. **182**, 1034 (2011) arXiv:1007.1327 [hep-ph].
128. N. Kidonakis, Phys. Rev. **D82**, 114030 (2010) [arXiv:1009.4935 [hep-ph]].
129. T. Becher, C. Lorentzen, and M.D. Schwartz, [arXiv:1106.4310 [hep-ph]].
130. I.W. Stewart, F.J. Tackmann, and W.J. Waalewijn, Phys. Rev. Lett. **106**, 032001 (2011) [arXiv:1005.4060 [hep-ph]].
131. T. Becher and M.D. Schwartz, JHEP **0807**, 034 (2008) [arXiv:0803.0342 [hep-ph]].
132. Y.-T. Chien and M.D. Schwartz, JHEP **1008**, 058 (2010) [arXiv:1005.1644 [hep-ph]].
133. P.F. Monni, T. Gehrmann, and G. Luisoni, JHEP **1108**, 010 (2011) [arXiv:1105.4560 [hep-ph]].
134. S. Moch and A. Vogt, Phys. Lett. **B631**, 48 (2005) [arXiv:hep-ph/0508265].
135. E. Laenen and L. Magnea, Phys. Lett. **B632**, 270 (2006) [arXiv:hep-ph/0508284].
136. A. Vogt, Phys. Lett. **B497**, 228 (2001) [hep-ph/0010146].
137. S. Catani *et al.*, JHEP **0307**, 028 (2003) [hep-ph/0306211].
138. T. Sjostrand *et al.*, Comput. Phys. Commun. **135**, 238 (2001) [arXiv:hep-ph/0010017].
139. T. Sjostrand, S. Mrenna, and P. Skands, JHEP **0605**, 026 (2006) [arXiv:hep-ph/0603175]; <http://projects.hepforge.org/pythia6/>.
140. T. Sjostrand, S. Mrenna, and P. Skands, Comput. Phys. Commun. **178**, 852 (2008) [arXiv:0710.3820 [hep-ph]]; <http://home.thep.lu.se/~torbjorn/Pythia.html>.
141. B.R. Webber, Nucl. Phys. **B238**, 492 (1984).
142. G. Corcella *et al.*, JHEP **0101**, 010 (2001) [arXiv:hep-ph/0011363]; <http://www.hep.phy.cam.ac.uk/theory/webber/Herwig/>.
143. M. Bahr *et al.*, Eur. Phys. J. **C58**, 639 (2008) [arXiv:0803.0883 [hep-ph]]; <http://projects.hepforge.org/herwig/>.
144. T. Gleisberg *et al.*, JHEP **0902**, 007 (2009) [arXiv:0811.4622 [hep-ph]]; <http://projects.hepforge.org/sherpa/>.
145. L. Lonnblad, Comput. Phys. Commun. **71**, 15 (1992).
146. A. Buckley *et al.*, Phys. Rept. **504**, 145 (2011) [arXiv:1101.2599 [hep-ph]].
147. B. Andersson *et al.*, Phys. Reports **97**, 31 (1983).
148. T. Sjostrand, Nucl. Phys. **B248**, 469 (1984).
149. T. Sjostrand and M. van Zijl, Phys. Rev. **D36**, 2019 (1987).
150. S. Catani *et al.*, JHEP **0111**, 063 (2001) [arXiv:hep-ph/0109231].
151. J. Alwall *et al.*, Eur. Phys. J. **C53**, 473 (2008) [arXiv:0706.2569 [hep-ph]].
152. S. Frixione and B.R. Webber, JHEP **0206**, 029 (2002) [arXiv:hep-ph/0204244].
153. P. Nason, JHEP **0411**, 040 (2004) [arXiv:hep-ph/0409146].
154. K. Hamilton and P. Nason, JHEP **1006**, 039 (2010) [arXiv:1004.1764 [hep-ph]].
155. S. Hoche *et al.*, [arXiv:1009.1127 [hep-ph]].
156. P.M. Stevenson, Phys. Lett. **B100**, 61 (1981).
157. P. M. Stevenson, Phys. Rev. **D23**, 2916 (1981).
158. G. Grunberg, Phys. Rev. **D29**, 2315 (1984).
159. S.J. Brodsky, G.P. Lepage, and P.B. Mackenzie, Phys. Rev. **D28**, 228 (1983).
160. M. Cacciari *et al.*, JHEP **0404**, 068 (2004) [arXiv:hep-ph/0303085].
161. M. Dasgupta and G.P. Salam, J. Phys. **G30**, R143 (2004) [arXiv:hep-ph/0312283].
162. S. Moretti, L. Lonnblad, and T. Sjostrand, JHEP **9808**, 001 (1998) [arXiv:hep-ph/9804296].
163. G.P. Salam, Eur. Phys. J. **C67**, 637 (2010) arXiv:0906.1833 [hep-ph].
164. S.D. Ellis *et al.*, Prog. in Part. Nucl. Phys. **60**, 484 (2008) [arXiv:0712.2447 [hep-ph]].
165. G.P. Salam and G. Soyez, JHEP **0705**, 086 (2007) [arXiv:0704.0292 [hep-ph]].
166. S. Catani *et al.*, Nucl. Phys. **B406**, 187 (1993).
167. S.D. Ellis and D.E. Soper, Phys. Rev. **D48**, 3160 (1993) [arXiv:hep-ph/9305266].
168. Y.L. Dokshitzer *et al.*, JHEP **9708**, 001 (1997) [arXiv:hep-ph/9707323].
169. M. Wobisch and T. Wengler, arXiv:hep-ph/9907280.

170. M. Cacciari, G.P. Salam, and G. Soyez, JHEP **0804**, 063 (2008) [arXiv:0802.1189 [hep-ph]].
171. M. Cacciari and G.P. Salam, Phys. Lett. **B641**, 57 (2006) [arXiv:hep-ph/0512210]; M. Cacciari, G.P. Salam, and G. Soyez, <http://fastjet.fr/>.
172. P.A. Delsart, K. Geerlins, and J. Huston, <http://projects.hepforge.org/spartyjet/>.
173. S. Brandt *et al.*, Phys. Lett. **12**, 57 (1964).
174. E. Farhi, Phys. Rev. Lett. **39**, 1587 (1977).
175. O. Biebel, Phys. Reports **340**, 165 (2001).
176. S. Kluth, Rept. on Prog. in Phys. **69**, 1771 (2006) [arXiv:hep-ex/0603011].
177. A. Banfi, G.P. Salam, and G. Zanderighi, JHEP **0408**, 062 (2004) [arXiv:hep-ph/0407287].
178. A. Banfi, G.P. Salam, and G. Zanderighi, JHEP **1006**, 038 (2010) [arXiv:1001.4082 [hep-ph]].
179. I.W. Stewart, F.J. Tackmann, and W.J. Waalewijn, Phys. Rev. Lett. **105**, 092002 (2010) [arXiv:1004.2489 [hep-ph]].
180. T. Aaltonen *et al.*, [CDF Collab.], Phys. Rev. **D83**, 112007 (2011) [arXiv:1103.5143 [hep-ex]].
181. V. Khachatryan *et al.*, [CMS Collab.], Phys. Lett. **B699**, 48 (2011) [arXiv:1102.0068 [hep-ex]].
182. D.E. Acosta *et al.*, [CDF Collab.], Phys. Rev. **D71**, 112002 (2005) [arXiv:hep-ex/0505013].
183. T. Aaltonen *et al.*, [CDF Collab.], Phys. Rev. **D78**, 072005 (2008) [arXiv:0806.1699 [hep-ex]].
184. J. Breitweg *et al.*, [ZEUS Collab.], Eur. Phys. J. **C2**, 61 (1998) [hep-ex/9710002].
185. C. Adloff *et al.*, [H1 Collab.], Nucl. Phys. **B545**, 3 (1999) [arXiv:hep-ex/9901010].
186. S. Chekanov *et al.*, [ZEUS Collab.], Nucl. Phys. **B700**, 3 (2004) [arXiv:hep-ex/0405065].
187. G. Aad *et al.*, [ATLAS Collab.], Phys. Rev. **D83**, 052003 (2011) [arXiv:1101.0070 [hep-ex]].
188. C. Glasman [H1 Collab. and ZEUS Collab.], Nucl. Phys. (Proc. Supp.) **191**, 121 (2009) [arXiv:0812.0757 [hep-ex]].
189. A. Abdesselam *et al.*, Eur. Phys. J. **C71**, 1661 (2011) [arXiv:1012.5412 [hep-ph]].
190. J.M. Campbell, J.W. Huston, and W.J. Stirling, Rept. on Prog. in Phys. **70**, 89 (2007) [arXiv:hep-ph/0611148].
191. M. Klein, R. Yoshida, Prog. in Part. Nucl. Phys. **61**, 343 (2008) [arXiv:0805.3334 [hep-ex]].
192. T. Gehrmann, PoS **DIS2010**, 004 (2010) [arXiv:1007.2107 [hep-ph]].
193. A. Bhatti and D. Lincoln, [arXiv:1002.1708 [hep-ex]].
194. M. Martinez, Eur. Phys. J. **C61**, 637 (2009).
195. F.D. Aaron *et al.*, [H1 Collab.], Eur. Phys. J. **C65**, 363 (2010) [arXiv:0904.3870 [hep-ex]].
196. F.D. Aaron *et al.*, [H1 Collab.], Eur. Phys. J. **C54**, 389 (2008) [arXiv:0711.2606 [hep-ex]].
197. S. Chekanov *et al.*, [ZEUS Collab.], Eur. Phys. J. **C52**, 515 (2007) [arXiv:0707.3093 [hep-ex]].
198. S. Chekanov *et al.*, [ZEUS Collab.], Phys. Rev. **D78**, 032004 (2008) [arXiv:0802.3955 [hep-ex]].
199. H. Abramowicz *et al.*, [ZEUS Collab.], Eur. Phys. J. **C70**, 965 (2010) [arXiv:1010.6167 [hep-ex]].
200. H. Abramowicz *et al.*, [ZEUS Collab.], Phys. Lett. **B691**, 127 (2010) [arXiv:1003.2923 [hep-ex]].
201. S. Chekanov *et al.*, [ZEUS Collab.], Nucl. Phys. **B792**, 1 (2008) [arXiv:0707.3749 [hep-ex]].
202. S. Chekanov *et al.*, [ZEUS Collab.], Phys. Rev. **D76**, 072011 (2007) [arXiv:0706.3809 [hep-ex]].
203. A. Aktas *et al.*, [H1 Collab.], Phys. Lett. **B639**, 21 (2006) [arXiv:hep-ex/0603014].
204. F.D. Aaron *et al.*, [H1 Collab.], Eur. Phys. J. **C70**, 15 (2010) [arXiv:1006.0946 [hep-ex]].
205. H. Abramowicz *et al.*, [ZEUS Collab.], Eur. Phys. J. **C71**, 1659 (2011) [arXiv:1104.5444 [hep-ex]].
206. A. Abulencia *et al.*, [CDF - Run II Collab.], Phys. Rev. **D75**, 092006 (2007) [Erratum-*ibid.* 119901] [arXiv:hep-ex/0701051].
207. V.M. Abazov *et al.*, [D0 Collab.], Phys. Rev. Lett. **101**, 062001 (2008) [arXiv:0802.2400 [hep-ex]].
208. V.M. Abazov *et al.*, [D0 Collab.], [arXiv:1110.3771 [hep-ex]].
209. G. Aad *et al.*, [Atlas Collab.], Eur. Phys. J. **C71**, 1512 (2011) [arXiv:1009.5908 [hep-ex]].
210. S. Chatrchyan *et al.*, [CMS Collab.], [arXiv:1106.0208 [hep-ex]].
211. M. Wobisch *et al.*, [fastNLO Collab.], [arXiv:1109.1310 [hep-ph]].
212. T. Aaltonen *et al.*, [CDF Collab.], Phys. Rev. **D79**, 112002 (2009) [arXiv:0812.4036 [hep-ex]].
213. V.M. Abazov *et al.*, [D0 Collab.], Phys. Rev. Lett. **103**, 191803 (2009) [arXiv:0906.4819 [hep-ex]].
214. V.M. Abazov *et al.*, [D0 Collab.], Phys. Lett. **B693**, 531 (2010) [arXiv:1002.4594 [hep-ex]].
215. S. Chatrchyan *et al.*, [CMS Collab.], Phys. Lett. **B700**, 187 (2011) [arXiv:1104.1693 [hep-ex]].
216. V. Khachatryan *et al.*, [CMS Collab.], Phys. Rev. Lett. **106**, 201804 (2011) [arXiv:1102.2020 [hep-ex]].
217. G. Aad *et al.*, [ATLAS Collab.], New J. Phys. **13**, 053044 (2011) [arXiv:1103.3864 [hep-ex]].
218. V.M. Abazov *et al.*, [D0 Collab.], Phys. Rev. Lett. **94**, 221801 (2005) [arXiv:hep-ex/0409040].
219. G. Aad *et al.*, [ATLAS Collab.], Phys. Rev. Lett. **106**, 172002 (2011) [arXiv:1102.2696 [hep-ex]].
220. V. Khachatryan *et al.*, [CMS Collab.], Phys. Rev. Lett. **106**, 122003 (2011) [arXiv:1101.5029 [hep-ex]].
221. V.M. Abazov *et al.*, [D0 Collab.], Phys. Lett. **B704**, 434 (2011) [arXiv:1104.1986 [hep-ex]].
222. ATLAS Collab., [arXiv:1107.2092 [hep-ex]].
223. S. Chatrchyan *et al.*, [CMS Collab.], Phys. Lett. **B702**, 336 (2011) [arXiv:1106.0647 [hep-ex]].
224. V.M. Abazov *et al.*, [D0 Collab.], Phys. Lett. **B666**, 435 (2008) [arXiv:0804.1107 [hep-ex]].
225. V.M. Abazov *et al.*, [D0 Collab.], Phys. Lett. **B669**, 278 (2008) [arXiv:0808.1296 [hep-ex]].
226. V.M. Abazov *et al.*, [D0 Collab.], Phys. Rev. Lett. **678**, 45 (2009) [arXiv:0903.1748 [hep-ex]].
227. T. Aaltonen *et al.*, [CDF Collab.], Phys. Rev. Lett. **100**, 102001 (2008) [arXiv:0711.3717 [hep-ex]].
228. T. Aaltonen *et al.*, [CDF Collab.], Phys. Rev. **D77**, 011108 (2008) [arXiv:0711.4044 [hep-ex]].
229. V.M. Abazov *et al.*, [D0 Collab.], Phys. Lett. **B682**, 370 (2010) [arXiv:0907.4286 [hep-ex]].
230. V.M. Abazov *et al.*, [D0 Collab.], Phys. Rev. Lett. **106**, 122001 (2011) [arXiv:1010.0262 [hep-ex]].
231. V.M. Abazov *et al.*, [D0 Collab.], [arXiv:1106.1457 [hep-ex]].
232. G. Aad *et al.*, [ATLAS Collab.], Phys. Lett. **B698**, 325 (2011) [arXiv:1012.5382 [hep-ex]].
233. G. Aad *et al.*, [ATLAS Collab.], [arXiv:1107.2381 [hep-ex]].
234. CDF Collab., public note 8418, July 2006; see also [http://www-cdf.fnal.gov/physics/new/qcd/abstracts/bjet\\_05.html](http://www-cdf.fnal.gov/physics/new/qcd/abstracts/bjet_05.html).
235. V.M. Abazov *et al.*, [D0 Collab.], Phys. Rev. Lett. **102**, 192002 (2009) [arXiv:0901.0739 [hep-ex]].
236. V.M. Abazov *et al.*, [D0 Collab.], Phys. Lett. **B666**, 23 (2008) [arXiv:0803.2259 [hep-ex]].
237. T. Aaltonen *et al.*, [CDF Collab.], Phys. Rev. Lett. **100**, 091803 (2008) [arXiv:0711.2901 [hep-ex]].

238. T. Aaltonen *et al.*, [CDF Collab.], Phys. Rev. **D79**, 052008 (2009) [arXiv:0812.4458 [hep-ex]].
239. T. Aaltonen *et al.*, [CDF Collab.], Phys. Rev. Lett. **104**, 131801 (2010) [arXiv:0909.1505 [hep-ex]].
240. V. M. Abazov *et al.* [ D0 Collab. ], Phys. Rev. **D83**, 031105 (2011) [arXiv:1010.6203 [hep-ex]].
241. G. Aad *et al.* [ATLAS Collab.] Phys. Lett. **B707**, 418 (2012) [arXiv:1109.1470 [hep-ex]].
242. G. Aad *et al.* [ATLAS Collab.] Phys. Lett. **B706**, 295 (2012) [arXiv:1109.1403 [hep-ex]].
243. S. Bethke, Prog. in Part. Nucl. Phys. **58**, 351 (2007) [arXiv:hep-ex/0606035].
244. S. Bethke, Eur. Phys. J. **C64**, 689 (2009) arXiv:0908.1135 [hep-ph].
245. S. Bethke, J. Phys. **G26**, R27 (2000) [arXiv:hep-ex/0004021].
246. M. Beneke and M. Jamin, JHEP **0809**, 044 (2008) [arXiv:0806.3156 [hep-ph]].
247. M. Davier *et al.*, Eur. Phys. J. **C56**, 305 (2008) [arXiv:0803.0979 [hep-ph]].
248. K. Maltman and T. Yavin, Phys. Rev. **D78**, 094020 (2008) [arXiv:0807.0650 [hep-ph]].
249. S. Narison, Phys. Lett. **B673**, 30 (2009) [arXiv:0901.3823 [hep-ph]].
250. I. Caprini and J. Fischer, Eur. Phys. J. **C64**, 35 (2009) [arXiv:0906.5211 [hep-ph]].
251. S. Menke, arXiv:0904.1796 [hep-ph].
252. A. Pich, arXiv:1107.1123 [hep-ph].
253. B.A. Magradze, arXiv:1112.5958 [hep-ph].
254. G. Abbas *et al.*, arXiv:1202.2672 [hep-ph].
255. D. Boito *et al.*, Phys. Rev. **D84**, 113006 (2011) arXiv:1110.1127 [hep-ph].
256. D. Boito *et al.*, arXiv:1203.3146 [hep-ph].
257. C. McNeile *et al.*, [HPQCD Collab.], Phys. Rev. **D82**, 034512 (2010) [arXiv:1004.4285 [hep-lat]].
258. C.T.H. Davies *et al.*, [HPQCD Collab., UKQCD Collab., and MILC Collab.], Phys. Rev. Lett. **92**, 022001 (2004) [arXiv:hep-lat/0304004].
259. K. Maltman, *et al.*, Phys. Rev. **D78**, 114504 (2008) [arXiv:0807.2020 [hep-lat]].
260. S. Aoki *et al.*, [PACS-CS Collab.], JHEP **0910**, 053 (2009), [arXiv:0906.3906 [hep-lat]].
261. E. Shintani *et al.*, [JLQCD Collab.], Phys. Rev. **D82**, 074505 (2010), [arXiv:1002.0371 [hep-lat]].
262. B. Blossier *et al.*, [ETM Collab.], arXiv:1201.5770 [hep-ph].
263. C. Glasman [H1 Collab. and ZEUS Collab.], J. Phys. Conf. Ser. **110** 022013 (2008) arXiv:0709.4426 [hep-ex]].
264. J. Blumlein, H. Bottcher, and A. Guffanti, Nucl. Phys. **B774**, 182 (2007) [arXiv:hep-ph/0607200].
265. S. Alekhin *et al.*, Phys. Rev. **D81**, 014032 (2010) [arXiv:0908.2766 [hep-ph]].
266. S. Alekhin, J. Blumlein, and S. Moch, arXiv:1202.2282 [hep-ph].
267. P. Jimenez-Delgado and E. Reya, Phys. Rev. **D79**, 074023 (2009) [arXiv:0810.4274 [hep-ph]].
268. A.D. Martin *et al.*, Eur. Phys. J. **C64**, 653 (2009) [arXiv:0905.3531 [hep-ph]].
269. R.D. Ball *et al.*, Phys. Lett. **B707**, 66 (2012) [arXiv:1110.2483 [hep-ph]].
270. R.S. Thorne, G. Watt, JHEP **1108**, 100 (2011) [arXiv:1106.5789 [hep-ph]].
271. S. Alekhin, J. Blumlein, and S.Moch, Eur. Phys. J. **C71**, 1723 (2011) [arXiv:1101.5261 [hep-ph]].
272. R.D. Ball *et al.*, Phys. Lett. **B704**, 36 (2011) [arXiv:1102.3182 [hep-ph]].
273. N. Brambilla *et al.*, Phys. Rev. **D75**, 074014 (2007) [arXiv:hep-ph/0702079].
274. G. Dissertori *et al.*, JHEP **0908**, 036 (2009) [arXiv:0906.3436 [hep-ph]].
275. G. Abbiendi *et al.*, Eur. Phys. J. **C71**, 1733 (2011), [arXiv:1101.1470 [hep-ex]].
276. S. Bethke *et al.*, [JADE Collab.], Eur. Phys. J. **C64**, 351 (2009) [arXiv:0810.1389 [hep-ex]].
277. G. Dissertori *et al.*, Phys. Rev. Lett. **104**, 072002 (2010) [arXiv:0910.4283 [hep-ph]].
278. R. Abbate *et al.*, Phys. Rev. **D83**, 074021 (2011) [arXiv:1006.3080 [hep-ph]].
279. M. Abazov *et al.*, D0 Collab., Phys. Rev. **D80**, 111107 (2009) [arXiv:0911.2710 [hep-ex]].
280. H. Flacher *et al.*, Eur. Phys. J. **C60**, 543 (2009), [arXiv:0811.0009 [hep-ph]].
281. M. Schmelling, Phys. Scripta **51**, 676 (1995).
282. S. Bethke *et al.*, *Workshop on precision measurements of  $\alpha_s$* , Munich, Feb. 9-11, 2011 [ arXiv:1110.0016 [hep-ph]].

## 10. ELECTROWEAK MODEL AND CONSTRAINTS ON NEW PHYSICS

Revised December 2011 by J. Erler (U. Mexico and Institute for Advanced Study) and P. Langacker (Princeton University and Institute for Advanced Study).

- 10.1 Introduction
- 10.2 Renormalization and radiative corrections
- 10.3 Low energy electroweak observables
- 10.4  $W$  and  $Z$  boson physics
- 10.5 Precision flavor physics
- 10.6 Experimental results
- 10.7 Constraints on new physics

### 10.1. Introduction

The standard model of the electroweak interactions (SM) [1] is based on the gauge group  $SU(2) \times U(1)$ , with gauge bosons  $W_\mu^i$ ,  $i = 1, 2, 3$ , and  $B_\mu$  for the  $SU(2)$  and  $U(1)$  factors, respectively, and the corresponding gauge coupling constants  $g$  and  $g'$ . The left-handed fermion fields of the  $i^{\text{th}}$  fermion family transform as doublets

$\Psi_i = \begin{pmatrix} \nu_i \\ \ell_i^- \end{pmatrix}$  and  $\begin{pmatrix} u_i \\ d_i^- \end{pmatrix}$  under  $SU(2)$ , where  $d_i' \equiv \sum_j V_{ij} d_j$ , and  $V$  is the Cabibbo-Kobayashi-Maskawa mixing matrix. (Constraints on  $V$  and tests of universality are discussed in Ref. 2 and in the Section on “The CKM Quark-Mixing Matrix”. The extension of the formalism to allow an analogous leptonic mixing matrix is discussed in the Section on “Neutrino Mass, Mixing, and Oscillations”.) The right-handed fields are  $SU(2)$  singlets. In the minimal model there are three fermion families.

A complex scalar Higgs doublet,  $\phi \equiv \begin{pmatrix} \phi^+ \\ \phi^0 \end{pmatrix}$ , is added to the model for mass generation through spontaneous symmetry breaking with potential\* given by,

$$V(\phi) = \mu^2 \phi^\dagger \phi + \frac{\lambda^2}{2} (\phi^\dagger \phi)^2. \quad (10.1)$$

For  $\mu^2$  negative,  $\phi$  develops a vacuum expectation value,  $v/\sqrt{2}$ , where  $v \approx 246.22$  GeV, breaking part of the electroweak (EW) gauge symmetry, after which only one neutral Higgs scalar,  $H$ , remains in the physical particle spectrum. In non-minimal models there are additional charged and neutral scalar Higgs particles [3].

After the symmetry breaking the Lagrangian for the fermion fields,  $\psi_i$ , is

$$\begin{aligned} \mathcal{L}_F = & \sum_i \bar{\psi}_i \left( i \not{\partial} - m_i - \frac{gm_i H}{2M_W} \right) \psi_i \\ & - \frac{g}{2\sqrt{2}} \sum_i \bar{\Psi}_i \gamma^\mu (1 - \gamma^5) (T^+ W_\mu^+ + T^- W_\mu^-) \Psi_i \\ & - e \sum_i q_i \bar{\psi}_i \gamma^\mu \psi_i A_\mu \\ & - \frac{g}{2 \cos \theta_W} \sum_i \bar{\psi}_i \gamma^\mu (g_V^i - g_A^i \gamma^5) \psi_i Z_\mu. \end{aligned} \quad (10.2)$$

$\theta_W \equiv \tan^{-1}(g'/g)$  is the weak angle;  $e = g \sin \theta_W$  is the positron electric charge; and  $A \equiv B \cos \theta_W + W^3 \sin \theta_W$  is the photon field ( $\gamma$ ).  $W^\pm \equiv (W^1 \mp iW^2)/\sqrt{2}$  and  $Z \equiv -B \sin \theta_W + W^3 \cos \theta_W$  are the charged and neutral weak boson fields, respectively. The Yukawa coupling of  $H$  to  $\psi_i$  in the first term in  $\mathcal{L}_F$ , which is flavor diagonal in the minimal model, is  $gm_i/2M_W$ . The boson masses in the EW sector are given (at tree level, *i.e.*, to lowest order in perturbation theory) by,

$$M_H = \lambda v, \quad (10.3a)$$

$$M_W = \frac{1}{2} g v = \frac{e v}{2 \sin \theta_W}, \quad (10.3b)$$

$$M_Z = \frac{1}{2} \sqrt{g^2 + g'^2} v = \frac{e v}{2 \sin \theta_W \cos \theta_W} = \frac{M_W}{\cos \theta_W}, \quad (10.3c)$$

$$M_\gamma = 0. \quad (10.3d)$$

\* There is no generally accepted convention to write the quartic term. Our numerical coefficient simplifies Eq. (10.3a) below and the squared coupling preserves the relation between the number of external legs and the power counting of couplings at a given loop order. This structure also naturally emerges from physics beyond the SM, such as supersymmetry.

The second term in  $\mathcal{L}_F$  represents the charged-current weak interaction [4–7], where  $T^+$  and  $T^-$  are the weak isospin raising and lowering operators. For example, the coupling of a  $W$  to an electron and a neutrino is

$$-\frac{e}{2\sqrt{2} \sin \theta_W} \left[ W_\mu^- \bar{e} \gamma^\mu (1 - \gamma^5) \nu + W_\mu^+ \bar{\nu} \gamma^\mu (1 - \gamma^5) e \right]. \quad (10.4)$$

For momenta small compared to  $M_W$ , this term gives rise to the effective four-fermion interaction with the Fermi constant given by  $G_F/\sqrt{2} = 1/2v^2 = g^2/8M_W^2$ .  $CP$  violation is incorporated into the EW model by a single observable phase in  $V_{ij}$ .

The third term in  $\mathcal{L}_F$  describes electromagnetic interactions (QED) [8–10], and the last is the weak neutral-current interaction [5–7]. The vector and axial-vector couplings are

$$g_V^i \equiv t_{3L}(i) - 2q_i \sin^2 \theta_W, \quad (10.5a)$$

$$g_A^i \equiv t_{3L}(i), \quad (10.5b)$$

where  $t_{3L}(i)$  is the weak isospin of fermion  $i$  ( $+1/2$  for  $u_i$  and  $\nu_i$ ;  $-1/2$  for  $d_i$  and  $e_i$ ) and  $q_i$  is the charge of  $\psi_i$  in units of  $e$ .

The first term in Eq. (10.2) also gives rise to fermion masses, and in the presence of right-handed neutrinos to Dirac neutrino masses. The possibility of Majorana masses is discussed in the Section on “Neutrino Mass, Mixing, and Oscillations”.

### 10.2. Renormalization and radiative corrections

In addition to the Higgs boson mass,  $M_H$ , the fermion masses and mixings, and the strong coupling constant,  $\alpha_s$ , the SM has three parameters. A particularly useful set contains the  $Z$  mass\*\*, the Fermi constant, and the fine structure constant, which will be discussed in turn:

The  $Z$  boson mass,  $M_Z = 91.1876 \pm 0.0021$  GeV, has been determined from the  $Z$  lineshape scan at LEP 1 [11].

The Fermi constant,  $G_F = 1.1663787(6) \times 10^{-5}$  GeV<sup>-2</sup>, is derived from the muon lifetime formula\*\*\*,

$$\frac{\hbar}{\tau_\mu} = \frac{G_F^2 m_\mu^5}{192\pi^3} F(\rho) \left[ 1 + H_1(\rho) \frac{\hat{\alpha}(m_\mu)}{\pi} + H_2(\rho) \frac{\hat{\alpha}^2(m_\mu)}{\pi^2} \right], \quad (10.6)$$

where  $\rho = m_e^2/m_\mu^2$ , and where

$$F(\rho) = 1 - 8\rho + 8\rho^3 - \rho^4 - 12\rho^2 \ln \rho = 0.99981295, \quad (10.7a)$$

$$\begin{aligned} H_1(\rho) = & \frac{25}{8} - \frac{\pi^2}{2} - \left( 9 + 4\pi^2 + 12 \ln \rho \right) \rho \\ & + 16\pi^2 \rho^{3/2} + \mathcal{O}(\rho^2) = -1.80793, \end{aligned} \quad (10.7b)$$

$$\begin{aligned} H_2(\rho) = & \frac{156815}{5184} - \frac{518}{81} \pi^2 - \frac{895}{36} \zeta(3) + \frac{67}{720} \pi^4 + \frac{53}{6} \pi^2 \ln 2 \\ & - (0.042 \pm 0.002)_{\text{had}} - \frac{5}{4} \pi^2 \sqrt{\rho} + \mathcal{O}(\rho) = 6.64, \end{aligned} \quad (10.7c)$$

$$\hat{\alpha}(m_\mu)^{-1} = \alpha^{-1} + \frac{1}{3\pi} \ln \rho + \mathcal{O}(\alpha) = 135.901 \quad (10.7d)$$

The massless corrections to  $H_1$  and  $H_2$  have been obtained in Refs. 13 and 14, respectively, where the term in parentheses is from the hadronic vacuum polarization [14]. The mass corrections to  $H_1$  have been known for some time [15], while those to  $H_2$  are more recent [16]. Notice the term linear in  $m_e$  whose appearance was

\*\* We emphasize that in the fits described in Sec. 10.6 and Sec. 10.7 the values of the SM parameters are affected by all observables that depend on them. This is of no practical consequence for  $\alpha$  and  $G_F$ , however, since they are very precisely known.

\*\*\* In the spirit of the Fermi theory, we incorporated the small propagator correction,  $3/5 m_\mu^2/M_W^2$ , into  $\Delta r$  (see below). This is also the convention adopted by the MuLan collaboration [12]. While this breaks with historical consistency, the numerical difference was negligible in the past.

unforeseen and can be traced to the use of the muon pole mass in the prefactor [16]. The remaining uncertainty in  $G_F$  is experimental and has recently been reduced by an order of magnitude by the MuLan collaboration [12] at the PSI.

The fine structure constant,  $\alpha = 1/137.035999074(44)$ , is currently dominated by the  $e^\pm$  anomalous magnetic moment [10]. In most EW renormalization schemes, it is convenient to define a running  $\alpha$  dependent on the energy scale of the process, with  $\alpha^{-1} \sim 137$  appropriate at very low energy, *i.e.* close to the Thomson limit. (The running has also been observed [17] directly.) For scales above a few hundred MeV this introduces an uncertainty due to the low energy hadronic contribution to vacuum polarization. In the modified minimal subtraction ( $\overline{\text{MS}}$ ) scheme [18] (used for this *Review*), and with  $\alpha_s(M_Z) = 0.120$ , we have  $\hat{\alpha}(m_\tau)^{-1} = 133.471 \pm 0.014$  and  $\hat{\alpha}(M_Z)^{-1} = 127.944 \pm 0.014$ . (In this Section we denote quantities defined in the modified minimal subtraction ( $\overline{\text{MS}}$ ) scheme by a caret; the exception is the strong coupling constant,  $\alpha_s$ , which will always correspond to the  $\overline{\text{MS}}$  definition and where the caret will be dropped.) The latter corresponds to a quark sector contribution (without the top) to the conventional (on-shell) QED coupling,  $\alpha(M_Z) = \frac{\alpha}{1 - \Delta\alpha(M_Z)}$ ,

of  $\Delta\alpha_{\text{had}}^{(5)}(M_Z) \approx 0.02772 \pm 0.00010$ . These values are updated from Ref. 19 with  $\Delta\alpha_{\text{had}}^{(5)}(M_Z)$  moved downwards and its uncertainty halved (partly due to a more precise charm quark mass). Its correlation with the  $\mu^\pm$  anomalous magnetic moment (see Sec. 10.5), as well as the non-linear  $\alpha_s$  dependence of  $\hat{\alpha}(M_Z)$  and the resulting correlation with the input variable  $\alpha_s$ , are fully taken into account in the fits. This is done by using as actual input (fit constraint) instead of  $\Delta\alpha_{\text{had}}^{(5)}(M_Z)$  the analogous low energy contribution by the three light quarks,  $\Delta\alpha_{\text{had}}^{(3)}(1.8 \text{ GeV}) = (55.50 \pm 0.78) \times 10^{-4}$  [20], and by calculating the perturbative and heavy quark contributions to  $\hat{\alpha}(M_Z)$  in each call of the fits according to Ref. 19. Part of the uncertainty ( $\pm 0.49 \times 10^{-4}$ ) is from  $e^+e^-$  annihilation data below 1.8 GeV and  $\tau$  decay data (including uncertainties from isospin breaking effects), but uncalculated higher order perturbative ( $\pm 0.41 \times 10^{-4}$ ) and non-perturbative ( $\pm 0.44 \times 10^{-4}$ ) QCD corrections and the  $\overline{\text{MS}}$  quark mass values (see below) also contribute. Various recent evaluations of  $\Delta\alpha_{\text{had}}^{(5)}$  are summarized in Table 10.1, where the leading order relation<sup>†</sup> between the  $\overline{\text{MS}}$  and on-shell definitions is given by,

$$\Delta\hat{\alpha}(M_Z) - \Delta\alpha(M_Z) = \frac{\alpha}{\pi} \left( \frac{100}{27} - \frac{1}{6} - \frac{7}{4} \ln \frac{M_Z^2}{M_W^2} \right) \approx 0.0072, \quad (10.8)$$

and where the first term is from fermions and the other two are from  $W^\pm$  loops which are usually excluded from the on-shell definition. Most of the older results relied on  $e^+e^- \rightarrow$  hadrons cross-section measurements up to energies of 40 GeV, which were somewhat higher than the QCD prediction, suggested stronger running, and were less precise. The most recent results typically assume the validity of perturbative QCD (PQCD) at scales of 1.8 GeV and above, and are in reasonable agreement with each other. There is, however, some discrepancy between analyses based on  $e^+e^- \rightarrow$  hadrons cross-section data and those based on  $\tau$  decay spectral functions [20]. The latter utilize data from OPAL [43], CLEO [44], ALEPH [45], and Belle [46] and imply lower central values for the extracted  $M_H$  of about 6%. This discrepancy is smaller than in the past and at least some of it appears to be experimental. The dominant  $e^+e^- \rightarrow \pi^+\pi^-$  cross-section was measured with the CMD-2 [47] and SND [48] detectors at the VEPP-2M  $e^+e^-$  collider at Novosibirsk and the results are (after an initial discrepancy due to a flaw in the Monte Carlo event generator used by SND) in good agreement with each other. As an alternative to cross-section scans, one can use the high statistics radiative return events at  $e^+e^-$  accelerators operating at resonances such as the  $\Phi$  or the  $\Upsilon(4S)$ . The method [49] is systematics limited but dominates

<sup>†</sup> Eq. (10.8) is for illustration only. Higher order contributions are directly evaluated in the  $\overline{\text{MS}}$  scheme using the FORTRAN package GAPP [21], including three-loop QED contributions of both leptons and quarks. The leptonic three-loop contribution in the on-shell scheme has been obtained in Ref. 22.

over the Novosibirsk data throughout. The BaBar collaboration [50] studied multi-hadron events radiatively returned from the  $\Upsilon(4S)$ , reconstructing the radiated photon and normalizing to  $\mu^\pm\gamma$  final states. Their result is higher compared to VEPP-2M and in fact agrees quite well with the  $\tau$  analysis including the energy dependence (shape). In contrast, the shape and smaller overall cross-section from the  $\pi^+\pi^-$  radiative return results from the  $\Phi$  obtained by the KLOE collaboration [51] differs significantly from what is observed by BaBar. The discrepancy originates from the kinematic region  $\sqrt{s} \gtrsim 0.6 \text{ GeV}$ , and is most pronounced for  $\sqrt{s} \gtrsim 0.85 \text{ GeV}$ . All measurements including older data [52] and multi-hadron final states (there are also discrepancies in the  $e^+e^- \rightarrow 2\pi^+2\pi^-$  channel [20]) are accounted for and corrections have been applied for missing channels [20]. Further improvement of this dominant theoretical uncertainty in the interpretation of precision data will require better measurements of the cross-section for  $e^+e^- \rightarrow$  hadrons below the charmonium resonances including multi-pion and other final states. To improve the precisions in  $\hat{m}_c(\hat{m}_c)$  and  $\hat{m}_b(\hat{m}_b)$  it would help to remeasure the threshold regions of the heavy quarks as well as the electronic decay widths of the narrow  $c\bar{c}$  and  $b\bar{b}$  resonances.

Further free parameters entering into Eq. (10.2) are the quark and lepton masses, where  $m_i$  is the mass of the  $i^{\text{th}}$  fermion  $\psi_i$ . For the quarks these are the current masses. For the light quarks, as described in the note on “Quark Masses” in the Quark Listings,  $\hat{m}_u = 2.5_{-0.8}^{+0.6} \text{ MeV}$ ,  $\hat{m}_d = 5.0_{-0.9}^{+0.7} \text{ MeV}$ , and  $\hat{m}_s = 100_{-20}^{+30} \text{ MeV}$ . These are running  $\overline{\text{MS}}$  masses evaluated at the scale  $\mu = 2 \text{ GeV}$ . For the heavier quarks we use QCD sum rule [53] constraints [54] and recalculate their masses in each call of our fits to account for their direct  $\alpha_s$  dependence. We find<sup>‡</sup>,  $\hat{m}_c(\mu = \hat{m}_c) = 1.267_{-0.040}^{+0.032} \text{ GeV}$  and  $\hat{m}_b(\mu = \hat{m}_b) = 4.197 \pm 0.025 \text{ GeV}$ , with a correlation of 24%.

The top quark “pole” mass (the quotation marks are a reminder that quarks do not form asymptotic states),  $m_t = 173.4 \pm 0.9 \text{ GeV}$ , is an average of published and preliminary CDF and DØ results from run I and II [56] with first results by the CMS [57] and ATLAS [58] collaborations averaged in ignoring correlations. To gauge the possible impact of the neglect of correlations involving the LHC experiments, we also averaged the results conservatively assuming that the entire 0.75 GeV systematic of the Tevatron average is fully correlated with a 0.75 GeV component in both CMS and ATLAS. Incidentally, this yields correlations of similar size as those between the two Tevatron experiments and the two Runs and reduces the central value by 0.15 GeV. Within round-off we expect a more refined average to coincide with ours. Our average<sup>§</sup> differs slightly from the value,  $m_t = 173.5 \pm 0.6 \pm 0.8 \text{ GeV}$ , which appears in the top quark Listings in this *Review* and which is based exclusively on published results. We are working, however, with  $\overline{\text{MS}}$  masses in all expressions to minimize theoretical uncertainties. Such a short distance mass definition (unlike the pole mass) is free from non-perturbative and renormalon [59] uncertainties. We therefore convert to the top quark  $\overline{\text{MS}}$  mass,

$$\hat{m}_t(\mu = \hat{m}_t) = m_t \left[ 1 - \frac{4}{3} \frac{\alpha_s}{\pi} + \mathcal{O}(\alpha_s^2) \right], \quad (10.9)$$

using the three-loop formula [60]. This introduces an additional uncertainty which we estimate to 0.5 GeV (the size of the three-loop term) and add in quadrature to the experimental pole mass error. This is convenient because we use the pole mass as an external constraint while fitting to the  $\overline{\text{MS}}$  mass. We are assuming that the kinematic

<sup>‡</sup> Other authors [55] advocate to evaluate and quote  $\hat{m}_c(\mu = 3 \text{ GeV})$  instead. We use  $\hat{m}_c(\mu = \hat{m}_c)$  because in the global analysis it is convenient to nullify any explicitly  $m_c$  dependent logarithms. Note also that our uncertainty for  $m_c$  (and to a lesser degree for  $m_b$ ) is larger than the one in Ref. 55, for example. The reason is that we determine the continuum contribution for charm pair production using only resonance data and theoretical consistency across various sum rule moments, and then use any difference to the experimental continuum data as an additional uncertainty. We also include an uncertainty for the condensate terms which grows rapidly for higher moments in the sum rule analysis.

<sup>§</sup> At the time of writing this review, the efforts to establish a top quark averaging group involving both the Tevatron and the LHC were still in progress. Therefore we perform a simplified average ourselves.

mass extracted from the collider events corresponds within this uncertainty to the pole mass. Using the BLM optimized [61] version of the two-loop perturbative QCD formula [62] (as we did in previous editions of this *Review*) gives virtually identical results. In summary, we will use  $m_t = 173.4 \pm 0.9$  (exp.)  $\pm 0.5$  (QCD) GeV =  $173.4 \pm 1.0$  GeV (together with  $M_H = 117$  GeV) for the numerical values quoted in Sec. 10.2–Sec. 10.5.

$\sin^2 \theta_W$  and  $M_W$  can be calculated from  $M_Z$ ,  $\hat{\alpha}(M_Z)$ , and  $G_F$ , when values for  $m_t$  and  $M_H$  are given; conversely (as is done at present),  $M_H$  can be constrained by  $\sin^2 \theta_W$  and  $M_W$ . The value of  $\sin^2 \theta_W$  is extracted from neutral-current processes (see Sec. 10.3) and  $Z$  pole observables (see Sec. 10.4) and depends on the renormalization prescription. There are a number of popular schemes [63–70] leading to values which differ by small factors depending on  $m_t$  and  $M_H$ . The notation for these schemes is shown in Table 10.1.

**Table 10.1:** Notations used to indicate the various schemes discussed in the text. Each definition of  $\sin^2 \theta_W$  leads to values that differ by small factors depending on  $m_t$  and  $M_H$ . Approximate values are also given for illustration.

Scheme	Notation	Value
On-shell	$s_W^2$	0.2231
NOV	$s_{M_Z}^2$	0.2310
$\overline{\text{MS}}$	$\hat{s}_Z^2$	0.2312
$\overline{\text{MS}}$ ND	$\hat{s}_{\text{ND}}^2$	0.2314
Effective angle	$\hat{s}_f^2$	0.2315

- (i) The on-shell scheme [63] promotes the tree-level formula  $\sin^2 \theta_W = 1 - M_W^2/M_Z^2$  to a definition of the renormalized  $\sin^2 \theta_W$  to all orders in perturbation theory, *i.e.*,  $\sin^2 \theta_W \rightarrow s_W^2 \equiv 1 - M_W^2/M_Z^2$ :

$$M_W = \frac{A_0}{s_W(1 - \Delta r)^{1/2}}, \quad M_Z = \frac{M_W}{c_W}, \quad (10.10)$$

where  $c_W \equiv \cos \theta_W$ ,  $A_0 = (\pi\alpha/\sqrt{2}G_F)^{1/2} = 37.28039(1)$  GeV, and  $\Delta r$  includes the radiative corrections relating  $\alpha$ ,  $\alpha(M_Z)$ ,  $G_F$ ,  $M_W$ , and  $M_Z$ . One finds  $\Delta r \sim \Delta r_0 - \rho_t/\tan^2 \theta_W$ , where  $\Delta r_0 = 1 - \alpha/\hat{\alpha}(M_Z) = 0.06635(10)$  is due to the running of  $\alpha$ , and  $\rho_t = 3G_F m_t^2/8\sqrt{2}\pi^2 = 0.00943(m_t/173.4 \text{ GeV})^2$  represents the dominant (quadratic)  $m_t$  dependence. There are additional contributions to  $\Delta r$  from bosonic loops, including those which depend logarithmically on  $M_H$ . One has  $\Delta r = 0.0358 \mp 0.0004 \pm 0.00010$ , where the first uncertainty is from  $m_t$  and the second is from  $\alpha(M_Z)$ . Thus the value of  $s_W^2$  extracted from  $M_Z$  includes an uncertainty ( $\mp 0.00012$ ) from the currently allowed range of  $m_t$ . This scheme is simple conceptually. However, the relatively large ( $\sim 3\%$ ) correction from  $\rho_t$  causes large spurious contributions in higher orders.

- (ii) A more precisely determined quantity  $s_{M_Z}^2$  [64] can be obtained from  $M_Z$  by removing the  $(m_t, M_H)$  dependent term from  $\Delta r$  [65], *i.e.*,

$$s_{M_Z}^2(1 - s_{M_Z}^2) \equiv \frac{\pi\alpha(M_Z)}{\sqrt{2}G_F M_Z^2}. \quad (10.11)$$

Using  $\alpha(M_Z)^{-1} = 128.93 \pm 0.02$  yields  $s_{M_Z}^2 = 0.23102 \mp 0.00005$ . The small uncertainty in  $s_{M_Z}^2$  compared to other schemes is because the  $m_t$  dependence has been removed by definition. However, the  $m_t$  uncertainty reemerges when other quantities (*e.g.*,  $M_W$  or other  $Z$  pole observables) are predicted in terms of  $M_Z$ .

Both  $s_W^2$  and  $s_{M_Z}^2$  depend not only on the gauge couplings but also on the spontaneous-symmetry breaking, and both definitions are awkward in the presence of any extension of the SM which perturbs the value of  $M_Z$  (or  $M_W$ ). Other definitions are motivated by the tree-level coupling constant definition  $\theta_W = \tan^{-1}(g'/g)$ :

- (iii) In particular, the modified minimal subtraction ( $\overline{\text{MS}}$ ) scheme introduces the quantity  $\sin^2 \hat{\theta}_W(\mu) \equiv \hat{g}'^2(\mu)/[\hat{g}^2(\mu) + \hat{g}'^2(\mu)]$ , where the couplings  $\hat{g}$  and  $\hat{g}'$  are defined by modified minimal subtraction and the scale  $\mu$  is conveniently chosen to be  $M_Z$  for many EW processes. The value of  $\hat{s}_Z^2 = \sin^2 \hat{\theta}_W(M_Z)$  extracted from  $M_Z$  is less sensitive than  $s_W^2$  to  $m_t$  (by a factor of  $\tan^2 \theta_W$ ), and is less sensitive to most types of new physics than  $s_W^2$  or  $s_{M_Z}^2$ . It is also very useful for comparing with the predictions of grand unification. There are actually several variant definitions of  $\sin^2 \hat{\theta}_W(M_Z)$ , differing according to whether or how finite  $\alpha \ln(m_t/M_Z)$  terms are decoupled (subtracted from the couplings). One cannot entirely decouple the  $\alpha \ln(m_t/M_Z)$  terms from all EW quantities because  $m_t \gg m_b$  breaks SU(2) symmetry. The scheme that will be adopted here decouples the  $\alpha \ln(m_t/M_Z)$  terms from the  $\gamma$ - $Z$  mixing [18,66], essentially eliminating any  $\ln(m_t/M_Z)$  dependence in the formulae for asymmetries at the  $Z$  pole when written in terms of  $\hat{s}_Z^2$ . (A similar definition is used for  $\hat{\alpha}$ .) The various definitions are related by

$$\hat{s}_Z^2 = c(m_t, M_H)s_W^2 = \bar{c}(m_t, M_H)s_{M_Z}^2, \quad (10.12)$$

where  $c = 1.0362 \pm 0.0004$  and  $\bar{c} = 1.0009 \mp 0.0002$ . The quadratic  $m_t$  dependence is given by  $c \sim 1 + \rho_t/\tan^2 \theta_W$  and  $\bar{c} \sim 1 - \rho_t/(1 - \tan^2 \theta_W)$ , respectively. The expressions for  $M_W$  and  $M_Z$  in the  $\overline{\text{MS}}$  scheme are

$$M_W = \frac{A_0}{\hat{s}_Z(1 - \Delta \hat{r}_W)^{1/2}}, \quad M_Z = \frac{M_W}{\hat{\rho}^{1/2} \hat{c}_Z}, \quad (10.13)$$

and one predicts  $\Delta \hat{r}_W = 0.06951 \pm 0.00001 \pm 0.00010$ .  $\Delta \hat{r}_W$  has no quadratic  $m_t$  dependence, because shifts in  $M_W$  are absorbed into the observed  $G_F$ , so that the error in  $\Delta \hat{r}_W$  is dominated by  $\Delta r_0 = 1 - \alpha/\hat{\alpha}(M_Z)$  which induces the second quoted uncertainty. The quadratic  $m_t$  dependence has been shifted into  $\hat{\rho} \sim 1 + \rho_t$ , where including bosonic loops,  $\hat{\rho} = 1.01051 \pm 0.00011$ . Quadratic  $M_H$  effects are deferred to two-loop order, while the leading logarithmic  $M_H$  effect is a good approximation only for large  $M_H$  values which are clearly disfavored by the precision data. As an illustration, the shift in  $M_W$  due to a large  $M_H$  (for fixed  $M_Z$ ) is given by

$$\begin{aligned} \Delta_H M_W &= -\frac{11\alpha}{96\pi} \frac{M_W}{c_W^2 - s_W^2} \ln \frac{M_H^2}{M_W^2} + \mathcal{O}(\alpha^2) \\ &\sim -200 \text{ MeV (for } M_H = 10 M_W). \end{aligned} \quad (10.14)$$

- (iv) A variant  $\overline{\text{MS}}$  quantity  $\hat{s}_{\text{ND}}^2$  (used in the 1992 edition of this *Review*) does not decouple the  $\alpha \ln(m_t/M_Z)$  terms [67]. It is related to  $\hat{s}_Z^2$  by

$$\hat{s}_Z^2 = \hat{s}_{\text{ND}}^2 / \left(1 + \frac{\hat{\alpha}}{\pi} d\right), \quad (10.15a)$$

$$d = \frac{1}{3} \left( \frac{1}{\hat{s}_Z^2} - \frac{8}{3} \right) \left[ \left(1 + \frac{\alpha_s}{\pi}\right) \ln \frac{m_t}{M_Z} - \frac{15\alpha_s}{8\pi} \right], \quad (10.15b)$$

Thus,  $\hat{s}_Z^2 - \hat{s}_{\text{ND}}^2 \approx -0.0002$ .

- (v) Yet another definition, the effective angle [68–70]  $\hat{s}_f^2$  for the  $Z$  vector coupling to fermion  $f$ , is based on  $Z$  pole observables and described below.

Experiments are at such level of precision that complete  $\mathcal{O}(\alpha)$  radiative corrections must be applied. For neutral-current and  $Z$  pole processes, these corrections are conveniently divided into two classes:

1. QED diagrams involving the emission of real photons or the exchange of virtual photons in loops, but not including vacuum polarization diagrams. These graphs often yield finite and gauge-invariant contributions to observable processes. However, they are dependent on energies, experimental cuts, *etc.*, and must be calculated individually for each experiment.
2. EW corrections, including  $\gamma\gamma$ ,  $\gamma Z$ ,  $ZZ$ , and  $WW$  vacuum polarization diagrams, as well as vertex corrections, box graphs,



*etc.*, involving virtual  $W$  and  $Z$  bosons. The one-loop corrections are included for all processes, and certain two-loop corrections are also important. In particular, two-loop corrections involving the top quark modify  $\rho_t$  in  $\hat{\rho}$ ,  $\Delta r$ , and elsewhere by

$$\rho_t \rightarrow \rho_t [1 + R(M_H, m_t) \rho_t / 3]. \quad (10.16)$$

$R(M_H, m_t)$  is best described as an expansion in  $M_Z^2/m_t^2$ . The unsuppressed terms were first obtained in Ref. 71, and are known analytically [72]. Contributions suppressed by  $M_Z^2/m_t^2$  were first studied in Ref. 73 with the help of small and large Higgs mass expansions, which can be interpolated. These contributions are about as large as the leading ones in Refs. 71 and 72. The complete two-loop calculation of  $\Delta r$  (without further approximation) has been performed in Refs. 74 and 75 for fermionic and purely bosonic diagrams, respectively. Similarly, the EW two-loop calculation for the relation between  $\overline{s}_Z^2$  and  $s_W^2$  is complete [76] including the recently obtained purely bosonic contribution [77]. For  $M_H$  above its lower direct limit,  $-17 < R < -13$ .

Mixed QCD-EW contributions to gauge boson self-energies of order  $\alpha\alpha_s m_t^2$  [78] and  $\alpha\alpha_s^2 m_t^2$  [79] increase the predicted value of  $m_t$  by 6%. This is, however, almost entirely an artifact of using the pole mass definition for  $m_t$ . The equivalent corrections when using the  $\overline{\text{MS}}$  definition  $\hat{m}_t(\hat{m}_t)$  increase  $m_t$  by less than 0.5%. The subleading  $\alpha\alpha_s$  corrections [80] are also included. Further three-loop corrections of order  $\alpha\alpha_s^2$  [81],  $\alpha^3 m_t^6$  [82,83], and  $\alpha^2 \alpha_s m_t^4$  (for  $M_H = 0$ ) [82], are rather small. The same is true for  $\alpha^3 M_H^4$  [84] corrections unless  $M_H$  approaches 1 TeV. Also known are the singlet contributions (pure gluonic intermediate states) of order  $\alpha\alpha_s^2$  [85] and  $\alpha\alpha_s^3$  [86]. Recently, the corresponding non-singlet contributions have been computed as well [87].

The leading EW two-loop terms for the  $Z \rightarrow b\bar{b}$ -vertex of  $\mathcal{O}(\alpha^2 m_t^4)$  have been obtained in Refs. 71 and 72, and the mixed QCD-EW contributions in Refs. 88 and 89. The authors of Ref. 90 completed the two-loop EW fermionic corrections to  $\overline{s}_Z^2$ . The  $\mathcal{O}(\alpha\alpha_s)$ -vertex corrections involving massless quarks [91] add coherently, resulting in a sizable effect and shift  $\alpha_s(M_Z)$  when extracted from  $Z$  lineshape observables (see Sec. 10.4) by  $\approx +0.0007$ .

Many of the EW corrections are absorbed into the renormalized Fermi constant defined in Eq. (10.6). Others modify the tree-level expressions for  $Z$  pole observables and neutral-current amplitudes. In particular, the relations in Eq. (10.5) now read,

$$\overline{g}_V^f = \sqrt{\rho_f} (t_{3L}^{(f)} - 2q_f \kappa_f \sin^2 \theta_W), \quad \overline{g}_A^f = \sqrt{\rho_f} t_{3L}^{(f)}, \quad (10.17)$$

where the EW radiative corrections have been absorbed into corrections  $\rho_f - 1$  and  $\kappa_f - 1$ , which depend on the fermion  $f$  and on the renormalization scheme. In the on-shell scheme, the quadratic  $m_t$  dependence is given by  $\rho_f \sim 1 + \rho_t$ ,  $\kappa_f \sim 1 + \rho_t / \tan^2 \theta_W$ , while in  $\overline{\text{MS}}$ ,  $\hat{\rho}_f \sim \hat{\kappa}_f \sim 1$ , for  $f \neq b$  ( $\hat{\rho}_b \sim 1 - \frac{4}{3}\rho_t$ ,  $\hat{\kappa}_b \sim 1 + \frac{2}{3}\rho_t$ ). In the  $\overline{\text{MS}}$  scheme the normalization is changed according to  $G_F M_Z^2 / 2\sqrt{2}\pi \rightarrow \hat{\alpha} / 4\hat{s}_Z^2 \hat{c}_Z^2$ . (If one continues to normalize amplitudes by  $G_F M_Z^2 / 2\sqrt{2}\pi$ , as in the 1996 edition of this *Review*, then  $\hat{\rho}_f$  contains an additional factor of  $\hat{\rho}(1 - \Delta\hat{\rho}_W)\hat{\alpha}/\alpha$ .) In practice, additional bosonic and fermionic loops, vertex corrections, leading higher order contributions, *etc.*, must be included. For example, in the  $\overline{\text{MS}}$  scheme one has  $\hat{\rho}_\ell = 0.9981$ ,  $\hat{\kappa}_\ell = 1.0013$ ,  $\hat{\rho}_b = 0.9869$ , and  $\hat{\kappa}_b = 1.0067$ . It is convenient to define an effective angle  $\overline{s}_Z^2 \equiv \sin^2 \overline{\theta}_W \equiv \hat{\kappa}_f \hat{s}_Z^2 = \kappa_f s_W^2$ , in terms of which  $\overline{g}_V^f$  and  $\overline{g}_A^f$  are given by  $\sqrt{\rho_f}$  times their tree-level formulae. Because  $\overline{g}_V^f$  is very small, not only  $A_{LR}^0 = A_e, A_{FB}^{(0,\ell)}$ , and  $\mathcal{P}_\tau$ , but also  $A_{FB}^{(0,b)}, A_{FB}^{(0,c)}, A_{FB}^{(0,s)}$ , and the hadronic asymmetries are mainly sensitive to  $\overline{s}_Z^2$ . One finds that  $\hat{\kappa}_f$  ( $f \neq b$ ) is almost independent of  $(m_t, M_H)$ , so that one can write

$$\overline{s}_\ell^2 \sim \hat{s}_Z^2 + 0.00029. \quad (10.18)$$

Thus, the asymmetries determine values of  $\overline{s}_\ell^2$  and  $\hat{s}_Z^2$  almost independent of  $m_t$ , while the  $\kappa$ 's for the other schemes are  $m_t$  dependent.

**Table 10.2:** Standard Model expressions for the neutral-current parameters for  $\nu$ -hadron,  $\nu$ - $e$ , and  $e^-$ -scattering processes.

At tree level,  $\rho = \kappa = 1$ ,  $\lambda = 0$ . If radiative corrections are included,  $\rho_{\nu N} = 1.0082$ ,  $\hat{\kappa}_{\nu N}(\langle Q^2 \rangle = -20 \text{ GeV}^2) = 0.9972$ ,  $\hat{\kappa}_{\nu N}(\langle Q^2 \rangle = -35 \text{ GeV}^2) = 0.9965$ ,  $\lambda_{uL} = -0.0031$ ,  $\lambda_{dL} = -0.0025$  and  $\lambda_R = 3.7 \times 10^{-5}$ . For  $\nu$ - $e$  scattering,  $\rho_{\nu e} = 1.0128$  and  $\hat{\kappa}_{\nu e} = 0.9963$  (at  $\langle Q^2 \rangle = 0$ ). For atomic parity violation and the polarized DIS experiment at SLAC,  $\rho'_e = 0.9887$ ,  $\rho_e = 1.0007$ ,  $\hat{\kappa}'_e = 1.0038$ ,  $\hat{\kappa}_e = 1.0297$ ,  $\lambda' = -1.8 \times 10^{-5}$ ,  $\lambda_u = -0.0118$  and  $\lambda_d = 0.0029$ . And for polarized Møller scattering with SLAC (JLab) kinematics,  $\lambda_e = -0.0002$  ( $\lambda_e = -0.0004$ ). The dominant  $m_t$  dependence is given by  $\rho \sim 1 + \rho_t$ , while  $\hat{\kappa} \sim 1$  ( $\overline{\text{MS}}$ ) or  $\kappa \sim 1 + \rho_t / \tan^2 \theta_W$  (on-shell).

Quantity	Standard Model Expression
$\epsilon_L(u)$	$\rho_{\nu N} \left( \frac{1}{2} - \frac{2}{3} \hat{\kappa}_{\nu N} \hat{s}_Z^2 \right) + \lambda_{uL}$
$\epsilon_L(d)$	$\rho_{\nu N} \left( -\frac{1}{2} + \frac{1}{3} \hat{\kappa}_{\nu N} \hat{s}_Z^2 \right) + \lambda_{dL}$
$\epsilon_R(u)$	$\rho_{\nu N} \left( -\frac{2}{3} \hat{\kappa}_{\nu N} \hat{s}_Z^2 \right) + \lambda_R$
$\epsilon_R(d)$	$\rho_{\nu N} \left( \frac{1}{3} \hat{\kappa}_{\nu N} \hat{s}_Z^2 \right) + 2\lambda_R$
$g_V^{\nu e}$	$\rho_{\nu e} \left( -\frac{1}{2} + 2\hat{\kappa}_{\nu e} \hat{s}_Z^2 \right)$
$g_A^{\nu e}$	$\rho_{\nu e} \left( -\frac{1}{2} \right)$
$C_{1u}$	$\rho'_e \left( -\frac{1}{2} + \frac{4}{3} \hat{\kappa}'_e \hat{s}_Z^2 \right) + \lambda'$
$C_{1d}$	$\rho'_e \left( \frac{1}{2} - \frac{2}{3} \hat{\kappa}'_e \hat{s}_Z^2 \right) - 2\lambda'$
$C_{2u}$	$\rho_e \left( -\frac{1}{2} + 2\hat{\kappa}_e \hat{s}_Z^2 \right) + \lambda_u$
$C_{2d}$	$\rho_e \left( \frac{1}{2} - 2\hat{\kappa}_e \hat{s}_Z^2 \right) + \lambda_d$
$C_{2e}$	$\rho_e \left( \frac{1}{2} - 2\hat{\kappa}_e \hat{s}_Z^2 \right) + \lambda_e$

Throughout this *Review* we utilize EW radiative corrections from the program GAPP [21], which works entirely in the  $\overline{\text{MS}}$  scheme, and which is independent of the package ZFITTER [70]. Another resource is the recently developed modular fitting toolkit Gfitter [92].

### 10.3. Low energy electroweak observables

In the following we discuss EW precision observables obtained at low momentum transfers [6], *i.e.*  $Q^2 \ll M_Z^2$ . It is convenient to write the four-fermion interactions relevant to  $\nu$ -hadron,  $\nu$ - $e$ , as well as parity violating  $e$ -hadron and  $e$ - $e$  neutral-current processes in a form that is valid in an arbitrary gauge theory (assuming massless left-handed neutrinos). One has,

$$-\mathcal{L}^{\nu h} = \frac{G_F}{\sqrt{2}} \bar{\nu} \gamma^\mu (1 - \gamma^5) \nu \times \sum_i [\epsilon_L(i) \bar{q}_i \gamma_\mu (1 - \gamma^5) q_i + \epsilon_R(i) \bar{q}_i \gamma_\mu (1 + \gamma^5) q_i], \quad (10.19)$$

$$-\mathcal{L}^{\nu e} = \frac{G_F}{\sqrt{2}} \bar{\nu}_\mu \gamma^\mu (1 - \gamma^5) \nu_\mu \bar{e} \gamma_\mu (g_V^{\nu e} - g_A^{\nu e} \gamma^5) e, \quad (10.20)$$

$$-\mathcal{L}^{eh} = -\frac{G_F}{\sqrt{2}} \sum_i \left[ C_{1i} \bar{e} \gamma_\mu \gamma^5 e \bar{q}_i \gamma^\mu q_i + C_{2i} \bar{e} \gamma_\mu e \bar{q}_i \gamma^\mu \gamma^5 q_i \right], \quad (10.21)$$

$$-\mathcal{L}^{ee} = -\frac{G_F}{\sqrt{2}} C_{2e} \bar{e} \gamma_\mu \gamma^5 e \bar{e} \gamma^\mu e, \quad (10.22)$$

where one must include the charged-current contribution for  $\nu_e$ - $e$  and  $\bar{\nu}_e$ - $e$  and the parity-conserving QED contribution for electron scattering.

The SM expressions for  $\epsilon_{L,R}(i)$ ,  $g_{V,A}^{\nu e}$ , and  $C_{ij}$  are given in Table 10.2. Note, that  $g_{V,A}^{\nu e}$  and the other quantities are coefficients of effective four-Fermi operators, which differ from the quantities defined in Eq. (10.5) in the radiative corrections and in the presence of possible physics beyond the SM.

**10.3.1. Neutrino scattering**: For a general review on  $\nu$ -scattering we refer to Ref. 93 (nonstandard neutrino scattering interactions are surveyed in Ref. 94).

The cross-section in the laboratory system for  $\nu_{\mu}e \rightarrow \nu_{\mu}e$  or  $\bar{\nu}_{\mu}e \rightarrow \bar{\nu}_{\mu}e$  elastic scattering [95] is

$$\frac{d\sigma_{\nu,\bar{\nu}}}{dy} = \frac{G_F^2 m_e E_\nu}{2\pi} \left[ (g_V^{\nu e} \pm g_A^{\nu e})^2 + (g_V^{\nu e} \mp g_A^{\nu e})^2 (1-y)^2 - (g_V^{\nu e 2} - g_A^{\nu e 2}) \frac{y m_e}{E_\nu} \right], \quad (10.23)$$

where the upper (lower) sign refers to  $\nu_{\mu}(\bar{\nu}_{\mu})e$ , and  $y \equiv T_e/E_\nu$  (which runs from 0 to  $(1 + m_e/2E_\nu)^{-1}$ ) is the ratio of the kinetic energy of the recoil electron to the incident  $\nu$  or  $\bar{\nu}$  energy. For  $E_\nu \gg m_e$  this yields a total cross-section

$$\sigma = \frac{G_F^2 m_e E_\nu}{2\pi} \left[ (g_V^{\nu e} \pm g_A^{\nu e})^2 + \frac{1}{3} (g_V^{\nu e} \mp g_A^{\nu e})^2 \right]. \quad (10.24)$$

The most accurate measurements [95–100] of  $\sin^2 \theta_W$  from  $\nu$ -lepton scattering (see Sec. 10.6) are from the ratio  $R \equiv \sigma_{\nu_{\mu}e}/\sigma_{\bar{\nu}_{\mu}e}$  in which many of the systematic uncertainties cancel. Radiative corrections (other than  $m_t$  effects) are small compared to the precision of present experiments and have negligible effect on the extracted  $\sin^2 \theta_W$ . The most precise experiment (CHARM II) [98] determined not only  $\sin^2 \theta_W$  but  $g_{V,A}^{\nu e}$  as well, which are shown in Fig. 10.1. The cross-sections for  $\nu_e e$  and  $\bar{\nu}_e e$  may be obtained from Eq. (10.23) by replacing  $g_{V,A}^{\nu e}$  by  $g_{V,A}^{\nu e} + 1$ , where the 1 is due to the charged-current contribution.

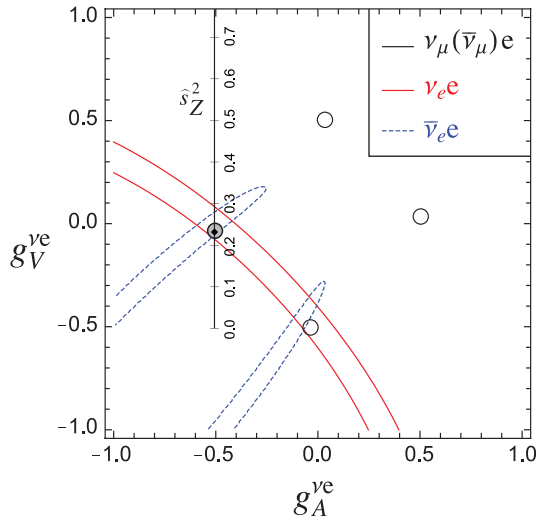


**Figure 10.1:** Allowed contours in  $g_A^{\nu e}$  vs.  $g_V^{\nu e}$  from neutrino-electron scattering and the SM prediction as a function of the weak mixing angle  $\hat{s}_Z^2$ . (The SM best fit value  $\hat{s}_Z^2 = 0.23116$  is also indicated.) The  $\nu_e e$  [99] and  $\bar{\nu}_e e$  [100] constraints are at  $1 \sigma$ , while each of the four equivalent  $\nu_{\mu}(\bar{\nu}_{\mu})e$  [95–98] solutions ( $g_{V,A} \rightarrow -g_{V,A}$  and  $g_{V,A} \rightarrow g_{A,V}$ ) are at 90% C.L. The global best fit region (shaded) almost exactly coincides with the corresponding  $\nu_{\mu}(\bar{\nu}_{\mu})e$  region. The solution near  $g_A = 0, g_V = -0.5$  is eliminated by  $e^+e^- \rightarrow \ell^+\ell^-$  data under the weak additional assumption that the neutral current is dominated by the exchange of a single  $Z$  boson.

A precise determination of the on-shell  $s_{W,V}^2$ , which depends only very weakly on  $m_t$  and  $M_H$ , is obtained from deep inelastic scattering (DIS) of neutrinos from (approximately) isoscalar targets [101]. The ratio  $R_{\nu} \equiv \sigma_{\nu N}^{NC}/\sigma_{\nu N}^{CC}$  of neutral-to-charged-current cross-sections has

been measured to 1% accuracy by CDHS [102] and CHARM [103] at CERN. CCFR [104] at Fermilab has obtained an even more precise result, so it is important to obtain theoretical expressions for  $R_{\nu}$  and  $R_{\bar{\nu}} \equiv \sigma_{\bar{\nu}N}^{NC}/\sigma_{\bar{\nu}N}^{CC}$  to comparable accuracy. Fortunately, many of the uncertainties from the strong interactions and neutrino spectra cancel in the ratio. A large theoretical uncertainty is associated with the  $c$ -threshold, which mainly affects  $\sigma^{CC}$ . Using the slow rescaling prescription [105] the central value of  $\sin^2 \theta_W$  from CCFR varies as  $0.0111(m_c [\text{GeV}] - 1.31)$ , where  $m_c$  is the effective mass which is numerically close to the  $\overline{\text{MS}}$  mass  $\hat{m}_c(\hat{m}_c)$ , but their exact relation is unknown at higher orders. For  $m_c = 1.31 \pm 0.24$  GeV (determined from  $\nu$ -induced dimuon production [106]) this contributes  $\pm 0.003$  to the total uncertainty  $\Delta \sin^2 \theta_W \sim \pm 0.004$ . (The experimental uncertainty is also  $\pm 0.003$ .) This uncertainty largely cancels, however, in the Paschos-Wolfenstein ratio [107],

$$R^- = \frac{\sigma_{\nu N}^{NC} - \sigma_{\bar{\nu}N}^{NC}}{\sigma_{\nu N}^{CC} - \sigma_{\bar{\nu}N}^{CC}}. \quad (10.25)$$

It was measured by Fermilab's NuTeV collaboration [108] for the first time, and required a high-intensity and high-energy anti-neutrino beam.

A simple zero<sup>th</sup>-order approximation is

$$R_{\nu} = g_L^2 + g_R^2 r, \quad R_{\bar{\nu}} = g_L^2 + \frac{g_R^2}{r}, \quad R^- = g_L^2 - g_R^2, \quad (10.26)$$

where

$$g_L^2 \equiv \epsilon_L(u)^2 + \epsilon_L(d)^2 \approx \frac{1}{2} - \sin^2 \theta_W + \frac{5}{9} \sin^4 \theta_W, \quad (10.27a)$$

$$g_R^2 \equiv \epsilon_R(u)^2 + \epsilon_R(d)^2 \approx \frac{5}{9} \sin^4 \theta_W, \quad (10.27b)$$

and  $r \equiv \sigma_{\bar{\nu}N}^{CC}/\sigma_{\nu N}^{CC}$  is the ratio of  $\bar{\nu}$  to  $\nu$  charged-current cross-sections, which can be measured directly. (In the simple parton model, ignoring hadron energy cuts,  $r \approx (\frac{1}{3} + \epsilon)/(\frac{1}{3} - \epsilon)$ , where  $\epsilon \sim 0.125$  is the ratio of the fraction of the nucleon's momentum carried by anti-quarks to that carried by quarks.) In practice, Eq. (10.26) must be corrected for quark mixing, quark sea effects,  $c$ -quark threshold effects, non-isoscalarity,  $W-Z$  propagator differences, the finite muon mass, QED and EW radiative corrections. Details of the neutrino spectra, experimental cuts,  $x$  and  $Q^2$  dependence of structure functions, and longitudinal structure functions enter only at the level of these corrections and therefore lead to very small uncertainties. CCFR quotes  $s_W^2 = 0.2236 \pm 0.0041$  for  $(m_t, M_H) = (175, 150)$  GeV with very little sensitivity to  $(m_t, M_H)$ .

The NuTeV collaboration found  $s_W^2 = 0.2277 \pm 0.0016$  (for the same reference values), which was  $3.0 \sigma$  higher than the SM prediction [108]. The deviation was in  $g_L^2$  (initially  $2.7 \sigma$  low) while  $g_R^2$  was consistent with the SM. Since then a number of experimental and theoretical developments changed the interpretation of the measured cross section ratios, affecting the extracted  $g_{L,R}^2$  (and thus  $s_W^2$ ) including their uncertainties and correlation. In the following paragraph we give a semi-quantitative and preliminary discussion of these effects, but we stress that the precise impact of them needs to be evaluated carefully by the collaboration with a new and self-consistent set of PDFs, including new radiative corrections, while simultaneously allowing isospin breaking and asymmetric strange seas. This is an effort which is currently on its way and until it is completed we do not include the NuTeV constraints on  $g_{L,R}^2$  in our default set of fits.

(i) In the original analysis NuTeV worked with a symmetric strange quark sea but subsequently measured [109] the difference between the strange and antistrange momentum distributions,  $S^- \equiv \int_0^1 dx x [s(x) - \bar{s}(x)] = 0.00196 \pm 0.00143$ , from dimuon events utilizing the first complete next-to-leading order QCD description [110] and parton distribution functions (PDFs) according to Ref. 111. The global PDF fits in Ref. 112 give somewhat smaller values,  $S^- = 0.0013(9)$  [ $S^- = 0.0010(13)$ ], where the semi-leptonic charmed-hadron branching ratio,  $B_{\mu} = 8.8 \pm 0.5\%$ , has [not] been used as an external constraint. The resulting  $S^-$  also depends on the PDF

model used and on whether theoretical arguments (see Ref. 113 and references therein) are invoked favoring a zero crossing of  $x[s(x) - \bar{s}(x)]$  at values much larger than seen by NuTeV and suggesting an effect of much smaller and perhaps negligible size. (ii) The measured branching ratio for  $K_{e3}$  decays enters crucially in the determination of the  $\nu_e(\bar{\nu}_e)$  contamination of the  $\nu_\mu(\bar{\nu}_\mu)$  beam. This branching ratio has moved from  $4.82 \pm 0.06\%$  at the time of the original publication [108] to the current value of  $5.07 \pm 0.04\%$ , *i.e.*, a change by more than  $4\sigma$ . This moves  $s_W^2$  about one standard deviation further away from the SM prediction while reducing the  $\nu_e(\bar{\nu}_e)$  uncertainty. (iii) PDFs seem to violate isospin symmetry at levels much stronger than generally expected [114]. A minimum  $\chi^2$  set of PDFs [115] allowing charge symmetry violation for both valence quarks [ $d_V^p(x) \neq u_V^n(x)$ ] and sea quarks [ $\bar{d}^p(x) \neq \bar{u}^n(x)$ ] shows a reduction in the NuTeV discrepancy by about  $1\sigma$ . But isospin symmetry violating PDFs are currently not well constrained phenomenologically and within uncertainties the NuTeV anomaly could be accounted for in full or conversely made larger [115]. Still, the leading contribution from quark mass differences turns out to be largely model-independent [116] (at least in sign) and a shift,  $\delta s_W^2 = -0.0015 \pm 0.0003$  [113], has been estimated. (iv) QED splitting effects also violate isospin symmetry with an effect on  $s_W^2$  whose sign (reducing the discrepancy) is model-independent. The corresponding shift of  $\delta s_W^2 = -0.0011$  has been calculated in Ref. 117 but has a large uncertainty. (v) Nuclear shadowing effects [118] are likely to affect the interpretation of the NuTeV result at some level, but the NuTeV collaboration argues that their data are dominated by values of  $Q^2$  at which nuclear shadowing is expected to be relatively small. However, another nuclear effect, the isovector EMC effect [119], is much larger (because it affects all neutrons in the nucleus, not just the excess ones) and model-independently works to reduce the discrepancy. It is estimated to lead to a shift of  $\delta s_W^2 = -0.0019 \pm 0.0006$  [113]. It would be important to verify and quantify this kind of effect experimentally, *e.g.*, in polarized electron scattering. (vi) The extracted  $s_W^2$  may also shift at the level of the quoted uncertainty when analyzed using the most recent QED and EW radiative corrections [120,121], as well as QCD corrections to the structure functions [122]. However, these are scheme-dependent and in order to judge whether they are significant they need to be adapted to the experimental conditions and kinematics of NuTeV, and have to be obtained in terms of observable variables and for the differential cross-sections. In addition, there is the danger of double counting some of the QED splitting effects. (vii) New physics could also affect  $g_{L,R}^2$  [123] but it is difficult to convincingly explain the entire effect that way.

### 10.3.2. Parity violation :

The SLAC polarized electron-deuteron DIS experiment [124] measured the right-left asymmetry,

$$A = \frac{\sigma_R - \sigma_L}{\sigma_R + \sigma_L}, \quad (10.28)$$

where  $\sigma_{R,L}$  is the cross-section for the deep-inelastic scattering of a right- or left-handed electron:  $e_{R,L}N \rightarrow eX$ . In the quark parton model,

$$\frac{A}{Q^2} = a_1 + a_2 \frac{1 - (1 - y)^2}{1 + (1 - y)^2}, \quad (10.29)$$

where  $Q^2 > 0$  is the momentum transfer and  $y$  is the fractional energy transfer from the electron to the hadrons. For the deuteron or other isoscalar targets, one has, neglecting the  $s$ -quark and anti-quarks,

$$a_1 = \frac{3G_F}{5\sqrt{2}\pi\alpha} \left( C_{1u} - \frac{1}{2}C_{1d} \right) \approx \frac{3G_F}{5\sqrt{2}\pi\alpha} \left( -\frac{3}{4} + \frac{5}{3}\sin^2\theta_W \right), \quad (10.30a)$$

$$a_2 = \frac{3G_F}{5\sqrt{2}\pi\alpha} \left( C_{2u} - \frac{1}{2}C_{2d} \right) \approx \frac{9G_F}{5\sqrt{2}\pi\alpha} \left( \sin^2\theta_W - \frac{1}{4} \right). \quad (10.30b)$$

In another polarized-electron scattering experiment on deuterons, but in the quasi-elastic kinematic regime, the SAMPLE experiment [125] at MIT-Bates extracted the combination  $C_{2u} - C_{2d}$  at  $Q^2$  values of  $0.1 \text{ GeV}^2$  and  $0.038 \text{ GeV}^2$ . What was actually determined were

nucleon form factors from which the quoted results were obtained by the removal of a multi-quark radiative correction [126]. Other linear combinations of the  $C_{iq}$  have been determined in polarized-lepton scattering at CERN in  $\mu$ -C DIS, at Mainz in  $e$ -Be (quasi-elastic), and at Bates in  $e$ -C (elastic). See the review articles in Refs. 127 and 128 for more details. Recent polarized electron asymmetry experiments, *i.e.*, SAMPLE, the PVA4 experiment at Mainz, and the HAPPEX and G0 experiments at Jefferson Lab, have focussed on the strange quark content of the nucleon. These are reviewed in Ref. 129, where it is shown that they can also provide significant constraints on  $C_{1u}$  and  $C_{1d}$  which complement those from atomic parity violation (see Fig. 10.2).

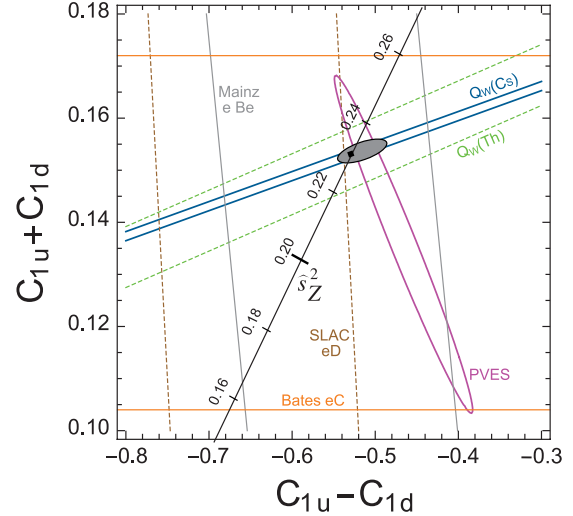


**Figure 10.2:** Constraints on the effective couplings,  $C_{1u}$  and  $C_{1d}$ , from recent (PVES) and older polarized parity violating electron scattering, and from atomic parity violation (APV) at  $1\sigma$ , as well as the 90% C.L. global best fit (shaded) and the SM prediction as a function of the weak mixing angle  $\hat{s}_W^2$ . (The SM best fit value  $\hat{s}_W^2 = 0.23116$  is also indicated.)

The parity violating asymmetry,  $A_{PV}$ , in fixed target polarized Moller scattering,  $e^-e^- \rightarrow e^-e^-$ , is defined as in Eq. (10.28) and reads [130],

$$\frac{A_{PV}}{Q^2} = -2C_{2e} \frac{G_F}{\sqrt{2}\pi\alpha} \frac{1 - y}{1 + y^4 + (1 - y)^4}, \quad (10.31)$$

where  $y$  is again the energy transfer. It has been measured at low  $Q^2 = 0.026 \text{ GeV}^2$  in the SLAC E158 experiment [131], with the result  $A_{PV} = (-1.31 \pm 0.14_{\text{stat.}} \pm 0.10_{\text{syst.}}) \times 10^{-7}$ . Expressed in terms of the weak mixing angle in the  $\overline{\text{MS}}$  scheme, this yields  $\hat{s}^2(Q^2) = 0.2403 \pm 0.0013$ , and established the scale dependence of the weak mixing angle (see Fig. 10.3) at the level of 6.4 standard deviations. One can also define the so-called weak charge of the electron (*cf.* Eq. (10.32) below) as  $Q_W(e) \equiv -2C_{2e} = -0.0403 \pm 0.0053$  (the implications are discussed in Ref. 133).

In a similar experiment and at about the same  $Q^2$ , Qweak at Jefferson Lab [136] will be able to measure the weak charge of the proton,  $Q_W(p) = -2[2C_{1u} + C_{1d}]$ , and  $\sin^2\theta_W$  in polarized  $ep$  scattering with relative precisions of 4% and 0.3%, respectively.

There are precise experiments measuring atomic parity violation (APV) [137] in cesium [138,139] (at the 0.4% level [138]), thallium [140], lead [141], and bismuth [142]. The EW physics is contained in the weak charges which are defined by,

$$Q_W(Z, N) \equiv -2[C_{1u}(2Z + N) + C_{1d}(Z + 2N)] \approx Z(1 - 4\sin^2\theta_W) - N. \quad (10.32)$$

*E.g.*,  $Q_W(^{133}\text{Cs})$  is extracted by measuring experimentally the ratio of the parity violating amplitude,  $E_{\text{PNC}}$ , to the Stark vector transition

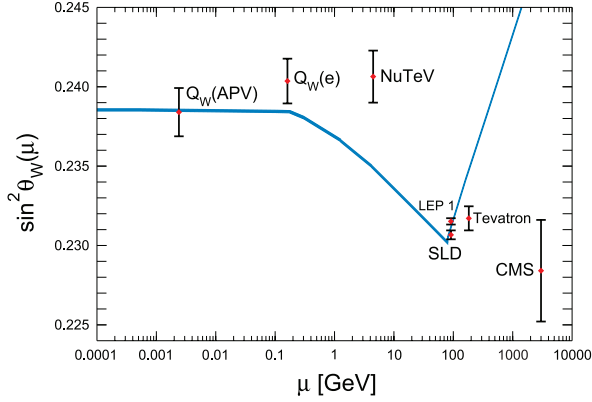


**Figure 10.3:** Scale dependence of the weak mixing angle defined in the  $\overline{\text{MS}}$  scheme [132] (for the scale dependence of the weak mixing angle defined in a mass-dependent renormalization scheme, see Ref. 133). The minimum of the curve corresponds to  $Q = M_W$ , below which we switch to an effective theory with the  $W^\pm$  bosons integrated out, and where the  $\beta$ -function for the weak mixing angle changes sign. At the location of the  $W$  boson mass and each fermion mass there are also discontinuities arising from scheme dependent matching terms which are necessary to ensure that the various effective field theories within a given loop order describe the same physics. However, in the  $\overline{\text{MS}}$  scheme these are very small numerically and barely visible in the figure provided one decouples quarks at  $Q = \hat{m}_q(\hat{m}_q)$ . The width of the curve reflects the theory uncertainty from strong interaction effects which at low energies is at the level of  $\pm 7 \times 10^{-5}$  [132]. Following the estimate [135] of the typical momentum transfer for parity violation experiments in Cs, the location of the APV data point is given by  $\mu = 2.4$  MeV. For NuTeV we display the updated value from Ref. 134 and chose  $\mu = \sqrt{20}$  GeV which is about half-way between the averages of  $\sqrt{Q^2}$  for  $\nu$  and  $\bar{\nu}$  interactions at NuTeV. The Tevatron measurements are strongly dominated by invariant masses of the final state dilepton pair of  $\mathcal{O}(M_Z)$  and can thus be considered as additional  $Z$  pole data points. However, for clarity we displayed the point horizontally to the right. Similar remarks apply to the first measurement at the LHC by the CMS collaboration.

polarizability,  $\beta$ , and by calculating theoretically  $E_{\text{PNC}}$  in terms of  $Q_W$ . One can then write,

$$Q_W = N \left( \frac{\text{Im } E_{\text{PNC}}}{\beta} \right)_{\text{exp.}} \left( \frac{|e| a_B Q_W}{\text{Im } E_{\text{PNC}} N} \right)_{\text{th.}} \left( \frac{\beta}{a_B^3} \right)_{\text{exp.+th.}} \left( \frac{a_B^2}{|e|} \right).$$

The uncertainties associated with atomic wave functions are quite small for cesium [143]. The semi-empirical value of  $\beta$  used in early analyses added another source of theoretical uncertainty [144]. However, the ratio of the off-diagonal hyperfine amplitude to the polarizability was subsequently measured directly by the Boulder group [145]. Combined with the precisely known hyperfine amplitude [146] one finds,  $\beta = 26.991 \pm 0.046$ , in excellent agreement with the earlier results, reducing the overall theory uncertainty (while slightly increasing the experimental error). The recent state-of-the-art many body calculation [147] yields,  $\text{Im } E_{\text{PNC}} = (0.8906 \pm 0.0026) \times 10^{-11} |e| a_B Q_W / N$ , while the two measurements [138,139] combine to give  $\text{Im } E_{\text{PNC}} / \beta = -1.5924 \pm 0.0055$  mV/cm, and we obtain  $Q_W(^{133}\text{Cs}) = -73.20 \pm 0.35$ . Thus, the various theoretical efforts in Refs. 147 and 148 together with an update of the SM calculation [149] including a very recent dispersion analysis of the  $\gamma Z$ -box contribution [150] removed an earlier  $2.3 \sigma$  deviation from the SM (see the year 2000 edition of this *Review*). The theoretical uncertainties are 3% for thallium [151] but larger for the other atoms. The Boulder experiment in cesium also observed the parity-violating weak corrections to the nuclear electromagnetic vertex (the anapole moment [152]).

In the future it could be possible to further reduce the theoretical

wave function uncertainties by taking the ratios of parity violation in different isotopes [137,153]. There would still be some residual uncertainties from differences in the neutron charge radii, however [154]. Experiments in hydrogen and deuterium are another possibility for reducing the atomic theory uncertainties [155], while measurements of single trapped radium ions are promising [156] because of the much larger parity violating effect.

## 10.4. $W$ and $Z$ boson physics

### 10.4.1. $e^+e^-$ scattering below the $Z$ pole :

The forward-backward asymmetry for  $e^+e^- \rightarrow \ell^+\ell^-$ ,  $\ell = \mu$  or  $\tau$ , is defined as

$$A_{FB} \equiv \frac{\sigma_F - \sigma_B}{\sigma_F + \sigma_B}, \quad (10.33)$$

where  $\sigma_F$  ( $\sigma_B$ ) is the cross-section for  $\ell^-$  to travel forward (backward) with respect to the  $e^-$  direction.  $A_{FB}$  and  $R$ , the total cross-section relative to pure QED, are given by

$$R = F_1, \quad A_{FB} = \frac{3 F_2}{4 F_1}, \quad (10.34)$$

where

$$F_1 = 1 - 2\chi_0 g_V^e g_V^\ell \cos \delta_R + \chi_0^2 (g_V^{e2} + g_A^{e2}) (g_V^{\ell 2} + g_A^{\ell 2}), \quad (10.35a)$$

$$F_2 = -2\chi_0 g_A^e g_A^\ell \cos \delta_R + 4\chi_0^2 g_A^e g_A^\ell g_V^e g_V^\ell, \quad (10.35b)$$

$$\tan \delta_R = \frac{M_Z \Gamma_Z}{M_Z^2 - s}, \quad \chi_0 = \frac{G_F}{2\sqrt{2}\pi\alpha} \frac{s M_Z^2}{[(M_Z^2 - s)^2 + M_Z^2 \Gamma_Z^2]^{1/2}}, \quad (10.36)$$

and where  $\sqrt{s}$  is the CM energy. Eqs. (10.35) are valid at tree level. If the data are radiatively corrected for QED effects (as described in Sec. 10.2), then the remaining EW corrections can be incorporated [157,158] (in an approximation adequate for existing PEP, PETRA, and TRISTAN data, which are well below the  $Z$  pole) by replacing  $\chi_0$  by  $\chi(s) \equiv (1 + \rho_\ell) \chi_0(s) \alpha/\alpha(s)$ , where  $\alpha(s)$  is the running QED coupling, and evaluating  $g_V$  in the  $\overline{\text{MS}}$  scheme. Reviews and formulae for  $e^+e^- \rightarrow$  hadrons may be found in Ref. 159.

### 10.4.2. $Z$ pole physics :

At LEP 1 and the SLC, there were high-precision measurements of various  $Z$  pole observables [11,160–166], as summarized in Table 10.4. These include the  $Z$  mass and total width,  $\Gamma_Z$ , and partial widths  $\Gamma(f\bar{f})$  for  $Z \rightarrow f\bar{f}$  where fermion  $f = e, \mu, \tau$ , hadrons,  $b$ , or  $c$ . It is convenient to use the variables  $M_Z, \Gamma_Z, R_\ell \equiv \Gamma(\text{had})/\Gamma(\ell^+\ell^-)$  ( $\ell = e, \mu, \tau$ ),  $\sigma_{\text{had}} \equiv 12\pi \Gamma(e^+e^-) \Gamma(\text{had})/M_Z^2 \Gamma_Z^2$ ,  $R_b \equiv \Gamma(b\bar{b})/\Gamma(\text{had})$ , and  $R_c \equiv \Gamma(c\bar{c})/\Gamma(\text{had})$ , most of which are weakly correlated experimentally. ( $\Gamma(\text{had})$  is the partial width into hadrons.) The three values for  $R_\ell$  are not inconsistent with lepton universality (although  $R_\tau$  is somewhat low compared to  $R_e$  and  $R_\mu$ ), but we use the general analysis in which the three observables are treated as independent. Similar remarks apply to  $A_{FB}^{0,\ell}$  defined in Eq. (10.39) ( $A_{FB}^{0,\tau}$  is somewhat high).  $\mathcal{O}(\alpha^3)$  QED corrections introduce a large anti-correlation ( $-30\%$ ) between  $\Gamma_Z$  and  $\sigma_{\text{had}}$ . The anti-correlation between  $R_b$  and  $R_c$  is  $-18\%$  [11]. The  $R_\ell$  are insensitive to  $m_t$  except for the  $Z \rightarrow b\bar{b}$  vertex and final state corrections and the implicit dependence through  $\sin^2 \theta_W$ . Thus, they are especially useful for constraining  $\alpha_s$ . The width for invisible decays [11],  $\Gamma(\text{inv}) = \Gamma_Z - 3\Gamma(\ell^+\ell^-) - \Gamma(\text{had}) = 499.0 \pm 1.5$  MeV, can be used to determine the number of neutrino flavors much lighter than  $M_Z/2$ ,  $N_\nu = \Gamma(\text{inv})/\Gamma^{\text{theory}}(\nu\bar{\nu}) = 2.984 \pm 0.009$  for  $(m_t, M_H) = (173.4, 117)$  GeV.

There were also measurements of various  $Z$  pole asymmetries. These include the polarization or left-right asymmetry

$$A_{LR} \equiv \frac{\sigma_L - \sigma_R}{\sigma_L + \sigma_R}, \quad (10.37)$$

where  $\sigma_L$  ( $\sigma_R$ ) is the cross-section for a left-(right)-handed incident electron.  $A_{LR}$  was measured precisely by the SLD collaboration at



the SLC [162], and has the advantages of being extremely sensitive to  $\sin^2 \theta_W$  and that systematic uncertainties largely cancel. In addition, SLD extracted the final-state couplings (defined below),  $A_b$ ,  $A_c$  [11],  $A_s$  [163],  $A_\tau$ , and  $A_\mu$  [164], from left-right forward-backward asymmetries, using

$$A_{LR}^{FB}(f) = \frac{\sigma_{LF}^f - \sigma_{LB}^f - \sigma_{RF}^f + \sigma_{RB}^f}{\sigma_{LF}^f + \sigma_{LB}^f + \sigma_{RF}^f + \sigma_{RB}^f} = \frac{3}{4} A_f, \quad (10.38)$$

where, for example,  $\sigma_{LF}^f$  is the cross-section for a left-handed incident electron to produce a fermion  $f$  traveling in the forward hemisphere. Similarly,  $A_\tau$  was measured at LEP 1 [11] through the negative total  $\tau$  polarization,  $\mathcal{P}_\tau$ , and  $A_e$  was extracted from the angular distribution of  $\mathcal{P}_\tau$ . An equation such as (10.38) assumes that initial state QED corrections, photon exchange,  $\gamma$ - $Z$  interference, the tiny EW boxes, and corrections for  $\sqrt{s} \neq M_Z$  are removed from the data, leaving the pure EW asymmetries. This allows the use of effective tree-level expressions,

$$A_{LR} = A_e P_e, \quad A_{FB} = \frac{3}{4} A_f \frac{A_e + P_e}{1 + P_e A_e}, \quad (10.39)$$

where

$$A_f \equiv \frac{2\hat{g}_V^f \hat{g}_A^f}{\hat{g}_V^{f2} + \hat{g}_A^{f2}}. \quad (10.40)$$

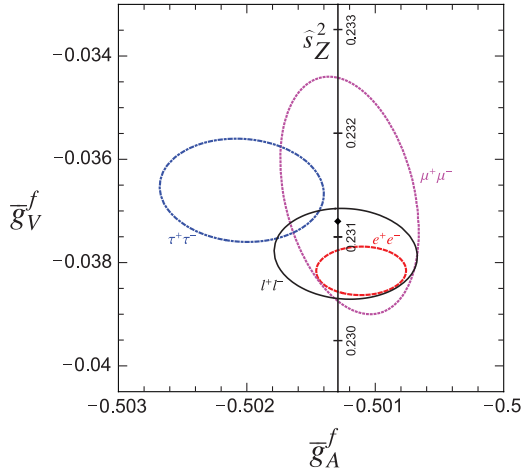


**Figure 10.4:**  $1\sigma$  (39.35% C.L.) contours for the  $Z$ -pole observables  $\hat{g}_A^f$  and  $\hat{g}_V^f$ ,  $f = e, \mu, \tau$  obtained at LEP and SLC [11], compared to the SM expectation as a function of  $\hat{s}_Z^2$ . (The SM best fit value  $\hat{s}_Z^2 = 0.23116$  is also indicated.) Also shown is the 90% CL allowed region in  $\hat{g}_{A,V}^\ell$  obtained assuming lepton universality.

$P_e$  is the initial  $e^-$  polarization, so that the second equality in Eq. (10.38) is reproduced for  $P_e = 1$ , and the  $Z$  pole forward-backward asymmetries at LEP 1 ( $P_e = 0$ ) are given by  $A_{FB}^{(0,f)} = \frac{3}{4} A_e A_f$  where  $f = e, \mu, \tau, b, c, s$  [165], and  $q$ , and where  $A_{FB}^{(0,q)}$  refers to the hadronic charge asymmetry. Corrections for  $t$ -channel exchange and  $s/t$ -channel interference cause  $A_{FB}^{(0,e)}$  to be strongly anti-correlated with  $R_e$  ( $-37\%$ ). The correlation between  $A_{FB}^{(0,b)}$  and  $A_{FB}^{(0,c)}$  amounts to 15%. The initial state coupling,  $A_e$ , was also determined through the left-right charge asymmetry [166] and in polarized Bhabha scattering [164] at the SLC.

As an example of the precision of the  $Z$ -pole observables, the values of  $\hat{g}_A^f$  and  $\hat{g}_V^f$ ,  $f = e, \mu, \tau, \ell$ , extracted from the LEP and SLC lineshape and asymmetry data is shown in Fig. 10.4, which should be compared with Fig. 10.1. (The two sets of parameters coincide in the SM at tree-level.)

As for hadron colliders, the forward-backward asymmetry,  $A_{FB}$ , for  $e^+e^-$  final states (with invariant masses restricted to or dominated

by values around  $M_Z$ ) in  $p\bar{p}$  collisions has been measured by the DØ [167] and CDF [168] collaborations and values for  $\hat{s}_\ell^2$  were extracted, which combine to  $\hat{s}_\ell^2 = 0.23200 \pm 0.00076$  (assuming common PDF uncertainties). By varying the invariant mass and the scattering angle (and assuming the electron couplings), information on the effective  $Z$  couplings to light quarks,  $\hat{g}_{V,A}^{u,d}$ , could also be obtained [167,169], but with large uncertainties and mutual correlations and not independently of  $\hat{s}_\ell^2$  above. Similar analyses have also been reported by the H1 and ZEUS collaborations at HERA [170] and by the LEP collaborations [11]. This kind of measurement is harder in the  $pp$  environment due to the difficulty to assign the initial quark and antiquark in the underlying Drell-Yan process to the protons. Nevertheless, the CMS collaboration [171] already reported a first measurement,  $\hat{s}_Z^2 = 0.2287 \pm 0.0032$ .

#### 10.4.3. LEP 2 :

LEP 2 [172] ran at several energies above the  $Z$  pole up to  $\sim 209$  GeV. Measurements were made of a number of observables, including the cross-sections for  $e^+e^- \rightarrow ff$  for  $f = q, \mu^-, \tau^-$ ; the differential cross-sections for  $f = e^-, \mu^-, \tau^-$ ;  $R_q$  for  $q = b, c$ ;  $A_{FB}(f)$  for  $f = \mu, \tau, b, c$ ;  $W$  branching ratios; and  $WW$ ,  $WW\gamma$ ,  $ZZ$ , single  $W$ , and single  $Z$  cross-sections. They are in good agreement with the SM predictions, with the exceptions of the total hadronic cross-section ( $1.7\sigma$  high),  $R_b$  ( $2.1\sigma$  low), and  $A_{FB}(b)$  ( $1.6\sigma$  low). Also, the negative result of the direct search for the SM Higgs boson excluded  $M_H$  values below 114.4 GeV at the 95% CL [173]. This result is complementary to and can be combined with [174] the limits inferred from the EW precision data.

The  $Z$  boson properties are extracted assuming the SM expressions for the  $\gamma$ - $Z$  interference terms. These have also been tested experimentally by performing more general fits [172,175] to the LEP 1 and LEP 2 data. Assuming family universality this approach introduces three additional parameters relative to the standard fit [11], describing the  $\gamma$ - $Z$  interference contribution to the total hadronic and leptonic cross-sections,  $J_{\text{had}}^{\text{tot}}$  and  $J_\ell^{\text{tot}}$ , and to the leptonic forward-backward asymmetry,  $J_\ell^{\text{fb}}$ . *E.g.*,

$$J_{\text{had}}^{\text{tot}} \sim g_V^\ell g_V^{\text{had}} = 0.277 \pm 0.065, \quad (10.41)$$

which is in agreement with the SM expectation [11] of  $0.21 \pm 0.01$ . These are valuable tests of the SM; but it should be cautioned that new physics is not expected to be described by this set of parameters, since (i) they do not account for extra interactions beyond the standard weak neutral-current, and (ii) the photonic amplitude remains fixed to its SM value.

Strong constraints on anomalous triple and quartic gauge couplings have been obtained at LEP 2 and the Tevatron as described in the Gauge & Higgs Bosons Particle Listings.

#### 10.4.4. $W$ and $Z$ decays :

The partial decay width for gauge bosons to decay into massless fermions  $f_1 \bar{f}_2$  (the numerical values include the small EW radiative corrections and final state mass effects) is given by

$$\Gamma(W^+ \rightarrow e^+ \nu_e) = \frac{G_F M_W^3}{6\sqrt{2}\pi} \approx 226.36 \pm 0.05 \text{ MeV}, \quad (10.42a)$$

$$\Gamma(W^+ \rightarrow u_i \bar{d}_j) = \frac{CG_F M_W^3}{6\sqrt{2}\pi} |V_{ij}|^2 \approx 706.34 \pm 0.16 \text{ MeV} |V_{ij}|^2, \quad (10.42b)$$

$$\Gamma(Z \rightarrow \psi_i \bar{\psi}_i) = \frac{CG_F M_Z^3}{6\sqrt{2}\pi} [g_V^{i2} + g_A^{i2}] \begin{cases} 167.22 \pm 0.01 \text{ MeV} (\nu\bar{\nu}), \\ 84.00 \pm 0.01 \text{ MeV} (e^+e^-), \\ 300.26 \pm 0.05 \text{ MeV} (u\bar{u}), \\ 383.04 \pm 0.05 \text{ MeV} (d\bar{d}), \\ 375.98 \mp 0.03 \text{ MeV} (b\bar{b}). \end{cases} \quad (10.42c)$$

For leptons  $C = 1$ , while for quarks

$$C = 3 \left[ 1 + \frac{\alpha_s(M_V)}{\pi} + 1.409 \frac{\alpha_s^2}{\pi^2} - 12.77 \frac{\alpha_s^3}{\pi^3} - 80.0 \frac{\alpha_s^4}{\pi^4} \right], \quad (10.43)$$

where the 3 is due to color and the factor in brackets represents the universal part of the QCD corrections [176] for massless quarks [177]. The  $\mathcal{O}(\alpha_s^4)$  contribution in Eq. (10.43) is recent [178]. The  $Z \rightarrow f\bar{f}$  widths contain a number of additional corrections: which are different for vector and axial-vector partial widths and are included through order  $\alpha_s^3$  and  $\hat{m}_q^4(M_Z^2)$  unless they are tiny; and singlet contributions starting from two-loop order which are large, strongly top quark mass dependent, family universal, and flavor non-universal [181]. The QED factor  $1 + 3\alpha q_f^2/4\pi$ , as well as two-loop order  $\alpha\alpha_s$  and  $\alpha^2$  self-energy corrections [182] are also included. Working in the on-shell scheme, *i.e.*, expressing the widths in terms of  $G_F M_{W,Z}^3$ , incorporates the largest radiative corrections from the running QED coupling [63,183]. EW corrections to the  $Z$  widths are then incorporated by replacing  $g_{V,A}^2$  by  $\bar{g}_{V,A}^2$ . Hence, in the on-shell scheme the  $Z$  widths are proportional to  $\rho_i \sim 1 + \rho_t$ . The  $\overline{\text{MS}}$  normalization accounts also for the leading EW corrections [68]. There is additional (negative) quadratic  $m_t$  dependence in the  $Z \rightarrow b\bar{b}$  vertex corrections [184] which causes  $\Gamma(b\bar{b})$  to decrease with  $m_t$ . The dominant effect is to multiply  $\Gamma(b\bar{b})$  by the vertex correction  $1 + \delta\rho_{b\bar{b}}$ , where  $\delta\rho_{b\bar{b}} \sim 10^{-2}(-\frac{1}{2}\frac{m_t^2}{M_Z^2} + \frac{1}{5})$ .

In practice, the corrections are included in  $\rho_b$  and  $\kappa_b$ , as discussed in Sec. 10.2.

For three fermion families the total widths are predicted to be

$$\Gamma_Z \approx 2.4960 \pm 0.0002 \text{ GeV}, \quad \Gamma_W \approx 2.0915 \pm 0.0005 \text{ GeV}. \quad (10.44)$$

We have assumed  $\alpha_s(M_Z) = 0.1200$ . An uncertainty in  $\alpha_s$  of  $\pm 0.002$  introduces an additional uncertainty of 0.06% in the hadronic widths, corresponding to  $\pm 1$  MeV in  $\Gamma_Z$ . These predictions are to be compared with the experimental results,  $\Gamma_Z = 2.4952 \pm 0.0023$  GeV [11] and  $\Gamma_W = 2.085 \pm 0.042$  GeV [185] (see the Gauge & Higgs Boson Particle Listings for more details).

## 10.5. Precision flavor physics

In addition to cross-sections, asymmetries, parity violation,  $W$  and  $Z$  decays, there is a large number of experiments and observables testing the flavor structure of the SM. These are addressed elsewhere in this *Review*, and are generally not included in this Section. However, we identify three precision observables with sensitivity to similar types of new physics as the other processes discussed here. The branching fraction of the flavor changing transition  $b \rightarrow s\gamma$  is of comparatively low precision, but since it is a loop-level process (in the SM) its sensitivity to new physics (and SM parameters, such as heavy quark masses) is enhanced. A discussion can be found in earlier editions of this *Review*. The  $\tau$ -lepton lifetime and leptonic branching ratios are primarily sensitive to  $\alpha_s$  and not affected significantly by many types of new physics. However, having an independent and reliable low energy measurement of  $\alpha_s$  in a global analysis allows the comparison with the  $Z$  lineshape determination of  $\alpha_s$  which shifts easily in the presence of new physics contributions. By far the most precise observable discussed here is the anomalous magnetic moment of the muon (the electron magnetic moment is measured to even greater precision and can be used to determine  $\alpha$ , but its new physics sensitivity is suppressed by an additional factor of  $m_e^2/m_\mu^2$ ). Its combined experimental and theoretical uncertainty is comparable to typical new physics contributions.

The extraction of  $\alpha_s$  from the  $\tau$  lifetime [186] is standing out from other determinations because of a variety of independent reasons: (i) the  $\tau$ -scale is low, so that upon extrapolation to the  $Z$  scale (where it can be compared to the theoretically clean  $Z$  lineshape determinations) the  $\alpha_s$  error shrinks by about an order of magnitude; (ii) yet, this scale is high enough that perturbation theory and the operator product expansion (OPE) can be applied; (iii) these observables are fully inclusive and thus free of fragmentation and hadronization effects that would have to be modeled or measured; (iv) duality violation (DV) effects are most problematic near the branch cut but there they are suppressed by a double zero at  $s = m_\tau^2$ ; (v) there are data [43] to constrain non-perturbative effects both within ( $\delta_{D=6,8}$ ) and breaking ( $\delta_{DV}$ ) the OPE; (vi) a complete four-loop order QCD calculation is available [178]; (vii) large effects associated

with the QCD  $\beta$ -function can be re-summed [187] in what has become known as contour improved perturbation theory (CIPT). However, while there is no doubt that CIPT shows faster convergence in the lower (calculable) orders, doubts have been cast on the method by the observation that at least in a specific model [188], which includes the exactly known coefficients and theoretical constraints on the large-order behavior, ordinary fixed order perturbation theory (FOPT) may nevertheless give a better approximation to the full result. We therefore use the expressions [54,177,178,189],

$$\tau_\tau = \hbar \frac{1 - \mathcal{B}_\tau^s}{\Gamma_\tau^e + \Gamma_\tau^\mu + \Gamma_\tau^{ud}} = 291.13 \pm 0.43 \text{ fs}, \quad (10.45)$$

$$\Gamma_\tau^{ud} = \frac{G_F^2 m_\tau^5 |V_{ud}|^2}{64\pi^3} S(m_\tau, M_Z) \left( 1 + \frac{3}{5} \frac{m_\tau^2 - m_\mu^2}{M_W^2} \right) \times \left[ 1 + \frac{\alpha_s(m_\tau)}{\pi} + 5.202 \frac{\alpha_s^2}{\pi^2} + 26.37 \frac{\alpha_s^3}{\pi^3} + 127.1 \frac{\alpha_s^4}{\pi^4} + \frac{\hat{\alpha}}{\pi} \left( \frac{85}{24} - \frac{\pi^2}{2} \right) + \delta_q \right], \quad (10.46)$$

and  $\Gamma_\tau^e$  and  $\Gamma_\tau^\mu$  can be taken from Eq. (10.6) with obvious replacements. The relative fraction of decays with  $\Delta S = -1$ ,  $\mathcal{B}_\tau^s = 0.0286 \pm 0.0007$ , is based on experimental data since the value for the strange quark mass,  $\hat{m}_s(m_\tau)$ , is not well known and the QCD expansion proportional to  $\hat{m}_s^2$  converges poorly and cannot be trusted.  $S(m_\tau, M_Z) = 1.01907 \pm 0.0003$  is a logarithmically enhanced EW correction factor with higher orders re-summed [190].  $\delta_q$  contains the dimension six and eight terms in the OPE, as well as DV effects,  $\delta_{D=6,8} + \delta_{DV} = -0.004 \pm 0.012$  [191]. Depending on how  $\delta_{D=6}$ ,  $\delta_{D=8}$ , and  $\delta_{DV}$  are extracted, there are strong correlations not only between them, but also with the gluon condensate ( $D = 4$ ) and possibly  $D > 8$  terms. These latter are suppressed in Eq. (10.46) by additional factors of  $\alpha_s$ , but not so for more general weight functions. A simultaneous fit to all non-perturbative terms [191] (as is necessary if one wants to avoid *ad hoc* assumptions) indicates that the  $\alpha_s$  errors may have been underestimated in the past. Higher statistics  $\tau$  decay data [45] and spectral functions from  $e^+e^-$  annihilation (providing a larger fit window and thus more discriminatory power and smaller correlations) are likely to reduce the  $\delta_q$  error in the future. Also included in  $\delta_q$  are quark mass effects and the  $D = 4$  condensate contributions. An uncertainty of similar size arises from the truncation of the FOPT series and is conservatively taken as the  $\alpha_s^4$  term (this is re-calculated in each call of the fits, leading to an  $\alpha_s$ -dependent and thus asymmetric error) until a better understanding of the numerical differences between FOPT and CIPT has been gained. Our perturbative error covers almost the entire range from using CIPT to assuming that the nearly geometric series in Eq. (10.46) continues to higher orders. The experimental uncertainty in Eq. (10.45), is from the combination of the two leptonic branching ratios with the direct  $\tau_\tau$ . Included are also various smaller uncertainties ( $\pm 0.5$  fs) from other sources which are dominated by the evolution from the  $Z$  scale. In total we obtain a  $\sim 2\%$  determination of  $\alpha_s(M_Z) = 0.1193_{-0.0020}^{+0.0022}$ , which corresponds to  $\alpha_s(m_\tau) = 0.327_{-0.016}^{+0.019}$ , and updates the result of Refs. 54 and 192. For more details, see Refs. 191 and 193 where the  $\tau$  spectral functions are used as additional input.

The world average of the muon anomalous magnetic moment<sup>‡</sup>,

$$a_\mu^{\text{exp}} = \frac{g_\mu - 2}{2} = (1165920.80 \pm 0.63) \times 10^{-9}, \quad (10.47)$$

is dominated by the final result of the E821 collaboration at BNL [194]. The QED contribution has been calculated to four

<sup>‡</sup> In what follows, we summarize the most important aspects of  $g_\mu - 2$ , and give some details about the evaluation in our fits. For more details see the dedicated contribution by A. Höcker and W. Marciano in this *Review*. There are some small numerical differences (at the level of 0.1 standard deviation), which are well understood and mostly arise because internal consistency of the fits requires the calculation of all observables from analytical expressions and common inputs and fit parameters, so that an independent evaluation is necessary for this Section. Note, that in the spirit of a global analysis based on all available information we have chosen here to average in the  $\tau$  decay data, as well.

loops [195] (fully analytically to three loops [196,197]), and the leading logarithms are included to five loops [198,199]. The estimated SM EW contribution [200–202],  $a_\mu^{\text{EW}} = (1.52 \pm 0.03) \times 10^{-9}$ , which includes leading two-loop [201] and three-loop [202] corrections, is at the level of twice the current uncertainty.

The limiting factor in the interpretation of the result are the uncertainties from the two- and three-loop hadronic contribution. *E.g.*, Ref. 20 obtained the value  $a_\mu^{\text{had}} = (69.23 \pm 0.42) \times 10^{-9}$  which combines CMD-2 [47] and SND [48]  $e^+e^- \rightarrow \text{hadrons}$  cross-section data with radiative return results from BaBar [50] and KLOE [51]. This value suggests a  $3.6 \sigma$  discrepancy between Eq. (10.47) and the SM prediction. An alternative analysis [20] using  $\tau$  decay data and isospin symmetry (CVC) yields  $a_\mu^{\text{had}} = (70.15 \pm 0.47) \times 10^{-9}$ . This result implies a smaller conflict ( $2.4 \sigma$ ) with Eq. (10.47). Thus, there is also a discrepancy between the spectral functions obtained from the two methods. For example, if one uses the  $e^+e^-$  data and CVC to predict the branching ratio for  $\tau^- \rightarrow \nu_\tau \pi^- \pi^0$  decays [20] we obtain an average of  $\mathcal{B}_{\text{CVC}} = 24.93 \pm 0.13 \pm 0.22_{\text{CVC}}$ , while the average of the directly measured branching ratio yields  $25.51 \pm 0.09$ , which is  $2.3 \sigma$  higher. It is important to understand the origin of this difference, but two observations point to the conclusion that at least some of it is experimental: (i) There is also a direct discrepancy of  $1.9 \sigma$  between  $\mathcal{B}_{\text{CVC}}$  derived from BaBar (which is not inconsistent with  $\tau$  decays) and KLOE. (ii) Isospin violating corrections have been studied in detail in Ref. 203 and found to be largely under control. The largest effect is due to higher-order EW corrections [204] but introduces a negligible uncertainty [190]. Nevertheless,  $a_\mu^{\text{had}}$  is often evaluated excluding the  $\tau$  decay data arguing [205] that CVC breaking effects (*e.g.*, through a relatively large mass difference between the  $\rho^\pm$  and  $\rho^0$  vector mesons) may be larger than expected. (This may also be relevant [205] in the context of the NuTeV result discussed above.) Experimentally [45], this mass difference is indeed larger than expected, but then one would also expect a significant width difference which is contrary to observation [45]. Fortunately, due to the suppression at large  $s$  (from where the conflicts originate) these problems are less pronounced as far as  $a_\mu^{\text{had}}$  is concerned. In the following we view all differences in spectral functions as (systematic) fluctuations and average the results.

An additional uncertainty is induced by the hadronic three-loop light-by-light scattering contribution. Two recent and inherently different model calculations yield  $a_\mu^{\text{LBS}} = (+1.36 \pm 0.25) \times 10^{-9}$  [206] and  $a_\mu^{\text{LBS}} = +1.37^{+0.15}_{-0.27} \times 10^{-9}$  [207] which are higher than previous evaluations [208,209]. The sign of this effect is opposite [208] to the one quoted in the 2002 edition of this *Review*, and has subsequently been confirmed by two other groups [209]. There is also the upper bound  $a_\mu^{\text{LBS}} < 1.59 \times 10^{-9}$  [207] but this requires an *ad hoc* assumption, too. The recent Ref. 210 quotes the value  $a_\mu^{\text{LBS}} = (+1.05 \pm 0.26) \times 10^{-9}$ , which we shift by  $2 \times 10^{-11}$  to account for the more accurate charm quark treatment of Ref. 207. We also increase the error to cover all evaluations, and we will use  $a_\mu^{\text{LBS}} = (+1.07 \pm 0.32) \times 10^{-9}$  in the fits.

Other hadronic effects at three-loop order contribute [211]  $a_\mu^{\text{had}}(\alpha^3) = (-1.00 \pm 0.06) \times 10^{-9}$ . Correlations with the two-loop hadronic contribution and with  $\Delta\alpha(M_Z)$  (see Sec. 10.2) were considered in Ref. 197 which also contains analytic results for the perturbative QCD contribution.

Altogether, the SM prediction is

$$a_\mu^{\text{theory}} = (1165918.41 \pm 0.48) \times 10^{-9}, \quad (10.48)$$

where the error is from the hadronic uncertainties excluding parametric ones such as from  $\alpha_s$  and the heavy quark masses. Using a correlation of about 84% from the data input to the vacuum polarization integrals [20], we estimate the correlation of the total (experimental plus theoretical) uncertainty in  $a_\mu$  with  $\Delta\alpha(M_Z)$  as 24%. The overall  $3.0 \sigma$  discrepancy between the experimental and theoretical  $a_\mu$  values could be due to fluctuations (the E821 result is statistics dominated) or underestimates of the theoretical uncertainties. On the other hand,  $g_\mu - 2$  is also affected by many types of new physics, such as supersymmetric models with large  $\tan\beta$  and moderately light

**Table 10.3:** Principal non- $Z$  pole observables, compared with the SM best fit predictions. The first  $M_W$  value is from the Tevatron [214] and the second one from LEP 2 [172].  $e$ -DIS [129] and the  $\nu$ -DIS constraints from CDHS [102], CHARM [103], and CCFR [104] are included, as well, but not shown in the Table. The world averages for  $g_{V,A}^{\nu e}$  are dominated by the CHARM II [98] results,  $g_V^{\nu e} = -0.035 \pm 0.017$  and  $g_A^{\nu e} = -0.503 \pm 0.017$ . The errors are the total (experimental plus theoretical) uncertainties. The  $\tau_\tau$  value is the  $\tau$  lifetime world average computed by combining the direct measurements with values derived from the leptonic branching ratios [54]; in this case, the theory uncertainty is included in the SM prediction. In all other SM predictions, the uncertainty is from  $M_Z$ ,  $M_H$ ,  $m_t$ ,  $m_b$ ,  $m_c$ ,  $\hat{\alpha}(M_Z)$ , and  $\alpha_s$ , and their correlations have been accounted for. The column denoted Pull gives the standard deviations for the principal fit with  $M_H$  free, while the column denoted Dev. (Deviation) is for  $M_H = 124.5 \text{ GeV}$  [215] fixed.

Quantity	Value	Standard Model	Pull	Dev.
$m_t$ [GeV]	$173.4 \pm 1.0$	$173.5 \pm 1.0$	-0.1	-0.3
$M_W$ [GeV]	$80.420 \pm 0.031$	$80.381 \pm 0.014$	1.2	1.6
	$80.376 \pm 0.033$		-0.2	0.2
$g_V^{\nu e}$	$-0.040 \pm 0.015$	$-0.0398 \pm 0.0003$	0.0	0.0
$g_A^{\nu e}$	$-0.507 \pm 0.014$	$-0.5064 \pm 0.0001$	0.0	0.0
$Q_W(e)$	$-0.0403 \pm 0.0053$	$-0.0474 \pm 0.0005$	1.3	1.3
$Q_W(\text{Cs})$	$-73.20 \pm 0.35$	$-73.23 \pm 0.02$	0.1	0.1
$Q_W(\text{Ti})$	$-116.4 \pm 3.6$	$-116.88 \pm 0.03$	0.1	0.1
$\tau_\tau$ [fs]	$291.13 \pm 0.43$	$290.75 \pm 2.51$	0.1	0.1
$\frac{1}{2}(g_\mu - 2 - \frac{\alpha}{\pi})$	$(4511.07 \pm 0.77) \times 10^{-9}$	$(4508.70 \pm 0.09) \times 10^{-9}$	3.0	3.0

superparticle masses [212]. Thus, the deviation could also arise from physics beyond the SM.

## 10.6. Global fit results

In this section we present the results of global fits to the experimental data discussed in Sec. 10.3–Sec. 10.5. For earlier analyses see Refs. 128 and 213.

The values for  $m_t$  [56–58],  $M_W$  [172,214], neutrino scattering [96–104], the weak charges of the electron [131], cesium [138,139] and thallium [140], the muon anomalous magnetic moment [194], and the  $\tau$  lifetime are listed in Table 10.3. Likewise, the principal  $Z$  pole observables can be found in Table 10.4 where the LEP 1 averages of the ALEPH, DELPHI, L3, and OPAL results include common systematic errors and correlations [11]. The heavy flavor results of LEP 1 and SLD are based on common inputs and correlated, as well [11]. Note that the values of  $\Gamma(\ell^+\ell^-)$ ,  $\Gamma(\text{had})$ , and  $\Gamma(\text{inv})$  are not independent of  $\Gamma_Z$ , the  $R_\ell$ , and  $\sigma_{\text{had}}$  and that the SM errors in those latter are largely dominated by the uncertainty in  $\alpha_s$ . Also shown in both Tables are the SM predictions for the values of  $M_Z$ ,  $M_H$ ,  $\alpha_s(M_Z)$ ,  $\Delta\alpha_{\text{had}}^{(3)}$  and the heavy quark masses shown in Table 10.5. The predictions result from a global least-square ( $\chi^2$ ) fit to all data using the minimization package MINUIT [216] and the EW library GAPP [21]. In most cases, we treat all input errors (the uncertainties of the values) as Gaussian. The reason is not that we assume that theoretical and systematic errors are intrinsically bell-shaped (which they are not) but because in most cases the input errors are combinations of many different (including statistical) error sources, which should yield approximately Gaussian *combined* errors by the large number theorem. Thus, if either the statistical components dominate or there are many components of similar size. An exception is the theory dominated error on the  $\tau$  lifetime, which we recalculate in each  $\chi^2$ -function call since it depends itself on  $\alpha_s$ . Sizes and shapes of the output errors (the uncertainties of the predictions and the SM fit parameters) are fully determined by the fit, and  $1 \sigma$  errors are defined to correspond to  $\Delta\chi^2 = \chi^2 - \chi_{\text{min}}^2 = 1$ , and do not necessarily correspond to the 68.3% probability range or the 39.3% probability contour (for 2 parameters).

**Table 10.4:** Principal  $Z$  pole observables and their SM predictions (*cf.* Table 10.3). The first  $\bar{s}_\ell^2(A_{FB}^{(0,g)})$  is the effective angle extracted from the hadronic charge asymmetry, the second is the combined value from  $D\bar{O}$  [167] and CDF [168], and the third is from CMS [171]. The three values of  $A_e$  are (i) from  $A_{LR}$  for hadronic final states [162]; (ii) from  $A_{LR}$  for leptonic final states and from polarized Bhabba scattering [164]; and (iii) from the angular distribution of the  $\tau$  polarization at LEP 1. The two  $A_\tau$  values are from SLD and the total  $\tau$  polarization, respectively.

Quantity	Value	Standard Model	Pull	Dev.
$M_Z$ [GeV]	$91.1876 \pm 0.0021$	$91.1874 \pm 0.0021$	0.1	0.0
$\Gamma_Z$ [GeV]	$2.4952 \pm 0.0023$	$2.4961 \pm 0.0010$	-0.4	-0.2
$\Gamma(\text{had})$ [GeV]	$1.7444 \pm 0.0020$	$1.7426 \pm 0.0010$	—	—
$\Gamma(\text{inv})$ [MeV]	$499.0 \pm 1.5$	$501.69 \pm 0.06$	—	—
$\Gamma(\ell^+\ell^-)$ [MeV]	$83.984 \pm 0.086$	$84.005 \pm 0.015$	—	—
$\sigma_{\text{had}}[\text{nb}]$	$41.541 \pm 0.037$	$41.477 \pm 0.009$	1.7	1.7
$R_e$	$20.804 \pm 0.050$	$20.744 \pm 0.011$	1.2	1.3
$R_\mu$	$20.785 \pm 0.033$	$20.744 \pm 0.011$	1.2	1.3
$R_\tau$	$20.764 \pm 0.045$	$20.789 \pm 0.011$	-0.6	-0.5
$R_b$	$0.21629 \pm 0.00066$	$0.21576 \pm 0.00004$	0.8	0.8
$R_c$	$0.1721 \pm 0.0030$	$0.17227 \pm 0.00004$	-0.1	-0.1
$A_{FB}^{(0,e)}$	$0.0145 \pm 0.0025$	$0.01633 \pm 0.00021$	-0.7	-0.7
$A_{FB}^{(0,\mu)}$	$0.0169 \pm 0.0013$		0.4	0.6
$A_{FB}^{(0,\tau)}$	$0.0188 \pm 0.0017$		1.5	1.6
$A_{FB}^{(0,b)}$	$0.0992 \pm 0.0016$	$0.1034 \pm 0.0007$	-2.6	-2.3
$A_{FB}^{(0,c)}$	$0.0707 \pm 0.0035$	$0.0739 \pm 0.0005$	-0.9	-0.8
$A_{FB}^{(0,s)}$	$0.0976 \pm 0.0114$	$0.1035 \pm 0.0007$	-0.5	-0.5
$\bar{s}_\ell^2(A_{FB}^{(0,g)})$	$0.2324 \pm 0.0012$	$0.23146 \pm 0.00012$	0.8	0.7
	$0.23200 \pm 0.00076$		0.7	0.6
	$0.2287 \pm 0.0032$		-0.9	-0.9
$A_e$	$0.15138 \pm 0.00216$	$0.1475 \pm 0.0010$	1.8	2.1
	$0.1544 \pm 0.0060$		1.1	1.3
	$0.1498 \pm 0.0049$		0.5	0.6
$A_\mu$	$0.142 \pm 0.015$		-0.4	-0.3
$A_\tau$	$0.136 \pm 0.015$		-0.8	-0.7
	$0.1439 \pm 0.0043$		-0.8	-0.7
$A_b$	$0.923 \pm 0.020$	$0.9348 \pm 0.0001$	-0.6	-0.6
$A_c$	$0.670 \pm 0.027$	$0.6680 \pm 0.0004$	0.1	0.1
$A_s$	$0.895 \pm 0.091$	$0.9357 \pm 0.0001$	-0.4	-0.4

The agreement is generally very good. Despite the few discrepancies discussed in the following, the fit describes well the data with a  $\chi^2/\text{d.o.f.} = 45.0/42$ . The probability of a larger  $\chi^2$  is 35%. Only the final result for  $g_\mu - 2$  from BNL and  $A_{FB}^{(0,b)}$  from LEP 1 are currently showing large ( $3.0\sigma$  and  $2.6\sigma$ ) deviations. In addition,  $A_{LR}^0$  (SLD) from hadronic final states differs by  $1.8\sigma$ .  $g_L^2$  from NuTeV is nominally in conflict with the SM, as well, but the precise status is under investigation (see Sec. 10.3).

$A_b$  can be extracted from  $A_{FB}^{(0,b)}$  when  $A_e = 0.1501 \pm 0.0016$  is taken from a fit to leptonic asymmetries (using lepton universality). The result,  $A_b = 0.881 \pm 0.017$ , is  $3.2\sigma$  below the SM prediction<sup>§</sup> and also  $1.6\sigma$  below  $A_b = 0.923 \pm 0.020$  obtained from  $A_{LR}^{FB}(b)$  at SLD. Thus, it appears that at least some of the problem in  $A_{FB}^{(0,b)}$  is experimental. Note, however, that the uncertainty in  $A_{FB}^{(0,b)}$  is strongly statistics dominated. The combined value,  $A_b = 0.899 \pm 0.013$  deviates by  $2.8\sigma$ .

<sup>§</sup> Alternatively, one can use  $A_\ell = 0.1481 \pm 0.0027$ , which is from LEP 1 alone and in excellent agreement with the SM, and obtain  $A_b = 0.893 \pm 0.022$  which is  $1.9\sigma$  low. This illustrates that some of the discrepancy is related to the one in  $A_{LR}$ .

It would be difficult to account for this  $4.0\%$  deviation by new physics that enters only at the level of radiative corrections since about a 20% correction to  $\bar{\kappa}_b$  would be necessary to account for the central value of  $A_b$  [217]. If this deviation is due to new physics, it is most likely of tree-level type affecting preferentially the third generation. Examples include the decay of a scalar neutrino resonance [218], mixing of the  $b$  quark with heavy exotics [219], and a heavy  $Z'$  with family-nonuniversal couplings [220,221]. It is difficult, however, to simultaneously account for  $R_b$ , which has been measured on the  $Z$  peak and off-peak [222] at LEP 1. An average of  $R_b$  measurements at LEP 2 at energies between 133 and 207 GeV is  $2.1\sigma$  below the SM prediction, while  $A_{FB}^{(b)}$  (LEP 2) is  $1.6\sigma$  low [172].

The left-right asymmetry,  $A_{LR}^0 = 0.15138 \pm 0.00216$  [162], based on all hadronic data from 1992–1998 differs  $1.8\sigma$  from the SM expectation of  $0.1475 \pm 0.0010$ . The combined value of  $A_\ell = 0.1513 \pm 0.0021$  from SLD (using lepton-family universality and including correlations) is also  $1.8\sigma$  above the SM prediction; but there is experimental agreement between this SLD value and the LEP 1 value,  $A_\ell = 0.1481 \pm 0.0027$ , obtained from a fit to  $A_{FB}^{(0,\ell)}$ ,  $A_e(\mathcal{P}_\tau)$ , and  $A_\tau(\mathcal{P}_\tau)$ , again assuming universality.

The observables in Table 10.3 and Table 10.4, as well as some other less precise observables, are used in the global fits described below. In all fits, the errors include full statistical, systematic, and theoretical uncertainties. The correlations on the LEP 1 lineshape and  $\tau$  polarization, the LEP/SLD heavy flavor observables, the SLD lepton asymmetries, and the deep inelastic and  $\nu$ - $e$  scattering observables, are included. The theoretical correlations between  $\Delta\alpha_{\text{had}}^{(5)}$  and  $g_\mu - 2$ , and between the charm and bottom quark masses, are also accounted for.

The data allow a simultaneous determination of  $M_Z$ ,  $M_H$ ,  $m_t$ , and the strong coupling  $\alpha_s(M_Z)$ . ( $\hat{m}_c$ ,  $\hat{m}_b$ , and  $\Delta\alpha_{\text{had}}^{(3)}$  are also allowed to float in the fits, subject to the theoretical constraints [19,54] described in Sec. 10.2. These are correlated with  $\alpha_s$ .)  $\alpha_s$  is determined mainly from  $R_\ell$ ,  $\Gamma_Z$ ,  $\sigma_{\text{had}}$ , and  $\tau_\tau$  and is only weakly correlated with the other variables. The global fit to all data, including the hadron collider average  $m_t = 173.4 \pm 1.0$  GeV, yields the result in Table 10.5 (the  $\overline{\text{MS}}$  top quark mass given there corresponds to  $m_t = 173.5 \pm 1.0$  GeV). The weak mixing angle is determined to

$$\hat{s}_Z^2 = 0.23116 \pm 0.00012, \quad s_W^2 = 0.22296 \pm 0.00028,$$

while the corresponding effective angle is related by Eq. (10.18), *i.e.*,  $\bar{s}_\ell^2 = 0.23146 \pm 0.00012$ .

As described in Sec. 10.2 and the paragraph following Eq. (10.47) in Sec. 10.5, there is considerable stress in the experimental  $e^+e^-$  spectral functions and also conflict when these are compared with  $\tau$  decay spectral functions. These are below or above the  $2\sigma$  level (depending on what is actually compared) but not larger than the deviations of some other quantities entering our analyses. The number and size of these deviations are not inconsistent with what one would expect to happen as a result of random fluctuations. It is nevertheless instructive to study the effect of doubling the uncertainty in  $\Delta\alpha_{\text{had}}^{(3)}(1.8 \text{ GeV}) = (55.50 \pm 0.78) \times 10^{-4}$ , (see Sec. 10.2) on the extracted Higgs mass. The result,  $M_H = 95_{-23}^{+28}$  GeV, demonstrates that the uncertainty in  $\Delta\alpha_{\text{had}}$  is currently of only secondary importance. Note also, that a shift of  $\pm 0.0001$  in  $\Delta\alpha_{\text{had}}^{(3)}(1.8 \text{ GeV})$  corresponds to a shift of  $\mp 5$  GeV in  $M_H$  or about one fifth of its total uncertainty. The hadronic contribution to  $\alpha(M_Z)$  is correlated with  $g_\mu - 2$  (see Sec. 10.5). The measurement of the latter is higher than the SM prediction, and its inclusion in the fit favors a larger  $\alpha(M_Z)$  and a lower  $M_H$  (currently by about 4 GeV).

The weak mixing angle can be determined from  $Z$  pole observables,  $M_W$ , and from a variety of neutral-current processes spanning a very wide  $Q^2$  range. The results (for the older low energy neutral-current data see Refs. 128 and 213) shown in Table 10.6 are in reasonable agreement with each other, indicating the quantitative success of the SM. The largest discrepancy is the value  $\hat{s}_Z^2 = 0.23193 \pm 0.00028$  from the forward-backward asymmetries into bottom and charm quarks, which is  $2.8\sigma$  above the value  $0.23116 \pm 0.00012$  from the



global fit to all data. Similarly,  $\hat{s}_Z^2 = 0.23067 \pm 0.00029$  from the SLD asymmetries (in both cases when combined with  $M_Z$ ) is 1.8  $\sigma$  low. The SLD result has the additional difficulty (within the SM) of implying very low and excluded [173] Higgs masses. This is also true for  $\hat{s}_Z^2 = 0.23098 \pm 0.00022$  from  $M_W$  and  $M_Z$  and — as a consequence — for the global fit. We have therefore included in Table 10.3 and Table 10.4 an additional column (denoted Deviation) indicating the deviations if  $M_H = 124.5$  GeV [215] is fixed.

**Table 10.5:** Principal SM fit result including mutual correlations (all masses in GeV). Note that  $\hat{m}_c(\hat{m}_c)$  induces a significant uncertainty in the running of  $\alpha$  beyond  $\Delta\alpha_{\text{had}}^{(3)}$  (1.8 GeV) resulting in a relatively large correlation with  $M_H$ . Since this effect is proportional to the quark’s electric charge squared it is much smaller for  $\hat{m}_b(\hat{m}_b)$ .

$M_Z$	$91.1874 \pm 0.0021$	1.00	-0.01	0.00	0.00	-0.01	0.00	0.14
$\hat{m}_t(\hat{m}_t)$	$163.71 \pm 0.95$	-0.01	1.00	0.01	-0.01	-0.15	0.00	0.31
$\hat{m}_b(\hat{m}_b)$	$4.197 \pm 0.025$	0.00	0.01	1.00	0.24	-0.04	0.01	0.04
$\hat{m}_c(\hat{m}_c)$	$1.266_{-0.040}^{+0.032}$	0.00	-0.01	0.24	1.00	0.09	0.03	0.14
$\alpha_s(M_Z)$	$0.1196 \pm 0.0017$	-0.01	-0.15	-0.04	0.09	1.00	-0.01	-0.05
$\Delta\alpha_{\text{had}}^{(3)}$ (1.8 GeV)	$0.00561 \pm 0.00008$	0.00	0.00	0.01	0.03	-0.01	1.00	-0.16
$M_H$	$99_{-23}^{+28}$	0.14	0.31	0.04	0.14	-0.05	-0.16	1.00

**Table 10.6:** Values of  $\hat{s}_Z^2$ ,  $s_W^2$ ,  $\alpha_s$ , and  $M_H$  [in GeV] for various (combinations of) observables. Unless indicated otherwise, the top quark mass,  $m_t = 173.4 \pm 1.0$  GeV, is used as an additional constraint in the fits. The (†) symbol indicates a fixed parameter.

Data	$\hat{s}_Z^2$	$s_W^2$	$\alpha_s(M_Z)$	$M_H$
All data	0.23116(12)	0.22295(28)	0.1196(17)	$99_{-23}^{+28}$
All indirect (no $m_t$ )	0.23118(14)	0.22285(35)	0.1197(17)	$134_{-65}^{+144}$
Z pole (no $m_t$ )	0.23121(17)	0.22318(60)	0.1197(28)	$102_{-51}^{+133}$
LEP 1 (no $m_t$ )	0.23152(20)	0.22383(67)	0.1213(30)	$191_{-105}^{+266}$
SLD + $M_Z$	0.23067(28)	0.22204(54)	0.1185 (†)	$39_{-19}^{+31}$
$A_{FB}^{(b,c)} + M_Z$	0.23193(28)	0.22494(76)	0.1185 (†)	$444_{-178}^{+300}$
$M_W + M_Z$	0.23098(22)	0.22262(47)	0.1185 (†)	$75_{-30}^{+39}$
$M_Z$	0.23124(5)	0.22318(13)	0.1185 (†)	124.5 (†)
$Q_W(e)$	0.2332(15)	0.2252(15)	0.1185 (†)	124.5 (†)
$Q_W$ (APV)	0.2311(16)	0.2230(17)	0.1185 (†)	124.5 (†)
$\nu_\mu$ -N DIS (isoscalar)	0.2332(39)	0.2251(39)	0.1185 (†)	124.5 (†)
Elastic $\nu_\mu(\bar{\nu}_\mu)$ -e	0.2311(77)	0.2230(77)	0.1185 (†)	124.5 (†)
e-D DIS (SLAC)	0.222(18)	0.214(18)	0.1185 (†)	124.5 (†)
Elastic $\nu_\mu(\bar{\nu}_\mu)$ -p	0.211(33)	0.203(33)	0.1185 (†)	124.5 (†)

The extracted Z pole value of  $\alpha_s(M_Z)$  is based on a formula with negligible theoretical uncertainty if one assumes the exact validity of the SM. One should keep in mind, however, that this value,  $\alpha_s(M_Z) = 0.1197 \pm 0.0028$ , is very sensitive to such types of new physics as non-universal vertex corrections. In contrast, the value derived from  $\tau$  decays,  $\alpha_s(M_Z) = 0.1193_{-0.0020}^{+0.0022}$ , is theory dominated but less sensitive to new physics. The two values are in remarkable agreement with each other. They are also in perfect agreement with the averages from jet-event shapes in  $e^+e^-$  annihilation

( $0.1172 \pm 0.0037$ ) and lattice simulations ( $0.1185 \pm 0.0007$ ), whereas the DIS average ( $0.1150 \pm 0.0021$ ) is somewhat lower. For more details, other determinations, and references, see Section 9 on “Quantum Chromodynamics” in this *Review*. Using  $\alpha(M_Z)$  and  $\hat{s}_Z^2$  as inputs, one can predict  $\alpha_s(M_Z)$  assuming grand unification. One predicts [223]  $\alpha_s(M_Z) = 0.130 \pm 0.001 \pm 0.01$  for the simplest theories based on the minimal supersymmetric extension of the SM, where the first (second) uncertainty is from the inputs (thresholds).

This is slightly larger, but consistent with the experimental  $\alpha_s(M_Z) = 0.1196 \pm 0.0017$  from the Z lineshape and the  $\tau$  lifetime, as well as with most other determinations. Non-supersymmetric unified theories predict the low value  $\alpha_s(M_Z) = 0.073 \pm 0.001 \pm 0.001$ . See also the note on “Supersymmetry” in the Searches Particle Listings.

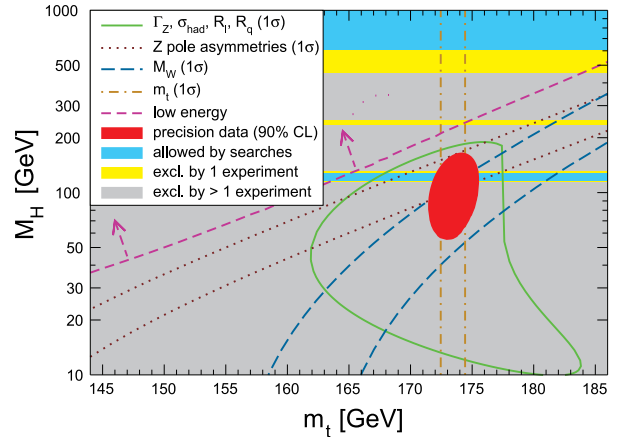


**Figure 10.5:** One-standard-deviation (39.35%) uncertainties in  $M_H$  as a function of  $m_t$  for various inputs, and the 90% CL region ( $\Delta\chi^2 = 4.605$ ) allowed by all data.  $\alpha_s(M_Z) = 0.1185$  is assumed except for the fits including the Z lineshape or low energy data. The bright (yellow) bands are excluded by one experiment and the remaining (gray) regions are ruled out by more than one experiment (95% CL).

The data indicate a preference for a small Higgs mass. There is a strong correlation between the quadratic  $m_t$  and logarithmic  $M_H$  terms in  $\hat{\rho}$  in all of the indirect data except for the  $Z \rightarrow b\bar{b}$  vertex. Therefore, observables (other than  $R_b$ ) which favor  $m_t$  values higher than the Tevatron range favor lower values of  $M_H$ .  $M_W$  has additional  $M_H$  dependence through  $\Delta\hat{r}_W$  which is not coupled to  $m_t^2$  effects. The strongest individual pulls toward smaller  $M_H$  are from  $M_W$  and

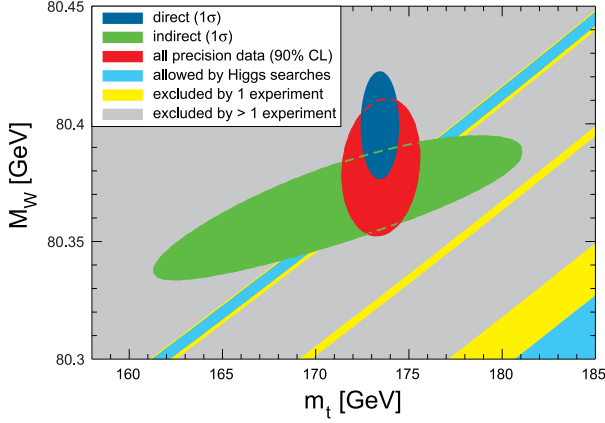


**Figure 10.6:** One-standard-deviation (39.35%) region in  $M_W$  as a function of  $m_t$  for the direct and indirect precision data, and the 90% CL region ( $\Delta\chi^2 = 4.605$ ) allowed by all precision data. The SM predictions are also indicated, where the blue bands for Higgs masses between 115.5 and 127 GeV and beyond 600 GeV are currently allowed at the 95% CL. The yellow bands are excluded by one experiment and the remaining (gray) regions are ruled out by more than one experiment (95% CL).

$A_{LR}^0$ , while  $A_{FB}^{(0,b)}$  favors higher values. The difference in  $\chi^2$  for the global fit is  $\Delta\chi^2 = \chi^2(M_H = 314 \text{ GeV}) - \chi_{\min}^2 = 25$ . Hence, the data favor a small value of  $M_H$ , as in supersymmetric extensions of the SM. The central value of the global fit result,  $M_H = 99_{-23}^{+28}$  GeV, is below the direct lower bound from LEP 2,  $M_H \geq 114.4$  GeV (95% CL) [173], which was very recently extended slightly by ATLAS to  $M_H \geq 115.5$  GeV [224].

The 90% central confidence range from all precision data is

$$68 \text{ GeV} \leq M_H \leq 155 \text{ GeV}. \quad (10.49)$$

Including the results of the direct searches at LEP 2 [173] and the Tevatron [225] as extra contributions to the likelihood function reduces the 95% upper limit to  $M_H \leq 150$  GeV. As two further refinements, we account for (i) theoretical uncertainties from uncalculated higher order contributions by allowing the  $T$  parameter (see next subsection) subject to the constraint  $T = 0 \pm 0.02$ , (ii) the  $M_H$  dependence of the correlation matrix which gives slightly more weight to lower Higgs masses [226]. The resulting limits at 95 (90, 99)% CL are, respectively,

$$M_H \leq 175 \text{ (148, 210) GeV}. \quad (10.50)$$

In their Higgs searches in  $pp$  collisions with CM energy of 7 TeV, both ATLAS [224] and CMS [227] find results consistent with Eq. (10.50) and currently report  $\gtrsim 2 \sigma$  excess fluctuation near  $M_H = 119.5$  GeV (CMS only),  $M_H = 124$  GeV (CMS), and  $M_H = 126$  GeV (ATLAS only). Of course, these excesses do not constitute a discovery. However, it is useful to take them at face value for comparison with the precision data in Table 10.3, Table 10.4, and Table 10.6. A combination of all available data yields (at the 68% CL) [215]

$$M_H = 124.5 \pm 0.8 \text{ GeV}. \quad (10.51)$$

The resulting probability distribution has a twin peak structure (besides a smaller maximum at  $M_H = 118.5$  GeV) with almost equal probability at  $M_H = 124$  GeV and  $M_H = 125$  GeV [215].

One can also carry out a fit to the indirect data alone, *i.e.*, without including the constraint,  $m_t = 173.4 \pm 1.0$  GeV, from the hadron colliders. (The indirect prediction is for the  $\overline{\text{MS}}$  mass,  $\hat{m}_t(\hat{m}_t) = 167.5_{-7.3}^{+8.9}$  GeV, which is in the end converted to the pole mass). One obtains  $m_t = 177.5_{-7.8}^{+9.4}$  GeV, in perfect agreement with the direct Tevatron/LHC average. Using this indirect top mass value, the tendency for a light Higgs persists and Eq. (10.49) becomes  $46 \text{ GeV} \leq M_H \leq 306 \text{ GeV}$ . The relations between  $M_H$  and  $m_t$  for various observables are shown in Fig. 10.5.

One can also determine the radiative correction parameters  $\Delta r$ : from the global fit one obtains  $\Delta r = 0.0352 \pm 0.0009$  and  $\Delta\hat{r}_W =$

**Table 10.7:** Values of the model-independent neutral-current parameters, compared with the SM predictions. There is a second  $g_{V,A}^{\nu e}$  solution, given approximately by  $g_{V,A}^{\nu e} \leftrightarrow g_{A,V}^{\nu e}$ , which is eliminated by  $e^+e^-$  data under the assumption that the neutral current is dominated by the exchange of a single  $Z$  boson. The  $\epsilon_L$ , as well as the  $\epsilon_R$ , are strongly correlated and non-Gaussian, so that for implementations we recommend the parametrization using  $g_i^2$  and  $\theta_i = \tan^{-1}[\epsilon_i(u)/\epsilon_i(d)]$ ,  $i = L$  or  $R$ . The analysis of more recent low energy experiments in polarized electron scattering performed in Ref. 129 is included by means of the two orthogonal constraints,  $\cos\gamma C_{1d} - \sin\gamma C_{1u} = 0.342 \pm 0.063$  and  $\sin\gamma C_{1d} + \cos\gamma C_{1u} = -0.0285 \pm 0.0043$ , where  $\tan\gamma \approx 0.445$ . In the SM predictions, the uncertainty is from  $M_Z$ ,  $M_H$ ,  $m_t$ ,  $m_b$ ,  $m_c$ ,  $\hat{\alpha}(M_Z)$ , and  $\alpha_s$ .

Quantity	Experimental Value	SM	Correlation		
$\epsilon_L(u)$	$0.328 \pm 0.016$	0.3461(1)	non-Gaussian		
$\epsilon_L(d)$	$-0.440 \pm 0.011$	-0.4292(1)			
$\epsilon_R(u)$	$-0.179 \pm 0.013$	-0.1549(1)			
$\epsilon_R(d)$	$-0.027_{-0.048}^{+0.077}$	0.0775			
$g_L^2$	$0.3009 \pm 0.0028$	0.3040(2)	small		
$g_R^2$	$0.0328 \pm 0.0030$	0.0300			
$\theta_L$	$2.50 \pm 0.035$	2.4630(1)			
$\theta_R$	$4.56_{-0.27}^{+0.42}$	5.1765			
$g_{V,A}^{\nu e}$	$-0.040 \pm 0.015$	-0.0399(2)	-0.05		
$g_{V,A}^{\nu e}$	$-0.507 \pm 0.014$	-0.5064(1)			
$C_{1u} + C_{1d}$	$0.1537 \pm 0.0011$	0.1530(1)	0.64	-0.18	-0.01
$C_{1u} - C_{1d}$	$-0.516 \pm 0.014$	-0.5300(3)		-0.27	-0.02
$C_{2u} + C_{2d}$	$-0.21 \pm 0.57$	-0.0089			-0.30
$C_{2u} - C_{2d}$	$-0.077 \pm 0.044$	-0.0627(5)			
$Q_W(e) = -2C_{2e}$	$-0.0403 \pm 0.0053$	-0.0474(5)			

$0.06945 \pm 0.00019$ .  $M_W$  measurements [172,214] (when combined with  $M_Z$ ) are equivalent to measurements of  $\Delta r = 0.0342 \pm 0.0015$ , which is  $0.9 \sigma$  below the result from all other data,  $\Delta r = 0.0358 \pm 0.0011$ . Fig. 10.6 shows the 1  $\sigma$  contours in the  $M_W$ - $m_t$  plane from the direct and indirect determinations, as well as the combined 90% CL region. The indirect determination uses  $M_Z$  from LEP 1 as input, which is defined assuming an  $s$ -dependent decay width.  $M_W$  then corresponds to the  $s$ -dependent width definition, as well, and can be directly compared with the results from the Tevatron and LEP 2 which have been obtained using the same definition. The difference to a constant width definition is formally only of  $\mathcal{O}(\alpha^2)$ , but is strongly enhanced since the decay channels add up coherently. It is about 34 MeV for  $M_Z$  and 27 MeV for  $M_W$ . The residual difference between working consistently with one or the other definition is about 3 MeV, *i.e.*, of typical size for non-enhanced  $\mathcal{O}(\alpha^2)$  corrections [74–77].

Most of the parameters relevant to  $\nu$ -hadron,  $\nu$ - $e$ ,  $e$ -hadron, and  $e^-e^\pm$  processes are determined uniquely and precisely from the data in “model-independent” fits (*i.e.*, fits which allow for an arbitrary EW gauge theory). The values for the parameters defined in Eqs. (10.19)–(10.22) are given in Table 10.7 along with the predictions of the SM. The agreement is very good. (The  $\nu$ -hadron results including the original NuTeV data can be found in the 2006 edition of this *Review*, and fits with modified NuTeV constraints in the 2008 and 2010 editions.) The off  $Z$  pole  $e^+e^-$  results are difficult to present in a model-independent way because  $Z$  propagator effects are non-negligible at TRISTAN, PETRA, PEP, and LEP 2 energies. However, assuming  $e$ - $\mu$ - $\tau$  universality, the low energy lepton asymmetries imply [159]  $4(g_A^e)^2 = 0.99 \pm 0.05$ , in good agreement with the SM prediction  $\simeq 1$ .

## 10.7. Constraints on new physics

The  $Z$  pole,  $W$  mass, and low energy data can be used to search for and set limits on deviations from the SM. We will mainly discuss the effects of exotic particles (with heavy masses  $M_{\text{new}} \gg M_Z$  in an expansion in  $M_Z/M_{\text{new}}$ ) on the gauge boson self-energies. (Brief remarks are made on new physics which is not of this type.) Most of the effects on precision measurements can be described by three gauge self-energy parameters  $S$ ,  $T$ , and  $U$ . We will define these, as well as related parameters, such as  $\rho_0$ ,  $\epsilon_i$ , and  $\hat{\epsilon}_i$ , to arise from new physics only. *I.e.*, they are equal to zero ( $\rho_0 = 1$ ) exactly in the SM, and do not include any (loop induced) contributions that depend on  $m_t$  or  $M_H$ , which are treated separately. Our treatment differs from most of the original papers.

Many extensions of the SM can be described by the  $\rho_0$  parameter,

$$\rho_0 \equiv \frac{M_W^2}{M_Z^2 \hat{c}_Z^2 \hat{\rho}}, \quad (10.52)$$

which describes new sources of SU(2) breaking that cannot be accounted for by the SM Higgs doublet or  $m_t$  effects.  $\hat{\rho}$  is calculated as in Eq. (10.13) assuming the validity of the SM. In the presence of  $\rho_0 \neq 1$ , Eq. (10.52) generalizes the second Eq. (10.13) while the first remains unchanged. Provided that the new physics which yields  $\rho_0 \neq 1$  is a small perturbation which does not significantly affect the radiative corrections,  $\rho_0$  can be regarded as a phenomenological parameter which multiplies  $G_F$  in Eqs. (10.19)–(10.22), (10.36), and  $\Gamma_Z$  in Eq. (10.42c). There are enough data to determine  $\rho_0$ ,  $M_H$ ,  $m_t$ , and  $\alpha_s$ , simultaneously. From the global fit,

$$\rho_0 = 1.0004_{-0.0004}^{+0.0003}, \quad (10.53)$$

$$115.5 \text{ GeV} \leq M_H \leq 127 \text{ GeV}, \quad (10.54)$$

$$m_t = 173.4 \pm 1.0 \text{ GeV}, \quad (10.55)$$

$$\alpha_s(M_Z) = 0.1195 \pm 0.0017, \quad (10.56)$$

where the limits on  $M_H$  are nominal direct search bounds at the 95% CL [173,224,227]. In addition, the LHC is not yet sensitive to very large values of  $M_H > 600$  GeV which are thus not ruled out either. In this very high mass scenario, we obtain,

$$\rho_0 = 1.0024_{-0.0003}^{+0.0010}, \quad (10.57)$$

$$0.6 \text{ TeV} \leq M_H \leq 1.2 \text{ TeV}, \quad (10.58)$$

$$\alpha_s(M_Z) = 0.1191 \pm 0.0016, \quad (10.59)$$

with the same  $m_t$ . Finally, if the direct search results are ignored entirely one finds  $M_H = 189_{-114}^{+568}$  GeV and  $\rho_0 = 1.0008_{-0.0011}^{+0.0020}$ . The result in Eq. (10.53) is slightly above but consistent with the SM expectation,  $\rho_0 = 1$ . It can be used to constrain higher-dimensional Higgs representations to have vacuum expectation values of less than a few percent of those of the doublets. Indeed, the relation between  $M_W$  and  $M_Z$  is modified if there are Higgs multiplets with weak isospin  $> 1/2$  with significant vacuum expectation values. For a general (charge-conserving) Higgs structure,

$$\rho_0 = \frac{\sum_i [t(i)t(i) - t_3(i)^2] |v_i|^2}{2 \sum_i t_3(i)^2 |v_i|^2}, \quad (10.60)$$

where  $v_i$  is the expectation value of the neutral component of a Higgs multiplet with weak isospin  $t(i)$  and third component  $t_3(i)$ . In order to calculate to higher orders in such theories one must define a set of four fundamental renormalized parameters which one may conveniently choose to be  $\alpha$ ,  $G_F$ ,  $M_Z$ , and  $M_W$ , since  $M_W$  and  $M_Z$  are directly measurable. Then  $\hat{s}_Z^2$  and  $\rho_0$  can be considered dependent parameters.

Eq. (10.53) can also be used to constrain other types of new physics. For example, non-degenerate multiplets of heavy fermions or scalars break the vector part of weak SU(2) and lead to a decrease in the value of  $M_Z/M_W$ . A non-degenerate SU(2) doublet ( $\begin{smallmatrix} f_1 \\ f_2 \end{smallmatrix}$ ) yields a positive contribution to  $\rho_0$  [228] of

$$\frac{C G_F}{8\sqrt{2}\pi^2} \Delta m^2, \quad (10.61)$$

where

$$\Delta m^2 \equiv m_1^2 + m_2^2 - \frac{4m_1^2 m_2^2}{m_1^2 - m_2^2} \ln \frac{m_1}{m_2} \geq (m_1 - m_2)^2, \quad (10.62)$$

and  $C = 1$  (3) for color singlets (triplets). Thus, in the presence of such multiplets,

$$\rho_0 = 1 + \frac{3 G_F}{8\sqrt{2}\pi^2} \sum_i \frac{C_i}{3} \Delta m_i^2, \quad (10.63)$$

where the sum includes fourth-family quark or lepton doublets, ( $\begin{smallmatrix} \nu \\ b \end{smallmatrix}$ ) or ( $\begin{smallmatrix} E^0 \\ E^- \end{smallmatrix}$ ), right-handed (mirror) doublets, non-degenerate vector-like fermion doublets (with an extra factor of 2), and scalar doublets such as ( $\begin{smallmatrix} \tilde{t} \\ \tilde{b} \end{smallmatrix}$ ) in Supersymmetry (in the absence of  $L$ - $R$  mixing).

Eq. (10.53) taken together with Eq. (10.63) implies at the 95% CL,

$$\sum_i \frac{C_i}{3} \Delta m_i^2 \leq (52 \text{ GeV})^2. \quad (10.64)$$

Non-degenerate multiplets usually imply  $\rho_0 > 1$ . Similarly, heavy  $Z'$  bosons decrease the prediction for  $M_Z$  due to mixing and generally lead to  $\rho_0 > 1$  [229]. On the other hand, additional Higgs doublets which participate in spontaneous symmetry breaking [230] or heavy lepton doublets involving Majorana neutrinos [231], both of which have more complicated expressions, as well as the vacuum expectation values of Higgs triplets or higher-dimensional representations can contribute to  $\rho_0$  with either sign. Allowing for the presence of heavy degenerate chiral multiplets (the  $S$  parameter, to be discussed below) affects the determination of  $\rho_0$  from the data, at present leading to a larger value (for fixed  $M_H$ ).

A number of authors [232–237] have considered the general effects on neutral-current and  $Z$  and  $W$  boson observables of various types of heavy (*i.e.*,  $M_{\text{new}} \gg M_Z$ ) physics which contribute to the  $W$  and  $Z$  self-energies but which do not have any direct coupling to the ordinary fermions. In addition to non-degenerate multiplets, which break the vector part of weak SU(2), these include heavy degenerate multiplets of chiral fermions which break the axial generators. The effects of one degenerate chiral doublet are small, but in Technicolor theories there may be many chiral doublets and therefore significant effects [232].

Such effects can be described by just three parameters,  $S$ ,  $T$ , and  $U$ , at the (EW) one-loop level. (Three additional parameters are needed if the new physics scale is comparable to  $M_Z$  [238]. Further generalizations, including effects relevant to LEP 2, are described in Ref. 239.)  $T$  is proportional to the difference between the  $W$  and  $Z$  self-energies at  $Q^2 = 0$  (*i.e.*, vector SU(2)-breaking), while  $S$  ( $S+U$ ) is associated with the difference between the  $Z$  ( $W$ ) self-energy at  $Q^2 = M_{Z,W}^2$  and  $Q^2 = 0$  (axial SU(2)-breaking). Denoting the contributions of new physics to the various self-energies by  $\Pi_{ij}^{\text{new}}$ , we have

$$\hat{\alpha}(M_Z) T \equiv \frac{\Pi_{WW}^{\text{new}}(0)}{M_W^2} - \frac{\Pi_{ZZ}^{\text{new}}(0)}{M_Z^2}, \quad (10.65a)$$

$$\begin{aligned} \hat{\alpha}(M_Z) S \equiv & \frac{\Pi_{ZZ}^{\text{new}}(M_Z^2) - \Pi_{ZZ}^{\text{new}}(0)}{4 \hat{s}_Z^2 \hat{c}_Z^2} - \frac{\Pi_{ZZ}^{\text{new}}(M_Z^2) - \Pi_{ZZ}^{\text{new}}(0)}{M_Z^2} \\ & - \frac{\hat{c}_Z^2 - \hat{s}_Z^2}{\hat{c}_Z \hat{s}_Z} \frac{\Pi_{Z\gamma}^{\text{new}}(M_Z^2)}{M_Z^2} - \frac{\Pi_{\gamma\gamma}^{\text{new}}(M_Z^2)}{M_Z^2}, \end{aligned} \quad (10.65b)$$

$$\begin{aligned} \hat{\alpha}(M_Z) (S+U) \equiv & \frac{\Pi_{WW}^{\text{new}}(M_Z^2) - \Pi_{WW}^{\text{new}}(0)}{4 \hat{s}_Z^2} - \frac{\Pi_{ZZ}^{\text{new}}(M_Z^2) - \Pi_{ZZ}^{\text{new}}(0)}{M_Z^2} \\ & - \frac{\hat{c}_Z}{\hat{s}_Z} \frac{\Pi_{Z\gamma}^{\text{new}}(M_Z^2)}{M_Z^2} - \frac{\Pi_{\gamma\gamma}^{\text{new}}(M_Z^2)}{M_Z^2}. \end{aligned} \quad (10.65c)$$

$S$ ,  $T$ , and  $U$  are defined with a factor proportional to  $\hat{\alpha}$  removed, so that they are expected to be of order unity in the presence of new physics. In the  $\overline{\text{MS}}$  scheme as defined in Ref. 66, the last two terms in Eqs. (10.65b) and (10.65c) can be omitted (as was done in some earlier

editions of this *Review*). These three parameters are related to other parameters ( $S_i, h_i, \hat{\epsilon}_i$ ) defined in Refs. [66,233,234] by

$$\begin{aligned} T &= h_V = \hat{\epsilon}_1 / \hat{\alpha}(M_Z), \\ S &= h_{AZ} = S_Z = 4 \hat{s}_Z^2 \hat{\epsilon}_3 / \hat{\alpha}(M_Z), \\ U &= h_{AW} - h_{AZ} = S_W - S_Z = -4 \hat{s}_Z^2 \hat{\epsilon}_2 / \hat{\alpha}(M_Z). \end{aligned} \quad (10.66)$$

A heavy non-degenerate multiplet of fermions or scalars contributes positively to  $T$  as

$$\rho_0 - 1 = \frac{1}{1 - \hat{\alpha}(M_Z)T} - 1 \simeq \hat{\alpha}(M_Z)T, \quad (10.67)$$

where  $\rho_0$  is given in Eq. (10.63). The effects of non-standard Higgs representations cannot be separated from heavy non-degenerate multiplets unless the new physics has other consequences, such as vertex corrections. Most of the original papers defined  $T$  to include the effects of loops only. However, we will redefine  $T$  to include all new sources of SU(2) breaking, including non-standard Higgs, so that  $T$  and  $\rho_0$  are equivalent by Eq. (10.67).

A multiplet of heavy degenerate chiral fermions yields

$$S = \frac{C}{3\pi} \sum_i (t_{3L}(i) - t_{3R}(i))^2, \quad (10.68)$$

where  $t_{3L,R}(i)$  is the third component of weak isospin of the left-(right-)handed component of fermion  $i$  and  $C$  is the number of colors. For example, a heavy degenerate ordinary or mirror family would contribute  $2/3\pi$  to  $S$ . In Technicolor models with QCD-like dynamics, one expects [232]  $S \sim 0.45$  for an iso-doublet of techni-fermions, assuming  $N_{TC} = 4$  techni-colors, while  $S \sim 1.62$  for a full techni-generation with  $N_{TC} = 4$ ;  $T$  is harder to estimate because it is model-dependent. In these examples one has  $S \geq 0$ . However, the QCD-like models are excluded on other grounds (flavor changing neutral-currents, and too-light quarks and pseudo-Goldstone bosons [240]). In particular, these estimates do not apply to models of walking Technicolor [240], for which  $S$  can be smaller or even negative [241]. Other situations in which  $S < 0$ , such as loops involving scalars or Majorana particles, are also possible [242]. The simplest origin of  $S < 0$  would probably be an additional heavy  $Z'$  boson [229], which could mimic  $S < 0$ . Supersymmetric extensions of the SM generally give very small effects. See Refs. 243 and 244 and the note on ‘‘Supersymmetry’’ in the Searches Particle Listings for a complete set of references.

Most simple types of new physics yield  $U = 0$ , although there are counter-examples, such as the effects of anomalous triple gauge vertices [234].

The SM expressions for observables are replaced by

$$\begin{aligned} M_Z^2 &= M_{Z0}^2 \frac{1 - \hat{\alpha}(M_Z)T}{1 - G_F M_{Z0}^2 S / 2\sqrt{2}\pi}, \\ M_W^2 &= M_{W0}^2 \frac{1}{1 - G_F M_{W0}^2 (S + U) / 2\sqrt{2}\pi}, \end{aligned} \quad (10.69)$$

where  $M_{Z0}$  and  $M_{W0}$  are the SM expressions (as functions of  $m_t$  and  $M_H$ ) in the  $\overline{\text{MS}}$  scheme. Furthermore,

$$\Gamma_Z = \frac{M_Z^3 \beta_Z}{1 - \hat{\alpha}(M_Z)T}, \quad \Gamma_W = M_W^3 \beta_W, \quad A_i = \frac{A_{i0}}{1 - \hat{\alpha}(M_Z)T}, \quad (10.70)$$

where  $\beta_Z$  and  $\beta_W$  are the SM expressions for the reduced widths  $\Gamma_{Z0}/M_{Z0}^3$  and  $\Gamma_{W0}/M_{W0}^3$ ,  $M_Z$  and  $M_W$  are the physical masses, and  $A_i$  ( $A_{i0}$ ) is a neutral-current amplitude (in the SM).

The data allow a simultaneous determination of  $\hat{s}_Z^2$  (from the  $Z$  pole asymmetries),  $S$  (from  $M_Z$ ),  $U$  (from  $M_W$ ),  $T$  (mainly from  $\Gamma_Z$ ),  $\alpha_s$  (from  $R_\ell$ ,  $\sigma_{\text{had}}$ , and  $\tau_\tau$ ), and  $m_t$  (from the hadron colliders), with little correlation among the SM parameters:

$$\begin{aligned} S &= 0.00_{-0.10}^{+0.11}, \\ T &= 0.02_{-0.12}^{+0.11}, \\ U &= 0.08 \pm 0.11, \end{aligned} \quad (10.71)$$

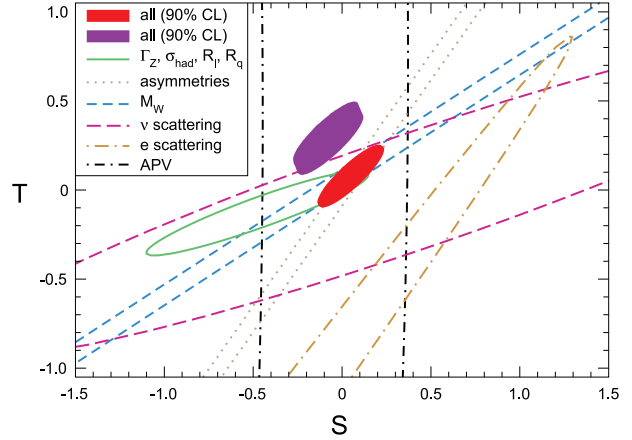


**Figure 10.7:**  $1\sigma$  constraints (39.35%) on  $S$  and  $T$  from various inputs combined with  $M_Z$ .  $S$  and  $T$  represent the contributions of new physics only. (Uncertainties from  $m_t$  are included in the errors.) The contours assume  $115.5 \text{ GeV} < M_H < 127 \text{ GeV}$  except for the larger (violet) one for all data which is for  $600 \text{ GeV} < M_H < 1 \text{ TeV}$ . Data sets not involving  $M_W$  are insensitive to  $U$ . Due to higher order effects, however,  $U = 0$  has to be assumed in all fits.  $\alpha_s$  is constrained using the  $\tau$  lifetime as additional input in all fits. The long-dashed (magenta) contour from  $\nu$  scattering is now consistent with the global average (see Sec. 10.3). The long-dash-dotted (orange) contour from polarized  $e$  scattering [129,131] is the upper tip of an elongated ellipse centered at around  $S = -14$  and  $T = -20$ . At first sight it looks as if it is deviating strongly but it is off by only  $1.8\sigma$ . This illusion arises because  $\Delta\chi^2 > 0.77$  everywhere on the visible part of the contour.

and  $\hat{s}_Z^2 = 0.23125 \pm 0.00016$ ,  $\alpha_s(M_Z) = 0.1197 \pm 0.0018$ ,  $m_t = 173.4 \pm 1.0 \text{ GeV}$ , where the uncertainties are from the inputs. We have used  $115.5 \text{ GeV} < M_H < 127 \text{ GeV}$  which is the allowed low mass window from LEP and the LHC. The SM parameters ( $U$ ) can be determined with no (little)  $M_H$  dependence. On the other hand,  $S$ ,  $T$ , and  $M_H$  cannot be obtained simultaneously from the precision data alone, because the Higgs boson loops themselves are resembled approximately by oblique effects. Negative (positive) contributions to the  $S$  ( $T$ ) parameter can weaken or entirely remove the strong constraints on  $M_H$  from the SM fits. Specific models in which a large  $M_H$  is compensated by new physics are reviewed in Ref. 245. The parameters in Eqs. (10.71), which by definition are due to new physics only, are in reasonable agreement with the SM values of zero. Fixing  $U = 0$  (as is also done in Fig. 10.7) moves  $S$  and  $T$  slightly upwards,

$$\begin{aligned} S &= 0.04 \pm 0.09, \\ T &= 0.07 \pm 0.08. \end{aligned} \quad (10.72)$$

The correlation between  $S$  and  $T$  in this fit amounts to 88%.

Using Eq. (10.67), the value of  $\rho_0$  corresponding to  $T$  in Eq. (10.71) is  $1.0001 \pm 0.0009$ , while the one corresponding to Eq. (10.72) is  $1.0005_{-0.0006}^{+0.0007}$ . The values of the  $\hat{\epsilon}$  parameters defined in Eq. (10.66) are

$$\begin{aligned} \hat{\epsilon}_3 &= 0.0000 \pm 0.0008, \\ \hat{\epsilon}_1 &= 0.0001 \pm 0.0009 \\ \hat{\epsilon}_2 &= -0.0006 \pm 0.0009. \end{aligned} \quad (10.73)$$

Unlike the original definition, we defined the quantities in Eqs. (10.73) to vanish identically in the absence of new physics and to correspond directly to the parameters  $S$ ,  $T$ , and  $U$  in Eqs. (10.71). There is a strong correlation (89%) between the  $S$  and  $T$  parameters. The  $U$  parameter is  $-49\%$  ( $-70\%$ ) anti-correlated with  $S$  ( $T$ ). The allowed regions in  $S$ - $T$  are shown in Fig. 10.7. From Eqs. (10.71) one obtains  $S \leq 0.17$  and  $T \leq 0.20$  at 95% CL.

If one assumes that the excess Higgs candidates seen at the LHC are statistical fluctuations then (in the presence of new physics significantly affecting gauge boson self-energies) there is still the possibility for a heavy Higgs scenario. If one fixes  $M_H = 600$  GeV (as is still allowed by direct searches) and requires the constraint  $S \geq 0$  (as is appropriate in QCD-like Technicolor models) then  $S \leq 0.13$  (Bayesian) or  $S \leq 0.11$  (frequentist). This rules out simple Technicolor models with many techni-doublets and QCD-like dynamics.

The  $S$  parameter can also be used to constrain the number of fermion families, *under the assumption* that there are no new contributions to  $T$  or  $U$  and therefore that any new families are degenerate; then an extra generation of SM fermions is excluded at the  $5.7 \sigma$  level corresponding to  $N_F = 2.91^{+0.19}_{-0.25}$  (with  $M_H$  in the allowed low mass window). This is in agreement with a fit to the number of light neutrinos,  $N_\nu = 2.989 \pm 0.007$ . However, the  $S$  parameter fits are valid even for a very heavy fourth family neutrino. This restriction can be relaxed by allowing  $T$  to vary as well, since  $T > 0$  is expected from a non-degenerate extra family. Fixing  $S = 2/3\pi$ , the global fit favors a fourth family contribution to  $T$  of  $0.21 \pm 0.04$ . However, the quality of the fit deteriorates ( $\Delta\chi^2 = 3.8$  relative to the SM fit with  $M_H$  forced not to drop below its ATLAS bound of 115.5 GeV) so that this tuned  $T$  scenario is also disfavored but less so than in the past. In fact, tuned mass splittings of the extra leptons and quarks [246] can yield fits with only moderately higher  $\chi^2$  values (by about 1 unit) than for the SM. A more detailed analysis is also required if the extra neutrino (or the extra down-type quark) is close to its direct mass limit [247]. Thus, a fourth family is disfavored but not excluded by the current EW precision data. Similar remarks apply to a heavy mirror family [248] involving right-handed SU(2) doublets and left-handed singlets. A more recent and detailed discussion can be found in Ref. 249. One important consequence of a heavy fourth family is to increase the Higgs production cross section by gluon fusion by a factor  $\sim 9$ , which considerably strengthens the exclusion limits from direct searches at the Tevatron [250] and LHC [251]. Additional heavy ordinary or mirror generations may also require large Yukawa and Higgs couplings that may lead to Landau poles at low scales [252]. In contrast, heavy degenerate non-chiral (also known as vector-like or exotic) multiplets, which are predicted in many grand unified theories [253] and other extensions of the SM, do not contribute to  $S$ ,  $T$ , and  $U$  (or to  $\rho_0$ ), and do not require large coupling constants. Such exotic multiplets may occur in partial families, as in  $E_6$  models, or as complete vector-like families [254].

There is no simple parametrization to describe the effects of every type of new physics on every possible observable. The  $S$ ,  $T$ , and  $U$  formalism describes many types of heavy physics which affect only the gauge self-energies, and it can be applied to all precision observables. However, new physics which couples directly to ordinary fermions, such as heavy  $Z'$  bosons [229], mixing with exotic fermions [255], or leptoquark exchange [172,256] cannot be fully parametrized in the  $S$ ,  $T$ , and  $U$  framework. It is convenient to treat these types of new physics by parameterizations that are specialized to that particular class of theories (*e.g.*, extra  $Z'$  bosons), or to consider specific models (which might contain, *e.g.*,  $Z'$  bosons and exotic fermions with correlated parameters). Fits to Supersymmetric models are described in Ref. 244. Models involving strong dynamics (such as (extended) Technicolor) for EW breaking are considered in Ref. 257. The effects of compactified extra spatial dimensions at the TeV scale are reviewed in Ref. 258, and constraints on Little Higgs models in Ref. 259. The implications of non-standard Higgs sectors, *e.g.*, involving Higgs singlets or triplets, are discussed in Ref. 260, while additional Higgs doublets are considered in Ref. 230. Limits on new four-Fermi operators and on leptoquarks using LEP 2 and lower energy data are given in Refs. 172 and 261. Constraints on various types of new physics are reviewed in Refs. [7,128,149,161,262,263], and implications for the LHC in Ref. 264.

An alternate formalism [265] defines parameters,  $\epsilon_1$ ,  $\epsilon_2$ ,  $\epsilon_3$ , and  $\epsilon_b$  in terms of the specific observables  $M_W/M_Z$ ,  $\Gamma_{\ell\ell}$ ,  $A_{FB}^{(0,\ell)}$ , and  $R_b$ . The definitions coincide with those for  $\hat{\epsilon}_i$  in Eqs. (10.65) and (10.66) for physics which affects gauge self-energies only, but the  $\epsilon$ 's now parametrize arbitrary types of new physics. However, the  $\epsilon$ 's are not related to other observables unless additional model-dependent

**Table 10.8:** 95% CL lower mass limits (in GeV) from low energy and  $Z$  pole data on various extra  $Z'$  gauge bosons, appearing in models of unification and string theory. More general parametrizations are described in Refs. 267 and 272. The EW results [273] are for Higgs sectors consisting of doublets and singlets only ( $\rho_0 = 1$ ) with unspecified  $U(1)'$  charges. The next two columns show the limits from ATLAS [274] and CMS [275] from the combination of both lepton channels. The CDF [276] and DØ [277] bounds from searches for  $\bar{p}p \rightarrow \mu^+\mu^-$  and  $e^+e^-$ , respectively, are listed in the next two columns, followed by the LEP 2  $e^+e^- \rightarrow f\bar{f}$  bounds [172] (assuming  $\theta = 0$ ). The Tevatron bounds would be moderately weakened if there are open supersymmetric or exotic decay channels [278]. The last column shows the  $1 \sigma$  ranges for  $M_H$  when it is left unconstrained in the EW fits.

$Z'$	EW	ATLAS	CMS	CDF	DØ	LEP 2	$M_H$
$Z_\chi$	1,141	1,640	–	930	903	673	$171^{+493}_{-89}$
$Z_\psi$	147	1,490	1,620	917	891	481	$97^{+31}_{-25}$
$Z_\eta$	427	1,540	–	938	923	434	$423^{+577}_{-350}$
$Z_{LR}$	998	–	–	–	–	804	$804^{+174}_{-35}$
$Z_S$	1,257	1,600	–	858	822	–	$149^{+353}_{-68}$
$Z_{SM}$	1,403	1,830	1,940	1,071	1,023	1,787	$331^{+669}_{-246}$
$Z_{string}$	1,362	–	–	–	–	–	$134^{+209}_{-58}$

assumptions are made. Another approach [266] parametrizes new physics in terms of gauge-invariant sets of operators. It is especially powerful in studying the effects of new physics on non-Abelian gauge vertices. The most general approach introduces deviation vectors [262]. Each type of new physics defines a deviation vector, the components of which are the deviations of each observable from its SM prediction, normalized to the experimental uncertainty. The length (direction) of the vector represents the strength (type) of new physics.

One of the best motivated kinds of physics beyond the SM besides Supersymmetry are extra  $Z'$  bosons [267]. They do not spoil the observed approximate gauge coupling unification, and appear copiously in many Grand Unified Theories (GUTs), most Superstring models [268], as well as in dynamical symmetry breaking [257] and Little Higgs models [259]. For example, the SO(10) GUT contains an extra U(1) as can be seen from its maximal subgroup,  $SU(5) \times U(1)_\chi$ . Similarly, the  $E_6$  GUT contains the subgroup  $SO(10) \times U(1)_\psi$ . The  $Z_\psi$  possesses only axial-vector couplings to the ordinary fermions, and its mass is generally less constrained. The  $Z_\eta$  boson is the linear combination  $\sqrt{3/8}Z_\chi - \sqrt{5/8}Z_\psi$ . The  $Z_{LR}$  boson occurs in left-right models with gauge group  $SU(3)_C \times SU(2)_L \times SU(2)_R \times U(1)_{B-L} \subset SO(10)$ , and the secluded  $Z_S$  emerges in a supersymmetric bottom-up scenario [269]. The sequential  $Z_{SM}$  boson is defined to have the same couplings to fermions as the SM  $Z$  boson. Such a boson is not expected in the context of gauge theories unless it has different couplings to exotic fermions than the ordinary  $Z$  boson. However, it serves as a useful reference case when comparing constraints from various sources. It could also play the role of an excited state of the ordinary  $Z$  boson in models with extra dimensions at the weak scale [258]. Finally, we consider a Superstring motivated  $Z_{string}$  boson appearing in a specific model [270]. The potential  $Z'$  boson is in general a superposition of the SM  $Z$  and the new boson associated with the extra U(1). The mixing angle  $\theta$  satisfies,

$$\tan^2 \theta = \frac{M_{Z'_0}^2 - M_Z^2}{M_{Z'}^2 - M_{Z'_0}^2},$$

where  $M_{Z'_0}$  is the SM value for  $M_Z$  in the absence of mixing. Note, that  $M_Z < M_{Z'_0}$ , and that the SM  $Z$  couplings are changed by the mixing. The couplings of the heavier  $Z'$  may also be modified by kinetic mixing [267,271]. If the Higgs U(1)' quantum numbers are

known, there will be an extra constraint,

$$\theta = C \frac{g_2}{g_1} \frac{M_Z^2}{M_{Z'}^2},$$

where  $g_{1,2}$  are the  $U(1)$  and  $U(1)'$  gauge couplings with  $g_2 = \sqrt{\frac{5}{3}} \sin \theta_W \sqrt{\lambda} g_1$  and  $g_1 = \sqrt{g^2 + g'^2}$ .  $\lambda \sim 1$  (which we assume) if the GUT group breaks directly to  $SU(3) \times SU(2) \times U(1) \times U(1)'$ .  $C$  is a function of vacuum expectation values. For minimal Higgs sectors it can be found in Ref. 229. Table 10.8 shows the 95% CL lower mass limits [273] for  $\rho_0 = 1$  and  $114.4 \text{ GeV} \leq M_H \leq 1 \text{ TeV}$ . The last column shows the  $1 \sigma$  ranges for  $M_H$  when it is left unconstrained. In cases of specific minimal Higgs sectors where  $C$  is known, the  $Z'$  mass limits from the EW precision data are generally pushed into the TeV region in which case they are still competitive with those from the LHC, and they are also competitive in the case of large  $g_2$  [279]. The limits on  $|\theta|$  are typically smaller than a few  $\times 10^{-3}$ . For more details see [267,273,280,281] and the note on “The  $Z'$  Searches” in the Gauge & Higgs Boson Particle Listings. Also listed in Table 10.8 are the direct lower limits on  $Z'$  production from the LHC [274,275] and the Tevatron [276,277], as well as the LEP 2 bounds [172].

#### Acknowledgments:

We are indebted to M. Davier, B. Malaescu, and K. Maltman for providing us with additional information about their work in a form suitable to be included in our fits. We also thank R. H. Bernstein, K. S. McFarland, H. Schellman, and G. P. Zeller for discussions on the NuTeV analysis. This work was supported in part by CONACyT (México) contract 82291-F and by PASPA (DGAPA-UNAM).

#### References:

1. S. L. Glashow, Nucl. Phys. **22**, 579 (1961);  
S. Weinberg, Phys. Rev. Lett. **19**, 1264 (1967);  
A. Salam, p. 367 of *Elementary Particle Theory*, ed.  
N. Svartholm (Almqvist and Wiksells, Stockholm, 1969);  
S.L. Glashow, J. Iliopoulos, and L. Maiani, Phys. Rev. **D2**,  
1285 (1970).
2. CKMfitter Group: J. Charles *et al.*, Eur. Phys. J. **C41**, 1  
(2005);  
CKMfitter Group: S. T'Jampens *et al.*, PoS **ICHEP2010**, 269  
(2010).
3. For reviews, see the Section on “Higgs Bosons: Theory and  
Searches” in this *Review*;  
J. Gunion *et al.*, *The Higgs Hunter's Guide*, (Addison-Wesley,  
Redwood City, 1990);  
M. Carena and H.E. Haber, Prog. in Part. Nucl. Phys. **50**, 63  
(2003);  
A. Djouadi, Phys. Reports **457**, 1 (2008).
4. For reviews, see E.D. Commins and P.H. Bucksbaum, *Weak  
Interactions of Leptons and Quarks*, (Cambridge Univ. Press,  
1983);  
G. Barbiellini and C. Santoni, Riv. Nuovo Cimento **9(2)**, 1  
(1986);  
N. Severijns, M. Beck, and O. Naviliat-Cuncic, Rev. Mod. Phys. **78**, 991 (2006);  
W. Fetscher and H.J. Gerber, p. 657 of Ref. 5;  
J. Deutsch and P. Quin, p. 706 of Ref. 5;  
P. Herczeg, p. 786 of Ref. 5;  
P. Herczeg, Prog. in Part. Nucl. Phys. **46**, 413 (2001).
5. *Precision Tests of the Standard Electroweak Model*, ed.  
P. Langacker (World Scientific, Singapore, 1995).
6. J. Erler and M.J. Ramsey-Musolf, Prog. in Part. Nucl. Phys. **54**, 351 (2005).
7. P. Langacker, *The Standard Model and Beyond*, (CRC Press,  
New York, 2009).
8. T. Kinoshita, *Quantum Electrodynamics*, (World Scientific,  
Singapore, 1990).
9. S. G. Karshenboim, Phys. Reports **422**, 1 (2005).
10. P.J. Mohr, B.N. Taylor, and D.B. Newell, Rev. Mod. Phys. **80**,  
633 (2008); for updates see  
<http://physics.nist.gov/cuu/Constants/>.
11. ALEPH, DELPHI, L3, OPAL, SLD, LEP Electroweak Working  
Group, SLD Electroweak and Heavy Flavour Groups: S. Schael  
*et al.*, Phys. Reports **427**, 257 (2006); for updates see  
<http://lepewwg.web.cern.ch/LEPEWWG/>.
12. MuLan: D. M. Webber *et al.*, Phys. Rev. Lett. **106**, 041803  
(2011).
13. T. Kinoshita and A. Sirlin, Phys. Rev. **113**, 1652 (1959).
14. T. van Ritbergen and R.G. Stuart, Nucl. Phys. **B564**, 343  
(2000);  
M. Steinhauser and T. Seidensticker, Phys. Lett. **B467**, 271  
(1999).
15. Y. Nir, Phys. Lett. **B221**, 184 (1989).
16. A. Pak and A. Czarnecki, Phys. Rev. Lett. **100**, 241807 (2008).
17. For a review, see S. Mele, [arXiv:hep-ex/0610037](https://arxiv.org/abs/hep-ex/0610037).
18. S. Fanchiotti, B. Kniehl, and A. Sirlin, Phys. Rev. **D48**, 307  
(1993) and references therein.
19. J. Erler, Phys. Rev. **D59**, 054008 (1999).
20. M. Davier *et al.*, Eur. Phys. J. **C71**, 1515 (2011);  
the quoted value uses additional information thankfully provided  
to us by the authors in a private communication.
21. J. Erler, [hep-ph/0005084](https://arxiv.org/abs/hep-ph/0005084).
22. M. Steinhauser, Phys. Lett. **B429**, 158 (1998).
23. A.D. Martin and D. Zeppenfeld, Phys. Lett. **B345**, 558 (1995).
24. S. Eidelman and F. Jegerlehner, Z. Phys. **C67**, 585 (1995).
25. B.V. Geshkenbein and V.L. Morgunov, Phys. Lett. **B352**, 456  
(1995).
26. H. Burkhardt and B. Pietrzyk, Phys. Lett. **B356**, 398 (1995).
27. M.L. Swartz, Phys. Rev. **D53**, 5268 (1996).
28. R. Alemany, M. Davier, and A. Höcker, Eur. Phys. J. **C2**, 123  
(1998).
29. N.V. Krasnikov and R. Rodenberg, Nuovo Cimento **111A**, 217  
(1998).
30. M. Davier and A. Höcker, Phys. Lett. **B419**, 419 (1998).
31. J.H. Kühn and M. Steinhauser, Phys. Lett. **B437**, 425 (1998).
32. M. Davier and A. Höcker, Phys. Lett. **B435**, 427 (1998).
33. S. Groote *et al.*, Phys. Lett. **B440**, 375 (1998).
34. A.D. Martin, J. Outhwaite, and M.G. Ryskin, Phys. Lett.  
**B492**, 69 (2000).
35. H. Burkhardt and B. Pietrzyk, Phys. Lett. **B513**, 46 (2001).
36. J.F. de Troconiz and F.J. Yndurain, Phys. Rev. **D65**, 093002  
(2002).
37. F. Jegerlehner, Nucl. Phys. Proc. Suppl. **126**, 325 (2004).
38. K. Hagiwara *et al.*, Phys. Rev. **D69**, 093003 (2004).
39. H. Burkhardt and B. Pietrzyk, Phys. Rev. **D72**, 057501 (2005).
40. K. Hagiwara *et al.*, Phys. Lett. **B649**, 173 (2007).
41. F. Jegerlehner, Nucl. Phys. Proc. Suppl. **181**, 135 (2008).
42. K. Hagiwara *et al.*, J. Phys. **G38**, 085003 (2011).
43. OPAL: K. Ackerstaff *et al.*, Eur. Phys. J. **C7**, 571 (1999).
44. CLEO: S. Anderson *et al.*, Phys. Rev. **D61**, 112002 (2000).
45. ALEPH: S. Schael *et al.*, Phys. Reports **421**, 191 (2005).
46. Belle: M. Fujikawa *et al.*: Phys. Rev. **D78**, 072006 (2008).
47. CMD-2: R.R. Akhmetshin *et al.*, Phys. Lett. **B578**, 285 (2004);  
CMD-2: V.M. Aulchenko *et al.*, JETP Lett. **82**, 743 (2005);  
CMD-2: R.R. Akhmetshin *et al.*, JETP Lett. **84**, 413 (2006);  
CMD-2: R.R. Akhmetshin *et al.*, Phys. Lett. **B648**, 28 (2007).
48. SND: M.N. Achasov *et al.*, Sov. Phys. JETP **103**, 380 (2006).
49. A.B. Arbuzov *et al.*, JHEP **9812**, 009 (1998);  
S. Binner, J.H. Kühn, and K. Melnikov, Phys. Lett. **B459**, 279  
(1999).
50. BaBar: B. Aubert *et al.*, Phys. Rev. **D70**, 072004 (2004);  
BaBar: B. Aubert *et al.*, Phys. Rev. **D71**, 052001 (2005);  
BaBar: B. Aubert *et al.*, Phys. Rev. **D73**, 052003 (2006);  
BaBar: B. Aubert *et al.*, Phys. Rev. **D76**, 092005 (2007);  
BaBar: B. Aubert *et al.*, Phys. Rev. Lett. **103**, 231801 (2009).
51. KLOE: F. Ambrosino *et al.*, Phys. Lett. **B670**, 285 (2009);  
KLOE: F. Ambrosino *et al.*, Phys. Lett. **B700**, 102 (2011).
52. See *e.g.*, CMD and OLYA: L.M. Barkov *et al.*, Nucl. Phys.  
**B256**, 365 (1985).
53. V.A. Novikov *et al.*, Phys. Reports **41**, 1 (1978).
54. J. Erler and M. Luo, Phys. Lett. **B558**, 125 (2003).
55. K. G. Chetyrkin *et al.*, Phys. Rev. **D80**, 074010 (2009).



56. Tevatron Electroweak Working Group, CDF and DØ: [arXiv:1107.5255 \[hep-ex\]](https://arxiv.org/abs/1107.5255).
57. CMS: [cdsweb.cern.ch/record/1356578/files/TOP-10-009-pas.pdf](https://cdsweb.cern.ch/record/1356578/files/TOP-10-009-pas.pdf).
58. ATLAS: [cdsweb.cern.ch/record/1376412/files/ATLAS-CONF-2011-120.pdf](https://cdsweb.cern.ch/record/1376412/files/ATLAS-CONF-2011-120.pdf).
59. M. Beneke, Phys. Reports **317**, 1 (1999).
60. K. G. Chetyrkin and M. Steinhauser, Nucl. Phys. **B573**, 617 (2000);  
K. Melnikov and T. van Ritbergen, Phys. Lett. **B482**, 99 (2000).
61. S.J. Brodsky, G.P. Lepage, and P.B. Mackenzie, Phys. Rev. **D28**, 228 (1983).
62. N. Gray *et al.*, Z. Phys. **C48**, 673 (1990).
63. A. Sirlin, Phys. Rev. **D22**, 971 (1980);  
D.C. Kennedy *et al.*, Nucl. Phys. **B321**, 83 (1989);  
D.Yu. Bardin *et al.*, Z. Phys. **C44**, 493 (1989);  
W. Hollik, Fortsch. Phys. **38**, 165 (1990);  
for reviews, see W. Hollik, pp. 37 and 117, and W. Marciano, p. 170 of Ref. 5.
64. V.A. Novikov, L.B. Okun, and M.I. Vysotsky, Nucl. Phys. **B397**, 35 (1993).
65. W. Hollik in Ref. 63 and references therein.
66. W.J. Marciano and J.L. Rosner, Phys. Rev. Lett. **65**, 2963 (1990).
67. G. Degrossi, S. Fanchiotti, and A. Sirlin, Nucl. Phys. **B351**, 49 (1991).
68. G. Degrossi and A. Sirlin, Nucl. Phys. **B352**, 342 (1991).
69. P. Gambino and A. Sirlin, Phys. Rev. **D49**, 1160 (1994).
70. ZFITTER: A.B. Arbuzov *et al.*, Comput. Phys. Commun. **174**, 728 (2006) and references therein.
71. R. Barbieri *et al.*, Nucl. Phys. **B409**, 105 (1993).
72. J. Fleischer, O.V. Tarasov, and F. Jegerlehner, Phys. Lett. **B319**, 249 (1993).
73. G. Degrossi, P. Gambino, and A. Vicini, Phys. Lett. **B383**, 219 (1996);  
G. Degrossi, P. Gambino, and A. Sirlin, Phys. Lett. **B394**, 188 (1997).
74. A. Freitas *et al.*, Phys. Lett. **B495**, 338 (2000) and *ibid.*, **570**, 260(E) (2003);  
M. Awramik and M. Czakon, Phys. Lett. **B568**, 48 (2003).
75. A. Freitas *et al.*, Nucl. Phys. **B632**, 189 (2002) and *ibid.*, **666**, 305(E) (2003);  
M. Awramik and M. Czakon, Phys. Rev. Lett. **89**, 241801 (2002);  
A. Onishchenko and O. Veretin, Phys. Lett. **B551**, 111 (2003).
76. M. Awramik *et al.*, Phys. Rev. Lett. **93**, 201805 (2004);  
W. Hollik, U. Meier, and S. Uccirati, Nucl. Phys. **B731**, 213 (2005).
77. M. Awramik, M. Czakon, and A. Freitas, JHEP **0611**, 048 (2006);  
W. Hollik, U. Meier, and S. Uccirati, Nucl. Phys. **B765**, 154 (2007).
78. A. Djouadi and C. Verzegnassi, Phys. Lett. **B195**, 265 (1987);  
A. Djouadi, Nuovo Cimento **100A**, 357 (1988).
79. K.G. Chetyrkin, J.H. Kühn, and M. Steinhauser, Phys. Lett. **B351**, 331 (1995);  
L. Avdeev *et al.*, Phys. Lett. **B336**, 560 (1994) and *ibid.*, **B349**, 597(E) (1995).
80. B.A. Kniehl, J.H. Kühn, and R.G. Stuart, Phys. Lett. **B214**, 621 (1988);  
B.A. Kniehl, Nucl. Phys. **B347**, 86 (1990);  
F. Halzen and B.A. Kniehl, Nucl. Phys. **B353**, 567 (1991);  
A. Djouadi and P. Gambino, Phys. Rev. **D49**, 3499 (1994) and *ibid.*, **53**, 4111(E) (1996).
81. K.G. Chetyrkin, J.H. Kühn, and M. Steinhauser, Phys. Rev. Lett. **75**, 3394 (1995).
82. J.J. van der Bij *et al.*, Phys. Lett. **B498**, 156 (2001).
83. M. Faisst *et al.*, Nucl. Phys. **B665**, 649 (2003).
84. R. Boughezal, J.B. Tausk, and J.J. van der Bij, Nucl. Phys. **B725**, 3 (2005).
85. A. Anselm, N. Dombey, and E. Leader, Phys. Lett. **B312**, 232 (1993).
86. Y. Schröder and M. Steinhauser, Phys. Lett. **B622**, 124 (2005).
87. K.G. Chetyrkin *et al.*, Phys. Rev. Lett. **97**, 102003 (2006);  
R. Boughezal and M. Czakon, Nucl. Phys. **B755**, 221 (2006).
88. J. Fleischer *et al.*, Phys. Lett. **B293**, 437 (1992);  
K.G. Chetyrkin, A. Kwiatkowski, and M. Steinhauser, Mod. Phys. Lett. **A8**, 2785 (1993).
89. R. Harlander, T. Seidensticker, and M. Steinhauser, Phys. Lett. **B426**, 125 (1998);  
J. Fleischer *et al.*, Phys. Lett. **B459**, 625 (1999).
90. M. Awramik *et al.*, Nucl. Phys. **B813**, 174 (2009).
91. A. Czarnecki and J.H. Kühn, Phys. Rev. Lett. **77**, 3955 (1996).
92. Gfitter: H. Flacher *et al.*, Eur. Phys. J. **C60**, 543 (2009).
93. J.M. Conrad, M.H. Shaevitz, and T. Bolton, Rev. Mod. Phys. **70**, 1341 (1998).
94. Z. Berezhiani and A. Rossi, Phys. Lett. **B535**, 207 (2002);  
S. Davidson *et al.*, JHEP **0303**, 011 (2003);  
A. Friedland, C. Lunardini and C. Pena-Garay, Phys. Lett. **B594**, 347 (2004).
95. J. Panman, p. 504 of Ref. 5.
96. CHARM: J. Dorenbosch *et al.*, Z. Phys. **C41**, 567 (1989).
97. CALO: L.A. Ahrens *et al.*, Phys. Rev. **D41**, 3297 (1990).
98. CHARM II: P. Vilain *et al.*, Phys. Lett. **B335**, 246 (1994).
99. ILM: R.C. Allen *et al.*, Phys. Rev. **D47**, 11 (1993);  
LSND: L.B. Auerbach *et al.*, Phys. Rev. **D63**, 112001 (2001).
100. TEXONO: M. Deniz *et al.*, Phys. Rev. **D81**, 072001 (2010).
101. For reviews, see G.L. Fogli and D. Haidt, Z. Phys. **C40**, 379 (1988);  
F. Perrier, p. 385 of Ref. 5.
102. CDHS: A. Blondel *et al.*, Z. Phys. **C45**, 361 (1990).
103. CHARM: J.V. Allaby *et al.*, Z. Phys. **C36**, 611 (1987).
104. CCFR: K.S. McFarland *et al.*, Eur. Phys. J. **C1**, 509 (1998).
105. R.M. Barnett, Phys. Rev. **D14**, 70 (1976);  
H. Georgi and H.D. Politzer, Phys. Rev. **D14**, 1829 (1976).
106. LAB-E: S.A. Rabinowitz *et al.*, Phys. Rev. Lett. **70**, 134 (1993).
107. E.A. Paschos and L. Wolfenstein, Phys. Rev. **D7**, 91 (1973).
108. NuTeV: G.P. Zeller *et al.*, Phys. Rev. Lett. **88**, 091802 (2002).
109. D. Mason *et al.*, Phys. Rev. Lett. **99**, 192001 (2007).
110. S. Kretzer, D. Mason, and F. Olness, Phys. Rev. **D65**, 074010 (2002).
111. J. Pumplin *et al.*, JHEP **0207**, 012 (2002);  
S. Kretzer *et al.*, Phys. Rev. Lett. **93**, 041802 (2004).
112. S. Alekhin, S.A. Kulagin, and R. Petti, Phys. Lett. **B675**, 433 (2009).
113. W. Bentz *et al.*, Phys. Lett. **B693**, 462 (2010).
114. E. Sather, Phys. Lett. **B274**, 433 (1992);  
E.N. Rodionov, A.W. Thomas, and J.T. Londergan, Mod. Phys. Lett. **A9**, 1799 (1994).
115. A.D. Martin *et al.*, Eur. Phys. J. **C35**, 325 (2004).
116. J.T. Londergan and A.W. Thomas, Phys. Rev. **D67**, 111901 (2003).
117. M. Glück, P. Jimenez-Delgado, and E. Reya, Phys. Rev. Lett. **95**, 022002 (2005).
118. S. Kumano, Phys. Rev. **D66**, 111301 (2002);  
S.A. Kulagin, Phys. Rev. **D67**, 091301 (2003);  
S.J. Brodsky, I. Schmidt, and J.J. Yang, Phys. Rev. **D70**, 116003 (2004);  
M. Hirai, S. Kumano, and T. H. Nagai, Phys. Rev. **D71**, 113007 (2005);  
G.A. Miller and A.W. Thomas, Int. J. Mod. Phys. A **20**, 95 (2005).
119. I.C. Cloet, W. Bentz, and A.W. Thomas, Phys. Rev. Lett. **102**, 252301 (2009).
120. K.P.O. Diener, S. Dittmaier, and W. Hollik, Phys. Rev. **D69**, 073005 (2004);  
A.B. Arbuzov, D.Y. Bardin, and L.V. Kalinovskaya, JHEP **0506**, 078 (2005);  
K. Park, U. Baur, and D. Wackerroth, [arXiv:0910.5013 \[hep-ph\]](https://arxiv.org/abs/0910.5013).

121. K.P.O. Diener, S. Dittmaier, and W. Hollik, *Phys. Rev.* **D72**, 093002 (2005).
122. B.A. Dobrescu and R.K. Ellis, *Phys. Rev.* **D69**, 114014 (2004).
123. For a review, see S. Davidson *et al.*, *JHEP* **0202**, 037 (2002).
124. SSF: C.Y. Prescott *et al.*, *Phys. Lett.* **B84**, 524 (1979).
125. E.J. Beise, M.L. Pitt, and D.T. Spayde, *Prog. in Part. Nucl. Phys.* **54**, 289 (2005).
126. S.L. Zhu *et al.*, *Phys. Rev.* **D62**, 033008 (2000).
127. P. Souder, p. 599 of Ref. 5.
128. P. Langacker, p. 883 of Ref. 5.
129. R.D. Young *et al.*, *Phys. Rev. Lett.* **99**, 122003 (2007).
130. E. Derman and W.J. Marciano, *Annals Phys.* **121**, 147 (1979).
131. E158: P.L. Anthony *et al.*, *Phys. Rev. Lett.* **95**, 081601 (2005).
132. J. Erler and M.J. Ramsey-Musolf, *Phys. Rev.* **D72**, 073003 (2005).
133. A. Czarnecki and W.J. Marciano, *Int. J. Mod. Phys. A* **15**, 2365 (2000).
134. K.S. McFarland, in the *Proceedings of DIS 2008*.
135. C. Bouchiat and C.A. Piketty, *Phys. Lett.* **B128**, 73 (1983).
136. Qweak: M.T. Gericke *et al.*, *AIP Conf. Proc.* **1149**, 237 (2009); the implications are discussed in Ref. 149.
137. For reviews and references to earlier work, see M.A. Bouchiat and L. Pottier, *Science* **234**, 1203 (1986); B.P. Masterson and C.E. Wieman, p. 545 of Ref. 5.
138. Cesium (Boulder): C.S. Wood *et al.*, *Science* **275**, 1759 (1997).
139. Cesium (Paris): J. Guéna, M. Lintz, and M.A. Bouchiat, *Phys. Rev.* **A71**, 042108 (2005).
140. Thallium (Oxford): N.H. Edwards *et al.*, *Phys. Rev. Lett.* **74**, 2654 (1995); Thallium (Seattle): P.A. Vetter *et al.*, *Phys. Rev. Lett.* **74**, 2658 (1995).
141. Lead (Seattle): D.M. Meekhof *et al.*, *Phys. Rev. Lett.* **71**, 3442 (1993).
142. Bismuth (Oxford): M.J.D. MacPherson *et al.*, *Phys. Rev. Lett.* **67**, 2784 (1991).
143. V.A. Dzuba, V.V. Flambaum, and O.P. Sushkov, *Phys. Lett.* **141A**, 147 (1989); S.A. Blundell, J. Sapirstein, and W.R. Johnson, *Phys. Rev.* **D45**, 1602 (1992); For reviews, see S.A. Blundell, W.R. Johnson, and J. Sapirstein, p. 577 of Ref. 5; J.S.M. Ginges and V.V. Flambaum, *Phys. Reports* **397**, 63 (2004); J. Guéna, M. Lintz, and M. A. Bouchiat, *Mod. Phys. Lett.* **A20**, 375 (2005); A. Derevianko and S.G. Porsev, *Eur. Phys. J. A* **32**, 517 (2007).
144. V.A. Dzuba, V.V. Flambaum, and O.P. Sushkov, *Phys. Rev.* **A56**, R4357 (1997).
145. S.C. Bennett and C.E. Wieman, *Phys. Rev. Lett.* **82**, 2484 (1999).
146. M.A. Bouchiat and J. Guéna, *J. Phys. (France)* **49**, 2037 (1988).
147. S. G. Porsev, K. Beloy, and A. Derevianko, *Phys. Rev. Lett.* **102**, 181601 (2009).
148. A. Derevianko, *Phys. Rev. Lett.* **85**, 1618 (2000); V.A. Dzuba, C. Harabati, and W.R. Johnson, *Phys. Rev.* **A63**, 044103 (2001); M.G. Kozlov, S.G. Porsev, and I.I. Tupitsyn, *Phys. Rev. Lett.* **86**, 3260 (2001); W.R. Johnson, I. Bednyakov, and G. Soff, *Phys. Rev. Lett.* **87**, 233001 (2001); A.I. Milstein and O.P. Sushkov, *Phys. Rev.* **A66**, 022108 (2002); V.A. Dzuba, V.V. Flambaum, and J.S. Ginges, *Phys. Rev.* **D66**, 076013 (2002); M.Y. Kuchiev and V.V. Flambaum, *Phys. Rev. Lett.* **89**, 283002 (2002); A.I. Milstein, O.P. Sushkov, and I.S. Terekhov, *Phys. Rev. Lett.* **89**, 283003 (2002); V.V. Flambaum and J.S.M. Ginges, *Phys. Rev.* **A72**, 052115 (2005).
149. J. Erler, A. Kurylov, and M.J. Ramsey-Musolf, *Phys. Rev.* **D68**, 016006 (2003).
150. P.G. Blunden, W. Melnitchouk, and A.W. Thomas, *Phys. Rev. Lett.* **107**, 081801 (2011).
151. V.A. Dzuba *et al.*, *J. Phys.* **B20**, 3297 (1987).
152. Ya.B. Zel'dovich, *Sov. Phys. JETP* **6**, 1184 (1958); for recent discussions, see V.V. Flambaum and D.W. Murray, *Phys. Rev.* **C56**, 1641 (1997); W.C. Haxton and C.E. Wieman, *Ann. Rev. Nucl. Part. Sci.* **51**, 261 (2001).
153. J.L. Rosner, *Phys. Rev.* **D53**, 2724 (1996).
154. S.J. Pollock, E.N. Fortson, and L. Willets, *Phys. Rev.* **C46**, 2587 (1992); B.Q. Chen and P. Vogel, *Phys. Rev.* **C48**, 1392 (1993).
155. R.W. Dunford and R.J. Holt, *J. Phys.* **G34**, 2099 (2007).
156. O.O. Versolato *et al.*, *Hyperfine Interact.* **199**, 9 (2011).
157. B.W. Lynn and R.G. Stuart, *Nucl. Phys.* **B253**, 216 (1985).
158. *Physics at LEP*, ed. J. Ellis and R. Peccei, CERN 86-02, Vol. 1.
159. PETRA: S.L. Wu, *Phys. Reports* **107**, 59 (1984); C. Kiesling, *Tests of the Standard Theory of Electroweak Interactions*, (Springer-Verlag, New York, 1988); R. Marshall, *Z. Phys.* **C43**, 607 (1989); Y. Mori *et al.*, *Phys. Lett.* **B218**, 499 (1989); D. Haidt, p. 203 of Ref. 5.
160. For reviews, see D. Schaile, p. 215, and A. Blondel, p. 277 of Ref. 5; P. Langacker [7]; and S. Riemann [161].
161. S. Riemann, Rept. on Prog. in Phys. **73**, 126201 (2010).
162. SLD: K. Abe *et al.*, *Phys. Rev. Lett.* **84**, 5945 (2000).
163. SLD: K. Abe *et al.*, *Phys. Rev. Lett.* **85**, 5059 (2000).
164. SLD: K. Abe *et al.*, *Phys. Rev. Lett.* **86**, 1162 (2001).
165. DELPHI: P. Abreu *et al.*, *Z. Phys.* **C67**, 1 (1995); OPAL: K. Ackerstaff *et al.*, *Z. Phys.* **C76**, 387 (1997).
166. SLD: K. Abe *et al.*, *Phys. Rev. Lett.* **78**, 17 (1997).
167. DØ: V.M. Abazov *et al.*, *Phys. Rev.* **D84**, 012007 (2011).
168. CDF: J. Han *et al.*, [arXiv:1110.0153](https://arxiv.org/abs/1110.0153) [hep-ex].
169. CDF: D. Acosta *et al.*, *Phys. Rev.* **D71**, 052002 (2005).
170. H1: A. Aktas *et al.*, *Phys. Lett.* **B632**, 35 (2006); H1 and ZEUS: Z. Zhang, *Nucl. Phys. Proc. Suppl.* **191**, 271 (2009).
171. CMS: S. Chatrchyan *et al.*, *Phys. Rev.* **D84**, 112002 (2011).
172. ALEPH, DELPHI, L3, OPAL, and LEP Electroweak Working Group: J. Alcarez *et al.*, [hep-ex/0612034](https://arxiv.org/abs/hep-ex/0612034).
173. ALEPH, DELPHI, L3, OPAL, and the LEP Working Group for Higgs Boson Searches: D. Abbaneo *et al.*, *Phys. Lett.* **B565**, 61 (2003).
174. J. Erler, *Phys. Rev.* **D81**, 051301 (R) (2010); see also Ref. 92.
175. A. Leike, T. Riemann, and J. Rose, *Phys. Lett.* **B273**, 513 (1991); T. Riemann, *Phys. Lett.* **B293**, 451 (1992).
176. A comprehensive report and further references can be found in K.G. Chetyrkin, J.H. Kühn, and A. Kwiatkowski, *Phys. Reports* **277**, 189 (1996).
177. J. Schwinger, *Particles, Sources, and Fields*, Vol. II, (Addison-Wesley, New York, 1973); K.G. Chetyrkin, A.L. Kataev, and F.V. Tkachev, *Phys. Lett.* **B85**, 277 (1979); M. Dine and J. Sapirstein, *Phys. Rev. Lett.* **43**, 668 (1979); W. Celmaster and R.J. Gonsalves, *Phys. Rev. Lett.* **44**, 560 (1980); S.G. Gorishnii, A.L. Kataev, and S.A. Larin, *Phys. Lett.* **B259**, 144 (1991); L.R. Surguladze, M.A. Samuel, *Phys. Rev. Lett.* **66**, 560 (1991) and *ibid.*, 2416(E).
178. P.A. Baikov, K.G. Chetyrkin, and J.H. Kühn, *Phys. Rev. Lett.* **101**, 012002 (2008).
179. W. Bernreuther and W. Wetzel, *Phys. Rev.* **D24**, 2724 (1982); B.A. Kniehl, *Phys. Lett.* **B237**, 127 (1990); K.G. Chetyrkin, *Phys. Lett.* **B307**, 169 (1993); A.H. Hoang *et al.*, *Phys. Lett.* **B338**, 330 (1994);



- S.A. Larin, T. van Ritbergen, and J.A.M. Vermaseren, Nucl. Phys. **B438**, 278 (1995).
180. T.H. Chang, K.J.F. Gaemers, and W.L. van Neerven, Nucl. Phys. **B202**, 407 (1980);  
J. Jersak, E. Laermann, and P.M. Zerwas, Phys. Rev. **D25**, 1218 (1982);  
S.G. Gorishnii, A.L. Kataev, and S.A. Larin, Nuovo Cimento **92**, 117 (1986);  
K.G. Chetyrkin and J.H. Kühn, Phys. Lett. **B248**, 359 (1990);  
K.G. Chetyrkin, J.H. Kühn, and A. Kwiatkowski, Phys. Lett. **B282**, 221 (1992);  
K.G. Chetyrkin and J.H. Kühn, Phys. Lett. **B406**, 102 (1997).
181. B.A. Kniehl and J.H. Kühn, Nucl. Phys. **B329**, 547 (1990);  
K.G. Chetyrkin and A. Kwiatkowski, Phys. Lett. **B319**, 307 (1993);  
S.A. Larin, T. van Ritbergen, and J.A.M. Vermaseren, Phys. Lett. **B320**, 159 (1994);  
K.G. Chetyrkin and O.V. Tarasov, Phys. Lett. **B327**, 114 (1994).
182. A.L. Kataev, Phys. Lett. **B287**, 209 (1992).
183. D. Albert *et al.*, Nucl. Phys. **B166**, 460 (1980);  
F. Jegerlehner, Z. Phys. **C32**, 425 (1986);  
A. Djouadi, J.H. Kühn, and P.M. Zerwas, Z. Phys. **C46**, 411 (1990);  
A. Borrelli *et al.*, Nucl. Phys. **B333**, 357 (1990).
184. A.A. Akhundov, D.Yu. Bardin, and T. Riemann, Nucl. Phys. **B276**, 1 (1986);  
W. Beenakker and W. Hollik, Z. Phys. **C40**, 141 (1988);  
B.W. Lynn and R.G. Stuart, Phys. Lett. **B352**, 676 (1990);  
J. Bernabeu, A. Pich, and A. Santamaria, Phys. Lett. **B200**, 569 (1988) and Nucl. Phys. **B363**, 326 (1991).
185. Tevatron Electroweak Working Group, CDF and DØ: 1003.2826 [hep-ex].
186. E. Braaten, S. Narison, and A. Pich, Nucl. Phys. **B373**, 581 (1992).
187. F. Le Diberder and A. Pich, Phys. Lett. **B286**, 147 (1992).
188. M. Beneke and M. Jamin, JHEP **0809**, 044 (2008).
189. E. Braaten and C.S. Li, Phys. Rev. **D42**, 3888 (1990).
190. J. Erler, Rev. Mex. Fis. **50**, 200 (2004).
191. D. Boito *et al.*, Phys. Rev. **D84**, 113006 (2011);  
D. Boito *et al.*, arXiv:1203.3146 [hep-ph].
192. J. Erler, arXiv:1102.5520 [hep-ph].
193. M. Davier *et al.*, Eur. Phys. J. **C56**, 305 (2008);  
K. Maltman and T. Yavin, Phys. Rev. **D78**, 094020 (2008).
194. E821: G.W. Bennett *et al.*, Phys. Rev. Lett. **92**, 161802 (2004).
195. T. Kinoshita and M. Nio, Phys. Rev. **D70**, 113001 (2004);  
M. Passera, J. Phys. **G31**, R75 (2005);  
T. Kinoshita, Nucl. Phys. Proc. Suppl. **144**, 206 (2005).
196. G. Li, R. Mendel, and M.A. Samuel, Phys. Rev. **D47**, 1723 (1993);  
S. Laporta and E. Remiddi, Phys. Lett. **B301**, 440 (1993);  
S. Laporta and E. Remiddi, Phys. Lett. **B379**, 283 (1996);  
A. Czarnecki and M. Skrzypek, Phys. Lett. **B449**, 354 (1999).
197. J. Erler and M. Luo, Phys. Rev. Lett. **87**, 071804 (2001).
198. A.L. Kataev, Nucl. Phys. Proc. Suppl. **155**, 369 (2006);  
T. Kinoshita and M. Nio, Phys. Rev. **D73**, 053007 (2006).
199. For reviews, see V.W. Hughes and T. Kinoshita, Rev. Mod. Phys. **71**, S133 (1999);  
A. Czarnecki and W.J. Marciano, Phys. Rev. **D64**, 013014 (2001);  
T. Kinoshita, J. Phys. **G29**, 9 (2003);  
M. Davier and W.J. Marciano, Ann. Rev. Nucl. Part. Sci. **54**, 115 (2004);  
J.P. Miller, E. de Rafael, and B.L. Roberts, Rept. Prog. Phys. **70**, 795 (2007);  
F. Jegerlehner, Acta Phys. Polon. **B38**, 3021 (2007).
200. S.J. Brodsky and J.D. Sullivan, Phys. Rev. **D156**, 1644 (1967);  
T. Burnett and M.J. Levine, Phys. Lett. **B24**, 467 (1967);  
R. Jackiw and S. Weinberg, Phys. Rev. **D5**, 2473 (1972);  
I. Bars and M. Yoshimura, Phys. Rev. **D6**, 374 (1972);  
K. Fujikawa, B.W. Lee, and A.I. Sanda, Phys. Rev. **D6**, 2923 (1972);  
G. Altarelli, N. Cabibbo, and L. Maiani, Phys. Lett. **B40**, 415 (1972);  
W.A. Bardeen, R. Gastmans, and B.E. Laurup, Nucl. Phys. **B46**, 315 (1972).
201. T.V. Kukhto *et al.*, Nucl. Phys. **B371**, 567 (1992);  
S. Peris, M. Perrottet, and E. de Rafael, Phys. Lett. **B355**, 523 (1995);  
A. Czarnecki, B. Krause, and W.J. Marciano, Phys. Rev. **D52**, 2619 (1995);  
A. Czarnecki, B. Krause, and W.J. Marciano, Phys. Rev. Lett. **76**, 3267 (1996).
202. G. Degrossi and G. Giudice, Phys. Rev. **D58**, 053007 (1998).
203. V. Cirigliano, G. Ecker, and H. Neufeld, JHEP **0208**, 002 (2002);  
K. Maltman and C.E. Wolfe, Phys. Rev. **D73**, 013004 (2006);  
M. Davier *et al.*, Eur. Phys. J. **C66**, 127 (2010).
204. W.J. Marciano and A. Sirlin, Phys. Rev. Lett. **61**, 1815 (1988).
205. S. Ghozzi and F. Jegerlehner, Phys. Lett. **B583**, 222 (2004).
206. K. Melnikov and A. Vainshtein, Phys. Rev. **D70**, 113006 (2004).
207. J. Erler and G. Toledo Sánchez, Phys. Rev. Lett. **97**, 161801 (2006).
208. M. Knecht and A. Nyffeler, Phys. Rev. **D65**, 073034 (2002).
209. M. Hayakawa and T. Kinoshita, hep-ph/0112102;  
J. Bijmens, E. Pallante, and J. Prades, Nucl. Phys. **B626**, 410 (2002);  
A recent discussion is in J. Bijmens and J. Prades, Mod. Phys. Lett. **A22**, 767 (2007).
210. J. Prades, E. de Rafael, and A. Vainshtein, 0901.0306 [hep-ph].
211. B. Krause, Phys. Lett. **B390**, 392 (1997).
212. J.L. Lopez, D.V. Nanopoulos, and X. Wang, Phys. Rev. **D49**, 366 (1994);  
for recent reviews, see Ref. 199.
213. U. Amaldi *et al.*, Phys. Rev. **D36**, 1385 (1987);  
G. Costa *et al.*, Nucl. Phys. **B297**, 244 (1988);  
P. Langacker and M. Luo, Phys. Rev. **D44**, 817 (1991);  
J. Erler and P. Langacker, Phys. Rev. **D52**, 441 (1995).
214. Tevatron Electroweak Working Group, CDF and DØ: 0908.1374 [hep-ex].
215. J. Erler, arXiv:1201.0695 [hep-ph].
216. F. James and M. Roos, Comput. Phys. Commun. **10**, 343 (1975).
217. For a more recent study, see J. Cao and J.M. Yang, JHEP **0812**, 006 (2008).
218. J. Erler, J.L. Feng, and N. Polonsky, Phys. Rev. Lett. **78**, 3063 (1997).
219. D. Choudhury, T.M.P. Tait, and C.E.M. Wagner, Phys. Rev. **D65**, 053002 (2002).
220. J. Erler and P. Langacker, Phys. Rev. Lett. **84**, 212 (2000).
221. P. Langacker and M. Plümacher, Phys. Rev. **D62**, 013006 (2000).
222. DELPHI: P. Abreu *et al.*, Eur. Phys. J. **C10**, 415 (1999).
223. P. Langacker and N. Polonsky, Phys. Rev. **D52**, 3081 (1995);  
J. Bagger, K.T. Matchev, and D. Pierce, Phys. Lett. **B348**, 443 (1995).
224. F. Gianotti, CERN public seminar, ATLAS-CONF-2011-163.
225. CDF and DØ: arXiv:1107.5518 [hep-ex].
226. J. Erler, Phys. Rev. **D63**, 071301 (R) (2001).
227. G. Tonelli, CERN public seminar, CMS-HIG-11-032.
228. M. Veltman, Nucl. Phys. **B123**, 89 (1977);  
M. Chanowitz, M.A. Furman, and I. Hinchliffe, Phys. Lett. **B78**, 285 (1978);  
The two-loop correction has been obtained by J.J. van der Bij and F. Hoogeveen, Nucl. Phys. **B283**, 477 (1987).
229. P. Langacker and M. Luo, Phys. Rev. **D45**, 278 (1992) and refs. therein.
230. A. Denner, R.J. Guth, and J.H. Kühn, Phys. Lett. **B240**, 438 (1990);  
W. Grimus *et al.*, J. Phys. G **35**, 075001 (2008);  
H. E. Haber and D. O'Neil, Phys. Rev. **D83**, 055017 (2011).

231. S. Bertolini and A. Sirlin, *Phys. Lett.* **B257**, 179 (1991).
232. M. Peskin and T. Takeuchi, *Phys. Rev. Lett.* **65**, 964 (1990); M. Peskin and T. Takeuchi, *Phys. Rev.* **D46**, 381 (1992); M. Golden and L. Randall, *Nucl. Phys.* **B361**, 3 (1991).
233. D. Kennedy and P. Langacker, *Phys. Rev.* **D44**, 1591 (1991).
234. G. Altarelli and R. Barbieri, *Phys. Lett.* **B253**, 161 (1990).
235. B. Holdom and J. Terning, *Phys. Lett.* **B247**, 88 (1990).
236. B.W. Lynn, M.E. Peskin, and R.G. Stuart, p. 90 of Ref. 158.
237. An alternative formulation is given by K. Hagiwara *et al.*, *Z. Phys.* **C64**, 559 (1994), and *ibid.*, **68**, 352(E) (1995); K. Hagiwara, D. Haidt, and S. Matsumoto, *Eur. Phys. J.* **C2**, 95 (1998).
238. I. Maksymyk, C.P. Burgess, and D. London, *Phys. Rev.* **D50**, 529 (1994); C.P. Burgess *et al.*, *Phys. Lett.* **B326**, 276 (1994).
239. R. Barbieri *et al.*, *Nucl. Phys.* **B703**, 127 (2004).
240. K. Lane, [hep-ph/0202255](https://arxiv.org/abs/hep-ph/0202255).
241. E. Gates and J. Terning, *Phys. Rev. Lett.* **67**, 1840 (1991); R. Sundrum and S.D.H. Hsu, *Nucl. Phys.* **B391**, 127 (1993); R. Sundrum, *Nucl. Phys.* **B395**, 60 (1993); M. Luty and R. Sundrum, *Phys. Rev. Lett.* **70**, 529 (1993); T. Appelquist and J. Terning, *Phys. Lett.* **B315**, 139 (1993); D.D. Dietrich, F. Sannino, and K. Tuominen, *Phys. Rev.* **D72**, 055001 (2005); N.D. Christensen and R. Shrock, *Phys. Lett.* **B632**, 92 (2006); M. Harada, M. Kurachi, and K. Yamawaki, *Prog. Theor. Phys.* **115**, 765 (2006).
242. H. Georgi, *Nucl. Phys.* **B363**, 301 (1991); M.J. Dugan and L. Randall, *Phys. Lett.* **B264**, 154 (1991).
243. R. Barbieri *et al.*, *Nucl. Phys.* **B341**, 309 (1990).
244. J. Erler and D.M. Pierce, *Nucl. Phys.* **B526**, 53 (1998); G.C. Cho and K. Hagiwara, *Nucl. Phys.* **B574**, 623 (2000); G. Altarelli *et al.*, *JHEP* **0106**, 018 (2001); S. Heinemeyer, W. Hollik, and G. Weiglein, *Phys. Reports* **425**, 265 (2006); S.P. Martin, K. Tobe, and J.D. Wells, *Phys. Rev.* **D71**, 073014 (2005); G. Marandella, C. Schappacher, and A. Strumia, *Nucl. Phys.* **B715**, 173 (2005); S. Heinemeyer *et al.*, *JHEP* **0608**, 052 (2006); M.J. Ramsey-Musolf and S. Su, *Phys. Reports* **456**, 1 (2008); J.R. Ellis *et al.*, *JHEP* **0708**, 083 (2007); A. Djouadi, *Phys. Reports* **459**, 1 (2008); S. Heinemeyer *et al.*, *JHEP* **0804**, 039 (2008).
245. M.E. Peskin and J.D. Wells, *Phys. Rev.* **D64**, 093003 (2001).
246. G.D. Kribs *et al.*, *Phys. Rev.* **D76**, 075016 (2007).
247. H.J. He, N. Polonsky, and S. Su, *Phys. Rev.* **D64**, 053004 (2001); V.A. Novikov *et al.*, *Sov. Phys. JETP* **76**, 127 (2002); S.S. Bulanov *et al.*, *Yad. Fiz.* **66**, 2219 (2003) and refs. therein.
248. J. Maalampi and M. Roos, *Phys. Reports* **186**, 53 (1990).
249. J. Erler and P. Langacker, *Phys. Rev. Lett.* **105**, 031801 (2010).
250. CDF and DØ: D. Benjamin, [arXiv:1108.3331 \[hep-ex\]](https://arxiv.org/abs/1108.3331).
251. ATLAS: <http://atlas.ch/news/2011/Higgs-note.pdf>.
252. Z. Murdock, S. Nandi and Z. Tavartkiladze, *Phys. Lett.* **B668**, 303 (2008).
253. For reviews, see the Section on “Grand Unified Theories” in this *Review*; P. Langacker, *Phys. Reports* **72**, 185 (1981); J.L. Hewett and T.G. Rizzo, *Phys. Reports* **183**, 193 (1989); for collider implications, see T.C. Andre and J.L. Rosner, *Phys. Rev.* **D69**, 035009 (2004); J. Kang, P. Langacker and B.D. Nelson, *Phys. Rev.* **D77**, 035003 (2008).
254. S.P. Martin, *Phys. Rev.* **D81**, 035004 (2010); P.W. Graham *et al.*, *Phys. Rev.* **D81**, 055016 (2010).
255. P. Langacker and D. London, *Phys. Rev.* **D38**, 886 (1988); D. London, p. 951 of Ref. 5; a recent analysis is F. del Aguila, J. de Blas and M. Perez-Victoria, *Phys. Rev.* **D78**, 013010 (2008).
256. M. Chemtob, *Prog. in Part. Nucl. Phys.* **54**, 71 (2005); R. Barbier *et al.*, *Phys. Reports* **420**, 1 (2005).
257. R.S. Chivukula and E.H. Simmons, *Phys. Rev.* **D66**, 015006 (2002); C.T. Hill and E.H. Simmons, *Phys. Reports* **381**, 235 (2003); R.S. Chivukula *et al.*, *Phys. Rev.* **D70**, 075008 (2004).
258. K. Agashe *et al.*, *JHEP* **0308**, 050 (2003); M. Carena *et al.*, *Phys. Rev.* **D68**, 035010 (2003); I. Gogoladze and C. Macesanu, *Phys. Rev.* **D74**, 093012 (2006); I. Antoniadis, [hep-th/0102202](https://arxiv.org/abs/hep-th/0102202) see also the note on “Extra Dimensions” in the Searches Particle Listings.
259. T. Han, H.E. Logan, and L.T. Wang, *JHEP* **0601**, 099 (2006); M. Perelstein, *Prog. in Part. Nucl. Phys.* **58**, 247 (2007).
260. E. Accomando *et al.*, [arXiv:hep-ph/0608079](https://arxiv.org/abs/hep-ph/0608079); V. Barger *et al.*, *Phys. Rev.* **D77**, 035005 (2008); W. Grimus *et al.*, *Nucl. Phys.* **B801**, 81 (2008); M. Maniatis, *Int. J. Mod. Phys.* **A25**, 3505 (2010); U. Ellwanger, C. Hugonie, and A.M. Teixeira, *Phys. Reports* **496**, 1 (2010); M.C. Chen, S. Dawson, and C.B. Jackson, *Phys. Rev.* **D78**, 093001 (2008).
261. G.C. Cho, K. Hagiwara, and S. Matsumoto, *Eur. Phys. J.* **C5**, 155 (1998); K. Cheung, *Phys. Lett.* **B517**, 167 (2001); Z. Han and W. Skiba, *Phys. Rev.* **D71**, 075009 (2005).
262. P. Langacker, M. Luo, and A.K. Mann, *Rev. Mod. Phys.* **64**, 87 (1992); M. Luo, p. 977 of Ref. 5.
263. F.S. Merritt *et al.*, p. 19 of *Particle Physics: Perspectives and Opportunities: Report of the DPF Committee on Long Term Planning*, ed. R. Peccei *et al.* (World Scientific, Singapore, 1995); M. Baak *et al.*, [arXiv:1107.0975 \[hep-ph\]](https://arxiv.org/abs/1107.0975).
264. D.E. Morrissey, T. Plehn, and T.M.P. Tait, [arXiv:0912.3259 \[hep-ph\]](https://arxiv.org/abs/0912.3259).
265. G. Altarelli, R. Barbieri, and S. Jadach, *Nucl. Phys.* **B369**, 3 (1992) and *ibid.*, **B376**, 444(E) (1992).
266. A. De Rújula *et al.*, *Nucl. Phys.* **B384**, 3 (1992); K. Hagiwara *et al.*, *Phys. Rev.* **D48**, 2182 (1993); C.P. Burgess *et al.*, *Phys. Rev.* **D49**, 6115 (1994); Z. Han and W. Skiba, *Phys. Rev.* **D71**, 075009 (2005); G. Cacciapaglia *et al.*, *Phys. Rev.* **D74**, 033011 (2006); V. Bernard *et al.*, *JHEP* **0801**, 015 (2008); Z. Han, *Int. J. Mod. Phys. A* **23**, 2653 (2008).
267. For reviews, see A. Leike, *Phys. Reports* **317**, 143 (1999); P. Langacker, *Rev. Mod. Phys.* **81**, 1199 (2009).
268. M. Cvetič and P. Langacker, *Phys. Rev.* **D54**, 3570 (1996).
269. J. Erler, P. Langacker, and T. Li, *Phys. Rev.* **D66**, 015002 (2002).
270. S. Chaudhuri *et al.*, *Nucl. Phys.* **B456**, 89 (1995); G. Cleaver *et al.*, *Phys. Rev.* **D59**, 055005 (1999).
271. B. Holdom, *Phys. Lett.* **B166**, 196 (1986).
272. M. Carena *et al.*, *Phys. Rev.* **D70**, 093009 (2004).
273. J. Erler, P. Langacker, S. Munir and E. Rojas, *JHEP* **0908**, 017 (2009).
274. ATLAS: G. Aad *et al.*, *Phys. Rev. Lett.* **107**, 272002 (2011).
275. CMS: [cdsweb.cern.ch/record/1369192/files/EXO-11-019-pas.pdf](https://cdsweb.cern.ch/record/1369192/files/EXO-11-019-pas.pdf).
276. CDF: T. Aaltonen *et al.*, *Phys. Rev. Lett.* **106**, 121801 (2011).
277. DØ: V.M. Abazov *et al.*, *Phys. Lett.* **B695**, 88 (2011).
278. J. Kang and P. Langacker, *Phys. Rev.* **D71**, 035014 (2005); C. -F. Chang, K. Cheung, and T. -C. Yuan, *JHEP* **1109**, 058 (2011).
279. J. Erler *et al.*, *JHEP* **1111**, 076 (2011).
280. F. del Aguila, J. de Blas, and M. Perez-Victoria, *JHEP* **1009**, 033 (2010).
281. T. Appelquist, B.A. Dobrescu, and A.R. Hopper, *Phys. Rev.* **D68**, 035012 (2003); R.S. Chivukula *et al.*, *Phys. Rev.* **D69**, 015009 (2004).

## 11. THE CKM QUARK-MIXING MATRIX

Revised March 2012 by A. Ceccucci (CERN), Z. Ligeti (LBNL), and Y. Sakai (KEK).

### 11.1. Introduction

The masses and mixings of quarks have a common origin in the Standard Model (SM). They arise from the Yukawa interactions with the Higgs condensate,

$$\mathcal{L}_Y = -Y_{ij}^d \overline{Q_{Li}^I} \phi d_{Rj}^I - Y_{ij}^u \overline{Q_{Li}^I} \epsilon \phi^* u_{Rj}^I + \text{h.c.}, \quad (11.1)$$

where  $Y^{u,d}$  are  $3 \times 3$  complex matrices,  $\phi$  is the Higgs field,  $i, j$  are generation labels, and  $\epsilon$  is the  $2 \times 2$  antisymmetric tensor.  $Q_{Li}^I$  are left-handed quark doublets, and  $d_{Rj}^I$  and  $u_{Rj}^I$  are right-handed down- and up-type quark singlets, respectively, in the weak-eigenstate basis. When  $\phi$  acquires a vacuum expectation value,  $\langle \phi \rangle = (0, v/\sqrt{2})$ , Eq. (11.1) yields mass terms for the quarks. The physical states are obtained by diagonalizing  $Y^{u,d}$  by four unitary matrices,  $V_{L,R}^{u,d}$ , as  $M_{\text{diag}}^f = V_L^f Y^f V_R^{f\dagger} (v/\sqrt{2})$ ,  $f = u, d$ . As a result, the charged-current  $W^\pm$  interactions couple to the physical  $u_{Lj}$  and  $d_{Lk}$  quarks with couplings given by

$$\frac{-g}{\sqrt{2}} (\overline{u}_L, \overline{c}_L, \overline{t}_L) \gamma^\mu W_\mu^+ V_{\text{CKM}} \begin{pmatrix} d_L \\ s_L \\ b_L \end{pmatrix} + \text{h.c.},$$

$$V_{\text{CKM}} \equiv V_L^u V_L^{d\dagger} = \begin{pmatrix} V_{ud} & V_{us} & V_{ub} \\ V_{cd} & V_{cs} & V_{cb} \\ V_{td} & V_{ts} & V_{tb} \end{pmatrix}. \quad (11.2)$$

This Cabibbo-Kobayashi-Maskawa (CKM) matrix [1,2] is a  $3 \times 3$  unitary matrix. It can be parameterized by three mixing angles and the  $CP$ -violating KM phase [2]. Of the many possible conventions, a standard choice has become [3]

$$V_{\text{CKM}} = \begin{pmatrix} c_{12}c_{13} & s_{12}c_{13} & s_{13}e^{-i\delta} \\ -s_{12}c_{23} - c_{12}s_{23}s_{13}e^{i\delta} & c_{12}c_{23} - s_{12}s_{23}s_{13}e^{i\delta} & s_{23}c_{13} \\ s_{12}s_{23} - c_{12}c_{23}s_{13}e^{i\delta} & -c_{12}s_{23} - s_{12}c_{23}s_{13}e^{i\delta} & c_{23}c_{13} \end{pmatrix}, \quad (11.3)$$

where  $s_{ij} = \sin \theta_{ij}$ ,  $c_{ij} = \cos \theta_{ij}$ , and  $\delta$  is the phase responsible for all  $CP$ -violating phenomena in flavor-changing processes in the SM. The angles  $\theta_{ij}$  can be chosen to lie in the first quadrant, so  $s_{ij}, c_{ij} \geq 0$ .

It is known experimentally that  $s_{13} \ll s_{23} \ll s_{12} \ll 1$ , and it is convenient to exhibit this hierarchy using the Wolfenstein parameterization. We define [4–6]

$$s_{12} = \lambda = \frac{|V_{us}|}{\sqrt{|V_{ud}|^2 + |V_{us}|^2}}, \quad s_{23} = A\lambda^2 = \lambda \left| \frac{V_{cb}}{V_{us}} \right|,$$

$$s_{13}e^{i\delta} = V_{ub}^* = A\lambda^3(\rho + i\eta) = \frac{A\lambda^3(\bar{\rho} + i\bar{\eta})\sqrt{1 - A^2\lambda^4}}{\sqrt{1 - \lambda^2[1 - A^2\lambda^4(\bar{\rho} + i\bar{\eta})]}}. \quad (11.4)$$

These relations ensure that  $\bar{\rho} + i\bar{\eta} = -(V_{ud}V_{ub}^*)/(V_{cd}V_{cb}^*)$  is phase-convention-independent, and the CKM matrix written in terms of  $\lambda$ ,  $A$ ,  $\bar{\rho}$ , and  $\bar{\eta}$  is unitary to all orders in  $\lambda$ . The definitions of  $\bar{\rho}, \bar{\eta}$  reproduce all approximate results in the literature. For example,  $\bar{\rho} = \rho(1 - \lambda^2/2 + \dots)$  and we can write  $V_{\text{CKM}}$  to  $\mathcal{O}(\lambda^4)$  either in terms of  $\bar{\rho}, \bar{\eta}$  or, traditionally,

$$V_{\text{CKM}} = \begin{pmatrix} 1 - \lambda^2/2 & \lambda & A\lambda^3(\rho - i\eta) \\ -\lambda & 1 - \lambda^2/2 & A\lambda^2 \\ A\lambda^3(1 - \rho - i\eta) & -A\lambda^2 & 1 \end{pmatrix} + \mathcal{O}(\lambda^4). \quad (11.5)$$

The CKM matrix elements are fundamental parameters of the SM, so their precise determination is important. The unitarity of the CKM matrix imposes  $\sum_i V_{ij}V_{ik}^* = \delta_{jk}$  and  $\sum_j V_{ij}V_{kj}^* = \delta_{ik}$ . The six vanishing combinations can be represented as triangles in a complex plane, of which the ones obtained by taking scalar products of neighboring rows or columns are nearly degenerate. The areas of all triangles are the same, half of the Jarlskog invariant,  $J$  [7], which

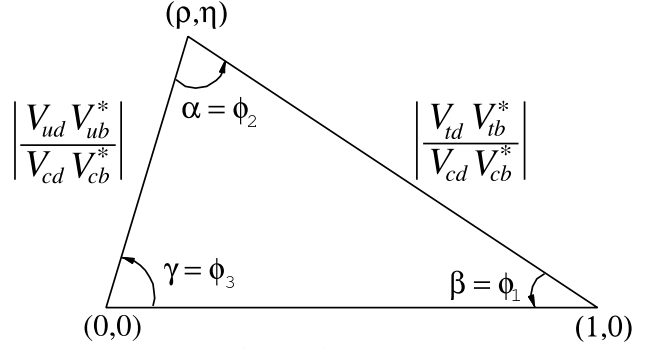


Figure 11.1: Sketch of the unitarity triangle.

is a phase-convention-independent measure of  $CP$  violation, defined by  $\text{Im}[V_{ij}V_{kl}V_{il}^*V_{kj}^*] = J \sum_{m,n} \epsilon_{ikm} \epsilon_{jln}$ .

The most commonly used unitarity triangle arises from

$$V_{ud}V_{ub}^* + V_{cd}V_{cb}^* + V_{td}V_{tb}^* = 0, \quad (11.6)$$

by dividing each side by the best-known one,  $V_{cd}V_{cb}^*$  (see Fig. 1). Its vertices are exactly  $(0,0)$ ,  $(1,0)$ , and, due to the definition in Eq. (11.4),  $(\bar{\rho}, \bar{\eta})$ . An important goal of flavor physics is to overconstrain the CKM elements, and many measurements can be conveniently displayed and compared in the  $\bar{\rho}, \bar{\eta}$  plane.

Processes dominated by loop contributions in the SM are sensitive to new physics, and can be used to extract CKM elements only if the SM is assumed. We describe such measurements assuming the SM in Sec. 11.2 and 11.3, give the global fit results for the CKM elements in Sec. 11.4, and discuss implications for new physics in Sec. 11.5.

### 11.2. Magnitudes of CKM elements

#### 11.2.1. $|V_{ud}|$ :

The most precise determination of  $|V_{ud}|$  comes from the study of superallowed  $0^+ \rightarrow 0^+$  nuclear beta decays, which are pure vector transitions. Taking the average of the twenty most precise determinations [8] yields

$$|V_{ud}| = 0.97425 \pm 0.00022. \quad (11.7)$$

The error is dominated by theoretical uncertainties stemming from nuclear Coulomb distortions and radiative corrections. A precise determination of  $|V_{ud}|$  is also obtained from the measurement of the neutron lifetime. The theoretical uncertainties are very small, but the determination is limited by the knowledge of the ratio of the axial-vector and vector couplings,  $g_A = G_A/G_V$  [9]. The PIBETA experiment [10] has improved the measurement of the  $\pi^+ \rightarrow \pi^0 e^+ \nu$  branching ratio to 0.6%, and quote  $|V_{ud}| = 0.9728 \pm 0.0030$ , in agreement with the more precise result listed above. The interest in this measurement is that the determination of  $|V_{ud}|$  is very clean theoretically, because it is a pure vector transition and is free from nuclear-structure uncertainties.

#### 11.2.2. $|V_{us}|$ :

The product of  $|V_{us}|$  and the form factor at  $q^2 = 0$ ,  $|V_{us}| f_+(0)$ , has been extracted traditionally from  $K_L^0 \rightarrow \pi e \nu$  decays in order to avoid isospin-breaking corrections ( $\pi^0 - \eta$  mixing) that affect  $K^\pm$  semileptonic decay, and the complications induced by a second (scalar) form factor present in the muonic decays. The last round of measurements has led to enough experimental constraints to justify the comparison between different decay modes. Systematic errors related to the experimental quantities, *e.g.*, the lifetime of neutral or charged kaons, and the form factor determinations for electron and muonic decays, differ among decay modes, and the consistency between different determinations enhances the confidence in the final result. For this reason, we follow the prescription [11] to average  $K_L^0 \rightarrow \pi e \nu$ ,  $K_L^0 \rightarrow \pi \mu \nu$ ,  $K^\pm \rightarrow \pi^0 e^\pm \nu$ ,  $K^\pm \rightarrow \pi^0 \mu^\pm \nu$  and  $K_S^0 \rightarrow \pi e \nu$ . The average of these five decay modes yields  $|V_{us}| f_+(0) = 0.21664 \pm 0.00048$ . Results obtained from each decay

mode, and exhaustive references to the experimental data, are listed for instance in Ref. [9]. The form factor value  $f_+(0) = 0.9644 \pm 0.0049$  [12] from a three-flavor unquenched lattice QCD calculation gives [9]  $|V_{us}| = 0.2246 \pm 0.0012$ . The broadly used classic calculation of  $f_+(0)$  [13] is in good agreement with this value, while other calculations [14] differ by as much as 2%.

The calculation of the ratio of the kaon and pion decay constants enables one to extract  $|V_{us}/V_{ud}|$  from  $K \rightarrow \mu\nu(\gamma)$  and  $\pi \rightarrow \mu\nu(\gamma)$ , where  $(\gamma)$  indicates that radiative decays are included [15]. The KLOE measurement of the  $K^+ \rightarrow \mu^+\nu(\gamma)$  branching ratio [16], combined with the lattice QCD calculation,  $f_K/f_\pi = 1.189 \pm 0.007$  [17], leads to  $|V_{us}| = 0.2259 \pm 0.0014$ , where the accuracy is limited by the knowledge of the ratio of the decay constants. The average of these two determinations is quoted by Ref. 9 as

$$|V_{us}| = 0.2252 \pm 0.0009. \quad (11.8)$$

The latest determination from hyperon decays can be found in Ref. 19. The authors focus on the analysis of the vector form factor, protected from first order  $SU(3)$  breaking effects by the Ademollo-Gatto theorem [20], and treat the ratio between the axial and vector form factors  $g_1/f_1$  as experimental input, thus avoiding first order  $SU(3)$  breaking effects in the axial-vector contribution. They find  $|V_{us}| = 0.2250 \pm 0.0027$ , although this does not include an estimate of the theoretical uncertainty due to second-order  $SU(3)$  breaking, contrary to Eq. (11.8). Concerning hadronic  $\tau$  decays to strange particles, the latest determinations based on LEP, BABAR, and Belle data yield  $|V_{us}| = 0.2208 \pm 0.0039$  [21]. A measurement of the ratio of branching fractions  $\mathcal{B}(\tau \rightarrow K\nu)/\mathcal{B}(\tau \rightarrow \pi\nu)$  by BABAR [22] combined with the above  $f_K/f_\pi$  value gives  $|V_{us}| = 0.2255 \pm 0.0024$ .

### 11.2.3. $|V_{cd}|$ :

The magnitude of  $V_{cd}$  can be extracted from semileptonic charm decays if theoretical knowledge of the form factors is available. Three-flavor unquenched lattice QCD calculations for  $D \rightarrow K\ell\nu$  and  $D \rightarrow \pi\ell\nu$  have been published [23]. Using these estimates and the average of recent CLEO-c [24] and Belle [25] measurements of  $D \rightarrow \pi\ell\nu$  decays, one obtains  $|V_{cd}| = 0.229 \pm 0.006 \pm 0.024$ , where the first uncertainty is experimental, and the second is from the theoretical uncertainty of the form factor.

This determination is not yet as precise as the one based on neutrino and antineutrino interactions. The difference of the ratio of double-muon to single-muon production by neutrino and antineutrino beams is proportional to the charm cross section off valence  $d$  quarks, and therefore to  $|V_{cd}|^2$  times the average semileptonic branching ratio of charm mesons,  $\mathcal{B}_\mu$ . The method was used first by CDHS [26] and then by CCFR [27,28] and CHARM II [29]. Averaging these results is complicated, not only because it requires assumptions about the scale of the QCD corrections, but also because  $\mathcal{B}_\mu$  is an effective quantity, which depends on the specific neutrino beam characteristics. Given that no new experimental input is available, we quote the average provided in a previous review,  $\mathcal{B}_\mu |V_{cd}|^2 = (0.463 \pm 0.034) \times 10^{-2}$  [30]. Analysis cuts make these experiments insensitive to neutrino energies smaller than 30 GeV. Thus,  $\mathcal{B}_\mu$  should be computed using only neutrino interactions with visible energy larger than 30 GeV. An appraisal [31] based on charm-production fractions measured in neutrino interactions [32,33] gives  $\mathcal{B}_\mu = 0.088 \pm 0.006$ . Data from the CHORUS experiment [34] are sufficiently precise to extract  $\mathcal{B}_\mu$  directly, by comparing the number of charm decays with a muon to the total number of charmed hadrons found in the nuclear emulsions. Requiring the visible energy to be larger than 30 GeV, CHORUS finds  $\mathcal{B}_\mu = 0.085 \pm 0.009 \pm 0.006$ . To extract  $|V_{cd}|$ , we use the average of these two determinations,  $\mathcal{B}_\mu = 0.087 \pm 0.005$ , and obtain

$$|V_{cd}| = 0.230 \pm 0.011. \quad (11.9)$$

### 11.2.4. $|V_{cs}|$ :

The determination of  $|V_{cs}|$  from neutrino and antineutrino scattering suffers from the uncertainty of the  $s$ -quark sea content. Measurements sensitive to  $|V_{cs}|$  from on-shell  $W^\pm$  decays were performed at LEP-2. The branching ratios of the  $W$  depend on the six CKM matrix elements involving quarks with masses smaller than  $M_W$ . The  $W$  branching ratio to each lepton flavor is given by  $1/\mathcal{B}(W \rightarrow \ell\bar{\nu}_\ell) = 3[1 + \sum_{u,c,d,s,b} |V_{ij}|^2 (1 + \alpha_s(m_W)/\pi)]$ . The measurement assuming lepton universality,  $\mathcal{B}(W \rightarrow \ell\bar{\nu}_\ell) = (10.83 \pm 0.07 \pm 0.07)\%$  [35], implies  $\sum_{u,c,d,s,b} |V_{ij}|^2 = 2.002 \pm 0.027$ . This is a precise test of unitarity, but only flavor-tagged  $W$ -decay measurements determine  $|V_{cs}|$  directly. DELPHI measured tagged  $W^+ \rightarrow c\bar{s}$  decays, obtaining  $|V_{cs}| = 0.94^{+0.32}_{-0.26} \pm 0.13$  [36]. Hereafter, the first error is statistical and the second is systematic, unless mentioned otherwise.

The direct determination of  $|V_{cs}|$  is possible from semileptonic  $D$  or leptonic  $D_s$  decays, using unquenched lattice QCD calculations of the semileptonic  $D$  form factor or the  $D_s$  decay constant. For muonic decays, the average of Belle [37], CLEO-c [38] and BABAR [39] gives  $\mathcal{B}(D_s^+ \rightarrow \mu^+\nu) = (5.90 \pm 0.33) \times 10^{-3}$  [41]. For decays with  $\tau$  leptons, the average of CLEO-c [38,42,43] and BABAR [39] gives  $\mathcal{B}(D_s^+ \rightarrow \tau^+\nu) = (5.29 \pm 0.28) \times 10^{-2}$  [41]. From each of these values, determinations of  $|V_{cs}|$  can be obtained by using the PDG values for the mass and lifetime of the  $D_s$ , the masses of the leptons, and  $f_{D_s} = (248.6 \pm 3.0)$  MeV [44]. The average of these determinations gives  $|V_{cs}| = 1.008 \pm 0.024$ , where the error is dominated by the lattice QCD determination of  $f_{D_s}$ . In semileptonic  $D$  decays, unquenched lattice QCD calculations have predicted the normalization and the shape (dependence on the invariant mass of the lepton pair,  $q^2$ ) of the form factors in  $D \rightarrow K\ell\nu$  and  $D \rightarrow \pi\ell\nu$  [23]. Using these theoretical results and the average of recent CLEO-c [24], Belle [25] and BABAR [45] measurements of  $B \rightarrow K\ell\nu$  decays, one obtains  $|V_{cs}| = 0.98 \pm 0.01 \pm 0.10$ , where the first error is experimental and the second, which is dominant, is from the theoretical uncertainty of the form factor. Averaging the determinations from leptonic and semileptonic decays, we find

$$|V_{cs}| = 1.006 \pm 0.023. \quad (11.10)$$

### 11.2.5. $|V_{cb}|$ :

This matrix element can be determined from exclusive and inclusive semileptonic decays of  $B$  mesons to charm. The inclusive determinations use the semileptonic decay rate measurement, together with the leptonic energy and the hadronic invariant-mass spectra. The theoretical foundation of the calculation is the operator product expansion [46,47]. It expresses the total rate and moments of differential energy and invariant-mass spectra as expansions in  $\alpha_s$ , and inverse powers of the heavy quark mass. The dependence on  $m_b$ ,  $m_c$ , and the parameters that occur at subleading order is different for different moments, and a large number of measured moments overconstrains all the parameters, and tests the consistency of the determination. The precise extraction of  $|V_{cb}|$  requires using a ‘‘threshold’’ quark mass definition [48,49]. Inclusive measurements have been performed using  $B$  mesons from  $Z^0$  decays at LEP, and at  $e^+e^-$  machines operated at the  $\Upsilon(4S)$ . At LEP, the large boost of  $B$  mesons from the  $Z^0$  allows the determination of the moments throughout phase space, which is not possible otherwise, but the large statistics available at the  $B$  factories lead to more precise determinations. An average of the measurements and a compilation of the references are provided by Ref. [50]:  $|V_{cb}| = (41.9 \pm 0.7) \times 10^{-3}$ .

Exclusive determinations are based on semileptonic  $B$  decays to  $D$  and  $D^*$ . In the  $m_{b,c} \gg \Lambda_{\text{QCD}}$  limit, all form factors are given by a single Isgur-Wise function [51], which depends on the product of the four-velocities of the  $B$  and  $D^{(*)}$  mesons,  $w = v \cdot v'$ . Heavy quark symmetry determines the normalization of the rate at  $w = 1$ , the maximum momentum transfer to the leptons, and  $|V_{cb}|$  is obtained from an extrapolation to  $w = 1$ . The exclusive determination,  $|V_{cb}| = (39.6 \pm 0.9) \times 10^{-3}$  [50], is less precise than the inclusive one because of the theoretical uncertainty in the form factor and the experimental uncertainty in the rate near  $w = 1$ . The  $V_{cb}$  and  $V_{ub}$  minireview [50] quotes a combination with a scaled error as

$$|V_{cb}| = (40.9 \pm 1.1) \times 10^{-3}. \quad (11.11)$$

### 11.2.6. $|V_{ub}|$ :

The determination of  $|V_{ub}|$  from inclusive  $B \rightarrow X_u \ell \bar{\nu}$  decay is complicated due to large  $B \rightarrow X_c \ell \bar{\nu}$  backgrounds. In most regions of phase space where the charm background is kinematically forbidden, the hadronic physics enters via unknown nonperturbative functions, so-called shape functions. (In contrast, the nonperturbative physics for  $|V_{cb}|$  is encoded in a few parameters.) At leading order in  $\Lambda_{\text{QCD}}/m_b$ , there is only one shape function, which can be extracted from the photon energy spectrum in  $B \rightarrow X_s \gamma$  [52,53], and applied to several spectra in  $B \rightarrow X_u \ell \bar{\nu}$ . The subleading shape functions are modeled in the current determinations. Phase space cuts for which the rate has only subleading dependence on the shape function are also possible [54]. The measurements of both the hadronic and the leptonic systems are important for an optimal choice of phase space. A different approach is to make the measurements more inclusive by extending them deeper into the  $B \rightarrow X_c \ell \bar{\nu}$  region, and thus reduce the theoretical uncertainties. Analyses of the electron-energy endpoint from CLEO [55], BABAR [56], and Belle [57] quote  $B \rightarrow X_u e \bar{\nu}$  partial rates for  $|\vec{p}_e| \geq 2.0 \text{ GeV}$  and  $1.9 \text{ GeV}$ , which are well below the charm endpoint. The large and pure  $B\bar{B}$  samples at the  $B$  factories permit the selection of  $B \rightarrow X_u \ell \bar{\nu}$  decays in events where the other  $B$  is fully reconstructed [58]. With this full-reconstruction tag method, the four-momenta of both the leptonic and the hadronic systems can be measured. It also gives access to a wider kinematic region because of improved signal purity. Ref. 50 quotes an inclusive average as  $|V_{ub}| = (4.41 \pm 0.15^{+0.15}_{-0.19}) \times 10^{-3}$ .

To extract  $|V_{ub}|$  from an exclusive channel, the form factors have to be known. Experimentally, better signal-to-background ratios are offset by smaller yields. The  $B \rightarrow \pi \ell \bar{\nu}$  branching ratio is now known to 5%. Unquenched lattice QCD calculations of the  $B \rightarrow \pi \ell \bar{\nu}$  form factor are available [59,60] for the high  $q^2$  region ( $q^2 > 16$  or  $18 \text{ GeV}^2$ ). A simultaneous fit to the experimental partial rates and lattice points versus  $q^2$  yields  $|V_{ub}| = (3.23 \pm 0.31) \times 10^{-3}$  [60]. Light-cone QCD sum rules are applicable for  $q^2 < 14 \text{ GeV}^2$  [61] and yield similar results.

The theoretical uncertainties in extracting  $|V_{ub}|$  from inclusive and exclusive decays are different. A combination of the determinations is quoted by Ref. [50] as

$$|V_{ub}| = (4.15 \pm 0.49) \times 10^{-3}. \quad (11.12)$$

A determination of  $|V_{ub}|$  not included in this average is obtained from  $\mathcal{B}(B \rightarrow \tau \bar{\nu}) = (1.67 \pm 0.30) \times 10^{-4}$  [40]. Using  $f_B = (190.6 \pm 4.6) \text{ MeV}$  [44], we find  $|V_{ub}| = (5.10 \pm 0.47) \times 10^{-3}$ . This decay rate is sensitive, for example, to tree-level charged Higgs contributions, and is higher than other  $|V_{ub}|$  determinations or the SM fit value.

### 11.2.7. $|V_{td}|$ and $|V_{ts}|$ :

The CKM elements  $|V_{td}|$  and  $|V_{ts}|$  are not likely to be precisely measurable in tree-level processes involving top quarks, so one has to rely on determinations from  $B$ - $\bar{B}$  oscillations mediated by box diagrams with top quarks, or loop-mediated rare  $K$  and  $B$  decays. Theoretical uncertainties in hadronic effects limit the accuracy of the current determinations. These can be reduced by taking ratios of processes that are equal in the flavor  $SU(3)$  limit to determine  $|V_{td}/V_{ts}|$ .

The mass difference of the two neutral  $B$  meson mass eigenstates is very well measured,  $\Delta m_d = (0.507 \pm 0.004) \text{ ps}^{-1}$  [62]. In the  $B_s^0$  system, the average of the CDF [63] and recent LHCb [64] measurements yields  $\Delta m_s = (17.719 \pm 0.043) \text{ ps}^{-1}$ . Using the unquenched lattice QCD calculations [44],  $f_{B_d} \sqrt{\widehat{B}_{B_d}} = (211 \pm 12) \text{ MeV}$ ,  $f_{B_s} \sqrt{\widehat{B}_{B_s}} = (248 \pm 15) \text{ MeV}$ , and assuming  $|V_{tb}| = 1$ , one finds

$$|V_{td}| = (8.4 \pm 0.6) \times 10^{-3}, \quad |V_{ts}| = (42.9 \pm 2.6) \times 10^{-3}. \quad (11.13)$$

The uncertainties are dominated by lattice QCD. Several uncertainties are reduced in the calculation of the ratio  $\xi = (f_{B_s} \sqrt{\widehat{B}_{B_s}})/(f_{B_d} \sqrt{\widehat{B}_{B_d}}) = 1.237 \pm 0.032$  [44], and therefore the constraint on  $|V_{td}/V_{ts}|$  from  $\Delta m_d/\Delta m_s$  is more reliable theoretically. These provide a new, theoretically clean, and significantly improved constraint

$$|V_{td}/V_{ts}| = 0.211 \pm 0.001 \pm 0.006. \quad (11.14)$$

The inclusive branching ratio  $\mathcal{B}(B \rightarrow X_s \gamma) = (3.55 \pm 0.26) \times 10^{-4}$  extrapolated to  $E_\gamma > E_0 = 1.6 \text{ GeV}$  [65] is also sensitive to  $V_{tb} V_{ts}^*$ . In addition to  $t$ -quark penguins, a large part of the sensitivity comes from charm contributions proportional to  $V_{cb} V_{cs}^*$  via the application of  $3 \times 3$  CKM unitarity (which is used here; any CKM determination from loop processes necessarily assumes the SM). With the NNLO calculation of  $\mathcal{B}(B \rightarrow X_s \gamma)_{E_\gamma > E_0}/\mathcal{B}(B \rightarrow X_c e \bar{\nu})$  [66], we obtain  $|V_{ts}/V_{cb}| = 1.04 \pm 0.05$ . The same CKM elements also determine the  $B_s \rightarrow \mu^+ \mu^-$  decay rate in the SM, and with the bounds approaching the SM level [67], this mode can soon provide a strong constraint.

A complementary determination of  $|V_{td}/V_{ts}|$  is possible from the ratio of  $B \rightarrow \rho \gamma$  and  $K^* \gamma$  rates. The ratio of the neutral modes is theoretically cleaner than that of the charged ones, because the poorly known spectator-interaction contribution is expected to be smaller ( $W$ -exchange vs. weak annihilation). For now, because of low statistics we average the charged and neutral rates assuming the isospin symmetry and heavy quark limit motivated relation,  $|V_{td}/V_{ts}|^2/\xi_\gamma^2 = [\Gamma(B^+ \rightarrow \rho^+ \gamma) + 2\Gamma(B^0 \rightarrow \rho^0 \gamma)]/[\Gamma(B^+ \rightarrow K^{*+} \gamma) + \Gamma(B^0 \rightarrow K^{*0} \gamma)] = (3.19 \pm 0.46)\%$  [65]. Here  $\xi_\gamma$  contains the poorly known hadronic physics. Using  $\xi_\gamma = 1.2 \pm 0.2$  [68], and combining the experimental and theoretical errors in quadrature, gives  $|V_{td}/V_{ts}| = 0.21 \pm 0.04$ .

A theoretically clean determination of  $|V_{td} V_{ts}^*|$  is possible from  $K^+ \rightarrow \pi^+ \nu \bar{\nu}$  decay [69]. Experimentally, only seven events have been observed [70] and the rate is consistent with the SM with large uncertainties. Much more data are needed for a precision measurement.

### 11.2.8. $|V_{tb}|$ :

The determination of  $|V_{tb}|$  from top decays uses the ratio of branching fractions  $R = \mathcal{B}(t \rightarrow Wb)/\mathcal{B}(t \rightarrow Wq) = |V_{tb}|^2/(\sum_q |V_{tq}|^2) = |V_{tb}|^2$ , where  $q = b, s, d$ . The CDF and DØ measurements performed on data collected during Run II of the Tevatron give  $|V_{tb}| > 0.78$  [71] and  $0.99 > |V_{tb}| > 0.90$  [72], respectively, at 95% CL. CMS recently measured the same quantity at 7 TeV and gives  $|V_{tb}| > 0.92$  [73] at 95% CL. The direct determination of  $|V_{tb}|$  without assuming unitarity is possible from the single top-quark-production cross section. The  $(2.71^{+0.44}_{-0.43}) \text{ pb}$  average cross section measured by DØ [74] and CDF [75,76] implies  $|V_{tb}| = 0.87 \pm 0.07$ . The recent CMS measurement,  $(83.6 \pm 29.8) \text{ pb}$  [77] at 7 TeV, implies  $|V_{tb}| = 1.14 \pm 0.22$ . The average of above gives

$$|V_{tb}| = 0.89 \pm 0.07. \quad (11.15)$$

An attempt at constraining  $|V_{tb}|$  from the precision electroweak data was made in Ref. 78. The result, mostly driven by the top-loop contributions to  $\Gamma(Z \rightarrow b\bar{b})$ , gives  $|V_{tb}| = 0.77^{+0.18}_{-0.24}$ .

## 11.3. Phases of CKM elements

As can be seen from Fig. 11.1, the angles of the unitarity triangle are

$$\begin{aligned} \beta &= \phi_1 = \arg\left(-\frac{V_{cd}V_{cb}^*}{V_{td}V_{tb}^*}\right), \\ \alpha &= \phi_2 = \arg\left(-\frac{V_{td}V_{tb}^*}{V_{ud}V_{ub}^*}\right), \\ \gamma &= \phi_3 = \arg\left(-\frac{V_{ud}V_{ub}^*}{V_{cd}V_{cb}^*}\right). \end{aligned} \quad (11.16)$$

Since  $CP$  violation involves phases of CKM elements, many measurements of  $CP$ -violating observables can be used to constrain these angles and the  $\bar{\rho}, \bar{\eta}$  parameters.

### 11.3.1. $\epsilon$ and $\epsilon'$ :

The measurement of  $CP$  violation in  $K^0$ - $\bar{K}^0$  mixing,  $|\epsilon| = (2.233 \pm 0.015) \times 10^{-3}$  [79], provides important information about the CKM matrix. In the SM, in the basis where  $V_{ud}V_{us}^*$  is real [80]

$$\begin{aligned} |\epsilon| = & \frac{G_F^2 f_K^2 m_K m_W^2}{12\sqrt{2}\pi^2 \Delta m_K} \widehat{B}_K \left\{ \eta_1 S(x_c) \text{Im}[(V_{cs}V_{cd}^*)^2] \right. \\ & \left. + \eta_2 S(x_t) \text{Im}[(V_{ts}V_{td}^*)^2] + 2\eta_3 S(x_c, x_t) \text{Im}(V_{cs}V_{cd}^*V_{ts}V_{td}^*) \right\}, \end{aligned} \quad (11.17)$$

where  $S$  is an Inami-Lim function [81],  $x_q = m_q^2/m_W^2$ , and  $\eta_i$  are perturbative QCD corrections. The constraint from  $\epsilon$  in the  $\bar{\rho}, \bar{\eta}$  plane is bounded by approximate hyperbolas. The dominant uncertainties are due to the bag parameter, for which we use  $\hat{B}_K = 0.7674 \pm 0.0099$  from lattice QCD [44], and the parametric uncertainty proportional to  $\sigma(A^4)$  from  $(V_{ts}V_{td}^*)^2$ , which is approximately  $\sigma(|V_{cb}|^4)$ .

The measurement of  $6 \operatorname{Re}(\epsilon'/\epsilon) = 1 - |\eta_{00}/\eta_{+-}|^2$ , where  $\eta_{00}$  and  $\eta_{+-}$  are the  $CP$ -violating amplitude ratios of  $K_S^0$  and  $K_L^0$  decays to two pions, provides a qualitative test of the CKM mechanism. Its nonzero experimental average,  $\operatorname{Re}(\epsilon'/\epsilon) = (1.67 \pm 0.23) \times 10^{-3}$  [79], demonstrates the existence of direct  $CP$  violation, a prediction of the KM ansatz. While  $\operatorname{Re}(\epsilon'/\epsilon) \propto \operatorname{Im}(V_{td}V_{ts}^*)$ , this quantity cannot easily be used to extract CKM parameters, because the electromagnetic penguin contributions tend to cancel the gluonic penguins for large  $m_t$  [82], thereby significantly increasing the hadronic uncertainties. Most estimates [83–86] agree with the observed value, indicating that  $\bar{\eta}$  is positive. Progress in lattice QCD, in particular finite-volume calculations [87,88], may eventually provide a determination of the  $K \rightarrow \pi\pi$  matrix elements.

### 11.3.2. $\beta / \phi_1$ :

#### 11.3.2.1. Charmonium modes:

$CP$ -violation measurements in  $B$ -meson decays provide direct information on the angles of the unitarity triangle, shown in Fig. 11.1. These overconstraining measurements serve to improve the determination of the CKM elements, or to reveal effects beyond the SM.

The time-dependent  $CP$  asymmetry of neutral  $B$  decays to a final state  $f$  common to  $B^0$  and  $\bar{B}^0$  is given by [89,90]

$$A_f = \frac{\Gamma(\bar{B}^0(t) \rightarrow f) - \Gamma(B^0(t) \rightarrow f)}{\Gamma(\bar{B}^0(t) \rightarrow f) + \Gamma(B^0(t) \rightarrow f)} = S_f \sin(\Delta m_d t) - C_f \cos(\Delta m_d t), \quad (11.18)$$

where

$$S_f = \frac{2 \operatorname{Im} \lambda_f}{1 + |\lambda_f|^2}, \quad C_f = \frac{1 - |\lambda_f|^2}{1 + |\lambda_f|^2}, \quad \lambda_f = \frac{q \bar{A}_f}{p A_f}. \quad (11.19)$$

Here,  $q/p$  describes  $B^0$ - $\bar{B}^0$  mixing and, to a good approximation in the SM,  $q/p = V_{tb}^* V_{td} / V_{ub} V_{ud}^* = e^{-2i\beta + \mathcal{O}(\lambda^4)}$  in the usual phase convention.  $A_f$  ( $\bar{A}_f$ ) is the amplitude of the  $B^0 \rightarrow f$  ( $\bar{B}^0 \rightarrow f$ ) decay. If  $f$  is a  $CP$  eigenstate, and amplitudes with one CKM phase dominate the decay, then  $|A_f| = |\bar{A}_f|$ ,  $C_f = 0$ , and  $S_f = \sin(\arg \lambda_f) = \eta_f \sin 2\phi$ , where  $\eta_f$  is the  $CP$  eigenvalue of  $f$  and  $2\phi$  is the phase difference between the  $B^0 \rightarrow f$  and  $B^0 \rightarrow \bar{B}^0 \rightarrow f$  decay paths. A contribution of another amplitude to the decay with a different CKM phase makes the value of  $S_f$  sensitive to relative strong interaction phases between the decay amplitudes (it also makes  $C_f \neq 0$  possible).

The  $b \rightarrow c\bar{c}s$  decays to  $CP$  eigenstates ( $B^0 \rightarrow$  charmonium  $K_{S,L}^0$ ) are the theoretically cleanest examples, measuring  $S_f = -\eta_f \sin 2\beta$ . The  $b \rightarrow sq\bar{q}$  penguin amplitudes have dominantly the same weak phase as the  $b \rightarrow c\bar{c}s$  tree amplitude. Since only  $\lambda^2$ -suppressed penguin amplitudes introduce a new  $CP$ -violating phase, amplitudes with a single weak phase dominate, and we expect  $|\bar{A}_{\psi K} / A_{\psi K} - 1| < 0.01$ . The  $e^+e^-$  asymmetric-energy  $B$ -factory experiments, BABAR [92] and Belle [93], provide precise measurements. The world average is [94]

$$\sin 2\beta = 0.679 \pm 0.020. \quad (11.20)$$

This measurement has a four-fold ambiguity in  $\beta$ , which can be resolved by a global fit as mentioned in Sec. 11.4. Experimentally, the two-fold ambiguity  $\beta \rightarrow \pi/2 - \beta$  (but not  $\beta \rightarrow \pi + \beta$ ) can be resolved by a time-dependent angular analysis of  $B^0 \rightarrow J/\psi K^{*0}$  [95,96], or a time-dependent Dalitz plot analysis of  $B^0 \rightarrow \bar{D}^0 h^0$  ( $h^0 = \pi^0, \eta, \omega$ ) with  $\bar{D}^0 \rightarrow K_S^0 \pi^+ \pi^-$  [97,98]. These results indicate that negative  $\cos 2\beta$  solutions are very unlikely, in agreement with the global CKM fit result.

The  $b \rightarrow c\bar{c}d$  mediated transitions, such as  $B^0 \rightarrow J/\psi \pi^0$  and  $B^0 \rightarrow D^{(*)+} D^{(*)-}$ , also measure approximately  $\sin 2\beta$ . However,

the dominant component of the  $b \rightarrow d$  penguin amplitude has a different CKM phase ( $V_{tb}^* V_{td}$ ) than the tree amplitude ( $V_{cb}^* V_{cd}$ ), and its magnitudes are of the same order in  $\lambda$ . Therefore, the effect of penguins could be large, resulting in  $S_f \neq -\eta_f \sin 2\beta$  and  $C_f \neq 0$ . These decay modes have also been measured by BABAR and Belle. The world averages [94],  $S_{J/\psi \pi^0} = -0.93 \pm 0.15$ ,  $S_{D^+ D^-} = -0.96 \pm 0.19$ , and  $S_{D^{*+} D^{*-}} = -0.77 \pm 0.14$  ( $\eta_f = +1$  for these modes), are consistent with  $\sin 2\beta$  obtained from  $B^0 \rightarrow$  charmonium  $K^0$  decays, and the  $C_f$ 's are consistent with zero, although the uncertainties are sizable.

The  $b \rightarrow c\bar{u}d$  decays,  $B^0 \rightarrow \bar{D}^0 h^0$  with  $\bar{D}^0 \rightarrow CP$  eigenstates, have no penguin contributions and provide theoretically clean  $\sin 2\beta$  measurements. BABAR measured  $S_{D^{(*)} h^0} = -0.56 \pm 0.25$  [91].

#### 11.3.2.2. Penguin-dominated modes:

The  $b \rightarrow s\bar{q}q$  penguin-dominated decays have the same CKM phase as the  $b \rightarrow c\bar{c}s$  tree level decays, up to corrections suppressed by  $\lambda^2$ , since  $V_{tb}^* V_{ts} = -V_{cb}^* V_{cs} [1 + \mathcal{O}(\lambda^2)]$ . Therefore, decays such as  $B^0 \rightarrow \phi K^0$  and  $\eta' K^0$  provide  $\sin 2\beta$  measurements in the SM. Any new physics contribution to the amplitude with a different weak phase would give rise to  $S_f \neq -\eta_f \sin 2\beta$ , and possibly  $C_f \neq 0$ . Therefore, the main interest in these modes is not simply to measure  $\sin 2\beta$ , but to search for new physics. Measurements of many other decay modes in this category, such as  $B \rightarrow \pi^0 K_S^0$ ,  $K_S^0 K_S^0 K_S^0$ , etc., have also been performed by BABAR and Belle. The results and their uncertainties are summarized in Fig. 12.3 and Table 12.1 of Ref. 90.

#### 11.3.3. $\alpha / \phi_2$ :

Since  $\alpha$  is the phase between  $V_{tb}^* V_{td}$  and  $V_{ub}^* V_{ud}$ , only time-dependent  $CP$  asymmetries in  $b \rightarrow u\bar{u}d$  decay dominated modes can directly measure  $\sin 2\alpha$ , in contrast to  $\sin 2\beta$ , where several different transitions can be used. Since  $b \rightarrow d$  penguin amplitudes have a different CKM phase than  $b \rightarrow u\bar{u}d$  tree amplitudes, and their magnitudes are of the same order in  $\lambda$ , the penguin contribution can be sizable, which makes the determination of  $\alpha$  complicated. To date,  $\alpha$  has been measured in  $B \rightarrow \pi\pi$ ,  $\rho\pi$  and  $\rho\rho$  decay modes.

##### 11.3.3.1. $B \rightarrow \pi\pi$ :

It is now experimentally well established that there is a sizable contribution of  $b \rightarrow d$  penguin amplitudes in  $B \rightarrow \pi\pi$  decays. Thus,  $S_{\pi^+ \pi^-}$  in the time-dependent  $B^0 \rightarrow \pi^+ \pi^-$  analysis does not measure  $\sin 2\alpha$ , but

$$S_{\pi^+ \pi^-} = \sqrt{1 - C_{\pi^+ \pi^-}^2} \sin(2\alpha + 2\Delta\alpha), \quad (11.21)$$

where  $2\Delta\alpha$  is the phase difference between  $e^{2i\gamma} \bar{A}_{\pi^+ \pi^-}$  and  $A_{\pi^+ \pi^-}$ . The value of  $\Delta\alpha$ , hence  $\alpha$ , can be extracted using the isospin relation among the amplitudes of  $B^0 \rightarrow \pi^+ \pi^-$ ,  $B^0 \rightarrow \pi^0 \pi^0$ , and  $B^+ \rightarrow \pi^+ \pi^0$  decays [99],

$$\frac{1}{\sqrt{2}} A_{\pi^+ \pi^-} + A_{\pi^0 \pi^0} - A_{\pi^+ \pi^0} = 0, \quad (11.22)$$

and a similar expression for the  $\bar{A}_{\pi\pi}$ 's. This method utilizes the fact that a pair of pions from  $B \rightarrow \pi\pi$  decay must be in a zero angular momentum state, and, because of Bose statistics, they must have even isospin. Consequently,  $\pi^0 \pi^{\pm}$  is in a pure isospin-2 state, while the penguin amplitudes only contribute to the isospin-0 final state. The latter does not hold for the electroweak penguin amplitudes, but their effect is expected to be small. The isospin analysis uses the world averages [94,100]  $S_{\pi^+ \pi^-} = -0.65 \pm 0.07$ ,  $C_{\pi^+ \pi^-} = -0.38 \pm 0.06$ , the branching fractions of all three modes, and the direct  $CP$  asymmetry  $C_{\pi^0 \pi^0} = -0.43_{-0.24}^{+0.25}$ . This analysis leads to 16 mirror solutions for  $0 \leq \alpha < 2\pi$ . Because of this, and the sizable experimental error of the  $B^0 \rightarrow \pi^0 \pi^0$  rate and  $CP$  asymmetry, only a loose constraint on  $\alpha$  can be obtained at present [101],  $0^\circ < \alpha < 7^\circ$ ,  $81^\circ < \alpha < 103^\circ$ ,  $121^\circ < \alpha < 150^\circ$ , and  $166^\circ < \alpha < 180^\circ$  at 68% CL.

### 11.3.3.2. $B \rightarrow \rho\rho$ :

The decay  $B^0 \rightarrow \rho^+\rho^-$  contains two vector mesons in the final state, which in general is a mixture of  $CP$ -even and  $CP$ -odd components. Therefore, it was thought that extracting  $\alpha$  from this mode would be complicated.

However, the longitudinal polarization fractions ( $f_L$ ) in  $B^+ \rightarrow \rho^+\rho^0$  and  $B^0 \rightarrow \rho^+\rho^-$  decays were measured to be close to unity [102], which implies that the final states are almost purely  $CP$ -even. Furthermore,  $\mathcal{B}(B^0 \rightarrow \rho^0\rho^0) = (0.73_{-0.28}^{+0.27}) \times 10^{-6}$  is much smaller than  $\mathcal{B}(B^0 \rightarrow \rho^+\rho^-) = (24.2_{-3.2}^{+3.1}) \times 10^{-6}$  and  $\mathcal{B}(B^+ \rightarrow \rho^+\rho^0) = (24.0_{-2.0}^{+1.9}) \times 10^{-6}$  [40], which implies that the effect of the penguin diagrams is small. The isospin analysis using the world averages,  $S_{\rho^+\rho^-} = -0.05 \pm 0.17$  and  $C_{\rho^+\rho^-} = -0.06 \pm 0.13$  [40], together with the time-dependent  $CP$  asymmetry,  $S_{\rho^0\rho^0} = -0.3 \pm 0.7$  and  $C_{\rho^0\rho^0} = -0.2 \pm 0.9$  [103], and the above-mentioned branching fractions, gives  $\alpha = (89.9 \pm 5.4)^\circ$  [101], with a mirror solution at  $3\pi/2 - \alpha$ . A possible small violation of Eq. (11.22) due to the finite width of the  $\rho$  [104] is neglected.

### 11.3.3.3. $B \rightarrow \rho\pi$ :

The final state in  $B^0 \rightarrow \rho^+\pi^-$  decay is not a  $CP$  eigenstate, but this decay proceeds via the same quark-level diagrams as  $B^0 \rightarrow \pi^+\pi^-$ , and both  $B^0$  and  $\bar{B}^0$  can decay to  $\rho^+\pi^-$ . Consequently, mixing-induced  $CP$  violations can occur in four decay amplitudes,  $B^0 \rightarrow \rho^\pm\pi^\mp$  and  $\bar{B}^0 \rightarrow \rho^\pm\pi^\mp$ . The time-dependent Dalitz plot analysis of  $B^0 \rightarrow \pi^+\pi^-\pi^0$  decays permits the extraction of  $\alpha$  with a single discrete ambiguity,  $\alpha \rightarrow \alpha + \pi$ , since one knows the variation of the strong phases in the interference regions of the  $\rho^+\pi^-$ ,  $\rho^-\pi^+$ , and  $\rho^0\pi^0$  amplitudes in the Dalitz plot [105]. The combination of Belle [106] and BABAR [107] measurements gives  $\alpha = (120_{-7}^{+11})^\circ$  [101]. This constraint is still moderate, and there are also solutions around  $30^\circ$  and  $90^\circ$  within  $2\sigma$  significance level.

Combining the above-mentioned three decay modes [101],  $\alpha$  is constrained as

$$\alpha = (89.0_{-4.2}^{+4.4})^\circ. \quad (11.23)$$

A different statistical approach [108] gives similar constraint from the combination of these measurements.

### 11.3.4. $\gamma / \phi_3$ :

By virtue of Eq. (11.16),  $\gamma$  does not depend on CKM elements involving the top quark, so it can be measured in tree-level  $B$  decays. This is an important distinction from the measurements of  $\alpha$  and  $\beta$ , and implies that the measurements of  $\gamma$  are unlikely to be affected by physics beyond the SM.

#### 11.3.4.1. $B^\pm \rightarrow DK^\pm$ :

The interference of  $B^- \rightarrow D^0K^-$  ( $b \rightarrow c\bar{u}s$ ) and  $B^- \rightarrow \bar{D}^0K^-$  ( $b \rightarrow \bar{u}cs$ ) transitions can be studied in final states accessible in both  $D^0$  and  $\bar{D}^0$  decays [89]. In principle, it is possible to extract the  $B$  and  $D$  decay amplitudes, the relative strong phases, and the weak phase  $\gamma$  from the data.

A practical complication is that the precision depends sensitively on the ratio of the interfering amplitudes

$$r_B = \left| \frac{A(B^- \rightarrow \bar{D}^0K^-)}{A(B^- \rightarrow D^0K^-)} \right|, \quad (11.24)$$

which is around 0.1–0.2. The original GLW method [109,110] considers  $D$  decays to  $CP$  eigenstates, such as  $B^\pm \rightarrow D_{CP}^{(*)}(\rightarrow \pi^+\pi^-)K^\pm$ . To alleviate the smallness of  $r_B$  and make the interfering amplitudes (which are products of the  $B$  and  $D$  decay amplitudes) comparable in magnitude, the ADS method [111] considers final states where Cabibbo-allowed  $\bar{D}^0$  and doubly-Cabibbo-suppressed  $D^0$  decays interfere. Extensive measurements have been made by the  $B$  factories [112,113], CDF [114] and LHCb [115] using both methods.

It was realized that both  $D^0$  and  $\bar{D}^0$  have large branching fractions to certain three-body final states, such as  $K_S\pi^+\pi^-$ , and the analysis can be optimized by studying the Dalitz plot dependence of the interferences [116,117]. The best present determination of  $\gamma$  comes from this method. Belle [118] and BABAR [119] obtained

$\gamma = (78_{-12}^{+11} \pm 4 \pm 9)^\circ$  and  $\gamma = (68 \pm 14 \pm 4 \pm 3)^\circ$ , respectively, where the last uncertainty is due to the  $D$ -decay modeling. The error is sensitive to the central value of the amplitude ratio  $r_B$  (and  $r_B^*$  for the  $D^*K$  mode), for which Belle found somewhat larger central values than BABAR. The same values of  $r_B^{(*)}$  enter the ADS analyses, and the data can be combined to fit for  $r_B^{(*)}$  and  $\gamma$ . The  $D^0\text{--}\bar{D}^0$  mixing has been neglected in all measurements, but its effect on  $\gamma$  is far below the present experimental accuracy [120], unless  $D^0\text{--}\bar{D}^0$  mixing is due to  $CP$ -violating new physics, in which case it can be included in the analysis [121].

Combining the GLW, ADS, and Dalitz analyses [101],  $\gamma$  is constrained as

$$\gamma = (68_{-11}^{+10})^\circ. \quad (11.25)$$

Similar results are found in Ref. [108].

#### 11.3.4.2. $B^0 \rightarrow D^{(*)\pm}\pi^\mp$ :

The interference of  $b \rightarrow u$  and  $b \rightarrow c$  transitions can be studied in  $\bar{B}^0 \rightarrow D^{(*)+}\pi^-$  ( $b \rightarrow c\bar{u}d$ ) and  $\bar{B}^0 \rightarrow B^0 \rightarrow D^{(*)+}\pi^-$  ( $\bar{b} \rightarrow \bar{u}c\bar{d}$ ) decays and their  $CP$  conjugates, since both  $B^0$  and  $\bar{B}^0$  decay to  $D^{(*)\pm}\pi^\mp$  (or  $D^\pm\rho^\mp$ , etc.). Since there are only tree and no penguin contributions to these decays, in principle, it is possible to extract from the four time-dependent rates the magnitudes of the two hadronic amplitudes, their relative strong phase, and the weak phase between the two decay paths, which is  $2\beta + \gamma$ .

A complication is that the ratio of the interfering amplitudes is very small,  $r_{D\pi} = A(B^0 \rightarrow D^+\pi^-)/A(\bar{B}^0 \rightarrow D^+\pi^-) = \mathcal{O}(0.01)$  (and similarly for  $r_{D^*\pi}$  and  $r_{D\rho}$ ), and therefore it has not been possible to measure it. To obtain  $2\beta + \gamma$ ,  $SU(3)$  flavor symmetry and dynamical assumptions have been used to relate  $A(\bar{B}^0 \rightarrow D^-\pi^+)$  to  $A(\bar{B}^0 \rightarrow D_s^-\pi^+)$ , so this measurement is not model-independent at present. Combining the  $D^\pm\pi^\mp$ ,  $D^{*\pm}\pi^\mp$  and  $D^\pm\rho^\mp$  measurements [122] gives  $\sin(2\beta + \gamma) > 0.68$  at 68% CL [101], consistent with the previously discussed results for  $\beta$  and  $\gamma$ . The amplitude ratio is much larger in the analogous  $B_s^0 \rightarrow D_s^\pm K^\mp$  decays, so it will be possible at LHCb to measure it and model-independently extract  $\gamma - 2\beta_s$  [123] (where  $\beta_s = \arg(-V_{ts}V_{tb}^*/V_{cs}V_{cb}^*)$  is related to the phase of  $B_s$  mixing).

## 11.4. Global fit in the Standard Model

Using the independently measured CKM elements mentioned in the previous sections, the unitarity of the CKM matrix can be checked. We obtain  $|V_{ud}|^2 + |V_{us}|^2 + |V_{ub}|^2 = 0.9999 \pm 0.0006$  (1st row),  $|V_{cd}|^2 + |V_{cs}|^2 + |V_{cb}|^2 = 1.067 \pm 0.047$  (2nd row),  $|V_{ud}|^2 + |V_{cd}|^2 + |V_{td}|^2 = 1.002 \pm 0.005$  (1st column), and  $|V_{us}|^2 + |V_{cs}|^2 + |V_{ts}|^2 = 1.065 \pm 0.046$  (2nd column), respectively. The uncertainties in the second row and column are dominated by that of  $|V_{cs}|$ . For the second row, a more stringent check is obtained from the measurement of  $\sum_{u,c,d,s,b} |V_{ij}|^2$  in Sec. 11.2.4 minus the sum in the first row above:  $|V_{cd}|^2 + |V_{cs}|^2 + |V_{cb}|^2 = 1.002 \pm 0.027$ . These provide strong tests of the unitarity of the CKM matrix. The sum of the three angles of the unitarity triangle,  $\alpha + \beta + \gamma = (178_{-12}^{+11})^\circ$ , is also consistent with the SM expectation.

The CKM matrix elements can be most precisely determined by a global fit that uses all available measurements and imposes the SM constraints (*i.e.*, three generation unitarity). The fit must also use theory predictions for hadronic matrix elements, which sometimes have significant uncertainties. There are several approaches to combining the experimental data. CKMfitter [6,101] and Ref. 124 (which develops [125,126] further) use frequentist statistics, while UTfit [108,127] uses a Bayesian approach. These approaches provide similar results.

The constraints implied by the unitarity of the three generation CKM matrix significantly reduce the allowed range of some of the CKM elements. The fit for the Wolfenstein parameters defined in Eq. (11.4) gives

$$\begin{aligned} \lambda &= 0.22535 \pm 0.00065, & A &= 0.811_{-0.012}^{+0.022}, \\ \bar{\rho} &= 0.131_{-0.013}^{+0.026}, & \bar{\eta} &= 0.345_{-0.014}^{+0.013}. \end{aligned} \quad (11.26)$$



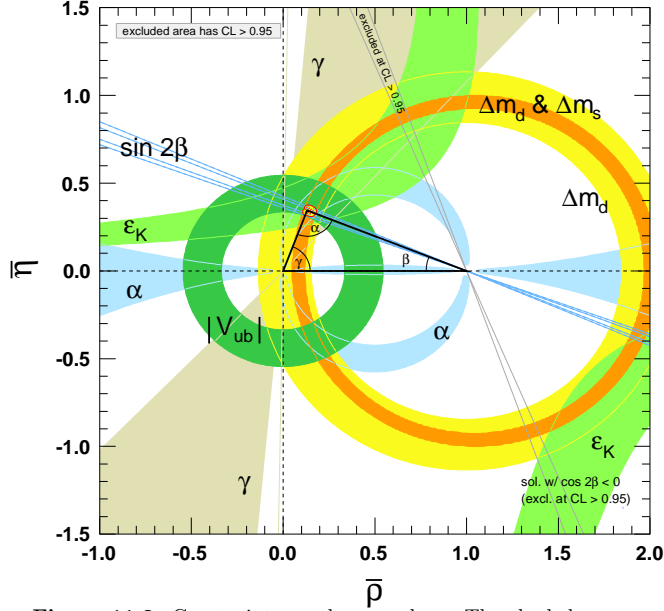


**Figure 11.2:** Constraints on the  $\bar{\rho}, \bar{\eta}$  plane. The shaded areas have 95% CL.

These values are obtained using the method of Refs. [6,101]. Using the prescription of Refs. [108,127] gives  $\lambda = 0.22535 \pm 0.00065$ ,  $A = 0.817 \pm 0.015$ ,  $\bar{\rho} = 0.136 \pm 0.018$ ,  $\bar{\eta} = 0.348 \pm 0.014$  [128]. The fit results for the magnitudes of all nine CKM elements are

$$V_{\text{CKM}} = \begin{pmatrix} 0.97427 \pm 0.00015 & 0.22534 \pm 0.00065 & 0.00351^{+0.00015}_{-0.00014} \\ 0.22520 \pm 0.00065 & 0.97344 \pm 0.00016 & 0.0412^{+0.0011}_{-0.0005} \\ 0.00867^{+0.00029}_{-0.00031} & 0.0404^{+0.0011}_{-0.0005} & 0.999146^{+0.000021}_{-0.000046} \end{pmatrix}, \quad (11.27)$$

and the Jarlskog invariant is  $J = (2.96^{+0.20}_{-0.16}) \times 10^{-5}$ .

Figure 11.2 illustrates the constraints on the  $\bar{\rho}, \bar{\eta}$  plane from various measurements and the global fit result. The shaded 95% CL regions all overlap consistently around the global fit region. This consistency gets noticeably worse if  $B \rightarrow \tau \bar{\nu}$  is included in the fit.

### 11.5. Implications beyond the SM

The effects in  $B$ ,  $K$ , and  $D$  decays and mixings due to high-scale physics ( $W$ ,  $Z$ ,  $t$ ,  $h$  in the SM, and new physics particles) can be parameterized by operators made of SM fields, obeying the  $SU(3) \times SU(2) \times U(1)$  gauge symmetry. The beyond SM (BSM) contributions to the coefficients of these operators are suppressed by powers of the scale of new physics. At lowest order, there are of order a hundred flavor-changing operators of dimension-6, and the observable effects of BSM interactions are encoded in their coefficients. In the SM, these coefficients are determined by just the four CKM parameters, and the  $W$ ,  $Z$ , and quark masses. For example,  $\Delta m_d$ ,  $\Gamma(B \rightarrow \rho \gamma)$ , and  $\Gamma(B \rightarrow X_d \ell^+ \ell^-)$  are all proportional to  $|V_{td} V_{tb}^*|^2$  in the SM, however, they may receive unrelated contributions from new physics. The new physics contributions may or may not obey the SM relations. (For example, the flavor sector of the MSSM contains 69  $CP$ -conserving parameters and 41  $CP$ -violating phases, *i.e.*, 40 new ones [129]). Thus, similar to the measurements of  $\sin 2\beta$  in tree- and loop-dominated decay modes, overconstraining measurements of the magnitudes and phases of flavor-changing neutral-current amplitudes give good sensitivity to new physics.

To illustrate the level of suppression required for BSM contributions, consider a class of models in which the unitarity of the CKM matrix is maintained, and the dominant effect of new physics is to modify the neutral meson mixing amplitudes [130] by  $(z_{ij}/\Lambda^2)(\bar{q}_i \gamma^\mu P_L q_j)^2$  (for recent reviews, see [131,132]). It is only known since the measurements of  $\gamma$  and  $\alpha$  that the SM gives the leading contribution to  $B^0 - \bar{B}^0$  mixing [6,133]. Nevertheless, new physics with a generic weak phase may still contribute to neutral meson mixings at a significant fraction of the SM [134,127]. The existing data imply that  $\Lambda/|z_{ij}|^{1/2}$  has to

exceed about  $10^4$  TeV for  $K^0 - \bar{K}^0$  mixing,  $10^3$  TeV for  $D^0 - \bar{D}^0$  mixing, 500 TeV for  $B^0 - \bar{B}^0$  mixing, and 100 TeV for  $B_s^0 - \bar{B}_s^0$  mixing [127,132]. (Some other operators are even better constrained [127].) The constraints are the strongest in the kaon sector, because the CKM suppression is the most severe. Thus, if there is new physics at the TeV scale,  $|z_{ij}| \ll 1$  is required. Even if  $|z_{ij}|$  are suppressed by a loop factor and  $|V_{ti}^* V_{tj}|^2$  (in the down quark sector), similar to the SM, one expects percent-level effects, which may be observable in forthcoming flavor physics experiments. To constrain such extensions of the SM, many measurements irrelevant for the SM-CKM fit, such as the  $CP$  asymmetry in semileptonic  $B_{d,s}^0$  decays,  $A_{\text{SL}}^{d,s}$ , are important [135]. A  $D^0$  measurement sensitive to the approximate linear combination  $0.6A_{\text{SL}}^d + 0.4A_{\text{SL}}^s$  shows a  $3.9\sigma$  hint of a deviation from the SM [136].

Many key measurements which are sensitive to BSM flavor physics are not useful to think about in terms of constraining the unitarity triangle in Fig. 11.1. For example, besides the angles in Eq. (11.16), a key quantity in the  $B_s$  system is  $\beta_s = \arg(-V_{ts} V_{tb}^* / V_{cs} V_{cb}^*)$ , which is the small,  $\lambda^2$ -suppressed, angle of a “squashed” unitarity triangle, obtained by taking the scalar product of the second and third columns. This angle can be measured via time-dependent  $CP$  violation in  $B_s^0 \rightarrow J/\psi \phi$ , similar to  $\beta$  in  $B^0 \rightarrow J/\psi K^0$ . Since the  $J/\psi \phi$  final state is not a  $CP$  eigenstate, an angular analysis of the decay products is needed to separate the  $CP$ -even and  $CP$ -odd components, which give opposite asymmetries. In the SM, the asymmetry for the  $CP$ -even part is  $2\beta_s$  (sometimes the notation  $\phi_s = -2\beta_s$  plus a possible BSM contribution to the  $B_s$  mixing phase is used). Checking if the data agrees with the SM prediction,  $\beta_s = 0.018 \pm 0.001$  [101], is another sensitive test of the SM. After the first  $CP$ -asymmetry measurements of  $B_s^0 \rightarrow J/\psi \phi$  hinted at a possible large deviation from the SM, the latest Tevatron results [137] are consistent with the SM, within the sizable uncertainties. So is the much more precise LHCb measurement obtained from  $1 \text{ fb}^{-1}$  data, including the  $J/\psi \pi \pi$  mode, yielding  $\beta_s = 0.001 \pm 0.044$  [138]. This uncertainty is still more than twice the SM central value and 40 times the SM uncertainty; thus a lot will be learned from higher precision measurements in the future.

In the kaon sector, the two measured  $CP$ -violating observables  $\epsilon$  and  $\epsilon'$  are tiny, so models in which all sources of  $CP$  violation are small were viable before the  $B$ -factory measurements. Since the measurement of  $\sin 2\beta$ , we know that  $CP$  violation can be an  $\mathcal{O}(1)$  effect, and only flavor mixing is suppressed between the three quark generations. Thus, many models with spontaneous  $CP$  violation are excluded. In the kaon sector, a very clean test of the SM will come from measurements of  $K^+ \rightarrow \pi^+ \nu \bar{\nu}$  and  $K_L^0 \rightarrow \pi^0 \nu \bar{\nu}$ . These loop-induced rare decays are sensitive to new physics, and will allow a determination of  $\beta$  independent of its value measured in  $B$  decays [139].

The CKM elements are fundamental parameters, so they should be measured as precisely as possible. The overconstraining measurements of  $CP$  asymmetries, mixing, semileptonic, and rare decays have started to severely constrain the magnitudes and phases of possible new physics contributions to flavor-changing interactions. When new particles are observed at the LHC, it will be important to know the flavor parameters as precisely as possible to understand the underlying physics.

### References:

1. N. Cabibbo, Phys. Rev. Lett. **10**, 531 (1963).
2. M. Kobayashi and T. Maskawa, Prog. Theor. Phys. **49**, 652 (1973).
3. L. L. Chau and W. Y. Keung, Phys. Rev. Lett. **53**, 1802 (1984).
4. L. Wolfenstein, Phys. Rev. Lett. **51**, 1945 (1983).
5. A. J. Buras *et al.*, Phys. Rev. **D50**, 3433 (1994) [hep-ph/9403384].
6. J. Charles *et al.* [CKMfitter Group], Eur. Phys. J. **C41**, 1 (2005) [hep-ph/0406184].
7. C. Jarlskog, Phys. Rev. Lett. **55**, 1039 (1985).
8. J. C. Hardy and I. S. Towner, Phys. Rev. **C70**, 055502 (2009) [arXiv:0812.1202 [nucl-ex]].
9. E. Blucher and W.J. Marciano, “ $V_{ud}, V_{us}$ , the Cabibbo Angle and CKM Unitarity,” in this Review.



10. D. Poganic *et al.*, Phys. Rev. Lett. **93**, 181803 (2004) [hep-ex/0312030].
11. M. Antonelli *et al.* [The FlaviaNet Kaon Working Group], arXiv:0801.1817; see also <http://www.lnf.infn.it/wg/vus>.
12. P. A. Boyle *et al.*, Phys. Rev. Lett. **100**, 141601 (2008) [arXiv:0710.5136].
13. H. Leutwyler and M. Roos, Z. Phys. **C25**, 91 (1984).
14. J. Bijnens and P. Talavera, Nucl. Phys. **B669**, 341 (2003) [hep-ph/0303103];  
M. Jamin *et al.*, JHEP **402**, 047 (2004) [hep-ph/0401080];  
V. Cirigliano *et al.*, JHEP **504**, 6 (2005) [hep-ph/0503108];  
C. Dawson *et al.*, PoS **LAT2005**, 337 (2005) [hep-lat/0510018];  
N. Tsutsui *et al.* [JLQCD Collab.], PoS **LAT2005**, 357 (2005) [hep-lat/0510068];  
M. Okamoto [Fermilab Lattice Collab.], hep-lat/0412044.
15. W. J. Marciano, Phys. Rev. Lett. **93**, 231803 (2004) [hep-ph/0402299].
16. F. Ambrosino *et al.* [KLOE Collab.], Phys. Lett. **B632**, 76 (2006) [hep-ex/0509045].
17. E. Follana *et al.* [HPQCD and UKQCD Collabs.], Phys. Rev. Lett. **100**, 062002 (2008) [arXiv:0706.1726].
18. C. Bernard *et al.* [MILC Collab.], PoS **LAT2007**, 090 (2006) [arXiv:0710.1118].
19. N. Cabibbo *et al.*, Ann. Rev. Nucl. and Part. Sci. **53**, 39 (2003) [hep-ph/0307298];  
Phys. Rev. Lett. **92**, 251803 (2004) [hep-ph/0307214].
20. M. Ademollo and R. Gatto, Phys. Rev. Lett. **13**, 264 (1964).
21. K. Maltman, AIP Conf. Proc. **1182**, 398 (2009) [arXiv:0906.5008 [hep-ph]]; K. Maltman *et al.*, Nucl. Phys. Proc. Suppl. **189**, 175 (2009) [arXiv:0906.1386]. Also, see E. Gamiz *et al.*, PoS **KAON2007**, 008 (2007) [arXiv:0709.0282].
22. B. Aubert [BABAR Collab.], arXiv:0912.0242.
23. C. Aubin *et al.* [Fermilab Lattice, MILC, and HPQCD Collabs.], Phys. Rev. Lett. **94**, 011601 (2005) [hep-ph/0408306].
24. D. Besson *et al.* [CLEO Collab.], Phys. Rev. **D80**, 032005 (2009) [arXiv:0906.2983].
25. L. Widhalm *et al.* [Belle Collab.], Phys. Rev. Lett. **97**, 061804 (2006) [hep-ex/0604049].
26. H. Abramowicz *et al.* [CHDS Collab.], Z. Phys. **C15**, 19 (1982).
27. S. A. Rabinowitz *et al.* [CCFR Collab.], Phys. Rev. Lett. **70**, 134 (1993).
28. A. O. Bazarko *et al.* [CCFR Collab.], Z. Phys. **C65**, 189 (1995) [hep-ex/9406007].
29. P. Vilain *et al.* [CHARM II Collab.], Eur. Phys. J. **C11**, 19 (1999).
30. F. J. Gilman *et al.*, Phys. Lett. **B592**, 793 (2004).
31. G. D. Lellis *et al.*, Phys. Rept. **399**, 227 (2004) [Erratum *ibid.* **411**, 323 (2005)].
32. N. Ushida *et al.* [Fermilab E531 Collab.], Phys. Lett. **B206**, 380 (1988).
33. T. Bolton, hep-ex/9708014.
34. A. Kayis-Topaksu *et al.* [CHORUS Collab.], Phys. Lett. **B626**, 24 (2005).
35. LEP  $W$  branching fraction results for this Review of Particle Physics, LEPEWWG/ XSEC/2005-01, <http://lepewwg.web.cern.ch/LEPEWWG/lepww/4f/Winter05/>.
36. P. Abreu *et al.* [DELPHI Collab.], Phys. Lett. **B439**, 209 (1998).
37. K. Abe *et al.* [Belle Collab.], Phys. Rev. Lett. **100**, 241801 (2008) [arXiv:0709.1340].
38. J. P. Alexander *et al.* [CLEO Collab.], Phys. Rev. **D79**, 052001 (2009) [arXiv:0901.1216].
39. P. del Amo Sanchez *et al.* [BABAR Collab.], Phys. Rev. **D82**, 091103 (2010) [arXiv:1008.4080].
40. Heavy Flavor Averaging Group, D. Asner *et al.*, arXiv:1010.1589 and <http://www.slac.stanford.edu/xorg/hfag/>.
41. Heavy Flavor Averaging Group [40], CHARM10 update for Charm Physics [http://www.slac.stanford.edu/xorg/hfag/charm/CHARM10/f.ds/results\\_20jan11.html](http://www.slac.stanford.edu/xorg/hfag/charm/CHARM10/f.ds/results_20jan11.html).
42. P.U.E. Onyisi *et al.* [CLEO Collab.], Phys. Rev. **D79**, 052002 (2009) [arXiv:0901.1147].
43. P. Naik *et al.* [CLEO Collab.], Phys. Rev. **D80**, 112004 (2009) [arXiv:0910.3602].
44. “2+1 Flavor Lattice QCD Averages: End of 2011” at <http://www.latticeaverages.org>; J. Laiho, E. Lunghi, and R.S. Van de Water, Phys. Rev. **D81**, 034503 (2010) [arXiv:0910.2928].
45. B. Aubert *et al.* [BABAR Collab.], Phys. Rev. **D76**, 052005 (2007) [arXiv:0704.0020].
46. I. I. Y. Bigi *et al.*, Phys. Rev. Lett. **71**, 496 (1993) [hep-ph/9304225].
47. A. V. Manohar and M. B. Wise, Phys. Rev. **D49**, 1310 (1994) [hep-ph/9308246].
48. I. I. Y. Bigi *et al.*, Phys. Rev. **D56**, 4017 (1997) [hep-ph/9704245].
49. A.H. Hoang *et al.*, Phys. Rev. **D59**, 074017 (1999) [hep-ph/9811239]; Phys. Rev. Lett. **82**, 277 (1999) [hep-ph/9809423]; A.H. Hoang and T. Teubner, Phys. Rev. **D60**, 114027 (1999) [hep-ph/9904468].
50. R. Kowalewski and T. Mannel, “Determination of  $V_{cb}$  and  $V_{ub}$ ,” in this Review.
51. N. Isgur and M.B. Wise, Phys. Lett. **B237**, 527 (1990); N. Isgur and M.B. Wise, Phys. Lett. **B232**, 113 (1989).
52. M. Neubert, Phys. Rev. **D49**, 3392 (1994) [hep-ph/9311325]; Phys. Rev. **D49**, 4623 (1994) [hep-ph/9312311].
53. I.I.Y. Bigi *et al.*, Int. J. Mod. Phys. **A9**, 2467 (1994) [hep-ph/9312359].
54. C.W. Bauer *et al.*, Phys. Lett. **B479**, 395 (2000) [hep-ph/0002161]; Phys. Rev. **D64**, 113004 (2001) [hep-ph/0107074].
55. A. Bornheim *et al.* [CLEO Collab.], Phys. Rev. Lett. **88**, 231803 (2002) [hep-ex/0202019].
56. B. Aubert *et al.* [BABAR Collab.], Phys. Rev. **D73**, 012006 (2006) [hep-ex/0509040].
57. A. Limosani *et al.* [Belle Collab.], Phys. Lett. **B621**, 28 (2005) [hep-ex/0504046].
58. P. Urquijo *et al.* [Belle Collab.], Phys. Rev. Lett. **104**, 021801 (2010) [arXiv:0907.0379];  
B. Aubert *et al.* [BABAR Collab.], Phys. Rev. Lett. **100**, 171802 (2008) [arXiv:0708.3702].
59. E. Dalgic *et al.*, Phys. Rev. **D73**, 074502 (2006) [Erratum *ibid.* **D75**, 119906 (2007)] [hep-lat/0601021].
60. J. A. Bailey *et al.* [Fermilab Lattice and MILC Collabs.], Phys. Rev. **D79**, 054507 (2009) [arXiv:0811.3640].
61. P. Ball and R. Zwicky, Phys. Rev. **D71**, 014015 (2005) [hep-ph/0406232].
62. O. Schneider, “ $B^0-\bar{B}^0$  mixing,” in this Review.
63. A. Abulencia *et al.* [CDF Collab.], Phys. Rev. Lett. **97**, 242003 (2006) [hep-ex/0609040].
64. R. Aaij *et al.* [LHCb Collab.], Phys. Lett. **B709**, 177 (2012) [arXiv:1112.4311]; LHCb-CONF-2011-050.
65. Heavy Flavor Averaging Group [40], and updates for Rare Decays: <http://www.slac.stanford.edu/xorg/hfag/rare/index.html>.
66. M. Misiak *et al.*, Phys. Rev. Lett. **98**, 022002 (2007) [hep-ph/0609232].
67. R. Aaij *et al.* [LHCb Collab.], arXiv:1203.4493; S. Chatrchyan *et al.* [CMS Collab.], arXiv:1203.3976; G. Aad *et al.* [ATLAS Collab.], arXiv:1204.0735.
68. B. Grinstein and D. Pirjol, Phys. Rev. **D62**, 093002 (2000) [hep-ph/0002216];  
A. Ali *et al.*, Phys. Lett. **B595**, 323 (2004) [hep-ph/0405075];  
M. Beneke *et al.*, Nucl. Phys. **B612**, 25 (2001) [hep-ph/0106067];  
S. W. Bosch and G. Buchalla, Nucl. Phys. **B621**, 459 (2002) [hep-ph/0106081];  
Z. Ligeti and M. B. Wise, Phys. Rev. **D60**, 117506 (1999) [hep-ph/9905277];  
D. Becirevic *et al.*, JHEP **305**, 7 (2003) [hep-lat/0301020];

- P. Ball *et al.*, Phys. Rev. **D75**, 054004 (2007) [hep-ph/0612081];  
W. Wang *et al.*, arXiv:0711.0432;  
C. D. Lu *et al.*, Phys. Rev. **D76**, 014013 (2007) [hep-ph/0701265].
69. A. J. Buras *et al.*, Phys. Rev. Lett. **95**, 261805 (2005) [hep-ph/0508165].
70. A.V. Artamonov *et al.* [E949 Collab.], Phys. Rev. Lett. **101**, 191802 (2008) [arXiv:0808.2459]; Phys. Rev. **D79**, 092004 (2009) [arXiv:0903.0030].
71. D. Acosta *et al.* [CDF Collab.], Phys. Rev. Lett. **95**, 102002 (2005) [hep-ex/0505091].
72. V.M. Abazov *et al.* [DØ Collab.], Phys. Rev. Lett. **107**, 121802 (2011) arXiv:1106.5436.
73. CMS-PAS-TOP-11-029 (2011) [CMS Collab.].
74. V. M. Abazov *et al.* [DØ Collab.], Phys. Rev. **D84**, 112001 (2011) [arXiv:1108.3091].
75. T. Aaltonen *et al.* [CDF Collab.], Phys. Rev. Lett. **103**, 092002 (2009) [arXiv:0903.0885]; T. Aaltonen *et al.* [CDF Collab.], Phys. Rev. **D82**, 112005 (2010) [arXiv:1004.1181].
76. T. Aaltonen *et al.* [CDF Collab.], Phys. Rev. **D81**, 072003 (2010) [arXiv:1001.4577].
77. S. Chatrchyan *et al.* [CMS Collab.], Phys. Rev. Lett. **107**, 091802 (2011) [arXiv:1106.3052].
78. J. Swain and L. Taylor, Phys. Rev. **D58**, 093006 (1998) [hep-ph/9712420].
79. “ $K_L^0$  meson” particle listing, in this *Review*.
80. G. Buchalla *et al.*, Rev. Mod. Phys. **68**, 1125 (1996) [hep-ph/9512380].
81. T. Inami and C. S. Lim, Prog. Theor. Phys. **65**, 297 (1981) [Erratum *ibid.* **65**, 1772 (1981)].
82. J. M. Flynn and L. Randall, Phys. Lett. **B224**, 221 (1989); G. Buchalla, A. J. Buras, and M. K. Harlander, Nucl. Phys. **B337**, 313 (1990).
83. M. Ciuchini *et al.*, Phys. Lett. **B301**, 263 (1993) [hep-ph/9212203]; A. J. Buras, M. Jamin, and M. E. Lautenbacher, Nucl. Phys. **B408**, 209 (1993) [hep-ph/9303284].
84. T. Hambye *et al.*, Nucl. Phys. **B564**, 391 (2000) [hep-ph/9906434].
85. S. Bertolini *et al.*, Phys. Rev. **D63**, 056009 (2001) [hep-ph/0002234].
86. A. Pich, hep-ph/0410215.
87. L. Lellouch and M. Luscher, Comm. Math. Phys. **219**, 31 (2001) [hep-lat/0003023].
88. C. h. Kim *et al.*, Nucl. Phys. **B727**, 218 (2005) [hep-lat/0507006].
89. A. B. Carter and A. I. Sanda, Phys. Rev. Lett. **45**, 952 (1980); Phys. Rev. **D23**, 1567 (1981).
90. A more detailed discussion and references can be found in: D. Kirkby and Y. Nir, “ $CP$  violation in meson decays,” in this *Review*.
91. B. Aubert *et al.* [BABAR Collab.], Phys. Rev. Lett. **99**, 081801 (2007) [arXiv:hep-ex/0703019].
92. B. Aubert *et al.* [BABAR Collab.], Phys. Rev. **D79**, 072009 (2009) [arXiv:0902.1708].
93. I. Adachi *et al.* [Belle Collab.], arXiv:1201.4643, to appear in Phys. Rev. Lett.
94. Heavy Flavor Averaging Group [40], Summer 2011 updates for Unitarity Triangle Parameters: <http://www.slac.stanford.edu/xorg/hfag/triangle/summer2011/index.shtml>.
95. B. Aubert *et al.* [BABAR Collab.], Phys. Rev. **D71**, 032005 (2005) [hep-ex/0411016].
96. R. Itoh *et al.* [Belle Collab.], Phys. Rev. Lett. **95**, 091601 (2005) [hep-ex/0504030].
97. P. Krokovny *et al.* [Belle Collab.], Phys. Rev. Lett. **97**, 081801 (2006) [hep-ex/0507065].
98. B. Aubert *et al.* [BABAR Collab.], Phys. Rev. Lett. **99**, 231802 (2007) [arXiv:0708.1544].
99. M. Gronau and D. London, Phys. Rev. Lett. **65**, 3381 (1990).
100. Inclusion of a recent LHCb result, R. Aaij *et al.*, LHCb-CONF-2012-007, gives a slightly changed value,  $C_{\pi\pi} = -0.36 \pm 0.06$ , and  $S_{\pi\pi}$  unchanged.
101. A. Höcker *et al.*, Eur. Phys. J. **C21**, 225 (2001) [hep-ph/0104062]; see also Ref. 6 and updates at <http://ckmfitter.in2p3.fr/>.
102. J. Zhang *et al.* [Belle Collab.], Phys. Rev. Lett. **91**, 221801 (2003) [hep-ex/0306007]; A. Somov *et al.* [Belle Collab.], Phys. Rev. Lett. **96**, 171801 (2006) [hep-ex/0601024]; B. Aubert *et al.* [BABAR Collab.], Phys. Rev. Lett. **97**, 261801 (2006) [hep-ex/0607092]; Phys. Rev. **D76**, 052007 (2007) [arXiv:0705.2157].
103. B. Aubert *et al.* [BABAR Collab.], Phys. Rev. **D78**, 071104 (2008) [arXiv:0807.4977].
104. A. F. Falk *et al.*, Phys. Rev. **D69**, 011502 (2004) [hep-ph/0310242].
105. H.R. Quinn and A.E. Snyder, Phys. Rev. **D48**, 2139 (1993).
106. A. Kusaka *et al.* [Belle Collab.], Phys. Rev. Lett. **98**, 221602 (2007) [hep-ex/0701015].
107. B. Aubert *et al.* [BABAR Collab.], Phys. Rev. **D76**, 102004 (2007) [hep-ex/0703008].
108. M. Bona *et al.* [UTfit Collab.], JHEP **507**, 28 (2005) [hep-ph/0501199], and updates at <http://www.utfit.org/>.
109. M. Gronau and D. London, Phys. Lett. **B253**, 483 (1991).
110. M. Gronau and D. Wyler, Phys. Lett. **B265**, 172 (1991).
111. D. Atwood *et al.*, Phys. Rev. Lett. **78**, 3257 (1997) [hep-ph/9612433]; Phys. Rev. **D63**, 036005 (2001) [hep-ph/0008090].
112. P. del Amo Sanchez *et al.* [BABAR Collab.], Phys. Rev. **D82**, 072004 (2010) [arXiv:1007.0504]; B. Aubert *et al.* [BABAR Collab.], Phys. Rev. **D78**, 092002 (2008) [arXiv:0807.2408]; Phys. Rev. **D80**, 092001 (2009) [arXiv:0909.3981]; P. del Amo Sanchez *et al.* Phys. Rev. **D82**, 072006 (2010) [arXiv:1006.4241]; J. P. Lees *et al.* Phys. Rev. **D84**, 012002 (2011) [arXiv:1104.4472].
113. K. Abe *et al.* [Belle Collab.], Phys. Rev. **D73**, 051106 (2006) [hep-ex/0601032]; Y. Horii *et al.*, Phys. Rev. Lett. **106**, 231803 (2011) [arXiv:1103.5951].
114. T. Aaltonen *et al.* [CDF Collab.], Phys. Rev. **D81**, 031105 (2010) [arXiv:0911.0425].
115. R. Aaij *et al.* [LHCb Collab.], arXiv:1203.3662.
116. A. Bondar, talk at the Belle analysis workshop, Novosibirsk, September 2002; A. Poluektov *et al.* [Belle Collab.], Phys. Rev. **D70**, 072003 (2004) [hep-ex/0406067].
117. A. Giri *et al.*, Phys. Rev. **D68**, 054018 (2003) [hep-ph/0303187].
118. A. Poluektov *et al.* [Belle Collab.], Phys. Rev. **D81**, 112002 (2010) [arXiv:1003.3360].
119. B. Aubert *et al.* [BABAR Collab.], Phys. Rev. Lett. **105**, 121801 (2010) [arXiv:1005.1096].
120. Y. Grossman *et al.*, Phys. Rev. **D72**, 031501 (2005) [hep-ph/0505270].
121. A. Amorim *et al.*, Phys. Rev. **D59**, 056001 (1999) [hep-ph/9807364].
122. B. Aubert *et al.* [BABAR Collab.], Phys. Rev. **D71**, 112003 (2005) [hep-ex/0504035]; Phys. Rev. **D73**, 111101 (2006) [hep-ex/0602049]; F.J. Ronga *et al.* [Belle Collab.], Phys. Rev. **D73**, 092003 (2006) [hep-ex/0604013]; S. Bahinipati *et al.* [Belle Collab.], Phys. Rev. **D84**, 021101 (2011) [arXiv:1102.0888].
123. R. Aleksan *et al.*, Z. Phys. **C54**, 653 (1992).
124. G. P. Dubois-Felsmann *et al.*, hep-ph/0308262.
125. “The BABAR physics book: Physics at an asymmetric B factory,” (P. F. Harrison and H. R. Quinn, eds.), SLAC-R-0504, 1998.
126. S. Plaszczynski and M. H. Schune, hep-ph/9911280.
127. M. Bona *et al.* [UTfit Collab.], JHEP **0803**, 049 (2008) [arXiv:0707.0636].
128. We thank the CKMfitter and UTfit groups for performing fits and preparing plots using input values from this *Review*.
129. H. E. Haber, Nucl. Phys. Proc. Supp. **62**, 469 (1998) [hep-ph/9709450]; Y. Nir, hep-ph/0109090.

- 
130. J. M. Soares and L. Wolfenstein, Phys. Rev. **D47**, 1021 (1993); T. Goto *et al.*, Phys. Rev. **D53**, 6662 (1996) [[hep-ph/9506311](#)]; J. P. Silva and L. Wolfenstein, Phys. Rev. **D55**, 5331 (1997) [[hep-ph/9610208](#)].
131. Y. Grossman, Z. Ligeti and Y. Nir, Prog. Theor. Phys. **122**, 125 (2009) [[arXiv:0904.4262](#)].
132. G. Isidori, Y. Nir and G. Perez, Ann. Rev. Nucl. and Part. Sci. **60**, 355 (2010) [[arXiv:1002.0900](#)].
133. Z. Ligeti, Int. J. Mod. Phys. **A20**, 5105 (2005) [[hep-ph/0408267](#)].
134. K. Agashe *et al.*, [hep-ph/0509117](#).
135. S. Laplace *et al.*, Phys. Rev. **D65**, 094040 (2002) [[hep-ph/0202010](#)].
136. V. M. Abazov *et al.* [DØ Collab.], Phys. Rev. **D84**, 052007 (2011) [[arXiv:1106.6308](#)].
137. V. M. Abazov *et al.* [DØ Collab.], Phys. Rev. **D85**, 032006 (2012) [[arXiv:1109.3166](#)]; T. Aaltonen *et al.* [CDF Collab.], CDF note 10778 (2012).
138. The LHCb Collab., LHCb-CONF-2012-002; R. Aaij *et al.* [LHCb Collab.], [arXiv:1204.5675](#).
139. G. Buchalla and A. J. Buras, Phys. Lett. **B333**, 221 (1994) [[hep-ph/9405259](#)].

12. *CP VIOLATION IN MESON DECAYS*

Revised May 2012 by D. Kirkby (UC Irvine) and Y. Nir (Weizmann Institute).

The *CP* transformation combines charge conjugation *C* with parity *P*. Under *C*, particles and antiparticles are interchanged, by conjugating all internal quantum numbers, *e.g.*,  $Q \rightarrow -Q$  for electromagnetic charge. Under *P*, the handedness of space is reversed,  $\vec{x} \rightarrow -\vec{x}$ . Thus, for example, a left-handed electron  $e_L^-$  is transformed under *CP* into a right-handed positron,  $e_R^+$ .

If *CP* were an exact symmetry, the laws of Nature would be the same for matter and for antimatter. We observe that most phenomena are *C*- and *P*-symmetric, and therefore, also *CP*-symmetric. In particular, these symmetries are respected by the gravitational, electromagnetic, and strong interactions. The weak interactions, on the other hand, violate *C* and *P* in the strongest possible way. For example, the charged *W* bosons couple to left-handed electrons,  $e_L^-$ , and to their *CP*-conjugate right-handed positrons,  $e_R^+$ , but to neither their *C*-conjugate left-handed positrons,  $e_L^+$ , nor their *P*-conjugate right-handed electrons,  $e_R^-$ . While weak interactions violate *C* and *P* separately, *CP* is still preserved in most weak interaction processes. The *CP* symmetry is, however, violated in certain rare processes, as discovered in neutral *K* decays in 1964 [1], and observed in recent years in *B* decays. A  $K_L$  meson decays more often to  $\pi^- e^+ \bar{\nu}_e$  than to  $\pi^+ e^- \nu_e$ , thus allowing electrons and positrons to be unambiguously distinguished, but the decay-rate asymmetry is only at the 0.003 level. The *CP*-violating effects observed in *B* decays are larger: the *CP* asymmetry in  $B^0/\bar{B}^0$  meson decays to *CP* eigenstates like  $J/\psi K_S$  is about 0.7 [2,3]. These effects are related to  $K^0 - \bar{K}^0$  and  $B^0 - \bar{B}^0$  mixing, but *CP* violation arising solely from decay amplitudes has also been observed, first in  $K \rightarrow \pi\pi$  decays [4–6], and more recently in various neutral *B* [7,8] and charged *B* [9–11] decays. Evidence for *CP* violation in the decay amplitude at a level higher than  $3\sigma$  (but still lower than  $5\sigma$ ) has also been achieved in neutral *D* [12] and  $B_s$  [13] decays. *CP* violation has not yet been observed in the lepton sector.

In addition to parity and to continuous Lorentz transformations, there is one other spacetime operation that could be a symmetry of the interactions: time reversal *T*,  $t \rightarrow -t$ . Violations of *T* symmetry have been observed in neutral *K* decays [14], and are expected as a corollary of *CP* violation if the combined *CPT* transformation is a fundamental symmetry of Nature [15]. All observations indicate that *CPT* is indeed a symmetry of Nature. Furthermore, one cannot build a Lorentz-invariant quantum field theory with a Hermitian Hamiltonian that violates *CPT*. (At several points in our discussion, we avoid assumptions about *CPT*, in order to identify cases where evidence for *CP* violation relies on assumptions about *CPT*.)

Within the Standard Model, *CP* symmetry is broken by complex phases in the Yukawa couplings (that is, the couplings of the Higgs scalar to quarks). When all manipulations to remove unphysical phases in this model are exhausted, one finds that there is a single *CP*-violating parameter [16]. In the basis of mass eigenstates, this single phase appears in the  $3 \times 3$  unitary matrix that gives the *W*-boson couplings to an up-type antiquark and a down-type quark. (If the Standard Model is supplemented with Majorana mass terms for the neutrinos, the analogous mixing matrix for leptons has three *CP*-violating phases.) The beautifully consistent and economical Standard-Model description of *CP* violation in terms of Yukawa couplings, known as the Kobayashi-Maskawa (KM) mechanism [16], agrees with all measurements to date. (The measurement of the dimuon asymmetry in semi-leptonic *b*-hadron decays deviates from the Standard Model prediction by  $3.9\sigma$  [17]. Pending confirmation, we do not discuss it further in this review.) Furthermore, one can fit the data allowing new physics contributions to loop processes to compete with, or even dominate over, the Standard Model ones [18,19]. Such an analysis provides a model-independent proof that the KM phase is different from zero, and that the matrix of three-generation quark mixing is the dominant source of *CP* violation in meson decays.

The current level of experimental accuracy and the theoretical uncertainties involved in the interpretation of the various observations leave room, however, for additional subdominant sources of *CP* violation from new physics. Indeed, almost all extensions of the

Standard Model imply that there are such additional sources. Moreover, *CP* violation is a necessary condition for baryogenesis, the process of dynamically generating the matter-antimatter asymmetry of the Universe [20]. Despite the phenomenological success of the KM mechanism, it fails (by several orders of magnitude) to accommodate the observed asymmetry [21]. This discrepancy strongly suggests that Nature provides additional sources of *CP* violation beyond the KM mechanism. (The evidence for neutrino masses implies that *CP* can be violated also in the lepton sector. This situation makes leptogenesis [22], a scenario where *CP*-violating phases in the Yukawa couplings of the neutrinos play a crucial role in the generation of the baryon asymmetry, a very attractive possibility.) The expectation of new sources motivates the large ongoing experimental effort to find deviations from the predictions of the KM mechanism.

*CP* violation can be experimentally searched for in a variety of processes, such as meson decays, electric dipole moments of neutrons, electrons and nuclei, and neutrino oscillations. Meson decays probe flavor-changing *CP* violation. The search for electric dipole moments may find (or constrain) sources of *CP* violation that, unlike the KM phase, are not related to flavor-changing couplings. Future searches for *CP* violation in neutrino oscillations might provide further input on leptogenesis.

The present measurements of *CP* asymmetries provide some of the strongest constraints on the weak couplings of quarks. Future measurements of *CP* violation in *K*, *D*, *B*, and  $B_s$  meson decays will provide additional constraints on the flavor parameters of the Standard Model, and can probe new physics. In this review, we give the formalism and basic physics that are relevant to present and near future measurements of *CP* violation in meson decays.

Before going into details, we list here the observables where *CP* violation has been observed at a level above  $5\sigma$  [23–25]:

- Indirect *CP* violation in  $K \rightarrow \pi\pi$  and  $K \rightarrow \pi\ell\nu$  decays, and in the  $K_L \rightarrow \pi^+ \pi^- e^+ e^-$  decay, is given by

$$|\epsilon| = (2.228 \pm 0.011) \times 10^{-3}. \quad (12.1)$$

- Direct *CP* violation in  $K \rightarrow \pi\pi$  decays is given by

$$\text{Re}(\epsilon'/\epsilon) = (1.65 \pm 0.26) \times 10^{-3}. \quad (12.2)$$

- *CP* violation in the interference of mixing and decay in the tree-dominated  $b \rightarrow c\bar{c}s$  transitions, such as  $B \rightarrow \psi K^0$ , is given by (we use  $K^0$  throughout to denote results that combine  $K_S$  and  $K_L$  modes, but use the sign appropriate to  $K_S$ ):

$$S_{\psi K^0} = +0.679 \pm 0.020. \quad (12.3)$$

- *CP* violation in the interference of mixing and decay in various modes related to  $b \rightarrow q\bar{q}s$  (penguin) transitions is given by

$$S_{\eta' K^0} = +0.59 \pm 0.07, \quad (12.4)$$

$$S_{\phi K^0} = +0.74_{-0.13}^{+0.11}, \quad (12.5)$$

$$S_{f_0 K^0} = +0.69_{-0.12}^{+0.10}, \quad (12.6)$$

$$S_{K^+ K^- K_S} = +0.68_{-0.10}^{+0.09}, \quad (12.7)$$

- *CP* violation in the interference of mixing and decay in the  $B \rightarrow \pi^+ \pi^-$  mode is given by

$$S_{\pi^+ \pi^-} = -0.65 \pm 0.07. \quad (12.8)$$

- Direct *CP* violation in the  $B \rightarrow \pi^+ \pi^-$  mode is given by

$$C_{\pi^+ \pi^-} = -0.36 \pm 0.06. \quad (12.9)$$

- *CP* violation in the interference of mixing and decay in various modes related to  $b \rightarrow c\bar{c}d$  transitions is given by

$$S_{\psi \pi^0} = -0.93 \pm 0.15, \quad (12.10)$$

$$S_{D^+ D^-} = -0.98 \pm 0.17. \quad (12.11)$$

$$S_{D^{*+} D^{*-}} = -0.77 \pm 0.10. \quad (12.12)$$

- Direct *CP* violation in the  $\overline{B}^0 \rightarrow K^- \pi^+$  mode is given by

$$\mathcal{A}_{K^\mp \pi^\pm} = -0.087 \pm 0.008. \quad (12.13)$$

- Direct *CP* violation in  $B^\pm \rightarrow D_+ K^\pm$  decays ( $D_+$  is the *CP*-even neutral  $D$  state) is given by

$$\mathcal{A}_{D_+ K^\pm} = +0.19 \pm 0.03. \quad (12.14)$$

### 12.1. Formalism

The phenomenology of *CP* violation is superficially different in  $K$ ,  $D$ ,  $B$ , and  $B_s$  decays. This is primarily because each of these systems is governed by a different balance between decay rates, oscillations, and lifetime splitting. However, the underlying mechanisms of *CP* violation are identical for all pseudoscalar mesons.

In this section, we present a general formalism for, and classification of, *CP* violation in the decay of a pseudoscalar meson  $M$  that might be a charged or neutral  $K$ ,  $D$ ,  $B$ , or  $B_s$  meson. Subsequent sections describe the *CP*-violating phenomenology, approximations, and alternative formalisms that are specific to each system.

**12.1.1. Charged- and neutral-meson decays:** We define decay amplitudes of  $M$  (which could be charged or neutral) and its *CP* conjugate  $\overline{M}$  to a multi-particle final state  $f$  and its *CP* conjugate  $\overline{f}$  as

$$\begin{aligned} A_f &= \langle f | \mathcal{H} | M \rangle, & \overline{A}_f &= \langle f | \mathcal{H} | \overline{M} \rangle, \\ A_{\overline{f}} &= \langle \overline{f} | \mathcal{H} | M \rangle, & \overline{A}_{\overline{f}} &= \langle \overline{f} | \mathcal{H} | \overline{M} \rangle, \end{aligned} \quad (12.15)$$

where  $\mathcal{H}$  is the Hamiltonian governing weak interactions. The action of *CP* on these states introduces phases  $\xi_M$  and  $\xi_f$  that depend on their flavor content, according to

$$CP|M\rangle = e^{+i\xi_M} |\overline{M}\rangle, \quad CP|f\rangle = e^{+i\xi_f} |\overline{f}\rangle, \quad (12.16)$$

with

$$CP|\overline{M}\rangle = e^{-i\xi_M} |M\rangle, \quad CP|\overline{f}\rangle = e^{-i\xi_f} |f\rangle \quad (12.17)$$

so that  $(CP)^2 = 1$ . The phases  $\xi_M$  and  $\xi_f$  are arbitrary and unphysical because of the flavor symmetry of the strong interaction. If *CP* is conserved by the dynamics,  $[CP, \mathcal{H}] = 0$ , then  $A_f$  and  $\overline{A}_{\overline{f}}$  have the same magnitude and an arbitrary unphysical relative phase

$$\overline{A}_{\overline{f}} = e^{i(\xi_f - \xi_M)} A_f. \quad (12.18)$$

**12.1.2. Neutral-meson mixing:** A state that is initially a superposition of  $M^0$  and  $\overline{M}^0$ , say

$$|\psi(0)\rangle = a(0)|M^0\rangle + b(0)|\overline{M}^0\rangle, \quad (12.19)$$

will evolve in time acquiring components that describe all possible decay final states  $\{f_1, f_2, \dots\}$ , that is,

$$|\psi(t)\rangle = a(t)|M^0\rangle + b(t)|\overline{M}^0\rangle + c_1(t)|f_1\rangle + c_2(t)|f_2\rangle + \dots \quad (12.20)$$

If we are interested in computing only the values of  $a(t)$  and  $b(t)$  (and not the values of all  $c_i(t)$ ), and if the times  $t$  in which we are interested are much larger than the typical strong interaction scale, then we can use a much simplified formalism [26]. The simplified time evolution is determined by a  $2 \times 2$  effective Hamiltonian  $\mathbf{H}$  that is not Hermitian, since otherwise the mesons would only oscillate and not decay. Any complex matrix, such as  $\mathbf{H}$ , can be written in terms of Hermitian matrices  $\mathbf{M}$  and  $\mathbf{\Gamma}$  as

$$\mathbf{H} = \mathbf{M} - \frac{i}{2} \mathbf{\Gamma}. \quad (12.21)$$

$\mathbf{M}$  and  $\mathbf{\Gamma}$  are associated with  $(M^0, \overline{M}^0) \leftrightarrow (M^0, \overline{M}^0)$  transitions via off-shell (dispersive), and on-shell (absorptive) intermediate states, respectively. Diagonal elements of  $\mathbf{M}$  and  $\mathbf{\Gamma}$  are associated with

the flavor-conserving transitions  $M^0 \rightarrow M^0$  and  $\overline{M}^0 \rightarrow \overline{M}^0$ , while off-diagonal elements are associated with flavor-changing transitions  $M^0 \leftrightarrow \overline{M}^0$ .

The eigenvectors of  $\mathbf{H}$  have well-defined masses and decay widths. To specify the components of the strong interaction eigenstates,  $M^0$  and  $\overline{M}^0$ , in the light ( $M_L$ ) and heavy ( $M_H$ ) mass eigenstates, we introduce three complex parameters:  $p$ ,  $q$ , and, for the case that both *CP* and *CPT* are violated in mixing,  $z$ :

$$\begin{aligned} |M_L\rangle &\propto p\sqrt{1-z}|M^0\rangle + q\sqrt{1+z}|\overline{M}^0\rangle \\ |M_H\rangle &\propto p\sqrt{1+z}|M^0\rangle - q\sqrt{1-z}|\overline{M}^0\rangle, \end{aligned} \quad (12.22)$$

with the normalization  $|q|^2 + |p|^2 = 1$  when  $z = 0$ . (Another possible choice, which is in standard usage for  $K$  mesons, defines the mass eigenstates according to their lifetimes:  $K_S$  for the short-lived and  $K_L$  for the long-lived state. The  $K_L$  is experimentally found to be the heavier state.)

The real and imaginary parts of the eigenvalues  $\omega_{L,H}$  corresponding to  $|M_{L,H}\rangle$  represent their masses and decay widths, respectively. The mass and width splittings are

$$\begin{aligned} \Delta m &\equiv m_H - m_L = \mathcal{R}e(\omega_H - \omega_L), \\ \Delta\Gamma &\equiv \Gamma_H - \Gamma_L = -2\mathcal{I}m(\omega_H - \omega_L). \end{aligned} \quad (12.23)$$

Note that here  $\Delta m$  is positive by definition, while the sign of  $\Delta\Gamma$  is to be experimentally determined. The sign of  $\Delta\Gamma$  has not yet been established for the  $B$  mesons, while  $\Delta\Gamma < 0$  is established for  $K$  and  $B_s$  mesons and  $\Delta\Gamma > 0$  is established for  $D$  mesons. The Standard Model predicts  $\Delta\Gamma < 0$  also for  $B$  mesons (for this reason,  $\Delta\Gamma = \Gamma_L - \Gamma_H$ , which is still a signed quantity, is often used in the  $B$  and  $B_s$  literature and is the convention used in the PDG experimental summaries).

Solving the eigenvalue problem for  $\mathbf{H}$  yields

$$\left(\frac{q}{p}\right)^2 = \frac{\mathbf{M}_{12}^* - (i/2)\mathbf{\Gamma}_{12}^*}{\mathbf{M}_{12} - (i/2)\mathbf{\Gamma}_{12}} \quad (12.24)$$

and

$$z \equiv \frac{\delta m - (i/2)\delta\Gamma}{\Delta m - (i/2)\Delta\Gamma}, \quad (12.25)$$

where

$$\delta m \equiv \mathbf{M}_{11} - \mathbf{M}_{22}, \quad \delta\Gamma \equiv \mathbf{\Gamma}_{11} - \mathbf{\Gamma}_{22} \quad (12.26)$$

are the differences in effective mass and decay-rate expectation values for the strong interaction states  $M^0$  and  $\overline{M}^0$ .

If either *CP* or *CPT* is a symmetry of  $\mathbf{H}$  (independently of whether  $T$  is conserved or violated), then the values of  $\delta m$  and  $\delta\Gamma$  are both zero, and hence  $z = 0$ . We also find that

$$\omega_H - \omega_L = 2\sqrt{\left(\mathbf{M}_{12} - \frac{i}{2}\mathbf{\Gamma}_{12}\right)\left(\mathbf{M}_{12}^* - \frac{i}{2}\mathbf{\Gamma}_{12}^*\right)}. \quad (12.27)$$

If either *CP* or  $T$  is a symmetry of  $\mathbf{H}$  (independently of whether *CPT* is conserved or violated), then  $\mathbf{\Gamma}_{12}/\mathbf{M}_{12}$  is real, leading to

$$\left(\frac{q}{p}\right)^2 = e^{2i\xi_M} \Rightarrow \left|\frac{q}{p}\right| = 1, \quad (12.28)$$

where  $\xi_M$  is the arbitrary unphysical phase introduced in Eq. (12.17). If, and only if, *CP* is a symmetry of  $\mathbf{H}$  (independently of *CPT* and  $T$ ), then both of the above conditions hold, with the result that the mass eigenstates are orthogonal

$$\langle M_H | M_L \rangle = |p|^2 - |q|^2 = 0. \quad (12.29)$$

**12.1.3. *CP-violating observables*** : All *CP*-violating observables in  $M$  and  $\bar{M}$  decays to final states  $f$  and  $\bar{f}$  can be expressed in terms of phase-convention-independent combinations of  $A_f$ ,  $\bar{A}_f$ ,  $A_{\bar{f}}$ , and  $\bar{A}_{\bar{f}}$ , together with, for neutral-meson decays only,  $q/p$ . *CP* violation in charged-meson decays depends only on the combination  $|\bar{A}_{\bar{f}}/A_f|$ , while *CP* violation in neutral-meson decays is complicated by  $M^0 \leftrightarrow \bar{M}^0$  oscillations, and depends, additionally, on  $|q/p|$  and on  $\lambda_f \equiv (q/p)(\bar{A}_f/A_f)$ .

The decay rates of the two neutral  $K$  mass eigenstates,  $K_S$  and  $K_L$ , are different enough ( $\Gamma_S/\Gamma_L \sim 500$ ) that one can, in most cases, actually study their decays independently. For neutral  $D$ ,  $B$ , and  $B_s$  mesons, however, values of  $\Delta\Gamma/\Gamma$  (where  $\Gamma \equiv (\Gamma_H + \Gamma_L)/2$ ) are relatively small, and so both mass eigenstates must be considered in their evolution. We denote the state of an initially pure  $|M^0\rangle$  or  $|\bar{M}^0\rangle$  after an elapsed proper time  $t$  as  $|M_{\text{phys}}^0(t)\rangle$  or  $|\bar{M}_{\text{phys}}^0(t)\rangle$ , respectively. Using the effective Hamiltonian approximation, but not assuming *CPT* is a good symmetry, we obtain

$$\begin{aligned} |M_{\text{phys}}^0(t)\rangle &= (g_+(t) + z g_-(t)) |M^0\rangle - \sqrt{1-z^2} \frac{q}{p} g_-(t) |\bar{M}^0\rangle, \\ |\bar{M}_{\text{phys}}^0(t)\rangle &= (g_+(t) - z g_-(t)) |\bar{M}^0\rangle - \sqrt{1-z^2} \frac{p}{q} g_-(t) |M^0\rangle, \end{aligned} \quad (12.30)$$

where

$$g_{\pm}(t) \equiv \frac{1}{2} \left( e^{-im_H t - \frac{1}{2}\Gamma_H t} \pm e^{-im_L t - \frac{1}{2}\Gamma_L t} \right) \quad (12.31)$$

and  $z = 0$  if either *CPT* or *CP* is conserved.

Defining  $x \equiv \Delta m/\Gamma$  and  $y \equiv \Delta\Gamma/(2\Gamma)$ , and assuming  $z = 0$ , one obtains the following time-dependent decay rates:

$$\begin{aligned} \frac{d\Gamma[M_{\text{phys}}^0(t) \rightarrow f]/dt}{e^{-\Gamma t} \mathcal{N}_f} &= \\ & \left( |A_f|^2 + |(q/p)\bar{A}_f|^2 \right) \cosh(y\Gamma t) + \left( |A_f|^2 - |(q/p)\bar{A}_f|^2 \right) \cos(x\Gamma t) \\ & + 2 \operatorname{Re} e((q/p)A_f^* \bar{A}_f) \sinh(y\Gamma t) - 2 \operatorname{Im}((q/p)A_f^* \bar{A}_f) \sin(x\Gamma t), \end{aligned} \quad (12.32)$$

$$\begin{aligned} \frac{d\Gamma[\bar{M}_{\text{phys}}^0(t) \rightarrow f]/dt}{e^{-\Gamma t} \mathcal{N}_f} &= \\ & \left( |(p/q)A_f|^2 + |\bar{A}_f|^2 \right) \cosh(y\Gamma t) - \left( |(p/q)A_f|^2 - |\bar{A}_f|^2 \right) \cos(x\Gamma t) \\ & + 2 \operatorname{Re} e((p/q)A_f \bar{A}_f^*) \sinh(y\Gamma t) - 2 \operatorname{Im}((p/q)A_f \bar{A}_f^*) \sin(x\Gamma t), \end{aligned} \quad (12.33)$$

where  $\mathcal{N}_f$  is a common, time-independent, normalization factor. Decay rates to the *CP*-conjugate final state  $\bar{f}$  are obtained analogously, with  $\mathcal{N}_f = \mathcal{N}_{\bar{f}}$  and the substitutions  $A_f \rightarrow A_{\bar{f}}$  and  $\bar{A}_f \rightarrow \bar{A}_{\bar{f}}$  in Eqs. (12.32, 12.33). Terms proportional to  $|A_f|^2$  or  $|\bar{A}_f|^2$  are associated with decays that occur without any net  $M \leftrightarrow \bar{M}$  oscillation, while terms proportional to  $|(q/p)\bar{A}_f|^2$  or  $|(p/q)A_f|^2$  are associated with decays following a net oscillation. The  $\sinh(y\Gamma t)$  and  $\sin(x\Gamma t)$  terms of Eqs. (12.32, 12.33) are associated with the interference between these two cases. Note that, in multi-body decays, amplitudes are functions of phase-space variables. Interference may be present in some regions but not others, and is strongly influenced by resonant substructure.

When neutral pseudoscalar mesons are produced coherently in pairs from the decay of a vector resonance,  $V \rightarrow M^0 \bar{M}^0$  (for example,  $\Upsilon(4S) \rightarrow B^0 \bar{B}^0$  or  $\phi \rightarrow K^0 \bar{K}^0$ ), the time-dependence of their subsequent decays to final states  $f_1$  and  $f_2$  has a similar form to Eqs. (12.32, 12.33):

$$\begin{aligned} \frac{d\Gamma[V_{\text{phys}}(t_1, t_2) \rightarrow f_1 f_2]/d(\Delta t)}{e^{-\Gamma|\Delta t|} \mathcal{N}_{f_1 f_2}} &= \\ & \left( |a_+|^2 + |a_-|^2 \right) \cosh(y\Gamma\Delta t) + \left( |a_+|^2 - |a_-|^2 \right) \cos(x\Gamma\Delta t) \\ & - 2 \operatorname{Re}(a_+^* a_-) \sinh(y\Gamma\Delta t) + 2 \operatorname{Im}(a_+^* a_-) \sin(x\Gamma\Delta t), \end{aligned} \quad (12.34)$$

where  $\Delta t \equiv t_2 - t_1$  is the difference in the production times,  $t_1$  and  $t_2$ , of  $f_1$  and  $f_2$ , respectively, and the dependence on the average decay time and on decay angles has been integrated out. The coefficients in Eq. (12.34) are determined by the amplitudes for no net oscillation from  $t_1 \rightarrow t_2$ ,  $\bar{A}_{f_1} A_{f_2}$ , and  $A_{f_1} \bar{A}_{f_2}$ , and for a net oscillation,  $(q/p)\bar{A}_{f_1} \bar{A}_{f_2}$  and  $(p/q)A_{f_1} A_{f_2}$ , via

$$\begin{aligned} a_+ &\equiv \bar{A}_{f_1} A_{f_2} - A_{f_1} \bar{A}_{f_2}, \\ a_- &\equiv -\sqrt{1-z^2} \left( \frac{q}{p} \bar{A}_{f_1} \bar{A}_{f_2} - \frac{p}{q} A_{f_1} A_{f_2} \right) + z (\bar{A}_{f_1} A_{f_2} + A_{f_1} \bar{A}_{f_2}). \end{aligned} \quad (12.35)$$

Assuming *CPT* conservation,  $z = 0$ , and identifying  $\Delta t \rightarrow t$  and  $f_2 \rightarrow f$ , we find that Eqs. (12.34) and (12.35) reduce to Eq. (12.32) with  $A_{f_1} = 0$ ,  $\bar{A}_{f_1} = 1$ , or to Eq. (12.33) with  $\bar{A}_{f_1} = 0$ ,  $A_{f_1} = 1$ . Indeed, such a situation plays an important role in experiments. Final states  $f_1$  with  $A_{f_1} = 0$  or  $\bar{A}_{f_1} = 0$  are called tagging states, because they identify the decaying pseudoscalar meson as, respectively,  $\bar{M}^0$  or  $M^0$ . Before one of  $M^0$  or  $\bar{M}^0$  decays, they evolve in phase, so that there is always one  $M^0$  and one  $\bar{M}^0$  present. A tagging decay of one meson sets the clock for the time evolution of the other: it starts at  $t_1$  as purely  $M^0$  or  $\bar{M}^0$ , with time evolution that depends only on  $t_2 - t_1$ .

When  $f_1$  is a state that both  $M^0$  and  $\bar{M}^0$  can decay into, then Eq. (12.34) contains interference terms proportional to  $A_{f_1} \bar{A}_{f_1} \neq 0$  that are not present in Eqs. (12.32, 12.33). Even when  $f_1$  is dominantly produced by  $M^0$  decays rather than  $\bar{M}^0$  decays, or vice versa,  $A_{f_1} \bar{A}_{f_1}$  can be non-zero owing to doubly-CKM-suppressed decays (with amplitudes suppressed by at least two powers of  $\lambda$  relative to the dominant amplitude, in the language of Section 12.3), and these terms should be considered for precision studies of *CP* violation in coherent  $V \rightarrow M^0 \bar{M}^0$  decays [27].

**12.1.4. *Classification of CP-violating effects*** : We distinguish three types of *CP*-violating effects in meson decays:

I. *CP* violation in decay is defined by

$$|\bar{A}_{\bar{f}}/A_f| \neq 1. \quad (12.36)$$

In charged meson decays, where mixing effects are absent, this is the only possible source of *CP* asymmetries:

$$A_{f\pm} \equiv \frac{\Gamma(M^- \rightarrow f^-) - \Gamma(M^+ \rightarrow f^+)}{\Gamma(M^- \rightarrow f^-) + \Gamma(M^+ \rightarrow f^+)} = \frac{|\bar{A}_{f-}/A_{f+}|^2 - 1}{|\bar{A}_{f-}/A_{f+}|^2 + 1}. \quad (12.37)$$

II. *CP* (and *T*) violation in mixing is defined by

$$|q/p| \neq 1. \quad (12.38)$$

In charged-current semileptonic neutral meson decays  $M, \bar{M} \rightarrow \ell^\pm X$  (taking  $|A_{\ell^+ X}| = |\bar{A}_{\ell^- X}|$  and  $A_{\ell^- X} = \bar{A}_{\ell^+ X} = 0$ , as is the case in the Standard Model, to lowest order in  $G_F$ , and in most of its reasonable extensions), this is the only source of *CP* violation, and can be measured via the asymmetry of “wrong-sign” decays induced by oscillations:

$$\begin{aligned} A_{\text{SL}}(t) &\equiv \frac{d\Gamma/dt[\bar{M}_{\text{phys}}^0(t) \rightarrow \ell^+ X] - d\Gamma/dt[M_{\text{phys}}^0(t) \rightarrow \ell^- X]}{d\Gamma/dt[\bar{M}_{\text{phys}}^0(t) \rightarrow \ell^+ X] + d\Gamma/dt[M_{\text{phys}}^0(t) \rightarrow \ell^- X]} \\ &= \frac{1 - |q/p|^4}{1 + |q/p|^4}. \end{aligned} \quad (12.39)$$

Note that this asymmetry of time-dependent decay rates is actually time-independent.

III. *CP* violation in interference between a decay without mixing,  $M^0 \rightarrow f$ , and a decay with mixing,  $M^0 \rightarrow \bar{M}^0 \rightarrow f$  (such an effect occurs only in decays to final states that are common to  $M^0$  and  $\bar{M}^0$ , including all *CP* eigenstates), is defined by

$$\operatorname{Im}(\lambda_f) \neq 0, \quad (12.40)$$

with

$$\lambda_f \equiv \frac{q \bar{A}_f}{p A_f}. \quad (12.41)$$

This form of  $CP$  violation can be observed, for example, using the asymmetry of neutral meson decays into final  $CP$  eigenstates  $f_{CP}$

$$\mathcal{A}_{f_{CP}}(t) \equiv \frac{d\Gamma/dt[\bar{M}_{\text{phys}}^0(t) \rightarrow f_{CP}] - d\Gamma/dt[M_{\text{phys}}^0(t) \rightarrow f_{CP}]}{d\Gamma/dt[\bar{M}_{\text{phys}}^0(t) \rightarrow f_{CP}] + d\Gamma/dt[M_{\text{phys}}^0(t) \rightarrow f_{CP}]}. \quad (12.42)$$

If  $\Delta\Gamma = 0$  and  $|q/p| = 1$ , as expected to a good approximation for  $B_d$  mesons, but not for  $K$  and  $B_s$  mesons, then  $\mathcal{A}_{f_{CP}}$  has a particularly simple form (see Eq. (12.86), below). If, in addition, the decay amplitudes fulfill  $|\bar{A}_{f_{CP}}| = |A_{f_{CP}}|$ , the interference between decays with and without mixing is the only source of the asymmetry and  $\mathcal{A}_{f_{CP}}(t) = \mathcal{I}m(\lambda_{f_{CP}}) \sin(x\Gamma t)$ .

Examples of these three types of  $CP$  violation will be given in Sections 12.4, 12.5, and 12.6.

## 12.2. Theoretical Interpretation: General Considerations

Consider the  $M \rightarrow f$  decay amplitude  $A_f$ , and the  $CP$  conjugate process,  $\bar{M} \rightarrow \bar{f}$ , with decay amplitude  $\bar{A}_{\bar{f}}$ . There are two types of phases that may appear in these decay amplitudes. Complex parameters in any Lagrangian term that contributes to the amplitude will appear in complex conjugate form in the  $CP$ -conjugate amplitude. Thus, their phases appear in  $A_f$  and  $\bar{A}_{\bar{f}}$  with opposite signs. In the Standard Model, these phases occur only in the couplings of the  $W^\pm$  bosons, and hence, are often called ‘‘weak phases.’’ The weak phase of any single term is convention-dependent. However, the difference between the weak phases in two different terms in  $A_f$  is convention-independent. A second type of phase can appear in scattering or decay amplitudes, even when the Lagrangian is real. Their origin is the possible contribution from intermediate on-shell states in the decay process. Since these phases are generated by  $CP$ -invariant interactions, they are the same in  $A_f$  and  $\bar{A}_{\bar{f}}$ . Usually the dominant rescattering is due to strong interactions; hence the designation ‘‘strong phases’’ for the phase shifts so induced. Again, only the relative strong phases between different terms in the amplitude are physically meaningful.

The ‘weak’ and ‘strong’ phases discussed here appear in addition to the ‘spurious’  $CP$ -transformation phases of Eq. (12.18). Those spurious phases are due to an arbitrary choice of phase convention, and do not originate from any dynamics or induce any  $CP$  violation. For simplicity, we set them to zero from here on.

It is useful to write each contribution  $a_i$  to  $A_f$  in three parts: its magnitude  $|a_i|$ , its weak phase  $\phi_i$ , and its strong phase  $\delta_i$ . If, for example, there are two such contributions,  $A_f = a_1 + a_2$ , we have

$$\begin{aligned} A_f &= |a_1|e^{i(\delta_1+\phi_1)} + |a_2|e^{i(\delta_2+\phi_2)}, \\ \bar{A}_{\bar{f}} &= |a_1|e^{i(\delta_1-\phi_1)} + |a_2|e^{i(\delta_2-\phi_2)}. \end{aligned} \quad (12.43)$$

Similarly, for neutral meson decays, it is useful to write

$$\mathbf{M}_{12} = |\mathbf{M}_{12}|e^{i\phi_M}, \quad \mathbf{\Gamma}_{12} = |\mathbf{\Gamma}_{12}|e^{i\phi_\Gamma}. \quad (12.44)$$

Each of the phases appearing in Eqs. (12.43, 12.44) is convention-dependent, but combinations such as  $\delta_1 - \delta_2$ ,  $\phi_1 - \phi_2$ ,  $\phi_M - \phi_\Gamma$ , and  $\phi_M + \phi_1 - \bar{\phi}_1$  (where  $\bar{\phi}_1$  is a weak phase contributing to  $\bar{A}_{\bar{f}}$ ) are physical.

It is now straightforward to evaluate the various asymmetries in terms of the theoretical parameters introduced here. We will do so with approximations that are often relevant to the most interesting measured asymmetries.

1. The  $CP$  asymmetry in charged meson decays [Eq. (12.37)] is given by

$$\mathcal{A}_{f^\pm} = -\frac{2|a_1 a_2| \sin(\delta_2 - \delta_1) \sin(\phi_2 - \phi_1)}{|a_1|^2 + |a_2|^2 + 2|a_1 a_2| \cos(\delta_2 - \delta_1) \cos(\phi_2 - \phi_1)}. \quad (12.45)$$

The quantity of most interest to theory is the weak phase difference  $\phi_2 - \phi_1$ . Its extraction from the asymmetry requires, however, that the amplitude ratio  $|a_2/a_1|$  and the strong phase difference  $\delta_2 - \delta_1$  are known. Both quantities depend on non-perturbative hadronic parameters that are difficult to calculate.

2. In the approximation that  $|\mathbf{\Gamma}_{12}/\mathbf{M}_{12}| \ll 1$  (valid for  $B$  and  $B_s$  mesons), the  $CP$  asymmetry in semileptonic neutral-meson decays [Eq. (12.39)] is given by

$$\mathcal{A}_{\text{SL}} = -\left| \frac{\mathbf{\Gamma}_{12}}{\mathbf{M}_{12}} \right| \sin(\phi_M - \phi_\Gamma). \quad (12.46)$$

The quantity of most interest to theory is the weak phase  $\phi_M - \phi_\Gamma$ . Its extraction from the asymmetry requires, however, that  $|\mathbf{\Gamma}_{12}/\mathbf{M}_{12}|$  is known. This quantity depends on long-distance physics that is difficult to calculate.

3. In the approximations that only a single weak phase contributes to decay,  $A_f = |a_f|e^{i(\delta_f+\phi_f)}$ , and that  $|\mathbf{\Gamma}_{12}/\mathbf{M}_{12}| = 0$ , we obtain  $|\lambda_f| = 1$ , and the  $CP$  asymmetries in decays to a final  $CP$  eigenstate  $f$  [Eq. (12.42)] with eigenvalue  $\eta_f = \pm 1$  are given by

$$\mathcal{A}_{f_{CP}}(t) = \mathcal{I}m(\lambda_f) \sin(\Delta mt) \quad \text{with} \quad \mathcal{I}m(\lambda_f) = \eta_f \sin(\phi_M + 2\phi_f). \quad (12.47)$$

Note that the phase so measured is purely a weak phase, and no hadronic parameters are involved in the extraction of its value from  $\mathcal{I}m(\lambda_f)$ .

The discussion above allows us to introduce another classification of  $CP$ -violating effects:

1. *Indirect CP violation* is consistent with taking  $\phi_M \neq 0$  and setting all other  $CP$  violating phases to zero.  $CP$  violation in mixing (type II) belongs to this class.
2. *Direct CP violation* cannot be accounted for by just  $\phi_M \neq 0$ .  $CP$  violation in decay (type I) belongs to this class.

As concerns type III  $CP$  violation, observing  $\eta_{f_1} \mathcal{I}m(\lambda_{f_1}) \neq \eta_{f_2} \mathcal{I}m(\lambda_{f_2})$  (for the same decaying meson and two different final  $CP$  eigenstates  $f_1$  and  $f_2$ ) would establish direct  $CP$  violation. The significance of this classification is related to theory. In superweak models [28],  $CP$  violation appears only in diagrams that contribute to  $\mathbf{M}_{12}$ , hence they predict that there is no direct  $CP$  violation. In most models and, in particular, in the Standard Model,  $CP$  violation is both direct and indirect. The experimental observation of  $\epsilon' \neq 0$  (see Section 12.4) excluded the superweak scenario.

## 12.3. Theoretical Interpretation: The KM Mechanism

Of all the Standard Model quark parameters, only the Kobayashi-Maskawa (KM) phase is  $CP$ -violating. Having a single source of  $CP$  violation, the Standard Model is very predictive for  $CP$  asymmetries: some vanish, and those that do not are correlated.

To be precise,  $CP$  could be violated also by strong interactions. The experimental upper bound on the electric-dipole moment of the neutron implies, however, that  $\theta_{\text{QCD}}$ , the non-perturbative parameter that determines the strength of this type of  $CP$  violation, is tiny, if not zero. (The smallness of  $\theta_{\text{QCD}}$  constitutes a theoretical puzzle, known as ‘the strong  $CP$  problem.’) In particular, it is irrelevant to our discussion of meson decays.

The charged current interactions (that is, the  $W^\pm$  interactions) for quarks are given by

$$-\mathcal{L}_{W^\pm} = \frac{g}{\sqrt{2}} \bar{u}_{Li} \gamma^\mu (V_{\text{CKM}})_{ij} d_{Lj} W_\mu^\pm + \text{h.c.} \quad (12.48)$$

Here  $i, j = 1, 2, 3$  are generation numbers. The Cabibbo-Kobayashi-Maskawa (CKM) mixing matrix for quarks is a  $3 \times 3$  unitary matrix [29]. Ordering the quarks by their masses, *i.e.*,  $(u_1, u_2, u_3) \rightarrow (u, c, t)$  and  $(d_1, d_2, d_3) \rightarrow (d, s, b)$ , the elements of  $V_{\text{CKM}}$  are written as follows:

$$V_{\text{CKM}} = \begin{pmatrix} V_{ud} & V_{us} & V_{ub} \\ V_{cd} & V_{cs} & V_{cb} \\ V_{td} & V_{ts} & V_{tb} \end{pmatrix}. \quad (12.49)$$

While a general  $3 \times 3$  unitary matrix depends on three real angles and six phases, the freedom to redefine the phases of the quark mass eigenstates can be used to remove five of the phases, leaving a single physical phase, the Kobayashi-Maskawa phase, that is responsible for all *CP* violation in meson decays in the Standard Model.

The fact that one can parametrize  $V_{\text{CKM}}$  by three real and only one imaginary physical parameters can be made manifest by choosing an explicit parametrization. The Wolfenstein parametrization [30,31] is particularly useful:

$$V_{\text{CKM}} = \begin{pmatrix} 1 - \frac{1}{2}\lambda^2 - \frac{1}{8}\lambda^4 & \lambda & A\lambda^3(\rho - i\eta) \\ -\lambda + \frac{1}{2}A^2\lambda^5[1 - 2(\rho + i\eta)] & 1 - \frac{1}{2}\lambda^2 - \frac{1}{8}\lambda^4(1 + 4A^2) & A\lambda^2 \\ A\lambda^3[1 - (1 - \frac{1}{2}\lambda^2)(\rho + i\eta)] & -A\lambda^2 + \frac{1}{2}A\lambda^4[1 - 2(\rho + i\eta)] & 1 - \frac{1}{2}A^2\lambda^4 \end{pmatrix}. \quad (12.50)$$

Here  $\lambda \approx 0.23$  (not to be confused with  $\lambda_f$ ), the sine of the Cabibbo angle, plays the role of an expansion parameter, and  $\eta$  represents the *CP*-violating phase. Terms of  $\mathcal{O}(\lambda^6)$  were neglected.

The unitarity of the CKM matrix,  $(VV^\dagger)_{ij} = (V^\dagger V)_{ij} = \delta_{ij}$ , leads to twelve distinct complex relations among the matrix elements. The six relations with  $i \neq j$  can be represented geometrically as triangles in the complex plane. Two of these,

$$\begin{aligned} V_{ud}V_{ub}^* + V_{cd}V_{cb}^* + V_{td}V_{tb}^* &= 0 \\ V_{td}V_{ud}^* + V_{ts}V_{us}^* + V_{tb}V_{ub}^* &= 0, \end{aligned}$$

have terms of equal order,  $\mathcal{O}(A\lambda^3)$ , and so have corresponding triangles whose interior angles are all  $\mathcal{O}(1)$  physical quantities that can be independently measured. The angles of the first triangle (see Fig. 12.1) are given by

$$\begin{aligned} \alpha \equiv \varphi_2 &\equiv \arg\left(-\frac{V_{td}V_{tb}^*}{V_{ud}V_{ub}^*}\right) \simeq \arg\left(-\frac{1 - \rho - i\eta}{\rho + i\eta}\right), \\ \beta \equiv \varphi_1 &\equiv \arg\left(-\frac{V_{cd}V_{cb}^*}{V_{td}V_{tb}^*}\right) \simeq \arg\left(\frac{1}{1 - \rho - i\eta}\right), \\ \gamma \equiv \varphi_3 &\equiv \arg\left(-\frac{V_{ud}V_{ub}^*}{V_{cd}V_{cb}^*}\right) \simeq \arg(\rho + i\eta). \end{aligned} \quad (12.51)$$

The angles of the second triangle are equal to  $(\alpha, \beta, \gamma)$  up to corrections of  $\mathcal{O}(\lambda^2)$ . The notations  $(\alpha, \beta, \gamma)$  and  $(\varphi_1, \varphi_2, \varphi_3)$  are both in common usage but, for convenience, we only use the first convention in the following.

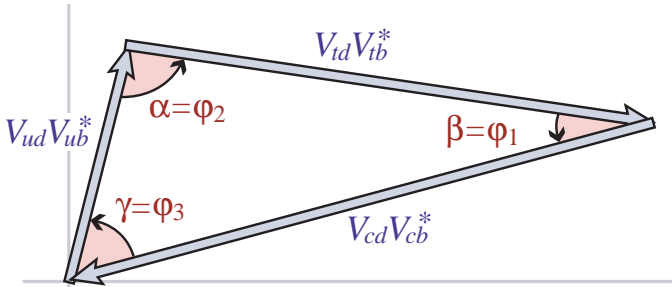


**Figure 12.1:** Graphical representation of the unitarity constraint  $V_{ud}V_{ub}^* + V_{cd}V_{cb}^* + V_{td}V_{tb}^* = 0$  as a triangle in the complex plane.

Another relation that can be represented as a triangle,

$$V_{us}V_{ub}^* + V_{cs}V_{cb}^* + V_{ts}V_{tb}^* = 0, \quad (12.52)$$

and, in particular, its small angle, of  $\mathcal{O}(\lambda^2)$ ,

$$\beta_s \equiv \arg\left(-\frac{V_{ts}V_{tb}^*}{V_{cs}V_{cb}^*}\right), \quad (12.53)$$

is convenient for analyzing *CP* violation in the  $B_s$  sector.

All unitarity triangles have the same area, commonly denoted by  $J/2$  [32]. If *CP* is violated,  $J$  is different from zero and can be taken as the single *CP*-violating parameter. In the Wolfenstein parametrization of Eq. (12.50),  $J \simeq \lambda^6 A^2 \eta$ .

## 12.4. *K* Decays

*CP* violation was discovered in  $K \rightarrow \pi\pi$  decays in 1964 [1]. The same mode provided the first evidence for direct *CP* violation [4–6].

The decay amplitudes actually measured in neutral  $K$  decays refer to the mass eigenstates  $K_L$  and  $K_S$ , rather than to the  $K$  and  $\bar{K}$  states referred to in Eq. (12.15). The final  $\pi^+\pi^-$  and  $\pi^0\pi^0$  states are *CP*-even. In the *CP* limit,  $K_S(K_L)$  would be *CP*-even (odd), and therefore would (would not) decay to two pions. We define *CP*-violating amplitude ratios for two-pion final states,

$$\eta_{00} \equiv \frac{\langle \pi^0\pi^0 | \mathcal{H} | K_L \rangle}{\langle \pi^0\pi^0 | \mathcal{H} | K_S \rangle}, \quad \eta_{+-} \equiv \frac{\langle \pi^+\pi^- | \mathcal{H} | K_L \rangle}{\langle \pi^+\pi^- | \mathcal{H} | K_S \rangle}. \quad (12.54)$$

Another important observable is the asymmetry of time-integrated semileptonic decay rates:

$$\delta_L \equiv \frac{\Gamma(K_L \rightarrow \ell^+\nu_\ell\pi^-) - \Gamma(K_L \rightarrow \ell^-\bar{\nu}_\ell\pi^+)}{\Gamma(K_L \rightarrow \ell^+\nu_\ell\pi^-) + \Gamma(K_L \rightarrow \ell^-\bar{\nu}_\ell\pi^+)}. \quad (12.55)$$

*CP* violation has been observed as an appearance of  $K_L$  decays to two-pion final states [23],

$$|\eta_{00}| = (2.221 \pm 0.011) \times 10^{-3} \quad |\eta_{+-}| = (2.232 \pm 0.011) \times 10^{-3} \quad (12.56)$$

$$|\eta_{00}/\eta_{+-}| = 0.9951 \pm 0.0008, \quad (12.57)$$

where the phase  $\phi_{ij}$  of the amplitude ratio  $\eta_{ij}$  has been determined both assuming *CPT* invariance:

$$\phi_{00} = (43.52 \pm 0.06)^\circ, \quad \phi_{+-} = (43.51 \pm 0.05)^\circ, \quad (12.58)$$

and without assuming *CPT* invariance:

$$\phi_{00} = (43.7 \pm 0.8)^\circ, \quad \phi_{+-} = (43.4 \pm 0.7)^\circ. \quad (12.59)$$

*CP* violation has also been observed in semileptonic  $K_L$  decays [23]

$$\delta_L = (3.32 \pm 0.06) \times 10^{-3}, \quad (12.60)$$

where  $\delta_L$  is a weighted average of muon and electron measurements, as well as in  $K_L$  decays to  $\pi^+\pi^-\gamma$  and  $\pi^+\pi^-e^+e^-$  [23]. *CP* violation in  $K \rightarrow 3\pi$  decays has not yet been observed [23,33].

Historically, *CP* violation in neutral  $K$  decays has been described in terms of parameters  $\epsilon$  and  $\epsilon'$ . The observables  $\eta_{00}$ ,  $\eta_{+-}$ , and  $\delta_L$  are related to these parameters, and to those of Section 12.1, by

$$\begin{aligned} \eta_{00} &= \frac{1 - \lambda_{\pi^0\pi^0}}{1 + \lambda_{\pi^0\pi^0}} = \epsilon - 2\epsilon', \\ \eta_{+-} &= \frac{1 - \lambda_{\pi^+\pi^-}}{1 + \lambda_{\pi^+\pi^-}} = \epsilon + \epsilon', \\ \delta_L &= \frac{1 - |q/p|^2}{1 + |q/p|^2} = \frac{2\mathcal{R}e(\epsilon)}{1 + |\epsilon|^2}, \end{aligned} \quad (12.61)$$

where, in the last line, we have assumed that  $|A_{\ell^+\nu_\ell\pi^-}| = |\bar{A}_{\ell^-\bar{\nu}_\ell\pi^+}|$  and  $|A_{\ell^-\bar{\nu}_\ell\pi^+}| = |\bar{A}_{\ell^+\nu_\ell\pi^-}| = 0$ . (The convention-dependent parameter  $\bar{\epsilon} \equiv (1 - q/p)/(1 + q/p)$ , sometimes used in the literature, is, in general, different from  $\epsilon$  but yields a similar expression,  $\delta_L = 2\mathcal{R}e(\bar{\epsilon})/(1 + |\bar{\epsilon}|^2)$ .) A fit to the  $K \rightarrow \pi\pi$  data yields [23]

$$|\epsilon| = (2.228 \pm 0.011) \times 10^{-3},$$

$$\mathcal{R}e(\epsilon'/\epsilon) = (1.65 \pm 0.26) \times 10^{-3}. \quad (12.62)$$

In discussing two-pion final states, it is useful to express the amplitudes  $A_{\pi^0\pi^0}$  and  $A_{\pi^+\pi^-}$  in terms of their isospin components via

$$\begin{aligned} A_{\pi^0\pi^0} &= \sqrt{\frac{1}{3}} |A_0| e^{i(\delta_0 + \phi_0)} - \sqrt{\frac{2}{3}} |A_2| e^{i(\delta_2 + \phi_2)}, \\ A_{\pi^+\pi^-} &= \sqrt{\frac{2}{3}} |A_0| e^{i(\delta_0 + \phi_0)} + \sqrt{\frac{1}{3}} |A_2| e^{i(\delta_2 + \phi_2)}, \end{aligned} \quad (12.63)$$



where we parameterize the amplitude  $A_I(\bar{A}_I)$  for  $K^0(\bar{K}^0)$  decay into two pions with total isospin  $I = 0$  or 2 as

$$\begin{aligned} A_I &\equiv \langle (\pi\pi)_I | \mathcal{H} | K^0 \rangle = |A_I| e^{i(\delta_I + \phi_I)}, \\ \bar{A}_I &\equiv \langle (\pi\pi)_I | \mathcal{H} | \bar{K}^0 \rangle = |A_I| e^{i(\delta_I - \phi_I)}. \end{aligned} \quad (12.64)$$

The smallness of  $|\eta_{00}|$  and  $|\eta_{+-}|$  allows us to approximate

$$\epsilon \simeq \frac{1}{2}(1 - \lambda_{(\pi\pi)_{I=0}}), \quad \epsilon' \simeq \frac{1}{6}(\lambda_{\pi^0\pi^0} - \lambda_{\pi^+\pi^-}). \quad (12.65)$$

The parameter  $\epsilon$  represents indirect  $CP$  violation, while  $\epsilon'$  parameterizes direct  $CP$  violation:  $\mathcal{R}e(\epsilon')$  measures  $CP$  violation in decay (type I),  $\mathcal{R}e(\epsilon)$  measures  $CP$  violation in mixing (type II), and  $\mathcal{I}m(\epsilon)$  and  $\mathcal{I}m(\epsilon')$  measure the interference between decays with and without mixing (type III).

The following expressions for  $\epsilon$  and  $\epsilon'$  are useful for theoretical evaluations:

$$\epsilon \simeq \frac{e^{i\pi/4} \mathcal{I}m(\mathbf{M}_{12})}{\sqrt{2} \Delta m}, \quad \epsilon' \simeq \frac{i}{\sqrt{2}} \left| \frac{A_2}{A_0} \right| e^{i(\delta_2 - \delta_0)} \sin(\phi_2 - \phi_0). \quad (12.66)$$

The expression for  $\epsilon$  is only valid in a phase convention where  $\phi_2 = 0$ , corresponding to a real  $V_{ud}V_{us}^*$ , and in the approximation that also  $\phi_0 = 0$ . The phase of  $\epsilon$ ,  $\arg(\epsilon) \approx \arctan(-2\Delta m/\Delta\Gamma)$ , is independent of the electroweak model and is experimentally determined to be about  $\pi/4$ . The calculation of  $\epsilon$  benefits from the fact that  $\mathcal{I}m(\mathbf{M}_{12})$  is dominated by short distance physics. Consequently, the main source of uncertainty in theoretical interpretations of  $\epsilon$  are the values of matrix elements, such as  $\langle K^0 | (\bar{s}d)_{V-A} (\bar{s}d)_{V-A} | \bar{K}^0 \rangle$ . The expression for  $\epsilon'$  is valid to first order in  $|A_2/A_0| \sim 1/20$ . The phase of  $\epsilon'$  is experimentally determined,  $\pi/2 + \delta_2 - \delta_0 \approx \pi/4$ , and is independent of the electroweak model. Note that, accidentally,  $\epsilon'/\epsilon$  is real to a good approximation.

A future measurement of much interest is that of  $CP$  violation in the rare  $K \rightarrow \pi\nu\bar{\nu}$  decays. The signal for  $CP$  violation is simply observing the  $K_L \rightarrow \pi^0\nu\bar{\nu}$  decay. The effect here is that of interference between decays with and without mixing (type III) [34]:

$$\frac{\Gamma(K_L \rightarrow \pi^0\nu\bar{\nu})}{\Gamma(K^+ \rightarrow \pi^+\nu\bar{\nu})} = \frac{1}{2} \left[ 1 + |\lambda_{\pi\nu\bar{\nu}}|^2 - 2\mathcal{R}e(\lambda_{\pi\nu\bar{\nu}}) \right] \simeq 1 - \mathcal{R}e(\lambda_{\pi\nu\bar{\nu}}), \quad (12.67)$$

where in the last equation we neglect  $CP$  violation in decay and in mixing (expected, model-independently, to be of order  $10^{-5}$  and  $10^{-3}$ , respectively). Such a measurement would be experimentally very challenging and theoretically very rewarding [35]. Similar to the  $CP$  asymmetry in  $B \rightarrow J/\psi K_S$ , the  $CP$  violation in  $K \rightarrow \pi\nu\bar{\nu}$  decay is predicted to be large (that is, the ratio in Eq. (12.67) is neither CKM- nor loop-suppressed) and can be very cleanly interpreted.

Within the Standard Model, the  $K_L \rightarrow \pi^0\nu\bar{\nu}$  decay is dominated by an intermediate top quark contribution and, consequently, can be interpreted in terms of CKM parameters [36]. (For the charged mode,  $K^+ \rightarrow \pi^+\nu\bar{\nu}$ , the contribution from an intermediate charm quark is not negligible, and constitutes a source of hadronic uncertainty.) In particular,  $\mathcal{B}(K_L \rightarrow \pi^0\nu\bar{\nu})$  provides a theoretically clean way to determine the Wolfenstein parameter  $\eta$  [37]:

$$\mathcal{B}(K_L \rightarrow \pi^0\nu\bar{\nu}) = \kappa_L [X(m_t^2/m_W^2)]^2 A^4 \eta^2, \quad (12.68)$$

where  $\kappa_L \sim 2 \times 10^{-10}$  incorporates the value of the four-fermion matrix element which is deduced, using isospin relations, from  $\mathcal{B}(K^+ \rightarrow \pi^0 e^+ \nu)$ , and  $X(m_t^2/m_W^2)$  is a known function of the top mass.

## 12.5. $D$ Decays

Evidence for  $D^0-\bar{D}^0$  mixing has been obtained in recent years [38–40]. The experimental constraints read [25,41]  $x \equiv \Delta m/\Gamma = 0.0063 \pm 0.0019$  and  $y \equiv \Delta\Gamma/(2\Gamma) = 0.0075 \pm 0.0012$ . Long-distance contributions make it difficult to calculate the Standard Model prediction for the  $D^0-\bar{D}^0$  mixing parameters. Therefore, the goal of the search for  $D^0-\bar{D}^0$  mixing is not to constrain the CKM parameters, but rather to probe new physics. Here  $CP$  violation plays an important role. Within the Standard Model, the  $CP$ -violating effects are predicted to be small, since the mixing and the relevant decays are described, to an excellent approximation, by physics of the first two generations. The expectation is that the Standard Model size of  $CP$  violation in  $D$  decays is of  $\mathcal{O}(10^{-3})$  or less, but theoretical work is ongoing to understand whether QCD effects can significantly enhance it. At present, the most sensitive searches involve the  $D \rightarrow K^+K^-$ ,  $D \rightarrow \pi^+\pi^-$  and  $D \rightarrow K^\pm\pi^\mp$  modes.

The neutral  $D$  mesons decay via a singly-Cabibbo-suppressed transition to the  $CP$  eigenstates  $K^+K^-$  and  $\pi^+\pi^-$ . These decays are dominated by Standard-Model tree diagrams. Thus, we can write, for  $f = K^+K^-$  or  $\pi^+\pi^-$ ,

$$\begin{aligned} A_f &= A_f^T e^{+i\phi_f^T} \left[ 1 + r_f e^{i(\delta_f + \phi_f)} \right], \\ \bar{A}_f &= A_f^T e^{-i\phi_f^T} \left[ 1 + r_f e^{i(\delta_f - \phi_f)} \right], \end{aligned} \quad (12.69)$$

where  $A_f^T e^{\pm i\phi_f^T}$  is the SM tree level contribution,  $\phi_f^T$  and  $\phi_f$  are weak,  $CP$  violating phases,  $\delta_f$  is a strong phase, and  $r_f$  is the ratio between a subleading ( $r_f \ll 1$ ) contribution with a weak phase different from  $\phi_f^T$  and the SM tree level contribution. Neglecting  $r_f$ ,  $\lambda_f$  is universal, and we can define a phase  $\phi_D$  via

$$\lambda_f \equiv -|q/p| e^{i\phi_D}. \quad (12.70)$$

(In the limit of  $CP$  conservation, choosing  $\phi_D = 0$  is equivalent to defining the mass eigenstates by their  $CP$  eigenvalue:  $|D_\mp\rangle = p|D^0\rangle \pm q|\bar{D}^0\rangle$ , with  $D_-(D_+)$  being the  $CP$ -odd ( $CP$ -even) state; that is, the state that does not (does) decay into  $K^+K^-$ .)

We define the time integrated  $CP$  asymmetry for a final  $CP$  eigenstate  $f$  as follows:

$$a_f \equiv \frac{\int_0^\infty \Gamma(D_{\text{phys}}^0(t) \rightarrow f) dt - \int_0^\infty \Gamma(\bar{D}_{\text{phys}}^0(t) \rightarrow f) dt}{\int_0^\infty \Gamma(D_{\text{phys}}^0(t) \rightarrow f) dt + \int_0^\infty \Gamma(\bar{D}_{\text{phys}}^0(t) \rightarrow f) dt}. \quad (12.71)$$

(This expression corresponds to the  $D$  meson being tagged at production, hence the integration goes from 0 to  $+\infty$ ; measurements are also possible with  $\psi(3770) \rightarrow D\bar{D}$ , in which case the integration goes from  $-\infty$  to  $+\infty$ .) We take  $x, y, r_f \ll 1$  and expand to leading order in these parameters. Then, we can separate the contribution to  $a_f$  to three parts [42],

$$a_f = a_f^d + a_f^m + a_f^i, \quad (12.72)$$

with the following underlying mechanisms:

1.  $a_f^d$  signals  $CP$  violation in decay (similar to Eq. (12.37)):

$$a_f^d = 2r_f \sin \phi_f \sin \delta_f. \quad (12.73)$$

2.  $a_f^m$  signals  $CP$  violation in mixing (similar to Eq. (12.46)). With our approximations, it is universal:

$$a_f^m = -\frac{y}{2} \left( \left| \frac{q}{p} \right| - \left| \frac{p}{q} \right| \right) \cos \phi_D. \quad (12.74)$$

3.  $a_f^i$  signals  $CP$  violation in the interference of mixing and decay (similar to Eq. (12.47)). With our approximations, it is universal:

$$a_f^i = \frac{x}{2} \left( \left| \frac{q}{p} \right| + \left| \frac{p}{q} \right| \right) \sin \phi_D. \quad (12.75)$$

One can isolate the effects of direct  $CP$  violation by taking the difference between the  $CP$  asymmetries in the  $K^+K^-$  and  $\pi^+\pi^-$  modes:

$$\Delta a_{CP} \equiv a_{K^+K^-} - a_{\pi^+\pi^-} = a_{K^+K^-}^d - a_{\pi^+\pi^-}^d, \quad (12.76)$$

where we neglected a residual, experiment-dependent, contribution from indirect  $CP$  violation due to the fact that there is a time dependent acceptance function that can be different for the  $K^+K^-$  and  $\pi^+\pi^-$  channels. Recently, evidence for such direct  $CP$  violation has been obtained [25]:

$$a_{K^+K^-}^d - a_{\pi^+\pi^-}^d = (-6.4 \pm 1.8) \times 10^{-3}. \quad (12.77)$$

One can also isolate the effects of indirect  $CP$  violation in the following way. Consider the time dependent decay rates in Eq. (12.32) and Eq. (12.33). The mixing processes modify the time dependence from a pure exponential. However, given the small values of  $x$  and  $y$ , the time dependences can be recast, to a good approximation, into purely exponential form, but with modified decay-rate parameters [43]:

$$\begin{aligned} \Gamma_{D^0 \rightarrow K^+K^-} &= \Gamma \times [1 + |q/p| (y \cos \phi_D - x \sin \phi_D)], \\ \Gamma_{\bar{D}^0 \rightarrow K^+K^-} &= \Gamma \times [1 + |p/q| (y \cos \phi_D + x \sin \phi_D)]. \end{aligned} \quad (12.78)$$

One can define  $CP$ -conserving and  $CP$ -violating combinations of these two observables (normalized to the true width  $\Gamma$ ):

$$\begin{aligned} y_{CP} &\equiv \frac{\Gamma_{\bar{D}^0 \rightarrow K^+K^-} + \Gamma_{D^0 \rightarrow K^+K^-} - 1}{2\Gamma} \\ &= (y/2) (|q/p| + |p/q|) \cos \phi_D - (x/2) (|q/p| - |p/q|) \sin \phi_D, \\ A_\Gamma &\equiv \frac{\Gamma_{D^0 \rightarrow K^+K^-} - \Gamma_{\bar{D}^0 \rightarrow K^+K^-}}{2\Gamma} \\ &= -(a^m + a^i). \end{aligned} \quad (12.79)$$

In the limit of  $CP$  conservation (and, in particular, within the Standard Model),  $y_{CP} = (\Gamma_+ - \Gamma_-)/2\Gamma$  (where  $\Gamma_+(\Gamma_-)$  is the decay width of the  $CP$ -even (-odd) mass eigenstate) and  $A_\Gamma = 0$ . Indeed, present measurements imply that  $CP$  violation is small [25],

$$\begin{aligned} y_{CP} &= + (1.06 \pm 0.21) \times 10^{-2}, \\ A_\Gamma &= + (0.03 \pm 0.23) \times 10^{-2}. \end{aligned}$$

The  $K^\pm\pi^\mp$  states are not  $CP$  eigenstates, but they are still common final states for  $D^0$  and  $\bar{D}^0$  decays. Since  $D^0(\bar{D}^0) \rightarrow K^-\pi^+$  is a Cabibbo-favored (doubly-Cabibbo-suppressed) process, these processes are particularly sensitive to  $x$  and/or  $y = \mathcal{O}(\lambda^2)$ . Taking into account that  $|\lambda_{K^-\pi^+}|, |\lambda_{K^+\pi^-}^{-1}| \ll 1$  and  $x, y \ll 1$ , assuming that there is no direct  $CP$  violation (these are Standard Model tree-level decays dominated by a single weak phase, and there is no contribution from penguin-like and chromomagnetic operators), and expanding the time-dependent rates for  $xt, yt \lesssim \Gamma^{-1}$ , one obtains

$$\begin{aligned} \Gamma[D_{\text{phys}}^0(t) \rightarrow K^+\pi^-] &= e^{-\Gamma t} |\bar{A}_{K^-\pi^+}|^2 \\ &\times \left[ r_d^2 + r_d \left| \frac{q}{p} \right| (y' \cos \phi_D - x' \sin \phi_D) \Gamma t + \left| \frac{q}{p} \right|^2 \frac{y^2 + x^2}{4} (\Gamma t)^2 \right], \\ \Gamma[\bar{D}_{\text{phys}}^0(t) \rightarrow K^-\pi^+] &= e^{-\Gamma t} |\bar{A}_{K^-\pi^+}|^2 \\ &\times \left[ r_d^2 + r_d \left| \frac{p}{q} \right| (y' \cos \phi_D + x' \sin \phi_D) \Gamma t + \left| \frac{p}{q} \right|^2 \frac{y^2 + x^2}{4} (\Gamma t)^2 \right], \end{aligned} \quad (12.80)$$

where

$$\begin{aligned} y' &\equiv y \cos \delta - x \sin \delta, \\ x' &\equiv x \cos \delta + y \sin \delta. \end{aligned} \quad (12.81)$$

The weak phase  $\phi_D$  is the same as that of Eq. (12.70) (a consequence of neglecting direct  $CP$  violation),  $\delta$  is a strong-phase difference for these processes, and  $r_d = \mathcal{O}(\tan^2 \theta_c)$  is the amplitude ratio,  $r_d = |\bar{A}_{K^-\pi^+}/A_{K^-\pi^+}| = |A_{K^+\pi^-}/\bar{A}_{K^+\pi^-}|$ , that is,  $\lambda_{K^-\pi^+} = r_d |q/p| e^{-i(\delta - \phi_D)}$  and  $\lambda_{K^+\pi^-}^{-1} = r_d |p/q| e^{-i(\delta + \phi_D)}$ . By fitting to the six coefficients of the various time-dependences, one can extract  $r_d$ ,  $|q/p|$ ,  $(x^2 + y^2)$ ,  $y' \cos \phi_D$ , and  $x' \sin \phi_D$ . In particular, finding  $CP$  violation ( $|q/p| \neq 1$  and/or  $\sin \phi_D \neq 0$ ) at a level much higher than  $10^{-3}$  would constitute evidence for new physics.

A fit to all data [25] yields no evidence for indirect  $CP$  violation:

$$\begin{aligned} 1 - |q/p| &= +0.12 \pm 0.17, \\ \phi_D &= -0.18 \pm 0.16. \end{aligned}$$

More details on various theoretical and experimental aspects of  $D^0 - \bar{D}^0$  mixing can be found in Ref. [44].

## 12.6. $B$ and $B_s$ Decays

The upper bound on the  $CP$  asymmetry in semileptonic  $B$  decays [24] implies that  $CP$  violation in  $B^0 - \bar{B}^0$  mixing is a small effect (we use  $\mathcal{A}_{\text{SL}}/2 \approx 1 - |q/p|$ , see Eq. (12.39)):

$$\mathcal{A}_{\text{SL}}^d = (-3.3 \pm 3.3) \times 10^{-3} \implies |q/p| = 1.0017 \pm 0.0017. \quad (12.82)$$

The Standard Model prediction is

$$\mathcal{A}_{\text{SL}}^d = \mathcal{O} \left[ (m_c^2/m_t^2) \sin \beta \right] \lesssim 0.001. \quad (12.83)$$

In models where  $\Gamma_{12}/\mathbf{M}_{12}$  is approximately real, such as the Standard Model, an upper bound on  $\Delta\Gamma/\Delta m \approx \text{Re}(\Gamma_{12}/\mathbf{M}_{12})$  provides yet another upper bound on the deviation of  $|q/p|$  from one. This constraint does not hold if  $\Gamma_{12}/\mathbf{M}_{12}$  is approximately imaginary. (An alternative parameterization uses  $q/p = (1 - \tilde{\epsilon}_B)/(1 + \tilde{\epsilon}_B)$ , leading to  $\mathcal{A}_{\text{SL}} \simeq 4\text{Re}(\tilde{\epsilon}_B)$ .)

The small deviation (less than one percent) of  $|q/p|$  from 1 implies that, at the present level of experimental precision,  $CP$  violation in  $B$  mixing is a negligible effect. Thus, for the purpose of analyzing  $CP$  asymmetries in hadronic  $B$  decays, we can use

$$\lambda_f = e^{-i\phi_{M(B)}} (\bar{A}_f/A_f), \quad (12.84)$$

where  $\phi_{M(B)}$  refers to the phase of  $\mathbf{M}_{12}$  appearing in Eq. (12.44) that is appropriate for  $B^0 - \bar{B}^0$  oscillations. Within the Standard Model, the corresponding phase factor is given by

$$e^{-i\phi_{M(B)}} = (V_{tb}^* V_{td}) / (V_{cb} V_{cd}^*). \quad (12.85)$$

Some of the most interesting decays involve final states that are common to  $B^0$  and  $\bar{B}^0$  [45,46]. It is convenient to rewrite Eq. (12.42) for  $B$  decays as [47–49]

$$\begin{aligned} A_f(t) &= S_f \sin(\Delta m t) - C_f \cos(\Delta m t), \\ S_f &\equiv \frac{2\text{Im}(\lambda_f)}{1 + |\lambda_f|^2}, \quad C_f \equiv \frac{1 - |\lambda_f|^2}{1 + |\lambda_f|^2}, \end{aligned} \quad (12.86)$$

where we assume that  $\Delta\Gamma = 0$  and  $|q/p| = 1$ . An alternative notation in use is  $A_f \equiv -C_f$ , but this  $A_f$  should not be confused with the  $A_f$  of Eq. (12.15).

A large class of interesting processes proceed via quark transitions of the form  $\bar{b} \rightarrow \bar{q}q\bar{q}'$  with  $q' = s$  or  $d$ . For  $q = c$  or  $u$ , there are contributions from both tree ( $t$ ) and penguin ( $p^{qu}$ , where  $q_u = u, c, t$  is the quark in the loop) diagrams (see Fig. 12.2) which carry different weak phases:

$$A_f = (V_{qb}^* V_{qq'}) t_f + \sum_{q_u=u,c,t} (V_{qub}^* V_{quq'}) p_f^{q_u}. \quad (12.87)$$

(The distinction between tree and penguin contributions is a heuristic one; the separation by the operator that enters is more precise. For a detailed discussion of the more complete operator product approach, which also includes higher order QCD corrections, see, for example, Ref. [50].) Using CKM unitarity, these decay amplitudes can always be written in terms of just two CKM combinations. For example, for  $f = \pi\pi$ , which proceeds via  $\bar{b} \rightarrow \bar{u}u\bar{d}$  transition, we can write

$$A_{\pi\pi} = (V_{ub}^*V_{ud})T_{\pi\pi} + (V_{tb}^*V_{td})P_{\pi\pi}^t, \quad (12.88)$$

where  $T_{\pi\pi} = t_{\pi\pi} + p_{\pi\pi}^u - p_{\pi\pi}^c$  and  $P_{\pi\pi}^t = p_{\pi\pi}^t - p_{\pi\pi}^c$ .  $CP$ -violating phases in Eq. (12.88) appear only in the CKM elements, so that

$$\frac{\bar{A}_{\pi\pi}}{A_{\pi\pi}} = \frac{(V_{ub}V_{ud}^*)T_{\pi\pi} + (V_{tb}V_{td}^*)P_{\pi\pi}^t}{(V_{ub}^*V_{ud})T_{\pi\pi} + (V_{tb}^*V_{td})P_{\pi\pi}^t}. \quad (12.89)$$

For  $f = J/\psi K$ , which proceeds via  $\bar{b} \rightarrow \bar{c}c\bar{s}$  transition, we can write

$$A_{\psi K} = (V_{cb}^*V_{cs})T_{\psi K} + (V_{ub}^*V_{us})P_{\psi K}^u, \quad (12.90)$$

where  $T_{\psi K} = t_{\psi K} + p_{\psi K}^c - p_{\psi K}^t$  and  $P_{\psi K}^u = p_{\psi K}^u - p_{\psi K}^t$ . A subtlety arises in this decay that is related to the fact that  $B^0$  decays into a final  $J/\psi K^0$  state while  $\bar{B}^0$  decays into a final  $J/\psi \bar{K}^0$  state. A common final state, *e.g.*,  $J/\psi K_S$ , is reached only via  $K^0 - \bar{K}^0$  mixing. Consequently, the phase factor (defined in Eq. (12.44)) corresponding to neutral  $K$  mixing,  $e^{-i\phi_{M(K)}} = (V_{cd}^*V_{cs})/(V_{cd}V_{cs}^*)$ , plays a role:

$$\frac{\bar{A}_{\psi K_S}}{A_{\psi K_S}} = -\frac{(V_{cb}V_{cs}^*)T_{\psi K} + (V_{ub}V_{us}^*)P_{\psi K}^u}{(V_{cb}^*V_{cs})T_{\psi K} + (V_{ub}^*V_{us})P_{\psi K}^u} \times \frac{V_{cd}^*V_{cs}}{V_{cd}V_{cs}^*}. \quad (12.91)$$

For  $q = s$  or  $d$ , there are only penguin contributions to  $A_f$ , that is,  $t_f = 0$  in Eq. (12.87). (The tree  $\bar{b} \rightarrow \bar{u}u\bar{q}$  transition followed by  $\bar{u}u \rightarrow \bar{q}q$  rescattering is included below in the  $P^u$  terms.) Again, CKM unitarity allows us to write  $A_f$  in terms of two CKM combinations. For example, for  $f = \phi K_S$ , which proceeds via  $\bar{b} \rightarrow \bar{s}s\bar{s}$  transition, we can write

$$\frac{\bar{A}_{\phi K_S}}{A_{\phi K_S}} = -\frac{(V_{cb}V_{cs}^*)P_{\phi K}^c + (V_{ub}V_{us}^*)P_{\phi K}^u}{(V_{cb}^*V_{cs})P_{\phi K}^c + (V_{ub}^*V_{us})P_{\phi K}^u} \times \frac{V_{cd}^*V_{cs}}{V_{cd}V_{cs}^*}, \quad (12.92)$$

where  $P_{\phi K}^c = p_{\phi K}^c - p_{\phi K}^t$  and  $P_{\phi K}^u = p_{\phi K}^u - p_{\phi K}^t$ .

Since the amplitude  $A_f$  involves two different weak phases, the corresponding decays can exhibit both  $CP$  violation in the interference of decays with and without mixing,  $S_f \neq 0$ , and  $CP$  violation in decays,  $C_f \neq 0$ . (At the present level of experimental precision, the contribution to  $C_f$  from  $CP$  violation in mixing is negligible, see Eq. (12.82).) If the contribution from a second weak phase is suppressed, then the interpretation of  $S_f$  in terms of Lagrangian  $CP$ -violating parameters is clean, while  $C_f$  is small. If such a second contribution is not suppressed,  $S_f$  depends on hadronic parameters and, if the relevant strong phase is large,  $C_f$  is large.

A summary of  $\bar{b} \rightarrow \bar{q}q\bar{q}'$  modes with  $q' = s$  or  $d$  is given in Table 12.1. The  $\bar{b} \rightarrow \bar{d}d\bar{q}$  transitions lead to final states that are similar to the  $\bar{b} \rightarrow \bar{u}u\bar{q}$  transitions and have similar phase dependence. Final states that consist of two-vector mesons ( $\psi\phi$  and  $\phi\phi$ ) are not  $CP$  eigenstates, and angular analysis is needed to separate the  $CP$ -even from the  $CP$ -odd contributions.

The cleanliness of the theoretical interpretation of  $S_f$  can be assessed from the information in the last column of Table 12.1. In case of small uncertainties, the expression for  $S_f$  in terms of CKM phases can be deduced from the fourth column of Table 12.1 in combination with Eq. (12.85) (and, for  $b \rightarrow \bar{q}q\bar{s}$  decays, the example in Eq. (12.91)). Here we consider several interesting examples.

For  $B \rightarrow J/\psi K_S$  and other  $\bar{b} \rightarrow \bar{c}c\bar{s}$  processes, we can neglect the  $P^u$  contribution to  $A_f$ , in the Standard Model, to an approximation that is better than one percent:

$$\lambda_{\psi K_S} = -e^{-2i\beta} \Rightarrow S_{\psi K_S} = \sin 2\beta, \quad C_{\psi K_S} = 0. \quad (12.93)$$

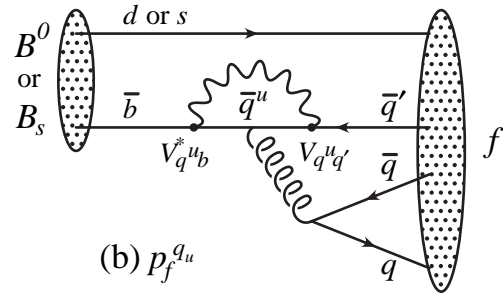
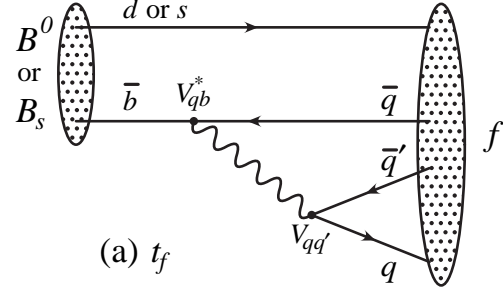


**Figure 12.2:** Feynman diagrams for (a) tree and (b) penguin amplitudes contributing to  $B^0 \rightarrow f$  or  $B_s \rightarrow f$  via a  $\bar{b} \rightarrow \bar{q}q\bar{q}'$  quark-level process.

**Table 12.1:** Summary of  $\bar{b} \rightarrow \bar{q}q\bar{q}'$  modes with  $q' = s$  or  $d$ . The second and third columns give examples of final hadronic states. The fourth column gives the CKM dependence of the amplitude  $A_f$ , using the notation of Eqs. (12.88, 12.90, 12.92), with the dominant term first and the subdominant second. The suppression factor of the second term compared to the first is given in the last column. “Loop” refers to a penguin versus tree-suppression factor (it is mode-dependent and roughly  $\mathcal{O}(0.2 - 0.3)$ ) and  $\lambda = 0.23$  is the expansion parameter of Eq. (12.50).

$\bar{b} \rightarrow \bar{q}q\bar{q}'$	$B^0 \rightarrow f$	$B_s \rightarrow f$	CKM dependence of $A_f$	Suppression
$\bar{b} \rightarrow \bar{c}c\bar{s}$	$\psi K_S$	$\psi\phi$	$(V_{cb}^*V_{cs})T + (V_{ub}^*V_{us})P^u$	loop $\times \lambda^2$
$\bar{b} \rightarrow \bar{s}s\bar{s}$	$\phi K_S$	$\phi\phi$	$(V_{cb}^*V_{cs})P^c + (V_{ub}^*V_{us})P^u$	$\lambda^2$
$\bar{b} \rightarrow \bar{u}u\bar{s}$	$\pi^0 K_S$	$K^+ K^-$	$(V_{cb}^*V_{cs})P^c + (V_{ub}^*V_{us})T$	$\lambda^2/\text{loop}$
$\bar{b} \rightarrow \bar{c}c\bar{d}$	$D^+ D^-$	$\psi K_S$	$(V_{cb}^*V_{cd})T + (V_{tb}^*V_{td})P^t$	loop
$\bar{b} \rightarrow \bar{s}s\bar{d}$	$K_S K_S$	$\phi K_S$	$(V_{tb}^*V_{td})P^t + (V_{cb}^*V_{cd})P^c$	$\lesssim 1$
$\bar{b} \rightarrow \bar{u}u\bar{d}$	$\pi^+ \pi^-$	$\rho^0 K_S$	$(V_{ub}^*V_{ud})T + (V_{tb}^*V_{td})P^t$	loop

In the presence of new physics,  $A_f$  is still likely to be dominated by the  $T$  term, but the mixing amplitude might be modified. We learn that, model-independently,  $C_f \approx 0$  while  $S_f$  cleanly determines the mixing phase ( $\phi_M - 2 \arg(V_{cb}V_{cd}^*)$ ). The experimental measurement [25],  $S_{\psi K} = 0.665 \pm 0.022$ , gave the first precision test of the Kobayashi-Maskawa mechanism, and its consistency with the predictions for  $\sin 2\beta$  makes it very likely that this mechanism is indeed the dominant source of  $CP$  violation in meson decays.

For  $B \rightarrow \phi K_S$  and other  $\bar{b} \rightarrow \bar{s}s\bar{s}$  processes (as well as some  $\bar{b} \rightarrow \bar{u}u\bar{s}$  processes), we can neglect the subdominant contributions, in the Standard Model, to an approximation that is good on the order of

a few percent:

$$\lambda_{\phi K_S} = -e^{-2i\beta} \Rightarrow S_{\phi K_S} = \sin 2\beta, \quad C_{\phi K_S} = 0. \quad (12.94)$$

In the presence of new physics, both  $A_f$  and  $M_{12}$  can get contributions that are comparable in size to those of the Standard Model and carry new weak phases. Such a situation gives several interesting consequences for penguin-dominated  $b \rightarrow q\bar{q}s$  decays ( $q = u, d, s$ ) to a final state  $f$ :

1. The value of  $-\eta_f S_f$  may be different from  $S_{\psi K_S}$  by more than a few percent, where  $\eta_f$  is the  $CP$  eigenvalue of the final state.
2. The values of  $\eta_f S_f$  for different final states  $f$  may be different from each other by more than a few percent (for example,  $S_{\phi K_S} \neq S_{\eta' K_S}$ ).
3. The value of  $C_f$  may be different from zero by more than a few percent.

While a clear interpretation of such signals in terms of Lagrangian parameters will be difficult because, under these circumstances, hadronic parameters do play a role, any of the above three options will clearly signal new physics. Fig. 12.3 summarizes the present experimental results: none of the possible signatures listed above is unambiguously established, but there is definitely still room for new physics.

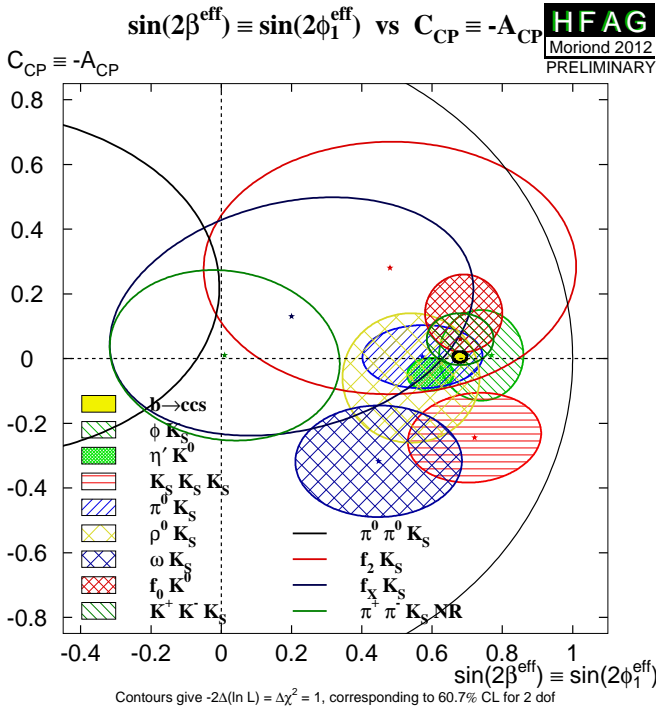


**Figure 12.3:** Summary of the results [25] of time-dependent analyses of  $b \rightarrow q\bar{q}s$  decays, which are potentially sensitive to new physics.

For  $B \rightarrow \pi\pi$  and other  $\bar{b} \rightarrow \bar{u}d$  processes, the penguin-to-tree ratio can be estimated using  $SU(3)$  relations and experimental data on related  $B \rightarrow K\pi$  decays. The result is that the suppression is on the order of 0.2–0.3 and so cannot be neglected. The expressions for  $S_{\pi\pi}$  and  $C_{\pi\pi}$  to leading order in  $R_{PT} \equiv (|V_{tb}V_{td}| P_{\pi\pi}^t)/(|V_{ub}V_{ud}| T_{\pi\pi})$  are:

$$\lambda_{\pi\pi} = e^{2i\alpha} \left[ (1 - R_{PT}e^{-i\alpha}) / (1 - R_{PT}e^{+i\alpha}) \right] \Rightarrow$$

$$S_{\pi\pi} \approx \sin 2\alpha + 2 \operatorname{Re}(R_{PT}) \cos 2\alpha \sin \alpha, \quad C_{\pi\pi} \approx 2 \operatorname{Im}(R_{PT}) \sin \alpha. \quad (12.95)$$

Note that  $R_{PT}$  is mode-dependent and, in particular, could be different for  $\pi^+\pi^-$  and  $\pi^0\pi^0$ . If strong phases can be neglected, then  $R_{PT}$  is real, resulting in  $C_{\pi\pi} = 0$ . The size of  $C_{\pi\pi}$  is an indicator of how large the strong phase is. The present experimental range is

$C_{\pi\pi} = -0.38 \pm 0.06$  [25]. As concerns  $S_{\pi\pi}$ , it is clear from Eq. (12.95) that the relative size or strong phase of the penguin contribution must be known to extract  $\alpha$ . This is the problem of penguin pollution.

The cleanest solution involves isospin relations among the  $B \rightarrow \pi\pi$  amplitudes [51]:

$$\frac{1}{\sqrt{2}} A_{\pi^+\pi^-} + A_{\pi^0\pi^0} = A_{\pi^+\pi^0}. \quad (12.96)$$

The method exploits the fact that the penguin contribution to  $P_{\pi\pi}^t$  is pure  $\Delta I = \frac{1}{2}$  (this is not true for the electroweak penguins which, however, are expected to be small), while the tree contribution to  $T_{\pi\pi}$  contains pieces which are both  $\Delta I = \frac{1}{2}$  and  $\Delta I = \frac{3}{2}$ . A simple geometric construction then allows one to find  $R_{PT}$  and extract  $\alpha$  cleanly from  $S_{\pi^+\pi^-}$ . The key experimental difficulty is that one must measure accurately the separate rates for  $B^0, \bar{B}^0 \rightarrow \pi^0\pi^0$ .

$CP$  asymmetries in  $B \rightarrow \rho\pi$  and  $B \rightarrow \rho\rho$  can also be used to determine  $\alpha$ . In particular, the  $B \rightarrow \rho\rho$  measurements are presently very significant in constraining  $\alpha$ . The extraction proceeds via isospin analysis similar to that of  $B \rightarrow \pi\pi$ . There are, however, several important differences. First, due to the finite width of the  $\rho$  mesons, a final  $(\rho\rho)_{I=1}$  state is possible [52]. The effect is, however, small, on the order of  $(\Gamma_\rho/m_\rho)^2 \sim 0.04$ . Second, due to the presence of three helicity states for the two-vector mesons, angular analysis is needed to separate the  $CP$ -even and  $CP$ -odd components. The theoretical expectation is, however, that the  $CP$ -odd component is small. This expectation is supported by experiments which find that the  $\rho^+\rho^-$  and  $\rho^\pm\rho^0$  modes are dominantly longitudinally polarized. Third, an important advantage of the  $\rho\rho$  modes is that the penguin contribution is expected to be small due to different hadronic dynamics. This expectation is confirmed by the smallness of  $\mathcal{B}(B^0 \rightarrow \rho^0\rho^0) = (0.73 \pm 0.28) \times 10^{-6}$  compared to  $\mathcal{B}(B^0 \rightarrow \rho^+\rho^-) = (24.2 \pm 3.1) \times 10^{-6}$ . Thus,  $S_{\rho^+\rho^-}$  is not far from  $\sin 2\alpha$ . Finally, both  $S_{\rho^0\rho^0}$  and  $C_{\rho^0\rho^0}$  are experimentally accessible, which may allow a precision determination of  $\alpha$ . The consistency between the range of  $\alpha$  determined by the  $B \rightarrow \pi\pi, \rho\pi, \rho\rho$  measurements and the range allowed by CKM fits (excluding these direct determinations) provides further support to the Kobayashi-Maskawa mechanism.

An interesting class of decay modes is that of the tree level decays  $B^\pm \rightarrow D^{(*)0}K^\pm$ . These decays provide golden methods for a clean determination of the angle  $\gamma$  [53–56]. The method uses the decays  $B^+ \rightarrow D^0K^+$ , which proceeds via the quark transition  $\bar{b} \rightarrow \bar{u}c\bar{s}$ , and  $B^+ \rightarrow \bar{D}^0K^+$ , which proceeds via the quark transition  $\bar{b} \rightarrow \bar{c}u\bar{s}$ , with the  $D^0$  and  $\bar{D}^0$  decaying into a common final state. The decays into common final states, such as  $(\pi^0 K_S) D K^+$ , involve interference effects between the two amplitudes, with sensitivity to the relative phase,  $\delta + \gamma$  ( $\delta$  is the relevant strong phase). The  $CP$ -conjugate processes are sensitive to  $\delta - \gamma$ . Measurements of branching ratios and  $CP$  asymmetries allow an extraction of  $\gamma$  and  $\delta$  from amplitude triangle relations. The extraction suffers from discrete ambiguities but involves no hadronic uncertainties. However, the smallness of the CKM-suppressed  $b \rightarrow u$  transitions makes it difficult at present to use the simplest methods [53–55] to determine  $\gamma$ . These difficulties are overcome (and the discrete ambiguities are removed) by performing a Dalitz plot analysis for multi-body  $D$  decays [56]. The consistency between the range of  $\gamma$  determined by the  $B \rightarrow DK$  measurements and the range allowed by CKM fits (excluding these direct determinations) provides further support to the Kobayashi-Maskawa mechanism.

The upper bound on the  $CP$  asymmetry in semileptonic  $B_s$  decays [25] implies that  $CP$  violation in  $B_s - \bar{B}_s$  mixing is a small effect:

$$\mathcal{A}_{SL}^s = (-10.5 \pm 6.4) \times 10^{-3} \Rightarrow |q/p| = 1.0052 \pm 0.0032. \quad (12.97)$$

Neglecting the deviation of  $|q/p|$  from 1, implies that we can use

$$\lambda_f = e^{-i\phi_M(B_s)} (\bar{A}_f/A_f). \quad (12.98)$$

Within the Standard Model,

$$e^{-i\phi_M(B_s)} = (V_{tb}^* V_{ts}) / (V_{tb} V_{ts}^*). \quad (12.99)$$

Note that  $\Delta\Gamma/\Gamma = 0.15 \pm 0.02$  [25] and therefore  $y$  should not be put to zero in Eqs. (12.32, 12.33). However,  $|q/p| = 1$  is expected to hold to an even better approximation than for  $B$  mesons. The  $B_s \rightarrow J/\psi\phi$  decay proceeds via the  $b \rightarrow c\bar{c}s$  transition. The  $CP$  asymmetry in this mode thus determines (with angular analysis to disentangle the  $CP$ -even and  $CP$ -odd components of the final state)  $\sin 2\beta_s$ , where  $\beta_s$  is defined in Eq. (12.53). The combination of CDF, D0 and LHCb measurements yields [25]

$$\beta_s = 0.07^{+0.06}_{-0.08}, \quad (12.100)$$

consistent with the Standard Model prediction,  $\beta_s = 0.018 \pm 0.001$  [18].

## 12.7. Summary and Outlook

$CP$  violation has been experimentally established in  $K$  and  $B$  meson decays. A full list of  $CP$  asymmetries that have been measured at a level higher than  $5\sigma$  is given in the introduction to this review. In Section 12.1.4 we introduced three types of  $CP$ -violating effects. Examples of these three types include the following:

1. All three types of  $CP$  violation have been observed in  $K \rightarrow \pi\pi$  decays:

$$\text{Re}(\epsilon') = \frac{1}{6} \left( \left| \frac{\bar{A}_{\pi^0\pi^0}}{A_{\pi^0\pi^0}} \right| - \left| \frac{\bar{A}_{\pi^+\pi^-}}{A_{\pi^+\pi^-}} \right| \right) = (2.5 \pm 0.4) \times 10^{-6} \quad (\text{I})$$

$$\text{Re}(\epsilon) = \frac{1}{2} \left( 1 - \left| \frac{q}{p} \right| \right) = (1.66 \pm 0.02) \times 10^{-3} \quad (\text{II})$$

$$\text{Im}(\epsilon) = -\frac{1}{2} \text{Im}(\lambda_{(\pi\pi)_{I=0}}) = (1.57 \pm 0.02) \times 10^{-3}. \quad (\text{III}) \quad (12.101)$$

2. Direct  $CP$  violation has been observed in, for example, the  $B^0 \rightarrow K^+\pi^-$  decays, while  $CP$  violation in interference of decays with and without mixing has been observed in, for example, the  $B \rightarrow J/\psi K_S$  decay:

$$A_{K^+\pi^-} = \frac{|\bar{A}_{K^-\pi^+}/A_{K^+\pi^-}|^2 - 1}{|\bar{A}_{K^-\pi^+}/A_{K^+\pi^-}|^2 + 1} = -0.087 \pm 0.008 \quad (\text{I})$$

$$S_{\psi K} = \text{Im}(\lambda_{\psi K}) = +0.679 \pm 0.020. \quad (\text{II}) \quad (12.102)$$

Based on Standard Model predictions, further observation of  $CP$  violation in  $D$ ,  $B$  and  $B_s$  decays seems promising for the near future, at both LHCb and a possible higher-luminosity asymmetric-energy B factory [58]. Observables that are subject to clean theoretical interpretation, such as  $S_{\psi K_S}$ ,  $\mathcal{B}(K_L \rightarrow \pi^0\nu\bar{\nu})$  and  $CP$  violation in  $B \rightarrow DK$  decays, are of particular value for constraining the values of the CKM parameters and probing the flavor sector of extensions to the Standard Model. Other probes of  $CP$  violation now being pursued experimentally include the electric dipole moments of the neutron and electron, and the decays of tau leptons. Additional processes that are likely to play an important role in future  $CP$  studies include top-quark production and decay, and neutrino oscillations.

All measurements of  $CP$  violation to date are consistent with the predictions of the Kobayashi-Maskawa mechanism of the Standard Model. Actually, it is now established that the KM mechanism plays a major role in the  $CP$  violation measured in meson decays. However, a dynamically-generated matter-antimatter asymmetry of the universe requires additional sources of  $CP$  violation, and such sources are naturally generated by extensions to the Standard Model. New sources might eventually reveal themselves as small deviations from the predictions of the KM mechanism in meson decay rates, or else might not be observable in meson decays at all, but observable with future probes such as neutrino oscillations or electric dipole moments. We cannot guarantee that new sources of  $CP$  violation will ever be found experimentally, but the fundamental nature of  $CP$  violation demands a vigorous effort.

A number of excellent reviews of  $CP$  violation are available [59–67], where the interested reader may find a detailed discussion of the various topics that are briefly reviewed here.

We thank Tim Gershon for significant contributions to the 2012 update.

## References:

1. J.H. Christenson *et al.*, Phys. Rev. Lett. **13**, 138 (1964).
2. B. Aubert *et al.*, [BABAR Collab.], Phys. Rev. Lett. **87**, 091801 (2001).
3. K. Abe *et al.*, [Belle Collab.], Phys. Rev. Lett. **87**, 091802 (2001).
4. H. Burkhardt *et al.*, [NA31 Collab.], Phys. Lett. **B206**, 169 (1988).
5. V. Fanti *et al.*, [NA48 Collab.], Phys. Lett. **B465**, 335 (1999).
6. A. Alavi-Harati *et al.*, [KTeV Collab.], Phys. Rev. Lett. **83**, 22 (1999).
7. B. Aubert *et al.*, [BABAR Collab.], Phys. Rev. Lett. **93**, 131801 (2004).
8. K. Abe *et al.*, [Belle Collab.], arXiv:hep-ex/0507045.
9. A. Poluektov *et al.*, [The Belle Collab.], Phys. Rev. **D81**, 112002 (2010).
10. P. del Amo Sanchez *et al.*, [BABAR Collab.], Phys. Rev. **D82**, 072004 (2010).
11. R. Aaij *et al.*, [LHCb Collab.], arXiv:1203.3662 [hep-ex].
12. R. Aaij *et al.*, [LHCb Collab.], Phys. Rev. Lett. **108**, 111602 (2012).
13. T. Aaltonen *et al.*, [CDF Collab.], Phys. Rev. Lett. **106**, 181802 (2011).
14. See results on the “Time reversal invariance,” within the review on “Tests of Conservation Laws,” in this *Review*.
15. See, for example, R. F. Streater and A. S. Wightman, *CPT, Spin and Statistics, and All That*, reprinted by Addison-Wesley, New York (1989).
16. M. Kobayashi and T. Maskawa, Prog. Theor. Phys. **49**, 652 (1973).
17. V. M. Abazov *et al.*, [D0 Collab.], Phys. Rev. **D82**, 032001 (2010); Phys. Rev. **D84**, 052007 (2011).
18. J. Charles *et al.*, [CKMfitter Group], Eur. Phys. J. **C41**, 1 (2005), updated results and plots available at: <http://ckmfitter.in2p3.fr>.
19. M. Bona *et al.*, [UTfit Collab.], JHEP **0603**, 080 (2006), updated results and plots available at: <http://babar.roma1.infn.it/ckm/>.
20. A.D. Sakharov, Pisma Zh. Eksp. Teor. Fiz. **5**, 32 (1967) [Sov. Phys. JETP Lett. **5**, 24 (1967)].
21. For a review, see *e.g.*, A. Riotto, “Theories of baryogenesis,” arXiv:hep-ph/9807454.
22. M. Fukugita and T. Yanagida, Phys. Lett. **B174**, 45 (1986).
23. See the  $K$ -Meson Listings in this *Review*.
24. See the  $B$ -Meson Listings in this *Review*.
25. D. Asner *et al.*, [HFAG Collab.], arXiv:1010.1589 [hep-ex], and online update at <http://www.slac.stanford.edu/xorg/hfag>.
26. V. Weisskopf and E. P. Wigner, Z. Phys. **63**, 54 (1930); Z. Phys. **65**, 18 (1930). [See also Appendix A of P.K. Kabir, *The CP Puzzle: Strange Decays of the Neutral Kaon*, Academic Press (1968)].
27. O. Long *et al.*, Phys. Rev. **D68**, 034010 (2003).
28. L. Wolfenstein, Phys. Rev. Lett. **13**, 562 (1964).
29. See the review on “Cabibbo-Kobayashi-Maskawa Mixing Matrix,” in this *Review*.
30. L. Wolfenstein, Phys. Rev. Lett. **51**, 1945 (1983).
31. A.J. Buras, M.E. Lautenbacher, and G. Ostermaier, Phys. Rev. **D50**, 3433 (1994).
32. C. Jarlskog, Phys. Rev. Lett. **55**, 1039 (1985).
33. See the review on “ $CP$  violation in  $K_S \rightarrow 3\pi$ ,” in this *Review*.
34. Y. Grossman and Y. Nir, Phys. Lett. **B398**, 163 (1997).
35. L.S. Littenberg, Phys. Rev. **D39**, 3322 (1989).
36. A.J. Buras, Phys. Lett. **B333**, 476 (1994).
37. G. Buchalla and A.J. Buras, Nucl. Phys. **B400**, 225 (1993).
38. B. Aubert *et al.*, [BABAR Collab.], Phys. Rev. Lett. **98**, 211802 (2007).
39. M. Staric *et al.*, [Belle Collab.], Phys. Rev. Lett. **98**, 211803 (2007).
40. T. Aaltonen *et al.*, [CDF Collab.], Phys. Rev. Lett. **100**, 121802 (2008).
41. See the  $D$ -Meson Listings in this *Review*.

42. Y. Grossman, A. L. Kagan and Y. Nir, Phys. Rev. **D75**, 036008 (2007).
43. S. Bergmann *et al.*, Phys. Lett. **B486**, 418 (2000).
44. See the review on " $D^0 - \bar{D}^0$  Mixing" in this *Review*.
45. A.B. Carter and A.I. Sanda, Phys. Rev. Lett. **45**, 952 (1980); Phys. Rev. **D23**, 1567 (1981).
46. I.I. Bigi and A.I. Sanda, Nucl. Phys. **B193**, 85 (1981).
47. I. Dunietz and J.L. Rosner, Phys. Rev. **D34**, 1404 (1986).
48. Ya.I. Azimov, N.G. Uraltsev, and V.A. Khoze, Sov. J. Nucl. Phys. **45**, 878 (1987) [*Yad. Fiz.* **45**, 1412 (1987)].
49. I.I. Bigi and A.I. Sanda, Nucl. Phys. **B281**, 41 (1987).
50. G. Buchalla, A.J. Buras, and M.E. Lautenbacher, Rev. Mod. Phys. **68**, 1125 (1996).
51. M. Gronau and D. London, Phys. Rev. Lett. **65**, 3381 (1990).
52. A. F. Falk *et al.*, Phys. Rev. **D69**, 011502 (2004).
53. M. Gronau and D. London, Phys. Lett. **B253**, 483 (1991).
54. M. Gronau and D. Wyler, Phys. Lett. **B265**, 172 (1991).
55. D. Atwood, I. Dunietz, and A. Soni, Phys. Rev. Lett. **78**, 3257 (1997).
56. A. Giri *et al.*, Phys. Rev. **D68**, 054018 (2003).
57. A.A. Alves *et al.*, [LHCb Collab.], "The LHCb Detector at the LHC," JINST **3** S08005 (2008).
58. M. Bona *et al.*, "SuperB: A High-Luminosity Asymmetric  $e^+e^-$  Super Flavor Factory. Conceptual Design Report," INFN/AE-07/2, SLAC-R-856, LAL-07-15 (2007) [arXiv:0709.0451](https://arxiv.org/abs/0709.0451).
59. G.C. Branco, L. Lavoura, and J.P. Silva, *CP Violation*, Oxford University Press, Oxford (1999).
60. I.I. Y. Bigi and A.I. Sanda, *CP Violation*, Cambridge Monogr., Part. Phys. Nucl. Phys. Cosmol. **9**, 1 (2000).
61. P.F. Harrison and H.R. Quinn, editors [BABAR Collab.], *The BABAR physics book: Physics at an asymmetric B factory*, SLAC-R-0504.
62. K. Anikeev *et al.*, [arXiv:hep-ph/0201071](https://arxiv.org/abs/hep-ph/0201071).
63. K. Kleinknecht, "Uncovering *CP* Violation," Springer tracts in modern physics **195** (2003).
64. H.R. Quinn and Y. Nir, "The Mystery of the Missing Antimatter," Princeton University Press, Princeton (2008).
65. J. Hewett *et al.*, [arXiv:hep-ph/0503261](https://arxiv.org/abs/hep-ph/0503261).
66. T.E. Browder *et al.*, Rev. Mod. Phys. **81**, 1887 (2009).
67. M. Ciuchini and A. Stocchi, Ann. Rev. Nucl. Part. Sci. **61**, 491 (2011).

## 13. NEUTRINO MASS, MIXING, AND OSCILLATIONS

Updated May 2012 by K. Nakamura (Kavli IPMU (WPI), U. Tokyo, KEK) and S.T. Petcov (SISSA/INFN Trieste, Kavli IPMU (WPI), U. Tokyo, Bulgarian Academy of Sciences).

The experiments with solar, atmospheric, reactor and accelerator neutrinos have provided compelling evidences for oscillations of neutrinos caused by nonzero neutrino masses and neutrino mixing. The data imply the existence of 3-neutrino mixing in vacuum. We review the theory of neutrino oscillations, the phenomenology of neutrino mixing, the problem of the nature - Dirac or Majorana, of massive neutrinos, the issue of CP violation in the lepton sector, and the current data on the neutrino masses and mixing parameters. The open questions and the main goals of future research in the field of neutrino mixing and oscillations are outlined.

### 13.1. Introduction: Massive neutrinos and neutrino mixing

It is a well-established experimental fact that the neutrinos and antineutrinos which take part in the standard charged current (CC) and neutral current (NC) weak interaction are of three varieties (types) or flavours: electron,  $\nu_e$  and  $\bar{\nu}_e$ , muon,  $\nu_\mu$  and  $\bar{\nu}_\mu$ , and tauon,  $\nu_\tau$  and  $\bar{\nu}_\tau$ . The notion of neutrino type or flavour is dynamical:  $\nu_e$  is the neutrino which is produced with  $e^+$ , or produces an  $e^-$  in CC weak interaction processes;  $\nu_\mu$  is the neutrino which is produced with  $\mu^+$ , or produces  $\mu^-$ , etc. The flavour of a given neutrino is Lorentz invariant. Among the three different flavour neutrinos and antineutrinos, no two are identical. Correspondingly, the states which describe different flavour neutrinos must be orthogonal (within the precision of the current data):  $\langle \nu_l | \nu_l \rangle = \delta_{ll}$ ,  $\langle \bar{\nu}_l | \bar{\nu}_l \rangle = \delta_{ll}$ ,  $\langle \bar{\nu}_l | \nu_l \rangle = 0$ .

It is also well-known from the existing data (all neutrino experiments were done so far with relativistic neutrinos or antineutrinos), that the flavour neutrinos  $\nu_l$  (antineutrinos  $\bar{\nu}_l$ ), are always produced in weak interaction processes in a state that is predominantly left-handed (LH) (right-handed (RH)). To account for this fact,  $\nu_l$  and  $\bar{\nu}_l$  are described in the Standard Model (SM) by a chiral LH flavour neutrino field  $\nu_{lL}(x)$ ,  $l = e, \mu, \tau$ . For massless  $\nu_l$ , the state of  $\nu_l$  ( $\bar{\nu}_l$ ) which the field  $\nu_{lL}(x)$  annihilates (creates) is with helicity (-1/2) (helicity +1/2). If  $\nu_l$  has a non-zero mass  $m(\nu_l)$ , the state of  $\nu_l$  ( $\bar{\nu}_l$ ) is a linear superposition of the helicity (-1/2) and (+1/2) states, but the helicity +1/2 state (helicity (-1/2) state) enters into the superposition with a coefficient  $\propto m(\nu_l)/E$ ,  $E$  being the neutrino energy, and thus is strongly suppressed. Together with the LH charged lepton field  $l_L(x)$ ,  $\nu_{lL}(x)$  forms an  $SU(2)_L$  doublet. In the absence of neutrino mixing and zero neutrino masses,  $\nu_{lL}(x)$  and  $l_L(x)$  can be assigned one unit of the additive lepton charge  $L_l$  and the three charges  $L_l$ ,  $l = e, \mu, \tau$ , are conserved by the weak interaction.

At present there is no compelling evidence for the existence of states of relativistic neutrinos (antineutrinos), which are predominantly right-handed,  $\nu_R$  (left-handed,  $\bar{\nu}_L$ ). If RH neutrinos and LH antineutrinos exist, their interaction with matter should be much weaker than the weak interaction of the flavour LH neutrinos  $\nu_l$  and RH antineutrinos  $\bar{\nu}_l$ , i.e.,  $\nu_R$  ( $\bar{\nu}_L$ ) should be “sterile” or “inert” neutrinos (antineutrinos) [1]. In the formalism of the Standard Model, the sterile  $\nu_R$  and  $\bar{\nu}_L$  can be described by  $SU(2)_L$  singlet RH neutrino fields  $\nu_{lR}(x)$ . In this case,  $\nu_{lR}$  and  $\bar{\nu}_L$  will have no gauge interactions, i.e., will not couple to the weak  $W^\pm$  and  $Z^0$  bosons. If present in an extension of the Standard Model, the RH neutrinos can play a crucial role i) in the generation of neutrino masses and mixing, ii) in understanding the remarkable disparity between the magnitudes of neutrino masses and the masses of the charged leptons and quarks, and iii) in the generation of the observed matter-antimatter asymmetry of the Universe (via the leptogenesis mechanism [2]). In this scenario which is based on the see-saw theory [3], there is a link between the generation of neutrino masses and the generation of the baryon asymmetry of the Universe. The simplest hypothesis (based on symmetry considerations) is that to each LH flavour neutrino field  $\nu_{lL}(x)$  there corresponds a RH neutrino field  $\nu_{lR}(x)$ ,  $l = e, \mu, \tau$ , although schemes with less (more) than three RH neutrinos are also being considered.

The experiments with solar, atmospheric and reactor neutrinos [4–16] have provided compelling evidences for the existence of neutrino oscillations [17,18], transitions in flight between the different flavour neutrinos  $\nu_e, \nu_\mu, \nu_\tau$  (antineutrinos  $\bar{\nu}_e, \bar{\nu}_\mu, \bar{\nu}_\tau$ ), caused by nonzero neutrino masses and neutrino mixing.

The existence of flavour neutrino oscillations implies that if a neutrino of a given flavour, say  $\nu_\mu$ , with energy  $E$  is produced in some weak interaction process, at a sufficiently large distance  $L$  from the  $\nu_\mu$  source the probability to find a neutrino of a different flavour, say  $\nu_\tau$ ,  $P(\nu_\mu \rightarrow \nu_\tau; E, L)$ , is different from zero.  $P(\nu_\mu \rightarrow \nu_\tau; E, L)$  is called the  $\nu_\mu \rightarrow \nu_\tau$  oscillation or transition probability. If  $P(\nu_\mu \rightarrow \nu_\tau; E, L) \neq 0$ , the probability that  $\nu_\mu$  will not change into a neutrino of a different flavour, i.e., the “ $\nu_\mu$  survival probability”  $P(\nu_\mu \rightarrow \nu_\mu; E, L)$ , will be smaller than one. If only muon neutrinos  $\nu_\mu$  are detected in a given experiment and they take part in oscillations, one would observe a “disappearance” of muon neutrinos on the way from the  $\nu_\mu$  source to the detector. Disappearance of the solar  $\nu_e$ , reactor  $\bar{\nu}_e$  and of atmospheric  $\nu_\mu$  and  $\bar{\nu}_\mu$  due to the oscillations have been observed respectively, in the solar neutrino [4–12], KamLAND [15,16] and Super-Kamokande [13,14] experiments. Strong evidences for disappearance of muon neutrinos due to oscillations were obtained also in the long-baseline accelerator neutrino experiments K2K [19] and MINOS [20,21]. As a consequence of the results of the experiments quoted above the existence of oscillations or transitions of the solar  $\nu_e$ , atmospheric  $\nu_\mu$  and  $\bar{\nu}_\mu$ , accelerator  $\nu_\mu$  (at  $L \sim 250$  km and  $L \sim 730$  km) and reactor  $\bar{\nu}_e$  (at  $L \sim 180$  km), driven by nonzero neutrino masses and neutrino mixing, was firmly established. There are strong indications that the solar  $\nu_e$  transitions are affected by the solar matter [22,23]. In June of 2011, the T2K [24] Collaboration reported indication of  $\nu_\mu \rightarrow \nu_e$  oscillations, i.e., “appearance” of  $\nu_e$  in a beam of  $\nu_\mu$  at a significance of  $2.5\sigma$ . Also MINOS [25] Collaboration obtained data consistent with  $\nu_\mu \rightarrow \nu_e$  oscillations. In March and April, 2012, the Daya Bay [26] and RENO [27] experiments reported strong evidence for reactor  $\bar{\nu}_e$  disappearance respectively at  $L \sim 1.65$  km and  $L \sim 1.38$  km and with statistical significance of  $5.2\sigma$  and  $4.9\sigma$ .

Oscillations of neutrinos are a consequence of the presence of flavour neutrino mixing, or lepton mixing, in vacuum. In the formalism of local quantum field theory, used to construct the Standard Model, this means that the LH flavour neutrino fields  $\nu_{lL}(x)$ , which enter into the expression for the lepton current in the CC weak interaction Lagrangian, are linear combinations of the fields of three (or more) neutrinos  $\nu_j$ , having masses  $m_j \neq 0$ :

$$\nu_{lL}(x) = \sum_j U_{lj} \nu_{jL}(x), \quad l = e, \mu, \tau, \quad (13.1)$$

where  $\nu_{jL}(x)$  is the LH component of the field of  $\nu_j$  possessing a mass  $m_j$  and  $U$  is a unitary matrix - the neutrino mixing matrix [1,17,18]. The matrix  $U$  is often called the Pontecorvo-Maki-Nakagawa-Sakata (PMNS) or Maki-Nakagawa-Sakata (MNS) mixing matrix. Obviously, Eq. (13.1) implies that the individual lepton charges  $L_l$ ,  $l = e, \mu, \tau$ , are not conserved.

All existing neutrino oscillation data, except for the LSND [28] and the MiniBooNE [29] results (see below), can be described assuming 3-flavour neutrino mixing in vacuum. The data on the invisible decay width of the  $Z^0$ -boson is compatible with only 3 light flavour neutrinos coupled to  $Z^0$  [30]. The number of massive neutrinos  $\nu_j$ ,  $n$ , can, in general, be bigger than 3,  $n > 3$ , if, for instance, there exist sterile neutrinos and they mix with the flavour neutrinos. It follows from the existing data that at least 3 of the neutrinos  $\nu_j$ , say  $\nu_1, \nu_2, \nu_3$ , must be light,  $m_{1,2,3} \lesssim 1$  eV, and must have different masses,  $m_1 \neq m_2 \neq m_3$ .

The short-baseline accelerator experiment LSND [28] observed a possible indication of  $\bar{\nu}_\mu \rightarrow \bar{\nu}_e$  oscillations. Performing a  $\bar{\nu}_\mu \rightarrow \bar{\nu}_e$  oscillation search, the MiniBooNE Collaboration reported a  $1.5\sigma$  excess of  $\bar{\nu}_e$  events [29], which is marginally consistent with the LSND indication of  $\bar{\nu}_\mu \rightarrow \bar{\nu}_e$  oscillations. However, in the MiniBooNE experiment no indications of  $\nu_\mu \rightarrow \nu_e$  oscillations were found so far [31]. Interpreting the LSND [28] and the MiniBooNE [29,31] results in terms of neutrino oscillations requires the introduction of at least two more light neutrinos with masses in the 1 eV range [32], and thus of two sterile neutrino fields which mix with the  $\nu_e$  and  $\nu_\mu$  fields.



However, further experimental investigations are definitely needed since the excess of  $\bar{\nu}_e$  events observed in the MiniBooNE experiment has a relatively low statistical significance.

Hints (at  $\sim 2.5\sigma$ ) for existence of additional light neutrinos beyond the three firmly established were obtained in the re-analysis [33] of the old short baseline (SBL) reactor  $\bar{\nu}_e$  oscillation data using the results of a new and very detailed calculation of the reactor  $\bar{\nu}_e$  fluxes [34]. The latter were found in Ref. 34 to be by approximately 3% larger than the fluxes calculated in Ref. 35 and widely used in the interpretation of the results of the SBL reactor  $\bar{\nu}_e$  oscillation experiments. It should be added that the results for the reactor  $\bar{\nu}_e$  fluxes have an uncertainty associated, *e.g.*, with the weak magnetism term contribution to the corresponding  $\beta$ -decay rates, which can be larger than the 3% difference between the “old” and “new” fluxes [36].

On the basis of the preceding discussion we can conclude that at present there are no compelling experimental evidences for the existence of more than 3 light neutrinos.

Being electrically neutral, the neutrinos with definite mass  $\nu_j$  can be Dirac fermions or Majorana particles [37,38]. The first possibility is realised when there exists a lepton charge carried by the neutrinos  $\nu_j$ , which is conserved by the particle interactions. This could be, *e.g.*, the total lepton charge  $L = L_e + L_\mu + L_\tau$ :  $L(\nu_j) = 1$ ,  $j = 1, 2, 3$ . In this case the neutrino  $\nu_j$  has a distinctive antiparticle  $\bar{\nu}_j$ :  $\bar{\nu}_j$  differs from  $\nu_j$  by the value of the lepton charge  $L$  it carries,  $L(\bar{\nu}_j) = -1$ . The massive neutrinos  $\nu_j$  can be Majorana particles if no lepton charge is conserved (see, *e.g.*, Ref. 39). A massive Majorana particle  $\chi_j$  is identical with its antiparticle  $\bar{\chi}_j$ :  $\chi_j \equiv \bar{\chi}_j$ . On the basis of the existing neutrino data it is impossible to determine whether the massive neutrinos are Dirac or Majorana fermions.

In the case of  $n$  neutrino flavours and  $n$  massive neutrinos, the  $n \times n$  unitary neutrino mixing matrix  $U$  can be parametrised by  $n(n-1)/2$  Euler angles and  $n(n+1)/2$  phases. If the massive neutrinos  $\nu_j$  are Dirac particles, only  $(n-1)(n-2)/2$  phases are physical and can be responsible for CP violation in the lepton sector. In this respect the neutrino (lepton) mixing with Dirac massive neutrinos is similar to the quark mixing. For  $n = 3$  there is just one CP violating phase in  $U$ , which is usually called “the Dirac CP violating phase.” CP invariance holds if (in a certain standard convention)  $U$  is real,  $U^* = U$ .

If, however, the massive neutrinos are Majorana fermions,  $\nu_j \equiv \chi_j$ , the neutrino mixing matrix  $U$  contains  $n(n-1)/2$  CP violation phases [40,41], *i.e.*, by  $(n-1)$  phases more than in the Dirac neutrino case: in contrast to Dirac fields, the massive Majorana neutrino fields cannot “absorb” phases. In this case  $U$  can be cast in the form [40]

$$U = V P \quad (13.2)$$

where the matrix  $V$  contains the  $(n-1)(n-2)/2$  Dirac CP violation phases, while  $P$  is a diagonal matrix with the additional  $(n-1)$  Majorana CP violation phases  $\alpha_{21}, \alpha_{31}, \dots, \alpha_{n1}$ ,

$$P = \text{diag} \left( 1, e^{i\frac{\alpha_{21}}{2}}, e^{i\frac{\alpha_{31}}{2}}, \dots, e^{i\frac{\alpha_{n1}}{2}} \right). \quad (13.3)$$

The Majorana phases will conserve CP if [42]  $\alpha_{j1} = \pi q_j$ ,  $q_j = 0, 1, 2$ ,  $j = 2, 3, \dots, n$ . In this case  $\exp[i(\alpha_{j1} - \alpha_{k1})] = \pm 1$  has a simple physical interpretation: this is the relative CP-parity of Majorana neutrinos  $\chi_j$  and  $\chi_k$ . The condition of CP invariance of the leptonic CC weak interaction in the case of mixing and massive Majorana neutrinos reads [39]:

$$U_{lj}^* = U_{lj} \rho_j, \quad \rho_j = \frac{1}{i} \eta_{CP}(\chi_j) = \pm 1, \quad (13.4)$$

where  $\eta_{CP}(\chi_j) = i\rho_j = \pm i$  is the CP parity of the Majorana neutrino  $\chi_j$  [42]. Thus, if CP invariance holds, the elements of  $U$  are either real or purely imaginary.

In the case of  $n = 3$  there are altogether 3 CP violation phases - one Dirac and two Majorana. Even in the mixing involving only 2 massive Majorana neutrinos there is one physical CP violation Majorana phase. In contrast, the CC weak interaction is automatically CP-invariant in the case of mixing of two massive Dirac neutrinos or of two quarks.

### 13.2. Neutrino oscillations in vacuum

Neutrino oscillations are a quantum mechanical consequence of the existence of nonzero neutrino masses and neutrino (lepton) mixing, Eq. (13.1), and of the relatively small splitting between the neutrino masses. The neutrino mixing and oscillation phenomena are analogous to the  $K^0 - \bar{K}^0$  and  $B^0 - \bar{B}^0$  mixing and oscillations.

In what follows we will present a simplified version of the derivation of the expressions for the neutrino and antineutrino oscillation probabilities. The complete derivation would require the use of the wave packet formalism for the evolution of the massive neutrino states, or, alternatively, of the field-theoretical approach, in which one takes into account the processes of production, propagation and detection of neutrinos [43].

Suppose the flavour neutrino  $\nu_l$  is produced in a CC weak interaction process and after a time  $T$  it is observed by a neutrino detector, located at a distance  $L$  from the neutrino source and capable of detecting also neutrinos  $\nu_{l'}$ ,  $l' \neq l$ . We will consider the evolution of the neutrino state  $|\nu_l\rangle$  in the frame in which the detector is at rest (laboratory frame). The oscillation probability, as we will see, is a Lorentz invariant quantity. If lepton mixing, Eq. (13.1), takes place and the masses  $m_j$  of all neutrinos  $\nu_j$  are sufficiently small, the state of the neutrino  $\nu_l$ ,  $|\nu_l\rangle$ , will be a coherent superposition of the states  $|\nu_j\rangle$  of neutrinos  $\nu_j$ :

$$|\nu_l\rangle = \sum_j U_{lj}^* |\nu_j; \vec{p}_j\rangle, \quad l = e, \mu, \tau, \quad (13.5)$$

where  $U$  is the neutrino mixing matrix and  $\vec{p}_j$  is the 4-momentum of  $\nu_j$  [44].

We will consider the case of relativistic neutrinos  $\nu_j$ , which corresponds to the conditions in both past and currently planned future neutrino oscillation experiments [46]. In this case the state  $|\nu_j; \vec{p}_j\rangle$  practically coincides with the helicity (-1) state  $|\nu_j, L; \vec{p}_j\rangle$  of the neutrino  $\nu_j$ , the admixture of the helicity (+1) state  $|\nu_j, R; \vec{p}_j\rangle$  in  $|\nu_j; \vec{p}_j\rangle$  being suppressed due to the factor  $\sim m_j/E_j$ , where  $E_j$  is the energy of  $\nu_j$ . If  $\nu_j$  are Majorana particles,  $\nu_j \equiv \chi_j$ , due to the presence of the helicity (+1) state  $|\chi_j, R; \vec{p}_j\rangle$  in  $|\chi_j; \vec{p}_j\rangle$ , the neutrino  $\nu_l$  can produce an  $l^+$  (instead of  $l^-$ ) when it interacts with nucleons. The cross section of such a  $|\Delta L_l| = 2$  process is suppressed by the factor  $(m_j/E_j)^2$ , which renders the process unobservable at present.

If the number  $n$  of massive neutrinos  $\nu_j$  is bigger than 3 due to a mixing between the active flavour and sterile neutrinos, one will have additional relations similar to that in Eq. (13.5) for the state vectors of the (predominantly LH) sterile antineutrinos. In the case of just one RH sterile neutrino field  $\nu_{sR}(x)$ , for instance, we will have in addition to Eq. (13.5):

$$|\bar{\nu}_{sL}\rangle = \sum_{j=1}^4 U_{sj}^* |\nu_j; \vec{p}_j\rangle \cong \sum_{j=1}^4 U_{sj}^* |\nu_j, L; \vec{p}_j\rangle, \quad (13.6)$$

where the neutrino mixing matrix  $U$  is now a  $4 \times 4$  unitary matrix.

For the state vector of RH flavour antineutrino  $\bar{\nu}_l$ , produced in a CC weak interaction process we similarly get:

$$|\bar{\nu}_l\rangle = \sum_j U_{lj} |\bar{\nu}_j; \vec{p}_j\rangle \cong \sum_{j=1} U_{lj} |\bar{\nu}_j, R; \vec{p}_j\rangle, \quad l = e, \mu, \tau, \quad (13.7)$$

where  $|\bar{\nu}_j, R; \vec{p}_j\rangle$  is the helicity (+1) state of the antineutrino  $\bar{\nu}_j$  if  $\nu_j$  are Dirac fermions, or the helicity (+1) state of the neutrino  $\nu_j \equiv \bar{\nu}_j \equiv \chi_j$  if the massive neutrinos are Majorana particles. Thus, in the latter case we have in Eq. (13.7):  $|\bar{\nu}_j; \vec{p}_j\rangle \cong |\nu_j, R; \vec{p}_j\rangle \equiv |\chi_j, R; \vec{p}_j\rangle$ . The presence of the matrix  $U$  in Eq. (13.7) (and not of  $U^*$ ) follows directly from Eq. (13.1).

We will assume in what follows that the spectrum of masses of neutrinos is not degenerate:  $m_j \neq m_k$ ,  $j \neq k$ . Then the states  $|\nu_j; \vec{p}_j\rangle$  in the linear superposition in the r.h.s. of Eq. (13.5) will have, in general, different energies and different momenta, independently of whether they are produced in a decay or interaction process:  $\vec{p}_j \neq \vec{p}_k$ , or  $E_j \neq E_k$ ,  $\mathbf{p}_j \neq \mathbf{p}_k$ ,  $j \neq k$ , where  $E_j = \sqrt{p_j^2 + m_j^2}$ ,  $p_j \equiv |\mathbf{p}_j|$ .



The deviations of  $E_j$  and  $p_j$  from the values for a massless neutrino  $E$  and  $p = E$  are proportional to  $m_j^2/E_0$ ,  $E_0$  being a characteristic energy of the process, and are extremely small. In the case of  $\pi^+ \rightarrow \mu^+ + \nu_\mu$  decay at rest, for instance, we have:  $E_j = E + m_j^2/(2m_\pi)$ ,  $p_j = E - \xi m_j^2/(2E)$ , where  $E = (m_\pi/2)(1 - m_\mu^2/m_\pi^2) \cong 30$  MeV,  $\xi = (1 + m_\mu^2/m_\pi^2)/2 \cong 0.8$ , and  $m_\mu$  and  $m_\pi$  are the  $\mu^+$  and  $\pi^+$  masses. Taking  $m_j = 1$  eV we find:  $E_j \cong E(1 + 1.2 \times 10^{-16})$  and  $p_j \cong E(1 - 4.4 \times 10^{-16})$ .

Suppose that the neutrinos are observed via a CC weak interaction process and that in the detector's rest frame they are detected after time  $T$  after emission, after traveling a distance  $L$ . Then the amplitude of the probability that neutrino  $\nu_{l'}$  will be observed if neutrino  $\nu_l$  was produced by the neutrino source can be written as [43,45,47]:

$$A(\nu_l \rightarrow \nu_{l'}) = \sum_j U_{l'j} D_j U_{jl}^\dagger, \quad l, l' = e, \mu, \tau, \quad (13.8)$$

where  $D_j = D_j(p_j; L, T)$  describes the propagation of  $\nu_j$  between the source and the detector,  $U_{jl}^\dagger$  and  $U_{l'j}$  are the amplitudes to find  $\nu_j$  in the initial and in the final flavour neutrino state, respectively. It follows from relativistic Quantum Mechanics considerations that [43,45]

$$D_j \equiv D_j(\vec{p}_j; L, T) = e^{-i\vec{p}_j(x_f - x_0)} = e^{-i(E_j T - p_j L)}, \quad p_j \equiv |\mathbf{p}_j|, \quad (13.9)$$

where [48]  $x_0$  and  $x_f$  are the space-time coordinates of the points of neutrino production and detection,  $T = (t_f - t_0)$  and  $L = \mathbf{k}(\mathbf{x}_f - \mathbf{x}_0)$ ,  $\mathbf{k}$  being the unit vector in the direction of neutrino momentum,  $\mathbf{p}_j = \mathbf{k}p_j$ . What is relevant for the calculation of the probability  $P(\nu_l \rightarrow \nu_{l'}) = |A(\nu_l \rightarrow \nu_{l'})|^2$  is the interference factor  $D_j D_k^*$  which depends on the phase

$$\begin{aligned} \delta\varphi_{jk} &= (E_j - E_k)T - (p_j - p_k)L = (E_j - E_k) \left[ T - \frac{E_j + E_k}{p_j + p_k} L \right] \\ &+ \frac{m_j^2 - m_k^2}{p_j + p_k} L. \end{aligned} \quad (13.10)$$

Some authors [49] have suggested that the distance traveled by the neutrinos  $L$  and the time interval  $T$  are related by  $T = (E_j + E_k)L/(p_j + p_k) = L/\bar{v}$ ,  $\bar{v} = (E_j/(E_j + E_k))v_j + (E_k/(E_j + E_k))v_k$  being the "average" velocity of  $\nu_j$  and  $\nu_k$ , where  $v_{j,k} = p_{j,k}/E_{j,k}$ . In this case the first term in the r.h.s. of Eq. (13.10) vanishes. The indicated relation has not emerged so far from any dynamical wave packet calculations. We arrive at the same conclusion concerning the term under discussion in Eq. (13.10) if one assumes [50] that  $E_j = E_k = E_0$ . Finally, it was proposed in Ref. 47 and Ref. 51 that the states of  $\nu_j$  and  $\bar{\nu}_j$  in Eq. (13.5) and Eq. (13.7) have the same 3-momentum,  $p_j = p_k = p$ . Under this condition the first term in the r.h.s. of Eq. (13.10) is negligible, being suppressed by the additional factor  $(m_j^2 + m_k^2)/p^2$  since for relativistic neutrinos  $L = T$  up to terms  $\sim m_{j,k}^2/p^2$ . We arrive at the same conclusion if  $E_j \neq E_k$ ,  $p_j \neq p_k$ ,  $j \neq k$ , and we take into account that neutrinos are relativistic and therefore, up to corrections  $\sim m_{j,k}^2/E_{j,k}^2$ , we have  $L \cong T$  (see, e.g., C. Giunti quoted in Ref. 43).

Although the cases considered above are physically quite different, they lead to the same result for the phase difference  $\delta\varphi_{jk}$ . Thus, we have:

$$\delta\varphi_{jk} \cong \frac{m_j^2 - m_k^2}{2p} L = 2\pi \frac{L}{L_{jk}^v} \text{sgn}(m_j^2 - m_k^2), \quad (13.11)$$

where  $p = (p_j + p_k)/2$  and

$$L_{jk}^v = 4\pi \frac{p}{|\Delta m_{jk}^2|} \cong 2.48 \text{ m} \frac{p[\text{MeV}]}{|\Delta m_{jk}^2|[\text{eV}^2]} \quad (13.12)$$

is the neutrino oscillation length associated with  $\Delta m_{jk}^2$ . We can safely neglect the dependence of  $p_j$  and  $p_k$  on the masses  $m_j$  and  $m_k$  and

consider  $p$  to be the zero neutrino mass momentum,  $p = E$ . The phase difference  $\delta\varphi_{jk}$ , Eq. (13.11), is Lorentz-invariant.

Eq. (13.9) corresponds to a plane-wave description of the propagation of neutrinos  $\nu_j$ . It accounts only for the movement of the center of the wave packet describing  $\nu_j$ . In the wave packet treatment of the problem, the interference between the states of  $\nu_j$  and  $\nu_k$  is subject to a number of conditions [43], the localisation condition and the condition of overlapping of the wave packets of  $\nu_j$  and  $\nu_k$  at the detection point being the most important. For relativistic neutrinos, the localisation condition in space, for instance, reads:  $\sigma_{xP}, \sigma_{xD} < L_{jk}^v/(2\pi)$ ,  $\sigma_{xP(D)}$  being the spatial width of the production (detection) wave packet. Thus, the interference will not be suppressed if the spatial width of the neutrino wave packets determined by the neutrino production and detection processes is smaller than the corresponding oscillation length in vacuum. In order for the interference to be nonzero, the wave packets describing  $\nu_j$  and  $\nu_k$  should also overlap in the point of neutrino detection. This requires that the spatial separation between the two wave packets at the point of neutrinos detection, caused by the two wave packets having different group velocities  $v_j \neq v_k$ , satisfies  $|(v_j - v_k)T| \ll \max(\sigma_{xP}, \sigma_{xD})$ . If the interval of time  $T$  is not measured,  $T$  in the preceding condition must be replaced by the distance  $L$  between the neutrino source and the detector (for further discussion see, e.g., Refs. [43,45,47]).

For the  $\nu_l \rightarrow \nu_{l'}$  and  $\bar{\nu}_l \rightarrow \bar{\nu}_{l'}$  oscillation probabilities we get from Eq. (13.8), Eq. (13.9), and Eq. (13.11):

$$\begin{aligned} P(\nu_l \rightarrow \nu_{l'}) &= \sum_j |U_{l'j}|^2 |U_{lj}|^2 + 2 \sum_{j>k} |U_{l'j} U_{lj}^* U_{lk} U_{lk}^*| \\ &\cos\left(\frac{\Delta m_{jk}^2}{2p} L - \phi_{l'l;jk}\right), \end{aligned} \quad (13.13)$$

$$\begin{aligned} P(\bar{\nu}_l \rightarrow \bar{\nu}_{l'}) &= \sum_j |U_{l'j}|^2 |U_{lj}|^2 + 2 \sum_{j>k} |U_{l'j} U_{lj}^* U_{lk} U_{lk}^*| \\ &\cos\left(\frac{\Delta m_{jk}^2}{2p} L + \phi_{l'l;jk}\right), \end{aligned} \quad (13.14)$$

where  $l, l' = e, \mu, \tau$  and  $\phi_{l'l;jk} = \arg(U_{l'j} U_{lj}^* U_{lk} U_{lk}^*)$ . It follows from Eq. (13.8) - Eq. (13.10) that in order for neutrino oscillations to occur, at least two neutrinos  $\nu_j$  should not be degenerate in mass and lepton mixing should take place,  $U \neq \mathbf{1}$ . The neutrino oscillations effects can be large if we have

$$\frac{|\Delta m_{jk}^2|}{2p} L = 2\pi \frac{L}{L_{jk}^v} \gtrsim 1, \quad j \neq k. \quad (13.15)$$

at least for one  $\Delta m_{jk}^2$ . This condition has a simple physical interpretation: the neutrino oscillation length  $L_{jk}^v$  should be of the order of, or smaller, than source-detector distance  $L$ , otherwise the oscillations will not have time to develop before neutrinos reach the detector.

We see from Eq. (13.13) and Eq. (13.14) that  $P(\nu_l \rightarrow \nu_{l'}) = P(\bar{\nu}_l \rightarrow \bar{\nu}_{l'})$ ,  $l, l' = e, \mu, \tau$ . This is a consequence of CPT invariance. The conditions of CP and T invariance read [40,52,53]:  $P(\nu_l \rightarrow \nu_{l'}) = P(\bar{\nu}_l \rightarrow \bar{\nu}_{l'})$ ,  $l, l' = e, \mu, \tau$  (CP),  $P(\nu_l \rightarrow \nu_{l'}) = P(\nu_{l'} \rightarrow \nu_l)$ ,  $P(\bar{\nu}_l \rightarrow \bar{\nu}_{l'}) = P(\bar{\nu}_{l'} \rightarrow \bar{\nu}_l)$ ,  $l, l' = e, \mu, \tau$  (T). In the case of CPT invariance, which we will assume to hold throughout this article, we get for the survival probabilities:  $P(\nu_l \rightarrow \nu_l) = P(\bar{\nu}_l \rightarrow \bar{\nu}_l)$ ,  $l, l' = e, \mu, \tau$ . Thus, the study of the "disappearance" of  $\nu_l$  and  $\bar{\nu}_l$ , caused by oscillations in vacuum, cannot be used to test whether CP invariance holds in the lepton sector. It follows from Eq. (13.13) and Eq. (13.14) that we can have CP violation effects in neutrino oscillations only if  $\phi_{l'l;jk} \neq \pi q$ ,  $q = 0, 1, 2$ , i.e., if  $U_{l'j} U_{lj}^* U_{lk} U_{lk}^*$ , and therefore  $U$  itself, is not real. As a measure of CP and T violation in neutrino oscillations we can consider the asymmetries:

$$A_{\text{CP}}^{(l'l)} \equiv P(\nu_l \rightarrow \nu_{l'}) - P(\bar{\nu}_l \rightarrow \bar{\nu}_{l'}), \quad A_{\text{T}}^{(l'l)} \equiv P(\nu_l \rightarrow \nu_{l'}) - P(\nu_{l'} \rightarrow \nu_l). \quad (13.16)$$

CPT invariance implies:  $A_{\text{CP}}^{(l'l)} = -A_{\text{CP}}^{(l'l)}$ ,  $A_{\text{T}}^{(l'l)} = P(\bar{\nu}_{l'} \rightarrow \bar{\nu}_l) - P(\bar{\nu}_l \rightarrow \bar{\nu}_{l'}) = A_{\text{CP}}^{(l'l)}$ . It follows further directly from Eq. (13.13) and Eq. (13.14) that

$$A_{\text{CP}}^{(l'l)} = 4 \sum_{j>k} \text{Im} \left( U_{l'j} U_{lj}^* U_{lk} U_{l'k}^* \right) \sin \frac{\Delta m_{jk}^2}{2p} L, \quad l, l' = e, \mu, \tau. \quad (13.17)$$

Eq. (13.2) and Eq. (13.13) - Eq. (13.14) imply that  $P(\nu_l \rightarrow \nu_{l'})$  and  $P(\bar{\nu}_l \rightarrow \bar{\nu}_{l'})$  do not depend on the Majorana CP violation phases in the neutrino mixing matrix  $U$  [40]. Thus, the experiments investigating the  $\nu_l \rightarrow \nu_{l'}$  and  $\bar{\nu}_l \rightarrow \bar{\nu}_{l'}$  oscillations,  $l, l' = e, \mu, \tau$ , cannot provide information on the nature - Dirac or Majorana, of massive neutrinos. The same conclusions hold also when the  $\nu_l \rightarrow \nu_{l'}$  and  $\bar{\nu}_l \rightarrow \bar{\nu}_{l'}$  oscillations take place in matter [54]. In the case of  $\nu_l \leftrightarrow \nu_{l'}$  and  $\bar{\nu}_l \leftrightarrow \bar{\nu}_{l'}$  oscillations in vacuum, only the Dirac phase(s) in  $U$  can cause CP violating effects leading to  $P(\nu_l \rightarrow \nu_{l'}) \neq P(\bar{\nu}_l \rightarrow \bar{\nu}_{l'})$ ,  $l \neq l'$ .

In the case of 3-neutrino mixing all different  $\text{Im}(U_{l'j} U_{lj}^* U_{lk} U_{l'k}^*) \neq 0$ ,  $l' \neq l = e, \mu, \tau$ ,  $j \neq k = 1, 2, 3$ , coincide up to a sign as a consequence of the unitarity of  $U$ . Therefore one has [55]:

$$A_{\text{CP}}^{(\mu e)} = -A_{\text{CP}}^{(\tau e)} = A_{\text{CP}}^{(\tau \mu)} = 4 J_{\text{CP}} \left( \sin \frac{\Delta m_{32}^2}{2p} L + \sin \frac{\Delta m_{21}^2}{2p} L + \sin \frac{\Delta m_{13}^2}{2p} L \right) \quad (13.18)$$

where

$$J_{\text{CP}} = \text{Im} \left( U_{\mu 3} U_{e 3}^* U_{e 2} U_{\mu 2}^* \right), \quad (13.19)$$

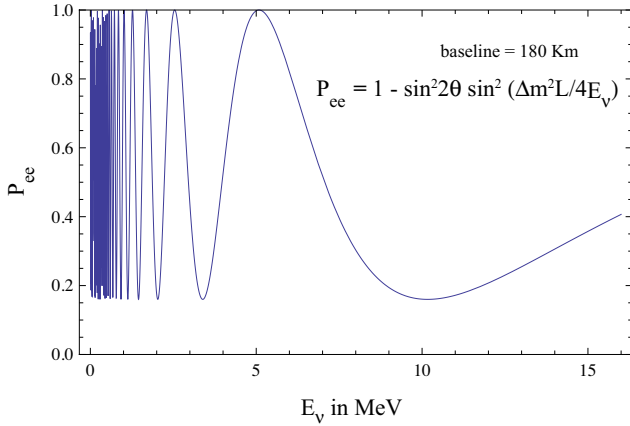


**Figure 13.1:** The  $\nu_e$  ( $\bar{\nu}_e$ ) survival probability  $P(\nu_e \rightarrow \nu_e) = P(\bar{\nu}_e \rightarrow \bar{\nu}_e)$ , Eq. (13.30), as a function of the neutrino energy for  $L = 180$  km,  $\Delta m^2 = 7.0 \times 10^{-5}$  eV<sup>2</sup> and  $\sin^2 2\theta = 0.84$  (from Ref. 62).

is the “rephasing invariant” associated with the Dirac CP violation phase in  $U$ . It is analogous to the rephasing invariant associated with the Dirac CP violating phase in the CKM quark mixing matrix [56]. It is clear from Eq. (13.18) that  $J_{\text{CP}}$  controls the magnitude of CP violation effects in neutrino oscillations in the case of 3-neutrino mixing. If  $\sin(\Delta m_{ij}^2/(2p))L \cong 0$  for  $(ij) = (32)$ , or  $(21)$ , or  $(13)$ , we get  $A_{\text{CP}}^{(l'l)} \cong 0$ . Thus, if as a consequence of the production, propagation and/or detection of neutrinos, effectively oscillations due only to one non-zero neutrino mass squared difference take place, the CP violating effects will be strongly suppressed. In particular, we get  $A_{\text{CP}}^{(l'l)} = 0$ , unless all three  $\Delta m_{ij}^2 \neq 0$ ,  $(ij) = (32)$ ,  $(21)$ ,  $(13)$ .

If the number of massive neutrinos  $n$  is equal to the number of neutrino flavours,  $n = 3$ , one has as a consequence of the unitarity of the neutrino mixing matrix:  $\sum_{l'=e,\mu,\tau} P(\nu_l \rightarrow \nu_{l'}) = 1$ ,  $l = e, \mu, \tau$ ,  $\sum_{l=e,\mu,\tau} P(\bar{\nu}_l \rightarrow \bar{\nu}_{l'}) = 1$ ,  $l' = e, \mu, \tau$ . Similar “probability conservation” equations hold for  $P(\bar{\nu}_l \rightarrow \bar{\nu}_{l'})$ . If, however, the number of light massive neutrinos is bigger than the number of flavour

neutrinos as a consequence, *e.g.*, of a flavour neutrino - sterile neutrino mixing, we would have  $\sum_{l'=e,\mu,\tau} P(\nu_l \rightarrow \nu_{l'}) = 1 - P(\nu_l \rightarrow \bar{\nu}_{sL})$ ,  $l = e, \mu, \tau$ , where we have assumed the existence of just one sterile neutrino. Obviously, in this case  $\sum_{l'=e,\mu,\tau} P(\nu_l \rightarrow \nu_{l'}) < 1$  if  $P(\nu_l \rightarrow \bar{\nu}_{sL}) \neq 0$ . The former inequality is used in the searches for oscillations between active and sterile neutrinos.

Consider next neutrino oscillations in the case of one neutrino mass squared difference “dominance”: suppose that  $|\Delta m_{j1}^2| \ll |\Delta m_{n1}^2|$ ,  $j = 2, \dots, (n-1)$ ,  $|\Delta m_{n1}^2| L/(2p) \gtrsim 1$  and  $|\Delta m_{j1}^2| L/(2p) \ll 1$ , so that  $\exp[i(\Delta m_{j1}^2 L/(2p))] \cong 1$ ,  $j = 2, \dots, (n-1)$ . Under these conditions we obtain from Eq. (13.13) and Eq. (13.14), keeping only the oscillating terms involving  $\Delta m_{n1}^2$ :

$$P(\nu_{l(l')} \rightarrow \nu_{l(l)}) \cong P(\bar{\nu}_{l(l')} \rightarrow \bar{\nu}_{l(l)}) \cong \delta_{ll'} - 2|U_{ln}|^2 \left[ \delta_{ll'} - |U_{l'n}|^2 \right] \left( 1 - \cos \frac{\Delta m_{n1}^2}{2p} L \right). \quad (13.20)$$

It follows from the neutrino oscillation data (Sections 13.4 and 13.5) that in the case of 3-neutrino mixing, one of the two independent neutrino mass squared differences, say  $\Delta m_{21}^2$ , is much smaller in absolute value than the second one,  $\Delta m_{31}^2$ :  $|\Delta m_{21}^2| \ll |\Delta m_{31}^2|$ . The data imply:

$$\begin{aligned} |\Delta m_{21}^2| &\cong 7.6 \times 10^{-5} \text{ eV}^2, \\ |\Delta m_{31}^2| &\cong 2.4 \times 10^{-3} \text{ eV}^2, \\ |\Delta m_{21}^2|/|\Delta m_{31}^2| &\cong 0.032. \end{aligned} \quad (13.21)$$

Neglecting the effects due to  $\Delta m_{21}^2$  we get from Eq. (13.20) by setting  $n = 3$  and choosing, *e.g.*, i)  $l = l' = e$  and ii)  $l = e(\mu)$ ,  $l' = \mu(e)$  [57]:

$$P(\nu_e \rightarrow \nu_e) = P(\bar{\nu}_e \rightarrow \bar{\nu}_e) \cong 1 - 2|U_{e3}|^2 \left( 1 - |U_{e3}|^2 \right) \left( 1 - \cos \frac{\Delta m_{31}^2}{2p} L \right), \quad (13.22)$$

$$\begin{aligned} P(\nu_{\mu(e)} \rightarrow \nu_{e(\mu)}) &\cong 2|U_{\mu 3}|^2 |U_{e 3}|^2 \left( 1 - \cos \frac{\Delta m_{31}^2}{2p} L \right) \\ &= \frac{|U_{\mu 3}|^2}{1 - |U_{e 3}|^2} P^{2\nu} \left( |U_{e 3}|^2, m_{31}^2 \right), \end{aligned} \quad (13.23)$$

**Table 13.1:** Sensitivity of different oscillation experiments.

Source	Type of $\nu$	$\bar{E}$ [MeV]	$L$ [km]	$\min(\Delta m^2)$ [eV <sup>2</sup> ]
Reactor	$\bar{\nu}_e$	$\sim 1$	1	$\sim 10^{-3}$
Reactor	$\bar{\nu}_e$	$\sim 1$	100	$\sim 10^{-5}$
Accelerator	$\nu_\mu, \bar{\nu}_\mu$	$\sim 10^3$	1	$\sim 1$
Accelerator	$\nu_\mu, \bar{\nu}_\mu$	$\sim 10^3$	1000	$\sim 10^{-3}$
Atmospheric $\nu$ 's	$\nu_{\mu,e}, \bar{\nu}_{\mu,e}$	$\sim 10^3$	$10^4$	$\sim 10^{-4}$
Sun	$\nu_e$	$\sim 1$	$1.5 \times 10^8$	$\sim 10^{-11}$

and  $P(\bar{\nu}_{\mu(e)} \rightarrow \bar{\nu}_{e(\mu)}) = P(\nu_{\mu(e)} \rightarrow \nu_{e(\mu)})$ . Here  $P^{2\nu}(|U_{e3}|^2, m_{31}^2)$  is the probability of the 2-neutrino transition  $\nu_e \rightarrow (s_{23}\nu_\mu + c_{23}\nu_\tau)$  due to  $\Delta m_{31}^2$  and a mixing with angle  $\theta_{13}$ , where

$$\begin{aligned} \sin^2 \theta_{13} &= |U_{e3}|^2, \quad s_{23}^2 \equiv \sin^2 \theta_{23} = \frac{|U_{\mu 3}|^2}{1 - |U_{e3}|^2}, \\ c_{23}^2 &\equiv \cos^2 \theta_{23} = \frac{|U_{\tau 3}|^2}{1 - |U_{e3}|^2}. \end{aligned} \quad (13.24)$$

Eq. (13.22) describes with a relatively high precision the oscillations of reactor  $\bar{\nu}_e$  on a distance  $L \sim 1$  km in the case of 3-neutrino mixing. It was used in the analysis of the data of the Chooz [58], Double Chooz [59], Daya Bay [26] and RENO [27] experiments. Eq. (13.20) with  $n = 3$  and  $l = l' = \mu$  describes with a relatively good precision the effects of oscillations of the accelerator  $\nu_\mu$ , seen in the K2K [19]

and MINOS [20,21] experiments. The  $\nu_\mu \rightarrow \nu_\tau$  oscillations, which the OPERA experiment [60,61] is aiming to detect, can be described by Eq. (13.20) with  $n = 3$  and  $l = \mu, l' = \tau$ . Finally, the probability Eq. (13.23) describes with a good precision the  $\nu_\mu \rightarrow \nu_e$  and  $\bar{\nu}_\mu \rightarrow \bar{\nu}_e$  oscillations under the conditions of the K2K experiment.

In certain cases the dimensions of the neutrino source,  $\Delta L$ , are not negligible in comparison with the oscillation length. Similarly, when analyzing neutrino oscillation data one has to include the energy resolution of the detector,  $\Delta E$ , etc. in the analysis. As can be shown [39], if  $2\pi\Delta L/L_{jk}^v \gg 1$ , and/or  $2\pi(L/L_{jk}^v)(\Delta E/E) \gg 1$ , the oscillating terms in the neutrino oscillation probabilities will be strongly suppressed. In this case (as well as in the case of sufficiently large separation of the  $\nu_j$  and  $\nu_k$  wave packets at the detection point) the interference terms in  $P(\nu_l \rightarrow \nu_{l'})$  and  $P(\bar{\nu}_l \rightarrow \bar{\nu}_{l'})$  will be negligibly small and the neutrino flavour conversion will be determined by the average probabilities:

$$\bar{P}(\nu_l \rightarrow \nu_{l'}) = \bar{P}(\bar{\nu}_l \rightarrow \bar{\nu}_{l'}) \cong \sum_j |U_{lj}|^2 |U_{l'j}|^2. \quad (13.25)$$

Suppose next that in the case of 3-neutrino mixing,  $|\Delta m_{21}^2| L/(2p) \sim 1$ , while at the same time  $|\Delta m_{31(32)}^2| L/(2p) \gg 1$ , and the oscillations due to  $\Delta m_{31}^2$  and  $\Delta m_{32}^2$  are strongly suppressed (averaged out) due to integration over the region of neutrino production, the energy resolution function, etc. In this case we get for the  $\nu_e$  and  $\bar{\nu}_e$  survival probabilities:

$$P(\nu_e \rightarrow \nu_e) = P(\bar{\nu}_e \rightarrow \bar{\nu}_e) \cong |U_{e3}|^4 + (1 - |U_{e3}|^2)^2 P^{2\nu}(\nu_e \rightarrow \nu_e), \quad (13.26)$$

$$P^{2\nu}(\nu_e \rightarrow \nu_e) = P^{2\nu}(\bar{\nu}_e \rightarrow \bar{\nu}_e) \equiv P_{ee}^{2\nu}(\theta_{12}, \Delta m_{21}^2) = 1 - \frac{1}{2} \sin^2 2\theta_{12} \left( 1 - \cos \frac{\Delta m_{21}^2 L}{2p} \right) \quad (13.27)$$

being the  $\nu_e$  and  $\bar{\nu}_e$  survival probability in the case of 2-neutrino oscillations “driven” by the angle  $\theta_{12}$  and  $\Delta m_{21}^2$ , with  $\theta_{12}$  determined by

$$\cos^2 \theta_{12} = \frac{|U_{e1}|^2}{1 - |U_{e3}|^2}, \quad \sin^2 \theta_{12} = \frac{|U_{e2}|^2}{1 - |U_{e3}|^2}. \quad (13.28)$$

Eq. (13.26) with  $P^{2\nu}(\bar{\nu}_e \rightarrow \bar{\nu}_e)$  given by Eq. (13.27) describes the effects of neutrino oscillations of reactor  $\bar{\nu}_e$  observed by the KamLAND experiment.

In the case of 3-neutrino mixing with  $0 < \Delta m_{21}^2 < |\Delta m_{31(32)}^2|$  and  $|U_{e3}|^2 = |\sin \theta_{13}|^2 \ll 1$  (see Section 13.6), one can identify  $\Delta m_{21}^2$  and  $\theta_{12}$  as the neutrino mass squared difference and mixing angle responsible for the solar  $\nu_e$  oscillations, and  $\Delta m_{31}^2$  and  $\theta_{23}$  as those associated with the dominant atmospheric  $\nu_\mu$  and  $\bar{\nu}_\mu$  oscillations. Thus,  $\theta_{12}$  and  $\theta_{23}$  are often called “solar” and “atmospheric” neutrino mixing angles and denoted as  $\theta_{12} = \theta_\odot$  and  $\theta_{23} = \theta_A$  (or  $\theta_{\text{atm}}$ ), while  $\Delta m_{21}^2$  and  $\Delta m_{31}^2$  are often referred to as the “solar” and “atmospheric” neutrino mass squared differences and denoted as  $\Delta m_{21}^2 \equiv \Delta m_\odot^2$  and  $\Delta m_{31}^2 \equiv \Delta m_A^2$  (or  $\Delta m_{\text{atm}}^2$ ).

The data of  $\nu$ -oscillations experiments is often analyzed assuming 2-neutrino mixing:

$$|\nu_l\rangle = |\nu_1\rangle \cos \theta + |\nu_2\rangle \sin \theta, \quad |\nu_x\rangle = -|\nu_1\rangle \sin \theta + |\nu_2\rangle \cos \theta, \quad (13.29)$$

where  $\theta$  is the neutrino mixing angle in vacuum and  $\nu_x$  is another flavour neutrino or sterile (anti-) neutrino,  $x = l' \neq l$  or  $\nu_x \equiv \bar{\nu}_{sL}$ . In this case we have [51]:

$$P^{2\nu}(\nu_l \rightarrow \nu_l) = 1 - \frac{1}{2} \sin^2 2\theta \left( 1 - \cos 2\pi \frac{L}{L^v} \right), \quad (13.30)$$

$$P^{2\nu}(\nu_l \rightarrow \nu_x) = 1 - P^{2\nu}(\nu_l \rightarrow \nu_l),$$

where  $L^v = 4\pi p/\Delta m^2$ ,  $\Delta m^2 = m_2^2 - m_1^2 > 0$ . Combining the CPT invariance constraints with the probability conservation one obtains:  $P(\nu_l \rightarrow \nu_x) = P(\bar{\nu}_l \rightarrow \bar{\nu}_x) = P(\nu_x \rightarrow \nu_l) = P(\bar{\nu}_x \rightarrow \bar{\nu}_l)$ .

These equalities and Eq. (13.30) with  $l = \mu$  and  $x = \tau$  were used, for instance, in the analysis of the Super-K atmospheric neutrino data [13], in which the first compelling evidence for oscillations of neutrinos was obtained. The probability  $P^{2\nu}(\nu_l \rightarrow \nu_x)$ , Eq. (13.30), depends on two factors: on  $(1 - \cos 2\pi L/L^v)$ , which exhibits oscillatory dependence on the distance  $L$  and on the neutrino energy  $p = E$  (hence the name “neutrino oscillations”), and on  $\sin^2 2\theta$ , which determines the amplitude of the oscillations. In order to have  $P^{2\nu}(\nu_l \rightarrow \nu_x) \cong 1$ , two conditions have to be fulfilled: one should have  $\sin^2 2\theta \cong 1$  and  $L^v \lesssim 2\pi L$  with  $\cos 2\pi L/L^v \cong -1$ . If  $L^v \gg 2\pi L$ , the oscillations do not have enough time to develop on the way to the neutrino detector and  $P(\nu_l \rightarrow \nu_x) \cong 0$ . This is illustrated in Fig. 1 showing the dependence of the probability  $P^{2\nu}(\nu_e \rightarrow \nu_e) = P^{2\nu}(\bar{\nu}_e \rightarrow \bar{\nu}_e)$  on the neutrino energy.

A given experiment searching for neutrino oscillations is specified, in particular, by the average energy of the neutrinos being studied,  $\bar{E}$ , and by the source-detector distance  $L$ . The requirement  $L_{jk}^v \lesssim 2\pi L$  determines the minimal value of a generic neutrino mass squared difference  $\Delta m^2 > 0$ , to which the experiment is sensitive (figure of merit of the experiment):  $\min(\Delta m^2) \sim 2\bar{E}/L$ . Because of the interference nature of neutrino oscillations, experiments can probe, in general, rather small values of  $\Delta m^2$  (see, e.g., Ref. 47). Values of  $\min(\Delta m^2)$ , characterizing qualitatively the sensitivity of different experiments are given in Table 1. They correspond to the reactor experiments Chooz ( $L \sim 1$  km) and KamLAND ( $L \sim 100$  km), to accelerator experiments - past ( $L \sim 1$  km), recent, current and future (K2K, MINOS, OPERA, T2K, NO $\nu$ A [63]),  $L \sim (300 \div 1000)$  km), to the Super-Kamiokande experiment studying atmospheric neutrino oscillations, and to the solar neutrino experiments.

### 13.3. Matter effects in neutrino oscillations

The presence of matter can change drastically the pattern of neutrino oscillations: neutrinos can interact with the particles forming the matter. Accordingly, the Hamiltonian of the neutrino system in matter  $H_m$ , differs from the Hamiltonian in vacuum  $H_0$ ,  $H_m = H_0 + H_{\text{int}}$ , where  $H_{\text{int}}$  describes the interaction of neutrinos with the particles of matter. When, for instance,  $\nu_e$  and  $\nu_\mu$  propagate in matter, they can scatter (due to  $H_{\text{int}}$ ) on the electrons ( $e^-$ ), protons ( $p$ ) and neutrons ( $n$ ) present in matter. The incoherent elastic and the quasi-elastic scattering, in which the states of the initial particles change in the process (destroying the coherence between the neutrino states), are not of interest - they have a negligible effect on the solar neutrino propagation in the Sun and on the solar, atmospheric and reactor neutrino propagation in the Earth [64]: even in the center of the Sun, where the matter density is relatively high ( $\sim 150$  g/cm $^3$ ), a  $\nu_e$  with energy of 1 MeV has a mean free path with respect to the indicated scattering processes  $\sim 10^{10}$  km. We recall that the solar radius is much smaller:  $R_\odot = 6.96 \times 10^5$  km. The oscillating  $\nu_e$  and  $\nu_\mu$  can scatter also elastically in the forward direction on the  $e^-$ ,  $p$  and  $n$ , with the momenta and the spin states of the particles remaining unchanged. In such a process the coherence of the neutrino states is preserved.

The  $\nu_e$  and  $\nu_\mu$  coherent elastic scattering on the particles of matter generates nontrivial indices of refraction of the  $\nu_e$  and  $\nu_\mu$  in matter [22]:  $\kappa(\nu_e) \neq 1$ ,  $\kappa(\nu_\mu) \neq 1$ . Most importantly, we have  $\kappa(\nu_e) \neq \kappa(\nu_\mu)$ . The difference  $\kappa(\nu_e) - \kappa(\nu_\mu)$  is determined essentially by the difference of the real parts of the forward  $\nu_e - e^-$  and  $\nu_\mu - e^-$  elastic scattering amplitudes [22]  $\text{Re}[F_{\nu_e e^-}(0)] - \text{Re}[F_{\nu_\mu e^-}(0)]$ : due to the flavour symmetry of the neutrino - quark (neutrino - nucleon) neutral current interaction, the forward  $\nu_e - p, n$  and  $\nu_\mu - p, n$  elastic scattering amplitudes are equal and therefore do not contribute to the difference of interest [65]. The imaginary parts of the forward scattering amplitudes (responsible, in particular, for decoherence effects) are proportional to the corresponding total scattering cross-sections and in the case of interest are negligible in comparison with the real parts. The real parts of the amplitudes  $F_{\nu_e e^-}(0)$  and  $F_{\nu_\mu e^-}(0)$  can be calculated in the Standard Model. To leading order in the Fermi constant  $G_F$ , only the term in  $F_{\nu_e e^-}(0)$  due to the diagram with exchange of a virtual  $W^\pm$ -boson contributes to  $F_{\nu_e e^-}(0) - F_{\nu_\mu e^-}(0)$ . One finds the following result

for  $\kappa(\nu_e) - \kappa(\nu_\mu)$  in the rest frame of the scatters [22,67,68]:

$$\begin{aligned}\kappa(\nu_e) - \kappa(\nu_\mu) &= \frac{2\pi}{p^2} \left( \text{Re} [F_{\nu_e e^-}(0)] - \text{Re} [F_{\nu_\mu e^-}(0)] \right) \\ &= -\frac{1}{p} \sqrt{2} G_F N_e, \end{aligned} \quad (13.31)$$

where  $N_e$  is the electron number density in matter. Given  $\kappa(\nu_e) - \kappa(\nu_\mu)$ , the system of evolution equations describing the  $\nu_e \leftrightarrow \nu_\mu$  oscillations in matter reads [22]:

$$i \frac{d}{dt} \begin{pmatrix} A_e(t, t_0) \\ A_\mu(t, t_0) \end{pmatrix} = \begin{pmatrix} -\epsilon(t) & \epsilon' \\ \epsilon' & \epsilon(t) \end{pmatrix} \begin{pmatrix} A_e(t, t_0) \\ A_\mu(t, t_0) \end{pmatrix} \quad (13.32)$$

where  $A_e(t, t_0)$  ( $A_\mu(t, t_0)$ ) is the amplitude of the probability to find  $\nu_e$  ( $\nu_\mu$ ) at time  $t$  of the evolution of the system if at time  $t_0 \leq t$  the neutrino  $\nu_e$  or  $\nu_\mu$  has been produced and

$$\epsilon(t) = \frac{1}{2} \left[ \frac{\Delta m^2}{2E} \cos 2\theta - \sqrt{2} G_F N_e(t) \right], \quad \epsilon' = \frac{\Delta m^2}{4E} \sin 2\theta. \quad (13.33)$$

The term  $\sqrt{2} G_F N_e(t)$  in  $\epsilon(t)$  accounts for the effects of matter on neutrino oscillations. The system of evolution equations describing the oscillations of antineutrinos  $\bar{\nu}_e \leftrightarrow \bar{\nu}_\mu$  in matter has exactly the same form except for the matter term in  $\epsilon(t)$  which changes sign. The effect of matter in neutrino oscillations is usually called the Mikheyev, Smirnov, Wolfenstein (or MSW) effect.

Consider first the case of  $\nu_e \leftrightarrow \nu_\mu$  oscillations in matter with constant density:  $N_e(t) = N_e = \text{const.}$  Due to the interaction term  $H_{int}$  in  $H_m$ , the eigenstates of the Hamiltonian of the neutrino system in vacuum,  $|\nu_{1,2}\rangle$  are not eigenstates of  $H_m$ . For the eigenstates  $|\nu_{1,2}^m\rangle$  of  $H_m$ , which diagonalize the evolution matrix in the r.h.s. of the system Eq. (13.32) we have:

$$|\nu_e\rangle = |\nu_1^m\rangle \cos \theta_m + |\nu_2^m\rangle \sin \theta_m, \quad |\nu_\mu\rangle = -|\nu_1^m\rangle \sin \theta_m + |\nu_2^m\rangle \cos \theta_m. \quad (13.34)$$

Here  $\theta_m$  is the neutrino mixing angle in matter [22],

$$\sin 2\theta_m = \frac{\tan 2\theta}{\sqrt{\left(1 - \frac{N_e}{N_e^{res}}\right)^2 + \tan^2 2\theta}}, \quad \cos 2\theta_m = \frac{1 - N_e/N_e^{res}}{\sqrt{\left(1 - \frac{N_e}{N_e^{res}}\right)^2 + \tan^2 2\theta}}, \quad (13.35)$$

where the quantity

$$N_e^{res} = \frac{\Delta m^2 \cos 2\theta}{2E\sqrt{2}G_F} \cong 6.56 \times 10^6 \frac{\Delta m^2 [\text{eV}^2]}{E [\text{MeV}]} \cos 2\theta \text{ cm}^{-3} N_A, \quad (13.36)$$

is called (for  $\Delta m^2 \cos 2\theta > 0$ ) “resonance density” [23,67],  $N_A$  being Avogadro’s number. The “adiabatic” states  $|\nu_{1,2}^m\rangle$  have energies  $E_{1,2}^m$  whose difference is given by

$$E_2^m - E_1^m = \frac{\Delta m^2}{2E} \left( \left(1 - \frac{N_e}{N_e^{res}}\right)^2 \cos^2 2\theta + \sin^2 2\theta \right)^{\frac{1}{2}} \equiv \frac{\Delta m^2}{2E}. \quad (13.37)$$

The probability of  $\nu_e \rightarrow \nu_\mu$  transition in matter with  $N_e = \text{const.}$  has the form [22,67]

$$\begin{aligned} P_m^{2\nu}(\nu_e \rightarrow \nu_\mu) &= |A_\mu(t)|^2 = \frac{1}{2} \sin^2 2\theta_m \left[ 1 - \cos 2\pi \frac{L}{L_m} \right] \\ L_m &= 2\pi / (E_2^m - E_1^m), \end{aligned} \quad (13.38)$$

where  $L_m$  is the oscillation length in matter. As Eq. (13.35) indicates, the dependence of  $\sin^2 2\theta_m$  on  $N_e$  has a resonance character [23]. Indeed, if  $\Delta m^2 \cos 2\theta > 0$ , for any  $\sin^2 2\theta \neq 0$  there exists a value of  $N_e$  given by  $N_e^{res}$ , such that when  $N_e = N_e^{res}$  we have  $\sin^2 2\theta_m = 1$  independently of the value of  $\sin^2 2\theta < 1$ . This implies that the presence of matter can lead to a strong enhancement of the oscillation probability  $P_m^{2\nu}(\nu_e \rightarrow \nu_\mu)$  even when the  $\nu_e \leftrightarrow \nu_\mu$  oscillations in vacuum are suppressed due to a small value of  $\sin^2 2\theta$ . For obvious reasons

$$N_e = N_e^{res} \equiv \frac{\Delta m^2 \cos 2\theta}{2E\sqrt{2}G_F}, \quad (13.39)$$

is called the “resonance condition” [23,67], while the energy at which Eq. (13.39) holds for given  $N_e$  and  $\Delta m^2 \cos 2\theta$ , is referred to as the “resonance energy”,  $E^{res}$ . The oscillation length at resonance is given by [23]  $L_m^{res} = L^v / \sin 2\theta$ , while the width in  $N_e$  of the resonance at half height reads  $\Delta N_e^{res} = 2N_e^{res} \tan 2\theta$ . Thus, if the mixing angle in vacuum is small, the resonance is narrow,  $\Delta N_e^{res} \ll N_e^{res}$ , and  $L_m^{res} \gg L^v$ . The energy difference  $E_2^m - E_1^m$  has a minimum at the resonance:  $(E_2^m - E_1^m)^{res} = \min (E_2^m - E_1^m) = (\Delta m^2 / (2E)) \sin 2\theta$ .

It is instructive to consider two limiting cases. If  $N_e \ll N_e^{res}$ , we have from Eq. (13.35) and Eq. (13.37),  $\theta_m \cong \theta$ ,  $L_m \cong L^v$  and neutrinos oscillate practically as in vacuum. In the limit  $N_e \gg N_e^{res}$ ,  $N_e^{res} \tan^2 2\theta$ , one finds  $\theta_m \cong \pi/2$  ( $\cos 2\theta_m \cong -1$ ) and the presence of matter suppresses the  $\nu_e \leftrightarrow \nu_\mu$  oscillations. In this case  $|\nu_e\rangle \cong |\nu_2^m\rangle$ ,  $|\nu_\mu\rangle = -|\nu_1^m\rangle$ , i.e.,  $\nu_e$  practically coincides with the heavier matter-eigenstate, while  $\nu_\mu$  coincides with the lighter one.

Since the neutral current weak interaction of neutrinos in the Standard Model is flavour symmetric, the formulae and results we have obtained are valid for the case of  $\nu_e - \nu_\tau$  mixing and  $\nu_e \leftrightarrow \nu_\tau$  oscillations in matter as well. The case of  $\nu_\mu - \nu_\tau$  mixing, however, is different: to a relatively good precision we have [69]  $\kappa(\nu_\mu) \cong \kappa(\nu_\tau)$  and the  $\nu_\mu \leftrightarrow \nu_\tau$  oscillations in the matter of the Earth and the Sun proceed practically as in vacuum [70].

The analogs of Eq. (13.35) to Eq. (13.38) for oscillations of antineutrinos,  $\bar{\nu}_e \leftrightarrow \bar{\nu}_\mu$ , in matter can formally be obtained by replacing  $N_e$  with  $(-N_e)$  in the indicated equations. It should be clear that depending on the sign of  $\Delta m^2 \cos 2\theta$ , the presence of matter can lead to resonance enhancement either of the  $\nu_e \leftrightarrow \nu_\mu$  or of the  $\bar{\nu}_e \leftrightarrow \bar{\nu}_\mu$  oscillations, but not of both types of oscillations [67]. For  $\Delta m^2 \cos 2\theta < 0$ , for instance, the matter can only suppress the  $\nu_e \rightarrow \nu_\mu$  oscillations, while it can enhance the  $\bar{\nu}_e \rightarrow \bar{\nu}_\mu$  transitions. This disparity between the behavior of neutrinos and that of antineutrinos is a consequence of the fact that the matter in the Sun or in the Earth we are interested in is not charge-symmetric (it contains  $e^-$ ,  $p$  and  $n$ , but does not contain their antiparticles) and therefore the oscillations in matter are neither CP- nor CPT- invariant [54]. Thus, even in the case of 2-neutrino mixing and oscillations we have, e.g.,  $P_m^{2\nu}(\nu_e \rightarrow \nu_\mu(\tau)) \neq P_m^{2\nu}(\bar{\nu}_e \rightarrow \bar{\nu}_\mu(\tau))$ .

The matter effects in the  $\nu_e \leftrightarrow \nu_\mu(\tau)$  ( $\bar{\nu}_e \leftrightarrow \bar{\nu}_\mu(\tau)$ ) oscillations will be invariant with respect to the operation of time reversal if the  $N_e$  distribution along the neutrino path is symmetric with respect to this operation [55,71]. The latter condition is fulfilled (to a good approximation) for the  $N_e$  distribution along a path of a neutrino crossing the Earth [72].

### 13.3.1. Effects of Earth matter on oscillations of neutrinos :

The formalism we have developed can be applied, e.g., to the study of matter effects in the  $\nu_e \leftrightarrow \nu_\mu(\tau)$  ( $\nu_\mu(\tau) \leftrightarrow \nu_e$ ) and  $\bar{\nu}_e \leftrightarrow \bar{\nu}_\mu(\tau)$  ( $\bar{\nu}_\mu(\tau) \leftrightarrow \bar{\nu}_e$ ) oscillations of neutrinos which traverse the Earth [73]. Indeed, the Earth density distribution in the existing Earth models [72] is assumed to be spherically symmetric and there are two major density structures - the core and the mantle, and a certain number of substructures (shells or layers). The Earth radius is  $R_\oplus = 6371$  km; the Earth core has a radius of  $R_c = 3486$  km, so the Earth mantle depth is 2885 km. For a spherically symmetric Earth density distribution, the neutrino trajectory in the Earth is specified by the value of the nadir angle  $\theta_n$  of the trajectory. For  $\theta_n \leq 33.17^\circ$ , or path lengths  $L \geq 10660$  km, neutrinos cross the Earth core. The path length for neutrinos which cross only the Earth mantle is given by  $L = 2R_\oplus \cos \theta_n$ . If neutrinos cross the Earth core, the lengths of the paths in the mantle,  $2L^{\text{man}}$ , and in the core,  $L^{\text{core}}$ , are determined by:  $L^{\text{man}} = R_\oplus \cos \theta_n - (R_c^2 - R_\oplus^2 \sin^2 \theta_n)^{\frac{1}{2}}$ ,  $L^{\text{core}} = 2(R_c^2 - R_\oplus^2 \sin^2 \theta_n)^{\frac{1}{2}}$ . The mean electron number densities in the mantle and in the core according to the PREM model read [72]:  $\bar{N}_e^{\text{man}} \cong 2.2 \text{ cm}^{-3} N_A$ ,  $\bar{N}_e^{\text{c}} \cong 5.4 \text{ cm}^{-3} N_A$ . Thus, we have  $\bar{N}_e^{\text{c}} \cong 2.5 \bar{N}_e^{\text{man}}$ . The change of  $\bar{N}_e$  from the mantle to the core can well be approximated by a step function [72]. The electron number density  $N_e$  changes relatively little around the indicated mean values along the trajectories of neutrinos which cross a substantial part of the Earth mantle, or the mantle and the core, and the two-layer constant density approximation,  $N_e^{\text{man}} = \text{const.} = \bar{N}_e^{\text{man}}$ ,  $N_e^{\text{c}} = \text{const.} = \bar{N}_e^{\text{c}}$ ,  $\bar{N}_e^{\text{man}}$  and  $\bar{N}_e^{\text{c}}$  being the mean densities along the given neutrino path in

the Earth, was shown to be sufficiently accurate in what concerns the calculation of neutrino oscillation probabilities [55,75,76] (and references quoted in [75,76]) in a large number of specific cases. This is related to the fact that the relatively small changes of density along the path of the neutrinos in the mantle (or in the core) take place over path lengths which are typically considerably smaller than the corresponding oscillation length in matter.

In the case of 3-neutrino mixing and for neutrino energies of  $E \gtrsim 2$  GeV, the effects due to  $\Delta m_{21}^2$  ( $|\Delta m_{21}^2| \ll |\Delta m_{31}^2|$ , see Eq. (13.21)) in the neutrino oscillation probabilities are sub-dominant and to leading order can be neglected: the corresponding resonance density  $|N_{e21}^{res}| \lesssim 0.25 \text{ cm}^{-3} N_A \ll \bar{N}_e^{man,c}$  and the Earth matter strongly suppresses the oscillations due to  $\Delta m_{21}^2$ . For oscillations in vacuum this approximation is valid as long as the leading order contribution due to  $\Delta m_{31}^2$  in the relevant probabilities is bigger than approximately  $10^{-3}$ . In this case the 3-neutrino  $\nu_e \rightarrow \nu_{\mu(\tau)}$  ( $\bar{\nu}_e \rightarrow \bar{\nu}_{\mu(\tau)}$ ) and  $\nu_{\mu(\tau)} \rightarrow \nu_e$  ( $\bar{\nu}_{\mu(\tau)} \rightarrow \bar{\nu}_e$ ) transition probabilities for neutrinos traversing the Earth, reduce effectively to a 2-neutrino transition probability (see, e.g., Refs. [76–78]), with  $\Delta m_{31}^2$  and  $\theta_{13}$  playing the role of the relevant 2-neutrino vacuum oscillation parameters. As will be discussed in Sections 13.6 and 13.7, the value of  $\sin^2 2\theta_{13}$  has been determined recently with a rather high precision in the Daya Bay [26] and RENO [27] experiments. The best fit values found in the two experiments read, respectively,  $\sin^2 2\theta_{13} = 0.092$  and  $0.113$ , while the  $3\sigma$  allowed range reported in [26] is  $0.04 \lesssim \sin^2 2\theta_{13} \lesssim 0.14$ . The 3-neutrino oscillation probabilities of the atmospheric and accelerator  $\nu_{e,\mu}$  having energy  $E$  and crossing the Earth along a trajectory characterized by a nadir angle  $\theta_n$ , for instance, have the following form:

$$P_m^{3\nu}(\nu_e \rightarrow \nu_e) \cong 1 - P_m^{2\nu}, \quad (13.40)$$

$$P_m^{3\nu}(\nu_e \rightarrow \nu_\mu) \cong P_m^{3\nu}(\nu_\mu \rightarrow \nu_e) \cong s_{23}^2 P_m^{2\nu}, \quad P_m^{3\nu}(\nu_e \rightarrow \nu_\tau) \cong c_{23}^2 P_m^{2\nu}, \quad (13.41)$$

$$P_m^{3\nu}(\nu_\mu \rightarrow \nu_\mu) \cong 1 - s_{23}^4 P_m^{2\nu} - 2c_{23}^2 s_{23}^2 \left[ 1 - Re(e^{-i\kappa} A_m^{2\nu}(\nu' \rightarrow \nu')) \right], \quad (13.42)$$

$$P_m^{3\nu}(\nu_\mu \rightarrow \nu_\tau) = 1 - P_m^{3\nu}(\nu_\mu \rightarrow \nu_\mu) - P_m^{3\nu}(\nu_\mu \rightarrow \nu_e). \quad (13.43)$$

Here  $P_m^{2\nu} \equiv P_m^{2\nu}(\Delta m_{31}^2, \theta_{13}; E, \theta_n)$  is the probability of the 2-neutrino  $\nu_e \rightarrow \nu' \equiv (s_{23}\nu_\mu + c_{23}\nu_\tau)$  oscillations in the Earth, and  $\kappa$  and  $A_m^{2\nu}(\nu' \rightarrow \nu') \equiv A_m^{2\nu}$  are known phase and 2-neutrino transition probability amplitude (see, e.g., Refs. [76,77]). We note that Eq. (13.40) to Eq. (13.42) are based only on the assumptions that  $|N_{e21}^{res}|$  is much smaller than the densities in the Earth mantle and core and that  $|\Delta m_{21}^2| \ll |\Delta m_{31}^2|$ , and does not rely on the constant density approximation. Similar results are valid for the corresponding antineutrino oscillation probabilities: one has just to replace  $P_m^{2\nu}$ ,  $\kappa$  and  $A_m^{2\nu}$  in the expressions given above with the corresponding quantities for antineutrinos (the latter are obtained from those for neutrinos by changing the sign in front of  $N_e$ ). Obviously, we have:  $P(\nu_{e(\mu)} \rightarrow \nu_{\mu(e)})$ ,  $P(\bar{\nu}_{e(\mu)} \rightarrow \bar{\nu}_{\mu(e)}) \leq \sin^2 \theta_{23}$ , and  $P(\nu_e \rightarrow \nu_\tau)$ ,  $P(\bar{\nu}_e \rightarrow \bar{\nu}_\tau) \leq \cos^2 \theta_{23}$ . The one  $\Delta m^2$  dominance approximation and correspondingly Eq. (13.40) to Eq. (13.43) were used by the Super-Kamiokande Collaboration in their 2006 neutrino oscillation analysis of the multi-GeV atmospheric neutrino data [79].

In the case of neutrinos crossing only the Earth mantle and in the constant density approximation,  $P_m^{2\nu}$  is given by the r.h.s. of Eq. (13.38) with  $\theta$  and  $\Delta m^2$  replaced by  $\theta_{13}$  and  $\Delta m_{31}^2$ , while for  $\kappa$  and  $A_m^{2\nu}$  we have (see, e.g., Ref. 76):

$$\kappa \cong \frac{1}{2} \left[ \frac{\Delta m_{31}^2}{2E} L + \sqrt{2} G_F \bar{N}_e^{man} L - \frac{\Delta M^2 L}{2E} \right],$$

$$A_m^{2\nu} = 1 + (e^{-i\frac{\Delta M^2 L}{2E}} - 1) \cos^2 \theta'_m, \quad (13.44)$$

where  $\Delta M^2$  is defined in Eq. (13.37) (with  $\theta = \theta_{13}$  and  $\Delta m^2 = \Delta m_{31}^2$ ),  $\theta'_m$  is the mixing angle in the mantle which coincides in vacuum with  $\theta_{13}$  (Eq. (13.35) with  $N_e = \bar{N}_e^{man}$  and  $\theta = \theta_{13}$ ), and  $L = 2R_\oplus \cos \theta_n$  is the distance the neutrino travels in the mantle.

It follows from Eq. (13.40) and Eq. (13.41) that for  $\Delta m_{31}^2 \cos 2\theta_{13} > 0$ , the oscillation effects of interest, e.g., in the  $\nu_{e(\mu)} \rightarrow \nu_{\mu(e)}$  and  $\nu_e \rightarrow \nu_\tau$  transitions will be maximal if  $P_m^{2\nu} \cong 1$ , i.e., if Eq. (13.39)

leading to  $\sin^2 2\theta_m \cong 1$  is fulfilled, and ii)  $\cos(\Delta M^2 L / (2E)) \cong -1$ . Given the value of  $\bar{N}_e^{man}$ , the first condition determines the neutrino's energy, while the second determines the path length  $L$ , for which one can have  $P_m^{2\nu} \cong 1$ . For  $\Delta m_{31}^2 \cong 2.4 \times 10^{-3} \text{ eV}^2$ ,  $\sin^2 2\theta_{13} \lesssim 0.14$  and  $\bar{N}_e^{man} \cong 2.2 \text{ N}_A \text{ cm}^{-3}$ , one finds that  $E_{res} \cong 7.2 \text{ GeV}$  and  $L \cong 2370 / \sin 2\theta_{13} \text{ km} \gtrsim 6267.3 \text{ km}$ . Since for neutrinos crossing only the mantle  $L \lesssim 10660 \text{ km}$ , the second condition can be satisfied only if  $\sin \theta_{13} \gtrsim 0.11$ , which falls in the range of the experimentally allowed values of  $\sin \theta_{13}$ . Thus, for  $\Delta m_{31}^2 > 0$ , the Earth matter effects can amplify  $P_m^{2\nu}$ , and therefore  $P(\nu_{e(\mu)} \rightarrow \nu_{\mu(e)})$  and  $P(\nu_e \rightarrow \nu_\tau)$ , maximally when the neutrinos cross only the mantle for  $E \sim 7 \text{ GeV}$  and  $L \gtrsim 5400 \text{ km}$ , or  $\cos \theta_n \gtrsim 0.43$ , provided  $\sin \theta_{13} \gtrsim 0.1$ . If  $\Delta m_{31}^2 < 0$  the same considerations apply for the corresponding antineutrino oscillation probabilities  $\bar{P}_m^{2\nu} = \bar{P}_m^{2\nu}(\bar{\nu}_e \rightarrow (s_{23}\bar{\nu}_\mu + c_{23}\bar{\nu}_\tau))$  and correspondingly for  $P(\bar{\nu}_{e(\mu)} \rightarrow \bar{\nu}_{\mu(e)})$  and  $P(\bar{\nu}_e \rightarrow \bar{\nu}_\tau)$ . For  $\Delta m_{31}^2 > 0$ , the  $\bar{\nu}_{e(\mu)} \rightarrow \bar{\nu}_{\mu(e)}$  and  $\bar{\nu}_e \rightarrow \bar{\nu}_\tau$  oscillations are suppressed by the Earth matter, while if  $\Delta m_{31}^2 < 0$ , the same conclusion holds for the  $\nu_{e(\mu)} \rightarrow \nu_{\mu(e)}$  and  $\nu_e \rightarrow \nu_\tau$  oscillations.

In the case of neutrinos crossing the Earth core, new resonance-like effects become possible in the  $\nu_\mu \rightarrow \nu_e$  and  $\nu_e \rightarrow \nu_{\mu(\tau)}$  (or  $\bar{\nu}_\mu \rightarrow \bar{\nu}_e$  and  $\bar{\nu}_e \rightarrow \bar{\nu}_{\mu(\tau)}$ ) transitions [75–77,80–82]. For  $\sin^2 \theta_{13} \lesssim 0.05$  and  $\Delta m_{31}^2 > 0$ , we can have [81]  $P_m^{2\nu}(\Delta m_{31}^2, \theta_{13}) \cong 1$ , and correspondingly maximal  $P_m^{3\nu}(\nu_e \rightarrow \nu_\mu) = P_m^{3\nu}(\nu_\mu \rightarrow \nu_e) \cong s_{23}^2$ , only due to the effect of maximal constructive interference between the amplitudes of the  $\nu_e \rightarrow \nu'$  transitions in the Earth mantle and in the Earth core. The effect differs from the MSW one and the enhancement happens in the case of interest at a value of the energy between the MSW resonance energies corresponding to the density in the mantle and that of the core, or at a value of the resonance density  $N_e^{res}$  which lies between the values of  $N_e$  in the mantle and in the core [75]. In Refs. [75,76] the enhancement was called “neutrino oscillation length resonance”, while in Refs. [77,80] the term “parametric resonance” for the same effect was used [83]. The *mantle-core enhancement effect* is caused by the existence (for a given neutrino trajectory through the Earth core) of points of resonance-like maximal neutrino conversion,  $P_m^{2\nu}(\Delta m_{31}^2, \theta_{13}) = 1$ , in the corresponding space of neutrino oscillation parameters [81]. For  $\Delta m_{31}^2 < 0$  the mantle-core enhancement can take place for the antineutrino transitions,  $\bar{\nu}_\mu \rightarrow \bar{\nu}_e$  and  $\bar{\nu}_e \rightarrow \bar{\nu}_{\mu(\tau)}$ .

A rather complete set of values of  $\Delta m_{31}^2/E > 0$  and  $\sin^2 2\theta_{13}$  for which  $P_m^{2\nu}(\Delta m_{31}^2, \theta_{13}) = 1$  was found in Ref. 81. The location of these points in the  $\Delta m_{31}^2/E - \sin^2 2\theta_{13}$  plane determines the regions in the plane where  $P_m^{2\nu}(\Delta m_{31}^2, \theta_{13})$  is large,  $P_m^{2\nu}(\Delta m_{31}^2, \theta_{13}) \gtrsim 0.5$ . These regions vary slowly with the nadir angle, being remarkably wide in the nadir angle and rather wide in the neutrino energy [81], so that the transitions of interest can produce noticeable effects in the measured observables. For  $\sin^2 \theta_{13} \lesssim 0.05$ , there are two sets of values of  $(\Delta m_{31}^2/E, \sin^2 \theta_{13})$  for which  $P_m^{2\nu}(\Delta m_{31}^2, \theta_{13}) = 1$ , and thus two regions in  $\Delta m_{31}^2/E - \sin^2 2\theta_{13}$  plane where  $P_m^{2\nu}(\Delta m_{31}^2, \theta_{13}) \gtrsim 0.5$ . For  $\Delta m_{31}^2 = 2.4 \times 10^{-3} \text{ eV}^2$  and nadir angle, e.g.,  $\theta_n = 0$  (Earth center crossing neutrinos), we have  $P_m^{2\nu}(\Delta m_{31}^2, \theta_{13}) = 1$  at  $(E, \sin^2 2\theta_{13}) = (3.3 \text{ GeV}, 0.034)$  and  $(5.0 \text{ GeV}, 0.15)$ . At the same time for  $E = 3.3 \text{ GeV}$  (5.0 GeV), the probability  $P_m^{2\nu}(\Delta m_{31}^2, \theta_{13}) \gtrsim 0.5$  for the values of  $\sin^2 2\theta_{13}$  from the interval  $0.02 \lesssim \sin^2 2\theta_{13} \lesssim 0.10$  ( $0.04 \lesssim \sin^2 2\theta_{13} \lesssim 0.26$ ). Similar results hold for neutrinos crossing the Earth core along the trajectories with  $\theta_n \neq 0$  (for further details see the last article in Ref. 81; see also the last article in Ref. 82).

The mantle-core enhancement of  $P_m^{2\nu}$  (or  $\bar{P}_m^{2\nu}$ ) is relevant, in particular, for the searches of sub-dominant  $\nu_{e(\mu)} \rightarrow \nu_{\mu(e)}$  (or  $\bar{\nu}_{e(\mu)} \rightarrow \bar{\nu}_{\mu(e)}$ ) oscillations of atmospheric neutrinos having energies  $E \gtrsim 2 \text{ GeV}$  and crossing the Earth core on the way to the detector (see Ref. 75 to Ref. 82 and the references quoted therein). The effects of Earth matter on the oscillations of atmospheric and accelerator neutrinos have not been observed so far. At present there are no compelling evidences for oscillations of the atmospheric  $\nu_e$  and/or  $\bar{\nu}_e$ .

The expression for the probability of the  $\nu_e \rightarrow \nu_\mu$  oscillations taking place in the Earth mantle in the case of 3-neutrino mixing, in which both neutrino mass squared differences  $\Delta m_{21}^2$  and  $\Delta m_{31}^2$  contribute and the CP violation effects due to the Dirac phase in the neutrino mixing matrix are taken into account, has the following

form in the constant density approximation and keeping terms up to second order in the two small parameters  $|\alpha| \equiv |\Delta m_{21}^2|/|\Delta m_{31}^2| \ll 1$  and  $\sin^2 \theta_{13} \ll 1$  [84]:

$$P_m^{3\nu \text{ man}}(\nu_e \rightarrow \nu_\mu) \cong P_0 + P_{\sin \delta} + P_{\cos \delta} + P_3. \quad (13.45)$$

Here

$$P_0 = \sin^2 \theta_{23} \frac{\sin^2 2\theta_{13}}{(A-1)^2} \sin^2[(A-1)\Delta]$$

$$P_3 = \alpha^2 \cos^2 \theta_{23} \frac{\sin^2 2\theta_{12}}{A^2} \sin^2(A\Delta), \quad (13.46)$$

$$P_{\sin \delta} = \alpha \frac{8 J_{CP}}{A(1-A)} (\sin \Delta) (\sin A\Delta) (\sin[(1-A)\Delta]), \quad (13.47)$$

$$P_{\cos \delta} = \alpha \frac{8 J_{CP} \cot \delta}{A(1-A)} (\cos \Delta) (\sin A\Delta) (\sin[(1-A)\Delta]), \quad (13.48)$$

where

$$\alpha = \frac{\Delta m_{21}^2}{\Delta m_{31}^2}, \quad \Delta = \frac{\Delta m_{31}^2 L}{4E}, \quad A = \sqrt{2} G_F N_e^{man} \frac{2E}{\Delta m_{31}^2}, \quad (13.49)$$

and  $\cot \delta = J_{CP}^{-1} \text{Re}(U_{\mu 3} U_{e 3}^* U_{e 2} U_{\mu 2}^*)$ ,  $J_{CP} = \text{Im}(U_{\mu 3} U_{e 3}^* U_{e 2} U_{\mu 2}^*)$ . The analytic expression for  $P_m^{3\nu \text{ man}}(\nu_e \rightarrow \nu_\mu)$  given above is valid for [84] neutrino path lengths in the mantle ( $L \leq 10660$  km) satisfying  $L \lesssim 10560$  km  $E[\text{GeV}] (7.6 \times 10^{-5} \text{ eV}^2 / \Delta m_{21}^2)$ , and energies  $E \gtrsim 0.34$  GeV  $(\Delta m_{21}^2 / 7.6 \times 10^{-5} \text{ eV}^2) (1.4 \text{ cm}^{-3} N_A / N_e^{man})$ . The expression for the  $\bar{\nu}_e \rightarrow \bar{\nu}_\mu$  oscillation probability can be obtained formally from that for  $P_m^{3\nu \text{ man}}(\nu_e \rightarrow \nu_\mu)$  by making the changes  $A \rightarrow -A$  and  $J_{CP} \rightarrow -J_{CP}$ , with  $J_{CP} \cot \delta \equiv \text{Re}(U_{\mu 3} U_{e 3}^* U_{e 2} U_{\mu 2}^*)$  remaining unchanged. The term  $P_{\sin \delta}$  in  $P_m^{3\nu \text{ man}}(\nu_e \rightarrow \nu_\mu)$  would be equal to zero if the Dirac phase in the neutrino mixing matrix  $U$  possesses a CP-conserving value. Even in this case, however, we have  $A_{CP}^{(\mu e) \text{ man}} \equiv (P_m^{3\nu \text{ man}}(\nu_e \rightarrow \nu_\mu) - P_m^{3\nu \text{ man}}(\bar{\nu}_e \rightarrow \bar{\nu}_\mu)) \neq 0$  due to the effects of the Earth matter. It will be important to experimentally disentangle the effects of the Earth matter and of  $J_{CP}$  in  $A_{CP}^{(\mu e) \text{ man}}$ : this will allow to get information about the Dirac CP violation phase in  $U$ . In the vacuum limit of  $N_e^{man} = 0$  ( $A = 0$ ) we have  $A_{CP}^{(\mu e) \text{ man}} = A_{CP}^{(\mu e)}$  (see Eq. (13.18)) and only the term  $P_{\sin \delta}$  contributes to the asymmetry  $A_{CP}^{(\mu e)}$ .

### 13.3.2. Oscillations of solar neutrinos :

Consider next the oscillations of solar  $\nu_e$  while they propagate from the central part of the Sun, where they are produced, to the surface of the Sun [23,74] (see also Ref. 22 and, *e.g.*, Ref. 85). Details concerning the production, spectrum, magnitude and particularities of the solar neutrino flux, the methods of detection of solar neutrinos, description of solar neutrino experiments and of the data they provided will be discussed in the next section (see also Ref. 86). The electron number density  $N_e$  changes considerably along the neutrino path in the Sun: it decreases monotonically from the value of  $\sim 100 \text{ cm}^{-3} N_A$  in the center of the Sun to 0 at the surface of the Sun. According to the contemporary solar models (see, *e.g.*, Ref. [86,87]),  $N_e$  decreases approximately exponentially in the radial direction towards the surface of the Sun:

$$N_e(t) = N_e(t_0) \exp\left\{-\frac{t-t_0}{r_0}\right\}, \quad (13.50)$$

where  $(t-t_0) \cong d$  is the distance traveled by the neutrino in the Sun,  $N_e(t_0)$  is the electron number density at the point of  $\nu_e$  production in the Sun,  $r_0$  is the scale-height of the change of  $N_e(t)$  and one has [86,87]  $r_0 \sim 0.1 R_\odot$ .

Consider the case of 2-neutrino mixing, Eq. (13.34). Obviously, if  $N_e$  changes with  $t$  (or equivalently with the distance) along the neutrino trajectory, the matter-eigenstates, their energies, the mixing angle and the oscillation length in matter, become, through their dependence on  $N_e$ , also functions of  $t$ :  $|\nu_{1,2}^m\rangle \equiv |\nu_{1,2}^m(t)\rangle$ ,  $E_{1,2}^m = E_{1,2}^m(t)$ ,  $\theta_m = \theta_m(t)$  and  $L_m = L_m(t)$ . It is not difficult to understand qualitatively the possible behavior of the neutrino system when solar neutrinos propagate from the center to the surface of the

Sun if one realizes that one is dealing effectively with a two-level system whose Hamiltonian depends on time and admits ‘‘jumps’’ from one level to the other (see Eq. (13.32)). Consider the case of  $\Delta m^2 \cos 2\theta > 0$ . Let us assume first for simplicity that the electron number density at the point of a solar  $\nu_e$  production in the Sun is much bigger than the resonance density,  $N_e(t_0) \gg N_e^{res}$ . Actually, this is one of the cases relevant to the solar neutrinos. In this case we have  $\theta_m(t_0) \cong \pi/2$  and the state of the electron neutrino in the initial moment of the evolution of the system practically coincides with the heavier of the two matter-eigenstates:

$$|\nu_e\rangle \cong |\nu_2^m(t_0)\rangle. \quad (13.51)$$

Thus, at  $t_0$  the neutrino system is in a state corresponding to the ‘‘level’’ with energy  $E_2^m(t_0)$ . When neutrinos propagate to the surface of the Sun they cross a layer of matter in which  $N_e = N_e^{res}$ : in this layer the difference between the energies of the two ‘‘levels’’ ( $E_2^m(t) - E_1^m(t)$ ) has a minimal value on the neutrino trajectory (Eq. (13.37) and Eq. (13.39)). Correspondingly, the evolution of the neutrino system can proceed basically in two ways. First, the system can stay on the ‘‘level’’ with energy  $E_2^m(t)$ , *i.e.*, can continue to be in the state  $|\nu_2^m(t)\rangle$  up to the final moment  $t_s$ , when the neutrino reaches the surface of the Sun. At the surface of the Sun  $N_e(t_s) = 0$  and therefore  $\theta_m(t_s) = \theta$ ,  $|\nu_{1,2}^m(t_s)\rangle \equiv |\nu_{1,2}\rangle$  and  $E_{1,2}^m(t_s) = E_{1,2}$ . Thus, in this case the state describing the neutrino system at  $t_0$  will evolve continuously into the state  $|\nu_2\rangle$  at the surface of the Sun. Using Eq. (13.29) with  $l = e$  and  $x = \mu$ , it is easy to obtain the probabilities to find  $\nu_e$  and  $\nu_\mu$  at the surface of the Sun:

$$P(\nu_e \rightarrow \nu_e; t_s, t_0) \cong |\langle \nu_e | \nu_2 \rangle|^2 = \sin^2 \theta$$

$$P(\nu_e \rightarrow \nu_\mu; t_s, t_0) \cong |\langle \nu_\mu | \nu_2 \rangle|^2 = \cos^2 \theta. \quad (13.52)$$

It is clear that under the assumption made and if  $\sin^2 \theta \ll 1$ , practically a total  $\nu_e \rightarrow \nu_\mu$  conversion is possible. This type of evolution of the neutrino system and the  $\nu_e \rightarrow \nu_\mu$  transitions taking place during the evolution, are called [23] ‘‘adiabatic.’’ They are characterized by the fact that the probability of the ‘‘jump’’ from the upper ‘‘level’’ (having energy  $E_2^m(t)$ ) to the lower ‘‘level’’ (with energy  $E_1^m(t)$ ),  $P'$ , or equivalently the probability of the  $\nu_2^m(t_0) \rightarrow \nu_1^m(t_s)$  transition,  $P' \equiv P'(\nu_2^m(t_0) \rightarrow \nu_1^m(t_s))$ , on the whole neutrino trajectory is negligible:

$$P' \equiv P'(\nu_2^m(t_0) \rightarrow \nu_1^m(t_s)) \cong 0 : \text{adiabatic transitions}. \quad (13.53)$$

The second possibility is realized if in the resonance region, where the two ‘‘levels’’ approach each other closest the system ‘‘jumps’’ from the upper ‘‘level’’ to the lower ‘‘level’’ and after that continues to be in the state  $|\nu_1^m(t)\rangle$  until the neutrino reaches the surface of the Sun. Evidently, now we have  $P' \equiv P'(\nu_2^m(t_0) \rightarrow \nu_1^m(t_s)) \sim 1$ . In this case the neutrino system ends up in the state  $|\nu_1^m(t_s)\rangle \equiv |\nu_1\rangle$  at the surface of the Sun and

$$P(\nu_e \rightarrow \nu_e; t_s, t_0) \cong |\langle \nu_e | \nu_1 \rangle|^2 = \cos^2 \theta$$

$$P(\nu_e \rightarrow \nu_\mu; t_s, t_0) \cong |\langle \nu_\mu | \nu_1 \rangle|^2 = \sin^2 \theta. \quad (13.54)$$

Obviously, if  $\sin^2 \theta \ll 1$ , practically no transitions of the solar  $\nu_e$  into  $\nu_\mu$  will occur. The considered regime of evolution of the neutrino system and the corresponding  $\nu_e \rightarrow \nu_\mu$  transitions are usually referred to as ‘‘extremely nonadiabatic.’’

Clearly, the value of the ‘‘jump’’ probability  $P'$  plays a crucial role in the the  $\nu_e \rightarrow \nu_\mu$  transitions: it fixes the type of the transition and determines to a large extent the  $\nu_e \rightarrow \nu_\mu$  transition probability [74,88,89]. We have considered above two limiting cases. Obviously, there exists a whole spectrum of possibilities since  $P'$  can have any value from 0 to  $\cos^2 \theta$  [90,91]. In general, the transitions are called ‘‘nonadiabatic’’ if  $P'$  is non-negligible.

Numerical studies have shown [23] that solar neutrinos can undergo both adiabatic and nonadiabatic  $\nu_e \rightarrow \nu_\mu$  transitions in the Sun and the matter effects can be substantial in the solar neutrino oscillations for  $10^{-8} \text{ eV}^2 \lesssim \Delta m^2 \lesssim 10^{-4} \text{ eV}^2$ ,  $10^{-4} \lesssim \sin^2 2\theta < 1.0$ .

The condition of adiabaticity of the solar  $\nu_e$  transitions in Sun can be written as [74,88]

$$\gamma(t) \equiv \sqrt{2} G_F \frac{(N_e^{res})^2}{|N_e(t)|} \tan^2 2\theta \left(1 + \tan^{-2} 2\theta_m(t)\right)^{\frac{3}{2}} \gg 1$$

adiabatic transitions, (13.55)

while if  $\gamma(t) \lesssim 1$  the transitions are nonadiabatic (see also Ref. 91), where  $\dot{N}_e(t) \equiv \frac{d}{dt} N_e(t)$ . Condition in Eq. (13.55) implies that the  $\nu_e \rightarrow \nu_{\mu(\tau)}$  transitions in the Sun will be adiabatic if  $N_e(t)$  changes sufficiently slowly along the neutrino path. In order for the transitions to be adiabatic, condition in Eq. (13.55) has to be fulfilled at any point of the neutrino's path in the Sun.

Actually, the system of evolution equations Eq. (13.32) can be solved exactly for  $N_e$  changing exponentially, Eq. (13.50), along the neutrino path in the Sun [90,92]. More specifically, the system in Eq. (13.32) is equivalent to one second order differential equation (with appropriate initial conditions). The latter can be shown [93] to coincide in form, in the case of  $N_e$  given by Eq. (13.50), with the Schroedinger equation for the radial part of the nonrelativistic wave function of the Hydrogen atom [94]. On the basis of the exact solution, which is expressed in terms of confluent hypergeometric functions, it was possible to derive a complete, simple and very accurate analytic description of the matter-enhanced transitions of solar neutrinos in the Sun for any values of  $\Delta m^2$  and  $\theta$  [22,90,91,95,96] (see also Refs. [23,74,89,97,98]).

The probability that a  $\nu_e$ , produced at time  $t_0$  in the central part of the Sun, will not transform into  $\nu_{\mu(\tau)}$  on its way to the surface of the Sun (reached at time  $t_s$ ) is given by

$$P_{\odot}^{2\nu}(\nu_e \rightarrow \nu_e; t_s, t_0) = \bar{P}_{\odot}^{2\nu}(\nu_e \rightarrow \nu_e; t_s, t_0) + \text{Oscillating terms.}$$

(13.56)

Here

$$\bar{P}_{\odot}^{2\nu}(\nu_e \rightarrow \nu_e; t_s, t_0) \equiv \bar{P}_{\odot} = \frac{1}{2} + \left(\frac{1}{2} - P'\right) \cos 2\theta_m(t_0) \cos 2\theta,$$

(13.57)

is the average survival probability for  $\nu_e$  having energy  $E \cong p$  [89], where

$$P' = \frac{\exp\left[-2\pi\tau_0 \frac{\Delta m^2}{2E} \sin^2 \theta\right] - \exp\left[-2\pi\tau_0 \frac{\Delta m^2}{2E}\right]}{1 - \exp\left[-2\pi\tau_0 \frac{\Delta m^2}{2E}\right]},$$

(13.58)

is [90] the ‘‘jump’’ probability for exponentially varying  $N_e$ , and  $\theta_m(t_0)$  is the mixing angle in matter at the point of  $\nu_e$  production [97]. The expression for  $\bar{P}_{\odot}^{2\nu}(\nu_e \rightarrow \nu_e; t_s, t_0)$  with  $P'$  given by Eq. (13.58) is valid for  $\Delta m^2 > 0$ , but for both signs of  $\cos 2\theta \neq 0$  [90,98]; it is valid for any given value of the distance along the neutrino trajectory and does not take into account the finite dimensions of the region of  $\nu_e$  production in the Sun. This can be done by integrating over the different neutrino paths, *i.e.*, over the region of  $\nu_e$  production.

The oscillating terms in the probability  $P_{\odot}^{2\nu}(\nu_e \rightarrow \nu_e; t_s, t_0)$  [95,93] were shown [96] to be strongly suppressed for  $\Delta m^2 \gtrsim 10^{-7} \text{ eV}^2$  by the various averagings one has to perform when analyzing the solar neutrino data. The current solar neutrino and KamLAND data suggest that  $\Delta m^2 \cong 7.6 \times 10^{-5} \text{ eV}^2$ . For  $\Delta m^2 \gtrsim 10^{-7} \text{ eV}^2$ , the averaging over the region of neutrino production in the Sun *etc.* renders negligible all interference terms which appear in the probability of  $\nu_e$  survival due to the  $\nu_e \leftrightarrow \nu_{\mu(\tau)}$  oscillations in vacuum taking place on the way of the neutrinos from the surface of the Sun to the surface of the Earth. Thus, the probability that  $\nu_e$  will remain  $\nu_e$  while it travels from the central part of the Sun to the surface of the Earth is effectively equal to the probability of survival of the  $\nu_e$  while it propagates from the central part to the surface of the Sun and is given by the average probability  $\bar{P}_{\odot}(\nu_e \rightarrow \nu_e; t_s, t_0)$  (determined by Eq. (13.57) and Eq. (13.58)).

If the solar  $\nu_e$  transitions are adiabatic ( $P' \cong 0$ ) and  $\cos 2\theta_m(t_0) \cong -1$  (*i.e.*,  $N_e(t_0)/|N_e^{res}| \gg 1, |\tan 2\theta|$ ), the  $\nu_e$  are born ‘‘above’’ (in  $N_e$ ) the resonance region), one has [23]

$$\bar{P}_{\odot}^{2\nu}(\nu_e \rightarrow \nu_e; t_s, t_0) \cong \frac{1}{2} - \frac{1}{2} \cos 2\theta. \quad (13.59)$$

The regime under discussion is realised for  $\sin^2 2\theta \cong 0.8$  (suggested by the data, Section 13.4), if  $E/\Delta m^2$  lies approximately in the range  $(2 \times 10^4 - 3 \times 10^7) \text{ MeV/eV}^2$  (see Ref. 91). This result is relevant for the interpretation of the Super-Kamiokande and SNO solar neutrino data. We see that depending on the sign of  $\cos 2\theta \neq 0$ ,  $\bar{P}_{\odot}^{2\nu}(\nu_e \rightarrow \nu_e)$  is either bigger or smaller than 1/2. It follows from the solar neutrino data that in the range of validity (in  $E/\Delta m^2$ ) of Eq. (13.59) we have  $\bar{P}_{\odot}^{2\nu}(\nu_e \rightarrow \nu_e) \cong 0.3$ . Thus, the possibility of  $\cos 2\theta \leq 0$  is ruled out by the data. Given the choice  $\Delta m^2 > 0$  we made, the data imply that  $\Delta m^2 \cos 2\theta > 0$ .

If  $E/\Delta m^2$  is sufficiently small so that  $N_e(t_0)/|N_e^{res}| \ll 1$ , we have  $P' \cong 0$ ,  $\theta_m(t_0) \cong \theta$  and the oscillations take place in the Sun as in vacuum [23]:

$$\bar{P}_{\odot}^{2\nu}(\nu_e \rightarrow \nu_e; t_s, t_0) \cong 1 - \frac{1}{2} \sin^2 2\theta, \quad (13.60)$$

which is the average two-neutrino vacuum oscillation probability. This expression describes with good precision the transitions of the solar  $\nu_e$  neutrinos (Section 13.4). The extremely nonadiabatic  $\nu_e$  transitions in the Sun, characterised by  $\gamma(t) \ll 1$ , are also described by the average vacuum oscillation probability (Eq. (13.60)) (for  $\Delta m^2 \cos 2\theta > 0$  in this case we have (see *e.g.*, Refs. [90,91])  $\cos 2\theta_m(t_0) \cong -1$  and  $P' \cong \cos^2 \theta$ ).

The probability of  $\nu_e$  survival in the case 3-neutrino mixing takes a simple form for  $|\Delta m_{31}^2| \cong 2.4 \times 10^{-3} \text{ eV}^2 \gg |\Delta m_{21}^2|$ . Indeed, for the energies of solar neutrinos  $E \lesssim 10 \text{ MeV}$ ,  $N_e^{res}$  corresponding to  $|\Delta m_{31}^2|$  satisfies  $N_e^{res} \gtrsim 10^3 \text{ cm}^{-3} N_A$  and is by a factor of 10 bigger than  $N_e$  in the center of the Sun. As a consequence, the oscillations due to  $\Delta m_{31}^2$  proceed as in vacuum. The oscillation length associated with  $|\Delta m_{31}^2|$  satisfies  $L_{31}^{\nu} \lesssim 10 \text{ km} \ll \Delta R$ ,  $\Delta R$  being the dimension of the region of  $\nu_e$  production in the Sun. We have for the different components of the solar  $\nu_e$  flux [86]  $\Delta R \cong (0.04 - 0.20) R_{\odot}$ . Therefore the averaging over  $\Delta R$  strongly suppresses the oscillations due to  $\Delta m_{31}^2$  and we get [78,99]:

$$P_{\odot}^{3\nu} \cong \sin^4 \theta_{13} + \cos^4 \theta_{13} P_{\odot}^{2\nu}(\Delta m_{21}^2, \theta_{12}; N_e \cos^2 \theta_{13}), \quad (13.61)$$

where  $P_{\odot}^{2\nu}(\Delta m_{21}^2, \theta_{12}; N_e \cos^2 \theta_{13})$  is given by Eq. (13.56) to Eq. (13.58) in which  $\Delta m^2 = \Delta m_{21}^2$ ,  $\theta = \theta_{12}$  and the solar  $e^-$  number density  $N_e$  is replaced by  $N_e \cos^2 \theta_{13}$ . Thus, the solar  $\nu_e$  transitions observed by the Super-Kamiokande and SNO experiments are described approximately by:

$$P_{\odot}^{3\nu} \cong \sin^4 \theta_{13} + \cos^4 \theta_{13} \sin^2 \theta_{12}. \quad (13.62)$$

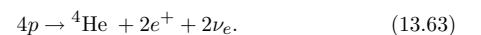
The data show that  $P_{\odot}^{3\nu} \cong 0.3$ , which is a strong evidence for matter effects in the solar  $\nu_e$  transitions [100] since in the case of oscillations in vacuum  $P_{\odot}^{3\nu} \cong \sin^4 \theta_{13} + (1 - 0.5 \sin^2 2\theta_{12}) \cos^4 \theta_{13} \gtrsim 0.49$ , where we have used  $\sin^2 \theta_{13} \lesssim 0.040$  and  $\sin^2 2\theta_{12} \lesssim 0.93$  (see Section 13.7).

## 13.4. Measurements of $\Delta m_{\odot}^2$ and $\theta_{\odot}$

### 13.4.1. Solar neutrino observations :

Observation of solar neutrinos directly addresses the theory of stellar structure and evolution, which is the basis of the standard solar model (SSM). The Sun as a well-defined neutrino source also provides extremely important opportunities to investigate nontrivial neutrino properties such as nonzero mass and mixing, because of the wide range of matter density and the great distance from the Sun to the Earth.

The solar neutrinos are produced by some of the fusion reactions in the pp chain or CNO cycle. The combined effect of these reactions is written as





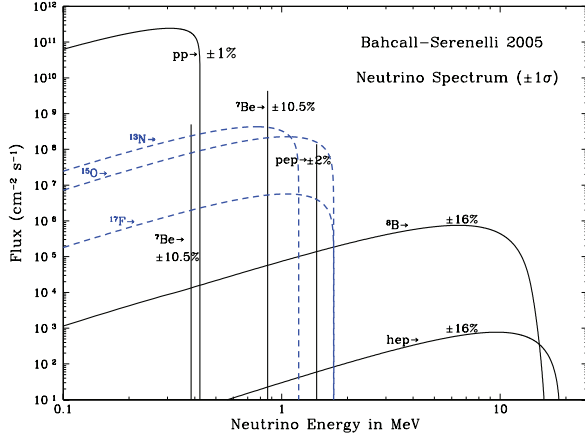


**Figure 13.2:** The solar neutrino spectrum predicted by the BS05(OP) standard solar model [101]. The neutrino fluxes are given in units of  $\text{cm}^{-2}\text{s}^{-1}\text{MeV}^{-1}$  for continuous spectra and  $\text{cm}^{-2}\text{s}^{-1}$  for line spectra. The numbers associated with the neutrino sources show theoretical errors of the fluxes. This figure is taken from the late John Bahcall's web site, <http://www.sns.ias.edu/~jnb/>.

Positrons annihilate with electrons. Therefore, when considering the solar thermal energy generation, a relevant expression is

$$4p + 2e^- \rightarrow {}^4\text{He} + 2\nu_e + 26.73 \text{ MeV} - E_\nu, \quad (13.64)$$

where  $E_\nu$  represents the energy taken away by neutrinos, with an average value being  $\langle E_\nu \rangle \sim 0.6$  MeV. There have been efforts to calculate solar neutrino fluxes from these reactions on the basis of SSM. A variety of input information is needed in the evolutionary calculations. The most elaborate SSM calculations have been developed by Bahcall and his collaborators, who define their SSM as the solar model which is constructed with the best available physics and input data. Therefore, their SSM calculations have been rather frequently updated. SSM's labelled as BS05(OP) [101], BSB06(GS) and BSB06(AGS) [87], and BPS08(GS) and BPS08(AGS) [102] represent some of recent model calculations. Here, "OP" means that newly calculated radiative opacities from the "Opacity Project" are used. The later models are also calculated with OP opacities. "GS" and "AGS" refer to old and new determinations of solar abundances of heavy elements. There are significant differences between the old, higher heavy element abundances (GS) and the new, lower heavy element abundances (AGS). The models with GS are consistent with helioseismological data, but the models with AGS are not.

The prediction of the BPS08(GS) model for the fluxes from neutrino-producing reactions is given in Table 13.2. Fig. 13.2 shows the solar-neutrino spectra calculated with the BS05(OP) model which is similar to the BPS08(GS) model. Here we note that in Ref. 103 the authors point out that electron capture on  ${}^{13}\text{N}$ ,  ${}^{15}\text{O}$ , and  ${}^{17}\text{F}$  produces line spectra of neutrinos, which have not been considered in the SSM calculations quoted above.

In 2011, a new SSM calculations [104] have been presented by A.M. Serenelli, W.C. Haxton, and C. Peña-Garay, by adopting the newly analyzed nuclear fusion cross sections. Their high metallicity SSM is labelled as SHP11(GS). For the same solar abundances as used in Ref. 101 and Ref. 87, the most significant change is a decrease of  ${}^8\text{B}$  flux by  $\sim 5\%$ .

So far, solar neutrinos have been observed by chlorine (Homestake) and gallium (SAGE, GALLEX, and GNO) radiochemical detectors and water Cherenkov detectors using light water (Kamiokande and Super-Kamiokande) and heavy water (SNO). Recently, a liquid scintillation detector (Borexino) successfully observed low energy solar neutrinos.

A pioneering solar neutrino experiment by Davis and collaborators at Homestake using the  ${}^{37}\text{Cl} - {}^{37}\text{Ar}$  method proposed by Pontecorvo [105] started in the late 1960's. This experiment exploited

**Table 13.2:** Neutrino-producing reactions in the Sun (first column) and their abbreviations (second column). The neutrino fluxes predicted by the BPS08(GS) model [102] are listed in the third column.

Reaction	Abbr.	Flux ( $\text{cm}^{-2} \text{s}^{-1}$ )
$pp \rightarrow d e^+ \nu$	<i>pp</i>	$5.97(1 \pm 0.006) \times 10^{10}$
$pe^- p \rightarrow d \nu$	<i>pep</i>	$1.41(1 \pm 0.011) \times 10^8$
${}^3\text{He} p \rightarrow {}^4\text{He} e^+ \nu$	<i>hep</i>	$7.90(1 \pm 0.15) \times 10^3$
${}^7\text{Be} e^- \rightarrow {}^7\text{Li} \nu + (\gamma)$	<i><math>{}^7\text{Be}</math></i>	$5.07(1 \pm 0.06) \times 10^9$
${}^8\text{B} \rightarrow {}^8\text{Be}^* e^+ \nu$	<i><math>{}^8\text{B}</math></i>	$5.94(1 \pm 0.11) \times 10^6$
${}^{13}\text{N} \rightarrow {}^{13}\text{C} e^+ \nu$	<i><math>{}^{13}\text{N}</math></i>	$2.88(1 \pm 0.15) \times 10^8$
${}^{15}\text{O} \rightarrow {}^{15}\text{N} e^+ \nu$	<i><math>{}^{15}\text{O}</math></i>	$2.15(1^{+0.17}_{-0.16}) \times 10^8$
${}^{17}\text{F} \rightarrow {}^{17}\text{O} e^+ \nu$	<i><math>{}^{17}\text{F}</math></i>	$5.82(1^{+0.19}_{-0.17}) \times 10^6$

$\nu_e$  absorption on  ${}^{37}\text{Cl}$  nuclei followed by the produced  ${}^{37}\text{Ar}$  decay through orbital  $e^-$  capture,

$$\nu_e + {}^{37}\text{Cl} \rightarrow {}^{37}\text{Ar} + e^- \quad (\text{threshold } 814 \text{ keV}). \quad (13.65)$$

The  ${}^{37}\text{Ar}$  atoms produced are radioactive, with a half life ( $\tau_{1/2}$ ) of 34.8 days. After an exposure of the detector for two to three times  $\tau_{1/2}$ , the reaction products were chemically extracted and introduced into a low-background proportional counter, where they were counted for a sufficiently long period to determine the exponentially decaying signal and a constant background. Solar-model calculations predict that the dominant contribution in the chlorine experiment came from  ${}^8\text{B}$  neutrinos, but  ${}^7\text{Be}$ , *pep*,  ${}^{13}\text{N}$ , and  ${}^{15}\text{O}$  neutrinos also contributed (for notations, refer to Table 13.2).

From the very beginning of the solar-neutrino observation [106], it was recognized that the observed flux was significantly smaller than the SSM prediction, provided nothing happens to the electron neutrinos after they are created in the solar interior. This deficit has been called "the solar-neutrino problem."

**Table 13.3:** Results from radiochemical solar-neutrino experiments. The predictions of a recent standard solar model BPS08(GS) are also shown. The first and the second errors in the experimental results are the statistical and systematic errors, respectively. SNU (Solar Neutrino Unit) is defined as  $10^{-36}$  neutrino captures per atom per second.

	${}^{37}\text{Cl} \rightarrow {}^{37}\text{Ar}$ (SNU)	${}^{71}\text{Ga} \rightarrow {}^{71}\text{Ge}$ (SNU)
Homestake [4]	$2.56 \pm 0.16 \pm 0.16$	–
GALLEX [8]	–	$77.5 \pm 6.2^{+4.3}_{-4.7}$
GALLEX- Reanalysis [107]	–	$73.4^{+6.1+3.7}_{-6.0-4.1}$
GNO [9]	–	$62.9^{+5.5}_{-5.3} \pm 2.5$
GNO+GALLEX [9]	–	$69.3 \pm 4.1 \pm 3.6$
GNO+GALLEX- Reanalysis [107]	–	$67.6^{+4.0+3.2}_{-4.0-3.2}$
SAGE [6]	–	$65.4^{+3.1+2.6}_{-3.0-2.8}$
SSM [BPS08(GS)] [102]	$8.46^{+0.87}_{-0.88}$	$127.9^{+8.1}_{-8.2}$

Gallium experiments (GALLEX and GNO at Gran Sasso in Italy and SAGE at Baksan in Russia) utilize the reaction

$$\nu_e + {}^{71}\text{Ga} \rightarrow {}^{71}\text{Ge} + e^- \quad (\text{threshold } 233 \text{ keV}). \quad (13.66)$$

They are sensitive to the most abundant *pp* solar neutrinos. The solar-model calculations predict that more than 80% of the capture



rate in gallium is due to low energy  $pp$  and  ${}^7\text{Be}$  solar neutrinos with the  $pp$  rate being about twice the  ${}^7\text{Be}$  rate. SAGE reported the first results in 1991 [108]. They observed the capture rate to be  $20_{-20}^{+15} \pm 32$  SNU, or a 90% confidence-level upper limit of 79 SNU. In 1992, GALLEX reported the observed capture rate of  $83 \pm 19 \pm 8$  SNU [7]. It was the first evidence for low-energy solar-neutrino observation. Later, SAGE observed similar flux [109] to GALLEX. The latest SAGE results are published in Ref. 6. The GALLEX Collaboration finished observations in early 1997 [8,107]. Since April, 1998, a newly defined collaboration, GNO (Gallium Neutrino Observatory) continued the observations until April 2003. The GNO results are published in Ref. 9. The GNO + GALLEX joint analysis results are also presented in Ref. 9 and Ref. 107. The results from radiochemical solar neutrino experiments are shown in Table 13.3.

In 1987, the Kamiokande experiment in Japan succeeded in real-time solar neutrino observation, utilizing  $\nu e$  scattering,

$$\nu_x + e^- \rightarrow \nu_x + e^-, \quad (13.67)$$

in a large water-Cherenkov detector. This experiment takes advantage of the directional correlation between the incoming neutrino and the recoil electron. This feature greatly helps the clear separation of the solar-neutrino signal from the background. The Kamiokande result gave the first direct evidence that neutrinos come from the direction of the Sun [110]. Later, the high-statistics Super-Kamiokande experiment [111–114] with a 50-kton water Cherenkov detector replaced the Kamiokande experiment. Due to the high thresholds (7 MeV in Kamiokande and 5 MeV at present in Super-Kamiokande) the experiments observe pure  ${}^8\text{B}$  solar neutrinos. It should be noted that the reaction (Eq. (13.67)) is sensitive to all active neutrinos,  $x = e, \mu,$  and  $\tau$ . However, the sensitivity to  $\nu_\mu$  and  $\nu_\tau$  is much smaller than the sensitivity to  $\nu_e$ ,  $\sigma(\nu_{\mu,\tau}e) \approx 0.16 \sigma(\nu_e e)$ .

In 1999, a new real time solar-neutrino experiment, SNO (Sudbury Neutrino Observatory), in Canada started observation. This experiment used 1000 tons of ultra-pure heavy water ( $\text{D}_2\text{O}$ ) contained in a spherical acrylic vessel, surrounded by an ultra-pure  $\text{H}_2\text{O}$  shield. SNO measured  ${}^8\text{B}$  solar neutrinos via the charged-current (CC) and neutral-current (NC) reactions

$$\nu_e + d \rightarrow e^- + p + p \quad (\text{CC}), \quad (13.68)$$

and

$$\nu_x + d \rightarrow \nu_x + p + n \quad (\text{NC}), \quad (13.69)$$

as well as  $\nu e$  scattering, (Eq. (13.67)). The CC reaction, (Eq. (13.68)), is sensitive only to  $\nu_e$ , while the NC reaction, (Eq. (13.69)), is sensitive to all active neutrinos. This is a key feature to solve the solar neutrino problem. If it is caused by flavour transitions such as neutrino oscillations, the solar neutrino fluxes measured by CC and NC reactions would show a significant difference.

The  $Q$ -value of the CC reaction is  $-1.4$  MeV and the  $e^-$  energy is strongly correlated with the  $\nu_e$  energy. Thus, the CC reaction provides an accurate measure of the shape of the  ${}^8\text{B}$  neutrino spectrum. The contributions from the CC reaction and  $\nu e$  scattering can be distinguished by using different  $\cos \theta$  distributions, where  $\theta$  is the angle of the  $e^-$  momentum with respect to the Sun-Earth axis. While the  $\nu e$  scattering events have a strong forward peak, CC events have an approximate angular distribution of  $1 - 1/3 \cos \theta$ .

The neutrino energy threshold of the NC reaction is 2.2 MeV. In the pure  $\text{D}_2\text{O}$  [11,12], the signal of the NC reaction was neutron capture in deuterium, producing a 6.25-MeV  $\gamma$ -ray. In this case, the capture efficiency was low and the deposited energy was close to the detection threshold of 5 MeV. In order to enhance both the capture efficiency and the total  $\gamma$ -ray energy (8.6 MeV), 2 tons of NaCl were added to the heavy water in the second phase of the experiment [115]. Subsequently NaCl was removed and an array of  ${}^3\text{He}$  neutron counters were installed for the third phase measurement [116]. These neutron counters provided independent NC measurement with different systematics from that of the second phase, and thus strengthened the reliability of the NC measurement. The SNO experiment completed data acquisition in 2006. Recently, the SNO group presented the

results of Phase I and Phase II joint analysis [117] as well as the results of a combined analysis of all three phases [118].

Table 13.4 shows the  ${}^8\text{B}$  solar neutrino results from real time experiments. The standard solar model predictions are also shown. Table 13.4 includes the results from the SNO group's recent joint analysis of the SNO Phase I and Phase II data with the analysis threshold as low as 3.5 MeV (effective electron kinetic energy) and significantly improved systematic uncertainties [117]. Also, the recent result from a combined analysis of all three phases [118] is included. It is seen from these tables that the results from all the solar-neutrino experiments, except SNO's NC result, indicate significantly less flux than expected from the solar-model predictions.

**Table 13.4:**  ${}^8\text{B}$  solar neutrino results from real time experiments. The predictions of BPS08(GS) and SHP11(GS) standard solar models are also shown. The first and the second errors in the experimental results are the statistical and systematic errors, respectively.

	Reaction	${}^8\text{B}$ $\nu$ flux ( $10^6 \text{cm}^{-2}\text{s}^{-1}$ )
Kamiokande [5]	$\nu e$	$2.80 \pm 0.19 \pm 0.33$
Super-K I [112,114]	$\nu e$	$2.38 \pm 0.02 \pm 0.08$
Super-K II [113,114]	$\nu e$	$2.41 \pm 0.05_{-0.15}^{+0.16}$
Super-K III [114]	$\nu e$	$2.32 \pm 0.04 \pm 0.05$
SNO Phase I [12]	CC	$1.76_{-0.05}^{+0.06} \pm 0.09$
(pure $\text{D}_2\text{O}$ )	$\nu e$	$2.39_{-0.23}^{+0.24} \pm 0.12$
	NC	$5.09_{-0.43-0.43}^{+0.44+0.46}$
SNO Phase II [115]	CC	$1.68 \pm 0.06_{-0.09}^{+0.08}$
(NaCl in $\text{D}_2\text{O}$ )	$\nu e$	$2.35 \pm 0.22 \pm 0.15$
	NC	$4.94 \pm 0.21_{-0.34}^{+0.38}$
SNO Phase III [116]	CC	$1.67_{-0.04-0.08}^{+0.05+0.07}$
( ${}^3\text{He}$ counters)	$\nu e$	$1.77_{-0.21-0.10}^{+0.24+0.09}$
	NC	$5.54_{-0.31-0.34}^{+0.33+0.36}$
SNO Phase I+II [117]	NC	$5.140_{-0.158-0.117}^{+0.160+0.132}$
	$\Phi_{\text{B}}$ from fit to all reacts.	$5.046_{-0.152-0.123}^{+0.159+0.107}$
SNO Phase I+II+III [118]	$\Phi_{\text{B}}$ from fit to all reacts.	$5.25 \pm 0.16_{-0.13}^{+0.11}$
Borexino [123]	$\nu e$	$2.4 \pm 0.4 \pm 0.1$
SSM [BPS08(GS)] [102]	–	$5.94(1 \pm 0.11)$
SSM [SHP11(GS)] [104]	–	$5.58(1 \pm 0.14)$

Another real time solar neutrino experiment, Borexino at Gran Sasso in Italy, started solar neutrino observation in 2007. This experiment measures solar neutrinos via  $\nu e$  scattering in 300 tons of ultra-pure liquid scintillator. With a detection threshold as low as 250 keV, the flux of monochromatic 0.862 MeV  ${}^7\text{Be}$  solar neutrinos has been directly observed for the first time (see Table 13.5). The observed energy spectrum shows the characteristic Compton-edge over the background [119,120]. Borexino also reported an observation of null day-night asymmetry of the  ${}^7\text{Be}$  neutrino flux,  $A_{dn} = 2(R_N - R_D)/(R_N + R_D) = 0.001 \pm 0.012 \pm 0.007$  [121], where  $R_N$  and  $R_D$  are the night and day count rates of  ${}^7\text{Be}$  neutrinos.

Further, Borexino measured the flux of monochromatic 1.44 MeV  $pep$  solar neutrinos [122]. The absence of the  $pep$  solar neutrino signal is disfavored at 98% CL. The  $pep$  solar neutrino flux measured via  $\nu e$  scattering (calculated from the measured interaction rate and the expected one with the assumption of no neutrino oscillations and the SHP11(GS) SSM [104], both given in [122]) is shown in Table 13.6 and compared with the SSM predictions. Also, an upper limit of the “unoscillated” CNO solar neutrino flux is determined [122] as  $< 7.7 \times 10^8 \text{cm}^{-2}\text{s}^{-1}$  (95% CL) by assuming the MSW large mixing angle solution with  $\Delta m_{21}^2 = (7.6 \pm 0.2) \times 10^{-5} \text{eV}^2$  and

$\tan^2\theta_{12} = 0.47^{+0.05}_{-0.04}$  and the SHP11(GS) SSM prediction [104] for the  $pep$   $\nu$  flux.

Borexino also measured  $^8\text{B}$  solar neutrinos with an energy threshold of 3 MeV [123]. Measurements of low energy solar neutrinos are important not only to test the SSM further, but also to study the MSW effect over the energy region spanning from sub-MeV to 10 MeV.

**Table 13.5:**  $^7\text{Be}$  solar neutrino result from Borexino [120]. The predictions of BPS08(GS) and SHP11(GS) standard solar models are also shown.

	Reaction	$^7\text{Be}$ $\nu$ flux ( $10^9\text{cm}^{-2}\text{s}^{-1}$ )
Borexino [120]	$\nu e$	$3.10 \pm 0.15$
SSM [BPS08(GS)] [102]	–	$5.07(1 \pm 0.06)$
SSM [SHP11(GS)] [104]	–	$5.00(1 \pm 0.07)$

**Table 13.6:**  $pep$  solar neutrino result from Borexino [122]. The predictions of BPS08(GS) and SHP11(GS) standard solar models are also shown.

	Reaction	$pep$ $\nu$ flux ( $10^8\text{cm}^{-2}\text{s}^{-1}$ )
Borexino [122]	$\nu e$	$1.0 \pm 0.2$
SSM [BPS08(GS)] [102]	–	$1.41(1 \pm 0.011)$
SSM [SHP11(GS)] [104]	–	$1.44(1 \pm 0.012)$

### 13.4.2. Evidence for solar neutrino flavour conversion :

Solar neutrino experiments achieved remarkable progress in the past ten years, and the solar-neutrino problem, which had remained unsolved for more than 30 years, has been understood as due to neutrino flavour conversion. In 2001, the initial SNO CC result combined with the Super-Kamiokande's high-statistics  $\nu e$  elastic scattering result [124] provided direct evidence for flavour conversion of solar neutrinos [11]. Later, SNO's NC measurements further strengthened this conclusion [12,115,116]. From the salt-phase measurement [115], the fluxes measured with CC, ES, and NC events were obtained as

$$\phi_{\text{SNO}}^{\text{CC}} = (1.68 \pm 0.06^{+0.08}_{-0.09}) \times 10^6 \text{cm}^{-2}\text{s}^{-1}, \quad (13.70)$$

$$\phi_{\text{SNO}}^{\text{ES}} = (2.35 \pm 0.22 \pm 0.15) \times 10^6 \text{cm}^{-2}\text{s}^{-1}, \quad (13.71)$$

$$\phi_{\text{SNO}}^{\text{NC}} = (4.94 \pm 0.21^{+0.38}_{-0.34}) \times 10^6 \text{cm}^{-2}\text{s}^{-1}, \quad (13.72)$$

where the first errors are statistical and the second errors are systematic. In the case of  $\nu_e \rightarrow \nu_{\mu,\tau}$  transitions, Eq. (13.72) is a mixing-independent result and therefore tests solar models. It shows good agreement with the  $^8\text{B}$  solar-neutrino flux predicted by the solar model [101]. Fig. 13.3 shows the salt phase result of  $\phi(\nu_{\mu}$  or  $\tau)$  versus the flux of electron neutrinos  $\phi(\nu_e)$  and the 68%, 95%, and 99% joint probability contours. The flux of non- $\nu_e$  active neutrinos,  $\phi(\nu_{\mu}$  or  $\tau)$ , can be deduced from these results. It is

$$\phi(\nu_{\mu} \text{ or } \tau) = (3.26 \pm 0.25^{+0.40}_{-0.35}) \times 10^6 \text{cm}^{-2}\text{s}^{-1}. \quad (13.73)$$

The non-zero  $\phi(\nu_{\mu}$  or  $\tau)$  is strong evidence for neutrino flavor conversion. These results are consistent with those expected from the LMA (large mixing angle) solution of solar neutrino oscillation in matter [22,23] with  $\Delta m_{21}^2 \sim 5 \times 10^{-5} \text{eV}^2$  and  $\tan^2\theta_{12} \sim 0.45$ . However, with the SNO data alone, the possibility of other solutions cannot be excluded with sufficient statistical significance.

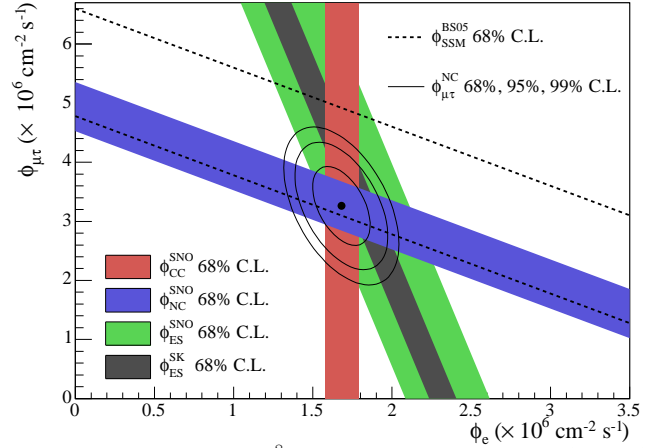


**Figure 13.3:** Fluxes of  $^8\text{B}$  solar neutrinos,  $\phi(\nu_e)$ , and  $\phi(\nu_{\mu}$  or  $\tau)$ , deduced from the SNO's CC, ES, and NC results of the salt phase measurement [115]. The Super-Kamiokande ES flux is from Ref. 125. The BS05(OP) standard solar model prediction [101] is also shown. The bands represent the  $1\sigma$  error. The contours show the 68%, 95%, and 99% joint probability for  $\phi(\nu_e)$  and  $\phi(\nu_{\mu}$  or  $\tau)$ . The figure is from Ref. 115.

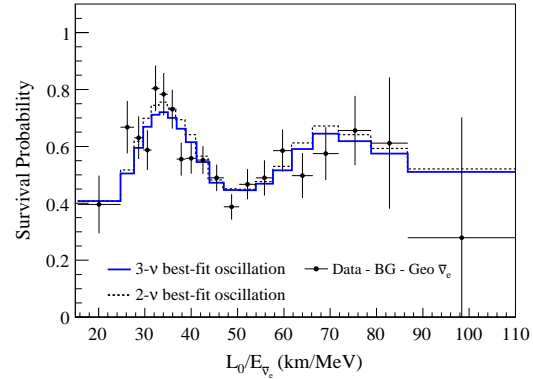


**Figure 14.4:** The ratio of the background and geoneutrino-subtracted  $\bar{\nu}_e$  spectrum to the predicted one without oscillations (survival probability) as a function of  $L_0/E$ , where  $L_0=180$  km. The histograms show the expected distributions based on the best-fit parameter values from the two- and three-flavor neutrino oscillation analyses. The figure is from Ref. 128.

### 13.4.3. KamLAND experiment :

KamLAND is a 1-kton ultra-pure liquid scintillator detector located at the old Kamiokande's site in Japan. The primary goal of the KamLAND experiment was a long-baseline (flux-weighted average distance of  $\sim 180$  km) neutrino oscillation studies using  $\bar{\nu}_e$ 's emitted from nuclear power reactors. The reaction  $\bar{\nu}_e + p \rightarrow e^+ + n$  is used to detect reactor  $\bar{\nu}_e$ 's and a delayed coincidence of the positron with a 2.2 MeV  $\gamma$ -ray from neutron capture on a proton is used to reduce the backgrounds. With the reactor  $\bar{\nu}_e$ 's energy spectrum ( $< 8$  MeV) and a prompt-energy analysis threshold of 2.6 MeV, this experiment has a sensitive  $\Delta m^2$  range down to  $\sim 10^{-5} \text{eV}^2$ . Therefore, if the LMA solution is the real solution of the solar neutrino problem, KamLAND should observe reactor  $\bar{\nu}_e$  disappearance, assuming CPT invariance.

The first KamLAND results [15] with 162 ton-yr exposure were reported in December 2002. The ratio of observed to expected (assuming no  $\bar{\nu}_e$  oscillations) number of events was

$$\frac{N_{\text{obs}} - N_{\text{BG}}}{N_{\text{NoOsc}}} = 0.611 \pm 0.085 \pm 0.041 \quad (13.74)$$

with obvious notation. This result showed clear evidence of an event deficit expected from neutrino oscillations. The 95% CL allowed

regions are obtained from the oscillation analysis with the observed event rates and positron spectrum shape. A combined global solar + KamLAND analysis showed that the LMA is a unique solution to the solar neutrino problem with  $> 5\sigma$  CL [126]. With increased statistics [16,127,128], KamLAND observed not only the distortion of the  $\bar{\nu}_e$  spectrum, but also for the first time the periodic feature of the  $\bar{\nu}_e$  survival probability expected from neutrino oscillations (see Fig. 13.4).

### 13.5. Measurements of $|\Delta m^2_{\Lambda}|$ and $\theta_{\Lambda}$

#### 13.5.1. Atmospheric neutrino results :

The first compelling evidence for the neutrino oscillation was presented by the Super-Kamiokande Collaboration in 1998 [13] from the observation of atmospheric neutrinos produced by cosmic-ray interactions in the atmosphere. The zenith-angle distributions of the  $\mu$ -like events which are mostly muon-neutrino and muon antineutrino initiated charged-current interactions, showed a clear deficit compared to the no-oscillation expectation. Note that a water Cherenkov detector cannot measure the charge of the final-state leptons, and therefore neutrino and antineutrino induced events cannot be discriminated. Neutrino events having their vertex in the 22.5 kton fiducial volume in Super-Kamiokande are classified into fully contained (FC) events and partially contained (PC) events. The FC events are required to have no activity in the anti-counter. Single-ring events have only one charged lepton which radiates Cherenkov light in the final state, and particle identification is particularly clean for single-ring FC events. A ring produced by an  $e$ -like ( $e^{\pm}, \gamma$ ) particle exhibits a more diffuse pattern than that produced by a  $\mu$ -like ( $\mu^{\pm}, \pi^{\pm}$ ) particle, since an  $e$ -like particle produces an electromagnetic shower and low-energy electrons suffer considerable multiple Coulomb scattering in water. All the PC events were assumed to be  $\mu$ -like since the PC events comprise a 98% pure charged-current  $\nu_{\mu}$  sample.

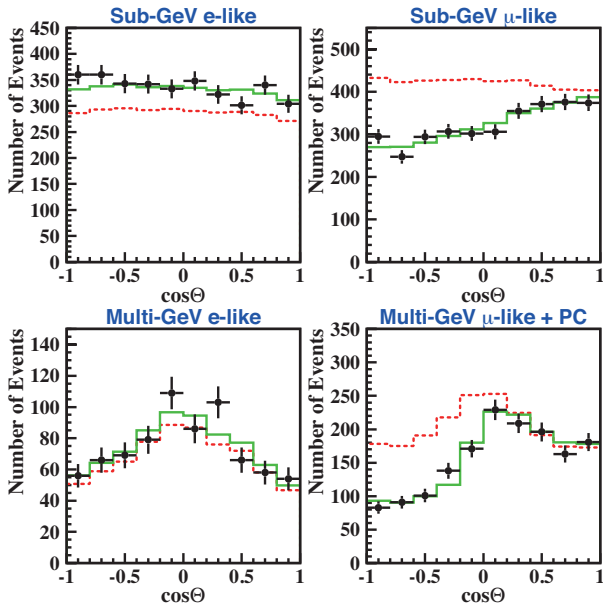


**Figure 13.5:** The zenith angle distributions for fully contained 1-ring  $e$ -like and  $\mu$ -like events with visible energy  $< 1.33$  GeV (sub-GeV) and  $> 1.33$  GeV (multi-GeV). For multi-GeV  $\mu$ -like events, a combined distribution with partially contained (PC) events is shown. The dotted histograms show the non-oscillated Monte Carlo events, and the solid histograms show the best-fit expectations for  $\nu_{\mu} \leftrightarrow \nu_{\tau}$  oscillations. (This figure is provided by the Super-Kamiokande Collab.)

Fig. 13.5 shows the zenith-angle distributions of  $e$ -like and  $\mu$ -like events from the SK-I measurement [129].  $\cos\theta = 1$  corresponds to the downward direction, while  $\cos\theta = -1$  corresponds to the upward

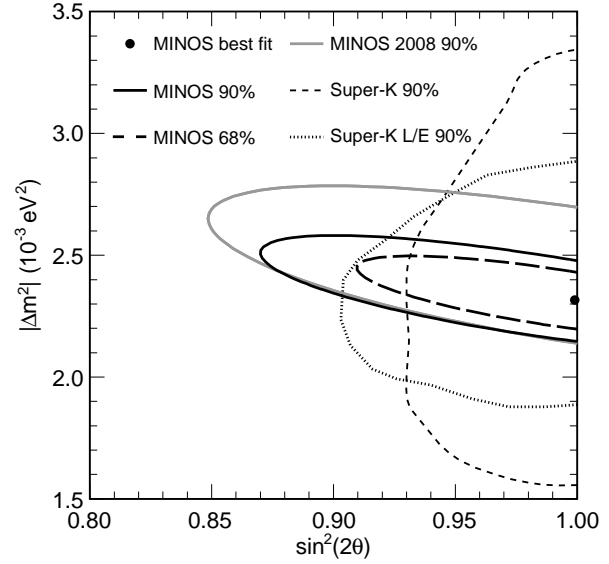


**Figure 13.6:** Allowed region for the  $\nu_{\mu} \leftrightarrow \nu_{\tau}$  oscillation parameters from the MINOS results published in 2011. The 68 % and 90 % CL allowed regions are shown together with the Super-Kamiokande and MINOS 2008 90% CL allowed regions. This figure is taken from Ref. 130.

direction. Events included in these plots are single-ring FC events subdivided into sub-GeV (visible energy  $< 1.33$  GeV) events and multi-GeV (visible energy  $> 1.33$  GeV) events. The zenith-angle distribution of the multi-GeV  $\mu$ -like events is shown combined with that of the PC events. The final-state leptons in these events have good directional correlation with the parent neutrinos. The dotted histograms show the Monte Carlo expectation for neutrino events. If the produced flux of atmospheric neutrinos of a given flavour remains unchanged at the detector, the data should have similar distributions to the expectation. However, the zenith-angle distribution of the  $\mu$ -like events shows a strong deviation from the expectation. On the other hand, the zenith-angle distribution of the  $e$ -like events is consistent with the expectation. This characteristic feature may be interpreted that muon neutrinos coming from the opposite side of the Earth's atmosphere, having travelled  $\sim 10,000$  km, oscillate into other neutrinos and disappeared, while oscillations still do not take place for muon neutrinos coming from above the detector, having travelled from a few to a few tens km. Disappeared muon neutrinos may have oscillated into tau neutrinos because there is no indication of electron neutrino appearance. The atmospheric neutrinos corresponding to the events shown in Fig. 13.5 have  $E = 1 \sim 10$  GeV. With  $L = 10000$  km, the hypothesis of neutrino oscillations suggests  $\Delta m^2 \sim 10^{-3} - 10^{-4} \text{ eV}^2$ . The solid histograms show the best-fit results of a two-neutrino oscillation analysis with the hypothesis of  $\nu_{\mu} \leftrightarrow \nu_{\tau}$ . For the allowed parameter region, see Fig. 13.6.

Also, a search for a  $\nu_{\tau}$  appearance signal by using the SK-I atmospheric neutrino data has been made by the Super-Kamiokande Collaboration [131], and no  $\nu_{\tau}$  appearance hypothesis is disfavored at  $2.4\sigma$ .

Although the SK-I atmospheric neutrino observations gave compelling evidence for muon neutrino disappearance which is consistent with two-neutrino oscillation  $\nu_{\mu} \leftrightarrow \nu_{\tau}$  [131], the question may be asked whether the observed muon neutrino disappearance is really due to neutrino oscillations. First, other exotic explanations such as neutrino decay [132] and quantum decoherence [133] cannot be completely ruled out from the zenith-angle distributions alone. To confirm neutrino oscillation, characteristic sinusoidal behavior of the conversion probability as a function of neutrino energy  $E$  for a fixed distance  $L$  in the case of long-baseline neutrino oscillation experiments, or as a function of  $L/E$  in the case of atmospheric neutrino experiments, should be observed. By selecting events with

high  $L/E$  resolution, evidence for the dip in the  $L/E$  distribution was observed at the right place expected from the interpretation of the SK-I data in terms of  $\nu_\mu \leftrightarrow \nu_\tau$  oscillations [14], see Fig. 13.7. This dip cannot be explained by alternative hypotheses of neutrino decay and neutrino decoherence, and they are excluded at more than  $3\sigma$  in comparison with the neutrino oscillation interpretation. For the constraints obtained from the  $L/E$  analysis, see Fig. 13.6.

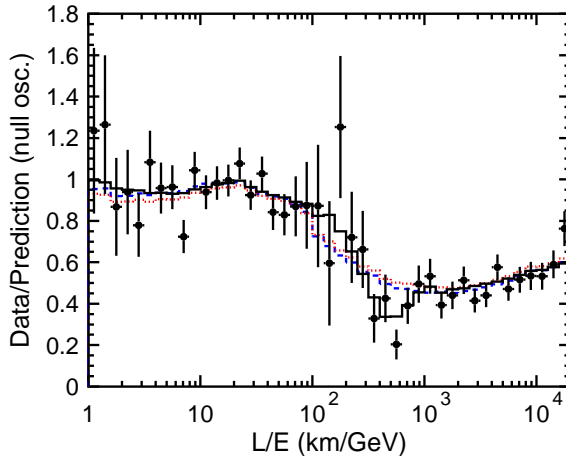


**Figure 13.7:** Results of the  $L/E$  analysis of SK-I atmospheric neutrino data. The points show the ratio of the data to the Monte Carlo prediction without oscillations, as a function of the reconstructed  $L/E$ . The error bars are statistical only. The solid line shows the best fit with 2-flavour  $\nu_\mu \leftrightarrow \nu_\tau$  oscillations. The dashed and dotted lines show the best fit expectations for neutrino decay and neutrino decoherence hypotheses, respectively. (From Ref. 14.)

### 13.5.2. Results from accelerator experiments :

The  $\Delta m^2 \geq 2 \times 10^{-3} \text{ eV}^2$  region can be explored by accelerator-based long-baseline experiments with typically  $E \sim 1 \text{ GeV}$  and  $L \sim$  several hundred km. With a fixed baseline distance and a narrower, well understood neutrino spectrum, the value of  $|\Delta m_A^2|$  and, with higher statistics, also the mixing angle, are potentially better constrained in accelerator experiments than from atmospheric neutrino observations.

The K2K (KEK-to-Kamioka) long-baseline neutrino oscillation experiment [19] is the first accelerator-based experiment with a neutrino path length extending hundreds of kilometers. K2K aimed at confirmation of the neutrino oscillation in  $\nu_\mu$  disappearance in the  $|\Delta m_A^2| \geq 2 \times 10^{-3} \text{ eV}^2$  region. A horn-focused wide-band muon neutrino beam having an average  $L/E_\nu \sim 200$  ( $L = 250 \text{ km}$ ,  $\langle E_\nu \rangle \sim 1.3 \text{ GeV}$ ), was produced by 12-GeV protons from the KEK-PS and directed to the Super-Kamiokande detector. The spectrum and profile of the neutrino beam were measured by a near neutrino detector system located 300 m downstream from the production target.

The construction of the K2K neutrino beam line and the near detector began before Super-Kamiokande's discovery of atmospheric neutrino oscillations. K2K experiment started data-taking in 1999 and was completed in 2004. The total number of protons on target (POT) for physics analysis amounted to  $0.92 \times 10^{20}$ . The observed number of beam-originated FC events in the 22.5 kton fiducial volume of Super-Kamiokande was 112, compared with an expectation of  $158.1_{-8.6}^{+9.2}$  events without oscillation. For 58 1-ring  $\mu$ -like subset of the data, the neutrino energy was reconstructed from measured muon momentum and angle, assuming CC quasi-elastic kinematics. The measured energy spectrum showed the distortion expected from neutrino oscillations. The probability that the observations are due to a statistical fluctuation instead of neutrino oscillation is 0.0015% or  $4.3 \sigma$  [19].

MINOS is the second long-baseline neutrino oscillation experiment with near and far detectors. Neutrinos are produced by the NuMI

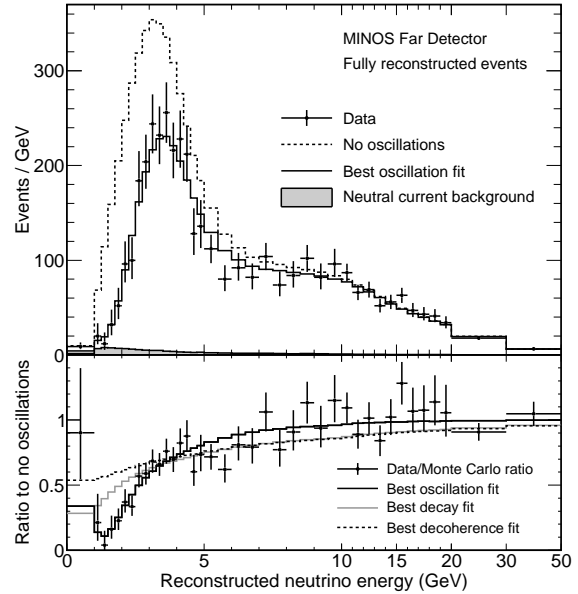


**Figure 13.8:** The top panel shows the energy spectra of fully reconstructed events in the MINOS far detector classified as CC interactions. The bottom panel shows the background subtracted ratios of data to the no-oscillation hypothesis. The best fit with the hypothesis of  $\nu_\mu \rightarrow \nu_\tau$  oscillations as well as the best fit to alternative models (neutrino decay and decoherence) is also shown. This figure is taken from Ref. 130.

(Neutrinos at the Main Injector) facility using 120 GeV protons from the Fermilab Main Injector. The far detector is a 5.4 kton (total mass) iron-scintillator tracking calorimeter with toroidal magnetic field, located underground in the Soudan mine. The baseline distance is 735 km. The near detector is also an iron-scintillator tracking calorimeter with toroidal magnetic field, with a total mass of 0.98 kton. The neutrino beam is a horn-focused wide-band beam. Its energy spectrum can be varied by moving the target position relative to the first horn and changing the horn current.

MINOS started the neutrino-beam run in 2005. Earlier  $\nu_\mu$  disappearance results were reported in Ref. 20 with  $1.27 \times 10^{20}$  POT and in Ref. 21 with  $3.36 \times 10^{20}$  POT. The updated results corresponding to a total POT of  $7.25 \times 10^{20}$  have been published recently [130]. Most of the data were taken with a “low-energy” option for the spectrum of the neutrino beam (the flux was enhanced in the 1-5 GeV energy range, peaking at 3 GeV). In the far detector, a total of 1986 fully reconstructed CC events were produced by the NuMI beam, compared to the unoscillated expectation of 2451 events. Fig. 13.8 shows the observed energy spectra and the expected spectra with no oscillation. Fig. 13.6 shows the 68% and 90% CL allowed regions obtained from the  $\nu_\mu \rightarrow \nu_\tau$  oscillation analysis. The results are compared with the 90% CL allowed regions obtained from the earlier MINOS [21], SK-I zenith-angle dependence [129,79], and the SK-I  $L/E$  analysis [14]. The MINOS results constrain the oscillation parameters as  $|\Delta m_A^2| = (2.32_{-0.08}^{+0.12}) \times 10^{-3} \text{ eV}^2$  and  $\sin^2 2\theta_A > 0.90$  at 90% CL. The alternative models to explain the  $\nu_\mu$  disappearance, neutrino decay and quantum decoherence of neutrinos, are disfavored at the  $7\sigma$  and  $9\sigma$ , respectively, by the MINOS data (see Fig. 13.8).

In addition to  $\nu_\mu$  disappearance, MINOS first observed muon antineutrino disappearance [134] with the NuMI beam line optimized for  $\bar{\nu}_\mu$  production. MINOS recently released  $\bar{\nu}_\mu$  disappearance result corresponding to POT =  $2.95 \times 10^{20}$  [135]. With increased statistics, the best-fit oscillation parameters are  $|\Delta \bar{m}_A^2| = (2.62_{-0.28}^{+0.31} \pm 0.09) \times 10^{-3} \text{ eV}^2$  and  $\sin^2 2\bar{\theta}_A = 0.95_{-0.11}^{+0.10} \pm 0.01$ , or  $\sin^2 2\bar{\theta}_A > 0.75$  at 90% CL. These results are consistent with their neutrino counterparts.

The regions of neutrino parameter space favored or excluded by various neutrino oscillation experiments are shown in Fig. 13.9.

Although the atmospheric neutrino oscillations and accelerator long-baseline  $\nu_\mu$  disappearance data are fully consistent with  $\nu_\mu \rightarrow \nu_\tau$



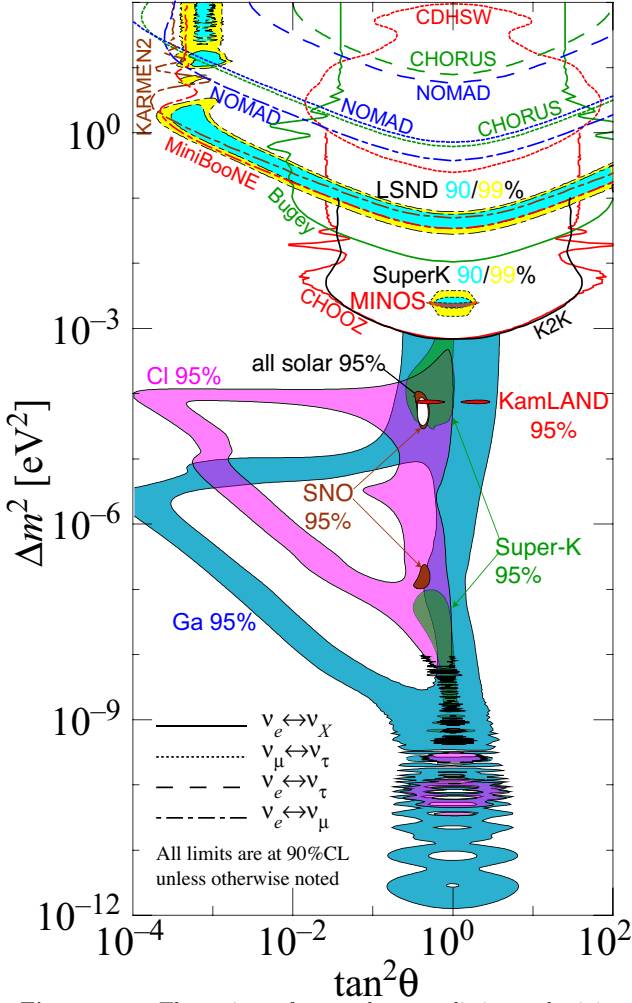


**Figure 13.9:** The regions of squared-mass splitting and mixing angle favored or excluded by various experiments based on two-flavor neutrino oscillation analyses. The figure was contributed by H. Murayama (University of California, Berkeley, and IPMU, University of Tokyo). References to the data used in the figure can be found at <http://hitoshi.berkeley.edu/neutrino>.

oscillations, appearance of  $\nu_\tau$  remained to be confirmed. For this purpose, a promising method is an accelerator long-baseline experiment using emulsion technique to identify short-lived  $\tau$  leptons event-by-event. The only experiment of this kind is OPERA with a neutrino source at CERN and a detector at Gran Sasso with the baseline distance of 730 km. The detector is a combination of the “Emulsion Cloud Chamber” and magnetized spectrometer. The CNGS (CERN Neutrinos to Gran Sasso) neutrino beam with  $\langle E_\nu \rangle = 17$  GeV is produced by high-energy protons from the CERN SPS. So far, OPERA reported observation of one  $\nu_\tau$  candidate in the hadronic decay channel of  $\tau$ , corresponding to an exposure of  $5.30 \times 10^{19}$  POT with a target mass of 1290 tons in 2008 and 2009 runs [60,61], with expectation of 1.65 signal events [61].

### 13.6. Measurements of $\theta_{13}$

Reactor  $\bar{\nu}_e$  disappearance experiments with  $L \sim 1$  km,  $\langle E \rangle \sim 3$  MeV are sensitive to  $\sim E/L \sim 3 \times 10^{-3}$  eV<sup>2</sup>  $\sim |\Delta m_{\Lambda}^2|$ . At this baseline distance, the reactor  $\bar{\nu}_e$  oscillations driven by  $\Delta m_{21}^2$  are negligible. Therefore, as can be seen from Eq. (13.22) and Eq. (13.24),  $\theta_{13}$  can be directly measured. A reactor neutrino oscillation experiment at the Chooz nuclear power station in France [58] was the first experiment of this kind. The detector was located in an underground laboratory with 300 mwe (meter water equivalent) rock overburden, at about 1 km from the neutrino source. It consisted of a central 5-ton target filled with 0.09% gadolinium loaded liquid scintillator,

surrounded by an intermediate 17-ton and outer 90-ton regions filled with undoped liquid scintillator. Reactor  $\bar{\nu}_e$ 's were detected via the reaction  $\bar{\nu}_e + p \rightarrow e^+ + n$ . Gd-doping was chosen to maximize the neutron capture efficiency. The Chooz experiment [58] found no evidence for  $\bar{\nu}_e$  disappearance. The 90% CL upper limit for  $|\Delta m_{\Lambda}^2| = 2.0 \times 10^{-3}$  eV<sup>2</sup> is  $\sin^2 2\theta_{13} < 0.19$ , and for the MINOS 2008 measurement [21] of  $|\Delta m_{\Lambda}^2| = 2.43 \times 10^{-3}$  eV it is  $\sin^2 2\theta_{13} < 0.15$ , both at 90% CL.

In the accelerator neutrino oscillation experiments with conventional neutrino beams,  $\theta_{13}$  can be measured using  $\nu_\mu \rightarrow \nu_e$  appearance. K2K was the first long-baseline experiment to search for  $\nu_e$  appearance signal due to the  $\nu_\mu \rightarrow \nu_e$  oscillations [136]. Based on the dominant term in the probability of  $\nu_\mu \rightarrow \nu_e$  oscillations (see Eq. (13.23) and Eq. (13.24)),

$$P(\nu_\mu \rightarrow \nu_e) = \sin^2 2\theta_{13} \cdot \sin^2 2\theta_{23} \cdot \sin^2(1.27\Delta m_{\Lambda}^2 L/E) \\ \sim \frac{1}{2} \sin^2 2\theta_{13} \sin^2(1.27\Delta m_{\Lambda}^2 L/E). \quad (13.75)$$

K2K set the 90% CL upper limit  $\sin^2 2\theta_{13} < 0.26$ .

By examining the expression for the probability of  $\nu_\mu \rightarrow \nu_e$  oscillations in matter (given by Eq. (13.45) in which the sign of the  $P_{\text{sin}\delta}$  term is flipped), however, it is understood that subleading terms could have rather large effects and the unknown CP-violating phase  $\delta$  causes uncertainties in determining the value of  $\theta_{13}$ . Actually, from the measurement of  $\nu_\mu \rightarrow \nu_e$  appearance,  $\theta_{13}$  is given as a function of  $\delta$  for a given sign of  $\Delta m_{\Lambda}^2$ , or of  $\Delta m_{32}^2 \cong \Delta m_{31}^2$ . (Also, deviations from maximal  $\theta_{23}$  mixing would cause a further uncertainty.) Therefore, a single experiment with a neutrino beam cannot determine the value of  $\theta_{13}$ , although it is possible to establish a non-zero  $\theta_{13}$ . In 2010, MINOS [137] set the limits for  $2 \sin^2 2\theta_{23} \sin^2 2\theta_{13}$  as a function of  $\delta$ . At  $\delta = 0$ , the 90% CL upper limit is 0.12 (0.20) for  $\Delta m_{\Lambda}^2 > 0$  ( $\Delta m_{\Lambda}^2 < 0$ ).

In 2011, experimental indications of  $\nu_\mu \rightarrow \nu_e$  oscillations and a non-zero  $\theta_{13}$  have been reported by the T2K [24] experiment. Also, MINOS [25] searched for  $\nu_\mu \rightarrow \nu_e$  appearance and disfavored the  $\theta_{13} = 0$  hypothesis at the 89% CL.

The T2K experiment is the first off-axis long-baseline neutrino oscillation experiment. The baseline distance is 295 km between the J-PARC in Tokai, Japan and Super-Kamiokande. A narrow-band  $\nu_\mu$  beam produced by 30 GeV protons from the J-PARC Main Ring is directed 2.5° off-axis to SK. With this configuration, the  $\nu_\mu$  beam is tuned to the first oscillation maximum. With  $1.43 \times 10^{20}$  POT, the T2K [24] Collaboration observed six candidate  $\nu_e$  events having all characteristics of being due to  $\nu_\mu \rightarrow \nu_e$  oscillations, while the expectation for  $\theta_{13} = 0$  is  $1.5 \pm 0.3$  events. The probability to observe six or more candidate events when  $1.5 \pm 0.3$  events are predicted is  $7 \times 10^{-3}$ , implying a non-zero  $\theta_{13}$  with statistical significance of  $2.5\sigma$ . At  $\delta = 0$ ,  $\sin^2 2\theta_{23} = 1$  and  $|\Delta m_{\Lambda}^2| = 2.4 \times 10^{-3}$  eV<sup>2</sup>, this result gives a best fit value of  $\sin^2 2\theta_{13} = 0.11$  (0.14) and a 90% CL interval of  $0.03$  (0.04)  $< \sin^2 2\theta_{13} < 0.28$  (0.34) for  $\Delta m_{\Lambda}^2 > 0$  ( $\Delta m_{\Lambda}^2 < 0$ ).

The MINOS Collaboration [25] also searched for the  $\nu_\mu \rightarrow \nu_e$  appearance signal. Though dependent on the definition of the signal, typically 62 candidate events are observed with an exposure of  $8.2 \times 10^{20}$  POT, while the expectation for  $\theta_{13} = 0$  is  $49.6 \pm 7.0 \pm 2.7$  events. At the 90% CL, the MINOS result implies that  $2 \sin^2 2\theta_{13} \sin^2 2\theta_{23} < 0.12$  (0.20) for  $\Delta m_{\Lambda}^2 > 0$  ( $\Delta m_{\Lambda}^2 < 0$ ) and  $\delta = 0$ , with a best fit value  $2 \sin^2 2\theta_{23} \sin^2 2\theta_{13} = 0.041^{+0.04}_{-0.031}$  ( $0.079^{+0.071}_{-0.053}$ ). The MINOS data disfavored the  $\theta_{13} = 0$  hypothesis at the 89% CL [25].

Recently, the three reactor neutrino experiments Double Chooz [59], Daya Bay [26], and RENO [27] reported their first results on reactor  $\bar{\nu}_e$  disappearance. Daya Bay and RENO measured reactor  $\bar{\nu}_e$ s with near and far detectors. The first results of Double Chooz was obtained with only a far detector, though this experiment is planning to have a near detector in 2012. The  $\bar{\nu}_e$  detectors of all the three experiments have similar structures; an antineutrino detector consisting of three layers and an optically independent outer veto detector. The innermost layer of the antineutrino detector is filled with Gd-doped liquid scintillator (LS), which is surrounded by a “ $\gamma$ -catcher” layer filled with Gd-free LS, and outside the  $\gamma$ -catcher is a buffer layer filled with mineral oil.

An outer veto detector is filled with purified water (Daya Bay and RENO) or LS (Double Chooz).

The Daya Bay experiment [26] measured  $\bar{\nu}_e$ s from the Daya Bay nuclear power complex (six 2.9 GW<sub>th</sub> reactors) in China with six functionally identical detectors deployed in two near (470 m and 576 m of flux-weighted baselines) and one far (1648 m) underground halls. With live time of 55 days, the ratio of the observed to expected number of  $\bar{\nu}_e$ s at the far hall is  $R = 0.940 \pm 0.011 \pm 0.004$  and the rate-only analysis yielded

$$\sin^2 2\theta_{13} = 0.092 \pm 0.016 \pm 0.005. \quad (13.76)$$

From this result,  $\theta_{13}$  is non-zero with a significance of  $5.2\sigma$ .

The RENO experiment [27] measured  $\bar{\nu}_e$ s from six 2.8 GW<sub>th</sub> reactors at Yonggwang Nuclear Power Plant in Korea with two identical detectors located at 294 m and 1383 m from the reactor array center. With 229 days of running time, the ratio of the observed to expected number of  $\bar{\nu}_e$ s in the far detector is  $R = 0.920 \pm 0.009 \pm 0.014$ , and from a rate-only analysis the following result is obtained:

$$\sin^2 2\theta_{13} = 0.113 \pm 0.013 \pm 0.019 \quad (13.77)$$

This result excludes the no-oscillation hypothesis at the  $4.9\sigma$  level.

The Double Chooz experiment [59] measured  $\bar{\nu}_e$ s from two 4.25 GW<sub>th</sub> reactors with a far detector at 1050 m from the two reactor cores. With 101 days of running, this experiment obtained  $\sin^2 2\theta_{13} = 0.086 \pm 0.041 \pm 0.030$ , or  $0.017 < \sin^2 2\theta_{13} < 0.16$  at the 90% CL, by analyzing the rate and energy spectrum of prompt positrons using the reactor  $\bar{\nu}_e$  spectrum of Ref. 36 and Ref. 34 and the Bugey4 rate measurement [138].

Turning to atmospheric and solar neutrino observations, Eq. (13.40) to Eq. (13.43) and Eq. (13.62) indicate that they are sensitive to  $\theta_{13}$  through sub-leading effects. So far, the SK, SNO, and KamLAND Collaborations presented their own  $\theta_{13}$  analyses by adding or updating their own data. In the atmospheric neutrino sector, the SK group analyzed its atmospheric neutrino data [79,139], and in the solar neutrino sector, SNO [117], SK [114], and KamLAND [128] analyzed the data from all solar neutrino experiments, with or without the KamLAND data, in terms of 3-neutrino oscillations. In addition, KamLAND [128] made a global analysis of all available neutrino data incorporating the Chooz, atmospheric and accelerator data. All these results are consistent with the recent results from accelerator [24,25] and reactor [59,26,27] experiments.

### 13.7. The three neutrino mixing

All existing compelling data on neutrino oscillations can be described assuming 3-flavour neutrino mixing in vacuum. This is the minimal neutrino mixing scheme which can account for the currently available data on the oscillations of the solar ( $\nu_e$ ), atmospheric ( $\nu_\mu$  and  $\bar{\nu}_\mu$ ), reactor ( $\bar{\nu}_e$ ) and accelerator ( $\nu_\mu$ ) neutrinos. The (left-handed) fields of the flavour neutrinos  $\nu_e$ ,  $\nu_\mu$  and  $\nu_\tau$  in the expression for the weak charged lepton current in the CC weak interaction Lagrangian, are linear combinations of the LH components of the fields of three massive neutrinos  $\nu_j$ :

$$\mathcal{L}_{CC} = -\frac{g}{\sqrt{2}} \sum_{l=e,\mu,\tau} \bar{l}_L(x) \gamma_\alpha \nu_{lL}(x) W^{\alpha\dagger}(x) + h.c.,$$

$$\nu_{lL}(x) = \sum_{j=1}^3 U_{lj} \nu_{jL}(x), \quad (13.78)$$

where  $U$  is the  $3 \times 3$  unitary neutrino mixing matrix [17,18]. The mixing matrix  $U$  can be parameterized by 3 angles, and, depending on whether the massive neutrinos  $\nu_j$  are Dirac or Majorana particles, by 1 or 3 CP violation phases [40,41]:

$$U = \begin{bmatrix} c_{12}c_{13} & s_{12}c_{13} & s_{13}e^{-i\delta} \\ -s_{12}c_{23} - c_{12}s_{23}s_{13}e^{i\delta} & c_{12}c_{23} - s_{12}s_{23}s_{13}e^{i\delta} & s_{23}c_{13} \\ s_{12}s_{23} - c_{12}c_{23}s_{13}e^{i\delta} & -c_{12}s_{23} - s_{12}c_{23}s_{13}e^{i\delta} & c_{23}c_{13} \end{bmatrix} \\ \times \text{diag}(1, e^{i\frac{\alpha_{21}}{2}}, e^{i\frac{\alpha_{31}}{2}}). \quad (13.79)$$

where  $c_{ij} = \cos \theta_{ij}$ ,  $s_{ij} = \sin \theta_{ij}$ , the angles  $\theta_{ij} = [0, \pi/2]$ ,  $\delta = [0, 2\pi]$  is the Dirac CP violation phase and  $\alpha_{21}$ ,  $\alpha_{31}$  are two Majorana CP violation phases. Thus, in the case of massive Dirac neutrinos, the neutrino mixing matrix  $U$  is similar, in what concerns the number of mixing angles and CP violation phases, to the CKM quark mixing matrix. The presence of two additional physical CP violation phases in  $U$  if  $\nu_j$  are Majorana particles is a consequence of the special properties of the latter (see, *e.g.*, Refs. [39,40]).

As we see, the fundamental parameters characterizing the 3-neutrino mixing are: i) the 3 angles  $\theta_{12}$ ,  $\theta_{23}$ ,  $\theta_{13}$ , ii) depending on the nature of massive neutrinos  $\nu_j$  - 1 Dirac ( $\delta$ ), or 1 Dirac + 2 Majorana ( $\delta, \alpha_{21}, \alpha_{31}$ ), CP violation phases, and iii) the 3 neutrino masses,  $m_1$ ,  $m_2$ ,  $m_3$ . Thus, depending on whether the massive neutrinos are Dirac or Majorana particles, this makes 7 or 9 additional parameters in the minimally extended Standard Model of particle interactions with massive neutrinos.

The neutrino oscillation probabilities depend (Section 13.2), in general, on the neutrino energy,  $E$ , the source-detector distance  $L$ , on the elements of  $U$  and, for relativistic neutrinos used in all neutrino experiments performed so far, on  $\Delta m_{ij}^2 \equiv (m_i^2 - m_j^2)$ ,  $i \neq j$ . In the case of 3-neutrino mixing there are only two independent neutrino mass squared differences, say  $\Delta m_{21}^2 \neq 0$  and  $\Delta m_{31}^2 \neq 0$ . The numbering of massive neutrinos  $\nu_j$  is arbitrary. It proves convenient from the point of view of relating the mixing angles  $\theta_{12}$ ,  $\theta_{23}$  and  $\theta_{13}$  to observables, to identify  $|\Delta m_{21}^2|$  with the smaller of the two neutrino mass squared differences, which, as it follows from the data, is responsible for the solar  $\nu_e$  and, the observed by KamLAND, reactor  $\bar{\nu}_e$  oscillations. We will number (just for convenience) the massive neutrinos in such a way that  $m_1 < m_2$ , so that  $\Delta m_{21}^2 > 0$ . With these choices made, there are two possibilities: either  $m_1 < m_2 < m_3$ , or  $m_3 < m_1 < m_2$ . Then the larger neutrino mass square difference  $|\Delta m_{31}^2|$  or  $|\Delta m_{32}^2|$ , can be associated with the experimentally observed oscillations of the atmospheric  $\nu_\mu$  and  $\bar{\nu}_\mu$  and accelerator  $\nu_\mu$ . The effects of  $\Delta m_{31}^2$  or  $\Delta m_{32}^2$  in the oscillations of solar  $\nu_e$ , and of  $\Delta m_{21}^2$  in the oscillations of atmospheric  $\nu_\mu$  and  $\bar{\nu}_\mu$  and of accelerator  $\nu_\mu$ , are relatively small and subdominant as a consequence of the facts that i)  $L$ ,  $E$  and  $L/E$  in the experiments with solar  $\nu_e$  and with atmospheric  $\nu_\mu$  and  $\bar{\nu}_\mu$  or accelerator  $\nu_\mu$ , are very different, ii) the conditions of production and propagation (on the way to the detector) of the solar  $\nu_e$  and of the atmospheric  $\nu_\mu$  and  $\bar{\nu}_\mu$  or accelerator  $\nu_\mu$ , are very different, and iii)  $|\Delta m_{21}^2|$  and  $|\Delta m_{31}^2|$  ( $|\Delta m_{32}^2|$ ) in the case of  $m_1 < m_2 < m_3$  ( $m_3 < m_1 < m_2$ ), as it follows from the data, differ by approximately a factor of 30,  $|\Delta m_{21}^2| \ll |\Delta m_{31(32)}^2|$ ,  $|\Delta m_{21}^2|/|\Delta m_{31(32)}^2| \cong 0.03$ . This implies that in both cases of  $m_1 < m_2 < m_3$  and  $m_3 < m_1 < m_2$  we have  $\Delta m_{32}^2 \cong \Delta m_{31}^2$  with  $|\Delta m_{31}^2 - \Delta m_{32}^2| = |\Delta m_{21}^2| \ll |\Delta m_{31,32}^2|$ .

It follows from the results of the Chooz experiment with reactor  $\bar{\nu}_e$  [58] and from the more recent data discussed in the preceding subsection that, in the convention we use, in which  $0 < \Delta m_{21}^2 < |\Delta m_{31(32)}^2|$ , the element  $|U_{e3}| = \sin \theta_{13}$  of the neutrino mixing matrix  $U$ , as the results of the Daya Bay and RENO experiments show, is small. This makes it possible to identify the angles  $\theta_{12}$  and  $\theta_{23}$  as the neutrino mixing angles associated with the solar  $\nu_e$  and the dominant atmospheric  $\nu_\mu$  (and  $\bar{\nu}_\mu$ ) oscillations, respectively. The angles  $\theta_{12}$  and  $\theta_{23}$  are often called ‘‘solar’’ and ‘‘atmospheric’’ neutrino mixing angles, and are often denoted as  $\theta_{12} = \theta_\odot$  and  $\theta_{23} = \theta_A$  (or  $\theta_{\text{atm}}$ ) while  $\Delta m_{21}^2$  and  $\Delta m_{31}^2$  are often referred to as the ‘‘solar’’ and ‘‘atmospheric’’ neutrino mass squared differences and are often denoted as  $\Delta m_{21}^2 \equiv \Delta m_\odot^2$ ,  $\Delta m_{31}^2 \equiv \Delta m_A^2$  (or  $\Delta m_{\text{atm}}^2$ ).

The solar neutrino data tell us that  $\Delta m_{21}^2 \cos 2\theta_{12} > 0$ . In the convention employed by us we have  $\Delta m_{21}^2 > 0$ . Correspondingly, in this convention one must have  $\cos 2\theta_{12} > 0$ .

Global analyses [140,141] of the existing neutrino oscillation data, including the T2K [24] and MINOS [25] (but not the Daya Bay [26] and RENO [27]) results, allowed us to determine the parameters which drive the solar neutrino and the dominant atmospheric neutrino oscillations,  $\Delta m_\odot^2 = \Delta m_{21}^2$ ,  $\theta_{12}$ , and  $|\Delta m_A^2| = |\Delta m_{31}^2| \cong |\Delta m_{32}^2|$ ,  $\theta_{23}$ , with a relatively good precision, and to establish that the angle  $\theta_{13} \neq 0$  at  $\gtrsim 99.73\%$  CL. The Daya Bay and RENO experiments provided a rather precise determination of the angle  $\theta_{13}$ . Analyses of

the global neutrino oscillation data, in which the Daya Bay and RENO results on  $\theta_{13}$  are also included, are lacking at present. Therefore we present in Table 13.7 the best fit values and the 99.73% CL allowed ranges of  $\Delta m_{21}^2$ ,  $\sin^2 \theta_{12}$ ,  $|\Delta m_{31(32)}^2|$ ,  $\sin^2 \theta_{23}$  and  $\sin^2 \theta_{13}$ , found in Ref. 140 as well as the PDG average [142] of the results of the three recent reactor experiments [26,27,59]. Since the PDG average of  $\sin^2 \theta_{13}$  is very close to that obtained in the global analysis in Ref. 140, and since the other oscillation parameter ranges are almost uncorrelated from  $\theta_{13}$ , we do not expect that the inclusion of the Daya Bay and RENO data will change significantly the results (neither the central values nor the errors) for  $\Delta m_{21}^2$ ,  $\sin^2 \theta_{12}$ ,  $|\Delta m_{31(32)}^2|$  and  $\sin^2 \theta_{23}$  obtained in Ref. 140. Obviously, the uncertainty in the value of  $\sin^2 \theta_{13}$  will shrink considerably. We note also that the results from Ref. 140 quoted in Table 13.7 are derived by marginalizing over  $\text{sgn}(\Delta m_{31}^2) = \pm 1$  and over  $\cos \delta = \pm 1$  and that the values (the values in brackets) of  $\sin^2 \theta_{12}$  and  $\sin^2 \theta_{13}$  are obtained in Ref. 140 using the reactor  $\bar{\nu}_e$  fluxes from Ref. 35 (from Ref. 34).

**Table 13.7:** The best-fit values and  $3\sigma$  allowed ranges of the 3-neutrino oscillation parameters, derived from a global fit of the current neutrino oscillation data, including the T2K and MINOS (but not the Daya Bay and RENO) results (from [140]). The PDG average of the results of the three recent reactor experiments [26,27,59] is given in the last line [142]. The values (values in brackets) of  $\sin^2 \theta_{12}$  and  $\sin^2 \theta_{13}$  are obtained using the “old” [35] (“new” [34]) reactor  $\bar{\nu}_e$  fluxes in the analysis.

Parameter	best-fit ( $\pm 1\sigma$ )	$3\sigma$
$\Delta m_{\odot}^2$ [ $10^{-5}$ eV <sup>2</sup> ]	$7.58_{-0.26}^{+0.22}$	6.99 – 8.18
$ \Delta m_{\text{A}}^2 $ [ $10^{-3}$ eV <sup>2</sup> ]	$2.35_{-0.09}^{+0.12}$	2.06 – 2.67
$\sin^2 \theta_{12}$	$0.306$ (0.312) $_{-0.015}^{+0.018}$	0.259 (0.265) – 0.359 (0.364)
$\sin^2 \theta_{23}$	$0.42_{-0.03}^{+0.08}$	0.34 – 0.64
$\sin^2 \theta_{13}$ [140]	$0.021$ (0.025) $_{-0.008}^{+0.007}$	0.001 (0.005) – 0.044 (0.050)
$\sin^2 \theta_{13}$ [142]	$0.0251 \pm 0.0034$	0.015 – 0.036

A combined analysis of the data on  $\theta_{13}$  from the T2K, MINOS, Double Chooz, Daya Bay and RENO experiments was performed in Ref. 145. The authors find that  $\theta_{13} \neq 0$  at  $7.7\sigma$ :

$$\sin^2 2\theta_{13} = 0.096 \pm 0.013 \quad (\pm 0.040) \text{ at } 1\sigma \quad (3\sigma) \quad (13.80)$$

In this analysis the positive or negative sign of  $\Delta m_{\text{A}}^2$  was used as input and the values of  $\sin^2 2\theta_{23}$  and  $|\Delta m_{\text{A}}^2|$  were varied imposing Gaussian priors based on the results of the atmospheric neutrino [139] and MINOS [130] experiments. The value of  $\sin^2 2\theta_{13}$  thus obtained showed a statistically insignificant dependence on the Dirac phase  $\delta$ .

It follows from the results given in Table 13.7 that  $\theta_{23} \cong \pi/4$ ,  $\theta_{12} \cong \pi/5.4$  and that  $\theta_{13} \cong \pi/20$ . Correspondingly, the pattern of neutrino mixing is drastically different from the pattern of quark mixing.

Note also that  $\Delta m_{21}^2$ ,  $\sin^2 \theta_{12}$ ,  $|\Delta m_{31(32)}^2|$ ,  $\sin^2 \theta_{23}$  and  $\sin^2 \theta_{13}$  are determined from the data with a  $1\sigma$  uncertainty ( $= 1/6$  of the  $3\sigma$  range) of approximately 2.6%, 5.4%, 4.3%, 12% and absolute error  $0.42 \times 10^{-2}$ , respectively.

The existing SK atmospheric neutrino, K2K and MINOS data do not allow to determine the sign of  $\Delta m_{31(32)}^2$ . Maximal solar neutrino mixing, *i.e.*,  $\theta_{12} = \pi/4$ , is ruled out at more than  $6\sigma$  by the data. Correspondingly, one has  $\cos 2\theta_{12} \geq 0.27$  (at 99.73% CL).

At present no experimental information on the Dirac and Majorana CP violation phases in the neutrino mixing matrix is available. Thus, the status of CP symmetry in the lepton sector is unknown. With  $\theta_{13} \neq 0$ , the Dirac phase  $\delta$  can generate CP violation effects in neutrino oscillations [40,52,53]. The magnitude of CP violation in  $\nu_l \rightarrow \nu_{l'}$  and  $\bar{\nu}_l \rightarrow \bar{\nu}_{l'}$  oscillations,  $l \neq l' = e, \mu, \tau$ , is determined, as we have seen, by the rephasing invariant  $J_{CP}$  (see Eq. (13.19)), which

in the “standard” parametrisation of the neutrino mixing matrix (Eq. (13.79)) has the form:

$$J_{CP} \equiv \text{Im}(U_{\mu 3} U_{e 3}^* U_{e 2} U_{\mu 2}^*) = \frac{1}{8} \cos \theta_{13} \sin 2\theta_{12} \sin 2\theta_{23} \sin 2\theta_{13} \sin \delta. \quad (13.81)$$

Thus, given the fact that  $\sin 2\theta_{12}$ ,  $\sin 2\theta_{23}$  and  $\sin 2\theta_{13}$  have been determined experimentally with a relatively good precision, the size of CP violation effects in neutrino oscillations depends essentially only on the magnitude of the currently unknown value of the Dirac phase  $\delta$ . The current data implies  $|J_{CP}| \lesssim 0.045$ , where we have used the  $3\sigma$  ranges of  $\sin^2 \theta_{12}$ ,  $\sin^2 \theta_{23}$  and  $\sin^2 \theta_{13}$  given in Table 13.7 and Eq. (13.76), respectively.

As we have indicated, the existing data do not allow one to determine the sign of  $\Delta m_{\text{A}}^2 = \Delta m_{31(2)}^2$ . In the case of 3-neutrino mixing, the two possible signs of  $\Delta m_{31(2)}^2$  correspond to two types of neutrino mass spectrum. In the widely used conventions of numbering the neutrinos with definite mass in the two cases, the two spectra read:

– *i) spectrum with normal ordering:*

$$m_1 < m_2 < m_3, \Delta m_{\text{A}}^2 = \Delta m_{21}^2 > 0,$$

$$\Delta m_{\odot}^2 \equiv \Delta m_{21}^2 > 0, m_{2(3)} = (m_1^2 + \Delta m_{21(31)}^2)^{\frac{1}{2}};$$

– *ii) spectrum with inverted ordering (IO):*

$$m_3 < m_1 < m_2, \Delta m_{\text{A}}^2 = \Delta m_{32}^2 < 0, \Delta m_{\odot}^2 \equiv \Delta m_{21}^2 > 0,$$

$$m_2 = (m_3^2 + \Delta m_{23}^2)^{\frac{1}{2}}, m_1 = (m_3^2 + \Delta m_{23}^2 - \Delta m_{21}^2)^{\frac{1}{2}}.$$

Depending on the values of the lightest neutrino mass [143],  $\min(m_j)$ , the neutrino mass spectrum can also be:

– *Normal Hierarchical (NH):*

$$m_1 \ll m_2 < m_3, m_2 \cong (\Delta m_{\odot}^2)^{\frac{1}{2}} \cong 0.0086 \text{ eV},$$

$$m_3 \cong |\Delta m_{\text{A}}^2|^{\frac{1}{2}} \cong 0.048 \text{ eV}; \text{ or}$$

– *Inverted Hierarchical (IH):*

$$m_3 \ll m_1 < m_2, \text{ with } m_{1,2} \cong |\Delta m_{\text{A}}^2|^{\frac{1}{2}} \cong 0.048 \text{ eV}; \text{ or}$$

– *Quasi-Degenerate (QD):*

$$m_1 \cong m_2 \cong m_3 \cong m_0, m_j^2 \gg |\Delta m_{\text{A}}^2|, m_0 \gtrsim 0.10 \text{ eV}.$$

All three types of spectrum are compatible with the existing constraints on the absolute scale of neutrino masses  $m_j$ . Information about the latter can be obtained, *e.g.*, by measuring the spectrum of electrons near the end point in  $^3\text{H}$   $\beta$ -decay experiments [146–149] and from cosmological and astrophysical data. The most stringent upper bounds on the  $\bar{\nu}_e$  mass were obtained in the Troitzk [147,148] experiment:

$$m_{\bar{\nu}_e} < 2.05 \text{ eV} \quad \text{at } 95\% \text{ CL}. \quad (13.82)$$

We have  $m_{\bar{\nu}_e} \cong m_{1,2,3}$  in the case of QD spectrum. The KATRIN experiment [149] is planned to reach sensitivity of  $m_{\bar{\nu}_e} \sim 0.20 \text{ eV}$ , *i.e.*, it will probe the region of the QD spectrum.

The Cosmic Microwave Background (CMB) data of the WMAP experiment, combined with supernovae data and data on galaxy clustering can be used to obtain an upper limit on the sum of neutrinos masses (see review on Cosmological Parameters [150] and, *e.g.*, Ref. 151). Depending on the model complexity and the input data used one obtains [151]:  $\sum_j m_j \lesssim (0.3 - 1.3) \text{ eV}$ , 95% CL.

It follows from these data that neutrino masses are much smaller than the masses of charged leptons and quarks. If we take as an indicative upper limit  $m_j \lesssim 0.5 \text{ eV}$ , we have  $m_j/m_{l,q} \lesssim 10^{-6}$ ,  $l = e, \mu, \tau$ ,  $q = d, s, b, u, c, t$ . It is natural to suppose that the remarkable smallness of neutrino masses is related to the existence of a new fundamental mass scale in particle physics, and thus to new physics beyond that predicted by the Standard Model.

### 13.7.1. The see-saw mechanism and the baryon asymmetry of the Universe :

A natural explanation of the smallness of neutrino masses is provided by the (type I) see-saw mechanism of neutrino mass generation [3]. An integral part of this rather simple mechanism [152] are the RH neutrinos  $\nu_{lR}$  (RH neutrino fields  $\nu_{lR}(x)$ ). The latter are assumed to possess a Majorana mass term as well as Yukawa type coupling  $\mathcal{L}_Y(x)$  with the Standard Model lepton and Higgs doublets,  $\psi_{lL}(x)$  and  $\Phi(x)$ , respectively,  $(\psi_{lL}(x))^T = (\nu_{lL}^T(x) \ l_l^T(x))$ ,  $l = e, \mu, \tau$ ,  $(\Phi(x))^T = (\Phi^{(0)} \ \Phi^{(-)})$ . In the basis in which the Majorana mass matrix of RH neutrinos is diagonal, we have:

$$\mathcal{L}_{Y,M}(x) = \left( \lambda_{il} \overline{N_{iR}}(x) \Phi^\dagger(x) \psi_{lL}(x) + \text{h.c.} \right) - \frac{1}{2} M_i \overline{N_i}(x) N_i(x), \quad (13.83)$$

where  $\lambda_{il}$  is the matrix of neutrino Yukawa couplings and  $N_i$  ( $N_i(x)$ ) is the heavy RH Majorana neutrino (field) possessing a mass  $M_i > 0$ . When the electroweak symmetry is broken spontaneously, the neutrino Yukawa coupling generates a Dirac mass term:  $m_{il}^D \overline{N_{iR}}(x) \nu_{lL}(x) + \text{h.c.}$ , with  $m^D = v\lambda$ ,  $v = 174$  GeV being the Higgs doublet v.e.v. In the case when the elements of  $m^D$  are much smaller than  $M_k$ ,  $|m_{il}^D| \ll M_k$ ,  $i, k = 1, 2, 3$ ,  $l = e, \mu, \tau$ , the interplay between the Dirac mass term and the mass term of the heavy (RH) Majorana neutrinos  $N_i$  generates an effective Majorana mass (term) for the LH flavour neutrinos [3]:  $m_{il}^{LL} \cong -(m^D)_{ij}^T M_j^{-1} m_{jl}^D$ . In grand unified theories,  $m^D$  is typically of the order of the charged fermion masses. In  $SO(10)$  theories, for instance,  $m^D$  coincides with the up-quark mass matrix. Taking indicatively  $m^{LL} \sim 0.1$  eV,  $m^D \sim 100$  GeV, one finds  $M \sim 10^{14}$  GeV, which is close to the scale of unification of the electroweak and strong interactions,  $M_{GUT} \cong 2 \times 10^{16}$  GeV. In GUT theories with RH neutrinos one finds that indeed the heavy Majorana neutrinos  $N_j$  naturally obtain masses which are by few to several orders of magnitude smaller than  $M_{GUT}$ . Thus, the enormous disparity between the neutrino and charged fermion masses is explained in this approach by the huge difference between effectively the electroweak symmetry breaking scale and  $M_{GUT}$ .

An additional attractive feature of the see-saw scenario is that the generation and smallness of neutrino masses is related via the leptogenesis mechanism [2] to the generation of the baryon asymmetry of the Universe. The Yukawa coupling in Eq. (13.83), in general, is not CP conserving. Due to this CP-nonconserving coupling the heavy Majorana neutrinos undergo, *e.g.*, the decays  $N_j \rightarrow l^+ + \Phi^{(-)}$ ,  $N_j \rightarrow l^- + \Phi^{(+)}$ , which have different rates:  $\Gamma(N_j \rightarrow l^+ + \Phi^{(-)}) \neq \Gamma(N_j \rightarrow l^- + \Phi^{(+)})$ . When these decays occur in the Early Universe at temperatures somewhat below the mass of, say,  $N_1$ , so that the latter are out of equilibrium with the rest of the particles present at that epoch, CP violating asymmetries in the individual lepton charges  $L_l$ , and in the total lepton charge  $L$ , of the Universe are generated. These lepton asymmetries are converted into a baryon asymmetry by  $(B - L)$  conserving, but  $(B + L)$  violating, sphaleron processes, which exist in the Standard Model and are effective at temperatures  $T \sim (100 - 10^{12})$  GeV. If the heavy neutrinos  $N_j$  have hierarchical spectrum,  $M_1 \ll M_2 \ll M_3$ , the observed baryon asymmetry can be reproduced provided the mass of the lightest one satisfies  $M_1 \gtrsim 10^9$  GeV [153]. Thus, in this scenario, the neutrino masses and mixing and the baryon asymmetry have the same origin - the neutrino Yukawa couplings and the existence of (at least two) heavy Majorana neutrinos. Moreover, quantitative studies based on recent advances in leptogenesis theory [154] have shown that the Dirac and/or Majorana phases in the neutrino mixing matrix  $U$  can provide the CP violation, necessary in leptogenesis for the generation of the observed baryon asymmetry of the Universe [155]. This implies, in particular, that if the CP symmetry is established not to hold in the lepton sector due to  $U$ , at least some fraction (if not all) of the observed baryon asymmetry might be due to the Dirac and/or Majorana CP violation present in the neutrino mixing.

### 13.7.2. The nature of massive neutrinos :

The experiments studying flavour neutrino oscillations cannot provide information on the nature - Dirac or Majorana, of massive neutrinos [40,54]. Establishing whether the neutrinos with definite mass  $\nu_j$  are Dirac fermions possessing distinct antiparticles, or Majorana fermions, i.e. spin 1/2 particles that are identical with their antiparticles, is of fundamental importance for understanding the origin of  $\nu$ -masses and mixing and the underlying symmetries of particle interactions (see *e.g.*, Ref. 66). The neutrinos with definite mass  $\nu_j$  will be Dirac fermions if the particle interactions conserve some additive lepton number, *e.g.*, the total lepton charge  $L = L_e + L_\mu + L_\tau$ . If no lepton charge is conserved,  $\nu_j$  will be Majorana fermions (see *e.g.*, Ref. 39). The massive neutrinos are predicted to be of Majorana nature by the see-saw mechanism of neutrino mass generation [3]. The observed patterns of neutrino mixing and of neutrino mass squared differences can be related to Majorana massive neutrinos and the existence of an approximate symmetry in the lepton sector corresponding, *e.g.*, to the conservation of the lepton charge  $L' = L_e - L_\mu - L_\tau$  [156]. Determining the nature of massive neutrinos  $\nu_j$  is one of the fundamental and most challenging problems in the future studies of neutrino mixing.

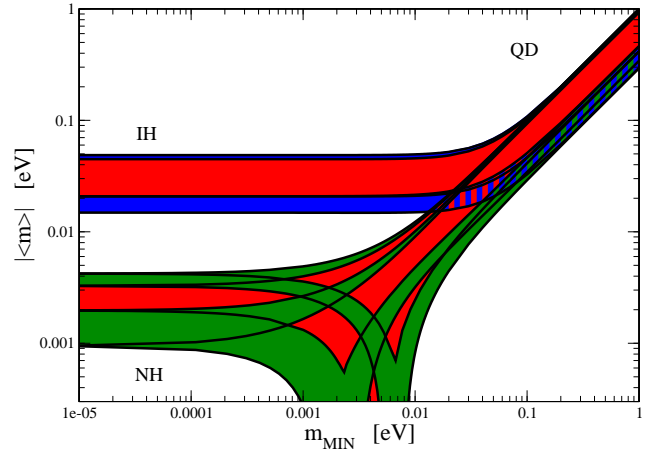


**Figure 13.10:** The effective Majorana mass  $|\langle m \rangle|$  (including a  $2\sigma$  uncertainty), as a function of  $\min(m_j)$  for  $\sin^2 \theta_{13} = 0.0236 \pm 0.0042$  [26] and  $\delta = 0$ . The figure is obtained using also the best fit values and  $1\sigma$  errors of  $\Delta m_{21}^2$ ,  $\sin^2 \theta_{12}$ , and  $|\Delta m_{31}^2| \cong |\Delta m_{32}^2|$  from Ref. 140 (given in Table 13.7). For  $\sin^2 \theta_{12}$  the results found with the “old” reactor  $\bar{\nu}_e$  fluxes [35] were employed. The phases  $\alpha_{21,31}$  are varied in the interval  $[0, \pi]$ . The predictions for the NH, IH and QD spectra are indicated. The red regions correspond to at least one of the phases  $\alpha_{21,31}$  and  $(\alpha_{31} - \alpha_{21})$  having a CP violating value, while the blue and green areas correspond to  $\alpha_{21,31}$  possessing CP conserving values. (Update by S. Pascoli of a figure from the last article quoted in Ref. 160.)

The Majorana nature of massive neutrinos  $\nu_j$  manifests itself in the existence of processes in which the total lepton charge  $L$  changes by two units:  $K^+ \rightarrow \pi^- + \mu^+ + \mu^+$ ,  $\mu^- + (A, Z) \rightarrow \mu^+ + (A, Z - 2)$ , *etc.* Extensive studies have shown that the only feasible experiments having the potential of establishing that the massive neutrinos are Majorana particles are at present the experiments searching for  $(\beta\beta)_{0\nu}$ -decay:  $(A, Z) \rightarrow (A, Z + 2) + e^- + e^-$  (see *e.g.*, Ref. 157). The observation of  $(\beta\beta)_{0\nu}$ -decay and the measurement of the corresponding half-life with sufficient accuracy, would not only be a proof that the total lepton charge is not conserved, but might also provide unique information on the i) type of neutrino mass spectrum (see, *e.g.*, Ref. 158), ii) Majorana phases in  $U$  [144,159] and iii) the absolute scale of neutrino masses (for details see Ref. 157 to Ref. 160 and references quoted therein).

Under the assumptions of 3- $\nu$  mixing, of massive neutrinos  $\nu_j$  being Majorana particles, and of  $(\beta\beta)_{0\nu}$ -decay generated only by the (V-A) charged current weak interaction via the exchange of the



three Majorana neutrinos  $\nu_j$  having masses  $m_j \lesssim$  few MeV, the  $(\beta\beta)_{0\nu}$ -decay amplitude has the form (see, *e.g.*, Ref. 39 and Ref. 157):  $A(\beta\beta)_{0\nu} \cong \langle m \rangle / M$ , where  $M$  is the corresponding nuclear matrix element which does not depend on the neutrino mixing parameters, and

$$\begin{aligned} |\langle m \rangle| &= \left| m_1 U_{e1}^2 + m_2 U_{e2}^2 + m_3 U_{e3}^2 \right| \\ &= \left| \left( m_1 c_{12}^2 + m_2 s_{12}^2 e^{i\alpha_{21}} \right) c_{13}^2 + m_3 s_{13}^2 e^{i(\alpha_{31}-2\delta)} \right|, \end{aligned} \quad (13.84)$$

is the effective Majorana mass in  $(\beta\beta)_{0\nu}$ -decay. In the case of CP-invariance one has [42],  $\eta_{21} \equiv e^{i\alpha_{21}} = \pm 1$ ,  $\eta_{31} \equiv e^{i\alpha_{31}} = \pm 1$ ,  $e^{-i2\delta} = 1$ . The three neutrino masses  $m_{1,2,3}$  can be expressed in terms of the two measured  $\Delta m_{jk}^2$  and, *e.g.*,  $\min(m_j)$ . Thus, given the neutrino oscillation parameters  $\Delta m_{21}^2$ ,  $\sin^2 \theta_{12}$ ,  $\Delta m_{31}^2$  and  $\sin^2 \theta_{13}$ ,  $|\langle m \rangle|$  is a function of the lightest neutrino mass  $\min(m_j)$ , the Majorana (and Dirac) CP violation phases in  $U$  and of the type of neutrino mass spectrum. In the case of NH, IH and QD spectrum we have (see, *e.g.*, Ref. 144 and Ref. 160):

$$|\langle m \rangle| \cong \left| \sqrt{\Delta m_{21}^2 s_{12}^2 c_{13}^2} + \sqrt{\Delta m_{31}^2 s_{13}^2 e^{i(\alpha_{31}-\alpha_{21}-2\delta)}} \right|, \quad \text{NH}, \quad (13.85)$$

$$|\langle m \rangle| \cong \tilde{m} \left( 1 - \sin^2 2\theta_{12} \sin^2 \frac{\alpha_{21}}{2} \right)^{\frac{1}{2}}, \quad \text{IH (IO) and QD}, \quad (13.86)$$

where  $\tilde{m} \equiv \sqrt{\Delta m_{23}^2 + m_3^2}$  and  $\tilde{m} \equiv m_0$  for IH (IO) and QD spectrum, respectively. In Eq. (13.86) we have exploited the fact that  $\sin^2 \theta_{13} \ll \cos 2\theta_{12}$ . The CP conserving values of the Majorana phases  $(\alpha_{31} - \alpha_{21})$  and  $\alpha_{21}$  determine the intervals of possible values of  $|\langle m \rangle|$ , corresponding to the different types of neutrino mass spectrum. Using the  $3\sigma$  ranges of the allowed values of the neutrino oscillation parameters from Table 13.7 and Eq. (13.76) one finds that: i)  $2.3 \times 10^{-4} \text{ eV} \lesssim |\langle m \rangle| \lesssim 5.0 \times 10^{-3} \text{ eV}$  in the case of NH spectrum; ii)  $\sqrt{\Delta m_{23}^2} \cos 2\theta_{12} \lesssim |\langle m \rangle| \lesssim \sqrt{\Delta m_{23}^2}$ , or  $1.3 \times 10^{-2} \text{ eV} \lesssim |\langle m \rangle| \lesssim 5.2 \times 10^{-2} \text{ eV}$  in the case of IH spectrum; iii)  $m_0 \cos 2\theta_{12} \lesssim |\langle m \rangle| \lesssim m_0$ , or  $2.8 \times 10^{-2} \text{ eV} \lesssim |\langle m \rangle| \lesssim m_0 \text{ eV}$ ,  $m_0 \gtrsim 0.10 \text{ eV}$ , in the case of QD spectrum. The difference in the ranges of  $|\langle m \rangle|$  in the cases of NH, IH and QD spectrum opens up the possibility to get information about the type of neutrino mass spectrum from a measurement of  $|\langle m \rangle|$  [158]. The predicted  $(\beta\beta)_{0\nu}$ -decay effective Majorana mass  $|\langle m \rangle|$  as a function of the lightest neutrino mass  $\min(m_j)$  is shown in Fig. 13.10.

### 13.8. Outlook

After the spectacular experimental progress made in the studies of neutrino oscillations, further understanding of the pattern of neutrino masses and neutrino mixing, of their origins and of the status of CP symmetry in the lepton sector requires an extensive and challenging program of research. The main goals of such a research program, outlined in the 2010 PDG edition of the Review of Particle Physics, included:

- Determining the nature - Dirac or Majorana, of massive neutrinos  $\nu_j$ . This is of fundamental importance for making progress in our understanding of the origin of neutrino masses and mixing and of the symmetries governing the lepton sector of particle interactions.
- Determination of the sign of  $\Delta m_{\Lambda}^2$  ( $\Delta m_{31}^2$ ) and of the type of neutrino mass spectrum.
- Determining or obtaining significant constraints on the absolute scale of neutrino masses.
- Measurement of, or improving by at least a factor of (5 - 10) the existing upper limit on, the small neutrino mixing angle  $\theta_{13}$ . Together with the Dirac CP-violating phase, the angle  $\theta_{13}$  determines the magnitude of CP-violation effects in neutrino oscillations.
- Determining the status of CP symmetry in the lepton sector.
- High precision measurement of  $\Delta m_{21}^2$ ,  $\theta_{12}$ , and  $|\Delta m_{31}^2|$ ,  $\theta_{23}$ .

- Understanding at a fundamental level the mechanism giving rise to neutrino masses and mixing and to  $L_1$ -non-conservation. This includes understanding the origin of the patterns of  $\nu$ -mixing and  $\nu$ -masses suggested by the data. Are the observed patterns of  $\nu$ -mixing and of  $\Delta m_{21,31}^2$  related to the existence of a new fundamental symmetry of particle interactions? Is there any relation between quark mixing and neutrino mixing, *e.g.*, does the relation  $\theta_{12} + \theta_c = \pi/4$ , where  $\theta_c$  is the Cabibbo angle, hold? What is the physical origin of CP violation phases in the neutrino mixing matrix  $U$ ? Is there any relation (correlation) between the (values of) CP violation phases and mixing angles in  $U$ ? Progress in the theory of neutrino mixing might also lead to a better understanding of the mechanism of generation of baryon asymmetry of the Universe.

The successful realization of this research program, which would be a formidable task and would require many years, already began during the last two years with the results of the T2K and MINOS experiments on the value of  $\theta_{13}$ , of the global analyses of the neutrino oscillation data, which showed that  $\theta_{13} \neq 0$  at  $3\sigma$ , and with the subsequent rather precise measurements of the value of  $\sin^2 2\theta_{13}$  in the Daya Bay and RENO experiments. Averaging the results of the three recent reactor experiments with the standard PDG method, one obtains  $\sin^2 2\theta_{13} = 0.098 \pm 0.013$  [142]. These results on  $\theta_{13}$  have far reaching implications. The measured relatively large value of  $\theta_{13}$  opens up the possibilities, in particular,

i) for searching for CP violation effects in neutrino oscillation experiments with high intensity accelerator neutrino beams, like T2K, NO $\nu$ A, etc. NO $\nu$ A [63], an off-axis  $\nu_e$  appearance experiment using the NuMI beam, is under construction and expected to be complete in 2014. The sensitivities of T2K and NO $\nu$ A on CP violation in neutrino oscillations are discussed in, *e.g.*, Ref. 162.

ii) for determining the sign of  $\Delta m_{32}^2$ , and thus the type of neutrino mass spectrum in the long baseline neutrino oscillation experiments at accelerators, in the experiments studying the oscillations of atmospheric neutrinos (see, *e.g.*, Ref. 82), as well as in experiments with reactor antineutrinos [161]. A value of  $\sin \theta_{13} \gtrsim 0.09$  is a necessary condition for a successful "flavoured" leptogenesis with hierarchical heavy Majorana neutrinos when the CP violation required for the generation of the matter-antimatter asymmetry of the Universe is provided entirely by the Dirac CP violating phase in the neutrino mixing matrix [155].

With the measurement of  $\theta_{13}$ , the first steps on the long "road" leading to a comprehensive understanding of the patterns of neutrino masses and mixing, of their origin and implications, were made.

### References:

1. B. Pontecorvo, Zh. Eksp. Teor. Fiz. **53**, 1717 (1967) [Sov. Phys. JETP **26**, 984 (1968)].
2. M. Fukugita and T. Yanagida, Phys. Lett. **B174**, 45 (1986); V.A. Kuzmin, V.A. Rubakov, and M.E. Shaposhnikov, Phys. Lett. **B155**, 36 (1985).
3. P. Minkowski, Phys. Lett. **B67**, 421 (1977); see also: M. Gell-Mann, P. Ramond, and R. Slansky in *Supergravity*, p. 315, edited by F. Nieuwenhuizen and D. Friedman, North Holland, Amsterdam, 1979; T. Yanagida, *Proc. of the Workshop on Unified Theories and the Baryon Number of the Universe*, edited by O. Sawada and A. Sugamoto, KEK, Japan 1979; R.N. Mohapatra and G. Senjanović, Phys. Rev. Lett. **44**, 912 (1980).
4. B.T. Cleveland *et al.*, Astrophys. J. **496**, 505 (1988).
5. Y. Fukuda *et al.*, [Super-Kamiokande Collab.], Phys. Rev. Lett. **77**, 1683 (1996).
6. J.N. Abdurashitov *et al.*, [SAGE Collab.], Phys. Rev. **C80**, 015807 (2009).
7. P. Anselmann *et al.*, [GALLEX Collab.], Phys. Lett. **B285**, 376 (1992).
8. W. Hampel *et al.*, [GALLEX Collab.], Phys. Lett. **B447**, 127 (1999).
9. M. Altmann *et al.*, [GNO Collab.], Phys. Lett. **B616**, 174 (2005).

10. S. Fukuda *et al.*, [Super-Kamiokande Collab.], Phys. Lett. **B539**, 179 (2002).
11. Q.R. Ahmad *et al.*, [SNO Collab.], Phys. Rev. Lett. **87**, 071301 (2001).
12. Q.R. Ahmad *et al.*, [SNO Collab.], Phys. Rev. Lett. **89**, 011301 (2002).
13. Y. Fukuda *et al.*, [Super-Kamiokande Collab.], Phys. Rev. Lett. **81**, 1562 (1998).
14. Y. Ashie *et al.*, [Super-Kamiokande Collab.], Phys. Rev. Lett. **93**, 101801 (2004).
15. K. Eguchi *et al.*, [KamLAND Collab.], Phys. Rev. Lett. **90**, 021802 (2003).
16. T. Araki *et al.*, [KamLAND Collab.], Phys. Rev. Lett. **94**, 081801 (2005).
17. B. Pontecorvo, Zh. Eksp. Teor. Fiz. **33**, 549 (1957) and **34**, 247 (1958).
18. Z. Maki, M. Nakagawa, and S. Sakata, Prog. Theor. Phys. **28**, 870 (1962).
19. M.H. Ahn *et al.*, [K2K Collab.], Phys. Rev. **D74**, 072003 (2006).
20. D.G. Michael *et al.*, [MINOS Collab.], Phys. Rev. Lett. **97**, 191801 (2006).
21. P. Adamson *et al.*, [MINOS Collab.], Phys. Rev. Lett. **101**, 131802 (2008).
22. L. Wolfenstein, Phys. Rev. **D17**, 2369 (1978); *Proc. of the 8th International Conference on Neutrino Physics and Astrophysics - "Neutrino'78"* (ed. E.C. Fowler, Purdue University Press, West Lafayette, 1978), p. C3.
23. S.P. Mikheev and A.Y. Smirnov, Sov. J. Nucl. Phys. **42**, 913 (1985); Nuovo Cimento **9C**, 17 (1986).
24. K. Abe *et al.*, [T2K Collab.], Phys. Rev. Lett. **107**, 041801 (2011).
25. P. Adamson *et al.*, [MINOS Collab.], Phys. Rev. Lett. **107**, 181802 (2011).
26. F.P. An *et al.*, [Daya Bay Collab.], Phys. Rev. Lett. **108**, 171803 (2012).
27. J.K. Ahn *et al.*, [RENO Collab.], Phys. Rev. Lett. **108**, 191802 (2012).
28. A. Aguilar *et al.*, [LSND Collab.], Phys. Rev. **D64**, 112007 (2001).
29. A.A. Aguilar-Arevalo *et al.*, [MiniBooNE Collab.], Phys. Rev. Lett. **105**, 181801 (2010).
30. D. Karlen in RPP2010.
31. A.A. Aguilar-Arevalo *et al.*, [MiniBooNE Collab.], Phys. Rev. Lett. **98**, 231801 (2007), and Phys. Rev. Lett. **102**, 101802 (2009).
32. J. Kopp, M. Maltoni and T. Schwetz, Phys. Rev. Lett. **107**, 091801 (2011), and references quoted therein.
33. G. Mention *et al.*, Phys. Rev. **D83**, 073006 (2011).
34. T.A. Mueller *et al.*, Phys. Rev. **C83**, 054615 (2011).
35. K. Schreckenbach *et al.*, Phys. Lett. **B160**, 325 (1985).
36. P. Huber, Phys. Rev. **C84**, 024617 (2011).
37. E. Majorana, Nuovo Cimento **5**, 171 (1937).
38. Majorana particles, in contrast to Dirac fermions, are their own antiparticles. An electrically charged particle (like the electron) cannot coincide with its antiparticle (the positron) which carries the opposite non-zero electric charge.
39. S.M. Bilenky and S.T. Petcov, Rev. Mod. Phys. **59**, 671 (1987).
40. S.M. Bilenky, J. Hosek, and S.T. Petcov, Phys. Lett. **B94**, 495 (1980).
41. J. Schechter and J.W.F. Valle, Phys. Rev. **D22**, 2227 (1980); M. Doi *et al.*, Phys. Lett. **B102**, 323 (1981).
42. L. Wolfenstein, Phys. Lett. **B107**, 77 (1981); S.M. Bilenky, N.P. Nedelcheva, and S.T. Petcov, Nucl. Phys. **B247**, 61 (1984); B. Kayser, Phys. Rev. **D30**, 1023 (1984).
43. S. Nussinov, Phys. Lett. **B63**, 201 (1976); B. Kayser, Phys. Rev. **D24**, 110 (1981); J. Rich, Phys. Rev. **D48**, 4318 (1993); H. Lipkin, Phys. Lett. **B348**, 604 (1995); W. Grimus and P. Stockinger, Phys. Rev. **D54**, 3414 (1996); L. Stodolski, Phys. Rev. **D58**, 036006 (1998); W. Grimus, P. Stockinger, and S. Mohanty, Phys. Rev. **D59**, 013011 (1999); L.B. Okun, Surv. High Energy Physics **15**, 75 (2000); J.-M. Levy, hep-ph/0004221 and arXiv:0901.0408; A.D. Dolgov, Phys. Reports **370**, 333 (2002); C. Giunti, Phys. Scripta **67**, 29 (2003) and Phys. Lett. **B17**, 103 (2004); M. Beuthe, Phys. Reports **375**, 105 (2003); H. Lipkin, Phys. Lett. **B642**, 366 (2006); S.M. Bilenky, F. von Feilitzsch, and W. Potzel, J. Phys. **G34**, 987 (2007); C. Giunti and C.W. Kim, *Fundamentals of Neutrino Physics and Astrophysics* (Oxford University Press, Oxford, 2007); E.Kh. Akhmedov, J. Kopp, and M. Lindner, JHEP **0805**, 005 (2008); E.Kh. Akhmedov and A.Yu. Smirnov, Phys. Atom. Nucl. **72**, 1363 (2009).
44. For the subtleties involved in the step leading from Eq. (13.1) to Eq. (13.5) see, *e.g.*, Ref. 45.
45. A.G. Cohen, S.L. Glashow, and Z. Ligeti, Phys. Lett. **B678**, 191 (2009).
46. The neutrino masses do not exceed approximately 1 eV,  $m_j \lesssim 1$ , while in neutrino oscillation experiments neutrinos with energy  $E \gtrsim 100$  keV are detected.
47. S.M. Bilenky and B. Pontecorvo, Phys. Reports **41**, 225 (1978).
48. In Eq. (13.9) we have neglected the possible instability of neutrinos  $\nu_j$ . In most theoretical models with nonzero neutrino masses and neutrino mixing, the predicted half life-time of neutrinos with mass of 1 eV exceeds the age of the Universe, see, *e.g.*, S.T. Petcov, Yad. Fiz. **25**, 641 (1977), (E) *ibid.*, **25** (1977) 1336 [Sov. J. Nucl. Phys. **25**, 340 (1977), (E) *ibid.*, **25**, (1977), 698], and Phys. Lett. **B115**, 401 (1982); W. Marciano and A.I. Sanda, Phys. Lett. **B67**, 303 (1977); P. Pal and L. Wolfenstein, Phys. Rev. **D25**, 766 (1982).
49. L.B. Okun (2000), J.-M. Levy (2000) and H. Lipkin (2006) quoted in Ref. 43 and Ref. 45.
50. The articles by L. Stodolsky (1998) and H. Lipkin (1995) quoted in Ref. 43.
51. V. Gribov and B. Pontecorvo, Phys. Lett. **B28**, 493 (1969).
52. N. Cabibbo, Phys. Lett. **B72**, 333 (1978).
53. V. Barger *et al.*, Phys. Rev. Lett. **45**, 2084 (1980).
54. P. Langacker *et al.*, Nucl. Phys. **B282**, 589 (1987).
55. P.I. Krastev and S.T. Petcov, Phys. Lett. **B205**, 84 (1988).
56. C. Jarlskog, Z. Phys. **C29**, 491 (1985).
57. A. De Rujula *et al.*, Nucl. Phys. **B168**, 54 (1980).
58. M. Apollonio *et al.*, [Chooze Collab.], Phys. Lett. **B466**, 415 (1999); Eur. Phys. J. **C27**, 331 (2003).
59. Y. Abe *et al.*, [Double Chooz Collab.], Phys. Rev. Lett. **108**, 131801 (2012).
60. N. Agafonova *et al.*, [OPERA Collab.], Phys. Lett. **B691**, 138 (2010).
61. N. Agafonova *et al.*, [OPERA Collab.], arXiv:1107.2594.
62. S. Goswami *et al.*, Nucl. Phys. (Proc. Supp.) **B143**, 121 (2005).
63. D.S. Ayres *et al.* [NO $\nu$ A Collab.], hep-ex/0503053.
64. These processes are important, however, for the supernova neutrinos see, *e.g.*, G. Raffelt, *Proc. International School of Physics "Enrico Fermi", CLII Course "Neutrino Physics"*, 23 July-2 August 2002, Varenna, Italy [hep-ph/0208024], and articles quoted therein.
65. We standardly assume that the weak interaction of the flavour neutrinos  $\nu_l$  and antineutrinos  $\bar{\nu}_l$  is described by the Standard Model (for alternatives see, *e.g.*, Ref. 22; M.M. Guzzo *et al.*, Phys. Lett. **B260**, 154 (1991); E. Roulet, Phys. Rev. **D44**, R935 (1991) and Ref. 66).
66. R. Mohapatra *et al.*, Rept. on Prog. in Phys. **70**, 1757 (2007); A. Bandyopadhyay *et al.*, Rept. on Prog. in Phys. **72**, 106201 (2009).
67. V. Barger *et al.*, Phys. Rev. **D22**, 2718 (1980).
68. P. Langacker, J.P. Leveille, and J. Sheiman, Phys. Rev. **D27**, 1228 (1983).
69. The difference between the  $\nu_\mu$  and  $\nu_\tau$  indices of refraction arises at one-loop level and can be relevant for the  $\nu_\mu - \nu_\tau$  oscillations in very dense media, like the core of supernovae, *etc.*; see F.J. Botella, C.S. Lim, and W.J. Marciano, Phys. Rev. **D35**, 896 (1987).
70. The relevant formulae for the oscillations between the  $\nu_e$  and a sterile neutrino  $\nu_s$ ,  $\nu_e \leftrightarrow \nu_s$ , can be obtained from those derived for the case of  $\nu_e \leftrightarrow \nu_{\mu(\tau)}$  oscillations by Refs. [54,68] replacing

- $N_e$  with  $(N_e - 1/2N_n)$ ,  $N_n$  being the neutron number density in matter.
71. T.K. Kuo and J. Pantaleone, Phys. Lett. **B198**, 406 (1987).
  72. A.D. Dziewonski and D.L. Anderson, Physics of the Earth and Planetary Interiors **25**, 297 (1981).
  73. The first studies of the effects of Earth matter on the oscillations of neutrinos were performed numerically in Refs. [67,74] and in E.D. Carlson, Phys. Rev. **D34**, 1454 (1986); A. Dar *et al.*, *ibid.*, **D35**, 3607 (1988); in Ref. 55 and in G. Auremma *et al.*, *ibid.*, **D37**, 665 (1988).
  74. A.Yu. Smirnov and S.P. Mikheev, *Proc. of the Vth Moriond Workshop* (eds. O. Fackler, J. Tran Thanh Van, Frontières, Gif-sur-Yvette, 1986), p. 355.
  75. S.T. Petcov, Phys. Lett. **B434**, 321 (1998), (E) *ibid.* **B444**, 584 (1998); see also: Nucl. Phys. (Proc. Supp.) **B77**, 93 (1999) and hep-ph/9811205.
  76. M.V. Chizhov, M. Maris, and S.T. Petcov, hep-ph/9810501.
  77. E.Kh. Akhmedov *et al.*, Nucl. Phys. **B542**, 3 (1999).
  78. S.T. Petcov, Phys. Lett. **B214**, 259 (1988).
  79. J. Hosaka *et al.*, [Super-Kamiokande Collab.], Phys. Rev. **D74**, 032002 (2006).
  80. E.Kh. Akhmedov, Nucl. Phys. **B538**, 25 (1999).
  81. M.V. Chizhov and S.T. Petcov, Phys. Rev. Lett. **83**, 1096 (1999) and Phys. Rev. Lett. **85**, 3979 (2000); Phys. Rev. **D63**, 073003 (2001).
  82. J. Bernabéu, S. Palomares-Ruiz, and S.T. Petcov, Nucl. Phys. **B669**, 255 (2003); S.T. Petcov and T. Schwetz, Nucl. Phys. **B740**, 1 (2006); R. Gandhi *et al.*, Phys. Rev. **D76**, 073012 (2007); E.Kh. Akhmedov, M. Maltoni, and A.Yu. Smirnov, JHEP **0705**, 077 (2007).
  83. The mantle-core enhancement maxima, *e.g.*, in  $P_m^{2\nu}(\nu_\mu \rightarrow \nu_\mu)$ , appeared in some of the early numerical calculations, but with incorrect interpretation (see, *e.g.*, the articles quoted in Ref. 73).
  84. M. Freund, Phys. Rev. **D64**, 053003 (2001).
  85. M.C. Gonzalez-Garcia and Y. Nir, Rev. Mod. Phys. **75**, 345 (2003); S.M. Bilenky, W. Grimus, and C. Giunti, Prog. in Part. Nucl. Phys. **43**, 1 (1999).
  86. J.N. Bahcall, *Neutrino Astrophysics*, Cambridge University Press, Cambridge, 1989; J.N. Bahcall and M. Pinsonneault, Phys. Rev. Lett. **92**, 121301 (2004).
  87. J.N. Bahcall, A.M. Serenelli, and S. Basu, Astrophys. J. Supp. **165**, 400 (2006).
  88. A. Messiah, *Proc. of the Vth Moriond Workshop* (eds. O. Fackler, J. Tran Thanh Van, Frontières, Gif-sur-Yvette, 1986), p. 373.
  89. S.J. Parke, Phys. Rev. Lett. **57**, 1275 (1986).
  90. S.T. Petcov, Phys. Lett. **B200**, 373 (1988).
  91. P.I. Krastev and S.T. Petcov, Phys. Lett. **B207**, 64 (1988); M. Bruggen, W.C. Haxton, and Y.-Z. Quian, Phys. Rev. **D51**, 4028 (1995).
  92. T. Kaneko, Prog. Theor. Phys. **78**, 532 (1987); S. Toshev, Phys. Lett. **B196**, 170 (1987); M. Ito, T. Kaneko, and M. Nakagawa, Prog. Theor. Phys. **79**, 13 (1988), (E) *ibid.*, **79**, 555 (1988).
  93. S.T. Petcov, Phys. Lett. **B406**, 355 (1997).
  94. C. Cohen-Tannoudji, B. Diu, and F. Laloe, *Quantum Mechanics*, Vol. 1 (Hermann, Paris, and John Wiley & Sons, New York, 1977).
  95. S.T. Petcov, Phys. Lett. **B214**, 139 (1988); E. Lisi *et al.*, Phys. Rev. **D63**, 093002 (2000); A. Friedland, Phys. Rev. **D64**, 013008 (2001).
  96. S.T. Petcov and J. Rich, Phys. Lett. **B224**, 401 (1989).
  97. An expression for the “jump” probability  $P'$  for  $N_e$  varying linearly along the neutrino path was derived in W.C. Haxton, Phys. Rev. Lett. **57**, 1271 (1986) and in Ref. 89 on the basis of the old Landau-Zener result: L.D. Landau, Phys. Z. USSR **1**, 426 (1932), C. Zener, Proc. R. Soc. A **137**, 696 (1932). An analytic description of the solar  $\nu_e$  transitions based on the Landau-Zener jump probability was proposed in Ref. 89 and in W.C. Haxton, Phys. Rev. **D35**, 2352 (1987). The precision limitations of this description, which is less accurate than that based on the exponential density approximation, were discussed in S.T. Petcov, Phys. Lett. **B191**, 299 (1987) and in Ref. 91.
  98. A. de Gouvea, A. Friedland, and H. Murayama, JHEP **0103**, 009 (2001).
  99. C.-S. Lim, Report BNL 52079, 1987; S.P. Mikheev and A.Y. Smirnov, Phys. Lett. **B200**, 560 (1988).
  100. G.L. Fogli *et al.*, Phys. Lett. **B583**, 149 (2004).
  101. J.N. Bahcall, A.M. Serenelli, and S. Basu, Astrophys. J. **621**, L85 (2005).
  102. C. Peña-Garay and A.M. Serenelli, arXiv:0811.2424.
  103. L.C. Stonehill, J.A. Formaggio, and R.G.H. Robertson, Phys. Rev. **C69**, 015801 (2004).
  104. A.M. Serenelli, W.C. Haxton, and C. Peña-Garay, Astrophys. J. **743**, 24 (2011).
  105. B. Pontecorvo, Chalk River Lab. report PD-205, 1946.
  106. D. Davis, Jr., D.S. Harmer, and K.C. Hoffman, Phys. Rev. Lett. **20**, 125 (1968).
  107. F. Kaether *et al.*, Phys. Lett. **B685**, 47 (2010). These authors reanalyzed a complete set of the GALLEX data with a method providing a better background reduction than that adopted in Ref. 8.
  108. A.I. Abazov *et al.*, [SAGE Collab.], Phys. Rev. Lett. **67**, 3332 (1991).
  109. J.N. Abdurashitov *et al.*, [SAGE Collab.], Phys. Lett. **B328**, 234 (1994).
  110. K.S. Hirata *et al.*, [Kamiokande Collab.], Phys. Rev. Lett. **63**, 16 (1989).
  111. Y. Fukuda *et al.*, [Super-Kamiokande Collab.], Phys. Rev. Lett. **81**, 1158 (1998).
  112. J. Hosaka *et al.*, [Super-Kamiokande Collab.], Phys. Rev. **D73**, 112001 (2006).
  113. J.P. Cravens *et al.*, [Super-Kamiokande Collab.], Phys. Rev. **D78**, 032002 (2008).
  114. K. Abe *et al.*, [Super-Kamiokande Collab.], Phys. Rev. **D83**, 052010 (2011).
  115. B. Aharmim *et al.*, [SNO Collab.], Phys. Rev. **C72**, 055502 (2005).
  116. B. Aharmim *et al.*, [SNO Collab.], Phys. Rev. Lett. **101**, 111301 (2008).
  117. B. Aharmim *et al.*, [SNO Collab.], Phys. Rev. **C81**, 055504 (2010).
  118. B. Aharmim *et al.*, [SNO Collab.], arXiv:1109.0763.
  119. C. Arpesella *et al.*, [Borexino Collab.], Phys. Lett. **B658**, 101 (2008); Phys. Rev. Lett. **101**, 091302 (2008).
  120. G. Bellini *et al.*, [Borexino Collab.], Phys. Rev. Lett. **107**, 141302 (2011).
  121. G. Bellini *et al.*, [Borexino Collab.], Phys. Lett. **B707**, 22 (2012).
  122. G. Bellini *et al.*, [Borexino Collab.], Phys. Rev. Lett. **108**, 051302 (2012).
  123. G. Bellini *et al.*, [Borexino Collab.], Phys. Rev. **D82**, 033006 (2010).
  124. Y. Fukuda *et al.*, [Super-Kamiokande Collab.], Phys. Rev. Lett. **86**, 5651 (2001).
  125. Y. Fukuda *et al.*, [Super-Kamiokande Collab.], Phys. Lett. **B539**, 179 (2002).
  126. G.L. Fogli *et al.*, Phys. Rev. **D67**, 073002 (2003); M. Maltoni, T. Schwetz, and J.W. Valle, Phys. Rev. **D67**, 093003 (2003); A. Bandyopadhyay *et al.*, Phys. Lett. **B559**, 121 (2003); J.N. Bahcall, M.C. Gonzalez-Garcia, and C. Peña-Garay, JHEP **0302**, 009 (2003); P.C. de Holanda and A.Y. Smirnov, JCAP **0302**, 001 (2003).
  127. S. Abe *et al.*, [KamLAND Collab.], Phys. Rev. Lett. **100**, 221803 (2008).
  128. A. Gando *et al.*, [KamLAND Collab.], Phys. Rev. **D83**, 052002 (2011).
  129. Y. Ashie *et al.*, [Super-Kamiokande Collab.], Phys. Rev. **D71**, 112005 (2005).
  130. P. Adamson *et al.*, [MINOS Collab.], Phys. Rev. Lett. **106**, 181801 (2011).

131. K. Abe *et al.*, [Super-Kamiokande Collab.], Phys. Rev. Lett. **97**, 171801 (2006).
132. V. Barger *et al.*, Phys. Rev. Lett. **82**, 2640 (1999).
133. E. Lisi *et al.*, Phys. Rev. Lett. **85**, 1166 (2000).
134. P. Adamson *et al.*, [MINOS Collab.], Phys. Rev. Lett. **107**, 021801 (2011).
135. P. Adamson *et al.*, [MINOS Collab.], Phys. Rev. Lett. **108**, 191801 (2012).
136. S. Yamamoto *et al.*, [K2K Collab.], Phys. Rev. Lett. **96**, 181801 (2006).
137. P. Adamson *et al.*, [MINOS Collab.], Phys. Rev. **D82**, 051102 (2010).
138. Y. Declais *et al.*, Phys. Lett. **B338**, 383 (1994).
139. R. Wendell *et al.*, [Super-Kamiokande Collab.], Phys. Rev. **D81**, 092004 (2010).
140. G.L. Fogli *et al.*, Phys. Rev. **D84**, 053007 (2011).
141. T. Schwetz, M Tórtola, and J.W.F. Valle, New J. Phys. **13**, 109401 (2011).
142. Neutrino Mixing section in the Lepton Particle Listings, RPP2012.
143. In the convention we use, the neutrino masses are not ordered in magnitude according to their index number:  $\Delta m_{31}^2 < 0$  corresponds to  $m_3 < m_1 < m_2$ . We can also number the massive neutrinos in such a way that one always has  $m_1 < m_2 < m_3$ , see, *e.g.*, Ref. 144.
144. S.M. Bilenky, S. Pascoli, and S.T. Petcov, Phys. Rev. **D64**, 053010 (2001), and *ibid.*, 113003.
145. P.A.N. Machado *et al.*, JHEP **1205**, 023 (2012).
146. F. Perrin, Comptes Rendus **197**, 868 (1933); E. Fermi, Nuovo Cim. **11**, 1 (1934).
147. V.N. Aseev *et al.*, Phys. Rev. **D84**, 112003 (2011).
148. V. Lobashev *et al.*, Nucl. Phys. **A719**, 153c, (2003).
149. K. Eitel *et al.*, Nucl. Phys. (Proc. Supp.) **B143**, 197 (2005).
150. O. Lahav and A.R. Liddle in RPP2010.
151. K.N. Abazajian *et al.*, Astopart. Phys. **35**, 177 (2011).
152. For alternative mechanisms of neutrino mass generation see, *e.g.*, the first article in Ref. 66 and references quoted therein.
153. S. Davidson and A. Ibarra, Phys. Lett. **B535**, 25 (2002).
154. A. Abada *et al.*, JCAP **0604**, 004 (2006); E. Nardi *et al.*, JHEP **0601**, 164 (2006).
155. S. Pascoli, S.T. Petcov, and A. Riotto, Phys. Rev. **D75**, 083511 (2007) and Nucl. Phys. **B774**, 1 (2007); E. Molinaro and S.T. Petcov, Phys. Lett. **B671**, 60 (2009).
156. S.T. Petcov, Phys. Lett. **B110**, 245 (1982); R. Barbieri *et al.*, JHEP **9812**, 017 (1998); P.H. Frampton, S.T. Petcov, and W. Rodejohann, Nucl. Phys. **B687**, 31 (2004).
157. A. Morales and J. Morales, Nucl. Phys. (Proc. Supp.) **B114**, 141 (2003); C. Aalseth *et al.*, hep-ph/0412300; S.R. Elliott and P. Vogel, Ann. Rev. Nucl. Part. Sci. **52**, 115 (2002).
158. S. Pascoli and S.T. Petcov, Phys. Lett. **B544**, 239 (2002); see also: S. Pascoli, S.T. Petcov, and L. Wolfenstein, Phys. Lett. **B524**, 319 (2002).
159. S.M. Bilenky *et al.*, Phys. Rev. **D54**, 4432 (1996).
160. S.M. Bilenky *et al.*, Phys. Lett. **B465**, 193 (1999); F. Vissani, JHEP **9906**, 022 (1999); K. Matsuda *et al.*, Phys. Rev. **D62**, 093001 (2000); K. Czakon *et al.*, hep-ph/0003161; H.V. Klapdor-Kleingrothaus, H. Päs and A.Yu. Smirnov, Phys. Rev. **D63**, 073005 (2001); S. Pascoli, S.T. Petcov and W. Rodejohann, Phys. Lett. **B549**, 177 (2002), and *ibid.* **B558**, 141 (2003); H. Murayama and Peña-Garay, Phys. Rev. **D69**, 031301 (2004); S. Pascoli, S.T. Petcov, and T. Schwetz, Nucl. Phys. **B734**, 24 (2006); M. Lindner, A. Merle, and W. Rodejohann, Phys. Rev. **D73**, 053005 (2006); A. Faessler *et al.*, Phys. Rev. **D79**, 053001 (2009); S. Pascoli and S.T. Petcov, Phys. Rev. **D77**, 113003 (2008); W. Rodejohann, Int. J. Mod. Phys. E **20**, 1833 (2011).
161. S.T. Petcov and M. Piai, Phys. Lett. **B533**, 94 (2002); S. Choubey, S.T. Petcov and M. Piai, Phys. Rev. **D68**, 113006 (2003); J. Learned *et al.*, Phys. Rev. **D78**, 071302 (2008); L. Zhan *et al.*, Phys. Rev. **D78**, 111103 (2008) and Phys. Rev. **D79**, 073007 (2009); P. Ghoshal and S.T. Petcov, JHEP **1103**, 058 (2011).
162. J. Bernabeu *et al.*, arXiv:1005.3146.

## 14. QUARK MODEL

Revised August 2011 by C. Amsler (University of Zürich), T. DeGrand (University of Colorado, Boulder), and B. Krusche (University of Basel).

### 14.1. Quantum numbers of the quarks

Quantum chromodynamics (QCD) is the theory of the strong interactions. QCD is a quantum field theory and its constituents are a set of fermions, the quarks, and gauge bosons, the gluons. Strongly interacting particles, the hadrons, are bound states of quark and gluon fields. As gluons carry no intrinsic quantum numbers beyond color charge, and because color is believed to be permanently confined, most of the quantum numbers of strongly interacting particles are given by the quantum numbers of their constituent quarks and antiquarks. The description of hadronic properties which strongly emphasizes the role of the minimum-quark-content part of the wave function of a hadron is generically called the quark model. It exists on many levels: from the simple, almost dynamics-free picture of strongly interacting particles as bound states of quarks and antiquarks, to more detailed descriptions of dynamics, either through models or directly from QCD itself. The different sections of this review survey the many approaches to the spectroscopy of strongly interacting particles which fall under the umbrella of the quark model.

Quarks are strongly interacting fermions with spin 1/2 and, by convention, positive parity. Antiquarks have negative parity. Quarks have the additive baryon number 1/3, antiquarks -1/3. Table 14.1 gives the other additive quantum numbers (flavors) for the three generations of quarks. They are related to the charge  $Q$  (in units of the elementary charge  $e$ ) through the generalized Gell-Mann-Nishijima formula

$$Q = I_z + \frac{B + S + C + B + T}{2}, \quad (14.1)$$

where  $B$  is the baryon number. The convention is that the *flavor* of a quark ( $I_z$ ,  $S$ ,  $C$ ,  $B$ , or  $T$ ) has the same sign as its *charge*  $Q$ . With this convention, any flavor carried by a charged meson has the same sign as its charge, *e.g.*, the strangeness of the  $K^+$  is +1, the bottomness of the  $B^+$  is +1, and the charm and strangeness of the  $D_s^-$  are each -1. Antiquarks have the opposite flavor signs.

### 14.2. Mesons

Mesons have baryon number  $B = 0$ . In the quark model, they are  $q\bar{q}'$  bound states of quarks  $q$  and antiquarks  $\bar{q}'$  (the flavors of  $q$  and  $q'$  may be different). If the orbital angular momentum of the  $q\bar{q}'$  state is  $\ell$ , then the parity  $P$  is  $(-1)^{\ell+1}$ . The meson spin  $J$  is given by the usual relation  $|\ell - s| \leq J \leq |\ell + s|$ , where  $s$  is 0 (antiparallel quark spins) or 1 (parallel quark spins). The charge conjugation, or  $C$ -parity  $C = (-1)^{\ell+s}$ , is defined only for the  $q\bar{q}$  states made of quarks and their own antiquarks. The  $C$ -parity can be generalized to the  $G$ -parity  $G = (-1)^{I+\ell+s}$  for mesons made of quarks and their own antiquarks (isospin  $I_z = 0$ ), and for the charged  $u\bar{d}$  and  $d\bar{u}$  states (isospin  $I = 1$ ).

**Table 14.1:** Additive quantum numbers of the quarks.

	$d$	$u$	$s$	$c$	$b$	$t$
$Q$ – electric charge	$-\frac{1}{3}$	$+\frac{2}{3}$	$-\frac{1}{3}$	$+\frac{2}{3}$	$-\frac{1}{3}$	$+\frac{2}{3}$
$I$ – isospin	$\frac{1}{2}$	$\frac{1}{2}$	0	0	0	0
$I_z$ – isospin $z$ -component	$-\frac{1}{2}$	$+\frac{1}{2}$	0	0	0	0
$S$ – strangeness	0	0	-1	0	0	0
$C$ – charm	0	0	0	+1	0	0
$B$ – bottomness	0	0	0	0	-1	0
$T$ – topness	0	0	0	0	0	+1

The mesons are classified in  $J^{PC}$  multiplets. The  $\ell = 0$  states are the pseudoscalars ( $0^{-+}$ ) and the vectors ( $1^{--}$ ). The orbital excitations  $\ell = 1$  are the scalars ( $0^{++}$ ), the axial vectors ( $1^{++}$ ) and ( $1^{+-}$ ), and the tensors ( $2^{++}$ ). Assignments for many of the known mesons are given in Tables 14.2 and 14.3. Radial excitations are denoted by the principal quantum number  $n$ . The very short lifetime of the  $t$  quark makes it likely that bound-state hadrons containing  $t$  quarks and/or antiquarks do not exist.

States in the natural spin-parity series  $P = (-1)^J$  must, according to the above, have  $s = 1$  and hence,  $CP = +1$ . Thus, mesons with natural spin-parity and  $CP = -1$  ( $0^{+-}$ ,  $1^{-+}$ ,  $2^{+-}$ ,  $3^{-+}$ , *etc.*) are forbidden in the  $q\bar{q}'$  model. The  $J^{PC} = 0^{-}$  state is forbidden as well. Mesons with such *exotic* quantum numbers may exist, but would lie outside the  $q\bar{q}'$  model (see section below on exotic mesons).

Following SU(3), the nine possible  $q\bar{q}'$  combinations containing the light  $u$ ,  $d$ , and  $s$  quarks are grouped into an octet and a singlet of light quark mesons:

$$3 \otimes \bar{3} = 8 \oplus 1. \quad (14.2)$$

A fourth quark such as charm  $c$  can be included by extending SU(3) to SU(4). However, SU(4) is badly broken owing to the much heavier  $c$  quark. Nevertheless, in an SU(4) classification, the sixteen mesons are grouped into a 15-plet and a singlet:

$$4 \otimes \bar{4} = 15 \oplus 1. \quad (14.3)$$

The *weight diagrams* for the ground-state pseudoscalar ( $0^{-+}$ ) and vector ( $1^{--}$ ) mesons are depicted in Fig. 14.1. The light quark mesons are members of nonets building the middle plane in Fig. 14.1(a) and (b).

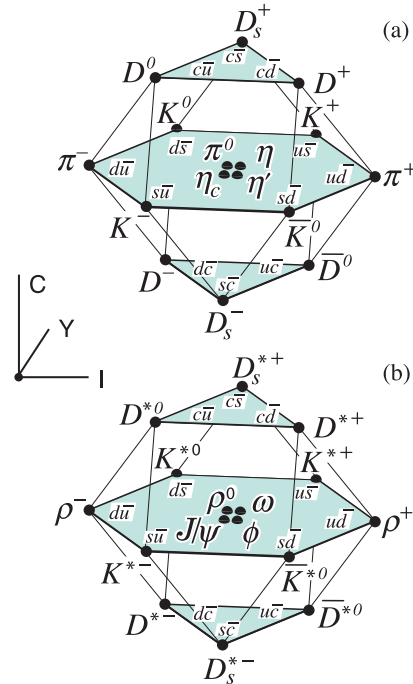


**Figure 14.1:** SU(4) weight diagram showing the 16-plets for the pseudoscalar (a) and vector mesons (b) made of the  $u$ ,  $d$ ,  $s$ , and  $c$  quarks as a function of isospin  $I$ , charm  $C$ , and hypercharge  $Y = S + B - \frac{C}{3}$ . The nonets of light mesons occupy the central planes to which the  $c\bar{c}$  states have been added.

Isoscalar states with the same  $J^{PC}$  will mix, but mixing between the two light quark isoscalar mesons, and the much heavier charmonium or bottomonium states, are generally assumed to be negligible. In the

**Table 14.2:** Suggested  $q\bar{q}$  quark-model assignments for some of the observed light mesons. Mesons in bold face are included in the Meson Summary Table. The wave functions  $f$  and  $f'$  are given in the text. The singlet-octet mixing angles from the quadratic and linear mass formulae are also given for the well established nonets. The classification of the  $0^{++}$  mesons is tentative and the mixing angle uncertain due to large uncertainties in some of the masses. Also, the  $f_0(1710)$  and  $f_0(1370)$  are expected to mix with the  $f_0(1500)$ . The latter is not in this table as it is hard to accommodate in the scalar nonet. The light scalars  $a_0(980)$ ,  $f_0(980)$ , and  $f_0(500)$  are often considered as meson-meson resonances or four-quark states, and are therefore not included in the table. See the “Note on Scalar Mesons” in the Meson Listings for details and alternative schemes.

$n^{2s+1}\ell_J$	$J^{PC}$	$l = 1$ $u\bar{d}, \bar{u}d, \frac{1}{\sqrt{2}}(d\bar{d} - u\bar{u})$	$l = \frac{1}{2}$ $u\bar{s}, d\bar{s}; \bar{d}s, -\bar{u}s$	$l = 0$ $f'$	$l = 0$ $f$	$\theta_{\text{quad}}$ [°]	$\theta_{\text{lin}}$ [°]
$1^1S_0$	$0^{-+}$	$\pi$	$K$	$\eta$	$\eta'(958)$	-11.5	-24.6
$1^3S_1$	$1^{--}$	$\rho(770)$	$K^*(892)$	$\phi(1020)$	$\omega(782)$	38.7	36.0
$1^1P_1$	$1^{+-}$	$b_1(1235)$	$K_{1B}^\dagger$	$h_1(1380)$	$h_1(1170)$		
$1^3P_0$	$0^{++}$	$a_0(1450)$	$K_0^*(1430)$	$f_0(1710)$	$f_0(1370)$		
$1^3P_1$	$1^{++}$	$a_1(1260)$	$K_{1A}^\dagger$	$f_1(1420)$	$f_1(1285)$		
$1^3P_2$	$2^{++}$	$a_2(1320)$	$K_2^*(1430)$	$f_2'(1525)$	$f_2(1270)$	29.6	28.0
$1^1D_2$	$2^{-+}$	$\pi_2(1670)$	$K_2(1770)^\dagger$	$\eta_2(1870)$	$\eta_2(1645)$		
$1^3D_1$	$1^{--}$	$\rho(1700)$	$K^*(1680)$		$\omega(1650)$		
$1^3D_2$	$2^{--}$		$K_2(1820)$				
$1^3D_3$	$3^{--}$	$\rho_3(1690)$	$K_3^*(1780)$	$\phi_3(1850)$	$\omega_3(1670)$	32.0	31.0
$1^3F_4$	$4^{++}$	$a_4(2040)$	$K_4^*(2045)$		$f_4(2050)$		
$1^3G_5$	$5^{--}$	$\rho_5(2350)$	$K_5^*(2380)$				
$1^3H_6$	$6^{++}$	$a_6(2450)$			$f_6(2510)$		
$2^1S_0$	$0^{-+}$	$\pi(1300)$	$K(1460)$	$\eta(1475)$	$\eta(1295)$		
$2^3S_1$	$1^{--}$	$\rho(1450)$	$K^*(1410)$	$\phi(1680)$	$\omega(1420)$		

† The  $1^{+\pm}$  and  $2^{-\pm}$  isospin  $\frac{1}{2}$  states mix. In particular, the  $K_{1A}$  and  $K_{1B}$  are nearly equal ( $45^\circ$ ) mixtures of the  $K_1(1270)$  and  $K_1(1400)$ . The physical vector mesons listed under  $1^3D_1$  and  $2^3S_1$  may be mixtures of  $1^3D_1$  and  $2^3S_1$ , or even have hybrid components.

**Table 14.3:**  $q\bar{q}$  quark-model assignments for the observed heavy mesons. Mesons in bold face are included in the Meson Summary Table.

$n^{2s+1}\ell_J$	$J^{PC}$	$l = 0$ $c\bar{c}$	$l = 0$ $b\bar{b}$	$l = \frac{1}{2}$ $c\bar{u}, \bar{c}d; \bar{c}u, \bar{c}d$	$l = 0$ $c\bar{s}; \bar{c}s$	$l = \frac{1}{2}$ $b\bar{u}, \bar{b}d; \bar{b}u, \bar{b}d$	$l = 0$ $b\bar{s}; \bar{b}s$	$l = 0$ $b\bar{c}; \bar{b}c$
$1^1S_0$	$0^{-+}$	$\eta_c(1S)$	$\eta_b(1S)$	$D$	$D_s^\pm$	$B$	$B_s^0$	$B_c^\pm$
$1^3S_1$	$1^{--}$	$J/\psi(1S)$	$\Upsilon(1S)$	$D^*$	$D_s^{*\pm}$	$B^*$	$B_s^*$	
$1^1P_1$	$1^{+-}$	$h_c(1P)$	$h_b(1P)$	$D_1(2420)$	$D_{s1}(2536)^\pm$	$B_1(5721)$	$B_{s1}(5830)^0$	
$1^3P_0$	$0^{++}$	$\chi_{c0}(1P)$	$\chi_{b0}(1P)$	$D_0^*(2400)$	$D_{s0}^*(2317)^\pm$			
$1^3P_1$	$1^{++}$	$\chi_{c1}(1P)$	$\chi_{b1}(1P)$	$D_1(2430)$	$D_{s1}(2460)^\pm$			
$1^3P_2$	$2^{++}$	$\chi_{c2}(1P)$	$\chi_{b2}(1P)$	$D_2^*(2460)$	$D_{s2}^*(2573)^\pm$	$B_2^*(5747)$	$B_{s2}^*(5840)^0$	
$1^3D_1$	$1^{--}$	$\psi(3770)$			$D_{s1}^*(2700)^\pm$			
$2^1S_0$	$0^{-+}$	$\eta_c(2S)$						
$2^3S_1$	$1^{--}$	$\psi(2S)$	$\Upsilon(2S)$					
$2^3P_{0,1,2}$	$0^{++}, 1^{++}, 2^{++}$	$\chi_{c2}(2P)$	$\chi_{b0,1,2}(2P)$					

† The masses of these states are considerably smaller than most theoretical predictions. They have also been considered as four-quark states (See the “Note on Non- $q\bar{q}$  Mesons” at the end of the Meson Listings). The open flavor states in the  $1^{+-}$  and  $1^{++}$  rows are mixtures of the  $1^{+\pm}$  states.

following, we shall use the generic names  $a$  for the  $I = 1$ ,  $K$  for the  $I = 1/2$ , and  $f$  and  $f'$  for the  $I = 0$  members of the light quark nonets. Thus, the physical isoscalars are mixtures of the SU(3) wave function  $\psi_8$  and  $\psi_1$ :

$$f' = \psi_8 \cos \theta - \psi_1 \sin \theta, \quad (14.4)$$

$$f = \psi_8 \sin \theta + \psi_1 \cos \theta, \quad (14.5)$$

where  $\theta$  is the nonet mixing angle and

$$\psi_8 = \frac{1}{\sqrt{6}}(u\bar{u} + d\bar{d} - 2s\bar{s}), \quad (14.6)$$

$$\psi_1 = \frac{1}{\sqrt{3}}(u\bar{u} + d\bar{d} + s\bar{s}). \quad (14.7)$$

These mixing relations are often rewritten to exhibit the  $u\bar{u} + d\bar{d}$  and  $s\bar{s}$  components which decouple for the ‘‘ideal’’ mixing angle  $\theta_i$ , such that  $\tan \theta_i = 1/\sqrt{2}$  (or  $\theta_i = 35.3^\circ$ ). Defining  $\alpha = \theta + 54.7^\circ$ , one obtains the physical isoscalar in the flavor basis

$$f' = \frac{1}{\sqrt{2}}(u\bar{u} + d\bar{d}) \cos \alpha - s\bar{s} \sin \alpha, \quad (14.8)$$

and its orthogonal partner  $f$  (replace  $\alpha$  by  $\alpha - 90^\circ$ ). Thus for ideal mixing ( $\alpha_i = 90^\circ$ ), the  $f'$  becomes pure  $s\bar{s}$  and the  $f$  pure  $u\bar{u} + d\bar{d}$ . The mixing angle  $\theta$  can be derived from the mass relation

$$\tan \theta = \frac{4m_K - m_a - 3m_{f'}}{2\sqrt{2}(m_a - m_K)}, \quad (14.9)$$

which also determines its sign or, alternatively, from

$$\tan^2 \theta = \frac{4m_K - m_a - 3m_{f'}}{-4m_K + m_a + 3m_f}. \quad (14.10)$$

Eliminating  $\theta$  from these equations leads to the sum rule [1]

$$(m_f + m_{f'})(4m_K - m_a) - 3m_f m_{f'} = 8m_K^2 - 8m_K m_a + 3m_a^2. \quad (14.11)$$

This relation is verified for the ground-state vector mesons. We identify the  $\phi(1020)$  with the  $f'$  and the  $\omega(783)$  with the  $f$ . Thus

$$\phi(1020) = \psi_8 \cos \theta_V - \psi_1 \sin \theta_V, \quad (14.12)$$

$$\omega(782) = \psi_8 \sin \theta_V + \psi_1 \cos \theta_V, \quad (14.13)$$

with the vector mixing angle  $\theta_V = 35^\circ$  from Eq. (14.9), very close to ideal mixing. Thus  $\phi(1020)$  is nearly pure  $s\bar{s}$ . For ideal mixing, Eq. (14.9) and Eq. (14.10) lead to the relations

$$m_K = \frac{m_f + m_{f'}}{2}, \quad m_a = m_f, \quad (14.14)$$

which are satisfied for the vector mesons.

The situation for the pseudoscalar and scalar mesons is not so clear cut, either theoretically or experimentally. For the pseudoscalars, the mixing angle is small. This can be understood qualitatively via gluon-line counting of the mixing process. The size of the mixing process between the nonstrange and strange mass bases scales as  $\alpha_s^2$ , not  $\alpha_s^3$ , because of two rather than three gluon exchange as it does for the vector mesons. It may also be that the lightest isoscalar pseudoscalars mix more strongly with excited states or with states of substantial non- $\bar{q}q$  content, as will be discussed below.

A variety of analysis methods lead to similar results: First, for these states, Eq. (14.11) is satisfied only approximately. Then Eq. (14.9) and Eq. (14.10) lead to somewhat different values for the mixing angle. Identifying the  $\eta$  with the  $f'$  one gets

$$\eta = \psi_8 \cos \theta_P - \psi_1 \sin \theta_P, \quad (14.15)$$

$$\eta' = \psi_8 \sin \theta_P + \psi_1 \cos \theta_P. \quad (14.16)$$

Following chiral perturbation theory, the meson masses in the mass formulae (Eq. (14.9) and Eq. (14.10)) might be replaced by their squares. Table 14.2 lists the mixing angle  $\theta_{\text{in}}$  from Eq. (14.10) and the corresponding  $\theta_{\text{quad}}$  obtained by replacing the meson masses by their squares throughout.

The pseudoscalar mixing angle  $\theta_P$  can also be measured by comparing the partial widths for radiative  $J/\psi$  decay into a vector and a pseudoscalar [2], radiative  $\phi(1020)$  decay into  $\eta$  and  $\eta'$  [3], or  $\bar{p}p$  annihilation at rest into a pair of vector and pseudoscalar or into two pseudoscalars [4,5]. One obtains a mixing angle between  $-10^\circ$  and  $-20^\circ$ . More recently, a lattice QCD simulation, Ref. 6, has successfully reproduced the masses of the  $\eta$  and  $\eta'$ , and as a byproduct find a mixing angle  $\theta_{\text{in}} = -14.1(2.8)^\circ$ . We return to this point in Sec. 14.6.

The nonet mixing angles can be measured in  $\gamma\gamma$  collisions, *e.g.*, for the  $0^{-+}$ ,  $0^{++}$ , and  $2^{++}$  nonets. In the quark model, the amplitude for the coupling of neutral mesons to two photons is proportional to  $\sum_i Q_i^2$ , where  $Q_i$  is the charge of the  $i$ -th quark. The  $2\gamma$  partial width of an isoscalar meson with mass  $m$  is then given in terms of the mixing angle  $\alpha$  by

$$\Gamma_{2\gamma} = C(5 \cos \alpha - \sqrt{2} \sin \alpha)^2 m^3, \quad (14.17)$$

for  $f'$  and  $f$  ( $\alpha \rightarrow \alpha - 90^\circ$ ). The coupling  $C$  may depend on the meson mass. It is often assumed to be a constant in the nonet. For the isovector  $a$ , one then finds  $\Gamma_{2\gamma} = 9 C m^3$ . Thus the members of an ideally mixed nonet couple to  $2\gamma$  with partial widths in the ratios  $f' : a = 25 : 2 : 9$ . For tensor mesons, one finds from the ratios of the measured  $2\gamma$  partial widths for the  $f_2(1270)$  and  $f_2'(1525)$  mesons a mixing angle  $\alpha_T$  of  $(81 \pm 1)^\circ$ , or  $\theta_T = (27 \pm 1)^\circ$ , in accord with the linear mass formula. For the pseudoscalars, one finds from the ratios of partial widths  $\Gamma(\eta' \rightarrow 2\gamma)/\Gamma(\eta \rightarrow 2\gamma)$  a mixing angle  $\theta_P = (-18 \pm 2)^\circ$ , while the ratio  $\Gamma(\eta' \rightarrow 2\gamma)/\Gamma(\pi^0 \rightarrow 2\gamma)$  leads to  $\sim -24^\circ$ . SU(3) breaking effects for pseudoscalars are discussed in Ref. 7.

**Table 14.4:** SU(3) couplings  $\gamma^2$  for quarkonium decays as a function of nonet mixing angle  $\alpha$ , up to a common multiplicative factor  $C$  ( $\phi \equiv 54.7^\circ + \theta_P$ ).

Isospin	Decay channel	$\gamma^2$
0	$\pi\pi$	$3 \cos^2 \alpha$
	$K\bar{K}$	$(\cos \alpha - \sqrt{2} \sin \alpha)^2$
	$\eta\eta$	$(\cos \alpha \cos^2 \phi - \sqrt{2} \sin \alpha \sin^2 \phi)^2$
	$\eta\eta'$	$\frac{1}{2} \sin^2 2\phi (\cos \alpha + \sqrt{2} \sin \alpha)^2$
1	$\eta\pi$	$2 \cos^2 \phi$
	$\eta'\pi$	$2 \sin^2 \phi$
	$K\bar{K}$	1
$\frac{1}{2}$	$K\pi$	$\frac{3}{2}$
	$K\eta$	$(\sin \phi - \frac{\cos \phi}{\sqrt{2}})^2$
	$K\eta'$	$(\cos \phi + \frac{\sin \phi}{\sqrt{2}})^2$

The partial width for the decay of a scalar or a tensor meson into a pair of pseudoscalar mesons is model-dependent. Following Ref. 8,

$$\Gamma = C \times \gamma^2 \times |F(q)|^2 \times q. \quad (14.18)$$

$C$  is a nonet constant,  $q$  the momentum of the decay products,  $F(q)$  a form factor, and  $\gamma^2$  the SU(3) coupling. The model-dependent form factor may be written as

$$|F(q)|^2 = q^{2\ell} \times \exp\left(-\frac{q^2}{8\beta^2}\right), \quad (14.19)$$

where  $\ell$  is the relative angular momentum between the decay products. The decay of a  $q\bar{q}$  meson into a pair of mesons involves the creation of a  $q\bar{q}$  pair from the vacuum, and SU(3) symmetry assumes that the

matrix elements for the creation of  $s\bar{s}$ ,  $u\bar{u}$ , and  $d\bar{d}$  pairs are equal. The couplings  $\gamma^2$  are given in Table 14.4, and their dependence upon the mixing angle  $\alpha$  is shown in Fig. 14.2 for isoscalar decays. The generalization to unequal  $s\bar{s}$ ,  $u\bar{u}$ , and  $d\bar{d}$  couplings is given in Ref. 8. An excellent fit to the tensor meson decay widths is obtained assuming SU(3) symmetry, with  $\beta \simeq 0.5$  GeV/c,  $\theta_V \simeq 26^\circ$  and  $\theta_P \simeq -17^\circ$  [8].

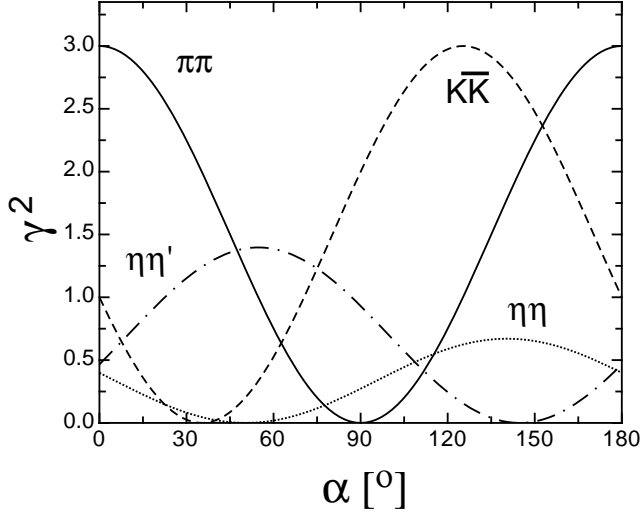


**Figure 14.2:** SU(3) couplings as a function of mixing angle  $\alpha$  for isoscalar decays, up to a common multiplicative factor  $C$  and for  $\theta_P = -17.3^\circ$ .

### 14.3. Exotic mesons

The existence of a light nonet composed of four quarks with masses below 1 GeV was suggested a long time ago [9]. Coupling two triplets of light quarks  $u$ ,  $d$ , and  $s$ , one obtains nine states, of which the six symmetric ( $uu$ ,  $dd$ ,  $ss$ ,  $ud+du$ ,  $us+su$ ,  $ds+sd$ ) form the six dimensional representation  $\mathbf{6}$ , while the three antisymmetric ( $ud-du$ ,  $us-su$ ,  $ds-sd$ ) form the three dimensional representation  $\bar{\mathbf{3}}$  of SU(3):

$$\mathbf{3} \otimes \mathbf{3} = \mathbf{6} \oplus \bar{\mathbf{3}}. \quad (14.20)$$

Combining with spin and color and requiring antisymmetry, one finds that the most deeply bound diquark (and hence the lightest) is the one in the  $\bar{\mathbf{3}}$  and spin singlet state. The combination of the diquark with an antiquark in the  $\mathbf{3}$  representation then gives a light nonet of four-quark scalar states. Letting the number of strange quarks determine the mass splitting, one obtains a mass inverted spectrum with a light isosinglet ( $u\bar{d}\bar{u}\bar{d}$ ), a medium heavy isodoublet (e.g.,  $u\bar{d}\bar{s}\bar{d}$ ) and a heavy isotriplet (e.g.,  $ds\bar{u}\bar{s}$ ) + isosinglet (e.g.,  $us\bar{u}\bar{s}$ ). It is then tempting to identify the lightest state with the  $f_0(500)$ , and the heaviest states with the  $a_0(980)$ , and  $f_0(980)$ . Then the meson with strangeness  $\kappa(800)$  would lie in between.

QCD predicts the existence of extra isoscalar mesons. In the pure gauge theory, they contain only gluons, and are called the glueballs. The ground state glueball is predicted by lattice gauge theories to be  $0^{++}$ , the first excited state  $2^{++}$ . Errors on the mass predictions are large. From Ref. 11 one obtains 1750 (50) (80) MeV for the mass of the lightest  $0^{++}$  glueball from quenched QCD. As an example for the glueball mass spectrum, we show in Fig. 14.3 a recent calculation from Ref. 10. A mass of 1710 MeV is predicted for the ground state, also with an error of about 100 MeV. Earlier work by other groups produced masses at 1650 MeV [12] and 1550 MeV [13] (see also [14]). The first excited state has a mass of about 2.4 GeV, and the lightest glueball with exotic quantum numbers ( $2^{+-}$ ) has a mass of about 4 GeV.

These calculations are made in the so-called “quenched approximation” which neglects  $q\bar{q}$  loops. However, both glue and  $q\bar{q}$  states will couple to singlet scalar mesons. Therefore glueballs will mix

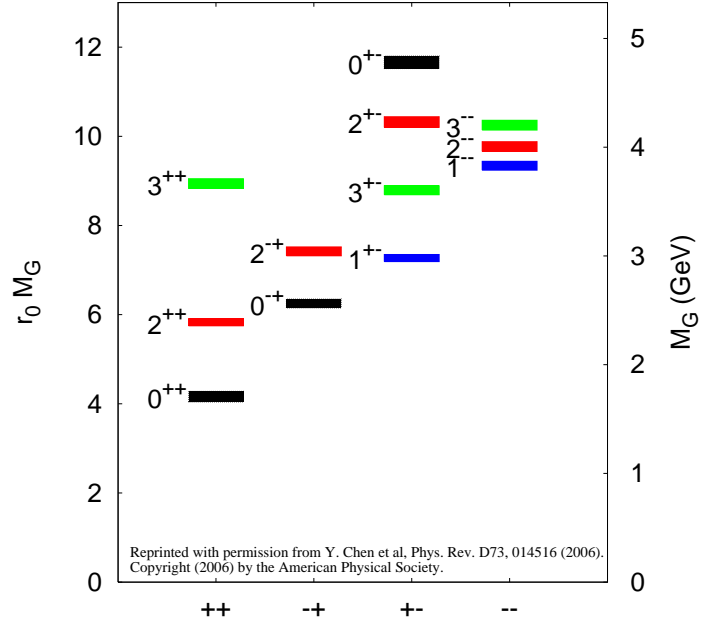


**Figure 14.3:** Predicted glueball mass spectrum from the lattice, in quenched approximation, (from Ref. 10).

with nearby  $q\bar{q}$  states of the same quantum numbers. For example, the two isoscalar  $0^{++}$  mesons around 1500 MeV will mix with the pure ground state glueball to generate the observed physical states  $f_0(1370)$ ,  $f_0(1500)$ , and  $f_0(1710)$  [8,15]. Lattice calculations are only beginning to include these effects. We return to a discussion of this point in Sec. 14.6.

The existence of three singlet scalar mesons around 1.5 GeV suggests additional degrees of freedom such as glue, since only two mesons are predicted in this mass range. The  $f_0(1500)$  [8,15] or, alternatively, the  $f_0(1710)$  [12], have been proposed as candidates for the scalar glueball, both states having considerable mixing also with the  $f_0(1370)$ . Other mixing schemes, in particular with the  $f_0(500)$  and the  $f_0(980)$ , have also been proposed (more details can be found in the “Note on Scalar Mesons” in the Meson Listings and in Ref. 16).

Mesons made of  $q\bar{q}$  pairs bound by excited gluons  $g$ , the hybrid states  $q\bar{q}g$ , are also predicted. They should lie in the 1.9 GeV mass region, according to gluon flux tube models [17]. Lattice QCD also predicts the lightest hybrid, an exotic  $1^{-+}$ , at a mass of 1.8 to 1.9 GeV [18]. However, the bag model predicts four nonets, among them an exotic  $1^{-+}$  around or above 1.4 GeV [19,20]. There are so far two candidates for exotic states with quantum numbers  $1^{-+}$ , the  $\pi_1(1400)$  and  $\pi_1(1600)$ , which could be hybrids or four-quark states (see the “Note on Non- $q\bar{q}$  Mesons” in the 2006 issue of this *Review* [21] and in Ref. 16).

### 14.4. Baryons: $qqq$ states

Baryons are fermions with baryon number  $B = 1$ , *i.e.*, in the most general case, they are composed of three quarks plus any number of quark - antiquark pairs. So far all established baryons are 3-quark ( $qqq$ ) configurations. The color part of their state functions is an SU(3) singlet, a completely antisymmetric state of the three colors. Since the quarks are fermions, the state function must be antisymmetric under interchange of any two equal-mass quarks (up and down quarks in the limit of isospin symmetry). Thus it can be written as

$$|qqq\rangle_A = |\text{color}\rangle_A \times |\text{space, spin, flavor}\rangle_S, \quad (14.21)$$

where the subscripts  $S$  and  $A$  indicate symmetry or antisymmetry under interchange of any two equal-mass quarks. Note the contrast with the state function for the three nucleons in  ${}^3\text{H}$  or  ${}^3\text{He}$ :

$$|NNN\rangle_A = |\text{space, spin, isospin}\rangle_A. \quad (14.22)$$

This difference has major implications for internal structure, magnetic moments, *etc.* (For a nice discussion, see Ref. 22.)



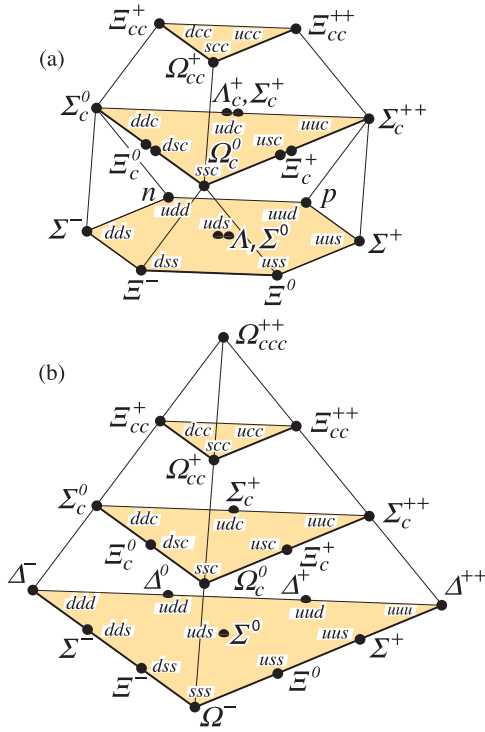


**Figure 14.4:** SU(4) multiplets of baryons made of  $u$ ,  $d$ ,  $s$ , and  $c$  quarks. (a) The 20-plet with an SU(3) octet. (b) The 20-plet with an SU(3) decuplet.

The “ordinary” baryons are made up of  $u$ ,  $d$ , and  $s$  quarks. The three flavors imply an approximate flavor SU(3), which requires that baryons made of these quarks belong to the multiplets on the right side of

$$\mathbf{3} \otimes \mathbf{3} \otimes \mathbf{3} = \mathbf{10}_S \oplus \mathbf{8}_M \oplus \mathbf{8}_M \oplus \mathbf{1}_A \quad (14.23)$$

(see Sec. 42, on “SU( $n$ ) Multiplets and Young Diagrams”). Here the subscripts indicate symmetric, mixed-symmetric, or antisymmetric states under interchange of any two quarks. The  $\mathbf{1}$  is a  $uds$  state ( $\Lambda_1$ ), and the octet contains a similar state ( $\Lambda_8$ ). If these have the same spin and parity, they can mix. The mechanism is the same as for the mesons (see above). In the ground state multiplet, the SU(3) flavor singlet  $\Lambda_1$  is forbidden by Fermi statistics. Section 41, on “SU(3) Isoscalar Factors and Representation Matrices,” shows how relative decay rates in, say,  $\mathbf{10} \rightarrow \mathbf{8} \otimes \mathbf{8}$  decays may be calculated.

The addition of the  $c$  quark to the light quarks extends the flavor symmetry to SU(4). However, due to the large mass of the  $c$  quark, this symmetry is much more strongly broken than the SU(3) of the three light quarks. Figures 14.4(a) and 14.4(b) show the SU(4) baryon multiplets that have as their bottom levels an SU(3) octet, such as the octet that includes the nucleon, or an SU(3) decuplet, such as the decuplet that includes the  $\Delta(1232)$ . All particles in a given SU(4) multiplet have the same spin and parity. The charmed baryons are discussed in more detail in the “Note on Charmed Baryons” in the Particle Listings. The addition of a  $b$  quark extends the flavor symmetry to SU(5); the existence of baryons with  $t$ -quarks is very unlikely due to the short lifetime of the top.

**Table 14.5:**  $N$  and  $\Delta$  states in the  $N=0,1,2$  harmonic oscillator bands.  $L^P$  denotes angular momentum and parity,  $S$  the three-quark spin and ‘sym’=A,S,M the symmetry of the spatial wave function. Only dominant components indicated. Assignments in the  $N=2$  band are partly tentative.

$N$	sym	$L^P$	$S$	$N(I = 1/2)$			$\Delta(I = 3/2)$		
2	A	$1^+$	$1/2$	$1/2^+$	$3/2^+$				
2	M	$2^+$	$3/2$	$1/2^+$	$3/2^+$	$5/2^+$	$7/2^+$		
2	M	$2^+$	$1/2$		$3/2^+$	$5/2^+$		$3/2^+$	$5/2^+$
2	M	$0^+$	$3/2$		$3/2^+$				
2	M	$0^+$	$1/2$	$1/2^+$			$1/2^+$		
				P <sub>11</sub> (1710)			P <sub>31</sub> (1750)		
2	S	$2^+$	$3/2$					$1/2^+$	$3/2^+$
								$5/2^+$	$7/2^+$
								P <sub>31</sub> (1910) P <sub>33</sub> (1920) F <sub>35</sub> (1905) F <sub>37</sub> (1950)	
2	S	$2^+$	$1/2$		$3/2^+$	$5/2^+$			
					P <sub>13</sub> (1720) F <sub>15</sub> (1680)				
2	S	$0^+$	$3/2$					$3/2^+$	
								P <sub>33</sub> (1600)	
2	S	$0^+$	$1/2$	$1/2^+$					
				P <sub>11</sub> (1440)					
1	M	$1^-$	$3/2$	$1/2^-$	$3/2^-$	$5/2^-$			
				S <sub>11</sub> (1650) D <sub>13</sub> (1700) D <sub>15</sub> (1675)					
1	M	$1^-$	$1/2$	$1/2^-$	$3/2^-$			$1/2^-$	$3/2^-$
				S <sub>11</sub> (1535) D <sub>13</sub> (1520)			S <sub>31</sub> (1620) D <sub>33</sub> (1700)		
0	S	$0^+$	$3/2$					$3/2^+$	
								P <sub>33</sub> (1232)	
0	S	$0^+$	$1/2$	$1/2^+$					
				P <sub>11</sub> (938)					

For the “ordinary” baryons (no  $c$  or  $b$  quark), flavor and spin may be combined in an approximate flavor-spin SU(6), in which the six basic states are  $d \uparrow, d \downarrow, \dots, s \downarrow$  ( $\uparrow, \downarrow$  = spin up, down). Then the baryons belong to the multiplets on the right side of

$$\mathbf{6} \otimes \mathbf{6} \otimes \mathbf{6} = \mathbf{56}_S \oplus \mathbf{70}_M \oplus \mathbf{70}_M \oplus \mathbf{20}_A. \quad (14.24)$$

These SU(6) multiplets decompose into flavor SU(3) multiplets as follows:

$$\mathbf{56} = {}^4\mathbf{10} \oplus {}^2\mathbf{8} \quad (14.25a)$$

$$\mathbf{70} = {}^2\mathbf{10} \oplus {}^4\mathbf{8} \oplus {}^2\mathbf{8} \oplus {}^2\mathbf{1} \quad (14.25b)$$

$$\mathbf{20} = {}^2\mathbf{8} \oplus {}^4\mathbf{1}, \quad (14.25c)$$

where the superscript  $(2S+1)$  gives the net spin  $S$  of the quarks for each particle in the SU(3) multiplet. The  $J^P = 1/2^+$  octet containing the nucleon and the  $J^P = 3/2^+$  decuplet containing the  $\Delta(1232)$  together make up the “ground-state” 56-plet, in which the orbital angular momenta between the quark pairs are zero (so that the spatial part of the state function is trivially symmetric). The  $\mathbf{70}$  and  $\mathbf{20}$  require some excitation of the spatial part of the state function in order to make the overall state function symmetric. States with nonzero orbital angular momenta are classified in SU(6)  $\otimes$  O(3) supermultiplets.

It is useful to classify the baryons into bands that have the same number  $N$  of quanta of excitation. Each band consists of a number of supermultiplets, specified by  $(D, L_N^P)$ , where  $D$  is the dimensionality of the SU(6) representation,  $L$  is the total quark orbital angular momentum, and  $P$  is the total parity. Supermultiplets contained in bands up to  $N = 12$  are given in Ref. 24. The  $N = 0$  band, which contains the nucleon and  $\Delta(1232)$ , consists only of the  $(56, 0_0^+)$  supermultiplet. The  $N = 1$  band consists only of the  $(70, 1_1^-)$  multiplet and contains the negative-parity baryons with masses below about 1.9 GeV. The  $N = 2$  band contains five supermultiplets:  $(56, 0_2^+)$ ,  $(70, 0_2^+)$ ,  $(56, 2_2^+)$ ,  $(70, 2_2^+)$ , and  $(20, 1_2^+)$ .

The wave functions of the non-strange baryons in the harmonic oscillator basis are often labeled by  $|X^{2S+1}L_\pi J^P\rangle$ , where  $S, L, J, P$  are as above,  $X = N$  or  $\Delta$ , and  $\pi = S, M$  or  $A$  denotes the symmetry of the spatial wave function. The possible model states for the bands with  $N=0,1,2$  are given in Table 14.5. The assignment of experimentally observed states is only complete and well established up to the  $N=1$  band. Some more tentative assignments for higher multiplets are suggested in Ref. 25.

In Table 14.6, quark-model assignments are given for many of the established baryons whose SU(6)  $\otimes$  O(3) compositions are relatively unmixed. One must, however, keep in mind that apart from the mixing of the  $\Lambda$  singlet and octet states, states with same  $J^P$  but different  $L, S$  combinations can also mix. In the quark model with one-gluon exchange motivated interactions, the size of the mixing is determined by the relative strength of the tensor term with respect to the contact term (see below). The mixing is more important for the decay patterns of the states than for their positions. An example are the lowest lying  $(70, 1_1^-)$  states with  $J^P=1/2^-$  and  $3/2^-$ . The physical states are:

$$|S_{11}(1535)\rangle = \cos(\Theta_S)|N^2P_M 1/2^-\rangle - \sin(\Theta_S)|N^4P_M 1/2^-\rangle \quad (14.26)$$

$$|D_{13}(1520)\rangle = \cos(\Theta_D)|N^2P_M 3/2^-\rangle - \sin(\Theta_D)|N^4P_M 3/2^-\rangle \quad (14.27)$$

and the orthogonal combinations for  $S_{11}(1650)$  and  $D_{13}(1700)$ . The mixing is large for the  $J^P=1/2^-$  states ( $\Theta_S \approx -32^\circ$ ), but small for the  $J^P=3/2^-$  states ( $\Theta_D \approx +6^\circ$ ) [26,31].

All baryons of the ground state multiplets are known. Many of their properties, in particular their masses, are in good agreement even with the most basic versions of the quark model, including harmonic (or linear) confinement and a spin-spin interaction, which is responsible for the octet - decuplet mass shifts. A consistent description of the ground-state electroweak properties, however, requires refined relativistic constituent quark models.

**Table 14.6:** Quark-model assignments for some of the known baryons in terms of a flavor-spin SU(6) basis. Only the dominant representation is listed. Assignments for several states, especially for the  $\Lambda(1810)$ ,  $\Lambda(2350)$ ,  $\Xi(1820)$ , and  $\Xi(2030)$ , are merely educated guesses.  $\dagger$  recent suggestions for assignments and re-assignments from ref. [28]. For assignments of the charmed baryons, see the “Note on Charmed Baryons” in the Particle Listings.

$J^P$	$(D, L_N^P)S$	Octet members			Singlets
$1/2^+$	$(56, 0_0^+)$	$1/2 N(939)$	$\Lambda(1116)$	$\Sigma(1193)$	$\Xi(1318)$
$1/2^+$	$(56, 0_2^+)$	$1/2 N(1440)$	$\Lambda(1600)$	$\Sigma(1660)$	$\Xi(1690)^\dagger$
$1/2^-$	$(70, 1_1^-)$	$1/2 N(1535)$	$\Lambda(1670)$	$\Sigma(1620)$	$\Xi(?)$ $\Lambda(1405)$
				$\Sigma(1560)^\dagger$	
$3/2^-$	$(70, 1_1^-)$	$1/2 N(1520)$	$\Lambda(1690)$	$\Sigma(1670)$	$\Xi(1820)$ $\Lambda(1520)$
$1/2^-$	$(70, 1_1^-)$	$3/2 N(1650)$	$\Lambda(1800)$	$\Sigma(1750)$	$\Xi(?)$
				$\Sigma(1620)^\dagger$	
$3/2^-$	$(70, 1_1^-)$	$3/2 N(1700)$	$\Lambda(?)$	$\Sigma(1940)^\dagger$	$\Xi(?)$
$5/2^-$	$(70, 1_1^-)$	$3/2 N(1675)$	$\Lambda(1830)$	$\Sigma(1775)$	$\Xi(1950)^\dagger$
$1/2^+$	$(70, 0_2^+)$	$1/2 N(1710)$	$\Lambda(1810)$	$\Sigma(1880)$	$\Xi(?)$ $\Lambda(1810)^\dagger$
$3/2^+$	$(56, 2_2^+)$	$1/2 N(1720)$	$\Lambda(1890)$	$\Sigma(?)$	$\Xi(?)$
$5/2^+$	$(56, 2_2^+)$	$1/2 N(1680)$	$\Lambda(1820)$	$\Sigma(1915)$	$\Xi(2030)$
$7/2^-$	$(70, 3_3^-)$	$1/2 N(2190)$	$\Lambda(?)$	$\Sigma(?)$	$\Xi(?)$ $\Lambda(2100)$
$9/2^-$	$(70, 3_3^-)$	$3/2 N(2250)$	$\Lambda(?)$	$\Sigma(?)$	$\Xi(?)$
$9/2^+$	$(56, 4_4^+)$	$1/2 N(2220)$	$\Lambda(2350)$	$\Sigma(?)$	$\Xi(?)$
Decuplet members					
$3/2^+$	$(56, 0_0^+)$	$3/2 \Delta(1232)$	$\Sigma(1385)$	$\Xi(1530)$	$\Omega(1672)$
$3/2^+$	$(56, 0_2^+)$	$3/2 \Delta(1600)$	$\Sigma(1690)^\dagger$	$\Xi(?)$	$\Omega(?)$
$1/2^-$	$(70, 1_1^-)$	$1/2 \Delta(1620)$	$\Sigma(1750)^\dagger$	$\Xi(?)$	$\Omega(?)$
$3/2^-$	$(70, 1_1^-)$	$1/2 \Delta(1700)$	$\Sigma(?)$	$\Xi(?)$	$\Omega(?)$
$5/2^+$	$(56, 2_2^+)$	$3/2 \Delta(1905)$	$\Sigma(?)$	$\Xi(?)$	$\Omega(?)$
$7/2^+$	$(56, 2_2^+)$	$3/2 \Delta(1950)$	$\Sigma(2030)$	$\Xi(?)$	$\Omega(?)$
$11/2^+$	$(56, 4_4^+)$	$3/2 \Delta(2420)$	$\Sigma(?)$	$\Xi(?)$	$\Omega(?)$

The situation for the excited states is much less clear. The assignment of some experimentally observed states with strange quarks to model configurations is only tentative and in many cases candidates are completely missing. Recently, Melde, Plessas and Sengl [28] have calculated baryon properties in relativistic constituent quark models, using one-gluon exchange and Goldstone-boson exchange for the modeling of the hyperfine interactions (see Sec. 14.5 on Dynamics). Both types of models give qualitatively comparable results, and underestimate in general experimentally observed decay widths. Nevertheless, in particular on the basis of the observed decay patterns, the authors have assigned some additional states with strangeness to the SU(3) multiplets and suggest re-assignments for a few others. Among the new assignments are states with weak experimental evidence (two or three star ratings) and partly without firm spin/parity assignments, so that further experimental efforts are necessary before final conclusions can be drawn. We have added their suggestions in Table 14.6.

In the non-strange sector there are two main problems which are illustrated in Fig. 14.5, where the experimentally observed excitation spectrum of the nucleon ( $N$  and  $\Delta$  resonances) is compared to the results of a typical quark model calculation [27]. The lowest states from the  $N=2$  band, the  $P_{11}(1440)$ , and the  $P_{33}(1600)$ , appear lower than the negative parity states from the  $N=1$  band (see Table 14.5) and much lower than predicted by most models. Also negative parity  $\Delta$  states from the  $N=3$  band ( $S_{31}(1900)$ ,  $D_{33}(1940)$ , and  $D_{35}(1930)$ ) are too low in energy. Part of the problem could be experimental. Among the negative parity  $\Delta$  states, only the  $D_{35}$  has three stars and

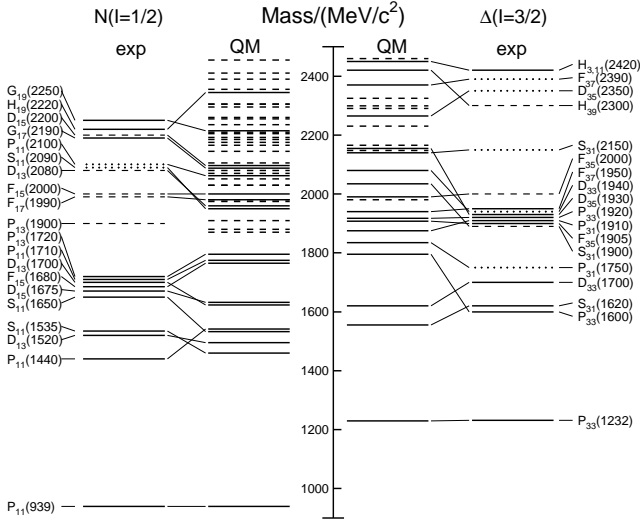


**Figure 14.5:** Excitation spectrum of the nucleon. Compared are the positions of the excited states identified in experiment, to those predicted by a relativized quark model calculation. Left hand side: isospin  $I = 1/2$   $N$ -states, right hand side: isospin  $I = 3/2$   $\Delta$ -states. Experimental: (columns labeled 'exp'), three- and four-star states are indicated by full lines (two-star dashed lines, one-star dotted lines). At the very left and right of the figure, the spectroscopic notation of these states is given. Quark model [27]: (columns labeled 'QM'), all states for the  $N=1,2$  bands, low-lying states for the  $N=3,4,5$  bands. Full lines: at least tentative assignment to observed states, dashed lines: so far no observed counterparts. Many of the assignments between predicted and observed states are highly tentative.

the uncertainty in the position of the  $P_{33}(1600)$  is large (1550 - 1700 MeV).

Furthermore, many more states are predicted than observed. This has been known for a long time as the 'missing resonance' problem [26]. Up to an excitation energy of 2.4 GeV, about 45  $N$  states are predicted, but only 12 are established (four- or three-star; see Note on  $N$  and  $\Delta$  Resonances for the rating of the status of resonances) and 7 are tentative (two- or one-star). Even for the  $N=2$  band, up to now only half of the predicted states have been observed. The most recent partial wave analysis of elastic pion scattering and charge exchange data by Arndt and collaborators [29] has made the situation even worse. They found no evidence for almost half of the states listed in this review (and included in Fig. 14.5). Such analyses are of course biased against resonances which couple only weakly to the  $N\pi$  channel. Quark model predictions for the couplings to other hadronic channels and to photons are given in Ref. 27. A large experimental effort is ongoing at several electron accelerators to study the baryon resonance spectrum with real and virtual photon-induced meson production reactions. This includes the search for as-yet-unobserved states, as well as detailed studies of the properties of the low lying states (decay patterns, electromagnetic couplings, magnetic moments, *etc.*) (see Ref. 30 for recent reviews). This experimental effort has currently entered its final phase with the measurement of single and double polarization observables for many different meson production channels, so that a much better understanding of the experimental spectrum can be expected for the near future.

In quark models, the number of excited states is determined by the effective degrees of freedom, while their ordering and decay properties are related to the residual quark - quark interaction. An overview of quark models for baryons is given in Ref. 31, a recent discussion of baryon spectroscopy is given in Ref. 25. The effective degrees of freedom in the standard nonrelativistic quark model are three equivalent valence quarks with one-gluon exchange-motivated, flavor-independent color-magnetic interactions. A different class of models uses interactions which give rise to a quark - diquark clustering

of the baryons (for a review see Ref. 32). If there is a tightly bound diquark, only two degrees of freedom are available at low energies, and thus *fewer* states are predicted. Furthermore, selection rules in the decay pattern may arise from the quantum numbers of the diquark. *More* states are predicted by collective models of the baryon like the algebraic approach in Ref. 33. In this approach, the quantum numbers of the valence quarks are distributed over a Y-shaped string-like configuration, and additional states arise *e.g.*, from vibrations of the strings. *More* states are also predicted in the framework of flux-tube models (see Ref. 34), which are motivated by lattice QCD. In addition to the quark degrees of freedom, flux-tubes responsible for the confinement of the quarks are considered as degrees of freedom. These models include hybrid baryons containing explicit excitations of the gluon fields. However, since all half integral  $J^P$  quantum numbers are possible for ordinary baryons, such 'exotics' will be very hard to identify, and probably always mix with ordinary states. So far, the experimentally observed number of states is still far lower even than predicted by the quark-diquark models.

Recently, the influence of chiral symmetry on the excitation spectrum of the nucleon has been hotly debated from a somewhat new perspective. Chiral symmetry, the fundamental symmetry of QCD, is strongly broken for the low lying states, resulting in large mass differences of parity partners like the  $J^P=1/2^+$   $P_{11}(938)$  ground state and the  $J^P=1/2^-$   $S_{11}(1535)$  excitation. However, at higher excitation energies there is some evidence for parity doublets and even some very tentative suggestions for full chiral multiplets of  $N^*$  and  $\Delta$  resonances. An effective restoration of chiral symmetry at high excitation energies due to a decoupling from the quark condensate of the vacuum has been discussed (see Ref. 35 for recent reviews) as a possible cause. In this case, the mass generating mechanisms for low and high lying states would be essentially different. As a further consequence, the parity doublets would decouple from pions, so that experimental bias would be worse. However, parity doublets might also arise from the spin-orbital dynamics of the 3-quark system. Presently, the status of data does not allow final conclusions.

The most recent developments on the theory side are the first unquenched lattice calculations for the excitation spectrum discussed in Sec. 14.6. The results are basically consistent with the level counting of  $SU(6) \otimes O(3)$  in the standard non-relativistic quark model and show no indication for quark-diquark structures or parity doubling. Consequently, there is as yet no indication from lattice that the mis-match between the excitation spectrum predicted by the standard quark model and experimental observations is due to inappropriate degrees of freedom in the quark model.

### 14.5. Dynamics

Quantum chromodynamics (QCD) is well-established as the theory for the strong interactions. As such, one of the goals of QCD is to predict the spectrum of strongly-interacting particles. To date, the only first-principles calculations of spectroscopy from QCD use lattice methods. These are the subject of Sec. 14.6. These calculations are difficult and unwieldy, and many interesting questions do not have a good lattice-based method of solution. Therefore, it is natural to build models, whose ingredients are abstracted from QCD, or from the low-energy limit of QCD (such as chiral Lagrangians) or from the data itself. The words "quark model" are a shorthand for such phenomenological models. Many specific quark models exist, but most contain a similar basic set of dynamical ingredients. These include:

- i) A confining interaction, which is generally spin-independent (*e.g.*, harmonic oscillator or linear confinement);
- ii) Different types of spin-dependent interactions:
  - a) commonly used is a color-magnetic flavor-independent interaction modeled after the effects of gluon exchange in QCD (see *e.g.*, Ref. 36). For example, in the  $S$ -wave states, there is a spin-spin hyperfine interaction of the form

$$H_{HF} = -\alpha_S M \sum_{i>j} (\vec{\sigma} \lambda_a)_i (\vec{\sigma} \lambda_a)_j, \quad (14.28)$$

where  $M$  is a constant with units of energy,  $\lambda_a$  ( $a = 1, \dots, 8$ ) is the set of  $SU(3)$  unitary spin matrices, defined in Sec. 41,

on “SU(3) Isoscalar Factors and Representation Matrices,” and the sum runs over constituent quarks or antiquarks. Spin-orbit interactions, although allowed, seem to be small in general, but a tensor term is responsible for the mixing of states with the same  $J^P$  but different  $L, S$  combinations.

b) other approaches include flavor-dependent short-range quark forces from instanton effects (see *e.g.*, Ref. 37). This interaction acts only on scalar, isoscalar pairs of quarks in a relative  $S$ -wave state:

$$\langle q^2; S, L, T | W | q^2; S, L, T \rangle = -4g\delta_{S,0}\delta_{L,0}\delta_{T,0}\mathcal{W} \quad (14.29)$$

where  $\mathcal{W}$  is the radial matrix element of the contact interaction.

c) a rather different and controversially discussed approach is based on flavor-dependent spin-spin forces arising from one-boson exchange. The interaction term is of the form:

$$H_{HF} \propto \sum_{i<j} V(\vec{r}_{ij}) \lambda_i^F \cdot \lambda_j^F \vec{\sigma}_i \cdot \vec{\sigma}_j \quad (14.30)$$

where the  $\lambda_i^F$  are in flavor space (see *e.g.*, Ref. 38).

- iii) A strange quark mass somewhat larger than the up and down quark masses, in order to split the SU(3) multiplets;
- iv) In the case of spin-spin interactions (ii,c), a flavor-symmetric interaction for mixing  $q\bar{q}$  configurations of different flavors (*e.g.*,  $u\bar{u} \leftrightarrow d\bar{d} \leftrightarrow s\bar{s}$ ), in isoscalar channels, so as to reproduce *e.g.*, the  $\eta - \eta'$  and  $\omega - \phi$  mesons.

These ingredients provide the basic mechanisms that determine the hadron spectrum in the standard quark model.

## 14.6. Lattice Calculations of Hadronic Spectroscopy

Lattice calculations are a major source of information about QCD masses and matrix elements. The necessary theoretical background is given in Sec. 17 of this *Review*. Here we confine ourselves to some general comments and illustrations of lattice calculations for spectroscopy.

In general, the cleanest lattice results come from computations of processes in which there is only one particle in the simulation volume. These quantities include masses of hadrons, simple decay constants, like pseudoscalar meson decay constants, and semileptonic form factors (such as the ones appropriate to  $B \rightarrow D\nu, K\nu, \pi\nu$ ). The cleanest predictions for masses are for states which have narrow decay widths and are far below any thresholds to open channels, since the effects of final state interactions are not yet under complete control on the lattice. As a simple corollary, the lightest state in a channel is easier to study than the heavier ones. “Difficult” states for the quark model (such as exotics) are also difficult for the lattice because of the lack of simple operators which couple well to them.

Good-quality modern lattice calculations will present multi-part error budgets with their predictions. A small part of the uncertainty is statistical, from sample size. Typically, the quoted statistical uncertainty includes uncertainty from a fit: it is rare that a simulation computes one global quantity which is the desired observable. Simulations which include virtual quark-antiquark pairs (also known as “dynamical quarks” or “sea quarks”) are often done at up and down quark mass values heavier than the experimental ones, and it is then necessary to extrapolate in these quark masses. Simulations can work at the physical values of the heavier quarks’ masses. They are always done at nonzero lattice spacing, and so it is necessary to extrapolate to zero lattice spacing. Some theoretical input is needed to do this. Much of the uncertainty in these extrapolations is systematic, from the choice of fitting function. Other systematics include the effect of finite simulation volume, the number of flavors of dynamical quarks actually simulated, and technical issues with how these dynamical quarks are included. The particular choice of a fiducial mass (to normalize other predictions) is not standardized; there are many possible choices, each with its own set of strengths and weaknesses, and determining it usually requires a second lattice simulation from that used to calculate the quantity under consideration.

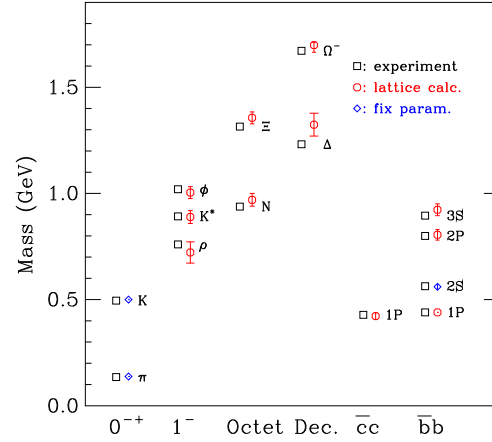


**Figure 14.6:** A recent calculation of spectroscopy with dynamical  $u, d,$  and  $s$  quarks. The pion and kaon fix the light quark masses. Only the mass splittings relative to the  $1S$  states in the heavy quark sectors are shown. The  $\Upsilon 2S - 1S$  splitting sets the overall energy scale.

A systematic error of major historical interest is the “quenched approximation,” in which dynamical quarks are simply left out of the simulation. This was done because the addition of these virtual pairs presented an expensive computational problem. No generally-accepted methodology has ever allowed one to correct for quenching effects, short of redoing all calculations with dynamical quarks. Recent advances in algorithms and computer hardware have rendered it obsolete.

With these brief remarks, we turn to examples. The field of lattice QCD simulations is vast, and so it is not possible to give a comprehensive review of them in a small space. The history of lattice QCD simulations is a story of thirty years of incremental improvements in physical understanding, algorithm development, and ever faster computers, which have combined to bring the field to a present state where it is possible to carry out very high quality calculations. We present a few representative illustrations, to show the current state of the art.

By far, the major part of all lattice spectroscopy is concerned with that of the light hadrons, and so we illustrate results from two groups. First, a recent calculation of spectroscopy with dynamical  $u, d,$  and  $s$  quarks is shown in Fig. 14.6. The pion and kaon masses are used to set the light quark masses. The  $\Upsilon 2S - 1S$  splitting is used to set the lattice spacing or equivalently, the overall energy scale in the lattice calculation. This is an updated figure from Ref. 39, using results from Ref. 41 and Ref. 42 (D. Toussaint, private communication).

These results come from simulations using dynamical up and down quarks which are heavier than their physical values. As a result, the error bars on all the particles which decay strongly and are above their decay thresholds (the vector mesons and the  $\Delta$ , for example) do not include the effect of coupling to the decay channels.

A more recent result by Ref. 40 goes farther, in that its simulations include the coupling of resonances to open channels in their analysis. Their plot of light hadron spectroscopy is shown in Fig. 14.7.

Flavor singlet mesons are at the frontier of lattice QCD calculations, because one must include the effects of “annihilation graphs,” for the valence  $q$  and  $\bar{q}$ . Recently, the RBC and UKQCD collaborations, Ref. 6, have reported a calculation of the  $\eta$  and  $\eta'$  mesons, finding masses of 573(6) and 947(142) MeV, respectively. The singlet-octet mixing angle (in the conventions of Table 14.2) is  $\theta_{in} = -14.1(2.8)^\circ$ .

The spectroscopy of mesons containing heavy quarks has become a truly high-precision endeavor. These simulations use Non-Relativistic QCD (NRQCD) or Heavy Quark Effective Theory (HQET), systematic expansions of the QCD Lagrangian in powers of the heavy quark velocity, or the heavy quark mass. Terms in the Lagrangian have obvious quark model analogs, but are derived directly from QCD. For example, the heavy quark potential is a derived quantity, extracted from simulations. Fig. 14.8 shows the mass spectrum for mesons containing at least one heavy ( $b$  or  $c$ ) quark from Ref. 42 and Ref. 43.

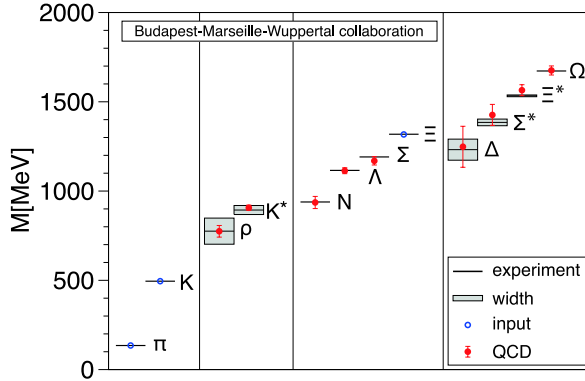


Figure 14.7: Light hadron spectroscopy from Ref. 40.

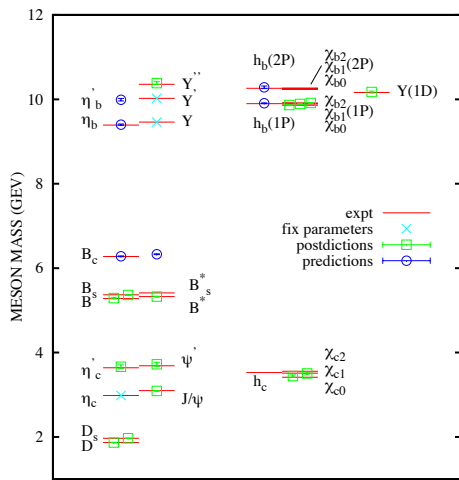


Figure 14.8: Spectroscopy for mesonic systems containing one or more heavy quarks (adapted from Ref. 42 and Ref. 43). Particles whose masses are used to fix lattice parameters are shown with crosses; the authors distinguish between “predictions” and “postdictions” of their calculation. Lines represent experiment.

The calculations use a discretization of nonrelativistic QCD for bottom quarks with charm and lighter quarks being handled with an improved relativistic action. Three flavors of light dynamical quarks are included.

Finally, Fig. 14.9 shows recent lattice calculations of singly and double charmed baryons. Here we are at the forefront of theory and experiment.

Recall that lattice calculations take operators which are interpolating fields with quantum numbers appropriate to the desired states, compute correlation functions of these operators, and fit the correlation functions to functional forms parameterized by a set of masses and matrix elements. As we move away from hadrons which can be created by the simplest quark model operators (appropriate to the lightest meson and baryon multiplets) we encounter a host of new problems: either no good interpolating fields, or too many possible interpolating fields, and many states with the same quantum numbers. Techniques for dealing with these interrelated problems vary from collaboration to collaboration, but all share common features: typically, correlation functions from many different interpolating fields are used, and the signal is extracted in what amounts to a variational calculation using the chosen operator basis. In addition to mass spectra, wave function information can be garnered from the form of the best variational wave function. Of course, the same problems which are present in the spectroscopy of the lightest hadrons (the need to extrapolate to infinite volume, physical values of the light quark masses, and zero lattice spacing) are also present. We briefly touch on three different kinds of hadrons: excited states of baryons, glueballs,

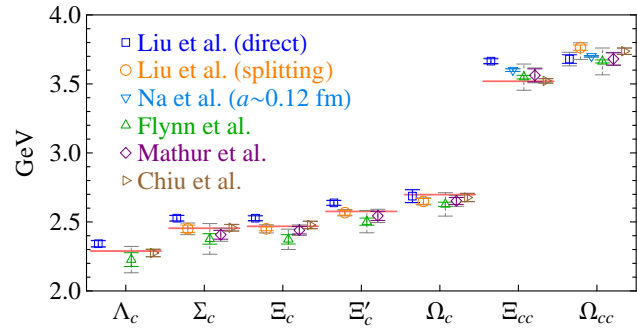


Figure 14.9: Lattice predictions for masses of charmed baryons. Data are Liu, *et al.*, Ref. 44; Na *et al.*, Ref. 45; Flynn *et al.*, Ref. 46; Mathur *et al.*, Ref. 47; and Chiu *et al.*, Ref. 48. The first two references use full QCD; the latter three are quenched. Two mass extractions are taken from Ref. 44; the lighter (orange) circular points come from a calculation of mass splittings while the darker (blue) square points are from a direct mass extrapolation. Lines are from experiment.

and hybrid mesons. The quality of the data is not as good as for the ground states, and so the results continue to evolve.

Ref. 49 is a good recent review of excited baryon spectroscopy. The interesting physics questions to be addressed are precisely those enumerated in the last section. An example of a recent calculation, due to Ref. 50 is shown in Fig. 14.10. Notice that the pion is not yet at its physical value. The lightest positive parity state is the nucleon, and the Roper resonance has not yet appeared as a light state.

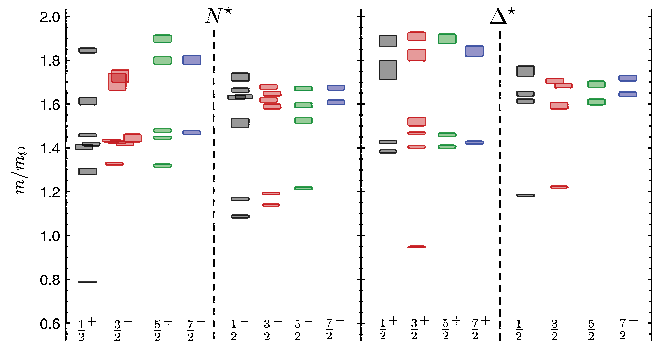
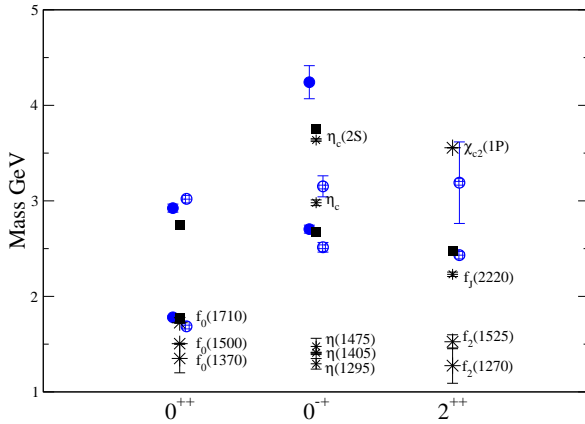


Figure 14.10: Spin-identified spectrum of nucleons and deltas, from lattices where  $m_\pi = 396$  MeV, in units of the calculated  $\Omega$  mass, from Ref. 50. The colors just correspond to the different  $J$  assignments: grey for  $J = 1/2$ , red for  $J = 3/2$ , green for  $J = 5/2$ , blue for  $J = 7/2$ .

Exotic mesons share the difficulties of ordinary excited states, and some recent calculations actually include both kinds of states in their combined fits. Ref. 51 provides a good summary of the theoretical and experimental situation regarding mesons with exotic quantum numbers, including a compilation of lattice data. The lightest exotics, the  $h_0$ ,  $\eta_1$ , and  $h_2$ , have long been targets of lattice studies. Recently, the authors of Ref. 52 have presented new results for isoscalar and isovector meson spectroscopy, which observe the three states around 2 GeV. Again, the light quark masses in the simulations are higher than in nature; the pion is at 396 MeV.

Finally, glueballs. In Fig. 14.3 we showed a figure from Ref. 10 showing a lattice prediction for the glueball mass spectrum in quenched approximation. A true QCD prediction of the glueball spectrum requires dynamical light quarks and (because glueball operators are intrinsically noisy) high statistics. Only recently have the first useful such calculations appeared. Fig. 14.11 shows results from Ref. 53, done with dynamical  $u$ ,  $d$  and  $s$  quarks at two lattice spacings, 0.123 and 0.092 fm, along with comparisons to the quenched lattice calculation of Ref. 11 and to experimental isosinglet mesons.

The dynamical simulation is, of course, not the last word on this subject, but it shows that the effects of quenching seem to be small.



**Figure 14.11:** Lattice QCD predictions for glueball masses. The open and closed circles are the larger and smaller lattice spacing data of the full QCD calculation of glueball masses of Ref. 53. Squares are the quenched data for glueball masses of Ref. 11. The bursts labeled by particle names are experimental states with the appropriate quantum numbers.

#### References:

1. J. Schwinger, Phys. Rev. Lett. **12**, 237 (1964).
2. A. Bramon *et al.*, Phys. Lett. **B403**, 339 (1997).
3. A. Aloisio *et al.*, Phys. Lett. **B541**, 45 (2002).
4. C. Amsler *et al.*, Phys. Lett. **B294**, 451 (1992).
5. C. Amsler, Rev. Mod. Phys. **70**, 1293 (1998).
6. N.H. Christ *et al.*, Phys. Rev. Lett. **105**, 241601 (2010) [arXiv:1002.2999 [hep-lat]].
7. T. Feldmann, Int. J. Mod. Phys. **A915**, 159 (2000).
8. C. Amsler and F.E. Close, Phys. Rev. **D53**, 295 (1996).
9. R.L. Jaffe, Phys. Rev. **D 15** 267, 281 (1977).
10. Y. Chen *et al.*, Phys. Rev. **D73**, 014516 (2006).
11. C. Morningstar and M. Peardon, Phys. Rev. **D60**, 034509 (1999).
12. W.J. Lee and D. Weingarten, Phys. Rev. **D61**, 014015 (2000).
13. G.S. Bali, *et. al.* Phys. Lett. **B309**, 378 (1993).
14. C. Michael, *AIP Conf. Proc.* **432**, 657 (1998).
15. F.E. Close and A. Kirk, Eur. Phys. J. **C21**, 531 (2001).
16. C. Amsler and N.A. Törnqvist, Phys. Reports **389**, 61 (2004).
17. N. Isgur and J. Paton, Phys. Rev. **D31**, 2910 (1985).
18. P. Lacock *et al.*, Phys. Lett. **B401**, 308 (1997);  
C. Bernard *et al.*, Phys. Rev. **D56**, 7039 (1997);  
C. Bernard *et al.*, Phys. Rev. **D68**, 074505 (2003).
19. M. Chanowitz and S. Sharpe, Nucl. Phys. **B222**, 211 (1983).
20. T. Barnes *et al.*, Nucl. Phys. **B224**, 241 (1983).
21. W.-M Yao *et al.*, J. Phys. **G33**, 1 (2006).
22. F.E. Close, in *Quarks and Nuclear Forces* (Springer-Verlag, 1982), p. 56.
23. Particle Data Group, Phys. Lett. **111B** (1982).
24. R.H. Dalitz and L.J. Reinders, in "Hadron Structure as Known from Electromagnetic and Strong Interactions," *Proceedings of the Hadron '77 Conference* (Veda, 1979), p. 11.
25. E. Klempt and J.M. Richard, Rev. Mod. Phys. **82**, 1095 (2010).
26. N. Isgur and G. Karl, Phys. Rev. **D18**, 4187 (1978); *ibid.*, **D19**, 2653 (1979); *ibid.*, **D20**, 1191 (1979);  
K.-T. Chao *et al.*, Phys. Rev. **D23**, 155 (1981).
27. S. Capstick and W. Roberts, Phys. Rev. **D49**, 4570 (1994); *ibid.*, **D57**, 4301 (1998); *ibid.*, **D58**, 074011 (1998).
28. T. Melde, W. Plessas, and B. Sengl, Phys. Rev. **D77**, 114002 (2008);  
S. Capstick, Phys. Rev. **D46**, 2864 (1992).
29. R.A. Arndt *et al.*, Phys. Rev. **C74**, 045205 (2006).
30. B. Krusche and S. Schadmand, Prog. Part. Nucl. Phys. **51**, 399 (2003);  
V.D. Burkert and T.-S.H. Lee, Int. J. Mod. Phys. **E13**, 1035 (2004).
31. S. Capstick and W. Roberts, Prog. Part. Nucl. Phys. **45**, 241 (2000);  
see also A.J.G. Hey and R.L. Kelly, Phys. Reports **96**, 71 (1983).
32. M. Anselmino *et al.*, Rev. Mod. Phys. **65**, 1199 (1993).
33. R. Bijker *et al.*, Ann. of Phys. **236** 69 (1994).
34. N. Isgur and J. Paton, Phys. Rev. **D31**, 2910 (1985);  
S. Capstick and P.R. Page, Phys. Rev. **C66**, 065204 (2002).
35. R.L. Jaffe, D. Pirjol, and A. Scardicchio, Phys. Rept. **435** 157 (2006);  
L. Ya. Glozman, Phys. Rept. **444**, 1 (2007).
36. A. De Rujula *et al.*, Phys. Rev. **D12**, 147 (1975).
37. W.H. Blask *et al.*, Z. Phys. **A337** 327 (1990);  
U. Löring *et al.*, Eur. Phys. J. **A10** 309 (2001);  
U. Löring *et al.*, Eur. Phys. J. **A10** 395 (2001); *ibid.*, **A10** 447 (2001).
38. L.Y. Glozman and D.O. Riska, Phys. Rept. **268**, 263 (1996);  
L.Y. Glozman *et al.*, Phys. Rev. **D58**, 094030 (1998).
39. C. Aubin *et al.* [MLC Collab.], Phys. Rev. **D70**, 094505 (2004) [arXiv:hep-lat/0407028].
40. S. Durr *et al.*, Science **322**, 1224 (2008) [arXiv:0906.3599 [hep-lat]].
41. C.T.H. Davies *et al.* [HPQCD Collaboration], Phys. Rev. Lett. **92**, 022001 (2004) [arXiv:hep-lat/0304004].
42. A. Gray *et al.*, Phys. Rev. **D72**, 094507 (2005) [hep-lat/0507013].
43. E.B. Gregory *et al.*, Phys. Rev. **D83**, 014506 (2011) [arXiv:1010.3848 [hep-lat]]; C.T.H. Davies *et al.*, Phys. Rev. **D82**, 114504 (2010) [arXiv:1008.4018 [hep-lat]]; E.B. Gregory *et al.*, Phys. Rev. Lett. **104**, 022001 (2010) [arXiv:0909.4462 [hep-lat]].
44. L. Liu *et al.*, Phys. Rev. **D81**, 094505 (2010) [arXiv:0909.3294 [hep-lat]].
45. H. Na and S.A. Gottlieb, PoS **LAT2007**, 124 (2007) [arXiv:0710.1422 [hep-lat]]; PoS **LATTICE2008**, 119 (2008) [arXiv:0812.1235 [hep-lat]].
46. J.M. Flynn, F. Mescia, and A.S.B. Tariq [UKQCD Collaboration], JHEP **0307**, 066 (2003) [arXiv:hep-lat/0307025].
47. N. Mathur, R. Lewis, and R. M. Woloshyn, Phys. Rev. **D66**, 014502 (2002) [arXiv:hep-ph/0203253].
48. T.W. Chiu and T.H. Hsieh, Nucl. Phys. A **755**, 471 (2005) [arXiv:hep-lat/0501021].
49. H.W. Lin, arXiv:1106.1608 [hep-lat].
50. R.G. Edwards *et al.*, arXiv:1104.5152 [hep-ph].
51. C.A. Meyer and Y. Van Haarlem, Phys. Rev. C **82**, 025208 (2010) [arXiv:1004.5516 [nucl-ex]].
52. J.J. Dudek *et al.*, Phys. Rev. D **83**, 111502 (2011) [arXiv:1102.4299 [hep-lat]]; J.J. Dudek *et al.*, Phys. Rev. D **82**, 034508 (2010) [arXiv:1004.4930 [hep-ph]]; J.J. Dudek *et al.*, Phys. Rev. Lett. **103**, 262001 (2009) [arXiv:0909.0200 [hep-ph]].
53. C.M. Richards *et al.*, [UKQCD Collaboration], Phys. Rev. D **82**, 034501 (2010) [arXiv:1005.2473 [hep-lat]].



## 15. GRAND UNIFIED THEORIES

Revised October 2011 by S. Raby (Ohio State University).

### 15.1. Grand Unification

#### 15.1.1. Standard Model : An Introduction :

In spite of all the successes of the Standard Model [SM] it is unlikely to be the final theory. It leaves many unanswered questions. Why the local gauge interactions  $SU(3)_C \times SU(2)_L \times U(1)_Y$  and why 3 families of quarks and leptons? Moreover why does one family consist of the states  $[Q, u^c, d^c; L, e^c]$  transforming as  $[(3, 2, 1/3), (\bar{3}, 1, -4/3), (\bar{3}, 1, 2/3); (1, 2, -1), (1, 1, 2)]$ , where  $Q = (u, d)$  and  $L = (\nu, e)$  are  $SU(2)_L$  doublets and  $u^c, d^c, e^c$  are charge conjugate  $SU(2)_L$  singlet fields with the  $U(1)_Y$  quantum numbers given? [We use the convention that electric charge  $Q_{EM} = T_{3L} + Y/2$  and all fields are left handed Weyl spinors.] Note the SM gauge interactions of quarks and leptons are completely fixed by their gauge charges. Thus if we understood the origin of this charge quantization, we would also understand why there are no fractionally charged hadrons. Finally, what is the origin of quark and lepton masses or the apparent hierarchy of family masses and quark and leptonic mixing angles? Perhaps if we understood this, we would also know the origin of CP violation, the solution to the strong CP problem, the origin of the cosmological matter - antimatter asymmetry. In addition, it lacks an explanation for the observed dark matter and dark energy of the universe.

The SM has 19 arbitrary parameters; their values are chosen to fit the data. Three arbitrary gauge couplings:  $g_3, g, g'$  (where  $g, g'$  are the  $SU(2)_L, U(1)_Y$  couplings, respectively) or equivalently  $\alpha_s = (g_3^2/4\pi), \alpha_{EM} = (e^2/4\pi)$  ( $e = g \sin\theta_W$ ) and  $\sin^2\theta_W = (g')^2/(g^2 + (g')^2)$ . In addition there are 13 parameters associated with the 9 charged fermion masses and the four mixing angles in the CKM matrix. The remaining 3 parameters are  $v, \lambda$  [the Higgs VEV and quartic coupling] (or equivalently  $M_Z, m_h^0$ ) and the QCD  $\theta$  parameter. In addition, data from neutrino oscillation experiments provide convincing evidence for neutrino masses. With 3 light Majorana neutrinos there are at least 9 additional parameters in the neutrino sector; 3 masses and 6 mixing angles and phases. In summary, the SM has too many arbitrary parameters and leaves open too many unresolved questions to be considered complete. These are the problems which grand unified theories hope to address.

#### 15.1.2. Charge Quantization :

In the Standard Model, quarks and leptons are on an equal footing; both fundamental particles without substructure. It is now clear that they may be two faces of the same coin; unified, for example, by extending QCD (or  $SU(3)_C$ ) to include leptons as the fourth color,  $SU(4)_C$  [1]. The complete Pati-Salam gauge group is  $SU(4)_C \times SU(2)_L \times SU(2)_R$  with the states of one family  $[(Q, L), (Q^c, L^c)]$  transforming as  $[(4, 2, 1), (\bar{4}, 1, \bar{2})]$  where  $Q^c = (d^c, u^c), L^c = (e^c, \nu^c)$  are doublets under  $SU(2)_R$ . Electric charge is now given by the relation  $Q_{EM} = T_{3L} + T_{3R} + 1/2(B - L)$  and  $SU(4)_C$  contains the subgroup  $SU(3)_C \times (B - L)$  where  $B$  ( $L$ ) is baryon (lepton) number. Note  $\nu^c$  has no SM quantum numbers and is thus completely "sterile". It is introduced to complete the  $SU(2)_R$  lepton doublet. This additional state is desirable when considering neutrino masses.

Although quarks and leptons are unified with the states of one family forming two irreducible representations of the gauge group; there are still 3 independent gauge couplings (two if one also imposes parity, i.e.  $L \leftrightarrow R$  symmetry). As a result the three low energy gauge couplings are still independent arbitrary parameters. This difficulty is resolved by embedding the SM gauge group into the simple unified gauge group, Georgi-Glashow  $SU(5)$ , with one universal gauge coupling  $\alpha_G$  defined at the grand unification scale  $M_G$  [2]. Quarks and leptons still sit in two irreducible representations, as before, with a  $\mathbf{10} = [Q, u^c, e^c]$  and  $\bar{\mathbf{5}} = [d^c, L]$ . Nevertheless, the three low energy gauge couplings are now determined in terms of two independent parameters :  $\alpha_G$  and  $M_G$ . Hence there is one prediction.

In order to break the electroweak symmetry at the weak scale and give mass to quarks and leptons, Higgs doublets are needed which can sit in either a  $\mathbf{5}_H$  or  $\bar{\mathbf{5}}_H$ . The additional 3 states are color triplet Higgs scalars. The couplings of these color triplets violate baryon and

lepton number and nucleons decay via the exchange of a single color triplet Higgs scalar. Hence in order not to violently disagree with the non-observation of nucleon decay, their mass must be greater than  $\sim 10^{11}$  GeV [3]. Moreover, in supersymmetric GUTs, in order to cancel anomalies as well as give mass to both up and down quarks, both Higgs multiplets  $\mathbf{5}_H, \bar{\mathbf{5}}_H$  are required. As we shall discuss later, nucleon decay now constrains the color triplet Higgs states in a SUSY GUT to have mass significantly greater than  $M_G$ .

Complete unification is possible with the symmetry group  $SO(10)$  with one universal gauge coupling  $\alpha_G$  and one family of quarks and leptons sitting in the 16 dimensional spinor representation  $\mathbf{16} = [\mathbf{10} + \bar{\mathbf{5}} + \mathbf{1}]$  [4]. The  $SU(5)$  singlet  $\mathbf{1}$  is identified with  $\nu^c$ . In Table 1 we present the states of one family of quarks and leptons, as they appear in the  $\mathbf{16}$ . It is an amazing and perhaps even profound fact that all the states of a single family of quarks and leptons can be represented digitally as a set of 5 zeros and/or ones or equivalently as the tensor product of 5 "spin"  $1/2$  states with  $\pm = |\pm \frac{1}{2} >$  and with the condition that we have an even number of  $|+ >$  spins. The first three "spins" correspond to  $SU(3)_C$  color quantum numbers, while the last two are  $SU(2)_L$  weak quantum numbers. In fact an  $SU(3)_C$  rotation just raises one color index and lowers another, thereby changing colors  $\{r, b, y\}$ . Similarly an  $SU(2)_L$  rotation raises one weak index and lowers another, thereby flipping the weak isospin from up to down or vice versa. In this representation weak hypercharge  $Y$  is given by the simple relation  $Y = -2/3(\sum \text{color spins}) + (\sum \text{weak spins})$ .  $SU(5)$  rotations [in particular, the ones NOT in  $SU(3)_C \times SU(2)_L \times U(1)_Y$ ] then raise (or lower) a color index, while at the same time lowering (or raising) a weak index. It is easy to see that such rotations can mix the states  $\{Q, u^c, e^c\}$  and  $\{d^c, L\}$  among themselves and  $\nu^c$  is a singlet. The new  $SO(10)$  rotations [not in  $SU(5)$ ] are then given by either raising or lowering any two spins. For example, by raising the two weak indices  $\nu^c$  rotates into  $e^c$ , etc.

**Table 15.1:** The quantum numbers of the  $\mathbf{16}$  dimensional representation of  $SO(10)$ .

State	Y	Color	Weak
$\nu^c$	0	---	--
$e^c$	2	---	++
$u_r$	1/3	+- -	-+
$d_r$	1/3	+- -	+-
$u_b$	1/3	-+ -	-+
$d_b$	1/3	-+ -	+-
$u_y$	1/3	-- +	-+
$d_y$	1/3	-- +	+-
$u_r^c$	-4/3	-+ +	--
$u_b^c$	-4/3	-+ +	--
$u_y^c$	-4/3	+ + -	--
$d_r^c$	2/3	-+ +	++
$d_b^c$	2/3	-+ +	++
$d_y^c$	2/3	+ + -	++
$\nu$	-1	+ + +	-+
$e$	-1	+ + +	+-

$SO(10)$  has two inequivalent maximal breaking patterns.  $SO(10) \rightarrow SU(5) \times U(1)_X$  and  $SO(10) \rightarrow SU(4)_C \times SU(2)_L \times SU(2)_R$ . In the first case we obtain Georgi-Glashow  $SU(5)$  if  $Q_{EM}$  is given in terms of  $SU(5)$  generators alone or so-called flipped  $SU(5)$  [5] if  $Q_{EM}$  is partly in  $U(1)_X$ . In the latter case we have the Pati-Salam symmetry. If  $SO(10)$  breaks directly to the SM at  $M_G$ , then we retain the prediction for gauge coupling unification. However more possibilities for breaking (hence more breaking scales and more parameters) are available in  $SO(10)$ . Nevertheless with one breaking pattern  $SO(10) \rightarrow SU(5) \rightarrow SM$ , where the last breaking scale is  $M_G$ , the predictions from gauge coupling unification are preserved. The Higgs multiplets in

minimal  $SO(10)$  are contained in the fundamental  $\mathbf{10}_H = [\mathbf{5}_H, \bar{\mathbf{5}}_H]$  representation. Note, only in  $SO(10)$  does the gauge symmetry distinguish quark and lepton multiplets from Higgs multiplets.

Finally, larger symmetry groups have been considered. For example,  $E(6)$  has a fundamental representation  $\mathbf{27}$  which under  $SO(10)$  transforms as a  $[\mathbf{16} + \mathbf{10} + \mathbf{1}]$ . The breaking pattern  $E(6) \rightarrow SU(3)_C \times SU(3)_L \times SU(3)_R$  is also possible. With the additional permutation symmetry  $Z(3)$  interchanging the three  $SU(3)$ s we obtain so-called “trification” [6] with a universal gauge coupling. The latter breaking pattern has been used in phenomenological analyses of the heterotic string [7]. However, in larger symmetry groups, such as  $E(6)$ ,  $SU(6)$ , etc., there are now many more states which have not been observed and must be removed from the effective low energy theory. In particular, three families of  $\mathbf{27}$ s in  $E(6)$  contain three Higgs type multiplets transforming as  $\mathbf{10}$ s of  $SO(10)$ . This makes these larger symmetry groups unattractive starting points for model building.

### 15.1.3. String Theory and Orbifold GUTs :

Orbifold compactification of the heterotic string [8–10], and recent field theoretic constructions known as orbifold GUTs [11], contain grand unified symmetries realized in 5 and 6 dimensions. However, upon compactifying all but four of these extra dimensions, only the MSSM is recovered as a symmetry of the effective four dimensional field theory.<sup>1</sup> These theories can retain many of the nice features of four dimensional SUSY GUTs, such as charge quantization, gauge coupling unification and sometimes even Yukawa unification; while at the same time resolving some of the difficulties of 4d GUTs, in particular problems with unwieldy Higgs sectors necessary for spontaneously breaking the GUT symmetry, and problems with doublet-triplet Higgs splitting or rapid proton decay. We will comment further on the corrections to the four dimensional GUT picture due to orbifold GUTs in the following sections. Finally, recent progress has been made in finding MSSM-like theories in the string landscape. This success is made possible by incorporating SUSY GUTs at an intermediate step in the construction. For a brief discussion, see Sec. 15.1.

### 15.1.4. Gauge coupling unification :

The biggest paradox of grand unification is to understand how it is possible to have a universal gauge coupling  $g_G$  in a grand unified theory [GUT] and yet have three unequal gauge couplings at the weak scale with  $g_3 > g > g'$ . The solution is given in terms of the concept of an effective field theory [EFT] [18]. The GUT symmetry is spontaneously broken at the scale  $M_G$  and all particles not in the SM obtain mass of order  $M_G$ . When calculating Green’s functions with external energies  $E \gg M_G$ , we can neglect the mass of all particles in the loop and hence all particles contribute to the renormalization group running of the universal gauge coupling. However, for  $E \ll M_G$  one can consider an effective field theory

<sup>1</sup> Also, in recent years there has been a great deal of progress in constructing three and four family models in Type IIA string theory with intersecting D6 branes [12]. Although these models can incorporate  $SU(5)$  or a Pati-Salam symmetry group in four dimensions, they typically have problems with gauge coupling unification. In the former case this is due to charged exotics which affect the RG running, while in the latter case the  $SU(4) \times SU(2)_L \times SU(2)_R$  symmetry never unifies. Local models, however, with D-branes at singularities have had some more success in obtaining gauge coupling unification [13]. Note, heterotic string theory models also exist whose low energy effective 4d field theory is a SUSY GUT [14]. These models have all the virtues and problems of 4d GUTs. Finally, many heterotic string models have been constructed with the standard model gauge symmetry in 4d and no intermediate GUT symmetry in less than 10d. Some minimal 3 family supersymmetric models have been constructed [15,16]. These theories may retain some of the symmetry relations of GUTs, however the unification scale would typically be the string scale, of order  $5 \times 10^{17}$  GeV, which is inconsistent with low energy data. A way out of this problem was discovered in the context of the strongly coupled heterotic string, defined in an effective 11 dimensions [17]. In this case the 4d Planck scale (which controls the value of the string scale) now unifies with the GUT scale.

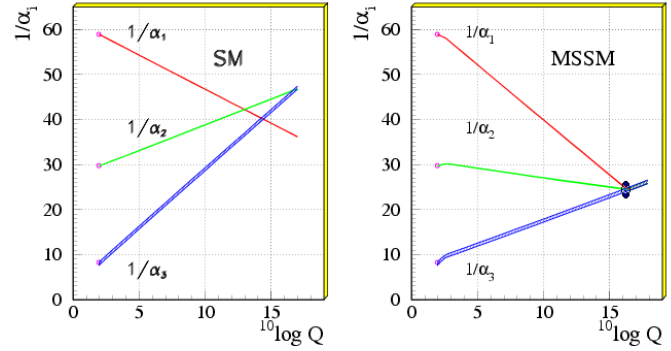


**Figure 15.1:** Gauge coupling unification in non-SUSY GUTs on the left vs. SUSY GUTs on the right using the LEP data as of 1991. Note, the difference in the running for SUSY is the inclusion of supersymmetric partners of standard model particles at scales of order a TeV (Fig. taken from Ref. 24). Given the present accurate measurements of the three low energy couplings, in particular  $\alpha_s(M_Z)$ , GUT scale threshold corrections are now needed to precisely fit the low energy data. The dark blob in the plot on the right represents these model dependent corrections.

including only the states with mass  $< E \ll M_G$ . The gauge symmetry of the EFT is  $SU(3)_C \times SU(2)_L \times U(1)_Y$  and the three gauge couplings renormalize independently. The states of the EFT include only those of the SM; 12 gauge bosons, 3 families of quarks and leptons and one or more Higgs doublets. At  $M_G$  the two effective theories [the GUT itself is most likely the EFT of a more fundamental theory defined at a higher scale] must give identical results; hence we have the boundary conditions  $g_3 = g_2 = g_1 \equiv g_G$  where at any scale  $\mu < M_G$  we have  $g_2 \equiv g$  and  $g_1 = \sqrt{5/3} g'$ . Then using two low energy couplings, such as  $\alpha_s(M_Z)$ ,  $\alpha_{EM}(M_Z)$ , the two independent parameters  $\alpha_G$ ,  $M_G$  can be fixed. The third gauge coupling,  $\sin^2 \theta_W$  in this case, is then predicted. This was the procedure up until about 1991 [19,20]. Subsequently, the uncertainties in  $\sin^2 \theta_W$  were reduced ten fold. Since then,  $\alpha_{EM}(M_Z)$ ,  $\sin^2 \theta_W$  have been used as input to predict  $\alpha_G$ ,  $M_G$  and  $\alpha_s(M_Z)$  [21].

We emphasize that the above boundary condition is only valid when using one loop renormalization group [RG] running. With precision electroweak data, however, it is necessary to use two loop RG running. Hence one must include one loop threshold corrections to gauge coupling boundary conditions at both the weak and GUT scales. In this case it is always possible to define the GUT scale as the point where  $\alpha_1(M_G) = \alpha_2(M_G) \equiv \tilde{\alpha}_G$  and  $\alpha_3(M_G) = \tilde{\alpha}_G (1 + \epsilon_3)$ . The threshold correction  $\epsilon_3$  is a logarithmic function of all states with mass of order  $M_G$  and  $\tilde{\alpha}_G = \alpha_G + \Delta$  where  $\alpha_G$  is the GUT coupling constant above  $M_G$  and  $\Delta$  is a one loop threshold correction. Note, the popular code “SOFTSUSY” [22] has defined the GUT scale in just this way. The value of  $\epsilon_3$  can be read off from the output data. To the extent that gauge coupling unification is perturbative, the GUT threshold corrections are small and calculable. This presumes that the GUT scale is sufficiently below the Planck scale or any other strong coupling extension of the GUT, such as a strongly coupled string theory.

Supersymmetric grand unified theories [SUSY GUTs] are an extension of non-SUSY GUTs [23]. The key difference between SUSY GUTs and non-SUSY GUTs is the low energy effective theory. The low energy effective field theory in a SUSY GUT is assumed to satisfy  $N=1$  supersymmetry down to scales of order the weak scale in addition to the SM gauge symmetry. Hence the spectrum includes all the SM states plus their supersymmetric partners. It also includes one pair (or more) of Higgs doublets; one to give mass to up-type quarks and the other to down-type quarks and charged leptons. Two doublets with opposite hypercharge  $Y$  are also needed to cancel fermionic triangle anomalies. Finally, it is important to recognize that a low energy SUSY breaking scale (the scale at which the SUSY partners of SM particles obtain mass) is necessary to solve the gauge hierarchy problem.



Simple non-SUSY  $SU(5)$  is ruled out; initially by the increased accuracy in the measurement of  $\sin^2 \theta_W$  and by early bounds on the proton lifetime (see below) [20]. However, by now LEP data [21] has conclusively shown that SUSY GUTs is the *new standard model*; by which we mean the theory used to guide the search for new physics beyond the present SM (see Fig. Fig. 15.1). SUSY extensions of the SM have the property that their effects decouple as the effective SUSY breaking scale is increased. Any theory beyond the SM must have this property simply because the SM works so well. However, the SUSY breaking scale cannot be increased with impunity, since this would reintroduce a gauge hierarchy problem. Unfortunately there is no clear-cut answer to the question, when is the SUSY breaking scale too high. A conservative bound would suggest that the third generation quarks and leptons must be lighter than about 1 TeV, in order that the one loop corrections to the Higgs mass from Yukawa interactions remains of order the Higgs mass bound itself.

At present gauge coupling unification within SUSY GUTs works extremely well. Exact unification at  $M_G$ , with two loop renormalization group running from  $M_G$  to  $M_Z$ , and one loop threshold corrections at the weak scale, fits to within  $3\sigma$  of the present precise low energy data. A small threshold correction at  $M_G$  ( $\epsilon_3 \sim -3\%$  to  $-4\%$ ) is sufficient to fit the low energy data precisely [25,26,27].<sup>2</sup> This may be compared to non-SUSY GUTs where the fit misses by  $\sim 12\sigma$  and a precise fit requires new weak scale states in incomplete GUT multiplets or multiple GUT breaking scales.<sup>3</sup>

Following the analysis of Ref. 27 let us try to understand the need for the GUT threshold correction and its order of magnitude. The renormalization group equations relate the low energy gauge coupling constants  $\alpha_i(M_Z)$ ,  $i = 1, 2, 3$  to the value of the unification scale  $\Lambda_U$  and the GUT coupling  $\alpha_U$  by the expression

$$\frac{1}{\alpha_i(M_Z)} = \frac{1}{\alpha_U} + \frac{b_i}{2\pi} \log \left( \frac{\Lambda_U}{M_Z} \right) + \delta_i \quad (15.1)$$

where  $\Lambda_U$  is the GUT scale evaluated at one loop and the threshold corrections,  $\delta_i$ , are given by  $\delta_i = \delta_i^{(2)} + \delta_i^{(l)} + \delta_i^{(g)}$  with  $\delta_i^{(2)}$  representing two loop running effects,  $\delta_i^{(l)}$  the light threshold corrections at the SUSY breaking scale and  $\delta_i^{(g)} = \delta_i^{(h)} + \delta_i^{(b)}$  representing GUT scale threshold corrections. Note, in this analysis, the two loop RG running is treated on the same footing as weak and GUT scale threshold corrections. One then obtains the prediction

$$(\alpha_3(M_Z) - \alpha_3^{LO}(M_Z))/\alpha_3^{LO}(M_Z) = -\alpha_3^{LO}(M_Z) \delta_s \quad (15.2)$$

where  $\alpha_3^{LO}(M_Z)$  is the leading order one loop RG result and  $\delta_s = \frac{1}{7}(5\delta_1 - 12\delta_2 + 7\delta_3)$  is the net threshold correction. [A similar formula applies at the GUT scale with the GUT threshold correction,  $\epsilon_3$ , given by  $\epsilon_3 = -\bar{\alpha}_G \delta_s^{(g)}$ .] Given the experimental inputs [31,32]:

$$\begin{aligned} \alpha_{em}^{-1}(M_Z) &= 127.916 \pm 0.015 \\ \sin^2 \theta_W(M_Z) &= 0.23116 \pm 0.00013 \\ \alpha_3(M_Z) &= 0.1184 \pm 0.0007 \end{aligned} \quad (15.3)$$

<sup>2</sup> This result implicitly assumes universal GUT boundary conditions for soft SUSY breaking parameters at  $M_G$ . In the simplest case we have a universal gaugino mass  $M_{1/2}$ , a universal mass for squarks and sleptons  $m_{16}$  and a universal Higgs mass  $m_{10}$ , as motivated by  $SO(10)$ . In some cases, threshold corrections to gauge coupling unification can be exchanged for threshold corrections to soft SUSY parameters. See for example, Ref. 28 and references therein.

<sup>3</sup> Non-SUSY GUTs with a more complicated breaking pattern can still fit the data. For example, non-SUSY  $SO(10) \rightarrow SU(4)_C \times SU(2)_L \times SU(2)_R \rightarrow SM$  with the second breaking scale of order an intermediate scale, determined by light neutrino masses using the see-saw mechanism, can fit the low energy data for gauge couplings [29] and at the same time survive nucleon decay bounds [30], discussed in the following section.

and taking into account the light threshold corrections, assuming an ensemble of 10 SUSY spectra [27] (corresponding to the Snowmass benchmark points), we have

$$\alpha_3^{LO}(M_Z) \approx 0.118 \quad (15.4)$$

and

$$\begin{aligned} \delta_s^{(2)} &\approx -0.82 \\ \delta_s^{(l)} &\approx -0.50 + \frac{19}{28\pi} \log \frac{M_{SUSY}}{M_Z}. \end{aligned}$$

For  $M_{SUSY} = 1$  TeV, we have  $\delta_s^{(2)} + \delta_s^{(l)} \approx -0.80$ . Since the one loop result  $\alpha_3^{LO}(M_Z)$  is very close to the experimental value, we need  $\delta_s \approx 0$  or equivalently,  $\delta_s^{(g)} \approx 0.80$ . This corresponds, at the GUT scale, to  $\epsilon_3 \approx -3\%$ . Note, this result depends implicitly on the assumption of universal soft SUSY breaking masses at the GUT scale, which directly affect the spectrum of SUSY particles at the weak scale. For example, if gaugino masses were not unified at  $M_G$  and, in particular, gluinos were lighter than winos at the weak scale, then it is possible that, due to weak scale threshold corrections, a much smaller or even slightly positive threshold correction at the GUT scale would be consistent with gauge coupling unification [34].

In four dimensional SUSY GUTs, the threshold correction  $\epsilon_3$  receives a positive contribution from Higgs doublets and triplets.<sup>4</sup> Thus a larger, negative contribution must come from the GUT breaking sector of the theory. This is certainly possible in specific  $SO(10)$  [35] or  $SU(5)$  [36] models, but it is clearly a significant constraint on the 4d GUT sector of the theory. In five or six dimensional orbifold GUTs, on the other hand, the ‘‘GUT scale’’ threshold correction comes from the Kaluza-Klein modes between the compactification scale,  $M_c$ , and the effective cutoff scale  $M_*$ .<sup>5</sup> Thus, in orbifold GUTs, gauge coupling unification at two loops is only consistent with the low energy data with a fixed value for  $M_c$  and  $M_*$ .<sup>6</sup> Typically, one finds  $M_c < M_G = 3 \times 10^{16}$  GeV, where  $M_G$  is the 4d GUT scale. Since the grand unified gauge bosons, responsible for nucleon decay, get mass at the compactification scale, the result  $M_c < M_G$  for orbifold GUTs has significant consequences for nucleon decay.

A few final comments are in order. We do not consider the scenario of split supersymmetry [39] in this review. In this scenario squarks and sleptons have mass at a scale  $\tilde{m} \gg M_Z$ , while gauginos and Higgsinos have mass of order the weak scale. Gauge coupling unification occurs at a scale of order  $10^{16}$  GeV, *provided that the scale  $\tilde{m}$  lies in the range  $10^3 - 10^{11}$  GeV* [40]. A serious complaint concerning the split SUSY scenario is that it does not provide a solution to the gauge hierarchy problem. Moreover, it is only consistent with grand unification if it also postulates an ‘‘intermediate’’ scale,  $\tilde{m}$ , for scalar masses. In addition, it is in conflict with  $b - \tau$  Yukawa unification, unless  $\tan \beta$  is fine-tuned to be close to 1 [40].<sup>7</sup>

<sup>4</sup> Note, the Higgs contribution is given by  $\epsilon_3 = \frac{3\bar{\alpha}_G}{5\pi} \log |\frac{\tilde{M}_t \gamma}{M_G}|$  where  $\tilde{M}_t$  is the effective color triplet Higgs mass (setting the scale for dimension 5 baryon and lepton number violating operators) and  $\gamma = \lambda_b/\lambda_t$  at  $M_G$ . Since  $\tilde{M}_t$  is necessarily greater than  $M_G$ , the Higgs contribution to  $\epsilon_3$  is positive.

<sup>5</sup> In string theory, the cutoff scale is the string scale.

<sup>6</sup> It is interesting to note that a ratio  $M_*/M_c \sim 100$ , needed for gauge coupling unification to work in orbifold GUTs is typically the maximum value for this ratio consistent with perturbativity [37]. In addition, in orbifold GUTs brane-localized gauge kinetic terms may destroy the successes of gauge coupling unification. However, for values of  $M_*/M_c = M_*\pi R \gg 1$  the unified bulk gauge kinetic terms can dominate over the brane-localized terms [38].

<sup>7</sup>  $b - \tau$  Yukawa unification only works for  $\tilde{m} < 10^4$  for  $\tan \beta \geq 1.5$ . This is because the effective theory between the gaugino mass scale and  $\tilde{m}$  includes only one Higgs doublet, as in the standard model. In this case, the large top quark Yukawa coupling tends to increase the ratio  $\lambda_b/\lambda_\tau$  as one runs down in energy below  $\tilde{m}$ . This is opposite to what happens in MSSM where the large top quark Yukawa coupling decreases the ratio  $\lambda_b/\lambda_\tau$  [41].

We have also neglected to discuss non-supersymmetric GUTs in four dimensions which still survive once one allows for several scales of GUT symmetry breaking [29]. Finally, it has been shown that non-supersymmetric GUTs in warped 5 dimensional orbifolds can be consistent with gauge coupling unification, assuming that the right-handed top quark and the Higgs doublets are composite-like objects with a compositeness scale of order a TeV [42]. However perturbative unification seems to fail.

### 15.1.5. Nucleon Decay :

Baryon number is necessarily violated in any GUT [43]. In  $SU(5)$ , nucleons decay via the exchange of gauge bosons with GUT scale masses, resulting in dimension 6 baryon number violating operators suppressed by  $(1/M_G^2)$ . The nucleon lifetime is calculable and given by  $\tau_N \propto M_G^4/(\alpha_G^2 m_p^5)$ . The dominant decay mode of the proton (and the baryon violating decay mode of the neutron), via gauge exchange, is  $p \rightarrow e^+ \pi^0$  ( $n \rightarrow e^+ \pi^-$ ). In any simple gauge symmetry, with one universal GUT coupling and scale  $(\alpha_G, M_G)$ , the nucleon lifetime from gauge exchange is calculable. Hence, the GUT scale may be directly observed via the extremely rare decay of the nucleon. Experimental searches for nucleon decay began with the Kolar Gold Mine, Homestake, Soudan, NUSEX, Frejus, HPW, and IMB detectors [19]. The present experimental bounds come from Super-Kamiokande and Soudan II. We discuss these results shortly. Non-SUSY GUTs are also ruled out by the non-observation of nucleon decay [20]. In SUSY GUTs, the GUT scale is of order  $3 \times 10^{16}$  GeV, as compared to the GUT scale in non-SUSY GUTs which is of order  $10^{15}$  GeV. Hence the dimension 6 baryon violating operators are significantly suppressed in SUSY GUTs [23] with  $\tau_p \sim 10^{34-38}$  yrs.

However, in SUSY GUTs there are additional sources for baryon number violation – dimension 4 and 5 operators [44]. Although our notation does not change, when discussing SUSY GUTs all fields are implicitly chiral superfields and the operators considered are the so-called F terms which contain two fermionic components and the rest scalars or products of scalars. Within the context of  $SU(5)$  the dimension 4 and 5 operators have the form  $(\mathbf{10} \mathbf{5} \mathbf{5}) \supset (u^c d^c d^c) + (Q L d^c) + (e^c L L)$  and  $(\mathbf{10} \mathbf{10} \mathbf{10} \mathbf{5}) \supset (Q Q Q L) + (u^c u^c d^c e^c) + B$  and  $L$  conserving terms, respectively. The dimension 4 operators are renormalizable with dimensionless couplings; similar to Yukawa couplings. On the other hand, the dimension 5 operators have a dimensionful coupling of order  $(1/M_G)$ .

The dimension 4 operators violate baryon number or lepton number, respectively, but not both. The nucleon lifetime is extremely short if both types of dimension 4 operators are present in the low energy theory. However both types can be eliminated by requiring R parity. In  $SU(5)$  the Higgs doublets reside in a  $\mathbf{5}_H$ ,  $\mathbf{5}_{\bar{H}}$  and R parity distinguishes the  $\mathbf{5}$  (quarks and leptons) from  $\mathbf{5}_H$  (Higgs). R parity [45] (or its cousin, family reflection symmetry (or *matter parity*) (see Dimopoulos and Georgi [23] and DRW [46]) takes  $F \rightarrow -F$ ,  $H \rightarrow H$  with  $F = \{\mathbf{10}, \mathbf{5}\}$ ,  $H = \{\mathbf{5}_H, \mathbf{5}_{\bar{H}}\}$ . This forbids the dimension 4 operator  $(\mathbf{10} \mathbf{5} \mathbf{5})$ , but allows the Yukawa couplings of the form  $(\mathbf{10} \mathbf{5} \mathbf{5}_{\bar{H}})$  and  $(\mathbf{10} \mathbf{10} \mathbf{5}_H)$ . It also forbids the dimension 3, lepton number violating, operator  $(\mathbf{5} \mathbf{5}_H) \supset (L H_u)$  with a coefficient with dimensions of mass which, like the  $\mu$  parameter, could be of order the weak scale and the dimension 5, baryon number violating, operator  $(\mathbf{10} \mathbf{10} \mathbf{10} \mathbf{5}_H) \supset (Q Q Q H_d) + \dots$ .

Note, in the MSSM it is possible to retain R parity violating operators at low energy as long as they violate either baryon number or lepton number only but not both. Such schemes are natural if one assumes a low energy symmetry, such as lepton number, baryon number, baryon triality [47] or proton hexality [48]. However these symmetries cannot be embedded in a GUT. Thus, in a SUSY GUT, only R parity can prevent all the dimension three and four baryon and lepton number violating operators. This does not mean to say that R parity is guaranteed to be satisfied in any GUT. For example the authors of Refs. [51,52] use constrained matter content to selectively generate safe effective R parity violating operators in a GUT. For a review on R parity violating interactions, see [53]. In Ref. [52], the authors show how to obtain the effective R parity violating operator  $O^{ijk} = (\mathbf{5}^j \cdot \mathbf{5}^k)_{\mathbf{15}} \cdot (\mathbf{10}^i \cdot \Sigma)_{15}$  where  $\Sigma$  is an  $SU(5)$  adjoint field and the subscripts 15, 15 indicate that the product of fields in parentheses

have been projected into these  $SU(5)$  directions. As a consequence the operator  $O^{ijk}$  is symmetric under interchange of the two  $\mathbf{5}$  states,  $O^{ijk} = O^{ikj}$ , and out of  $\mathbf{10} \mathbf{5} \mathbf{5}$  only the lepton number/R parity violating operator  $QL\bar{D}$  survives.

Note also, R parity distinguishes Higgs multiplets from ordinary families. In  $SU(5)$ , Higgs and quark/lepton multiplets have identical quantum numbers; while in  $E(6)$ , Higgs and families are unified within the fundamental  $\mathbf{27}$  representation. Only in  $SO(10)$  are Higgs and ordinary families distinguished by their gauge quantum numbers. Moreover the  $Z(4)$  center of  $SO(10)$  distinguishes  $\mathbf{10}$ s from  $\mathbf{16}$ s and can be associated with R parity [49].

Dimension 5 baryon number violating operators may be forbidden at tree level by symmetries in  $SU(5)$ , etc. These symmetries are typically broken however by the VEVs responsible for the color triplet Higgs masses. Consequently these dimension 5 operators are generically generated via color triplet Higgsino exchange. Hence, the color triplet partners of Higgs doublets must necessarily obtain mass of order the GUT scale. [It is also important to note that Planck or string scale physics may independently generate dimension 5 operators, even without a GUT. These contributions must be suppressed by some underlying symmetry; for example, the same flavor symmetry which may be responsible for hierarchical fermion Yukawa matrices.]

The dominant decay modes from dimension 5 operators are  $p \rightarrow K^+ \bar{\nu}$  ( $n \rightarrow K^0 \bar{\nu}$ ). This is due to a simple symmetry argument; the operators  $(Q_i Q_j Q_k L_l)$ ,  $(u_i^c u_j^c d_k^c e_l^c)$  (where  $i, j, k, l = 1, 2, 3$  are family indices and color and weak indices are implicit) must be invariant under  $SU(3)_C$  and  $SU(2)_L$ . As a result their color and weak doublet indices must be anti-symmetrized. However since these operators are given by bosonic superfields, they must be totally symmetric under interchange of all indices. Thus the first operator vanishes for  $i = j = k$  and the second vanishes for  $i = j$ . Hence a second or third generation member must exist in the final state [46].

Recent Super-Kamiokande bounds on the proton lifetime severely constrain these dimension 6 and 5 operators with (172.8 kt-yr) of data they find  $\tau_{(p \rightarrow e^+ \pi^0)} > 1.0 \times 10^{34}$  yrs,  $\tau_{(p \rightarrow K^+ \bar{\nu})} > 3.3 \times 10^{33}$  yrs and  $\tau_{(n \rightarrow e^+ \pi^-)} > 2 \times 10^{33}$  yrs at (90% CL) [54]. These constraints are now sufficient to rule out minimal SUSY  $SU(5)$  [55].<sup>8</sup> Non-minimal Higgs sectors in  $SU(5)$  or  $SO(10)$  theories still survive [26,36]. The upper bound on the proton lifetime from these theories are approximately a factor of 10 above the experimental bounds. They are also being pushed to their theoretical limits. Hence if SUSY GUTs are correct, then nucleon decay must be seen soon.

Is there a way out of this conclusion? Orbifold GUTs and string theories, see Sec. 15.1, contain grand unified symmetries realized in higher dimensions. In the process of compactification and GUT symmetry breaking, color triplet Higgs states are removed (projected out of the massless sector of the theory). In addition, the same projections typically rearrange the quark and lepton states so that the massless states which survive emanate from different GUT multiplets. In these models, proton decay due to dimension 5 operators can be severely suppressed or eliminated completely. However, proton decay due to dimension 6 operators may be enhanced, since the gauge bosons mediating proton decay obtain mass at the compactification scale,  $M_C$ , which is typically less than the 4d GUT scale (see the discussion at the end of Sec. 15.1), or suppressed, if the states of one family come from different irreducible representations. Which effect dominates is a model dependent issue. In some complete 5d orbifold

<sup>8</sup> This conclusion relies on the mild assumption that the three-by-three matrices diagonalizing squark and slepton mass matrices are not so different from their fermionic partners. It has been shown that if this caveat is violated, then dimension five proton decay in minimal SUSY  $SU(5)$  may not be ruled out [56]. This is however a very fine-tuned resolution of the problem. Another possible way out is to allow for a more complicated  $SU(5)$  breaking Higgs sector in the otherwise minimal model [57]. I have also implicitly assumed a hierarchical structure for Yukawa matrices in this analysis. It is however possible to fine-tune a hierarchical structure for quarks and leptons which baffles the family structure. In this case it is possible to avoid the present constraints on minimal SUSY  $SU(5)$ , for example see [58].

GUT models [59,27] the lifetime for the decay  $\tau(p \rightarrow e^+\pi^0)$  can be near the excluded bound of  $1 \times 10^{34}$  years with, however, large model dependent and/or theoretical uncertainties. In other cases, the modes  $p \rightarrow K^+\bar{\nu}$  and  $p \rightarrow K^0\mu^+$  may be dominant [27]. To summarize, in either 4d or orbifold string/field theories, nucleon decay remains a premier signature for SUSY GUTs. Moreover, the observation of nucleon decay may distinguish extra-dimensional orbifold GUTs from four dimensional ones.

As a final note, in orbifold GUTs or string theory new discrete symmetries consistent with SUSY GUTs can forbid all dimension 3 and 4 baryon [B] and lepton [L] number violating operators and even forbid the mu term and dimension 5 B and L violating operators to all orders in perturbation theory [50]. The mu term and dimension 5 B and L violating operators may then be generated, albeit sufficiently suppressed, via non-perturbative effects. The simplest example of this is a  $Z_4^R$  symmetry which is the unique discrete R symmetry consistent with  $SO(10)$  [50]. In this case, proton decay is completely dominated by dimension 6 operators.

Before concluding the topic of baryon number violation, consider the status of  $\Delta B = 2$  neutron- anti-neutron oscillations. Generically the leading operator for this process is the dimension 9 six quark operator  $G_{(\Delta B=2)}(u^c d^c d^c u^c d^c d^c)$  with dimensionful coefficient  $G_{(\Delta B=2)} \sim 1/M^5$ . The present experimental bound  $\tau_{n-\bar{n}} \geq 0.86 \times 10^8$  sec. at 90% CL [60] probes only up to the scale  $M \leq 10^6$  GeV. For  $M \sim M_G$ ,  $n - \bar{n}$  oscillations appear to be unobservable for any GUT (for a recent discussion see [61]).

### 15.1.6. Yukawa coupling unification :

#### 15.1.6.1. 3rd generation, $b - \tau$ or $t - b - \tau$ unification:

If quarks and leptons are two sides of the same coin, related by a new grand unified gauge symmetry, then that same symmetry relates the Yukawa couplings (and hence the masses) of quarks and leptons. In  $SU(5)$ , there are two independent renormalizable Yukawa interactions given by  $\lambda_t(\mathbf{10} \mathbf{10} \mathbf{5}_H) + \lambda(\mathbf{10} \mathbf{5} \mathbf{5}_H)$ . These contain the SM interactions  $\lambda_t(\mathbf{Q} u^c \mathbf{H}_u) + \lambda(\mathbf{Q} d^c \mathbf{H}_d + \mathbf{e}^c \mathbf{L} \mathbf{H}_d)$ . Hence, at the GUT scale we have the tree level relation,  $\lambda_b = \lambda_\tau \equiv \lambda$  [41]. In  $SO(10)$  there is only one independent renormalizable Yukawa interaction given by  $\lambda(\mathbf{16} \mathbf{16} \mathbf{10}_H)$  which gives the tree level relation,  $\lambda_t = \lambda_b = \lambda_\tau \equiv \lambda$  [62,63]. Note, in the discussion above we assume the minimal Higgs content with Higgs in  $\mathbf{5}, \bar{\mathbf{5}}$  for  $SU(5)$  and  $\mathbf{10}$  for  $SO(10)$ . With Higgs in higher dimensional representations there are more possible Yukawa couplings [75,76,77].

In order to make contact with the data, one now renormalizes the top, bottom and  $\tau$  Yukawa couplings, using two loop RG equations, from  $M_G$  to  $M_Z$ . One then obtains the running quark masses  $m_t(M_Z) = \lambda_t(M_Z) v_u$ ,  $m_b(M_Z) = \lambda_b(M_Z) v_d$  and  $m_\tau(M_Z) = \lambda_\tau(M_Z) v_d$  where  $\langle H_u^0 \rangle \equiv v_u = \sin \beta v/\sqrt{2}$ ,  $\langle H_d^0 \rangle \equiv v_d = \cos \beta v/\sqrt{2}$ ,  $v_u/v_d \equiv \tan \beta$  and  $v \sim 246$  GeV is fixed by the Fermi constant,  $G_\mu$ .

Including one loop threshold corrections at  $M_Z$  and additional RG running, one finds the top, bottom and  $\tau$  pole masses. In SUSY,  $b - \tau$  unification has two possible solutions with  $\tan \beta \sim 1$  or 40 – 50. The small  $\tan \beta$  solution is now disfavored by the LEP limit,  $\tan \beta > 2.4$  [64].<sup>9</sup> The large  $\tan \beta$  limit overlaps the  $SO(10)$  symmetry relation.

When  $\tan \beta$  is large there are significant weak scale threshold corrections to down quark and charged lepton masses from either gluino and/or chargino loops [66]. Yukawa unification (consistent with low energy data) is only possible in a restricted region of SUSY parameter space with important consequences for SUSY searches [67]. More recent analyses of Yukawa unification can be found in Refs. [68,69,70,71]. There seems to be at least four possible choices of soft SUSY breaking parameters which fit the data, possibly more. Each case then leads to a distinct sparticle spectrum and phenomenology for LHC and dark matter experiments. They correspond to:

<sup>9</sup> However, this bound disappears if one takes  $M_{SUSY} = 2$  TeV and  $m_t = 180$  GeV [65]. This apparent loop hole is now inconsistent with the observed top quark mass.

- universal squark and slepton masses ( $m_{16}$ ), universal A parameter ( $A_0$ ) and gaugino masses ( $M_{1/2}$ ), and non-universal Higgs masses ( $m_{H_u}, m_{H_d}$ ) with “just-so” splitting [67,68].
- a universal squark and slepton mass term for the first two families ( $m_{16_{1,2}}$ ) which is larger than the universal scalar mass for the third family ( $m_{16_3}$ ), universal A parameter ( $A_0$ ) and gaugino masses ( $M_{1/2}$ ) and universal Higgs mass term ( $m_{10}$ ). However all scalar masses then receive a D-term contribution to their masses given by the  $U(1)$  from  $SO(10)$  which commutes with  $SU(5)$ . This is of the form

$$\begin{aligned} m_Q^2 &= m_E^2 = m_U^2 = m_{16}^2 + M_D^2, \\ m_D^2 &= m_L^2 = m_{16}^2 - 3M_D^2, \\ m_{\bar{\nu}}^2 &= m_{16}^2 + 5M_D^2, \\ m_{H_{u,d}}^2 &= m_{10}^2 \mp 2M_D^2. \end{aligned}$$

This is the so-called “DR3 splitting” [69]. The R is associated with taking into account the renormalization group [RG] running of the right-handed neutrino from the GUT scale to the nominal value of its mass of order  $10^{10-14}$  GeV, as indicated by light neutrino masses via the See-Saw mechanism. This RG running contributes to an additional splitting of the  $H_u$  and  $H_d$  masses [67].

- universal squark and slepton masses ( $m_0$ ), split Higgs masses and non-universal gaugino masses satisfying ( $M_1 = \frac{3}{5}M_2 + \frac{2}{5}M_3$ ), and  $\mu, M_2 < 0$  [70], and
- universal squark and slepton mass term ( $m_{16}$ ), A parameter ( $A_0$ ), Higgs mass term ( $m_{10}$ ). All scalar masses then receive a D-term contribution to their masses given by the  $U(1)$  from  $SO(10)$  which commutes with  $SU(5)$ , as above. Finally, non-universal gaugino masses satisfying ( $M_3 : M_2 : M_1 = 2 : -3 : -1$ ) with  $M_3 > 0$  and  $\mu < 0$  [71].

#### 15.1.6.2. Three families:

Simple Yukawa unification is not possible for the first two generations of quarks and leptons. Consider the  $SU(5)$  GUT scale relation  $\lambda_b = \lambda_\tau$ . If extended to the first two generations one would have  $\lambda_s = \lambda_\mu$ ,  $\lambda_d = \lambda_e$  which gives  $\lambda_s/\lambda_d = \lambda_\mu/\lambda_e$ . The last relation is a renormalization group invariant and is thus satisfied at any scale. In particular, at the weak scale one obtains  $m_s/m_d = m_\mu/m_e$  which is in serious disagreement with the data with  $m_s/m_d \sim 20$  and  $m_\mu/m_e \sim 200$ . An elegant solution to this problem was given by Georgi and Jarlskog [72]. For a recent analysis in the context of supersymmetric GUTs, see Ref. [73]. Of course, a three family model must also give the observed CKM mixing in the quark sector. Note, although there are typically many more parameters in the GUT theory above  $M_G$ , it is possible to obtain effective low energy theories with many fewer parameters making strong predictions for quark and lepton masses.

Three family models which make significant predictions for low energy experiments have been constructed in the context of supersymmetric GUTs. It is important to note that grand unification alone is not sufficient to obtain predictive theories of fermion masses and mixing angles. Other ingredients are needed. In one approach additional global family symmetries are introduced (non-abelian family symmetries can significantly reduce the number of arbitrary parameters in the Yukawa matrices). These family symmetries constrain the set of effective higher dimensional fermion mass operators. In addition, sequential breaking of the family symmetry is correlated with the hierarchy of fermion masses. Three-family models exist which fit all the data, including neutrino masses and mixing [74]. In a completely separate approach for  $SO(10)$  models, the Standard Model Higgs bosons are contained in the higher dimensional Higgs representations including the  $\mathbf{10}, \overline{\mathbf{126}}$  and/or  $\mathbf{120}$ . Such theories have been shown to make predictions for neutrino masses and mixing angles [75–77]. A recent paper on this subject argues the necessity of split supersymmetry [78].

### 15.1.7. Neutrino Masses :

Atmospheric and solar neutrino oscillations, along with long baseline accelerator and reactor experiments, require neutrino masses. Adding three “sterile” neutrinos  $\nu^c$  with the Yukawa coupling  $\lambda_\nu$  ( $\nu^c \mathbf{L} \mathbf{H}_u$ ), one easily obtains three massive Dirac neutrinos with mass  $m_\nu = \lambda_\nu v_u$ .<sup>10</sup> However in order to obtain a tau neutrino with mass of order 0.1 eV, one needs  $\lambda_{\nu\tau}/\lambda_\tau \leq 10^{-10}$ . The see-saw mechanism, on the other hand, can naturally explain such small neutrino masses [79,80]. Since  $\nu^c$  has no SM quantum numbers, there is no symmetry (other than global lepton number) which prevents the mass term  $\frac{1}{2} \nu^c M \nu^c$ . Moreover one might expect  $M \sim M_G$ . Heavy “sterile” neutrinos can be integrated out of the theory, defining an effective low energy theory with only light active Majorana neutrinos with the effective dimension 5 operator  $\frac{1}{2} (\mathbf{L} \mathbf{H}_u) \lambda_\nu^T M^{-1} \lambda_\nu (\mathbf{L} \mathbf{H}_u)$ . This then leads to a  $3 \times 3$  Majorana neutrino mass matrix  $\mathbf{m} = m_\nu^T M^{-1} m_\nu$ .

Atmospheric neutrino oscillations require neutrino masses with  $\Delta m_\nu^2 \sim 3 \times 10^{-3} \text{ eV}^2$  with maximal mixing, in the simplest two neutrino scenario. With hierarchical neutrino masses  $m_{\nu\tau} = \sqrt{\Delta m_\nu^2} \sim 0.055 \text{ eV}$ . Moreover via the “see-saw” mechanism  $m_{\nu\tau} = m_t(m_t)^2/(3M)$ . Hence one finds  $M \sim 2 \times 10^{14} \text{ GeV}$ ; remarkably close to the GUT scale. Note we have related the neutrino Yukawa coupling to the top quark Yukawa coupling  $\lambda_{\nu\tau} = \lambda_t$  at  $M_G$  as given in  $SO(10)$  or  $SU(4) \times SU(2)_L \times SU(2)_R$ . However at low energies they are no longer equal and we have estimated this RG effect by  $\lambda_{\nu\tau}(M_Z) \approx \lambda_t(M_Z)/\sqrt{3}$ .

Neutrinos pose a special problem for SUSY GUTs. The question is why are the quark mixing angles in the CKM matrix small, while there are two large lepton mixing angles in the PMNS matrix. For a recent discussion of neutrino masses and mixing angles, see Refs. [81] and [82]. For SUSY GUT models which fit quark and lepton masses, see Ref. [74]. Finally, for a compilation of the range of SUSY GUT predictions for neutrino mixing, see [83].

### 15.1.8. Selected Topics :

#### 15.1.8.1. Magnetic Monopoles:

In the broken phase of a GUT there are typically localized classical solutions carrying magnetic charge under an unbroken  $U(1)$  symmetry [84]. These magnetic monopoles with mass of order  $M_G/\alpha_G$  are produced during the GUT phase transition in the early universe. The flux of magnetic monopoles is experimentally found to be less than  $\sim 10^{-16} \text{ cm}^{-2} \text{ s}^{-1} \text{ sr}^{-1}$  [85]. Many more are however predicted, hence the GUT monopole problem. In fact, one of the original motivations for an inflationary universe is to solve the monopole problem by invoking an epoch of rapid inflation after the GUT phase transition [86]. This would have the effect of diluting the monopole density as long as the reheat temperature is sufficiently below  $M_G$ . Other possible solutions to the monopole problem include: sweeping them away by domain walls [87],  $U(1)$  electromagnetic symmetry breaking at high temperature [88] or GUT symmetry non-restoration [89]. Parenthetically, it was also shown that GUT monopoles can catalyze nucleon decay [90]. A significantly lower bound on the monopole flux can then be obtained by considering X-ray emission from radio pulsars due to monopole capture and the subsequent nucleon decay catalysis [91].

#### 15.1.8.2. Baryogenesis via Leptogenesis:

Baryon number violating operators in  $SU(5)$  or  $SO(10)$  preserve the global symmetry  $B - L$ . Hence the value of the cosmological  $B - L$  density is an initial condition of the theory and is typically assumed to be zero. On the other hand, anomalies of the electroweak symmetry violate  $B + L$  while also preserving  $B - L$ . Hence thermal fluctuations in the early universe, via so-called sphaleron processes, can drive  $B + L$  to zero, washing out any net baryon number generated in the early universe at GUT temperatures.

<sup>10</sup> Note, these “sterile” neutrinos are quite naturally identified with the right-handed neutrinos necessarily contained in complete families of  $SO(10)$  or Pati-Salam.

One way out of this dilemma is to generate a net  $B - L$  dynamically in the early universe. We have just seen that neutrino oscillations suggest a new scale of physics of order  $10^{14} \text{ GeV}$ . This scale is associated with heavy Majorana neutrinos with mass  $M$ . If in the early universe, the decay of the heavy neutrinos is out of equilibrium and violates both lepton number and CP, then a net lepton number may be generated. This lepton number will then be partially converted into baryon number via electroweak processes [92].

#### 15.1.8.3. GUT symmetry breaking:

The grand unification symmetry is necessarily broken spontaneously. Scalar potentials (or superpotentials) exist whose vacua spontaneously break  $SU(5)$  and  $SO(10)$ . These potentials are ad hoc (just like the Higgs potential in the SM) and therefore it is hoped that they may be replaced with better motivated sectors. Gauge coupling unification now tests GUT breaking sectors, since it is one of the two dominant corrections to the GUT threshold correction  $\epsilon_3$ . The other dominant correction comes from the Higgs sector and doublet-triplet splitting. This latter contribution is always positive  $\epsilon_3 \propto \ln(M_T/M_G)$  (where  $M_T$  is an effective color triplet Higgs mass), while the low energy data typically requires  $\epsilon_3 < 0$ . Hence the GUT breaking sector must provide a significant (of order -8%) contribution to  $\epsilon_3$  to be consistent with the Super-K bound on the proton lifetime [35,26,36,74].

In string theory (and GUTs in extra-dimensions), GUT breaking may occur due to boundary conditions in the compactified dimensions [8,11]. This is still ad hoc. The major benefit is that it does not require complicated GUT breaking sectors.

#### 15.1.8.4. Doublet-triplet splitting:

The minimal supersymmetric standard model has a  $\mu$  problem; why is the coefficient of the bilinear Higgs term in the superpotential  $\mu (\mathbf{H}_u \mathbf{H}_d)$  of order the weak scale when, since it violates no low energy symmetry, it could be as large as  $M_G$ . In a SUSY GUT, the  $\mu$  problem is replaced by the problem of *doublet-triplet* splitting — giving mass of order  $M_G$  to the color triplet Higgs and mass  $\mu$  to the Higgs doublets. Several mechanisms for natural doublet-triplet splitting have been suggested, such as the sliding singlet [93], missing partner or missing VEV [94], and pseudo-Nambu-Goldstone boson mechanisms. Particular examples of the missing partner mechanism for  $SU(5)$  [36], the missing VEV mechanism for  $SO(10)$  [74,26] and the pseudo-Nambu-Goldstone boson mechanism for  $SU(6)$  [95] have been shown to be consistent with gauge coupling unification and proton decay. There are also several mechanisms for explaining why  $\mu$  is of order the SUSY breaking scale [96]. Finally, for a recent review of the  $\mu$  problem and some suggested solutions in SUSY GUTs and string theory, see Ref. [97,10,98,50] and references therein.

Once again, in string theory (and orbifold GUTs), the act of breaking the GUT symmetry via orbifolding projects certain states out of the theory. It has been shown that it is possible to remove the color triplet Higgs while retaining the Higgs doublets in this process. Hence the doublet-triplet splitting problem is finessed. As discussed earlier (see Sec. 15.1), this can have the effect of eliminating the contribution of dimension 5 operators to nucleon decay.

#### 15.1.9. String theory :

String theory has made significant progress in locating the minimal supersymmetric standard model [MSSM] in the string landscape. Random searches for MSSM-like models have found some success, see for example Ref. 99. However, recently a solid leap forward has been made by imposing a supersymmetric GUT locally in the extra dimensions of the string. Many MSSM-like models have been found in  $E(8) \times E(8)$  heterotic orbifold constructions [100–103] or more recently on smooth Calabi-Yau three-folds [104]. See also in F theory constructions [105–107]. There appear, however, to be some problems associated with large threshold corrections to gauge coupling unification in the F theory constructions which make use of a non-vanishing hypercharge field strength to break  $SU(5)$  to  $SU(3)_C \times SU(2)_L \times U(1)_Y$  [108]. Nevertheless, a SUSY GUT guarantees the correct particle content of the Standard Model and also allows for reasonable looking hierarchical Yukawa matrices. For a more detailed discussion, see [109].

## 15.2. Conclusion

Grand unification of the strong and electroweak interactions requires that the three low energy gauge couplings unify (up to small threshold corrections) at a unique scale,  $M_G$ . Supersymmetric grand unified theories provide, by far, the most predictive and economical framework allowing for perturbative unification.

The three pillars of SUSY GUTs are:

- gauge coupling unification at  $M_G \sim 3 \times 10^{16}$  GeV;
- low-energy supersymmetry [with a large SUSY desert], and
- nucleon decay.

The first prediction has already been verified (see Fig. Fig. 15.1). Perhaps the next two will soon appear. Whether or not Yukawa couplings unify is more model dependent. Nevertheless, the “digital” 16 dimensional representation of quarks and leptons in  $SO(10)$  is very compelling and may yet lead to an understanding of fermion masses and mixing angles.

In any event, the experimental verification of the first three pillars of SUSY GUTs would forever change our view of Nature. Moreover, the concomitant evidence for a vast SUSY desert would expose a huge lever arm for discovery. For then it would become clear that experiments probing the TeV scale could reveal physics at the GUT scale and perhaps beyond. Of course, some questions will still remain: Why do we have three families of quarks and leptons? How is the grand unified symmetry and possible family symmetries chosen by Nature? At what scale might stringy physics become relevant? Etc.

### References:

1. J. Pati and A. Salam, Phys. Rev. **D8**, 1240 (1973);  
For more discussion on the standard charge assignments in this formalism, see A. Davidson, Phys. Rev. **D20**, 776 (1979); and R.N. Mohapatra and R.E. Marshak, Phys. Lett. **B91**, 222 (1980).
2. H. Georgi and S.L. Glashow, Phys. Rev. Lett. **32**, 438 (1974).
3. E. Golowich, Phys. Rev. **D24**, 2899 (1981).
4. H. Georgi, Particles and Fields, *Proceedings of the APS Div. of Particles and Fields*, ed. C. Carlson, p. 575 (1975);  
H. Fritzsch and P. Minkowski, Ann. Phys. **93**, 193 (1975).
5. S.M. Barr, Phys. Lett. **B112**, 219 (1982).
6. A. de Rujula *et al.*, *5th Workshop on Grand Unification*, ed. K. Kang *et al.*, World Scientific, Singapore (1984), p. 88;  
See also earlier paper by Y. Achiman and B. Stech, p. 303, “New Phenomena in Lepton-Hadron Physics,” ed. D.E.C. Fries and J. Wess, Plenum, NY (1979).
7. B.R. Greene *et al.*, Nucl. Phys. **B278**, 667 (1986);  
*ibid.*, Nucl. Phys. **B292**, 606 (1987);  
B.R. Greene *et al.*, Nucl. Phys. **B325**, 101 (1989);  
J.E. Kim, Phys. Lett. **B591**, 119 (2004).
8. P. Candelas *et al.*, Nucl. Phys. **B258**, 46 (1985);  
L.J. Dixon *et al.*, Nucl. Phys. **B261**, 678 (1985);  
*ibid.*, Nucl. Phys. **B274**, 285 (1986);  
L. E. Ibanez *et al.*, Phys. Lett. **B187**, 25 (1987);  
*ibid.*, Phys. Lett. **B191**, 282 (1987);  
J.E. Kim *et al.*, Nucl. Phys. **B712**, 139 (2005).
9. T. Kobayashi *et al.*, Phys. Lett. **B593**, 262 (2004);  
S. Forste *et al.*, Phys. Rev. **D70**, 106008 (2004);  
T. Kobayashi *et al.*, Nucl. Phys. **B704**, 3 (2005);  
W. Buchmuller *et al.*, Nucl. Phys. **B712**, 139 (2005);  
W. Buchmuller *et al.*, Phys. Rev. Lett. **96**, 121602 (2006);  
*ibid.*, Nucl. Phys. **B785**, 149 (2007);  
O. Lebedev, *et al.*, Phys. Lett. **B645**, 88 (2007);  
J. E. Kim, J. H. Kim and B. Kyae, JHEP **0706**, 034 (2007);  
O. Lebedev, *et al.*, Phys. Rev. **D77**, 046013 (2008).
10. E. Witten, [hep-ph/0201018];  
M. Dine *et al.*, Phys. Rev. **D66**, 115001 (2002), [hep-ph/0206268].
11. Y. Kawamura, Prog. Theor. Phys. **103**, 613 (2000);  
*ibid.*, **105**, 999 (2001);  
G. Altarelli *et al.*, Phys. Lett. **B5111**, 257 (2001);  
L.J. Hall *et al.*, Phys. Rev. **D64**, 055003 (2001);  
A. Hebecker and J. March-Russell, Nucl. Phys. **B613**, 3 (2001);  
T. Asaka *et al.*, Phys. Lett. **B523**, 199 (2001);  
L.J. Hall *et al.*, Phys. Rev. **D65**, 035008 (2002);  
R. Dermisek and A. Mafi, Phys. Rev. **D65**, 055002 (2002);  
H.D. Kim and S. Raby, JHEP **0301**, 056 (2003).
12. For a recent review see, R. Blumenhagen *et al.*, “Toward realistic intersecting D-brane models,” hep-th/0502005.
13. M.J. Dolan, S. Krippendorff, and F. Quevedo, JHEP **1110**, 024 (2011).
14. G. Aldazabal *et al.*, Nucl. Phys. **B452**, 3 (1995);  
Z. Kakushadze and S.H.H. Tye, Phys. Rev. **D54**, 7520 (1996);  
Z. Kakushadze *et al.*, Int. J. Mod. Phys. **A13**, 2551 (1998).
15. G. B. Cleaver *et al.*, Int. J. Mod. Phys. **A16**, 425 (2001), hep-ph/9904301;  
*ibid.*, Nucl. Phys. **B593**, 471 (2001) hep-ph/9910230.
16. V. Braun *et al.*, Phys. Lett. **B618**, 252 (2005), hep-th/0501070;  
*ibid.*, JHEP **506**, 039 (2005), [hep-th/0502155].
17. E. Witten, Nucl. Phys. **B471**, 135 (1996), [hep-th/9602070].
18. H. Georgi *et al.*, Phys. Rev. Lett. **33**, 451 (1974);  
See also the definition of effective field theories by S. Weinberg, Phys. Lett. **91B**, 51 (1980).
19. See talks on proposed and running nucleon decay experiments, and theoretical talks by P. Langacker, p. 131, and W.J. Marciano and A. Sirlin, p. 151, in *The Second Workshop on Grand Unification*, eds. J.P. Leveille *et al.*, Birkhäuser, Boston (1981).
20. W.J. Marciano, p. 190, *Eighth Workshop on Grand Unification*, ed. K. Wali, World Scientific Publishing Co., Singapore (1987).
21. U. Amaldi *et al.*, Phys. Lett. **B260**, 447 (1991);  
J. Ellis *et al.*, Phys. Lett. **B260**, 131 (1991);  
P. Langacker and M. Luo, Phys. Rev. **D44**, 817 (1991);  
P. Langacker and N. Polonsky, Phys. Rev. **D47**, 4028 (1993);  
M. Carena *et al.*, Nucl. Phys. **B406**, 59 (1993);  
see also the review by S. Dimopoulos *et al.*, Physics Today, p. 25 October (1991).
22. B.C. Allanach, Comput. Phys. Commun. **143**, 305 (2002) [hep-ph/0104145].
23. S. Dimopoulos *et al.*, Phys. Rev. **D24**, 1681 (1981);  
S. Dimopoulos and H. Georgi, Nucl. Phys. **B193**, 150 (1981);  
L. Ibanez and G.G. Ross, Phys. Lett. **105B**, 439 (1981);  
N. Sakai, Z. Phys. **C11**, 153 (1981);  
M.B. Einhorn and D.R.T. Jones, Nucl. Phys. **B196**, 475 (1982);  
W.J. Marciano and G. Senjanovic, Phys. Rev. **D25**, 3092 (1982).
24. D.I. Kazakov, Lectures given at the European School on High Energy Physics, Aug.-Sept. 2000, Caramulo, Portugal [hep-ph/0012288v2].
25. V. Lucas and S. Raby, Phys. Rev. **D54**, 2261 (1996) [hep-ph/9601303];  
T. Blazek *et al.*, Phys. Rev. **D56**, 6919 (1997) [hep-ph/9611217];  
G. Altarelli *et al.*, JHEP **0011**, 040 (2000) [hep-ph/0007254].
26. R. Dermisek *et al.*, Phys. Rev. **D63**, 035001 (2001);  
K.S. Babu *et al.*, Nucl. Phys. **B566**, 33 (2000).
27. M. L. Alciati *et al.*, JHEP **0503**, 054 (2005) [hep-ph/0501086].
28. G. Anderson *et al.*, eConf **C960625**, SUP107 (1996) [hep-ph/9609457].
29. R.N. Mohapatra and M.K. Parida, Phys. Rev. **D47**, 264 (1993).
30. D.G. Lee *et al.*, Phys. Rev. **D51**, 229 (1995).
31. Eur. Phys. J. **C64**, 689 (2009).
32. K. Nakamura *et al.*, (Particle Data Group), J. Phys. **G37**, 075021 (2010).
33. K. Nakamura *et al.*, (Particle Data Group), J. Phys. **G37**, 075021 (2010).
34. S. Raby *et al.*, Phys. Lett. **B687**, 342 (2010) [arXiv:0911.4249 [hep-ph]].
35. K.S. Babu and S.M. Barr, Phys. Rev. **D48**, 5354 (1993);  
V. Lucas and S. Raby, Phys. Rev. **D54**, 2261 (1996);  
S.M. Barr and S. Raby, Phys. Rev. Lett. **79**, 4748 (1997) and references therein.

36. G. Altarelli *et al.*, JHEP **0011**, 040 (2000) See also earlier papers by A. Masiero *et al.*, Phys. Lett. **B115**, 380 (1982); B. Grinstein, Nucl. Phys. **B206**, 387 (1982).
37. K.R. Dienes *et al.*, Phys. Rev. Lett. **91**, 061601 (2003).
38. L. J. Hall *et al.*, Phys. Rev. **D64**, 055003 (2001).
39. N. Arkani-Hamed and S. Dimopoulos, JHEP **0506**, 073 (2005) [hep-th/0405159].
40. G.F. Giudice and A. Romanino, Nucl. Phys. **B699**, 65 (2004) [Erratum: *ibid.*, Nucl. Phys. **B706**, 65 (2005)] [hep-ph/0406088].
41. M. Chanowitz *et al.*, Nucl. Phys. **B135**, 66 (1978); For the corresponding SUSY analysis, see M. Einhorn and D.R.T. Jones, Nucl. Phys. **B196**, 475 (1982); K. Inoue *et al.*, Prog. Theor. Phys. **67**, 1889 (1982); L. E. Ibanez and C. Lopez, Phys. Lett. **B126**, 54 (1983); *ibid.*, Nucl. Phys. **B233**, 511 (1984).
42. K. Agashe *et al.*, [hep-ph/0502222].
43. M. Gell-Mann *et al.*, in *Supergravity*, eds. P. van Nieuwenhuizen and D.Z. Freedman, North-Holland, Amsterdam, 1979, p. 315.
44. S. Weinberg, Phys. Rev. **D26**, 287 (1982); N. Sakai and T. Yanagida, Nucl. Phys. **B197**, 533 (1982).
45. G. Farrar and P. Fayet, Phys. Lett. **B76**, 575 (1978).
46. S. Dimopoulos *et al.*, Phys. Lett. **112B**, 133 (1982); J. Ellis *et al.*, Nucl. Phys. **B202**, 43 (1982).
47. L.E. Ibanez and G.G. Ross, Nucl. Phys. **B368**, 3 (1992).
48. H. K. Dreiner, C. Luhn, and M. Thormeier, Phys. Rev. **D73**, 075007 (2006).
49. For a recent discussion, see C.S. Aulakh *et al.*, Nucl. Phys. **B597**, 89 (2001).
50. H. M. Lee *et al.*, Phys. Lett. **B694**, 491 (2011); R. Kappl *et al.*, Nucl. Phys. **B847**, 325 (2011); H. M. Lee *et al.*, Nucl. Phys. **B850**, 1 (2011).
51. R. Barbieri *et al.*, Phys. Lett. **B407**, 250 (1997).
52. G. F. Giudice and R. Rattazzi, Phys. Lett. **B406**, 321 (1997).
53. R. Barbier *et al.*, Phys. Rev. **420**, 1 (2005).
54. Makoto Miura [Super-Kamiokande Collab.], ICHEP 2010.
55. T. Goto and T. Nihei, Phys. Rev. **D59**, 115009 (1999) [hep-ph/9808255]; H. Murayama and A. Pierce, Phys. Rev. **D65**, 055009 (2002) hep-ph/0108104.
56. B. Bajc *et al.*, Phys. Rev. **D66**, 075005 (2002) [hep-ph/0204311].
57. J.L. Chkareuli and I.G. Gogoladze, Phys. Rev. **D58**, 055011 (1998) [hep-ph/9803335].
58. K.S. Choi, Phys. Lett. **B668**, 392 (2008).
59. L.J. Hall and Y. Nomura, Phys. Rev. **D66**, 075004 (2002); H.D. Kim *et al.*, JHEP **0505**, 036 (2005).
60. M. Baldoceolin *et al.*, Z. Phys. **C63**, 409 (1994).
61. K. S. Babu and R. N. Mohapatra, Phys. Lett. **B518**, 269 (2001) [hep-ph/0108089].
62. H. Georgi and D.V. Nanopoulos, Nucl. Phys. **B159**, 16 (1979); J. Harvey *et al.*, Phys. Lett. **B92**, 309 (1980); *ibid.*, Nucl. Phys. **B199**, 223 (1982).
63. T. Banks, Nucl. Phys. **B303**, 172 (1988); M. Olechowski and S. Pokorski, Phys. Lett. **B214**, 393 (1988); S. Pokorski, Nucl. Phys. (Proc. Supp.) **B13**, 606 (1990); B. Ananthanarayan *et al.*, Phys. Rev. **D44**, 1613 (1991); Q. Shafi and B. Ananthanarayan, ICTP Summer School lectures (1991); S. Dimopoulos *et al.*, Phys. Rev. Lett. **68**, 1984 (1992); *ibid.*, Phys. Rev. **D45**, 4192 (1992); G. Anderson *et al.*, Phys. Rev. **D47**, 3702 (1993); B. Ananthanarayan *et al.*, Phys. Lett. **B300**, 245 (1993); G. Anderson *et al.*, Phys. Rev. **D49**, 3660 (1994); B. Ananthanarayan *et al.*, Phys. Rev. **D50**, 5980 (1994).
64. LEP Higgs Working Group and ALEPH Collab. and DELPHI Collab. and L3 Collab. and OPAL Collab., Preliminary results, [hep-ex/0107030] (2001).
65. M. Carena and H.E. Haber, Prog. in Part. Nucl. Phys. **50**, 63 (2003) [hep-ph/0208209].
66. L.J. Hall *et al.*, Phys. Rev. **D50**, 7048 (1994); M. Carena *et al.*, Nucl. Phys. **B419**, 213 (1994); R. Rattazzi and U. Sarid, Nucl. Phys. **B501**, 297 (1997).
67. Blazek *et al.*, Phys. Rev. Lett. **88**, 111804 (2002) [hep-ph/0107097]; *ibid.*, Phys. Rev. **D65**, 115004 (2002) [hep-ph/0201081]; K. Tobe and J. D. Wells, Nucl. Phys. **B663**, 123 (2003) [hep-ph/0301015]; D. Auto *et al.*, JHEP **0306**, 023 (2003) [hep-ph/0302155]; R. Dermisek *et al.*, JHEP **0304**, 037 (2003); *ibid.*, JHEP **0509**, 029 (2005).
68. W. Altmannshofer *et al.*, Phys. Lett. **B668**, 385 (2008); D. Guadagnoli *et al.*, JHEP **0910**, 059 (2009).
69. H. Baer *et al.*, JHEP **0810**, 079 (2008); H. Baer *et al.*, JHEP **0909**, 005 (2009).
70. I. Gogoladze *et al.*, JHEP **1012**, 055 (2010); S. Dar *et al.*, [arXiv:1105.5122 [hep-ph]]; I. Gogoladze *et al.*, [arXiv:1107.1228 [hep-ph]].
71. M. Badziak, M. Olechowski, and S. Pokorski, JHEP **1108**, 147 (2011).
72. H. Georgi and C. Jarlskog, Phys. Lett. **B86**, 297 (1979).
73. S. Antusch and M. Spinrath, Phys. Rev. **D79**, 095004 (2009).
74. K.S. Babu and R.N. Mohapatra, Phys. Rev. Lett. **74**, 2418 (1995); V. Lucas and S. Raby, Phys. Rev. **D54**, 2261 (1996); T. Blažek *et al.*, Phys. Rev. **D56**, 6919 (1997); R. Barbieri *et al.*, Nucl. Phys. **B493**, 3 (1997); T. Blazek *et al.*, Phys. Rev. **D60**, 113001 (1999); *ibid.*, Phys. Rev. **D62**, 055001 (2000); Q. Shafi and Z. Tavartkiladze, Phys. Lett. **B487**, 145 (2000); C.H. Albright and S.M. Barr, Phys. Rev. Lett. **85**, 244 (2000); K.S. Babu *et al.*, Nucl. Phys. **B566**, 33 (2000); M. -C. Chen and K. T. Mahanthappa, Phys. Rev. **D62**, 113007 (2000); G. Altarelli *et al.*, Ref. 36; Z. Berezhiani and A. Rossi, Nucl. Phys. **B594**, 113 (2001); C. H. Albright and S. M. Barr, Phys. Rev. **D64**, 073010 (2001); M. -C. Chen, K. T. Mahanthappa, Int. J. Mod. Phys. **A18**, 5819 (2003); R. Dermisek and S. Raby, Phys. Lett. **B622**, 327 (2005); R. Dermisek *et al.*, Phys. Rev. **D74**, 035011 (2006); M. Albrecht *et al.*, JHEP **0710**, 055 (2007); K. S. Babu *et al.*, JHEP **1006**, 084 (2010).
75. G. Lazarides *et al.*, Nucl. Phys. **B181**, 287 (1981); T. E. Clark *et al.*, Phys. Lett. **B115**, 26 (1982); K. S. Babu and R. N. Mohapatra, Phys. Rev. Lett. **70**, 2845 (1993).
76. B. Bajc *et al.*, Phys. Rev. Lett. **90**, 051802 (2003).
77. H. S. Goh *et al.*, Phys. Lett. **B570**, 215 (2003) [hep-ph/0303055]; *ibid.*, Phys. Rev. **D68**, 115008 (2003) [hep-ph/0308197]; B. Dutta *et al.*, Phys. Rev. **D69**, 115014 (2004) [hep-ph/0402113]; S. Bertolini and M. Malinsky, [hep-ph/0504241]; K. S. Babu and C. Macesanu, [hep-ph/0505200].
78. B. Bajc *et al.*, JHEP **0811**, 007 (2008).
79. P. Minkowski, Phys. Lett. **B67**, 421 (1977).
80. T. Yanagida, in *Proceedings of the Workshop on the Unified Theory and the Baryon Number of the Universe*, eds. O. Sawada and A. Sugamoto, KEK report No. 79-18, Tsukuba, Japan, 1979; S. Glashow, Quarks and leptons, published in *Proceedings of the Cargèse Lectures*, M. Levy (ed.), Plenum Press, New York, (1980); M. Gell-Mann *et al.*, in *Supergravity*, ed. P. van Nieuwenhuizen *et al.*, North-Holland, Amsterdam, (1979), p. 315; R.N. Mohapatra and G. Senjanovic, Phys. Rev. Lett. **44**, 912 (1980).
81. G.L. Fogli *et al.*, Phys. Rev. **D84**, 053007 (2011).
82. T. Schwetz, M. Tortola, and J.W.F. Valle, New J. Phys. **13**, 109401 (2011), [arXiv:1108.1376 [hep-ph]].

83. C.H. Albright and M.-C. Chen, Phys. Rev. **D74**, 113006 (2006).
84. G. 't Hooft, Nucl. Phys. **B79**, 276 (1974);  
A.M. Polyakov, Pis'ma Zh. Eksp. Teor. Fiz. **20**, 430 (1974) [JETP Lett. **20**, 194 (1974)];  
For a pedagogical introduction, see S. Coleman, in *Aspects of Symmetry*, Selected Erice Lectures, Cambridge University Press, Cambridge, (1985), and P. Goddard and D. Olive, Rep. Prog. Phys. **41**, 1357 (1978).
85. I. De Mitri, (MACRO Collab.), Nucl. Phys. (Proc. Suppl.) **B95**, 82 (2001).
86. For a review, see A.D. Linde, *Particle Physics and Inflationary Cosmology*, Harwood Academic, Switzerland (1990).
87. G. R. Dvali *et al.*, Phys. Rev. Lett. **80**, 2281 (1998) [hep-ph/9710301].
88. P. Langacker and S. Y. Pi, Phys. Rev. Lett. **45**, 1 (1980).
89. G. R. Dvali *et al.*, Phys. Rev. Lett. **75**, 4559 (1995) [hep-ph/9507230].
90. V. Rubakov, Nucl. Phys. **B203**, 311 (1982), Institute of Nuclear Research Report No. P-0211, Moscow (1981), unpublished;  
C. Callan, Phys. Rev. **D26**, 2058 (1982);  
F. Wilczek, Phys. Rev. Lett. **48**, 1146 (1982);  
See also, S. Dawson and A.N. Schellekens, Phys. Rev. **D27**, 2119 (1983).
91. K. Freese *et al.*, Phys. Rev. Lett. **51**, 1625 (1983).
92. M. Fukugita and T. Yanagida, Phys. Lett. **B174**, 45 (1986);  
See also the recent review by W. Buchmuller *et al.*, hep-ph/0502169 and references therein.
93. E. Witten, Phys. Lett. **105B**, 267 (1981).
94. S. Dimopoulos and F. Wilczek, *Proceedings Erice Summer School*, ed. A. Zichichi (1981);  
K.S. Babu and S.M. Barr, Phys. Rev. **D50**, 3529 (1994).
95. R. Barbieri *et al.*, Nucl. Phys. **B391**, 487 (1993);  
Z. Berezhiani *et al.*, Nucl. Phys. **B444**, 61 (1995);  
Q. Shafi and Z. Tavartkiladze, Phys. Lett. **B522**, 102 (2001).
96. G.F. Giudice and A. Masiero, Phys. Lett. **B206**, 480 (1988);  
J.E. Kim and H.P. Nilles, Mod. Phys. Lett. **A9**, 3575 (1994).
97. L. Randall and C. Csaki, hep-ph/9508208.
98. A. Hebecker *et al.*, [arXiv:0801.4101 [hep-ph]];  
F. Brümmer *et al.*, JHEP **08**, 011 (2009);  
F. Brümmer *et al.*, JHEP **04**, 006 (2010).
99. T. P. T. Dijkstra *et al.*, Phys. Lett. **B609**, 408 (2005).
100. T. Kobayashi *et al.*, Phys. Lett. **B593**, 262 (2004);  
*ibid.*, Nucl. Phys. **B704**, 3 (2005).
101. W. Buchmuller *et al.*, Phys. Rev. Lett. **96**, 121602 (2006);  
*ibid.*, Nucl. Phys. **B785**, 149 (2007).
102. O. Lebedev *et al.*, Phys. Lett. **B645**, 88 (2007);  
*ibid.*, [arXiv:0708.2691 [hep-th]];  
O. Lebedev *et al.*, Phys. Lett. **B668**, 331 (2008).
103. J. E. Kim *et al.*, JHEP **0706**, 034 (2007);  
J. E. Kim and B. Kyae, Phys. Rev. **D77**, 106008 (2008).
104. L. B. Anderson *et al.*, [arXiv:1106.4804 [hep-th]].
105. C. Beasley *et al.*, JHEP **01**, 058 (2009);  
R. Donagi and M. Wijnholt, [arXiv:0802.2969 [hep-th]];  
C. Beasley *et al.*, JHEP **01**, 059 (2009);  
R. Donagi and M. Wijnholt, [arXiv:0808.2223 [hep-th]];  
R. Blumenhagen *et al.*, [arXiv:0811.2936 [hep-th]].
106. C. M. Chen and Y. C. Chung, Nucl. Phys. **B824**, 273 (2010).
107. J. Marsano *et al.*, JHEP **0908**, 030 (2009).
108. R. Blumenhagen, Phys. Rev. Lett. **102**, 071601 (2009).
109. S. Raby, Rept. on Prog. in Phys. **74**, 036901 (2011).

## 16. HEAVY-QUARK AND SOFT-COLLINEAR EFFECTIVE THEORY

Written August 2011 by C.W. Bauer (LBNL) and M. Neubert (U. Mainz).

### 16.1. Effective Field Theories

Quantum field theories represent the most precise computational tool for describing physics at the highest energies. One of their characteristic features is that they almost inevitably involve multiple length scales. When trying to determine the value of an observable, quantum field theory demands that all possible virtual states and hence all particles be included in the calculation. Since these particles have widely different masses, the final prediction is sensitive to many scales. This fact represents a formidable challenge from a practical point of view. No realistic quantum field theories can be solved exactly, so that one has to resort to approximation schemes; these, however, are typically most straightforward when only a single scale is involved at a time.

Effective field theories (EFTs) provide a general theoretical framework to deal with the multi-scale problems of realistic quantum field theories. This framework aims to reduce such problems to a combination of separate and simpler single-scale problems; simultaneously, however, it provides an organizational scheme whereby the other scales are not omitted but allowed to play their role in a separate step of the computation. The philosophy and basic principles of this approach are very generic, and correspondingly EFTs represent a widely used method in many different areas of high-energy physics, from the low energy scales of atomic and nuclear physics to the high energy scales of (partly yet unknown) elementary particle physics. EFTs can play a role both within analytic perturbative computations and in the context of non-perturbative numerical simulations; see [1–3] for some early references. One of the simplest applications of EFTs to particle physics is to describe an underlying theory that is only probed at energy scales  $E < \Lambda$ . Any particle with mass  $m > \Lambda$  cannot be produced as a real state and therefore only leads to short-distance virtual effects. Thus, one can construct an effective theory in which the quantum fluctuations of such heavy particles are “integrated out” from the generating functional integral for Green functions. This results in a simpler theory containing only those degrees of freedom that are relevant to the energy scales under consideration. In fact, the standard model of particle physics itself is widely viewed as an EFT of some yet unknown, more fundamental theory.

The development of any effective theory starts by identifying the degrees of freedom that are relevant to describe the physics at a given energy (or length) scale, and constructing the Lagrangian describing the interactions among these fields. Short-distance quantum fluctuations associated with much smaller length scales are absorbed into the coefficients of the various operators in the effective Lagrangian. These coefficients are determined in a matching procedure, by requiring that the EFT reproduces the matrix elements of the full theory up to power corrections. In many cases the effective Lagrangian exhibits enhanced symmetries compared with the fundamental theory, allowing for simple and sometimes striking predictions relating different observables.

### 16.2. Heavy-Quark Effective Theory

Heavy-quark systems provide prime examples for applications of the EFT technology, because the hierarchy  $m_Q \gg \Lambda_{\text{QCD}}$  (with  $Q = b, c$ ) provides a natural separation of scales. Physics at the scale  $m_Q$  is of a short-distance nature and can be treated perturbatively, while for heavy-quark systems there is always also some hadronic physics governed by the confinement scale  $\Lambda_{\text{QCD}}$ . Being able to separate the short-distance and long-distance effects associated with these two scales is crucial for any quantitative description in heavy-quark physics. For instance, if the long-distance hadronic matrix elements are obtained from lattice QCD, then it is necessary to analytically compute the short-distance effects, which come from short-wavelength modes that do not fit on present-day lattices. In many other instances, the long-distance hadronic physics can be encoded in a small number of universal parameters.

#### 16.2.1. General idea and derivation of the effective

**Lagrangian**: The simplest effective theory for heavy-quark systems is the heavy-quark effective theory (HQET) [4–7] (see [8,9] for detailed discussions). It provides a simplified description of the soft interactions of a single heavy quark interacting with soft, light partons. This includes the interactions that bind the heavy quark with other light partons inside heavy mesons ( $B, B^*, \dots$ ) and baryons ( $\Lambda_b, \Sigma_b, \dots$ ).

A softly interacting heavy quark is nearly on-shell. Its momentum may be decomposed as  $p_Q = m_Q v + k$ , where  $v$  is the 4-velocity of the hadron containing the heavy quark, and the “residual momentum”  $k \sim \Lambda_{\text{QCD}}$  results from the soft interactions of the heavy quark with its environment. In the limit  $m_Q \gg \Lambda_{\text{QCD}}$ , the soft interactions do not change the 4-velocity of the heavy quark, which is therefore a conserved quantum number that is often used as a label on the effective heavy-quark fields. A nearly on-shell Dirac spinor has two large and two small components. We define

$$Q(x) = e^{-im_Q v \cdot x} [h_v(x) + H_v(x)], \quad (16.1)$$

where

$$h_v(x) = e^{im_Q v \cdot x} \frac{1 + \not{v}}{2} Q(x), \quad H_v(x) = e^{im_Q v \cdot x} \frac{1 - \not{v}}{2} Q(x) \quad (16.2)$$

are the large (“upper”) and small (“lower”) components of the Dirac spinor, respectively. The extraction of the phase factor in Eq. (16.1) implies that the fields  $h_v$  and  $H_v$  carry the residual momentum  $k$ . These fields obey the projection relations  $\not{v} h_v = h_v$  and  $\not{v} H_v = -H_v$ . Inserting these definitions into the Dirac Lagrangian yields

$$\mathcal{L}_Q = \bar{h}_v i v \cdot D h_v + \bar{H}_v (-i v \cdot D - 2m_Q) H_v + \bar{h}_v i \overleftrightarrow{D} H_v + \bar{H}_v i \overleftrightarrow{D} h_v, \quad (16.3)$$

where  $i \overleftrightarrow{D}^\mu = i D^\mu - v^\mu i v \cdot D$  is the “spatial” covariant derivative (note that  $v^\mu = (1, \vec{0})$  in the heavy-hadron rest frame). The interpretation of Eq. (16.3) is that the field  $h_v$  describes a massless fermion, while  $H_v$  describes a heavy fermion with mass  $2m_Q$ . Both modes are coupled to each other via the last two terms. Soft interactions cannot excite the heavy fermion, so we integrate it out from the generating functional of the theory. The light field which remains describes the fluctuations of the heavy quark about its mass shell. Solving the classical equation of motion for the field  $H_v$  yields

$$H_v = \frac{1}{2m_Q + i v \cdot D} i \overleftrightarrow{D} h_v = \frac{1}{2m_Q} \sum_{n=0}^{\infty} \left( -\frac{i v \cdot D}{2m_Q} \right)^n i \overleftrightarrow{D} h_v, \quad (16.4)$$

which implies  $H_v = O(\Lambda_{\text{QCD}}/m_Q) h_v$ , provided the residual momenta are small. The effective Lagrangian of HQET is obtained by inserting this result into Eq. (16.3). At subleading order in  $1/m_Q$  one finds

$$\mathcal{L}_{\text{HQET}} = \bar{h}_v i v \cdot D_s h_v + \frac{1}{2m_Q} \times \left[ \bar{h}_v (i \overleftrightarrow{D}_s)^2 h_v + C_{\text{mag}}(\mu) \frac{g}{2} \bar{h}_v \sigma_{\mu\nu} G_s^{\mu\nu} h_v \right] + \dots \quad (16.5)$$

Note that the covariant derivative  $i D_s^\mu = i \partial^\mu + g A_s^\mu$  contains only the soft gluon field. Hard gluons have been integrated out, and their effects are contained in the Wilson coefficients of the various operators in the effective Lagrangian. From the leading operator one derives the Feynman rules of HQET. The new operators entering at subleading order are referred to as the “kinetic energy” and “chromo-magnetic interaction”. The kinetic-energy operator corresponds to the first correction term in the Taylor expansion of the relativistic energy  $E = m_Q + \vec{p}^2/2m_Q + \dots$ . Lorentz invariance, which is encoded as a reparametrization invariance of the effective Lagrangian [10], ensures that its Wilson coefficient is not renormalized ( $C_{\text{kin}} \equiv 1$ ). The coefficient of the chromo-magnetic operator,  $C_{\text{mag}}(\mu) = 1 + \mathcal{O}(\alpha_s)$ , receives corrections starting at one-loop order.



**16.2.2. Spin-flavor symmetry and applications in spectroscopy :** The leading term in the HQET Lagrangian exhibits a global spin-flavor symmetry. Its physical meaning is that, in the infinite mass limit, the properties of hadronic systems containing a single heavy quark are insensitive to the spin and flavor of the heavy quark [11,12]. The spin symmetry results from the fact that there appear no Dirac matrices in the leading term in the effective Lagrangian Eq. (16.5), implying that the interactions of the heavy quark with soft gluons leave its spin unchanged. The flavor symmetry arises since the mass of the heavy quark does not appear at leading order. When there are  $n_Q$  heavy quarks moving at the same velocity, one can simply extend Eq. (16.5) by summing over  $n_Q$  identical terms for heavy-quark fields  $h_v^i$ . The result is invariant under rotations in flavor space. When combined with the spin symmetry, the symmetry group becomes promoted to  $SU(2n_Q)$ . The flavor symmetry is broken by the operators arising at order  $1/m_Q$  and higher. However, at first order only the chromo-magnetic operator breaks the spin symmetry.

The spin-flavor symmetry leads to many interesting relations between the properties of hadrons containing a heavy quark. The most direct consequences concern the spectroscopy of such states [13]. In the heavy-quark limit, the spin of the heavy quark and the total angular momentum  $j$  of the light degrees of freedom are separately conserved by the strong interactions. Because of heavy-quark symmetry, the dynamics is independent of the spin and mass of the heavy quark. Hadronic states can thus be classified by the quantum numbers (flavor, spin, parity, etc.) of the light degrees of freedom. The spin symmetry predicts that, for fixed  $j \neq 0$ , there is a doublet of degenerate states with total spin  $J = j \pm 1/2$ . The flavor symmetry relates the properties of states with different heavy quark flavor. In the case of the ground-state mesons containing a heavy quark, the light degrees of freedom have the quantum numbers of an antiquark, and the degenerate states are the pseudoscalar ( $J = 0$ ) and vector ( $J = 1$ ) mesons. Their masses are split by hyperfine corrections of order  $1/m_Q$ , such that one expects  $m_{B^*} - m_B = O(1/m_b)$  and  $m_{D^*} - m_D = O(1/m_c)$ . It follows that  $m_{B^*}^2 - m_B^2 \simeq m_{D^*}^2 - m_D^2 \simeq \text{const}$ . The data are compatible with this result:  $m_{B^*}^2 - m_B^2 \simeq 0.49 \text{ GeV}^2$  and  $m_{D^*}^2 - m_D^2 \simeq 0.55 \text{ GeV}^2$ .

**16.2.3. Weak decay form factors :** Of particular interest are the relations between the weak decay form factors of heavy mesons, which parametrize hadronic matrix elements of currents between two meson states containing a heavy quark. These relations have been derived by Isgur and Wise [12], generalizing ideas developed by Nussinov and Wetzel [14] and Voloshin and Shifman [15]. For the purpose of this discussion, it is convenient to work with a mass-independent normalization of meson states and use velocity rather than momentum variables.

Consider the elastic scattering of a pseudoscalar meson,  $P(v) \rightarrow P(v')$ , induced by an external vector current coupled to the heavy quark contained in  $P$ , which acts as a color source moving with the meson's velocity  $v$ . The action of the current is to replace instantaneously the color source by one moving at velocity  $v'$ . Soft gluons need to be exchanged in order to rearrange the light degrees of freedom and build the final state meson moving at velocity  $v'$ . This rearrangement leads to a form factor suppression. The important observation is that, in the  $m_Q \rightarrow \infty$  limit, the form factor can only depend on the Lorentz boost  $\gamma = v \cdot v'$  connecting the rest frames of the initial and final-state mesons (as long as  $\gamma = \mathcal{O}(1)$ ). In the effective theory, which provides the appropriate framework to consider the limit  $m_Q \rightarrow \infty$  with the quark velocities kept fixed, the hadronic matrix element describing the scattering process can be written as

$$\langle P(v') | \bar{h}_{v'} \gamma^\mu h_v | P(v) \rangle = \xi(v \cdot v') (v + v')^\mu, \quad (16.6)$$

with a form factor  $\xi(v \cdot v')$  that is real and does not depend on  $m_Q$ . By flavor symmetry, the form factor remains identical when one replaces the heavy quark  $Q$  in one of the meson states by a heavy quark  $Q'$  of a different flavor, thereby turning  $P$  into another pseudoscalar meson  $P'$ . At the same time, the current becomes a flavor-changing vector current. This universal form factor is called the Isgur-Wise function [12]. For equal velocities the vector current  $J^\mu = \bar{h}_v \gamma^\mu h_v$  is conserved in the effective theory, irrespective of the

flavor of the heavy quarks. The corresponding conserved charges are the generators of the flavor symmetry. It follows that the Isgur-Wise function is normalized at the point of equal velocities:  $\xi(1) = 1$ . Since  $E_{\text{recoil}} = m_{P'}(v \cdot v' - 1)$  is the recoil energy of the daughter meson  $P'$  in the rest frame of the parent meson  $P$ , the point  $v \cdot v' = 1$  is referred to as the zero recoil limit. The heavy-quark spin symmetry leads to additional relations among weak decay form factors. It can be used to relate matrix elements involving vector mesons to those involving pseudoscalar mesons, which once again can be described completely in terms of the universal Isgur-Wise function.

These form factor relations imposed by heavy-quark symmetry describe the semileptonic decay processes  $\bar{B} \rightarrow D \ell \bar{\nu}$  and  $\bar{B} \rightarrow D^* \ell \bar{\nu}$  in the limit of infinite heavy-quark masses. They are model-independent consequences of QCD. The known normalization of the Isgur-Wise function at zero recoil can be used to obtain a model-independent measurement of the element  $|V_{cb}|$  of the Cabibbo-Kobayashi-Maskawa (CKM) matrix. The semileptonic decay  $\bar{B} \rightarrow D^* \ell \bar{\nu}$  is ideally suited for this purpose [16]. Experimentally, this is a particularly clean mode, since the reconstruction of the  $D^*$  meson mass provides a powerful rejection against background. From the theoretical point of view, it is ideal since the decay rate at zero recoil is protected by Luke's theorem against first-order power corrections in  $1/m_Q$  [17]. This is described in more detail in Section 11 of the PDG Book.

**16.2.4. Decoupling transformation :** At leading order in  $1/m_Q$ , the couplings of soft gluons to heavy quarks in the effective Lagrangian Eq. (16.5) can be removed by the field redefinition  $h_v(x) = Y_v(x) h_v^{(0)}(x)$ , where  $Y_v(x)$  denotes a time-like Wilson line along the direction of  $v$ , extending from minus infinity to the point  $x$ . In terms of the new fields, the HQET Lagrangian becomes

$$\mathcal{L}_{\text{HQET}} = \bar{h}_v^{(0)} i v \cdot \partial h_v^{(0)} + O(1/m_Q). \quad (16.7)$$

At leading order in  $1/m_Q$ , this is a free theory as far as the strong interactions of heavy quarks are concerned. However, the theory is nevertheless non-trivial in the presence of external sources. Consider, e.g., the case of a weak-interaction heavy-quark current

$$\bar{h}_{v'} \gamma^\mu (1 - \gamma_5) h_v = \bar{h}_{v'}^{(0)} \gamma^\mu (1 - \gamma_5) Y_{v'}^\dagger Y_v h_v^{(0)}, \quad (16.8)$$

where  $v$  and  $v'$  are the velocities of the heavy mesons containing the heavy quarks. Unless the two velocities are equal, the object  $Y_{v'}^\dagger Y_v$  is non-trivial, and hence the soft gluons do not decouple from the heavy quarks inside the current operator. One may interpret  $Y_{v'}^\dagger Y_v$  as a Wilson loop with a cusp at the point  $x$ , where the two paths parallel to the different velocity vectors intersect. The presence of the cusp leads to non-trivial ultra-violet behavior (for  $v \neq v'$ ), which is described by a cusp anomalous dimension  $\Gamma_c(v \cdot v')$  that was calculated at two-loop order in [18]. It coincides with the velocity-dependent anomalous dimension of heavy-quark currents, which was rediscovered later in the context of HQET [19]. The interpretation of heavy quarks as Wilson lines is a useful tool, which was put forward in some of the very first papers on the subject [4]. This technology will be useful in the study of the interactions of heavy quarks with collinear degrees of freedom discussed later in this review.

**16.2.5. Heavy-quark expansion for inclusive decays :** The theoretical description of inclusive decays of hadrons containing a heavy quark exploits two observations [20–24]: bound-state effects related to the initial state can be calculated using the heavy-quark expansion, and the fact that the final state consists of a sum over many hadronic channels eliminates the sensitivity to the properties of individual final-state hadrons. The second feature rests on the hypothesis of quark-hadron duality, i.e. the assumption that decay rates are calculable in QCD after a smearing procedure has been applied [25]. In semileptonic decays, the integration over the lepton spectrum provides a smearing over the invariant hadronic mass of the final state (global duality). For nonleptonic decays, where the total hadronic mass is fixed, the summation over many hadronic final states provides an averaging (local duality).

Using the optical theorem, the inclusive decay width of a hadron  $H_b$  containing a  $b$  quark can be written in the form

$$\Gamma(H_b) = \frac{1}{M_{H_b}} \text{Im} \langle H_b | i \int d^4x T \{ \mathcal{H}_{\text{eff}}(x), \mathcal{H}_{\text{eff}}(0) \} | H_b \rangle. \quad (16.9)$$

The effective weak Hamiltonian for  $b$ -quark decays consists of dimension-6 four-fermion operators and dipole operators [80]. It follows that the leading contributions to the inclusive decay rate in Eq. (16.9) arise from two-loop diagrams. Because of the large mass of the  $b$  quark, the momenta flowing through the internal propagators are large. It is thus possible to construct an operator-product expansion (OPE) for the transition operator, in which it is represented as a series of local operators containing two  $b$ -quark fields. The operator with the lowest dimension is  $\bar{b}b$ . The next non-trivial operator has dimension 5 and contains the gluon field. It arises from diagrams in which a soft gluon is emitted from one of the internal lines of the two-loop diagrams. From dimension 6 on, an increasing number of operators appears. For dimensional reasons, the matrix elements of higher-dimensional operators are suppressed by inverse powers of the  $b$ -quark mass. Thus, the total inclusive decay rate of a hadron  $H_b$  can be written as [21,47]

$$\Gamma(H_b) = \frac{G_F^2 m_b^5 |V_{cb}|^2}{192\pi^3} \times \left\{ c_3 \langle \bar{b}b \rangle + c_5 \frac{\langle \bar{b} g \sigma_{\mu\nu} G^{\mu\nu} b \rangle}{m_b^2} + \sum_n c_6^{(n)} \frac{\langle O_6^{(n)} \rangle}{m_b^3} + \dots \right\}, \quad (16.10)$$

where the prefactor arises from the loop integrations,  $c_i$  are calculable coefficient functions, and  $\langle O_i \rangle$  are the (normalized) forward matrix elements between  $H_b$  states. These matrix elements can be systematically expanded in powers of  $1/m_b$  using HQET. The result is [21,47]

$$\langle \bar{b}b \rangle = 1 - \frac{\mu_\pi^2(H_b) - \mu_G^2(H_b)}{2m_b^2} + \dots, \quad \langle \bar{b} g \sigma_{\mu\nu} G^{\mu\nu} b \rangle = \frac{2\mu_G^2(H_b)}{m_b^2} + \dots, \quad (16.11)$$

where  $\mu_\pi^2(H_b)$  and  $\mu_G^2(H_b)$  are the matrix elements of the heavy-quark kinetic energy and chromomagnetic interaction inside the hadron  $H_b$ , respectively [27]. For the ground-state heavy mesons and baryons, one can extract  $\mu_G^2(B) = 3(m_{B^*}^2 - m_B^2)/4 \simeq 0.36 \text{ GeV}^2$  and  $\mu_G^2(\Lambda_b) = 0$  from spectroscopy.

From the fully inclusive width Eq. (16.10) one can obtain the lifetime of a heavy hadron via  $\tau(H_b) = 1/\Gamma(H_b)$ . Due to the universality of the leading term in the heavy-quark expansion, lifetime ratios such as  $\tau(B^-)/\tau(\bar{B}^0)$ ,  $\tau(B_s^0)/\tau(\bar{B}^0)$ , and  $\tau(\Lambda_b)/\tau(\bar{B}^0)$  are particularly sensitive to the hadronic parameters determining the power corrections in the expansion. In order to understand these ratios theoretically, it is necessary to include phase-space enhanced power corrections of order  $(\Lambda_{\text{QCD}}/m_b)^3$  as well as short-distance perturbative effects in the calculation [28,29].

A formula analogous to Eq. (16.10) can be derived for differential distributions in specific inclusive decay processes, assuming that these distributions are integrated over sufficiently large portions of phase space to ensure quark-hadron duality. Important examples are the distributions in lepton energy ( $d\Gamma/dE_\ell$ ) or lepton invariant mass ( $d\Gamma/dq^2$ ), as well as moments of the invariant hadronic mass distribution, in the semileptonic processes  $\bar{B} \rightarrow X_u \ell \bar{\nu}$  and  $\bar{B} \rightarrow X_c \ell \bar{\nu}$ , as well as the photon energy spectrum ( $d\Gamma/dE_\gamma$ ) in the radiative process  $\bar{B} \rightarrow X_s \gamma$ . While the latter process is primarily used to test the Standard Model and search for hints of new physics, an analysis of decay distributions in the semileptonic processes can be employed to perform a global fit determining the CKM matrix elements  $|V_{ub}|$  and  $|V_{cb}|$  along with heavy-quark parameters such as the masses  $m_b$ ,  $m_c$  and the hadronic parameters  $\mu_\pi^2(B)$ ,  $\mu_G^2(B)$ . These determinations provide some of the most accurate values for these parameters [30].

**16.2.6. Shape functions and non-local power corrections :** In certain regions of phase space, in which the hadronic final state in an inclusive heavy-hadron decay is made up of light energetic partons, the local OPE for inclusive decays must be replaced by a more complicated expansion involving hadronic matrix elements of non-local light-ray operators [52,53]. Prominent examples are the radiative decay  $\bar{B} \rightarrow X_s \gamma$  for large photon energy  $E_\gamma$  near  $m_B/2$ , and the semileptonic decay  $\bar{B} \rightarrow X_u \ell \bar{\nu}$  at large lepton energy or small hadronic invariant mass. In these cases, the differential decay rates at leading order in the heavy-quark expansion can be written in the factorized form  $d\Gamma \propto H J \otimes S$  [33], where the hard function  $H$  and the jet function  $J$  are calculable in perturbation theory. The characteristic scales for these functions are set by  $m_b$  and  $(m_b \Lambda_{\text{QCD}})^{1/2}$ , respectively. The soft function

$$S(\omega) = \int \frac{dt}{4\pi} e^{-i\omega t} \langle \bar{B}(v) | \bar{h}_v(tn) Y_n(tn) Y_n^\dagger(0) h_v(0) | \bar{B}(v) \rangle \quad (16.12)$$

is a genuinely non-perturbative object, called the shape function [52,53]. Here  $Y_n$  are soft Wilson lines along a light-like direction  $n$  aligned with the momentum of the hadronic final-state jet. The jet function and the shape function share a common variable  $\omega \sim \Lambda_{\text{QCD}}$ , and the symbol  $\otimes$  denotes a convolution in this variable.

While the hard function is different for the two decays, the jet and soft functions are identical at leading order in  $\Lambda_{\text{QCD}}/m_Q$ . This is particularly important for the soft function. It is this shape function that introduces non-perturbative physics into the theoretical predictions for the cross sections of  $\bar{B} \rightarrow X_s \gamma$  and  $\bar{B} \rightarrow X_u \ell \bar{\nu}$  in the regions of experimental interest. The fact that both decays depend on the same non-perturbative function made it possible to determine this non-perturbative information from the measured shape of the photon spectrum in  $\bar{B} \rightarrow X_s \gamma$ , allowing for a better understanding of the process used to determine the CKM element  $|V_{ub}|$ . In higher orders of the heavy-quark expansion, an increasing number of subleading jet and soft functions is required to describe the decay distributions [34]. These have been analyzed in detail at order  $1/m_b$  [35–37]. The technology for deriving the corresponding factorization theorems relies on SCET, which is discussed below.

### 16.3. Soft-Collinear Effective Theory

As discussed in the previous section, soft gluons that bind a heavy quark inside a heavy meson cannot change the virtuality of that heavy quark by a significant amount. The ratio of  $\Lambda_{\text{QCD}}/m_Q$  provided the expansion parameter in HQET, which is a small parameter since  $m_Q \gg \Lambda_{\text{QCD}}$ . This obviously does not work when considering light quarks. However, if the energy  $Q$  of the quarks is large, the ratio  $\Lambda_{\text{QCD}}/Q$  provides a small parameter which can be used to construct an effective theory. One major difference to HQET is that light energetic quarks cannot only emit soft gluons, but they can also emit collinear gluons (an energetic gluon in the same direction as the original quark), without parametrically changing their virtuality. Thus, to fully reproduce the long-distance physics of energetic quarks requires that one includes their interactions with both soft and collinear particles. The resulting effective theory is therefore called soft-collinear effective theory (SCET) [38–40].

SCET is applicable for processes containing particles with energy much in excess of their mass, and it has therefore a wide range of applications. In this brief review we will outline the main features of this effective theory and mention a few selected applications.

**16.3.1. General idea of the expansion :** Consider a quark with energy  $Q$  and virtuality  $m \ll Q$ , moving along the direction  $\vec{n}$ . It is convenient to parameterize the momentum  $p_n$  of this particle in terms of its light-cone components, defined by  $(p_n^-, p_n^+, p_n^\perp) = (\vec{n} \cdot p_n, n \cdot p_n, p_n^\perp)$ , where  $n^\mu = (1, \vec{n})$  and  $\bar{n}^\mu = (1, -\vec{n})$  are light-like 4-vectors, and  $n \cdot p_\perp = \bar{n} \cdot p_\perp = 0$ . A subscript  $n$  has been added to the momentum to identify it as a collinear particle in direction  $n$  (more precisely, a particle with energy much larger than its virtuality moving along a direction  $\vec{n}$ ). In terms of these light-cone components, the virtuality satisfies  $m^2 = p_n^+ p_n^- + p_n^{\perp 2}$ . The individual components of the momentum satisfy

$$(p_n^-, p_n^+, p_n^\perp) \sim (Q, m^2/Q, m) \equiv Q(1, \lambda^2, \lambda), \quad (16.13)$$

where  $\lambda = m/Q$  is the expansion parameter of SCET.

The virtuality of such an energetic particle remains parametrically unchanged if it interacts with energetic particles in the same direction  $n$ , or with soft particles with momentum scaling as

$$(p_s^-, p_s^+, p_s^\perp) \sim Q(\lambda^2, \lambda^2, \lambda^2). \quad (16.14)$$

Thus, it is the interactions of collinear and soft degrees of freedom that give rise to the long-distance physics. SCET, which is constructed to reproduce this long-distance dynamics, is therefore an effective theory describing the interactions of collinear and soft particles.

The above power counting treats the soft momentum to be of order  $m^2/Q$ , where  $m$  denotes the mass of a collinear system. If the mass of the collinear system is of order  $\Lambda_{\text{QCD}}$ , as would be the case for a single energetic hadron, this power counting is no longer applicable, since  $\Lambda_{\text{QCD}}$  provides a natural cutoff to QCD and the soft momentum cannot be below this scale. To describe such systems requires a modified version of SCET, called SCET<sub>II</sub>, in which the scaling of the soft modes is  $Q(\lambda, \lambda, \lambda)$ . In this review we will focus only on SCET with the scaling discussed before, which is sometimes called SCET<sub>I</sub>.

**16.3.2. Leading-order Lagrangian :** The derivation of the SCET Lagrangian follows similar steps as the derivation of the HQET Lagrangian in Section 16.2.1, but care has to be taken to properly account for the interactions of collinear fields with one another. We begin by deriving the Lagrangian for a theory containing only a single type of collinear degrees of freedom. We are interested in the interactions of fermion fields  $q_n(x)$  with gluon fields  $A_n(x)$ , which have collinear momentum in the same light-like direction  $n$ . Similar to HQET, one can separate the full QCD field into two components,  $q_n(x) = \psi_n(x) + \Xi_n(x)$ , where

$$\psi_n(x) = \frac{\not{n}\not{\bar{n}}}{4} q_n(x), \quad \Xi_n(x) = \frac{\not{n}\not{\bar{n}}}{4} q_n(x).$$

In terms of these fields, the QCD Lagrangian is

$$\begin{aligned} \mathcal{L}_n = & \bar{\psi}_n(x) \frac{\not{n}}{2} i n \cdot D_n \psi_n(x) + \bar{\Xi}_n(x) \frac{\not{n}}{2} i \bar{n} \cdot D_n \Xi_n(x) \\ & + \bar{\psi}_n(x) i \not{D}_n^\perp \Xi_n(x) + \bar{\Xi}_n(x) i \not{D}_n^\perp \psi_n(x), \end{aligned} \quad (16.15)$$

where we have defined the transverse derivative  $D_n^{\perp\mu} = D_n^\mu - \frac{n^\mu}{2} \bar{n} \cdot D_n - \frac{\bar{n}^\mu}{2} n \cdot D_n$ . Since  $\bar{n} \cdot p_n \gg 1$  the field  $\Xi_n(x)$  has no pole in its propagator, similar to the field  $H_v(x)$  in Eq. (16.3). It can therefore be integrated out using its equation of motion. Inserting this back into Eq. (16.15), we find

$$\mathcal{L}_n = \bar{\psi}_n(x) \left[ i n \cdot D_n + i \not{D}_n^\perp \frac{1}{i \bar{n} \cdot D_n} i \not{D}_n^\perp \right] \frac{\not{n}}{2} \psi_n(x). \quad (16.16)$$

While this Lagrangian leads to the correct Feynman rules of SCET, there is one feature that warrants extra discussion. In contrast to the Lagrangian of HQET given in Eq. (16.5), where the derivative scales like the residual momentum  $k$  of the heavy quark, the derivatives in Eq. (16.16) pick up both the large momentum components of order  $Q$  and  $Q\lambda$ , as well as the residual momentum of order  $Q\lambda^2$ . One can separate the large and residual momentum components using a procedure similar to the HQET case. Separating the collinear momentum into a “label” and a residual component,  $p^\mu = P^\mu + k^\mu$ , and performing a phase redefinition on the collinear fields  $\psi_n(x) = e^{iP \cdot x} \xi_n(x)$ , derivatives acting on the fields  $\xi_n(x)$  now only pick out the residual momentum. Since the label momentum in SCET is not conserved as in HQET, one defines a label operator  $\mathcal{P}^\mu$  acting as  $\mathcal{P}^\mu \xi_n(x) = P^\mu \xi_n(x)$  [39], as well as a corresponding covariant label operator  $i \mathcal{D}_n^\mu = \mathcal{P}^\mu + g A_n(x)$ .

The final step to complete the Lagrangian of SCET is to include the interactions of collinear fields with soft fields. These interactions can be included by adding the soft gluons to the covariant derivatives, while preserving the power counting. This leads to the final SCET Lagrangian [39–41]

$$\mathcal{L}_n = \bar{\xi}_n(x) \left[ i n \cdot D_n + g n \cdot A_s + i \not{D}_n^\perp \frac{1}{i \bar{n} \cdot D_n} i \not{D}_n^\perp \right] \frac{\not{n}}{2} \xi_n(x). \quad (16.17)$$

The leading-order Lagrangian describing collinear fields in different light-like directions is simply given by the sum of the Lagrangians for each direction  $n$  separately, i.e.  $\mathcal{L} = \sum_n \mathcal{L}_n$ . The soft gluons are the same in each individual Lagrangian. An alternative way to understand the separation between large and small momentum components is to derive the Lagrangian of SCET in position space. In this case no label operators are required to describe interactions in SCET, and the dependence on short-distance effects is contained in non-localities at short distances. An important difference between SCET and HQET is that the SCET Lagrangian is not corrected by short distance fluctuations [42].

**16.3.3. Collinear gauge invariance and Wilson lines :** An important aspect of SCET is the gauge structure of the theory. Because the effective field operators in SCET describe modes with certain momentum scalings, the effective Lagrangian respects only residual gauge symmetries. One of them satisfies the collinear scaling

$$(\bar{n} \cdot \partial_n, n \cdot \partial_n, \partial_n^\perp) U_n(x) \sim Q(1, \lambda^2, \lambda) U_n(x), \quad (16.18)$$

and one the soft scaling

$$(\bar{n} \cdot \partial_n, n \cdot \partial_n, \partial_n^\perp) U_s(x) \sim Q(\lambda^2, \lambda^2, \lambda^2) U_s(x). \quad (16.19)$$

The fact that collinear fields in different directions do not transform under the same gauge transformations implies that each collinear sector, containing particles with large momenta along a certain direction, has to be separately gauge invariant. This is achieved by the introduction of collinear Wilson lines [39]

$$W_n(x) = P \exp \left[ -ig \int_{-\infty}^0 ds \bar{n} \cdot A_n(s \bar{n} + x) \right], \quad (16.20)$$

which transform under collinear gauge transformations according to  $W_n \rightarrow U_n W_n$ . Thus, the combination  $\chi_n \equiv W_n^\dagger \psi_n$  is gauge invariant. In a similar manner, one can define the gauge-invariant gluon field  $B_n^\mu = g^{-1} W_n^\dagger i D_n^\mu W_n$  [43]. Operators in SCET are typically constructed from such gauge-invariant collinear fields.

**16.3.4. Decoupling of soft gluons :** Soft gluons in SCET couple to collinear quarks only through the term  $\bar{\xi}_n g n \cdot A_s \frac{\not{n}}{2} \xi_n$  in the effective Lagrangian in Eq. (16.17). This coupling is similar to the coupling of soft gluons to heavy quarks in HQET, and soft gluons in SCET can be decoupled from collinear fields in a way similar as explained in Section 16.2.4. Written in terms of the redefined fields

$$\psi_n(x) = Y_n(x) \psi_n^{(0)}(x), \quad A_n(x) = Y_n(x) A_n^{(0)}(x) Y_n^\dagger(x), \quad (16.21)$$

the soft gluons decouple from the SCET Lagrangian [40]. This fact greatly facilitates proofs of factorization theorems in SCET.

**16.3.5. Factorization Theorems :** One of the important applications of SCET is to understand how to factorize cross sections involving energetic particles in different directions into simpler pieces that can either be calculated perturbatively or determined from data. Factorization theorems have been around for much longer than SCET. For a review on the subject, see [44]. However, the effective theory allows for a conceptually simpler understanding of certain classes of factorization theorems [45], since most simplifications happen already at the level of the Lagrangian. The discussion in this section is valid to leading order in the power counting of the effective theory.

As discussed in the previous section, the Lagrangian of SCET does not involve any couplings between collinear degrees of freedom in different light-like directions, or between soft and collinear degrees of freedom after the field redefinition Eq. (16.21) has been performed. An operator describing the scattering and production of collinear partons at short distances can thus be written as

$$\langle O(x) \rangle \simeq C_O(\mu) \times$$

$$\left\langle \mathcal{C}_{n_a}^{(0)}(x) \mathcal{C}_{n_b}^{(0)}(x) \mathcal{C}_{n_1}^{(0)}(x) \dots \mathcal{C}_{n_N}^{(0)}(x) [\mathcal{Y}_{n_a} \mathcal{Y}_{n_b} \mathcal{Y}_{n_1} \dots \mathcal{Y}_{n_N}](x) \right\rangle_\mu. \quad (16.22)$$

Here  $\mathcal{C}_n(x)$  denotes a gauge-invariant combination of collinear fields (either quark or gluon fields) in the direction  $n$ , and the matching coefficient accounting for short-distance effects is denoted by  $C_O$ . The soft Wilson lines can either be in a color triplet or color octet representation, and are collectively denoted by  $\mathcal{Y}_n$ . Both the matrix elements and the coefficient  $C_O$  depend on the renormalization scale  $\mu$ .

Having defined the operator mediating a given process, one can calculate the cross section by squaring the operator, taking the forward matrix element and integrating over the phase space of all final-state particles. The absence of interactions between collinear degrees of freedom moving along different directions or soft degrees of freedom implies that the forward matrix element of the operator can be factorized as

$$\begin{aligned} \langle \text{in} | O(x) O^\dagger(0) | \text{in} \rangle &= \langle \text{in}_a | \mathcal{C}_{n_a}(x) \mathcal{C}_{n_a}^\dagger(0) | \text{in}_a \rangle \langle \text{in}_b | \mathcal{C}_{n_b}(x) \mathcal{C}_{n_b}^\dagger(0) | \text{in}_b \rangle \\ &\times \langle 0 | \mathcal{C}_{n_1}(x) \mathcal{C}_{n_1}^\dagger(0) | 0 \rangle \cdots \langle 0 | \mathcal{C}_{n_N}(x) \mathcal{C}_{n_N}^\dagger(0) | 0 \rangle \\ &\times \langle 0 | [\mathcal{Y}_{n_a} \cdots \mathcal{Y}_{n_N}](x) [\mathcal{Y}_{n_a} \cdots \mathcal{Y}_{n_N}]^\dagger(0) | 0 \rangle. \end{aligned} \quad (16.23)$$

Thus, the matrix element required for the differential cross section has factorized into a product of simpler structures, each of which can be evaluated separately.

For most applications the matrix elements of incoming collinear fields are non-perturbative objects given in terms of the well-known parton distribution functions, while the matrix elements of outgoing collinear fields are determined by perturbatively calculable jet functions  $J_i(\mu)$ . Finally, the vacuum matrix element of the soft Wilson lines defines a so-called soft function, commonly denoted by  $S(\mu)$ . The common dependence on  $x$  in the above equation implies that in momentum space the various components of the factorization theorem are convoluted with one another. Deriving this convolution requires a careful treatment of the phase-space integration, in particular treating the large and residual components of each momentum appropriately.

Putting all information together, the differential cross section can be written as

$$d\sigma \sim H(\mu) \otimes [f_{p_1/P}(\mu) f_{p_2/P}(\mu)] \otimes [J_1(\mu) \cdots J_N(\mu)] \otimes S(\mu). \quad (16.24)$$

The hard coefficient is equal to the square of the matching coefficient,  $H(\mu) = |C_O(\mu)|^2$ . It should be mentioned that the most difficult part of traditional factorization proofs involves showing that so-called Glauber gluons do not spoil the above factorization theorem. This question has not yet been fully addressed in the context of SCET.

**16.3.6. Resummation of large logarithms:** SCET can be used to sum the large logarithmic terms that arise in perturbative calculations. In general, perturbation theory will generate a logarithmic dependence on any ratio of scales  $r$  in a problem, and for processes that involve initial or final states with energy much in excess of their mass there are two powers of logarithms for every power of the strong coupling constant. Thus, for widely separated scales these large logarithms can spoil fixed-order perturbation theory, and a much better convergence is achieved by expanding in  $\alpha_s$ , but holding  $\alpha_s \log^2 r$  fixed, such that the first term in the new expansion resums powers of  $\alpha_s \log^2 r$  to all orders. More precisely, a proper resummation requires to sum logarithms of the form  $\alpha_s^n \log^m r$  with  $m \leq n + 1$  in the logarithm of a cross-section.

The important ingredient in achieving this resummation is the fact that SCET factorizes a given cross section into simpler pieces, as discussed in the previous section. Each of the ingredients of the factorization theorem depends on a single physical scale, and the only dependence on that scale can arise through logarithms of its ratio with the renormalization scale  $\mu$ . Thus, for each of the components in the factorization theorem one can choose a renormalization scale  $\mu$  for which the large logarithmic terms are absent.

Of course, the factorization formula requires a common renormalization scale  $\mu$  in all its components, and one therefore has to use the RG to evolve the various component functions from their preferred

scale to the common scale  $\mu$ . For example, for the hard coefficient  $H(\mu)$ , the RG equation can be written as

$$\mu \frac{d}{d\mu} H(\mu) = \gamma_H(\mu) H(\mu). \quad (16.25)$$

In general, the anomalous dimension is of the form  $\gamma_H(\mu) = c_H \Gamma_{\text{cusp}}(\alpha_s) \log(Q/\mu) + \gamma(\alpha_s)$ , where  $c_H$  is a process-dependent coefficient and  $\Gamma_{\text{cusp}}$  denotes the so-called cusp anomalous dimension [18,46]. The non-cusp part of the anomalous dimension  $\gamma$  is again process dependent. The presence of a logarithm of the hard scale  $Q$  in the anomalous dimension is characteristic of Sudakov problems and arises since the perturbative series contains double logarithms of scale ratios. The anomalous dimension  $\gamma_H$  is known at two-loop order for arbitrary  $n$ -parton amplitudes containing massless or massive external partons [47–50]. Solving the RG equation yields

$$H(\mu) = U_H(\mu, \mu_h) H(\mu_h), \quad (16.26)$$

which can be used to write the hard function at a scale  $\mu_h \sim Q$ , where its perturbative expression does not contain any large logarithms, in terms of the common renormalization scale  $\mu$ . The RG evolution factor  $U_H(\mu, \mu_h)$  sums logarithms of the form  $\mu/\mu_h$ . By calculating the anomalous dimension  $\gamma_H(\mu)$  to higher and higher orders in perturbation theory, one can resum more and more logarithms in the evolution kernel. The RG equations for the jet and soft functions are more complicated, since they involve convolutions over the relevant momentum variables.

**16.3.7. Applications:** Most of the applications of SCET are either in flavor physics, where the decay of a heavy  $B$  meson can give rise to energetic light partons, or in collider physics, where the presence of jets naturally leads to collimated sets of energetic particles. For several of these applications alternative approaches existed before the invention of SCET, but the effective theory has opened up alternative ways to understand the physics of these processes. There are, however, many examples for which SCET has allowed new insights that were not available or possible without the effective theory. In particular, it has provided a field-theoretic basis for the QCD factorization approach to exclusive, non-leptonic decays of  $B$  mesons [51]. Using SCET methods, proofs of factorization were derived for the color-allowed decay  $\bar{B}^0 \rightarrow D^+ \pi^-$  [52], the color-suppressed decay  $\bar{B}^0 \rightarrow D^0 \pi^0$  [53], and the radiative decay  $\bar{B} \rightarrow K^* \gamma$  [54]. Further examples are factorization theorems and the resummation of endpoint logarithms for quarkonia production [55], factorization theorems for cross sections defined through jet algorithms [56], the resummation of large logarithmic terms for the thrust [57] and jet broadening [58] distributions in  $e^+e^-$  annihilation beyond NLL order, the development of new factorizable observables to veto extra jets [59], all-orders factorization theorems for processes containing electroweak Sudakov logarithms [60], as well as the resummation of threshold (soft gluon) logarithms for several important processes at hadron colliders [61,62]. We describe two of these applications in more detail.

Event-shape distributions, in particular the thrust distribution, have been measured to high accuracy at LEP [63]. Comparing these data to precise theoretical predictions allows for a determination of the strong coupling constant  $\alpha_s$ . For small values of  $\tau \equiv 1 - T$ , the distribution can be factorized into the form [64,65]

$$\frac{1}{Q\sigma_0} \frac{d\sigma}{d\tau} = H(\mu) \int ds \int dk J(s, \mu) S(Q\tau - s/Q - k, \mu). \quad (16.27)$$

Here  $Q$  denotes the center-of-mass energy of the collision,  $\sigma_0$  is the total hadronic cross section, and  $H$ ,  $J$  and  $S$  are the hard, jet and soft functions in SCET. Large logarithms of the form  $(\alpha_s^n \ln^{2n-1} \tau)/\tau$  become important and have to be resummed. Furthermore, for  $\tau \sim \Lambda_{\text{QCD}}/Q$  non-perturbative effects in the soft function become important. Using SCET the resummation of these large logarithms has been performed to  $\text{N}^3\text{LL}$ , which is two orders beyond what was previously available [57]. The factorization in the effective theory has also allowed to include the non-perturbative physics through a shape function, very similar to the  $B$ -physics case discussed above.

The known perturbative effects for large values of  $\tau$  can be included by matching the SCET result to the known two-loop spectrum [66,67]. Comparing the predicted to the measured thrust distribution allows for a precise determination of the strong coupling constant  $\alpha_s$  [68].

For quarkonium produced in  $e^+e^-$  annihilation or photo-production, large logarithms arise in the region of phase space where the energy of the produced  $Q\bar{Q}$  state is close to its maximum value. In this region the quarkonium is predominantly produced in a color-octet configuration and recoils against a collinear hadronic system. Then logarithms of the form  $\log(1 - E_\Psi/E_{\max})$  as well as non-perturbative effects become important and should be included in attempts to describe the data. While some of these issues had been addressed without the use of an effective theory (see [69] and references therein), a complete treatment of the endpoint region has only been achieved using SCET [55]. It was shown that including both effects consistently, theory and data can be brought into better agreement.

#### 16.4. Open issues and perspectives

HQET has successfully passed many experimental tests, and there are not too many open questions that still need to be addressed. One issue that has not been derived from first principles is quark-hadron duality. The validity of global duality (at energies even lower than those relevant in  $B$  decays) has been tested experimentally using high-precision data on semileptonic  $B$  decays and on hadronic  $\tau$  decays, and there has been good agreement between theory and data. However, assigning a theoretical uncertainty to possible duality violations is difficult. Another known issue is that the measured value of the CKM element  $|V_{cb}|$  is different depending of whether one uses inclusive or exclusive  $B$  decays to derive it (see the relevant section in the Particle Data Book). Both measurements rely on the heavy-quark limit, and the uncertainties quoted include the effects from power corrections arising from the finite  $b$ -quark mass.

SCET, on the other hand, is still an active field of research, and there are several open questions that need to be answered. In this review we have not discussed any issues having to do with SCET<sub>II</sub>, which is the appropriate effective theory describing the interactions of collinear particles with soft particles having momentum scaling as  $Q(\lambda, \lambda, \lambda)$ . This is important, for example, to describe exclusive decays of  $B$  mesons into light, energetic mesons, or in collider-physics applications such as the  $p_T$  resummation for Drell-Yan production. There are still open issues in how to properly formulate SCET<sub>II</sub>, which are under active investigation. They include the treatment of endpoint singularities of convolution integrals, double counting between overlapping momentum regions, and the breakdown of the naive factorization of soft and collinear modes due to quantum effects. Glauber gluons are known to affect factorization theorems, but how to properly include them in SCET is still an open question.

#### References:

1. E. Witten, Nucl. Phys. B **122**, 109 (1977).
2. S. Weinberg, Phys. Lett. B **91**, 51 (1980).
3. L.J. Hall, Nucl. Phys. B **178**, 75 (1981).
4. E. Eichten and B. Hill, Phys. Lett. B **234**, 511 (1990).
5. H. Georgi, Phys. Lett. B **240**, 447 (1990).
6. B. Grinstein, Nucl. Phys. B **339**, 253 (1990).
7. T. Mannel, W. Roberts, and Z. Ryzak, Nucl. Phys. B **368**, 204 (1992).
8. M. Neubert, Phys. Rept. **245**, 259 (1994) [[hep-ph/9306320](#)].
9. A.V. Manohar and M.B. Wise, Camb. Monogr. Part. Phys. Nucl. Phys. Cosmol. **10**, 1 (2000).
10. M.E. Luke and A.V. Manohar, Phys. Lett. B **286**, 348 (1992) [[hep-ph/9205228](#)].
11. E.V. Shuryak, Phys. Lett. B **93**, 134 (1980).
12. N. Isgur and M.B. Wise, Phys. Lett. B **232**, 113 (1989); Phys. Lett. B **237**, 527 (1990).
13. N. Isgur and M.B. Wise, Phys. Rev. Lett. **66**, 1130 (1991).
14. S. Nussinov and W. Wetzel, Phys. Rev. D **36**, 130 (1987).
15. M.A. Shifman and M.B. Voloshin, Sov. J. Nucl. Phys. **45**, 292 (1987); Sov. J. Nucl. Phys. **47**, 511 (1988).
16. M. Neubert, Phys. Lett. B **264**, 455 (1991).
17. M.E. Luke, Phys. Lett. B **252**, 447 (1990).
18. G.P. Korchemsky and A.V. Radyushkin, Nucl. Phys. B **283**, 342 (1987).
19. A.F. Falk *et al.*, Nucl. Phys. B **343**, 1 (1990).
20. J. Chay, H. Georgi, and B. Grinstein, Phys. Lett. B **247**, 399 (1990).
21. I.I.Y. Bigi, N.G. Uraltsev, and A.I. Vainshtein, Phys. Lett. B **293**, 430 (1992) [[hep-ph/9207214](#)]; I.I.Y. Bigi *et al.*, Phys. Rev. Lett. **71**, 496 (1993) [[hep-ph/9304225](#)].
22. A.V. Manohar and M.B. Wise, Phys. Rev. D **49**, 1310 (1994) [[hep-ph/9308246](#)].
23. T. Mannel, Nucl. Phys. B **413**, 396 (1994) [[hep-ph/9308262](#)].
24. A.F. Falk, M.E. Luke, and M.J. Savage, Phys. Rev. D **49**, 3367 (1994) [[hep-ph/9308288](#)].
25. E.C. Poggio, H.R. Quinn, and S. Weinberg, Phys. Rev. D **13**, 1958 (1976).
26. G. Buchalla, A.J. Buras, and M.E. Lautenbacher, Rev. Mod. Phys. **68**, 1125 (1996) [[hep-ph/9512380](#)].
27. A.F. Falk and M. Neubert, Phys. Rev. D **47**, 2965 (1993) [[hep-ph/9209268](#)].
28. M. Neubert and C.T. Sachrajda, Nucl. Phys. B **483**, 339 (1997) [[hep-ph/9603202](#)].
29. M. Beneke, G. Buchalla and I. Dunietz, Phys. Rev. D **54**, 4419 (1996) [[hep-ph/9605259](#)].
30. C.W. Bauer *et al.*, Phys. Rev. D **70**, 094017 (2004) [[hep-ph/0408002](#)].
31. M. Neubert, Phys. Rev. D **49**, 4623 (1994) [[hep-ph/9312311](#)].
32. I.I.Y. Bigi *et al.*, Int. J. Mod. Phys. A **9**, 2467 (1994) [[hep-ph/9312359](#)].
33. G. P. Korchemsky and G.F. Sterman, Phys. Lett. B **340**, 96 (1994) [[hep-ph/9407344](#)].
34. C.W. Bauer, M.E. Luke, and T. Mannel, Phys. Rev. D **68**, 094001 (2003) [[hep-ph/0102089](#)].
35. K.S.M. Lee and I.W. Stewart, Nucl. Phys. B **721**, 325 (2005) [[hep-ph/0409045](#)].
36. S.W. Bosch, M. Neubert, and G. Paz, JHEP **0411**, 073 (2004) [[hep-ph/0409115](#)].
37. M. Beneke *et al.*, JHEP **0506**, 071 (2005) [[hep-ph/0411395](#)].
38. C. W. Bauer, S. Fleming, and M.E. Luke, Phys. Rev. D **63**, 014006 (2000) [[hep-ph/0005275](#)]; C.W. Bauer *et al.*, Phys. Rev. D **63**, 114020 (2001) [[hep-ph/0011336](#)].
39. C.W. Bauer and I.W. Stewart, Phys. Lett. B **516**, 134 (2001) [[hep-ph/0107001](#)].
40. C.W. Bauer, D. Pirjol, and I.W. Stewart, Phys. Rev. D **65**, 054022 (2002) [[hep-ph/0109045](#)].
41. J. Chay and C. Kim, Phys. Rev. D **65**, 114016 (2002) [[hep-ph/0201197](#)].
42. M. Beneke *et al.*, Nucl. Phys. B **643**, 431 (2002) [[hep-ph/0206152](#)].
43. R.J. Hill and M. Neubert, Nucl. Phys. B **657**, 229 (2003) [[hep-ph/0211018](#)].
44. J. C. Collins, D.E. Soper, and G.F. Sterman, Adv. Ser. Direct. High Energy Phys. **5**, 1 (1988) [[hep-ph/0409313](#)].
45. C.W. Bauer *et al.*, Phys. Rev. D **66**, 014017 (2002) [[hep-ph/0202088](#)].
46. I.A. Korchemskaya and G.P. Korchemsky, Phys. Lett. B **287**, 169 (1992).
47. T. Becher and M. Neubert, Phys. Rev. Lett. **102**, 162001 (2009) [[arXiv:0901.0722](#)] [[hep-ph](#)].
48. E. Gardi and L. Magnea, JHEP **0903**, 079 (2009) [[arXiv:0901.1091](#)] [[hep-ph](#)].
49. A. Mitov, G.F. Sterman, and I. Sung, Phys. Rev. D **79**, 094015 (2009) [[arXiv:0903.3241](#)] [[hep-ph](#)].
50. A. Ferroglia *et al.*, Phys. Rev. Lett. **103**, 201601 (2009) [[arXiv:0907.4791](#)] [[hep-ph](#)].
51. M. Beneke *et al.*, Phys. Rev. Lett. **83**, 1914 (1999) [[hep-ph/9905312](#)].
52. C.W. Bauer, D. Pirjol, and I.W. Stewart, Phys. Rev. Lett. **87**, 201806 (2001) [[hep-ph/0107002](#)].
53. S. Mantry, D. Pirjol, and I.W. Stewart, Phys. Rev. D **68**, 114009 (2003) [[hep-ph/0306254](#)].

54. T. Becher, R.J. Hill, and M. Neubert, Phys. Rev. D **72**, 094017 (2005) [[hep-ph/0503263](#)].
55. S. Fleming, A.K. Leibovich, and T. Mehen, Phys. Rev. D **68**, 094011 (2003) [[hep-ph/0306139](#)].
56. C.W. Bauer, A. Hornig, and F.J. Tackmann, Phys. Rev. D **79**, 114013 (2009) [[arXiv:0808.2191](#) [[hep-ph](#)]].
57. T. Becher and M.D. Schwartz, JHEP **0807**, 034 (2008) [[arXiv:0803.0342](#) [[hep-ph](#)]].
58. T. Becher, G. Bell, and M. Neubert, Phys. Lett. B **704**, 276 (2011) [[arXiv:1104.4108](#) [[hep-ph](#)]].
59. I.W. Stewart, F.J. Tackmann, and W.J. Waalewijn, Phys. Rev. D **81**, 094035 (2010) [[arXiv:0910.0467](#) [[hep-ph](#)]].
60. J.-y. Chiu, R. Kelley, and A.V. Manohar, Phys. Rev. D **78**, 073006 (2008) [[arXiv:0806.1240](#) [[hep-ph](#)]].
61. T. Becher, M. Neubert, and G. Xu, JHEP **0807**, 030 (2008) [[arXiv:0710.0680](#) [[hep-ph](#)]].
62. V. Ahrens *et al.*, Eur. Phys. J. C **62**, 333 (2009) [[arXiv:0809.4283](#) [[hep-ph](#)]]; V. Ahrens *et al.*, JHEP **1009**, 097 (2010) [[arXiv:1003.5827](#) [[hep-ph](#)]].
63. For a review, see: S. Kluth, Rept. Prog. Phys. **69**, 1771 (2006) [[hep-ex/0603011](#)].
64. G.P. Korchemsky and G.F. Sterman, Nucl. Phys. B **555**, 335 (1999) [[hep-ph/9902341](#)]; G.P. Korchemsky and S. Tafat, JHEP **0010**, 010 (2000) [[hep-ph/0007005](#)].
65. C.F. Berger and G.F. Sterman, JHEP **0309**, 058 (2003) [[hep-ph/0307394](#)].
66. A. Gehrmann-De Ridder *et al.*, Phys. Rev. Lett. **99**, 132002 (2007) [[arXiv:0707.1285](#) [[hep-ph](#)]].
67. S. Weinzierl, Phys. Rev. Lett. **101**, 162001 (2008) [[arXiv:0807.3241](#) [[hep-ph](#)]].
68. R. Abbate *et al.*, Phys. Rev. **D83**, 074021 (2011) [[arXiv:1006.3080](#) [[hep-ph](#)]].
69. B.A. Kniehl and G. Kramer, Phys. Rev. D **56**, 5820 (1997) [[hep-ph/9706369](#)].

## 17. LATTICE QUANTUM CHROMODYNAMICS

Written September 2011 by S. Hashimoto (KEK), J. Laiho (University of Glasgow) and S.R. Sharpe (University of Washington).

### 17.1. Lattice regularization of QCD

Gauge theories form the building blocks of the Standard Model. While the SU(2) and U(1) parts have weak couplings and can be studied accurately with perturbative methods, the SU(3) component—QCD—is only amenable to a perturbative treatment at high energies. The growth of the coupling constant in the infrared—the flip-side of asymptotic freedom—requires the use of non-perturbative methods to determine the low energy properties of QCD. Lattice gauge theory, proposed by K. Wilson in 1974 [1], provides such a method, for it gives a non-perturbative definition of vector-like gauge field theories like QCD. In lattice regularized QCD—commonly called lattice QCD or LQCD—Euclidean space-time is discretized, usually on a hypercubic lattice with lattice spacing  $a$ , with quark fields placed on sites and gauge fields on the links between sites. The lattice spacing plays the role of the ultraviolet regulator, rendering the quantum field theory finite. The continuum theory is recovered by taking the limit of vanishing lattice spacing, which can be reached by tuning the bare coupling constant to zero according to the renormalization group.

Unlike dimensional regularization, which is commonly used in continuum QCD calculations, the definition of LQCD does not rely on the perturbative expansion. Indeed, LQCD allows non-perturbative calculations by numerical evaluation of the path integral that defines the theory.

Practical LQCD calculations are limited by the availability of computational resources and the efficiency of algorithms. Because of this, LQCD results come with both statistical and systematic errors, the former arising from the use of Monte-Carlo integration, the latter, for example, from the use of non-zero values of  $a$ . There are also different ways in which the QCD action can be discretized, and all must give consistent results in the continuum limit. It is the purpose of this review to provide an outline of the methods of LQCD, with particular focus on applications to particle physics, and an overview of the various sources of error. This should allow the reader to better understand the LQCD results that are presented in other sections for a variety of quantities (quark masses, the hadron spectrum and several electroweak matrix elements). For more extensive explanations the reader should consult the available text books, the most up-to-date of which are Refs. [2,3,4].

#### 17.1.1. Gauge invariance, gluon fields and the gluon action :

A key feature of the lattice formulation of QCD is that it preserves gauge invariance. This is in contrast to perturbative calculations, where gauge fixing is an essential step. The preservation of gauge invariance leads to considerable simplifications, e.g. restricting the form of operators that can mix under renormalization.

The gauge transformations of lattice quark fields are just as in the continuum:  $q(x) \rightarrow V(x)q(x)$  and  $\bar{q}(x) \rightarrow \bar{q}(x)V^\dagger(x)$ , with  $V(x)$  an arbitrary element of SU(3). The only difference is that the Euclidean space-time positions  $x$  are restricted to lie on the sites of the lattice, i.e.  $x = a(n_1, n_2, n_3, n_4)$  for a hypercubic lattice, with the  $n_j$  being integers. Quark bilinears involving different lattice points can be made gauge invariant by introducing the gluon field  $U_\mu(x)$ . For example, for adjacent points the bilinear is  $\bar{q}(x)U_\mu(x)q(x+a\hat{\mu})$ , with  $\hat{\mu}$  the unit vector in the  $\mu$ 'th direction. (This form is used in the construction of the lattice covariant derivative.) The gluon field (or “gauge link”) is an element of the group, SU(3), in contrast to the continuum field  $A_\mu$  which takes values in the Lie algebra. The bilinear is invariant if  $U_\mu$  transforms as  $U_\mu(x) \rightarrow V(x)U_\mu(x)V^\dagger(x+a\hat{\mu})$ . The lattice gluon field is naturally associated with the link joining  $x$  and  $x+a\hat{\mu}$ , and corresponds in the continuum to a Wilson line connecting these two points,  $P \exp(i \int_x^{x+a\hat{\mu}} dx_\mu A_\mu^{\text{cont}}(x))$  (where  $P$  indicates a path-ordered integral, and the superscript on  $A_\mu$  indicates that it is a continuum field). The trace of a product of the  $U_\mu(x)$  around any closed loop is easily seen to be gauge invariant and is the lattice version of a Wilson loop.

The simplest possible gauge action, usually called the Wilson gauge action, is given by the product of gauge links around elementary

plaquettes:

$$S_g = \beta \sum_{x,\mu\nu} [1 - \text{ReTr}[U_\mu(x)U_\nu(x+a\hat{\mu})U_\mu^\dagger(x+a\hat{\nu})U_\nu^\dagger(x)]/3]. \quad (17.1)$$

For small  $a$ , assuming that the fields are slowly varying, one can expand the action in powers of  $a$  using  $U_\mu(x) = \exp(iaA_\mu(x))$ . Keeping only the leading non-vanishing term, and replacing the sum with an integral, one finds the continuum form,

$$S_g \rightarrow \int d^4x \frac{1}{4g_{\text{lat}}^2} \text{Tr}[F_{\mu\nu}^2(x)], \quad (F_{\mu\nu} = \partial_\mu A_\nu - \partial_\nu A_\mu + i[A_\mu, A_\nu]) \quad (17.2)$$

as long as one chooses  $\beta = 6/g_{\text{lat}}^2$  for the lattice coupling. In this expression,  $g_{\text{lat}}$  is the bare coupling constant in the lattice scheme, which can be related (by combining continuum and lattice perturbation theory) to a more conventional coupling constant such as that in the  $\overline{\text{MS}}$  scheme (see Sec. 17.3.4 below).

In practice, the lattice spacing  $a$  is non-zero, leading to discretization errors. In particular, the lattice breaks Euclidean rotational invariance (which is the Euclidean version of Lorentz invariance) down to a discrete hypercubic subgroup. One wants to reduce discretization errors as much as possible. A very useful tool in this regard is the Symanzik effective action: the interactions of quarks and gluons with momenta low compared to the lattice cutoff ( $|p| \ll 1/a$ ) are described by a continuum action consisting of the standard continuum terms (e.g. the gauge action given in Eq. (17.2)) augmented by higher dimensional operators suppressed by powers of  $a$  [5]. For the Wilson lattice gauge action, the leading correction comes in at  $\mathcal{O}(a^2)$ . It takes the form  $\sum_j a^2 \mathcal{O}_6^{(j)}$ , with the sum running over all dimension-six operators  $\mathcal{O}_6^{(j)}$  allowed by the lattice symmetries. Some of these operators violate Euclidean invariance, and all of them lead to discretization errors proportional to  $a^2$ . These errors can, however, be reduced by adding corresponding operators to the lattice action and tuning their coefficients to eliminate the dimension-six operators in the effective action to a given order in perturbation theory. This is the idea of the Symanzik improvement program [5]. In the case of the gauge action, one adds loops involving six gauge links (as opposed to the four links needed for the original plaquette action, Eq. (17.1)) to define the  $\mathcal{O}(a^2)$  improved (or “Symanzik”) action [6]. In practical implementations, the improvement is either at tree-level (so that residual errors are proportional to  $\alpha_s a^2$ , where the coupling is evaluated at a scale  $\sim 1/a$ ), or at one loop order (errors proportional to  $\alpha_s^2 a^2$ ). Another popular choice is motivated by studies of renormalization group (RG) flow. It has the same terms as the  $\mathcal{O}(a^2)$  improved action but with different coefficients, and is called the RG-improved or “Iwasaki” action [7].

#### 17.1.2. Lattice fermions :

Naive discretization of the continuum fermion action  $S_f = \int d^4x \bar{q}[i\partial_\mu \gamma_\mu + m]q$ , in which one replaces the derivative  $\partial_\mu q$  by a discrete difference  $[q(x+a\hat{\mu}) - q(x-a\hat{\mu})]/2a$ , leads to the fermion doubling problem—the resulting action describes  $2^d$  equivalent fermion fields in the continuum limit in  $d$  dimensions. The appearance of the extra “doubler” fermions is related to the deeper theoretical problem of formulating chirally symmetric fermions on the lattice. This is encapsulated by the Nielsen-Ninomiya theorem [8]: one cannot define lattice fermions having exact, continuum-like chiral symmetry without producing doublers. Naive lattice fermions do have chiral symmetry but at the cost of introducing 15 unwanted doublers (for  $d = 4$ ).

The doubling problem has been addressed in various ways, each coming with different pros and cons. Wilson fermions [1] add a term proportional to  $a\bar{q}\Delta q$  to the fermion action (the “Wilson term”—in which  $\Delta$  is a covariant lattice Laplacian). This gives a mass of  $\mathcal{O}(1/a)$  to the doublers, so that they decouple in the continuum limit. The Wilson term, however, violates chiral symmetry, and also introduces discretization errors linear in  $a$ . A commonly used variant that eliminates the  $\mathcal{O}(a)$  discretization error is the  $\mathcal{O}(a)$ -improved Wilson (or “clover”) fermion [9]. In this application of Symanzik improvement, methods have been developed to remove  $\mathcal{O}(a)$  terms to all orders in perturbation theory using auxiliary simulations to tune parameters (“non-perturbative improvement”) [10].

The advantages of Wilson fermions are their theoretical simplicity and relatively small computational cost. The disadvantage is their lack of chiral symmetry, which makes them difficult to use in cases where mixing with wrong chirality operators can occur, particularly if this involves divergences proportional to powers of  $1/a$ . A related problem is potential numerical instabilities due to spurious near-zero modes. Ongoing work has, however, been successful at ameliorating these problems and increasing the range of quantities for which Wilson fermions can be used.

Twisted-mass fermions [11] are a variant of Wilson fermions which remove the numerical instability problem by treating two flavors of fermions together and adding an isospin-breaking mass term (the “twisted mass” term). Another advantage of this approach is that all errors linear in  $a$  are automatically removed (without the need for tuning of parameters) by a clever choice of twisted mass and operators.

Staggered fermions are a reduced version of naive fermions in which there is only a single fermion Dirac component on each lattice site, with the full Dirac structure built up from neighboring sites [12]. They have the advantages of being somewhat faster to simulate than Wilson-like fermions, of preserving some chiral symmetry, and of having discretization errors of  $\mathcal{O}(a^2)$ . Their disadvantage is that they retain some of the doublers (3 for  $d = 4$ ). The action thus describes four degenerate fermions in the continuum limit. The resulting SU(4) flavor symmetry is usually called “taste symmetry”, and the preserved chiral symmetry in this formulation has non-singlet taste. Practical applications usually introduce one staggered fermion for each physical flavor, and remove contributions from the unwanted tastes by taking the fourth-root of the fermion determinant appearing in the path integral. The validity of this “rooting” procedure is not obvious because taste symmetry is violated for non-zero lattice spacing. Theoretical arguments, supported by numerical evidence, suggest that the procedure is valid as long as one takes the continuum limit before approaching the light quark mass region [13].

Just as for Wilson fermions, the staggered action can be improved, so as to reduce discretization errors. The widely used “asqtad” action [14] removes tree-level  $\mathcal{O}(a^2)$  errors, and leads to substantial reduction in the breaking of taste symmetry. More recently, a highly improved staggered quark (“HISQ”) action has been introduced [15], which further reduces taste symmetry-breaking and can also be used for heavy quarks such as charm.

There is an important class of lattice fermions that possess a continuum-like chiral symmetry without introducing unwanted doublers. The Dirac operator  $D$  for these fermions satisfies the Ginsparg-Wilson relation  $D\gamma_5 + \gamma_5 D = aD\gamma_5 D$  [16]. In the continuum, the right-hand-side vanishes due to chiral symmetry. On the lattice, it is non-vanishing, but with a particular form (with two factors of  $D$ ) that restricts the violations of chiral symmetry in Ward-Takahashi identities to short-distance terms that do not contribute to physical matrix elements. In fact, one can define a modified chiral transformation on the lattice (by including dependence on the gauge fields) such that “Ginsparg-Wilson fermions” have an exact chiral symmetry [17]. The net result is that such fermions essentially have the same properties under chiral transformations as do continuum fermions. Their leading discretization errors are of  $\mathcal{O}(a^2)$ .

Two types of Ginsparg-Wilson fermions are being used in large-scale projects. The first are Domain-wall fermions (DWF). These are defined on a five-dimensional space, in which the fifth dimension is fictitious [18]. The action is chosen so that the low-lying modes are chiral, with left- and right-handed modes localized on opposite four-dimensional surfaces. For an infinite fifth dimension, these fermions satisfy the Ginsparg-Wilson relation. In practice, the fifth dimension is kept finite, and there remains a small, controllable violation of chiral symmetry. The second type are Overlap fermions. These appeared from a completely different context and have an explicit form that exactly satisfies the Ginsparg-Wilson relation [19]. Their numerical implementation requires an approximation of the matrix sign function of a Wilson-like fermion operator, which is costly, instead of treating five-dimensional fields in the case of DWF.

As noted above, each fermion formulation has its own advantages and disadvantages. For instance, domain-wall and overlap fermions are

theoretically preferred as they have chiral symmetry without doublers, but their computational cost is at least an order of magnitude greater than for other choices. If the physics application of interest does not require near-exact chiral symmetry, there is no strong motivation to use these expensive formulations. On the other hand, there is a class of applications (including the calculation of the  $\Delta I = 1/2$  amplitude for  $K \rightarrow \pi\pi$  decays and the S-parameter [20]) where chiral symmetry plays an essential role and for which the use of Ginsparg-Wilson fermions is strongly favored.

### 17.1.3. Heavy quarks on the lattice :

The fermion formulations described in the previous subsection are useful only for quarks whose masses are small compared to the lattice cutoff,  $m \lesssim 1/a$ . This is because there are discretization errors proportional to powers of  $am$ , and if  $am \gtrsim 1$  these errors are large and uncontrolled. Present LQCD simulations typically have cutoffs in the range of  $1/a = 2 - 4$  GeV (corresponding to  $a \approx 0.1 - 0.05$  fm), so that bottom quarks (with  $m_b \approx 4.5$  GeV) require alternative discretizations while charm quarks ( $m_c \approx 1.5$  GeV) are a borderline case.

For the charm quark, a straightforward approach is to simultaneously reduce the lattice spacing and to improve the fermion action so as to reduce the size of errors proportional to powers of  $am_c$ . This approach has, for example, been followed successfully by the HPQCD collaboration using the HISQ action [15]. It is important to note, however, that reducing  $a$  increases the computational cost because an increased number of lattice points are needed for the same physical volume. One cannot reduce the spatial size below  $2 - 3$  fm without introducing finite volume errors. Present lattices have sizes up to  $\sim 64^3 \times 144$  (with the long direction being Euclidean time), and thus allow a lattice cutoff up to  $1/a \sim 4$  GeV.

Other choices for the heavy quark action are motivated by effective field theories. For a bottom quark in heavy-light hadrons, one can use Heavy Quark Effective Theory (HQET) to expand about the infinite quark-mass limit, in which the bottom quark is a static color source [21]. Corrections, proportional to powers of  $1/m_b$ , can be introduced as operator insertions, with coefficients that can be determined non-perturbatively using existing techniques [22].

Another way of introducing the  $1/m_b$  corrections is to include the relevant terms in the effective action. This leads to a non-relativistic QCD (NRQCD) action, in which the heavy quark is described by a two-component spinor [23]. This approach has the advantage over HQET that it can also be used for heavy-heavy systems, such as the Upsilon states. A disadvantage is that some of the parameters in this effective theory are determined perturbatively (in practice at tree-level, or in some cases at one-loop), which limits the precision of the final results. Although discretization effects can be controlled within NRQCD, at fine enough lattice spacings the NRQCD effective theory no longer applies since power divergent terms become important, and taking the continuum limit would require fine-tuning a large number of couplings non-perturbatively.

This problem can be avoided if one uses HQET power counting to reduce heavy-quark discretization effects. This can be accomplished by tuning the parameters of an improved Wilson quark action so that the leading HQET corrections to the static quark limit are correctly accounted for. As the lattice spacing becomes finer, the action smoothly goes over to that of a light Wilson quark action, where the continuum limit can be taken as usual. In principle, one can improve the action in the heavy quark regime up to arbitrarily high orders using HQET, but so far large-scale simulations have typically used clover improved Wilson quarks, where tuning the parameters of the action corresponds to including all corrections through next-to-leading order in HQET. Three different methods for tuning the parameters of the clover action are being used: the Fermilab [24], Tsukuba [25] and Columbia [26] approaches. An advantage of this HQET approach is that the  $c$  and  $b$  quarks can be treated on the same footing. On the other hand, as in NRQCD the tuning of the parameters in the effective action is typically done perturbatively, though a first attempt to tune them non-perturbatively has been made [27].



#### 17.1.4. Basic inputs for lattice calculations :

Since LQCD is a regularization of QCD, the number of input parameters is the same as for continuum QCD—the strong coupling constant  $\alpha_s = g^2/(4\pi)$ , the quark masses for each flavor, and the CP violating phase  $\theta$ . The  $\theta$  parameter is usually assumed to be zero, while the other parameters must be determined using experimental inputs.

**17.1.4.1. Lattice spacing:** In QCD, the coupling constant is a function of scale. With lattice regularization, this scale is the inverse lattice spacing  $1/a$ , and choosing the bare coupling constant is equivalent to fixing the lattice spacing.

In principle,  $a$  can be determined using any dimensionful quantity measured by experiments. For example, using the mass of hadron  $H$  one has  $a = (am_H)^{\text{lat}}/m_H^{\text{exp}}$ . (Of course, one must first tune the quark masses to their physical values, as discussed below.) In practice, one chooses quantities that can be calculated accurately on the lattice, and that are only weakly dependent on the light quark masses. The latter property minimizes errors from extrapolating to the physical light quark masses or from mistuning of these masses. Two commonly used choices are the spin-averaged 1S-1P or 1S-2S splittings in the Upsilon system, and the mass of the  $\Omega^-$  baryon. The former has the advantage that it is insensitive to the  $b$ -quark mass, but the disadvantage that it requires a discretized heavy quark action.

The determination of  $a$  using quantities involving light (up and down) quarks—such as the nucleon mass or the pion decay constant—is more challenging. Most current lattice simulations are done using light quark masses heavier than those in nature. One thus has to extrapolate the lattice data towards the physical quark masses. This “chiral extrapolation” is non-trivial because the quark mass dependence may involve non-analytic terms due to the loops of nearly massless pions, as predicted by Chiral Perturbation Theory (ChPT) [28].

**17.1.4.2. Light quark masses:** In LQCD simulations, the up, down and strange quarks are usually referred to as the light quarks, in the sense that  $m_q < \Lambda_{\text{QCD}}$ . (The standard definition of  $\Lambda_{\text{QCD}}$  is given in the “Quantum Chromodynamics” review; in this review we are using it only to indicate the approximate non-perturbative scale of QCD.) This condition is stronger than that used above to distinguish quarks with small discretization errors,  $m_q < 1/a$ . Loop effects from light quarks must be included in the simulations to accurately represent QCD. At present, most simulations are done in the isospin symmetric limit  $m_u = m_d \equiv m_\ell$ , and are often referred to as “ $N_f = 2 + 1$ ” simulations. Precision is now reaching the point where isospin breaking effects, as well as those of electromagnetism (EM) must be included. This can be done approximately using ChPT and other theoretical input, but ultimately one needs to simulate directly with  $m_u \neq m_d$  and including QED corrections. Such work is now beginning.

To tune  $m_\ell$  and  $m_s$  to their physical values, the most commonly used quantities are, respectively,  $m_\pi$  and  $m_K$ . If the scale is being set by  $m_\Omega$ , then one adjusts the lattice light quark masses until the ratios  $m_\pi/m_\Omega$  and  $m_K/m_\Omega$  take their physical values. At leading order in ChPT, one has the Gell-Mann-Oakes-Renner relations  $m_{\pi_0}^2 \propto (m_u + m_d)$  and  $m_{K^0}^2 \propto (m_d + m_s)$ , which shows the sensitivity of these quantities to the quark masses. In practice one uses higher order ChPT (or other fit functions) to extrapolate or interpolate the lattice results so as to match the desired ratios, correcting for the (small) effects of isospin breaking and electromagnetic corrections. Most present calculations need to extrapolate to the physical value of  $m_\ell$ , while simulating directly at or near to the physical value of  $m_s$ .

**17.1.4.3. Heavy quark masses:** Heavy quarks ( $c$  and  $b$ ) are usually treated only as valence quarks, with no loop effects included. Generically, the errors introduced by this approximation are  $\sim \alpha_s(m_c)\Lambda_{\text{QCD}}^2/m_c^2$  and are small. For high precision, however, dynamical charm quarks may be necessary, and simulations are beginning to include them.

The heavy quark masses can be tuned by setting heavy-heavy or heavy-light meson masses to their experimental values. For the charm quark, for example, one could use the  $J/\psi$  or the  $D_s$  meson.

Consistency between these two determinations provides an important check on the lattice formulation used for the heavy quark [29].

#### 17.1.5. Sources of systematic error :

Lattice results have statistical and systematic errors that must be quantified for any calculation in order for the result to be a useful input to phenomenology. The statistical error is due to the use of Monte Carlo importance sampling to evaluate the path integral (a method discussed below) and is the most straightforward error to estimate. There are, in addition, a number of systematic errors that are always present to some degree in lattice calculations, although the size of any given error depends on the particular quantity under consideration and the parameters of the lattices being used. The most common lattice errors are reviewed below.

**17.1.5.1. Continuum limit:** Physical results are obtained in the limit that the lattice spacing  $a$  goes to zero. The Symanzik effective theory determines the scaling of lattice errors with  $a$ . Most lattice calculations use improved actions with leading discretization errors of  $\mathcal{O}(a^2\Lambda^2)$  or  $\mathcal{O}(\alpha_s a\Lambda)$ , where  $\Lambda$  is a typical momentum scale in the system. Knowledge of the scaling of the leading discretization errors allows controlled extrapolation to  $a = 0$  when multiple lattice spacings are available, as in current state-of-the-art calculations. Residual errors arise from the exclusion of subleading  $a$  dependence from the fits.

For many quantities the typical momentum scale in the system is  $\sim \Lambda_{\text{QCD}} \approx 300$  MeV. Discretization errors are expected to be larger for quantities involving larger scales, for example form factors or decays involving particles with momenta larger than  $\Lambda_{\text{QCD}}$ .

**17.1.5.2. Infinite volume limit:** LQCD calculations are necessarily carried out in finite space-time boxes, leading to departures of physical quantities (masses, decay constants, etc.) from their measured, infinite volume values. These finite-volume shifts are an important systematic that must be estimated and minimized.

Typical lattices are asymmetric, with  $N_s$  points in the three spatial directions and  $N_t$  in the (Euclidean) temporal direction. The spatial and temporal sizes in physical units are thus  $L_s = aN_s$  and  $L_t = aN_t$ , respectively. (Anisotropic lattice spacings are also sometimes used, as discussed below in Sec. 17.3.1.) Typically,  $L_t \geq 2L_s$ , so that the dominant impact of using finite volume is from the presence of a finite spatial box.

At present, high-precision LQCD calculations are of quantities involving no more than a single particle in initial and final states. For such quantities, once the volume exceeds about 2 fm (so that the particle is not “squeezed”), the dominant finite-volume effect comes from virtual pions wrapping around the lattice in the spatial directions. This effect is exponentially suppressed as the volume becomes large, roughly as  $\sim \exp(-m_\pi L_s)$ , and has been estimated using ChPT [30] or other methods [31]. The estimates suggest that finite volume shifts are sub-percent effects when  $m_\pi L_s \gtrsim 4$ , and most large-scale simulations use lattices satisfying this condition. This becomes challenging as one approaches the physical pion mass, for which  $L_s \gtrsim 5$  fm is required. At present, this can only be achieved by using relatively coarse lattices,  $a \gtrsim 0.07$  fm.

Finite volume errors are usually determined by repeating the simulations on two or more different volumes (with other parameters fixed). If different volumes are not available, the ChPT estimate can be used, often inflated to account for the fact that the ChPT calculation is truncated at some order.

In the future, LQCD calculations involving more than a single hadron will become increasingly precise. Examples include the calculation of resonance parameters and  $K \rightarrow \pi\pi$  amplitudes. Finite volume effects are much larger in these cases, with power-law terms (e.g.  $1/L_s^3$ ) in addition to exponential dependence. Indeed, as will be discussed in Sec. 17.2.4, one can use the volume dependence to indirectly extract infinite-volume quantities such as scattering lengths. Doing so, however, requires a set of lattice volumes satisfying  $m_\pi L_s \gtrsim 4$  and is thus more challenging than for single-particle quantities.

**17.1.5.3. Chiral extrapolation:** An important source of systematic error in most LQCD calculations is the need to extrapolate in  $m_u$  and  $m_d$  (or, equivalently, in  $m_\pi$ ). To do this, one needs a functional form that is, at least approximately, valid for pion masses ranging from the unphysical values used in simulations down to the physical value. A theoretically favored choice is to use the predictions of SU(3) or SU(2) ChPT. This is a valid description of QCD for  $m_q \ll \Lambda_{QCD}$  (or  $m_\pi \ll m_\rho$ ), but it is not known *a priori* the extent to which it applies at larger pion masses. This concern is exacerbated in practice since one must truncate the ChPT expressions, typically at one-loop or two-loop order. Experience to date suggests that one-loop expressions are not sufficiently accurate if  $m_\pi \gtrsim 400$  MeV [32].

Another choice of fit function is based on the observation that one does not need to extrapolate to the chiral limit, but only to the physical, non-zero, value of  $m_\pi$ , and thus an analytic description might suffice. In practice, of course, one must truncate the analytic form at low order, and a concern is whether the curvature from known non-analytic terms is adequately reproduced.

In either approach, extrapolation errors are estimated by varying the fit function and the number of data points included. We also note that, in many calculations, additional input to the chiral extrapolation is obtained from “partially quenched” results in which the valence and sea-quark masses differ [33].

Very recently, simulations with physical light quark masses (except that  $m_u = m_d = (m_u^{\text{phys}} + m_d^{\text{phys}})/2$ ) have been undertaken [34]. This is a major step forward as it removes the need for chiral extrapolation. As noted above, such simulations require large boxes, and thus very large lattices, and to date the results have been used to compute a limited number of observables. In the future, however, such simulations will play an increasingly important role in the determination of physical quantities.

**17.1.5.4. Operator matching:** Many of the quantities that LQCD can calculate precisely involve hadronic matrix elements of operators from the electroweak Hamiltonian. Examples include the pion and kaon decay constants, semileptonic form factors and the kaon mixing parameter  $B_K$  (the latter defined in Eq. (17.12)). The operators in the lattice matrix elements are defined in the lattice regularization scheme. To be used in tests of the Standard Model, however, they must be matched to the continuum regularization scheme in which the corresponding Wilson coefficients have been calculated. The only case in which such matching is not needed is if the operator is a conserved or partially conserved current. Similar matching is also needed for the conversion of lattice bare quark masses to those in the continuum  $\overline{\text{MS}}$  scheme.

Three methods are used to calculate the matching factors: perturbation theory (usually to one- or two-loop order), non-perturbative renormalization (NPR) using Landau-gauge quark and gluon propagators [35], and NPR using gauge-invariant methods based on the Schrödinger functional [36]. The NPR methods replace truncation errors (which can only be approximately estimated) by statistical and systematic errors which can be determined reliably and systematically reduced.

A common issue that arises in many such calculations (e.g. for quark masses and  $B_K$ ) is that, using NPR, one ends up with operators regularized in a MOM-like (or Schrödinger functional) scheme, rather than the  $\overline{\text{MS}}$  scheme mostly used for calculating the Wilson coefficients. To make contact with this scheme requires a purely continuum perturbative matching calculation. The resultant truncation error can, however, be minimized by pushing up the momentum scale at which the matching is done using step-scaling techniques as part of the NPR calculation [37]. It should also be noted that this final step in the conversion to the  $\overline{\text{MS}}$  scheme could be avoided if continuum calculations used a MOM-like scheme.

## 17.2. Methods and status

Once the lattice action is chosen, it is straightforward to define the quantum theory using the path integral formulation. The Euclidean-space partition function is

$$Z = \int [dU] \prod_f [dq_f][d\bar{q}_f] e^{-S_g[U] - \sum_f \bar{q}_f (D[U] + m_f) q_f}, \quad (17.3)$$

where link variables are integrated over the SU(3) manifold,  $q_f$  and  $\bar{q}_f$  are Grassmann (anticommuting) quark and antiquark fields of flavor  $f$ , and  $D[U]$  is the chosen lattice Dirac operator with  $m_f$  the quark mass in lattice units. Integrating out the quark and antiquark fields, one arrives at a form suitable for simulation:

$$Z = \int [dU] e^{-S_g[U]} \prod_f \det(D[U] + m_f). \quad (17.4)$$

The building blocks for calculations are expectation values of multi-local gauge-invariant operators,

$$\begin{aligned} \langle \mathcal{O}(U, q, \bar{q}) \rangle &= \\ (1/Z) \int [dU] \prod_f [dq_f][d\bar{q}_f] \mathcal{O}(U, q, \bar{q}) e^{-S_g[U] - \sum_f \bar{q}_f (D[U] + m_f) q_f}. \end{aligned} \quad (17.5)$$

If the operators depend on the (anti-)quark fields  $q_f$  and  $\bar{q}_f$ , then integrating these fields out leads not only to the fermion determinant but also, through Wick’s theorem, a series of quark “propagators”,  $(D[U] + m_f)^{-1}$ , connecting the positions of the fields.

### 17.2.1. Monte-Carlo method:

Since the number of integration variables  $U$  is huge ( $N_s^3 \times N_t \times 4 \times 9$ ), direct numerical integration is impractical and one has to use Monte-Carlo techniques. In this method, one generates a Markov chain of gauge configurations (a “configuration” being the set of  $U$ ’s on all links) distributed according to the probability measure  $[dU] e^{-S_g[U]} \prod_f \det(D[U] + m_f)$ . Once the configurations are generated, expectation values  $\langle \mathcal{O}(U, q, \bar{q}) \rangle$  are calculated by averaging over those configurations. In this way the configurations can be used repeatedly for many different calculations, and there are several large collections of ensembles of configurations (with a range of values of  $a$ , lattice sizes and quark masses) that are generally available. As the number of the configurations,  $N$ , is increased, the error decreases as  $1/\sqrt{N}$ , as long as the configurations are statistically independent.

The most challenging part of the generation of gauge configurations is the need to include the fermion determinant. Direct evaluation of the determinant is not feasible, as it requires  $\mathcal{O}((N_s^3 \times N_t)^3)$  computations. Instead, one rewrites it in terms of “pseudofermion” fields  $\phi$  (auxiliary fermion fields with bosonic statistics). For example, for two degenerate quarks one has

$$\det(D[U] + m_f)^2 = \int [d\phi] e^{-\phi^\dagger (D[U] + m_f)^{-2} \phi}. \quad (17.6)$$

By treating the pseudofermions as additional integration variables in the path integral, one obtains a totally bosonic representation. The price one pays is that the pseudofermion effective action is highly non-local since it includes the inverse Dirac operator  $(D[U] + m_f)^{-1}$ . Thus, the large sparse matrix  $(D[U] + m)$  has to be inverted every time one needs an evaluation of the effective action.

Present simulations generate gauge configurations using the Hybrid Monte Carlo (HMC) algorithm [38], or variants thereof. This algorithm combines molecular dynamics (MD) evolution in a fictitious time (which is also discretized) with a Metropolis “accept-reject” step. It makes a global update of the configuration, and is made exact by the Metropolis step. In its original form it can be used only for two degenerate flavors, but extensions (particularly the rational HMC [39]) are available for single flavors. Considerable speed-up of the algorithms has been achieved over the last two decades using a variety of techniques.

All these algorithms spend the bulk of their computational time on the repeated inversion of  $(D[U] + m)$  acting on a source (which

is required at every step of the MD evolution). Inversions are done using iterative algorithms such as the conjugate gradient algorithm and its generalizations. In this class of algorithms, computational cost is proportional to the condition number of the matrix, which is the ratio of maximum and minimum eigenvalues. For  $(D[U] + m)$  the smallest eigenvalue is  $\approx m$ , so the condition number and cost are inversely proportional to the quark mass. This is a major reason why simulations at the physical quark mass are challenging. Recent algorithmic improvements, however, promise to significantly reduce or remove this problem.

A practical concern is the inevitable presence of correlations between configurations in the Markov chain. These are characterized by an autocorrelation length in the fictitious MD time. One aims to use configurations separated in MD time by greater than this autocorrelation length. In practice, it is difficult to measure this length accurately, and this leads to some uncertainty in the resulting statistical errors.

For most of the applications of LQCD discussed in this review, the cost of generating gauge configurations is larger than that of performing the “measurements” on those configurations. The computational cost of the HMC and related algorithms grows with the lattice volume,  $V_{\text{lat}} = N_s^3 N_t$ , as  $V_{\text{lat}}^{5/4}$  [40]. This provides a (time-dependent) limit on the largest lattice volumes that can be simulated. At present, the largest lattices being used have  $N_s = 64$  and  $N_t = 144$ . Typically one aims to create an ensemble of  $\sim 10^3$  statistically independent configurations at each choice of parameters ( $a$ ,  $m_q$  and  $V_{\text{lat}}$ ). For most physical quantities of interest, this is sufficient to make the resulting statistical errors smaller than or comparable to the systematic errors.

### 17.2.2. Two-point functions :

One can extract properties of stable hadrons using two-point correlation functions,  $\langle O_X(x) O_Y^\dagger(0) \rangle$ . Here  $O_{X,Y}(x)$  are operators that have non-zero overlaps with the hadronic state of interest  $|H\rangle$ , *i.e.*  $\langle 0|O_{X,Y}(x)|H\rangle \neq 0$ . One usually Fourier-transforms in the spatial directions and considers correlators as a function of Euclidean time:

$$C_{XY}(t; \vec{p}) = \sum_{\vec{x}} \langle O_X(t, \vec{x}) O_Y^\dagger(0) \rangle e^{-i\vec{p}\cdot\vec{x}}. \quad (17.7)$$

(Here and throughout this section all quantities are expressed in dimensionless lattice units, so that, for example,  $\vec{p} = a\vec{p}_{\text{phys}}$ .) By inserting a complete set of states having spatial momentum  $\vec{p}$ , the two-point function can be written as

$$C_{XY}(t; \vec{p}) = \sum_{i=0}^{\infty} \frac{1}{2E_i(\vec{p})} \langle 0|O_X(0)|H_i(\vec{p})\rangle \langle H_i(\vec{p})|O_Y^\dagger(0)|0\rangle e^{-E_i(\vec{p})t}, \quad (17.8)$$

where the energy of the  $i$ -th state  $E_i(\vec{p})$  appears as an eigenvalue of the time evolution operator  $e^{-Ht}$  in the Euclidean time direction. The factor of  $1/[2E_i(\vec{p})]$  is due to the relativistic normalization used for the states. For large enough  $t$ , the dominant contribution is that of the lowest energy state  $|H_0(\vec{p})\rangle$ :

$$C_{XY}(t) \xrightarrow{t \rightarrow \infty} \frac{1}{2E_0(\vec{p})} \langle 0|O_X(0)|H_0(\vec{p})\rangle \langle H_0(\vec{p})|O_Y^\dagger(0)|0\rangle e^{-E_0(\vec{p})t}. \quad (17.9)$$

One can thus obtain the energy  $E_0(\vec{p})$ , which equals the hadron mass  $m_H$  when  $\vec{p} = 0$ , and the product of matrix elements  $\langle 0|O_X(0)|H_i(\vec{p})\rangle \langle H_i(\vec{p})|O_Y^\dagger(0)|0\rangle$ .

This method can be used to determine the masses of all the stable mesons and baryons by making appropriate choices of operators. For example, if one uses the axial current,  $O_X = O_Y = A_\mu = \bar{d}\gamma_\mu\gamma_5 u$ , then one can determine  $m_{\pi^+}$  from the rate of exponential fall-off, and in addition the decay constant  $f_\pi$  from the coefficient of the exponential. A complication arises for states with high spins ( $j \geq 4$  for bosons) because the spatial rotation group on the lattice is a discrete subgroup of the continuum group  $\text{SO}(3)$ . This implies that lattice operators, even when chosen to lie in irreducible representations of the lattice rotation group, have overlap with states that have a number of values of  $j$  in the continuum limit [41]. For example  $j = 0$  operators can

also create mesons with  $j = 4$ . A method to overcome this problem has recently been introduced [42].

The expression given above for the correlator  $C_{XY}(t; \vec{p})$  shows how, in principle, one can determine the energies of the excited hadron states having the same quantum numbers as the operators  $O_{X,Y}$ , by fitting the correlation function to a sum of exponentials. In practice, this usually requires using a large basis of operators and adopting the variational approach such as that of Ref. [43]. One can also use an anisotropic lattice in which  $a_t$ , the lattice spacing in the time direction, is smaller than its spatial counterpart  $a_s$ . This allows better separation of the different exponentials. Using a combination of these and other technical improvements extensive excited-state spectra have recently been obtained [42,44].

### 17.2.3. Three-point functions :

Weak matrix elements needed to calculate semileptonic form factors and neutral meson mixing amplitudes can be computed from three-point correlation functions. We discuss here, as a representative example, the  $D \rightarrow K$  amplitude. As in the case of two-point correlation functions one constructs operators  $O_D$  and  $O_K$  having overlap, respectively, with the  $D$  and  $K$  mesons. We are interested in calculating the matrix element  $\langle K|V_\mu|D\rangle$ , with  $V_\mu = \bar{c}\gamma_\mu s$  the vector current. To obtain this, we use the three-point correlator

$$C_{KV_\mu D}(t_x, t_y; \vec{p}) = \sum_{\vec{x}, \vec{y}} \langle O_K(t_x, \vec{x}) V_\mu(0) O_D^\dagger(t_y, \vec{y}) \rangle e^{-i\vec{p}\cdot\vec{x}}, \quad (17.10)$$

and focus on the limit  $t_x \rightarrow \infty$ ,  $t_y \rightarrow -\infty$ . In this example we set the  $D$ -meson at rest while the kaon carries three-momentum  $\vec{p}$ . Momentum conservation then implies that the weak operator  $V_\mu$  inserts three-momentum  $-\vec{p}$ . Inserting a pair of complete sets of states between each pair of operators, we find

$$C_{KV_\mu D}(t_x, t_y; \vec{p}) = \sum_{i,j} \frac{1}{2m_{D_i} 2E_{K_j}(\vec{p})} e^{-m_{D_i} t_x - E_{K_j}(\vec{p}) |t_y|} \times \\ \times \langle 0|O_K(t_x, \vec{x})|K_i(\vec{p})\rangle \langle K_i(\vec{p})|V_\mu(0)|D_j(\vec{0})\rangle \langle D_j(\vec{0})|O_D^\dagger(0)|0\rangle. \quad (17.11)$$

The matrix element  $\langle K_i(\vec{p})|V_\mu(0)|D_j(\vec{0})\rangle$  can then be extracted, since all other quantities in this expression can be obtained from two-point correlation functions. Typically one is interested in the weak matrix elements of ground states, such as the lightest pseudoscalar mesons. In the limit of large separation between the three operators in Euclidean time, the three-point correlation function yields the weak matrix element of the transition between ground states.

### 17.2.4. Scattering amplitudes and resonances :

The methods described thus far yield matrix elements involving single, stable particles (where by stable here we mean absolutely stable to strong interaction decays). Most of the particles listed in the Review of Particle Properties are, however, unstable—they are resonances decaying into final states consisting of multiple strongly interacting particles. LQCD simulations cannot directly calculate resonance properties, but methods have been developed to do so indirectly for resonances coupled to two-particle final states in the elastic regime [45].

The difficulty faced by LQCD calculations is that, to obtain resonance properties, or, more generally, scattering phase-shifts, one must calculate multiparticle scattering amplitudes in momentum space and put the external particles on their mass-shells. This requires analytically continuing from Euclidean to Minkowski momenta. Although it is straightforward in LQCD to generalize the methods described above to calculate four- and higher-point correlation functions, one necessarily obtains them at a discrete and finite set of Euclidean momenta. Analytic continuation to  $p_E^2 = -m^2$  is then an ill-posed and numerically unstable problem. The same problem arises for single-particle states, but can be overcome by picking out the exponential fall-off of the Euclidean correlator, as described above. With a multi-particle state, however, there is no corresponding trick, except for two particles at threshold [46].

What LQCD can calculate are the energies of the eigenstates of the QCD Hamiltonian in a finite box. The energies of states containing two stable particles, e.g. two pions, clearly depend on the interactions between the particles. It is possible to invert this dependence and, with plausible assumptions, determine the scattering phase-shifts at a discrete set of momenta from a calculation of the two-particle energy levels for a variety of spatial volumes [45]. This is a challenging calculation, but it has recently been carried through for pions with  $m_\pi \sim 300 - 400$  MeV for the  $I = 2$   $\pi\pi$  system (where there is no resonance) [47] and for the  $I = 1$  system, where the parameters of the  $\rho$  resonance can be determined from the phase shifts (ignoring the small inelasticity) [48,49]. Extensions to nucleon interactions are also being actively studied [50].

It is also possible to extend the methodology to calculate electroweak decay amplitudes to two particles below the inelastic threshold, e.g.  $\Gamma(K \rightarrow \pi\pi)$  [51]. First results using this methodology are now appearing. An extension to decays above the elastic threshold, e.g. hadronic  $B$  decays, has yet to be formulated.

### 17.2.5. Status of LQCD simulations :

Until the 1990s, most large-scale lattice simulations were limited to the “quenched” approximation, wherein the fermion determinant is omitted from the path integral. While much of the basic methodology was developed in this era, the results obtained had uncontrolled systematic errors and were not suitable for use in placing precision constraints on the Standard Model. During the 1990s, more extensive simulations including the fermion determinant (also known as simulations with “dynamical” fermions) were begun, but with unphysically high quark masses ( $m_\ell \sim 50 - 100$  MeV), such that the extrapolation to the physical light quark masses was a source of large systematic errors [52]. In the last 5-10 years, advances in both algorithms and computers have allowed simulations to reach much smaller quark masses ( $m_\ell \sim 10 - 20$  MeV) and even, as noted above, to work at the physical light quark mass [34]. The net effect is that LQCD calculations of selected quantities now have all sources of error controlled and small, such that they can be used effectively in phenomenological analyses.

On a more qualitative level, analytic and numerical results from LQCD have demonstrated that QCD confines color and spontaneously breaks chiral symmetry. Confinement can be seen as a linearly rising potential between heavy quark and anti-quark in the absence of quark loops. Analytically, this can be shown in the strong coupling limit  $g_{\text{lat}} \rightarrow \infty$  [1]. At weaker couplings there are precise numerical calculations of the potential that clearly show that this behavior persists in the continuum limit [2,3,4].

Chiral symmetry breaking was also demonstrated in the strong coupling limit on the lattice [12,53], and there have been a number of numerical studies showing that this holds also in the continuum limit. The accumulation of low-lying modes of the Dirac operator, which is the analog of Cooper pair condensation in superconductors, has been observed, yielding a determination of the chiral condensate [54]. Many relations among physical quantities that can be derived under the assumption of broken chiral symmetry have been confirmed by a number of lattice groups.

## 17.3. Physics applications

In this section we describe the main applications of LQCD that are both computationally mature and relevant for the determination of particle properties.

A general feature to keep in mind is that, since there are many different choices for lattice actions, all of which lead to the same continuum theory, a crucial test is that results for any given quantity are consistent. In many cases, different lattice calculations are completely independent and often have very different systematic errors. Thus final agreement, if found, is a highly non-trivial check, just as it is for different experimental measurements.

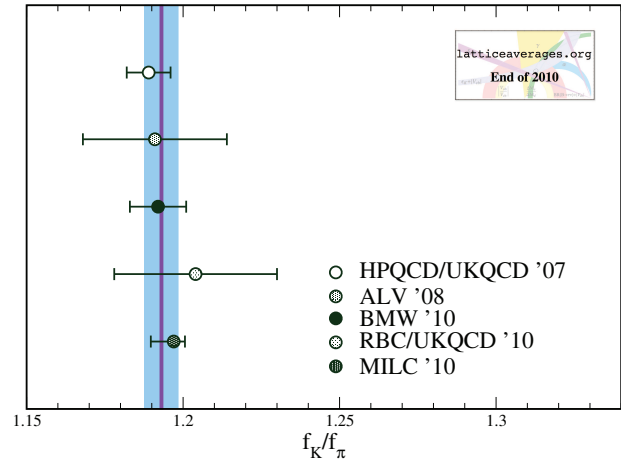


**Figure 17.1:** Results for  $f_K/f_\pi$  from simulations with  $N_f = 2 + 1$ . These are from the HPQCD/UKQCD [29], ALV [58], BMW [60], RBC/UKQCD [61] and MILC [62] collaborations. The resulting average is  $1.1931 \pm 0.0053$ .

### 17.3.1. Spectrum :

The most basic prediction of LQCD is of the hadron spectrum. Once the input parameters are fixed as described in Sec. 17.1.4, the masses or resonance parameters of all other states can be predicted. This includes hadrons composed of light ( $u$ ,  $d$  and  $s$ ) quarks, as well as heavy-light and heavy-heavy hadrons. It also includes quark-model exotics (e.g.  $J^{PC} = 1^{-+}$  mesons) and glueballs. Thus, in principle, LQCD calculations should be able to reproduce many of the experimental results compiled in the Review of Particle Properties. Doing so would test both that the error budgets of LQCD calculations are accurate and that QCD indeed describes the strong interactions in the low-energy domain. The importance of the latter test can hardly be overstated.

What is the status of this fundamental test? As discussed in Sec. 17.2, LQCD calculations are most straightforward for stable, low-lying hadrons. Resonances which can decay into only two particles are more challenging, though ultimately tractable, while those with decays to more than two particles are not yet accessible. It is also more challenging to calculate masses of flavor singlet states (which can annihilate into purely gluonic intermediate states) than those of flavor non-singlets. The present status for light hadrons is that fully controlled results are available for the masses of the octet light baryons, while results with less than complete control are available for the decuplet baryon resonances, the vector meson resonances and the  $\eta$  and  $\eta'$ . There are more extensive results for heavy-light ( $D$  and  $B$  systems) and heavy-heavy ( $J/\psi$  and  $\Upsilon$  systems). All present results, which are discussed in the “Quark Model” review, are consistent with experimental values.

### 17.3.2. Decay constants and bag parameters :

The pseudoscalar decay constants can be determined from two point correlation functions involving the axial-vector current, as discussed in Sec. 17.2.2. The decay constant  $f_P$  of a meson  $P$  is extracted from the weak matrix element involving the axial-vector current using the relation  $\langle 0 | A_\mu(x) | P(\vec{p}) \rangle = f_P p_\mu \exp(-ip \cdot x)$ , where  $p_\mu$  is the momentum of  $P$  and  $A_\mu(x)$  is the axial-vector current. For the pion and kaon decay constants, this calculation is by now straightforward. The ratio  $f_K/f_\pi$  is especially important for the extraction of  $|V_{us}|/|V_{ud}|$  from experiment, and many of the systematic errors in the lattice calculation cancel or are significantly reduced when forming the ratio. A number of lattice groups have calculated this ratio with precision at the percent level or better; all the results are in good agreement, with sub-percent precision in the world average [55,56]. A recent summary from Ref. [57] is shown in Fig. 17.1.

The heavy-light decay constants  $f_D$  and  $f_{D_s}$  involve a charm valence quark, which requires special treatment because of the relatively large charm quark mass. The different approaches in use have been discussed in Sec. 17.1.3. The HISQ action allows the charm quark to be treated in the same way as the light quarks, and has enabled HPQCD to quote precise values for the charm decay constants [29]. Calculations using less improved quark actions give consistent results, but with larger errors [59,63].

The bottom meson decay constants  $f_B$  and  $f_{B_s}$  require a valence  $b$  quark. Lattice calculations of these quantities are available using the Fermilab formulation or NRQCD to treat the bottom quark (from Refs. [64] and [65], respectively), or using an interpolation between results from around  $m_c$  to infinite quark mass [66].

The kaon bag parameter  $B_K$  is needed to turn the precise measurement of CP-violation in kaon mixing into a constraint on the Standard Model. It is defined by

$$\frac{8}{3}m_K^2 f_K^2 B_K(\mu) = \langle \bar{K}^0 | Q_{\Delta S=2}(\mu) | K^0 \rangle, \quad (17.12)$$

where  $m_K$  is the kaon mass,  $f_K$  is the kaon decay constant,  $Q_{\Delta S=2} = \bar{s}\gamma_\mu(1-\gamma_5)d\bar{s}\gamma_\mu(1-\gamma_5)d$  is the four-quark operator of the effective electroweak Hamiltonian and  $\mu$  is the renormalization scale. The short distance contribution to the electroweak Hamiltonian can be calculated perturbatively, but the long-distance matrix element parameterized by  $B_K$  must be computed using non-perturbative methods. In order to be of use to phenomenology, the renormalization factor of the four-quark operator must be matched to a continuum renormalization scheme, e.g. to  $\overline{MS}$ , as described in Sec. 17.1.5.4. Determinations with percent-level precision using different fermion actions are now available with DWF [67], staggered fermions [68], DWF valence on staggered sea quarks [69], twisted mass fermions [70] and Wilson fermions [71]. The results are all consistent.

The bag parameters for  $B$  and  $B_s$  meson mixing are defined analogously to that of kaon mixing. The  $B$  and  $B_s$  mesons contain a valence  $b$ -quark so that calculations of these quantities must use one of the methods for heavy quarks described above. These quantities have been calculated by HPQCD using NRQCD for the  $b$ -quark [65]. The ratio  $\xi = f_{B_s}\sqrt{B_{B_s}}/(f_B\sqrt{B_B})$  is especially useful in CKM studies because many of the lattice systematic uncertainties cancel in the ratio, including most of the operator matching needed to convert to a continuum scheme. The dominant error in the ratio is the error associated with the chiral extrapolation of the light quark masses. The ratio  $\xi$  has been calculated in unquenched LQCD using different treatments for the  $b$ -quark [65,72], with results that are consistent.

The results discussed in this section are used in the reviews “The CKM Quark-Mixing Matrix,” “ $V_{ud}, V_{us}$ , the Cabibbo Angle and CKM Unitarity,” and “ $B_0 - \bar{B}_0$  Mixing.”

### 17.3.3. Form factors ( $K \rightarrow \pi\ell\nu$ , $D \rightarrow K\ell\nu$ , $B \rightarrow \pi\ell\nu$ , $B \rightarrow D^{(*)}\ell\nu$ ):

Semileptonic decay rates can be used to extract CKM matrix elements once the semileptonic form factors are known from lattice calculations. For example, the matrix element of a pseudoscalar meson  $P$  undergoing semileptonic decay to another pseudoscalar meson  $D$  is mediated by the vector current, and can be written in terms of form factors as

$$\langle D(p_D) | V_\mu | P(p_P) \rangle = f_+(q^2)(p_D + p_P - \Delta)_\mu + f_0(q^2)\Delta_\mu, \quad (17.13)$$

where  $q = p_D - p_P$ ,  $\Delta_\mu = (m_D^2 - m_P^2)q_\mu/q^2$  and  $V_\mu$  is the quark vector current. The shape of the form factor is typically well determined by experiment, and the value of  $f_+(q^2)$  at some reference value of  $q^2$  is needed from the lattice in order to extract CKM matrix elements. Typically  $f_+(q^2)$  dominates the decay rate, since the contribution from  $f_0(q^2)$  is suppressed when the final state lepton is light.

The form factor  $f_+(0)$  for  $K \rightarrow \pi\ell\nu$  decays is highly constrained by the Ademollo-Gatto theorem [73] and chiral symmetry. Old estimates using chiral perturbation theory combined with quark models quote sub-percent precision [74], though they suffer from some model dependence. The lattice has now matched this precision while also

eliminating the model dependence; good agreement with the old estimate is found [75,76].

Charm meson semileptonic decays have been calculated by different groups using methods similar to those used for charm decay constants, and results are steadily improving in precision [77,78,79]. For semileptonic decays involving a bottom quark, one uses HQET or NRQCD to control the discretization errors of the bottom quark. The form factors for the semileptonic decay  $B \rightarrow \pi\ell\nu$  have been calculated in unquenched lattice QCD by two groups: HPQCD [80] and the Fermilab/MILC Collaborations [81]. These  $B$  semileptonic form factors are difficult to calculate at low  $q^2$ , i.e. when the momentum transfer to the leptons is small and the pion carries significant momentum. The low  $q^2$  region has large discretization errors and very large statistical errors, while the high  $q^2$  region is much more accessible to the lattice. For experiment, the opposite is true. To combine lattice and experimental results it has proved helpful to use the  $z$ -parameter expansion [82]. This provides a theoretically constrained parameterization of the entire  $q^2$  range, and allows one to obtain  $|V_{ub}|$  with minimal model dependence [83,81].

The semileptonic decays  $B \rightarrow D\ell\nu$  and  $B \rightarrow D^*\ell\nu$  can be used to extract  $|V_{cb}|$  once the corresponding form factors are known. At present only one unquenched calculation exists for the  $B \rightarrow D^*\ell\nu$  form factor, where the Fermilab formulation of the heavy quark was adopted [84]. This calculation is done at zero-recoil because that is where the lattice systematic errors are smallest. Calculations of the necessary form factors for both processes at non-zero recoil have been done in the quenched approximation [85]. using a step-scaling approach for the heavy quarks. Lattice calculations at non-zero recoil are needed in order to decrease the error associated with the extrapolation of the experimental data to the zero-recoil point.

The results discussed in this section are used in the reviews “The CKM Quark-Mixing Matrix,” “ $V_{ud}, V_{us}$ , the Cabibbo Angle and CKM Unitarity,” and “ $V_{cb}$  and  $V_{ub}$  CKM Matrix Elements.”

### 17.3.4. Strong coupling constant :

As explained in Sec. 17.1.4.1, for a given lattice action, the choice of bare lattice coupling constant,  $g_{\text{lat}}$ , determines the lattice spacing  $a$ . If one then calculates  $a$  as described in Sec. 17.1.4.1, one knows the strong coupling constant in the bare lattice scheme at the scale  $1/a$ ,  $\alpha_{\text{lat}} = g_{\text{lat}}^2/(4\pi)$ . This is not, however, useful for comparing to results for  $\alpha_s$  obtained from experiment. This is because the latter results give  $\alpha_s$  in the  $\overline{MS}$  scheme, and the conversion factor between these two schemes is known to converge extremely poorly in perturbation theory. Instead one must use a method which directly determines  $\alpha_s$  in a scheme closer to  $\overline{MS}$ .

Several such methods have been used, all following a similar strategy. One calculates a short-distance quantity  $K$  both perturbatively ( $K^{\text{PT}}$ ) and non-perturbatively ( $K^{\text{NP}}$ ) on the lattice, and requires equality:  $K^{\text{NP}} = K^{\text{PT}} = \sum_{i=0}^n c_i \alpha_s^i$ . Solving this equation one obtains  $\alpha_s$  at a scale related to the quantity being used. Often,  $\alpha_s$  thus obtained is not defined in the conventional  $\overline{MS}$  scheme, and one has to convert among the different schemes using perturbation theory. Unlike for the bare lattice scheme, the required conversion factors are reasonably convergent. As a final step, one uses the renormalization group to run the resulting coupling to a canonical scale (such as  $M_Z$ ).

In the work of the HPQCD collaboration [86], the short-distance quantities are Wilson loops of several sizes and their ratios, which are perturbatively calculated to  $\mathcal{O}(\alpha_s^3)$  using the  $V$ -scheme defined through the heavy quark potential. The coefficients of even higher orders are estimated with the lattice data at various values of  $a$ .

Another choice of short-distance quantities are current-current correlators. Appropriate moments of these correlators are ultraviolet finite, and by matching lattice results to the *continuum* perturbative predictions, one can directly extract the  $\overline{MS}$  coupling. The JLQCD collaboration [87] uses this approach with light overlap fermions, while the HPQCD collaboration uses charm-quark correlators and HISQ fermions [88].

With a definition of  $\alpha_s$  given using the Schrödinger functional, one can non-perturbatively control the evolution of  $\alpha_s$  to high-energy scales, such as 100 GeV, where the perturbative expansion converges

very well. This method developed by the ALPHA collaboration [37] has been applied to 2+1-flavor QCD by the PACS-CS collaboration [89].

Results are summarized in the review of “Quantum Chromodynamics”.

### 17.3.5. Quark masses :

Once the quark mass parameters are tuned in the lattice action, the remaining task is to convert them to those of the conventional definition. Since the quarks do not appear as asymptotic states due to confinement, the pole mass of the quark propagator is not a physical quantity. Instead, one defines the quark mass after subtracting the ultra-violet divergences in some particular way. The conventional choice is again the  $\overline{\text{MS}}$  scheme at a canonical scale such as 2 or 3 GeV.

As discussed in Sec. 17.1.5.4, one must convert the lattice bare quark mass to that in the  $\overline{\text{MS}}$  scheme. The most common approaches used for doing so are perturbation theory and the NPR method, the latter using an RI/MOM intermediate scheme.

Alternatively, one can use a definition based on the Schrödinger functional, which allows one to evolve the quark mass to a high scale non-perturbatively [90]. In practice, one can reach scales as high as  $\sim 100$  GeV, at which matching to the  $\overline{\text{MS}}$  scheme can be reliably calculated in perturbation theory.

Another approach available for heavy quarks is to match current-current correlators at short distances calculated on the lattice to those obtained in continuum perturbation theory in the  $\overline{\text{MS}}$  scheme. This has allowed an accurate determination of  $m_c(\overline{\text{MS}})$  [91].

Results are summarized in the review of “Quark Masses”.

### 17.3.6. Other applications :

In this review we have concentrated on applications of LQCD that are relevant to the quantities discussed in the Review of Particle Properties. We have not discussed at all several other applications which are being actively pursued by simulations. Here we list the major such applications. The reader can consult the texts [2,3,4] for further details.

LQCD can be used, in principle, to simulate QCD at non-zero temperature and density, and in particular to study how confinement and chiral-symmetry breaking are lost as  $T$  and  $\mu$  (the chemical potential) are increased. This is of relevance to heavy-ion collisions, the early Universe and neutron-star structure. In practice, finite temperature simulations are computationally tractable and relatively mature, while simulations at finite  $\mu$  suffer from a “sign problem” and are at a rudimentary stage.

Another topic under active investigation is nucleon structure (generalized structure functions) and inter-nucleon interactions.

Finally, we note that there is much recent interest in studying QCD-like theories with more fermions, possibly in other representations of the gauge group. The main interest is to find nearly conformal theories which might be candidates for “walking technicolor” models.

## 17.4. Outlook

While LQCD calculations have made major strides in the last decade, and are now playing an important role in constraining the Standard Model, there are many calculations that could be done in principle but are not yet mature due to limitations in computational resources. As we move to exascale resources (e.g.  $10^{18}$  floating point operations per second), the list of mature calculations will grow. Examples that we expect to mature in the next few years are results for excited hadrons, including quark-model exotics;  $\langle N|\bar{s}s|N\rangle$  and related matrix elements (needed for dark-matter searches); results for moments of structure functions;  $K \rightarrow \pi\pi$  amplitudes (allowing a prediction of  $\epsilon'/\epsilon$  from the Standard Model);  $\bar{K} \leftrightarrow K$  and  $\bar{B} \leftrightarrow B$  mixing amplitudes from operators arising in models of new physics (allowing one to constrain these models in a manner complementary to the direct searches at the LHC); hadronic vacuum polarization contributions to muon  $g-2$ , the running of  $\alpha_{\text{EM}}$  and  $\alpha_s$ ;  $\pi \rightarrow \gamma\gamma$  and related amplitudes; and perhaps the long-distance contribution to  $\bar{K} \leftrightarrow K$  mixing and the light-by-light contribution to muon  $g-2$ . There will also be steady improvement in the precision attained

for the mature quantities discussed above. As already noted, this will ultimately require simulations with  $m_u \neq m_d$  and including electromagnetic effects.

## 17.5. Acknowledgments

We are grateful to Jean-Francois Arguin, Christine Davies, Max Hansen, Andreas Kronfeld, Laurent Lellouch, Vittorio Lubicz and Paul Mackenzie for comments.

### References:

1. K.G. Wilson, Phys. Rev. **D10**, 2445 (1974).
2. T. Degrand and C. DeTar, “Lattice Methods for Quantum Chromodynamics,” *World Scientific* (2006).
3. C. Gattringer and C.B. Lang, *Quantum Chromodynamics on the Lattice: An Introductory Presentation*, Springer (2009).
4. “Modern Perspectives in Lattice QCD: quantum field theory and high performance computing,” (Lecture notes of the Les Houches Summer School, Vol. 93) eds. L. Lellouch *et al.*, Oxford Univ. Press. (Aug. 2011).
5. K. Symanzik, Nucl. Phys. **B226**, 187 (1983); Nucl. Phys. **B226**, 205 (1983).
6. M. Lüscher & P. Weisz, Commun. Math. Phys. **97**, 59 (1985).
7. Y. Iwasaki, UT-HEP-118.
8. H.B. Nielsen & M. Ninomiya, Phys. Lett. **B105**, 219 (1981).
9. B. Sheikholeslami and R. Wohlert, Nucl. Phys. B **259**, 572 (1985).
10. K. Jansen *et al.*, Phys. Lett. **B372**, 275 (1996).
11. R. Frezzotti & G. C. Rossi, JHEP **0408**, 007 (2004).
12. L. Susskind, Phys. Rev. D **16**, 3031 (1977).
13. M. Golterman, PoS **CONFINEMENT8**, 014 (2008).
14. G.P. Lepage, Phys. Rev. D **59**, 074502 (1999).
15. E. Follana *et al.* [HPQCD & UKQCD Collabs.], Phys. Rev. D **75**, 054502 (2007).
16. P.H. Ginsparg & K. G. Wilson, Phys. Rev. D **25**, 2649 (1982).
17. M. Luscher, Phys. Lett. B **428**, 342 (1998).
18. D.B. Kaplan, Phys. Lett. B **288**, 342 (1992); Y. Shamir, Nucl. Phys. B **406**, 90 (1993); Nucl. Phys. B **417**, 167 (1994).
19. H. Neuberger, Phys. Lett. B **417**, 141 (1998) Phys. Lett. B **427**, 353 (1998).
20. E. Shintani *et al.* [JLQCD Collab.], Phys. Rev. Lett. **101**, 242001 (2008).
21. E. Eichten & B.R. Hill, Phys. Lett. B **234**, 511 (1990).
22. J. Heitger & R. Sommer [ALPHA Collab.], JHEP **0402**, 022 (2004); B. Blossier *et al.* [ALPHA Collab.], JHEP **1012**, 039 (2010).
23. B.A. Thacker & G. P. Lepage, Phys. Rev. D **43**, 196 (1991); G.P. Lepage *et al.*, Phys. Rev. D **46**, 4052 (1992).
24. A.X. El-Khadra *et al.*, Phys. Rev. D **55**, 3933 (1997).
25. S. Aoki *et al.*, Prog. Theor. Phys. **109**, 383 (2003).
26. N.H. Christ *et al.*, Phys. Rev. D **76**, 074505 (2007).
27. H.W. Lin & N. Christ, Phys. Rev. D **76**, 074506 (2007).
28. For lecture notes on applications of Chiral Perturbation Theory to lattice QCD, see S. R. Sharpe, arXiv:hep-lat/0607016 and M. Golterman in Ref. 4.
29. E. Follana *et al.* [HPQCD & UKQCD Collabs.], Phys. Rev. Lett. **100**, 062002 (2008); C.T.H. Davies *et al.* [HPQCD Collab.], Phys. Rev. **D82**, 114504 (2010).
30. G. Colangelo *et al.*, Nucl. Phys. **B721**, 136 (2005).
31. M. Lüscher, Commun. Math. Phys. **104**, 177 (1986).
32. J. Noaki *et al.* [JLQCD & TWQCD Collabs.], Phys. Rev. Lett. **101**, 202004 (2008).
33. C.W. Bernard & M.F.L. Golterman, Phys. Rev. **D49**, 486 (1994); S.R. Sharpe, Phys. Rev. **D56**, 7052 (1997); S.R. Sharpe & N. Shore, Phys. Rev. **D62**, 094503 (2000).
34. S. Aoki *et al.* [PACS-CS Collab.], Phys. Rev. D **81**, 074503 (2010); S. Durr *et al.*, Phys. Lett. B **701**, 265 (2011).
35. G. Martinelli *et al.*, Nucl. Phys. B **445**, 81 (1995).
36. M. Lüscher *et al.*, Nucl. Phys. **B384**, 168 (1992).
37. M. Lüscher *et al.*, Nucl. Phys. B **413**, 481 (1994); M. Della Morte *et al.*, [ALPHA Collab.], Nucl. Phys. B **713**, 378 (2005).
38. S. Duane *et al.*, Phys. Lett. B **195**, 216 (1987).

39. M.A. Clark & A. D. Kennedy, Phys. Rev. Lett. **98**, 051601 (2007).
40. M. Creutz, Phys. Rev. **D38**, 1228 (1988); R. Gupta *et al.*, Phys. Rev. **D38**, 1278 (1988).
41. J.E. Mandula *et al.*, Nucl. Phys. **B228**, 91 (1983); J.E. Mandula and E. Shpiz, Nucl. Phys. **B232**, 180 (1984).
42. J.J. Dudek *et al.*, Phys. Rev. **D82**, 034508 (2010); J.J. Dudek *et al.*, Phys. Rev. **D83**, 111502 (2011); R.G. Edwards *et al.*, [arXiv:1104.5152 [hep-ph]].
43. M. Lüscher & U. Wolff, Nucl. Phys. **B339**, 222 (1990).
44. G.P. Engel *et al.* [Bern-Graz-Regensburg Collab.], Phys. Rev. **D82**, 034505 (2010).
45. M. Lüscher, Commun. Math. Phys. **105**, 153-188 (1986); Nucl. Phys. **B354**, 531-578 (1991) and **B364**, 237-254 (1991).
46. L. Maiani & M. Testa, Phys. Lett. **B245**, 585-590 (1990).
47. K. Sasaki & N. Ishizuka, Phys. Rev. **D78**, 014511 (2008); J.J. Dudek *et al.*, Phys. Rev. **D83**, 071504 (2011); S.R. Beane *et al.*, [arXiv:1107.5023 [hep-lat]].
48. S. Aoki *et al.* [CP-PACS Collab.], Phys. Rev. **D76**, 094506 (2007); M. Gockeler *et al.* [QCDSF Collab.], PoS **LATTICE2008**, 136 (2008); X. Feng *et al.*, Phys. Rev. **D83**, 094505 (2011); S. Aoki *et al.* [PACS-CS Collab.], [arXiv:1106.5365 [hep-lat]].
49. S. Durr *et al.*, Science **322**, 1224 (2008).
50. S.R. Beane *et al.*, Int. J. Mod. Phys. **E17**, 1157 (2008).
51. L. Lellouch & M. Lüscher, Commun. Math. Phys. **219**, 31 (2001).
52. C. Bernard *et al.*, Nucl. Phys. Proc. Suppl. **119**, 170 (2003).
53. J.M. Blairon *et al.*, Nucl. Phys. **B180**, 439 (1981).
54. H. Fukaya *et al.* [JLQCD Collab.], Phys. Rev. Lett. **104**, 122002 (2010); H. Fukaya *et al.* [JLQCD & TWQCD Collabs.], Phys. Rev. **D83**, 074501 (2011).
55. J. Laiho *et al.*, Phys. Rev. **D81**, 034503 (2010).
56. G. Colangelo *et al.*, Eur. Phys. J. **C71**, 1695 (2011).
57. J. Laiho *et al.*, [latticeaverages.org](http://latticeaverages.org).
58. C. Aubin *et al.*, PoS **LATTICE2008**, 105 (2008).
59. C. Aubin *et al.*, Phys. Rev. Lett. **95**, 122002 (2005).
60. S. Durr *et al.*, Phys. Rev. **D81**, 054507 (2010).
61. Y. Aoki *et al.* [RBC & UKQCD Collabs.], Phys. Rev. **D83**, 074508 (2011).
62. A. Bazavov *et al.* [MILC Collab.], PoS **LATTICE2010**, 074 (2010).
63. B. Blossier *et al.* [ETM Collab.], JHEP **0907**, 043 (2009).
64. C. Bernard *et al.*, PoS **LATTICE2008**, 278 (2008).
65. E. Gamiz *et al.* [HPQCD Collab.], Phys. Rev. **D80**, 014503 (2009).
66. B. Blossier *et al.* [ETM Collab.], JHEP **1004**, 049 (2010); P. Dimopoulos *et al.* [ETM Collab.], [arXiv:1107.1441 [hep-lat]].
67. Y. Aoki *et al.*, [arXiv:1012.4178 [hep-lat]].
68. T. Bae *et al.*, Phys. Rev. **D82**, 114509 (2010).
69. C. Aubin *et al.*, Phys. Rev. **D81**, 014507 (2010).
70. M. Constantinou *et al.* [ETM Collab.], Phys. Rev. **D83**, 014505 (2011).
71. S. Durr *et al.*, [arXiv:1106.3230 [hep-lat]].
72. R.T. Evans *et al.*, PoS **LATTICE2008**, 052 (2008); C. Albertus *et al.*, Phys. Rev. **D82**, 014505 (2010).
73. M. Ademollo & R. Gatto, Phys. Rev. Lett. **13**, 264 (1964).
74. H. Leutwyler & M. Roos, Z. Phys. **C25**, 91 (1984).
75. P.A. Boyle *et al.*, Eur. Phys. J. **C69**, 159 (2010).
76. V.ubicz *et al.* [ETM Collab.], Phys. Rev. **D80**, 111502 (2009).
77. H. Na *et al.* [HPQCD Collab.], Phys. Rev. **D82**, 114506 (2010).
78. S. Di Vita *et al.* [ETM Collab.], PoS **LAT2010** (2011).
79. C. Aubin *et al.* [Fermilab Lattice, MILC and HPQCD Collab.], Phys. Rev. Lett. **94**, 011601 (2005).
80. E. Dalgic *et al.* [HPQCD Collab.], Phys. Rev. **D73**, 074502 (2006).
81. J.A. Bailey *et al.*, Phys. Rev. **D79**, 054507 (2009).
82. C. Bourrely *et al.*, Nucl. Phys. **B189**, 157 (1981); C.G. Boyd *et al.*, Phys. Rev. Lett. **74**, 4603 (1995); T. Becher & R.J. Hill, Phys. Lett. **B633**, 61 (2006); C. Bourrely *et al.*, Phys. Rev. **D79**, 013008 (2009).
83. M.C. Arnesen *et al.*, Phys. Rev. Lett. **95**, 071802 (2005).
84. C. Bernard *et al.*, Phys. Rev. **D79**, 014506 (2009); J.A. Bailey *et al.* [Fermilab Lattice & MILC Collabs.], PoS **LATTICE2010**, 311 (2010).
85. G.M. de Divitiis *et al.*, Phys. Lett. **B655**, 45 (2007); Nucl. Phys. **B807**, 373 (2009).
86. C.T.H. Davies *et al.* [HPQCD Collab.], Phys. Rev. D **78**, 114507 (2008).
87. E. Shintani *et al.*, Phys. Rev. D **82**, 074505 (2010).
88. C. McNeile *et al.*, [HPQCD Collab.], Phys. Rev. D **82**, 034512 (2010).
89. S. Aoki *et al.* [PACS-CS Collab.], JHEP **0910**, 053 (2009).
90. S. Capitani *et al.* [ALPHA Collab.], Nucl. Phys. B **544**, 669 (1999).
91. I. Allison *et al.* [HPQCD Collab.], Phys. Rev. **D78**, 054513 (2008).

## 18. STRUCTURE FUNCTIONS

Updated July 2011 by B. Foster (University of Hamburg/DESY), A.D. Martin (University of Durham), and M.G. Vincter (Carleton University).

## 18.1. Deep inelastic scattering

High-energy lepton-nucleon scattering (deep inelastic scattering) plays a key role in determining the partonic structure of the proton. The process  $\ell N \rightarrow \ell' X$  is illustrated in Fig. 18.1. The filled circle in this figure represents the internal structure of the proton which can be expressed in terms of structure functions.

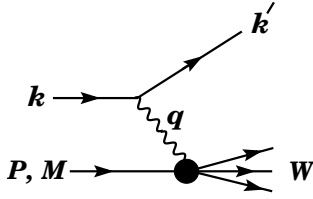


**Figure 18.1:** Kinematic quantities for the description of deep inelastic scattering. The quantities  $k$  and  $k'$  are the four-momenta of the incoming and outgoing leptons,  $P$  is the four-momentum of a nucleon with mass  $M$ , and  $W$  is the mass of the recoiling system  $X$ . The exchanged particle is a  $\gamma$ ,  $W^\pm$ , or  $Z$ ; it transfers four-momentum  $q = k - k'$  to the nucleon.

Invariant quantities:

$\nu = \frac{q \cdot P}{M} = E - E'$  is the lepton's energy loss in the nucleon rest frame (in earlier literature sometimes  $\nu = q \cdot P$ ). Here,  $E$  and  $E'$  are the initial and final lepton energies in the nucleon rest frame.

$Q^2 = -q^2 = 2(EE' - \vec{k} \cdot \vec{k}') - m_\ell^2 - m_{\ell'}^2$  where  $m_\ell(m_{\ell'})$  is the initial (final) lepton mass. If  $EE' \sin^2(\theta/2) \gg m_\ell^2, m_{\ell'}^2$ , then  $\approx 4EE' \sin^2(\theta/2)$ , where  $\theta$  is the lepton's scattering angle with respect to the lepton beam direction.

$x = \frac{Q^2}{2M\nu}$  where, in the parton model,  $x$  is the fraction of the nucleon's momentum carried by the struck quark.

$y = \frac{q \cdot P}{k \cdot P} = \frac{\nu}{E}$  is the fraction of the lepton's energy lost in the nucleon rest frame.

$W^2 = (P + q)^2 = M^2 + 2M\nu - Q^2$  is the mass squared of the system  $X$  recoiling against the scattered lepton.

$s = (k + P)^2 = \frac{Q^2}{xy} + M^2 + m_\ell^2$  is the center-of-mass energy squared of the lepton-nucleon system.

The process in Fig. 18.1 is called deep ( $Q^2 \gg M^2$ ) inelastic ( $W^2 \gg M^2$ ) scattering (DIS). In what follows, the masses of the initial and scattered leptons,  $m_\ell$  and  $m_{\ell'}$ , are neglected.

## 18.1.1. DIS cross sections :

$$\frac{d^2\sigma}{dx dy} = x(s - M^2) \frac{d^2\sigma}{dx dQ^2} = \frac{2\pi M\nu}{E'} \frac{d^2\sigma}{d\Omega_{N\text{rest}} dE'} . \quad (18.1)$$

In lowest-order perturbation theory, the cross section for the scattering of polarized leptons on polarized nucleons can be expressed in terms of the products of leptonic and hadronic tensors associated with the coupling of the exchanged bosons at the upper and lower vertices in Fig. 18.1 (see Refs. 1–4)

$$\frac{d^2\sigma}{dx dy} = \frac{2\pi y \alpha^2}{Q^4} \sum_j \eta_j L_j^{\mu\nu} W_{\mu\nu}^j . \quad (18.2)$$

For neutral-current processes, the summation is over  $j = \gamma, Z$  and  $\gamma Z$  representing photon and  $Z$  exchange and the interference between

them, whereas for charged-current interactions there is only  $W$  exchange,  $j = W$ . (For transverse nucleon polarization, there is a dependence on the azimuthal angle of the scattered lepton.)  $L_{\mu\nu}$  is the lepton tensor associated with the coupling of the exchange boson to the leptons. For incoming leptons of charge  $e = \pm 1$  and helicity  $\lambda = \pm 1$ ,

$$\begin{aligned} L_{\mu\nu}^\gamma &= 2 \left( k_\mu k'_\nu + k'_\mu k_\nu - k \cdot k' g_{\mu\nu} - i\lambda \varepsilon_{\mu\nu\alpha\beta} k^\alpha k'^\beta \right), \\ L_{\mu\nu}^{\gamma Z} &= (g_V^e + e\lambda g_A^e) L_{\mu\nu}^\gamma, \quad L_{\mu\nu}^Z = (g_V^e + e\lambda g_A^e)^2 L_{\mu\nu}^\gamma, \\ L_{\mu\nu}^W &= (1 + e\lambda)^2 L_{\mu\nu}^\gamma, \end{aligned} \quad (18.3)$$

where  $g_V^e = -\frac{1}{2} + 2\sin^2\theta_W$ ,  $g_A^e = -\frac{1}{2}$ .

Although here the helicity formalism is adopted, an alternative approach is to express the tensors in Eq. (18.3) in terms of the polarization of the lepton.

The factors  $\eta_j$  in Eq. (18.2) denote the ratios of the corresponding propagators and couplings to the photon propagator and coupling squared

$$\begin{aligned} \eta_\gamma &= 1 \quad ; \quad \eta_{\gamma Z} = \left( \frac{G_F M_Z^2}{2\sqrt{2}\pi\alpha} \right) \left( \frac{Q^2}{Q^2 + M_Z^2} \right); \\ \eta_Z &= \eta_{\gamma Z}^2 \quad ; \quad \eta_W = \frac{1}{2} \left( \frac{G_F M_W^2}{4\pi\alpha} \frac{Q^2}{Q^2 + M_W^2} \right)^2 . \end{aligned} \quad (18.4)$$

The hadronic tensor, which describes the interaction of the appropriate electroweak currents with the target nucleon, is given by

$$W_{\mu\nu} = \frac{1}{4\pi} \int d^4z e^{iq \cdot z} \langle P, S | [J_\mu^\dagger(z), J_\nu(0)] | P, S \rangle, \quad (18.5)$$

where  $S$  denotes the nucleon-spin 4-vector, with  $S^2 = -M^2$  and  $S \cdot P = 0$ .

## 18.2. Structure functions of the proton

The structure functions are defined in terms of the hadronic tensor (see Refs. 1–3)

$$\begin{aligned} W_{\mu\nu} &= \left( -g_{\mu\nu} + \frac{q_\mu q_\nu}{q^2} \right) F_1(x, Q^2) + \frac{\hat{P}_\mu \hat{P}_\nu}{P \cdot q} F_2(x, Q^2) \\ &\quad - i\varepsilon_{\mu\nu\alpha\beta} \frac{q^\alpha P^\beta}{2P \cdot q} F_3(x, Q^2) \\ &\quad + i\varepsilon_{\mu\nu\alpha\beta} \frac{q^\alpha}{P \cdot q} \left[ S^\beta g_1(x, Q^2) + \left( S^\beta - \frac{S \cdot q}{P \cdot q} P^\beta \right) g_2(x, Q^2) \right] \\ &\quad + \frac{1}{P \cdot q} \left[ \frac{1}{2} (\hat{P}_\mu \hat{S}_\nu + \hat{S}_\mu \hat{P}_\nu) - \frac{S \cdot q}{P \cdot q} \hat{P}_\mu \hat{P}_\nu \right] g_3(x, Q^2) \\ &\quad + \frac{S \cdot q}{P \cdot q} \left[ \frac{\hat{P}_\mu \hat{P}_\nu}{P \cdot q} g_4(x, Q^2) + \left( -g_{\mu\nu} + \frac{q_\mu q_\nu}{q^2} \right) g_5(x, Q^2) \right] \end{aligned} \quad (18.6)$$

where

$$\hat{P}_\mu = P_\mu - \frac{P \cdot q}{q^2} q_\mu, \quad \hat{S}_\mu = S_\mu - \frac{S \cdot q}{q^2} q_\mu . \quad (18.7)$$

In Ref. 2, the definition of  $W_{\mu\nu}$  with  $\mu \leftrightarrow \nu$  is adopted, which changes the sign of the  $\varepsilon_{\mu\nu\alpha\beta}$  terms in Eq. (18.6), although the formulae given here below are unchanged. Ref. 1 tabulates the relation between the structure functions defined in Eq. (18.6) and other choices available in the literature.

The cross sections for neutral- and charged-current deep inelastic scattering on unpolarized nucleons can be written in terms of the structure functions in the generic form

$$\begin{aligned} \frac{d^2\sigma^i}{dx dy} &= \frac{4\pi\alpha^2}{xyQ^2} \eta^i \left\{ \left( 1 - y - \frac{x^2 y^2 M^2}{Q^2} \right) F_2^i \right. \\ &\quad \left. + y^2 x F_1^i \mp \left( y - \frac{y^2}{2} \right) x F_3^i \right\}, \end{aligned} \quad (18.8)$$



where  $i = \text{NC}, \text{CC}$  corresponds to neutral-current ( $eN \rightarrow eX$ ) or charged-current ( $eN \rightarrow \nu X$  or  $\nu N \rightarrow eX$ ) processes, respectively. For incoming neutrinos,  $L_{\mu\nu}^W$  of Eq. (18.3) is still true, but with  $e, \lambda$  corresponding to the outgoing charged lepton. In the last term of Eq. (18.8), the  $-$  sign is taken for an incoming  $e^+$  or  $\bar{\nu}$  and the  $+$  sign for an incoming  $e^-$  or  $\nu$ . The factor  $\eta^{\text{NC}} = 1$  for unpolarized  $e^\pm$  beams, whereas\*

$$\eta^{\text{CC}} = (1 \pm \lambda)^2 \eta_W \quad (18.9)$$

with  $\pm$  for  $\ell^\pm$ ; and where  $\lambda$  is the helicity of the incoming lepton and  $\eta_W$  is defined in Eq. (18.4); for incoming neutrinos  $\eta^{\text{CC}} = 4\eta_W$ . The CC structure functions, which derive exclusively from  $W$  exchange, are

$$F_1^{\text{CC}} = F_1^W, \quad F_2^{\text{CC}} = F_2^W, \quad xF_3^{\text{CC}} = xF_3^W. \quad (18.10)$$

The NC structure functions  $F_2^\gamma, F_2^{\gamma Z}, F_2^Z$  are, for  $e^\pm N \rightarrow e^\pm X$ , given by Ref. 5,

$$F_2^{\text{NC}} = F_2^\gamma - (g_V^e \pm \lambda g_A^e) \eta_{\gamma Z} F_2^{\gamma Z} + (g_V^e + g_A^e \pm 2\lambda g_V^e g_A^e) \eta_Z F_2^Z \quad (18.11)$$

and similarly for  $F_1^{\text{NC}}$ , whereas

$$xF_3^{\text{NC}} = -(g_A^e \pm \lambda g_V^e) \eta_{\gamma Z} xF_3^{\gamma Z} + [2g_V^e g_A^e \pm \lambda(g_V^e + g_A^e)] \eta_Z xF_3^Z. \quad (18.12)$$

The polarized cross-section difference

$$\Delta\sigma = \sigma(\lambda_n = -1, \lambda_\ell) - \sigma(\lambda_n = 1, \lambda_\ell), \quad (18.13)$$

where  $\lambda_\ell, \lambda_n$  are the helicities ( $\pm 1$ ) of the incoming lepton and nucleon, respectively, may be expressed in terms of the five structure functions  $g_{1,\dots,5}(x, Q^2)$  of Eq. (18.6). Thus,

$$\begin{aligned} \frac{d^2 \Delta\sigma^i}{dx dy} &= \frac{8\pi\alpha^2}{xyQ^2} \eta^i \left\{ -\lambda_\ell y \left( 2 - y - 2x^2 y^2 \frac{M^2}{Q^2} \right) x g_1^i + \lambda_\ell 4x^3 y^2 \frac{M^2}{Q^2} g_2^i \right. \\ &+ 2x^2 y \frac{M^2}{Q^2} \left( 1 - y - x^2 y^2 \frac{M^2}{Q^2} \right) g_3^i \\ &\left. - \left( 1 + 2x^2 y \frac{M^2}{Q^2} \right) \left[ \left( 1 - y - x^2 y^2 \frac{M^2}{Q^2} \right) g_4^i + x y^2 g_5^i \right] \right\} \quad (18.14) \end{aligned}$$

with  $i = \text{NC}$  or  $\text{CC}$  as before. The Eq. (18.13) corresponds to the difference of antiparallel minus parallel spins of the incoming particles for  $e^-$  or  $\nu$  initiated reactions, but the difference of parallel minus antiparallel for  $e^+$  or  $\bar{\nu}$  initiated processes. For longitudinal nucleon polarization, the contributions of  $g_2$  and  $g_3$  are suppressed by powers of  $M^2/Q^2$ . These structure functions give an unsuppressed contribution to the cross section for transverse polarization [1], but in this case the cross-section difference vanishes as  $M/Q \rightarrow 0$ .

Because the same tensor structure occurs in the spin-dependent and spin-independent parts of the hadronic tensor of Eq. (18.6) in the  $M^2/Q^2 \rightarrow 0$  limit, the differential cross-section difference of Eq. (18.14) may be obtained from the differential cross section Eq. (18.8) by replacing

$$F_1 \rightarrow -g_5, \quad F_2 \rightarrow -g_4, \quad F_3 \rightarrow 2g_1, \quad (18.15)$$

and multiplying by two, since the total cross section is the average over the initial-state polarizations. In this limit, Eq. (18.8) and Eq. (18.14) may be written in the form

$$\begin{aligned} \frac{d^2 \sigma^i}{dx dy} &= \frac{2\pi\alpha^2}{xyQ^2} \eta^i \left[ Y_+ F_2^i \mp Y_- x F_3^i - y^2 F_L^i \right], \\ \frac{d^2 \Delta\sigma^i}{dx dy} &= \frac{4\pi\alpha^2}{xyQ^2} \eta^i \left[ -Y_+ g_4^i \mp Y_- 2x g_1^i + y^2 g_L^i \right], \quad (18.16) \end{aligned}$$

with  $i = \text{NC}$  or  $\text{CC}$ , where  $Y_\pm = 1 \pm (1 - y)^2$  and

$$F_L^i = F_2^i - 2x F_1^i, \quad g_L^i = g_4^i - 2x g_5^i. \quad (18.17)$$

In the naive quark-parton model, the analogy with the Callan-Gross relations [6]  $F_L^i = 0$ , are the Dicus relations [7]  $g_L^i = 0$ . Therefore, there are only two independent polarized structure functions:  $g_1$  (parity conserving) and  $g_5$  (parity violating), in analogy with the unpolarized structure functions  $F_1$  and  $F_3$ .

### 18.2.1. Structure functions in the quark-parton model :

In the quark-parton model [8,9], contributions to the structure functions  $F^i$  and  $g^i$  can be expressed in terms of the quark distribution functions  $q(x, Q^2)$  of the proton, where  $q = u, \bar{u}, d, \bar{d}$  etc. The quantity  $q(x, Q^2) dx$  is the number of quarks (or antiquarks) of designated flavor that carry a momentum fraction between  $x$  and  $x + dx$  of the proton's momentum in a frame in which the proton momentum is large.

For the neutral-current processes  $ep \rightarrow eX$ ,

$$\begin{aligned} [F_2^\gamma, F_2^{\gamma Z}, F_2^Z] &= x \sum_q [e_q^2, 2e_q g_V^q, g_V^{q2} + g_A^{q2}] (q + \bar{q}), \\ [F_3^\gamma, F_3^{\gamma Z}, F_3^Z] &= \sum_q [0, 2e_q g_A^q, 2g_V^q g_A^q] (q - \bar{q}), \\ [g_1^\gamma, g_1^{\gamma Z}, g_1^Z] &= \frac{1}{2} \sum_q [e_q^2, 2e_q g_V^q, g_V^{q2} + g_A^{q2}] (\Delta q + \Delta \bar{q}), \\ [g_5^\gamma, g_5^{\gamma Z}, g_5^Z] &= \sum_q [0, e_q g_A^q, g_V^q g_A^q] (\Delta q - \Delta \bar{q}), \quad (18.18) \end{aligned}$$

where  $g_V^q = \pm \frac{1}{2} - 2e_q \sin^2 \theta_W$  and  $g_A^q = \pm \frac{1}{2}$ , with  $\pm$  according to whether  $q$  is a  $u$ - or  $d$ -type quark respectively. The quantity  $\Delta q$  is the difference  $q \uparrow - q \downarrow$  of the distributions with the quark spin parallel and antiparallel to the proton spin.

For the charged-current processes  $e^- p \rightarrow \nu X$  and  $\bar{\nu} p \rightarrow e^+ X$ , the structure functions are:

$$\begin{aligned} F_2^{W^-} &= 2x(u + \bar{d} + \bar{s} + c \dots), \\ F_3^{W^-} &= 2(u - \bar{d} - \bar{s} + c \dots), \\ g_1^{W^-} &= (\Delta u + \Delta \bar{d} + \Delta \bar{s} + \Delta c \dots), \\ g_5^{W^-} &= (-\Delta u + \Delta \bar{d} + \Delta \bar{s} - \Delta c \dots), \quad (18.19) \end{aligned}$$

where only the active flavors are to be kept and where CKM mixing has been neglected. For  $e^+ p \rightarrow \bar{\nu} X$  and  $\nu p \rightarrow e^- X$ , the structure functions  $F^{W^+}, g^{W^+}$  are obtained by the flavor interchanges  $d \leftrightarrow u, s \leftrightarrow c$  in the expressions for  $F^{W^-}, g^{W^-}$ . The structure functions for scattering on a neutron are obtained from those of the proton by the interchange  $u \leftrightarrow d$ . For both the neutral- and charged-current processes, the quark-parton model predicts  $2xF_1^i = F_2^i$  and  $g_4^i = 2xg_5^i$ .

Neglecting masses, the structure functions  $g_2$  and  $g_3$  contribute only to scattering from transversely polarized nucleons (for which  $S \cdot q = 0$ ), and have no simple interpretation in terms of the quark-parton model. They arise from off-diagonal matrix elements  $\langle P, \lambda' | [J_\mu^\dagger(z), J_\nu(0)] | P, \lambda \rangle$ , where the proton helicities satisfy  $\lambda' \neq \lambda$ . In fact, the leading-twist contributions to both  $g_2$  and  $g_3$  are both twist-2 and twist-3, which contribute at the same order of  $Q^2$ . The Wandzura-Wilczek relation [10] expresses the twist-2 part of  $g_2$  in terms of  $g_1$  as

$$g_2^i(x) = -g_1^i(x) + \int_x^1 \frac{dy}{y} g_1^i(y). \quad (18.20)$$

However, the twist-3 component of  $g_2$  is unknown. Similarly, there is a relation expressing the twist-2 part of  $g_3$  in terms of  $g_4$ . A complete set of relations, including  $M^2/Q^2$  effects, can be found in Ref. 11.

### 18.2.2. Structure functions and QCD :

One of the most striking predictions of the quark-parton model is that the structure functions  $F_i, g_i$  scale, i.e.,  $F_i(x, Q^2) \rightarrow F_i(x)$  in the Bjorken limit that  $Q^2$  and  $\nu \rightarrow \infty$  with  $x$  fixed [12]. This property is related to the assumption that the transverse momentum of the partons in the infinite-momentum frame of the proton is small. In QCD, however, the radiation of hard gluons from the quarks violates this assumption, leading to logarithmic scaling violations, which are particularly large at small  $x$ , see Fig. 18.2. The radiation of gluons produces the evolution of the structure functions. As  $Q^2$  increases, more and more gluons are radiated, which in turn split into  $q\bar{q}$  pairs. This process leads both to the softening of the initial quark momentum distributions and to the growth of the gluon density and the  $q\bar{q}$  sea as  $x$  decreases.

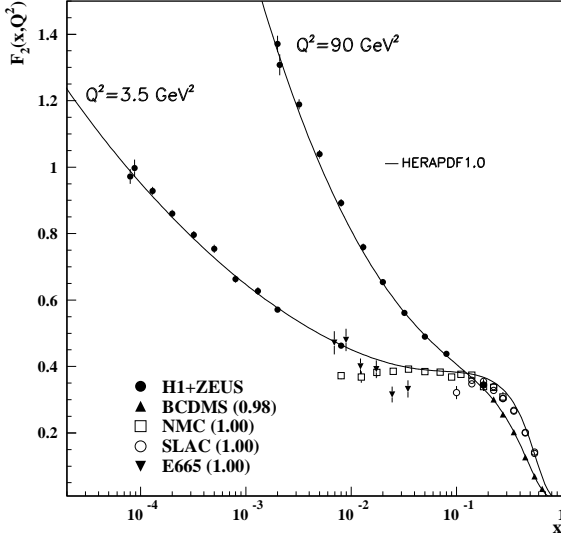


**Figure 18.2:** The proton structure function  $F_2^p$  given at two  $Q^2$  values ( $3.5 \text{ GeV}^2$  and  $90 \text{ GeV}^2$ ), which exhibit scaling at the ‘pivot’ point  $x \sim 0.14$ . See the captions in Fig. 18.8 and Fig. 18.10 for the references of the data. The various data sets have been renormalized by the factors shown in brackets in the key to the plot, which were globally determined in the full HERAPDF analysis [46]. In practice, data for the reduced cross section,  $F_2(x, Q^2) - (y^2/Y_+ )F_L(x, Q^2)$ , are fitted, rather than  $F_2$  and  $F_L$  separately.

In QCD, the above process is described in terms of scale-dependent parton distributions  $f_a(x, \mu^2)$ , where  $a = g$  or  $q$  and, typically,  $\mu$  is the scale of the probe  $Q$ . For  $Q^2 \gg M^2$ , the structure functions are of the form

$$F_i = \sum_a C_i^a \otimes f_a, \quad (18.21)$$

where  $\otimes$  denotes the convolution integral

$$C \otimes f = \int_x^1 \frac{dy}{y} C(y) f\left(\frac{x}{y}\right), \quad (18.22)$$

and where the coefficient functions  $C_i^a$  are given as a power series in  $\alpha_s$ . The parton distribution  $f_a$  corresponds, at a given  $x$ , to the density of parton  $a$  in the proton integrated over transverse momentum  $k_t$  up to  $\mu$ . Its evolution in  $\mu$  is described in QCD by a DGLAP equation (see Refs. 14–17) which has the schematic form

$$\frac{\partial f_a}{\partial \ln \mu^2} \sim \frac{\alpha_s(\mu^2)}{2\pi} \sum_b (P_{ab} \otimes f_b), \quad (18.23)$$

where the  $P_{ab}$ , which describe the parton splitting  $b \rightarrow a$ , are also given as a power series in  $\alpha_s$ . Although perturbative QCD can predict, via Eq. (18.23), the evolution of the parton distribution functions from a particular scale,  $\mu_0$ , these DGLAP equations cannot predict them *a priori* at any particular  $\mu_0$ . Thus they must be measured at a starting point  $\mu_0$  before the predictions of QCD can be compared to the data at other scales,  $\mu$ . In general, all observables involving a hard hadronic interaction (such as structure functions) can be expressed as a convolution of calculable, process-dependent coefficient functions and these universal parton distributions, e.g. Eq. (18.21).

It is often convenient to write the evolution equations in terms of the gluon, non-singlet ( $q^{NS}$ ) and singlet ( $q^S$ ) quark distributions, such that

$$q^{NS} = q_i - \bar{q}_i \quad (\text{or } q_i - q_j), \quad q^S = \sum_i (q_i + \bar{q}_i). \quad (18.24)$$

The non-singlet distributions have non-zero values of flavor quantum numbers, such as isospin and baryon number. The DGLAP evolution

equations then take the form

$$\frac{\partial q^{NS}}{\partial \ln \mu^2} = \frac{\alpha_s(\mu^2)}{2\pi} P_{qq} \otimes q^{NS},$$

$$\frac{\partial}{\partial \ln \mu^2} \begin{pmatrix} q^S \\ g \end{pmatrix} = \frac{\alpha_s(\mu^2)}{2\pi} \begin{pmatrix} P_{qq} & 2n_f P_{qg} \\ P_{gq} & P_{gg} \end{pmatrix} \otimes \begin{pmatrix} q^S \\ g \end{pmatrix}, \quad (18.25)$$

where  $P$  are splitting functions that describe the probability of a given parton splitting into two others, and  $n_f$  is the number of (active) quark flavors. The leading-order Altarelli-Parisi [16] splitting functions are

$$P_{qq} = \frac{4}{3} \left[ \frac{1+x^2}{(1-x)} \right]_+ = \frac{4}{3} \left[ \frac{1+x^2}{(1-x)_+} \right] + 2\delta(1-x), \quad (18.26)$$

$$P_{gq} = \frac{1}{2} \left[ x^2 + (1-x)^2 \right], \quad (18.27)$$

$$P_{gq} = \frac{4}{3} \left[ \frac{1+(1-x)^2}{x} \right], \quad (18.28)$$

$$P_{gg} = 6 \left[ \frac{1-x}{x} + x(1-x) + \frac{x}{(1-x)_+} \right] + \left[ \frac{11}{2} - \frac{n_f}{3} \right] \delta(1-x), \quad (18.29)$$

where the notation  $[F(x)]_+$  defines a distribution such that for any sufficiently regular test function,  $f(x)$ ,

$$\int_0^1 dx f(x) [F(x)]_+ = \int_0^1 dx (f(x) - f(1)) F(x). \quad (18.30)$$

In general, the splitting functions can be expressed as a power series in  $\alpha_s$ . The series contains both terms proportional to  $\ln \mu^2$  and to  $\ln 1/x$ . The leading-order DGLAP evolution sums up the  $(\alpha_s \ln \mu^2)^n$  contributions, while at next-to-leading order (NLO) the sum over the  $\alpha_s(\alpha_s \ln \mu^2)^{n-1}$  terms is included [18,19]. In fact, the NNLO contributions to the splitting functions and the DIS coefficient functions are now also all known [20–22].

In the kinematic region of very small  $x$ , it is essential to sum leading terms in  $\ln 1/x$ , independent of the value of  $\ln \mu^2$ . At leading order, LLx, this is done by the BFKL equation for the unintegrated distributions (see Refs. [23,24]). The leading-order  $(\alpha_s \ln(1/x))^n$  terms result in a power-like growth,  $x^{-\omega}$  with  $\omega = (12\alpha_s \ln 2)/\pi$ , at asymptotic values of  $\ln 1/x$ . More recently, the next-to-leading  $\ln 1/x$  (NLLx) contributions have become available [25,26]. They are so large (and negative) that the result appears to be perturbatively unstable. Methods, based on a combination of collinear and small  $x$  resummations, have been developed which reorganize the perturbative series into a more stable hierarchy [27–30]. There are indications that small  $x$  resummations become necessary for real precision for  $x \lesssim 10^{-3}$  at low scales. On the other hand, there is no convincing indication that, for  $Q^2 \gtrsim 2 \text{ GeV}^2$ , we have entered the ‘non-linear’ regime where the gluon density is so high that gluon-gluon recombination effects become significant.

The precision of the contemporary experimental data demands that at least NLO, and preferably NNLO, DGLAP evolution be used in comparisons between QCD theory and experiment. Beyond the leading order, it is necessary to specify, and to use consistently, both a renormalization and a factorization scheme. The renormalization scheme used is almost universally the modified minimal subtraction ( $\overline{\text{MS}}$ ) scheme [31,32]. There are two popular choices for factorization scheme, in which the form of the correction for each structure function is different. The most-used factorization scheme is again  $\overline{\text{MS}}$  [33]. However, sometimes the DIS [34] scheme is adopted, in which there are no higher-order corrections to the  $F_2$  structure function. The two schemes differ in how the non-divergent pieces are assimilated in the parton distribution functions.

The  $u$ ,  $d$ , and  $s$  quarks are taken to be massless, and the effects of the  $c$  and  $b$ -quark masses have been studied up to NNLO, for example, in [35–42]. An approach using a ‘general mass variable flavor number scheme’ (GM-VFNS) is now generally adopted, in which evolution

**Table 18.1:** The main processes relevant to global PDF analyses, ordered in three groups: fixed-target experiments, HERA and the  $p\bar{p}$  Tevatron ( $pp$  LHC). For each process we give an indication of their dominant partonic subprocesses, the primary partons which are probed and the approximate range of  $x$  constrained by the data. The Table is adapted from [13].

Process	Subprocess	Partons	$x$ range
$\ell^\pm \{p, n\} \rightarrow \ell^\pm X$	$\gamma^* q \rightarrow q$	$q, \bar{q}, g$	$x \gtrsim 0.01$
$\ell^\pm n/p \rightarrow \ell^\pm X$	$\gamma^* d/u \rightarrow d/u$	$d/u$	$x \gtrsim 0.01$
$pp \rightarrow \mu^+ \mu^- X$	$u\bar{u}, d\bar{d} \rightarrow \gamma^*$	$\bar{q}$	$0.015 \lesssim x \lesssim 0.35$
$pn/pp \rightarrow \mu^+ \mu^- X$	$(u\bar{d})/(u\bar{u}) \rightarrow \gamma^*$	$\bar{d}/\bar{u}$	$0.015 \lesssim x \lesssim 0.35$
$\nu(\bar{\nu}) N \rightarrow \mu^-(\mu^+) X$	$W^* q \rightarrow q'$	$q, \bar{q}$	$0.01 \lesssim x \lesssim 0.5$
$\nu N \rightarrow \mu^- \mu^+ X$	$W^* s \rightarrow c$	$s$	$0.01 \lesssim x \lesssim 0.2$
$\bar{\nu} N \rightarrow \mu^+ \mu^- X$	$W^* \bar{s} \rightarrow \bar{c}$	$\bar{s}$	$0.01 \lesssim x \lesssim 0.2$
$e^\pm p \rightarrow e^\pm X$	$\gamma^* q \rightarrow q$	$g, q, \bar{q}$	$0.0001 \lesssim x \lesssim 0.1$
$e^+ p \rightarrow \bar{\nu} X$	$W^+ \{d, s\} \rightarrow \{u, c\}$	$d, s$	$x \gtrsim 0.01$
$e^\pm p \rightarrow e^\pm c\bar{c}X, e^\pm b\bar{b}X$	$\gamma^* c \rightarrow c, \gamma^* g \rightarrow c\bar{c}$	$c, b, g$	$0.0001 \lesssim x \lesssim 0.01$
$e^\pm p \rightarrow \text{jet}+X$	$\gamma^* g \rightarrow q\bar{q}$	$g$	$0.01 \lesssim x \lesssim 0.1$
$p\bar{p}, pp \rightarrow \text{jet}+X$	$gg, qg, q\bar{q} \rightarrow 2j$	$g, q$	$0.005 \lesssim x \lesssim 0.5$
$p\bar{p} \rightarrow (W^\pm \rightarrow \ell^\pm \nu) X$	$ud \rightarrow W^+, \bar{u}\bar{d} \rightarrow W^-$	$u, d, \bar{u}, \bar{d}$	$x \gtrsim 0.05$
$pp \rightarrow (W^\pm \rightarrow \ell^\pm \nu) X$	$u\bar{d} \rightarrow W^+, d\bar{u} \rightarrow W^-$	$u, d, \bar{u}, \bar{d}$	$x \gtrsim 0.001$
$p\bar{p}(pp) \rightarrow (Z \rightarrow \ell^+ \ell^-) X$	$uu, dd, \dots (u\bar{u}, \dots) \rightarrow Z$	$u, d, \dots$	$x \gtrsim 0.001$
$pp \rightarrow (\gamma^* \rightarrow \ell^+ \ell^-) X$	$u\bar{u}, d\bar{d}, \dots \rightarrow \gamma^*$	$\bar{q}$	$x \gtrsim 10^{-5}$
$pp \rightarrow b\bar{b} X$	$gg \rightarrow b\bar{b}$	$g$	$x \gtrsim 10^{-5}$
$pp \rightarrow \gamma X$	$gq \rightarrow \gamma q, g\bar{q} \rightarrow \gamma\bar{q}$	$g$	$x \gtrsim 0.005$

with  $n_f = 3$  is matched to that with  $n_f = 4$  at the charm threshold, with an analogous matching at the bottom threshold.

The discussion above relates to the  $Q^2$  behavior of leading-twist (twist-2) contributions to the structure functions. Higher-twist terms, which involve their own non-perturbative input, exist. These die off as powers of  $Q$ ; specifically twist- $n$  terms are damped by  $1/Q^{n-2}$ . The higher-twist terms appear to be numerically unimportant for  $Q^2$  above a few  $\text{GeV}^2$ , except for  $x$  close to 1.

### 18.3. Determination of parton distributions

The parton distribution functions (PDFs) can be determined from data for deep inelastic lepton-nucleon scattering and for related hard-scattering processes initiated by nucleons. Table 18.1 highlights some processes and their primary sensitivity to PDFs. The kinematic ranges of fixed-target and collider experiments are complementary (as is shown in Fig. 18.3), which enables the determination of PDFs over a wide range in  $x$  and  $Q^2$ . As precise LHC data for  $W^\pm$ ,  $Z$ ,  $\gamma$ , jet,  $b\bar{b}$  and  $t\bar{t}$  production become available, the kinematic reach of the data will further widen, and tighter constraints on the PDFs are expected.

Recent determinations of the unpolarized PDF's have been made by six groups: MSTW [13], CT(EQ) [43], NNPDF [44,45], HERAPDF [46], ABKM [47] and GJR [48,49]. Distinguishing features of the various analyses have been reviewed in [50,51]. Most groups use input PDFs of the form  $x f = x^a(\dots)(1-x)^b$  with 10-25 free parameters in total. Note, however, that NNPDF combine a Monte Carlo representation of the probability measure in the space of PDFs with the use of neural networks to give a set of unbiased input distributions, while GJR generate 'dynamical' PDFs from a valence-like input at some very low starting scale,  $Q_0^2 = 0.5 \text{ GeV}^2$ . All groups, except CT, present PDFs at NLO and NNLO. The results of one analysis are shown in Fig. 18.4 at scales  $\mu^2 = 10$  and  $10^4 \text{ GeV}^2$ .

MSTW, CT and NNPDF are 'global' analyses in that they fit to a full range of the types of data that are available (and use GM-VFNS). The most recent determinations of these three groups have converged, so that now a reasonable agreement has been achieved between the resulting PDFs, the value obtained for  $\alpha_s(M_Z^2)$ , and their predictions for the LHC. The values of  $\alpha_s$  found by MSTW [13,52] may be taken

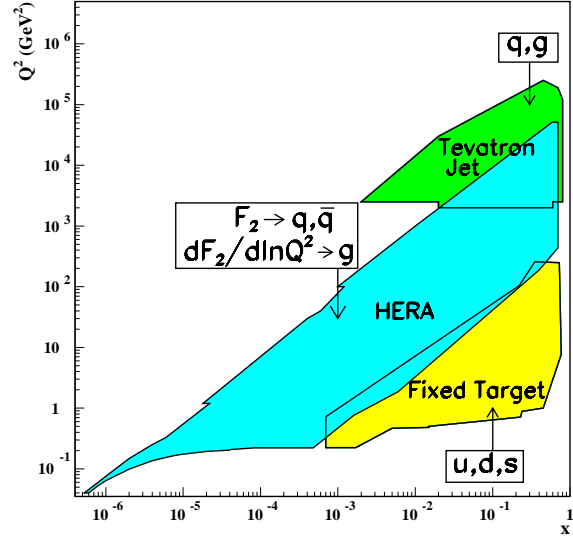


**Figure 18.3:** Kinematic domains in  $x$  and  $Q^2$  probed by fixed-target and collider experiments, shown together with the parton distributions that are most strongly constrained by the indicated regions.

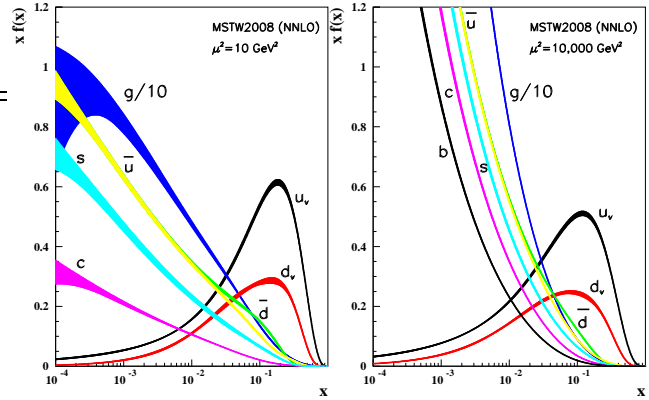


**Figure 18.4:** Distributions of  $x$  times the unpolarized parton distributions  $f(x)$  (where  $f = u_v, d_v, \bar{u}, \bar{d}, s, c, b, g$ ) and their associated uncertainties using the NNLO MSTW2008 parameterization [13] at a scale  $\mu^2 = 10 \text{ GeV}^2$  and  $\mu^2 = 10,000 \text{ GeV}^2$ .

as representative of that found in global fits to DIS and related hard scattering data

$$\text{NLO} : \alpha_s(M_Z^2) = 0.1202_{-0.0015}^{+0.0012} \pm 0.003,$$

$$\text{NNLO} : \alpha_s(M_Z^2) = 0.1171 \pm 0.0014 \pm 0.002,$$

where the first error (at 68% C.L.) corresponds to the uncertainties in the data fitted and the second is an estimate of the theory error (that is, the uncertainty which might be expected at higher orders).

The PDFs of the remaining three groups are obtained without including the Tevatron  $W, Z$  production data; and the HERAPDF and ABKM groups do not fit to the Tevatron jet data. The importance of carefully including the latter data is discussed in detail in [53], and is shown to be responsible for the anomalously low value of  $\alpha_s$  found by ABKM [47].

Spin-dependent (or polarized) PDFs have been obtained through NLO global analyses which include measurements of the  $g_1$  structure function in inclusive polarized DIS, 'flavour-tagged' semi-inclusive DIS data, and results from polarized  $pp$  scattering at RHIC. Recent NLO analyses are given in Refs. [54–57]. Improved parton-to-hadron fragmentation functions, needed to describe the semi-inclusive DIS data, can be found in [58–60]. Fig. 18.5 shows several global analyses at a scale of  $2.5 \text{ GeV}^2$  along with the data from semi-inclusive DIS.

Comprehensive sets of PDFs are available as program-callable functions from the HepData website [66], which includes comparison graphics of PDFs, and from the LHAPDF library [67], which can be linked directly into a users programme to provide access to recent PDFs in a standard format.

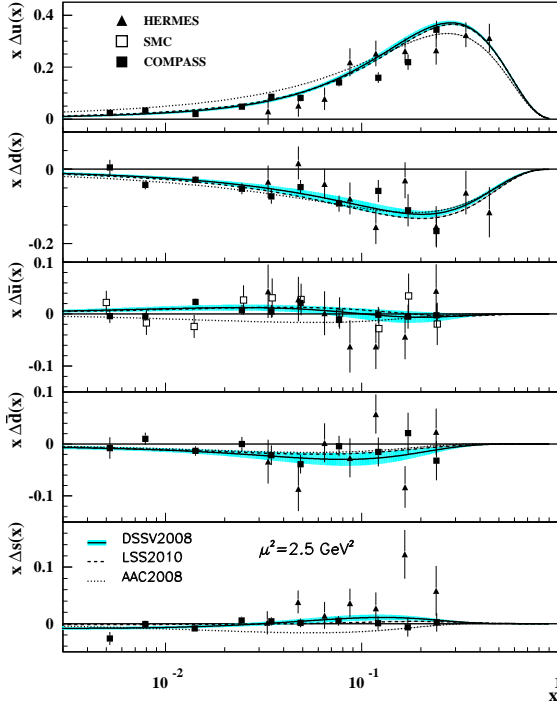


**Figure 18.5:** Distributions of  $x$  times the polarized parton distributions  $\Delta q(x)$  (where  $q = u, d, \bar{u}, \bar{d}, s$ ) using the LSS2010 [57], AAC2008 [54], and DSSV2008 [55] parameterizations at a scale  $\mu^2 = 2.5 \text{ GeV}^2$ , showing the error corridor of the latter set (corresponding to a one-unit increase in  $\chi^2$ ). See also BB2010 [56]. Points represent data from semi-inclusive positron (HERMES [61,62]) and muon (SMC [63] and COMPASS [64,65]) deep inelastic scattering given at  $Q^2 = 2.5 \text{ GeV}^2$ . SMC results are extracted under the assumption that  $\Delta \bar{u}(x) = \Delta \bar{d}(x)$ .

#### 18.4. The hadronic structure of the photon

Besides the *direct* interactions of the photon, it is possible for it to fluctuate into a hadronic state via the process  $\gamma \rightarrow q\bar{q}$ . While in this state, the partonic content of the photon may be *resolved*, for example, through the process  $e^+e^- \rightarrow e^+e^-\gamma^* \rightarrow e^+e^-X$ , where the virtual photon emitted by the DIS lepton probes the hadronic structure of the quasi-real photon emitted by the other lepton. The perturbative LO contributions,  $\gamma \rightarrow q\bar{q}$  followed by  $\gamma^*q \rightarrow q$ , are subject to QCD corrections due to the coupling of quarks to gluons.

Often the equivalent-photon approximation is used to express the differential cross section for deep inelastic electron–photon scattering in terms of the structure functions of the transverse quasi-real photon times a flux factor  $N_\gamma^T$  (for these incoming quasi-real photons of transverse polarization)

$$\frac{d^2\sigma}{dx dQ^2} = N_\gamma^T \frac{2\pi\alpha^2}{xQ^4} \left[ \left(1 + (1-y)^2\right) F_2^\gamma(x, Q^2) - y^2 F_L^\gamma(x, Q^2) \right],$$

where we have used  $F_2^\gamma = 2xF_T^\gamma + F_L^\gamma$ , not to be confused with  $F_2^\gamma$  of Sec. 18.2. Complete formulae are given, for example, in the comprehensive review of Ref. 68.

The hadronic photon structure function,  $F_2^\gamma$ , evolves with increasing  $Q^2$  from the ‘hadron-like’ behavior, calculable via the vector-meson-dominance model, to the dominating ‘point-like’ behaviour, calculable in perturbative QCD. Due to the point-like coupling, the logarithmic evolution of  $F_2^\gamma$  with  $Q^2$  has a *positive* slope for all values of  $x$ , see Fig. 18.15. The ‘loss’ of quarks at large  $x$  due to gluon radiation is over-compensated by the ‘creation’ of quarks via the point-like  $\gamma \rightarrow q\bar{q}$  coupling. The logarithmic evolution was first predicted in the quark–parton model ( $\gamma^*\gamma \rightarrow q\bar{q}$ ) [69,70], and then in QCD in the limit of large  $Q^2$  [71]. The evolution is now known to NLO [72–74]. NLO data analyses to determine the parton densities of the photon can be found in [75–77].

#### 18.5. Diffractive DIS (DDIS)

Some 10% of DIS events are diffractive,  $\gamma^*p \rightarrow X + p$ , in which the slightly deflected proton and the cluster  $X$  of outgoing hadrons are well-separated in rapidity. Besides  $x$  and  $Q^2$ , two extra variables are needed to describe a DDIS event: the fraction  $x_{IP}$  of the proton’s momentum transferred across the rapidity gap and  $t$ , the square of the 4-momentum transfer of the proton. The DDIS data [78–83] are usually analyzed using two levels of factorization. First, the diffractive structure function  $F_2^D$  satisfies *collinear factorization*, and can be expressed as the convolution [84]

$$F_2^D = \sum_{a=q,g} C_2^a \otimes f_{a/p}^D, \quad (18.31)$$

with the same coefficient functions as in DIS (see Eq. (18.21)), and where the diffractive parton distributions  $f_{a/p}^D$  ( $a = q, g$ ) satisfy DGLAP evolution. Second, *Regge factorization* is assumed [85],

$$f_{a/p}^D(x_{IP}, t, z, \mu^2) = f_{IP/p}(x_{IP}, t) f_{a/IP}(z, \mu^2), \quad (18.32)$$

where  $f_{a/IP}$  are the parton densities of the Pomeron, which itself is treated like a hadron, and  $z \in [x/x_{IP}, 1]$  is the fraction of the Pomeron’s momentum carried by the parton entering the hard subprocess. The Pomeron flux factor  $f_{IP/p}(x_{IP}, t)$  is taken from Regge phenomenology. There are also secondary Reggeon contributions to Eq. (18.32). A sample of the  $t$ -integrated diffractive parton densities, obtained in this way, is shown in Fig. 18.6.

Although collinear factorization holds as  $\mu^2 \rightarrow \infty$ , there are non-negligible corrections for finite  $\mu^2$  and small  $x_{IP}$ . Besides the *resolved* interactions of the Pomeron, the perturbative QCD Pomeron may also interact *directly* with the hard subprocess, giving rise to an inhomogeneous evolution equation for the diffractive parton densities analogous to the photon case. The results of the MRW analysis [87], which includes these contributions, are also shown in Fig. 18.6. Unlike the inclusive case, the diffractive parton densities cannot be directly used to calculate diffractive hadron–hadron cross sections, since account must first be taken of ‘soft’ rescattering effects.

#### 18.6. Generalized parton distributions

The parton distributions of the proton of Sec. 18.3 are given by the diagonal matrix elements  $\langle P, \lambda | \hat{O} | P, \lambda \rangle$ , where  $P$  and  $\lambda$  are the 4-momentum and helicity of the proton, and  $\hat{O}$  is a twist-2 quark or gluon operator. However, there is new information in the so-called generalised parton distributions (GPDs) defined in terms of the off-diagonal matrix elements  $\langle P', \lambda' | \hat{O} | P, \lambda \rangle$ ; see Refs. 89–93 for reviews. Unlike the diagonal PDFs, the GPDs cannot be regarded as parton densities, but are to be interpreted as probability amplitudes.

The physical significance of GPDs is best seen using light-cone coordinates,  $z^\pm = (z^0 \pm z^3)/\sqrt{2}$ , and in the light-cone gauge,  $A^+ = 0$ . It is conventional to define the generalised quark distributions in terms of quark operators at light-like separation

$$\begin{aligned} F_q(x, \xi, t) &= \frac{1}{2} \int \frac{dz^-}{2\pi} e^{ix\bar{P}^+z^-} \langle P' | \bar{\psi}(-z/2) \gamma^+ \psi(z/2) | P \rangle \Big|_{z^+ = z^1 = z^2 = 0} \\ &= \frac{1}{2P^+} \left( H_q(x, \xi, t) \bar{u}(P') \gamma^+ u(P) + E_q(x, \xi, t) \bar{u}(P') \frac{i\sigma^{+\alpha} \Delta_\alpha}{2m} u(P) \right) \end{aligned} \quad (18.34)$$

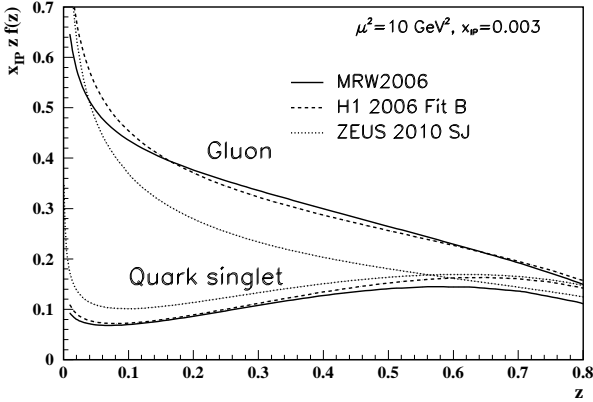


**Figure 18.6:** Diffractive parton distributions,  $x_{IP} z f_a^D$ , obtained from fitting to the ZEUS data with  $Q^2 > 5 \text{ GeV}^2$  [86], H1 data with  $Q^2 > 8.5 \text{ GeV}^2$  assuming Regge factorization [81], and using a more perturbative QCD approach [87]. Only the Pomeron contributions are shown and not the secondary Reggeon contributions, which are negligible at the value of  $x_P = 0.003$  chosen here. The H1 2007 Jets distribution [88] is similar to H1 2006 Fit B.

with  $\bar{P} = (P + P')/2$  and  $\Delta = P' - P$ , and where we have suppressed the helicity labels of the protons and spinors. We now have two extra kinematic variables:

$$t = \Delta^2, \quad \xi = -\Delta^+ / (P + P')^+. \quad (18.35)$$

We see that  $-1 \leq \xi \leq 1$ . Similarly, we may define GPDs  $\bar{H}_q$  and  $\bar{E}_q$  with an additional  $\gamma_5$  between the quark operators in Eq. (18.33); and also an analogous set of gluon GPDs,  $H_g$ ,  $E_g$ ,  $\bar{H}_g$  and  $\bar{E}_g$ . After a Fourier transform with respect to the transverse components of  $\Delta$ , we are able to describe the spatial distribution of partons in the impact parameter plane in terms of GPDs [94,95].

For  $P' = P$ ,  $\lambda' = \lambda$  the matrix elements reduce to the ordinary PDFs of Sec. 18.2.1

$$H_q(x, 0, 0) = q(x), \quad H_q(-x, 0, 0) = -\bar{q}(x), \quad H_g(x, 0, 0) = xg(x), \quad (18.36)$$

$$\bar{H}_q(x, 0, 0) = \Delta q(x), \quad \bar{H}_q(-x, 0, 0) = \Delta \bar{q}(x), \quad \bar{H}_g(x, 0, 0) = x\Delta g(x), \quad (18.37)$$

where  $\Delta q = q \uparrow - q \downarrow$  as in Eq. (18.18). No corresponding relations exist for  $E$ ,  $\bar{E}$  as they decouple in the forward limit,  $\Delta = 0$ .

$H_q, E_g$  are even functions of  $x$ , and  $\bar{H}_g, \bar{E}_g$  are odd functions of  $x$ . We can introduce valence and ‘singlet’ quark distributions which are even and odd functions of  $x$  respectively. For example

$$H_q^V(x, \xi, t) \equiv H_q(x, \xi, t) + H_q(-x, \xi, t) = H_q^V(-x, \xi, t), \quad (18.38)$$

$$H_q^S(x, \xi, t) \equiv H_q(x, \xi, t) - H_q(-x, \xi, t) = -H_q^S(-x, \xi, t). \quad (18.39)$$

All the GPDs satisfy relations of the form

$$H(x, -\xi, t) = H(x, \xi, t) \quad \text{and} \quad H(x, -\xi, t)^* = H(x, \xi, t), \quad (18.40)$$

and so are real-valued functions. Moreover, the moments of GPDs, that is the  $x$  integrals of  $x^n H_q$  etc., are *polynomials* in  $\xi$  of order  $n + 1$ . Another important property of GPDs are Ji’s sum rules [89]

$$\frac{1}{2} \int_{-1}^1 dx \, x (H_q(x, \xi, t) + E_q(x, \xi, t)) = J_q(t), \quad (18.41)$$

where  $J_q(0)$  is the total angular momentum carried by quarks and antiquarks of flavour  $q$ , with a similar relation for gluons.

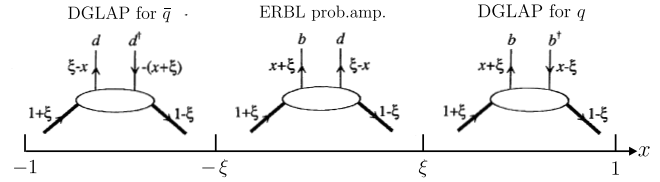


**Figure 18.7:** Schematic diagrams of the three distinct kinematic regions of (the imaginary part of)  $H_q$ . The proton and quark momentum fractions refer to  $\bar{P}^+$ , and  $x$  covers the interval  $(-1,1)$ . In the ERBL domain the GPDs are generalisations of distribution amplitudes which occur in processes such as  $p\bar{p} \rightarrow J/\psi$ .

To visualize the physical content of  $H_q$ , we Fourier expand  $\psi$  and  $\bar{\psi}$  in terms of quark, antiquark creation ( $b, d$ ) and annihilation ( $b^\dagger, d^\dagger$ ) operators, and sketch the result in Fig. 18.7. There are two types of domain: (i) the time-like or ‘annihilation’ domain, with  $|x| < |\xi|$ , where the GPDs describe the wave functions of a  $t$ -channel  $q\bar{q}$  (or gluon) pair and evolve according to modified ERBL equations [96,97]; (ii) the space-like or ‘scattering’ domain, with  $|x| > |\xi|$ , where the GPDs generalise the familiar  $\bar{q}, q$  (and gluon) PDFs and describe ‘deeply virtual Compton scattering’ ( $\gamma^* p \rightarrow \gamma p$ ),  $\gamma p \rightarrow J/\psi p$ , etc., and evolve according to modified DGLAP equations. The splitting functions for the evolution of GPDs are known to NLO [98].

GPDs describe new aspects of proton structure and must be determined from experiment. We can parametrise them in terms of ‘double distributions’ [99,100], which reduce to diagonal PDFs as  $\xi \rightarrow 0$ . With an additional physically reasonable ‘Regge’ assumption of no extra singularity at  $\xi = 0$ , GPDs at low  $\xi$  are uniquely given in terms of diagonal PDFs to  $O(\xi)$ , and have been used [101] to describe  $\gamma p \rightarrow J/\psi p$  data. Alternatively, flexible  $SO(3)$ -based parametrisations have been used to determine GPDs from DVCS data [102].

\* The value of  $\eta^{\text{CC}}$  deduced from Ref. 1 is found to be a factor of two too small;  $\eta^{\text{CC}}$  of Eq. (18.9) agrees with Refs. [2,3].

## References:

1. J. Blümlein and N. Kochelev, Nucl. Phys. **B498**, 285 (1997).
2. S. Forte *et al.*, Nucl. Phys. **B602**, 585 (2001).
3. M. Anselmino *et al.*, Z. Phys. **C64**, 267 (1994).
4. M. Anselmino *et al.*, Phys. Rep. **261**, 1 (1995).
5. M. Klein and T. Riemann, Z. Phys. **C24**, 151 (1984).
6. C.G. Callan and D.J. Gross, Phys. Rev. Lett. **22**, 156 (1969).
7. D.A. Dicus, Phys. Rev. **D5**, 1367 (1972).
8. J.D. Bjorken and E.A. Paschos, Phys. Rev. **185**, 1975 (1969).
9. R.P. Feynman, Photon Hadron Interactions (Benjamin, New York, 1972).
10. S. Wandzura and F. Wilczek, Phys. Rev. **B72**, 195 (1977).
11. J. Blümlein and A. Tkabladze, Nucl. Phys. **B553**, 427 (1999).
12. J.D. Bjorken, Phys. Rev. **179**, 1547 (1969).
13. MSTW, A.D. Martin *et al.*, Eur. Phys. J. **C63**, 189 (2009).
14. V.N. Gribov and L.N. Lipatov, Sov. J. Nucl. Phys. **15**, 438 (1972).
15. L.N. Lipatov, Sov. J. Nucl. Phys. **20**, 95 (1975).
16. G. Altarelli and G. Parisi, Nucl. Phys. **B126**, 298 (1977).
17. Yu.L. Dokshitzer, Sov. Phys. JETP **46**, 641 (1977).
18. G. Curci *et al.*, Nucl. Phys. **B175**, 27 (1980); W. Furmanski, and R. Petronzio, Phys. Lett. **B97**, 437 (1980).
19. R.K. Ellis *et al.*, QCD and Collider Physics (Cambridge UP, 1996).
20. E.B. Zijlstra and W.L. van Neerven, Phys. Lett. **B272**, 127 (1991); Phys. Lett. **B273**, 476 (1991); Phys. Lett. **B297**, 377 (1992); Nucl. Phys. **B383**, 525 (1992).
21. S. Moch and J.A.M. Vermaseren, Nucl. Phys. **B573**, 853 (2000).
22. S. Moch *et al.*, Nucl. Phys. **B688**, 101 (2004); Nucl. Phys. **B691**, 129 (2004); Phys. Lett. **B606**, 123 (2005); Nucl. Phys. **B724**, 3 (2005).

23. E.A. Kuraev *et al.*, Phys. Lett. **B60**, 50 (1975); Sov. Phys. JETP **44**, 443 (1976); Sov. Phys. JETP **45**, 199 (1977).
24. Ya.Ya. Balitsky and L.N. Lipatov, Sov. J. Nucl. Phys. **28**, 822 (1978).
25. V.S. Fadin, and L.N. Lipatov, Phys. Lett. **B429**, 127 (1998).
26. G. Camici and M. Ciafaloni, Phys. Lett. **B412**, 396 (1997), erratum-Phys. Lett. **B147**, 390 (1997); Phys. Lett. **B430**, 349 (1998).
27. M. Ciafaloni *et al.*, Phys. Rev. **D60**, 114036 (1999); JHEP **0007** 054 (2000).
28. M. Ciafaloni *et al.*, Phys. Lett. **B576**, 143 (2003); Phys. Rev. **D68**, 114003 (2003).
29. G. Altarelli *et al.*, Nucl. Phys. **B742**, 1 (2006); Nucl. Phys. **B799**, 199 (2008).
30. C.D. White and R.S. Thorne, Phys. Rev. **D75**, 034005 (2007).
31. G. 't Hooft and M. Veltman, Nucl. Phys. **B44**, 189 (1972).
32. G. 't Hooft, Nucl. Phys. **B61**, 455 (1973).
33. W.A. Bardeen *et al.*, Phys. Rev. **D18**, 3998 (1978).
34. G. Altarelli *et al.*, Nucl. Phys. **B143**, 521 (1978) and erratum: Nucl. Phys. **B146**, 544 (1978).
35. M.A.G. Aivazis *et al.*, Phys. Rev. **D50**, 3102 (1994).
36. J.C. Collins, Phys. Rev. **D58**, 094002 (1998).
37. A. Chuvakin *et al.*, Phys. Rev. **D61**, 096004 (2000).
38. R.S. Thorne and R.G. Roberts, Eur. Phys. J. **C19**, 339 (2001).
39. S. Kretzer *et al.*, Phys. Rev. **D69**, 114005 (2004).
40. R.S. Thorne, Phys. Rev. **D73**, 054019 (2006).
41. R.S. Thorne and W.-K. Tung, Proc. 4th HERA-LHC Workshop, [arXiv:0809.0714](https://arxiv.org/abs/0809.0714).
42. S. Forte *et al.*, Nucl. Phys. **B834**, 116 (2010).
43. H.-L. Lai *et al.*, Phys. Rev. **D82**, 074024 (2010).
44. R.D. Ball *et al.*, Nucl. Phys. **B849**, 296 (2011).
45. R.D. Ball *et al.*, [arXiv:1107.2652](https://arxiv.org/abs/1107.2652).
46. F.D. Aaron *et al.*, JHEP **1001**, 109 (2010).
47. S. Alekhin, *et al.*, Phys. Rev. **D81**, 014032 (2010).
48. M. Glück *et al.*, Eur. Phys. J. **C53**, 355 (2008).
49. P. Jimenez-Delgado and E. Reya, Phys. Rev. **D79**, 074023 (2009).
50. A. De Roeck and R.S. Thorne, [arXiv:1103.0555](https://arxiv.org/abs/1103.0555).
51. G. Watt, [arXiv:1106.5788](https://arxiv.org/abs/1106.5788).
52. MSTW, A.D. Martin *et al.*, Eur. Phys. J. **C64**, 653 (2009).
53. R.S. Thorne and G. Watt, [arXiv:1106.5789](https://arxiv.org/abs/1106.5789).
54. M. Hirai *et al.*, Nucl. Phys. **B813**, 106 (2009).
55. D. de Florian *et al.*, Phys. Rev. Lett. **101**, 072001 (2008); Phys. Rev. **D80**, 034030 (2009).
56. J. Blümlein and H. Böttcher, Nucl. Phys. **B841**, 205 (2010).
57. E. Leader *et al.*, Phys. Rev. **D82**, 114018 (2010).
58. D. de Florian *et al.*, Phys. Rev. **D75**, 114010 (2007); Phys. Rev. **D76**, 074033 (2007).
59. S. Albino *et al.*, Nucl. Phys. **B803**, 42 (2008).
60. M. Hirai and S. Kumano, [arXiv:1106.1553](https://arxiv.org/abs/1106.1553).
61. HERMES, A. Airpetian *et al.*, Phys. Rev. Lett. **92**, 012005 (2004); A. Airpetian *et al.*, Phys. Rev. **D71**, 012003 (2005).
62. HERMES, A. Airpetian *et al.*, Phys. Lett. **B666**, 446 (2008).
63. SMC, B. Adeva *et al.*, Phys. Lett. **B420**, 180 (1998).
64. COMPASS, M. Alekseev *et al.*, Phys. Lett. **B680**, 217 (2009).
65. COMPASS, M. Alekseev *et al.*, Phys. Lett. **B693**, 227 (2010).
66. <http://hepdata.cedar.ac.uk/pdfs>.
67. <http://projects.hepforge.org/lhapdf>, see [hep-ph/0508110](https://arxiv.org/abs/hep-ph/0508110).
68. R. Nisius, Phys. Reports **332**, 165 (2000).
69. T.F. Walsh and P.M. Zerwas, Phys. Lett. **B44**, 195 (1973).
70. R.L. Kingsley, Nucl. Phys. **B60**, 45 (1973).
71. E. Witten, Nucl. Phys. **B120**, 189 (1977).
72. W.A. Bardeen and A.J. Buras, Phys. Rev. **D20**, 166 (1979), erratum Phys. Rev. **D21**, 2041 (1980).
73. M. Fontannaz and E. Pilon, Phys. Rev. **D45**, 382 (1992), erratum Phys. Rev. **D46**, 484 (1992).
74. M. Glück *et al.*, Phys. Rev. **D45**, 3986 (1992).
75. F. Cornet *et al.*, Phys. Rev. **D70**, 093004 (2004).
76. P. Aurenche, *et al.*, Eur. Phys. J. **C44**, 395 (2005).
77. W. Slominski *et al.*, Eur. Phys. J. **C45**, 633 (2006).
78. ZEUS, S. Chekanov *et al.*, Eur. Phys. J. **C38**, 43 (2004).
79. ZEUS, S. Chekanov *et al.*, Nucl. Phys. **B713**, 3 (2005).
80. H1, A. Aktas *et al.*, Eur. Phys. J. **C48**, 749 (2006).
81. H1, A. Aktas *et al.*, Eur. Phys. J. **C48**, 715 (2006).
82. ZEUS, S. Chekanov *et al.*, Nucl. Phys. **B816**, 1 (2009).
83. H1, F.D. Aaron *et al.*, Eur. Phys. J. **C71**, 1578 (2011).
84. J. C. Collins, Phys. Rev. **D57**, 3051 (1998); Erratum Phys. Rev. **D61**, 019902 (2000).
85. G. Ingelman and P. E. Schlein, Phys. Lett. **B152**, 256 (1985).
86. ZEUS, S. Chekanov *et al.*, Nucl. Phys. **B831**, 1 (2010).
87. A. D. Martin, M. G. Ryskin and G. Watt, Phys. Lett. **B644**, 131 (2007).
88. H1, A. Aktas *et al.*, JHEP **0710**, 042 (2007).
89. X. Ji, J. Phys. **G24**, 1181 (1998).
90. K. Goeke *et al.*, Prog. in Part. Nucl. Phys. **47**, 401 (2001).
91. M. Diehl, Phys. Rept. **388**, 41 (2003).
92. A.V. Belitsky and A.V. Radyushkin, Phys. Rept. **418**, 1 (2005).
93. S. Boffi and B. Pasquini, Riv. Nuovo Cimento **30**, 387 (2007).
94. M. Burkardt, Int. J. Mod. Phys. **A18**, 173 (2003).
95. M. Diehl, Eur. Phys. J. **C25**, 223 (2002).
96. A.V. Efremov and A.V. Radyushkin, Phys. Lett. **B94**, 245 (1980).
97. G.P. Lepage and S.J. Brodsky, Phys. Rev. **D22**, 2157 (1980).
98. A.V. Belitsky *et al.*, Phys. Lett. **B493**, 341 (2000).
99. A.V. Radyushkin, Phys. Rev. **D59**, 014030 (1999).
100. A.V. Radyushkin, Phys. Lett. **B449**, 81 (1999).
101. A.D. Martin *et al.*, Eur. Phys. J. **C63**, 57 (2009).
102. K. Kumerički and D. Müller, Nucl. Phys. **B841**, 1 (2010).

NOTE: THE FIGURES IN THIS SECTION ARE INTENDED TO SHOW THE REPRESENTATIVE DATA. THEY ARE NOT MEANT TO BE COMPLETE COMPILATIONS OF ALL THE WORLD'S RELIABLE DATA.

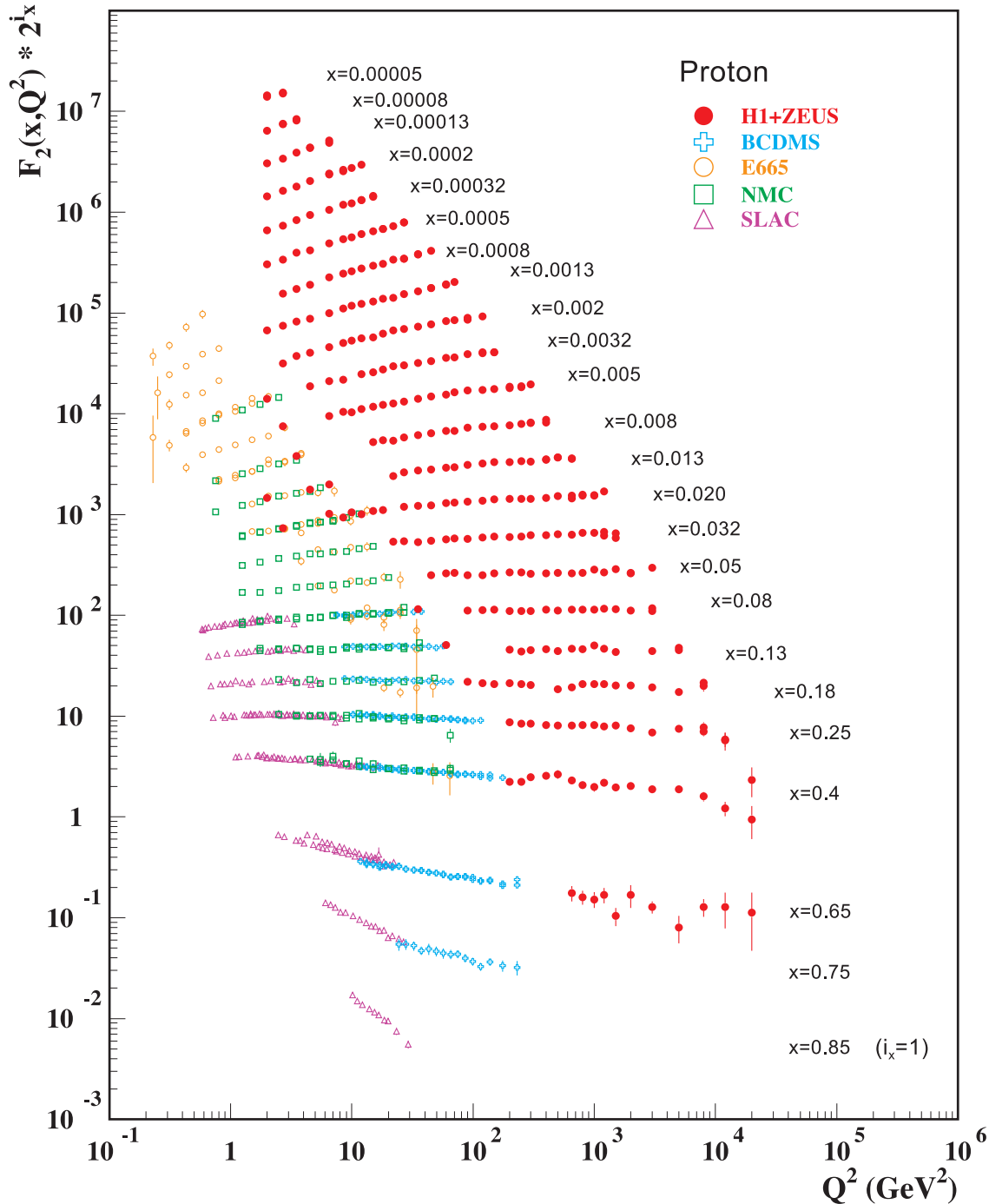


**Figure 18.8:** The proton structure function  $F_2^p$  measured in electromagnetic scattering of electrons and positrons on protons (collider experiments H1 and ZEUS for  $Q^2 \geq 2$  GeV $^2$ ), in the kinematic domain of the HERA data (see Fig. 18.10 for data at smaller  $x$  and  $Q^2$ ), and for electrons (SLAC) and muons (BCDMS, E665, NMC) on a fixed target. Statistical and systematic errors added in quadrature are shown. The data are plotted as a function of  $Q^2$  in bins of fixed  $x$ . Some points have been slightly offset in  $Q^2$  for clarity. The H1+ZEUS combined binning in  $x$  is used in this plot; all other data are rebinned to the  $x$  values of these data. For the purpose of plotting,  $F_2^p$  has been multiplied by  $2^{i_x}$ , where  $i_x$  is the number of the  $x$  bin, ranging from  $i_x = 1$  ( $x = 0.85$ ) to  $i_x = 24$  ( $x = 0.00005$ ). References: **H1 and ZEUS**—F.D. Aaron *et al.*, JHEP **1001**, 109 (2010); **BCDMS**—A.C. Benvenuti *et al.*, Phys. Lett. **B223**, 485 (1989) (as given in [66]) ; **E665**—M.R. Adams *et al.*, Phys. Rev. **D54**, 3006 (1996); **NMC**—M. Arneodo *et al.*, Nucl. Phys. **B483**, 3 (1997); **SLAC**—L.W. Whitlow *et al.*, Phys. Lett. **B282**, 475 (1992).

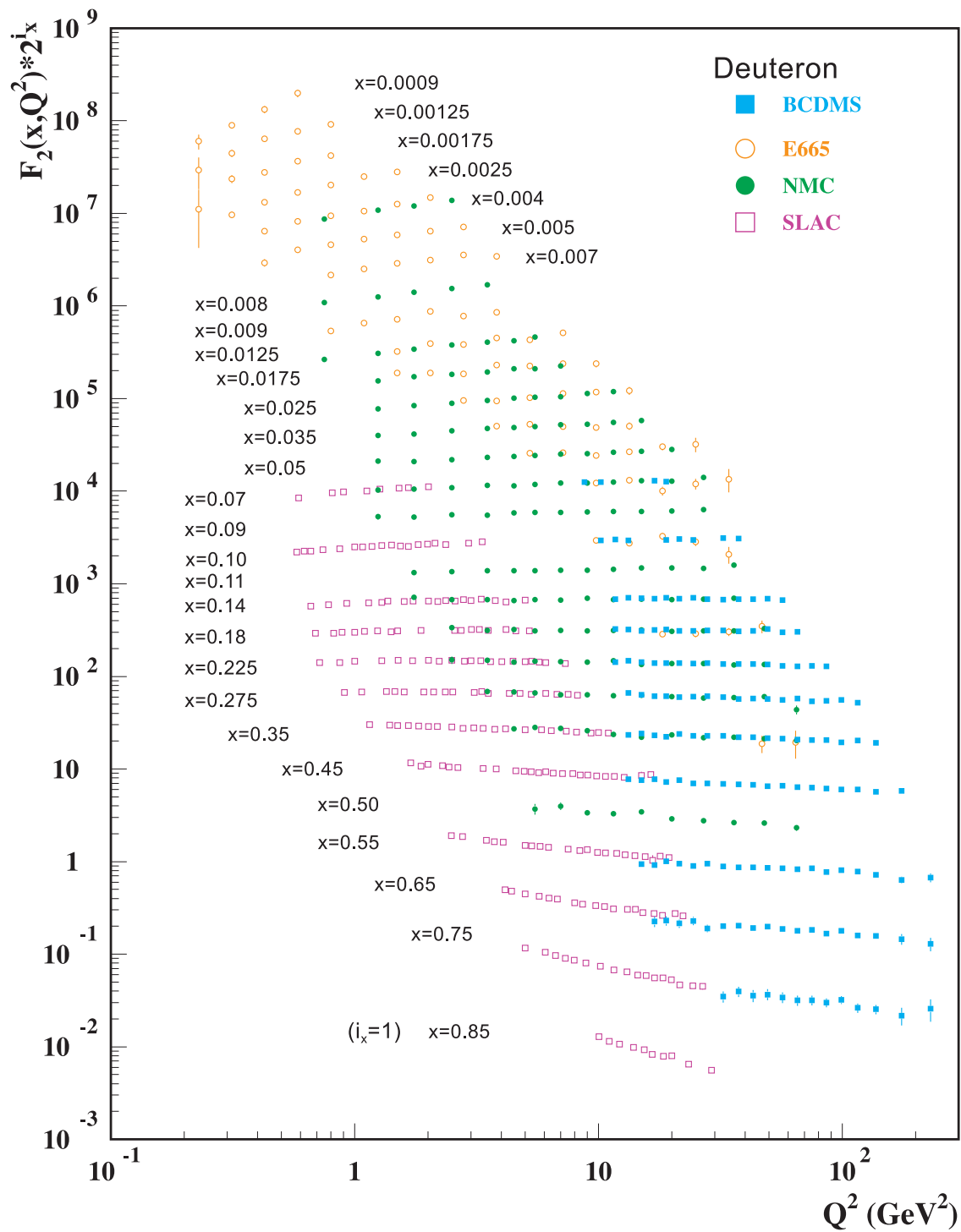


**Figure 18.9:** The deuteron structure function  $F_2^d$  measured in electromagnetic scattering of electrons (SLAC) and muons (BCDMS, E665, NMC) on a fixed target, shown as a function of  $Q^2$  for bins of fixed  $x$ . Statistical and systematic errors added in quadrature are shown. For the purpose of plotting,  $F_2^d$  has been multiplied by  $2^{i_x}$ , where  $i_x$  is the number of the  $x$  bin, ranging from 1 ( $x = 0.85$ ) to 29 ( $x = 0.0009$ ). References: **BCDMS**—A.C. Benvenuti *et al.*, Phys. Lett. **B237**, 592 (1990). **E665**, **NMC**, **SLAC**—same references as Fig. 18.8.



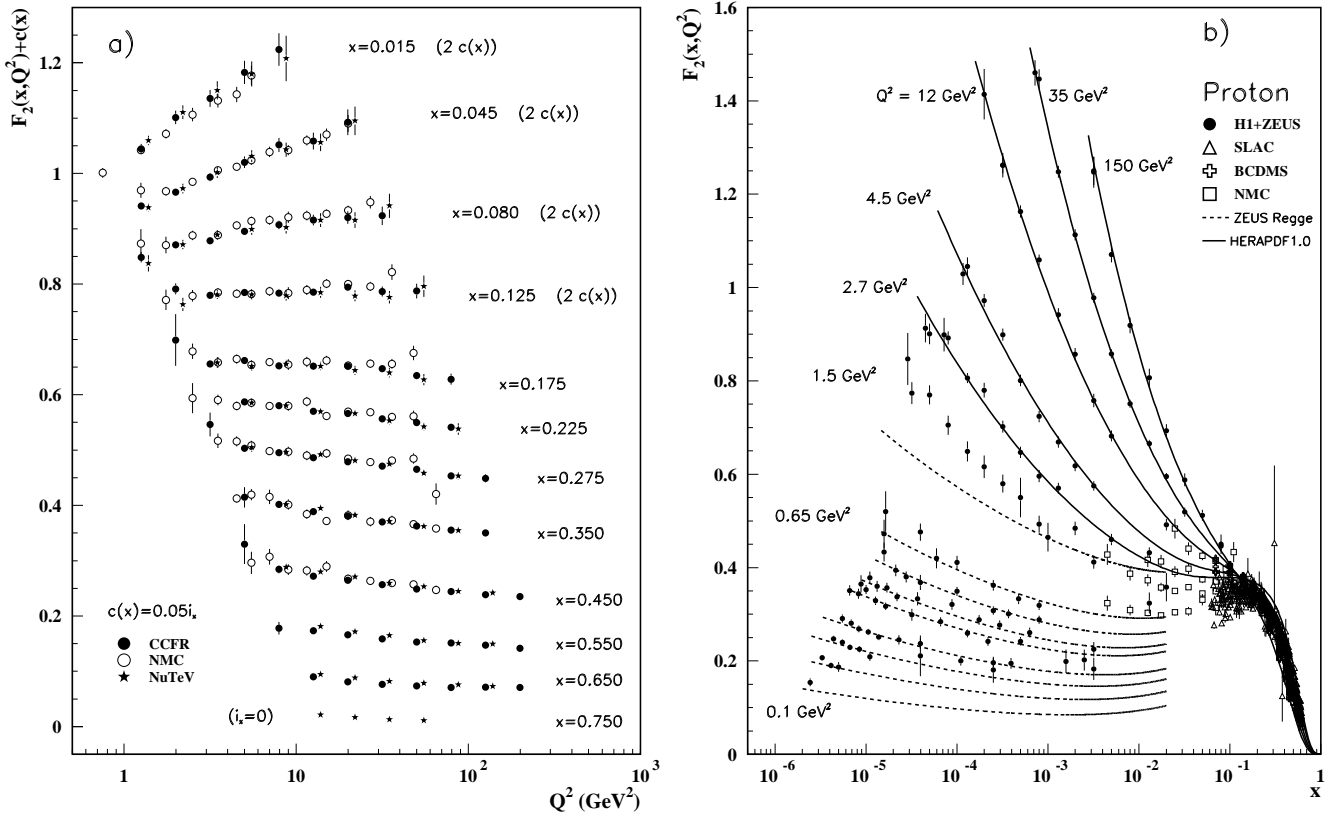


**Figure 18.10:** a) The deuteron structure function  $F_2$  measured in deep inelastic scattering of muons on a fixed target (NMC) is compared to the structure function  $F_2$  from neutrino-iron scattering (CCFR and NuTeV) using  $F_2^\mu = (5/18)F_2^p - x(s + \bar{s})/6$ , where heavy-target effects have been taken into account. The data are shown versus  $Q^2$ , for bins of fixed  $x$ . The NMC data have been rebinned to CCFR and NuTeV  $x$  values. For the purpose of plotting, a constant  $c(x) = 0.05i_x$  is added to  $F_2$ , where  $i_x$  is the number of the  $x$  bin, ranging from 0 ( $x = 0.75$ ) to 7 ( $x = 0.175$ ). For  $i_x = 8$  ( $x = 0.125$ ) to 11 ( $x = 0.015$ ),  $2c(x)$  has been added. References: NMC—M. Arneodo *et al.*, Nucl. Phys. **B483**, 3 (1997); CCFR/NuTeV—U.K. Yang *et al.*, Phys. Rev. Lett. **86**, 2741 (2001); NuTeV—M. Tzanov *et al.*, Phys. Rev. **D74**, 012008 (2006).

b) The proton structure function  $F_2^p$  mostly at small  $x$  and  $Q^2$ , measured in electromagnetic scattering of electrons and positrons (H1, ZEUS), electrons (SLAC), and muons (BCDMS, NMC) on protons. Lines are ZEUS Regge and HERAPDF parameterizations for lower and higher  $Q^2$ , respectively. The width of the bins can be up to 10% of the stated  $Q^2$ . Some points have been slightly offset in  $x$  for clarity. References: H1 and ZEUS—F.D. Aaron *et al.*, JHEP **1001**, 109 (2010) (for both data and HERAPDF parameterization); ZEUS—J. Breitweg *et al.*, Phys. Lett. **B487**, 53 (2000) (ZEUS Regge parameterization); BCDMS, NMC, SLAC—same references as Fig. 18.8.

Statistical and systematic errors added in quadrature are shown for both plots.

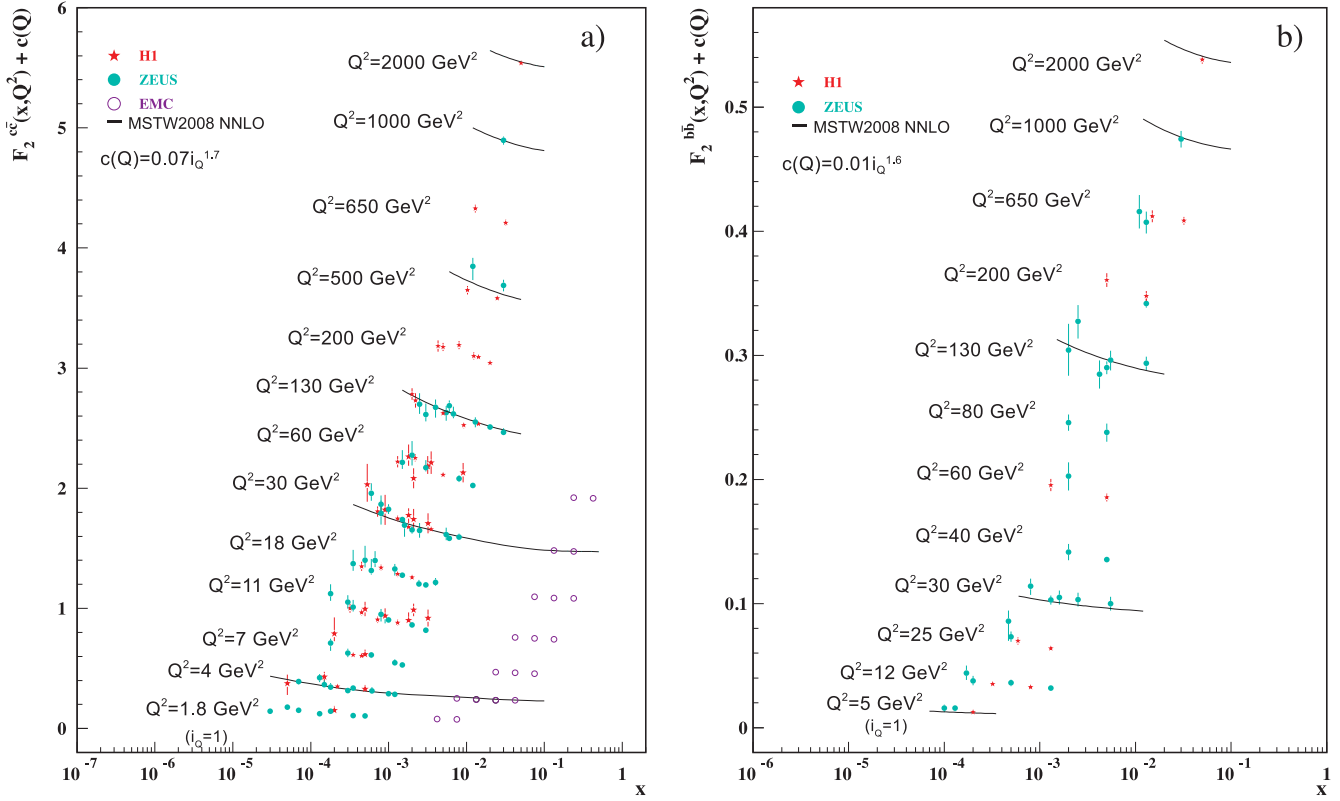


**Figure 18.11:** a) The charm quark structure function  $F_2^{c\bar{c}}(x)$ , i.e. that part of the inclusive structure function  $F_2^p$  arising from the production of charm quarks, measured in electromagnetic scattering of positrons on protons (H1, ZEUS) and muons on iron (EMC). For the purpose of plotting, a constant  $c(Q) = 0.07i_Q^{1.7}$  is added to  $F_2^{c\bar{c}}$  where  $i_Q$  is the number of the  $Q^2$  bin, ranging from 1 ( $Q^2 = 1.8 \text{ GeV}^2$ ) to 13 ( $Q^2 = 2000 \text{ GeV}^2$ ). References: **ZEUS**—J. Breitweg *et al.*, *Eur. Phys. J.* **C12**, 35 (2000); S. Chekanov *et al.*, *Phys. Rev.* **D69**, 012004 (2004); S. Chekanov *et al.*, *JHEP* **07**, 074 (2007); S. Chekanov *et al.*, *Eur. Phys. J.* **C65**, 65 (2010); **H1**—C. Adloff *et al.*, *Z. Phys.* **C72**, 593 (1996); C. Adloff *et al.*, *Phys. Lett.* **B528**, 199 (2002); F.D. Aaron *et al.*, *Phys. Lett.* **B686**, 91 (2010); F.D. Aaron *et al.*, *Eur. Phys. J.* **C65**, 89 (2010); **EMC**—J.J. Aubert *et al.*, *Nucl. Phys.* **B213**, 31 (1983).

b) The bottom quark structure function  $F_2^{b\bar{b}}(x)$ . For the purpose of plotting, a constant  $c(Q) = 0.01i_Q^{1.6}$  is added to  $F_2^{b\bar{b}}$  where  $i_Q$  is the number of the  $Q^2$  bin, ranging from 1 ( $Q^2 = 5 \text{ GeV}^2$ ) to 12 ( $Q^2 = 2000 \text{ GeV}^2$ ). References: **ZEUS**—S. Chekanov *et al.*, *Eur. Phys. J.* **C65**, 65 (2010); H. Abramowicz *et al.*, *Eur. Phys. J.* **C69**, 347 (2010); H. Abramowicz *et al.*, *Eur. Phys. J.* **C71**, 1573 (2010); **H1**—F.D. Aaron *et al.*, *Eur. Phys. J.* **C65**, 89 (2010).

For both plots, statistical and systematic errors added in quadrature are shown. The data are given as a function of  $x$  in bins of  $Q^2$ . Points may have been slightly offset in  $x$  for clarity. Some data have been rebinned to common  $Q^2$  values. Also shown is the MSTW2008 parameterization given at several  $Q^2$  values (A.D. Martin *et al.*, *Eur. Phys. J.* **C63**, 189 (2009)).

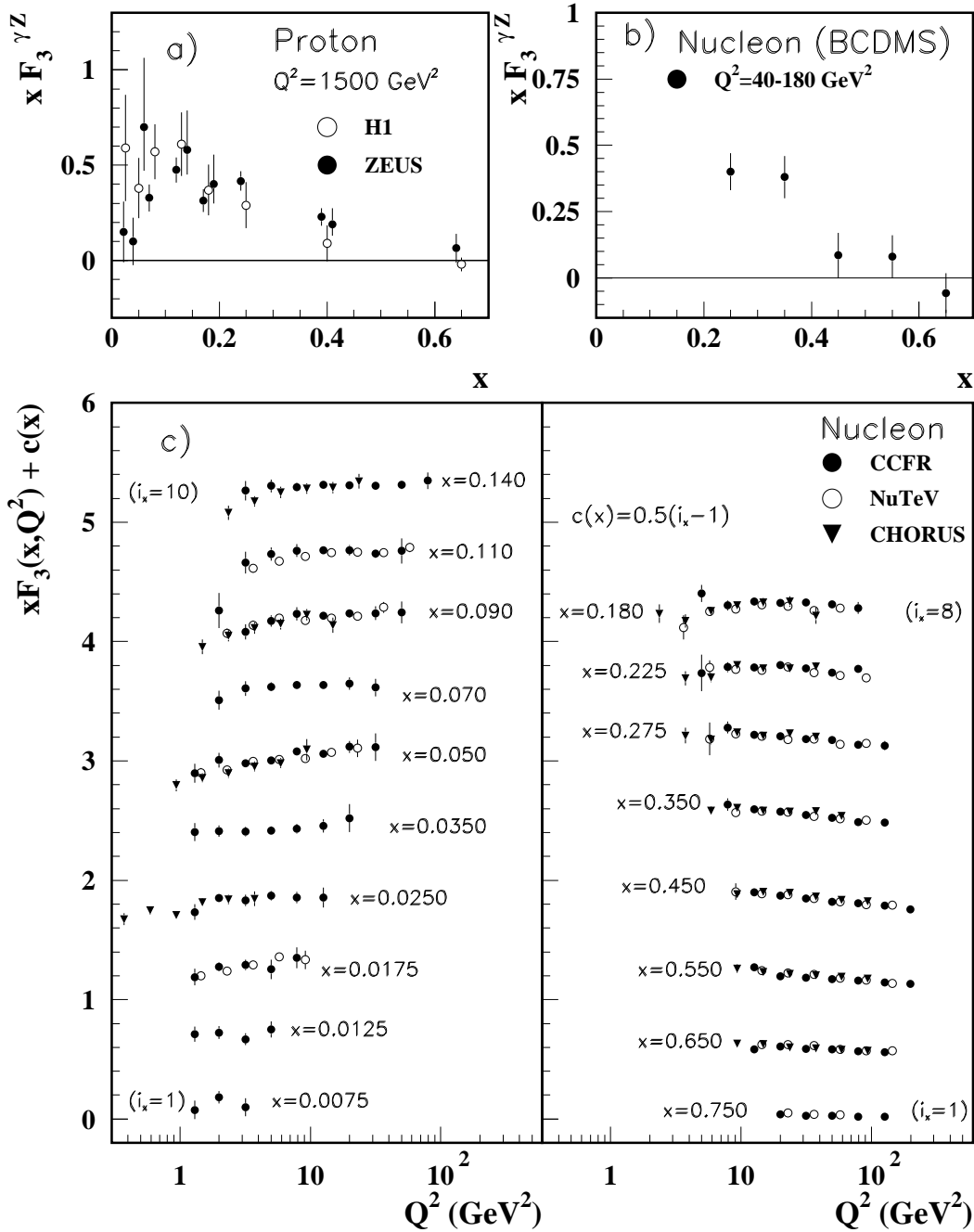


**Figure 18.12:** The structure function  $x F_3^{\gamma Z}$  measured in electroweak scattering of **a)** electrons on protons (H1 and ZEUS) and **b)** muons on carbon (BCDMS). The ZEUS points have been slightly offset in  $x$  for clarity. References: **H1**—C. Adloff *et al.*, *Eur. Phys. J. C* **30**, 1 (2003); **ZEUS**—S. Chekanov *et al.*, *Eur. Phys. J. C* **28**, 175 (2003); S. Chekanov *et al.*, *Eur. Phys. J. C* **62**, 625 (2009); **BCDMS**—A. Argento *et al.*, *Phys. Lett. B* **140**, 142 (1984).

**c)** The structure function  $x F_3$  of the nucleon measured in  $\nu$ -Fe scattering. The data are plotted as a function of  $Q^2$  in bins of fixed  $x$ . For the purpose of plotting, a constant  $c(x) = 0.5(i_x - 1)$  is added to  $x F_3$ , where  $i_x$  is the number of the  $x$  bin as shown in the plot. The NuTeV and CHORUS points have been shifted to the nearest corresponding  $x$  bin as given in the plot and slightly offset in  $Q^2$  for clarity. References: **CCFR**—W.G. Seligman *et al.*, *Phys. Rev. Lett.* **79**, 1213 (1997); **NuTeV**—M. Tzanov *et al.*, *Phys. Rev. D* **74**, 012008 (2006); **CHORUS**—G. Önengüt *et al.*, *Phys. Lett. B* **632**, 65 (2006).

Statistical and systematic errors added in quadrature are shown for all plots.

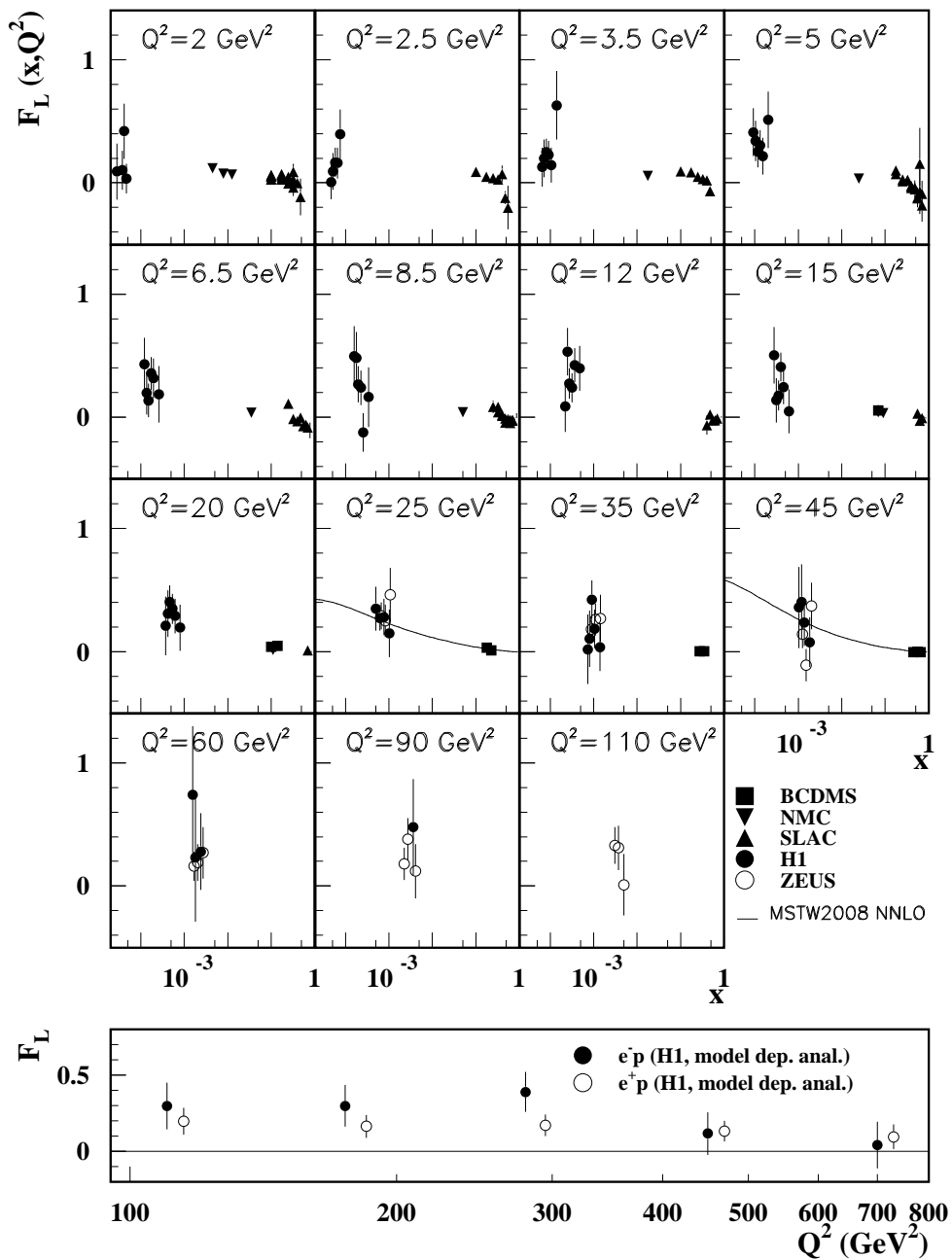


**Figure 18.13:** Top panel: The longitudinal structure function  $F_L$  as a function of  $x$  in bins of fixed  $Q^2$  measured on the proton (except for the SLAC data which also contain deuterium data). BCDMS, NMC, and SLAC results are from measurements of  $R$  (the ratio of longitudinal to transverse photon absorption cross sections) which are converted to  $F_L$  by using the BCDMS parameterization of  $F_2$  (A.C. Benvenuti *et al.*, Phys. Lett. **B223**, 485 (1989)). It is assumed that the  $Q^2$  dependence of the fixed-target data is small within a given  $Q^2$  bin. Some of the other data may have been rebinned to common  $Q^2$  values. Also shown is the MSTW2008 parameterization given at two  $Q^2$  values (A.D. Martin *et al.*, Eur. Phys. J. **C63**, 189 (2009)). References: **H1**—F.D. Aaron *et al.*, Phys. Lett. **B665**, 139 (2008); F.D. Aaron *et al.*, Eur. Phys. J. **C71**, 1579 (2011); **ZEUS**—S. Chekanov *et al.*, Phys. Lett. **B682**, 8 (2009); **BCDMS**—A. Benvenuti *et al.*, Phys. Lett. **B223**, 485 (1989); **NMC**—M. Arneodo *et al.*, Nucl. Phys. **B483**, 3 (1997); **SLAC**—L.W. Whitlow *et al.*, Phys. Lett. **B250**, 193 (1990) and numerical values from the thesis of L.W. Whitlow (SLAC-357).

Bottom panel: Higher  $Q^2$  values of the longitudinal structure function  $F_L$  as a function of  $Q^2$  given at the measured  $x$  for  $e^+/e^-$ -proton scattering. Points have been slightly offset in  $Q^2$  for clarity. References: **H1**—C. Adloff *et al.*, Eur. Phys. J. **C30**, 1 (2003).

The H1 results shown in the bottom plot require the assumption of the validity of the QCD form for the  $F_2$  structure function in order to extract  $F_L$ . Statistical and systematic errors added in quadrature are shown for both plots.

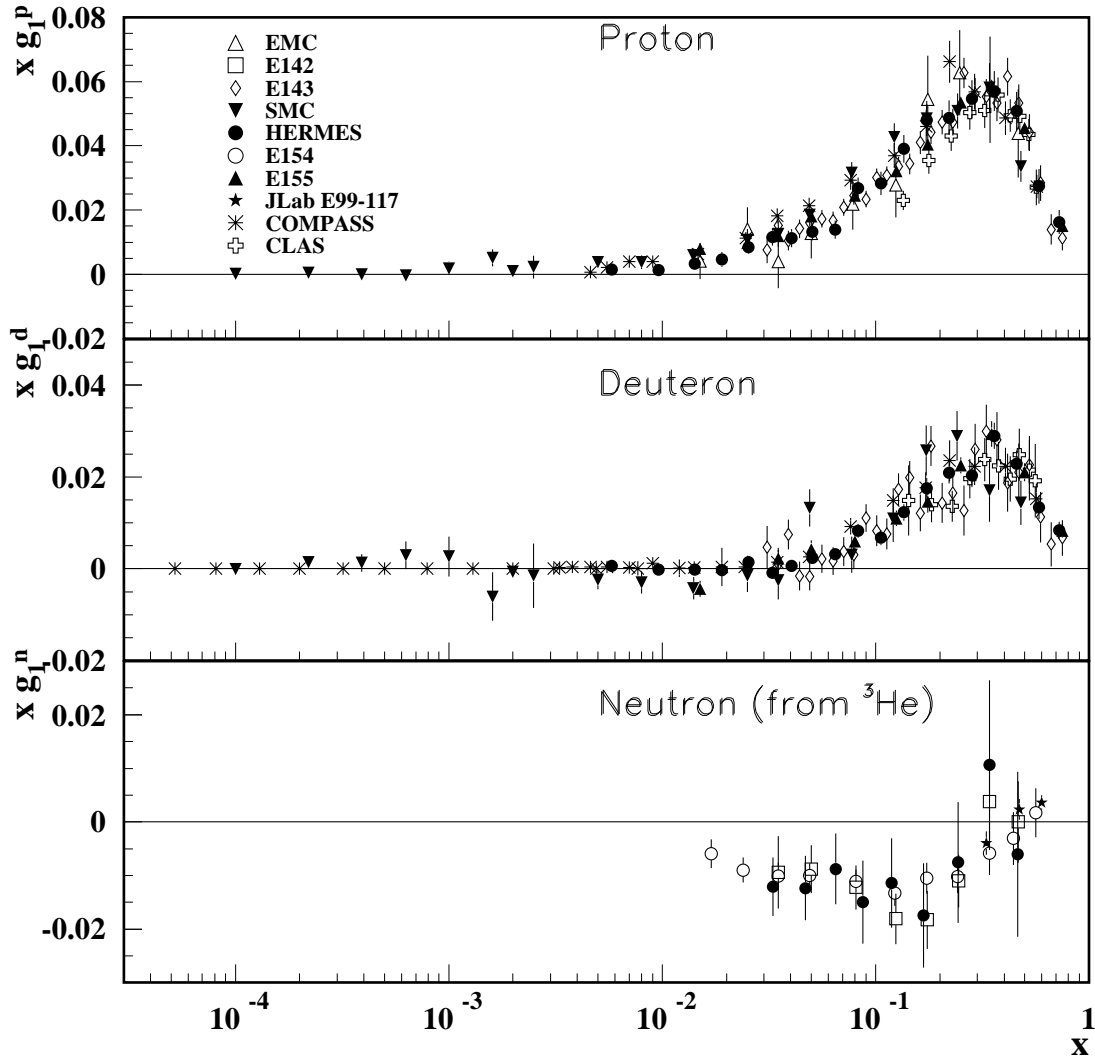


**Figure 18.14:** The spin-dependent structure function  $xg_1(x)$  of the proton, deuteron, and neutron (from  $^3\text{He}$  target) measured in deep inelastic scattering of polarized electrons/positrons: E142 ( $Q^2 \sim 0.3 - 10 \text{ GeV}^2$ ), E143 ( $Q^2 \sim 0.3 - 10 \text{ GeV}^2$ ), E154 ( $Q^2 \sim 1 - 17 \text{ GeV}^2$ ), E155 ( $Q^2 \sim 1 - 40 \text{ GeV}^2$ ), JLab E99-117 ( $Q^2 \sim 2.71 - 4.83 \text{ GeV}^2$ ), HERMES ( $Q^2 \sim 0.18 - 20 \text{ GeV}^2$ ), CLAS ( $Q^2 \sim 1 - 5 \text{ GeV}^2$ ) and muons: EMC ( $Q^2 \sim 1.5 - 100 \text{ GeV}^2$ ), SMC ( $Q^2 \sim 0.01 - 100 \text{ GeV}^2$ ), COMPASS ( $Q^2 \sim 0.001 - 100 \text{ GeV}^2$ ), shown at the measured  $Q^2$  (except for EMC data given at  $Q^2 = 10.7 \text{ GeV}^2$  and E155 data given at  $Q^2 = 5 \text{ GeV}^2$ ). Note that  $g_1^n(x)$  may also be extracted by taking the difference between  $g_1^d(x)$  and  $g_1^p(x)$ , but these values have been omitted in the bottom plot for clarity. Statistical and systematic errors added in quadrature are shown. References: **EMC**—J. Ashman *et al.*, Nucl. Phys. **B328**, 1 (1989); **E142**—P.L. Anthony *et al.*, Phys. Rev. **D54**, 6620 (1996); **E143**—K. Abe *et al.*, Phys. Rev. **D58**, 112003 (1998); **SMC**—B. Adeva *et al.*, Phys. Rev. **D58**, 112001 (1998), B. Adeva *et al.*, Phys. Rev. **D60**, 072004 (1999) and Erratum-Phys. Rev. **D62**, 079902 (2000); **HERMES**—A. Airapetian *et al.*, Phys. Rev. **D75**, 012007 (2007) and K. Ackerstaff *et al.*, Phys. Lett. **B404**, 383 (1997); **E154**—K. Abe *et al.*, Phys. Rev. Lett. **79**, 26 (1997); **E155**—P.L. Anthony *et al.*, Phys. Lett. **B463**, 339 (1999) and P.L. Anthony *et al.*, Phys. Lett. **B493**, 19 (2000); **Jlab-E99-117**—X. Zheng *et al.*, Phys. Rev. **C70**, 065207 (2004); **COMPASS**—V.Yu. Alexakhin *et al.*, Phys. Lett. **B647**, 8 (2007), E.S. Ageev *et al.*, Phys. Lett. **B647**, 330 (2007), and M.G. Alekseev *et al.*, Phys. Lett. **B690**, 466 (2010); **CLAS**—K.V. Dharmawardane *et al.*, Phys. Lett. **B641**, 11 (2006) (which also includes resonance region data not shown on this plot).

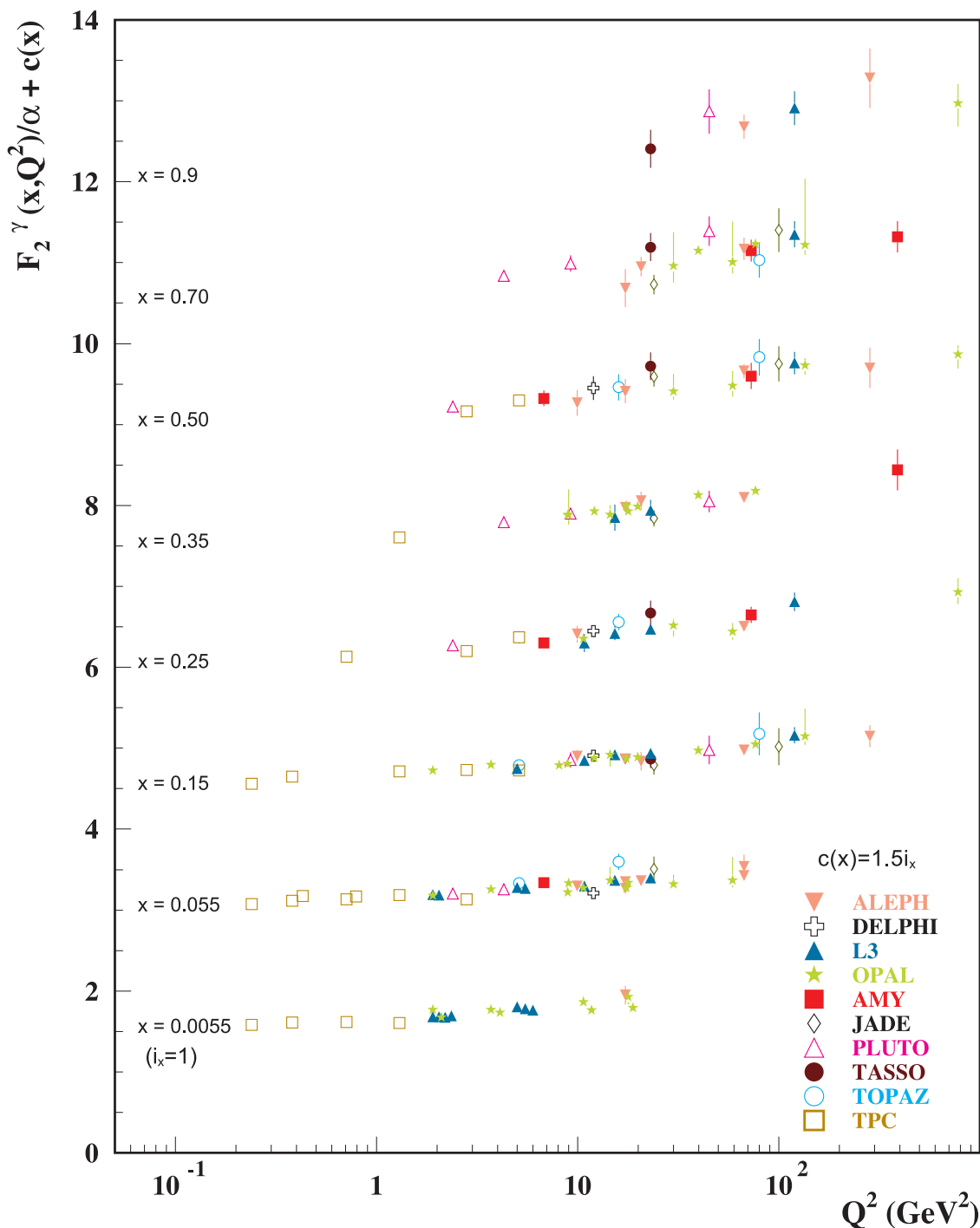


**Figure 18.15:** The hadronic structure function of the photon  $F_2^\gamma$  divided by the fine structure constant  $\alpha$  measured in  $e^+e^-$  scattering, shown as a function of  $Q^2$  for bins of  $x$ . Data points have been shifted to the nearest corresponding  $x$  bin as given in the plot. Some points have been offset in  $Q^2$  for clarity. Statistical and systematic errors added in quadrature are shown. For the purpose of plotting, a constant  $c(x) = 1.5i_x$  is added to  $F_2^\gamma/\alpha$  where  $i_x$  is the number of the  $x$  bin, ranging from 1 ( $x = 0.0055$ ) to 8 ( $x = 0.9$ ). References: **ALEPH**–R. Barate *et al.*, Phys. Lett. **B458**, 152 (1999); A. Heister *et al.*, Eur. Phys. J. **C30**, 145 (2003); **DELPHI**–P. Abreu *et al.*, Z. Phys. **C69**, 223 (1995); **L3**–M. Acciarri *et al.*, Phys. Lett. **B436**, 403 (1998); M. Acciarri *et al.*, Phys. Lett. **B447**, 147 (1999); M. Acciarri *et al.*, Phys. Lett. **B483**, 373 (2000); **OPAL**–A. Ackerstaff *et al.*, Phys. Lett. **B411**, 387 (1997); A. Ackerstaff *et al.*, Z. Phys. **C74**, 33 (1997); G. Abbiendi *et al.*, Eur. Phys. J. **C18**, 15 (2000); G. Abbiendi *et al.*, Phys. Lett. **B533**, 207 (2002) (note that there is overlap of the data samples in these last two papers); **AMY**–S.K. Sahu *et al.*, Phys. Lett. **B346**, 208 (1995); T. Kojima *et al.*, Phys. Lett. **B400**, 395 (1997); **JADE**–W. Bartel *et al.*, Z. Phys. **C24**, 231 (1984); **PLUTO**–C. Berger *et al.*, Phys. Lett. **142B**, 111 (1984); C. Berger *et al.*, Nucl. Phys. **B281**, 365 (1987); **TASSO**–M. Althoff *et al.*, Z. Phys. **C31**, 527 (1986); **TOPAZ**–K. Muramatsu *et al.*, Phys. Lett. **B332**, 477 (1994); **TPC/Two Gamma**–H. Aihara *et al.*, Z. Phys. **C34**, 1 (1987).

## 19. FRAGMENTATION FUNCTIONS IN $e^+e^-$ , $ep$ AND $pp$ COLLISIONS

Revised August 2011 by O. Biebel (Ludwig-Maximilians-Universität, Munich, Germany), D. de Florian (Dep. de Física, FCEyN-UBA, Buenos Aires, Argentina), D. Milstead (Fysikum, Stockholms Universitet, Sweden), and A. Vogt (Dep. of Mathematical Sciences, University of Liverpool, UK).

### 19.1. Introduction to fragmentation

The term ‘fragmentation functions’ is widely used for two related if conceptually different sets of functions describing final-state single particle energy distributions in hard scattering processes (see Refs. [1,2] for introductory reviews, and Refs. [3,4] for summaries of recent experimental and theoretical research in this field).

The first are cross-section observables such as the functions  $F_{T,L,A}(x,s)$  in semi-inclusive  $e^+e^-$  annihilation at center-of-mass (CM) energy  $\sqrt{s}$  via an intermediate photon or  $Z$ -boson,  $e^+e^- \rightarrow \gamma/Z \rightarrow h+X$ , given by

$$\frac{1}{\sigma_0} \frac{d^2\sigma^h}{dx d\cos\theta} = \frac{3}{8}(1 + \cos^2\theta)F_T^h + \frac{3}{4}\sin^2\theta F_L^h + \frac{3}{4}\cos\theta F_A^h. \quad (19.1)$$

Here  $x = 2E_h/\sqrt{s} \leq 1$  is the scaled energy of the hadron  $h$  (in practice the approximation  $x \simeq x_p = 2p_h/\sqrt{s}$  is often used), and  $\theta$  is its angle relative to the electron beam in the CM frame. Eq. (19.1) is the most general form for unpolarized inclusive single-particle production via vector bosons [5]. The transverse and longitudinal fragmentation functions  $F_T$  and  $F_L$  represent the contributions from  $\gamma/Z$  polarizations transverse or longitudinal with respect to the direction of motion of the hadron. The parity-violating term with the asymmetric fragmentation function  $F_A$  arises from the interference between vector and axial-vector contributions. Normalization factors  $\sigma_0$  used in the literature range from the total cross section  $\sigma_{\text{tot}}$  for  $e^+e^- \rightarrow$  hadrons, including all weak and QCD contributions, to  $\sigma_0 = 4\pi\alpha^2 N_c/3s$  with  $N_c = 3$ , the lowest-order QED cross section for  $e^+e^- \rightarrow \mu^+\mu^-$  times the number of colors  $N_c$ . LEP1 measurements of all three fragmentation functions are shown in Fig. 19.1.

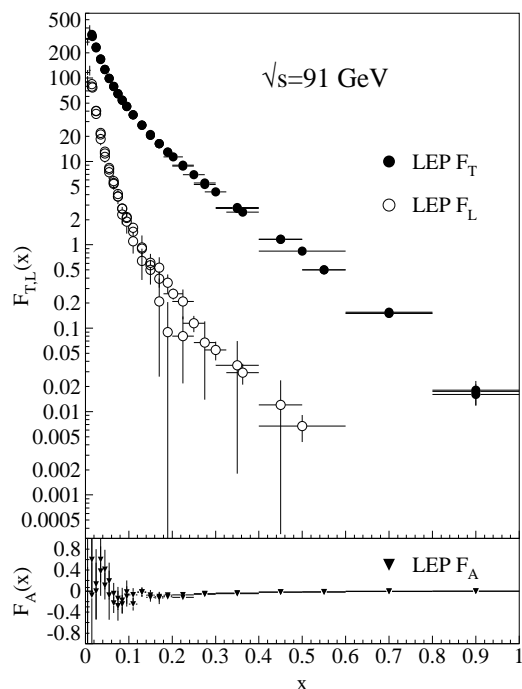


**Figure 19.1:** LEP1 measurements of total transverse ( $F_T$ ), longitudinal ( $F_L$ ), and asymmetric ( $F_A$ ) fragmentation functions [6–8]. Data points with relative errors greater than 100% are omitted.

Integration of Eq. (19.1) over  $\theta$  yields the total fragmentation function  $F^h = F_T^h + F_L^h$ ,

$$\frac{1}{\sigma_0} \frac{d\sigma^h}{dx} = F^h(x,s) = \sum_i \int_x^1 \frac{dz}{z} C_i(z, \alpha_s(\mu), \frac{s}{\mu^2}) D_i^h(\frac{x}{z}, \mu^2) + \mathcal{O}(\frac{1}{\sqrt{s}}) \quad (19.2)$$

with  $i = u, \bar{u}, d, \bar{d}, \dots, g$ . Here we have introduced the second set of functions mentioned in the first paragraph, the parton fragmentation functions (or fragmentation densities)  $D_i^h$ . These functions are the final-state analogue of the initial-state parton distributions addressed in Section 18 of this *Review*. Due to the different sign of the squared four-momentum  $q^2$  of the intermediate gauge boson these two sets of distributions are also referred to as the timelike ( $e^+e^-$  annihilation,  $q^2 > 0$ ) and spacelike (deep-inelastic scattering (DIS),  $q^2 < 0$ ) parton distributions. The function  $D_i^h(z, \mu^2)$  encodes the

probability that the parton  $i$  fragments into a hadron  $h$  carrying a fraction  $z$  of the parton’s momentum. Beyond the leading order (LO) of perturbative QCD these universal functions are factorization-scheme dependent, with ‘reasonable’ scheme choices retaining certain quark-parton-model (QPM) constraints such as the momentum sum rule

$$\sum_h \int_0^1 dz z D_i^h(z, \mu^2) = 1. \quad (19.3)$$

The dependence of the functions  $D_i^h$  on the factorization (or fragmentation) scale  $\mu^2$  (in Eq. (19.2) and below identified with the renormalization scale) is discussed in Section 19.2.

The second ingredient in Eq. (19.2), and analogous expressions for the functions  $F_{T,L,A}$ , are the observable-dependent coefficient functions  $C_i$ . At the zeroth order in the strong coupling  $\alpha_s$  the coefficient functions  $C_g$  for gluons are zero, while for (anti-)quarks  $C_i = g_i(s)\delta(1-z)$  except for  $F_L$ , where  $g_i(s)$  is the appropriate electroweak coupling. In particular,  $g_i(s)$  is proportional to the squared charge of the quark  $i$  at  $s \ll M_Z^2$ , when weak effects can be neglected. The full electroweak prefactors  $g_i(s)$  can be found in Ref. [5]. The power corrections in Eq. (19.2) arise from quark and hadron mass terms and from non-perturbative effects.

Measurements of fragmentation in lepton-hadron and hadron-hadron scattering are complementary to those in  $e^+e^-$  annihilation. The latter provides a clean environment (no initial-state hadron remnant) and stringent constraints on the combinations  $D_{q_i}^h + D_{\bar{q}_i}^h$ . However  $e^+e^-$  annihilation is far less sensitive to  $D_g^h$  and insensitive to the charge asymmetries  $D_{q_i}^h - D_{\bar{q}_i}^h$ . These quantities are best constrained in proton-(anti-)proton and electron-proton scattering, respectively. Especially the latter provides a more complicated environment with which it is possible to study the influence on the fragmentation process from initial state QCD radiation, the partonic and spin structure of the hadron target, and the target remnant system (see Ref. [9] for a comprehensive review of the measurements and models of fragmentation in lepton-hadron scattering).

Moreover, unlike  $e^+e^-$  annihilation where  $q^2 = s$  is fixed by the collider energy, lepton-hadron scattering has two independent scales,  $Q^2 = -q^2$  and the invariant mass  $W^2$  of the hadronic final state, which both can vary by several orders of magnitudes for a given CM energy, thus allowing the study of fragmentation in different environments by a single experiment. E.g., in photoproduction the exchanged photon is quasi-real ( $Q^2 \approx 0$ ) leading to processes akin to hadron-hadron scattering. In DIS ( $Q^2 \gg 1 \text{ GeV}^2$ ), using the QPM, the hadronic fragments of the struck quark can be directly compared with quark fragmentation in  $e^+e^-$  in a suitable frame. Results from lepton-hadron experiments quoted in this report primarily concern fragmentation in the DIS regime. Studies performed by lepton-hadron experiments of fragmentation with photoproduction data containing high transverse momentum jets or particles are also reported, when these are directly comparable to DIS and  $e^+e^-$  results.

Fragmentation studies at HERA are usually performed in one of two frames in which the target hadron and the exchanged boson are collinear. The hadronic center-of-mass frame (HCMS) is defined

as the rest system of the exchanged boson and incoming hadron, with the  $z^*$ -axis defined along the direction of the exchanged boson. The positive  $z^*$  direction defines the so-called current region. Fragmentation measurements performed in the HCMS often use the Feynman- $x$  variable  $x_F = 2p_z^*/W$ , where  $p_z^*$  is the longitudinal momentum of the particle in this frame. As  $W$  is the invariant mass of the hadronic final state,  $x_F$  ranges between  $-1$  and  $1$ .

The Breit system [10] is connected to the HCMS by a longitudinal boost such that the time component of  $q$  vanishes, i.e.,  $q = (0, 0, 0, -Q)$ . In the QPM, the struck parton then has the longitudinal momentum  $Q/2$  which becomes  $-Q/2$  after the collision. As compared with the HCMS, the current region of the Breit frame is more closely matched to the partonic scattering process, and is thus appropriate for direct comparisons of fragmentation functions in DIS with those from  $e^+e^-$  annihilation. The variable  $x_p = 2p^*/Q$  is used at HERA for measurements in the Breit frame, ensuring rather directly comparable DIS and  $e^+e^-$  results, where  $p^*$  is the particle's momentum in the current region of the Breit frame.

## 19.2. Scaling violation

The simplest parton-model approach would predict scale-independent  $x$ -distributions ('scaling') for both the fragmentation function  $F^h$  and the parton fragmentation functions  $D_i^h$ . Perturbative QCD corrections lead, after factorization of the final-state collinear singularities for light partons, to logarithmic scaling violations via the evolution equations

$$\frac{\partial}{\partial \ln \mu^2} D_i(x, \mu^2) = \sum_j \int_x^1 \frac{dz}{z} P_{ji}(z, \alpha_s(\mu^2)) D_j\left(\frac{x}{z}, \mu^2\right). \quad (19.4)$$

Usually this system of equations is decomposed into a  $2 \times 2$  flavour-singlet sector comprising gluon and the sum of all quark and antiquark fragmentation functions, and scalar ('non-singlet') equations for quark-antiquark and flavour differences. Notice that the singlet splitting-function matrix is now  $P_{ji}$ , rather than  $P_{ij}$  as for the initial-state parton distributions, since  $D_j$  represents the fragmentation of the final parton.

The splitting functions in Eq. (19.4) have perturbative expansion of the form

$$P_{ji}(z, \alpha_s) = \frac{\alpha_s}{2\pi} P_{ji}^{(0)}(z) + \left(\frac{\alpha_s}{2\pi}\right)^2 P_{ji}^{(1)}(z) + \left(\frac{\alpha_s}{2\pi}\right)^3 P_{ji}^{(2)}(z) + \dots \quad (19.5)$$

where the leading-order (LO) functions  $P^{(0)}(z)$  [11,12] are the same as those for the initial-state parton distributions. The next-to-leading order (NLO) corrections  $P^{(1)}(z)$  have been calculated in Refs. [13–17] (there are well-known misprints in the journal version of Ref. [14]). Ref. [17] also includes the spin-dependent case. These functions are different from, but related to their space-like counterparts, see also Ref. [18]. These relations have facilitated recent calculations of the next-to-next-to-leading order (NNLO) quantities  $P_{qq}^{(2)}(z)$  and  $P_{gg}^{(2)}(z)$  in Eq. (19.5) [19,20]. The corresponding off-diagonal quantities  $P_{qg}^{(2)}$  and  $P_{gq}^{(2)}$  were recently obtained in Ref. [21] by using similar relations supplemented with constraints from the momentum sum rule Eq. (19.3) [20] and the supersymmetric limit. An uncertainty, which does not affect the logarithmic behaviour at small and large momentum fractions, still remains on the  $P_{gg}^{(2)}$  kernel. All these results refer to the standard  $\overline{\text{MS}}$  scheme, with the exception of Refs. [16], with a fixed number  $n_f$  of light flavours. The NLO treatment of flavour thresholds in the evolution has been addressed in Ref. [22].

The QCD parts of the coefficient functions for  $F_{T,L,A}(x, s)$  in Eq. (19.1) and the total fragmentation function  $F_2^h \equiv F^h$  in Eq. (19.2) are given by

$$C_{a,i}(z, \alpha_s) = (1 - \delta_{aL}) \delta_{iq} + \frac{\alpha_s}{2\pi} c_{a,i}^{(1)}(z) + \left(\frac{\alpha_s}{2\pi}\right)^2 c_{a,i}^{(2)}(z) + \dots \quad (19.6)$$

The first-order corrections have been calculated a long time ago in Refs. [23], and the second-order terms in [24]. The latter results have recently been verified (and some typos corrected) in Refs. [19,25]. Thus the coefficient functions are known to NNLO except for  $F_L$  where the leading contribution is of order  $\alpha_s$ .

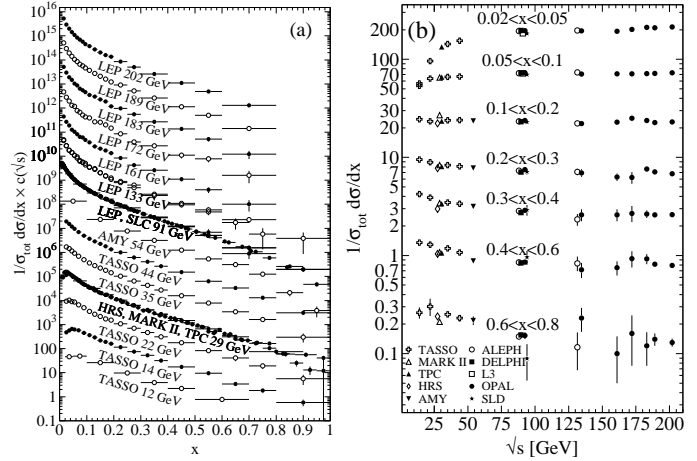


**Figure 19.2:** The  $e^+e^-$  fragmentation function for all charged particles is shown [8, 26–42] (a) for different CM energies  $\sqrt{s}$  versus  $x$  and (b) for various ranges of  $x$  versus  $\sqrt{s}$ . For the purpose of plotting (a), the distributions were scaled by  $c(\sqrt{s}) = 10^i$  with  $i$  ranging from  $i = 0$  ( $\sqrt{s} = 12$  GeV) to  $i = 13$  ( $\sqrt{s} = 202$  GeV).

The effect of the evolution is similar in the timelike and spacelike cases: as the scale increases, one observes a scaling violation in which the  $x$ -distribution is shifted towards lower values. This can be seen from Fig. 19.2 where a large amount of measurements of the total fragmentation function in  $e^+e^-$  annihilation are summarized. QCD analyses of these data are discussed in Section 19.5 below.

Unlike the splitting functions in Eq. (19.5), see Refs. [18–20], the coefficient functions for  $F_{2,T,A}$  in Eq. (19.6) show a threshold enhancement with terms up to  $\alpha_s^n (1-z)^{-1} \ln^{2n-1}(1-z)$ . Such logarithms can be resummed to all orders in  $\alpha_s$  using standard soft-gluon techniques [43–45]. Recently this resummation has been extended to the subleading (and for  $F_L$  leading) class  $\alpha_s^k \ln^k(1-z)$  of large- $x$  logarithms [46,47].

In Refs. [23] the NLO coefficient functions have been calculated also for single hadron production in lepton-proton scattering,  $ep \rightarrow e + h + X$ . More recently corresponding results have been obtained for the case that a non-vanishing transverse momentum is required in the HCMS frame [48].

Scaling violations in DIS are shown in Fig. 19.3 for both HCMS and Breit frame. In Fig. 1.3(a) the distribution in terms of  $x_F = 2p_z^*/W$  shows a steeper slope in  $ep$  data than for the lower-energy  $\mu p$  data for  $x_F > 0.15$ , indicating the scaling violations. At smaller values of  $x_F$  in the current jet region, the multiplicity of particles substantially increases with  $W$  owing to the increased phase space available for the fragmentation process. The EMC data access both the current region and the region of the fragmenting target remnant system. At higher values of  $|x_F|$ , due to the extended nature of the remnant, the multiplicity in the target region far exceeds that in the current region. For acceptance reasons the remnant hemisphere of the HCMS is only accessible by the lower-energy fixed-target experiments.

Using hadrons from the current hemisphere in the Breit frame, measurements of fragmentation functions and the production properties of particles in  $ep$  scattering have been made by Refs. [53–58]. Fig. 19.3(b) compares results from  $ep$  scattering and  $e^+e^-$  experiments, the latter results are halved as they cover both event hemispheres. The agreement between the DIS and  $e^+e^-$  results is fairly good. However, processes in DIS which are not present in  $e^+e^-$  annihilation, such as boson-gluon fusion and initial state QCD radiation, can depopulate the current region. These effects become most prominent at low values of  $Q$  and  $x_p$ . Hence, when compared with  $e^+e^-$  annihilation data at  $\sqrt{s} = 5.2, 6.5$  GeV [60] not shown here, the DIS particle rates tend to lie below those from  $e^+e^-$  annihilation. A recent ZEUS study [61] finds that the direct comparability of the  $ep$  data to  $e^+e^-$  results at low scales is improved if twice the energy in the current hemisphere of



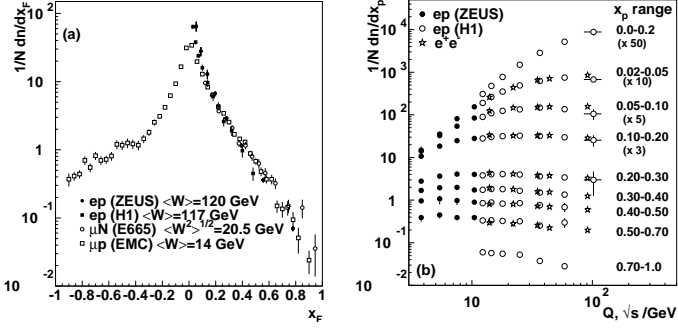


**Figure 19.3:** (a) The distribution  $1/N \cdot dN/dx_F$  for all charged particles in DIS lepton-hadron experiments at different values of  $W$ , and measured in the HCMS [49–52]. (b) Scaling violations of the fragmentation function for all charged particles in the current region of the Breit frame of DIS [53,58] and in  $e^+e^-$  interactions [41,59]. The data are shown as a function of  $\sqrt{s}$  for  $e^+e^-$  results, and as a function of  $Q$  for the DIS results, each within the same indicated intervals of the scaled momentum  $x_p$ . The data for the four lowest intervals of  $x_p$  are multiplied by factors 50, 10, 5, and 3, respectively for clarity.

the Breit frame,  $2E_B^{\text{CF}}$ , is used instead of  $Q$  as the fragmentation scale.

### 19.3. Fragmentation functions for small particle momenta

The higher-order timelike splitting functions in Eq. (19.5) are very singular at small  $x$ . They show a double-logarithmic (LL) enhancement with leading terms of the form  $\alpha_s^n \ln^{2n-2} x$  corresponding to poles  $\alpha_s^n (N-1)^{1-2n}$  for the Mellin moments

$$P^{(n)}(N) = \int_0^1 dx x^{N-1} P^{(n)}(x). \quad (19.7)$$

Despite large cancellations between leading and non-leading logarithms at non-asymptotic value of  $x$ , the resulting small- $x$  rise in the timelike splitting functions dwarfs that of their spacelike counterparts in the evolution of the parton distributions in Section 18 of this *Review*, see Fig. 1 of Ref. [20]. Consequently the fixed-order approximation to the evolution breaks down orders of magnitude in  $x$  earlier in fragmentation than in DIS.

The pattern of the known coefficients and other considerations suggest that the LL terms sum to all-order expressions without any pole at  $N=1$  such as [62,63]

$$P_{gg}^{\text{LL}}(N) = -\frac{1}{4}(N-1 - \sqrt{(N-1)^2 - 24\alpha_s/\pi}). \quad (19.8)$$

Keeping the first three terms in the resulting expansion of Eq. (19.4) around  $N=1$  yields a Gaussian in the variable  $\xi = \ln(1/x)$  for the small- $x$  fragmentation functions,

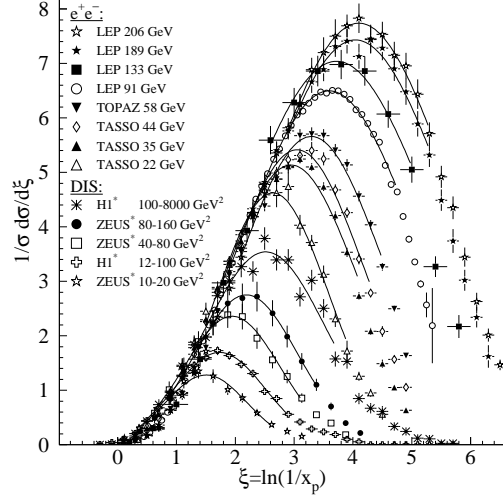
$$xD(x, s) \propto \exp\left[-\frac{1}{2\sigma^2}(\xi - \xi_p)^2\right], \quad (19.9)$$

with the peak position and width varying with the energy as [64] (see also Ref. [2])

$$\xi_p \simeq \frac{1}{4} \ln\left(\frac{s}{\Lambda^2}\right), \quad \sigma \propto \left[\ln\left(\frac{s}{\Lambda^2}\right)\right]^{3/4}. \quad (19.10)$$

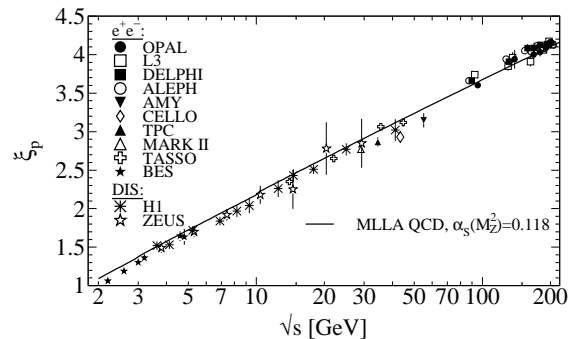
Next-to-leading order corrections to the above predictions have been calculated [65]. In the method of Ref. [66], see also Refs. [67,68], the corrections are included in an analytical form known as the ‘modified leading logarithmic approximation’ (MLLA). Alternatively they can be used to compute higher-moment corrections to the shape in Eq. (19.9) [69]. Double-logarithmic contributions to the gluonic coefficient were derived in the standard  $\overline{\text{MS}}$  scheme in Ref. [70]. The resummation of the dominant small  $x$  terms for the flavour-singlet splitting kernels and coefficient functions was recently studied in [71].

Fig. 19.4 shows the  $\xi$  distribution for charged particles produced in the current region of the Breit frame in DIS and in  $e^+e^-$  annihilation. Consistent with Eq. (19.9) (the ‘hump backed plateau’) and Eq. (19.10) the distributions have a Gaussian shape with the peak position and area increasing with the CM energy ( $e^+e^-$ ) and  $Q^2$  (DIS).



**Figure 19.4:** Distribution of  $\xi = \ln(1/x_p)$  at several CM energies ( $e^+e^-$ ) [26–28,33–36,41,72–75] and intervals of  $Q^2$  (DIS) [56,57]. At each energy only one representative measurement is displayed. For clarity some measurements at intermediate CM energies ( $e^+e^-$ ) or  $Q^2$  ranges (DIS) are not shown. The DIS measurements (\*) have been scaled by a factor of 2 for direct comparability with the  $e^+e^-$  results. Fits of simple Gaussian functions are overlaid for illustration.

The predicted energy dependence Eq. (19.10) of the peak in the  $\xi$  distribution is explained by soft gluon coherence (angular ordering) which correctly predicts the suppression of hadron production at small  $x$ . Of course, a decrease at very small  $x$  is expected on purely kinematical grounds, but this would occur at particle energies proportional to their masses, *i.e.*, at  $x \propto m/\sqrt{s}$  and hence  $\xi \sim \frac{1}{2} \ln s$ . Thus, if the suppression were purely kinematic, the peak position  $\xi_p$  would vary twice as rapidly with the energy, which is ruled out by the data in Fig. 19.5. The  $e^+e^-$  and DIS data agree well with each other, demonstrating the universality of hadronization, and the MLLA prediction. Measurements of the higher moments of the  $\xi$  distribution in  $e^+e^-$  [41,75–77] and DIS [57] have also been performed and show consistency with each other.



**Figure 19.5:** Evolution of the peak position,  $\xi_p$ , of the  $\xi$  distribution with the CM energy  $\sqrt{s}$ . The MLLA QCD prediction using  $\alpha_s(s = M_Z^2) = 0.118$  is superimposed to the data of Refs. [26,28,29,32–34,36,41,55,56,73,74,77–85].

### 19.4. Fragmentation models

Although the scaling violation can be calculated perturbatively, the actual form of the parton fragmentation functions is non-perturbative. Perturbative evolution gives rise to a shower of quarks and gluons (partons). Multi-parton final states from leading and higher order matrix element calculations are linked to these parton showers using factorization prescriptions, also called matching schemes, see Ref. [86] for an overview. Phenomenological schemes are then used to model the carry-over of parton momenta and flavor to the hadrons. Two of the very popular models are the *string fragmentation* [87,88], implemented in the JETSET [89], PYTHIA [90] and UCLA [91] Monte Carlo event generation programs, and the *cluster fragmentation* of the HERWIG [92] and SHERPA [93] Monte Carlo event generators. For details see Chap. 38 of this *Review*.

### 19.5. Quark and gluon fragmentation functions

The fragmentation functions are solutions to the evolution equations Eq. (19.4), but need to be parametrized at some initial scale  $\mu_0^2$  (usually around 1 GeV<sup>2</sup> for light quarks and gluons and  $m_Q^2$  for heavy quarks). A usual parametrization for light hadrons is [94–100]

$$D_i^h(x, \mu_0^2) = N x^\alpha (1-x)^\beta \left(1 + \gamma(1-x)^\delta\right), \quad (19.11)$$

where the normalization  $N$ , and the parameters  $\alpha$ ,  $\beta$ ,  $\gamma$  and  $\delta$  in general depend on the energy scale  $\mu_0^2$ , and also on the type of the parton,  $i$ , and the hadron,  $h$ . Frequently the term involving  $\gamma$  and  $\delta$  is left out [96–99]. Heavy flavor fragmentation into heavy mesons is discussed in Sec. 19.9. The parameters of Eq. (19.11) (see [94–99]) are obtained by performing global fits to data on various hadron types for different combinations of partons and hadrons in  $e^+e^-$ , lepton-hadron and hadron-hadron collisions.

Data from  $e^+e^-$  annihilation present the cleanest experimental source for the measurement of fragmentation functions, but can not contribute to disentangle quark from antiquark distributions. Since the bulk of the  $e^+e^-$  annihilation data is obtained at the mass of the  $Z$ -boson, where the electroweak couplings are roughly the same for the different partons, it provides the most precise determination of the flavor-singlet quark fragmentation. Flavor tagged results [101], distinguishing between the light quark, charm and bottom contributions are of particular value for flavor decomposition, even though those measurements can not be unambiguously interpreted in perturbative QCD.

The most relevant source for quark-antiquark (and also flavor) separation is provided by data from semi-inclusive DIS (SIDIS). Semi-inclusive measurements are usually performed at much lower scales than for  $e^+e^-$  annihilation. The inclusion of SIDIS data in global fits allows for a wider coverage in the evolution of the fragmentation functions, resulting at the same time in a stringent test of the universality of these distributions. Charged-hadron production data in hadronic collisions also presents a sensitivity on (anti-)quark fragmentation functions.

The gluon fragmentation function  $D_g(x)$  can be extracted, in principle, from the longitudinal fragmentation function  $F_L$  in Eq. (19.2), as the coefficient functions  $C_{L,i}$  for quarks and gluons are comparable at order  $\alpha_s$ . However at NLO, *i.e.*, including the  $\mathcal{O}(\alpha_s^2)$  coefficient functions  $C_{L,i}^{(2)}$  [24], quark fragmentation is dominant in  $F_L$  over a large part of the kinematic range, reducing the sensitivity on  $D_g$ . This distribution could be determined also analyzing the evolution of the fragmentation functions. This possibility is limited by the lack of sufficiently precise data at energy scales away from the  $Z$ -resonance and the dominance of the quark contributions and at medium and large values of  $x$ .

$D_g$  can also be deduced from the fragmentation of three-jet events in which the gluon jet is identified, for example, by tagging the other two jets with heavy quark decays. To leading order, the measured distributions of  $x = E_{\text{had}}/E_{\text{jet}}$  for particles in gluon jets can be identified directly with the gluon fragmentation functions  $D_g(x)$ . At higher orders the theoretical interpretation of this observable is ambiguous.

A direct constraint on  $D_g$  is provided by  $pp, p\bar{p} \rightarrow hX$  data. At variance with  $e^+e^-$  annihilation and SIDIS, for this process gluon fragmentation starts to contribute at the lowest order in the coupling constant, introducing a strong sensitivity on  $D_g$ . At large  $x \gtrsim 0.5$ , where information from  $e^+e^-$  is sparse, data from hadronic colliders facilitate significantly improved extractions of  $D_g$  [94,95].

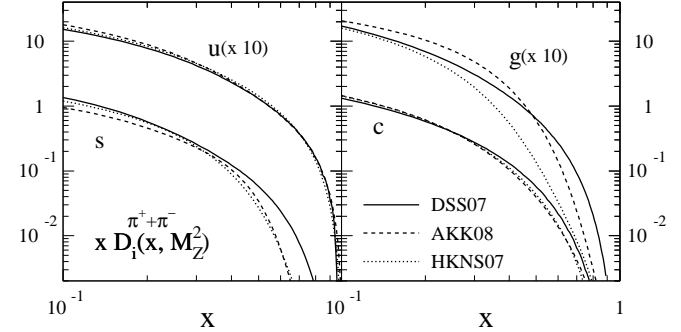


**Figure 19.6:** Comparison of up, strange, charm and gluon NLO fragmentation functions for  $\pi^+ + \pi^-$  at the mass of the  $Z$ . The different lines correspond to the result of the most recent analyses performed in Refs. [94,95,99].

A comparison of recent fits of NLO fragmentation functions for  $\pi^+ + \pi^-$  obtained by DSS07 [94], AKK08 [95] and HKNS07 [99] is shown in Fig. 19.6. Differences between the sets are large especially for the gluon fragmentation function over the full range of  $x$  and for the quark distribution at large momentum fractions. Those discrepancies can be considered as a first estimate of the present uncertainties involved in the extraction of the fragmentation functions. The differences are even larger for other species of hadrons like kaons and protons [94,95,99].

### 19.6. Identified particles in $e^+e^-$ and semi-inclusive DIS

A great wealth of measurements of  $e^+e^-$  fragmentation into identified particles exists. A collection of references for data on fragmentation into identified particles is given on Table 46.1. Representative of this body of data is Fig. 19.7 which shows fragmentation functions as the scaled momentum spectra of charged particles at several CM energies.

Quantitative results of studies of scaling violation in  $e^+e^-$  fragmentation have been reported in [6,39,103,104]. The values of  $\alpha_s$  obtained are consistent with the world average (see review on QCD in Section 9 of this *Review*).

Many studies have been made of identified particles produced in lepton-hadron scattering, although fewer particle species have been measured than in  $e^+e^-$  collisions. References [105–110] and [111–117] are representative of the data from fixed target and  $ep$  collider experiments, respectively.

QCD calculations performed at NLO provide an overall good description of the HERA data [52,53,57,112,118,119] for both SIDIS [120] and the hadron transverse momentum distribution [48] in the kinematic regions in which the calculations are predictive.

Fig. 19.8(a) compares lower-energy fixed-target and HERA data on strangeness production, showing that the HERA spectra have substantially increased multiplicities, albeit with insufficient statistical precision to study scaling violations. The fixed-target data show that the  $\Lambda$  rate substantially exceeds the  $\bar{\Lambda}$  rate in the remnant region, owing to the conserved baryon number from the baryon target. Fig. 19.8(b) shows neutral and charged pion fragmentation functions  $1/N \cdot dn/dz$ , where  $z$  is defined as the ratio of the pion energy to that of the exchanged boson, both measured in the laboratory frame. Results are shown from HERMES and the EMC experiments, where HERMES data have been evolved with NLO QCD to  $\langle Q^2 \rangle = 25$  GeV<sup>2</sup> in order to be consistent with the EMC. Each of the experiments uses various kinematic cuts to ensure that the measured particles lie in

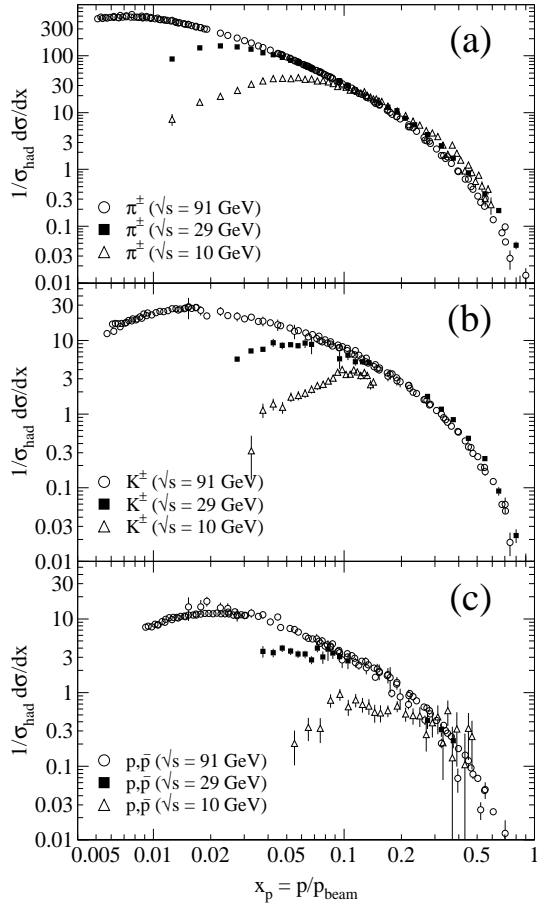


**Figure 19.7:** Scaled momentum spectra of (a)  $\pi^\pm$ , (b)  $K^\pm$ , and (c)  $p/\bar{p}$  at  $\sqrt{s} = 10, 29, \text{ and } 91 \text{ GeV}$  [38,42,82,102].

the region which is expected to be associated with the struck quark. In the DIS kinematic regime accessed at these experiments, and over the range in  $z$  shown in Fig. 19.8, the  $z$  and  $x_F$  variables have similar values [49]. The precision data on identified particles can be used in the study of the quark flavor content of the proton [121].

Data on identified particle production can aid the investigation of the universality of jet fragmentation in  $e^+e^-$  and DIS. The strangeness suppression factor  $\gamma_s$ , as derived principally from tuning the Lund string model [88] within JETSET [89], is typically found to be around 0.3 in  $e^+e^-$  experiments [72], although values closer to 0.2 [122] have also been obtained. A number of measurements of so-called  $V^0$ -particles ( $K^0$ ,  $\Lambda^0$ ) and the relative rates of  $V^0$ 's and inclusively produced charged particles have been performed at HERA [111,113,117] and fixed target experiments [105]. These typically favour a stronger suppression ( $\gamma_s \approx 0.2$ ) than usually obtained from  $e^+e^-$  data although values close to 0.3 have also been obtained [123,124].

However, when comparing the description of QCD-based models for lepton-hadron interactions and  $e^+e^-$  collisions, it is important to note that the overall description by event generators of inclusively produced hadronic final states is more accurate in  $e^+e^-$  collisions than lepton-hadron interactions [125]. Predictions of particle rates in lepton-hadron scattering are affected by uncertainties in the modelling of the parton composition of the proton and photon, the extended target remnant, and initial and final state QCD radiation. Furthermore, the tuning of event generators for  $e^+e^-$  collisions is typically based on a larger set of parameters and uses more observables [72] than are used when optimizing models for lepton-hadron data [126].

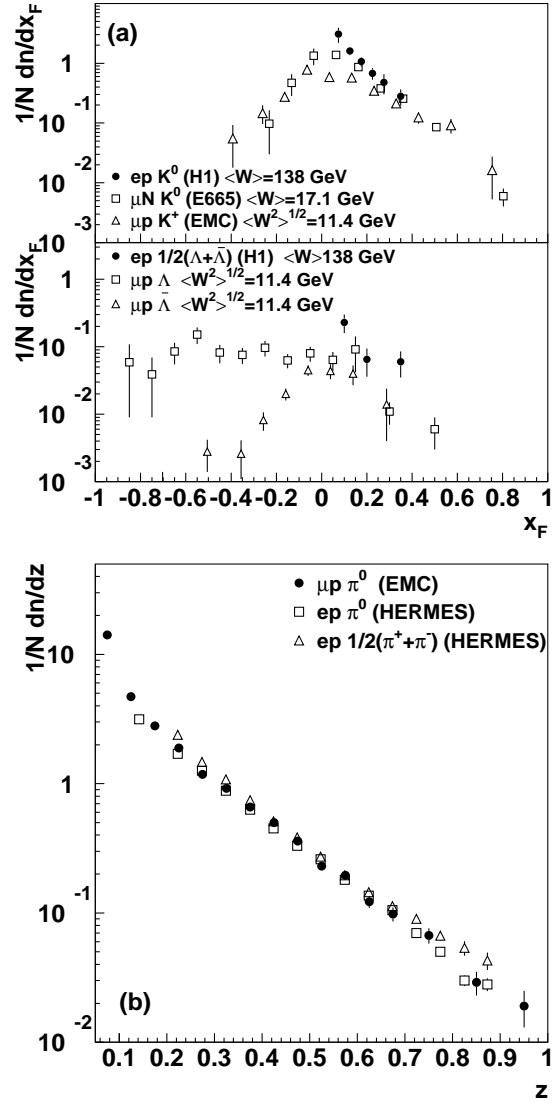


**Figure 19.8:** (a)  $1/N \cdot dn/dx_F$  for identified strange particles in DIS at various values of  $W$  [105,108,111]. (b)  $1/N \cdot dn/dz$  for measurements of pions from fixed-target DIS experiment [106,109,110].

## 19.7. Fragmentation in hadron-hadron collisions

An extensive set on high-transverse momentum ( $p_T$ ) single-inclusive hadron data has been collected in  $h_1 h_2 \rightarrow hX$  scattering processes, both at high energy colliders and fixed-target experiments [127–145]. Only the transverse momentum  $p_T$  is considered in hadron-hadron collisions because of lack of knowledge of the longitudinal momentum of the hard subprocess. Fig. 19.9 shows a compilation of neutral pion and charged hadron production data for energies in the range  $\sqrt{s} \approx 23 - 800 \text{ GeV}$ .

The differential cross-section for high-transverse momentum distributions has been computed to next-to-leading order accuracy in perturbative QCD [146]. NLO calculations yield a good description of the collider data, but significantly under-predict the cross-section for several fixed-target energy data sets [147,148]. Data collected at high energy colliders are either included in global fit analyses or used as a test for the universality of fragmentation functions.

Different strategies have been developed to ameliorate the theoretical description at fixed-target energies. A possible phenomenological approach involves the introduction of a non-perturbative intrinsic partonic transverse momentum [145,149,150]. From the perturbative side, the resummation of the dominant higher order corrections at

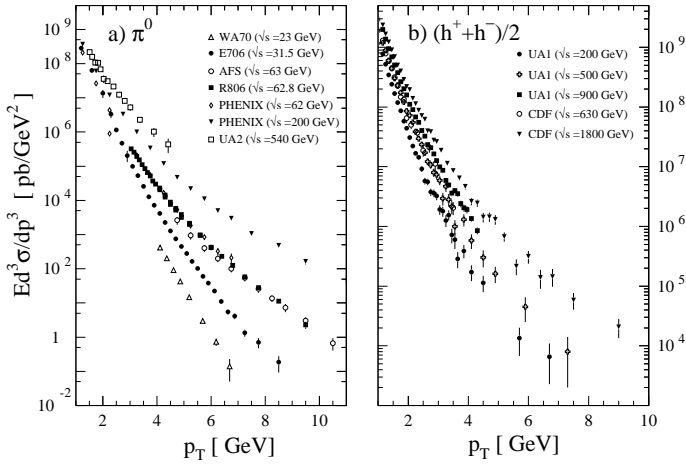


**Figure 19.9:** Selection of inclusive (a)  $\pi^0$  and (b) charged-hadron production data from  $pp$  [135,142–145] and  $p\bar{p}$  [127,130,133] collisions.

threshold produces an enhancement of the theoretical calculation that significantly improves the description of the data [151,152].

Measurements of hadron production in longitudinally polarized  $pp$  collisions are used mainly in the determination of the polarized gluon distribution in the proton [153,154].

Hadron production provides a critical observable for probing the high energy-density matter produced in heavy-ion collisions. Measurements at colliders show a suppression of inclusive hadron yields at high transverse momentum for  $AA$  collisions compared to  $pp$  scattering, indicating the formation of a dense medium opaque to quark and gluons, see e.g. [155].

## 19.8. Spin-dependent fragmentation

Measurements of charged-hadron production in unpolarized lepton-hadron scattering provide a unique tool to perform a flavor-separation determination of polarized parton densities from DIS interactions with longitudinally polarized targets [156–160].

Polarized scattering presents the possibility to measure the spin transfer from the struck quark to the final hadron, and thus develop spin-dependent fragmentation functions [161,162]. Early measurements of the longitudinal spin transfer to Lambda hyperons have been presented in [163,164]. This process is also useful in the study of the quark transversity distribution [165], which describes the probability of finding a transversely polarized quark with its spin aligned or anti-aligned with the spin of a transversely polarized nucleon. The transversity function is chiral-odd, and therefore not accessible through measurements of inclusive lepton-hadron scattering. Semi-inclusive DIS, in which another chiral-odd observable may be involved, provides a valuable tool to probe transversity. The Collins fragmentation function [166] relates the transverse polarization of the quark to that of the final hadron. It is chiral-odd and naive T-odd, leading to a characteristic single spin asymmetry in the azimuthal angular distribution of the produced hadron in the hadron scattering plane. Azimuthal angular distributions in semi-inclusive DIS can also be produced by other processes requiring non-polarized fragmentation functions, like the Sivers mechanism [167].

A number of experiments have measured these asymmetries [168–178]. Collins and Sivers asymmetries have been shown experimentally to be non zero by the HERMES measurements on transversely polarized proton targets [169–171]. Independent information on the Collins function has been provided by the BELLE Collaboration [172–173]. Measurements performed by the COMPASS collaboration on deuteron targets show results compatible with zero for both asymmetries [174–176].

## 19.9. Heavy quark fragmentation

It was recognized very early [179] that a heavy flavored meson should retain a large fraction of the momentum of the primordial heavy quark, and therefore its fragmentation function should be much harder than that of a light hadron. In the limit of a very heavy quark, one expects the fragmentation function for a heavy quark to go into any heavy hadron to be peaked near  $x = 1$ .

When the heavy quark is produced at a momentum much larger than its mass, one expects important perturbative effects, enhanced by powers of the logarithm of the transverse momentum over the heavy quark mass, to intervene and modify the shape of the fragmentation function. In leading logarithmic order (*i.e.*, including all powers of  $\alpha_s \log m_Q/p_T$ ), the total (*i.e.*, summed over all hadron types) perturbative fragmentation function is simply obtained by solving the leading evolution equation for fragmentation functions, Eq. (19.4), with the initial condition at a scale  $\mu^2 = m_Q^2$  given by  $D_Q(z, m_Q^2) = \delta(1-z)$  and  $D_i(z, m_Q^2) = 0$  for  $i \neq Q$  (here  $D_i(z)$ , stands for the probability to produce a heavy quark  $Q$  from parton  $i$  with a fraction  $z$  of the parton momentum).

Several extensions of the leading logarithmic result have appeared in the literature. Next-to-leading-log (NLL) order results for the perturbative heavy quark fragmentation function have been obtained in [180]. The resummation of the dominant logarithmic contributions at large  $z$  was performed in [43] to next-to-leading-log accuracy. Fixed-order calculations of the fragmentation function at order  $\alpha_s^2$  in  $e^+e^-$  annihilation have appeared in [181] while the initial condition for the perturbative heavy quark fragmentation function has been extended to NNLO in [182].

Inclusion of non-perturbative effects in the calculation of the heavy-quark fragmentation function is done by convoluting the perturbative result with a phenomenological non-perturbative form [183–188], see also section 17.8 of [189]. The parameters entering the non-perturbative forms are fitted together with some model of hard radiation, which can be either a shower Monte Carlo, a leading-log or NLL calculation (which may or may not include Sudakov resummation), or a fixed order calculation [181,190].

A more conventional approach [191] involves the introduction of a unique set of heavy quark fragmentation functions of non-perturbative nature that obey the usual massless evolution equations in Eq. (19.4). Finite mass terms of the form  $(m_Q/p_T)^n$  are kept in the corresponding short distance coefficient function for each scattering process. Within this approach, the initial condition for the perturbative fragmentation function provides the term needed to define the correct subtraction scheme to match the massless limit for the coefficient function (see e.g. [192]). Such implementation is in line with the variable flavor number scheme introduced for parton distributions functions, as described in Section 18 of this *Review*.

High statistics data for charmed mesons production near the  $\Upsilon$  resonance (excluding decay products of  $B$  mesons) have been published [193,194]. They include results for  $D$  and  $D^*$ ,  $D_s$  (see also [195,196]) and  $\Lambda_c$ . Shown in Fig. 19.10(a) are the CLEO and BELLE inclusive cross-sections times branching ratio  $\mathcal{B}$ ,  $s \cdot \mathcal{B} d\sigma/dx_p$ , for the production of  $D^0$  and  $D^{*+}$ . The variable  $x_p$  approximates the light-cone momentum fraction  $z$ , but is not identical to it. The two measurements are consistent with each other.

The branching ratio  $\mathcal{B}$  represents  $D^0 \rightarrow K^-\pi^+$  for the  $D^0$  results and for the  $D^{*+}$  the product branching fraction:  $D^{*+} \rightarrow D^0\pi^+$ ,  $D^0 \rightarrow K^-\pi^+$ . Given the high precision of CLEO’s and BELLE’s data, a superposition of different parametric forms for the non-perturbative contribution is needed to obtain a good fit [22]. Older studies are reported in Refs. [197–199]. Charmed meson spectra on the  $Z$  peak have been published by OPAL and ALEPH [200,201].

Charm quark production has also been extensively studied at HERA by the H1 and ZEUS collaborations. Measurements have been made of  $D^{*\pm}$ ,  $D^\pm$ , and  $D_s^\pm$  mesons; see, for example, Refs. [202,203]. The production of the  $\Lambda_c$  baryon has also been studied [204].

Experimental studies of the fragmentation function for  $b$  quarks, shown in Fig. 19.10(b), have been performed at LEP and SLD [205–207]. Commonly used methods identify the  $B$  meson

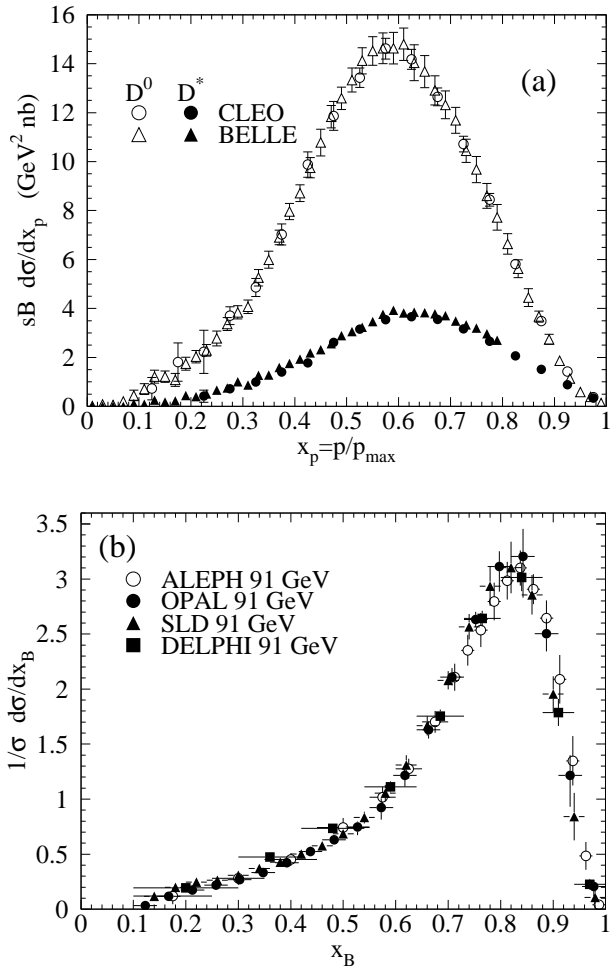


**Figure 19.10:** (a) Efficiency-corrected inclusive cross-section measurements for the production of  $D^0$  and  $D^{*+}$  in  $e^+e^-$  measurements at  $\sqrt{s} \approx 10.6$  GeV, excluding  $B$  decay products [193,194]. (b) Measured  $e^+e^-$  fragmentation function of  $b$  quarks into  $B$  hadrons at  $\sqrt{s} \approx 91$  GeV [206].

through its semileptonic decay or based upon tracks emerging from the  $B$  secondary vertex. The studies in [206] fit the  $B$  spectrum using a Monte Carlo shower model supplemented with non-perturbative fragmentation functions yielding consistent results.

The experiments measure primarily the spectrum of  $B$  mesons. This defines a fragmentation function which includes the effect of the decay of higher mass excitations, like the  $B^*$  and  $B^{**}$ . In the literature, there is sometimes ambiguity in what is defined to be the bottom fragmentation function. Instead of using what is directly measured (*i.e.*, the  $B$  meson spectrum) corrections are applied to account for  $B^*$  or  $B^{**}$  production in some cases. For a more detailed discussion see section 17.8 of [189].

Heavy-flavor production in  $e^+e^-$  collisions is the primary source of information for the role of fragmentation effects in heavy-flavor production in hadron-hadron and lepton-hadron collisions. The QCD calculations tend to underestimate the data in certain regions of phase space. The discrepancy observed between theoretical calculations and the measured  $B$  meson spectrum at the hadron colliders [208] is substantially reduced when a more refined use of information on heavy flavor production from  $e^+e^-$  data is made [209] and when up-to-date parton distributions and strong coupling constant values are considered [210].

Both bottomed- and charmed-mesons spectra have been measured at the Tevatron with unprecedented accuracy [211]. The measured spectra are in good agreement with QCD calculations (including non-perturbative fragmentation effects inferred from  $e^+e^-$  data [212]),

no longer supporting the previously reported discrepancies [208].

The HERA collaborations have produced a number of measurements of beauty production; see, for example, Refs. [202,213–215]. As for the Tevatron data, the HERA results are described well by QCD-based calculations using fragmentation models optimised with  $e^+e^-$  data.

Besides degrading the fragmentation function by gluon radiation, QCD evolution can also generate soft heavy quarks, increasing in the small  $x$  region as  $\sqrt{s}$  increases. Several theoretical studies are available on the issue of how often  $b\bar{b}$  or  $c\bar{c}$  pairs are produced indirectly, via a gluon splitting mechanism [216–218]. Experimental results from studies on charm and bottom production via gluon splitting, given in [201,219–223], yield weighted averages of  $\pi_{g \rightarrow c\bar{c}} = 3.05 \pm 0.45\%$  and  $\pi_{g \rightarrow b\bar{b}} = 0.277 \pm 0.072\%$ , respectively.

#### References:

1. G. Altarelli, Phys. Reports **81**, 1 (1982).
2. R.K. Ellis *et al.*, *QCD and Collider Physics*, Cambridge University Press (1996).
3. S. Albino *et al.*, arXiv:0804.2021 [hep-ph].
4. F. Arleo, Eur. Phys. J. **C61**, 603 (2009).
5. P. Nason and B.R. Webber, Nucl. Phys. **B421**, 473 (1994); Erratum *ibid.* **B480**, 755 (1996).
6. D. Barate *et al.*, [ALEPH Collab.], Phys. Lett. **B357**, 487 (1995); Erratum *ibid.*, **B364**, 247 (1995).
7. R. Akers *et al.*, [OPAL Collab.], Z. Phys. **C68**, 203 (1995).
8. P. Abreu *et al.*, [DELPHI Collab.], Eur. Phys. J. **C6**, 19 (1999).
9. W. Kittel and E.A. De Wolf, *Soft Multihadron Dynamics*, World Scientific (2005).
10. H.F. Jones, Nuovo Cimento **40A**, 1018 (1965); K.H. Streng *et al.*, Z. Phys. **C2**, 237 (1979).
11. V.N. Gribov and L.N. Lipatov, Sov. J. Nucl. Phys. **15**, 438 (1972); V.N. Gribov and L.N. Lipatov, Sov. J. Nucl. Phys. **15**, 675 (1972); G. Altarelli and G. Parisi, Nucl. Phys. **B126**, 298 (1977); Yu.L. Dokshitzer, Sov. Phys. JETP Lett. **46**, 641 (1977).
12. H. Georgi and H.D. Politzer, Nucl. Phys. **B136**, 445 (1978); J.F. Owens, Phys. Lett. **B76**, 85 (1978); T. Uematsu, Phys. Lett. **B79**, 97 (1978).
13. G. Curci *et al.*, Nucl. Phys. **B175**, 27 (1980).
14. W. Furmanski and R. Petronzio, Phys. Lett. **97B**, 437 (1980).
15. E.G. Floratos *et al.*, Nucl. Phys. **B192**, 417 (1981); T. Munehisa *et al.*, Prog. Theor. Phys. **67**, 609 (1982).
16. J. Kalinowski *et al.*, Nucl. Phys. **B181**, 221 (1981); J. Kalinowski *et al.*, Nucl. Phys. **B181**, 253 (1981).
17. M. Stratmann and W. Vogelsang, Nucl. Phys. **B496**, 41 (1997).
18. Yu.L. Dokshitzer *et al.*, Phys. Lett. **B634**, 504 (2006).
19. A. Mitov *et al.*, Phys. Lett. **B638**, 61 (2006).
20. S. Moch and A. Vogt, Phys. Lett. **B659**, 290 (2008).
21. A.A. Almasy, A. Vogt, and S. Moch, arXiv:1107.2263 [hep-ph].
22. M. Cacciari *et al.*, JHEP **0604**, 006 (2006).
23. G. Altarelli *et al.*, Nucl. Phys. **B160**, 301 (1979); R. Baier and K. Fey, Z. Phys. **C2**, 339 (1979).
24. P.J. Rijken and W.L. van Neerven, Phys. Lett. **B386**, 422 (1996); P.J. Rijken and W.L. van Neerven, Phys. Lett. **B392**, 207 (1997); P.J. Rijken and W.L. van Neerven, Nucl. Phys. **B487**, 233 (1997).
25. A. Mitov and S. Moch, Nucl. Phys. **B751**, 18 (2006).
26. D. Buskulic *et al.*, [ALEPH Collab.], Z. Phys. **C73**, 409 (1997).
27. E. Barate *et al.*, [ALEPH Collab.], Phys. Reports **294**, 1 (1998).
28. B. Adeva *et al.*, [L3 Collab.], Phys. Lett. **B259**, 199 (1991).
29. Y.K. Li *et al.*, [AMY Collab.], Phys. Rev. **D41**, 2675 (1990).
30. D. Bender *et al.*, [HRS Collab.], Phys. Rev. **D31**, 1 (1984).
31. G.S. Abrams *et al.*, Mark II Collab., Phys. Rev. Lett. **64**, 1334 (1990).
32. A. Petersen *et al.*, [Mark II Collab.], Phys. Rev. **D37**, 1 (1988).

33. R. Akers *et al.*, [OPAL Collab.], *Z. Phys.* **C72**, 191 (1996).
34. K. Ackerstaff *et al.*, [OPAL Collab.], *Z. Phys.* **C75**, 193 (1997).
35. K. Ackerstaff *et al.*, [OPAL Collab.], *Eur. Phys. J.* **C7**, 369 (1998).
36. G. Abbiendi *et al.*, [OPAL Collab.], *Eur. Phys. J.* **C16**, 185 (2000);  
G. Abbiendi *et al.*, [OPAL Collab.], *Eur. Phys. J.* **C27**, 467 (2003).
37. G. Abbiendi *et al.*, [OPAL Collab.], *Eur. Phys. J.* **C37**, 25 (2004).
38. K. Abe *et al.*, [SLD Collab.], *Phys. Rev.* **D69**, 072003 (2004).
39. P. Abreu *et al.*, [DELPHI Collab.], *Phys. Lett.* **B398**, 194 (1997).
40. R. Brandelik *et al.*, [TASSO Collab.], *Phys. Lett.* **B114**, 65 (1982).
41. W. Braunschweig *et al.*, [TASSO Collab.], *Z. Phys.* **C47**, 187 (1990).
42. H. Aihara *et al.*, [TPC Collab.], *Phys. Rev. Lett.* **61**, 1263 (1988).
43. M. Cacciari and S. Catani, *Nucl. Phys.* **B617**, 253 (2001).
44. J. Blümlein and V. Ravindran, *Phys. Lett.* **B640**, 40 (2006).
45. S. Moch and A. Vogt, *Phys. Lett.* **B680**, 239 (2009).
46. S. Moch and A. Vogt, *JHEP* **0911**, 099 (2009).
47. A. Vogt, *Phys. Lett.* **B691**, 77 (2010).
48. P. Aurenche *et al.*, *Eur. Phys. J.* **C34**, 277 (2004);  
A. Daleo *et al.*, *Phys. Rev.* **D71**, 034013 (2005);  
B.A. Kniehl *et al.*, *Nucl. Phys.* **B711**, 345 (2005);  
Erratum *ibid.* **B720**, 231 (2005).
49. M.R. Adams *et al.*, [E665 Collab.], *Phys. Lett.* **B272**, 163 (1991).
50. M. Arneodo *et al.*, [EMC Collab.], *Z. Phys.* **C35**, 417 (1987).
51. I. Abt *et al.*, [H1 Collab.], *Z. Phys.* **C63**, 377 (1994).
52. M. Derrick *et al.*, [ZEUS Collab.], *Z. Phys.* **C70**, 1 (1996).
53. J. Breitweg *et al.*, [ZEUS Collab.], *Phys. Lett.* **B414**, 428 (1997).
54. S. Aid *et al.*, [H1 Collab.], *Nucl. Phys.* **B445**, 3 (1995).
55. M. Derrick *et al.*, [ZEUS Collab.], *Z. Phys.* **C67**, 93 (1995).
56. C. Adloff *et al.*, [H1 Collab.], *Nucl. Phys.* **B504**, 3 (1997).
57. J. Breitweg *et al.*, [ZEUS Collab.], *Eur. Phys. J.* **C11**, 251 (1999).
58. F.D. Aaron *et al.*, [H1 Collab.], *Phys. Lett.* **B654**, 148 (2007).
59. P. Abreu *et al.*, [DELPHI Collab.], *Phys. Lett.* **B311**, 408 (1993).
60. J.F. Patrick *et al.*, [MARK II Collab.], *Phys. Rev. Lett.* **49**, 1232, (1982).
61. S. Chekanov *et al.*, [ZEUS Collab.], *JHEP* **0608**, 061 (2008).
62. A.H. Mueller, *Phys. Lett.* **B104**, 161 (1981).
63. A. Bassetto *et al.*, *Nucl. Phys.* **B207**, 189 (1982).
64. Yu.L. Dokshitzer *et al.*, *Z. Phys.* **C15**, 324 (1982).
65. A.H. Mueller, *Nucl. Phys.* **B213**, 85 (1983);  
Erratum in *ibid.* **B241**, 141 (196).
66. Yu.L. Dokshitzer *et al.*, *Int. J. Mod. Phys.* **A7**, 1875 (1992).
67. Yu.L. Dokshitzer *et al.*, *Basics of Perturbative QCD*, Editions Frontières (1991).
68. V.A. Khoze and W. Ochs, *Int. J. Mod. Phys.* **A12**, 2949 (1997).
69. C.P. Fong and B.R. Webber, *Nucl. Phys.* **B355**, 54 (1992).
70. S. Albino *et al.*, *Nucl. Phys.* **B851**, 86 (2011).
71. A. Vogt, [arXiv:1108.2993 \[hep-ph\]](https://arxiv.org/abs/1108.2993).
72. DELPHI Collab.: P. Abreu *et al.*, *Z. Phys.* **C73**, 11 (1996).
73. DELPHI Collab.: P. Abreu *et al.*, *Z. Phys.* **C73**, 229 (1997).
74. L3 Collab.: P. Achard *et al.*, *Phys. Reports* **399**, 71 (2004).
75. TOPAZ Collab.: R. Itoh *et al.*, *Phys. Lett.* **B345**, 335 (1995).
76. TASSO Collab.: W. Braunschweig *et al.*, *Z. Phys.* **C22**, 307 (1990).
77. OPAL Collab.: M.Z. Akrawy *et al.*, *Phys. Lett.* **B247**, 617 (1990).
78. BES Collab.: J.Z. Bai *et al.*, *Phys. Rev.* **D69**, 072002 (2004).
79. ALEPH Collab.: D. Buskulic *et al.*, *Z. Phys.* **C55**, 209 (1992).
80. ALEPH Collab.: A. Heister *et al.*, *Eur. Phys. J.* **C35**, 457 (2004).
81. DELPHI Collab.: P. Abreu *et al.*, *Phys. Lett.* **B275**, 231 (1992).
82. DELPHI Collab.: P. Abreu *et al.*, *Eur. Phys. J.* **C5**, 585 (1998).
83. DELPHI Collab.: P. Abreu *et al.*, *Phys. Lett.* **B459**, 397 (1999).
84. L3 Collab.: M. Acciarri *et al.*, *Phys. Lett.* **B444**, 569 (1998).
85. TPC/TWO-GAMMA Collab.: H. Aihara *et al.*, LBL 23737.
86. S. Höche *et al.*, [arXiv:hep-ph/0602031](https://arxiv.org/abs/hep-ph/0602031);  
J. Alwall *et al.*, *Eur. Phys. J.* **C53**, 473 (2008);  
S. Mrenna and P. Richardson, *JHEP* **0405**, 040 (2004).
87. X. Artru and G. Mennessier, *Nucl. Phys.* **B70**, 93 (1974).
88. B. Andersson *et al.*, *Phys. Reports* **97**, 31 (1983).
89. T. Sjöstrand and M. Bengtsson, *Comp. Phys. Comm.* **43**, 367 (1987);  
T. Sjöstrand, *Comp. Phys. Comm.* **82**, 74 (1994).
90. T. Sjöstrand, S. Mrenna, P. Skands, *JHEP* **0605**, 026 (2006);  
T. Sjöstrand, S. Mrenna, P. Skands, *Comp. Phys. Comm.* **178**, 852 (2008).
91. S. Chun and C. Buchanan, *Phys. Reports* **292**, 239 (1998).
92. G. Marchesini *et al.*, *Comp. Phys. Comm.* **67**, 465 (1992);  
G. Corcella *et al.*, *JHEP* **0101**, 010 (2001);  
M. Bähr *et al.*, *Eur. Phys. J.* **C58**, 639 (2008).
93. T. Gleisberg *et al.*, *JHEP* **0902**, 007 (2009).
94. D. de Florian *et al.*, *Phys. Rev.* **D76**, 074033 (2007);  
D. de Florian *et al.*, *Phys. Rev.* **D75**, 114010 (2007).
95. S. Albino *et al.*, *Nucl. Phys.* **B803**, 42 (2008).
96. S. Kretzer *et al.*, *Eur. Phys. J.* **C22**, 269 (2001).
97. S. Kretzer, *Phys. Rev.* **D62**, 054001 (2000).
98. L. Bourhis *et al.*, *Eur. Phys. J.* **C19**, 89 (2001).
99. M. Hirai *et al.*, *Phys. Rev.* **D75**, 094009 (2007).
100. C. Aidala *et al.*, *Phys. Rev.* **D83**, 034002 (2011).
101. ALEPH Collab.: R. Barate *et al.*, *Eur. Phys. J.* **C17**, 1 (2000);  
OPAL Collab.: R. Akers *et al.*, *Z. Phys.* **C68**, 179 (1995);  
OPAL Collab.: G. Abbiendi *et al.*, *Eur. Phys. J.* **C11**, 217 (1999).
102. ALEPH Collab.: D. Buskulic *et al.*, *Z. Phys.* **C66**, 355 (1995);  
ARGUS Collab.: H. Albrecht *et al.*, *Z. Phys.* **C44**, 547 (1989);  
OPAL Collab.: R. Akers *et al.*, *Z. Phys.* **C63**, 181 (1994);  
SLD Collab.: K. Abe *et al.*, *Phys. Rev.* **D59**, 052001 (1999).
103. DELPHI Collab.: P. Abreu *et al.*, *Eur. Phys. J.* **C13**, 573 (2000).
104. B.A. Kniehl *et al.*, *Phys. Rev. Lett.* **85**, 5288 (2000).
105. E665 Collab.: M.R. Adams *et al.*, *Z. Phys.* **C61**, 539 (1994).
106. EMC Collab.: J.J. Aubert *et al.*, *Z. Phys.* **C18**, 189 (1983);  
EMC Collab.: M. Arneodo *et al.*, *Phys. Lett.* **B150**, 458 (1985).
107. EMC Collab.: M. Arneodo *et al.*, *Z. Phys.* **C33**, 167 (1986).
108. EMC Collab.: M. Arneodo *et al.*, *Z. Phys.* **C34**, 283 (1987).
109. HERMES Collab.: A. Airapetian *et al.*, *Eur. Phys. J.* **C21**, 599 (2001).
110. T.P. McPharlin *et al.*, *Phys. Lett.* **B90**, 479 (1980).
111. H1 Collab.: S. Aid *et al.*, *Nucl. Phys.* **B480**, 3 (1996).
112. H1 Collab.: C. Adloff *et al.*, *Eur. Phys. J.* **C18**, 293 (2000);  
H1 Collab.: A. Aktas *et al.*, *Eur. Phys. J.* **C36**, 413 (2004).
113. ZEUS Collab.: M. Derrick *et al.*, *Z. Phys.* **C68**, 29 (1995);  
ZEUS Collab.: J. Breitweg *et al.*, *Eur. Phys. J.* **C2**, 77 (1998).
114. ZEUS Collab.: S. Chekanov *et al.*, *Phys. Lett.* **B553**, 141 (2003).
115. ZEUS Collab.: S. Chekanov *et al.*, *Nucl. Phys.* **B786**, 181 (2007).
116. H1 Collab.: F. D. Aaron *et al.*, *Eur. Phys. J.* **C61**, 185 (2009).
117. H1 Collab.: F. D. Aaron *et al.*, *Phys. Lett.* **B673**, 119 (2009).
118. P. Dixon *et al.*, *J. Phys.* **G25**, 1453 (1999).
119. H1 Collab.: C. Adloff *et al.*, *Phys. Lett.* **B462**, 440 (1999).
120. D. Graudenz, *Fortsch. Phys.* **45**, 629 (1997).
121. S. Albino *et al.*, *Phys. Rev.* **D75**, 034018 (2007).
122. OPAL Collab.: P.D. Acton *et al.*, *Phys. Lett.* **B305**, 407 (1993).
123. E632 Collab.: D. DeProspero *et al.*, *Phys. Rev.* **D50**, 6691 (1994).
124. ZEUS Collab.: S. Chekanov *et al.*, *Eur. Phys. J.* **C51**, 1 (2007).
125. G. Grindhammer *et al.*, in: *Proceedings of the Workshop on Monte Carlo Generators for HERA Physics*, Hamburg, Germany, 1998/1999.
126. N. Brook *et al.*, in: *Proceedings of the Workshop for Future HERA Physics at HERA*, Hamburg, Germany, 1996.
127. CDF Collab.: F. Abe *et al.*, *Phys. Rev. Lett.* **61**, 1819 (1988).

128. CDF Collab.: D. E. Acosta *et al.*, Phys. Rev. **D72**, 052001 (2005).
129. UA1 Collab.: G. Arnison *et al.*, Phys. Lett. **B118**, 167 (1982).
130. UA1 Collab.: C. Albajar *et al.*, Nucl. Phys. **B335**, 261 (1990).
131. UA1 Collab.: G. Bocquet *et al.*, Phys. Lett. **B366**, 434 (1996).
132. UA2 Collab.:M. Banner *et al.*, Phys. Lett. **B122**, 322 (1983).
133. UA2 Collab.:M. Banner *et al.*, Phys. Lett. **B115**, 59 (1982).
134. UA2 Collab.:M. Banner *et al.*, Z. Phys. **C27**, 329 (1985).
135. PHENIX Collab.: S. S. Adler *et al.*, Phys. Rev. Lett. **91**, 241803 (2003).
136. BRAHMS Collab.: I. Arsene *et al.*, Phys. Rev. Lett. **98**, 252001 (2007).
137. STAR Collab.: J. Adams *et al.*, Phys. Lett. **B637**, 161 (2006).
138. STAR Collab.: J. Adams *et al.*, Phys. Rev. Lett. **97**, 152302 (2006).
139. STAR Collab.: B. I. Abelev *et al.*, Phys. Rev. **C75**, 064901 (2007).
140. E706 Collab.: L. Apanasevich *et al.*, Phys. Rev. Lett. **81**, 2642 (1998).
141. UA6 Collab.: G. Balocchi *et al.*, Phys. Lett. **B436**, 222 (1998).
142. WA70 Collab.: M. Bonesini *et al.*, Z. Phys. **C38**, 371 (1988).
143. AFS Collab.: E. Anassontzis *et al.*, Sov. J. Nucl. Phys. **51**, 836 (1990).
144. R806 Collab.: C. Kourkoumelis *et al.*, Z. Phys. **C5**, 95 (1980).
145. E706 Collab.: L. Apanasevich *et al.*, Phys. Rev. **D68**, 052001 (2003).
146. F. Aversa *et al.*, Nucl. Phys. **B327**, 105 (1989);  
D. de Florian, Phys. Rev. **D67**, 054004 (2003);  
B. Jager *et al.*, Phys. Rev. **D67**, 054005 (2003).
147. U. Baur *et al.*, [arXiv:hep-ph/0005226](https://arxiv.org/abs/hep-ph/0005226).
148. P. Aurenche *et al.*, Eur. Phys. J. **C13**, 347 (2000).
149. L. Apanasevich *et al.*, Phys. Rev. **D59**, 074007 (1999).
150. U. D'Alesio and F. Murgia, Phys. Rev. **D70**, 074009 (2004).
151. D. de Florian and W. Vogelsang, Phys. Rev. **D71**, 114004 (2005).
152. L. G. Almeida *et al.*, Phys. Rev. **D80**, 074016 (2009).
153. PHENIX Collab.: A. Adare *et al.*, Phys. Rev. **D76**, 051106 (2007).
154. PHENIX Collab.: A. Adare *et al.*, Phys. Rev. **D79**, 012003 (2009).
155. PHENIX Collab.: K. Adcox *et al.*, Phys. Rev. Lett. **88**, 022301 (2002);  
STAR Collab.: C. Adler *et al.*, Phys. Rev. Lett. **90**, 082302 (2003).
156. COMPASS Collab.: M. Alekseev *et al.*, Phys. Lett. **B660**, 458, (2008).
157. HERMES Collab.: A. Airapetian *et al.*, Phys. Rev. **D71**, 012003 (2005).
158. SMC Collab.: B. Adeva *et al.*, Phys. Lett. **B420**, 180 (1998).
159. HERMES Collab.: A. Airapetian *et al.*, Phys. Lett. **B666**, 446 (2008).
160. D. de Florian *et al.*, Phys. Rev. Lett. **101**, 072001 (2008).
161. P.J. Mulders and R.D. Tangerman, Nucl. Phys. **B461**, 197 (1996);  
Erratum *ibid.*, **B484**, 538 (1997).
162. R. Jacob, Nucl. Phys. **A711**, 35 (2002).
163. COMPASS Collab.: M. Alekseev *et al.*, Eur. Phys. J. **C64**, 171 (2009).
164. HERMES Collab.: A. Airapetian *et al.*, Phys. Rev. **D74**, 072004 (2006).
165. J.P. Ralston and D.E. Soper, Nucl. Phys. **B152**, 109 (1979).
166. J. Collins, Nucl. Phys. **B396**, 161 (1993).
167. D. Sivers, Phys. Rev. **D43**, 261 (1991).
168. CLAS Collab.: H. Avakian *et al.*, Phys. Rev. **D69**, 112004 (2004).
169. HERMES Collab.: A. Airapetian *et al.*, Phys. Rev. Lett. **84**, 4047 (2000).
170. HERMES Collab.: A. Airapetian *et al.*, Phys. Rev. **D64**, 097101 (2001).
171. HERMES Collab.: A. Airapetian *et al.*, Phys. Rev. Lett. **94**, 012002 (2005).
172. BELLE Collab.: K. Abe *et al.*, Phys. Rev. Lett. **96**, 232002 (2006).
173. BELLE Collab.: K. Abe *et al.*, Phys. Rev. **D78**, 032011 (2008).
174. COMPASS Collab.: V.Y. Alexakhin *et al.*, Phys. Rev. Lett. **94**, 202002 (2005).
175. COMPASS Collab.: V.Y. Alexakhin *et al.*, Nucl. Phys. **B765**, 31 (2007).
176. COMPASS Collab.: M. Alekseev *et al.*, Phys. Lett. **B673**, 127 (2009).
177. COMPASS Collab.: M. Alekseev *et al.*, Phys. Lett. **B692**, 240 (2010).
178. COMPASS Collab.: M. Alekseev *et al.*, Eur. Phys. J. **C70**, 39 (2010).
179. V.A. Khoze *et al.*, *Proceedings, Conference on High-Energy Physics, Tbilisi 1976*;  
J.D. Bjorken, Phys. Rev. **D17**, 171 (1978).
180. B. Mele and P. Nason, Phys. Lett. **B245**, 635 (1990);  
B. Mele and P. Nason, Nucl. Phys. **B361**, 626 (1991).
181. P. Nason and C. Oleari, Phys. Lett. **B418**, 199 (1998);  
P. Nason and C. Oleari, Phys. Lett. **B447**, 327 (1999);  
P. Nason and C. Oleari, Nucl. Phys. **B565**, 245 (2000).
182. K. Melnikov and A. Mitov, Phys. Rev. **D70**, 034027 (2004).
183. C. Peterson *et al.*, Phys. Rev. **D27**, 105 (1983).
184. V.G. Kartvelishvili *et al.*, Phys. Lett. **B78**, 615 (1978).
185. P. Collins and T. Spiller, J. Phys. **G11**, 1289 (1985).
186. G. Colangelo and P. Nason, Phys. Lett. **B285**, 167 (1992).
187. M.G. Bowler, Z. Phys. **C11**, 169 (1981).
188. E. Braaten *et al.*, Phys. Rev. **D51**, 4819 (1995).
189. Particle Data Group: C. Amsler *et al.*, Phys. Lett. **B667**, 1 (2008).
190. J. Chrin, Z. Phys. **C36**, 163 (1987).
191. J. Collins, Phys. Rev. **D58**, 094002 (1998).
192. B.A. Kniehl *et al.*, Eur. Phys. J. **C41**, 199 (2005).
193. CLEO Collab.: M. Artuso *et al.*, Phys. Rev. **D70**, 112001 (2004).
194. BELLE Collab.: R. Seuster *et al.*, Phys. Rev. **D73**, 032002 (2006).
195. CLEO Collab.: R.A. Briere *et al.*, Phys. Rev. **D62**, 112003 (2000).
196. BABAR Collab.: B. Aubert *et al.*, Phys. Rev. **D65**, 091104 (2002).
197. CLEO Collab.: D. Bortoletto *et al.*, Phys. Rev. **D37**, 1719 (1988).
198. ARGUS Collab.: H. Albrecht *et al.*, Z. Phys. **C52**, 353 (1991).
199. ARGUS Collab.: H. Albrecht *et al.*, Z. Phys. **C54**, 1 (1992).
200. OPAL Collab.: G. Alexander *et al.*, Z. Phys. **C69**, 543 (1996).
201. ALEPH Collab.: R. Barate *et al.*, Phys. Lett. **B561**, 213 (2003).
202. H1 Collab.: F.D. Aaron *et al.*, Eur. Phys. J. **C65**, 89 (2010).
203. ZEUS Collab.: S. Chekanov *et al.*, JHEP **0707**, 074 (2007);  
ZEUS Collab.: S. Chekanov *et al.*, JHEP **0904**, 82 (2009);  
ZEUS Collab.: S. Chekanov *et al.*, Eur. Phys. J. **C63**, 171 (2009);  
H1 Collab.: A. Aktas *et al.*, Eur. Phys. J. **C51**, 271 (2007);  
H1 Collab.: F. D. Aaron *et al.*, Eur. Phys. J. **C59**, 589 (2009).
204. ZEUS Collab.: S. Chekanov *et al.*, Eur. Phys. J. **C44**, 351 (2005).
205. ALEPH Collab.: D. Buskulic *et al.*, Phys. Lett. **B357**, 699 (1995).
206. ALEPH Collab.: A. Heister *et al.*, Phys. Lett. **B512**, 30 (2001);  
DELPHI Collab.: J. Abdallah *et al.*, Eur. Phys. J. **C71**, 1557 (2011);  
OPAL Collab.: G. Abbiendi *et al.*, Eur. Phys. J. **C29**, 463 (2003);  
SLD Collab.: K. Abe *et al.*, Phys. Rev. **D65**, 092006 (2002);  
Erratum *ibid.*, **D66**, 079905 (2002).
207. L3 Collab.: B. Adeva *et al.*, Phys. Lett. **B261**, 177 (1991).
208. CDF Collab.: F. Abe *et al.*, Phys. Rev. Lett. **71**, 500 (1993);  
CDF Collab.: F. Abe *et al.*, Phys. Rev. Lett. **71**, 2396 (1993);  
CDF Collab.: F. Abe *et al.*, Phys. Rev. **D50**, 4252 (1994);  
CDF Collab.: F. Abe *et al.*, Phys. Rev. Lett. **75**, 1451 (1995);  
CDF Collab.: D. Acosta *et al.*, Phys. Rev. **D66**, 032002 (2002);

- CDF Collab.: D. Acosta *et al.*, Phys. Rev. **D65**, 052005 (2002);  
D0 Collab.: S. Abachi *et al.*, Phys. Rev. Lett. **74**, 3548 (1995);  
UA1 Collab.: C. Albajar *et al.*, Phys. Lett. **B186**, 237 (1987);  
UA1 Collab.: C. Albajar *et al.*, Phys. Lett. **B256**, 121 (1991);  
Erratum *ibid.*, **B272**, 497 (1991).
209. M. Cacciari and P. Nason, Phys. Rev. Lett. **89**, 122003 (2002).  
210. B.A. Kniehl *et al.*, Phys. Rev. **D77**, 014011 (2008).  
211. CDF Collab.: D. Acosta *et al.*, Phys. Rev. Lett. **91**, 241804 (2003);  
CDF Collab.: D. Acosta *et al.*, Phys. Rev. **D71**, 032001 (2005).  
212. M. Cacciari and P. Nason, JHEP **0309**, 006 (2003);  
M. Cacciari *et al.*, JHEP **0407**, 033 (2004);  
B.A. Kniehl *et al.*, Phys. Rev. Lett. **96**, 012001 (2006).
213. ZEUS Collab.: S. Chekanov *et al.*, Phys. Rev. **D78**, 072001 (2008).  
214. ZEUS Collab.: S. Chekanov *et al.*, JHEP **0902**, 032 (2009).  
215. H1 Collab.: A. Aktas *et al.*, Eur. Phys. J. **C47**, 597 (2006).  
216. A.H. Mueller and P. Nason, Nucl. Phys. **B266**, 265 (1986);  
M.L. Mangano and P. Nason, Phys. Lett. **B285**, 160 (1992).  
217. M.H. Seymour, Nucl. Phys. **B436**, 163 (1995).  
218. D.J. Miller and M.H. Seymour, Phys. Lett. **B435**, 213 (1998).  
219. ALEPH Collab.: R. Barate *et al.*, Phys. Lett. **B434**, 437 (1998).  
220. DELPHI Collab.: P. Abreu *et al.*, Phys. Lett. **B405**, 202 (1997).  
221. L3 Collab.: M. Acciarri *et al.*, Phys. Lett. **B476**, 243 (2000).  
222. OPAL Collab.: G. Abbiendi *et al.*, Eur. Phys. J. **C13**, 1 (2000).  
223. SLD Collab.: K. Abe *et al.*, SLAC-PUB-8157, hep-ex/9908028.



## 20. EXPERIMENTAL TESTS OF GRAVITATIONAL THEORY

Revised October 2011 by T. Damour (IHES, Bures-sur-Yvette, France).

Einstein's General Relativity, the current "standard" theory of gravitation, describes gravity as a universal deformation of the Minkowski metric:

$$g_{\mu\nu}(x^\lambda) = \eta_{\mu\nu} + h_{\mu\nu}(x^\lambda), \text{ where } \eta_{\mu\nu} = \text{diag}(-1, +1, +1, +1). \quad (20.1)$$

General Relativity is classically defined by two postulates. One postulate states that the Lagrangian density describing the propagation and self-interaction of the gravitational field is

$$\mathcal{L}_{\text{Ein}}[g_{\mu\nu}] = \frac{c^4}{16\pi G_N} \sqrt{g} g^{\mu\nu} R_{\mu\nu}(g), \quad (20.2)$$

$$R_{\mu\nu}(g) = \partial_\alpha \Gamma_{\mu\nu}^\alpha - \partial_\nu \Gamma_{\mu\alpha}^\alpha + \Gamma_{\alpha\beta}^\beta \Gamma_{\mu\nu}^\alpha - \Gamma_{\alpha\nu}^\beta \Gamma_{\mu\beta}^\alpha, \quad (20.3)$$

$$\Gamma_{\mu\nu}^\lambda = \frac{1}{2} g^{\lambda\sigma} (\partial_\mu g_{\nu\sigma} + \partial_\nu g_{\mu\sigma} - \partial_\sigma g_{\mu\nu}), \quad (20.4)$$

where  $G_N$  is Newton's constant,  $g = -\det(g_{\mu\nu})$ , and  $g^{\mu\nu}$  is the matrix inverse of  $g_{\mu\nu}$ . A second postulate states that  $g_{\mu\nu}$  couples universally, and minimally, to all the fields of the Standard Model by replacing everywhere the Minkowski metric  $\eta_{\mu\nu}$ . Schematically (suppressing matrix indices and labels for the various gauge fields and fermions and for the Higgs doublet),

$$\begin{aligned} \mathcal{L}_{\text{SM}}[\psi, A_\mu, H, g_{\mu\nu}] = & -\frac{1}{4} \sum \sqrt{g} g^{\mu\alpha} g^{\nu\beta} F_{\mu\nu}^a F_{\alpha\beta}^a \\ & - \sum \sqrt{g} \bar{\psi} \gamma^\mu D_\mu \psi \\ & - \frac{1}{2} \sqrt{g} g^{\mu\nu} D_\mu \bar{H} D_\nu H - \sqrt{g} V(H) \\ & - \sum \lambda \sqrt{g} \bar{\psi} H \psi, \end{aligned} \quad (20.5)$$

where  $\gamma^\mu \gamma^\nu + \gamma^\nu \gamma^\mu = 2g^{\mu\nu}$ , and where the covariant derivative  $D_\mu$  contains, besides the usual gauge field terms, a spin-dependent gravitational contribution. From the total action follow Einstein's field equations,

$$R_{\mu\nu} - \frac{1}{2} R g_{\mu\nu} = \frac{8\pi G_N}{c^4} T_{\mu\nu}. \quad (20.6)$$

Here  $R = g^{\mu\nu} R_{\mu\nu}$ ,  $T_{\mu\nu} = g_{\mu\alpha} g_{\nu\beta} T^{\alpha\beta}$ , and  $T^{\mu\nu} = (2/\sqrt{g}) \delta \mathcal{L}_{\text{SM}} / \delta g_{\mu\nu}$  is the (symmetric) energy-momentum tensor of the Standard Model matter. The theory is invariant under arbitrary coordinate transformations:  $x'^\mu = f^\mu(x^\nu)$ . To solve the field equations Eq. (20.6), one needs to fix this coordinate gauge freedom. *E.g.*, the "harmonic gauge" (which is the analogue of the Lorenz gauge,  $\partial_\mu A^\mu = 0$ , in electromagnetism) corresponds to imposing the condition  $\partial_\nu (\sqrt{g} g^{\mu\nu}) = 0$ .

In this *Review*, we only consider the classical limit of gravitation (*i.e.* classical matter and classical gravity). Considering quantum matter in a classical gravitational background already poses interesting challenges, notably the possibility that the zero-point fluctuations of the matter fields generate a nonvanishing vacuum energy density  $\rho_{\text{vac}}$ , corresponding to a term  $-\sqrt{g} \rho_{\text{vac}}$  in  $\mathcal{L}_{\text{SM}}$  [1]. This is equivalent to adding a "cosmological constant" term  $+\Lambda g_{\mu\nu}$  on the left-hand side of Einstein's equations Eq. (20.6), with  $\Lambda = 8\pi G_N \rho_{\text{vac}}/c^4$ . Recent cosmological observations (see the following *Reviews*) suggest a positive value of  $\Lambda$  corresponding to  $\rho_{\text{vac}} \approx (2.3 \times 10^{-3} \text{eV})^4$ . Such a small value has a negligible effect on the tests discussed below.

### 20.1. Experimental tests of the coupling between matter and gravity

The universality of the coupling between  $g_{\mu\nu}$  and the Standard Model matter postulated in Eq. (20.5) ("Equivalence Principle") has many observable consequences [2,3]. First, it predicts that the outcome of a local non-gravitational experiment, referred to local standards, does not depend on where, when, and in which locally inertial frame, the experiment is performed. This means, for instance, that local experiments should neither feel the cosmological evolution of the universe (constancy of the "constants"), nor exhibit preferred directions in spacetime (isotropy of space, local Lorentz

invariance). These predictions are consistent with many experiments and observations. Stringent limits on a possible time variation of the basic coupling constants have been obtained by analyzing a natural fission reactor phenomenon which took place at Oklo, Gabon, two billion years ago [4,5]. These limits are at the  $1 \times 10^{-7}$  level for the fractional variation of the fine-structure constant  $\alpha_{\text{em}}$  [5], and at the  $4 \times 10^{-9}$  level for the fractional variation of the ratio between the light quark masses and  $\Lambda_{QCD}$  [6]. The determination of the lifetime of Rhenium 187 from isotopic measurements of some meteorites dating back to the formation of the solar system (about 4.6 Gyr ago) yields comparably strong limits [7]. Measurements of absorption lines in astronomical spectra also give stringent limits on the variability of both  $\alpha_{\text{em}}$  (at the  $10^{-5}$  level [8]), and  $\mu = m_p/m_e$ , *e.g.*

$$|\Delta\mu/\mu| < 1.8 \times 10^{-6} (95\% \text{ C.L.}), \quad (20.7)$$

at a redshift  $z = 0.68466$  [9], and  $\Delta\mu/\mu = (0.3 \pm 3.2_{\text{stat}} \pm 1.9_{\text{sys}}) \times 10^{-6}$  at the large redshift  $z = 2.811$  [10]. Direct laboratory limits on the (present) time variation of  $\alpha_{\text{em}}$  (based on monitoring the frequency ratio of several different atomic clocks) have recently reached the level [11]:

$$\dot{\alpha}_{\text{em}}/\alpha_{\text{em}} = (-1.6 \pm 2.3) \times 10^{-17} \text{yr}^{-1}.$$

There are also experimental limits on a possible dependence of coupling constants on the gravitational potential [12]. See [13] for a review of the issue of "variable constants."

The highest precision tests of the isotropy of space have been performed by looking for possible quadrupolar shifts of nuclear energy levels [14]. The (null) results can be interpreted as testing the fact that the various pieces in the matter Lagrangian Eq. (20.5) are indeed coupled to one and the same external metric  $g_{\mu\nu}$  to the  $10^{-29}$  level. For astrophysical constraints on possible Planck-scale violations of Lorentz invariance, see Ref. 15.

The universal coupling to  $g_{\mu\nu}$  postulated in Eq. (20.5) implies that two (electrically neutral) test bodies dropped at the same location and with the same velocity in an external gravitational field fall in the same way, independently of their masses and compositions. The universality of the acceleration of free fall has been verified at the  $10^{-13}$  level for laboratory bodies, notably Beryllium and Titanium test bodies [16],

$$(\Delta a/a)_{\text{BeTi}} = (0.3 \pm 1.8) \times 10^{-13}, \quad (20.8)$$

as well as for the gravitational accelerations of the Earth and the Moon toward the Sun [17],

$$(\Delta a/a)_{\text{EarthMoon}} = (-1.0 \pm 1.4) \times 10^{-13}. \quad (20.9)$$

The latter result constrains not only how  $g_{\mu\nu}$  couples to matter, but also how it couples to itself [18] ("strong equivalence principle"; see Eq. (20.15) below, and the end of the section on binary pulsar tests). See also Ref. 19 for a review of torsion balance experiments.

Finally, Eq. (20.5) also implies that two identically constructed clocks located at two different positions in a static external Newtonian potential  $U(\mathbf{x}) = \sum G_N m/r$  exhibit, when intercompared by means of electromagnetic signals, the (apparent) difference in clock rate,  $\tau_1/\tau_2 = \nu_2/\nu_1 = 1 + [U(\mathbf{x}_1) - U(\mathbf{x}_2)]/c^2 + O(1/c^4)$ , independently of their nature and constitution. This universal gravitational redshift of clock rates has been verified at the  $10^{-4}$  level by comparing a hydrogen-maser clock flying on a rocket up to an altitude  $\sim 10,000$  km to a similar clock on the ground [20]. The redshift due to a height change of only 33 cm has been recently detected by comparing two optical clocks based on  $^{27}\text{Al}^+$  ions [21].

## 20.2. Tests of the dynamics of the gravitational field in the weak field regime

The effect on matter of one-graviton exchange, *i.e.*, the interaction Lagrangian obtained when solving Einstein's field equations Eq. (20.6) written in, say, the harmonic gauge at first order in  $h_{\mu\nu}$ ,

$$\square h_{\mu\nu} = -\frac{16\pi G_N}{c^4}(T_{\mu\nu} - \frac{1}{2}T\eta_{\mu\nu}) + O(h^2) + O(hT), \quad (20.10)$$

reads  $-(8\pi G_N/c^4)T^{\mu\nu}\square^{-1}(T_{\mu\nu} - \frac{1}{2}T\eta_{\mu\nu})$ . For a system of  $N$  moving

point masses, with free Lagrangian  $L^{(1)} = \sum_{A=1}^N -m_A c^2 \sqrt{1 - v_A^2/c^2}$ , this interaction, expanded to order  $v^2/c^2$ , reads (with  $r_{AB} \equiv |\mathbf{x}_A - \mathbf{x}_B|$ ,  $\mathbf{n}_{AB} \equiv (\mathbf{x}_A - \mathbf{x}_B)/r_{AB}$ )

$$L^{(2)} = \frac{1}{2} \sum_{A \neq B} \frac{G_N m_A m_B}{r_{AB}} \left[ 1 + \frac{3}{2c^2}(v_A^2 + v_B^2) - \frac{7}{2c^2}(\mathbf{v}_A \cdot \mathbf{v}_B) - \frac{1}{2c^2}(\mathbf{n}_{AB} \cdot \mathbf{v}_A)(\mathbf{n}_{AB} \cdot \mathbf{v}_B) + O\left(\frac{1}{c^4}\right) \right]. \quad (20.11)$$

The two-body interactions, Eq. (20.11), exhibit  $v^2/c^2$  corrections to Newton's  $1/r$  potential induced by spin-2 exchange ("gravito-magnetism"). Consistency at the "post-Newtonian" level  $v^2/c^2 \sim G_N m/r c^2$  requires that one also considers the three-body interactions induced by some of the three-graviton vertices and other nonlinearities (terms  $O(h^2)$  and  $O(hT)$  in Eq. (20.10)),

$$L^{(3)} = -\frac{1}{2} \sum_{B \neq A \neq C} \frac{G_N^2 m_A m_B m_C}{r_{AB} r_{AC} c^2} + O\left(\frac{1}{c^4}\right). \quad (20.12)$$

All currently performed gravitational experiments in the solar system, including perihelion advances of planetary orbits, the bending and delay of electromagnetic signals passing near the Sun, and very accurate ranging data to the Moon obtained by laser echoes, are compatible with the post-Newtonian results Eqs. (20.10)–(20.12). The "gravito-magnetic" interactions  $\propto v_A v_B$  contained in Eq. (20.11) are involved in many of these experimental tests. They have been particularly tested in lunar laser ranging data [17], in the LAGEOS satellite observations [22], and in the dedicated Gravity Probe B mission [23].

Similar to what is done in discussions of precision electroweak experiments, it is useful to quantify the significance of precision gravitational experiments by parameterizing plausible deviations from General Relativity. The addition of a mass-term in Einstein's field equations leads to a score of theoretical difficulties which have not yet received any consensual solution. We shall, therefore, not consider here the ill-defined "mass of the graviton" as a possible deviation parameter from General Relativity (see, however, Ref. 24). Deviations from Einstein's pure spin-2 theory are then defined by adding new, bosonic light or massless, macroscopically coupled fields. The possibility of new gravitational-strength couplings leading (on small, and possibly large, scales) to deviations from Einsteinian (and Newtonian) gravity is suggested by String Theory [25], and by Brane World ideas [26]. For reviews of experimental constraints on Yukawa-type additional interactions, see Refs. [19,27]. Recent experiments have set limits on non-Newtonian forces below 0.056 mm [28].

Here, we shall focus on the parametrization of long-range deviations from relativistic gravity obtained by adding a strictly massless (*i.e.* without self-interaction  $V(\varphi) = 0$ ) scalar field  $\varphi$  coupled to the trace of the energy-momentum tensor  $T = g_{\mu\nu} T^{\mu\nu}$  [29]. The most general such theory contains an arbitrary function  $a(\varphi)$  of the scalar field, and can be defined by the Lagrangian

$$\mathcal{L}_{\text{tot}}[g_{\mu\nu}, \varphi, \psi, A_\mu, H] = \frac{c^4}{16\pi G} \sqrt{g}(R(g_{\mu\nu}) - 2g^{\mu\nu} \partial_\mu \varphi \partial_\nu \varphi) + \mathcal{L}_{\text{SM}}[\psi, A_\mu, H, \tilde{g}_{\mu\nu}], \quad (20.13)$$

where  $G$  is a "bare" Newton constant, and where the Standard Model matter is coupled not to the "Einstein" (pure spin-2) metric  $g_{\mu\nu}$ , but to the conformally related ("Jordan-Fierz") metric  $\tilde{g}_{\mu\nu} = \exp(2a(\varphi))g_{\mu\nu}$ . The scalar field equation  $\square_g \varphi = -(4\pi G/c^4)\alpha(\varphi)T$  displays  $\alpha(\varphi) \equiv \partial a(\varphi)/\partial \varphi$  as the basic (field-dependent) coupling between  $\varphi$  and matter [30]. The one-parameter ( $\omega$ ) Jordan-Fierz-Brans-Dicke theory [29] is the special case  $a(\varphi) = \alpha_0 \varphi$  leading to a field-independent coupling  $\alpha(\varphi) = \alpha_0$  (with  $\alpha_0^2 = 1/(2\omega + 3)$ ). The addition of a self-interaction term  $V(\varphi)$  in Eq. (20.13) introduces new phenomenological possibilities; notably the "chameleon mechanism" [31].

In the weak-field slow-motion limit appropriate to describing gravitational experiments in the solar system, the addition of  $\varphi$  modifies Einstein's predictions only through the appearance of two "post-Einstein" dimensionless parameters:  $\bar{\gamma} = -2\alpha_0^2/(1 + \alpha_0^2)$  and  $\bar{\beta} = +\frac{1}{2}\beta_0\alpha_0^2/(1 + \alpha_0^2)^2$ , where  $\alpha_0 \equiv \alpha(\varphi_0)$ ,  $\beta_0 \equiv \partial\alpha(\varphi_0)/\partial\varphi_0$ ,  $\varphi_0$  denoting the vacuum expectation value of  $\varphi$ . These parameters show up also naturally (in the form  $\gamma_{\text{PPN}} = 1 + \bar{\gamma}$ ,  $\beta_{\text{PPN}} = 1 + \bar{\beta}$ ) in phenomenological discussions of possible deviations from General Relativity [2]. The parameter  $\bar{\gamma}$  measures the admixture of spin 0 to Einstein's graviton, and contributes an extra term  $+\bar{\gamma}(\mathbf{v}_A - \mathbf{v}_B)^2/c^2$  in the square brackets of the two-body Lagrangian Eq. (20.11). The parameter  $\bar{\beta}$  modifies the three-body interaction Eq. (20.12) by an overall multiplicative factor  $1 + 2\bar{\beta}$ . Moreover, the combination  $\eta \equiv 4\bar{\beta} - \bar{\gamma}$  parameterizes the lowest order effect of the self-gravity of orbiting masses by modifying the Newtonian interaction energy terms in Eq. (20.11) into  $G_{AB} m_A m_B / r_{AB}$ , with a body-dependent gravitational "constant"  $G_{AB} = G_N [1 + \eta(E_A^{\text{grav}}/m_A c^2 + E_B^{\text{grav}}/m_B c^2) + O(1/c^4)]$ , where  $G_N = G \exp[2a(\varphi_0)](1 + \alpha_0^2)$  and where  $E_A^{\text{grav}}$  denotes the gravitational binding energy of body  $A$ .

The best current limits on the post-Einstein parameters  $\bar{\gamma}$  and  $\bar{\beta}$  are (at the 68% confidence level):

$$\bar{\gamma} = (2.1 \pm 2.3) \times 10^{-5}, \quad (20.14)$$

deduced from the additional Doppler shift experienced by radio-wave beams connecting the Earth to the Cassini spacecraft when they passed near the Sun [32], and

$$4\bar{\beta} - \bar{\gamma} = (4.4 \pm 4.5) \times 10^{-4}, \quad (20.15)$$

from Lunar Laser Ranging measurements [17] of a possible polarization of the Moon toward the Sun [18]. More stringent limits on  $\bar{\gamma}$  are obtained in models (*e.g.*, string-inspired ones [25]) where scalar couplings violate the Equivalence Principle.

## 20.3. Tests of the dynamics of the gravitational field in the radiative and/or strong field regimes

The discovery of pulsars (*i.e.*, rotating neutron stars emitting a beam of radio noise) in gravitationally bound orbits [33,34] has opened up an entirely new testing ground for relativistic gravity, giving us an experimental handle on the regime of radiative and/or strong gravitational fields. In these systems, the finite velocity of propagation of the gravitational interaction between the pulsar and its companion generates damping-like terms at order  $(v/c)^5$  in the equations of motion [35]. These damping forces are the local counterparts of the gravitational radiation emitted at infinity by the system ("gravitational radiation reaction"). They cause the binary orbit to shrink and its orbital period  $P_b$  to decrease. The remarkable stability of pulsar clocks has allowed one to measure the corresponding very small orbital period decay  $\dot{P}_b \equiv dP_b/dt \sim -(v/c)^5 \sim -10^{-12}$  in several binary systems, thereby giving us a direct experimental confirmation of the propagation properties of the gravitational field, and, in particular, an experimental confirmation that the speed of propagation of gravity is equal to the velocity of light to better than a part in a thousand. In addition, the surface gravitational potential of a neutron star  $h_{00}(R) \simeq 2Gm/c^2 R \simeq 0.4$  being a factor  $\sim 10^8$  higher than the surface potential of the Earth, and a mere factor 2.5 below the black hole limit ( $h_{00}(R) = 1$ ), pulsar data have allowed one to obtain several accurate tests of the strong-gravitational-field regime, as we discuss next.

Binary pulsar timing data record the times of arrival of successive electromagnetic pulses emitted by a pulsar orbiting around the center of mass of a binary system. After correcting for the Earth motion around the Sun and for the dispersion due to propagation in the interstellar plasma, the time of arrival of the  $N$ th pulse  $t_N$  can be described by a generic, parameterized “timing formula” [36] whose functional form is common to the whole class of tensor-scalar gravitation theories:

$$t_N - t_0 = F[T_N(\nu_p, \dot{\nu}_p, \ddot{\nu}_p); \{p^K\}; \{p^{PK}\}]. \quad (20.16)$$

Here,  $T_N$  is the pulsar proper time corresponding to the  $N$ th turn given by  $N/2\pi = \nu_p T_N + \frac{1}{2}\dot{\nu}_p T_N^2 + \frac{1}{6}\ddot{\nu}_p T_N^3$  (with  $\nu_p \equiv 1/P_p$  the spin frequency of the pulsar, *etc.*),  $\{p^K\} = \{P_b, T_0, e, \omega_0, x\}$  is the set of “Keplerian” parameters (notably, orbital period  $P_b$ , eccentricity  $e$ , periastron longitude  $\omega_0$  and projected semi-major axis  $x = a \sin i/c$ ), and  $\{p^{PK}\} = \{k, \gamma_{\text{timing}}, \dot{P}_b, r, s, \delta\theta, \dot{e}, \dot{x}\}$  denotes the set of (separately measurable) “post-Keplerian” parameters. Most important among these are: the fractional periastron advance per orbit  $k \equiv \dot{\omega}P_b/2\pi$ , a dimensionful time-dilation parameter  $\gamma_{\text{timing}}$ , the orbital period derivative  $\dot{P}_b$ , and the “range” and “shape” parameters of the gravitational time delay caused by the companion,  $r$  and  $s$ .

Without assuming any specific theory of gravity, one can phenomenologically analyze the data from any binary pulsar by least-squares fitting the observed sequence of pulse arrival times to the timing formula Eq. (20.16). This fit yields the “measured” values of the parameters  $\{\nu_p, \dot{\nu}_p, \ddot{\nu}_p\}$ ,  $\{p^K\}$ ,  $\{p^{PK}\}$ . Now, each specific relativistic theory of gravity predicts that, for instance,  $k$ ,  $\gamma_{\text{timing}}$ ,  $\dot{P}_b$ ,  $r$  and  $s$  (to quote parameters that have been successfully measured from some binary pulsar data) are some theory-dependent functions of the Keplerian parameters and of the (unknown) masses  $m_1, m_2$  of the pulsar and its companion. For instance, in General Relativity, one finds (with  $M \equiv m_1 + m_2$ ,  $n \equiv 2\pi/P_b$ )

$$\begin{aligned} k^{\text{GR}}(m_1, m_2) &= 3(1 - e^2)^{-1} (G_N M n / c^3)^{2/3}, \\ \gamma_{\text{timing}}^{\text{GR}}(m_1, m_2) &= e n^{-1} (G_N M n / c^3)^{2/3} m_2 (m_1 + 2m_2) / M^2, \\ \dot{P}_b^{\text{GR}}(m_1, m_2) &= - (192\pi/5) (1 - e^2)^{-7/2} \left( 1 + \frac{73}{24} e^2 + \frac{37}{96} e^4 \right) \\ &\quad \times (G_N M n / c^3)^{5/3} m_1 m_2 / M^2, \\ r(m_1, m_2) &= G_N m_2 / c^3, \\ s(m_1, m_2) &= n x (G_N M n / c^3)^{-1/3} M / m_2. \end{aligned} \quad (20.17)$$

In tensor-scalar theories, each of the functions  $k^{\text{theory}}(m_1, m_2)$ ,  $\gamma_{\text{timing}}^{\text{theory}}(m_1, m_2)$ ,  $\dot{P}_b^{\text{theory}}(m_1, m_2)$ , *etc.*, is modified by quasi-static strong field effects (associated with the self-gravities of the pulsar and its companion), while the particular function  $\dot{P}_b^{\text{theory}}(m_1, m_2)$  is further modified by radiative effects (associated with the spin 0 propagator) [30,37,38].

Let us give some highlights of the current experimental situation (see Ref. 39 for a more extensive review). In the first discovered binary pulsar PSR1913 + 16 [33,34], it has been possible to measure with accuracy *three* post-Keplerian parameters:  $k$ ,  $\gamma_{\text{timing}}$  and  $\dot{P}_b$ . The three equations  $k^{\text{measured}} = k^{\text{theory}}(m_1, m_2)$ ,  $\gamma_{\text{timing}}^{\text{measured}} = \gamma_{\text{timing}}^{\text{theory}}(m_1, m_2)$ ,  $\dot{P}_b^{\text{measured}} = \dot{P}_b^{\text{theory}}(m_1, m_2)$  determine, for each given theory, three curves in the two-dimensional mass plane. This yields *one* (combined radiative/strong-field) test of the specified theory, according to whether the three curves meet at one point, as they should. After subtracting a small ( $\sim 10^{-14}$  level in  $\dot{P}_b^{\text{obs}} = (-2.423 \pm 0.001) \times 10^{-12}$ ), but significant, Newtonian perturbing effect caused by the Galaxy [40], one finds that General Relativity passes this  $(k - \gamma_{\text{timing}} - \dot{P}_b)_{1913+16}$  test with complete success at the  $10^{-3}$  level [34,41,42]

$$\left[ \frac{\dot{P}_b^{\text{obs}} - \dot{P}_b^{\text{galactic}}}{\dot{P}_b^{\text{GR}}[k^{\text{obs}}, \gamma_{\text{timing}}^{\text{obs}}]} \right]_{1913+16} = 0.997 \pm 0.002. \quad (20.18)$$

Here  $\dot{P}_b^{\text{GR}}[k^{\text{obs}}, \gamma_{\text{timing}}^{\text{obs}}]$  is the result of inserting in  $\dot{P}_b^{\text{GR}}(m_1, m_2)$  the values of the masses predicted by the two equations  $k^{\text{obs}} =$

$k^{\text{GR}}(m_1, m_2)$ ,  $\gamma_{\text{timing}}^{\text{obs}} = \gamma_{\text{timing}}^{\text{GR}}(m_1, m_2)$ . This yields experimental evidence for the reality of gravitational radiation damping forces at the  $(-3 \pm 2) \times 10^{-3}$  level.

The discovery of the binary pulsar PSR1534 + 12 [43] has allowed one to measure *five* post-Keplerian parameters:  $k$ ,  $\gamma_{\text{timing}}$ ,  $r$ ,  $s$ , and (with less accuracy)  $\dot{P}_b$  [44,45]. This allows one to obtain *three* (five observables minus two masses) tests of relativistic gravity. Two among these tests probe strong field gravity, without mixing of radiative effects [44]. General Relativity passes all these tests within the measurement accuracy. The most precise of the new, pure strong-field tests is the one obtained by combining the measurements of  $k$ ,  $\gamma$ , and  $s$ . Using the most recent data [45], one finds agreement at the 1% level:

$$\left[ \frac{s^{\text{obs}}}{s^{\text{GR}}[k^{\text{obs}}, \gamma_{\text{timing}}^{\text{obs}}]} \right]_{1534+12} = 1.000 \pm 0.007. \quad (20.19)$$

The discovery of the binary pulsar PSR J1141 – 6545 [46] (whose companion is probably a white dwarf) has allowed one to measure *four* observable parameters:  $k$ ,  $\gamma_{\text{timing}}$ ,  $\dot{P}_b$  [47,48], and the parameter  $s$  [49,48]. The latter parameter (which is equal to the sine of the inclination angle,  $s = \sin i$ ) was consistently measured in two ways: from a scintillation analysis [49], and from timing measurements [48]. General Relativity passes all the corresponding tests within measurement accuracy. See Fig. 20.1 which uses the (more precise) scintillation measurement of  $s = \sin i$ .

The discovery of the remarkable *double* binary pulsar PSR J0737 – 3039 A and B [50,51] has led to the measurement of *seven* independent parameters [52,53]: five of them are the post-Keplerian parameters  $k$ ,  $\gamma_{\text{timing}}$ ,  $r$ ,  $s$  and  $\dot{P}_b$  entering the relativistic timing formula of the fast-spinning pulsar PSR J0737 – 3039 A, a sixth is the ratio  $R = x_B/x_A$  between the projected semi-major axis of the more slowly spinning companion pulsar PSR J0737 – 3039 B, and that of PSR J0737 – 3039 A. [The theoretical prediction for the ratio  $R = x_B/x_A$ , considered as a function of the (inertial) masses  $m_1 = m_A$  and  $m_2 = m_B$ , is  $R^{\text{theory}} = m_1/m_2 + O((v/c)^4)$  [36], independently of the gravitational theory considered.] Finally, the seventh parameter  $\Omega_{\text{SO,B}}$  is the angular rate of (spin-orbit) precession of PSR J0737 – 3039 B around the total angular momentum [53]. These seven measurements give us *five* tests of relativistic gravity [52,54]. General Relativity passes all those tests with flying colors (see Fig. 20.1). Let us highlight here two of them.

One test is a new, precise confirmation of the reality of gravitational radiation

$$\left[ \frac{\dot{P}_b^{\text{obs}}}{\dot{P}_b^{\text{GR}}[k^{\text{obs}}, R^{\text{obs}}]} \right]_{0737-3039} = 1.003 \pm 0.014. \quad (20.20)$$

Another one is an accurate ( $5 \times 10^{-4}$  level) new strong-field confirmation of General Relativity:

$$\left[ \frac{s^{\text{obs}}}{s^{\text{GR}}[k^{\text{obs}}, R^{\text{obs}}]} \right]_{0737-3039} = 0.99987 \pm 0.00050. \quad (20.21)$$

Fig. 20.1 illustrates all the tests of strong-field and radiative gravity derived from the above-mentioned binary pulsars:  $(3 - 2 =)$  one test from PSR1913 + 16,  $(5 - 2 =)$  3 tests from PSR1534 + 12,  $(4 - 2 =)$  2 tests from PSR J1141 – 6545, and  $(7 - 2 =)$  5 tests from PSR J0737 – 3039.

Data from several nearly circular binary systems (made of a neutron star and a white dwarf) have also led to strong-field confirmations (at the  $4.6 \times 10^{-3}$  level) of the ‘strong equivalence principle,’ *i.e.*, the fact that neutron stars and white dwarfs fall with the same acceleration in the gravitational field of the Galaxy [55,56]. The measurements of  $\dot{P}_b$  in some pulsar-white dwarf systems lead to strong constraints on the variation of Newton’s  $G_N$ , and on the existence of gravitational dipole radiation [57,58]. In addition, arrays of millisecond pulsars are sensitive detectors of (very low frequency) gravitational waves [59].

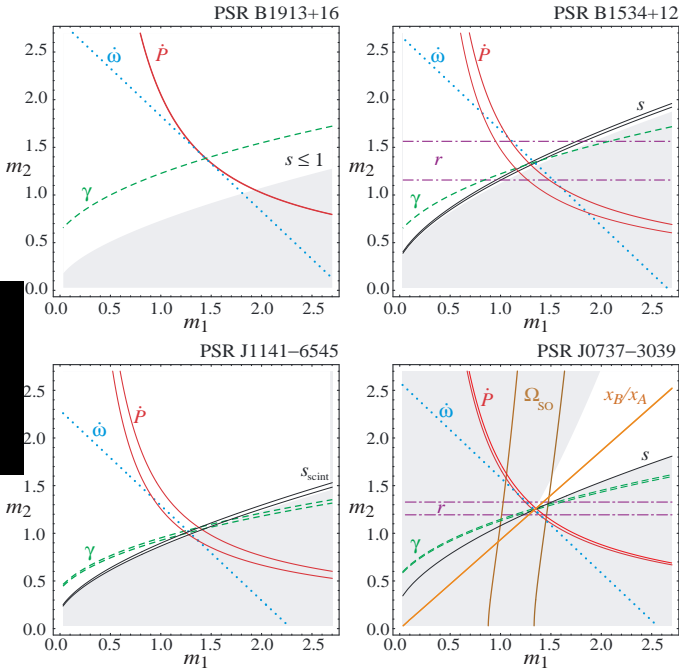


**Figure 20.1:** Illustration of the *eleven* tests of relativistic gravity obtained in the four different binary pulsar systems: PSR1913 + 16 (one test), PSR1534 + 12 (3 tests), PSR J1141 – 6545 (2 tests), and PSR J0737 – 3039 A,B (5 tests). Each curve (or strip) in the mass plane corresponds to the interpretation, within General Relativity, of some observable parameter among:  $\dot{P}_b$ ,  $k \equiv \dot{\omega}P_b/2\pi$ ,  $\gamma_{\text{timing}}$ ,  $r$ ,  $s = \sin i$ ,  $\Omega_{\text{SO,B}}$  and  $R$ . (Figure updated from [61]; courtesy of G. Esposito-Farèse.)

They constrain the contribution  $\Omega_{gw}(f)$  to the critical cosmological density of a stochastic background of gravitational waves to the level  $\Omega_{gw}(1/(\text{Syr})) < 2 \times 10^{-8} h^{-2}$  [60] (here,  $h$  denotes the normalized Hubble expansion rate).

The constraints on tensor-scalar theories provided by the various binary-pulsar “experiments” have been analyzed in [38,61,62] and shown to exclude a large portion of the parameter space allowed by solar-system tests. Finally, measurements over several years of the pulse profiles of various pulsars have detected secular profile changes compatible with the prediction [63] that the general relativistic spin-orbit coupling should cause a secular change in the orientation of the pulsar beam with respect to the line of sight (“geodetic precession”). Such confirmations of general-relativistic spin-orbit effects were obtained in PSR 1913+16 [64], PSR B1534+12 [65], PSR J1141–6545 [66], and PSR J0737 – 3039 [53].

The tests considered above have examined the gravitational interaction on scales between a fraction of a millimeter and a few astronomical units. On the other hand, the general relativistic action on light and matter of an external gravitational field have been verified on much larger scales in many gravitational lensing systems. For quantitative tests on kiloparsec scales see Ref. 67. Some tests on cosmological scales are also available [68].

## 20.4. Conclusions

All present experimental tests are compatible with the predictions of the current “standard” theory of gravitation: Einstein’s General Relativity. The universality of the coupling between matter and gravity (Equivalence Principle) has been verified around the  $10^{-13}$  level. Solar system experiments have tested the weak-field predictions of Einstein’s theory at the  $10^{-4}$  level (and down to the  $2 \times 10^{-5}$  level for the post-Einstein parameter  $\bar{\gamma}$ ). The propagation properties of relativistic gravity, as well as several of its strong-field aspects, have been verified at the  $10^{-3}$  level in binary pulsar experiments. Recent laboratory experiments have also set strong constraints on sub-millimeter modifications of Newtonian gravity.

## References:

1. S. Weinberg, *Rev. Mod. Phys.* **61**, 1 (1989).
2. C.M. Will, *Theory and Experiment in Gravitational Physics* (Cambridge University Press, Cambridge, 1993); and *Living Rev. Rel.* **9**, 3 (2006).
3. T. Damour, in *Gravitation and Quantizations*, eds. B. Julia and J. Zinn-Justin, Les Houches, Session LVII (Elsevier, Amsterdam, 1995), pp. 1–61.
4. A.I. Shlyakhter, *Nature* **264**, 340 (1976).
5. T. Damour and F. Dyson, *Nucl. Phys.* **B480**, 37 (1996); C.R. Gould, E.I. Sharapov, and S.K. Lamoreaux, *Phys. Rev. C* **74**, 024607 (2006); Yu. V. Petrov *et al.*, *Phys. Rev. C* **74**, 064610 (2006).
6. V.V. Flambaum and R.B. Wiringa, *Phys. Rev.* **C79**, 034302 (2009).
7. K.A. Olive *et al.*, *Phys. Rev.* **D66**, 045022 (2002); K.A. Olive *et al.*, *Phys. Rev. D* **69**, 027701 (2004).
8. J.K. Webb *et al.*, *Phys. Rev. Lett.* **87**, 091301 (2001); M.T. Murphy, J.K. Webb, and V.V. Flambaum, *Mon. Not. Roy. Astron. Soc.* **384**, 1053 (2008).
9. M.T. Murphy *et al.*, *Science* **320**, 1611 (2008).
10. J.A. King *et al.*, *Mon. Not. Roy. Astron. Soc.* in press [[arXiv:1106.5786](https://arxiv.org/abs/1106.5786) [[astro-ph.CO](https://arxiv.org/abs/1106.5786)]].
11. T. Rosenband *et al.*, *Science*, **319**, 1808 (2008).
12. T.M. Fortier *et al.*, *Phys. Rev. Lett.* **98**, 070801 (2007); S. Blatt *et al.*, *Phys. Rev. Lett.* **100**, 140801 (2008); T. Dent, *Phys. Rev. Lett.* **101**, 041102 (2008).
13. J.-P. Uzan, *Living Rev. Rel.* **14**, 2 (2011).
14. T.E. Chupp *et al.*, *Phys. Rev. Lett.* **63**, 1541 (1989); M. Smiciklas *et al.*, [[arXiv:1106.0738](https://arxiv.org/abs/1106.0738) [[physics.atom-ph](https://arxiv.org/abs/1106.0738)]].
15. T. Jacobson, S. Liberati, and D. Mattingly, *Annals Phys.* **321**, 150 (2006).
16. S. Schlamminger *et al.*, *Phys. Rev. Lett.* **100**, 041101 (2008).
17. J.G. Williams, S.G. Turyshev, and D.H. Boggs, *Phys. Rev. Lett.* **93**, 261101 (2004); and *Int. J. Mod. Phys. D* **18**, 1129 (2009).
18. K. Nordtvedt, *Phys. Rev.* **170**, 1186 (1968).
19. E.G. Adelberger *et al.*, *Prog. Part. Nucl. Phys.* **62**, 102 (2009).
20. R.F.C. Vessot and M.W. Levine, *Gen. Rel. Grav.* **10**, 181 (1978); R.F.C. Vessot *et al.*, *Phys. Rev. Lett.* **45**, 2081 (1980).
21. C.W. Chou *et al.*, *Science* **329**, 1630 (2010).
22. I. Ciufolini and E. C. Pavlis, *Nature* **431**, 958 (2004).
23. C.W.F. Everitt *et al.*, *Phys. Rev. Lett.* **106**, 221101 (2011).
24. A.S. Goldhaber and M.M. Nieto, *Rev. Mod. Phys.* **82**, 939 (2010).
25. T.R. Taylor and G. Veneziano, *Phys. Lett.* **B213**, 450 (1988); T. Damour and A.M. Polyakov, *Nucl. Phys.* **B423**, 532 (1994); S. Dimopoulos and G. Giudice, *Phys. Lett.* **B379**, 105 (1996); I. Antoniadis, S. Dimopoulos, and G. Dvali, *Nucl. Phys.* **B516**, 70 (1998).
26. V.A. Rubakov, *Phys. Usp* **44**, 871 (2001); R. Maartens and K. Koyama, *Living Rev. Rel.* **13**, 5 (2010).
27. R. D. Newman *et al.*, *Space Sci. Rev.* **148**, 175 (2009).
28. D. J. Kapner *et al.*, *Phys. Rev. Lett.* **98**, 021101 (2007).
29. P. Jordan, *Schwerkraft und Weltall* (Vieweg, Braunschweig, 1955); M. Fierz, *Helv. Phys. Acta* **29**, 128 (1956); C. Brans and R.H. Dicke, *Phys. Rev.* **124**, 925 (1961).
30. T. Damour and G. Esposito-Farèse, *Class. Quantum Grav.* **9**, 2093 (1992).
31. J. Khoury and A. Weltman, *Phys. Rev. Lett.* **93**, 171104 (2004).
32. B. Bertotti, L. Iess, and P. Tortora, *Nature*, **425**, 374 (2003).
33. R.A. Hulse, *Rev. Mod. Phys.* **66**, 699 (1994).
34. J.H. Taylor, *Rev. Mod. Phys.* **66**, 711 (1994).
35. T. Damour and N. Deruelle, *Phys. Lett.* **A87**, 81 (1981); T. Damour, *C.R. Acad. Sci. Paris* **294**, 1335 (1982).
36. T. Damour and N. Deruelle, *Ann. Inst. H. Poincaré A*, **44**, 263 (1986); T. Damour and J.H. Taylor, *Phys. Rev.* **D45**, 1840 (1992).
37. C.M. Will and H.W. Zaglauer, *Astrophys. J.* **346**, 366 (1989).
38. T. Damour and G. Esposito-Farèse, *Phys. Rev.* **D54**, 1474 (1996); and *Phys. Rev.* **D58**, 042001 (1998).

39. I.H. Stairs, *Living Rev. Rel.* **6** 5 (2003).
40. T. Damour and J.H. Taylor, *Astrophys. J.* **366**, 501 (1991).
41. J.M. Weisberg and J.H. Taylor, in *Radio Pulsars, ASP Conference Series* **328**, 25 (2005); [astro-ph/0407149](#).
42. J.M. Weisberg, D.J. Nice, and J.H. Taylor, *Astrophys. J.* **722**, 1030-1034 (2010).
43. A. Wolszczan, *Nature* **350**, 688 (1991).
44. J.H. Taylor *et al.*, *Nature* **355**, 132 (1992).
45. I.H. Stairs *et al.*, *Astrophys. J.* **505**, 352 (1998);  
I.H. Stairs *et al.*, *Astrophys. J.* **581**, 501 (2002).
46. V.M. Kaspi *et al.*, *Astrophys. J.* **528**, 445 (2000).
47. M. Bailes *et al.*, *Astrophys. J.* **595**, L49 (2003).
48. N.D.R. Bhat, M. Bailes and J.P.W. Verbiest, *Phys. Rev.* **D77**, 124017 (2008).
49. S.M. Ord *et al.*, *Astrophys. J.* **574**, L75 (2002).
50. M. Burgay *et al.*, *Nature* **426**, 531 (2003).
51. A.G. Lyne *et al.*, *Science* **303**, 1153 (2004).
52. M. Kramer *et al.*, *Science* **314**, 97 (2006).
53. R.P. Breton *et al.*, *Science* **321**, 104 (2008).
54. M. Kramer and N. Wex, *Class. Quant. Grav.* **26**, 073001 (2009).
55. T. Damour and G. Schäfer, *Phys. Rev. Lett.* **66**, 2549 (1991).
56. M.E. Gonzalez *et al.*, [[arXiv:1109.5638 \[astro-ph.HE\]](#)].
57. J.P.W. Verbiest *et al.*, *Astrophys. J.*, **679**, 675 (2008).
58. K. Lazaridis *et al.*, *Mon. Not. Roy. Astron. Soc.* **400**, 805 (2009).
59. A.N. Lommen and D.C. Backer, *Bulletin of the American Astronomical Society* **33**, 1347 (2001); and *Astrophys. J.* **562**, 297 (2001).
60. F.A. Jenet *et al.*, *Astrophys. J.* **653**, 1571 (2006).
61. G. Esposito-Farèse, in *Proceedings of the 10th Marcel Grossmann Meeting on Recent Developments in Theoretical and Experimental General Relativity*, edited by M. Novello *et al.*, (World Scientific, 2006), part A, pp 647-666.
62. G. Esposito-Farèse, in *Mass and Motion in General Relativity*, eds L. Blanchet *et al.*, series *Fundam. Theor. Phys.* **162** (Springer, Dordrecht, 2011) 461-489.
63. T. Damour and R. Ruffini, *C. R. Acad. Sc. Paris* **279**, série A, 971 (1974);  
B.M. Barker and R.F. O'Connell, *Phys. Rev.* **D12**, 329 (1975).
64. M. Kramer, *Astrophys. J.* **509**, 856 (1998);  
J.M. Weisberg and J.H. Taylor, *Astrophys. J.* **576**, 942 (2002).
65. I.H. Stairs, S.E. Thorsett, and Z. Arzoumanian, *Phys. Rev. Lett.* **93**, 141101 (2004).
66. A.W. Hotan, M. Bailes, and S.M. Ord, *Astrophys. J.* **624**, 906 (2005).
67. A.S. Bolton, S. Rappaport, and S. Burles, *Phys. Rev.* **D74**, 061501 (2006); T.L. Smith, [arXiv:0907.4829 \[astro-ph.CO\]](#);  
J. Schwab, A.S. Bolton and S.A. Rappaport, *Astrophys. J.* **708**, 750-757 (2010).
68. J. -P. Uzan, *Gen. Rel. Grav.* **42**, 2219-2246 (2010).

## 21. BIG-BANG COSMOLOGY

Revised September 2011 by K.A. Olive (University of Minnesota) and J.A. Peacock (University of Edinburgh).

### 21.1. Introduction to Standard Big-Bang Model

The observed expansion of the Universe [1,2,3] is a natural (almost inevitable) result of any homogeneous and isotropic cosmological model based on general relativity. However, by itself, the Hubble expansion does not provide sufficient evidence for what we generally refer to as the Big-Bang model of cosmology. While general relativity is in principle capable of describing the cosmology of any given distribution of matter, it is extremely fortunate that our Universe appears to be homogeneous and isotropic on large scales. Together, homogeneity and isotropy allow us to extend the Copernican Principle to the Cosmological Principle, stating that all spatial positions in the Universe are essentially equivalent.

The formulation of the Big-Bang model began in the 1940s with the work of George Gamow and his collaborators, Alpher and Herman. In order to account for the possibility that the abundances of the elements had a cosmological origin, they proposed that the early Universe which was once very hot and dense (enough so as to allow for the nucleosynthetic processing of hydrogen), and has expanded and cooled to its present state [4,5]. In 1948, Alpher and Herman predicted that a direct consequence of this model is the presence of a relic background radiation with a temperature of order a few K [6,7]. Of course this radiation was observed 16 years later as the microwave background radiation [8]. Indeed, it was the observation of the 3 K background radiation that singled out the Big-Bang model as the prime candidate to describe our Universe. Subsequent work on Big-Bang nucleosynthesis further confirmed the necessity of our hot and dense past. (See the review on BBN—Sec. 22 of this *Review* for a detailed discussion of BBN.) These relativistic cosmological models face severe problems with their initial conditions, to which the best modern solution is inflationary cosmology, discussed in Sec. 21.3.5. If correct, these ideas would strictly render the term ‘Big Bang’ redundant, since it was first coined by Hoyle to represent a criticism of the lack of understanding of the initial conditions.

#### 21.1.1. The Robertson-Walker Universe :

The observed homogeneity and isotropy enable us to describe the overall geometry and evolution of the Universe in terms of two cosmological parameters accounting for the spatial curvature and the overall expansion (or contraction) of the Universe. These two quantities appear in the most general expression for a space-time metric which has a (3D) maximally symmetric subspace of a 4D space-time, known as the Robertson-Walker metric:

$$ds^2 = dt^2 - R^2(t) \left[ \frac{dr^2}{1 - kr^2} + r^2 (d\theta^2 + \sin^2 \theta d\phi^2) \right] \quad (21.1)$$

Note that we adopt  $c = 1$  throughout. By rescaling the radial coordinate, we can choose the curvature constant  $k$  to take only the discrete values  $+1$ ,  $-1$ , or  $0$  corresponding to closed, open, or spatially flat geometries. In this case, it is often more convenient to re-express the metric as

$$ds^2 = dt^2 - R^2(t) \left[ d\chi^2 + S_k^2(\chi) (d\theta^2 + \sin^2 \theta d\phi^2) \right], \quad (21.2)$$

where the function  $S_k(\chi)$  is  $(\sin \chi, \chi, \sinh \chi)$  for  $k = (+1, 0, -1)$ . The coordinate  $r$  (in Eq. (21.1)) and the ‘angle’  $\chi$  (in Eq. (21.2)) are both dimensionless; the dimensions are carried by  $R(t)$ , which is the cosmological scale factor which determines proper distances in terms of the comoving coordinates. A common alternative is to define a dimensionless scale factor,  $a(t) = R(t)/R_0$ , where  $R_0 \equiv R(t_0)$  is  $R$  at the present epoch. It is also sometimes convenient to define a dimensionless or conformal time coordinate,  $\eta$ , by  $d\eta = dt/R(t)$ . Along constant spatial sections, the proper time is defined by the time coordinate,  $t$ . Similarly, for  $dt = d\theta = d\phi = 0$ , the proper distance is given by  $R(t)\chi$ . For standard texts on cosmological models see *e.g.*, Refs. [9–16].

#### 21.1.2. The redshift :

The cosmological redshift is a direct consequence of the Hubble expansion, determined by  $R(t)$ . A local observer detecting light from a distant emitter sees a redshift in frequency. We can define the redshift as

$$z \equiv \frac{\nu_1 - \nu_2}{\nu_2} \simeq \frac{v_{12}}{c}, \quad (21.3)$$

where  $\nu_1$  is the frequency of the emitted light,  $\nu_2$  is the observed frequency and  $v_{12}$  is the relative velocity between the emitter and the observer. While the definition,  $z = (\nu_1 - \nu_2)/\nu_2$  is valid on all distance scales, relating the redshift to the relative velocity in this simple way is only true on small scales (*i.e.*, less than cosmological scales) such that the expansion velocity is non-relativistic. For light signals, we can use the metric given by Eq. (21.1) and  $ds^2 = 0$  to write

$$\frac{v_{12}}{c} = \dot{R} \delta r = \frac{\dot{R}}{R} \delta t = \frac{\delta R}{R} = \frac{R_2 - R_1}{R_1}, \quad (21.4)$$

where  $\delta r(\delta t)$  is the radial coordinate (temporal) separation between the emitter and observer. Thus, we obtain the simple relation between the redshift and the scale factor

$$1 + z = \frac{\nu_1}{\nu_2} = \frac{R_2}{R_1}. \quad (21.5)$$

This result does not depend on the non-relativistic approximation.

#### 21.1.3. The Friedmann-Lemaître equations of motion :

The cosmological equations of motion are derived from Einstein’s equations

$$\mathcal{R}_{\mu\nu} - \frac{1}{2}g_{\mu\nu}\mathcal{R} = 8\pi G_N T_{\mu\nu} + \Lambda g_{\mu\nu}. \quad (21.6)$$

Gliner [17] and Zeldovich [18] have pioneered the modern view, in which the  $\Lambda$  term is taken to the rhs and interpreted as an effective energy–momentum tensor  $T_{\mu\nu}$  for the vacuum of  $\Lambda g_{\mu\nu}/8\pi G_N$ . It is common to assume that the matter content of the Universe is a perfect fluid, for which

$$T_{\mu\nu} = -pg_{\mu\nu} + (p + \rho)u_\mu u_\nu, \quad (21.7)$$

where  $g_{\mu\nu}$  is the space-time metric described by Eq. (21.1),  $p$  is the isotropic pressure,  $\rho$  is the energy density and  $u = (1, 0, 0, 0)$  is the velocity vector for the isotropic fluid in co-moving coordinates. With the perfect fluid source, Einstein’s equations lead to the Friedmann-Lemaître equations

$$H^2 \equiv \left( \frac{\dot{R}}{R} \right)^2 = \frac{8\pi G_N \rho}{3} - \frac{k}{R^2} + \frac{\Lambda}{3}, \quad (21.8)$$

and

$$\frac{\ddot{R}}{R} = \frac{\Lambda}{3} - \frac{4\pi G_N}{3}(\rho + 3p), \quad (21.9)$$

where  $H(t)$  is the Hubble parameter and  $\Lambda$  is the cosmological constant. The first of these is sometimes called the Friedmann equation. Energy conservation via  $T^{\mu\nu}_{;\mu} = 0$ , leads to a third useful equation [which can also be derived from Eq. (21.8) and Eq. (21.9)]

$$\dot{\rho} = -3H(\rho + p). \quad (21.10)$$

Eq. (21.10) can also be simply derived as a consequence of the first law of thermodynamics.

Eq. (21.8) has a simple classical mechanical analog if we neglect (for the moment) the cosmological term  $\Lambda$ . By interpreting  $-k/R^2$  Newtonianly as a ‘total energy’, then we see that the evolution of the Universe is governed by a competition between the potential energy,  $8\pi G_N \rho/3$ , and the kinetic term  $(\dot{R}/R)^2$ . For  $\Lambda = 0$ , it is clear that the Universe must be expanding or contracting (except at the turning point prior to collapse in a closed Universe). The ultimate fate of the Universe is determined by the curvature constant  $k$ . For  $k = +1$ , the Universe will recollapse in a finite time, whereas for  $k = 0, -1$ , the Universe will expand indefinitely. These simple conclusions can be altered when  $\Lambda \neq 0$  or more generally with some component with  $(\rho + 3p) < 0$ .

#### 21.1.4. Definition of cosmological parameters :

In addition to the Hubble parameter, it is useful to define several other measurable cosmological parameters. The Friedmann equation can be used to define a critical density such that  $k = 0$  when  $\Lambda = 0$ ,

$$\begin{aligned} \rho_c &\equiv \frac{3H^2}{8\pi G_N} = 1.88 \times 10^{-26} h^2 \text{ kg m}^{-3} \\ &= 1.05 \times 10^{-5} h^2 \text{ GeV cm}^{-3}, \end{aligned} \quad (21.11)$$

where the scaled Hubble parameter,  $h$ , is defined by

$$\begin{aligned} H &\equiv 100 h \text{ km s}^{-1} \text{ Mpc}^{-1} \\ \Rightarrow H^{-1} &= 9.78 h^{-1} \text{ Gyr} \\ &= 2998 h^{-1} \text{ Mpc}. \end{aligned} \quad (21.12)$$

The cosmological density parameter  $\Omega_{\text{tot}}$  is defined as the energy density relative to the critical density,

$$\Omega_{\text{tot}} = \rho/\rho_c. \quad (21.13)$$

Note that one can now rewrite the Friedmann equation as

$$k/R^2 = H^2(\Omega_{\text{tot}} - 1). \quad (21.14)$$

From Eq. (21.14), one can see that when  $\Omega_{\text{tot}} > 1$ ,  $k = +1$  and the Universe is closed, when  $\Omega_{\text{tot}} < 1$ ,  $k = -1$  and the Universe is open, and when  $\Omega_{\text{tot}} = 1$ ,  $k = 0$ , and the Universe is spatially flat.

It is often necessary to distinguish different contributions to the density. It is therefore convenient to define present-day density parameters for pressureless matter ( $\Omega_m$ ) and relativistic particles ( $\Omega_r$ ), plus the quantity  $\Omega_\Lambda = \Lambda/3H^2$ . In more general models, we may wish to drop the assumption that the vacuum energy density is constant, and we therefore denote the present-day density parameter of the vacuum by  $\Omega_v$ . The Friedmann equation then becomes

$$k/R_0^2 = H_0^2(\Omega_m + \Omega_r + \Omega_v - 1), \quad (21.15)$$

where the subscript 0 indicates present-day values. Thus, it is the sum of the densities in matter, relativistic particles, and vacuum that determines the overall sign of the curvature. Note that the quantity  $-k/R_0^2 H_0^2$  is sometimes referred to as  $\Omega_k$ . This usage is unfortunate: it encourages one to think of curvature as a contribution to the energy density of the Universe, which is not correct.

#### 21.1.5. Standard Model solutions :

Much of the history of the Universe in the standard Big-Bang model can be easily described by assuming that either matter or radiation dominates the total energy density. During inflation and again today the expansion rate for the Universe is accelerating, and domination by a cosmological constant or some other form of dark energy should be considered. In the following, we shall delineate the solutions to the Friedmann equation when a single component dominates the energy density. Each component is distinguished by an equation of state parameter  $w = p/\rho$ .

##### 21.1.5.1. Solutions for a general equation of state:

Let us first assume a general equation of state parameter for a single component,  $w$  which is constant. In this case, Eq. (21.10) can be written as  $\dot{\rho} = -3(1+w)\rho\dot{R}/R$  and is easily integrated to yield

$$\rho \propto R^{-3(1+w)}. \quad (21.16)$$

Note that at early times when  $R$  is small, the less singular curvature term  $k/R^2$  in the Friedmann equation can be neglected so long as  $w > -1/3$ . Curvature domination occurs at rather late times (if a cosmological constant term does not dominate sooner). For  $w \neq -1$ , one can insert this result into the Friedmann equation Eq. (21.8), and if one neglects the curvature and cosmological constant terms, it is easy to integrate the equation to obtain,

$$R(t) \propto t^{2/[3(1+w)]}. \quad (21.17)$$

##### 21.1.5.2. A Radiation-dominated Universe:

In the early hot and dense Universe, it is appropriate to assume an equation of state corresponding to a gas of radiation (or relativistic particles) for which  $w = 1/3$ . In this case, Eq. (21.16) becomes  $\rho \propto R^{-4}$ . The ‘extra’ factor of  $1/R$  is due to the cosmological redshift; not only is the number density of particles in the radiation background decreasing as  $R^{-3}$  since volume scales as  $R^3$ , but in addition, each particle’s energy is decreasing as  $E \propto \nu \propto R^{-1}$ . Similarly, one can substitute  $w = 1/3$  into Eq. (21.17) to obtain

$$R(t) \propto t^{1/2}; \quad H = 1/2t. \quad (21.18)$$

##### 21.1.5.3. A Matter-dominated Universe:

At relatively late times, non-relativistic matter eventually dominates the energy density over radiation (see Sec. 21.3.8). A pressureless gas ( $w = 0$ ) leads to the expected dependence  $\rho \propto R^{-3}$  from Eq. (21.16) and, if  $k = 0$ , we get

$$R(t) \propto t^{2/3}; \quad H = 2/3t. \quad (21.19)$$

##### 21.1.5.4. A Universe dominated by vacuum energy:

If there is a dominant source of vacuum energy,  $V_0$ , it would act as a cosmological constant with  $\Lambda = 8\pi G_N V_0$  and equation of state  $w = -1$ . In this case, the solution to the Friedmann equation is particularly simple and leads to an exponential expansion of the Universe

$$R(t) \propto e^{\sqrt{\Lambda/3}t}. \quad (21.20)$$

A key parameter is the equation of state of the vacuum,  $w \equiv p/\rho$ : this need not be the  $w = -1$  of  $\Lambda$ , and may not even be constant [19,20,21]. There is now much interest in the more general possibility of a dynamically evolving vacuum energy, for which the name ‘dark energy’ has become commonly used. A variety of techniques exist whereby the vacuum density as a function of time may be measured, usually expressed as the value of  $w$  as a function of epoch [22,23]. The best current measurement for the equation of state (assumed constant, but without assuming zero curvature) is  $w = -1.00 \pm 0.06$  [24]. Unless stated otherwise, we will assume that the vacuum energy is a cosmological constant with  $w = -1$  exactly.

The presence of vacuum energy can dramatically alter the fate of the Universe. For example, if  $\Lambda < 0$ , the Universe will eventually recollapse independent of the sign of  $k$ . For large values of  $\Lambda > 0$  (larger than the Einstein static value needed to halt any cosmological expansion or contraction), even a closed Universe will expand forever. One way to quantify this is the deceleration parameter,  $q_0$ , defined as

$$q_0 = -\left. \frac{R\ddot{R}}{\dot{R}^2} \right|_0 = \frac{1}{2}\Omega_m + \Omega_r + \frac{(1+3w)}{2}\Omega_v. \quad (21.21)$$

This equation shows us that  $w < -1/3$  for the vacuum may lead to an accelerating expansion. To the continuing astonishment of cosmologists, such an effect has been observed; one piece of direct evidence is the Supernova Hubble diagram [26–32] (see Fig. 21.1 below); current data indicate that vacuum energy is indeed the largest contributor to the cosmological density budget, with  $\Omega_v = 0.73 \pm 0.03$  and  $\Omega_m = 0.27 \pm 0.03$  if  $k = 0$  is assumed (7-year mean WMAP) [24].

The existence of this constituent is without doubt the greatest puzzle raised by the current cosmological model; the final section of this review discusses some of the ways in which the vacuum-energy problem is being addressed.

## 21.2. Introduction to Observational Cosmology

### 21.2.1. Fluxes, luminosities, and distances :

The key quantities for observational cosmology can be deduced quite directly from the metric.

(1) The *proper* transverse size of an object seen by us to subtend an angle  $d\psi$  is its comoving size  $d\psi S_k(\chi)$  times the scale factor at the time of emission:

$$d\ell = d\psi R_0 S_k(\chi)/(1+z) . \quad (21.22)$$

(2) The apparent flux density of an object is deduced by allowing its photons to flow through a sphere of current radius  $R_0 S_k(\chi)$ ; but photon energies and arrival rates are redshifted, and the bandwidth  $d\nu$  is reduced. The observed photons at frequency  $\nu_0$  were emitted at frequency  $\nu_0(1+z)$ , so the flux density is the luminosity at this frequency, divided by the total area, divided by  $1+z$ :

$$S_\nu(\nu_0) = \frac{L_\nu([1+z]\nu_0)}{4\pi R_0^2 S_k^2(\chi)(1+z)} . \quad (21.23)$$

These relations lead to the following common definitions:

$$\begin{aligned} \text{angular-diameter distance: } D_A &= (1+z)^{-1} R_0 S_k(\chi) \\ \text{luminosity distance: } D_L &= (1+z) R_0 S_k(\chi) . \end{aligned} \quad (21.24)$$

These distance-redshift relations are expressed in terms of observables by using the equation of a null radial geodesic ( $R(t)d\chi = dt$ ) plus the Friedmann equation:

$$\begin{aligned} R_0 d\chi &= \frac{1}{H(z)} dz = \frac{1}{H_0} \left[ (1 - \Omega_m - \Omega_v - \Omega_r)(1+z)^2 \right. \\ &\quad \left. + \Omega_v(1+z)^{3+3w} + \Omega_m(1+z)^3 + \Omega_r(1+z)^4 \right]^{-1/2} dz . \end{aligned} \quad (21.25)$$

The main scale for the distance here is the Hubble length,  $1/H_0$ .

The flux density is the product of the specific intensity  $I_\nu$  and the solid angle  $d\Omega$  subtended by the source:  $S_\nu = I_\nu d\Omega$ . Combining the angular size and flux-density relations thus gives the relativistic version of surface-brightness conservation:

$$I_\nu(\nu_0) = \frac{B_\nu([1+z]\nu_0)}{(1+z)^3} , \quad (21.26)$$

where  $B_\nu$  is surface brightness (luminosity emitted into unit solid angle per unit area of source). We can integrate over  $\nu_0$  to obtain the corresponding total or bolometric formula:

$$I_{\text{tot}} = \frac{B_{\text{tot}}}{(1+z)^4} . \quad (21.27)$$

This cosmology-independent form expresses Liouville's Theorem: photon phase-space density is conserved along rays.

### 21.2.2. Distance data and geometrical tests of cosmology :

In order to confront these theoretical predictions with data, we have to bridge the divide between two extremes. Nearby objects may have their distances measured quite easily, but their radial velocities are dominated by deviations from the ideal Hubble flow, which typically have a magnitude of several hundred  $\text{km s}^{-1}$ . On the other hand, objects at redshifts  $z \gtrsim 0.01$  will have observed recessional velocities that differ from their ideal values by  $\lesssim 10\%$ , but absolute distances are much harder to supply in this case. The traditional solution to this problem is the construction of the distance ladder: an interlocking set of methods for obtaining relative distances between various classes of object, which begins with absolute distances at the 10 to 100 pc level, and terminates with galaxies at significant redshifts. This is reviewed in the review on Cosmological Parameters—Sec. 23 of this *Review*.

By far the most exciting development in this area has been the use of type Ia Supernovae (SNe), which now allow measurement of relative distances with 5% precision. In combination with Cepheid data from the HST and a direct geometrical distance to the maser

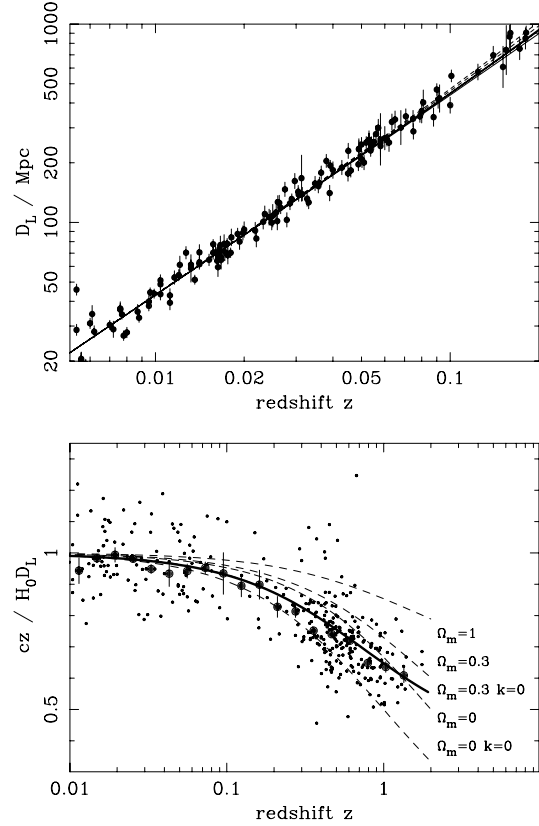


**Figure 21.1:** The type Ia supernova Hubble diagram [26–30]. The first panel shows that for  $z \ll 1$  the large-scale Hubble flow is indeed linear and uniform; the second panel shows an expanded scale, with the linear trend divided out, and with the redshift range extended to show how the Hubble law becomes nonlinear. ( $\Omega_r = 0$  is assumed.) Larger points with errors show median values in redshift bins. Comparison with the prediction of Friedmann-Lemaître models appears to favor a vacuum-dominated Universe.

galaxy NGC4258, SNe results extend the distance ladder to the point where deviations from uniform expansion are negligible, leading to the best existing direct value for  $H_0$ :  $73.8 \pm 2.4 \text{ km s}^{-1} \text{ Mpc}^{-1}$  [25]. Better still, the analysis of high- $z$  SNe has allowed the first meaningful test of cosmological geometry to be carried out: as shown in Fig. 21.1 and Fig. 21.2, a combination of supernova data and measurements of microwave-background anisotropies strongly favors a  $k = 0$  model dominated by vacuum energy. (See the review on Cosmological Parameters—Sec. 23 of this *Review* for a more comprehensive review of Hubble parameter determinations.)

### 21.2.3. Age of the Universe :

The most striking conclusion of relativistic cosmology is that the Universe has not existed forever. The dynamical result for the age of the Universe may be written as

$$\begin{aligned} H_0 t_0 &= \int_0^\infty \frac{dz}{(1+z)H(z)} \\ &= \int_0^\infty \frac{dz}{(1+z) [(1+z)^2(1+\Omega_m z) - z(2+z)\Omega_v]^{1/2}} , \end{aligned} \quad (21.28)$$

where we have neglected  $\Omega_r$  and chosen  $w = -1$ . Over the range of interest ( $0.1 \lesssim \Omega_m \lesssim 1$ ,  $|\Omega_v| \lesssim 1$ ), this exact answer may be approximated to a few % accuracy by

$$H_0 t_0 \simeq \frac{2}{3} (0.7\Omega_m + 0.3 - 0.3\Omega_v)^{-0.3} . \quad (21.29)$$



For the special case that  $\Omega_m + \Omega_v = 1$ , the integral in Eq. (21.28) can be expressed analytically as

$$H_0 t_0 = \frac{2}{3\sqrt{\Omega_v}} \ln \frac{1 + \sqrt{\Omega_v}}{\sqrt{1 - \Omega_v}} \quad (\Omega_m < 1). \quad (21.30)$$

The most accurate means of obtaining ages for astronomical objects is based on the natural clocks provided by radioactive decay. The use of these clocks is complicated by a lack of knowledge of the initial conditions of the decay. In the Solar System, chemical fractionation of different elements helps pin down a precise age for the pre-Solar nebula of 4.6 Gyr, but for stars it is necessary to attempt an a priori calculation of the relative abundances of nuclei that result from supernova explosions. In this way, a lower limit for the age of stars in the local part of the Milky Way of about 11 Gyr is obtained [36,37].

The other major means of obtaining cosmological age estimates is based on the theory of stellar evolution. In principle, the main-sequence turnoff point in the color-magnitude diagram of a globular cluster should yield a reliable age. However, these have been controversial owing to theoretical uncertainties in the evolution model, as well as observational uncertainties in the distance, dust extinction, and metallicity of clusters. The present consensus favors ages for the oldest clusters of about 12 Gyr [38,39].

These methods are all consistent with the age deduced from studies of structure formation, using the microwave background and large-scale structure:  $t_0 = 13.77 \pm 0.13$  Gyr [24], where the extra accuracy comes at the price of assuming the Cold Dark Matter model to be true.

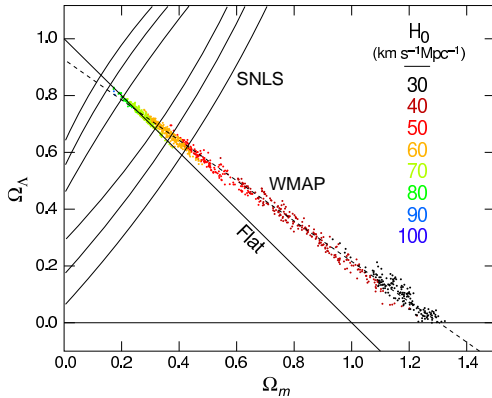


**Figure 21.2:** Likelihood-based probability densities on the plane  $\Omega_\Lambda$  (i.e.,  $\Omega_v$  assuming  $w = -1$ ) vs  $\Omega_m$ . The colored Monte-Carlo points derive from WMAP [34] and show that the CMB alone requires a flat universe  $\Omega_v + \Omega_m \simeq 1$  if the Hubble constant is not too high. The SNe Ia results [35] very nearly constrain the orthogonal combination  $\Omega_v - \Omega_m$ . The intersection of these constraints is the most direct (but far from the only) piece of evidence favoring a flat model with  $\Omega_m \simeq 0.25$ .

#### 21.2.4. Horizon, isotropy, flatness problems :

For photons, the radial equation of motion is just  $c dt = R d\chi$ . How far can a photon get in a given time? The answer is clearly

$$\Delta\chi = \int_{t_1}^{t_2} \frac{dt}{R(t)} \equiv \Delta\eta, \quad (21.31)$$

i.e., just the interval of conformal time. We can replace  $dt$  by  $dR/\dot{R}$ , which the Friedmann equation says is  $\propto dR/\sqrt{\rho R^2}$  at early times. Thus, this integral converges if  $\rho R^2 \rightarrow \infty$  as  $t_1 \rightarrow 0$ , otherwise it diverges. Provided the equation of state is such that  $\rho$  changes faster than  $R^{-2}$ , light signals can only propagate a finite distance between the Big Bang and the present; there is then said to be a particle horizon. Such a horizon therefore exists in conventional Big-Bang models, which are dominated by radiation ( $\rho \propto R^{-4}$ ) at early times.

At late times, the integral for the horizon is largely determined by the matter-dominated phase, for which

$$D_H = R_0 \chi_H \equiv R_0 \int_0^{t(z)} \frac{dt}{R(t)} \simeq \frac{6000}{\sqrt{\Omega_z}} h^{-1} \text{Mpc} \quad (z \gg 1). \quad (21.32)$$

The horizon at the time of formation of the microwave background ('last scattering':  $z \simeq 1100$ ) was thus of order 100 Mpc in size, subtending an angle of about  $1^\circ$ . Why then are the large number of causally disconnected regions we see on the microwave sky all at the same temperature? The Universe is very nearly isotropic and homogeneous, even though the initial conditions appear not to permit such a state to be constructed.

A related problem is that the  $\Omega = 1$  Universe is unstable:

$$\Omega(a) - 1 = \frac{\Omega - 1}{1 - \Omega + \Omega_v a^2 + \Omega_m a^{-1} + \Omega_r a^{-2}}, \quad (21.33)$$

where  $\Omega$  with no subscript is the total density parameter, and  $a(t) = R(t)/R_0$ . This requires  $\Omega(t)$  to be unity to arbitrary precision as the initial time tends to zero; a universe of non-zero curvature today requires very finely tuned initial conditions.

### 21.3. The Hot Thermal Universe

#### 21.3.1. Thermodynamics of the early Universe :

As alluded to above, we expect that much of the early Universe can be described by a radiation-dominated equation of state. In addition, through much of the radiation-dominated period, thermal equilibrium is established by the rapid rate of particle interactions relative to the expansion rate of the Universe (see Sec. 21.3.3 below). In equilibrium, it is straightforward to compute the thermodynamic quantities,  $\rho$ ,  $p$ , and the entropy density,  $s$ . In general, the energy density for a given particle type  $i$  can be written as

$$\rho_i = \int E_i dn_{q_i}, \quad (21.34)$$

with the density of states given by

$$dn_{q_i} = \frac{g_i}{2\pi^2} (\exp[(E_{q_i} - \mu_i)/T_i] \pm 1)^{-1} q_i^2 dq_i, \quad (21.35)$$

where  $g_i$  counts the number of degrees of freedom for particle type  $i$ ,  $E_{q_i}^2 = m_i^2 + q_i^2$ ,  $\mu_i$  is the chemical potential, and the  $\pm$  corresponds to either Fermi or Bose statistics. Similarly, we can define the pressure of a perfect gas as

$$p_i = \frac{1}{3} \int \frac{q_i^2}{E_i} dn_{q_i}. \quad (21.36)$$

The number density of species  $i$  is simply

$$n_i = \int dn_{q_i}, \quad (21.37)$$

and the entropy density is

$$s_i = \frac{\rho_i + p_i - \mu_i n_i}{T_i}. \quad (21.38)$$

In the Standard Model, a chemical potential is often associated with baryon number, and since the net baryon density relative to the photon density is known to be very small (of order  $10^{-10}$ ), we can neglect any such chemical potential when computing total thermodynamic quantities.

For photons, we can compute all of the thermodynamic quantities rather easily. Taking  $g_i = 2$  for the 2 photon polarization states, we have (in units where  $\hbar = k_B = 1$ )

$$\rho_\gamma = \frac{\pi^2}{15} T^4; \quad p_\gamma = \frac{1}{3} \rho_\gamma; \quad s_\gamma = \frac{4\rho_\gamma}{3T}; \quad n_\gamma = \frac{2\zeta(3)}{\pi^2} T^3, \quad (21.39)$$

with  $2\zeta(3)/\pi^2 \simeq 0.2436$ . Note that Eq. (21.10) can be converted into an equation for entropy conservation. Recognizing that  $\dot{p} = s\dot{T}$ , Eq. (21.10) becomes

$$d(sR^3)/dt = 0. \quad (21.40)$$

For radiation, this corresponds to the relationship between expansion and cooling,  $T \propto R^{-1}$  in an adiabatically expanding universe. Note also that both  $s$  and  $n_\gamma$  scale as  $T^3$ .

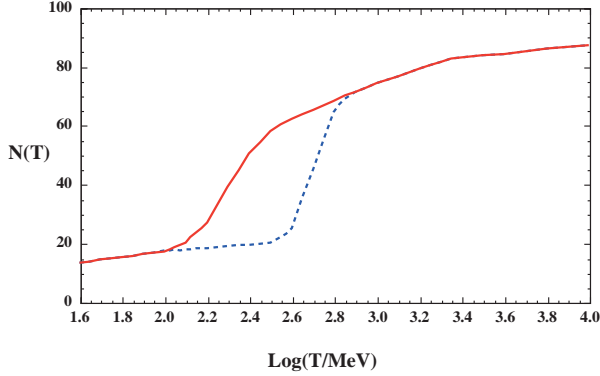


**Figure 21.3:** The effective numbers of relativistic degrees of freedom as a function of temperature. The sharp drop corresponds to the quark-hadron transition. The solid curve assume a QCD scale of 150 MeV, while the dashed curve assumes 450 MeV.

### 21.3.2. Radiation content of the Early Universe :

At the very high temperatures associated with the early Universe, massive particles are pair produced, and are part of the thermal bath. If for a given particle species  $i$  we have  $T \gg m_i$ , then we can neglect the mass in Eq. (21.34) to Eq. (21.38), and the thermodynamic quantities are easily computed as in Eq. (21.39). In general, we can approximate the energy density (at high temperatures) by including only those particles with  $m_i \ll T$ . In this case, we have

$$\rho = \left( \sum_B g_B + \frac{7}{8} \sum_F g_F \right) \frac{\pi^2}{30} T^4 \equiv \frac{\pi^2}{30} N(T) T^4, \quad (21.41)$$

where  $g_{B(F)}$  is the number of degrees of freedom of each boson (fermion) and the sum runs over all boson and fermion states with  $m \ll T$ . The factor of  $7/8$  is due to the difference between the Fermi and Bose integrals. Eq. (21.41) defines the effective number of degrees of freedom,  $N(T)$ , by taking into account new particle degrees of freedom as the temperature is raised. This quantity is plotted in Fig. 21.3 [40].

The value of  $N(T)$  at any given temperature depends on the particle physics model. In the standard  $SU(3) \times SU(2) \times U(1)$  model, we can specify  $N(T)$  up to temperatures of  $O(100)$  GeV. The change in  $N$  (ignoring mass effects) can be seen in the table below.

Temperature	New Particles	$4N(T)$
$T < m_e$	$\gamma$ 's + $\nu$ 's	29
$m_e < T < m_\mu$	$e^\pm$	43
$m_\mu < T < m_\pi$	$\mu^\pm$	57
$m_\pi < T < T_c^\dagger$	$\pi$ 's	69
$T_c < T < m_{\text{strange}}$	$\pi$ 's + $u, \bar{u}, d, \bar{d}$ + gluons	205
$m_s < T < m_{\text{charm}}$	$s, \bar{s}$	247
$m_c < T < m_\tau$	$c, \bar{c}$	289
$m_\tau < T < m_{\text{bottom}}$	$\tau^\pm$	303
$m_b < T < m_{W,Z}$	$b, \bar{b}$	345
$m_{W,Z} < T < m_{\text{Higgs}}$	$W^\pm, Z$	381
$m_H < T < m_{\text{top}}$	$H^0$	385
$m_t < T$	$t, \bar{t}$	427

$^\dagger T_c$  corresponds to the confinement-deconfinement transition between quarks and hadrons.

At higher temperatures,  $N(T)$  will be model-dependent. For example, in the minimal  $SU(5)$  model, one needs to add 24 states to  $N(T)$  for the  $X$  and  $Y$  gauge bosons, another 24 from the adjoint Higgs, and another 6 (in addition to the 4 already counted in  $W^\pm, Z$ , and  $H$ ) from the  $\bar{\mathbf{5}}$  of Higgs. Hence for  $T > m_X$  in minimal  $SU(5)$ ,  $N(T) = 160.75$ . In a supersymmetric model this would at least double, with some changes possibly necessary in the table if the lightest supersymmetric particle has a mass below  $m_t$ .

In the radiation-dominated epoch, Eq. (21.10) can be integrated (neglecting the  $T$ -dependence of  $N$ ) giving us a relationship between the age of the Universe and its temperature

$$t = \left( \frac{90}{32\pi^3 G_N N(T)} \right)^{1/2} T^{-2}. \quad (21.42)$$

Put into a more convenient form

$$t T_{\text{MeV}}^2 = 2.4 [N(T)]^{-1/2}, \quad (21.43)$$

where  $t$  is measured in seconds and  $T_{\text{MeV}}$  in units of MeV.

**21.3.3. Neutrinos and equilibrium :** Due to the expansion of the Universe, certain rates may be too slow to either establish or maintain equilibrium. Quantitatively, for each particle  $i$ , as a minimal condition for equilibrium, we will require that some rate  $\Gamma_i$  involving that type be larger than the expansion rate of the Universe or

$$\Gamma_i > H. \quad (21.44)$$

Recalling that the age of the Universe is determined by  $H^{-1}$ , this condition is equivalent to requiring that on average, at least one interaction has occurred over the lifetime of the Universe.

A good example for a process which goes in and out of equilibrium is the weak interactions of neutrinos. On dimensional grounds, one can estimate the thermally averaged scattering cross section

$$\langle \sigma v \rangle \sim O(10^{-2}) T^2 / m_W^4 \quad (21.45)$$

for  $T \lesssim m_W$ . Recalling that the number density of leptons is  $n \propto T^3$ , we can compare the weak interaction rate,  $\Gamma_{\text{wk}} \sim n \langle \sigma v \rangle$ , with the expansion rate,

$$H = \left( \frac{8\pi G_N \rho}{3} \right)^{1/2} = \left( \frac{8\pi^3}{90} N(T) \right)^{1/2} T^2 / M_{\text{P}} \sim 1.66 N(T)^{1/2} T^2 / M_{\text{P}}, \quad (21.46)$$

where the Planck mass  $M_{\text{P}} = G_N^{-1/2} = 1.22 \times 10^{19}$  GeV.

Neutrinos will be in equilibrium when  $\Gamma_{\text{wk}} > H$  or

$$T > (500 m_W^4 / M_{\text{P}})^{1/3} \sim 1 \text{ MeV}. \quad (21.47)$$

However, this condition assumes  $T \ll m_W$ ; for higher temperatures, we should write  $\langle \sigma v \rangle \sim O(10^{-2}) / T^2$ , so that  $\Gamma \sim 10^{-2} T$ . Thus, in the very early stages of expansion, at temperatures  $T \gtrsim 10^{-2} M_{\text{P}} / \sqrt{N}$ , equilibrium will not have been established.

Having attained a quasi-equilibrium stage, the Universe then cools further to the point where the interaction and expansion timescales match once again. The temperature at which these rates are equal is commonly referred to as the neutrino decoupling or freeze-out temperature and is defined by  $\Gamma_{\text{wk}}(T_d) = H(T_d)$ . For  $T < T_d$ , neutrinos drop out of equilibrium. The Universe becomes transparent to neutrinos and their momenta simply redshift with the cosmic expansion. The effective neutrino temperature will simply fall with  $T \sim 1/R$ .

Soon after decoupling,  $e^\pm$  pairs in the thermal background begin to annihilate (when  $T \lesssim m_e$ ). Because the neutrinos are decoupled, the energy released due to annihilation heats up the photon background relative to the neutrinos. The change in the photon temperature can be easily computed from entropy conservation. The neutrino entropy must be conserved separately from the entropy of interacting particles. A straightforward computation yields

$$T_\nu = (4/11)^{1/3} T_\gamma \simeq 1.9 \text{ K}. \quad (21.48)$$

Today, the total entropy density is therefore given by

$$s = \frac{4}{3} \frac{\pi^2}{30} \left( 2 + \frac{21}{4} (T_\nu / T_\gamma)^3 \right) T_\gamma^3 = \frac{4}{3} \frac{\pi^2}{30} \left( 2 + \frac{21}{11} \right) T_\gamma^3 = 7.04 n_\gamma. \quad (21.49)$$

Similarly, the total relativistic energy density today is given by

$$\rho_r = \frac{\pi^2}{30} \left[ 2 + \frac{21}{4} (T_\nu/T_\gamma)^4 \right] T_\gamma^4 \simeq 1.68 \rho_\gamma. \quad (21.50)$$

In practice, a small correction is needed to this, since neutrinos are not totally decoupled at  $e^\pm$  annihilation: the effective number of massless neutrino species is 3.04, rather than 3 [41].

This expression ignores neutrino rest masses, but current oscillation data require at least one neutrino eigenstate to have a mass exceeding 0.05 eV. In this minimal case,  $\Omega_\nu h^2 = 5 \times 10^{-4}$ , so the neutrino contribution to the matter budget would be negligibly small (which is our normal assumption). However, a nearly degenerate pattern of mass eigenstates could allow larger densities, since oscillation experiments only measure differences in  $m^2$  values. Note that a 0.05-eV neutrino has  $kT_\nu = m_\nu$  at  $z \simeq 297$ , so the above expression for the total present relativistic density is really only an extrapolation. However, neutrinos are almost certainly relativistic at all epochs where the radiation content of the Universe is dynamically significant.

### 21.3.4. Field Theory and Phase transitions :

It is very likely that the Universe has undergone one or more phase transitions during the course of its evolution [42–45]. Our current vacuum state is described by  $SU(3)_c \times U(1)_{em}$ , which in the Standard Model is a remnant of an unbroken  $SU(3)_c \times SU(2)_L \times U(1)_Y$  gauge symmetry. Symmetry breaking occurs when a non-singlet gauge field (the Higgs field in the Standard Model) picks up a non-vanishing vacuum expectation value, determined by a scalar potential. For example, a simple (non-gauged) potential describing symmetry breaking is  $V(\phi) = \frac{1}{4}\lambda\phi^4 - \frac{1}{2}\mu^2\phi^2 + V(0)$ . The resulting expectation value is simply  $\langle\phi\rangle = \mu/\sqrt{\lambda}$ .

In the early Universe, finite temperature radiative corrections typically add terms to the potential of the form  $\phi^2 T^2$ . Thus, at very high temperatures, the symmetry is restored and  $\langle\phi\rangle = 0$ . As the Universe cools, depending on the details of the potential, symmetry breaking will occur via a first order phase transition in which the field tunnels through a potential barrier, or via a second order transition in which the field evolves smoothly from one state to another (as would be the case for the above example potential).

The evolution of scalar fields can have a profound impact on the early Universe. The equation of motion for a scalar field  $\phi$  can be derived from the energy-momentum tensor

$$T_{\mu\nu} = \partial_\mu\phi\partial_\nu\phi - \frac{1}{2}g_{\mu\nu}\partial_\rho\phi\partial^\rho\phi - g_{\mu\nu}V(\phi). \quad (21.51)$$

By associating  $\rho = T_{00}$  and  $p = R^{-2}(t)T_{ii}$  we have

$$\begin{aligned} \rho &= \frac{1}{2}\dot{\phi}^2 + \frac{1}{2}R^{-2}(t)(\nabla\phi)^2 + V(\phi) \\ p &= \frac{1}{2}\dot{\phi}^2 - \frac{1}{6}R^{-2}(t)(\nabla\phi)^2 - V(\phi), \end{aligned} \quad (21.52)$$

and from Eq. (21.10) we can write the equation of motion (by considering a homogeneous region, we can ignore the gradient terms)

$$\ddot{\phi} + 3H\dot{\phi} = -\partial V/\partial\phi. \quad (21.53)$$

### 21.3.5. Inflation :

In Sec. 21.2.4, we discussed some of the problems associated with the standard Big-Bang model. However, during a phase transition, our assumptions of an adiabatically expanding universe are generally not valid. If, for example, a phase transition occurred in the early Universe such that the field evolved slowly from the symmetric state to the global minimum, the Universe may have been dominated by the vacuum energy density associated with the potential near  $\phi \simeq 0$ . During this period of slow evolution, the energy density due to radiation will fall below the vacuum energy density,  $\rho \ll V(0)$ . When this happens, the expansion rate will be dominated by the constant  $V(0)$ , and we obtain the exponentially expanding solution given in Eq. (21.20). When the field evolves towards the global minimum it will

begin to oscillate about the minimum, energy will be released during its decay, and a hot thermal universe will be restored. If released fast enough, it will produce radiation at a temperature  $NT_R^4 \lesssim V(0)$ . In this reheating process, entropy has been created and the final value of  $RT$  is greater than the initial value of  $RT$ . Thus, we see that, during a phase transition, the relation  $RT \sim$  constant need not hold true. This is the basis of the inflationary Universe scenario [46–48].

If, during the phase transition, the value of  $RT$  changed by a factor of  $O(10^{29})$ , the cosmological problems discussed above would be solved. The observed isotropy would be generated by the immense expansion; one small causal region could get blown up, and thus our entire visible Universe would have been in thermal contact some time in the past. In addition, the density parameter  $\Omega$  would have been driven to 1 (with exponential precision). Density perturbations will be stretched by the expansion,  $\lambda \sim R(t)$ . Thus it will appear that  $\lambda \gg H^{-1}$  or that the perturbations have left the horizon, where in fact the size of the causally connected region is now no longer simply  $H^{-1}$ . However, not only does inflation offer an explanation for large scale perturbations, it also offers a source for the perturbations themselves through quantum fluctuations.

Early models of inflation were based on a first order phase transition of a Grand Unified Theory [49]. Although these models led to sufficient exponential expansion, completion of the transition through bubble percolation did not occur, and lack of bubble collisions meant that the interior of the bubbles was not reheated. Subsequent models of inflation [50,51] considered second-order transitions within Grand Unified theories, thus successfully ending inflation with reheating from oscillations of the scalar field. But these models predicted too high an amplitude of relic density fluctuations. As a result, current models of inflation postulate second-order transitions in a completely new scalar field: the inflaton,  $\phi$ . The potential of this field,  $V(\phi)$ , needs to have a very low gradient and curvature in order to match observed metric fluctuations.

In viable inflation models of this type, reheated bubbles again typically do not percolate, so inflation is ‘eternal’ and continues with exponential expansion in the region outside bubbles. These causally disconnected bubble universes constitute a ‘multiverse’, where low-energy physics can vary between different bubbles. This has led to a controversial ‘anthropic’ approach to cosmology [82–84], where observer selection within the multiverse can be introduced as a means of understanding e.g. why the observed level of vacuum energy is so low (because larger values suppress growth of structure).

### 21.3.6. Baryogenesis :

The Universe appears to be populated exclusively with matter rather than antimatter. Indeed antimatter is only detected in accelerators or in cosmic rays. However, the presence of antimatter in the latter is understood to be the result of collisions of primary particles in the interstellar medium. There is in fact strong evidence against primary forms of antimatter in the Universe. Furthermore, the density of baryons compared to the density of photons is extremely small,  $\eta \sim 10^{-10}$ .

The production of a net baryon asymmetry requires baryon number violating interactions,  $C$  and  $CP$  violation and a departure from thermal equilibrium [52]. The first two of these ingredients are expected to be contained in grand unified theories as well as in the non-perturbative sector of the Standard Model, the third can be realized in an expanding universe where as we have seen interactions come in and out of equilibrium.

There are several interesting and viable mechanisms for the production of the baryon asymmetry. While, we can not review any of them here in any detail, we mention some of the important scenarios. In all cases, all three ingredients listed above are incorporated. One of the first mechanisms was based on the out of equilibrium decay of a massive particle such as a superheavy GUT gauge of Higgs boson [53,54]. A novel mechanism involving the decay of flat directions in supersymmetric models is known as the Affleck-Dine scenario [55]. There is also the possibility of generating the baryon asymmetry at the electro-weak scale using the non-perturbative interactions of sphalerons [56]. Because these interactions conserve the sum of baryon and lepton number,  $B + L$ , it is possible to first

generate a lepton asymmetry (*e.g.*, by the out-of-equilibrium decay of a superheavy right-handed neutrino), which is converted to a baryon asymmetry at the electro-weak scale [57]. This mechanism is known as lepto-baryogenesis.

### 21.3.7. Nucleosynthesis :

An essential element of the standard cosmological model is Big-Bang nucleosynthesis (BBN), the theory which predicts the abundances of the light element isotopes D,  $^3\text{He}$ ,  $^4\text{He}$ , and  $^7\text{Li}$ . Nucleosynthesis takes place at a temperature scale of order 1 MeV. The nuclear processes lead primarily to  $^4\text{He}$ , with a primordial mass fraction of about 25%. Lesser amounts of the other light elements are produced: about  $10^{-5}$  of D and  $^3\text{He}$  and about  $10^{-10}$  of  $^7\text{Li}$  by number relative to H. The abundances of the light elements depend almost solely on one key parameter, the baryon-to-photon ratio,  $\eta$ . The nucleosynthesis predictions can be compared with observational determinations of the abundances of the light elements. Consistency between theory and observations leads to a conservative range of

$$5.1 \times 10^{-10} < \eta < 6.5 \times 10^{-10} . \quad (21.54)$$

$\eta$  is related to the fraction of  $\Omega$  contained in baryons,  $\Omega_b$ ,

$$\Omega_b = 3.66 \times 10^7 \eta h^{-2} , \quad (21.55)$$

or  $10^{10} \eta = 274 \Omega_b h^2$ . The WMAP result [24] for  $\Omega_b h^2$  of  $0.0225 \pm 0.0006$  translates into a value of  $\eta = 6.16 \pm 0.15$ . This result can be used to ‘predict’ the light element abundance which can in turn be compared with observation [58]. The resulting D/H abundance is in excellent agreement with that found in quasar absorption systems. It is in reasonable agreement with the helium abundance observed in extra-galactic HII regions (once systematic uncertainties are accounted for), but is in poor agreement with the Li abundance observed in the atmospheres of halo dwarf stars [59]. (See the review on BBN—Sec. 22 of this *Review* for a detailed discussion of BBN or references [60,61].)

### 21.3.8. The transition to a matter-dominated Universe :

In the Standard Model, the temperature (or redshift) at which the Universe undergoes a transition from a radiation dominated to a matter dominated Universe is determined by the amount of dark matter. Assuming three nearly massless neutrinos, the energy density in radiation at temperatures  $T \ll 1$  MeV, is given by

$$\rho_r = \frac{\pi^2}{30} \left[ 2 + \frac{21}{4} \left( \frac{4}{11} \right)^{4/3} \right] T^4 . \quad (21.56)$$

In the absence of non-baryonic dark matter, the matter density can be written as

$$\rho_m = m_N \eta n_\gamma , \quad (21.57)$$

where  $m_N$  is the nucleon mass. Recalling that  $n_\gamma \propto T^3$  [cf. Eq. (21.39)], we can solve for the temperature or redshift at the matter-radiation equality when  $\rho_r = \rho_m$ ,

$$T_{eq} = 0.22 m_N \eta \quad \text{or} \quad (1 + z_{eq}) = 0.22 \eta \frac{m_N}{T_0} , \quad (21.58)$$

where  $T_0$  is the present temperature of the microwave background. For  $\eta = 6.2 \times 10^{-10}$ , this corresponds to a temperature  $T_{eq} \simeq 0.13$  eV or  $(1 + z_{eq}) \simeq 550$ . A transition this late is very problematic for structure formation (see Sec. 21.4.5).

The redshift of matter domination can be pushed back significantly if non-baryonic dark matter is present. If instead of Eq. (21.57), we write

$$\rho_m = \Omega_m \rho_c \left( \frac{T}{T_0} \right)^3 , \quad (21.59)$$

we find that

$$T_{eq} = 0.9 \frac{\Omega_m \rho_c}{T_0^3} \quad \text{or} \quad (1 + z_{eq}) = 2.4 \times 10^4 \Omega_m h^2 . \quad (21.60)$$

## 21.4. The Universe at late times

### 21.4.1. The CMB :

One form of the infamous Olbers’ paradox says that, in Euclidean space, surface brightness is independent of distance. Every line of sight will terminate on matter that is hot enough to be ionized and so scatter photons:  $T \gtrsim 10^3$  K; the sky should therefore shine as brightly as the surface of the Sun. The reason the night sky is dark is entirely due to the expansion, which cools the radiation temperature to 2.73 K. This gives a Planck function peaking at around 1 mm to produce the microwave background (CMB).

The CMB spectrum is a very accurate match to a Planck function [62]. (See the review on CBR—Sec. 25 of this *Review*.) The COBE estimate of the temperature is [63]

$$T = 2.7255 \pm 0.0006 \text{ K} . \quad (21.61)$$

The lack of any distortion of the Planck spectrum is a strong physical constraint. It is very difficult to account for in any expanding universe other than one that passes through a hot stage. Alternative schemes for generating the radiation, such as thermalization of starlight by dust grains, inevitably generate a superposition of temperatures. What is required in addition to thermal equilibrium is that  $T \propto 1/R$ , so that radiation from different parts of space appears identical.

Although it is common to speak of the CMB as originating at ‘recombination,’ a more accurate terminology is the era of ‘last scattering.’ In practice, this takes place at  $z \simeq 1100$ , almost independently of the main cosmological parameters, at which time the fractional ionization is very small. This occurred when the age of the Universe was a few hundred thousand years. (See the review on CBR—Sec. 25 of this *Review* for a full discussion of the CMB.)

### 21.4.2. Matter in the Universe :

One of the main tasks of cosmology is to measure the density of the Universe, and how this is divided between dark matter and baryons. The baryons consist partly of stars, with  $0.002 \lesssim \Omega_* \lesssim 0.003$  [64] but mainly inhabit the intergalactic medium (IGM). One powerful way in which this can be studied is via the absorption of light from distant luminous objects such as quasars. Even very small amounts of neutral hydrogen can absorb rest-frame UV photons (the Gunn-Peterson effect), and should suppress the continuum by a factor  $\exp(-\tau)$ , where

$$\tau \simeq 10^{4.62} h^{-1} \left[ \frac{n_{\text{HI}}(z)/m^{-3}}{(1+z)\sqrt{1+\Omega_m z}} \right] , \quad (21.62)$$

and this expression applies while the Universe is matter dominated ( $z \gtrsim 1$  in the  $\Omega_m = 0.3$   $\Omega_v = 0.7$  model). It is possible that this general absorption has now been seen at  $z = 6.2 - 6.4$  [65]. In any case, the dominant effect on the spectrum is a ‘forest’ of narrow absorption lines, which produce a mean  $\tau = 1$  in the Ly $\alpha$  forest at about  $z = 3$ , and so we have  $\Omega_{\text{HI}} \simeq 10^{-6.7} h^{-1}$ . This is such a small number that clearly the IGM is very highly ionized at these redshifts.

The Ly $\alpha$  forest is of great importance in pinning down the abundance of deuterium. Because electrons in deuterium differ in reduced mass by about 1 part in 4000 compared to hydrogen, each absorption system in the Ly $\alpha$  forest is accompanied by an offset deuterium line. By careful selection of systems with an optimal HI column density, a measurement of the D/H ratio can be made. This has now been done in 7 quasars, with relatively consistent results [66]. Combining these determinations with the theory of primordial nucleosynthesis yields a baryon density of  $\Omega_b h^2 = 0.019 - 0.024$  (95% confidence). (See also the review on BBN—Sec. 22 of this *Review*.)

Ionized IGM can also be detected in emission when it is densely clumped, via bremsstrahlung radiation. This generates the spectacular X-ray emission from rich clusters of galaxies. Studies of this phenomenon allow us to achieve an accounting of the total baryonic material in clusters. Within the central  $\simeq 1$  Mpc, the masses in stars, X-ray emitting gas and total dark matter can be determined with reasonable accuracy (perhaps 20% rms), and this allows a minimum baryon fraction to be determined [67,68]:

$$\frac{M_{\text{baryons}}}{M_{\text{total}}} \gtrsim 0.009 + (0.066 \pm 0.003) h^{-3/2} . \quad (21.63)$$

Because clusters are the largest collapsed structures, it is reasonable to take this as applying to the Universe as a whole. This equation implies a minimum baryon fraction of perhaps 12% (for reasonable  $h$ ), which is too high for  $\Omega_m = 1$  if we take  $\Omega_b h^2 \simeq 0.02$  from nucleosynthesis. This is therefore one of the more robust arguments in favor of  $\Omega_m \simeq 0.3$ . (See the review on Cosmological Parameters—Sec. 23 of this *Review*.) This argument is also consistent with the inference on  $\Omega_m$  that can be made from Fig. 21.2.

This method is much more robust than the older classical technique for weighing the Universe: ‘ $L \times M/L$ .’ The overall light density of the Universe is reasonably well determined from redshift surveys of galaxies, so that a good determination of mass  $M$  and luminosity  $L$  for a single object suffices to determine  $\Omega_m$  if the mass-to-light ratio is universal.

#### 21.4.3. Gravitational lensing :

A robust method for determining masses in cosmology is to use gravitational light deflection. Most systems can be treated as a geometrically thin gravitational lens, where the light bending is assumed to take place only at a single distance. Simple geometry then determines a mapping between the coordinates in the intrinsic source plane and the observed image plane:

$$\alpha(D_L \theta_I) = \frac{D_S}{D_{LS}} (\theta_I - \theta_S), \quad (21.64)$$

where the angles  $\theta_I, \theta_S$  and  $\alpha$  are in general two-dimensional vectors on the sky. The distances  $D_{LS}$  etc. are given by an extension of the usual distance-redshift formula:

$$D_{LS} = \frac{R_0 S_k (\chi_S - \chi_L)}{1 + z_S}. \quad (21.65)$$

This is the angular-diameter distance for objects on the source plane as perceived by an observer on the lens.

Solutions of this equation divide into weak lensing, where the mapping between source plane and image plane is one-to-one, and strong lensing, in which multiple imaging is possible. For circularly-symmetric lenses, an on-axis source is multiply imaged into a ‘caustic’ ring, whose radius is the Einstein radius:

$$\begin{aligned} \theta_E &= \left( 4GM \frac{D_{LS}}{D_L D_S} \right)^{1/2} \\ &= \left( \frac{M}{10^{11.09} M_\odot} \right)^{1/2} \left( \frac{D_L D_S / D_{LS}}{\text{Gpc}} \right)^{-1/2} \text{ arcsec}. \end{aligned} \quad (21.66)$$

The observation of ‘arcs’ (segments of near-perfect Einstein rings) in rich clusters of galaxies has thus given very accurate masses for the central parts of clusters—generally in good agreement with other indicators, such as analysis of X-ray emission from the cluster IGM [69].

Gravitational lensing has also developed into a particularly promising probe of cosmological structure on 10 to 100 Mpc scales. Weak image distortions manifest themselves as an additional ellipticity of galaxy images (‘shear’), which can be observed by averaging many images together (the corresponding flux amplification is less readily detected). The result is a ‘cosmic shear’ field of order 1% ellipticity, coherent over scales of around 30 arcmin, which is directly related to the cosmic mass field, without any astrophysical uncertainties. For this reason, weak lensing is seen as potentially the cleanest probe of matter fluctuations, next to the CMB. Already, impressive results have been obtained in measuring cosmological parameters, based on survey data from only  $\sim 50 \text{ deg}^2$  [85]. The particular current strength of this technique is the ability to measure the amplitude of mass fluctuations; this can be deduced from the CMB only subject to uncertainty over the optical depth due to Thomson scattering after reionization.

#### 21.4.4. Density Fluctuations :

The overall properties of the Universe are very close to being homogeneous; and yet telescopes reveal a wealth of detail on scales varying from single galaxies to large-scale structures of size exceeding 100 Mpc. The existence of these structures must be telling us something important about the initial conditions of the Big Bang, and about the physical processes that have operated subsequently. This motivates the study of the density perturbation field, defined as

$$\delta(\mathbf{x}) \equiv \frac{\rho(\mathbf{x}) - \langle \rho \rangle}{\langle \rho \rangle}. \quad (21.67)$$

A critical feature of the  $\delta$  field is that it inhabits a universe that is isotropic and homogeneous in its large-scale properties. This suggests that the statistical properties of  $\delta$  should also be statistically homogeneous—*i.e.*, it is a stationary random process.

It is often convenient to describe  $\delta$  as a Fourier superposition:

$$\delta(\mathbf{x}) = \sum \delta_{\mathbf{k}} e^{-i\mathbf{k} \cdot \mathbf{x}}. \quad (21.68)$$

We avoid difficulties with an infinite universe by applying periodic boundary conditions in a cube of some large volume  $V$ . The cross-terms vanish when we compute the variance in the field, which is just a sum over modes of the power spectrum

$$\langle \delta^2 \rangle = \sum |\delta_{\mathbf{k}}|^2 \equiv \sum P(k). \quad (21.69)$$

Note that the statistical nature of the fluctuations must be isotropic, so we write  $P(k)$  rather than  $P(\mathbf{k})$ . The  $\langle \dots \rangle$  average here is a volume average. Cosmological density fields are an example of an ergodic process, in which the average over a large volume tends to the same answer as the average over a statistical ensemble.

The statistical properties of discrete objects sampled from the density field are often described in terms of  $N$ -point correlation functions, which represent the excess probability over random for finding one particle in each of  $N$  boxes in a given configuration. For the 2-point case, the correlation function is readily shown to be identical to the autocorrelation function of the  $\delta$  field:  $\xi(r) = \langle \delta(x)\delta(x+r) \rangle$ .

The power spectrum and correlation function are Fourier conjugates, and thus are equivalent descriptions of the density field (similarly,  $k$ -space equivalents exist for the higher-order correlations). It is convenient to take the limit  $V \rightarrow \infty$  and use  $k$ -space integrals, defining a dimensionless power spectrum, which measures the contribution to the fractional variance in density per unit logarithmic range of scale, as  $\Delta^2(k) = d\langle \delta^2 \rangle / d \ln k = V k^3 P(k) / 2\pi^2$ :

$$\xi(r) = \int \Delta^2(k) \frac{\sin kr}{kr} d \ln k; \quad \Delta^2(k) = \frac{2}{\pi} k^3 \int_0^\infty \xi(r) \frac{\sin kr}{kr} r^2 dr. \quad (21.70)$$

For many years, an adequate approximation to observational data on galaxies was  $\xi = (r/r_0)^{-\gamma}$ , with  $\gamma \simeq 1.8$  and  $r_0 \simeq 5 h^{-1} \text{ Mpc}$ . Modern surveys are now able to probe into the large-scale linear regime where unaltered traces of the curved post-recombination spectrum can be detected [70,71,72].

#### 21.4.5. Formation of cosmological structure :

The simplest model for the generation of cosmological structure is gravitational instability acting on some small initial fluctuations (for the origin of which a theory such as inflation is required). If the perturbations are adiabatic (*i.e.*, fractionally perturb number densities of photons and matter equally), the linear growth law for matter perturbations is simple:

$$\delta \propto \begin{cases} a^2(t) & (\text{radiation domination; } \Omega_r = 1) \\ a(t) & (\text{matter domination; } \Omega_m = 1). \end{cases} \quad (21.71)$$

For low density universes, the present-day amplitude is suppressed by a factor  $g(\Omega)$ , where

$$g(\Omega) \simeq \frac{5}{2} \Omega_m \left[ \Omega_m^{4/7} - \Omega_v + (1 + \Omega_m/2)(1 + \frac{1}{70} \Omega_v) \right]^{-1} \quad (21.72)$$

is an accurate fit for models with matter plus cosmological constant. The alternative perturbation mode is isocurvature: only the equation of state changes, and the total density is initially unperturbed. These modes perturb the total entropy density, and thus induce additional large-scale CMB anisotropies [73]. Although the character of perturbations in the simplest inflationary theories are purely adiabatic, correlated adiabatic and isocurvature modes are predicted in many models; the simplest example is the curvaton, which is a scalar field that decays to yield a perturbed radiation density. If the matter content already exists at this time, the overall perturbation field will have a significant isocurvature component. Such a prediction is inconsistent with current CMB data [74], and most analyses of CMB and LSS data assume the adiabatic case to hold exactly.

Linear evolution preserves the shape of the power spectrum. However, a variety of processes mean that growth actually depends on the matter content:

- (1) Pressure opposes gravity effectively for wavelengths below the horizon length while the Universe is radiation dominated. The *comoving* horizon size at  $z_{\text{eq}}$  is therefore an important scale:
 
$$D_H(z_{\text{eq}}) = \frac{2(\sqrt{2}-1)}{(\Omega_m z_{\text{eq}})^{1/2} H_0} = \frac{16.0}{\Omega_m h^2} \text{Mpc} . \quad (21.73)$$
- (2) At early times, dark matter particles will undergo free streaming at the speed of light, and so erase all scales up to the horizon—a process that only ceases when the particles go nonrelativistic. For light massive neutrinos, this happens at  $z_{\text{eq}}$ ; all structure up to the horizon-scale power-spectrum break is in fact erased. Hot(cold) dark matter models are thus sometimes dubbed large(small)-scale damping models.
- (3) A further important scale arises where photon diffusion can erase perturbations in the matter–radiation fluid; this process is named Silk damping.

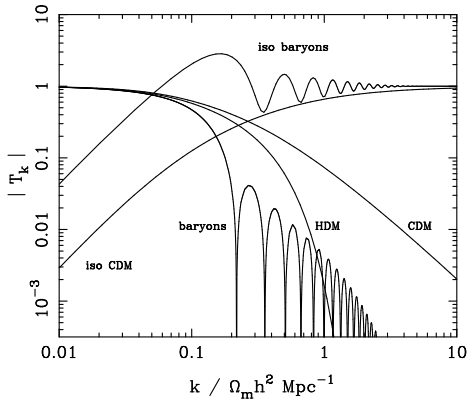


**Figure 21.4:** A plot of transfer functions for various models. For adiabatic models,  $T_k \rightarrow 1$  at small  $k$ , whereas the opposite is true for isocurvature models. For dark-matter models, the characteristic wavenumber scales proportional to  $\Omega_m h^2$ . The scaling for baryonic models does not obey this exactly; the plotted cases correspond to  $\Omega_m = 1$ ,  $h = 0.5$ .

The overall effect is encapsulated in the transfer function, which gives the ratio of the late-time amplitude of a mode to its initial value (see Fig. 21.4). The overall power spectrum is thus the primordial power-law, times the square of the transfer function:

$$P(k) \propto k^n T_k^2 . \quad (21.74)$$

The most generic power-law index is  $n = 1$ : the ‘Zeldovich’ or ‘scale-invariant’ spectrum. Inflationary models tend to predict a small ‘tilt’:  $|n - 1| \lesssim 0.03$  [12,13]. On the assumption that the dark matter is cold, the power spectrum then depends on 5 parameters:  $n$ ,  $h$ ,  $\Omega_b$ ,  $\Omega_{\text{cdm}}$  ( $\equiv \Omega_m - \Omega_b$ ) and an overall amplitude. The latter is often specified as  $\sigma_8$ , the linear-theory fractional rms in density when a spherical filter of radius  $8 h^{-1} \text{Mpc}$  is applied in linear theory. This

scale can be probed directly via weak gravitational lensing, and also via its effect on the abundance of rich galaxy clusters. The favored value is approximately [34,75]

$$\sigma_8 \simeq (0.803 \pm 0.011) (\Omega_m/0.25)^{-0.47} . \quad (21.75)$$

A direct measure of mass inhomogeneity is valuable, since the galaxies inevitably are biased with respect to the mass. This means that the fractional fluctuations in galaxy number,  $\delta n/n$ , may differ from the mass fluctuations,  $\delta\rho/\rho$ . It is commonly assumed that the two fields obey some proportionality on large scales where the fluctuations are small,  $\delta n/n = b\delta\rho/\rho$ , but even this is not guaranteed [76].

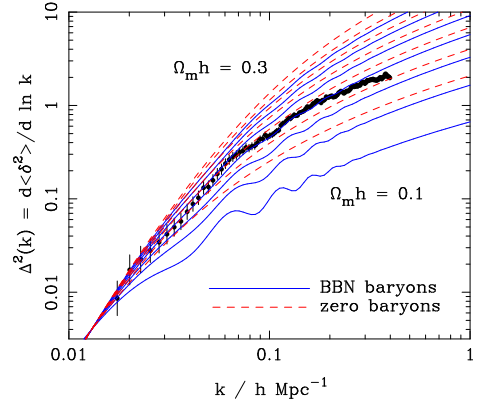


**Figure 21.5:** The galaxy power spectrum from the 2dFGRS [71], shown in dimensionless form,  $\Delta^2(k) \propto k^3 P(k)$ . The solid points with error bars show the power estimate. The window function correlates the results at different  $k$  values, and also distorts the large-scale shape of the power spectrum. An approximate correction for the latter effect has been applied. The solid and dashed lines show various CDM models, all assuming  $n = 1$ . For the case with non-negligible baryon content, a big-bang nucleosynthesis value of  $\Omega_b h^2 = 0.02$  is assumed, together with  $h = 0.7$ . A good fit is clearly obtained for  $\Omega_m h \simeq 0.2$ .

The main shape of the transfer function is a break around the horizon scale at  $z_{\text{eq}}$ , which depends just on  $\Omega_m h$  when wavenumbers are measured in observable units ( $h \text{Mpc}^{-1}$ ). For reasonable baryon content, weak oscillations in the transfer function are also expected, and these BAOs (Baryon Acoustic Oscillations) have been clearly detected [77,78]. As well as directly measuring the baryon fraction, the scale of the oscillations directly measures the acoustic horizon at decoupling; this can be used as an additional standard ruler for cosmological tests, and the BAO method is likely to be important in future large galaxy surveys. Overall, current power-spectrum data [70,71,72] favor  $\Omega_m h \simeq 0.20$  and a baryon fraction of about 0.15 for  $n = 1$  (see Fig. 21.5).

In principle, accurate data over a wide range of  $k$  could determine both  $\Omega h$  and  $n$ , but in practice there is a strong degeneracy between these. In order to constrain  $n$  itself, it is necessary to examine data on anisotropies in the CMB.

#### 21.4.6. CMB anisotropies :

The CMB has a clear dipole anisotropy, of magnitude  $1.23 \times 10^{-3}$ . This is interpreted as being due to the Earth’s motion, which is equivalent to a peculiar velocity for the Milky Way of

$$v_{\text{MW}} \simeq 600 \text{ km s}^{-1} \quad \text{towards } (\ell, b) \simeq (270^\circ, 30^\circ) . \quad (21.76)$$

All higher-order multipole moments of the CMB are however much smaller (of order  $10^{-5}$ ), and interpreted as signatures of density fluctuations at last scattering ( $\simeq 1100$ ). To analyze these, the sky is expanded in spherical harmonics as explained in the review on CBR–Sec. 25 of this *Review*. The dimensionless power per  $\ln k$  or ‘bandpower’ for the CMB is defined as

$$\mathcal{T}^2(\ell) = \frac{\ell(\ell+1)}{2\pi} C_\ell . \quad (21.77)$$



This function encodes information from the three distinct mechanisms that cause CMB anisotropies:

- (1) Gravitational (Sachs–Wolfe) perturbations. Photons from high-density regions at last scattering have to climb out of potential wells, and are thus redshifted.
- (2) Intrinsic (adiabatic) perturbations. In high-density regions, the coupling of matter and radiation can compress the radiation also, giving a higher temperature.
- (3) Velocity (Doppler) perturbations. The plasma has a non-zero velocity at recombination, which leads to Doppler shifts in frequency and hence shifts in brightness temperature.

Because the potential fluctuations obey Poisson’s equation,  $\nabla^2\Phi = 4\pi G\rho\delta$ , and the velocity field satisfies the continuity equation  $\nabla \cdot \mathbf{u} = -\dot{\delta}$ , the resulting different powers of  $k$  ensure that the Sachs-Wolfe effect dominates on large scales and adiabatic effects on small scales.

The relation between angle and comoving distance on the last-scattering sphere requires the comoving angular-diameter distance to the last-scattering sphere; because of its high redshift, this is effectively identical to the horizon size at the present epoch,  $D_H$ :

$$\begin{aligned} D_H &= \frac{2}{\Omega_m H_0} \quad (\Omega_v = 0) \\ D_H &\simeq \frac{2}{\Omega_m^{0.4} H_0} \quad (\text{flat} : \Omega_m + \Omega_v = 1). \end{aligned} \quad (21.78)$$

These relations show how the CMB is strongly sensitive to curvature: the horizon length at last scattering is  $\propto 1/\sqrt{\Omega_m}$ , so that this subtends an angle that is virtually independent of  $\Omega_m$  for a flat model. Observations of a peak in the CMB power spectrum at relatively large scales ( $\ell \simeq 225$ ) are thus strongly inconsistent with zero- $\Lambda$  models with low density: current CMB + BAO +SN data require  $\Omega_m + \Omega_v = 1.006 \pm 0.007$  [24]. (See *e.g.*, Fig. 21.2).

In addition to curvature, the CMB encodes information about several other key cosmological parameters. Within the compass of simple adiabatic CDM models, there are 9 of these:

$$\omega_c, \omega_b, \Omega_t, h, \tau, n_s, n_t, r, Q. \quad (21.79)$$

The symbol  $\omega$  denotes the physical density,  $\Omega h^2$ : the transfer function depends only on the densities of CDM ( $\omega_c$ ) and baryons ( $\omega_b$ ). Transcribing the power spectrum at last scattering into an angular power spectrum brings in the total density parameter ( $\Omega_t \equiv \Omega_m + \Omega_v = \Omega_c + \Omega_b + \Omega_v$ ) and  $h$ : there is an exact geometrical degeneracy [79] between these that keeps the angular-diameter distance to last scattering invariant, so that models with substantial spatial curvature and large vacuum energy cannot be ruled out without prior knowledge of the Hubble parameter. Alternatively, the CMB alone cannot measure the Hubble parameter.

The other main parameter degeneracy involves the tensor contribution to the CMB anisotropies. These are important at large scales (up to the horizon scales); for smaller scales, only scalar fluctuations (density perturbations) are important. Each of these components is characterized by a spectral index,  $n$ , and a ratio between the power spectra of tensors and scalars ( $r$ ). See the review on Cosmological Parameters—Sec. 23 of this *Review* for a technical definition of the  $r$  parameter. Finally, the overall amplitude of the spectrum must be specified ( $Q$ ), together with the optical depth to Compton scattering owing to recent reionization ( $\tau$ ). The tensor degeneracy operates as follows: the main effect of adding a large tensor contribution is to reduce the contrast between low  $\ell$  and the peak at  $\ell \simeq 225$  (because the tensor spectrum has no acoustic component). The required height of the peak can be recovered by increasing  $n_s$  to increase the small-scale power in the scalar component; this in turn over-predicts the power at  $\ell \sim 1000$ , but this effect can be counteracted by raising the baryon density [80]. In order to break this degeneracy, additional data are required. For example, an excellent fit to the CMB data is obtained with a scalar-only model with zero curvature and  $\omega_b = 0.0225$ ,  $\omega_c = 0.1120$ ,  $h = 0.704$ ,  $n_s = 0.967$  [24]. However, this is indistinguishable from a model where tensors dominate at  $\ell \lesssim 100$ ,

if we raise  $\omega_b$  to 0.03 and  $n_s$  to 1.2. This baryon density is too high for nucleosynthesis, which disfavors the high-tensor solution [81].

The reason the tensor component is introduced, and why it is so important, is that it is the only non-generic prediction of inflation. Slow-roll models of inflation involve two dimensionless parameters:

$$\epsilon \equiv \frac{M_{\text{P}}^2}{16\pi} \left( \frac{V'}{V} \right)^2, \quad \eta \equiv \frac{M_{\text{P}}^2}{8\pi} \left( \frac{V''}{V} \right), \quad (21.80)$$

where  $V$  is the inflaton potential, and dashes denote derivatives with respect to the inflation field. In terms of these, the tensor-to-scalar ratio is  $r \simeq 16\epsilon$ , and the spectral indices are  $n_s = 1 - 6\epsilon + 2\eta$  and  $n_t = -2\epsilon$ . The natural expectation of inflation is that the quasi-exponential phase ends once the slow-roll parameters become significantly non-zero, so that both  $n_s \neq 1$  and a significant tensor component are expected. These prediction can be avoided in some models, but it is undeniable that observation of such features would be a great triumph for inflation. Cosmology therefore stands at a fascinating point given that the most recent CMB data appear to reject the zero-tensor  $n_s = 1$  model at around  $2.4\sigma$ :  $n_s = 0.967 \pm 0.014$  [24]. If we insist on  $n_s = 1$ , then a very substantial tensor fraction would be required ( $r \simeq 0.2$ ), although the fit is better with  $r = 0$ . Assuming that no systematic error in this result can be identified, cosmology has passed a critical hurdle; the years ahead will be devoted to the task of breaking the tensor degeneracy — for which the main tool will be the polarization of the CMB [14].

#### 21.4.7. Probing dark energy and the nature of gravity :

The most radical element of our current cosmological model is the dark energy that accelerates the expansion. The energy density of this component is approximately  $(2.4 \text{ meV})^4$  (for  $w = -1$ ,  $\Omega_v = 0.75$ ,  $h = 0.73$ ), or roughly  $10^{-123} M_{\text{P}}^4$ , and such an un-naturally small number is hard to understand. Various quantum effects (most simply zero-point energy) should make contributions to the vacuum energy density: these may be truncated by new physics at high energy, but this presumably occurs at  $> 1 \text{ TeV}$  scales, not meV; thus the apparent energy scale of the vacuum is at least  $10^{15}$  times smaller than its natural value. This situation is well analysed in [82], which lists extreme escape routes — especially the multiverse viewpoint, according to which low values of  $\Lambda$  are rare, but high values suppress the formation of structure and observers. It is certainly impressive that Weinberg used such reasoning to predict the value of  $\Lambda$  before any data strongly indicated a non-zero value.

But it may be that the phenomenon of dark energy is entirely illusory. The necessity for this constituent arises from using the Friedmann equation to describe the evolution of the cosmic expansion; if this equation is incorrect, it would require the replacement of Einstein’s relativistic theory of gravity with some new alternative. A frontier of current cosmological research is to distinguish these possibilities [87,88]. We also note that it has been suggested that dark energy might be an illusion even within general relativity, owing to an incorrect treatment of averaging in an inhomogeneous Universe [89,90]. Many would argue that a standard Newtonian treatment of such issues should be adequate inside the cosmological horizon, but debate on this issue continues.

Dark Energy can differ from a classical cosmological constant in being a dynamical phenomenon [33,91], *e.g.*, a rolling scalar field (sometimes dubbed ‘quintessence’). Empirically, this means that it is endowed with two thermodynamic properties that astronomers can try to measure: the bulk equation of state and the sound speed. If the sound speed is close to the speed of light, the effect of this property is confined to very large scales, and mainly manifests itself in the large-angle multipoles of the CMB anisotropies [92]. The equation of state parameter governs the rate of change of the vacuum density:  $d \ln \rho_v / d \ln a = -3(1+w)$ , so it can be accessed via the evolving expansion rate,  $H(a)$ . This can be measured most cleanly by using the inbuilt natural ruler of large-scale structure: the Baryon Acoustic Oscillation horizon scale [93]:

$$D_{\text{BAO}} \simeq 147 (\Omega_m h^2 / 0.13)^{-0.25} (\Omega_b h^2 / 0.023)^{-0.08} \text{ Mpc}. \quad (21.81)$$

$H(a)$  is measured by radial clustering, since  $dr/dz = c/H$ ; clustering in the plane of the sky measures the integral of this. The expansion

rate is also measured by the growth of density fluctuations, where the pressure-free growth equation for the density perturbation is  $\delta + 2H(a)\dot{\delta} = 4\pi G\rho_0\delta$ . Thus, both the scale and amplitude of density fluctuations are sensitive to  $w(a)$  – but only weakly. These observables change by only typically 0.2% for a 1% change in  $w$ . Current constraints [24] are  $-1.11 < w < -0.89$  (95% confidence), so a substantial improvement will require us to limit systematics in data to a few parts in 1000.

Testing whether theories of gravity require revision can also be done using data on cosmological inhomogeneities. Two separate issues arise, concerning the metric perturbation potentials  $\Psi$  and  $\Phi$ , which affect respectively the time and space parts of the metric. In Einstein gravity, these potentials are both equal to the Newtonian gravitational potential, which satisfies Poisson's equation:  $\nabla^2\Phi/a^2 = 4\pi G\bar{\rho}\delta$ . Empirically, modifications of gravity require us to explore a change with scale and with time of the 'slip' ( $\Psi/\Phi$ ) and the effective  $G$  on the rhs of the Poisson equation. The former aspect can only be probed via gravitational lensing, whereas the latter can be addressed on 10-100 Mpc scales via the growth of clustering. Various schemes for parameterising modified gravity exist, but a practical approach is to assume that the growth rate can be tied to the density parameter:  $d\ln\delta/d\ln a = \Omega_m(a)$  [94]. The parameter  $\gamma$  is close to 0.55 for standard relativistic gravity, but can differ by around 0.1 from this value in many non-standard models. Clearly this parameterization is incomplete, since it explicitly rejects the possibility of early dark energy ( $\Omega_m(a) \rightarrow 1$  as  $a \rightarrow 0$ ), but it is a convenient way of capturing the power of various experiments. Current data are consistent with standard  $\Lambda$ CDM [86], and exclude variations in slip or effective  $G$  of larger than a few times 10%.

Current planning envisages a set of satellite probes that, a decade hence, will pursue these fundamental tests via gravitational lensing measurements over thousands of square degrees,  $> 10^8$  redshifts, and photometry of  $> 1000$  supernovae (WFIRST in the USA, Euclid in Europe) [22,23]. These experiments will measure both  $w$  and the perturbation growth rate to an accuracy of around 1%. The outcome will be either a validation of the standard relativistic vacuum-dominated big bang cosmology at a level of precision far beyond anything attempted to date, or the opening of entirely new directions in cosmological models.

#### References:

1. V.M. Slipher, *Pop. Astr.* **23**, 21 (1915).
2. K. Lundmark, *MNRAS* **84**, 747 (1924).
3. E. Hubble and M.L. Humason, *Astrophys. J.* **74**, 43 (1931).
4. G. Gamow, *Phys. Rev.* **70**, 572 (1946).
5. R.A. Alpher *et al.*, *Phys. Rev.* **73**, 803 (1948).
6. R.A. Alpher and R.C. Herman, *Phys. Rev.* **74**, 1737 (1948).
7. R.A. Alpher and R.C. Herman, *Phys. Rev.* **75**, 1089 (1949).
8. A.A. Penzias and R.W. Wilson, *Astrophys. J.* **142**, 419 (1965).
9. P.J.E. Peebles, *Principles of Physical Cosmology*, Princeton University Press (1993).
10. G. Börner, *The Early Universe: Facts and Fiction*, Springer-Verlag (1988).
11. E.W. Kolb and M.S. Turner, *The Early Universe*, Addison-Wesley (1990).
12. J.A. Peacock, *Cosmological Physics*, Camb. Univ. Press (1999).
13. A.R. Liddle and D. Lyth, *Cosmological Inflation and Large-Scale Structure*, Cambridge University Press (2000).
14. S. Dodelson, *Modern Cosmology*, Academic Press (2003).
15. V. Mukhanov, *Physical Foundations of Cosmology*, Cambridge University Press (2005).
16. S. Weinberg, *Cosmology*, Oxford Press (2008).
17. E.B. Gliner, *Sov. Phys. JETP* **22**, 378 (1966).
18. Y.B. Zeldovich, (1967), *Sov. Phys. Usp.* **11**, 381 (1968).
19. P.M. Garnavich *et al.*, *Astrophys. J.* **507**, 74 (1998).
20. S. Perlmutter *et al.*, *Phys. Rev. Lett.* **83**, 670 (1999).
21. I. Maor *et al.*, *Phys. Rev.* **D65**, 123003 (2002).
22. A. Albrecht *et al.*, *astro-ph/0609591*.
23. J. Peacock *et al.*, *astro-ph/0610906*.
24. E. Komatsu *et al.*, *Astrophys. J. Supp.* **191**, 18 (2011).
25. A.G. Riess *et al.*, *Astrophys. J.* **730**, 119 (2011).
26. A.G. Riess *et al.*, *Astrophys. J.* **116**, 1009 (1998).
27. S. Perlmutter *et al.*, *Astrophys. J.* **517**, 565 (1999).
28. A.G. Riess, *Pub. Astron. Soc. Pac.* **112**, 1284 (2000).
29. A.G. Riess *et al.*, *Astrophys. J.* **659**, 98 (2007).
30. T.M. Davis *et al.*, *Astrophys. J.* **666**, 716 (2007).
31. J.L. Tonry *et al.*, *Astrophys. J.* **594**, 1 (2003).
32. M. Kowalski *et al.*, *Astrophys. J.* **686**, 749 (2008).
33. I. Zlatev *et al.*, *Phys. Rev. Lett.* **82**, 896 (1999).
34. D.N. Spergel *et al.*, *Astrophys. J. Supp.* **170**, 377 (2007).
35. P. Astier *et al.*, *Astron. & Astrophys.* **447**, 31 (2006).
36. J.A. Johnson and M. Bolte, *Astrophys. J.* **554**, 888 (2001).
37. R. Cayrel *et al.*, *Nature* **409**, 691 (2001).
38. R. Jimenez and P. Padoan, *Astrophys. J.* **498**, 704 (1998).
39. E. Carretta *et al.*, *Astrophys. J.* **533**, 215 (2000).
40. M. Srednicki *et al.*, *Nucl. Phys.* **B310**, 693 (1988).
41. G. Mangano *et al.*, *Phys. Lett.* **B534**, 8 (2002).
42. A. Linde, *Phys. Rev.* **D14**, 3345 (1976).
43. A. Linde, *Rept. on Prog. in Phys.* **42**, 389 (1979).
44. C.E. Vayonakis, *Surv. High Energy Physics* **5**, 87 (1986).
45. S.A. Bonometto and A. Masiero, *Nuovo Cimento* **9N5**, 1 (1986).
46. A. Linde, *Part. Phys. & Inflat. Cosmology*, Harwood (1990).
47. K.A. Olive, *Phys. Reports* **190**, 3345 (1990).
48. D. Lyth and A. Riotto, *Phys. Reports* **314**, 1 (1999).
49. A.H. Guth, *Phys. Rev.* **D23**, 347 (1981).
50. A.D. Linde, *Phys. Lett.* **108B**, 389 (1982).
51. A. Albrecht & P.J. Steinhardt, *Phys. Rev. Lett.* **48**, 1220 (1982).
52. A.D. Sakharov, *Sov. Phys. JETP Lett.* **5**, 24 (1967).
53. S. Weinberg, *Phys. Rev. Lett.* **42**, 850 (1979).
54. D. Toussaint *et al.*, *Phys. Rev.* **D19**, 1036 (1979).
55. I. Affleck and M. Dine, *Nucl. Phys.* **B249**, 361 (1985).
56. V. Kuzmin *et al.*, *Phys. Lett.* **B155**, 36 (1985).
57. M. Fukugita and T. Yanagida, *Phys. Lett.* **B174**, 45 (1986).
58. R.H. Cyburt *et al.*, *Phys. Lett.* **B567**, 227 (2003).
59. R.H. Cyburt *et al.*, *JCAP* **0811**, 012 (2008).
60. K.A. Olive *et al.*, *Phys. Reports* **333**, 389 (2000).
61. J. M. O'meara *et al.*, *Astrophys. J.* **649**, L61 (2006).
62. D.J. Fixsen *et al.*, *Astrophys. J.* **473**, 576 (1996).
63. J.C. Mather *et al.*, *Astrophys. J.* **512**, 511 (1999).
64. S.M. Cole *et al.*, *MNRAS* **326**, 255 (2001).
65. A. Mesinger and Z. Haiman, *Astrophys. J.* **660**, 923 (2007).
66. M. Pettini *et al.*, *MNRAS* **391**, 1499 (2008).
67. S.D.M. White *et al.*, *Nature* **366**, 429 (1993).
68. S.W. Allen *et al.*, *MNRAS* **334**, L11 (2002).
69. S.W. Allen, *MNRAS* **296**, 392 (1998).
70. W.J. Percival *et al.*, *MNRAS* **327**, 1297 (2001).
71. S.M. Cole *et al.*, *MNRAS* **362**, 505 (2005).
72. W.J. Percival *et al.*, *Astrophys. J.* **657**, 645 (2007).
73. G. Efstathiou and J.R. Bond, *MNRAS* **218**, 103 (1986).
74. C. Gordon and A. Lewis, *Phys. Rev.* **D67**, 123513 (2003).
75. A. Vikhlinin *et al.*, *Astrophys. J.* **692**, 1060 (2009).
76. A. Dekel and O. Lahav, *Astrophys. J.* **520**, 24 (1999).
77. W.J. Percival *et al.*, *MNRAS* **381**, 1053 (2007).
78. W.J. Percival *et al.*, *MNRAS* **401**, 2148 (2010).
79. G. Efstathiou and J.R. Bond, *MNRAS* **304**, 75 (1999).
80. G.P. Efstathiou *et al.*, *MNRAS* **330**, L29 (2002).
81. G.P. Efstathiou, *MNRAS* **332**, 193 (2002).
82. S. Weinberg, *Rev. Mod. Phys.* **60**, 1 (1989).
83. L. Susskind, *hep-th/0302219* (2003).
84. B. Carr, *Universe or multiverse?* C.U.P. (2007).
85. L. Fu *et al.*, *Astron. & Astrophys.* **479**, 9 (2008).
86. S.F. Daniel *et al.*, *Phys. Rev.* **D81**, 123508 (2010).
87. W. Hu and I. Sawicki, *Phys. Rev.* **D76**, 4043 (2007).
88. B. Jain and P. Zhang, *Phys. Rev.* **D78**, 3503 (2008).
89. D.L. Wiltshire, *Phys. Rev. Lett.* **99**, 251101 (2007).
90. T. Buchert, *Gen. Rel. Grav.* **40**, 467 (2008).
91. C. Armendariz-Picon, V. Mukhanov, and P.J. Steinhardt, *Phys. Rev.* **D63**, 3510 (2001).
92. S. DeDeo, R.R. Caldwell, and P.J. Steinhardt, *Phys. Rev.* **D67**, 3509 (2003).
93. W. Hu, *arXiv:astro-ph/0407158* (2004).
94. E. Linder, *Phys. Rev.* **D72**, 43529 (2005).



## 22. BIG-BANG NUCLEOSYNTHESIS

Revised August 2011 by B.D. Fields (Univ. of Illinois) and S. Sarkar (Univ. of Oxford).

Big-Bang nucleosynthesis (BBN) offers the deepest reliable probe of the early Universe, being based on well-understood Standard Model physics [1–8]. Predictions of the abundances of the light elements, D,  $^3\text{He}$ ,  $^4\text{He}$ , and  $^7\text{Li}$ , synthesized at the end of the ‘first three minutes’, are in good overall agreement with the primordial abundances inferred from observational data, thus validating the standard hot Big-Bang cosmology (see [9] for a review). This is particularly impressive given that these abundances span nine orders of magnitude – from  $^4\text{He}/\text{H} \sim 0.08$  down to  $^7\text{Li}/\text{H} \sim 10^{-10}$  (ratios by number). Thus BBN provides powerful constraints on possible deviations from the standard cosmology, and on new physics beyond the Standard Model [4–7].

### 22.1. Theory

The synthesis of the light elements is sensitive to physical conditions in the early radiation-dominated era at a temperature  $T \sim 1$  MeV, corresponding to an age  $t \sim 1$  s. At higher temperatures, weak interactions were in thermal equilibrium, thus fixing the ratio of the neutron and proton number densities to be  $n/p = e^{-Q/T}$ , where  $Q = 1.293$  MeV is the neutron-proton mass difference. As the temperature dropped, the neutron-proton inter-conversion rate,  $\Gamma_{n \leftrightarrow p} \sim G_F^2 T^5$ , fell faster than the Hubble expansion rate,  $H \sim \sqrt{g_* G_N} T^2$ , where  $g_*$  counts the number of relativistic particle species determining the energy density in radiation (see ‘Big Bang Cosmology’ review). This resulted in departure from chemical equilibrium (‘freeze-out’) at  $T_{\text{fr}} \sim (g_* G_N / G_F^4)^{1/6} \simeq 1$  MeV. The neutron fraction at this time,  $n/p = e^{-Q/T_{\text{fr}}} \simeq 1/6$ , is thus sensitive to every known physical interaction, since  $Q$  is determined by both strong and electromagnetic interactions while  $T_{\text{fr}}$  depends on the weak as well as gravitational interactions. Moreover, the sensitivity to the Hubble expansion rate affords a probe of *e.g.*, the number of relativistic neutrino species [10]. After freeze-out, the neutrons were free to  $\beta$ -decay, so the neutron fraction dropped to  $n/p \simeq 1/7$  by the time nuclear reactions began. A simplified analytic model of freeze-out yields the  $n/p$  ratio to an accuracy of  $\sim 1\%$  [11,12].

The rates of these reactions depend on the density of baryons (strictly speaking, nucleons), which is usually expressed normalized to the relic blackbody photon density as  $\eta \equiv n_b/n_\gamma$ . As we shall see, all the light-element abundances can be explained with  $\eta_{10} \equiv \eta \times 10^{10}$  in the range 5.1–6.5 (95% CL). With  $n_\gamma$  fixed by the present CMB temperature 2.725 K (see ‘Cosmic Microwave Background’ review), this can be stated as the allowed range for the baryon mass density today,  $\rho_b = (3.5\text{--}4.5) \times 10^{-31}$  g cm $^{-3}$ , or as the baryonic fraction of the critical density,  $\Omega_b = \rho_b/\rho_{\text{crit}} \simeq \eta_{10} h^{-2}/274 = (0.019\text{--}0.024)h^{-2}$ , where  $h \equiv H_0/100$  km s $^{-1}$  Mpc $^{-1} = 0.72 \pm 0.08$  is the present Hubble parameter (see Cosmological Parameters review).

The nucleosynthesis chain begins with the formation of deuterium in the process  $p(n,\gamma)\text{D}$ . However, photo-dissociation by the high number density of photons delays production of deuterium (and other complex nuclei) well after  $T$  drops below the binding energy of deuterium,  $\Delta_{\text{D}} = 2.23$  MeV. The quantity  $\eta^{-1}e^{-\Delta_{\text{D}}/T}$ , *i.e.*, the number of photons per baryon above the deuterium photo-dissociation threshold, falls below unity at  $T \simeq 0.1$  MeV; nuclei can then begin to form without being immediately photo-dissociated again. Only 2-body reactions, such as  $\text{D}(p,\gamma)^3\text{He}$ ,  $^3\text{He}(\text{D},p)^4\text{He}$ , are important because the density by this time has become rather low – comparable to that of air!

Nearly all neutrons end up bound in the most stable light element  $^4\text{He}$ . Heavier nuclei do not form in any significant quantity both because of the absence of stable nuclei with mass number 5 or 8 (which impedes nucleosynthesis via  $n^4\text{He}$ ,  $p^4\text{He}$  or  $^4\text{He}^4\text{He}$  reactions), and the large Coulomb barriers for reactions such as  $^3\text{He}(^4\text{He},\gamma)^7\text{Li}$  and  $^3\text{He}(^4\text{He},\gamma)^7\text{Be}$ . Hence the primordial mass fraction of  $^4\text{He}$ , conventionally referred to as  $Y_p$ , can be estimated by the simple counting argument

$$Y_p = \frac{2(n/p)}{1+n/p} \simeq 0.25. \quad (22.1)$$

There is little sensitivity here to the actual nuclear reaction rates, which are, however, important in determining the other ‘left-over’

abundances: D and  $^3\text{He}$  at the level of a few times  $10^{-5}$  by number relative to H, and  $^7\text{Li}/\text{H}$  at the level of about  $10^{-10}$  (when  $\eta_{10}$  is in the range 1–10). These values can be understood in terms of approximate analytic arguments [12,13]. The experimental parameter most important in determining  $Y_p$  is the neutron lifetime,  $\tau_n$ , which normalizes (the inverse of)  $\Gamma_{n \leftrightarrow p}$ . The experimental uncertainty in  $\tau_n$  has been thought small, at  $\tau_n = 885.7 \pm 0.8$  s but recent measurements and re-analyses suggest possible systematic errors  $\sim 6$  times larger (see *N Baryons Listing*).

The elemental abundances shown in Fig. 22.1 as a function of  $\eta_{10}$  were calculated [14] using an updated version [15] of the Wagoner code [1]; other modern versions [16,17] are publicly available. The  $^4\text{He}$  curve includes small corrections due to radiative processes at zero and finite temperatures [18], non-equilibrium neutrino heating during  $e^\pm$  annihilation [19], and finite nucleon mass effects [20]; the range reflects primarily the  $2\sigma$  uncertainty in the neutron lifetime. The spread in the curves for D,  $^3\text{He}$ , and  $^7\text{Li}$  corresponds to the  $2\sigma$  uncertainties in nuclear cross sections, as estimated by Monte Carlo methods [21–22]. The input nuclear data have been carefully reassessed [14, 23–27], leading to improved precision in the abundance predictions. In particular, the uncertainty in  $^7\text{Li}/\text{H}$  at interesting values of  $\eta$  has been reduced recently by a factor  $\sim 2$ , a consequence of a similar reduction in the error budget [28] for the dominant mass-7 production channel  $^3\text{He}(^4\text{He},\gamma)^7\text{Be}$ . Polynomial fits to the predicted abundances and the error correlation matrix have been given [22,29]. The boxes in Fig. 22.1 show the observationally inferred primordial abundances with their associated statistical and systematic uncertainties, as discussed below.

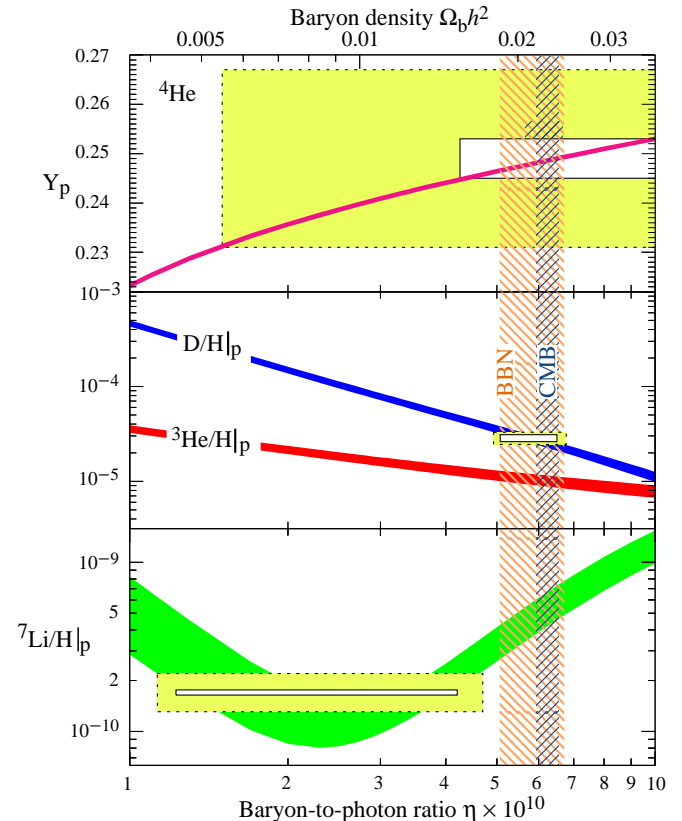


**Figure 22.1:** The abundances of  $^4\text{He}$ , D,  $^3\text{He}$ , and  $^7\text{Li}$  as predicted by the standard model of Big-Bang nucleosynthesis [14] – the bands show the 95% CL range. Boxes indicate the observed light element abundances (smaller boxes:  $\pm 2\sigma$  statistical errors; larger boxes:  $\pm 2\sigma$  statistical and systematic errors). The narrow vertical band indicates the CMB measure of the cosmic baryon density, while the wider band indicates the BBN concordance range (both at 95% CL).

## 22.2. Light Element Abundances

BBN theory predicts the universal abundances of D,  $^3\text{He}$ ,  $^4\text{He}$ , and  $^7\text{Li}$ , which are essentially fixed by  $t \sim 180$  s. Abundances are, however, usually observed at much later epochs, after stellar nucleosynthesis has commenced. The ejected remains of this stellar processing can alter the light element abundances from their primordial values, and also produce heavy elements such as C, N, O, and Fe ('metals'). Thus, one seeks astrophysical sites with low metal abundances, in order to measure light element abundances which are closer to primordial. For all of the light elements, systematic errors are an important (and often dominant) limitation to the precision with which primordial abundances can be inferred.

High-resolution spectra reveal the presence of D in high-redshift, low-metallicity quasar absorption systems via its isotope-shifted Lyman- $\alpha$  absorption [30–33]. It is believed that there are no astrophysical sources of deuterium [34], so any detection provides a lower limit to primordial D/H, and thus an upper limit on  $\eta$ ; for example, the local interstellar value of  $\text{D}/\text{H}|_{\text{p}} = (1.56 \pm 0.04) \times 10^{-5}$  [35] requires  $\eta_{10} \leq 9$ . Recent observations find an unexpected scatter of a factor of  $\sim 2$  [36], as well as correlations with heavy element abundances which suggest that interstellar D may suffer stellar processing (astration), but also partly reside in dust particles which evade gas-phase observations. This is supported by a measurement in the lower halo [37], which indicates that the Galactic D abundance has been reduced by a factor of only  $1.12 \pm 0.13$  since its formation. For the high-redshift systems, conventional models of galactic nucleosynthesis (chemical evolution) do not predict either of these effects for D/H [38].

The observed extragalactic D values are bracketed by the non-detection of D in a high-redshift system,  $\text{D}/\text{H}|_{\text{p}} < 6.7 \times 10^{-5}$  at  $1\sigma$  [39], and low values in some (damped Lyman- $\alpha$ ) systems [30,31]. Averaging the seven most precise observations of deuterium in quasar absorption systems gives  $\text{D}/\text{H} = (2.82 \pm 0.12) \times 10^{-5}$ , where the error is statistical only [32,33]. However, there remains concern over systematic errors, the dispersion between the values being much larger than is expected from the individual measurement errors ( $\chi^2 = 17.7$  for  $\nu = 6$  d.o.f.). Increasing the error by a factor  $\sqrt{\chi^2/\nu}$  gives, as shown in Fig. 22.1:

$$\text{D}/\text{H}|_{\text{p}} = (2.82 \pm 0.21) \times 10^{-5}. \quad (22.2)$$

$^4\text{He}$  can be observed in clouds of ionized hydrogen (H II regions), the most metal-poor of which are in dwarf galaxies. There is now a large body of data on  $^4\text{He}$  and CNO in such systems [40]. These data confirm that the small stellar contribution to helium is positively correlated with metal production. Extrapolating to zero metallicity gives the primordial  $^4\text{He}$  abundance [41]

$$Y_{\text{p}} = 0.249 \pm 0.009. \quad (22.3)$$

Here the latter error is a careful (and significantly enlarged) estimate of the systematic uncertainties which dominate, and is based on the scatter in different analyses of the physical properties of the H II regions [40,41]. Other recent extrapolations to zero metallicity give  $Y_{\text{p}} = 0.247 \pm 0.001$  or  $0.252 \pm 0.001$  depending on which set of He I emissivities are used [42], and  $Y_{\text{p}} = 0.248 \pm 0.003$  [43]. These are consistent (given the systematic errors) with the above estimate [41], which appears in Fig. 22.1. The CMB damping tail (see Cosmic Microwave Background review) is sensitive to the primordial  $^4\text{He}$  abundance [44]. Recent measurements find  $Y_{\text{p}} = 0.296 \pm 0.030$  [45], consistent with the above; future *Planck* measurements should tighten this result.

As we will see in more detail below, the primordial abundance of lithium now plays a central role in BBN, and possibly points to new physics. The systems best suited for Li observations are metal-poor stars in the spheroid (Pop II) of our Galaxy, which have metallicities going down to at least  $10^{-4}$ , and perhaps  $10^{-5}$  of the Solar value [46]. Observations have long shown [47–51] that Li does not vary significantly in Pop II stars with metallicities  $\lesssim 1/30$  of Solar — the 'Spite plateau' [47]. Precision data suggest a small but significant correlation between Li and Fe [48], which

can be understood as the result of Li production from Galactic cosmic rays [49]. Extrapolating to zero metallicity, one arrives at a primordial value  $\text{Li}/\text{H}|_{\text{p}} = (1.23 \pm 0.06^{+0.68}_{-0.32}) \times 10^{-10}$  [50], where the first error given is statistical and is very small due to the relatively large sample of 22 stars used. One source of systematic error stems from the differences in techniques used to determine the physical parameters (*e.g.*, the temperature) of the stellar atmosphere in which the Li absorption line is formed. Alternative analyses, using methods that give systematically higher temperatures, and in some cases different stars and stellar systems (globular clusters), yield  $\text{Li}/\text{H}|_{\text{p}} = (2.19 \pm 0.28) \times 10^{-10}$  [51],  $\text{Li}/\text{H}|_{\text{p}} = (2.34 \pm 0.32) \times 10^{-10}$  [52], and  $\text{Li}/\text{H}|_{\text{p}} = (1.26 \pm 0.26) \times 10^{-10}$  [53]; the differences with [50] indicate a systematic uncertainty of a factor of  $\sim 2$ . Moreover, it is possible that the Li in Pop II stars has been partially destroyed, due to mixing of the outer layers with the hotter interior [54]. Such processes can be constrained by the absence of significant scatter in Li versus Fe [48], and by observations of the fragile isotope  $^6\text{Li}$  [49]. Nevertheless, some depletion is likely to exist: a factor as large as  $\sim 1.8$  has been suggested [55] (and recent observations find a puzzling drop in Li/H in ultra-metal-poor stars [56]). Including these systematics, we estimate a primordial Li range which spans the ranges above, as shown in Fig. 22.1:

$$\text{Li}/\text{H}|_{\text{p}} = (1.7 \pm 0.06 \pm 0.44) \times 10^{-10}. \quad (22.4)$$

Stellar determination of Li abundances typically sum over both stable isotopes  $^6\text{Li}$  and  $^7\text{Li}$ . Recent high-precision measurements are sensitive to the tiny isotopic shift in Li absorption (which manifests itself in the shape of the blended, thermally broadened line) and indicate  $^6\text{Li}/^7\text{Li} \leq 0.15$  [57]. This confirms that  $^7\text{Li}$  is dominant, but surprisingly there is indication of a  $^6\text{Li}$  plateau (analogous to the  $^7\text{Li}$  plateau) which suggests a significant primordial  $^6\text{Li}$  abundance. However, caution must be exercised since convective motions in the star can generate similar asymmetries in the line shape, hence the deduced  $^6\text{Li}$  abundance is presently best interpreted as an upper limit [58].

Turning to  $^3\text{He}$ , the only data available are from the Solar system and (high-metallicity) H II regions in our Galaxy [59]. This makes inferring the primordial abundance difficult, a problem compounded by the fact that stellar nucleosynthesis models for  $^3\text{He}$  are in conflict with observations [60]. Consequently, it is no longer appropriate to use  $^3\text{He}$  as a cosmological probe; instead, one might hope to turn the problem around and constrain stellar astrophysics using the predicted primordial  $^3\text{He}$  abundance [61].

## 22.3. Concordance, Dark Matter, and the CMB

We now use the observed light element abundances to test the theory. We first consider standard BBN, which is based on Standard Model physics alone, so  $N_{\nu} = 3$  and the only free parameter is the baryon-to-photon ratio  $\eta$ . (The implications of BBN for physics beyond the Standard Model will be considered below, §4). Thus, any abundance measurement determines  $\eta$ , while additional measurements overconstrain the theory and thereby provide a consistency check.

First we note that the overlap in the  $\eta$  ranges spanned by the larger boxes in Fig. 22.1 indicates overall concordance. More quantitatively, when we account for theoretical uncertainties, as well as the statistical and systematic errors in observations, there is acceptable agreement among the abundances when

$$5.1 \leq \eta_{10} \leq 6.5 \text{ (95\% CL)}. \quad (22.5)$$

However, the agreement is much less satisfactory if we use only the quoted statistical errors in the observations. In particular, as seen in Fig. 22.1, D and  $^4\text{He}$  are consistent with each other, but favor a value of  $\eta$  which is higher by a factor of at least 2.4, and by at least  $\sim 4.2\sigma$  from that indicated by the  $^7\text{Li}$  abundance determined in stars. Furthermore, if the  $^6\text{Li}$  plateau [57] reflects a primordial component, it is  $\sim 1000$  times that expected in standard BBN; both these "lithium problems" may indicate new physics (see below).

Even so, the overall concordance is remarkable: using well-established microphysics we have extrapolated back to an age of  $\sim 1$  s

to correctly predict light element abundances spanning 9 orders of magnitude. This is a major success for the standard cosmology, and inspires confidence in extrapolation back to still earlier times.

This concordance provides a measure of the baryon content

$$0.019 \leq \Omega_b h^2 \leq 0.024 \text{ (95\% CL)}, \quad (22.6)$$

a result that plays a key role in our understanding of the matter budget of the Universe. First we note that  $\Omega_b \ll 1$ , *i.e.*, baryons cannot close the Universe [62]. Furthermore, the cosmic density of (optically) luminous matter is  $\Omega_{\text{lum}} \simeq 0.0024 h^{-1}$  [63], so that  $\Omega_b \gg \Omega_{\text{lum}}$ : most baryons are optically dark, probably in the form of a diffuse intergalactic medium [64]. Finally, given that  $\Omega_m \sim 0.3$  (see Dark Matter and Cosmological Parameters reviews), we infer that most matter in the Universe is not only dark, but also takes some non-baryonic (more precisely, non-nucleonic) form.

The BBN prediction for the cosmic baryon density can be tested through precision observations of CMB temperature fluctuations (see Cosmic Microwave Background review). One can determine  $\eta$  from the amplitudes of the acoustic peaks in the CMB angular power spectrum [65], making it possible to compare two measures of  $\eta$  using very different physics, at two widely separated epochs. In the standard cosmology, there is no change in  $\eta$  between BBN and CMB decoupling, thus, a comparison of  $\eta_{\text{BBN}}$  and  $\eta_{\text{CMB}}$  is a key test. Agreement would endorse the standard picture while disagreement could point to new physics during/between the BBN and CMB epochs.

The release of the WMAP results was a landmark event in this test of BBN. As with other cosmological parameter determinations from CMB data, the derived  $\eta_{\text{CMB}}$  depends on the adopted priors [66], in particular the form assumed for the power spectrum of primordial density fluctuations. If this is taken to be a scale-free power-law, the five-year WMAP data imply  $\Omega_b h^2 = 0.02273 \pm 0.00062$  or  $\eta_{10} = 6.23 \pm 0.17$  [67] as shown in Fig. 22.1. Other assumptions for the shape of the power spectrum can lead to baryon densities as low as  $\Omega_b h^2 = 0.0175 \pm 0.0007$  [68]. Thus, outstanding uncertainties regarding priors are a source of systematic error which presently exceeds the statistical error in the prediction for  $\eta$ .

It is remarkable that the CMB estimate of the baryon density is consistent with the BBN range quoted in Eq. (22.6), and in very good agreement with the value inferred from recent high-redshift D/H measurements [33] and  ${}^4\text{He}$  determinations; together these observations span diverse environments from redshifts  $z = 1000$  to the present.

Bearing in mind the importance of priors, the promise of precision determinations of the baryon density using the CMB motivates the use of this value as an input to BBN calculations. Within the context of the Standard Model, BBN then becomes a zero-parameter theory, and the light element abundances are completely determined to within the uncertainties in  $\eta_{\text{CMB}}$  and the BBN theoretical errors. Comparison with the observed abundances then can be used to test the astrophysics of post-BBN light element evolution [71]. Alternatively, one can consider possible physics beyond the Standard Model (*e.g.*, which might change the expansion rate during BBN) and then use all of the abundances to test such models; this is the subject of our final section.

## 22.4. The Lithium Problem

As Fig. 22.1 shows, stellar Li/H measurements are inconsistent with the CMB (and D/H), given the error budgets we have quoted. Recent updates in nuclear cross sections, stellar abundance systematics, and the WMAP results all *increase* the discrepancy to as much as  $5.3\sigma$ , depending on the stellar abundance analysis adopted. [14].

The question then becomes more pressing as to whether this mismatch comes from systematic errors in the observed abundances, and/or uncertainties in stellar astrophysics or nuclear inputs, or whether there might be new physics at work [7]. Nucleosynthesis models in which the baryon-to-photon ratio is inhomogeneous can alter abundances for a given  $\eta_{\text{BBN}}$ , but will overproduce  ${}^7\text{Li}$  [69]. Entropy generation by some non-standard process could have decreased  $\eta$  between the BBN era and CMB decoupling, however the lack of

spectral distortions in the CMB rules out any significant energy injection upto a redshift  $z \sim 10^7$  [70]. The most intriguing resolution of the lithium problem thus involves new physics during BBN [5–6].

For now this is a central unresolved issue in BBN. Nevertheless, the remarkable concordance between the CMB and D/H, as well as  ${}^4\text{He}$ , remain as non-trivial successes, and open windows onto the early Universe and particle physics, as we now discuss.

## 22.5. Beyond the Standard Model

Given the simple physics underlying BBN, it is remarkable that it still provides the most effective test for the cosmological viability of ideas concerning physics beyond the Standard Model. Although baryogenesis and inflation must have occurred at higher temperatures in the early Universe, we do not as yet have ‘standard models’ for these, so BBN still marks the boundary between the established and the speculative in Big Bang cosmology. It might appear possible to push the boundary back to the quark-hadron transition at  $T \sim \Lambda_{\text{QCD}}$ , or electroweak symmetry breaking at  $T \sim 1/\sqrt{G_{\text{F}}}$ ; however, so far no observable relics of these epochs have been identified, either theoretically or observationally. Thus, although the Standard Model provides a precise description of physics up to the Fermi scale, cosmology cannot be traced in detail before the BBN era.

Limits on particle physics beyond the Standard Model come mainly from the observational bounds on the  ${}^4\text{He}$  abundance. This is proportional to the  $n/p$  ratio which is determined when the weak-interaction rates fall behind the Hubble expansion rate at  $T_{\text{fr}} \sim 1 \text{ MeV}$ . The presence of additional neutrino flavors (or of any other relativistic species) at this time increases  $g_*$ , hence the expansion rate, leading to a larger value of  $T_{\text{fr}}$ ,  $n/p$ , and therefore  $Y_{\text{p}}$  [10,72]. In the Standard Model, the number of relativistic particle species at 1 MeV is  $g_* = 5.5 + \frac{7}{4}N_\nu$ , where the factor 5.5 accounts for photons and  $e^\pm$ , and  $N_\nu$  is the *effective* number of (nearly massless) neutrino flavors (see Big Bang Cosmology review). The helium curves in Fig. 22.1 were computed taking  $N_\nu = 3$ ; small corrections for non-equilibrium neutrino heating [19] are included in the thermal evolution and lead to an effective  $N_\nu = 3.04$  compared to assuming instantaneous neutrino freezeout (see, *e.g.*, Big Bang Cosmology review). The computed  ${}^4\text{He}$  abundance scales as  $\Delta Y_{\text{p}} \simeq 0.013 \Delta N_\nu$  [11]. Clearly the central value for  $N_\nu$  from BBN will depend on  $\eta$ , which is independently determined (with weaker sensitivity to  $N_\nu$ ) by the adopted D or  ${}^7\text{Li}$  abundance. For example, if the best value for the observed primordial  ${}^4\text{He}$  abundance is 0.249, then, for  $\eta_{10} \sim 6$ , the central value for  $N_\nu$  is very close to 3. This limit depends sensitively on the adopted light element abundances, particularly  $Y_{\text{p}}$ . A maximum likelihood analysis on  $\eta$  and  $N_\nu$  based on the above  ${}^4\text{He}$  and D abundances finds the (correlated) 95% CL ranges to be  $4.9 < \eta_{10} < 7.1$  and  $1.8 < N_\nu < 4.5$  [73]. Similar results were obtained in another study [74] which presented a simpler method to extract such bounds based on  $\chi^2$  statistics, given a set of input abundances. Using the CMB determination of  $\eta$  improves the constraints: including the most recent WMAP data yields  $N_\nu < 4.2$  (95% CL) [75]. It is also worth noting that CMB damping tail measurements alone now find  $N_\nu = 3.85 \pm 0.62$  [45].

Just as one can use the measured helium abundance to place limits on  $g_*$  [72], any changes in the strong, weak, electromagnetic, or gravitational coupling constants, arising *e.g.*, from the dynamics of new dimensions, can be similarly constrained [76], as can be any speed-up of the expansion rate in *e.g.* scalar-tensor theories of gravity [77].

The limits on  $N_\nu$  can be translated into limits on other types of particles or particle masses that would affect the expansion rate of the Universe during nucleosynthesis. For example, consider ‘sterile’ neutrinos with only right-handed interactions of strength  $G_{\text{R}} < G_{\text{F}}$ . Such particles would decouple at higher temperature than (left-handed) neutrinos, so their number density ( $\propto T^3$ ) relative to neutrinos would be reduced by any subsequent entropy release, *e.g.*, due to annihilations of massive particles that become non-relativistic between the two decoupling temperatures. Thus (relativistic) particles with less than full strength weak interactions contribute less to the energy density than particles that remain in equilibrium up to the time of nucleosynthesis [78]. If we impose  $N_\nu < 4$  as an

illustrative constraint, then the three right-handed neutrinos must have a temperature  $3(T_{\nu_R}/T_{\nu_L})^4 < 1$ . Since the temperature of the decoupled  $\nu_R$ 's is determined by entropy conservation (see Big Bang Cosmology review),  $T_{\nu_R}/T_{\nu_L} = [(43/4)/g_*(T_d)]^{1/3} < 0.76$ , where  $T_d$  is the decoupling temperature of the  $\nu_R$ 's. This requires  $g_*(T_d) > 24$ , so decoupling must have occurred at  $T_d > 140$  MeV. The decoupling temperature is related to  $G_R$  through  $(G_R/G_F)^2 \sim (T_d/3 \text{ MeV})^{-3}$ , where 3 MeV is the decoupling temperature for  $\nu_L$ 's. This yields a limit  $G_R \lesssim 10^{-2} G_F$ . The above argument sets lower limits on the masses of new  $Z'$  gauge bosons to which right-handed neutrinos would be coupled in models of superstrings [79], or extended technicolor [80]. Similarly a Dirac magnetic moment for neutrinos, which would allow the right-handed states to be produced through scattering and thus increase  $g_*$ , can be significantly constrained [81], as can any new interactions for neutrinos which have a similar effect [82]. Right-handed states can be populated directly by helicity-flip scattering if the neutrino mass is large enough, and this property has been used to infer a bound of  $m_{\nu\tau} \lesssim 1$  MeV taking  $N_\nu < 4$  [83]. If there is mixing between active and sterile neutrinos then the effect on BBN is more complicated [84].

The limit on the expansion rate during BBN can also be translated into bounds on the mass/lifetime of non-relativistic particles which decay during BBN. This results in an even faster speed-up rate, and typically also change the entropy [85]. If the decays include Standard Model particles, the resulting electromagnetic [86–87] and/or hadronic [88] cascades can strongly perturb the light elements, which leads to even stronger constraints. Such arguments have been applied to rule out a MeV mass  $\nu_\tau$ , which decays during nucleosynthesis [89].

Such arguments have proved very effective in constraining supersymmetry. For example, if the gravitino is very light and contributes to  $g_*$ , the illustrative BBN limit  $N_\nu < 4$  requires its mass to exceed  $\sim 1$  eV [90]. Alternatively, much recent interest has focussed on the case in which the next-to-lightest supersymmetric particle is metastable and decays during or after BBN. The constraints on unstable particles discussed above imply stringent bounds on the allowed abundance of such particles [88]; if the metastable particle is charged (*e.g.*, the stau), then it is possible for it to form atom-like electromagnetic bound states with nuclei, and the resulting impact on light elements can be quite complex [91]. Such decays can destroy  ${}^7\text{Li}$  and/or produce  ${}^6\text{Li}$ , leading to a possible supersymmetric solution to the lithium problems noted above [92] (see [5] for a review). In addition, these arguments impose powerful constraints on supersymmetric inflationary cosmology [87–88], in particular thermal leptogenesis [93]. These can be evaded only if the gravitino is massive enough to decay before BBN, *i.e.*,  $m_{3/2} \gtrsim 50$  TeV [94] (which would be unnatural), or if it is in fact the lightest supersymmetric particle and thus stable [87,95]. Similar constraints apply to moduli – very weakly coupled fields in string theory which obtain an electroweak-scale mass from supersymmetry breaking [96].

Finally, we mention that BBN places powerful constraints on the possibility that there are new large dimensions in nature, perhaps enabling the scale of quantum gravity to be as low as the electroweak scale [97]. Thus, Standard Model fields may be localized on a ‘brane,’ while gravity alone propagates in the ‘bulk.’ It has been further noted that the new dimensions may be non-compact, even infinite [98], and the cosmology of such models has attracted considerable attention. The expansion rate in the early Universe can be significantly modified, so BBN is able to set interesting constraints on such possibilities [99].

## References:

- R.V. Wagoner *et al.*, *Astrophys. J.* **148**, 3 (1967).
- G. Steigman, *Ann. Rev. Nucl. and Part. Sci.* **57**, 463 (2007).
- F. Iocco, *Phys. Reports* **472**, 1 (2009).
- S. Sarkar, *Rept. on Prog. in Phys.* **59**, 1493 (1996).
- K. Jedamzik and M. Pospelov, *New J. Phys.* **11**, 105028 (2009).
- M. Pospelov and J. Pradler, *Ann. Rev. Nucl. and Part. Sci.* **60**, 539 (2010).
- B.D. Fields, *Ann. Rev. Nucl. and Part. Sci.* **61**, in press (2011).
- D.N. Schramm and M.S. Turner, *Rev. Mod. Phys.* **70**, 303 (1998).
- K.A. Olive *et al.*, *Phys. Reports* **333**, 389 (2000).
- P.J.E. Peebles, *Phys. Rev. Lett.* **16**, 411 (1966).
- J. Bernstein *et al.*, *Rev. Mod. Phys.* **61**, 25 (1989).
- S. Mukhanov, *Int. J. Theor. Phys.* **143**, 669 (2004).
- R. Esmailzadeh *et al.*, *Astrophys. J.* **378**, 504 (1991).
- R.H. Cyburt *et al.*, *JCAP* **0811**, 012 (2008).
- R.H. Cyburt *et al.*, *New Astron.* **6**, 215 (2001).
- L. Kawano, FERMILAB-PUB-92/04-A.
- O. Pisanti *et al.*, *Comput. Phys. Commun.* **178**, 956 (2008).
- S. Esposito *et al.*, *Nucl. Phys.* **B568**, 421 (2000).
- S. Dodelson and M.S. Turner, *Phys. Rev.* **D46**, 3372 (1992).
- D. Seckel, [hep-ph/9305311](#);  
R. Lopez and M.S. Turner, *Phys. Rev.* **D59**, 103502 (1999).
- M.S. Smith *et al.*, *Astrophys. J. Supp.* **85**, 219 (1993).
- G. Fiorentini *et al.*, *Phys. Rev.* **D58**, 063506 (1998).
- K.M. Nollett and S. Burles, *Phys. Rev.* **D61**, 123505 (2000).
- R.H. Cyburt, *Phys. Rev.* **D70**, 023505 (2004).
- P.D. Serpico *et al.*, *JCAP* **12**, 010 (2004).
- A. Coc *et al.*, *Astrophys. J. Supp.*, submitted (2011).
- R.N. Boyd *et al.*, *Phys. Rev.* **D82**, 105005 (2010).
- R.H. Cyburt and B. Davids, *Phys. Rev.* **C78**, 012 (2008).
- K.M. Nollett *et al.*, *Astrophys. J. Lett.* **552**, L1 (2001).
- S. D’Odorico *et al.*, *Astron. & Astrophys.* **368**, L21 (2001).
- M. Pettini and D. Bowen, *Astrophys. J.* **560**, 41 (2001).
- J.M. O’Meara *et al.*, *Astrophys. J. Lett.* **649**, L61 (2006).
- M. Pettini *et al.*, *MNRAS* **391**, 1499 (2008).
- R.I. Epstein *et al.*, *Nature* **263**, 198 (1976).
- B.E. Wood *et al.*, *Astrophys. J.* **609**, 838 (2004).
- J.L. Linsky *et al.*, *Astrophys. J.* **647**, 1106 (2006).
- B.D. Savage *et al.*, *Astrophys. J.* **659**, 1222 (2007).
- B.D. Fields, *Astrophys. J.* **456**, 678 (1996).
- D. Kirkman *et al.*, *Astrophys. J.* **529**, 655 (2000).
- Y.I. Izotov *et al.*, *Astrophys. J.* **527**, 757 (1999).
- K.A. Olive and E. Skillman, *Astrophys. J.* **617**, 29 (2004).
- Y.I. Izotov *et al.*, *Astrophys. J.* **662**, 15 (2007).
- M. Peimbert *et al.*, *Astrophys. J.* **667**, 636 (2007).
- R. Trotta and S.H. Hansen, *Phys. Rev.* **D69**, 023509 (2004).
- R. Keisler *et al.*, *Astrophys. J.* submitted (2011),  
[arXiv:1105.3182](#).
- N. Christlieb *et al.*, *Nature* **419**, 904 (2002).
- M. Spite and F. Spite, *Nature* **297**, 483 (1982).
- S.G. Ryan *et al.*, *Astrophys. J.* **523**, 654 (1999).
- E. Vangioni-Flam *et al.*, *New Astron.* **4**, 245 (1999).
- S.G. Ryan *et al.*, *Astrophys. J. Lett.* **530**, L57 (2000).
- P. Bonifacio *et al.*, *Astron. & Astrophys.* **390**, 91 (2002).
- J. Meléndez and I. Ramirez, *Astrophys. J. Lett.* **615**, 33 (2004).
- P. Bonifacio *et al.*, *Astron. & Astrophys.* **462**, 851 (2007).
- M.H. Pinsonneault *et al.*, *Astrophys. J.* **574**, 389 (2002).
- A.J. Korn *et al.*, *Nature* **442**, 657 (2006).
- W. Aoki, *Astrophys. J.* **698**, 1803 (2009);  
A. Hosford *et al.*, *Astron. Astrophys.*, **493**, 601 (2009);  
J. Melendez *et al.*, *Astron. Astrophys.*, **515**, L3 (2010);  
L. Sbordone *et al.*, *Astron. Astrophys.*, **522**, A26 (2010).
- M. Asplund *et al.*, *Astrophys. J.* **644**, 229 (2006).
- R. Cayrel *et al.*, *Astron. & Astrophys.* **473**, L37 (2007).
- T.M. Bania *et al.*, *Nature* **415**, 54 (2002).
- K.A. Olive *et al.*, *Astrophys. J.* **479**, 752 (1997).
- E. Vangioni-Flam *et al.*, *Astrophys. J.* **585**, 611 (2003).
- H. Reeves *et al.*, *Astrophys. J.* **179**, 909 (1973).
- M. Fukugita and P.J.E. Peebles, *Astrophys. J.* **616**, 643 (2004).
- R. Cen and J.P. Ostriker, *Astrophys. J.* **514**, 1 (1999).
- G. Jungman *et al.*, *Phys. Rev.* **D54**, 1332 (1996).
- M. Tegmark *et al.*, *Phys. Rev.* **D63**, 043007 (2001).
- J. Dunkley *et al.*, *Astrophys. J. Supp.* **180**, 306 (2009).
- P. Hunt and S. Sarkar, *Phys. Rev.* **D76**, 123504 (2007).
- K. Jedamzik and J.B. Rehm, *Phys. Rev.* **D64**, 023510 (2001).
- D.J. Fixsen *et al.*, *Astrophys. J.* **473**, 576 (1996).
- R.H. Cyburt *et al.*, *Phys. Lett.* **B567**, 227 (2003).
- G. Steigman *et al.*, *Phys. Lett.* **B66**, 202 (1977).
- R.H. Cyburt *et al.*, *Astropart. Phys.* **23**, 313 (2005).
- E. Lisi *et al.*, *Phys. Rev.* **D59**, 123520 (1999).
- G. Mangano and P.D. Serpico, *Phys. Lett.* **B701**, 296 (2011).

76. E.W. Kolb *et al.*, Phys. Rev. **D33**, 869 (1986);  
F.S. Accetta *et al.*, Phys. Lett. **B248**, 146 (1990);  
B.A. Campbell and K.A. Olive, Phys. Lett. **B345**, 429 (1995);  
K.M. Nollett and R. Lopez, Phys. Rev. **D66**, 063507 (2002);  
C. Bambi *et al.*, Phys. Rev. **D71**, 123524 (2005).
77. A. Coc *et al.*, Phys. Rev. **D73**, 083525 (2006).
78. K.A. Olive *et al.*, Nucl. Phys. **B180**, 497 (1981).
79. J. Ellis *et al.*, Phys. Lett. **B167**, 457 (1986).
80. L.M. Krauss *et al.*, Phys. Rev. Lett. **71**, 823 (1993).
81. J.A. Morgan, Phys. Lett. **B102**, 247 (1981).
82. E.W. Kolb *et al.*, Phys. Rev. **D34**, 2197 (1986);  
J.A. Grifols and E. Massó, Mod. Phys. Lett. **A2**, 205 (1987);  
K.S. Babu *et al.*, Phys. Rev. Lett. **67**, 545 (1991).
83. A.D. Dolgov *et al.*, Nucl. Phys. **B524**, 621 (1998).
84. K. Enqvist *et al.*, Nucl. Phys. **B373**, 498 (1992);  
A.D. Dolgov, Phys. Reports **370**, 333 (2002).
85. K. Sato and M. Kobayashi, Prog. Theor. Phys. **58**, 1775 (1977);  
D.A. Dicus *et al.*, Phys. Rev. **D17**, 1529 (1978);  
R.J. Scherrer and M.S. Turner, Astrophys. J. **331**, 19 (1988).
86. D. Lindley, MNRAS **188**, 15 (1979); Astrophys. J. **294**, 1 (1985).
87. J. Ellis *et al.*, Nucl. Phys. **B259**, 175 (1985);  
J. Ellis *et al.*, Nucl. Phys. **B373**, 399 (1992);  
R.H. Cyburt *et al.*, Phys. Rev. **D67**, 103521 (2003).
88. M.H. Reno and D. Seckel, Phys. Rev. **D37**, 3441 (1988);  
S. Dimopoulos *et al.*, Nucl. Phys. **B311**, 699 (1989);  
K. Kohri *et al.*, Phys. Rev. **D71**, 083502 (2005).
89. S. Sarkar and A.M. Cooper, Phys. Lett. **B148**, 347 (1984).
90. J.A. Grifols *et al.*, Phys. Lett. **B400**, 124 (1997).
91. M. Pospelov *et al.*, Phys. Rev. Lett. **98**, 231301 (2007);  
R.H. Cyburt *et al.*, JCAP **11**, 014 (2006);  
M. Kawasaki *et al.*, Phys. Lett. **B649**, 436 (2007).
92. K. Jedamzik *et al.*, JCAP **07**, 007 (2006).
93. S. Davidson *et al.*, Phys. Rev. **466**, 105 (2008).
94. S. Weinberg, Phys. Rev. Lett. **48**, 1303 (1979).
95. M. Bolz *et al.*, Nucl. Phys. **B606**, 518 (2001).
96. G. Coughlan *et al.*, Phys. Lett. **B131**, 59 (1983).
97. N. Arkani-Hamed *et al.*, Phys. Rev. **D59**, 086004 (1999).
98. L. Randall and R. Sundrum, Phys. Rev. Lett. **83**, 3370 (1999).
99. J.M. Cline *et al.*, Phys. Rev. Lett. **83**, 4245 (1999);  
P. Binetruy *et al.*, Phys. Lett. **B477**, 285 (2000).

## 23. THE COSMOLOGICAL PARAMETERS

Updated September 2011, by O. Lahav (University College London) and A.R. Liddle (University of Sussex).

### 23.1. Parametrizing the Universe

Rapid advances in observational cosmology have led to the establishment of a precision cosmological model, with many of the key cosmological parameters determined to one or two significant figure accuracy. Particularly prominent are measurements of cosmic microwave background (CMB) anisotropies, led by the seven-year results from the Wilkinson Microwave Anisotropy Probe (WMAP) [1–3]. However the most accurate model of the Universe requires consideration of a wide range of different types of observation, with complementary probes providing consistency checks, lifting parameter degeneracies, and enabling the strongest constraints to be placed.

The term ‘cosmological parameters’ is forever increasing in its scope, and nowadays includes the parametrization of some functions, as well as simple numbers describing properties of the Universe. The original usage referred to the parameters describing the global dynamics of the Universe, such as its expansion rate and curvature. Also now of great interest is how the matter budget of the Universe is built up from its constituents: baryons, photons, neutrinos, dark matter, and dark energy. We need to describe the nature of perturbations in the Universe, through global statistical descriptors such as the matter and radiation power spectra. There may also be parameters describing the physical state of the Universe, such as the ionization fraction as a function of time during the era since recombination. Typical comparisons of cosmological models with observational data now feature between five and ten parameters.

#### 23.1.1. The global description of the Universe :

Ordinarily, the Universe is taken to be a perturbed Robertson–Walker space-time with dynamics governed by Einstein’s equations. This is described in detail by Olive and Peacock in this volume. Using the density parameters  $\Omega_i$  for the various matter species and  $\Omega_\Lambda$  for the cosmological constant, the Friedmann equation can be written

$$\sum_i \Omega_i + \Omega_\Lambda - 1 = \frac{k}{R^2 H^2}, \quad (23.1)$$

where the sum is over all the different species of material in the Universe. This equation applies at any epoch, but later in this article we will use the symbols  $\Omega_i$  and  $\Omega_\Lambda$  to refer to the present values. A typical collection would be baryons, photons, neutrinos, and dark matter (given charge neutrality, the electron density is guaranteed to be too small to be worth considering separately and is included with the baryons).

The complete present state of the homogeneous Universe can be described by giving the current values of all the density parameters and of the Hubble parameter  $h$ . These also allow us to track the history of the Universe back in time, at least until an epoch where interactions allow interchanges between the densities of the different species, which is believed to have last happened at neutrino decoupling, shortly before Big Bang Nucleosynthesis (BBN). To probe further back into the Universe’s history requires assumptions about particle interactions, and perhaps about the nature of physical laws themselves.

#### 23.1.2. Neutrinos :

The standard neutrino sector has three flavors. For neutrinos of mass in the range  $5 \times 10^{-4}$  eV to 1 MeV, the density parameter in neutrinos is predicted to be

$$\Omega_\nu h^2 = \frac{\sum m_\nu}{93 \text{ eV}}, \quad (23.2)$$

where the sum is over all families with mass in that range (higher masses need a more sophisticated calculation). We use units with  $c = 1$  throughout. Results on atmospheric and Solar neutrino oscillations [4] imply non-zero mass-squared differences between the three neutrino flavors. These oscillation experiments cannot tell us the absolute neutrino masses, but within the simple assumption of a mass hierarchy suggest a lower limit of approximately 0.05 eV on the sum of the neutrino masses.

For a total mass as small as 0.1 eV, this could have a potentially observable effect on the formation of structure, as neutrino free-streaming damps the growth of perturbations. Present cosmological observations have shown no convincing evidence of any effects from either neutrino masses or an otherwise non-standard neutrino sector, and impose quite stringent limits, which we summarize in Section 23.3.4. Accordingly, the usual assumption is that the masses are too small to have a significant cosmological impact at present data accuracy. However, we note that the inclusion of neutrino mass as a free parameter can affect the derived values of other cosmological parameters.

The cosmological effect of neutrinos can also be modified if the neutrinos have decay channels, or if there is a large asymmetry in the lepton sector manifested as a different number density of neutrinos versus anti-neutrinos. This latter effect would need to be of order unity to be significant (rather than the  $10^{-9}$  seen in the baryon sector), which may be in conflict with nucleosynthesis [5].

#### 23.1.3. Inflation and perturbations :

A complete model of the Universe should include a description of deviations from homogeneity, at least in a statistical way. Indeed, some of the most powerful probes of the parameters described above come from the evolution of perturbations, so their study is naturally intertwined in the determination of cosmological parameters.

There are many different notations used to describe the perturbations, both in terms of the quantity used to describe the perturbations and the definition of the statistical measure. We use the dimensionless power spectrum  $\Delta^2$  as defined in Olive and Peacock (also denoted  $\mathcal{P}$  in some of the literature). If the perturbations obey Gaussian statistics, the power spectrum provides a complete description of their properties.

From a theoretical perspective, a useful quantity to describe the perturbations is the curvature perturbation  $\mathcal{R}$ , which measures the spatial curvature of a comoving slicing of the space-time. A case of particular interest is the Harrison–Zel’dovich spectrum, which corresponds to a constant  $\Delta_{\mathcal{R}}^2$ . More generally, one can approximate the spectrum by a power-law, writing

$$\Delta_{\mathcal{R}}^2(k) = \Delta_{\mathcal{R}}^2(k_*) \left[ \frac{k}{k_*} \right]^{n-1}, \quad (23.3)$$

where  $n$  is known as the spectral index, always defined so that  $n = 1$  for the Harrison–Zel’dovich spectrum, and  $k_*$  is an arbitrarily chosen scale. The initial spectrum, defined at some early epoch of the Universe’s history, is usually taken to have a simple form such as this power-law, and we will see that observations require  $n$  close to one, which corresponds to the perturbations in the curvature being independent of scale. Subsequent evolution will modify the spectrum from its initial form.

The simplest viable mechanism for generating the observed perturbations is the inflationary cosmology, which posits a period of accelerated expansion in the Universe’s early stages [6,7]. It is a useful working hypothesis that this is the sole mechanism for generating perturbations, and it may further be assumed to be the simplest class of inflationary model, where the dynamics are equivalent to that of a single scalar field  $\phi$  slowly rolling on a potential  $V(\phi)$ . One may seek to verify that this simple picture can match observations and to determine the properties of  $V(\phi)$  from the observational data. Alternatively, more complicated models, perhaps motivated by contemporary fundamental physics ideas, may be tested on a model-by-model basis.

Inflation generates perturbations through the amplification of quantum fluctuations, which are stretched to astrophysical scales by the rapid expansion. The simplest models generate two types, density perturbations which come from fluctuations in the scalar field and its corresponding scalar metric perturbation, and gravitational waves which are tensor metric fluctuations. The former experience gravitational instability and lead to structure formation, while the latter can influence the CMB anisotropies. Defining slow-roll parameters, with primes indicating derivatives with respect to the scalar field, as

$$\epsilon = \frac{m_{\text{Pl}}^2}{16\pi} \left( \frac{V'}{V} \right)^2 ; \quad \eta = \frac{m_{\text{Pl}}^2}{8\pi} \frac{V''}{V}, \quad (23.4)$$

which should satisfy  $\epsilon, |\eta| \ll 1$ , the spectra can be computed using the slow-roll approximation as

$$\Delta_{\mathcal{R}}^2(k) \simeq \frac{8}{3m_{\text{Pl}}^4} \frac{V}{\epsilon} \Big|_{k=aH} ; \quad \Delta_{\text{grav}}^2(k) \simeq \frac{128}{3m_{\text{Pl}}^4} V \Big|_{k=aH}. \quad (23.5)$$

In each case, the expressions on the right-hand side are to be evaluated when the scale  $k$  is equal to the Hubble radius during inflation. The symbol ‘ $\simeq$ ’ here indicates use of the slow-roll approximation, which is expected to be accurate to a few percent or better.

From these expressions, we can compute the spectral indices

$$n \simeq 1 - 6\epsilon + 2\eta \quad ; \quad n_{\text{grav}} \simeq -2\epsilon. \quad (23.6)$$

Another useful quantity is the ratio of the two spectra, defined by

$$r \equiv \frac{\Delta_{\text{grav}}^2(k_*)}{\Delta_{\mathcal{R}}^2(k_*)}. \quad (23.7)$$

This convention matches that used by WMAP [2] (there are some alternative historical definitions which lead to a slightly different prefactor in the following equation). We have

$$r \simeq 16\epsilon \simeq -8n_{\text{grav}}, \quad (23.8)$$

which is known as the consistency equation.

In general, one could consider corrections to the power-law approximation, which we discuss later. However, for now we make the working assumption that the spectra can be approximated by power laws. The consistency equation shows that  $r$  and  $n_{\text{grav}}$  are not independent parameters, and so the simplest inflation models give initial conditions described by three parameters, usually taken as  $\Delta_{\mathcal{R}}^2$ ,  $n$ , and  $r$ , all to be evaluated at some scale  $k_*$ , usually the ‘statistical center’ of the range explored by the data. Alternatively, one could use the parametrization  $V$ ,  $\epsilon$ , and  $\eta$ , all evaluated at a point on the putative inflationary potential.

After the perturbations are created in the early Universe, they undergo a complex evolution up until the time they are observed in the present Universe. While the perturbations are small, this can be accurately followed using a linear theory numerical code such as CMBFAST or CAMB [8]. This works right up to the present for the CMB, but for density perturbations on small scales non-linear evolution is important and can be addressed by a variety of semi-analytical and numerical techniques. However the analysis is made, the outcome of the evolution is in principle determined by the cosmological model, and by the parameters describing the initial perturbations, and hence can be used to determine them.

Of particular interest are CMB anisotropies. Both the total intensity and two independent polarization modes are predicted to have anisotropies. These can be described by the radiation angular power spectra  $C_\ell$  as defined in the article of Scott and Smoot in this volume, and again provide a complete description if the density perturbations are Gaussian.

#### 23.1.4. The standard cosmological model :

We now have most of the ingredients in place to describe the cosmological model. Beyond those of the previous subsections, there are two parameters which are essential: a measure of the ionization state of the Universe and the galaxy bias parameter. The Universe is known to be highly ionized at low redshifts (otherwise radiation from distant quasars would be heavily absorbed in the ultra-violet), and the ionized electrons can scatter microwave photons altering the pattern of observed anisotropies. The most convenient parameter to describe this is the optical depth to scattering  $\tau$  (*i.e.*, the probability that a given photon scatters once); in the approximation of instantaneous and complete reionization, this could equivalently be described by the redshift of reionization  $z_{\text{ion}}$ . The bias parameter, described fully later, is needed to relate the observed galaxy power spectrum to the predicted dark matter power spectrum. The basic set of cosmological parameters is therefore as shown in Table 23.1. The spatial curvature does not appear in the list, because it can be determined from the other parameters using Eq. (23.1) (and is assumed zero for the observed

values shown). The total present matter density  $\Omega_{\text{m}} = \Omega_{\text{cdm}} + \Omega_{\text{b}}$  is sometimes used in place of the dark matter density.

Most attention to date has been on parameter estimation, where a set of parameters is chosen by hand and the aim is to constrain them. Interest has been growing towards the higher-level inference problem of model selection, which compares different choices of parameter sets. Bayesian inference offers an attractive framework for cosmological model selection, setting a tension between model predictiveness and ability to fit the data.

**Table 23.1:** The basic set of cosmological parameters. We give values (with some additional rounding) as obtained using a fit of a spatially-flat  $\Lambda$ CDM cosmology with a power-law initial spectrum to WMAP7 data alone: Table 10, left column of Ref. 2. Tensors are assumed zero except in quoting a limit on them. The exact values and uncertainties depend on both the precise data-sets used and the choice of parameters allowed to vary. Limits on  $\Omega_\Lambda$  and  $h$  weaken if the Universe is not assumed flat. The density perturbation amplitude is specified by the derived parameter  $\sigma_8$ . Uncertainties are one-sigma/68% confidence unless otherwise stated.

Parameter	Symbol	Value
Hubble parameter	$h$	$0.704 \pm 0.025$
Cold dark matter density	$\Omega_{\text{cdm}}$	$\Omega_{\text{cdm}} h^2 = 0.112 \pm 0.006$
Baryon density	$\Omega_{\text{b}}$	$\Omega_{\text{b}} h^2 = 0.0225 \pm 0.0006$
Cosmological constant	$\Omega_\Lambda$	$0.73 \pm 0.03$
Radiation density	$\Omega_{\text{r}}$	$\Omega_{\text{r}} h^2 = 2.47 \times 10^{-5}$
Neutrino density	$\Omega_\nu$	See Sec. 23.1.2
Density perturb. amplitude at $k = 0.002 \text{Mpc}^{-1}$	$\Delta_{\mathcal{R}}^2$	$(2.43 \pm 0.11) \times 10^{-9}$
Density perturb. spectral index	$n$	$0.967 \pm 0.014$
Tensor to scalar ratio	$r$	$r < 0.36$ (95% conf.)
Ionization optical depth	$\tau$	$0.088 \pm 0.015$
Bias parameter	$b$	See Sec. 23.3.4

As described in Sec. 23.4, models based on these eleven parameters are able to give a good fit to the complete set of high-quality data available at present, and indeed some simplification is possible. Observations are consistent with spatial flatness, and indeed the inflation models so far described automatically generate negligible spatial curvature, so we can set  $k = 0$ ; the density parameters then must sum to unity, and so one can be eliminated. The neutrino energy density is often not taken as an independent parameter. Provided the neutrino sector has the standard interactions, the neutrino energy density, while relativistic, can be related to the photon density using thermal physics arguments, and it is currently difficult to see the effect of the neutrino mass, although observations of large-scale structure have already placed interesting upper limits. This reduces the standard parameter set to nine. In addition, there is no observational evidence for the existence of tensor perturbations (though the upper limits are fairly weak), and so  $r$  could be set to zero. Presently  $n$  is in a somewhat uncertain position regarding whether it needs to be varied in a fit, or can be set to the Harrison–Zel’dovich value  $n = 1$ . Parameter estimation [3] indicates  $n = 1$  is disfavoured at over  $2\text{-}\sigma$ , but Bayesian model selection techniques [9] suggest the data is not conclusive. With  $n$  set to one, this leaves seven parameters, which is the smallest set that can usefully be compared to the present cosmological data set. This model (usually with  $n$  kept as a parameter) is referred to by various names, including  $\Lambda$ CDM, the concordance cosmology, and the standard cosmological model.

Of these parameters, only  $\Omega_{\text{r}}$  is accurately measured directly. The radiation density is dominated by the energy in the CMB, and the COBE satellite FIRAS experiment determined its temperature to be  $T = 2.7255 \pm 0.0006 \text{K}$  [10], corresponding to  $\Omega_{\text{r}} = 2.47 \times 10^{-5} h^{-2}$ . It typically need not be varied in fitting other data. If galaxy clustering

data are not included in a fit, then the bias parameter is also unnecessary.

In addition to this minimal set, there is a range of other parameters which might prove important in future as the data-sets further improve, but for which there is so far no direct evidence, allowing them to be set to a specific value for now. We discuss various speculative options in the next section. For completeness at this point, we mention one other interesting parameter, the helium fraction, which is a non-zero parameter that can affect the CMB anisotropies at a subtle level. Presently, BBN provides the best measurement of this parameter (see the Fields and Sarkar article in this volume), and it is usually fixed in microwave anisotropy studies, but the data are just reaching a level where allowing its variation may become mandatory.

### 23.1.5. Derived parameters :

The parameter list of the previous subsection is sufficient to give a complete description of cosmological models which agree with observational data. However, it is not a unique parametrization, and one could instead use parameters derived from that basic set. Parameters which can be obtained from the set given above include the age of the Universe, the present horizon distance, the present neutrino background temperature, the epoch of matter–radiation equality, the epochs of recombination and decoupling, the epoch of transition to an accelerating Universe, the baryon-to-photon ratio, and the baryon to dark matter density ratio. In addition, the physical densities of the matter components,  $\Omega_i h^2$ , are often more useful than the density parameters. The density perturbation amplitude can be specified in many different ways other than the large-scale primordial amplitude, for instance, in terms of its effect on the CMB, or by specifying a short-scale quantity, a common choice being the present linear-theory mass dispersion on a scale of  $8 h^{-1} \text{Mpc}$ , known as  $\sigma_8$ , whose WMAP7 value is  $0.81 \pm 0.03$  [2].

Different types of observation are sensitive to different subsets of the full cosmological parameter set, and some are more naturally interpreted in terms of some of the derived parameters of this subsection than on the original base parameter set. In particular, most types of observation feature degeneracies whereby they are unable to separate the effects of simultaneously varying several of the base parameters.

## 23.2. Extensions to the standard model

This section discusses some ways in which the standard model could be extended. At present, there is no positive evidence in favor of any of these possibilities, which are becoming increasingly constrained by the data, though there always remains the possibility of trace effects at a level below present observational capability.

### 23.2.1. More general perturbations :

The standard cosmology assumes adiabatic, Gaussian perturbations. Adiabaticity means that all types of material in the Universe share a common perturbation, so that if the space-time is foliated by constant-density hypersurfaces, then all fluids and fields are homogeneous on those slices, with the perturbations completely described by the variation of the spatial curvature of the slices. Gaussianity means that the initial perturbations obey Gaussian statistics, with the amplitudes of waves of different wavenumbers being randomly drawn from a Gaussian distribution of width given by the power spectrum. Note that gravitational instability generates non-Gaussianity; in this context, Gaussianity refers to a property of the initial perturbations, before they evolve significantly.

The simplest inflation models, based on one dynamical field, predict adiabatic perturbations and a level of non-Gaussianity which is too small to be detected by any experiment so far conceived. For present data, the primordial spectra are usually assumed to be power laws.

#### 23.2.1.1. Non-power-law spectra:

For typical inflation models, it is an approximation to take the spectra as power laws, albeit usually a good one. As data quality improves, one might expect this approximation to come under pressure, requiring a more accurate description of the initial spectra, particularly for the density perturbations. In general, one can expand  $\ln \Delta_{\mathcal{R}}^2$  as

$$\ln \Delta_{\mathcal{R}}^2(k) = \ln \Delta_{\mathcal{R}}^2(k_*) + (n_* - 1) \ln \frac{k}{k_*} + \frac{1}{2} \left. \frac{dn}{d \ln k} \right|_* \ln^2 \frac{k}{k_*} + \dots, \quad (23.9)$$

where the coefficients are all evaluated at some scale  $k_*$ . The term  $dn/d \ln k|_*$  is often called the running of the spectral index [11]. Once non-power-law spectra are allowed, it is necessary to specify the scale  $k_*$  at which the spectral index is defined.

#### 23.2.1.2. Isocurvature perturbations:

An isocurvature perturbation is one which leaves the total density unperturbed, while perturbing the relative amounts of different materials. If the Universe contains  $N$  fluids, there is one growing adiabatic mode and  $N - 1$  growing isocurvature modes (for reviews see Ref. 12 and Ref. 7). These can be excited, for example, in inflationary models where there are two or more fields which acquire dynamically-important perturbations. If one field decays to form normal matter, while the second survives to become the dark matter, this will generate a cold dark matter isocurvature perturbation.

In general, there are also correlations between the different modes, and so the full set of perturbations is described by a matrix giving the spectra and their correlations. Constraining such a general construct is challenging, though constraints on individual modes are beginning to become meaningful, with no evidence that any other than the adiabatic mode must be non-zero.

#### 23.2.1.3. Seeded perturbations:

An alternative to laying down perturbations at very early epochs is that they are seeded throughout cosmic history, for instance by topological defects such as cosmic strings. It has long been excluded that these are the sole original of structure, but they could contribute part of the perturbation signal, current limits being approximately ten percent [13]. In particular, cosmic defects formed in a phase transition ending inflation is a plausible scenario for such a contribution.

#### 23.2.1.4. Non-Gaussianity:

Multi-field inflation models can also generate primordial non-Gaussianity (reviewed, *e.g.*, in Ref. 7). The extra fields can either be in the same sector of the underlying theory as the inflaton, or completely separate, an interesting example of the latter being the curvaton model [14]. Current upper limits on non-Gaussianity are becoming stringent, but there remains much scope to push down those limits and perhaps reveal trace non-Gaussianity in the data. If non-Gaussianity is observed, its nature may favor an inflationary origin, or a different one such as topological defects.

### 23.2.2. Dark matter properties :

Dark matter properties are discussed in the article by Drees and Gerbier in this volume. The simplest assumption concerning the dark matter is that it has no significant interactions with other matter, and that its particles have a negligible velocity as far as structure formation is concerned. Such dark matter is described as ‘cold,’ and candidates include the lightest supersymmetric particle, the axion, and primordial black holes. As far as astrophysicists are concerned, a complete specification of the relevant cold dark matter properties is given by the density parameter  $\Omega_{\text{cdm}}$ , though those seeking to directly detect it are as interested in its interaction properties.

Cold dark matter is the standard assumption and gives an excellent fit to observations, except possibly on the shortest scales where there remains some controversy concerning the structure of dwarf galaxies and possible substructure in galaxy halos. It has long been excluded for all the dark matter to have a large velocity dispersion, so-called ‘hot’ dark matter, as it does not permit galaxies to form; for thermal relics the mass must be below about 1 keV to satisfy this



constraint, though relics produced non-thermally, such as the axion, need not obey this limit. However, in future further parameters might need to be introduced to describe dark matter properties relevant to astrophysical observations. Suggestions which have been made include a modest velocity dispersion (warm dark matter) and dark matter self-interactions. There remains the possibility that the dark matter comprises two separate components, *e.g.*, a cold one and a hot one, an example being if massive neutrinos have a non-negligible effect.

### 23.2.3. Dark energy :

While the standard cosmological model given above features a cosmological constant, in order to explain observations indicating that the Universe is presently accelerating, further possibilities exist under the general heading ‘dark energy’.<sup>†</sup> One possibility, usually called quintessence, is that a scalar field is responsible, with the mechanism mimicking that of early Universe inflation [15]. As described by Olive and Peacock, a fairly model-independent description of dark energy can be given using the equation of state parameter  $w$ , with  $w = -1$  corresponding to a cosmological constant and  $w$  potentially varying with redshift. For high-precision predictions of CMB anisotropies, the scalar-field description has the advantage of a self-consistent evolution of the ‘sound speed’ associated with the dark energy perturbations.

A competing possibility is that the observed acceleration is due to a modification of gravity, *i.e.*, the left-hand side of Einstein’s equation rather than the right (for a review see Ref. 16). Observations of expansion kinematics alone cannot distinguish these two possibilities, but probes of the growth rate of structure formation may be able to. It is possible that certain modified theories of gravity could explain the late-time acceleration of the Universe without recourse to any dark energy or cosmological constant. In a ‘Newtonian’ gauge the perturbed metric can be written with two potentials. Non-relativistic particles only respond to the temporal one, essentially the Newtonian potential, while relativistic particles, *e.g.*, photons, respond to the full metric in the form of the sum of the two potentials. In standard general relativity the two potentials are the same (in absence of anisotropic stress). Measurements of redshift distortions from spectroscopic surveys and weak lensing from imaging surveys can in principle distinguish between the Dark Energy and Modified Gravity alternatives (*e.g.*, Ref. 17).

While present observations are consistent with a cosmological constant, to test dark energy models  $w$  must be varied. The most popular option is  $w(a) = w_0 + (1 - a)w_a$  with  $w_0$  and  $w_a$  constants to be determined [18]. Additionally the weak energy condition  $w \geq -1$  may be imposed. Future data may require a more sophisticated parametrization of the dark energy, including its sound speed which influences structure formation.

### 23.2.4. Complex ionization history :

The full ionization history of the Universe is given by the ionization fraction as a function of redshift  $z$ . The simplest scenario takes the ionization to have the small residual value left after recombination up to some redshift  $z_{\text{ion}}$ , at which point the Universe instantaneously reionizes completely. Then there is a one-to-one correspondence between  $\tau$  and  $z_{\text{ion}}$  (that relation, however, also depending on other cosmological parameters). An accurate treatment of this process will track separate histories for hydrogen and helium. While currently rapid ionization appears to be a good approximation, as data improve a more complex ionization history may need to be considered.

### 23.2.5. Varying ‘constants’ :

Variation of the fundamental constants of Nature over cosmological times is another possible enhancement of the standard cosmology. There is a long history of study of variation of the gravitational constant  $G$ , and more recently attention has been drawn to the possibility of small fractional variations in the fine-structure constant. There is presently no observational evidence for the former, which is tightly constrained by a variety of measurements. Evidence for

the latter has been claimed from studies of spectral line shifts in quasar spectra at redshifts of order two [19], but this is presently controversial and in need of further observational study.

### 23.2.6. Cosmic topology :

The usual hypothesis is that the Universe has the simplest topology consistent with its geometry, for example that a flat Universe extends forever. Observations cannot tell us whether that is true, but they can test the possibility of a non-trivial topology on scales up to roughly the present Hubble scale. Extra parameters would be needed to specify both the type and scale of the topology, for example, a cuboidal topology would need specification of the three principal axis lengths. At present, there is no direct evidence for cosmic topology, though the low values of the observed cosmic microwave quadrupole and octupole have been cited as a possible signature [20].

## 23.3. Probes

The goal of the observational cosmologist is to utilize astronomical information to derive cosmological parameters. The transformation from the observables to the key parameters usually involves many assumptions about the nature of the objects, as well as about the nature of the dark matter. Below we outline the physical processes involved in each probe, and the main recent results. The first two subsections concern probes of the homogeneous Universe, while the remainder consider constraints from perturbations.

In addition to statistical uncertainties we note three sources of systematic uncertainties that will apply to the cosmological parameters of interest: (i) due to the assumptions on the cosmological model and its priors (*i.e.*, the number of assumed cosmological parameters and their allowed range); (ii) due to the uncertainty in the astrophysics of the objects (*e.g.*, light curve fitting for supernovae or the mass–temperature relation of galaxy clusters); and (iii) due to instrumental and observational limitations (*e.g.*, the effect of ‘seeing’ on weak gravitational lensing measurements, or beam shape on CMB anisotropy measurements).

### 23.3.1. Direct measures of the Hubble constant :

In 1929, Edwin Hubble discovered the law of expansion of the Universe by measuring distances to nearby galaxies. The slope of the relation between the distance and recession velocity is defined to be the Hubble constant  $H_0$ . Astronomers argued for decades on the systematic uncertainties in various methods and derived values over the wide range,  $40 \text{ km s}^{-1} \text{ Mpc}^{-1} \lesssim H_0 \lesssim 100 \text{ km s}^{-1} \text{ Mpc}^{-1}$ .

One of the most reliable results on the Hubble constant comes from the Hubble Space Telescope Key Project [21]. This study used the empirical period–luminosity relations for Cepheid variable stars to obtain distances to 31 galaxies, and calibrated a number of secondary distance indicators—Type Ia Supernovae (SNe Ia), the Tully–Fisher relation, surface-brightness fluctuations, and Type II Supernovae—measured over distances of 400 to 600 Mpc. They estimated  $H_0 = 72 \pm 3$  (statistical)  $\pm 7$  (systematic)  $\text{km s}^{-1} \text{ Mpc}^{-1}$ .<sup>‡</sup>

A recent study [22] of over 600 Cepheids in the host galaxies of eight recent SNe Ia, observed with an improved camera on board the Hubble Space Telescope, was used to calibrate the magnitude–redshift relation for 240 SNe Ia. This yielded an even more accurate figure,  $H_0 = 73.8 \pm 2.4 \text{ km s}^{-1} \text{ Mpc}^{-1}$  (including both statistical and systematic errors). The major sources of uncertainty in this result are due to the heavy element abundance of the Cepheids and the distance to the fiducial nearby galaxy, the Large Magellanic Cloud, relative to which all Cepheid distances are measured. It is impressive that this result is in such good agreement with the result derived from the WMAP CMB measurements combined with other probes (see Table 23.2).

<sup>‡</sup> Unless stated otherwise, all quoted uncertainties in this article are one-sigma/68% confidence. Cosmological parameters often have significantly non-Gaussian uncertainties. Throughout we have rounded central values, and especially uncertainties, from original sources in cases where they appear to be given to excessive precision.

<sup>†</sup> It is actually the negative pressure of this material, not its energy, that is responsible for giving the acceleration. Furthermore, while generally in physics matter and energy are interchangeable terms, dark matter and dark energy are quite distinct concepts.

### 23.3.2. Supernovae as cosmological probes :

The relation between observed flux and the intrinsic luminosity of an object depends on the luminosity distance  $D_L$ , which in turn depends on cosmological parameters:

$$D_L = (1+z)r_e(z), \quad (23.10)$$

where  $r_e(z)$  is the coordinate distance. For example, in a flat Universe

$$r_e(z) = \int_0^z \frac{dz'}{H(z')}. \quad (23.11)$$

For a general dark energy equation of state  $w(z) = p_{de}(z)/\rho_{de}(z)$ , the Hubble parameter is, still considering only the flat case,

$$\frac{H^2(z)}{H_0^2} = (1+z)^3 \Omega_m + \Omega_{de} \exp[3X(z)], \quad (23.12)$$

where

$$X(z) = \int_0^z [1+w(z')](1+z')^{-1} dz', \quad (23.13)$$

and  $\Omega_{de}$  is the present density parameter of the dark energy component. If a general equation of state is allowed, then one has to solve for  $w(z)$  (parametrized, for example, as  $w(z) = w = \text{const.}$ , or  $w(z) = w_0 + w_1 z$ ) as well as for  $\Omega_{de}$ .

Empirically, the peak luminosity of SNe Ia can be used as an efficient distance indicator (*e.g.*, Ref. 23). The favorite theoretical explanation for SNe Ia is the thermonuclear disruption of carbon-oxygen white dwarfs. Although not perfect ‘standard candles,’ it has been demonstrated that by correcting for a relation between the light curve shape, color, and the luminosity at maximum brightness, the dispersion of the measured luminosities can be greatly reduced. There are several possible systematic effects which may affect the accuracy of the use of SNe Ia as distance indicators, *e.g.*, evolution with redshift and interstellar extinction in the host galaxy and in the Milky Way.

Two major studies, the Supernova Cosmology Project and the High- $z$  Supernova Search Team, found evidence for an accelerating Universe [24], interpreted as due to a cosmological constant or a dark energy component. Representative results from the ‘Union sample’ [25] of over 300 SNe Ia are shown in Fig. 23.1 (see also further results in Ref. 26). When combined with the CMB data (which indicates flatness, *i.e.*,  $\Omega_m + \Omega_\Lambda \approx 1$ ), the best-fit values are  $\Omega_m \approx 0.3$  and  $\Omega_\Lambda \approx 0.7$ . Most results in the literature are consistent with the  $w = -1$  cosmological constant case. As an example of recent results, the SNLS3 team found, for a constant equation of state parameter,  $w = -0.91^{+0.16}_{-0.20}$  (stat.)  $^{+0.07}_{-0.14}$  (sys.) [27]. This includes a correction for the recently-discovered relationship between host galaxy mass and supernova absolute brightness. This agrees with earlier results [25,28]. Future experiments will aim to set constraints on the cosmic equation of state  $w(z)$ , though given the integral relation between the luminosity distance and  $w(z)$  it is not straightforward to recover  $w(z)$  (*e.g.*, Ref. 29).

### 23.3.3. Cosmic microwave background :

The physics of the CMB is described in detail by Scott and Smoot in this volume. Before recombination, the baryons and photons are tightly coupled, and the perturbations oscillate in the potential wells generated primarily by the dark matter perturbations. After decoupling, the baryons are free to collapse into those potential wells. The CMB carries a record of conditions at the time of last scattering, often called primary anisotropies. In addition, it is affected by various processes as it propagates towards us, including the effect of a time-varying gravitational potential (the integrated Sachs–Wolfe effect), gravitational lensing, and scattering from ionized gas at low redshift.

The primary anisotropies, the integrated Sachs–Wolfe effect, and scattering from a homogeneous distribution of ionized gas, can all be calculated using linear perturbation theory. Available codes include CMBFAST and CAMB [8], the latter widely used embedded within the analysis package CosmoMC [30]. Gravitational lensing is also calculated in these codes. Secondary effects such as inhomogeneities in the reionization process, and scattering from gravitationally-collapsed gas (the Sunyaev–Zel’dovich effect), require more complicated, and more uncertain, calculations.

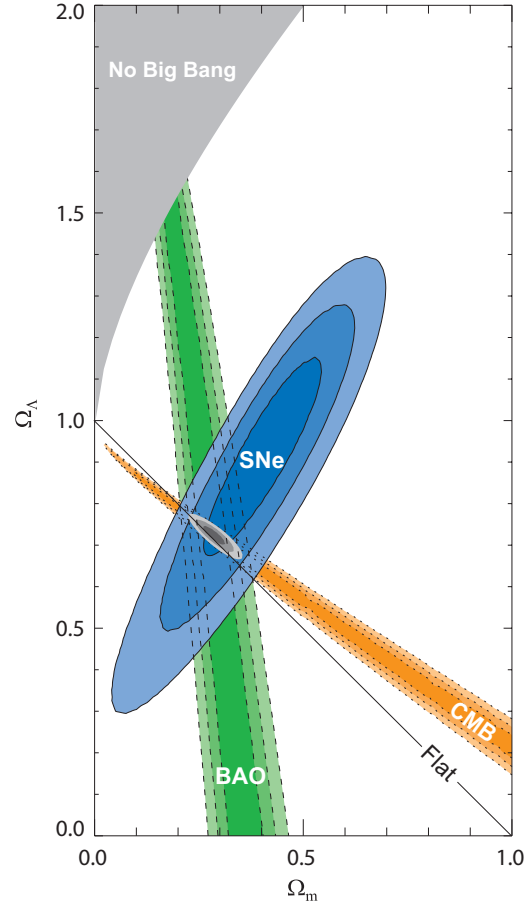


**Figure 23.1:** Confidence level contours of 68.3%, 95.4% and 99.7% in the  $\Omega_\Lambda$ - $\Omega_m$  plane from the CMB, BAOs and the Union SNe Ia set, as well as their combination (assuming  $w = -1$ ). [Courtesy of Kowalski *et al.* [25]]

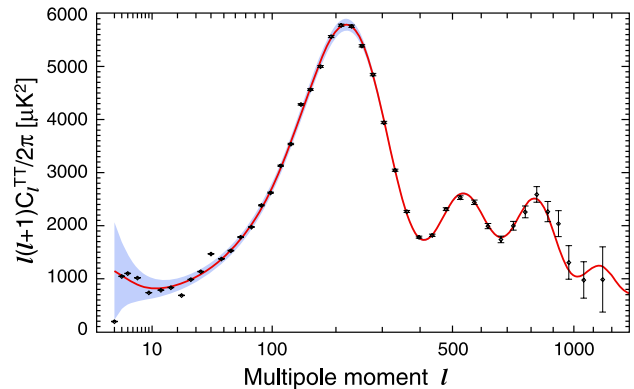


**Figure 23.2:** The angular power spectrum of the CMB temperature anisotropies from WMAP7, from Ref. 2. The grey band indicates the cosmic variance uncertainty. The solid line shows the prediction from the best-fitting  $\Lambda$ CDM model. [Figure courtesy NASA/WMAP Science Team.]

The upshot is that the detailed pattern of anisotropies depends on all of the cosmological parameters. In a typical cosmology, the anisotropy power spectrum [usually plotted as  $\ell(\ell+1)C_\ell$ ] features a flat plateau at large angular scales (small  $\ell$ ), followed by a series of oscillatory features at higher angular scales, the first and most prominent being at around one degree ( $\ell \simeq 200$ ). These features, known as acoustic peaks, represent the oscillations of the photon-baryon fluid around the time of decoupling. Some features can be

closely related to specific parameters—for instance, the location of the first peak probes the spatial geometry, while the relative heights of the peaks probes the baryon density—but many other parameters combine to determine the overall shape.

The seven-year data release from the WMAP satellite [1], henceforth WMAP7, has provided the most powerful results to date on the spectrum of CMB anisotropies, with a precision determination of the temperature power spectrum up to  $\ell \simeq 900$ , shown in Fig. 23.2, as well as measurements of the spectrum of  $E$ -polarization anisotropies and the correlation spectrum between temperature and polarization (those spectra having first been detected by DASI [31]). These are consistent with models based on the parameters we have described, and provide accurate determinations of many of those parameters [2].

WMAP7 provides an exquisite measurement of the location of the first acoustic peak, determining the angular-diameter distance of the last-scattering surface. In combination with other data this strongly constrains the spatial geometry, in a manner consistent with spatial flatness and excluding significantly-curved Universes. WMAP7 also gives a precision measurement of the age of the Universe. It gives a baryon density consistent with, and at higher precision than, that coming from BBN. It affirms the need for both dark matter and dark energy. It shows no evidence for dynamics of the dark energy, being consistent with a pure cosmological constant ( $w = -1$ ). The density perturbations are consistent with a power-law primordial spectrum, with indications that the spectral slope may be less than the Harrison–Zel’dovich value  $n = 1$  [2]. There is no indication of tensor perturbations, but the upper limit is quite weak. WMAP7’s current best-fit for the reionization optical depth,  $\tau = 0.088$ , is in reasonable agreement with models of how early structure formation induces reionization.

WMAP7 is consistent with other experiments and its dynamic range can be enhanced by including information from small-angle CMB experiments such as ACBAR, QUaD, the South Pole Telescope (SPT), and the Atacama Cosmology Telescope (ACT), which gives extra constraining power on some parameters. ACT has also announced the first detection of gravitational lensing of the CMB from the four-point correlation of temperature variations [32], agreeing with the expected effect in the standard cosmology.

### 23.3.4. Galaxy clustering :

The power spectrum of density perturbations depends on the nature of the dark matter. Within the  $\Lambda$ CDM model, the power spectrum shape depends primarily on the primordial power spectrum and on the combination  $\Omega_m h$  which determines the horizon scale at matter–radiation equality, with a subdominant dependence on the baryon density.

The matter distribution is most easily probed by observing the galaxy distribution, but this must be done with care as the galaxies do not perfectly trace the dark matter distribution. Rather, they are a ‘biased’ tracer of the dark matter. The need to allow for such bias is emphasized by the observation that different types of galaxies show bias with respect to each other. In particular scale-dependent and stochastic biasing may introduce a systematic effect on the determination of cosmological parameters from redshift surveys. Prior knowledge from simulations of galaxy formation or from gravitational lensing data could help to quantify biasing. Furthermore, the observed 3D galaxy distribution is in redshift space, *i.e.*, the observed redshift is the sum of the Hubble expansion and the line-of-sight peculiar velocity, leading to linear and non-linear dynamical effects which also depend on the cosmological parameters. On the largest length scales, the galaxies are expected to trace the location of the dark matter, except for a constant multiplier  $b$  to the power spectrum, known as the linear bias parameter. On scales smaller than  $20 h^{-1}$  Mpc or so, the clustering pattern is ‘squashed’ in the radial direction due to coherent infall, which depends approximately on the parameter  $\beta \equiv \Omega_m^{0.6}/b$  (on these shorter scales, more complicated forms of biasing are not excluded by the data). On scales of a few  $h^{-1}$  Mpc, there is an effect of elongation along the line of sight (colloquially known as the ‘finger of God’ effect) which depends on the galaxy velocity dispersion.

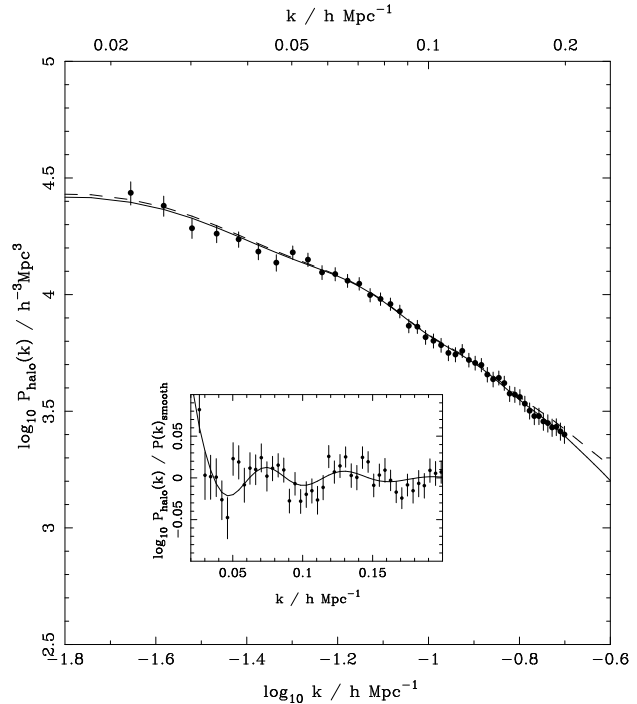


**Figure 23.3:** The galaxy power spectrum from the SDSS LRGs. The best-fit LRG+WMAP  $\Lambda$ CDM model is shown for two sets of nuisance parameters (solid and dashed lines). The BAO inset shows the same data and model divided by a spline fit to the smooth component. [Figure courtesy B. Reid/W. Percival; see Ref. 35.]

#### 23.3.4.1. Baryonic Acoustic Oscillations (BAOs):

The Fourier power spectra of the 2-degree Field (2dF) Galaxy Redshift Survey and the Sloan Digital Sky Survey (SDSS) are well fitted by a  $\Lambda$ CDM model and both surveys show evidence for BAOs [33,34]. Further analyses used the Luminous Red Galaxies (LRGs) in the SDSS 7th Data Release [35], shown in Fig. 23.3. Combining the so-called ‘halo’ power spectrum measurement with the then-current WMAP5 results, for the flat  $\Lambda$ CDM model they find  $\Omega_m = 0.289 \pm 0.019$  and  $H_0 = 69.4 \pm 1.6 \text{ km s}^{-1} \text{ Mpc}^{-1}$ . A new survey, WiggleZ, combined with the 6dF and SDSS-LRG surveys, CMB and SNIa data, yields a constant equation of state  $w = -1.03 \pm 0.08$  for a flat universe, consistent with a cosmological constant. However, allowing for epoch-dependent  $w(a) = w_0 + (1-a)w_a$  they find that the uncertainties are much larger,  $w_0 = -1.09 \pm 0.17$  and  $w_a = 0.19 \pm 0.69$  [36]. Further BAO results are expected from the BOSS survey.

#### 23.3.4.2. Integrated Sachs–Wolfe effect:

The integrated Sachs–Wolfe (ISW) effect, described in the article by Scott and Smoot, is the change in CMB photon energy when propagating through the changing gravitational potential wells of developing cosmic structures. In linear theory, the ISW signal is expected in universes where there is dark energy, curvature or modified gravity. Correlating the large-angle CMB anisotropies with very large scale structures, first proposed in Ref. 37, has provided results which vary from no detection of this effect to  $4\sigma$  detection [38,39].

#### 23.3.4.3. Limits on neutrino mass from galaxy surveys and other probes:

Large-scale structure data can put an upper limit on  $\Omega_\nu$  due to the neutrino ‘free streaming’ effect [40–43]. Upper limits on neutrino mass are commonly estimated by comparing the observed galaxy power spectrum with a four-component model of baryons, cold dark matter, a cosmological constant, and massive neutrinos. Such analyses also assume that the primordial power spectrum is adiabatic, scale-invariant, and Gaussian. Potential systematic effects include biasing of the galaxy distribution and non-linearities of the

power spectrum. An upper limit can also be derived from CMB anisotropies alone, but it is typically not below 2 eV [44]. Additional cosmological data sets can improve the results. Recent results using a photometric redshift sample of LRGs combined with WMAP, BAO, Hubble constant and SNe Ia data brought the upper limit on the total neutrino mass down to 0.28 eV [45], with a similar result for a combination of other data sets [46]. As the lower limit on neutrino mass from terrestrial experiments is 0.05 eV, it looks promising that cosmological surveys will detect the neutrino mass. Another probe of neutrino mass is the intergalactic medium, which manifests itself in quasar absorption lines (the Lyman- $\alpha$  forest), yielding from the SDSS flux power spectrum an upper limit of 0.9 eV (95% confidence) [47].

### 23.3.5. Clusters of galaxies :

A cluster of galaxies is a large collection of galaxies held together by their mutual gravitational attraction. The largest ones are around  $10^{15}$  Solar masses, and are the largest gravitationally-collapsed structures in the Universe. Even at the present epoch they are relatively rare, with only a few percent of galaxies being in clusters. They provide various ways to study the cosmological parameters.

The first objects of a given kind form at the rare high peaks of the density distribution, and if the primordial density perturbations are Gaussian distributed, their number density is exponentially sensitive to the size of the perturbations, and hence can strongly constrain it. Clusters are an ideal application in the present Universe. They are usually used to constrain the amplitude  $\sigma_8$ , as a box of side  $8 h^{-1}$  Mpc contains about the right amount of material to form a cluster. The most useful observations at present are of X-ray emission from hot gas lying within the cluster, whose temperature is typically a few keV, and which can be used to estimate the mass of the cluster. A theoretical prediction for the mass function of clusters can come either from semi-analytic arguments or from numerical simulations. The same approach can be adopted at high redshift (which for clusters means redshifts of order one) to attempt to measure  $\sigma_8$  at an earlier epoch. The evolution of  $\sigma_8$  is primarily driven by the value of the matter density  $\Omega_m$ , with a sub-dominant dependence on the dark energy properties.

At present, the main uncertainty is the relation between the observed gas temperature and the cluster mass, despite extensive study using simulations. Mantz *et al.* [48] used a large sample of X-ray selected clusters to find  $\sigma_8 = 0.82 \pm 0.05$ ,  $\Omega_m = 0.23 \pm 0.04$ , and  $w = -1.01 \pm 0.20$  for a constant dark energy equation of state  $w$ . This agrees well with the values predicted in cosmologies compatible with WMAP7.

A further use of clusters is to measure the ratio of baryon to dark matter mass, through modelling of the way the hot cluster gas is confined by the total gravitational potential. Allen *et al.* [49] give examples of constraints that can be obtained this way on both dark matter and dark energy using Chandra data across a range of redshifts.

### 23.3.6. Clustering in the inter-galactic medium :

It is commonly assumed, based on hydrodynamic simulations, that the neutral hydrogen in the inter-galactic medium (IGM) can be related to the underlying mass distribution. It is then possible to estimate the matter power spectrum on scales of a few megaparsecs from the absorption observed in quasar spectra, the so-called Lyman- $\alpha$  forest. The usual procedure is to measure the power spectrum of the transmitted flux, and then to infer the mass power spectrum. Photo-ionization heating by the ultraviolet background radiation and adiabatic cooling by the expansion of the Universe combine to give a simple power-law relation between the gas temperature and the baryon density. It also follows that there is a power-law relation between the optical depth  $\tau$  and  $\rho_b$ . Therefore, the observed flux  $F = \exp(-\tau)$  is strongly correlated with  $\rho_b$ , which itself traces the mass density. The matter and flux power spectra can be related by

$$P_m(k) = b^2(k) P_F(k), \quad (23.14)$$

where  $b(k)$  is a bias function which is calibrated from simulations. Croft *et al.* [50] derived cosmological parameters from Keck Telescope observations of the Lyman- $\alpha$  forest at redshifts  $z = 2$  to 4. Their

derived power spectrum corresponds to that of a CDM model, which is in good agreement with the 2dF galaxy power spectrum. A recent study using VLT spectra [51] agrees with the flux power spectrum of Ref. 50. This method depends on various assumptions. Seljak *et al.* [52] pointed out that uncertainties are sensitive to the range of cosmological parameters explored in the simulations, and the treatment of the mean transmitted flux. Nevertheless, this method has the potential of measuring accurately the power spectrum of mass perturbations in a different way to other methods.

### 23.3.7. Gravitational lensing :

Images of background galaxies are distorted by the gravitational effect of mass variations along the line of sight. Deep gravitational potential wells such as galaxy clusters generate ‘strong lensing’, leading to arcs, arclets and multiple images, while more moderate perturbations give rise to ‘weak lensing’. Weak lensing is now widely used to measure the mass power spectrum in selected regions of the sky (see Ref. 53 for recent reviews). As the signal is weak, the image of deformed galaxy shapes (the ‘shear map’) must be analyzed statistically to measure the power spectrum, higher moments, and cosmological parameters.

The shear measurements are mainly sensitive to the combination of  $\Omega_m$  and the amplitude  $\sigma_8$ . For example, the weak lensing signal detected by the CFHT Legacy Survey has been analyzed to yield  $\sigma_8(\Omega_m/0.25)^{0.64} = 0.78 \pm 0.04$  [54] and  $\sigma_8(\Omega_m/0.24)^{0.59} = 0.84 \pm 0.05$  [55] assuming a  $\Lambda$ CDM model. Earlier results are summarized in Ref. 53. There are various systematic effects in the interpretation of weak lensing, *e.g.*, due to atmospheric distortions during observations, the redshift distribution of the background galaxies, the intrinsic correlation of galaxy shapes, and non-linear modeling uncertainties.

### 23.3.8. Peculiar velocities :

Deviations from the Hubble flow directly probe the mass perturbations in the Universe, and hence provide a powerful probe of the dark matter [56]. Peculiar velocities are deduced from the difference between the redshift and the distance of a galaxy. The observational difficulty is in accurately measuring distances to galaxies. Even the best distance indicators (*e.g.*, the Tully–Fisher relation) give an uncertainty of 15% per galaxy, hence limiting the application of the method at large distances. Peculiar velocities are mainly sensitive to  $\Omega_m$ , not to  $\Omega_\Lambda$  or dark energy. While at present cosmological parameters derived from peculiar velocities are strongly affected by random and systematic errors, a new generation of surveys may improve their accuracy. Three promising approaches are the 6dF near-infrared survey of 15,000 peculiar velocities, peculiar velocities of SNe Ia, and the kinematic Sunyaev–Zel’dovich effect.

There is also a renewed interest in ‘redshift distortion’. As the measured redshift of a galaxy is the sum of its redshift due to the Hubble expansion and its peculiar velocity, this distortion depends on cosmological parameters [57] via the perturbation growth rate  $f(z) = d \ln \delta / d \ln a \approx \Omega^\gamma(z)$ , where  $\gamma = 0.55$  for a concordance  $\Lambda$ CDM model, and is different for a modified gravity model. Recent observational results [58,59] show that by measuring  $f(z)$  with redshift it is feasible to constrain  $\gamma$  and rule out certain modified gravity models.

## 23.4. Bringing observations together

Although it contains two ingredients—dark matter and dark energy—which have not yet been verified by laboratory experiments, the  $\Lambda$ CDM model is almost universally accepted by cosmologists as the best description of the present data. The basic ingredients are given by the parameters listed in Sec. 23.1.4, with approximate values of some of the key parameters being  $\Omega_b \approx 0.05$ ,  $\Omega_{\text{cdm}} \approx 0.23$ ,  $\Omega_\Lambda \approx 0.72$ , and a Hubble constant  $h \approx 0.70$ . The spatial geometry is very close to flat (and usually assumed to be precisely flat), and the initial perturbations Gaussian, adiabatic, and nearly scale-invariant.

The most powerful single experiment is WMAP7, which on its own supports all these main tenets. Values for some parameters, as given in Larson *et al.* [2] and Komatsu *et al.* [3], are reproduced in Table 23.2. These particular results presume a flat Universe. The

constraints are somewhat strengthened by adding additional data-sets, as shown in the Table, though most of the constraining power resides in the WMAP7 data.

**Table 23.2:** Parameter constraints reproduced from Larson *et al.* [2] and Komatsu *et al.* [3], with some additional rounding. All columns assume the  $\Lambda$ CDM cosmology with a power-law initial spectrum, no tensors, spatial flatness, and a cosmological constant as dark energy. Above the line are the six parameter combinations actually fit to the data; those below the line are derived from these. Two different data combinations are shown to highlight the extent to which this choice matters. The first column is WMAP7 alone, while the second column shows a combination of WMAP7 with BAO and  $H_0$  data as described in Ref. 3. The perturbation amplitude  $\Delta_{\mathcal{R}}^2$  is specified at the scale  $0.002 \text{ Mpc}^{-1}$ . Uncertainties are shown at 68% confidence.

	WMAP7 alone	WMAP7 + BAO + $H_0$
$\Omega_b h^2$	$0.0225 \pm 0.0006$	$0.0226 \pm 0.0005$
$\Omega_{\text{cdm}} h^2$	$0.112 \pm 0.006$	$0.113 \pm 0.004$
$\Omega_\Lambda$	$0.73 \pm 0.03$	$0.725 \pm 0.016$
$n$	$0.967 \pm 0.014$	$0.968 \pm 0.012$
$\tau$	$0.088 \pm 0.015$	$0.088 \pm 0.014$
$\Delta_{\mathcal{R}}^2 \times 10^9$	$2.43 \pm 0.11$	$2.43 \pm 0.09$
$h$	$0.704 \pm 0.025$	$0.702 \pm 0.014$
$\sigma_8$	$0.81 \pm 0.03$	$0.816 \pm 0.024$
$\Omega_m h^2$	$0.134 \pm 0.006$	$0.135 \pm 0.004$

If the assumption of spatial flatness is lifted, it turns out that WMAP7 on its own only weakly constrains the spatial curvature, due to a parameter degeneracy in the angular-diameter distance. However inclusion of other data readily removes this, *e.g.*, inclusion of BAO and  $H_0$  data, plus the assumption that the dark energy is a cosmological constant, yields a constraint on  $\Omega_{\text{tot}} \equiv \sum \Omega_i + \Omega_\Lambda$  of  $\Omega_{\text{tot}} = 1.002 \pm 0.011$  [3]. Results of this type are normally taken as justifying the restriction to flat cosmologies.

The baryon density  $\Omega_b$  is now measured with quite high accuracy from the CMB and large-scale structure, and is consistent with the determination from BBN; Fields and Sarkar in this volume quote the range  $0.019 \leq \Omega_b h^2 \leq 0.024$  (95% confidence).

While  $\Omega_\Lambda$  is measured to be non-zero with very high confidence, there is no evidence of evolution of the dark energy density. The WMAP team find the constraint  $w = -0.98 \pm 0.05$  on a constant equation of state from a compilation of data including SNe Ia, with the cosmological constant case  $w = -1$  giving an excellent fit to the data. Allowing more complicated forms of dark energy weakens the limits.

The data provide strong support for the main predictions of the simplest inflation models: spatial flatness and adiabatic, Gaussian, nearly scale-invariant density perturbations. But it is disappointing that there is no sign of primordial gravitational waves, with WMAP7 alone providing only an upper limit  $r < 0.36$  at 95% confidence [2] (this assumes no running, weakening to 0.49 if running is allowed). The spectral index  $n$  is placed in an interesting position, with indications that  $n < 1$  is required by the data. However, the confidence with which  $n = 1$  is ruled out is still rather weak, and in our view it is premature to conclude that  $n = 1$  is no longer viable.

Tests have been made for various types of non-Gaussianity, a particular example being a parameter  $f_{\text{NL}}$  which measures a quadratic contribution to the perturbations. Various non-gaussianity shapes are possible (see Ref. 3 for details), and current constraints on the popular ‘local’, ‘equilateral’, and ‘orthogonal’ types are  $-10 < f_{\text{NL}}^{\text{local}} < 74$ ,

$-210 < f_{\text{NL}}^{\text{equil}} < 270$ , and  $-410 < f_{\text{NL}}^{\text{orthog}} < 6$  at 95% confidence (these look weak, but prominent non-Gaussianity requires the product  $f_{\text{NL}} \Delta_{\mathcal{R}}$  to be large, and  $\Delta_{\mathcal{R}}$  is of order  $10^{-5}$ ). There is presently no secure indication of primordial non-gaussianity.

One parameter which is very robust is the age of the Universe, as there is a useful coincidence that for a flat Universe the position of the first peak is strongly correlated with the age. The WMAP7 result is  $13.77 \pm 0.13$  Gyr (assuming flatness). This is in good agreement with the ages of the oldest globular clusters and radioactive dating.

### 23.5. Outlook for the future

The concordance model is now well established, and there seems little room left for any dramatic revision of this paradigm. A measure of the strength of that statement is how difficult it has proven to formulate convincing alternatives.

Should there indeed be no major revision of the current paradigm, we can expect future developments to take one of two directions. Either the existing parameter set will continue to prove sufficient to explain the data, with the parameters subject to ever-tightening constraints, or it will become necessary to deploy new parameters. The latter outcome would be very much the more interesting, offering a route towards understanding new physical processes relevant to the cosmological evolution. There are many possibilities on offer for striking discoveries, for example:

- The cosmological effects of a neutrino mass may be unambiguously detected, shedding light on fundamental neutrino properties;
- Compelling detection of deviations from scale-invariance in the initial perturbations would indicate dynamical processes during perturbation generation by, for instance, inflation;
- Detection of primordial non-Gaussianities would indicate that non-linear processes influence the perturbation generation mechanism;
- Detection of variation in the dark-energy density (*i.e.*,  $w \neq -1$ ) would provide much-needed experimental input into the nature of the properties of the dark energy.

These provide more than enough motivation for continued efforts to test the cosmological model and improve its accuracy.

Over the coming years, there are a wide range of new observations which will bring further precision to cosmological studies. Indeed, there are far too many for us to be able to mention them all here, and so we will just highlight a few areas.

The CMB observations will improve in several directions. A current frontier is the study of polarization, first detected in 2002 by DASI and for which power spectrum measurements have now been made by several experiments. Future measurements may be able to separately detect the two modes of polarization. Another area of development is pushing accurate power spectrum measurements to smaller angular scales, currently well underway with ACT and SPT. Finally, we mention the *Planck* satellite, launched in 2009, which is making high-precision all-sky maps of temperature and polarization, utilizing a very wide frequency range to improve understanding of foreground contaminants, and to compile a large sample of clusters via the Sunyaev–Zel’dovich effect. Its main cosmological results will be published in early 2013.

An impressive array of ground-based dark energy surveys are also already operational, under construction, or proposed, including ground-based imaging surveys the Dark Energy Survey, Pan-STARRS, and LSST, spectroscopic surveys such as BigBOSS and DESpec, and proposed space missions Euclid and WFIRST.

An exciting new area for the future will be radio surveys of the redshifted 21-cm line of hydrogen. Because of the intrinsic narrowness of this line, by tuning of the bandpass the emission from narrow redshift slices of the Universe will be measured to extremely high redshift, probing the details of the reionization process at redshifts up to perhaps 20. LOFAR is the first instrument able to do this and is at an advanced construction and commissioning stage. In the longer term, the Square Kilometer Array (SKA) will take these studies to a precision level.

The above future surveys will address fundamental questions of physics well beyond just testing the ‘concordance’  $\Lambda$ CDM model and minor variations. By learning about both the geometry of the universe and the growth of perturbations, it will be possible to test theories of modified gravity and inhomogeneous universes.

The development of the first precision cosmological model is a major achievement. However, it is important not to lose sight of the motivation for developing such a model, which is to understand the underlying physical processes at work governing the Universe’s evolution. On that side, progress has been much less dramatic. For instance, there are many proposals for the nature of the dark matter, but no consensus as to which is correct. The nature of the dark energy remains a mystery. Even the baryon density, now measured to an accuracy of a few percent, lacks an underlying theory able to predict it even within orders of magnitude. Precision cosmology may have arrived, but at present many key questions remain to motivate and challenge the cosmology community.

#### References:

1. N. Jarosik *et al.*, *Astrophys. J. Supp.* **192**, 14 (2011).
2. D. Larson *et al.*, *Astrophys. J. Supp.* **192**, 16 (2011).
3. E. Komatsu *et al.*, *Astrophys. J. Supp.* **192**, 18 (2011).
4. S. Fukuda *et al.*, *Phys. Rev. Lett.* **85**, 3999 (2000);  
Q.R. Ahmad *et al.*, *Phys. Rev. Lett.* **87**, 071301 (2001).
5. A.D. Dolgov *et al.*, *Nucl. Phys.* **B632**, 363 (2002).
6. E.W. Kolb and M.S. Turner, *The Early Universe*, Addison–Wesley (Redwood City, 1990).
7. D.H. Lyth and A.R. Liddle, *The Primordial Density Perturbation*, Cambridge University Press (2009).
8. U. Seljak and M. Zaldarriaga, *Astrophys. J.* **469**, 1 (1996);  
A. Lewis, A. Challinor and A. Lasenby, *Astrophys. J.* **538**, 473 (2000).
9. D. Parkinson and A.R. Liddle, *Phys. Rev.* **D82**, 103533 (2010).
10. D. Fixsen, *Astrophys. J.* **707**, 916 (2009).
11. A. Kosowsky and M.S. Turner, *Phys. Rev.* **D52**, 1739 (1995).
12. K.A. Malik and D. Wands, *Phys. Reports* **475**, 1 (2009).
13. N. Bevis *et al.*, *Phys. Rev. Lett.* **100**, 021301 (2008);  
L. Pogosian *et al.*, *JCAP* **0902**, 013 (2009);  
R. Battye and A. Moss, *Phys. Rev.* **D82**, 023521 (2010).
14. D.H. Lyth and D. Wands, *Phys. Lett.* **B524**, 5 (2002);  
K. Enqvist and M.S. Sloth, *Nucl. Phys.* **B626**, 395 (2002);  
T. Moroi and T. Takahashi, *Phys. Lett.* **B522**, 215 (2001).
15. B. Ratra and P.J.E. Peebles, *Phys. Rev.* **D37**, 3406 (1988);  
C. Wetterich, *Nucl. Phys.* **B302**, 668 (1988).
16. T. Clifton *et al.*, *arXiv:1106.2476*.
17. B. Jain and P. Zhang, *Phys. Rev.* **D78**, 063503 (2008).
18. M. Chevallier and D. Polarski, *Int. J. Mod. Phys.* **D10**, 213 (2001);  
E.V. Linder, *Phys. Rev. Lett.* **90**, 091301 (2003).
19. J.K. Webb *et al.*, *Phys. Rev. Lett.* **82**, 884 (1999);  
J.K. Webb *et al.*, *Ap. Space Sci.* **283**, 565 (2003);  
H. Chand *et al.*, *Astron. & Astrophys.* **417**, 853 (2004);  
R. Srianand *et al.*, *Phys. Rev. Lett.* **92**, 121302 (2004).
20. J. Levin, *Phys. Reports* **365**, 251 (2002).
21. W.L. Freedman *et al.*, *Astrophys. J.* **553**, 47 (2001).
22. A.G. Riess *et al.*, *Astrophys. J.* **730**, 119 (2011).
23. B. Leibundgut, *Ann. Rev. Astron. Astrophys.* **39**, 67 (2001).
24. A.G. Riess *et al.*, *Astron. J.* **116**, 1009 (1998);  
P. Garnavich *et al.*, *Astrophys. J.* **509**, 74 (1998);  
S. Perlmutter *et al.*, *Astrophys. J.* **517**, 565 (1999).
25. M. Kowalski *et al.*, *Astrophys. J.* **686**, 749 (2008).
26. A.G. Riess *et al.*, *Astrophys. J.* **659**, 98 (2007);  
S. Jha *et al.*, *Astrophys. J.* **659**, 122 (2007);  
W.M. Wood-Vasey *et al.*, *Astrophys. J.* **666**, 694 (2007);  
M. Hicken *et al.*, *Astrophys. J.* **700**, 1097 (2009);  
R. Amanullah *et al.*, *Astrophys. J.* **716**, 712 (2010).
27. A. Conley *et al.*, *Astrophys. J. Supp.* **192**, 1 (2011);  
M. Sullivan *et al.*, *Astrophys. J.* **737**, 102 (2011).
28. R. Kessler *et al.*, *Astrophys. J. Supp.* **185**, 32 (2009).
29. I. Maor *et al.*, *Phys. Rev.* **D65**, 123003 (2002).
30. A. Lewis and S. Bridle, *Phys. Rev.* **D66**, 103511 (2002).
31. J. Kovac *et al.*, *Nature* **420**, 772 (2002).
32. S. Das *et al.*, *Phys. Rev. Lett.* **107**, 021301 (2011).
33. D. Eisenstein *et al.*, *Astrophys. J.* **633**, 560 (2005).
34. S. Cole *et al.*, *MNRAS* **362**, 505 (2005).
35. B. Reid *et al.*, *MNRAS* **404**, 60 (2010);  
W.J. Percival *et al.*, *MNRAS* **401**, 2148 (2010).
36. C. Blake *et al.*, *MNRAS* in press, *arXiv:1108.2635*.
37. R.G. Crittenden and N. Turok, *Phys. Rev. Lett.* **75**, 2642 (1995).
38. S.P. Boughn and R.G. Crittenden, *Nature* **427**, 45 (2004).
39. F.-X. Dupe *et al.*, *A&A*, in press, *arXiv:1010.2192*.
40. W. Hu *et al.*, *Phys. Rev. Lett.* **80**, 5255 (1998).
41. J. Lesgourgues and S. Pastor, *Phys. Reports* **429**, 307 (2006).
42. S. Hannestad, *JCAP* **0305**, 004 (2003).
43. O. Elgaroy and O. Lahav, *New J. Phys.* **7**, 61 (2005).
44. K. Ichikawa *et al.*, *Phys. Rev.* **D71**, 043001 (2005).
45. S. Thomas, F.B. Abdalla, and O. Lahav, *Phys. Rev. Lett.* **105**, 031301 (2010).
46. B.A. Reid *et al.*, *JCAP* **1001**, 003 (2010).
47. M. Viel, M.G. Haehnelt, and V. Springel, *JCAP* **06**, 015 (2010).
48. A. Mantz *et al.*, *MNRAS* **406**, 1759 (2010).
49. S.W. Allen *et al.*, *MNRAS* **383**, 879 (2008).
50. R.A.C. Croft *et al.*, *Astrophys. J.* **581**, 20 (2002).
51. S. Kim *et al.*, *MNRAS* **347**, 355 (2004).
52. U. Seljak *et al.*, *MNRAS* **342**, L79 (2003);  
U. Seljak *et al.*, *Phys. Rev.* **D71**, 103515 (2005).
53. A. Refregier, *Ann. Rev. Astron. Astrophys.* **41**, 645 (2003);  
H. Hoekstra and B. Jain, *Ann. Rev. Nucl. and Part. Sci.* **58**, 99 (2008);  
R. Massey *et al.*, *Nature* **445**, 286, (2007).
54. L. Fu *et al.*, *Astron. & Astrophys.* **479**, 9 (2008).
55. J. Benjamin *et al.*, *MNRAS* **381**, 702 (2007).
56. A. Dekel, *Ann. Rev. Astron. Astrophys.* **32**, 371 (1994).
57. N. Kaiser, *MNRAS* **227**, 1 (1987).
58. L. Guzzo *et al.*, *Nature* **451**, 541 (2008).
59. A. Nusser and M. Davis, *Astrophys. J.* **736**, 93 (2011).

## 24. DARK MATTER

Revised September 2011 by M. Drees (Bonn University) and G. Gerbier (Saclay, CEA).

### 24.1. Theory

#### 24.1.1. Evidence for Dark Matter :

The existence of Dark (*i.e.*, non-luminous and non-absorbing) Matter (DM) is by now well established [1,2]. The earliest, and perhaps still most convincing, evidence for DM came from the observation that various luminous objects (stars, gas clouds, globular clusters, or entire galaxies) move faster than one would expect if they only felt the gravitational attraction of other visible objects. An important example is the measurement of galactic rotation curves. The rotational velocity  $v$  of an object on a stable Keplerian orbit with radius  $r$  around a galaxy scales like  $v(r) \propto \sqrt{M(r)/r}$ , where  $M(r)$  is the mass inside the orbit. If  $r$  lies outside the visible part of the galaxy and mass tracks light, one would expect  $v(r) \propto 1/\sqrt{r}$ . Instead, in most galaxies one finds that  $v$  becomes approximately constant out to the largest values of  $r$  where the rotation curve can be measured; in our own galaxy,  $v \simeq 240$  km/s at the location of our solar system, with little change out to the largest observable radius. This implies the existence of a *dark halo*, with mass density  $\rho(r) \propto 1/r^2$ , *i.e.*,  $M(r) \propto r$ ; at some point  $\rho$  will have to fall off faster (in order to keep the total mass of the galaxy finite), but we do not know at what radius this will happen. This leads to a lower bound on the DM mass density,  $\Omega_{\text{DM}} \gtrsim 0.1$ , where  $\Omega_X \equiv \rho_X/\rho_{\text{crit}}$ ,  $\rho_{\text{crit}}$  being the critical mass density (*i.e.*,  $\Omega_{\text{tot}} = 1$  corresponds to a flat Universe).

The observation of clusters of galaxies tends to give somewhat larger values,  $\Omega_{\text{DM}} \simeq 0.2$ . These observations include measurements of the peculiar velocities of galaxies in the cluster, which are a measure of their potential energy if the cluster is virialized; measurements of the *X-ray* temperature of hot gas in the cluster, which again correlates with the gravitational potential felt by the gas; and—most directly—studies of (weak) gravitational lensing of background galaxies on the cluster.

A particularly compelling example involves the bullet cluster (1E0657-558) which recently (on cosmological time scales) passed through another cluster. As a result, the hot gas forming most of the clusters' baryonic mass was shocked and decelerated, whereas the galaxies in the clusters proceeded on ballistic trajectories. Gravitational lensing shows that most of the total mass also moved ballistically, indicating that DM self-interactions are indeed weak [1].

The currently most accurate, if somewhat indirect, determination of  $\Omega_{\text{DM}}$  comes from global fits of cosmological parameters to a variety of observations; see the Section on Cosmological Parameters for details. For example, using measurements of the anisotropy of the cosmic microwave background (CMB) and of the spatial distribution of galaxies, Ref. 3 finds a density of cold, non-baryonic matter

$$\Omega_{\text{nbm}} h^2 = 0.112 \pm 0.006, \quad (24.1)$$

where  $h$  is the Hubble constant in units of 100 km/(s·Mpc). Some part of the baryonic matter density [3],

$$\Omega_{\text{b}} h^2 = 0.022 \pm 0.001, \quad (24.2)$$

may well contribute to (baryonic) DM, *e.g.*, MACHOs [4] or cold molecular gas clouds [5].

The DM density in the “neighborhood” of our solar system is also of considerable interest. This was first estimated as early as 1922 by J.H. Jeans, who analyzed the motion of nearby stars transverse to the galactic plane [2]. He concluded that in our galactic neighborhood, the average density of DM must be roughly equal to that of luminous matter (stars, gas, dust). Remarkably enough, the most recent estimate, based on a detailed model of our galaxy constrained by a host of observables including the galactic rotation curve, finds a quite similar result for the smooth component of the local Dark Matter density [6]:

$$\rho_{\text{DM}}^{\text{local}} = (0.39 \pm 0.03) \frac{\text{GeV}}{\text{cm}^3}. \quad (24.3)$$

This value may have to be increased by a factor of  $1.2 \pm 0.2$  since the baryons in the galactic disk, in which the solar system is located, also increase the local DM density [7]. Small substructures (minihaloes, streams) are not likely to change the local DM density significantly [1].

#### 24.1.2. Candidates for Dark Matter :

Analyses of structure formation in the Universe indicate that most DM should be “cold” or “cool”, *i.e.*, should have been non-relativistic at the onset of galaxy formation (when there was a galactic mass inside the causal horizon) [1]. This agrees well with the upper bound [3] on the contribution of light neutrinos to Eq. (24.1),

$$\Omega_{\nu} h^2 \leq 0.0062 \quad 95\% \text{ CL}. \quad (24.4)$$

Candidates for non-baryonic DM in Eq. (24.1) must satisfy several conditions: they must be stable on cosmological time scales (otherwise they would have decayed by now), they must interact very weakly with electromagnetic radiation (otherwise they wouldn't qualify as *dark matter*), and they must have the right relic density. Candidates include primordial black holes, axions, sterile neutrinos, and weakly interacting massive particles (WIMPs).

Primordial black holes must have formed before the era of Big-Bang nucleosynthesis, since otherwise they would have been counted in Eq. (24.2) rather than Eq. (24.1). Such an early creation of a large number of black holes is possible only in certain somewhat contrived cosmological models [8].

The existence of axions [9] was first postulated to solve the strong *CP* problem of QCD; they also occur naturally in superstring theories. They are pseudo Nambu-Goldstone bosons associated with the (mostly) spontaneous breaking of a new global “Peccei-Quinn” (PQ)  $U(1)$  symmetry at scale  $f_a$ ; see the Section on Axions in this *Review* for further details. Although very light, axions would constitute cold DM, since they were produced non-thermally. At temperatures well above the QCD phase transition, the axion is massless, and the axion field can take any value, parameterized by the “misalignment angle”  $\theta_i$ . At  $T \lesssim 1$  GeV, the axion develops a mass  $m_a$  due to instanton effects. Unless the axion field happens to find itself at the minimum of its potential ( $\theta_i = 0$ ), it will begin to oscillate once  $m_a$  becomes comparable to the Hubble parameter  $H$ . These coherent oscillations transform the energy originally stored in the axion field into physical axion quanta. The contribution of this mechanism to the present axion relic density is [1]

$$\Omega_a h^2 = \kappa_a \left( f_a / 10^{12} \text{ GeV} \right)^{1.175} \theta_i^2, \quad (24.5)$$

where the numerical factor  $\kappa_a$  lies roughly between 0.5 and a few. If  $\theta_i \sim \mathcal{O}(1)$ , Eq. (24.5) will saturate Eq. (24.1) for  $f_a \sim 10^{11}$  GeV, comfortably above laboratory and astrophysical constraints [9]; this would correspond to an axion mass around 0.1 meV. However, if the post-inflationary reheat temperature  $T_R > f_a$ , cosmic strings will form during the PQ phase transition at  $T \simeq f_a$ . Their decay will give an additional contribution to  $\Omega_a$ , which is often bigger than that in Eq. (24.5) [1], leading to a smaller preferred value of  $f_a$ , *i.e.*, larger  $m_a$ . On the other hand, values of  $f_a$  near the Planck scale become possible if  $\theta_i$  is for some reason very small.

“Sterile”  $SU(2) \times U(1)_Y$  singlet neutrinos with keV masses [10] could alleviate the “cusp/core problem” [1] of cold DM models. If they were produced non-thermally through mixing with standard neutrinos, they would eventually decay into a standard neutrino and a photon.

Weakly interacting massive particles (WIMPs)  $\chi$  are particles with mass roughly between 10 GeV and a few TeV, and with cross sections of approximately weak strength. Within standard cosmology, their present relic density can be calculated reliably if the WIMPs were in thermal and chemical equilibrium with the hot “soup” of Standard Model (SM) particles after inflation. In this case, their density would become exponentially (Boltzmann) suppressed at  $T < m_\chi$ . The WIMPs therefore drop out of thermal equilibrium (“freeze out”) once the rate of reactions that change SM particles into WIMPs or vice

versa, which is proportional to the product of the WIMP number density and the WIMP pair annihilation cross section into SM particles  $\sigma_A$  times velocity, becomes smaller than the Hubble expansion rate of the Universe. After freeze out, the co-moving WIMP density remains essentially constant; if the Universe evolved adiabatically after WIMP decoupling, this implies a constant WIMP number to entropy density ratio. Their present relic density is then approximately given by (ignoring logarithmic corrections) [11]

$$\Omega_\chi h^2 \simeq \text{const.} \cdot \frac{T_0^3}{M_{\text{Pl}}^3 \langle \sigma_A v \rangle} \simeq \frac{0.1 \text{ pb} \cdot c}{\langle \sigma_A v \rangle}. \quad (24.6)$$

Here  $T_0$  is the current CMB temperature,  $M_{\text{Pl}}$  is the Planck mass,  $c$  is the speed of light,  $\sigma_A$  is the total annihilation cross section of a pair of WIMPs into SM particles,  $v$  is the relative velocity between the two WIMPs in their cms system, and  $\langle \dots \rangle$  denotes thermal averaging. Freeze out happens at temperature  $T_F \simeq m_\chi/20$  almost independently of the properties of the WIMP. This means that WIMPs are already non-relativistic when they decouple from the thermal plasma; it also implies that Eq. (24.6) is applicable if  $T_R > T_F$ . Notice that the 0.1 pb in Eq. (24.6) contains factors of  $T_0$  and  $M_{\text{Pl}}$ ; it is, therefore, quite intriguing that it “happens” to come out near the typical size of weak interaction cross sections.

The seemingly most obvious WIMP candidate is a heavy neutrino. However, an SU(2) doublet neutrino will have too small a relic density if its mass exceeds  $M_Z/2$ , as required by LEP data. One can suppress the annihilation cross section, and hence increase the relic density, by postulating mixing between a heavy SU(2) doublet and some sterile neutrino. However, one also has to require the neutrino to be stable; it is not obvious why a massive neutrino should not be allowed to decay.

The currently best motivated WIMP candidate is, therefore, the lightest superparticle (LSP) in supersymmetric models [12] with exact R-parity (which guarantees the stability of the LSP). Searches for exotic isotopes [13] imply that a stable LSP has to be neutral. This leaves basically two candidates among the superpartners of ordinary particles, a sneutrino, and a neutralino. The negative outcome of various WIMP searches (see below) rules out “ordinary” sneutrinos as primary component of the DM halo of our galaxy. (In models with gauge-mediated SUSY breaking, the lightest “messenger sneutrino” could make a good WIMP [14].) The most widely studied WIMP is therefore the lightest neutralino. Detailed calculations [1] show that the lightest neutralino will have the desired thermal relic density Eq. (24.1) in at least four distinct regions of parameter space.  $\chi$  could be (mostly) a bino or photino (the superpartner of the  $U(1)_Y$  gauge boson and photon, respectively), if both  $\chi$  and some sleptons have mass below  $\sim 150$  GeV, or if  $m_\chi$  is close to the mass of some sfermion (so that its relic density is reduced through co-annihilation with this sfermion), or if  $2m_\chi$  is close to the mass of the CP-odd Higgs boson present in supersymmetric models. Finally, Eq. (24.1) can also be satisfied if  $\chi$  has a large higgsino or wino component.

Many non-supersymmetric extensions of the Standard Model also contain viable WIMP candidates [1]. Examples are the lightest  $T$ -odd particle in “Little Higgs” models with conserved  $T$ -parity, or “techni-baryons” in scenarios with an additional, strongly interacting (“technicolor” or similar) gauge group.

There also exist models where the DM particles, while interacting only weakly with ordinary matter, have quite strong interactions within an extended “dark sector” of the theory. These were motivated by measurements by the PAMELA, ATIC and Fermi satellites indicating excesses in the cosmic  $e^+$  and/or  $e^-$  fluxes at high energies. However, these excesses are relative to background estimates that are clearly too simplistic (*e.g.*, neglecting primary sources of electrons and positrons, and modeling the galaxy as a homogeneous cylinder). Moreover, the excesses, if real, are far too large to be due to usual WIMPs, but can be explained by astrophysical sources. It therefore seems unlikely that they are due to Dark Matter [15]. Similarly, claims of positive signals for direct WIMP detection by the DAMA and, more recently, CoGeNT and CRESST collaborations (see below) led to the development of tailor-made models to alleviate tensions with null experiments. Since we are not convinced that these data indeed signal WIMP detection, and these models (some of which were quickly

excluded by improved measurements) lack independent motivation, we will not discuss them any further in this Review.

Although thermally produced WIMPs are attractive DM candidates because their relic density naturally has at least the right order of magnitude, non-thermal production mechanisms have also been suggested, *e.g.*, LSP production from the decay of some moduli fields [16], from the decay of the inflaton [17], or from the decay of “ $Q$ -balls” (non-topological solitons) formed in the wake of Affleck-Dine baryogenesis [18]. Although LSPs from these sources are typically highly relativistic when produced, they quickly achieve kinetic (but not chemical) equilibrium if  $T_R$  exceeds a few MeV [19] (but stays below  $m_\chi/20$ ). They therefore also contribute to cold DM. Finally, if the WIMPs aren’t their own antiparticles, an asymmetry between WIMPs and antiWIMPs might have been created in the early Universe, possibly by the same (unknown) mechanism that created the baryon antibaryon asymmetry. In such “asymmetric DM” models [20] the WIMP antiWIMP annihilation cross section  $\langle \sigma_A v \rangle$  should be significantly larger than  $1 \text{ pb} \cdot c$ , cf Eq. (24.6).

Primary black holes (as MACHOs), axions, sterile neutrinos, and WIMPs are all (in principle) detectable with present or near-future technology (see below). There are also particle physics DM candidates which currently seem almost impossible to detect, unless they decay; the present lower limit on their lifetime is of order  $10^{25}$  to  $10^{26}$  s for 100 GeV particles. These include the gravitino (the spin-3/2 superpartner of the graviton) [1], states from the “hidden sector” thought responsible for supersymmetry breaking [14], and the axino (the spin-1/2 superpartner of the axion) [1].

## 24.2. Experimental detection of Dark Matter

### 24.2.1. The case of baryonic matter in our galaxy :

The search for hidden galactic baryonic matter in the form of MAssive Compact Halo Objects (MACHOs) has been initiated following the suggestion that they may represent a large part of the galactic DM and could be detected through the microlensing effect [4]. The MACHO, EROS, and OGLE collaborations have performed a program of observation of such objects by monitoring the luminosity of millions of stars in the Large and Small Magellanic Clouds for several years. EROS concluded that MACHOs cannot contribute more than 8% to the mass of the galactic halo [21], while MACHO observed a signal at 0.4 solar mass and put an upper limit of 40%. Overall, this strengthens the need for non-baryonic DM, also supported by the arguments developed above.

### 24.2.2. Axion searches :

Axions can be detected by looking for  $a \rightarrow \gamma$  conversion in a strong magnetic field [1]. Such a conversion proceeds through the loop-induced  $a\gamma\gamma$  coupling, whose strength  $g_{a\gamma\gamma}$  is an important parameter of axion models. There currently are two experiments searching for axionic DM. They both employ high quality cavities. The cavity “Q factor” enhances the conversion rate on resonance, *i.e.*, for  $m_a(c^2 + v_a^2/2) = \hbar\omega_{\text{res}}$ . One then needs to scan the resonance frequency in order to cover a significant range in  $m_a$  or, equivalently,  $f_a$ . The bigger of the two experiments, the ADMX experiment [22], originally situated at the LLNL in California but now running at the University of Washington, started taking data in the first half of 1996. It now uses SQUIDs as first-stage amplifiers; their extremely low noise temperature (1.2 K) enhances the conversion signal. Published results [23], combining data taken with conventional amplifiers and SQUIDs, exclude axions with mass between 1.9 and 3.53  $\mu\text{eV}$ , corresponding to  $f_a \simeq 4 \cdot 10^{13}$  GeV, for an assumed local DM density of 0.45  $\text{GeV}/\text{cm}^3$ , if  $g_{a\gamma\gamma}$  is near the upper end of the theoretically expected range. An about five times better limit on  $g_{a\gamma\gamma}$  was achieved [24] for  $1.98 \mu\text{eV} \leq m_a \leq 2.18 \mu\text{eV}$ , if a large fraction of the local DM density is due to a single flow of axions with very low velocity dispersion. The ADMX experiment is being upgraded by reducing the cavity and SQUID temperature from the current 1.2 K to about 0.1 K. This should increase the frequency scanning speed for given sensitivity by more than two orders of magnitude, or increase the sensitivity for fixed observation time.



The smaller “CARRACK” experiment now being developed in Kyoto, Japan [25] uses Rydberg atoms (atoms excited to a very high state,  $n = 111$ ) to detect the microwave photons that would result from axion conversion. This allows almost noise-free detection of single photons. Their ultimate goal is to probe the range between 2 and 50  $\mu\text{eV}$  with sensitivity to all plausible axion models, if axions form most of DM.

### 24.2.3. Searches for keV Neutrinos :

Relic keV neutrinos  $\nu_s$  can only be detected if they mix with the ordinary neutrinos. This mixing leads to radiative  $\nu_s \rightarrow \nu\gamma$  decays, with lifetime  $\tau_{\nu_s} \simeq 1.8 \cdot 10^{21} \text{ s} \cdot (\sin\theta)^{-2} \cdot (1 \text{ keV}/m_{\nu_s})^5$ , where  $\theta$  is the mixing angle [10]. This gives rise to a flux of mono-energetic photons with  $E_\gamma = m_{\nu_s}/2$ , which might be observable by *X-ray* satellites. In the simplest case the relic  $\nu_s$  are produced only by oscillations of standard neutrinos. Assuming that all lepton-antilepton asymmetries are well below  $10^{-3}$ , the  $\nu_s$  relic density can then be computed uniquely in terms of the mixing angle  $\theta$  and the mass  $m_{\nu_s}$ . The combination of lower bounds on  $m_{\nu_s}$  from analyses of structure formation (in particular, the Ly $\alpha$  “forest”) and upper bounds on *X-ray* fluxes from various (clusters of) galaxies exclude this scenario if  $\nu_s$  forms all of DM. This conclusion can be evaded if  $\nu_s$  forms only part of DM, and/or if there is a lepton asymmetry  $\geq 10^{-3}$  (i.e. some 7 orders of magnitude above the observed baryon-antibaryon asymmetry), and/or if there is an additional source of  $\nu_s$  production in the early Universe, e.g. from the decay of heavier particles [10].

### 24.2.4. Basics of direct WIMP search :

As stated above, WIMPs should be gravitationally trapped inside galaxies and should have the adequate density profile to account for the observed rotational curves. These two constraints determine the main features of experimental detection of WIMPs, which have been detailed in the reviews in [1].

Their mean velocity inside our galaxy relative to its center is expected to be similar to that of stars, *i.e.*, a few hundred kilometers per second at the location of our solar system. For these velocities, WIMPs interact with ordinary matter through elastic scattering on nuclei. With expected WIMP masses in the range 10 GeV to 10 TeV, typical nuclear recoil energies are of order of 1 to 100 keV.

The shape of the nuclear recoil spectrum results from a convolution of the WIMP velocity distribution, usually taken as a Maxwellian distribution in the galactic rest frame, shifted into the Earth rest frame, with the angular scattering distribution, which is isotropic to first approximation but forward-peaked for high nuclear mass (typically higher than Ge mass) due to the nuclear form factor. Overall, this results in a roughly exponential spectrum. The higher the WIMP mass, the higher the mean value of the exponential. This points to the need for low nuclear recoil energy threshold detectors.

On the other hand, expected interaction rates depend on the product of the local WIMP flux and the interaction cross section. The first term is fixed by the local density of dark matter, taken as 0.39 GeV/cm<sup>3</sup> [see Eq. (24.3)], the mean WIMP velocity, typically 220 km/s, the galactic escape velocity, typically 544 km/s [26] and the mass of the WIMP. The expected interaction rate then mainly depends on two unknowns, the mass and cross section of the WIMP (with some uncertainty [6] due to the halo model). This is why the experimental observable, which is basically the scattering rate as a function of energy, is usually expressed as a contour in the WIMP mass–cross section plane.

The cross section depends on the nature of the couplings. For non-relativistic WIMPs, one in general has to distinguish spin-independent and spin-dependent couplings. The former can involve scalar and vector WIMP and nucleon currents (vector currents are absent for Majorana WIMPs, *e.g.*, the neutralino), while the latter involve axial vector currents (and obviously only exist if  $\chi$  carries spin). Due to coherence effects, the spin-independent cross section scales approximately as the square of the mass of the nucleus, so higher mass nuclei, from Ge to Xe, are preferred for this search. For spin-dependent coupling, the cross section depends on the nuclear spin factor; used target nuclei include <sup>19</sup>F, <sup>23</sup>Na, <sup>73</sup>Ge, <sup>127</sup>I, <sup>129</sup>Xe, <sup>131</sup>Xe, and <sup>133</sup>Cs.

Cross sections calculated in MSSM models [27] induce rates of at most 1 evt day<sup>-1</sup> kg<sup>-1</sup> of detector, much lower than the usual radioactive backgrounds. This indicates the need for underground laboratories to protect against cosmic ray induced backgrounds, and for the selection of extremely radio-pure materials.

The typical shape of exclusion contours can be anticipated from this discussion: at low WIMP mass, the sensitivity drops because of the detector energy threshold, whereas at high masses, the sensitivity also decreases because, for a fixed mass density, the WIMP flux decreases  $\propto 1/m_\chi$ . The sensitivity is best for WIMP masses near the mass of the recoiling nucleus.

Two important points are to be kept in mind when comparing exclusion curves from various experiments between them or with positive indications of a signal.

For an experiment with a fixed nuclear recoil energy threshold, the lower is the considered WIMP mass, the lower is the fraction of the spectrum to which the experiment is sensitive. This fraction may be extremely small in some cases. For instance CoGeNT [28], using a Germanium detector with an energy threshold of around 2 keV, is sensitive to about 10 % of the total recoil spectrum of a 7 GeV WIMP, while for XENON100 [29], using a liquid Xenon detector with a threshold of 8.4 keV, this fraction is only 0.05 % (that is the extreme tail of the distribution), for the same WIMP mass. The two experiments are then sensitive to very different parts of the WIMP velocity distribution.

A second important point to consider is the energy resolution of the detector. Again at low WIMP mass, the expected roughly exponential spectrum is very steep and when the characteristic energy of the exponential becomes of the same order as the energy resolution, the energy smearing becomes important. In particular, a significant fraction of the expected spectrum below effective threshold is smeared above threshold, increasing artificially the sensitivity. For instance, a Xenon detector with a threshold of 8 keV and infinitely good resolution is actually insensitive to a 7 GeV mass WIMP, because the expected energy distribution has a cut-off at roughly 5 keV. When folding in the experimental resolution of XENON100 (corresponding to a photostatistics of 0.5 photoelectron per keV), then around 1 % of the signal is smeared above 5 keV and 0.05 % above 8 keV. Setting reliable cross section limits in this mass range thus requires a complete understanding of the response of the detector at energies well below the nominal threshold.

In order to homogenize the reliability of the presented exclusion curves, and save the reader the trouble of performing tedious (though easy to do) calculations, we propose to set cross section limits only for WIMP mass above a “WIMP safe” minimal mass value defined as the maximum of 1) the mass where the increase of sensitivity from infinite resolution to actual experimental resolution is not more than a factor two, and 2) the mass where the experiment is sensitive to at least 1 % of the total WIMP signal recoil spectrum. These recommendations are irrespective of the content of the experimental data obtained by the experiments.

### 24.2.5. Status and prospects of direct WIMP searches :

Given the intense activity of the field, readers interested in more details than the ones given below may refer to [1], as well as to presentations at recent conferences [30].

The first searches have been performed with ultra-pure semiconductors installed in pure lead and copper shields in underground environments. Combining a priori excellent energy resolutions and very pure detector material, they produced the first limits on WIMP searches (Heidelberg-Moscow, IGEX, COSME-II, HDMS) [1]. Planned experiments using several tens of kg to a ton of Germanium run at liquid nitrogen temperature (designed for double-beta decay search)—GERDA, MAJORANA—are based in addition on passive reduction of the external and internal electromagnetic and neutron background by using segmented detectors, minimal detector housing, close electronics, pulse shape discrimination and large liquid nitrogen or argon shields. Their sensitivity to WIMP interactions will depend on their ability to lower the energy threshold sufficiently, while keeping the background rate small.

The use of so called Point Contact Germanium detectors, with a very small capacitance allowing to reach sub-keV thresholds, has given rise to new results. The CoGeNT collaboration [31] has operated a single 440 g Germanium detector with an effective threshold of 400 eV in the Soudan Underground Laboratory for 56 days [28]. After applying a rise time cut on the pulse shapes in order to remove the surface interactions known to suffer from incomplete charge collection, the resulting spectrum below 4 keV is said by the authors to exhibit an irreducible excess of events, with energy spectrum roughly exponential, compatible with a light mass WIMP in the 7-11 GeV range, and cross section around  $10^{-4}$  pb. However, this conclusion crucially depends on the energy dependent rise time cut applied to the data and a sizeable leaking of surface events into the kept spectrum cannot be excluded. The authors acknowledge themselves that a possible instrumental effect, leading to such an excess, is worth investigating. Nevertheless, considerable attention has been paid to the WIMP interpretation, largely due to the temptation to consider it as a confirmation of the low mass WIMP DAMA/LIBRA solution, without channeling (see below). A recent unpublished analysis, presented at the TAUP 2011 conference, indicates a reduction of the claimed signal by a factor 10. Further results [32] based on data accumulated during one year led to the claim of a 2.8 sigma modulation said to be compatible with a WIMP. Here again, the claim is considerably weakened by the fact that the amplitude of the curve describing the expected WIMP modulation in the 0.5-3 keV bin is too high by roughly a factor 2 (or more, if the unmodulated “signal” has to be reduced) and wrongly leads to the conclusion that the modulation is compatible with a standard WIMP in a standard halo. This is also noted in [33].

A new consortium, CDEX/TEXONO, plans to build a 10 kg array of small and very low (200 eV) threshold detectors, and to operate them in the new Chinese Jinping underground laboratory, the deepest in the world.

In order to make further progress in the reliability of any claimed signal, active background rejection and signal identification questions have to be addressed. This is the focus of a growing number of investigations and improvements. Active background rejection in detectors relies on the relatively small ionization in nuclear recoils due to their low velocity. This induces a reduction (“quenching”) of the ionization/scintillation signal for nuclear recoil signal events relative to  $e$  or  $\gamma$  induced backgrounds. Energies calibrated with gamma sources are then called “electron equivalent energies” (keVee unit used below). This effect has been both calculated and measured [1]. It is exploited in cryogenic detectors described later. In scintillation detectors, it induces in addition a difference in decay times of pulses induced by  $e/\gamma$  events vs nuclear recoils. In most cases, due to the limited resolution and discrimination power of this technique at low energies, this effect allows only a statistical background rejection. It has been used in NaI(Tl) (DAMA, LIBRA, NAIAD, Saclay NaI), in CsI(Tl) (KIMS), and Xe (ZEPLIN-I) [1,30]. Pulse shape discrimination is particularly efficient in liquid argon. Using a high energy threshold, it has been used for an event by event discrimination by the WARP experiment, but the high threshold also leads to a moderate signal sensitivity. No observation of nuclear recoils has been reported by these experiments.

Two experimental signatures are predicted for true WIMP signals. One is a strong daily forward/backward asymmetry of the nuclear recoil direction, due to the alternate sweeping of the WIMP cloud by the rotating Earth. Detection of this effect requires gaseous detectors or anisotropic response scintillators (stilbene). The second is a few percent annual modulation of the recoil rate due to the Earth speed adding to or subtracting from the speed of the Sun. This tiny effect can only be detected with large masses; nuclear recoil identification should also be performed, as the otherwise much larger background may also be subject to seasonal modulation.

The DAMA collaboration has reported results from a total of 6 years exposure with the LIBRA phase involving 250 kg of detectors, plus the earlier 6 years exposure of the original DAMA/NaI experiment with 100 kg of detectors [34], for a cumulated exposure of 1.17 t-y. They observe an annual modulation of the signal in the 2 to 6 keVee bin, with the expected period (1 year) and phase (maximum around June 2), at  $8.9 \sigma$  level. If interpreted within the standard halo model described above, two possible explanations have been proposed: a

WIMP with  $m_\chi \simeq 50$  GeV and  $\sigma_{\chi p} \simeq 7 \cdot 10^{-6}$  pb (central values) or at low mass, in the 6 to 10 GeV range with  $\sigma_{\chi p} \sim 10^{-3}$  pb; the cross section could be somewhat lower if there is a significant channeling effect [1].

Interpreting these observations as positive WIMP signal raises several issues of internal consistency. First, the proposed WIMP solutions would induce a sizeable fraction of nuclear recoils in the total measured rate in the 2 to 6 keVee bin. No pulse shape analysis has been reported by the authors to check whether the unmodulated signal was detectable this way. Secondly, the residual  $e/\gamma$ -induced background, inferred by subtracting the signal predicted by the WIMP interpretation from the data, has an unexpected shape [35], starting near zero at threshold and quickly rising to reach its maximum near 3 to 3.5 keVee; from general arguments one would expect the background (e.g. due to electronic noise) to increase towards the threshold. Finally, the amplitude of the annual modulation shows a somewhat troublesome tendency to decrease with time. The original DAMA data, taken 1995 to 2001, gave an amplitude of the modulation of  $20.0 \pm 3.2$  in units of  $10^{-3}$  counts/(kg·day·keVee), in the 2-6 keVee bin. During the first phase of DAMA/LIBRA, covering data taken between 2003 and 2007, this amplitude became  $10.7 \pm 1.9$ , and in the second phase of DAMA/LIBRA, covering data taken between 2007 and 2009, it further decreased to  $8.5 \pm 2.2$ . The ratio of amplitudes inferred from the DAMA/LIBRA phase 2 and original DAMA data is  $0.43 \pm 0.13$ , differing from the expected value of 1 by more than 4 standard deviations. (The results for the DAMA/LIBRA phase 2 have been calculated by us using published results for the earlier data alone [36] as well as for the latest grand total [34].) Similar conclusions can be drawn from analyses of the 2-4 and 2-5 keVee bins.

Concerning compatibility with other experiments (see below), the high mass solution is clearly excluded by several null observations (CDMS, EDELWEISS, XENON), while possibly a small parameter space remains available for the low mass solution (according to [35] this possibility is excluded if the energy spectrum measured by DAMA/LIBRA is taken into account). It should be noted that these comparisons have to make assumptions about the WIMP velocity distribution (see above), but varying this within reasonable limits does not resolve the tension [35]. Moreover, one usually assumes that the WIMP scatters elastically, and that the spin-independent cross section for scattering off protons and neutrons is roughly the same. These assumptions are satisfied by all models we know that are either relatively simple (i.e. do not introduce many new particles) or have independent motivation (e.g. attempting to solve the hierarchy problem). As noted earlier, recently models have been constructed where these assumptions do not hold, but at least some of these are no longer able to make the WIMP interpretation of the DAMA(/LIBRA) observations compatible with all null results from other experiments. Finally, appealing to spin-dependent interactions does not help, either [37], in view of null results from direct searches as well as limits on neutrino fluxes from the Sun (see the subsection on indirect WIMP detection below).

No other annual modulation analysis with comparable sensitivity has been reported by any experiment. ANAIS [30], a 100 kg NaI(Tl) project planned to be run at the Canfranc lab, is in the phase of crystal selection and purification. DM-ice is a new project with the aim of checking the DAMA/LIBRA modulation signal in the southern hemisphere. It will consist of 250 kg of NaI(Tl) installed in the heart of the IceCube array. The counting rate of crystals from the previous NAIAD array recently measured in situ is currently dominated by internal radioactivity.

KIMS [38], an experiment operating 12 crystals of CsI(Tl) with a total mass of 104.4 kg in the Yang Yang laboratory in Korea, has accumulated several years of continuous operation. They should soon be able to set an upper limit on annual modulation amplitude lower than DAMA value if no annual modulation is present, or confirm the DAMA value at  $3 \sigma$ .

At mK temperature, the simultaneous measurement of the phonon and ionization signals in semiconductor detectors permits event by event discrimination between nuclear and electronic recoils down to 5 to 10 keV recoil energy. This feature is being used by the CDMS [30] and EDELWEISS [30] collaborations. Surface interactions,

exhibiting incomplete charge collection, are an important residual background, which is treated by two different techniques: CDMS uses the timing information of the phonon pulse, while EDELWEISS uses the ionization pulses in an interleaved electrodes scheme. New limits on the spin-independent coupling of WIMPs were obtained by CDMS, after operating 19 Germanium cryogenic detectors at the Soudan mine during new runs involving a total exposure of around 612 kg·d (around 300 kg·d fiducial) [39]. Two events were found in the pre-defined signal region, while 0.9 background event were expected. Given these figures, no observation of a signal is claimed. While this data set alone provided a worse limit than the previous runs, the combined data sets provide an improved upper limit on the spin-independent cross section for the scattering of a 70 GeV/ $c^2$  WIMP on a nucleon of  $3.8 \times 10^{-8}$  pb, at 90% CL. The “WIMP safe” minimal mass (see the discussion at the end of sec. 1.2.4) of this analysis is about 12 GeV.

An independent analysis of data at low energy (i.e. above 2 keV recoil energy) has also been performed by CDMS [40]. From the knowledge of the quenching factor of Germanium recoils down to 2 keV recoil energy, the energy spectrum is reconstructed using only the measured phonon energy. The obtained spectrum, once corrected for quenching, has a shape somewhat similar to that reported by CoGeNT, but with a lower amplitude (especially for one of the detector modules, which was used to set the limit) so that CDMS concludes that their data are inconsistent with the original WIMP interpretation of the CoGeNT data (note that both detectors use the same target material, so this comparison really is model-independent), as well as with the standard WIMP interpretation of the DAMA data. New detectors with interleaved electrode schemes are being built.

EDELWEISS has operated ten 400 g Germanium detectors equipped with different thermal sensors and an interdigitised charge collection electrode scheme, during one year at the Laboratoire Souterrain de Modane [41]. A total of 5 events were observed in the signal region for a fiducial exposure of 384 kg·d, while 3 events were expected from backgrounds. No WIMP signal was claimed. A similar sensitivity to CDMS is obtained at high mass, while the high 20 keV analysis threshold induces a somewhat poorer limit at masses lower than 50 GeV. New larger detectors with a complete coverage of the crystal with annular electrodes, and better rejection of non-recoil events are being built.

Given their similar sensitivities, the two collaborations combined their data sets. Using a simple combination method, a gain of 1.6 relative to the best limit has been obtained at WIMP masses larger than 700 GeV, and an improved limit of  $3.3 \times 10^{-8}$  pb for a 90 GeV WIMP mass [42].

The cryogenic experiment CRESST [30] uses the scintillation of  $\text{CaWO}_4$  as second variable for background discrimination. CRESST has recently submitted for publication [43] the result of the analysis of 730 kg·d exposure performed with 8 detectors. The observation of 67 events in the signal region does not match the about 40 expected background events, originating from  $e/\gamma$  leakage, neutron recoils, as well as leakage from  $\alpha$  and Pb recoils. The event excess is said to be compatible with WIMPs. A likelihood method provides two solutions, respectively for 12 and 25 GeV masses, stating also that the background hypothesis alone is more than 4 sigma away from the observed data. However, some other potential sources of background are insufficiently addressed, like “no-light” events, a category of events which previously plagued the sensitivity of this experiment.

Other inorganic scintillators are also being explored, e.g. by the ROSEBUD collaboration [30].

The experimental programs of CDMS II, EDELWEISS II and CRESST II aim at an increase of sensitivity by a factor of 10, by operating around 40 kg of detectors. The next stage SuperCDMS and EURECA-I (a combination of EDELWEISS and CRESST) projects will involve typically 150 kg of detectors. Then GEODM and EURECA-2 will turn to 1 t goals.

Noble gas detectors for dark matter detection are now being developed rapidly by several groups [1]. Dual (liquid and gas) phase detectors allow to measure both the primary scintillation and the ionization electrons drifted through the liquid and amplified in the gas, which is used for background rejection.

The XENON collaboration [30] has successfully operated the 161 kg XENON100 setup at Gran Sasso laboratory during a 100 day data taking period. Within a fiducial mass of 48 kg, 3 events were observed in the signal region, while 1.8 were expected, out of which 1.2 originate from a sizeable contamination of Krypton 85 in the liquid [29]. This allowed to set the best limits at all masses on spin-independent interactions of WIMPs, with a minimum of cross section at  $7.0 \times 10^{-9}$  pb for a mass of 50 GeV. However, the reliability of limits set at masses lower than 10 GeV, especially wrt the relative light efficiency factor, have been discussed in the community. Moreover, as underlined near the end of section 1.2.4, the limits at low mass can be set *only* thanks to the poor energy resolution at threshold  $-8.4$  keV— due to the low photoelectron yield of 0.5 pe/keV. With infinite energy resolution, a Xe detector *with the same threshold of 8.4 keV* is not sensitive to a WIMP mass of 7 GeV. Folding in the XENON100 resolution, the expected fraction of a 7 GeV WIMP signal above 8.4 keV is around 0.05 % (in strong contrast with the 10 % to which CoGeNT is sensitive). If one follows the recommendation made above, the “WIMP safe” minimal mass for XENON100 is around 12 GeV.

A reanalysis of part of the XENON10 data [44], using the ionization signal only, with an ionization yield of around 3.5 electron/keV at a threshold of 1.4 keV, sets a more convincing limit in the 7 GeV range, about one order of magnitude below the original CoGeNT claim (see above). The “WIMP safe” minimal mass for this XENON10 analysis is around 5 GeV. The XENON10 limit for spin dependent WIMPs with pure neutron couplings is still the best published limit at all masses [45] (but likely to be soon superseded by an analysis of XENON100 data). XENON1t, the successor of XENON100 planned to be run at Gran Sasso lab, is in its preparation phase. One should note that, presumably, the planned increase of distance between planes of PMT’s will lead to a lower photoelectron yield for scintillation light than at XENON100. This was the case when going from XENON10 (around 1 pe/keV) to XENON100 (around 0.5 pe/keV). For comparison, a 0.25 pe yield per keV would correspond to a “WIMP safe” mass of order of 20 GeV.

A new liquid Xenon based project, PANDA-X, with pancake geometry, planned to be housed in the new Jinping lab, will perform a dedicated low mass WIMP search.

ZEPLIN III [30], using a similar principle and with an active mass of 12 kg of Xenon, operated in the Boulby laboratory, has been upgraded for a lower background, has acquired new data, and is now stopped. XMASS [30] in Japan is close to operate a single-phase 800 kg detector (100 kg fiducial mass) installed in a large pure water shield at the SuperKamiokande site. With no pulse shape analysis, the expected performance relies heavily on the self-shielding effect to lower the background [1].

The LUX detector [1], a 300 kg double phase Xenon detector, planned to be operated in the new SURF (previous Sanford) laboratory in US, is in the commissioning phase, in a water shield at surface, before transport underground to the 4850 level.

The WARP collaboration [30] is currently installing a 100 l Argon detector at the Gran Sasso laboratory. Thanks to a double-background rejection method based on the asymmetry between scintillating and ionizing pulses and extremely efficient pulse shape discrimination of scintillating pulses, it looks possible to achieve very high background rejection, even in the presence of the radioactive isotope  $^{39}\text{Ar}$ . The ArDM project [30] is using a similar technique with a much larger (1,100 kg) mass. It should be installed soon and take data at the newly opened Canfranc laboratory. MiniCLEAN and DEAP-3600 [30], both measuring only scintillation signals in spherical geometries in single phase mode, are being assembled at SNOLab and will operate respectively 500 kg of Ar/Ne and 3600 kg of Ar [1]. DARK SIDE [30], is another Argon based, double phase project, involving in a first step about 50 kg of  $^{39}\text{Ar}$  depleted Argon, to be installed in Gran Sasso lab.

The low pressure Time Projection Chamber technique is the only convincing way to measure the direction of nuclear recoils and prove the galactic origin of a possible signal [1]. The DRIFT collaboration [30] has operated a 1  $\text{m}^3$  volume detector in the UK Boulby mine. Though the background due to internal radon contamination was lowered, no new competitive limit has yet been

set. The MIMAC collaboration [30] is investigating a sub-keV energy threshold TPC detector. Additional sensitive measurements of Fluor nuclei quenching factor and recoil imaging have been performed recently by this group down to few keV. A 2.5 l 1000 channel prototype is going to be operated soon in the Fréjus laboratory. Other groups developing similar techniques, though with lower sensitivity, are DMTPC in the US and NewAge in Japan.

The following more unconventional detectors use  $^{19}\text{F}$  nuclei to set limits on the spin dependent coupling of WIMPs, with less than kg mass detectors. The bubble chamber like detector, COUPP [30], run at Fermilab, has provided a new limit [46] for spin dependent proton coupling WIMPs for masses above 20 GeV, superseding an earlier KIMS result. PICASSO [30], a superheated droplet detector run at SNOLAB, obtained a better limit below 20 GeV on the same type of WIMPs [47]. Finally, SIMPLE [30], a similar experiment run at Laboratoire Souterrain de Rustrel, submitted results for publication that claim to provide the currently best limit on the spin-dependent WIMP-proton cross section for all WIMP masses [48].

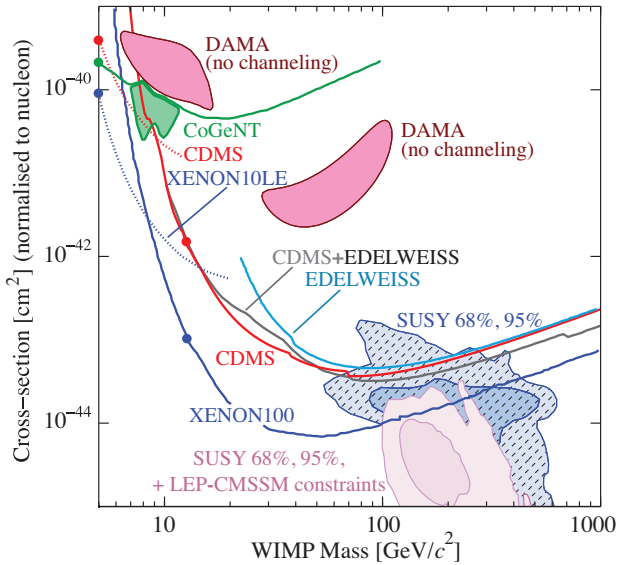


**Figure 24.1:** Cross sections (normalised to nucleon assuming  $A^2$  dependence, see section 1.2.4) for spin independent coupling versus mass diagrams. References to the experimental results are given in the text. The big dots on some curves show the “WIMP safe” minimal mass for the corresponding experimental result (see details in text). DAMA candidates region (no channeling) are from [50], shaded 68% and 95% regions are SUSY predictions by [51], together with recent constraints (crosshatched 68% and 95% regions) set by LHC experiments (CMSSM) [52]. Here equal cross sections for scattering from protons and neutrons have been assumed.

Figures 24.1 and 24.2 illustrate the limits and positive claims for cross sections, normalised to nucleon, for spin independent and spin dependent couplings, respectively, as functions of WIMP mass, where only the two currently best limits are presented. Also shown are constraints from indirect observations (see the next section) and typical regions of SUSY models, before and after recent LHC results. These figures have been made with the `dmtools` web page, thanks to the very efficient collaboration of `dmtools` team [55].

Sensitivities down to  $\sigma_{\chi p}$  of  $10^{-10}$  pb, as needed to probe large regions of MSSM parameter space [27], will be reached with detectors of typical masses of 1 ton, assuming nearly perfect background discrimination capabilities. Note that the expected WIMP rate is then 5 evts/ton/year for Ge. The ultimate neutron background will only be identified by its multiple interactions in a finely segmented or multiple-interaction-sensitive detector, and/or by operating detectors containing different target materials within the same set-up. Larger mass projects are envisaged by the DARWIN European consortium

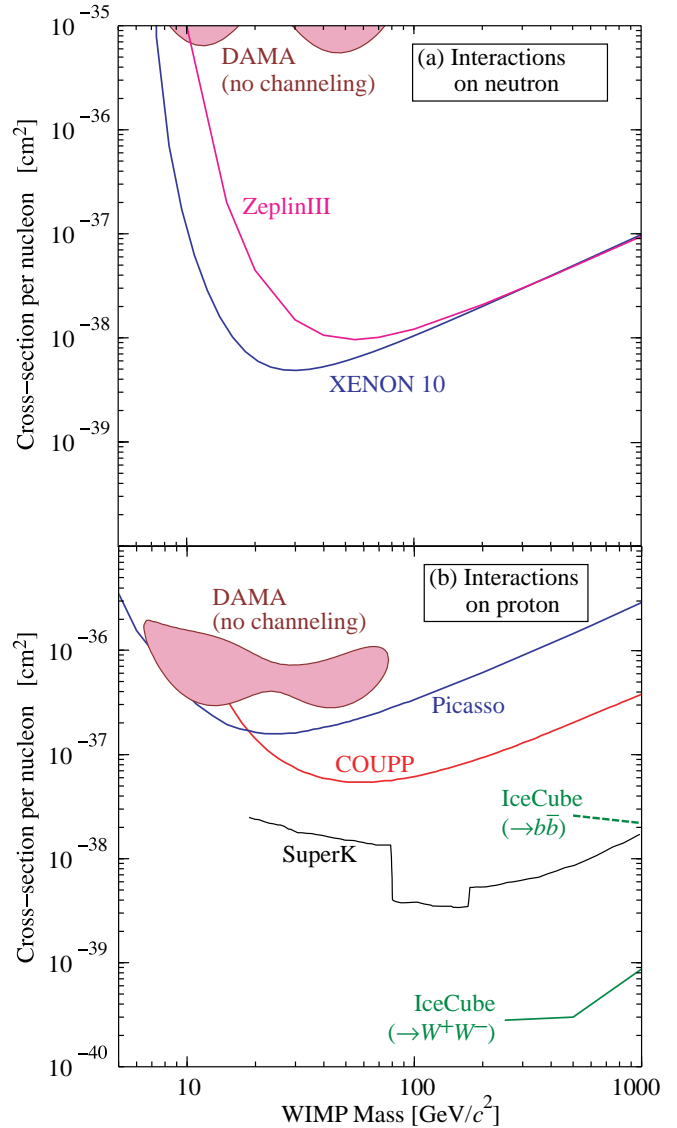


**Figure 24.2:** Cross sections for spin dependent coupling versus mass diagrams. References to the experimental results are given in the text. The DAMA candidates region (no channeling) are from [50]: (a) interactions on neutron; (b) interactions on proton.

and the MAX project in the US (liquid Xe and Ar multiton project) [30].

#### 24.2.6. Status and prospects of indirect WIMP searches :

WIMPs can annihilate and their annihilation products can be detected; these include neutrinos, gamma rays, positrons, antiprotons, and antinuclei [1]. These methods are complementary to direct detection and might be able to explore higher masses and different coupling scenarios. “Smoking gun” signals for indirect detection are GeV neutrinos coming from the center of the Sun or Earth, and monoenergetic photons from WIMP annihilation in space.

WIMPs can be slowed down, captured, and trapped in celestial objects like the Earth or the Sun, thus enhancing their density and their probability of annihilation. This is a source of muon neutrinos which can interact in the Earth. Upward going muons can then be detected in large neutrino telescopes such as MACRO, BAKSAN, SuperKamiokande, Baikal, AMANDA, ANTARES, NESTOR, and the large sensitive area IceCube [1]. The best upper limit for relatively soft muons, of  $\approx 1000$  muons/km<sup>2</sup>/year for muons with energy above  $\sim 2$  GeV [53], comes from SuperKamiokande [30] using through-going muons. For more energetic muons a slightly more stringent limit

has been set by IceCube22 (using 22 strings), e.g. excluding a flux above 610 muons/km<sup>2</sup>/year from the Sun for a WIMP model with average muon energy of 150 GeV [54]. In the framework of the MSSM and with standard halo velocity profiles, only the limits from the Sun, which mostly probe spin-dependent couplings, are competitive with direct WIMP search limits. IceCube80 [30] will increase this sensitivity by a factor  $\simeq 5$  at masses higher than 200 GeV while IceCube Deep Core will allow to reach masses down to 50 GeV [1].

WIMP annihilation in the halo can give a continuous spectrum of gamma rays and (at one-loop level) also monoenergetic photon contributions from the  $\gamma\gamma$  and  $\gamma Z$  channels. These channels also allow to search for WIMPs for which direct detection experiments have little sensitivity, e.g., almost pure higgsinos. However, the size of this signal depends very strongly on the halo model, but is expected to be most prominent near the galactic center. The central region of our galaxy hosts a strong TeV point source discovered [56] by the H.E.S.S. Cherenkov telescope [57]. Moreover, FERMI/LAT [30] data revealed a new extended source of GeV photons near the galactic center above and below the galactic plane [58]. Both of these sources are most likely of astrophysical origin. The presence of these unexpected backgrounds makes it more difficult to discover WIMPs in this channel, and no convincing signal has been claimed. FERMI/LAT observations of the galactic halo are in agreement with predictions based on purely astrophysical sources (in contrast to a re-analysis of earlier EGRET data [59]), and rule out many WIMP models that were constructed to explain the PAMELA and FERMI/LAT excesses in the  $e^\pm$  channel [60]. Similarly, Cherenkov telescope and FERMI/LAT observations of nearby dwarf galaxies, globular clusters, and clusters of galaxies only yielded upper limits on photon fluxes from WIMP annihilation. While limits from individual observations are still above the predictions of most WIMP models, a very recent combination [61] of limits from dwarf galaxies excludes WIMPs annihilating hadronically with the standard cross section needed for thermal relics, if the WIMP mass is below 25 GeV; assumptions are annihilation from an  $S$ -wave initial state, and a dark matter density distribution scaling like the inverse of the distance from the center of the dwarf galaxy at small radii.

Antiparticles arise as additional WIMP annihilation products in the halo. To date the best measurement of the antiproton flux comes from the PAMELA satellite [30], and covers kinetic energies between 60 MeV and 180 GeV [62]. The result is in good agreement with secondary production and propagation models. These data exclude WIMP models that attempt to explain the  $e^\pm$  excesses via annihilation into  $W^\pm$  or  $Z^0$  boson pairs; however, largely due to systematic uncertainties they do not significantly constrain conventional WIMP models.

The best measurements of the positron (and electron) flux at (tens of) GeV energies again comes from PAMELA [63], showing a rather marked rise of the positron fraction between 10 and 100 GeV. The observed spectrum falls within the one order of magnitude span (largely due to differences in the propagation model used) of positron fraction values predicted by secondary production models [64]. Measurements of the total electron+positrons energy spectrum by ATIC [65], FERMI/LAT [66] and H.E.S.S. [67] between 100 and 1000 GeV also exceed the predicted purely secondary spectrum, but with very large dispersion of the magnitude of these excesses. While it has been recognized that astrophysical sources may account for all these features, many ad-hoc Dark Matter models have been built to account for these excesses. As mentioned in section 1, given the amount of jerking and twisting needed to build such models not to contradict any observation, it seems very unlikely that Dark Matter is at the origin of these excesses.

Last but not least, an antideuteron signal [1], as potentially observable by AMS2 or PAMELA, could constitute a signal for WIMP annihilation in the halo.

An interesting comparison of respective sensitivities to MSSM parameter space of future direct and various indirect searches has been performed with the DARKSUSY tool [68]. A web-based up-to-date collection of results from direct WIMP searches, theoretical predictions, and sensitivities of future experiments can be found in [55]. Also, the web page [69] allows to make predictions for WIMP

signals in various experiments, within a variety of SUSY models and to extract limits from simply parametrised data. Integrated analysis of all data from direct and indirect WIMP detection, and also from LHC experiments should converge to a comprehensive approach, required to fully unravel the mysteries of dark matter.

#### References:

- For details, recent reviews and many more references about particle dark matter, see G. Bertone, *Particle Dark Matter* (Cambridge University Press, 2010).
- For a brief but delightful history of DM, see V. Trimble, in *Proceedings of the First International Symposium on Sources of Dark Matter in the Universe*, Bel Air, California, 1994, published by World Scientific, Singapore (ed. D.B. Cline). See also the recent review G. Bertone, D. Hooper, and J. Silk, *Phys. Rep.* **405**, 279 (2005).
- See *Cosmological Parameters* in this Review.
- B. Paczynski, *Astrophys. J.* **304**, 1 (1986); K. Griest, *Astrophys. J.* **366**, 412 (1991).
- F. De Paolis *et al.*, *Phys. Rev. Lett.* **74**, 14 (1995).
- R. Catena and P. Ullio, *JCAP* **1008**, 004 (2010).
- M. Pato *et al.*, *Phys. Rev.* **D82**, 023531 (2010).
- K. Kohri, D.H. Lyth, and A. Melchiorri, *JCAP* **0804**, 038 (2008).
- See *Axions and Other Very Light Bosons* in this Review.
- A. Kusenko, *Phys. Reports* **481**, 1 (2009).
- E.W. Kolb and M.E. Turner, *The Early Universe*, Addison-Wesley (1990).
- For a general introduction to SUSY, see the section devoted in this Review of *Particle Physics*. For a review of SUSY Dark Matter, see G. Jungman, M. Kamionkowski, and K. Griest, *Phys. Reports* **267**, 195 (1996).
- See *Searches for WIMPs and Other Particles* in this Review.
- S. Dimopoulos, G.F. Giudice, and A. Pomarol, *Phys. Lett.* **B389**, 37 (1996).
- M. Cirelli and J.M. Cline, *Phys. Rev.* **D82**, 023503 (2010).
- T. Moroi and L. Randall, *Nucl. Phys.* **B570**, 455 (2000).
- R. Allahverdi and M. Drees, *Phys. Rev. Lett.* **89**, 091302 (2002).
- M. Fujii and T. Yanagida, *Phys. Lett.* **B542**, 80 (2002).
- J. Hisano, K. Kohri, and M.M. Nojiri, *Phys. Lett.* **B505**, 169 (2001).
- D.E. Kaplan, M.A. Luty, and K.M. Zurek, *Phys. Rev.* **D79**, 115016 (2009).
- MACHO Collab., C. Alcock *et al.*, *Astrophys. J.* **542**, 257 (2000); EROS Collab., *AA* **469**, 387 (2007); OGLE Collab., [arXiv:1106.2925 \[astro-ph.GA\]](https://arxiv.org/abs/1106.2925), (MNRAS, to appear).
- <http://www.phys.washington.edu/groups/admx/home.html>.
- S.J. Asztalos *et al.*, *Phys. Rev.* **D69**, 011101 (2004); S.J. Asztalos *et al.*, *Phys. Rev. Lett.* **104**, 041301 (2010).
- L.D. Duffy *et al.*, *Phys. Rev.* **D74**, 012006 (2006).
- M. Shibata *et al.*, *J. Low Temp. Phys.* **151**, 1043 (2008); M. Tada *et al.*, *Phys. Lett.* **A349**, 488 (2006).
- M.C. Smith *et al.*, *Mon. Not. R. Astron. Soc.* **379**, 755 (2007).
- J. Ellis *et al.*, *Phys. Rev.* **D77**, 065026 (2008).
- C.E. Aalseth *et al.*, *Phys. Rev. Lett.* **106**, 131301 (2011).
- XENON100 Collab., E. Aprile *et al.*, [arXiv:1104.2549](https://arxiv.org/abs/1104.2549), submitted to PRL.
- A very useful collection of web links to the homepages of Dark Matter related conferences, and of experiments searching for WIMP Dark Matter, is the “Dark Matter Portal” at <http://lpsc.in2p3.fr/mayet/dm.php>.
- <http://cogent.pnnl.gov/>.
- C.E. Aalseth *et al.*, *Phys. Rev. Lett.* **107**, 141301 (2011).
- P.J. Fox *et al.*, [arXiv:1107.0717v2](https://arxiv.org/abs/1107.0717v2);
- T. Schwetz and J. Zupan, *JCAP* **1108**, 008 (2011).
- DAMA Collab., R. Bernabei *et al.*, *Eur. Phys. J.* **C67**, 39 (2010).
- M. Fairbairn and T. Schwetz, *JCAP* **0901**, 037 (2009).
- DAMA Collab., R. Bernabei *et al.*, *Eur. Phys. J.* **C56**, 333 (2008).
- C.J. Copi and L.M. Krauss, *New Astron. Rev.* **49**, 185 (2005).

38. [http://q2c.snu.ac.kr/KIMS/KIMS\\_index.htm](http://q2c.snu.ac.kr/KIMS/KIMS_index.htm).
39. CDMS Collab., Z. Ahmed *et al.*, *Science* **327**, 1619 (2010).
40. CDMS Collab., Z. Ahmed *et al.*, *Phys. Rev. Lett.* **06**, 131302 (2011).
41. EDELWEISS Collab., E. Armengaud *et al.*, *Phys. Lett.* **B702**, 329 (2011).
42. EDELWEISS and CDMS Collab., Z. Ahmed *et al.*, *Phys. Rev.* **84**, 011102 (2011).
43. CRESST Collab., G. Angloher *et al.*, [arXiv:1109.0702](https://arxiv.org/abs/1109.0702) [[astro-ph.CO](https://arxiv.org/abs/1109.0702)].
44. XENON10 Collab., J. Angle *et al.*, *Phys. Rev. Lett.* **107**, 051301 (2011).
45. XENON10 Collab., J. Angle *et al.*, *Phys. Rev. Lett.* **101**, 091301 (2008).
46. E. Behnke *et al.*, *Phys. Rev. Lett.* **106**, 021303 (2011).
47. S. Archambault *et al.*, *Phys. Lett.* **B682**, 185 (2009).
48. M. Felizardo *et al.*, [arXiv:1106.3014](https://arxiv.org/abs/1106.3014) [[astro-ph.CO](https://arxiv.org/abs/1106.3014)].
49. ZEPLIN Collab., V. N. Lebedenko *et al.*, *Phys. Rev. Lett.* **103**, 151302 (2009).
50. C. Savage *et al.*, *JCAP* **0904**, 010, 2009.
51. R. Trotta *et al.*, *JHEP* **0812** 024, 2008.
52. O. Buchmueller *et al.*, *Eur. Phys. J.* **C71**, 1634 (2011).
53. SuperKamiokande Collab., S. Desai *et al.*, *Phys. Rev.* **D70**, 083523 (2004).
54. IceCube Collab., R. Abbasi *et al.*, *Phys. Rev. Lett.* **102**, 201302 (2009).
55. <http://dmtools.brown.edu>; <http://dmtools.brown.edu:8080/>.
56. H.E.S.S. Collab., F. Aharonian *et al.*, *Astron. Astrophys.* **503**, 817 (2009); H.E.S.S. Collab., F. Acero *et al.*, *MNRAS* **402**, 1877 (2010).
57. <http://www.mpi-hd.mpg.de/hfm/HESS/>.
58. M. Su, T.R. Slatyer, and D.P. Finkbeiner, *Astrophys. J.* **724**, 1044 (2010).
59. W. de Boer *et al.*, *Astron. Astrophys.* **444**, 51 (2005), and *Phys. Lett.* **B636**, 13 (2006).
60. A.A. Abdo *et al.*, *JCAP* **1004**, 014 (2010).
61. Fermi-LAT Collab., M. Ackermann *et al.*, [arXiv:1108.3546](https://arxiv.org/abs/1108.3546) [[astro-ph](https://arxiv.org/abs/1108.3546)].
62. PAMELA Collab., O. Adriani *et al.*, *Phys. Rev. Lett.* **105**, 121101 (2010).
63. PAMELA collab., O. Adriani *et al.*, *Nature* **458**, 607 (2009).
64. T. Delahaye *et al.*, *Astronomy and Astrophysics* **501**, 821 (2009).
65. ATIC collab., J. Chang *et al.*, *Nature (London)* **456**, 362 (2008).
66. FERMI/LAT collab., A.A. Abdo *et al.*, *Phys. Rev. Lett.* **102**, 181101 (2009).
67. HESS collab., F. Aharonian *et al.*, *Phys. Rev. Lett.* **101**, 261104 (2008).
68. DARKSUSY site: <http://www.physto.se/edsjo/darksusy/>.
69. ILIAS web page: <http://pisrv0.pit.physik.uni-tuebingen.de.darkmatter/>.

## 25. COSMIC MICROWAVE BACKGROUND

Revised August 2011 by D. Scott (University of British Columbia) and G.F. Smoot (UCB/LBNL).

### 25.1. Introduction

The energy content in radiation from beyond our Galaxy is dominated by the cosmic microwave background (CMB), discovered in 1965 [1]. The spectrum of the CMB is well described by a blackbody function with  $T = 2.7255$  K, this spectral form being one of the main pillars of the hot Big Bang model for the early Universe. The lack of any observed deviations from a blackbody spectrum constrains physical processes over cosmic history at redshifts  $z \lesssim 10^7$  (see earlier versions of this review). All viable cosmological models predict a very nearly Planckian spectrum inside the current observational limits.

Another observable quantity inherent in the CMB is the variation in temperature (or intensity) from one part of the microwave sky to another [2]. Since the first detection of these anisotropies by the COBE satellite [3], there has been intense activity to map the sky at increasing levels of sensitivity and angular resolution by ground-based and balloon-borne measurements. These were joined in 2003 by the first results from NASA's Wilkinson Microwave Anisotropy Probe (WMAP) [4], which were improved upon by analysis of the 3-year, 5-year, and 7-year WMAP data [5,6,7]. Together these observations have led to a stunning confirmation of the 'Standard Model of Cosmology.' In combination with other astrophysical data, the CMB anisotropy measurements place quite precise constraints on a number of cosmological parameters, and have launched us into an era of precision cosmology. This is expected to continue with the improved capabilities of ESA's *Planck* satellite [8,9].

### 25.2. Description of CMB Anisotropies

Observations show that the CMB contains anisotropies at the  $10^{-5}$  level, over a wide range of angular scales. These anisotropies are usually expressed by using a spherical harmonic expansion of the CMB sky:

$$T(\theta, \phi) = \sum_{\ell m} a_{\ell m} Y_{\ell m}(\theta, \phi).$$

The vast majority of the cosmological information is contained in the temperature 2-point function, *i.e.*, the variance as a function only of angular separation, since we notice no preferred direction. Equivalently, the power per unit  $\ln \ell$  is  $\ell \sum_m |a_{\ell m}|^2 / 4\pi$ .

#### 25.2.1. The Monopole :

The CMB has a mean temperature of  $T_\gamma = 2.7255 \pm 0.0006$  K ( $1\sigma$ ) [10], which can be considered as the monopole component of CMB maps,  $a_{00}$ . Since all mapping experiments involve difference measurements, they are insensitive to this average level. Monopole measurements can only be made with absolute temperature devices, such as the FIRAS instrument on the COBE satellite [11]. Such measurements of the spectrum are consistent with a blackbody distribution over more than three decades in frequency (with some recent evidence for deviation at low frequencies [12]). A blackbody of the measured temperature corresponds to  $n_\gamma = (2\zeta(3)/\pi^2) T_\gamma^3 \simeq 411 \text{ cm}^{-3}$  and  $\rho_\gamma = (\pi^2/15) T_\gamma^4 \simeq 4.64 \times 10^{-34} \text{ g cm}^{-3} \simeq 0.260 \text{ eV cm}^{-3}$ .

#### 25.2.2. The Dipole :

The largest anisotropy is in the  $\ell = 1$  (dipole) first spherical harmonic, with amplitude  $3.355 \pm 0.008$  mK [6]. The dipole is interpreted to be the result of the Doppler shift caused by the solar system motion relative to the nearly isotropic blackbody field, as broadly confirmed by measurements of the radial velocities of local galaxies (although with some debate [13]). The motion of an observer with velocity  $\beta \equiv v/c$  relative to an isotropic Planckian radiation field of temperature  $T_0$  produces a Doppler-shifted temperature pattern

$$\begin{aligned} T(\theta) &= T_0(1 - \beta^2)^{1/2} / (1 - \beta \cos \theta) \\ &\simeq T_0 \left( 1 + \beta \cos \theta + \left( \beta^2/2 \right) \cos 2\theta + O(\beta^3) \right). \end{aligned}$$

At every point in the sky, one observes a blackbody spectrum, with temperature  $T(\theta)$ . The spectrum of the dipole is the differential of a blackbody spectrum, as confirmed by Ref. 14.

The implied velocity for the solar system barycenter is  $v = 369.0 \pm 0.9 \text{ km s}^{-1}$ , assuming a value  $T_0 = T_\gamma$ , towards  $(\ell, b) = (263.99^\circ \pm 0.14^\circ, 48.26^\circ \pm 0.03^\circ)$  [6,15]. Such a solar system motion implies a velocity for the Galaxy and the Local Group of galaxies relative to the CMB. The derived value is  $v_{\text{LG}} = 627 \pm 22 \text{ km s}^{-1}$  towards  $(\ell, b) = (276^\circ \pm 3^\circ, 30^\circ \pm 3^\circ)$ , where most of the error comes from uncertainty in the velocity of the solar system relative to the Local Group.

The dipole is a frame-dependent quantity, and one can thus determine the 'absolute rest frame' as that in which the CMB dipole would be zero. Our velocity relative to the Local Group, as well as the velocity of the Earth around the Sun, and any velocity of the receiver relative to the Earth, is normally removed for the purposes of CMB anisotropy study.

#### 25.2.3. Higher-Order Multipoles :

The variations in the CMB temperature maps at higher multipoles ( $\ell \geq 2$ ) are interpreted as being mostly the result of perturbations in the density of the early Universe, manifesting themselves at the epoch of the last scattering of the CMB photons. In the hot Big Bang picture, the expansion of the Universe cools the plasma so that by a redshift  $z \simeq 1100$  (with little dependence on the details of the model), the hydrogen and helium nuclei can bind electrons into neutral atoms, a process usually referred to as recombination [16]. Before this epoch, the CMB photons are tightly coupled to the baryons, while afterwards they can freely stream towards us.

Theoretical models generally predict that the  $a_{\ell m}$  modes are Gaussian random fields to high precision, *e.g.*, standard slow-roll inflation's non-Gaussian contribution is expected to be one or two orders of magnitude below current observational limits [17]. Although non-Gaussianity of various forms is possible in early Universe models, tests show that Gaussianity is an extremely good simplifying approximation [18], with only some relatively weak indications of non-Gaussianity or statistical anisotropy at large scales. Such signatures found in existing WMAP data are generally considered to be subtle foreground or instrumental artifacts [19].

A statistically isotropic sky means that all  $m$ 's are equivalent, *i.e.*, there is no preferred axis. Together with the assumption of Gaussian statistics, the variance of the temperature field (or equivalently the power spectrum in  $\ell$ ) then fully characterizes the anisotropies. The power summed over all  $m$ 's at each  $\ell$  is  $(2\ell + 1)C_\ell / (4\pi)$ , where  $C_\ell \equiv \langle |a_{\ell m}|^2 \rangle$ . Thus averages of  $a_{\ell m}$ 's over  $m$  can be used as estimators of the  $C_\ell$ 's to constrain their expectation values, which are the quantities predicted by a theoretical model. For an idealized full-sky observation, the variance of each measured  $C_\ell$  (*i.e.*, the variance of the variance) is  $[2/(2\ell + 1)]C_\ell^2$ . This sampling uncertainty (known as 'cosmic variance') comes about because each  $C_\ell$  is  $\chi^2$  distributed with  $(2\ell + 1)$  degrees of freedom for our observable volume of the Universe. For fractional sky coverage,  $f_{\text{sky}}$ , this variance is increased by  $1/f_{\text{sky}}$  and the modes become partially correlated.

It is important to understand that theories predict the expectation value of the power spectrum, whereas our sky is a single realization. Hence the cosmic variance is an unavoidable source of uncertainty when constraining models; it dominates the scatter at lower  $\ell$ 's, while the effects of instrumental noise and resolution dominate at higher  $\ell$ 's [20].

#### 25.2.4. Angular Resolution and Binning :

There is no one-to-one conversion between multipole  $\ell$  and the angle subtended by a particular spatial scale projected onto the sky. However, a single spherical harmonic  $Y_{\ell m}$  corresponds to angular variations of  $\theta \sim \pi/\ell$ . CMB maps contain anisotropy information from the size of the map (or in practice some fraction of that size) down to the beam-size of the instrument,  $\sigma$ . One can think of the effect of a Gaussian beam as rolling off the power spectrum with the function  $e^{-\ell(\ell+1)\sigma^2}$ .

For less than full sky coverage, the  $\ell$  modes become correlated. Hence, experimental results are usually quoted as a series of 'band powers', defined as estimators of  $\ell(\ell + 1)C_\ell/2\pi$  over different ranges of  $\ell$ . Because of the strong foreground signals in the Galactic Plane, even 'all-sky' surveys, such as WMAP and *Planck* involve a cut sky. The amount of binning required to obtain uncorrelated estimates of power also depends on the map size.

### 25.3. Cosmological Parameters

The current ‘Standard Model’ of cosmology contains around 10 free parameters (see The Cosmological Parameters—Sec. 23 of this *Review*). The basic framework is the Friedmann-Robertson-Walker (FRW) metric (*i.e.*, a universe that is approximately homogeneous and isotropic on large scales), with density perturbations laid down at early times and evolving into today’s structures (see Big-Bang cosmology—Sec. 21 of this *Review*). The most general possible set of density variations is a linear combination of an adiabatic density perturbation and some isocurvature perturbations. Adiabatic means that there is no change to the entropy per particle for each species, *i.e.*,  $\delta\rho/\rho$  for matter is  $(3/4)\delta\rho/\rho$  for radiation. Isocurvature means that the set of individual density perturbations adds to zero, for example, matter perturbations compensate radiation perturbations so that the total energy density remains unperturbed, *i.e.*,  $\delta\rho$  for matter is  $-\delta\rho$  for radiation. These different modes give rise to distinct (temporal) phases during growth, with those of the adiabatic scenario being strongly preferred by the data. Models that generate mainly isocurvature type perturbations (such as most topological defect scenarios) are no longer considered to be viable. However, an admixture of the adiabatic mode with up to about 10% isocurvature contribution is still allowed [21].

Within the adiabatic family of models, there is, in principle, a free function describing the variation of comoving curvature perturbations,  $\mathcal{R}(\mathbf{x}, t)$ . The great virtue of  $\mathcal{R}$  is that it is constant in time for a purely adiabatic perturbation. There are physical reasons to anticipate that the variance of these perturbations will be described well by a power-law in scale, *i.e.*, in Fourier space  $\langle |\mathcal{R}|_k^2 \rangle \propto k^{n-4}$ , where  $k$  is wavenumber and  $n$  is the usual definition of spectral index. So-called ‘scale-invariant’ initial conditions (meaning gravitational potential fluctuations which are independent of  $k$ ) correspond to  $n = 1$ . In inflationary models [22], perturbations are generated by quantum fluctuations, which are set by the energy scale of inflation, together with the slope and higher derivatives of the inflationary potential. One generally expects that the Taylor series expansion of  $\ln \mathcal{R}_k(\ln k)$  has terms of steadily decreasing size. For the simplest models, there are thus two parameters describing the initial conditions for density perturbations: the amplitude and slope of the power spectrum. These can be explicitly defined, for example, through:

$$\Delta_{\mathcal{R}}^2 \equiv (k^3/2\pi^2) \langle |\mathcal{R}|_k^2 \rangle = A (k/k_0)^{n-1},$$

with  $A \equiv \Delta_{\mathcal{R}}^2(k_0)$  and  $k_0 = 0.002 \text{ Mpc}^{-1}$ , say. There are many other equally valid definitions of the amplitude parameter (see also Sec. 21 and Sec. 23 of this *Review*), and we caution that the relationships between some of them can be cosmology-dependent. In ‘slow roll’ inflationary models, this normalization is proportional to the combination  $V^3/(V')^2$ , for the inflationary potential  $V(\phi)$ . The slope  $n$  also involves  $V''$ , and so the combination of  $A$  and  $n$  can, in principle, constrain potentials.

Inflation generates tensor (gravitational wave) modes, as well as scalar (density perturbation) modes. This fact introduces another parameter, measuring the amplitude of a possible tensor component, or equivalently the ratio of the tensor to scalar contributions. The tensor amplitude is  $A_T \propto V$ , and thus one expects a larger gravitational wave contribution in models where inflation happens at higher energies. The tensor power spectrum also has a slope, often denoted  $n_T$ , but since this seems unlikely to be measured in the near future, it is sufficient for now to focus only on the amplitude of the gravitational wave component. It is most common to define the tensor contribution through  $r$ , the ratio of tensor to scalar perturbation spectra at some small value of  $k$  (although sometimes it is defined in terms of the ratio of contributions at  $\ell = 2$ ). Different inflationary potentials will lead to different predictions, *e.g.*, for  $\lambda\phi^4$  inflation with 50 e-folds,  $r = 0.32$ , and for  $m^2\phi^2$  inflation  $r \simeq 0.15$ , while other models can have arbitrarily small values of  $r$ . In any case, whatever the specific definition, and whether they come from inflation or something else, the ‘initial conditions’ give rise to a minimum of 3 parameters:  $A$ ,  $n$ , and  $r$ .

The background cosmology requires an expansion parameter (the Hubble Constant,  $H_0$ , often represented through  $H_0 = 100 h \text{ km s}^{-1} \text{ Mpc}^{-1}$ ) and several parameters to describe the matter

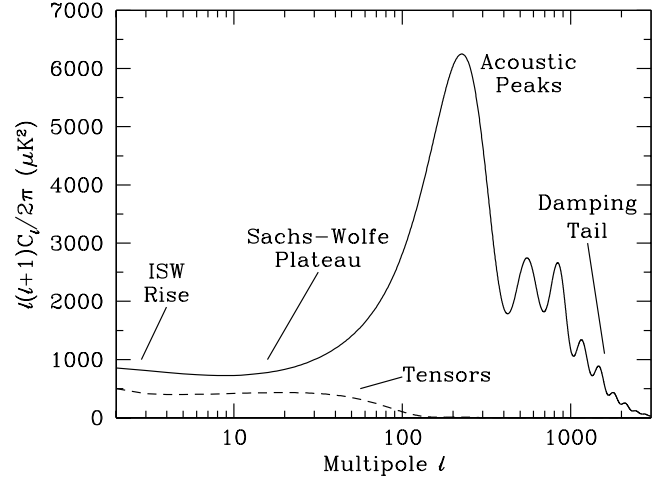


**Figure 25.1:** The theoretical CMB anisotropy power spectrum, using a standard  $\Lambda$ CDM model from CMBFAST. The  $x$ -axis is logarithmic here. The regions, each covering roughly a decade in  $\ell$ , are labeled as in the text: the ISW rise; Sachs-Wolfe plateau; acoustic peaks; and damping tail. Also shown is the shape of the tensor (gravitational wave) contribution, with an arbitrary normalization.

and energy content of the Universe. These are usually given in terms of the critical density, *i.e.*, for species ‘ $x$ ’,  $\Omega_x \equiv \rho_x/\rho_{\text{crit}}$ , where  $\rho_{\text{crit}} \equiv 3H_0^2/8\pi G$ . Since physical densities  $\rho_x \propto \Omega_x h^2 \equiv \omega_x$  are what govern the physics of the CMB anisotropies, it is these  $\omega$ ’s that are best constrained by CMB data. In particular CMB, observations constrain  $\Omega_b h^2$  for baryons and  $\Omega_m h^2$  for baryons plus cold dark matter.

The contribution of a cosmological constant  $\Lambda$  (or other form of dark energy) is usually included via a parameter which quantifies the curvature,  $\Omega_K \equiv 1 - \Omega_{\text{tot}}$ , where  $\Omega_{\text{tot}} = \Omega_m + \Omega_\Lambda$ . The radiation content, while in principle a free parameter, is precisely enough determined by the measurement of  $T_\gamma$ , and makes a  $< 10^{-4}$  contribution to  $\Omega_{\text{tot}}$  today.

The main effect of astrophysical processes on the  $C_\ell$ ’s comes through reionization. The Universe became reionized at some redshift  $z_i$ , long after recombination, affecting the CMB through the integrated Thomson scattering optical depth:

$$\tau = \int_0^{z_i} \sigma_T n_e(z) \frac{dt}{dz} dz,$$

where  $\sigma_T$  is the Thomson cross-section,  $n_e(z)$  is the number density of free electrons (which depends on astrophysics), and  $dt/dz$  is fixed by the background cosmology. In principle,  $\tau$  can be determined from the small-scale matter power spectrum, together with the physics of structure formation and feedback processes. However, this is a sufficiently intricate calculation that  $\tau$  needs to be considered as a free parameter.

Thus, we have eight basic cosmological parameters:  $A$ ,  $n$ ,  $r$ ,  $h$ ,  $\Omega_b h^2$ ,  $\Omega_m h^2$ ,  $\Omega_{\text{tot}}$ , and  $\tau$ . One can add additional parameters to this list, particularly when using the CMB in combination with other data sets. The next most relevant ones might be:  $\Omega_\nu h^2$ , the massive neutrino contribution;  $w$  ( $\equiv p/\rho$ ), the equation of state parameter for the dark energy; and  $dn/d \ln k$ , measuring deviations from a constant spectral index. To these 11 one could of course add further parameters describing additional physics, such as details of the reionization process, features in the initial power spectrum, a sub-dominant contribution of isocurvature modes, *etc.*

As well as these underlying parameters, there are other quantities that can be obtained from them. Such derived parameters include the actual  $\Omega$ ’s of the various components (*e.g.*,  $\Omega_m$ ), the variance of density perturbations at particular scales (*e.g.*,  $\sigma_8$ ), the age of the Universe today ( $t_0$ ), the age of the Universe at recombination, reionization, *etc.*



## 25.4. Physics of Anisotropies

The cosmological parameters affect the anisotropies through the well understood physics of the evolution of linear perturbations within a background FRW cosmology. There are very effective, fast, and publicly available software codes for computing the CMB anisotropy, polarization, and matter power spectra, *e.g.*, CMBFAST [23] and CAMB [24]. These have been tested over a wide range of cosmological parameters and are considered to be accurate to better than the 1% level [25].

A description of the physics underlying the  $C_\ell$ 's can be separated into three main regions, as shown in Fig. 25.1.

### 25.4.1. The ISW rise, $\ell \lesssim 10$ , and Sachs-Wolfe plateau, $10 \lesssim \ell \lesssim 100$ :

The horizon scale (or more precisely, the angle subtended by the Hubble radius) at last scattering corresponds to  $\ell \simeq 100$ . Anisotropies at larger scales have not evolved significantly, and hence directly reflect the ‘initial conditions’.  $\delta T/T = -(1/5)\mathcal{R}(\mathbf{x}_{\text{LSS}}) \simeq (1/3)\delta\phi/c^2$ , here  $\delta\phi$  is the perturbation to the gravitational potential, evaluated on the last scattering surface (LSS). This is a result of the combination of gravitational redshift and intrinsic temperature fluctuations and is usually referred to as the Sachs-Wolfe effect [26].

Assuming that a nearly scale-invariant spectrum of curvature and corresponding density perturbations was laid down at early times (*i.e.*,  $n \simeq 1$ , meaning equal power per decade in  $k$ ), then  $\ell(\ell+1)C_\ell \simeq \text{constant}$  at low  $\ell$ 's. This effect is hard to see unless the multipole axis is plotted logarithmically (as in Fig. 25.1, but not Fig. 25.2).

Time variation of the potentials (*i.e.*, time-dependent metric perturbations) leads to an upturn in the  $C_\ell$ 's in the lowest several multipoles; any deviation from a total equation of state  $w = 0$  has such an effect. So the dominance of the dark energy at low redshift makes the lowest  $\ell$ 's rise above the plateau. This is sometimes called the integrated Sachs-Wolfe effect (or ISW rise), since it comes from the line integral of  $\dot{\phi}$ ; it has been confirmed through correlations between the large-angle anisotropies and large-scale structure [27]. Specific models can also give additional contributions at low  $\ell$  (*e.g.*, perturbations in the dark energy component itself [28]), but typically these are buried in the cosmic variance.

In principle, the mechanism that produces primordial perturbations could generate scalar, vector, and tensor modes. However, the vector (vorticity) modes decay with the expansion of the Universe. The tensors (transverse trace-free perturbations to the metric) generate temperature anisotropies through the integrated effect of the locally anisotropic expansion of space. Since the tensor modes also redshift away after they enter the horizon, they contribute only to angular scales above about  $1^\circ$  (see Fig. 25.1). Hence some fraction of the low  $\ell$  signal could be due to a gravitational wave contribution, although small amounts of tensors are essentially impossible to discriminate from other effects that might raise the level of the plateau. However, the tensors *can* be distinguished using polarization information (see Sec. 25.6).

### 25.4.2. The acoustic peaks, $100 \lesssim \ell \lesssim 1000$ :

On sub-degree scales, the rich structure in the anisotropy spectrum is the consequence of gravity-driven acoustic oscillations occurring before the atoms in the Universe became neutral. Perturbations inside the horizon at last scattering have been able to evolve causally and produce anisotropy at the last scattering epoch, which reflects this evolution. The frozen-in phases of these sound waves imprint a dependence on the cosmological parameters, which gives CMB anisotropies their great constraining power.

The underlying physics can be understood as follows. Before the Universe became neutral, the proton-electron plasma was tightly coupled to the photons, and these components behaved as a single ‘photon-baryon fluid.’ Perturbations in the gravitational potential, dominated by the dark matter component, were steadily evolving. They drove oscillations in the photon-baryon fluid, with photon pressure providing most of the restoring force and baryons giving some additional inertia. The perturbations were quite small in amplitude,  $O(10^{-5})$ , and so evolved linearly. That means each Fourier mode developed independently, and hence can be described by a driven harmonic oscillator, with frequency determined by the sound speed in

the fluid. Thus the fluid density underwent oscillations, giving time variations in temperature. These combine with a velocity effect which is  $\pi/2$  out of phase and has its amplitude reduced by the sound speed.

After the Universe recombined, the radiation decoupled from the baryons and could travel freely towards us. At that point, the phases of the oscillations were frozen-in, and became projected on the sky as a harmonic series of peaks. The main peak is the mode that went through  $1/4$  of a period, reaching maximal compression. The even peaks are maximal *under*-densities, which are generally of smaller amplitude because the rebound has to fight against the baryon inertia. The troughs, which do not extend to zero power, are partially filled by the Doppler effect because they are at the velocity maxima.

The physical length scale associated with the peaks is the sound horizon at last scattering, which can be straightforwardly calculated. This length is projected onto the sky, leading to an angular scale that depends on the geometry of space, as well as the distance to last scattering. Hence the angular position of the peaks is a sensitive probe of the spatial curvature of the Universe (*i.e.*,  $\Omega_{\text{tot}}$ ), with the peaks lying at higher  $\ell$  in open universes and lower  $\ell$  in closed geometry.

One additional effect arises from reionization at redshift  $z_1$ . A fraction of photons ( $\tau$ ) will be isotropically scattered at  $z < z_1$ , partially erasing the anisotropies at angular scales smaller than those subtended by the Hubble radius at  $z_1$ . This corresponds typically to  $\ell$ 's above about a few 10s, depending on the specific reionization model. The acoustic peaks are therefore reduced by a factor  $e^{-2\tau}$  relative to the plateau.

These peaks were a clear theoretical prediction going back to about 1970 [29]. One can think of them as a snapshot of stochastic standing waves. Since the physics governing them is simple and their structure rich, then one can see how they encode extractable information about the cosmological parameters. Their empirical existence started to become clear around 1994 [30], and the emergence, over the following decade, of a coherent series of acoustic peaks and troughs is a triumph of modern cosmology. This picture has received further confirmation with the detection in the power spectrum of galaxies (at redshifts close to zero) of the imprint of these same acoustic oscillations in the baryon component [33–33].

### 25.4.3. The damping tail, $\ell \gtrsim 1000$ :

The recombination process is not instantaneous, which imparts a thickness to the last scattering surface. This leads to a damping of the anisotropies at the highest  $\ell$ 's, corresponding to scales smaller than that subtended by this thickness. One can also think of the photon-baryon fluid as having imperfect coupling, so that there is diffusion between the two components, and hence the amplitudes of the oscillations decrease with time. These effects lead to a damping of the  $C_\ell$ 's, sometimes called Silk damping [34], which cuts off the anisotropies at multipoles above about 2000.

An extra effect at high  $\ell$ 's comes from gravitational lensing, caused mainly by non-linear structures at low redshift. The  $C_\ell$ 's are convolved with a smoothing function in a calculable way, partially flattening the peaks, generating a power-law tail at the highest multipoles, and complicating the polarization signal [35]. The effects of lensing on the CMB have recently been detected by correlating temperature gradients and small-scale filtered anisotropies from WMAP with lensing potentials traced using galaxies [36], as well as through the effect on the shape of the  $C_\ell$ 's [37] and directly through the CMB 4-point function [38]. This is an example of a ‘secondary effect,’ *i.e.*, the processing of anisotropies due to relatively nearby structures (see Sec. 25.7.2). Galaxies and clusters of galaxies give several such effects; all are expected to be of low amplitude and typically affect only the highest  $\ell$ 's, but they carry additional cosmological information and will be increasingly important as experiments push to higher sensitivity and angular resolution [39].

### 25.5. Current Anisotropy Data

There has been a steady improvement in the quality of CMB data that has led to the development of the present-day cosmological model. Probably the most robust constraints currently available come from the combination of the WMAP 7-year data [40] with smaller scale results from the ACT [41] and SPT [42] experiments (together with constraints from other cosmological data-sets). We plot power spectrum estimates from these experiments, as well as ACBAR [43] and QUAD [44] in Fig. 25.2. Other recent experiments also give powerful constraints, which are quite consistent with what we describe below. There have been some comparisons among data-sets [45], which indicate very good agreement, both in maps and in derived power spectra (up to systematic uncertainties in the overall calibration for some experiments). This makes it clear that systematic effects are largely under control. However, a fully self-consistent joint analysis of all the current data-sets has not been attempted, one of the reasons being that it would require a careful treatment of the overlapping sky coverage.

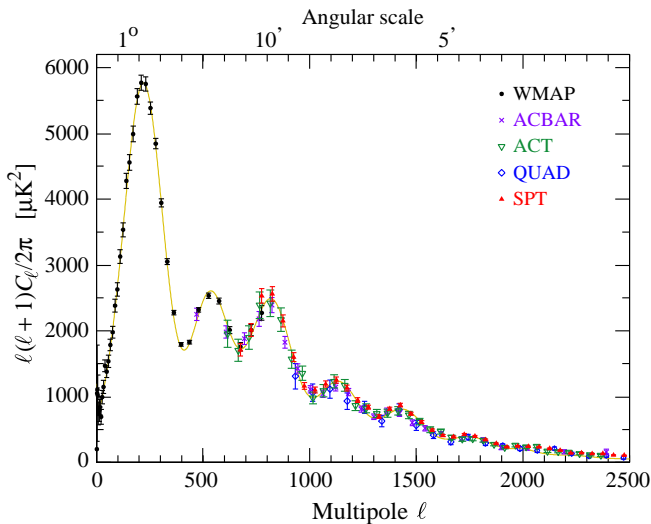


**Figure 25.2:** Band-power estimates from the WMAP, ACBAR, ACT, QUAD, and SPT experiments (omitting some band-powers which have larger error bars). Note that the widths of the  $\ell$ -bands vary between experiments and have not been plotted. This figure represents only a selection of available experimental results, with some other data-sets being of similar quality. The multipole axis here is linear, so the Sachs-Wolfe plateau is hard to see. However, the acoustic peaks and damping region are very clearly observed, with no need for a theoretical curve to guide the eye; the curve plotted is a best-fit model from WMAP plus other CMB data. At high  $\ell$  there is some departure from the model due to secondary anisotropies.

The band-powers shown in Fig. 25.2 are in very good agreement with a ‘ $\Lambda$ CDM’ model. As described earlier, several of the peaks and troughs are quite apparent. For details of how these estimates were arrived at, the strength of any correlations between band-powers and other information required to properly interpret them, the original papers should be consulted.

### 25.6. CMB Polarization

Since Thomson scattering of an anisotropic radiation field also generates linear polarization, the CMB is predicted to be polarized at the level of roughly 5% of the temperature anisotropies [46]. Polarization is a spin-2 field on the sky, and the algebra of the modes in  $\ell$ -space is strongly analogous to spin-orbit coupling in quantum mechanics [47]. The linear polarization pattern can be decomposed in a number of ways, with two quantities required for each pixel in a map, often given as the  $Q$  and  $U$  Stokes parameters. However, the most intuitive and physical decomposition is a geometrical one, splitting the polarization pattern into a part that comes from a

divergence (often referred to as the ‘ $E$ -mode’) and a part with a curl (called the ‘ $B$ -mode’) [48]. More explicitly, the modes are defined in terms of second derivatives of the polarization amplitude, with the Hessian for the  $E$ -modes having principle axes in the same sense as the polarization, while the  $B$ -mode pattern can be thought of as a  $45^\circ$  rotation of the  $E$ -mode pattern. Globally one sees that the  $E$ -modes have  $(-1)^\ell$  parity (like the spherical harmonics), while the  $B$ -modes have  $(-1)^{\ell+1}$  parity.

The existence of this linear polarization allows for six different cross power spectra to be determined from data that measure the full temperature and polarization anisotropy information. Parity considerations make two of these zero, and we are left with four potential observables:  $C_\ell^{\text{TT}}$ ,  $C_\ell^{\text{TE}}$ ,  $C_\ell^{\text{EE}}$ , and  $C_\ell^{\text{BB}}$ . Because scalar perturbations have no handedness, the  $B$ -mode power spectrum can only be sourced by vectors or tensors. Moreover, since inflationary scalar perturbations give only  $E$ -modes, while tensors generate roughly equal amounts of  $E$ - and  $B$ -modes, then the determination of a non-zero  $B$ -mode signal is a way to measure the gravitational wave contribution (and thus potentially derive the energy scale of inflation), even if it is rather weak. However, one must first eliminate the foreground contributions and other systematic effects down to very low levels.

The oscillating photon-baryon fluid also results in a series of acoustic peaks in the polarization  $C_\ell$ ’s. The main ‘EE’ power spectrum has peaks that are out of phase with those in the ‘TT’ spectrum, because the polarization anisotropies are sourced by the fluid velocity. The ‘TE’ part of the polarization and temperature patterns comes from correlations between density and velocity perturbations on the last scattering surface, which can be both positive and negative, and is of larger amplitude than the EE signal. There is no polarization Sachs-Wolfe effect, and hence no large-angle plateau. However, scattering during a recent period of reionization can create a polarization ‘bump’ at large angular scales.

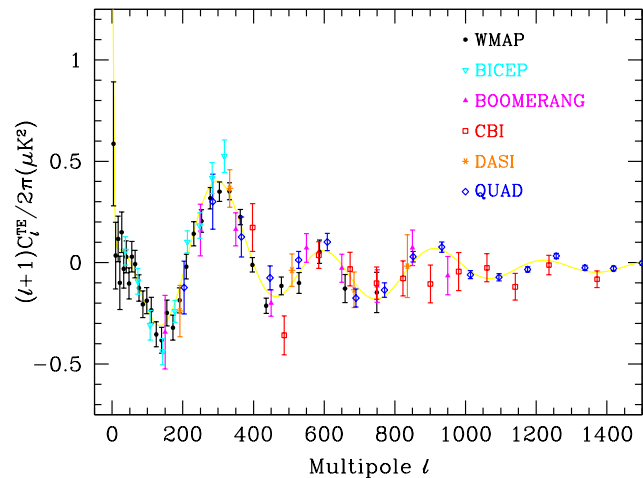


**Figure 25.3:** Cross power spectrum of the temperature anisotropies and  $E$ -mode polarization signal from WMAP, together with estimates from BICEP, BOOMERANG, CBI, DASI, and QUAD, several of which extend to higher  $\ell$ . Note that the  $y$ -axis here is not multiplied by the additional  $\ell$ , which helps to show both the large and small angular scale features.

Because the polarization anisotropies have only a fraction of the amplitude of the temperature anisotropies, they took longer to detect. The first measurement of a polarization signal came in 2002 from the DASI experiment [49], which provided a convincing detection, confirming the general paradigm, but of low enough significance that it lent little constraint to models. As well as the  $E$ -mode signal, DASI also made a statistical detection of the TE correlation.

The TE signal has now been mapped out quite accurately through data from WMAP [50], together with the BICEP [51], BOOMERANG [52], CBI [53], DASI [54], and QUAD [55] experiments, which are shown in Fig. 25.3. The anti-correlation

at  $\ell \simeq 150$  and the peak at  $\ell \simeq 300$  are now quite distinct. The measured shape of the cross-correlation power spectrum provides supporting evidence for the adiabatic nature of the perturbations, as well as directly constraining the thickness of the last scattering surface. Since the polarization anisotropies are generated in this scattering surface, the existence of correlations at angles above about a degree demonstrates that there were super-Hubble fluctuations at the recombination epoch. The sign of this correlation also confirms the adiabatic paradigm.

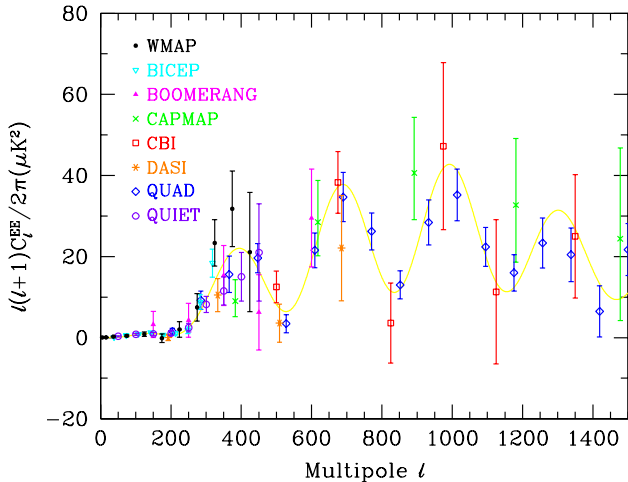


**Figure 25.4:** Power spectrum of  $E$ -mode polarization from several different experiments, plotted along with a theoretical model which fits WMAP plus other CMB data. Note that the widths of the bands have been suppressed for clarity, but that in some cases they are almost as wide as the features in the power spectrum.

Experimental band-powers for  $C_\ell^{EE}$  from WMAP plus BICEP [51], BOOMERANG [56], CAPMAP [57], CBI [53], DASI [54], QUAD [55] and QUIET [58] are shown in Fig. 25.4. Without the benefit of correlating with the temperature anisotropies (*i.e.*, measuring  $C_\ell^{TE}$ ), the polarization anisotropies are very weak and challenging to measure. Nevertheless, there is a highly significant overall detection which is consistent with expectation. The data convincingly show the peak at  $\ell \simeq 140$  (hard to see on this scale), the next peak at  $\ell \simeq 400$  (corresponding to the first trough in  $C_\ell^{TT}$ ) and the generally oscillatory structure.

Several experiments have reported upper limits on  $C_\ell^{BB}$ , but they are currently not very constraining. This situation should change as increasingly ambitious experiments report results.

The most distinctive novel from the polarization measurements is at the largest angular scales ( $\ell < 10$ ) in  $C_\ell^{TE}$ , where there is an excess signal compared to that expected from the temperature power spectrum alone. This is precisely the signal anticipated from an early period of reionization, arising from Doppler shifts during the partial scattering at  $z < z_i$ . The effect is also confirmed in the WMAP  $C_\ell^{EE}$  results at  $\ell = 2-7$  [50]. The amplitude of the signal indicates that the first stars, presumably the source of the ionizing radiation, formed around  $z \simeq 10$  (although the uncertainty is still quite large). Since this corresponds to scattering optical depth  $\tau \simeq 0.1$ , then roughly 10% of CMB photons were re-scattered at the reionization epoch, with the other 90% last scattering at  $z \simeq 1100$ .

## 25.7. Complications

There are a number of issues which complicate the interpretation of CMB anisotropy data (and are considered to be *signal* by many astrophysicists), some of which we sketch out below.

### 25.7.1. Foregrounds :

The microwave sky contains significant emission from our Galaxy and from extra-galactic sources [59,60]. Fortunately, the frequency dependence of these various sources is in general substantially different from that of the CMB anisotropy signals. The combination of Galactic synchrotron, bremsstrahlung, and dust emission reaches a minimum at a wavelength of roughly 3 mm (or about 100 GHz). As one moves to greater angular resolution, the minimum moves to slightly higher frequencies, but becomes more sensitive to unresolved (point-like) sources.

At frequencies around 100 GHz, and for portions of the sky away from the Galactic Plane, the foregrounds are typically 1 to 10% of the CMB anisotropies. By making observations at multiple frequencies, it is relatively straightforward to separate the various components and determine the CMB signal to the few per cent level. For greater sensitivity, it is necessary to use the spatial information and statistical properties of the foregrounds to separate them from the CMB.

The foregrounds for CMB polarization follow a similar pattern, but are less well studied, and are intrinsically more complicated. WMAP has shown that the polarized foregrounds dominate at large angular scales, and that they must be well characterized in order to be discriminated [60]. Whether it is possible to achieve sufficient separation to detect  $B$ -mode CMB polarization is still an open question. However, for the time being, foreground contamination is not a fundamental limit for CMB experiments.

### 25.7.2. Secondary Anisotropies :

With increasingly precise measurements of the primary anisotropies, there is growing theoretical and experimental interest in ‘secondary anisotropies,’ pushing experiments to higher angular resolution and sensitivity. These secondary effects arise from the processing of the CMB due to ionization history and the evolution of structure, including gravitational lensing and patchy reionization effects [61]. Additional information can thus be extracted about the Universe at  $z \ll 1000$ . This tends to be most effectively done through correlating CMB maps with other cosmological probes of structure. Secondary signals are also typically non-Gaussian, unlike the primary CMB anisotropies.

A secondary signal of great current interest is the Sunyaev-Zeldovich (SZ) effect [62], which is Compton scattering ( $\gamma e \rightarrow \gamma' e'$ ) of the CMB photons by hot electron gas. This creates spectral distortions by transferring energy from the electrons to the photons. It is particularly important for clusters of galaxies, through which one observes a partially Comptonized spectrum, resulting in a decrement at radio wavelengths and an increment in the submillimeter.

The imprint on the CMB sky is of the form  $\Delta T/T = y f(x)$ , with the  $y$ -parameter being the integral of Thomson optical depth times  $kT_e/m_e c^2$  through the cluster, and  $f(x)$  describing the frequency dependence. This is simply  $x \coth(x/2) - 4$  for a non-relativistic gas (the electron temperature in a cluster is typically a few keV), where the dimensionless frequency  $x \equiv h\nu/kT_e$ . As well as this ‘thermal’ SZ effect, there is also a smaller ‘kinetic’ effect due to the bulk motion of the cluster gas, giving  $\Delta T/T \sim \tau(v/c)$ , with either sign, but having the same spectrum as the primary CMB anisotropies.

A significant advantage in finding galaxy clusters this way is that the SZ effect is largely independent of redshift, so in principle clusters can be found to arbitrarily large distances. The SZ effect can be used to find and study individual clusters, and to obtain estimates of the Hubble constant. There is also the potential to constrain the equation of state of the dark energy through counts of detected clusters as a function of redshift [63]. Many experiments are currently in operation which will probe clusters in this way. The promise of the method has been realized through detections of clusters purely through the SZ effect, by SPT [64], ACT [65] and *Planck* [66].

### 25.7.3. Higher-order Statistics :

Although most of the CMB anisotropy information is contained in the power spectra, there will also be weak signals present in higher-order statistics. These can measure any primordial non-Gaussianity in the perturbations, as well as non-linear growth of the fluctuations on small scales and other secondary effects (plus residual foreground contamination of course). Although there are an infinite variety of ways in which the CMB could be non-Gaussian [17], there is a

generic form to consider for the initial conditions, where a quadratic contribution to the curvature perturbations is parameterized through a dimensionless number  $f_{\text{NL}}$ . This weakly non-linear component can be constrained using measurements of the bispectrum or Minkowski functionals, for example. The constraints depend on the shape of the triangles in harmonic space, and it has become common to distinguish the ‘local’ or ‘squeezed’ configuration (in which one side is much smaller than the other two) from the ‘equilateral’ configuration. The results from the WMAP team are  $-10 < f_{\text{NL}} < 74$  (95% confidence region), for the local mode and  $-214 < f_{\text{NL}} < 266$  for the equilateral mode [40]. Different estimators used by other authors give results of similar magnitude [67].

The level of  $f_{\text{NL}}$  expected is small, so that a detection of  $f_{\text{NL}} \gtrsim 10$  would rule out all single field, slow-roll inflationary models. However, with the capabilities of *Planck* and other future experiments, it seems that a measurement of primordial non-Gaussianity may be feasible for a wide class of models, and therefore much effort is expected to be devoted to predictions and measurements in the coming years.

## 25.8. Constraints on Cosmologies

The most striking outcome of the newer experimental results is that the standard cosmological paradigm is in very good shape. A large amount of high precision data on the power spectrum is adequately fit with fewer than 10 free parameters. The framework is that of FRW models, which have nearly flat geometry, containing dark matter and dark energy, and with adiabatic perturbations having close to scale invariant initial conditions.

Within this basic picture, the values of the cosmological parameters can be constrained. Of course, much more stringent bounds can be placed on models which cover a restricted parameter space, *e.g.*, assuming that  $\Omega_{\text{tot}} = 1$ ,  $n = 1$  or  $r = 0$ . More generally, the constraints depend upon the adopted prior probability distributions, even if they are implicit, for example by restricting the parameter freedom or their ranges (particularly where likelihoods peak near the boundaries), or by using different choices of other data in combination with the CMB. When the data become even more precise, these considerations will be less important, but for now we caution that restrictions on model space and choice of priors need to be kept in mind when adopting specific parameter values and uncertainties.

There are some combinations of parameters that fit the CMB anisotropies almost equivalently. For example, there is a nearly exact geometric degeneracy, where any combination of  $\Omega_{\text{m}}$  and  $\Omega_{\Lambda}$  that gives the same angular diameter distance to last scattering will give nearly identical  $C_{\ell}$ 's. There are also other less exact degeneracies among the parameters. Such degeneracies can be broken when using the CMB results in combination with other cosmological data-sets. Particularly useful are complementary constraints from galaxy clustering, the abundance of galaxy clusters, baryon acoustic oscillations, weak gravitational lensing measurements, Type Ia supernova distances, and the distribution of Lyman  $\alpha$  forest clouds. For an overview of some of these other cosmological constraints, see The Cosmological Parameters—Sec. 23 of this *Review*.

The 7-year WMAP data alone, within the context of a six parameter family of models (which fixes  $\Omega_{\text{tot}} = 1$  and  $r = 0$ ), yield the following results [50]:  $A = (2.43 \pm 0.11) \times 10^{-9}$ ;  $n = 0.967 \pm 0.014$ ;  $h = 0.704 \pm 0.025$ ;  $\Omega_{\text{b}}h^2 = 0.0225 \pm 0.0006$ ;  $\Omega_{\text{m}}h^2 = 0.134 \pm 0.006$ ; and  $\tau = 0.088 \pm 0.015$ . There has been little substantive change compared with earlier results, although it is now possible to obtain this 6-parameter set without using additional cosmological data-sets. Compared with the earliest WMAP results, the better measurement of the third acoustic peak, together with improved understanding of calibration issues has led to tighter error bars on dark matter density and overall normalization. The evidence for non-zero reionization optical depth is now very compelling, while the evidence for  $n < 1$  is still only at the roughly  $3\sigma$  level.

Other combinations of data, *e.g.*, including additional CMB measurements, or using other cosmological data-sets, lead to consistent results to those given above, sometimes with smaller error bars, and with the precise values depending on data selection [33,55,68,42] (see Sec. 23 of this *Review*). Note that for  $h$ , the CMB data alone provide only a very weak constraint, unless spatial flatness or some other cosmological data are used. For  $\Omega_{\text{b}}h^2$ , the precise value depends

sensitively on how much freedom is allowed in the shape of the primordial power spectrum (see Sec. 22 of this *Review*). The addition of other data-sets also allows for constraints to be placed on further parameters.

For  $\Omega_{\text{tot}}$ , perhaps the best WMAP constraint is  $1.002 \pm 0.006$  [40], from the combination with Hubble constant [22] and baryon acoustic oscillation [33] constraints (and setting  $w = -1$ ). The 95% confidence upper limit on  $r$  is 0.36 using WMAP alone [50], tightening to  $r < 0.17$  with the addition of other data [42]. This limit depends on how the slope  $n$  is restricted and whether  $dn/d\ln k \neq 0$  is allowed. Nevertheless, it is clear that  $\lambda\phi^4$  (sometimes called self-coupled) inflation is disfavored by the data, while the  $m^2\phi^2$  (sometimes called mass term) inflationary model is still allowed [40]. Gravitational wave constraints coming directly from  $B$ -mode limits are at the level of  $r < 0.73$  [51].

There are also constraints on parameters over and above the basic eight that we have described, usually requiring extra cosmological data to break degeneracies. For example, the addition of the dark energy equation of state  $w$  adds the partial degeneracy of being able to fit a ridge in  $(w, h)$  space, extending to low values of both parameters. This degeneracy is broken when the CMB is used in combination with independent  $H_0$  limits, or other data. For example, WMAP plus baryon acoustic oscillation and supernova data [70] yields  $w = -1.00 \pm 0.06$ , even without assuming flatness.

For the optical depth  $\tau$ , the best-fit corresponds to a reionization redshift centered on 10.5 in the best-fit cosmology, and assuming instantaneous reionization. This redshift appears to be higher than that suggested from studies of absorption in high- $z$  quasar spectra [71], perhaps indicating that the process of reionization was complex. The important constraint provided by CMB polarization, in combination with astrophysical measurements, allows us to investigate how the first stars formed and brought about the end of the cosmic dark ages.

## 25.9. Particle Physics Constraints

CMB data are beginning to put limits on parameters which are directly relevant for particle physics models. For example, there is a limit on the neutrino contribution  $\Omega_{\nu}h^2 < 0.0062$  (95% confidence) from a combination of WMAP and other data [18]. This directly implies a limit on neutrino mass,  $\sum m_{\nu} < 0.58$  eV, assuming the usual number density of fermions which decoupled when they were relativistic. Some tighter constraints can be derived using the CMB in combination with other data-sets [72].

The current suite of data suggests that  $n < 1$ , with a best-fitting value about 0.03 below unity. If borne out, this would be quite constraining for inflationary models. Moreover, it gives a real target for  $B$ -mode searches, since the value of  $r$  in simple models may be in the range of detectability, *e.g.*,  $r \sim 0.12$  for  $m^2\phi^2$  inflation if  $n \simeq 0.97$ . In addition, a combination of the WMAP data with other data-sets constrains the running of the spectral index, although at the moment there is no evidence for  $dn/d\ln k \neq 0$  [40].

One other possible hint of new physics lies in the fact that the quadrupole seems anomalously low and also appears remarkably well aligned with the octupole. Additionally there is some weak evidence for a large scale modulation of the smaller-scale power [73]. These effects might be expected in a universe which has a large-scale cut-off, or anisotropy in the initial power spectrum, or is topologically non-trivial. However, cosmic variance, a posteriori statistics, possible foregrounds, apparent correlations between modes (as mentioned in Sec. 25.2), *etc.*, limit the significance of these anomalies, and for now the general view is that such features are not unreasonably unlikely within the  $\Lambda$ CDM paradigm [19].

It is also possible to put limits on other pieces of physics [74], for example the neutrino chemical potentials, contribution of warm dark matter, decaying particles, parity violation, time variation of the fine-structure constant, topological defects, or physics beyond general relativity. Further particle physics constraints will follow as the anisotropy measurements increase in precision.

Careful measurement of the CMB power spectra and non-Gaussianity can in principle put constraints on physics at the highest energies, including ideas of string theory, extra dimensions, colliding branes, *etc.* At the moment any calculation of predictions appears to be far from definitive. However, there is a great deal of activity on

implications of string theory for the early Universe, and hence a very real chance that there might be observational implications for specific scenarios.

### 25.10. Fundamental Lessons

More important than the precise values of parameters is what we have learned about the general features which describe our observable Universe. Beyond the basic hot Big Bang picture, the CMB has taught us that:

- The Universe recombined at  $z \simeq 1100$  and started to become ionized again at  $z \simeq 10$ .
- The geometry of the Universe is close to flat.
- Both dark matter and dark energy are required.
- Gravitational instability is sufficient to grow all of the observed large structures in the Universe.
- Topological defects were not important for structure formation.
- There are ‘synchronized’ super-Hubble modes generated in the early Universe.
- The initial perturbations were predominantly adiabatic in nature.
- The perturbations had close to Gaussian (*i.e.*, maximally random) initial conditions.

It is very tempting to make an analogy between the status of the cosmological ‘Standard Model’ and that of particle physics (see earlier Sections of this *Review*). In cosmology there are about 10 free parameters, each of which is becoming well determined, and with a great deal of consistency between different measurements. However, none of these parameters can be calculated from a fundamental theory, and so hints of the bigger picture, ‘physics beyond the Standard Model,’ are being searched for with ever more ambitious experiments.

Despite this analogy, there are some basic differences. For one thing, many of the cosmological parameters change with cosmic epoch, and so the measured values are simply the ones determined today, and hence they are not ‘constants,’ like particle masses for example (although they *are* deterministic, so that if one knows their values at one epoch, they can be calculated at another). Moreover, the parameter set is not as well defined as it is in the particle physics Standard Model; different researchers will not necessarily agree on which parameters should be considered as free, and the set can be extended as the quality of the data improves. In addition, parameters like  $\tau$ , which come from astrophysics, are in principle calculable from known physical processes. On top of all this, other parameters might be ‘stochastic’ in that they may be fixed only in our observable patch of the Universe or among certain vacuum states in the ‘Landscape’ [76].

In a more general sense, the cosmological ‘Standard Model’ is much further from the underlying ‘fundamental theory,’ which will ultimately provide the values of the parameters from first principles. Nevertheless, any genuinely complete ‘theory of everything’ must include an explanation for the values of these cosmological parameters as well as the parameters of the Standard Model of particle physics.

### 25.11. Future Directions

Given the significant progress in measuring the CMB sky, which has been instrumental in tying down the cosmological model, what can we anticipate for the future? There will be a steady improvement in the precision and confidence with which we can determine the appropriate cosmological parameters. Ground-based experiments operating at smaller angular scales will continue to place tighter constraints on the damping tail. New polarization experiments will push down the limits on primordial  $B$ -modes. The third generation CMB satellite mission, *Planck*, was launched successfully in May 2009, and has already led to many papers on foregrounds and secondary anisotropies [9]. Cosmological results from the primary CMB anisotropies are expected from *Planck* in early 2013 and are keenly anticipated.

Despite the increasing improvement in the results, the addition of the latest experiments has not significantly changed the established cosmological model. It is, therefore, appropriate to ask: what should we expect to come from *Planck* and from other future experiments? *Planck* certainly has the advantage of high sensitivity and a full-sky survey. A precise measurement of the third acoustic peak provides

a good determination of the matter density; this can only be done by measurements which are accurate relative to the first two peaks (which themselves constrain the curvature and the baryon density). A detailed measurement of the damping tail region will also significantly improve the determination of  $n$  and any running of the slope. *Planck* should be capable of measuring  $C_\ell^{\text{EE}}$  quite well, providing both a strong check on the cosmological Standard Model and extra constraints that will improve parameter estimation.

A set of cosmological parameters is now known to roughly 10% accuracy, and that may seem sufficient for many people. However, we should certainly demand more of measurements which describe *the entire observable Universe!* Hence a lot of activity in the coming years will continue to focus on determining those parameters with increasing precision. This necessarily includes testing for consistency among different predictions of the cosmological Standard Model, and searching for signals which might require additional physics.

A second area of focus will be the smaller scale anisotropies and ‘secondary effects.’ There is a great deal of information about structure formation at  $z \ll 1000$  encoded in the CMB sky. This may involve higher-order statistics as well as spectral signatures, with many new experiments targeting the galaxy cluster SZ effect. Such investigations can also provide constraints on the dark energy equation of state, for example. *Planck*, as well as new telescopes aimed at the highest  $\ell$ ’s, should be able to make a lot of progress in this arena.

A third direction is increasingly sensitive searches for specific signatures of physics at the highest energies. The most promising of these may be the primordial gravitational wave signals in  $C_\ell^{\text{BB}}$ , which could be a probe of the  $\sim 10^{16}$  GeV energy range. As well as *Planck*, there are several ground- and balloon-based experiments underway which are designed to search for the polarization  $B$ -modes. Whether the amplitude of the effect coming from inflation will be detectable is unclear, but the prize makes the effort worthwhile, and the indications that  $n \simeq 0.95$  give some genuine optimism that  $r$  (the tensor to scalar ratio) may be of order 0.1, and hence within reach soon.

Anisotropies in the CMB have proven to be the premier probe of cosmology and the early Universe. Theoretically the CMB involves well understood physics in the linear regime, and is under very good calculational control. A substantial and improving set of observational data now exists. Systematics appear to be under control and not a limiting factor. And so for the next few years we can expect an increasing amount of cosmological information to be gleaned from CMB anisotropies, with the prospect also of some genuine surprises.

### References:

1. A.A. Penzias and R. Wilson, *Astrophys. J.* **142**, 419 (1965); R.H. Dicke *et al.*, *Astrophys. J.* **142**, 414 (1965).
2. M. White, D. Scott, and J. Silk, *Ann. Rev. Astron. & Astrophys.* **32**, 329 (1994); W. Hu and S. Dodelson, *Ann. Rev. Astron. & Astrophys.* **40**, 171 (2002).
3. G.F. Smoot *et al.*, *Astrophys. J.* **396**, L1 (1992).
4. C.L. Bennett *et al.*, *Astrophys. J. Supp.* **148**, 1 (2003).
5. N. Jarosik *et al.*, *Astrophys. J. Supp.* **170**, 263 (2007).
6. G. Hinshaw *et al.*, *Astrophys. J. Supp.* **180**, 225 (2009).
7. N. Jarosik *et al.*, *Astrophys. J. Supp.* **192**, 14 (2011).
8. J.A. Tauber *et al.*, *Astron. & Astrophys.* **520**, 1 (2010).
9. *Planck Collab.*, *Astron. & Astrophys.* in press, [arXiv:1101.2022](https://arxiv.org/abs/1101.2022).
10. D.J. Fixsen, *Astrophys. J.* **707**, 916 (2009).
11. J.C. Mather *et al.*, *Astrophys. J.* **512**, 511 (1999).
12. D.J. Fixsen *et al.*, *Astrophys. J.* **734**, 5 (2011).
13. R. Watkins, H.A. Feldman, and M.J. Hudson, *MNRAS* **392**, 743 (2009).
14. D.J. Fixsen *et al.*, *Astrophys. J.* **420**, 445 (1994).
15. D.J. Fixsen *et al.*, *Astrophys. J.* **473**, 576 (1996); A. Kogut *et al.*, *Astrophys. J.* **419**, 1 (1993).
16. S. Seager, D.D. Sasselov, and D. Scott, *Astrophys. J. Supp.* **128**, 407 (2000).
17. N. Bartolo *et al.*, *Phys. Rep.* **402**, 103 (2004).
18. E. Komatsu *et al.*, *Astrophys. J. Supp.* **180**, 330 (2009).
19. C.L. Bennett *et al.*, *Astrophys. J. Supp.* **192**, 17 (2011).
20. L. Knox, *Phys. Rev.* **D52**, 4307 (1995).

21. I. Sollom, A. Challinor, and M.P. Hobson, *Phys. Rev.* **D79**, 123521 (2009).
22. A.R. Liddle and D.H. Lyth, *Cosmological Inflation and Large-Scale Structure*, Cambridge University Press (2000).
23. U. Seljak and M. Zaldarriaga, *Astrophys. J.* **469**, 437 (1996).
24. A. Lewis, A. Challinor, and A. Lasenby, *Astrophys. J.* **538**, 473 (2000).
25. U. Seljak *et al.*, *Phys. Rev.* **D68**, 083507 (2003).
26. R.K. Sachs and A.M. Wolfe, *Astrophys. J.* **147**, 73 (1967).
27. R. Crittenden and N. Turok, *Phys. Rev. Lett.* **76**, 575 (1996); T. Giannantonio *et al.*, *Phys. Rev.* **D77**, 123520 (2008); S. Ho *et al.*, *Phys. Rev.* **D78**, 043519 (2008).
28. W. Hu *et al.*, *Phys. Rev.* **D59**, 023512 (1999).
29. P.J.E. Peebles and J.T. Yu, *Astrophys. J.* **162**, 815 (1970); R.A. Sunyaev and Ya.B. Zel'dovich, *Astrophys. & Space Sci.* **7**, 3 (1970).
30. D. Scott, J. Silk, and M. White, *Science* **268**, 829 (1995).
31. D.J. Eisenstein, *New Astron. Rev.* **49**, 360 (2005).
32. W.J. Percival *et al.*, *MNRAS* **381**, 1053 (2007).
33. W.J. Percival *et al.*, *MNRAS* **401**, 2148 (2010).
34. J. Silk, *Astrophys. J.* **151**, 459 (1968).
35. M. Zaldarriaga and U. Seljak, *Phys. Rev.* **D58**, 023003 (1998); A. Lewis and A. Challinor, *Phys. Rep.* **429**, 1 (2006).
36. K.M. Smith, O. Zahn, and O. Doré, *Phys. Rev.* **D76**, 3510 (2007); C.M. Hirata *et al.*, *Phys. Rev.* **D78**, 043520 (2008).
37. E. Shirokoff *et al.*, *Astrophys. J.* **736**, 61 (2011).
38. S. Das *et al.*, *Phys. Rev. Lett.* **107**, 021301 (2011).
39. N. Sehgal *et al.*, *Astrophys. J.* **709**, 920 (2010).
40. E. Komatsu *et al.*, *Astrophys. J. Supp.* **192**, 18 (2011).
41. S. Das *et al.*, *Astrophys. J.* **729**, 62 (2011).
42. R. Keisler *et al.*, [arXiv:1105.3182](https://arxiv.org/abs/1105.3182).
43. C.L. Reichardt *et al.*, *Astrophys. J.* **694**, 1200 (2009).
44. J.R. Hinderks *et al.*, *Astrophys. J.* **692**, 1221 (2009); R.B. Friedman *et al.*, *Astrophys. J.* **700**, L187 (2009).
45. M.E. Abroe *et al.*, *Astrophys. J.* **605**, 607 (2004); J.W. Fowler *et al.*, *Astrophys. J.* **722**, 1148 (2010).
46. W. Hu and M. White, *New Astron.* **2**, 323 (1997).
47. W. Hu and M. White, *Phys. Rev.* **D56**, 596 (1997).
48. M. Zaldarriaga and U. Seljak, *Phys. Rev.* **D55**, 1830 (1997); M. Kamionkowski, A. Kosowsky, and A. Stebbins, *Phys. Rev.* **D55**, 7368 (1997).
49. J. Kovac *et al.*, *Nature*, **420**, 772 (2002).
50. D. Larson *et al.*, *Astrophys. J. Supp.* **192**, 16 (2011).
51. H.C. Chiang *et al.*, *Astrophys. J.* **711**, 1123 (2010).
52. F. Piacentini *et al.*, *Astrophys. J.* **647**, 833 (2006).
53. J.L. Sievers *et al.*, *Astrophys. J.* **660**, 976 (2007).
54. E.M. Leitch *et al.*, *Astrophys. J.* **624**, 10 (2005).
55. M.L. Brown *et al.*, *Astrophys. J.* **705**, 978 (2009).
56. T.E. Montroy *et al.*, *Astrophys. J.* **647**, 813 (2006).
57. C. Bischoff *et al.*, *Astrophys. J.* **684**, 771 (2008).
58. QUIET Collab., [arXiv:1012.5348](https://arxiv.org/abs/1012.5348).
59. M. Tegmark *et al.*, *Astrophys. J.* **530**, 133 (2000).
60. B. Gold *et al.*, *Astrophys. J. Supp.* **192**, 15 (2011).
61. N. Aghanim, S. Majumdar, and J. Silk, *Rept. Prog. Phys.*, **71**, 066902 (2008); M. Millea *et al.*, [arXiv:1102.5195](https://arxiv.org/abs/1102.5195).
62. R.A. Sunyaev and Ya.B. Zel'dovich, *Ann. Rev. Astron. Astrophys.* **18**, 537 (1980); M. Birkinshaw, *Phys. Rep.* **310**, 98 (1999).
63. J.E. Carlstrom, G.P. Holder, and E.D. Reese, *Ann. Rev. Astron. & Astrophys.* **40**, 643 (2002).
64. R. Williamson *et al.*, *Astrophys. J.* **738**, 139 (2011).
65. T.A. Marriage *et al.*, *Astrophys. J.* **737**, 61 (2011).
66. Planck Collab., *Astron. & Astrophys.* in press, [arXiv:1101.2024](https://arxiv.org/abs/1101.2024).
67. K.M. Smith, L. Senatore, and M. Zaldarriaga, *J. Cosm. & Astropart. Phys.* **09**, 006; A. Curto *et al.*, *Mon. Not. R. Astron. Soc.* in press, [arXiv:1105.6106](https://arxiv.org/abs/1105.6106).
68. J. Dunkley *et al.*, *Astrophys. J. Supp.* **180**, 306 (2009).
69. A.G. Riess *et al.*, *Astrophys. J.* **699**, 539 (2009).
70. M. Hicken *et al.*, *Astrophys. J.* **700**, 1097 (2009).
71. X. Fan, C.L. Carilli, and B. Keating, *Ann. Rev. Astron. & Astrophys.* **44**, 415 (2006).
72. U. Seljak, A. Slosar, and P. McDonald, *J. Cosm. & Astropart. Phys.* **10**, 014 (2006); S.A. Thomas, F.B. Abdalla, and O. Lahav, *Phys. Rev. Lett.* **105**, 031301 (2010); S. Hannestad *et al.*, *J. Cosm. & Astropart.* **08**, 001 (2010).
73. J. Hoftuft *et al.*, *Astrophys. J.* **699**, 985 (2009); D. Hanson and A. Lewis, *Phys. Rev.* **D80**, 063004 (2010).
74. M. Kamionkowski and A. Kosowsky, *Ann. Rev. Nucl. Part. Sci.* **49**, 77 (1999); A. Lasenby, *Space Sci. Rev.* **148**, 329 (2009).
75. R. Maartens, *Living Rev. Rel.* **7**, 7 (2004).
76. R. Bousso and J. Polchinski, *JHEP* **0006**, 006 (2000); L. Susskind, *The Davis Meeting On Cosmic Inflation* (2003), [hep-th/0302219](https://arxiv.org/abs/hep-th/0302219).



## 26. COSMIC RAYS

Revised August 2011 by J.J. Beatty (Ohio State Univ.) and J. Matthews (Louisiana State Univ. and Southern Univ.); revised August 2009 by T.K. Gaisser and T. Stanev (Bartol Research Inst., Univ. of Delaware).

### 26.1. Primary spectra

The cosmic radiation incident at the top of the terrestrial atmosphere includes all stable charged particles and nuclei with lifetimes of order  $10^6$  years or longer. Technically, “primary” cosmic rays are those particles accelerated at astrophysical sources and “secondaries” are those particles produced in interaction of the primaries with interstellar gas. Thus electrons, protons and helium, as well as carbon, oxygen, iron, and other nuclei synthesized in stars, are primaries. Nuclei such as lithium, beryllium, and boron (which are not abundant end-products of stellar nucleosynthesis) are secondaries. Antiprotons and positrons are also in large part secondary. Whether a small fraction of these particles may be primary is a question of current interest.

Apart from particles associated with solar flares, the cosmic radiation comes from outside the solar system. The incoming charged particles are “modulated” by the solar wind, the expanding magnetized plasma generated by the Sun, which decelerates and partially excludes the lower energy galactic cosmic rays from the inner solar system. There is a significant anticorrelation between solar activity (which has an alternating eleven-year cycle) and the intensity of the cosmic rays with energies below about 10 GeV. In addition, the lower-energy cosmic rays are affected by the geomagnetic field, which they must penetrate to reach the top of the atmosphere. Thus the intensity of any component of the cosmic radiation in the GeV range depends both on the location and time.

There are four different ways to describe the spectra of the components of the cosmic radiation: (1) By particles per unit rigidity. Propagation (and probably also acceleration) through cosmic magnetic fields depends on gyroradius or *magnetic rigidity*,  $R$ , which is gyroradius multiplied by the magnetic field strength:

$$R = \frac{pc}{Ze} = r_L B. \quad (26.1)$$

(2) By particles per energy-per-nucleon. Fragmentation of nuclei propagating through the interstellar gas depends on energy per nucleon, since that quantity is approximately conserved when a nucleus breaks up on interaction with the gas. (3) By nucleons per energy-per-nucleon. Production of secondary cosmic rays in the atmosphere depends on the intensity of nucleons per energy-per-nucleon, approximately independently of whether the incident nucleons are free protons or bound in nuclei. (4) By particles per energy-per-nucleus. Air shower experiments that use the atmosphere as a calorimeter generally measure a quantity that is related to total energy per particle.

The units of differential intensity  $I$  are  $[\text{m}^{-2} \text{s}^{-1} \text{sr}^{-1} \mathcal{E}^{-1}]$ , where  $\mathcal{E}$  represents the units of one of the four variables listed above.

The intensity of primary nucleons in the energy range from several GeV to somewhat beyond 100 TeV is given approximately by

$$I_N(E) \approx 1.8 \times 10^4 (E/1 \text{ GeV})^{-\alpha} \frac{\text{nucleons}}{\text{m}^2 \text{ s sr GeV}}, \quad (26.2)$$

where  $E$  is the energy-per-nucleon (including rest mass energy) and  $\alpha$  ( $\equiv \gamma + 1$ ) = 2.7 is the differential spectral index of the cosmic ray flux and  $\gamma$  is the integral spectral index. About 79% of the primary nucleons are free protons and about 70% of the rest are nucleons bound in helium nuclei. The fractions of the primary nuclei are nearly constant over this energy range (possibly with small but interesting variations). Fractions of both primary and secondary incident nuclei are listed in Table 26.1. Figure 26.1 shows the major components for energies greater than 2 GeV/nucleon.

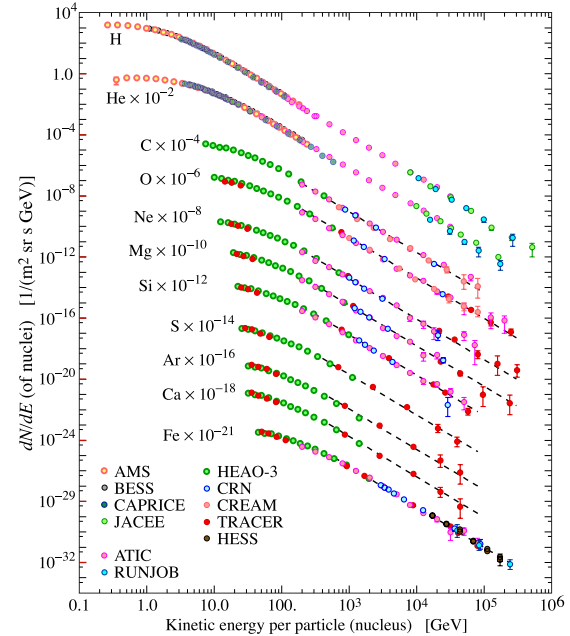


**Figure 26.1:** Fluxes of nuclei of the primary cosmic radiation in particles per energy-per-nucleus are plotted vs energy-per-nucleus using data from Refs. [1–12]. The figure was created by P. Boyle and D. Muller.

The composition and energy spectra of nuclei are typically interpreted in the context of propagation models, in which the sources of the primary cosmic radiation are located within the galaxy [16]. The ratio of secondary to primary nuclei is observed to decrease with increasing energy, a fact interpreted to mean that the lifetime of cosmic rays in the galaxy decreases with energy. Measurements of radioactive “clock” isotopes in the low energy cosmic radiation are consistent with a lifetime in the galaxy of about 15 Myr.

**Table 26.1:** Relative abundances  $F$  of cosmic-ray nuclei at 10.6 GeV/nucleon normalized to oxygen ( $\equiv 1$ ) [6]. The oxygen flux at kinetic energy of 10.6 GeV/nucleon is  $3.26 \times 10^{-2} (\text{m}^2 \text{ s sr GeV/nucleon})^{-1}$ . Abundances of hydrogen and helium are from Refs. [2,3]. Note that one can not use these values to extend the cosmic ray flux to high energy because the power law indices for each element may differ slightly.

$Z$	Element	$F$	$Z$	Element	$F$
1	H	540	13–14	Al-Si	0.19
2	He	26	15–16	P-S	0.03
3–5	Li-B	0.40	17–18	Cl-Ar	0.01
6–8	C-O	2.20	19–20	K-Ca	0.02
9–10	F-Ne	0.30	21–25	Sc-Mn	0.05
11–12	Na-Mg	0.22	26–28	Fe-Ni	0.12

Cosmic rays are nearly isotropic at most energies due to diffusive propagation in the galactic magnetic field. Milagro [13], IceCube [14], and The Tibet-III air shower array [15] have observed anisotropy at the level of about  $10^{-3}$  for cosmic rays with energy of a few TeV, possibly due to nearby sources.

The spectrum of electrons and positrons incident at the top of the atmosphere is expected to steepen by one power of  $E$  at an energy of  $\sim 5$  GeV because of the strong synchrotron energy loss in the galactic magnetic fields. The ATIC experiment [21] measured an excess of electrons above 100 GeV followed by a steepening above 1,000 GeV. The Fermi/LAT  $\gamma$ -ray observatory confirmed the relatively

flat electron spectrum [23] without confirming the peak of the ATIC excess at  $\sim 800$  GeV.

The PAMELA satellite experiment [24] measured the positron to electron ratio to increase above 10 GeV instead of the expected decrease [25] at higher energy. The structure in the electron spectrum as well as the increase in the positron fraction could be related to contributions from individual nearby sources emerging above a background suppressed at high energy by synchrotron losses [26]. The low positron to electron ratio below 10 GeV is due to the new solar magnetic field polarity after the year 2001.

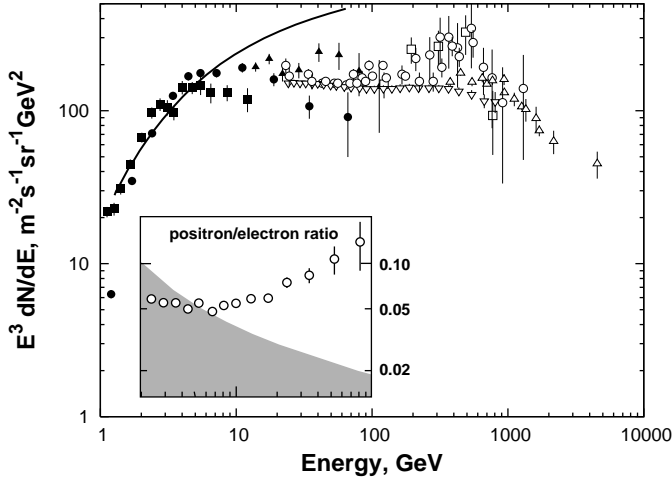


**Figure 26.2:** Differential spectrum of electrons plus positrons multiplied by  $E^3$  (data from [17–23]). The line shows the proton spectrum multiplied by 0.01. The inset shows the positron to electron ratio measured by PAMELA [24] compared to the expected decrease [25].

The ratio of antiprotons to protons is  $\sim 2 \times 10^{-4}$  [27] at around 10–20 GeV, and there is clear evidence [28] for the kinematic suppression at lower energy that is the signature of secondary antiprotons. The  $\bar{p}/p$  ratio also shows a strong dependence on the phase and polarity of the solar cycle [29] in the opposite sense to that of the positron fraction. There is at this time no evidence for a significant primary component of antiprotons. No antihelium or antideuteron has been found in the cosmic radiation. The best measured upper limit on the ratio antihelium/helium is currently approximately  $1 \times 10^{-7}$  [30]. The upper limit on the flux of antideuterons around 1 GeV/nucleon is approximately  $2 \times 10^{-4} (\text{m}^2 \text{ s sr GeV/nucleon})^{-1}$  [31].

## 26.2. Cosmic rays in the atmosphere

Figure 26.3 shows the vertical fluxes of the major cosmic ray components in the atmosphere in the energy region where the particles are most numerous (except for electrons, which are most numerous near their critical energy, which is about 81 MeV in air). Except for protons and electrons near the top of the atmosphere, all particles are produced in interactions of the primary cosmic rays in the air. Muons and neutrinos are products of the decay chain of charged mesons, while electrons and photons originate in decays of neutral mesons.

Most measurements are made at ground level or near the top of the atmosphere, but there are also measurements of muons and electrons from airplanes and balloons. Fig. 26.3 includes recent measurements of negative muons [32–36]. Since  $\mu^+(\mu^-)$  are produced in association with  $\nu_\mu(\bar{\nu}_\mu)$ , the measurement of muons near the maximum of the intensity curve for the parent pions serves to calibrate the atmospheric  $\nu_\mu$  beam [37]. Because muons typically lose almost 2 GeV in passing through the atmosphere, the comparison near the production altitude is important for the sub-GeV range of  $\nu_\mu(\bar{\nu}_\mu)$  energies.

The flux of cosmic rays through the atmosphere is described by a set of coupled cascade equations with boundary conditions at the

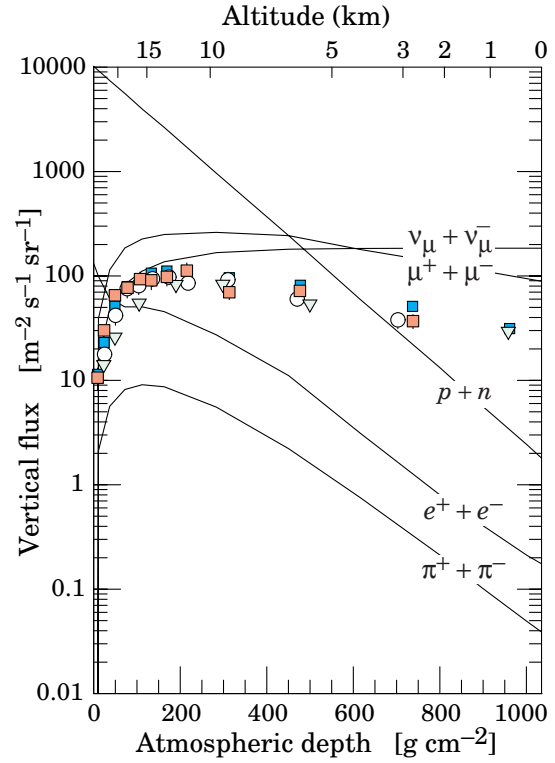


**Figure 26.3:** Vertical fluxes of cosmic rays in the atmosphere with  $E > 1$  GeV estimated from the nucleon flux of Eq. (26.2). The points show measurements of negative muons with  $E_\mu > 1$  GeV [32–36].

top of the atmosphere to match the primary spectrum. Numerical or Monte Carlo calculations are needed to account accurately for decay and energy-loss processes, and for the energy-dependences of the cross sections and of the primary spectral index  $\gamma$ . Approximate analytic solutions are, however, useful in limited regions of energy [38,39]. For example, the vertical intensity of charged pions with energy  $E_\pi \ll \epsilon_\pi = 115$  GeV is

$$I_\pi(E_\pi, X) \approx \frac{Z_{N\pi}}{\lambda_N} I_N(E_\pi, 0) e^{-X/\Lambda} \frac{X E_\pi}{\epsilon_\pi}, \quad (26.3)$$

where  $\Lambda$  is the characteristic length for exponential attenuation of the parent nucleon flux in the atmosphere. This expression has a maximum at  $X = \Lambda \approx 121 \pm 4 \text{ g cm}^{-2}$  [40], which corresponds to an altitude of 15 kilometers. The quantity  $Z_{N\pi}$  is the spectrum-weighted moment of the inclusive distribution of charged pions in interactions of nucleons with nuclei of the atmosphere. The intensity of low-energy pions is much less than that of nucleons because  $Z_{N\pi} \approx 0.079$  is small and because most pions with energy much less than the critical energy  $\epsilon_\pi$  decay rather than interact.

## 26.3. Cosmic rays at the surface

**26.3.1. Muons:** Muons are the most numerous charged particles at sea level (see Fig. 26.3). Most muons are produced high in the atmosphere (typically 15 km) and lose about 2 GeV to ionization before reaching the ground. Their energy and angular distribution reflect a convolution of the production spectrum, energy loss in the atmosphere, and decay. For example, 2.4 GeV muons have a decay length of 15 km, which is reduced to 8.7 km by energy loss. The mean energy of muons at the ground is  $\approx 4$  GeV. The energy spectrum is almost flat below 1 GeV, steepens gradually to reflect the primary spectrum in the 10–100 GeV range, and steepens further at higher energies because pions with  $E_\pi > \epsilon_\pi$  tend to interact in the atmosphere before they decay. Asymptotically ( $E_\mu \gg 1$  TeV), the energy spectrum of atmospheric muons is one power steeper than the primary spectrum.



The integral intensity of vertical muons above 1 GeV/c at sea level is  $\approx 70 \text{ m}^{-2}\text{s}^{-1}\text{sr}^{-1}$  [41,42], with recent measurements [43–45] favoring a lower normalization by 10–15%. Experimentalists are familiar with this number in the form  $I \approx 1 \text{ cm}^{-2} \text{ min}^{-1}$  for horizontal detectors. The overall angular distribution of muons at the ground is  $\propto \cos^2 \theta$ , which is characteristic of muons with  $E_\mu \sim 3 \text{ GeV}$ . At lower energy the angular distribution becomes increasingly steep, while at higher energy it flattens, approaching a  $\sec \theta$  distribution for  $E_\mu \gg \epsilon_\pi$  and  $\theta < 70^\circ$ .

Figure 26.4 shows the muon energy spectrum at sea level for two angles. At large angles low energy muons decay before reaching the surface and high energy pions decay before they interact, thus the average muon energy increases. An approximate extrapolation formula valid when muon decay is negligible ( $E_\mu > 100/\cos \theta \text{ GeV}$ ) and the curvature of the Earth can be neglected ( $\theta < 70^\circ$ ) is

$$\frac{dN_\mu}{dE_\mu d\Omega} \approx \frac{0.14 E_\mu^{-2.7}}{\text{cm}^2 \text{ s sr GeV}} \times \left\{ \frac{1}{1 + \frac{1.1 E_\mu \cos \theta}{115 \text{ GeV}}} + \frac{0.054}{1 + \frac{1.1 E_\mu \cos \theta}{850 \text{ GeV}}} \right\}, \quad (26.4)$$

where the two terms give the contribution of pions and charged kaons. Eq. (26.4) neglects a small contribution from charm and heavier flavors which is negligible except at very high energy [50].

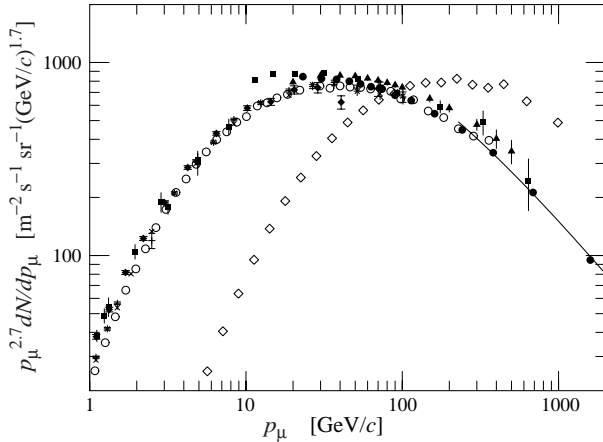


**Figure 26.4:** Spectrum of muons at  $\theta = 0^\circ$  ( $\blacklozenge$  [41],  $\blacksquare$  [46],  $\blacktriangledown$  [47],  $\blacktriangle$  [48],  $\times$ ,  $+$  [43],  $\circ$  [44], and  $\bullet$  [45] and  $\theta = 75^\circ$   $\diamond$  [49]). The line plots the result from Eq. (26.4) for vertical showers.

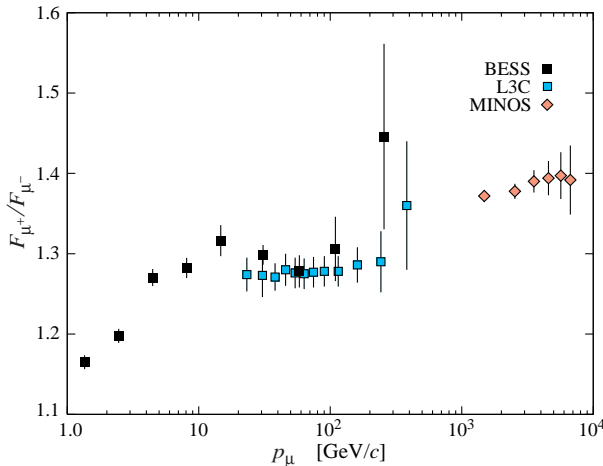


**Figure 26.5:** Muon charge ratio as a function of the muon momentum from Refs. [44,45,51].

The muon charge ratio reflects the excess of  $\pi^+$  over  $\pi^-$  and  $K^+$  over  $K^-$  in the forward fragmentation region of proton initiated interactions together with the fact that there are more protons than neutrons in the primary spectrum. The increase with energy of  $\mu^+/\mu^-$  shown in Fig. 26.5 reflects the increasing importance of kaons in the TeV range [51] and indicates a significant contribution of associated production by cosmic-ray protons ( $p \rightarrow \Lambda + K^+$ ). The same process is even more important for atmospheric neutrinos at high energy.

**26.3.2. Electromagnetic component:** At the ground, this component consists of electrons, positrons, and photons primarily from cascades initiated by decay of neutral and charged mesons. Muon decay is the dominant source of low-energy electrons at sea level. Decay of neutral pions is more important at high altitude or when the energy threshold is high. Knock-on electrons also make a small contribution at low energy [52]. The integral vertical intensity of electrons plus positrons is very approximately 30, 6, and  $0.2 \text{ m}^{-2}\text{s}^{-1}\text{sr}^{-1}$  above 10, 100, and 1000 MeV respectively [42,53], but the exact numbers depend sensitively on altitude, and the angular dependence is complex because of the different altitude dependence of the different sources of electrons [52–54]. The ratio of photons to electrons plus positrons is approximately 1.3 above 1 GeV and 1.7 below the critical energy [54].

**26.3.3. Protons:** Nucleons above 1 GeV/c at ground level are degraded remnants of the primary cosmic radiation. The intensity is approximately  $I_N(E, 0) \times \exp(-X/\cos \theta \Lambda)$  for  $\theta < 70^\circ$ . At sea level, about 1/3 of the nucleons in the vertical direction are neutrons (up from  $\approx 10\%$  at the top of the atmosphere as the  $n/p$  ratio approaches equilibrium). The integral intensity of vertical protons above 1 GeV/c at sea level is  $\approx 0.9 \text{ m}^{-2}\text{s}^{-1}\text{sr}^{-1}$  [42,55].

## 26.4. Cosmic rays underground

Only muons and neutrinos penetrate to significant depths underground. The muons produce tertiary fluxes of photons, electrons, and hadrons.

**26.4.1. Muons:** As discussed in Section 30.6 of this *Review*, muons lose energy by ionization and by radiative processes: bremsstrahlung, direct production of  $e^+e^-$  pairs, and photonuclear interactions. The total muon energy loss may be expressed as a function of the amount of matter traversed as

$$-\frac{dE_\mu}{dX} = a + b E_\mu, \quad (26.5)$$

where  $a$  is the ionization loss and  $b$  is the fractional energy loss by the three radiation processes. Both are slowly varying functions of energy. The quantity  $\epsilon \equiv a/b$  ( $\approx 500 \text{ GeV}$  in standard rock) defines a critical energy below which continuous ionization loss is more important than radiative losses. Table 26.2 shows  $a$  and  $b$  values for standard rock, and  $b$  for ice, as a function of muon energy. The second column of Table 26.2 shows the muon range in standard rock ( $A = 22$ ,  $Z = 11$ ,  $\rho = 2.65 \text{ g cm}^{-3}$ ). These parameters are quite sensitive to the chemical composition of the rock, which must be evaluated for each location.

**Table 26.2:** Average muon range  $R$  and energy loss parameters  $a$  and  $b$  calculated for standard rock [56] and the total energy loss parameter  $b$  for ice. Range is given in km-water-equivalent, or  $10^5 \text{ g cm}^{-2}$ .

$E_\mu$ GeV	$R$ km.w.e.	$a$ MeV $\text{g}^{-1} \text{cm}^2$	$b_{\text{brems}}$ —	$b_{\text{pair}}$ $10^{-6} \text{ g}^{-1} \text{cm}^2$	$b_{\text{nucl}}$ $10^{-6} \text{ g}^{-1} \text{cm}^2$	$\sum b_i$ —	$\sum b(\text{ice})$ —
10	0.05	2.17	0.70	0.70	0.50	1.90	1.66
100	0.41	2.44	1.10	1.53	0.41	3.04	2.51
1000	2.45	2.68	1.44	2.07	0.41	3.92	3.17
10000	6.09	2.93	1.62	2.27	0.46	4.35	3.78

The intensity of muons underground can be estimated from the muon intensity in the atmosphere and their rate of energy loss. To the extent that the mild energy dependence of  $a$  and  $b$  can be neglected, Eq. (26.5) can be integrated to provide the following relation between the energy  $E_{\mu,0}$  of a muon at production in the atmosphere and its average energy  $E_{\mu}$  after traversing a thickness  $X$  of rock (or ice or water):

$$E_{\mu,0} = (E_{\mu} + \epsilon) e^{bX} - \epsilon. \quad (26.6)$$

Especially at high energy, however, fluctuations are important and an accurate calculation requires a simulation that accounts for stochastic energy-loss processes [57].

There are two depth regimes for which Eq. (26.6) can be simplified. For  $X \ll b^{-1} \approx 2.5$  km water equivalent,  $E_{\mu,0} \approx E_{\mu}(X) + aX$ , while for  $X \gg b^{-1}$   $E_{\mu,0} \approx (\epsilon + E_{\mu}(X)) \exp(bX)$ . Thus at shallow depths the differential muon energy spectrum is approximately constant for  $E_{\mu} < aX$  and steepens to reflect the surface muon spectrum for  $E_{\mu} > aX$ , whereas for  $X > 2.5$  km.w.e. the differential spectrum underground is again constant for small muon energies but steepens to reflect the surface muon spectrum for  $E_{\mu} > \epsilon \approx 0.5$  TeV. In the deep regime the shape is independent of depth although the intensity decreases exponentially with depth. In general the muon spectrum at slant depth  $X$  is

$$\frac{dN_{\mu}(X)}{dE_{\mu}} = \frac{dN_{\mu}}{dE_{\mu,0}} \frac{dE_{\mu,0}}{dE_{\mu}} = \frac{dN_{\mu}}{dE_{\mu,0}} e^{bX}, \quad (26.7)$$

where  $E_{\mu,0}$  is the solution of Eq. (26.6) in the approximation neglecting fluctuations.

Fig. 26.6 shows the vertical muon intensity versus depth. In constructing this “depth-intensity curve,” each group has taken account of the angular distribution of the muons in the atmosphere, the map of the overburden at each detector, and the properties of the local medium in connecting measurements at various slant depths and zenith angles to the vertical intensity. Use of data from a range of angles allows a fixed detector to cover a wide range of depths. The flat portion of the curve is due to muons produced locally by charged-current interactions of  $\nu_{\mu}$ . The inset shows the vertical intensity curve for water and ice published in Refs. [59–62]. It is not as steep as the one for rock because of the lower muon energy loss in water.

#### 26.4.2. Neutrinos:

Because neutrinos have small interaction cross sections, measurements of atmospheric neutrinos require a deep detector to avoid backgrounds. There are two types of measurements: contained (or semi-contained) events, in which the vertex is determined to originate inside the detector, and neutrino-induced muons. The latter are muons that enter the detector from zenith angles so large (*e.g.*, nearly horizontal or upward) that they cannot be muons produced in the atmosphere. In neither case is the neutrino flux measured directly. What is measured is a convolution of the neutrino flux and cross section with the properties of the detector (which includes the surrounding medium in the case of entering muons).

Contained and semi-contained events reflect neutrinos in the sub-GeV to multi-GeV region where the product of increasing cross section and decreasing flux is maximum. In the GeV region the neutrino flux and its angular distribution depend on the geomagnetic location of the detector and, to a lesser extent, on the phase of the solar cycle. Naively, we expect  $\nu_{\mu}/\nu_e = 2$  from counting neutrinos of the two flavors coming from the chain of pion and muon decay. Contrary to expectation, however, the numbers of the two classes of events are similar rather than different by a factor of two. This is now understood to be a consequence of neutrino flavor oscillations [70]. (See the article on neutrino properties in this *Review*.)

Two well-understood properties of atmospheric cosmic rays provide a standard for comparison of the measurements of atmospheric neutrinos to expectation. These are the “ $\sec\theta$  effect” and the “east-west effect” [69]. The former refers originally to the enhancement of the flux of  $> 10$  GeV muons (and neutrinos) at large zenith angles because the parent pions propagate more in the low density

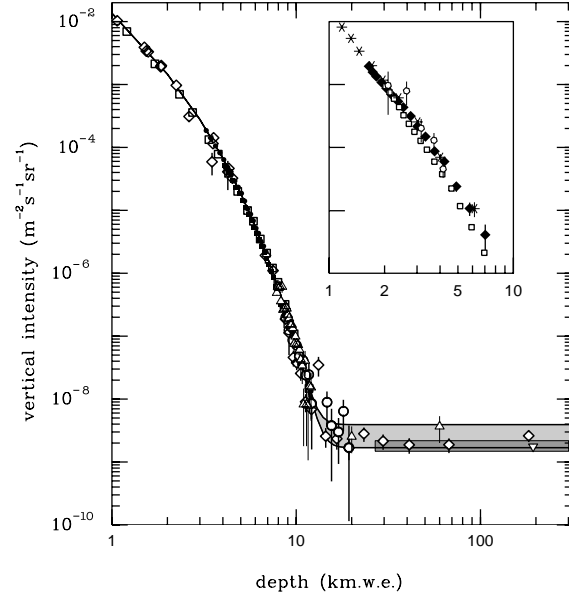


**Figure 26.6:** Vertical muon intensity vs depth (1 km.w.e. =  $10^5$  g  $\text{cm}^{-2}$  of standard rock). The experimental data are from:  $\diamond$ : the compilations of Crouch [58],  $\square$ : Baksan [63],  $\circ$ : LVD [64],  $\bullet$ : MACRO [65],  $\blacksquare$ : Frejus [66], and  $\triangle$ : SNO [67]. The shaded area at large depths represents neutrino-induced muons of energy above 2 GeV. The upper line is for horizontal neutrino-induced muons, the lower one for vertically upward muons. Darker shading shows the muon flux measured by the SuperKamiokande experiment. The inset shows the vertical intensity curve for water and ice published in Refs. [59–62].

upper atmosphere where decay is enhanced relative to interaction. For neutrinos from muon decay, the enhancement near the horizontal becomes important for  $E_{\nu} > 1$  GeV and arises mainly from the increased pathlength through the atmosphere for muon decay in flight. Fig. 26.7 from Ref. 68 shows a comparison between measurement and expectation for the zenith angle dependence of multi-GeV electron-like (mostly  $\nu_e$ ) and muon-like (mostly  $\nu_{\mu}$ ) events separately. The  $\nu_e$  show an enhancement near the horizontal and approximate equality for nearly upward ( $\cos\theta \approx -1$ ) and nearly downward ( $\cos\theta \approx 1$ ) events. There is, however, a very significant deficit of upward ( $\cos\theta < 0$ )  $\nu_{\mu}$  events, which have long pathlengths comparable to the radius of the Earth. This feature is the principal signature for oscillations [70].

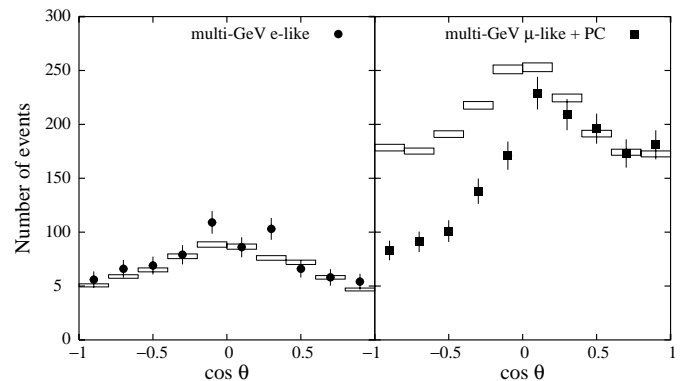


**Figure 26.7:** Zenith-angle dependence of multi-GeV neutrino interactions from SuperKamiokande [68]. The shaded boxes show the expectation in the absence of any oscillations.

Muons that enter the detector from outside after production in charged-current interactions of neutrinos naturally reflect a higher energy portion of the neutrino spectrum than contained events because

**Table 26.3:** Measured fluxes ( $10^{-9} \text{ m}^{-2} \text{ s}^{-1} \text{ sr}^{-1}$ ) of neutrino-induced muons as a function of the effective minimum muon energy  $E_\mu$ .

$E_\mu >$	1 GeV	1 GeV	1 GeV	2 GeV	3 GeV	3 GeV
Ref.	CWI [71]	Baksan [72]	MACRO [73]	IMB [74]	Kam [75]	SuperK [76]
$F_\mu$	$2.17 \pm 0.21$	$2.77 \pm 0.17$	$2.29 \pm 0.15$	$2.26 \pm 0.11$	$1.94 \pm 0.12$	$1.74 \pm 0.07$

the muon range increases with energy as well as the cross section. The relevant energy range is  $\sim 10 < E_\nu < 1000$  GeV, depending somewhat on angle. Neutrinos in this energy range show a  $\sec\theta$  effect similar to muons (see Eq. (26.4)). This causes the flux of horizontal neutrino-induced muons to be approximately a factor two higher than the vertically upward flux. The upper and lower edges of the horizontal shaded region in Fig. 26.6 correspond to horizontal and vertical intensities of neutrino-induced muons. Table 26.3 gives the measured fluxes of upward-moving neutrino-induced muons averaged over the lower hemisphere. Generally the definition of minimum muon energy depends on where it passes through the detector. The tabulated effective minimum energy estimates the average over various accepted trajectories.

## 26.5. Air showers

So far we have discussed inclusive or uncorrelated fluxes of various components of the cosmic radiation. An air shower is caused by a single cosmic ray with energy high enough for its cascade to be detectable at the ground. The shower has a hadronic core, which acts as a collimated source of electromagnetic subshowers, generated mostly from  $\pi^0 \rightarrow \gamma\gamma$  decays. The resulting electrons and positrons are the most numerous charged particles in the shower. The number of muons, produced by decays of charged mesons, is an order of magnitude lower. Air showers spread over a large area on the ground, and arrays of detectors operated for long times are useful for studying cosmic rays with primary energy  $E_0 > 100$  TeV, where the low flux makes measurements with small detectors in balloons and satellites difficult.

Greisen [77] gives the following approximate expressions for the numbers and lateral distributions of particles in showers at ground level. The total number of muons  $N_\mu$  with energies above 1 GeV is

$$N_\mu(> 1 \text{ GeV}) \approx 0.95 \times 10^5 \left( N_e / 10^6 \right)^{3/4}, \quad (26.8)$$

where  $N_e$  is the total number of charged particles in the shower (not just  $e^\pm$ ). The number of muons per square meter,  $\rho_\mu$ , as a function of the lateral distance  $r$  (in meters) from the center of the shower is

$$\rho_\mu = \frac{1.25 N_\mu}{2\pi \Gamma(1.25)} \left( \frac{1}{320} \right)^{1.25} r^{-0.75} \left( 1 + \frac{r}{320} \right)^{-2.5}, \quad (26.9)$$

where  $\Gamma$  is the gamma function. The number density of charged particles is

$$\rho_e = C_1(s, d, C_2) x^{(s-2)} (1+x)^{(s-4.5)} (1+C_2 x^d). \quad (26.10)$$

Here  $s$ ,  $d$ , and  $C_2$  are parameters in terms of which the overall normalization constant  $C_1(s, d, C_2)$  is given by

$$C_1(s, d, C_2) = \frac{N_e}{2\pi r_1^2} [B(s, 4.5 - 2s) + C_2 B(s + d, 4.5 - d - 2s)]^{-1}, \quad (26.11)$$

where  $B(m, n)$  is the beta function. The values of the parameters depend on shower size ( $N_e$ ), depth in the atmosphere, identity of the primary nucleus, etc. For showers with  $N_e \approx 10^6$  at sea level, Greisen uses  $s = 1.25$ ,  $d = 1$ , and  $C_2 = 0.088$ . Finally,  $x$  is  $r/r_1$ , where  $r_1$  is the Molière radius, which depends on the density of the atmosphere and hence on the altitude at which showers are detected. At sea level  $r_1 \approx 78$  m. It increases with altitude as the air density decreases. (See

the section on electromagnetic cascades in the article on the passage of particles through matter in this *Review*).

The lateral spread of a shower is determined largely by Coulomb scattering of the many low-energy electrons and is characterized by the Molière radius. The lateral spread of the muons ( $\rho_\mu$ ) is larger and depends on the transverse momenta of the muons at production as well as multiple scattering.

There are large fluctuations in development from shower to shower, even for showers of the same energy and primary mass—especially for small showers, which are usually well past maximum development when observed at the ground. Thus the shower size  $N_e$  and primary energy  $E_0$  are only related in an average sense, and even this relation depends on depth in the atmosphere. One estimate of the relation is [84]

$$E_0 \sim 3.9 \times 10^6 \text{ GeV} (N_e / 10^6)^{0.9} \quad (26.12)$$

for vertical showers with  $10^{14} < E < 10^{17}$  eV at 920 g  $\text{cm}^{-2}$  (965 m above sea level). As  $E_0$  increases the shower maximum (on average) moves down into the atmosphere and the relation between  $N_e$  and  $E_0$  changes. Moreover, because of fluctuations,  $N_e$  as a function of  $E_0$  is not correctly obtained by inverting Eq. (26.12). At the maximum of shower development, there are approximately 2/3 particles per GeV of primary energy.

There are three common types of air shower detectors: shower arrays that study the shower size  $N_e$  and the lateral distribution on the ground, Cherenkov detectors that detect the Cherenkov radiation emitted by the charged particles of the shower, and fluorescence detectors that study the nitrogen fluorescence excited by the charged particles in the shower. The fluorescence light is emitted isotropically so the showers can be observed from the side. Detailed simulations and cross-calibrations between different types of detectors are necessary to establish the primary energy spectrum from air-shower experiments.

Figure 26.8 shows the “all-particle” spectrum. The differential energy spectrum has been multiplied by  $E^{2.6}$  in order to display the features of the steep spectrum that are otherwise difficult to discern. The steepening that occurs between  $10^{15}$  and  $10^{16}$  eV is known as the *knee* of the spectrum. The feature around  $10^{18.5}$  eV is called the *ankle* of the spectrum.

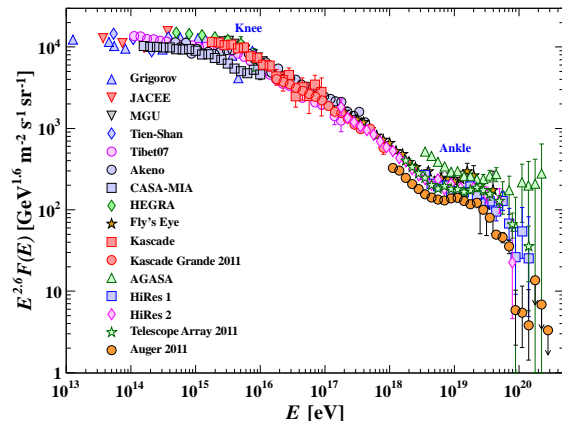


**Figure 26.8:** The all-particle spectrum as a function of  $E$  (energy-per-nucleus) from air shower measurements [79–90,100–104].

Measurements of flux with small air shower experiments in the knee region differ by as much as a factor of two, indicative of systematic uncertainties in interpretation of the data. (For a review see Ref. 78.) In establishing the spectrum shown in Fig. 26.8, efforts have been made to minimize the dependence of the analysis on the primary composition. Ref. 87 uses an unfolding procedure to obtain the spectra of the individual components, giving a result for the all-particle spectrum between  $10^{15}$  and  $10^{17}$  eV that lies toward the upper range of the data shown in Fig. 26.8. In the energy range above  $10^{17}$  eV, the fluorescence technique [89] is particularly useful because it can establish the primary energy in a model-independent way by observing most of the longitudinal development of each shower, from which  $E_0$  is obtained by integrating the energy deposition in the atmosphere. The result, however, depends strongly on the light absorption in the atmosphere and the calculation of the detector's aperture.

Assuming the cosmic ray spectrum below  $10^{18}$  eV is of galactic origin, the *knee* could reflect the fact that most cosmic accelerators in the galaxy have reached their maximum energy. Some types of expanding supernova remnants, for example, are estimated not to be able to accelerate protons above energies in the range of  $10^{15}$  eV. Effects of propagation and confinement in the galaxy [91] also need to be considered. The KASCADE-Grande experiment [90] has reported observation of a second steepening of the spectrum near  $8 \times 10^{16}$  eV, with evidence that this structure is accompanied a transition to heavy primaries.

Concerning the ankle, one possibility is that it is the result of a higher energy population of particles overtaking a lower energy population, for example an extragalactic flux beginning to dominate over the galactic flux (e.g. Ref. 89). Another possibility is that the dip structure in the region of the ankle is due to  $\gamma p \rightarrow e^+ + e^-$  energy losses of extragalactic protons on the 2.7 K cosmic microwave radiation (CMB) [93]. This dip structure has been cited as a robust signature of both the protonic and extragalactic nature of the highest energy cosmic rays [92]. If this interpretation is correct, then the galactic cosmic rays do not contribute significantly to the flux above  $10^{18}$  eV, consistent with the maximum expected range of acceleration by supernova remnants.

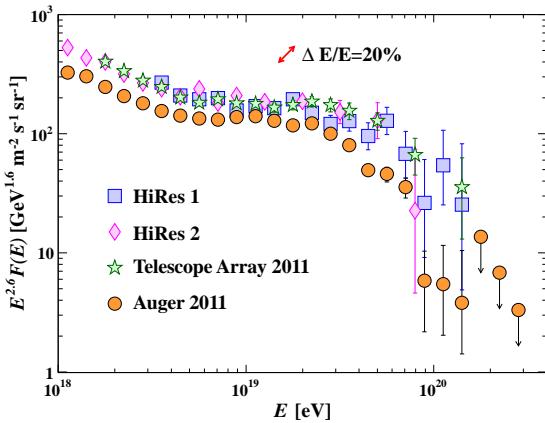


**Figure 26.9:** Expanded view of the highest energy portion of the cosmic-ray spectrum from data of HiRes 1&2 [101], the Telescope Array [103], and the Auger Observatory [104]. The HiRes stereo spectrum [112] is consistent with the HiRes 1&2 monocular results. The differential cosmic ray flux is multiplied by  $E^{2.6}$ . The red arrow indicates the change in the plotted data for a systematic shift in the energy scale of 20%.

The energy-dependence of the composition from the knee through the ankle is useful in discriminating between these two viewpoints, since a heavy composition above  $10^{18}$  eV is inconsistent with the formation of the ankle by pair production losses on the CMB.

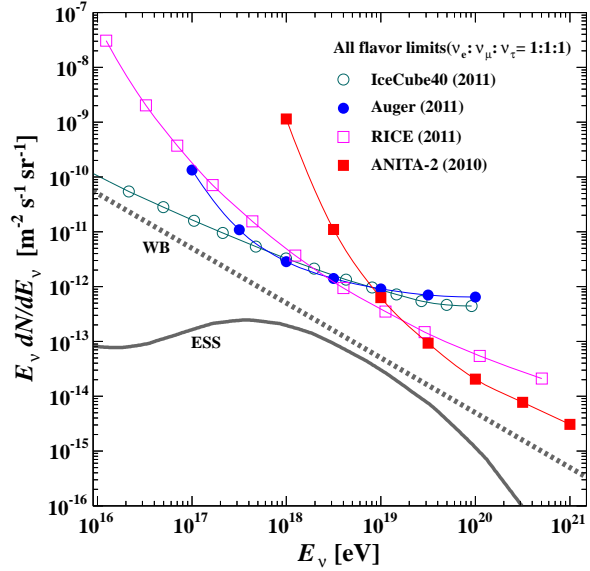


**Figure 26.10:** Differential limits on the flux of cosmogenic neutrinos set by four neutrino experiments. The curves show the Waxman-Bahcall benchmark flux (WB, [111]) and a representative midrange model for the expected flux of cosmogenic neutrinos (ESS, [110]). The expected flux is uncertain by over an order of magnitude in either direction.

The HiRes and Auger experiments, however, present very different interpretations of data on the depth of shower maximum  $X_{max}$ , a quantity that correlates strongly with the interaction cross section of the primary particle. If these results are interpreted using standard extrapolations of measured proton and nuclear cross sections, then the HiRes data [94] is consistent with the ultrahigh-energy cosmic ray (UHECR) composition getting lighter and containing only protons and helium above  $10^{19}$  eV, while Auger [95,96] sees a composition getting lighter up to  $2 \times 10^{18}$  eV and becoming heavier after that, intermediate between protons and iron at  $3 \times 10^{19}$  eV. This may mean that the extragalactic cosmic rays have a mixed composition at acceleration similar to the GeV galactic cosmic rays. It is important to note that the measurements of  $X_{max}$  may be interpreted with equal validity in terms of a changing proton-air cross-section and no change in composition.

If the cosmic ray flux at the highest energies is cosmological in origin, there should be a rapid steepening of the spectrum (called the GZK feature) around  $5 \times 10^{19}$  eV, resulting from the onset of inelastic interactions of UHE cosmic rays with the cosmic microwave background [97,98]. Photo-dissociation of heavy nuclei in the mixed composition model [99] would have a similar effect. UHECR experiments have detected events of energy above  $10^{20}$  eV [89,100–102]. The AGASA experiment [100] did not observe the expected GZK feature. The HiRes fluorescence experiment [101,112] has detected evidence of the GZK suppression, and the Auger observatory [102–104] has presented spectra showing this suppression based on surface detector measurements calibrated against its fluorescence detector using events detected in hybrid mode, i.e. with both the surface and the fluorescence detectors. Recent observations by the Telescope Array [103] also exhibit this suppression.

Figure 26.9 gives an expanded view of the high energy end of the spectrum, showing only the more recent data. This figure shows the differential flux multiplied by  $E^{2.6}$ . The experiments are consistent in normalization if one takes quoted systematic errors in the energy scales into account. The continued power law type of flux beyond the GZK cutoff previously claimed by the AGASA experiment [100] is not supported by the HiRes, Telescope Array, and Auger data.

One half of the energy that UHECR protons lose in photoproduction interactions that cause the GZK effects ends up in neutrinos [105].

Measuring this *cosmogenic* neutrino flux above  $10^{18}$  eV would help resolve the UHECR uncertainties mentioned above. The magnitude of this flux depends strongly on the cosmic ray spectrum at acceleration, the cosmic ray composition, and the cosmological evolution of the cosmic ray sources. In the case that UHECR have mixed composition only the proton fraction would produce cosmogenic neutrinos. Heavy nuclei propagation produces mostly  $\bar{\nu}_e$  at lower energy from neutron decay.

The expected rate of cosmogenic neutrinos is lower than current limits obtained by IceCube [106], the Auger observatory [108], RICE [107], and ANITA-2 [109], which are shown in Figure 26.10 together with a model for cosmogenic neutrino production [110] and the Waxman-Bahcall benchmark flux of neutrinos produced in cosmic ray sources [111]. At production, the dominant component of neutrinos comes from  $\pi^\pm$  decays and has flavor content  $\nu_e : \nu_\mu : \nu_\tau = 1 : 2 : 0$ . After oscillations, the arriving cosmogenic neutrinos are expected to be an equal mixture of all three flavors. The sensitivity of each experiment depends on neutrino flavor. IceCube, RICE, and ANITA are sensitive to all three flavors, and the sensitivity to different flavors is energy dependent. The limit of Auger is only for  $\nu_\tau$  and  $\bar{\nu}_\tau$  which should be about 1/3 of the total neutrino flux after oscillations, so this limit is plotted multiplied by a factor of three for comparison with the other limits and with the theoretical estimates.

#### References:

1. M. Boezio *et al.*, *Astropart. Phys.* **19**, 583 (2003).
2. AMS Collab., *Phys. Lett.* **B490**, 27 (2000); *Phys. Lett.* **B494**, 193 (2000).
3. T. Sanuki *et al.*, *Astrophys. J.* **545**, 1135 (2000).
4. S. Haino *et al.*, *Phys. Lett.* **B594**, 35 (2004).
5. H.S. Ahn *et al.*, *Astrophys. J.* **707**, 593 (2000).
6. J.J. Engelmann *et al.*, *Astron. & Astrophys.* **233**, 96 (1990).
7. D. Müller *et al.*, *Ap J*, **374**, 356 (1991).
8. M. Ave *et al.*, *Astrophys. J.* **678**, 262 (2008).
9. A.D. Panov *et al.*, *Bull Russian Acad of Science, Physics*, **71**, 494 (2007).
10. V.A. Derbina *et al.*, *Astrophys. J.* **628**, L41 (2005).
11. K. Asakimori *et al.* (JACEE Collab.), *Astrophys. J.* **502**, 278 (1998).
12. F. Aharonian *et al.* (HESS Collab.), *Phys. Rev.* **D75**, 042004 (2007).
13. A.A. Abdo *et al.*, *Astrophys. J.* **698**, 2121 (2009).
14. R. Abbasi *et al.*, *Astrophys. J.* **718**, L194 (2010).
15. M. Amenomori *et al.*, *Astrophys. J.* **711**, 119 (2010).
16. A.W. Strong *et al.*, *Ann. Rev. Nucl. and Part. Sci.* **57**, 285 (2007).
17. M.A. DuVernois *et al.*, *Astrophys. J.* **559**, 296 (2000).
18. S. Torii *et al.*, *Astrophys. J.* **559**, 973 (2001).
19. M. Boezio *et al.*, *Astrophys. J.* **532**, 635 (2000).
20. K. Yoshida *et al.*, *Adv. Spa. Research*, **42**, 1670 (2008).
21. J. Chang *et al.* (ATIC Collab.), *Nature* **456**, 362 (2008).
22. F. Aharonian *et al.* (HESS Collab.), *Phys. Rev. Lett.* **101**, 261104 (2008) and [arXiv:0905.0105](https://arxiv.org/abs/0905.0105).
23. A.A. Abdo *et al.* (Fermi/LAT Collab.), *Phys. Rev. Lett.* **102**, 181101 (2009).
24. O. Adriani *et al.* (Pamela Collab.), *Nature* **458**, 607 (2009); *Phys. Rev. Lett.* **102**, 051101 (2009).
25. I.V. Moskalenko and A.W. Strong, *Astrophys. J.* **493**, 694 (1998).
26. J. Nishimura *et al.*, *Adv. Space Research* **19**, 767 (1997).
27. A.S. Beach *et al.*, *Phys. Rev. Lett.* **87**, 271101 (2001).
28. A. Yamamoto *et al.*, *Adv. Space Research* (2007) in press.
29. Y. Asaoka *et al.*, *Phys. Rev. Lett.* **88**, 51101 (2002).
30. K. Abe *et al.*, [arXiv:1201.2967v1](https://arxiv.org/abs/1201.2967v1) (2012).
31. H. Fuke *et al.*, *Phys. Rev. Lett.* **95**, 081101 (2005).
32. R. Bellotti *et al.*, *Phys. Rev.* **D53**, 35 (1996).
33. R. Bellotti *et al.*, *Phys. Rev.* **D60**, 052002 (1999).
34. M. Boezio *et al.*, *Phys. Rev.* **D62**, 032007 (2000); M. Boezio *et al.*, *Phys. Rev.* **D67**, 072003 (2003).
35. S. Coutu *et al.*, *Phys. Rev.* **D62**, 032001 (2000).
36. S. Haino *et al.*, *Phys. Lett.* **B594**, 35 (2004).
37. T. Sanuki *et al.*, *Phys. Rev.* **D75**, 043005 (2007).
38. T.K. Gaisser, *Cosmic Rays and Particle Physics*, Cambridge University Press (1990).
39. P. Lipari, *Astropart. Phys.* **1**, 195 (1993).
40. E. Mocchiutto *et al.*, in *Proc. 28th Int. Cosmic Ray Conf.*, Tsukuba, 1627 (2003).
41. M.P. De Pascale *et al.*, *J. Geophys. Res.* **98**, 3501 (1993).
42. P.K.F. Grieder, *Cosmic Rays at Earth*, Elsevier Science (2001).
43. J. Kremer *et al.*, *Phys. Rev. Lett.* **83**, 4241 (1999).
44. S. Haino *et al.* (BESS Collab.), *Phys. Lett.* **B594**, 35 (2004).
45. P. Archard *et al.* (L3+C Collab.), *Phys. Lett.* **B598**, 15 (2004).
46. O.C. Allkofer, K. Carstensen, and W.D. Dau, *Phys. Lett.* **B36**, 425 (1971).
47. B.C. Rastin, *J. Phys.* **G10**, 1609 (1984).
48. C.A. Ayre *et al.*, *J. Phys.* **G1**, 584 (1975).
49. H. Jokisch *et al.*, *Phys. Rev.* **D19**, 1368 (1979).
50. C.G.S. Costa, *Astropart. Phys.* **16**, 193 (2001).
51. P. Adamson *et al.* (MINOS Collab.), *Phys. Rev.* **D76**, 052003 (2007).
52. S. Hayakawa, *Cosmic Ray Physics*, Wiley, Interscience, New York (1969).
53. R.R. Daniel and S.A. Stephens, *Revs. Geophysics & Space Sci.* **12**, 233 (1974).
54. K.P. Beuermann and G. Wibberenz, *Can. J. Phys.* **46**, S1034 (1968).
55. I.S. Diggory *et al.*, *J. Phys.* **A7**, 741 (1974).
56. D.E. Groom, N.V. Mokhov, and S.I. Striganov, "Muon stopping-power and range tables," *Atomic Data and Nuclear Data Tables*, **78**, 183 (2001).
57. P. Lipari and T. Stanev, *Phys. Rev.* **D44**, 3543 (1991).
58. M. Crouch, in *Proc. 20th Int. Cosmic Ray Conf.*, Moscow, **6**, 165 (1987).
59. I.A. Belolaptikov *et al.*, *Astropart. Phys.* **7**, 263 (1997).
60. J. Babson *et al.*, *Phys. Rev.* **D42**, 3613 (1990).
61. P. Desiati *et al.*, in *Proc. 28th Int. Cosmic Ray Conf.*, Tsukuba, 1373 (2003).
62. T. Pradier *et al.* (ANTARES Collab.), [arXiv:0805.2545](https://arxiv.org/abs/0805.2545) and 31st ICRC, 7-15 July 2009, Łódź, Poland (paper #0340).
63. Yu.M. Andreev, V.I. Gurentzov, and I.M. Kogai, in *Proc. 20th Int. Cosmic Ray Conf.*, Moscow, **6**, 200 (1987).
64. M. Aglietta *et al.* (LVD Collab.), *Astropart. Phys.* **3**, 311 (1995).
65. M. Ambrosio *et al.* (MACRO Collab.), *Phys. Rev.* **D52**, 3793 (1995).
66. Ch. Berger *et al.* (Frejus Collab.), *Phys. Rev.* **D40**, 2163 (1989).
67. C. Waltham *et al.*, in *Proc. 27th Int. Cosmic Ray Conf.*, Hamburg, 991 (2001).
68. Y. Ashie *et al.* (SuperKamiokande Collab.), *Phys. Rev.* **D71**, 112005 (2005).
69. T. Futagami *et al.*, *Phys. Rev. Lett.* **82**, 5194 (1999).
70. Y. Fukuda *et al.*, *Phys. Rev. Lett.* **81**, 1562 (1998).
71. F. Reines *et al.*, *Phys. Rev. Lett.* **15**, 429 (1965).
72. M.M. Boliev *et al.*, in *Proc. 3rd Int. Workshop on Neutrino Telescopes* (ed. Milla Baldo Ceolin), 235 (1991).
73. M. Ambrosio *et al.*, (MACRO) *Phys. Lett.* **B434**, 451 (1998). The number quoted for MACRO is the average over 90% of the lower hemisphere,  $\cos\theta < -0.1$ ; see F. Ronga *et al.*, [hep-ex/9905025](https://arxiv.org/abs/hep-ex/9905025).
74. R. Becker-Szendy *et al.*, *Phys. Rev. Lett.* **69**, 1010 (1992); *Proc. 25th Int. Conf. High-Energy Physics*, Singapore (eds. K.K. Phua and Y. Yamaguchi, World Scientific), 662 (1991).
75. S. Hatakeyama *et al.*, *Phys. Rev. Lett.* **81**, 2016 (1998).
76. Y. Fukuda *et al.*, *Phys. Rev. Lett.* **82**, 2644 (1999).
77. K. Greisen, *Ann. Rev. Nucl. Sci.* **10**, 63 (1960).
78. S.P. Swordy *et al.*, *Astropart. Phys.* **18**, 129 (2002).
79. N.L. Grigorov *et al.*, *Yad. Fiz.* **11**, 1058 (1970) and *Proc. 12th Int. Cosmic Ray Conf.*, Hobart, **2**, 206 (1971).
80. K. Asakimori *et al.*, *Proc. 23rd Int. Cosmic Ray Conf.*, Calgary, **2**, 25 (1993); *Proc. 22nd Int. Cosmic Ray Conf.*, Dublin, **2**, 57 and 97 (1991).
81. T.V. Danilova *et al.*, *Proc. 15th Int. Cosmic Ray Conf.*, Plovdiv, **8**, 129 (1977).

82. Yu. A. Fomin *et al.*, *Proc. 22nd Int. Cosmic Ray Conf.*, Dublin, **2**, 85 (1991).
83. M. Amenomori *et al.*, *Astrophys. J.* **461**, 408 (1996).
84. M. Nagano *et al.*, *J. Phys.* **G10**, 1295 (1984).
85. F. Arqueros *et al.*, *Astron. & Astrophys.* **359**, 682 (2000).
86. M.A.K. Glasmacher *et al.*, *Astropart. Phys.* **10**, 291 (1999).
87. T. Antoni *et al.* (KASCADE Collab.), *Astropart. Phys.* **24**, 1 (2005).
88. M. Amenomori *et al.*, *Proc. 30th Int. Cosmic Ray Conf.*, (Merida, Yucatan, 2007), paper 0277.
89. D.J. Bird *et al.*, *Astrophys. J.* **424**, 491 (1994).
90. W.D. Apel *et al.* *Phys. Rev. Lett.* **107**, 171104 (2011).
91. V.S. Ptuskin *et al.*, *Astron. & Astrophys.* **268**, 726 (1993).
92. V.S. Berezinsky and S.I. Grigor'eva, *Astron. & Astrophys.* **199**, 1 (1988).
93. V. Berezinsky, A. Gazizov, and S. Grigorieva, *Phys. Rev.* **D74**, 043005 (2006).
94. R.U. Abbasi *et al.* (The HiRes Collab.), *Astrophys. J.* **622**, 910 (2005).
95. M. Unger *et al.* (Auger Collab.), *Proc. 30th Int. Cosmic Ray Conf.*, Merida, Mexico, 2007 ([arXiv:0706.1495](https://arxiv.org/abs/0706.1495)).
96. J. Abraham *et al.* (Auger Collab.), *Proc. 31st Int. Cosmic Ray Conf.*, Lodz, Poland, 2009; ([arXiv:0906.2319](https://arxiv.org/abs/0906.2319)).
97. K. Greisen, *Phys. Rev. Lett.* **16**, 748 (1966).
98. G.T. Zatsepin and V.A. Kuz'min, *Sov. Phys. JETP Lett.* **4**, 78 (1966).
99. D. Allard *et al.*, *Astron. & Astrophys.* **443**, L29 (2005).
100. M. Takeda *et al.* (The AGASA Collab.), *Astropart. Phys.* **19**, 447 (2003).
101. R. Abbasi *et al.* (HiRes Collab.), *Phys. Rev. Lett.* **100**, 101101 (2008).
102. J. Abraham *et al.* (Auger Collab.), *Phys. Rev. Lett.* **101**, 061101 (2008).
103. Y. Tsunesada *et al.* (Telescope Array Collab.), in *Proc. 32nd Int. Cosmic Ray Conf.*, Beijing, China ([arXiv:1111.2507v1](https://arxiv.org/abs/1111.2507v1)).
104. P. Abreu *et al.* (Auger Collab.), in *Proc. 32nd Int. Cosmic Ray Conf.*, Beijing, China ([arXiv:1107.4809](https://arxiv.org/abs/1107.4809)).
105. V.S. Berezinsky and G.T. Zatsepin, *Phys. Lett.* **B28**, 423 (1969).
106. R. Abbasi *et al.* (IceCube Collab.) *Phys. Rev.* **D83**, 092003 (2011).
107. I. Kravchenko *et al.* (RICE Collab.), *Phys. Rev.* **D73**, 082002 (2006);  
I. Kravchenko *et al.* [arXiv:1106.1164](https://arxiv.org/abs/1106.1164) (2011).
108. J. Abraham *et al.* (Auger Collab.), *Phys. Rev. Lett.* **100**, 211101 (2008);  
P. Abreu *et al.* (Auger Collab.), in *Proc. 32nd Int. Cosmic Ray Conf.*, Beijing, China ([arXiv:1107.4805](https://arxiv.org/abs/1107.4805)).
109. P. Gorham *et al.* (ANITA Collab.), *Phys. Rev.* **D82**, 022004 (2010);  
P. Gorham *et al.* (ANITA Collab.) ([arXiv:1011.5004](https://arxiv.org/abs/1011.5004)).
110. R. Engel, D. Seckel, and T. Stanev, *Phys. Rev.* **D64**, 09310 (2001).
111. E. Waxman and J. Bahcall, *Phys. Rev.* **D59**, 023002 (1999).
112. R.U. Abbasi *et al.* (HiRes Collab.), *Astropart. Phys.* **32**, 53 (2009).

## 27. ACCELERATOR PHYSICS OF COLLIDERS

Revised July 2011 by D.A. Edwards (DESY) and M.J. Syphers (MSU).

### 27.1. Luminosity

This article provides background for the High-Energy Collider Parameter Tables that follow. The number of events,  $N_{exp}$ , is the product of the cross section of interest,  $\sigma_{exp}$ , and the time integral over the instantaneous *luminosity*,  $\mathcal{L}$ :

$$N_{exp} = \sigma_{exp} \times \int \mathcal{L}(t) dt. \quad (27.1)$$

Today's colliders all employ bunched beams. If two bunches containing  $n_1$  and  $n_2$  particles collide head-on with frequency  $f$ , a basic expression for the luminosity is

$$\mathcal{L} = f \frac{n_1 n_2}{4\pi\sigma_x\sigma_y} \quad (27.2)$$

where  $\sigma_x$  and  $\sigma_y$  characterize the rms transverse beam sizes in the horizontal (bend) and vertical directions. In this form it is assumed that the bunches are identical in transverse profile, that the profiles are Gaussian and independent of position along the bunch, and the particle distributions are not altered during bunch crossing.

Whatever the distribution at the source, by the time the beam reaches high energy, the normal form is a useful approximation as suggested by the  $\sigma$ -notation. In the case of an electron storage ring, synchrotron radiation leads to a Gaussian distribution in equilibrium, but even in the absence of radiation the central limit theorem of probability and the diminished importance of space charge effects produces a similar result.

The luminosity may be obtained directly by measurement of the beam properties in Eq. (27.2), but the beam measurements are apt to interfere with data acquisition, so this method though valuable to establish collider performance is not suitable for continuous use. A similar expression to Eq. (27.1) with  $N_{ref}$  from a known reference cross section,  $\sigma_{ref}$ , may be used to determine  $\sigma_{exp}$  according to  $\sigma_{exp} = (N_{exp}/N_{ref})\sigma_{ref}$ .

In the Tables, luminosity is stated in units of  $\text{cm}^{-2}\text{s}^{-1}$ . Integrated luminosity, on the other hand is usually quoted as the inverse of the standard measures of cross section such as femtobarns and, recently, attobarns.

Subsequent sections in this report enlarge briefly on the dynamics behind collider design, comment on the realization of collider performance in a selection of today's facilities, and end with some remarks on future possibilities.

### 27.2. Beam Dynamics

The first concern of beam dynamics is stability. While a reference particle proceeds along the design, or reference, trajectory other particles in the bunch are to remain close by. Assume that the reference particle carries a right-handed Cartesian coordinate system, with the  $z$ -coordinate pointed in the direction of motion along the reference trajectory. The independent variable is the distance  $s$  of the reference particle along this trajectory rather than time, and for simplicity this path is taken to be planar. The transverse coordinates are  $x$  and  $y$ , where  $\{x, z\}$  defines the plane of the reference trajectory.

Several time scales are involved, and the approximations used in writing the equations of motion reflect that circumstance. All of today's high energy colliders are alternating gradient synchrotrons [1,2], and the shortest time scale is that associated with transverse stability, the betatron oscillations, so called because of their analysis for the betatron accelerator species years ago. The linearized equations of motion of a particle displaced from the reference particle are

$$\begin{aligned} x'' + K_x x &= 0, & K_x &\equiv \frac{e}{p} \frac{\partial B}{\partial x} + \frac{1}{\rho^2} \\ y'' + K_y y &= 0, & K_y &\equiv -\frac{e}{p} \frac{\partial B}{\partial x} \\ z' &= -x/\rho \end{aligned} \quad (27.3)$$

where the magnetic field  $B(s)$  is only in the  $y$  direction, contains only dipole and quadrupole terms, and is treated as static here. The radius of curvature due to the field on the reference orbit is  $\rho$ ;  $p$  and  $e$  are the particle's momentum and charge respectively. The prime denotes  $d/ds$ .

The equations for  $x$  and  $y$  are those of harmonic oscillators but with restoring force periodic in  $s$ , that is, they are instances of Hill's equation. The solution may be written in the form

$$\begin{aligned} x(s) &= A_x \sqrt{\beta_x} \cos \psi_x \\ x'(s) &= -\frac{A_x}{\sqrt{\beta_x}} [\alpha \cos \psi_x + \sin \psi_x] \end{aligned} \quad (27.4)$$

where  $A_x$  is a constant of integration,  $\alpha \equiv -(1/2)d\beta_x(s)/ds$ , and the envelope of the motion is modulated by the *amplitude function*,  $\beta_x$ . A solution of the same form describes the motion in  $y$ . The subscripts will be suppressed in the following discussion.

The amplitude function satisfies

$$2\beta\beta'' - \beta'^2 + 4\beta^2 K = 4, \quad (27.5)$$

and in a region free of magnetic field it should be noted that the solution of Eq. (27.5) is a parabola. Expressing  $A$  in terms of  $x$ ,  $x'$  yields

$$\begin{aligned} A^2 &= \gamma x^2 + 2\alpha x x' + \beta x'^2 \\ &= \frac{1}{\beta} [x^2 + (\alpha x + \beta x')^2] \end{aligned} \quad (27.6)$$

with  $\gamma \equiv (1 + \alpha^2)/\beta$ . In a single pass system such as a linac, the *Courant-Snyder parameters*  $\alpha$ ,  $\beta$ ,  $\gamma$  may be selected to match the  $x x'$  distribution of the input beam; in a recursive system, the parameters are usually defined by the structure rather than by the beam.

The relationships between the parameters and the structure may be seen by treatment of a simple *lattice* consisting of equally spaced thin lens quadrupoles equal in magnetic field gradient magnitude but alternating in sign. For this discussion, the weak focusing effects of the bending magnets may be neglected. The propagation of  $X \equiv \{x, x'\}$  through a repetition period may be written  $X_2 = M X_1$ , with the matrix  $M = FODO$  composed of the matrices

$$F = \begin{pmatrix} 1 & 0 \\ -1/f & 1 \end{pmatrix}, \quad D = \begin{pmatrix} 1 & 0 \\ 1/f & 1 \end{pmatrix}, \quad O = \begin{pmatrix} 1 & L \\ 0 & 1 \end{pmatrix},$$

where  $f$  is the magnitude of the focal length and  $L$  the lens spacing. Then

$$M = \begin{pmatrix} 1 + \frac{L}{f} & 2L + \frac{L^2}{f} \\ -\frac{L}{f^2} & 1 - \frac{L}{f} - \frac{L^2}{f^2} \end{pmatrix}. \quad (27.7)$$

The matrix for  $y$  is identical in form differing only by a change in sign of terms linear in  $f$ . An eigenvector-eigenvalue analysis of the matrix  $M$  shows that the motion is stable provided  $f > L/2$ . While that criterion is easily met, in practice instability may be caused by many other factors, including the beam-beam interaction itself.

Standard focus-drift-defocus-drift, or *FODO*, cells such as characterized in simple form by Eq. (27.7) occupy most of the layout of a large collider ring and may be used to set the scale of the amplitude function and related phase advance. Conversion of Eq. (27.4) to a matrix form equivalent to Eq. (27.7) gives

$$M = \begin{pmatrix} c + \alpha s & \beta s \\ -\gamma s & c - \alpha s \end{pmatrix} \quad (27.8)$$

where  $c \equiv \cos \Delta\psi$ ,  $s \equiv \sin \Delta\psi$ , and the relation between structure and amplitude function is specified by setting the values of the latter to be the same at both ends of the cell. By comparison of Eq. (27.7) and Eq. (27.8) one finds  $c = 1 - L^2/(2f^2)$ , so the choice  $f = L/\sqrt{2}$  would give a phase advance  $\Delta\psi$  of 90 degrees for the standard cell. The amplitude function – a maximum at the focusing quadrupole – would then be  $2.7L$ , illustrating the relationship of alternating gradient focusing amplitudes to relatively local aspects of the design. Other functions such as injection, extraction, and HEP experiments



are included by lattice sections matched to the  $\beta$ ,  $\alpha$  standard cell parameters at the insertion points.

The phase advances according to  $d\psi/ds = 1/\beta$ ; that is,  $\beta$  also plays the role of a local  $\lambda/2\pi$ , and the *tune*,  $\nu$ , is the number of such oscillations per turn about the closed path. In the neighborhood of an interaction point (IP), the beam optics of the ring is configured so as to produce a near focus; the value of the amplitude function at this point is designated  $\beta^*$ .

The motion as it develops with  $s$  describes an ellipse in  $\{x, x' \equiv dx/ds\}$  phase space the area of which is  $\pi A^2$ , where  $A$  is the constant in Eq. (27.4). If the interior of that ellipse is populated by an ensemble of non-interacting particles, that area, given the name *emittance* and denoted by  $\varepsilon$ , would change only with energy. For a beam with a Gaussian distribution in  $x, x'$ , the area containing one standard deviation  $\sigma_x$  is the definition of emittance in the Tables:

$$\varepsilon_x \equiv \pi \frac{\sigma_x^2}{\beta_x}, \quad (27.9)$$

with a corresponding expression in the other transverse direction,  $y$ . This definition includes 39% of the beam. For most of the entries in the Tables the standard deviation is used as the beam radius.

To complete the coordinates used to describe the motion, we take as the variable conjugate to  $z$  the fractional momentum deviation  $\delta p/p$  from that of the reference particle. Radiofrequency electric fields in the  $s$  direction provide a means for longitudinal oscillations, and the frequency determines the bunch length. The frequency of this system appears in the Tables as does the rms value of  $\delta p/p$  characterized as “energy spread” of the beam.

For HEP bunch length is a significant quantity for a variety of reasons, but in the present context if the bunch length becomes larger than  $\beta^*$  the luminosity is adversely affected. This is because  $\beta$  grows parabolically as one proceeds away from the interaction point and so the beam size increases thus lowering the contribution to the luminosity from such locations. This is often called the “hourglass” effect.

The other major external electromagnetic field interaction in the single particle context is the production of synchrotron radiation due to centripetal acceleration, given by the Larmor formula multiplied by a relativistic magnification factor of  $\gamma^4$  [3]. In the case of electron rings this process determines the equilibrium emittance through a balance between radiation damping and excitation of oscillations, and further serves as the barrier to future higher energy versions in this variety of collider.

### 27.3. Impediments to High Luminosity

Eq. (27.2) can be recast in terms of emittances and amplitude functions as

$$\mathcal{L} = f \frac{n_1 n_2}{4 \sqrt{\varepsilon_x \beta_x^* \varepsilon_y \beta_y^*}}. \quad (27.10)$$

So to achieve high luminosity, all one has to do is make high population bunches of low emittance collide at high frequency at locations where the beam optics provides as low values of the amplitude functions as possible.

Such expressions as Eq. (27.10) of the luminosity are special cases of the more general forms available elsewhere [4]. But while there are no fundamental limits to the process, there are certainly challenges. Here we have space to mention only a few of these. The beam-beam tune shift appears in the Tables. A bunch in beam 1 presents a (nonlinear) lens to a particle in beam 2 resulting in changes to the particle’s transverse tune with a range characterized by the parameter [4]

$$\xi_{y,2} = \frac{r_e n_1 \beta_{y,2}^*}{2\pi \gamma_2 \sigma_{y,1} (\beta_{x,1} + \sigma_{y,1})} \quad (27.11)$$

where  $r_e = e^2/(4\pi\epsilon_0 mc^2)$  is the classical radius of the electron. The transverse oscillations are susceptible to resonant perturbations from a variety of sources such as imperfections in the magnetic guide field, so certain values of the tune must be avoided. Accordingly, the tune spread arising from  $\xi$  is limited, but limited to a value difficult to

predict. But a glance at the Tables shows that electrons are more forgiving than protons thanks to the damping effects of synchrotron radiation; the  $\xi$ -values for the former are about an order of magnitude larger than those for protons.

A subject of present intense interest is the *electron-cloud effect* [5,6]; actually a variety of related processes come under this heading. They typically involve a buildup of electron density in the vacuum chamber due to emission from the chamber walls stimulated by electrons or photons originating from the beam itself. For instance, there is a process closely resembling the multipacting effects familiar from radiofrequency system commissioning. Low energy electrons are ejected from the walls by photons from positron or proton beam-produced synchrotron radiation. These electrons are accelerated toward a beam bunch, but by the time they reach the center of the vacuum chamber the bunch has gone and so the now-energetic electrons strike the opposite wall to produce more secondaries. These secondaries are now accelerated by a subsequent bunch, and so on. Among the disturbances that this electron accumulation can produce is enhancement of the tune spread within the bunch; the near-cancellation of bunch-induced electric and magnetic fields is no longer in effect.

The benefits of low emittance are clear in Eq. (27.10). For electron synchrotrons, radiation damping provides an automatic route. For hadrons, particularly antiprotons, two inventions have played a prominent role. Stochastic cooling [7] was employed first in the *SppS* and subsequently in the Tevatron. Electron cooling [8] was also used in the Tevatron complex to great advantage. Further innovations are underway due to the needs of potential future projects; these are noted in the final section.

### 27.4. Comments on Present Facilities

Collider accelerator physics of course goes far beyond the elements of the preceding sections. In this section elaboration is made on various issues associated with some of the recently operating colliders, particularly factors which impact integrated luminosity. The various colliders utilizing hadrons have important unique differences and hence are broken out separately. As space is limited, general references are provided where much further information can be obtained.

**27.4.1. LHC:** [9] The superconducting Large Hadron Collider is the world’s highest energy collider. Operation for HEP is currently conducted with 3.5 TeV protons in each beam. Progress is rapid and current status is best checked at the Web site referenced in the heading of this subsection. To meet its luminosity goals the LHC will have to contend with a high beam current of 0.5 A, leading to stored energies of several hundred MJ per beam. Component protection, beam collimation, and controlled energy deposition will be given very high priorities. Additionally, at energies of 5-7 TeV per particle, synchrotron radiation will move from being a curiosity to a challenge in a hadron accelerator for the first time. At design beam current the system must remove roughly 7 kW at 1.8 K due to synchrotron radiation. As the photons are emitted their interactions with the vacuum chamber wall can generate free electrons, with consequent “electron cloud” development. Much care was taken to design a special liner for the chamber to mitigate this issue.

The two proton beams are contained in separate pipes throughout most of the circumference, but naturally must be brought together into a single pipe at the interaction points. The large number of bunches, and subsequent short bunch spacing, would lead to approximately 30 head-on collisions through 120 m of common beam pipe at each IP. Thus, a small crossing angle is employed, which reduces the luminosity by about 15%. Still, the bunches moving in one direction will have long-range encounters with the counter-rotating bunches and the resulting perturbations of the particle motion constitute a continued course of study. Initial luminosity measurements were made by the “van der Meer scan” as was done long ago on the ISR [10]. The detectors will have measurements based on a reference cross section; for an example see the discussion in the ATLAS design report [11]. The Tables also show the performance anticipated for Pb-Pb collisions. The ALICE [12] experiment is designed to concentrate on these high energy-density phenomena.



In the coming years, an ambitious upgrade program, Super LHC [13], has as its target an order-of-magnitude increase in luminosity.

**27.4.2. Tevatron :** [14] The first superconducting synchrotron in history, the Tevatron was the highest energy collider for 25 years. Operation was terminated in September 2011. The route to high integrated luminosity in the Tevatron was governed by the antiproton production rate, the turn-around time to produce another store, and the resulting optimization of store time. The overall reliability of the accelerator complex plays a crucial role, as it can take many hours to produce an adequate number of antiprotons for collisions.

Unlike the LHC, the beams in the Tevatron circulated in a single vacuum pipe and thus were placed on separated orbits which wrap around each other in a helical pattern outside of the interaction regions. Hence, long-range encounters played an important role here as well, though the effects could be different from the LHC where the encounters are more or less “in phase” with each other through a single interaction region. In the Tevatron, the 70 long-range encounters were distributed about the synchrotron and their mitigation was limited by the available aperture.

In recent years the antiproton bunch intensities approached those of the proton bunches, and their emittances were greatly reduced using improved beam cooling, so much so that detrimental effects on the proton beam became apparent. The antiproton beam emittance was adjusted prior to collision conditions to optimize the proton bunch lifetime during the store [15]. The Tevatron ultimately achieved luminosities a factor of 400 over the original design specification.

**27.4.3.  $e^+e^-$  Rings :** As should be expected, synchrotron radiation plays a major role in the design and optimization of  $e^+e^-$  colliders. While vacuum stability and electron clouds can be of concern in the positron rings, synchrotron radiation along with the restoration of longitudinal momentum by the RF system have the positive effect of generating very small transverse beam sizes and small momentum spread. Further reduction of beam size at the interaction points using standard beam optics techniques and successfully contending with high beam currents has led to record luminosities in these rings, far exceeding those of hadron colliders. To maximize integrated luminosity the beam can be “topped off” by injecting new particles without removing existing ones – a feature difficult to imitate in hadron colliders.

Asymmetric energies of the two beams have allowed for the enhancement of  $B$ -physics research and for interesting interaction region designs. As the bunch spacing can be quite short, the lepton beams sometimes pass through each other at an angle and hence have reduced luminosity. Recently, however, the invention of high frequency “crab crossing” schemes have produced full restoration of the luminous region. KEK-B has attained over  $1 \text{ fb}^{-1}$  of integrated luminosity in a single day, and its upgrade plans are aiming for initial luminosities of  $8 \times 10^{35} \text{ cm}^{-2}\text{s}^{-1}$  [16].

**27.4.4. HERA :** [17] Now decommissioned, HERA was the first facility to employ both applications of superconductivity: magnets and accelerating structures. Its next-generation cold-iron superconducting magnets for the proton beam were the culmination of lessons learned from the Tevatron experience and extensive development of the technology since then. The HERA team felt comfortable with a larger dynamic range of the magnet system, enabling the use of the existing DESY complex for injection. Though the HERA magnets could reach fields consistent with energies above 1 TeV, other accelerator systems precluded operation above 920 GeV.

The lepton beams (positrons or electrons) were provided by the existing complex, and were accelerated to 27.5 GeV using conventional magnets. The interaction region where the beams had common vacuum chambers had the interesting feature that the lepton beam could be manipulated without detrimental effects on the proton beam due to the large difference in magnetic rigidity. A 4-times higher frequency RF system was used at collision to generate shorter bunches, thus helping alleviate the hour glass effect at the collision points. As in any high energy lepton storage ring, the lepton beam naturally would become transversely polarized (within about 40 minutes, for

HERA). “Spin rotators” were implemented on either side of an IP to produce longitudinal polarization at the experiment.

**27.4.5. RHIC :** [18] The Relativistic Heavy Ion Collider employs superconducting magnets, and collides combinations of fully-stripped ions such as H-H (p-p), Au-Au, Cu-Cu, and d-Au.

The high charge per particle (+79 for gold, for instance) makes intra-beam scattering of particles within the bunch of special concern, even for seemingly modest bunch intensities. Another special feature of accelerating heavy ions in RHIC is that the beams experience a “transition energy” during acceleration – a point where the derivative with respect to momentum of the revolution period is zero. This is more typical of low-energy accelerators, where the necessary phase jump required of the RF system is implemented rapidly and little time is spent near this condition. In the case of RHIC with heavy ions, the superconducting magnets do not ramp very quickly and the period of time spent crossing transition is long and must be dealt with carefully. For p-p operation the beams are always above their transition energy and so this condition is completely avoided.

RHIC is also distinctive in its ability to accelerate and collide polarized proton beams. As proton beam polarization must be maintained from its low-energy source, successful acceleration through the myriad of depolarizing resonance conditions in high energy circular accelerators has taken years to accomplish. An energy of 250 GeV per proton with  $\sim 48\%$  final polarization per beam has been realized.

## 27.5. Future Prospects

Present design activity emphasizes a lepton collider as the next major HEP project contingent upon the initial results from the LHC. Synchrotron radiation precludes a higher energy successor to LEP. Four alternatives are noted in this section: two approaches to an electron-positron linear collider, a muon ring collider, and potential use of plasma acceleration.

**27.5.1. Electron-Positron Linear Colliders :** A major problem confronting a high energy, high luminosity single pass collider design is the power requirement, so measures must be taken to keep the demand within bounds as illustrated in a transformed Eq. (27.2) as developed in the *TESLA Design Report* [19]:

$$\mathcal{L} = \frac{1}{4\pi r_e^{3/2}} \frac{P_b}{E_{cm}} \left( \frac{\pi \delta_E}{\gamma \varepsilon_y} \right)^{1/2} H_D. \quad (27.12)$$

Here,  $P_b$  is the total power of both beams and  $E_{cm}$  their cms energy. Management of  $P_b$  leads to an upward push on the product of collision frequency and bunch population with an attendant rise in the energy radiated due to the electromagnetic field of one bunch acting on the particles of the other. The fractional spread in the collision energy that results from this radiation is represented by  $\delta_E$  and keeping a significant fraction of the luminosity within a percent or so of the nominal energy represents a design goal. A consequence is the use of flat beams, where  $\delta_E$  is managed by the beam width, and luminosity adjusted by the beam height, thus the explicit appearance of the vertical emittance  $\varepsilon_y$ . The final factor in Eq. (27.12),  $H_D$ , represents the enhancement of luminosity due to the pinch effect during bunch crossing.

The approach designated by the International Linear Collider (ILC) is presented in the Tables, and the contrast with the collision-point parameters of the circular colliders is striking, though reminiscent in direction of those of the SLAC Linear Collider that are no longer shown. The ILC *Reference Design Report* [20] has a baseline cms energy of 500 GeV with upgrade provision for 1 TeV, and luminosity comparable to the LHC. The ILC is based on superconducting accelerating structures of the 1.3 GHz TESLA variety.

At CERN, a design effort is underway on the Compact Linear Collider (CLIC), each linac of which is itself a two-beam accelerator, in that a high energy, low current beam is fed by a low energy, high current driver [21]. The CLIC design employs normal conducting 12 GHz accelerating structures at a gradient of 100 MeV/m, some three times the current capability of the superconducting ILC cavities. The design cms energy is 3 TeV.

**27.5.2. Muon Collider**: The muon to electron mass ratio of 210 implies less concern about synchrotron radiation by a factor of about  $2 \times 10^9$  and its  $1.6 \mu\text{s}$  lifetime means that it will last for some  $150B$  turns in a ring about half of which is occupied by bend magnets with average field  $B$  (tesla). Design effort became serious in the mid 1990s and a collider outline emerged quickly [22].

Removal of the synchrotron radiation barrier reduces collider facility scale to a level compatible with on-site placement at some locations. If a Higgs particle is detected the  $(m_\mu/m_e)^2$  cross section advantage in s-channel production would be valuable. And a neutrino factory could potentially be realized in the course of construction [23].

The challenges to luminosity achievement were clear and very attractive for R&D: targetting, collection, and emittance reduction are three that come immediately to mind. The proton source needs to deliver a beam power of several MW, collection would be aided by magnetic fields common on neutron stars (though scaled back for application on earth), and the emittance requirements have inspired fascinating investigations into phase space manipulation that are finding application in other facilities. A summary of the status may be found in a presentation to the HEPAP P5 Panel [24].

**27.5.3. Plasma Acceleration**: At the 1956 CERN Symposium, a paper by Veksler in which he suggested acceleration of protons to the TeV scale using a bunch of electrons anticipated current interest in plasma acceleration [25]. A half-century later this is more than a suggestion, with the demonstration, as a striking example, of energy enhancement of 28.5 GeV at SLAC [26].

How plasma acceleration will find application in an HEP facility is not yet clear, given the necessity of coordinating multiple plasma chambers. Active R&D is underway; for recent discussion of parameters for a laser-plasma based electron positron collider, see, for example, relevant papers in an Advanced Accelerator Concepts Workshop [27].

#### References:

1. E.D. Courant and H.S. Snyder, *Ann. Phys.* **3**, 1 (1958). This is the classic article on the alternating gradient synchrotron.
2. A.W. Chao and M. Tigner (eds.), *Handbook of Accelerator Physics and Engineering*, World Science Publishing Co. (Singapore, 2nd printing, 2002.), Sec. 2.1, 2.2.
3. H. Wiedemann, *Handbook of Accelerator Physics and Engineering*, *ibid*, Sec. 3.1.
4. M. A. Furman and M. S. Zisman, *Handbook of Accelerator Physics and Engineering*, *ibid*, Sec. 4.1.
5. M.A. Furman, *Handbook of Accelerator Physics and Engineering*, *ibid*, Sec. 2.5.11.
6. <http://ab-abp-rlc.web.cern.ch/ab-abp-rlc-ecloud/>. This site contains many references as well as videos of electron cloud simulations.
7. D.Möhl *et al.*, *Phys. Rep.* **58**, 73 (1980).
8. G.I. Budker, *Proc. Int. Symp. Electron & Positron Storage Rings* (1966).
9. Detailed information from the multi-volume design report to present status may be found at <http://lhcb.web.cern.ch/lhcb/>.
10. S. van der Meer, "Calibration of the Effective Beam Height at the ISR," CERN-ISR-PO/68-(1968).
11. <http://atlas.web.cern.ch/Atlas/GROUPS/PHYSICS/TDR/access.html>.
12. <http://aliceinfo.cern.ch/Public/Welcome.html>.
13. <http://project-slhcb.web.cern.ch/project-slhcb/about/>.
14. H.T. Edwards, "The Tevatron Energy Doubler: A Superconducting Accelerator," *Ann. Rev. Nucl. Part. Sci.* **35**, 605 (1985).
15. C. Gattuso, M. Convery, and M. Syphers, "Optimization of integrated luminosity in the Tevatron," FERMILAB-CONF-09-132-AD (Apr 2009).
16. An overview of electron-positron colliders past and present may be found in ICFA Beam Dynamics Newsletter No. 46, April 2009, <http://www-bd.fnal.gov/icfabd/>. A day-by-day account of the luminosity progress at KEK-B may be found at [http://belle.kek.jp/bdocs/lumi\\_belle.png](http://belle.kek.jp/bdocs/lumi_belle.png).
17. Brief history at [http://en.wikipedia.org/wiki/Hadron\\_Elektron\\_Ring\\_Anlage](http://en.wikipedia.org/wiki/Hadron_Elektron_Ring_Anlage).
18. M. Harrison, T. Ludlam, and S. Ozaki, eds, "Special Issue: The Relativistic Heavy Ion Collider Project: RHIC and its Detectors," *Nuc. Inst. & Meth. in Phys. Research A* **499** (2003).
19. [http://tesla.desy.de/new\\_pages/TDR\\_CD/start.html](http://tesla.desy.de/new_pages/TDR_CD/start.html).
20. <http://www.linearcollider.org/cms/>.
21. <http://clic-study.web.cern.ch/>.
22. Robert B. Palmer, Alvin Tollestrup, and Andrew Sessler, MC-047, [http://www.fnal.gov/projects/muon\\_collider/notes/fnal\\_notes.html](http://www.fnal.gov/projects/muon_collider/notes/fnal_notes.html).
23. [http://en.wikipedia.org/wiki/Neutrino\\_Factory](http://en.wikipedia.org/wiki/Neutrino_Factory).
24. <http://www.cap.bnl.gov/mumu/polit/palmer-p5.pdf>.
25. V.I. Veksler, CERN Symposium on High Energy Accelerators and Pion Physics, 11–23 June 1956, p. 80. This paper may be downloaded from <http://cdsweb.cern.ch/record/1241563?ln=en>.
26. <http://slac.stanford.edu/grp/arb/siemann.pdf>.
27. Advanced Accelerator Concepts, edited by C. Schroeder, W. Leemans, and E. Esarey, *AIP Conference Proceedings 1086*, Santa Cruz CA 27 July – 2 August 2008.

HIGH-ENERGY COLLIDER PARAMETERS:  $e^+e^-$  Colliders (I)

Updated in early 2012 with numbers received from representatives of the colliders (contact J. Beringer, LBNL). The table shows parameter values as achieved by January 1, 2012. Quantities are, where appropriate, r.m.s.; unless noted otherwise, energies refer to beam energy;  $H$  and  $V$  indicate horizontal and vertical directions; s.c. stands for superconducting. Parameters for the defunct SPEAR, DORIS, PETRA, PEP, SLC, TRISTAN, and VEPP-2M colliders may be found in our 1996 edition (Phys. Rev. D54, 1 July 1996, Part I).

	VEPP-2000 (Novosibirsk)	VEPP-4M (Novosibirsk)	BEPC (China)	BEPC-II (China)	DAΦNE (Frascati)
Physics start date	2010	1994	1989	2008	1999
Physics end date	—	—	2005	—	—
Maximum beam energy (GeV)	1.0	6	2.5	1.89 (2.3 max)	0.510
Delivered integrated luminosity per exp. ( $\text{fb}^{-1}$ )	0.030	0.027	0.11	3.74	$\approx 4.7$ in 2001-2007 2.7 w/crab-waist
Luminosity ( $10^{30} \text{ cm}^{-2}\text{s}^{-1}$ )	100	20	12.6 at 1.843 GeV 5 at 1.55 GeV	649	453
Time between collisions ( $\mu\text{s}$ )	0.04	0.6	0.8	0.008	0.0027
Full crossing angle ( $\mu$ rad)	0	0	0	$2.2 \times 10^4$	$5 \times 10^4$
Energy spread (units $10^{-3}$ )	0.64	1	0.58 at 2.2 GeV	0.52	0.40
Bunch length (cm)	4	5	$\approx 5$	$\approx 1.5$	low current: 1 at 15mA: 2
Beam radius ( $10^{-6}$ m)	125 (round)	$H$ : 1000 $V$ : 30	$H$ : 890 $V$ : 37	$H$ : 380 $V$ : 5.7	$H$ : 260 $V$ : 4.8
Free space at interaction point (m)	$\pm 1$	$\pm 2$	$\pm 2.15$	$\pm 0.63$	$\pm 0.295$
Luminosity lifetime (hr)	continuous	2	7–12	1.5	0.2
Turn-around time (min)	continuous	18	32	26	2 (topping up)
Injection energy (GeV)	0.2–1.0	1.8	1.55	1.89	on energy
Transverse emittance ( $10^{-9}\pi$ rad-m)	$H$ : 250 $V$ : 250	$H$ : 200 $V$ : 20	$H$ : 660 $V$ : 28	$H$ : 144 $V$ : 2.2	$H$ : 260 $V$ : 2.6
$\beta^*$ , amplitude function at interaction point (m)	$H$ : 0.06 – 0.11 $V$ : 0.06 – 0.10	$H$ : 0.75 $V$ : 0.05	$H$ : 1.2 $V$ : 0.05	$H$ : 1.0 $V$ : 0.015	$H$ : 0.26 $V$ : 0.009
Beam-beam tune shift per crossing (units $10^{-4}$ )	$H$ : 750 $V$ : 750	500	350	327	440
RF frequency (MHz)	172	180	199.53	499.8	356
Particles per bunch (units $10^{10}$ )	16	15	20 at 2 GeV 11 at 1.55 GeV	4.1	$e^-$ : 3.2 $e^+$ : 2.1
Bunches per ring per species	1	2	1	88	100 to 105 (120 buckets)
Average beam current per species (mA)	150	80	40 at 2 GeV 22 at 1.55 GeV	725	$e^-$ : 1500 $e^+$ : 1000
Circumference or length (km)	0.024	0.366	0.2404	0.23753	0.098
Interaction regions	2	1	2	1	1
Magnetic length of dipole (m)	1.2	2	1.6	outer ring: 1.6 inner ring: 1.41	outer ring: 1.2 inner ring: 1
Length of standard cell (m)	12	7.2	6.6	outer ring: 6.6 inner ring: 6.2	n/a
Phase advance per cell (deg)	$H$ : 738 $V$ : 378	65	$\approx 60$	60–90 non-standard cells	—
Dipoles in ring	8	78	40 + 4 weak	84 + 8 weak	8
Quadrupoles in ring	20	150	68	134+2 s.c.	48
Peak magnetic field (T)	2.4	0.6	0.903 at 2.8 GeV	outer ring: 0.677 inner ring: 0.766	1.2

HIGH-ENERGY COLLIDER PARAMETERS:  $e^+e^-$  Colliders (II)

Updated in early 2012 with numbers received from representatives of the colliders (contact J. Beringer, LBNL). For existing colliders, the table shows parameter values as achieved by January 1, 2012. For future colliders, design values are quoted. Quantities are, where appropriate, r.m.s.; unless noted otherwise, energies refer to beam energy;  $H$  and  $V$  indicate horizontal and vertical directions; s.c. stands for superconducting.

	CESR (Cornell)	CESR-C (Cornell)	LEP (CERN)	ILC (TBD)	CLIC (TBD)
Physics start date	1979	2002	1989	TBD	TBD
Physics end date	2002	2008	2000	—	—
Maximum beam energy (GeV)	6	6	100 - 104.6	250 (upgradeable to 500)	1500 (first phase: 250)
Delivered integrated luminosity per exp. ( $\text{fb}^{-1}$ )	41.5	2.0	0.221 at Z peak 0.501 at 65 – 100 GeV 0.275 at >100 GeV	—	—
Luminosity ( $10^{30} \text{ cm}^{-2}\text{s}^{-1}$ )	1280 at 5.3 GeV	76 at 2.08 GeV	24 at Z peak 100 at > 90 GeV	$1.5 \times 10^4$	$6 \times 10^4$
Time between collisions ( $\mu\text{s}$ )	0.014 to 0.22	0.014 to 0.22	22	$0.55^\dagger$	$0.0005^\ddagger$
Full crossing angle ( $\mu$ rad)	$\pm 2000$	$\pm 3300$	0	14000	20000
Energy spread (units $10^{-3}$ )	0.6 at 5.3 GeV	0.82 at 2.08 GeV	0.7→1.5	1	3.4
Bunch length (cm)	1.8	1.2	1.0	0.03	0.0044
Beam radius ( $\mu\text{m}$ )	$H$ : 460 $V$ : 4	$H$ : 340 $V$ : 6.5	$H$ : 200 → 300 $V$ : 2.5 → 8	$H$ : 0.474 $V$ : 0.0059	$H$ : 0.045 * $V$ : 0.0009
Free space at interaction point (m)	$\pm 2.2$ ( $\pm 0.6$ to REC quads)	$\pm 2.2$ ( $\pm 0.3$ to PM quads)	$\pm 3.5$	$\pm 3.5$	$\pm 3.5$
Luminosity lifetime (hr)	2–3	2–3	20 at Z peak 10 at > 90 GeV	n/a	n/a
Turn-around time (min)	5 (topping up)	1.5 (topping up)	50	n/a	n/a
Injection energy (GeV)	1.8–6	1.5–6	22	n/a	n/a
Transverse emittance ( $10^{-9}\pi$ rad-m)	$H$ : 210 $V$ : 1	$H$ : 120 $V$ : 3.5	$H$ : 20–45 $V$ : 0.25 → 1	$H$ : 0.02 $V$ : $7 \times 10^{-5}$	$H$ : $2.2 \times 10^{-4}$ $V$ : $6.8 \times 10^{-6}$
$\beta^*$ , amplitude function at interaction point (m)	$H$ : 1.0 $V$ : 0.018	$H$ : 0.94 $V$ : 0.012	$H$ : 1.5 $V$ : 0.05	$H$ : 0.01 $V$ : $5 \times 10^{-4}$	$H$ : 0.0069 $V$ : $6.8 \times 10^{-5}$
Beam-beam tune shift per crossing (units $10^{-4}$ )	$H$ : 250 $V$ : 620	$e^-$ : 420 ( $H$ ), 280 ( $V$ ) $e^+$ : 410 ( $H$ ), 270 ( $V$ )	830	n/a	7.7
RF frequency (MHz)	500	500	352.2	1300	11994
Particles per bunch (units $10^{10}$ )	1.15	4.7	45 in collision 60 in single beam	2	0.37
Bunches per ring per species	9 trains of 5 bunches	8 trains of 3 bunches	4 trains of 1 or 2	1312	312 (in train)
Average beam current per species (mA)	340	72	4 at Z peak 4→6 at > 90 GeV	6 (in pulse)	1205 (in train)
Beam polarization (%)	—	—	55 at 45 GeV 5 at 61 GeV	$e^-$ : > 80% $e^+$ : > 60%	$e^-$ : 70% at IP
Circumference or length (km)	0.768	0.768	26.66	31	48
Interaction regions	1	1	4	1	1
Magnetic length of dipole (m)	1.6–6.6	1.6–6.6	11.66/pair	n/a	n/a
Length of standard cell (m)	16	16	79	n/a	n/a
Phase advance per cell (deg)	45–90 (no standard cell)	45–90 (no standard cell)	102/90	n/a	n/a
Dipoles in ring	86	84	3280 + 24 inj. + 64 weak	n/a	n/a
Quadrupoles in ring	101 + 4 s.c.	101 + 4 s.c.	520 + 288 + 8 s.c.	n/a	n/a
Peak magnetic field (T)	0.3 / 0.8 at 8 GeV	0.3 / 0.8 at 8 GeV, 2.1 wigglers at 1.9 GeV	0.135	n/a	n/a

$^\dagger$ Time between bunch trains: 200ms.

$^\ddagger$ Time between bunch trains: 20ms.

\*Effective beam size including non-linear and chromatic effects.

HIGH-ENERGY COLLIDER PARAMETERS:  $e^+e^-$  Colliders (III)

Updated in early 2012 with numbers received from representatives of the colliders (contact J. Beringer, LBNL). For existing colliders, the table shows parameter values as achieved by January 1, 2012. For future colliders, design values are quoted. Quantities are, where appropriate, r.m.s.; unless noted otherwise, energies refer to beam energy;  $H$  and  $V$  indicate horizontal and vertical directions; s.c. stands for superconducting.

	KEKB (KEK)	PEP-II (SLAC)	SuperB (Italy)	SuperKEKB (KEK)
Physics start date	1999	1999	TBD	2015
Physics end date	2010	2008	—	—
Maximum beam energy (GeV)	$e^-$ : 8.33 (8.0 nominal) $e^+$ : 3.64 (3.5 nominal)	$e^-$ : 7–12 (9.0 nominal) $e^+$ : 2.5–4 (3.1 nominal) (nominal $E_{cm} = 10.5$ GeV)	$e^-$ : 4.2 $e^+$ : 6.7	$e^-$ : 7 $e^+$ : 4
Delivered integrated luminosity per exp. ( $\text{fb}^{-1}$ )	1040	557	—	—
Luminosity ( $10^{30} \text{ cm}^{-2}\text{s}^{-1}$ )	21083	12069 (design: 3000)	$1.0 \times 10^6$	$8 \times 10^5$
Time between collisions ( $\mu\text{s}$ )	0.00590 or 0.00786	0.0042	0.0042	0.004
Full crossing angle ( $\mu$ rad)	$\pm 11000^\dagger$	0	$\pm 33000$	$\pm 41500$
Energy spread (units $10^{-3}$ )	0.7	$e^-/e^+$ : 0.61/0.77	$e^-/e^+$ : 0.73/0.64	$e^-/e^+$ : 0.64/0.81
Bunch length (cm)	0.65	$e^-/e^+$ : 1.1/1.0	0.5	$e^-/e^+$ : 0.5/0.6
Beam radius ( $\mu\text{m}$ )	H: 124 ( $e^-$ ), 117 ( $e^+$ ) V: 1.9	H: 157 V: 4.7	H: 9 ( $e^-$ ), 7 ( $e^+$ ) V: 0.04	$e^-$ : 11 (H), 0.062 (V) $e^+$ : 10 (H), 0.048 (V)
Free space at interaction point (m)	+0.75/−0.58 (+300/−500) mrad cone	$\pm 0.2$ , $\pm 300$ mrad cone	$\pm 0.35$	$e^-$ : +1.20/−1.28, $e^+$ : +0.78/−0.73 (+300/−500) mrad cone
Luminosity lifetime (hr)	continuous	continuous	continuous	continuous
Turn-around time (min)	continuous	continuous	continuous	continuous
Injection energy (GeV)	$e^-/e^+$ : 8/3.5	2.5–12	$e^-/e^+$ : 4.2/6.7	$e^-/e^+$ : 7/4
Transverse emittance ( $10^{-9}\pi$ rad-m)	$e^-$ : 24 (57*) (H), 0.61 (V) $e^+$ : 18 (55*) (H), 0.56 (V)	$e^-$ : 48 (H), 1.8 (V) $e^+$ : 24 (H), 1.8 (V)	$e^-$ : 2.5 (H), 0.006 (V) $e^+$ : 2.0 (H), 0.005 (V)	$e^-$ : 4.6 (H), 0.013 (V) $e^+$ : 3.2 (H), 0.0086 (V)
$\beta^*$ , amplitude function at interaction point (m)	$e^-$ : 1.2 (0.27*) (H), 0.0059 (V) $e^+$ : 1.2 (0.23*) (H), 0.0059 (V)	$e^-$ : 0.50 (H), 0.012 (V) $e^+$ : 0.50 (H), 0.012 (V)	$e^-$ : 0.032 (H), 0.00021 (V) $e^+$ : 0.026 (H), 0.00025 (V)	$e^-$ : 0.025 (H), $3 \times 10^{-4}$ (V) $e^+$ : 0.032 (H), $2.7 \times 10^{-4}$ (V)
Beam-beam tune shift per crossing (units $10^{-4}$ )	$e^-$ : 1020 (H), 900 (V) $e^+$ : 1270 (H), 1290 (V)	$e^-$ : 703 (H), 498 (V) $e^+$ : 510 (H), 727 (V)	20 (H), 950 (V)	$e^-$ : 12 (H), 807 (V) $e^+$ : 28 (H), 881 (V)
RF frequency (MHz)	508.887	476	476	508.887
Particles per bunch (units $10^{10}$ )	$e^-/e^+$ : 4.7/6.4	$e^-/e^+$ : 5.2/8.0	$e^-/e^+$ : 6.5/5.1	$e^-/e^+$ : 6.53/9.04
Bunches per ring per species	1585	1732	978	2500
Average beam current per species (mA)	$e^-/e^+$ : 1188/1637	$e^-/e^+$ : 1960/3026	$e^-/e^+$ : 1900/2400	$e^-/e^+$ : 2600/3600
Beam polarization (%)	—	—	$> 80$ ( $e^-$ )	—
Circumference or length (km)	3.016	2.2	1.258	3.016
Interaction regions	1	1	1	1
Magnetic length of dipole (m)	$e^-/e^+$ : 5.86/0.915	$e^-/e^+$ : 5.4/0.45	$e^-/e^+$ : 0.9/5.4	$e^-/e^+$ : 5.9/4.0
Length of standard cell (m)	$e^-/e^+$ : 75.7/76.1	15.2	40	$e^-/e^+$ : 75.7/76.1
Phase advance per cell (deg)	450	$e^-/e^+$ : 60/90	360 (V), 1080 (H)	450
Dipoles in ring	$e^-/e^+$ : 116/112	$e^-/e^+$ : 192/192	$e^-/e^+$ : 186/102	$e^-/e^+$ : 116/112
Quadrupoles in ring	$e^-/e^+$ : 452/452	$e^-/e^+$ : 290/326	$e^-/e^+$ : 290/300	$e^-/e^+$ : 466/460
Peak magnetic field (T)	$e^-/e^+$ : 0.25/0.72	$e^-/e^+$ : 0.18/0.75	$e^-/e^+$ : 0.52/0.25	$e^-/e^+$ : 0.22/0.19

$\dagger$ KEKB was operated with crab crossing from 2007 to 2010.

\*With dynamic beam-beam effect.

HIGH-ENERGY COLLIDER PARAMETERS:  $ep$ ,  $\bar{p}p$ ,  $pp$  Colliders

Updated in early 2012 with numbers received from representatives of the colliders (contact J. Beringer, LBNL). The table shows parameter values as achieved by January 1, 2012. For LHC, the parameters expected for running in 2012 and nominal values are also given. Quantities are, where appropriate, r.m.s.; unless noted otherwise, energies refer to beam energy;  $H$  and  $V$  indicate horizontal and vertical directions; s.c. stands for superconducting; pk and avg denote peak and average values.

	HERA (DESY)	TEVATRON* (Fermilab)	RHIC (Brookhaven)	LHC (CERN)		
Physics start date	1992	1987	2001	2009	2012 (expected)	nominal
Physics end date	2007	2011	—	—		
Particles collided	$ep$	$p\bar{p}$	$pp$ (polarized)	$pp$		
Maximum beam energy (TeV)	$e$ : 0.030 $p$ : 0.92	0.980	0.25 48% polarization	3.5	4.0	7.0
Delivered integrated luminosity per exp. ( $\text{fb}^{-1}$ )	0.8	12	up to 0.14 at 100 GeV/n up to 0.15 at 200 GeV/n	up to 5.6	—	—
Luminosity ( $10^{30} \text{ cm}^{-2}\text{s}^{-1}$ )	75	431	145 (pk) 90 (avg)	$3.7 \times 10^3$	$5 \times 10^3$	$1.0 \times 10^4$
Time between collisions (ns)	96	396	107	49.90	49.90	24.95
Full crossing angle ( $\mu$ rad)	0	0	0	240	$\approx 300$	$\approx 300$
Energy spread (units $10^{-3}$ )	$e$ : 0.91 $p$ : 0.2	0.14	0.15	0.116	0.116	0.113
Bunch length (cm)	$e$ : 0.83 $p$ : 8.5	$p$ : 50 $\bar{p}$ : 45	70	9	9	7.5
Beam radius ( $10^{-6}$ m)	$e$ : 110( $H$ ), 30( $V$ ) $p$ : 111( $H$ ), 30( $V$ )	$p$ : 28 $\bar{p}$ : 16	90	26	20	16.6
Free space at interaction point (m)	$\pm 2$	$\pm 6.5$	16	38	38	38
Initial luminosity decay time, $-L/(dL/dt)$ (hr)	10	6 (avg)	5.5	8	8	14.9
Turn-around time (min)	$e$ : 75, $p$ : 135	90	200	$\approx 180$	$\approx 180$	$\approx 180$
Injection energy (TeV)	$e$ : 0.012 $p$ : 0.040	0.15	0.023	0.450	0.450	0.450
Transverse emittance ( $10^{-9}\pi$ rad-m)	$e$ : 20( $H$ ), 3.5( $V$ ) $p$ : 5( $H$ ), 5( $V$ )	$p$ : 3 $\bar{p}$ : 1	15	0.7	0.6	0.5
$\beta^*$ , ampl. function at interaction point (m)	$e$ : 0.6( $H$ ), 0.26( $V$ ) $p$ : 2.45( $H$ ), 0.18( $V$ )	0.28	0.6	1.0	0.6	0.55
Beam-beam tune shift per crossing (units $10^{-4}$ )	$e$ : 190( $H$ ), 450( $V$ ) $p$ : 12( $H$ ), 9( $V$ )	$p$ : 120 $\bar{p}$ : 120	50	23	60	34
RF frequency (MHz)	$e$ : 499.7 $p$ : 208.2/52.05	53	accel: 9 store: 28	400.8	400.8	400.8
Particles per bunch (units $10^{10}$ )	$e$ : 3 $p$ : 7	$p$ : 26 $\bar{p}$ : 9	16.5	15	15	11.5
Bunches per ring per species	$e$ : 189 $p$ : 180	36	109	1380	1380	2808
Average beam current per species (mA)	$e$ : 40 $p$ : 90	$p$ : 70 $\bar{p}$ : 24	180	374	374	584
Circumference (km)	6.336	6.28	3.834	26.659		
Interaction regions	2 colliding beams 1 fixed target ( $e$ beam)	2 high $\mathcal{L}$	6 total, 2 high $\mathcal{L}$	4 total, 2 high $\mathcal{L}$		
Magnetic length of dipole (m)	$e$ : 9.185 $p$ : 8.82	6.12	9.45	14.3		
Length of standard cell (m)	$e$ : 23.5 $p$ : 47	59.5	29.7	106.90		
Phase advance per cell (deg)	$e$ : 60 $p$ : 90	67.8	84	90		
Dipoles in ring	$e$ : 396 $p$ : 416	774	192 per ring + 12 common	1232 main dipoles		
Quadrupoles in ring	$e$ : 580 $p$ : 280	216	246 per ring	482 2-in-1 24 1-in-1		
Magnet type	$e$ : C-shaped $p$ : s.c., collared, cold iron	s.c. $\cos\theta$ warm iron	s.c. $\cos\theta$ cold iron	s.c. 2 in 1 cold iron		
Peak magnetic field (T)	$e$ : 0.274, $p$ : 5	4.4	3.5	8.3		

\*Additional TEVATRON parameters:  $\bar{p}$  source accum. rate:  $25 \times 10^{10} \text{ hr}^{-1}$ ; max. no. of  $\bar{p}$  stored:  $3.4 \times 10^{12}$  (Accumulator),  $6.1 \times 10^{12}$  (Recycler).

## HIGH-ENERGY COLLIDER PARAMETERS: Heavy Ion Colliders

Updated in early 2012 with numbers received from representatives of the colliders (contact J. Beringer, LBNL). The table shows parameter values as achieved by January 1, 2012. For LHC, the parameters expected for running in 2012 and nominal values are also given. Quantities are, where appropriate, r.m.s.; unless noted otherwise, energies refer to beam energy; s.c. stands for superconducting; pk and avg denote peak and average values.

	RHIC (Brookhaven)			LHC (CERN)		
	2000	2004	2002	2010	2012 (expected)	nominal
Physics start date	2000	2004	2002	2010	2012 (expected)	nominal
Physics end date	—			—		
Particles collided	Au Au	Cu Cu	d Au	Pb Pb	p Pb	Pb Pb
Maximum beam energy (TeV/n)	0.1	0.1	0.1	1.38	<i>p</i> : 4 <i>Pb</i> : 1.58	2.76
$\sqrt{s_{NN}}$ (TeV)	0.2	0.2	0.2	2.76	5.0	5.5
Delivered int. nucleon-pair lumin. per exp. ( $\text{pb}^{-1}$ )	up to 568 (at 100 GeV/n)	up to 65 (at 100 GeV/n)	up to 103 (at 100 GeV/n)	$\approx 7.4$	—	—
Luminosity ( $10^{27} \text{ cm}^{-2}\text{s}^{-1}$ )	5.0 (pk) 3.0 (avg)	20 (pk) 0.8 (avg)	270 (pk) 140 (avg)	0.5	85	1.0
Time between collisions (ns)	107	321	107	199.6	99.8	99.8
Full crossing angle ( $\mu$ rad)	0	0	0	160	160	$\leq 100$
Energy spread (units $10^{-3}$ )	0.75	0.75	0.75	0.11	0.11	0.11
Bunch length (cm)	30	30	30	9.7	<i>p</i> : 9 <i>Pb</i> : 9.7	7.9
Beam radius ( $10^{-6}$ m)	135	145	145	50	23	15.9
Free space at interaction point (m)	16	16	16	38	38	38
Initial luminosity decay time, $-L/(dL/dt)$ (hr)	1.2	1.8	1.5	5	$\approx 8$	$10.9 - 3.6^{\ddagger}$
Turn-around time (min)	100	145	145	180	$\approx 200$	$\approx 180$
Injection energy (TeV)	0.011 TeV/n	0.011 TeV/n	0.012 TeV/n	0.177 TeV/n	<i>p</i> : 0.45 TeV/n <i>Pb</i> : 0.177 TeV/n	0.177 TeV/n
Transverse emittance ( $10^{-9}\pi$ rad-m)	23	23	25	1.0	0.9	0.5
$\beta^*$ , ampl. function at interaction point (m)	0.75	0.9	0.85	1.0	0.6	0.5
Beam-beam tune shift per crossing (units $10^{-4}$ )	16	30	d: 21 Au: 17	3	4	2
RF frequency (MHz)	accel: 28 store: 197	accel: 28 store: 197	accel: 28 store: 197	400.8	400.8	400.8
Particles per bunch (units $10^{10}$ )	0.13	0.45	d: 10 Au: 0.1	0.011 (r.m.s.)	<i>p</i> : 1.1 <i>Pb</i> : 0.008	0.007
Bunches per ring per species	111	37	95	356	560	592
Average beam current per species (mA)	145	60	d: 119 Au: 94	6.85	<i>p</i> : 11 <i>Pb</i> : 9.9	6.12
Circumference (km)	3.834			26.659		
Interaction regions	6 total, 2 high $\mathcal{L}$			1 dedicated +2	3 high $\mathcal{L}$ +1	1 dedicated +2
Magnetic length of dipole (m)	9.45			14.3		
Length of standard cell (m)	29.7			106.90		
Phase advance per cell (deg)	93	84	d: 84 Au: 93	90		
Dipoles in ring	192 per ring + 12 common			1232 main dipoles		
Quadrupoles in ring	246 per ring			482 2-in-1 24 1-in-1		
Magnet type	s.c. $\cos\theta$ cold iron			s.c. 2 in 1 cold iron		
Peak magnetic field (T)	3.5			8.3		

$\ddagger$ For 1 - 3 experiments.

## 29. NEUTRINO BEAM LINES AT HIGH-ENERGY PROTON SYNCHROTRONS

Created in May 2012 with numbers verified by representatives of the synchrotrons (contact C.-J. Lin, LBNL). For existing (future) neutrino beam lines the latest achieved (design) values are given.

The main source of neutrinos at proton synchrotrons is from the decay of pions and kaons produced by protons striking a nuclear target. There are different schemes to focus the secondary particles to enhance neutrino flux and/or tune the neutrino energy profile. In wide-band beams (WBB), the neutrino parent mesons are focused over a wide momentum range to obtain maximum neutrino intensity. In narrow-band beams (NBB), the secondary particles are first momentum-selected to produce a monochromatic parent beam. Another approach to generate a narrow-band neutrino spectrum is to select neutrinos that decay off-axis relative to the momentum of the parent mesons. For a comprehensive review of the topic, including other historical neutrino beam lines, see the article by S. E. Kopp, "Accelerator-based neutrino beams," Phys. Rept. **439**, 101 (2007).

	PS (CERN)				SPS (CERN)				PS (KEK)	Main Ring (JPARC)
	1963	1969	1972	1983	1977	1977	1995	2006	1999	2009
Date	1963	1969	1972	1983	1977	1977	1995	2006	1999	2009
Proton Kinetic Energy (GeV)	20.6	20.6	26	19	350	350	450	400	12	30 (50)
Protons per Pulse ( $10^{12}$ )	0.7	0.6	5	5	10	10	18	50	6	135 (330)
Cycle Time (s)	3	2.3	-	-	-	-	14.4	6	2.2	2.56 (3.5)
Beam Power (kW)	0.8	0.9	-	-	-	-	55	510	5	250 (750)
Secondary Focussing	1-horn WBB	3-horn WBB	2-horn WBB	bare target	dichromatic NBB	2-horn WBB	2-horn WBB	2-horn WBB	2-horn WBB	3-horn off-axis
Decay Pipe Length (m)	60	60	60	45	290	290	290	994	200	96
$\langle E_\nu \rangle$ (GeV)	1.5	1.5	1.5	1	50,150 <sup>†</sup>	20	24.3	17	1.3	0.6
Experiments	HLBC, Spark Ch.	HLBC, Spark Ch.	GGM, Aachen-Padova	CDHS, CHARM	CDHS, CHARM, BEBC	GGM, CDHS, CHARM, BEBC	NOMAD, CHORUS	OPERA, INCARUS	K2K	T2K

	Main Ring (Fermilab)							Booster (Fermilab)	Main Injector (Fermilab)	
	1975	1975	1974	1979	1976	1991	1998	2002	2005	2013
Date	1975	1975	1974	1979	1976	1991	1998	2002	2005	2013
Proton Kinetic Energy (GeV)	300,400	300,400	300	400	350	800	800	8	120	120
Protons per Pulse ( $10^{12}$ )	10	10	10	10	13	10	12	4.5	37	(49)
Cycle Time (s)	-	-	-	-	-	60	60	0.5	2	(1.333)
Beam Power (kW)	-	-	-	-	-	20	25	12	350	(700)
Secondary Focussing	bare target	quad trip., SSBT	dichromatic NBB	2-horn WBB	1-horn WBB	quad trip.	SSQT WBB	1-horn WBB	2-horn WBB	2-horn off-axis
Decay Pipe Length (m)	350	350	400	400	400	400	400	50	675	675
$\langle E_\nu \rangle$ (GeV)	40	50,180 <sup>†</sup>	50,180 <sup>†</sup>	25	100	90,260	70,180	1	3-20 <sup>‡</sup>	2
Experiments	HPWF	CITF, HPWF	CITF, HPWF, 15' BC	15' BC	HPWF 15' BC	15' BC, CCFRR	NuTeV	MiniBooNE, SciBooNE	MINOS, MINERνA	NOνA, MINERνA, MINOS+

<sup>†</sup>Pion and kaon peaks in the momentum-selected channel.

<sup>‡</sup>Tunable WBB energy spectrum.



## 30. PASSAGE OF PARTICLES THROUGH MATTER

Revised January 2012 by H. Bichsel (University of Washington),  
D.E. Groom (LBNL), and S.R. Klein (LBNL).

30. PASSAGE OF PARTICLES THROUGH MATTER . . . . .	323
30.1. Notation . . . . .	323
30.2. Electronic energy loss by heavy particles . . . . .	323
30.2.1. Moments and cross sections . . . . .	323
30.2.2. Stopping power at intermediate energies . . . . .	324
30.2.3. Energy loss at low energies . . . . .	326
30.2.4. Density effect . . . . .	326
30.2.5. Energetic knock-on electrons ( $\delta$ rays) . . . . .	326
30.2.6. Restricted energy loss rates for relativistic ionizing particles . . . . .	327
30.2.7. Fluctuations in energy loss . . . . .	327
30.2.8. Energy loss in mixtures and compounds . . . . .	328
30.2.9. Ionization yields . . . . .	328
30.3. Multiple scattering through small angles . . . . .	328
30.4. Photon and electron interactions in matter . . . . .	329
30.4.1. Radiation length . . . . .	329
30.4.2. Energy loss by electrons . . . . .	330
30.4.3. Critical energy . . . . .	331
30.4.4. Energy loss by photons . . . . .	332
30.4.5. Bremsstrahlung and pair production at very high energies . . . . .	332
30.4.6. Photonuclear and electronuclear interactions at still higher energies . . . . .	332
30.5. Electromagnetic cascades . . . . .	333
30.6. Muon energy loss at high energy . . . . .	334
30.7. Cherenkov and transition radiation . . . . .	335
30.7.1. Optical Cherenkov radiation . . . . .	335
30.7.2. Coherent radio Cherenkov radiation . . . . .	335
30.7.3. Transition radiation . . . . .	336

## 30.1. Notation

**Table 30.1:** Summary of variables used in this section. The kinematic variables  $\beta$  and  $\gamma$  have their usual meanings.

Symbol	Definition	Units or Value
$\alpha$	Fine structure constant ( $e^2/4\pi\epsilon_0\hbar c$ )	1/137.035 999 11(46)
$M$	Incident particle mass	MeV/ $c^2$
$E$	Incident part. energy $\gamma Mc^2$	MeV
$T$	Kinetic energy	MeV
$m_e c^2$	Electron mass $\times c^2$	0.510 998 918(44) MeV
$r_e$	Classical electron radius $e^2/4\pi\epsilon_0 m_e c^2$	2.817 940 325(28) fm
$N_A$	Avogadro's number	$6.022 1415(10) \times 10^{23}$ mol $^{-1}$
$ze$	Charge of incident particle	
$Z$	Atomic number of absorber	
$A$	Atomic mass of absorber	g mol $^{-1}$
$K/A$	$4\pi N_A r_e^2 m_e c^2 / A$	0.307 075 MeV g $^{-1}$ cm $^2$ for $A = 1$ g mol $^{-1}$
$I$	Mean excitation energy	eV ( <i>Nota bene!</i> )
$\delta(\beta\gamma)$	Density effect correction to ionization energy loss	
$\hbar\omega_p$	Plasma energy ( $\sqrt{4\pi N_e r_e^3} m_e c^2 / \alpha$ )	$\sqrt{\rho(Z/A)} \times 28.816$ eV ( $\rho$ in g cm $^{-3}$ )
$N_e$	Electron density	(units of $r_e$ ) $^{-3}$
$w_j$	Weight fraction of the $j$ th element in a compound or mixture	
$n_j$	$\alpha$ number of $j$ th kind of atoms in a compound or mixture	
—	$4\alpha r_e^2 N_A / A$	(716.408 g cm $^{-2}$ ) $^{-1}$ for $A = 1$ g mol $^{-1}$
$X_0$	Radiation length	g cm $^{-2}$
$E_c$	Critical energy for electrons	MeV
$E_{\mu c}$	Critical energy for muons	GeV
$E_s$	Scale energy $\sqrt{4\pi/\alpha} m_e c^2$	21.2052 MeV
$R_M$	Molière radius	g cm $^{-2}$

## 30.2. Electronic energy loss by heavy particles [1–34]

## 30.2.1. Moments and cross sections :

The electronic interactions of fast charged particles with speed  $v = \beta c$  occur in *single collisions with energy losses*  $E$  [1], leading to ionization, atomic, or collective excitation. Most frequently the energy losses are small (for 90% of all collisions the energy losses are less than 100 eV). In thin absorbers few collisions will take place and the total energy loss will show a large variance [1]; also see Sec. 30.2.7 below. For particles with charge  $ze$  more massive than electrons (“heavy” particles), scattering from free electrons is adequately described by the Rutherford differential cross section [2], \* †

$$\frac{d\sigma_R(E; \beta)}{dE} = \frac{2\pi r_e^2 m_e c^2 z^2}{\beta^2} \frac{(1 - \beta^2 E/T_{\max})}{E^2}, \quad (30.1)$$

where  $T_{\max}$  is the maximum energy transfer possible in a single collision. But in matter electrons are not free.  $E$  must be finite and depends on atomic and bulk structure. For electrons bound

\* For spin 0 particles. The  $\beta$  dependence in the parentheses is different for spin 1/2 and spin 1 particles, but it is not important except at energies far above atomic binding energies.

† In high-energy physics  $E$  normally means total energy,  $T + mc^2$ . In stopping power discussions,  $E$  means kinetic energy, and we follow that convention (with some inconsistency).

in atoms Bethe [3] used “Born Theorie” to obtain the differential cross section

$$\frac{d\sigma_B(E; \beta)}{dE} = \frac{d\sigma_R(E, \beta)}{dE} B(E). \quad (30.2)$$

Examples of  $B(E)$  and  $d\sigma_B/dE$  can be seen in Figs. 5 and 6 of Ref. 1.

of a few %. With the symbol definitions and values given in Table 30.1, the units are  $\text{MeV g}^{-1}\text{cm}^2$ . At the lower limit the projectile velocity becomes comparable to atomic electron “velocities” (Sec. 30.2.3), and at the upper limit radiative effects begin to be important (Sec. 30.6). Both limits are  $Z$  dependent.

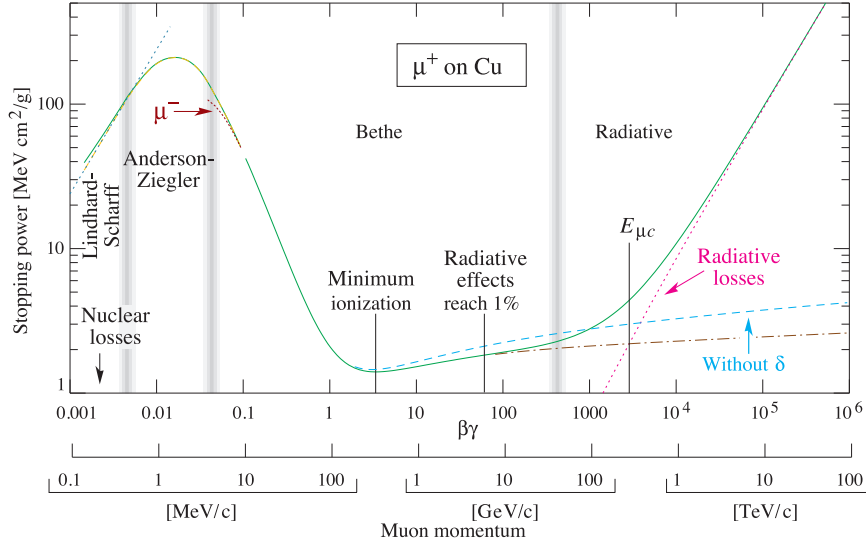


**Fig. 30.1:** Stopping power ( $= -dE/dx$ ) for positive muons in copper as a function of  $\beta\gamma = p/Mc$  over nine orders of magnitude in momentum (12 orders of magnitude in kinetic energy). Solid curves indicate the total stopping power. Data below the break at  $\beta\gamma \approx 0.1$  are taken from ICRU 49 [4], and data at higher energies are from Ref. 5. Vertical bands indicate boundaries between different approximations discussed in the text. The short dotted lines labeled “ $\mu^-$ ” illustrate the “Barkas effect,” the dependence of stopping power on projectile charge at very low energies [6].

Bethe’s theory extends only to some energy above which atomic effects were not important. The free-electron cross section (Eq. (30.1)) can be used to extend the cross section to  $T_{\max}$ . At high energies  $\sigma_B$  is further modified by polarization of the medium, and this “density effect,” discussed in Sec. 30.2.4, must also be included. Less important corrections are discussed below.

The mean number of collisions with energy loss between  $E$  and  $E + dE$  occurring in a distance  $\delta x$  is  $N_e \delta x (d\sigma/dE) dE$ , where  $d\sigma(E; \beta)/dE$  contains all contributions. It is convenient to define the moments

$$M_j(\beta) = N_e \delta x \int E^j \frac{d\sigma(E; \beta)}{dE} dE, \quad (30.3)$$

so that  $M_0$  is the mean number of collisions in  $\delta x$ ,  $M_1$  is the mean energy loss in  $\delta x$ ,  $M_2 - M_1^2$  is the variance, *etc.* The number of collisions is Poisson-distributed with mean  $M_0$ .  $N_e$  is either measured in electrons/g ( $N_e = N_A Z/A$ ) or electrons/cm<sup>3</sup> ( $N_e = N_A \rho Z/A$ ). The former is used throughout this chapter, since quantities of interest ( $dE/dx$ ,  $X_0$ , *etc.*) vary smoothly with composition when there is no density dependence.

### 30.2.2. Stopping power at intermediate energies :

The mean rate of energy loss by moderately relativistic charged heavy particles,  $M_1/\delta x$ , is well-described by the “Bethe” equation,

$$-\left\langle \frac{dE}{dx} \right\rangle = K z^2 \frac{Z}{A} \frac{1}{\beta^2} \left[ \frac{1}{2} \ln \frac{2m_e c^2 \beta^2 \gamma^2 T_{\max}}{I^2} - \beta^2 - \frac{\delta(\beta\gamma)}{2} \right]. \quad (30.4)$$

It describes the mean rate of energy loss in the region  $0.1 \lesssim \beta\gamma \lesssim 1000$  for intermediate- $Z$  materials with an accuracy

Here  $T_{\max}$  is the maximum kinetic energy which can be imparted to a free electron in a single collision, and the other variables are defined in Table 30.1. A minor dependence on  $M$  at the highest energies is introduced through  $T_{\max}$ , but for all practical purposes  $\langle dE/dx \rangle$  in a given material is a function of  $\beta$  alone.

For heavy projectiles, like ions, additional terms are required to account for higher-order photon coupling to the target, and to account for the finite size of the target radius. These can change  $dE/dx$  by a factor of two or more for the heaviest nuclei in certain kinematic regimes [7].

Few concepts in high-energy physics are as misused as  $\langle dE/dx \rangle$ . The main problem is that the mean is weighted by very rare events with large single-collision energy deposits. Even with samples of hundreds of events a dependable value for the mean energy loss cannot be obtained. Far better and more easily measured is the most probable energy loss, discussed in Sec. 30.2.7. The most probable energy loss in a detector is considerably below the mean given by the Bethe equation.

In a TPC (Sec. 31.6.5), the mean of 50%–70% of the samples with the smallest signals is often used as an estimator.

Although it must be used with cautions and caveats,  $\langle dE/dx \rangle$  as described in Eq. (30.4) still forms the basis of much of our understanding of energy loss by charged particles. Extensive tables are available [5,4, [pdg.lbl.gov/AtomicNuclearProperties/](http://pdg.lbl.gov/AtomicNuclearProperties/)].

The function as computed for muons on copper is shown as the “Bethe” region of Fig. 30.1. Mean energy loss behavior below this region is discussed in Sec. 30.2.3, and the radiative effects at high energy are discussed in Sec. 30.6. Only in the Bethe region is it a function of  $\beta$  alone; the mass dependence

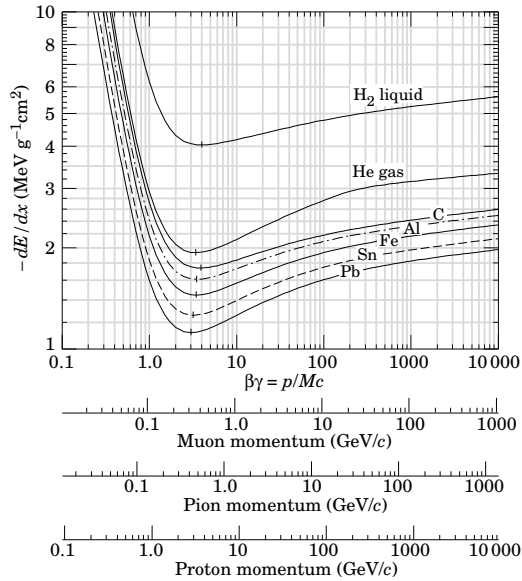


**Figure 30.2:** Mean energy loss rate in liquid (bubble chamber) hydrogen, gaseous helium, carbon, aluminum, iron, tin, and lead. Radiative effects, relevant for muons and pions, are not included. These become significant for muons in iron for  $\beta\gamma \gtrsim 1000$ , and at lower momenta for muons in higher- $Z$  absorbers. See Fig. 30.23.

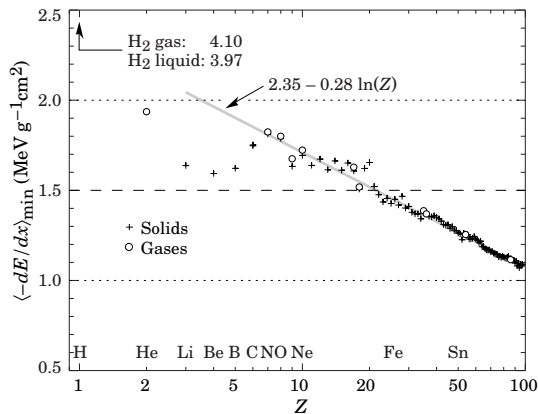


**Figure 30.3:** Stopping power at minimum ionization for the chemical elements. The straight line is fitted for  $Z > 6$ . A simple functional dependence on  $Z$  is not to be expected, since  $\langle -dE/dx \rangle$  also depends on other variables.

is more complicated elsewhere. The stopping power in several other materials is shown in Fig. 30.2. Except in hydrogen, particles with the same velocity have similar rates of energy loss in different materials, although there is a slow decrease in the rate of energy loss with increasing  $Z$ . The qualitative behavior difference at high energies between a gas (He in the figure) and the other materials shown in the figure is due to the density-effect correction,  $\delta(\beta\gamma)$ , discussed in Sec. 30.2.4. The stopping power functions are characterized by broad minima whose position drops from  $\beta\gamma = 3.5$  to  $3.0$  as  $Z$  goes from 7 to 100. The values of minimum ionization as a function of atomic number are shown in Fig. 30.3.

In practical cases, most relativistic particles (*e.g.*, cosmic-ray muons) have mean energy loss rates close to the minimum; they are “minimum-ionizing particles,” or mip’s.

Eq. (30.4) may be integrated to find the total (or partial) “continuous slowing-down approximation” (CSDA) range  $R$  for

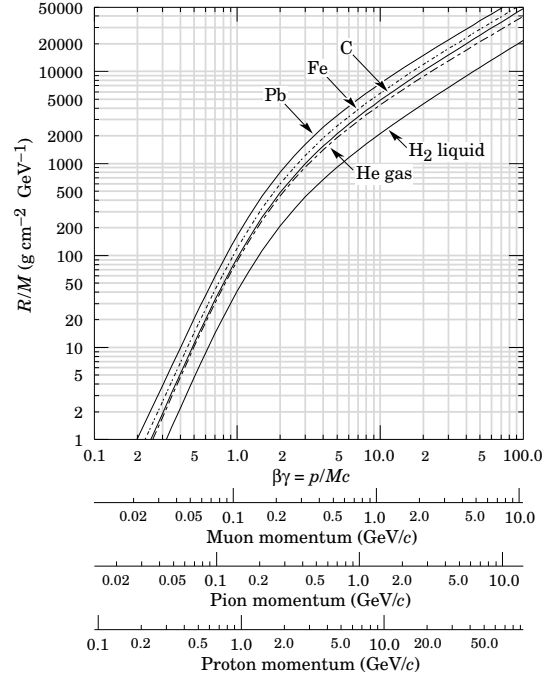


**Figure 30.4:** Range of heavy charged particles in liquid (bubble chamber) hydrogen, helium gas, carbon, iron, and lead. For example: For a  $K^+$  whose momentum is 700 MeV/c,  $\beta\gamma = 1.42$ . For lead we read  $R/M \approx 396$ , and so the range is  $195 \text{ g cm}^{-2}$ .

a particle which loses energy only through ionization and atomic excitation. Since  $dE/dx$  depends only on  $\beta$ ,  $R/M$  is a function of  $E/M$  or  $pc/M$ . In practice, range is a useful concept only for low-energy hadrons ( $R \lesssim \lambda_I$ , where  $\lambda_I$  is the nuclear interaction length), and for muons below a few hundred GeV (above which radiative effects dominate).  $R/M$  as a function of  $\beta\gamma = p/Mc$  is shown for a variety of materials in Fig. 30.4.

The mass scaling of  $dE/dx$  and range is valid for the electronic losses described by the Bethe equation, but not for radiative losses, relevant only for muons and pions.

For a particle with mass  $M$  and momentum  $M\beta\gamma c$ ,  $T_{\max}$  is given by

$$T_{\max} = \frac{2m_e c^2 \beta^2 \gamma^2}{1 + 2\gamma m_e/M + (m_e/M)^2}. \quad (30.5)$$

In older references [2,8] the “low-energy” approximation  $T_{\max} = 2m_e c^2 \beta^2 \gamma^2$ , valid for  $2\gamma m_e/M \ll 1$ , is often implicit. For a pion in copper, the error thus introduced into  $dE/dx$  is greater than 6% at 100 GeV.

At energies of order 100 GeV, the maximum 4-momentum transfer to the electron can exceed 1 GeV/c, where hadronic structure effects significantly modify the cross sections. This problem has been investigated by J.D. Jackson [9], who concluded that for hadrons (but not for large nuclei) corrections to  $dE/dx$  are negligible below energies where radiative effects dominate. While the cross section for rare hard collisions is modified, the average stopping power, dominated by many softer collisions, is almost unchanged.

“The determination of the mean excitation energy is the principal non-trivial task in the evaluation of the Bethe stopping-power formula” [10]. Recommended values have varied substantially with time. Estimates based on experimental stopping-power measurements for protons, deuterons, and alpha particles and on oscillator-strength distributions and dielectric-response functions were given in ICRU 49 [4]. See also ICRU

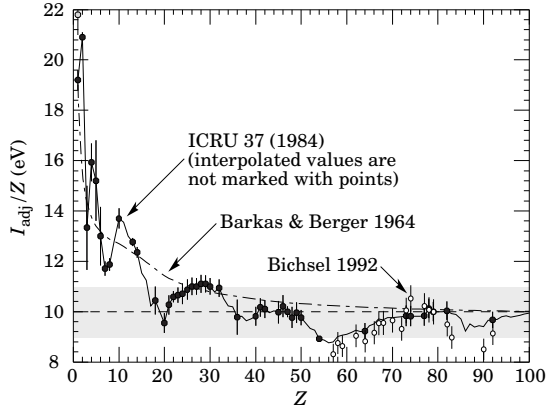


**Figure 30.5:** Mean excitation energies (divided by  $Z$ ) as adopted by the ICRU [11]. Those based on experimental measurements are shown by symbols with error flags; the interpolated values are simply joined. The grey point is for liquid  $H_2$ ; the black point at 19.2 eV is for  $H_2$  gas. The open circles show more recent determinations by Bichsel [13]. The dotted curve is from the approximate formula of Barkas [14] used in early editions of this *Review*.

37 [11]. These values, shown in Fig. 30.5, have since been widely used. Machine-readable versions can also be found [12]. These values are widely used.

**30.2.3. Energy loss at low energies :** Shell corrections  $C/Z$  must be included in the square brackets of Eq. (30.4) [4,11,13,14] to correct for atomic binding having been neglected in calculating some of the contributions to Eq. (30.4). The Barkas form [14] was used in generating Fig. 30.1. For copper it contributes about 1% at  $\beta\gamma = 0.3$  (kinetic energy 6 MeV for a pion), and the correction decreases very rapidly with increasing energy.

Equation 30.2, and therefore Eq. (30.4), are based on a first-order Born approximation. Higher-order corrections, again important only at lower energies, are normally included by adding the “Bloch correction”  $z^2 L_2(\beta)$  inside the square brackets (Eq.(2.5) in [4]).

An additional “Barkas correction”  $zL_1(\beta)$  reduces the stopping power for a negative particle below that for a positive particle with the same mass and velocity. In a 1956 paper, Barkas *et al.* noted that negative pions had a longer range than positive pions [6]. The effect has been measured for a number of negative/positive particle pairs, including a detailed study with antiprotons [15].

A detailed discussion of low-energy corrections to the Bethe formula is given in ICRU Report 49 [4]. When the corrections are properly included, the Bethe treatment is accurate to about 1% down to  $\beta \approx 0.05$ , or about 1 MeV for protons.

For  $0.01 < \beta < 0.05$ , there is no satisfactory theory. For protons, one usually relies on the phenomenological fitting formulae developed by Andersen and Ziegler [4,16]. As shown in ICRU 49 [4] (using data taken from Ref. 16), the nuclear plus electronic proton stopping power in copper is  $113 \text{ MeV cm}^2 \text{ g}^{-1}$  at  $T = 10 \text{ keV}$ , rises to a maximum of  $210 \text{ MeV cm}^2 \text{ g}^{-1}$  at 100–150 keV, then falls to  $120 \text{ MeV cm}^2 \text{ g}^{-1}$  at 1 MeV.

For particles moving more slowly than  $\approx 0.01c$  (more or less the velocity of the outer atomic electrons), Lindhard has been quite successful in describing electronic stopping power, which is proportional to  $\beta$  [17]. Finally, we note that at even lower energies, *e.g.*, for protons of less than several hundred eV, non-ionizing nuclear recoil energy loss dominates the total energy loss [4,17,18].

**30.2.4. Density effect :** As the particle energy increases, its electric field flattens and extends, so that the distant-collision contribution to Eq. (30.4) increases as  $\ln \beta\gamma$ . However, real media become polarized, limiting the field extension and effectively truncating this part of the logarithmic rise [2–8,19–21]. At very high energies,

$$\delta/2 \rightarrow \ln(\hbar\omega_p/I) + \ln \beta\gamma - 1/2, \quad (30.6)$$

where  $\delta(\beta\gamma)/2$  is the density effect correction introduced in Eq. (30.4) and  $\hbar\omega_p$  is the plasma energy defined in Table 30.1. A comparison with Eq. (30.4) shows that  $|dE/dx|$  then grows as  $\ln \beta\gamma$  rather than  $\ln \beta^2\gamma^2$ , and that the mean excitation energy  $I$  is replaced by the plasma energy  $\hbar\omega_p$ . The ionization stopping power as calculated with and without the density effect correction is shown in Fig. 30.1. Since the plasma frequency scales as the square root of the electron density, the correction is much larger for a liquid or solid than for a gas, as is illustrated by the examples in Fig. 30.2.

The density effect correction is usually computed using Sternheimer’s parameterization [19]:

$$\delta(\beta\gamma) = \begin{cases} 2(\ln 10)x - \bar{C} & \text{if } x \geq x_1; \\ 2(\ln 10)x - \bar{C} + a(x_1 - x)^k & \text{if } x_0 \leq x < x_1; \\ 0 & \text{if } x < x_0 \text{ (nonconductors);} \\ \delta_0 10^{2(x-x_0)} & \text{if } x < x_0 \text{ (conductors)} \end{cases} \quad (30.7)$$

Here  $x = \log_{10} \eta = \log_{10}(p/Mc)$ .  $\bar{C}$  (the negative of the  $C$  used in Ref. 19) is obtained by equating the high-energy case of Eq. (30.7) with the limit given in Eq. (30.6). The other parameters are adjusted to give a best fit to the results of detailed calculations for momenta below  $Mc \exp(x_1)$ . Parameters for elements and nearly 200 compounds and mixtures of interest are published in a variety of places, notably in Ref. 21. A recipe for finding the coefficients for nontabulated materials is given by Sternheimer and Peierls [22], and is summarized in Ref. 5.

The remaining relativistic rise comes from the  $\beta^2\gamma^2$  growth of  $T_{\max}$ , which in turn is due to (rare) large energy transfers to a few electrons. When these events are excluded, the energy deposit in an absorbing layer approaches a constant value, the Fermi plateau (see Sec. 30.2.6 below). At extreme energies (*e.g.*,  $> 332 \text{ GeV}$  for muons in iron, and at a considerably higher energy for protons in iron), radiative effects are more important than ionization losses. These are especially relevant for high-energy muons, as discussed in Sec. 30.6.

**30.2.5. Energetic knock-on electrons ( $\delta$  rays) :** The distribution of secondary electrons with kinetic energies  $T \gg I$  is [2]

$$\frac{d^2 N}{dT dx} = \frac{1}{2} K z^2 \frac{Z}{A} \frac{1}{\beta^2} \frac{F(T)}{T^2} \quad (30.8)$$

for  $I \ll T \leq T_{\max}$ , where  $T_{\max}$  is given by Eq. (30.5). Here  $\beta$  is the velocity of the primary particle. The factor  $F$  is spin-dependent, but is about unity for  $T \ll T_{\max}$ . For spin-0 particles  $F(T) = (1 - \beta^2 T/T_{\max})$ ; forms for spins 1/2 and 1 are also given by Rossi [2] (Sec. 2.3, Eqns. 7 and 8). For incident electrons, the indistinguishability of projectile and target means that the range of  $T$  extends only to half the kinetic energy of the incident particle. Additional formulae are given in Ref. 23. Equation (30.8) is inaccurate for  $T$  close to  $I$  [24].

$\delta$  rays of even modest energy are rare. For a  $\beta \approx 1$  particle, for example, on average only one collision with  $T_e > 10 \text{ keV}$  will occur along a path length of 90 cm of Ar gas [1].

A  $\delta$  ray with kinetic energy  $T_e$  and corresponding momentum  $p_e$  is produced at an angle  $\theta$  given by

$$\cos \theta = (T_e/p_e)(p_{\max}/T_{\max}), \quad (30.9)$$

where  $p_{\max}$  is the momentum of an electron with the maximum possible energy transfer  $T_{\max}$ .

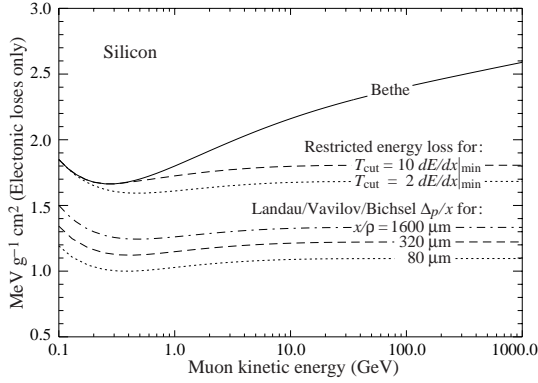


**Figure 30.6:** Bethe  $dE/dx$ , two examples of restricted energy loss, and the Landau most probable energy per unit thickness in silicon. The change of  $\Delta_p/x$  with thickness  $x$  illustrates its  $a \ln x + b$  dependence. Minimum ionization ( $dE/dx|_{\min}$ ) is  $1.664 \text{ MeV g}^{-1} \text{ cm}^2$ . Radiative losses are excluded. The incident particles are muons.

**30.2.6. Restricted energy loss rates for relativistic ionizing particles:** Further insight can be obtained by examining the mean energy deposit by an ionizing particle when energy transfers are restricted to  $T \leq T_{\text{cut}} \leq T_{\text{max}}$ . The restricted energy loss rate is

$$-\frac{dE}{dx}\Big|_{T < T_{\text{cut}}} = Kz^2 \frac{Z}{A} \frac{1}{\beta^2} \left[ \frac{1}{2} \ln \frac{2m_e c^2 \beta^2 \gamma^2 T_{\text{cut}}}{I^2} - \frac{\beta^2}{2} \left( 1 + \frac{T_{\text{cut}}}{T_{\text{max}}} \right) - \frac{\delta}{2} \right]. \quad (30.10)$$

This form approaches the normal Bethe function (Eq. (30.4)) as  $T_{\text{cut}} \rightarrow T_{\text{max}}$ . It can be verified that the difference between Eq. (30.4) and Eq. (30.10) is equal to  $\int_{T_{\text{cut}}}^{T_{\text{max}}} T(d^2N/dTdx)dT$ , where  $d^2N/dTdx$  is given by Eq. (30.8).

Since  $T_{\text{cut}}$  replaces  $T_{\text{max}}$  in the argument of the logarithmic term of Eq. (30.4), the  $\beta\gamma$  term producing the relativistic rise in the close-collision part of  $dE/dx$  is replaced by a constant, and  $|dE/dx|_{T < T_{\text{cut}}}$  approaches the constant “Fermi plateau.” (The density effect correction  $\delta$  eliminates the explicit  $\beta\gamma$  dependence produced by the distant-collision contribution.) This behavior is illustrated in Fig. 30.6, where restricted loss rates for two examples of  $T_{\text{cut}}$  are shown in comparison with the full Bethe  $dE/dx$  and the Landau-Vavilov most probable energy loss (to be discussed in Sec. 30.2.7 below).

**30.2.7. Fluctuations in energy loss:** For detectors of moderate thickness  $x$  (e.g. scintillators or LAr cells),\* the energy loss probability distribution  $f(\Delta; \beta\gamma, x)$  is adequately described by the highly-skewed Landau (or Landau-Vavilov) distribution [25,26]. The most probable energy loss is [27]

$$\Delta_p = \xi \left[ \ln \frac{2m_e c^2 \beta^2 \gamma^2}{I} + \ln \frac{\xi}{I} + j - \beta^2 - \delta(\beta\gamma) \right], \quad (30.11)$$

where  $\xi = (K/2) \langle Z/A \rangle (x/\beta^2) \text{ MeV}$  for a detector with a thickness  $x$  in  $\text{g cm}^{-2}$ , and  $j = 0.200$  [27]. † While  $dE/dx$  is independent of thickness,  $\Delta_p/x$  scales as  $a \ln x + b$ . The density correction  $\delta(\beta\gamma)$  was not included in Landau’s or Vavilov’s work, but it was later included by Bichsel [27]. The high-energy

behavior of  $\delta(\beta\gamma)$  (Eq. (30.6)) is such that

$$\Delta_p \xrightarrow{\beta\gamma \gtrsim 100} \xi \left[ \ln \frac{2m_e c^2 \xi}{(\hbar\omega_p)^2} + j \right]. \quad (30.12)$$

Thus the Landau-Vavilov most probable energy loss, like the restricted energy loss, reaches a Fermi plateau. The Bethe  $dE/dx$  and Landau-Vavilov-Bichsel  $\Delta_p/x$  in silicon are shown as a function of muon energy in Fig. 30.6. The energy deposit in the  $1600 \mu\text{m}$  case is roughly the same as in a  $3 \text{ mm}$  thick plastic scintillator.

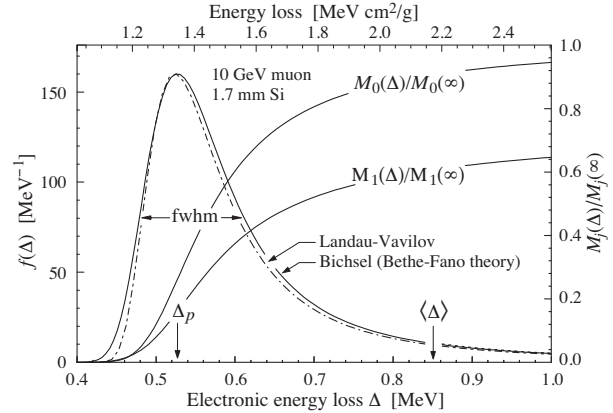


**Figure 30.7:** Electronic energy deposit distribution for a 10 GeV muon traversing 1.7 mm of silicon, the stopping power equivalent of about 0.3 cm of PVC scintillator [1,13,29]. The Landau-Vavilov function (dot-dashed) uses a Rutherford cross section without atomic binding corrections but with a kinetic energy transfer limit of  $T_{\text{max}}$ . The solid curve was calculated using Bethe-Fano theory.  $M_0(\Delta)$  and  $M_1(\Delta)$  are the cumulative 0th moment (mean number of collisions) and 1st moment (mean energy loss) in crossing the silicon. (See Sec. 30.2.1. The fwhm of the Landau-Vavilov function is about  $4\xi$  for detectors of moderate thickness.  $\Delta_p$  is the most probable energy loss, and  $\langle\Delta\rangle$  divided by the thickness is the Bethe  $\langle dE/dx \rangle$ .)

The distribution function for the energy deposit by a 10 GeV muon going through a detector of about this thickness is shown in Fig. 30.7. In this case the most probable energy loss is 62% of the mean ( $M_1(\langle\Delta\rangle)/M_1(\infty)$ ). Folding in experimental resolution displaces the peak of the distribution, usually toward a higher value. 90% of the collisions ( $M_1(\langle\Delta\rangle)/M_1(\infty)$ ) contribute to energy deposits below the mean. It is the very rare high-energy-transfer collisions, extending to  $T_{\text{max}}$  at several GeV, that drives the mean into the tail of the distribution. *The mean of the energy loss given by the Bethe equation, Eq. (30.4), is thus ill-defined experimentally and is not useful for describing energy loss by single particles.\** It rises as  $\ln \beta\gamma$  because  $T_{\text{max}}$  increases as  $\beta^2 \gamma^2$ . The large single-collision energy transfers that increasingly extend the long tail are rare, making the mean of an experimental distribution consisting of a few hundred events subject to large fluctuations and sensitive to cuts. *The most probable energy loss should be used.†*

The Landau distribution fails to describe energy loss in thin absorbers such as gas TPC cells [1] and Si detectors [27], as shown clearly in Fig. 1 of Ref. 1 for an argon-filled TPC cell. Also

\* It does find application in dosimetry, where only bulk deposit is relevant.

† An alternative approach is taken in TPC analysis, where some fraction of the highest energy deposit signals along a track, e.g. 20%, are discarded before taking the average.

\*  $G \lesssim 0.05\text{--}0.1$ , where  $G$  is given by Rossi [Ref. 2, Eq. 2.7.10]. It is Vavilov’s  $\kappa$  [26].

† Rossi [2], Talman [28], and others give somewhat different values for  $j$ . The most probable loss is not sensitive to its value.



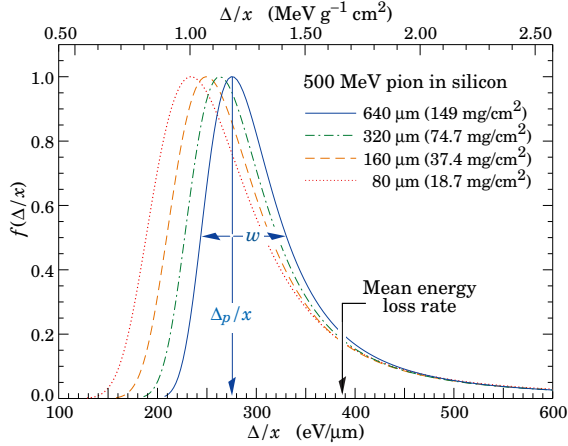


**Figure 30.8:** Straggling functions in silicon for 500 MeV pions, normalized to unity at the most probable value  $\delta_p/x$ . The width  $w$  is the full width at half maximum.

see Talman [28]. While  $\Delta_p/x$  may be calculated adequately with Eq. (30.11), the distributions are significantly wider than the Landau width  $w = 4\xi$  [Ref. 27, Fig. 15]. Examples for 500 MeV pions incident on thin silicon detectors are shown in Fig. 30.8. For very thick absorbers the distribution is less skewed but never approaches a Gaussian.

The most probable energy loss, scaled to the mean loss at minimum ionization, is shown in Fig. 30.9 for several silicon detector thicknesses.

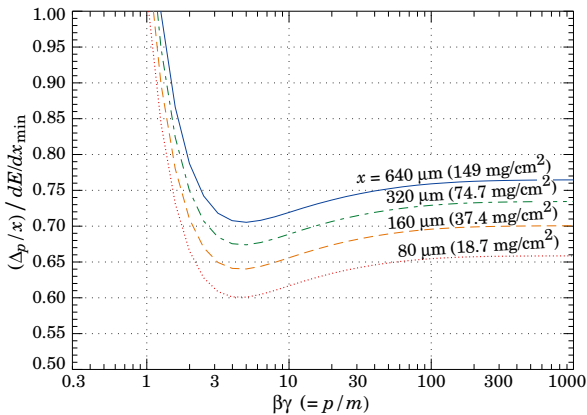


**Figure 30.9:** Most probable energy loss in silicon, scaled to the mean loss of a minimum ionizing particle,  $388 \text{ eV}/\mu\text{m}$  ( $1.66 \text{ MeV g}^{-1} \text{ cm}^2$ ).

**30.2.8. Energy loss in mixtures and compounds :** A mixture or compound can be thought of as made up of thin layers of pure elements in the right proportion (Bragg additivity). In this case,

$$\frac{dE}{dx} = \sum w_j \left. \frac{dE}{dx} \right|_j, \quad (30.13)$$

where  $dE/dx|_j$  is the mean rate of energy loss (in  $\text{MeV g cm}^{-2}$ ) in the  $j$ th element. Eq. (30.4) can be inserted into Eq. (30.13) to find expressions for  $\langle Z/A \rangle$ ,  $\langle I \rangle$ , and  $\langle \delta \rangle$ ; for example,  $\langle Z/A \rangle = \sum w_j Z_j/A_j = \sum n_j Z_j / \sum n_j A_j$ . However,  $\langle I \rangle$  as defined this way is an underestimate, because in a compound electrons are more tightly bound than in the free elements, and  $\langle \delta \rangle$  as calculated this way has little relevance, because it is the electron density that matters. If possible, one uses the tables given in Refs. 21 and 30, which include effective excitation energies and interpolation coefficients for calculating the density effect correction for the chemical elements and nearly 200 mixtures and com-

pounds. If a compound or mixture is not found, then one uses the recipe for  $\delta$  given in Ref. 22 (repeated in Ref. 5), and calculates  $\langle I \rangle$  according to the discussion in Ref. 10. (Note the “13%” rule!)

**30.2.9. Ionization yields :** Physicists frequently relate total energy loss to the number of ion pairs produced near the particle’s track. This relation becomes complicated for relativistic particles due to the wandering of energetic knock-on electrons whose ranges exceed the dimensions of the fiducial volume. For a qualitative appraisal of the nonlocality of energy deposition in various media by such modestly energetic knock-on electrons, see Ref. 31. The mean local energy dissipation per local ion pair produced,  $W$ , while essentially constant for relativistic particles, increases at slow particle speeds [32]. For gases,  $W$  can be surprisingly sensitive to trace amounts of various contaminants [32]. Furthermore, ionization yields in practical cases may be greatly influenced by such factors as subsequent recombination [33].

### 30.3. Multiple scattering through small angles

A charged particle traversing a medium is deflected by many small-angle scatters. Most of this deflection is due to Coulomb scattering from nuclei, and hence the effect is called multiple Coulomb scattering. (However, for hadronic projectiles, the strong interactions also contribute to multiple scattering.) The Coulomb scattering distribution is well represented by the theory of Molière [35]. It is roughly Gaussian for small deflection angles, but at larger angles (greater than a few  $\theta_0$ , defined below) it behaves like Rutherford scattering, with larger tails than does a Gaussian distribution.

If we define

$$\theta_0 = \theta_{\text{plane}}^{\text{rms}} = \frac{1}{\sqrt{2}} \theta_{\text{space}}^{\text{rms}}. \quad (30.14)$$

then it is sufficient for many applications to use a Gaussian approximation for the central 98% of the projected angular distribution, with a width given by [36,37]

$$\theta_0 = \frac{13.6 \text{ MeV}}{\beta c p} z \sqrt{x/X_0} \left[ 1 + 0.038 \ln(x/X_0) \right]. \quad (30.15)$$

Here  $p$ ,  $\beta c$ , and  $z$  are the momentum, velocity, and charge number of the incident particle, and  $x/X_0$  is the thickness of the scattering medium in radiation lengths (defined below). This value of  $\theta_0$  is from a fit to Molière distribution for singly charged particles with  $\beta = 1$  for all  $Z$ , and is accurate to 11% or better for  $10^{-3} < x/X_0 < 100$ .

Eq. (30.15) describes scattering from a single material, while the usual problem involves the multiple scattering of a particle traversing many different layers and mixtures. Since it is from a fit to a Molière distribution, it is incorrect to add the individual  $\theta_0$  contributions in quadrature; the result is systematically too small. It is much more accurate to apply Eq. (30.15) once, after finding  $x$  and  $X_0$  for the combined scatterer.

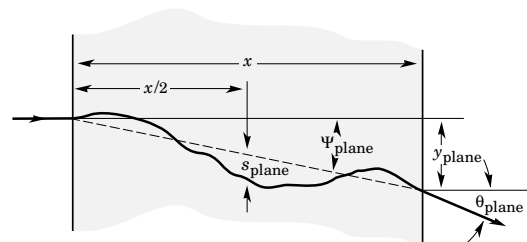


**Figure 30.10:** Quantities used to describe multiple Coulomb scattering. The particle is incident in the plane of the figure.

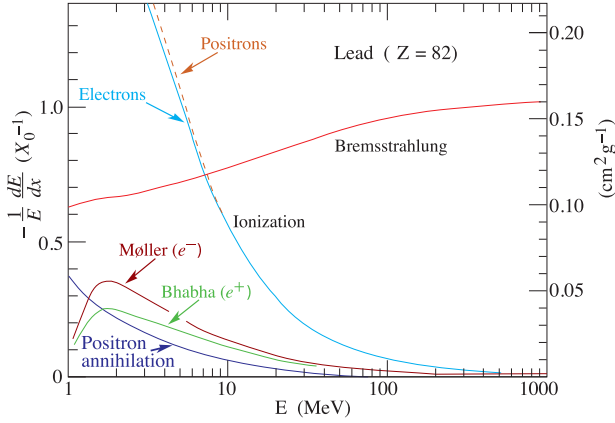


**Figure 30.11:** Fractional energy loss per radiation length in lead as a function of electron or positron energy. Electron (positron) scattering is considered as ionization when the energy loss per collision is below 0.255 MeV, and as Møller (Bhabha) scattering when it is above. Adapted from Fig. 3.2 from Messel and Crawford, *Electron-Photon Shower Distribution Function Tables for Lead, Copper, and Air Absorbers*, Pergamon Press, 1970. Messel and Crawford use  $X_0(\text{Pb}) = 5.82 \text{ g/cm}^2$ , but we have modified the figures to reflect the value given in the Table of Atomic and Nuclear Properties of Materials ( $X_0(\text{Pb}) = 6.37 \text{ g/cm}^2$ ).

The nonprojected (space) and projected (plane) angular distributions are given approximately by [35]

$$\frac{1}{2\pi\theta_0^2} \exp\left[-\frac{\theta_{\text{space}}^2}{2\theta_0^2}\right] d\Omega, \quad (30.16)$$

$$\frac{1}{\sqrt{2\pi}\theta_0} \exp\left[-\frac{\theta_{\text{plane}}^2}{2\theta_0^2}\right] d\theta_{\text{plane}}, \quad (30.17)$$

where  $\theta$  is the deflection angle. In this approximation,  $\theta_{\text{space}}^2 \approx (\theta_{\text{plane},x}^2 + \theta_{\text{plane},y}^2)$ , where the  $x$  and  $y$  axes are orthogonal to the direction of motion, and  $d\Omega \approx d\theta_{\text{plane},x} d\theta_{\text{plane},y}$ . Deflections into  $\theta_{\text{plane},x}$  and  $\theta_{\text{plane},y}$  are independent and identically distributed.

Fig. 30.10 shows these and other quantities sometimes used to describe multiple Coulomb scattering. They are

$$\psi_{\text{plane}}^{\text{rms}} = \frac{1}{\sqrt{3}} \theta_{\text{plane}}^{\text{rms}} = \frac{1}{\sqrt{3}} \theta_0, \quad (30.18)$$

$$y_{\text{plane}}^{\text{rms}} = \frac{1}{\sqrt{3}} x \theta_{\text{plane}}^{\text{rms}} = \frac{1}{\sqrt{3}} x \theta_0, \quad (30.19)$$

$$s_{\text{plane}}^{\text{rms}} = \frac{1}{4\sqrt{3}} x \theta_{\text{plane}}^{\text{rms}} = \frac{1}{4\sqrt{3}} x \theta_0. \quad (30.20)$$

All the quantitative estimates in this section apply only in the limit of small  $\theta_{\text{plane}}^{\text{rms}}$  and in the absence of large-angle scatters. The random variables  $s$ ,  $\psi$ ,  $y$ , and  $\theta$  in a given plane are correlated. Obviously,  $y \approx x\psi$ . In addition,  $y$  and  $\theta$  have the correlation coefficient  $\rho_{y\theta} = \sqrt{3}/2 \approx 0.87$ . For Monte Carlo generation of a joint ( $y_{\text{plane}}, \theta_{\text{plane}}$ ) distribution, or for other calculations, it may be most convenient to work with independent Gaussian random variables ( $z_1, z_2$ ) with mean zero and variance one, and then set

$$y_{\text{plane}} = z_1 x \theta_0 (1 - \rho_{y\theta}^2)^{1/2} / \sqrt{3} + z_2 \rho_{y\theta} x \theta_0 / \sqrt{3} \quad (30.21)$$

$$= z_1 x \theta_0 / \sqrt{12} + z_2 x \theta_0 / 2; \quad (30.22)$$

$$\theta_{\text{plane}} = z_2 \theta_0. \quad (30.23)$$

Note that the second term for  $y_{\text{plane}}$  equals  $x \theta_{\text{plane}}/2$  and represents the displacement that would have occurred had the deflection  $\theta_{\text{plane}}$  all occurred at the single point  $x/2$ .

For heavy ions the multiple Coulomb scattering has been measured and compared with various theoretical distributions [38].

## 30.4. Photon and electron interactions in matter

**30.4.1. Radiation length:** High-energy electrons predominantly lose energy in matter by bremsstrahlung, and high-energy photons by  $e^+e^-$  pair production. The characteristic amount of matter traversed for these related interactions is called the radiation length  $X_0$ , usually measured in  $\text{g cm}^{-2}$ . It is both (a) the mean distance over which a high-energy electron loses all but  $1/e$  of its energy by bremsstrahlung, and (b)  $\frac{7}{9}$  of the mean free path for pair production by a high-energy photon [39]. It is also the appropriate scale length for describing high-energy electromagnetic cascades.  $X_0$  has been calculated and tabulated by Y.S. Tsai [40]:

$$\frac{1}{X_0} = 4\alpha r_e^2 \frac{N_A}{A} \left\{ Z^2 [L_{\text{rad}} - f(Z)] + Z L'_{\text{rad}} \right\}. \quad (30.24)$$

For  $A = 1 \text{ g mol}^{-1}$ ,  $4\alpha r_e^2 N_A/A = (716.408 \text{ g cm}^{-2})^{-1}$ .  $L_{\text{rad}}$  and  $L'_{\text{rad}}$  are given in Table 30.2. The function  $f(Z)$  is an infinite sum, but for elements up to uranium can be represented to 4-place accuracy by

$$f(Z) = a^2 \left[ (1 + a^2)^{-1} + 0.20206 - 0.0369 a^2 + 0.0083 a^4 - 0.002 a^6 \right], \quad (30.25)$$

where  $a = \alpha Z$  [41].

**Table 30.2:** Tsai's  $L_{\text{rad}}$  and  $L'_{\text{rad}}$ , for use in calculating the radiation length in an element using Eq. (30.24).

Element	$Z$	$L_{\text{rad}}$	$L'_{\text{rad}}$
H	1	5.31	6.144
He	2	4.79	5.621
Li	3	4.74	5.805
Be	4	4.71	5.924
Others	$> 4$	$\ln(184.15 Z^{-1/3})$	$\ln(1194 Z^{-2/3})$

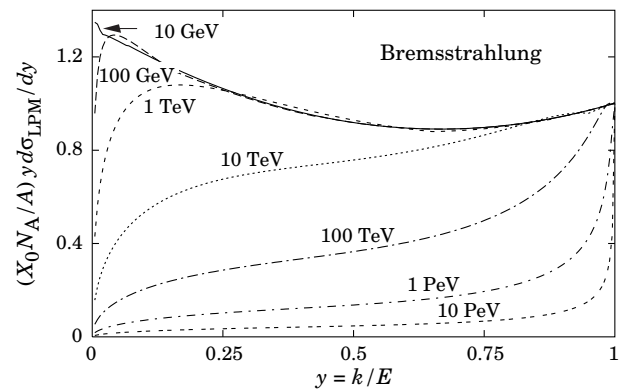


**Figure 30.12:** The normalized bremsstrahlung cross section  $k d\sigma_{\text{LPM}}/dk$  in lead versus the fractional photon energy  $y = k/E$ . The vertical axis has units of photons per radiation length.

The radiation length in a mixture or compound may be approximated by

$$1/X_0 = \sum w_j / X_j, \quad (30.26)$$

where  $w_j$  and  $X_j$  are the fraction by weight and the radiation length for the  $j$ th element.

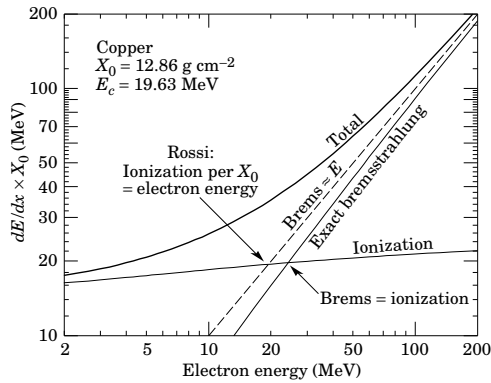


Figure 30.13: Two definitions of the critical energy  $E_c$ .

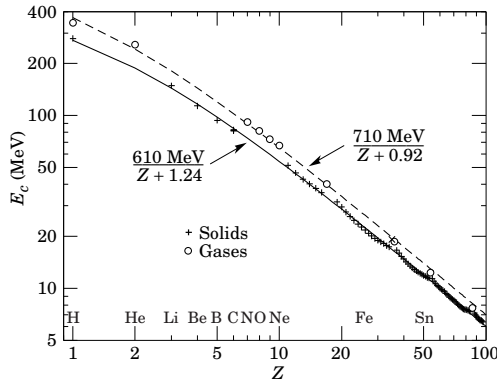


Figure 30.14: Electron critical energy for the chemical elements, using Rossi's definition [2]. The fits shown are for solids and liquids (solid line) and gases (dashed line). The rms deviation is 2.2% for the solids and 4.0% for the gases. (Computed with code supplied by A. Fassó.)

**30.4.2. Energy loss by electrons:** At low energies electrons and positrons primarily lose energy by ionization, although other processes (Møller scattering, Bhabha scattering,  $e^+$  annihilation) contribute, as shown in Fig. 30.11. While ionization loss rates rise logarithmically with energy, bremsstrahlung losses rise nearly linearly (fractional loss is nearly independent of energy), and dominates above a few tens of MeV in most materials (See Sec. 30.4.3 below.)

Ionization loss by electrons and positrons differ somewhat, and both differ from loss by heavy particles because of the kinematics, spin, and the identity of the incident electron with the electrons which it ionizes. Complete discussions and tables can be found in Refs. 10, 11, and 30.

At very high energies and except at the high-energy tip of the bremsstrahlung spectrum, the cross section can be approximated in the “complete screening case” as [40]

$$\frac{d\sigma}{dk} = (1/k)4\alpha r_e^2 \left\{ \left( \frac{4}{3} - \frac{4}{3}y + y^2 \right) [Z^2(L_{\text{rad}} - f(Z)) + Z L'_{\text{rad}}] + \frac{1}{9}(1-y)(Z^2 + Z) \right\}, \quad (30.27)$$

where  $y = k/E$  is the fraction of the electron's energy transferred to the radiated photon. At small  $y$  (the “infrared limit”) the term on the second line ranges from 1.7% (low  $Z$ ) to 2.5% (high  $Z$ ) of the total. If it is ignored and the first line simplified with the definition of  $X_0$  given in Eq. (30.24), we have

$$\frac{d\sigma}{dk} = \frac{A}{X_0 N_A k} \left( \frac{4}{3} - \frac{4}{3}y + y^2 \right). \quad (30.28)$$

This cross section (times  $k$ ) is shown by the top curve in Fig. 30.12.

This formula is accurate except in near  $y = 1$ , where

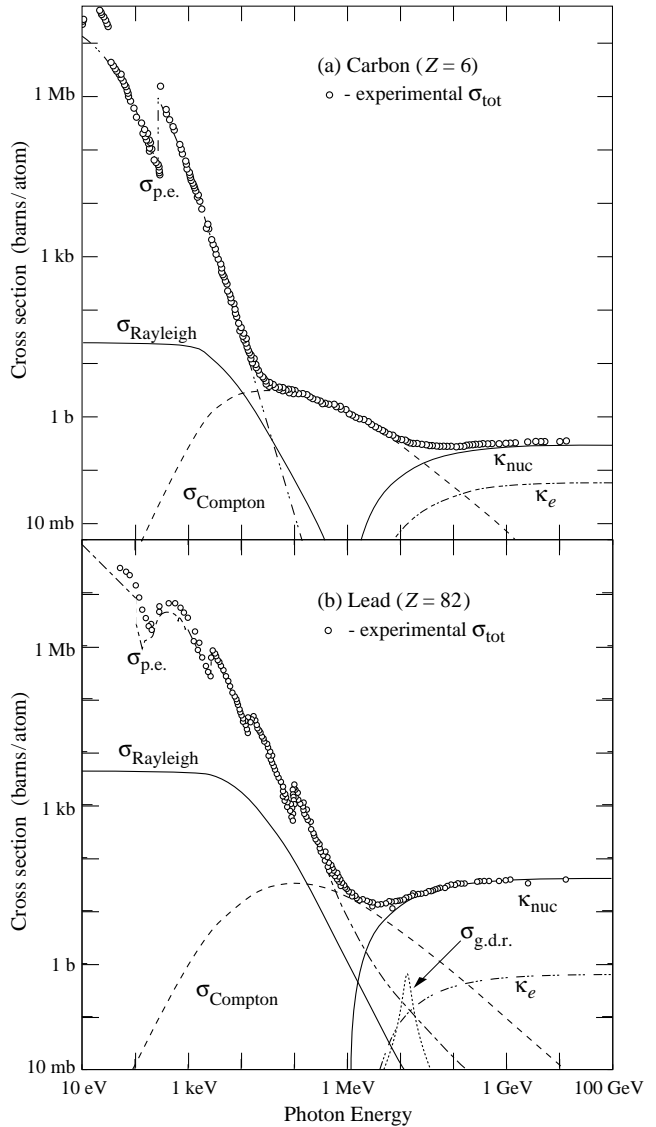


Figure 30.15: Photon total cross sections as a function of energy in carbon and lead, showing the contributions of different processes [48]:

- $\sigma_{\text{p.e.}}$  = Atomic photoelectric effect (electron ejection, photon absorption)
- $\sigma_{\text{Rayleigh}}$  = Rayleigh (coherent) scattering—atom neither ionized nor excited
- $\sigma_{\text{Compton}}$  = Incoherent scattering (Compton scattering off an electron)
- $\kappa_{\text{nuc}}$  = Pair production, nuclear field
- $\kappa_e$  = Pair production, electron field
- $\sigma_{\text{g.d.r.}}$  = Photonuclear interactions, most notably the Giant Dipole Resonance [49]. In these interactions, the target nucleus is broken up.

Original figures through the courtesy of John H. Hubbell (NIST).

screening may become incomplete, and near  $y = 0$ , where the infrared divergence is removed by the interference of bremsstrahlung amplitudes from nearby scattering centers (the LPM effect) [42,43] and dielectric suppression [44,45]. These and other suppression effects in bulk media are discussed in Sec. 30.4.5.

With decreasing energy ( $E \lesssim 10$  GeV) the high- $y$  cross section drops and the curves become rounded as  $y \rightarrow 1$ . Curves of this



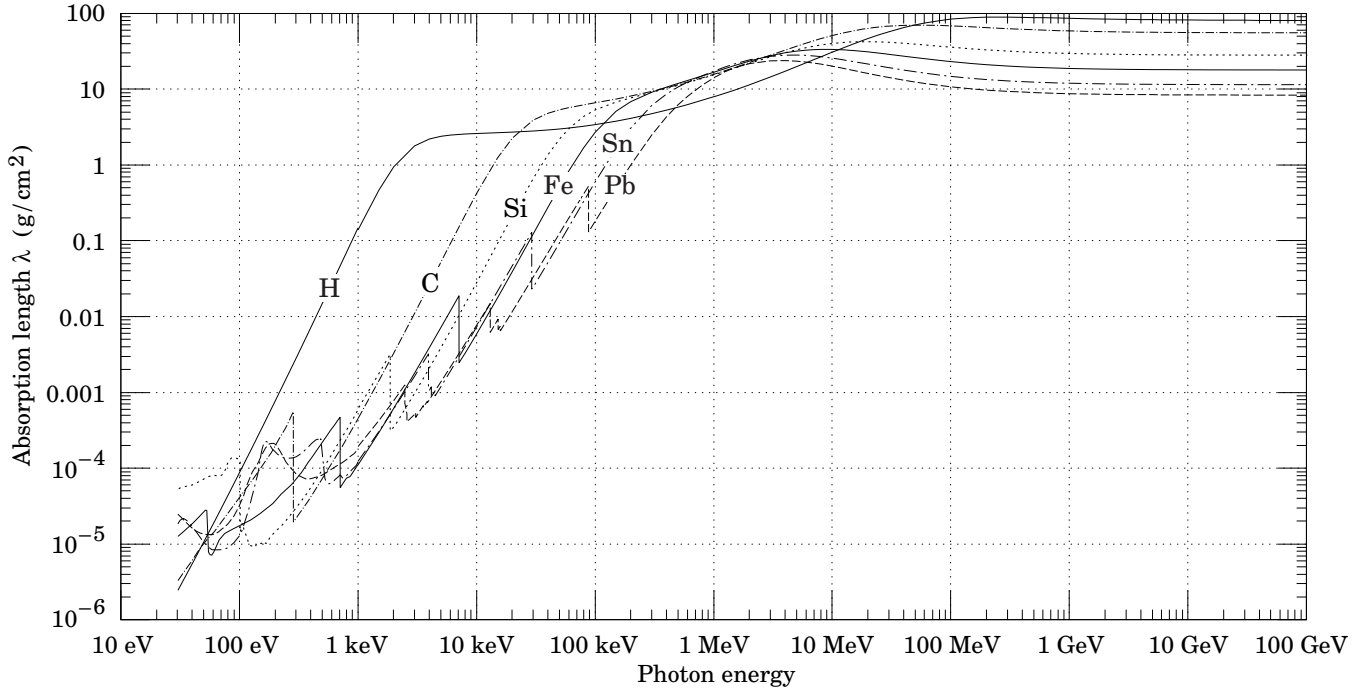


**Fig. 30.16:** The photon mass attenuation length (or mean free path)  $\lambda = 1/(\mu/\rho)$  for various elemental absorbers as a function of photon energy. The mass attenuation coefficient is  $\mu/\rho$ , where  $\rho$  is the density. The intensity  $I$  remaining after traversal of thickness  $t$  (in mass/unit area) is given by  $I = I_0 \exp(-t/\lambda)$ . The accuracy is a few percent. For a chemical compound or mixture,  $1/\lambda_{\text{eff}} \approx \sum_{\text{elements}} w_Z/\lambda_Z$ , where  $w_Z$  is the proportion by weight of the element with atomic number  $Z$ . The processes responsible for attenuation are given in Fig. 30.11. Since coherent processes are included, not all these processes result in energy deposition. The data for  $30 \text{ eV} < E < 1 \text{ keV}$  are obtained from [http://www-cxro.lbl.gov/optical\\_constants](http://www-cxro.lbl.gov/optical_constants) (courtesy of Eric M. Gullikson, LBNL). The data for  $1 \text{ keV} < E < 100 \text{ GeV}$  are from <http://physics.nist.gov/PhysRefData>, through the courtesy of John H. Hubbell (NIST).

familiar shape can be seen in Rossi [2] (Figs. 2.11.2,3); see also the review by Koch & Motz [46].

Except at these extremes, and still in the complete-screening approximation, the number of photons with energies between  $k_{\text{min}}$  and  $k_{\text{max}}$  emitted by an electron travelling a distance  $d \ll X_0$  is

$$N_\gamma = \frac{d}{X_0} \left[ \frac{4}{3} \ln \left( \frac{k_{\text{max}}}{k_{\text{min}}} \right) - \frac{4(k_{\text{max}} - k_{\text{min}})}{3E} + \frac{k_{\text{max}}^2 - k_{\text{min}}^2}{2E^2} \right]. \quad (30.29)$$

**30.4.3. Critical energy:** An electron loses energy by bremsstrahlung at a rate nearly proportional to its energy, while the ionization loss rate varies only logarithmically with the electron energy. The *critical energy*  $E_c$  is sometimes defined as the energy at which the two loss rates are equal [47]. Among alternate definitions is that of Rossi [2], who defines the critical energy as the energy at which the ionization loss per radiation length is equal to the electron energy. Equivalently, it is the same as the first definition with the approximation  $|dE/dx|_{\text{brems}} \approx E/X_0$ . This form has been found to describe transverse electromagnetic shower development more accurately (see below). These definitions are illustrated in the case of copper in Fig. 30.13.

The accuracy of approximate forms for  $E_c$  has been limited by the failure to distinguish between gases and solid or liquids, where there is a substantial difference in ionization at the relevant energy because of the density effect. We distinguish these two cases in Fig. 30.14. Fits were also made with functions of the form  $a/(Z+b)^\alpha$ , but  $\alpha$  was found to be essentially unity. Since  $E_c$  also depends on  $A$ ,  $I$ , and other factors, such forms are at best approximate.

Values of  $E_c$  for both electrons and positrons in more than 300 materials can be found at [pdg.lbl.gov/AtomicNuclearProperties](http://pdg.lbl.gov/AtomicNuclearProperties).

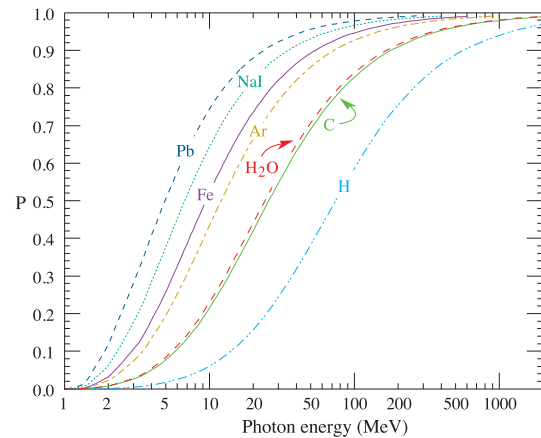


**Figure 30.17:** Probability  $P$  that a photon interaction will result in conversion to an  $e^+e^-$  pair. Except for a few-percent contribution from photonuclear absorption around 10 or 20 MeV, essentially all other interactions in this energy range result in Compton scattering off an atomic electron. For a photon attenuation length  $\lambda$  (Fig. 30.16), the probability that a given photon will produce an electron pair (without first Compton scattering) in thickness  $t$  of absorber is  $P[1 - \exp(-t/\lambda)]$ .

**30.4.4. Energy loss by photons :** Contributions to the photon cross section in a light element (carbon) and a heavy element (lead) are shown in Fig. 30.15. At low energies it is seen that the photoelectric effect dominates, although Compton scattering, Rayleigh scattering, and photonuclear absorption also contribute. The photoelectric cross section is characterized by discontinuities (absorption edges) as thresholds for photoionization of various atomic levels are reached. Photon attenuation lengths for a variety of elements are shown in Fig. 30.16, and data for  $30 \text{ eV} < k < 100 \text{ GeV}$  for all elements is available from the web pages given in the caption. Here  $k$  is the photon energy.

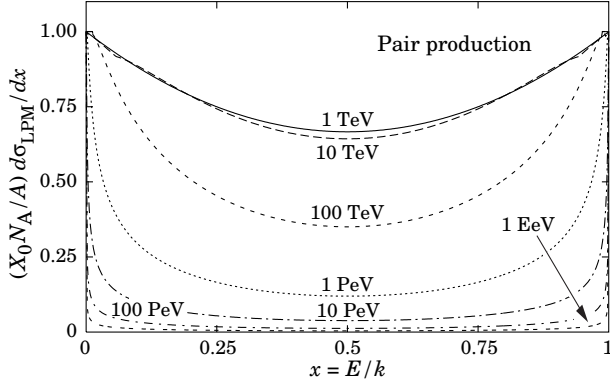


**Figure 30.18:** The normalized pair production cross section  $d\sigma_{LPM}/dy$ , versus fractional electron energy  $x = E/k$ .

The increasing domination of pair production as the energy increases is shown in Fig. 30.17. Using approximations similar to those used to obtain Eq. (30.28), Tsai's formula for the differential cross section [40] reduces to

$$\frac{d\sigma}{dx} = \frac{A}{X_0 N_A} \left[ 1 - \frac{4}{3}x(1-x) \right] \quad (30.30)$$

in the complete-screening limit valid at high energies. Here  $x = E/k$  is the fractional energy transfer to the pair-produced electron (or positron), and  $k$  is the incident photon energy. The cross section is very closely related to that for bremsstrahlung, since the Feynman diagrams are variants of one another. The cross section is of necessity symmetric between  $x$  and  $1-x$ , as can be seen by the solid curve in Fig. 30.18. See the review by Motz, Olsen, & Koch for a more detailed treatment [50].

Eq. (30.30) may be integrated to find the high-energy limit for the total  $e^+e^-$  pair-production cross section:

$$\sigma = \frac{7}{9} (A/X_0 N_A). \quad (30.31)$$

Equation Eq. (30.31) is accurate to within a few percent down to energies as low as 1 GeV, particularly for high- $Z$  materials.

**30.4.5. Bremsstrahlung and pair production at very high energies :** At ultrahigh energies, Eqns. 30.27–30.31 will fail because of quantum mechanical interference between amplitudes from different scattering centers. Since the longitudinal momentum transfer to a given center is small ( $\propto k/E(E-k)$ , in the case of bremsstrahlung), the interaction is spread over a comparatively long distance called the formation length ( $\propto E(E-k)/k$ ) via the uncertainty principle. In alternate language, the formation length is the distance over which the highly relativistic electron and the photon “split apart.” The interference is usually destructive. Calculations of the “Landau-Pomeranchuk-Migdal” (LPM) effect may be made semi-classically based on the average multiple scattering, or more rigorously using a quantum transport approach [42,43].

In amorphous media, bremsstrahlung is suppressed if the photon energy  $k$  is less than  $E^2/(E + E_{LPM})$  [43], where\*

$$E_{LPM} = \frac{(m_e c^2)^2 \alpha X_0}{4\pi \hbar c \rho} = (7.7 \text{ TeV/cm}) \times \frac{X_0}{\rho}. \quad (30.32)$$

Since physical distances are involved,  $X_0/\rho$ , in cm, appears. The energy-weighted bremsstrahlung spectrum for lead,  $k d\sigma_{LPM}/dk$ , is shown in Fig. 30.12. With appropriate scaling by  $X_0/\rho$ , other materials behave similarly.

For photons, pair production is reduced for  $E(k-E) > k E_{LPM}$ . The pair-production cross sections for different photon energies are shown in Fig. 30.18.

If  $k \ll E$ , several additional mechanisms can also produce suppression. When the formation length is long, even weak factors can perturb the interaction. For example, the emitted photon can coherently forward scatter off of the electrons in the media. Because of this, for  $k < \omega_p E/m_e \sim 10^{-4}$ , bremsstrahlung is suppressed by a factor  $(km_e/\omega_p E)^2$  [45]. Magnetic fields can also suppress bremsstrahlung.

In crystalline media, the situation is more complicated, with coherent enhancement or suppression possible. The cross section depends on the electron and photon energies and the angles between the particle direction and the crystalline axes [52].

**30.4.6. Photonuclear and electronuclear interactions at still higher energies :** At still higher photon and electron energies, where the bremsstrahlung and pair production cross-sections are heavily suppressed by the LPM effect, photonuclear and electronuclear interactions predominate over electromagnetic interactions.

At photon energies above about  $10^{20}$  eV, for example, photons usually interact hadronically. The exact cross-over energy depends on the model used for the photonuclear interactions. At still higher energies ( $\gtrsim 10^{23}$  eV), photonuclear interactions can become coherent, with the photon interaction spread over multiple nuclei. Essentially, the photon coherently converts to a  $\rho^0$ , in a process that is somewhat similar to kaon regeneration [53]. These processes are illustrated in Fig. 30.19.

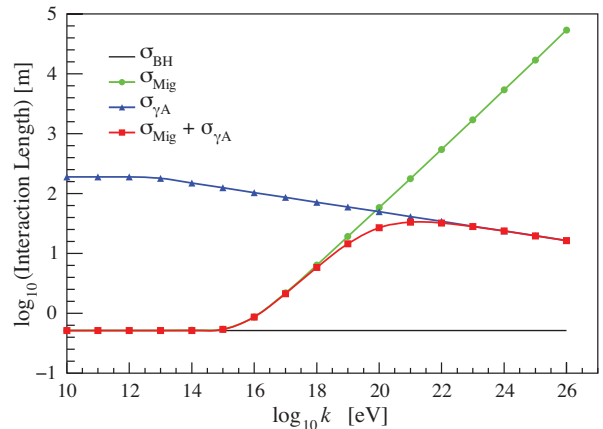


**Figure 30.19:** Interaction length for a photon in ice as a function of photon energy for the Bethe-Heitler (BH), LPM (Mig) and photonuclear ( $\gamma A$ ) cross sections [53]. The Bethe-Heitler interaction length is  $9X_0/7$ , and  $X_0$  is 0.393 m in ice.

Similar processes occur for electrons. As electron energies increase and the LPM effect suppresses bremsstrahlung,

\* This definition differs from that of Ref. 51 by a factor of two.  $E_{LPM}$  scales as the 4th power of the mass of the incident particle, so that  $E_{LPM} = (1.4 \times 10^{10} \text{ TeV/cm}) \times X_0/\rho$  for a muon.

electronuclear interactions become more important. At energies above  $10^{21}$  eV, these electronuclear interactions dominate electron energy loss [53].

### 30.5. Electromagnetic cascades

When a high-energy electron or photon is incident on a thick absorber, it initiates an electromagnetic cascade as pair production and bremsstrahlung generate more electrons and photons with lower energy. The longitudinal development is governed by the high-energy part of the cascade, and therefore scales as the radiation length in the material. Electron energies eventually fall below the critical energy, and then dissipate their energy by ionization and excitation rather than by the generation of more shower particles. In describing shower behavior, it is therefore convenient to introduce the scale variables

$$t = x/X_0, \quad y = E/E_c, \quad (30.33)$$

so that distance is measured in units of radiation length and energy in units of critical energy.

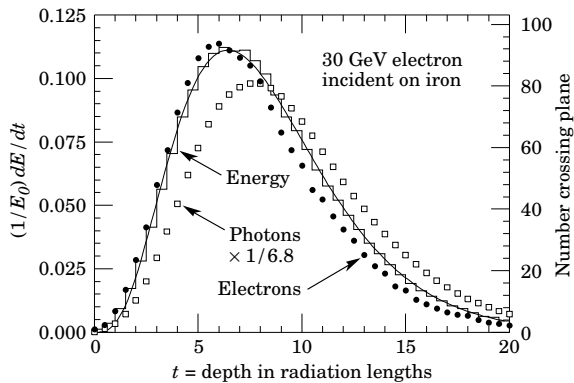


**Figure 30.20:** An EGS4 simulation of a 30 GeV electron-induced cascade in iron. The histogram shows fractional gamma energy deposition per radiation length, and the curve is a gamma-function fit to the distribution. Circles indicate the number of electrons with total energy greater than 1.5 MeV crossing planes at  $X_0/2$  intervals (scale on right) and the squares the number of photons with  $E \geq 1.5$  MeV crossing the planes (scaled down to have same area as the electron distribution).

Longitudinal profiles from an EGS4 [54] simulation of a 30 GeV electron-induced cascade in iron are shown in Fig. 30.20. The number of particles crossing a plane (very close to Rossi's  $\Pi$  function [2]) is sensitive to the cutoff energy, here chosen as a total energy of 1.5 MeV for both electrons and photons. The electron number falls off more quickly than energy deposition. This is because, with increasing depth, a larger fraction of the cascade energy is carried by photons. Exactly what a calorimeter measures depends on the device, but it is not likely to be exactly any of the profiles shown. In gas counters it may be very close to the electron number, but in glass Cherenkov detectors and other devices with “thick” sensitive regions it is closer to the energy deposition (total track length). In such detectors the signal is proportional to the “detectable” track length  $T_d$ , which is in general less than the total track length  $T$ . Practical devices are sensitive to electrons with energy above some detection threshold  $E_d$ , and  $T_d = T F(E_d/E_c)$ . An analytic form for  $F(E_d/E_c)$  obtained by Rossi [2] is given by Fabjan [55]; see also Amaldi [56].

The mean longitudinal profile of the energy deposition in an electromagnetic cascade is reasonably well described by a gamma

distribution [57]:

$$\frac{dE}{dt} = E_0 b \frac{(bt)^{a-1} e^{-bt}}{\Gamma(a)} \quad (30.34)$$

The maximum  $t_{\max}$  occurs at  $(a-1)/b$ . We have made fits to shower profiles in elements ranging from carbon to uranium, at energies from 1 GeV to 100 GeV. The energy deposition profiles are well described by Eq. (30.34) with

$$t_{\max} = (a-1)/b = 1.0 \times (\ln y + C_j), \quad j = e, \gamma, \quad (30.35)$$

where  $C_e = -0.5$  for electron-induced cascades and  $C_\gamma = +0.5$  for photon-induced cascades. To use Eq. (30.34), one finds  $(a-1)/b$  from Eq. (30.35) and Eq. (30.33), then finds  $a$  either by assuming  $b \approx 0.5$  or by finding a more accurate value from Fig. 30.21. The results are very similar for the electron number profiles, but there is some dependence on the atomic number of the medium. A similar form for the electron number maximum was obtained by Rossi in the context of his “Approximation B,” [2] (see Fabjan’s review in Ref. 55), but with  $C_e = -1.0$  and  $C_\gamma = -0.5$ ; we regard this as superseded by the EGS4 result.

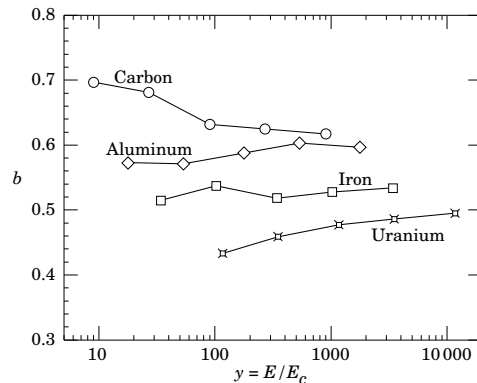


**Figure 30.21:** Fitted values of the scale factor  $b$  for energy deposition profiles obtained with EGS4 for a variety of elements for incident electrons with  $1 \leq E_0 \leq 100$  GeV. Values obtained for incident photons are essentially the same.

The “shower length”  $X_s = X_0/b$  is less conveniently parameterized, since  $b$  depends upon both  $Z$  and incident energy, as shown in Fig. 30.21. As a corollary of this  $Z$  dependence, the number of electrons crossing a plane near shower maximum is underestimated using Rossi’s approximation for carbon and seriously overestimated for uranium. Essentially the same  $b$  values are obtained for incident electrons and photons. For many purposes it is sufficient to take  $b \approx 0.5$ .

The length of showers initiated by ultra-high energy photons and electrons is somewhat greater than at lower energies since the first or first few interaction lengths are increased via the mechanisms discussed above.

The gamma function distribution is very flat near the origin, while the EGS4 cascade (or a real cascade) increases more rapidly. As a result Eq. (30.34) fails badly for about the first two radiation lengths; it was necessary to exclude this region in making fits.

Because fluctuations are important, Eq. (30.34) should be used only in applications where average behavior is adequate. Grindhammer *et al.* have developed fast simulation algorithms in which the variance and correlation of  $a$  and  $b$  are obtained by fitting Eq. (30.34) to individually simulated cascades, then generating profiles for cascades using  $a$  and  $b$  chosen from the correlated distributions [58].

The transverse development of electromagnetic showers in different materials scales fairly accurately with the *Molière radius*  $R_M$ , given by [59,60]

$$R_M = X_0 E_s / E_c, \quad (30.36)$$

where  $E_s \approx 21$  MeV (Table 30.1), and the Rossi definition of  $E_c$  is used.

In a material containing a weight fraction  $w_j$  of the element with critical energy  $E_{cj}$  and radiation length  $X_j$ , the Molière radius is given by

$$\frac{1}{R_M} = \frac{1}{E_s} \sum \frac{w_j E_{cj}}{X_j}. \quad (30.37)$$

Measurements of the lateral distribution in electromagnetic cascades are shown in Refs. 59 and 60. On the average, only 10% of the energy lies outside the cylinder with radius  $R_M$ . About 99% is contained inside of  $3.5R_M$ , but at this radius and beyond composition effects become important and the scaling with  $R_M$  fails. The distributions are characterized by a narrow core, and broaden as the shower develops. They are often represented as the sum of two Gaussians, and Grindhammer [58] describes them with the function

$$f(r) = \frac{2r R^2}{(r^2 + R^2)^2}, \quad (30.38)$$

where  $R$  is a phenomenological function of  $x/X_0$  and  $\ln E$ .

At high enough energies, the LPM effect (Sec. 30.4.5) reduces the cross sections for bremsstrahlung and pair production, and hence can cause significant elongation of electromagnetic cascades [43].

### 30.6. Muon energy loss at high energy

At sufficiently high energies, radiative processes become more important than ionization for all charged particles. For muons and pions in materials such as iron, this “critical energy” occurs at several hundred GeV. (There is no simple scaling with particle mass, but for protons the “critical energy” is much, much higher.) Radiative effects dominate the energy loss of energetic muons found in cosmic rays or produced at the newest accelerators. These processes are characterized by small cross sections, hard spectra, large energy fluctuations, and the associated generation of electromagnetic and (in the case of photonuclear interactions) hadronic showers [61–69]. As a consequence, at these energies the treatment of energy loss as a uniform and continuous process is for many purposes inadequate.

It is convenient to write the average rate of muon energy loss as [70]

$$-dE/dx = a(E) + b(E) E. \quad (30.39)$$

Here  $a(E)$  is the ionization energy loss given by Eq. (30.4), and  $b(E)$  is the sum of  $e^+e^-$  pair production, bremsstrahlung, and photonuclear contributions. To the approximation that these slowly-varying functions are constant, the mean range  $x_0$  of a muon with initial energy  $E_0$  is given by

$$x_0 \approx (1/b) \ln(1 + E_0/E_{\mu c}), \quad (30.40)$$

where  $E_{\mu c} = a/b$ . Fig. 30.22 shows contributions to  $b(E)$  for iron. Since  $a(E) \approx 0.002$  GeV  $g^{-1} cm^2$ ,  $b(E)E$  dominates the energy loss above several hundred GeV, where  $b(E)$  is nearly constant. The rates of energy loss for muons in hydrogen, uranium, and iron are shown in Fig. 30.23 [5].

The “muon critical energy”  $E_{\mu c}$  can be defined more exactly as the energy at which radiative and ionization losses are equal, and can be found by solving  $E_{\mu c} = a(E_{\mu c})/b(E_{\mu c})$ . This definition corresponds to the solid-line intersection in Fig. 30.13, and is different from the Rossi definition we used for electrons. It serves the same function: below  $E_{\mu c}$  ionization losses dominate, and above  $E_{\mu c}$  radiative effects dominate. The dependence of  $E_{\mu c}$  on atomic number  $Z$  is shown in Fig. 30.24.

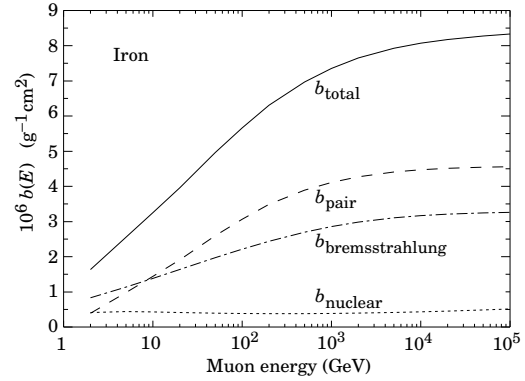


**Figure 30.22:** Contributions to the fractional energy loss by muons in iron due to  $e^+e^-$  pair production, bremsstrahlung, and photonuclear interactions, as obtained from Groom *et al.* [5] except for post-Born corrections to the cross section for direct pair production from atomic electrons.

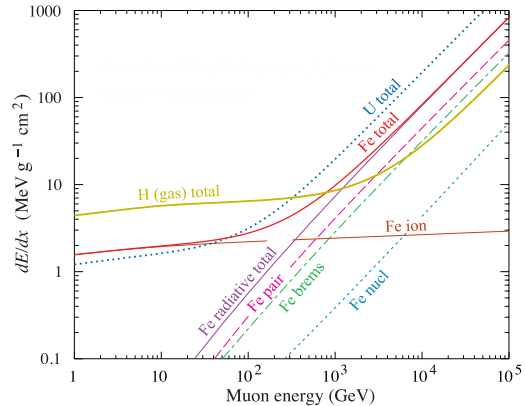


**Figure 30.23:** The average energy loss of a muon in hydrogen, iron, and uranium as a function of muon energy. Contributions to  $dE/dx$  in iron from ionization and the processes shown in Fig. 30.22 are also shown.

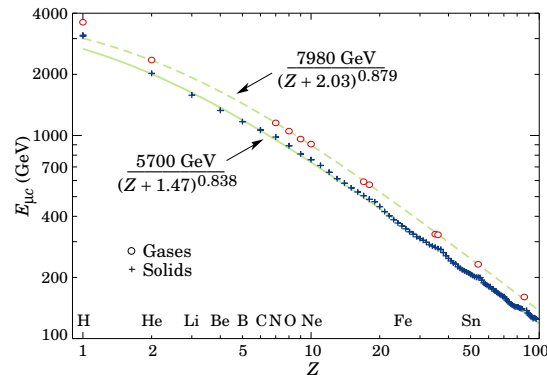


**Figure 30.24:** Muon critical energy for the chemical elements, defined as the energy at which radiative and ionization energy loss rates are equal [5]. The equality comes at a higher energy for gases than for solids or liquids with the same atomic number because of a smaller density effect reduction of the ionization losses. The fits shown in the figure exclude hydrogen. Alkali metals fall 3–4% above the fitted function, while most other solids are within 2% of the function. Among the gases the worst fit is for radon (2.7% high).

The radiative cross sections are expressed as functions of the fractional energy loss  $\nu$ . The bremsstrahlung cross section goes roughly as  $1/\nu$  over most of the range, while for the pair production case the distribution goes as  $\nu^{-3}$  to  $\nu^{-2}$  [71]. “Hard” losses are therefore more probable in bremsstrahlung, and in fact energy losses due to pair production may very nearly be treated as continuous. The simulated [69] momentum distribution of an incident 1 TeV/c muon beam after it crosses 3 m of iron is shown in Fig. 30.25. The most probable loss is 8 GeV, or  $3.4 \text{ MeV g}^{-1}\text{cm}^2$ . The full width at half maximum is 9 GeV/c, or 0.9%. The radiative tail is almost entirely due to bremsstrahlung, although most of the events in which more than 10% of the incident energy lost experienced relatively hard photonuclear interactions. The latter can exceed detector resolution [72], necessitating the reconstruction of lost energy. Tables [5] list the stopping power as  $9.82 \text{ MeV g}^{-1}\text{cm}^2$  for a 1 TeV muon, so that the mean loss should be  $23 \text{ GeV}$  ( $\approx 23 \text{ GeV}/c$ ), for a final momentum of 977 GeV/c, far below the peak. This agrees with the indicated mean calculated from the simulation. Electromagnetic and hadronic cascades in detector materials can obscure muon tracks in detector planes and reduce tracking efficiency [73].

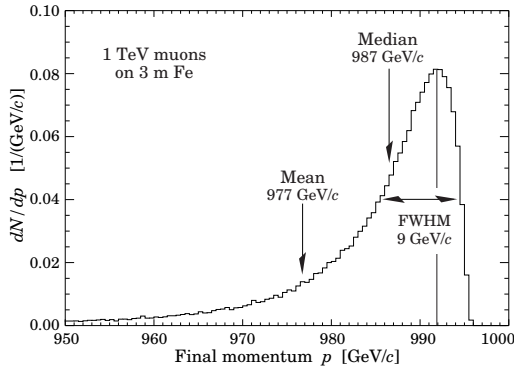


**Figure 30.25:** The momentum distribution of 1 TeV/c muons after traversing 3 m of iron as calculated with the MARS15 Monte Carlo code [69] by S.I. Striganov [5].

### 30.7. Cherenkov and transition radiation [74,75,34]

A charged particle radiates if its velocity is greater than the local phase velocity of light (Cherenkov radiation) or if it crosses suddenly from one medium to another with different optical properties (transition radiation). Neither process is important for energy loss, but both are used in high-energy and cosmic-ray physics detectors.

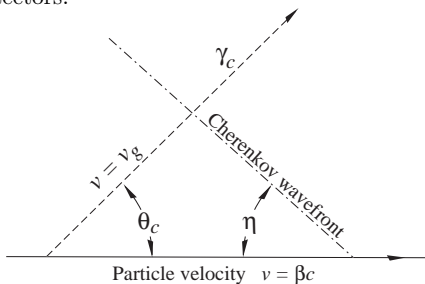


**Figure 30.26:** Cherenkov light emission and wavefront angles. In a dispersive medium,  $\theta_c + \eta \neq 90^\circ$ .

**30.7.1. Optical Cherenkov radiation :** The angle  $\theta_c$  of Cherenkov radiation, relative to the particle’s direction, for a particle with velocity  $\beta c$  in a medium with index of refraction  $n$  is

$$\begin{aligned} \cos \theta_c &= (1/n\beta) \\ \text{or } \tan \theta_c &= \sqrt{\beta^2 n^2 - 1} \\ &\approx \sqrt{2(1 - 1/n\beta)} \quad \text{for small } \theta_c, \text{ e.g. in gas} \end{aligned} \quad (30.41)$$

The threshold velocity  $\beta_t$  is  $1/n$ , and  $\gamma_t = 1/(1 - \beta_t^2)^{1/2}$ . Therefore,  $\beta_t \gamma_t = 1/(2\delta + \delta^2)^{1/2}$ , where  $\delta = n - 1$ . Values of  $\delta$  for various commonly used gases are given as a function of pressure and wavelength in Ref. 76. For values at atmospheric pressure, see Table 6.1. Data for other commonly used materials are given in Ref. 77.

Practical Cherenkov radiator materials are dispersive. Let  $\omega$  be the photon’s frequency, and let  $k = 2\pi/\lambda$  be its wavenumber. The photons propagate at the group velocity  $v_g = d\omega/dk = c/[n(\omega) + \omega(dn/d\omega)]$ . In a non-dispersive medium, this simplifies to  $v_g = c/n$ .

In his classical paper, Tamm [78] showed that for dispersive media the radiation is concentrated in a thin conical shell whose vertex is at the moving charge, and whose opening half-angle  $\eta$  is given by

$$\begin{aligned} \cot \eta &= \left[ \frac{d}{d\omega} (\omega \tan \theta_c) \right]_{\omega_0} \\ &= \left[ \tan \theta_c + \beta^2 \omega n(\omega) \frac{dn}{d\omega} \cot \theta_c \right]_{\omega_0}, \end{aligned} \quad (30.42)$$

where  $\omega_0$  is the central value of the small frequency range under consideration. (See Fig. 30.26.) This cone has a opening half-angle  $\eta$ , and, unless the medium is non-dispersive ( $dn/d\omega = 0$ ),  $\theta_c + \eta \neq 90^\circ$ . The Cherenkov wavefront ‘sideslips’ along with the particle [79]. This effect may have timing implications for ring imaging Cherenkov counters [80], but it is probably unimportant for most applications.

The number of photons produced per unit path length of a particle with charge  $ze$  and per unit energy interval of the photons is

$$\begin{aligned} \frac{d^2 N}{dE dx} &= \frac{\alpha z^2}{hc} \sin^2 \theta_c = \frac{\alpha^2 z^2}{r_e m_e c^2} \left( 1 - \frac{1}{\beta^2 n^2(E)} \right) \\ &\approx 370 \sin^2 \theta_c(E) \text{ eV}^{-1} \text{ cm}^{-1} \quad (z = 1), \end{aligned} \quad (30.43)$$

or, equivalently,

$$\frac{d^2 N}{dx d\lambda} = \frac{2\pi \alpha z^2}{\lambda^2} \left( 1 - \frac{1}{\beta^2 n^2(\lambda)} \right). \quad (30.44)$$

The index of refraction  $n$  is a function of photon energy  $E = \hbar\omega$ , as is the sensitivity of the transducer used to detect the light. For practical use, Eq. (30.43) must be multiplied by the the transducer response function and integrated over the region for which  $\beta n(\omega) > 1$ . Further details are given in the discussion of Cherenkov detectors in the Particle Detectors section (Sec. 31 of this Review).

When two particles are close together (lateral separation  $\lesssim 1$  wavelength), the electromagnetic fields from the particles may add coherently, affecting the Cherenkov radiation. Because of their opposite charges, the radiation from an  $e^+e^-$  pair at close separation is suppressed compared to two independent leptons [81].

### 30.7.2. Coherent radio Cherenkov radiation :

Coherent Cherenkov radiation is produced by many charged particles with a non-zero net charge moving through matter on an approximately common “wavefront”—for example, the electrons and positrons in a high-energy electromagnetic cascade. The signals can be visible above backgrounds for shower energies as low as  $10^{17}$  eV; see Sec. 32.3.2 for more details. The



phenomenon is called the Askaryan effect [82]. Near the end of a shower, when typical particle energies are below  $E_c$  (but still relativistic), a charge imbalance develops. The photons can Compton-scatter atomic electrons, and positrons can annihilate with atomic electrons to contribute even more photons which can in turn Compton scatter. These processes result in a roughly 20% excess of electrons over positrons in a shower. The net negative charge leads to coherent radio Cherenkov emission. The radiation includes a component from the decelerating charges (as in bremsstrahlung). Because the emission is coherent, the electric field strength is proportional to the shower energy and the signal power increases as its square. The electric field strength also increases linearly with frequency, up to a maximum frequency determined by the lateral spread of the shower. This cutoff occurs at about 1 GHz in ice, and scales inversely with the Moliere radius. At low frequencies, the radiation is roughly isotropic, but, as the frequency rises toward the cutoff frequency, the radiation becomes increasingly peaked around the Cherenkov angle. The radiation is linearly polarized in the plane containing the shower axis and the photon direction. A measurement of the signal polarization can be used to help determine the shower direction. The characteristics of this radiation have been nicely demonstrated in a series of experiments at SLAC [83]. A detailed discussion of the radiation can be found in Ref. 84.

**30.7.3. Transition radiation:** The energy radiated when a particle with charge  $ze$  crosses the boundary between vacuum and a medium with plasma frequency  $\omega_p$  is

$$I = \alpha z^2 \gamma \hbar \omega_p / 3, \quad (30.45)$$

where

$$\hbar \omega_p = \sqrt{4\pi N_e r_e^3} m_e c^2 / \alpha = \sqrt{\rho \text{ (in g/cm}^3\text{)} \langle Z/A \rangle} \times 28.81 \text{ eV}. \quad (30.46)$$

For styrene and similar materials,  $\hbar \omega_p \approx 20$  eV; for air it is 0.7 eV.

The number spectrum  $dN_\gamma/d(\hbar\omega)$  diverges logarithmically at low energies and decreases rapidly for  $\hbar\omega/\gamma\hbar\omega_p > 1$ . About half the energy is emitted in the range  $0.1 \leq \hbar\omega/\gamma\hbar\omega_p \leq 1$ . Inevitable absorption in a practical detector removes the divergence. For a particle with  $\gamma = 10^3$ , the radiated photons are in the soft x-ray range 2 to 40 keV. The  $\gamma$  dependence of the emitted energy thus comes from the hardening of the spectrum rather than from an increased quantum yield.

The number of photons with energy  $\hbar\omega > \hbar\omega_0$  is given by the answer to problem 13.15 in Ref. 34,

$$N_\gamma(\hbar\omega > \hbar\omega_0) = \frac{\alpha z^2}{\pi} \left[ \left( \ln \frac{\gamma \hbar \omega_p}{\hbar \omega_0} - 1 \right)^2 + \frac{\pi^2}{12} \right], \quad (30.47)$$

within corrections of order  $(\hbar\omega_0/\gamma\hbar\omega_p)^2$ . The number of photons above a fixed energy  $\hbar\omega_0 \ll \gamma\hbar\omega_p$  thus grows as  $(\ln \gamma)^2$ , but the number above a fixed fraction of  $\gamma\hbar\omega_p$  (as in the example above) is constant. For example, for  $\hbar\omega > \gamma\hbar\omega_p/10$ ,  $N_\gamma = 2.519 \alpha z^2 / \pi = 0.59\% \times z^2$ .

The particle stays “in phase” with the x ray over a distance called the formation length,  $d(\omega)$ . Most of the radiation is produced in a distance  $d(\omega) = (2c/\omega)(1/\gamma^2 + \theta^2 + \omega_p^2/\omega^2)^{-1}$ . Here  $\theta$  is the x-ray emission angle, characteristically  $1/\gamma$ . For  $\theta = 1/\gamma$  the formation length has a maximum at  $d(\gamma\omega_p/\sqrt{2}) = \gamma c/\sqrt{2}\omega_p$ . In practical situations it is tens of  $\mu\text{m}$ .

Since the useful x-ray yield from a single interface is low, in practical detectors it is enhanced by using a stack of  $N$  foil radiators—foils  $L$  thick, where  $L$  is typically several formation lengths—separated by gas-filled gaps. The amplitudes at successive interfaces interfere to cause oscillations about the single-interface spectrum. At increasing frequencies above the position of the last interference maximum ( $L/d(\omega) = \pi/2$ ), the formation zones, which have opposite phase, overlap more and

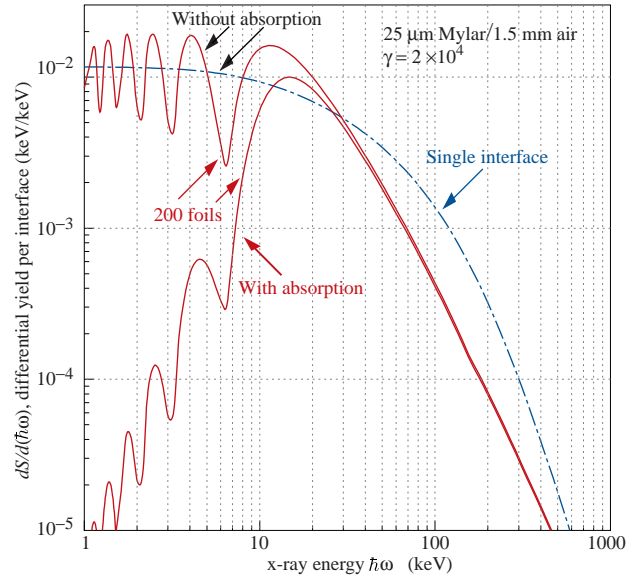


**Figure 30.27:** X-ray photon energy spectra for a radiator consisting of 200 25  $\mu\text{m}$  thick foils of Mylar with 1.5 mm spacing in air (solid lines) and for a single surface (dashed line). Curves are shown with and without absorption. Adapted from Ref. 85.

more and the spectrum saturates,  $dI/d\omega$  approaching zero as  $L/d(\omega) \rightarrow 0$ . This is illustrated in Fig. 30.27 for a realistic detector configuration.

For regular spacing of the layers fairly complicated analytic solutions for the intensity have been obtained [85]. (See also Ref. 86 and references therein.) Although one might expect the intensity of coherent radiation from the stack of foils to be proportional to  $N^2$ , the angular dependence of the formation length conspires to make the intensity  $\propto N$ .

#### References:

1. H. Bichsel, Nucl. Instrum. Methods **A562**, 154 (2006).
2. B. Rossi, *High Energy Particles*, Prentice-Hall, Inc., Englewood Cliffs, NJ, 1952.
3. H.A. Bethe, *Zur Theorie des Durchgangs schneller Korpuskularstrahlen durch Materie*, H. Bethe, Ann. Phys. **5**, 325 (1930).
4. “Stopping Powers and Ranges for Protons and Alpha Particles,” ICRU Report No. 49 (1993); Tables and graphs of these data are available at <http://physics.nist.gov/PhysRefData/>.
5. D.E. Groom, N.V. Mokhov, and S.I. Striganov, “Muon stopping-power and range tables: 10 MeV–100 TeV,” Atomic Data and Nuclear Data Tables **78**, 183–356 (2001). Since submission of this paper it has become likely that post-Born corrections to the direct pair production cross section should be made. Code used to make Figs. 30.22–30.24 included these corrections [D.Yu. Ivanov *et al.*, Phys. Lett. **B442**, 453 (1998)]. The effect is negligible except at high  $Z$ . (It is less than 1% for iron.); More extensive printable and machine-readable tables are given at <http://pdg.lbl.gov/AtomicNuclearProperties/>.
6. W.H. Barkas, W. Birnbaum, and F.M. Smith, Phys. Rev. **101**, 778 (1956).
7. J. Lindhard and A. H. Sorensen, Phys. Rev. **A53**, 2443 (1996).
8. U. Fano, Ann. Rev. Nucl. Sci. **13**, 1 (1963).
9. J.D. Jackson, Phys. Rev. **D59**, 017301 (1999).

10. S.M. Seltzer and M.J. Berger, *Int. J. of Applied Rad.* **33**, 1189 (1982).
11. "Stopping Powers for Electrons and Positrons," ICRU Report No. 37 (1984).
12. <http://physics.nist.gov/PhysRefData/XrayMassCoef/tab3.htm>
13. H. Bichsel, *Phys. Rev.* **A46**, 5761 (1992).
14. W.H. Barkas and M.J. Berger, *Tables of Energy Losses and Ranges of Heavy Charged Particles*, NASA-SP-3013 (1964).
15. S.P. Möller *et al.*, *Phys. Rev.* **A56**, 2930 (1997).
16. H.H. Andersen and J.F. Ziegler, *Hydrogen: Stopping Powers and Ranges in All Elements*. Vol. 3 of *The Stopping and Ranges of Ions in Matter* (Pergamon Press 1977).
17. J. Lindhard, *Kgl. Danske Videnskab. Selskab, Mat.-Fys. Medd.* **28**, No. 8 (1954);  
J. Lindhard, M. Scharff, and H.E. Schiøtt, *Kgl. Danske Videnskab. Selskab, Mat.-Fys. Medd.* **33**, No. 14 (1963).
18. J.F. Ziegler, J.F. Biersac, and U. Littmark, *The Stopping and Range of Ions in Solids*, Pergamon Press 1985.
19. R.M. Sternheimer, *Phys. Rev.* **88**, 851 (1952).
20. A. Crispin and G.N. Fowler, *Rev. Mod. Phys.* **42**, 290 (1970).
21. R.M. Sternheimer, S.M. Seltzer, and M.J. Berger, "The Density Effect for the Ionization Loss of Charged Particles in Various Substances," *Atomic Data and Nuclear Data Tables* **30**, 261 (1984). Minor errors are corrected in Ref. 5. Chemical composition for the tabulated materials is given in Ref. 10.
22. R.M. Sternheimer and R.F. Peierls, *Phys. Rev.* **B3**, 3681 (1971).
23. For unit-charge projectiles, see E.A. Uehling, *Ann. Rev. Nucl. Sci.* **4**, 315 (1954). For highly charged projectiles, see J.A. Doggett and L.V. Spencer, *Phys. Rev.* **103**, 1597 (1956). A Lorentz transformation is needed to convert these center-of-mass data to knock-on energy spectra.
24. N.F. Mott and H.S.W. Massey, *The Theory of Atomic Collisions*, Oxford Press, London, 1965.
25. L.D. Landau, *J. Exp. Phys. (USSR)* **8**, 201 (1944).
26. P.V. Vavilov, *Sov. Phys. JETP* **5**, 749 (1957).
27. H. Bichsel, *Rev. Mod. Phys.* **60**, 663 (1988).
28. R. Talman, *Nucl. Instrum. Methods* **159**, 189 (1979).
29. H. Bichsel, Ch. 87 in the *Atomic, Molecular and Optical Physics Handbook*, G.W.F. Drake, editor (Am. Inst. Phys. Press, Woodbury NY, 1996).
30. S.M. Seltzer and M.J. Berger, *Int. J. of Applied Rad.* **35**, 665 (1984). This paper corrects and extends the results of Ref. 10.
31. L.V. Spencer "Energy Dissipation by Fast Electrons," Nat'l Bureau of Standards Monograph No. 1 (1959).
32. "Average Energy Required to Produce an Ion Pair," ICRU Report No. 31 (1979).
33. N. Hadley *et al.*, "List of Poisoning Times for Materials," Lawrence Berkeley Lab Report TPC-LBL-79-8 (1981).
34. J.D. Jackson, *Classical Electrodynamics*, 3rd edition, (John Wiley and Sons, New York, 1998).
35. H.A. Bethe, *Phys. Rev.* **89**, 1256 (1953). A thorough review of multiple scattering is given by W.T. Scott, *Rev. Mod. Phys.* **35**, 231 (1963). However, the data of Shen *et al.*, (*Phys. Rev.* **D20**, 1584 (1979)) show that Bethe's simpler method of including atomic electron effects agrees better with experiment than does Scott's treatment. For a thorough discussion of simple formulae for single scatters and methods of compounding these into multiple-scattering formulae, see W.T. Scott, *Rev. Mod. Phys.* **35**, 231 (1963). Detailed summaries of formulae for computing single scatters are given in J.W. Motz, H. Olsen, and H.W. Koch, *Rev. Mod. Phys.* **36**, 881 (1964).
36. V.L. Highland, *Nucl. Instrum. Methods* **129**, 497 (1975); *Nucl. Instrum. Methods* **161**, 171 (1979).
37. G.R. Lynch and O.I. Dahl, *Nucl. Instrum. Methods* **B58**, 6 (1991).
38. M. Wong *et al.*, *Med. Phys.* **17**, 163 (1990).
39. E. Segré, *Nuclei and Particles*, New York, Benjamin (1964) p. 65 ff.
40. Y.S. Tsai, *Rev. Mod. Phys.* **46**, 815 (1974).
41. H. Davies, H.A. Bethe, and L.C. Maximon, *Phys. Rev.* **93**, 788 (1954).
42. L.D. Landau and I.J. Pomeranchuk, *Dokl. Akad. Nauk. SSSR* **92**, 535 (1953); **92**, 735 (1953). These papers are available in English in L. Landau, *The Collected Papers of L.D. Landau*, Pergamon Press, 1965; A.B. Migdal, *Phys. Rev.* **103**, 1811 (1956).
43. S. Klein, *Rev. Mod. Phys.* **71**, 1501 (1999).
44. M.L. Ter-Mikaelian, *SSSR* **94**, 1033 (1954); M.L. Ter-Mikaelian, *High Energy Electromagnetic Processes in Condensed Media* (John Wiley and Sons, New York, 1972).
45. P. Anthony *et al.*, *Phys. Rev. Lett.* **76**, 3550 (1996).
46. H.W. Koch and J.W. Motz, *Rev. Mod. Phys.* **31**, 920 (1959).
47. M.J. Berger & S.M. Seltzer, "Tables of Energy Losses and Ranges of Electrons and Positrons," National Aeronautics and Space Administration Report NASA-SP-3012 (Washington DC 1964).
48. Data from J.H. Hubbell, H. Gimm, and I. Øverbø, *J. Phys. Chem. Ref. Data* **9**, 1023 (1980); parameters for  $\sigma_{g,d.r.}$  from A. Veyssiere *et al.*, *Nucl. Phys.* **A159**, 561 (1970). Curves for these and other elements, compounds, and mixtures may be obtained from <http://physics.nist.gov/PhysRefData>. The photon total cross section is approximately flat for at least two decades beyond the energy range shown.
49. B.L. Berman and S.C. Fultz, *Rev. Mod. Phys.* **47**, 713 (1975).
50. J.W. Motz, H.A. Olsen, and H.W. Koch, *Rev. Mod. Phys.* **41**, 581 (1969).
51. P. Anthony *et al.*, *Phys. Rev. Lett.* **75**, 1949 (1995).
52. U.I. Uggerhoj, *Rev. Mod. Phys.* **77**, 1131 (2005).
53. L. Gerhardt and S.R. Klein, *Phys. Rev.* **D82**, 074017 (2010).
54. W.R. Nelson, H. Hirayama, and D.W.O. Rogers, "The EGS4 Code System," SLAC-265, Stanford Linear Accelerator Center (Dec. 1985).
55. *Experimental Techniques in High Energy Physics*, ed. T. Ferbel (Addison-Wesley, Menlo Park CA 1987).
56. U. Amaldi, *Phys. Scripta* **23**, 409 (1981).
57. E. Longo and I. Sestili, *Nucl. Instrum. Methods* **128**, 283 (1975).
58. G. Grindhammer *et al.*, in *Proceedings of the Workshop on Calorimetry for the Supercollider*, Tuscaloosa, AL, March 13-17, 1989, edited by R. Donaldson and M.G.D. Gilchrist (World Scientific, Teaneck, NJ, 1989), p. 151.
59. W.R. Nelson *et al.*, *Phys. Rev.* **149**, 201 (1966).
60. G. Bathow *et al.*, *Nucl. Phys.* **B20**, 592 (1970).
61. H.A. Bethe and W. Heitler, *Proc. Roy. Soc.* **A146**, 83 (1934);  
H.A. Bethe, *Proc. Cambridge Phil. Soc.* **30**, 542 (1934).
62. A.A. Petrukhin and V.V. Shestakov, *Can. J. Phys.* **46**, S377 (1968).
63. V.M. Galitskii and S.R. Kel'ner, *Sov. Phys. JETP* **25**, 948 (1967).
64. S.R. Kel'ner and Yu.D. Kotov, *Sov. J. Nucl. Phys.* **7**, 237 (1968).

65. R.P. Kokoulin and A.A. Petrukhin, in *Proceedings of the International Conference on Cosmic Rays*, Hobart, Australia, August 16–25, 1971, Vol. 4, p. 2436.
66. A.I. Nikishov, *Sov. J. Nucl. Phys.* **27**, 677 (1978).
67. Y.M. Andreev *et al.*, *Phys. Atom. Nucl.* **57**, 2066 (1994).
68. L.B. Bezrukov and E.V. Bugaev, *Sov. J. Nucl. Phys.* **33**, 635 (1981).
69. N.V. Mokhov, “The MARS Code System User’s Guide,” Fermilab-FN-628 (1995);  
N.V. Mokhov *et al.*, *Radiation Protection and Dosimetry*, vol. 116, part 2, pp. 99 (2005);  
Fermilab-Conf-04/053 (2004);  
N.V. Mokhov *et al.*, in *Proc. of Intl. Conf. on Nuclear Data for Science and Tech.* (Santa Fe, NM, 2004), AIP Conf. Proc. 769, part 2, p. 1618;  
Fermilab-Conf-04/269-AD (2004);  
<http://www-ap.fnal.gov/MARS/>.
70. P.H. Barrett *et al.*, *Rev. Mod. Phys.* **24**, 133 (1952).
71. A. Van Ginneken, *Nucl. Instrum. Methods* **A251**, 21 (1986).
72. U. Becker *et al.*, *Nucl. Instrum. Methods* **A253**, 15 (1986).
73. J.J. Eastman and S.C. Loken, in *Proceedings of the Workshop on Experiments, Detectors, and Experimental Areas for the Supercollider*, Berkeley, CA, July 7–17, 1987, edited by R. Donaldson and M.G.D. Gilchriese (World Scientific, Singapore, 1988), p. 542.
74. *Methods of Experimental Physics*, L.C.L. Yuan and C.-S. Wu, editors, Academic Press, 1961, Vol. 5A, p. 163.
75. W.W.M. Allison and P.R.S. Wright, “The Physics of Charged Particle Identification:  $dE/dx$ , Cherenkov Radiation, and Transition Radiation,” p. 371 in *Experimental Techniques in High Energy Physics*, T. Ferbel, editor, (Addison-Wesley 1987).
76. E.R. Hayes, R.A. Schluter, and A. Tamosaitis, “Index and Dispersion of Some Cherenkov Counter Gases,” ANL-6916 (1964).
77. T. Ypsilantis, “Particle Identification at Hadron Colliders,” CERN-EP/89-150 (1989), or ECFA 89-124, **2** 661 (1989).
78. I. Tamm, *J. Phys. U.S.S.R.*, **1**, 439 (1939).
79. H. Motz and L.I. Schiff, *Am. J. Phys.* **21**, 258 (1953).
80. B.N. Ratcliff, *Nucl. Instrum. Meth.* **A502**, 211 (2003).
81. S.K. Mandal, S.R. Klein, and J. D. Jackson, *Phys. Rev.* **D72**, 093003 (2005).
82. G.A. Askaryan, *Sov. Phys. JETP* **14**, 441 (1962).
83. P.W. Gorham *et al.*, *Phys. Rev.* **D72**, 023002 (2005).
84. E. Zas, F. Halzen, and T. Stanev, *Phys. Rev. D* **45**, 362(1992).
85. M.L. Cherry, *Phys. Rev.* **D10**, 3594–3607 (1974);  
M.L. Cherry, *Phys. Rev.* **D17**, 2245–2260 (1978).
86. B. Dolgoshein, *Nucl. Instrum. Methods* **A326**, 434–469 (1993).



## 31. PARTICLE DETECTORS AT ACCELERATORS

Revised 2011. See the various sections for authors.

31. PARTICLE DETECTORS AT ACCELERATORS . . . . .	339
31.1. Introduction . . . . .	339
31.2. Photon detectors . . . . .	339
31.2.1. Vacuum photodetectors . . . . .	340
31.2.1.1. Photomultiplier tubes . . . . .	340
31.2.1.2. Microchannel plates . . . . .	341
31.2.1.3. Hybrid photon detectors . . . . .	341
31.2.2. Gaseous photon detectors . . . . .	341
31.2.3. Solid-state photon detectors . . . . .	341
31.3. Organic scintillators . . . . .	342
31.3.1. Scintillation mechanism . . . . .	343
31.3.2. Caveats and cautions . . . . .	343
31.3.3. Scintillating and wavelength-shifting fibers . . . . .	343
31.4. Inorganic scintillators: . . . . .	344
31.5. Cherenkov detectors . . . . .	346
31.6. Gaseous detectors . . . . .	348
31.6.1. Energy loss and charge transport in gases . . . . .	348
31.6.2. Multi-Wire Proportional and Drift Chambers . . . . .	350
31.6.3. High Rate Effects . . . . .	351
31.6.4. Micro-Pattern Gas Detectors . . . . .	351
31.6.5. Time-projection chambers . . . . .	353
31.6.6. Transition radiation detectors (TRD's) . . . . .	354
31.6.7. Resistive-plate chambers . . . . .	355
31.7. Semiconductor detectors . . . . .	356
31.7.1. Materials Requirements . . . . .	356
31.7.2. Detector Configurations . . . . .	356
31.7.3. Signal Formation . . . . .	357
31.7.4. Radiation Damage . . . . .	357
31.8. Low-noise electronics . . . . .	357
31.9. Calorimeters . . . . .	360
31.9.1. Electromagnetic calorimeters . . . . .	360
31.9.2. Hadronic calorimeters . . . . .	361
31.9.3. Free electron drift velocities in liquid ionization chambers . . . . .	363
31.10. Superconducting magnets for collider detectors . . . . .	363
31.10.1. Solenoid Magnets . . . . .	363
31.10.2. Properties of collider detector magnets . . . . .	364
31.10.3. Toroidal magnets . . . . .	365
31.11. Measurement of particle momenta in a uniform magnetic field . . . . .	365
References . . . . .	365

## 31.1. Introduction

This review summarizes the detector technologies employed at accelerator particle physics experiments. Several of these detectors are also used in a non-accelerator context and examples of such applications will be provided. The detector techniques which are specific to non-accelerator particle physics experiments are the subject of Chap. 32. More detailed discussions of detectors and their underlying physics can be found in books by Ferbel [1], Kleinknecht [2], Knoll [3], Green [4], Leroy & Rancoita [5], and Grupen [6].

In Table 31.1 are given typical resolutions and deadtimes of common charged particle detectors. The quoted numbers are usually based on typical devices, and should be regarded only as rough approximations for new designs. The spatial resolution refers to the intrinsic detector resolution, i.e. without multiple scattering. We note that analog detector readout can provide better spatial resolution than digital readout by measuring the deposited charge in neighboring channels. Quoted ranges attempt to be representative of both possibilities. The time resolution is defined by how accurately the time at which a particle crossed the detector can be determined. The deadtime is the minimum separation in time between two resolved hits on the same channel. Typical performance of calorimetry and particle identification are provided in the relevant sections below.

**Table 31.1:** Typical resolutions and deadtimes of common charged particle detectors. Revised November 2011.

Detector Type	Intrinsic Spatial Resolution (rms)	Time Resolution	Dead Time
Resistive plate chamber	$\lesssim 10$ mm	1–2 ns	—
Streamer chamber	$300 \mu\text{m}^a$	$2 \mu\text{s}$	100 ms
Liquid argon drift [7]	$\sim 175\text{--}450 \mu\text{m}$	$\sim 200$ ns	$\sim 2 \mu\text{s}$
Scintillation tracker	$\sim 100 \mu\text{m}$	$100 \text{ps}/n^b$	10 ns
Bubble chamber	$10\text{--}150 \mu\text{m}$	1 ms	$50 \text{ms}^c$
Proportional chamber	$50\text{--}100 \mu\text{m}^d$	2 ns	20–200 ns
Drift chamber	$50\text{--}100 \mu\text{m}$	$2 \text{ns}^e$	20–100 ns
Micro-pattern gas detectors	$30\text{--}40 \mu\text{m}$	$< 10$ ns	10–100 ns
Silicon strip	pitch/(3 to 7) <sup>f</sup>	few ns <sup>g</sup>	$\lesssim 50 \text{ns}^g$
Silicon pixel	$\lesssim 10 \mu\text{m}$	few ns <sup>g</sup>	$\lesssim 50 \text{ns}^g$
Emulsion	$1 \mu\text{m}$	—	—

<sup>a</sup>  $300 \mu\text{m}$  is for 1 mm pitch (wirespacing/ $\sqrt{12}$ ).

<sup>b</sup>  $n$  = index of refraction.

<sup>c</sup> Multiple pulsing time.

<sup>d</sup> Delay line cathode readout can give  $\pm 150 \mu\text{m}$  parallel to anode wire.

<sup>e</sup> For two chambers.

<sup>f</sup> The highest resolution (“7”) is obtained for small-pitch detectors ( $\lesssim 25 \mu\text{m}$ ) with pulse-height-weighted center finding.

<sup>g</sup> Limited by the readout electronics [8].

## 31.2. Photon detectors

Updated August 2011 by D. Chakraborty (Northern Illinois U) and T. Sumiyoshi (Tokyo Metro U).

Most detectors in high-energy, nuclear, and astrophysics rely on the detection of photons in or near the visible range,  $100 \text{nm} \lesssim \lambda \lesssim 1000 \text{nm}$ , or  $E \approx$  a few eV. This range covers scintillation and Cherenkov radiation as well as the light detected in many astronomical observations.

Generally, photodetection involves generating a detectable electrical signal proportional to the (usually very small) number of incident photons. The process involves three distinct steps:

1. Generation of a primary photoelectron or electron-hole ( $e-h$ ) pair by an incident photon by the photoelectric or photoconductive effect,
2. Amplification of the p.e. signal to detectable levels by one or more multiplicative bombardment steps and/or an avalanche process (usually), and,

3. Collection of the secondary electrons to form the electrical signal. The important characteristics of a photodetector include the following in statistical averages:

1. Quantum efficiency (QE or  $\epsilon_Q$ ): the number of primary photoelectrons generated per incident photon ( $0 \leq \epsilon_Q \leq 1$ ; in silicon more than one  $e$ - $h$  pair per incident photon can be generated for  $\lambda \lesssim 165$  nm),
2. Collection efficiency (CE or  $\epsilon_C$ ): the overall acceptance factor other than the generation of photoelectrons ( $0 \leq \epsilon_C \leq 1$ ),
3. Gain ( $G$ ): the number of electrons collected for each photoelectron generated,
4. Dark current or dark noise: the electrical signal when there is no photon,
5. Energy resolution: electronic noise (ENC or  $N_e$ ) and statistical fluctuations in the amplification process compound the Poisson distribution of  $n_\gamma$  photons from a given source:

$$\frac{\sigma(E)}{\langle E \rangle} = \sqrt{\frac{f_N}{n_\gamma \epsilon_Q \epsilon_C} + \left( \frac{N_e}{G n_\gamma \epsilon_Q \epsilon_C} \right)^2}, \quad (31.1)$$

- where  $f_N$ , or the excess noise factor (ENF), is the contribution to the energy distribution variance due to amplification statistics [9],
6. Dynamic range: the maximum signal available from the detector (this is usually expressed in units of the response to noise-equivalent power, or NEP, which is the optical input power that produces a signal-to-noise ratio of 1),
  7. Time dependence of the response: this includes the transit time, which is the time between the arrival of the photon and the electrical pulse, and the transit time spread, which contributes to the pulse rise time and width, and
  8. Rate capability: inversely proportional to the time needed, after the arrival of one photon, to get ready to receive the next.

requirements, power consumption, calibration needs, aging, cost, and so on. Several technologies employing different phenomena for the three steps described above, and many variants within each, offer a wide range of solutions to choose from. The salient features of the main technologies and the common variants are described below. Some key characteristics are summarized in Table 31.2.

**31.2.1. Vacuum photodetectors:** Vacuum photodetectors can be broadly subdivided into three types: photomultiplier tubes, microchannel plates, and hybrid photodetectors.

**31.2.1.1. Photomultiplier tubes:** A versatile class of photon detectors, vacuum photomultiplier tubes (PMT) has been employed by a vast majority of all particle physics experiments to date [9]. Both “transmission-” and “reflection-type” PMT’s are widely used. In the former, the photocathode material is deposited on the inside of a transparent window through which the photons enter, while in the latter, the photocathode material rests on a separate surface that the incident photons strike. The cathode material has a low work function, chosen for the wavelength band of interest. When a photon hits the cathode and liberates an electron (the photoelectric effect), the latter is accelerated and guided by electric fields to impinge on a secondary-emission electrode, or dynode, which then emits a few ( $\sim 5$ ) secondary electrons. The multiplication process is repeated typically 10 times in series to generate a sufficient number of electrons, which are collected at the anode for delivery to the external circuit. The total gain of a PMT depends on the applied high voltage  $V$  as  $G = AV^{kn}$ , where  $k \approx 0.7$ – $0.8$  (depending on the dynode material),  $n$  is the number of dynodes in the chain, and  $A$  a constant (which also depends on  $n$ ). Typically,  $G$  is in the range of  $10^5$ – $10^6$ . Pulse risetimes are usually in the few nanosecond range. With *e.g.* two-level discrimination the effective time resolution can be much better.

**Table 31.2:** Representative characteristics of some photodetectors commonly used in particle physics. The time resolution of the devices listed here vary in the 10–2000 ps range.

Type	$\lambda$ (nm)	$\epsilon_Q \epsilon_C$	Gain	Risetime (ns)	Area (mm <sup>2</sup> )	1-p.e noise (Hz)	HV (V)	Price (USD)
PMT*	115–1700	0.15–0.25	$10^3$ – $10^7$	0.7–10	$10^2$ – $10^5$	$10$ – $10^4$	500–3000	100–5000
MCP*	100–650	0.01–0.10	$10^3$ – $10^7$	0.15–0.3	$10^2$ – $10^4$	0.1–200	500–3500	10–6000
HPD*	115–850	0.1–0.3	$10^3$ – $10^4$	7	$10^2$ – $10^5$	$10$ – $10^3$	$\sim 2 \times 10^4$	$\sim 600$
GPM*	115–500	0.15–0.3	$10^3$ – $10^6$	$O(0.1)$	$O(10)$	$10$ – $10^3$	300–2000	$O(10)$
APD	300–1700	$\sim 0.7$	$10$ – $10^8$	$O(1)$	$10$ – $10^3$	$1$ – $10^3$	400–1400	$O(100)$
PPD	320–900	0.15–0.3	$10^5$ – $10^6$	$\sim 1$	1–10	$O(10^6)$	30–60	$O(100)$
VLPC	500–600	$\sim 0.9$	$\sim 5 \times 10^4$	$\sim 10$	1	$O(10^4)$	$\sim 7$	$\sim 1$

\*These devices often come in multi-anode configurations. In such cases, area, noise, and price are to be considered on a “per readout-channel” basis.

The QE is a strong function of the photon wavelength ( $\lambda$ ), and is usually quoted at maximum, together with a range of  $\lambda$  where the QE is comparable to its maximum. Spatial uniformity and linearity with respect to the number of photons are highly desirable in a photodetector’s response.

Optimization of these factors involves many trade-offs and vary widely between applications. For example, while a large gain is desirable, attempts to increase the gain for a given device also increases the ENF and after-pulsing (“echos” of the main pulse). In solid-state devices, a higher QE often requires a compromise in the timing properties. In other types, coverage of large areas by focusing increases the transit time spread.

Other important considerations also are highly application-specific. These include the photon flux and wavelength range, the total area to be covered and the efficiency required, the volume available to accommodate the detectors, characteristics of the environment such as chemical composition, temperature, magnetic field, ambient background, as well as ambient radiation of different types and, mode of operation (continuous or triggered), bias (high-voltage)

A large variety of PMT’s, including many just recently developed, covers a wide span of wavelength ranges from infrared (IR) to extreme ultraviolet (XUV) [10]. They are categorized by the window materials, photocathode materials, dynode structures, anode configurations, *etc.* Common window materials are borosilicate glass for IR to near-UV, fused quartz and sapphire ( $\text{Al}_2\text{O}_3$ ) for UV, and  $\text{MgF}_2$  or LiF for XUV. The choice of photocathode materials include a variety of mostly Cs- and/or Sb-based compounds such as CsI, CsTe, bi-alkali (SbRbCs, SbKCs), multi-alkali ( $\text{SbNa}_2\text{KCs}$ ), GaAs(Cs), GaAsP, *etc.* Sensitive wavelengths and peak quantum efficiencies for these materials are summarized in Table 31.3. Typical dynode structures used in PMT’s are circular cage, line focusing, box and grid, venetian blind, and fine mesh. In some cases, limited spatial resolution can be obtained by using a mosaic of multiple anodes. Fast PMT’s with very large windows—measuring up to 508 mm across—have been developed in recent years for detection of Cherenkov radiation in neutrino experiments such as Super-Kamiokande and KamLAND among many others. Specially prepared low-radioactivity glass is used to make these PMT’s, and they are also able to withstand the high pressure of

the surrounding liquid.

PMT's are vulnerable to magnetic fields—sometimes even the geomagnetic field causes large orientation-dependent gain changes. A high-permeability metal shield is often necessary. However, proximity-focused PMT's, *e.g.* the fine-mesh types, can be used even in a high magnetic field ( $\geq 1$  T) if the electron drift direction is parallel to the field. CMS uses custom-made vacuum phototriodes (VPT) mounted on the back face of projective lead tungstate crystals to detect scintillation light in the endcap sections of its electromagnetic calorimeters, which are inside a 3.8 T superconducting solenoid. A VPT employs a single dynode (thus,  $G \approx 10$ ) placed close to the photocathode, and a mesh anode plane between the two, to help it cope with the strong magnetic field, which is not too unfavorably oriented with respect to the photodetector axis in the endcaps (within  $25^\circ$ ), but where the radiation level is too high for Avalanche Photodiodes (APD's) like those used in the barrel section.

**31.2.1.2. Microchannel plates:** A typical Microchannel plate (MCP) photodetector consists of one or more  $\sim 2$  mm thick glass plates with densely packed  $O(10 \mu\text{m})$ -diameter cylindrical holes, or “channels”, sitting between the transmission-type photocathode and anode planes, separated by  $O(1 \text{ mm})$  gaps. Instead of discrete dynodes, the inner surface of each cylindrical tube serves as a continuous dynode for the entire cascade of multiplicative bombardments initiated by a photoelectron. Gain fluctuations can be minimized by operating in a saturation mode, whence each channel is only capable of a binary output, but the sum of all channel outputs remains proportional to the number of photons received so long as the photon flux is low enough to ensure that the probability of a single channel receiving more than one photon during a single time gate is negligible. MCP's are thin, offer good spatial resolution, have excellent time resolution ( $\sim 20$  ps), and can tolerate random magnetic fields up to 0.1 T and axial fields up to  $\sim 1$  T. However, they suffer from relatively long recovery time per channel and short lifetime. MCP's are widely employed as image-intensifiers, although not so much in HEP or astrophysics.

**31.2.1.3. Hybrid photon detectors:** Hybrid photon detectors (HPD) combine the sensitivity of a vacuum PMT with the excellent spatial and energy resolutions of a Si sensor [11]. A single photoelectron ejected from the photocathode is accelerated through a potential difference of  $\sim 20$  kV before it impinges on the silicon sensor/anode. The gain nearly equals the maximum number of  $e$ - $h$  pairs that could be created from the entire kinetic energy of the accelerated electron:  $G \approx eV/w$ , where  $e$  is the electronic charge,  $V$  is the applied potential difference, and  $w \approx 3.7$  eV is the mean energy required to create an  $e$ - $h$  pair in Si at room temperature. Since the gain is achieved in a single step, one might expect to have the excellent resolution of a simple Poisson statistic with large mean, but in fact it is even better, thanks to the Fano effect discussed in Sec. 31.7.

Low-noise electronics must be used to read out HPD's if one intends to take advantage of the low fluctuations in gain, *e.g.* when counting small numbers of photons. HPD's can have the same  $\epsilon_Q \epsilon_C$  and window geometries as PMT's and can be segmented down to  $\sim 50 \mu\text{m}$ . However, they require rather high biases and will not function in a magnetic field. The exception is proximity-focused devices ( $\Rightarrow$  no (de)magnification) in an axial field. With time resolutions of  $\sim 10$  ps and superior rate capability, proximity-focused HPD's can be an alternative to MCP's. Current applications of HPD's include the CMS hadronic calorimeter and the RICH detector in LHCb. Large-size HPD's with sophisticated focusing may be suitable for future water Cherenkov experiments.

Hybrid APD's (HAPD's) add an avalanche multiplication step following the electron bombardment to boost the gain by a factor of  $\sim 50$ . This affords a higher gain and/or lower electrical bias, but also degrades the signal definition.

**Table 31.3:** Properties of photocathode and window materials commonly used in vacuum photodetectors [10].

Photocathode material	$\lambda$ (nm)	Window material	Peak $\epsilon_Q$ ( $\lambda/\text{nm}$ )
CsI	115–200	MgF <sub>2</sub>	0.11 (140)
CsTe	115–320	MgF <sub>2</sub>	0.14 (240)
Bi-alkali	300–650	Borosilicate	0.27 (390)
	160–650	Synthetic Silica	0.27 (390)
“Ultra Bi-alkali”	300–650	Borosilicate	0.43 (350)
	160–650	Synthetic Silica	0.43 (350)
Multi-alkali	300–850	Borosilicate	0.20 (360)
	160–850	Synthetic Silica	0.20 (360)
GaAs(Cs)*	160–930	Synthetic Silica	0.23 (280)
GaAsP(Cs)	300–750	Borosilicate	0.50 (500)
InP/InGaAsP <sup>†</sup>	350–1700	Borosilicate	0.01 (1100)

\*Reflection type photocathode is used. <sup>†</sup>Requires cooling to  $\sim -80^\circ\text{C}$ .

**31.2.2. Gaseous photon detectors:** In gaseous photomultipliers (GPM) a photoelectron in a suitable gas mixture initiates an avalanche in a high-field region, producing a large number of secondary impact-ionization electrons. In principle the charge multiplication and collection processes are identical to those employed in gaseous tracking detectors such as multiwire proportional chambers, micromesh gaseous detectors (Micromegas), or gas electron multipliers (GEM). These are discussed in Sec. 31.6.4.

The devices can be divided into two types depending on the photocathode material. One type uses solid photocathode materials much in the same way as PMT's. Since it is resistant to gas mixtures typically used in tracking chambers, CsI is a common choice. In the other type, photoionization occurs on suitable molecules vaporized and mixed in the drift volume. Most gases have photoionization work functions in excess of 10 eV, which would limit their sensitivity to wavelengths far too short. However, vapors of TMAE (tetrakis dimethyl-amine ethylene) or TEA (tri-ethyl-amine), which have smaller work functions (5.3 eV for TMAE and 7.5 eV for TEA), are suited for XUV photon detection [12]. Since devices like GEM's offer sub-mm spatial resolution, GPM's are often used as position-sensitive photon detectors. They can be made into flat panels to cover large areas ( $O(1 \text{ m}^2)$ ), can operate in high magnetic fields, and are relatively inexpensive. Many of the ring imaging Cherenkov (RICH) detectors to date have used GPM's for the detection of Cherenkov light [13]. Special care must be taken to suppress the photon-feedback process in GPM's. It is also important to maintain high purity of the gas as minute traces of O<sub>2</sub> can significantly degrade the detection efficiency.

**31.2.3. Solid-state photon detectors:** In a phase of rapid development, solid-state photodetectors are competing with vacuum- or gas-based devices for many existing applications and making way for a multitude of new ones. Compared to traditional vacuum- and gaseous photodetectors, solid-state devices are more compact, lightweight, rugged, tolerant to magnetic fields, and often cheaper. They also allow fine pixelization, are easy to integrate into large systems, and can operate at low electric potentials, while matching or exceeding most performance criteria. They are particularly well suited for detection of  $\gamma$ - and X-rays. Except for applications where coverage of very large areas or dynamic range is required, solid-state detectors are proving to be the better choice. Some hybrid devices attempt to combine the best features of different technologies while applications of nanotechnology are opening up exciting new possibilities.

Silicon photodiodes (PD) are widely used in high-energy physics as particle detectors and in a great number of applications (including solar cells!) as light detectors. The structure is discussed in some detail in Sec. 31.7. In its simplest form, the PD is a reverse-biased  $p$ - $n$  junction. Photons with energies above the indirect bandgap energy (wavelengths shorter than about 1050 nm, depending on the temperature) can create  $e$ - $h$  pairs (the photoconductive effect), which are collected on the  $p$  and  $n$  sides, respectively. Often, as in the PD's

used for crystal scintillator readout in CLEO, L3, Belle, BaBar, and GLAST, intrinsic silicon is doped to create a *p-i-n* structure. The reverse bias increases the thickness of the depleted region; in the case of these particular detectors, to full depletion at a depth of about 100  $\mu\text{m}$ . Increasing the depletion depth decreases the capacitance (and hence electronic noise) and extends the red response. Quantum efficiency can exceed 90%, but falls toward the red because of the increasing absorption length of light in silicon. The absorption length reaches 100  $\mu\text{m}$  at 985 nm. However, since  $G = 1$ , amplification is necessary. Optimal low-noise amplifiers are slow, but, even so, noise limits the minimum detectable signal in room-temperature devices to several hundred photons.

Very large arrays containing  $O(10^7)$  of  $O(10 \mu\text{m}^2)$ -sized photodiodes pixelizing a plane are widely used to photograph all sorts of things from everyday subjects at visible wavelengths to crystal structures with X-rays and astronomical objects from infrared to UV. To limit the number of readout channels, these are made into charge-coupled devices (CCD), where pixel-to-pixel signal transfer takes place over thousands of synchronous cycles with sequential output through shift registers [14]. Thus, high spatial resolution is achieved at the expense of speed and timing precision. Custom-made CCD's have virtually replaced photographic plates and other imagers for astronomy and in spacecraft. Typical QE's exceed 90% over much of the visible spectrum, and "thick" CCD's have useful QE up to  $\lambda = 1 \mu\text{m}$ . Active Pixel Sensor (APS) arrays with a preamplifier on each pixel and CMOS processing afford higher speeds, but are challenged at longer wavelengths. Much R&D is underway to overcome the limitations of both CCD and CMOS imagers.

In APD's, an exponential cascade of impact ionizations initiated by the original photogenerated *e-h* pair under a large reverse-bias voltage leads to an avalanche breakdown [15]. As a result, detectable electrical response can be obtained from low-intensity optical signals down to single photons. Excellent junction uniformity is critical, and a guard ring is generally used as a protection against edge breakdown. Well-designed APD's, such as those used in CMS' crystal-based electromagnetic calorimeter, have achieved  $\epsilon_Q \epsilon_C \approx 0.7$  with sub-ns response time. The sensitive wavelength window and gain depend on the semiconductor used. The gain is typically 10–200 in linear and up to  $10^8$  in Geiger mode of operation. Stability and close monitoring of the operating temperature are important for linear-mode operation, and substantial cooling is often necessary. Position-sensitive APD's use time information at multiple anodes to calculate the hit position.

One of the most promising recent developments in the field is that of devices consisting of large arrays ( $O(10^3)$ ) of tiny APD's packed over a small area ( $O(1 \text{ mm}^2)$ ) and operated in a limited Geiger mode [16]. Among different names used for this class of photodetectors, "PPD" (for "Pixelized Photon Detector") is most widely accepted (formerly "SiPM"). Although each cell only offers a binary output, linearity with respect to the number of photons is achieved by summing the cell outputs in the same way as with a MCP in saturation mode (see above). PPD's are being adopted as the preferred solution for various purposes including medical imaging, *e.g.* positron emission tomography (PET). These compact, rugged, and economical devices allow auto-calibration through decent separation of photoelectron peaks and offer gains of  $O(10^6)$  at a moderate bias voltage ( $\sim 50 \text{ V}$ ). However, the single-photoelectron noise of a PPD, being the logical "or" of  $O(10^3)$  Geiger APD's, is rather large:  $O(1 \text{ MHz/mm}^2)$  at room temperature. PPD's are particularly well-suited for applications where triggered pulses of several photons are expected over a small area, *e.g.* fiber-guided scintillation light. Intense R&D is expected to lower the noise level and improve radiation hardness, resulting in coverage of larger areas and wider applications. Attempts are being made to combine the fabrication of the sensors and the front-end electronics (ASIC) in the same process with the goal of making PPD's and other finely pixelized solid-state photodetectors extremely easy to use.

Of late, much R&D has been directed to *p-i-n* diode arrays based on thin polycrystalline diamond films formed by chemical vapor deposition (CVD) on a hot substrate ( $\sim 1000 \text{ K}$ ) from a hydrocarbon-containing gas mixture under low pressure ( $\sim 100 \text{ mbar}$ ). These devices have maximum sensitivity in the extreme- to moderate-UV

region [17]. Many desirable characteristics, including high tolerance to radiation and temperature fluctuations, low dark noise, blindness to most of the solar radiation spectrum, and relatively low cost make them ideal for space-based UV/XUV astronomy, measurement of synchrotron radiation, and luminosity monitoring at (future) lepton collider(s).

Visible-light photon counters (VLPC) utilize the formation of an impurity band only 50 meV below the conduction band in As-doped Si to generate strong ( $G \approx 5 \times 10^4$ ) yet sharp response to single photons with  $\epsilon_Q \approx 0.9$  [18]. The smallness of the band gap considerably reduces the gain dispersion. Only a very small bias ( $\sim 7 \text{ V}$ ) is needed, but high sensitivity to infrared photons requires cooling below 10 K. The dark noise increases sharply and exponentially with both temperature and bias. The Run 2 DØ detector used 86000 VLPC's to read the optical signal from its scintillating-fiber tracker and scintillator-strip preshower detectors.

### 31.3. Organic scintillators

Revised August 2011 by Kurtis F. Johnson (FSU).

Organic scintillators are broadly classed into three types, crystalline, liquid, and plastic, all of which utilize the ionization produced by charged particles (see Sec. 30.2 of this *Review*) to generate optical photons, usually in the blue to green wavelength regions [19]. Plastic scintillators are by far the most widely used, liquid organic scintillator is finding increased use, and crystal organic scintillators are practically unused in high-energy physics. Plastic scintillator densities range from 1.03 to 1.20  $\text{g cm}^{-3}$ . Typical photon yields are about 1 photon per 100 eV of energy deposit [20]. A one-cm-thick scintillator traversed by a minimum-ionizing particle will therefore yield  $\approx 2 \times 10^4$  photons. The resulting photoelectron signal will depend on the collection and transport efficiency of the optical package and the quantum efficiency of the photodetector.

Organic scintillator does not respond linearly to the ionization density. Very dense ionization columns emit less light than expected on the basis of  $dE/dx$  for minimum-ionizing particles. A widely used semi-empirical model by Birks posits that recombination and quenching effects between the excited molecules reduce the light yield [21]. These effects are more pronounced the greater the density of the excited molecules. Birks' formula is

$$\frac{d\mathcal{L}}{dx} = \mathcal{L}_0 \frac{dE/dx}{1 + k_B dE/dx}, \quad (31.2)$$

where  $\mathcal{L}$  is the luminescence,  $\mathcal{L}_0$  is the luminescence at low specific ionization density, and  $k_B$  is Birks' constant, which must be determined for each scintillator by measurement. Decay times are in the ns range; rise times are much faster. The high light yield and fast response time allow the possibility of sub-ns timing resolution [22]. The fraction of light emitted during the decay "tail" can depend on the exciting particle. This allows pulse shape discrimination as a technique to carry out particle identification. Because of the hydrogen content (carbon to hydrogen ratio  $\approx 1$ ) plastic scintillator is sensitive to proton recoils from neutrons. Ease of fabrication into desired shapes and low cost has made plastic scintillator a common detector element. In the form of scintillating fiber it has found widespread use in tracking and calorimetry [23].

Demand for large volume detectors has lead to increased use of liquid organic scintillator, which has the same scintillation mechanism as plastic scintillator, due to its cost advantage. The containment vessel defines the detector shape; photodetectors or waveshifters may be immersed in the liquid.

### 31.3.1. Scintillation mechanism :

A charged particle traversing matter leaves behind it a wake of excited molecules. Certain types of molecules, however, will release a small fraction ( $\approx 3\%$ ) of this energy as optical photons. This process, scintillation, is especially marked in those organic substances which contain aromatic rings, such as polystyrene (PS) and polyvinyltoluene (PVT). Liquids which scintillate include toluene, xylene and pseudocumene.

In fluorescence, the initial excitation takes place via the absorption of a photon, and de-excitation by emission of a longer wavelength photon. Fluors are used as “wavelength shifters” to shift scintillation light to a more convenient wavelength. Occurring in complex molecules, the absorption and emission are spread out over a wide band of photon energies, and have some overlap, that is, there is some fraction of the emitted light which can be re-absorbed [24]. This “self-absorption” is undesirable for detector applications because it causes a shortened attenuation length. The wavelength difference between the major absorption and emission peaks is called the Stokes shift. It is usually the case that the greater the Stokes shift, the smaller the self-absorption thus, a large Stokes shift is a desirable property for a fluor.

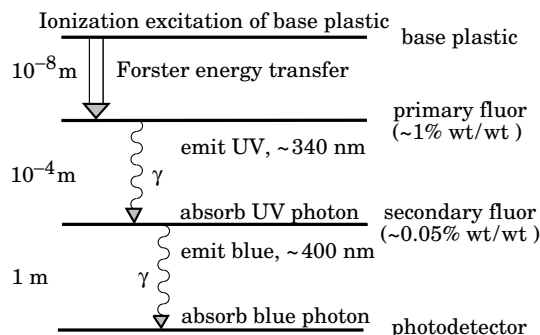


**Figure 31.1:** Cartoon of scintillation “ladder” depicting the operating mechanism of organic scintillator. Approximate fluor concentrations and energy transfer distances for the separate sub-processes are shown.

The plastic scintillators used in high-energy physics are binary or ternary solutions of selected fluors in a plastic base containing aromatic rings. (See the appendix in Ref. 25 for a comprehensive list of components.) Virtually all plastic scintillators contain as a base either PVT or PS. PVT-based scintillator can be up to 50% brighter.

Ionization in the plastic base produces UV photons with short attenuation length (several mm). Longer attenuation lengths are obtained by dissolving a “primary” fluor in high concentration (1% by weight) into the base, which is selected to efficiently re-radiate absorbed energy at wavelengths where the base is more transparent (see Fig. 31.1).

The primary fluor has a second important function. The decay time of the scintillator base material can be quite long – in pure polystyrene it is 16 ns, for example. The addition of the primary fluor in high concentration can shorten the decay time by an order of magnitude and increase the total light yield. At the concentrations used (1% and greater), the average distance between a fluor molecule and an excited base unit is around 100 Å, much less than a wavelength of light. At these distances the predominant mode of energy transfer from base to fluor is not the radiation of a photon, but a resonant dipole-dipole interaction, first described by Foerster, which strongly couples the base and fluor [26]. The strong coupling sharply increases the speed and the light yield of the plastic scintillators.

Unfortunately, a fluor which fulfills other requirements is usually not completely adequate with respect to emission wavelength or attenuation length, so it is necessary to add yet another wavelength shifter (the “secondary” fluor), at fractional percent levels, and occasionally a third (not shown in Fig. 31.1).

External wavelength shifters are widely used to aid light collection in complex geometries. Scintillation light is captured by a lightpipe

comprising a wave-shifting fluor dissolved in a nonscintillating base. The wavelength shifter must be insensitive to ionizing radiation and Cherenkov light. A typical wavelength shifter uses an acrylic base because of its good optical qualities, a single fluor to shift the light emerging from the plastic scintillator to the blue-green, and contains ultra-violet absorbing additives to deaden response to Cherenkov light.

### 31.3.2. Caveats and cautions :

Plastic scintillators are reliable, robust, and convenient. However, they possess quirks to which the experimenter must be alert. Exposure to solvent vapors, high temperatures, mechanical flexing, irradiation, or rough handling will aggravate the process. A particularly fragile region is the surface which can “craze” develop microcracks which degrade its transmission of light by total internal reflection. Crazeing is particularly likely where oils, solvents, or *fingerprints* have contacted the surface.

They have a long-lived luminescence which does not follow a simple exponential decay. Intensities at the  $10^{-4}$  level of the initial fluorescence can persist for hundreds of ns [19,27].

They will decrease their light yield with increasing partial pressure of oxygen. This can be a 10% effect in an artificial atmosphere [28]. It is not excluded that other gases may have similar quenching effects.

Their light yield may be changed by a magnetic field. The effect is very nonlinear and apparently not all types of plastic scintillators are so affected. Increases of  $\approx 3\%$  at 0.45 T have been reported [29]. Data are sketchy and mechanisms are not understood.

Irradiation of plastic scintillators creates color centers which absorb light more strongly in the UV and blue than at longer wavelengths. This poorly understood effect appears as a reduction both of light yield and attenuation length. Radiation damage depends not only on the integrated dose, but on the dose rate, atmosphere, and temperature, before, during and after irradiation, as well as the materials properties of the base such as glass transition temperature, polymer chain length, *etc.* Annealing also occurs, accelerated by the diffusion of atmospheric oxygen and elevated temperatures. The phenomena are complex, unpredictable, and not well understood [30]. Since color centers are less disruptive at longer wavelengths, the most reliable method of mitigating radiation damage is to shift emissions at every step to the longest practical wavelengths, *e.g.*, utilize fluors with large Stokes shifts (aka the “Better red than dead” strategy).

### 31.3.3. Scintillating and wavelength-shifting fibers :

The clad optical fiber comprising scintillator and wavelength shifter (WLS) is particularly useful [31]. Since the initial demonstration of the scintillating fiber (SCIFI) calorimeter [32], SCIFI techniques have become mainstream [33]. SCIFI calorimeters are fast, dense, radiation hard, and can have leadglass-like resolution. SCIFI trackers can handle high rates and are radiation tolerant, but the low photon yield at the end of a long fiber (see below) forces the use of sensitive photodetectors. WLS scintillator readout of a calorimeter allows a very high level of hermeticity since the solid angle blocked by the fiber on its way to the photodetector is very small. The sensitive region of scintillating fibers can be controlled by splicing them onto clear (non-scintillating/non-WLS) fibers.

A typical configuration would be fibers with a core of polystyrene-based scintillator or WLS (index of refraction  $n = 1.59$ ), surrounded by a cladding of PMMA ( $n = 1.49$ ) a few microns thick, or, for added light capture, with another cladding of fluorinated PMMA with  $n = 1.42$ , for an overall diameter of 0.5 to 1 mm. The fiber is drawn from a boule and great care is taken during production to ensure that the intersurface between the core and the cladding has the highest possible uniformity and quality, so that the signal transmission via total internal reflection has a low loss. The fraction of generated light which is transported down the optical pipe is denoted the capture fraction and is about 6% for the single-clad fiber and 10% for the double-clad fiber. The number of photons from the fiber available at the photodetector is always smaller than desired, and increasing the light yield has proven difficult. A minimum-ionizing particle traversing a high-quality 1 mm diameter fiber perpendicular to its axis will produce fewer than 2000 photons, of which about 200 are captured. Attenuation may eliminate 95% of these photons in a large collider tracker.

A scintillating or WLS fiber is often characterized by its attenuation

length, over which the signal is attenuated to  $1/e$  of its original value. Many factors determine the attenuation length, including the importance of re-absorption of emitted photons by the polymer base or dissolved fluors, the level of crystallinity of the base polymer, and the quality of the total internal reflection boundary [34]. Attenuation lengths of several meters are obtained by high quality fibers. However, it should be understood that the attenuation length is not the sole measure of fiber quality. Among other things, it is not constant with distance from the excitation source and it is wavelength dependent.

### 31.4. Inorganic scintillators:

Revised September 2009 by R.-Y. Zhu (California Institute of Technology) and C.L. Woody (BNL).

Inorganic crystals form a class of scintillating materials with much higher densities than organic plastic scintillators (typically  $\sim 4\text{--}8\text{ g/cm}^3$ ) with a variety of different properties for use as scintillation detectors. Due to their high density and high effective atomic number, they can be used in applications where high stopping power or a high conversion efficiency for electrons or photons is required. These include total absorption electromagnetic calorimeters (see Sec. 31.9.1), which consist of a totally active absorber (as opposed to a sampling calorimeter), as well as serving as gamma ray detectors over a wide range of energies. Many of these crystals also have very high light output, and can therefore provide excellent energy resolution down to very low energies ( $\sim$  few hundred keV).

Some crystals are intrinsic scintillators in which the luminescence is produced by a part of the crystal lattice itself. However, other crystals require the addition of a dopant, typically fluorescent ions such as thallium (Tl) or cerium (Ce) which is responsible for producing the scintillation light. However, in both cases, the scintillation mechanism is the same. Energy is deposited in the crystal by ionization, either directly by charged particles, or by the conversion of photons into electrons or positrons which subsequently produce ionization. This energy is transferred to the luminescent centers which then radiate scintillation photons. The efficiency  $\eta$  for the conversion of energy deposit in the crystal to scintillation light can be expressed by the relation [35]

$$\eta = \beta \cdot S \cdot Q \quad (31.3)$$

where  $\beta$  is the efficiency of the energy conversion process,  $S$  is the efficiency of energy transfer to the luminescent center, and  $Q$  is the quantum efficiency of the luminescent center. The value of  $\eta$  ranges between 0.1 and  $\sim 1$  depending on the crystal, and is the main factor in determining the intrinsic light output of the scintillator. In addition, the scintillation decay time is primarily determined by the energy transfer and emission process. The decay time of the scintillator is mainly dominated by the decay time of the luminescent center. For example, in the case of thallium doped sodium iodide (NaI(Tl)), the value of  $\eta$  is  $\sim 0.5$ , which results in a light output  $\sim 40,000$  photons per MeV of energy deposit. This high light output is largely due to the high quantum efficiency of the thallium ion ( $Q \sim 1$ ), but the decay time is rather slow ( $\tau \sim 250$  ns).

Table 31.4 lists the basic properties of some commonly used inorganic crystal scintillators. NaI(Tl) is one of the most common and widely used scintillators, with an emission that is well matched to a bi-alkali photomultiplier tube, but it is highly hygroscopic and difficult to work with, and has a rather low density. CsI(Tl) has high light yield, an emission that is well matched to solid state photodiodes, and is mechanically robust (high plasticity and resistance to cracking). However, it needs careful surface treatment and is slightly hygroscopic. Compared with CsI(Tl), pure CsI has identical mechanical properties, but faster emission at shorter wavelengths and light output approximately an order of magnitude lower. BaF<sub>2</sub> has a fast component with a sub-nanosecond decay time, and is the fastest known scintillator. However, it also has a slow component with a much longer decay time ( $\sim 630$  ns). Bismuth germanate (Bi<sub>4</sub>Ge<sub>3</sub>O<sub>12</sub> or BGO) has a high density, and consequently a short radiation length  $X_0$  and Molière radius  $R_M$ . BGO's emission is well-matched to the spectral sensitivity of photodiodes, and it is easy to handle and not hygroscopic. Lead tungstate (PbWO<sub>4</sub> or PWO) has a very high density, with a very short  $X_0$  and  $R_M$ , but its intrinsic light yield is rather low.

Cerium doped lutetium oxyorthosilicate (Lu<sub>2</sub>SiO<sub>5</sub>:Ce, or LSO:Ce) [36] and cerium doped lutetium-yttrium oxyorthosilicate (Lu<sub>2(1-x)</sub>Y<sub>2x</sub>SiO<sub>5</sub>, LYSO:Ce) [37] are dense crystal scintillators which have a high light yield and a fast decay time. Only properties of LSO:Ce is listed in Table 31.4 since the properties of LYSO:Ce are similar to that of LSO:Ce except a little lower density than LSO:Ce depending on the yttrium fraction in LYSO:Ce. This material is also featured with excellent radiation hardness [38], so is expected to be used where extraordinary radiation hardness is required.

Table 31.4 also includes cerium doped lanthanum tri-halides, such as LaBr<sub>3</sub> [39], which is brighter and faster than LSO:Ce, but it is highly hygroscopic and has a lower density. The FWHM energy resolution measured for this material coupled to a PMT with bi-alkali photocathode for 0.662 MeV  $\gamma$ -rays from a <sup>137</sup>Cs source is about 3%, which is the best among all inorganic crystal scintillators. For this reason, LaBr<sub>3</sub> is expected to be widely used in applications where a good energy resolution for low energy photons are required, such as homeland security.

Beside the crystals listed in Table 31.4, a number of new crystals are being developed that may have potential applications in high energy or nuclear physics. Of particular interest is the family of yttrium and lutetium perovskites, which include YAP (YAlO<sub>3</sub>:Ce) and LuAP (LuAlO<sub>3</sub>:Ce) and their mixed compositions. These have been shown to be linear over a large energy range [40], and have the potential for providing extremely good intrinsic energy resolution. In addition, other fluoride crystals such as CeF<sub>3</sub> have been shown to provide excellent energy resolution in calorimeter applications.

Aiming at the best jet-mass resolution inorganic scintillators are being investigated for HEP calorimeters with dual readout for both Cherenkov and scintillation light to be used at future linear colliders. These materials may be used for an electromagnetic calorimeter [41] or a homogeneous hadronic calorimetry (HHCAL) detector concept, including both electromagnetic and hadronic parts [42]. Because of the unprecedented volume (70 to 100 m<sup>3</sup>) foreseen for the HHCAL detector concept the materials must be (1) dense (to minimize the leakage) and (2) cost-effective. It should also be UV transparent (for effective collection of the Cherenkov light) and allow for a clear discrimination between the Cherenkov and scintillation light. The preferred scintillation light is thus at a longer wavelength, and not necessarily bright or fast. Dense crystals, scintillating glasses and ceramics offer a very attractive implementation for this detector concept. Inorganic crystals being investigated are lead fluoride (PbF<sub>2</sub>), lead chloride fluoride (PbFCl) and BSO [43].

Table 31.4 gives the light output of other crystals relative to NaI(Tl) and their dependence to the temperature variations measured for crystal samples of 1.5  $X_0$  cube with a Tyvek paper wrapping and a full end face coupled to a photodetector [44]. The quantum efficiencies of the photodetector is taken out to facilitate a direct comparison of crystal's light output. However, the useful signal produced by a scintillator is usually quoted in terms of the number of photoelectrons per MeV produced by a given photodetector. The relationship between the number of photons/MeV produced and photoelectrons/MeV detected involves the factors for the light collection efficiency  $L$  and the quantum efficiency  $QE$  of the photodetector:

$$N_{p.e.}/\text{MeV} = L \cdot QE \cdot N_{\gamma}/\text{MeV} \quad (31.4)$$

$L$  includes the transmission of scintillation light within the crystal (*i.e.*, the bulk attenuation length of the material), reflections and scattering from the surfaces, and the size and shape of the crystal. These factors can vary considerably depending on the sample, but can be in the range of  $\sim 10\text{--}60\%$ . The internal light transmission depends on the intrinsic properties of the material, *e.g.* the density and type of the scattering centers and defects that can produce internal absorption within the crystal, and can be highly affected by factors such as radiation damage, as discussed below.

The quantum efficiency depends on the type of photodetector used to detect the scintillation light, which is typically  $\sim 15\text{--}20\%$  for photomultiplier tubes and  $\sim 70\%$  for silicon photodiodes for visible wavelengths. The quantum efficiency of the detector is usually highly wavelength dependent and should be matched to the particular crystal of interest to give the highest quantum yield at the wavelength

corresponding to the peak of the scintillation emission. Fig. 31.2 shows the quantum efficiencies of two photodetectors, a Hamamatsu R2059 PMT with bi-alkali cathode and quartz window and a Hamamatsu S8664 avalanche photodiode (APD) as a function of wavelength. Also shown in the figure are emission spectra of three crystal scintillators, BGO, LSO:Ce/LYSO:Ce and CsI(Tl), and the numerical values of the emission weighted quantum efficiency. The area under each emission spectrum is proportional to crystal's light yield, as shown in Table 31.4, where the quantum efficiencies of the photodetector has been taken out. Results with different photodetectors can be significantly different. For example, the response of CsI(Tl) relative to NaI(Tl) with a standard photomultiplier tube with a bi-alkali photo-cathode, e.g. Hamamatsu R2059, would be 45 rather than 165 because of the photomultiplier's low quantum efficiency at longer wavelengths. For scintillators which emit in the UV, a detector with a quartz window should be used.

For very low energy applications (typically below 1 MeV), non-proportionality of the scintillation light yield may be important. It has been known for a long time that the conversion factor between the energy deposited in a crystal scintillator and the number of photons produced is not constant. It is also known that the energy resolution measured by all crystal scintillators for low energy  $\gamma$ -rays is significantly worse than the contribution from photo-electron statistics alone, indicating an intrinsic contribution from the scintillator itself. Precision measurement using low energy electron beam shows that this non-proportionality is crystal dependent [45]. Recent study on this issue also shows that this effect is also sample dependent even for the same crystal [46]. Further work is therefore needed to fully understand this subject.

One important issue related to the application of a crystal scintillator is its radiation hardness. Stability of its light output, or the ability to track and monitor the variation of its light output in a radiation environment, is required for high resolution and precision calibration [47]. All known crystal scintillators suffer from radiation damage. A common damage phenomenon is the appearance of radiation induced absorption caused by the formation of color centers originated from the impurities or point defects in the crystal. This radiation induced absorption reduces the light attenuation length in the crystal, and hence its light output. For crystals with high defect density, a severe reduction of light attenuation length may cause a distortion of the light response uniformity, leading to a degradation of the energy resolution. Additional radiation damage effects may include a reduced intrinsic scintillation light yield (damage to the luminescent centers) and an increased phosphorescence (afterglow). For crystals to be used in the construction a high precision calorimeter in a radiation environment, its scintillation mechanism must not be damaged and its light attenuation length in the expected radiation environment must be long enough so that its light response uniformity, and thus its energy resolution, does not change [48].

Most of the crystals listed in Table 31.4 have been used in high energy or nuclear physics experiments when the ultimate energy resolution for electrons and photons is desired. Examples are the Crystal Ball NaI(Tl) calorimeter at SPEAR, the L3 BGO calorimeter at LEP, the CLEO CsI(Tl) calorimeter at CESR, the KTeV CsI calorimeter at the Tevatron, the BaBar, BELLE and BES II CsI(Tl) calorimeters at PEP-II, KEK and BEPC III. Because of its high density and relative low cost, PWO calorimeters are widely used by CMS and ALICE at LHC, by CLAS and PrimEx at CEBAF, and by PANDA at GSI. Recently, investigations have been made aiming at using LSO:Ce or LYSO:Ce crystals for future high energy or nuclear physics experiments [38].

**Table 31.4:** Properties of several inorganic crystal scintillators. Most of the notation is defined in Sec. 6 of this *Review*.

Parameter:	$\rho$	MP	$X_0^*$	$R_M^*$	$dE^*/dx$	$\lambda_I^*$	$\tau_{\text{decay}}$	$\lambda_{\text{max}}$	$n^{\ddagger}$	Relative output <sup>†</sup>	Hygro-scopic <sup>‡</sup>	$d(LY)/dT$
Units:	g/cm <sup>3</sup>	°C	cm	cm	MeV/cm	cm	ns	nm		%/°C <sup>‡</sup>		%/°C <sup>‡</sup>
NaI(Tl)	3.67	651	2.59	4.13	4.8	42.9	245	410	1.85	100	yes	-0.2
BGO	7.13	1050	1.12	2.23	9.0	22.8	300	480	2.15	21	no	-0.9
BaF <sub>2</sub>	4.89	1280	2.03	3.10	6.5	30.7	650 <sup>s</sup> 0.9 <sup>f</sup>	300 <sup>s</sup> 220 <sup>f</sup>	1.50	36 <sup>s</sup> 4.1 <sup>f</sup>	no	-1.9 <sup>s</sup> 0.1 <sup>f</sup>
CsI(Tl)	4.51	621	1.86	3.57	5.6	39.3	1220	550	1.79	165	slight	0.4
CsI(pure)	4.51	621	1.86	3.57	5.6	39.3	30 <sup>s</sup> 6 <sup>f</sup>	420 <sup>s</sup> 310 <sup>f</sup>	1.95	3.6 <sup>s</sup> 1.1 <sup>f</sup>	slight	-1.4
PbWO <sub>4</sub>	8.3	1123	0.89	2.00	10.1	20.7	30 <sup>s</sup> 10 <sup>f</sup>	425 <sup>s</sup> 420 <sup>f</sup>	2.20	0.3 <sup>s</sup> 0.077 <sup>f</sup>	no	-2.5
LSO(Ce)	7.40	2050	1.14	2.07	9.6	20.9	40	402	1.82	85	no	-0.2
LaBr <sub>3</sub> (Ce)	5.29	788	1.88	2.85	6.9	30.4	20	356	1.9	130	yes	0.2

\* Numerical values calculated using formulae in this review.

<sup>‡</sup> Refractive index at the wavelength of the emission maximum.

<sup>†</sup> Relative light output measured for samples of 1.5  $X_0$  cube with a Tyvek paper wrapping and a full end face coupled to a photodetector. The quantum efficiencies of the photodetector are taken out.

<sup>‡</sup> Variation of light yield with temperature evaluated at the room temperature.

*f* = fast component, *s* = slow component



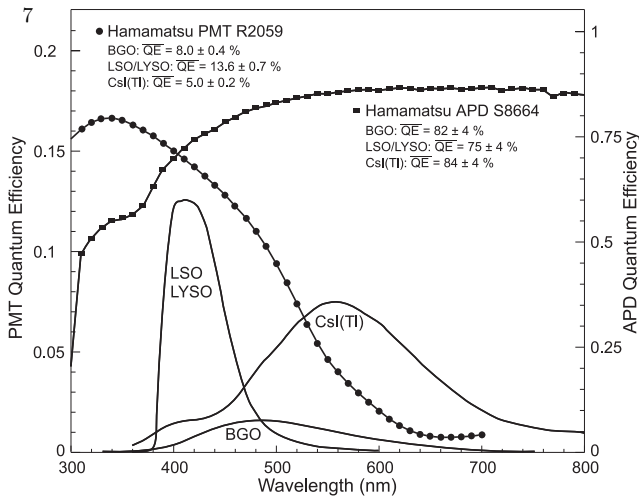


**Figure 31.2:** The quantum efficiencies of two photodetectors, a Hamamatsu R2059 PMT with bi-alkali cathode and a Hamamatsu S8664 avalanche photodiode (APD), are shown as a function of wavelength. Also shown in the figure are emission spectra of three crystal scintillators, BGO, LSO and CsI(Tl), and the numerical values of the emission weighted quantum efficiencies. The area under each emission spectrum is proportional to crystal's light yield.

### 31.5. Cherenkov detectors

Revised September 2009 by B.N. Ratcliff (SLAC).

Although devices using Cherenkov radiation are often thought of as only particle identification (PID) detectors, in practice they are used over a broader range of applications including; (1) fast particle counters; (2) hadronic PID; and (3) tracking detectors performing complete event reconstruction. Examples of applications from each category include; (1) the BaBar luminosity detector [49]; (2) the hadronic PID detectors at the B factory detectors—DIRC in BaBar [50] and the aerogel threshold Cherenkov in Belle [51]; and (3) large water Cherenkov counters such as Super-Kamiokande [53]. Cherenkov counters contain two main elements; (1) a radiator through which the charged particle passes, and (2) a photodetector. As Cherenkov radiation is a weak source of photons, light collection and detection must be as efficient as possible. The refractive index  $n$  and the particle's path length through the radiator  $L$  appear in the Cherenkov relations allowing the tuning of these quantities for particular applications.

Cherenkov detectors utilize one or more of the properties of Cherenkov radiation discussed in the Passages of Particles through Matter section (Sec. 30 of this *Review*): the prompt emission of a light pulse; the existence of a velocity threshold for radiation; and the dependence of the Cherenkov cone half-angle  $\theta_c$  and the number of emitted photons on the velocity of the particle and the refractive index of the medium.

The number of photoelectrons ( $N_{p.e.}$ ) detected in a given device is

$$N_{p.e.} = L \frac{\alpha^2 z^2}{r_e m_e c^2} \int \epsilon(E) \sin^2 \theta_c(E) dE, \quad (31.5)$$

where  $\epsilon(E)$  is the efficiency for collecting the Cherenkov light and transducing it into photoelectrons, and  $\alpha^2/(r_e m_e c^2) = 370 \text{ cm}^{-1} \text{ eV}^{-1}$ .

The quantities  $\epsilon$  and  $\theta_c$  are functions of the photon energy  $E$ . As the typical energy dependent variation of the index of refraction is modest, a quantity called the *Cherenkov detector quality factor*  $N_0$  can be defined as

$$N_0 = \frac{\alpha^2 z^2}{r_e m_e c^2} \int \epsilon dE, \quad (31.6)$$

so that, taking  $z = 1$  (the usual case in high-energy physics),

$$N_{p.e.} \approx L N_0 (\sin^2 \theta_c). \quad (31.7)$$

This definition of the quality factor  $N_0$  is not universal, nor, indeed, very useful for those common situations where  $\epsilon$  factorizes as  $\epsilon = \epsilon_{\text{coll}} \epsilon_{\text{det}}$  with the geometrical photon collection efficiency ( $\epsilon_{\text{coll}}$ ) varying substantially for different tracks while the photon detector efficiency ( $\epsilon_{\text{det}}$ ) remains nearly track independent. In this case, it can be useful to explicitly remove ( $\epsilon_{\text{coll}}$ ) from the definition of  $N_0$ . A typical value of  $N_0$  for a photomultiplier (PMT) detection system working in the visible and near UV, and collecting most of the Cherenkov light, is about  $100 \text{ cm}^{-1}$ . Practical counters, utilizing a variety of different photodetectors, have values ranging between about  $30$  and  $180 \text{ cm}^{-1}$ . Radiators can be chosen from a variety of transparent materials (Sec. 30 of this *Review* and Table 6.1). In addition to refractive index, the choice requires consideration of factors such as material density, radiation length and radiation hardness, transmission bandwidth, absorption length, chromatic dispersion, optical workability (for solids), availability, and cost. When the momenta of particles to be identified is high, the refractive index must be set close to one, so that the photon yield per unit length is low and a long particle path in the radiator is required. Recently, the gap in refractive index that has traditionally existed between gases and liquid or solid materials has been partially closed with transparent *silica aerogels* with indices that range between about 1.007 and 1.13.

Cherenkov counters may be classified as either *imaging* or *threshold* types, depending on whether they do or do not make use of Cherenkov angle ( $\theta_c$ ) information. Imaging counters may be used to track particles as well as identify them. The recent development of very fast photodetectors such as micro-channel plate PMTs (MCP PMT) (see Sec. 31.2 of this *Review*) also potentially allows very fast Cherenkov based time of flight (TOF) detectors of either class [57].

*Threshold* Cherenkov detectors [54], in their simplest form, make a yes/no decision based on whether the particle is above or below the Cherenkov threshold velocity  $\beta_t = 1/n$ . A straightforward enhancement of such detectors uses the number of observed photoelectrons (or a calibrated pulse height) to discriminate between species or to set probabilities for each particle species [55]. This strategy can increase the momentum range of particle separation by a modest amount (to a momentum some 20% above the threshold momentum of the heavier particle in a typical case).

Careful designs give  $\langle \epsilon_{\text{coll}} \rangle \gtrsim 90\%$ . For a photomultiplier with a typical bi-alkali cathode,  $\int \epsilon_{\text{det}} dE \approx 0.27 \text{ eV}$ , so that

$$N_{p.e.}/L \approx 90 \text{ cm}^{-1} (\sin^2 \theta_c) \quad (\text{i.e., } N_0 = 90 \text{ cm}^{-1}). \quad (31.8)$$

Suppose, for example, that  $n$  is chosen so that the threshold for species  $a$  is  $p_t$ ; that is, at this momentum species  $a$  has velocity  $\beta_a = 1/n$ . A second, lighter, species  $b$  with the same momentum has velocity  $\beta_b$ , so  $\cos \theta_c = \beta_a/\beta_b$ , and

$$N_{p.e.}/L \approx 90 \text{ cm}^{-1} \frac{m_a^2 - m_b^2}{p_t^2 + m_a^2}. \quad (31.9)$$

For  $K/\pi$  separation at  $p = p_t = 1(5) \text{ GeV}/c$ ,  $N_{p.e.}/L \approx 16(0.8) \text{ cm}^{-1}$  for  $\pi$ 's and (by design) 0 for  $K$ 's.

For limited path lengths  $N_{p.e.}$  will usually be small. The overall efficiency of the device is controlled by Poisson fluctuations, which can be especially critical for separation of species where one particle type is dominant. Moreover, the effective number of photoelectrons is often less than the average number calculated above due to additional equivalent noise from the photodetector (see the discussion of the excess noise factor in Sec. 31.2 of this *Review*). It is common to design for at least 10 photoelectrons for the high velocity particle in order to obtain a robust counter. As rejection of the particle that is below threshold depends on *not* seeing a signal, electronic and other background noise can be important. Physics sources of light production for the below threshold particle, such as decay to an above threshold particle or the production of delta rays in the radiator, often limit the separation attainable, and need to be carefully considered. Well designed, modern multi-channel counters, such as the ACC at Belle [51], can attain adequate particle separation performance over a substantial momentum range for essentially the full solid angle of the spectrometer.



*Imaging* counters make the most powerful use of the information available by measuring the ring-correlated angles of emission of the individual Cherenkov photons. Since low-energy photon detectors can measure only the position (and, perhaps, a precise detection time) of the individual Cherenkov photons (not the angles directly), the photons must be “imaged” onto a detector so that their angles can be derived [56]. Typically the optics map the Cherenkov cone onto (a portion of) a distorted “circle” at the photodetector. Though the imaging process is directly analogous to familiar imaging techniques used in telescopes and other optical instruments, there is a somewhat bewildering variety of methods used in a wide variety of counter types with different names. Some of the imaging methods used include (1) focusing by a lens; (2) proximity focusing (i.e., focusing by limiting the emission region of the radiation); and (3) focusing through an aperture (a pinhole). In addition, the prompt Cherenkov emission coupled with the speed of modern photon detectors allows the use of (4) time imaging, a method which is little used in conventional imaging technology. Finally, (5) correlated tracking (and event reconstruction) can be performed in large water counters by combining the individual space position and time of each photon together with the constraint that Cherenkov photons are emitted from each track at the same polar angle (Sec. 32.3.1 of this *Review*).

In a simple model of an imaging PID counter, the fractional error on the particle velocity ( $\delta_\beta$ ) is given by

$$\delta_\beta \approx \frac{\sigma_\beta}{\beta} = \tan \theta_c \sigma(\theta_c) \quad , \quad (31.10)$$

where

$$\sigma(\theta_c) = \frac{\langle \sigma(\theta_i) \rangle}{\sqrt{N_{p.e.}}} \oplus C \quad , \quad (31.11)$$

and  $\langle \sigma(\theta_i) \rangle$  is the average single photoelectron resolution, as defined by the optics, detector resolution and the intrinsic chromaticity spread of the radiator index of refraction averaged over the photon detection bandwidth.  $C$  combines a number of other contributions to resolution including, (1) correlated terms such as tracking, alignment, and multiple scattering, (2) hit ambiguities, (3) background hits from random sources, and (4) hits coming from other tracks. The actual separation performance is also limited by physics effects such as decays in flight and particle interactions in the material of the detector. In many practical cases, the performance is limited by these effects.

For a  $\beta \approx 1$  particle of momentum ( $p$ ) well above threshold entering a radiator with index of refraction ( $n$ ), the number of  $\sigma$  separation ( $N_\sigma$ ) between particles of mass  $m_1$  and  $m_2$  is approximately

$$N_\sigma \approx \frac{|m_1^2 - m_2^2|}{2p^2 \sigma(\theta_c) \sqrt{n^2 - 1}} \quad . \quad (31.12)$$

In practical counters, the angular resolution term  $\sigma(\theta_c)$  varies between about 0.1 and 5 mrad depending on the size, radiator, and photodetector type of the particular counter. The range of momenta over which a particular counter can separate particle species extends from the point at which the number of photons emitted becomes sufficient for the counter to operate efficiently as a threshold device ( $\sim 20\%$  above the threshold for the lighter species) to the value in the imaging region given by the equation above. For example, for  $\sigma(\theta_c) = 2\text{mrad}$ , a fused silica radiator ( $n = 1.474$ ), or a fluorocarbon gas radiator ( $\text{C}_5\text{F}_{12}$ ,  $n = 1.0017$ ), would separate  $\pi/K$ 's from the threshold region starting around 0.15(3) GeV/ $c$  through the imaging region up to about 4.2(18) GeV/ $c$  at better than  $3\sigma$ .

Many different imaging counters have been built during the last several decades [57]. Among the earliest examples of this class of counters are the very limited acceptance Differential Cherenkov detectors, designed for particle selection in high momentum beam lines. These devices use optical focusing and/or geometrical masking to select particles having velocities in a specified region. With careful design, a velocity resolution of  $\sigma_\beta/\beta \approx 10^{-4}$ – $10^{-5}$  can be obtained [54].

Practical multi-track Ring-Imaging Cherenkov detectors (generically called RICH counters) are a more recent development. RICH counters are sometimes further classified by ‘generations’ that differ based on historical timing, performance, design, and photodetection techniques.

Prototypical examples of first generation RICH counters are those used in the DELPHI and SLD detectors at the LEP and SLC Z factory  $e^+e^-$  colliders [57]. They have both liquid ( $\text{C}_6\text{F}_{14}$ ,  $n = 1.276$ ) and gas ( $\text{C}_5\text{F}_{12}$ ,  $n = 1.0017$ ) radiators, the former being proximity imaged with the latter using mirrors. The phototransducers are a TPC/wire-chamber combination. They are made sensitive to photons by doping the TPC gas (usually, ethane/methane) with  $\sim 0.05\%$  TMAE (tetrakis(dimethylamino)ethylene). Great attention to detail is required, (1) to avoid absorbing the UV photons to which TMAE is sensitive, (2) to avoid absorbing the single photoelectrons as they drift in the long TPC, and (3) to keep the chemically active TMAE vapor from interacting with materials in the system. In spite of their unforgiving operational characteristics, these counters attained good  $e/\pi/K/p$  separation over wide momentum ranges (from about 0.25 to 20 GeV/ $c$ ) during several years of operation at LEP and SLC. Related but smaller acceptance devices include the OMEGA RICH at the CERN SPS, and the RICH in the balloon-borne CAPRICE detector [57].

Later generation counters [57] generally operate at much higher rates, with more detection channels, than the first generation detectors just described. They also utilize faster, more forgiving photon detectors, covering different photon detection bandwidths. Radiator choices have broadened to include materials such as lithium fluoride, fused silica, and aerogel. Vacuum based photodetection systems (*e.g.*, single or multi anode PMTs, MCP PMTs, or hybrid photodiodes (HPD)) have become increasingly common (see Sec. 31.2 of this *Review*). They handle high rates, and can be used with a wide choice of radiators. Examples include (1) the SELEX RICH at Fermilab, which mirror focuses the Cherenkov photons from a neon radiator onto a camera array made of  $\sim 2000$  PMTs to separate hadrons over a wide momentum range (to well above 200 GeV/ $c$  for heavy hadrons); (2) the HERMES RICH at HERA, which mirror focuses photons from  $\text{C}_4\text{F}_{10}$  ( $n = 1.00137$ ) and aerogel ( $n = 1.0304$ ) radiators within the same volume onto a PMT camera array to separate hadrons in the momentum range from 2 to 15 GeV/ $c$ ; and (3) the LHCb detector now being brought into operation at the LHC. It uses two separate counters. One volume, like HERMES, contains two radiators (aerogel and  $\text{C}_4\text{F}_{10}$ ) while the second volume contains  $\text{CF}_4$ . Photons are mirror focused onto detector arrays of HPDs to cover a  $\pi/K$  separation momentum range between 1 and 150 GeV/ $c$ .

Other fast detection systems that use solid cesium iodide (CsI) photocathodes or triethylamine (TEA) doping in proportional chambers are useful with certain radiator types and geometries. Examples include (1) the CLEO-III RICH at CESR that uses a LiF radiator with TEA doped proportional chambers; (2) the ALICE detector at the LHC that uses proximity focused liquid ( $\text{C}_6\text{F}_{14}$ ) radiators and solid CSI photocathodes (similar photodetectors have been used for several years by the HADES and COMPASS detectors), and the hadron blind detector (HBD) in the PHENIX detector at RHIC that couples a low index  $\text{CF}_4$  radiator to a photodetector based on electron multiplier (GEM) chambers with reflective CSI photocathodes [57].

A DIRC (Detection [of] Internally Reflected Cherenkov [light]) is a distinctive, compact RICH subtype first used in the BaBar detector [52]. A DIRC “inverts” the usual RICH principle for use of light from the radiator by collecting and imaging the total internally reflected light rather than the transmitted light. It utilizes the optical material of the radiator in two ways, simultaneously; first as a Cherenkov radiator, and second, as a light pipe. The magnitudes of the photon angles are preserved during transport by the flat, rectangular cross section radiators, allowing the photons to be efficiently transported to a detector outside the path of the particle where they may be imaged in up to three independent dimensions (the usual two in space and, due to the long photon paths lengths, one in time). Because the index of refraction in the radiator is large ( $\sim 1.48$  for fused silica), the momentum range with good  $\pi/K$  separation is rather low. The BaBar DIRC range extends up to  $\sim 4$  GeV/ $c$ . It is plausible, but difficult, to extend it up to about 10 GeV/ $c$  with an improved design. New DIRC detectors are being developed that take advantage of the new, very fast, pixelated photodetectors becoming available, such as flat panel PMTs and MCP PMTs. They

typically utilize either time imaging or mirror focused optics, or both, leading not only to a precision measurement of the Cherenkov angle, but in some cases, to a precise measurement of the particle time of flight, and/or to correction of the chromatic dispersion in the radiator. Examples include (1) the time of propagation (TOP) counter being developed for the BELLE-II upgrade at KEKB which emphasizes precision timing for both Cherenkov imaging and TOF; (2) the full 3-dimensional imaging FDIRC for the SuperB detector at the Italian SuperB collider which uses precision timing not only for improving the angle reconstruction and TOF, but also to correct the chromatic dispersion; and (3) the DIRCs being developed for the PANDA detector at FAIR that use elegant focusing optics and fast timing [57].

### 31.6. Gaseous detectors

**31.6.1. Energy loss and charge transport in gases :** Revised March 2010 by F. Sauli (CERN) and M. Titov (CEA Saclay).

Gas-filled detectors localize the ionization produced by charged particles, generally after charge multiplication. The statistics of ionization processes having asymmetries in the ionization trails, affect the coordinate determination deduced from the measurement of drift time, or of the center of gravity of the collected charge. For thin gas layers, the width of the energy loss distribution can be larger than its average, requiring multiple sample or truncated mean analysis to achieve good particle identification. In the truncated mean method for calculating  $\langle dE/dx \rangle$ , the ionization measurements along the track length are broken into many samples and then a fixed fraction of high-side (and sometimes also low-side) values are rejected [58].

The energy loss of charged particles and photons in matter is discussed in Sec. 30. Table 31.5 provides values of relevant parameters in some commonly used gases at NTP (normal temperature, 20° C, and pressure, 1 atm) for unit-charge minimum-ionizing particles (MIPs) [59–65]. Values often differ, depending on the source, so those in the table should be taken only as approximate. For different conditions and for mixtures, and neglecting internal energy transfer processes (*e.g.*, Penning effect), one can scale the density,  $N_P$ , and  $N_T$  with temperature and pressure assuming a perfect gas law.

**Table 31.5:** Properties of noble and molecular gases at normal temperature and pressure (NTP: 20° C, one atm).  $E_X$ ,  $E_I$ : first excitation, ionization energy;  $W_I$ : average energy per ion pair;  $dE/dx|_{\min}$ ,  $N_P$ ,  $N_T$ : differential energy loss, primary and total number of electron-ion pairs per cm, for unit charge minimum ionizing particles.

Gas	Density, mg cm <sup>-3</sup>	$E_x$ eV	$E_I$ eV	$W_I$ eV	$dE/dx _{\min}$ keV cm <sup>-1</sup>	$N_P$ cm <sup>-1</sup>	$N_T$ cm <sup>-1</sup>
He	0.179	19.8	24.6	41.3	0.32	3.5	8
Ne	0.839	16.7	21.6	37	1.45	13	40
Ar	1.66	11.6	15.7	26	2.53	25	97
Xe	5.495	8.4	12.1	22	6.87	41	312
CH <sub>4</sub>	0.667	8.8	12.6	30	1.61	28	54
C <sub>2</sub> H <sub>6</sub>	1.26	8.2	11.5	26	2.91	48	112
iC <sub>4</sub> H <sub>10</sub>	2.49	6.5	10.6	26	5.67	90	220
CO <sub>2</sub>	1.84	7.0	13.8	34	3.35	35	100
CF <sub>4</sub>	3.78	10.0	16.0	54	6.38	63	120

When an ionizing particle passes through the gas it creates electron-ion pairs, but often the ejected electrons have sufficient energy to further ionize the medium. As shown in Table 31.5, the total number of electron-ion pairs ( $N_T$ ) is usually a few times larger than the number of primaries ( $N_P$ ).

The probability for a released electron to have an energy  $E$  or larger follows an approximate  $1/E^2$  dependence (Rutherford law), shown in Fig. 31.3 for Ar/CH<sub>4</sub> at NTP (dotted line, left scale). More detailed estimates taking into account the electronic structure of the medium are shown in the figure, for three values of the particle velocity factor  $\beta\gamma$  [60]. The dot-dashed line provides, on the right scale, the

practical range of electrons (including scattering) of energy  $E$ . As an example, about 0.6% of released electrons have 1 keV or more energy, substantially increasing the ionization loss rate. The practical range of 1 keV electrons in argon (dot-dashed line, right scale) is 70  $\mu$ m and this can contribute to the error in the coordinate determination.

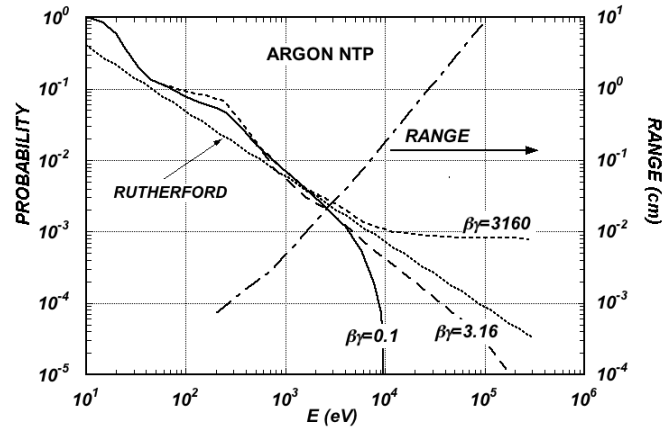


**Figure 31.3:** Probability of single collisions in which released electrons have an energy  $E$  or larger (left scale) and practical range of electrons in Ar/CH<sub>4</sub> (P10) at NTP (dot-dashed curve, right scale) [60].

The number of electron-ion pairs per primary ionization, or cluster size, has an exponentially decreasing probability; for argon, there is about 1% probability for primary clusters to contain ten or more electron-ion pairs [61].

Once released in the gas, and under the influence of an applied electric field, electrons and ions drift in opposite directions and diffuse towards the electrodes. The scattering cross section is determined by the details of atomic and molecular structure. Therefore, the drift velocity and diffusion of electrons depend very strongly on the nature of the gas, specifically on the inelastic cross-section involving the rotational and vibrational levels of molecules. In noble gases, the inelastic cross section is zero below excitation and ionization thresholds. Large drift velocities are achieved by adding polyatomic gases (usually CH<sub>4</sub>, CO<sub>2</sub>, or CF<sub>4</sub>) having large inelastic cross sections at moderate energies, which results in “cooling” electrons into the energy range of the Ramsauer-Townsend minimum (at  $\sim 0.5$  eV) of the elastic cross-section of argon. The reduction in both the total electron scattering cross-section and the electron energy results in a large increase of electron drift velocity (for a compilation of electron-molecule cross sections see Ref. 62). Another principal role of the polyatomic gas is to absorb the ultraviolet photons emitted by the excited noble gas atoms. Extensive collections of experimental data [63] and theoretical calculations based on transport theory [64] permit estimates of drift and diffusion properties in pure gases and their mixtures. In a simple approximation, gas kinetic theory provides the drift velocity  $v$  as a function of the mean collision time  $\tau$  and the electric field  $E$ :  $v = eE\tau/m_e$  (Townsend’s expression). Values of drift velocity and diffusion for some commonly used gases at NTP are given in Fig. 31.4 and Fig. 31.5. These have been computed with the MAGBOLTZ program [65]. For different conditions, the horizontal axis must be scaled inversely with the gas density. Standard deviations for longitudinal ( $\sigma_L$ ) and transverse diffusion ( $\sigma_T$ ) are given for one cm of drift, and scale with the the square root of the drift distance. Since the collection time is inversely proportional to the drift velocity, diffusion is less in gases such as CF<sub>4</sub> that have high drift velocities. In the presence of an external magnetic field, the Lorentz force acting on electrons between collisions deflects the drifting electrons and modifies the drift properties. The electron trajectories, velocities and diffusion parameters can be computed with MAGBOLTZ. A simple theory, the friction force model, provides an expression for the vector drift velocity  $v$  as a function of electric and magnetic field vectors  $\mathbf{E}$  and  $\mathbf{B}$ , of the

Larmor frequency  $\omega = eB/m_e$ , and of the mean collision time  $\tau$ :

$$v = \frac{e}{m_e} \frac{\tau}{1 + \omega^2 \tau^2} \left( E + \frac{\omega \tau}{B} (E \times B) + \frac{\omega^2 \tau^2}{B^2} (E \cdot B) B \right) \quad (31.13)$$

To a good approximation, and for moderate fields, one can assume that the energy of the electrons is not affected by  $B$ , and use for  $\tau$  the values deduced from the drift velocity at  $B = 0$  (the Townsend expression). For  $E$  perpendicular to  $B$ , the drift angle to the relative to the electric field vector is  $\tan \theta_B = \omega \tau$  and  $v = (E/B)(\omega \tau / \sqrt{1 + \omega^2 \tau^2})$ . For parallel electric and magnetic fields, drift velocity and longitudinal diffusion are not affected, while the transverse diffusion can be strongly reduced:  $\sigma_T(B) = \sigma_T(B=0) / \sqrt{1 + \omega^2 \tau^2}$ . The dotted line in Fig. 31.5 represents  $\sigma_T$  for the classic Ar/CH<sub>4</sub> (90:10) mixture at 4 T. Large values of  $\omega \tau \sim 20$  at 5 T are consistent with the measurement of diffusion coefficient in Ar/CF<sub>4</sub>/iC<sub>4</sub>H<sub>10</sub> (95:3:2). This reduction is exploited in time projection chambers (Sec. 31.6.5) to improve spatial resolution.

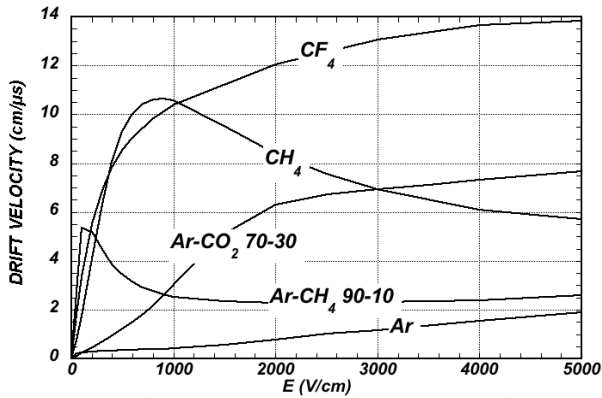


Figure 31.4: Computed electron drift velocity as a function of electric field in several gases at NTP and  $B = 0$  [65].

In mixtures containing electronegative molecules, such as O<sub>2</sub> or H<sub>2</sub>O, electrons can be captured to form negative ions. Capture cross-sections are strongly energy-dependent, and therefore the capture probability is a function of applied field. For example, the electron is attached to the oxygen molecule at energies below 1 eV. The three-body electron attachment coefficients may differ greatly for the same additive in different mixtures. As an example, at moderate fields (up to 1 kV/cm) the addition of 0.1% of oxygen to an Ar/CO<sub>2</sub> mixture results in an electron capture probability about twenty times larger than the same addition to Ar/CH<sub>4</sub>.

Carbon tetrafluoride is not electronegative at low and moderate fields, making its use attractive as drift gas due to its very low diffusion. However, CF<sub>4</sub> has a large electron capture cross section at fields above  $\sim 8$  kV/cm, before reaching avalanche field strengths. Depending on detector geometry, some signal reduction and resolution loss can be expected using this gas.

If the electric field is increased sufficiently, electrons gain enough energy between collisions to ionize molecules. Above a gas-dependent threshold, the mean free path for ionization,  $\lambda_i$ , decreases exponentially with the field; its inverse,  $\alpha = 1/\lambda_i$ , is the first Townsend coefficient. In wire chambers, most of the increase of avalanche particle density occurs very close to the anode wires, and a simple electrostatic consideration shows that the largest fraction of the detected signal is due to the motion of positive ions receding from the wires. The electron component, although very fast, contributes very little to the signal. This determines the characteristic shape of the detected signals in the proportional mode: a fast rise followed by a gradual increase. The slow component, the so-called “ion tail” that limits the time resolution of the detector, is usually removed by differentiation of the signal. In uniform fields,  $N_0$  initial electrons multiply over a length  $x$  forming an electron avalanche of size  $N = N_0 e^{\alpha x}$ ;  $N/N_0$  is the gain of the detector. Fig. 31.6 shows examples of Townsend coefficients for several gas mixtures, computed with MAGBOLTZ [65].

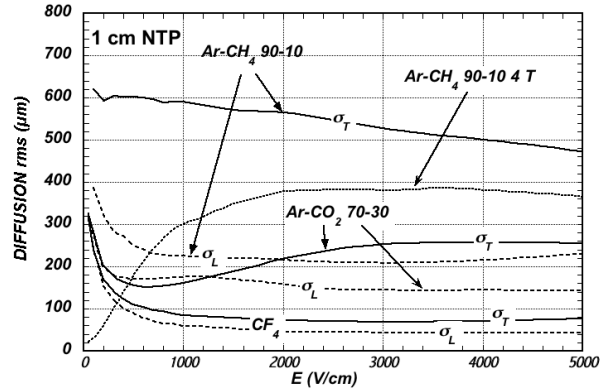


Figure 31.5: Electron longitudinal diffusion ( $\sigma_L$ ) (dashed lines) and transverse diffusion ( $\sigma_T$ ) (full lines) for 1 cm of drift at NTP and  $B = 0$ . The dotted line shows  $\sigma_T$  for the P10 mixture at 4 T [65].

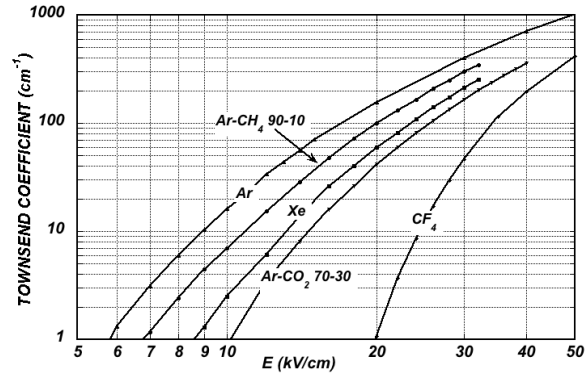


Figure 31.6: Computed first Townsend coefficient  $\alpha$  as a function of electric field in several gases at NTP [65].

Positive ions released by the primary ionization or produced in the avalanches drift and diffuse under the influence of the electric field. Negative ions may also be produced by electron attachment to gas molecules. The drift velocity of ions in the fields encountered in gaseous detectors (up to few kV/cm) is typically about three orders of magnitude less than for electrons. The ion mobility  $\mu$ , the ratio of drift velocity to electric field, is constant for a given ion type up to very high fields. Values of mobility at NTP for ions in their own and other gases are given in Table 31.6 [66]. For different temperatures and pressures, the mobility can be scaled inversely with the density assuming an ideal gas law. For mixtures, due to a very effective charge transfer mechanism, only ions with the lowest ionization potential survive after a short path in the gas. Both the lateral and transverse diffusion of ions are proportional to the square root of the drift time, with a coefficient that depends on temperature but not on the ion mass. Accumulation of ions in the gas drift volume may induce field distortions (see Sec. 31.6.5).

Table 31.6: Mobility of ions in gases at NTP [66].

Gas	Ion	Mobility $\mu$ (cm <sup>2</sup> V <sup>-1</sup> s <sup>-1</sup> )
He	He <sup>+</sup>	10.4
Ne	Ne <sup>+</sup>	4.7
Ar	Ar <sup>+</sup>	1.54
Ar/CH <sub>4</sub>	CH <sub>4</sub> <sup>+</sup>	1.87
Ar/CO <sub>2</sub>	CO <sub>2</sub> <sup>+</sup>	1.72
CH <sub>4</sub>	CH <sub>4</sub> <sup>+</sup>	2.26
CO <sub>2</sub>	CO <sub>2</sub> <sup>+</sup>	1.09

**31.6.2. Multi-Wire Proportional and Drift Chambers :** Revised March 2010 by Fabio Sauli (CERN) and Maxim Titov (CEA Saclay).

Single-wire counters that detect the ionization produced in a gas by a charged particle, followed by charge multiplication and collection around a thin wire have been used for decades. Good energy resolution is obtained in the proportional amplification mode, while very large saturated pulses can be detected in the streamer and Geiger modes [3].

Multiwire proportional chambers (MWPCs) [67,68], introduced in the late '60's, detect, localize and measure energy deposit by charged particles over large areas. A mesh of parallel anode wires at a suitable potential, inserted between two cathodes, acts almost as a set of independent proportional counters (see Fig. 31.7a). Electrons released in the gas volume drift towards the anodes and produce avalanches in the increasing field. Analytic expressions for the electric field can be found in many textbooks. The fields close to the wires  $E(r)$ , in the drift region  $E_D$ , and the capacitance  $C$  per unit length of anode wire are approximately given by

$$E(r) = \frac{CV_0}{2\pi\epsilon_0} \frac{1}{r} \quad E_D = \frac{CV_0}{2\epsilon_0 s} \quad C = \frac{2\pi\epsilon_0}{\pi(\ell/s) - \ln(2\pi a/s)}, \quad (31.14)$$

where  $r$  is the distance from the center of the anode,  $s$  the wire spacing,  $\ell$  and  $V_0$  the distance and potential difference between anode and cathode, and  $a$  the anode wire radius.

Because of electrostatic forces, anode wires are in equilibrium only for a perfect geometry. Small deviations result in forces displacing the wires alternatively below and above the symmetry plane, sometimes with catastrophic results. These displacement forces are countered by the mechanical tension of the wire, up to a maximum unsupported stable length,  $L_M$  [58], above which the wire deforms:

$$L_M = \frac{s}{CV_0} \sqrt{4\pi\epsilon_0 T_M} \quad (31.15)$$

The maximum tension  $T_M$  depends on the wire diameter and modulus of elasticity. Table 31.7 gives approximate values for tungsten and the corresponding maximum stable wire length under reasonable assumptions for the operating voltage ( $V_0 = 5$  kV) [69]. Internal supports and spacers can be used in the construction of longer detectors to overcome limits on the wire length imposed by Eq. (31.15).

**Table 31.7:** Maximum tension  $T_M$  and stable unsupported length  $L_M$  for tungsten wires with spacing  $s$ , operated at  $V_0 = 5$  kV. No safety factor is included.

Wire diameter ( $\mu\text{m}$ )	$T_M$ (newton)	$s$ (mm)	$L_M$ (cm)
10	0.16	1	25
20	0.65	2	85

Detection of charge on the wires over a predefined threshold provides the transverse coordinate to the wire with an accuracy comparable to that of the wire spacing. The coordinate along each wire can be obtained by measuring the ratio of collected charge at the two ends of resistive wires. Making use of the charge profile induced on segmented cathodes, the so-called center-of gravity (COG) method, permits localization of tracks to sub-mm accuracy. Due to the statistics of energy loss and asymmetric ionization clusters, the position accuracy is  $\sim 50 \mu\text{m}$  rms for tracks perpendicular to the wire plane, but degrades to  $\sim 250 \mu\text{m}$  at  $30^\circ$  to the normal [70]. The intrinsic bi-dimensional characteristic of the COG readout has found numerous applications in medical imaging.

Drift chambers, developed in the early '70's, can be used to estimate the longitudinal position of a track by exploiting the arrival time of electrons at the anodes if the time of interaction is known [71]. The distance between anode wires is usually several cm, allowing coverage of large areas at reduced cost. In the original design, a thicker wire (the field wire) at the proper voltage, placed between the anode wires, reduces the field at the mid-point between anodes and improves

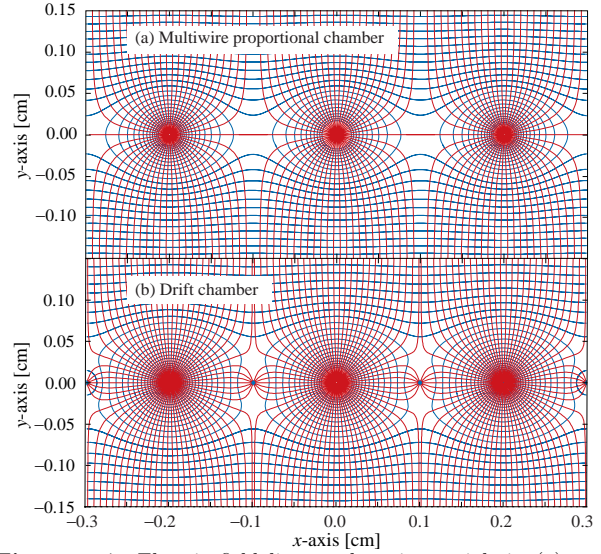


**Figure 31.7:** Electric field lines and equipotentials in (a) a multiwire proportional chamber and (b) a drift chamber.

charge collection (Fig. 31.7b). In some drift chamber designs, and with the help of suitable voltages applied to field-shaping electrodes, the electric field structure is adjusted to improve the linearity of space-to-drift-time relation, resulting in better spatial resolution [72].

Drift chambers can reach a longitudinal spatial resolution from timing measurement of order  $100 \mu\text{m}$  (rms) or better for minimum ionizing particles, depending on the geometry and operating conditions. However, a degradation of resolution is observed [73] due to primary ionization statistics for tracks close to the anode wires, caused by the spread in arrival time of the nearest ionization clusters. The effect can be reduced by operating the detector at higher pressures. Sampling the drift time on rows of anodes led to the concept of multiple arrays such as the multi-drift module [74] and the JET chamber [75]. A measurement of drift time, together with the recording of charge sharing from the two ends of the anode wires provides the coordinates of segments of tracks. The total charge gives information on the differential energy loss and is exploited for particle identification. The time projection chamber (TPC) [76] combines a measurement of drift time and charge induction on cathodes, to obtain excellent tracking for high multiplicity topologies occurring at moderate rates (see Sec. 31.6.5). In all cases, a good knowledge of electron drift velocity and diffusion properties is required. This has to be combined with the knowledge of the electric fields in the structures, computed with commercial or custom-developed software [65,77]. For an overview of detectors exploiting the drift time for coordinate measurement see Refs. 6 and 58.

Multiwire and drift chambers have been operated with a variety of gas fillings and operating modes, depending on experimental requirements. The so-called "Magic Gas," a mixture of argon, isobutane and Freon [68], permits very high and saturated gains ( $\sim 10^6$ ). This gas mixture was used in early wire chambers, but was found to be susceptible to severe aging processes. With present-day electronics, proportional gains around  $10^4$  are sufficient for detection of minimum ionizing particles, and noble gases with moderate amounts of polyatomic gases, such as methane or carbon dioxide, are used.

Although very powerful in terms of performance, multi-wire structures have reliability problems when used in harsh or hard-to-access environments, since a single broken wire can disable the entire detector. Introduced in the '80's, straw and drift tube systems make use of large arrays of wire counters encased in individual enclosures, each acting as an independent wire counter [78]. Techniques for low-cost mass production of these detectors have been developed for large experiments, such as the Transition Radiation Tracker and the Drift Tubes arrays for CERN's LHC experiments [79].

**31.6.3. High Rate Effects** : Revised March 2010 by Fabio Sauli (CERN) and Maxim Titov (CEA Saclay).

The production of positive ions in the avalanches and their slow drift before neutralization result in a rate-dependent accumulation of positive charge in the detector. This may result in significant field distortion, gain reduction and degradation of spatial resolution. As shown in Fig. 31.8 [80], the proportional gain drops above a charge production rate around  $10^9$  electrons per second and mm of wire, independently of the avalanche size. For a proportional gain of  $10^4$  and 100 electrons per track, this corresponds to a particle flux of  $10^3 \text{ s}^{-1} \text{ mm}^{-1}$  (1 kHz/mm<sup>2</sup> for 1 mm wire spacing).

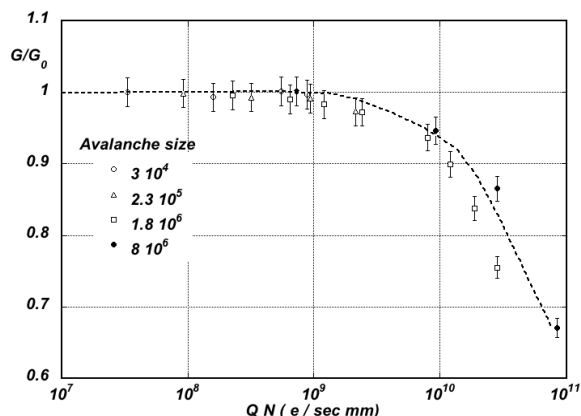


**Figure 31.8:** Charge rate dependence of normalized gas gain  $G/G_0$  (relative to zero counting rate) in proportional thin-wire detectors [80].  $Q$  is the total charge in single avalanche;  $N$  is the particle rate per wire length.

At high radiation fluxes, a fast degradation of detectors due to the formation of polymers deposits (aging) is often observed. The process has been extensively investigated, often with conflicting results. Several causes have been identified, including organic pollutants and silicone oils. Addition of small amounts of water in many (but not all) cases has been shown to extend the lifetime of the detectors. Addition of fluorinated gases (*e.g.*,  $\text{CF}_4$ ) or oxygen may result in an etching action that can overcome polymer formation, or even eliminate already existing deposits. However, the issue of long-term survival of gas detectors with these gases is controversial [81]. Under optimum operating conditions, a total collected charge of a few coulombs per cm of wire can usually be reached before noticeable degradation occurs. This corresponds, for one mm spacing and at a gain of  $10^4$ , to a total particle flux of  $\sim 10^{14}$  MIPs/cm<sup>2</sup>.

**31.6.4. Micro-Pattern Gas Detectors** : Revised March 2010 by Fabio Sauli (CERN) and Maxim Titov (CEA Saclay)

Despite various improvements, position-sensitive detectors based on wire structures are limited by basic diffusion processes and space charge effects to localization accuracies of 50–100  $\mu\text{m}$  [82]. Modern photolithographic technology led to the development of novel Micro-Pattern Gas Detector (MPGD) concepts [83], revolutionizing cell size limitations for many gas detector applications. By using pitch size of a few hundred  $\mu\text{m}$ , an order of magnitude improvement in granularity over wire chambers, these detectors offer intrinsic high rate capability ( $> 10^6 \text{ Hz/mm}^2$ ), excellent spatial resolution ( $\sim 30 \mu\text{m}$ ), multi-particle resolution ( $\sim 500 \mu\text{m}$ ), and single photo-electron time resolution in the ns range.

The Micro-Strip Gas Chamber (MSGC), invented in 1988, was the first of the micro-structure gas chambers [84]. It consists of a set of tiny parallel metal strips laid on a thin resistive support, alternatively connected as anodes and cathodes. Owing to the small anode-to-cathode distance ( $\sim 100 \mu\text{m}$ ), the fast collection of positive ions reduces space charge build-up, and provides a greatly increased rate capability. Unfortunately, the fragile electrode structure of the MSGC turned out to be easily destroyed by discharges induced by heavily ionizing particles [85]. Nevertheless, detailed studies of their properties, and in particular, on the radiation-induced processes

leading to discharge breakdown, led to the development of the more powerful devices: GEM and Micromegas. These have improved reliability and radiation hardness. The absence of space-charge effects in GEM detectors at the highest rates reached so far and the fine granularity of MPGDs improve the maximum rate capability by more than two orders of magnitude (Fig. 31.9) [72,86]. Even larger rate capability has been reported for Micromegas [87].

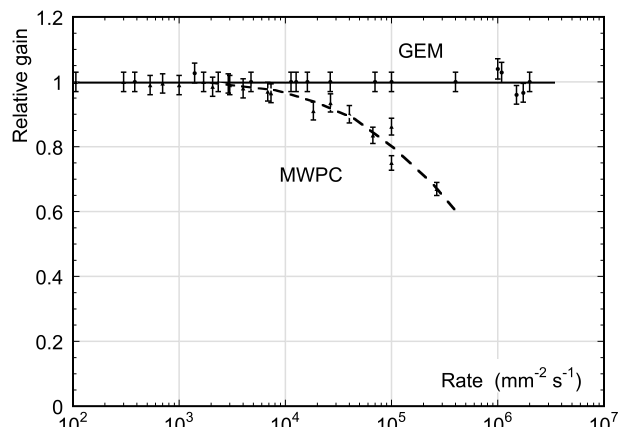


**Figure 31.9:** Normalized gas gain as a function of particle rate for MWPC [72] and GEM [86].

The Gas Electron Multiplier (GEM) detector consists of a thin-foil copper-insulator-copper sandwich chemically perforated to obtain a high density of holes in which avalanches occur [88]. The hole diameter is typically between 25  $\mu\text{m}$  and 150  $\mu\text{m}$ , while the corresponding distance between holes varies between 50  $\mu\text{m}$  and 200  $\mu\text{m}$ . The central insulator is usually (in the original design) the polymer Kapton, with a thickness of 50  $\mu\text{m}$ . Application of a potential difference between the two sides of the GEM generates the electric fields indicated in Fig. 31.10. Each hole acts as an independent proportional counter. Electrons released by the primary ionization particle in the upper conversion region (above the GEM foil) drift into the holes, where charge multiplication occurs in the high electric field (50–70 kV/cm). Most of avalanche electrons are transferred into the gap below the GEM. Several GEM foils can be cascaded, allowing the multi-layer GEM detectors to operate at overall gas gain above  $10^4$  in the presence of highly ionizing particles, while strongly reducing the risk of discharges. This is a major advantage of the GEM technology [89]. Localization can then be performed by collecting the charge on a patterned one- or two-dimensional readout board of arbitrary pattern, placed below the last GEM.

The micro-mesh gaseous structure (Micromegas) is a thin parallel-plate avalanche counter, as shown in Fig. 31.11 [90]. It consists of a drift region and a narrow multiplication gap (25–150  $\mu\text{m}$ ) between a thin metal grid (micromesh) and the readout electrode (strips or pads of conductor printed on an insulator board). Electrons from the primary ionization drift through the holes of the mesh into the narrow multiplication gap, where they are amplified. The electric field is homogeneous both in the drift (electric field  $\sim 1 \text{ kV/cm}$ ) and amplification (50–70 kV/cm) gaps. In the narrow multiplication region, gain variations due to small variations of the amplification gap are approximately compensated by an inverse variation of the amplification coefficient, resulting in a more uniform gain. The small amplification gap produces a narrow avalanche, giving rise to excellent spatial resolution: 12  $\mu\text{m}$  accuracy, limited by the micro-mesh pitch, has been achieved for MIPs, as well as very good time resolution and energy resolution ( $\sim 12\%$  FWHM with 6 keV x rays) [91].

The performance and robustness of GEM and Micromegas have encouraged their use in high-energy and nuclear physics, UV and visible photon detection, astroparticle and neutrino physics, neutron detection and medical physics. Most structures were originally optimized for high-rate particle tracking in nuclear and high-energy physics experiments. COMPASS, a high-luminosity experiment at CERN, pioneered the use of large-area ( $\sim 40 \times 40 \text{ cm}^2$ ) GEM and



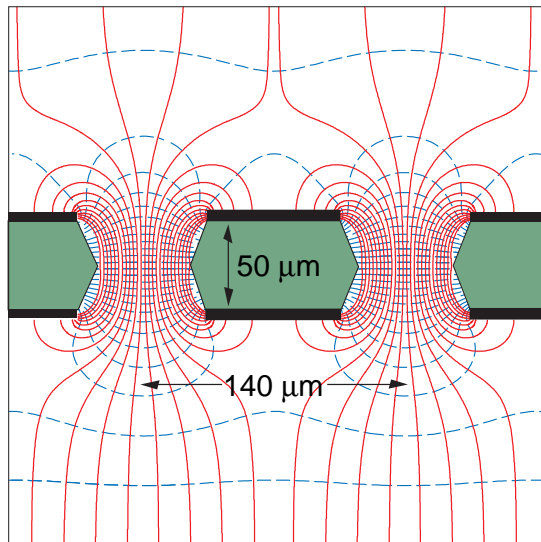


**Figure 31.10:** Schematic view and typical dimensions of the hole structure in the GEM amplification cell. Electric field lines (solid) and equipotentials (dashed) are shown.

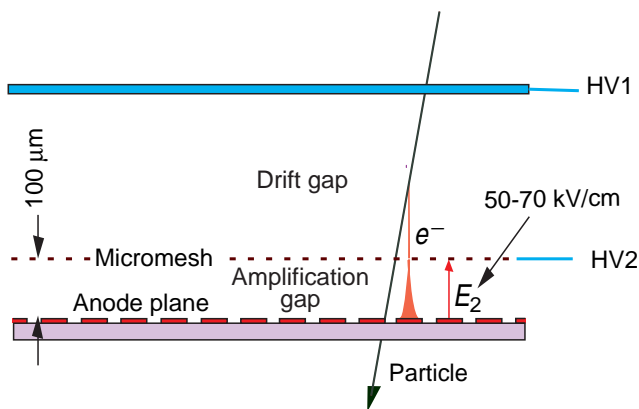


**Figure 31.11:** Schematic drawing of the Micromegas detector.

Micromegas detectors close to the beam line with particle rates of  $25 \text{ kHz/mm}^2$ . Both technologies achieved a tracking efficiency of close to 100% at gas gains of about  $10^4$ , a spatial resolution of  $70\text{--}100 \mu\text{m}$  and a time resolution of  $\sim 10 \text{ ns}$ . GEM detectors are also used for triggering in the LHCb Muon System and for tracking in the TOTEM Telescopes. Both GEM and Micromegas devices are foreseen for the upgrade of the LHC experiments and for one of the readout options for the Time Projection Chamber (TPC) at the International Linear Collider (ILC). The development of new fabrication techniques—“bulk” Micromegas technology [92] and single-mask GEMs [93]—is a big step toward industrial production of large-size MPGDs. In some applications requiring very large-area coverage with moderate spatial resolution, coarse macro-patterned detectors, such as Thick GEMs (THGEM) [94] or patterned resistive-plate devices [95] might offer economically interesting solutions.

Sensitive and low-noise electronics enlarge the range of the MPGD applications. Recently, the GEM and Micromegas detectors were read out by high-granularity ( $\sim 50 \mu\text{m}$  pitch) CMOS chips assembled directly below the GEM or Micromegas amplification structures [96]. These detectors use the bump-bonding pads of a pixel chip as an integrated charge collecting anode. With this arrangement signals are induced at the input gate of a charge-sensitive preamplifier (top metal layer of the CMOS chip). Every pixel is then directly connected to the amplification and digitization circuits, integrated in the underlying active layers of the CMOS technology, yielding timing and charge measurements as well as precise spatial information in 3D.

The operation of a MPGD with a Timepix CMOS chip has

demonstrated the possibility of reconstructing 3D-space points of individual primary electron clusters with  $\sim 30 \mu\text{m}$  spatial resolution and event-time resolution with nanosecond precision. This has become indispensable for tracking and triggering and also for discriminating between ionizing tracks and photon conversions. The GEM, in conjunction with a CMOS ASIC,\* can directly view the absorption process of a few keV x-ray quanta and simultaneously reconstruct the direction of emission, which is sensitive to the x-ray polarization. Thanks to these developments, a micro-pattern device with finely segmented CMOS readout can serve as a high-precision “electronic bubble chamber.” This may open new opportunities for x-ray polarimeters, detection of weakly interacting massive particles (WIMPs) and axions, Compton telescopes, and 3D imaging of nuclear recoils.

An elegant solution for the construction of the Micromegas with pixel readout is the integration of the amplification grid and CMOS chip by means of an advanced “wafer post-processing” technology [97]. This novel concept is called “Ingrid” (see Fig. 31.12). With this technique, the structure of a thin ( $1 \mu\text{m}$ ) aluminum grid is fabricated on top of an array of insulating pillars, which stands  $\sim 50 \mu\text{m}$  above the CMOS chip. The sub- $\mu\text{m}$  precision of the grid dimensions and avalanche gap size results in a uniform gas gain. The grid hole size, pitch and pattern can be easily adapted to match the geometry of any pixel readout chip.

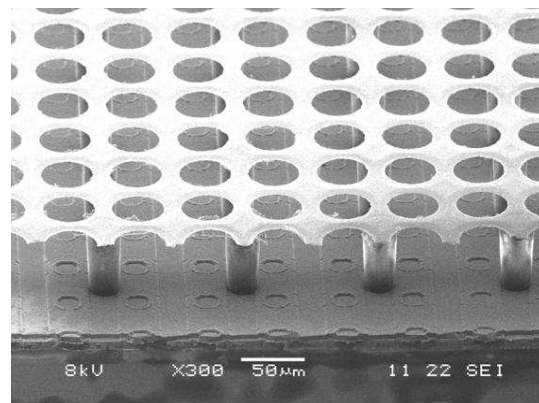


**Figure 31.12:** Photo of the Micromegas “Ingrid” detector. The grid holes can be accurately aligned with readout pixels of CMOS chip. The insulating pillars are centered between the grid holes, thus avoiding dead regions.

Recent developments in radiation hardness research with state-of-the-art MPGDs are reviewed in Ref. 98. Earlier aging studies of GEM and Micromegas concepts revealed that they might be even less vulnerable to radiation-induced performance degradation than standard silicon microstrip detectors.

The RD51 collaboration was established in 2008 to further advance technological developments of micro-pattern detectors and associated electronic-readout systems for applications in basic and applied research [99].

\* Application Specific Integrated Circuit

**31.6.5. Time-projection chambers :** Reviser October 2011 by D. Karlen (U. of Victoria and TRIUMF, Canada)

The Time Projection Chamber (TPC) concept, invented by David Nygren in the late 1970's [76], is the basis for charged particle tracking in a large number of particle and nuclear physics experiments. A uniform electric field drifts tracks of electrons produced by charged particles traversing a medium, either gas or liquid, towards a surface segmented into 2D readout pads. The signal amplitudes and arrival times are recorded to provide full 3D measurements of the particle trajectories. The intrinsic 3D segmentation gives the TPC a distinct advantage over other large volume tracking detector designs which record information only in a 2D projection with less overall segmentation, particularly for pattern recognition in events with large numbers of particles.

Gaseous TPC's are often designed to operate within a strong magnetic field (typically parallel to the drift field) so that particle momenta can be estimated from the track curvature. For this application, precise spatial measurements in the plane transverse to the magnetic field are most important. Since the amount of ionization along the length of the track depends on the velocity of the particle, ionization and momentum measurements can be combined to identify the types of particles observed in the TPC. The estimator for the energy deposit by a particle is usually formed as the truncated mean of the energy deposits, using the 50%–70% of the samples with the smallest signals. Variance due to energetic  $\delta$ -ray production is thus reduced.

Gas amplification of  $10^3$ – $10^4$  at the readout endplate is usually required in order to provide signals with sufficient amplitude for conventional electronics to sense the drifted ionization. Until recently, the gas amplification system used in TPC's have exclusively been planes of anode wires operated in proportional mode placed close to the readout pads. Performance has been recently improved by replacing these wire planes with micro-pattern gas detectors, namely GEM [88] and Micromegas [90] devices. Advances in electronics miniaturization have been important in this development, allowing pad areas to be reduced to the  $10 \text{ mm}^2$  scale or less, well matched to the narrow extent of signals produced with micro-pattern gas detectors. Presently, the ultimate in fine segmentation TPC readout are silicon sensors, with  $0.05 \text{ mm} \times 0.05 \text{ mm}$  pixels, in combination with GEM or Micromegas [100]. With such fine granularity it is possible to count the number of ionization clusters along the length of a track which, in principle, can improve the particle identification capability.

Examples of two modern large volume gaseous TPC's are shown in Fig. 31.13 and Fig. 31.14. The particle identification performance is illustrated in Fig. 31.15, for the original TPC in the PEP-4/9 experiment [101].

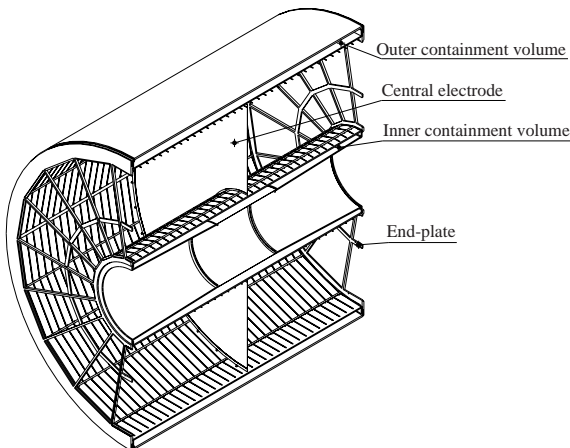


**Figure 31.13:** The ALICE TPC shown in a cutaway view [102]. The drift volume is 5 m long with a 5 m diameter. Gas amplification is provided by planes of anode wires.

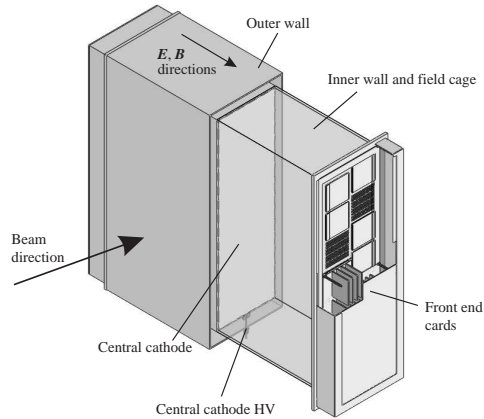


**Figure 31.14:** One of the 3 TPC modules for the near detector of the T2K experiment [103]. The drift volume is  $2 \text{ m} \times 2 \text{ m} \times 0.8 \text{ m}$ . Micromegas devices are used for gas amplification and readout.

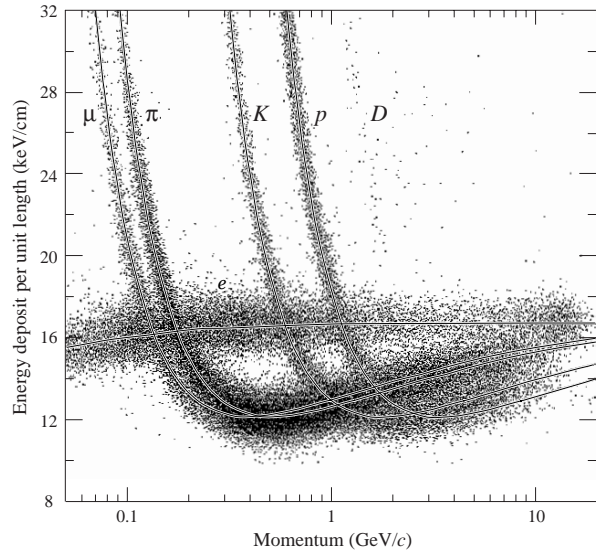


**Figure 31.15:** The PEP4/9-TPC energy deposit measurements (185 samples, 8.5 atm Ar-CH<sub>4</sub> 80:20). The ionization rate at the Fermi plateau (at high  $\beta$ ) is 1.4 times that for the minimum at lower  $\beta$ . This ratio increases to 1.6 at atmospheric pressure.

The greatest challenges for a large TPC arise from the long drift distance, typically 100 times further than in a comparable wire chamber design. In particular, the long drift distance can make the device sensitive to small distortions in the electric field. Distortions can arise from a number of sources, such as imperfections in the TPC construction, deformations of the readout surface, or the presence of ions in the active medium.

For a gaseous TPC operated in a magnetic field, the electron drift velocity  $v$  is defined by Eq. (31.13). With a strong magnetic field parallel to the electric field and a gas with a large value of  $\omega\tau$  (also favored to reduce transverse diffusion as discussed below), the transverse displacements of the drifting electrons due to electric field distortions are reduced. In this mode of operation, it is essential to precisely map the magnetic field as the electron drift lines closely follow the magnetic field lines. Corrections for electric and/or magnetic field non-uniformities can be determined from control samples of electrons produced by ionizing the gas with UV laser beams, from photoelectrons produced on the cathode, or from tracks emanating from calibration reactions.

The long drift distance means that there is a delay, typically 10–100  $\mu\text{s}$  in a large gaseous TPC, for signals to arrive at the endplate. For experiments with shorter intervals between events, this

can produce ambiguities in the starting time for the drift of ionization. This can be resolved by matching the TPC data with that from an auxiliary detector providing additional spatial or timing information.

In a gaseous TPC, the motion of positive ions is much slower than the electrons, and so the positive ions produced by many events may exist in the active volume. Of greatest concern is the ions produced in the gas amplification stage. Large gaseous TPC's built until now with wire planes have included a gating grid that prevent the positive ions from escaping into the drift volume in the interval between event triggers. Micro-pattern gas detectors release much less positive ions than wire planes operating at the same gain, which may allow operation of a TPC without a gating grid.

Given the long drift distance in a large TPC, the active medium must remain very pure, as small amounts of contamination can absorb the ionization signal. For example, in a typical large gaseous TPC,  $O_2$  must be kept below a few parts in  $10^5$ , otherwise a large fraction of the drifting electrons will become attached. Special attention must be made in the choice of construction materials in order to avoid the release of other electronegative contaminants.

Diffusion degrades the position information of ionization that drifts a long distance. For a gaseous TPC, the effect can be alleviated by the choice of a gas with low intrinsic diffusion or by operating in a strong magnetic field parallel to the drift field with a gas which exhibits a significant reduction in transverse diffusion with magnetic field. For typical operation without magnetic field, the transverse extent of the electrons,  $\sigma_{Dx}$ , is a few mm after drifting 1 m due to diffusion. With a strong magnetic field,  $\sigma_{Dx}$  can be reduced by as much as a factor of 10,

$$\sigma_{Dx}(B)/\sigma_{Dx}(0) = \frac{1}{\sqrt{1 + \omega^2 \tau^2}} \quad (31.16)$$

where  $\omega\tau$  is defined above. The diffusion limited position resolution from the information collected by a single row of pads is

$$\sigma_x = \frac{\sigma_{Dx}}{\sqrt{n}} \quad (31.17)$$

where  $n$  is the effective number of electrons collected by the pad row, giving an ultimate single row resolution of order  $100 \mu\text{m}$ .

Diffusion is significantly reduced in a negative-ion TPC [104], which uses a special gas mixture that attaches electrons immediately as they are produced. The drifting negative ions exhibit much less diffusion than electrons. The slow drift velocity and small  $\omega\tau$  of negative ions must be compatible with the experimental environment.

The spatial resolution achieved by a TPC is determined by a number of factors in addition to diffusion. Non-uniform ionization along the length of the track is a particularly important factor, and is responsible for the so-called “track angle” and “ $\mathbf{E} \times \mathbf{B}$ ” effects. If the boundaries between pads in a row are not parallel to the track, the ionization fluctuations will increase the variance in the position estimate from that row. For this reason, experiments with a preferred track direction should have pad boundaries aligned with that direction. Traditional TPC's with wire plane amplification suffer from the effects of non-parallel electric and magnetic fields near the wires that rotate ionization segments, thereby degrading the resolution because of the non-uniform ionization. Micro-pattern gas detectors exhibit a much smaller  $\mathbf{E} \times \mathbf{B}$  effect, since their feature size is much smaller than that of a wire grid.

**31.6.6. Transition radiation detectors (TRD's):** Written August 2007 by P. Nevski (BNL) and A. Romaniouk (Moscow Eng. & Phys. Inst.)

Transition radiation (TR) x rays are produced when a highly relativistic particle ( $\gamma \gtrsim 10^3$ ) crosses a refractive index interface, as discussed in Sec. 30.7. The x rays, ranging from a few keV to a few dozen keV, are emitted at a characteristic angle  $1/\gamma$  from the particle trajectory. Since the TR yield is about 1% per boundary crossing, radiation from multiple surface crossings is used in practical detectors. In the simplest concept, a detector module might consist of low- $Z$  foils followed by a high- $Z$  active layer made of proportional counters filled with a Xe-rich gas mixture. The atomic number considerations follow from the dominant photoelectric absorption cross section per atom going roughly as  $Z^n/E_x^3$ , where  $n$  varies between 4 and 5 over

the region of interest, and the x-ray energy is  $E_x$ .<sup>\*</sup> To minimize self-absorption, materials such as polypropylene, Mylar, carbon, and (rarely) lithium are used as radiators. The TR signal in the active regions is in most cases superimposed upon the particle's ionization losses. These drop a little faster than  $Z/A$  with increasing  $Z$ , providing another reason for active layers with high  $Z$ .

The TR intensity for a single boundary crossing always increases with  $\gamma$ , but for multiple boundary crossings interference leads to saturation near a Lorentz factor  $\gamma_{\text{sat}} = 0.6 \omega_1 \sqrt{\ell_1 \ell_2} / c$  [105], where  $\omega_1$  is the radiator plasma frequency,  $\ell_1$  is its thickness, and  $\ell_2$  the spacing. In most of the detectors used in particle physics the radiator parameters are chosen to provide  $\gamma_{\text{sat}} \approx 2000$ . Those detectors normally work as threshold devices, ensuring the best electron/pion separation in the momentum range  $1 \text{ GeV}/c \lesssim p \lesssim 150 \text{ GeV}/c$ .

One can distinguish two design concepts—“thick” and “thin” detectors:

1. The radiator, optimized for a minimum total radiation length at maximum TR yield and total TR absorption, consists of few hundred foils (for instance 300  $20 \mu\text{m}$  thick polypropylene foils). A dominant fraction of the soft TR photons is absorbed in the radiator itself. To increase the average TR photon energy further, part of the radiator far from the active layers is often made of thicker foils. The detector thickness, about 2 cm for Xe-filled gas chambers, is optimized to absorb the shaped x-ray spectrum. A classical detector is composed of several similar modules which respond nearly independently. Such detectors were used in the NA34 [106], and are being used in the ALICE experiment [107].
2. In another TRD concept a fine granular radiator/detector structure exploits the soft part of the TR spectrum more efficiently. This can be achieved, for instance, by distributing small-diameter straw-tube detectors uniformly or in thin layers throughout the radiator material (foils or fibers). Even with a relatively thin radiator stack, radiation below 5 keV is mostly lost in the radiators themselves. However for photon energies above this value the absorption becomes smaller and the radiation can be registered by several consecutive detector layers, thus creating a strong TR build-up effect. Descriptions of detectors using this approach can be found in both accelerator and space experiments [107]. For example, in the ATLAS TR tracker charged particles cross about 35 effective straw tube layers embedded in the radiator material [107]. The effective thickness of the Xe gas per straw is about 2.3 mm and the average number of foils per straw is about 40 with an effective foil thickness of about  $20 \mu\text{m}$ .

Both TR photon absorption and the TR build-up significantly affect the detector performance. Although the values mentioned above are typical for most of the plastic radiators used with Xe-based detectors, they vary significantly depending on detector parameters: radiator material, thickness and spacing, the construction of the sensitive chambers, their position, *etc.* Thus careful simulations are usually needed to build a detector optimized for a particular application.

The discrimination between electrons and pions can be based on the charge deposition measured in each detection module, on the number of clusters—energy depositions observed above an optimal threshold (usually in the 5 to 7 keV region), or on more sophisticated methods analyzing the pulse shape as a function of time. The total energy measurement technique is more suitable for thick gas volumes, which absorb most of the TR radiation and where the ionization loss fluctuations are small. The cluster-counting method works better for detectors with thin gas layers, where the fluctuations of the ionization losses are big. Cluster-counting replaces the Landau-Vavilov distribution of background ionization energy losses with the Poisson statistics of  $\delta$ -electrons, responsible for the distribution tails. The latter distribution is narrower than the Landau-Vavilov distribution.

The major factor in the performance of any TRD is its overall length. This is illustrated in Fig. 31.16, which shows, for a variety of detectors, the pion efficiency at a fixed electron efficiency of 90% as a function of the overall detector length. The experimental data, covering a range of particle energies from a few GeV to 40 GeV, are

<sup>\*</sup> Photon absorption coefficients for the elements (via a NIST link), and  $dE/dx|_{\text{min}}$  and plasma energies for many materials are given in [pdg.lbl.gov/AtomicNuclearProperties](http://pdg.lbl.gov/AtomicNuclearProperties).



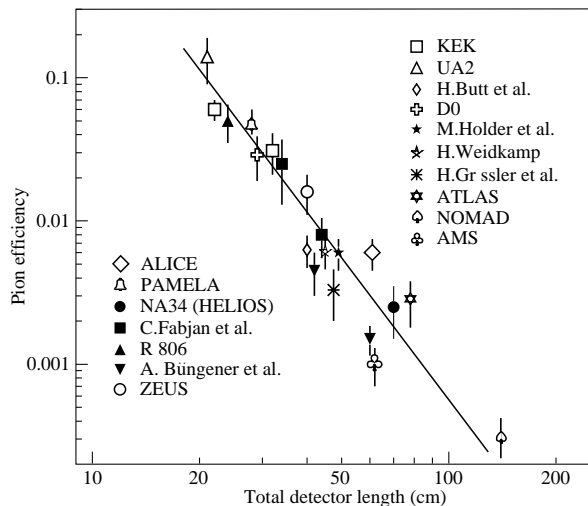


**Figure 31.16:** Pion efficiency measured (or predicted) for different TRDs as a function of the detector length for a fixed electron efficiency of 90%. The plot is taken from [106] with efficiencies of more recent detectors added [107].

rescaled to an energy of 10 GeV when possible. Phenomenologically, the rejection power against pions increases as  $5 \cdot 10^{L/38}$ , where the range of validity is  $L \approx 20\text{--}100$  cm.

Many recent TRDs combine particle identification with charged-track measurement in the same detector [107]. This provides a powerful tool for electron identification even at very high particle densities. Another example of this combination is described by Brigida *et al.* in Ref. 107. In this work Si-microstrip detectors operating in a magnetic field are used both for particle and TR detection. The excellent coordinate resolution of the Si detectors allows spatial separation of the TR photons from particle ionization tracks with relatively modest distances between radiator and detector.

Recent TRDs for particle astrophysics are designed to directly measure the Lorentz factor of high-energy nuclei by using the quadratic dependence of the TR yield on nuclear charge; see Cherry and Müller papers in Ref. 107. The radiator configuration  $(\ell_1, \ell_2)$  is tuned to extend the TR yield rise up to  $\gamma \lesssim 10^5$  using more energetic part of the TR spectrum (up to 100 keV). Exotic radiator materials such as aluminum and unusual TR detection methods (Compton scattering) are used such cases.

**31.6.7. Resistive-plate chambers :** Revised September 2007 by H.R. Band (U. Wisconsin).

The resistive-plate chamber (RPC) was developed by Santonico and Cardarelli in the early 1980's [108] as a low-cost alternative to large scintillator planes.\* Most commonly, an RPC is constructed from two parallel high-resistivity ( $10^9\text{--}10^{13}$   $\Omega\text{-cm}$ ) glass or phenolic (Bakelite)/melamine laminate plates with a few-mm gap between them which is filled with atmospheric-pressure gas. The gas is chosen to absorb UV photons in order to limit transverse growth of discharges. The backs of the plates are coated with a lower-resistivity paint or ink ( $\sim 10^5$   $\Omega/\square$ ), and a high potential (7–12 kV) is maintained between them. The passage of a charged particle initiates an electric discharge, whose size and duration are limited since the current reduces the local potential to below that needed to maintain the discharge. The sensitivity of the detector outside of this region is unaffected. The signal readout is via capacitive coupling to metallic strips on both sides of the detector which are separated from the high voltage coatings by thin insulating sheets. The  $x$  and  $y$  position of the discharge can be measured if the strips on opposite sides of the gap are orthogonal. When operated in streamer mode, the induced signals on the strips can be quite large ( $\sim 300$  mV), making sensitive electronics unnecessary. An example of an RPC structure is shown in Fig. 31.17.

\* It was based on earlier work on a spark counter with one high-resistivity plate [109].

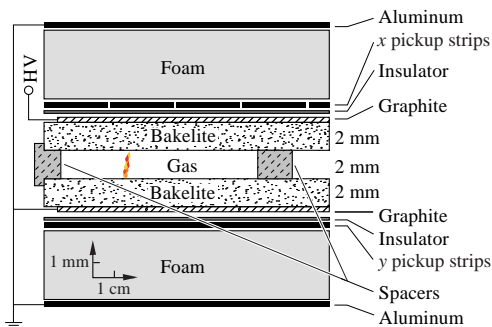


**Figure 31.17:** Schematic cross section of a typical RPC, in this case the single-gap streamer-mode BaBar RPC.

RPC's have inherent rate limitations since the time needed to re-establish the field after a discharge is proportional to the chamber capacitance and plate resistance. The average charge per streamer is 100–1000 pC. Typically, the efficiency of streamer-mode glass RPC's begins to fall above  $\sim 0.4$  Hz/cm<sup>2</sup>. Because of Bakelite's lower bulk resistivity, Bakelite RPC's can be efficient at 10–100 Hz/cm<sup>2</sup>. The need for higher rate capability led to the development of avalanche-mode RPC's, in which the gas and high voltage have been tuned to limit the growth of the electric discharge, preventing streamer formation. Typical avalanche-mode RPC's have a signal charge of about 10 pC and can be efficient at 1 kHz/cm<sup>2</sup>. The avalanche discharge produces a much smaller induced signal on the pickup strips ( $\sim 1$  mV) than streamers, and thus requires a more sophisticated and careful electronic design.

Many variations of the initial RPC design have been built for operation in either mode. Efficiencies of  $\geq 92\%$  for single gaps can be improved by the use of two or more gas gaps with shared pickup strips. Non-flammable and more environmentally friendly gas mixtures have been developed. In streamer mode, various mixtures of argon with isobutane and tetrafluoroethane have been used. For avalanche mode operation, a gas mixture of tetrafluoroethane ( $\text{C}_2\text{H}_2\text{F}_4$ ) with 2–5% isobutane and 0.4–10% sulfur hexafluoride ( $\text{SF}_6$ ) is typical. An example of large-scale RPC use is provided by the muon system being built for the ATLAS detector, where three layers of pairs of RPC's are used to trigger the drift tube arrays between the pairs. The total area is about 10,000 m<sup>2</sup>. These RPC's provide a spatial resolution of 1 cm and a time resolution of 1 ns at an efficiency  $\geq 99\%$ .

Developments of multiple-gap RPC's [110] lead to RPC designs with much better timing resolution ( $\sim 50$  ps) for use in time-of-flight particle identification systems. A pioneering design used by the HARP experiment [111] has two sets of 2 thin gas gaps (0.3 mm) separated by thin (0.7 mm) glass plates. The outer plates are connected to high voltage and ground while the inner plate is electrically isolated and floats to a stable equilibrium potential. The observed RPC intrinsic time resolution of 127 ps may have been limited by amplifier noise. Fonte provides useful review [112] of other RPC designs.

Operational experience with RPC's has been mixed. Several experiments (*e.g.*, L3 and HARP) have reported reliable performance. However, the severe problems experienced with the BaBar RPC's have raised concerns about the long-term reliability of Bakelite RPC's.

Glass RPC's have had fewer problems, as seen by the history of the BELLE chambers. A rapid growth in the noise rate and leakage current in some of the BELLE glass RPC's was observed during commissioning. It was found that water vapor in the input gas was reacting with fluorine (produced by the disassociation of the tetrafluoroethane in the streamers) to produce hydrofluoric acid. The acid etched the glass surfaces, leading to increased noise rates and lower efficiencies. The use of copper gas piping to insure the dryness of the input gas stopped the problem. The BELLE RPC's have now operated reliably for more than 5 years.

Several different failure modes diagnosed in the first-generation BaBar Bakelite RPC's caused the average efficiency of the barrel RPC's to fall from  $\geq 90\%$  to 35% in five years. The linseed oil which is used in Bakelite RPC's to coat the inner surface [113] had not been completely cured. Under warm conditions (32°C)

and high voltage, oil collected on the spacers between the gaps or formed oil-drop bridges between the gaps. This led to large leakage currents (50–100  $\mu\text{A}$  in some chambers) which persisted even when the temperature was regulated at 20°C. In addition, the graphite layer used to distribute the high voltage over the Bakelite became highly resistive (100 k $\Omega/\square \rightarrow$  10 M $\Omega/\square$ ), resulting in lowered efficiency in some regions and the complete death of whole chambers.

The BaBar problems and the proposed use of Bakelite RPC's in the LHC detectors prompted detailed studies of RPC aging and have led to improved construction techniques and a better understanding of RPC operational limits. The graphite layer has been improved and should be stable with integrated currents of  $\lesssim 600 \text{ mC/cm}^2$ . Molded gas inlets and improved cleanliness during construction have reduced the noise rate of new chambers. Unlike glass RPC's, Bakelite RPC's have been found to require humid input gases to prevent drying of the Bakelite (increasing the bulk resistivity) which would decrease the rate capability. Second-generation BaBar RPC's incorporating many of the above improvements have performed reliably for over two years [114].

With many of these problems solved, new-generation RPC's are now being or soon will be used in about a dozen cosmic-ray and HEP detectors. Their comparatively low cost, ease of construction, good time resolution, high efficiency, and moderate spatial resolution make them attractive in many situations, particularly those requiring fast timing and/or large-area coverage.

### 31.7. Semiconductor detectors

Updated August 2011 by H. Spieler.

Semiconductor detectors provide a unique combination of energy and position resolution. In collider detectors they are most widely used as position sensing devices and photodetectors (Sec. 31.2). Integrated circuit technology allows the formation of high-density micron-scale electrodes on large (15–20 cm diameter) wafers, providing excellent position resolution. Furthermore, the density of silicon and its small ionization energy yield adequate signals with active layers only 100–300  $\mu\text{m}$  thick, so the signals are also fast (typically tens of ns). The high energy resolution is a key parameter in x-ray, gamma, and charged particle spectroscopy, *e.g.*, in neutrinoless double beta decay searches. Silicon and germanium are the most commonly used materials, but gallium-arsenide, CdTe, CdZnTe, and other materials are also useful. CdZnTe provides a higher stopping power and the ratio of Cd to Zn concentrations changes the bandgap. Ge detectors are commonly operated at liquid nitrogen temperature to reduce the bias current, which depends exponentially on temperature. Semiconductor detectors depend crucially on low-noise electronics (see Sec. 31.8), so the detection sensitivity is determined by signal charge and capacitance. For a comprehensive discussion of semiconductor detectors and electronics see Ref. 115.

#### 31.7.1. Materials Requirements :

Semiconductor detectors are essentially solid state ionization chambers. Absorbed energy forms electron-hole pairs, *i.e.*, negative and positive charge carriers, which under an applied electric field move towards their respective collection electrodes, where they induce a signal current. The energy required to form an electron-hole pair is proportional to the bandgap. In tracking detectors the energy loss in the detector should be minimal, whereas for energy spectroscopy the stopping power should be maximized, so for gamma rays high- $Z$  materials are desirable.

Measurements on silicon photodiodes [116] show that for photon energies below 4 eV one electron-hole ( $e-h$ ) pair is formed per incident photon. The mean energy  $E_i$  required to produce an  $e-h$  pair peaks at 4.4 eV for a photon energy around 6 eV. Above  $\sim 1.5$  keV it assumes a constant value, 3.67 eV at room temperature. It is larger than the bandgap energy because momentum conservation requires excitation of lattice vibrations (phonons). For minimum-ionizing particles, the most probable charge deposition in a 300  $\mu\text{m}$  thick silicon detector is about 3.5 fC (22000 electrons). Other typical ionization energies are 2.96 eV in Ge, 4.2 eV in GaAs, and 4.43 eV in CdTe.

Since both electronic and lattice excitations are involved, the variance in the number of charge carriers  $N = E/E_i$  produced by an absorbed energy  $E$  is reduced by the Fano factor  $F$  (about 0.1 in Si and Ge). Thus,  $\sigma_N = \sqrt{FN}$  and the energy resolution

$\sigma_E/E = \sqrt{FE_i/E}$ . However, the measured signal fluctuations are usually dominated by electronic noise or energy loss fluctuations in the detector. The electronic noise contributions depend on the pulse shaping in the signal processing electronics, so the choice of the shaping time is critical (see Sec. 31.8).

A smaller bandgap would produce a larger signal and improve energy resolution, but the intrinsic resistance of the material is critical. Thermal excitation, given by the Fermi-Dirac distribution, promotes electrons into the conduction band, so the thermally excited carrier concentration increases exponentially with decreasing bandgaps. In pure Si the carrier concentration is  $\sim 10^{10} \text{ cm}^{-3}$  at 300 K, corresponding to a resistivity  $\rho \approx 400 \text{ k}\Omega \text{ cm}$ . In reality, crystal imperfections and minute impurity concentrations limit Si carrier concentrations to  $\sim 10^{11} \text{ cm}^{-3}$  at 300 K, corresponding to a resistivity  $\rho \approx 40 \text{ k}\Omega \text{ cm}$ . In practice, resistivities up to 20 k $\Omega \text{ cm}$  are available, with mass production ranging from 5 to 10 k $\Omega \text{ cm}$ . Signal currents at keV scale energies are of order  $\mu\text{A}$ . However, for a resistivity of  $10^4 \Omega \text{ cm}$  a 300  $\mu\text{m}$  thick sensor with 1  $\text{cm}^2$  area would have a resistance of 300  $\Omega$ , so 30 V would lead to a current flow of 100 mA and a power dissipation of 3 W. On the other hand, high-quality single crystals of Si and Ge can be grown economically with suitably large volumes, so to mitigate the effect of resistivity one resorts to reverse-biased diode structures. Although this reduces the bias current relative to a resistive material, the thermally excited leakage current can still be excessive at room temperature, so Ge diodes are typically operated at liquid nitrogen temperature (77 K).

A major effort is to find high- $Z$  materials with a bandgap that is sufficiently high to allow room-temperature operation while still providing good energy resolution. Compound semiconductors, *e.g.*, CdZnTe, can allow this, but typically suffer from charge collection problems, characterized by the product  $\mu\tau$  of mobility and carrier lifetime. In Si and Ge  $\mu\tau > 1 \text{ cm}^2 \text{ V}^{-1}$  for both electrons and holes, whereas in compound semiconductors it is in the range  $10^{-3}$ – $10^{-8}$ . Since for holes  $\mu\tau$  is typically an order of magnitude smaller than for electrons, detector configurations where the electron contribution to the charge signal dominates—*e.g.*, strip or pixel structures—can provide better performance.

#### 31.7.2. Detector Configurations :

A  $p-n$  junction operated at reverse bias forms a sensitive region depleted of mobile charge and sets up an electric field that sweeps charge liberated by radiation to the electrodes. Detectors typically use an asymmetric structure, *e.g.*, a highly doped  $p$  electrode and a lightly doped  $n$  region, so that the depletion region extends predominantly into the lightly doped volume.

In a planar device the thickness of the depleted region is

$$W = \sqrt{2\epsilon(V + V_{bi})/Ne} = \sqrt{2\rho\mu\epsilon(V + V_{bi})}, \quad (31.18)$$

where  $V$  = external bias voltage

$V_{bi}$  = “built-in” voltage ( $\approx 0.5$  V for resistivities typically used in Si detectors)

$N$  = doping concentration

$e$  = electronic charge

$\epsilon$  = dielectric constant =  $11.9 \epsilon_0 \approx 1 \text{ pF/cm}$  in Si

$\rho$  = resistivity (typically 1–10 k $\Omega \text{ cm}$  in Si)

$\mu$  = charge carrier mobility

= 1350  $\text{cm}^2 \text{ V}^{-1} \text{ s}^{-1}$  for electrons in Si

= 450  $\text{cm}^2 \text{ V}^{-1} \text{ s}^{-1}$  for holes in Si

In Si

$$W = 0.5 [\mu\text{m}/\sqrt{\Omega \cdot \text{cm} \cdot \text{V}}] \times \sqrt{\rho(V + V_{bi})} \text{ for } n\text{-type Si, and}$$

$$W = 0.3 [\mu\text{m}/\sqrt{\Omega \cdot \text{cm} \cdot \text{V}}] \times \sqrt{\rho(V + V_{bi})} \text{ for } p\text{-type Si.}$$

The conductive  $p$  and  $n$  regions together with the depleted volume form a capacitor with the capacitance per unit area

$$C = \epsilon/W \approx 1 [\text{pF/cm}]/W \text{ in Si.} \quad (31.19)$$

In strip and pixel detectors the capacitance is dominated by the fringing capacitance. For example, the strip-to-strip Si fringing capacitance is  $\sim 1$ – $1.5 \text{ pF cm}^{-1}$  of strip length at a strip pitch of 25–50  $\mu\text{m}$ .

Large volume ( $\sim 10^2\text{--}10^3\text{ cm}^3$ ) Ge detectors are commonly configured as coaxial detectors, *e.g.*, a cylindrical n-type crystal with 5–10 cm diameter and 10 cm length with an inner 5–10 mm diameter n<sup>+</sup> electrode and an outer p<sup>+</sup> layer forming the diode junction. Ge can be grown with very low impurity levels,  $10^9\text{--}10^{10}\text{ cm}^{-3}$  (HPGe), so these large volumes can be depleted with several kV.

### 31.7.3. Signal Formation :

The signal pulse shape depends on the instantaneous carrier velocity  $v(x) = \mu E(x)$  and the electrode geometry, which determines the distribution of induced charge (*e.g.*, see Ref. 115, pp. 71–83). Charge collection time decreases with increasing bias voltage, and can be reduced further by operating the detector with “overbias,” *i.e.*, a bias voltage exceeding the value required to fully deplete the device. The collection time is limited by velocity saturation at high fields (in Si approaching  $10^7\text{ cm/s}$  at  $E > 10^4\text{ V/cm}$ ); at an average field of  $10^4\text{ V/cm}$  the collection time is about 15 ps/ $\mu\text{m}$  for electrons and 30 ps/ $\mu\text{m}$  for holes. In typical fully-depleted detectors 300  $\mu\text{m}$  thick, electrons are collected within about 10 ns, and holes within about 25 ns.

Position resolution is limited by transverse diffusion during charge collection (typically 5  $\mu\text{m}$  for 300  $\mu\text{m}$  thickness) and by knock-on electrons. Resolutions of 2–4  $\mu\text{m}$  (rms) have been obtained in beam tests. In magnetic fields, the Lorentz drift deflects the electron and hole trajectories and the detector must be tilted to reduce spatial spreading (see “Hall effect” in semiconductor textbooks).

Electrodes can be in the form of cm-scale pads, strips, or  $\mu\text{m}$ -scale pixels. Various readout structures have been developed for pixels, *e.g.*, CCDs, DEPFETs, monolithic pixel devices that integrate sensor and electronics (MAPS), and hybrid pixel devices that utilize separate sensors and readout ICs connected by two-dimensional arrays of solder bumps. For an overview and further discussion see Ref. 115.

In gamma ray spectroscopy ( $E_\gamma > 10^2\text{ keV}$ ) Compton scattering dominates, so for a significant fraction of events the incident gamma energy is not completely absorbed, *i.e.*, the Compton scattered photon escapes from the detector and the energy deposited by the Compton electron is only a fraction of the total. Distinguishing multi-interaction events, *e.g.*, multiple Compton scatters with a final photoelectric absorption, from single Compton scatters allows background suppression. Since the individual interactions take place in different parts of the detector volume, these events can be distinguished by segmenting the outer electrode of a coaxial detector and analyzing the current pulse shapes. The different collection times can be made more distinguishable by using “point” electrodes, where most of the signal is induced when charges are close to the electrode, similarly to strip or pixel detectors. Charge clusters arriving from different positions in the detector will arrive at different times and produce current pulses whose major components are separated in time. Point electrodes also reduce the electrode capacitance, which reduces electronic noise, but careful design is necessary to avoid low-field regions in the detector volume.

**31.7.4. Radiation Damage :** Radiation damage occurs through two basic mechanisms:

1. Bulk damage due to displacement of atoms from their lattice sites. This leads to increased leakage current, carrier trapping, and build-up of space charge that changes the required operating voltage. Displacement damage depends on the nonionizing energy loss and the energy imparted to the recoil atoms, which can initiate a chain of subsequent displacements, *i.e.*, damage clusters. Hence, it is critical to consider both particle type and energy.
2. Surface damage due to charge build-up in surface layers, which leads to increased surface leakage currents. In strip detectors the inter-strip isolation is affected. The effects of charge build-up are strongly dependent on the device structure and on fabrication details. Since the damage is proportional to the absorbed energy (when ionization dominates), the dose can be specified in rad (or Gray) independent of particle type.

The increase in reverse bias current due to bulk damage is  $\Delta I_r = \alpha\Phi$  per unit volume, where  $\Phi$  is the particle fluence and  $\alpha$  the damage coefficient ( $\alpha \approx 3 \times 10^{-17}\text{ A/cm}$  for minimum ionizing protons

and pions after long-term annealing;  $\alpha \approx 2 \times 10^{-17}\text{ A/cm}$  for 1 MeV neutrons). The reverse bias current depends strongly on temperature

$$\frac{I_R(T_2)}{I_R(T_1)} = \left(\frac{T_2}{T_1}\right)^2 \exp\left[-\frac{E}{2k}\left(\frac{T_1 - T_2}{T_1 T_2}\right)\right], \quad (31.20)$$

where  $E = 1.2\text{ eV}$ , so rather modest cooling can reduce the current substantially ( $\sim 6$ -fold current reduction in cooling from room temperature to  $0^\circ\text{C}$ ).

Displacement damage forms acceptor-like states. These trap electrons, building up a negative space charge, which in turn requires an increase in the applied voltage to sweep signal charge through the detector thickness. This has the same effect as a change in resistivity, *i.e.*, the required voltage drops initially with fluence, until the positive and negative space charge balance and very little voltage is required to collect all signal charge. At larger fluences the negative space charge dominates, and the required operating voltage increases ( $V \propto N$ ). The safe limit on operating voltage ultimately limits the detector lifetime. Strip detectors specifically designed for high voltages have been extensively operated at bias voltages  $> 500\text{ V}$ . Since the effect of radiation damage depends on the electronic activity of defects, various techniques have been applied to neutralize the damage sites. For example, additional doping with oxygen can increase the allowable charged hadron fluence roughly three-fold [117]. Detectors with columnar electrodes normal to the surface can also extend operational lifetime [118]. The increase in leakage current with fluence, on the other hand, appears to be unaffected by resistivity and whether the material is n or p-type. At fluences beyond  $10^{15}\text{ cm}^{-2}$  decreased carrier lifetime becomes critical [119,120].

Strip and pixel detectors have remained functional at fluences beyond  $10^{15}\text{ cm}^{-2}$  for minimum ionizing protons. At this damage level, charge loss due to recombination and trapping becomes significant and the high signal-to-noise ratio obtainable with low-capacitance pixel structures extends detector lifetime. The higher mobility of electrons makes them less sensitive to carrier lifetime than holes, so detector configurations that emphasize the electron contribution to the charge signal are advantageous, *e.g.*, n<sup>+</sup> strips or pixels on a p- or n-substrate. The occupancy of the defect charge states is strongly temperature dependent; competing processes can increase or decrease the required operating voltage. It is critical to choose the operating temperature judiciously ( $-10$  to  $0^\circ\text{C}$  in typical collider detectors) and limit warm-up periods during maintenance. For a more detailed summary see Ref. 121 and the web-sites of the ROSE and RD50 collaborations at <http://RD48.web.cern.ch/rd48> and <http://RD50.web.cern.ch/rd50>. Materials engineering, *e.g.*, introducing oxygen interstitials, can improve certain aspects and is under investigation. At high fluences diamond is an alternative, but operates as an insulator rather than a reverse-biased diode.

Currently, the lifetime of detector systems is still limited by the detectors; in the electronics use of standard “deep submicron” CMOS fabrication processes with appropriately designed circuitry has increased the radiation resistance to fluences  $> 10^{15}\text{ cm}^{-2}$  of minimum ionizing protons or pions. For a comprehensive discussion of radiation effects see Ref. 122.

### 31.8. Low-noise electronics

Revised August 2011 by H. Spieler.

Many detectors rely critically on low-noise electronics, either to improve energy resolution or to allow a low detection threshold. A typical detector front-end is shown in Fig. 31.18.

The detector is represented by a capacitance  $C_d$ , a relevant model for most detectors. Bias voltage is applied through resistor  $R_b$  and the signal is coupled to the preamplifier through a blocking capacitor  $C_c$ . The series resistance  $R_s$  represents the sum of all resistances present in the input signal path, *e.g.* the electrode resistance, any input protection networks, and parasitic resistances in the input transistor. The preamplifier provides gain and feeds a pulse shaper, which tailors the overall frequency response to optimize signal-to-noise ratio while limiting the duration of the signal pulse to accommodate the signal pulse rate. Even if not explicitly stated, all amplifiers provide some form of pulse shaping due to their limited frequency response.

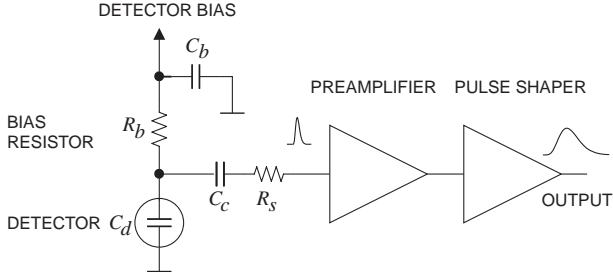


Figure 31.18: Typical detector front-end circuit.

The equivalent circuit for the noise analysis (Fig. 31.19) includes both current and voltage noise sources. The leakage current of a semiconductor detector, for example, fluctuates due to electron emission statistics. The statistical fluctuations in the charge measurement will scale with the square root of the total number of recorded charges, so this noise contribution increases with the width of the shaped output pulse. This “shot noise”  $i_{nd}$  is represented by a current noise generator in parallel with the detector. Resistors exhibit noise due to thermal velocity fluctuations of the charge carriers. This yields a constant noise power density vs. frequency, so increasing the bandwidth of the shaped output pulse, *i.e.* reducing the shaping time, will increase the noise. This noise source can be modeled either as a voltage or current generator. Generally, resistors shunting the input act as noise current sources and resistors in series with the input act as noise voltage sources (which is why some in the detector community refer to current and voltage noise as “parallel” and “series” noise). Since the bias resistor effectively shunts the input, as the capacitor  $C_b$  passes current fluctuations to ground, it acts as a current generator  $i_{nb}$  and its noise current has the same effect as the shot noise current from the detector. Any other shunt resistances can be incorporated in the same way. Conversely, the series resistor  $R_s$  acts as a voltage generator. The electronic noise of the amplifier is described fully by a combination of voltage and current sources at its input, shown as  $e_{na}$  and  $i_{na}$ .

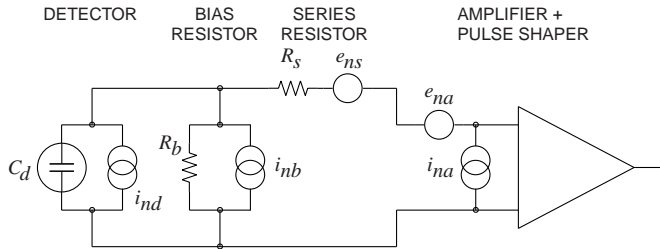


Figure 31.19: Equivalent circuit for noise analysis.

Shot noise and thermal noise have a “white” frequency distribution, *i.e.* the spectral power densities  $dP_n/df \propto di_n^2/df \propto de_n^2/df$  are constant with the magnitudes

$$\begin{aligned} i_{nd}^2 &= 2eI_d, \\ i_{nb}^2 &= \frac{4kT}{R_b}, \\ e_{ns}^2 &= 4kTR_s, \end{aligned} \quad (31.21)$$

where  $e$  is the electronic charge,  $I_d$  the detector bias current,  $k$  the Boltzmann constant and  $T$  the temperature. Typical amplifier noise parameters  $e_{na}$  and  $i_{na}$  are of order  $\text{nV}/\sqrt{\text{Hz}}$  and  $\text{pA}/\sqrt{\text{Hz}}$ . Trapping and detrapping processes in resistors, dielectrics and semiconductors can introduce additional fluctuations whose noise power frequently exhibits a  $1/f$  spectrum. The spectral density of the  $1/f$  noise voltage is

$$e_{nf}^2 = \frac{A_f}{f}, \quad (31.22)$$

where the noise coefficient  $A_f$  is device specific and of order  $10^{-10}$ – $10^{-12} \text{ V}^2$ .

A fraction of the noise current flows through the detector capacitance, resulting in a frequency-dependent noise voltage  $i_n/(\omega C_d)$ , which is added to the noise voltage in the input circuit. Thus, the current noise contribution increases with lowering frequency, so its contribution increases with shaping pulse width. Since the individual noise contributions are random and uncorrelated, they add in quadrature. The total noise at the output of the pulse shaper is obtained by integrating over the full bandwidth of the system. Superimposed on repetitive detector signal pulses of constant magnitude, purely random noise produces a Gaussian signal distribution.

Since radiation detectors typically convert the deposited energy into charge, the system’s noise level is conveniently expressed as an equivalent noise charge  $Q_n$ , which is equal to the detector signal that yields a signal-to-noise ratio of one. The equivalent noise charge is commonly expressed in Coulombs, the corresponding number of electrons, or the equivalent deposited energy (eV). For a capacitive sensor

$$Q_n^2 = i_n^2 F_i T_S + e_n^2 F_v \frac{C^2}{T_S} + F_{vf} A_f C^2, \quad (31.23)$$

where  $C$  is the sum of all capacitances shunting the input,  $F_i$ ,  $F_v$ , and  $F_{vf}$  depend on the shape of the pulse determined by the shaper and  $T_s$  is a characteristic time, for example, the peaking time of a semi-gaussian pulse or the sampling interval in a correlated double sampler. The form factors  $F_i$ ,  $F_v$  are easily calculated

$$F_i = \frac{1}{2T_S} \int_{-\infty}^{\infty} [W(t)]^2 dt, \quad F_v = \frac{T_S}{2} \int_{-\infty}^{\infty} \left[ \frac{dW(t)}{dt} \right]^2 dt, \quad (31.24)$$

where for time-invariant pulse-shaping  $W(t)$  is simply the system’s impulse response (the output signal seen on an oscilloscope) for a short input pulse with the peak output signal normalized to unity. For more details see Refs. 123 and 124.

A pulse shaper formed by a single differentiator and integrator with equal time constants has  $F_i = F_v = 0.9$  and  $F_{vf} = 4$ , independent of the shaping time constant. The overall noise bandwidth, however, depends on the time constant, *i.e.* the characteristic time  $T_s$ . The contribution from noise currents increases with shaping time, *i.e.*, pulse duration, whereas the voltage noise decreases with increasing shaping time. Noise with a  $1/f$  spectrum depends only on the ratio of upper to lower cutoff frequencies (integrator to differentiator time constants), so for a given shaper topology the  $1/f$  contribution to  $Q_n$  is independent of  $T_s$ . Furthermore, the contribution of noise voltage sources to  $Q_n$  increases with detector capacitance. Pulse shapers can be designed to reduce the effect of current noise, *e.g.*, mitigate radiation damage. Increasing pulse symmetry tends to decrease  $F_i$  and increase  $F_v$  (*e.g.*, to 0.45 and 1.0 for a shaper with one  $CR$  differentiator and four cascaded integrators). For the circuit shown in Fig. 31.19,

$$\begin{aligned} Q_n^2 &= \left( 2eI_d + 4kT/R_b + i_{na}^2 \right) F_i T_S \\ &\quad + (4kTR_s + e_{na}^2) F_v C_d^2 / T_S + F_{vf} A_f C_d^2. \end{aligned} \quad (31.25)$$

As the characteristic time  $T_S$  is changed, the total noise goes through a minimum, where the current and voltage contributions are equal. Fig. 31.20 shows a typical example. At short shaping times the current noise dominates, whereas at long shaping times the current noise takes over. The noise minimum is flattened by the presence of  $1/f$  noise. Increasing the detector capacitance will increase the voltage noise and shift the noise minimum to longer shaping times.

For quick estimates, one can use the following equation, which assumes an FET amplifier (negligible  $i_{na}$ ) and a simple  $CR$ – $RC$  shaper with time constants  $\tau$  (equal to the peaking time):

$$\begin{aligned} (Q_n/e)^2 &= 12 \left[ \frac{1}{\text{nA} \cdot \text{ns}} \right] I_d \tau + 6 \times 10^5 \left[ \frac{\text{k}\Omega}{\text{ns}} \right] \frac{\tau}{R_b} \\ &\quad + 3.6 \times 10^4 \left[ \frac{\text{ns}}{(\text{pF})^2 (\text{nV})^2 / \text{Hz}} \right] e_n^2 \frac{C^2}{\tau}. \end{aligned} \quad (31.26)$$

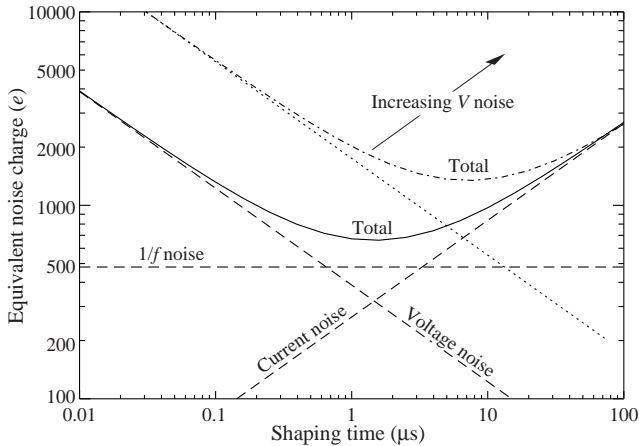


**Figure 31.20:** Equivalent noise charge vs shaping time. Changing the voltage or current noise contribution shifts the noise minimum. Increased voltage noise is shown as an example.

Noise is improved by reducing the detector capacitance and leakage current, judiciously selecting all resistances in the input circuit, and choosing the optimum shaping time constant.

The noise parameters of the amplifier depend primarily on the input device. In field effect transistors, the noise current contribution is very small, so reducing the detector leakage current and increasing the bias resistance will allow long shaping times with correspondingly lower noise. In bipolar transistors, the base current sets a lower bound on the noise current, so these devices are best at short shaping times. In special cases where the noise of a transistor scales with geometry, *i.e.*, decreasing noise voltage with increasing input capacitance, the lowest noise is obtained when the input capacitance of the transistor is equal to the detector capacitance, albeit at the expense of power dissipation. Capacitive matching is useful with field-effect transistors, but not bipolar transistors. In bipolar transistors, the minimum obtainable noise is independent of shaping time, but only at the optimum collector current  $I_C$ , which does depend on shaping time.

$$Q_{n,\min}^2 = 4kT \frac{C}{\sqrt{\beta_{DC}}} \sqrt{F_i F_v} \text{ at } I_c = \frac{kT}{e} C \sqrt{\beta_{DC}} \sqrt{\frac{F_v}{F_i}} \frac{1}{T_S}, \quad (31.27)$$

where  $\beta_{DC}$  is the DC current gain. For a  $CR$ - $RC$  shaper and  $\beta_{DC} = 100$ ,

$$Q_{n,\min}/e \approx 250 \sqrt{C/\text{pF}}. \quad (31.28)$$

Practical noise levels range from  $\sim 1e$  for CCD's at long shaping times to  $\sim 10^4 e$  in high-capacitance liquid argon calorimeters. Silicon strip detectors typically operate at  $\sim 10^3$  electrons, whereas pixel detectors with fast readout provide noise of several hundred electrons.

In timing measurements, the slope-to-noise ratio must be optimized, rather than the signal-to-noise ratio alone, so the rise time  $t_r$  of the pulse is important. The "jitter"  $\sigma_t$  of the timing distribution is

$$\sigma_t = \frac{\sigma_n}{(dS/dt)_{S_T}} \approx \frac{t_r}{S/N}, \quad (31.29)$$

where  $\sigma_n$  is the rms noise and the derivative of the signal  $dS/dt$  is evaluated at the trigger level  $S_T$ . To increase  $dS/dt$  without incurring excessive noise, the amplifier bandwidth should match the rise-time of the detector signal. The 10 to 90% rise time of an amplifier with bandwidth  $f_U$  is  $0.35/f_U$ . For example, an oscilloscope with 350 MHz bandwidth has a 1 ns rise time. When amplifiers are cascaded, which is invariably necessary, the individual rise times add in quadrature.

$$t_r \approx \sqrt{t_{r1}^2 + t_{r2}^2 + \dots + t_{rn}^2}. \quad (31.30)$$

Increasing signal-to-noise ratio also improves time resolution, so minimizing the total capacitance at the input is also important. At high signal-to-noise ratios, the time jitter can be much smaller than the rise time. The timing distribution may shift with signal

level ("walk"), but this can be corrected by various means, either in hardware or software [8].

The basic principles discussed above apply to both analog and digital signal processing. In digital signal processing the pulse shaper shown in Fig. 31.18 is replaced by an analog to digital converter (ADC) followed by a digital processor that determines the pulse shape. Digital signal processing allows great flexibility in implementing filtering functions. The software can be changed readily to adapt to a wide variety of operating conditions and it is possible to implement filters that are impractical or even impossible using analog circuitry. However, this comes at the expense of increased circuit complexity and increased demands on the ADC compared to analog shaping.

If the sampling rate of the ADC is too low, high frequency components will be transferred to lower frequencies ("aliasing"). The sampling rate of the ADC must be high enough to capture the maximum frequency component of the input signal. Apart from missing information on the fast components of the pulse, undersampling introduces spurious artifacts. If the frequency range of the input signal is much greater, the noise at the higher frequencies will be transferred to lower frequencies and increase the noise level in the frequency range of pulses formed in the subsequent digital shaper. The Nyquist criterion states that the sampling frequency must be at least twice the maximum relevant input frequency. This requires that the bandwidth of the circuitry preceding the ADC must be limited. The most reliable technique is to insert a low-pass filter.

The digitization process also introduces inherent noise, since the voltage range  $\Delta V$  corresponding to a minimum bit introduces quasi-random fluctuations relative to the exact amplitude

$$\sigma_n = \frac{\Delta V}{\sqrt{12}}. \quad (31.31)$$

When the Nyquist condition is fulfilled the noise bandwidth  $\Delta f_n$  is spread nearly uniformly and extends to 1/2 the sampling frequency  $f_S$ , so the spectral noise density

$$e_n = \frac{\sigma_n}{\sqrt{\Delta f_n}} = \frac{\Delta V}{\sqrt{12}} \cdot \frac{1}{\sqrt{f_S/2}} = \frac{\Delta V}{\sqrt{6} f_S}. \quad (31.32)$$

Sampling at a higher frequency spreads the total noise over a larger frequency range, so oversampling can be used to increase the effective resolution. In practice, this quantization noise is increased by differential nonlinearity. Furthermore, the equivalent input noise of ADCs is often rather high, so the overall gain of the stages preceding the ADC must be sufficiently large for the preamplifier input noise to override.

When implemented properly, digital signal processing provides significant advantages in systems where the shape of detector signal pulses changes greatly, for example in large semiconductor detectors for gamma rays or in gaseous detectors (*e.g.* TPCs) where the duration of the current pulse varies with drift time, which can range over orders of magnitude. Where is analog signal processing best (most efficient)? In systems that require fast time response the high power requirements of high-speed ADCs are prohibitive. Systems that are not sensitive to pulse shape can use fixed shaper constants and rather simple filters, which can be either continuous or sampled. In high density systems that require small circuit area and low power (*e.g.* strip and pixel detectors), analog filtering often yields the required response and tends to be most efficient.

For a more detailed introduction to detector signal processing and electronics see Ref. 115.



### 31.9. Calorimeters

A calorimeter is designed to measure the energy deposition and its direction for a contained electromagnetic (EM) or hadronic shower. The characteristic interaction distance for an electromagnetic interaction is the radiation length  $X_0$ , which ranges from  $13.8 \text{ g cm}^{-2}$  in iron to  $6.0 \text{ g cm}^{-2}$  in uranium.\* Similarly, the characteristic nuclear interaction length  $\lambda_I$  varies from  $132.1 \text{ g cm}^{-2}$  (Fe) to  $209 \text{ g cm}^{-2}$  (U).† In either case, a calorimeter must be many interaction lengths deep, where “many” is determined by physical size, cost, and other factors. EM calorimeters tend to be  $15\text{--}30 X_0$  deep, while hadronic calorimeters are usually compromised at  $5\text{--}8 \lambda_I$ . In real experiments there is likely to be an EM calorimeter in front of the hadronic section, which in turn has less sampling density in the back, so the hadronic cascade occurs in a succession of different structures.

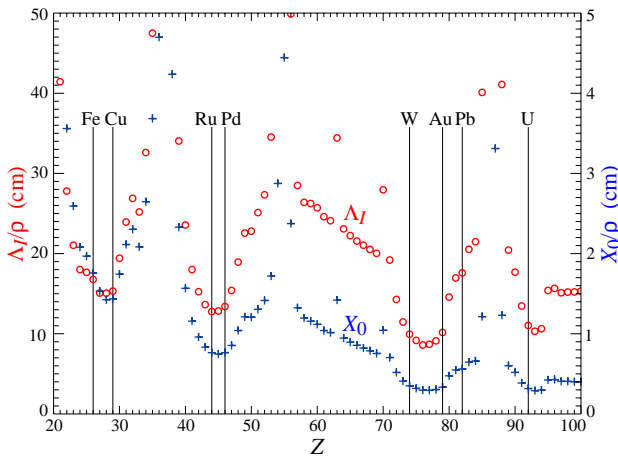


**Figure 31.21:** Nuclear interaction length  $\lambda_I/\rho$  (circles) and radiation length  $X_0/\rho$  (+’s) in cm for the chemical elements with  $Z > 20$  and  $\lambda_I < 50$  cm.

In all cases there is a premium on small  $\lambda_I/\rho$  and  $X_0/\rho$  (both with units of length). These quantities are shown for  $Z > 20$  for the chemical elements in Fig. 31.21. For the hadronic case, metallic absorbers in the W–Au region are best, followed by U. The Ru–Pd region elements are rare and expensive. Lead is a bad choice. Given cost considerations, Fe and Cu might be appropriate choices. For EM calorimeters high  $Z$  is preferred, and lead is not a bad choice.

These considerations are for *sampling calorimeters* consisting of metallic absorber sandwiched or (threaded) with an active material which generates signal. The active medium may be a scintillator, an ionizing noble liquid, a gas chamber, a semiconductor, or a Cherenkov radiator. The average interaction length is thus greater than that of the absorber alone, sometimes substantially so.

There are also *homogeneous calorimeters*, in which the entire volume is sensitive, *i.e.*, contributes signal. Homogeneous calorimeters (so far usually electromagnetic) may be built with inorganic heavy (high density, high  $\langle Z \rangle$ ) scintillating crystals, or non-scintillating Cherenkov radiators such as lead glass and lead fluoride. Scintillation light and/or ionization in noble liquids can be detected. Nuclear interaction lengths in inorganic crystals range from  $17.8 \text{ cm}$  ( $\text{LuAlO}_3$ ) to  $42.2 \text{ cm}$  ( $\text{NaI}$ ). Popular choices have been BGO with  $\lambda_I = 22.3 \text{ cm}$  and  $X_0 = 1.12 \text{ cm}$ , and  $\text{PbWO}_4$  ( $20.3 \text{ cm}$  and  $0.89 \text{ cm}$ ). Properties of these and other commonly used inorganic crystal scintillators can be found in Table 31.4.

#### 31.9.1. Electromagnetic calorimeters :

Revised October 2009 by R.-Y. Zhu (California Inst. of Technology).

The development of electromagnetic showers is discussed in the section on “Passage of Particles Through Matter” (Sec. 30 of this *Review*).

Formulae are given which approximately describe average showers, but since the physics of electromagnetic showers is well understood, detailed and reliable Monte Carlo simulation is possible. EGS4 [125] and GEANT [126] have emerged as the standards.

There are homogeneous and sampling electromagnetic calorimeters. In a homogeneous calorimeter the entire volume is sensitive, *i.e.*, contributes signal. Homogeneous electromagnetic calorimeters may be built with inorganic heavy (high- $Z$ ) scintillating crystals such as BGO, CsI, NaI, and PWO, non-scintillating Cherenkov radiators such as lead glass and lead fluoride, or ionizing noble liquids. Properties of commonly used inorganic crystal scintillators can be found in Table 31.4. A sampling calorimeter consists of an active medium which generates signal and a passive medium which functions as an absorber. The active medium may be a scintillator, an ionizing noble liquid, a gas chamber, or a semiconductor. The passive medium is usually a material of high density, such as lead, iron, copper, or depleted uranium.

The energy resolution  $\sigma_E/E$  of a calorimeter can be parametrized as  $a/\sqrt{E} \oplus b \oplus c/E$ , where  $\oplus$  represents addition in quadrature and  $E$  is in GeV. The stochastic term  $a$  represents statistics-related fluctuations such as intrinsic shower fluctuations, photoelectron statistics, dead material at the front of the calorimeter, and sampling fluctuations. For a fixed number of radiation lengths, the stochastic term  $a$  for a sampling calorimeter is expected to be proportional to  $\sqrt{t/f}$ , where  $t$  is plate thickness and  $f$  is sampling fraction [127,128]. While  $a$  is at a few percent level for a homogeneous calorimeter, it is typically 10% for sampling calorimeters. The main contributions to the systematic, or constant, term  $b$  are detector non-uniformity and calibration uncertainty. In the case of the hadronic cascades discussed below, non-compensation also contributes to the constant term. One additional contribution to the constant term for calorimeters built for modern high-energy physics experiments, operated in a high-beam intensity environment, is radiation damage of the active medium. This can be minimized by developing radiation-hard active media [48] and by frequent *in situ* calibration and monitoring [47,128]. With effort, the constant term  $b$  can be reduced to below one percent. The term  $c$  is due to electronic noise summed over readout channels within a few Molière radii. The best energy resolution for electromagnetic shower measurement is obtained in total absorption homogeneous calorimeters, *e.g.* calorimeters built with heavy crystal scintillators. These are used when ultimate performance is pursued.

The position resolution depends on the effective Molière radius and the transverse granularity of the calorimeter. Like the energy resolution, it can be factored as  $a/\sqrt{E} \oplus b$ , where  $a$  is a few to  $20 \text{ mm}$  and  $b$  can be as small as a fraction of mm for a dense calorimeter with fine granularity. Electromagnetic calorimeters may also provide direction measurement for electrons and photons. This is important for photon-related physics when there are uncertainties in event origin, since photons do not leave information in the particle tracking system. Typical photon angular resolution is about  $45 \text{ mrad}/\sqrt{E}$ , which can be provided by implementing longitudinal segmentation [129] for a sampling calorimeter or by adding a preshower detector [130] for a homogeneous calorimeter without longitudinal segmentation.

Novel technologies have been developed for electromagnetic calorimetry. New heavy crystal scintillators, such as PWO and LSO:Ce (see Sec. 31.4), have attracted much attention for homogeneous calorimetry. In some cases, such as PWO, it has received broad applications in high-energy and nuclear physics experiments. The “spaghetti” structure has been developed for sampling calorimetry with scintillating fibers as the sensitive medium. The “accordion” structure has been developed for sampling calorimetry with ionizing noble liquid as the sensitive medium. Table 31.8 provides a brief description of typical electromagnetic calorimeters built recently for high-energy physics experiments. Also listed in this table are calorimeter depths in radiation lengths ( $X_0$ ) and the achieved energy resolution. Whenever possible, the performance of calorimeters *in*

\*  $X_0 = 120 \text{ g cm}^{-2} Z^{-2/3}$  to better than 5% for  $Z > 23$ .

†  $\lambda_I = 37.8 \text{ g cm}^{-2} A^{0.312}$  to within 0.8% for  $Z > 15$ .

**Table 31.8:** Resolution of typical electromagnetic calorimeters.  $E$  is in GeV.

Technology (Experiment)	Depth	Energy resolution	Date
NaI(Tl) (Crystal Ball)	$20X_0$	$2.7\%/E^{1/4}$	1983
$\text{Bi}_4\text{Ge}_3\text{O}_{12}$ (BGO) (L3)	$22X_0$	$2\%/\sqrt{E} \oplus 0.7\%$	1993
CsI (KTeV)	$27X_0$	$2\%/\sqrt{E} \oplus 0.45\%$	1996
CsI(Tl) (BaBar)	$16\text{--}18X_0$	$2.3\%/E^{1/4} \oplus 1.4\%$	1999
CsI(Tl) (BELLE)	$16X_0$	$1.7\%$ for $E_\gamma > 3.5$ GeV	1998
$\text{PbWO}_4$ (PWO) (CMS)	$25X_0$	$3\%/\sqrt{E} \oplus 0.5\% \oplus 0.2/E$	1997
Lead glass (OPAL)	$20.5X_0$	$5\%/\sqrt{E}$	1990
Liquid Kr (NA48)	$27X_0$	$3.2\%/\sqrt{E} \oplus 0.42\% \oplus 0.09/E$	1998
Scintillator/depleted U (ZEUS)	$20\text{--}30X_0$	$18\%/\sqrt{E}$	1988
Scintillator/Pb (CDF)	$18X_0$	$13.5\%/\sqrt{E}$	1988
Scintillator fiber/Pb spaghetti (KLOE)	$15X_0$	$5.7\%/\sqrt{E} \oplus 0.6\%$	1995
Liquid Ar/Pb (NA31)	$27X_0$	$7.5\%/\sqrt{E} \oplus 0.5\% \oplus 0.1/E$	1988
Liquid Ar/Pb (SLD)	$21X_0$	$8\%/\sqrt{E}$	1993
Liquid Ar/Pb (H1)	$20\text{--}30X_0$	$12\%/\sqrt{E} \oplus 1\%$	1998
Liquid Ar/depl. U (DØ)	$20.5X_0$	$16\%/\sqrt{E} \oplus 0.3\% \oplus 0.3/E$	1993
Liquid Ar/Pb accordion (ATLAS)	$25X_0$	$10\%/\sqrt{E} \oplus 0.4\% \oplus 0.3/E$	1996

*situ* is quoted, which is usually in good agreement with prototype test beam results as well as EGS or GEANT simulations, provided that all systematic effects are properly included. Detailed references on detector design and performance can be found in Appendix C of reference [128] and Proceedings of the International Conference series on Calorimetry in Particle Physics.

### 31.9.2. Hadronic calorimeters : [1–5,128]

Revised October 2011 by D. E. Groom (LBNL).

Most large hadron calorimeters are parts of large  $4\pi$  detectors at colliding beam facilities. At present these are sampling calorimeters: plates of absorber (Fe, Pb, Cu, or occasionally U or W) alternating with plastic scintillators (plates, tiles, bars), liquid argon (LAr), or gaseous detectors. The ionization is measured directly, as in LAr calorimeters, or via scintillation light observed by photodetectors (usually PMT's). Wavelength-shifting fibers are often used to solve difficult problems of geometry and light collection uniformity. Silicon sensors are being studied for ILC detectors; in this case  $e$ - $h$  pairs are collected. There are as many variants of these schemes as there are calorimeters, including variations in geometry of the absorber and sensors, *e.g.*, scintillating fibers threading an absorber [131], and the “accordion” LAr detector, with zig-zag absorber plates to minimize channeling effects. Another departure from the traditional sandwich structure is the LAr-tube design shown in Fig. 31.22(a).

A relatively new variant is the detection of Cerenkov light in hadron calorimetry. Such a calorimeter is sensitive to  $e^\pm$ 's in the EM showers plus a few relativistic pions. An example is the radiation-hard forward calorimeter in CMS, with iron absorber and quartz fiber readout by PMT's.

Ideally the calorimeter is segmented in  $\phi$  and  $\theta$  (or  $\eta = -\ln \tan(\theta/2)$ ). Fine segmentation, while desirable, is limited by cost, readout complexity, practical geometry, and the transverse size of the cascades—but see [132]. An example, a wedge of the ATLAS central barrel calorimeter, is shown in Fig. 31.22(b).

In an inelastic hadronic collision a significant fraction  $f_{em}$  of the energy is removed from further hadronic interaction by the production of secondary  $\pi^0$ 's and  $\eta$ 's, whose decay photons generate high-energy electromagnetic (EM) showers. Charged secondaries ( $\pi^\pm$ ,  $p$ , ...) deposit energy via ionization and excitation, but also interact with

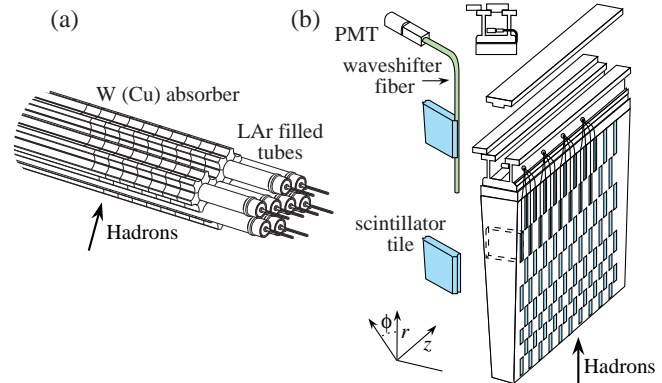


**Figure 31.22:** (a) ATLAS forward hadronic calorimeter structure (FCal2, 3). Tubes containing LAr are embedded in a mainly tungsten matrix. (b) ATLAS central calorimeter wedge; iron with plastic scintillator tile with wavelength-shifting fiber readout.

nuclei, producing spallation protons and neutrons, evaporation neutrons, and spallation products. The charged collision products produce detectable ionization, as do the showering  $\gamma$ -rays from the prompt de-excitation of highly excited nuclei. The recoiling nuclei generate little or no detectable signal. The neutrons lose kinetic energy in elastic collisions over hundreds of ns, gradually thermalize, and are captured, with the production of more  $\gamma$ -rays—usually outside the acceptance gate of the electronics. Between endothermic spallation losses, nuclear recoils, and late neutron capture, a significant fraction of the hadronic energy (20%–40%, depending on the absorber and energy of the incident particle) is invisible.

In contrast to EM showers, hadronic cascade processes are characterized by the production of relatively few high-energy particles. The lost energy and  $f_{em}$ , the  $\pi^0 \rightarrow \gamma\gamma$  fraction are highly variable from event to event. Until there is event-by-event knowledge of both the invisible energy loss and EM deposit (to be discussed below), the energy resolution of a hadron calorimeter will remain significantly worse than that of an EM calorimeter.

It has been shown by a simple induction argument, and verified by experiment, that the decrease in the average value of the hadronic energy fraction ( $\langle f_h \rangle = 1 - \langle f_{em} \rangle$ ) as the projectile energy  $E$  increases is fairly well described by the power law [133,135]

$$\langle f_h \rangle \approx (E/E_0)^{m-1} \quad (\text{for } E > E_0), \quad (31.33)$$

at least up to a few hundred GeV. The exponent  $m$  depends logarithmically on the mean multiplicity and the mean fractional loss to  $\pi^0$  production in a single interaction. It is in the range 0.80–0.87, but must be obtained experimentally for each calorimeter configuration.  $E_0$  is roughly the energy for the onset of inelastic collisions. It is 1 GeV or a little less for incident pions [133].

In a hadron-nucleus collision a large fraction of the incident energy is carried by a “leading particle” with the same quark content as the incident hadron. If the projectile is a charged pion, the leading particle is usually a pion, which can be neutral and hence contributes to the EM sector. This is not true for incident protons. The result is an increased mean hadronic fraction for incident protons: in Eq. (31.34b)  $E_0 \approx 2.6$  GeV [133,134,136].

The EM energy deposit is usually detected more efficiently than the hadronic energy deposit. If the detection efficiency for the EM sector is  $e$  and that for the hadronic sector is  $h$ , then the ratio of the mean response to a pion to that for an electron is

$$\pi/e = \langle f_{em} \rangle + \langle f_h \rangle h/e = 1 - (1 - h/e) \langle f_h \rangle \quad (31.34a)$$

$$\approx 1 - (1 - h/e)(E/E_0)^{m-1}. \quad (31.34b)$$

If  $h \neq e$  the hadronic response is not a linear function of energy. Only the product  $(1 - h/e)E_0^{1-m}$  can be obtained by measuring  $\pi/e$  as a function of energy. Since  $1 - m$  is small and  $E_0 \approx 1$  GeV for the usual pion-induced cascades, this fact is usually ignored and  $h/e$  is reported.

The discussion above assumes an idealized calorimeter, with the same structure throughout and without leakage. “Real” calorimeters

usually have an EM detector in front and a coarse “catcher” in the back. Complete containment is generally impractical.

By definition,  $0 \leq f_{em} \leq 1$ . Its variance changes only slowly with energy, but perforce  $\langle f_{em} \rangle \rightarrow 1$  as the projectile energy increases. An empirical power law  $\sigma_{f_{em}} = (E/E_1)^{1-\ell}$  (where  $\ell < 1$ ) describes the energy dependence adequately and has the right asymptotic properties. For  $h/e \neq 1$ , fluctuations in  $f_{em}$  significantly contribute to the resolution, in particular contributing a larger fraction of the variance at high energies. Since the  $f_{em}$  distribution has a tail on the high side, the calorimeter response is non-Gaussian with a high-energy tail if  $h/e < 1$ . *Noncompensation* ( $h/e \neq 1$ ) thus seriously degrades resolution as well as producing a nonlinear response.

It is clearly desirable to *compensate* the response, *i.e.*, to design the calorimeter such that  $h/e = 1$ . This is possible only with a sampling calorimeter, where several variables can be chosen or tuned:

1. Decrease the EM sensitivity. EM cross sections increase with  $Z$ ,<sup>†</sup> and most of the energy in an EM shower is deposited by low-energy electrons. A disproportionate fraction of the EM energy is thus deposited in the higher- $Z$  absorber. Lower- $Z$  cladding, such as the steel cladding on ZEUS U plates, preferentially absorbs low-energy  $\gamma$ 's in EM showers and thus also lowers the electronic response. G10 signal boards in the DØ calorimeters had the same effect. The degree of EM signal suppression can be somewhat controlled by tuning the sensor/absorber thickness ratio.
2. Increase the hadronic sensitivity. The abundant neutrons produced in the cascade have a large  $n$ - $p$  scattering cross section, with the production of low-energy scattered protons in hydrogenous sampling materials such as butane-filled proportional counters or plastic scintillator. (When scattering from a nucleus with mass number  $A$ , a neutron can at most lose  $4/(1+A)^2$  of its kinetic energy.) The down side in the scintillator case is that the signal from a highly-ionizing proton stub can be reduced by as much as 90% by recombination and quenching (Birk's Law, Eq. (31.2)).
3. Fabjan and Willis proposed that the additional signal generated in the aftermath of fission in  $^{238}\text{U}$  absorber plates should compensate nuclear fluctuations [137]. The production of fission fragments due to fast  $n$  capture was later observed [138]. However, while a very large amount of energy is released, it is mostly carried by low-velocity, very highly ionizing fission fragments which produce very little observable signal because of recombination and quenching. The approach seemed promising for awhile. But, for example, much of the compensation observed with the ZEUS  $^{238}\text{U}$ /scintillator calorimeter was mainly the result of methods 2 and 3 above.

Motivated very much by the work of Brau, Gabriel, Brückmann, and Wigmans [139], several groups built calorimeters which were very nearly compensating. The degree of compensation was sensitive to the acceptance gate width, and so could be somewhat further tuned. These included

- a) HELIOS with 2.5 mm thick scintillator plates sandwiched between 2 mm thick  $^{238}\text{U}$  plates (one of several structures);  $\sigma/E = 0.34/\sqrt{E}$  was obtained,
- b) ZEUS, 2.6 cm thick scintillator plates between 3.3 mm  $^{238}\text{U}$  plates;  $\sigma/E = 0.35/\sqrt{E}$ ,
- c) a ZEUS prototype with 10 mm Pb plates and 2.5 mm scintillator sheets;  $\sigma/E = 0.44/\sqrt{E}$ , and
- d) DØ, where the sandwich cell consists of a 4–6 mm thick  $^{238}\text{U}$  plate, 2.3 mm LAr, a G-10 signal board, and another 2.3 mm LAr gap. Given geometrical and cost constraints, the calorimeters used in modern collider detectors are not compensating:  $h/e \approx 0.7$ , for the ATLAS central barrel calorimeter, is typical.

A more versatile approach to compensation is provided by a *dual-readout calorimeter*, in which the signal is sensed by two readout systems with highly contrasting  $h/e$ . Although the concept is more than two decades old [140], it has only recently been implemented by the DREAM collaboration [141]. The test beam calorimeter consisted of copper tubes, each filled with scintillator and quartz fibers. If the two signals  $Q$  and  $S$  (quartz and scintillator) are both normalized to

electron response, then for each event Eq. (31.34) takes the form:

$$\begin{aligned} Q &= E[f_{em} + h/e|_Q(1 - f_{em})] \\ S &= E[f_{em} + h/e|_S(1 - f_{em})] \end{aligned} \quad (31.35)$$

These equations are linear in  $1/E$  and  $f_{em}$ , and are easily solved to obtain estimators of the *corrected* energy and  $f_{em}$  for each event. Both are subject to resolution effects, but effects due to fluctuations in  $f_{em}$  are eliminated. The solution for the corrected energy is given by [135]:

$$E = \frac{RS - Q}{R - 1}, \text{ where } R = \frac{1 - h/e|_Q}{1 - h/e|_S} \quad (31.36)$$

$R$  is the energy-independent slope of the event locus on a plot of  $Q$  vs  $S$ . It can be found either from the fitted slope or by measuring  $\pi/e$  as a function of  $E$ .

Although the usually-dominant contribution of the  $f_{em}$  distribution to the resolution can be minimized by compensation or the use of dual calorimetry, there remain significant contributions to the resolution:

1. Incomplete corrections for leakage, differences in light collection efficiency, and electronics calibration.
2. Readout transducer shot noise (usually photoelectron statistics), plus electronic noise.
3. Sampling fluctuations. Only a small part of the energy takes place in the scintillator or other sensor, and that fraction is subject to large fluctuations. This can be as high as  $40\%/\sqrt{E}$  (lead/scintillator). It is even greater in the Fe/scint case because of the very small sampling fraction (if the calorimeter is to be compensating), and substantially lower in a U/scint calorimeter. It is obviously zero for a homogeneous calorimeter.
4. Intrinsic fluctuations. The many ways ionization can be produced in a hadronic shower have different detection efficiencies and are subject to stochastic fluctuations. In particular, a very large fraction of the hadronic energy ( $\sim 20\%$  for Fe/scint,  $\sim 40\%$  for U/scint) is “invisible,” going into nuclear dissociation, thermalized neutrons, etc. The lost fraction depends on readout—it will be greater for a Cherenkov readout, less for a heterogeneous active medium such as organic scintillator.

Except in a sampling calorimeter especially designed for the purpose, sampling and intrinsic resolution contributions cannot be separated. This may have been best studied by Drews *et al.* [142], who used a calorimeter in which even- and odd-numbered scintillators were separately read out. Sums and differences of the variances were used to separate sampling and intrinsic contributions.

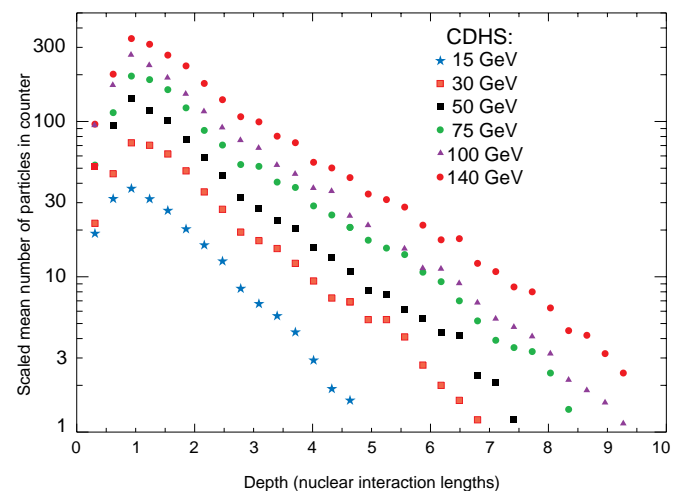


**Figure 31.23:** Mean profiles of  $\pi^+$  (mostly) induced cascades in the CDHS neutrino detector [143].

The fractional resolution can be represented by

$$\frac{\sigma}{E} = \frac{\alpha_1(E)}{\sqrt{E}} \oplus \left| 1 - \frac{h}{e} \right| \left( \frac{E}{E_1} \right)^{1-\ell} \quad (31.37)$$

<sup>†</sup> The asymptotic pair-production cross section scales roughly as  $Z^{0.75}$ , and  $|dE/dx|$  slowly decreases with increasing  $Z$ .



The coefficient  $a_1$  is expected to have mild energy dependence for a number of reasons. For example, the sampling variance is  $(\pi/e)E$  rather than  $E$ .  $(E/E_1)^{1-\ell}$  is the parameterization of  $\sigma_{fem}$  discussed above. At a time when data were of lower quality, a plot of  $(\sigma/E)^2$  vs  $1/E$  was apparently well-described by a straight line (constant  $a_1$ ) with a finite intercept—the square of the right term in Eq. (31.37), then called “the constant term.” Modern data show the slight downturn [131].

After the first interaction of the incident hadron, the average longitudinal distribution rises to a smooth peak. The peak position increases slowly with energy. The distribution becomes a reasonably exponential after several interaction length. Examples from the CDHS magnetized iron-scintillator sandwich calorimeter test beam calibration runs [143] are shown in Fig. 31.23. Proton-induced cascades are somewhat shorter and broader than pion-induced cascades [136]. A gamma distribution fairly well describes the longitudinal development of an EM shower, as discussed in Sec. 30.5. Following this logic, Bock *et al.* suggested that the profile of a hadronic cascade could be fitted by the sum of two gamma distributions, one with a characteristic length  $X_0$  and the other with length  $\lambda_I$  [144]. Fits to this 4-parameter function are commonly used, *e.g.*, by the ATLAS Tilecal collaboration [136]. If the interaction point is not known (the usual case), the distribution must be convoluted with an exponential in the interaction length of the incident particle. Adragna *et al.* give an analytic form for the convoluted function [136].

The transverse energy deposit is characterized by a central core dominated by EM cascades, together with a wide “skirt” produced by wide-angle hadronic interactions [145].

The CALICE collaboration has tested a “tracking” calorimeter (AHCAL) with highly granular scintillator readout [132]. Since the position of the first interaction is observed, the average longitudinal and radial shower distributions are obtained.

### 31.9.3. Free electron drift velocities in liquid ionization chambers :

Written August 2009 by W. Walkowiak (U. Siegen)

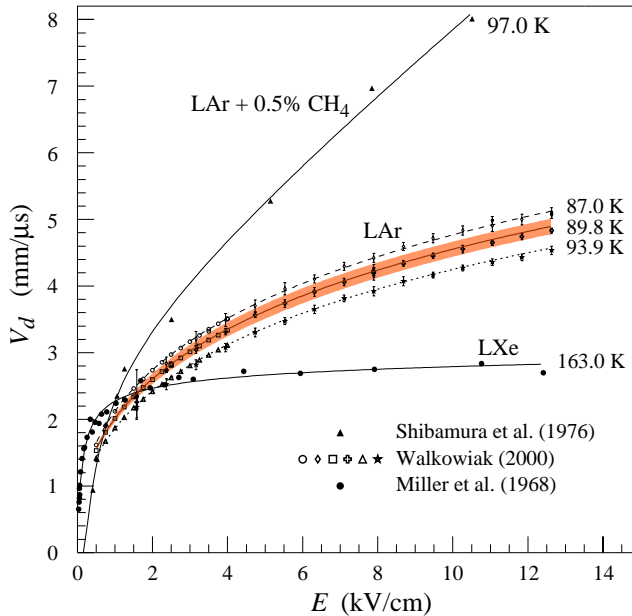


**Figure 31.24:** Drift velocity of free electrons as a function of electric field strength for LAr [146], LAr + 0.5% CH<sub>4</sub> [148] and LXe [147]. The average temperatures of the liquids are indicated. Results of a fit to an empirical function [152] are superimposed. In case of LAr at 91 K the error band for the global fit [146] including statistical and systematic errors as well as correlations of the data points is given. Only statistical errors are shown for the individual LAr data points.

Drift velocities of free electrons in LAr [146] are given as a function of electric field strength for different temperatures of the medium in

Fig. 31.24. The drift velocities in LAr have been measured using a double-gridded drift chamber with electrons produced by a laser pulse on a gold-plated cathode. The average temperature gradient of the drift velocity of the free electrons in LAr is described [146] by

$$\frac{\Delta v_d}{\Delta T v_d} = (-1.72 \pm 0.08) \%/\text{K}.$$

Earlier measurements [147–150] used different techniques and show systematic deviations of the drift velocities for free electrons which cannot be explained by the temperature dependence mentioned above.

Drift velocities of free electrons in LXe [148] as a function of electric field strength are also displayed in Fig. 31.24. The drift velocity saturates for  $|E| > 3$  kV/cm, and decreases with increasing temperature for LXe as well as measured *e.g.* by [151].

The addition of small concentrations of other molecules like N<sub>2</sub>, H<sub>2</sub> and CH<sub>4</sub> in solution to the liquid typically increases the drift velocities of free electrons above the saturation value [148,149], see example for CH<sub>4</sub> admixture to LAr in Fig. 31.24. Therefore, actual drift velocities are critically dependent on even small additions or contaminations.

## 31.10. Superconducting magnets for collider detectors

Revised September 2011 by A. Yamamoto (KEK); revised October 2001 by R.D. Kephart (FNAL)

**31.10.1. Solenoid Magnets :** In all cases SI unit are assumed, so that the magnetic field,  $B$ , is in Tesla, the stored energy,  $E$ , is in joules, the dimensions are in meters, and  $\mu_0 = 4\pi \times 10^{-7}$ .

The magnetic field ( $B$ ) in an ideal solenoid with a flux return iron yoke, in which the magnetic field is  $< 2$  T, is given by

$$B = \mu_0 n I \quad (31.38)$$

where  $n$  is the number of turns/meter and  $I$  is the current. In an air-core solenoid, the central field is given by

$$B(0,0) = \mu_0 n I \frac{L}{\sqrt{L^2 + 4R^2}}, \quad (31.39)$$

where  $L$  is the coil length and  $R$  is the coil radius.

In most cases, momentum analysis is made by measuring the circular trajectory of the passing particles according to  $p = mv\gamma = qrB$ , where  $p$  is the momentum,  $m$  the mass,  $q$  the charge,  $r$  the bending radius. The sagitta,  $s$ , of the trajectory is given by

$$s = qB\ell^2/8p, \quad (31.40)$$

where  $\ell$  is the path length in the magnetic field. In a practical momentum measurement in colliding beam detectors, it is more effective to increase the magnetic volume than the field strength, since

$$dp/p \propto p/B\ell^2, \quad (31.41)$$

where  $\ell$  corresponds to the solenoid coil radius  $R$ . The energy stored in the magnetic field of any magnet is calculated by integrating  $B^2$  over all space:

$$E = \frac{1}{2\mu_0} \int B^2 dV \quad (31.42)$$

If the coil thin, (which is the case if it is to superconducting coil), then

$$E \approx (B^2/2\mu_0)\pi R^2 L. \quad (31.43)$$

For a detector in which the calorimetry is outside the aperture of the solenoid, the coil must be thin in terms of radiation and absorption lengths. This usually means that the coil is superconducting and that the vacuum vessel encasing it is of minimum real thickness and fabricated of a material with long radiation length. There are two major contributors to the thickness of a thin solenoid:

**Table 31.9:** Progress of superconducting magnets for particle physics detectors.

Experiment	Laboratory	$B$ [T]	Radius [m]	Length [m]	Energy [MJ]	$X/X_0$	$E/M$ [kJ/kg]
TOPAZ*	KEK	1.2	1.45	5.4	20	0.70	4.3
CDF*	Tsukuba/Fermi	1.5	1.5	5.07	30	0.84	5.4
VENUS*	KEK	0.75	1.75	5.64	12	0.52	2.8
AMY*	KEK	3	1.29	3	40	†	
CLEO-II*	Cornell	1.5	1.55	3.8	25	2.5	3.7
ALEPH*	Saclay/CERN	1.5	2.75	7.0	130	2.0	5.5
DELPHI*	RAL/CERN	1.2	2.8	7.4	109	1.7	4.2
ZEUS*	INFN/DESY	1.8	1.5	2.85	11	0.9	5.5
H1*	RAL/DESY	1.2	2.8	5.75	120	1.8	4.8
BaBar*	INFN/SLAC	1.5	1.5	3.46	27	†	3.6
D0*	Fermi	2.0	0.6	2.73	5.6	0.9	3.7
BELLE*	KEK	1.5	1.8	4	42	†	5.3
BES-III	IHEP	1.0	1.475	3.5	9.5	†	2.6
ATLAS-CS	ATLAS/CERN	2.0	1.25	5.3	38	0.66	7.0
ATLAS-BT	ATLAS/CERN	1	4.7–9.75	26	1080	(Toroid)†	
ATLAS-ET	ATLAS/CERN	1	0.825–5.35	5	2 × 250	(Toroid)†	
CMS	CMS/CERN	4	6	12.5	2600	†	12

\* No longer in service

† EM calorimeter is inside solenoid, so small  $X/X_0$  is not a goal

- 1) The conductor consisting of the current-carrying superconducting material (usually NbTi/Cu) and the quench protecting stabilizer (usually aluminum) are wound on the inside of a structural support cylinder (usually aluminum also). The coil thickness scales as  $B^2R$ , so the thickness in radiation lengths ( $X_0$ ) is

$$t_{\text{coil}}/X_0 = (R/\sigma_h X_0)(B^2/2\mu_0), \quad (31.44)$$

where  $t_{\text{coil}}$  is the physical thickness of the coil,  $X_0$  the average radiation length of the coil/stabilizer material, and  $\sigma_h$  is the hoop stress in the coil [155].  $B^2/2\mu_0$  is the magnetic pressure. In large detector solenoids, the aluminum stabilizer and support cylinders dominate the thickness; the superconductor (NbTi/Cu) contributes a smaller fraction. The main coil and support cylinder components typically contribute about 2/3 of the total thickness in radiation lengths.

- 2) Another contribution to the material comes from the outer cylindrical shell of the vacuum vessel. Since this shell is susceptible to buckling collapse, its thickness is determined by the diameter, length and the modulus of the material of which it is fabricated. The outer vacuum shell represents about 1/3 of the total thickness in radiation length.

### 31.10.2. Properties of collider detector magnets :

The physical dimensions, central field stored energy and thickness in radiation lengths normal to the beam line of the superconducting solenoids associated with the major collider are given in Table 31.9 [154]. Fig. 31.25 shows thickness in radiation lengths as a function of  $B^2R$  in various collider detector solenoids.

The ratio of stored energy to cold mass ( $E/M$ ) is a useful performance measure. It can also be expressed as the ratio of the stress,  $\sigma_h$ , to twice the equivalent density,  $\rho$ , in the coil [155]:

$$\frac{E}{M} = \frac{\int (B^2/2\mu_0)dV}{\rho V_{\text{coil}}} \approx \frac{\sigma_h}{2\rho} \quad (31.45)$$

The  $E/M$  ratio in the coil is approximately equivalent to  $H$ ,\* the enthalpy of the coil, and it determines the average coil temperature rise after energy absorption in a quench:

$$E/M = H(T_2) - H(T_1) \approx H(T_2) \quad (31.46)$$

\* The enthalpy, or heat content, is called  $H$  in the thermodynamics literature. It is not to be confused with the magnetic field intensity  $B/\mu$ .

where  $T_2$  is the average coil temperature after the full energy absorption in a quench, and  $T_1$  is the initial temperature.  $E/M$  ratios of 5, 10, and 20 kJ/kg correspond to  $\sim 65$ ,  $\sim 80$ , and  $\sim 100$  K, respectively. The  $E/M$  ratios of various detector magnets are shown in Fig. 31.26 as a function of total stored energy. One would like the cold mass to be as small as possible to minimize the thickness, but temperature rise during a quench must also be minimized. An  $E/M$  ratio as large as 12 kJ/kg is designed into the CMS solenoid, with the possibility that about half of the stored energy can go to an external dump resistor. Thus the coil temperature can be kept below 80 K if the energy extraction system work well. The limit is set by the maximum temperature that the coil design can tolerate during a quench. This maximum local temperature should be  $< 130$  K (50 K + 80 K), so that thermal expansion effects in the coil are manageable.

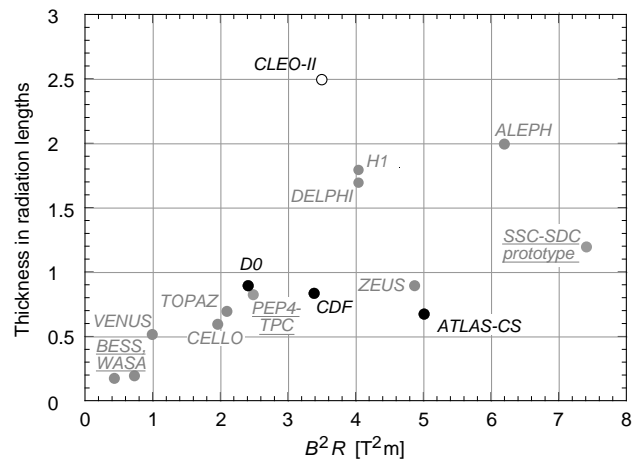


**Figure 31.25:** Magnet wall thickness in radiation length as a function of  $B^2R$  for various detector solenoids. Gray entries are for magnets no longer in use, and entries underlined are not listed in Table 31.9. Open circles are for magnets not designed to be “thin.” The SSC-SDC prototype provided important R&D for LHC magnets.

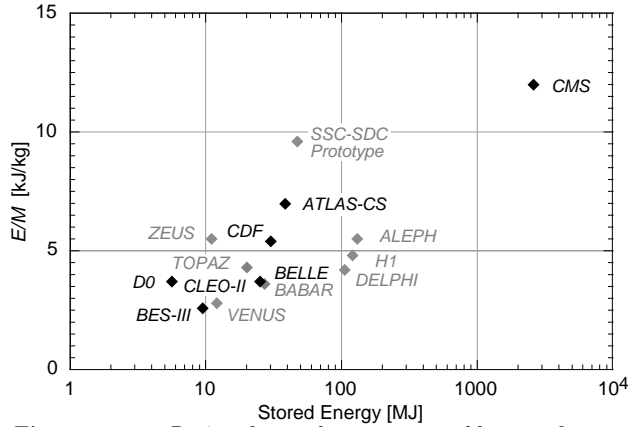


**Figure 31.26:** Ratio of stored energy to cold mass for major detector solenoids. Gray indicates magnets no longer in operation.

### 31.10.3. Toroidal magnets :

Toroidal coils uniquely provide a closed magnetic field without the necessity of an iron flux-return yoke. Because no field exists at the collision point and along the beam line, there is, in principle, no effect on the beam. On the other hand, the field profile generally has  $1/r$  dependence. The particle momentum may be determined by measurements of the deflection angle combined with the sagitta. The deflection (bending) power  $BL$  is

$$BL \approx \int_{R_i}^{R_0} \frac{B_i R_i dR}{R \sin \theta} = \frac{B_i R_i}{\sin \theta} \ln(R_0/R_i), \quad (31.47)$$

where  $R_i$  is the inner coil radius,  $R_0$  is the outer coil radius, and  $\theta$  is the angle between the particle trajectory and the beam line axis. The momentum resolution given by the deflection may be expressed as

$$\frac{\Delta p}{p} \propto \frac{p}{BL} \approx \frac{p \sin \theta}{B_i R_i \ln(R_0/R_i)}. \quad (31.48)$$

The momentum resolution is better in the forward/backward (smaller  $\theta$ ) direction. The geometry has been found to be optimal when  $R_0/R_i \approx 3-4$ . In practical designs, the coil is divided into 6–12 lumped coils in order to have reasonable acceptance and accessibility. This causes the coil design to be much more complex. The mechanical structure needs to sustain the decentering force between adjacent coils, and the peak field in the coil is 3–5 times higher than the useful magnetic field for the momentum analysis [153].

### 31.11. Measurement of particle momenta in a uniform magnetic field [156,157]

The trajectory of a particle with momentum  $p$  (in GeV/c) and charge  $ze$  in a constant magnetic field  $\vec{B}$  is a helix, with radius of curvature  $R$  and pitch angle  $\lambda$ . The radius of curvature and momentum component perpendicular to  $\vec{B}$  are related by

$$p \cos \lambda = 0.3 z B R, \quad (31.49)$$

where  $B$  is in tesla and  $R$  is in meters.

The distribution of measurements of the curvature  $k \equiv 1/R$  is approximately Gaussian. The curvature error for a large number of uniformly spaced measurements on the trajectory of a charged particle in a uniform magnetic field can be approximated by

$$(\delta k)^2 = (\delta k_{\text{res}})^2 + (\delta k_{\text{ms}})^2, \quad (31.50)$$

where  $\delta k$  = curvature error

$\delta k_{\text{res}}$  = curvature error due to finite measurement resolution

$\delta k_{\text{ms}}$  = curvature error due to multiple scattering.

If many ( $\geq 10$ ) uniformly spaced position measurements are made along a trajectory in a uniform medium,

$$\delta k_{\text{res}} = \frac{\epsilon}{L'^2} \sqrt{\frac{720}{N+4}}, \quad (31.51)$$

where  $N$  = number of points measured along track

$L'$  = the projected length of the track onto the bending plane

$\epsilon$  = measurement error for each point, perpendicular to the trajectory.

If a vertex constraint is applied at the origin of the track, the coefficient under the radical becomes 320.

For arbitrary spacing of coordinates  $s_i$  measured along the projected trajectory and with variable measurement errors  $\epsilon_i$  the curvature error  $\delta k_{\text{res}}$  is calculated from:

$$(\delta k_{\text{res}})^2 = \frac{4}{w} \frac{V_{ss}}{V_{ss} V_s^2 s^2 - (V_{ss^2})^2}, \quad (31.52)$$

where  $V$  are covariances defined as  $V_{s^m s^n} = \langle s^m s^n \rangle - \langle s^m \rangle \langle s^n \rangle$  with  $\langle s^m \rangle = w^{-1} \sum (s_i^m / \epsilon_i^2)$  and  $w = \sum \epsilon_i^{-2}$ .

The contribution due to multiple Coulomb scattering is approximately

$$\delta k_{\text{ms}} \approx \frac{(0.016)(\text{GeV}/c)z}{Lp\beta \cos^2 \lambda} \sqrt{\frac{L}{X_0}}, \quad (31.53)$$

where  $p$  = momentum (GeV/c)

$z$  = charge of incident particle in units of  $e$

$L$  = the total track length

$X_0$  = radiation length of the scattering medium (in units of length; the  $X_0$  defined elsewhere must be multiplied by density)

$\beta$  = the kinematic variable  $v/c$ .

More accurate approximations for multiple scattering may be found in the section on Passage of Particles Through Matter (Sec. 30 of this Review). The contribution to the curvature error is given approximately by  $\delta k_{\text{ms}} \approx 8s_{\text{plane}}^{\text{rms}}/L^2$ , where  $s_{\text{plane}}^{\text{rms}}$  is defined there.

#### References:

1. *Experimental Techniques in High Energy Physics*, T. Ferbel (ed.) (Addison-Wesley, Menlo Park, CA, 1987).
2. K. Kleinknecht, *Detectors for Particle Radiation*, Cambridge University Press (1998).
3. G.F. Knoll, *Radiation Detection and Measurement*, 3rd edition, John Wiley & Sons, New York (1999).
4. D.R. Green, *The Physics of Particle Detectors*, Cambridge Monographs on Particle Physics, Nuclear Physics and Cosmology, # 12, Cambridge University Press (2000).
5. C. Leroy & P.-G. Rancoita, *Principles of Radiation Interaction in Matter and Detection*, (World Scientific, Singapore, 2004).
6. C. Grupen, *Particle Detectors, Cambridge Monographs on Particle Physics, Nuclear Physics and Cosmology*, Cambridge University Press (2008).
7. [Icarus Collaboration], ICARUS-TM/2001-09; LGNS-EXP 13/89 add 2-01.
8. H. Spieler, IEEE Trans. **NS29**, 1142 (1982).
9. K. Arisaka, Nucl. Instrum. Methods **A442**, 80 (2000).
10. K.K. Hamamatsu, Electron Tube Division, *Photomultiplier Tubes: Basics and Applications*, 3rd edition (2006); Can be found under "Photomultiplier Tube Handbook" at [http://sales.hamamatsu.com/assets/applications/ETD/pmt\\_handbook/pmt\\_handbook\\_complete.pdf](http://sales.hamamatsu.com/assets/applications/ETD/pmt_handbook/pmt_handbook_complete.pdf).
11. A. Braem *et al.*, Nucl. Instrum. Methods **A518**, 574 (2004).
12. R. Arnold *et al.*, Nucl. Instrum. Methods **A314**, 465 (1992).
13. P. Mangeot *et al.*, Nucl. Instrum. Methods **A216**, 79 (1983); R. Apsimon *et al.*, IEEE. Trans. Nucl. Sci. **33**, 122 (1986); R. Arnold *et al.*, Nucl. Instrum. Methods **A270**, 255 (1988); D. Aston *et al.*, Nucl. Instrum. Methods **A283**, 582 (1989).
14. J. Janesick *Scientific charge-coupled devices*, SPIE Press, Bellingham, WA (2001).
15. R. Haitz *et al.*, J. Appl. Phys. **36**, 3123 (1965); R. McIntyre, IEEE Trans. Electron Devices **13**, 164 (1966); H. Dautet *et al.*, Applied Optics, **32**, (21), 3894 (1993); Perkin-Elmer Optoelectronics, *Avalanche Photodiodes: A User's Guide*.
16. P. Buzhan *et al.*, Nucl. Instrum. Methods **A504**, 48 (2003); Z. Sadygov *et al.*, Nucl. Instrum. Methods **A504**, 301 (2003);

- V. Golovin and V. Saveliev, Nucl. Instrum. Methods **A518**, 560 (2004).
17. M. Landstrass *et al.*, Diam. & Rel. Matter, **2**, 1033 (1993); R. McKeag and R. Jackman, Diam. & Rel. Matter, **7**, 513 (1998); R. Brascia *et al.*, Phys. Stat. Sol. **199**, 113 (2003).
  18. M. Petrov, M. Stapelbroek, and W. Kleinhans, Appl. Phys. Lett. **51**, 406 (1987); M. Atac, M. Petrov, IEEE Trans. Nucl. Sci. **36**, 163 (1989); M. Atac *et al.*, Nucl. Instrum. Methods **A314**, 56 (1994).
  19. J.B. Birks, *The Theory and Practice of Scintillation Counting*, (Pergamon, London, 1964).
  20. D. Clark, Nucl. Instrum. Methods **117**, 295 (1974).
  21. J.B. Birks, Proc. Phys. Soc. **A64**, 874 (1951).
  22. B. Bengston and M. Moszynski, Nucl. Instrum. Methods **117**, 227 (1974); J. Bialkowski, *et al.*, Nucl. Instrum. Methods **117**, 221 (1974).
  23. C. P. Achenbach, "Active optical fibres in modern particle physics experiments," arXiv:nucl-ex/0404008v1.
  24. I.B. Berlman, *Handbook of Fluorescence Spectra of Aromatic Molecules*, 2nd edition (Academic Press, New York, 1971).
  25. C. Zorn, in *Instrumentation in High Energy Physics*, ed. F. Sauli, (1992, World Scientific, Singapore) pp. 218–279.
  26. T. Foerster, Ann. Phys. **2**, 55 (1948).
  27. J.M. Fluornoy, *Conference on Radiation-Tolerant Plastic Scintillators and Detectors*, K.F. Johnson and R.L. Clough editors, Rad. Phys. and Chem., **41** 389 (1993).
  28. D. Horstman and U. Holm, *ibid.*, 395.
  29. D. Blomker, *et al.*, Nucl. Instrum. Methods **A311**, 505 (1992); J. Mainusch, *et al.*, Nucl. Instrum. Methods **A312**, 451 (1992).
  30. *Conference on Radiation-Tolerant Plastic Scintillators and Detectors*, K.F. Johnson and R.L. Clough editors, Rad. Phys. and Chem., **41** (1993).
  31. S.R. Borenstein and R.C. Strand, IEEE Trans. Nuc. Sci. **NS-31(1)**, 396 (1984).
  32. P. Sonderegger, Nucl. Instrum. Methods **A257**, 523 (1987).
  33. Achenbach, *ibid.*
  34. C.M. Hawkes, *et al.*, Nucl. Instrum. Methods **A292**, 329 (1990).
  35. A. Lempicki *et al.*, Nucl. Instrum. Methods **A333**, 304 (1993); G. Blasse, *Proceedings of the Crystal 2000 International Workshop on Heavy Scintillators for Scientific and Industrial Applications*, Chamonix, France, Sept. (1992), Edition Frontieres.
  36. C. Melcher and J. Schweitzer, Nucl. Instrum. Methods **A314**, 212 (1992).
  37. D.W. Cooke *et al.*, J. Appl. Phys. **88**, 7360 (2000); T. Kimble, M Chou, and B.H.T. Chai, in *Proc. IEEE Nuclear Science Symposium Conference* (2002).
  38. J.M. Chen *et al.*, IEEE Trans. Nuc. Sci. **NS-54(3)**, 718 (2007) and **NS-54(4)**, 1319 (2007).
  39. E.V.D. van Loef *et al.*, Nucl. Instrum. Methods **A486**, 254 (2002).
  40. C. Kuntner *et al.*, Nucl. Instrum. Methods **A493**, 131 (2002).
  41. N. Akchurin *et al.*, Nucl. Instrum. Methods **A595**, 359 (2008).
  42. A. Para, FERMILAB-CONF-11-519-CD; H. Wenzel *et al.*, FERMILAB-PUB-11-531-CD-E.
  43. R.-Y. Zhu, Journal of Physics: Conference Series **160**, 012017 (2009).
  44. R.H. Mao, L.Y. Zhang, and R.Y. Zhu, IEEE Trans. Nuc. Sci. **NS-55(4)**, 2425 (2008).
  45. B.D. Rooney and J.D. Valentine, IEEE Trans. Nuc. Sci. **NS-44(3)**, 509 (1997).
  46. W.W. Moses *et al.*, IEEE Trans. Nuc. Sci. **NS-55(3)**, 1049 (2008).
  47. G. Gratta, H. Newman, and R.Y. Zhu, Ann. Rev. Nucl. and Part. Sci. **44**, 453 (1994).
  48. R.Y. Zhu, Nucl. Instrum. Methods **A413**, 297 (1998).
  49. S. Ecklund, *et al.*, Nucl. Instrum. Methods **A463**, 68 (2001).
  50. B. Aubert, *et al.*, [BaBar Collaboration], Nucl. Instrum. Methods **A479**, 1 (2002).
  51. A. Abashian, *et al.*, Nucl. Instrum. Methods **A479**, 117 (2002).
  52. I. Adam, *et al.*, Nucl. Instrum. Methods **A538**, 281 (2005).
  53. M. Shiozawa, [Super-Kamiokande Collaboration], Nucl. Instrum. Methods **A433**, 240 (1999).
  54. J. Litt and R. Meunier, Ann. Rev. Nucl. Sci. **23**, 1 (1973).
  55. D. Bartlett, *et al.*, Nucl. Instrum. Methods **A260**, 55 (1987).
  56. B. Ratcliff, Nucl. Instrum. Methods **A502**, 211 (2003).
  57. See the RICH Workshop series: Nucl. Instrum. Methods **A343**, 1 (1993); Nucl. Instrum. Methods **A371**, 1 (1996); Nucl. Instrum. Methods **A433**, 1 (1999); Nucl. Instrum. Methods **A502**, 1 (2003); Nucl. Instrum. Methods **A553**, 1 (2005); Nucl. Instrum. Methods **A595**, 1 (2008).
  58. W. Blum, W. Riegler, and L. Rolandi, *Particle Detection with Drift Chambers* (Springer-Verlag, 2008).
  59. L.G. Christophorou, *Atomic and Molecular Radiation Physics* (Wiley, 1971); I.B. Smirnov, Nucl. Instrum. Methods **A554**, 474 (2005); J. Berkowitz, *Atomic and Molecular Photo Absorption* (Academic Press, 2002); <http://pdg.lbl.gov/2007/AtomicNuclearProperties>.
  60. H. Bichsel, Nucl. Instrum. Methods **A562**, 154 (2006).
  61. H. Fischle *et al.*, Nucl. Instrum. Methods **A301**, 202 (1991).
  62. <http://rjd.web.cern.ch/rjd/cgi-bin/cross>.
  63. A. Peisert and F. Sauli, "Drift and Diffusion of Electrons in Gases," CERN 84-08 (1984).
  64. S. Biagi, Nucl. Instrum. Methods **A421**, 234 (1999).
  65. <http://consult.cern.ch/writeup/magboltz/>.
  66. E. McDaniel and E. Mason, *The Mobility and Diffusion of Ions in Gases* (Wiley, 1973); G. Shultz *et al.*, Rev. Phys. Appl. **12**, 67 (1977).
  67. G. Charpak *et al.*, Nucl. Instrum. Methods **A62**, 262 (1968).
  68. G. Charpak and F. Sauli, Ann. Rev. Nucl. Sci. **34**, 285 (1984).
  69. F. Sauli, "Principles of Operation of Multiwire Proportional and Drift Chambers," in *Experimental Techniques in High Energy Physics*, T. Ferbel (ed.) (Addison-Wesley, Menlo Park, CA, 1987).
  70. G. Charpak *et al.*, Nucl. Instrum. Methods **A167**, 455 (1979).
  71. A.H. Walenta *et al.*, Nucl. Instrum. Methods **A92**, 373 (1971).
  72. A. Breskin *et al.*, Nucl. Instrum. Methods **A124**, 189 (1975).
  73. A. Breskin *et al.*, Nucl. Instrum. Methods **A156**, 147 (1978).
  74. R. Bouclier *et al.*, Nucl. Instrum. Methods **A265**, 78 (1988).
  75. H. Drumm *et al.*, Nucl. Instrum. Methods **A176**, 333 (1980).
  76. D.R. Nygren & J.N. Marx, Phys. Today **31N10**, 46 (1978).
  77. <http://www.ansoft.com>.
  78. P. Beringer *et al.*, Nucl. Instrum. Methods **A254**, 542 (1987).
  79. J. Virdee, Phys. Rep. 403-404, 401 (2004).
  80. H. Walenta, Phys. Scripta **23**, 354 (1981).
  81. J. Va'vra, Nucl. Instrum. Methods **A515**, 1 (2003); M. Titov, "Radiation damage and long-term aging in gas detectors," arXiv:physics/0403055.
  82. M. Aleksa *et al.*, Nucl. Instrum. Methods **A446**, 435 (2000).
  83. F. Sauli and A. Sharma, Ann. Rev. Nucl. Part. Sci. **49**, 341 (1999).
  84. A. Oed, Nucl. Instrum. Methods **A263**, 351 (1988); A. Barr *et al.*, Nucl. Phys. B (Proc. Suppl.), **61B**, 264 (1988).
  85. Y. Bagaturia *et al.*, Nucl. Instrum. Methods **A490**, 223 (2002).
  86. J. Benloch *et al.*, IEEE Trans. Nucl. Sci., **NS-45** (1998) 234.
  87. Y. Giomataris, Nucl. Instrum. Methods **A419**, 239 (1998).
  88. F. Sauli, Nucl. Instrum. Methods **A386**, 531 (1997); A. Bressan *et al.*, Nucl. Instrum. Methods **A425**, 262 (1999).
  89. S. Bachmann *et al.*, Nucl. Instrum. Methods **A479**, 294 (2002); A. Bressan *et al.*, Nucl. Instrum. Methods **A424**, 321 (1999).
  90. Y. Giomataris *et al.*, Nucl. Instrum. Methods **A376**, 29 (1996).
  91. J. Derre *et al.*, Nucl. Instrum. Methods **A459**, 523 (2001); G. Charpak *et al.*, Nucl. Instrum. Methods **A478**, 26 (2002).
  92. I. Giomataris *et al.*, Nucl. Instrum. Methods **A560**, 405 (2006).
  93. S. Duarte Pinto *et al.*, IEEE NSS/MIC Conference Record (2008).
  94. L. Periale *et al.*, Nucl. Instrum. Methods **A478**, 377 (2002); R. Chechik *et al.*, Nucl. Instrum. Methods **A535**, 303 (2004); A. Breskin *et al.*, Nucl. Instrum. Methods **A598**, 107 (2009).
  95. A. Di Mauro *et al.*, Nucl. Instrum. Methods **A581**, 225 (2007).

96. R. Bellazzini *et al.*, Nucl. Instrum. Methods **A535**, 477 (2004); M. Campbell *et al.*, Nucl. Instrum. Methods **A540**, 295 (2005); A. Bamberger *et al.*, Nucl. Instrum. Methods **A573**, 361 (2007); T. Kim *et al.*, Nucl. Instrum. Methods **A599**, 173 (2008).
97. M. Chefdeville *et al.*, Nucl. Instrum. Methods **A556**, 490 (2006).
98. M. Titov, arXiv: physics/0403055; *Proc. of the Workshop of the INFN ELOISATRON Project*, "Innovative Detectors For Super-Colliders," Erice, Italy, Sept. 28–Oct. 4 (2003).
99. <http://rd51-public.web.cern.ch/RD51-Public>.
100. P. Colas *et al.*, Nucl. Instrum. Methods **A535**, 506 (2004); M. Campbell *et al.*, Nucl. Instrum. Methods **A540**, 295 (2005).
101. H. Aihara *et al.*, IEEE Trans. **NS30**, 63 (1983).
102. J. Alme *et al.*, Nucl. Instrum. Methods **A622**, 316 (2010).
103. N. Abgrall *et al.*, Nucl. Instrum. Methods **A637**, 25 (2011).
104. C.J. Martoff *et al.*, Nucl. Instrum. Methods **A440**, 355 (2000).
105. X. Artru *et al.*, Phys. Rev. **D12**, 1289 (1975); G.M. Garibian *et al.*, Nucl. Instrum. Methods **125**, 133 (1975).
106. B. Dolgoshein, Nucl. Instrum. Methods **A326**, 434 (1993).
107. *TRDs for the Third Millennium: Proc. 2nd Workshop on Advanced Transition Radiation Detectors for Accelerator and Space Applications*, Nucl. Instrum. Methods **A522**, 1 (2004).
108. R. Santonico and R. Cardarelli, Nucl. Instrum. Methods **A187**, 377 (1981).
109. V.V. Parkhomchuk, Yu.N. Pestov, and N.V. Petrovykh, Nucl. Instrum. Methods **93**, 269 (1971).
110. E. Cerron Zeballos *et al.*, Nucl. Instrum. Methods **A374**, 132 (1996).
111. V. Ammosov *et al.*, Nucl. Instrum. Methods **A578**, 119 (2007).
112. P. Fonte, IEEE. Trans. Nucl. Sci. **49**, 881 (2002).
113. M. Abbrescia *et al.*, Nucl. Instrum. Methods **A394**, 13 (1997).
114. F. Anulli *et al.*, Nucl. Instrum. Methods **A552**, 276 (2005).
115. H. Spieler, *Semiconductor Detector Systems*, Oxford Univ. Press, Oxford (2005).
116. F. Scholze *et al.*, Nucl. Instrum. Methods **A439**, 208 (2000).
117. G. Lindström *et al.*, Nucl. Instrum. Methods **A465**, 60 (2001).
118. C. Da Via *et al.*, Nucl. Instrum. Methods **A509**, 86 (2003).
119. G. Kramberger *et al.*, Nucl. Instrum. Methods **A481**, 297 (2002).
120. O. Krasel *et al.*, IEEE Trans. Nucl. Sci. **NS-51/6,3055** (2004).
121. G. Lindström *et al.*, Nucl. Instrum. Methods **A426**, 1 (1999).
122. A. Holmes-Siedle and L. Adams, *Handbook of Radiation Effects*, 2nd ed., Oxford 2002.
123. V. Radeka, IEEE Trans. Nucl. Sci. **NS-15/3**, 455 (1968); V. Radeka, IEEE Trans. Nucl. Sci. **NS-21**, 51 (1974).
124. F.S. Goulding, Nucl. Instrum. Methods **100**, 493 (1972); F.S. Goulding and D.A. Landis, IEEE Trans. Nucl. Sci. **NS-29**, 1125 (1982).
125. W.R. Nelson, H. Hirayama, and D.W.O. Rogers, "The EGS4 Code System," SLAC-265, Stanford Linear Accelerator Center (Dec. 1985).
126. R. Brun *et al.*, *GEANT3*, CERN DD/EE/84-1 (1987).
127. D. Hitlin *et al.*, Nucl. Instrum. Methods **137**, 225 (1976). See also W. J. Willis and V. Radeka, Nucl. Instrum. Methods **120**, 221 (1974), for a more detailed discussion.
128. R. Wigmans, *Calorimetry: Energy Measurement in Particle Physics*, Inter. Series of Monographs on Phys. **107**, Clarendon, Oxford (2000).
129. ATLAS Collaboration, *The ATLAS Liquid Argon Calorimeter Technical Design Report*, CERN/LHCC 96-41 (1996).
130. CMS Collaboration, *The CMS Electromagnetic Calorimeter Technical Design Report*, CERN/LHCC 97-33 (1997).
131. N. Akchurin, *et al.*, Nucl. Instrum. Methods **A399**, 202 (1997).
132. N. Feege, Submitted to *Proc. 2nd Inter. Conf. Advances Nucl. Instr.* (ANIMMA 2011) (arXiv:1109.1982).
133. T.A. Gabriel *et al.*, Nucl. Instrum. Methods **A338**, 336 (1994).
134. N. Akchurin, *et al.*, Nucl. Instrum. Methods **A408**, 380 (1998); An energy-independent analysis of these data is given in Ref. 135.
135. D.E. Groom, Nucl. Instrum. Methods **A572**, 633 (2007); Erratum: D.E. Groom, Nucl. Instrum. Methods **A593**, 638 (2008).
136. P. Adragna *et al.*, Nucl. Instrum. Methods **A615**, 158 (2010).
137. C.W. Fabjan *et al.*, Phys. Lett. **B60**, 105 (1975).
138. C. Leroy, J. Sirois, and R. Wigmans, Nucl. Instrum. Methods **A252**, 4 (1986).
139. J.E. Brau and T.A. Gabriel, Nucl. Instrum. Methods **A238**, 489 (1985); H. Brückmann and H. Kowalski, ZEUS Int. Note 86/026 DESY, Hamburg (1986); R. Wigmans, Nucl. Instrum. Methods **A259**, 389 (1987); R. Wigmans, Nucl. Instrum. Methods **A265**, 273 (1988).
140. P. Mockett, "A review of the physics and technology of high-energy calorimeter devices," *Proc. 11th SLAC Summer Inst. Part. Phys.*, July 1983, SLAC Report No. 267 (July 1983), p. 42, [www.slac.stanford.edu/pubs/confproc/ssi83/ssi83-008.html](http://www.slac.stanford.edu/pubs/confproc/ssi83/ssi83-008.html).
141. R. Wigmans, "Quartz Fibers and the Prospects for Hadron Calorimetry at the 1% Resolution Level," *Proc. 7th Inter. Conf. on Calorimetry in High Energy Physics*, Tucson, AZ, Nov. 9–14, 1997, eds. E. Cheu *et al.*, (World Scientific, River Edge, NJ, 1998), p. 182; N. Akchurin *et al.*, Nucl. Instrum. Methods **A537**, 537 (2005).
142. G. Drews, *et al.*, Nucl. Instr. and Meth. A **335**, 335 (1990).
143. M. Holder *et al.*, Nucl. Instrum. Methods **151**, 69 (1978).
144. R.K. Bock, T. Hansl-Kozanecka, and T.P. Shah, Nucl. Instrum. Methods **186**, 533 (1981); Y.A. Kulchitsky and V.B. Vinogradov, Nucl. Instrum. Methods **A455**, 499 (2000).
145. D. Acosta *et al.*, Nucl. Instrum. Methods **A316**, 184 (1997).
146. W. Walkowiak, Nucl. Instrum. Methods **A449**, 288 (2000).
147. L.S. Miller *et al.*, Phys. Rev. **166**, 871 (1968).
148. E. Shibamura *et al.*, Nucl. Instrum. Methods **A316**, 184 (1975).
149. K. Yoshino *et al.*, Phys. Rev. **A14**, 438 (1976).
150. A.O. Allen *et al.*, "Drift mobilities and conduction band energies of excess electrons in dielectric liquids," NSRDS-NBS-58 (1976).
151. P. Benetti *et al.*, Nucl. Instrum. Methods **A32**, 361 (1993).
152. A.M. Kalinin *et al.*, "Temperature and electric field strength dependence of electron drift velocity in liquid argon," ATLAS Internal Note, ATLAS-LARG-NO-058, CERN (1996).
153. T. Taylor, Phys. Scr. **23**, 459 (1980).
154. A. Yamamoto, Nucl. Instr. Meth. **A494**, 255 (2003).
155. A. Yamamoto, Nucl. Instr. Meth. **A453**, 445 (2000).
156. R.L. Gluckstern, Nucl. Instrum. Methods **24**, 381 (1963).
157. V. Karimäki, Nucl. Instrum. Methods **A410**, 284 (1998).

## 32. PARTICLE DETECTORS FOR NON-ACCELERATOR PHYSICS

Updated 2011 (see the various sections for authors).

32. PARTICLE DETECTORS FOR NON-ACCELERATOR PHYSICS . . . . .	368
32.1. Introduction . . . . .	368
32.2. High-energy cosmic-ray hadron and gamma-ray detectors . . . . .	368
32.2.1. Atmospheric fluorescence detectors . . . . .	368
32.2.2. Atmospheric Cherenkov telescopes for high-energy $\gamma$ -ray astronomy . . . . .	369
32.3. Large neutrino detectors . . . . .	370
32.3.1. Deep liquid detectors for rare processes . . . . .	370
32.3.1.1. Liquid scintillator detectors . . . . .	371
32.3.1.2. Water Cherenkov detectors . . . . .	371
32.3.2. Coherent radio Cherenkov radiation detectors . . . . .	372
32.3.2.1. The Moon as a target . . . . .	372
32.3.2.2. The ANITA balloon experiment . . . . .	373
32.3.2.3. Active Volume Detectors . . . . .	373
32.4. Large time-projection chambers for rare event detection . . . . .	373
32.5. Sub-Kelvin detectors . . . . .	375
32.5.1. Thermal Phonons . . . . .	375
32.5.2. Athermal Phonons and Superconducting Quasiparticles . . . . .	377
32.5.3. Ionization and Scintillation . . . . .	377
32.6. Low-radioactivity background techniques . . . . .	377
32.6.1. Defining the problem . . . . .	377
32.6.2. Environmental radioactivity . . . . .	378
32.6.3. Radioimpurities in detector or shielding components . . . . .	378
32.6.4. Radon and its progeny . . . . .	378
32.6.5. Cosmic rays . . . . .	379
32.6.6. Neutrons . . . . .	379

### 32.1. Introduction

Non-accelerator experiments have become increasingly important in particle physics. These include classical cosmic ray experiments, neutrino oscillation measurements, and searches for double-beta decay, dark matter candidates, and magnetic monopoles. The experimental methods are sometimes those familiar at accelerators (plastic scintillators, drift chambers, TRD's, *etc.*) but there is also instrumentation either not found at accelerators or applied in a radically different way. Examples are atmospheric scintillation detectors (Fly's Eye), massive Cherenkov detectors (Super-Kamiokande, IceCube), ultracold solid state detectors (CDMS). And, except for the cosmic ray detectors, radiologically ultra-pure materials are required.

In this section, some more important detectors special to terrestrial non-accelerator experiments are discussed. Techniques used in both accelerator and non-accelerator experiments are described in Sec. 28, Particle Detectors at Accelerators, some of which have been modified to accommodate the non-accelerator nuances.

Space-based detectors also use some unique instrumentation, but these are beyond the present scope of RPP.

### 32.2. High-energy cosmic-ray hadron and gamma-ray detectors

#### 32.2.1. Atmospheric fluorescence detectors :

Updated August 2011 by L.R. Wiencke (Colorado School of Mines).

Cosmic-ray fluorescence detectors (FD) use the atmosphere as a giant calorimeter to measure isotropic scintillation light that traces the development profiles of extensive air showers (EAS). The EASs observed are produced by the interactions of high-energy ( $E > 10^{17}$  eV) subatomic particles in the stratosphere and upper troposphere, independent of the primary species. Experiments with FDs include the pioneering Fly's Eye [1], HiRes [2], the Telescope Array [3], and the Pierre Auger Observatory [4]. The proposed JEM-EUSO [5] FD would tilt down to sweep across a much larger area from space.

The scintillation light is emitted between 290 and 430 nm (Fig. 32.1), when relativistic charged particles, primarily electrons and positrons, excite nitrogen molecules in air, resulting in transitions of the 1P and 2P systems. Reviews and references for the pioneering and ongoing laboratory measurements of fluorescence yield,  $Y(\lambda, P, T, u)$ , including dependence on wavelength ( $\lambda$ ), temperature ( $T$ ), pressure ( $p$ ), and humidity ( $u$ ) may be found in Refs. 6 and 7.

An FD element (telescope) consists of a non-tracking spherical mirror (3.5–13 m<sup>2</sup> and less than astronomical quality), a close-packed "camera" of PMTs (for example, Hamamatsu R9508 or Photonis XP3062) near the focal plane, and flash ADC readout system with a pulse and track-finding trigger scheme [8]. Simple reflector optics (12° × 16° degree field of view (FOV) on 256 PMTs) and Schmidt optics (30° × 30° FOV on 440 PMTs), including a correcting element, have been used. Segmented mirrors have been fabricated from slumped or slumped/polished glass with anodized aluminium coating and from chemically anodized AlMgSiO<sub>5</sub> affixed to shaped aluminum. A broadband UV filter (custom fabricated or Schott MUG-6) covers the camera face or much larger entrance aperture to reduce background light such as starlight, airglow, man-made light pollution, and airplane strobelights.

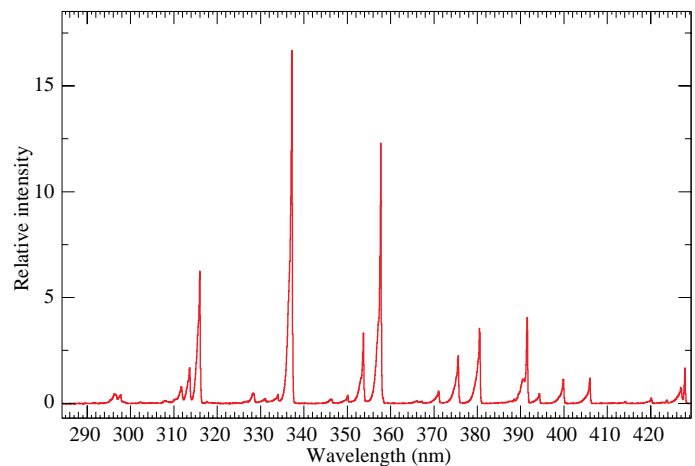


**Figure 32.1:** Measured fluorescence spectrum excited by 3 MeV electrons in dry air at 800 hPa and 293 K [9].

At 10<sup>20</sup> eV, where the flux drops below 1 EAS/km<sup>2</sup>century, the aperture for an eye of adjacent FD telescopes that span the horizon can reach 10<sup>4</sup> km<sup>2</sup> sr. FD operation requires (nearly) moonless nights and clear atmospheric conditions, which imposes a duty cycle of about 10%. Arrangements of LEDs, calibrated diffuse sources [10], pulsed UV



lasers [11], LIDARs\* and cloud monitors are used for photometric calibration, atmospheric calibration [12], and determination of exposure [13].

The EAS generates a track consistent with a light source moving at  $v = c$  across the FOV. The number of photons ( $N_\gamma$ ) as a function of atmospheric depth ( $X$ ) can be expressed as [7]

$$\frac{dN_\gamma}{dX} = \frac{dE_{\text{dep}}^{\text{tot}}}{dX} \int Y(\lambda, P, T, u) \cdot \tau_{\text{atm}}(\lambda, X) \cdot \varepsilon_{\text{FD}}(\lambda) d\lambda, \quad (32.1)$$

where  $\tau_{\text{atm}}(\lambda, X)$  is atmospheric transmission, including wavelength ( $\lambda$ ) dependence, and  $\varepsilon_{\text{FD}}(\lambda)$  is FD efficiency.  $\varepsilon_{\text{FD}}(\lambda)$  includes geometric factors and collection efficiency of the optics, quantum efficiency of the PMTs, and other throughput factors. The typical systematic uncertainties,  $Y$  (10–15%),  $\tau_{\text{atm}}$  (10%) and  $\varepsilon_{\text{FD}}$  (photometric calibration 10%), currently dominate the total reconstructed EAS energy uncertainty.  $\Delta E/E$  of 20–25% is possible, provided the geometric fit of the EAS axis is constrained by multi-eye stereo projection, or by timing from a colocated sparse array of surface detectors.

Analysis methods to reconstruct the EAS profile and deconvolute the contributions of re-scattered scintillation light, and direct and scattered Cherenkov light are described in [1] and more recently in [14]. The EAS energy is typically obtained by integrating over the Gaisser-Hillas function [15]

$$E_{\text{cal}} = \int_0^\infty w_{\text{max}} \left( \frac{X - X_0}{X_{\text{max}} - X_0} \right)^{(X_{\text{max}} - X_0)/\lambda} e^{-(X_{\text{max}} - X)/\lambda} dX, \quad (32.2)$$

where  $X_{\text{max}}$  is the depth at which the shower reaches its maximum energy deposit  $w_{\text{max}}$ .  $X_0$  and  $\lambda$  are two shape parameters.

### 32.2.2. Atmospheric Cherenkov telescopes for high-energy $\gamma$ -ray astronomy :

Written August 2009 by J. Holder (Bartol Research Inst., Univ. of Delaware).

A wide variety of astrophysical objects are now known to produce high-energy  $\gamma$ -ray photons. Leptonic or hadronic particle populations, accelerated to relativistic energies in the source, produce  $\gamma$  rays typically through inverse Compton boosting of ambient photons, or through the decay of neutral pions produced in hadronic interactions. At energies below  $\sim 30$  GeV,  $\gamma$ -ray emission can be detected directly using satellite or balloon-borne instrumentation, with an effective area approximately equal to the size of the detector ( $< 1 \text{ m}^2$ ). At higher energies, a technique with much larger effective collection area is required to measure astrophysical  $\gamma$ -ray fluxes, which decrease rapidly with increasing energy. Atmospheric Cherenkov detectors achieve effective collection areas of  $\sim 10^5 \text{ m}^2$  by employing the Earth's atmosphere as an intrinsic part of the detection technique.

As described in Chapter 26, a hadronic cosmic ray or high energy  $\gamma$ -ray incident on the Earth's atmosphere triggers a particle cascade, or air shower. Relativistic charged particles in the cascade produce Cherenkov radiation, which is emitted along the shower direction, resulting in a light pool on the ground with a radius of  $\sim 130 \text{ m}$ . Cherenkov light is produced throughout the cascade development, with the maximum emission occurring when the number of particles in the cascade is largest, at an altitude of  $\sim 10 \text{ km}$  for primary energies of 100 GeV–1 TeV. Following absorption and scattering in the atmosphere, the Cherenkov light at ground level peaks at a wavelength,  $\lambda \approx 300\text{--}350 \text{ nm}$ . The photon density is typically  $\sim 100$  photons/ $\text{m}^2$  at 1 TeV, arriving in a brief flash of a few nanoseconds duration. This Cherenkov pulse can be detected from any point within the light pool radius by using large reflecting surfaces to focus the Cherenkov light on to fast photon detectors (Fig. 32.2).

Modern atmospheric Cherenkov telescopes, such as those built and operated by the H.E.S.S. [17], MAGIC [18] and VERITAS [16] collaborations, consist of large ( $> 100 \text{ m}^2$ ) segmented mirrors on steerable altitude-azimuth mounts. A camera, made from an array of

up to 1000 photomultiplier tubes (PMTs) covering a field-of-view of up to  $5.0^\circ$  in diameter, is placed at the mirror focus and used to record a Cherenkov image of each air shower. Images are recorded at a rate of a few hundred Hz, the vast majority of which are due to showers with hadronic cosmic-ray primaries. The shape and orientation of the Cherenkov images are used to discriminate  $\gamma$ -ray photon events from this cosmic-ray background, and to reconstruct the photon energy and arrival direction.  $\gamma$ -ray images result from purely electromagnetic cascades and appear as narrow, elongated ellipses in the camera plane. The long axis of the ellipse corresponds to the vertical extension of the air shower, and points back towards the source position in the field-of-view. If multiple telescopes are used to view the same shower (“stereoscopy”), the source position is simply the intersection point of the various image axes. Cosmic-ray primaries produce secondaries with large transverse momenta, which initiate sub-showers. Their images are consequently wider and less regular than those with  $\gamma$ -ray primaries and, since the original charged particle has been deflected by galactic magnetic fields before reaching the Earth, the images have no preferred orientation.

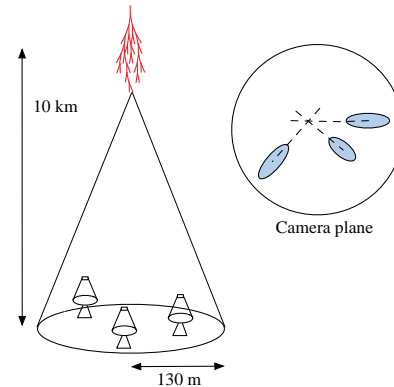


**Figure 32.2:** A schematic illustration of an atmospheric Cherenkov telescope array. The primary particle initiates an air shower, resulting in a cone of Cherenkov radiation. Telescopes within the Cherenkov light pool record elliptical images; the intersection of the long axes of these images indicates the arrival direction of the primary, and hence the location of a  $\gamma$ -ray source in the sky.

The measurable differences in Cherenkov image orientation and morphology provide the background discrimination which makes ground-based  $\gamma$ -ray astronomy possible. For point-like sources, such as distant Active Galactic Nuclei (AGNs), modern instruments can reject up to 99.999% of the triggered cosmic-ray events, while retaining up to 50% of the  $\gamma$ -ray population. In the case of spatially extended sources, such as Galactic supernova remnants (SNR), the background rejection is less efficient, but the technique can be used to produce  $\gamma$ -ray maps of the emission from the source. The angular resolution depends upon the energy of the primary  $\gamma$ -ray, but is typically  $0.1^\circ$  per event (68% containment radius) at energies above a few hundred GeV.

The total Cherenkov yield from the air shower is proportional to the energy of the primary particle. The image intensity, combined with the reconstructed distance of the shower core from each telescope, can therefore be used to estimate the primary energy. The energy resolution of this technique, also energy-dependent, is typically 15–20% at energies above a few hundred GeV. Energy spectra of  $\gamma$ -ray sources can be measured over a wide range; potentially from  $\sim 50$  GeV to  $\sim 100$  TeV, depending upon the instrument characteristics, source strength, and exposure time. To a first approximation, the lower energy threshold at the trigger level,  $E_T$ , depends upon the mirror area,  $A$ , the photon collection efficiency,  $\eta(\lambda)$ , the Cherenkov light yield,  $C(\lambda)$ , the night sky background light,  $B(\lambda)$ , the solid angle,  $\Omega$ , and the trigger resolving time,  $\tau$ , as follows [19]:

$$E_T \propto \frac{1}{C(\lambda)} \sqrt{\frac{B(\lambda)\Omega\tau}{\eta(\lambda)A}} \quad (32.3)$$

\* This acronym for “Light Detection and Ranging,” refers here to systems that measure atmospheric properties from the light scattered backwards from laser pulses directed into the sky.

In practice, this function may be modified by the properties of the detector; for example, by complex, multi-level, combinatorial trigger systems and highly pixellated fields of view. In addition, the useful scientific threshold, after the application of analysis cuts to select  $\gamma$ -ray events, is always somewhat higher than this.

The first astrophysical source to be convincingly detected using the imaging atmospheric Cherenkov technique was the Crab Nebula [20], with a flux of  $2.1 \times 10^{-11}$  photons  $\text{cm}^{-2} \text{s}^{-1}$  above 1 TeV [21]. Modern arrays have sensitivity sufficient to detect sources with 1% of the Crab Nebula's flux in a few tens of hours, and the TeV source catalog now consists of more than 80 sources. The majority of these have been detected by scanning the Galactic plane from the southern hemisphere with the H.E.S.S. telescope array [22].

### 32.3. Large neutrino detectors

Large water Cherenkov and scintillator detectors (see Table 32.1) usually consist of a volume of transparent liquid viewed by photomultiplier tubes (PMTs) (see Sec. 31.2); the liquid serves as active target. PMT hit charges and times are recorded and digitized, and triggering is usually based on coincidence of PMTs hits within a time window comparable to the detector's light-crossing time. Because photosensors lining an inner surface represent a driving cost that scales as surface area, very large volumes can be used for comparatively reasonable cost. Some detectors are segmented into subvolumes individually viewed by PMTs, and may include other detector elements (*e.g.*, tracking detectors). Devices to increase light collection, *e.g.*, reflectors or waveshifter plates, may be employed. A common configuration is to have at least one concentric outer layer of liquid material separated from the inner part of the detector to serve as shielding against ambient background. If optically separated and

**Table 32.1:** Properties of large detectors for rare processes. If total target mass is divided into large submodules, the number of subdetectors is indicated in parentheses.

Detector	Fid. mass, kton (modules)	PMTs (diameter, cm)	$\xi$	p.e./MeV	Dates
Baksan	0.33, scint (3150)	1/module (15)	segmented	40	1980–
MACRO	0.6, scint (476)	2-4/module (20)	segmented	18	1989–2000
LVD	1, scint. (840)	3/module (15)	segmented	15	1992–
KamLAND	1, scint	1325(43)+554(51)*	34%	460	2002–
Borexino	0.1, scint	2212 (20)	30%	500	2007–
SNO+	0.78, scint	9438 (20)	54%	400–900	Future
CHOOZ	0.005, scint (Gd)	192 (20)	15%	130	1997–1998
Double Chooz	0.020, scint (Gd)(2)	534/module (20)	13%	180	2011–
Daya Bay	0.160, scint (Gd)(8)	192/module (20)	5.6% <sup>†</sup>	100	2011–
RENO	0.030, scint (Gd)(2)	342/module (25)	12.6%	100	2011–
IMB-1	3.3, H <sub>2</sub> O	2048 (12.5)	1%	0.25	1982–1985
IMB-2	3.3, H <sub>2</sub> O	2048 (20)	4.5%	1.1	1987–1990
Kam I	0.88/0.78, H <sub>2</sub> O	1000/948 (50)	20%	3.4	1983–1985
Kam II	1.04, H <sub>2</sub> O	948 (50)	20%	3.4	1986–1990
Kam III	1.04, H <sub>2</sub> O	948 (50)	20% <sup>‡</sup>	4.3	1990–1995
SK I	22.5, H <sub>2</sub> O	11146 (50)	39%	6	1996–2001
SK II	22.5, H <sub>2</sub> O	5182 (50)	19%	3	2002–2005
SK III+	22.5, H <sub>2</sub> O	11129 (50)	39%	6	2006–
SNO	1, D <sub>2</sub> O/1.7, H <sub>2</sub> O	9438 (20)	31% <sup>§</sup>	9	1999–2006

\* The 51 cm PMTs were added in 2003.

† The effective Daya Bay coverage is 12% with top and bottom reflectors.

‡ The effective Kamiokande III coverage was 25% with light collectors.

§ The effective SNO coverage was 54% with light collectors.

#### 32.3.1. Deep liquid detectors for rare processes :

Revised November 2011 by K. Scholberg & C.W. Walter (Duke University)

Deep, large detectors for rare processes tend to be multi-purpose with physics reach that includes not only solar, reactor, supernova and atmospheric neutrinos, but also searches for baryon number violation, searches for exotic particles such as magnetic monopoles, and neutrino and cosmic ray astrophysics in different energy regimes. The detectors may also serve as targets for long-baseline neutrino beams for neutrino oscillation physics studies. In general, detector design considerations can be divided into high- and low-energy regimes, for which background and event reconstruction issues differ. The high-energy regime, from about 100 MeV to a few hundred GeV, is relevant for proton decay searches, atmospheric neutrinos and high-energy astrophysical neutrinos. The low-energy regime (a few tens of MeV or less) is relevant for supernova, solar, reactor and geological neutrinos.

instrumented with PMTs, an outer layer may also serve as an active veto against entering cosmic rays and other background events. The PMTs for large detectors typically range in size from 20 cm to 50 cm diameter, and typical quantum efficiencies are in the 20–25% range. The active liquid volume requires purification and there may be continuous recirculation of liquid. For large homogeneous detectors, the event interaction vertex is determined using relative timing of PMT hits, and energy deposition is determined from the number of recorded photoelectrons. A “fiducial volume” is usually defined within the full detector volume, some distance away from the PMT array. Inside the fiducial volume, enough PMTs are illuminated per event that reconstruction is considered reliable, and furthermore, entering background from the enclosing walls is suppressed by a buffer of self-shielding. PMT and detector optical parameters are calibrated using laser, LED, or other light sources. Quality of event reconstruction typically depends on photoelectron yield, pixelization and timing.



Because in most cases one is searching for rare events, large detectors are usually sited underground to reduce cosmic-ray related background (see Chapter 26). The minimum depth required varies according to the physics goals [23].

### 32.3.1.1. Liquid scintillator detectors:

Past and current large underground detectors based on hydrocarbon scintillators include LVD, MACRO, Baksan, Borexino, KamLAND and SNO+. Experiments at nuclear reactors include CHOOZ, Double CHOOZ, Daya Bay, and RENO. Organic liquid scintillators (see Sec. 31.3.0) for large detectors are chosen for high light yield and attenuation length, good stability, compatibility with other detector materials, high flash point, low toxicity, appropriate density for mechanical stability, and low cost. They may be doped with waveshifters and stabilizing agents. Popular choices are pseudocumene (1,2,4-trimethylbenzene) with a few g/L of the PPO (2,5-diphenyloxazole) fluor, and linear alkylbenzene (LAB). In a typical detector configuration there will be active or passive regions of undoped scintillator, non-scintillating mineral oil or water surrounding the inner neutrino target volume. A thin vessel or balloon made of nylon, acrylic or other material transparent to scintillation light may contain the inner target; if the scintillator is buoyant with respect to its buffer, ropes may hold the balloon in place. For phototube surface coverages in the 20–40% range, yields in the few hundreds of photoelectrons per MeV of energy deposition can be obtained. Typical energy resolution is about  $7\%/\sqrt{E(\text{MeV})}$ , and typical position reconstruction resolution is a few tens of cm at  $\sim 1$  MeV, scaling as  $\sim N^{-1/2}$ , where  $N$  is the number of photoelectrons detected.

Shallow detectors for reactor neutrino oscillation experiments require excellent muon veto capabilities. For  $\bar{\nu}_e$  detection via inverse beta decay on free protons,  $\bar{\nu}_e + p \rightarrow n + e^+$ , the neutron is captured by a proton on a  $\sim 180 \mu\text{s}$  timescale, resulting in a 2.2 MeV  $\gamma$  ray, observable by Compton scattering and which can be used as a tag in coincidence with the positron signal. The positron annihilation  $\gamma$  rays may also contribute. Inverse beta decay tagging may be improved by addition of Gd at  $\sim 0.1\%$  by mass, which for natural isotope abundance has a  $\sim 49,000$  barn cross-section for neutron capture (in contrast to the 0.3 barn cross-section for capture on free protons). Gd capture takes  $\sim 30 \mu\text{s}$ , and is followed by a cascade of  $\gamma$  rays adding up to about 8 MeV. Gadolinium doping of scintillator requires specialized formulation to ensure adequate attenuation length and stability.

Scintillation detectors have an advantage over water Cherenkov detectors in the lack of Cherenkov threshold and the high light yield. However, scintillation light emission is nearly isotropic, and therefore directional capabilities are relatively weak. Liquid scintillator is especially suitable for detection of low-energy events. Radioactive backgrounds are a serious issue, and include long-lived cosmogenics. To go below a few MeV, very careful selection of materials and purification of the scintillator is required (see Sec. 32.6). Fiducialization and tagging can reduce background. A recent idea, not yet realized, is to dissolve neutrinoless double beta decay ( $0\nu\beta\beta$ ) isotopes in scintillator (for instance  $^{150}\text{Nd}$  in SNO+). Although energy resolution is poor compared to typical  $0\nu\beta\beta$  search experiments, the quantity of isotope could be so large that the kinematic signature of  $0\nu\beta\beta$  would be visible as a clear feature in the spectrum.

### 32.3.1.2. Water Cherenkov detectors:

Very large-imaging water detectors reconstruct ten-meter-scale Cherenkov rings produced by charged particles (see Sec. 31.5.0). The first such large detectors were IMB and Kamiokande. The only currently existing instance of this class of detector, with fiducial volume of 22.5 kton and total mass of 50 kton, is Super-Kamiokande (Super-K). For volumes of this scale, absorption and scattering of Cherenkov light are non-negligible, and a wavelength-dependent factor  $\exp(-d/L(\lambda))$  (where  $d$  is the distance from emission to the sensor and  $L(\lambda)$  is the attenuation length of the medium) must be included in the integral of Eq. (31.5) for the photoelectron yield. Attenuation lengths on the order of 100 meters have been achieved.

Cherenkov detectors are excellent electromagnetic calorimeters, and the number of Cherenkov photons produced by an  $e/\gamma$  is nearly proportional to its kinetic energy. For massive particles, the number of photons produced is also related to the energy, but not linearly. For any type of particle, the *visible energy*  $E_{\text{vis}}$  is defined as the

energy of an electron which would produce the same number of Cherenkov photons. The number of collected photoelectrons depends on the scattering and attenuation in the water along with the photocathode coverage, quantum efficiency and the optical parameters of any external light collection systems or protective material surrounding them. Event-by-event corrections are made for geometry and attenuation. For a typical case, in water  $N_{\text{p.e.}} \sim 15 \xi E_{\text{vis}}(\text{MeV})$ , where  $\xi$  is the effective fractional photosensor coverage. Cherenkov photoelectron yield per MeV of energy is relatively small compared to that for scintillator, *e.g.*,  $\sim 6$  pe/MeV for Super-K with a PMT surface coverage of  $\sim 40\%$ . In spite of light yield and Cherenkov threshold issues, the intrinsic directionality of Cherenkov light allows individual particle tracks to be reconstructed. Vertex and direction fits are performed using PMT hit charges and times, requiring that the hit pattern be consistent with a Cherenkov ring.

High-energy ( $\sim 100$  MeV or more) neutrinos from the atmosphere or beams interact with nucleons; for the nucleons bound inside the  $^{16}\text{O}$  nucleus, the nuclear effects both at the interaction, and as the particles leave the nucleus must be considered when reconstructing the interaction. Various event topologies can be distinguished by their timing and fit patterns, and by presence or absence of light in a veto. “Fully-contained” events are those for which the neutrino interaction final state particles do not leave the inner part of the detector; these have their energies relatively well measured. Neutrino interactions for which the lepton is not contained in the inner detector sample have higher-energy parent neutrino energy distributions. For example, in “partially-contained” events, the neutrino interacts inside the inner part of the detector but the lepton (almost always a muon, since only muons are penetrating) exits. “Upward-going muons” can arise from neutrinos which interact in the rock below the detector and create muons which enter the detector and either stop, or go all the way through (entering downward-going muons cannot be distinguished from cosmic rays). At high energies, multi-photoelectron hits are likely and the charge collected by each PMT (rather than the number of PMTs firing) must be used; this degrades the energy resolution to approximately  $2\%/\sqrt{\xi E_{\text{vis}}(\text{GeV})}$ . The absolute energy scale in this regime can be known to  $\approx 2\text{--}3\%$  using cosmic-ray muon energy deposition, Michel electrons and  $\pi^0$  from atmospheric neutrino interactions. Typical vertex resolutions for GeV energies are a few tens of cm [24]. Angular resolution for determination of the direction of a charged particle track is a few degrees. For a neutrino interaction, because some final-state particles are usually below Cherenkov threshold, knowledge of direction of the incoming neutrino direction itself is generally worse than that of the lepton direction, and dependent on neutrino energy.

Multiple particles in an interaction (so long as they are above Cherenkov threshold) may be reconstructed, allowing for the exclusive reconstruction of final states. In searches for proton decay, multiple particles can be kinematically reconstructed to form a decaying nucleon. High-quality particle identification is also possible:  $\gamma$  rays and electrons shower, and electrons scatter, which results in fuzzy rings, whereas muons, pions and protons make sharp rings. These patterns can be quantitatively separated with high reliability using maximum likelihood methods [25]. A  $e/\mu$  misidentification probability of  $\sim 0.4\%/\xi$  in the sub-GeV range is consistent with the performance of several experiments for  $4\% < \xi < 40\%$ . Sources of background for high energy interactions include misidentified cosmic muons and anomalous light patterns when the PMTs sometimes “flash” and emit photons themselves. The latter class of events can be removed using its distinctive PMT signal patterns, which may be repeated. More information about high energy event selection and reconstruction may be found in reference [26].

In spite of the fairly low light yield, large water Cherenkov detectors may be employed for reconstructing low-energy events, down to *e.g.*  $\sim 4\text{--}5$  MeV for Super-K [27]. Low-energy neutrino interactions of solar neutrinos in water are predominantly elastic scattering off atomic electrons; single electron events are then reconstructed. At solar neutrino energies, the visible energy resolution ( $\sim 30\%/\sqrt{\xi E_{\text{vis}}(\text{MeV})}$ ) is about 20% worse than photoelectron counting statistics would imply. Using an electron LINAC and/or nuclear sources, 0.5–1.5% determination of the absolute energy scale

has been achieved at solar neutrino energies. Angular resolution is limited by multiple scattering in this energy regime (25–30°). At these energies, radioactive backgrounds become a dominant issue. These backgrounds include radon in the water itself or emanated by detector materials, and  $\gamma$  rays from the rock and detector materials. In the few to tens of MeV range, radioactive products of cosmic ray muon-induced spallation are troublesome, and are removed by proximity in time and space to preceding muons, at some cost in dead time.

The Sudbury Neutrino Observatory (SNO) detector [28] is the only instance of a large heavy water detector and deserves mention here. In addition to an outer 1.7 kton of light water, SNO contained 1 kton of D<sub>2</sub>O, giving it unique sensitivity to neutrino neutral current ( $\nu_x + d \rightarrow \nu_x + p + n$ ), and charged current ( $\nu_e + d \rightarrow p + p + e^-$ ) deuteron breakup reactions. The neutrons were detected in three ways: In the first phase, via the reaction  $n + d \rightarrow t + \gamma + 6.25$  MeV; Cherenkov radiation from electrons Compton-scattered by the  $\gamma$  rays was observed. In the second phase, NaCl was dissolved in the water. <sup>35</sup>Cl captures neutrons,  $n + ^{35}\text{Cl} \rightarrow ^{36}\text{Cl} + \gamma + 8.6$  MeV. The  $\gamma$  rays were observed via Compton scattering. In a final phase, specialized low-background <sup>3</sup>He counters (“neutral current detectors” or NCDs) were deployed in the detector. These detected neutrons via  $n + ^3\text{He} \rightarrow p + t + 0.76$  MeV, and ionization charge from energy loss of the products was recorded in proportional counters.

### 32.3.2. Coherent radio Cherenkov radiation detectors :

Written October 2011 by S.R. Klein (LBNL)

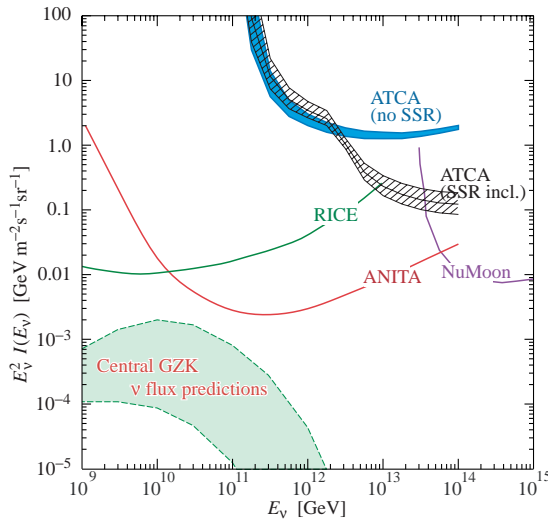


**Figure 32.3:** Representative  $\nu$  flux limits from radio-detection experiments, illustrating the energy ranges for different techniques. Shown are limits from the Rice, ANITA, NuMoon and Lunaska (ATCA) collaborations. NuMoon and Lunaska are low and high frequency lunar scans respectively, showing the strengths of the two different frequency bands. The two separate limits for ATCA are for different models of the lunar regolith; their separation is a measure of the resultant uncertainty. Also shown, for comparison is the mid-range of flux predictions for GZK neutrinos from Ref. 34.

Radio detectors sensitive to coherent Cherenkov radiation provide an attractive way to search for ultra-high energy cosmic neutrinos. These neutrinos are the only long-range probe of the ultra-high energy cosmos. Protons and heavier nuclei with energies  $\gtrsim 5 \times 10^{19}$  eV are limited to ranges of less than 100 Mpc by interactions with CMB photons (the GZK effect [29]), and gamma rays pair-produce from the CMB. The decay products of the particles produced in the hadronic interactions include neutrinos. To detect a useful number of these “GZK neutrinos” annually (assuming that ultra-high energy cosmic rays are protons) requires a detector of about 100 km<sup>3</sup> in volume. This is too big for an optical Cherenkov detector. Optical attenuation lengths are less than 200 m in ice or water, so a 100 km<sup>3</sup> detector would require a prohibitive number of sensors.

Electromagnetic and hadronic showers produce radio pulses via the Askaryan effect [30], as discussed in Sec. 30. The shower contains more electrons than positrons, leading to coherent emission. The electric field strength is proportional to the neutrino energy; the radiated power goes as its square. Detectors with antennas placed in the active volume have thresholds around 10<sup>17</sup> eV.

The electric field strength increases linearly with frequency, up to a cut-off wavelength set by the transverse size of the shower. The cut-off is about 1 GHz in ice, and 2.5 GHz in rock/lunar regolith. The broadband spectrum argues for a wide detection bandwidth, but, dispersion during signal transmission can cause technical challenges. The angular distribution depends on the frequency. Near the cutoff frequency, radiation is emitted in a narrow cone, centered around the Cherenkov angle (about 56° in ice) [31]. At lower frequencies, the angular distribution broadens, eventually becoming largely isotropic. The signal is linearly polarized in the plane containing the shower direction and the photon direction. This polarization is a useful check that any observed signal is indeed coherent Cherenkov radiation. Polarization measurements can be used to help reconstruct the neutrino direction.

Radiodetection requires a dielectric medium, with a long absorption length for radio waves. The huge target volumes require that this be a commonly available natural material, usually Antarctic ice or the lunar regolith [32].

When viewed from near the Cherenkov angle, the experimental signal is a short wideband radio pulse coming from a shower-sized region within a solid. The initial pulse width is  $\approx 1$  ns, but it may be broadened by dispersion as it propagates. As long as the dispersion can be accounted for, a large bandwidth detector is the most sensitive. Because the angular distribution depends on the frequency, spectral information can be used to help reconstruct the neutrino direction.

Radio detectors have observed cosmic-ray air showers in the atmosphere. The physics of radio-wave generation in air showers is more complex because there are contributions due to charge separation by charged particles, and from synchrotron radiation from  $e^\pm$ , both due to the Earth’s magnetic field. Several experiments have also set limits on radiation due to magnetic monopoles.

#### 32.3.2.1. The Moon as a target:

Because of its large size and non-conducting regolith, and the availability of large radio-telescopes, the moon is an attractive target [33]; several representative lunar experiments are listed in Table 32.2. Conventional radio-telescopes are reasonably well suited to lunar neutrino searches, with natural beam widths not too dissimilar from the size of the Moon. Still, there are some experimental challenges in understanding the signal. The composition of the lunar regolith is not well known, and the attenuation length for radio waves must be estimated. An attenuation length of 9/f(GHz) (m) is often used. The big limitation of lunar experiments is that the 240,000 km target-antenna separation leads to neutrino energy thresholds far above 10<sup>20</sup> eV.

**Table 32.2:** Experiments that have set limits on neutrino interactions in the Moon; current limits are shown in Fig. 32.3 [32].

Experiment	Year	Dish Size	Frequency	Bandwidth	Obs. Time
Parkes	1995	64 m	1425 MHz	500 MHz	10 hrs
Glue	1999+	70 m, 34 m	2200 MHz	40-150 MHz	120 hrs
NuMoon	2008	11×25 m	115–180 MHz	—	50 hrs
Lunaska	2008	3×22 m	1200–1800 MHz	—	6 nights
Resun	2008	4×25 m	1450 MHz	50 MHz	45 hours

The frequency range affects the sensitive volume. At low frequencies, radiation is relatively isotropic, so signals can be detected from most of the Moon’s surface, for most angles of incidence. At higher frequencies, the signal is stronger, but radiation is concentrated near the Cherenkov angle, and the geometry limits the sensitivity to interactions near the Moon’s limb, where the neutrino also arrives within a fairly narrow angular range. The larger high-frequency attenuation limits the depth that can be probed.

So, higher frequency searches probe lower neutrino energies, but lower frequency searches can set tighter flux limits on high-energy neutrinos. An alternative approach, increasingly viable with modern technology, is to search over a wide frequency range. This introduces a technical challenge in the form of dispersion (frequency dependent time delays) in the ionosphere. The Parkes experiment pioneered the use of de-dispersion filters; this has been taken to a high art by the Lunaska collaboration.

Lunar experiments use several techniques to reject backgrounds, which are mostly anthropogenic. Many experiments use multiple antennas, separated by at least hundreds of meters; by requiring a coincidence within a small time window, anthropogenic noise can be rejected. An alternative approach is to use beam forming with multiple receivers in a single antenna, to ensure that the signal points back to the moon. The limits set by representative lunar experiments are shown in Fig. 32.3.

These efforts have considerable scope for expansion. In the near future, several large radio detector arrays should reach significantly lower limits. The LOFAR array is beginning to take data with 36 detector clusters spread over Northwest Europe. In the longer term, the Square Kilometer Array (SKA) with 1 km<sup>2</sup> effective area will push thresholds down to near 10<sup>20</sup> eV.

### 32.3.2.2. The ANITA balloon experiment:

To reduce the energy threshold, it is necessary to reduce the antenna-target separation. Most of these experiments use Antarctic ice as a medium. One such experiment is the ANITA balloon experiment which made two flights around Antarctica, floating at an altitude around 35 km [34]. Its 40 (32 in the first flight) dual-polarization horn antennas scanned the surrounding ice, out to the horizon (650 km away). Because of the small angle of incidence, ANITA was able to make use of polarization information;  $\nu$  signals should be vertically polarized, while most background from cosmic-ray air showers is expected to be horizontally polarized. By using the several-meter separation between antennas, ANITA achieved a pointing accuracy of 0.2-0.4<sup>o</sup> in elevation, and 0.5-1.1<sup>o</sup> in azimuth.

Antarctic experiments must consider the inhomogeneities in the ice: varying density in the upper ice (the firn) and the variation in radio attenuation length with temperature. ANITA also had to consider the surface roughness, which affects the transition from ice to air. All of these affect the propagation of radio-waves from the  $\nu$ -induced shower to the antennas.

The ‘firn’ is the top 100-200 m of Antarctic ice, where there is a transition from packed snow at the surface to solid ice (density 0.92 g/cm<sup>3</sup>) below, where the density increases gradually with depth. The index of refraction depends on the density, so radio waves bend downward in the firn. This bending reduces the effectiveness of surface or aerial antennas. The thickness of the firn varies with location; it is thicker in central Antarctica than in the coastal ice sheets.

The attenuation length of radio waves depends on the frequency and ice temperature, with attenuation higher in warmer ice. A recent measurement, by the ARA collaboration at the South Pole found an average attenuation length of 670<sup>+180</sup><sub>-66</sub> m [35]. On the Ross Ice Shelf, ARIANNA finds attenuation lengths of 300-500 m, depending on frequency [36].

ANITA verified the accuracy of their calibrations by observing radio sources that they buried in the ice. ANITA has also recently observed radio waves from cosmic-ray air showers; these showers are differentiated from neutrino showers on the basis of the radio polarization and zenith angle distribution [37].

As with the lunar experiments, ANITA had to contend with anthropogenic backgrounds. They used their good pointing accuracy to remove all candidate events that pointed toward known or suspected areas of human habitation. The limit from their two flights is shown in Fig. 32.3. These are the most stringent limits on GZK neutrinos to date. Because of the significant target to detector separation, ANITA is most sensitive at energies above 10<sup>19</sup> eV, above the peak of the GZK neutrino spectrum.

### 32.3.2.3. Active Volume Detectors:

The use of radio antennas located in the active volume was pioneered by the RICE experiment, which buried radio antennas in holes drilled for AMANDA [38] at the South Pole. RICE was comprised of 18 half-wave dipole antennas, sensitive from 200 MHz to 1 GHz, buried between 100 and 300 m deep. Each antenna fed an in-situ preamplifier which transmitted the signals to surface digitizing electronics. The array triggered when four or more stations fired discriminators within 1.2  $\mu$ s, giving it a threshold of about 10<sup>17</sup> eV.

Two groups are prototyping detectors, with the goal of a detector with an active volume in the 100 km<sup>3</sup> range. Both techniques are modular, so the detector volume scales roughly linearly with the available funding. The Askaryan Radio Array (ARA) is located at the South Pole, while the Antarctic Ross Iceshelf ANTenna Neutrino Array (ARIANNA) is on the Ross Ice Shelf. Both experiments use local triggers based on a coincidence between multiple antennas in a single station/cluster.

One big difference between the two experiments is the depth of their antennas. ARA buries antennas up to 200 m deep in the ice, to avoid the firn. Because of the refraction, a surface antenna cannot ‘see’ a signal from a near-surface interaction some distance away. Burying antennas avoids this problem. However, drilling holes has costs, and the limited hole diameter (15 cm in ARA) requires compromises between antenna design (particularly for horizontally polarized waves), mechanical support, power and communications. In contrast, ARIANNA places antennas in shallow, near-surface holes. This greatly simplifies deployment and avoid limitations on antenna design, but at a cost of reduced sensitivity to neutrino interactions near the surface.

The current ARA proposal, ARA-37 [35], calls for an array of 37 stations, each consisting of 16 embedded antennas deployed up to 200 m deep below the firn in several 15-cm diameter boreholes. ARA will detect signals in the frequency range from 150 to 850 MHz for vertical polarization, and 250 MHz to 850 MHz for horizontal polarization. ARA plans to use bicone antennas for vertical polarization, and quad-slotted cylinders for horizontal polarization. The collaboration uses notch filters and surface veto antennas to eliminate most anthropogenic noise, and vetos events when aircraft are in the area, or weather balloons are being launched.

ARIANNA will be located in Moore’s Bay, on the Ross Ice Shelf, where  $\approx$  575 m of ice sits atop the Ross Sea [36]. The site was chosen because the ice-seawater interface is smooth there, so the interface acts as a mirror for radio waves. The major advantage of this approach is that ARIANNA is sensitive to downward going neutrinos, and should be able to see more of the Cherenkov cone for horizontal neutrinos. One disadvantage of the site is that the ice is warmer, so the radio attenuation length will be shorter. Each ARIANNA station will use 8 log-periodic dipole antennas, pointing downward and arranged in an octagon. The multiple antennas allow for single-station directional and polarization measurements. The ARIANNA site is about 110 km from McMurdo station, and is shielded by Minna Bluff.

## 32.4. Large time-projection chambers for rare event detection

Written August 2009 by M. Heffner (LLNL).

The Time Projection Chamber (TPC) concept (Sec. 31.6.5) has been applied to many projects outside of particle physics and the accelerator-based experiments for which it was initially developed. TPCs in non-accelerator particle physics experiments are principally focused on rare event detection (*e.g.*, neutrino and dark matter experiments) and the physics of these experiments can place dramatically different constraints on the TPC design (only extensions of the traditional TPCs are discussed here). The drift gas or liquid is usually the target or matter under observation and due to very low signal rates a TPC with the largest possible active mass is desired. The large mass complicates particle tracking of short and sometimes very low-energy particles. Other special design issues include efficient light collection, background rejection, internal triggering, and optimal energy resolution.

Backgrounds from  $\gamma$  rays and neutrons are significant design issues in the construction of these TPCs. These are generally placed

deep underground to shield them from cosmogenic particles and are surrounded with shielding to reduce radiation from the local surroundings. The construction materials are carefully screened for radiopurity, as they are in close contact with the active mass and can be a significant source of background. The TPC excels in reducing this internal background because the mass inside the field cage forms one monolithic volume from which fiducial cuts can be made *ex post facto* to isolate quiet drift mass. The liquid (gas) can be circulated and purified to a very high level. Self-shielding in these large mass systems can be significant and the effect improves with density and size. (See Sec. 32.6.)

The liquid-phase TPC can have a high density at low pressure that results in very good self-shielding and compact installation with lightweight containment. The down sides are the need for cryogenics, slower charge drift, tracks shorter than typical electron diffusion distances, lower-energy resolution (*e.g.*, xenon) and limited charge readout options. Slower charge drift requires long electron lifetimes, placing strict limits on the oxygen and other impurities with high electron affinity. A significant variation of the liquid-phase TPC that improves the charge readout is the dual-phase TPC, where a gas phase layer is formed above the liquid into which the drifting electrons are extracted and amplified, typically with electroluminescence (*i.e.*, secondary scintillation or proportional scintillation (Fig. 32.4)). The careful transfer of electrons across the phase boundary requires careful control of its position and setting up an appropriate electric field.

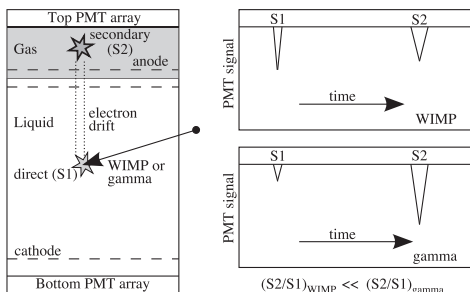


**Figure 32.4:** The configuration of a dual phase detector is shown on the left with the locations of where the primary and secondary light are generated. On the right is a schematic view of the signals of both an electron and nuclear interaction illustrating the discrimination power of this method. This figure is slightly modified from Ref. 39.

A high-pressure gas phase TPC has no cryogenics and density is easily optimized for the signal, but a large heavy-pressure vessel is required. Although self shielding is reduced, it can in some cases approach that of the liquid phase; in xenon at 50 atm the density is about half that of water or about 1/6 of liquid xenon. A significant feature of high pressure xenon gas is the energy resolution. Below a density of about  $0.5 \text{ g cm}^{-3}$  the intrinsic resolution is only a few times that of high purity germanium [40]. A neutrinoless double beta decay ( $0\nu 2\beta$ ) search with a TPC operated below this density limit could enjoy excellent energy resolution and maintain particle tracking for background rejection.

An observable interaction with the TPC results in a charged particle that travels in the drift matter, exciting and ionizing the atoms until the initial energy is converted into ionization, scintillation, or heat with relatively large fluctuations around the mean. Rare-event TPCs can be designed to detect scintillation light as well as charge to exploit the anti-correlation to improve energy resolution and/or signal to noise [41]. An electric drift field separates the electrons and positive ions from the ionization although the separation is not complete and some electrons are captured, exciting atoms and releasing more light than the primary excitation alone. The average partition between the scintillation and ionization can be manipulated to increase the ionization (at the expense of scintillation) by a number of methods, such as increasing the strength of the electric field up to saturation of the ionization yield, increasing the temperature to enhance the diffusion of the ionized electrons, and adding dopants

such as triethylamine that can be photoionized by the scintillation photons releasing more ionization.

Scintillation light is typically collected with photomultiplier tubes (PMTs) and avalanche photo diodes (APDs) although any fast (compared to the ionization drift speed) light collector capable of detecting the typically UV photons, maintaining high radiopurity, and perhaps withstanding pressure would work. (CCDs are slow and therefore only record two dimensions, integrating over the time direction. Some of the 3D information can be recovered by a few PMTs.) In most cases, coating the optics or adding a wavelength shifter is required [41], although some work has been done to directly readout the 175 nm light from xenon with a silicon detector. In a typical cylindrical geometry, the light detectors are placed at the ends on an equipotential of the field cage simplifying the design, but limiting the collection efficiency. The field cage can be made of UV-reflective materials such as Teflon, to increase the light-collection efficiency.

Charge collection can be accomplished with proportional avalanche in the manner used in a traditional TPC (even in the liquid state), although the final signal suffers from rather large fluctuations caused by small fluctuations early in the avalanche that are amplified by the process. Inductive readout of passing charges and direct collection of the unamplified charge do not rely on an avalanche, and are effective where energy resolution is of paramount importance, but depend on low-noise amplifiers and relatively large signals (*e.g.*, in  $0\nu 2\beta$  decay).

Electroluminescence can be used to proportionally amplify the drifted ionization, and it does not suffer the fluctuations of an avalanche or the small signals of direct collection. It works by setting up at the positive end of the drift volume parallel meshes or wire arrays with an electric field larger than the drift field, but less than the field needed for avalanche. In xenon, this is  $3\text{--}6 \text{ kV cm}^{-1} \text{ bar}^{-1}$  for good energy resolution. Eq. (32.4) shows the dependence of the yield ( $Y$ ) in xenon in units of photons/(electron cm bar) as a function of pressure ( $p$ ) in units of bar and electric field ( $E$ ) in units of kV/cm [42]:

$$Y/p = 140 E/p - 116 . \quad (32.4)$$

The amplification can be adjusted with the length of the electroluminescence region, pressure and electric field.

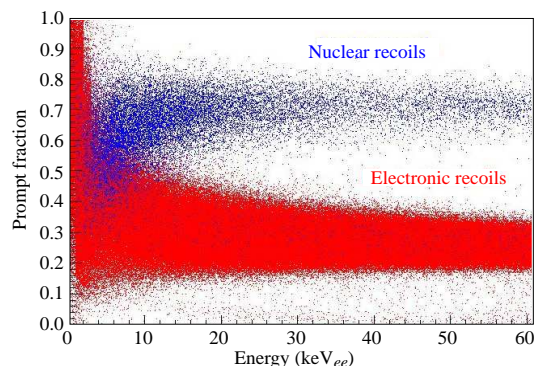


**Figure 32.5:** An example of pulse-shape discrimination of nuclear recoils and electrons in argon. The prompt fraction is a measure of the pulse shape that clearly separates the two interactions down to very low energy. Figure from Ref. 43.

Differentiation of nuclear and electron recoils at low-energy deposition is important as a means of background rejection. The nuclear recoil deposits a higher density of ionization than an electron recoil and this results in a higher geminate recombination resulting in a higher output of primary scintillation and lower charge. The ratio of scintillation to charge can be used to distinguish the two. In the case of an electroluminescence readout, this is done simply with the ratio of primary light to secondary light. Optically transparent grids with PMT or APD readout combine to make an elegant setup wherein the same array can measure the primary scintillation (S1), and the electroluminescence (S2) eliminating the necessity of two sets of readout detectors. Fig. 32.4 illustrates this method that works in

the gas phase and in dual phase detectors. The time evolution of the primary light is also affected by the type of recoil that results from different populations of excimers in the singlet and triplet states [43]. This alone has resulted in excellent discrimination, particularly in gasses where the decay times are significantly different (see Table 32.3). An example of the discrimination is displayed in Fig. 32.5, where nuclear recoils and electrons can be identified down to 10's of keV<sub>ee</sub>, in argon. Nuclear recoils deposit less ionization than electrons at a given energy. For this reason, nuclear recoil energy is typically reported in equivalent electron energy loss, keV<sub>ee</sub>, when compared with electrons.

The composition of the drift matter is an important choice in TPC design, and the noble gasses are frequently selected as the bulk element in the mix (Table 32.3). The noble gasses have no electron affinity in the ground state, resulting in good free-electron lifetime and a good amount of scintillation that is useful for particle identification and  $t_0$  determination. In the case of argon and xenon, the low average energy to produce an ion pair results in good energy resolution. The noble gasses are easily purified to a high level that, combined with moderate cost, enables the construction of large monolithic detectors. Of the noble gasses one isotope of xenon (<sup>136</sup>Xe) is a candidate for ( $0\nu 2\beta$ ).

**Table 32.3:** Properties of the noble gasses typically used in non-accelerator TPCs [44,45].  $W$  is the average energy spent to produce one electron ion pair.

Element	$W$ (eV)	photon yield ( $\gamma$ /keV)	wave- length (nm)	decay time (fast/slow)	cost* (\$/kg)
Helium	46.0	50	80	10 ns/1.6 $\mu$ s	\$52
Neon	36.6	30	77	10 ns/3.9 $\mu$ s	\$330
Argon	26.4	40	128	4 ns/1.6 $\mu$ s	\$5
Xenon	21.7	42	175	4 ns/22 ns	\$1200

\* Prices from chemcool.com as updated in 2011.

The negative-ion TPC [46] uses an electronegative gas (*e.g.*, CS<sub>2</sub>) either as the drift gas or as a dopant to the drift gas that captures the primary electrons, forming negative ions that drift in the electric field. Upon reaching the gas-gain region of the TPC, the electron is stripped from the ion in the high electric field, and the electron avalanches in the normal manner. The larger mass of the the negative ion keeps the kinetic energy of the ion thermal at high electric fields, and therefore such a TPC exhibits far less diffusion. The reduction of diffusion over large distance (time) enables detailed tracking of small tracks in a large volume without the benefit of a magnetic field to limit diffusion (which would be prohibitively expensive for a large volume). The trade-off is orders-of-magnitude slower drift, placing a limit on the trigger rate.

### 32.5. Sub-Kelvin detectors

Written September 2009 by S. Golwala (Caltech).

Detectors operating below 1 K, also known as “low-temperature” or “cryogenic” detectors, use  $\lesssim$ meV quanta (phonons, superconducting quasiparticles) to provide better energy resolution than is typically available from conventional technologies. Such resolution can provide unique advantages to applications reliant on energy resolution, such as beta-decay experiments seeking to measure the  $\nu_e$  mass or searches for neutrinoless double-beta decay. In addition, the sub-Kelvin mode is combined with conventional (eV quanta) ionization or scintillation measurements to provide discrimination of nuclear recoils from electron recoils, critical for searches for WIMP dark matter and for coherent neutrino-nucleus scattering. We describe the techniques in generic fashion in the text and provide a list of experiments using these techniques in An excellent review [47] is available that covers this material and other applications of low-temperature detectors. The proceedings of the Low Temperature Detectors Workshops are also useful [48].

#### 32.5.1. Thermal Phonons :

The most basic kind of low-temperature detector employs a dielectric absorber coupled to a thermal bath via a weak link. A thermistor monitors the temperature of the absorber. The energy  $E$  deposited by a particle interaction causes a calorimetric temperature change by increasing the population of thermal phonons. The fundamental sensitivity is

$$\sigma_E^2 = \xi^2 kT [TC(T) + \beta E], \quad (32.5)$$

where  $C$  is the heat capacity of the detector,  $T$  is the temperature of operation,  $k$  is Boltzmann's constant, and  $\xi$  is a dimensionless factor of order unity that is precisely calculable from the nature of the thermal link and the non-thermodynamic noises (*e.g.*, Johnson and/or readout noise). The first term is imposed by statistical fluctuations in the number of thermally excited phonons and on the energy in the absorber due to exchange with the thermal bath (see, *e.g.*, Ref. 49 and references therein). The second term is due to statistical fluctuations in the number of phonons excited by the absorbed radiation. The factor  $\beta$  is also dimensionless and  $\mathcal{O}(1)$  and is also precisely calculable from the nature of the thermal link. The ratio of the second term to the first term is equal to the fractional absorber temperature change due to an energy deposition. Thus, the second term becomes appreciable when this fractional temperature change is appreciable, at which point nonlinear effects also come into play. The energy resolution typically acquires an additional energy dependence due to deviations from an ideal calorimetric model that cause position and/or energy dependence in the signal shape.

The rise time of response is limited by the internal thermal conductivity of the absorber. The decay time constant, describing the time required for the absorbed energy to flow out to the bath, is  $\tau = C/G$ , where  $G$  is the thermal conductance of the weak link. The above formula immediately suggests the use of crystalline dielectric absorbers and low temperatures because of the linear factor of  $T$  and because  $C$  for crystalline dielectrics drops as  $T^3$  for  $T$  well below the material's Debye temperature ( $\Theta_D$ , typically hundreds of K). Specifically, the Debye model indicates that a crystal consisting of  $N$  atoms has

$$C = \frac{12\pi^4}{5} N k \left( \frac{T}{\Theta_D} \right)^3 \quad (32.6)$$

which gives  $\sigma_E = 5.2\xi$  eV for 1 kg of germanium operated at  $T = 10$  mK. (For a detector of this size the 2nd term in Eq. (32.5) is negligible.) In practice, a number of factors degrade the above result by about an order of magnitude (thermistor heat capacity and power dissipation, readout noise, *etc.*), but the predicted energy resolution for such a large mass remains attractive.

Neutron-transmutation-doped (NTD) germanium and implanted silicon semiconductors are used for thermistors. Conduction is via phonon-assisted hopping between impurity sites, yielding an exponentially decreasing resistance as a function of temperature,  $R(T)$ , with negative slope,  $dR/dT$ . Attachment to the absorber is usually by eutectic bonding or epoxy or by direct implantation into the absorber. Another type of temperature sensor is the superconducting phase-transition thermometers (SPT) or transition-edge sensor (TES). A SPT or TES is a superconducting film operated in the transition from superconductive to normal resistance at the transition temperature,  $T_c$ , where its resistance is a strong function of temperature with positive  $dR/dT$ . This can provide strong electrothermal negative feedback, which improves linearity, speeds up response, and mitigates variations in  $T_c$  among multiple TESs on the same absorber. Nb<sub>x</sub>Si<sub>1-x</sub> is another thermistor material that ranges between the semiconducting and superconducting regimes as a function of the stoichiometry (defined by  $x$ ). SPTs/ TESs and Nb<sub>x</sub>Si<sub>1-x</sub> thermistors are frequently deposited directly onto the absorber by sputtering or evaporation.

The readout method depends on the type of thermometer used. Doped semiconductors typically have high impedances and are well matched to low-noise JFET-based readout while SPTs/ TESs are low-impedance devices requiring SQUID amplifiers.

**Table 32.4:** Selected experiments using sub-Kelvin detectors. The table is not exhaustive. Operation mode, detector and excitation sensor construction, baseline energy resolution, and energy resolution at a particular energy of interest  $E_0$  are given. We quote the energy and energy resolution for “total” phonon signal, where the total phonon signal includes both recoil energy and, where relevant, drift heating. Ionization and scintillation energies are normalized so that, for electron recoils, the energy in these channels is equal to the recoil energy (“electron-equivalent” energies). For scintillation energy, this is the electron-equivalent energy deposited in the target detector, not the energy received by the photon absorber. Approximate dates of operation are also given. Key to comments: “a-Si” and “a-Ge” = amorphous silicon or germanium layers in ionization electrodes. “H-a-Si” = hydrogenated amorphous silicon. “P-implanted” = phosphorous implantation. “Interdig.” = interdigitated ionization electrode design that provides some  $z$  information from ionization signal asymmetry. “Surface-event discrimination” = ability to reject events near surfaces that suffer reduced ionization yield and can be misidentified as WIMPs. “w/phonons” = using athermal phonon pulse rising edge (faster for surface events). “w/ioniz. asym.” = using the asymmetry of the ionization signal on electrodes on opposite faces of interdigitated-electrode detectors. “w/phonon asym.” = using the asymmetry of the phonon signal detected on opposite detector faces. “U” = not known by author. SuperCDMS energy resolutions have not been fully reported yet but are likely no worse than CDMS II.

Experiment	technique	substrate + mass	sensor	$\Delta E_{FWHM}$ [keV]		$E_0$ [keV]	comments
				at $E=0$	at $E_0$		
WIMP dark matter							
CDMS I (1996–2000)	thermal	Ge	NTD Ge	0.3	0.7	12	nuclear recoil
	phonon, ionization	0.16 kg	thermistor, H-a-Si/Al electrode	0.9	1.1	10.4	discrimination w/ionization yield
CDMS II (2001–2008)	athermal	Ge	tungsten	0.4	2.4	20.7	CDMS I+
	phonon, ionization	0.25 kg	TES, a-Si/Al electrode	0.7	0.8	10.4	surface-event discrimination w/phonons
SuperCDMS- SNOLAB, in develop- ment	athermal	Ge	tungsten	0.4	U	U	CDMS II+
	phonon, ionization	0.64 kg	TES, a-Si/Al interdig.	0.7	U	U	surface-event discr.w/ioniz.+ phonon $z$ asym.
EDELWEISS I (1996–2005)	thermal	Ge	NTD Ge	2.3	2.3	24.2	nuclear recoil
	phonon, ionization	0.32 kg	thermistor, a-Si/Al a-Ge/Al	1.1	1.1	10.4	discrimination w/ionization yield
EDELWEISS II (2006–)	thermal	Ge	NTD Ge	3.6	3.6	38.0	EDELWEISS I
	phonon, ionization	0.4 kg	thermistor, a-Si/Al interdig.	1.0	1.0	10.4	+surface-event discrimination w/ioniz.asym.
CRESST I (1996–2002)	athermal	Al <sub>2</sub> O <sub>3</sub>	tungsten	0.20	0.24	1.5	no NR discr.
	phonon	0.26 kg	SPT				
CRESST II (2003–)	athermal	CaWO <sub>4</sub>	tungsten	0.3	0.3	8.1	NR discr.
	phonon, scint.	0.3 kg (ZnWO <sub>4</sub> )	SPT (target and photon abs.)	1.0	3.5	10	w/scint. yield
$\alpha$ decay							
ROSEBUD (1996–)	athermal	BGO	NTD Ge	6	5500	18	$\alpha$ discr.
	phonon, scint.	46 g	thermistor (target & photon abs.)	U	U	U	w/scint. yield, first det. of <sup>209</sup> Bi $\alpha$ decay
$\beta$ decay							
Oxford <sup>63</sup> Ni (1994–1995)	athermal phonon	InSb 3.3 g	Al STJ	1.24	1.24	67	
MARE (2009–)	thermal phonon	AgReO <sub>4</sub> 0.5 mg	P-implanted Si thermistor	U	0.033	2.6	
$0\nu\beta\beta$ decay							
CUORE (2003–)	thermal phonon	TeO <sub>2</sub> * 0.75 kg	NTD Ge thermistor	U	7	2527	

\* The CUORE energy resolution is worse than can be obtained with Ge diode detectors.



### 32.5.2. Athermal Phonons and Superconducting Quasiparticles :

The advantage of thermal phonons is also a disadvantage: energy resolution degrades as  $\sqrt{M}$  where  $M$  is the detector mass. This motivates the use of athermal phonons. There are three steps in the development of the phonon signal. The recoiling particle deposits energy along its track, with the majority going directly into phonons. (A minority of the energy goes directly into scintillation and ionization. Energy deposited in ionization is recovered when the carriers recombine.) The recoil and bandgap energy scales (keV and higher, and eV, respectively) are much larger than phonon energies (meV), so the full energy spectrum of phonons is populated, with phase space favoring the most energetic phonons. However, these initial energetic phonons do not propagate because of isotopic scattering (scattering due to variations in lattice ion atomic mass, rate  $\propto \nu^4$  where  $\nu$  is the phonon frequency) and anharmonic decay (scattering wherein a single phonon splits into two phonons, rate  $\propto \nu^5$ ). Anharmonic decay downshifts the phonon spectrum, which increases the phonon mean free path, so that eventually phonons can propagate the characteristic dimension of the detector. These phonons travel quasiballistically, preserve information about the position of the parent interaction, and are not affected by an increase in detector mass (modulo the concomitant larger distance to the surface where they can be sensed). Anharmonic decay continues until a thermal distribution is reached ( $\mu\text{eV}$  at mK temperatures), which is exhibited as a thermal increase in the temperature of the detector. If one can detect the athermal phonons at the crystal surface, keep the density of such sensors fixed as the detector surface area increases with mass, and the crystals are pure enough that the athermal phonons can propagate to the surface prior to thermalization, then an increase in detector mass need not degrade energy resolution, and can in fact improve position reconstruction. Sensors for athermal phonons are similar to those for superconducting quasiparticles described below.

Another mode is detection of superconducting quasiparticles in superconducting crystals. Energy absorption breaks superconducting Cooper pairs and yields quasiparticles, electron-like excitations that can diffuse through the material and that recombine after the quasiparticle lifetime. In crystals with very large mean free path against scattering, the diffusion length (distance traveled in a quasiparticle lifetime) is large enough (mm to cm) that the quasiparticles reach the surface and can be detected, usually in a superconducting tunnel junction (STJ) or TES/SPT.

A similar technique is applied to detect athermal phonons. Athermal phonons reaching a superconducting film on the detector surface generate quasiparticles as above. Such thin films have diffusion lengths much shorter than for superconducting crystalline substrates, only of order  $100\ \mu\text{m}$  to 1 mm. Thus, the superconducting film must be segmented on this length scale and have a quasiparticle sensor for each segment. The sensors may, however, be connected in series or parallel in large groups to reduce readout channel count.

The readout for athermal phonon and quasiparticle sensing depends on the type of quasiparticle detector. Tunnel junctions match well to JFET-based readouts, while TESs/SPTs use SQUID amplifiers.

### 32.5.3. Ionization and Scintillation :

While ionization and scintillation detectors usually operate at much higher temperatures, ionization and scintillation can be measured at low temperature and can be combined with a “sub-Kelvin” technique to discriminate nuclear recoils from background interactions producing electron recoils, which is critical for WIMP searches and coherent neutrino-nucleus scattering. With ionization, such techniques are based on Lindhard theory [50], which predicts substantially reduced ionization yield for nuclear recoils relative to electron recoils. For scintillation, application of Birks’ law (Sec. 31.3.0) yields a similar prediction. (The reduced ionization or scintillation yield for nuclear recoils is frequently referred to as “quenching”.)

Specifically, consider the example of measuring thermal phonons and ionization. All the deposited energy eventually appears in the thermal phonon channel, regardless of recoil type (modulo some loss to permanent crystal defect creation). Thus, the ionization yield—the number of charge pairs detected per unit detected energy in phonons—provides a means to discriminate nuclear recoils from

electron recoils. Similar discrimination is observed with athermal phonons and ionization and with phonons and scintillation.

In semiconducting materials of sufficient purity—germanium and silicon—electron-hole pairs created by recoiling particles can be drifted to surface electrodes by applying an electric field, similar to how this is done at 77 K in high-purity germanium photon spectrometers (Sec. 31.7). There are three important differences, however, that result in the use of low fields—of order 1 V/cm—instead of the hundreds to thousands of V/cm used in 77 K detectors. First, high fields are required at 77 K to deplete the active volume of thermally excited mobile carriers. At low temperature and in crystals of purity high enough to drift ionization with negligible trapping, the population of thermally excited carriers is exponentially suppressed due to the low ambient thermal energy. Second, high fields in 77 K operation prevent trapping of drifting carriers on ionized impurities and crystalline defects and/or overcome space charge effects. At low temperatures, ionized impurities and space charge can be neutralized (using free charge created by photons from LEDs or radioactive sources) and remain in this state for minutes to hours. This reduces trapping exponentially and allows low-field drift. Third, a high field in a sub-Kelvin detector would result in a massive phonon signal from the drifting carriers, fully correlated with the ionization signal and thereby eliminating nuclear recoil discrimination. Readout of the charge signal is typically done with a conventional JFET-based transimpedance amplifier.

A number of materials that scintillate on their own (*i.e.*, without doping) continue to do so at low temperatures, including  $\text{BaF}_2$ , BGO,  $\text{CaWO}_4$ ,  $\text{ZnWO}_4$ ,  $\text{PbWO}_4$ , and other tungstates and molybdates. In and of itself, there is little advantage to a low-temperature scintillation measurement because detecting the scintillation is nontrivial, the quanta are large, and the detection efficiency is usually poor. Such techniques are pursued only in order to obtain nuclear-recoil discrimination. Conventional photodetectors do not operate at such low temperatures, so one typically detects the scintillation photons in an adjacent low-temperature detector that is thermally disconnected from but resides in an optically reflective cavity with the target detector.

## 32.6. Low-radioactivity background techniques

Written August 2009 by A. Piepke (University of Alabama).

The physics reach of low-energy rare event searches *e.g.* for dark matter, neutrino oscillations, or double beta decay is often limited by background caused by radioactivity. Depending on the chosen detector design, the separation of the physics signal from this unwanted interference can be achieved on an event-by-event basis by active event tagging, utilizing some unique event feature, or by reducing the radiation background by appropriate shielding and material selection. In both cases, the background rate is proportional to the flux of background-creating radiation. Its reduction is thus essential for realizing the full physics potential of the experiment. In this context, “low energy” may be defined as the regime of natural, anthropogenic, or cosmogenic radioactivity, all at energies up to about 10 MeV. Following the classification of [51], sources of background may be categorized into the following classes:

1. environmental radioactivity,
2. radioimpurities in detector or shielding components,
3. radon and its progeny,
4. cosmic rays,
5. neutrons from natural fission, ( $\alpha$ ,  $n$ ) reactions and from cosmic-ray muon spallation and capture.

**32.6.1. Defining the problem :** The application defines the requirements. Background goals can be as demanding as a few low-energy events per year in a ton-size detector. The strength of the physics signal to be measured can often be estimated theoretically or from limits derived by earlier experiments. The experiments are then designed for the desired signal-to-background ratio. This requires finding the right balance between clarity of measurement, ease of construction, and budget. In a practical sense, it is important to formulate background goals that are sufficient for the task at hand but doable, in a finite time. It is now standard practice to use a detector simulation to translate the background requirements into

limits for the radioactivity content of various detector components, requirements for the radiation shielding, and allowable cosmic-ray flux. This strategy allows identifying the most critical components early and the allocation of analysis and development resources accordingly. The CERN code GEANT4 is a widely used tool for this task. It contains sufficient nuclear physics to allow accurate background estimations. Custom-written event generators, modeling particle correlations in complex decay schemes, are used as well.

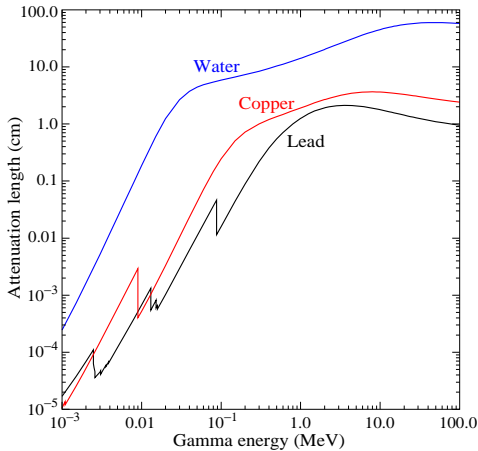


**Figure 32.6:**  $\gamma$ -ray attenuation lengths in some common shielding materials. The mass attenuation data has been taken from the NIST data base XCOM; see “Atomic Nuclear Properties” at [pdg.lbl.gov](http://pdg.lbl.gov).

**32.6.2. Environmental radioactivity:** The long-lived natural radioisotopes  $^{40}\text{K}$ ,  $^{232}\text{Th}$ , and  $^{238}\text{U}$  have average abundances of 2.4, 9.6 and 2.7 ppm in the earth’s crust, with large local variations. In most applications,  $\gamma$  radiation emitted by natural radioactivity constitutes the dominant contribution to the local radiation field. Typical low-background applications require levels of natural radioactivity on the order of ppb or ppt in the detector components. Passive or active shielding is used to suppress external  $\gamma$  radiation down to that level. Fig. 32.6 shows the energy-dependent attenuation length  $\lambda(E_\gamma)$  as a function of  $\gamma$  ray energy  $E_\gamma$  for three common shielding materials (water, copper, lead). The thickness  $\ell$  required to reduce the external flux by a factor  $f > 1$  is estimated assuming exponential damping:

$$\ell = \lambda(E_\gamma) \cdot \ln f. \quad (32.7)$$

At 100 keV, a typical energy scale for dark matter searches (or 2.615 MeV, for a typical double-beta decay experiment), attenuation by a factor  $f = 10^5$  requires 67(269) cm of  $\text{H}_2\text{O}$ , 2.8(34) cm of Cu, or 0.18(23) cm of Pb. Such estimates allows for an order-of-magnitude estimate of the experiment dimensions. A precise estimation of the leakage of external  $\gamma$  radiation, including scattering and the effect of energy cuts, requires Monte Carlo simulations and determination of the radioactivity present in the laboratory. Detailed modeling of the  $\gamma$  flux in a large laboratory, or inside hermetic shielding, needs to cope with very small detector-hit efficiencies. It is often advantageous to calculate solid angle and mass attenuation separately. This approach reduces the computation time required for a statistically meaningful number of detector hits to manageable levels.

Because of its low density, water has relatively long attenuation lengths, resulting in rather voluminous shields. However, because water can be obtained relatively cheaply in large amounts, it has become the medium of choice for most large detectors. Water purification technology is effective and commercially available, an important consideration in view of the intrinsic radioactivity of the shield, to be discussed below. High-purity water, instrumented with photo multiplier tubes, can further serve as a Cherenkov cosmic-ray veto detector. Liquefied gases are being used for shielding as well.

### 32.6.3. Radioimpurities in detector or shielding components

: After suppressing the effect of external radioactivity, radioactive impurities contained in the detector components or attached to its surfaces become important. Any material is radioactive at some level. The activity can be natural, cosmogenic, or man-made. The determination of the activity content of a specific material or component requires case-by-case analysis, and is almost never obtainable from the manufacturer. However, there are some general rules than can be used to guide the pre-selection. For detectors designed to look for electrons (for example in double-beta decay searches or neutrino detection via inverse beta decay or elastic scattering), this is the principal source of background. For devices detecting nuclear recoils (for example in dark matter searches), this is often of secondary importance as ionization signals can be actively suppressed on an event-by-event basis.

For natural radioactivity, a rule of thumb is that synthetic substances are cleaner than natural materials. Typically, more highly processed materials have lower activity content. Substances with smaller chemical reactivity tend to be cleaner. The refining process tends to remove K, Th, and U. For example, Al is often found to contain considerable amounts of Th and U, while electrolytic Cu is very low in primordial activities. Plastics or liquid hydrocarbons, having been refined by distillation, are often quite radiopure. Tabulated radioactivity screening results for a wide range of materials can be found in Refs. 52 and 53.

The long-lived  $^{238}\text{U}$  daughter  $^{210}\text{Pb}$  ( $T_{1/2}=22.3$  y) is found in all shielding lead, and is a background concern at low energies. This is due to the relatively high endpoint energy ( $Q_\beta=1.162$  MeV) of its beta-unstable daughter  $^{210}\text{Bi}$ . Lead parts made from selected low-U ores have specific activities of about 5–30 mBq/kg. For lower activity, ancient lead (for example from Roman ships) has been used. Because the ore processing and lead refining removed most of the  $^{238}\text{U}$ , the  $^{210}\text{Pb}$  decayed during the long waiting time to the level supported by the U-content of the refined lead. Lining the lead with copper to range out the low-energy radiation is another remedy. However, intermediate  $Z$  materials are an activation risk when handled above ground, as will be discussed below.  $^{210}\text{Pb}$  is also found in solders.

The fission product  $^{137}\text{Cs}$  can be found attached to the surface of materials. The radioactive noble gas  $^{85}\text{Kr}$ , released into the atmosphere by nuclear reactors and nuclear fuel re-processing, is also important, especially due to its high solubility in organic materials. Post-World War II steel typically contains a few tens of mBq/kg of  $^{60}\text{Co}$ .

Surface activity is not a material property but is added during manufacturing and handling. It can often be effectively removed by etching. Installation of low-background detectors is often done in clean rooms to avoid this contamination. Surface contamination can be quantified by means of wipe-testing with acid or alcohol wetted Whatman 41 filters. The paper filters are ashed after wiping and the residue is digested in acid. Subsequent analysis by means of mass spectroscopy or neutron activation analysis is capable of detecting less than 1 pg/cm<sup>2</sup> of Th and U. The most demanding low-rate experiments require screening of *all* components, which can be a time consuming task. The requirements for activity characterization depend on the experiment and the location and amount of a particular component. Monte Carlo simulations are used to quantify these requirements. Activities of the order  $\mu\text{Bq/kg}$  or even below may need to be detected in the process. At such level of sensitivity, the characterization becomes a challenging problem in itself. Low-background  $\alpha$ ,  $\beta$ , and  $\gamma$  ray counting, mass spectroscopy, and neutron activation analysis are used.

**32.6.4. Radon and its progeny:** The noble gas  $^{222}\text{Rn}$ , a pure  $\alpha$ -emitter, is a  $^{238}\text{U}$  decay product. Due to its half-life of 3.8 d it is released by surface soil and is found in the atmosphere everywhere.  $^{220}\text{Rn}$  ( $^{232}\text{Th}$  decay product) is unimportant because of its short half-life.  $^{222}\text{Rn}$  activity in air ranges from 10 to 100 mBq/L outdoors and 100 to thousands of mBq/L indoors. The natural radon concentration depends on the weather and shows daily and seasonal variations. Radon levels are lowest above the oceans. For electron detectors, it is not the Rn itself that creates background, but its progeny  $^{214}\text{Pb}$ ,  $^{214}\text{Bi}$ ,  $^{210}\text{Bi}$ , which emit energetic beta and  $\gamma$  radiation. Thus, not



only the detector itself has to be separated from contact with air, but also internal voids in the shield which contain air can be a background concern. Radon is quite soluble in water and even more so in organic solvents. For large liquid scintillation detectors, radon mobility due to convection and diffusion is a concern. To define a scale: typical double-beta-decay searches are disturbed by a  $\mu\text{Bq}$  (or 1/11.6 d) activity of  $^{222}\text{Rn}$  contained in the detector medium. This corresponds to a steady-state population of 0.5 atoms in 50  $\mu\text{L}$  of air (assuming 20 mBq/L of radon in the air). The criteria for leak tightness are thus quite demanding. The decay of Rn itself is a concern for some recoil type detectors, as nuclear recoil energies in  $\alpha$  decays are substantial (76 keV in case of  $^{222}\text{Rn}$ ).

Low-activity detectors are often kept sealed from the air and continuously flushed with boil-off nitrogen, which contains only small amounts of Rn. For the most demanding applications, the nitrogen is purified by multiple distillations. Then only the Rn outgassing of the piping (due to its U internal content) determines the radon concentration. Radon diffuses readily through thin plastic barriers. If the detector is to be isolated from its environment by means of a membrane, the right choice of material is important [54].

If energies below 1 MeV are to be measured, additional care has to be taken to avoid plate-out of the long-lived radon daughter  $^{210}\text{Pb}$  on the surfaces. This can be reduced by keeping the parts under a protective low-radon cover gas.

Radon can be detected even at the level of few atoms with solid state, scintillation, or gas detectors by exploiting the fast decay sequences of  $^{214}\text{Bi}$  and  $^{214}\text{Po}$ . The efficiency of these devices is sometimes boosted by electrostatic collection of charged radon into a small detector.

**32.6.5. Cosmic rays:** Cosmic radiation, discussed in detail in Chapter 26, is a source of background for just about any non-accelerator experiment. Primary cosmic rays are about 90% protons, 9% alpha particles, and the rest heavier nuclei (Fig. 26.1). They are totally attenuated within the first few  $\text{hg}/\text{cm}^2$  of atmospheric thickness. At sea level secondary particles ( $\pi^\pm : p : e^\pm : n : \mu^\pm$ ) are observed with relative intensities (1 : 13 : 340 : 480 : 1420) for  $E < 1 \text{ GeV}$  (Ref. 55; also see Fig. 26.3).

All but the muon and the neutron components are readily absorbed by overburden such as building ceilings and passive shielding. Only if there is very little overburden (less than a few  $\times 10 \text{ g cm}^{-2}$  in rock) do pions and protons need to be considered when estimating the production rate of cosmogenic radioactivity.

Sensitive experiments are thus operated deep underground where essentially only muons penetrate. As shown in Fig. 26.6, the muon intensity falls off rapidly with depth. Active detection systems capable of tagging events correlated in time with cosmic-ray activity are needed, depending on the overburden. Such experiments are described in Sec. 32.3.1.

The muonic background is only related to low-radioactivity techniques insofar as photonuclear interactions of muons can produce long-lived radioactivity. This happens at any depth, and it constitutes an essentially irreducible background.

Cosmogenic activation of components brought from the surface is also an issue. Proper management of parts and materials above ground during machining and detector assembly minimizes the accumulation of long-lived activity. Cosmogenic activation is most important for intermediate  $Z$  materials such as Cu and Fe. For the most demanding applications, metals are stored and transported under sufficient shielding to stop the hadronic component of the cosmic rays. Parts, *e.g.*, the nickel tubes for the  $^3\text{He}$  counters in SNO, can be stored underground for long periods before being used. Underground machine shops are also sometimes used to limit the duration of exposure at the surface.

**32.6.6. Neutrons:** Neutrons contribute to the background of low-energy experiments in different ways: directly through nuclear recoil in the detector medium, and indirectly, through the production of radio nuclides inside the detector and its components. The latter mechanism allows even remote materials to contribute to the background by means of penetrating  $\gamma$  radiation, since inelastic scattering of fast neutrons or radiative capture of slow neutrons can result in the emission of  $\gamma$  radiation. Neutrons are thus an important source of

low-energy background. They are produced in different ways:

1. At the earth's surface neutrons are the most frequent cosmic-ray secondaries other than muons;
2. Energetic tertiary neutrons are produced by cosmic-ray muons in nuclear spallation reactions with the detector and laboratory walls;
3. In high  $Z$  materials, often used in radiation shields, nuclear capture of negative muons results in emission of neutrons;
4. Natural radioactivity has a neutron component through spontaneous fission and  $(\alpha, n)$ -reactions.

A calculation with the hadronic simulation code FLUKA, using the known energy distribution of secondary neutrons at the earth's surface [56], yields a mass attenuation of 1.5  $\text{hg}/\text{cm}^2$  in concrete for secondary neutrons. If energy-dependent neutron-capture cross sections are known, then such calculations can be used to obtain the production rate of radio nuclides.

At an overburden of only few meters, water equivalent neutron production by muons becomes the dominant mechanism. Neutron production rates are high in high- $Z$  shielding materials. A high- $Z$  radiation shield, discussed earlier as being effective in reducing background due to external radioactivity, thus acts as a source for cosmogenic tertiary high-energy neutrons. Depending on the overburden and the radioactivity content of the laboratory, there is an optimal shielding thickness. Water shields, although bulky, are an attractive alternative due to their low neutron production yield and self-shielding.

Neutron shields made from plastic or water are commonly used to reduce the neutron flux. The shield is sometimes doped with a substance having a high thermal neutron capture cross section (such as boron) to absorb thermal neutrons more quickly. The hydrogen serves as a target for elastic scattering, and is effective in reducing the neutron energy. Neutrons from natural radioactivity have relatively low energies and can be effectively suppressed by a neutron shield. Such a neutron shield should be inside the lead to be effective for tertiary neutrons. However, this is rarely done as it increases the neutron production target (in form of the passive shield), and costs increase as the cube of the dimensions. An active cosmic-ray veto is an effective solution, correlating a neutron with its parent muon. This solution works best if the veto system is as far removed from the detector as feasible (outside the radiation shield) to correlate as many background-producing muons with neutrons as possible. The vetoed time after a muon hit needs to be sufficiently long to assure neutron thermalization. The average thermalization and capture time in lead is about 900  $\mu\text{s}$  [51]. The veto-induced deadtime, and hence muon hit rate on the veto detector, is the limiting factor for the physical size of the veto system (besides the cost). The background caused by neutron-induced radioactivity with live times exceeding the veto time cannot be addressed in this way. Moving the detector deep underground, and thus reducing the muon flux, is the only technique addressing all sources of neutron background.

#### References:

1. R.M. Baltrusaitis *et al.*, Nucl. Instrum. Methods **A20**, 410 (1985).
2. T. Abu-Zayyad *et al.*, Nucl. Instrum. Methods **A450**, 253 (2000).
3. T. Nonaka *et al.*, Nucl. Phys. B Proc. Suppl. **190**, 26, (2009).
4. J. Abraham *et al.*, [Pierre Auger Collab.], Nucl. Instrum. Methods **A620**, 227 (2010).
5. Y. Takahashi and the JEM-EUSO Collab., New J. Phys. **11**, 065009 (2009).
6. F. Arqueros, J. Hrandel, and B. Keilhauer, Nucl. Instrum. Methods **A597**, 23 (2008).
7. F. Arqueros, J. Hrandel, and B. Keilhauer, Nucl. Instrum. Methods **A597**, 1 (2008).
8. J. Boyer *et al.*, Nucl. Instrum. Methods **A482**, 457 (2002); M. Kleifges for the Pierre Auger Collab., Nucl. Instrum. Methods **A518**, 180 (2004).
9. M. Ave *et al.*, [AIRFLY Collab.], Astropart. Phys. **28**, 41 (2007).
10. J.T. Brack *et al.*, Astropart. Phys. **20**, 653, (2004).
11. B. Fick *et al.*, JINST **1**, 11003, (2006).

12. J. Abraham *et al.*, [Pierre Auger Collab.], *Astropart. Phys.* **33**, 108 (2010).
13. J. Abraham *et al.*, [Pierre Auger Collab.], *Astropart. Phys.* **34**, 368 (2011).
14. M. Unger *et al.*, *Nucl. Instrum. Methods* **A588**, 433 (2008).
15. T.K. Gaisser and A.M. Hillas, *Proc. 15th Int. Cosmic Ray Conf.* (Plovdiv, Bulgaria, 13–26 Aug. 1977).
16. J. Holder *et al.*, *Proc. 4th International Meeting on High Energy Gamma-Ray Astron.*, eds. F.A. Aharonian, W. Hofmann, and F. Rieger, *AIP Conf. Proc.* **1085**, 657 (2008).
17. J.A. Hinton, *New Astron. Rev.* **48**, 331 (2004).
18. J. Albert *et al.*, *Astrophys. J.* **674**, 1037 (2008).
19. Lectures given at the International Heraeus Summer School, “Physics with Cosmic Accelerators,” Bad Honnef, Germany, July 5–16 (2004), [astro-ph/0508253](#).
20. T.C. Weekes *et al.*, *Astrophys. J.* **342**, 379 (1989).
21. A.M. Hillas *et al.*, *Astrophys. J.* **503**, 744 (1998).
22. F.A. Aharonian, *et al.*, *Astrophys. J.* **636**, 777 (2006).
23. L.A. Bernstein *et al.*, “Report on the Depth Requirements for a Massive Detector at Homestake” (2009); [arXiv:0907.4183](#).
24. Y. Ashie *et al.*, *Phys. Rev.* **D71**, 112005 (2005).
25. S. Kasuga *et al.*, *Phys. Lett.* **B374**, 238 (1996).
26. M. Shiozawa, *Nucl. Instrum. Methods* **A433**, 240 (1999).
27. J. Hosaka *et al.*, *Phys. Rev.* **D73**, 112001 (2006).
28. J. Boger *et al.*, *Nucl. Instrum. Methods* **A449**, 172 (2000).
29. K. Griesen, *Phys. Rev. Lett.* **16**, 748 (1966); G.T. Zatsepin and V.A. Kuzmin, *JETP Lett.* **4**, 78 (1966).
30. G.A. Askaryan, *JETP* **14** 441 (1962); G.A. Askaryan *JETP* **21**, 658 (1965).
31. D. Saltzberg *et al.*, *Phys. Rev. Lett.* **86**, 2802 (2001); O. Scholten *et al.*, *J. Phys. Conf. Ser.* **81**, 012004 (2007).
32. S.R. Klein, [arXiv:1012.1407](#).
33. R.D. Dagkesamanskii and I.M. Zheleznykh, *Sov. Phys. JETP Lett.* **50**, 233 (1989).
34. P. Gorham *et al.*, *Phys. Rev. Lett.* **103** 051103 (2009). The published limit is corrected in an erratum, P. Gorham *et al.*, [arXiv:1011.5004](#).
35. P. Allison *et al.*, [arXiv:1105.2854](#); P. Allison *et al.*, *Nucl. Instrum. & Meth.* **A604**, S64 (2009); the ARA Collaboration, presented at the *2011 Intl. Cosmic Ray Conf.*
36. L. Gerhardt *et al.*, *Nucl. Instrum. Methods* **A624**, 85-91 (2010); S. Barwick, preprint [arXiv:astro-ph/0610631](#); T. Barella, S. Barwick, and D. Saltzberg, *J. Glaciology* **57**, 61 (2011).
37. S. Hoover *et al.*, *Phys. Rev. Lett.* **105**, 151101 (2010).
38. I. Kravchenko *et al.*, *Phys. Rev.* **D73**, 082002 (2006); I. Kravchenko *et al.*, *Astropart. Phys.* **19**, 15 (2003).
39. M. Schaumann, “The XENON 100 Dark Matter Experiment,” *10th Conf. on the Intersections of Part. & Nucl. Phys.*, (2009), to be published in *AIP Conf. Proc.*
40. A. Bolotnikov and B. Ramsey, *Nucl. Instrum. Methods* **A496**, 360 (1997).
41. E. Aprile *et al.*, *Phys. Rev.* **B76**, 014115 (2007).
42. C.M.B. Monteiro *et al.*, “Secondary scintillation yield in pure xenon,” *JINST* **2** P05001 (2007), doi 10.1088/1748-0221/2/05/P05001.
43. W.H. Lippincott *et al.*, *Phys. Rev.* **C78**, 035801 (2008).
44. W. Blum and L. Rolandi, *Particle Detection with Drift Chambers*, Springer-Verlag (1994).
45. R.S. Chandrasekharan, “Noble Gas Scintillation-Based Radiation Portal Monitor and Active Interrogation Systems,” *IEEE Nucl. Sci. Symposium Conference Record* (2006).
46. C.J. Martoff *et al.*, *Nucl. Instrum. Methods* **A440**, 355 (2000).
47. *Cryogenic Particle Detection*, ed. by C. Enss, (Springer-Verlag: Berlin, 2005).
48. *Proc. 13th Inter. Workshop on Low Temperature Detectors*, *AIP Conference Proc.* (2009); see also *Proceedings* of previous occurrences of this workshop.
49. S.H. Moseley, J.C. Mather, and D. McCammon, *J. Appl. Phys.* **56**, 1257 (1984).
50. J. Lindhard *et al.*, *Mat. Fys. Medd. K. Dan. Vidensk. Selsk.* **33**, 10 (1963).
51. G. Heusser, *Ann. Rev. Nucl. and Part. Sci.* **45**, 543 (1995).
52. P. Jagam and J.J. Simpson, *Nucl. Instrum. Methods* **A324**, 389 (1993).
53. D.S. Leonard *et al.*, *Nucl. Instrum. Methods* **A591**, 490 (2008).
54. M. Wojcik *et al.*, *Nucl. Instrum. Methods* **A449**, 158 (2000).
55. National Council on Radiation Protection and Measurement, Report 94, Bethesda, MD (1987).
56. M.S. Gordon *et al.*, *IEEE Trans.* **NS51**, 3427 (2004).

## 33. RADIOACTIVITY AND RADIATION PROTECTION

Revised August 2011 by S. Roesler and M. Silari (CERN).

### 33.1. Definitions [1,2]

#### 33.1.1. Physical quantities :

• **Fluence,  $\Phi$**  (unit:  $1/\text{m}^2$ ): The fluence is the quotient of  $dN$  by  $da$ , where  $dN$  is the number of particles incident upon a small sphere of cross-sectional area  $da$

$$\Phi = dN/da . \quad (33.1)$$

In dosimetric calculations, fluence is frequently expressed in terms of the lengths of the particle trajectories. It can be shown that the fluence,  $\Phi$ , is given by

$$\Phi = dl/dV,$$

where  $dl$  is the sum of the particle trajectory lengths in the volume  $dV$ .

• **Absorbed dose,  $D$**  (unit: gray,  $1 \text{ Gy}=1 \text{ J/kg}=100 \text{ rad}$ ): The absorbed dose is the energy imparted by ionizing radiation in a volume element of a specified material divided by the mass of this volume element.

• **Kerma,  $K$**  (unit: gray): Kerma is the sum of the initial kinetic energies of all charged particles liberated by indirectly ionizing radiation in a volume element of the specified material divided by the mass of this volume element.

• **Linear energy transfer,  $L$  or  $LET$**  (unit:  $\text{J/m}$ , often given in  $\text{keV}/\mu\text{m}$ ): The linear energy transfer is the mean energy,  $dE$ , lost by a charged particle owing to collisions with electrons in traversing a distance  $dl$  in matter. *Low-LET radiation*: x rays and gamma rays (accompanied by charged particles due to interactions with the surrounding medium) or light charged particles such as electrons that produce sparse ionizing events far apart at a molecular scale ( $L < 10 \text{ keV}/\mu\text{m}$ ). *High-LET radiation*: neutrons and heavy charged particles that produce ionizing events densely spaced at a molecular scale ( $L > 10 \text{ keV}/\mu\text{m}$ ).

• **Activity,  $A$**  (unit: becquerel,  $1 \text{ Bq}=1/\text{s}=27 \text{ picocurie}$ ): Activity is the expectation value of the number of nuclear decays occurring in a given quantity of material per unit time.

#### 33.1.2. Protection quantities :

Protection quantities are dose quantities developed for radiological protection that allow quantification of the extent of exposure of the human body to ionizing radiation from both whole and partial body external irradiation and from intakes of radionuclides.

• **Organ absorbed dose,  $D_T$**  (unit: gray): The mean absorbed dose in an organ or tissue  $T$  of mass  $m_T$  is defined as

$$D_T = \frac{1}{m_T} \int_{m_T} D dm .$$

• **Equivalent dose,  $H_T$**  (unit: sievert,  $1 \text{ Sv}=100 \text{ rem}$ ): The equivalent dose  $H_T$  in an organ or tissue  $T$  is equal to the sum of the absorbed doses  $D_{T,R}$  in the organ or tissue caused by different radiation types  $R$  weighted with so-called radiation weighting factors  $w_R$ :

$$H_T = \sum_R w_R \times D_{T,R} . \quad (33.2)$$

It expresses long-term risks (primarily cancer and leukemia) from low-level chronic exposure. The values for  $w_R$  recommended by ICRP [2] are given in Table 33.1.

• **Effective dose,  $E$**  (unit: sievert): The sum of the equivalent doses, weighted by the tissue weighting factors  $w_T$  ( $\sum_T w_T = 1$ ) of several organs and tissues  $T$  of the body that are considered to be most sensitive [2], is called “effective dose”:

$$E = \sum_T w_T \times H_T . \quad (33.3)$$

**Table 33.1:** Radiation weighting factors,  $w_R$ .

Radiation type	$w_R$
Photons, electrons and muons	1
Neutrons, $E_n < 1 \text{ MeV}$	$2.5 + 18.2 \times \exp[-(\ln E_n)^2/6]$
$1 \text{ MeV} \leq E_n \leq 50 \text{ MeV}$	$5.0 + 17.0 \times \exp[-(\ln(2E_n))^2/6]$
$E_n > 50 \text{ MeV}$	$2.5 + 3.25 \times \exp[-(\ln(0.04E_n))^2/6]$
Protons and charged pions	2
Alpha particles, fission fragments, heavy ions	20

#### 33.1.3. Operational quantities :

The body-related protection quantities, equivalent dose and effective dose, are not measurable in practice. Therefore, operational quantities are used for the assessment of effective dose or mean equivalent doses in tissues or organs. These quantities aim to provide a conservative estimate for the value of the protection quantity.

• **Ambient dose equivalent,  $H^*(10)$**  (unit: sievert): The dose equivalent at a point in a radiation field that would be produced by the corresponding expanded and aligned field in a 30 cm diameter sphere of unit density tissue (ICRU sphere) at a depth of 10 mm on the radius vector opposing the direction of the aligned field. Ambient dose equivalent is the operational quantity for *area monitoring*.

• **Personal dose equivalent,  $H_p(d)$**  (unit: sievert): The dose equivalent in ICRU tissue at an appropriate depth,  $d$ , below a specified point on the human body. The specified point is normally taken to be where the individual dosimeter is worn. For the assessment of effective dose,  $H_p(10)$  with a depth  $d = 10 \text{ mm}$  is chosen, and for the assessment of the dose to the skin and to the hands and feet the personal dose equivalent,  $H_p(0.07)$ , with a depth  $d = 0.07 \text{ mm}$ , is used. Personal dose equivalent is the operational quantity for *individual monitoring*.

#### 33.1.4. Dose conversion coefficients :

Dose conversion coefficients allow direct calculation of protection or operational quantities from particle fluence and are functions of particle type, energy and irradiation configuration. The most common coefficients are those for effective dose and ambient dose equivalent. The former are based on simulations in which the dose to organs of anthropomorphic phantoms is calculated for approximate actual conditions of exposure, such as irradiation of the front of the body (antero-posterior irradiation) or isotropic irradiation.

Conversion coefficients from fluence to effective dose are given for anterior-posterior irradiation and various particles in Fig. 33.1 [3]. For example, the effective dose from an anterior-posterior irradiation in a field of 1-MeV neutrons with a fluence of 1 neutron per  $\text{cm}^2$  is about 290 pSv. In Monte Carlo simulations such coefficients allow multiplication with fluence at scoring time such that effective dose to a human body at the considered location is directly obtained.

### 33.2. Radiation levels [4]

• **Natural background radiation:** On a worldwide average, the annual whole-body dose equivalent due to all sources of natural background radiation ranges from 1.0 to 13 mSv (0.1–1.3 rem) with an annual average of 2.4 mSv [5]. In certain areas values up to 50 mSv (5 rem) have been measured. A large fraction (typically more than 50%) originate from inhaled natural radioactivity, mostly radon and radon daughters. The latter can vary by more than one order of magnitude: it is 0.1–0.2 mSv in open areas, 2 mSv on average in a house and more than 20 mSv in poorly ventilated mines.

• **Cosmic ray background radiation:** At sea level, the whole-body dose equivalent due to cosmic ray background radiation is dominated by muons; at higher altitudes also nucleons contribute. Dose equivalent rates range from less than 0.1  $\mu\text{Sv/h}$  at sea level to a few  $\mu\text{Sv/h}$  at aircraft altitudes. Details on cosmic ray fluence levels are given in the Cosmic Rays section (Sec. 26 of this Review).

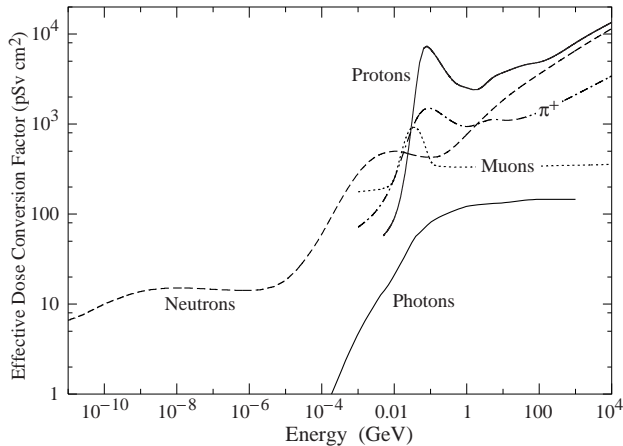


**Figure 33.1:** Fluence to effective dose conversion coefficients for anterior-posterior irradiation and various particles [3].

• **Fluence to deposit one Gy:** *Charged particles:* The fluence necessary to deposit a dose of one Gy (in units of  $\text{cm}^{-2}$ ) is about  $6.24 \times 10^9 / (dE/dx)$ , where  $dE/dx$  (in units of  $\text{MeV g}^{-1} \text{cm}^2$ ) is the mean energy loss rate that may be obtained from Figs. 30.2 and 30.4 in Sec. 30 of this *Review*, and from <http://pdg.lbl.gov/AtomicNuclearProperties>. For example, it is approximately  $3.5 \times 10^9 \text{ cm}^{-2}$  for minimum-ionizing singly-charged particles in carbon. *Photons:* This fluence is about  $6.24 \times 10^9 / (Ef/\ell)$  for photons of energy  $E$  (in MeV), an attenuation length  $\ell$  (in  $\text{g cm}^{-2}$ ), and a fraction  $f \lesssim 1$ , expressing the fraction of the photon energy deposited in a small volume of thickness  $\ll \ell$  but large enough to contain the secondary electrons. For example, it is approximately  $2 \times 10^{11} \text{ cm}^{-2}$  for 1 MeV photons on carbon ( $f \approx 1/2$ ).

### 33.3. Health effects of ionizing radiation

Radiation can cause two types of health effects, deterministic and stochastic:

- **Deterministic effects** are tissue reactions which cause injury to a population of cells if a given threshold of absorbed dose is exceeded. The severity of the reaction increases with dose. The quantity in use for tissue reactions is the absorbed dose,  $D$ . When particles other than photons and electrons (low-LET radiation) are involved, a Relative Biological Effectiveness (RBE)-weighted dose may be used. The RBE of a given radiation is the reciprocal of the ratio of the absorbed dose of that radiation to the absorbed dose of a reference radiation (usually x rays) required to produce the same degree of biological effect. It is a complex quantity that depends on many factors such as cell type, dose rate, fractionation, etc.
- **Stochastic effects** are malignant diseases and heritable effects for which the probability of an effect occurring, but not its severity, is a function of dose without threshold.
- **Lethal dose:** The whole-body dose from penetrating ionizing radiation resulting in 50% mortality in 30 days (assuming no medical treatment) is 2.5–4.5 Gy (250–450 rad)<sup>†</sup>, as measured internally on the body longitudinal center line. The surface dose varies due to variable body attenuation and may be a strong function of energy.
- **Cancer induction:** The cancer induction probability is about 5% per Sv on average for the entire population [2].
- **Recommended effective dose limits:** The International Commission on Radiological Protection (ICRP) recommends a limit for radiation workers of 20 mSv effective dose per year averaged over 5 years, with the provision that the dose should not exceed 50 mSv in any single year [2]. The limit in the EU-countries and Switzerland is 20 mSv per year, in the U.S. it is 50 mSv per year (5 rem per year). Many physics laboratories in the U.S. and elsewhere set lower limits. The effective dose limit for general public is typically 1 mSv per year.

<sup>†</sup> RBE-weighted when necessary

### 33.4. Prompt neutrons at accelerators

Neutrons dominate the particle environment outside thick shielding (e.g., > 1 m of concrete) for high energy (> a few hundred MeV) electron and hadron accelerators.

#### 33.4.1. Electron accelerators :

At electron accelerators, neutrons are generated via photonuclear reactions from bremsstrahlung photons. In the photon energy range from threshold (few MeV) to about 30 MeV, neutron production is via the Giant Dipole Resonance (GDR) mechanism. The reaction consists in a collective excitation of the nucleus, in which neutrons and protons oscillate in the direction of the photon electric field. The oscillation is damped by friction in a few cycles, with the photon energy being transferred to the nucleus in a process similar to evaporation. Nucleons emitted in the dipolar interaction have an anisotropic angular distribution, with a maximum at  $90^\circ$ , while those leaving the nucleus as a result of evaporation are emitted isotropically with a Maxwellian energy distribution described as [6]:

$$\frac{dN}{dE_n} = \frac{E_n}{T^2} e^{-E_n/T}, \quad (33.4)$$

where  $T$  is a nuclear ‘temperature’ (in units of MeV) characteristic of the particular target nucleus and its excitation energy. For heavy nuclei the ‘temperature’ generally lies in the range of  $T = 0.5\text{--}1.0$  MeV. For higher energy photons, the quasi-deuteron (between about 30 MeV and 250 MeV), delta resonance (250 MeV–1.2 GeV) and vector meson dominance ( $\gtrsim 1.2$  GeV) mechanisms become important.

Neutron yields from semi-infinite targets per kW of electron beam power are plotted in Fig. 33.2 as a function of the electron beam energy [6].

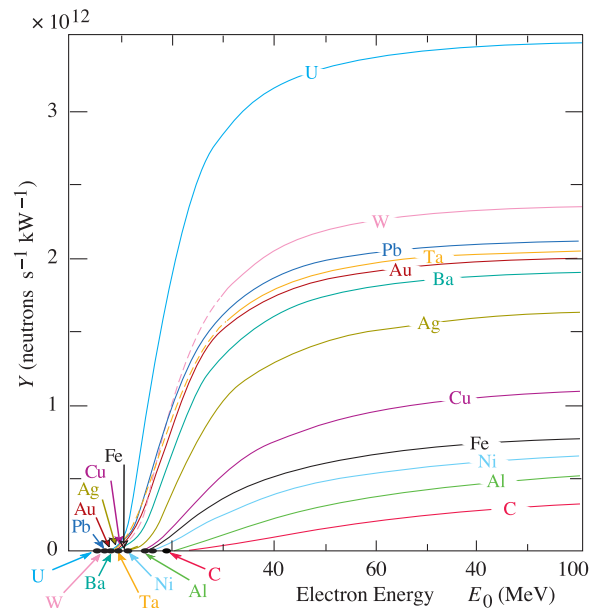


**Figure 33.2:** Neutron yields from semi-infinite targets per kW of electron beam power, as a function of the electron beam energy, disregarding target self-shielding [6].

Typical neutron energy spectra outside of concrete (80 cm thick,  $2.35 \text{ g/cm}^3$ ) and iron (40 cm thick) shields are shown in Fig. 33.3. In order to compare these spectra to those caused by proton beams (see below) the spectra are scaled by a factor of 100, which roughly corresponds to the difference in the high energy hadronic cross sections for photons and hadrons (e.g., the fine structure constant). The shape of these spectra are generally characterized by a low-energy peak at around 1 MeV (evaporation neutrons) and a high-energy shoulder at around 70–80 MeV. In case of concrete shielding, the spectrum also shows a pronounced peak at thermal neutron energies.

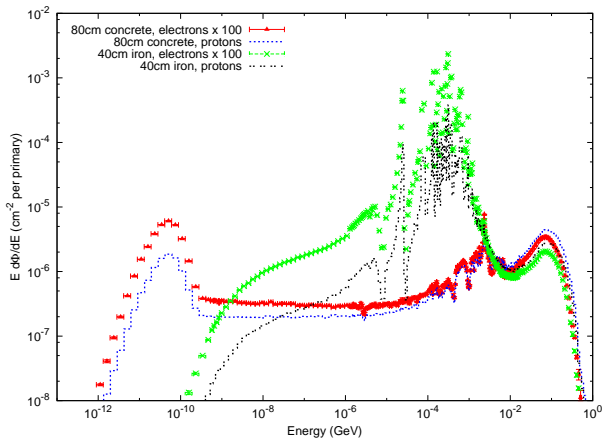


**Figure 33.3:** Neutron energy spectra calculated with the FLUKA code [7,8] from 25 GeV proton and electron beams on a thick copper target. Spectra are evaluated at 90° to the beam direction behind 80 cm of concrete or 40 cm of iron. All spectra are normalized per beam particle. In addition, spectra for electron beam are multiplied by a factor of 100.

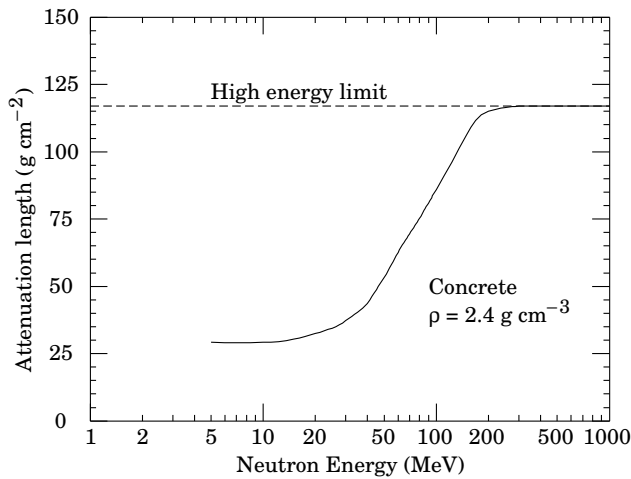


**Figure 33.4:** The variation of the attenuation length for mono-energetic neutrons in concrete as a function of neutron energy [9].

**33.4.2. Proton accelerators :**

At proton accelerators, neutron yields emitted per incident proton by different target materials are roughly independent of proton energy between 20 MeV and 1 GeV, and are given by the ratio C : Al : Cu-Fe : Sn : Ta-Pb = 0.3 : 0.6 : 1.0 : 1.5 : 1.7 [9]. Above about 1 GeV, the neutron yield is proportional to  $E^m$ , where  $0.80 \leq m \leq 0.85$  [10].

Typical neutron energy spectra outside of concrete and iron shielding are shown in Fig. 33.3. Here, the radiation fields are caused by a 25 GeV proton beam interacting with a thick copper target. The comparison of these spectra with those for an electron beam of the same energy reflects the difference in the hadronic cross sections between photons and hadrons above a few 100 MeV. Differences are increasing towards lower energies because of different interaction mechanisms. Furthermore, the slight shift in energy above about 100 MeV follows from the fact that the energies of the interacting photons are lower than 25 GeV. Apart from this the shapes of the two spectra are similar.

The neutron-attenuation length is shown in Fig. 33.4 for concrete and mono-energetic broad-beam conditions. As can be seen in the figure it reaches a value of about 117 g/cm<sup>2</sup> above 200 MeV. As the cascade through thick shielding is carried by high-energy particles this value is equal to the equilibrium attenuation length at 90 degrees in concrete.

**33.5. Photon sources**

The dose equivalent rate in tissue (in mSv/h) from a gamma point source emitting one photon of energy  $E$  (in MeV) per second at a distance of 1 m is  $4.6 \times 10^{-9} \mu_{en}/\rho E$ , where  $\mu_{en}/\rho$  is the mass energy absorption coefficient. The latter has a value of  $0.029 \pm 0.004 \text{ cm}^2/\text{g}$  for photons in tissue over an energy range between 60 keV and 2 MeV (see Ref. 11 for tabulated values).

Similarly, the dose equivalent rate in tissue (in mSv/h) at the surface of a semi-infinite slab of uniformly activated material containing 1 Bq/g of a gamma emitter of energy  $E$  (in MeV) is  $2.9 \times 10^{-4} R_\mu E$ , where  $R_\mu$  is the ratio of the mass energy absorption coefficients of the photons in tissue and in the material.

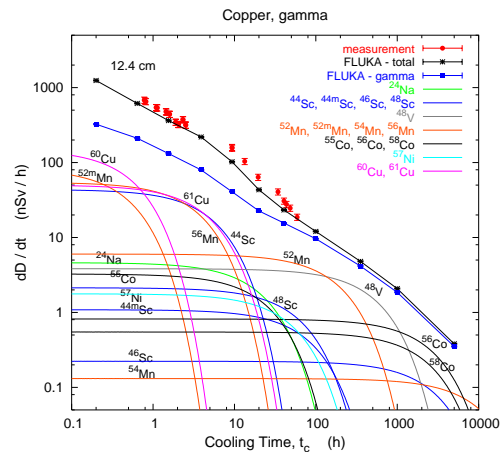


**Figure 33.5:** Contribution of individual gamma-emitting nuclides to the total dose rate at 12.4 cm distance to an activated copper sample [12].

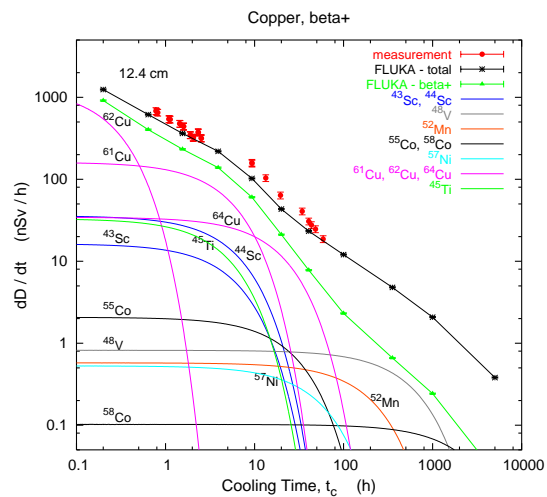


**Figure 33.6:** Contribution of individual positron-emitting nuclides to the total dose rate at 12.4 cm distance to an activated copper sample [12].

**33.6. Accelerator-induced radioactivity**

Typical medium- and long-lived activation products in metallic components of accelerators are <sup>22</sup>Na, <sup>46</sup>Sc, <sup>48</sup>V, <sup>51</sup>Cr, <sup>54</sup>Mn, <sup>55</sup>Fe, <sup>59</sup>Fe, <sup>56</sup>Co, <sup>57</sup>Co, <sup>58</sup>Co, <sup>60</sup>Co, <sup>63</sup>Ni and <sup>65</sup>Zn. Gamma-emitting nuclides dominate doses by external irradiation at longer decay times (more than one day) while at short decay times  $\beta^+$  emitters are also important (through photons produced by  $\beta^+$  annihilation). Due to their short range,  $\beta^-$  emitters are relevant, for example, only for

dose to the skin and eyes or for doses due to inhalation or ingestion. Fig. 33.5 and Fig. 33.6 show the contributions of gamma and  $\beta^+$  emitters to the total dose rate at 12.4 cm distance to an activated copper sample [12]. Typically, dose rates at a certain decay time are mainly determined by radionuclides having a half-life of the order of the decay time. Extended irradiation periods might be an exception to this general rule as in this case the activity of long-lived nuclides can build up sufficiently so that it dominates that one of short-lived even at short cooling times.

Activation in concrete is dominated by  $^{24}\text{Na}$  (short decay times) and  $^{22}\text{Na}$  (long decay times). Both nuclides can be produced either by low-energy neutron reactions on the sodium-component in the concrete or by spallation reactions on silicon and calcium. At long decay times nuclides of radiological interest in activated concrete can also be  $^{60}\text{Co}$ ,  $^{152}\text{Eu}$ ,  $^{154}\text{Eu}$  and  $^{134}\text{Cs}$ , all of which produced by  $(n,\gamma)$ -reactions with traces of natural cobalt, europium and cesium. Thus, such trace elements might be important even if their content in concrete is only a few parts per million or less by weight.

The explicit simulation of radionuclide production with general-purpose Monte Carlo codes has become the most commonly applied method to calculate induced radioactivity and its radiological consequences. Nevertheless, other more approximative approaches, such as “ $\omega$ -factors” [9], can still be useful for fast order-of-magnitude estimates. These  $\omega$ -factors give the dose rate per unit star density (inelastic reactions above a certain energy threshold, e.g. 50 MeV) on contact to an extended, uniformly activated object after a 30-day irradiation and 1-day decay. For steel or iron,  $\omega \simeq 3 \times 10^{-12}$  (Sv  $\text{cm}^3/\text{star}$ ). This does not include possible contributions from thermal-neutron activation.

#### References:

1. International Commission on Radiation Units and Measurements, *Fundamental Quantities and Units for Ionizing Radiation*, ICRU Report 60 (1998).
2. ICRP Publication 103, *The 2007 Recommendations of the International Commission on Radiological Protection*, Annals of the ICRP, Elsevier (2007).
3. M. Pelliccioni, *Radiation Protection Dosimetry* **88**, 279 (2000).
4. E. Pochin, *Nuclear Radiation: Risks and Benefits*, Clarendon Press, Oxford, 1983.
5. United Nations, *Report of the United Nations Scientific Committee on the Effect of Atomic Radiation*, General Assembly, Official Records A/63/46 (2008).
6. W.P. Swanson, *Radiological Safety Aspects of the Operation of Electron Linear Accelerators*, IAEA Technical Reports Series No. 188 (1979).
7. A. Ferrari, *et al.*, FLUKA, A Multi-particle Transport Code (Program Version 2005), CERN-2005-010 (2005).
8. G. Battistoni, *et al.*, The FLUKA code: Description and benchmarking, *Proceedings of the Hadronic Shower Simulation Workshop 2006*, Fermilab 6–8 September 2006, M. Albrow, R. Raja, eds., *AIP Conference Proceeding 896*, 31–49, (2007).
9. R.H. Thomas and G.R. Stevenson, *Radiological Safety Aspects of the Operation of Proton Accelerators*, IAEA Technical Report Series No. 283 (1988).
10. T.A. Gabriel, *et al.*, *Nucl. Instrum. Methods* **A338**, 336 (1994).
11. <http://physics.nist.gov/PhysRefData/XrayMassCoef/cover.html>.
12. S. Roesler, *et al.*, “Simulation of Remanent Dose Rates and Benchmark Measurements at the CERN-EU High Energy Reference Field Facility,” in *Proceedings of the Sixth International Meeting on Nuclear Applications of Accelerator Technology*, San Diego, CA, 1-5 June 2003, 655–662 (2003).

## 34. COMMONLY USED RADIOACTIVE SOURCES

Table 34.1. Revised November 1993 by E. Browne (LBNL).

Nuclide	Half-life	Particle			Photon	
		Type of decay	Energy (MeV)	Emission prob.	Energy (MeV)	Emission prob.
$^{22}_{11}\text{Na}$	2.603 y	$\beta^+$ , EC	0.545	90%	0.511 Annih. 1.275 100%	
$^{54}_{25}\text{Mn}$	0.855 y	EC			0.835 100% Cr K x rays 26%	
$^{55}_{26}\text{Fe}$	2.73 y	EC			Mn K x rays: 0.00590 24.4% 0.00649 2.86%	
$^{57}_{27}\text{Co}$	0.744 y	EC			0.014 9% 0.122 86% 0.136 11% Fe K x rays 58%	
$^{60}_{27}\text{Co}$	5.271 y	$\beta^-$	0.316	100%	1.173 100% 1.333 100%	
$^{68}_{32}\text{Ge}$	0.742 y	EC			Ga K x rays 44%	
-----						
$\rightarrow ^{68}_{31}\text{Ga}$		$\beta^+$ , EC	1.899	90%	0.511 Annih. 1.077 3%	
$^{90}_{38}\text{Sr}$	28.5 y	$\beta^-$	0.546	100%		
-----						
$\rightarrow ^{90}_{39}\text{Y}$		$\beta^-$	2.283	100%		
$^{106}_{44}\text{Ru}$	1.020 y	$\beta^-$	0.039	100%		
-----						
$\rightarrow ^{106}_{45}\text{Rh}$		$\beta^-$	3.541	79%	0.512 21% 0.622 10%	
$^{109}_{48}\text{Cd}$	1.267 y	EC	0.063 $e^-$ 0.084 $e^-$ 0.087 $e^-$	41% 45% 9%	0.088 3.6% Ag K x rays 100%	
$^{113}_{50}\text{Sn}$	0.315 y	EC	0.364 $e^-$ 0.388 $e^-$	29% 6%	0.392 65% In K x rays 97%	
$^{137}_{55}\text{Cs}$	30.2 y	$\beta^-$	0.514 1.176	94% 6%	0.662 85%	
$^{133}_{56}\text{Ba}$	10.54 y	EC	0.045 $e^-$ 0.075 $e^-$	50% 6%	0.081 34% 0.356 62% Cs K x rays 121%	
$^{207}_{83}\text{Bi}$	31.8 y	EC	0.481 $e^-$ 0.975 $e^-$ 1.047 $e^-$	2% 7% 2%	0.569 98% 1.063 75% 1.770 7% Pb K x rays 78%	
$^{228}_{90}\text{Th}$	1.912 y	$6\alpha$ : $3\beta^-$ :	5.341 to 8.785 0.334 to 2.246		0.239 44% 0.583 31% 2.614 36%	
-----						
$(\rightarrow ^{224}_{88}\text{Ra} \rightarrow ^{220}_{86}\text{Rn} \rightarrow ^{216}_{84}\text{Po} \rightarrow ^{212}_{82}\text{Pb} \rightarrow ^{212}_{83}\text{Bi} \rightarrow ^{212}_{84}\text{Po})$						
$^{241}_{95}\text{Am}$	432.7 y	$\alpha$	5.443 5.486	13% 85%	0.060 36% Np L x rays 38%	
$^{241}\text{Am/Be}$	432.2 y	$6 \times 10^{-5}$ neutrons (4–8 MeV) and $4 \times 10^{-5}$ $\gamma$ 's (4.43 MeV) per Am decay				
$^{244}_{96}\text{Cm}$	18.11 y	$\alpha$	5.763 5.805	24% 76%	Pu L x rays $\sim$ 9%	
$^{252}_{98}\text{Cf}$	2.645 y	$\alpha$ (97%) Fission (3.1%)	6.076 6.118	15% 82%		
-----						
$\approx 20$ $\gamma$ 's/fission; 80% < 1 MeV $\approx 4$ neutrons/fission; $\langle E_n \rangle = 2.14$ MeV						

“Emission probability” is the probability per decay of a given emission; because of cascades these may total more than 100%. Only principal emissions are listed. EC means electron capture, and  $e^-$  means monoenergetic internal conversion (Auger) electron. The intensity of 0.511 MeV  $e^+e^-$  annihilation photons depends upon the number of stopped positrons. Endpoint  $\beta^\pm$  energies are listed. In some cases when energies are closely spaced, the  $\gamma$ -ray values are approximate weighted averages. Radiation from short-lived daughter isotopes is included where relevant.

Half-lives, energies, and intensities are from E. Browne and R.B. Firestone, *Table of Radioactive Isotopes* (John Wiley & Sons, New York, 1986), recent *Nuclear Data Sheets*, and *X-ray and Gamma-ray Standards for Detector Calibration*, IAEA-TECDOC-619 (1991).

Neutron data are from *Neutron Sources for Basic Physics and Applications* (Pergamon Press, 1983).

## 35. PROBABILITY

Revised September 2011 by G. Cowan (RHUL).

## 35.1. General [1–8]

An abstract definition of probability can be given by considering a set  $S$ , called the sample space, and possible subsets  $A, B, \dots$ , the interpretation of which is left open. The probability  $P$  is a real-valued function defined by the following axioms due to Kolmogorov [9]:

1. For every subset  $A$  in  $S$ ,  $P(A) \geq 0$ ;
2. For disjoint subsets (*i.e.*,  $A \cap B = \emptyset$ ),  $P(A \cup B) = P(A) + P(B)$ ;
3.  $P(S) = 1$ .

In addition, one defines the conditional probability  $P(A|B)$  (read  $P$  of  $A$  given  $B$ ) as

$$P(A|B) = \frac{P(A \cap B)}{P(B)}. \quad (35.1)$$

From this definition and using the fact that  $A \cap B$  and  $B \cap A$  are the same, one obtains *Bayes' theorem*,

$$P(A|B) = \frac{P(B|A)P(A)}{P(B)}. \quad (35.2)$$

From the three axioms of probability and the definition of conditional probability, one obtains the *law of total probability*,

$$P(B) = \sum_i P(B|A_i)P(A_i), \quad (35.3)$$

for any subset  $B$  and for disjoint  $A_i$  with  $\cup_i A_i = S$ . This can be combined with Bayes' theorem (Eq. (35.2)) to give

$$P(A|B) = \frac{P(B|A)P(A)}{\sum_i P(B|A_i)P(A_i)}, \quad (35.4)$$

where the subset  $A$  could, for example, be one of the  $A_i$ .

The most commonly used interpretation of the subsets of the sample space are outcomes of a repeatable experiment. The probability  $P(A)$  is assigned a value equal to the limiting frequency of occurrence of  $A$ . This interpretation forms the basis of *frequentist statistics*.

The subsets of the sample space can also be interpreted as *hypotheses*, *i.e.*, statements that are either true or false, such as ‘The mass of the  $W$  boson lies between 80.3 and 80.5 GeV.’ In the frequency interpretation, such statements are either always or never true, *i.e.*, the corresponding probabilities would be 0 or 1. Using *subjective probability*, however,  $P(A)$  is interpreted as the degree of belief that the hypothesis  $A$  is true. Subjective probability is used in *Bayesian* (as opposed to frequentist) statistics. Bayes' theorem can be written

$$P(\text{theory}|\text{data}) \propto P(\text{data}|\text{theory})P(\text{theory}), \quad (35.5)$$

where ‘theory’ represents some hypothesis and ‘data’ is the outcome of the experiment. Here  $P(\text{theory})$  is the *prior* probability for the theory, which reflects the experimenter's degree of belief before carrying out the measurement, and  $P(\text{data}|\text{theory})$  is the probability to have gotten the data actually obtained, given the theory, which is also called the *likelihood*.

Bayesian statistics provides no fundamental rule for obtaining the prior probability, which may depend on previous measurements, theoretical prejudices, *etc.* Once this has been specified, however, Eq. (35.5) tells how the probability for the theory must be modified in the light of the new data to give the *posterior* probability,  $P(\text{theory}|\text{data})$ . As Eq. (35.5) is stated as a proportionality, the probability must be normalized by summing (or integrating) over all possible hypotheses.

## 35.2. Random variables

A *random variable* is a numerical characteristic assigned to an element of the sample space. In the frequency interpretation of probability, it corresponds to an outcome of a repeatable experiment. Let  $x$  be a possible outcome of an observation. If  $x$  can take on any value from a continuous range, we write  $f(x; \theta)dx$  as the probability that the measurement's outcome lies between  $x$  and  $x + dx$ . The function  $f(x; \theta)$  is called the *probability density function* (p.d.f.), which may depend on one or more parameters  $\theta$ . If  $x$  can take on only discrete values (*e.g.*, the non-negative integers), then  $f(x; \theta)$  is itself a probability.

The p.d.f. is always normalized to unit area (unit sum, if discrete). Both  $x$  and  $\theta$  may have multiple components and are then often written as vectors. If  $\theta$  is unknown, we may wish to estimate its value from a given set of measurements of  $x$ ; this is a central topic of *statistics* (see Sec. 36).

The *cumulative distribution function*  $F(a)$  is the probability that  $x \leq a$ :

$$F(a) = \int_{-\infty}^a f(x) dx. \quad (35.6)$$

Here and below, if  $x$  is discrete-valued, the integral is replaced by a sum. The endpoint  $a$  is expressly included in the integral or sum. Then  $0 \leq F(x) \leq 1$ ,  $F(x)$  is nondecreasing, and  $P(a < x \leq b) = F(b) - F(a)$ . If  $x$  is discrete,  $F(x)$  is flat except at allowed values of  $x$ , where it has discontinuous jumps equal to  $f(x)$ .

Any function of random variables is itself a random variable, with (in general) a different p.d.f. The *expectation value* of any function  $u(x)$  is

$$E[u(x)] = \int_{-\infty}^{\infty} u(x) f(x) dx, \quad (35.7)$$

assuming the integral is finite. For  $u(x)$  and  $v(x)$ , any two functions of  $x$ ,  $E[u + v] = E[u] + E[v]$ . For  $c$  and  $k$  constants,  $E[cu + k] = cE[u] + k$ .

The  $n^{\text{th}}$  moment of a random variable  $x$  is

$$\alpha_n \equiv E[x^n] = \int_{-\infty}^{\infty} x^n f(x) dx, \quad (35.8a)$$

and the  $n^{\text{th}}$  central moment of  $x$  (or moment about the mean,  $\alpha_1$ ) is

$$m_n \equiv E[(x - \alpha_1)^n] = \int_{-\infty}^{\infty} (x - \alpha_1)^n f(x) dx. \quad (35.8b)$$

The most commonly used moments are the mean  $\mu$  and variance  $\sigma^2$ :

$$\mu \equiv \alpha_1, \quad (35.9a)$$

$$\sigma^2 \equiv V[x] \equiv m_2 = \alpha_2 - \mu^2. \quad (35.9b)$$

The mean is the location of the ‘center of mass’ of the p.d.f., and the variance is a measure of the square of its width. Note that  $V[cx + k] = c^2V[x]$ . It is often convenient to use the *standard deviation* of  $x$ ,  $\sigma$ , defined as the square root of the variance.

Any odd moment about the mean is a measure of the skewness of the p.d.f. The simplest of these is the dimensionless coefficient of skewness  $\gamma_1 = m_3/\sigma^3$ .

The fourth central moment  $m_4$  provides a convenient measure of the tails of a distribution. For the Gaussian distribution (see Sec. 35.4), one has  $m_4 = 3\sigma^4$ . The *kurtosis* is defined as  $\gamma_2 = m_4/\sigma^4 - 3$ , *i.e.*, it is zero for a Gaussian, positive for a *leptokurtic* distribution with longer tails, and negative for a *platykurtic* distribution with tails that die off more quickly than those of a Gaussian.

The *quantile*  $x_\alpha$  is the value of the random variable  $x$  at which the cumulative distribution is equal to  $\alpha$ . That is, the quantile is the inverse of the cumulative distribution function, *i.e.*,  $x_\alpha = F^{-1}(\alpha)$ . An important special case is the *median*,  $x_{\text{med}}$ , defined by  $F(x_{\text{med}}) = 1/2$ , *i.e.*, half the probability lies above and half lies below  $x_{\text{med}}$ . (More rigorously,  $x_{\text{med}}$  is a median if  $P(x \geq x_{\text{med}}) \geq 1/2$  and  $P(x \leq x_{\text{med}}) \geq 1/2$ . If only one value exists, it is called ‘the median.’)

Under a monotonic change of variable  $x \rightarrow y(x)$ , the quantiles of a distribution (and hence also the median) obey  $y_\alpha = y(x_\alpha)$ . In



general the expectation value and *mode* (most probable value) of a distribution do not, however, transform in this way.

Let  $x$  and  $y$  be two random variables with a *joint* p.d.f.  $f(x, y)$ . The *marginal* p.d.f. of  $x$  (the distribution of  $x$  with  $y$  unobserved) is

$$f_1(x) = \int_{-\infty}^{\infty} f(x, y) dy, \tag{35.10}$$

and similarly for the marginal p.d.f.  $f_2(y)$ . The *conditional* p.d.f. of  $y$  given fixed  $x$  (with  $f_1(x) \neq 0$ ) is defined by  $f_3(y|x) = f(x, y)/f_1(x)$ , and similarly  $f_4(x|y) = f(x, y)/f_2(y)$ . From these, we immediately obtain Bayes' theorem (see Eqs. (35.2) and (35.4)),

$$f_4(x|y) = \frac{f_3(y|x)f_1(x)}{f_2(y)} = \frac{f_3(y|x)f_1(x)}{\int f_3(y|x')f_1(x') dx'}. \tag{35.11}$$

The mean of  $x$  is

$$\mu_x = \int_{-\infty}^{\infty} \int_{-\infty}^{\infty} x f(x, y) dx dy = \int_{-\infty}^{\infty} x f_1(x) dx, \tag{35.12}$$

and similarly for  $y$ . The *covariance* of  $x$  and  $y$  is

$$\text{cov}[x, y] = E[(x - \mu_x)(y - \mu_y)] = E[xy] - \mu_x \mu_y. \tag{35.13}$$

A dimensionless measure of the covariance of  $x$  and  $y$  is given by the *correlation coefficient*,

$$\rho_{xy} = \text{cov}[x, y] / \sigma_x \sigma_y, \tag{35.14}$$

where  $\sigma_x$  and  $\sigma_y$  are the standard deviations of  $x$  and  $y$ . It can be shown that  $-1 \leq \rho_{xy} \leq 1$ .

Two random variables  $x$  and  $y$  are *independent* if and only if

$$f(x, y) = f_1(x)f_2(y). \tag{35.15}$$

If  $x$  and  $y$  are independent, then  $\rho_{xy} = 0$ ; the converse is not necessarily true. If  $x$  and  $y$  are independent,  $E[u(x)v(y)] = E[u(x)]E[v(y)]$ , and  $V[x + y] = V[x] + V[y]$ ; otherwise,  $V[x + y] = V[x] + V[y] + 2\text{cov}[x, y]$ , and  $E[uv]$  does not necessarily factorize.

Consider a set of  $n$  continuous random variables  $\mathbf{x} = (x_1, \dots, x_n)$  with joint p.d.f.  $f(\mathbf{x})$ , and a set of  $n$  new variables  $\mathbf{y} = (y_1, \dots, y_n)$ , related to  $\mathbf{x}$  by means of a function  $\mathbf{y}(\mathbf{x})$  that is one-to-one, *i.e.*, the inverse  $\mathbf{x}(\mathbf{y})$  exists. The joint p.d.f. for  $\mathbf{y}$  is given by

$$g(\mathbf{y}) = f(\mathbf{x}(\mathbf{y}))|J|, \tag{35.16}$$

where  $|J|$  is the absolute value of the determinant of the square matrix  $J_{ij} = \partial x_i / \partial y_j$  (the Jacobian determinant). If the transformation from  $\mathbf{x}$  to  $\mathbf{y}$  is not one-to-one, the  $\mathbf{x}$ -space must be broken into regions where the function  $\mathbf{y}(\mathbf{x})$  can be inverted, and the contributions to  $g(\mathbf{y})$  from each region summed.

Given a set of functions  $\mathbf{y} = (y_1, \dots, y_m)$  with  $m < n$ , one can construct  $n - m$  additional independent functions, apply the procedure above, then integrate the resulting  $g(\mathbf{y})$  over the unwanted  $y_i$  to find the marginal distribution of those of interest.

For a one-to-one transformation of discrete random variables, simply substitute; no Jacobian is necessary because now  $f$  is a probability rather than a probability density. If the transformation is not one-to-one, then sum the probabilities for all values of the original variable that contribute to a given value of the transformed variable. If  $f$  depends on a set of parameters  $\theta$ , a change to a different parameter set  $\eta(\theta)$  is made by simple substitution; no Jacobian is used.

### 35.3. Characteristic functions

The characteristic function  $\phi(u)$  associated with the p.d.f.  $f(x)$  is essentially its Fourier transform, or the expectation value of  $e^{iux}$ :

$$\phi(u) = E[e^{iux}] = \int_{-\infty}^{\infty} e^{iux} f(x) dx. \tag{35.17}$$

Once  $\phi(u)$  is specified, the p.d.f.  $f(x)$  is uniquely determined and vice versa; knowing one is equivalent to the other. Characteristic functions are useful in deriving a number of important results about moments and sums of random variables.

It follows from Eqs. (35.8a) and (35.17) that the  $n^{\text{th}}$  moment of a random variable  $x$  that follows  $f(x)$  is given by

$$i^{-n} \left. \frac{d^n \phi}{du^n} \right|_{u=0} = \int_{-\infty}^{\infty} x^n f(x) dx = \alpha_n. \tag{35.18}$$

Thus it is often easy to calculate all the moments of a distribution defined by  $\phi(u)$ , even when  $f(x)$  cannot be written down explicitly.

If the p.d.f.s  $f_1(x)$  and  $f_2(y)$  for independent random variables  $x$  and  $y$  have characteristic functions  $\phi_1(u)$  and  $\phi_2(u)$ , then the characteristic function of the weighted sum  $ax + by$  is  $\phi_1(au)\phi_2(bu)$ . The rules of addition for several important distributions (*e.g.*, that the sum of two Gaussian distributed variables also follows a Gaussian distribution) easily follow from this observation.

Let the (partial) characteristic function corresponding to the conditional p.d.f.  $f_2(x|z)$  be  $\phi_2(u|z)$ , and the p.d.f. of  $z$  be  $f_1(z)$ . The characteristic function after integration over the conditional value is

$$\phi(u) = \int \phi_2(u|z)f_1(z) dz. \tag{35.19}$$

Suppose we can write  $\phi_2$  in the form

$$\phi_2(u|z) = A(u)e^{ig(u)z}. \tag{35.20}$$

Then

$$\phi(u) = A(u)\phi_1(g(u)). \tag{35.21}$$

The cumulants (semi-invariants)  $\kappa_n$  of a distribution with characteristic function  $\phi(u)$  are defined by the relation

$$\phi(u) = \exp \left[ \sum_{n=1}^{\infty} \frac{\kappa_n}{n!} (iu)^n \right] = \exp \left( i\kappa_1 u - \frac{1}{2}\kappa_2 u^2 + \dots \right). \tag{35.22}$$

The values  $\kappa_n$  are related to the moments  $\alpha_n$  and  $m_n$ . The first few relations are

$$\begin{aligned} \kappa_1 &= \alpha_1 (= \mu, \text{ the mean}) \\ \kappa_2 &= m_2 = \alpha_2 - \alpha_1^2 (= \sigma^2, \text{ the variance}) \\ \kappa_3 &= m_3 = \alpha_3 - 3\alpha_1\alpha_2 + 2\alpha_1^3. \end{aligned} \tag{35.23}$$

### 35.4. Some probability distributions

Table 35.1 gives a number of common probability density functions and corresponding characteristic functions, means, and variances. Further information may be found in Refs. [1–8], [17], and [11], which has particularly detailed tables. Monte Carlo techniques for generating each of them may be found in our Sec. 37.4 and in Ref. 17. We comment below on all except the trivial uniform distribution.

#### 35.4.1. Binomial distribution :

A random process with exactly two possible outcomes which occur with fixed probabilities is called a *Bernoulli* process. If the probability of obtaining a certain outcome (a “success”) in an individual trial is  $p$ , then the probability of obtaining exactly  $r$  successes ( $r = 0, 1, 2, \dots, N$ ) in  $N$  independent trials, without regard to the order of the successes and failures, is given by the binomial distribution  $f(r; N, p)$  in Table 35.1. If  $r$  and  $s$  are binomially distributed with parameters  $(N_r, p)$  and  $(N_s, p)$ , then  $t = r + s$  follows a binomial distribution with parameters  $(N_r + N_s, p)$ .

**Table 35.1.** Some common probability density functions, with corresponding characteristic functions and means and variances. In the Table,  $\Gamma(k)$  is the gamma function, equal to  $(k - 1)!$  when  $k$  is an integer;  ${}_1F_1$  is the confluent hypergeometric function of the 1st kind [11].

Distribution	Probability density function $f$ (variable; parameters)	Characteristic function $\phi(u)$	Mean	Variance $\sigma^2$
Uniform	$f(x; a, b) = \begin{cases} 1/(b - a) & a \leq x \leq b \\ 0 & \text{otherwise} \end{cases}$	$\frac{e^{ibu} - e^{iau}}{(b - a)iu}$	$\frac{a + b}{2}$	$\frac{(b - a)^2}{12}$
Binomial	$f(r; N, p) = \frac{N!}{r!(N - r)!} p^r q^{N-r}$ $r = 0, 1, 2, \dots, N; \quad 0 \leq p \leq 1; \quad q = 1 - p$	$(q + pe^{iu})^N$	$Np$	$Npq$
Poisson	$f(n; \nu) = \frac{\nu^n e^{-\nu}}{n!}; \quad n = 0, 1, 2, \dots; \quad \nu > 0$	$\exp[\nu(e^{iu} - 1)]$	$\nu$	$\nu$
Normal (Gaussian)	$f(x; \mu, \sigma^2) = \frac{1}{\sigma\sqrt{2\pi}} \exp(-(x - \mu)^2/2\sigma^2)$ $-\infty < x < \infty; \quad -\infty < \mu < \infty; \quad \sigma > 0$	$\exp(i\mu u - \frac{1}{2}\sigma^2 u^2)$	$\mu$	$\sigma^2$
Multivariate Gaussian	$f(\mathbf{x}; \boldsymbol{\mu}, V) = \frac{1}{(2\pi)^n \sqrt{ V }} \times \exp[-\frac{1}{2}(\mathbf{x} - \boldsymbol{\mu})^T V^{-1}(\mathbf{x} - \boldsymbol{\mu})]$ $-\infty < x_j < \infty; \quad -\infty < \mu_j < \infty; \quad  V  > 0$	$\exp[i\boldsymbol{\mu} \cdot \mathbf{u} - \frac{1}{2}\mathbf{u}^T V \mathbf{u}]$	$\boldsymbol{\mu}$	$V_{jk}$
$\chi^2$	$f(z; n) = \frac{z^{n/2-1} e^{-z/2}}{2^{n/2} \Gamma(n/2)}; \quad z \geq 0$	$(1 - 2iu)^{-n/2}$	$n$	$2n$
Student's $t$	$f(t; n) = \frac{1}{\sqrt{n\pi}} \frac{\Gamma[(n+1)/2]}{\Gamma(n/2)} \left(1 + \frac{t^2}{n}\right)^{-(n+1)/2}$ $-\infty < t < \infty; \quad n$ not required to be integer	—	0 for $n > 1$	$n/(n - 2)$ for $n > 2$
Gamma	$f(x; \lambda, k) = \frac{x^{k-1} \lambda^k e^{-\lambda x}}{\Gamma(k)}; \quad 0 \leq x < \infty;$ $k$ not required to be integer	$(1 - iu/\lambda)^{-k}$	$k/\lambda$	$k/\lambda^2$
Beta	$f(x; \alpha, \beta) = \frac{\Gamma(\alpha + \beta)}{\Gamma(\alpha)\Gamma(\beta)} x^{\alpha-1} (1 - x)^{\beta-1}$ $0 \leq x \leq 1$	${}_1F_1(\alpha; \alpha + \beta; iu)$	$\frac{\alpha}{\alpha + \beta}$	$\frac{\alpha\beta}{(\alpha + \beta)^2(\alpha + \beta + 1)}$

**35.4.2. Poisson distribution :**

The Poisson distribution  $f(n; \nu)$  gives the probability of finding exactly  $n$  events in a given interval of  $x$  (e.g., space or time) when the events occur independently of one another and of  $x$  at an average rate of  $\nu$  per the given interval. The variance  $\sigma^2$  equals  $\nu$ . It is the limiting case  $p \rightarrow 0, N \rightarrow \infty, Np = \nu$  of the binomial distribution. The Poisson distribution approaches the Gaussian distribution for large  $\nu$ .

For example, a large number of radioactive nuclei of a given type will result in a certain number of decays in a fixed time interval. If this interval is small compared to the mean lifetime, then the probability for a given nucleus to decay is small, and thus the number of decays in the time interval is well modeled as a Poisson variable.

**35.4.3. Normal or Gaussian distribution :**

The normal (or Gaussian) probability density function  $f(x; \mu, \sigma^2)$  given in Table 35.1 has mean  $E[x] = \mu$  and variance  $V[x] = \sigma^2$ . Comparison of the characteristic function  $\phi(u)$  given in Table 35.1 with Eq. (35.22) shows that all cumulants  $\kappa_n$  beyond  $\kappa_2$  vanish; this is a unique property of the Gaussian distribution. Some other properties are:

$P(x \text{ in range } \mu \pm \sigma) = 0.6827,$   
 $P(x \text{ in range } \mu \pm 0.6745\sigma) = 0.5,$   
 $E[|x - \mu|] = \sqrt{2/\pi}\sigma = 0.7979\sigma,$   
 half-width at half maximum =  $\sqrt{2 \ln 2}\sigma = 1.177\sigma.$

For a Gaussian with  $\mu = 0$  and  $\sigma^2 = 1$  (the *standard* Gaussian), the cumulative distribution, Eq. (35.6), is related to the error function  $\text{erf}(y)$  by

$$F(x; 0, 1) = \frac{1}{2} \left[ 1 + \text{erf}(x/\sqrt{2}) \right]. \tag{35.24}$$

The error function and standard Gaussian are tabulated in many references (e.g., Ref. [11,12]) and are available in software packages such as ROOT [5]. For a mean  $\mu$  and variance  $\sigma^2$ , replace  $x$  by  $(x - \mu)/\sigma$ . The probability of  $x$  in a given range can be calculated with Eq. (36.55).

For  $x$  and  $y$  independent and normally distributed,  $z = ax + by$  follows  $f(z; a\mu_x + b\mu_y, a^2\sigma_x^2 + b^2\sigma_y^2)$ ; that is, the weighted means and variances add.

The Gaussian derives its importance in large part from the *central limit theorem*:

If independent random variables  $x_1, \dots, x_n$  are distributed according to *any* p.d.f. with finite mean and variance, then the sum  $y = \sum_{i=1}^n x_i$  will have a p.d.f. that approaches a Gaussian for large  $n$ . If the p.d.f.s of the  $x_i$  are not identical, the theorem still holds under somewhat more restrictive conditions. The mean and variance are given by the sums of corresponding terms from the individual  $x_i$ . Therefore, the sum of a large number of fluctuations  $x_i$  will be distributed as a Gaussian, even if the  $x_i$  themselves are not.

(Note that the *product* of a large number of random variables is not Gaussian, but its logarithm is. The p.d.f. of the product is *log-normal*. See Ref. 8 for details.)

For a set of  $n$  Gaussian random variables  $\mathbf{x}$  with means  $\boldsymbol{\mu}$  and covariances  $V_{ij} = \text{cov}[x_i, x_j]$ , the p.d.f. for the one-dimensional

Gaussian is generalized to

$$f(\mathbf{x}; \boldsymbol{\mu}, V) = \frac{1}{(2\pi)^{n/2} \sqrt{|V|}} \exp \left[ -\frac{1}{2} (\mathbf{x} - \boldsymbol{\mu})^T V^{-1} (\mathbf{x} - \boldsymbol{\mu}) \right], \quad (35.25)$$

where the determinant  $|V|$  must be greater than 0. For diagonal  $V$  (independent variables),  $f(\mathbf{x}; \boldsymbol{\mu}, V)$  is the product of the p.d.f.s of  $n$  Gaussian distributions. For  $n = 2$ ,  $f(\mathbf{x}; \boldsymbol{\mu}, V)$  is

$$f(x_1, x_2; \mu_1, \mu_2, \sigma_1, \sigma_2, \rho) = \frac{1}{2\pi\sigma_1\sigma_2\sqrt{1-\rho^2}} \times \exp \left\{ \frac{-1}{2(1-\rho^2)} \left[ \frac{(x_1 - \mu_1)^2}{\sigma_1^2} - \frac{2\rho(x_1 - \mu_1)(x_2 - \mu_2)}{\sigma_1\sigma_2} + \frac{(x_2 - \mu_2)^2}{\sigma_2^2} \right] \right\}. \quad (35.26)$$

The characteristic function for the multivariate Gaussian is

$$\phi(\mathbf{u}; \boldsymbol{\mu}, V) = \exp \left[ i\boldsymbol{\mu} \cdot \mathbf{u} - \frac{1}{2} \mathbf{u}^T V \mathbf{u} \right]. \quad (35.27)$$

If the components of  $\mathbf{x}$  are independent, then Eq. (35.27) is the product of the c.f.s of  $n$  Gaussians.

For a multi-dimensional Gaussian distribution for variables  $x_i$ ,  $i = 1, \dots, n$ , the marginal distribution for any single  $x_i$  is a one-dimensional Gaussian with mean  $\mu_i$  and variance  $V_{ii}$ .  $V$  is  $n \times n$ , symmetric, and positive definite. For any vector  $\mathbf{X}$ , the quadratic form  $\mathbf{X}^T V^{-1} \mathbf{X} = C$ , where  $C$  is any positive number, traces an  $n$ -dimensional ellipsoid as  $\mathbf{X}$  varies. If  $X_i = x_i - \mu_i$ , then  $C$  is a random variable obeying the  $\chi^2$  distribution with  $n$  degrees of freedom, discussed in the following section. The probability that  $\mathbf{X}$  corresponding to a set of Gaussian random variables  $x_i$  lies outside the ellipsoid characterized by a given value of  $C$  ( $= \chi^2$ ) is given by  $1 - F_{\chi^2}(C; n)$ , where  $F_{\chi^2}$  is the cumulative  $\chi^2$  distribution. This may be read from Fig. 36.1. For example, the “ $s$ -standard-deviation ellipsoid” occurs at  $C = s^2$ . For the two-variable case ( $n = 2$ ), the point  $\mathbf{X}$  lies outside the one-standard-deviation ellipsoid with 61% probability. The use of these ellipsoids as indicators of probable error is described in Sec. 36.3.2.4; the validity of those indicators assumes that  $\boldsymbol{\mu}$  and  $V$  are correct.

#### 35.4.4. $\chi^2$ distribution :

If  $x_1, \dots, x_n$  are independent Gaussian random variables, the sum  $z = \sum_{i=1}^n (x_i - \mu_i)^2 / \sigma_i^2$  follows the  $\chi^2$  p.d.f. with  $n$  degrees of freedom, which we denote by  $\chi^2(n)$ . More generally, for  $n$  correlated Gaussian variables as components of a vector  $\mathbf{X}$  with covariance matrix  $V$ ,  $z = \mathbf{X}^T V^{-1} \mathbf{X}$  follows  $\chi^2(n)$  as in the previous section. For a set of  $z_i$ , each of which follows  $\chi^2(n_i)$ ,  $\sum z_i$  follows  $\chi^2(\sum n_i)$ . For large  $n$ , the  $\chi^2$  p.d.f. approaches a Gaussian with a mean and variance give by  $\mu = n$  and  $\sigma^2 = 2n$ , respectively (here the formulae for  $\mu$  and  $\sigma^2$  are valid for all  $n$ ).

The  $\chi^2$  p.d.f. is often used in evaluating the level of compatibility between observed data and a hypothesis for the p.d.f. that the data might follow. This is discussed further in Sec. 36.2.2 on tests of goodness-of-fit.

#### 35.4.5. Student's $t$ distribution :

Suppose that  $y$  and  $x_1, \dots, x_n$  are independent and Gaussian distributed with mean 0 and variance 1. We then define

$$z = \sum_{i=1}^n x_i^2 \quad \text{and} \quad t = \frac{y}{\sqrt{z/n}}. \quad (35.28)$$

The variable  $z$  thus follows a  $\chi^2(n)$  distribution. Then  $t$  is distributed according to Student's  $t$  distribution with  $n$  degrees of freedom,  $f(t; n)$ , given in Table 35.1.

The Student's  $t$  distribution resembles a Gaussian but has wider tails. As  $n \rightarrow \infty$ , the distribution approaches a Gaussian. If  $n = 1$ , it is a *Cauchy* or *Breit-Wigner* distribution. This distribution is symmetric about zero (its mode), but the expectation value is undefined. For the Student's  $t$ , the mean is well defined only for  $n > 1$  and the variance is finite only for  $n > 2$ , so the central limit theorem is

not applicable to sums of random variables following the  $t$  distribution for  $n = 1$  or 2.

As an example, consider the *sample mean*  $\bar{x} = \sum x_i/n$  and the *sample variance*  $s^2 = \sum (x_i - \bar{x})^2 / (n - 1)$  for normally distributed  $x_i$  with unknown mean  $\mu$  and variance  $\sigma^2$ . The sample mean has a Gaussian distribution with a variance  $\sigma^2/n$ , so the variable  $(\bar{x} - \mu) / \sqrt{\sigma^2/n}$  is normal with mean 0 and variance 1. The quantity  $(n - 1)s^2 / \sigma^2$  is independent of this and follows  $\chi^2(n - 1)$ . The ratio

$$t = \frac{(\bar{x} - \mu) / \sqrt{\sigma^2/n}}{\sqrt{(n - 1)s^2 / \sigma^2(n - 1)}} = \frac{\bar{x} - \mu}{\sqrt{s^2/n}} \quad (35.29)$$

is distributed as  $f(t; n - 1)$ . The unknown variance  $\sigma^2$  cancels, and  $t$  can be used to test the hypothesis that the true mean is some particular value  $\mu$ .

In Table 35.1,  $n$  in  $f(t; n)$  is not required to be an integer. A Student's  $t$  distribution with non-integral  $n > 0$  is useful in certain applications.

#### 35.4.6. Gamma distribution :

For a process that generates events as a function of  $x$  (e.g., space or time) according to a Poisson distribution, the distance in  $x$  from an arbitrary starting point (which may be some particular event) to the  $k^{\text{th}}$  event follows a *gamma* distribution,  $f(x; \lambda, k)$ . The Poisson parameter  $\mu$  is  $\lambda$  per unit  $x$ . The special case  $k = 1$  (i.e.,  $f(x; \lambda, 1) = \lambda e^{-\lambda x}$ ) is called the *exponential* distribution. A sum of  $k'$  exponential random variables  $x_i$  is distributed as  $f(\sum x_i; \lambda, k')$ .

The parameter  $k$  is not required to be an integer. For  $\lambda = 1/2$  and  $k = n/2$ , the gamma distribution reduces to the  $\chi^2(n)$  distribution.

#### 35.4.7. Beta distribution :

The beta distribution describes a continuous random variable  $x$  in the interval  $[0, 1]$ ; this can easily be generalized by scaling and translation to have arbitrary endpoints. In Bayesian inference about the parameter  $p$  of a binomial process, if the prior p.d.f. is a beta distribution  $f(p; \alpha, \beta)$  then the observation of  $r$  successes out of  $N$  trials gives a posterior beta distribution  $f(p; r + \alpha, N - r + \beta)$  (Bayesian methods are discussed further in Sec. 36). The uniform distribution is a beta distribution with  $\alpha = \beta = 1$ .

#### References:

1. H. Cramér, *Mathematical Methods of Statistics*, (Princeton Univ. Press, New Jersey, 1958).
2. A. Stuart and J.K. Ord, *Kendall's Advanced Theory of Statistics*, Vol. 1 *Distribution Theory* 6th Ed., (Halsted Press, New York, 1994), and earlier editions by Kendall and Stuart.
3. F.E. James, *Statistical Methods in Experimental Physics*, 2nd Ed., (World Scientific, Singapore, 2006).
4. L. Lyons, *Statistics for Nuclear and Particle Physicists*, (Cambridge University Press, New York, 1986).
5. B.R. Roe, *Probability and Statistics in Experimental Physics*, 2nd Ed., (Springer, New York, 2001).
6. R.J. Barlow, *Statistics: A Guide to the Use of Statistical Methods in the Physical Sciences*, (John Wiley, New York, 1989).
7. S. Brandt, *Data Analysis*, 3rd Ed., (Springer, New York, 1999).
8. G. Cowan, *Statistical Data Analysis*, (Oxford University Press, Oxford, 1998).
9. A.N. Kolmogorov, *Grundbegriffe der Wahrscheinlichkeitsrechnung*, (Springer, Berlin, 1933); *Foundations of the Theory of Probability*, 2nd Ed., (Chelsea, New York 1956).
10. Ch. Walck, *Hand-book on Statistical Distributions for Experimentalists*, University of Stockholm Internal Report SUF-PFY/96-01, available from [www.physto.se/~walck](http://www.physto.se/~walck).
11. M. Abramowitz and I. Stegun, eds., *Handbook of Mathematical Functions*, (Dover, New York, 1972).
12. F.W.J. Olver et al., eds., *NIST Handbook of Mathematical Functions*, (Cambridge University Press, 2010); a companion Digital Library of Mathematical Functions is available at [dlmf.nist.gov](http://dlmf.nist.gov).
13. Rene Brun and Fons Rademakers, *Nucl. Inst. Meth. A* **389**, 81 (1997); see also [root.cern.ch](http://root.cern.ch).
14. The CERN Program Library (CERNLIB); see [cernlib.web.cern.ch/cernlib](http://cernlib.web.cern.ch/cernlib).

## 36. STATISTICS

Revised September 2011 by G. Cowan (RHUL).

This chapter gives an overview of statistical methods used in high-energy physics. In statistics, we are interested in using a given sample of data to make inferences about a probabilistic model, *e.g.*, to assess the model's validity or to determine the values of its parameters. There are two main approaches to statistical inference, which we may call frequentist and Bayesian. In frequentist statistics, probability is interpreted as the frequency of the outcome of a repeatable experiment. The most important tools in this framework are parameter estimation, covered in Section 36.1, and statistical tests, discussed in Section 36.2. Frequentist confidence intervals, which are constructed so as to cover the true value of a parameter with a specified probability, are treated in Section 36.3.2. Note that in frequentist statistics one does not define a probability for a hypothesis or for a parameter.

Frequentist statistics provides the usual tools for reporting the outcome of an experiment objectively, without needing to incorporate prior beliefs concerning the parameter being measured or the theory being tested. As such, they are used for reporting most measurements and their statistical uncertainties in high-energy physics.

In Bayesian statistics, the interpretation of probability is more general and includes *degree of belief* (called subjective probability). One can then speak of a probability density function (p.d.f.) for a parameter, which expresses one's state of knowledge about where its true value lies. Bayesian methods allow for a natural way to input additional information, which in general may be subjective; in fact they *require* the *prior* p.d.f. as input for the parameters, *i.e.*, the degree of belief about the parameters' values before carrying out the measurement. Using Bayes' theorem Eq. (35.4), the prior degree of belief is updated by the data from the experiment. Bayesian methods for interval estimation are discussed in Sections 36.3.1 and 36.3.2.6

Bayesian techniques are often used to treat systematic uncertainties, where the author's beliefs about, say, the accuracy of the measuring device may enter. Bayesian statistics also provides a useful framework for discussing the validity of different theoretical interpretations of the data. This aspect of a measurement, however, will usually be treated separately from the reporting of the result. In some analyses, both the frequentist and Bayesian approaches are used together. One may, for example, treat systematic uncertainties in a model using Bayesian methods, but then construct a frequentist statistical test of that model.

For many inference problems, the frequentist and Bayesian approaches give similar numerical answers, even though they are based on fundamentally different interpretations of probability. For small data samples, however, and for measurements of a parameter near a physical boundary, the different approaches may yield different results, so we are forced to make a choice. For a discussion of Bayesian vs. non-Bayesian methods, see references written by a statistician [1], by a physicist [2], or the more detailed comparison in Ref. 3.

Following common usage in physics, the word "error" is often used in this chapter to mean "uncertainty." More specifically it can indicate the size of an interval as in "the standard error" or "error propagation," where the term refers to the standard deviation of an estimator.

### 36.1. Parameter estimation

Here we review *point estimation* of parameters, first with an overview of the frequentist approach and its two most important methods, maximum likelihood and least squares, treated in Sections 36.1.2 and 36.1.3. The Bayesian approach is outlined in Sec. 36.1.4.

An estimator  $\hat{\theta}$  (written with a hat) is a function of the data used to estimate the value of the parameter  $\theta$ . Sometimes the word 'estimate' is used to denote the value of the estimator when evaluated with given data. There is no fundamental rule dictating how an estimator must be constructed. One tries, therefore, to choose that estimator which has the best properties. The most important of these are (a) *consistency*, (b) *bias*, (c) *efficiency*, and (d) *robustness*.

(a) An estimator is said to be *consistent* if the estimate  $\hat{\theta}$  converges to the true value  $\theta$  as the amount of data increases. This property is so important that it is possessed by all commonly used estimators.

(b) The *bias*,  $b = E[\hat{\theta}] - \theta$ , is the difference between the expectation value of the estimator and the true value of the parameter.

The expectation value is taken over a hypothetical set of similar experiments in which  $\hat{\theta}$  is constructed in the same way. When  $b = 0$ , the estimator is said to be unbiased. The bias depends on the chosen metric, *i.e.*, if  $\hat{\theta}$  is an unbiased estimator of  $\theta$ , then  $\hat{\theta}^2$  is not in general an unbiased estimator for  $\theta^2$ . If we have an estimate  $\hat{b}$  for the bias, we can subtract it from  $\hat{\theta}$  to obtain a new  $\hat{\theta}' = \hat{\theta} - \hat{b}$ . The estimate  $\hat{b}$  may, however, be subject to statistical or systematic uncertainties that are larger than the bias itself, so that the new  $\hat{\theta}'$  may not be better than the original.

(c) *Efficiency* is the ratio of the minimum possible variance for any estimator of  $\theta$  to the variance  $V[\hat{\theta}]$  of the estimator actually used. Under rather general conditions, the minimum variance is given by the Rao-Cramér-Frechet bound,

$$\sigma_{\min}^2 = \left(1 + \frac{\partial b}{\partial \theta}\right)^2 / I(\theta), \quad (36.1)$$

where

$$I(\theta) = E \left[ \left( \frac{\partial}{\partial \theta} \sum_i \ln f(x_i; \theta) \right)^2 \right] \quad (36.2)$$

is the *Fisher information*. The sum is over all data, assumed independent, and distributed according to the p.d.f.  $f(x; \theta)$ ,  $b$  is the bias, if any, and the allowed range of  $x$  must not depend on  $\theta$ .

The *mean-squared error*,

$$\text{MSE} = E[(\hat{\theta} - \theta)^2] = V[\hat{\theta}] + b^2, \quad (36.3)$$

is a measure of an estimator's quality which combines bias and variance.

(d) *Robustness* is the property of being insensitive to departures from assumptions in the p.d.f., *e.g.*, owing to uncertainties in the distribution's tails.

Simultaneously optimizing for all the measures of estimator quality described above can lead to conflicting requirements. For example, there is in general a trade-off between bias and variance. For some common estimators, the properties above are known exactly. More generally, it is possible to evaluate them by Monte Carlo simulation. Note that they will often depend on the unknown  $\theta$ .

#### 36.1.1. Estimators for mean, variance and median :

Suppose we have a set of  $N$  independent measurements,  $x_i$ , assumed to be unbiased measurements of the same unknown quantity  $\mu$  with a common, but unknown, variance  $\sigma^2$ . Then

$$\hat{\mu} = \frac{1}{N} \sum_{i=1}^N x_i \quad (36.4)$$

$$\hat{\sigma}^2 = \frac{1}{N-1} \sum_{i=1}^N (x_i - \hat{\mu})^2 \quad (36.5)$$

are unbiased estimators of  $\mu$  and  $\sigma^2$ . The variance of  $\hat{\mu}$  is  $\sigma^2/N$  and the variance of  $\hat{\sigma}^2$  is

$$V[\hat{\sigma}^2] = \frac{1}{N} \left( m_4 - \frac{N-3}{N-1} \sigma^4 \right), \quad (36.6)$$

where  $m_4$  is the 4th central moment of  $x$ . For Gaussian distributed  $x_i$ , this becomes  $2\sigma^4/(N-1)$  for any  $N \geq 2$ , and for large  $N$ , the standard deviation of  $\hat{\sigma}$  (the "error of the error") is  $\sigma/\sqrt{2N}$ . Again, if the  $x_i$  are Gaussian,  $\hat{\mu}$  is an efficient estimator for  $\mu$ , and the estimators  $\hat{\mu}$  and  $\hat{\sigma}^2$  are uncorrelated. Otherwise the arithmetic mean (36.4) is not necessarily the most efficient estimator; this is discussed further in Sec. 8.7 of Ref. 4.

If  $\sigma^2$  is known, it does not improve the estimate  $\hat{\mu}$ , as can be seen from Eq. (36.4); however, if  $\mu$  is known, substitute it for  $\hat{\mu}$  in Eq. (36.5) and replace  $N-1$  by  $N$  to obtain an estimator of  $\sigma^2$  still

with zero bias but smaller variance. If the  $x_i$  have different, known variances  $\sigma_i^2$ , then the weighted average

$$\hat{\mu} = \frac{1}{w} \sum_{i=1}^N w_i x_i \quad (36.7)$$

is an unbiased estimator for  $\mu$  with a smaller variance than an unweighted average; here  $w_i = 1/\sigma_i^2$  and  $w = \sum_i w_i$ . The standard deviation of  $\hat{\mu}$  is  $1/\sqrt{w}$ .

As an estimator for the median  $x_{\text{med}}$ , one can use the value  $\hat{x}_{\text{med}}$  such that half the  $x_i$  are below and half above (the sample median). If the sample median lies between two observed values, it is set by convention halfway between them. If the p.d.f. of  $x$  has the form  $f(x - \mu)$  and  $\mu$  is both mean and median, then for large  $N$  the variance of the sample median approaches  $1/[4Nf^2(0)]$ , provided  $f(0) > 0$ . Although estimating the median can often be more difficult computationally than the mean, the resulting estimator is generally more robust, as it is insensitive to the exact shape of the tails of a distribution.

### 36.1.2. The method of maximum likelihood :

Suppose we have a set of  $N$  measured quantities  $\mathbf{x} = (x_1, \dots, x_N)$  described by a joint p.d.f.  $f(\mathbf{x}; \boldsymbol{\theta})$ , where  $\boldsymbol{\theta} = (\theta_1, \dots, \theta_n)$  is set of  $n$  parameters whose values are unknown. The *likelihood function* is given by the p.d.f. evaluated with the data  $\mathbf{x}$ , but viewed as a function of the parameters, *i.e.*,  $L(\boldsymbol{\theta}) = f(\mathbf{x}; \boldsymbol{\theta})$ . If the measurements  $x_i$  are statistically independent and each follow the p.d.f.  $f(x; \boldsymbol{\theta})$ , then the joint p.d.f. for  $\mathbf{x}$  factorizes and the likelihood function is

$$L(\boldsymbol{\theta}) = \prod_{i=1}^N f(x_i; \boldsymbol{\theta}). \quad (36.8)$$

The method of maximum likelihood takes the estimators  $\hat{\boldsymbol{\theta}}$  to be those values of  $\boldsymbol{\theta}$  that maximize  $L(\boldsymbol{\theta})$ .

Note that the likelihood function is *not* a p.d.f. for the parameters  $\boldsymbol{\theta}$ ; in frequentist statistics this is not defined. In Bayesian statistics, one can obtain the posterior p.d.f. for  $\boldsymbol{\theta}$  from the likelihood, but this requires multiplying by a prior p.d.f. (see Sec. 36.3.1).

It is usually easier to work with  $\ln L$ , and since both are maximized for the same parameter values  $\boldsymbol{\theta}$ , the maximum likelihood (ML) estimators can be found by solving the *likelihood equations*,

$$\frac{\partial \ln L}{\partial \theta_i} = 0, \quad i = 1, \dots, n. \quad (36.9)$$

Often the solution must be found numerically. Maximum likelihood estimators are important because they are approximately unbiased and efficient for large data samples, under quite general conditions, and the method has a wide range of applicability.

In evaluating the likelihood function, it is important that any normalization factors in the p.d.f. that involve  $\boldsymbol{\theta}$  be included. However, we will only be interested in the maximum of  $L$  and in ratios of  $L$  at different values of the parameters; hence any multiplicative factors that do not involve the parameters that we want to estimate may be dropped, including factors that depend on the data but not on  $\boldsymbol{\theta}$ .

Under a one-to-one change of parameters from  $\boldsymbol{\theta}$  to  $\boldsymbol{\eta}$ , the ML estimators  $\hat{\boldsymbol{\theta}}$  transform to  $\boldsymbol{\eta}(\hat{\boldsymbol{\theta}})$ . That is, the ML solution is invariant under change of parameter. However, other properties of ML estimators, in particular the bias, are not invariant under change of parameter.

The inverse  $V^{-1}$  of the covariance matrix  $V_{ij} = \text{cov}[\hat{\theta}_i, \hat{\theta}_j]$  for a set of ML estimators can be estimated by using

$$(\hat{V}^{-1})_{ij} = - \frac{\partial^2 \ln L}{\partial \theta_i \partial \theta_j} \Big|_{\hat{\boldsymbol{\theta}}}. \quad (36.10)$$

For finite samples, however, Eq. (36.10) can result in an underestimate of the variances. In the large sample limit (or in a linear model with Gaussian errors),  $L$  has a Gaussian form and  $\ln L$  is (hyper)parabolic. In this case, it can be seen that a numerically equivalent way of

determining  $s$ -standard-deviation errors is from the contour given by the  $\boldsymbol{\theta}'$  such that

$$\ln L(\boldsymbol{\theta}') = \ln L_{\text{max}} - s^2/2, \quad (36.11)$$

where  $\ln L_{\text{max}}$  is the value of  $\ln L$  at the solution point (compare with Eq. (36.58)). The extreme limits of this contour on the  $\theta_i$  axis give an approximate  $s$ -standard-deviation confidence interval for  $\theta_i$  (see Section 36.3.2.4).

In the case where the size  $n$  of the data sample  $x_1, \dots, x_n$  is small, the unbinned maximum likelihood method, *i.e.*, use of equation (36.8), is preferred since binning can only result in a loss of information, and hence larger statistical errors for the parameter estimates. The sample size  $n$  can be regarded as fixed, or the analyst can choose to treat it as a Poisson-distributed variable; this latter option is sometimes called “extended maximum likelihood” (see, *e.g.*, Refs. [6–8]).

If the sample is large, it can be convenient to bin the values in a histogram, so that one obtains a vector of data  $\mathbf{n} = (n_1, \dots, n_N)$  with expectation values  $\boldsymbol{\nu} = E[\mathbf{n}]$  and probabilities  $f(\mathbf{n}; \boldsymbol{\nu})$ . Then one may maximize the likelihood function based on the contents of the bins (so  $i$  labels bins). This is equivalent to maximizing the likelihood ratio  $\lambda(\boldsymbol{\theta}) = f(\mathbf{n}; \boldsymbol{\nu}(\boldsymbol{\theta}))/f(\mathbf{n}; \mathbf{n})$ , or to minimizing the equivalent quantity  $-2 \ln \lambda(\boldsymbol{\theta})$ . For independent Poisson distributed  $n_i$  this is [9]

$$-2 \ln \lambda(\boldsymbol{\theta}) = 2 \sum_{i=1}^N \left[ \nu_i(\boldsymbol{\theta}) - n_i + n_i \ln \frac{n_i}{\nu_i(\boldsymbol{\theta})} \right], \quad (36.12)$$

where for bins with  $n_i = 0$ , the last term in (36.12) is zero. The expression (36.12) without the terms  $\nu_i - n_i$  also gives  $-2 \ln \lambda(\boldsymbol{\theta})$  for multinomially distributed  $n_i$ , *i.e.*, when the total number of entries is regarded as fixed. In the limit of zero bin width, maximizing (36.12) is equivalent to maximizing the unbinned likelihood function (36.8).

A benefit of binning is that it allows for a goodness-of-fit test (see Sec. 36.2.2). Assuming the model is correct, then according to Wilks’ theorem, for sufficiently large  $\nu_i$  and providing certain regularity conditions are met, the minimum of  $-2 \ln \lambda$  as defined by Eq. (36.12) follows a  $\chi^2$  distribution (see, *e.g.*, Ref. 3). If there are  $N$  bins and  $m$  fitted parameters, then the number of degrees of freedom for the  $\chi^2$  distribution is  $N - m$  if the data are treated as Poisson-distributed, and  $N - m - 1$  if the  $n_i$  are multinomially distributed.

Suppose the  $n_i$  are Poisson-distributed and the overall normalization  $\nu_{\text{tot}} = \sum_i \nu_i$  is taken as an adjustable parameter, so that  $\nu_i = \nu_{\text{tot}} p_i(\boldsymbol{\theta})$ , where the probability to be in the  $i$ th bin,  $p_i(\boldsymbol{\theta})$ , does not depend on  $\nu_{\text{tot}}$ . Then by minimizing Eq. (36.12), one obtains that the area under the fitted function is equal to the sum of the histogram contents, *i.e.*,  $\sum_i \nu_i = \sum_i n_i$ . This is not the case for parameter estimation methods based on a least-squares procedure with traditional weights (see, *e.g.*, Ref. 8).

### 36.1.3. The method of least squares :

The *method of least squares* (LS) coincides with the method of maximum likelihood in the following special case. Consider a set of  $N$  independent measurements  $y_i$  at known points  $x_i$ . The measurement  $y_i$  is assumed to be Gaussian distributed with mean  $F(x_i; \boldsymbol{\theta})$  and known variance  $\sigma_i^2$ . The goal is to construct estimators for the unknown parameters  $\boldsymbol{\theta}$ . The likelihood function contains the sum of squares

$$\chi^2(\boldsymbol{\theta}) = -2 \ln L(\boldsymbol{\theta}) + \text{constant} = \sum_{i=1}^N \frac{(y_i - F(x_i; \boldsymbol{\theta}))^2}{\sigma_i^2}. \quad (36.13)$$

The set of parameters  $\boldsymbol{\theta}$  which maximize  $L$  is the same as those which minimize  $\chi^2$ .

The minimum of Equation (36.13) defines the least-squares estimators  $\hat{\boldsymbol{\theta}}$  for the more general case where the  $y_i$  are not Gaussian distributed as long as they are independent. If they are not independent but rather have a covariance matrix  $V_{ij} = \text{cov}[y_i, y_j]$ , then the LS estimators are determined by the minimum of

$$\chi^2(\boldsymbol{\theta}) = (\mathbf{y} - \mathbf{F}(\boldsymbol{\theta}))^T V^{-1} (\mathbf{y} - \mathbf{F}(\boldsymbol{\theta})), \quad (36.14)$$

where  $\mathbf{y} = (y_1, \dots, y_N)$  is the vector of measurements,  $\mathbf{F}(\boldsymbol{\theta})$  is the corresponding vector of predicted values (understood as a column vector in (36.14)), and the superscript  $T$  denotes the transposed (*i.e.*, row) vector.

In many practical cases, one further restricts the problem to the situation where  $F(x_i; \boldsymbol{\theta})$  is a linear function of the parameters, *i.e.*,

$$F(x_i; \boldsymbol{\theta}) = \sum_{j=1}^m \theta_j h_j(x_i). \tag{36.15}$$

Here the  $h_j(x)$  are  $m$  linearly independent functions, *e.g.*,  $1, x, x^2, \dots, x^{m-1}$ , or Legendre polynomials. We require  $m < N$  and at least  $m$  of the  $x_i$  must be distinct.

Minimizing  $\chi^2$  in this case with  $m$  parameters reduces to solving a system of  $m$  linear equations. Defining  $H_{ij} = h_j(x_i)$  and minimizing  $\chi^2$  by setting its derivatives with respect to the  $\theta_i$  equal to zero gives the LS estimators,

$$\hat{\boldsymbol{\theta}} = (H^T V^{-1} H)^{-1} H^T V^{-1} \mathbf{y} \equiv D \mathbf{y}. \tag{36.16}$$

The covariance matrix for the estimators  $U_{ij} = \text{cov}[\hat{\theta}_i, \hat{\theta}_j]$  is given by

$$U = D V D^T = (H^T V^{-1} H)^{-1}, \tag{36.17}$$

or equivalently, its inverse  $U^{-1}$  can be found from

$$(U^{-1})_{ij} = \frac{1}{2} \frac{\partial^2 \chi^2}{\partial \theta_i \partial \theta_j} \Big|_{\boldsymbol{\theta}=\hat{\boldsymbol{\theta}}} = \sum_{k,l=1}^N h_i(x_k) (V^{-1})_{kl} h_j(x_l). \tag{36.18}$$

The LS estimators can also be found from the expression

$$\hat{\boldsymbol{\theta}} = U \mathbf{g}, \tag{36.19}$$

where the vector  $\mathbf{g}$  is defined by

$$g_i = \sum_{j,k=1}^N y_j h_i(x_k) (V^{-1})_{jk}. \tag{36.20}$$

For the case of uncorrelated  $y_i$ , for example, one can use (36.19) with

$$(U^{-1})_{ij} = \sum_{k=1}^N \frac{h_i(x_k) h_j(x_k)}{\sigma_k^2}, \tag{36.21}$$

$$g_i = \sum_{k=1}^N \frac{y_k h_i(x_k)}{\sigma_k^2}. \tag{36.22}$$

Expanding  $\chi^2(\boldsymbol{\theta})$  about  $\hat{\boldsymbol{\theta}}$ , one finds that the contour in parameter space defined by

$$\chi^2(\boldsymbol{\theta}) = \chi^2(\hat{\boldsymbol{\theta}}) + 1 = \chi_{\min}^2 + 1 \tag{36.23}$$

has tangent planes located at approximately plus-or-minus-one standard deviation  $\sigma_{\hat{\theta}}$  from the LS estimates  $\boldsymbol{\theta}$ .

In constructing the quantity  $\chi^2(\boldsymbol{\theta})$ , one requires the variances or, in the case of correlated measurements, the covariance matrix. Often these quantities are not known *a priori* and must be estimated from the data; an important example is where the measured value  $y_i$  represents a counted number of events in the bin of a histogram. If, for example,  $y_i$  represents a Poisson variable, for which the variance is equal to the mean, then one can either estimate the variance from the predicted value,  $F(x_i; \boldsymbol{\theta})$ , or from the observed number itself,  $y_i$ . In the first option, the variances become functions of the fitted parameters, which may lead to calculational difficulties. The second option can be undefined if  $y_i$  is zero, and in both cases for small  $y_i$ , the variance will be poorly estimated. In either case, one should constrain the normalization of the fitted curve to the correct value, *i.e.*, one should determine the area under the fitted curve directly from the number of entries in the histogram (see Ref. 8, Section 7.4). A further alternative is to use the method of maximum likelihood; for binned data this can be done by minimizing Eq. (36.12)

As the minimum value of the  $\chi^2$  represents the level of agreement between the measurements and the fitted function, it can be used for assessing the goodness-of-fit; this is discussed further in Section 36.2.2.

### 36.1.4. The Bayesian approach :

In the frequentist methods discussed above, probability is associated only with data, not with the value of a parameter. This is no longer the case in Bayesian statistics, however, which we introduce in this section. Bayesian methods are considered further in Sec. 36.3.1 for interval estimation and in Sec. 36.2.3 for model selection. For general introductions to Bayesian statistics see, *e.g.*, Refs. [20–23].

Suppose the outcome of an experiment is characterized by a vector of data  $\mathbf{x}$ , whose probability distribution depends on an unknown parameter (or parameters)  $\boldsymbol{\theta}$  that we wish to determine. In Bayesian statistics, all knowledge about  $\boldsymbol{\theta}$  is summarized by the posterior p.d.f.  $p(\boldsymbol{\theta}|\mathbf{x})$ , whose integral over any given region gives the degree of belief for  $\boldsymbol{\theta}$  to take on values in that region, given the data  $\mathbf{x}$ . It is obtained by using Bayes' theorem,

$$p(\boldsymbol{\theta}|\mathbf{x}) = \frac{L(\mathbf{x}|\boldsymbol{\theta})\pi(\boldsymbol{\theta})}{\int L(\mathbf{x}|\boldsymbol{\theta}')\pi(\boldsymbol{\theta}') d\boldsymbol{\theta}'}, \tag{36.24}$$

where  $L(\mathbf{x}|\boldsymbol{\theta})$  is the likelihood function, *i.e.*, the joint p.d.f. for the data viewed as a function of  $\boldsymbol{\theta}$ , evaluated with the data actually obtained in the experiment, and  $\pi(\boldsymbol{\theta})$  is the prior p.d.f. for  $\boldsymbol{\theta}$ . Note that the denominator in Eq. (36.24) serves to normalize the posterior p.d.f. to unity.

As it can be difficult to report the full posterior p.d.f.  $p(\boldsymbol{\theta}|\mathbf{x})$ , one would usually summarize it with statistics such as the mean (or median), and covariance matrix. In addition one may construct intervals with a given probability content, as is discussed in Sec. 36.3.1 on Bayesian interval estimation.

#### 36.1.4.1. Priors:

Bayesian statistics supplies no unique rule for determining the prior  $\pi(\boldsymbol{\theta})$ ; this reflects the experimenter's subjective degree of belief (or state of knowledge) about  $\boldsymbol{\theta}$  before the measurement was carried out. For the result to be of value to the broader community, whose members may not share these beliefs, it is important to carry out a sensitivity analysis, that is, to show how the result changes under a reasonable variation of the prior probabilities.

One might like to construct  $\pi(\boldsymbol{\theta})$  to represent complete ignorance about the parameters by setting it equal to a constant. A problem here is that if the prior p.d.f. is flat in  $\boldsymbol{\theta}$ , then it is not flat for a nonlinear function of  $\boldsymbol{\theta}$ , and so a different parametrization of the problem would lead in general to a non-equivalent posterior p.d.f.

For the special case of a constant prior, one can see from Bayes' theorem (36.24) that the posterior is proportional to the likelihood, and therefore the mode (peak position) of the posterior is equal to the ML estimator. The posterior mode, however, will change in general upon a transformation of parameter. A summary statistic other than the mode may be used as the Bayesian estimator, such as the median, which is invariant under parameter transformation. But this will not in general coincide with the ML estimator.

The difficult and subjective nature of encoding personal knowledge into priors has led to what is called *objective Bayesian statistics*, where prior probabilities are based not on an actual degree of belief but rather derived from formal rules. These give, for example, priors which are invariant under a transformation of parameters or which result in a maximum gain in information for a given set of measurements. For an extensive review see, *e.g.*, Ref. 24.

Objective priors do not in general reflect degree of belief, but they could in some cases be taken as possible, although perhaps extreme, subjective priors. The posterior probabilities as well therefore do not necessarily reflect a degree of belief. However one may regard investigating a variety of objective priors to be an important part of the sensitivity analysis. Furthermore, use of objective priors with Bayes' theorem can be viewed as a recipe for producing estimators or intervals which have desirable frequentist properties.

An important procedure for deriving objective priors is due to Jeffreys. According to *Jeffreys' rule* one takes the prior as

$$\pi(\boldsymbol{\theta}) \propto \sqrt{\det(I(\boldsymbol{\theta}))}, \tag{36.25}$$

where

$$I_{ij}(\boldsymbol{\theta}) = -E \left[ \frac{\partial^2 \ln L(\mathbf{x}|\boldsymbol{\theta})}{\partial \theta_i \partial \theta_j} \right] = - \int \frac{\partial^2 \ln L(\mathbf{x}|\boldsymbol{\theta})}{\partial \theta_i \partial \theta_j} L(\mathbf{x}|\boldsymbol{\theta}) d\mathbf{x} \quad (36.26)$$

is the *Fisher information matrix*. One can show that the Jeffreys prior leads to inference that is invariant under a transformation of parameters. One should note that the Jeffreys prior depends on the likelihood function, and thus contains information about the measurement model itself, which goes beyond one's degree of belief about the value of a parameter. As examples, the Jeffreys prior for the mean  $\mu$  of a Gaussian distribution is a constant, and for the mean of a Poisson distribution one finds  $\pi(\mu) \propto 1/\sqrt{\mu}$ .

Neither the constant nor  $1/\sqrt{\mu}$  priors can be normalized to unit area and are said to be *improper*. This can be allowed because the prior always appears multiplied by the likelihood function, and if the likelihood falls off sufficiently quickly then one may have a normalizable posterior density.

An important type of objective prior is the reference prior due to Bernardo and Berger [25]. To find the reference prior for a given problem one considers the Kullback-Leibler divergence  $D_n[\pi, p]$  of the posterior  $p(\boldsymbol{\theta}|\mathbf{x})$  relative to a prior  $\pi(\boldsymbol{\theta})$ , obtained from a set of data  $\mathbf{x} = (x_1, \dots, x_n)$ , which are assumed to consist of  $n$  independent and identically distributed values of  $x$ :

$$D_n[\pi, p] = \int p(\boldsymbol{\theta}|\mathbf{x}) \ln \frac{p(\boldsymbol{\theta}|\mathbf{x})}{\pi(\boldsymbol{\theta})} d\boldsymbol{\theta}. \quad (36.27)$$

This is effectively a measure of the gain in information provided by the data. The reference prior is chosen so that the expectation value of this information gain is maximized for the limiting case of  $n \rightarrow \infty$ , where the expectation is computed with respect to the marginal distribution of the data,

$$p(\mathbf{x}) = \int L(\mathbf{x}|\boldsymbol{\theta}) \pi(\boldsymbol{\theta}) d\boldsymbol{\theta}. \quad (36.28)$$

For a single, continuous parameter the reference prior is usually identical to Jeffreys' prior. In the multiparameter case an iterative algorithm exists, which requires sorting the parameters by order of inferential importance. Often the result does not depend on this order, but when it does, this can be part of a robustness analysis. Further discussion and applications to particle physics problems can be found in Ref. 26.

#### 36.1.4.2. Bayesian treatment of nuisance parameters:

Bayesian statistics provides a framework for incorporating systematic uncertainties into a result. Suppose, for example, that a model depends not only on parameters of interest  $\boldsymbol{\theta}$ , but on *nuisance parameters*  $\boldsymbol{\nu}$ , whose values are known with some limited accuracy. For a single nuisance parameter  $\nu$ , for example, one might have a p.d.f. centered about its nominal value with a certain standard deviation  $\sigma_\nu$ . Often a Gaussian p.d.f. provides a reasonable model for one's degree of belief about a nuisance parameter; in other cases, more complicated shapes may be appropriate. If, for example, the parameter represents a non-negative quantity then a log-normal or gamma p.d.f. can be a more natural choice than a Gaussian truncated at zero. The likelihood function, prior, and posterior p.d.f.s then all depend on both  $\boldsymbol{\theta}$  and  $\boldsymbol{\nu}$ , and are related by Bayes' theorem, as usual. One can obtain the posterior p.d.f. for  $\boldsymbol{\theta}$  alone by integrating over the nuisance parameters, *i.e.*,

$$p(\boldsymbol{\theta}|\mathbf{x}) = \int p(\boldsymbol{\theta}, \boldsymbol{\nu}|\mathbf{x}) d\boldsymbol{\nu}. \quad (36.29)$$

Such integrals can often not be carried out in closed form, and if the number of nuisance parameters is large, then they can be difficult to compute with standard Monte Carlo methods. *Markov Chain Monte Carlo* (MCMC) is often used for computing integrals of this type (see Sec. 37.5).

If the prior joint p.d.f. for  $\boldsymbol{\theta}$  and  $\boldsymbol{\nu}$  factorizes, then integrating the posterior p.d.f. over  $\boldsymbol{\nu}$  is equivalent to replacing the likelihood function by the *marginal likelihood* (see Ref. 27),

$$L_m(\mathbf{x}|\boldsymbol{\theta}) = \int L(\mathbf{x}|\boldsymbol{\theta}, \boldsymbol{\nu}) \pi(\boldsymbol{\nu}) d\boldsymbol{\nu}. \quad (36.30)$$

The marginal likelihood can also be used together with frequentist methods that employ the likelihood function such as ML estimation of parameters. The results then have a mixed frequentist/Bayesian character, where the systematic uncertainty due to limited knowledge of the nuisance parameters is built in (see Ref. 28). Although this may make it more difficult to disentangle statistical from systematic effects, such a hybrid approach may satisfy the objective of reporting the result in a convenient way. The marginal likelihood may be compared with the profile likelihood, which is discussed in Sec. 36.3.2.3.

#### 36.1.5. Propagation of errors :

Consider a set of  $n$  quantities  $\boldsymbol{\theta} = (\theta_1, \dots, \theta_n)$  and a set of  $m$  functions  $\boldsymbol{\eta}(\boldsymbol{\theta}) = (\eta_1(\boldsymbol{\theta}), \dots, \eta_m(\boldsymbol{\theta}))$ . Suppose we have estimated  $\hat{\boldsymbol{\theta}} = (\hat{\theta}_1, \dots, \hat{\theta}_n)$ , using, say, maximum-likelihood or least-squares, and we also know or have estimated the covariance matrix  $V_{ij} = \text{cov}[\hat{\theta}_i, \hat{\theta}_j]$ . The goal of *error propagation* is to determine the covariance matrix for the functions,  $U_{ij} = \text{cov}[\hat{\eta}_i, \hat{\eta}_j]$ , where  $\hat{\boldsymbol{\eta}} = \boldsymbol{\eta}(\hat{\boldsymbol{\theta}})$ . In particular, the diagonal elements  $U_{ii} = V[\hat{\eta}_i]$  give the variances. The new covariance matrix can be found by expanding the functions  $\boldsymbol{\eta}(\boldsymbol{\theta})$  about the estimates  $\hat{\boldsymbol{\theta}}$  to first order in a Taylor series. Using this one finds

$$U_{ij} \approx \sum_{k,l} \frac{\partial \eta_i}{\partial \theta_k} \frac{\partial \eta_j}{\partial \theta_l} \Big|_{\hat{\boldsymbol{\theta}}} V_{kl}. \quad (36.31)$$

This can be written in matrix notation as  $U \approx AVA^T$  where the matrix of derivatives  $A$  is

$$A_{ij} = \frac{\partial \eta_i}{\partial \theta_j} \Big|_{\hat{\boldsymbol{\theta}}}, \quad (36.32)$$

and  $A^T$  is its transpose. The approximation is exact if  $\boldsymbol{\eta}(\boldsymbol{\theta})$  is linear (it holds, for example, in equation (36.17)). If this is not the case, the approximation can break down if, for example,  $\boldsymbol{\eta}(\boldsymbol{\theta})$  is significantly nonlinear close to  $\hat{\boldsymbol{\theta}}$  in a region of a size comparable to the standard deviations of  $\hat{\boldsymbol{\theta}}$ .

## 36.2. Statistical tests

In addition to estimating parameters, one often wants to assess the validity of certain statements concerning the data's underlying distribution. Frequentist *hypothesis tests*, described in Sec. 36.2.1, provide a rule for accepting or rejecting hypotheses depending on the outcome of a measurement. In *significance tests*, covered in Sec. 36.2.2, one gives the probability to obtain a level of incompatibility with a certain hypothesis that is greater than or equal to the level observed with the actual data. In the Bayesian approach, the corresponding procedure is based fundamentally on the posterior probabilities of the competing hypotheses. In Sec. 36.2.3 we describe a related construct called the Bayes factor, which can be used to quantify the degree to which the data prefer one or another hypothesis.

#### 36.2.1. Hypothesis tests :

Consider an experiment whose outcome is characterized by a vector of data  $\mathbf{x}$ . A *hypothesis* is a statement about the distribution of  $\mathbf{x}$ . It could, for example, define completely the p.d.f. for the data (a simple hypothesis), or it could specify only the functional form of the p.d.f., with the values of one or more parameters left open (a composite hypothesis).

A *statistical test* is a rule that states for which values of  $\mathbf{x}$  a given hypothesis (often called the null hypothesis,  $H_0$ ) should be rejected. This is done by defining a region of  $\mathbf{x}$ -space called the critical region,  $w$ , such that there is no more than a specified probability under  $H_0$ ,  $\alpha$ , called the *size* or *significance level* of the test, to find  $\mathbf{x} \in w$ . If the data are discrete, it may not be possible to find a critical region with exact probability content  $\alpha$ , and thus we require  $P(\mathbf{x} \in w | H_0) \leq \alpha$ . If the data are observed in the critical region,  $H_0$  is rejected.

There are in general a large (often infinite) number of regions of the data space that have probability content  $\alpha$  and thus qualify as possible critical regions. To choose one of them one should take into account the probabilities for the data predicted by some alternative hypothesis (or set of alternatives)  $H_1$ . Rejecting  $H_0$  if it is true is

called a *type-I error*, and occurs by construction with probability no greater than  $\alpha$ . Not rejecting  $H_0$  if an alternative  $H_1$  is true is called a *type-II error*, and for a given test this will have a certain probability  $\beta$ . The quantity  $1 - \beta$  is called the *power* of the test of  $H_0$  with respect to the alternative  $H_1$ . A strategy for defining the critical region can therefore be to maximize the power with respect to some alternative (or alternatives) given a fixed size  $\alpha$ .

In high-energy physics, the components of  $\mathbf{x}$  might represent the measured properties of candidate events, and the critical region is defined by the cuts that one imposes in order to reject background and thus accept events likely to be of a certain desired type. Here  $H_0$  could represent the background hypothesis and the alternative  $H_1$  could represent the sought after signal. In other cases,  $H_0$  could be the hypothesis that an entire event sample consists of background events only, and the alternative  $H_1$  may represent the hypothesis of a mixture of background and signal.

Often rather than using the full set of quantities  $\mathbf{x}$ , it is convenient to define a *test statistic*,  $t$ , which can be a single number, or in any case a vector with fewer components than  $\mathbf{x}$ . Each hypothesis for the distribution of  $\mathbf{x}$  will determine a distribution for  $t$ , and the acceptance region in  $\mathbf{x}$ -space will correspond to a specific range of values of  $t$ .

To maximize the power of a test of  $H_0$  with respect to the alternative  $H_1$ , the *Neyman–Pearson lemma* states that the critical region  $w$  should be chosen such that for all data values  $\mathbf{x}$  inside  $w$ , the ratio

$$\lambda(\mathbf{x}) = \frac{f(\mathbf{x}|H_1)}{f(\mathbf{x}|H_0)}, \quad (36.33)$$

is greater than a given constant, the value of which is determined by the size of the test  $\alpha$ . Here  $H_0$  and  $H_1$  must be simple hypotheses, i.e., they should not contain undetermined parameters.

The lemma is equivalent to the statement that (36.33) represents the optimal test statistic where the critical region is defined by a single cut on  $\lambda$ . This test will lead to the maximum power (e.g., probability to reject the background hypothesis if the signal hypothesis is true) for a given probability  $\alpha$  to reject the background hypothesis if it is in fact true. It can be difficult in practice, however, to determine  $\lambda(\mathbf{x})$ , since this requires knowledge of the joint p.d.f.s  $f(\mathbf{x}|H_0)$  and  $f(\mathbf{x}|H_1)$ .

In the usual case where the likelihood ratio (36.33) cannot be used explicitly, there exist a variety of other multivariate classifiers that effectively separate different types of events. Methods often used in HEP include *neural networks* or *Fisher discriminants* (see Ref. 10). Recently, further classification methods from machine-learning have been applied in HEP analyses; these include *probability density estimation (PDE)* techniques, *kernel-based PDE (KDE or Parzen window)*, *support vector machines*, and *decision trees*. Techniques such as “boosting” and “bagging” can be applied to combine a number of classifiers into a stronger one with greater stability with respect to fluctuations in the training data. Descriptions of these methods can be found in [11–13], and *Proceedings of the PHYSTAT* conference series [14]. Software for HEP includes the *TMVA* [15] and *StatPatternRecognition* [16] packages.

### 36.2.2. Significance tests :

Often one wants to quantify the level of agreement between the data and a hypothesis without explicit reference to alternative hypotheses. This can be done by defining a statistic  $t$ , which is a function of the data whose value reflects in some way the level of agreement between the data and the hypothesis. The analyst must decide what values of the statistic correspond to better or worse levels of agreement with the hypothesis in question; for many goodness-of-fit statistics, there is an obvious choice.

The hypothesis in question, say,  $H_0$ , will determine the p.d.f.  $g(t|H_0)$  for the statistic. The significance of a discrepancy between the data and what one expects under the assumption of  $H_0$  is quantified by giving the  $p$ -value, defined as the probability to find  $t$  in the region of equal or lesser compatibility with  $H_0$  than the level of compatibility observed with the actual data. For example, if  $t$  is defined such that large values correspond to poor agreement with the hypothesis, then

the  $p$ -value would be

$$p = \int_{t_{\text{obs}}}^{\infty} g(t|H_0) dt, \quad (36.34)$$

where  $t_{\text{obs}}$  is the value of the statistic obtained in the actual experiment.

The  $p$ -value should not be confused with the size (significance level) of a test, or the confidence level of a confidence interval (Section 36.3), both of which are pre-specified constants. We may formulate a hypothesis test, however, by defining the critical region to correspond to the data outcomes that give the lowest  $p$ -values, so that finding  $p < \alpha$  implies that the data outcome was in the critical region. When constructing a  $p$ -value, one generally takes the region of data space deemed to have lower compatibility with the model being tested to have higher compatibility with a given alternative, and thus the corresponding test will have a high power with respect to this alternative.

The  $p$ -value is a function of the data, and is therefore itself a random variable. If the hypothesis used to compute the  $p$ -value is true, then for continuous data,  $p$  will be uniformly distributed between zero and one. Note that the  $p$ -value is not the probability for the hypothesis; in frequentist statistics, this is not defined. Rather, the  $p$ -value is the probability, under the assumption of a hypothesis  $H_0$ , of obtaining data at least as incompatible with  $H_0$  as the data actually observed.

When searching for a new phenomenon, one tries to reject the hypothesis  $H_0$  that the data are consistent with known, e.g., Standard Model processes. If the  $p$ -value of  $H_0$  is sufficiently low, then one is willing to accept that some alternative hypothesis is true. Often one converts the  $p$ -value into an equivalent significance  $Z$ , defined so that a  $Z$  standard deviation upward fluctuation of a Gaussian random variable would have an upper tail area equal to  $p$ , i.e.,

$$Z = \Phi^{-1}(1 - p). \quad (36.35)$$

Here  $\Phi$  is the cumulative distribution of the Standard Gaussian, and  $\Phi^{-1}$  is its inverse (quantile) function. Often in HEP, the level of significance where an effect is said to qualify as a discovery is  $Z = 5$ , i.e., a  $5\sigma$  effect, corresponding to a  $p$ -value of  $2.87 \times 10^{-7}$ . One’s actual degree of belief that a new process is present, however, will depend in general on other factors as well, such as the plausibility of the new signal hypothesis and the degree to which it can describe the data, one’s confidence in the model that led to the observed  $p$ -value, and possible corrections for multiple observations out of which one focuses on the smallest  $p$ -value obtained (the “look-elsewhere effect”). For a review of how to incorporate systematic uncertainties into  $p$ -values see, e.g., Ref. 17; a computationally fast method that provides an approximate correction for the look-elsewhere effect is described in Ref. 18.

When estimating parameters using the method of least squares, one obtains the minimum value of the quantity  $\chi^2$  (36.13). This statistic can be used to test the *goodness-of-fit*, i.e., the test provides a measure of the significance of a discrepancy between the data and the hypothesized functional form used in the fit. It may also happen that no parameters are estimated from the data, but that one simply wants to compare a histogram, e.g., a vector of Poisson distributed numbers  $\mathbf{n} = (n_1, \dots, n_N)$ , with a hypothesis for their expectation values  $\nu_i = E[n_i]$ . As the distribution is Poisson with variances  $\sigma_i^2 = \nu_i$ , the  $\chi^2$  (36.13) becomes *Pearson’s  $\chi^2$  statistic*,

$$\chi^2 = \sum_{i=1}^N \frac{(n_i - \nu_i)^2}{\nu_i}. \quad (36.36)$$

If the hypothesis  $\boldsymbol{\nu} = (\nu_1, \dots, \nu_N)$  is correct, and if the expected values  $\nu_i$  in (36.36) are sufficiently large (or equivalently, if the measurements  $n_i$  can be treated as following a Gaussian distribution), then the  $\chi^2$  statistic will follow the  $\chi^2$  p.d.f. with the number of degrees of freedom equal to the number of measurements  $N$  minus the number of fitted parameters.



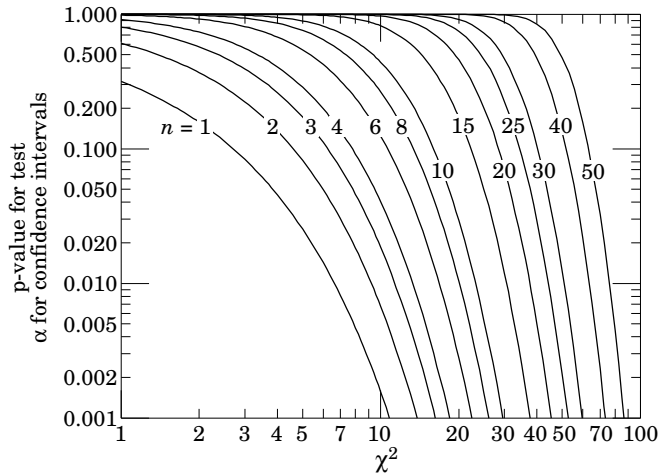


**Figure 36.1:** One minus the  $\chi^2$  cumulative distribution,  $1 - F(\chi^2; n)$ , for  $n$  degrees of freedom. This gives the  $p$ -value for the  $\chi^2$  goodness-of-fit test as well as one minus the coverage probability for confidence regions (see Sec. 36.3.2.4).

Alternatively, one may fit parameters and evaluate goodness-of-fit by minimizing  $-2 \ln \lambda$  from Eq. (36.12). One finds that the distribution of this statistic approaches the asymptotic limit faster than does Pearson's  $\chi^2$ , and thus computing the  $p$ -value with the  $\chi^2$  p.d.f. will in general be better justified (see Ref. 9 and references therein).

Assuming the goodness-of-fit statistic follows a  $\chi^2$  p.d.f., the  $p$ -value for the hypothesis is then

$$p = \int_{\chi^2}^{\infty} f(z; n_d) dz, \quad (36.37)$$

where  $f(z; n_d)$  is the  $\chi^2$  p.d.f. and  $n_d$  is the appropriate number of degrees of freedom. Values can be obtained from Fig. 36.1 or from the ROOT function `TMath::Prob`. If the conditions for using the  $\chi^2$  p.d.f. do not hold, the statistic can still be defined as before, but its p.d.f. must be determined by other means in order to obtain the  $p$ -value, e.g., using a Monte Carlo calculation.

Since the mean of the  $\chi^2$  distribution is equal to  $n_d$ , one expects in a “reasonable” experiment to obtain  $\chi^2 \approx n_d$ . Hence the quantity  $\chi^2/n_d$  is sometimes reported. Since the p.d.f. of  $\chi^2/n_d$  depends on  $n_d$ , however, one must report  $n_d$  as well if one wishes to determine the  $p$ -value. The  $p$ -values obtained for different values of  $\chi^2/n_d$  are shown in Fig. 36.2.

If one finds a  $\chi^2$  value much greater than  $n_d$ , and a correspondingly small  $p$ -value, one may be tempted to expect a high degree of uncertainty for any fitted parameters. Poor goodness-of-fit, however, does not mean that one will have large statistical errors for parameter estimates. If, for example, the error bars (or covariance matrix) used in constructing the  $\chi^2$  are underestimated, then this will lead to underestimated statistical errors for the fitted parameters. The standard deviations of estimators that one finds from, say, Eq. (36.11) reflect how widely the estimates would be distributed if one were to repeat the measurement many times, assuming that the hypothesis and measurement errors used in the  $\chi^2$  are also correct. They do not include the systematic error which may result from an incorrect hypothesis or incorrectly estimated measurement errors in the  $\chi^2$ .

### 36.2.3. Bayesian model selection :

In Bayesian statistics, all of one's knowledge about a model is contained in its posterior probability, which one obtains using Bayes' theorem (36.24). Thus one could reject a hypothesis  $H$  if its posterior probability  $P(H|\mathbf{x})$  is sufficiently small. The difficulty here is that  $P(H|\mathbf{x})$  is proportional to the prior probability  $P(H)$ , and there will not be a consensus about the prior probabilities for the existence of new phenomena. Nevertheless one can construct a quantity called the Bayes factor (described below), which can be used to quantify the

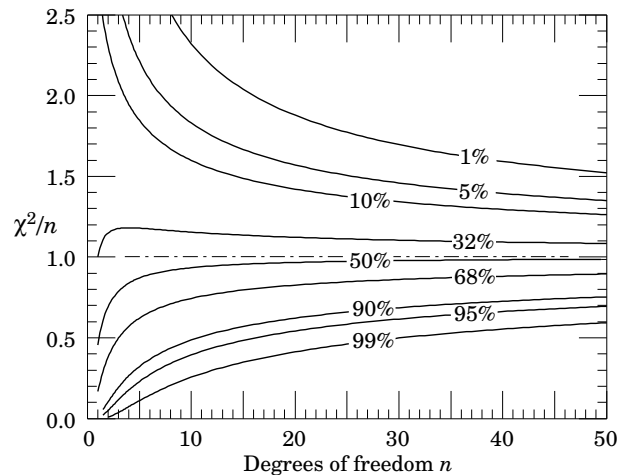


**Figure 36.2:** The ‘reduced’  $\chi^2$ , equal to  $\chi^2/n$ , for  $n$  degrees of freedom. The curves show as a function of  $n$  the  $\chi^2/n$  that corresponds to a given  $p$ -value.

degree to which the data prefer one hypothesis over another, and is independent of their prior probabilities.

Consider two models (hypotheses),  $H_i$  and  $H_j$ , described by vectors of parameters  $\theta_i$  and  $\theta_j$ , respectively. Some of the components will be common to both models and others may be distinct. The full prior probability for each model can be written in the form

$$\pi(H_i, \theta_i) = P(H_i)\pi(\theta_i|H_i), \quad (36.38)$$

Here  $P(H_i)$  is the overall prior probability for  $H_i$ , and  $\pi(\theta_i|H_i)$  is the normalized p.d.f. of its parameters. For each model, the posterior probability is found using Bayes' theorem,

$$P(H_i|\mathbf{x}) = \frac{\int L(\mathbf{x}|\theta_i, H_i)P(H_i)\pi(\theta_i|H_i) d\theta_i}{P(\mathbf{x})}, \quad (36.39)$$

where the integration is carried out over the internal parameters  $\theta_i$  of the model. The ratio of posterior probabilities for the models is therefore

$$\frac{P(H_i|\mathbf{x})}{P(H_j|\mathbf{x})} = \frac{\int L(\mathbf{x}|\theta_i, H_i)\pi(\theta_i|H_i) d\theta_i}{\int L(\mathbf{x}|\theta_j, H_j)\pi(\theta_j|H_j) d\theta_j} \frac{P(H_i)}{P(H_j)}. \quad (36.40)$$

The Bayes factor is defined as

$$B_{ij} = \frac{\int L(\mathbf{x}|\theta_i, H_i)\pi(\theta_i|H_i) d\theta_i}{\int L(\mathbf{x}|\theta_j, H_j)\pi(\theta_j|H_j) d\theta_j}. \quad (36.41)$$

This gives what the ratio of posterior probabilities for models  $i$  and  $j$  would be if the overall prior probabilities for the two models were equal. If the models have no nuisance parameters i.e., no internal parameters described by priors, then the Bayes factor is simply the likelihood ratio. The Bayes factor therefore shows by how much the probability ratio of model  $i$  to model  $j$  changes in the light of the data, and thus can be viewed as a numerical measure of evidence supplied by the data in favour of one hypothesis over the other.

Although the Bayes factor is by construction independent of the overall prior probabilities  $P(H_i)$  and  $P(H_j)$ , it does require priors for all internal parameters of a model, i.e., one needs the functions  $\pi(\theta_i|H_i)$  and  $\pi(\theta_j|H_j)$ . In a Bayesian analysis where one is only interested in the posterior p.d.f. of a parameter, it may be acceptable to take an unnormalizable function for the prior (an improper prior) as long as the product of likelihood and prior can be normalized. But improper priors are only defined up to an arbitrary multiplicative constant, and so the Bayes factor would depend on this constant. Furthermore, although the range of a constant normalized prior is unimportant for parameter determination (provided it is wider than the likelihood), this is not so for the Bayes factor when such a prior

is used for only one of the hypotheses. So to compute a Bayes factor, all internal parameters must be described by normalized priors that represent meaningful probabilities over the entire range where they are defined.

An exception to this rule may be considered when the identical parameter appears in the models for both numerator and denominator of the Bayes factor. In this case one can argue that the arbitrary constants would cancel. One must exercise some caution, however, as parameters with the same name and physical meaning may still play different roles in the two models.

Both integrals in equation (36.41) are of the form

$$m = \int L(\mathbf{x}|\boldsymbol{\theta})\pi(\boldsymbol{\theta}) d\boldsymbol{\theta}, \tag{36.42}$$

which is called the *marginal likelihood* (or in some fields called the *evidence*). A review of Bayes factors including a discussion of computational issues can be found in Ref. 30.

### 36.3. Intervals and limits

When the goal of an experiment is to determine a parameter  $\theta$ , the result is usually expressed by quoting, in addition to the point estimate, some sort of interval which reflects the statistical precision of the measurement. In the simplest case, this can be given by the parameter’s estimated value  $\hat{\theta}$  plus or minus an estimate of the standard deviation of  $\hat{\theta}$ ,  $\sigma_{\hat{\theta}}$ . If, however, the p.d.f. of the estimator is not Gaussian or if there are physical boundaries on the possible values of the parameter, then one usually quotes instead an interval according to one of the procedures described below.

In reporting an interval or limit, the experimenter may wish to

- communicate as objectively as possible the result of the experiment;
- provide an interval that is constructed to cover the true value of the parameter with a specified probability;
- provide the information needed by the consumer of the result to draw conclusions about the parameter or to make a particular decision;
- draw conclusions about the parameter that incorporate stated prior beliefs.

With a sufficiently large data sample, the point estimate and standard deviation (or for the multiparameter case, the parameter estimates and covariance matrix) satisfy essentially all of these goals. For finite data samples, no single method for quoting an interval will achieve all of them.

In addition to the goals listed above, the choice of method may be influenced by practical considerations such as ease of producing an interval from the results of several measurements. Of course the experimenter is not restricted to quoting a single interval or limit; one may choose, for example, first to communicate the result with a confidence interval having certain frequentist properties, and then in addition to draw conclusions about a parameter using a judiciously chosen subjective Bayesian prior.

It is recommended, however, that there be a clear separation between these two aspects of reporting a result. In the remainder of this section, we assess the extent to which various types of intervals achieve the goals stated here.

#### 36.3.1. Bayesian intervals :

As described in Sec. 36.1.4, a Bayesian posterior probability may be used to determine regions that will have a given probability of containing the true value of a parameter. In the single parameter case, for example, an interval (called a Bayesian or credible interval)  $[\theta_{lo}, \theta_{up}]$  can be determined which contains a given fraction  $1 - \alpha$  of the posterior probability, *i.e.*,

$$1 - \alpha = \int_{\theta_{lo}}^{\theta_{up}} p(\boldsymbol{\theta}|\mathbf{x}) d\boldsymbol{\theta}. \tag{36.43}$$

Sometimes an upper or lower limit is desired, *i.e.*,  $\theta_{lo}$  or  $\theta_{up}$  can be set to a physical boundary or to plus or minus infinity. In other cases, one

might choose  $\theta_{lo}$  and  $\theta_{up}$  such that  $p(\boldsymbol{\theta}|\mathbf{x})$  is higher everywhere inside the interval than outside; these are called *highest posterior density* (HPD) intervals. Note that HPD intervals are not invariant under a nonlinear transformation of the parameter.

If a parameter is constrained to be non-negative, then the prior p.d.f. can simply be set to zero for negative values. An important example is the case of a Poisson variable  $n$ , which counts signal events with unknown mean  $s$ , as well as background with mean  $b$ , assumed known. For the signal mean  $s$ , one often uses the prior

$$\pi(s) = \begin{cases} 0 & s < 0 \\ 1 & s \geq 0 \end{cases}. \tag{36.44}$$

This prior is regarded as providing an interval whose frequentist properties can be studied, rather than as representing a degree of belief. In the absence of a clear discovery, (*e.g.*, if  $n = 0$  or if in any case  $n$  is compatible with the expected background), one usually wishes to place an upper limit on  $s$  (see, however, Sec. 36.3.2.6 on “flip-flopping” concerning frequentist coverage). Using the likelihood function for Poisson distributed  $n$ ,

$$L(n|s) = \frac{(s + b)^n}{n!} e^{-(s+b)}, \tag{36.45}$$

along with the prior (36.44) in (36.24) gives the posterior density for  $s$ . An upper limit  $s_{up}$  at confidence level (or here, rather, credibility level)  $1 - \alpha$  can be obtained by requiring

$$1 - \alpha = \int_{-\infty}^{s_{up}} p(s|n) ds = \frac{\int_{-\infty}^{s_{up}} L(n|s) \pi(s) ds}{\int_{-\infty}^{\infty} L(n|s) \pi(s) ds}, \tag{36.46}$$

where the lower limit of integration is effectively zero because of the cut-off in  $\pi(s)$ . By relating the integrals in Eq. (36.46) to incomplete gamma functions, the equation reduces to

$$\alpha = e^{-s_{up}} \frac{\sum_{m=0}^n (s_{up} + b)^m / m!}{\sum_{m=0}^n b^m / m!}. \tag{36.47}$$

This must be solved numerically for the limit  $s_{up}$ . For the special case of  $b = 0$ , the sums can be related to the quantile  $F_{\chi^2}^{-1}$  of the  $\chi^2$  distribution (inverse of the cumulative distribution) to give

$$s_{up} = \frac{1}{2} F_{\chi^2}^{-1}(1 - \alpha; n_d), \tag{36.48}$$

where the number of degrees of freedom is  $n_d = 2(n + 1)$ . The quantile of the  $\chi^2$  distribution can be obtained using the ROOT function `TMath::ChisquareQuantile`. It so happens that for the case of  $b = 0$ , the upper limits from Eq. (36.48) coincide numerically with the values of the frequentist upper limits discussed in Section 36.3.2.5. Values for  $1 - \alpha = 0.9$  and  $0.95$  are given by the values  $\nu_{up}$  in Table 36.3. The frequentist properties of confidence intervals for the Poisson mean in this way are discussed in Refs. [2] and [19].

As in any Bayesian analysis, it is important to show how the result would change if one uses different prior probabilities. For example, one could consider the Jeffreys prior as described in Sec. 36.1.4. For this problem one finds the Jeffreys prior  $\pi(s) \propto 1/\sqrt{s + b}$  for  $s \geq 0$  and zero otherwise. As with the constant prior, one would not regard this as representing one’s prior beliefs about  $s$ , both because it is improper and also as it depends on  $b$ . Rather it is used with Bayes’ theorem to produce an interval whose frequentist properties can be studied.

#### 36.3.2. Frequentist confidence intervals :

The unqualified phrase “confidence intervals” refers to frequentist intervals obtained with a procedure due to Neyman [29], described below. These are intervals (or in the multiparameter case, regions) constructed so as to include the true value of the parameter with a probability greater than or equal to a specified level, called the *coverage probability*. In this section, we discuss several techniques for producing intervals that have, at least approximately, this property.

**36.3.2.1. The Neyman construction for confidence intervals:**

Consider a p.d.f.  $f(x; \theta)$  where  $x$  represents the outcome of the experiment and  $\theta$  is the unknown parameter for which we want to construct a confidence interval. The variable  $x$  could (and often does) represent an estimator for  $\theta$ . Using  $f(x; \theta)$ , we can find for a pre-specified probability  $1 - \alpha$ , and for every value of  $\theta$ , a set of values  $x_1(\theta, \alpha)$  and  $x_2(\theta, \alpha)$  such that

$$P(x_1 < x < x_2; \theta) = 1 - \alpha = \int_{x_1}^{x_2} f(x; \theta) dx . \quad (36.49)$$

This is illustrated in Fig. 36.3: a horizontal line segment  $[x_1(\theta, \alpha), x_2(\theta, \alpha)]$  is drawn for representative values of  $\theta$ . The union of such intervals for all values of  $\theta$ , designated in the figure as  $D(\alpha)$ , is known as the *confidence belt*. Typically the curves  $x_1(\theta, \alpha)$  and  $x_2(\theta, \alpha)$  are monotonic functions of  $\theta$ , which we assume for this discussion.

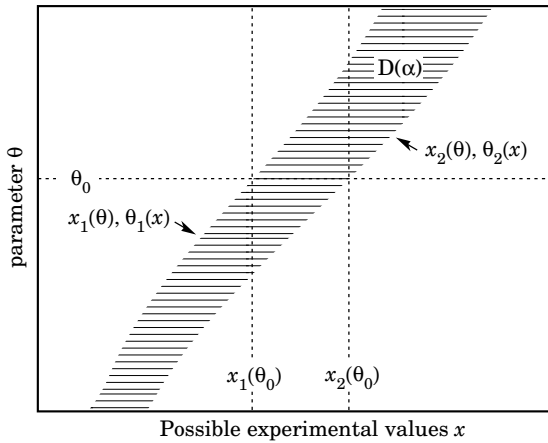


**Figure 36.3:** Construction of the confidence belt (see text).

Upon performing an experiment to measure  $x$  and obtaining a value  $x_0$ , one draws a vertical line through  $x_0$ . The confidence interval for  $\theta$  is the set of all values of  $\theta$  for which the corresponding line segment  $[x_1(\theta, \alpha), x_2(\theta, \alpha)]$  is intercepted by this vertical line. Such confidence intervals are said to have a *confidence level* (CL) equal to  $1 - \alpha$ .

Now suppose that the true value of  $\theta$  is  $\theta_0$ , indicated in the figure. We see from the figure that  $\theta_0$  lies between  $\theta_1(x)$  and  $\theta_2(x)$  if and only if  $x$  lies between  $x_1(\theta_0)$  and  $x_2(\theta_0)$ . The two events thus have the same probability, and since this is true for any value  $\theta_0$ , we can drop the subscript 0 and obtain

$$1 - \alpha = P(x_1(\theta) < x < x_2(\theta)) = P(\theta_2(x) < \theta < \theta_1(x)) . \quad (36.50)$$

In this probability statement,  $\theta_1(x)$  and  $\theta_2(x)$ , *i.e.*, the endpoints of the interval, are the random variables and  $\theta$  is an unknown constant. If the experiment were to be repeated a large number of times, the interval  $[\theta_1, \theta_2]$  would vary, covering the fixed value  $\theta$  in a fraction  $1 - \alpha$  of the experiments.

The condition of coverage in Eq. (36.49) does not determine  $x_1$  and  $x_2$  uniquely, and additional criteria are needed. One possibility is to choose *central intervals* such that the probabilities excluded below  $x_1$  and above  $x_2$  are each  $\alpha/2$ . In other cases, one may want to report only an upper or lower limit, in which case the probability excluded below  $x_1$  or above  $x_2$  can be set to zero. Another principle based on *likelihood ratio ordering* for determining which values of  $x$  should be included in the confidence belt is discussed below.

When the observed random variable  $x$  is continuous, the coverage probability obtained with the Neyman construction is  $1 - \alpha$ , regardless of the true value of the parameter. If  $x$  is discrete, however, it is not possible to find segments  $[x_1(\theta, \alpha), x_2(\theta, \alpha)]$  that satisfy Eq. (36.49) exactly for all values of  $\theta$ . By convention, one constructs the confidence belt requiring the probability  $P(x_1 < x < x_2)$  to be *greater than or equal to*  $1 - \alpha$ . This gives confidence intervals that include the true parameter with a probability greater than or equal to  $1 - \alpha$ .

An equivalent method of constructing confidence intervals is to consider a test (see Sec. 36.2) of the hypothesis that the parameter's true value is  $\theta$  (assume one constructs a test for all physical values of  $\theta$ ). One then excludes all values of  $\theta$  where the hypothesis would be rejected at a significance level less than  $\alpha$ . The remaining values constitute the confidence interval at confidence level  $1 - \alpha$ .

In this procedure, one is still free to choose the test to be used; this corresponds to the freedom in the Neyman construction as to which values of the data are included in the confidence belt. One possibility is to use a test statistic based on the *likelihood ratio*,

$$\lambda = \frac{f(x; \theta)}{f(x; \hat{\theta})} , \quad (36.51)$$

where  $\hat{\theta}$  is the value of the parameter which, out of all allowed values, maximizes  $f(x; \theta)$ . This results in the intervals described in Ref. 31 by Feldman and Cousins. The same intervals can be obtained from the Neyman construction described above by including in the confidence belt those values of  $x$  which give the greatest values of  $\lambda$ .

**36.3.2.2. Parameter exclusion in cases of low sensitivity:**

An important example of a statistical test arises in the search for a new signal process. Suppose the parameter  $\mu$  is defined such that it is proportional to the signal cross section. A statistical test may be carried out for hypothesized values of  $\mu$ , which may be done by computing a  $p$ -value,  $p_\mu$ , for each hypothesized  $\mu$ . Those values not rejected in a test of size  $\alpha$ , *i.e.*, for which one does not find  $p_\mu < \alpha$ , constitute a confidence interval with confidence level  $1 - \alpha$ .

In general one will find that for some regions in the parameter space of the signal model, the predictions for data are almost indistinguishable from those of the background-only model. This corresponds to the case where  $\mu$  is very small, as would occur, *e.g.*, if one searches for a Higgs boson with a mass so high that its production rate in a given experiment is negligible. That is, one has essentially no experimental sensitivity to such a model.

One would prefer that if the sensitivity to a model (or a point in a model's parameter space) is very low, then it should not be excluded. Even if the outcomes predicted with or without signal are identical, however, the probability to reject the signal model will equal  $\alpha$ , the type-I error rate. As one often takes  $\alpha$  to be 5%, this would mean that in a large number of searches covering a broad range of a signal model's parameter space, there would inevitably be excluded regions in which the experimental sensitivity is very small, and thus one may question whether it is justified to regard such parameter values as disfavored.

Exclusion of models to which one has little or no sensitivity occurs, for example, if the data fluctuate very low relative to the expectation of the background-only hypothesis. In this case the resulting upper limit on the predicted rate (cross section) of a signal model may be anomalously low. As a means of controlling this effect one often determines the mean or median limit under assumption of the background-only hypothesis using a simplified Monte Carlo simulation of the experiment. An upper limit found significantly below the background-only expectation may indicate a strong downward fluctuation of the data, or perhaps as well an incorrect estimate of the background rate.

The CL<sub>s</sub> method aims to mitigate the problem of excluding models to which one is not sensitive by effectively penalizing the  $p$ -value of a tested parameter by an amount that increases with decreasing sensitivity [32,33]. The procedure is based on a statistic called CL<sub>s</sub>, which is defined as

$$CL_s = \frac{p_\mu}{1 - p_0} , \quad (36.52)$$

where  $p_0$  is the  $p$ -value of the background-only hypothesis. In the usual formulation of the method, the  $p$ -values for  $\mu$  and 0 are defined using a single test statistic, and the definition of CL<sub>s</sub> above assumes this statistic is continuous; more details can be found in Refs. [32,33].

A point in a model's parameter space is regarded as excluded if one finds  $CL_s < \alpha$ . As the denominator in Eq. (36.52) is always less than or equal to unity, the exclusion criterion based on CL<sub>s</sub>

is more stringent than the usual requirement  $p_\mu < \alpha$ . In this sense the CL<sub>s</sub> procedure is conservative, and the coverage probability of the corresponding intervals will exceed the nominal confidence level  $1 - \alpha$ . If the experimental sensitivity to a given value of  $\mu$  is very low, then one finds that as  $p_\mu$  decreases, so does the denominator  $1 - p_0$ , and thus the condition  $CL_s < \alpha$  is effectively prevented from being satisfied. In this way the exclusion of parameters in the case of low sensitivity is suppressed.

The CL<sub>s</sub> procedure has the attractive feature that the resulting intervals coincide with those obtained from the Bayesian method in two important cases: the mean value of a Poisson or Gaussian distributed measurement with a constant prior. The CL<sub>s</sub> intervals overcover for all values of the parameter  $\mu$ , however, by an amount that depends on  $\mu$ .

The problem of excluding parameter values to which one has little sensitivity is particularly acute when one wants to set a one-sided limit, e.g., an upper limit on a cross section. Here one tests a value of a rate parameter  $\mu$  against the alternative of a lower rate, and therefore the critical region of the test is taken to correspond to data outcomes with a low event yield. If the number of events found in the search region fluctuates low enough, however, it can happen that all physically meaningful signal parameter values, including those to which one has very little sensitivity, are rejected by the test. Another solution to the problem, therefore, is to replace the one-sided test by one based on the likelihood ratio, where the critical region is not restricted to low rates. This is the approach followed in the Feldman-Cousins procedure described above. Further properties of Feldman-Cousins intervals are discussed below in Section 36.3.2.6.

**36.3.2.3. Profile likelihood and treatment of nuisance parameters:**

As mentioned in Section 36.3.1, one may have a model containing parameters that must be determined from data, but which are not of any interest in the final result (nuisance parameters). Suppose the likelihood  $L(\theta, \nu)$  depends on parameters of interest  $\theta$  and nuisance parameters  $\nu$ . The nuisance parameters can be effectively removed from the problem by constructing the *profile likelihood*, defined by

$$L_p(\theta) = L(\theta, \hat{\nu}(\theta)), \tag{36.53}$$

where  $\hat{\nu}(\theta)$  is given by the  $\nu$  that maximizes the likelihood for fixed  $\theta$ . The profile likelihood may then be used to construct tests of intervals for the parameters of interest. This is in contrast to the marginal likelihood (36.30) used in the Bayesian approach. For example, one may construct the profile likelihood ratio,

$$\lambda_p(\theta) = \frac{L_p(\theta)}{L_p(\hat{\theta}, \hat{\nu})}, \tag{36.54}$$

where  $\hat{\theta}$  and  $\hat{\nu}$  are the ML estimators. The ratio  $\lambda_p$  can be used in place of the likelihood ratio (36.51) for inference about  $\theta$ . The resulting intervals for the parameters of interest are not guaranteed to have the exact coverage probability for all values of the nuisance parameters, but in cases of practical interest the approximation is found to be very good. Further discussion on use of the profile likelihood can be found in, e.g., Refs. [37–39] and other contributions to the PHYSTAT conferences [14].

**36.3.2.4. Gaussian distributed measurements:**

An important example of constructing a confidence interval is when the data consists of a single random variable  $x$  that follows a Gaussian distribution; this is often the case when  $x$  represents an estimator for a parameter and one has a sufficiently large data sample. If there is more than one parameter being estimated, the multivariate Gaussian is used. For the univariate case with known  $\sigma$ ,

$$1 - \alpha = \frac{1}{\sqrt{2\pi}\sigma} \int_{\mu-\delta}^{\mu+\delta} e^{-(x-\mu)^2/2\sigma^2} dx = \text{erf}\left(\frac{\delta}{\sqrt{2}\sigma}\right) \tag{36.55}$$

is the probability that the measured value  $x$  will fall within  $\pm\delta$  of the true value  $\mu$ . From the symmetry of the Gaussian with respect to  $x$  and  $\mu$ , this is also the probability for the interval  $x \pm \delta$  to include  $\mu$ . Fig. 36.4 shows a  $\delta = 1.64\sigma$  confidence interval unshaded. The choice  $\delta = \sigma$  gives an interval called the *standard error* which has  $1 - \alpha = 68.27\%$  if  $\sigma$  is known. Values of  $\alpha$  for other frequently used choices of  $\delta$  are given in Table 36.1.

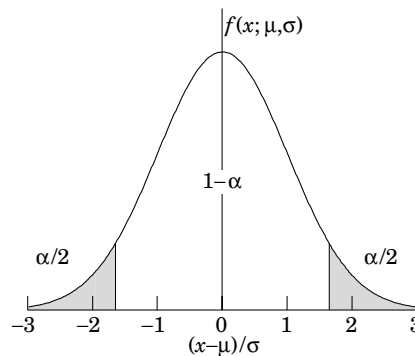


**Figure 36.4:** Illustration of a symmetric 90% confidence interval (unshaded) for a measurement of a single quantity with Gaussian errors. Integrated probabilities, defined by  $\alpha = 0.1$ , are as shown.

**Table 36.1:** Area of the tails  $\alpha$  outside  $\pm\delta$  from the mean of a Gaussian distribution.

$\alpha$	$\delta$	$\alpha$	$\delta$
0.3173	$1\sigma$	0.2	$1.28\sigma$
$4.55 \times 10^{-2}$	$2\sigma$	0.1	$1.64\sigma$
$2.7 \times 10^{-3}$	$3\sigma$	0.05	$1.96\sigma$
$6.3 \times 10^{-5}$	$4\sigma$	0.01	$2.58\sigma$
$5.7 \times 10^{-7}$	$5\sigma$	0.001	$3.29\sigma$
$2.0 \times 10^{-9}$	$6\sigma$	$10^{-4}$	$3.89\sigma$

We can set a one-sided (upper or lower) limit by excluding above  $x + \delta$  (or below  $x - \delta$ ). The values of  $\alpha$  for such limits are half the values in Table 36.1.

The relation (36.55) can be re-expressed using the cumulative distribution function for the  $\chi^2$  distribution as

$$\alpha = 1 - F(\chi^2; n), \tag{36.56}$$

for  $\chi^2 = (\delta/\sigma)^2$  and  $n = 1$  degree of freedom. This can be obtained from Fig. 36.1 on the  $n = 1$  curve or by using the ROOT function `TMath::Prob`.

For multivariate measurements of, say,  $n$  parameter estimates  $\hat{\theta} = (\hat{\theta}_1, \dots, \hat{\theta}_n)$ , one requires the full covariance matrix  $V_{ij} = \text{cov}[\hat{\theta}_i, \hat{\theta}_j]$ , which can be estimated as described in Sections 36.1.2 and 36.1.3. Under fairly general conditions with the methods of maximum-likelihood or least-squares in the large sample limit, the estimators will be distributed according to a multivariate Gaussian centered about the true (unknown) values  $\theta$ , and furthermore, the likelihood function itself takes on a Gaussian shape.

The standard error ellipse for the pair  $(\hat{\theta}_i, \hat{\theta}_j)$  is shown in Fig. 36.5, corresponding to a contour  $\chi^2 = \chi^2_{\min} + 1$  or  $\ln L = \ln L_{\max} - 1/2$ . The ellipse is centered about the estimated values  $\hat{\theta}$ , and the tangents to the ellipse give the standard deviations of the estimators,  $\sigma_i$  and  $\sigma_j$ . The angle of the major axis of the ellipse is given by

$$\tan 2\phi = \frac{2\rho_{ij}\sigma_i\sigma_j}{\sigma_j^2 - \sigma_i^2}, \tag{36.57}$$

where  $\rho_{ij} = \text{cov}[\hat{\theta}_i, \hat{\theta}_j]/\sigma_i\sigma_j$  is the correlation coefficient.

The correlation coefficient can be visualized as the fraction of the distance  $\sigma_i$  from the ellipse’s horizontal center-line at which the ellipse becomes tangent to vertical, i.e., at the distance  $\rho_{ij}\sigma_i$  below the center-line as shown. As  $\rho_{ij}$  goes to  $+1$  or  $-1$ , the ellipse thins to a diagonal line.

It could happen that one of the parameters, say,  $\theta_j$ , is known from previous measurements to a precision much better than  $\sigma_j$ , so that the current measurement contributes almost nothing to the knowledge of  $\theta_j$ . However, the current measurement of  $\theta_i$  and its dependence on  $\theta_j$  may still be important. In this case, instead of quoting both parameter

**Table 36.2:**  $\Delta\chi^2$  or  $2\Delta\ln L$  corresponding to a coverage probability  $1 - \alpha$  in the large data sample limit, for joint estimation of  $m$  parameters.

$(1 - \alpha)$ (%)	$m = 1$	$m = 2$	$m = 3$
68.27	1.00	2.30	3.53
90.	2.71	4.61	6.25
95.	3.84	5.99	7.82
95.45	4.00	6.18	8.03
99.	6.63	9.21	11.34
99.73	9.00	11.83	14.16

estimates and their correlation, one sometimes reports the value of  $\theta_i$ , which minimizes  $\chi^2$  at a fixed value of  $\theta_j$ , such as the PDG best value. This  $\theta_i$  value lies along the dotted line between the points where the ellipse becomes tangent to vertical, and has statistical error  $\sigma_{\text{inner}}$  as shown on the figure, where  $\sigma_{\text{inner}} = (1 - \rho_{ij}^2)^{1/2}\sigma_i$ . Instead of the correlation  $\rho_{ij}$ , one reports the dependency  $d\hat{\theta}_i/d\theta_j$  which is the slope of the dotted line. This slope is related to the correlation coefficient by  $d\hat{\theta}_i/d\theta_j = \rho_{ij} \times \frac{\sigma_i}{\sigma_j}$ .

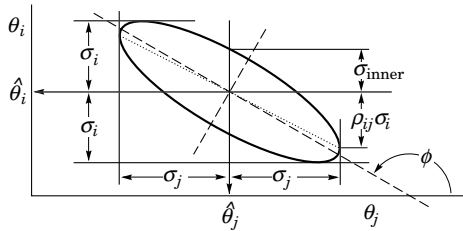


**Figure 36.5:** Standard error ellipse for the estimators  $\hat{\theta}_i$  and  $\hat{\theta}_j$ . In this case the correlation is negative.

As in the single-variable case, because of the symmetry of the Gaussian function between  $\theta$  and  $\hat{\theta}$ , one finds that contours of constant  $\ln L$  or  $\chi^2$  cover the true values with a certain, fixed probability. That is, the confidence region is determined by

$$\ln L(\theta) \geq \ln L_{\text{max}} - \Delta \ln L, \tag{36.58}$$

or where a  $\chi^2$  has been defined for use with the method of least-squares,

$$\chi^2(\theta) \leq \chi^2_{\text{min}} + \Delta\chi^2. \tag{36.59}$$

Values of  $\Delta\chi^2$  or  $2\Delta\ln L$  are given in Table 36.2 for several values of the coverage probability and number of fitted parameters.

For finite non-Gaussian data samples, the probability for the regions determined by equations (36.58) or (36.59) to cover the true value of  $\theta$  will depend on  $\theta$ , so these are not exact confidence regions according to our previous definition. Nevertheless, they can still have a coverage probability only weakly dependent on the true parameter, and approximately as given in Table 36.2. In any case, the coverage probability of the intervals or regions obtained according to this procedure can in principle be determined as a function of the true parameter(s), for example, using a Monte Carlo calculation.

One of the practical advantages of intervals that can be constructed from the log-likelihood function or  $\chi^2$  is that it is relatively simple to produce the interval for the combination of several experiments. If  $N$  independent measurements result in log-likelihood functions  $\ln L_i(\theta)$ , then the combined log-likelihood function is simply the sum,

$$\ln L(\theta) = \sum_{i=1}^N \ln L_i(\theta). \tag{36.60}$$

This can then be used to determine an approximate confidence interval or region with Eq. (36.58), just as with a single experiment.

**36.3.2.5. Poisson or binomial data:**

Another important class of measurements consists of counting a certain number of events,  $n$ . In this section, we will assume these are all events of the desired type, *i.e.*, there is no background. If  $n$  represents the number of events produced in a reaction with cross section  $\sigma$ , say, in a fixed integrated luminosity  $\mathcal{L}$ , then it follows a Poisson distribution with mean  $\nu = \sigma\mathcal{L}$ . If, on the other hand, one has selected a larger sample of  $N$  events and found  $n$  of them to have a particular property, then  $n$  follows a binomial distribution where the parameter  $p$  gives the probability for the event to possess the property in question. This is appropriate, *e.g.*, for estimates of branching ratios or selection efficiencies based on a given total number of events.

For the case of Poisson distributed  $n$ , the upper and lower limits on the mean value  $\nu$  can be found from the Neyman procedure to be

$$\nu_{\text{lo}} = \frac{1}{2}F_{\chi^2}^{-1}(\alpha_{\text{lo}}; 2n), \tag{36.61a}$$

$$\nu_{\text{up}} = \frac{1}{2}F_{\chi^2}^{-1}(1 - \alpha_{\text{up}}; 2(n + 1)), \tag{36.61b}$$

where the upper and lower limits are at confidence levels of  $1 - \alpha_{\text{lo}}$  and  $1 - \alpha_{\text{up}}$ , respectively, and  $F_{\chi^2}^{-1}$  is the quantile of the  $\chi^2$  distribution (inverse of the cumulative distribution). The quantiles  $F_{\chi^2}^{-1}$  can be obtained from standard tables or from the ROOT routine `TMath::ChisquareQuantile`. For central confidence intervals at confidence level  $1 - \alpha$ , set  $\alpha_{\text{lo}} = \alpha_{\text{up}} = \alpha/2$ .

**Table 36.3:** Lower and upper (one-sided) limits for the mean  $\nu$  of a Poisson variable given  $n$  observed events in the absence of background, for confidence levels of 90% and 95%.

$n$	$1 - \alpha = 90\%$		$1 - \alpha = 95\%$	
	$\nu_{\text{lo}}$	$\nu_{\text{up}}$	$\nu_{\text{lo}}$	$\nu_{\text{up}}$
0	–	2.30	–	3.00
1	0.105	3.89	0.051	4.74
2	0.532	5.32	0.355	6.30
3	1.10	6.68	0.818	7.75
4	1.74	7.99	1.37	9.15
5	2.43	9.27	1.97	10.51
6	3.15	10.53	2.61	11.84
7	3.89	11.77	3.29	13.15
8	4.66	12.99	3.98	14.43
9	5.43	14.21	4.70	15.71
10	6.22	15.41	5.43	16.96

It happens that the upper limit from Eq. (36.61b) coincides numerically with the Bayesian upper limit for a Poisson parameter, using a uniform prior p.d.f. for  $\nu$ . Values for confidence levels of 90% and 95% are shown in Table 36.3. For the case of binomially distributed  $n$  successes out of  $N$  trials with probability of success  $p$ , the upper and lower limits on  $p$  are found to be

$$p_{\text{lo}} = \frac{nF_F^{-1}[\alpha_{\text{lo}}; 2n, 2(N - n + 1)]}{N - n + 1 + nF_F^{-1}[\alpha_{\text{lo}}; 2n, 2(N - n + 1)]}, \tag{36.62a}$$

$$p_{\text{up}} = \frac{(n + 1)F_F^{-1}[1 - \alpha_{\text{up}}; 2(n + 1), 2(N - n)]}{(N - n) + (n + 1)F_F^{-1}[1 - \alpha_{\text{up}}; 2(n + 1), 2(N - n)]}. \tag{36.62b}$$

Here  $F_F^{-1}$  is the quantile of the  $F$  distribution (also called the Fisher–Snedecor distribution; see Ref. 4).

**36.3.2.6. Difficulties with intervals near a boundary:**

A number of issues arise in the construction and interpretation of confidence intervals when the parameter can only take on values in a restricted range. An important example is where the mean of a Gaussian variable is constrained on physical grounds to be non-negative. This arises, for example, when the square of the neutrino mass is estimated from  $\hat{m}^2 = \hat{E}^2 - \hat{p}^2$ , where  $\hat{E}$  and  $\hat{p}$  are independent, Gaussian-distributed estimates of the energy and momentum. Although the true  $m^2$  is constrained to be positive, random errors in  $\hat{E}$  and  $\hat{p}$  can easily lead to negative values for the estimate  $\hat{m}^2$ .

If one uses the prescription given above for Gaussian distributed measurements, which says to construct the interval by taking the estimate plus-or-minus-one standard deviation, then this can give intervals that are partially or entirely in the unphysical region. In fact, by following strictly the Neyman construction for the central confidence interval, one finds that the interval is truncated below zero; nevertheless an extremely small or even a zero-length interval can result.

An additional important example is where the experiment consists of counting a certain number of events,  $n$ , which is assumed to be Poisson-distributed. Suppose the expectation value  $E[n] = \nu$  is equal to  $s + b$ , where  $s$  and  $b$  are the means for signal and background processes, and assume further that  $b$  is a known constant. Then  $\hat{s} = n - b$  is an unbiased estimator for  $s$ . Depending on true magnitudes of  $s$  and  $b$ , the estimate  $\hat{s}$  can easily fall in the negative region. Similar to the Gaussian case with the positive mean, the central confidence interval or even the interval that gives the upper limit for  $s$  may be of zero length.

An additional difficulty arises when a parameter estimate is not significantly far away from the boundary, in which case it is natural to report a one-sided confidence interval (often an upper limit). It is straightforward to force the Neyman prescription to produce only an upper limit by setting  $x_2 = \infty$  in Eq. (36.49). Then  $x_1$  is uniquely determined and the upper limit can be obtained. If, however, the data come out such that the parameter estimate is not so close to the boundary, one might wish to report a central confidence interval (*i.e.*, an interval based on a two-sided test with equal upper and lower tail areas). As pointed out by Feldman and Cousins [31], however, if the decision to report an upper limit or two-sided interval is made by looking at the data (“flip-flopping”), then in general there will be parameter values for which the resulting intervals have a coverage probability less than  $1 - \alpha$ .

With the confidence intervals suggested in [31], the prescription determines whether the interval is one- or two-sided in a way which preserves the coverage probability (and are thus said to be *unified*) and in addition they avoid the problem of null intervals. The intervals based on the Feldman-Cousins prescription are of this type. For a given choice of  $1 - \alpha$ , if the parameter estimate is sufficiently close to the boundary, the method gives a one-sided limit. In the case of a Poisson variable in the presence of background, for example, this would occur if the number of observed events is compatible with the expected background. For parameter estimates increasingly far away from the boundary, *i.e.*, for increasing signal significance, the interval makes a smooth transition from one- to two-sided, and far away from the boundary, one obtains a central interval.

The intervals according to this method for the mean of Poisson variable in the absence of background are given in Table 36.4. (Note that  $\alpha$  in Ref. 31 is defined following Neyman [29] as the coverage probability; this is opposite the modern convention used here in which the coverage probability is  $1 - \alpha$ .) The values of  $1 - \alpha$  given here refer to the coverage of the true parameter by the whole interval  $[\nu_1, \nu_2]$ . In Table 36.3 for the one-sided upper limit, however,  $1 - \alpha$  refers to the probability to have  $\nu_{\text{up}} \geq \nu$  (or  $\nu_{\text{lo}} \leq \nu$  for lower limits).

A potential difficulty with unified intervals arises if, for example, one constructs such an interval for a Poisson parameter  $s$  of some yet to be discovered signal process with, say,  $1 - \alpha = 0.9$ . If the true signal parameter is zero, or in any case much less than the expected background, one will usually obtain a one-sided upper limit on  $s$ . In a certain fraction of the experiments, however, a two-sided interval

**Table 36.4:** Unified confidence intervals  $[\nu_1, \nu_2]$  for the mean of a Poisson variable given  $n$  observed events in the absence of background, for confidence levels of 90% and 95%.

$n$	$1 - \alpha = 90\%$		$1 - \alpha = 95\%$	
	$\nu_1$	$\nu_2$	$\nu_1$	$\nu_2$
0	0.00	2.44	0.00	3.09
1	0.11	4.36	0.05	5.14
2	0.53	5.91	0.36	6.72
3	1.10	7.42	0.82	8.25
4	1.47	8.60	1.37	9.76
5	1.84	9.99	1.84	11.26
6	2.21	11.47	2.21	12.75
7	3.56	12.53	2.58	13.81
8	3.96	13.99	2.94	15.29
9	4.36	15.30	4.36	16.77
10	5.50	16.50	4.75	17.82

for  $s$  will result. Since, however, one typically chooses  $1 - \alpha$  to be only 0.9 or 0.95 when setting limits, the value  $s = 0$  may be found below the lower edge of the interval before the existence of the effect is well established. It must then be communicated carefully that in excluding  $s = 0$  from the interval, one is not necessarily claiming to have discovered the effect.

It must then be communicated carefully that in excluding  $s = 0$  at, say, 90 or 95% confidence level from the interval, one is not necessarily claiming to have discovered the effect, for which one would usually require a higher level of significance (*e.g.*,  $5\sigma$ ).

The intervals constructed according to the unified procedure in Ref. 31 for a Poisson variable  $n$  consisting of signal and background have the property that for  $n = 0$  observed events, the upper limit decreases for increasing expected background. This is counter-intuitive, since it is known that if  $n = 0$  for the experiment in question, then no background was observed, and therefore one may argue that the expected background should not be relevant. The extent to which one should regard this feature as a drawback is a subject of some controversy (see, *e.g.*, Ref. 36).

Another possibility is to construct a Bayesian interval as described in Section 36.3.1. The presence of the boundary can be incorporated simply by setting the prior density to zero in the unphysical region. More specifically, the prior may be chosen using formal rules such as the reference prior or Jeffreys prior mentioned in Sec. 36.1.4. The use of such priors is currently receiving increased attention in HEP.

In HEP a widely used prior for the mean  $\mu$  of a Poisson distributed measurement has been uniform for  $\mu \geq 0$ . This prior does not follow from any fundamental rule nor can it be regarded as reflecting a reasonable degree of belief, since the prior probability for  $\mu$  to lie between any two finite limits is zero. It is more appropriately regarded as a procedure for obtaining intervals with frequentist properties that can be investigated. The resulting upper limits have a coverage probability that depends on the true value of the Poisson parameter, and is nowhere smaller than the stated probability content. Lower limits and two-sided intervals for the Poisson mean based on flat priors undercover, however, for some values of the parameter, although to an extent that in practical cases may not be too severe [2,19]. Intervals constructed in this way have the advantage of being easy to derive; if several independent measurements are to be combined then one simply multiplies the likelihood functions (cf. Eq. (36.60)).

An additional alternative is presented by the intervals found from the likelihood function or  $\chi^2$  using the prescription of Equations (36.58) or (36.59). However, the coverage probability is not, in general, independent of the true parameter, and these intervals can for some parameter values undercover. The coverage probability can, of course, be determined with some extra effort and reported with the result. These intervals are also invariant under transformation of the

parameter; this is not true for Bayesian intervals with a conventional flat prior, because a uniform distribution in, say,  $\theta$  will not be uniform if transformed to  $1/\theta$ . A study of the coverage of different intervals for a Poisson parameter can be found in [34]. Use of the likelihood function to determine approximate confidence intervals is discussed further in [35].

In any case, it is important to always report sufficient information so that the result can be combined with other measurements. Often this means giving an unbiased estimator and its standard deviation, even if the estimated value is in the unphysical region.

It can also be useful with a frequentist interval to calculate its subjective probability content using the posterior p.d.f. based on one or several reasonable guesses for the prior p.d.f. If it turns out to be significantly less than the stated confidence level, this warns that it would be particularly misleading to draw conclusions about the parameter's value from the interval alone.

#### References:

1. B. Efron, Am. Stat. **40**, 11 (1986).
2. R.D. Cousins, Am. J. Phys. **63**, 398 (1995).
3. A. Stuart, J.K. Ord, and S. Arnold, *Kendall's Advanced Theory of Statistics*, Vol. 2A: *Classical Inference and the Linear Model*, 6th ed., Oxford Univ. Press (1999), and earlier editions by Kendall and Stuart. The likelihood-ratio ordering principle is described at the beginning of Ch. 23. Chapter 26 compares different schools of statistical inference.
4. F.E. James, *Statistical Methods in Experimental Physics*, 2nd ed., (World Scientific, Singapore, 2007).
5. H. Cramér, *Mathematical Methods of Statistics*, Princeton Univ. Press, New Jersey (1958).
6. L. Lyons, *Statistics for Nuclear and Particle Physicists*, (Cambridge University Press, New York, 1986).
7. R. Barlow, Nucl. Instrum. Methods **A297**, 496 (1990).
8. G. Cowan, *Statistical Data Analysis*, (Oxford University Press, Oxford, 1998).
9. For a review, see S. Baker and R. Cousins, Nucl. Instrum. Methods **221**, 437 (1984).
10. For information on neural networks and related topics, see e.g., C.M. Bishop, *Neural Networks for Pattern Recognition*, Clarendon Press, Oxford (1995); C. Peterson and T. Rognvaldsson, An Introduction to Artificial Neural Networks, in *Proceedings of the 1991 CERN School of Computing*, C. Verkerk (ed.), CERN 92-02 (1992).
11. T. Hastie, R. Tibshirani, and J. Friedman, *The Elements of Statistical Learning* (2nd edition, Springer, New York, 2009).
12. A. Webb, *Statistical Pattern Recognition*, 2nd ed., (Wiley, New York, 2002).
13. L.I. Kuncheva, *Combining Pattern Classifiers*, (Wiley, New York, 2004).
14. Links to the *Proceedings of the PHYSTAT* conference series (Durham 2002, Stanford 2003, Oxford 2005, and Geneva 2007) can be found at [phystat.org](http://phystat.org).
15. A. Höcker *et al.*, *TMVA Users Guide*, [physics/0703039\(2007\)](http://physics/0703039(2007);); software available from [tmva.sf.net](http://tmva.sf.net).
16. I. Narsky, *StatPatternRecognition: A C++ Package for Statistical Analysis of High Energy Physics Data*, [physics/0507143\(2005\)](http://physics/0507143(2005);); software avail. from [sourceforge.net/projects/statpatrec](http://sourceforge.net/projects/statpatrec).
17. L. Demortier, *P-Values and Nuisance Parameters*, *Proceedings of PHYSTAT 2007*, CERN-2008-001, p. 23.
18. E. Gross and O. Vitells, Eur. Phys. J. **C70**, 525 (2010); [arXiv:1005.1891](http://arxiv.org/abs/1005.1891).
19. B.P. Roe and M.B. Woodroffe, Phys. Rev. **D63**, 13009 (2000).
20. A. O'Hagan and J.J. Forster, *Bayesian Inference*, (2nd edition, volume 2B of *Kendall's Advanced Theory of Statistics*, Arnold, London, 2004).
21. Devinderjit Sivia and John Skilling, *Data Analysis: A Bayesian Tutorial*, (Oxford University Press, 2006).
22. P.C. Gregory, *Bayesian Logical Data Analysis for the Physical Sciences*, (Cambridge University Press, 2005).
23. J.M. Bernardo and A.F.M. Smith, *Bayesian Theory*, (Wiley, 2000).
24. Robert E. Kass and Larry Wasserman, *The Selection of Prior Distributions by Formal Rules*, J. Am. Stat. Assoc. **91**, 1343 (1996).
25. J.M. Bernardo, J. R. Statist. Soc. **B41**, 113 (1979); J.M. Bernardo and J.O. Berger, J. Am. Stat. Assoc. **84**, 200 (1989). See also J.M. Bernardo, *Reference Analysis*, in *Handbook of Statistics*, 25 (D.K. Dey and C.R. Rao, eds.), 17-90, Elsevier (2005) and references therein.
26. L. Demortier, S. Jain, and H. Prosper, Phys. Rev. **D 82**, 034002 (2010); [arXiv:1002.1111](http://arxiv.org/abs/1002.1111).
27. P.H. Garthwaite, I.T. Jolliffe, and B. Jones, *Statistical Inference*, (Prentice Hall, 1995).
28. R.D. Cousins and V.L. Highland, *Incorporating systematic uncertainties into an upper limit*, Nucl. Instrum. Methods **A320**, 331 (1992).
29. J. Neyman, Phil. Trans. Royal Soc. London, Series A, **236**, 333 (1937), reprinted in *A Selection of Early Statistical Papers on J. Neyman*, (University of California Press, Berkeley, 1967).
30. Robert E. Kass and Adrian E. Raftery, *Bayes Factors*, J. Am. Stat. Assoc. **90**, 773 (1995).
31. G.J. Feldman and R.D. Cousins, Phys. Rev. **D57**, 3873 (1998). This paper does not specify what to do if the ordering principle gives equal rank to some values of  $x$ . Eq. 21.6 of Ref. 3 gives the rule: all such points are included in the acceptance region (the domain  $D(\alpha)$ ). Some authors have assumed the contrary, and shown that one can then obtain null intervals.
32. A.L. Read, *Modified frequentist analysis of search results (the  $CL_s$  method)*, in F. James, L. Lyons, and Y. Perrin (eds.), *Workshop on Confidence Limits*, CERN Yellow Report 2000-005, available through [cdsweb.cern.ch](http://cdsweb.cern.ch).
33. T. Junk, Nucl. Instrum. Methods **A434**, 435 (1999).
34. Joel Heinrich, *Coverage of Error Bars for Poisson Data*, CDF Statistics Note 6438, [www-cdf.fnal.gov/publications/cdf6438.coverage.pdf](http://www-cdf.fnal.gov/publications/cdf6438.coverage.pdf) (2003).
35. F. Porter, Nucl. Instrum. Methods **A368**, 793 (1996).
36. Workshop on Confidence Limits, CERN, 17-18 Jan. 2000, [www.cern.ch/CERN/Divisions/EP/Events/CLW/](http://www.cern.ch/CERN/Divisions/EP/Events/CLW/). The proceedings, F. James, L. Lyons, and Y. Perrin (eds.), CERN Yellow Report 2000-005, are available through [cdsweb.cern.ch](http://cdsweb.cern.ch). See also the Fermilab workshop at [conferences.fnal.gov/c12k/](http://conferences.fnal.gov/c12k/).
37. N. Reid, *Likelihood Inference in the Presence of Nuisance Parameters*, *Proceedings of PHYSTAT2003*, L. Lyons, R. Mount, and R. Reitmeyer, eds., eConf C030908, Stanford, 2003.
38. W.A. Rolke, A.M. Lopez, and J. Conrad, Nucl. Instrum. Methods **A551**, 493 (2005); [physics/0403059](http://physics/0403059).
39. Glen Cowan *et al.*, Eur. Phys. J. **C71**, 1554 (2011).

### 37. MONTE CARLO TECHNIQUES

Revised September 2011 by G. Cowan (RHUL).

Monte Carlo techniques are often the only practical way to evaluate difficult integrals or to sample random variables governed by complicated probability density functions. Here we describe an assortment of methods for sampling some commonly occurring probability density functions.

#### 37.1. Sampling the uniform distribution

Most Monte Carlo sampling or integration techniques assume a “random number generator,” which generates uniform statistically independent values on the half open interval  $[0, 1)$ ; for reviews see, e.g., [1,2].

Uniform random number generators are available in software libraries such as CERNLIB [3], CLHEP [4], and ROOT [5]. For example, in addition to a basic congruential generator `TRandom` (see below), ROOT provides three more sophisticated routines: `TRandom1` implements the RANLUX generator [6] based on the method by Lüscher, and allows the user to select different quality levels, trading off quality with speed; `TRandom2` is based on the maximally equidistributed combined Tausworthe generator by L’Ecuyer [7]; the `TRandom3` generator implements the Mersenne twister algorithm of Matsumoto and Nishimura [8]. All of the algorithms produce a periodic sequence of numbers, and to obtain effectively random values, one must not use more than a small subset of a single period. The Mersenne twister algorithm has an extremely long period of  $2^{19937} - 1$ .

The performance of the generators can be investigated with tests such as DIEHARD [9] or TestU01 [10]. Many commonly available congruential generators fail these tests and often have sequences (typically with periods less than  $2^{32}$ ), which can be easily exhausted on modern computers. A short period is a problem for the `TRandom` generator in ROOT, which, however, has the advantage that its state is stored in a single 32-bit word. The generators `TRandom1`, `TRandom2`, or `TRandom3` have much longer periods, with `TRandom3` being recommended by the ROOT authors as providing the best combination of speed and good random properties. For further information see, e.g., Ref. 11.

#### 37.2. Inverse transform method

If the desired probability density function is  $f(x)$  on the range  $-\infty < x < \infty$ , its cumulative distribution function (expressing the probability that  $x \leq a$ ) is given by Eq. (35.6). If  $a$  is chosen with probability density  $f(a)$ , then the integrated probability up to point  $a$ ,  $F(a)$ , is itself a random variable which will occur with uniform probability density on  $[0, 1]$ . Suppose  $u$  is generated according to a uniformly distributed in  $(0, 1)$ . If  $x$  can take on any value, and ignoring the endpoints, we can then find a unique  $x$  chosen from the p.d.f.  $f(x)$  for a given  $u$  if we set

$$u = F(x), \tag{37.1}$$

provided we can find an inverse of  $F$ , defined by

$$x = F^{-1}(u). \tag{37.2}$$

This method is shown in Fig. 37.1a. It is most convenient when one can calculate by hand the inverse function of the indefinite integral of  $f$ . This is the case for some common functions  $f(x)$  such as  $\exp(x)$ ,  $(1 - x)^n$ , and  $1/(1 + x^2)$  (Cauchy or Breit-Wigner), although it does not necessarily produce the fastest generator. Standard libraries contain software to implement this method numerically, working from functions or histograms in one or more dimensions, e.g., the UNU.RAN package [12], available in ROOT.

For a discrete distribution,  $F(x)$  will have a discontinuous jump of size  $f(x_k)$  at each allowed  $x_k, k = 1, 2, \dots$ . Choose  $u$  from a uniform distribution on  $(0, 1)$  as before. Find  $x_k$  such that

$$F(x_{k-1}) < u \leq F(x_k) \equiv \text{Prob}(x \leq x_k) = \sum_{i=1}^k f(x_i); \tag{37.3}$$

then  $x_k$  is the value we seek (note:  $F(x_0) \equiv 0$ ). This algorithm is illustrated in Fig. 37.1b.

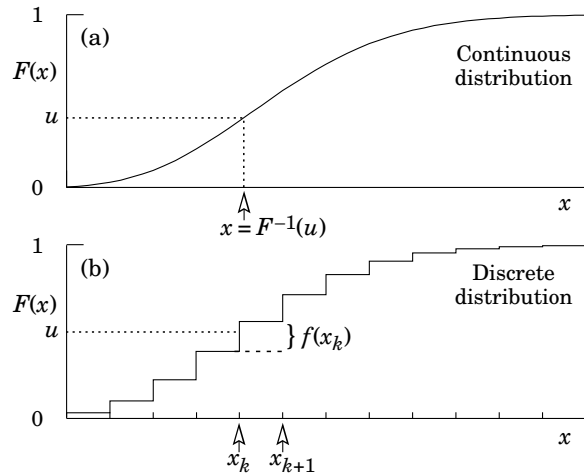


**Figure 37.1:** Use of a random number  $u$  chosen from a uniform distribution  $(0, 1)$  to find a random number  $x$  from a distribution with cumulative distribution function  $F(x)$ .

#### 37.3. Acceptance-rejection method (Von Neumann)

Very commonly an analytic form for  $F(x)$  is unknown or too complex to work with, so that obtaining an inverse as in Eq. (37.2) is impractical. We suppose that for any given value of  $x$ , the probability density function  $f(x)$  can be computed, and further that enough is known about  $f(x)$  that we can enclose it entirely inside a shape which is  $C$  times an easily generated distribution  $h(x)$ , as illustrated in Fig. 37.2. That is,  $Ch(x) \geq f(x)$  must hold for all  $x$ .

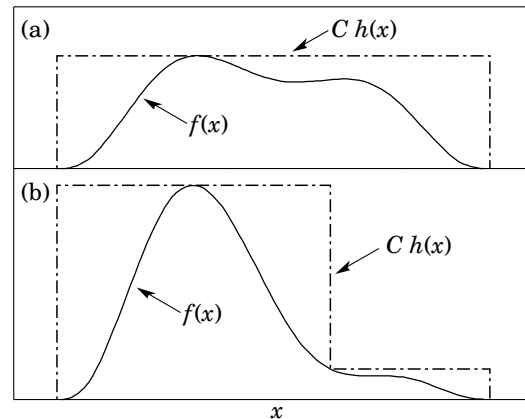


**Figure 37.2:** Illustration of the acceptance-rejection method. Random points are chosen inside the upper bounding figure, and rejected if the ordinate exceeds  $f(x)$ . The lower figure illustrates a method to increase the efficiency (see text).

Frequently  $h(x)$  is uniform or is a normalized sum of uniform distributions. Note that both  $f(x)$  and  $h(x)$  must be normalized to unit area, and therefore, the proportionality constant  $C > 1$ . To generate  $f(x)$ , first generate a candidate  $x$  according to  $h(x)$ . Calculate  $f(x)$  and the height of the envelope  $Ch(x)$ ; generate  $u$  and test if  $uCh(x) \leq f(x)$ . If so, accept  $x$ ; if not reject  $x$  and try again. If we regard  $x$  and  $uCh(x)$  as the abscissa and ordinate of a point in a two-dimensional plot, these points will populate the entire area  $Ch(x)$  in a smooth manner; then we accept those which fall under  $f(x)$ . The efficiency is the ratio of areas, which must equal  $1/C$ ; therefore we must keep  $C$  as close as possible to 1.0. Therefore, we try to choose  $Ch(x)$  to be as close to  $f(x)$  as convenience dictates, as in the lower part of Fig. 37.2.



### 37.4. Algorithms

Algorithms for generating random numbers belonging to many different distributions are given for example by Press [13], Ahrens and Dieter [14], Rubinstein [15], Devroye [16], Walck [17] and Gentle [18]. For many distributions, alternative algorithms exist, varying in complexity, speed, and accuracy. For time-critical applications, these algorithms may be coded in-line to remove the significant overhead often encountered in making function calls.

In the examples given below, we use the notation for the variables and parameters given in Table 35.1. Variables named “ $u$ ” are assumed to be independent and uniform on  $[0,1]$ . Denominators must be verified to be non-zero where relevant.

#### 37.4.1. Exponential decay :

This is a common application of the inverse transform method, and uses the fact that if  $u$  is uniformly distributed in  $[0,1]$ , then  $(1-u)$  is as well. Consider an exponential p.d.f.  $f(t) = (1/\tau) \exp(-t/\tau)$  that is truncated so as to lie between two values,  $a$  and  $b$ , and renormalized to unit area. To generate decay times  $t$  according to this p.d.f., first let  $\alpha = \exp(-a/\tau)$  and  $\beta = \exp(-b/\tau)$ ; then generate  $u$  and let

$$t = -\tau \ln(\beta + u(\alpha - \beta)). \quad (37.4)$$

For  $(a,b) = (0, \infty)$ , we have simply  $t = -\tau \ln u$ . (See also Sec. 37.4.6.)

#### 37.4.2. Isotropic direction in 3D :

Isotropy means the density is proportional to solid angle, the differential element of which is  $d\Omega = d(\cos\theta)d\phi$ . Hence  $\cos\theta$  is uniform  $(2u_1 - 1)$  and  $\phi$  is uniform  $(2\pi u_2)$ . For alternative generation of  $\sin\phi$  and  $\cos\phi$ , see the next subsection.

#### 37.4.3. Sine and cosine of random angle in 2D :

Generate  $u_1$  and  $u_2$ . Then  $v_1 = 2u_1 - 1$  is uniform on  $(-1,1)$ , and  $v_2 = 2u_2$  is uniform on  $(0,1)$ . Calculate  $r^2 = v_1^2 + v_2^2$ . If  $r^2 > 1$ , start over. Otherwise, the sine ( $S$ ) and cosine ( $C$ ) of a random angle (*i.e.*, uniformly distributed between zero and  $2\pi$ ) are given by

$$S = 2v_1v_2/r^2 \quad \text{and} \quad C = (v_1^2 - v_2^2)/r^2. \quad (37.5)$$

#### 37.4.4. Gaussian distribution :

If  $u_1$  and  $u_2$  are uniform on  $(0,1)$ , then

$$z_1 = \sin(2\pi u_1) \sqrt{-2 \ln u_2} \quad \text{and} \quad z_2 = \cos(2\pi u_1) \sqrt{-2 \ln u_2} \quad (37.6)$$

are independent and Gaussian distributed with mean 0 and  $\sigma = 1$ .

There are many variants of this basic algorithm, which may be faster. For example, construct  $v_1 = 2u_1 - 1$  and  $v_2 = 2u_2 - 1$ , which are uniform on  $(-1,1)$ . Calculate  $r^2 = v_1^2 + v_2^2$ , and if  $r^2 > 1$  start over. If  $r^2 < 1$ , it is uniform on  $(0,1)$ . Then

$$z_1 = v_1 \sqrt{\frac{-2 \ln r^2}{r^2}} \quad \text{and} \quad z_2 = v_2 \sqrt{\frac{-2 \ln r^2}{r^2}} \quad (37.7)$$

are independent numbers chosen from a normal distribution with mean 0 and variance 1.  $z'_i = \mu + \sigma z_i$  distributes with mean  $\mu$  and variance  $\sigma^2$ .

For a multivariate Gaussian with an  $n \times n$  covariance matrix  $V$ , one can start by generating  $n$  independent Gaussian variables,  $\{\eta_j\}$ , with mean 0 and variance 1 as above. Then the new set  $\{x_i\}$  is obtained as  $x_i = \mu_i + \sum_j L_{ij} \eta_j$ , where  $\mu_i$  is the mean of  $x_i$ , and  $L_{ij}$  are the components of  $L$ , the unique lower triangular matrix that fulfils  $V = LL^T$ . The matrix  $L$  can be easily computed by the following recursive relation (Cholesky's method):

$$L_{jj} = \left( V_{jj} - \sum_{k=1}^{j-1} L_{jk}^2 \right)^{1/2}, \quad (37.8a)$$

$$L_{ij} = \frac{V_{ij} - \sum_{k=1}^{j-1} L_{ik} L_{jk}}{L_{jj}}, \quad j = 1, \dots, n; \quad i = j + 1, \dots, n, \quad (37.8b)$$

where  $V_{ij} = \rho_{ij} \sigma_i \sigma_j$  are the components of  $V$ . For  $n = 2$  one has

$$L = \begin{pmatrix} \sigma_1 & 0 \\ \rho \sigma_2 & \sqrt{1 - \rho^2} \sigma_2 \end{pmatrix}, \quad (37.9)$$

and therefore the correlated Gaussian variables are generated as  $x_1 = \mu_1 + \sigma_1 \eta_1$ ,  $x_2 = \mu_2 + \rho \sigma_2 \eta_1 + \sqrt{1 - \rho^2} \sigma_2 \eta_2$ .

#### 37.4.5. $\chi^2(n)$ distribution :

To generate a variable following the  $\chi^2$  distribution for  $n$  degrees of freedom, use the Gamma distribution with  $k = n/2$  and  $\lambda = 1/2$  using the method of Sec. 37.4.6.

#### 37.4.6. Gamma distribution :

All of the following algorithms are given for  $\lambda = 1$ . For  $\lambda \neq 1$ , divide the resulting random number  $x$  by  $\lambda$ .

- If  $k = 1$  (the *exponential* distribution), accept  $x = -\ln u$ . (See also Sec. 37.4.1.)

- If  $0 < k < 1$ , initialize with  $v_1 = (e + k)/e$  (with  $e = 2.71828\dots$  being the natural log base). Generate  $u_1, u_2$ . Define  $v_2 = v_1 u_1$ .

**Case 1:**  $v_2 \leq 1$ . Define  $x = v_2^{1/k}$ . If  $u_2 \leq e^{-x}$ , accept  $x$  and stop, else restart by generating new  $u_1, u_2$ .

**Case 2:**  $v_2 > 1$ . Define  $x = -\ln([v_1 - v_2]/k)$ . If  $u_2 \leq x^{k-1}$ , accept  $x$  and stop, else restart by generating new  $u_1, u_2$ . Note that, for  $k < 1$ , the probability density has a pole at  $x = 0$ , so that return values of zero due to underflow must be accepted or otherwise dealt with.

- Otherwise, if  $k > 1$ , initialize with  $c = 3k - 0.75$ . Generate  $u_1$  and compute  $v_1 = u_1(1 - u_1)$  and  $v_2 = (u_1 - 0.5)\sqrt{c/v_1}$ . If  $x = k + v_2 - 1 \leq 0$ , go back and generate new  $u_1$ ; otherwise generate  $u_2$  and compute  $v_3 = 64v_1^3 u_2^2$ . If  $v_3 \leq 1 - 2v_2^2/x$  or if  $\ln v_3 \leq 2\{[k-1] \ln[x/(k-1)] - v_2\}$ , accept  $x$  and stop; otherwise go back and generate new  $u_1$ .

#### 37.4.7. Binomial distribution :

Begin with  $k = 0$  and generate  $u$  uniform in  $[0,1]$ . Compute  $P_k = (1-p)^n$  and store  $P_k$  into  $B$ . If  $u \leq B$  accept  $r_k = k$  and stop. Otherwise, increment  $k$  by one; compute the next  $P_k$  as  $P_k \cdot (p/(1-p)) \cdot (n-k)/(k+1)$ ; add this to  $B$ . Again, if  $u \leq B$ , accept  $r_k = k$  and stop, otherwise iterate until a value is accepted. If  $p > 1/2$ , it will be more efficient to generate  $r$  from  $f(r; n, q)$ , *i.e.*, with  $p$  and  $q$  interchanged, and then set  $r_k = n - r$ .

#### 37.4.8. Poisson distribution :

Iterate until a successful choice is made: Begin with  $k = 1$  and set  $A = 1$  to start. Generate  $u$ . Replace  $A$  with  $uA$ ; if now  $A < \exp(-\mu)$ , where  $\mu$  is the Poisson parameter, accept  $n_k = k - 1$  and stop. Otherwise increment  $k$  by 1, generate a new  $u$  and repeat, always starting with the value of  $A$  left from the previous try.

Note that the Poisson generator used in ROOT's `TRandom` classes before version 5.12 (including the derived classes `TRandom1`, `TRandom2`, `TRandom3`) as well as the routine `RNPSSN` from CERNLIB, use a Gaussian approximation when  $\mu$  exceeds a given threshold. This may be satisfactory (and much faster) for some applications. To do this, generate  $z$  from a Gaussian with zero mean and unit standard deviation; then use  $x = \max(0, [\mu + z\sqrt{\mu} + 0.5])$  where  $[\ ]$  signifies the greatest integer  $\leq$  the expression. The routines from Numerical Recipes [13] and CLHEP's routine `RandPoisson` do not make this approximation (see, *e.g.*, Ref. 11).

#### 37.4.9. Student's $t$ distribution :

Generate  $u_1$  and  $u_2$  uniform in  $(0,1)$ ; then  $t = \sin(2\pi u_1)[n(u_2^{-2/n} - 1)]^{1/2}$  follows the Student's  $t$  distribution for  $n > 0$  degrees of freedom ( $n$  not necessarily an integer).

Alternatively, generate  $x$  from a Gaussian with mean 0 and  $\sigma^2 = 1$  according to the method of 37.4.4. Next generate  $y$ , an independent gamma random variate, according to 37.4.6 with  $\lambda = 1/2$  and  $k = n/2$ . Then  $z = x/\sqrt{y/n}$  is distributed as a  $t$  with  $n$  degrees of freedom.

For the special case  $n = 1$ , the Breit-Wigner distribution, generate  $u_1$  and  $u_2$ ; set  $v_1 = 2u_1 - 1$  and  $v_2 = 2u_2 - 1$ . If  $v_1^2 + v_2^2 \leq 1$  accept  $z = v_1/v_2$  as a Breit-Wigner distribution with unit area, center at 0.0, and FWHM 2.0. Otherwise start over. For center  $M_0$  and FWHM  $\Gamma$ , use  $W = z\Gamma/2 + M_0$ .

### 37.4.10. Beta distribution :

The choice of an appropriate algorithm for generation of beta distributed random numbers depends on the values of the parameters  $\alpha$  and  $\beta$ . For, e.g.,  $\alpha = 1$ , one can use the transformation method to find  $x = 1 - u^{1/\beta}$ , and similarly if  $\beta = 1$  one has  $x = u^{1/\alpha}$ . For more general cases see, e.g., Refs. [17,18] and references therein.

### 37.5. Markov Chain Monte Carlo

In applications involving generation of random numbers following a multivariate distribution with a high number of dimensions, the transformation method may not be possible and the acceptance-rejection technique may have too low of an efficiency to be practical. If it is not required to have independent random values, but only that they follow a certain distribution, then Markov Chain Monte Carlo (MCMC) methods can be used. In depth treatments of MCMC can be found, e.g., in the texts by Robert and Casella [19], Liu [20], and the review by Neal [21].

MCMC is particularly useful in connection with Bayesian statistics, where a p.d.f.  $p(\boldsymbol{\theta})$  for an  $n$ -dimensional vector of parameters  $\boldsymbol{\theta} = (\theta_1, \dots, \theta_n)$  is obtained, and one needs the marginal distribution of a subset of the components. Here one samples  $\boldsymbol{\theta}$  from  $p(\boldsymbol{\theta})$  and simply records the marginal distribution for the components of interest.

A simple and broadly applicable MCMC method is the Metropolis-Hastings algorithm, which allows one to generate multidimensional points  $\boldsymbol{\theta}$  distributed according to a target p.d.f. that is proportional to a given function  $p(\boldsymbol{\theta})$ . It is not necessary to have  $p(\boldsymbol{\theta})$  normalized to unit area, which is useful in Bayesian statistics, as posterior probability densities are often determined only up to an unknown normalization constant.

To generate points that follow  $p(\boldsymbol{\theta})$ , one first needs a proposal p.d.f.  $q(\boldsymbol{\theta}; \boldsymbol{\theta}_0)$ , which can be (almost) any p.d.f. from which independent random values  $\boldsymbol{\theta}$  can be generated, and which contains as a parameter another point in the same space  $\boldsymbol{\theta}_0$ . For example, a multivariate Gaussian centered about  $\boldsymbol{\theta}_0$  can be used. Beginning at an arbitrary starting point  $\boldsymbol{\theta}_0$ , the Hastings algorithm iterates the following steps:

1. Generate a value  $\boldsymbol{\theta}$  using the proposal density  $q(\boldsymbol{\theta}; \boldsymbol{\theta}_0)$ ;
2. Form the Hastings test ratio,  $\alpha = \min \left[ 1, \frac{p(\boldsymbol{\theta})q(\boldsymbol{\theta}_0; \boldsymbol{\theta})}{p(\boldsymbol{\theta}_0)q(\boldsymbol{\theta}; \boldsymbol{\theta}_0)} \right]$ ;
3. Generate a value  $u$  uniformly distributed in  $[0, 1]$ ;
4. If  $u \leq \alpha$ , take  $\boldsymbol{\theta}_1 = \boldsymbol{\theta}$ . Otherwise, repeat the old point, i.e.,  $\boldsymbol{\theta}_1 = \boldsymbol{\theta}_0$ .
5. Set  $\boldsymbol{\theta}_0 = \boldsymbol{\theta}_1$  and return to step 1.

If one takes the proposal density to be symmetric in  $\boldsymbol{\theta}$  and  $\boldsymbol{\theta}_0$ , then this is the *Metropolis-Hastings* algorithm, and the test ratio becomes  $\alpha = \min[1, p(\boldsymbol{\theta})/p(\boldsymbol{\theta}_0)]$ . That is, if the proposed  $\boldsymbol{\theta}$  is at a value of probability higher than  $\boldsymbol{\theta}_0$ , the step is taken. If the proposed step is rejected, the old point is repeated.

Methods for assessing and optimizing the performance of the algorithm are discussed in, e.g., Refs. [19–21]. One can, for example, examine the autocorrelation as a function of the lag  $k$ , i.e., the correlation of a sampled point with that  $k$  steps removed. This should decrease as quickly as possible for increasing  $k$ .

Generally one chooses the proposal density so as to optimize some quality measure such as the autocorrelation. For certain problems it has been shown that one achieves optimal performance when the acceptance fraction, that is, the fraction of points with  $u \leq \alpha$ , is around 40%. This can be adjusted by varying the width of the proposal density. For example, one can use for the proposal p.d.f. a multivariate Gaussian with the same covariance matrix as that of the target p.d.f., but scaled by a constant.

#### References:

1. F. James, *Comp. Phys. Comm.* **60**, 329 (1990).
2. P. L'Ecuyer, *Proc. 1997 Winter Simulation Conference*, IEEE Press, Dec. 1997, 127–134.
3. The CERN Program Library (CERNLIB); see [cernlib.web.cern.ch/cernlib](http://cernlib.web.cern.ch/cernlib).
4. Leif Lönnblad, *Comp. Phys. Comm.* **84**, 307 (1994).
5. Rene Brun and Fons Rademakers, *Nucl. Inst. Meth.* **A389**, 81 (1997); see also [root.cern.ch](http://root.cern.ch).
6. F. James, *Comp. Phys. Comm.* **79**, 111 (1994), based on M. Lüscher, *Comp. Phys. Comm.* **79**, 100 (1994).
7. P. L'Ecuyer, *Mathematics of Computation*, **65**, 213 (1996) and **65**, 225 (1999).
8. M. Matsumoto and T. Nishimura, *ACM Transactions on Modeling and Computer Simulation*, Vol. 8, No. 1, January 1998, 3–30.
9. Much of DIEHARD is described in: G. Marsaglia, *A Current View of Random Number Generators*, keynote address, *Computer Science and Statistics: 16th Symposium on the Interface*, Elsevier (1985).
10. P. L'Ecuyer and R. Simard, *ACM Transactions on Mathematical Software* **33**, 4, Article 1, December 2007.
11. J. Heinrich, CDF Note CDF/MEMO/STATISTICS/PUBLIC/8032, 2006.
12. UNU.RAN is described at [statmath.wu.ac.at/software/unuran](http://statmath.wu.ac.at/software/unuran); see also W. Hörmann, J. Leydold, and G. Derflinger, *Automatic Nonuniform Random Variate Generation*, (Springer, New York, 2004).
13. W.H. Press *et al.*, *Numerical Recipes*, 3rd edition, (Cambridge University Press, New York, 2007).
14. J.H. Ahrens and U. Dieter, *Computing* **12**, 223 (1974).
15. R.Y. Rubinstein, *Simulation and the Monte Carlo Method*, (John Wiley and Sons, Inc., New York, 1981).
16. L. Devroye, *Non-Uniform Random Variate Generation*, (Springer-Verlag, New York, 1986); available online at [cg.scs.carleton.ca/~luc/rnbookindex.html](http://cg.scs.carleton.ca/~luc/rnbookindex.html).
17. C. Walck, *Handbook on Statistical Distributions for Experimentalists*, University of Stockholm Internal Report SUF-PFY/96-01, available from [www.physto.se/~walck](http://www.physto.se/~walck).
18. J.E. Gentle, *Random Number Generation and Monte Carlo Methods*, 2nd ed., (Springer, New York, 2003).
19. C.P. Robert and G. Casella, *Monte Carlo Statistical Methods*, 2nd ed., (Springer, New York, 2004).
20. J.S. Liu, *Monte Carlo Strategies in Scientific Computing*, (Springer, New York, 2001).
21. R.M. Neal, *Probabilistic Inference Using Markov Chain Monte Carlo Methods*, Technical Report CRG-TR-93-1, Dept. of Computer Science, University of Toronto, available from [www.cs.toronto.edu/~radford/res-mcmc.html](http://www.cs.toronto.edu/~radford/res-mcmc.html).

## 38. MONTE CARLO EVENT GENERATORS

Written January 2012 by P. Nason (INFN, Milan) and P.Z. Skands (CERN).

General-purpose Monte Carlo (GPMC) generators like HERWIG [1], HERWIG++ [2], PYTHIA 6 [3], PYTHIA 8 [4], and SHERPA [5], provide fully exclusive modeling of high-energy collisions. They play an essential role in QCD modeling (in particular for aspects beyond fixed-order perturbative QCD), in data analysis, where they are used together with detector simulation to provide a realistic estimate of the detector response to collision events, and in the planning of new experiments, where they are used to estimate signals and backgrounds in high-energy processes. They are built from several components, that describe the physics starting from very short distance scales, up to the typical scale of hadron formation and decay. Since QCD is weakly interacting at short distances (below a femtometer), the components of the GPMC dealing with short-distance physics are based upon perturbation theory. At larger distances, all soft hadronic phenomena, like hadronization and the formation of the underlying event, cannot be computed from first principles, and one must rely upon QCD-inspired models.

The purpose of this review is to illustrate the main components of these generators. It is divided into four sections. The first one deals with short-distance, perturbative phenomena. The basic concepts leading to the simulations of the dominant QCD processes are illustrated here. In the second section, hadronization phenomena are treated. The two most popular hadronization models for the formation of primary hadrons, the string and cluster models, are illustrated. The basics of the implementation of primary-hadron decays into stable ones is also illustrated here. In the third section, models for soft hadron physics are discussed. These include models for the underlying event, and for minimum-bias interactions. Issues of Bose-Einstein and color-reconnection effects are also discussed here. The fourth section briefly introduces the problem of MC tuning.

We use natural units throughout, such that  $c = 1$  and  $\hbar = 1$ , with energy, momenta and masses measured in GeV, and time and distances measured in  $\text{GeV}^{-1}$ .

### 38.1. Short-distance physics in GPMC generators

The short-distance components of a GPMC generator deal with the computation of the primary process at hand, with decays of short-lived particles, and with the generation of QCD and QED radiation, on time scales below  $1/\Lambda$ , with  $\Lambda$  denoting a typical hadronic scale of a few hundred MeV, corresponding roughly to an inverse femtometer. In  $e^+e^-$  annihilation, for example, the short-distance physics describes the evolution of the system from the instant when the  $e^+e^-$  pair annihilates up to a time when the size of the produced system is just below a femtometer.

In the present discussion we take the momentum scale of the primary process to be  $Q \gg \Lambda$ , so that the corresponding time and distance scale  $1/Q$  is small. Soft- and collinear-safe inclusive observables, such as total decay widths or inclusive cross sections, can be reliably computed in QCD perturbation theory (pQCD), with the perturbative expansion truncated at any fixed order  $n$ , and the remainder suppressed by  $\alpha_S(Q)^{n+1}$ .

Less inclusive observables, however, can receive large enhancements that destroy the convergence of the fixed-order expansion. This is due to the presence of collinear and infrared singularities in QCD. Thus, for example, a correction in which a parton from the primary interaction splits collinearly into two partons of comparable energy, is of order  $\alpha_S(Q) \ln(Q/\Lambda)$ , where the logarithm arises from an integral over a singularity regulated by the hadronic scale  $\Lambda$ . Since  $\alpha_S(Q) \propto 1/\ln(Q/\Lambda)$ , the corresponding cross section receives a correction of order unity. Two subsequent collinear splittings yield  $\alpha_S^2(Q) \ln^2(Q/\Lambda)$ , and so on. Thus, corrections of order unity arise at all orders in perturbation theory. The dominant region of phase space is the one where radiation is strongly ordered in a measure of hardness and/or angle. This means that, from a typical final-state configuration, by clustering together final-state parton pairs with, say, the smallest angle, recursively, we can reconstruct a branching tree, that may be viewed as the splitting history of the event. This history necessarily has some dependence on which measure is used to

order the clusterings. However, strong ordering in energy times angle, in virtuality or in transverse momenta are in fact equivalent in the dominant region. In fact, in the small-angle limit, the virtuality  $t$  of a parton of energy  $E$ , splitting into two on-shell partons is given by

$$t = E^2 z(1-z)(1-\cos\theta) \approx \frac{z(1-z)}{2} E^2 \theta^2, \quad (38.1)$$

where  $z$  and  $1-z$  are the energy fractions carried by the produced partons, and  $\theta$  is their relative angle. The transverse momentum of the final partons relative to the direction of the incoming one is given by

$$p_T^2 \approx z^2(1-z)^2 E^2 \theta^2. \quad (38.2)$$

Thus, significant differences between these measures only arise in regions with very small  $z$  or  $1-z$  values. In QCD, because of soft divergences, these regions are in fact important, and the choice of the appropriate ordering variable is very relevant (see Sec. 38.3).

The so called KLN theorem [6,7] guarantees that large logarithmically divergent corrections, arising from final-state collinear splitting and from soft emissions, cancel against the virtual corrections in the total cross section, order by order in perturbation theory. Furthermore, the factorization theorem guarantees that initial-state collinear singularities can be factorized into the parton density functions (PDFs). Therefore, the cross section for the basic process remains accurate up to corrections of higher orders in  $\alpha_S(Q)$ , provided it is interpreted as an inclusive cross section, rather than as a bare partonic cross section. Thus, for example, the leading order (LO) cross section for  $e^+e^- \rightarrow q\bar{q}$  is a good LO estimate of the  $e^+e^-$  cross section for the production of a pair of quarks accompanied by an arbitrary number of collinear and soft gluons, but is not a good estimate of the cross section for the production of a  $q\bar{q}$  pair with no extra radiation.

Shower algorithms are used to compute the cross section for generic hard processes including all leading-logarithmic (LL) corrections. These algorithms begin with the generation of the kinematics of the basic process, performed with a probability proportional to its LO partonic cross section, which is interpreted physically as the inclusive cross section for the basic process, followed by an arbitrary sequence of small-angle splittings. A probability is then assigned to each splitting sequence. Thus, the initial LO cross section is partitioned into the cross sections for a multitude of final states of arbitrary multiplicity. The sum of all these partial cross sections equals that of the primary process. This property of the GPMCs reflects the KLN cancellation mentioned earlier, and it is often called “unitarity of the shower process”, a name that reminds us that the KLN cancellation itself is a consequence of unitarity. The fact that a quantum mechanical process can be described in terms of composition of probabilities, rather than amplitudes, follows from the LL approximation. In fact, in the dominant, strongly ordered region, subsequent splittings are separated by increasingly large times and distances, and this suppresses interference effects.

We now illustrate the basic parton-shower algorithm, as first introduced in Ref. 8. The purpose of this illustration is to give a schematic representation of how shower algorithms work, to introduce some concepts that will be referred to in the following, and to show the relationship between shower algorithms and Feynman-diagram results. For simplicity, we consider the example of  $e^+e^-$  annihilation into  $q\bar{q}$  pairs. With each dominant (i.e. strongly ordered) final-state configuration one can associate a unique ordered tree diagram, by recursively clustering together final-state parton pairs with the smallest angle, and ending up with the hard production vertex (i.e. the  $\gamma^* \rightarrow q\bar{q}$ ). The momenta of all intermediate lines of the tree diagram are then uniquely determined from the final-state momenta. Virtualities in the graph are also strongly ordered. One assigns to each splitting vertex a virtuality  $t$ , equal to the invariant mass of the pair of generated partons, the energy fractions  $z$  and  $1-z$  of the two generated partons, and the azimuth  $\phi$  of the splitting process with respect to the momentum of the incoming parton. For definiteness, we assume that  $z$  and  $\phi$  are defined in the center-of-mass (CM) frame of the  $e^+e^-$  collision, although other definitions are possible that differ only beyond the LL approximation. The differential cross section for

a given final state is given by the product of the differential cross section for the initial  $e^+e^- \rightarrow q\bar{q}$  process, multiplied by a factor

$$\Delta_i(t, t') \frac{\alpha_S(t)}{2\pi} P_{i,jk}(z) \frac{dt}{t} \frac{d\phi}{2\pi} \quad (38.3)$$

for each intermediate line ending in a splitting vertex. We have denoted with  $t'$  the maximal virtuality that is allowed for the line, with  $t$  its virtuality, and  $z$  and  $\phi$  refer to the splitting process.  $\Delta(t, t')$  is the so-called Sudakov form factor

$$\Delta_i(t, t') = \exp \left[ - \int_t^{t'} \frac{dq^2}{q^2} \frac{\alpha_S(q^2)}{2\pi} \sum_{jk} P_{i,jk}(z) dz \frac{d\phi}{2\pi} \right]. \quad (38.4)$$

The suffixes  $i$  and  $jk$  represent the parton species of the incoming and final partons, respectively, and  $P_{i,jk}(z)$  are the Altarelli-Parisi [9] splitting kernels. Final-state lines that do not undergo any further splitting are associated with a factor

$$\Delta_i(t_0, t'), \quad (38.5)$$

where  $t_0$  is an infrared cutoff defined by the shower hadronization scale (at which the charges are screened by hadronization) or, for an unstable particle, its width (a source cannot emit radiation with a period exceeding its lifetime).

Notice that the definition of the Sudakov form factor is such that

$$\Delta_i(t_2, t_1) + \int_{t_2}^{t_1} \frac{dt}{t} dz \frac{d\phi}{2\pi} \sum_{jk} \Delta_i(t, t_1) \frac{\alpha_S(t)}{2\pi} P_{i,jk}(z) = 1. \quad (38.6)$$

This implies that the cross section for developing the shower up to a given stage does not depend on what happens next, since subsequent factors for further splitting or not splitting add up to one.

The shower cross section can then be formulated in a probabilistic way. The Sudakov form factor  $\Delta_i(t_2, t_1)$  is interpreted as the probability for a splitting *not* to occur, for a parton of type  $i$ , starting from a branching vertex at the scale  $t_1$ , down to a scale  $t_2$ . Notice that  $0 < \Delta_i(t_2, t_1) \leq 1$ , where the upper extreme is reached for  $t_2 = t_1$ , and the lower extreme is approached for  $t_2 = t_0$ . From Eq. (38.4), it seems that the Sudakov form factor should vanish if  $t_2 = 0$ . However, because of the presence of the running coupling in the integrand,  $t_2$  cannot be taken smaller than some cutoff scale of the order of  $\Lambda$ , so that at its lower extreme the Sudakov form factor is small, but not zero. Event generation then proceeds as follows. One gets a uniform random number  $0 \leq r \leq 1$ , and seeks a solution of the equation  $r = \Delta_i(t_2, t_1)$  as a function of  $t_2$ . If  $r$  is too small and no solution exists, no splitting is generated, and the line is interpreted as a final parton. If a solution  $t_2$  exists, a branching is generated at the scale  $t_2$ . Its  $z$  value and the final parton species  $jk$  are generated with a probability proportional to  $P_{i,jk}(z)$ . The azimuth is generated uniformly. This procedure is started with both the initial quark and the antiquark, and is applied recursively to all generated partons, thus producing two shower cascades. It may generate an arbitrary number of partons, and it stops when no final-state partons undergo further splitting.

We emphasize that the shower cross section described above can be derived from perturbative QCD by keeping only the collinear-dominant real and virtual contributions to the cross section. In particular, up to terms that vanish after azimuthal averaging, the product of the cross section for the basic process, times the factors

$$\frac{\alpha_S}{2\pi} \frac{dt}{t} dz \frac{d\phi}{2\pi} P_{i,jk}(z) \quad (38.7)$$

at each branching vertex, gives the leading collinear contribution to the tree-level cross section for the same process. The dominant virtual corrections in the same approximation are provided by the running coupling at each vertex and by the Sudakov form factors in the intermediate lines.

**38.1.1. Angular correlations :** In gluon splitting processes ( $g \rightarrow q\bar{q}$ ,  $g \rightarrow gg$ ) in the collinear approximation, the distribution of the split pair is not uniform in azimuth, and the Altarelli-Parisi splitting functions are recovered only after azimuthal averaging. This dependence is due to the interference of positive and negative helicity states for the gluon that undergoes splitting. Spin correlations propagate through the splitting process, and determine acausal correlations of the EPR kind [10]. A method to partially account for these effects was introduced in Ref. 11, in which the azimuthal correlation between two successive splittings is computed by averaging over polarizations. This can then be applied at each branching step. Acausal correlations are argued to be small, and are discarded with this method, that is still used in the PYTHIA code [139]. A method that fully includes spin correlation effects was later proposed by Collins [12], and has been implemented in the fortran HERWIG code [13].

**38.1.2. Initial-state radiation :** Initial-state radiation (ISR) arises because incoming charged particles can radiate before entering the hard-scattering process. In doing so, they acquire a non-vanishing transverse momentum, and their virtuality becomes negative (spacelike). The dominant logarithmic region is the collinear one, where virtualities become larger and larger in absolute value with each emission, up to a limit given by the hardness of the basic process itself. A shower that starts by considering the highest virtualities first would thus have to work backward in time for ISR. A corresponding backwards-evolution algorithm was formulated by Sjöstrand [14], and was basically adopted in all shower models.

The key point in backwards evolution is that the evolution probability depends on the amount of partons that could have given rise to the one being evolved. This is reflected by introducing the ratio of the PDF after the branching to the PDF before the branching in the definition of the backward-evolution Sudakov form factor,

$$\Delta_i^{\text{ISR}}(t, t') = \exp \left[ - \int_{t'}^t \frac{dt''}{t''} \frac{\alpha_S(t'')}{2\pi} \int_x^1 \frac{dz}{z} \sum_{jk} P_{j,ik}(z) \frac{f_j(t'', x/z)}{f_i(t'', x)} \right]. \quad (38.8)$$

Notice that there are two uses of the PDFs: they are used to compute the cross section for the basic hard process, and they control ISR via backward evolution. Since the evolution is generated with leading-logarithmic accuracy, it is acceptable to use two different PDF sets for these two tasks, provided they agree at the LO level.

In the context of GPMC evolution, each ISR emission generates a finite amount of transverse momentum. Details on how the recoils generated by these transverse “kicks” are distributed among other partons in the event, in particular the ones involved in the hard process, constitute one of the main areas of difference between existing algorithms, see Ref. 15. An additional  $\mathcal{O}(1 \text{ GeV})$  of “primordial  $k_T$ ” is typically added, to represent the sum of unresolved and/or non-perturbative motion below the shower cutoff scale.

**38.1.3. Soft emissions and QCD coherence :** In massless field theories like QCD, there are two sources of large logarithms of infrared origin. One has to do with collinear singularities, which arise when two final-state particles become collinear, or when a final-state particle becomes collinear to an initial-state one. The other has to do with the emission of soft gluons at arbitrary angles. Because of that, it turns out that in QCD perturbation theory two powers of large logarithms can arise for each power of  $\alpha_S$ . The expansion in leading soft and collinear logarithms is often referred to as the double-logarithmic expansion.

Within the conventional parton-shower formalism, based on collinear factorization, it was shown in a sequel of publications (see Ref. 16 and references therein) that the double-logarithmic region can be correctly described by using the angle of the emissions as the ordering variable, rather than the virtuality, and that the argument of  $\alpha_S$  at the splitting vertex should be the relative parton transverse momentum after the splitting. Physically, the ordering in angle approximates the coherent interference arising from large-angle soft emission from a bunch of collinear partons. Without this effect,

the particle multiplicity would grow too rapidly with energy, in conflict with  $e^+e^-$  data. For this reason, angular ordering is used as the evolution variable in both the HERWIG [16] and HERWIG++ [17] programs, and an angular veto is imposed on the virtuality-ordered evolution in PYTHIA 6 [18].

A radical alternative formulation of QCD cascades first proposed in Ref. 19 focuses upon soft emission, rather than collinear emission, as the basic splitting mechanism. It then becomes natural to consider a branching process where it is a parton pair (i.e. a dipole) rather than a single parton, that emits a soft parton. Adding a suitable correction for non-soft, collinear partons, one can achieve in this framework the correct logarithmic structure for both soft and collinear emissions in the limit of large number of colors  $N_c$ , without any explicit angular-ordering requirement. The ARIADNE [20] and VINCIA [21] programs are based on this approach. In SHERPA, the default shower [22] is also of a dipole type [23], while the  $p_\perp$ -ordered showers in PYTHIA 6 and 8 represent a hybrid, combining collinear splitting kernels with dipole kinematics [24].

**38.1.4. Massive quarks :** Quark masses act as cut-off on collinear singularities. If the mass of a quark is below, or of the order of  $\Lambda$ , its effect in the shower is small. For larger quark masses, like in  $c$  or  $b$  production, it is the mass, rather than the typical hadronic scale, that cuts off collinear radiation. For a quark with energy  $E$  and mass  $m_Q$ , the divergent behavior  $d\theta/\theta$  of the collinear splitting process is regulated for  $\theta \leq \theta_0 = m_Q/E$ . We thus expect less collinear activity for heavy quarks than for light ones, which in turn is the reason why heavy quarks carry a larger fraction of the momentum acquired in the hard production process.

This feature can be implemented with different levels of sophistication. Using the fact that soft emission exhibits a zero at zero emission angle, older parton shower algorithms simply limited the shower emission to be not smaller than the angle  $\theta_0$ . More modern approaches are used in both PYTHIA, where mass effects are included using a kind of matrix-element correction method [25], and in HERWIG++ and SHERPA, where a generalization of the Altarelli-Parisi splitting kernel is used for massive quarks [26].

**38.1.5. Color information :** Shower MC generators track large- $N_c$  color information during the development of the shower. In the large- $N_c$  limit, a quark is represented by a color line, i.e. a line with an arrow in the direction of the shower development, an antiquark by an anticolor line, with the arrow in the opposite direction, and a gluon by a pair of color-anticolor lines. The rules for color propagation are:

$$\begin{array}{c} \rightarrow e e e \rightarrow \quad e e e \leftarrow \quad e e e \rightarrow \\ \rightarrow e e e \rightarrow \quad e e e \leftarrow \quad e e e \rightarrow \end{array} \quad (38.9)$$

At the end of the shower development, partons are connected by color lines. We can have a quark directly connected by a color line to an antiquark, or via an arbitrary number of intermediate gluons, as shown in Fig. 38.1.

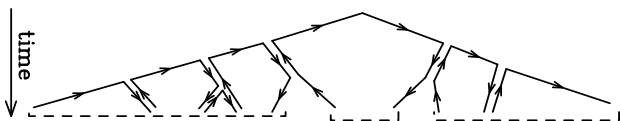


**Figure 38.1:** Color development of a shower in  $e^+e^-$  annihilation. Systems of color-connected partons are indicated by the dashed lines.

It is also possible for a set of gluons to be connected cyclically in color, as e.g. in the decay  $\Upsilon \rightarrow ggg$ .

The color information is used in angular-ordered showers, where the angle of color-connected partons determines the initial angle for the shower development, and in dipole showers, where dipoles are always color-connected partons. It is also used in hadronization models, where the initial strings or clusters used for hadronization are formed by systems of color-connected partons.

**38.1.6. Electromagnetic corrections :** The physics of photon emission from light charged particles can also be treated with a shower MC algorithm. A high-energy electron, for example, is accompanied by bremsstrahlung photons, which considerably affect its dynamics. Also here, similarly to the QCD case, electromagnetic corrections are of order  $\alpha_{em} \ln Q/m_e$ , or even of order  $\alpha_{em} \ln Q/m_e \ln E_\gamma/E$  in the region where soft photon emission is important, so that their inclusion in the simulation process is mandatory. This can be done with a Monte Carlo algorithm. In case of photons emitted by leptons, at variance with the QCD case, the shower can be continued down to values of the lepton virtuality that are arbitrarily close to its mass shell. In practice, photon radiation must be cut off below a certain energy, in order for the shower algorithm to terminate. Therefore, there is always a minimum energy for emitted photons that depends upon the implementations (and so does the MC truth for a charged lepton). In the case of electrons, this energy is typically of the order of its mass. Electromagnetic radiation below this scale is not enhanced by collinear singularities, and is thus bound to be soft, so that the electron momentum is not affected by it.

For photons emitted from quarks, we have instead the obvious limitation that the photon wavelength cannot exceed the typical hadronic size. Longer-wavelength photons are in fact emitted by hadrons, rather than quarks. This last effect is in practice never modeled by existing shower MC implementations. Thus, electromagnetic radiation from quarks is cut off at a typical hadronic scale.

**38.1.7. Beyond-the-Standard-Model Physics :** The inclusion of processes for physics beyond the Standard Model (BSM) in event generators is to some extent just a matter of implementing the relevant hard processes and (chains of) decays, with the level of difficulty depending on the complexity of the model and the degree of automation [27,28]. Notable exceptions are long-lived colored particles [29], particles in exotic color representations, and particles showering under new gauge symmetries, with a growing set of implementations documented in the individual GPMC manuals. Further complications that may be relevant are finite-width effects (discussed in Sec. 38.1.8) and the assumed threshold behavior.

In addition to code-specific implementations [15], there are a few commonly adopted standards that are useful for transferring information and events between codes. Currently, the most important of these is the Les Houches Event File (LHEF) standard [30], normally used to transfer parton-level events from a hard-process generator to a shower generator. Another important standard is the Supersymmetry Les Houches Accord (SLHA) format [31], originally used to transfer information on supersymmetric particle spectra and couplings, but by now extended to apply also to more general BSM frameworks and incorporated within the LHEF standard [32].

**38.1.8. Decay Chains and Particle Widths :** In most BSM processes and some SM ones, an important aspect of the event simulation is how decays of short-lived particles, such as top quarks, electroweak and Higgs bosons, and new BSM resonances, are handled. We here briefly summarize the spectrum of possibilities, but emphasize that there is no universal standard. Users are advised to check whether the treatment of a given code is adequate for the physics study at hand.

The appearance of an unstable resonance as a physical particle at some intermediate stage of the event generation implies that its production and decay processes are treated as being factorized. This is valid up to corrections of order  $\Gamma/m_0$ , with  $\Gamma$  the width and  $m_0$  the pole mass. States whose widths are a substantial fraction of their mass should not be treated as “physical particles,” but rather as intrinsically off-shell internal propagator lines.

For states treated as physical particles, two aspects are relevant: the mass distribution of the decaying particle itself and the distributions of its decay products. For the former, matrix-element generators often use a simple  $\delta$  function at  $m_0$ . The next level up, typically used in GPMCs, is to use a Breit-Wigner distribution (relativistic or non-relativistic), which formally resums higher-order virtual corrections to the mass distribution. Note, however, that this still only generates an

improved picture for *moderate* fluctuations away from  $m_0$ . Similarly to above, particles that are significantly off-shell (in units of  $\Gamma$ ) should not be treated as resonant, but rather as internal off-shell propagator lines. In most GPMCs, further refinements are included, for instance by letting  $\Gamma$  be a function of  $m$  (“running widths”) and by limiting the magnitude of the allowed fluctuations away from  $m_0$ .

For the distributions of the decay products, the simplest treatment is again to assign them their respective  $m_0$  values, with a uniform phase-space distribution. A more sophisticated treatment distributes the decay products according to the differential decay matrix elements, capturing at least the internal dynamics and helicity structure of the decay process, including EPR-like correlations. Further refinements include polarizations of the external states [33] and assigning the decay products their own Breit-Wigner distributions, the latter of which opens the possibility to include also intrinsically off-shell decay channels, like  $H \rightarrow WW^*$ .

During subsequent showering of the decay products, most parton-shower models will preserve their total invariant mass, so as not to skew the original resonance shape.

When computing partial widths and/or modifying decay tables, one should be aware of the danger of double-counting intermediate on-shell particles, see Sec. 38.2.3.

**38.1.9. Matching with Matrix Elements** : Shower algorithms are based upon a combination of the collinear (small-angle) and soft (small-energy) approximations and are thus inaccurate for hard, large-angle emissions. They also lack next-to-leading order (NLO) corrections to the basic process.

Traditional GPMCs, like HERWIG and PYTHIA, have included for a long time the so called Matrix Element Corrections (MEC), first formulated in Ref. 34 with later developments summarized in Ref. 15. They are available for processes involving two incoming and one outgoing or one incoming and two outgoing particles, like DIS, vector boson and Higgs production and decays, and top decays. The MEC corrects the emission of the hardest jets at large angles, so that it becomes exact at leading order.

In the past decade, considerable progress has taken place in order to improve the parton shower description of hard collisions, in two different directions: the so called Matrix Elements and Parton Shower matching (ME+PS from now on), and the matching of NLO calculations and Parton Showers (NLO+PS).

The ME+PS method allows one to use tree-level matrix elements for hard, large-angle emissions. It was first formulated in the so-called CKKW paper [35], and several variants have appeared, including the CKKW-L, MLM, and pseudoshower methods, see Refs. 36, 15 for summaries. Truncated showers are required [37] in order to maintain color coherence when interfacing matrix-element calculations to angular-ordered parton showers using these methods. It is also important to ensure consistent  $\alpha_S$  choices between the real (ME-driven) and virtual (PS-driven) corrections [38].

In the ME+PS method one typically starts by generating exact matrix elements for the production of the basic process plus a certain number  $\leq n$  of other partons. A minimum separation is imposed on the produced partons, requiring, for example, that the relative transverse momentum in any pair of partons is above a given cut  $Q_{\text{cut}}$ . One then reweights these amplitudes in such a way that, in the strongly ordered region, the virtual effects that are included in the shower algorithm (i.e. running couplings and Sudakov form factors) are also accounted for. At this stage the generated configurations are tree-level accurate at large angle, and at small angle they match the results of the shower algorithm, except that there are no emissions below the scale  $Q_{\text{cut}}$ , and no final states with more than  $n$  partons. These kinematic configurations are thus fed into a GPMC, that must generate all splittings with relative transverse momentum below the scale  $Q_{\text{cut}}$ , for initial events with less than  $n$  partons, or below the scale of the smallest pair transverse momentum, for events with exactly  $n$  partons. The matching parameter  $Q_{\text{cut}}$  must be chosen to be large enough for fixed-order perturbation theory to hold, but small enough so that the shower is accurate for emissions below it. Notice that the accuracy achieved with MEC is equivalent to that of ME+PS

with  $n = 1$ , where MEC has the advantage of not having a matching parameter  $Q_{\text{cut}}$ .

The popularity of the ME+PS method is due to the fact that processes with many jets appear often as background of new physics searches. These jets are typically required to be well separated, and to have large transverse momenta. These kinematical configurations, away from the small-angle region, are precisely those where GPMCs fail to be accurate, and it is thus mandatory to describe them using exact tree-level matrix element calculations.

The NLO+PS methods extend the accuracy of the generation of the basic process at the NLO level in QCD. They must thus include the radiation of an extra parton with full tree-level accuracy, since this radiation constitutes a NLO correction to the basic process. They must also include NLO virtual corrections. They can be viewed as an extension of the MEC method with the inclusion of NLO virtual corrections. They are however more general, since they are applicable to processes of arbitrary complexity. Two of these methods are now widely used: MC@NLO [39] and POWHEG [37,40], with several alternative methods now also being pursued, see Ref. 15 and references therein.

NLO+PS generators should produce NLO accurate distributions for inclusive quantities, and should generate the hardest jet with tree-level accuracy even at large angle. It should be recalled, though, that in  $2 \rightarrow 1$  processes like  $Z/W$  production, GPMCs including MEC and weighted by a constant  $K$  factor may perform nearly as well, and, if suitably tuned, may even yield a better description of data. It may thus be wise to consider tuning also the NLO+PS generators for these processes.

ME+PS generators should be preferred over NLO+PS ones when one needs an accurate description of hard, large-angle emissions, beyond the hardest jet. Attempts to merge ME+PS and NLO+PS, in order to get event samples that have the advantage of both methods have appeared, see Refs. 41, 15, and references therein.

Several ME+PS implementations use existing LO generators, like ALPGEN [42], MADGRAPH [43], and others summarized in Ref. 36, for the calculation of the matrix element, and feed the partonic events to a GPMC like PYTHIA or HERWIG using the Les Houches Interface for User Processes (LHI/LHEF) [44,30]. SHERPA and HERWIG++ also include their own matrix-element generators and matching algorithms.

Several NLO+PS processes are implemented in the MC@NLO program [39], together with the new AMC@NLO development [45], and in the POWHEG BOX framework [40]. Again, SHERPA and HERWIG++, also include their own POWHEG implementation, suitably adapted with the inclusion of vetoed and truncated showers, for several processes.

## 38.2. Hadronization Models

In the context of event generators, *hadronization* denotes the process by which a set of colored partons (*after* showering) is transformed into a set of color-singlet *primary* hadrons, which may then subsequently decay further. This non-perturbative transition takes place at the *hadronization scale*  $Q_{\text{had}}$ , which by construction is identical to the infrared cutoff of the parton shower. In the absence of a first-principles solution to the relevant dynamics, event generators use QCD-inspired phenomenological models to describe this transition.

A key difference between MC hadronization models and the fragmentation-function (FF) formalism used to describe inclusive hadron spectra in perturbative QCD (see Chap. 9 of PDG book) is that the former is always defined at the hadronization scale, while the latter can be defined at an arbitrary perturbative scale  $Q$ . They can therefore only be compared directly if the perturbative evolution between  $Q$  and  $Q_{\text{had}}$  is taken into account. FFs are calculable in pQCD, given a non-perturbative initial condition obtained by fits to hadron spectra. In the MC context, one can prove that the correct QCD evolution of the FFs arises from the shower formalism, with the hadronization model providing an explicit parametrization of the non-perturbative component. It should be kept in mind, however, that the MC modeling of shower and hadronization includes much more information on the final state since it is fully exclusive (i.e., it addresses all particles in the final state explicitly), while FFs only describe inclusive spectra. This exclusivity also enables MC models to



make use of the color-flow information coming from the perturbative shower evolution (see Sec. 38.1.5) to determine between which partons the confining potentials should arise.

If one had an exact hadronization model, its dependence upon the hadronization scale  $Q_{\text{had}}$  would be compensated by the corresponding scale dependence of the shower algorithm, which stops generating branchings at the scale  $Q_{\text{had}}$ . However, due to their complicated and fully exclusive nature, it is generally not possible to enforce this compensation automatically in MC models of hadronization. One must therefore be aware that the model must be “retuned” by hand if changes are made to the perturbative evolution, in particular if the infrared cutoff is modified. Tuning is discussed briefly in Sec. 38.4.

An important result in “quenched” lattice QCD (see Chap. 17 of PDG book) is that the potential of the color-dipole field between a charge and an anticharge appears to grow linearly with the separation of the charges, at distances greater than about a femtometer. This is known as “linear confinement”, and it forms the starting point for the *string model of hadronization*, discussed below in Sec. 38.2.1. Alternatively, a property of perturbative QCD called “preconfinement” is the basis of the *cluster model of hadronization*, discussed in Sec. 38.2.2.

Finally, it should be emphasized that the so-called “parton level” that can be obtained by switching off hadronization in a GPMC, is not a universal concept, since each model defines the hadronization scale differently (e.g. by a cutoff in  $p_{\perp}$ , invariant mass, etc., with different tunes using different values for the cutoff). Comparisons to distributions at this level may therefore be used to provide an idea of the overall impact of hadronization corrections within a given model, but should be avoided in the context of physical observables.

**38.2.1. The String Model:** Starting from early concepts [46], several hadronization models based on strings have been proposed [15]. Of these, the most widely used today is the so-called Lund model [47,48], implemented in PYTHIA [139,140]. We concentrate on that particular model here, though many of the overall concepts would be shared by any string-inspired method.

Consider a color-connected quark-antiquark pair with no intermediate gluons emerging from the parton shower (like the  $\bar{q}q$  pair in the center of Fig. 38.1), e.g. a red  $q$  and an antired  $\bar{q}$ . As the charges move apart, linear confinement implies that a potential  $V(r) = \kappa r$  is reached for large distances  $r$ . (At short distances, there is a Coulomb term  $\propto 1/r$  as well, but this is neglected in the Lund string.) This potential describes a string with tension  $\kappa \sim 1 \text{ GeV/fm} \sim 0.2 \text{ GeV}^2$ . The physical picture is that of a color flux tube being stretched between the  $q$  and the  $\bar{q}$ .

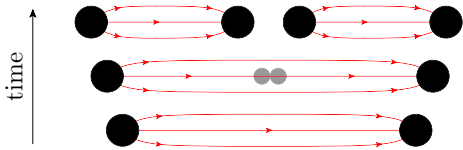


**Figure 38.2:** Illustration of string breaking by quark pair-creation in the string field.

As the string grows, the non-perturbative creation of quark-antiquark pairs can break the string, via the process  $(q\bar{q}) \rightarrow (q\bar{q}') + (q'\bar{q})$ , illustrated in Fig. 38.2. More complicated color-connected quark-antiquark configurations involving intermediate gluons (like the  $\bar{q}gggq$  and  $\bar{q}gq$  systems on the left and right part of Fig. 38.1) are treated by representing gluons as transverse “kinks.” Thus soft gluons effectively build up a transverse structure in the originally one-dimensional object, with infinitely soft ones smoothly absorbed into the string. For strings with finite-energy kinks, the space-time evolution is slightly more involved [48], but the main point is that there are no separate free parameters for gluon jets. Differences with respect to quark fragmentation arise simply because quarks are only connected to a single string piece, while gluons have one on either side, increasing their relative energy loss (per unit

invariant time) by a factor of 2, similar to the ratio of color Casimirs  $C_A/C_F = 2.25$ .

Since the string breaks are causally disconnected (as can be realized from space-time diagrams [48]), they do not have to be considered in any specific time-ordered sequence. In the Lund model, the string breaks are generated starting with the leading (“outermost”) hadrons, containing the endpoint quarks, and iterating inwards towards the center of the string, alternating randomly between the left and right sides. One can thereby split off a single on-shell hadron in each step, making it straightforward to ensure that only states consistent with known hadron states are produced.

For each breakup vertex, quantum mechanical tunneling is assumed to control the masses and  $p_{\perp}$  kicks that can be produced, leading to a Gaussian suppression

$$\text{Prob}(m_q^2, p_{\perp q}^2) \propto \exp\left(\frac{-\pi m_q^2}{\kappa}\right) \exp\left(\frac{-\pi p_{\perp q}^2}{\kappa}\right), \quad (38.10)$$

where  $m_q$  is the mass of the produced quark flavor and  $p_{\perp}$  is the non-perturbative transverse momentum imparted to it by the breakup process (the antiquark has the same mass and opposite  $p_{\perp}$ ), with a universal average value of  $\langle p_{\perp q}^2 \rangle = \kappa/\pi \sim (250 \text{ MeV})^2$ . The charm and bottom masses are sufficiently heavy that they are not produced at all in the soft fragmentation. The transverse direction is defined with respect to the string axis, so the  $p_{\perp}$  in a frame where the string is moving will be modified by a Lorentz boost. Note that the effective amount of “non-perturbative”  $p_{\perp}$ , in a Monte Carlo model with a fixed shower cutoff  $Q_{\text{had}}$ , may be larger than the purely non-perturbative  $\kappa/\pi$  above, to account for effects of additional unresolved soft-gluon radiation below  $Q_{\text{had}}$ . In principle, the magnitude of this additional component should scale with the cutoff, but in practice it is up to the user to enforce this by retuning the relevant parameter when changing the hadronization scale.

Since quark masses are difficult to define for light quarks, the value of the strangeness suppression is determined from experimental observables, such as the  $K/\pi$  and  $K^*/\rho$  ratios. The parton-shower evolution generates a small amount of strangeness as well, through perturbative  $g \rightarrow s\bar{s}$  splittings. The optimal value for the non-perturbative  $2s/(u+d)$  ratio should therefore exhibit a mild anticorrelation with the amount of quarks produced in the perturbative stage.

Baryon production can also be incorporated, by allowing string breaks to produce pairs of *diquarks*, loosely bound states of two quarks in an overall  $\bar{3}$  representation. Again, since diquark masses are difficult to define, the relative rate of diquark to quark production is extracted, e.g. from the  $p/\pi$  ratio, and since the perturbative shower splittings do not produce diquarks, the effective value for this parameter is mildly correlated with the amount of  $g \rightarrow q\bar{q}$  splittings occurring on the shower side. More advanced scenarios for baryon production have also been proposed, see Ref. 48. Within the PYTHIA framework, a fragmentation model including baryon string junctions [49] is also available.

The next step of the algorithm is the assignment of the produced quarks within hadron multiplets. Using a nonrelativistic classification of spin states, the fragmenting  $q$  may combine with the  $\bar{q}'$  from a newly created breakup to produce a meson — or baryon, if diquarks are involved — of a given valence quark spin  $S$  and angular momentum  $L$ . The lowest-lying pseudoscalar and vector meson multiplets, and spin-1/2 and -3/2 baryons, are assumed to dominate in a string framework<sup>1</sup>, but individual rates are not predicted by the model. This is therefore the sector that contains the largest amount of free parameters.

<sup>1</sup> The PYTHIA implementation includes the lightest pseudoscalar and vector mesons, with the four  $L = 1$  multiplets (scalar, tensor, and 2 pseudovectors) available but disabled by default, largely because several states are poorly known and thus may result in a worse overall description when included. For baryons, the lightest spin-1/2 and -3/2 multiplets are included.

From spin counting, the ratio  $V/P$  of vectors to pseudoscalars is expected to be 3, but in practice this is only approximately true for  $B$  mesons. For lighter flavors, the difference in phase space caused by the  $V$ - $P$  mass splittings implies a suppression of vector production. When extracting the corresponding parameters from data, it is advisable to begin with the heaviest states, since so-called feed-down from the decays of higher-lying hadron states complicates the extraction for lighter particles, see Sec. 38.2.3. For diquarks, separate parameters control the relative rates of spin-1 diquarks vs. spin-0 ones and, likewise, have to be extracted from data.

With  $p_{\perp}^2$  and  $m^2$  now fixed, the final step is to select the fraction,  $z$ , of the fragmenting endpoint quark's longitudinal momentum that is carried by the created hadron, an aspect for which the string model is highly predictive. The requirement that the fragmentation be independent of the sequence in which breakups are considered (causality) imposes a "left-right symmetry" on the possible form of the fragmentation function,  $f(z)$ , with the solution

$$f(z) \propto \frac{1}{z} (1-z)^a \exp\left(-\frac{b(m_h^2 + p_{\perp h}^2)}{z}\right), \quad (38.11)$$

which is known as the Lund symmetric fragmentation function (normalized to unit integral). The dimensionless parameter  $a$  dampens the hard tail of the fragmentation function, towards  $z \rightarrow 1$ , and may in principle be flavor-dependent, while  $b$ , with dimension  $\text{GeV}^{-2}$ , is a universal constant related to the string tension [48] which determines the behavior in the soft limit,  $z \rightarrow 0$ . Note that the explicit mass dependence in  $f(z)$  implies a harder fragmentation function for heavier hadrons (in the rest frame of the string).

As a by-product, the probability distribution in invariant time  $\tau$  of  $q'\bar{q}$  breakup vertices, or equivalently  $\Gamma = (\kappa\tau)^2$ , is also obtained, with  $dP/d\Gamma \propto \Gamma^a \exp(-b\Gamma)$  implying an area law for the color flux, and the average breakup time lying along a hyperbola of constant invariant time  $\tau_0 \sim 10^{-23}\text{s}$  [48].

For massive endpoints (e.g.  $c$  and  $b$  quarks, or hypothetical hadronizing new-physics particles), which do not move along straight lightcone sections, the exponential suppression with string area leads to modifications of the form  $f(z) \rightarrow f(z)/z^{bm_Q^2}$ , with  $m_Q$  the mass of the heavy quark [50]. Although different forms can also be used to describe inclusive heavy-meson spectra (see Sec 19.9 of PDG book), such choices are not consistent with causality in the string framework and hence are theoretically disfavored in this context, one well-known example being the Peterson formula [51],

$$f(z) \propto \frac{1}{z} \left(1 - \frac{1}{z} - \frac{\epsilon_Q}{1-z}\right)^{-2}, \quad (38.12)$$

with  $\epsilon_Q$  a free parameter expected to scale  $\propto 1/m_Q^2$ .

**38.2.2. The Cluster Model:** The cluster hadronization model is based on *preconfinement*, i.e., on the observation [52,53] that the color structure of a perturbative QCD shower evolution at any scale  $Q_0$  is such that color-singlet subsystems of partons (labeled "clusters") occur with a universal invariant mass distribution that only depends on  $Q_0$  and on  $\Lambda_{\text{QCD}}$ , not on the starting scale  $Q$ , for  $Q \gg Q_0 \gg \Lambda_{\text{QCD}}$ . Further, this mass distribution is power-suppressed at large masses.

Following early models based on this universality [8,54], the cluster model developed by Webber [55] has for many years been a hallmark of the HERWIG and HERWIG++ generators, with an alternative implementation [56] now available in the SHERPA generator. The key idea, in addition to preconfinement, is to force "by hand" all gluons to split into quark-antiquark pairs at the end of the parton shower. Compared with the string description, this effectively amounts to viewing gluons as "seeds" for string breaks, rather than as kinks in a continuous object. After the splittings, a new set of low-mass color-singlet clusters is obtained, formed only by quark-antiquark pairs. These can be decayed to on-shell hadrons in a simple manner.

The algorithm starts by generating the forced  $g \rightarrow q\bar{q}$  breakups, and by assigning flavors and momenta to the produced quark pairs. For a typical shower cutoff corresponding to a gluon virtuality

of  $Q_{\text{had}} \sim 1\text{GeV}$ , the  $p_{\perp}$  generated by the splittings can be neglected. The constituent light-quark masses,  $m_{u,d} \sim 300\text{MeV}$  and  $m_s \sim 450\text{MeV}$ , imply a suppression (typically even an absence) of strangeness production. In principle, the model also allows for diquarks to be produced at this stage, but due to the larger constituent masses this would only become relevant for shower cutoffs larger than  $1\text{GeV}$ .

If a cluster formed in this way has an invariant mass above some cutoff value, typically 3–4 GeV, it is forced to undergo sequential  $1 \rightarrow 2$  cluster breakups, along an axis defined by the constituent partons of the original cluster, until all sub-cluster masses fall below the cutoff value. Due to the preservation of the original axis in these breakups, this treatment has some resemblance to the string-like picture.

Next, on the low-mass side of the spectrum, some clusters are allowed to decay directly to a single hadron, with nearby clusters absorbing any excess momentum. This improves the description of the high- $z$  part of the fragmentation spectrum — where the hadron carries almost all the momentum of its parent jet — at the cost of introducing one additional parameter, controlling the probability for single-hadron cluster decay.

Having obtained a final distribution of small-mass clusters, now with a strict cutoff at 3–4 GeV and with the component destined to decay to single hadrons already removed, the remaining clusters are interpreted as a smoothed-out spectrum of excited mesons, each of which decays isotropically to two hadrons, with relative probabilities proportional to the available phase space for each possible two-hadron combination that is consistent with the cluster's internal flavors, including spin degeneracy. It is important that all the light members (containing only  $uds$ ) of each hadron multiplet be included, as the absence of members can lead to unphysical isospin or SU(3) flavor violation. Typically, the lightest pseudoscalar, vector, scalar, even and odd charge conjugation pseudovector, and tensor multiplets of light mesons are included. In addition, some excited vector multiplets of light mesons may be available. For baryons, usually only the lightest octet, decuplet and singlet baryons are present, although both the HERWIG++ and SHERPA implementations now include some heavier baryon multiplets as well.

Contrary to the case in the string model, the mechanism of phase-space suppression employed here leads to a natural enhancement of the lighter pseudoscalars, and no parameters beyond the spectrum of hadron masses need to be introduced at this point. The phase space also limits the transverse momenta of the produced hadrons relative to the jet axis.

Note that, since the masses and decays of excited heavy-flavor hadrons in particular are not well known, there is some freedom in the model to adjust these, which in turn will affect their relative phase-space populations.

**38.2.3. Hadron and  $\tau$  Decays:** Of the so-called primary hadrons, originating directly from string breaks and/or cluster decays (see above), many are unstable and so decay further, until a set of particles is obtained that can be considered stable on time scales relevant to the given measurement<sup>2</sup>. The decay modeling can therefore have a significant impact on final particle yields and spectra, especially for the lowest-lying hadronic states, which receive the largest relative contributions from decays (feed-down). Note that the interplay between primary production and feed-down implies that the hadronization parameters should be retuned if significant changes to the decay treatment are made.

Particle summary tables, such as those given elsewhere in this *Review*, represent a condensed summary of the available experimental measurements and hence may be incomplete and/or exhibit inconsistencies within the experimental precision. In an MC decay package, on the other hand, all information must be quantified and consistent, with all branching ratios summing to unity.

<sup>2</sup> E.g., a typical hadron-collider definition of a "stable particle" is  $c\tau \geq 10\text{mm}$ , which includes the weakly-decaying strange hadrons ( $K$ ,  $\Lambda$ ,  $\Sigma^{\pm}$ ,  $\bar{\Sigma}^{\pm}$ ,  $\Xi$ ,  $\Omega$ ).



When adapting particle summary information for use in a decay package, a number of choices must therefore be made. The amount of ambiguity increases as more excited hadron multiplets are added to the simulation, about which less and less is known from experiment, with each GPMC making its own choices.

A related choice is how to distribute the decay products differentially in phase space, in particular which matrix elements to use. Historically, MC generators contained matrix elements only for selected (generator-specific) classes of hadron and  $\tau$  decays, coupled with a Breit-Wigner smearing of the masses, truncated at the edges of the physical decay phase space (the treatment of decay thresholds can be important for certain modes [15]). A more sophisticated treatment can then be obtained by reweighting the generated events using the obtained particle four-momenta and/or by using specialized external packages such as EVTGEN [57] for hadron decays and TAUOLA [58] for  $\tau$  decays.

More recently, HERWIG++ and SHERPA include helicity-dependence in  $\tau$  decays [59,60], with a more limited treatment available in PYTHIA 8 [140]. The HERWIG++ and SHERPA generators have also included significantly improved internal simulations of hadronic decays, which include spin correlations between those decays for which matrix elements are used.

HERWIG++ and PYTHIA include the probability for  $B$  mesons to oscillate into  $\bar{B}$  ones before decay. SHERPA and EVTGEN also include CP-violating effects and, for common decay modes of the neutral meson and its antiparticle, the interference between the direct decay and oscillation followed by decay.

We end on a note of warning on double counting. This may occur if a particle can decay via an intermediate on-shell resonance. An example is  $a_1 \rightarrow \pi\pi\pi$  which may proceed via  $a_1 \rightarrow \rho\pi$ ,  $\rho \rightarrow \pi\pi$ . If these decay channels of the  $a_1$  are both included, each with their full partial width, a double counting of the on-shell  $a_1 \rightarrow \rho\pi$  contribution would result. Such cases are normally dealt with consistently in the default MC generator packages, so this warning is mostly relevant for users that wish to edit decay tables on their own.

### 38.3. Models for Soft Hadron-Hadron Physics

**38.3.1. Minimum-Bias and Diffraction:** The term “minimum bias” (MB) originates from the experimental requirement of a minimal number of tracks (or hits) in a given instrumented region. In order to make MC predictions for such observables, all possible contributions to the relevant phase-space region must be accounted for. There are essentially four types of physics processes, which together make up the total hadron-hadron ( $hh$ ) cross section: 1) elastic scattering<sup>3</sup>:  $hh \rightarrow hh$ , 2) single diffractive dissociation:  $hh \rightarrow h + \text{gap} + X$ , with  $X$  denoting anything that is not the original beam particle, and “gap” denoting a rapidity region devoid of observed activity; 3) double diffractive dissociation:  $hh \rightarrow X + \text{gap} + X$ , and 4) inelastic non-diffractive scattering: everything else. A fifth class may also be defined, called central diffraction ( $hh \rightarrow h + \text{gap} + X + \text{gap} + h$ ). Some differences exist between theoretical and experimental terminology [61]. In the experimental setting, diffraction is defined by an observable gap, of some minimal size in rapidity. In the MC context, each diffractive physics process typically produces a whole spectrum of gaps, with small ones suppressed but not excluded.

The inelastic non-diffractive part of the cross section is typically modeled either by smoothly regulating and extending the perturbative QCD scattering cross sections all the way to zero  $p_\perp$  [62] (PYTHIA 6, PYTHIA 8, and SHERPA), or by regulating the QCD cross sections with a sharp cutoff [63] (HERWIG+JIMMY) and adding a separate class of intrinsically soft scatterings below that scale [64] (HERWIG++). See also Sec. 38.3.2. In all cases, the three most important ingredients are: 1) the IR regularization of the perturbative scattering cross sections, including their PDF dependence, 2) the assumed matter distribution of the colliding hadrons, possibly including multi-parton correlations [49] and/or  $x$  dependence [65], and 3) additional soft-QCD effects

such as color reconnections and/or other collective effects, discussed in Sec. 38.3.3.

Currently, there are essentially three methods for simulating diffraction in the main MC models: 1) in PYTHIA 6, one picks a diffractive mass according to parametrized cross sections  $\propto dM^2/M^2$  [66]. This mass is represented as a string, which is fragmented as described in Sec. 38.2.1, though differences in the effective scale of the hadronization may necessitate a (re)tuning of the fragmentation parameters for diffraction; 2) in PYTHIA 8, the high-mass tail beyond  $M \sim 10$  GeV is augmented by a partonic description in terms of pomeron PDFs [67], allowing diffractive jet production including showers and underlying event [68]; 3) the PHOJET and DPMJET programs also include central diffraction and rely directly on a formulation in terms of pomerons (color-singlet multi-gluon states) [69–71]. Cut pomerons correspond to exchanges of soft gluons while uncut ones give elastic and diffractive topologies as well as virtual corrections that help preserve unitarity. So-called “hard pomerons” provide a transition to the perturbative regime. Fragmentation is still handled using the Lund string model, so there is some overlap with the above models at the hadronization stage. In addition, a pomeron-based package exists for HERWIG [72], and an effort is underway to construct an MC implementation of the “KMR” model [73] within the SHERPA generator. Color reconnections (Sec. 38.3.3) may also play a role in creating rapidity gaps and the underlying event (Sec. 38.3.2) in destroying them.

**38.3.2. Underlying Event and Jet Pedestals:** In the event-generator context, the term underlying event (UE) denotes any additional activity *beyond* the basic process and its associated ISR and FSR activity. The dominant contribution to this is believed to come from additional color exchanges between the beam particles, which can be represented either as multiple parton-parton interactions (MPI) or as so-called cut pomerons (Sec. 38.3.1). The experimentally observed fact that the UE is more active than MB events at the same CM energy is called the “jet pedestal” effect.

The most easily identifiable consequence of MPI is arguably the possibility of observing several hard parton-parton interactions in one and the same hadron-hadron event. This tends to produce largely uncorrelated back-to-back jet pairs, with each pair having a small value of  $\text{sum}(\vec{p}_\perp)$ . For comparison, jets from bremsstrahlung tend to be aligned with the direction of their parent initial- or final-state partons. The fraction of MPI that give rise to additional reconstructible jets is, however, quite small. Soft interactions that do not give rise to observable jets are much more plentiful, and can give significant corrections to the color flow and total scattered energy of the event. This affects the final-state activity in a more global way, increasing multiplicity and summed  $E_T$  distributions, and contributing to the break-up of the beam remnants in the forward direction.

The first detailed Monte Carlo model for perturbative MPI was proposed in Ref. 62, and with some variation this still forms the basis for most modern implementations. Some useful additional references can be found in Ref. 15. The first crucial observation is that the  $t$ -channel propagators appearing in perturbative QCD  $2 \rightarrow 2$  scattering almost go on shell at low  $p_\perp$ , causing the differential cross sections to become very large, behaving roughly as

$$d\sigma_{2 \rightarrow 2} \propto \frac{dt}{t^2} \sim \frac{dp_\perp^2}{p_\perp^4}. \quad (38.13)$$

This cross section is an inclusive number. Thus, if a single hadron-hadron event contains two parton-parton interactions, it will “count” twice in  $\sigma_{2 \rightarrow 2}$  but only once in  $\sigma_{\text{tot}}$ , and so on. In the limit that all the interactions are independent and equivalent, one would have

$$\sigma_{2 \rightarrow 2}(p_{\perp \text{min}}) = \langle n \rangle (p_{\perp \text{min}}) \sigma_{\text{tot}}, \quad (38.14)$$

with  $\langle n \rangle (p_{\perp \text{min}})$  giving the average of a Poisson distribution in the number of parton-parton interactions above  $p_{\perp \text{min}}$  per hadron-hadron collision,

$$\mathcal{P}_n(p_{\perp \text{min}}) = \frac{\langle n \rangle (p_{\perp \text{min}})^n \exp(-\langle n \rangle (p_{\perp \text{min}}))}{n!}. \quad (38.15)$$

<sup>3</sup> The QED elastic-scattering cross section diverges and is normally a non-default option in MC models.

This simple argument in fact expresses unitarity; instead of the total interaction cross section diverging as  $p_{\perp\min} \rightarrow 0$  (which would violate unitarity), we have restated the problem so that it is now the *number of MPI per collision* that diverges, with the total cross section remaining finite. At LHC energies, the  $2 \rightarrow 2$  scattering cross sections computed using the full LO QCD cross section folded with modern PDFs becomes larger than the total  $pp$  one for  $p_{\perp}$  values of order 4–5 GeV [74]. One therefore expects the average number of perturbative MPI to exceed unity at around that scale.

Two important ingredients remain to fully regulate the remaining divergence. Firstly, the interactions cannot use up more momentum than is available in the parent hadron. This suppresses the large- $n$  tail of the estimate above. In PYTHIA-based models, the MPI are ordered in  $p_{\perp}$ , and the parton densities for each successive interaction are explicitly constructed so that the sum of  $x$  fractions can never be greater than unity. In the HERWIG models, instead the uncorrelated estimate of  $\langle n \rangle$  above is used as an initial guess, but the generation of actual MPI is stopped once the energy-momentum conservation limit is reached.

The second ingredient invoked to suppress the number of interactions, at low  $p_{\perp}$  and  $x$ , is color screening; if the wavelength  $\sim 1/p_{\perp}$  of an exchanged colored parton becomes larger than a typical color-anticolor separation distance, it will only see an *average* color charge that vanishes in the limit  $p_{\perp} \rightarrow 0$ , hence leading to suppressed interactions. This provides an infrared cutoff for MPI similar to that provided by the hadronization scale for parton showers. A first estimate of the color-screening cutoff would be the proton size,  $p_{\perp\min} \approx \hbar/r_p \approx 0.3 \text{ GeV} \approx \Lambda_{\text{QCD}}$ , but empirically this appears to be far too low. In current models, one replaces the proton radius  $r_p$  in the above formula by a “typical color screening distance,” i.e., an average size of a region within which the net compensation of a given color charge occurs. This number is not known from first principles [73] and is perceived of simply as an effective cutoff parameter. The simplest choice is to introduce a step function  $\Theta(p_{\perp} - p_{\perp\min})$ . Alternatively, one may note that the jet cross section is divergent like  $\alpha_s^2(p_{\perp}^2)/p_{\perp}^4$ , cf. Eq. (38.13), and that therefore a factor

$$\frac{\alpha_s^2(p_{\perp 0}^2 + p_{\perp 1}^2)}{\alpha_s^2(p_{\perp 1}^2)} \frac{p_{\perp 1}^4}{(p_{\perp 0}^2 + p_{\perp 1}^2)^2} \quad (38.16)$$

would smoothly regulate the divergences, now with  $p_{\perp 0}$  as the free parameter. Regardless of whether it is imposed as a smooth (PYTHIA and SHERPA) or steep (HERWIG++) function, this is effectively the main “tuning” parameter in such models.

Note that the numerical value obtained for the cross section depends upon the PDF set used, and therefore the optimal value to use for the cutoff will also depend on this choice. Note also that the cutoff does not have to be energy-independent. Higher energies imply that parton densities can be probed at smaller  $x$  values, where the number of partons rapidly increases. Partons then become closer packed and the color screening distance  $d$  decreases. The uncertainty on the energy and/or  $x$  scaling of the cutoff is a major concern when extrapolating between different collider energies [75].

We now turn to the origin of the observational fact that hard jets appear to sit on top of a higher “pedestal” of underlying activity than events with no hard jets. This is interpreted as a consequence of impact-parameter-dependence: in peripheral collisions, only a small fraction of events contain any high- $p_{\perp}$  activity, whereas central collisions are more likely to contain at least one hard scattering; a high- $p_{\perp}$  triggered sample will therefore be biased towards small impact parameters,  $b$ . The ability of a model to describe the shape of the pedestal (e.g. to describe both MB and UE distributions simultaneously) therefore depends upon its modeling of the  $b$ -dependence, and correspondingly the impact-parameter shape constitutes another main tuning parameter.

For each impact parameter  $b$ , the number of interactions  $\tilde{n}(b)$  can then still be assumed to be distributed according to Eq. (38.15), again modulo momentum conservation, but now with the mean value of the Poisson distribution depending on impact parameter,  $\langle \tilde{n}(b) \rangle$ . This causes the final  $n$ -distribution (integrated over  $b$ ) to be wider than a Poissonian.

Finally, there are two perturbative modeling aspects which go beyond the introduction of MPI themselves: 1) parton showers off the MPI, and 2) perturbative parton-rescattering effects. Without showers, MPI models would generate very sharp peaks for back-to-back MPI jets, caused by unshowered partons passed directly to the hadronization model. However, with the exception of the oldest PYTHIA6 model, all GPMC models do include such showers [15], and hence should exhibit more realistic (i.e., broader and more decorrelated) MPI jets. On the initial-state side, the main questions are whether and how correlated multi-parton densities are taken into account and, as discussed previously, how the showers are regulated at low  $p_{\perp}$  and/or low  $x$ . Although none of the MC models currently impose a rigorous correlated multi-parton evolution, all of them include some elementary aspects. The most significant for parton-level results is arguably momentum conservation, which is enforced explicitly in all the models. The so-called “interleaved” models [24] attempt to go a step further, generating an explicitly correlated multi-parton evolution in which flavor sum rules are imposed to conserve, e.g. the total numbers of valence and sea quarks [49].

Perturbative rescattering in the final state can occur if partons are allowed to undergo several distinct interactions, with showering activity possibly taking place in-between. This has so far not been studied extensively, but a first exploratory model is available [76]. In the initial state, parton rescattering/recombination effects have so far not been included in any of the GPMC models.

**38.3.3. Bose-Einstein and Color-Reconnection Effects :** In the context of  $e^+e^-$  collisions, Bose-Einstein (BE) correlations have mostly been discussed as a source of uncertainty on high-precision  $W$  mass determinations at LEP [77]. In hadron-hadron (and nucleus-nucleus) collisions, however, BE correlations are used extensively to study the space-time structure of hadronizing matter (“femtoscopy”).

In MC models of hadronization, each string break and/or particle/cluster decay is normally factorized from all other ones. This reduces the number of variables that must be considered simultaneously, but also makes the introduction of correlations among particles from different breaks/decays intrinsically difficult to address. In the context of GPMCs, a few semi-classical models are available within the PYTHIA 6 and 8 generators [78], in which the BE effect is mimicked by an attractive interaction between pairs of identical particles in the final state, with no higher correlations included. This “force” acts after the decays of very short-lived particles, like  $\rho$ , but before decays of longer-lived ones, like  $\pi^0$ . The main differences between the variants of this model is the assumed shape of the correlation function and how overall momentum conservation is handled.

As discussed in Sec. 38.2, leading-color (“planar”) color flows are used to set up the hadronizing systems (clusters or strings) at the hadronization stage. If the systems do not overlap significantly in space and time, subleading-color ambiguities and/or non-perturbative reconstructions are expected to be small. However, if the density of displaced color charges is sufficiently high that several systems can overlap significantly, full-color and/or reconnection effects should become progressively larger.

In the specific context of MPI, a crucial question is how color is neutralized *between* different MPI systems, including the remnants. The large rapidity differences involved imply large invariant masses (though normally low  $p_{\perp}$ ), and hence large amounts of (soft) particle production. Indeed, in the context of soft-inclusive physics, it is these “inter-system” strings/clusters that furnish the dominant particle-production mechanism, and hence their modeling is an essential part of the soft-physics description, affecting topics such as MB/UE multiplicity and  $p_{\perp}$  distributions, rapidity gaps, and precision mass measurements. A more comprehensive review of color-reconnection effects can be found in Ref. 15.

### 38.4. Parameters and Tuning

The achievable accuracy in GPMC models depends both on the inclusiveness of the chosen observable and on the sophistication of the simulation. An important driver for the latter is obviously the development of improved theoretical models, discussed in the preceding sections; but it also depends crucially on the available constraints on the remaining free parameters. Using existing data to constrain these is referred to as generator tuning.

Although MC models may appear to have a bewildering array of adjustable parameters, most of them only control relatively small (exclusive) details of the event generation. The majority of the (inclusive) physics is determined by only a few, very important ones, such as the value of  $\alpha_s$ , in the perturbative domain, and the properties of the non-perturbative fragmentation functions, in the non-perturbative one. One may therefore take a factorized approach, first constraining the perturbative parameters and thereafter the non-perturbative ones, each ordered in a measure of their relative significance to the overall modeling.

At LO $\times$ LL, perturbation theory is doing well if it agrees with an IR safe measurement within 10%. It would therefore not make much sense to tune a GPMC beyond roughly 5% (it might even be dangerous, due to overfitting). The advent of NLO Monte Carlos may reduce this number slightly, but only for quantities for which one expects NLO precision. For LO Monte Carlos, distributions should be normalized to unity, since the NLO normalization is not tunable. For quantities governed by non-perturbative physics, uncertainties are larger. For some quantities, e.g. ones for which the underlying modeling is known to be poor, an order-of-magnitude agreement or worse may have to be accepted.

In the context of LO $\times$ LL GPMC tuning, subleading aspects of coupling-constant and PDF choices are relevant. In particular, one should be aware that the choice of QCD  $\Lambda$  parameter  $\Lambda_{MC} = 1.569\Lambda_{\overline{MS}}$  (for 5 active flavors) improves the predictions of coherent shower algorithms at the NLL level [79], and hence this scheme is typically considered the baseline for shower tuning. The question of LO vs. NLO PDFs is more involved [15], but it should be emphasized that the low- $x$  gluon in particular is important for determining the level of the underlying event in MPI models (Sec. 38.3.2), and hence the MB/UE tuning (and energy scaling [75]) is linked to the choice of PDF in such models. Further issues and an example of a specific recipe that could be followed in a realistic set-up can be found in Ref. 80.

Recent years have seen the emergence of automated tools that attempt to reduce the amount of both computer and manpower required for tuning [81]. Automating the human expert input is more difficult. In the tools currently on the market, this question is addressed by a combination of input solicited from the generator authors (e.g., which parameters and ranges to consider, which observables constitute a complete set, etc) and a set of weights determining the relative priority given to each bin in each distribution. The field is still burgeoning, however, and future sophistications are to be expected. Nevertheless, the overall quality of the automated tunes appear to at least be competitive with the manual ones.

#### References:

- G. Corcella *et al.*, JHEP **0101**, 010 (2001), [hep-ph/0011363](#).
- M.Bähr *et al.*, Eur. Phys. J. **C58**, 639 (2008), [arXiv:0803.0883](#).
- T. Sjöstrand, S. Mrenna, and P. Z. Skands, JHEP **05**, 026 (2006), [hep-ph/0603175](#).
- T. Sjöstrand, S. Mrenna, and P. Z. Skands, Comp. Phys. Comm. **178**, 852 (2008), [arXiv:0710.3820](#).
- T. Gleisberg *et al.*, JHEP **0402**, 056 (2004), [hep-ph/0311263](#).
- T. Kinoshita, J. Math. Phys. **3**, 650 (1962).
- T. Lee and M. Nauenberg, Phys. Rev. **133**, 1549 (1964).
- G.C. Fox and S. Wolfram, Nucl. Phys. **B168**, 285 (1980).
- G. Altarelli and G. Parisi, Nucl. Phys. **B126**, 298 (1977).
- A. Einstein, B. Podolsky, and N. Rosen, Phys. Rev. **47**, 777 (1935).
- B.R. Webber, Phys. Lett. **B193**, 91 (1987).
- J.C. Collins, Nucl. Phys. **B304**, 794 (1988).
- I.G. Knowles, Comp. Phys. Comm. **58**, 271 (1990).
- T. Sjöstrand, Phys. Lett. **B157**, 321 (1985).
- A. Buckley *et al.*, Phys. Reports **504**, 145 (2011), [1101.2599](#).
- G. Marchesini and B.R. Webber, Nucl. Phys. **B310**, 461 (1988).
- S. Gieseke, P. Stephens, and B. Webber, JHEP **0312**, 045 (2003), [hep-ph/0310083](#).
- M. Bengtsson and T. Sjöstrand, Nucl. Phys. **B289**, 810 (1987).
- G. Gustafson and U. Pettersson, Nucl. Phys. **B306**, 746 (1988).
- L. Lönnblad, Comp. Phys. Comm. **71**, 15 (1992).
- W.T. Giele, D.A. Kosower, and P.Z. Skands, Phys. Rev. **D78**, 014026 (2008), [arXiv:0707.3652](#).
- S. Schumann and F. Krauss, JHEP **0803**, 038 (2008), [arXiv:0709.1027](#).
- Z. Nagy and D.E. Soper, JHEP **0510**, 024 (2005), [hep-ph/0503053](#).
- T. Sjöstrand and P.Z. Skands, Eur. Phys. J. **C39**, 129 (2005), [hep-ph/0408302](#).
- E. Norrbin and T. Sjöstrand, Nucl. Phys. **B603**, 297 (2001), [hep-ph/0010012](#).
- S. Catani *et al.*, Nucl. Phys. **B627**, 189 (2002), [hep-ph/0201036](#).
- A. Semenov, Comp. Phys. Comm. **180**, 431 (2009), [0805.0555](#).
- N.D. Christensen and C. Duhr, Comp. Phys. Comm. **180**, 1614 (2009), [arXiv:0806.4194](#).
- M. Fairbairn *et al.*, Phys. Reports **438**, 1 (2007), [hep-ph/0611040](#).
- J. Alwall *et al.*, Comp. Phys. Comm. **176**, 300 (2007), [hep-ph/0609017](#).
- P.Z. Skands *et al.*, JHEP **0407**, 036 (2004), [hep-ph/0311123](#).
- J. Alwall *et al.*, (2007), [arXiv:0712.3311](#).
- P. Richardson, JHEP **0111**, 029 (2001), [hep-ph/0110108](#).
- M. Bengtsson and T. Sjöstrand, Phys. Lett. **B185**, 435 (1987).
- S. Catani *et al.*, JHEP **11**, 063 (2001), [hep-ph/0109231](#).
- J. Alwall *et al.*, Eur. Phys. J. **C53**, 473 (2008), [arXiv:0706.2569](#).
- P. Nason, JHEP **11**, 040 (2004), [hep-ph/0409146](#).
- B. Cooper *et al.*, (2011), [arXiv:1109.5295](#).
- S. Frixione and B.R. Webber, JHEP **06**, 029 (2002), [hep-ph/0204244](#).
- S. Alioli *et al.*, JHEP **1006**, 043 (2010), [arXiv:1002.2581](#).
- S. Alioli, K. Hamilton, and E. Re, (2001), [arXiv:1108.0909](#).
- M.L. Mangano *et al.*, JHEP **0307**, 001 (2003), [hep-ph/0206293](#).
- J. Alwall *et al.*, JHEP **1106**, 128 (2011), [arXiv:1106.0522](#).
- E. Boos *et al.*, (2007), [hep-ph/0109068](#).
- V. Hirschi *et al.*, JHEP **1105**, 044 (2011), [arXiv:1103.0621](#).
- X. Artru and G. Mennessier, Nucl. Phys. **B70**, 93 (1974).
- B. Andersson *et al.*, Phys. Reports **97**, 31 (1983).
- B. Andersson, Camb. Monogr. Part. Phys. Nucl. Phys. Cosmol. **7** (1997).
- T. Sjöstrand and P.Z. Skands, JHEP **0403**, 053 (2004), [hep-ph/0402078](#).
- M. Bowler, Z. Phys. **C11**, 169 (1981).
- C. Peterson *et al.*, Phys. Rev. **D27**, 105 (1983).
- D. Amati and G. Veneziano, Phys. Lett. **B83**, 87 (1979).
- A. Bassetto, M. Ciafaloni, and G. Marchesini, Phys. Lett. **B83**, 207 (1979).
- R.D. Field and S. Wolfram, Nucl. Phys. **B213**, 65 (1983).
- B.R. Webber, Nucl. Phys. **B238**, 492 (1984).
- J.-C. Winter, F. Krauss, and G. Soff, Eur. Phys. J. **C36**, 381 (2004), [hep-ph/0311085](#).
- D. Lange, Nucl. Instrum. Methods **A462**, 152 (2001).
- S. Jadach *et al.*, Comp. Phys. Comm. **76**, 361 (1993).
- D. Grellscheid and P. Richardson, (2007), [arXiv:0710.1951](#).
- T. Gleisberg *et al.*, JHEP **0902**, 007 (2009), [arXiv:0811.4622](#).
- V. Khoze *et al.*, Eur. Phys. J. **C69**, 85 (2010), [arXiv:1005.4839](#).
- T. Sjöstrand and M. van Zijl, Phys. Rev. **D36**, 2019 (1987).
- J.M. Butterworth, J.R. Forshaw, and M.H. Seymour, Z. Phys. **C72**, 637 (1996), [hep-ph/9601371](#).
- M. Bähr *et al.*, (2009), [arXiv:0905.4671](#).
- R. Corke and T. Sjöstrand, JHEP **1105**, 009 (2011), [1101.5953](#).
- G.A. Schuler and T. Sjöstrand, Phys. Rev. **D49**, 2257 (1994).
- G. Ingelman and P. Schlein, Phys. Lett. **B152**, 256 (1985).
- S. Navin, (2010), [arXiv:1005.3894](#).

69. P. Aurenche *et al.*, *Comp. Phys. Comm.* **83**, 107 (1994), [hep-ph/9402351](#).
70. F.W. Bopp, R. Engel, and J. Ranft, (1998), [hep-ph/9803437](#).
71. S. Roesler, R. Engel, and J. Ranft, p. 1033 (2000), [hep-ph/0012252](#).
72. B.E. Cox and J.R. Forshaw, *Comp. Phys. Comm.* **144**, 104 (2002), [hep-ph/0010303](#).
73. M. Ryskin, A. Martin, and V. Khoze, *Eur. Phys. J.* **C71**, 1617 (2011), [arXiv:1102.2844](#).
74. M. Bähr, J.M. Butterworth, and M.H. Seymour, *JHEP* **01**, 065 (2009), [arXiv:0806.2949](#).
75. H. Schulz and P.Z. Skands, *Eur. Phys. J.* **C71**, 1644 (2011), [arXiv:1103.3649](#).
76. R. Corke and T. Sjöstrand, *JHEP* **01**, 035 (2009), [0911.1901](#).
77. LEP Electroweak Working Group, (2005), [hep-ex/0511027](#).
78. L. Lönnblad and T. Sjöstrand, *Eur. Phys. J.* **C2**, 165 (1998), [hep-ph/9711460](#).
79. S. Catani, B. R. Webber, and G. Marchesini, *Nucl. Phys.* **B349**, 635 (1991).
80. P.Z. Skands, (2011), [arXiv:1104.2863](#).
81. A. Buckley *et al.*, *Eur. Phys. J.* **C65**, 331 (2010), [0907.2973](#).

## 39. MONTE CARLO PARTICLE NUMBERING SCHEME

Revised April 2012 by J.-F. Arguin (LBNL, U. Montreal), L. Garren (Fermilab), F. Krauss (Durham U.), C.-J. Lin (LBNL), S. Navas (U. Granada), P. Richardson (Durham U.), and T. Sjöstrand (Lund U.).

The Monte Carlo particle numbering scheme presented here is intended to facilitate interfacing between event generators, detector simulators, and analysis packages used in particle physics. The numbering scheme was introduced in 1988 [1] and a revised version [2,3] was adopted in 1998 in order to allow systematic inclusion of quark model states which are as yet undiscovered and hypothetical particles such as SUSY particles. The numbering scheme is used in several event generators, *e.g.* HERWIG, PYTHIA, and SHERPA, and interfaces, *e.g.* /HEPEVT/ and HepMC.

The general form is a 7-digit number:

$$\pm n n_r n_L n_{q_1} n_{q_2} n_{q_3} n_J .$$

This encodes information about the particle's spin, flavor content, and internal quantum numbers. The details are as follows:

1. Particles are given positive numbers, antiparticles negative numbers. The PDG convention for mesons is used, so that  $K^+$  and  $B^+$  are particles.
2. Quarks and leptons are numbered consecutively starting from 1 and 11 respectively; to do this they are first ordered by family and within families by weak isospin.
3. In composite quark systems (diquarks, mesons, and baryons)  $n_{q_{1-3}}$  are quark numbers used to specify the quark content, while the rightmost digit  $n_J = 2J + 1$  gives the system's spin (except for the  $K_S^0$  and  $K_L^0$ ). The scheme does not cover particles of spin  $J > 4$ .
4. Diquarks have 4-digit numbers with  $n_{q_1} \geq n_{q_2}$  and  $n_{q_3} = 0$ .
5. The numbering of mesons is guided by the nonrelativistic ( $L$ - $S$  decoupled) quark model, as listed in Tables 14.2 and 14.3.
  - a. The numbers specifying the meson's quark content conform to the convention  $n_{q_1} = 0$  and  $n_{q_2} \geq n_{q_3}$ . The special case  $K_L^0$  is the sole exception to this rule.
  - b. The quark numbers of flavorless, light ( $u, d, s$ ) mesons are: 11 for the member of the isotriplet ( $\pi^0, \rho^0, \dots$ ), 22 for the lighter isosinglet ( $\eta, \omega, \dots$ ), and 33 for the heavier isosinglet ( $\eta', \phi, \dots$ ). Since isosinglet mesons are often large mixtures of  $u\bar{u} + d\bar{d}$  and  $s\bar{s}$  states, 22 and 33 are assigned by mass and do not necessarily specify the dominant quark composition.
  - c. The special numbers 310 and 130 are given to the  $K_S^0$  and  $K_L^0$  respectively.
  - d. The fifth digit  $n_L$  is reserved to distinguish mesons of the same total ( $J$ ) but different spin ( $S$ ) and orbital ( $L$ ) angular momentum quantum numbers. For  $J > 0$  the numbers are: ( $L, S$ ) = ( $J - 1, 1$ )  $n_L = 0$ , ( $J, 0$ )  $n_L = 1$ , ( $J, 1$ )  $n_L = 2$  and ( $J + 1, 1$ )  $n_L = 3$ . For the exceptional case  $J = 0$  the numbers are ( $0, 0$ )  $n_L = 0$  and ( $1, 1$ )  $n_L = 1$  (*i.e.*  $n_L = L$ ). See Table 39.1.

**Table 39.1:** Meson numbering logic. Here  $qq$  stands for  $n_{q_2} n_{q_3}$ .

$J$	$L = J - 1, S = 1$			$L = J, S = 0$			$L = J, S = 1$			$L = J + 1, S = 1$		
	code	$J^{PC}$	$L$	code	$J^{PC}$	$L$	code	$J^{PC}$	$L$	code	$J^{PC}$	$L$
0	—	—	—	00qq1	0 <sup>++</sup>	0	—	—	—	10qq1	0 <sup>++</sup>	1
1	00qq3	1 <sup>+-</sup>	0	10qq3	1 <sup>+-</sup>	1	20qq3	1 <sup>++</sup>	1	30qq3	1 <sup>+-</sup>	2
2	00qq5	2 <sup>++</sup>	1	10qq5	2 <sup>+-</sup>	2	20qq5	2 <sup>+-</sup>	2	30qq5	2 <sup>++</sup>	3
3	00qq7	3 <sup>+-</sup>	2	10qq7	3 <sup>+-</sup>	3	20qq7	3 <sup>++</sup>	3	30qq7	3 <sup>+-</sup>	4
4	00qq9	4 <sup>++</sup>	3	10qq9	4 <sup>+-</sup>	4	20qq9	4 <sup>+-</sup>	4	30qq9	4 <sup>++</sup>	5

- e. If a set of physical mesons correspond to a (non-negligible) mixture of basis states, differing in their internal quantum numbers, then the lightest physical state gets the smallest basis state number. For example the  $K_1(1270)$  is numbered 10313 ( $1^1P_1 K_{1B}$ ) and the  $K_1(1400)$  is numbered 20313 ( $1^3P_1 K_{1A}$ ).

- f. The sixth digit  $n_r$  is used to label mesons radially excited above the ground state.
- g. Numbers have been assigned for complete  $n_r = 0$   $S$ - and  $P$ -wave multiplets, even where states remain to be identified.
- h. In some instances assignments within the  $q\bar{q}$  meson model are only tentative; here best guess assignments are made.
- i. Many states appearing in the Meson Listings are not yet assigned within the  $q\bar{q}$  model. Here  $n_{q_{2-3}}$  and  $n_J$  are assigned according to the state's likely flavors and spin; all such unassigned light isoscalar states are given the flavor code 22. Within these groups  $n_L = 0, 1, 2, \dots$  is used to distinguish states of increasing mass. These states are flagged using  $n = 9$ . It is to be expected that these numbers will evolve as the nature of the states are elucidated. Codes are assigned to all mesons which are listed in the one-page table at the end of the Meson Summary Table as long as they have a preferred or established spin. Additional heavy meson states expected from heavy quark spectroscopy are also assigned codes.

6. The numbering of baryons is again guided by the nonrelativistic quark model, see Table 14.6. This numbering scheme is illustrated through a few examples in Table 39.2.
  - a. The numbers specifying a baryon's quark content are such that in general  $n_{q_1} \geq n_{q_2} \geq n_{q_3}$ .
  - b. Two states exist for  $J = 1/2$  baryons containing 3 different types of quarks. In the lighter baryon ( $\Lambda, \Xi, \Omega, \dots$ ) the light quarks are in an antisymmetric ( $J = 0$ ) state while for the heavier baryon ( $\Sigma^0, \Xi', \Omega', \dots$ ) they are in a symmetric ( $J = 1$ ) state. In this situation  $n_{q_2}$  and  $n_{q_3}$  are reversed for the lighter state, so that the smaller number corresponds to the lighter baryon.
  - c. For excited baryons a scheme is adopted, where the  $n_r$  label is used to denote the excitation bands in the harmonic oscillator model, see Sec. 14.4. Using the notation employed there,  $n_r$  is given by the  $N$ -index of the  $D_N$  band identifier.
  - d. Further degeneracies of excited hadron multiplets with the same excitation number  $n_r$  and spin  $J$  are lifted by labelling such multiplets with the  $n_L$  index according to their mass, as given by its  $N$  or  $\Delta$ -equivalent.
  - e. In such excited multiplets extra singlets may occur, the  $\Lambda(1520)$  being a prominent example. In such cases the ordering is reversed such that the heaviest quark label is pushed to the last position:  $n_{q_3} > n_{q_1} > n_{q_2}$ .
  - f. For pentaquark states  $n = 9$ ,  $n_r n_L n_{q_1} n_{q_2}$  gives the four quark numbers in order  $n_r \geq n_L \geq n_{q_1} \geq n_{q_2}$ ,  $n_{q_3}$  gives the antiquark number, and  $n_J = 2J + 1$ , with the assumption that  $J = 1/2$  for the states currently reported.
7. The gluon, when considered as a gauge boson, has official number 21. In codes for glueballs, however, 9 is used to allow a notation in close analogy with that of hadrons.
8. The pomeron and odderon trajectories and a generic reggeon trajectory of states in QCD are assigned codes 990, 9990, and 110 respectively, where the final 0 indicates the indeterminate nature of the spin, and the other digits reflect the expected "valence" flavor content. We do not attempt a complete classification of all reggeon trajectories, since there is currently no need to distinguish a specific such trajectory from its lowest-lying member.
9. Two-digit numbers in the range 21–30 are provided for the Standard Model gauge bosons and Higgs.
10. Codes 81–100 are reserved for generator-specific pseudoparticles and concepts.
11. The search for physics beyond the Standard Model is an active area, so these codes are also standardized as far as possible.
  - a. A standard fourth generation of fermions is included by analogy with the first three.
  - b. The graviton and the boson content of a two-Higgs-doublet scenario and of additional  $SU(2) \times U(1)$  groups are found in the range 31–40.
  - c. "One-of-a-kind" exotic particles are assigned numbers in the range 41–80.
  - d. Fundamental supersymmetric particles are identified by adding a nonzero  $n$  to the particle number. The superpartner of a boson or a left-handed fermion has  $n = 1$  while the

**Table 39.2:** Some examples of octet (top) and decuplet (bottom) members for the numbering scheme for excited baryons. Here  $qqq$  stands for  $n_{q_1}n_{q_2}n_{q_3}$ . See the text for the definition of the notation. The numbers in parenthesis correspond to the mass of the baryons. The states marked as (?) are not experimentally confirmed.

$J^P$	$(D, L_N^P)$	$n_r n_L n_{q_1} n_{q_2} n_{q_3} n_J$	$N$	$\Lambda_8$	$\Sigma$	$\Xi$	$\Lambda_1$
Octet			211,221	312	311,321,322	331,332	213
$1/2^+$	$(\mathbf{56}, \mathbf{0}_0^+)$	00qqq2	(939)	(1116)	(1193)	(1318)	—
$1/2^+$	$(\mathbf{56}, \mathbf{0}_2^+)$	20qqq2	(1440)	(1600)	(1660)	(1690)	—
$1/2^+$	$(\mathbf{70}, \mathbf{0}_2^+)$	21qqq2	(1710)	(1810)	(1880)	(?)	(?)
$1/2^-$	$(\mathbf{70}, \mathbf{1}_1^-)$	10qqq2	(1535)	(1670)	(1620)	(1750)	(1405)
$J^P$	$(D, L_N^P)$	$n_r n_L n_{q_1} n_{q_2} n_{q_3} n_J$	$\Delta$	$\Sigma$	$\Xi$	$\Omega$	
Decuplet			111,211,221,222	311,321,322	331,332	333	
$3/2^+$	$(\mathbf{56}, \mathbf{0}_0^+)$	00qqq4	(1232)	(1385)	(1530)	(1672)	
$3/2^+$	$(\mathbf{56}, \mathbf{0}_2^+)$	20qqq4	(1600)	(1690)	(?)	(?)	
$1/2^-$	$(\mathbf{70}, \mathbf{1}_1^-)$	11qqq2	(1620)	(1750)	(?)	(?)	
$3/2^-$	$(\mathbf{70}, \mathbf{1}_1^-)$	12qqq4	(1700)	(?)	(?)	(?)	

- superpartner of a right-handed fermion has  $n = 2$ . When mixing occurs, such as between the winos and charged Higgsinos to give charginos, or between left and right sfermions, the lighter physical state is given the smaller basis state number.
- e. Technicolor states have  $n = 3$ , with technifermions treated like ordinary fermions. States which are ordinary color singlets have  $n_r = 0$ . Color octets have  $n_r = 1$ . If a state has non-trivial quantum numbers under the topcolor groups  $SU(3)_1 \times SU(3)_2$ , the quantum numbers are specified by  $\text{tech}, i, j$ , where  $i$  and  $j$  are 1 or 2.  $n_L$  is then  $2i + j$ . The colon,  $V_8$ , is a heavy gluon color octet and thus is 3100021.
- f. Excited (composite) quarks and leptons are identified by setting  $n = 4$  and  $n_r = 0$ .
- g. Within several scenarios of new physics, it is possible to have colored particles sufficiently long-lived for color-singlet hadronic states to form around them. In the context of supersymmetric scenarios, these states are called  $R$ -hadrons, since they carry odd  $R$ -parity.  $R$ -hadron codes, defined here, should be viewed as templates for corresponding codes also in other scenarios, for any long-lived particle that is either an unflavored color octet or a flavored color triplet. The  $R$ -hadron code is obtained by combining the SUSY particle code with a code for the light degrees of freedom, with as many intermediate zeros removed from the former as required to make place for the latter at the end. (To exemplify, a sparticle  $n00000n_{\tilde{q}}$  combined with quarks  $q_1$  and  $q_2$  obtains code  $n00n_{\tilde{q}}n_{q_1}n_{q_2}n_J$ .) Specifically, the new-particle spin decouples in the limit of large masses, so that the final  $n_J$  digit is defined by the spin state of the light-quark system alone. An appropriate number of  $n_q$  digits is used to define the ordinary-quark content. As usual, 9 rather than 21 is used to denote a gluon/gluino in composite states. The sign of the hadron agrees with that of the constituent new particle (a color triplet) where there is a distinct new antiparticle, and else is defined as for normal hadrons. Particle names are  $R$  with the flavor content as lower index.
- h. A black hole in models with extra dimensions has code 5000040. Kaluza-Klein excitations in models with extra dimensions have  $n = 5$  or  $n = 6$ , to distinguish excitations of left- or right-handed fermions or, in case of mixing, the lighter or heavier state (cf. 11d). The nonzero  $n_r$  digit gives the radial excitation number, in scenarios where the level spacing allow these to be distinguished. Should the model also contain supersymmetry, excited SUSY states would be denoted by an  $n_r > 0$ , with  $n = 1$  or 2 as usual. Should some colored states be long-lived enough that hadrons would form around them, the coding strategy of 11g applies, with the initial two  $nn_r$  digits preserved in the combined code.

- i. Magnetic monopoles and dyons are assumed to have one unit of Dirac monopole charge and a variable integer number  $n_{q_1}n_{q_2}n_{q_3}$  units of electric charge. Codes  $411n_{q_1}n_{q_2}n_{q_3}0$  are then used when the magnetic and electrical charge sign agree and  $412n_{q_1}n_{q_2}n_{q_3}0$  when they disagree, with the overall sign of the particle set by the magnetic charge. For now no spin information is provided.

12. Occasionally program authors add their own states. To avoid confusion, these should be flagged by setting  $nn_r = 99$ .
13. Concerning the non-99 numbers, it may be noted that only quarks, excited quarks, squarks, and diquarks have  $n_{q_3} = 0$ ; only diquarks, baryons (including pentaquarks), and the odderon have  $n_{q_1} \neq 0$ ; and only mesons, the reggeon, and the pomeron have  $n_{q_1} = 0$  and  $n_{q_2} \neq 0$ . Concerning mesons (not antimessons), if  $n_{q_1}$  is odd then it labels a quark and an antiquark if even.
14. Nuclear codes are given as 10-digit numbers  $\pm 10LZZZAAAI$ . For a (hyper)nucleus consisting of  $n_p$  protons,  $n_n$  neutrons and  $n_\Lambda$   $\Lambda$ 's,  $A = n_p + n_n + n_\Lambda$  gives the total baryon number,  $Z = n_p$  the total charge and  $L = n_\Lambda$  the total number of strange quarks.  $I$  gives the isomer level, with  $I = 0$  corresponding to the ground state and  $I > 0$  to excitations, see [4], where states denoted  $m, n, p, q$  translate to  $I = 1 - 4$ . As examples, the deuteron is 1000010020 and  $^{235}\text{U}$  is 1000922350. To avoid ambiguities, nuclear codes should not be applied to a single hadron, like  $p$ ,  $n$  or  $\Lambda^0$ , where quark-contents-based codes already exist.

This text and full lists of particle numbers, including excited baryons particles from physics beyond the standard model, can be found on the WWW [5]. The StdHep Monte Carlo standardization project [6] maintains the list of PDG particle numbers, as well as numbering schemes from most event generators and software to convert between the different schemes.

#### References:

1. G.P. Yost *et al.*, Particle Data Group, Phys. Lett. **B204**, 1 (1988).
2. I.G. Knowles *et al.*, in “Physics at LEP2”, CERN 96-01, v. 2, p. 103.
3. C. Caso *et al.*, Particle Data Group, Eur. Phys. J. **C3**, 1 (1998).
4. G. Audi *et al.*, Nucl. Phys. **A729**, 3 (2003) See also [http://www.nndc.bnl.gov/amdc/web/nubase\\_en.html](http://www.nndc.bnl.gov/amdc/web/nubase_en.html).
5. <http://pdg.lbl.gov/current/mc-particle-id/>.
6. L. Garren, StdHep, Monte Carlo Standardization at FNAL, Fermilab PM0091 and StdHep WWW site: <http://cepa.fnal.gov/psm/stdhep/>.

**QUARKS**

$d$	1
$u$	2
$s$	3
$c$	4
$b$	5
$t$	6
$b'$	7
$t'$	8

**LEPTONS**

$e^-$	11
$\nu_e$	12
$\mu^-$	13
$\nu_\mu$	14
$\tau^-$	15
$\nu_\tau$	16
$\tau'^-$	17
$\nu_{\tau'}$	18

**GAUGE AND HIGGS BOSONS**

$g$	(9) 21
$\gamma$	22
$Z^0$	23
$W^+$	24
$h^0/H_1^0$	25
$Z'/Z_2^0$	32
$Z''/Z_3^0$	33
$W'/W_2^+$	34
$H^0/H_2^0$	35
$A^0/H_3^0$	36
$H^+$	37

**SPECIAL PARTICLES**

$G$ (graviton)	39
$R^0$	41
$LQ^c$	42
<i>reggeon</i>	110
<i>pomeron</i>	990
<i>odderon</i>	9990

for MC internal  
use 81–100

**DIQUARKS**

$(dd)_1$	1103
$(ud)_0$	2101
$(ud)_1$	2103
$(uu)_1$	2203
$(sd)_0$	3101
$(sd)_1$	3103
$(su)_0$	3201
$(su)_1$	3203
$(ss)_1$	3303
$(cd)_0$	4101
$(cd)_1$	4103
$(cu)_0$	4201
$(cu)_1$	4203
$(cs)_0$	4301
$(cs)_1$	4303
$(cc)_1$	4403
$(bd)_0$	5101
$(bd)_1$	5103
$(bu)_0$	5201
$(bu)_1$	5203
$(bs)_0$	5301
$(bs)_1$	5303
$(bc)_0$	5401
$(bc)_1$	5403
$(bb)_1$	5503

**SUSY****PARTICLES**

$\tilde{d}_L$	1000001
$\tilde{u}_L$	1000002
$\tilde{s}_L$	1000003
$\tilde{c}_L$	1000004
$\tilde{b}_1$	1000005 <sup>a</sup>
$\tilde{t}_1$	1000006 <sup>a</sup>
$\tilde{e}_L$	1000011
$\tilde{\nu}_{eL}$	1000012
$\tilde{\mu}_L$	1000013
$\tilde{\nu}_{\mu L}$	1000014
$\tilde{\tau}_1$	1000015 <sup>a</sup>
$\tilde{\nu}_{\tau L}$	1000016
$\tilde{d}_R$	2000001
$\tilde{u}_R$	2000002
$\tilde{s}_R$	2000003
$\tilde{c}_R$	2000004
$\tilde{b}_2$	2000005 <sup>a</sup>
$\tilde{t}_2$	2000006 <sup>a</sup>
$\tilde{e}_R$	2000011
$\tilde{\mu}_R$	2000013
$\tilde{\tau}_2$	2000015 <sup>a</sup>
$\tilde{g}$	1000021
$\tilde{\chi}_1^0$	1000022 <sup>b</sup>
$\tilde{\chi}_2^0$	1000023 <sup>b</sup>
$\tilde{\chi}_1^+$	1000024 <sup>b</sup>
$\tilde{\chi}_3^0$	1000025 <sup>b</sup>
$\tilde{\chi}_4^0$	1000035 <sup>b</sup>
$\tilde{\chi}_2^+$	1000037 <sup>b</sup>
$\tilde{G}$	1000039

**LIGHT  $I = 1$  MESONS**

$\pi^0$	111
$\pi^+$	211
$a_0(980)^0$	9000111
$a_0(980)^+$	9000211
$\pi(1300)^0$	100111
$\pi(1300)^+$	100211
$a_0(1450)^0$	10111
$a_0(1450)^+$	10211
$\pi(1800)^0$	9010111
$\pi(1800)^+$	9010211
$\rho(770)^0$	113
$\rho(770)^+$	213
$b_1(1235)^0$	10113
$b_1(1235)^+$	10213
$a_1(1260)^0$	20113
$a_1(1260)^+$	20213
$\pi_1(1400)^0$	9000113
$\pi_1(1400)^+$	9000213
$\rho(1450)^0$	100113
$\rho(1450)^+$	100213
$\pi_1(1600)^0$	9010113
$\pi_1(1600)^+$	9010213
$a_1(1640)^0$	9020113
$a_1(1640)^+$	9020213
$\rho(1700)^0$	30113
$\rho(1700)^+$	30213
$\rho(1900)^0$	9030113
$\rho(1900)^+$	9030213
$\rho(2150)^0$	9040113
$\rho(2150)^+$	9040213
$a_2(1320)^0$	115
$a_2(1320)^+$	215
$\pi_2(1670)^0$	10115
$\pi_2(1670)^+$	10215
$a_2(1700)^0$	9000115
$a_2(1700)^+$	9000215
$\pi_2(2100)^0$	9010115
$\pi_2(2100)^+$	9010215
$\rho_3(1690)^0$	117
$\rho_3(1690)^+$	217
$\rho_3(1990)^0$	9000117
$\rho_3(1990)^+$	9000217
$\rho_3(2250)^0$	9010117
$\rho_3(2250)^+$	9010217
$a_4(2040)^0$	119
$a_4(2040)^+$	219

**LIGHT  $I = 0$  MESONS**

$(u\bar{u}, d\bar{d}, \text{ and } s\bar{s} \text{ Admixtures})$	
$\eta$	221
$\eta'(958)$	331
$f_0(600)$	9000221
$f_0(980)$	9010221
$\eta(1295)$	100221
$f_0(1370)$	10221
$\eta(1405)$	9020221
$\eta(1475)$	100331
$f_0(1500)$	9030221
$f_0(1710)$	10331
$\eta(1760)$	9040221
$f_0(2020)$	9050221
$f_0(2100)$	9060221
$f_0(2200)$	9070221
$\eta(2225)$	9080221
$\omega(782)$	223
$\phi(1020)$	333
$h_1(1170)$	10223
$f_1(1285)$	20223
$h_1(1380)$	10333
$f_1(1420)$	20333
$\omega(1420)$	100223
$f_1(1510)$	9000223
$h_1(1595)$	9010223
$\omega(1650)$	30223
$\phi(1680)$	100333
$f_2(1270)$	225
$f_2(1430)$	9000225
$f_2'(1525)$	335
$f_2(1565)$	9010225
$f_2(1640)$	9020225
$\eta_2(1645)$	10225
$f_2(1810)$	9030225
$\eta_2(1870)$	10335
$f_2(1910)$	9040225
$f_2(1950)$	9050225
$f_2(2010)$	9060225
$f_2(2150)$	9070225
$f_2(2300)$	9080225
$f_2(2340)$	9090225
$\omega_3(1670)$	227
$\phi_3(1850)$	337
$f_4(2050)$	229
$f_J(2220)$	9000229
$f_4(2300)$	9010229

STRANGE MESONS		CHARMED MESONS		$c\bar{c}$ MESONS		LIGHT BARYONS		BOTTOM BARYONS	
$K_L^0$	130	$D^+$	411	$\eta_c(1S)$	441	$p$	2212	$\Lambda_b^0$	5122
$K_S^0$	310	$D^0$	421	$\chi_{c0}(1P)$	10441	$n$	2112	$\Sigma_b^-$	5112
$K^0$	311	$D_0^*(2400)^+$	10411	$\eta_c(2S)$	100441	$\Delta^{++}$	2224	$\Sigma_b^0$	5212
$K^+$	321	$D_0^*(2400)^0$	10421	$J/\psi(1S)$	443	$\Delta^+$	2214	$\Sigma_b^+$	5222
$K_0^*(800)^0$	9000311	$D^*(2010)^+$	413	$h_c(1P)$	10443	$\Delta^0$	2114	$\Sigma_b^{*-}$	5114
$K_0^*(800)^+$	9000321	$D^*(2007)^0$	423	$\chi_{c1}(1P)$	20443	$\Delta^-$	1114	$\Sigma_b^{*0}$	5214
$K_0^*(1430)^0$	10311	$D_1(2420)^+$	10413	$\psi(2S)$	100443	<b>STRANGE BARYONS</b>			
$K_0^*(1430)^+$	10321	$D_1(2420)^0$	10423	$\psi(3770)$	30443	$\Lambda$	3122	$\Sigma_b^{*+}$	5224
$K(1460)^0$	100311	$D_1(H)^+$	20413	$\psi(4040)$	9000443	$\Sigma^+$	3222	$\Xi_b^-$	5132
$K(1460)^+$	100321	$D_1(2430)^0$	20423	$\psi(4160)$	9010443	$\Sigma^0$	3212	$\Xi_b^0$	5232
$K(1830)^0$	9010311	$D_2^*(2460)^+$	415	$\psi(4415)$	9020443	$\Sigma^-$	3112	$\Xi_b^{*-}$	5312
$K(1830)^+$	9010321	$D_2^*(2460)^0$	425	$\chi_{c2}(1P)$	445	$\Sigma^{*+}$	3224 <sup>c</sup>	$\Xi_b^0$	5322
$K_0^*(1950)^0$	9020311	$D_s^+$	431	$\chi_{c2}(2P)$	100445	$\Sigma^{*0}$	3214 <sup>c</sup>	$\Xi_b^-$	5314
$K_0^*(1950)^+$	9020321	$D_{s0}^*(2317)^+$	10431	<b><math>b\bar{b}</math> MESONS</b>				$\Sigma^{*-}$	3114 <sup>c</sup>
$K^*(892)^0$	313	$D_s^{*+}$	433	$\eta_b(1S)$	551	$\Xi^0$	3322	$\Xi_b^{*0}$	5324
$K^*(892)^+$	323	$D_{s1}(2536)^+$	10433	$\chi_{b0}(1P)$	10551	$\Xi^-$	3312	$\Omega_b^-$	5332
$K_1(1270)^0$	10313	$D_{s1}(2460)^+$	20433	$\eta_b(2S)$	100551	$\Xi^{*0}$	3324 <sup>c</sup>	$\Omega_b^{*-}$	5334
$K_1(1270)^+$	10323	$D_{s2}^*(2573)^+$	435	$\chi_{b0}(2P)$	110551	$\Xi^{*-}$	3314 <sup>c</sup>	$\Xi_{bc}^0$	5142
$K_1(1400)^0$	20313	<b>BOTTOM MESONS</b>				$\eta_b(3S)$	200551	$\Xi_{bc}^+$	5242
$K_1(1400)^+$	20323	$B^0$	511	$\chi_{b0}(3P)$	210551	$\Lambda_c^+$	4122	$\Xi_{bc}^0$	5412
$K^*(1410)^0$	100313	$B^+$	521	$\Upsilon(1S)$	553	$\Sigma_c^{++}$	4222	$\Xi_{bc}^{*0}$	5414
$K^*(1410)^+$	100323	$B_0^{*0}$	10511	$h_b(1P)$	10553	$\Sigma_c^+$	4212	$\Xi_{bc}^{*+}$	5424
$K_1(1650)^0$	9000313	$B_0^{*+}$	10521	$\chi_{b1}(1P)$	20553	$\Sigma_c^0$	4112	$\Omega_{bc}^0$	5342
$K_1(1650)^+$	9000323	$B^{*0}$	513	$\Upsilon_1(1D)$	30553	$\Sigma_c^{*+}$	4224	$\Omega_{bc}^{\prime 0}$	5432
$K^*(1680)^0$	30313	$B^{*+}$	523	$\Upsilon(2S)$	100553	$\Sigma_c^{*0}$	4114	$\Omega_{bc}^{\prime +}$	5434
$K^*(1680)^+$	30323	$B_1(L)^0$	10513	$h_b(2P)$	110553	$\Sigma_c^+$	4214	$\Omega_{bc}^{\prime 0}$	5432
$K_2^*(1430)^0$	315	$B_1(L)^+$	10523	$\chi_{b1}(2P)$	120553	$\Sigma_c^{*0}$	4114	$\Omega_{bcc}^+$	5442
$K_2^*(1430)^+$	325	$B_1(H)^0$	20513	$\Upsilon_1(2D)$	130553	$\Xi_c^+$	4232	$\Omega_{bcc}^{*+}$	5444
$K_2(1580)^0$	9000315	$B_1(H)^+$	20523	$\Upsilon(3S)$	200553	$\Xi_c^0$	4132	$\Xi_{bb}^-$	5512
$K_2(1580)^+$	9000325	$B_2^0$	515	$h_b(3P)$	210553	$\Xi_c^{\prime 0}$	4312	$\Xi_{bb}^0$	5522
$K_2(1770)^0$	10315	$B_2^{*+}$	525	$\chi_{b1}(3P)$	220553	$\Xi_c^{*+}$	4324	$\Xi_{bb}^{*-}$	5514
$K_2(1770)^+$	10325	$B_s^0$	531	$\Upsilon(4S)$	300553	$\Xi_c^{*0}$	4314	$\Xi_{bb}^{*0}$	5524
$K_2(1820)^0$	20315	$B_{s0}^{*0}$	10531	$\Upsilon(10860)$	9000553	$\Omega_c^0$	4332	$\Omega_{bb}^-$	5532
$K_2(1820)^+$	20325	$B_s^{*0}$	533	$\Upsilon(11020)$	9010553	$\Omega_c^{*0}$	4334	$\Omega_{bb}^{*-}$	5534
$K_2^*(1980)^0$	9010315	$B_{s1}(L)^0$	10533	$\chi_{b2}(1P)$	555	$\Xi_{cc}^+$	4412	$\Omega_{bbb}^0$	5542
$K_2^*(1980)^+$	9010325	$B_{s1}(H)^0$	20533	$\eta_{b2}(1D)$	10555	$\Xi_{cc}^{*+}$	4422	$\Omega_{bbb}^{*0}$	5544
$K_2(2250)^0$	9020315	$B_{s2}^{*0}$	535	$\Upsilon_2(1D)$	20555	$\Xi_{cc}^{*+}$	4414	$\Omega_{bbb}^-$	5554
$K_2(2250)^+$	9020325	$B_c^+$	541	$\chi_{b2}(2P)$	100555	$\Xi_{cc}^{*+}$	4424		
$K_3^*(1780)^0$	317	$B_{c0}^{*+}$	10541	$\eta_{b2}(2D)$	110555	$\Omega_{cc}^+$	4432		
$K_3^*(1780)^+$	327	$B_c^{*+}$	543	$\Upsilon_2(2D)$	120555	$\Omega_{cc}^{*+}$	4434		
$K_3(2320)^0$	9010317	$B_{c1}(L)^+$	10543	$\chi_{b2}(3P)$	200555	$\Omega_{ccc}^{*+}$	4444		
$K_3(2320)^+$	9010327	$B_{c1}(H)^+$	20543	$\Upsilon_3(1D)$	557				
$K_4^*(2045)^0$	319	$B_{c2}^{*+}$	545	$\Upsilon_3(2D)$	100557				
$K_4^*(2045)^+$	329								
$K_4(2500)^0$	9000319								
$K_4(2500)^+$	9000329								

**Footnotes to the Tables:**

- a) Particular in the third generation, the left and right sfermion states may mix, as shown. The lighter mixed state is given the smaller number.
- b) The physical  $\tilde{\chi}$  states are admixtures of the pure  $\tilde{\gamma}$ ,  $\tilde{Z}^0$ ,  $\tilde{W}^+$ ,  $\tilde{H}_1^0$ ,  $\tilde{H}_2^0$ , and  $\tilde{H}^+$  states.
- c)  $\Sigma^*$  and  $\Xi^*$  are alternate names for  $\Sigma(1385)$  and  $\Xi(1530)$ .



40. CLEBSCH-GORDAN COEFFICIENTS, SPHERICAL HARMONICS, AND  $d$  FUNCTIONS

Note: A square-root sign is to be understood over every coefficient, e.g., for  $-8/15$  read  $-\sqrt{8/15}$ .

Notation:

$J$	$J$	...
$M$	$M$	...

$m_1$	$m_2$	Coefficients
$m_1$	$m_2$	
$\vdots$	$\vdots$	
$\vdots$	$\vdots$	

$$Y_1^0 = \sqrt{\frac{3}{4\pi}} \cos \theta$$

$$Y_1^1 = -\sqrt{\frac{3}{8\pi}} \sin \theta e^{i\phi}$$

$$Y_2^0 = \sqrt{\frac{5}{4\pi}} \left( \frac{3}{2} \cos^2 \theta - \frac{1}{2} \right)$$

$$Y_2^1 = -\sqrt{\frac{15}{8\pi}} \sin \theta \cos \theta e^{i\phi}$$

$$Y_2^2 = \frac{1}{4} \sqrt{\frac{15}{2\pi}} \sin^2 \theta e^{2i\phi}$$

$1/2 \times 1/2$	$2 \times 1/2$	$3/2 \times 1/2$	$3/2 \times 1$	$2 \times 1$	$1 \times 1$
------------------	----------------	------------------	----------------	--------------	--------------

$$Y_\ell^{-m} = (-1)^m Y_\ell^{m*}$$

$$d_{m,0}^\ell = \sqrt{\frac{4\pi}{2\ell+1}} Y_\ell^m e^{-im\phi}$$

$$\langle j_1 j_2 m_1 m_2 | j_1 j_2 J M \rangle$$

$$= (-1)^{J-j_1-j_2} \langle j_2 j_1 m_2 m_1 | j_2 j_1 J M \rangle$$

$$d_{m',m}^j = (-1)^{m-m'} d_{m,m'}^j = d_{-m,-m'}^j$$

$3/2 \times 3/2$	$d_{1,0}^1 = \cos \theta$	$d_{1/2,1/2}^{1/2} = \cos \frac{\theta}{2}$	$d_{1,1}^1 = \frac{1+\cos \theta}{2}$
$2 \times 3/2$	$d_{1/2,-1/2}^{1/2} = -\sin \frac{\theta}{2}$	$d_{1,0}^1 = -\frac{\sin \theta}{\sqrt{2}}$	$d_{1,-1}^1 = \frac{1-\cos \theta}{2}$

$$d_{3/2,3/2}^{3/2} = \frac{1+\cos \theta}{2} \cos \frac{\theta}{2}$$

$$d_{3/2,1/2}^{3/2} = -\sqrt{3} \frac{1+\cos \theta}{2} \sin \frac{\theta}{2}$$

$$d_{3/2,-1/2}^{3/2} = \sqrt{3} \frac{1-\cos \theta}{2} \cos \frac{\theta}{2}$$

$$d_{3/2,-3/2}^{3/2} = -\frac{1-\cos \theta}{2} \sin \frac{\theta}{2}$$

$$d_{1/2,1/2}^{3/2} = \frac{3 \cos \theta - 1}{2} \cos \frac{\theta}{2}$$

$$d_{1/2,-1/2}^{3/2} = -\frac{3 \cos \theta + 1}{2} \sin \frac{\theta}{2}$$

$$d_{2,2}^2 = \left( \frac{1+\cos \theta}{2} \right)^2$$

$$d_{2,1}^2 = -\frac{1+\cos \theta}{2} \sin \theta$$

$$d_{2,0}^2 = \frac{\sqrt{6}}{4} \sin^2 \theta$$

$$d_{2,-1}^2 = -\frac{1-\cos \theta}{2} \sin \theta$$

$$d_{2,-2}^2 = \left( \frac{1-\cos \theta}{2} \right)^2$$

$$d_{1,1}^2 = \frac{1+\cos \theta}{2} (2 \cos \theta - 1)$$

$$d_{1,0}^2 = -\sqrt{\frac{3}{2}} \sin \theta \cos \theta$$

$$d_{1,-1}^2 = \frac{1-\cos \theta}{2} (2 \cos \theta + 1)$$

$$d_{0,0}^2 = \left( \frac{3}{2} \cos^2 \theta - \frac{1}{2} \right)$$

Figure 40.1: The sign convention is that of Wigner (Group Theory, Academic Press, New York, 1959), also used by Condon and Shortley (The Theory of Atomic Spectra, Cambridge Univ. Press, New York, 1953), Rose (Elementary Theory of Angular Momentum, Wiley, New York, 1957), and Cohen (Tables of the Clebsch-Gordan Coefficients, North American Rockwell Science Center, Thousand Oaks, Calif., 1974).

## 41. SU(3) ISOSCALAR FACTORS AND REPRESENTATION MATRICES

Written by R.L. Kelly (LBNL).

The most commonly used SU(3) isoscalar factors, corresponding to the singlet, octet, and decuplet content of  $8 \otimes 8$  and  $10 \otimes 8$ , are shown at the right. The notation uses particle names to identify the coefficients, so that the pattern of relative couplings may be seen at a glance. We illustrate the use of the coefficients below. See J.J de Swart, Rev. Mod. Phys. **35**, 916 (1963) for detailed explanations and phase conventions.

A  $\sqrt{\quad}$  is to be understood over every integer in the matrices; the exponent 1/2 on each matrix is a reminder of this. For example, the  $\Xi \rightarrow \Omega K$  element of the  $10 \rightarrow 10 \otimes 8$  matrix is  $-\sqrt{6}/\sqrt{24} = -1/2$ .

Intramultiplet relative decay strengths may be read directly from the matrices. For example, in decuplet  $\rightarrow$  octet + octet decays, the ratio of  $\Omega^* \rightarrow \Xi \bar{K}$  and  $\Delta \rightarrow N\pi$  partial widths is, from the  $10 \rightarrow 8 \times 8$  matrix,

$$\frac{\Gamma(\Omega^* \rightarrow \Xi \bar{K})}{\Gamma(\Delta \rightarrow N\pi)} = \frac{12}{6} \times (\text{phase space factors}). \quad (41.1)$$

Including isospin Clebsch-Gordan coefficients, we obtain, e.g.,

$$\frac{\Gamma(\Omega^{*-} \rightarrow \Xi^0 K^-)}{\Gamma(\Delta^+ \rightarrow p \pi^0)} = \frac{1/2}{2/3} \times \frac{12}{6} \times p.s.f. = \frac{3}{2} \times p.s.f. \quad (41.2)$$

Partial widths for  $8 \rightarrow 8 \otimes 8$  involve a linear superposition of  $8_1$  (symmetric) and  $8_2$  (antisymmetric) couplings. For example,

$$\Gamma(\Xi^* \rightarrow \Xi \pi) \sim \left( -\sqrt{\frac{9}{20}} g_1 + \sqrt{\frac{3}{12}} g_2 \right)^2. \quad (41.3)$$

The relations between  $g_1$  and  $g_2$  (with de Swart's normalization) and the standard  $D$  and  $F$  couplings that appear in the interaction Lagrangian,

$$\mathcal{L} = -\sqrt{2} D \text{Tr}(\{\bar{B}, B\}M) + \sqrt{2} F \text{Tr}([\bar{B}, B]M), \quad (41.4)$$

where  $[\bar{B}, B] \equiv \bar{B}B - B\bar{B}$  and  $\{\bar{B}, B\} \equiv \bar{B}B + B\bar{B}$ , are

$$D = \frac{\sqrt{30}}{40} g_1, \quad F = \frac{\sqrt{6}}{24} g_2. \quad (41.5)$$

Thus, for example,

$$\Gamma(\Xi^* \rightarrow \Xi \pi) \sim (F - D)^2 \sim (1 - 2\alpha)^2, \quad (41.6)$$

where  $\alpha \equiv F/(D + F)$ . (This definition of  $\alpha$  is de Swart's. The alternative  $D/(D + F)$ , due to Gell-Mann, is also used.)

The generators of SU(3) transformations,  $\lambda_a$  ( $a = 1, 8$ ), are  $3 \times 3$  matrices that obey the following commutation and anticommutation relationships:

$$[\lambda_a, \lambda_b] \equiv \lambda_a \lambda_b - \lambda_b \lambda_a = 2i f_{abc} \lambda_c \quad (41.7)$$

$$\{\lambda_a, \lambda_b\} \equiv \lambda_a \lambda_b + \lambda_b \lambda_a = \frac{4}{3} \delta_{ab} I + 2d_{abc} \lambda_c, \quad (41.8)$$

where  $I$  is the  $3 \times 3$  identity matrix, and  $\delta_{ab}$  is the Kronecker delta symbol. The  $f_{abc}$  are odd under the permutation of any pair of indices, while the  $d_{abc}$  are even. The nonzero values are

$1 \rightarrow 8 \otimes 8$

$$(\Lambda) \rightarrow (N \bar{K} \Sigma \pi \Lambda \eta \Xi K) = \frac{1}{\sqrt{8}} (2 \ 3 \ -1 \ -2)^{1/2}$$

$8_1 \rightarrow 8 \otimes 8$

$$\begin{pmatrix} N \\ \Sigma \\ \Lambda \\ \Xi \end{pmatrix} \rightarrow \begin{pmatrix} N\pi & N\eta & \Sigma K & \Lambda K \\ N\bar{K} & \Sigma\pi & \Lambda\pi & \Sigma\eta & \Xi K \\ N\bar{K} & \Sigma\pi & \Lambda\eta & \Xi K \\ \Sigma\bar{K} & \Lambda\bar{K} & \Xi\pi & \Xi\eta \end{pmatrix} = \frac{1}{\sqrt{20}} \begin{pmatrix} 9 & -1 & -9 & -1 \\ -6 & 0 & 4 & 4 & -6 \\ 2 & -12 & -4 & -2 \\ 9 & -1 & -9 & -1 \end{pmatrix}^{1/2}$$

$8_2 \rightarrow 8 \otimes 8$

$$\begin{pmatrix} N \\ \Sigma \\ \Lambda \\ \Xi \end{pmatrix} \rightarrow \begin{pmatrix} N\pi & N\eta & \Sigma K & \Lambda K \\ N\bar{K} & \Sigma\pi & \Lambda\pi & \Sigma\eta & \Xi K \\ N\bar{K} & \Sigma\pi & \Lambda\eta & \Xi K \\ \Sigma\bar{K} & \Lambda\bar{K} & \Xi\pi & \Xi\eta \end{pmatrix} = \frac{1}{\sqrt{12}} \begin{pmatrix} 3 & 3 & 3 & -3 \\ 2 & 8 & 0 & 0 & -2 \\ 6 & 0 & 0 & 6 \\ 3 & 3 & 3 & -3 \end{pmatrix}^{1/2}$$

$10 \rightarrow 8 \otimes 8$

$$\begin{pmatrix} \Delta \\ \Sigma \\ \Xi \\ \Omega \end{pmatrix} \rightarrow \begin{pmatrix} N\pi & \Sigma K \\ N\bar{K} & \Sigma\pi & \Lambda\pi & \Sigma\eta & \Xi K \\ \Sigma\bar{K} & \Lambda\bar{K} & \Xi\pi & \Xi\eta \\ \Xi\bar{K} \end{pmatrix} = \frac{1}{\sqrt{12}} \begin{pmatrix} -6 & 6 \\ -2 & 2 & -3 & 3 & 2 \\ 3 & -3 & 3 & 3 \\ 12 \end{pmatrix}^{1/2}$$

$8 \rightarrow 10 \otimes 8$

$$\begin{pmatrix} N \\ \Sigma \\ \Lambda \\ \Xi \end{pmatrix} \rightarrow \begin{pmatrix} \Delta\pi & \Sigma K \\ \Delta\bar{K} & \Sigma\pi & \Sigma\eta & \Xi K \\ \Sigma\pi & \Sigma\pi & \Xi K \\ \Sigma\bar{K} & \Xi\pi & \Xi\eta & \Omega K \end{pmatrix} = \frac{1}{\sqrt{15}} \begin{pmatrix} -12 & 3 \\ 8 & -2 & -3 & 2 \\ -9 & 6 \\ 3 & -3 & -3 & 6 \end{pmatrix}^{1/2}$$

$10 \rightarrow 10 \otimes 8$

$$\begin{pmatrix} \Delta \\ \Sigma \\ \Xi \\ \Omega \end{pmatrix} \rightarrow \begin{pmatrix} \Delta\pi & \Delta\eta & \Sigma K \\ \Delta\bar{K} & \Sigma\pi & \Sigma\eta & \Xi K \\ \Sigma\bar{K} & \Xi\pi & \Xi\eta & \Omega K \\ \Xi\bar{K} & \Omega\eta \end{pmatrix} = \frac{1}{\sqrt{24}} \begin{pmatrix} 15 & 3 & -6 \\ 8 & 8 & 0 & -8 \\ 12 & 3 & -3 & -6 \\ 12 & -12 \end{pmatrix}^{1/2}$$

$abc$	$f_{abc}$	$abc$	$d_{abc}$	$abc$	$d_{abc}$
123	1	118	$1/\sqrt{3}$	355	1/2
147	1/2	146	1/2	366	-1/2
156	-1/2	157	1/2	377	-1/2
246	1/2	228	$1/\sqrt{3}$	448	$-1/(2\sqrt{3})$
257	1/2	247	-1/2	558	$-1/(2\sqrt{3})$
345	1/2	256	1/2	668	$-1/(2\sqrt{3})$
367	-1/2	338	$1/\sqrt{3}$	778	$-1/(2\sqrt{3})$
458	$\sqrt{3}/2$	344	1/2	888	$-1/\sqrt{3}$
678	$\sqrt{3}/2$				

The  $\lambda_a$ 's are

$$\lambda_1 = \begin{pmatrix} 0 & 1 & 0 \\ 1 & 0 & 0 \\ 0 & 0 & 0 \end{pmatrix} \quad \lambda_2 = \begin{pmatrix} 0 & -i & 0 \\ i & 0 & 0 \\ 0 & 0 & 0 \end{pmatrix} \quad \lambda_3 = \begin{pmatrix} 1 & 0 & 0 \\ 0 & -1 & 0 \\ 0 & 0 & 0 \end{pmatrix}$$

$$\lambda_4 = \begin{pmatrix} 0 & 0 & 1 \\ 0 & 0 & 0 \\ 1 & 0 & 0 \end{pmatrix} \quad \lambda_5 = \begin{pmatrix} 0 & 0 & -i \\ 0 & 0 & 0 \\ i & 0 & 0 \end{pmatrix} \quad \lambda_6 = \begin{pmatrix} 0 & 0 & 0 \\ 0 & 0 & 1 \\ 0 & 1 & 0 \end{pmatrix}$$

$$\lambda_7 = \begin{pmatrix} 0 & 0 & 0 \\ 0 & 0 & -i \\ 0 & i & 0 \end{pmatrix} \quad \lambda_8 = \frac{1}{\sqrt{3}} \begin{pmatrix} 1 & 0 & 0 \\ 0 & 1 & 0 \\ 0 & 0 & -2 \end{pmatrix}$$

Equation (41.7) defines the Lie algebra of SU(3). A general  $d$ -dimensional representation is given by a set of  $d \times d$  matrices satisfying Eq. (41.7) with the  $f_{abc}$  given above. Equation (41.8) is specific to the defining 3-dimensional representation.

## 42. SU(n) MULTIPLETS AND YOUNG DIAGRAMMS

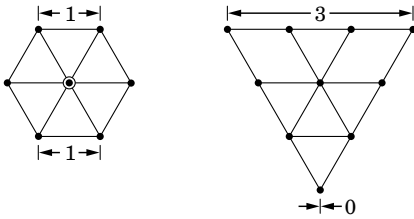
Written by C.G. Wohl (LBNL).

This note tells (1) how SU(n) particle multiplets are identified or labeled, (2) how to find the number of particles in a multiplet from its label, (3) how to draw the Young diagram for a multiplet, and (4) how to use Young diagrams to determine the overall multiplet structure of a composite system, such as a 3-quark or a meson-baryon system.

In much of the literature, the word “representation” is used where we use “multiplet,” and “tableau” is used where we use “diagram.”

### 42.1. Multiplet labels

An SU(n) multiplet is uniquely identified by a string of (n-1) nonnegative integers: (α, β, γ, ...). Any such set of integers specifies a multiplet. For an SU(2) multiplet such as an isospin multiplet, the single integer α is the number of steps from one end of the multiplet to the other (i.e., it is one fewer than the number of particles in the multiplet). In SU(3), the two integers α and β are the numbers of steps across the top and bottom levels of the multiplet diagram. Thus the labels for the SU(3) octet and decuplet



are (1,1) and (3,0). For larger n, the interpretation of the integers in terms of the geometry of the multiplets, which exist in an (n-1)-dimensional space, is not so readily apparent.

The label for the SU(n) singlet is (0, 0, ..., 0). In a flavor SU(n), the n quarks together form a (1, 0, ..., 0) multiplet, and the n antiquarks belong to a (0, ..., 0, 1) multiplet. These two multiplets are conjugate to one another, which means their labels are related by (α, β, ...) ↔ (... , β, α).

### 42.2. Number of particles

The number of particles in a multiplet, N = N(α, β, ...), is given as follows (note the pattern of the equations).

In SU(2), N = N(α) is

$$N = \frac{(\alpha + 1)}{1} \tag{42.1}$$

In SU(3), N = N(α, β) is

$$N = \frac{(\alpha + 1)}{1} \cdot \frac{(\beta + 1)}{1} \cdot \frac{(\alpha + \beta + 2)}{2} \tag{42.2}$$

In SU(4), N = N(α, β, γ) is

$$N = \frac{(\alpha + 1)}{1} \cdot \frac{(\beta + 1)}{1} \cdot \frac{(\gamma + 1)}{1} \cdot \frac{(\alpha + \beta + 2)}{2} \cdot \frac{(\beta + \gamma + 2)}{2} \cdot \frac{(\alpha + \beta + \gamma + 3)}{3} \tag{42.3}$$

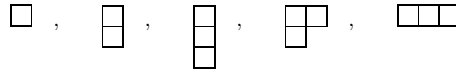
Note that in Eq. (42.3) there is no factor with (α + γ + 2): only a consecutive sequence of the label integers appears in any factor. One more example should make the pattern clear for any SU(n). In SU(5), N = N(α, β, γ, δ) is

$$N = \frac{(\alpha + 1)}{1} \cdot \frac{(\beta + 1)}{1} \cdot \frac{(\gamma + 1)}{1} \cdot \frac{(\delta + 1)}{1} \cdot \frac{(\alpha + \beta + 2)}{2} \cdot \frac{(\beta + \gamma + 2)}{2} \cdot \frac{(\gamma + \delta + 2)}{2} \cdot \frac{(\alpha + \beta + \gamma + 3)}{3} \cdot \frac{(\beta + \gamma + \delta + 3)}{3} \cdot \frac{(\alpha + \beta + \gamma + \delta + 4)}{4} \tag{42.4}$$

From the symmetry of these equations, it is clear that multiplets that are conjugate to one another have the same number of particles, but so can other multiplets. For example, the SU(4) multiplets (3,0,0) and (1,1,0) each have 20 particles. Try the equations and see.

### 42.3. Young diagrams

A Young diagram consists of an array of boxes (or some other symbol) arranged in one or more left-justified rows, with each row being at least as long as the row beneath. The correspondence between a diagram and a multiplet label is: The top row juts out α boxes to the right past the end of the second row, the second row juts out β boxes to the right past the end of the third row, etc. A diagram in SU(n) has at most n rows. There can be any number of “completed” columns of n boxes buttressing the left of a diagram; these don’t affect the label. Thus in SU(3) the diagrams



represent the multiplets (1,0), (0,1), (0,0), (1,1), and (3,0). In any SU(n), the quark multiplet is represented by a single box, the antiquark multiplet by a column of (n-1) boxes, and a singlet by a completed column of n boxes.

### 42.4. Coupling multiplets together

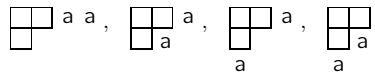
The following recipe tells how to find the multiplets that occur in coupling two multiplets together. To couple together more than two multiplets, first couple two, then couple a third with each of the multiplets obtained from the first two, etc.

First a definition: A sequence of the letters a, b, c, ... is admissible if at any point in the sequence at least as many a’s have occurred as b’s, at least as many b’s have occurred as c’s, etc. Thus abcd and aabc are admissible sequences and abb and acb are not. Now the recipe:

(a) Draw the Young diagrams for the two multiplets, but in one of the diagrams replace the boxes in the first row with a’s, the boxes in the second row with b’s, etc. Thus, to couple two SU(3) octets (such as the π-meson octet and the baryon octet), we start with and

. The unlettered diagram forms the upper left-hand corner of all the enlarged diagrams constructed below.

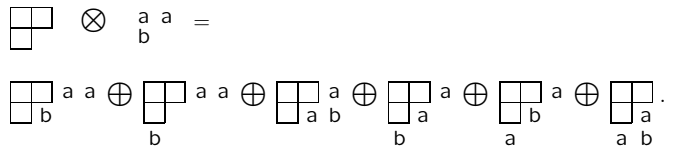
(b) Add the a’s from the lettered diagram to the right-hand ends of the rows of the unlettered diagram to form all possible legitimate Young diagrams that have no more than one a per column. In general, there will be several distinct diagrams, and all the a’s appear in each diagram. At this stage, for the coupling of the two SU(3) octets, we have:



(c) Use the b’s to further enlarge the diagrams already obtained, subject to the same rules. Then throw away any diagram in which the full sequence of letters formed by reading right to left in the first row, then the second row, etc., is not admissible.

(d) Proceed as in (c) with the c’s (if any), etc.

The final result of the coupling of the two SU(3) octets is:



Here only the diagrams with admissible sequences of a’s and b’s and with fewer than four rows (since n = 3) have been kept. In terms of multiplet labels, the above may be written

$$(1, 1) \otimes (1, 1) = (2, 2) \oplus (3, 0) \oplus (0, 3) \oplus (1, 1) \oplus (1, 1) \oplus (0, 0) .$$

In terms of numbers of particles, it may be written

$$8 \otimes 8 = 27 \oplus 10 \oplus \overline{10} \oplus 8 \oplus 8 \oplus 1 .$$

The product of the numbers on the left here is equal to the sum on the right, a useful check. (See also Sec. 14 on the Quark Model.)

## 43. KINEMATICS

Revised January 2000 by J.D. Jackson (LBNL) and June 2008 by D.R. Tovey (Sheffield).

Throughout this section units are used in which  $\hbar = c = 1$ . The following conversions are useful:  $\hbar c = 197.3$  MeV fm,  $(\hbar c)^2 = 0.3894$  (GeV)<sup>2</sup> mb.

## 43.1. Lorentz transformations

The energy  $E$  and 3-momentum  $\mathbf{p}$  of a particle of mass  $m$  form a 4-vector  $p = (E, \mathbf{p})$  whose square  $p^2 \equiv E^2 - |\mathbf{p}|^2 = m^2$ . The velocity of the particle is  $\boldsymbol{\beta} = \mathbf{p}/E$ . The energy and momentum  $(E^*, \mathbf{p}^*)$  viewed from a frame moving with velocity  $\boldsymbol{\beta}_f$  are given by

$$\begin{pmatrix} E^* \\ p_{\parallel}^* \end{pmatrix} = \begin{pmatrix} \gamma_f & -\gamma_f \boldsymbol{\beta}_f \\ -\gamma_f \boldsymbol{\beta}_f & \gamma_f \end{pmatrix} \begin{pmatrix} E \\ p_{\parallel} \end{pmatrix}, \quad p_T^* = p_T, \quad (43.1)$$

where  $\gamma_f = (1 - \beta_f^2)^{-1/2}$  and  $p_T$  ( $p_{\parallel}$ ) are the components of  $\mathbf{p}$  perpendicular (parallel) to  $\boldsymbol{\beta}_f$ . Other 4-vectors, such as the space-time coordinates of events, of course transform in the same way. The scalar product of two 4-momenta  $p_1 \cdot p_2 = E_1 E_2 - \mathbf{p}_1 \cdot \mathbf{p}_2$  is invariant (frame independent).

## 43.2. Center-of-mass energy and momentum

In the collision of two particles of masses  $m_1$  and  $m_2$  the total center-of-mass energy can be expressed in the Lorentz-invariant form

$$\begin{aligned} E_{\text{cm}} &= \left[ (E_1 + E_2)^2 - (\mathbf{p}_1 + \mathbf{p}_2)^2 \right]^{1/2}, \\ &= \left[ m_1^2 + m_2^2 + 2E_1 E_2 (1 - \beta_1 \beta_2 \cos \theta) \right]^{1/2}, \end{aligned} \quad (43.2)$$

where  $\theta$  is the angle between the particles. In the frame where one particle (of mass  $m_2$ ) is at rest (lab frame),

$$E_{\text{cm}} = (m_1^2 + m_2^2 + 2E_{1\text{lab}} m_2)^{1/2}. \quad (43.3)$$

The velocity of the center-of-mass in the lab frame is

$$\boldsymbol{\beta}_{\text{cm}} = \mathbf{p}_{\text{lab}} / (E_{1\text{lab}} + m_2), \quad (43.4)$$

where  $\mathbf{p}_{\text{lab}} \equiv \mathbf{p}_{1\text{lab}}$  and

$$\gamma_{\text{cm}} = (E_{1\text{lab}} + m_2) / E_{\text{cm}}. \quad (43.5)$$

The c.m. momenta of particles 1 and 2 are of magnitude

$$p_{\text{cm}} = p_{\text{lab}} \frac{m_2}{E_{\text{cm}}}. \quad (43.6)$$

For example, if a 0.80 GeV/c kaon beam is incident on a proton target, the center of mass energy is 1.699 GeV and the center of mass momentum of either particle is 0.442 GeV/c. It is also useful to note that

$$E_{\text{cm}} dE_{\text{cm}} = m_2 dE_{1\text{lab}} = m_2 \beta_{1\text{lab}} dp_{\text{lab}}. \quad (43.7)$$

## 43.3. Lorentz-invariant amplitudes

The matrix elements for a scattering or decay process are written in terms of an invariant amplitude  $-i\mathcal{M}$ . As an example, the  $S$ -matrix for  $2 \rightarrow 2$  scattering is related to  $\mathcal{M}$  by

$$\begin{aligned} \langle p'_1 p'_2 | S | p_1 p_2 \rangle &= I - i(2\pi)^4 \delta^4(p_1 + p_2 - p'_1 - p'_2) \\ &\times \frac{\mathcal{M}(p_1, p_2; p'_1, p'_2)}{(2E_1)^{1/2} (2E_2)^{1/2} (2E'_1)^{1/2} (2E'_2)^{1/2}}. \end{aligned} \quad (43.8)$$

The state normalization is such that

$$\langle p' | p \rangle = (2\pi)^3 \delta^3(\mathbf{p} - \mathbf{p}'). \quad (43.9)$$

## 43.4. Particle decays

The partial decay rate of a particle of mass  $M$  into  $n$  bodies in its rest frame is given in terms of the Lorentz-invariant matrix element  $\mathcal{M}$  by

$$d\Gamma = \frac{(2\pi)^4}{2M} |\mathcal{M}|^2 d\Phi_n(P; p_1, \dots, p_n), \quad (43.10)$$

where  $d\Phi_n$  is an element of  $n$ -body phase space given by

$$d\Phi_n(P; p_1, \dots, p_n) = \delta^4(P - \sum_{i=1}^n p_i) \prod_{i=1}^n \frac{d^3 p_i}{(2\pi)^3 2E_i}. \quad (43.11)$$

This phase space can be generated recursively, viz.

$$\begin{aligned} d\Phi_n(P; p_1, \dots, p_n) &= d\Phi_j(q; p_1, \dots, p_j) \\ &\times d\Phi_{n-j+1}(P; q, p_{j+1}, \dots, p_n) (2\pi)^3 dq^2, \end{aligned} \quad (43.12)$$

where  $q^2 = (\sum_{i=1}^j E_i)^2 - |\sum_{i=1}^j \mathbf{p}_i|^2$ . This form is particularly useful in the case where a particle decays into another particle that subsequently decays.

**43.4.1. Survival probability:** If a particle of mass  $M$  has mean proper lifetime  $\tau$  ( $= 1/\Gamma$ ) and has momentum  $(E, \mathbf{p})$ , then the probability that it lives for a time  $t_0$  or greater before decaying is given by

$$P(t_0) = e^{-t_0 \Gamma / \gamma} = e^{-M t_0 \Gamma / E}, \quad (43.13)$$

and the probability that it travels a distance  $x_0$  or greater is

$$P(x_0) = e^{-M x_0 \Gamma / |\mathbf{p}|}. \quad (43.14)$$

## 43.4.2. Two-body decays:

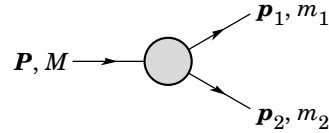


Figure 43.1: Definitions of variables for two-body decays.

In the rest frame of a particle of mass  $M$ , decaying into 2 particles labeled 1 and 2,

$$E_1 = \frac{M^2 - m_2^2 + m_1^2}{2M}, \quad (43.15)$$

$$|\mathbf{p}_1| = |\mathbf{p}_2|$$

$$= \frac{[(M^2 - (m_1 + m_2)^2)(M^2 - (m_1 - m_2)^2)]^{1/2}}{2M}, \quad (43.16)$$

and

$$d\Gamma = \frac{1}{32\pi^2} |\mathcal{M}|^2 \frac{|\mathbf{p}_1|}{M^2} d\Omega, \quad (43.17)$$

where  $d\Omega = d\phi_1 d(\cos \theta_1)$  is the solid angle of particle 1. The invariant mass  $M$  can be determined from the energies and momenta using Eq. (43.2) with  $M = E_{\text{cm}}$ .

## 43.4.3. Three-body decays:

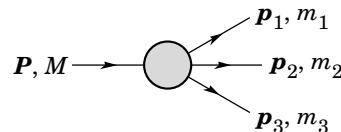


Figure 43.2: Definitions of variables for three-body decays.

Defining  $p_{ij} = p_i + p_j$  and  $m_{ij}^2 = p_{ij}^2$ , then  $m_{12}^2 + m_{23}^2 + m_{13}^2 = M^2 + m_1^2 + m_2^2 + m_3^2$  and  $m_{12}^2 = (P - p_3)^2 = M^2 + m_3^2 - 2ME_3$ , where  $E_3$  is the energy of particle 3 in the rest frame of  $M$ . In that frame, the momenta of the three decay particles lie in a plane. The relative orientation of these three momenta is fixed if their energies are known. The momenta can therefore be specified in space by giving three Euler angles  $(\alpha, \beta, \gamma)$  that specify the orientation of the final system relative to the initial particle [1]. Then

$$d\Gamma = \frac{1}{(2\pi)^5} \frac{1}{16M} |\mathcal{M}|^2 dE_1 dE_2 d\alpha d(\cos\beta) d\gamma. \quad (43.18)$$

Alternatively

$$d\Gamma = \frac{1}{(2\pi)^5} \frac{1}{16M^2} |\mathcal{M}|^2 |\mathbf{p}_1^*| |\mathbf{p}_3| dm_{12} d\Omega_1^* d\Omega_3, \quad (43.19)$$

where  $(|\mathbf{p}_1^*|, \Omega_1^*)$  is the momentum of particle 1 in the rest frame of 1 and 2, and  $\Omega_3$  is the angle of particle 3 in the rest frame of the decaying particle.  $|\mathbf{p}_1^*|$  and  $|\mathbf{p}_3|$  are given by

$$|\mathbf{p}_1^*| = \frac{[(m_{12}^2 - (m_1 + m_2)^2)(m_{12}^2 - (m_1 - m_2)^2)]^{1/2}}{2m_{12}}, \quad (43.20a)$$

and

$$|\mathbf{p}_3| = \frac{[(M^2 - (m_{12} + m_3)^2)(M^2 - (m_{12} - m_3)^2)]^{1/2}}{2M}. \quad (43.20b)$$

[Compare with Eq. (43.16).]

If the decaying particle is a scalar or we average over its spin states, then integration over the angles in Eq. (43.18) gives

$$\begin{aligned} d\Gamma &= \frac{1}{(2\pi)^3} \frac{1}{8M} |\overline{\mathcal{M}}|^2 dE_1 dE_2 \\ &= \frac{1}{(2\pi)^3} \frac{1}{32M^3} |\overline{\mathcal{M}}|^2 dm_{12}^2 dm_{23}^2. \end{aligned} \quad (43.21)$$

This is the standard form for the Dalitz plot.

**43.4.3.1. Dalitz plot:** For a given value of  $m_{12}^2$ , the range of  $m_{23}^2$  is determined by its values when  $\mathbf{p}_2$  is parallel or antiparallel to  $\mathbf{p}_3$ :

$$(m_{23}^2)_{\max} = (E_2^* + E_3^*)^2 - \left( \sqrt{E_2^{*2} - m_2^2} - \sqrt{E_3^{*2} - m_3^2} \right)^2, \quad (43.22a)$$

$$(m_{23}^2)_{\min} = (E_2^* + E_3^*)^2 - \left( \sqrt{E_2^{*2} - m_2^2} + \sqrt{E_3^{*2} - m_3^2} \right)^2. \quad (43.22b)$$

Here  $E_2^* = (m_{12}^2 - m_1^2 + m_2^2)/2m_{12}$  and  $E_3^* = (M^2 - m_{12}^2 - m_3^2)/2m_{12}$  are the energies of particles 2 and 3 in the  $m_{12}$  rest frame. The scatter plot in  $m_{12}^2$  and  $m_{23}^2$  is called a Dalitz plot. If  $|\overline{\mathcal{M}}|^2$  is constant, the allowed region of the plot will be uniformly populated with events [see Eq. (43.21)]. A nonuniformity in the plot gives immediate information on  $|\mathcal{M}|^2$ . For example, in the case of  $D \rightarrow K\pi\pi$ , bands appear when  $m_{(K\pi)} = m_{K^*(892)}$ , reflecting the appearance of the decay chain  $D \rightarrow K^*(892)\pi \rightarrow K\pi\pi$ .

#### 43.4.4. Kinematic limits :

**43.4.4.1. Three-body decays:** In a three-body decay (Fig. 43.2) the maximum of  $|\mathbf{p}_3|$ , [given by Eq. (43.20)], is achieved when  $m_{12} = m_1 + m_2$ , *i.e.*, particles 1 and 2 have the same vector velocity in the rest frame of the decaying particle. If, in addition,  $m_3 > m_1, m_2$ , then  $|\mathbf{p}_3|_{\max} > |\mathbf{p}_1|_{\max}, |\mathbf{p}_2|_{\max}$ . The distribution of  $m_{12}$  values possesses an end-point or maximum value at  $m_{12} = M - m_3$ . This can be used to constrain the mass difference of a parent particle and one invisible decay product.

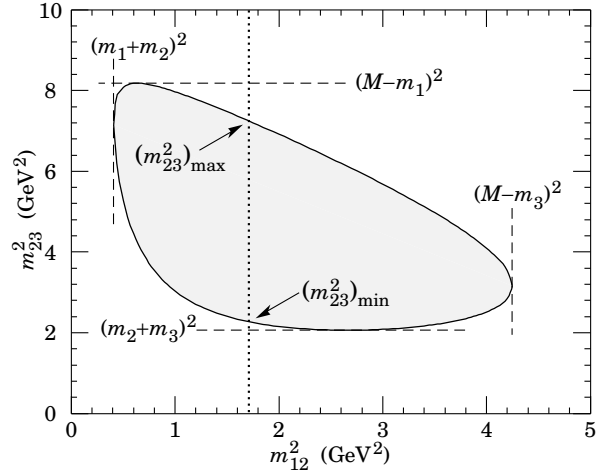


**Figure 43.3:** Dalitz plot for a three-body final state. In this example, the state is  $\pi^+K^0p$  at 3 GeV. Four-momentum conservation restricts events to the shaded region.

#### 43.4.4.2. Sequential two-body decays:

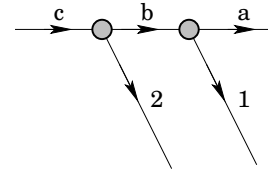


**Figure 43.4:** Particles participating in sequential two-body decay chain. Particles labeled 1 and 2 are visible while the particle terminating the chain (a) is invisible.

When a heavy particle initiates a sequential chain of two-body decays terminating in an invisible particle, constraints on the masses of the states participating in the chain can be obtained from end-points and thresholds in invariant mass distributions of the aggregated decay products. For the two-step decay chain depicted in Fig. 43.4 the invariant mass distribution of the two visible particles possesses an end-point given by:

$$(m_{12}^{\max})^2 = \frac{(m_c^2 - m_b^2)(m_b^2 - m_a^2)}{m_b^2}, \quad (43.23)$$

provided particles 1 and 2 are massless. If visible particle 1 has non-zero mass  $m_1$  then Eq. (43.23) is replaced by

$$(m_{12}^{\max})^2 = m_1^2 + \frac{(m_c^2 - m_b^2)}{2m_b^2} \times \left( m_1^2 + m_b^2 - m_a^2 + \sqrt{(-m_1^2 + m_b^2 - m_a^2)^2 - 4m_1^2 m_a^2} \right). \quad (43.24)$$

See Refs. 2 and 3 for other cases.

**43.4.5. Multibody decays :** The above results may be generalized to final states containing any number of particles by combining some of the particles into “effective particles” and treating the final states as 2 or 3 “effective particle” states. Thus, if  $p_{ijk\dots} = p_i + p_j + p_k + \dots$ , then

$$m_{ijk\dots} = \sqrt{p_{ijk\dots}^2}, \quad (43.25)$$

and  $m_{ijk\dots}$  may be used in place of *e.g.*,  $m_{12}$  in the relations in Sec. 43.4.3 or Sec. 43.4.4 above.

## 43.5. Cross sections

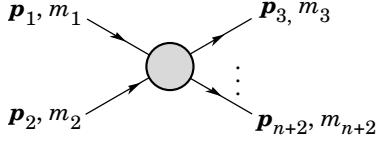


**Figure 43.5:** Definitions of variables for production of an  $n$ -body final state.

The differential cross section is given by

$$d\sigma = \frac{(2\pi)^4 |\mathcal{M}|^2}{4\sqrt{(p_1 \cdot p_2)^2 - m_1^2 m_2^2}} \times d\Phi_n(p_1 + p_2; p_3, \dots, p_{n+2}). \quad (43.26)$$

[See Eq. (43.11).] In the rest frame of  $m_2$ (lab),

$$\sqrt{(p_1 \cdot p_2)^2 - m_1^2 m_2^2} = m_2 p_{1\text{lab}}; \quad (43.27a)$$

while in the center-of-mass frame

$$\sqrt{(p_1 \cdot p_2)^2 - m_1^2 m_2^2} = p_{1\text{cm}} \sqrt{s}. \quad (43.27b)$$

## 43.5.1. Two-body reactions :

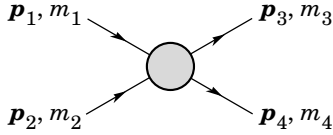


**Figure 43.6:** Definitions of variables for a two-body final state.

Two particles of momenta  $p_1$  and  $p_2$  and masses  $m_1$  and  $m_2$  scatter to particles of momenta  $p_3$  and  $p_4$  and masses  $m_3$  and  $m_4$ ; the Lorentz-invariant Mandelstam variables are defined by

$$s = (p_1 + p_2)^2 = (p_3 + p_4)^2 = m_1^2 + 2E_1 E_2 - 2\mathbf{p}_1 \cdot \mathbf{p}_2 + m_2^2, \quad (43.28)$$

$$t = (p_1 - p_3)^2 = (p_2 - p_4)^2 = m_1^2 - 2E_1 E_3 + 2\mathbf{p}_1 \cdot \mathbf{p}_3 + m_3^2, \quad (43.29)$$

$$u = (p_1 - p_4)^2 = (p_2 - p_3)^2 = m_1^2 - 2E_1 E_4 + 2\mathbf{p}_1 \cdot \mathbf{p}_4 + m_4^2, \quad (43.30)$$

and they satisfy

$$s + t + u = m_1^2 + m_2^2 + m_3^2 + m_4^2. \quad (43.31)$$

The two-body cross section may be written as

$$\frac{d\sigma}{dt} = \frac{1}{64\pi s} \frac{1}{|\mathbf{p}_{1\text{cm}}|^2} |\mathcal{M}|^2. \quad (43.32)$$

In the center-of-mass frame

$$t = (E_{1\text{cm}} - E_{3\text{cm}})^2 - (p_{1\text{cm}} - p_{3\text{cm}})^2 - 4p_{1\text{cm}} p_{3\text{cm}} \sin^2(\theta_{\text{cm}}/2) = t_0 - 4p_{1\text{cm}} p_{3\text{cm}} \sin^2(\theta_{\text{cm}}/2), \quad (43.33)$$

where  $\theta_{\text{cm}}$  is the angle between particle 1 and 3. The limiting values  $t_0$  ( $\theta_{\text{cm}} = 0$ ) and  $t_1$  ( $\theta_{\text{cm}} = \pi$ ) for  $2 \rightarrow 2$  scattering are

$$t_0(t_1) = \left[ \frac{m_1^2 - m_3^2 - m_2^2 + m_4^2}{2\sqrt{s}} \right]^2 - (p_{1\text{cm}} \mp p_{3\text{cm}})^2. \quad (43.34)$$

In the literature the notation  $t_{\text{min}}$  ( $t_{\text{max}}$ ) for  $t_0$  ( $t_1$ ) is sometimes used, which should be discouraged since  $t_0 > t_1$ . The center-of-mass energies and momenta of the incoming particles are

$$E_{1\text{cm}} = \frac{s + m_1^2 - m_2^2}{2\sqrt{s}}, \quad E_{2\text{cm}} = \frac{s + m_2^2 - m_1^2}{2\sqrt{s}}, \quad (43.35)$$

For  $E_{3\text{cm}}$  and  $E_{4\text{cm}}$ , change  $m_1$  to  $m_3$  and  $m_2$  to  $m_4$ . Then

$$p_{i\text{cm}} = \sqrt{E_{i\text{cm}}^2 - m_i^2} \text{ and } p_{1\text{cm}} = \frac{p_{1\text{lab}} m_2}{\sqrt{s}}. \quad (43.36)$$

Here the subscript lab refers to the frame where particle 2 is at rest. [For other relations see Eqs. (43.2)–(43.4).]

**43.5.2. Inclusive reactions :** Choose some direction (usually the beam direction) for the  $z$ -axis; then the energy and momentum of a particle can be written as

$$E = m_T \cosh y, \quad p_x, p_y, p_z = m_T \sinh y, \quad (43.37)$$

where  $m_T$ , conventionally called the ‘transverse mass’, is given by

$$m_T^2 = m^2 + p_x^2 + p_y^2. \quad (43.38)$$

and the rapidity  $y$  is defined by

$$y = \frac{1}{2} \ln \left( \frac{E + p_z}{E - p_z} \right)$$

$$= \ln \left( \frac{E + p_z}{m_T} \right) = \tanh^{-1} \left( \frac{p_z}{E} \right). \quad (43.39)$$

Note that the definition of the transverse mass in Eq. (43.38) differs from that used by experimentalists at hadron colliders (see Sec. 43.6.1 below). Under a boost in the  $z$ -direction to a frame with velocity  $\beta$ ,  $y \rightarrow y - \tanh^{-1} \beta$ . Hence the shape of the rapidity distribution  $dN/dy$  is invariant, as are differences in rapidity. The invariant cross section may also be rewritten

$$E \frac{d^3\sigma}{d^3p} = \frac{d^3\sigma}{d\phi dy p_T dp_T} \Rightarrow \frac{d^2\sigma}{\pi dy d(p_T^2)}. \quad (43.40)$$

The second form is obtained using the identity  $dy/dp_z = 1/E$ , and the third form represents the average over  $\phi$ .

Feynman’s  $x$  variable is given by

$$x = \frac{p_z}{p_{z\text{max}}} \approx \frac{E + p_z}{(E + p_z)_{\text{max}}} \quad (p_T \ll |p_z|). \quad (43.41)$$

In the c.m. frame,

$$x \approx \frac{2p_{z\text{cm}}}{\sqrt{s}} = \frac{2m_T \sinh y_{\text{cm}}}{\sqrt{s}} \quad (43.42)$$

and

$$= (y_{\text{cm}})_{\text{max}} = \ln(\sqrt{s}/m). \quad (43.43)$$

The invariant mass  $M$  of the two-particle system described in Sec. 43.4.2 can be written in terms of these variables as

$$M^2 = m_1^2 + m_2^2 + 2[E_T(1)E_T(2) \cosh \Delta y - \mathbf{p}_T(1) \cdot \mathbf{p}_T(2)], \quad (43.44)$$

where

$$E_T(i) = \sqrt{|\mathbf{p}_T(i)|^2 + m_i^2}, \quad (43.45)$$

and  $\mathbf{p}_T(i)$  denotes the transverse momentum vector of particle  $i$ .

For  $p \gg m$ , the rapidity [Eq. (43.39)] may be expanded to obtain

$$y = \frac{1}{2} \ln \frac{\cos^2(\theta/2) + m^2/4p^2 + \dots}{\sin^2(\theta/2) + m^2/4p^2 + \dots} \approx -\ln \tan(\theta/2) \equiv \eta \quad (43.46)$$

where  $\cos \theta = p_z/p$ . The pseudorapidity  $\eta$  defined by the second line is approximately equal to the rapidity  $y$  for  $p \gg m$  and  $\theta \gg 1/\gamma$ , and in any case can be measured when the mass and momentum of the particle are unknown. From the definition one can obtain the identities

$$\sinh \eta = \cot \theta, \quad \cosh \eta = 1/\sin \theta, \quad \tanh \eta = \cos \theta. \quad (43.47)$$

**43.5.3. Partial waves :** The amplitude in the center of mass for elastic scattering of spinless particles may be expanded in Legendre polynomials

$$f(k, \theta) = \frac{1}{k} \sum_{\ell} (2\ell + 1) a_{\ell} P_{\ell}(\cos \theta), \quad (43.48)$$

where  $k$  is the c.m. momentum,  $\theta$  is the c.m. scattering angle,  $a_{\ell} = (\eta_{\ell} e^{2i\delta_{\ell}} - 1)/2i$ ,  $0 \leq \eta_{\ell} \leq 1$ , and  $\delta_{\ell}$  is the phase shift of the  $\ell^{\text{th}}$  partial wave. For purely elastic scattering,  $\eta_{\ell} = 1$ . The differential cross section is

$$\frac{d\sigma}{d\Omega} = |f(k, \theta)|^2. \quad (43.49)$$

The optical theorem states that

$$\sigma_{\text{tot}} = \frac{4\pi}{k} \text{Im} f(k, 0), \quad (43.50)$$

and the cross section in the  $\ell^{\text{th}}$  partial wave is therefore bounded:

$$\sigma_{\ell} = \frac{4\pi}{k^2} (2\ell + 1) |a_{\ell}|^2 \leq \frac{4\pi(2\ell + 1)}{k^2}. \quad (43.51)$$

The evolution with energy of a partial-wave amplitude  $a_{\ell}$  can be displayed as a trajectory in an Argand plot, as shown in Fig. 43.7.

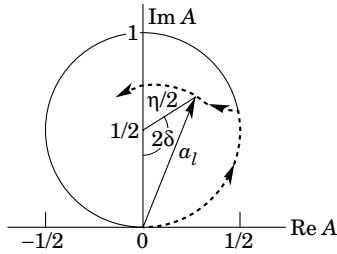


**Figure 43.7:** Argand plot showing a partial-wave amplitude  $a_{\ell}$  as a function of energy. The amplitude leaves the unitary circle where inelasticity sets in ( $\eta_{\ell} < 1$ ).

The usual Lorentz-invariant matrix element  $\mathcal{M}$  (see Sec. 43.3 above) for the elastic process is related to  $f(k, \theta)$  by

$$\mathcal{M} = -8\pi\sqrt{s} f(k, \theta), \quad (43.52)$$

so

$$\sigma_{\text{tot}} = -\frac{1}{2p_{\text{lab}} m_2} \text{Im} \mathcal{M}(t = 0), \quad (43.53)$$

where  $s$  and  $t$  are the center-of-mass energy squared and momentum transfer squared, respectively (see Sec. 43.4.1).

**43.5.3.1. Resonances:** The Breit-Wigner (nonrelativistic) form for an elastic amplitude  $a_{\ell}$  with a resonance at c.m. energy  $E_R$ , elastic width  $\Gamma_{\text{el}}$ , and total width  $\Gamma_{\text{tot}}$  is

$$a_{\ell} = \frac{\Gamma_{\text{el}}/2}{E_R - E - i\Gamma_{\text{tot}}/2}, \quad (43.54)$$

where  $E$  is the c.m. energy. As shown in Fig. 43.8, in the absence of background the elastic amplitude traces a counterclockwise circle with center  $ix_{\text{el}}/2$  and radius  $x_{\text{el}}/2$ , where the elasticity  $x_{\text{el}} = \Gamma_{\text{el}}/\Gamma_{\text{tot}}$ . The amplitude has a pole at  $E = E_R - i\Gamma_{\text{tot}}/2$ .

The spin-averaged Breit-Wigner cross section for a spin- $J$  resonance produced in the collision of particles of spin  $S_1$  and  $S_2$  is

$$\sigma_{BW}(E) = \frac{(2J+1)}{(2S_1+1)(2S_2+1)} \frac{\pi}{k^2} \frac{B_{\text{in}} B_{\text{out}} \Gamma_{\text{tot}}^2}{(E - E_R)^2 + \Gamma_{\text{tot}}^2/4}, \quad (43.55)$$

where  $k$  is the c.m. momentum,  $E$  is the c.m. energy, and  $B_{\text{in}}$  and  $B_{\text{out}}$  are the branching fractions of the resonance into the entrance and exit channels. The  $2S+1$  factors are the multiplicities of the incident spin states, and are replaced by 2 for photons. This expression is valid only for an isolated state. If the width is not small,  $\Gamma_{\text{tot}}$  cannot be treated as a constant independent of  $E$ . There are many other forms for  $\sigma_{BW}$ , all of which are equivalent to the one given here in the narrow-width case. Some of these forms may be more appropriate if the resonance is broad.

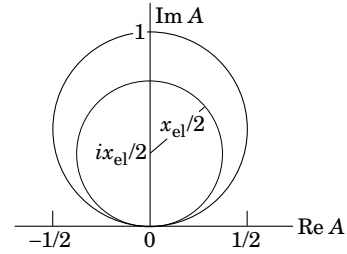


**Figure 43.8:** Argand plot for a resonance.

The relativistic Breit-Wigner form corresponding to Eq. (43.54) is:

$$a_{\ell} = \frac{-m\Gamma_{\text{el}}}{s - m^2 + im\Gamma_{\text{tot}}}. \quad (43.56)$$

A better form incorporates the known kinematic dependences, replacing  $m\Gamma_{\text{tot}}$  by  $\sqrt{s}\Gamma_{\text{tot}}(s)$ , where  $\Gamma_{\text{tot}}(s)$  is the width the resonance particle would have if its mass were  $\sqrt{s}$ , and correspondingly  $m\Gamma_{\text{el}}$  by  $\sqrt{s}\Gamma_{\text{el}}(s)$  where  $\Gamma_{\text{el}}(s)$  is the partial width in the incident channel for a mass  $\sqrt{s}$ :

$$a_{\ell} = \frac{-\sqrt{s}\Gamma_{\text{el}}(s)}{s - m^2 + i\sqrt{s}\Gamma_{\text{tot}}(s)}. \quad (43.57)$$

For the  $Z$  boson, all the decays are to particles whose masses are small enough to be ignored, so on dimensional grounds  $\Gamma_{\text{tot}}(s) = \sqrt{s}\Gamma_0/m_Z$ , where  $\Gamma_0$  defines the width of the  $Z$ , and  $\Gamma_{\text{el}}(s)/\Gamma_{\text{tot}}(s)$  is constant. A full treatment of the line shape requires consideration of dynamics, not just kinematics. For the  $Z$  this is done by calculating the radiative corrections in the Standard Model.

## 43.6. Transverse variables

At hadron colliders, a significant and unknown proportion of the energy of the incoming hadrons in each event escapes down the beam-pipe. Consequently if invisible particles are created in the final state, their net momentum can only be constrained in the plane transverse to the beam direction. Defining the  $z$ -axis as the beam direction, this net momentum is equal to the missing transverse energy vector

$$\mathbf{E}_T^{\text{miss}} = -\sum_i \mathbf{p}_T(i), \quad (43.58)$$

where the sum runs over the transverse momenta of all visible final state particles.

### 43.6.1. Single production with semi-invisible final state :

Consider a single heavy particle of mass  $M$  produced in association with visible particles which decays as in Fig. 43.1 to two particles, of which one (labeled particle 1) is invisible. The mass of the parent particle can be constrained with the quantity  $M_T$  defined by

$$M_T^2 \equiv [E_T(1) + E_T(2)]^2 - [\mathbf{p}_T(1) + \mathbf{p}_T(2)]^2 = m_1^2 + m_2^2 + 2[E_T(1)E_T(2) - \mathbf{p}_T(1) \cdot \mathbf{p}_T(2)], \quad (43.59)$$

where

$$\mathbf{p}_T(1) = \mathbf{E}_T^{\text{miss}}. \quad (43.60)$$

This quantity is called the ‘transverse mass’ by hadron collider experimentalists but it should be noted that it is quite different from that used in the description of inclusive reactions [Eq. (43.38)]. The distribution of event  $M_T$  values possesses an end-point at  $M_T^{\text{max}} = M$ . If  $m_1 = m_2 = 0$  then

$$M_T^2 = 2|\mathbf{p}_T(1)||\mathbf{p}_T(2)|(1 - \cos\phi_{12}), \quad (43.61)$$

where  $\phi_{ij}$  is defined as the angle between particles  $i$  and  $j$  in the transverse plane.

## 43.6.2. Pair production with semi-invisible final states :

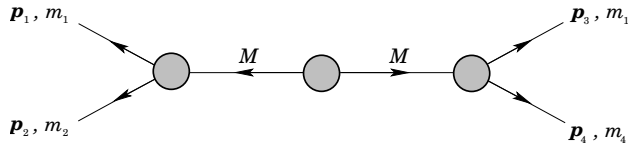


**Figure 43.9:** Definitions of variables for pair production of semi-invisible final states. Particles 1 and 3 are invisible while particles 2 and 4 are visible.

Consider two identical heavy particles of mass  $M$  produced such that their combined center-of-mass is at rest in the transverse plane (Fig. 43.9). Each particle decays to a final state consisting of an invisible particle of fixed mass  $m_1$  together with an additional visible particle.  $M$  and  $m_1$  can be constrained with the variables  $M_{T2}$  and  $M_{CT}$  which are defined in Refs. [4] and [5].

**References:**

1. See, for example, J.J. Sakurai, *Modern Quantum Mechanics*, Addison-Wesley (1985), p. 172, or D.M. Brink and G.R. Satchler, *Angular Momentum*, 2nd ed., Oxford University Press (1968), p. 20.
2. I. Hinchliffe *et al.*, Phys. Rev. **D55**, 5520 (1997).
3. B.C. Allanach *et al.*, JHEP **0009**, 004 (2000).
4. C.G. Lester and D.J. Summers, Phys. Lett. **B463**, 99 (1999).
5. D.R. Tovey, JHEP **0804**, 034 (2008).



## 44. CROSS-SECTION FORMULAE FOR SPECIFIC PROCESSES

Revised October 2009 by H. Baer (University of Oklahoma) and R.N. Cahn (LBNL).

### PART I: STANDARD MODEL PROCESSES

Setting aside leptoproduction (for which, see Sec. 16 of this *Review*), the cross sections of primary interest are those with light incident particles,  $e^+e^-$ ,  $\gamma\gamma$ ,  $q\bar{q}$ ,  $gq$ ,  $gg$ , etc., where  $g$  and  $q$  represent gluons and light quarks. The produced particles include both light particles and heavy ones -  $t$ ,  $W$ ,  $Z$ , and the Higgs boson  $H$ . We provide the production cross sections calculated within the Standard Model for several such processes.

#### 44.1. Resonance Formation

Resonant cross sections are generally described by the Breit-Wigner formula (Sec. 18 of this *Review*).

$$\sigma(E) = \frac{2J+1}{(2S_1+1)(2S_2+1)} \frac{4\pi}{k^2} \left[ \frac{\Gamma^2/4}{(E-E_0)^2 + \Gamma^2/4} \right] B_{in} B_{out}, \quad (44.1)$$

where  $E$  is the c.m. energy,  $J$  is the spin of the resonance, and the number of polarization states of the two incident particles are  $2S_1+1$  and  $2S_2+1$ . The c.m. momentum in the initial state is  $k$ ,  $E_0$  is the c.m. energy at the resonance, and  $\Gamma$  is the full width at half maximum height of the resonance. The branching fraction for the resonance into the initial-state channel is  $B_{in}$  and into the final-state channel is  $B_{out}$ . For a narrow resonance, the factor in square brackets may be replaced by  $\pi\Gamma\delta(E-E_0)/2$ .

#### 44.2. Production of light particles

The production of point-like, spin-1/2 fermions in  $e^+e^-$  annihilation through a virtual photon,  $e^+e^- \rightarrow \gamma^* \rightarrow ff$ , at c.m. energy squared  $s$  is given by

$$\frac{d\sigma}{d\Omega} = N_c \frac{\alpha^2}{4s} \beta [1 + \cos^2\theta + (1-\beta^2)\sin^2\theta] Q_f^2, \quad (44.2)$$

where  $\beta$  is  $v/c$  for the produced fermions in the c.m.,  $\theta$  is the c.m. scattering angle, and  $Q_f$  is the charge of the fermion. The factor  $N_c$  is 1 for charged leptons and 3 for quarks. In the ultrarelativistic limit,  $\beta \rightarrow 1$ ,

$$\sigma = N_c Q_f^2 \frac{4\pi\alpha^2}{3s} = N_c Q_f^2 \frac{86.8 \text{ nb}}{s(\text{GeV}^2)}. \quad (44.3)$$

The cross section for the annihilation of a  $q\bar{q}$  pair into a distinct pair  $q'\bar{q}'$  through a gluon is completely analogous up to color factors, with the replacement  $\alpha \rightarrow \alpha_s$ . Treating all quarks as massless, averaging over the colors of the initial quarks and defining  $t = -s\sin^2(\theta/2)$ ,  $u = -s\cos^2(\theta/2)$ , one finds [1]

$$\frac{d\sigma}{d\Omega}(q\bar{q} \rightarrow q'\bar{q}') = \frac{\alpha_s^2}{9s} \frac{t^2 + u^2}{s^2}. \quad (44.4)$$

Crossing symmetry gives

$$\frac{d\sigma}{d\Omega}(qq' \rightarrow qq') = \frac{\alpha_s^2}{9s} \frac{s^2 + u^2}{t^2}. \quad (44.5)$$

If the quarks  $q$  and  $q'$  are identical, we have

$$\frac{d\sigma}{d\Omega}(q\bar{q} \rightarrow q\bar{q}) = \frac{\alpha_s^2}{9s} \left[ \frac{t^2 + u^2}{s^2} + \frac{s^2 + u^2}{t^2} - \frac{2u^2}{3st} \right], \quad (44.6)$$

and by crossing

$$\frac{d\sigma}{d\Omega}(qq \rightarrow qq) = \frac{\alpha_s^2}{9s} \left[ \frac{t^2 + s^2}{u^2} + \frac{s^2 + u^2}{t^2} - \frac{2s^2}{3ut} \right]. \quad (44.7)$$

Annihilation of  $e^+e^-$  into  $\gamma\gamma$  has the cross section

$$\frac{d\sigma}{d\Omega}(e^+e^- \rightarrow \gamma\gamma) = \frac{\alpha^2}{2s} \frac{u^2 + t^2}{tu}. \quad (44.8)$$

The related QCD process also has a triple-gluon coupling. The cross section is

$$\frac{d\sigma}{d\Omega}(q\bar{q} \rightarrow gg) = \frac{8\alpha_s^2}{27s} (t^2 + u^2) \left( \frac{1}{tu} - \frac{9}{4s^2} \right). \quad (44.9)$$

The crossed reactions are

$$\frac{d\sigma}{d\Omega}(gq \rightarrow gq) = \frac{\alpha_s^2}{9s} (s^2 + u^2) \left( -\frac{1}{su} + \frac{9}{4t^2} \right) \quad (44.10)$$

and

$$\frac{d\sigma}{d\Omega}(gg \rightarrow q\bar{q}) = \frac{\alpha_s^2}{24s} (t^2 + u^2) \left( \frac{1}{tu} - \frac{9}{4s^2} \right). \quad (44.11)$$

Finally,

$$\frac{d\sigma}{d\Omega}(gg \rightarrow gg) = \frac{9\alpha_s^2}{8s} \left( 3 - \frac{ut}{s^2} - \frac{su}{t^2} - \frac{st}{u^2} \right). \quad (44.12)$$

Lepton-quark scattering is analogous (neglecting  $Z$  exchange)

$$\frac{d\sigma}{d\Omega}(e_q \rightarrow e_q) = \frac{\alpha^2}{2s} e_q^2 \frac{s^2 + u^2}{t^2}. \quad (44.13)$$

where  $e_q$  is the charge of the quark. For neutrino scattering with the four-Fermi interaction

$$\frac{d\sigma}{d\Omega}(\nu d \rightarrow \ell^- u) = \frac{G_F^2 s}{4\pi^2}, \quad (44.14)$$

where the Cabibbo angle suppression is ignored. Similarly

$$\frac{d\sigma}{d\Omega}(\nu \bar{u} \rightarrow \ell^+ \bar{d}) = \frac{G_F^2 s}{4\pi^2} \frac{(1 + \cos\theta)^2}{4}. \quad (44.15)$$

To obtain the formulae for deep inelastic scattering (presented in more detail in Section 16) we consider quarks of type  $i$  carrying a fraction  $x = Q^2/(2M\nu)$  of the nucleon's energy, where  $\nu = E - E'$  is the energy lost by the lepton in the nucleon rest frame. With  $y = \nu/E$  we have the correspondences

$$\begin{aligned} 1 + \cos\theta &\rightarrow 2(1-y), \\ d\Omega_{cm} &\rightarrow 4\pi f_i(x) dx dy, \end{aligned} \quad (44.16)$$

where the latter incorporates the quark distribution,  $f_i(x)$ . In this way we find

$$\begin{aligned} \frac{d\sigma}{dx dy}(eN \rightarrow eX) &= \frac{4\pi\alpha^2 xs}{Q^4} \frac{1}{2} \left[ 1 + (1-y)^2 \right] \\ &\times \left[ \frac{4}{9}(u(x) + \bar{u}(x) + \dots) + \frac{1}{9}(d(x) + \bar{d}(x) + \dots) \right] \end{aligned} \quad (44.17)$$

where now  $s = 2ME$  is the cm energy squared for the electron-nucleon collision and we have suppressed contributions from higher mass quarks.

Similarly,

$$\frac{d\sigma}{dx dy}(\nu N \rightarrow \ell^- X) = \frac{G_F^2 xs}{\pi} [(d(x) + \dots) + (1-y)^2(\bar{u}(x) + \dots)] \quad (44.18)$$

and

$$\frac{d\sigma}{dx dy}(\bar{\nu} N \rightarrow \ell^+ X) = \frac{G_F^2 xs}{\pi} [\bar{d}(x) + \dots + (1-y)^2(u(x) + \dots)]. \quad (44.19)$$

Quasi-elastic neutrino scattering ( $\nu_\mu n \rightarrow \mu^- p$ ,  $\bar{\nu}_\mu p \rightarrow \mu^+ n$ ) is directly related to the crossed reaction, neutron decay. The formula for the differential cross section is presented, for example, in N.J. Baker *et al.*, Phys. Rev. **D23**, 2499 (1981).

### 44.3. Hadroproduction of heavy quarks

For hadroproduction of heavy quarks  $Q = c, b, t$ , it is important to include mass effects in the formulae. For  $q\bar{q} \rightarrow Q\bar{Q}$ , one has

$$\frac{d\sigma}{d\Omega}(q\bar{q} \rightarrow Q\bar{Q}) = \frac{\alpha_s^2}{9s^3} \left[ (m_Q^2 - t)^2 + (m_Q^2 - u)^2 + 2m_Q^2 s \right], \quad (44.20)$$

while for  $gg \rightarrow Q\bar{Q}$  one has

$$\begin{aligned} \frac{d\sigma}{d\Omega}(gg \rightarrow Q\bar{Q}) = & \frac{\alpha_s^2}{32s} \left[ \frac{6}{s^2} (m_Q^2 - t)(m_Q^2 - u) - \frac{m_Q^2(s - 4m_Q^2)}{3(m_Q^2 - t)(m_Q^2 - u)} + \right. \\ & \frac{4}{3} \frac{(m_Q^2 - t)(m_Q^2 - u) - 2m_Q^2(m_Q^2 + t)}{(m_Q^2 - t)^2} \\ & + \frac{4}{3} \frac{(m_Q^2 - t)(m_Q^2 - u) - 2m_Q^2(m_Q^2 + u)}{(m_Q^2 - u)^2} \\ & - \left[ 3 \frac{(m_Q^2 - t)(m_Q^2 - u) + m_Q^2(u - t)}{s(m_Q^2 - t)} \right. \\ & \left. \left. - 3 \frac{(m_Q^2 - t)(m_Q^2 - u) + m_Q^2(t - u)}{s(m_Q^2 - u)} \right] \right]. \quad (44.21) \end{aligned}$$

### 44.4. Production of Weak Gauge Bosons

#### 44.4.1. $W$ and $Z$ resonant production :

Resonant production of a single  $W$  or  $Z$  is governed by the partial widths

$$\Gamma(W \rightarrow \ell_i \bar{\nu}_i) = \frac{\sqrt{2} G_F m_W^3}{12\pi} \quad (44.22)$$

$$\Gamma(W \rightarrow q_i \bar{q}_j) = 3 \frac{\sqrt{2} G_F |V_{ij}|^2 m_W^3}{12\pi} \quad (44.23)$$

$$\begin{aligned} \Gamma(Z \rightarrow f\bar{f}) = & N_c \frac{\sqrt{2} G_F m_Z^3}{6\pi} \\ & \times \left[ (T_3 - Q_f \sin^2 \theta_W)^2 + (Q_f \sin \theta_W)^2 \right]. \quad (44.24) \end{aligned}$$

The weak mixing angle is  $\theta_W$ . The CKM matrix elements are indicated by  $V_{ij}$  and  $N_c$  is 3 for  $q\bar{q}$  final states and 1 for leptonic final states.

The full differential cross section for  $f_i \bar{f}_j \rightarrow (W, Z) \rightarrow f'_i \bar{f}'_j$  is given by

$$\begin{aligned} \frac{d\sigma}{d\Omega} = & \frac{N_c^f}{N_c^i} \cdot \frac{1}{256\pi^2 s} \cdot \frac{s^2}{(s - M^2)^2 + s\Gamma^2} \\ & \times \left[ (L^2 + R^2)(L'^2 + R'^2)(1 + \cos^2 \theta) \right. \\ & \left. + (L^2 - R^2)(L'^2 - R'^2) 2 \cos \theta \right] \quad (44.25) \end{aligned}$$

where  $M$  is the mass of the  $W$  or  $Z$ . The couplings for the  $W$  are  $L = (8G_F m_W^2 / \sqrt{2})^{1/2} V_{ij} / \sqrt{2}$ ;  $R = 0$  where  $V_{ij}$  is the corresponding CKM matrix element, with an analogous expression for  $L'$  and  $R'$ . For  $Z$ , the couplings are  $L = (8G_F m_Z^2 / \sqrt{2})^{1/2} (T_3 - \sin^2 \theta_W Q)$ ;  $R = -(8G_F m_Z^2 / \sqrt{2})^{1/2} \sin^2 \theta_W Q$ , where  $T_3$  is the weak isospin of the initial left-handed fermion and  $Q$  is the initial fermion's electric charge. The expressions for  $L'$  and  $R'$  are analogous. The color factors  $N_c^{i,f}$  are 3 for initial or final quarks and 1 for initial or final leptons.

#### 44.4.2. Production of pairs of weak gauge bosons :

The cross section for  $f\bar{f} \rightarrow W^+ W^-$  is given in term of the couplings of the left-handed and right-handed fermion  $f$ ,  $\ell = 2(T_3 - Qx_W)$ ,  $r = -2Qx_W$ , where  $T_3$  is the third component of weak isospin for the left-handed  $f$ ,  $Q$  is its electric charge (in units of the proton charge), and  $x_W = \sin^2 \theta_W$ :

$$\begin{aligned} \frac{d\sigma}{dt} = & \frac{2\pi\alpha^2}{N_c s^2} \left\{ \left[ \left( Q + \frac{\ell + r}{4x_W} \frac{s}{s - m_Z^2} \right)^2 + \left( \frac{\ell - r}{4x_W} \frac{s}{s - m_Z^2} \right)^2 \right] A(s, t, u) \right. \\ & + \frac{1}{2x_W} \left( Q + \frac{\ell}{2x_W} \frac{s}{s - m_Z^2} \right) (\Theta(-Q)I(s, t, u) - \Theta(Q)I(s, u, t)) \\ & \left. + \frac{1}{8x_W^2} (\Theta(-Q)E(s, t, u) + \Theta(Q)E(s, u, t)) \right\}, \quad (44.26) \end{aligned}$$

where  $\Theta(x)$  is 1 for  $x > 0$  and 0 for  $x < 0$ , and where

$$\begin{aligned} A(s, t, u) = & \left( \frac{tu}{m_W^4} - 1 \right) \left( \frac{1}{4} - \frac{m_W^2}{s} + 3 \frac{m_W^4}{s^2} \right) + \frac{s}{m_W^2} - 4, \\ I(s, t, u) = & \left( \frac{tu}{m_W^4} - 1 \right) \left( \frac{1}{4} - \frac{m_W^2}{2s} - \frac{m_W^4}{st} \right) + \frac{s}{m_W^2} - 2 + 2 \frac{m_W^2}{t}, \\ E(s, t, u) = & \left( \frac{tu}{m_W^4} - 1 \right) \left( \frac{1}{4} + \frac{m_W^4}{t^2} \right) + \frac{s}{m_W^2}, \quad (44.27) \end{aligned}$$

and  $s, t, u$  are the usual Mandelstam variables with  $s = (p_f + p_{\bar{f}})^2$ ,  $t = (p_f - p_{W^-})^2$ ,  $u = (p_f - p_{W^+})^2$ . The factor  $N_c$  is 3 for quarks and 1 for leptons.

The analogous cross-section for  $q_i \bar{q}_j \rightarrow W^\pm Z^0$  is

$$\begin{aligned} \frac{d\sigma}{dt} = & \frac{\pi\alpha^2 |V_{ij}|^2}{6s^2 x_W^2} \left\{ \left( \frac{1}{s - m_W^2} \right)^2 \left[ \left( \frac{9 - 8x_W}{4} \right) (ut - m_W^2 m_Z^2) \right. \right. \\ & \left. \left. + (8x_W - 6) s (m_W^2 + m_Z^2) \right] \right. \\ & + \left[ \frac{ut - m_W^2 m_Z^2 - s(m_W^2 + m_Z^2)}{s - m_W^2} \right] \left[ \frac{\ell_j}{t} - \frac{\ell_i}{u} \right] \\ & \left. + \frac{ut - m_W^2 m_Z^2}{4(1 - x_W)} \left[ \frac{\ell_j^2}{t^2} + \frac{\ell_i^2}{u^2} \right] + \frac{s(m_W^2 + m_Z^2)}{2(1 - x_W)} \frac{\ell_i \ell_j}{tu} \right\}, \quad (44.28) \end{aligned}$$

where  $\ell_i$  and  $\ell_j$  are the couplings of the left-handed  $q_i$  and  $q_j$  as defined above. The CKM matrix element between  $q_i$  and  $q_j$  is  $V_{ij}$ .

The cross section for  $q_i \bar{q}_i \rightarrow Z^0 Z^0$  is

$$\frac{d\sigma}{dt} = \frac{\pi\alpha^2}{96} \frac{\ell_i^4 + r_i^4}{x_W^2 (1 - x_W^2)^2 s^2} \left[ \frac{t}{u} + \frac{u}{t} + \frac{4m_Z^2 s}{tu} - m_Z^4 \left( \frac{1}{t^2} + \frac{1}{u^2} \right) \right]. \quad (44.29)$$

### 44.5. Production of Higgs Bosons

#### 44.5.1. Resonant Production :

The Higgs boson of the Standard Model can be produced resonantly in the collisions of quarks, leptons,  $W$  or  $Z$  bosons, gluons, or photons. The production cross section is thus controlled by the partial width of the Higgs boson into the entrance channel and its total width. The branching fractions for the Standard Model Higgs boson are shown in Fig. 1 of the ‘‘Searches for Higgs bosons’’ review in the Particle Listings section, as a function of the Higgs boson mass. The partial widths are given by the relations

$$\Gamma(H \rightarrow f\bar{f}) = \frac{G_F m_f^2 m_H N_c}{4\pi\sqrt{2}} \left( 1 - 4m_f^2/m_H^2 \right)^{3/2}, \quad (44.30)$$

$$\Gamma(H \rightarrow W^+ W^-) = \frac{G_F m_H^3 \beta_W}{32\pi\sqrt{2}} \left( 4 - 4a_W + 3a_W^2 \right), \quad (44.31)$$

$$\Gamma(H \rightarrow ZZ) = \frac{G_F m_H^3 \beta_Z}{64\pi\sqrt{2}} \left( 4 - 4a_Z + 3a_Z^2 \right), \quad (44.32)$$

where  $N_c$  is 3 for quarks and 1 for leptons and where  $a_W = 1 - \beta_W^2 = 4m_W^2/m_H^2$  and  $a_Z = 1 - \beta_Z^2 = 4m_Z^2/m_H^2$ . The decay to two gluons proceeds through quark loops, with the  $t$  quark dominating [2]. Explicitly,

$$\Gamma(H \rightarrow gg) = \frac{\alpha_s^2 G_F m_H^3}{36\pi^3 \sqrt{2}} \left| \sum_q I(m_q^2/m_H^2) \right|^2, \quad (44.33)$$

where  $I(z)$  is complex for  $z < 1/4$ . For  $z < 2 \times 10^{-3}$ ,  $|I(z)|$  is small so the light quarks contribute negligibly. For  $m_H < 2m_t$ ,  $z > 1/4$  and

$$I(z) = 3 \left[ 2z + 2z(1-4z) \left( \sin^{-1} \frac{1}{2\sqrt{z}} \right)^2 \right], \quad (44.34)$$

which has the limit  $I(z) \rightarrow 1$  as  $z \rightarrow \infty$ .

#### 44.5.2. Higgs Boson Production in $W^*$ and $Z^*$ decay :

The Standard Model Higgs boson can be produced in the decay of a virtual  $W$  or  $Z$  ("Higgsstrahlung") [3,4]: In particular, if  $k$  is the c.m. momentum of the Higgs boson,

$$\sigma(q_i \bar{q}_j \rightarrow WH) = \frac{\pi \alpha^2 |V_{ij}|^2}{36 \sin^4 \theta_W} \frac{2k}{\sqrt{s}} \frac{k^2 + 3m_W^2}{(s - m_W^2)^2} \quad (44.35)$$

$$\sigma(f \bar{f} \rightarrow ZH) = \frac{2\pi \alpha^2 (\ell_f^2 + r_f^2)}{48 N_c \sin^4 \theta_W \cos^4 \theta_W} \frac{2k}{\sqrt{s}} \frac{k^2 + 3m_Z^2}{(s - m_Z^2)^2}, \quad (44.36)$$

where  $\ell$  and  $r$  are defined as above.

#### 44.5.3. $W$ and $Z$ Fusion :

Just as high-energy electrons can be regarded as sources of virtual photon beams, at very high energies they are sources of virtual  $W$  and  $Z$  beams. For Higgs boson production, it is the longitudinal components of the  $W$ s and  $Z$ s that are important [5]. The distribution of longitudinal  $W$ s carrying a fraction  $y$  of the electron's energy is [6]

$$f(y) = \frac{g^2}{16\pi^2} \frac{1-y}{y}, \quad (44.37)$$

where  $g = e/\sin \theta_W$ . In the limit  $s \gg m_H \gg m_W$ , the partial decay rate is  $\Gamma(H \rightarrow W_L W_L) = (g^2/64\pi)(m_H^3/m_W^2)$  and in the equivalent  $W$  approximation [7]

$$\sigma(e^+ e^- \rightarrow \bar{\nu}_e \nu_e H) = \frac{1}{16m_W^2} \left( \frac{\alpha}{\sin^2 \theta_W} \right)^3 \times \left[ \left( 1 + \frac{m_H^2}{s} \right) \log \frac{s}{m_H^2} - 2 + 2 \frac{m_H^2}{s} \right]. \quad (44.38)$$

There are significant corrections to this relation when  $m_H$  is not large compared to  $m_W$  [8]. For  $m_H = 150$  GeV, the estimate is too high by 51% for  $\sqrt{s} = 1000$  GeV, 32% too high at  $\sqrt{s} = 2000$  GeV, and 22% too high at  $\sqrt{s} = 4000$  GeV. Fusion of  $ZZ$  to make a Higgs boson can be treated similarly. Identical formulae apply for Higgs production in the collisions of quarks whose charges permit the emission of a  $W^+$  and a  $W^-$ , except that QCD corrections and CKM matrix elements are required. Even in the absence of QCD corrections, the fine-structure constant ought to be evaluated at the scale of the collision, say  $m_W$ . All quarks contribute to the  $ZZ$  fusion process.

#### 44.6. Inclusive hadronic reactions

One-particle inclusive cross sections  $E d^3\sigma/d^3p$  for the production of a particle of momentum  $p$  are conveniently expressed in terms of rapidity  $y$  (see above) and the momentum  $p_T$  transverse to the beam direction (in the c.m.):

$$E \frac{d^3\sigma}{d^3p} = \frac{d^3\sigma}{d\phi dy p_T dp_T^2}. \quad (44.39)$$

In appropriate circumstances, the cross section may be decomposed as a partonic cross section multiplied by the probabilities of finding partons of the prescribed momenta:

$$\sigma_{\text{hadronic}} = \sum_{ij} \int dx_1 dx_2 f_i(x_1) f_j(x_2) d\hat{\sigma}_{\text{partonic}}, \quad (44.40)$$

The probability that a parton of type  $i$  carries a fraction of the incident particle's that lies between  $x_1$  and  $x_1 + dx_1$  is  $f_i(x_1)dx_1$  and similarly for partons in the other incident particle. The partonic collision is specified by its c.m. energy squared  $\hat{s} = x_1 x_2 s$  and the momentum transfer squared  $\hat{t}$ . The final hadronic state is more conveniently specified by the rapidities  $y_1, y_2$  of the two jets resulting from the collision and the transverse momentum  $p_T$ . The connection between the differentials is

$$dx_1 dx_2 d\hat{t} = dy_1 dy_2 \frac{\hat{s}}{s} dp_T^2, \quad (44.41)$$

so that

$$\frac{d^3\sigma}{dy_1 dy_2 dp_T^2} = \frac{\hat{s}}{s} \left[ f_i(x_1) f_j(x_2) \frac{d\hat{\sigma}}{d\hat{t}}(\hat{s}, \hat{t}, \hat{u}) + f_i(x_2) f_j(x_1) \frac{d\hat{\sigma}}{d\hat{t}}(\hat{s}, \hat{u}, \hat{t}) \right], \quad (44.42)$$

where we have taken into account the possibility that the incident parton types might arise from either incident particle. The second term should be dropped if the types are identical:  $i = j$ .

#### 44.7. Two-photon processes

In the Weizsäcker-Williams picture, a high-energy electron beam is accompanied by a spectrum of virtual photons of energies  $\omega$  and invariant-mass squared  $q^2 = -Q^2$ , for which the photon number density is

$$dn = \frac{\alpha}{\pi} \left[ 1 - \frac{\omega}{E} + \frac{\omega^2}{E^2} - \frac{m_e^2 \omega^2}{Q^2 E^2} \right] \frac{d\omega dQ^2}{\omega Q^2}, \quad (44.43)$$

where  $E$  is the energy of the electron beam. The cross section for  $e^+ e^- \rightarrow e^+ e^- X$  is then [9]

$$d\sigma_{e^+ e^- \rightarrow e^+ e^- X}(s) = dn_1 dn_2 d\sigma_{\gamma\gamma \rightarrow X}(W^2), \quad (44.44)$$

where  $W^2 = m_X^2$ . Integrating from the lower limit  $Q^2 =$

$m_e^2 \frac{\omega_i^2}{E_i(E_i - \omega_i)}$  to a maximum  $Q^2$  gives

$$\sigma_{e^+ e^- \rightarrow e^+ e^- X}(s) = \frac{\alpha^2}{\pi^2} \int_{z_{th}}^1 \frac{dz}{z} \times \left[ \left( \ln \frac{Q_{max}^2}{zm_e^2} - 1 \right)^2 f(z) + \frac{1}{3} (\ln z)^3 \right] \sigma_{\gamma\gamma \rightarrow X}(zs), \quad (44.45)$$

where

$$f(z) = \left( 1 + \frac{1}{2}z \right)^2 \ln(1/z) - \frac{1}{2}(1-z)(3+z). \quad (44.46)$$

The appropriate value of  $Q_{max}^2$  depends on the properties of the produced system  $X$ . For production of hadronic systems,  $Q_{max}^2 \approx m_\rho^2$ , while for lepton-pair production,  $Q^2 \approx W^2$ . For production of a resonance with spin  $J \neq 1$ , we have

$$\sigma_{e^+e^- \rightarrow e^+e^-R}(s) = (2J+1) \frac{8\alpha^2 \Gamma_{R \rightarrow \gamma\gamma}}{m_R^3} \times \left[ f(m_R^2/s) \left( \ln \frac{m_V^2 s}{m_e^2 m_R^2} - 1 \right)^2 - \frac{1}{3} \left( \ln \frac{s}{M_R^2} \right)^3 \right], \quad (44.47)$$

where  $m_V$  is the mass that enters into the form factor for the  $\gamma\gamma \rightarrow R$  transition, typically  $m_\rho$ .

## PART II: PROCESSES BEYOND THE STANDARD MODEL

### 44.8. Production of supersymmetric particles

In supersymmetric (SUSY) theories (see Supersymmetric Particle Searches in this *Review*), every boson has a fermionic superpartner, and every fermion has a bosonic superpartner. The minimal supersymmetric Standard Model (MSSM) is a direct supersymmetrization of the Standard Model (SM), although a second Higgs doublet is needed to avoid triangle anomalies [10]. Under soft SUSY breaking, superpartner masses are lifted above the SM particle masses. In weak scale SUSY, the superpartners are invoked to stabilize the weak scale under radiative corrections, so the superpartners are expected to have masses of order the TeV scale.

#### 44.8.1. Gluino and squark production :

The superpartners of gluons are the color octet, spin- $\frac{1}{2}$  gluinos ( $\tilde{g}$ ), while each helicity component of quark flavor has a spin-0 squark partner, e.g.  $\tilde{q}_L$  and  $\tilde{q}_R$ . Third generation left- and right- squarks are expected to have large mixing, resulting in mass eigenstates  $\tilde{q}_1$  and  $\tilde{q}_2$ , with  $m_{\tilde{q}_1} < m_{\tilde{q}_2}$  (here,  $q$  denotes any of the SM flavors of quarks and  $\tilde{q}_i$  the corresponding flavor and type ( $i = L, R$  or  $1, 2$ ) of squark). Gluino pair production ( $\tilde{g}\tilde{g}$ ) takes place via either glue-gluon or quark-antiquark annihilation [11].

The subprocess cross sections are usually presented as differential distributions in the Mandelstam variables  $s$ ,  $t$  and  $u$ . Note that for a  $2 \rightarrow 2$  scattering subprocess  $ab \rightarrow cd$ , the Mandelstam variable  $s = (p_a + p_b)^2 = (p_c + p_d)^2$ , where  $p_a$  is the 4-momentum of particle  $a$ , and so forth. The variable  $t = (p_c - p_a)^2$ , where  $c$  and  $a$  are taken conventionally to be the most similar particles in the subprocess. The variable  $u$  would then be equal to  $(p_d - p_a)^2$ . Note that since  $s$ ,  $t$  and  $u$  are squares of 4-vectors, they are invariants in any inertial reference frame.

Gluino pair production at hadron colliders is described by:

$$\begin{aligned} \frac{d\sigma}{dt}(gg \rightarrow \tilde{g}\tilde{g}) &= \frac{9\pi\alpha_s^2}{4s^2} \left\{ \frac{2(m_g^2 - t)(m_g^2 - u)}{s^2} \right. \\ &+ \frac{(m_g^2 - t)(m_g^2 - u) - 2m_g^2(m_g^2 + t)}{(m_g^2 - t)^2} \\ &+ \frac{(m_g^2 - t)(m_g^2 - u) - 2m_g^2(m_g^2 + u)}{(m_g^2 - u)^2} + \frac{m_g^2(s - 4m_g^2)}{(m_g^2 - t)(m_g^2 - u)} \\ &\left. - \frac{(m_g^2 - t)(m_g^2 - u) + m_g^2(u - t)}{s(m_g^2 - t)} - \frac{(m_g^2 - t)(m_g^2 - u) + m_g^2(t - u)}{s(m_g^2 - u)} \right\}, \quad (44.48) \end{aligned}$$

where  $\alpha_s$  is the strong fine structure constant. Also,

$$\begin{aligned} \frac{d\sigma}{dt}(q\bar{q} \rightarrow \tilde{g}\tilde{g}) &= \frac{8\pi\alpha_s^2}{9s^2} \left\{ \frac{4}{3} \left( \frac{m_g^2 - t}{m_q^2 - t} \right)^2 + \frac{4}{3} \left( \frac{m_g^2 - u}{m_q^2 - u} \right)^2 \right. \\ &+ \frac{3}{s^2} \left[ (m_g^2 - t)^2 + (m_g^2 - u)^2 + 2m_g^2 s \right] - 3 \frac{(m_g^2 - t)^2 + m_g^2 s}{s(m_q^2 - t)} \\ &\left. - 3 \frac{(m_g^2 - u)^2 + m_g^2 s}{s(m_q^2 - u)} + \frac{1}{3} \frac{m_g^2 s}{(m_q^2 - t)(m_q^2 - u)} \right\}. \quad (44.49) \end{aligned}$$

Gluinos can also be produced in association with squarks:  $\tilde{g}\tilde{q}_i$  production, where  $\tilde{q}_i$  represents any of the various types (left-, right- or mixed) and flavors of squarks. The subprocess cross section is independent of whether the squark is the right-, left- or mixed type:

$$\begin{aligned} \frac{d\sigma}{dt}(gq \rightarrow \tilde{g}\tilde{q}_i) &= \frac{\pi\alpha_s^2}{24s^2} \left[ \frac{16}{3}(s^2 + (m_{\tilde{q}_i}^2 - u)^2) + \frac{4}{3}s(m_{\tilde{q}_i}^2 - u) \right] \\ &\times \left( (m_g^2 - u)^2 + (m_{\tilde{q}_i}^2 - m_g^2)^2 + \frac{2sm_g^2(m_{\tilde{q}_i}^2 - m_g^2)}{(m_g^2 - t)} \right). \quad (44.50) \end{aligned}$$

There are many different subprocesses for production of squark pairs. Since left- and right- squarks generally have different masses and different decay patterns, we present the differential cross section for each subprocess of  $\tilde{q}_i$  ( $i = L, R$  or  $1, 2$ ) separately. (In early literature, the following formulae were often combined into a single equation which didn't differentiate the various squark types.) The result for  $gg \rightarrow \tilde{q}_i\tilde{q}_i$  is:

$$\begin{aligned} \frac{d\sigma}{dt}(gg \rightarrow \tilde{q}_i\tilde{q}_i) &= \frac{\pi\alpha_s^2}{4s^2} \left\{ \frac{1}{3} \left( \frac{m_q^2 + t}{m_q^2 - t} \right)^2 + \frac{1}{3} \left( \frac{m_q^2 + u}{m_q^2 - u} \right)^2 \right. \\ &+ \frac{3}{32s^2} \left( 8s(4m_q^2 - s) + 4(u - t)^2 \right) + \frac{7}{12} \\ &- \frac{1}{48} \frac{(4m_q^2 - s)^2}{(m_q^2 - t)(m_q^2 - u)} \\ &+ \frac{3}{32} \frac{[(t - u)(4m_q^2 + 4t - s) - 2(m_q^2 - u)(6m_q^2 + 2t - s)]}{s(m_q^2 - t)} \\ &+ \frac{3}{32} \frac{[(u - t)(4m_q^2 + 4u - s) - 2(m_q^2 - t)(6m_q^2 + 2u - s)]}{s(m_q^2 - u)} \\ &\left. + \frac{7}{96} \frac{[4m_q^2 + 4t - s]}{m_q^2 - t} + \frac{7}{96} \frac{[4m_q^2 + 4u - s]}{m_q^2 - u} \right\}, \quad (44.51) \end{aligned}$$

which has an obvious  $u \leftrightarrow t$  symmetry.

For  $q\bar{q} \rightarrow \tilde{q}_i\tilde{q}_i$  with the same initial and final state flavors, we have

$$\begin{aligned} \frac{d\sigma}{dt}(q\bar{q} \rightarrow \tilde{q}_i\tilde{q}_i) &= \frac{2\pi\alpha_s^2}{9s^2} \left\{ \frac{1}{(t - m_q^2)^2} + \frac{2}{s^2} - \frac{2/3}{s(t - m_q^2)} \right\} \\ &\times \left[ -st - (t - m_{\tilde{q}_i}^2)^2 \right], \quad (44.52) \end{aligned}$$

while if initial and final state flavors are different ( $q\bar{q} \rightarrow \tilde{q}_i\tilde{q}_j$ ) we instead have

$$\frac{d\sigma}{dt}(q\bar{q} \rightarrow \tilde{q}_i\tilde{q}_j) = \frac{4\pi\alpha_s^2}{9s^4} \left[ -st - (t - m_{\tilde{q}_i}^2)^2 \right]. \quad (44.53)$$

If the two initial state quarks are of different flavors, then we have

$$\frac{d\sigma}{dt}(q\bar{q}' \rightarrow \tilde{q}_i\tilde{q}_j) = \frac{2\pi\alpha_s^2 - st - (t - m_{\tilde{q}_i}^2)^2}{9s^2 (t - m_q^2)^2}. \quad (44.54)$$

If the initial quarks are of different flavor and final state squarks are of different type ( $i \neq j$ ) then

$$\frac{d\sigma}{dt}(q\bar{q}' \rightarrow \tilde{q}_i\tilde{q}_j) = \frac{2\pi\alpha_s^2}{9s^2} \frac{m_g^2 s}{(t - m_q^2)^2}. \quad (44.55)$$

For same-flavor initial state quarks, but final state unlike-type squarks, we also have

$$\frac{d\sigma}{dt}(q\bar{q} \rightarrow \tilde{q}_i\tilde{q}_j) = \frac{2\pi\alpha_s^2}{9s^2} \frac{m_g^2 s}{(t - m_q^2)^2}. \quad (44.56)$$

There also exist cross sections for quark-quark annihilation to squark pairs. For same flavor quark-quark annihilation to same flavor/same type final state squarks,

$$\begin{aligned} \frac{d\sigma}{dt}(qq \rightarrow \tilde{q}_i \tilde{q}_i) &= \\ &= \frac{\pi\alpha_s^2 m_g^2 s}{9s^2} \left\{ \frac{1}{(t-m_g^2)^2} + \frac{1}{(u-m_g^2)^2} - \frac{2/3}{(t-m_g^2)(u-m_g^2)} \right\}, \end{aligned} \quad (44.57)$$

while if the final type squarks are different ( $i \neq j$ ), we have

$$\begin{aligned} \frac{d\sigma}{dt}(qq \rightarrow \tilde{q}_i \tilde{q}_j) &= \\ \frac{2\pi\alpha_s^2}{9s^2} \left\{ \frac{[-st - (t-m_{\tilde{q}_i}^2)(t-m_{\tilde{q}_j}^2)]}{(t-m_g^2)} + \frac{[-su - (u-m_{\tilde{q}_i}^2)(u-m_{\tilde{q}_j}^2)]}{(u-m_g^2)} \right\}. \end{aligned} \quad (44.58)$$

If initial/final state flavors are different, but final state squark types are the same, then

$$\frac{d\sigma}{dt}(qq' \rightarrow \tilde{q}_i \tilde{q}_i) = \frac{2\pi\alpha_s^2 m_g^2 s}{9s^2 (t-m_g^2)^2}. \quad (44.59)$$

If initial quark flavors are different and final squark types are different, then

$$\frac{d\sigma}{dt}(qq' \rightarrow \tilde{q}_i \tilde{q}_j) = \frac{2\pi\alpha_s^2 (-st - (t-m_{\tilde{q}_i}^2)(t-m_{\tilde{q}_j}^2))}{9s^2 (t-m_g^2)^2}. \quad (44.60)$$

#### 44.8.2. Gluino and squark associated production :

In the MSSM, the charged spin- $\frac{1}{2}$  winos and higgsinos mix to make chargino states  $\chi_{1,2}^{\pm}$ , with  $m_{\chi_1^{\pm}} < m_{\chi_2^{\pm}}$ . The spin- $\frac{1}{2}$  neutral bino, wino and higgsino fields mix to give four neutralino mass eigenstates  $\chi_{1,2,3,4}^0$  ordered according to mass. We sometimes denote the charginos and neutralinos collectively as -inos for notational simplicity

For gluino and squark production in association with charginos and neutralinos [12], the quark-squark-neutralino couplings\* are defined by the interaction Lagrangian terms  $\mathcal{L}_{f\tilde{f}\tilde{\chi}_i^0} = \left[ iA_{\tilde{\chi}_i^0}^f \tilde{f}_L^\dagger \tilde{\chi}_i^0 P_L f + iB_{\tilde{\chi}_i^0}^f \tilde{f}_R^\dagger \tilde{\chi}_i^0 P_R f + \text{h.c.} \right]$ , where  $A_{\tilde{\chi}_i^0}^f$  and  $B_{\tilde{\chi}_i^0}^f$  are coupling constants involving gauge couplings, neutralino mixing elements and in the case of third generation fermions, Yukawa couplings. Their form depends on the conventions used for setting up the MSSM Lagrangian, and can be found in various reviews [13] and textbooks [14,15].  $P_L$  and  $P_R$  are the usual left- and right-spinor projection operators and  $f$  denotes any of the SM fermions  $u, d, e, \nu_e, \dots$ . The fermion-sfermion- chargino couplings have the form  $\mathcal{L} = \left[ iA_{\tilde{\chi}_i^{\pm}}^d \tilde{u}_L^\dagger \tilde{\chi}_i^{\pm} P_L d + iA_{\tilde{\chi}_i^{\pm}}^u \tilde{d}_L^\dagger \tilde{\chi}_i^{\pm} P_L u + \text{h.c.} \right]$  for  $u$  and  $d$  quarks, where the  $A_{\tilde{\chi}_i^{\pm}}^d$  and  $A_{\tilde{\chi}_i^{\pm}}^u$  couplings are again convention-dependent, and can be found in textbooks. The superscript  $c$  denotes ‘‘charge conjugate spinor’’, defined by  $\psi^c \equiv C\bar{\psi}^T$ .

The subprocess cross sections for chargino-squark associated production occur via squark exchange and are given by

$$\frac{d\sigma}{dt}(\bar{u}g \rightarrow \tilde{\chi}_i^- \tilde{d}_L) = \frac{\alpha_s}{24s^2} |A_{\tilde{\chi}_i^-}^u|^2 \psi(m_{\tilde{d}_L}, m_{\tilde{\chi}_i^-}, t), \quad (44.61)$$

$$\frac{d\sigma}{dt}(dg \rightarrow \tilde{\chi}_i^- \tilde{u}_L) = \frac{\alpha_s}{24s^2} |A_{\tilde{\chi}_i^-}^d|^2 \psi(m_{\tilde{u}_L}, m_{\tilde{\chi}_i^-}, t), \quad (44.62)$$

\* The couplings  $A_{\tilde{\chi}_i^0}^f$  and  $B_{\tilde{\chi}_i^0}^f$  are given explicitly in Ref. 15 in Eq. (8.87). Also, the couplings  $A_{\tilde{\chi}_i^{\pm}}^d$  and  $A_{\tilde{\chi}_i^{\pm}}^u$  are given in Eq. (8.93). The couplings  $X_i^j$  and  $Y_i^j$  are given by Eq. (8.103), while the  $x_i$  and  $y_i$  couplings are given in Eq. (8.100). Finally, the couplings  $W_{ij}$  are given in Eq. (8.101).

while neutralino-squark production is given by

$$\frac{d\sigma}{dt}(qg \rightarrow \tilde{\chi}_i^0 \tilde{q}) = \frac{\alpha_s}{24s^2} \left( |A_{\tilde{\chi}_i^0}^q|^2 + |B_{\tilde{\chi}_i^0}^q|^2 \right) \psi(m_{\tilde{q}}, m_{\tilde{\chi}_i^0}, t), \quad (44.63)$$

where

$$\begin{aligned} \psi(m_1, m_2, t) &= \frac{s+t-m_1^2}{2s} - \frac{m_1^2(m_2^2-t)}{(m_1^2-t)^2} \\ &+ \frac{t(m_2^2-m_1^2) + m_2^2(s-m_2^2+m_1^2)}{s(m_1^2-t)}. \end{aligned} \quad (44.64)$$

Here, the variable  $t$  is given by the square of ‘‘squark-minus-quark’’ four-momentum. The neutralino-gluino associated production cross section also occurs via squark exchange and is given by

$$\begin{aligned} \frac{d\sigma}{dt}(q\bar{q} \rightarrow \tilde{\chi}_i^0 \tilde{g}) &= \frac{\alpha_s}{18s^2} \left( |A_{\tilde{\chi}_i^0}^q|^2 + |B_{\tilde{\chi}_i^0}^q|^2 \right) \left[ \frac{(m_{\tilde{\chi}_i^0}^2-t)(m_g^2-t)}{(m_g^2-t)^2} \right. \\ &+ \left. \frac{(m_{\tilde{\chi}_i^0}^2-u)(m_g^2-u)}{(m_g^2-u)^2} - \frac{2\eta_i \eta_{\tilde{g}} m_{\tilde{g}} m_{\tilde{\chi}_i^0} s}{(m_g^2-t)(m_g^2-u)} \right], \end{aligned} \quad (44.65)$$

where  $\eta_i$  is the sign of the neutralino mass eigenvalue and  $\eta_{\tilde{g}}$  is the sign of the gluino mass eigenvalue. We also have chargino-gluino associated production:

$$\begin{aligned} \frac{d\sigma}{dt}(\bar{u}d \rightarrow \tilde{\chi}_i^- \tilde{g}) &= \frac{\alpha_s}{18s^2} \left[ |A_{\tilde{\chi}_i^-}^u|^2 \frac{(m_{\tilde{\chi}_i^-}^2-t)(m_g^2-t)}{(m_{\tilde{d}_L}^2-t)^2} \right. \\ &+ |A_{\tilde{\chi}_i^-}^d|^2 \frac{(m_{\tilde{\chi}_i^-}^2-u)(m_g^2-u)}{(m_{\tilde{u}_L}^2-u)^2} + \left. \frac{2\eta_{\tilde{g}} \text{Re}(A_{\tilde{\chi}_i^-}^u A_{\tilde{\chi}_i^-}^d) m_{\tilde{g}} m_{\tilde{\chi}_i^-} s}{(m_{\tilde{d}_L}^2-t)(m_{\tilde{u}_L}^2-u)} \right], \end{aligned} \quad (44.66)$$

where  $\hat{t} = (\tilde{g} - d)^2$  and in the third term one must take the real part of the in general complex coupling constant product.

#### 44.8.3. Slepton and sneutrino production :

The subprocess cross section for  $\tilde{\ell}_L \tilde{\nu}_{\ell L}$  production ( $\ell = e$  or  $\mu$ ) occurs via  $s$ -channel  $W$  exchange and is given by

$$\frac{d\sigma}{dt}(d\bar{u} \rightarrow \tilde{\ell}_L \tilde{\nu}_{\ell L}) = \frac{g^4 |D_W(s)|^2}{192\pi s^2} \left( tu - m_{\tilde{\ell}_L}^2 m_{\tilde{\nu}_{\ell L}}^2 \right), \quad (44.67)$$

where  $D_W(s) = 1/(s - M_W^2 + iM_W\Gamma_W)$  is the  $W$ -boson propagator denominator. The production of  $\tilde{\tau}_1 \tilde{\nu}_{\tau}$  is given as above, but replacing  $m_{\tilde{\ell}_L} \rightarrow m_{\tilde{\tau}_1}$ ,  $m_{\tilde{\nu}_{\ell L}} \rightarrow m_{\tilde{\nu}_{\tau}}$  and multiplying by an overall factor of  $\cos^2 \theta_{\tau}$  (where  $\theta_{\tau}$  is the tau-slepton mixing angle). Similar substitutions hold for  $\tilde{\tau}_2 \tilde{\nu}_{\tau}$  production, except the overall factor is  $\sin^2 \theta_{\tau}$ .

**Table 44.1:** The constants  $\alpha_f$  and  $\beta_f$  that appear in in the SM neutral current Lagrangian. Here  $t \equiv \tan \theta_W$  and  $c \equiv \cot \theta_W$ .

$f$	$q_f$	$\alpha_f$	$\beta_f$
$\ell$	-1	$\frac{1}{4}(3t-c)$	$\frac{1}{4}(t+c)$
$\nu_{\ell}$	0	$\frac{1}{4}(t+c)$	$-\frac{1}{4}(t+c)$
$u$	$\frac{2}{3}$	$-\frac{5}{12}t + \frac{1}{4}c$	$-\frac{1}{4}(t+c)$
$d$	$-\frac{1}{3}$	$\frac{1}{12}t - \frac{1}{4}c$	$\frac{1}{4}(t+c)$

The subprocess cross section for  $\tilde{\ell}_L \bar{\ell}_L$  production occurs via  $s$ -channel  $\gamma$  and  $Z$  exchange, and depends on the neutral current interaction, with fermion couplings to  $\gamma$  and  $Z^0$  given by  $\mathcal{L}_{\text{neutral}} = -e q_f \bar{f} \gamma^\mu f A_\mu + e \bar{f} \gamma^\mu (\alpha_f + \beta_f \gamma_5) f Z_\mu$  (with values of  $q_f$ ,  $\alpha_f$ , and  $\beta_f$  given in Table 44.1.

The subprocess cross section is given by

$$\frac{d\sigma}{dt}(q\bar{q} \rightarrow \tilde{\ell}_L \bar{\ell}_L) = \frac{e^4}{24\pi s^2} (tu - m_{\tilde{\ell}_L}^4) \times \left\{ \frac{q_\ell^2 q_q^2}{s^2} + (\alpha_\ell - \beta_\ell)^2 (\alpha_q^2 + \beta_q^2) |D_Z(s)|^2 + \frac{2q_\ell q_q \alpha_q (\alpha_\ell - \beta_\ell) (s - M_Z^2)}{s} |D_Z(s)|^2 \right\}, \quad (44.68)$$

where  $D_Z(s) = 1/(s - M_Z^2 + iM_Z\Gamma_Z)$ . The cross section for sneutrino production is given by the same formula, but with  $\alpha_\ell$ ,  $\beta_\ell$ ,  $q_\ell$  and  $m_{\tilde{\ell}_L}$  replaced by  $\alpha_\nu$ ,  $\beta_\nu$ , 0 and  $m_{\tilde{\nu}_L}$ , respectively. The cross section for  $\tilde{\tau}_1 \bar{\tau}_1$  production is obtained by replacing  $m_{\tilde{\ell}_L} \rightarrow m_{\tilde{\tau}_1}$  and  $\beta_\ell \rightarrow \beta_\ell \cos 2\theta_\tau$ .

The cross section for  $\tilde{\ell}_R \bar{\ell}_R$  production is given by substituting  $\alpha_\ell - \beta_\ell \rightarrow \alpha_\ell + \beta_\ell$  and  $m_{\tilde{\ell}_L} \rightarrow m_{\tilde{\ell}_R}$  in the equation above. The cross section for  $\tilde{\tau}_2 \bar{\tau}_2$  production is obtained from the formula for  $\tilde{\ell}_R \bar{\ell}_R$  production by replacing  $m_{\tilde{\ell}_R} \rightarrow m_{\tilde{\tau}_2}$  and  $\beta_\ell \rightarrow \beta_\ell \cos 2\theta_\tau$ .

Finally, the cross section for  $\tilde{\tau}_1 \bar{\tau}_2$  production occurs only via  $Z$  exchange, and is given by

$$\frac{d\sigma}{dt}(q\bar{q} \rightarrow \tilde{\tau}_1 \bar{\tau}_2) = \frac{d\sigma}{dt}(q\bar{q} \rightarrow \tilde{\tau}_1 \bar{\tau}_2) = \frac{e^4}{24\pi s^2} (\alpha_q^2 + \beta_q^2) \beta_\ell^2 \sin^2 2\theta_\tau |D_Z(s)|^2 (ut - m_{\tilde{\tau}_1}^2 m_{\tilde{\tau}_2}^2). \quad (44.69)$$

#### 44.8.4. Chargino and neutralino pair production :

##### 44.8.4.1. $\tilde{\chi}_i^- \tilde{\chi}_j^0$ production:

The subprocess cross section for  $d\bar{u} \rightarrow \tilde{\chi}_i^- \tilde{\chi}_j^0$  depends on Lagrangian couplings  $\mathcal{L}_{W\bar{u}d} = -\frac{g}{\sqrt{2}} \bar{u} \gamma_\mu P_L d W^{+\mu} + \text{h.c.}$ ,  $\mathcal{L}_{W\tilde{\chi}_i^- \tilde{\chi}_j^0} = -g(-i)^\theta_j \bar{\tilde{\chi}}_i^- [X_i^j + Y_i^j \gamma_5] \gamma_\mu \tilde{\chi}_j^0 W^{-\mu} + \text{h.c.}$ ,  $\mathcal{L}_{q\tilde{q}\tilde{\chi}_i^-} = iA_{\tilde{\chi}_i^-}^d \bar{u} \tilde{\chi}_i^- P_L d + iA_{\tilde{\chi}_i^-}^u \bar{d} \tilde{\chi}_i^- P_L u + \text{h.c.}$  and  $\mathcal{L}_{q\tilde{q}\tilde{\chi}_j^0} = iA_{\tilde{\chi}_j^0}^q \bar{q} \tilde{\chi}_j^0 P_L q + \text{h.c.}$ . Contributing diagrams include  $W$  exchange and also  $\tilde{d}_L$  and  $\tilde{u}_L$  squark exchange. The  $X_i^j$  and  $Y_i^j$  couplings are new, and again convention-dependent: the cross section formulae works if the interaction Lagrangian is written in the above form, so that the couplings can be suitably extracted. The term  $\theta_j = 0$  (1) if  $m_{\tilde{\chi}_j^0} > 0$  ( $< 0$ ); it comes about because the neutralino field must be re-defined by a  $-i\gamma_5$  transformation if its mass eigenvalue is negative [15]. The subprocess cross section is given in terms of dot products of four momenta, where particle labels are used to denote their four-momenta; note that all mass terms in the cross section formulae are positive definite, so that the signs of mass eigenstates have been absorbed into the Lagrangian couplings, as for instance in Ref. [15]. We then have

$$\frac{d\sigma}{dt}(d\bar{u} \rightarrow \tilde{\chi}_i^- \tilde{\chi}_j^0) = \frac{1}{192\pi s^2} \left[ T_W + T_{\tilde{d}_L} + T_{\tilde{u}_L} + T_{W\tilde{d}_L} + T_{W\tilde{u}_L} + T_{\tilde{d}_L \tilde{u}_L} \right] \quad (44.70)$$

where

$$T_W = 8g^4 |D_W(s)|^2 \left\{ [X_i^j + Y_i^j \gamma_5] (\tilde{\chi}_j^0 \cdot d\tilde{\chi}_i^- \cdot \bar{u} + \tilde{\chi}_j^0 \cdot \bar{u}\tilde{\chi}_i^- \cdot d) + 2(X_i^j Y_i^j) (\tilde{\chi}_j^0 \cdot d\tilde{\chi}_i^- \cdot \bar{u} - \tilde{\chi}_j^0 \cdot \bar{u}\tilde{\chi}_i^- \cdot d) + [X_i^j - Y_i^j \gamma_5] m_{\tilde{\chi}_i^-} m_{\tilde{\chi}_j^0} d \cdot \bar{u} \right\}, \quad (44.71)$$

$$T_{\tilde{d}_L} = \frac{4|A_{\tilde{\chi}_i^-}^u|^2 |A_{\tilde{\chi}_j^0}^d|^2}{[(\tilde{\chi}_i^- - \bar{u})^2 - m_{\tilde{d}_L}^2]^2} d \cdot \tilde{\chi}_j^0 \tilde{\chi}_i^- \cdot \bar{u}, \quad (44.72)$$

$$T_{\tilde{u}_L} = \frac{4|A_{\tilde{\chi}_i^-}^d|^2 |A_{\tilde{\chi}_j^0}^u|^2}{[(\tilde{\chi}_j^0 - \bar{u})^2 - m_{\tilde{u}_L}^2]^2} \bar{u} \cdot \tilde{\chi}_j^0 \tilde{\chi}_i^- \cdot d \quad (44.73)$$

$$T_{W\tilde{d}_L} = \frac{-\sqrt{2}g^2 \text{Re}[A_{\tilde{\chi}_j^0}^{d*} A_{\tilde{\chi}_i^-}^u (-i)^\theta_j] (s - M_W^2) |D_W(s)|^2}{(\tilde{\chi}_i^- - \bar{u})^2 - m_{\tilde{d}_L}^2} \times \left\{ 8(X_i^j + Y_i^j) \tilde{\chi}_j^0 \cdot d\bar{u} \cdot \tilde{\chi}_i^- + 4(X_i^j - Y_i^j) m_{\tilde{\chi}_i^-} m_{\tilde{\chi}_j^0} d \cdot \bar{u} \right\} \quad (44.74)$$

$$T_{W\tilde{u}_L} = \frac{\sqrt{2}g^2 \text{Re}[A_{\tilde{\chi}_i^-}^{d*} A_{\tilde{\chi}_j^0}^u (-i)^\theta_j] (s - M_W^2) |D_W(s)|^2}{(\tilde{\chi}_j^0 - \bar{u})^2 - m_{\tilde{u}_L}^2} \times \left\{ 8(X_i^j - Y_i^j) \tilde{\chi}_j^0 \cdot \bar{u}d \cdot \tilde{\chi}_i^- + 4(X_i^j + Y_i^j) m_{\tilde{\chi}_i^-} m_{\tilde{\chi}_j^0} d \cdot \bar{u} \right\} \quad (44.75)$$

and

$$T_{\tilde{d}_L \tilde{u}_L} = -\frac{4\text{Re}[A_{\tilde{\chi}_j^0}^d A_{\tilde{\chi}_i^-}^{u*} A_{\tilde{\chi}_i^-}^{d*} A_{\tilde{\chi}_j^0}^u] m_{\tilde{\chi}_i^-} m_{\tilde{\chi}_j^0} d \cdot \bar{u}}{[(\tilde{\chi}_i^- - \bar{u})^2 - m_{\tilde{d}_L}^2][(\tilde{\chi}_j^0 - \bar{u})^2 - m_{\tilde{u}_L}^2]}. \quad (44.76)$$

##### 44.8.4.2. Chargino pair production:

The subprocess cross section for  $d\bar{d} \rightarrow \tilde{\chi}_i^- \tilde{\chi}_i^+$  ( $i = 1, 2$ ) depends on Lagrangian couplings  $\mathcal{L} = e\tilde{\chi}_i^- \gamma_\mu \tilde{\chi}_i^+ A^\mu - e \cot \theta_W \tilde{\chi}_i^- \gamma_\mu (x_i - y_i \gamma_5) \tilde{\chi}_i^+ Z^\mu$  and also  $\mathcal{L} \ni iA_{\tilde{\chi}_i^-}^d \bar{u} \tilde{\chi}_i^- P_L d + iA_{\tilde{\chi}_i^-}^u \bar{d} \tilde{\chi}_i^- P_L u + \text{h.c.}$ . Contributing diagrams include  $s$ -channel  $\gamma$ ,  $Z^0$  exchange and  $t$ -channel  $\tilde{u}_L$  exchange [16,17]. The couplings  $x_i$  and  $y_i$  are again new and as usual convention-dependent.

The subprocess cross section is given by

$$\frac{d\sigma}{dt}(d\bar{d} \rightarrow \tilde{\chi}_i^- \tilde{\chi}_i^+) = \frac{1}{192\pi s^2} [T_\gamma + T_Z + T_{\tilde{u}_L} + T_{\gamma Z} + T_{\gamma \tilde{u}_L} + T_{Z\tilde{u}_L}] \quad (44.77)$$

where

$$T_\gamma = \frac{32e^4 q_d^2}{s^2} \left[ d \cdot \tilde{\chi}_i^+ \bar{d} \cdot \tilde{\chi}_i^- + d \cdot \tilde{\chi}_i^- \bar{d} \cdot \tilde{\chi}_i^+ + m_{\tilde{\chi}_i^-}^2 d \cdot \bar{d} \right] \quad (44.78)$$

$$T_Z = 32e^4 \cot^2 \theta_W |D_Z(s)|^2$$

$$\left\{ (\alpha_d^2 + \beta_d^2) (x_i^2 + y_i^2) \left[ d \cdot \tilde{\chi}_i^+ \bar{d} \cdot \tilde{\chi}_i^- + d \cdot \tilde{\chi}_i^- \bar{d} \cdot \tilde{\chi}_i^+ + m_{\tilde{\chi}_i^-}^2 d \cdot \bar{d} \right] \mp 4\alpha_d \beta_d x_i y_i \left[ d \cdot \tilde{\chi}_i^+ \bar{d} \cdot \tilde{\chi}_i^- - d \cdot \tilde{\chi}_i^- \bar{d} \cdot \tilde{\chi}_i^+ \right] - 2y_i^2 (\alpha_d^2 + \beta_d^2) m_{\tilde{\chi}_i^-}^2 d \cdot \bar{d} \right\}, \quad (44.79)$$

$$T_{\tilde{u}_L} = \frac{4|A_{\tilde{\chi}_i^-}^d|^4}{[(d - \tilde{\chi}_i^-)^2 - m_{\tilde{u}_L}^2]^2} d \cdot \tilde{\chi}_i^- \bar{d} \cdot \tilde{\chi}_i^+ \quad (44.80)$$

$$T_{\gamma Z} = \frac{64e^4 \cot \theta_W q_d (s - M_Z^2) |D_Z(s)|^2}{s} \times \left\{ \alpha_d x_i \left( d \cdot \tilde{\chi}_i^+ \bar{d} \cdot \tilde{\chi}_i^- + d \cdot \tilde{\chi}_i^- \bar{d} \cdot \tilde{\chi}_i^+ + m_{\tilde{\chi}_i^-}^2 d \cdot \bar{d} \right) \pm \beta_d y_i \left( d \cdot \tilde{\chi}_i^- \bar{d} \cdot \tilde{\chi}_i^+ - d \cdot \tilde{\chi}_i^+ \bar{d} \cdot \tilde{\chi}_i^- \right) \right\} \quad (44.81)$$

$$T_{\gamma \tilde{u}_L} = \mp \frac{8e^2 q_d}{s} \frac{|A_{\tilde{\chi}_i^-}^d|^2}{[(d - \tilde{\chi}_i^-)^2 - m_{\tilde{u}_L}^2]} \left\{ 2\bar{d} \cdot \tilde{\chi}_i^+ d \cdot \tilde{\chi}_i^- + m_{\tilde{\chi}_i^-}^2 d \cdot \bar{d} \right\} \quad (44.82)$$

and

$$T_{Z\tilde{u}_L} = \mp 8e^2 \cot \theta_W |D_Z(s)|^2 \frac{|A_{\tilde{\chi}_i^-}^d|^2 (s - M_Z^2)}{[(d - \tilde{\chi}_i^-)^2 - m_{\tilde{u}_L}^2]} (\alpha_d - \beta_d) \\ \times \left\{ 2(x_i \mp y_i) d \cdot \tilde{\chi}_i^- \bar{d} \cdot \tilde{\chi}_i^+ + m_{\tilde{\chi}_i^-}^2 (x_i \pm y_i) d \cdot \bar{d} \right\} \quad (44.83)$$

using the upper of the sign choices.

The cross section for  $u\bar{u} \rightarrow \tilde{\chi}_i^+ \tilde{\chi}_i^-$  can be obtained from the above by replacing  $\alpha_d \rightarrow \alpha_u$ ,  $\beta_d \rightarrow \beta_u$ ,  $q_d \rightarrow q_u$ ,  $\tilde{u}_L \rightarrow \tilde{d}_L$ ,  $A_{\tilde{\chi}_i^-}^d \rightarrow A_{\tilde{\chi}_i^-}^u$ ,  $d \rightarrow \bar{u}$ ,  $\bar{d} \rightarrow u$  and adopting the lower of the sign choices everywhere.

The cross section for  $q\bar{q} \rightarrow \tilde{\chi}_1^- \tilde{\chi}_2^+$ ,  $\tilde{\chi}_1^+ \tilde{\chi}_2^-$  can occur via  $Z$  and  $\tilde{q}_L$  exchange. It is usually much smaller than  $\tilde{\chi}_{1,2}^- \tilde{\chi}_{1,2}^+$  production, so the cross section will not be presented here. It can be found in Appendix A of Ref. 15.

#### 44.8.4.3. Neutralino pair production:

Neutralino pair production via  $q\bar{q}$  fusion takes place via  $s$ -channel  $Z$  exchange plus  $t$ - and  $u$ -channel left- and right- squark exchange (5 diagrams) [17,18]. The Lagrangian couplings (see previous footnote\*) needed include terms given above plus terms of the form  $\mathcal{L} = W_{ij} \tilde{\chi}_i^0 \gamma^\mu (\gamma_5)^{\theta_i + \theta_j + 1} \tilde{\chi}_j^0 Z^\mu$ . The couplings  $W_{ij}$  depend only on the *higgsino* components of the neutralinos  $i$  and  $j$ . The subprocess cross section is given by:

$$\frac{d\sigma}{dt}(q\bar{q} \rightarrow \tilde{\chi}_i^0 \tilde{\chi}_j^0) = \frac{1}{192\pi s^2} [T_Z + T_{\tilde{q}_L} + T_{\tilde{q}_R} + T_{Z\tilde{q}_L} + T_{Z\tilde{q}_R}] \quad (44.84)$$

where

$$T_Z = 128e^2 |W_{ij}|^2 (\alpha_q^2 + \beta_q^2) |D_Z(s)|^2 \\ \left[ q \cdot \tilde{\chi}_i^0 \bar{q} \cdot \tilde{\chi}_j^0 + q \cdot \tilde{\chi}_j^0 \bar{q} \cdot \tilde{\chi}_i^0 - \eta_i \eta_j m_{\tilde{\chi}_i^0} m_{\tilde{\chi}_j^0} q \cdot \bar{q} \right], \quad (44.85)$$

$$T_{\tilde{q}_L} = 4 |A_{\tilde{\chi}_i^0}^q|^2 |A_{\tilde{\chi}_j^0}^q|^2 \left\{ \frac{q \cdot \tilde{\chi}_i^0 \bar{q} \cdot \tilde{\chi}_j^0}{[(\tilde{\chi}_i^0 - q)^2 - m_{\tilde{q}_L}^2]^2} + \frac{q \cdot \tilde{\chi}_j^0 \bar{q} \cdot \tilde{\chi}_i^0}{[(\tilde{\chi}_j^0 - q)^2 - m_{\tilde{q}_L}^2]^2} \right. \\ \left. - \eta_i \eta_j \frac{m_{\tilde{\chi}_i^0} m_{\tilde{\chi}_j^0} q \cdot \bar{q}}{[(\tilde{\chi}_i^0 - q)^2 - m_{\tilde{q}_L}^2][(\tilde{\chi}_j^0 - q)^2 - m_{\tilde{q}_L}^2]} \right\} \quad (44.86)$$

$$T_{\tilde{q}_R} = 4 |B_{\tilde{\chi}_i^0}^q|^2 |B_{\tilde{\chi}_j^0}^q|^2 \left\{ \frac{q \cdot \tilde{\chi}_i^0 \bar{q} \cdot \tilde{\chi}_j^0}{[(\tilde{\chi}_i^0 - q)^2 - m_{\tilde{q}_R}^2]^2} + \frac{q \cdot \tilde{\chi}_j^0 \bar{q} \cdot \tilde{\chi}_i^0}{[(\tilde{\chi}_j^0 - q)^2 - m_{\tilde{q}_R}^2]^2} \right. \\ \left. - \eta_i \eta_j \frac{m_{\tilde{\chi}_i^0} m_{\tilde{\chi}_j^0} q \cdot \bar{q}}{[(\tilde{\chi}_i^0 - q)^2 - m_{\tilde{q}_R}^2][(\tilde{\chi}_j^0 - q)^2 - m_{\tilde{q}_R}^2]} \right\} \quad (44.87)$$

$$T_{Z\tilde{q}_L} = 16e(\alpha_q - \beta_q)(s - M_Z^2) |D_Z(s)|^2 \\ \left\{ \frac{\text{Re}(W_{ij} A_{\tilde{\chi}_i^0}^{q*} A_{\tilde{\chi}_j^0}^q)}{[(\tilde{\chi}_i^0 - q)^2 - m_{\tilde{q}_L}^2]} \left[ 2q \cdot \tilde{\chi}_i^0 \bar{q} \cdot \tilde{\chi}_j^0 - \eta_i \eta_j m_{\tilde{\chi}_i^0} m_{\tilde{\chi}_j^0} q \cdot \bar{q} \right] \right. \\ \left. + \eta_i \eta_j \frac{\text{Re}(W_{ij} A_{\tilde{\chi}_i^0}^q A_{\tilde{\chi}_j^0}^{q*})}{[(\tilde{\chi}_j^0 - q)^2 - m_{\tilde{q}_L}^2]} \left[ 2q \cdot \tilde{\chi}_j^0 \bar{q} \cdot \tilde{\chi}_i^0 - \eta_i \eta_j m_{\tilde{\chi}_i^0} m_{\tilde{\chi}_j^0} q \cdot \bar{q} \right] \right\} \quad (44.88)$$

$$T_{Z\tilde{q}_R} = 16e(\alpha_q + \beta_q)(s - M_Z^2) |D_Z(s)|^2 \\ \left\{ \frac{\text{Re}(W_{ij} B_{\tilde{\chi}_i^0}^{q*} B_{\tilde{\chi}_j^0}^q)}{[(\tilde{\chi}_i^0 - q)^2 - m_{\tilde{q}_R}^2]} \left[ 2q \cdot \tilde{\chi}_i^0 \bar{q} \cdot \tilde{\chi}_j^0 - \eta_i \eta_j m_{\tilde{\chi}_i^0} m_{\tilde{\chi}_j^0} q \cdot \bar{q} \right] \right. \\ \left. - \frac{\text{Re}(W_{ij} B_{\tilde{\chi}_i^0}^q B_{\tilde{\chi}_j^0}^{q*})}{[(\tilde{\chi}_j^0 - q)^2 - m_{\tilde{q}_R}^2]} \left[ 2q \cdot \tilde{\chi}_j^0 \bar{q} \cdot \tilde{\chi}_i^0 - \eta_i \eta_j m_{\tilde{\chi}_i^0} m_{\tilde{\chi}_j^0} q \cdot \bar{q} \right] \right\}. \quad (44.89)$$

As before,  $\eta_i = \pm 1$  corresponding to whether the neutralino mass eigenvalue is positive or negative. When  $i = j$  in the above formula, one must remember to integrate over just  $2\pi$  steradians of solid angle to avoid double counting in the total cross section.

## 44.9. Universal extra dimensions

In the Universal Extra Dimension (UED) model of Ref. [19] (see Ref. [20] for a review of models with extra spacetime dimensions), the Standard Model is embedded in a five dimensional theory, where the fifth dimension is compactified on an  $S_1/Z_2$  orbifold. Each SM chirality state is then the zero mode of an infinite tower of Kaluza-Klein excitations labelled by  $n = 0 - \infty$ . A KK parity is usually assumed to hold, where each state is assigned KK-parity  $P = (-1)^n$ . If the compactification scale is around a TeV, then the  $n = 1$  (or even higher) KK modes may be accessible to collider searches.

Of interest for hadron colliders are the production of massive  $n \geq 1$  quark or gluon pairs. These production cross sections have been calculated in Ref. [21,22]. We list here results for the  $n = 1$  case only with  $M_1 = 1/R$  ( $R$  is the compactification radius) and  $s$ ,  $t$  and  $u$  are the usual Mandelstam variables; more general formulae can be found in Ref. [22]. The superscript  $*$  stands for any KK excited state, while  $\bullet$  stands for left chirality states and  $\circ$  stands for right chirality states.

$$\frac{d\sigma}{dt} = \frac{1}{16\pi s^2} T \quad (44.90)$$

where

$$T(q\bar{q} \rightarrow g^* g^*) = \frac{2g_s^4}{27} \left[ M_1^2 \left( -\frac{4s^3}{t'^2 u'^2} + \frac{57s}{t'u'} - \frac{108}{s} \right) \right. \\ \left. + \frac{20s^2}{t'u'} - 93 + \frac{108t'u'}{s^2} \right] \quad (44.91)$$

and

$$T(gg \rightarrow g^* g^*) = \\ \frac{9g_s^4}{27} \left[ 3M_1^4 \frac{s^2 + t'^2 + u'^2}{t'^2 u'^2} - 3M_1^2 \frac{s^2 + t'^2 + u'^2}{st'u'} + 1 \right. \\ \left. + \frac{(s^2 + t'^2 + u'^2)^3}{4s^2 t'^2 u'^2} - \frac{t'u'}{s^2} \right] \quad (44.92)$$

where  $t' = t - M_1^2$  and  $u' = u - M_1^2$ .

Also,

$$T(q\bar{q} \rightarrow q_1^* \bar{q}_1^*) = \frac{4g_s^4}{9} \left[ \frac{2M_1^2}{s} + \frac{t'^2 + u'^2}{s^2} \right],$$

$$T(q\bar{q} \rightarrow q_1^* \bar{q}_1^*) = \frac{g_s^4}{9} \left[ 2M_1^2 \left( \frac{4}{s} + \frac{s}{t'^2} - \frac{1}{t'} \right) \right. \\ \left. + \frac{23}{6} + \frac{2s^2}{t'^2} + \frac{8s}{3t'} + \frac{6t'}{s} + \frac{8t'^2}{s^2} \right],$$

$$T(qq \rightarrow q_1^* \bar{q}_1^*) = \frac{g_s^4}{27} \left[ M_1^2 \left( 6 \frac{t'}{u'^2} + 6 \frac{u'}{t'^2} - \frac{s}{t'u'} \right) \right. \\ \left. + 2 \left( 3 \frac{t'^2}{u'^2} + 3 \frac{u'^2}{t'^2} + 4 \frac{s^2}{t'u'} - 5 \right) \right],$$

$$T(gg \rightarrow q_1^* \bar{q}_1^*) = g_s^4 \left[ M_1^4 \frac{4}{t'u'} \left( \frac{s^2}{6t'u'} - \frac{3}{8} \right) \right. \\ \left. + M_1^2 \frac{4}{s} \left( \frac{s^2}{6t'u'} - \frac{3}{8} \right) + \frac{s^2}{6t'u'} - \frac{17}{24} + \frac{3t'u'}{4s^2} \right],$$

$$T(gq \rightarrow g^* q_1^*) = \frac{-g_s^4}{3} \left[ \frac{5s^2}{12t'^2} + \frac{s^3}{t'^2 u'} + \frac{11s u'}{6t'^2} + \frac{5u'^2}{12t'^2} + \frac{u'^3}{st'^2} \right],$$

$$T(qq' \rightarrow q_1^* \bar{q}_1^*) = \frac{g_s^4}{18} \left[ 4M_1^4 \frac{s}{t'^2} + 5 + 4 \frac{s^2}{t'^2} + 8 \frac{s}{t'} \right],$$

$$T(qq' \rightarrow q_1^* \bar{q}_1^*) = \frac{2g_s^4}{9} \left[ -M_1^2 \frac{s}{t'^2} + \frac{1}{4} + \frac{s^2}{t'^2} \right],$$

$$T(qq \rightarrow q_1^{\bullet} q_1^{\circ}) = \frac{g_s^4}{9} \left[ M_1^2 \left( \frac{2s^3}{t'^2 u'^2} - \frac{4s}{t' u'} \right) + 2 \frac{s^4}{t'^2 u'^2} - 8 \frac{s^2}{t' u'} + 5 \right],$$

$$T(q\bar{q}' \rightarrow q_1^{\bullet} \bar{q}_1^{\circ}) = \frac{g_s^4}{9} \left[ 2M_1^2 \left( \frac{1}{t'} + \frac{u'}{t'^2} \right) + \frac{5}{2} + \frac{4u'}{t'} + \frac{2u'^2}{t'^2} \right],$$

and

$$T(qq' \rightarrow q_1^{\bullet} q_1^{\circ}) = \frac{g_s^4}{9} \left[ -2M_1^2 \left( \frac{1}{t'} + \frac{u'}{t'^2} \right) + \frac{1}{2} + \frac{2u'^2}{t'^2} \right].$$

#### 44.10. Large extra dimensions

In the ADD theory [23] with large extra dimensions (LED), the SM particles are confined to a 3-brane, while gravity propagates in the bulk. It is assumed that the  $n$  extra dimensions are compactified on an  $n$ -dimensional torus of volume  $(2\pi r)^n$ , so that the fundamental  $4+n$  dimensional Planck scale  $M_*$  is related to the usual 4-dimensional Planck scale  $M_{Pl}$  by  $M_{Pl}^2 = M_*^{n+2} (2\pi r)^n$ . If  $M_* \sim 1$  TeV, then the  $M_W - M_{Pl}$  hierarchy problem is just due to gravity propagating in the large extra dimensions.

In these theories, the KK-excited graviton states  $G_{\mu\nu}^n$  for  $n = 1 - \infty$  can be produced at collider experiments. The graviton couplings to matter are suppressed by  $1/M_{Pl}$ , so that graviton emission cross sections  $d\sigma/dt \sim 1/M_{Pl}^2$ . However, the mass splittings between the excited graviton states can be tiny, so the graviton eigenstates are usually approximated by a continuum distribution. A summation (integration) over all allowed graviton emissions ends up cancelling the  $1/M_{Pl}^2$  factor, so that observable cross section rates can be attained. Some of the fundamental production formulae for a KK graviton (denoted  $G$ ) of mass  $m$  at hadron colliders include the subprocesses

$$\frac{d\sigma_m}{dt}(f\bar{f} \rightarrow \gamma G) = \frac{\alpha Q_f^2}{16N_f} \frac{1}{sM_{Pl}^2} F_1\left(\frac{t}{s}, \frac{m^2}{s}\right), \quad (44.93)$$

where  $Q_f$  is the charge of fermion  $f$  and  $N_f$  is the number of QCD colors of  $f$ . Also,

$$\frac{d\sigma_m}{dt}(q\bar{q} \rightarrow gG) = \frac{\alpha_s}{36} \frac{1}{sM_{Pl}^2} F_1\left(\frac{t}{s}, \frac{m^2}{s}\right), \quad (44.94)$$

$$\frac{d\sigma_m}{dt}(qq \rightarrow qG) = \frac{\alpha_s}{96} \frac{1}{sM_{Pl}^2} F_2\left(\frac{t}{s}, \frac{m^2}{s}\right), \quad (44.95)$$

$$\frac{d\sigma_m}{dt}(gg \rightarrow gG) = \frac{3\alpha_s}{16} \frac{1}{sM_{Pl}^2} F_3\left(\frac{t}{s}, \frac{m^2}{s}\right), \quad (44.96)$$

where

$$F_1(x, y) = \frac{1}{x(y-1-x)} \left[ -4x(1+x)(1+2x+2x^2) + y(1+6x+18x^2+16x^3) - 6y^2x(1+2x) + y^3(1+4x) \right] \quad (44.97)$$

$$F_2(x, y) = -(y-1-x) F_1\left(\frac{x}{y-1-x}, \frac{y}{y-1-x}\right) \quad (44.98)$$

and

$$F_3(x, y) = \frac{1}{x(y-1-x)} \left[ 1 + 2x + 3x^2 + 2x^3 + x^4 - 2y(1+x^3) + 3y^2(1+x^2) - 2y^3(1+x) + y^4 \right]. \quad (44.99)$$

These formulae must then be multiplied by the graviton density of states formula  $dN = S_{n-1} \frac{M_{Pl}^2}{M_*^{n+2}} m^{n-1} dm$  to gain the cross section

$$\frac{d^2\sigma}{dt dm} = S_{n-1} \frac{M_{Pl}^2}{M_*^{n+2}} m^{n-1} \frac{d\sigma_m}{dt} \quad (44.100)$$

where  $S_n = \frac{(2\pi)^{n/2}}{\Gamma(n/2)}$  is the surface area of an  $n$ -dimensional sphere of unit radius.

Virtual graviton processes can also be searched for at colliders. For instance, in Ref. [24] the cross section for Drell-Yan production of lepton pairs via gluon fusion was calculated, where it is found that, in the center-of-mass system

$$\frac{d\sigma}{dz}(gg \rightarrow \ell^+ \ell^-) = \frac{\lambda^2 s^3}{64\pi M_*^8} (1-z^2)(1+z^2) \quad (44.101)$$

where  $z = \cos\theta$  and  $\lambda$  is a model-dependent coupling constant  $\sim 1$ . Formulae for Drell-Yan production via  $q\bar{q}$  fusion can also be found in Ref. [24,25].

#### 44.11. Warped extra dimensions

In the Randall-Sundrum model [26] of warped extra dimensions, the arena for physics is a 5-d anti-deSitter ( $AdS_5$ ) spacetime, for which a non-factorizable metric exists with a metric warp factor  $e^{-2\sigma(\phi)}$ . It is assumed that two opposite tension 3-branes exist within  $AdS_5$  at the two ends of an  $S_1/Z_2$  orbifold parametrized by co-ordinate  $\phi$  which runs from  $0 - \pi$ . The 4-D solution of the Einstein equations yields  $\sigma(\phi) = kr_c|\phi|$ , where  $r_c$  is the compactification radius of the extra dimension and  $k \sim M_{Pl}$ . The 4-D effective action allows one to identify  $\bar{M}_{Pl}^2 = \frac{M^3}{k}(1 - e^{-2kr_c\pi})$ , where  $M$  is the 5-D Planck scale. Physical particles on the TeV scale (SM) brane have mass  $m = e^{-kr_c\pi} m_0$ , where  $m_0$  is a fundamental mass of order the Planck scale. Thus, the weak scale-Planck scale hierarchy occurs due to the existence of the exponential warp factor if  $kr_c \sim 12$ .

In the simplest versions of the RS model, the TeV-scale brane contains only SM particles plus a tower of KK gravitons. The RS gravitons have mass  $m_n = kx_n e^{-kr_c\pi}$ , where the  $x_i$  are roots of Bessel functions  $J_1(x_n) = 0$ , with  $x_1 \simeq 3.83$ ,  $x_2 \simeq 7.02$  etc. While the RS zero-mode graviton couplings suppressed by  $1/\bar{M}_{Pl}$  and are thus inconsequential for collider searches, the  $n=1$  and higher modes have couplings suppressed instead by  $\Lambda_\pi = e^{-kr_c\pi} \bar{M}_{Pl} \sim TeV$ . The  $n=1$  RS graviton should have width  $\Gamma_1 = \rho m_1 x_1^2 (k/\bar{M}_{Pl})^2$ , where  $\rho$  is a constant depending on how many decay modes are open. The formulae for dilepton production via virtual RS graviton exchange can be gained from the above formulae for the ADD scenario via the replacement [27]

$$\frac{\lambda}{M_*^4} \rightarrow \frac{i^2}{8\Lambda_\pi^2} \sum_{n=1}^{\infty} \frac{1}{s - m_n^2 + im_n\Gamma_n}. \quad (44.102)$$

#### References:

1. J.F. Owens *et al.*, Phys. Rev. **D18**, 1501 (1978). Note that cross section given in previous editions of RPP for  $gg \rightarrow q\bar{q}$  lacked a factor of  $\pi$ .
2. F. Wilczek, Phys. Rev. Lett. **39**, 1304 (1977).
3. B.L. Ioffe and V.Khoze, Leningrad Report 274, 1976; Sov. J. Nucl. Phys. **9**, 50 (1978).
4. J. Ellis *et al.*, Nucl. Phys. **B106**, 292 (1976).
5. R.N. Cahn and S. Dawson, Phys. Lett. **B136**, 196 (1984), erratum, Phys. Lett. **B138**, 464 (1984).
6. S. Dawson, Nucl. Phys. **B249**, 42 (1985).
7. M.S. Chanowitz and M.K. Gaillard, Phys. Lett. **B142**, 85 (1984).
8. R.N. Cahn, Nucl. Phys. **B255**, 341 (1985).
9. For an exhaustive treatment, see V.M. Budnev *et al.*, Phys. Reports **15C**, 181 (1975).
10. See *e.g.* H. Haber, *Supersymmetry, Part I (Theory)*, this Review.
11. P.R. Harrison and C.H. Llewellyn Smith, Nucl. Phys. **B213**, 223 (1983), Erratum-*ibid.*, **B223**, 542 (1983); S. Dawson, E. Eichten, and C. Quigg, Phys. Rev. **D31**, 1581 (1985); V. Barger *et al.*, Phys. Rev. **D31**, 528 (1985); H. Baer and X. Tata, Phys. Lett. **B160**, 159 (1985).
12. H. Baer, D. Karatas, and X. Tata, Phys. Rev. **D42**, 2259 (1990).
13. H. Haber and G. Kane, Phys. Rept. **117**, 75 (1985).
14. Theory and Phenomenology of Sparticles, M. Drees, R. Godbole, and P. Roy (World Scientific) 2005.



15. Weak Scale Supersymmetry: From Superfields to Scattering Events, H. Baer and X. Tata (Cambridge University Press) 2006.
16. A. Bartl, H. Fraas, and W. Majerotto, *Z. Phys.* **C30**, 441 (1986).
17. H. Baer *et al.*, *Int. J. Mod. Phys.* **A4**, 4111 (1989).
18. A. Bartl, H. Fraas, and W. Majerotto, *Nucl. Phys.* **B278**, 1 (1986).
19. T. Appelquist, H.C. Cheng, and B. Dobrescu, *Phys. Rev.* **D64**, 035002 (2001).
20. For a review of models with extra spacetime dimensions, see G. Giudice and J. Wells, *Extra Dimensions*, this *Review*.
21. J.M. Smillie and B.R. Webber, *JHEP* **0510**, 069 (2005).
22. C. Macesanu, C.D. McMullen, and S. Nandi, *Phys. Rev.* **D66**, 015009 (2002).
23. N. Arkani-Hamed, S. Dimopoulos, and G. Dvali, *Phys. Lett.* **B429**, 263 (1998) and *Phys. Rev.* **D59**, 086004 (1999).
24. J. L. Hewett, *Phys. Rev. Lett.* **82**, 4765 (1999).
25. G. Giudice, R. Rattazzi, and J. Wells, *Nucl. Phys.* **B544**, 3 (1999); E.A. Mirabelli, M. Perelstein, and M.E. Peskin, *Phys. Rev. Lett.* **82**, 2236 (1999); T. Han, J. Lykken, and R. Zhang, *Phys. Rev.* **D59**, 105006 (1999).
26. L. Randall and R.S. Sundrum, *Phys. Rev. Lett.* **83**, 3370 (1999).
27. H. Davoudiasl, J.L. Hewett, and T.G. Rizzo, *Phys. Rev. Lett.* **84**, 2080 (2000).

## 45. NEUTRINO CROSS SECTION MEASUREMENTS

Written in April 2012 by G.P. Zeller (Fermilab).

Neutrino interaction cross sections are an essential ingredient in most neutrino experiments. Interest in neutrino scattering has recently increased due to the need for such information in the interpretation of neutrino oscillation data. Scattering results on both charged current (CC) and neutral current (NC) neutrino channels have been collected over many decades using a variety of targets, analysis techniques, and detector technologies. With the advent of intense neutrino sources for oscillation measurements, experiments are remeasuring these cross sections with a renewed appreciation for nuclear effects<sup>†</sup> and precise knowledge of their incoming neutrino fluxes. This review summarizes accelerator-based neutrino cross section measurements made in the  $\sim 0.1 - 300$  GeV range with an emphasis on inclusive, quasi-elastic, and single pion production processes (areas where we have the most experimental input at present). For a more comprehensive discussion of neutrino interaction cross sections, including neutrino-electron scattering and lower energy measurements, the reader is directed to a recent review of this subject [1].

by NuTeV [2] and at lower energies on argon by ArgoNeuT [3]. At high energy, the inclusive cross section is dominated by deep inelastic scattering (DIS). Several high energy neutrino experiments have measured the DIS cross sections for specific final states, for example opposite-sign dimuon production. The most recent dimuon cross section measurements include those from CHORUS [4], NOMAD [5], and NuTeV [6]. At lower neutrino energies, the inclusive cross section is largely a combination of quasi-elastic scattering and resonance production processes, two areas we will turn to next.

## 45.2. Quasi-elastic scattering

Historically, neutrino (or antineutrino) quasi-elastic scattering refers to the processes,  $\nu_\mu n \rightarrow \mu^- p$  and  $\bar{\nu}_\mu p \rightarrow \mu^+ n$ , where a charged lepton and single nucleon are ejected in the elastic interaction of a neutrino (or antineutrino) with a nucleon in the target material. This is the final state one would strictly observe, for example, in scattering off of a free nucleon target. QE scattering is important as it is the dominant neutrino interaction at energies less than about 1 GeV and is a large signal sample in many neutrino oscillation experiments.

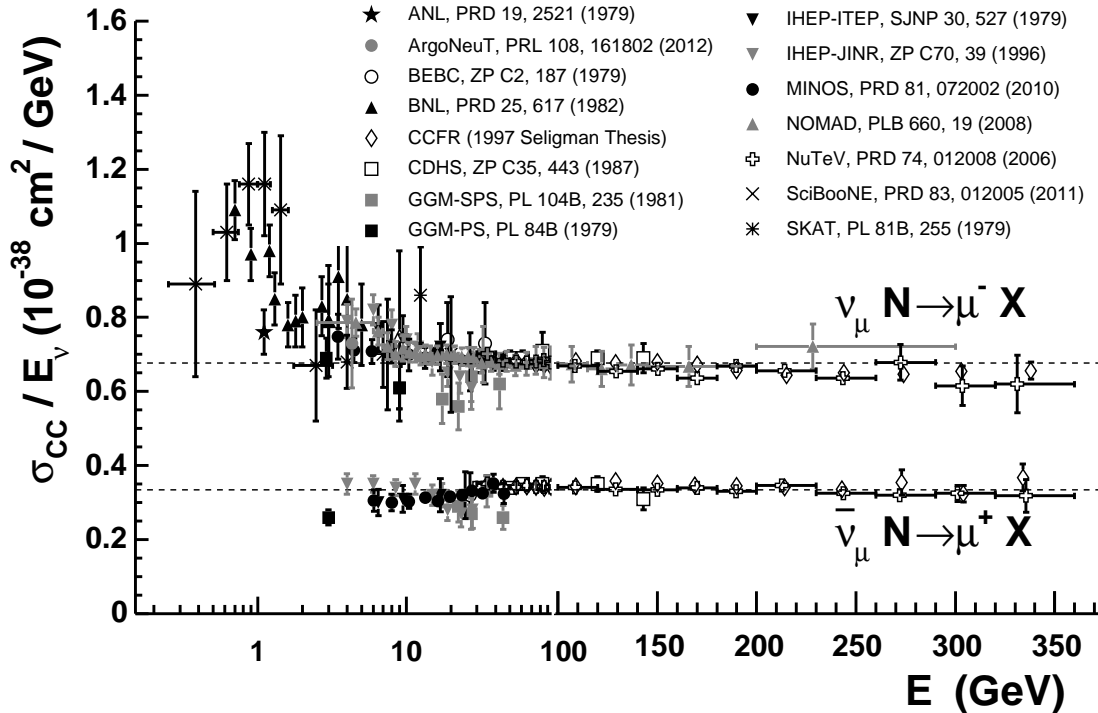


Fig. 45.1: Measurements of  $\nu_\mu$  and  $\bar{\nu}_\mu$  CC inclusive scattering cross sections divided by neutrino energy as a function of neutrino energy. Note the transition between logarithmic and linear scales occurring at 100 GeV. Neutrino-nucleon cross sections are typically twice as large as the corresponding antineutrino cross sections, though this difference can be larger at lower energies. NC cross sections (not shown) are generally smaller (but non-negligible) compared to their CC counterparts.

## 45.1. Inclusive Scattering

Over the years, many experiments have measured the total cross section for neutrino ( $\nu_\mu N \rightarrow \mu^- X$ ) and antineutrino ( $\bar{\nu}_\mu N \rightarrow \mu^+ X$ ) scattering off nucleons covering a broad range of energies (Fig. 45.1). As can be seen, the inclusive cross section approaches a linear dependence on neutrino energy. Such behavior is expected for point-like scattering of neutrinos from quarks, an assumption which breaks down at lower energies.

To provide a more complete picture, differential cross sections for such inclusive scattering processes have also been reported on iron

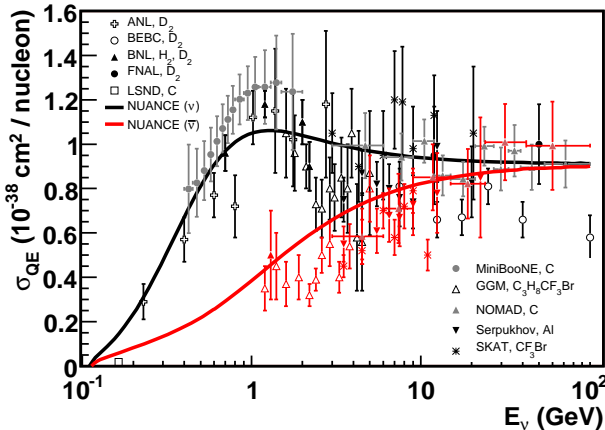
<sup>†</sup> Kinematic and final state effects which impact neutrino scattering off nuclei. Note that most modern neutrino experiments use nuclear targets to increase their event yields.

Fig. 45.2 displays the current status of existing measurements of  $\nu_\mu$  and  $\bar{\nu}_\mu$  QE scattering cross sections as a function of neutrino energy. In this plot, and all others in this review, the prediction from a representative neutrino event generator (NUANCE) [7] provides a theoretical comparator. Other generators and more sophisticated calculations exist which can give different predictions [8].

In many of these initial measurements of the neutrino QE cross section, bubble chamber experiments typically employed light targets ( $H_2$  or  $D_2$ ) and required both the detection of the final state muon and single nucleon<sup>‡</sup>; thus the final state was clear and elastic kinematic conditions could be verified. The situation is more complicated of course for heavier nuclear targets. In this case, nuclear effects can

<sup>‡</sup> In the case of  $D_2$ , many experiments additionally observed the spectator proton.

impact the size and shape of the cross section as well as the final state kinematics and topology. Due to intranuclear rescattering and the possible effects of correlations between target nucleons, additional nucleons may be ejected in the final state; hence, a QE interaction on a nuclear target does not always imply the ejection of a *single* nucleon. Thus, one needs to take some care in defining what one means by neutrino QE scattering when scattering off targets heavier than  $H_2$  or  $D_2$ . Adding to the complexity, recent measurements [9] of the  $\nu_\mu$  QE scattering cross section on carbon at low energy have observed a significantly larger than expected cross section, an enhancement believed to be signaling the presence of sizable nuclear effects. Such cross sections have also been reported for the first time in the form of double-differential distributions [9], thus reducing the model-dependence of the data and allowing a much more stringent test of the underlying nuclear theory. The impact of nuclear effects on neutrino QE scattering has been the subject of intense theoretical scrutiny over the past year [19] with potential implications on nucleon ejection [20], neutrino energy reconstruction [21], and the neutrino/antineutrino cross section ratio [22]. The reader is referred to a recent review of the situation in [23]. Additional measurements are clearly needed before a complete understanding is achieved. In addition to such CC investigations, measurements of the NC counterpart of this channel have also been performed. The most recent NC elastic scattering cross section measurements include those from BNL E734 [24] and MiniBooNE [25]. A number of measurements of the Cabibbo-suppressed antineutrino QE hyperon production cross section have additionally been reported [18,26], although none in recent years.



**Figure 45.2:** Measurements of  $\nu_\mu$  (black) and  $\bar{\nu}_\mu$  (red) quasi-elastic scattering cross sections (per nucleon) as a function of neutrino energy. Data on a variety of nuclear targets are shown, including measurements from ANL [10], BEBC [11], BNL [12], FNAL [13], Gargamelle [14], LSND [15], MiniBooNE [9], NOMAD [16], Serpukhov [17], and SKAT [18]. Also shown is the QE free nucleon scattering prediction [7] assuming  $M_A = 1.0$  GeV. This prediction is significantly altered by nuclear corrections in the case of neutrino-nucleus scattering. Care should be taken in interpreting measurements on targets heavier than deuterium.

### 45.3. Pion Production

In addition to such elastic processes, neutrinos can also inelastically scatter producing a nucleon excited state ( $\Delta$ ,  $N^*$ ). Such baryonic resonances quickly decay, most often to a nucleon and single pion final state. Fig. 45.3 and Fig. 45.4 show a collection of resonance single pion production cross section data for both CC and NC neutrino scattering. Decades ago, BEBC, FNAL, Gargamelle, and SKAT also performed similar measurements for antineutrinos [27]. Most often these experiments reported measurements of NC/CC single pion cross section ratios [28].

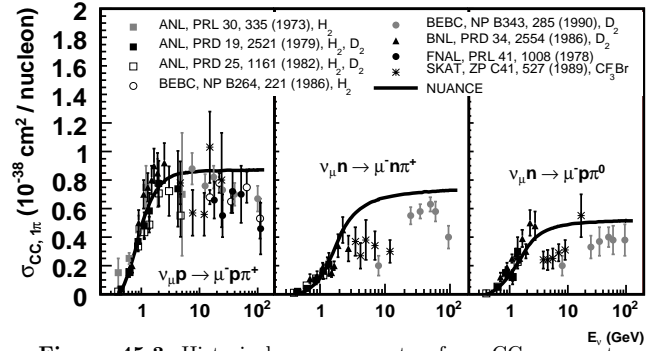


**Figure 45.3:** Historical measurements of  $\nu_\mu$  CC resonant single pion production. The data appear as reported by the experiments; no additional corrections have been applied to account for differing nuclear targets or invariant mass ranges. The free scattering prediction is from [7] with  $M_A = 1.1$  GeV. Note that other absolute measurements have been made by MiniBooNE [30] but cannot be directly compared with this historical data - the modern measurements are more inclusive and have quantified the production of pions leaving the target nucleus rather than specific  $\pi + N$  final states as identified at the neutrino interaction vertex.

It should be noted that baryonic resonances can also decay to multi-pion, other mesonic ( $K$ ,  $\eta$ ,  $\rho$ , etc.), and even photon final states. Experimental results for these channels are typically sparse or non-existent [1]; however, photon production processes can be an important background for  $\nu_\mu \rightarrow \nu_e$  appearance searches and thus have become the focus of some recent experimental investigations [29].

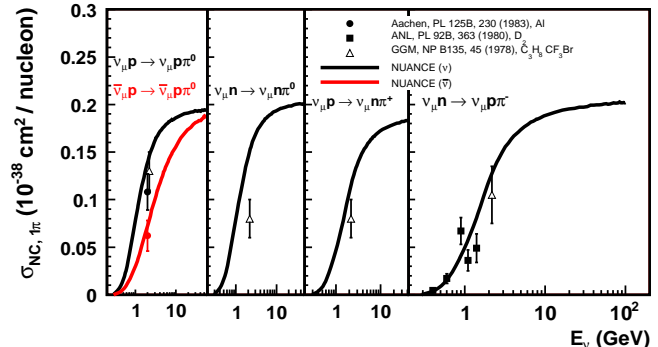


**Figure 45.4:** Same as Fig. 45.3 but for NC neutrino (black) and antineutrino (red) scattering. The Gargamelle measurements come from a re-analysis of this data [31]. Note that more recent absolute measurements exist [32] but cannot be directly compared with this data for the same reasons as in Fig. 45.3.

In addition to resonance production processes, neutrinos can also coherently scatter off of the entire nucleus and produce a distinctly forward-scattered single pion final state. Both CC ( $\nu_\mu A \rightarrow \mu^- A \pi^+$ ,  $\bar{\nu}_\mu A \rightarrow \mu^+ A \pi^-$ ) and NC ( $\nu_\mu A \rightarrow \nu_\mu A \pi^0$ ,  $\bar{\nu}_\mu A \rightarrow \bar{\nu}_\mu A \pi^0$ ) processes are possible in this case. The level of coherent pion production is predicted to be small compared to incoherent processes [33], but observations exist across a broad energy range and on multiple nuclear targets [34–36]. Most of these measurements have been performed at energies above 2 GeV, but several modern experiments have started to search for coherent pion production at lower neutrino energies, including K2K [37], MiniBooNE [38], and SciBooNE [39].

As with QE scattering, a new appreciation for the significance of nuclear effects has surfaced in pion production channels, again due to the use of heavy targets in modern neutrino experiments. Many experiments have been careful to report cross sections for various detected final states, thereby not correcting for large and uncertain nuclear effects (e.g., pion rescattering, charge exchange, and absorption) which can introduce unwanted sources of uncertainty and

model dependence. Recent measurements of single pion cross sections, as published by K2K [40], MiniBooNE [41], and SciBooNE [42], take the form of ratios with respect to QE or CC inclusive scattering samples. Providing the most comprehensive survey of neutrino single pion production to date, MiniBooNE has recently published a total of 16 single- and double-differential cross sections for both the final state muon (in the case of CC scattering) and pion in these interactions; thus, providing the first measurements of these distributions [30,32]. Regardless of the interaction channel, such differential cross section measurements (in terms of observed final state particle kinematics) are now preferred for their reduced model dependence and for the additional kinematic information they provide. Such a new direction has been the focus of modern measurements as opposed to the reporting of (model-dependent) cross sections as a function of neutrino energy. Together with similar results for other interaction channels, a better understanding and modeling of nuclear effects will be possible moving forward.

#### 45.4. Outlook

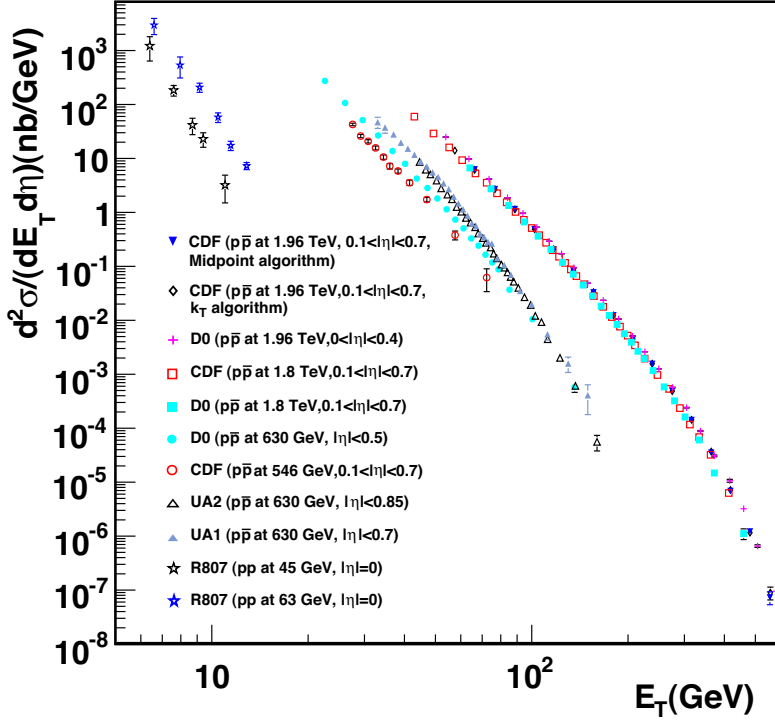
Coming soon, additional neutrino and antineutrino cross section measurements in the few-GeV energy range are anticipated from ArgoNeuT, MiniBooNE, MINOS, NOMAD, and SciBooNE. In addition, a few new experiments are now collecting data or will soon be commissioning their detectors. Analysis of a broad energy range of data on a variety of targets in the MINER $\nu$ A experiment will provide the most detailed analysis yet of nuclear effects in neutrino interactions. Data from ICARUS and MicroBooNE will probe deeper into complex neutrino final states using the superior capabilities of liquid argon time projection chambers, while the T2K and NO $\nu$ A near detectors will collect high statistics samples in intense neutrino beams. Together, these investigations should significantly advance our understanding of neutrino-nucleus scattering in the years to come.

#### References:

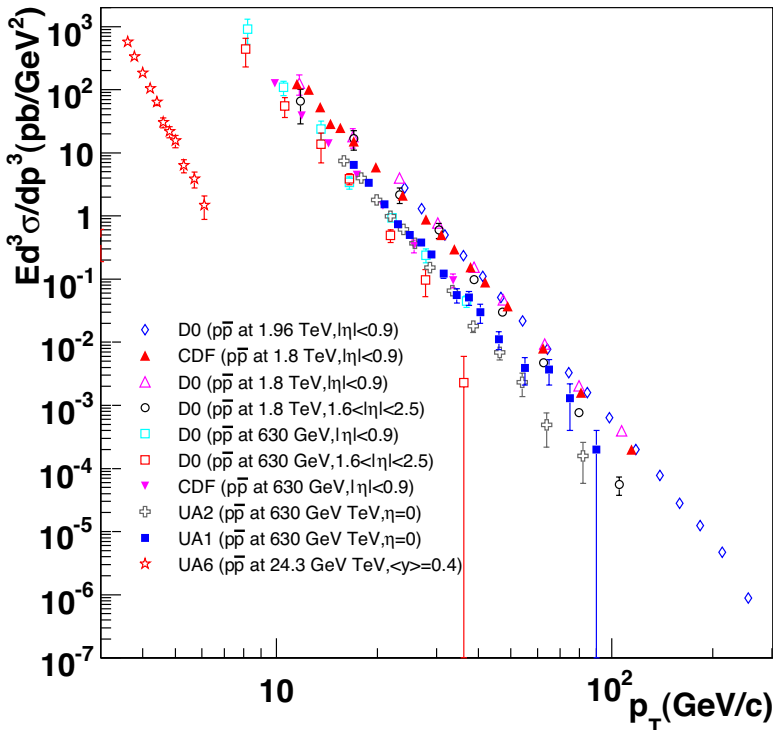
- J.A. Formaggio and G.P. Zeller, "From eV to EeV: Neutrino Cross Sections Across Energy Scales", to be published in *Rev. Mod. Phys.* (2012).
- M. Tzanov *et al.*, *Phys. Rev.* **D74**, 012008 (2006).
- C. Anderson *et al.*, *Phys. Rev. Lett.* **108**, 161802 (2012).
- A. Kayis-Topaksu *et al.*, *Nucl. Phys.* **B798**, 1 (2008).
- P. Astier *et al.*, *Phys. Lett.* **B486**, 35 (2000).
- D. Mason *et al.*, *Phys. Rev. Lett.* **99**, 192001 (2007).
- D. Casper, *Nucl. Phys. (Proc. Supp.)* **112**, 161 (2002), default v3 NUANCE.
- R. Tacik, *AIP Conf. Proc.* **1405**, 229 (2011); S. Boyd *et al.*, *AIP Conf. Proc.* **1189**, 60 (2009).
- A.A. Aguilar-Arevalo *et al.*, *Phys. Rev.* **D81**, 092005 (2010).
- S.J. Barish *et al.*, *Phys. Rev.* **D16**, 3103 (1977).
- D. Allasia *et al.*, *Nucl. Phys.* **B343**, 285 (1990).
- N.J. Baker *et al.*, *Phys. Rev.* **D23**, 2499 (1981); G. Fanourakis *et al.*, *Phys. Rev.* **D21**, 562 (1980).
- T. Kitagaki *et al.*, *Phys. Rev.* **D28**, 436 (1983).
- S. Bonetti *et al.*, *Nuovo Cimento* **A38**, 260 (1977); N. Armenise *et al.*, *Nucl. Phys.* **B152**, 365 (1979).
- L.B. Auerbach *et al.*, *Phys. Rev.* **C66**, 015501 (2002).
- V. Lyubushkin *et al.*, *Eur. Phys. J.* **C63**, 355 (2009).
- S.V. Belikov *et al.*, *Z. Phys.* **A320**, 625 (1985).
- J. Brunner *et al.*, *Z. Phys.* **C45**, 551 (1990).
- U. Mosel, [arXiv:1111.1732](https://arxiv.org/abs/1111.1732) [nucl-th]; M. Martini *et al.*, [arXiv:1110.0221](https://arxiv.org/abs/1110.0221) [nucl-th]; J.T. Sobczyk, [arXiv:1109.1081](https://arxiv.org/abs/1109.1081) [hep-ex]; A. Meucci *et al.*, *Phys. Rev. Lett.* **107**, 172501 (2011); J.E. Amaro *et al.*, *Phys. Rev.* **D84**, 033004 (2011); A. Meucci *et al.*, *Phys. Rev.* **C83**, 064614 (2011); A. Ankowski *et al.*, *Phys. Rev.* **C83**, 054616 (2011); E. Fernandez-Martinez *et al.*, *Phys. Rev.* **B697**, 477 (2011); J.E. Amaro *et al.*, *Phys. Lett.* **B696**, 151 (2011).
- J.T. Sobczyk, [arXiv:1201.3673](https://arxiv.org/abs/1201.3673) [hep-ph].
- J. Nieves *et al.*, [arXiv:1204.5404](https://arxiv.org/abs/1204.5404) [hep-ph]; O. Lalakulich *et al.*, [arXiv:1203.2935](https://arxiv.org/abs/1203.2935) [nucl-th]; M. Martini *et al.*, [arXiv:1202.4745](https://arxiv.org/abs/1202.4745) [hep-ph]; J. Nieves *et al.*, *Phys. Lett.* **B707**, 72 (2012); T. Lietner and U. Mosel, *Phys. Rev.* **C81**, 064614 (2010); A.V. Butkevich, *Phys. Rev.* **C78**, 015501 (2008).
- J.E. Amaro *et al.*, [arXiv:1112.2123](https://arxiv.org/abs/1112.2123) [nucl-th]; A. Bodek *et al.*, *Eur. Phys. J.* **C71**, 1726 (2011); J. Nieves *et al.*, [arXiv:1102.2777](https://arxiv.org/abs/1102.2777) [hep-ph]; M. Martini *et al.*, *Phys. Rev.* **C81**, 045502 (2010).
- H. Gallagher, G. Garvey, and G.P. Zeller, *Ann. Rev. Nucl. and Part. Sci.* **61**, 355 (2011).
- L.A. Ahrens *et al.*, *Phys. Rev.* **D35**, 785 (1987).
- A.A. Aguilar-Arevalo *et al.*, *Phys. Rev.* **D82**, 092005 (2010).
- V.V. Ammosov *et al.*, *Z. Phys.* **C36**, 377 (1987); O. Erriques *et al.*, *Phys. Lett.* **70B**, 383 (1977); T. Eichten *et al.*, *Phys. Lett.* **40B**, 593 (1972).
- D. Allasia *et al.*, *Nucl. Phys.* **B343**, 285 (1990); H.J. Grabosch *et al.*, *Z. Phys.* **C41**, 527 (1989); G.T. Jones *et al.*, *Z. Phys.* **C43**, 527 (1998); P. Allen *et al.*, *Nucl. Phys.* **B264**, 221 (1986); S.J. Barish *et al.*, *Phys. Lett.* **B91**, 161 (1980); T. Bolognese *et al.*, *Phys. Lett.* **B81**, 393 (1979).
- M. Derrick *et al.*, *Phys. Rev.* **D23**, 569 (1981); W. Krenz *et al.*, *Nucl. Phys.* **B135**, 45 (1978); W. Lee *et al.*, *Phys. Rev. Lett.* **38**, 202 (1977); S.J. Barish *et al.*, *Phys. Rev. Lett.* **33**, 448 (1974).
- C.T. Kullenberg *et al.*, *Phys. Lett.* **B706**, 268 (2012).
- A.A. Aguilar-Arevalo *et al.*, *Phys. Rev.* **D83**, 052009 (2011); A.A. Aguilar-Arevalo *et al.*, *Phys. Rev.* **D83**, 052007 (2011).
- E. Hawker, *Proceedings of the 2nd International Workshop on Neutrino-Nucleus Interactions in the Few-GeV Region*, Irvine, CA, 2002, unpublished, <http://www.ps.uci.edu/nuint/proceedings/hawker.pdf>.
- A.A. Aguilar-Arevalo *et al.*, *Phys. Rev.* **D81**, 013005 (2010).
- L. Alvarez-Ruso, *AIP Conf. Proc.* **1405**, 140 (2011).
- for a compilation of historical data, see P. Villain *et al.*, *Phys. Lett.* **B313**, 267 (1993).
- D. Cherdack, *AIP Conf. Proc.* **1405**, 115 (2011).
- C.T. Kullenberg *et al.*, *Phys. Lett.* **B682**, 177 (2009).
- M. Hasegawa *et al.*, *Phys. Rev. Lett.* **95**, 252301 (2005).
- A.A. Aguilar-Arevalo *et al.*, *Phys. Lett.* **B664**, 41 (2008).
- Y. Kurimoto *et al.*, *Phys. Rev.* **D81**, 111102 (R) (2010); K. Hiraide *et al.*, *Phys. Rev.* **D78**, 112004 (2008).
- C. Mariani *et al.*, *Phys. Rev.* **D83**, 054023 (2011); A. Rodriguez *et al.*, *Phys. Rev.* **D78**, 032003 (2008); S. Nakayama *et al.*, *Phys. Lett.* **B619**, 255 (2005).
- A.A. Aguilar-Arevalo *et al.*, *Phys. Rev. Lett.* **103**, 081801 (2009).
- Y. Kurimoto *et al.*, *Phys. Rev.* **D81**, 033004 (2010).

## 46. PLOTS OF CROSS SECTIONS AND RELATED QUANTITIES

(For neutrino plots, see review article "Neutrino Cross Section Measurements" by G.P. Zeller in this edition of RPP)

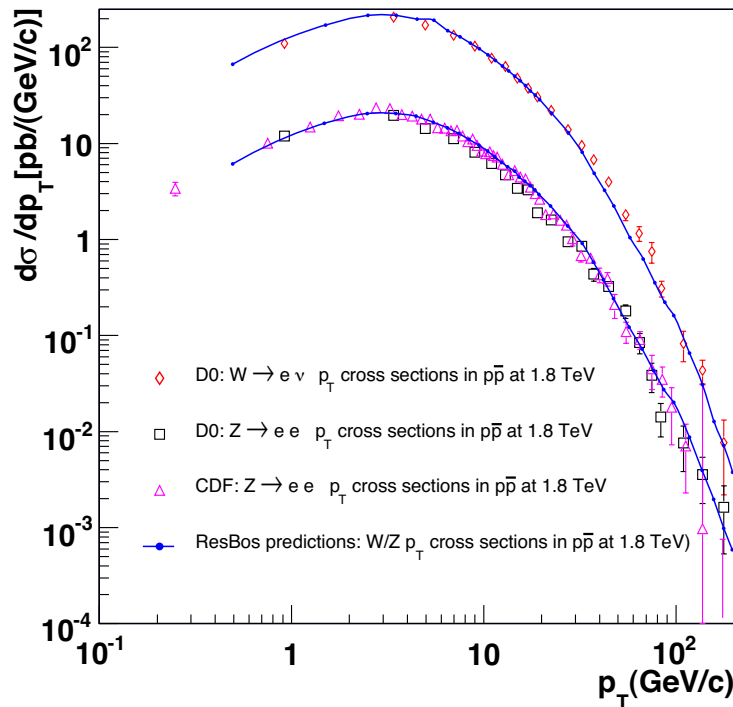
Jet Production in  $pp$  and  $\bar{p}p$  Interactions

**Figure 46.1:** Inclusive differential jet cross sections plotted as a function of the jet transverse energy. The CDF and D0 measurements use a cone algorithm of radius 0.7 for all results shown except for the CDF measurements at 1.96 TeV which also use  $k_T$  with a D parameter of 0.7 and midpoint algorithms. The cone/ $k_T$  results should be similar if  $R_{cone} = D$ . UA1 (UA2) uses a non-iterative cone algorithm with a radius of 1.0 (1.3). Recent NLO QCD predictions (such as CTEQ6M) provide a good description of the CDF and D0 jet cross sections, Rept. on Prog. in Phys. **70**, 89 (2007). Comparisons with the older cross sections are more difficult due to the nature of the jet algorithms used. CDF: Phys. Rev. **D75**, 092006 (2007), Phys. Rev. **D64**, 032001 (2001), Phys. Rev. Lett. **70**, 1376 (1993); D0: Phys. Rev. **D64**, 032003 (2001); UA2: Phys. Lett. **B257**, 232 (1991); UA1: Phys. Lett. **B172**, 461 (1986); R807: Phys. Lett. **B123**, 133 (1983). (Courtesy of J. Huston, Michigan State University, 2010.)

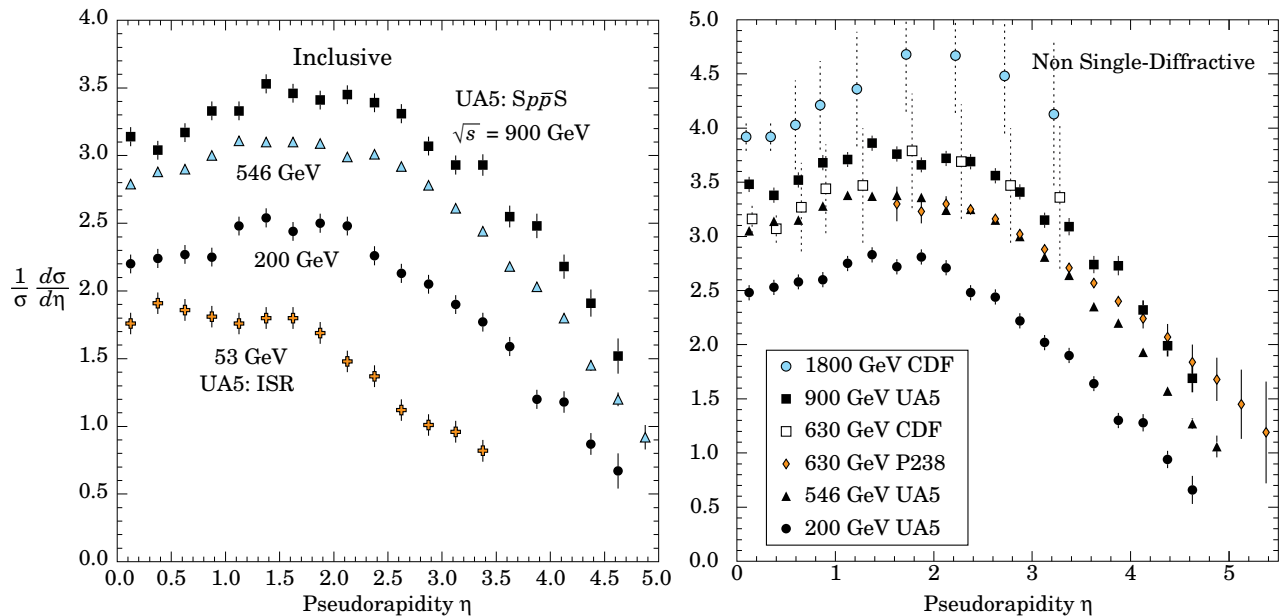
Direct  $\gamma$  Production in  $\bar{p}p$  Interactions

**Figure 46.2:** Isolated photon cross sections plotted as a function of the photon transverse momentum. The errors are either statistical only (CDF, D0 (1.96 TeV), UA1, UA2, UA6) or uncorrelated (D0 1.8 TeV, 630 GeV). The data are generally in good agreement with NLO QCD predictions, albeit with a tendency for the data to be above (below) the theory for lower (large) transverse momenta, Phys. Rev. **D59**, 074007 (1999). D0: Phys. Lett. **B639**, 151 (2006), Phys. Rev. Lett. **87**, 251805 (2001); CDF: Phys. Rev. **D65**, 112003 (2002); UA6: Phys. Lett. **B206**, 163 (1988); UA1: Phys. Lett. **B209**, 385 (1988); UA2: Phys. Lett. **B288**, 386 (1992). (Courtesy of J. Huston, Michigan State University, 2007.)

## Differential Cross Section for W and Z Boson Production



**Figure 46.3:** Differential cross sections for W and Z production shown as a function of the boson transverse momentum. The D0 results include only the statistical error while the CDF results include all errors except for the 3.9% integrated luminosity error. The results are in good agreement with theoretical predictions that include both the effects of NLO corrections and of  $q_T$  resummation, such as the ResBos (Phys. Rev. **D67**, 073016 (2003)) predictions indicated on the plot. **D0:** Phys. Lett. **B513**, 292 (2001), Phys. Rev. Lett. **84**, 2792 (2000). **CDF:** Phys. Rev. Lett. **84**, 845 (2000). (Courtesy of J. Huston, Michigan State University, 2007)

Pseudorapidity Distributions in  $\bar{p}p$  Interactions

**Figure 46.4:** Charged particle pseudorapidity distributions in  $\bar{p}p$  collisions for  $53 \text{ GeV} \leq \sqrt{s} \leq 1800 \text{ GeV}$ . UA5 data from the  $S\bar{p}pS$  are taken from G.J. Alner *et al.*, Z. Phys. **C33**, 1 (1986), and from the ISR from K. Alpgöard *et al.*, Phys. Lett. **112B**, 193 (1982). The UA5 data are shown for both the full inelastic cross section and with singly diffractive events excluded. Additional non single-diffractive measurements are available from CDF at the Tevatron, F. Abe *et al.*, Phys. Rev. **D41**, 2330 (1990) and Experiment P238 at the  $S\bar{p}pS$ , R. Harr *et al.*, Phys. Lett. **B401**, 176 (1997). (Courtesy of D.R. Ward, Cambridge Univ., 1999)

Average Hadron Multiplicities in Hadronic  $e^+e^-$  Annihilation Events

**Table 46.1:** Average hadron multiplicities per hadronic  $e^+e^-$  annihilation event at  $\sqrt{s} \approx 10, 29\text{--}35, 91,$  and  $130\text{--}200$  GeV. The rates given include decay products from resonances with  $c\tau < 10$  cm, and include the corresponding anti-particle state. Correlations of the systematic uncertainties were considered for the calculation of the averages. (Updated May 2010 by O. Biebel, LMU, Munich)

Particle	$\sqrt{s} \approx 10$ GeV	$\sqrt{s} = 29\text{--}35$ GeV	$\sqrt{s} = 91$ GeV	$\sqrt{s} = 130\text{--}200$ GeV
<b>Pseudoscalar mesons:</b>				
$\pi^+$	$6.6 \pm 0.2$	$10.3 \pm 0.4$	$17.02 \pm 0.19$	$21.24 \pm 0.39$
$\pi^0$	$3.2 \pm 0.3$	$5.83 \pm 0.28$	$9.42 \pm 0.32$	
$K^+$	$0.90 \pm 0.04$	$1.48 \pm 0.09$	$2.228 \pm 0.059$	$2.82 \pm 0.19$
$K^0$	$0.91 \pm 0.05$	$1.48 \pm 0.07$	$2.049 \pm 0.026$	$2.10 \pm 0.12$
$\eta$	$0.20 \pm 0.04$	$0.61 \pm 0.07$	$1.049 \pm 0.080$	
$\eta(958)$	$0.03 \pm 0.01$	$0.26 \pm 0.10$	$0.152 \pm 0.020$	
$D^+$	$0.194 \pm 0.019^{(a)}$	$0.17 \pm 0.03$	$0.175 \pm 0.016$	
$D^0$	$0.446 \pm 0.032^{(a)}$	$0.45 \pm 0.07$	$0.454 \pm 0.030$	
$D_s^+$	$0.063 \pm 0.014^{(a)}$	$0.45 \pm 0.20^{(b)}$	$0.131 \pm 0.021$	
$B^{(c)}$	—	—	$0.165 \pm 0.026^{(d)}$	
$B^+$	—	—	$0.178 \pm 0.006^{(d)}$	
$B_s^0$	—	—	$0.057 \pm 0.013^{(d)}$	
<b>Scalar mesons:</b>				
$f_0(980)$	$0.024 \pm 0.006$	$0.05 \pm 0.02^{(e)}$	$0.146 \pm 0.012$	
$a_0(980)^\pm$	—	—	$0.27 \pm 0.11^{(f)}$	
<b>Vector mesons:</b>				
$\rho(770)^0$	$0.35 \pm 0.04$	$0.81 \pm 0.08$	$1.231 \pm 0.098$	
$\rho(770)^\pm$	—	—	$2.40 \pm 0.43^{(f)}$	
$\omega(782)$	$0.30 \pm 0.08$	—	$1.016 \pm 0.065$	
$K^*(892)^+$	$0.27 \pm 0.03$	$0.64 \pm 0.05$	$0.715 \pm 0.059$	
$K^*(892)^0$	$0.29 \pm 0.03$	$0.56 \pm 0.06$	$0.738 \pm 0.024$	
$\phi(1020)$	$0.044 \pm 0.003$	$0.085 \pm 0.011$	$0.0963 \pm 0.0032$	
$D^*(2010)^+$	$0.177 \pm 0.022^{(a)}$	$0.43 \pm 0.07$	$0.1937 \pm 0.0057^{(g)}$	
$D^*(2007)^0$	$0.168 \pm 0.019^{(a)}$	$0.27 \pm 0.11$	—	
$D_s^*(2112)^+$	$0.048 \pm 0.014^{(a)}$	—	$0.101 \pm 0.048^{(h)}$	
$B^* (i)$	—	—	$0.288 \pm 0.026$	
$J/\psi(1S)$	$0.00050 \pm 0.00005^{(a)}$	—	$0.0052 \pm 0.0004^{(j)}$	
$\psi(2S)$	—	—	$0.0023 \pm 0.0004^{(j)}$	
$\Upsilon(1S)$	—	—	$0.00014 \pm 0.00007^{(j)}$	
<b>Pseudovector mesons:</b>				
$f_1(1285)$	—	—	$0.165 \pm 0.051$	
$f_1(1420)$	—	—	$0.056 \pm 0.012$	
$\chi_{c1}(3510)$	—	—	$0.0041 \pm 0.0011^{(j)}$	
<b>Tensor mesons:</b>				
$f_2(1270)$	$0.09 \pm 0.02$	$0.14 \pm 0.04$	$0.166 \pm 0.020$	
$f_2'(1525)$	—	—	$0.012 \pm 0.006$	
$K_2^*(1430)^+$	—	$0.09 \pm 0.03$	—	
$K_2^*(1430)^0$	—	$0.12 \pm 0.06$	$0.084 \pm 0.022$	
$B^{** (k)}$	—	—	$0.118 \pm 0.024$	
$D_{s1}^\pm$	—	—	$0.0052 \pm 0.0011^{(\ell)}$	
$D_{s2}^{*\pm}$	—	—	$0.0083 \pm 0.0031^{(\ell)}$	
<b>Baryons:</b>				
$p$	$0.253 \pm 0.016$	$0.640 \pm 0.050$	$1.050 \pm 0.032$	$1.41 \pm 0.18$
$\Lambda$	$0.080 \pm 0.007$	$0.205 \pm 0.010$	$0.3915 \pm 0.0065$	$0.39 \pm 0.03$
$\Sigma^0$	$0.023 \pm 0.008$	—	$0.076 \pm 0.011$	
$\Sigma^-$	—	—	$0.081 \pm 0.010$	
$\Sigma^+$	—	—	$0.107 \pm 0.011$	
$\Sigma^\pm$	—	—	$0.174 \pm 0.009$	
$\Xi^-$	$0.0059 \pm 0.0007$	$0.0176 \pm 0.0027$	$0.0258 \pm 0.0010$	
$\Delta(1232)^{++}$	$0.040 \pm 0.010$	—	$0.085 \pm 0.014$	
$\Sigma(1385)^-$	$0.006 \pm 0.002$	$0.017 \pm 0.004$	$0.0240 \pm 0.0017$	
$\Sigma(1385)^+$	$0.005 \pm 0.001$	$0.017 \pm 0.004$	$0.0239 \pm 0.0015$	
$\Sigma(1385)^\pm$	$0.0106 \pm 0.0020$	$0.033 \pm 0.008$	$0.0462 \pm 0.0028$	
$\Xi(1530)^0$	$0.0015 \pm 0.0006$	—	$0.0068 \pm 0.0006$	
$\Omega^-$	$0.0007 \pm 0.0004$	$0.014 \pm 0.007$	$0.0016 \pm 0.0003$	
$\Lambda_c^+$	$0.074 \pm 0.031^{(m)}$	$0.110 \pm 0.050$	$0.078 \pm 0.017$	
$\Lambda_b^0$	—	—	$0.031 \pm 0.016$	
$\Sigma_c^{++}, \Sigma_c^0$	$0.014 \pm 0.007$	—	—	
$\Lambda(1520)$	$0.008 \pm 0.002$	—	$0.0222 \pm 0.0027$	

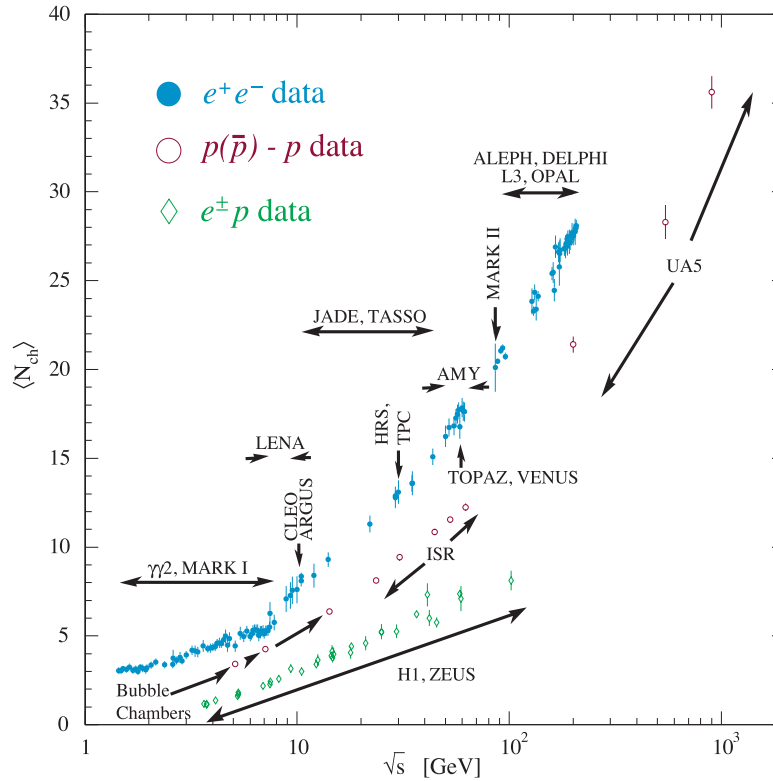
## Notes for Table 46.1:

- (a)  $\sigma_{\text{had}} = 3.33 \pm 0.05 \pm 0.21$  nb (CLEO: Phys. Rev. **D29**, 1254 (1984)) has been used in converting the measured cross sections to average hadron multiplicities.
- (b)  $B(D_s \rightarrow \eta\pi, \eta'\pi)$  was used (RPP 1994).
- (c) Comprises both charged and neutral  $B$  meson states.
- (d) The Standard Model  $B(Z \rightarrow b\bar{b}) = 0.217$  was used.
- (e)  $x_p = p/p_{\text{beam}} > 0.1$  only.
- (f) Both charge states.
- (g)  $B(D^*(2010)^+ \rightarrow D^0\pi^+) \times B(D^0 \rightarrow K^-\pi^+)$  has been used (RPP 2000).
- (h)  $B(D_s^* \rightarrow D_s^+\gamma)$ ,  $B(D_s^+ \rightarrow \phi\pi^+)$ ,  $B(\phi \rightarrow K^+K^-)$  have been used (RPP 1998).
- (i) Any charge state (i.e.,  $B_d^*$ ,  $B_u^*$ , or  $B_s^*$ ).
- (j)  $B(Z \rightarrow \text{hadrons}) = 0.699$  was used (RPP 1994).
- (k) Any charge state (i.e.,  $B_d^{**}$ ,  $B_u^{**}$ , or  $B_s^{**}$ ).
- (l) Assumes  $B(D_{s1}^+ \rightarrow D^{*+}K^0 + D^{*0}K^+) = 100\%$  and  $B(D_{s2}^+ \rightarrow D^0K^+) = 45\%$ .
- (m) The value was derived from the cross section of  $\Lambda_c^+ \rightarrow p\pi K$  using (a) and assuming the branching fraction to be  $(5.0 \pm 1.3)\%$  (RPP 2004).

## References for Table 46.1:

- RPP 1992: Phys. Rev. **D45** (1992) and references therein.
- RPP 1994: Phys. Rev. **D50**, 1173 (1994) and references therein.
- RPP 1996: Phys. Rev. **D54**, 1 (1996) and references therein.
- RPP 1998: Eur. Phys. J. **C3**, 1 (1998) and references therein.
- RPP 2000: Eur. Phys. J. **C15**, 1 (2000) and references therein.
- RPP 2002: Phys. Rev. **D66**, 010001 (2002) and references therein.
- RPP 2004: Phys. Lett. **B592**, 1 (2004) and references therein.
- RPP 2006: J. Phys. **G33**, 1 (2006) and references therein.
- RPP 2008: Phys. Lett. **B667**, 1 (2008) and references therein.
- R. Marshall, Rept. on Prog. in Phys. **52**, 1329 (1989). A. De Angelis, J. Phys. **G19**, 1233 (1993) and references therein.
- ALEPH: D. Buskulic *et al.*: Phys. Lett. **B295**, 396 (1992); Z. Phys. **C64**, 361 (1994); **C69**, 15 (1996); **C69**, 379 (1996); **C73**, 409 (1997); and R. Barate *et al.*: Z. Phys. **C74**, 451 (1997); Phys. Reports **294**, 1 (1998); Eur. Phys. J. **C5**, 205 (1998); **C16**, 597 (2000); **C16**, 613 (2000); and A. Heister *et al.*: Phys. Lett. **B526**, 34 (2002); **B528**, 19 (2002).
- ARGUS: H. Albrecht *et al.*: Phys. Lett. **230B**, 169 (1989); Z. Phys. **C44**, 547 (1989); **C46**, 15 (1990); **C54**, 1 (1992); **C58**, 199 (1993); **C61**, 1 (1994); Phys. Rep. **276**, 223 (1996).
- BaBar: B. Aubert *et al.*: Phys. Rev. Lett. **87**, 162002 (2001); Phys. Rev. **D65**, 091104 (2002).
- Belle: K. Abe *et al.*, Phys. Rev. Lett. **88**, 052001 (2002); and R. Seuster *et al.*, Phys. Rev. **D73**, 032002 (2006).
- CELLO: H.J. Behrend *et al.*: Z. Phys. **C46**, 397 (1990); **C47**, 1 (1990).
- CLEO: D. Bortoletto *et al.*, Phys. Rev. **D37**, 1719 (1988); erratum *ibid.* **D39**, 1471 (1989); and M. Artuso *et al.*, Phys. Rev. **D70**, 112001 (2004).
- Crystal Ball: Ch. Bieler *et al.*, Z. Phys. **C49**, 225 (1991).
- DELPHI: P. Abreu *et al.*: Z. Phys. **C57**, 181 (1993); **C59**, 533 (1993); **C61**, 407 (1994); **C65**, 587 (1995); **C67**, 543 (1995); **C68**, 353 (1995); **C73**, 61 (1996); Nucl. Phys. **B444**, 3 (1995); Phys. Lett. **B341**, 109 (1994); **B345**, 598 (1995); **B361**, 207 (1995); **B372**, 172 (1996); **B379**, 309 (1996); **B416**, 233 (1998); **B449**, 364 (1999); **B475**, 429 (2000); Eur. Phys. J. **C6**, 19 (1999); **C5**, 585 (1998); **C18**, 203 (2000); and J. Abdallah *et al.*, Phys. Lett. **B569**, 129 (2003); Phys. Lett. **B576**, 29 (2003); Eur. Phys. J. **C44**, 299 (2005); and W. Adam *et al.*: Z. Phys. **C69**, 561 (1996); **C70**, 371 (1996).
- HRS: S. Abachi *et al.*, Phys. Rev. Lett. **57**, 1990 (1986); and M. Derrick *et al.*, Phys. Rev. **D35**, 2639 (1987).
- L3: M. Acciarri *et al.*: Phys. Lett. **B328**, 223 (1994); **B345**, 589 (1995); **B371**, 126 (1996); **B371**, 137 (1996); **B393**, 465 (1997); **B404**, 390 (1997); **B407**, 351 (1997); **B407**, 389 (1997), erratum *ibid.* **B427**, 409 (1998); **B453**, 94 (1999); **B479**, 79 (2000).
- MARK II: H. Schellman *et al.*, Phys. Rev. **D31**, 3013 (1985); and G. Wormser *et al.*, Phys. Rev. Lett. **61**, 1057 (1988).
- JADE: W. Bartel *et al.*, Z. Phys. **C20**, 187 (1983); and D.D. Pietzl *et al.*, Z. Phys. **C46**, 1 (1990).
- OPAL: R. Akers *et al.*: Z. Phys. **C63**, 181 (1994); **C66**, 555 (1995); **C67**, 389 (1995); **C68**, 1 (1995); and G. Alexander *et al.*: Phys. Lett. **B358**, 162 (1995); Z. Phys. **C70**, 197 (1996); **C72**, 1 (1996); **C72**, 191 (1996); **C73**, 569 (1997); **C73**, 587 (1997); Phys. Lett. **B370**, 185 (1996); and K. Ackerstaff *et al.*: Z. Phys. **C75**, 192 (1997); Phys. Lett. **B412**, 210 (1997); Eur. Phys. J. **C1**, 439 (1998); **C4**, 19 (1998); **C5**, 1 (1998); **C5**, 411 (1998); and G. Abbiendi *et al.*: Eur. Phys. J. **C16**, 185 (2000); **C17**, 373 (2000).
- PLUTO: Ch. Berger *et al.*, Phys. Lett. **104B**, 79 (1981).
- SLD: K. Abe, Phys. Rev. **D59**, 052001 (1999); Phys. Rev. **D69**, 072003 (2004).
- TASSO: H. Aihara *et al.*, Z. Phys. **C27**, 27 (1985).
- TPC: H. Aihara *et al.*, Phys. Rev. Lett. **53**, 2378 (1984).



Average  $e^+e^-$ ,  $pp$ , and  $p\bar{p}$  Multiplicity

**Figure 46.5:** Average multiplicity as a function of  $\sqrt{s}$  for  $e^+e^-$  and  $p\bar{p}$  annihilations, and  $pp$  and  $ep$  collisions. The indicated errors are statistical and systematic errors added in quadrature, except when no systematic errors are given. Files of the data shown in this figure are given in <http://pdg.lbl.gov/current/avg-multiplicity/>.

$e^+e^-$ : Most  $e^+e^-$  measurements include contributions from  $K_S^0$  and  $\Lambda$  decays. The  $\gamma\gamma 2$  and MARK I measurements contain a systematic 5% error. Points at identical energies have been spread horizontally for clarity:

**ALEPH:** D. Buskulic *et al.*, Z. Phys. **C69**, 15 (1995); and Z. Phys. **C73**, 409 (1997);  
A. Heister *et al.*, Eur. Phys. J. **C35**, 457 (2004).

**ARGUS:** H. Albrecht *et al.*, Z. Phys. **C54**, 13 (1992).

**DELPHI:** P. Abreu *et al.*, Eur. Phys. J. **C6**, 19 (1999); Phys. Lett. **B372**, 172 (1996); Phys. Lett. **B416**, 233 (1998); and Eur. Phys. J. **C18**, 203 (2000).

**L3:** M. Acciarri *et al.*, Phys. Lett. **B371**, 137 (1996); Phys. Lett. **B404**, 390 (1997); and Phys. Lett. **B444**, 569 (1998);  
P. Achard *et al.*, Phys. Reports **339**, 71 (2004).

**OPAL:** G. Abbiendi *et al.*, Eur. Phys. J. **C16**, 185 (2000); and Eur. Phys. J. **C37**, 25 (2004);  
K. Ackerstaff *et al.*, Z. Phys. **C75**, 193 (1997);  
P.D. Acton *et al.*, Z. Phys. **C53**, 539 (1992) and references therein;  
R. Akers *et al.*, Z. Phys. **C68**, 203 (1995).

**TOPAZ:** K. Nakabayashi *et al.*, Phys. Lett. **B413**, 447 (1997).

**VENUS:** K. Okabe *et al.*, Phys. Lett. **B423**, 407 (1998).

$e^\pm p$ : Multiplicities have been measured in the current fragmentation region of the Breit frame:

**H1:** C. Adloff *et al.*, Nucl. Phys. **B504**, 3 (1997); F.D. Aaron *et al.*, Phys. Lett. **B654**, 148 (2007).

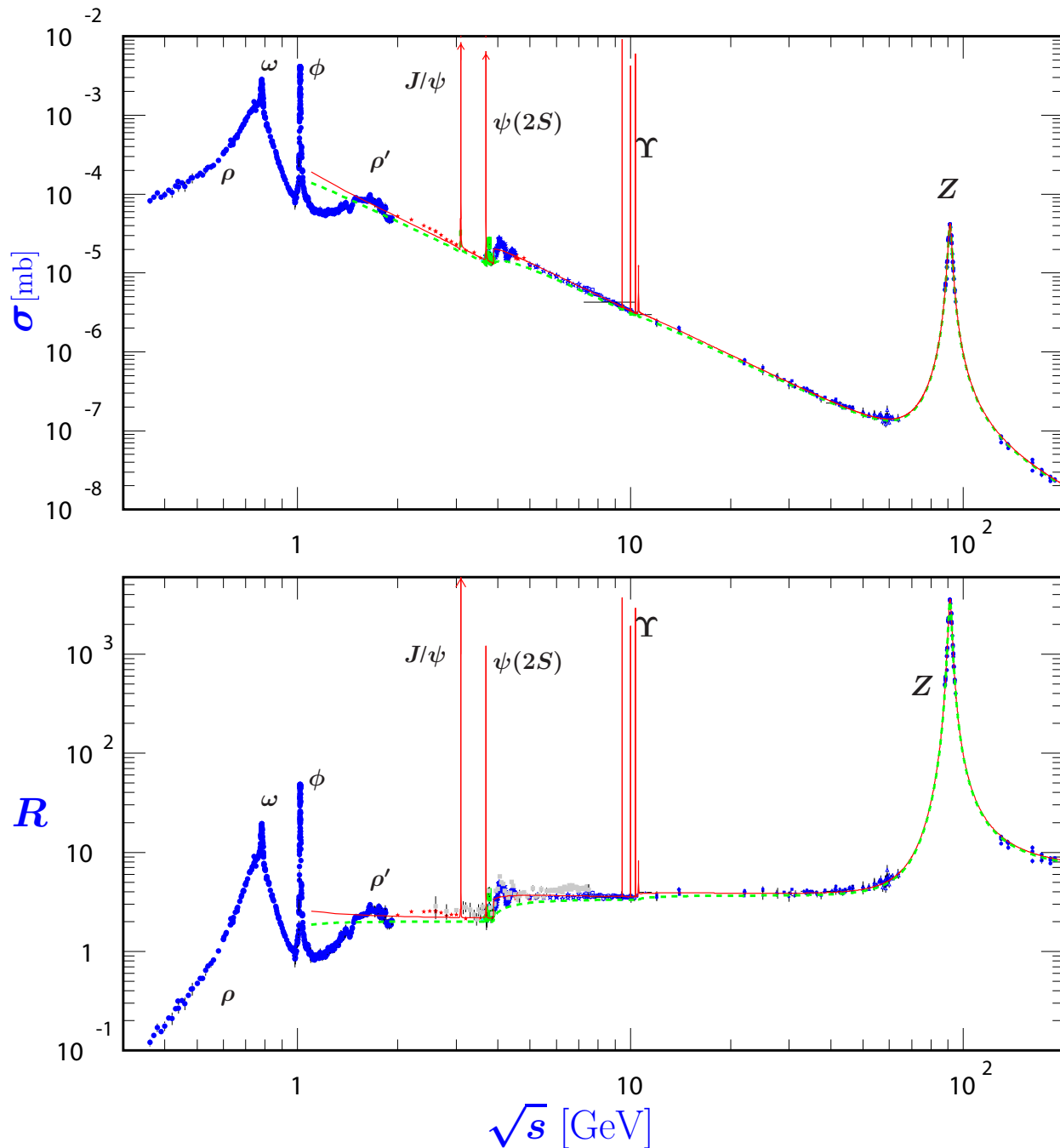
**ZEUS:** J. Breitweg *et al.*, Eur. Phys. J. **C11**, 251 (1999);  
S. Chekanov *et al.*, Phys. Lett. **B510**, 36 (2001).

$p(\bar{p})$ : The errors of the  $p(\bar{p})$  measurements are the quadratically added statistical and systematic errors, except for the bubble chamber measurements for which only statistical errors are given in the references. The values measured by UA5 exclude single diffractive dissociation:  
**bubble chamber:** J. Benecke *et al.*, Nucl. Phys. **B76**, 29 (1976); W.M. Morse *et al.*, Phys. Rev. **D15**, 66 (1977).

**ISR:** A. Breakstone *et al.*, Phys. Rev. **D30**, 528 (1984).

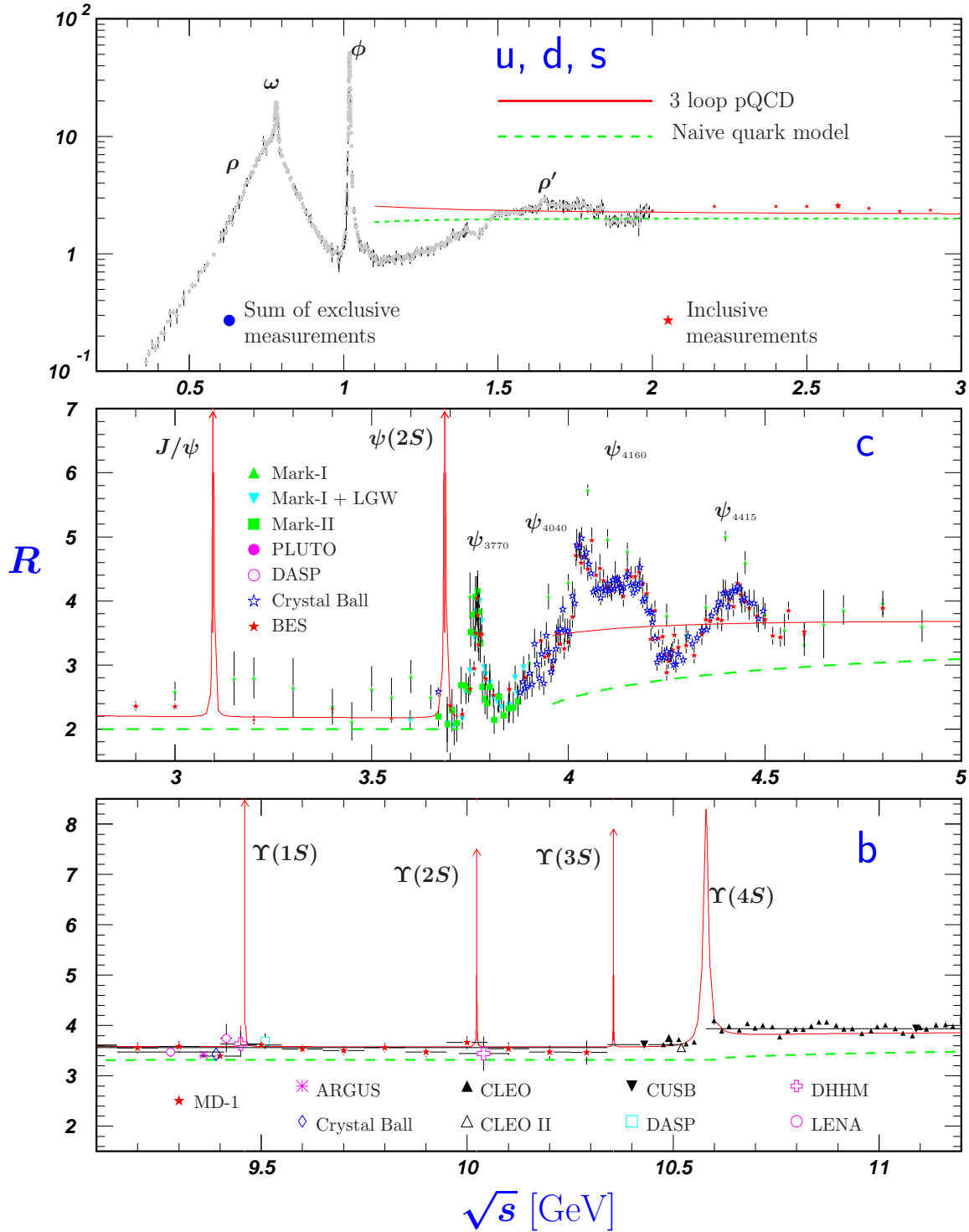
**UA5:** G.J. Alner *et al.*, Phys. Lett. **167B**, 476 (1986);  
R.E. Ansorge *et al.*, Z. Phys. **C43**, 357 (1989).

(Courtesy of O. Biebel, LMU, Munich, 2010)

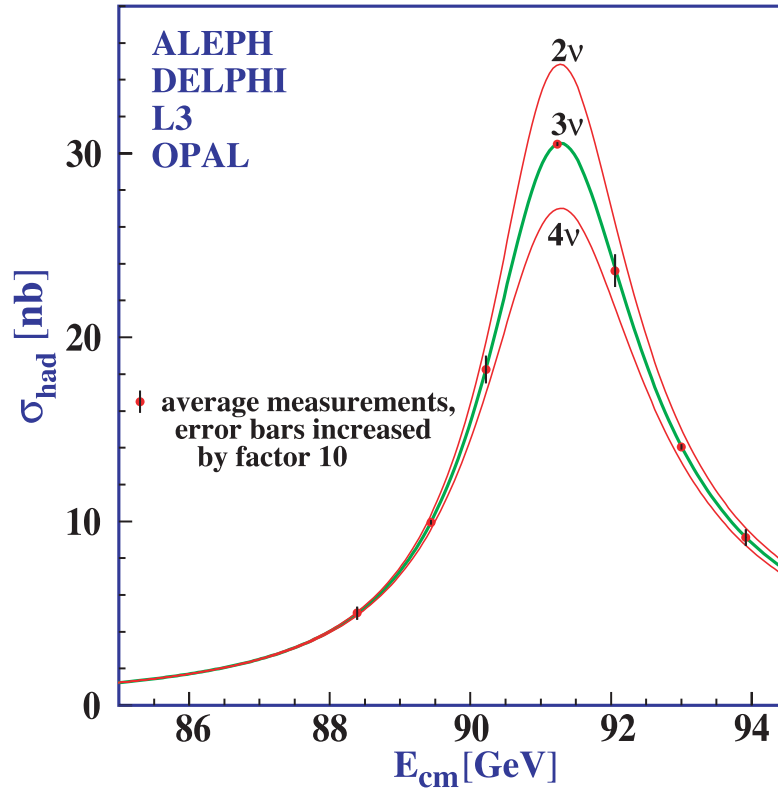
$\sigma$  and  $R$  in  $e^+e^-$  Collisions

**Figure 46.6:** World data on the total cross section of  $e^+e^- \rightarrow \text{hadrons}$  and the ratio  $R(s) = \sigma(e^+e^- \rightarrow \text{hadrons}, s) / \sigma(e^+e^- \rightarrow \mu^+\mu^-, s)$ .  $\sigma(e^+e^- \rightarrow \text{hadrons}, s)$  is the experimental cross section corrected for initial state radiation and electron-positron vertex loops,  $\sigma(e^+e^- \rightarrow \mu^+\mu^-, s) = 4\pi\alpha^2(s)/3s$ . Data errors are total below 2 GeV and statistical above 2 GeV. The curves are an educative guide: the broken one (green) is a naive quark-parton model prediction, and the solid one (red) is 3-loop pQCD prediction (see “Quantum Chromodynamics” section of this Review, Eq. (9.7) or, for more details, K. G. Chetyrkin *et al.*, Nucl. Phys. **B586**, 56 (2000) (Erratum *ibid.* **B634**, 413 (2002))). Breit-Wigner parameterizations of  $J/\psi$ ,  $\psi(2S)$ , and  $\Upsilon(nS)$ ,  $n = 1, 2, 3, 4$  are also shown. The full list of references to the original data and the details of the  $R$  ratio extraction from them can be found in [arXiv:hep-ph/0312114]. Corresponding computer-readable data files are available at <http://pdg.lbl.gov/current/xsect/>. (Courtesy of the COMPAS (Protvino) and HEPDATA (Durham) Groups, May 2010.)

### $R$ in Light-Flavor, Charm, and Beauty Threshold Regions



**Figure 46.7:**  $R$  in the light-flavor, charm, and beauty threshold regions. Data errors are total below 2 GeV and statistical above 2 GeV. The curves are the same as in Fig. 46.6. **Note:** CLEO data above  $\Upsilon(4S)$  were not fully corrected for radiative effects, and we retain them on the plot only for illustrative purposes with a normalization factor of 0.8. The full list of references to the original data and the details of the  $R$  ratio extraction from them can be found in [arXiv:hep-ph/0312114]. The computer-readable data are available at <http://pdg.lbl.gov/current/xsect/>. (Courtesy of the COMPAS (Protvino) and HEPDATA (Durham) Groups, May 2010.)

Annihilation Cross Section Near  $M_Z$ 

**Figure 46.8:** Combined data from the ALEPH, DELPHI, L3, and OPAL Collaborations for the cross section in  $e^+e^-$  annihilation into hadronic final states as a function of the center-of-mass energy near the Z pole. The curves show the predictions of the Standard Model with two, three, and four species of light neutrinos. The asymmetry of the curve is produced by initial-state radiation. Note that the error bars have been increased by a factor ten for display purposes. References:

**ALEPH:** R. Barate *et al.*, Eur. Phys. J. **C14**, 1 (2000).

**DELPHI:** P. Abreu *et al.*, Eur. Phys. J. **C16**, 371 (2000).

**L3:** M. Acciarri *et al.*, Eur. Phys. J. **C16**, 1 (2000).

**OPAL:** G. Abbiendi *et al.*, Eur. Phys. J. **C19**, 587 (2001).

**Combination:** The ALEPH, DELPHI, L3, OPAL, SLD Collaborations, the LEP Electroweak Working Group, and the SLD Electroweak and Heavy Flavor Groups, Phys. Rept. **427**, 257 (2006) [[arXiv:hep-ex/0509008](https://arxiv.org/abs/hep-ex/0509008)].

(Courtesy of M. Grünewald and the LEP Electroweak Working Group, 2007)

**Table 46.2: Total hadronic cross section.** Analytic  $S$ -matrix and Regge theory suggest a variety of parameterizations of total cross sections at high energies with different areas of applicability and fits quality.

A ranking procedure, based on measures of different aspects of the quality of the fits to the current evaluated experimental database, allows one to single out the following parameterization of highest rank [1]

$$\sigma^{ab} = Z^{ab} + B^{ab} \log^2(s/s_M) + Y_1^{ab}(s_M/s)^{\eta_1} - Y_2^{ab}(s_M/s)^{\eta_2} \quad \sigma^{\bar{a}b} = Z^{ab} + B^{ab} \log^2(s/s_M) + Y_1^{ab}(s_M/s)^{\eta_1} + Y_2^{ab}(s_M/s)^{\eta_2},$$

where  $Z^{ab}$ ,  $B^{a(p,n,\gamma^*)} = \pi \frac{(hc)^2}{M^2}$ ,  $B^{ad} = \lambda \pi \frac{(hc)^2}{M^2}$  (dimensionless factor  $\lambda$  introduced to test the universality for nuclei targets),  $Y_i^{ab}$  are in mb;  $s$ ,  $s_M = (m_a + m_b + M)^2$  are in  $\text{GeV}^2$ ;  $m_a$ ,  $m_b$ , [ $m_{\gamma^*} = m_{\rho(770)}$ ] are the masses of initial state particles, and  $M$  – the mass parameter defining the rate of universal rise of the cross sections are all in  $\text{GeV}$ . Parameters  $M$ ,  $\eta_1$  and  $\eta_2$  are universal for all collisions considered. Terms  $Z^{ab} + B^{ab} \log^2(s/s_M)$  represent the pomerons. The exponents  $\eta_1$  and  $\eta_2$  represent lower-lying C-even and C-odd exchanges, respectively. In addition to total cross sections  $\sigma$ , the measured ratios of the real-to-imaginary parts of the forward scattering amplitudes  $\rho = \text{Re}(T)/\text{Im}(T)$  are included in the fits by using  $s$  to  $u$  crossing symmetry and differential dispersion relations.

Exact factorization hypothesis was used for both  $Z^{ab}$  and  $B^{ab} \log^2(s/s_M)$  to extend the universal rise of the total hadronic cross sections to the  $\gamma p \rightarrow \text{hadrons}$  and  $\gamma \gamma \rightarrow \text{hadrons}$  collisions. This results in substitutions:  $Z^{\gamma p} + \pi \frac{(hc)^2}{M^2} \log^2(s/s_M) \Rightarrow \delta [Z^{pp} + \pi \frac{(hc)^2}{M^2} \log^2(s/s_M)]$ , and  $Z^{\gamma \gamma} + \pi \frac{(hc)^2}{M^2} \log^2(s/s_M) \Rightarrow \delta^2 [Z^{pp} + \pi \frac{(hc)^2}{M^2} \log^2(s/s_M)]$ , with the additional parameter  $\delta$ . Simultaneous fit was made to the 2011-updated data for all collisions listed in the central column of the table. The total number of adjusted parameters is **34**. Asymptotic parameters ( $Z$ ,  $M$ ,  $\lambda$ ,  $\delta$ ,  $\eta_1$ ,  $\eta_2$ ) thus obtained were then fixed and used as inputs to fits by groups to check a stability of the whole situation with description of the high energy data. Results are shown in the right hand part of the table. All fits included data above  $\sqrt{s_{\min}} = 5 \text{ GeV}$  with overall  $\chi^2/\text{dof} = 0.96$ .

$M=2.15(2)$ , $\eta_1=0.462(2)$ , $\eta_2=0.550(5)$			Beam/ Target	$\delta=0.003056(15)$ , $\lambda=1.630(35)$			$\chi^2/\text{dof}$ by groups
$Z$	$Y_1$	$Y_2$		$Z$	$Y_1$	$Y_2$	
34.71(15)	12.72(19)	7.35(8)	$\bar{p}(p)/p$	34.71(15)	12.72(6)	7.35(7)	
35.00(18)	12.19(34)	6.62(16)	$\bar{p}(p)n$	35.00(16)	12.19(45)	6.6(2)	1.051
34.9(1.4)	-55(23)	-57(24)	$\Sigma^-/p$	34.9(1.4)	-55(6)	-57(8)	0.558
19.02(13)	9.22(16)	1.75(3)	$\pi^\pm/p$	19.02(13)	9.22(3)	1.75(3)	1.020
16.55(9)	4.02(14)	3.39(4)	$K^\pm/p$	16.55(9)	4.02(3)	3.39(3)	
16.49(10)	3.44(19)	1.82(7)	$K^\pm/n$	16.49(6)	3.44(16)	1.82(7)	0.737
	0.0128(12)		$\gamma/p$		0.00128(4)		
	$-0.034(0.183) \cdot 10^{-4}$		$\gamma/\gamma$		$-0.034(166) \cdot 10^{-4}$		0.722
65.02(38)	29.04(44)	14.9(2)	$\bar{p}(p)/d$	65.02(16)	29.04(39)	14.9(2)	1.524
37.06(30)	18.28(41)	0.34(9)	$\pi^\pm/d$	37.06(7)	18.28(19)	0.34(9)	0.747
32.34(22)	7.33(34)	5.59(9)	$K^\pm/d$	32.34(6)	7.33(16)	5.59(7)	0.819

The fitted functions are shown in the following figures, along with one-standard-deviation error bands. Whenever the reduced  $\chi^2$  is greater than one, a scale factor has been included to evaluate the parameter values and to draw the error bands. Where appropriate, statistical and systematic errors were combined quadratically in constructing weights for all fits. Only statistical error bars are shown on the plots. Vertical arrows indicate lower limits on the  $p_{\text{lab}}$  or  $\sqrt{s}$  range used in the fits. Database used in the fits now includes  $pp$  data from TOTEM experiment [2] and new data in the RHIC energy range from ARGO-YBJ cosmic ray experiment [3]. The modifications of the universal asymptotic term are motivated by ideas, suggestions and results from the old and recent papers [4-13]. Computer-readable data files are available at <http://pdg.lbl.gov/current/xsect/>. (Courtesy of the COMPAS group, IHEP, Protvino, April 2012)

#### References:

1. J.R. Cudell *et al.* (COMPETE Collab.), Phys. Rev. **D65**, 074024 (2002).
2. G. Antchev *et al.* (TOTEM Collaboration), Europhys. Lett. **96**, 21002 (2011).
3. G. Aielli *et al.* (ARGO-YBJ Collaboration), Phys. Rev. **D80**, 092004 (2009).
4. K. Igi and M. Ishida, Phys. Rev. **D66**, 034023 (2002), Phys. Lett. **B622**, 286 (2005).
5. M. M. Block and F. Halzen, Phys. Rev. **D70**, 091901 (2004), Phys. Rev. **D72**, 036006 (2005).
6. M. Ishida and K. Igi, Prog. Theor. Phys. Suppl. **187**, 297 (2011).
7. M. Ishida and V. Barger, Phys. Rev. D **84**, 014027 (2011).
8. F. Halzen, K. Igi, M. Ishida and C. S. Kim, Phys. Rev. **D85**, 074020 (2012).
9. S. S. Gershtein, A. A. Logunov, Sov. J. Nucl. Phys. **39**, 960 (1984) [Yad. Fiz. **39**, 1514 (1984)].
10. E. Iancu and R. Venugopalan, In Hwa, R.C. (ed.) *et al.*: *Quark gluon plasma* 249-3363 [hep-ph/0303204].
11. L. Frankfurt, M. Strikman, and M. Zhalov, Phys. Lett. **B616**, 59 (2005).
12. Y. I. Azimov, Phys. Rev. **D84**, 056012 (2011).
13. D. A. Fagundes, M. J. Menon and P. V. R. G. Silva, Nucl. Phys. **A880**, 1-11 (2012).

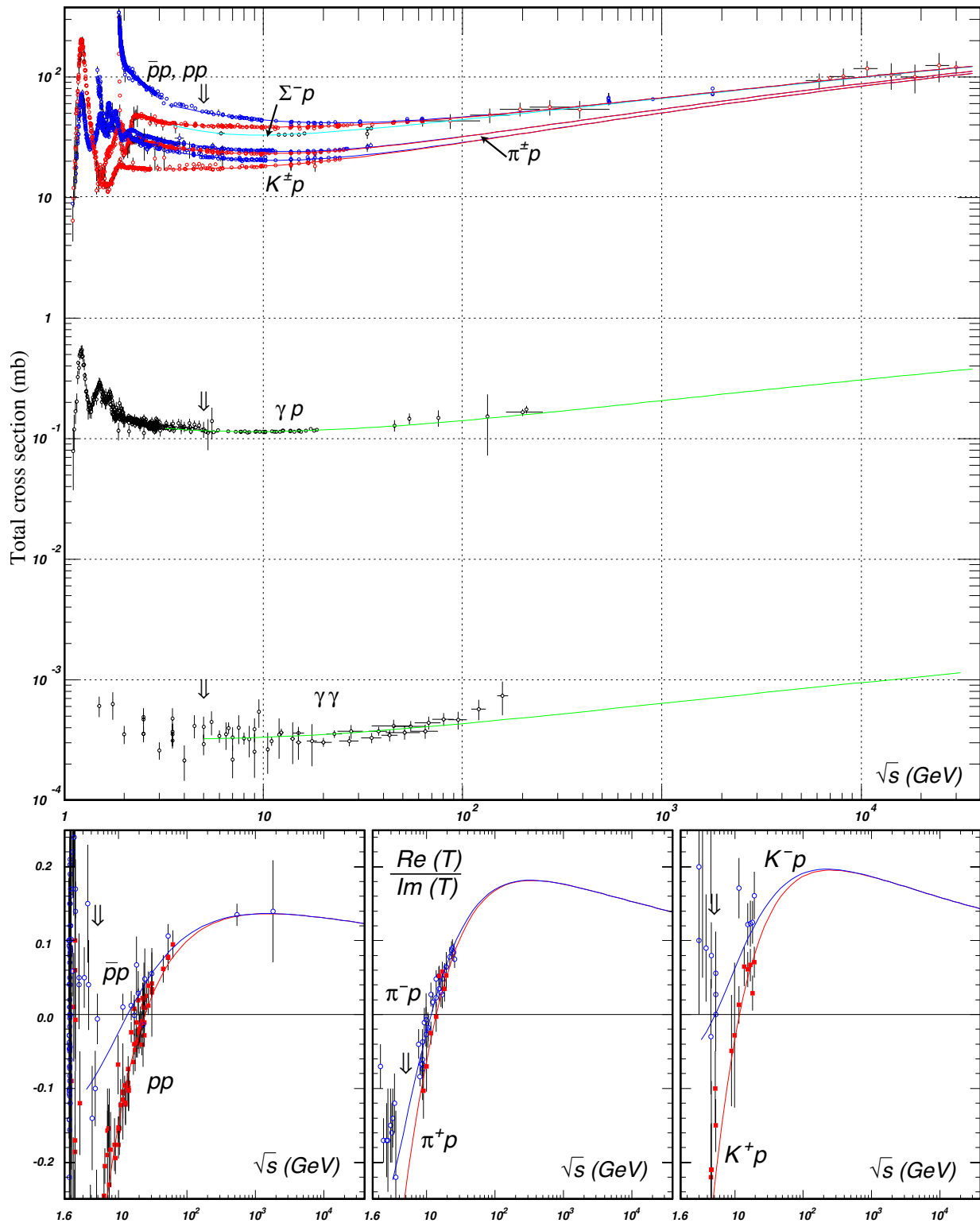


**Figure 46.9:** Summary of hadronic,  $\gamma p$ , and  $\gamma\gamma$  total cross sections, and ratio of the real to imaginary parts of the forward hadronic amplitudes. Corresponding computer-readable data files may be found at <http://pdg.lbl.gov/current/xsect/>. (Courtesy of the COMPAS group, IHEP, Protvino, April 2012.)

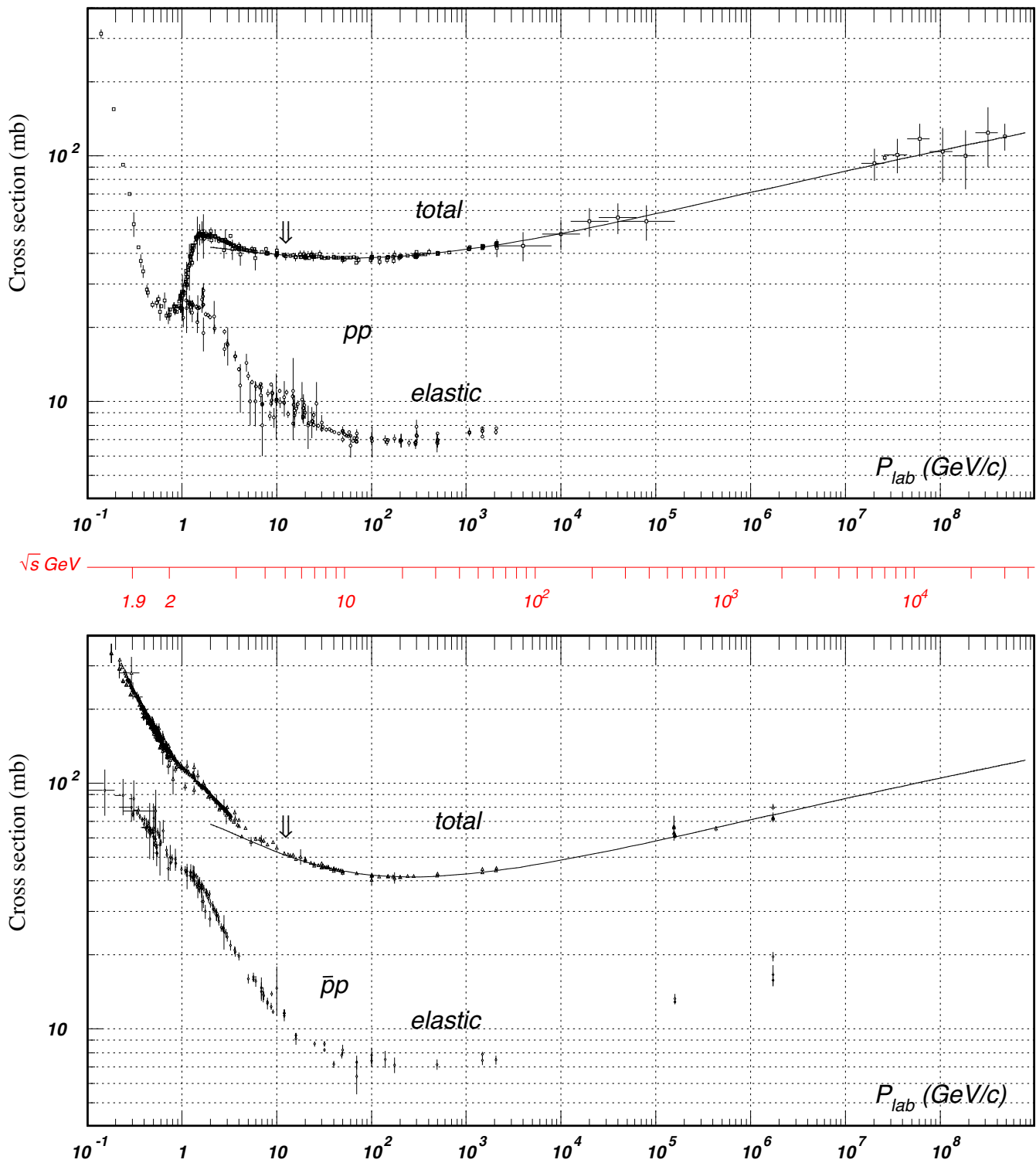


**Figure 46.10:** Total and elastic cross sections for  $pp$  and  $\bar{p}p$  collisions as a function of laboratory beam momentum and total center-of-mass energy. Corresponding computer-readable data files may be found at <http://pdg.lbl.gov/current/xsect/>. (Courtesy of the COMPAS group, IHEP, Protvino, April 2012)

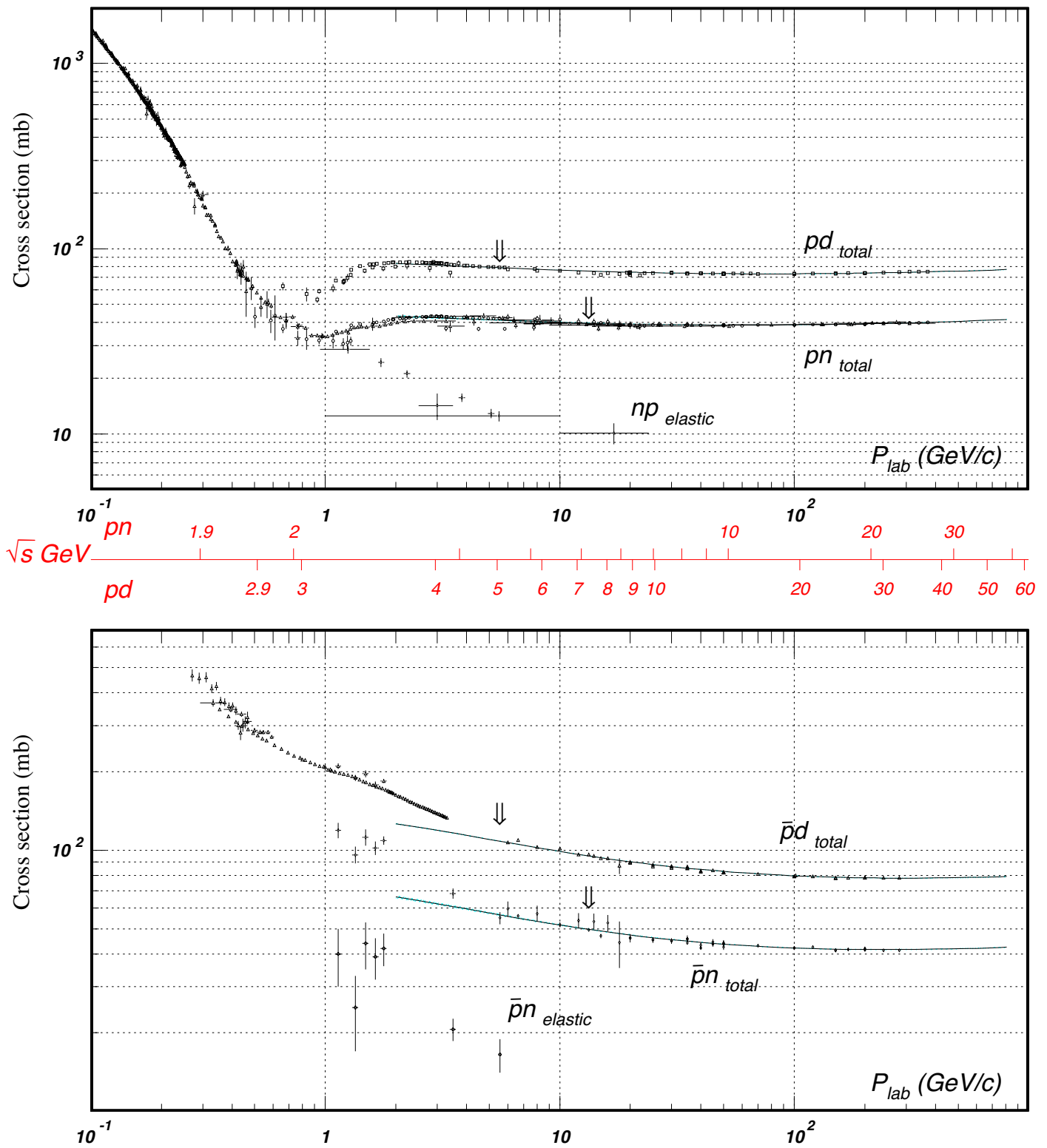


**Figure 46.11:** Total and elastic cross sections for  $pd$  (total only),  $np$ ,  $\bar{p}d$  (total only), and  $\bar{p}n$  collisions as a function of laboratory beam momentum and total center-of-mass energy. Corresponding computer-readable data files may be found at <http://pdg.lbl.gov/current/xsect/>. (Courtesy of the COMPAS Group, IHEP, Protvino, April 2012)



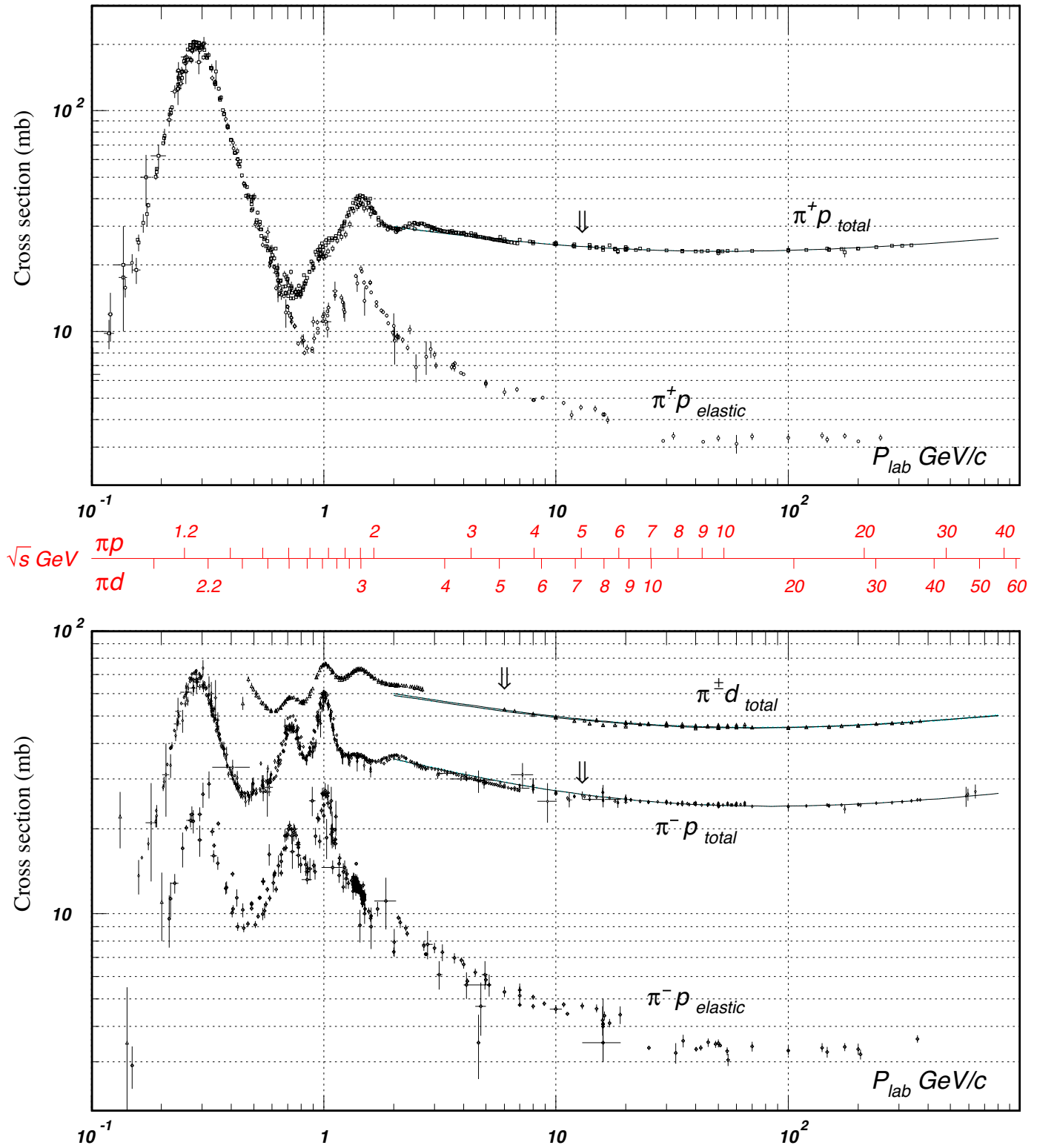


**Figure 46.12:** Total and elastic cross sections for  $\pi^\pm p$  and  $\pi^\pm d$  (total only) collisions as a function of laboratory beam momentum and total center-of-mass energy. Corresponding computer-readable data files may be found at <http://pdg.lbl.gov/current/xsect/>. (Courtesy of the COMPAS Group, IHEP, Protvino, April 2012)

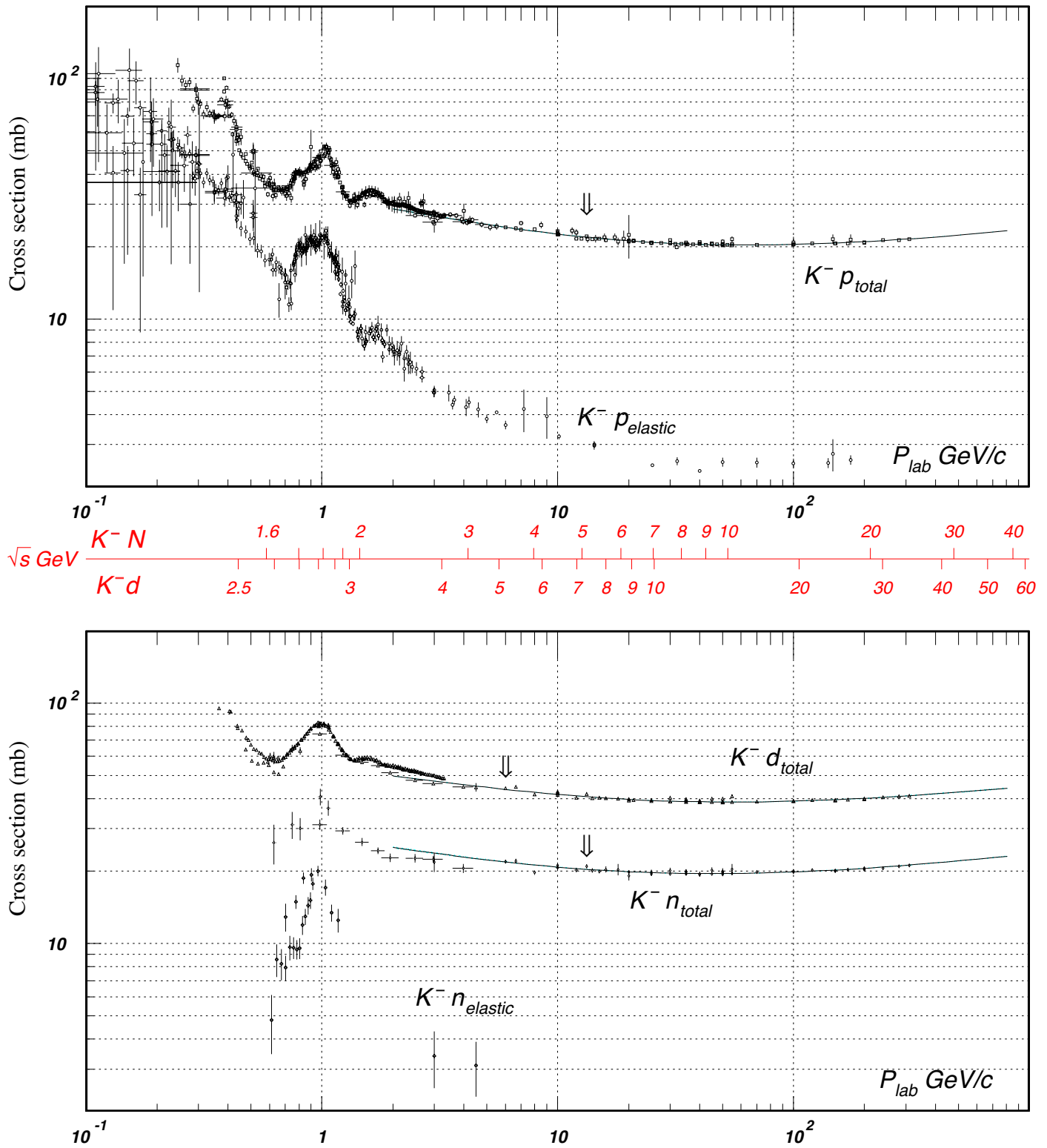


**Figure 46.13:** Total and elastic cross sections for  $K^-p$  and  $K^-d$  (total only), and  $K^-n$  collisions as a function of laboratory beam momentum and total center-of-mass energy. Corresponding computer-readable data files may be found at <http://pdg.lbl.gov/current/xsect/>. (Courtesy of the COMPAS Group, IHEP, Protvino, April 2012)

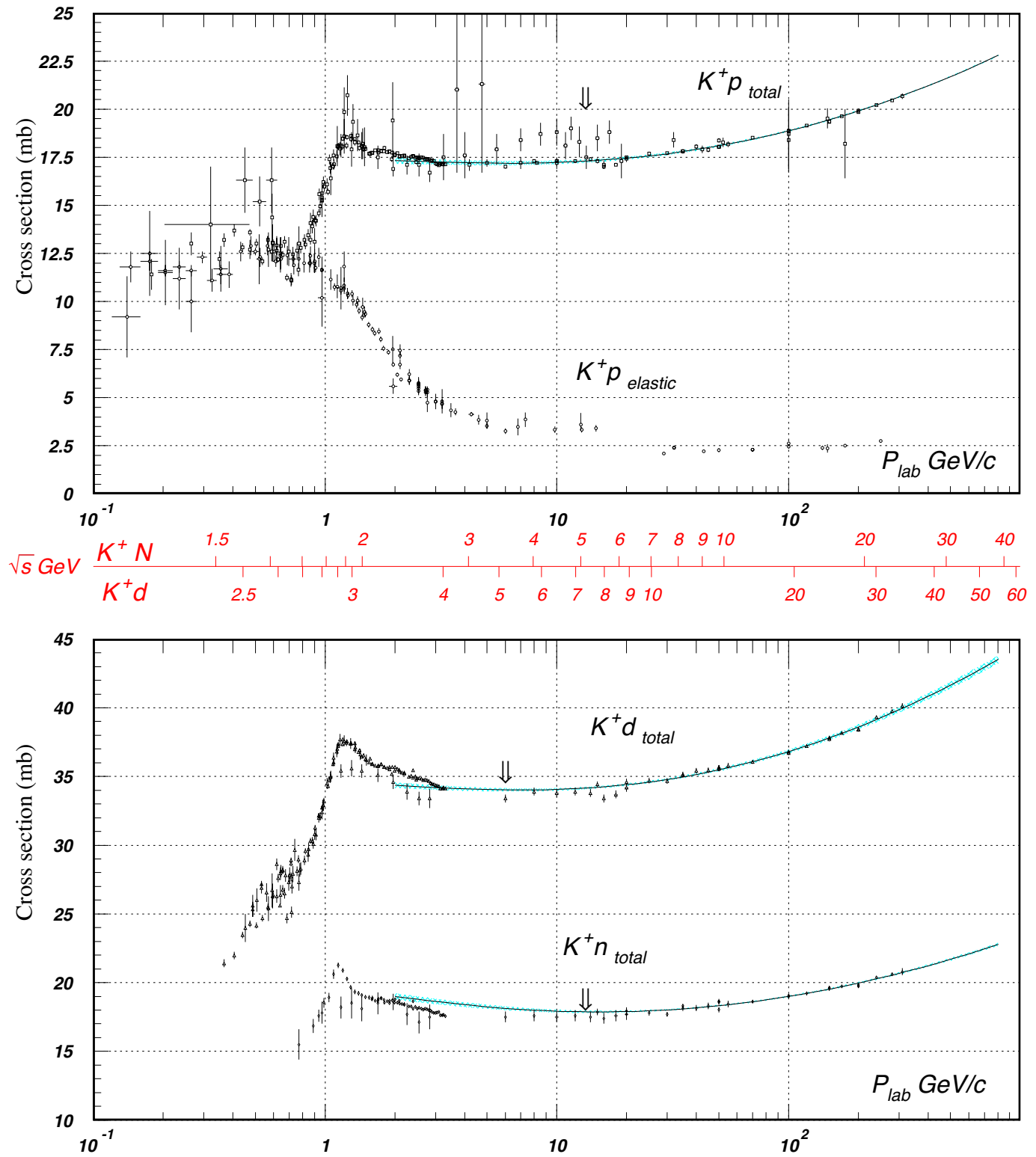


**Figure 46.14:** Total and elastic cross sections for  $K^+p$  and total cross sections for  $K^+d$  and  $K^+n$  collisions as a function of laboratory beam momentum and total center-of-mass energy. Corresponding computer-readable data files may be found at <http://pdg.lbl.gov/current/xsect/>. (Courtesy of the COMPAS Group, IHEP, Protvino, April 2012)

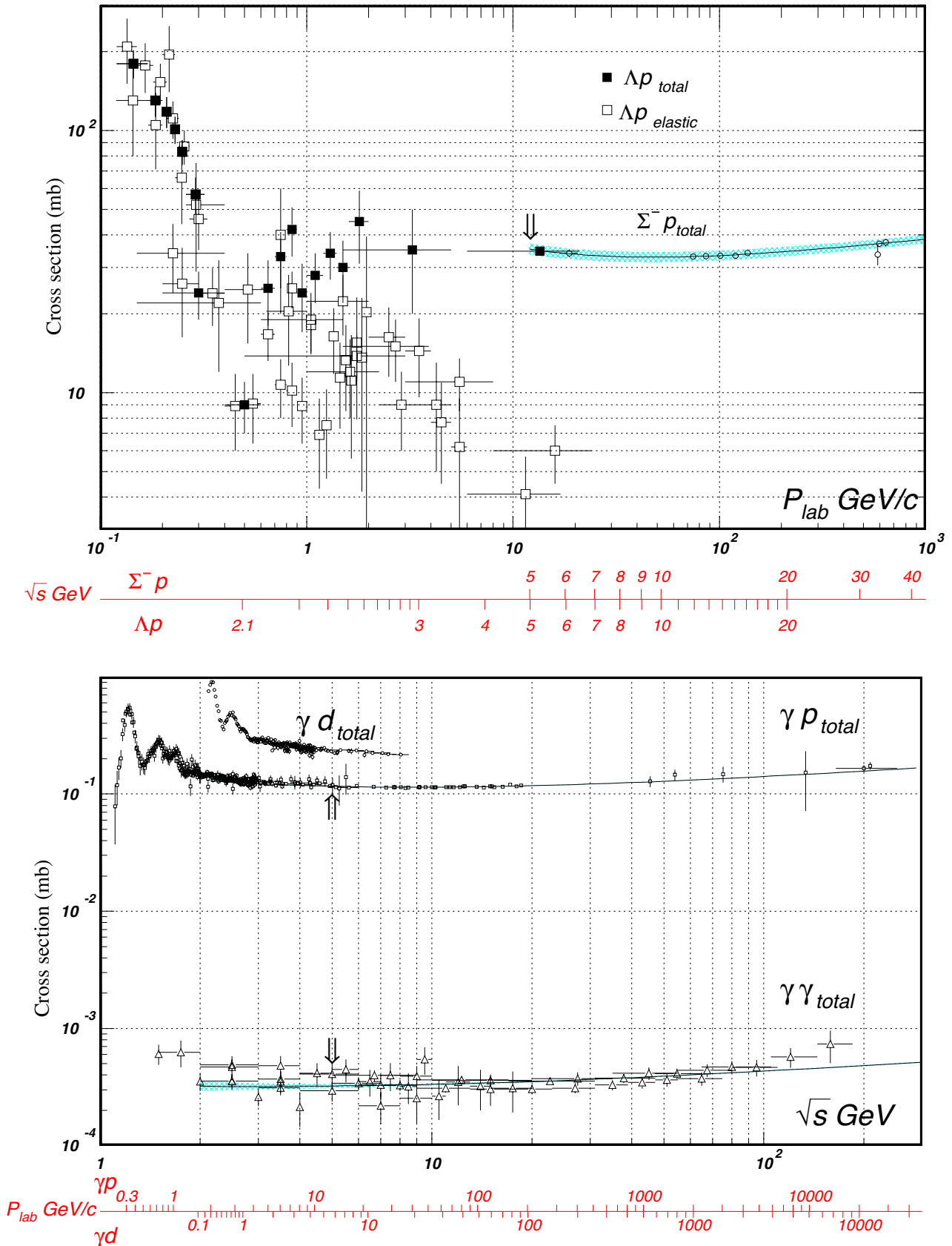
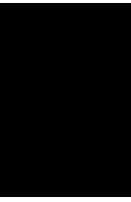


**Figure 46.15:** Total and elastic cross sections for  $\Lambda p$ , total cross section for  $\Sigma^- p$ , and total hadronic cross sections for  $\gamma d$ ,  $\gamma p$ , and  $\gamma\gamma$  collisions as a function of laboratory beam momentum and the total center-of-mass energy. Corresponding computer-readable data files may be found at <http://pdg.lbl.gov/current/xsect/>. (Courtesy of the COMPAS group, IHEP, Protvino, April 2012)

**INTRODUCTION TO THE PARTICLE LISTINGS**

Illustrative key . . . . .	457
Abbreviations . . . . .	458





# Illustrative Key to the Particle Listings

Name of particle. "Old" name used before 1986 renaming scheme also given if different. See the section "Naming Scheme for Hadrons" for details.

**$a_0(1200)$**

$$I^G(J^{PC}) = 1^-(0^+ +)$$

Particle quantum numbers (where known).

OMITTED FROM SUMMARY TABLE  
Evidence not compelling, may be a kinematic effect.

Indicates particle omitted from Particle Physics Summary Table, implying particle's existence is not confirmed.

Quantity tabulated below.

## $a_0(1200)$ MASS

Top line gives our best value (and error) of quantity tabulated here, based on weighted average of measurements used. Could also be from fit, best limit, estimate, or other evaluation. See next page for details.

VALUE (MeV)	EVTS	DOCUMENT ID	TECN	CHG	COMMENT
<b>1206 ± 7 OUR AVERAGE</b>					
1210 ± 8 ± 9	3000	FENNER 87	MMS	-	3.5 $\pi^- p$
1198 ± 10		PIERCE 83	ASPK	+	2.1 $K^- p$
1216 ± 11 ± 9	1500	MERRILL 81	HBC	0	3.2 $K^- p$
1192 ± 16		LYNCH 81	HBC	±	2.7 $\pi^- p$

General comments on particle.

Footnote number linking measurement to text of footnote.

<sup>1</sup>Systematic error was added quadratically by us in our 1986 edition.

"Document id" for this result; full reference given below.

Measurement technique. (See abbreviations on next page.)

## $a_0(1200)$ WIDTH

Number of events above background.

Measured value used in averages, fits, limits, etc.

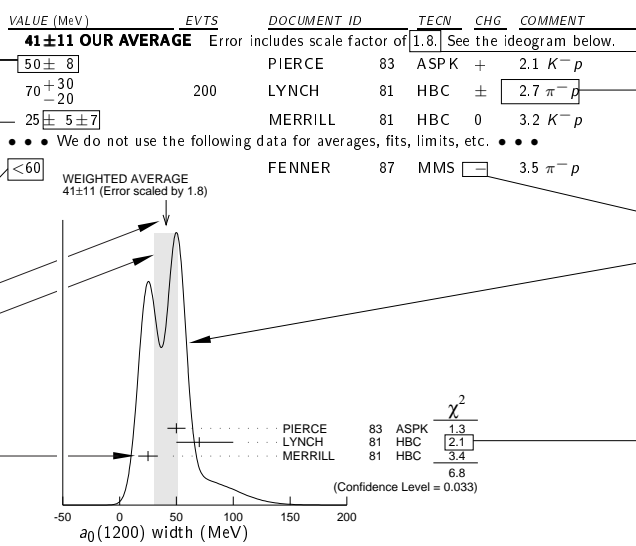
Error in measured value (often statistical only; followed by systematic if separately known; the two are combined in quadrature for averaging and fitting.)

Measured value *not* used in averages, fits, limits, etc. See the Introductory Text for explanations.

Arrow points to weighted average.

Shaded pattern extends  $\pm 1\sigma$  (scaled by "scale factor" S) from weighted average.

Value and error for each experiment.



Scale factor > 1 indicates possibly inconsistent data.

Reaction producing particle, or general comments.

"Change bar" indicates result added or changed since previous edition.

Charge(s) of particle(s) detected.

Ideogram to display possibly inconsistent data. Curve is sum of Gaussians, one for each experiment (area of Gaussian = 1/error; width of Gaussian = ±error). See Introductory Text for discussion.

Contribution of experiment to  $\chi^2$  (if no entry present, experiment not used in calculating  $\chi^2$  or scale factor because of very large error).

## $a_0(1200)$ DECAY MODES

Partial decay mode (labeled by  $\Gamma_i$ ).

Mode	Fraction ( $\Gamma_i/\Gamma$ )	Scale factor/ Confidence level
$\Gamma_1$ $3\pi$	(65.2 ± 1.3) %	S=1.7
$\Gamma_2$ $K\bar{K}$	(34.8 ± 1.3) %	S=1.7
$\Gamma_3$ $\eta\pi^\pm$	< 4.9 × 10 <sup>-4</sup>	CL=95%

Our best value for branching fraction as determined from data averaging, fitting, evaluating, limit selection, etc. This list is basically a compact summary of results in the Branching Ratio section below.

## $a_0(1200)$ BRANCHING RATIOS

Branching ratio.

Our best value (and error) of quantity tabulated, as determined from constrained fit (using *all significant* measured branching ratios for this particle).

Weighted average of measurements of this ratio only.

Footnote (referring to LYNCH 81).

Confidence level for measured upper limit.

References, ordered inversely by year, then author.

"Document id" used on data entries above.

Journal, report, preprint, etc. (See abbreviations on next page.)

VALUE	DOCUMENT ID	TECN	CHG	COMMENT
<b>0.652 ± 0.013 OUR FIT</b>				Error includes scale factor of 1.7.
<b>0.643 ± 0.010 OUR AVERAGE</b>				
0.64 ± 0.01	PIERCE 83	ASPK	+	2.1 $K^- p$
0.74 ± 0.06	MERRILL 81	HBC	0	3.2 $K^- p$
0.48 ± 0.15	<sup>2</sup> LYNCH 81	HBC	±	2.7 $\pi^- p$
<sup>2</sup> Data has questionable background subtraction.				

VALUE	DOCUMENT ID	TECN	CHG	COMMENT
<b>0.348 ± 0.013 OUR FIT</b>				Error includes scale factor of 1.7.
<b>0.35 ± 0.05</b>	PIERCE 83	ASPK	+	2.1 $K^- p$

VALUE	DOCUMENT ID	TECN	CHG	COMMENT
<b>0.535 ± 0.030 OUR FIT</b>				Error includes scale factor of 1.7.
<b>0.50 ± 0.03</b>	MERRILL 81	HBC	0	3.2 $K^- p$

VALUE (units 10 <sup>-4</sup> )	CL%	DOCUMENT ID	TECN	CHG	COMMENT
<b>&lt;3.5</b>	95	PIERCE 83	ASPK	+	2.1 $K^- p$

$\Gamma_2/\Gamma$

Branching ratio in terms of partial decay mode(s)  $\Gamma_i$  above.

$\Gamma_2/\Gamma_1$

0.71  $\Gamma_3/\Gamma$

## $a_0(1200)$ REFERENCES

FENNER 87	PRL 55 14	H. Fenner et al.	(SLAC)
PIERCE 83	PL 123B 230	J.H. Pierce	(FNAL) JUP
LYNCH 81	PR D24 610	G.R. Lynch et al.	(CLEO Collab.)
MERRILL 81	PRL 47 143	D.W. Merrill et al.	(SACL, CERN)

Partial list of author(s) in addition to first author.

Quantum number determinations in this reference.

Institution(s) of author(s). (See abbreviations on next page.)

# Abbreviations Used in the Particle Listings

## Indicator of Procedure Used to Obtain Our Result

OUR AVERAGE	From a weighted average of selected data.
OUR FIT	From a constrained or overdetermined multiparameter fit of selected data.
OUR EVALUATION	Not from a direct measurement, but evaluated from measurements of other quantities.
OUR ESTIMATE	Based on the observed range of the data. Not from a formal statistical procedure.
OUR LIMIT	For special cases where the limit is evaluated by us from measured ratios or other data. Not from a direct measurement.

## Measurement Techniques

(i.e., Detectors and Methods of Analysis)

ACCM	ACCMOR Collaboration
ADMX	Axion Dark Matter Experiment
AEMS	Argonne effective mass spectrometer
ALEP	ALEPH – CERN LEP detector
ALPS	Photon regeneration experiment
AMND	AMANDA South Pole neutrino detector
AMY	AMY detector at KEK-TRISTAN
ANIT	Antarctic Impulsive Transient Antenna balloon mission
APEX	FNAL APEX Collab.
ARG	ARGUS detector at DORIS
ARGD	Fit to semicircular amplitude path on Argand diagram
ASP	Anomalous single-photon detector
ASPK	Automatic spark chambers
ASTE	ASTERIX detector at LEAR
ASTR	Astronomy
ATLS	ATLAS detector at CERN LHC
B787	BNL experiment 787 detector
B791	BNL experiment 791 detector
B845	BNL experiment 845 detector
B852	BNL E-852
B865	BNL E865 detector
B871	BNL experiment 871 detector
B949	BNL E949 detector at AGS
BABR	BaBar Collab.
BAKS	Baksan underground scintillation telescope
BC	Bubble chamber
BDMP	Beam dump
BEAT	CERN BEATRICE Collab.
BEBC	Big European bubble chamber at CERN
BELL	Belle Collab.
BES	BES Beijing Spectrometer at Beijing Electron-Positron Collider
BES2	BES Beijing Spectrometer at Beijing Electron-Positron Collider
BES3	BES Beijing Spectrometer at Beijing Electron-Positron Collider
BIS2	BIS-2 spectrometer at Serpukhov
BKEI	BENKEI spectrometer system at KEK Proton Synchrotron
BOLO	Bolometer, a cryogenic thermal detector
BONA	Bonanza nonmagnetic detector at DORIS
BORX	BOREXINO
BPWA	Barrelet-zero partial-wave analysis
CALO	Calorimeter
CAST	CAST experiment at CERN
CBAL	Crystal Ball detector at SLAC-SPEAR or DORIS
CBAR	Crystal Barrel detector at CERN-LEAR
CBOX	Crystal Box at LAMPF
CBTP	CBELSA/TAPS Collaboration
CC	Cloud chamber
CCFR	Columbia-Chicago-Fermilab-Rochester detector
CDF	Collider detector at Fermilab
CDF2	CDF-II Collab.
CDHS	CDHS neutrino detector at CERN
CDM2	CDMS II, Cryogenic Dark Matter Search at Soudan Underground Lab.
CDMS	CDMS Collab.
CELL	CELLO detector at DESY
CGNT	CoGeNT dark matter search experiment
CHER	Cherenkov detector
CHM2	CHARM-II neutrino detector (glass) at CERN
CHOZ	Nuclear Power Station near Chooz, France
CHRM	CHARM neutrino detector (marble) at CERN
CHRS	CHORUS Collaboration – CERNS SPS
CIB	Cosmic Infrared Background
CIBS	CERN-IHEP boson spectrometer
CLAS	Jefferson CLAS Collab.
CLE2	CLEO II detector at CESR

CLE3	CLEO III detector at CESR
CLEO	Cornell magnetic detector at CESR
CMB	Cosmic Microwave Background
CMD	Cryogenic magnetic detector at VEPP-2M, Novosibirsk
CMD2	Cryogenic magnetic detector 2 at VEPP-2M, Novosibirsk
CMS	CMS detector at CERN LHC
CNTR	Counters
COMP	COMPASS experiment at the CERN SPS
COSM	Cosmology and astrophysics
COSY	COSY-TOF Collaboration
COUP	COUPP (the Chicagoland Observatory for Underground Particle Physics) Collab.
CPLR	CLEAR Collaboration
CRES	CRESST cryogenic detector
CRYB	Crystal Ball at BNL
CRYM	Crystal Ball detector at Mainz Microtron MAMI
CSB2	Columbia U. - Stony Brook BGO calorimeter inserted in NaI array
CSME	COSME Collaboration
CUOR	CUORICINO experiment at Gran Sasso Laboratory.
CUSB	Columbia U. - Stony Brook segmented NaI detector at CESR
D0	D0 detector at Fermilab Tevatron Collider
DAMA	DAMA, dark matter detector at Gran Sasso National Lab.
DASP	DESY double-arm spectrometer
DAYA	Daya Bay Collaboration
DBC	Deuterium bubble chamber
DCHZ	Double Chooz Collaboration
DLCO	DELCO detector at SLAC-SPEAR or SLAC-PEP
DLPH	DELPHI detector at LEP
DM1	Magnetic detector no. 1 at Orsay DCI collider
DM2	Magnetic detector no. 2 at Orsay DCI collider
DMTP	Dark Matter Time Projection Chamber (DMTPC) directional detection experiment
DONU	DONUT Collab.
DPWA	Energy-dependent partial-wave analysis
E621	Fermilab E621 detector
E653	Fermilab E653 detector
E665	Fermilab E665 detector
E687	Fermilab E687 detector
E691	Fermilab E691 detector
E705	Fermilab E705 Spectrometer-Calorimeter
E731	Fermilab E731 Spectrometer-Calorimeter
E756	Fermilab E756 detector
E760	Fermilab E760 detector
E761	Fermilab E761 detector
E771	Fermilab E771 detector
E773	Fermilab E773 Spectrometer-Calorimeter
E789	Fermilab E789 detector
E791	Fermilab E791 detector
E799	Fermilab E799 Spectrometer-Calorimeter
E835	Fermilab E835 detector
EDE2	EDELWEISS II dark matter search Collaboration
EDEL	EDELWEISS dark matter search Collaboration
EHS	Four-pi detector at CERN
ELEC	Electronic combination
EMC	European muon collaboration detector at CERN
EMUL	Emulsions
FAST	Fiber Active Scintillator Target detector at PSI
FBC	Freon bubble chamber
FENI	FENICE (at the ADONE collider of Frascati)
FIT	Fit to previously existing data
FLAT	Large Area Telescope onboard the Fermi Gamma-Ray Space Telescope
FMPS	Fermilab Multiparticle Spectrometer
FOCS	FNAL E831 FOCUS Collab.
FRAB	ADONE $B\bar{B}$ group detector
FRAG	ADONE $\gamma\gamma$ group detector
FRAM	ADONE MEA group detector
FREJ	FREJUS Collaboration – modular flash chamber detector (calorimeter)
FRMI	Fermi large area telescope (Fermi-LAT)
GA24	Hodoscope Cherenkov $\gamma$ calorimeter (IHEP GAMS-2000) (CERN GAMS-4000)
GALX	GALLEX solar neutrino detector in the Gran Sasso Underground Lab.
GAM2	IHEP hodoscope Cherenkov $\gamma$ calorimeter GAMS-2000
GAM4	CERN hodoscope Cherenkov $\gamma$ calorimeter GAMS-4000
GAMS	IHEP hodoscope Cherenkov $\gamma$ calorimeter GAMS-4 $\pi$
GNO	Gallium Neutrino Observatory in the Gran Sasso Underground Lab.



## Abbreviations Used in the Particle Listings

GOLI	CERN Goliath spectrometer	MRKJ	Mark-J detector at DESY
GRAL	GRAAL Collaboration	MRS	Magnetic resonance spectrometer
H1	H1 detector at DESY/HERA	MUG2	MUON(g-2)
HBC	Hydrogen bubble chamber	MWPC	Multi-Wire Proportional Chamber
HDHC	Hydrogen and deuterium bubble chambers	NA14	CERN NA14
HDMO	Heidelberg-Moscow Experiment	NA31	CERN NA31 Spectrometer-Calorimeter
HDMS	Heidelberg Dark Matter Search Experiment	NA32	CERN NA32 Spectrometer
HEBC	Helium bubble chamber	NA48	CERN NA48 Collaboration
HEPT	Helium proportional tubes	NA49	CERN NA49 Collaboration
HERB	HERA-B detector at DESY/HERA	NA60	CERN NA60 Collaboration
HERM	HERMES detector at DESY/HERA	NA62	CERN NA62 Experiment
HESS	High Energy Stereoscopic System gamma-ray instrument	NAGE	NEWAGE, New generation WIMP-search experiment with advanced gaseous tracking
HFS	Hyperfine structure	NAIA	NAIAD (NaI Advanced Detector) dark matter search experiment
HLBC	Heavy-liquid bubble chamber	ND	NaI detector at VEPP-2M, Novosibirsk
HOME	Homestake underground scintillation detector	NICE	Serpukhov nonmagnetic precision spectrometer
HPGE	High-purity Germanium detector	NMR	Nuclear magnetic resonance
HPW	Harvard-Pennsylvania-Wisconsin detector	NOMD	NOMAD Collaboration, CERN SPS
HRS	SLAC high-resolution spectrometer	NTEV	NuTeV Collab. at Fermilab
HYBR	Hybrid: bubble chamber + electronics	NUSX	Mont Blanc NUSEX underground detector
HYCP	HyperCP Collab. (FNAL E-871)	OBLX	OBELIX detector at LEAR
ICAR	ICARUS experiment at Gran Sasso Laboratory.	OLYA	Detector at VEPP-2M and VEPP-4, Novosibirsk
ICCB	IceCube neutrino detector at South Pole	OMEG	CERN OMEGA spectrometer
IGEX	IGEX Collab.	OPAL	OPAL detector at LEP
IMB	Irvine-Michigan-Brookhaven underground Cherenkov detector	OSPK	Optical spark chamber
IMB3	Irvine-Michigan-Brookhaven underground Cherenkov detector	PIBE	The PIBETA detector at the Paul Scherrer Institute (PSI), Switzerland.
INDU	Magnetic induction	PICA	PICASSO dark matter search experiment
IPWA	Energy-independent partial-wave analysis	PLAS	Plastic detector
ISTR	IHEP ISTR+ spectrometer-calorimeter	PLUT	DESY PLUTO detector
JADE	JADE detector at DESY	PRMX	The PRIMEX detector in Hall B at TJNAF
K246	KEK E246 detector with polarimeter	PWA	Partial-wave analysis
K2K	KEK to Super-Kamiokande	REDE	Resonance depolarization
K391	KEK E391a detector	RENO	RENO Collaboration
K470	KEK-E470 Stopping K detector	RICE	Radio Ice Cherenkov Experiment
KAM2	KAMIOKANDE-II underground Cherenkov detector	RVUE	Review of previous data
KAMI	KAMIOKANDE underground Cherenkov detector	SAGE	US - Russian Gallium Experiment
KAR2	KARMEN2 calorimeter at the ISIS neutron spallation source at Rutherford	SELX	FNAL SELEX Collab.
KARM	KARMEN calorimeter at the ISIS neutron spallation source at Rutherford	SFM	CERN split-field magnet
KEDR	detector operating at VEPP-4M collider (Novosibirsk)	SHF	SLAC Hybrid Facility Photon Collaboration
KIMS	Korea Invisible Mass Search experiment at YangYang, Korea	SIGM	Serpukhov CERN-IHEP magnetic spectrometer (SIGMA)
KLND	KamLand Collab. (Japan)	SILI	Silicon detector
KLOE	KLOE detector at DAFNE (the Frascati e+e- collider Italy)	SIMP	SIMPLE, dark matter detector at Laboratori Nazionali del Sud
KOLR	Kolar Gold Field underground detector	SKAM	Super-Kamiokande Collab.
KTEV	KTeV Collaboration	SLAX	Solar Axion Experiment in Canfranc Underground Laboratory
L3	L3 detector at LEP	SLD	SLC Large Detector for e+e- colliding beams at SLAC
LASS	Large-angle superconducting solenoid spectrometer at SLAC	SMPL	SIMPLE, Superheated Instrument for Massive Particle Experiments
LATT	Lattice calculations	SND	Novosibirsk Spherical neutral detector at VEPP-2M
LEBC	Little European bubble chamber at CERN	SNDR	SINDRUM spectrometer at PSI
LEGS	BNL LEGS Collab.	SNO	SNO Collaboration (Sudbury Neutrino Observatory)
LENA	Nonmagnetic lead-glass NaI detector at DORIS	SOU2	Soudan 2 underground detector
LEP	From combination of all 4 LEP experiments: ALEPH, DELPHI, L3, OPAL	SODU	Soudan underground detector
LEPS	Low-Energy Pion Spectrometer at the Paul Scherrer Institute	SPEC	Spectrometer
LGW	Lead Glass Wall collaboration at SPEAR/SLAC	SPED	From maximum of speed plot or resonant amplitude
LHCb	LHCb detector at CERN LHC	SPHR	Bonn SAPHIR Collab.
LSD	Mont Blanc liquid scintillator detector	SPNX	SPHINX spectrometer at IHEP accelerator
LSND	Liquid Scintillator Neutrino Detector	SPRK	Spark chamber
MAC	MAC detector at PEP/SLAC	SQID	SQUID device
MBOO	Fermilab MiniBooNE neutrino experiment	STRC	Streamer chamber
MBR	Molecular beam resonance technique	SVD2	SVD-2 experiment at IHEP, Protvino
MCRO	MACRO detector in Gran Sasso	T2K	T2K Collaboration
MD1	Magnetic detector at VEPP-4, Novosibirsk	TASS	DESY TASSO detector
MDRP	Millikan drop measurement	TEVA	Combined analysis of CDF and DØ experiments
MEG	Muon to electron conversion detector at PSI	TEXO	TEXONO Collab., ultra low energy Ge detector at Kuo-Sheng Laboratory
MICA	Underground mica deposits	THEO	Theoretical or heavily model-dependent result
MINS	Fermilab MINOS experiment	TNF	TNF-IHEP facility at 70 GeV IHEP accelerator
MIRA	MIRABELLE Liquid-hydrogen bubble chamber	TOF	Time-of-flight
MLEV	Magnetic levitation	TOPZ	TOPAZ detector at KEK-TRISTAN
MMS	Missing mass spectrometer	TPC	TPC detector at PEP/SLAC
MPS	Multiparticle spectrometer at BNL	TPS	Tagged photon spectrometer at Fermilab
MPS2	Multiparticle spectrometer upgrade at BNL	TRAP	Penning trap
MPSF	Multiparticle spectrometer at Fermilab	TWST	TWIST spectrometer at TRIUMF
MPWA	Model-dependent partial-wave analysis	UA1	UA1 detector at CERN
MRK1	SLAC Mark-I detector	UA2	UA2 detector at CERN
MRK2	SLAC Mark-II detector	UA5	UA5 detector at CERN
MRK3	SLAC Mark-III detector		

## Abbreviations Used in the Particle Listings

UCNA	UCNA collaboration using polarized ultracold neutrons at LANSCE
UKDM	UK Dark Matter Collab.
VES	Vertex Spectrometer Facility at 70 GeV IHEP accelerator
VLBI	Very Long Baseline Interferometer
VNS	VENUS detector at KEK-TRISTAN
WA75	CERN WA75 experiment
WA82	CERN WA82 experiment
WA89	CERN WA89 experiment
WARP	Liquid argon detector for CDM searches at Gran Sasso
WASA	WASA detector at CELSIUS, Uppsala and at COSY, Juelich
WIRE	Wire chamber
X100	XENON100 dark matter search experiment at Gran Sasso National Laboratory
XE10	XENON10 experiment at Gran Sasso National Laboratory
XEBC	Xenon bubble chamber
ZEP2	ZEPLIN-II dark matter detector
ZEP3	ZEPLIN-III dark matter detector at Palmer Underground Lab.
ZEPL	ZEPLIN-I galactic dark matter detector
ZEUS	ZEUS detector at DESY/HERA

### Conferences

Conferences are generally referred to by the location at which they were held (e.g., HAMBURG, TORONTO, CORNELL, BRIGHTON, etc.).

### Journals

AA	Astronomy and Astrophysics
ADVP	Advances in Physics
AFIS	Anales de Fisica
AJP	American Journal of Physics
AL	Astronomy Letters
ANP	Annals of Physics
ANPL	Annals of Physics (Leipzig)
ANYAS	Annals of the New York Academy of Sciences
AP	Atomic Physics
APAH	Acta Physica Academiae Scientiarum Hungaricae
APJ	Astrophysical Journal
APJS	Astrophysical Journal Suppl.
APP	Acta Physica Polonica
APS	Acta Physica Slovaca
ARNPS	Annual Review of Nuclear and Particle Science
ARNS	Annual Review of Nuclear Science
ASP	Astroparticle Physics
BAPS	Bulletin of the American Physical Society
BASUP	Bulletin of the Academy of Science, USSR (Physics)
CJNP	Chinese Journal of Nuclear Physics
CJP	Canadian Journal of Physics
CNPP	Comments on Nuclear and Particle Physics
CTP	Communications in Theoretical Physics
CZJP	Czechoslovak Journal of Physics
DANS	Doklady Akademii nauk SSSR
EPJ	The European Physical Journal
EPL	Europhysics Letters
FECAF	Fizika Elementarnykh Chastits i Atomnogo Yadra
HADJ	Hadronic Journal
IJMP	International Journal of Modern Physics
JAP	Journal of Applied Physics
JCAP	Journal of Cosmology and Astroparticle Physics
JETP	English Translation of Soviet Physics ZETF
JETPL	English Translation of Soviet Physics ZETF Letters
JHEP	Journal of High Energy Physics
JINR	Joint Inst. for Nuclear Research
JINRRC	JINR Rapid Communications
JPA	Journal of Physics, A
JPB	Journal of Physics, B
JPCRD	Journal of Physical and Chemical Reference Data
JPG	Journal of Physics, G
JPSJ	Journal of the Physical Society of Japan
LCN	Lettere Nuovo Cimento
MNRAS	Monthly Notices of the Royal Astronomical Society
MPL	Modern Physics Letters
NAT	Nature
NC	Nuovo Cimento
NIM	Nuclear Instruments and Methods
NJP	New Journal of Physics
NP	Nuclear Physics

NPBPS	Nuclear Physics B Proceedings Supplement
PAN	Physics of Atomic Nuclei (formerly SJNP)
PD	Physics Doklady (Magazine)
PDAT	Physik Daten
PL	Physics Letters
PN	Particles and Nuclei
PPCF	Plasma Physics and Controlled Fusion
PPN	Physics of Particles and Nuclei (formerly SJNP)
PPNL	Physics of Particles and Nuclei Letters
PPNP	Progress in Particles and Nuclear Physics
PPSL	Proc. of the Physical Society of London
PR	Physical Review
PRAM	Pramana
PRL	Physical Review Letters
PRPL	Physics Reports (Physics Letters C)
PRSE	Proc. of the Royal Society of Edinburgh
PRSL	Proc. of the Royal Society of London, Section A
PS	Physica Scripta
PTP	Progress of Theoretical Physics
PTPS	Progress of Theoretical Physics Supplement
PTRSL	Phil. Trans. Royal Society of London
RA	Radiochimica Acta
RMP	Reviews of Modern Physics
RNC	La Rivista del Nuovo Cimento
RPP	Reports on Progress in Physics
RRP	Revue Roumaine de Physique
SCI	Science
SJNP	Soviet Journal of Nuclear Physics
SJPN	Soviet Journal of Particles and Nuclei
SPD	Soviet Physics Doklady (Magazine)
SPU	Soviet Physics - Uspekhi
UFN	Usp. Fiz. Nauk - Russian version of SPU
YAF	Yadernaya Fizika
ZETF	Zhurnal Eksperimental'noi i Teoreticheskoi Fiziki
ZETFP	Zhurnal Eksperimental'noi i Teoreticheskoi Fiziki, Pis'ma Redakts
ZNAT	Zeitschrift fur Naturforschung
ZPHY	Zeitschrift fur Physik

### Institutions

AACH	Phys. Inst. der Techn. Hochschule <b>Aachen</b> (Historical, use for general Inst. der Techn. Hochschule)	Aachen, Germany
AACH1	I Phys. Inst. B, RWTH <b>Aachen</b>	Aachen, Germany
AACH3	III Phys. Inst. A, RWTH <b>Aachen</b> Univ.	Aachen, Germany
AACHT	Inst. für Theoretische Teilchenphysik & Kosmologie, RWTH <b>Aachen</b>	Aachen, Germany
AARH	Univ. of <b>Aarhus</b>	Aarhus C, Denmark
ABO	<b>Åbo</b> Akademi Univ.	Turku, Finland
ADEL	<b>Adelphi</b> Univ.	Garden City, NY, USA
ADLD	The Univ. of <b>Adelaide</b> ; Centre for Subatomic Structure of Matter (CSSM); Dept. of Physics	Adelaide, SA, Australia
AERE	Atomic Energy Research Estab.	Didcot, United Kingdom
AFRR	<b>Armed Forces</b> Radiobiology Res. Inst.	Bethesda, MD, USA
AHMED	Physical Research Lab.	<b>Ahmedabad</b> , Gujarat, India
AICH	<b>Aichi</b> Univ. of Education	Aichi, Japan
AKIT	<b>Akita</b> Univ.	Akita, Japan
ALAH	Univ. of <b>Alabama (Huntsville)</b>	Huntsville, AL, USA
ALAT	Univ. of <b>Alabama (Tuscaloosa)</b>	Tuscaloosa, AL, USA
ALBA	<b>SUNY at Albany</b>	Albany, NY, USA
ALBE	Univ. of <b>Alberta</b>	Edmonton, AB, Canada
AMES	<b>Ames Lab.</b>	Ames, IA, USA
AMHT	<b>Amherst</b> College	Amherst, MA, USA
AMST	Univ. van <b>Amsterdam</b>	GL Amsterdam, The Netherlands
ANIK	<b>NIKHEF</b>	<b>Amsterdam</b> , The Netherlands

## Abbreviations Used in the Particle Listings

ANKA	Middle East Technical Univ.; Dept. of Physics; Experimental HEP Lab	Ankara, Turkey	BRUXT	Univ. Libre de Bruxelles; Physique Théorique	Bruxelles, Belgium
ANL	Argonne National Lab.; High Energy Physics Division, Bldg. 362; Physics Division, Bldg. 203	Argonne, IL, USA	BUCH	Univ. of Bucharest	Bucharest-Magurele, Romania
ANSM	St. Anselm Coll.	Manchester, NH, USA	BUDA	KFKI Research Inst. for Particle & Nuclear Physics	Budapest, Hungary
ARCBO	Arecibo Observatory	Arecibo, PR, USA	BUFF	SUNY at Buffalo	Buffalo, NY, USA
ARIZ	Univ. of Arizona	Tucson, AZ, USA	BURE	Inst. des Hautes Etudes Scientifiques	Bures-sur-Yvette, France
ARZS	Arizona State Univ.	Tempe, AZ, USA	CAEN	Lab. de Physique Corpusculaire, ENSICAEN	Caen, France
ASCI	Russian Academy of Sciences	Moscow, Russian Federation	CAGL	Univ. degli Studi di Cagliari	Monserrato (CA), Italy
AST	Inst. of Phys.	Nankang, Taipei, Taiwan	CAIR	Cairo University	Orman, Giza, Cairo, Egypt
ATEN	NCSR "Demokritos"	Aghia Paraskevi, Greece	CAIW	Carnegie Inst. of Washington	Washington, DC, USA
ATHU	Univ. of Athens	Athens, Greece	CALC	Univ. of Calcutta	Calcutta, India
AUCK	Univ. of Auckland	Auckland, New Zealand	CAMB	DAMTP	Cambridge, United Kingdom
BAKU	Natl. Azerbaijan Academy of Sciences, Inst. of Physics	Baku, Azerbaijan	CAMP	Univ. Estadual de Campinas (UNICAMP)	Campinas, SP, Brasil
BANG	Indian Inst. of Science	Bangalore, India	CANB	Australian National Univ.	Canberra, ACT, Australia
BANGB	Bangabasi College	Calcutta, India	CANTB	Inst. de Física de Cantabria (CSIC-Univ. Cantabria)	Santander, Spain
BARC	Univ. Autónoma de Barcelona	Bellaterra (Barcelona), Spain	CAPE	University of Cape Town	Rondebosch, Cape Town, South Africa
BARI	Univ. e del Politecnico di Bari	Bari, Italy	CARA	Univ. Central de Venezuela	Caracas, Venezuela
BART	Univ. of Delaware; Bartol Research Inst.	Newark, DE, USA	CARL	Carleton Univ.	Ottawa, ON, Canada
BASL	Inst. für Physik der Univ. Basel	Basel, Switzerland	CARLC	Carleton College	Northfield, MN, USA
BAYR	Univ. Bayreuth	Bayreuth, Germany	CASE	Case Western Reserve Univ.	Cleveland, OH, USA
BCEN	Centre d'Etudes Nucleaires de Bordeaux-Gradignan	Gradignan, France	CAST	China Center of Advanced Science and Technology	Beijing, China
BCIP	Natl. Inst. for Physics & Nuclear Eng. "Horia Hulubei" (IFIN-HH)	Bucharest-Magurele, Romania	CATA	Univ. di Catania	Catania, Italy
BEIJ	Beijing Univ.	Beijing, China	CATH	Catholic Univ. of America	Washington, DC, USA
BELJT	Inst. of Theoretical Physics	Beijing, China	CAVE	Cavendish Lab.	Cambridge, United Kingdom
BELG	Inter-University Inst. for High Energies (ULB-VUB)	Brussel, Belgium	CBNM	CBNM	Geel, Belgium
BELL	AT & T Bell Labs	Murray Hill, NJ, USA	CCAC	Allegheny College	Meadville, PA, USA
BERG	Univ. of Bergen	Bergen, Norway	CDEF	Univ. Paris VII, Denis Diderot	Paris, France
BERL	DESY, Deutsches Elektronen-Synchrotron	Zeuthen, Germany	CEA	Cambridge Electron Accelerator (Historical in Review)	Cambridge, MA, USA
BERN	Univ. of Berne	Berne, Switzerland	CEADE	Center for Apl. Studies for Nuclear Physics	Havana, Cuba
BGNA	Univ. di Bologna, & INFN, Sezione di Bologna; Via Irnerio, 46, I-40126 Bologna; Viale C. Berti Pichat, n. 6/2	Bologna, Italy	CEBAF	Jefferson Lab—Thomas Jefferson National Accelerator Facility	Newport News, VA, USA
BHAB	Bhabha Atomic Research Center	Trombay, Bombay, India	CENG	Centre d'Etudes Nucleaires	Grenoble, France
BHEP	Inst. of High Energy Physics	Beijing, China	CERN	CERN, European Organization for Nuclear Research	Genève, Switzerland
BIEL	Univ. Bielefeld	Bielefeld, Germany	CFPA	Univ. of California, (Berkeley)	Berkeley, CA, USA
BING	SUNY at Binghamton	Binghamton, NY, USA	CHIC	Univ. of Chicago	Chicago, IL, USA
BIRK	Birkbeck College, Univ. of London	London, United Kingdom	CIAE	China Institute of Atomic Energy	Beijing, China
BIRM	Univ. of Birmingham	Edgbaston, Birmingham, United Kingdom	CINC	Univ. of Cincinnati	Cincinnati, OH, USA
BLSU	Bloomsburg Univ.	Bloomsburg, PA, USA	CINV	CINVESTAV-IPN, Centro de Investigacion y de Estudios Avanzados del IPN	México, DF, Mexico
BNL	Brookhaven National Lab.	Upton, NY, USA	CIT	California Inst. of Tech.	Pasadena, CA, USA
BOCH	Ruhr Univ. Bochum	Bochum, Germany	CLER	Univ. de Clermont-Ferrand	Aubière, France
BOHR	Niels Bohr Inst.	Copenhagen Ø, Denmark	CLEV	Cleveland State Univ.	Cleveland, OH, USA
BOIS	Boise State Univ.	Boise, ID, USA	CMNS	Comenius Univ. (FMFI UK)	Bratislava, Slovakia
BOMB	Univ. of Bombay	Bombay, India	CMU	Carnegie Mellon Univ.	Pittsburgh, PA, USA
BONN	Univ. of Bonn	Bonn, Germany	CNEA	Comisión Nacional de Energía Atómica	Buenos Aires, Argentina
BORD	Univ. de Bordeaux I	Gradignan, France	CNRC	Centre for Research in Particle Physics	Ottawa, ON, Canada
BOSE	S.N. Bose National Centre for Basis Sciences	Calcutta, India	COIM	Univ. de Coimbra	Coimbra, Portugal
BOSK	"Rudjer Bošković" Inst.	Zagreb, Croatia	COLO	Univ. of Colorado	Boulder, CO, USA
BOST	Boston Univ.	Boston, MA, USA	COLU	Columbia Univ.	New York, NY, USA
BRAN	Brandeis Univ.	Waltham, MA, USA	CONC	Concordia University	Montreal, PQ, Canada
BRCO	Univ. of British Columbia	Vancouver, BC, Canada	CORN	Cornell Univ.	Ithaca, NY, USA
BRIS	Univ. of Bristol	Bristol, United Kingdom	COSU	Colorado State Univ.	Fort Collins, CO, USA
BROW	Brown Univ.	Providence, RI, USA	CPPM	Centre National de la Recherche Scientifique, Luminy	Marseille, France
BRUN	Brunel Univ.	Uxbridge, Middlesex, United Kingdom	CRAC	Henryk Niewodnicza'nski Inst. of Nuclear Physics	Kraków, Poland
BRUX	Univ. Libre de Bruxelles; Service de Physique des Particules Élémentaires	Bruxelles, Belgium	CRNL	Chalk River Labs.	Chalk River, ON, Canada
			CSOK	Oklahoma Central State Univ.	Edmond, OK, USA

## Abbreviations Used in the Particle Listings

CST	Univ. of <b>Science and Technology</b> of China	<b>Hefei</b> , Anhui 230026, China	HAWN	<b>Hahn-Meitner</b> Inst. Berlin GmbH	Berlin, Germany
CSULB	<b>California</b> State Univ.	Long Beach, CA, USA	HAIF	<b>Technion</b> – Israel Inst. of Tech.	Technion, Haifa, Israel
CSUS	<b>California</b> State Univ.	Sacramento, USA	HAMB	Univ. <b>Hamburg</b>	Hamburg, Germany
CUNY	<b>City College</b> of New York	New York, NY, USA	HANN	Univ. <b>Hannover</b>	Hannover, Germany
CURCP	Univ. <b>Pierre et Marie Curie</b> (Paris VI), LCP	Paris, France	HARC	<b>Houston Advanced Research Ctr.</b>	The Woodlands, TX, USA
CURIN	Univ. <b>Pierre et Marie Curie</b> (Paris VI), LPNHE	Paris, France	HARV	<b>Harvard</b> Univ.	Cambridge, MA, USA
CURIT	Univ. <b>Pierre et Marie Curie</b> (Paris VI), LPTHE	Paris, France	HAWA	Univ. of <b>Hawai'i</b>	Honolulu, HI, USA
DALH	<b>Dalhousie</b> Univ.	Halifax, NS, Canada	HEBR	<b>Hebrew</b> Univ.	Jerusalem, Israel
DARE	<b>Daresbury</b> Lab	Cheshire, United Kingdom	HEID	Univ. <b>Heidelberg</b> ; (unspecified division) (Historical in <i>Review</i> )	Heidelberg, Germany
DARM	Tech. Hochschule <b>Darmstadt</b>	Darmstadt, Germany	HEIDH	Ruprecht-Karls Univ. <b>Heidelberg</b>	Heidelberg, Germany
DELA	Univ. of <b>Delaware</b> ; Dept. of Physics & Astronomy	Newark, DE, USA	HEIDP	Univ. <b>Heidelberg</b> ; Physikalisches Inst.	Heidelberg, Germany
DELH	Univ. of <b>Delhi</b>	Delhi, India	HEIDT	Univ. <b>Heidelberg</b> ; Inst. für Theoretische Physik	Heidelberg, Germany
DESY	<b>DESY</b> , Deutsches Elektronen-Synchrotron	<b>Hamburg</b> , Germany	HELH	Univ. of <b>Helsinki</b> ; Dept. of Phys., High Energy Phys. Div. (SEFO); Dept. of Phys., Theor. Phys. Div. (TFO); Helsinki Institute of Physics (HIP)	University of Helsinki, Finland
DFAB	Escuela de Ingenieros	<b>Bilbao</b> , Spain	HIRO	<b>Hiroshima</b> Univ.	Higashi-Hiroshima, Japan
DOE	<b>Department of Energy</b>	Washington, DC, USA	HOUS	Univ. of <b>Houston</b>	Houston, TX, USA
DORT	Technische Univ. <b>Dortmund</b>	Dortmund, Germany	HPC	<b>Hewlett-Packard</b> Corp.	Cupertino, CA, USA
DUKE	<b>Duke</b> Univ.	Durham, NC, USA	HSCA	<b>Harvard-Smithsonian</b> Center for Astrophysics	Cambridge, MA, USA
DURH	Univ. of <b>Durham</b>	Durham, United Kingdom	IAS	<b>Inst. for Advanced Study</b>	Princeton, NJ, USA
DUUC	<b>University College</b> Dublin	Dublin, Ireland	IASD	<b>Dublin</b> Inst. for Advanced Studies	Dublin, Ireland
EDIN	Univ. of <b>Edinburgh</b>	Edinburgh, United Kingdom	IBAR	<b>Ibaraki</b> Univ.	Ibaraki, Japan
EFI	Univ. of Chicago, <b>The Enrico Fermi Inst.</b>	<b>Chicago</b> , IL, USA	IBM	<b>IBM</b> Corp.	Palo Alto, CA, USA
ELMT	<b>Elmhurst</b> College	Elmhurst, IL, USA	IBMY	<b>IBM</b>	Yorktown Heights, NY, USA
ENSP	<b>l'Ecole Normale Supérieure</b>	<b>Paris</b> , France	IBS	Inst. for <b>Boson Studies</b>	Pasadena, CA, USA
EOTV	<b>Eötvös</b> University	Budapest, Hungary	ICEPP	The Univ. of <b>Tokyo</b>	Tokyo, Japan
EPOL	<b>École Polytechnique</b>	<b>Palaiseau</b> , France	ICRR	Univ. of <b>Tokyo</b>	Chiba, Japan
ERLA	Univ. <b>Erlangen-Nurnberg</b>	Erlangen, Germany	ICTP	<b>Abdus Salam</b> International Centre for Theoretical Physics	<b>Trieste</b> , Italy
ETH	Univ. <b>Zürich</b>	Zürich, Switzerland	IFIC	<b>IFIC</b> (Instituto de Física Corpuscular)	<b>Valencia</b> , Spain
FERR	Univ. di <b>Ferrara</b>	Ferrara, Italy	IFRJ	Univ. Federal do <b>Rio de Janeiro</b>	Rio de Janeiro, RJ, Brasil
FIRZ	Univ. degli Studi di <b>Firenze</b>	Sesto Fiorentino, Italy	IIT	<b>Illinois Inst. of Tech.</b>	Chicago, IL, USA
FISK	<b>Fisk</b> Univ.	Nashville, TN, USA	ILL	Univ. of <b>Illinois at Urbana-Champaign</b>	Urbana, IL, USA
FLOP	Univ. of <b>Florida</b>	Gainesville, FL, USA	ILLC	Univ. of <b>Illinois at Chicago</b>	Chicago, IL, USA
FNAL	<b>Fermilab</b>	Batavia, IL, USA	ILLG	Inst. <b>Laue-Langevin</b>	Grenoble, France
FOM	<b>FOM</b> , Stichting voor Fundamenteel Onderzoek der Materie	JP <b>Utrecht</b> , The Netherlands	IND	<b>Indiana</b> Univ.	Bloomington, IN, USA
FRAN	<b>Frankfurt Inst. for Advanced Studies (FIAS)</b>	Frankfurt am Main, Germany	INEL	E G and G <b>Idaho</b> , Inc.	Idaho Falls, ID, USA
FRAS	Lab. Nazionali di <b>Frascati</b> dell'INFN	Frascati (Roma), Italy	INFN	Ist. Nazionale di Fisica Nucleare (Generic INFN, unknown location)	Various places, Italy
FREIB	<b>Albert-Ludwigs</b> Univ.	<b>Freiburg</b> , Germany	INNS	Univ. of <b>Innsbruck</b>	<b>Innsbruck</b> , Austria
FREIE	<b>Freie</b> Univ. Berlin	Berlin, Germany	INPK	Inst. of Nuclear Physics	<b>Kraków</b> , Poland
FRIB	Univ. de <b>Fribourg</b>	Fribourg, Switzerland	INRM	<b>INR</b> , Inst. for Nucl. Research	<b>Moscow</b> , Russian Federation
FSU	<b>Florida State</b> Univ.; High Energy Physics	Tallahassee, FL, USA	INUS	<b>KEK</b> , High Energy Accelerator Research Organization	Tokyo, Japan
FSUSC	<b>Florida State</b> Univ.; SCS (School of Computational Science)	Tallahassee, FL, USA	IOAN	Univ. of <b>Ioannina</b>	Ioannina, Greece
FUKI	<b>Fukui</b> Univ.	Fukui, Japan	IOFF	A.F. <b>Ioffe</b> Phys. Tech. Inst.	St. <b>Petersburg</b> , Russian Federation
FUKU	<b>Fukushima</b> Univ.	Fukushima, Japan	IOWA	Univ. of <b>Iowa</b>	Iowa City, IA, USA
GENO	Univ. di <b>Genova</b>	Genova, Italy	IPN	<b>IPN</b> , Inst. de Phys. Nucl.	<b>Orsay</b> , France
GEOR	<b>Georgian Academy of Sciences</b>	Tbilisi, Republic of Georgia	IPNP	Univ. Pierre et Marie Curie ( <b>Paris VI</b> )	Paris, France
GESC	<b>General Electric</b> Co.	Schenectady, NY, USA	IRAD	Inst. du Radium (Historical)	<b>Paris</b> , France
GEVA	Univ. de <b>Genève</b>	Genève, Switzerland	ISNG	Lab. de Physique Subatomique et de Cosmologie ( <b>LPSC</b> )	<b>Grenoble</b> , France
GIES	Univ. <b>Giessen</b>	Giessen, Germany	ISU	<b>Iowa State</b> Univ.	Ames, IA, USA
GIFU	<b>Gifu</b> Univ.	Gifu, Japan	ISUT	Isfahan University of Technology	Isfahan, Iran
GLAS	Univ. of <b>Glasgow</b>	Glasgow, United Kingdom	ITEP	<b>ITEP</b> , Inst. of Theor. and Exp. Physics	<b>Moscow</b> , Russian Federation
GMAS	<b>George Mason</b> Univ.	Fairfax, VA, USA	ITHA	<b>Ithaca</b> College	Ithaca, NY, USA
GOET	Univ. <b>Göttingen</b>	Göttingen, Germany			
GRAN	Univ. de <b>Granada</b>	Granada, Spain			
GRAZ	Univ. <b>Graz</b>	Graz, Austria			
GRON	Univ. of <b>Groningen</b>	Groningen, The Netherlands			
GSCO	<b>Geological Survey of Canada</b>	Ottawa, ON, Canada			
GSI	GSI Helmholtzzentrum für Schwerionenforschung GmbH	<b>Darmstadt</b> , Germany			
GUAN	Univ. de <b>Guanajuato</b>	León, Gto., Mexico			
GUEL	Univ. of <b>Guelph</b>	Guelph, ON, Canada			
GWU	<b>George Washington</b> Univ.	Washington, DC, USA			

# Abbreviations Used in the Particle Listings

IUPU	<b>Indiana Univ., Purdue Univ. Indianapolis</b>	Indianapolis, IN, USA	LISBT	Centro de Física Teórica de Partículas ( <b>CFTP</b> )	<b>Lisboa</b> , Portugal
JADA	<b>Jadavpur Univ.</b>	Calcutta, India	LIVP	Univ. of <b>Liverpool</b>	Liverpool, United Kingdom
JAGL	<b>Jagiellonian Univ.</b>	Kraków, Poland	LLL	<b>Lawrence Livermore Lab.</b> (Old name for LLNL)	Livermore, CA, USA
JHU	<b>Johns Hopkins Univ.</b>	Baltimore, MD, USA	LLNL	<b>Lawrence Livermore National Lab.</b>	Livermore, CA, USA
JINR	<b>JINR</b> , Joint Inst. for Nucl. Research	<b>Dubna</b> , Russian Federation	LOCK	<b>Lockheed Palo Alto Res. Lab</b>	Palo Alto, CA, USA
JULI	Forschungszentrum <b>Jülich</b>	Jülich, Germany	LOIC	<b>Imperial College of Science Tech. &amp; Medicine</b>	London, United Kingdom
JYV	Univ. of <b>Jyväskylä</b>	Jyväskylä, Finland	LOQM	<b>Queen Mary, Univ. of London</b>	London, United Kingdom
KAGO	Univ. of <b>Kagoshima</b>	Kagoshima-shi, Japan	LOUC	<b>University College London</b>	London, United Kingdom
KANS	Univ. of <b>Kansas</b>	Lawrence, KS, USA	LOUV	Univ. Catholique de <b>Louvain</b>	Louvain-la-Neuve, Belgium
KARL	Univ. <b>Karlsruhe</b> (Historical in <i>Review</i> )	Karlsruhe, Germany	LOWC	<b>Westfield College</b> (Historical, see LOQM (Queen Mary and Westfield joined))	London, United Kingdom
KARLE	<b>Karlsruhe Inst. of Technology (KIT)</b> ; Inst. for Experimental Nuclear Physics	Karlsruhe, Germany	LRL	U.C. Lawrence Radiation Lab. (Old name for LBL)	<b>Berkeley</b> , CA, USA
KARLK	<b>Karlsruhe Inst. of Technology (KIT)</b>	Eggenstein-Leopoldshafen, Germany	LSU	<b>Louisiana State Univ.</b>	Baton Rouge, LA, USA
KARLT	<b>Karlsruhe Inst. of Technology (KIT)</b> ; Inst. for Theoretical Physics	Karlsruhe, Germany	LUND	<b>Fysiska Institutionen</b>	<b>Lund</b> , Sweden
KAZA	<b>Kazakh Inst. of High Energy Physics</b>	Alma Ata, Kazakhstan	LUND	<b>Lund Univ.</b>	Lund, Sweden
KEK	<b>KEK</b> , High Energy Accelerator Research Organization	Ibaraki-ken, Japan	LYON	Institute de Physique Nucléaire de <b>Lyon (IPN)</b>	Villeurbanne, France
KENT	Univ. of <b>Kent</b>	Canterbury, United Kingdom	MADE	<b>UAM/CSIC</b> , Inst. de Física Teórica	<b>Madrid</b> , Cantoblanco, Spain
KEYN	<b>Open Univ.</b>	Milton Keynes, United Kingdom	MADR	<b>C.I.E.M.A.T</b>	<b>Madrid</b> , Spain
KFTI	<b>Kharkov Inst. of Physics and Tech.</b> (NSC KIPT)	Kharkov, Ukraine	MADU	Univ. Autónoma de <b>Madrid</b>	Cantoblanco, Madrid, Spain
KIAE	<b>Kurchatov Inst.</b>	<b>Moscow</b> , Russian Federation	MANI	Univ. of <b>Manitoba</b>	Winnipeg, MB, Canada
KIAM	<b>Keldysh Inst. of Applied Math., Acad. Sci., Russia</b>	<b>Moscow</b> , Russian Federation	MANZ	<b>Johannes-Gutenberg- Univ.</b> ; Inst. für Kernphysik, J.-J.-Becher-Weg 45; Inst. für Physik, Staudingerweg 7	<b>Mainz</b> , Germany
KIDR	<b>Vinča Inst. of Nuclear Sciences</b>	Belgrade, Serbia	MARB	Univ. <b>Marburg</b>	Marburg, Germany
KIEV	<b>Institute for Nuclear Research</b>	<b>Kyiv</b> , Ukraine	MARS	Centre de Physique des Particules de <b>Marseille</b>	Marseille, France
KINK	<b>Kinki Univ.</b>	Osaka, Japan	MASA	Univ. of <b>Massachusetts Amherst</b>	<b>Amherst</b> , MA, USA
KNTY	Univ. of <b>Kentucky</b>	Lexington, KY, USA	MASB	Univ. of <b>Massachusetts Boston</b>	<b>Boston</b> , MA, USA
KOBE	<b>Kobe Univ.</b>	Kobe, Japan	MASD	Univ. of <b>Massachusetts Dartmouth</b>	North <b>Dartmouth</b> , MA, USA
KOMAB	Univ. of <b>Tokyo, Komaba</b>	Tokyo, Japan	MCGI	<b>McGill Univ.</b>	Montreal, QC, Canada
KONAN	<b>Konan Univ.</b>	Kobe, Japan	MCHS	Univ. of <b>Manchester</b>	Manchester, United Kingdom
KOSI	Inst. of Experimental Physics <b>SAS</b>	<b>Košice</b> , Slovakia	MCMS	<b>McMaster Univ.</b>	Hamilton, ON, Canada
KYOT	<b>Kyoto Univ.</b> ; Dept. of Physics, Graduate School of Science	Kyoto, Japan	MEHTA	<b>Harish-Chandra Research Inst.</b>	Allahabad, India
KYOTU	<b>Kyoto Univ.</b> ; <b>Yukawa Inst. for Theor. Physics</b>	Kyoto, Japan	MEIS	<b>Meisei Univ.</b>	Tokyo, Japan
KYUN	<b>Kyungpook National Univ.</b>	Daegu, Republic of Korea	MELB	Univ. of <b>Melbourne</b> ; ARC Ctr. of Excellence for Part. Phys. at Terascale; Exper. & Theor. Particle Physics Research Groups	Victoria, Australia
KYUSH	<b>Kyushu Univ.</b> ; Elementary Particle Theory Group; Exp. Particle Physics Group	Fukuoka, Japan	MEUD	Observatoire de <b>Meudon</b>	Meudon, France
LALO	<b>LAL</b> , Laboratoire de l'Accélérateur Linéaire	<b>Orsay</b> , France	MICH	Univ. of <b>Michigan</b>	Ann Arbor, MI, USA
LANC	<b>Lancaster Univ.</b>	Lancaster, United Kingdom	MILA	Univ. di <b>Milano</b>	Milano, Italy
LANL	<b>Los Alamos National Lab.</b> (LANL)	Los Alamos, NM, USA	MILAI	<b>INFN</b> , Sez. di <b>Milano</b>	Milano, Italy
LAPP	<b>LAPP</b> , Lab. d'Annecy-le-Vieux de Phys. des Particules	<b>Annecy-le-Vieux</b> , France	MINN	Univ. of <b>Minnesota</b>	Minneapolis, MN, USA
LASL	U.C. <b>Los Alamos Scientific Lab.</b> (Old name for LANL)	Los Alamos, NM, USA	MIPT	Moscow Institute of Physics and Technology	Moscow, Russian Federation
LATV	<b>Latvian State Univ.</b>	Riga, Latvia	MISS	Univ. of <b>Mississippi</b>	University, MS, USA
LAUS	EPFL <b>Lausanne</b>	Lausanne, Switzerland	MISSR	Univ. of <b>Missouri</b>	Rolla, MO, USA
LAVL	Univ. <b>Laval</b>	Quebec, QC, Canada	MIT	<b>MIT Massachusetts Inst. of Technology</b>	Cambridge, MA, USA
LBL	<b>Lawrence Berkeley National Lab.</b>	Berkeley, CA, USA	MIU	<b>Maharishi International Univ.</b>	Fairfield, IA, USA
LCGT	Univ. di <b>Torino</b>	Turin, Italy	MIYA	<b>Miyazaki Univ.</b>	Miyazaki-shi, Japan
LEBD	<b>Lebedev Physical Inst.</b>	<b>Moscow</b> , Russian Federation	MONP	Univ. de <b>Montpellier II</b>	Montpellier, France
LECE	Univ. di <b>Lecce</b>	Lecce, Italy	MONS	Univ. of <b>Mons</b>	<b>Mons</b> , Belgium
LEED	Univ. of <b>Leeds</b>	Leeds, United Kingdom	MONT	Univ. de <b>Montréal</b> ; Pavillon René-J.-A.-Lévesque	Montréal, PQ, Canada
LEGN	Lab. Naz. di Legnaro	<b>Legnaro</b> , Italy	MONTC	Univ. de <b>Montréal</b> ; Centre de recherches mathématiques	Montréal, PQ, Canada
LEHI	<b>Lehigh Univ.</b>	Bethlehem, PA, USA	MOSU	<b>Skobeltsyn Inst. of Nuclear Physics</b> , Lomonosov Moscow State Univ.; Experimental HEP Division; Theoretical HEP Division	<b>Moscow</b> , Russian Federation
LEHM	<b>Lehman College of CUNY</b>	Bronx, NY, USA	MPCM	Max Planck Inst. für Chemie	<b>Mainz</b> , Germany
LEID	Univ. <b>Leiden</b>	Leiden, The Netherlands			
LEMO	<b>Le Moyne Coll.</b>	Syracuse, NY, USA			
LEUV	Katholieke Univ. <b>Leuven</b>	Leuven, Belgium			
LINZ	Univ. <b>Linz</b>	Linz, Austria			
LISB	Inst. Nacional de Investigacion Científica	<b>Lisboa</b> CODEX, Portugal			

## Abbreviations Used in the Particle Listings

MPEI	<b>Moscow Physical Engineering Inst.</b>	Moscow, Russian Federation	ORST	<b>Oregon State Univ.</b>	Corvallis, OR, USA
MPIA	<b>Max-Planck-Institute für Astrophysik</b>	Garching, Germany	OSAK	<b>Osaka Univ.</b>	Osaka, Japan
MPIH	<b>Max-Planck-Inst. für Kernphysik</b>	<b>Heidelberg</b> , Germany	OSKC	<b>Osaka City Univ.</b>	Osaka-shi, Japan
MPIM	<b>Max-Planck-Inst. für Physik</b>	<b>München</b> , Germany	OSLO	<b>Univ. of Oslo</b>	Oslo, Norway
MSU	<b>Michigan State Univ.</b>	East Lansing, MI, USA	OSU	<b>Ohio State Univ.</b>	Columbus, OH, USA
MTHO	<b>Mount Holyoke College</b>	South Hadley, MA, USA	OTTA	<b>Univ. of Ottawa</b>	Ottawa, ON, Canada
MULH	<b>Centre Univ. du Haut-Rhin</b>	Mulhouse, France	OXF	<b>University of Oxford</b>	Oxford, United Kingdom
MUNI	<b>Ludwig-Maximilians-Univ. München</b>	Garching, Germany	OXFTP	<b>Univ. of Oxford</b>	Oxford, United Kingdom
MUNT	<b>Tech. Univ. München</b>	Garching, Germany	PADO	<b>Univ. degli Studi di Padova</b>	Padova, Italy
MURA	<b>Midwestern Univ. Research Assoc. (Historical in <i>Review</i>)</b>	Stroughton, WI, USA	PARIN	<b>LPNHE, IN<sup>2</sup>P<sup>3</sup>/CNRS</b>	Paris, France
MURC	<b>Univ. of Murcia</b>	Murcia, Spain	PARIS	<b>Univ. de Paris (Historical)</b>	Paris, France
NAAS	<b>North America Aviation Science Center (Historical in <i>Review</i>)</b>	Thousand Oaks, CA, USA	PARIT	<b>Univ. Paris VII, LPTHE</b>	Paris, France
NAGO	<b>Nagoya Univ.</b>	Nagoya, Japan	PARM	<b>INFN, Gruppo Collegato di Parma</b>	Parma, Italy
NAPL	<b>Univ. di Napoli "Federico II"</b>	Napoli, Italy	PAST	<b>Institut Pasteur</b>	Paris, France
NASA	<b>NASA</b>	Greenbelt, MD, USA	PATR	<b>Univ. of Patras</b>	Patras, Greece
NBS	<b>U.S. National Bureau of Standards (Old name for NIST)</b>	Gaithersburg, MD, USA	PAVI	<b>Univ. di Pavia</b>	Pavia, Italy
NBSB	<b>National Inst. Standards Tech.</b>	Boulder, CO, USA	PAVII	<b>INFN, Sez. di Pavia</b>	Pavia, Italy
NCAR	<b>National Center for Atmospheric Research</b>	Boulder, CO, USA	PENN	<b>Univ. of Pennsylvania</b>	Philadelphia, PA, USA
NCSU	<b>North Carolina State Univ.</b>	<b>Raleigh</b> , NC, USA	PGIA	<b>INFN, Sezione di Perugia</b>	Perugia, Italy
NDAM	<b>Univ. of Notre Dame</b>	Notre Dame, IN, USA	PISA	<b>Univ. di Pisa</b>	Pisa, Italy
NEAS	<b>Northeastern Univ.</b>	Boston, MA, USA	PISAI	<b>INFN, Sez. di Pisa</b>	Pisa, Italy
NEBR	<b>Univ. of Nebraska</b>	Lincoln, NE, USA	PITT	<b>Univ. of Pittsburgh</b>	Pittsburgh, PA, USA
NEUC	<b>Univ. de Neuchâtel</b>	Neuchâtel, Switzerland	PLAT	<b>SUNY at Plattsburgh</b>	Plattsburgh, NY, USA
NICEA	<b>Univ. de Nice</b>	Nice, France	PLRM	<b>Univ. di Palermo</b>	Palermo, Italy
NICEO	<b>Observatoire de Nice</b>	Nice, France	PNL	<b>Battelle Memorial Inst.</b>	Richland, WA, USA
NIHO	<b>Nihon Univ.</b>	Tokyo, Japan	PNPI	<b>Petersburg Nuclear Physics Inst. of Russian Academy of Sciences</b>	Gatchina, Russian Federation
NIIG	<b>Niigata Univ.</b>	Niigata, Japan	PPA	<b>Princeton-Penn. Proton Accelerator (Historical in <i>Review</i>)</b>	Princeton, NJ, USA
NIJM	<b>Radboud Univ. Nijmegen</b>	<b>ED Nijmegen</b> , The Netherlands	PRAG	<b>Inst. of Physics, ASCR</b>	Prague, Czech Republic
NIRS	<b>Nat. Inst. Radiological Sciences</b>	<b>Chiba</b> , Japan	PRIN	<b>Princeton Univ.</b>	Princeton, NJ, USA
NIST	<b>National Institute of Standards &amp; Technology</b>	Gaithersburg, MD, USA	PSI	<b>Paul Scherrer Inst.</b>	Villigen PSI, Switzerland
NIU	<b>Northern Illinois Univ.</b>	De Kalb, IL, USA	PSLL	<b>Physical Science Lab</b>	Las Cruces, NM, USA
NMSU	<b>New Mexico State Univ.; Dept. of Physics, MSC 3D; Part. &amp; Nucl. Phys. Group, Box 30001/Dept.</b>	Las Cruces, NM, USA	PSU	<b>Penn State Univ.</b>	University Park, PA, USA
NORD	<b>Nordita</b>	Stockholm, Sweden	PUCB	<b>Pontificia Univ. Católica do Rio de Janeiro</b>	Rio de Janeiro, RJ, Brasil
NOTT	<b>Univ. of Nottingham</b>	Nottingham, United Kingdom	PUEB	<b>Univ. Autonoma de Puebla</b>	Puebla, Pue, Mexico
NOVM	<b>Inst. of Mathematics</b>	<b>Novosibirsk</b> , Russian Federation	PURD	<b>Purdue Univ.</b>	West Lafayette, IN, USA
NOVO	<b>BINP, Budker Inst. of Nuclear Physics</b>	<b>Novosibirsk</b> , Russian Federation	QUKI	<b>Queen's Univ.</b>	Kingston, ON, Canada
NPOL	<b>Polytechnic of North London</b>	London, United Kingdom	RAL	<b>Rutherford Appleton Lab.</b>	Didcot, Oxfordshire, United Kingdom
NRL	<b>Naval Research Lab</b>	Washington, DC, USA	REGE	<b>Univ. Regensburg</b>	Regensburg, Germany
NSF	<b>National Science Foundation</b>	Arlington, VA, USA	REHO	<b>Weizmann Inst. of Science</b>	Rehovot, Israel
NTHU	<b>National Tsing Hua Univ.</b>	Hsinchu, Taiwan	REZ	<b>Nuclear Physics Inst. AVČR</b>	Řež, Czech Republic
NTUA	<b>National Tech. Univ. of Athens</b>	Athens, Greece	RHBL	<b>Royal Holloway, Univ. of London</b>	Egham, Surrey, United Kingdom
NWES	<b>Northwestern Univ.</b>	Evanston, IL, USA	RHEL	<b>Rutherford High Energy Lab (Old name for RAL)</b>	Chilton, Didcot, Oxon., United Kingdom
NYU	<b>New York Univ.</b>	New York, NY, USA	RICE	<b>Rice Univ.</b>	Houston, TX, USA
OBER	<b>Oberlin College</b>	Oberlin, OH, USA	RIKEN	<b>Riken Nishina Center for Accelerator-Based Science</b>	Saitama, Japan
OCH	<b>Ochanomizu Univ.</b>	Tokyo, Japan	RIKK	<b>Rikkyo Univ.</b>	Tokyo, Japan
OHIO	<b>Ohio Univ.</b>	Athens, OH, USA	RIS	<b>Rowland Inst. for Science</b>	Cambridge, MA, USA
OKAY	<b>Okayama Univ.</b>	Okayama, Japan	RISC	<b>Rockwell International</b>	Thousand Oaks, CA, USA
OKLA	<b>Univ. of Oklahoma</b>	Norman, OK, USA	RISL	<b>Universities Research Reactor</b>	Risley, Warrington, United Kingdom
OKSU	<b>Oklahoma State Univ.</b>	Stillwater, OK, USA	RISO	<b>Riso National Laboratory</b>	Roskilde, Denmark
OREG	<b>Univ. of Oregon; Inst. of Theoretical Science; U.O. Center for High Energy Physics</b>	Eugene, OR, USA	RL	<b>Rutherford High Energy Lab (Old name for RAL)</b>	Chilton, Didcot, Oxon., United Kingdom
ORNL	<b>Oak Ridge National Laboratory</b>	Oak Ridge, TN, USA	RMCS	<b>Royal Military Coll. of Science</b>	Swindon, Wilts., United Kingdom
ORSAY	<b>Univ. de Paris Sud</b>	<b>Orsay CEDEX</b> , France	ROCH	<b>Univ. of Rochester</b>	Rochester, NY, USA
			ROCK	<b>Rockefeller Univ.</b>	New York, NY, USA
			ROMA	<b>Univ. di Roma (Historical)</b>	Roma, Italy
			ROMA2	<b>Univ. di Roma, "Tor Vergata"</b>	Roma, Italy
			ROMAI	<b>INFN, Sez. di Roma</b>	Roma, Italy
			ROSE	<b>Rose-Hulman Inst. of Technology</b>	Terre Haute IN, USA
			RPI	<b>Rensselaer Polytechnic Inst.</b>	Troy, NY, USA
			RUTG	<b>Rutgers, the State Univ. of New Jersey</b>	Piscataway, NJ, USA
			SACL	<b>CEA Saclay, IRFU</b>	Gif-sur-Yvette, France
			SACLD	<b>CEA Saclay (Essonne)</b>	Gif-sur-Yvette, France
			SAGA	<b>Saga Univ.</b>	Saga-shi, Japan

## Abbreviations Used in the Particle Listings

SAHA	<b>Saha</b> Inst. of Nuclear Physics	Bidhan Nagar, Calcutta, India	TEXA	Univ. of <b>Texas</b> at <b>Austin</b>	Austin, TX, USA
SANG	<b>Kyoto Sangyo</b> Univ.	Kyoto-shi, Japan	TGAK	<b>Tokyo Gakugei</b> Univ.	Tokyo, Japan
SANI	Ist. Superiore di Sanità	<b>Roma</b> , Italy	TGU	<b>Tohoku Gakuin</b> Univ.	Miyagi, Japan
SASK	Univ. of <b>Saskatchewan</b>	Saskatoon, SK, Canada	THES	Aristotle Univ. of <b>Thessaloniki</b> (AUTH)	Thessaloniki, Greece
SASSO	Lab. Naz. <b>Gran Sasso</b> dell'INFN	<b>Assergi</b> (AQ), Italy	TINT	<b>Tokyo Inst. of Technology</b>	Tokyo, Japan
SAVO	Univ. de <b>Savoie</b>	Chambery, France	TISA	<b>Sagamihara</b> Inst. of Space & Astronautical Sci.	Kanagawa, Japan
SBER	<b>California</b> State Univ.	<b>San Bernardino</b> , CA, USA	TMSK	<b>Tomsk</b> Polytechnic Univ.	<b>Tomsk</b> , Russian Federation
SCHAF	W.J. <b>Schafer</b> Assoc.	Livermore, DA, USA	TMTC	<b>Tokyo Metropolitan</b> Coll. Tech.	Tokyo, Japan
SCIT	<b>Science</b> Univ. of <b>Tokyo</b>	Tokyo, Japan	TMU	<b>Tokyo Metropolitan Univ.</b>	Tokyo, Japan
SCOT	<b>Scottish</b> Univ. Research and Reactor Ctr.	Glasgow, United Kingdom	TNTO	Univ. of <b>Toronto</b>	Toronto, ON, Canada
SCUC	Univ. of <b>South Carolina</b>	Columbia, SC, USA	TOHO	<b>Toho</b> Univ.	Chiba, Japan
SEAT	<b>Seattle Pacific</b> Coll.	Seattle, WA, USA	TOHOK	<b>Tohoku</b> Univ.	Sendai, Japan
SEIB	Austrian Research Center, <b>Seibersdorf</b> LTD.	Seibersdorf, Austria	TOKA	<b>Tokai</b> Univ.	Shimizu, Japan
SEOI	<b>Korea</b> Univ.; Dept. of Physics; HEP Group	Seoul, Republic of Korea	TOKAH	<b>Tokai</b> Univ.	Hiratsuka, Japan
SEOUL	<b>Seoul</b> National Univ.; Center for Theoretical Physics; Dept. of Physics & Astronomy, Coll. of Natural Sciences	Seoul, Republic of Korea	TOKMS	Univ. of <b>Tokyo</b> ; Meson Science Laboratory	Tokyo, Japan
SERP	<b>IHEP</b> , Inst. for High Energy Physics	Protvino, Russian Federation	TOKU	Univ. of <b>Tokushima</b>	Tokushima-shi, Japan
SETO	<b>Seton Hall</b> Univ.	South Orange, NJ, USA	TOKY	Univ. of <b>Tokyo</b> ; High-Energy Physics Theory Group	Tokyo, Japan
SFLA	Univ. of <b>South Florida</b>	Tampa, FL, USA	TOKYC	Univ. of <b>Tokyo</b> ; Dept. of Chemistry	Tokyo, Japan
SFRA	<b>Simon Fraser</b> University	Burnaby, BC, Canada	TORI	Univ. degli Studi di <b>Torino</b>	Torino, Italy
SFSU	<b>California</b> State Univ.	<b>San Francisco</b> , CA, USA	TPTI	<b>Uzbek</b> Academy of Sciences	<b>Tashkent</b> , Republic of Uzbekistan
SHAMS	<b>Ain Shams</b> University	Abbassia, Cairo, Egypt	TRIN	Trinity College <b>Dublin</b>	Dublin, Ireland
SHEF	Univ. of <b>Sheffield</b>	Sheffield, United Kingdom	TRIU	<b>TRIUMF</b>	Vancouver, BC, Canada
SHMP	Univ. of <b>Southampton</b>	Southampton, United Kingdom	TRST	Univ. di <b>Trieste</b>	Trieste, Italy
SIEG	Univ. <b>Siegen</b>	Siegen, Germany	TRSTI	<b>INFN</b> , Sez. di <b>Trieste</b>	Trieste, Italy
SILES	Univ. of <b>Silesia</b>	Katowice, Poland	TRSTT	Univ. degli Studi di <b>Trieste</b>	<b>Trieste</b> , Italy
SIN	Swiss Inst. of Nuclear Research (Old name for VILL)	<b>Villigen</b> , Switzerland	TSUK	Univ. of <b>Tsukuba</b>	Ibaraki-ken, Japan
SING	<b>National Univ.</b> of Singapore	Kent Ridge, Singapore	TTAM	<b>Tamagawa</b> Univ.	Tokyo, Japan
SISSA	Scuola Internazionale Superiore di Studi Avanzati	<b>Trieste</b> , Italy	TUAT	<b>Tokyo</b> Univ. of Agriculture Tech.	Tokyo, Japan
SLAC	<b>SLAC National Accelerator Laboratory</b>	Menlo Park, CA, USA	TUBIN	Univ. <b>Tübingen</b>	Tübingen, Germany
SLOV	Inst. of Physics, Slovak Acad. of Sciences	<b>Bratislava</b> 45, Slovakia	TUFTS	<b>Tufts</b> Univ.	Medford, MA, USA
SMU	<b>Southern Methodist</b> Univ.	Dallas, TX, USA	TUW	<b>Technische</b> Univ. <b>Wien</b>	Vienna, Austria
SNSP	<b>Scuola Normale Superiore</b>	<b>Pisa</b> , Italy	TUZL	<b>Tuzla</b> Univ.	Tuzla, Argentina
SOFI	Inst. for Nuclear Research and Nuclear Energy	<b>Sofia</b> , Bulgaria	UBA	Univ. de <b>Buenos Aires</b>	Buenos Aires, Argentina
SOFU	Univ. of <b>Sofia</b> "St. Kliment Ohridski"	Sofia, Bulgaria	UCB	Univ. of <b>California</b> ( <b>Berkeley</b> )	Berkeley, CA, USA
SPAUL	Univ. de <b>São Paulo</b>	São Paulo, SP, Brasil	UCD	Univ. of <b>California</b> ( <b>Davis</b> )	Davis, CA, USA
SPIFT	Inst. de Física Teórica ( <b>IFT</b> )	<b>São Paulo</b> , SP, Brasil	UCI	Univ. of <b>California</b> ( <b>Irvine</b> )	Irvine, CA, USA
SSL	Univ. of <b>California</b> ( <b>Berkeley</b> )	Berkeley, CA, USA	UCLA	Univ. of <b>California</b> ( <b>Los Angeles</b> )	Los Angeles, CA, USA
STAN	<b>Stanford</b> Univ.	Stanford, CA, USA	UCND	<b>Union Carbide</b> Corp.	Oak Ridge, TN, USA
STEV	<b>Stevens</b> Inst. of Tech.	Hoboken, NJ, USA	UCR	Univ. of <b>California</b> ( <b>Riverside</b> )	Riverside, CA, USA
STLO	<b>St. Louis</b> Univ.	St. Louis, MO, USA	UCSB	Univ. of <b>California</b> ( <b>Santa Barbara</b> ); Physics Dept., High Energy Physics Experiment	Santa Barbara, CA, USA
STOH	<b>Stockholm</b> Univ.	Stockholm, Sweden	UCSBT	Univ. of <b>California</b> ( <b>Santa Barbara</b> ); Kavli Inst. for Theoretical Physics	Santa Barbara, CA, USA
STON	<b>SUNY at Stony Brook</b>	Stony Brook, NY, USA	UCSC	Univ. of <b>California</b> ( <b>Santa Cruz</b> )	Santa Cruz, CA, USA
STRB	Inst. Pluridisciplinaire Hubert Curien ( <b>CNRS</b> )	<b>Strasbourg</b> , France	UCSD	Univ. of <b>California</b> ( <b>San Diego</b> )	La Jolla, CA, USA
STUT	Univ. <b>Stuttgart</b>	Stuttgart, Germany	UGAZ	Univ. of <b>Gaziantep</b>	Gaziantep, Turkey
STUTM	Max-Planck-Inst.	<b>Stuttgart</b> , Germany	UMD	Univ. of <b>Maryland</b>	College Park, MD, USA
SUGI	<b>Sugiyama Jogakuen</b> Univ.	Aichi, Japan	UNAM	Univ. Nac. Autónoma de México ( <b>UNAM</b> )	<b>México</b> , DF, Mexico
SURR	Univ. of <b>Surrey</b>	Guildford, Surrey, United Kingdom	UNAM	Univ. Nacional Autónoma de México ( <b>UNAM</b> )	<b>México</b> , DF, Mexico
SUSS	Univ. of <b>Sussex</b>	Brighton, United Kingdom	UNC	Univ. of <b>North Carolina</b>	Greensboro, NC, USA
SVR	<b>Savannah</b> River Labs.	Aiken, SC, USA	UNCCH	Univ. of <b>North Carolina</b> at <b>Chapel Hill</b>	Chapel Hill, NC, USA
SYDN	Univ. of <b>Sydney</b>	Sydney, NSW, Australia	UNCS	<b>Union</b> College	Schenectady, NY, USA
SYRA	<b>Syracuse</b> Univ.	Syracuse, NY, USA	UNESP	UNESP	Botucatu, Brasil
TAJK	Acad. Sci., Tadjik SSR	<b>Dushanbe</b> , Tadjikistan	UNH	Univ. of <b>New Hampshire</b>	Durham, NH, USA
TAMU	<b>Texas A&amp;M</b> Univ.	College Station, TX, USA	UNM	Univ. of <b>New Mexico</b>	Albuquerque, NM, USA
TATA	<b>Tata</b> Inst. of Fundamental Research	Bombay, India	UOEH	Univ. of Occupational and Environmental Health	<b>Kitakyushu</b> , Japan
TBIL	<b>Tbilisi State University</b>	Tbilisi, Republic of Georgia	UPNJ	<b>Uppsala</b> College	East Orange, NJ, USA
TELA	<b>Tel-Aviv</b> Univ.	Tel Aviv, Israel	UPPS	<b>Uppsala</b> Univ.	<b>Uppsala</b> , Sweden
TELE	<b>Teledyne Brown</b> Engineering	Huntsville, AL, USA			
TEMP	<b>Temple</b> Univ.	Philadelphia, PA, USA			
TENN	Univ. of <b>Tennessee</b>	Knoxville, TN, USA			

## Abbreviations Used in the Particle Listings

UPR	Univ. of <b>Puerto Rico</b>	<b>Rio Piedras</b> , PR, USA	WAYN	<b>Wayne State Univ.</b>	Detroit, MI, USA
URI	Univ. of <b>Rhode Island</b>	Kingston, RI, USA	WESL	<b>Wesleyan Univ.</b>	Middletown, CT, USA
USC	Univ. of <b>Southern California</b>	Los Angeles, CA, USA	WIEN	Univ. <b>Wien</b>	Vienna, Austria
USF	Univ. of <b>San Francisco</b>	San Francisco, CA, USA	WILL	Coll. of <b>William and Mary</b>	Williamsburg, VA, USA
UTAH	Univ. of <b>Utah</b>	Salt Lake City, UT, USA	WINR	National Centre for Nuclear Research	<b>Warsaw</b> , Poland
UTRE	Univ. of <b>Utrecht</b>	Utrecht, The Netherlands	WISC	Univ. of <b>Wisconsin</b>	Madison, WI, USA
UTRO	<b>Norwegian Univ. of Science &amp; Technology</b>	Trondheim, Norway	WITW	Univ. of the <b>Witwatersrand</b>	Wits, South Africa
UVA	Univ. of <b>Virginia</b>	Charlottesville, VA, USA	WMIU	<b>Western Michigan Univ.</b>	Kalamazoo, MI, USA
UZINR	Acad. Sci., <b>Ukrainian SSR</b>	<b>Uzhgorod</b> , Ukraine	WONT	The Univ. of <b>Western Ontario</b>	London, ON, Canada
VALE	Univ. de <b>Valencia</b> ; Dept. Física Teórica, Fac. de Física; Dept. Ing. Electronica, ETSE	Burjassot, <b>Valencia</b> , Spain	WOOD	<b>Woodstock College</b> (No longer in existence)	Woodstock, MD, USA
VALP	<b>Valparaiso Univ.</b>	Valparaiso, IN, USA	WUPP	<b>Bergische Univ.</b> Wuppertal	<b>Wuppertal</b> , Germany
VAND	<b>Vanderbilt Univ.</b>	Nashville, TN, USA	WURZ	Univ. <b>Würzburg</b>	Würzburg, Germany
VASS	<b>Vassar College</b>	Poughkeepsie, NY, USA	WUSL	<b>Washington Univ.</b>	St. Louis, MO, USA
VICT	Univ. of <b>Victoria</b>	Victoria, BC, Canada	WYOM	Univ. of <b>Wyoming</b>	Laramie, WY, USA
VIEN	Inst. für Hochenergiephysik (HEPHY)	<b>Vienna</b> , Austria	YALE	<b>Yale Univ.</b>	New Haven, CT, USA
VILL	<b>ETH Zürich</b>	Zürich, Switzerland	YARO	<b>Yaroslavl State Univ.</b>	Yaroslavl, Russian Federation
VPI	<b>Virginia Tech.</b>	Blacksburg, VA, USA	YCC	<b>Yokohama Coll. of Commerce</b>	Yokohama, Japan
VRIJ	<b>Vrije Univ.</b>	HV <b>Amsterdam</b> , The Netherlands	YERE	<b>Yerevan Physics Inst.</b>	Yerevan, Armenia
WABRNE	Eidgenössisches Amt für Messwesen	<b>Waber</b> , Switzerland	YOKO	<b>Yokohama National Univ.</b>	Yokohama-shi, Japan
WARS	Univ. of <b>Warsaw</b>	Warsaw, Poland	YORKC	<b>York Univ.</b>	Toronto, Canada
WASCR	<b>Waseda Univ.</b> ; Cosmic Ray Division	Tokyo, Japan	ZAGR	<b>Zagreb Univ.</b>	Zagreb, Croatia
WASH	Univ. of <b>Washington</b> ; Elem. Particle Experiment (EPE); Particle Astrophysics (PA)	Seattle, WA, USA	ZARA	Univ. de <b>Zaragoza</b>	Zaragoza, Spain
WASU	<b>Waseda Univ.</b> ; Dept. of Physics, High Energy Physics Group	Tokyo, Japan	ZEEM	Univ. van <b>Amsterdam</b>	TV Amsterdam, The Netherlands
			ZHZH	<b>Zhengzhou Univ.</b>	Zhengzhou, Henan, China
			ZURI	Univ. <b>Zürich</b>	Zürich, Switzerland

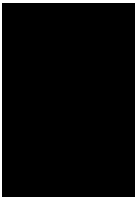


## GAUGE AND HIGGS BOSONS

$\gamma$ . . . . .	469
$g$ (gluon) . . . . .	469
graviton . . . . .	470
$W$ . . . . .	470
$Z$ . . . . .	478
Higgs Bosons — $H^0$ and $H^\pm$ . . . . .	501
Heavy Bosons Other than Higgs Bosons . . . . .	543
Axions ( $A^0$ ) and Other Very Light Bosons . . . . .	562

### Notes in the Gauge and Higgs Boson Listings

The Mass of the $W$ Boson (rev.) . . . . .	470
Triple Gauge Couplings (rev.) . . . . .	474
Anomalous $W/Z$ Quartic Couplings (rev.) . . . . .	477
The $Z$ Boson . . . . .	478
Anomalous $ZZ\gamma$ , $Z\gamma\gamma$ , and $ZZV$ Couplings (rev.) . . . . .	498
Anomalous $W/Z$ Quartic Couplings . . . . .	499
Searches for Higgs Bosons (rev.) . . . . .	501
The $W'$ Searches (rev.) . . . . .	543
The $Z'$ Searches (rev.) . . . . .	547
Leptoquarks (rev.) . . . . .	555
Axions and Other Very Light Bosons (rev.) . . . . .	562





See key on page 457

# Gauge & Higgs Boson Particle Listings

$\gamma, g$

## GAUGE AND HIGGS BOSONS



$$I(J^{PC}) = 0,1(1^{--})$$

### $\gamma$ MASS

Results prior to 2008 are critiqued in GOLDHABER 10.

The following conversions are useful:  $1 \text{ eV} = 1.783 \times 10^{-33} \text{ g} = 1.957 \times 10^{-6} m_e$ ;  $\lambda_C = 1.973 \times 10^{-7} \text{ m}$ .

VALUE (eV)	CL%	DOCUMENT ID	TECN	COMMENT
$< 1$	$\times 10^{-18}$	1 RYUTOV 07		MHD of solar wind
••• We do not use the following data for averages, fits, limits, etc. •••				
$< 1$	$\times 10^{-26}$	2 ACCIOLY 10		Anomalous mag. mom.
		3 ADELBERGER 07A		Galactic field existence if Higgs mass
$< 1.4$	$\times 10^{-7}$	ACCIOLY 04		Dispersion of GHz radio waves by sun
$< 2$	$\times 10^{-16}$	FULLEKRUG 04		Speed of 5-50 Hz radiation in atmosphere
$< 7$	$\times 10^{-19}$	4 LUO 03		Modulation torsion balance
$< 1$	$\times 10^{-17}$	5 LAKES 98		Torque on toroid balance
$< 6$	$\times 10^{-17}$	6 RYUTOV 97		MHD of solar wind
$< 9$	$\times 10^{-16}$	7 FISCHBACH 94		Earth magnetic field
$< (4.73 \pm 0.45) \times 10^{-12}$		8 CHERNIKOV 92	SQID	Ampere-law null test
$< (9.0 \pm 8.1) \times 10^{-10}$		9 RYAN 85		Coulomb-law null test
$< 3$	$\times 10^{-27}$	10 CHIBISOV 76		Galactic magnetic field
$< 6$	$\times 10^{-16}$	99.7 DAVIS 75		Jupiter magnetic field
$< 7.3$	$\times 10^{-16}$	HOLLWEG 74		Alfvén waves
$< 6$	$\times 10^{-17}$	11 FRANKEN 71		Low freq. res. cir.
$< 1$	$\times 10^{-14}$	WILLIAMS 71	CNTR	Tests Gauss law
$< 2.3$	$\times 10^{-15}$	GOLDHABER 68		Satellite data
$< 6$	$\times 10^{-15}$	11 PATEL 65		Satellite data
$< 6$	$\times 10^{-15}$	GINTSBURG 64		Satellite data

- RYUTOV 07 extends the method of RYUTOV 97 to the radius of Pluto's orbit.
- ACCIOLY 10 limits come from possible alterations of anomalous magnetic moment of electron and gravitational deflection of electromagnetic radiation. Reported limits are not "claimed" by the authors and in any case are not competitive.
- When trying to measure  $m$  one must distinguish between measurements performed on large and small scales. If the photon acquires mass by the Higgs mechanism, the large-scale behavior of the photon might be effectively Maxwellian. If, on the other hand, one postulates the Proca regime for all scales, the very existence of the galactic field implies  $m < 10^{-26} \text{ eV}$ , as correctly calculated by YAMAGUCHI 59 and CHIBISOV 76.
- LUO 03 determine a limit on  $\mu^2 A < 1.1 \times 10^{-11} \text{ T m/m}^2$  (with  $\mu^{-1}$ =characteristic length for photon mass;  $A$ =ambient vector potential) — similar to the LAKES 98 technique. Unlike LAKES 98 who used static, the authors used dynamic torsion balance. Assuming  $A$  to be  $10^{12} \text{ T m}$ , they obtain  $\mu < 1.2 \times 10^{-51} \text{ g}$ , equivalent to  $6.7 \times 10^{-19} \text{ eV}$ . The rotating modified Cavendish balance removes dependence on the direction of  $A$ . GOLDHABER 03 argue that because plasma current effects are neglected, the LUO 03 limit does not provide the best available limit on  $\mu^2 A$  nor a reliable limit at all on  $\mu$ . The reason is that the  $A$  associated with cluster magnetic fields could become arbitrarily small in plasma voids, whose existence would be compatible with present knowledge. LUO 03B reply that fields of distant clusters are not accurately mapped, but assert that a zero  $A$  is unlikely given what we know about the magnetic field in our galaxy.
- LAKES 98 reports limits on torque on a toroid Cavendish balance, obtaining a limit on  $\mu^2 A < 2 \times 10^{-9} \text{ Tm/m}^2$  via the Maxwell-Proca equations, where  $\mu^{-1}$  is the characteristic length associated with the photon mass and  $A$  is the ambient vector potential in the Lorentz gauge. Assuming  $A \approx 1 \times 10^{12} \text{ Tm}$  due to cluster fields he obtains  $\mu^{-1} > 2 \times 10^{10} \text{ m}$ , corresponding to  $\mu < 1 \times 10^{-17} \text{ eV}$ . A more conservative limit, using  $A \approx (1 \mu\text{G}) \times (600 \text{ pc})$  based on the galactic field, is  $\mu^{-1} > 1 \times 10^9 \text{ m}$  or  $\mu < 2 \times 10^{-16} \text{ eV}$ .
- RYUTOV 97 uses a magnetohydrodynamics argument concerning survival of the Sun's field to the radius of the Earth's orbit. "To reconcile observations to theory, one has to reduce [the photon mass] by approximately an order of magnitude compared with" DAVIS 75.
- FISCHBACH 94 report  $< 8 \times 10^{-16}$  with unknown CL. We report Bayesian CL used elsewhere in these Listings and described in the Statistics section.
- CHERNIKOV 92 measures the photon mass at 1.24 K, following a theoretical suggestion that electromagnetic gauge invariance might break down at some low critical temperature. See the erratum for a correction, included here, to the published result.
- RYAN 85 measures the photon mass at 1.36 K (see the footnote to CHERNIKOV 92).
- CHIBISOV 76 depends in critical way on assumptions such as applicability of virial theorem. Some of the arguments given only in unpublished references.
- See criticism questioning the validity of these results in GOLDHABER 71, PARK 71 and KROLL 71. See also review GOLDHABER 71B.

### $\gamma$ CHARGE

OKUN 06 has argued that schemes in which all photons are charged are inconsistent. He says that if a neutral photon is also admitted to avoid this problem, then other problems emerge, such as those connected with the emission and absorption of charged photons by charged particles. He concludes that in the absence of a self-consistent phenomenological basis, interpretation of experimental data is at best difficult.

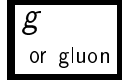
VALUE (e)	CHARGE	DOCUMENT ID	TECN	COMMENT
$< 1 \times 10^{-46}$	mixed	12 ALTSCHUL 07b	VLBI	Aharonov-Bohm effect
$< 1 \times 10^{-35}$	single	13 CAPRINI 05	CMB	Isotropy constraint

••• We do not use the following data for averages, fits, limits, etc. •••

- $< 1 \times 10^{-32}$  single 12 ALTSCHUL 07b VLBI Aharonov-Bohm effect
  - $< 3 \times 10^{-33}$  mixed 14 KOBYCHEV 05 VLBI Smear as function of B-E $_{\gamma}$
  - $< 4 \times 10^{-31}$  single 14 KOBYCHEV 05 VLBI Deflection as function of B-E $_{\gamma}$
  - $< 8.5 \times 10^{-17}$  15 SEMERTZIDIS 03 Laser light deflection in B-field
  - $< 3 \times 10^{-28}$  single 16 SIVARAM 95 CMB For  $\Omega_M = 0.3, h^2 = 0.5$
  - $< 5 \times 10^{-30}$  17 RAFFELT 94 TOF Pulsar  $f_1 - f_2$
  - $< 2 \times 10^{-28}$  18 COCCONI 92 VLBA radio telescope resolution
  - $< 2 \times 10^{-32}$  COCCONI 88 TOF Pulsar  $f_1 - f_2$  TOF
- 12 ALTSCHUL 07b looks for Aharonov-Bohm phase shift in addition to geometric phase shift in radio interference fringes (VSOP mission).
- 13 CAPRINI 05 uses isotropy of the cosmic microwave background to place stringent limits on possible charge asymmetry of the Universe. Charge limits are set on the photon, neutrino, and dark matter particles. Valid if charge asymmetries produced by different particles are not anticorrelated.
- 14 KOBYCHEV 05 considers a variety of observable effects of photon charge for extragalactic compact radio sources. Best limits if source observed through a foreground cluster of galaxies.
- 15 SEMERTZIDIS 03 reports the first laboratory limit on the photon charge in the last 30 years. Straightforward improvements in the apparatus could attain a sensitivity of  $10^{-20} \text{ e}$ .
- 16 SIVARAM 95 requires that CMB photon charge density not overwhelm gravity. Result scales as  $\Omega_M h^2$ .
- 17 RAFFELT 94 notes that COCCONI 88 neglects the fact that the time delay due to dispersion by free electrons in the interstellar medium has the same photon energy dependence as that due to bending of a charged photon in the magnetic field. His limit is based on the assumption that the entire observed dispersion is due to photon charge. It is a factor of 200 less stringent than the COCCONI 88 limit.
- 18 See COCCONI 92 for less stringent limits in other frequency ranges. Also see RAFFELT 94 note.

### $\gamma$ REFERENCES

ACCIOLY 10	PR D82 065026	A. Accioly, J. Helayel-Neto, E. Scatena (LABEX+)
GOLDHABER 10	RMP 82 939	A.F. Goldhaber, M.M. Nieto (STON, LANL)
ADELBERGER 07A	PRL 98 010402	E. Adelberger, G. Dvali, A. Gruzinov (WASH, NYU)
ALTSCHUL 07b	PRL 98 261801	B. Altschul (IND)
Also	ASP 29 290	B. Altschul (SUC)
RYUTOV 07	PPCF 49 B429	D.D. Ryutov (LLNL)
OKUN 06	APP B37 565	L.B. Okun (ITEP)
CAPRINI 05	JCAP 0502 006	C. Caprini, P.G. Ferreira (GEVA, OXFTP)
KOBYCHEV 05	AL 31 147	V.V. Kobychiev, S.B. Popov (KIEV, PADO)
ACCIOLY 04	PR D69 107501	A. Accioly, R. Paszko
FULLEKRUG 04	PRL 93 043901	M. Fullekrug
GOLDHABER 03	PRL 91 149101	A.S. Goldhaber, M.M. Nieto
LUO 03	PRL 90 081801	J. Luo et al.
LUO 03B	PRL 91 149102	J. Luo et al.
SEMERTZIDIS 03	PR D67 017701	Y.K. Semertzidis, G.T. Danby, D.M. Lazarus
LAKES 98	PRL 80 1826	R. Lakes (WISC)
RYUTOV 97	PPCF 39 A73	D.D. Ryutov (LLNL)
SIVARAM 95	AJP 63 473	C. Sivaram (BANG)
FISCHBACH 94	PRL 73 514	E. Fischbach et al. (PURD, JHU+)
RAFFELT 94	PR D50 7729	G. Raffelt (MPIM)
CHERNIKOV 92	PRL 68 3383	M.A. Chernikov et al. (ETH)
Also	PRL 69 2939 (erratum)	M.A. Chernikov et al. (ETH)
COCCONI 92	AJP 60 750	G. Cocconi (CERN)
COCCONI 88	PL B206 705	G. Cocconi (CERN)
RYAN 85	PR D32 802	J.J. Ryan, F. Accetta, R.H. Austin (PRIN)
CHIBISOV 76	SU 19 624	G.V. Chibisov (LEBD)
Translated from	UFN 119 551.	
DAVIS 75	PRL 35 1402	L. Davis, A.S. Goldhaber, M.M. Nieto (CIT, STON+)
HOLLWEG 74	PRL 32 961	J.V. Hollweg (NCAR)
FRANKEN 71	PRL 26 115	P.A. Franken, G.W. Ampulski (MICH)
GOLDHABER 71	PRL 26 1390	A.S. Goldhaber, M.M. Nieto (STON, BOHR, UCSB)
GOLDHABER 71B	RMP 43 277	A.S. Goldhaber, M.M. Nieto (STON, BOHR, UCSB)
KROLL 71	PRL 26 1395	N.M. Kroll (SLAC)
PARK 71	PRL 26 1393	D. Park, E.R. Williams (WILC)
WILLIAMS 71	PRL 26 721	E.R. Williams, J.E. Faller, H.A. Hill (WESL)
GOLDHABER 68	PRL 21 567	A.S. Goldhaber, M.M. Nieto (STON)
PATEL 65	PL 14 105	V.L. Patel (DUKE)
GINTSBURG 64	Sov. Astr. AJ7 536	M.A. Gintsburg (ASCI)
YAMAGUCHI 59	PTPS 11 37	Y. Yamaguchi



or gluon

$$I(J^P) = 0(1^-)$$

SU(3) color octet

Mass  $m = 0$ . Theoretical value. A mass as large as a few MeV may not be precluded, see YNDURAIN 95.

VALUE	DOCUMENT ID	TECN	COMMENT
••• We do not use the following data for averages, fits, limits, etc. •••			
	ABREU 92E	DLPH	Spin 1, not 0
	ALEXANDER 91H	OPAL	Spin 1, not 0
	BEHREND 82D	CELL	Spin 1, not 0
	BERGER 80D	PLUT	Spin 1, not 0
	BRANDELIK 80C	TASS	Spin 1, not 0

### gluon REFERENCES

YNDURAIN 95	PL B345 524	F.J. Yndurain (MADU)
ABREU 92E	PL B274 498	P. Abreu et al. (DELPHI Collab.)
ALEXANDER 91H	ZPHY C52 543	G. Alexander et al. (OPAL Collab.)
BEHREND 82D	PL B110 329	H.J. Behrend et al. (CELLO Collab.)
BERGER 80D	PL B97 459	C. Berger et al. (PLUTO Collab.)
BRANDELIK 80C	PL B97 453	R. Brandelik et al. (TASSO Collab.)

# Gauge & Higgs Boson Particle Listings

## graviton, $W$

graviton

 $J = 2$ 

### graviton MASS

All of the following limits are obtained assuming Yukawa potential in weak field limit. VANDAM 70 argue that a massive field cannot approach general relativity in the zero-mass limit; however, see GOLDHABER 10 and references therein.  $h_0$  is the Hubble constant in units of  $100 \text{ km s}^{-1} \text{ Mpc}^{-1}$ .

The following conversions are useful:  $1 \text{ eV} = 1.783 \times 10^{-33} \text{ g} = 1.957 \times 10^{-6} m_e$ ;  $\lambda_C = 1.973 \times 10^{-7} \text{ m}$ .

VALUE (eV)	DOCUMENT ID	COMMENT
$< 7 \times 10^{-32}$	1 CHOUDHURY 04	Weak gravitational lensing
$< 7.6 \times 10^{-20}$	2 FINN 02	Binary Pulsars
$< 2 \times 10^{-29} h_0^{-1}$	3 DAMOUR 91	Binary pulsar PSR 1913+16
$< 7 \times 10^{-28}$	GOLDHABER 74	Rich clusters
$< 8 \times 10^4$	HARE 73	Galaxy
	HARE 73	$2\gamma$ decay

<sup>1</sup> CHOUDHURY 04 sets limits based on nonobservation of a distortion in the measured values of the variance of the power spectrum.

<sup>2</sup> FINN 02 analyze the orbital decay rates of PSR B1913+16 and PSR B1534+12 with a possible graviton mass as a parameter. The combined frequentist mass limit is at 90%CL.

<sup>3</sup> DAMOUR 91 is an analysis of the orbital period change in binary pulsar PSR 1913+16, and confirms the general relativity prediction to 0.8%. "The theoretical importance of the [rate of orbital period decay] measurement has long been recognized as a direct confirmation that the gravitational interaction propagates with velocity  $c$  (which is the immediate cause of the appearance of a damping force in the binary pulsar system) and thereby as a test of the existence of gravitational radiation and of its quadrupolar nature." TAYLOR 93 adds that orbital parameter studies now agree with general relativity to 0.5%, and set limits on the level of scalar contribution in the context of a family of tensor [spin 2]-biscalar theories.

### graviton REFERENCES

GOLDHABER 10	RMP 82 939	A.F. Goldhaber, M.M. Nieto	(STON, LANL)
CHOUDHURY 04	ASP 21 559	S.R. Choudhury et al.	(DELPH, MELB)
FINN 02	PR D65 044022	L.S. Finn, P.J. Sutton	
TAYLOR 93	NAT 355 132	J.W. Taylor et al.	(PRIN, ARCO, BURE+J)
DAMOUR 91	APJ 366 501	T. Damour, J.H. Taylor	(BURE, MEUD, PRIN)
GOLDHABER 74	PR D9 1119	A.S. Goldhaber, M.M. Nieto	(LANL, STON)
HARE 73	CJP 51 431	M.G. Hare	(SASK)
VANDAM 70	NP B22 397	H. van Dam, M. Veltman	(UTRE)

W

 $J = 1$ 

### THE MASS AND WIDTH OF THE W BOSON

Revised March 2012 by M.W. Gr unewald (U Ghent) and A. Gurtu (King Abdulaziz University).

Precision determination of the W-mass is of great importance in testing the internal consistency of the Standard Model and, together with other electroweak data, in constraining the mass of the undiscovered Higgs boson. From the time of its discovery in 1983, the W-boson has been studied and its mass determined in  $p\bar{p}$  and  $e^+e^-$  interactions; it is currently studied in  $pp$  interactions at the LHC. The W mass and width definition used here corresponds to a Breit-Wigner with mass-dependent width.

Production of on-shell W bosons at hadron colliders is tagged by the high  $p_T$  charged lepton from its decay. Owing to the unknown parton-parton effective energy and missing energy in the longitudinal direction, the collider experiments reconstruct the transverse mass of the W, and derive the W mass from comparing the transverse mass distribution with Monte Carlo predictions as a function of  $M_W$ . These analyses use the electron and muon decay modes of the W boson.

In the  $e^+e^-$  collider (LEP) a precise knowledge of the beam energy enables one to determine the  $e^+e^- \rightarrow W^+W^-$  cross section as a function of center of mass energy, as well as

to reconstruct the W mass precisely from its decay products, even if one of them decays leptonically. Close to the  $W^+W^-$  threshold (161 GeV), the dependence of the W-pair production cross section on  $M_W$  is large, and this was used to determine  $M_W$ . At higher energies (172 to 209 GeV) this dependence is much weaker and W-bosons were directly reconstructed and the mass determined as the invariant mass of its decay products, improving the resolution with a kinematic fit.

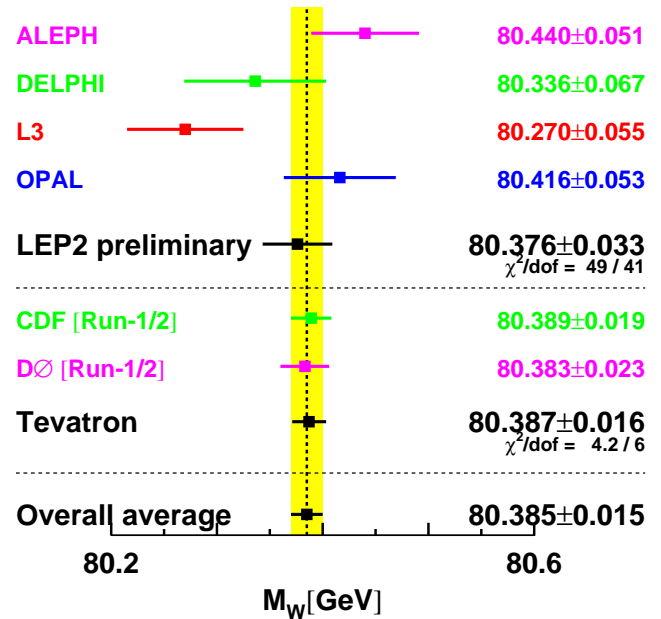


Figure 1: Measurements of the W-boson mass by the LEP and Tevatron experiments.

In order to compute the LEP average W mass, each experiment provided its measured W mass for the  $q\bar{q}q\bar{q}$  and  $q\bar{q}\ell\bar{\nu}_\ell$ ,  $\ell = e, \mu, \tau$  channels at each center-of-mass energy, along with a detailed break-up of errors: statistical, uncorrelated, partially correlated and fully correlated systematics [1]. These have been combined to obtain a LEP W mass of  $M_W = 80.376 \pm 0.033 \text{ GeV}$ . Errors due to uncertainties in LEP energy (9 MeV), and possible effect of color reconnection (CR) and Bose-Einstein correlations (BEC) between quarks from different W's (8 MeV) are included. The mass difference between  $q\bar{q}q\bar{q}$  and  $q\bar{q}\ell\bar{\nu}_\ell$  final states (due to possible CR and BEC effects) is  $-12 \pm 45 \text{ MeV}$ . In a similar manner, the width results obtained at LEP have been combined, resulting in  $\Gamma_W = 2.196 \pm 0.083 \text{ GeV}$  [1].

The two Tevatron experiments have also identified common systematic errors. Between the two experiments, uncertainties due to the parton distribution functions, radiative corrections, and choice of mass (width) in the width (mass) measurements are treated as correlated. An average W mass of  $M_W = 80.420 \pm 0.031 \text{ GeV}$  [2] and a W width of  $\Gamma_W = 2.046 \pm 0.049 \text{ GeV}$  [3] are obtained. Errors of 12 MeV (20 MeV) and 9 MeV (7 MeV) accounting for PDF and radiative correction

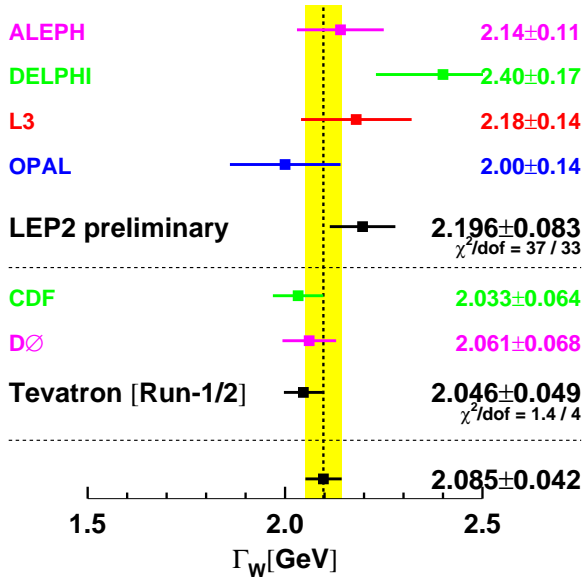


Figure 2: Measurements of the  $W$ -boson width by the LEP and Tevatron experiments.

uncertainties in the mass (width) combination dominate the correlated uncertainties.

At the 2012 winter conferences, the CDF and D0 experiments have presented new results for the mass of the  $W$  boson based on  $2 - 4 \text{ fb}^{-1}$  of Run-II data,  $80.387 \pm 0.019 \text{ GeV}$  [4] and  $80.375 \pm 0.023 \text{ GeV}$  [5], respectively. The  $W$ -mass determination from the Tevatron experiments has thus become very precise. Combining all Tevatron results from Run-I and Run-II using an improved treatment of correlations, a new average of  $80.387 \pm 0.016 \text{ GeV}$  is obtained [6], with common uncertainties of 10 MeV (PDF) and 4 MeV (radiative corrections).

The LEP and Tevatron results on mass and width, which are based on all results available, are compared in Fig. 1 and Fig. 2. Good agreement between the results is observed. Combining these results, assuming no common systematic uncertainties between the LEP and the Tevatron measurements, yields an average  $W$  mass of  $M_W = 80.385 \pm 0.015 \text{ GeV}$  and a  $W$  width of  $\Gamma_W = 2.085 \pm 0.042 \text{ GeV}$ .

The Standard Model prediction from the electroweak fit, using  $Z$ -pole data plus  $m_{\text{top}}$  measurement, gives a  $W$ -boson mass of  $M_W = 80.365 \pm 0.020 \text{ GeV}$  and a  $W$ -boson width of  $\Gamma_W = 2.091 \pm 0.002 \text{ GeV}$  [7].

## References

1. The LEP Collaborations: ALEPH, DELPHI, L3, OPAL, the LEP Electroweak Working Group, CERN-PH-EP/2006-042, hep-ex/0612034 (December 2006).
2. The Tevatron Electroweak Working Group, for the CDF and DØ Collaborations: *Updated Combination of CDF and DØ Results for the Mass of the W Boson*, August 2009, arXiv:0908.1374 [hep-ex].
3. The Tevatron Electroweak Working Group, for the CDF and DØ Collaborations: *Combination of CDF and DØ*

*Results on the Width of the W Boson*, March 2010, arXiv:1003.2826 [hep-ex].

4. The CDF Collaboration, *Precise measurement of the  $W$ -boson mass with the CDF II detector*, arXiv:1203.0275 [hep-ex], Phys. Rev. Lett. **108**, 151803 (2012).
5. The DØ Collaboration, *Measurement of the  $W$  Boson Mass with the DØ Detector*, arXiv:1203.0293 [hep-ex], Phys. Rev. Lett. **108**, 151804 (2012).
6. The Tevatron Electroweak Working Group, for the CDF and DØ Collaborations: *2012 Update of the Combination of CDF and DØ Results for the Mass of the W Boson*, March 2012, arXiv:1204.0042 [hep-ex].
7. The ALEPH, CDF, D0, DELPHI, L3, OPAL, SLD Collaborations, the LEP Electroweak Working Group, the Tevatron Electroweak Working Group, and the SLD electroweak and heavy flavour groups, CERN-PH-EP/2010-095, arXiv:1012.2367 [hep-ex] (December 2010).

## W MASS

The  $W$ -mass listed here corresponds to the mass parameter in a Breit-Wigner distribution with mass-dependent width. To obtain the world average, common systematic uncertainties between experiments are properly taken into account. The LEP-2 average  $W$  mass based on published results is  $80.376 \pm 0.033 \text{ GeV}$  [CERN-PH-EP/2006-042]. The combined Tevatron data yields an average  $W$  mass of  $80.387 \pm 0.016 \text{ GeV}$  [FERMLAB-TM-2532-E].

OUR FIT uses these average LEP and Tevatron mass values and combines them assuming no correlations.

VALUE (GeV)	EVTS	DOCUMENT ID	TECN	COMMENT
<b>80.385 ± 0.015 OUR FIT</b>				
80.387 ± 0.019	1095k	1 AALTONEN	12E CDF	$E_{\text{cm}}^{\text{PD}} = 1.96 \text{ TeV}$
80.367 ± 0.026	1677k	2 ABAZOV	12F D0	$E_{\text{cm}}^{\text{PD}} = 1.96 \text{ TeV}$
80.401 ± 0.043	500k	3 ABAZOV	09AB D0	$E_{\text{cm}}^{\text{PD}} = 1.96 \text{ TeV}$
80.336 ± 0.055 ± 0.039	10.3k	4 ABDALLAH	08A DLPH	$E_{\text{cm}}^{\text{PD}} = 161-209 \text{ GeV}$
80.415 ± 0.042 ± 0.031	11830	5 ABBIENDI	06 OPAL	$E_{\text{cm}}^{\text{PD}} = 170-209 \text{ GeV}$
80.270 ± 0.046 ± 0.031	9909	6 ACHARD	06 L3	$E_{\text{cm}}^{\text{PD}} = 161-209 \text{ GeV}$
80.440 ± 0.043 ± 0.027	8692	7 SCHAEEL	06 ALEP	$E_{\text{cm}}^{\text{PD}} = 161-209 \text{ GeV}$
80.483 ± 0.084	49247	8 ABAZOV	02D D0	$E_{\text{cm}}^{\text{PD}} = 1.8 \text{ TeV}$
80.433 ± 0.079	53841	9 AFFOLDER	01E CDF	$E_{\text{cm}}^{\text{PD}} = 1.8 \text{ TeV}$
••• We do not use the following data for averages, fits, limits, etc. •••				
80.413 ± 0.034 ± 0.034	115k	10 AALTONEN	07F CDF	$E_{\text{cm}}^{\text{PD}} = 1.96 \text{ TeV}$
82.87 ± 1.82 ± $\begin{smallmatrix} 0.30 \\ -0.16 \end{smallmatrix}$	1500	11 AKTAS	06 H1	$e^{\pm} p \rightarrow \bar{\nu}_e(\nu_e)X$ , $\sqrt{s} \approx 300 \text{ GeV}$
80.3 ± 2.1 ± 1.2 ± 1.0	645	12 CHEKANOV	02C ZEUS	$e^{-} p \rightarrow \nu_e X$ , $\sqrt{s} = 318 \text{ GeV}$
81.4 ± $\begin{smallmatrix} 2.7 \\ 2.6 \end{smallmatrix}$ ± $\begin{smallmatrix} 3.3 \\ 3.0 \end{smallmatrix}$	1086	13 BREITWEG	00D ZEUS	$e^{+} p \rightarrow \bar{\nu}_e X$ , $\sqrt{s} \approx 300 \text{ GeV}$
80.84 ± 0.22 ± 0.83	2065	14 ALITTI	92B UA2	See $W/Z$ ratio below
80.79 ± 0.31 ± 0.84		15 ALITTI	90B UA2	$E_{\text{cm}}^{\text{PD}} = 546,630 \text{ GeV}$
80.0 ± 3.3 ± 2.4	22	16 ABE	89I CDF	$E_{\text{cm}}^{\text{PD}} = 1.8 \text{ TeV}$
82.7 ± 1.0 ± 2.7	149	17 ALBAJAR	89 UA1	$E_{\text{cm}}^{\text{PD}} = 546,630 \text{ GeV}$
81.8 ± $\begin{smallmatrix} 6.0 \\ -5.3 \end{smallmatrix}$ ± 2.6	46	18 ALBAJAR	89 UA1	$E_{\text{cm}}^{\text{PD}} = 546,630 \text{ GeV}$
89 ± 3 ± 6	32	19 ALBAJAR	89 UA1	$E_{\text{cm}}^{\text{PD}} = 546,630 \text{ GeV}$
81. ± 5.	6	ARNISON	83 UA1	$E_{\text{cm}}^{\text{PD}} = 546 \text{ GeV}$
80. ± $\begin{smallmatrix} 10. \\ -6. \end{smallmatrix}$	4	BANNER	83B UA2	Repl. by ALITTI 90B

<sup>1</sup> AALTONEN 12E select 470k  $W \rightarrow e\nu$  decays and 625k  $W \rightarrow \mu\nu$  decays in  $2.2 \text{ fb}^{-1}$  of Run-II data. The mass is determined using the transverse mass, transverse lepton momentum and transverse missing energy distributions, accounting for correlations. This result supersedes AALTONEN 07F.

<sup>2</sup> ABAZOV 12F select 1677k  $W \rightarrow e\nu$  decays in  $4.3 \text{ fb}^{-1}$  of Run-II data. The mass is determined using the transverse mass and transverse lepton momentum distributions, accounting for correlations.

<sup>3</sup> ABAZOV 09AB study the transverse mass, transverse electron momentum, and transverse missing energy in a sample of 0.5 million  $W \rightarrow e\nu$  decays selected in Run-II data. The quoted result combines all three methods, accounting for correlations.

<sup>4</sup> ABDALLAH 08A use direct reconstruction of the kinematics of  $W^+ W^- \rightarrow q\bar{q}\ell\nu$  and  $W^+ W^- \rightarrow q\bar{q}q\bar{q}$  events for energies 172 GeV and above. The  $W$  mass was also extracted from the dependence of the  $WW$  cross section close to the production threshold and combined appropriately to obtain the final result. The systematic error includes  $\pm 0.025 \text{ GeV}$  due to final state interactions and  $\pm 0.009 \text{ GeV}$  due to LEP energy uncertainty.

<sup>5</sup> ABBIENDI 06 use direct reconstruction of the kinematics of  $W^+ W^- \rightarrow q\bar{q}\ell\nu\ell$  and  $W^+ W^- \rightarrow q\bar{q}q\bar{q}$  events. The result quoted here is obtained combining this mass value with the results using  $W^+ W^- \rightarrow \nu\ell\ell\nu\rho$  events in the energy range 183-207

# Gauge & Higgs Boson Particle Listings

## W

GeV (ABBIENDI 03c) and the dependence of the  $WW$  production cross-section on  $m_W$  at threshold. The systematic error includes  $\pm 0.009$  GeV due to the uncertainty on the LEP beam energy.

- <sup>6</sup> ACHARD 06 use direct reconstruction of the kinematics of  $W^+W^- \rightarrow q\bar{q}\ell\nu_\ell$  and  $W^+W^- \rightarrow q\bar{q}q\bar{q}$  events in the C.M. energy range 189–209 GeV. The result quoted here is obtained combining this mass value with those obtained from a direct  $W$  mass reconstruction at 172 and 183 GeV and with those from the dependence of the  $WW$  production cross-section on  $m_W$  at 161 and 172 GeV (ACCIARRI 99).
- <sup>7</sup> SCHAEEL 06 use direct reconstruction of the kinematics of  $W^+W^- \rightarrow q\bar{q}\ell\nu_\ell$  and  $W^+W^- \rightarrow q\bar{q}q\bar{q}$  events in the C.M. energy range 183–209 GeV. The result quoted here is obtained combining this mass value with those obtained from the dependence of the  $W$  pair production cross-section on  $m_W$  at 161 and 172 GeV (BARATE 97 and BARATE 97s respectively). The systematic error includes  $\pm 0.009$  GeV due to possible effects of final state interactions in the  $q\bar{q}q\bar{q}$  channel and  $\pm 0.009$  GeV due to the uncertainty on the LEP beam energy.
- <sup>8</sup> ABAZOV 02D improve the measurement of the  $W$ -boson mass including  $W \rightarrow e\nu_e$  events in which the electron is close to a boundary of a central electromagnetic calorimeter module. Properly combining the results obtained by fitting  $m_T(W)$ ,  $p_T(e)$ , and  $p_T(\nu)$ , this sample provides a mass value of  $80.574 \pm 0.405$  GeV. The value reported here is a combination of this measurement with all previous  $D0$   $W$ -boson mass measurements.
- <sup>9</sup> AFFOLDER 01E fit the transverse mass spectrum of 30115  $W \rightarrow e\nu_e$  events ( $M_W = 80.473 \pm 0.065 \pm 0.092$  GeV) and of 14740  $W \rightarrow \mu\nu_\mu$  events ( $M_W = 80.465 \pm 0.100 \pm 0.103$  GeV) obtained in the run IB (1994–95). Combining the electron and muon results, accounting for correlated uncertainties, yields  $M_W = 80.470 \pm 0.089$  GeV. They combine this value with their measurement of ABE 95P reported in run IA (1992–93) to obtain the quoted value.
- <sup>10</sup> AALTONEN 07F obtain high purity  $W \rightarrow e\nu_e$  and  $W \rightarrow \mu\nu_\mu$  candidate samples totaling 63,964 and 51,128 events respectively. The  $W$  mass value quoted above is derived by simultaneously fitting the transverse mass and the lepton, and neutrino  $p_T$  distributions.
- <sup>11</sup> AKTAS 06 fit the  $Q^2$  dependence ( $300 < Q^2 < 30,000$  GeV<sup>2</sup>) of the charged-current differential cross section with a propagator mass. The first error is experimental and the second corresponds to uncertainties due to input parameters and model assumptions.
- <sup>12</sup> CHEKA NOV 02c fit the  $Q^2$  dependence ( $200 < Q^2 < 60000$  GeV<sup>2</sup>) of the charged-current differential cross sections with a propagator mass fit. The last error is due to the uncertainty on the probability density functions.
- <sup>13</sup> BREITWEG 00D fit the  $Q^2$  dependence ( $200 < Q^2 < 22500$  GeV<sup>2</sup>) of the charged-current differential cross sections with a propagator mass fit. The last error is due to the uncertainty on the probability density functions.
- <sup>14</sup> ALITTI 92B result has two contributions to the systematic error ( $\pm 0.83$ ); one ( $\pm 0.81$ ) cancels in  $m_W/m_Z$  and one ( $\pm 0.17$ ) is noncancelling. These were added in quadrature. We choose the ALITTI 92B value without using the LEP  $m_Z$  value, because we perform our own combined fit.
- <sup>15</sup> There are two contributions to the systematic error ( $\pm 0.84$ ): one ( $\pm 0.81$ ) which cancels in  $m_W/m_Z$  and one ( $\pm 0.21$ ) which is non-cancelling. These were added in quadrature.
- <sup>16</sup> ABE 89i systematic error dominated by the uncertainty in the absolute energy scale.
- <sup>17</sup> ALBAJAR 89 result is from a total sample of 299  $W \rightarrow e\nu$  events.
- <sup>18</sup> ALBAJAR 89 result is from a total sample of 67  $W \rightarrow \mu\nu$  events.
- <sup>19</sup> ALBAJAR 89 result is from  $W \rightarrow \tau\nu$  events.

### W/Z MASS RATIO

VALUE	EVTS	DOCUMENT ID	TECN	COMMENT
<b>0.8819 ± 0.0012 OUR AVERAGE</b>				
0.8821 ± 0.0011 ± 0.0008	28323	<sup>20</sup> ABBOTT	98N D0	$E_{cm}^{p\bar{p}} = 1.8$ TeV
0.88114 ± 0.00154 ± 0.00252	5982	<sup>21</sup> ABBOTT	98P D0	$E_{cm}^{p\bar{p}} = 1.8$ TeV
0.8813 ± 0.0036 ± 0.0019	156	<sup>22</sup> ALITTI	92B UA2	$E_{cm}^{p\bar{p}} = 630$ GeV
<sup>20</sup> ABBOTT 98N obtain this from a study of 28323 $W \rightarrow e\nu_e$ and 3294 $Z \rightarrow e^+e^-$ decays. Of this latter sample, 2179 events are used to calibrate the electron energy scale.				
<sup>21</sup> ABBOTT 98P obtain this from a study of 5982 $W \rightarrow e\nu_e$ events. The systematic error includes an uncertainty of $\pm 0.00175$ due to the electron energy scale.				
<sup>22</sup> Scale error cancels in this ratio.				

### $m_Z - m_W$

VALUE (GeV)	DOCUMENT ID	TECN	COMMENT
<b>10.4 ± 1.4 ± 0.8</b>	ALBAJAR 89	UA1	$E_{cm}^{p\bar{p}} = 546,630$ GeV
• • • We do not use the following data for averages, fits, limits, etc. • • •			
11.3 ± 1.3 ± 0.9	ANSARI 87	UA2	$E_{cm}^{p\bar{p}} = 546,630$ GeV

### $m_{W^+} - m_{W^-}$

Test of  $CPT$  invariance.

VALUE (GeV)	EVTS	DOCUMENT ID	TECN	COMMENT
<b>-0.19 ± 0.58</b>	1722	ABE	90G CDF	$E_{cm}^{p\bar{p}} = 1.8$ TeV

### W WIDTH

The  $W$  width listed here corresponds to the width parameter in a Breit-Wigner distribution with mass-dependent width. To obtain the world average, common systematic uncertainties between experiments are properly taken into account. The LEP-2 average  $W$  width based on published results is  $2.196 \pm 0.083$  GeV [CERN-PH-EP/2006-042]. The combined Tevatron data yields an average  $W$  width of  $2.046 \pm 0.049$  GeV [FERMILAB-TM-2460-E].

OUR FIT uses these average LEP and Tevatron width values and combines them assuming no correlations.

VALUE (GeV)	EVTS	DOCUMENT ID	TECN	COMMENT
<b>2.085 ± 0.042 OUR FIT</b>				
2.028 ± 0.072	5272	<sup>23</sup> ABAZOV	09AK D0	$E_{cm}^{p\bar{p}} = 1.96$ GeV
2.032 ± 0.045 ± 0.057	6055	<sup>24</sup> AALTONEN	08B CDF	$E_{cm}^{p\bar{p}} = 1.96$ TeV
2.404 ± 0.140 ± 0.101	10.3k	<sup>25</sup> ABDALLAH	08A DLPH	$E_{cm}^{e\bar{e}} = 183$ –209 GeV
1.996 ± 0.096 ± 0.102	10729	<sup>26</sup> ABBIENDI	06 OPAL	$E_{cm}^{e\bar{e}} = 170$ –209 GeV
2.18 ± 0.11 ± 0.09	9795	<sup>27</sup> ACHARD	06 L3	$E_{cm}^{e\bar{e}} = 172$ –209 GeV
2.14 ± 0.09 ± 0.06	8717	<sup>28</sup> SCHAEEL	06 ALEP	$E_{cm}^{e\bar{e}} = 183$ –209 GeV
2.23 +0.15 -0.14 ± 0.10	294	<sup>29</sup> ABAZOV	02E D0	Direct meas.
2.05 ± 0.10 ± 0.08	662	<sup>30</sup> AFFOLDER	00M CDF	Direct meas.
• • • We do not use the following data for averages, fits, limits, etc. • • •				
2.152 ± 0.066	79176	<sup>31</sup> ABBOTT	00B D0	Extracted value
2.064 ± 0.060 ± 0.059		<sup>32</sup> ABE	95W CDF	Extracted value
2.10 +0.14 -0.13 ± 0.09	3559	<sup>33</sup> ALITTI	92 UA2	Extracted value
2.18 +0.26 -0.24 ± 0.04		<sup>34</sup> ALBAJAR	91 UA1	Extracted value

- <sup>23</sup> ABAZOV 09AK obtain this result fitting the high-end tail (100–200 GeV) of the transverse mass spectrum in  $W \rightarrow e\nu$  decays.
- <sup>24</sup> AALTONEN 08B obtain this result fitting the high-end tail (90–200 GeV) of the transverse mass spectrum in semileptonic  $W \rightarrow e\nu_e$  and  $W \rightarrow \mu\nu_\mu$  decays.
- <sup>25</sup> ABDALLAH 08A use direct reconstruction of the kinematics of  $W^+W^- \rightarrow q\bar{q}\ell\nu$  and  $W^+W^- \rightarrow q\bar{q}q\bar{q}$  events. The systematic error includes  $\pm 0.065$  GeV due to final state interactions.
- <sup>26</sup> ABBIENDI 06 use direct reconstruction of the kinematics of  $W^+W^- \rightarrow q\bar{q}\ell\nu_\ell$  and  $W^+W^- \rightarrow q\bar{q}q\bar{q}$  events. The systematic error includes  $\pm 0.003$  GeV due to the uncertainty on the LEP beam energy.
- <sup>27</sup> ACHARD 06 use direct reconstruction of the kinematics of  $W^+W^- \rightarrow q\bar{q}\ell\nu_\ell$  and  $W^+W^- \rightarrow q\bar{q}q\bar{q}$  events in the C.M. energy range 189–209 GeV. The result quoted here is obtained combining this value of the width with the result obtained from a direct  $W$  mass reconstruction at 172 and 183 GeV (ACCIARRI 99).
- <sup>28</sup> SCHAEEL 06 use direct reconstruction of the kinematics of  $W^+W^- \rightarrow q\bar{q}\ell\nu_\ell$  and  $W^+W^- \rightarrow q\bar{q}q\bar{q}$  events. The systematic error includes  $\pm 0.05$  GeV due to possible effects of final state interactions in the  $q\bar{q}q\bar{q}$  channel and  $\pm 0.01$  GeV due to the uncertainty on the LEP beam energy.
- <sup>29</sup> ABAZOV 02E obtain this result fitting the high-end tail (90–200 GeV) of the transverse-mass spectrum in semileptonic  $W \rightarrow e\nu_e$  decays.
- <sup>30</sup> AFFOLDER 00M fit the high transverse mass (100–200 GeV)  $W \rightarrow e\nu_e$  and  $W \rightarrow \mu\nu_\mu$  events to obtain  $\Gamma(W) = 2.04 \pm 0.11(\text{stat}) \pm 0.09(\text{syst})$  GeV. This is combined with the earlier CDF measurement (ABE 95c) to obtain the quoted result.
- <sup>31</sup> ABBOTT 00B measure  $R = 10.43 \pm 0.27$  for the  $W \rightarrow e\nu_e$  decay channel. They use the SM theoretical predictions for  $\sigma(W)/\sigma(Z)$  and  $\Gamma(W \rightarrow e\nu_e)$  and the world average for  $\Gamma(Z \rightarrow e^+e^-)$ . The value quoted here is obtained combining this result ( $2.169 \pm 0.070$  GeV) with that of ABBOTT 99H.
- <sup>32</sup> ABE 95W measured  $R = 10.90 \pm 0.32 \pm 0.29$ . They use  $m_W = 80.23 \pm 0.18$  GeV,  $\sigma(W)/\sigma(Z) = 3.35 \pm 0.03$ ,  $\Gamma(W \rightarrow e\nu) = 225.9 \pm 0.9$  MeV,  $\Gamma(Z \rightarrow e^+e^-) = 83.98 \pm 0.18$  MeV, and  $\Gamma(Z) = 2.4969 \pm 0.0038$  GeV.
- <sup>33</sup> ALITTI 92 measured  $R = 10.4 +0.7 -0.6 \pm 0.3$ . The values of  $\sigma(Z)$  and  $\sigma(W)$  come from  $O(\alpha_s^2)$  calculations using  $m_W = 80.14 \pm 0.27$  GeV, and  $m_Z = 91.175 \pm 0.021$  GeV along with the corresponding value of  $\sin^2\theta_W = 0.2274$ . They use  $\sigma(W)/\sigma(Z) = 3.26 \pm 0.07 \pm 0.05$  and  $\Gamma(Z) = 2.487 \pm 0.010$  GeV.
- <sup>34</sup> ALBAJAR 91 measured  $R = 9.5 +1.1 -1.0$  (stat. + syst.).  $\sigma(W)/\sigma(Z)$  is calculated in QCD at the parton level using  $m_W = 80.18 \pm 0.28$  GeV and  $m_Z = 91.172 \pm 0.031$  GeV along with  $\sin^2\theta_W = 0.2322 \pm 0.0014$ . They use  $\sigma(W)/\sigma(Z) = 3.23 \pm 0.05$  and  $\Gamma(Z) = 2.498 \pm 0.020$  GeV. This measurement is obtained combining both the electron and muon channels.

### W+ DECAY MODES

$W^-$  modes are charge conjugates of the modes below.

Mode	Fraction ( $\Gamma_i/\Gamma$ )	Confidence level
$\Gamma_1$ $\ell^+\nu$	[a] (10.80 ± 0.09) %	
$\Gamma_2$ $e^+\nu$	(10.75 ± 0.13) %	
$\Gamma_3$ $\mu^+\nu$	(10.57 ± 0.15) %	
$\Gamma_4$ $\tau^+\nu$	(11.25 ± 0.20) %	
$\Gamma_5$ hadrons	(67.60 ± 0.27) %	
$\Gamma_6$ $\pi^+\gamma$	< 8	$\times 10^{-5}$ 95%
$\Gamma_7$ $D_s^+\gamma$	< 1.3	$\times 10^{-3}$ 95%
$\Gamma_8$ $c\bar{X}$	(33.4 ± 2.6) %	
$\Gamma_9$ $c\bar{s}$	(31 +13 -11) %	
$\Gamma_{10}$ invisible	[b] (1.4 ± 2.9) %	

[a]  $\ell$  indicates each type of lepton ( $e$ ,  $\mu$ , and  $\tau$ ), not sum over them.

[b] This represents the width for the decay of the  $W$  boson into a charged particle with momentum below detectability,  $p < 200$  MeV.

## W PARTIAL WIDTHS

 $\Gamma(\text{invisible})$  $\Gamma_{10}$ 

This represents the width for the decay of the  $W$  boson into a charged particle with momentum below detectability,  $p < 200$  MeV.

VALUE (MeV)	DOCUMENT ID	TECN	COMMENT
$30^{+52}_{-48} \pm 33$	35 BARATE	99i ALEP	$E_{\text{cm}}^{ee} = 161+172+183$ GeV

• • • We do not use the following data for averages, fits, limits, etc. • • •

	36 BARATE	99L ALEP	$E_{\text{cm}}^{ee} = 161+172+183$ GeV
--	-----------	----------	--

35 BARATE 99i measure this quantity using the dependence of the total cross section  $\sigma_{WW}$  upon a change in the total width. The fit is performed to the  $WW$  measured cross sections at 161, 172, and 183 GeV. This partial width is  $< 139$  MeV at 95%CL.

36 BARATE 99L use  $W$ -pair production to search for effectively invisible  $W$  decays, tagging with the decay of the other  $W$  boson to Standard Model particles. The partial width for effectively invisible decay is  $< 27$  MeV at 95%CL.

## W BRANCHING RATIOS

Overall fits are performed to determine the branching ratios of the  $W$ . LEP averages on  $W \rightarrow e\nu_e$ ,  $W \rightarrow \mu\nu_\mu$ , and  $W \rightarrow \tau\nu_\tau$ , and their correlations are first obtained by combining results from the four experiments taking properly into account the common systematics. The procedure is described in the note LEPEWWG/XSEC/2001-02, 30 March 2001, at <http://lepewwg.web.cern.ch/LEPEWWG/lepww/4f/PDG01>. The LEP average values so obtained, using published data, are given in the note LEPEWWG/XSEC/2005-01 accessible at <http://lepewwg.web.cern.ch/LEPEWWG/lepww/4f/PDG05/>. These results, together with results from the  $p\bar{p}$  colliders are then used in fits to obtain the world average  $W$  branching ratios. A first fit determines three individual leptonic branching ratios,  $B(W \rightarrow e\nu_e)$ ,  $B(W \rightarrow \mu\nu_\mu)$ , and  $B(W \rightarrow \tau\nu_\tau)$ . This fit has a  $\chi^2=7.9$  for 9 degrees of freedom. The correlation coefficients between the branching fractions are 0.08 ( $e-\mu$ ),  $-0.21$  ( $e-\tau$ ),  $-0.14$  ( $\mu-\tau$ ). A second fit assumes lepton universality and determines the leptonic branching ratio  $B(W \rightarrow \ell\nu_\ell)$  and the hadronic branching ratio is derived as  $B(W \rightarrow \text{hadrons}) = 1-3B(W \rightarrow \ell\nu)$ . This fit has a  $\chi^2=15.5$  for 11 degrees of freedom.

The LEP  $W \rightarrow \ell\nu$  data are obtained by the Collaborations using individual leptonic channels and are, therefore, not included in the overall fits to avoid double counting.

Note: The LEP combination including the new OPAL results, ABBIENDI 07A, could not be performed in time for this Review. Thus, the OUR FIT values quoted below use the previous OPAL results as in ABBIENDI,G 00.

 $\Gamma(\ell^+ \nu)/\Gamma_{\text{total}}$  $\Gamma_1/\Gamma$ 

$\ell$  indicates average over  $e$ ,  $\mu$ , and  $\tau$  modes, not sum over modes.

VALUE (units $10^{-2}$ )	EVTS	DOCUMENT ID	TECN	COMMENT
<b>10.80 ± 0.09 OUR FIT</b>				
10.86 ± 0.12 ± 0.08	16438	ABBIENDI	07A OPAL	$E_{\text{cm}}^{ee} = 161-209$ GeV
10.85 ± 0.14 ± 0.08	13600	ABDALLAH	04G DLPH	$E_{\text{cm}}^{ee} = 161-209$ GeV
10.83 ± 0.14 ± 0.10	11246	ACHARD	04J L3	$E_{\text{cm}}^{ee} = 161-209$ GeV
10.96 ± 0.12 ± 0.05	16116	SCHAEAL	04A ALEP	$E_{\text{cm}}^{ee} = 183-209$ GeV

• • • We do not use the following data for averages, fits, limits, etc. • • •

11.02 ± 0.52	11858	37 ABBOTT	99H D0	$E_{\text{cm}}^{p\bar{p}} = 1.8$ TeV
10.4 ± 0.8	3642	38 ABE	92i CDF	$E_{\text{cm}}^{p\bar{p}} = 1.8$ TeV

37 ABBOTT 99H measure  $R \equiv [\sigma_{W} B(W \rightarrow \ell\nu_\ell)] / [\sigma_Z B(Z \rightarrow \ell\ell)] = 10.90 \pm 0.52$  combining electron and muon channels. They use  $M_W = 80.39 \pm 0.06$  GeV and the SM theoretical predictions for  $\sigma(W)/\sigma(Z)$  and  $B(Z \rightarrow \ell\ell)$ .

38 1216 ± 38 $^{+27}_{-31}$   $W \rightarrow \mu\nu$  events from ABE 92i and 2426  $W \rightarrow e\nu$  events of ABE 91c. ABE 92i give the inverse quantity as  $9.6 \pm 0.7$  and we have inverted.

 $\Gamma(e^+ \nu)/\Gamma_{\text{total}}$  $\Gamma_2/\Gamma$ 

VALUE (units $10^{-2}$ )	EVTS	DOCUMENT ID	TECN	COMMENT
<b>10.75 ± 0.13 OUR FIT</b>				
10.71 ± 0.25 ± 0.11	2374	ABBIENDI	07A OPAL	$E_{\text{cm}}^{ee} = 161-209$ GeV
10.55 ± 0.31 ± 0.14	1804	ABDALLAH	04G DLPH	$E_{\text{cm}}^{ee} = 161-209$ GeV
10.78 ± 0.29 ± 0.13	1576	ACHARD	04J L3	$E_{\text{cm}}^{ee} = 161-209$ GeV
10.78 ± 0.27 ± 0.10	2142	SCHAEAL	04A ALEP	$E_{\text{cm}}^{ee} = 183-209$ GeV

• • • We do not use the following data for averages, fits, limits, etc. • • •

10.61 ± 0.28	39 ABAZOV	04D TEVA	$E_{\text{cm}}^{p\bar{p}} = 1.8$ TeV
--------------	-----------	----------	--------------------------------------

39 ABAZOV 04D take into account all correlations to properly combine the CDF (ABE 95W) and DØ (ABBOTT 00B) measurements of the ratio  $R$  in the electron channel. The ratio  $R$  is defined as  $[\sigma_W \cdot B(W \rightarrow e\nu_e)] / [\sigma_Z \cdot B(Z \rightarrow ee)]$ . The combination gives  $R^{\text{TeVatron}} = 10.59 \pm 0.23$ .  $\sigma_W / \sigma_Z$  is calculated at next-to-next-to-leading order (3.360 ± 0.051). The branching fraction  $B(Z \rightarrow ee)$  is taken from this Review as (3.363 ± 0.004)%.

 $\Gamma(\mu^+ \nu)/\Gamma_{\text{total}}$  $\Gamma_3/\Gamma$ 

VALUE (units $10^{-2}$ )	EVTS	DOCUMENT ID	TECN	COMMENT
<b>10.57 ± 0.15 OUR FIT</b>				
10.78 ± 0.24 ± 0.10	2397	ABBIENDI	07A OPAL	$E_{\text{cm}}^{ee} = 161-209$ GeV
10.65 ± 0.26 ± 0.08	1998	ABDALLAH	04G DLPH	$E_{\text{cm}}^{ee} = 161-209$ GeV
10.03 ± 0.29 ± 0.12	1423	ACHARD	04J L3	$E_{\text{cm}}^{ee} = 161-209$ GeV
10.87 ± 0.25 ± 0.08	2216	SCHAEAL	04A ALEP	$E_{\text{cm}}^{ee} = 183-209$ GeV

 $\Gamma(\tau^+ \nu)/\Gamma_{\text{total}}$  $\Gamma_4/\Gamma$ 

VALUE (units $10^{-2}$ )	EVTS	DOCUMENT ID	TECN	COMMENT
<b>11.25 ± 0.20 OUR FIT</b>				
11.14 ± 0.31 ± 0.17	2177	ABBIENDI	07A OPAL	$E_{\text{cm}}^{ee} = 161-209$ GeV
11.46 ± 0.39 ± 0.19	2034	ABDALLAH	04G DLPH	$E_{\text{cm}}^{ee} = 161-209$ GeV
11.89 ± 0.40 ± 0.20	1375	ACHARD	04J L3	$E_{\text{cm}}^{ee} = 161-209$ GeV
11.25 ± 0.32 ± 0.20	2070	SCHAEAL	04A ALEP	$E_{\text{cm}}^{ee} = 183-209$ GeV

 $\Gamma(\text{hadrons})/\Gamma_{\text{total}}$  $\Gamma_5/\Gamma$ 

OUR FIT value is obtained by a fit to the lepton branching ratio data assuming lepton universality.

VALUE (units $10^{-2}$ )	EVTS	DOCUMENT ID	TECN	COMMENT
<b>67.60 ± 0.27 OUR FIT</b>				
67.41 ± 0.37 ± 0.23	16438	ABBIENDI	07A OPAL	$E_{\text{cm}}^{ee} = 161-209$ GeV
67.45 ± 0.41 ± 0.24	13600	ABDALLAH	04G DLPH	$E_{\text{cm}}^{ee} = 161-209$ GeV
67.50 ± 0.42 ± 0.30	11246	ACHARD	04J L3	$E_{\text{cm}}^{ee} = 161-209$ GeV
67.13 ± 0.37 ± 0.15	16116	SCHAEAL	04A ALEP	$E_{\text{cm}}^{ee} = 183-209$ GeV

 $\Gamma(\mu^+ \nu)/\Gamma(e^+ \nu)$  $\Gamma_3/\Gamma_2$ 

VALUE	EVTS	DOCUMENT ID	TECN	COMMENT
<b>0.983 ± 0.018 OUR FIT</b>				
0.89 ± 0.10	13k	40 ABACHI	95D D0	$E_{\text{cm}}^{p\bar{p}} = 1.8$ TeV
1.02 ± 0.08	1216	41 ABE	92i CDF	$E_{\text{cm}}^{p\bar{p}} = 1.8$ TeV
1.00 ± 0.14 ± 0.08	67	ALBAJAR	89 UA1	$E_{\text{cm}}^{p\bar{p}} = 546, 630$ GeV

• • • We do not use the following data for averages, fits, limits, etc. • • •

1.24 $^{+0.6}_{-0.4}$	14	ARNISON	84D UA1	Repl. by ALBAJAR 89
-----------------------	----	---------	---------	---------------------

40 ABACHI 95D obtain this result from the measured  $\sigma_W B(W \rightarrow \mu\nu) = 2.09 \pm 0.23 \pm 0.11$  nb and  $\sigma_W B(W \rightarrow e\nu) = 2.36 \pm 0.07 \pm 0.13$  nb in which the first error is the combined statistical and systematic uncertainty, the second reflects the uncertainty in the luminosity.

41 ABE 92i obtain  $\sigma_W B(W \rightarrow \mu\nu) = 2.21 \pm 0.07 \pm 0.21$  and combine with ABE 91c  $\sigma_W B(W \rightarrow e\nu)$  to give a ratio of the couplings from which we derive this measurement.

 $\Gamma(\tau^+ \nu)/\Gamma(e^+ \nu)$  $\Gamma_4/\Gamma_2$ 

VALUE	EVTS	DOCUMENT ID	TECN	COMMENT
<b>1.046 ± 0.023 OUR FIT</b>				
0.961 ± 0.061	980	42 ABBOTT	00D D0	$E_{\text{cm}}^{p\bar{p}} = 1.8$ TeV
0.94 ± 0.14	179	43 ABE	92E CDF	$E_{\text{cm}}^{p\bar{p}} = 1.8$ TeV
1.04 ± 0.08 ± 0.08	754	44 ALITTI	92F UA2	$E_{\text{cm}}^{p\bar{p}} = 630$ GeV
1.02 ± 0.20 ± 0.12	32	ALBAJAR	89 UA1	$E_{\text{cm}}^{p\bar{p}} = 546, 630$ GeV

• • • We do not use the following data for averages, fits, limits, etc. • • •

0.995 ± 0.112 ± 0.083	198	ALITTI	91C UA2	Repl. by ALITTI 92F
1.02 ± 0.20 ± 0.10	32	ALBAJAR	87 UA1	Repl. by ALBAJAR 89

42 ABBOTT 00D measure  $\sigma_W \times B(W \rightarrow \tau\nu_\tau) = 2.22 \pm 0.09 \pm 0.10 \pm 0.10$  nb. Using the ABBOTT 00B result  $\sigma_W \times B(W \rightarrow e\nu_e) = 2.31 \pm 0.01 \pm 0.05 \pm 0.10$  nb, they quote the ratio of the couplings from which we derive this measurement.

43 ABE 92E use two procedures for selecting  $W \rightarrow \tau\nu_\tau$  events. The missing  $E_T$  trigger leads to  $132 \pm 14 \pm 8$  events and the  $\tau$  trigger to  $47 \pm 9 \pm 4$  events. Proper statistical and systematic correlations are taken into account to arrive at  $\sigma_B(W \rightarrow \tau\nu) = 2.05 \pm 0.27$  nb. Combined with ABE 91C result on  $\sigma_B(W \rightarrow e\nu)$ , ABE 92E quote a ratio of the couplings from which we derive this measurement.

44 This measurement is derived by us from the ratio of the couplings of ALITTI 92F.

 $\Gamma(\pi^+ \gamma)/\Gamma(e^+ \nu)$  $\Gamma_6/\Gamma_2$ 

VALUE	CL%	DOCUMENT ID	TECN	COMMENT
$< 7 \times 10^{-4}$	95	ABE	98H CDF	$E_{\text{cm}}^{p\bar{p}} = 1.8$ TeV
$< 4.9 \times 10^{-3}$	95	45 ALITTI	92D UA2	$E_{\text{cm}}^{p\bar{p}} = 630$ GeV
$< 5.8 \times 10^{-3}$	95	46 ALBAJAR	90 UA1	$E_{\text{cm}}^{p\bar{p}} = 546, 630$ GeV

45 ALITTI 92D limit is  $3.8 \times 10^{-3}$  at 90%CL.

46 ALBAJAR 90 obtain  $< 0.048$  at 90%CL.

 $\Gamma(D_s^+ \gamma)/\Gamma(e^+ \nu)$  $\Gamma_7/\Gamma_2$ 

VALUE	CL%	DOCUMENT ID	TECN	COMMENT
$< 1.2 \times 10^{-2}$	95	ABE	98P CDF	$E_{\text{cm}}^{p\bar{p}} = 1.8$ TeV

 $\Gamma(cX)/\Gamma(\text{hadrons})$  $\Gamma_8/\Gamma_5$ 

VALUE	EVTS	DOCUMENT ID	TECN	COMMENT
<b>0.49 ± 0.04 OUR AVERAGE</b>				
0.481 ± 0.042 ± 0.032	3005	47 ABBIENDI	00V OPAL	$E_{\text{cm}}^{ee} = 183 + 189$ GeV
0.51 ± 0.05 ± 0.03	746	48 BARATE	99M ALEP	$E_{\text{cm}}^{ee} = 172 + 183$ GeV

## Gauge &amp; Higgs Boson Particle Listings

## W

<sup>47</sup> ABBIENDI 00v tag  $W \rightarrow cX$  decays using measured jet properties, lifetime information, and leptons produced in charm decays. From this result, and using the additional measurements of  $\Gamma(W)$  and  $B(W \rightarrow \text{hadrons})$ ,  $|V_{cs}|$  is determined to be  $0.969 \pm 0.045 \pm 0.036$ .

<sup>48</sup> BARATE 99M tag  $c$  jets using a neural network algorithm. From this measurement  $|V_{cs}|$  is determined to be  $1.00 \pm 0.11 \pm 0.07$ .

$R_{cs} = \Gamma(c\bar{s})/\Gamma(\text{hadrons})$				$\Gamma_9/\Gamma_5$
VALUE	DOCUMENT ID	TECN	COMMENT	
$0.46^{+0.18}_{-0.14} \pm 0.07$	49 ABREU	98N	DLPH	$E_{cm}^{ee} = 161+172$ GeV

<sup>49</sup> ABREU 98N tag  $c$  and  $s$  jets by identifying a charged kaon as the highest momentum particle in a hadronic jet. They also use a lifetime tag to independently identify a  $c$  jet, based on the impact parameter distribution of charged particles in a jet. From this measurement  $|V_{cs}|$  is determined to be  $0.94^{+0.32}_{-0.26} \pm 0.13$ .

## AVERAGE PARTICLE MULTIPLICITIES IN HADRONIC W DECAY

Summed over particle and antiparticle, when appropriate.

$\langle N_{\pi^\pm} \rangle$				
VALUE	DOCUMENT ID	TECN	COMMENT	
$15.70 \pm 0.35$	50 ABREU,P	00F	DLPH	$E_{cm}^{ee} = 189$ GeV

<sup>50</sup> ABREU,P 00F measure  $\langle N_{\pi^\pm} \rangle = 31.65 \pm 0.48 \pm 0.76$  and  $15.51 \pm 0.38 \pm 0.40$  in the fully hadronic and semileptonic final states respectively. The value quoted is a weighted average without assuming any correlations.

$\langle N_{K^\pm} \rangle$				
VALUE	DOCUMENT ID	TECN	COMMENT	
$2.20 \pm 0.19$	51 ABREU,P	00F	DLPH	$E_{cm}^{ee} = 189$ GeV

<sup>51</sup> ABREU,P 00F measure  $\langle N_{K^\pm} \rangle = 4.38 \pm 0.42 \pm 0.12$  and  $2.23 \pm 0.32 \pm 0.17$  in the fully hadronic and semileptonic final states respectively. The value quoted is a weighted average without assuming any correlations.

$\langle N_p \rangle$				
VALUE	DOCUMENT ID	TECN	COMMENT	
$0.92 \pm 0.14$	52 ABREU,P	00F	DLPH	$E_{cm}^{ee} = 189$ GeV

<sup>52</sup> ABREU,P 00F measure  $\langle N_p \rangle = 1.82 \pm 0.29 \pm 0.16$  and  $0.94 \pm 0.23 \pm 0.06$  in the fully hadronic and semileptonic final states respectively. The value quoted is a weighted average without assuming any correlations.

$\langle N_{\text{charged}} \rangle$				
VALUE	DOCUMENT ID	TECN	COMMENT	
$19.39 \pm 0.08$ OUR AVERAGE				
$19.38 \pm 0.05 \pm 0.08$	53 ABBIENDI	06A	OPAL	$E_{cm}^{ee} = 189-209$ GeV
$19.44 \pm 0.17$	54 ABREU,P	00F	DLPH	$E_{cm}^{ee} = 183+189$ GeV
$19.3 \pm 0.3 \pm 0.3$	55 ABBIENDI	99N	OPAL	$E_{cm}^{ee} = 183$ GeV
$19.23 \pm 0.74$	56 ABREU	98c	DLPH	$E_{cm}^{ee} = 172$ GeV

<sup>53</sup> ABBIENDI 06A measure  $\langle N_{\text{charged}} \rangle = 38.74 \pm 0.12 \pm 0.26$  when both  $W$  bosons decay hadronically and  $\langle N_{\text{charged}} \rangle = 19.39 \pm 0.11 \pm 0.09$  when one  $W$  boson decays semileptonically. The value quoted here is obtained under the assumption that there is no color reconnection between  $W$  bosons; the value is a weighted average taking into account correlations in the systematic uncertainties.

<sup>54</sup> ABREU,P 00F measure  $\langle N_{\text{charged}} \rangle = 39.12 \pm 0.33 \pm 0.36$  and  $38.11 \pm 0.57 \pm 0.44$  in the fully hadronic final states at 189 and 183 GeV respectively, and  $\langle N_{\text{charged}} \rangle = 19.49 \pm 0.31 \pm 0.27$  and  $19.78 \pm 0.49 \pm 0.43$  in the semileptonic final states. The value quoted is a weighted average without assuming any correlations.

<sup>55</sup> ABBIENDI 99N use the final states  $W^+W^- \rightarrow q\bar{q}\ell\bar{\nu}_\ell$  to derive this value.

<sup>56</sup> ABREU 98c combine results from both the fully hadronic as well semileptonic  $WW$  final states after demonstrating that the  $W$  decay charged multiplicity is independent of the topology within errors.

## TRIPLE GAUGE COUPLINGS (TGC'S)

Revised March 2012 by M.W. Grunewald (U. Ghent) and A. Gurtu (King Abdulaziz University).

Fourteen independent couplings, 7 each for  $ZWW$  and  $\gamma WW$ , completely describe the  $VWW$  vertices within the most general framework of the electroweak Standard Model (SM) consistent with Lorentz invariance and  $U(1)$  gauge invariance. Of each of the 7 TGC's, 3 conserve  $C$  and  $P$  individually, 3 violate  $CP$ , and one TGC violates  $C$  and  $P$  individually while conserving  $CP$ . Assumption of  $C$  and  $P$  conservation and electromagnetic gauge invariance reduces the independent  $VWW$  couplings to five: one common set [1,2] is  $(\kappa_\gamma, \kappa_Z, \lambda_\gamma, \lambda_Z, g_1^Z)$ , where  $\kappa_\gamma = \kappa_Z = g_1^Z = 1$  and  $\lambda_\gamma = \lambda_Z = 0$  in the Standard Model at the tree level. The parameters  $\kappa_Z$  and  $\lambda_Z$  are related to the other three due to constraints

of gauge invariance as follows:  $\kappa_Z = g_1^Z - (\kappa_\gamma - 1) \tan^2 \theta_W$  and  $\lambda_Z = \lambda_\gamma$ , where  $\theta_W$  is the weak mixing angle. The  $W$  magnetic dipole moment,  $\mu_W$ , and the  $W$  electric quadrupole moment,  $q_W$ , are expressed as  $\mu_W = e(1 + \kappa_\gamma + \lambda_\gamma)/2M_W$  and  $q_W = -e(\kappa_\gamma - \lambda_\gamma)/M_W^2$ .

Precision measurements of suitable observables at LEP1 has already led to an exploration of much of the TGC parameter space. At LEP2, the  $VWW$  coupling arises in  $W$ -pair production via  $s$ -channel exchange, or in single  $W$  production via the radiation of a virtual photon off the incident  $e^+$  or  $e^-$ . At the Tevatron and the LHC, hard-photon bremsstrahlung off a produced  $W$  or  $Z$  signals the presence of a triple-gauge vertex. In order to extract the value of one TGC, the others are generally kept fixed to their SM values.

While most analyses use the above gauge constraints in the extraction of TGCs, one analysis of  $W$ -pair events also determines the real and imaginary parts of all 14 couplings using unconstrained single-parameter fits [3]. The results are consistent.

## References

1. K. Hagiwara *et al.*, Nucl. Phys. **B282**, 253 (1987).
2. G. Gounaris *et al.*, CERN 96-01 p. 525.
3. S. Schael *et al.* (ALEPH Collab.), Phys. Lett. **B614**, 7 (2005).

 $g_1^Z$ 

OUR FIT below is obtained by combining the measurements taking into account properly the common systematic errors (see LEPEWWG/TGC/2005-01 at <http://lepewwg.web.cern.ch/LEPEWWG/lepww/tgcl>).

VALUE	EVTS	DOCUMENT ID	TECN	COMMENT
$0.984^{+0.022}_{-0.019}$ OUR FIT				
$0.975^{+0.033}_{-0.030}$	7872	57 ABDALLAH	10	DLPH $E_{cm}^{ee} = 189-209$ GeV
$1.001 \pm 0.027 \pm 0.013$	9310	58 SCHAEEL	05A	ALEP $E_{cm}^{ee} = 183-209$ GeV
$0.987^{+0.034}_{-0.033}$	9800	59 ABBIENDI	04D	OPAL $E_{cm}^{ee} = 183-209$ GeV
$0.966^{+0.034}_{-0.032} \pm 0.015$	8325	60 ACHARD	04D	L3 $E_{cm}^{ee} = 161-209$ GeV
••• We do not use the following data for averages, fits, limits, etc. •••				
	34	61 ABAZOV	11	D0 $E_{cm}^{pp} = 1.96$ TeV
	334	62 AALTONEN	10K	CDF $E_{cm}^{pp} = 1.96$ TeV
$1.04 \pm 0.09$		63 ABAZOV	09AD	D0 $E_{cm}^{pp} = 1.96$ TeV
		64 ABAZOV	09AJ	D0 $E_{cm}^{pp} = 1.96$ TeV
$1.07^{+0.08}_{-0.12}$	1880	65 ABDALLAH	08C	DLPH Superseded by ABDALLAH 10
	13	66 ABAZOV	07z	D0 $E_{cm}^{pp} = 1.96$ TeV
	2.3	67 ABAZOV	05s	D0 $E_{cm}^{pp} = 1.96$ TeV
$0.98 \pm 0.07 \pm 0.01$	2114	68 ABREU	01i	DLPH $E_{cm}^{ee} = 183+189$ GeV
	331	69 ABBOTT	99i	D0 $E_{cm}^{pp} = 1.8$ TeV

<sup>57</sup> ABDALLAH 10 use data on the final states  $e^+e^- \rightarrow jj\ell\nu, jjjj, jjX, \ell X$ , at center-of-mass energies between 189-209 GeV at LEP2, where  $j = \text{jet}$ ,  $\ell = \text{lepton}$ , and  $X$  represents missing momentum. The fit is carried out keeping all other parameters fixed at their SM values.

<sup>58</sup> SCHAEEL 05A study single-photon, single- $W$ , and  $WW$ -pair production from 183 to 209 GeV. The result quoted here is derived from the  $WW$ -pair production sample. Each parameter is determined from a single-parameter fit in which the other parameters assume their Standard Model values.

<sup>59</sup> ABBIENDI 04d combine results from  $W^+W^-$  in all decay channels. Only  $CP$ -conserving couplings are considered and each parameter is determined from a single-parameter fit in which the other parameters assume their Standard Model values. The 95% confidence interval is  $0.923 < g_1^Z < 1.054$ .

<sup>60</sup> ACHARD 04d study  $WW$ -pair production, single- $W$  production and single-photon production with missing energy from 189 to 209 GeV. The result quoted here is obtained from the  $WW$ -pair production sample including data from 161 to 183 GeV, ACCIARRI 99q. Each parameter is determined from a single-parameter fit in which the other parameters assume their Standard Model values.

<sup>61</sup> ABAZOV 11 study the  $p\bar{p} \rightarrow 3\ell\nu$  process arising in  $WZ$  production. They observe 34  $WZ$  candidates with an estimated background of 6 events. An analysis of the  $p_T$  spectrum of the  $Z$  boson leads to a 95% C.L. limit of  $0.944 < g_1^Z < 1.154$ , for a form factor  $\Lambda = 2$  TeV.



- <sup>62</sup> AALTONEN 10K study  $p\bar{p} \rightarrow W^+W^-$  with  $W \rightarrow e/\mu\nu$ . The  $p_T$  of the leading (second) lepton is required to be  $> 20$  (10) GeV. The final number of events selected is 654 of which  $320 \pm 47$  are estimated to be background. The 95% C.L. interval is  $0.76 < g_1^Z < 1.34$  for  $\Lambda = 1.5$  TeV and  $0.78 < g_1^Z < 1.30$  for  $\Lambda = 2$  TeV.
- <sup>63</sup> ABAZOV 09AD study the  $p\bar{p} \rightarrow \ell\nu 2$ jet process arising in  $WW$  and  $WZ$  production. They select 12,473 (14,392) events in the electron (muon) channel with an expected di-boson signal of 436 (527) events. The results on the anomalous couplings are derived from an analysis of the  $p_T$  spectrum of the 2-jet system and quoted at 68% C.L. and for a form factor of 2 TeV. This measurement is not used for obtaining the mean as it is for a specific form factor. The 95% confidence interval is  $0.88 < g_1^Z < 1.20$ .
- <sup>64</sup> ABAZOV 09AJ study the  $p\bar{p} \rightarrow 2\ell 2\nu$  process arising in  $WW$  production. They select 100 events with an expected  $WW$  signal of 65 events. An analysis of the  $p_T$  spectrum of the two charged leptons leads to 95% C.L. limits of  $0.86 < g_1^Z < 1.3$ , for a form factor  $\Lambda = 2$  TeV.
- <sup>65</sup> ABDALLAH 08c determine this triple gauge coupling from the measurement of the spin density matrix elements in  $e^+e^- \rightarrow W^+W^- \rightarrow (qq)(\ell\nu)$ , where  $\ell = e$  or  $\mu$ . Values of all other couplings are fixed to their standard model values.
- <sup>66</sup> ABAZOV 07z set limits on anomalous TGCs using the measured cross section and  $p_T(Z)$  distribution in  $WZ$  production with both the  $W$  and the  $Z$  decaying leptonically into electrons and muons. Setting the other couplings to their standard model values, the 95% C.L. limit for a form factor scale  $\Lambda = 2$  TeV is  $0.86 < g_1^Z < 1.35$ .
- <sup>67</sup> ABAZOV 05s study  $p\bar{p} \rightarrow WZ$  production with a subsequent trilepton decay to  $\ell\nu\ell'\bar{\nu}$  ( $\ell$  and  $\ell' = e$  or  $\mu$ ). Three events (estimated background  $0.71 \pm 0.08$  events) with  $WZ$  decay characteristics are observed from which they derive limits on the anomalous  $WWZ$  couplings. The 95% C.L. limit for a form factor scale  $\Lambda = 1.5$  TeV is  $0.51 < g_1^Z < 1.66$ , fixing  $\lambda_Z$  and  $\kappa_Z$  to their Standard Model values.
- <sup>68</sup> ABREU 01i combine results from  $e^+e^-$  interactions at 189 GeV leading to  $W^+W^-$  and  $W\nu_e$  final states with results from ABREU 99L at 183 GeV. The 95% confidence interval is  $0.84 < g_1^Z < 1.13$ .
- <sup>69</sup> ABBOTT 99i perform a simultaneous fit to the  $W\gamma$ ,  $WW \rightarrow$  dilepton,  $WW/WZ \rightarrow e\nu jj$ ,  $WW/WZ \rightarrow \mu\nu jj$ , and  $WZ \rightarrow$  trilepton data samples. For  $\Lambda = 2.0$  TeV, the 95%CL limits are  $0.63 < g_1^Z < 1.57$ , fixing  $\lambda_Z$  and  $\kappa_Z$  to their Standard Model values, and assuming Standard Model values for the  $WW\gamma$  couplings.

 $\kappa_\gamma$ 

OUR FIT below is obtained by combining the measurements taking into account properly the common systematic errors (see LEPEWWG/TGC/2005-01 at <http://lepewwg.web.cern.ch/LEPEWWG/lepww/tgc/>).

VALUE	EVTS	DOCUMENT ID	TECN	COMMENT
<b><math>0.973^{+0.044}_{-0.045}</math> OUR FIT</b>				
$1.024^{+0.077}_{-0.081}$	7872	70 ABDALLAH	10 DLPH	$E_{cm}^{ee} = 189-209$ GeV
$0.971 \pm 0.055 \pm 0.030$	10689	71 SCHAEEL	05A ALEP	$E_{cm}^{ee} = 183-209$ GeV
$0.88^{+0.09}_{-0.08}$	9800	72 ABBIENDI	04D OPAL	$E_{cm}^{ee} = 183-209$ GeV
$1.013^{+0.067}_{-0.064} \pm 0.026$	10575	73 ACHARD	04D L3	$E_{cm}^{ee} = 161-209$ GeV
• • • We do not use the following data for averages, fits, limits, etc. • • •				
		74 ABAZOV	11AC D0	$E_{cm}^{pp} = 1.96$ TeV
		75 CHATRCHYAN	11M CMS	$E_{cm}^{pp} = 7$ TeV
	334	76 AALTONEN	10K CDF	$E_{cm}^{pp} = 1.96$ TeV
	53	77 AARON	09B H1	$E_{cm}^{ep} = 0.3$ TeV
$1.07^{+0.26}_{-0.29}$		78 ABAZOV	09AD D0	$E_{cm}^{pp} = 1.96$ TeV
		79 ABAZOV	09AJ D0	$E_{cm}^{pp} = 1.96$ TeV
		80 ABAZOV	08R D0	$E_{cm}^{pp} = 1.96$ TeV
$0.68^{+0.17}_{-0.15}$	1880	81 ABDALLAH	08c DLPH	Superseded by ABDAL-LAH 10
	1617	82 AALTONEN	07L CDF	$E_{cm}^{pp} = 1.96$ GeV
	17	83 ABAZOV	06H D0	$E_{cm}^{pp} = 1.96$ TeV
	141	84 ABAZOV	05J D0	$E_{cm}^{pp} = 1.96$ TeV
$1.25^{+0.21}_{-0.20} \pm 0.06$	2298	85 ABREU	01i DLPH	$E_{cm}^{ee} = 183+189$ GeV
		86 BREITWEG	00 ZEUS	$e^+p \rightarrow e^+W^\pm X$ , $\sqrt{s} \approx 300$ GeV
$0.92 \pm 0.34$	331	87 ABBOTT	99i D0	$E_{cm}^{pp} = 1.8$ TeV
		70 ABDALLAH	10	use data on the final states $e^+e^- \rightarrow jj\ell\nu, jjjj, jjX, \ell X$ , at center-of-mass energies between 189–209 GeV at LEP2, where $j =$ jet, $\ell =$ lepton, and $X$ represents missing momentum. The fit is carried out keeping all other parameters fixed at their SM values.
		71 SCHAEEL	05A	study single-photon, single- $W$ , and $WW$ -pair production from 183 to 209 GeV. Each parameter is determined from a single-parameter fit in which the other parameters assume their Standard Model values.
		72 ABBIENDI	04D	combine results from $W^+W^-$ in all decay channels. Only $CP$ -conserving couplings are considered and each parameter is determined from a single-parameter fit in which the other parameters assume their Standard Model values. The 95% confidence interval is $0.73 < \kappa_\gamma < 1.07$ .
		73 ACHARD	04D	study $W^+W^-$ pair production, single- $W$ production and single-photon production with missing energy from 189 to 209 GeV. The result quoted here is obtained including data from 161 to 183 GeV, ACCIARRI 99q. Each parameter is determined from a single-parameter fit in which the other parameters assume their Standard Model values.
		74 ABAZOV	11ac	study $W\gamma$ production in $p\bar{p}$ collisions at 1.96 TeV, with the $W$ decay products containing an electron or a muon. They select 196 (363) events in the electron (muon) mode, with a SM expectation of 190 (372) events. A likelihood fit to the photon $E_T$ spectrum above 15 GeV yields at 95% C.L. the result: $0.6 < \kappa_\gamma < 1.4$ for a formfactor $\Lambda = 2$ TeV.

- <sup>75</sup> CHATRCHYAN 11M study  $W\gamma$  production in  $pp$  collisions at  $\sqrt{s} = 7$  TeV using  $36 \text{ pb}^{-1}$   $pp$  data with the  $W$  decaying to electron and muon. The total cross section is measured for photon transverse energy  $E_T^\gamma > 10$  GeV and spatial separation from charged leptons in the plane of pseudo rapidity and azimuthal angle  $\Delta R(\ell, \gamma) > 0.7$ . The number of candidate (background) events is 452 ( $228 \pm 21$ ) for the electron channel and 520 ( $277 \pm 25$ ) for the muon channel. Setting other couplings to their standard model value, they derive a 95% CL limit of  $-0.11 < \kappa_\gamma < 2.04$ .
- <sup>76</sup> AALTONEN 10K study  $p\bar{p} \rightarrow W^+W^-$  with  $W \rightarrow e/\mu\nu$ . The  $p_T$  of the leading (second) lepton is required to be  $> 20$  (10) GeV. The final number of events selected is 654 of which  $320 \pm 47$  are estimated to be background. The 95% C.L. interval is  $0.37 < \kappa_\gamma < 1.72$  for  $\Lambda = 1.5$  TeV and  $0.43 < \kappa_\gamma < 1.65$  for  $\Lambda = 2$  TeV.
- <sup>77</sup> AARON 09B study single- $W$  production in  $ep$  collisions at 0.3 TeV C.M. energy. They select 53  $W \rightarrow e/\mu$  events with a standard model expectation of  $54.1 \pm 7.4$  events. Fitting the transverse momentum spectrum of the hadronic recoil system they obtain a 95% C.L. limit of  $-3.7 < \kappa_\gamma < -1.5$  or  $0.3 < \kappa_\gamma < 1.5$ , where the ambiguity is due to the quadratic dependence of the cross section to the coupling parameter.
- <sup>78</sup> ABAZOV 09AD study the  $p\bar{p} \rightarrow \ell\nu 2$ jet process arising in  $WW$  and  $WZ$  production. They select 12,473 (14,392) events in the electron (muon) channel with an expected di-boson signal of 436 (527) events. The results on the anomalous couplings are derived from an analysis of the  $p_T$  spectrum of the 2-jet system and quoted at 68% C.L. and for a form factor of 2 TeV. This measurement is not used for obtaining the mean as it is for a specific form factor. The 95% confidence interval is  $0.56 < \kappa_\gamma < 1.55$ .
- <sup>79</sup> ABAZOV 09AJ study the  $p\bar{p} \rightarrow 2\ell 2\nu$  process arising in  $WW$  production. They select 100 events with an expected  $WW$  signal of 65 events. An analysis of the  $p_T$  spectrum of the two charged leptons leads to 95% C.L. limits of  $0.46 < \kappa_\gamma < 1.83$ , for a form factor  $\Lambda = 2$  TeV.
- <sup>80</sup> ABAZOV 08R use  $0.7 \text{ fb}^{-1}$   $p\bar{p}$  data at  $\sqrt{s} = 1.96$  TeV to select 263  $W\gamma + X$  events, of which 187 constitute signal, with the  $W$  decaying into an electron or a muon, which is required to be well separated from a photon with  $E_T > 9$  GeV. A likelihood fit to the photon  $E_T$  spectrum yields a 95% CL limit  $0.49 < \kappa_\gamma < 1.51$  with other couplings fixed to their Standard Model values.
- <sup>81</sup> ABDALLAH 08c determine this triple gauge coupling from the measurement of the spin density matrix elements in  $e^+e^- \rightarrow W^+W^- \rightarrow (qq)(\ell\nu)$ , where  $\ell = e$  or  $\mu$ . Values of all other couplings are fixed to their standard model values.
- <sup>82</sup> AALTONEN 07L set limits on anomalous TGCs using the  $p_T(W)$  distribution in  $WW$  and  $WZ$  production with the  $W$  decaying to an electron or muon and the  $Z$  to 2 jets. Setting other couplings to their standard model value, the 95% C.L. limits are  $0.54 < \kappa_\gamma < 1.39$  for a form factor scale  $\Lambda = 1.5$  TeV.
- <sup>83</sup> ABAZOV 06H study  $p\bar{p} \rightarrow WW$  production with a subsequent decay  $WW \rightarrow e^+\nu_e e^-\bar{\nu}_e$ ,  $WW \rightarrow e^+\nu_e \mu^+\bar{\nu}_\mu$  or  $WW \rightarrow \mu^+\nu_\mu \mu^-\bar{\nu}_\mu$ . The 95% C.L. limit for a form factor scale  $\Lambda = 1$  TeV is  $-0.05 < \kappa_\gamma < 2.29$ , fixing  $\lambda_\gamma = 0$ . With the assumption that the  $WW\gamma$  and  $WWZ$  couplings are equal the 95% C.L. one-dimensional limit ( $\Lambda = 2$  TeV) is  $0.68 < \kappa < 1.45$ .
- <sup>84</sup> ABAZOV 05i perform a likelihood fit to the photon  $E_T$  spectrum of  $W\gamma + X$  events, where the  $W$  decays to an electron or muon which is required to be well separated from the photon. For  $\Lambda = 2.0$  TeV the 95% CL limits are  $0.12 < \kappa_\gamma < 1.96$ . In the fit  $\lambda_\gamma$  is kept fixed to its Standard Model value.
- <sup>85</sup> ABREU 01i combine results from  $e^+e^-$  interactions at 189 GeV leading to  $W^+W^-$ ,  $W\nu_e$ , and  $\nu\bar{\nu}$  final states with results from ABREU 99L at 183 GeV. The 95% confidence interval is  $0.87 < \kappa_\gamma < 1.68$ .
- <sup>86</sup> BREITWEG 00 search for  $W$  production in events with large hadronic  $p_T$ . For  $p_T > 20$  GeV, the upper limit on the cross section gives the 95%CL limit  $-3.7 < \kappa_\gamma < 2.5$  (for  $\lambda_\gamma = 0$ ).
- <sup>87</sup> ABBOTT 99i perform a simultaneous fit to the  $W\gamma$ ,  $WW \rightarrow$  dilepton,  $WW/WZ \rightarrow e\nu jj$ ,  $WW/WZ \rightarrow \mu\nu jj$ , and  $WZ \rightarrow$  trilepton data samples. For  $\Lambda = 2.0$  TeV, the 95%CL limits are  $0.75 < \kappa_\gamma < 1.39$ .

 $\lambda_\gamma$ 

OUR FIT below is obtained by combining the measurements taking into account properly the common systematic errors (see LEPEWWG/TGC/2005-01 at <http://lepewwg.web.cern.ch/LEPEWWG/lepww/tgc/>).

VALUE	EVTS	DOCUMENT ID	TECN	COMMENT
<b><math>-0.028^{+0.020}_{-0.021}</math> OUR FIT</b>				
$0.002 \pm 0.035$	7872	88 ABDALLAH	10 DLPH	$E_{cm}^{ee} = 189-209$ GeV
$-0.012 \pm 0.027 \pm 0.011$	10689	89 SCHAEEL	05A ALEP	$E_{cm}^{ee} = 183-209$ GeV
$-0.060^{+0.034}_{-0.033}$	9800	90 ABBIENDI	04D OPAL	$E_{cm}^{ee} = 183-209$ GeV
$-0.021^{+0.035}_{-0.034} \pm 0.017$	10575	91 ACHARD	04D L3	$E_{cm}^{ee} = 161-209$ GeV
• • • We do not use the following data for averages, fits, limits, etc. • • •				
		92 ABAZOV	11AC D0	$E_{cm}^{pp} = 1.96$ TeV
		93 CHATRCHYAN	11M CMS	$E_{cm}^{pp} = 7$ TeV
	53	94 AARON	09B H1	$E_{cm}^{ep} = 0.3$ TeV
$0.00 \pm 0.06$		95 ABAZOV	09AD D0	$E_{cm}^{pp} = 1.96$ TeV
		96 ABAZOV	09AJ D0	$E_{cm}^{pp} = 1.96$ TeV
		97 ABAZOV	08R D0	$E_{cm}^{pp} = 1.96$ TeV
$0.16^{+0.12}_{-0.13}$	1880	98 ABDALLAH	08c DLPH	Superseded by ABDAL-LAH 10
	1617	99 AALTONEN	07L CDF	$E_{cm}^{pp} = 1.96$ GeV
	17	100 ABAZOV	06H D0	$E_{cm}^{pp} = 1.96$ TeV
	141	101 ABAZOV	05J D0	$E_{cm}^{pp} = 1.96$ TeV
$0.05 \pm 0.09 \pm 0.01$	2298	102 ABREU	01i DLPH	$E_{cm}^{ee} = 183+189$ GeV
		103 BREITWEG	00 ZEUS	$e^+p \rightarrow e^+W^\pm X$ , $\sqrt{s} \approx 300$ GeV
$0.00^{+0.10}_{-0.09}$	331	104 ABBOTT	99i D0	$E_{cm}^{pp} = 1.8$ TeV

## Gauge &amp; Higgs Boson Particle Listings

## W

- 88 ABDALLAH 10 use data on the final states  $e^+e^- \rightarrow jj\ell\nu, jjjj, jjX, \ell X$ , at center-of-mass energies between 189–209 GeV at LEP2, where  $j = \text{jet}$ ,  $\ell = \text{lepton}$ , and  $X$  represents missing momentum. The fit is carried out keeping all other parameters fixed at their SM values.
- 89 SCHAE 05A study single-photon, single- $W$ , and  $WW$ -pair production from 183 to 209 GeV. Each parameter is determined from a single-parameter fit in which the other parameters assume their Standard Model values.
- 90 ABBIENDI 04D combine results from  $W^+W^-$  in all decay channels. Only  $CP$ -conserving couplings are considered and each parameter is determined from a single-parameter fit in which the other parameters assume their Standard Model values. The 95% confidence interval is  $-0.13 < \lambda_\gamma < 0.01$ .
- 91 ACHARD 04D study  $WW$ -pair production, single- $W$  production and single-photon production with missing energy from 189 to 209 GeV. The result quoted here is obtained including data from 161 to 183 GeV, ACCIARRI 99Q. Each parameter is determined from a single-parameter fit in which the other parameters assume their Standard Model values.
- 92 ABAZOV 11AC study  $W\gamma$  production in  $p\bar{p}$  collisions at 1.96 TeV, with the  $W$  decay products containing an electron or a muon. They select 196 (363) events in the electron (muon) mode, with a SM expectation of 190 (372) events. A likelihood fit to the photon  $E_T$  spectrum above 15 GeV yields at 95% C.L. the result:  $-0.08 < \lambda_\gamma < 0.07$  for a form factor  $\Lambda = 2$  TeV.
- 93 CHATRCHYAN 11M study  $W\gamma$  production in  $pp$  collisions at  $\sqrt{s} = 7$  TeV using 36 pb $^{-1}$   $pp$  data with the  $W$  decaying to electron and muon. The total cross section is measured for photon transverse energy  $E_T^\gamma > 10$  GeV and spatial separation from charged leptons in the plane of pseudo rapidity and azimuthal angle  $\Delta R(\ell, \gamma) > 0.7$ . The number of candidate (background) events is 452 ( $228 \pm 21$ ) for the electron channel and 520 ( $277 \pm 25$ ) for the muon channel. Setting other couplings to their standard model value, they derive a 95% CL limit of  $-0.18 < \lambda_\gamma < 0.17$ .
- 94 AARON 09B study single- $W$  production in  $e p$  collisions at 0.3 TeV C.M. energy. They select 53  $W \rightarrow e/\mu$  events with a standard model expectation of  $54.1 \pm 7.4$  events. Fitting the transverse momentum spectrum of the hadronic recoil system they obtain a 95% C.L. limit of  $-2.5 < \lambda_\gamma < 2.5$ .
- 95 ABAZOV 09AD study the  $p\bar{p} \rightarrow \ell\nu 2\text{jet}$  process arising in  $WW$  and  $WZ$  production. They select 12,473 (14,392) events in the electron (muon) channel with an expected di-boson signal of 436 (527) events. The results on the anomalous couplings are derived from an analysis of the  $p_T$  spectrum of the 2-jet system and quoted at 68% C.L. and for a form factor of 2 TeV. This measurement is not used for obtaining the mean as it is for a specific form factor. The 95% confidence interval is  $-0.10 < \lambda_\gamma < 0.11$ .
- 96 ABAZOV 09AJ study the  $p\bar{p} \rightarrow 2\ell 2\nu$  process arising in  $WW$  production. They select 100 events with an expected  $WW$  signal of 65 events. An analysis of the  $p_T$  spectrum of the two charged leptons leads to 95% C.L. limits of  $-0.14 < \lambda_\gamma < 0.18$ , for a form factor  $\Lambda = 2$  TeV.
- 97 ABAZOV 08R use 0.7 fb $^{-1}$   $p\bar{p}$  data at  $\sqrt{s} = 1.96$  TeV to select 263  $W\gamma + X$  events, of which 187 constitute signal, with the  $W$  decaying into an electron or a muon, which is required to be well separated from a photon with  $E_T > 9$  GeV. A likelihood fit to the photon  $E_T$  spectrum yields a 95% CL limit  $-0.12 < \lambda_\gamma < 0.13$  with other couplings fixed to their Standard Model values.
- 98 ABDALLAH 08C determine this triple gauge coupling from the measurement of the spin density matrix elements in  $e^+e^- \rightarrow W^+W^- \rightarrow (qq)(\ell\nu)$ , where  $\ell = e$  or  $\mu$ . Values of all other couplings are fixed to their standard model values.
- 99 AALTONEN 07L set limits on anomalous TGCs using the  $p_T(W)$  distribution in  $WW$  and  $WZ$  production with the  $W$  decaying to an electron or muon and the  $Z$  to 2 jets. Setting other couplings to their standard model value, the 95% C.L. limits are  $-0.18 < \lambda_\gamma < 0.17$  for a form factor scale  $\Lambda = 1.5$  TeV.
- 100 ABAZOV 06H study  $p\bar{p} \rightarrow WW$  production with a subsequent decay  $WW \rightarrow e^+\nu_e e^-\bar{\nu}_e, WW \rightarrow e^\pm\nu_e\mu^\mp\nu_\mu$  or  $WW \rightarrow \mu^+\nu_\mu\mu^-\bar{\nu}_\mu$ . The 95% C.L. limit for a form factor scale  $\Lambda = 1$  TeV is  $-0.97 < \lambda_\gamma < 1.04$ , fixing  $\kappa_\gamma=1$ . With the assumption that the  $WW\gamma$  and  $WWZ$  couplings are equal the 95% C.L. one-dimensional limit ( $\Lambda = 2$  TeV) is  $-0.29 < \lambda < 0.30$ .
- 101 ABAZOV 05J perform a likelihood fit to the photon  $E_T$  spectrum of  $W\gamma + X$  events, where the  $W$  decays to an electron or muon which is required to be well separated from the photon. For  $\Lambda = 2.0$  TeV the 95% CL limits are  $-0.20 < \lambda_\gamma < 0.20$ . In the fit  $\kappa_\gamma$  is kept fixed to its Standard Model value.
- 102 ABREU 01I combine results from  $e^+e^-$  interactions at 189 GeV leading to  $W^+W^-$ ,  $W\nu_\mu$ , and  $\nu\bar{\nu}\gamma$  final states with results from ABREU 99L at 183 GeV. The 95% confidence interval is  $-0.11 < \lambda_\gamma < 0.23$ .
- 103 BREITWEG 00 search for  $W$  production in events with large hadronic  $p_T$ . For  $p_T > 20$  GeV, the upper limit on the cross section gives the 95%CL limit  $-3.2 < \lambda_\gamma < 3.2$  for  $\kappa_\gamma$  fixed to its Standard Model value.
- 104 ABBOTT 99I perform a simultaneous fit to the  $W\gamma, WW \rightarrow$  dilepton,  $WW/WZ \rightarrow e\nu jj, WW/WZ \rightarrow \mu\nu jj$ , and  $WZ \rightarrow$  trilepton data samples. For  $\Lambda = 2.0$  TeV, the 95%CL limits are  $-0.18 < \lambda_\gamma < 0.19$ .

 $\kappa_Z$ 

This coupling is  $CP$ -conserving ( $C$ - and  $P$ -separately conserving).

VALUE	EVTS	DOCUMENT ID	TECN	COMMENT
<b><math>0.924 \pm 0.059 \pm 0.024</math></b>	7171	105 ACHARD	04D L3	$E_{cm}^{ee} = 189\text{--}209$ GeV
• • • We do not use the following data for averages, fits, limits, etc. • • •				
	34	106 ABAZOV	11 D0	$E_{cm}^{pp} = 1.96$ TeV
	17	107 ABAZOV	06H D0	$E_{cm}^{pp} = 1.96$ TeV
	2.3	108 ABAZOV	05S D0	$E_{cm}^{pp} = 1.96$ TeV

- 105 ACHARD 04D study  $WW$ -pair production, single- $W$  production and single-photon production with missing energy from 189 to 209 GeV. The result quoted here is obtained using the  $WW$ -pair production sample. Each parameter is determined from a single-parameter fit in which the other parameters assume their Standard Model values.

- 106 ABAZOV 11 study the  $p\bar{p} \rightarrow 3\ell\nu$  process arising in  $WZ$  production. They observe 34  $WZ$  candidates with an estimated background of 6 events. An analysis of the  $p_T$  spectrum of the  $Z$  boson leads to a 95% C.L. limit of  $0.600 < \kappa_Z < 1.675$ , for a form factor  $\Lambda = 2$  TeV.

- 107 ABAZOV 06H study  $p\bar{p} \rightarrow WW$  production with a subsequent decay  $WW \rightarrow e^+\nu_e e^-\bar{\nu}_e, WW \rightarrow e^\pm\nu_e\mu^\mp\nu_\mu$  or  $WW \rightarrow \mu^+\nu_\mu\mu^-\bar{\nu}_\mu$ . The 95% C.L. limit for a form factor scale  $\Lambda = 2$  TeV is  $0.55 < \kappa_Z < 1.55$ , fixing  $\lambda_Z=0$ . With the assumption that the  $WW\gamma$  and  $WWZ$  couplings are equal the 95% C.L. one-dimensional limit ( $\Lambda = 2$  TeV) is  $0.68 < \kappa < 1.45$ .

- 108 ABAZOV 05S study  $p\bar{p} \rightarrow WZ$  production with a subsequent trilepton decay to  $\ell\nu\ell'\bar{\nu}'$  ( $\ell$  and  $\ell' = e$  or  $\mu$ ). Three events (estimated background  $0.71 \pm 0.08$  events) with  $WZ$  decay characteristics are observed from which they derive limits on the anomalous  $WWZ$  couplings. The 95% CL limit for a form factor scale  $\Lambda = 1$  TeV is  $-1.0 < \kappa_Z < 3.4$ , fixing  $\lambda_Z$  and  $g_1^Z$  to their Standard Model values.

 $\lambda_Z$ 

This coupling is  $CP$ -conserving ( $C$ - and  $P$ -separately conserving).

VALUE	EVTS	DOCUMENT ID	TECN	COMMENT
<b><math>-0.088 \pm 0.060 \pm 0.023</math></b>	7171	109 ACHARD	04D L3	$E_{cm}^{ee} = 189\text{--}209$ GeV
• • • We do not use the following data for averages, fits, limits, etc. • • •				
	34	110 ABAZOV	11 D0	$E_{cm}^{pp} = 1.96$ TeV
	334	111 AALTONEN	10K CDF	$E_{cm}^{pp} = 1.96$ TeV
	13	112 ABAZOV	07Z D0	$E_{cm}^{pp} = 1.96$ TeV
	17	113 ABAZOV	06H D0	$E_{cm}^{pp} = 1.96$ TeV
	2.3	114 ABAZOV	05S D0	$E_{cm}^{pp} = 1.96$ TeV

- 109 ACHARD 04D study  $WW$ -pair production, single- $W$  production and single-photon production with missing energy from 189 to 209 GeV. The result quoted here is obtained using the  $WW$ -pair production sample. Each parameter is determined from a single-parameter fit in which the other parameters assume their Standard Model values.

- 110 ABAZOV 11 study the  $p\bar{p} \rightarrow 3\ell\nu$  process arising in  $WZ$  production. They observe 34  $WZ$  candidates with an estimated background of 6 events. An analysis of the  $p_T$  spectrum of the  $Z$  boson leads to a 95% C.L. limit of  $-0.077 < \lambda_Z < 0.093$ , for a form factor  $\Lambda = 2$  TeV.

- 111 AALTONEN 10K study  $p\bar{p} \rightarrow W^+W^-$  with  $W \rightarrow e/\mu\nu$ . The  $p_T$  of the leading (second) lepton is required to be  $> 20$  (10) GeV. The final number of events selected is 654 of which  $320 \pm 47$  are estimated to be background. The 95% C.L. interval is  $-0.16 < \lambda_Z < 0.16$  for  $\Lambda = 1.5$  TeV and  $-0.14 < \lambda_Z < 0.15$  for  $\Lambda = 2$  TeV.

- 112 ABAZOV 07Z set limits on anomalous TGCs using the measured cross section and  $p_T(Z)$  distribution in  $WZ$  production with both the  $W$  and the  $Z$  decaying leptonically into electrons and muons. Setting the other couplings to their standard model values, the 95% C.L. limit for a form factor scale  $\Lambda = 2$  TeV is  $-0.17 < \lambda_Z < 0.21$ .

- 113 ABAZOV 06H study  $p\bar{p} \rightarrow WW$  production with a subsequent decay  $WW \rightarrow e^+\nu_e e^-\bar{\nu}_e, WW \rightarrow e^\pm\nu_e\mu^\mp\nu_\mu$  or  $WW \rightarrow \mu^+\nu_\mu\mu^-\bar{\nu}_\mu$ . The 95% C.L. limit for a form factor scale  $\Lambda = 2$  TeV is  $-0.39 < \lambda_Z < 0.39$ , fixing  $\kappa_Z=1$ . With the assumption that the  $WW\gamma$  and  $WWZ$  couplings are equal the 95% C.L. one-dimensional limit ( $\Lambda = 2$  TeV) is  $-0.29 < \lambda < 0.30$ .

- 114 ABAZOV 05S study  $p\bar{p} \rightarrow WZ$  production with a subsequent trilepton decay to  $\ell\nu\ell'\bar{\nu}'$  ( $\ell$  and  $\ell' = e$  or  $\mu$ ). Three events (estimated background  $0.71 \pm 0.08$  events) with  $WZ$  decay characteristics are observed from which they derive limits on the anomalous  $WWZ$  couplings. The 95% CL limit for a form factor scale  $\Lambda = 1.5$  TeV is  $-0.48 < \lambda_Z < 0.48$ , fixing  $g_1^Z$  and  $\kappa_Z$  to their Standard Model values.

 $g_5^Z$ 

This coupling is  $CP$ -conserving but  $C$ - and  $P$ -violating.

VALUE	EVTS	DOCUMENT ID	TECN	COMMENT
<b><math>0.93 \pm 0.09</math> OUR AVERAGE</b>				Error includes scale factor of 1.1.
$0.96 \pm 0.13$	9800	115 ABBIENDI	04D OPAL	$E_{cm}^{ee} = 183\text{--}209$ GeV
$1.00 \pm 0.13 \pm 0.05$	7171	116 ACHARD	04D L3	$E_{cm}^{ee} = 189\text{--}209$ GeV
$0.56 \pm 0.23 \pm 0.12$	1154	117 ACCIARRI	99Q L3	$E_{cm}^{ee} = 161+172 + 183$ GeV

• • • We do not use the following data for averages, fits, limits, etc. • • •

$0.84 \pm 0.23$  118 EBOLI 00 THEO LEP1, SLC+ Tevatron

- 115 ABBIENDI 04D combine results from  $W^+W^-$  in all decay channels. Only  $CP$ -conserving couplings are considered and each parameter is determined from a single-parameter fit in which the other parameters assume their Standard Model values. The 95% confidence interval is  $0.72 < g_5^Z < 1.21$ .

- 116 ACHARD 04D study  $WW$ -pair production, single- $W$  production and single-photon production with missing energy from 189 to 209 GeV. The result quoted here is obtained using the  $WW$ -pair production sample. Each parameter is determined from a single-parameter fit in which the other parameters assume their Standard Model values.

- 117 ACCIARRI 99Q study  $W$ -pair, single- $W$ , and single photon events.

- 118 EBOLI 00 extract this indirect value of the coupling studying the non-universal one-loop contributions to the experimental value of the  $Z \rightarrow b\bar{b}$  width ( $\Lambda=1$  TeV is assumed).

 $g_4^Z$ 

This coupling is  $CP$ -violating ( $C$ -violating and  $P$ -conserving).

VALUE	EVTS	DOCUMENT ID	TECN	COMMENT
<b><math>-0.30 \pm 0.17</math> OUR AVERAGE</b>				
$-0.39 \pm 0.19$	1880	119 ABDALLAH	08C DLPH	$E_{cm}^{ee} = 189\text{--}209$ GeV
$-0.02 \pm 0.32$	1065	120 ABBIENDI	01H OPAL	$E_{cm}^{ee} = 189$ GeV

- 119 ABDALLAH 08C determine this triple gauge coupling from the measurement of the spin density matrix elements in  $e^+e^- \rightarrow W^+W^- \rightarrow (qq)(\ell\nu)$ , where  $\ell = e$  or  $\mu$ . Values of all other couplings are fixed to their standard model values.

- 120 ABBIENDI 01H study  $W$ -pair events, with one leptonically and one hadronically decaying  $W$ . The coupling is extracted using information from the  $W$  production angle together with decay angles from the leptonically decaying  $W$ .

$\tilde{\kappa}_Z$   
This coupling is  $CP$ -violating ( $C$ -conserving and  $P$ -violating).

VALUE	EVTS	DOCUMENT ID	TECN	COMMENT
$-0.12^{+0.06}_{-0.04}$ OUR AVERAGE				
$-0.09^{+0.08}_{-0.05}$	1880	121 ABDALLAH	08c DLPH	$E_{\text{cm}}^{\text{ee}} = 189\text{--}209$ GeV
$-0.20^{+0.10}_{-0.07}$	1065	122 ABBIENDI	01H OPAL	$E_{\text{cm}}^{\text{ee}} = 189$ GeV
• • • We do not use the following data for averages, fits, limits, etc. • • •				
		123 BLINOV	11 LEP	$E_{\text{cm}}^{\text{ee}} = 183\text{--}207$ GeV
121 ABDALLAH 08c determine this triple gauge coupling from the measurement of the spin density matrix elements in $e^+e^- \rightarrow W^+W^- \rightarrow (qq)(\ell\nu)$ , where $\ell = e$ or $\mu$ . Values of all other couplings are fixed to their standard model values.				
122 ABBIENDI 01H study $W$ -pair events, with one leptonically and one hadronically decaying $W$ . The coupling is extracted using information from the $W$ production angle together with decay angles from the leptonically decaying $W$ .				
123 BLINOV 11 use the LEP-average $e^+e^- \rightarrow W^+W^-$ cross section data for $\sqrt{s} = 183\text{--}207$ GeV to determine an upper limit on the TGC $\tilde{\kappa}_Z$ . The average values of the cross sections as well as their correlation matrix, and standard model expectations of the cross sections are taken from the LEPEWWG note hep-ex/0612034. At 95% confidence level $ \tilde{\kappa}_Z  < 0.13$ .				

$\tilde{\lambda}_Z$   
This coupling is  $CP$ -violating ( $C$ -conserving and  $P$ -violating).

VALUE	EVTS	DOCUMENT ID	TECN	COMMENT
$-0.09 \pm 0.07$ OUR AVERAGE				
$-0.08 \pm 0.07$	1880	124 ABDALLAH	08c DLPH	$E_{\text{cm}}^{\text{ee}} = 189\text{--}209$ GeV
$-0.18^{+0.24}_{-0.16}$	1065	125 ABBIENDI	01H OPAL	$E_{\text{cm}}^{\text{ee}} = 189$ GeV
• • • We do not use the following data for averages, fits, limits, etc. • • •				
		126 BLINOV	11 LEP	$E_{\text{cm}}^{\text{ee}} = 183\text{--}207$ GeV
124 ABDALLAH 08c determine this triple gauge coupling from the measurement of the spin density matrix elements in $e^+e^- \rightarrow W^+W^- \rightarrow (qq)(\ell\nu)$ , where $\ell = e$ or $\mu$ . Values of all other couplings are fixed to their standard model values.				
125 ABBIENDI 01H study $W$ -pair events, with one leptonically and one hadronically decaying $W$ . The coupling is extracted using information from the $W$ production angle together with decay angles from the leptonically decaying $W$ .				
126 BLINOV 11 use the LEP-average $e^+e^- \rightarrow W^+W^-$ cross section data for $\sqrt{s} = 183\text{--}207$ GeV to determine an upper limit on the TGC $\tilde{\lambda}_Z$ . The average values of the cross sections as well as their correlation matrix, and standard model expectations of the cross sections are taken from the LEPEWWG note hep-ex/0612034. At 95% confidence level $ \tilde{\lambda}_Z  < 0.31$ .				

### W ANOMALOUS MAGNETIC MOMENT

The full magnetic moment is given by  $\mu_W = e(1+\kappa+\lambda)/2m_W$ . In the Standard Model, at tree level,  $\kappa=1$  and  $\lambda=0$ . Some papers have defined  $\Delta\kappa = 1-\kappa$  and assume that  $\lambda=0$ . Note that the electric quadrupole moment is given by  $-e(\kappa-\lambda)/m_W^2$ . A description of the parameterization of these moments and additional references can be found in HAGIWARA 87 and BAUR 88. The parameter  $\Lambda$  appearing in the theoretical limits below is a regularization cutoff which roughly corresponds to the energy scale where the structure of the  $W$  boson becomes manifest.

VALUE ( $e/2m_W$ )	EVTS	DOCUMENT ID	TECN	COMMENT
$2.22^{+0.20}_{-0.19}$	2298	127 ABREU	01i DLPH	$E_{\text{cm}}^{\text{ee}} = 183\text{--}189$ GeV
• • • We do not use the following data for averages, fits, limits, etc. • • •				
		128 ABE	95c CDF	
		129 ALITTI	92c UA2	
		130 SAMUEL	92 THEO	
		131 SAMUEL	91 THEO	
		132 GRIFOLS	88 THEO	
		133 GROTCHE	87 THEO	
		134 VANDERBIJ	87 THEO	
		135 GRAU	85 THEO	
		136 SUZUKI	85 THEO	
		137 HERZOG	84 THEO	

- 127 ABREU 01i combine results from  $e^+e^-$  interactions at 189 GeV leading to  $W^+W^-$ ,  $W\nu_e$ , and  $\nu\bar{\nu}\gamma$  final states with results from ABREU 99L at 183 GeV to determine  $\Delta g_1^Z$ ,  $\Delta\kappa_\gamma$ , and  $\lambda_\gamma$ .  $\Delta\kappa_\gamma$  and  $\lambda_\gamma$  are simultaneously floated in the fit to determine  $\mu_W$ .
- 128 ABE 95c report  $-1.3 < \kappa < 3.2$  for  $\lambda=0$  and  $-0.7 < \lambda < 0.7$  for  $\kappa=1$  in  $p\bar{p} \rightarrow e\nu_e\gamma X$  and  $\mu\nu_\mu\gamma X$  at  $\sqrt{s} = 1.8$  TeV.
- 129 ALITTI 92c measure  $\kappa = 1^{+2.6}_{-2.2}$  and  $\lambda = 0^{+1.7}_{-1.8}$  in  $p\bar{p} \rightarrow e\nu\gamma + X$  at  $\sqrt{s} = 630$  GeV. At 95%CL they report  $-3.5 < \kappa < 5.9$  and  $-3.6 < \lambda < 3.5$ .
- 130 SAMUEL 92 use preliminary CDF and UA2 data and find  $-2.4 < \kappa < 3.7$  at 96%CL and  $-3.1 < \lambda < 4.2$  at 95%CL respectively. They use data for  $W\gamma$  production and radiative  $W$  decay.
- 131 SAMUEL 91 use preliminary CDF data for  $p\bar{p} \rightarrow W\gamma X$  to obtain  $-11.3 \leq \Delta\kappa \leq 10.9$ . Note that their  $\kappa = 1 - \Delta\kappa$ .
- 132 GRIFOLS 88 uses deviation from  $\rho$  parameter to set limit  $\Delta\kappa \lesssim 65 (M_W^2/\Lambda^2)$ .
- 133 GROTCHE 87 finds the limit  $-37 < \Delta\kappa < 73.5$  (90% CL) from the experimental limits on  $e^+e^- \rightarrow \nu\bar{\nu}\gamma$  assuming three neutrino generations and  $-19.5 < \Delta\kappa < 56$  for four generations. Note their  $\Delta\kappa$  has the opposite sign as our definition.

- 134 VANDERBIJ 87 uses existing limits to the photon structure to obtain  $|\Delta\kappa| < 33 (m_W/\Lambda)$ . In addition VANDERBIJ 87 discusses problems with using the  $\rho$  parameter of the Standard Model to determine  $\Delta\kappa$ .
- 135 GRAU 85 uses the muon anomaly to derive a coupled limit on the anomalous magnetic dipole and electric quadrupole ( $\lambda$ ) moments  $1.05 > \Delta\kappa \ln(\Lambda/m_W) + \lambda/2 > -2.77$ . In the Standard Model  $\lambda = 0$ .
- 136 SUZUKI 85 uses partial-wave unitarity at high energies to obtain  $|\Delta\kappa| \lesssim 190 (m_W/\Lambda)^2$ . From the anomalous magnetic moment of the muon, SUZUKI 85 obtains  $|\Delta\kappa| \lesssim 2.2/\ln(\Lambda/m_W)$ . Finally SUZUKI 85 uses deviations from the  $\rho$  parameter and obtains a very qualitative, order-of-magnitude limit  $|\Delta\kappa| \lesssim 150 (m_W/\Lambda)^4$  if  $|\Delta\kappa| \ll 1$ .
- 137 HERZOG 84 consider the contribution of  $W$ -boson to muon magnetic moment including anomalous coupling of  $WW\gamma$ . Obtain a limit  $-1 < \Delta\kappa < 3$  for  $\Lambda \gtrsim 1$  TeV.

### ANOMALOUS W/Z QUARTIC COUPLINGS

Revised March 2012 by M.W. Grünewald (U. Ghent) and A. Gurtu (King Abdulaziz University).

The Standard Model quartic couplings,  $WWWW$ ,  $WWZZ$ ,  $WWZ\gamma$ ,  $WW\gamma\gamma$ , and  $ZZ\gamma\gamma$  lead to negligible effects at LEP energies, while they are important at a TeV Linear Collider. Outside the Standard Model framework, possible quartic couplings,  $a_0, a_c, a_n$ , are expressed in terms of the following dimension-6 operators [1,2];

$$L_6^0 = -\frac{e^2}{16\Lambda^2} a_0 F^{\mu\nu} F_{\mu\nu} \vec{W}^\alpha \cdot \vec{W}_\alpha$$

$$L_6^c = -\frac{e^2}{16\Lambda^2} a_c F^{\mu\alpha} F_{\mu\beta} \vec{W}^\beta \cdot \vec{W}_\alpha$$

$$L_6^n = -i\frac{e^2}{16\Lambda^2} a_n \epsilon_{ijk} W_{\mu\alpha}^{(i)} W_\nu^{(j)} W^{(k)\alpha} F^{\mu\nu}$$

$$\tilde{L}_6^0 = -\frac{e^2}{16\Lambda^2} \tilde{a}_0 F^{\mu\nu} \tilde{F}_{\mu\nu} \vec{W}^\alpha \cdot \vec{W}_\alpha$$

$$\tilde{L}_6^n = -i\frac{e^2}{16\Lambda^2} \tilde{a}_n \epsilon_{ijk} W_{\mu\alpha}^{(i)} W_\nu^{(j)} W^{(k)\alpha} \tilde{F}^{\mu\nu}$$

where  $F, W$  are photon and  $W$  fields,  $L_6^0$  and  $L_6^c$  conserve  $C, P$  separately ( $\tilde{L}_6^0$  conserves only  $C$ ) and generate anomalous  $W^+W^-\gamma\gamma$  and  $ZZ\gamma\gamma$  couplings,  $L_6^n$  violates  $CP$  ( $\tilde{L}_6^n$  violates both  $C$  and  $P$ ) and generates an anomalous  $W^+W^-Z\gamma$  coupling, and  $\Lambda$  is an energy scale for new physics. For the  $ZZ\gamma\gamma$  coupling the  $CP$ -violating term represented by  $L_6^n$  does not contribute. These couplings are assumed to be real and to vanish at tree level in the Standard Model.

Within the same framework as above, a more recent description of the quartic couplings [3] treats the anomalous parts of the  $WW\gamma\gamma$  and  $ZZ\gamma\gamma$  couplings separately leading to two sets parameterized as  $a_0^V/\Lambda^2$  and  $a_c^V/\Lambda^2$ , where  $V = W$  or  $Z$ .

At LEP the processes studied in search of these quartic couplings are  $e^+e^- \rightarrow WW\gamma$ ,  $e^+e^- \rightarrow \gamma\gamma\nu\bar{\nu}$ , and  $e^+e^- \rightarrow Z\gamma\gamma$  and limits are set on the quantities  $a_0^W/\Lambda^2, a_c^W/\Lambda^2, a_n/\Lambda^2$ . The characteristics of the first process depend on all the three couplings whereas those of the latter two depend only on the two  $CP$ -conserving couplings. The sensitive measured variables are the cross sections for these processes as well as the energy and angular distributions of the photon and recoil mass to the photon pair.

### References

- G. Belanger and F. Boudjema, Phys. Lett. **B288**, 201 (1992).
- J.W. Stirling and A. Werthenbach, Eur. Phys. J. **C14**, 103 (2000);  
J.W. Stirling and A. Werthenbach, Phys. Lett. **B466**, 369 (1999);  
A. Denner *et al.*, Eur. Phys. J. **C20**, 201 (2001);  
G. Montagna *et al.*, Phys. Lett. **B515**, 197 (2001).
- G. Belanger *et al.*, Eur. Phys. J. **C13**, 283 (2000).



the effective electroweak mixing angle  $\sin^2\bar{\theta}_W$  and the rates of  $Z$  decay to  $b$ - and  $c$ -quarks, owing to availability of polarized electron beams, small beam size, and stable beam spot.

The  $Z$ -boson properties reported in this section may broadly be categorized as:

- The standard ‘lineshape’ parameters of the  $Z$  consisting of its mass,  $M_Z$ , its total width,  $\Gamma_Z$ , and its partial decay widths,  $\Gamma(\text{hadrons})$ , and  $\Gamma(\ell\bar{\ell})$  where  $\ell = e, \mu, \tau, \nu$ ;
- $Z$  asymmetries in leptonic decays and extraction of  $Z$  couplings to charged and neutral leptons;
- The  $b$ - and  $c$ -quark-related partial widths and charge asymmetries which require special techniques;
- Determination of  $Z$  decay modes and the search for modes that violate known conservation laws;
- Average particle multiplicities in hadronic  $Z$  decay;
- $Z$  anomalous couplings.

The effective vector and axial-vector coupling constants describing the  $Z$ -to-fermion coupling are also measured in  $p\bar{p}$  and  $ep$  collisions at the Tevatron and at HERA. The corresponding cross-section formulae are given in Section 39 (Cross-section formulae for specific processes) and Section 16 (Structure Functions) in this *Review*. In this minireview, we concentrate on the measurements in  $e^+e^-$  collisions at LEP and SLC.

The standard ‘lineshape’ parameters of the  $Z$  are determined from an analysis of the production cross sections of these final states in  $e^+e^-$  collisions. The  $Z \rightarrow \nu\bar{\nu}(\gamma)$  state is identified directly by detecting single photon production and indirectly by subtracting the visible partial widths from the total width. Inclusion in this analysis of the forward-backward asymmetry of charged leptons,  $A_{FB}^{(0,\ell)}$ , of the  $\tau$  polarization,  $P(\tau)$ , and its forward-backward asymmetry,  $P(\tau)^{fb}$ , enables the separate determination of the effective vector ( $\bar{g}_V$ ) and axial vector ( $\bar{g}_A$ ) couplings of the  $Z$  to these leptons and the ratio ( $\bar{g}_V/\bar{g}_A$ ), which is related to the effective electroweak mixing angle  $\sin^2\bar{\theta}_W$  (see the ‘‘Electroweak Model and Constraints on New Physics’’ review).

Determination of the  $b$ - and  $c$ -quark-related partial widths and charge asymmetries involves tagging the  $b$  and  $c$  quarks for which various methods are employed: requiring the presence of a high momentum prompt lepton in the event with high transverse momentum with respect to the accompanying jet; impact parameter and lifetime tagging using precision vertex measurement with high-resolution detectors; application of neural-network techniques to classify events as  $b$  or non- $b$  on a statistical basis using event-shape variables; and using the presence of a charmed meson ( $D/D^*$ ) or a kaon as a tag.

### **Z-parameter determination**

LEP was run at energy points on and around the  $Z$  mass (88–94 GeV) constituting an energy ‘scan.’ The shape of the cross-section variation around the  $Z$  peak can be described by a Breit-Wigner *ansatz* with an energy-dependent

total width [1–3]. The **three** main properties of this distribution, viz., the **position** of the peak, the **width** of the distribution, and the **height** of the peak, determine respectively the values of  $M_Z$ ,  $\Gamma_Z$ , and  $\Gamma(e^+e^-) \times \Gamma(f\bar{f})$ , where  $\Gamma(e^+e^-)$  and  $\Gamma(f\bar{f})$  are the electron and fermion partial widths of the  $Z$ . The quantitative determination of these parameters is done by writing analytic expressions for these cross sections in terms of the parameters, and fitting the calculated cross sections to the measured ones by varying these parameters, taking properly into account all the errors. Single-photon exchange ( $\sigma_\gamma^0$ ) and  $\gamma$ - $Z$  interference ( $\sigma_{\gamma Z}^0$ ) are included, and the large ( $\sim 25\%$ ) initial-state radiation (ISR) effects are taken into account by convoluting the analytic expressions over a ‘Radiator Function’ [1–5]  $H(s, s')$ . Thus for the process  $e^+e^- \rightarrow f\bar{f}$ :

$$\sigma_f(s) = \int H(s, s') \sigma_f^0(s') ds' \quad (1)$$

$$\sigma_f^0(s) = \sigma_Z^0 + \sigma_\gamma^0 + \sigma_{\gamma Z}^0 \quad (2)$$

$$\sigma_Z^0 = \frac{12\pi}{M_Z^2} \frac{\Gamma(e^+e^-)\Gamma(f\bar{f})}{\Gamma_Z^2} \frac{s \Gamma_Z^2}{(s - M_Z^2)^2 + s^2 \Gamma_Z^2 / M_Z^2} \quad (3)$$

$$\sigma_\gamma^0 = \frac{4\pi\alpha^2(s)}{3s} Q_f^2 N_c^f \quad (4)$$

$$\sigma_{\gamma Z}^0 = -\frac{2\sqrt{2}\alpha(s)}{3} (Q_f G_F N_c^f \mathcal{G}_V^e \mathcal{G}_V^f) \times \frac{(s - M_Z^2) M_Z^2}{(s - M_Z^2)^2 + s^2 \Gamma_Z^2 / M_Z^2} \quad (5)$$

where  $Q_f$  is the charge of the fermion,  $N_c^f = 3$  for quarks and 1 for leptons, and  $\mathcal{G}_V^f$  is the vector coupling of the  $Z$  to the fermion-antifermion pair  $f\bar{f}$ .

Since  $\sigma_{\gamma Z}^0$  is expected to be much less than  $\sigma_Z^0$ , the LEP Collaborations have generally calculated the interference term in the framework of the Standard Model. This fixing of  $\sigma_{\gamma Z}^0$  leads to a tighter constraint on  $M_Z$ , and consequently a smaller error on its fitted value. It is possible to relax this constraint and carry out the fit within the S-matrix framework, which is briefly described in the next section.

In the above framework, the QED radiative corrections have been explicitly taken into account by convoluting over the ISR and allowing the electromagnetic coupling constant to run [6]:  $\alpha(s) = \alpha/(1 - \Delta\alpha)$ . On the other hand, weak radiative corrections that depend upon the assumptions of the electroweak theory and on the values of  $M_{\text{top}}$  and  $M_{\text{Higgs}}$  are accounted for by **absorbing them into the couplings**, which are then called the *effective* couplings  $\mathcal{G}_V$  and  $\mathcal{G}_A$  (or alternatively the effective parameters of the  $\star$  scheme of Kennedy and Lynn [7].)

$\mathcal{G}_V^f$  and  $\mathcal{G}_A^f$  are complex numbers with small imaginary parts. As experimental data does not allow simultaneous extraction of both real and imaginary parts of the effective couplings, the convention  $g_A^f = \text{Re}(\mathcal{G}_A^f)$  and  $g_V^f = \text{Re}(\mathcal{G}_V^f)$  is used and the imaginary parts are added in the fitting code [4].

Defining

$$A_f = 2 \frac{g_V^f \cdot g_A^f}{(g_V^f)^2 + (g_A^f)^2} \quad (6)$$

# Gauge & Higgs Boson Particle Listings

## Z

the lowest-order expressions for the various lepton-related asymmetries on the  $Z$  pole are [8–10]  $A_{FB}^{(0,\ell)} = (3/4)A_e A_f$ ,  $P(\tau) = -A_\tau$ ,  $P(\tau)^{fb} = -(3/4)A_e$ ,  $A_{LR} = A_e$ . The full analysis takes into account the energy-dependence of the asymmetries. Experimentally  $A_{LR}$  is defined as  $(\sigma_L - \sigma_R)/(\sigma_L + \sigma_R)$ , where  $\sigma_{L(R)}$  are the  $e^+e^- \rightarrow Z$  production cross sections with left- (right)-handed electrons.

The definition of the partial decay width of the  $Z$  to  $f\bar{f}$  includes the effects of QED and QCD final-state corrections, as well as the contribution due to the imaginary parts of the couplings:

$$\Gamma(f\bar{f}) = \frac{G_F M_Z^3}{6\sqrt{2}\pi} N_c^f \left( |g_A^f|^2 R_A^f + |g_V^f|^2 R_V^f \right) + \Delta_{ew/QCD} \quad (7)$$

where  $R_V^f$  and  $R_A^f$  are radiator factors to account for final state QED and QCD corrections, as well as effects due to nonzero fermion masses, and  $\Delta_{ew/QCD}$  represents the non-factorizable electroweak/QCD corrections.

### S-matrix approach to the Z

While most experimental analyses of LEP/SLC data have followed the ‘Breit-Wigner’ approach, an alternative S-matrix-based analysis is also possible. The  $Z$ , like all unstable particles, is associated with a complex pole in the S matrix. The pole position is process-independent and gauge-invariant. The mass,  $\bar{M}_Z$ , and width,  $\bar{\Gamma}_Z$ , can be defined in terms of the pole in the energy plane via [11–14]

$$\bar{s} = \bar{M}_Z^2 - i\bar{M}_Z\bar{\Gamma}_Z \quad (8)$$

leading to the relations

$$\begin{aligned} \bar{M}_Z &= M_Z / \sqrt{1 + \Gamma_Z^2/M_Z^2} \\ &\approx M_Z - 34.1 \text{ MeV} \end{aligned} \quad (9)$$

$$\begin{aligned} \bar{\Gamma}_Z &= \Gamma_Z / \sqrt{1 + \Gamma_Z^2/M_Z^2} \\ &\approx \Gamma_Z - 0.9 \text{ MeV} . \end{aligned} \quad (10)$$

The L3 and OPAL Collaborations at LEP (ACCIARRI 00Q and ABBIENDI 04G) have analyzed their data using the S-matrix approach as defined in Eq. (8), in addition to the conventional one. They observe a downward shift in the  $Z$  mass as expected.

### Handling the large-angle $e^+e^-$ final state

Unlike other  $f\bar{f}$  decay final states of the  $Z$ , the  $e^+e^-$  final state has a contribution not only from the  $s$ -channel but also from the  $t$ -channel and  $s$ - $t$  interference. The full amplitude is not amenable to fast calculation, which is essential if one has to carry out minimization fits within reasonable computer time. The usual procedure is to calculate the non- $s$  channel part of the cross section separately using the Standard Model programs ALIBABA [15] or TOPAZ0 [16], with the measured value of  $M_{\text{top}}$ , and  $M_{\text{Higgs}} = 150$  GeV, and add it to the  $s$ -channel cross section calculated as for other channels. This leads to two additional sources of error in the analysis: firstly,

the theoretical calculation in ALIBABA itself is known to be accurate to  $\sim 0.5\%$ , and secondly, there is uncertainty due to the error on  $M_{\text{top}}$  and the unknown value of  $M_{\text{Higgs}}$  (100–1000 GeV). These errors are propagated into the analysis by including them in the systematic error on the  $e^+e^-$  final state. As these errors are common to the four LEP experiments, this is taken into account when performing the LEP average.

### Errors due to uncertainty in LEP energy determination [17–22]

The systematic errors related to the LEP energy measurement can be classified as:

- The absolute energy scale error;
- Energy-point-to-energy-point errors due to the non-linear response of the magnets to the exciting currents;
- Energy-point-to-energy-point errors due to possible higher-order effects in the relationship between the dipole field and beam energy;
- Energy reproducibility errors due to various unknown uncertainties in temperatures, tidal effects, corrector settings, RF status, *etc.*

Precise energy calibration was done outside normal data-taking using the resonant depolarization technique. Run-time energies were determined every 10 minutes by measuring the relevant machine parameters and using a model which takes into account all the known effects, including leakage currents produced by trains in the Geneva area and the tidal effects due to gravitational forces of the Sun and the Moon. The LEP Energy Working Group has provided a covariance matrix from the determination of LEP energies for the different running periods during 1993–1995 [17].

### Choice of fit parameters

The LEP Collaborations have chosen the following primary set of parameters for fitting:  $M_Z$ ,  $\Gamma_Z$ ,  $\sigma_{\text{hadron}}^0$ ,  $R(\text{lepton})$ ,  $A_{FB}^{(0,\ell)}$ , where  $R(\text{lepton}) = \Gamma(\text{hadrons})/\Gamma(\text{lepton})$ ,  $\sigma_{\text{hadron}}^0 = 12\pi\Gamma(e^+e^-)\Gamma(\text{hadrons})/M_Z^2\Gamma_Z^2$ . With a knowledge of these fitted parameters and their covariance matrix, any other parameter can be derived. The main advantage of these parameters is that they form a physics motivated set of parameters with much reduced correlations.

Thus, the most general fit carried out to cross section and asymmetry data determines the **nine parameters**:  $M_Z$ ,  $\Gamma_Z$ ,  $\sigma_{\text{hadron}}^0$ ,  $R(e)$ ,  $R(\mu)$ ,  $R(\tau)$ ,  $A_{FB}^{(0,e)}$ ,  $A_{FB}^{(0,\mu)}$ ,  $A_{FB}^{(0,\tau)}$ . Assumption of lepton universality leads to a **five-parameter fit** determining  $M_Z$ ,  $\Gamma_Z$ ,  $\sigma_{\text{hadron}}^0$ ,  $R(\text{lepton})$ ,  $A_{FB}^{(0,\ell)}$ .

### Combining results from LEP and SLC experiments

With a steady increase in statistics over the years and improved understanding of the common systematic errors between LEP experiments, the procedures for combining results have evolved continuously [23]. The Line Shape Sub-group of the LEP Electroweak Working Group investigated the effects of these common errors, and devised a combination procedure

for the precise determination of the  $Z$  parameters from LEP experiments. Using these procedures, this note also gives the results after combining the final parameter sets from the four experiments, and these are the results quoted as the fit results in the  $Z$  listings below. Transformation of variables leads to values of derived parameters like partial decay widths and branching ratios to hadrons and leptons. Finally, transforming the LEP combined nine parameter set to  $(M_Z, \Gamma_Z, \sigma_{\text{hadron}}^{\circ}, g_A^f, g_V^f, f = e, \mu, \tau)$  using the average values of lepton asymmetry parameters  $(A_e, A_\mu, A_\tau)$  as constraints, leads to the best fitted values of the vector and axial-vector couplings  $(g_V, g_A)$  of the charged leptons to the  $Z$ .

Brief remarks on the handling of common errors and their magnitudes are given below. The identified common errors are those coming from

- (a) LEP energy-calibration uncertainties, and
- (b) the theoretical uncertainties in (i) the luminosity determination using small angle Bhabha scattering, (ii) estimating the non-s channel contribution to large angle Bhabha scattering, (iii) the calculation of QED radiative effects, and (iv) the parametrization of the cross section in terms of the parameter set used.

#### Common LEP energy errors

All the collaborations incorporate in their fit the full LEP energy error matrix as provided by the LEP energy group for their intersection region [17]. The effect of these errors is separated out from that of other errors by carrying out fits with energy errors scaled up and down by  $\sim 10\%$  and redoing the fits. From the observed changes in the overall error matrix, the covariance matrix of the common energy errors is determined. Common LEP energy errors lead to uncertainties on  $M_Z$ ,  $\Gamma_Z$ , and  $\sigma_{\text{hadron}}^{\circ}$  of 1.7, 1.2 MeV, and 0.011 nb, respectively.

#### Common luminosity errors

BHLUMI 4.04 [24] is used by all LEP collaborations for small-angle Bhabha scattering leading to a common uncertainty in their measured cross sections of 0.061% [25]. BHLUMI does not include a correction for production of light fermion pairs. OPAL explicitly corrects for this effect and reduces their luminosity uncertainty to 0.054%, which is taken fully correlated with the other experiments. The other three experiments among themselves have a common uncertainty of 0.061%.

#### Common non-s channel uncertainties

The same standard model programs ALIBABA [15] and TOPAZ0 [16] are used to calculate the non-s channel contribution to the large angle Bhabha scattering [26]. As this contribution is a function of the  $Z$  mass, which itself is a variable in the fit, it is parametrized as a function of  $M_Z$  by each collaboration to properly track this contribution as  $M_Z$  varies in the fit. The common errors on  $R_e$  and  $A_{FB}^{(0,e)}$  are 0.024 and 0.0014 respectively, and are correlated between them.

#### Common theoretical uncertainties: QED

There are large initial-state photon and fermion pair radiation effects near the  $Z$  resonance, for which the best currently

available evaluations include contributions up to  $\mathcal{O}(\alpha^3)$ . To estimate the remaining uncertainties, different schemes are incorporated in the standard model programs ZFITTER [5], TOPAZ0 [16], and MIZA [27]. Comparing the different options leads to error estimates of 0.3 and 0.2 MeV on  $M_Z$  and  $\Gamma_Z$  respectively, and of 0.02% on  $\sigma_{\text{hadron}}^{\circ}$ .

#### Common theoretical uncertainties: parametrization of lineshape and asymmetries

To estimate uncertainties arising from ambiguities in the model-independent parametrization of the differential cross-section near the  $Z$  resonance, results from TOPAZ0 and ZFITTER were compared by using ZFITTER to fit the cross sections and asymmetries calculated using TOPAZ0. The resulting uncertainties on  $M_Z$ ,  $\Gamma_Z$ ,  $\sigma_{\text{hadron}}^{\circ}$ ,  $R(\text{lepton})$ , and  $A_{FB}^{(0,\ell)}$  are 0.1 MeV, 0.1 MeV, 0.001 nb, 0.004, and 0.0001 respectively.

Thus, the overall theoretical errors on  $M_Z$ ,  $\Gamma_Z$ ,  $\sigma_{\text{hadron}}^{\circ}$  are 0.3 MeV, 0.2 MeV, and 0.008 nb respectively; on each  $R(\text{lepton})$  is 0.004 and on each  $A_{FB}^{(0,\ell)}$  is 0.0001. Within the set of three  $R(\text{lepton})$ 's and the set of three  $A_{FB}^{(0,\ell)}$ 's, the respective errors are fully correlated.

All the theory-related errors mentioned above utilize Standard Model programs which need the Higgs mass and running electromagnetic coupling constant as inputs; uncertainties on these inputs will also lead to common errors. All LEP collaborations used the same set of inputs for Standard Model calculations:  $M_Z = 91.187$  GeV, the Fermi constant  $G_F = (1.16637 \pm 0.00001) \times 10^{-5}$  GeV $^{-2}$  [28],  $\alpha^{(5)}(M_Z) = 1/128.877 \pm 0.090$  [29],  $\alpha_s(M_Z) = 0.119$  [30],  $M_{\text{top}} = 174.3 \pm 5.1$  GeV [30] and  $M_{\text{Higgs}} = 150$  GeV. The only observable effect, on  $M_Z$ , is due to the variation of  $M_{\text{Higgs}}$  between 100–1000 GeV (due to the variation of the  $\gamma/Z$  interference term which is taken from the Standard Model):  $M_Z$  changes by +0.23 MeV per unit change in  $\log_{10} M_{\text{Higgs}}/\text{GeV}$ , which is not an error but a correction to be applied once  $M_{\text{Higgs}}$  is determined. The effect is much smaller than the error on  $M_Z$  ( $\pm 2.1$  MeV).

#### Methodology of combining the LEP experimental results

The LEP experimental results actually used for combination are slightly modified from those published by the experiments (which are given in the Listings below). This has been done in order to facilitate the procedure by making the inputs more consistent. These modified results are given explicitly in [23]. The main differences compared to the published results are (a) consistent use of ZFITTER 6.23 and TOPAZ0 (the published ALEPH results used ZFITTER 6.10); (b) use of the combined energy-error matrix, which makes a difference of 0.1 MeV on the  $M_Z$  and  $\Gamma_Z$  for L3 only as at that intersection the RF modeling uncertainties are the largest.

Thus, nine-parameter sets from all four experiments with their covariance matrices are used together with all the common errors correlations. A grand covariance matrix,  $V$ , is constructed and a combined nine-parameter set is obtained by

# Gauge & Higgs Boson Particle Listings

## Z

minimizing  $\chi^2 = \Delta^T V^{-1} \Delta$ , where  $\Delta$  is the vector of residuals of the combined parameter set to the results of individual experiments. Imposing lepton universality in the combination results in the combined five parameter set.

### Study of $Z \rightarrow b\bar{b}$ and $Z \rightarrow c\bar{c}$

In the sector of  $c$ - and  $b$ -physics, the LEP experiments have measured the ratios of partial widths  $R_b = \Gamma(Z \rightarrow b\bar{b})/\Gamma(Z \rightarrow \text{hadrons})$ , and  $R_c = \Gamma(Z \rightarrow c\bar{c})/\Gamma(Z \rightarrow \text{hadrons})$ , and the forward-backward (charge) asymmetries  $A_{FB}^{b\bar{b}}$  and  $A_{FB}^{c\bar{c}}$ . The SLD experiment at SLC has measured the ratios  $R_c$  and  $R_b$  and, utilizing the polarization of the electron beam, was able to obtain the final state coupling parameters  $A_b$  and  $A_c$  from a measurement of the left-right forward-backward asymmetry of  $b$ - and  $c$ -quarks. The high precision measurement of  $R_c$  at SLD was made possible owing to the small beam size and very stable beam spot at SLC, coupled with a highly precise CCD pixel detector. Several of the analyses have also determined other quantities, in particular the semileptonic branching ratios,  $B(b \rightarrow \ell^-)$ ,  $B(b \rightarrow c \rightarrow \ell^+)$ , and  $B(c \rightarrow \ell^+)$ , the average time-integrated  $B^0\bar{B}^0$  mixing parameter  $\bar{\chi}$  and the probabilities for a  $c$ -quark to fragment into a  $D^+$ , a  $D_s$ , a  $D^{*+}$ , or a charmed baryon. The latter measurements do not concern properties of the  $Z$  boson, and hence they do not appear in the Listing below. However, for completeness, we will report at the end of this minireview their values as obtained fitting the data contained in the Z section. All these quantities are correlated with the electroweak parameters, and since the mixture of  $b$  hadrons is different from the one at the  $\Upsilon(4S)$ , their values might differ from those measured at the  $\Upsilon(4S)$ .

All the above quantities are correlated to each other since:

- Several analyses (for example the lepton fits) determine more than one parameter simultaneously;
- Some of the electroweak parameters depend explicitly on the values of other parameters (for example  $R_b$  depends on  $R_c$ );
- Common tagging and analysis techniques produce common systematic uncertainties.

The LEP Electroweak Heavy Flavour Working Group has developed [31] a procedure for combining the measurements taking into account known sources of correlation. The combining procedure determines fourteen parameters: the six parameters of interest in the electroweak sector,  $R_b$ ,  $R_c$ ,  $A_{FB}^{b\bar{b}}$ ,  $A_{FB}^{c\bar{c}}$ ,  $A_b$  and  $A_c$  and, in addition,  $B(b \rightarrow \ell^-)$ ,  $B(b \rightarrow c \rightarrow \ell^+)$ ,  $B(c \rightarrow \ell^+)$ ,  $\bar{\chi}$ ,  $f(D^+)$ ,  $f(D_s)$ ,  $f(c_{\text{baryon}})$  and  $P(c \rightarrow D^{*+}) \times B(D^{*+} \rightarrow \pi^+ D^0)$ , to take into account their correlations with the electroweak parameters. Before the fit both the peak and off-peak asymmetries are translated to the common energy  $\sqrt{s} = 91.26$  GeV using the predicted energy-dependence from ZFITTER [5].

### Summary of the measurements and of the various kinds of analysis

The measurements of  $R_b$  and  $R_c$  fall into two classes. In the first, named single-tag measurement, a method for selecting

$b$  and  $c$  events is applied and the number of tagged events is counted. A second technique, named double-tag measurement, has the advantage that the tagging efficiency is directly derived from the data thereby reducing the systematic error on the measurement.

The measurements in the  $b$ - and  $c$ -sector can be essentially grouped in the following categories:

- Lifetime (and lepton) double-tagging measurements of  $R_b$ . These are the most precise measurements of  $R_b$  and obviously dominate the combined result. The main sources of systematics come from the charm contamination and from estimating the hemisphere  $b$ -tagging efficiency correlation;
- Analyses with  $D/D^{*\pm}$  to measure  $R_c$ . These measurements make use of several different tagging techniques (inclusive/exclusive double tag, exclusive double tag, reconstruction of all weakly decaying charmed states) and no assumptions are made on the energy-dependence of charm fragmentation;
- A measurement of  $R_c$  using single leptons and assuming  $B(b \rightarrow c \rightarrow \ell^+)$ ;
- Lepton fits which use hadronic events with one or more leptons in the final state to measure the asymmetries  $A_{FB}^{b\bar{b}}$  and  $A_{FB}^{c\bar{c}}$ . Each analysis usually gives several other electroweak parameters. The dominant sources of systematics are due to lepton identification, to other semileptonic branching ratios and to the modeling of the semileptonic decay;
- Measurements of  $A_{FB}^{b\bar{b}}$  using lifetime tagged events with a hemisphere charge measurement. These measurements dominate the combined result;
- Analyses with  $D/D^{*\pm}$  to measure  $A_{FB}^{c\bar{c}}$  or simultaneously  $A_{FB}^{b\bar{b}}$  and  $A_{FB}^{c\bar{c}}$ ;
- Measurements of  $A_b$  and  $A_c$  from SLD, using several tagging methods (lepton, kaon,  $D/D^*$ , and vertex mass). These quantities are directly extracted from a measurement of the left-right forward-backward asymmetry in  $c\bar{c}$  and  $b\bar{b}$  production using a polarized electron beam.

### Averaging procedure

All the measurements are provided by the LEP and SLD Collaborations in the form of tables with a detailed breakdown of the systematic errors of each measurement and its dependence on other electroweak parameters.

The averaging proceeds via the following steps:

- Define and propagate a consistent set of external inputs such as branching ratios, hadron lifetimes, fragmentation models *etc.* All the measurements are checked to ensure that all use a common set of assumptions (for instance, since the QCD corrections for the forward-backward asymmetries are strongly dependent on the experimental conditions, the data are corrected before combining);



- Form the full (statistical and systematic) covariance matrix of the measurements. The systematic correlations between different analyses are calculated from the detailed error breakdown in the measurement tables. The correlations relating several measurements made by the same analysis are also used;
- Take into account any explicit dependence of a measurement on the other electroweak parameters. As an example of this dependence, we illustrate the case of the double-tag measurement of  $R_b$ , where  $c$ -quarks constitute the main background. The normalization of the charm contribution is not usually fixed by the data and the measurement of  $R_b$  depends on the assumed value of  $R_c$ , which can be written as:

$$R_b = R_b^{\text{meas}} + a(R_c) \frac{(R_c - R_c^{\text{used}})}{R_c}, \quad (11)$$

where  $R_b^{\text{meas}}$  is the result of the analysis which assumed a value of  $R_c = R_c^{\text{used}}$  and  $a(R_c)$  is the constant which gives the dependence on  $R_c$ ;

- Perform a  $\chi^2$  minimization with respect to the combined electroweak parameters.

After the fit the average peak asymmetries  $A_{FB}^{c\bar{c}}$  and  $A_{FB}^{b\bar{b}}$  are corrected for the energy shift from 91.26 GeV to  $M_Z$  and for QED (initial state radiation),  $\gamma$  exchange, and  $\gamma Z$  interference effects, to obtain the corresponding pole asymmetries  $A_{FB}^{0,c}$  and  $A_{FB}^{0,b}$ .

This averaging procedure, using the fourteen parameters described above, and applied to the data contained in the Z particle listing below, gives the following results (where the last 8 parameters do not depend directly on the Z):

$$R_b^0 = 0.21629 \pm 0.00066$$

$$R_c^0 = 0.1721 \pm 0.0030$$

$$A_{FB}^{0,b} = 0.0992 \pm 0.0016$$

$$A_{FB}^{0,c} = 0.0707 \pm 0.0035$$

$$A_b = 0.923 \pm 0.020$$

$$A_c = 0.670 \pm 0.027$$

$$B(b \rightarrow \ell^-) = 0.1071 \pm 0.0022$$

$$B(b \rightarrow c \rightarrow \ell^+) = 0.0801 \pm 0.0018$$

$$B(c \rightarrow \ell^+) = 0.0969 \pm 0.0031$$

$$\bar{\chi} = 0.1250 \pm 0.0039$$

$$f(D^+) = 0.235 \pm 0.016$$

$$f(D_s) = 0.126 \pm 0.026$$

$$P(c_{\text{baryon}}) = 0.093 \pm 0.022$$

$$P(c \rightarrow D^{*+}) \times B(D^{*+} \rightarrow \pi^+ D^0) = 0.1622 \pm 0.0048$$

Among the non-electroweak observables, the B semileptonic branching fraction  $B(b \rightarrow \ell^-)$  is of special interest, since the dominant error source on this quantity is the dependence on the semileptonic decay model for  $b \rightarrow \ell^-$ , with  $\Delta B(b \rightarrow \ell^-)_{b \rightarrow \ell^- \text{-model}} = 0.0012$ . Extensive studies have been made to understand the size of this error. Among the electroweak quantities, the quark asymmetries with leptons depend also on the semileptonic decay model, while the asymmetries using other methods usually do not. The fit implicitly requires that the different methods give consistent results and this effectively constrains the decay model, and thus reduces in principle the error from this source in the fit result.

To obtain a conservative estimate of the modelling error, the above fit has been repeated removing all asymmetry measurements. The results of the fit on B-decay related observables are [23]:  $B(b \rightarrow \ell^-) = 0.1069 \pm 0.0022$ , with  $\Delta B(b \rightarrow \ell^-)_{b \rightarrow \ell^- \text{-model}} = 0.0013$ ,  $B(b \rightarrow c \rightarrow \ell^+) = 0.0802 \pm 0.0019$  and  $\bar{\chi} = 0.1259 \pm 0.0042$ .

## References

1. R.N. Cahn, Phys. Rev. **D36**, 2666 (1987).
2. F.A. Berends *et al.*, “Z Physics at LEP 1,” CERN Report 89-08 (1989), Vol. 1, eds. G. Altarelli, R. Kleiss, and C. Verzegnassi, p. 89.
3. A. Borrelli *et al.*, Nucl. Phys. **B333**, 357 (1990).
4. D. Bardin and G. Passarino, “Upgrading of Precision Calculations for Electroweak Observables,” hep-ph/9803425; D. Bardin, G. Passarino, and M. Grunewald, “Precision Calculation Project Report,” hep-ph/9902452.
5. D. Bardin *et al.*, Z. Phys. **C44**, 493 (1989); Comp. Phys. Comm. **59**, 303 (1990); D. Bardin *et al.*, Nucl. Phys. **B351**, 1 (1991); Phys. Lett. **B255**, 290 (1991), and CERN-TH/6443/92 (1992); Comp. Phys. Comm. **133**, 229 (2001).
6. G. Burgers *et al.*, “Z Physics at LEP 1,” CERN Report 89-08 (1989), Vol. 1, eds. G. Altarelli, R. Kleiss, and C. Verzegnassi, p. 55.
7. D.C. Kennedy and B.W. Lynn, Nucl. Phys. **B322**, 1 (1989).
8. M. Consoli *et al.*, “Z Physics at LEP 1,” CERN Report 89-08 (1989), Vol. 1, eds. G. Altarelli, R. Kleiss, and C. Verzegnassi, p. 7.
9. M. Bohm *et al.*, *ibid*, p. 203.
10. S. Jadach *et al.*, *ibid*, p. 235.
11. R. Stuart, Phys. Lett. **B262**, 113 (1991).
12. A. Sirlin, Phys. Rev. Lett. **67**, 2127 (1991).
13. A. Leike, T. Riemann, and J. Rose, Phys. Lett. **B273**, 513 (1991).
14. See also D. Bardin *et al.*, Phys. Lett. **B206**, 539 (1988).
15. W. Beenakker, F.A. Berends, and S.C. van der Marck, Nucl. Phys. **B349**, 323 (1991).
16. G. Montagna *et al.*, Nucl. Phys. **B401**, 3 (1993); Comp. Phys. Comm. **76**, 328 (1993); Comp. Phys. Comm. **93**, 120 (1996); G. Montagna *et al.*, Comp. Phys. Comm. **117**, 278 (1999).
17. R. Assmann *et al.*, (Working Group on LEP Energy), Eur. Phys. J. **C6**, 187 (1999).

## Gauge &amp; Higgs Boson Particle Listings

## Z

18. R. Assmann *et al.*, (Working Group on LEP Energy), *Z. Phys.* **C66**, 567 (1995).
19. L. Arnaudon *et al.*, (Working Group on LEP Energy and LEP Collabs.), *Phys. Lett.* **B307**, 187 (1993).
20. L. Arnaudon *et al.*, (Working Group on LEP Energy), CERN-PPE/92-125 (1992).
21. L. Arnaudon *et al.*, *Phys. Lett.* **B284**, 431 (1992).
22. R. Bailey *et al.*, 'LEP Energy Calibration' CERN-SL-90-95-AP, Proceedings of the "2<sup>nd</sup> European Particle Accelerator Conference," Nice, France, 12–16 June 1990, pp. 1765-1767.
23. The LEP Collabs.: ALEPH, DELPHI, L3, OPAL, and the LEP Electroweak Working Group: CERN-PH-EP/2007-039 (2007); CERN-PH-EP/2006-042 (2006).  
The LEP Collabs.: ALEPH, DELPHI, L3, OPAL, the LEP Electroweak Working Group, and the SLD Heavy Flavour Group: *Phys. Reports* **427**, 257 (2006); CERN-PH-EP/2005-051 (2005); CERN-PH-EP/2004-069 (2004); CERN-EP/2003-091 (2003); CERN-EP/2002-091 (2002); CERN-EP/2001-098 (2001); CERN-EP/2001-021 (2001); CERN-EP/2000-016 (1999); CERN-EP/99-15 (1998); CERN-PPE/97-154 (1997); CERN-PPE/96-183 (1996); CERN-PPE/95-172 (1995); CERN-PPE/94-187 (1994); CERN-PPE/93-157 (1993).
24. S. Jadach *et al.*, BHLUMI 4.04, *Comp. Phys. Comm.* **102**, 229 (1997);  
S. Jadach and O. Nicosini, Event generators for Bhabha scattering, in *Physics at LEP2*, CERN-96-01 Vol. 2, February 1996.
25. B.F.L. Ward *et al.*, *Phys. Lett.* **B450**, 262 (1999).
26. W. Beenakker and G. Passarino, *Phys. Lett.* **B425**, 199 (1998).
27. M. Martinez *et al.*, *Z. Phys.* **C49**, 645 (1991);  
M. Martinez and F. Teubert, *Z. Phys.* **C65**, 267 (1995), updated with results summarized in S. Jadach, B. Pietrzyk, and M. Skrzypek, *Phys. Lett.* **B456**, 77 (1999) and Reports of the working group on precision calculations for the Z resonance, CERN 95-03, ed. D. Bardin, W. Hollik, and G. Passarino, and references therein.
28. T. van Ritbergen and R. Stuart, *Phys. Lett.* **B437**, 201 (1998); *Phys. Rev. Lett.* **82**, 488 (1999).
29. S. Eidelman and F. Jegerlehner, *Z. Phys.* **C67**, 585 (1995);  
M. Steinhauser, *Phys. Lett.* **B429**, 158 (1998).
30. Particle Data Group (D.E. Groom *et al.*), *Eur. Phys. J.* **C15**, 1 (2000).
31. The LEP Experiments: ALEPH, DELPHI, L3, and OPAL *Nucl. Instrum. Methods* **A378**, 101 (1996).

## Z MASS

OUR FIT is obtained using the fit procedure and correlations as determined by the LEP Electroweak Working Group (see the note "The Z boson" and ref. LEP-SLC 06). The fit is performed using the Z mass and width, the Z hadronic pole cross section, the ratios of hadronic to leptonic partial widths, and the Z pole forward-backward lepton asymmetries. This set is believed to be most free of correlations.

The Z-boson mass listed here corresponds to the mass parameter in a Breit-Wigner distribution with mass dependent width. The value is 34 MeV greater than the real part of the position of the pole (in the energy-squared plane) in the Z-boson propagator. Also the LEP experiments have generally assumed a fixed value of the  $\gamma - Z$  interferences term based on the standard model. Keeping this term as free parameter leads to a somewhat larger error on the fitted Z mass. See ACCIARRI 00q and ABBIENDI 04g for a detailed investigation of both these issues.

VALUE (GeV)	EVTS	DOCUMENT ID	TECN	COMMENT
<b>91.1876 ± 0.0021 OUR FIT</b>				
91.1852 ± 0.0030	4.57M	<sup>1</sup> ABBIENDI	01A OPAL	$E_{cm}^{ee} = 88-94$ GeV
91.1863 ± 0.0028	4.08M	<sup>2</sup> ABREU	00F DLPH	$E_{cm}^{ee} = 88-94$ GeV
91.1898 ± 0.0031	3.96M	<sup>3</sup> ACCIARRI	00C L3	$E_{cm}^{ee} = 88-94$ GeV
91.1885 ± 0.0031	4.57M	<sup>4</sup> BARATE	00C ALEP	$E_{cm}^{ee} = 88-94$ GeV
• • • We do not use the following data for averages, fits, limits, etc. • • •				
91.1872 ± 0.0033		<sup>5</sup> ABBIENDI	04G OPAL	$E_{cm}^{ee} =$ LEP1 + 130-209 GeV
91.272 ± 0.032 ± 0.033		<sup>6</sup> ACHARD	04C L3	$E_{cm}^{ee} = 183-209$ GeV
91.1875 ± 0.0039	3.97M	<sup>7</sup> ACCIARRI	00Q L3	$E_{cm}^{ee} =$ LEP1 + 130-189 GeV
91.151 ± 0.008		<sup>8</sup> MIYABAYASHI	95 TOPZ	$E_{cm}^{ee} = 57.8$ GeV
91.74 ± 0.28 ± 0.93	156	<sup>9</sup> ALITTI	92B UA2	$E_{cm}^{pp} = 630$ GeV
90.9 ± 0.3 ± 0.2	188	<sup>10</sup> ABE	89C CDF	$E_{cm}^{pp} = 1.8$ TeV
91.14 ± 0.12	480	<sup>11</sup> ABRAMS	89B MRK2	$E_{cm}^{ee} = 89-93$ GeV
93.1 ± 1.0 ± 3.0	24	<sup>12</sup> ALBAJAR	89 UA1	$E_{cm}^{pp} = 546,630$ GeV

<sup>1</sup> ABBIENDI 01A error includes approximately 2.3 MeV due to statistics and 1.8 MeV due to LEP energy uncertainty.

<sup>2</sup> The error includes 1.6 MeV due to LEP energy uncertainty.

<sup>3</sup> The error includes 1.8 MeV due to LEP energy uncertainty.

<sup>4</sup> BARATE 00C error includes approximately 2.4 MeV due to statistics, 0.2 MeV due to experimental systematics, and 1.7 MeV due to LEP energy uncertainty.

<sup>5</sup> ABBIENDI 04G obtain this result using the S-matrix formalism for a combined fit to their cross section and asymmetry data at the Z peak and their data at 130-209 GeV. The authors have corrected the measurement for the 34 MeV shift with respect to the Breit-Wigner fits.

<sup>6</sup> ACHARD 04C select  $e^+e^- \rightarrow Z\gamma$  events with hard initial-state radiation. Z decays to  $q\bar{q}$  and muon pairs are considered. The fit results obtained in the two samples are found consistent to each other and combined considering the uncertainty due to ISR modelling as fully correlated.

<sup>7</sup> ACCIARRI 00q interpret the s-dependence of the cross sections and lepton forward-backward asymmetries in the framework of the S-matrix formalism. They fit to their cross section and asymmetry data at high energies, using the results of S-matrix fits to Z-peak data (ACCIARRI 00c) as constraints. The 130-189 GeV data constrains the  $\gamma/Z$  interference term. The authors have corrected the measurement for the 34.1 MeV shift with respect to the Breit-Wigner fits. The error contains a contribution of  $\pm 2.3$  MeV due to the uncertainty on the  $\gamma/Z$  interference.

<sup>8</sup> MIYABAYASHI 95 combine their low energy total hadronic cross-section measurement with the ACTON 93d data and perform a fit using an S-matrix formalism. As expected, this result is below the mass values obtained with the standard Breit-Wigner parametrization.

<sup>9</sup> Enters fit through W/Z mass ratio given in the W Particle Listings. The ALITTI 92b systematic error ( $\pm 0.93$ ) has two contributions: one ( $\pm 0.92$ ) cancels in  $m_W/m_Z$  and one ( $\pm 0.12$ ) is noncancelling. These were added in quadrature.

<sup>10</sup> First error of ABE 89 is combination of statistical and systematic contributions; second is mass scale uncertainty.

<sup>11</sup> ABRAMS 89b uncertainty includes 35 MeV due to the absolute energy measurement.

<sup>12</sup> ALBAJAR 89 result is from a total sample of 33  $Z \rightarrow e^+e^-$  events.

## Z WIDTH

OUR FIT is obtained using the fit procedure and correlations as determined by the LEP Electroweak Working Group (see the note "The Z boson" and ref. LEP-SLC 06).

VALUE (GeV)	EVTS	DOCUMENT ID	TECN	COMMENT
<b>2.4952 ± 0.0023 OUR FIT</b>				
2.4948 ± 0.0041	4.57M	<sup>13</sup> ABBIENDI	01A OPAL	$E_{cm}^{ee} = 88-94$ GeV
2.4876 ± 0.0041	4.08M	<sup>14</sup> ABREU	00F DLPH	$E_{cm}^{ee} = 88-94$ GeV
2.5024 ± 0.0042	3.96M	<sup>15</sup> ACCIARRI	00C L3	$E_{cm}^{ee} = 88-94$ GeV
2.4951 ± 0.0043	4.57M	<sup>16</sup> BARATE	00C ALEP	$E_{cm}^{ee} = 88-94$ GeV
• • • We do not use the following data for averages, fits, limits, etc. • • •				
2.4943 ± 0.0041		<sup>17</sup> ABBIENDI	04G OPAL	$E_{cm}^{ee} =$ LEP1 + 130-209 GeV
2.5025 ± 0.0041	3.97M	<sup>18</sup> ACCIARRI	00Q L3	$E_{cm}^{ee} =$ LEP1 + 130-189 GeV
2.50 ± 0.21 ± 0.06		<sup>19</sup> ABREU	96R DLPH	$E_{cm}^{ee} = 91.2$ GeV
3.8 ± 0.8 ± 1.0	188	ABE	89C CDF	$E_{cm}^{pp} = 1.8$ TeV
2.42 +0.45 -0.35	480	<sup>20</sup> ABRAMS	89B MRK2	$E_{cm}^{ee} = 89-93$ GeV
2.7 +1.2 -1.0 ± 1.3	24	<sup>21</sup> ALBAJAR	89 UA1	$E_{cm}^{pp} = 546,630$ GeV
2.7 ± 2.0 ± 1.0	25	<sup>22</sup> ANSARI	87 UA2	$E_{cm}^{pp} = 546,630$ GeV

<sup>13</sup> ABBIENDI 01A error includes approximately 3.6 MeV due to statistics, 1 MeV due to event selection systematics, and 1.3 MeV due to LEP energy uncertainty.

<sup>14</sup> The error includes 1.2 MeV due to LEP energy uncertainty.

<sup>15</sup> The error includes 1.3 MeV due to LEP energy uncertainty.

<sup>16</sup> BARATE 00C error includes approximately 3.8 MeV due to statistics, 0.9 MeV due to experimental systematics, and 1.3 MeV due to LEP energy uncertainty.

<sup>17</sup> ABBIENDI 04G obtain this result using the S-matrix formalism for a combined fit to their cross section and asymmetry data at the Z peak and their data at 130-209 GeV. The authors have corrected the measurement for the 1 MeV shift with respect to the Breit-Wigner fits.

<sup>18</sup> ACCIARRI 00q interpret the s-dependence of the cross sections and lepton forward-backward asymmetries in the framework of the S-matrix formalism. They fit to their

cross section and asymmetry data at high energies, using the results of S-matrix fits to Z-peak data (ACCIARRI 00c) as constraints. The 130–189 GeV data constrains the  $\gamma/Z$  interference term. The authors have corrected the measurement for the 0.9 MeV shift with respect to the Breit-Wigner fits.

- <sup>19</sup> ABREU 96R obtain this value from a study of the interference between initial and final state radiation in the process  $e^+e^- \rightarrow Z \rightarrow \mu^+\mu^-$ .
- <sup>20</sup> ABRAMS 89B uncertainty includes 50 MeV due to the miniSAM background subtraction error.
- <sup>21</sup> ALBAJAR 89 result is from a total sample of 33  $Z \rightarrow e^+e^-$  events.
- <sup>22</sup> Quoted values of ANSARI 87 are from direct fit. Ratio of Z and W production gives either  $\Gamma(Z) < (1.09 \pm 0.07) \times \Gamma(W)$ , CL = 90% or  $\Gamma(Z) = (0.82^{+0.19}_{-0.14} \pm 0.06) \times \Gamma(W)$ . Assuming Standard-Model value  $\Gamma(W) = 2.65$  GeV then gives  $\Gamma(Z) < 2.89 \pm 0.19$  or  $= 2.17^{+0.50}_{-0.37} \pm 0.16$ .

Z DECAY MODES

Mode	Fraction ( $\Gamma_i/\Gamma$ )	Scale factor/ Confidence level
$\Gamma_1$ $e^+e^-$	( 3.363 $\pm$ 0.004 ) %	
$\Gamma_2$ $\mu^+\mu^-$	( 3.366 $\pm$ 0.007 ) %	
$\Gamma_3$ $\tau^+\tau^-$	( 3.370 $\pm$ 0.008 ) %	
$\Gamma_4$ $\ell^+\ell^-$	[a] ( 3.3658 $\pm$ 0.0023 ) %	
$\Gamma_5$ invisible	(20.00 $\pm$ 0.06 ) %	
$\Gamma_6$ hadrons	(69.91 $\pm$ 0.06 ) %	
$\Gamma_7$ $(u\bar{u} + c\bar{c})/2$	(11.6 $\pm$ 0.6 ) %	
$\Gamma_8$ $(d\bar{d} + s\bar{s} + b\bar{b})/3$	(15.6 $\pm$ 0.4 ) %	
$\Gamma_9$ $c\bar{c}$	(12.03 $\pm$ 0.21 ) %	
$\Gamma_{10}$ $b\bar{b}$	(15.12 $\pm$ 0.05 ) %	
$\Gamma_{11}$ $b\bar{b}b\bar{b}$	( 3.6 $\pm$ 1.3 ) $\times 10^{-4}$	
$\Gamma_{12}$ $ggg$	< 1.1	% CL=95%
$\Gamma_{13}$ $\pi^0\gamma$	< 5.2	$\times 10^{-5}$ CL=95%
$\Gamma_{14}$ $\eta\gamma$	< 5.1	$\times 10^{-5}$ CL=95%
$\Gamma_{15}$ $\omega\gamma$	< 6.5	$\times 10^{-4}$ CL=95%
$\Gamma_{16}$ $\eta'(958)\gamma$	< 4.2	$\times 10^{-5}$ CL=95%
$\Gamma_{17}$ $\gamma\gamma$	< 5.2	$\times 10^{-5}$ CL=95%
$\Gamma_{18}$ $\gamma\gamma\gamma$	< 1.0	$\times 10^{-5}$ CL=95%
$\Gamma_{19}$ $\pi^\pm W^\mp$	[b] < 7	$\times 10^{-5}$ CL=95%
$\Gamma_{20}$ $\rho^\pm W^\mp$	[b] < 8.3	$\times 10^{-5}$ CL=95%
$\Gamma_{21}$ $J/\psi(1S)X$	( 3.51 $^{+0.23}_{-0.25}$ ) $\times 10^{-3}$	S=1.1
$\Gamma_{22}$ $\psi(2S)X$	( 1.60 $\pm$ 0.29 ) $\times 10^{-3}$	
$\Gamma_{23}$ $\chi_{c1}(1P)X$	( 2.9 $\pm$ 0.7 ) $\times 10^{-3}$	
$\Gamma_{24}$ $\chi_{c2}(1P)X$	< 3.2	$\times 10^{-3}$ CL=90%
$\Gamma_{25}$ $\Upsilon(1S)X + \Upsilon(2S)X + \Upsilon(3S)X$	( 1.0 $\pm$ 0.5 ) $\times 10^{-4}$	
$\Gamma_{26}$ $\Upsilon(1S)X$	< 4.4	$\times 10^{-5}$ CL=95%
$\Gamma_{27}$ $\Upsilon(2S)X$	< 1.39	$\times 10^{-4}$ CL=95%
$\Gamma_{28}$ $\Upsilon(3S)X$	< 9.4	$\times 10^{-5}$ CL=95%
$\Gamma_{29}$ $(D^0/\bar{D}^0)X$	(20.7 $\pm$ 2.0 ) %	
$\Gamma_{30}$ $D^\pm X$	(12.2 $\pm$ 1.7 ) %	
$\Gamma_{31}$ $D^*(2010)^\pm X$	[b] (11.4 $\pm$ 1.3 ) %	
$\Gamma_{32}$ $D_{s1}(2536)^\pm X$	( 3.6 $\pm$ 0.8 ) $\times 10^{-3}$	
$\Gamma_{33}$ $D_{sJ}(2573)^\pm X$	( 5.8 $\pm$ 2.2 ) $\times 10^{-3}$	
$\Gamma_{34}$ $D^*(2629)^\pm X$	searched for	
$\Gamma_{35}$ $BX$		
$\Gamma_{36}$ $B^*X$		
$\Gamma_{37}$ $B^+X$	[c] ( 6.08 $\pm$ 0.13 ) %	
$\Gamma_{38}$ $B_s^0X$	[c] ( 1.59 $\pm$ 0.13 ) %	
$\Gamma_{39}$ $B_c^\pm X$	searched for	
$\Gamma_{40}$ $A_c^\pm X$	( 1.54 $\pm$ 0.33 ) %	
$\Gamma_{41}$ $\Xi_c^0 X$	seen	
$\Gamma_{42}$ $\Xi_b X$	seen	
$\Gamma_{43}$ $b$ -baryon X	[c] ( 1.38 $\pm$ 0.22 ) %	
$\Gamma_{44}$ anomalous $\gamma$ + hadrons	[d] < 3.2	$\times 10^{-3}$ CL=95%
$\Gamma_{45}$ $e^+e^-\gamma$	[d] < 5.2	$\times 10^{-4}$ CL=95%
$\Gamma_{46}$ $\mu^+\mu^-\gamma$	[d] < 5.6	$\times 10^{-4}$ CL=95%
$\Gamma_{47}$ $\tau^+\tau^-\gamma$	[d] < 7.3	$\times 10^{-4}$ CL=95%
$\Gamma_{48}$ $\ell^+\ell^-\gamma\gamma$	[e] < 6.8	$\times 10^{-6}$ CL=95%
$\Gamma_{49}$ $q\bar{q}\gamma\gamma$	[e] < 5.5	$\times 10^{-6}$ CL=95%
$\Gamma_{50}$ $\nu\bar{\nu}\gamma\gamma$	[e] < 3.1	$\times 10^{-6}$ CL=95%
$\Gamma_{51}$ $e^\pm\mu^\mp$	LF [b] < 1.7	$\times 10^{-6}$ CL=95%
$\Gamma_{52}$ $e^\pm\tau^\mp$	LF [b] < 9.8	$\times 10^{-6}$ CL=95%
$\Gamma_{53}$ $\mu^\pm\tau^\mp$	LF [b] < 1.2	$\times 10^{-5}$ CL=95%
$\Gamma_{54}$ $p e$	L,B < 1.8	$\times 10^{-6}$ CL=95%
$\Gamma_{55}$ $p \mu$	L,B < 1.8	$\times 10^{-6}$ CL=95%

- [a]  $\ell$  indicates each type of lepton ( $e, \mu, \text{ and } \tau$ ), not sum over them.
- [b] The value is for the sum of the charge states or particle/antiparticle states indicated.
- [c] This value is updated using the product of (i) the  $Z \rightarrow b\bar{b}$  fraction from this listing and (ii) the  $b$ -hadron fraction in an unbiased sample of weakly decaying  $b$ -hadrons produced in Z-decays provided by the Heavy Flavor Averaging Group (HFAG, [http://www.slac.stanford.edu/xorg/hfag/osc/PGD\\_2009/#FRA CZ](http://www.slac.stanford.edu/xorg/hfag/osc/PGD_2009/#FRA CZ)).
- [d] See the Particle Listings below for the  $\gamma$  energy range used in this measurement.
- [e] For  $m_{\gamma\gamma} = (60 \pm 5)$  GeV.

Z PARTIAL WIDTHS

$\Gamma(e^+e^-)$   $\Gamma_1$   
 For the LEP experiments, this parameter is not directly used in the overall fit but is derived using the fit results; see the note "The Z boson" and ref. LEP-SLC 06.

VALUE (MeV)	EVTS	DOCUMENT ID	TECN	COMMENT
<b>83.91 <math>\pm</math> 0.12 OUR FIT</b>				
83.66 $\pm$ 0.20	137.0K	ABBIENDI	01A OPAL	$E_{cm}^{ee} = 88-94$ GeV
83.54 $\pm$ 0.27	117.8k	ABREU	00F DLPH	$E_{cm}^{ee} = 88-94$ GeV
84.16 $\pm$ 0.22	124.4k	ACCIARRI	00c L3	$E_{cm}^{ee} = 88-94$ GeV
83.88 $\pm$ 0.19		BARATE	00c ALEP	$E_{cm}^{ee} = 88-94$ GeV
82.89 $\pm$ 1.20 $\pm$ 0.89		<sup>23</sup> ABE	95J SLD	$E_{cm}^{ee} = 91.31$ GeV

<sup>23</sup> ABE 95J obtain this measurement from Bhabha events in a restricted fiducial region to improve systematics. They use the values 91.187 and 2.489 GeV for the Z mass and total decay width to extract this partial width.

$\Gamma(\mu^+\mu^-)$   $\Gamma_2$   
 This parameter is not directly used in the overall fit but is derived using the fit results; see the note "The Z boson" and ref. LEP-SLC 06.

VALUE (MeV)	EVTS	DOCUMENT ID	TECN	COMMENT
<b>83.99 <math>\pm</math> 0.18 OUR FIT</b>				
84.03 $\pm$ 0.30	182.8K	ABBIENDI	01A OPAL	$E_{cm}^{ee} = 88-94$ GeV
84.48 $\pm$ 0.40	157.6k	ABREU	00F DLPH	$E_{cm}^{ee} = 88-94$ GeV
83.95 $\pm$ 0.44	113.4k	ACCIARRI	00c L3	$E_{cm}^{ee} = 88-94$ GeV
84.02 $\pm$ 0.28		BARATE	00c ALEP	$E_{cm}^{ee} = 88-94$ GeV

$\Gamma(\tau^+\tau^-)$   $\Gamma_3$   
 This parameter is not directly used in the overall fit but is derived using the fit results; see the note "The Z boson" and ref. LEP-SLC 06.

VALUE (MeV)	EVTS	DOCUMENT ID	TECN	COMMENT
<b>84.08 <math>\pm</math> 0.22 OUR FIT</b>				
83.94 $\pm$ 0.41	151.5K	ABBIENDI	01A OPAL	$E_{cm}^{ee} = 88-94$ GeV
83.71 $\pm$ 0.58	104.0k	ABREU	00F DLPH	$E_{cm}^{ee} = 88-94$ GeV
84.23 $\pm$ 0.58	103.0k	ACCIARRI	00c L3	$E_{cm}^{ee} = 88-94$ GeV
84.38 $\pm$ 0.31		BARATE	00c ALEP	$E_{cm}^{ee} = 88-94$ GeV

$\Gamma(\ell^+\ell^-)$   $\Gamma_4$   
 In our fit  $\Gamma(\ell^+\ell^-)$  is defined as the partial Z width for the decay into a pair of massless charged leptons. This parameter is not directly used in the 5-parameter fit assuming lepton universality but is derived using the fit results. See the note "The Z boson" and ref. LEP-SLC 06.

VALUE (MeV)	EVTS	DOCUMENT ID	TECN	COMMENT
<b>83.984 <math>\pm</math> 0.086 OUR FIT</b>				
83.82 $\pm$ 0.15	471.3K	ABBIENDI	01A OPAL	$E_{cm}^{ee} = 88-94$ GeV
83.85 $\pm$ 0.17	379.4k	ABREU	00F DLPH	$E_{cm}^{ee} = 88-94$ GeV
84.14 $\pm$ 0.17	340.8k	ACCIARRI	00c L3	$E_{cm}^{ee} = 88-94$ GeV
84.02 $\pm$ 0.15	500k	BARATE	00c ALEP	$E_{cm}^{ee} = 88-94$ GeV

$\Gamma(\text{invisible})$   $\Gamma_5$   
 We use only direct measurements of the invisible partial width using the single photon channel to obtain the average value quoted below. OUR FIT value is obtained as a difference between the total and the observed partial widths assuming lepton universality.

VALUE (MeV)	EVTS	DOCUMENT ID	TECN	COMMENT
<b>499.0 <math>\pm</math> 1.5 OUR FIT</b>				
<b>503 <math>\pm</math> 16 OUR AVERAGE</b> Error includes scale factor of 1.2.				
498 $\pm$ 12 $\pm$ 12	1791	ACCIARRI	98G L3	$E_{cm}^{ee} = 88-94$ GeV
539 $\pm$ 26 $\pm$ 17	410	AKERS	95c OPAL	$E_{cm}^{ee} = 88-94$ GeV
450 $\pm$ 34 $\pm$ 34	258	BUSKULIC	93L ALEP	$E_{cm}^{ee} = 88-94$ GeV
540 $\pm$ 80 $\pm$ 40	52	ADEVA	92 L3	$E_{cm}^{ee} = 88-94$ GeV

- • • We do not use the following data for averages, fits, limits, etc. • • •
- 498.1  $\pm$  2.6 <sup>24</sup> ABBIENDI 01A OPAL  $E_{cm}^{ee} = 88-94$  GeV
- 498.1  $\pm$  3.2 <sup>24</sup> ABREU 00F DLPH  $E_{cm}^{ee} = 88-94$  GeV
- 499.1  $\pm$  2.9 <sup>24</sup> ACCIARRI 00c L3  $E_{cm}^{ee} = 88-94$  GeV
- 499.1  $\pm$  2.5 <sup>24</sup> BARATE 00c ALEP  $E_{cm}^{ee} = 88-94$  GeV

<sup>24</sup> This is an indirect determination of  $\Gamma(\text{invisible})$  from a fit to the visible Z decay modes.

## Gauge &amp; Higgs Boson Particle Listings

## Z

 $\Gamma(\text{hadrons})$  $\Gamma_6$ 

This parameter is not directly used in the 5-parameter fit assuming lepton universality, but is derived using the fit results. See the note "The Z boson" and ref. LEP-SLC 06.

VALUE (MeV)	EVTS	DOCUMENT ID	TECN	COMMENT
<b>1744.4 ± 2.0 OUR FIT</b>				
1745.4 ± 3.5	4.10M	ABBIENDI	01A OPAL	$E_{\text{cm}}^{\text{ee}} = 88\text{--}94$ GeV
1738.1 ± 4.0	3.70M	ABREU	00F DLPH	$E_{\text{cm}}^{\text{ee}} = 88\text{--}94$ GeV
1751.1 ± 3.8	3.54M	ACCIARRI	00c L3	$E_{\text{cm}}^{\text{ee}} = 88\text{--}94$ GeV
1744.0 ± 3.4	4.07M	BARATE	00c ALEP	$E_{\text{cm}}^{\text{ee}} = 88\text{--}94$ GeV

## Z BRANCHING RATIOS

OUR FIT is obtained using the fit procedure and correlations as determined by the LEP Electroweak Working Group (see the note "The Z boson" and ref. LEP-SLC 06).

 $\Gamma(\text{hadrons})/\Gamma(e^+e^-)$  $\Gamma_6/\Gamma_1$ 

VALUE	EVTS	DOCUMENT ID	TECN	COMMENT
<b>20.804 ± 0.050 OUR FIT</b>				
20.902 ± 0.084	137.0K	<sup>25</sup> ABBIENDI	01A OPAL	$E_{\text{cm}}^{\text{ee}} = 88\text{--}94$ GeV
20.88 ± 0.12	117.8k	ABREU	00F DLPH	$E_{\text{cm}}^{\text{ee}} = 88\text{--}94$ GeV
20.816 ± 0.089	124.4k	ACCIARRI	00c L3	$E_{\text{cm}}^{\text{ee}} = 88\text{--}94$ GeV
20.677 ± 0.075		<sup>26</sup> BARATE	00c ALEP	$E_{\text{cm}}^{\text{ee}} = 88\text{--}94$ GeV
• • • We do not use the following data for averages, fits, limits, etc. • • •				
27.0 $\begin{smallmatrix} +11.7 \\ -8.8 \end{smallmatrix}$	12	<sup>27</sup> ABRAMS	89D MRK2	$E_{\text{cm}}^{\text{ee}} = 89\text{--}93$ GeV

<sup>25</sup> ABBIENDI 01A error includes approximately 0.067 due to statistics, 0.040 due to event selection systematics, 0.027 due to the theoretical uncertainty in  $t$ -channel prediction, and 0.014 due to LEP energy uncertainty.

<sup>26</sup> BARATE 00c error includes approximately 0.062 due to statistics, 0.033 due to experimental systematics, and 0.026 due to the theoretical uncertainty in  $t$ -channel prediction.

<sup>27</sup> ABRAMS 89D have included both statistical and systematic uncertainties in their quoted errors.

 $\Gamma(\text{hadrons})/\Gamma(\mu^+\mu^-)$  $\Gamma_6/\Gamma_2$ 

OUR FIT is obtained using the fit procedure and correlations as determined by the LEP Electroweak Working Group (see the note "The Z boson" and ref. LEP-SLC 06).

VALUE	EVTS	DOCUMENT ID	TECN	COMMENT
<b>20.785 ± 0.033 OUR FIT</b>				
20.811 ± 0.058	182.8K	<sup>28</sup> ABBIENDI	01A OPAL	$E_{\text{cm}}^{\text{ee}} = 88\text{--}94$ GeV
20.65 ± 0.08	157.6k	ABREU	00F DLPH	$E_{\text{cm}}^{\text{ee}} = 88\text{--}94$ GeV
20.861 ± 0.097	113.4k	ACCIARRI	00c L3	$E_{\text{cm}}^{\text{ee}} = 88\text{--}94$ GeV
20.799 ± 0.056		<sup>29</sup> BARATE	00c ALEP	$E_{\text{cm}}^{\text{ee}} = 88\text{--}94$ GeV
• • • We do not use the following data for averages, fits, limits, etc. • • •				
18.9 $\begin{smallmatrix} +7.1 \\ -5.3 \end{smallmatrix}$	13	<sup>30</sup> ABRAMS	89D MRK2	$E_{\text{cm}}^{\text{ee}} = 89\text{--}93$ GeV

<sup>28</sup> ABBIENDI 01A error includes approximately 0.050 due to statistics and 0.027 due to event selection systematics.

<sup>29</sup> BARATE 00c error includes approximately 0.053 due to statistics and 0.021 due to experimental systematics.

<sup>30</sup> ABRAMS 89D have included both statistical and systematic uncertainties in their quoted errors.

 $\Gamma(\text{hadrons})/\Gamma(\tau^+\tau^-)$  $\Gamma_6/\Gamma_3$ 

OUR FIT is obtained using the fit procedure and correlations as determined by the LEP Electroweak Working Group (see the note "The Z boson" and ref. LEP-SLC 06).

VALUE	EVTS	DOCUMENT ID	TECN	COMMENT
<b>20.764 ± 0.045 OUR FIT</b>				
20.832 ± 0.091	151.5K	<sup>31</sup> ABBIENDI	01A OPAL	$E_{\text{cm}}^{\text{ee}} = 88\text{--}94$ GeV
20.84 ± 0.13	104.0k	ABREU	00F DLPH	$E_{\text{cm}}^{\text{ee}} = 88\text{--}94$ GeV
20.792 ± 0.133	103.0k	ACCIARRI	00c L3	$E_{\text{cm}}^{\text{ee}} = 88\text{--}94$ GeV
20.707 ± 0.062		<sup>32</sup> BARATE	00c ALEP	$E_{\text{cm}}^{\text{ee}} = 88\text{--}94$ GeV
• • • We do not use the following data for averages, fits, limits, etc. • • •				
15.2 $\begin{smallmatrix} +4.8 \\ -3.9 \end{smallmatrix}$	21	<sup>33</sup> ABRAMS	89D MRK2	$E_{\text{cm}}^{\text{ee}} = 89\text{--}93$ GeV

<sup>31</sup> ABBIENDI 01A error includes approximately 0.055 due to statistics and 0.071 due to event selection systematics.

<sup>32</sup> BARATE 00c error includes approximately 0.054 due to statistics and 0.033 due to experimental systematics.

<sup>33</sup> ABRAMS 89D have included both statistical and systematic uncertainties in their quoted errors.

 $\Gamma(\text{hadrons})/\Gamma(e^+\ell^-)$  $\Gamma_6/\Gamma_4$ 

$\ell$  indicates each type of lepton ( $e$ ,  $\mu$ , and  $\tau$ ), not sum over them.

Our fit result is obtained requiring lepton universality.

VALUE	EVTS	DOCUMENT ID	TECN	COMMENT
<b>20.767 ± 0.025 OUR FIT</b>				
20.823 ± 0.044	471.3K	<sup>34</sup> ABBIENDI	01A OPAL	$E_{\text{cm}}^{\text{ee}} = 88\text{--}94$ GeV
20.730 ± 0.060	379.4k	ABREU	00F DLPH	$E_{\text{cm}}^{\text{ee}} = 88\text{--}94$ GeV
20.810 ± 0.060	340.8k	ACCIARRI	00c L3	$E_{\text{cm}}^{\text{ee}} = 88\text{--}94$ GeV
20.725 ± 0.039	500k	<sup>35</sup> BARATE	00c ALEP	$E_{\text{cm}}^{\text{ee}} = 88\text{--}94$ GeV
• • • We do not use the following data for averages, fits, limits, etc. • • •				
18.9 $\begin{smallmatrix} +3.6 \\ -3.2 \end{smallmatrix}$	46	ABRAMS	89B MRK2	$E_{\text{cm}}^{\text{ee}} = 89\text{--}93$ GeV

<sup>34</sup> ABBIENDI 01A error includes approximately 0.034 due to statistics and 0.027 due to event selection systematics.

<sup>35</sup> BARATE 00c error includes approximately 0.033 due to statistics, 0.020 due to experimental systematics, and 0.005 due to the theoretical uncertainty in  $t$ -channel prediction.

 $\Gamma(\text{hadrons})/\Gamma_{\text{total}}$  $\Gamma_6/\Gamma$ 

This parameter is not directly used in the overall fit but is derived using the fit results; see the note "The Z boson" and ref. LEP-SLC 06.

VALUE (%)	DOCUMENT ID
<b>69.911 ± 0.056 OUR FIT</b>	

 $\Gamma(e^+e^-)/\Gamma_{\text{total}}$  $\Gamma_1/\Gamma$ 

This parameter is not directly used in the overall fit but is derived using the fit results; see the note "The Z boson" and ref. LEP-SLC 06.

VALUE (%)	DOCUMENT ID
<b>(3363.2 ± 4.2) × 10<sup>-3</sup> OUR FIT</b>	

 $\Gamma(\mu^+\mu^-)/\Gamma_{\text{total}}$  $\Gamma_2/\Gamma$ 

This parameter is not directly used in the overall fit but is derived using the fit results; see the note "The Z boson" and ref. LEP-SLC 06.

VALUE (%)	DOCUMENT ID
<b>(3366.2 ± 6.6) × 10<sup>-3</sup> OUR FIT</b>	

 $\Gamma(\mu^+\mu^-)/\Gamma(e^+e^-)$  $\Gamma_2/\Gamma_1$ 

This parameter is not directly used in the overall fit but is derived using the fit results; see the note "The Z boson" and ref. LEP-SLC 06.

VALUE	DOCUMENT ID
<b>1.0009 ± 0.0028 OUR FIT</b>	

 $\Gamma(\tau^+\tau^-)/\Gamma_{\text{total}}$  $\Gamma_3/\Gamma$ 

This parameter is not directly used in the overall fit but is derived using the fit results; see the note "The Z boson" and ref. LEP-SLC 06.

VALUE (%)	DOCUMENT ID
<b>(3369.6 ± 8.3) × 10<sup>-3</sup> OUR FIT</b>	

 $\Gamma(\tau^+\tau^-)/\Gamma(e^+e^-)$  $\Gamma_3/\Gamma_1$ 

This parameter is not directly used in the overall fit but is derived using the fit results; see the note "The Z boson" and ref. LEP-SLC 06.

VALUE	DOCUMENT ID
<b>1.0019 ± 0.0032 OUR FIT</b>	

 $\Gamma(e^+\ell^-)/\Gamma_{\text{total}}$  $\Gamma_4/\Gamma$ 

$\ell$  indicates each type of lepton ( $e$ ,  $\mu$ , and  $\tau$ ), not sum over them.

Our fit result assumes lepton universality.

This parameter is not directly used in the overall fit but is derived using the fit results; see the note "The Z boson" and ref. LEP-SLC 06.

VALUE (%)	DOCUMENT ID
<b>(3365.8 ± 2.3) × 10<sup>-3</sup> OUR FIT</b>	

 $\Gamma(\text{invisible})/\Gamma_{\text{total}}$  $\Gamma_5/\Gamma$ 

See the data, the note, and the fit result for the partial width,  $\Gamma_5$ , above.

VALUE (%)	DOCUMENT ID
<b>20.000 ± 0.055 OUR FIT</b>	

 $\Gamma((u\bar{u} + c\bar{c})/2)/\Gamma(\text{hadrons})$  $\Gamma_7/\Gamma_6$ 

This quantity is the branching ratio of  $Z \rightarrow$  "up-type" quarks to  $Z \rightarrow$  hadrons. Except ACKERSTAFF 97T the values of  $Z \rightarrow$  "up-type" and  $Z \rightarrow$  "down-type" branchings are extracted from measurements of  $\Gamma(\text{hadrons})$ , and  $\Gamma(Z \rightarrow \gamma + \text{jets})$  where  $\gamma$  is a high-energy ( $>5$  or  $7$  GeV) isolated photon. As the experiments use different procedures and slightly different values of  $M_Z$ ,  $\Gamma(\text{hadrons})$  and  $\alpha_S$  in their extraction procedures, our average has to be taken with caution.

VALUE	DOCUMENT ID	TECN	COMMENT
<b>0.166 ± 0.009 OUR AVERAGE</b>			
0.172 $\begin{smallmatrix} +0.011 \\ -0.010 \end{smallmatrix}$	<sup>36</sup> ABBIENDI	04E OPAL	$E_{\text{cm}}^{\text{ee}} = 91.2$ GeV
0.160 ± 0.019 ± 0.019	<sup>37</sup> ACKERSTAFF 97T	OPAL	$E_{\text{cm}}^{\text{ee}} = 88\text{--}94$ GeV
0.137 $\begin{smallmatrix} +0.038 \\ -0.054 \end{smallmatrix}$	<sup>38</sup> ABREU	95x DLPH	$E_{\text{cm}}^{\text{ee}} = 88\text{--}94$ GeV
0.137 ± 0.033	<sup>39</sup> ADRIANI	93 L3	$E_{\text{cm}}^{\text{ee}} = 91.2$ GeV

<sup>36</sup> ABBIENDI 04E select photons with energy  $> 7$  GeV and use  $\Gamma(\text{hadrons}) = 1744.4 \pm 2.0$  MeV and  $\alpha_S = 0.1172 \pm 0.002$  to obtain  $\Gamma_u = 300^{+19}_{-18}$  MeV.

<sup>37</sup> ACKERSTAFF 97T measure  $\Gamma_{u\bar{u}}/(\Gamma_{d\bar{d}} + \Gamma_{u\bar{u}} + \Gamma_{s\bar{s}}) = 0.258 \pm 0.031 \pm 0.032$ . To obtain this branching ratio authors use  $R_c + R_b = 0.380 \pm 0.010$ . This measurement is fully negatively correlated with the measurement of  $\Gamma_{d\bar{d}s\bar{s}}/(\Gamma_{d\bar{d}} + \Gamma_{u\bar{u}} + \Gamma_{s\bar{s}})$  given in the next data block.

<sup>38</sup> ABREU 95x use  $M_Z = 91.187 \pm 0.009$  GeV,  $\Gamma(\text{hadrons}) = 1725 \pm 12$  MeV and  $\alpha_S = 0.123 \pm 0.005$ . To obtain this branching ratio we divide their value of  $C_{2/3} = 0.91 \pm 0.25$  by their value of  $(3C_{1/3} + 2C_{2/3}) = 6.66 \pm 0.05$ .

<sup>39</sup> ADRIANI 93 use  $M_Z = 91.181 \pm 0.022$  GeV,  $\Gamma(\text{hadrons}) = 1742 \pm 19$  MeV and  $\alpha_S = 0.125 \pm 0.009$ . To obtain this branching ratio we divide their value of  $C_{2/3} = 0.92 \pm 0.22$  by their value of  $(3C_{1/3} + 2C_{2/3}) = 6.720 \pm 0.076$ .

$\Gamma((d\bar{d}+s\bar{s}+b\bar{b})/3)/\Gamma(\text{hadrons})$  $\Gamma_8/\Gamma_6$ 

This quantity is the branching ratio of  $Z \rightarrow$  "down-type" quarks to  $Z \rightarrow$  hadrons. Except ACKERSTAFF 97T the values of  $Z \rightarrow$  "up-type" and  $Z \rightarrow$  "down-type" branchings are extracted from measurements of  $\Gamma(\text{hadrons})$ , and  $\Gamma(Z \rightarrow \gamma + \text{jets})$  where  $\gamma$  is a high-energy ( $> 7$  GeV) isolated photon. As the experiments use different procedures and slightly different values of  $M_Z$ ,  $\Gamma(\text{hadrons})$  and  $\alpha_s$  in their extraction procedures, our average has to be taken with caution.

VALUE	DOCUMENT ID	TECN	COMMENT
<b>0.223 ± 0.006 OUR AVERAGE</b>			
0.218 ± 0.007	40	ABBIENDI 04E	OPAL $E_{\text{cm}}^{\text{ee}} = 91.2$ GeV
0.230 ± 0.010 ± 0.010	41	ACKERSTAFF 97T	OPAL $E_{\text{cm}}^{\text{ee}} = 88\text{--}94$ GeV
0.243 +0.036 -0.026	42	ABREU 95x	DLPH $E_{\text{cm}}^{\text{ee}} = 88\text{--}94$ GeV
0.243 ± 0.022	43	ADRIANI 93	L3 $E_{\text{cm}}^{\text{ee}} = 91.2$ GeV

- 40 ABBIENDI 04E select photons with energy  $> 7$  GeV and use  $\Gamma(\text{hadrons}) = 1744.4 \pm 2.0$  MeV and  $\alpha_s = 0.1172 \pm 0.002$  to obtain  $\Gamma_d = 381 \pm 12$  MeV.
- 41 ACKERSTAFF 97T measure  $\Gamma_{d\bar{d},s\bar{s}}/(\Gamma_{d\bar{d}} + \Gamma_{u\bar{u}} + \Gamma_{s\bar{s}}) = 0.371 \pm 0.016 \pm 0.016$ . To obtain this branching ratio authors use  $R_C + R_b = 0.380 \pm 0.010$ . This measurement is fully negatively correlated with the measurement of  $\Gamma_{u\bar{u}}/(\Gamma_{d\bar{d}} + \Gamma_{u\bar{u}} + \Gamma_{s\bar{s}})$  presented in the previous data block.
- 42 ABREU 95x use  $M_Z = 91.187 \pm 0.009$  GeV,  $\Gamma(\text{hadrons}) = 1725 \pm 12$  MeV and  $\alpha_s = 0.123 \pm 0.005$ . To obtain this branching ratio we divide their value of  $C_{1/3} = 1.62^{+0.24}_{-0.17}$  by their value of  $(3C_{1/3} + 2C_{2/3}) = 6.66 \pm 0.05$ .
- 43 ADRIANI 93 use  $M_Z = 91.181 \pm 0.022$  GeV,  $\Gamma(\text{hadrons}) = 1742 \pm 19$  MeV and  $\alpha_s = 0.125 \pm 0.009$ . To obtain this branching ratio we divide their value of  $C_{1/3} = 1.63 \pm 0.15$  by their value of  $(3C_{1/3} + 2C_{2/3}) = 6.720 \pm 0.076$ .

 $R_C = \Gamma(c\bar{c})/\Gamma(\text{hadrons})$  $\Gamma_9/\Gamma_6$ 

OUR FIT is obtained by a simultaneous fit to several  $c$ - and  $b$ -quark measurements as explained in the note "The Z boson" and ref. LEP-SLC 06.

The Standard Model predicts  $R_C = 0.1723$  for  $m_t = 174.3$  GeV and  $M_H = 150$  GeV.

VALUE	DOCUMENT ID	TECN	COMMENT
<b>0.1721 ± 0.0030 OUR FIT</b>			
0.1744 ± 0.0031 ± 0.0021	44	ABE 05F	SLD $E_{\text{cm}}^{\text{ee}} = 91.28$ GeV
0.1665 ± 0.0051 ± 0.0081	45	ABREU 00	DLPH $E_{\text{cm}}^{\text{ee}} = 88\text{--}94$ GeV
0.1698 ± 0.0069	46	BARATE 00B	ALEP $E_{\text{cm}}^{\text{ee}} = 88\text{--}94$ GeV
0.180 ± 0.011 ± 0.013	47	ACKERSTAFF 98E	OPAL $E_{\text{cm}}^{\text{ee}} = 88\text{--}94$ GeV
0.167 ± 0.011 ± 0.012	48	ALEXANDER 96R	OPAL $E_{\text{cm}}^{\text{ee}} = 88\text{--}94$ GeV

- • • We do not use the following data for averages, fits, limits, etc. • • •
- 49 ABREU 95D DLPH  $E_{\text{cm}}^{\text{ee}} = 88\text{--}94$  GeV
- 44 ABE 05F use hadronic Z decays collected during 1996–98 to obtain an enriched sample of  $c\bar{c}$  events using a double tag method. The single  $c$ -tag is obtained with a neural network trained to perform flavor discrimination using as input several signatures (corrected secondary vertex mass, vertex decay length, multiplicity and total momentum of the hemisphere). A multitag approach is used, defining 4 regions of the output value of the neural network and  $R_C$  is extracted from a simultaneous fit to the count rates of the 4 different tags. The quoted systematic error includes an uncertainty of  $\pm 0.0006$  due to the uncertainty on  $R_b$ .
- 45 ABREU 00 obtain this result properly combining the measurement from the  $D^{*+}$  production rate ( $R_C = 0.1610 \pm 0.0104 \pm 0.0077 \pm 0.0043$  (BR)) with that from the overall charm counting ( $R_C = 0.1692 \pm 0.0047 \pm 0.0063 \pm 0.0074$  (BR)) in  $c\bar{c}$  events. The systematic error includes an uncertainty of  $\pm 0.0054$  due to the uncertainty on the charmed hadron branching fractions.
- 46 BARATE 00B use exclusive decay modes to independently determine the quantities  $R_C \times f(c \rightarrow X)$ ,  $X = D^0, D^+, D_s^+$ , and  $A_c$ . Estimating  $R_C \times f(c \rightarrow \Xi_c/\Omega_c) = 0.0034$ , they simply sum over all the charm decays to obtain  $R_C = 0.1738 \pm 0.0047 \pm 0.0088 \pm 0.0075$  (BR). This is combined with all previous ALEPH measurements (BARATE 98T and BUSKULIC 94G,  $R_C = 0.1681 \pm 0.0054 \pm 0.0062$ ) to obtain the quoted value.
- 47 ACKERSTAFF 98E use an inclusive/exclusive double tag. In one jet  $D^{*\pm}$  mesons are exclusively reconstructed in several decay channels and in the opposite jet a slow pion (opposite charge inclusive  $D^{*\pm}$ ) tag is used. The  $b$  content of this sample is measured by the simultaneous detection of a lepton in one jet and an inclusively reconstructed  $D^{*\pm}$  meson in the opposite jet. The systematic error includes an uncertainty of  $\pm 0.006$  due to the external branching ratios.
- 48 ALEXANDER 96R obtain this value via direct charm counting, summing the partial contributions from  $D^0, D^+, D_s^+$ , and  $A_c^+$ , and assuming that strange-charmed baryons account for the 15% of the  $A_c^+$  production. An uncertainty of  $\pm 0.005$  due to the uncertainties in the charm hadron branching ratios is included in the overall systematics.
- 49 ABREU 95D perform a maximum likelihood fit to the combined  $p$  and  $p_T$  distributions of single and dilepton samples. The second error includes an uncertainty of  $\pm 0.0124$  due to models and branching ratios.

 $R_b = \Gamma(b\bar{b})/\Gamma(\text{hadrons})$  $\Gamma_{10}/\Gamma_6$ 

OUR FIT is obtained by a simultaneous fit to several  $c$ - and  $b$ -quark measurements as explained in the note "The Z boson" and ref. LEP-SLC 06.

The Standard Model predicts  $R_b = 0.21581$  for  $m_t = 174.3$  GeV and  $M_H = 150$  GeV.

VALUE	DOCUMENT ID	TECN	COMMENT
<b>0.21629 ± 0.00066 OUR FIT</b>			
0.21594 ± 0.00094 ± 0.00075	50	ABE 05F	SLD $E_{\text{cm}}^{\text{ee}} = 91.28$ GeV
0.2174 ± 0.0015 ± 0.0028	51	ACCIARRI 00	L3 $E_{\text{cm}}^{\text{ee}} = 89\text{--}93$ GeV
0.2178 ± 0.0011 ± 0.0013	52	ABBIENDI 99B	OPAL $E_{\text{cm}}^{\text{ee}} = 88\text{--}94$ GeV
0.21634 ± 0.00067 ± 0.00060	53	ABREU 99B	DLPH $E_{\text{cm}}^{\text{ee}} = 88\text{--}94$ GeV
0.2159 ± 0.0009 ± 0.0011	54	BARATE 97F	ALEP $E_{\text{cm}}^{\text{ee}} = 88\text{--}94$ GeV

- • • We do not use the following data for averages, fits, limits, etc. • • •

0.2145 ± 0.0089 ± 0.0067	55	ABREU 95D	DLPH $E_{\text{cm}}^{\text{ee}} = 88\text{--}94$ GeV
0.219 ± 0.006 ± 0.005	56	BUSKULIC 94G	ALEP $E_{\text{cm}}^{\text{ee}} = 88\text{--}94$ GeV
0.251 ± 0.049 ± 0.030	57	JACOBSEN 91	MRK2 $E_{\text{cm}}^{\text{ee}} = 91$ GeV

- 50 ABE 05F use hadronic Z decays collected during 1996–98 to obtain an enriched sample of  $b\bar{b}$  events using a double tag method. The single  $b$ -tag is obtained with a neural network trained to perform flavor discrimination using as input several signatures (corrected secondary vertex mass, vertex decay length, multiplicity and total momentum of the hemisphere; the key tag is obtained requiring the secondary vertex corrected mass to be above the  $D$ -meson mass). ABE 05F obtain  $R_b = 0.21604 \pm 0.00098 \pm 0.00074$  where the systematic error includes an uncertainty of  $\pm 0.00012$  due to the uncertainty on  $R_C$ . The value reported here is obtained properly combining with ABE 98D. The quoted systematic error includes an uncertainty of  $\pm 0.00012$  due to the uncertainty on  $R_C$ .
- 51 ACCIARRI 00 obtain this result using a double-tagging technique, with a high  $p_T$  lepton tag and an impact parameter tag in opposite hemispheres.
- 52 ABBIENDI 99B tag  $Z \rightarrow b\bar{b}$  decays using leptons and/or separated decay vertices. The  $b$ -tagging efficiency is measured directly from the data using a double-tagging technique.
- 53 ABREU 99B obtain this result combining in a multivariate analysis several tagging methods (impact parameter and secondary vertex reconstruction, complemented by event shape variables). For  $R_C$  different from its Standard Model value of 0.172,  $R_b$  varies as  $-0.024 \times (R_C - 0.172)$ .
- 54 BARATE 97F combine the lifetime-mass hemisphere tag (BARATE 97E) with event shape information and lepton tag to identify  $Z \rightarrow b\bar{b}$  candidates. They further use  $c$ - and  $u$  $d$ -selection tags to identify the background. For  $R_C$  different from its Standard Model value of 0.172,  $R_b$  varies as  $-0.019 \times (R_C - 0.172)$ .
- 55 ABREU 95D perform a maximum likelihood fit to the combined  $p$  and  $p_T$  distributions of single and dilepton samples. The second error includes an uncertainty of  $\pm 0.0023$  due to models and branching ratios.
- 56 BUSKULIC 94G perform a simultaneous fit to the  $p$  and  $p_T$  spectra of both single and dilepton events.
- 57 JACOBSEN 91 tagged  $b\bar{b}$  events by requiring coincidence of  $\geq 3$  tracks with significant impact parameters using vertex detector. Systematic error includes lifetime and decay uncertainties ( $\pm 0.014$ ).

 $\Gamma(b\bar{b}b\bar{b})/\Gamma(\text{hadrons})$  $\Gamma_{11}/\Gamma_6$ 

VALUE (units $10^{-4}$ )	DOCUMENT ID	TECN	COMMENT
<b>5.2 ± 1.9 OUR AVERAGE</b>			
3.6 ± 1.7 ± 2.7	58	ABBIENDI 01G	OPAL $E_{\text{cm}}^{\text{ee}} = 88\text{--}94$ GeV
6.0 ± 1.9 ± 1.4	59	ABREU 99U	DLPH $E_{\text{cm}}^{\text{ee}} = 88\text{--}94$ GeV

- 58 ABBIENDI 01G use a sample of four-jet events from hadronic Z decays. To enhance the  $b\bar{b}b\bar{b}$  signal, at least three of the four jets are required to have a significantly detached secondary vertex.
- 59 ABREU 99U force hadronic Z decays into 3 jets to use all the available phase space and require a  $b$  tag for every jet. This decay mode includes primary and secondary 4b production, e.g. from gluon splitting to  $b\bar{b}$ .

 $\Gamma(gg)/\Gamma(\text{hadrons})$  $\Gamma_{12}/\Gamma_6$ 

VALUE	CL%	DOCUMENT ID	TECN	COMMENT
<b>&lt; 1.6 × 10<sup>-2</sup></b>	95	60	ABREU 96S	DLPH $E_{\text{cm}}^{\text{ee}} = 88\text{--}94$ GeV

- 60 This branching ratio is slightly dependent on the jet-finder algorithm. The value we quote is obtained using the JADE algorithm, while using the DURHAM algorithm ABREU 96S obtain an upper limit of  $1.5 \times 10^{-2}$ .

 $\Gamma(\pi^0\gamma)/\Gamma_{\text{total}}$  $\Gamma_{13}/\Gamma$ 

VALUE	CL%	DOCUMENT ID	TECN	COMMENT
<b>&lt; 5.2 × 10<sup>-5</sup></b>	95	61	ACCIARRI 95G	L3 $E_{\text{cm}}^{\text{ee}} = 88\text{--}94$ GeV
< 5.5 × 10 <sup>-5</sup>	95	ABREU 94B	DLPH $E_{\text{cm}}^{\text{ee}} = 88\text{--}94$ GeV	
< 2.1 × 10 <sup>-4</sup>	95	DECAMP 92	ALEP $E_{\text{cm}}^{\text{ee}} = 88\text{--}94$ GeV	
< 1.4 × 10 <sup>-4</sup>	95	AKRAWY 91F	OPAL $E_{\text{cm}}^{\text{ee}} = 88\text{--}94$ GeV	

- 61 This limit is for both decay modes  $Z \rightarrow \pi^0\gamma/\gamma\gamma$  which are indistinguishable in ACCIARRI 95G.

 $\Gamma(\eta\gamma)/\Gamma_{\text{total}}$  $\Gamma_{14}/\Gamma$ 

VALUE	CL%	DOCUMENT ID	TECN	COMMENT
< 7.6 × 10 <sup>-5</sup>	95	ACCIARRI 95G	L3 $E_{\text{cm}}^{\text{ee}} = 88\text{--}94$ GeV	
< 8.0 × 10 <sup>-5</sup>	95	ABREU 94B	DLPH $E_{\text{cm}}^{\text{ee}} = 88\text{--}94$ GeV	
<b>&lt; 5.1 × 10<sup>-5</sup></b>	95	DECAMP 92	ALEP $E_{\text{cm}}^{\text{ee}} = 88\text{--}94$ GeV	
< 2.0 × 10 <sup>-4</sup>	95	AKRAWY 91F	OPAL $E_{\text{cm}}^{\text{ee}} = 88\text{--}94$ GeV	

 $\Gamma(\omega\gamma)/\Gamma_{\text{total}}$  $\Gamma_{15}/\Gamma$ 

VALUE	CL%	DOCUMENT ID	TECN	COMMENT
<b>&lt; 6.5 × 10<sup>-4</sup></b>	95	ABREU 94B	DLPH $E_{\text{cm}}^{\text{ee}} = 88\text{--}94$ GeV	

 $\Gamma(\eta'(958)\gamma)/\Gamma_{\text{total}}$  $\Gamma_{16}/\Gamma$ 

VALUE	CL%	DOCUMENT ID	TECN	COMMENT
<b>&lt; 4.2 × 10<sup>-5</sup></b>	95	DECAMP 92	ALEP $E_{\text{cm}}^{\text{ee}} = 88\text{--}94$ GeV	

 $\Gamma(\gamma\gamma)/\Gamma_{\text{total}}$  $\Gamma_{17}/\Gamma$ 

VALUE	CL%	DOCUMENT ID	TECN	COMMENT
<b>&lt; 5.2 × 10<sup>-5</sup></b>	95	62	ACCIARRI 95G	L3 $E_{\text{cm}}^{\text{ee}} = 88\text{--}94$ GeV
< 5.5 × 10 <sup>-5</sup>	95	ABREU 94B	DLPH $E_{\text{cm}}^{\text{ee}} = 88\text{--}94$ GeV	
< 1.4 × 10 <sup>-4</sup>	95	AKRAWY 91F	OPAL $E_{\text{cm}}^{\text{ee}} = 88\text{--}94$ GeV	

- 62 This limit is for both decay modes  $Z \rightarrow \pi^0\gamma/\gamma\gamma$  which are indistinguishable in ACCIARRI 95G.

## Gauge &amp; Higgs Boson Particle Listings

## Z

$\Gamma(\gamma\gamma)/\Gamma_{\text{total}}$					$\Gamma_{18}/\Gamma$
VALUE	CL%	DOCUMENT ID	TECN	COMMENT	
$<1.0 \times 10^{-5}$	95	<sup>63</sup> ACCIARRI	95c L3	$E_{\text{cm}}^{\text{e}} = 88-94$ GeV	
$<1.7 \times 10^{-5}$	95	<sup>63</sup> ABREU	94B DLPH	$E_{\text{cm}}^{\text{e}} = 88-94$ GeV	
$<6.6 \times 10^{-5}$	95	AKRAWY	91F OPAL	$E_{\text{cm}}^{\text{e}} = 88-94$ GeV	

<sup>63</sup> Limit derived in the context of composite Z model.

$\Gamma(\pi^{\pm} W^{\mp})/\Gamma_{\text{total}}$					$\Gamma_{19}/\Gamma$
VALUE	CL%	DOCUMENT ID	TECN	COMMENT	
$<7 \times 10^{-5}$	95	DECAMP	92 ALEP	$E_{\text{cm}}^{\text{e}} = 88-94$ GeV	

The value is for the sum of the charge states indicated.

$\Gamma(\rho^{\pm} W^{\mp})/\Gamma_{\text{total}}$					$\Gamma_{20}/\Gamma$
VALUE	CL%	DOCUMENT ID	TECN	COMMENT	
$<8.3 \times 10^{-5}$	95	DECAMP	92 ALEP	$E_{\text{cm}}^{\text{e}} = 88-94$ GeV	

The value is for the sum of the charge states indicated.

$\Gamma(J/\psi(1S)X)/\Gamma_{\text{total}}$					$\Gamma_{21}/\Gamma$
VALUE (units $10^{-3}$ )	EVTS	DOCUMENT ID	TECN	COMMENT	

**$3.51^{+0.23}_{-0.25}$  OUR AVERAGE** Error includes scale factor of 1.1.

$3.21 \pm 0.21^{+0.19}_{-0.28}$	553	<sup>64</sup> ACCIARRI	99F L3	$E_{\text{cm}}^{\text{e}} = 88-94$ GeV
$3.9 \pm 0.2 \pm 0.3$	511	<sup>65</sup> ALEXANDER	96B OPAL	$E_{\text{cm}}^{\text{e}} = 88-94$ GeV
$3.73 \pm 0.39 \pm 0.36$	153	<sup>66</sup> ABREU	94P DLPH	$E_{\text{cm}}^{\text{e}} = 88-94$ GeV

<sup>64</sup> ACCIARRI 99F combine  $\mu^+\mu^-$  and  $e^+e^- J/\psi(1S)$  decay channels. The branching ratio for prompt  $J/\psi(1S)$  production is measured to be  $(2.1 \pm 0.6 \pm 0.4^{+0.4}_{-0.2}(\text{theor.})) \times 10^{-4}$ .

<sup>65</sup> ALEXANDER 96B identify  $J/\psi(1S)$  from the decays into lepton pairs.  $(4.8 \pm 2.4)\%$  of this branching ratio is due to prompt  $J/\psi(1S)$  production (ALEXANDER 96N).

<sup>66</sup> Combining  $\mu^+\mu^-$  and  $e^+e^-$  channels and taking into account the common systematic errors.  $(7.7^{+6.3}_{-5.4})\%$  of this branching ratio is due to prompt  $J/\psi(1S)$  production.

$\Gamma(\psi(2S)X)/\Gamma_{\text{total}}$					$\Gamma_{22}/\Gamma$
VALUE (units $10^{-3}$ )	EVTS	DOCUMENT ID	TECN	COMMENT	
<b><math>1.60 \pm 0.29</math> OUR AVERAGE</b>					
$1.6 \pm 0.5 \pm 0.3$	39	<sup>67</sup> ACCIARRI	97J L3	$E_{\text{cm}}^{\text{e}} = 88-94$ GeV	
$1.6 \pm 0.3 \pm 0.2$	46.9	<sup>68</sup> ALEXANDER	96B OPAL	$E_{\text{cm}}^{\text{e}} = 88-94$ GeV	
$1.60 \pm 0.73 \pm 0.33$	5.4	<sup>69</sup> ABREU	94P DLPH	$E_{\text{cm}}^{\text{e}} = 88-94$ GeV	

<sup>67</sup> ACCIARRI 97J measure this branching ratio via the decay channel  $\psi(2S) \rightarrow \ell^+\ell^- (\ell = \mu, e)$ .

<sup>68</sup> ALEXANDER 96B measure this branching ratio via the decay channel  $\psi(2S) \rightarrow J/\psi\pi^+\pi^-$ , with  $J/\psi \rightarrow \ell^+\ell^-$ .

<sup>69</sup> ABREU 94P measure this branching ratio via decay channel  $\psi(2S) \rightarrow J/\psi\pi^+\pi^-$ , with  $J/\psi \rightarrow \mu^+\mu^-$ .

$\Gamma(\chi_{c1}(1P)X)/\Gamma_{\text{total}}$					$\Gamma_{23}/\Gamma$
VALUE (units $10^{-3}$ )	EVTS	DOCUMENT ID	TECN	COMMENT	
<b><math>2.9 \pm 0.7</math> OUR AVERAGE</b>					
$2.7 \pm 0.6 \pm 0.5$	33	<sup>70</sup> ACCIARRI	97J L3	$E_{\text{cm}}^{\text{e}} = 88-94$ GeV	
$5.0 \pm 2.1^{+1.5}_{-0.9}$	6.4	<sup>71</sup> ABREU	94P DLPH	$E_{\text{cm}}^{\text{e}} = 88-94$ GeV	

<sup>70</sup> ACCIARRI 97J measure this branching ratio via the decay channel  $\chi_{c1} \rightarrow J/\psi + \gamma$ , with  $J/\psi \rightarrow \ell^+\ell^- (\ell = \mu, e)$ . The  $M(\ell^+\ell^-\gamma) - M(\ell^+\ell^-)$  mass difference spectrum is fitted with two gaussian shapes for  $\chi_{c1}$  and  $\chi_{c2}$ .

<sup>71</sup> This branching ratio is measured via the decay channel  $\chi_{c1} \rightarrow J/\psi + \gamma$ , with  $J/\psi \rightarrow \mu^+\mu^-$ .

$\Gamma(\chi_{c2}(1P)X)/\Gamma_{\text{total}}$					$\Gamma_{24}/\Gamma$
VALUE	CL%	DOCUMENT ID	TECN	COMMENT	
$<3.2 \times 10^{-3}$	90	<sup>72</sup> ACCIARRI	97J L3	$E_{\text{cm}}^{\text{e}} = 88-94$ GeV	

<sup>72</sup> ACCIARRI 97J derive this limit via the decay channel  $\chi_{c2} \rightarrow J/\psi + \gamma$ , with  $J/\psi \rightarrow \ell^+\ell^- (\ell = \mu, e)$ . The  $M(\ell^+\ell^-\gamma) - M(\ell^+\ell^-)$  mass difference spectrum is fitted with two gaussian shapes for  $\chi_{c1}$  and  $\chi_{c2}$ .

$\Gamma(\Upsilon(1S)X + \Upsilon(2S)X + \Upsilon(3S)X)/\Gamma_{\text{total}}$					$\Gamma_{25}/\Gamma = (\Gamma_{26} + \Gamma_{27} + \Gamma_{28})/\Gamma$
VALUE (units $10^{-4}$ )	EVTS	DOCUMENT ID	TECN	COMMENT	
<b><math>1.0 \pm 0.4 \pm 0.22</math></b>	6.4	<sup>73</sup> ALEXANDER	96F OPAL	$E_{\text{cm}}^{\text{e}} = 88-94$ GeV	

<sup>73</sup> ALEXANDER 96F identify the  $\Upsilon$  (which refers to any of the three lowest bound states) through its decay into  $e^+e^-$  and  $\mu^+\mu^-$ . The systematic error includes an uncertainty of  $\pm 0.2$  due to the production mechanism.

$\Gamma(\Upsilon(1S)X)/\Gamma_{\text{total}}$					$\Gamma_{26}/\Gamma$
VALUE	CL%	DOCUMENT ID	TECN	COMMENT	
$<4.4 \times 10^{-5}$	95	<sup>74</sup> ACCIARRI	99F L3	$E_{\text{cm}}^{\text{e}} = 88-94$ GeV	

<sup>74</sup> ACCIARRI 99F search for  $\Upsilon(1S)$  through its decay into  $\ell^+\ell^- (\ell = e \text{ or } \mu)$ .

$\Gamma(\Upsilon(2S)X)/\Gamma_{\text{total}}$					$\Gamma_{27}/\Gamma$
VALUE	CL%	DOCUMENT ID	TECN	COMMENT	
$<13.9 \times 10^{-5}$	95	<sup>75</sup> ACCIARRI	97R L3	$E_{\text{cm}}^{\text{e}} = 88-94$ GeV	

<sup>75</sup> ACCIARRI 97R search for  $\Upsilon(2S)$  through its decay into  $\ell^+\ell^- (\ell = e \text{ or } \mu)$ .

$\Gamma(\Upsilon(3S)X)/\Gamma_{\text{total}}$					$\Gamma_{28}/\Gamma$
VALUE	CL%	DOCUMENT ID	TECN	COMMENT	
$<9.4 \times 10^{-5}$	95	<sup>76</sup> ACCIARRI	97R L3	$E_{\text{cm}}^{\text{e}} = 88-94$ GeV	

<sup>76</sup> ACCIARRI 97R search for  $\Upsilon(3S)$  through its decay into  $\ell^+\ell^- (\ell = e \text{ or } \mu)$ .

$\Gamma((D^0/\bar{D}^0)X)/\Gamma(\text{hadrons})$					$\Gamma_{29}/\Gamma_6$
VALUE	EVTS	DOCUMENT ID	TECN	COMMENT	
<b><math>0.296 \pm 0.019 \pm 0.021</math></b>	369	<sup>77</sup> ABREU	93I DLPH	$E_{\text{cm}}^{\text{e}} = 88-94$ GeV	

<sup>77</sup> The  $(D^0/\bar{D}^0)$  states in ABREU 93I are detected by the  $K\pi$  decay mode. This is a corrected result (see the erratum of ABREU 93I).

$\Gamma(D^{\pm}X)/\Gamma(\text{hadrons})$					$\Gamma_{30}/\Gamma_6$
VALUE	EVTS	DOCUMENT ID	TECN	COMMENT	
<b><math>0.174 \pm 0.016 \pm 0.018</math></b>	539	<sup>78</sup> ABREU	93I DLPH	$E_{\text{cm}}^{\text{e}} = 88-94$ GeV	

<sup>78</sup> The  $D^{\pm}$  states in ABREU 93I are detected by the  $K\pi\pi$  decay mode. This is a corrected result (see the erratum of ABREU 93I).

$\Gamma(D^*(2010)^{\pm}X)/\Gamma(\text{hadrons})$					$\Gamma_{31}/\Gamma_6$
VALUE	EVTS	DOCUMENT ID	TECN	COMMENT	

The value is for the sum of the charge states indicated.

<b><math>0.163 \pm 0.019</math> OUR AVERAGE</b>					
$0.155 \pm 0.010 \pm 0.013$	358	<sup>79</sup> ABREU	93I DLPH	$E_{\text{cm}}^{\text{e}} = 88-94$ GeV	
$0.21 \pm 0.04$	362	<sup>80</sup> DECAMP	91J ALEP	$E_{\text{cm}}^{\text{e}} = 88-94$ GeV	

<sup>79</sup>  $D^*(2010)^{\pm}$  in ABREU 93I are reconstructed from  $D^0\pi^{\pm}$ , with  $D^0 \rightarrow K^-\pi^+$ . The new CLEO II measurement of  $B(D^{*\pm} \rightarrow D^0\pi^{\pm}) = (68.1 \pm 1.6)\%$  is used. This is a corrected result (see the erratum of ABREU 93I).

<sup>80</sup> DECAMP 91J report  $B(D^*(2010)^+ \rightarrow D^0\pi^+) B(D^0 \rightarrow K^-\pi^+) \Gamma(D^*(2010)^{\pm}X) / \Gamma(\text{hadrons}) = (5.11 \pm 0.34) \times 10^{-3}$ . They obtained the above number assuming  $B(D^0 \rightarrow K^-\pi^+) = (3.62 \pm 0.34 \pm 0.44)\%$  and  $B(D^*(2010)^+ \rightarrow D^0\pi^+) = (55 \pm 4)\%$ . We have rescaled their original result of  $0.26 \pm 0.05$  taking into account the new CLEO II branching ratio  $B(D^*(2010)^+ \rightarrow D^0\pi^+) = (68.1 \pm 1.6)\%$ .

$\Gamma(D_{s1}(2536)^{\pm}X)/\Gamma(\text{hadrons})$					$\Gamma_{32}/\Gamma_6$
VALUE (%)	EVTS	DOCUMENT ID	TECN	COMMENT	
<b><math>0.52 \pm 0.09 \pm 0.06</math></b>	92	<sup>81</sup> HEISTER	02B ALEP	$E_{\text{cm}}^{\text{e}} = 88-94$ GeV	

$D_{s1}(2536)^{\pm}$  is an expected orbitally-excited state of the  $D_s$  meson.

<sup>81</sup> HEISTER 02B reconstruct this meson in the decay modes  $D_{s1}(2536)^{\pm} \rightarrow D^{*\pm}K^0$  and  $D_{s1}(2536)^{\pm} \rightarrow D^{*0}K^{\pm}$ . The quoted branching ratio assumes that the decay width of the  $D_{s1}(2536)$  is saturated by the two measured decay modes.

$\Gamma(D_{sJ}(2573)^{\pm}X)/\Gamma(\text{hadrons})$					$\Gamma_{33}/\Gamma_6$
VALUE (%)	EVTS	DOCUMENT ID	TECN	COMMENT	
<b><math>0.83 \pm 0.29^{+0.07}_{-0.13}</math></b>	64	<sup>82</sup> HEISTER	02B ALEP	$E_{\text{cm}}^{\text{e}} = 88-94$ GeV	

$D_{sJ}(2573)^{\pm}$  is an expected orbitally-excited state of the  $D_s$  meson.

<sup>82</sup> HEISTER 02B reconstruct this meson in the decay mode  $D_{sJ}(2573)^{\pm} \rightarrow D^0K^{\pm}$ . The quoted branching ratio assumes that the detected decay mode represents 45% of the full decay width.

$\Gamma(D^{*'}(2629)^{\pm}X)/\Gamma(\text{hadrons})$					$\Gamma_{34}/\Gamma_6$
VALUE	EVTS	DOCUMENT ID	TECN	COMMENT	
<b><math>0.75 \pm 0.04</math> OUR AVERAGE</b>					
$0.760 \pm 0.036 \pm 0.083$		<sup>84</sup> ACKERSTAFF	97M OPAL	$E_{\text{cm}}^{\text{e}} = 88-94$ GeV	
$0.771 \pm 0.026 \pm 0.070$		<sup>85</sup> BUSKULIC	96D ALEP	$E_{\text{cm}}^{\text{e}} = 88-94$ GeV	
$0.72 \pm 0.03 \pm 0.06$		<sup>86</sup> ABREU	95R DLPH	$E_{\text{cm}}^{\text{e}} = 88-94$ GeV	
$0.76 \pm 0.08 \pm 0.06$	1378	<sup>87</sup> ACCIARRI	95B L3	$E_{\text{cm}}^{\text{e}} = 88-94$ GeV	

$D^{*'}(2629)^{\pm}$  is a predicted radial excitation of the  $D^*(2010)^{\pm}$  meson.

<sup>83</sup> ABBIENDI 01N searched for the decay mode  $D^{*'}(2629)^{\pm} \rightarrow D^{*\pm}\pi^+\pi^-$  with  $D^{*'} \rightarrow D^0\pi^+$ , and  $D^0 \rightarrow K^-\pi^+$ . They quote a 95% CL limit for  $Z \rightarrow D^{*'}(2629)^{\pm} \times B(D^{*'}(2629)^+ \rightarrow D^{*+}\pi^+\pi^-) < 3.1 \times 10^{-3}$ .

$\Gamma(B^*X)/[\Gamma(BX) + \Gamma(B^*X)]$					$\Gamma_{36}/(\Gamma_{35} + \Gamma_{36})$
VALUE	EVTS	DOCUMENT ID	TECN	COMMENT	
<b><math>0.75 \pm 0.04</math> OUR AVERAGE</b>					
$0.760 \pm 0.036 \pm 0.083$		<sup>84</sup> ACKERSTAFF	97M OPAL	$E_{\text{cm}}^{\text{e}} = 88-94$ GeV	
$0.771 \pm 0.026 \pm 0.070$		<sup>85</sup> BUSKULIC	96D ALEP	$E_{\text{cm}}^{\text{e}} = 88-94$ GeV	
$0.72 \pm 0.03 \pm 0.06$		<sup>86</sup> ABREU	95R DLPH	$E_{\text{cm}}^{\text{e}} = 88-94$ GeV	
$0.76 \pm 0.08 \pm 0.06$	1378	<sup>87</sup> ACCIARRI	95B L3	$E_{\text{cm}}^{\text{e}} = 88-94$ GeV	

As the experiments assume different values of the  $b$ -baryon contribution, our average should be taken with caution.

<sup>84</sup> ACKERSTAFF 97M use an inclusive  $B$  reconstruction method and assume a  $(13.2 \pm 4.1)\%$   $b$ -baryon contribution. The value refers to a  $b$ -flavored meson mixture of  $B_U, B_D,$  and  $B_S$ .

<sup>85</sup> BUSKULIC 96D use an inclusive reconstruction of  $B$  hadrons and assume a  $(12.2 \pm 4.3)\%$   $b$ -baryon contribution. The value refers to a  $b$ -flavored mixture of  $B_U, B_D,$  and  $B_S$ .

<sup>86</sup> ABREU 95R use an inclusive  $B$ -reconstruction method and assume a  $(10 \pm 4)\%$   $b$ -baryon contribution. The value refers to a  $b$ -flavored meson mixture of  $B_U, B_D,$  and  $B_S$ .

<sup>87</sup> ACCIARRI 95B assume a 9.4%  $b$ -baryon contribution. The value refers to a  $b$ -flavored mixture of  $B_U, B_D,$  and  $B_S$ .

See key on page 457

## Gauge &amp; Higgs Boson Particle Listings

Z

 $\Gamma(B^+X)/\Gamma(\text{hadrons})$   $\Gamma_{37}/\Gamma_6$ 

"OUR EVALUATION" is obtained using our current values for  $f(\bar{b} \rightarrow B^+)$  and  $R_b = \Gamma(b\bar{b})/\Gamma(\text{hadrons})$ . We calculate  $\Gamma(B^+X)/\Gamma(\text{hadrons}) = R_b \times f(\bar{b} \rightarrow B^+)$ . The decay fraction  $f(\bar{b} \rightarrow B^+)$  was provided by the Heavy Flavor Averaging Group (HFAG, [http://www.slac.stanford.edu/xorg/hfag/osc/PDG\\_2009/#FRACZ](http://www.slac.stanford.edu/xorg/hfag/osc/PDG_2009/#FRACZ)).

VALUE	DOCUMENT ID	TECN	COMMENT
<b>0.0869 ± 0.0019 OUR EVALUATION</b>			
<b>0.0887 ± 0.0030</b>	88 ABDALLAH	03k DLPH	$E_{\text{cm}}^{\text{ee}} = 88\text{--}94$ GeV

88 ABDALLAH 03k measure the production fraction of  $B^+$  mesons in hadronic Z decays ( $f(B^+) = (40.99 \pm 0.82 \pm 1.11)\%$ ). The value quoted here is obtained multiplying this production fraction by our value of  $R_b = \Gamma(b\bar{b})/\Gamma(\text{hadrons})$ .

 $\Gamma(B_s^0X)/\Gamma(\text{hadrons})$   $\Gamma_{38}/\Gamma_6$ 

"OUR EVALUATION" is obtained using our current values for  $f(\bar{b} \rightarrow B_s^0)$  and  $R_b = \Gamma(b\bar{b})/\Gamma(\text{hadrons})$ . We calculate  $\Gamma(B_s^0X)/\Gamma(\text{hadrons}) = R_b \times f(\bar{b} \rightarrow B_s^0)$ . The decay fraction  $f(\bar{b} \rightarrow B_s^0)$  was provided by the Heavy Flavor Averaging Group (HFAG, [http://www.slac.stanford.edu/xorg/hfag/osc/PDG\\_2009/#FRACZ](http://www.slac.stanford.edu/xorg/hfag/osc/PDG_2009/#FRACZ)).

VALUE	DOCUMENT ID	TECN	COMMENT
<b>0.0227 ± 0.0019 OUR EVALUATION</b>			
seen	89 ABREU	92M DLPH	$E_{\text{cm}}^{\text{ee}} = 88\text{--}94$ GeV
seen	90 ACTON	92N OPAL	$E_{\text{cm}}^{\text{ee}} = 88\text{--}94$ GeV
seen	91 BUSKULIC	92E ALEP	$E_{\text{cm}}^{\text{ee}} = 88\text{--}94$ GeV

89 ABREU 92M reported value is  $\Gamma(B_s^0X) * B(B_s^0 \rightarrow D_s \mu \nu_\mu X) * B(D_s \rightarrow \phi\pi)/\Gamma(\text{hadrons}) = (18 \pm 8) \times 10^{-5}$ .

90 ACTON 92N find evidence for  $B_s^0$  production using  $D_s$ - $\ell$  correlations, with  $D_s^+ \rightarrow \phi\pi^+$  and  $K^*(892)K^+$ . Assuming  $R_b$  from the Standard Model and averaging over the  $e$  and  $\mu$  channels, authors measure the product branching fraction to be  $f(\bar{b} \rightarrow B_s^0) \times B(B_s^0 \rightarrow D_s^+ \ell^+ \nu_\ell X) \times B(D_s^+ \rightarrow \phi\pi^+) = (3.9 \pm 1.1 \pm 0.8) \times 10^{-4}$ .

91 BUSKULIC 92E find evidence for  $B_s^0$  production using  $D_s$ - $\ell$  correlations, with  $D_s^+ \rightarrow \phi\pi^+$  and  $K^*(892)K^+$ . Using  $B(D_s^+ \rightarrow \phi\pi^+) = (2.7 \pm 0.7)\%$  and summing up the  $e$  and  $\mu$  channels, the weighted average product branching fraction is measured to be  $B(\bar{b} \rightarrow B_s^0) \times B(B_s^0 \rightarrow D_s^+ \ell^+ \nu_\ell X) = 0.040 \pm 0.011^{+0.010}_{-0.012}$ .

 $\Gamma(B_c^+X)/\Gamma(\text{hadrons})$   $\Gamma_{39}/\Gamma_6$ 

VALUE	DOCUMENT ID	TECN	COMMENT
searched for	92 ACKERSTAFF	98o OPAL	$E_{\text{cm}}^{\text{ee}} = 88\text{--}94$ GeV
searched for	93 ABREU	97E DLPH	$E_{\text{cm}}^{\text{ee}} = 88\text{--}94$ GeV
searched for	94 BARATE	97H ALEP	$E_{\text{cm}}^{\text{ee}} = 88\text{--}94$ GeV

92 ACKERSTAFF 98o searched for the decay modes  $B_c \rightarrow J/\psi\pi^+$ ,  $J/\psi a_1^+$ , and  $J/\psi\ell^+\nu_\ell$ , with  $J/\psi \rightarrow \ell^+\ell^-$ ,  $\ell = e, \mu$ . The number of candidates (background) for the three decay modes is  $2(0.63 \pm 0.2)$ ,  $0(1.10 \pm 0.22)$ , and  $1(0.82 \pm 0.19)$  respectively. Interpreting the  $2B_c \rightarrow J/\psi\pi^+$  candidates as signal, they report  $\Gamma(B_c^+X) \times B(B_c \rightarrow J/\psi\pi^+)/\Gamma(\text{hadrons}) = (3.8^{+5.0}_{-2.4} \pm 0.5) \times 10^{-5}$ . Interpreted as background, the 90% CL bounds are  $\Gamma(B_c^+X) \times B(B_c \rightarrow J/\psi\pi^+)/\Gamma(\text{hadrons}) < 1.06 \times 10^{-4}$ ,  $\Gamma(B_c^+X) \times B(B_c \rightarrow J/\psi a_1^+)/\Gamma(\text{hadrons}) < 5.29 \times 10^{-4}$ ,  $\Gamma(B_c^+X) \times B(B_c \rightarrow J/\psi\ell^+\nu_\ell)/\Gamma(\text{hadrons}) < 6.96 \times 10^{-5}$ .

93 ABREU 97E searched for the decay modes  $B_c \rightarrow J/\psi\pi^+$ ,  $J/\psi\ell^+\nu_\ell$ , and  $J/\psi(3\pi^+)$ , with  $J/\psi \rightarrow \ell^+\ell^-$ ,  $\ell = e, \mu$ . The number of candidates (background) for the three decay modes is  $1(1.7)$ ,  $0(0.3)$ , and  $1(2.3)$  respectively. They report the following 90% CL limits:  $\Gamma(B_c^+X) \times B(B_c \rightarrow J/\psi\pi^+)/\Gamma(\text{hadrons}) < (1.05\text{--}0.84) \times 10^{-4}$ ,  $\Gamma(B_c^+X) \times B(B_c \rightarrow J/\psi\ell^+\nu_\ell)/\Gamma(\text{hadrons}) < (5.8\text{--}5.0) \times 10^{-5}$ ,  $\Gamma(B_c^+X) \times B(B_c \rightarrow J/\psi(3\pi^+))/\Gamma(\text{hadrons}) < 1.75 \times 10^{-4}$ , where the ranges are due to the predicted  $B_c$  lifetime (0.4–1.4) ps.

94 BARATE 97H searched for the decay modes  $B_c \rightarrow J/\psi\pi^+$  and  $J/\psi\ell^+\nu_\ell$  with  $J/\psi \rightarrow \ell^+\ell^-$ ,  $\ell = e, \mu$ . The number of candidates (background) for the two decay modes is  $0(0.44)$  and  $2(0.81)$  respectively. They report the following 90% CL limits:  $\Gamma(B_c^+X) \times B(B_c \rightarrow J/\psi\pi^+)/\Gamma(\text{hadrons}) < 3.6 \times 10^{-5}$  and  $\Gamma(B_c^+X) \times B(B_c \rightarrow J/\psi\ell^+\nu_\ell)/\Gamma(\text{hadrons}) < 5.2 \times 10^{-5}$ .

 $\Gamma(\Lambda_c^+X)/\Gamma(\text{hadrons})$   $\Gamma_{40}/\Gamma_6$ 

VALUE	DOCUMENT ID	TECN	COMMENT
<b>0.022 ± 0.005 OUR AVERAGE</b>			
0.024 ± 0.005 ± 0.006	95 ALEXANDER	96R OPAL	$E_{\text{cm}}^{\text{ee}} = 88\text{--}94$ GeV
0.021 ± 0.003 ± 0.005	96 BUSKULIC	96Y ALEP	$E_{\text{cm}}^{\text{ee}} = 88\text{--}94$ GeV

95 ALEXANDER 96R measure  $R_b \times f(b \rightarrow \Lambda_c^+X) \times B(\Lambda_c^+ \rightarrow pK^-\pi^+) = (0.122 \pm 0.023 \pm 0.010)\%$  in hadronic Z decays; the value quoted here is obtained using our best value  $B(\Lambda_c^+ \rightarrow pK^-\pi^+) = (5.0 \pm 1.3)\%$ . The first error is the total experiment's error and the second error is the systematic error due to the branching fraction uncertainty.

96 BUSKULIC 96Y obtain the production fraction of  $\Lambda_c^+$  baryons in hadronic Z decays  $f(b \rightarrow \Lambda_c^+X) = 0.110 \pm 0.014 \pm 0.006$  using  $B(\Lambda_c^+ \rightarrow pK^-\pi^+) = (4.4 \pm 0.6)\%$ ; we have rescaled using our best value  $B(\Lambda_c^+ \rightarrow pK^-\pi^+) = (5.0 \pm 1.3)\%$  obtaining  $f(b \rightarrow \Lambda_c^+X) = 0.097 \pm 0.013 \pm 0.025$  where the first error is their total experiment's error and the second error is the systematic error due to the branching fraction uncertainty. The value quoted here is obtained multiplying this production fraction by our value of  $R_b = \Gamma(b\bar{b})/\Gamma(\text{hadrons})$ .

 $\Gamma(\Xi_c^0X)/\Gamma(\text{hadrons})$   $\Gamma_{41}/\Gamma_6$ 

VALUE	DOCUMENT ID	TECN	COMMENT
••• We do not use the following data for averages, fits, limits, etc. •••			
seen	97 ABDALLAH	05c DLPH	$E_{\text{cm}}^{\text{ee}} = 88\text{--}94$ GeV
97 ABDALLAH 05c searched for the charmed strange baryon $\Xi_c^0$ in the decay channel $\Xi_c^0 \rightarrow \Xi^-\pi^+$ ( $\Xi^- \rightarrow \Lambda\pi^-$ ). The production rate is measured to be $f_{\Xi_c^0} \times B(\Xi_c^0 \rightarrow \Xi^-\pi^+) = (4.7 \pm 1.4 \pm 1.1) \times 10^{-4}$ per hadronic Z decay.			

 $\Gamma(\Xi_b^-X)/\Gamma(\text{hadrons})$   $\Gamma_{42}/\Gamma_6$ 

Here  $\Xi_b^-$  is used as a notation for the strange  $b$ -baryon states  $\Xi_b^-$  and  $\Xi_b^0$ .

VALUE	DOCUMENT ID	TECN	COMMENT
••• We do not use the following data for averages, fits, limits, etc. •••			
seen	98 ABDALLAH	05c DLPH	$E_{\text{cm}}^{\text{ee}} = 88\text{--}94$ GeV
seen	99 BUSKULIC	96T ALEP	$E_{\text{cm}}^{\text{ee}} = 88\text{--}94$ GeV
seen	100 ABREU	95V DLPH	$E_{\text{cm}}^{\text{ee}} = 88\text{--}94$ GeV

98 ABDALLAH 05c searched for the beauty strange baryon  $\Xi_b^-$  in the inclusive semileptonic decay channel  $\Xi_b^- \rightarrow \Xi^-\ell^-\bar{\nu}_\ell X$ . Evidence for the  $\Xi_b^-$  production is seen from the observation of  $\Xi^+$  production accompanied by a lepton of the same sign. From the excess of "right-sign" pairs  $\Xi^+\ell^+$  compared to "wrong-sign" pairs  $\Xi^+\ell^-$  the production rate is measured to be  $B(b \rightarrow \Xi_b^-) \times B(\Xi_b^- \rightarrow \Xi^-\ell^-\bar{\nu}_\ell X) = (3.0 \pm 1.0 \pm 0.3) \times 10^{-4}$  per lepton species, averaged over electrons and muons.

99 BUSKULIC 96T investigate  $\Xi$ -lepton correlations and find a significant excess of "right-sign" pairs  $\Xi^+\ell^+$  compared to "wrong-sign" pairs  $\Xi^+\ell^-$ . This excess is interpreted as evidence for  $\Xi_b^-$  semileptonic decay. The measured product branching ratio is  $B(b \rightarrow \Xi_b^-) \times B(\Xi_b^- \rightarrow X_c X \ell^-\bar{\nu}_\ell) \times B(X_c \rightarrow \Xi^-\ell^+ X') = (5.4 \pm 1.1 \pm 0.8) \times 10^{-4}$  per lepton species, averaged over electrons and muons, with  $X_c$  a charmed baryon.

100 ABREU 95V observe an excess of "right-sign" pairs  $\Xi^+\ell^+$  compared to "wrong-sign" pairs  $\Xi^+\ell^-$  in jets; this excess is interpreted as evidence for the beauty strange baryon  $\Xi_b^-$  production, with  $\Xi_b^- \rightarrow \Xi^-\ell^-\bar{\nu}_\ell X$ . They find that the probability for this signal to come from non  $b$ -baryon decays is less than  $5 \times 10^{-4}$  and that  $\Lambda_b$  decays can account for less than 10% of these events. The  $\Xi_b^-$  production rate is then measured to be  $B(b \rightarrow \Xi_b^-) \times B(\Xi_b^- \rightarrow \Xi^-\ell^-\bar{\nu}_\ell X) = (5.9 \pm 2.1 \pm 1.0) \times 10^{-4}$  per lepton species, averaged over electrons and muons.

 $\Gamma(b\text{-baryon } X)/\Gamma(\text{hadrons})$   $\Gamma_{43}/\Gamma_6$ 

"OUR EVALUATION" is obtained using our current values for  $f(b \rightarrow b\text{-baryon})$  and  $R_b = \Gamma(b\bar{b})/\Gamma(\text{hadrons})$ . We calculate  $\Gamma(b\text{-baryon } X)/\Gamma(\text{hadrons}) = R_b \times f(b \rightarrow b\text{-baryon})$ . The decay fraction  $f(b \rightarrow b\text{-baryon})$  was provided by the Heavy Flavor Averaging Group (HFAG, [http://www.slac.stanford.edu/xorg/hfag/osc/PDG\\_2009](http://www.slac.stanford.edu/xorg/hfag/osc/PDG_2009)).

VALUE	DOCUMENT ID	TECN	COMMENT
<b>0.0197 ± 0.0032 OUR EVALUATION</b>			
<b>0.0221 ± 0.0015 ± 0.0058</b>	101 BARATE	98V ALEP	$E_{\text{cm}}^{\text{ee}} = 88\text{--}94$ GeV

101 BARATE 98V use the overall number of identified protons in  $b$ -hadron decays to measure  $f(b \rightarrow b\text{-baryon}) = 0.102 \pm 0.007 \pm 0.027$ . They assume  $\text{BR}(b\text{-baryon} \rightarrow pX) = (58 \pm 6)\%$  and  $\text{BR}(B_c^0 \rightarrow pX) = (8.0 \pm 4.0)\%$ . The value quoted here is obtained multiplying this production fraction by our value of  $R_b = \Gamma(b\bar{b})/\Gamma(\text{hadrons})$ .

 $\Gamma(\text{anomalous } \gamma + \text{hadrons})/\Gamma_{\text{total}}$   $\Gamma_{44}/\Gamma$ 

Limits on additional sources of prompt photons beyond expectations for final-state bremsstrahlung.

VALUE	CL%	DOCUMENT ID	TECN	COMMENT
<b>&lt;3.2 × 10<sup>-3</sup></b>	95	102 AKRAWY	90I OPAL	$E_{\text{cm}}^{\text{ee}} = 88\text{--}94$ GeV
102 AKRAWY 90I report $\Gamma(\gamma X) < 8.2$ MeV at 95%CL. They assume a three-body $\gamma\gamma\bar{q}$ distribution and use $E(\gamma) > 10$ GeV.				

 $\Gamma(e^+e^- \gamma)/\Gamma_{\text{total}}$   $\Gamma_{45}/\Gamma$ 

VALUE	CL%	DOCUMENT ID	TECN	COMMENT
<b>&lt;5.2 × 10<sup>-4</sup></b>	95	103 ACTON	91B OPAL	$E_{\text{cm}}^{\text{ee}} = 91.2$ GeV
103 ACTON 91B looked for isolated photons with $E > 2\%$ of beam energy ( $> 0.9$ GeV).				

 $\Gamma(\mu^+\mu^-\gamma)/\Gamma_{\text{total}}$   $\Gamma_{46}/\Gamma$ 

VALUE	CL%	DOCUMENT ID	TECN	COMMENT
<b>&lt;5.6 × 10<sup>-4</sup></b>	95	104 ACTON	91B OPAL	$E_{\text{cm}}^{\text{ee}} = 91.2$ GeV
104 ACTON 91B looked for isolated photons with $E > 2\%$ of beam energy ( $> 0.9$ GeV).				

 $\Gamma(\tau^+\tau^-\gamma)/\Gamma_{\text{total}}$   $\Gamma_{47}/\Gamma$ 

VALUE	CL%	DOCUMENT ID	TECN	COMMENT
<b>&lt;7.3 × 10<sup>-4</sup></b>	95	105 ACTON	91B OPAL	$E_{\text{cm}}^{\text{ee}} = 91.2$ GeV
105 ACTON 91B looked for isolated photons with $E > 2\%$ of beam energy ( $> 0.9$ GeV).				

 $\Gamma(\ell^+\ell^-\gamma)/\Gamma_{\text{total}}$   $\Gamma_{48}/\Gamma$ 

The value is the sum over  $\ell = e, \mu, \tau$ .

VALUE	CL%	DOCUMENT ID	TECN	COMMENT
<b>&lt;6.8 × 10<sup>-6</sup></b>	95	106 ACTON	93E OPAL	$E_{\text{cm}}^{\text{ee}} = 88\text{--}94$ GeV
106 For $m_{\gamma\gamma} = 60 \pm 5$ GeV.				

 $\Gamma(q\bar{q}\gamma\gamma)/\Gamma_{\text{total}}$   $\Gamma_{49}/\Gamma$ 

VALUE	CL%	DOCUMENT ID	TECN	COMMENT
<b>&lt;5.5 × 10<sup>-6</sup></b>	95	107 ACTON	93E OPAL	$E_{\text{cm}}^{\text{ee}} = 88\text{--}94$ GeV
107 For $m_{\gamma\gamma} = 60 \pm 5$ GeV.				

# Gauge & Higgs Boson Particle Listings

## Z

### $\Gamma(\nu\bar{\nu}\gamma\gamma)/\Gamma_{total}$ $\Gamma_{50}/\Gamma$

VALUE	CL%	DOCUMENT ID	TECN	COMMENT
$<3.1 \times 10^{-6}$	95	108 ACTON	93E OPAL	$E_{cm}^{ee} = 88-94$ GeV

108 For  $m_{\gamma\gamma} = 60 \pm 5$  GeV.

### $\Gamma(e^{\pm}\mu^{\mp})/\Gamma_{total}$ $\Gamma_{51}/\Gamma$

Test of lepton family number conservation. The value is for the sum of the charge states indicated.

VALUE	CL%	DOCUMENT ID	TECN	COMMENT
$<2.5 \times 10^{-6}$	95	ABREU	97C DLPH	$E_{cm}^{ee} = 88-94$ GeV
$<1.7 \times 10^{-6}$	95	AKERS	95W OPAL	$E_{cm}^{ee} = 88-94$ GeV
$<0.6 \times 10^{-5}$	95	ADRIANI	93I L3	$E_{cm}^{ee} = 88-94$ GeV
$<2.6 \times 10^{-5}$	95	DECAMP	92 ALEP	$E_{cm}^{ee} = 88-94$ GeV

### $\Gamma(e^{\pm}\mu^{\mp})/\Gamma(e^{+}e^{-})$ $\Gamma_{51}/\Gamma_1$

Test of lepton family number conservation. The value is for the sum of the charge states indicated.

VALUE	CL%	DOCUMENT ID	TECN	COMMENT
$<0.07$	90	ALBAJAR	89 UA1	$E_{cm}^{p\bar{p}} = 546,630$ GeV

### $\Gamma(e^{\pm}\tau^{\mp})/\Gamma_{total}$ $\Gamma_{52}/\Gamma$

Test of lepton family number conservation. The value is for the sum of the charge states indicated.

VALUE	CL%	DOCUMENT ID	TECN	COMMENT
$<2.2 \times 10^{-5}$	95	ABREU	97C DLPH	$E_{cm}^{ee} = 88-94$ GeV
$<9.8 \times 10^{-6}$	95	AKERS	95W OPAL	$E_{cm}^{ee} = 88-94$ GeV
$<1.3 \times 10^{-5}$	95	ADRIANI	93I L3	$E_{cm}^{ee} = 88-94$ GeV
$<1.2 \times 10^{-4}$	95	DECAMP	92 ALEP	$E_{cm}^{ee} = 88-94$ GeV

### $\Gamma(\mu^{\pm}\tau^{\mp})/\Gamma_{total}$ $\Gamma_{53}/\Gamma$

Test of lepton family number conservation. The value is for the sum of the charge states indicated.

VALUE	CL%	DOCUMENT ID	TECN	COMMENT
$<1.2 \times 10^{-5}$	95	ABREU	97C DLPH	$E_{cm}^{ee} = 88-94$ GeV
$<1.7 \times 10^{-5}$	95	AKERS	95W OPAL	$E_{cm}^{ee} = 88-94$ GeV
$<1.9 \times 10^{-5}$	95	ADRIANI	93I L3	$E_{cm}^{ee} = 88-94$ GeV
$<1.0 \times 10^{-4}$	95	DECAMP	92 ALEP	$E_{cm}^{ee} = 88-94$ GeV

### $\Gamma(pe)/\Gamma_{total}$ $\Gamma_{54}/\Gamma$

Test of baryon number and lepton number conservations. Charge conjugate states are implied.

VALUE	CL%	DOCUMENT ID	TECN	COMMENT
$<1.8 \times 10^{-6}$	95	109 ABBIENDI	99I OPAL	$E_{cm}^{ee} = 88-94$ GeV

109 ABBIENDI 99i give the 95%CL limit on the partial width  $\Gamma(Z^0 \rightarrow pe) < 4.6$  KeV and we have transformed it into a branching ratio.

### $\Gamma(p\mu)/\Gamma_{total}$ $\Gamma_{55}/\Gamma$

Test of baryon number and lepton number conservations. Charge conjugate states are implied.

VALUE	CL%	DOCUMENT ID	TECN	COMMENT
$<1.8 \times 10^{-6}$	95	110 ABBIENDI	99I OPAL	$E_{cm}^{ee} = 88-94$ GeV

110 ABBIENDI 99i give the 95%CL limit on the partial width  $\Gamma(Z^0 \rightarrow p\mu) < 4.4$  KeV and we have transformed it into a branching ratio.

## AVERAGE PARTICLE MULTIPLICITIES IN HADRONIC Z DECAY

Summed over particle and antiparticle, when appropriate.

### $\langle N_{\eta} \rangle$

VALUE	DOCUMENT ID	TECN	COMMENT
<b><math>20.97 \pm 0.02 \pm 1.15</math></b>	ACKERSTAFF 98A	OPAL	$E_{cm}^{ee} = 91.2$ GeV

### $\langle N_{\pi^{\pm}} \rangle$

VALUE	DOCUMENT ID	TECN	COMMENT
<b><math>17.03 \pm 0.16</math> OUR AVERAGE</b>			
$17.007 \pm 0.209$	ABE	04C SLD	$E_{cm}^{ee} = 91.2$ GeV
$17.26 \pm 0.10 \pm 0.88$	ABREU	98L DLPH	$E_{cm}^{ee} = 91.2$ GeV
$17.04 \pm 0.31$	BARATE	98V ALEP	$E_{cm}^{ee} = 91.2$ GeV
$17.05 \pm 0.43$	AKERS	94P OPAL	$E_{cm}^{ee} = 91.2$ GeV

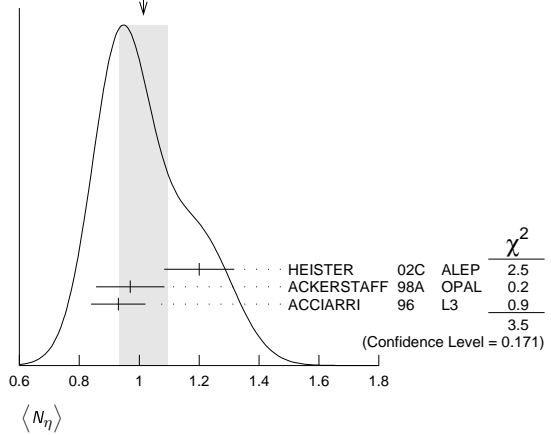
### $\langle N_{\pi^0} \rangle$

VALUE	DOCUMENT ID	TECN	COMMENT
<b><math>9.76 \pm 0.26</math> OUR AVERAGE</b>			
$9.55 \pm 0.06 \pm 0.75$	ACKERSTAFF 98A	OPAL	$E_{cm}^{ee} = 91.2$ GeV
$9.63 \pm 0.13 \pm 0.63$	BARATE	97J ALEP	$E_{cm}^{ee} = 91.2$ GeV
$9.90 \pm 0.02 \pm 0.33$	ACCIARRI	96 L3	$E_{cm}^{ee} = 91.2$ GeV
$9.2 \pm 0.2 \pm 1.0$	ADAM	96 DLPH	$E_{cm}^{ee} = 91.2$ GeV

### $\langle N_{\eta} \rangle$

VALUE	DOCUMENT ID	TECN	COMMENT
<b><math>1.01 \pm 0.08</math> OUR AVERAGE</b>	Error includes scale factor of 1.3. See the ideogram below.		
$1.20 \pm 0.04 \pm 0.11$	HEISTER	02C ALEP	$E_{cm}^{ee} = 91.2$ GeV
$0.97 \pm 0.03 \pm 0.11$	ACKERSTAFF	98A OPAL	$E_{cm}^{ee} = 91.2$ GeV
$0.93 \pm 0.01 \pm 0.09$	ACCIARRI	96 L3	$E_{cm}^{ee} = 91.2$ GeV

WEIGHTED AVERAGE  
1.01±0.08 (Error scaled by 1.3)



### $\langle N_{\rho^{\pm}} \rangle$

VALUE	DOCUMENT ID	TECN	COMMENT
<b><math>2.57 \pm 0.15</math> OUR AVERAGE</b>			
$2.59 \pm 0.03 \pm 0.16$	111 BEDDALL	09	ALEPH archive, $E_{cm}^{ee} = 91.2$ GeV
$2.40 \pm 0.06 \pm 0.43$	ACKERSTAFF	98A OPAL	$E_{cm}^{ee} = 91.2$ GeV

111 BEDDALL 09 analyse 3.2 million hadronic Z decays as archived by ALEPH collaboration and report a value of  $2.59 \pm 0.03 \pm 0.15 \pm 0.04$ . The first error is statistical, the second systematic, and the third arises from extrapolation to full phase space. We combine the systematic errors in quadrature.

### $\langle N_{\rho^0} \rangle$

VALUE	DOCUMENT ID	TECN	COMMENT
<b><math>1.24 \pm 0.10</math> OUR AVERAGE</b>	Error includes scale factor of 1.1.		
$1.19 \pm 0.10$	ABREU	99J DLPH	$E_{cm}^{ee} = 91.2$ GeV
$1.45 \pm 0.06 \pm 0.20$	BUSKULIC	96H ALEP	$E_{cm}^{ee} = 91.2$ GeV

### $\langle N_{\eta'} \rangle$

VALUE	DOCUMENT ID	TECN	COMMENT
<b><math>1.02 \pm 0.06</math> OUR AVERAGE</b>			
$1.00 \pm 0.03 \pm 0.06$	HEISTER	02C ALEP	$E_{cm}^{ee} = 91.2$ GeV
$1.04 \pm 0.04 \pm 0.14$	ACKERSTAFF	98A OPAL	$E_{cm}^{ee} = 91.2$ GeV
$1.17 \pm 0.09 \pm 0.15$	ACCIARRI	97D L3	$E_{cm}^{ee} = 91.2$ GeV

### $\langle N_{\eta' \prime} \rangle$

VALUE	DOCUMENT ID	TECN	COMMENT
<b><math>0.17 \pm 0.05</math> OUR AVERAGE</b>	Error includes scale factor of 2.4.		
$0.14 \pm 0.01 \pm 0.02$	ACKERSTAFF	98A OPAL	$E_{cm}^{ee} = 91.2$ GeV
$0.25 \pm 0.04$	112 ACCIARRI	97D L3	$E_{cm}^{ee} = 91.2$ GeV
$0.068 \pm 0.018 \pm 0.016$	113 BUSKULIC	92D ALEP	$E_{cm}^{ee} = 91.2$ GeV

112 ACCIARRI 97D obtain this value averaging over the two decay channels  $\eta' \rightarrow \pi^+ \pi^- \eta'$  and  $\eta' \rightarrow \rho^0 \gamma$ .

113 BUSKULIC 92D obtain this value for  $x > 0.1$ .

### $\langle N_{\eta(980)} \rangle$

VALUE	DOCUMENT ID	TECN	COMMENT
<b><math>0.147 \pm 0.011</math> OUR AVERAGE</b>			
$0.164 \pm 0.021$	ABREU	99J DLPH	$E_{cm}^{ee} = 91.2$ GeV
$0.141 \pm 0.007 \pm 0.011$	ACKERSTAFF	98Q OPAL	$E_{cm}^{ee} = 91.2$ GeV

### $\langle N_{\eta_0(980)^{\pm}} \rangle$

VALUE	DOCUMENT ID	TECN	COMMENT
<b><math>0.27 \pm 0.04 \pm 0.10</math></b>			
	ACKERSTAFF	98A OPAL	$E_{cm}^{ee} = 91.2$ GeV



See key on page 457

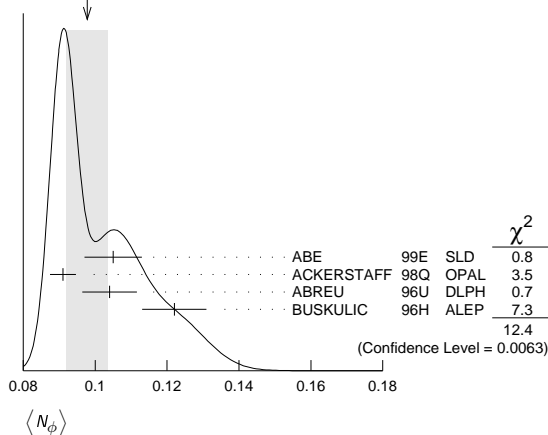
# Gauge & Higgs Boson Particle Listings

Z

## $\langle N_\phi \rangle$

VALUE	DOCUMENT ID	TECN	COMMENT
<b>0.098 ± 0.006 OUR AVERAGE</b>	Error includes scale factor of 2.0. See the ideogram below.		
0.105 ± 0.008	ABE	99E SLD	$E_{cm}^{ee} = 91.2$ GeV
0.091 ± 0.002 ± 0.003	ACKERSTAFF	98Q OPAL	$E_{cm}^{ee} = 91.2$ GeV
0.104 ± 0.003 ± 0.007	ABREU	96U DLPH	$E_{cm}^{ee} = 91.2$ GeV
0.122 ± 0.004 ± 0.008	BUSKULIC	96H ALEP	$E_{cm}^{ee} = 91.2$ GeV

WEIGHTED AVERAGE  
0.098 ± 0.006 (Error scaled by 2.0)



## $\langle N_{f_2(1270)} \rangle$

VALUE	DOCUMENT ID	TECN	COMMENT
<b>0.169 ± 0.025 OUR AVERAGE</b>	Error includes scale factor of 1.4.		
0.214 ± 0.038	ABREU	99J DLPH	$E_{cm}^{ee} = 91.2$ GeV
0.155 ± 0.011 ± 0.018	ACKERSTAFF	98Q OPAL	$E_{cm}^{ee} = 91.2$ GeV

## $\langle N_{f_1(1285)} \rangle$

VALUE	DOCUMENT ID	TECN	COMMENT
<b>0.165 ± 0.051</b>	114 ABDALLAH	03H DLPH	$E_{cm}^{ee} = 91.2$ GeV

114 ABDALLAH 03H assume a  $K\bar{K}\pi$  branching ratio of  $(9.0 \pm 0.4)\%$ .

## $\langle N_{f_1(1420)} \rangle$

VALUE	DOCUMENT ID	TECN	COMMENT
<b>0.056 ± 0.012</b>	115 ABDALLAH	03H DLPH	$E_{cm}^{ee} = 91.2$ GeV

115 ABDALLAH 03H assume a  $K\bar{K}\pi$  branching ratio of 100%.

## $\langle N_{f_2'(1525)} \rangle$

VALUE	DOCUMENT ID	TECN	COMMENT
<b>0.012 ± 0.006</b>	ABREU	99J DLPH	$E_{cm}^{ee} = 91.2$ GeV

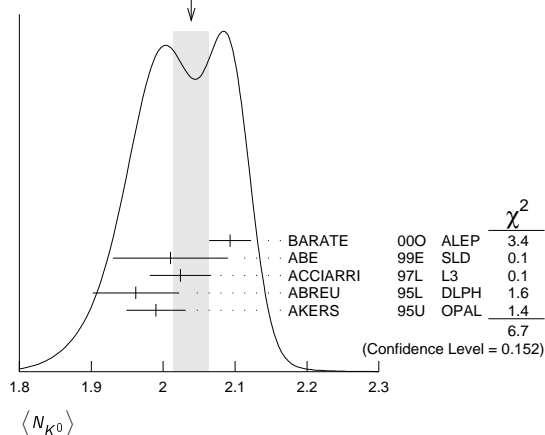
## $\langle N_{K^\pm} \rangle$

VALUE	DOCUMENT ID	TECN	COMMENT
<b>2.24 ± 0.04 OUR AVERAGE</b>			
2.203 ± 0.071	ABE	04C SLD	$E_{cm}^{ee} = 91.2$ GeV
2.21 ± 0.05 ± 0.05	ABREU	98L DLPH	$E_{cm}^{ee} = 91.2$ GeV
2.26 ± 0.12	BARATE	98V ALEP	$E_{cm}^{ee} = 91.2$ GeV
2.42 ± 0.13	AKERS	94P OPAL	$E_{cm}^{ee} = 91.2$ GeV

## $\langle N_{K^0} \rangle$

VALUE	DOCUMENT ID	TECN	COMMENT
<b>2.039 ± 0.025 OUR AVERAGE</b>	Error includes scale factor of 1.3. See the ideogram below.		
2.093 ± 0.004 ± 0.029	BARATE	00O ALEP	$E_{cm}^{ee} = 91.2$ GeV
2.01 ± 0.08	ABE	99E SLD	$E_{cm}^{ee} = 91.2$ GeV
2.024 ± 0.006 ± 0.042	ACCIARRI	97L L3	$E_{cm}^{ee} = 91.2$ GeV
1.962 ± 0.022 ± 0.056	ABREU	95L DLPH	$E_{cm}^{ee} = 91.2$ GeV
1.99 ± 0.01 ± 0.04	AKERS	95U OPAL	$E_{cm}^{ee} = 91.2$ GeV

WEIGHTED AVERAGE  
2.039 ± 0.025 (Error scaled by 1.3)



## $\langle N_{K^*(892)^\pm} \rangle$

VALUE	DOCUMENT ID	TECN	COMMENT
<b>0.72 ± 0.05 OUR AVERAGE</b>			
0.712 ± 0.031 ± 0.059	ABREU	95L DLPH	$E_{cm}^{ee} = 91.2$ GeV
0.72 ± 0.02 ± 0.08	ACTON	93 OPAL	$E_{cm}^{ee} = 91.2$ GeV

## $\langle N_{K^*(892)^0} \rangle$

VALUE	DOCUMENT ID	TECN	COMMENT
<b>0.739 ± 0.022 OUR AVERAGE</b>			
0.707 ± 0.041	ABE	99E SLD	$E_{cm}^{ee} = 91.2$ GeV
0.74 ± 0.02 ± 0.02	ACKERSTAFF	97S OPAL	$E_{cm}^{ee} = 91.2$ GeV
0.77 ± 0.02 ± 0.07	ABREU	96U DLPH	$E_{cm}^{ee} = 91.2$ GeV
0.83 ± 0.01 ± 0.09	BUSKULIC	96H ALEP	$E_{cm}^{ee} = 91.2$ GeV
0.97 ± 0.18 ± 0.31	ABREU	93 DLPH	$E_{cm}^{ee} = 91.2$ GeV

## $\langle N_{K_2^*(1430)} \rangle$

VALUE	DOCUMENT ID	TECN	COMMENT
<b>0.073 ± 0.023</b>	ABREU	99J DLPH	$E_{cm}^{ee} = 91.2$ GeV
0.19 ± 0.04 ± 0.06	116 AKERS	95X OPAL	$E_{cm}^{ee} = 91.2$ GeV

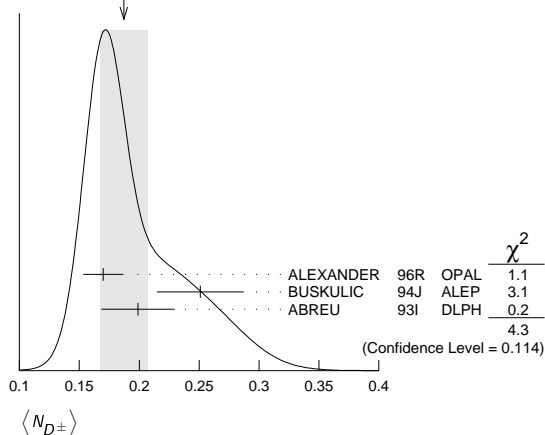
••• We do not use the following data for averages, fits, limits, etc. •••  
116 AKERS 95x obtain this value for  $x < 0.3$ .

## $\langle N_{D^\pm} \rangle$

VALUE	DOCUMENT ID	TECN	COMMENT
<b>0.187 ± 0.020 OUR AVERAGE</b>	Error includes scale factor of 1.5. See the ideogram below.		
0.170 ± 0.009 ± 0.014	ALEXANDER	96R OPAL	$E_{cm}^{ee} = 91.2$ GeV
0.251 ± 0.026 ± 0.025	BUSKULIC	94J ALEP	$E_{cm}^{ee} = 91.2$ GeV
0.199 ± 0.019 ± 0.024	117 ABREU	93I DLPH	$E_{cm}^{ee} = 91.2$ GeV

117 See ABREU 95 (erratum).

WEIGHTED AVERAGE  
0.187 ± 0.020 (Error scaled by 1.5)



# Gauge & Higgs Boson Particle Listings

## Z

### $\langle N_{D^0} \rangle$

VALUE	DOCUMENT ID	TECN	COMMENT
<b>0.462 ± 0.026 OUR AVERAGE</b>			
0.465 ± 0.017 ± 0.027	ALEXANDER 96R	OPAL	$E_{cm}^{ee} = 91.2$ GeV
0.518 ± 0.052 ± 0.035	BUSKULIC 94J	ALEP	$E_{cm}^{ee} = 91.2$ GeV
0.403 ± 0.038 ± 0.044	118 ABREU 93I	DLPH	$E_{cm}^{ee} = 91.2$ GeV

118 See ABREU 95 (erratum).

### $\langle N_{D_s^\pm} \rangle$

VALUE	DOCUMENT ID	TECN	COMMENT
<b>0.131 ± 0.010 ± 0.018</b>	ALEXANDER 96R	OPAL	$E_{cm}^{ee} = 91.2$ GeV

### $\langle N_{D^*(2010)^\pm} \rangle$

VALUE	DOCUMENT ID	TECN	COMMENT
<b>0.183 ± 0.008 OUR AVERAGE</b>			
0.1854 ± 0.0041 ± 0.0091	119 ACKERSTAFF 98E	OPAL	$E_{cm}^{ee} = 91.2$ GeV
0.187 ± 0.015 ± 0.013	BUSKULIC 94J	ALEP	$E_{cm}^{ee} = 91.2$ GeV
0.171 ± 0.012 ± 0.016	120 ABREU 93I	DLPH	$E_{cm}^{ee} = 91.2$ GeV

119 ACKERSTAFF 98E systematic error includes an uncertainty of ±0.0069 due to the branching ratios  $B(D^{*+} \rightarrow D^0 \pi^+) = 0.683 \pm 0.014$  and  $B(D^0 \rightarrow K^- \pi^+) = 0.0383 \pm 0.0012$ .

120 See ABREU 95 (erratum).

### $\langle N_{D_{s1}(2536)^+} \rangle$

VALUE (units $10^{-3}$ )	DOCUMENT ID	TECN	COMMENT
<b>2.9<sup>+0.7</sup><sub>-0.6</sub> ± 0.2</b>	121 ACKERSTAFF 97W	OPAL	$E_{cm}^{ee} = 91.2$ GeV

121 ACKERSTAFF 97W obtain this value for  $x > 0.6$  and with the assumption that its decay width is saturated by the  $D^*K$  final states.

### $\langle N_{B^*} \rangle$

VALUE	DOCUMENT ID	TECN	COMMENT
<b>0.28 ± 0.01 ± 0.03</b>	122 ABREU 95R	DLPH	$E_{cm}^{ee} = 91.2$ GeV

122 ABREU 95R quote this value for a flavor-averaged excited state.

### $\langle N_{J/\psi(1S)} \rangle$

VALUE	DOCUMENT ID	TECN	COMMENT
<b>0.0056 ± 0.0003 ± 0.0004</b>	123 ALEXANDER 96B	OPAL	$E_{cm}^{ee} = 91.2$ GeV

123 ALEXANDER 96B identify  $J/\psi(1S)$  from the decays into lepton pairs.

### $\langle N_{\psi(2S)} \rangle$

VALUE	DOCUMENT ID	TECN	COMMENT
<b>0.0023 ± 0.0004 ± 0.0003</b>	ALEXANDER 96B	OPAL	$E_{cm}^{ee} = 91.2$ GeV

### $\langle N_p \rangle$

VALUE	DOCUMENT ID	TECN	COMMENT
<b>1.046 ± 0.026 OUR AVERAGE</b>			
1.054 ± 0.035	ABE 04C	SLD	$E_{cm}^{ee} = 91.2$ GeV
1.08 ± 0.04 ± 0.03	ABREU 98L	DLPH	$E_{cm}^{ee} = 91.2$ GeV
1.00 ± 0.07	BARATE 98V	ALEP	$E_{cm}^{ee} = 91.2$ GeV
0.92 ± 0.11	AKERS 94P	OPAL	$E_{cm}^{ee} = 91.2$ GeV

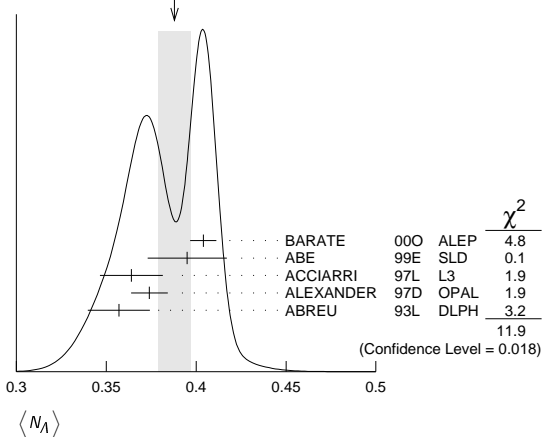
### $\langle N_{\Delta(1232)^{++}} \rangle$

VALUE	DOCUMENT ID	TECN	COMMENT
<b>0.087 ± 0.033 OUR AVERAGE</b>	Error includes scale factor of 2.4.		
0.079 ± 0.009 ± 0.011	ABREU 95W	DLPH	$E_{cm}^{ee} = 91.2$ GeV
0.22 ± 0.04 ± 0.04	ALEXANDER 95D	OPAL	$E_{cm}^{ee} = 91.2$ GeV

### $\langle N_\Lambda \rangle$

VALUE	DOCUMENT ID	TECN	COMMENT
<b>0.388 ± 0.009 OUR AVERAGE</b>	Error includes scale factor of 1.7. See the ideogram below.		
0.404 ± 0.002 ± 0.007	BARATE 00O	ALEP	$E_{cm}^{ee} = 91.2$ GeV
0.395 ± 0.022	ABE 99E	SLD	$E_{cm}^{ee} = 91.2$ GeV
0.364 ± 0.004 ± 0.017	ACCIARRI 97L	L3	$E_{cm}^{ee} = 91.2$ GeV
0.374 ± 0.002 ± 0.010	ALEXANDER 97D	OPAL	$E_{cm}^{ee} = 91.2$ GeV
0.357 ± 0.003 ± 0.017	ABREU 93L	DLPH	$E_{cm}^{ee} = 91.2$ GeV

WEIGHTED AVERAGE  
0.388±0.009 (Error scaled by 1.7)



### $\langle N_{\Lambda(1520)} \rangle$

VALUE	DOCUMENT ID	TECN	COMMENT
<b>0.0224 ± 0.0027 OUR AVERAGE</b>			
0.029 ± 0.005 ± 0.005	ABREU 00P	DLPH	$E_{cm}^{ee} = 91.2$ GeV
0.0213 ± 0.0021 ± 0.0019	ALEXANDER 97D	OPAL	$E_{cm}^{ee} = 91.2$ GeV

### $\langle N_{\Sigma^+} \rangle$

VALUE	DOCUMENT ID	TECN	COMMENT
<b>0.107 ± 0.010 OUR AVERAGE</b>			
0.114 ± 0.011 ± 0.009	ACCIARRI 00J	L3	$E_{cm}^{ee} = 91.2$ GeV
0.099 ± 0.008 ± 0.013	ALEXANDER 97E	OPAL	$E_{cm}^{ee} = 91.2$ GeV

### $\langle N_{\Sigma^-} \rangle$

VALUE	DOCUMENT ID	TECN	COMMENT
<b>0.082 ± 0.007 OUR AVERAGE</b>			
0.081 ± 0.002 ± 0.010	ABREU 00P	DLPH	$E_{cm}^{ee} = 91.2$ GeV
0.083 ± 0.006 ± 0.009	ALEXANDER 97E	OPAL	$E_{cm}^{ee} = 91.2$ GeV

### $\langle N_{\Sigma^+ + \Sigma^-} \rangle$

VALUE	DOCUMENT ID	TECN	COMMENT
<b>0.181 ± 0.018 OUR AVERAGE</b>			
0.182 ± 0.010 ± 0.016	124 ALEXANDER 97E	OPAL	$E_{cm}^{ee} = 91.2$ GeV
0.170 ± 0.014 ± 0.061	ABREU 95O	DLPH	$E_{cm}^{ee} = 91.2$ GeV

124 We have combined the values of  $\langle N_{\Sigma^+} \rangle$  and  $\langle N_{\Sigma^-} \rangle$  from ALEXANDER 97E adding the statistical and systematic errors of the two final states separately in quadrature. If isospin symmetry is assumed this value becomes  $0.174 \pm 0.010 \pm 0.015$ .

### $\langle N_{\Sigma^0} \rangle$

VALUE	DOCUMENT ID	TECN	COMMENT
<b>0.076 ± 0.010 OUR AVERAGE</b>			
0.095 ± 0.015 ± 0.013	ACCIARRI 00J	L3	$E_{cm}^{ee} = 91.2$ GeV
0.071 ± 0.012 ± 0.013	ALEXANDER 97E	OPAL	$E_{cm}^{ee} = 91.2$ GeV
0.070 ± 0.010 ± 0.010	ADAM 96B	DLPH	$E_{cm}^{ee} = 91.2$ GeV

### $\langle N_{(\Sigma^+ + \Sigma^- + \Sigma^0)/3} \rangle$

VALUE	DOCUMENT ID	TECN	COMMENT
<b>0.084 ± 0.005 ± 0.008</b>	ALEXANDER 97E	OPAL	$E_{cm}^{ee} = 91.2$ GeV

### $\langle N_{\Sigma(1385)^+} \rangle$

VALUE	DOCUMENT ID	TECN	COMMENT
<b>0.0239 ± 0.0009 ± 0.0012</b>	ALEXANDER 97D	OPAL	$E_{cm}^{ee} = 91.2$ GeV

### $\langle N_{\Sigma(1385)^-} \rangle$

VALUE	DOCUMENT ID	TECN	COMMENT
<b>0.0240 ± 0.0010 ± 0.0014</b>	ALEXANDER 97D	OPAL	$E_{cm}^{ee} = 91.2$ GeV

### $\langle N_{\Sigma(1385)^+ + \Sigma(1385)^-} \rangle$

VALUE	DOCUMENT ID	TECN	COMMENT
<b>0.046 ± 0.004 OUR AVERAGE</b>	Error includes scale factor of 1.6.		
0.0479 ± 0.0013 ± 0.0026	ALEXANDER 97D	OPAL	$E_{cm}^{ee} = 91.2$ GeV
0.0382 ± 0.0028 ± 0.0045	ABREU 95O	DLPH	$E_{cm}^{ee} = 91.2$ GeV

### $\langle N_{\Xi^-} \rangle$

VALUE	DOCUMENT ID	TECN	COMMENT
<b>0.0258 ± 0.0009 OUR AVERAGE</b>			
0.0247 ± 0.0009 ± 0.0025	ABDALLAH 06E	DLPH	$E_{cm}^{ee} = 91.2$ GeV
0.0259 ± 0.0004 ± 0.0009	ALEXANDER 97D	OPAL	$E_{cm}^{ee} = 91.2$ GeV

$\langle N_{\Xi(1530)^0} \rangle$

VALUE	DOCUMENT ID	TECN	COMMENT
<b>0.0059 ± 0.0011 OUR AVERAGE</b>	Error includes scale factor of 2.3.		
0.0045 ± 0.0005 ± 0.0006	ABDALLAH 05c	DLPH	$E_{cm}^{ee} = 91.2$ GeV
0.0068 ± 0.0005 ± 0.0004	ALEXANDER 97D	OPAL	$E_{cm}^{ee} = 91.2$ GeV

$\langle N_{\Omega^-} \rangle$

VALUE	DOCUMENT ID	TECN	COMMENT
<b>0.00164 ± 0.00028 OUR AVERAGE</b>			
0.0018 ± 0.0003 ± 0.0002	ALEXANDER 97D	OPAL	$E_{cm}^{ee} = 91.2$ GeV
0.0014 ± 0.0002 ± 0.0004	ADAM 96B	DLPH	$E_{cm}^{ee} = 91.2$ GeV

$\langle N_{\Lambda^+} \rangle$

VALUE	DOCUMENT ID	TECN	COMMENT
<b>0.078 ± 0.012 ± 0.012</b>	ALEXANDER 96R	OPAL	$E_{cm}^{ee} = 91.2$ GeV

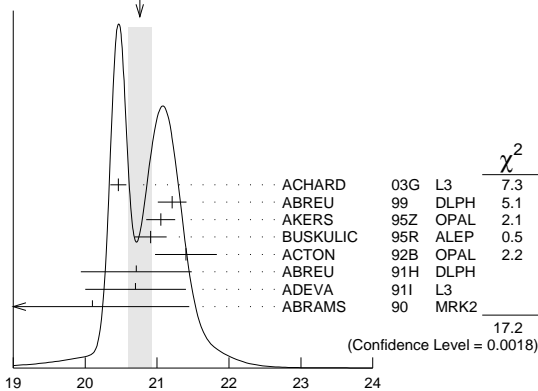
$\langle N_D^- \rangle$

VALUE (units $10^{-6}$ )	DOCUMENT ID	TECN	COMMENT
<b>0.078 ± 0.012 ± 0.012</b>	ALEXANDER 96R	OPAL	$E_{cm}^{ee} = 91.2$ GeV
• • • We do not use the following data for averages, fits, limits, etc. • • •			
5.9 ± 1.8 ± 0.5	125 SCHAEEL 06A	ALEP	$E_{cm}^{ee} = 91.2$ GeV

$\langle N_{charged} \rangle$

VALUE	DOCUMENT ID	TECN	COMMENT
<b>20.76 ± 0.16 OUR AVERAGE</b>	Error includes scale factor of 2.1. See the ideogram below.		
20.46 ± 0.01 ± 0.11	ACHARD 03G	L3	$E_{cm}^{ee} = 91.2$ GeV
21.21 ± 0.01 ± 0.20	ABREU 99	DLPH	$E_{cm}^{ee} = 91.2$ GeV
21.05 ± 0.20	AKERS 95Z	OPAL	$E_{cm}^{ee} = 91.2$ GeV
20.91 ± 0.03 ± 0.22	BUSKULIC 95R	ALEP	$E_{cm}^{ee} = 91.2$ GeV
21.40 ± 0.43	ACTON 92B	OPAL	$E_{cm}^{ee} = 91.2$ GeV
20.71 ± 0.04 ± 0.77	ABREU 91H	DLPH	$E_{cm}^{ee} = 91.2$ GeV
20.7 ± 0.7	ADEVA 91I	L3	$E_{cm}^{ee} = 91.2$ GeV
20.1 ± 1.0 ± 0.9	ABRAMS 90	MRK2	$E_{cm}^{ee} = 91.1$ GeV

WEIGHTED AVERAGE  
20.76 ± 0.16 (Error scaled by 2.1)



Z HADRONIC POLE CROSS SECTION

OUR FIT is obtained using the fit procedure and correlations as determined by the LEP Electroweak Working Group (see the note "The Z boson" and ref. LEP-SLC 06). This quantity is defined as

$$\sigma_h^0 = \frac{12\pi}{M_Z^2} \frac{\Gamma(e^+e^-)\Gamma(\text{hadrons})}{\Gamma_Z^2}$$

It is one of the parameters used in the Z lineshape fit.

VALUE (nb)	EVTS	DOCUMENT ID	TECN	COMMENT
<b>41.541 ± 0.037 OUR FIT</b>				
41.501 ± 0.055	4.10M	126 ABBIENDI 01A	OPAL	$E_{cm}^{ee} = 88-94$ GeV
41.578 ± 0.069	3.70M	ABREU 00F	DLPH	$E_{cm}^{ee} = 88-94$ GeV
41.535 ± 0.055	3.54M	ACCIARRI 00c	L3	$E_{cm}^{ee} = 88-94$ GeV
41.559 ± 0.058	4.07M	127 BARATE 00c	ALEP	$E_{cm}^{ee} = 88-94$ GeV
• • • We do not use the following data for averages, fits, limits, etc. • • •				
42 ± 4	450	ABRAMS 89B	MRK2	$E_{cm}^{ee} = 89.2-93.0$ GeV

126 ABBIENDI 01A error includes approximately 0.031 due to statistics, 0.033 due to event selection systematics, 0.029 due to uncertainty in luminosity measurement, and 0.011 due to LEP energy uncertainty.

127 BARATE 00c error includes approximately 0.030 due to statistics, 0.026 due to experimental systematics, and 0.025 due to uncertainty in luminosity measurement.

Z VECTOR COUPLINGS

These quantities are the effective vector couplings of the Z to charged leptons. Their magnitude is derived from a measurement of the Z lineshape and the forward-backward lepton asymmetries as a function of energy around the Z mass. The relative sign among the vector to axial-vector couplings is obtained from a measurement of the Z asymmetry parameters,  $A_{e^+}$ ,  $A_{\mu^+}$ , and  $A_{\tau^+}$ . By convention the sign of  $g_A^e$  is fixed to be negative (and opposite to that of  $g_V^e$  obtained using  $\nu_e$  scattering measurements). For the light quarks, the sign of the couplings is assigned consistently with this assumption. The fit values quoted below correspond to global nine- or five-parameter fits to lineshape, lepton forward-backward asymmetry, and  $A_{e^+}$ ,  $A_{\mu^+}$ , and  $A_{\tau^+}$  measurements. See the note "The Z boson" and ref. LEP-SLC 06 for details. Where  $p\bar{p}$  and  $e p$  data is quoted, OUR FIT value corresponds to a weighted average of this with the LEP/SLD fit result.

$g_V^e$

VALUE	EVTS	DOCUMENT ID	TECN	COMMENT
<b>-0.03817 ± 0.00047 OUR FIT</b>				
-0.058 ± 0.016 ± 0.007	5026	128 ACOSTA 05M	CDF	$E_{cm}^{p\bar{p}} = 1.96$ TeV
-0.0346 ± 0.0023	137.0K	129 ABBIENDI 01o	OPAL	$E_{cm}^{ee} = 88-94$ GeV
-0.0412 ± 0.0027	124.4k	130 ACCIARRI 00c	L3	$E_{cm}^{ee} = 88-94$ GeV
-0.0400 ± 0.0037		BARATE 00c	ALEP	$E_{cm}^{ee} = 88-94$ GeV
-0.0414 ± 0.0020	131	ABE 95J	SLD	$E_{cm}^{ee} = 91.31$ GeV

128 ACOSTA 05M determine the forward-backward asymmetry of  $e^+e^-$  pairs produced via  $q\bar{q} \rightarrow Z/\gamma^* \rightarrow e^+e^-$  in 15  $M(e^+e^-)$  effective mass bins ranging from 40 GeV to 600 GeV. These results are used to obtain the vector and axial-vector couplings of the Z to  $e^+e^-$ , assuming the quark couplings are as predicted by the standard model. Higher order radiative corrections have not been taken into account.

129 ABBIENDI 01o use their measurement of the  $\tau$  polarization in addition to the lineshape and forward-backward lepton asymmetries.

130 ACCIARRI 00c use their measurement of the  $\tau$  polarization in addition to forward-backward lepton asymmetries.

131 ABE 95J obtain this result combining polarized Bhabha results with the  $A_{LR}$  measurement of ABE 94c. The Bhabha results alone give  $-0.0507 \pm 0.0096 \pm 0.0020$ .

$g_V^{\mu}$

VALUE	EVTS	DOCUMENT ID	TECN	COMMENT
<b>-0.0367 ± 0.0023 OUR FIT</b>				
-0.0388 <sup>+0.0060</sup> <sub>-0.0064</sub>	182.8K	132 ABBIENDI 01o	OPAL	$E_{cm}^{ee} = 88-94$ GeV
-0.0386 ± 0.0073	113.4k	133 ACCIARRI 00c	L3	$E_{cm}^{ee} = 88-94$ GeV
-0.0362 ± 0.0061		BARATE 00c	ALEP	$E_{cm}^{ee} = 88-94$ GeV
• • • We do not use the following data for averages, fits, limits, etc. • • •				
-0.0413 ± 0.0060	66143	134 ABBIENDI 01k	OPAL	$E_{cm}^{ee} = 89-93$ GeV

132 ABBIENDI 01o use their measurement of the  $\tau$  polarization in addition to the lineshape and forward-backward lepton asymmetries.

133 ACCIARRI 00c use their measurement of the  $\tau$  polarization in addition to forward-backward lepton asymmetries.

134 ABBIENDI 01k obtain this from an angular analysis of the muon pair asymmetry which takes into account effects of initial state radiation on an event by event basis and of initial-final state interference.

$g_V^e$

VALUE	EVTS	DOCUMENT ID	TECN	COMMENT
<b>-0.0366 ± 0.0010 OUR FIT</b>				
-0.0365 ± 0.0023	151.5K	135 ABBIENDI 01o	OPAL	$E_{cm}^{ee} = 88-94$ GeV
-0.0384 ± 0.0026	103.0k	136 ACCIARRI 00c	L3	$E_{cm}^{ee} = 88-94$ GeV
-0.0361 ± 0.0068		BARATE 00c	ALEP	$E_{cm}^{ee} = 88-94$ GeV
135 ABBIENDI 01o use their measurement of the $\tau$ polarization in addition to the lineshape and forward-backward lepton asymmetries.				
136 ACCIARRI 00c use their measurement of the $\tau$ polarization in addition to forward-backward lepton asymmetries.				

$g_V^e$

VALUE	EVTS	DOCUMENT ID	TECN	COMMENT
<b>-0.03783 ± 0.00041 OUR FIT</b>				
-0.0358 ± 0.0014	471.3K	137 ABBIENDI 01o	OPAL	$E_{cm}^{ee} = 88-94$ GeV
-0.0397 ± 0.0020	379.4k	138 ABREU 00F	DLPH	$E_{cm}^{ee} = 88-94$ GeV
-0.0397 ± 0.0017	340.8k	139 ACCIARRI 00c	L3	$E_{cm}^{ee} = 88-94$ GeV
-0.0383 ± 0.0018	500k	BARATE 00c	ALEP	$E_{cm}^{ee} = 88-94$ GeV
137 ABBIENDI 01o use their measurement of the $\tau$ polarization in addition to the lineshape and forward-backward lepton asymmetries.				
138 Using forward-backward lepton asymmetries.				
139 ACCIARRI 00c use their measurement of the $\tau$ polarization in addition to forward-backward lepton asymmetries.				

$g_V^e$

VALUE	EVTS	DOCUMENT ID	TECN	COMMENT
<b>0.25<sup>+0.07</sup><sub>-0.06</sub> OUR AVERAGE</b>				
0.201 ± 0.112	156k	140 ABAZOV 11D	D0	$E_{cm}^{p\bar{p}} = 1.97$ TeV
0.27 ± 0.13	1500	141 AKTAS 06	H1	$e^{\pm}p \rightarrow \mathcal{P}_e(\nu_e)X$ , $\sqrt{s} \approx 300$ GeV
0.24 <sup>+0.28</sup> <sub>-0.11</sub>		142 LEP-SLC 06		$E_{cm}^{ee} = 88-94$ GeV
0.399 <sup>+0.152</sup> <sub>-0.188</sub> ± 0.066	5026	143 ACOSTA 05M	CDF	$E_{cm}^{p\bar{p}} = 1.96$ TeV

## Gauge &amp; Higgs Boson Particle Listings

Z

- 140 ABAZOV 11d study  $p\bar{p} \rightarrow Z/\gamma^* e^+ e^-$  events using  $5 \text{ fb}^{-1}$  data at  $\sqrt{s} = 1.96 \text{ TeV}$ . The candidate events are selected by requiring two isolated electromagnetic showers with  $E_T > 25 \text{ GeV}$ , at least one electron in the central region and the di-electron mass in the range 50–1000 GeV. From the forward-backward asymmetry, determined as a function of the di-electron mass, they derive the axial and vector couplings of the  $u$ - and  $d$ -quarks and the value of  $\sin^2\theta_{eff}^e = 0.2309 \pm 0.0008(\text{stat}) \pm 0.0006(\text{syst})$ .
- 141 AKTAS 06 fit the neutral current ( $1.5 \leq Q^2 \leq 30,000 \text{ GeV}^2$ ) and charged current ( $1.5 \leq Q^2 \leq 15,000 \text{ GeV}^2$ ) differential cross sections. In the determination of the  $u$ -quark couplings the electron and  $d$ -quark couplings are fixed to their standard model values.
- 142 LEP-SLC 06 is a combination of the results from LEP and SLC experiments using light quark tagging.  $s$ - and  $d$ -quark couplings are assumed to be identical.
- 143 ACOSTA 05M determine the forward-backward asymmetry of  $e^+ e^-$  pairs produced via  $q\bar{q} \rightarrow Z/\gamma^* \rightarrow e^+ e^-$  in 15  $M(e^+ e^-)$  effective mass bins ranging from 40 GeV to 600 GeV. These results are used to obtain the vector and axial-vector couplings of the Z to the light quarks, assuming the electron couplings are as predicted by the Standard Model. Higher order radiative corrections have not been taken into account.

$g_V^d$	VALUE	EVTS	DOCUMENT ID	TECN	COMMENT
	<b>-0.33</b>				<b>OUR AVERAGE</b>
	$-0.351 \pm 0.251$	156k	144 ABAZOV	11D D0	$E_{cm}^{p\bar{p}} = 1.97 \text{ TeV}$
	$-0.33 \pm 0.33$	1500	145 AKTAS	06 H1	$e^\pm p \rightarrow \mathcal{P}_e(\nu_e)X$ , $\sqrt{s} \approx 300 \text{ GeV}$
	$-0.33$		146 LEP-SLC	06	$E_{cm}^{ee} = 88-94 \text{ GeV}$
	$-0.226 \pm 0.635$	5026	147 ACOSTA	05M CDF	$E_{cm}^{p\bar{p}} = 1.96 \text{ TeV}$

- 144 ABAZOV 11d study  $p\bar{p} \rightarrow Z/\gamma^* e^+ e^-$  events using  $5 \text{ fb}^{-1}$  data at  $\sqrt{s} = 1.96 \text{ TeV}$ . The candidate events are selected by requiring two isolated electromagnetic showers with  $E_T > 25 \text{ GeV}$ , at least one electron in the central region and the di-electron mass in the range 50–1000 GeV. From the forward-backward asymmetry, determined as a function of the di-electron mass, they derive the axial and vector couplings of the  $u$ - and  $d$ -quarks and the value of  $\sin^2\theta_{eff}^e = 0.2309 \pm 0.0008(\text{stat}) \pm 0.0006(\text{syst})$ .
- 145 AKTAS 06 fit the neutral current ( $1.5 \leq Q^2 \leq 30,000 \text{ GeV}^2$ ) and charged current ( $1.5 \leq Q^2 \leq 15,000 \text{ GeV}^2$ ) differential cross sections. In the determination of the  $d$ -quark couplings the electron and  $u$ -quark couplings are fixed to their standard model values.
- 146 LEP-SLC 06 is a combination of the results from LEP and SLC experiments using light quark tagging.  $s$ - and  $d$ -quark couplings are assumed to be identical.
- 147 ACOSTA 05M determine the forward-backward asymmetry of  $e^+ e^-$  pairs produced via  $q\bar{q} \rightarrow Z/\gamma^* \rightarrow e^+ e^-$  in 15  $M(e^+ e^-)$  effective mass bins ranging from 40 GeV to 600 GeV. These results are used to obtain the vector and axial-vector couplings of the Z to the light quarks, assuming the electron couplings are as predicted by the Standard Model. Higher order radiative corrections have not been taken into account.

## Z AXIAL-VECTOR COUPLINGS

These quantities are the effective axial-vector couplings of the Z to charged leptons. Their magnitude is derived from a measurement of the Z lineshape and the forward-backward lepton asymmetries as a function of energy around the Z mass. The relative sign among the vector to axial-vector couplings is obtained from a measurement of the Z asymmetry parameters,  $A_e$ ,  $A_\mu$ , and  $A_\tau$ . By convention the sign of  $g_A^e$  is fixed to be negative (and opposite to that of  $g^{e^*}$  obtained using  $\nu_e$  scattering measurements). For the light quarks, the sign of the couplings is assigned consistently with this assumption. The fit values quoted below correspond to global nine- or five-parameter fits to lineshape, lepton forward-backward asymmetry, and  $A_e$ ,  $A_\mu$ , and  $A_\tau$  measurements. See the note "The Z boson" and ref. LEP-SLC 06 for details. Where  $p\bar{p}$  and  $e p$  data is quoted, OUR FIT value corresponds to a weighted average of this with the LEP/SLD fit result.

$g_A^e$	VALUE	EVTS	DOCUMENT ID	TECN	COMMENT
	<b>-0.50111</b>				<b>OUR FIT</b>
	$-0.528 \pm 0.123 \pm 0.059$	5026	148 ACOSTA	05M CDF	$E_{cm}^{p\bar{p}} = 1.96 \text{ TeV}$
	$-0.50062 \pm 0.00062$	137.0K	149 ABBIENDI	01o OPAL	$E_{cm}^{ee} = 88-94 \text{ GeV}$
	$-0.5015 \pm 0.0007$	124.4k	150 ACCIARRI	00c L3	$E_{cm}^{ee} = 88-94 \text{ GeV}$
	$-0.50166 \pm 0.00057$		BARATE	00c ALEP	$E_{cm}^{ee} = 88-94 \text{ GeV}$
	$-0.4977 \pm 0.0045$		151 ABE	95j SLD	$E_{cm}^{ee} = 91.31 \text{ GeV}$

- 148 ACOSTA 05M determine the forward-backward asymmetry of  $e^+ e^-$  pairs produced via  $q\bar{q} \rightarrow Z/\gamma^* \rightarrow e^+ e^-$  in 15  $M(e^+ e^-)$  effective mass bins ranging from 40 GeV to 600 GeV. These results are used to obtain the vector and axial-vector couplings of the Z to  $e^+ e^-$ , assuming the quark couplings are as predicted by the standard model. Higher order radiative corrections have not been taken into account.
- 149 ABBIENDI 01o use their measurement of the  $\tau$  polarization in addition to the lineshape and forward-backward lepton asymmetries.
- 150 ACCIARRI 00c use their measurement of the  $\tau$  polarization in addition to forward-backward lepton asymmetries.
- 151 ABE 95j obtain this result combining polarized Bhabha results with the  $A_{LR}$  measurement of ABE 94c. The Bhabha results alone give  $-0.4968 \pm 0.0039 \pm 0.0027$ .

$g_A^u$	VALUE	EVTS	DOCUMENT ID	TECN	COMMENT
	<b>-0.50120</b>				<b>OUR FIT</b>
	$-0.50117 \pm 0.00099$	182.8K	152 ABBIENDI	01o OPAL	$E_{cm}^{ee} = 88-94 \text{ GeV}$
	$-0.5009 \pm 0.0014$	113.4k	153 ACCIARRI	00c L3	$E_{cm}^{ee} = 88-94 \text{ GeV}$
	$-0.50046 \pm 0.00093$		BARATE	00c ALEP	$E_{cm}^{ee} = 88-94 \text{ GeV}$
	$-0.520 \pm 0.015$	66143	154 ABBIENDI	01k OPAL	$E_{cm}^{ee} = 89-93 \text{ GeV}$

- • • We do not use the following data for averages, fits, limits, etc. • • •
- 152 ABBIENDI 01o use their measurement of the  $\tau$  polarization in addition to the lineshape and forward-backward lepton asymmetries.
- 153 ACCIARRI 00c use their measurement of the  $\tau$  polarization in addition to forward-backward lepton asymmetries.
- 154 ABBIENDI 01k obtain this from an angular analysis of the muon pair asymmetry which takes into account effects of initial state radiation on an event by event basis and of initial-final state interference.

$g_A^t$	VALUE	EVTS	DOCUMENT ID	TECN	COMMENT
	<b>-0.50204</b>				<b>OUR FIT</b>
	$-0.50165 \pm 0.00124$	151.5K	155 ABBIENDI	01o OPAL	$E_{cm}^{ee} = 88-94 \text{ GeV}$
	$-0.5023 \pm 0.0017$	103.0k	156 ACCIARRI	00c L3	$E_{cm}^{ee} = 88-94 \text{ GeV}$
	$-0.50216 \pm 0.00100$		BARATE	00c ALEP	$E_{cm}^{ee} = 88-94 \text{ GeV}$

- 155 ABBIENDI 01o use their measurement of the  $\tau$  polarization in addition to the lineshape and forward-backward lepton asymmetries.
- 156 ACCIARRI 00c use their measurement of the  $\tau$  polarization in addition to forward-backward lepton asymmetries.

$g_A^b$	VALUE	EVTS	DOCUMENT ID	TECN	COMMENT
	<b>-0.50123</b>				<b>OUR FIT</b>
	$-0.50089 \pm 0.00045$	471.3K	157 ABBIENDI	01o OPAL	$E_{cm}^{ee} = 88-94 \text{ GeV}$
	$-0.5007 \pm 0.0005$	379.4k	ABREU	00f DLPH	$E_{cm}^{ee} = 88-94 \text{ GeV}$
	$-0.50153 \pm 0.00053$	340.8k	158 ACCIARRI	00c L3	$E_{cm}^{ee} = 88-94 \text{ GeV}$
	$-0.50150 \pm 0.00046$	500k	BARATE	00c ALEP	$E_{cm}^{ee} = 88-94 \text{ GeV}$

- 157 ABBIENDI 01o use their measurement of the  $\tau$  polarization in addition to the lineshape and forward-backward lepton asymmetries.
- 158 ACCIARRI 00c use their measurement of the  $\tau$  polarization in addition to forward-backward lepton asymmetries.

$g_A^s$	VALUE	EVTS	DOCUMENT ID	TECN	COMMENT
	<b>0.50</b>				<b>OUR AVERAGE</b>
	$0.501 \pm 0.110$	156k	159 ABAZOV	11D D0	$E_{cm}^{p\bar{p}} = 1.97 \text{ TeV}$
	$0.57 \pm 0.08$	1500	160 AKTAS	06 H1	$e^\pm p \rightarrow \mathcal{P}_e(\nu_e)X$ , $\sqrt{s} \approx 300 \text{ GeV}$
	$0.47$		161 LEP-SLC	06	$E_{cm}^{ee} = 88-94 \text{ GeV}$
	$0.441 \pm 0.207$	5026	162 ACOSTA	05M CDF	$E_{cm}^{p\bar{p}} = 1.96 \text{ TeV}$

- 159 ABAZOV 11d study  $p\bar{p} \rightarrow Z/\gamma^* e^+ e^-$  events using  $5 \text{ fb}^{-1}$  data at  $\sqrt{s} = 1.96 \text{ TeV}$ . The candidate events are selected by requiring two isolated electromagnetic showers with  $E_T > 25 \text{ GeV}$ , at least one electron in the central region and the di-electron mass in the range 50–1000 GeV. From the forward-backward asymmetry, determined as a function of the di-electron mass, they derive the axial and vector couplings of the  $u$ - and  $d$ -quarks and the value of  $\sin^2\theta_{eff}^e = 0.2309 \pm 0.0008(\text{stat}) \pm 0.0006(\text{syst})$ .
- 160 AKTAS 06 fit the neutral current ( $1.5 \leq Q^2 \leq 30,000 \text{ GeV}^2$ ) and charged current ( $1.5 \leq Q^2 \leq 15,000 \text{ GeV}^2$ ) differential cross sections. In the determination of the  $u$ -quark couplings the electron and  $d$ -quark couplings are fixed to their standard model values.
- 161 LEP-SLC 06 is a combination of the results from LEP and SLC experiments using light quark tagging.  $s$ - and  $d$ -quark couplings are assumed to be identical.
- 162 ACOSTA 05M determine the forward-backward asymmetry of  $e^+ e^-$  pairs produced via  $q\bar{q} \rightarrow Z/\gamma^* \rightarrow e^+ e^-$  in 15  $M(e^+ e^-)$  effective mass bins ranging from 40 GeV to 600 GeV. These results are used to obtain the vector and axial-vector couplings of the Z to the light quarks, assuming the electron couplings are as predicted by the Standard Model. Higher order radiative corrections have not been taken into account.

$g_A^d$	VALUE	EVTS	DOCUMENT ID	TECN	COMMENT
	<b>-0.523</b>				<b>OUR AVERAGE</b>
	$-0.497 \pm 0.165$	156k	163 ABAZOV	11D D0	$E_{cm}^{p\bar{p}} = 1.97 \text{ TeV}$
	$-0.80 \pm 0.24$	1500	164 AKTAS	06 H1	$e^\pm p \rightarrow \mathcal{P}_e(\nu_e)X$ , $\sqrt{s} \approx 300 \text{ GeV}$
	$-0.52$		165 LEP-SLC	06	$E_{cm}^{ee} = 88-94 \text{ GeV}$
	$-0.016 \pm 0.346$	5026	166 ACOSTA	05M CDF	$E_{cm}^{p\bar{p}} = 1.96 \text{ TeV}$

- 163 ABAZOV 11d study  $p\bar{p} \rightarrow Z/\gamma^* e^+ e^-$  events using  $5 \text{ fb}^{-1}$  data at  $\sqrt{s} = 1.96 \text{ TeV}$ . The candidate events are selected by requiring two isolated electromagnetic showers with  $E_T > 25 \text{ GeV}$ , at least one electron in the central region and the di-electron mass in the range 50–1000 GeV. From the forward-backward asymmetry, determined as a function of the di-electron mass, they derive the axial and vector couplings of the  $u$ - and  $d$ -quarks and the value of  $\sin^2\theta_{eff}^e = 0.2309 \pm 0.0008(\text{stat}) \pm 0.0006(\text{syst})$ .

- <sup>164</sup> AKTAS 06 fit the neutral current ( $1.5 \leq Q^2 \leq 30,000 \text{ GeV}^2$ ) and charged current ( $1.5 \leq Q^2 \leq 15,000 \text{ GeV}^2$ ) differential cross sections. In the determination of the  $d$ -quark couplings the electron and  $u$ -quark couplings are fixed to their standard model values.
- <sup>165</sup> LEP-SLC 06 is a combination of the results from LEP and SLC experiments using light quark tagging.  $s$ - and  $d$ -quark couplings are assumed to be identical.
- <sup>166</sup> ACOSTA 05M determine the forward-backward asymmetry of  $e^+e^-$  pairs produced via  $q\bar{q} \rightarrow Z/\gamma^* \rightarrow e^+e^-$  in 15  $M(e^+e^-)$  effective mass bins ranging from 40 GeV to 600 GeV. These results are used to obtain the vector and axial-vector couplings of the Z to the light quarks, assuming the electron couplings are as predicted by the Standard Model. Higher order radiative corrections have not been taken into account.

### Z COUPLINGS TO NEUTRAL LEPTONS

Averaging over neutrino species, the invisible Z decay width determines the effective neutrino coupling  $g^{\nu_e}$ . For  $g^{\nu_e}$  and  $g^{\nu_\mu}$ ,  $\nu_e e$  and  $\nu_\mu e$  scattering results are combined with  $g_A^e$  and  $g_V^e$  measurements at the Z mass to obtain  $g^{\nu_e}$  and  $g^{\nu_\mu}$  following NOVIKOV 93c.

$g^{\nu_e}$	VALUE	DOCUMENT ID	TECN	COMMENT
<b>0.50076 ± 0.00076</b>	167	LEP-SLC	06	$E_{\text{cm}}^{\text{ee}} = 88\text{--}94 \text{ GeV}$

<sup>167</sup> From invisible Z-decay width.

$g^{\nu_\mu}$	VALUE	DOCUMENT ID	TECN	COMMENT
<b>0.528 ± 0.085</b>	168	VILAIN	94	CHM2 From $\nu_\mu e$ and $\nu_e e$ scattering

<sup>168</sup> VILAIN 94 derive this value from their value of  $g^{\nu_\mu}$  and their ratio  $g^{\nu_e}/g^{\nu_\mu} = 1.05^{+0.15}_{-0.18}$ .

$g^{\nu_\mu}$	VALUE	DOCUMENT ID	TECN	COMMENT
<b>0.502 ± 0.017</b>	169	VILAIN	94	CHM2 From $\nu_\mu e$ scattering

<sup>169</sup> VILAIN 94 derive this value from their measurement of the couplings  $g_A^{e\nu_\mu} = -0.503 \pm 0.017$  and  $g_V^{e\nu_\mu} = -0.035 \pm 0.017$  obtained from  $\nu_\mu e$  scattering. We have re-evaluated this value using the current PDG values for  $g_A^e$  and  $g_V^e$ .

### Z ASYMMETRY PARAMETERS

For each fermion-antifermion pair coupling to the Z these quantities are defined as

$$A_f = \frac{2g_V^f g_A^f}{(g_V^f)^2 + (g_A^f)^2}$$

where  $g_V^f$  and  $g_A^f$  are the effective vector and axial-vector couplings. For their relation to the various lepton asymmetries see the note "The Z boson" and ref. LEP-SLC 06.

### $A_e$

Using polarized beams, this quantity can also be measured as  $(\sigma_L - \sigma_R)/(\sigma_L + \sigma_R)$ , where  $\sigma_L$  and  $\sigma_R$  are the  $e^+e^-$  production cross sections for Z bosons produced with left-handed and right-handed electrons respectively.

VALUE	EVTS	DOCUMENT ID	TECN	COMMENT
<b>0.1515 ± 0.0019 OUR AVERAGE</b>				
0.1454 ± 0.0108 ± 0.0036	144810	170	ABBIENDI	01o OPAL $E_{\text{cm}}^{\text{ee}} = 88\text{--}94 \text{ GeV}$
0.1516 ± 0.0021	559000	171	ABE	01B SLD $E_{\text{cm}}^{\text{ee}} = 91.24 \text{ GeV}$
0.1504 ± 0.0068 ± 0.0008		172	HEISTER	01 ALEP $E_{\text{cm}}^{\text{ee}} = 88\text{--}94 \text{ GeV}$
0.1382 ± 0.0116 ± 0.0005	105000	173	ABREU	00E DLPH $E_{\text{cm}}^{\text{ee}} = 88\text{--}94 \text{ GeV}$
0.1678 ± 0.0127 ± 0.0030	137092	174	ACCIARRI	98H L3 $E_{\text{cm}}^{\text{ee}} = 88\text{--}94 \text{ GeV}$
0.162 ± 0.041 ± 0.014	89838	175	ABE	97 SLD $E_{\text{cm}}^{\text{ee}} = 91.27 \text{ GeV}$
0.202 ± 0.038 ± 0.008		176	ABE	95J SLD $E_{\text{cm}}^{\text{ee}} = 91.31 \text{ GeV}$

<sup>170</sup> ABBIENDI 01o fit for  $A_e$  and  $A_\tau$  from measurements of the  $\tau$  polarization at varying  $\tau$  production angles. The correlation between  $A_e$  and  $A_\tau$  is less than 0.03.

<sup>171</sup> ABE 01B use the left-right production and left-right forward-backward decay asymmetries in leptonic Z decays to obtain a value of  $0.1544 \pm 0.0060$ . This is combined with left-right production asymmetry measurement using hadronic Z decays (ABE 00B) to obtain the quoted value.

<sup>172</sup> HEISTER 01 obtain this result fitting the  $\tau$  polarization as a function of the polar production angle of the  $\tau$ .

<sup>173</sup> ABREU 00E obtain this result fitting the  $\tau$  polarization as a function of the polar  $\tau$  production angle. This measurement is a combination of different analyses (exclusive  $\tau$  decay modes, inclusive hadronic 1-prong reconstruction, and a neural network analysis).

<sup>174</sup> Derived from the measurement of forward-backward  $\tau$  polarization asymmetry.

<sup>175</sup> ABE 97 obtain this result from a measurement of the observed left-right charge asymmetry,  $A_Q^{\text{obs}} = 0.225 \pm 0.056 \pm 0.019$ , in hadronic Z decays. If they combine this value of  $A_Q^{\text{obs}}$  with their earlier measurement of  $A_{LR}^{\text{obs}}$  they determine  $A_e$  to be  $0.1574 \pm 0.0197 \pm 0.0067$  independent of the beam polarization.

<sup>176</sup> ABE 95J obtain this result from polarized Bhabha scattering.

### $A_\mu$

This quantity is directly extracted from a measurement of the left-right forward-backward asymmetry in  $\mu^+\mu^-$  production at SLC using a polarized electron beam. This double asymmetry eliminates the dependence on the Z- $e$ - $e$  coupling parameter  $A_e$ .

VALUE	EVTS	DOCUMENT ID	TECN	COMMENT
<b>0.142 ± 0.015</b>	16844	177	ABE	01B SLD $E_{\text{cm}}^{\text{ee}} = 91.24 \text{ GeV}$

<sup>177</sup> ABE 01B obtain this direct measurement using the left-right production and left-right forward-backward polar angle asymmetries in  $\mu^+\mu^-$  decays of the Z boson obtained with a polarized electron beam.

### $A_\tau$

The LEP Collaborations derive this quantity from the measurement of the  $\tau$  polarization in  $Z \rightarrow \tau^+\tau^-$ . The SLD Collaboration directly extracts this quantity from its measured left-right forward-backward asymmetry in  $Z \rightarrow \tau^+\tau^-$  produced using a polarized  $e^-$  beam. This double asymmetry eliminates the dependence on the Z- $e$ - $e$  coupling parameter  $A_e$ .

VALUE	EVTS	DOCUMENT ID	TECN	COMMENT
<b>0.143 ± 0.004 OUR AVERAGE</b>				
0.1456 ± 0.0076 ± 0.0057	144810	178	ABBIENDI	01o OPAL $E_{\text{cm}}^{\text{ee}} = 88\text{--}94 \text{ GeV}$
0.136 ± 0.015	16083	179	ABE	01B SLD $E_{\text{cm}}^{\text{ee}} = 91.24 \text{ GeV}$
0.1451 ± 0.0052 ± 0.0029		180	HEISTER	01 ALEP $E_{\text{cm}}^{\text{ee}} = 88\text{--}94 \text{ GeV}$
0.1359 ± 0.0079 ± 0.0055	105000	181	ABREU	00E DLPH $E_{\text{cm}}^{\text{ee}} = 88\text{--}94 \text{ GeV}$
0.1476 ± 0.0088 ± 0.0062	137092		ACCIARRI	98H L3 $E_{\text{cm}}^{\text{ee}} = 88\text{--}94 \text{ GeV}$

<sup>178</sup> ABBIENDI 01o fit for  $A_e$  and  $A_\tau$  from measurements of the  $\tau$  polarization at varying  $\tau$  production angles. The correlation between  $A_e$  and  $A_\tau$  is less than 0.03.

<sup>179</sup> ABE 01B obtain this direct measurement using the left-right production and left-right forward-backward polar angle asymmetries in  $\tau^+\tau^-$  decays of the Z boson obtained with a polarized electron beam.

<sup>180</sup> HEISTER 01 obtain this result fitting the  $\tau$  polarization as a function of the polar production angle of the  $\tau$ .

<sup>181</sup> ABREU 00E obtain this result fitting the  $\tau$  polarization as a function of the polar  $\tau$  production angle. This measurement is a combination of different analyses (exclusive  $\tau$  decay modes, inclusive hadronic 1-prong reconstruction, and a neural network analysis).

### $A_s$

The SLD Collaboration directly extracts this quantity by a simultaneous fit to four measured  $s$ -quark polar angle distributions corresponding to two states of  $e^-$  polarization (positive and negative) and to the  $K^+K^-$  and  $K^\pm K_S^0$  strange particle tagging modes in the hadronic final states.

VALUE	EVTS	DOCUMENT ID	TECN	COMMENT
<b>0.895 ± 0.066 ± 0.062</b>	2870	182	ABE	00D SLD $E_{\text{cm}}^{\text{ee}} = 91.2 \text{ GeV}$

<sup>182</sup> ABE 00D tag  $Z \rightarrow s\bar{s}$  events by an absence of B or D hadrons and the presence in each hemisphere of a high momentum  $K^\pm$  or  $K_S^0$ .

### $A_c$

This quantity is directly extracted from a measurement of the left-right forward-backward asymmetry in  $c\bar{c}$  production at SLC using polarized electron beam. This double asymmetry eliminates the dependence on the Z- $e$ - $e$  coupling parameter  $A_e$ . OUR FIT is obtained by a simultaneous fit to several  $c$ - and  $b$ -quark measurements as explained in the note "The Z boson" and ref. LEP-SLC 06.

VALUE	EVTS	DOCUMENT ID	TECN	COMMENT
<b>0.670 ± 0.027 OUR FIT</b>				
0.6712 ± 0.0224 ± 0.0157		183	ABE	05 SLD $E_{\text{cm}}^{\text{ee}} = 91.24 \text{ GeV}$
• • • We do not use the following data for averages, fits, limits, etc. • • •				
0.583 ± 0.055 ± 0.055		184	ABE	02G SLD $E_{\text{cm}}^{\text{ee}} = 91.24 \text{ GeV}$
0.688 ± 0.041		185	ABE	01c SLD $E_{\text{cm}}^{\text{ee}} = 91.25 \text{ GeV}$

<sup>183</sup> ABE 05 use hadronic Z decays collected during 1996–98 to obtain an enriched sample of  $c\bar{c}$  events tagging on the invariant mass of reconstructed secondary decay vertices. The charge of the underlying  $c$ -quark is obtained with an algorithm that takes into account the net charge of the vertex as well as the charge of tracks emanating from the vertex and identified as kaons. This yields (9970 events)  $A_c = 0.6747 \pm 0.0290 \pm 0.0233$ . Taking into account all correlations with earlier results reported in ABE 02G and ABE 01c, they obtain the quoted overall SLD result.

<sup>184</sup> ABE 02c tag  $b$  and  $c$  quarks through their semileptonic decays into electrons and muons. A maximum likelihood fit is performed to extract simultaneously  $A_b$  and  $A_c$ .

<sup>185</sup> ABE 01c tag  $Z \rightarrow c\bar{c}$  events using two techniques: exclusive reconstruction of  $D^{*+}$ ,  $D^+$  and  $D^0$  mesons and the soft pion tag for  $D^{*+} \rightarrow D^0\pi^+$ . The large background from D mesons produced in  $b\bar{b}$  events is separated efficiently from the signal using precision vertex information. When combining the  $A_c$  values from these two samples, care is taken to avoid double counting of events common to the two samples, and common systematic errors are properly taken into account.

### $A_b$

This quantity is directly extracted from a measurement of the left-right forward-backward asymmetry in  $b\bar{b}$  production at SLC using polarized electron beam. This double asymmetry eliminates the dependence on the Z- $e$ - $e$  coupling parameter  $A_e$ . OUR FIT is obtained by a simultaneous fit to several  $c$ - and  $b$ -quark measurements as explained in the note "The Z boson" and ref. LEP-SLC 06.

VALUE	EVTS	DOCUMENT ID	TECN	COMMENT
<b>0.923 ± 0.020 OUR FIT</b>				
0.9170 ± 0.0147 ± 0.0145		186	ABE	05 SLD $E_{\text{cm}}^{\text{ee}} = 91.24 \text{ GeV}$
• • • We do not use the following data for averages, fits, limits, etc. • • •				
0.907 ± 0.020 ± 0.024	48028	187	ABE	03F SLD $E_{\text{cm}}^{\text{ee}} = 91.24 \text{ GeV}$
0.919 ± 0.030 ± 0.024		188	ABE	02G SLD $E_{\text{cm}}^{\text{ee}} = 91.24 \text{ GeV}$
0.855 ± 0.088 ± 0.102	7473	189	ABE	99L SLD $E_{\text{cm}}^{\text{ee}} = 91.27 \text{ GeV}$

## Gauge &amp; Higgs Boson Particle Listings

## Z

- <sup>186</sup> ABE 05 use hadronic Z decays collected during 1996–98 to obtain an enriched sample of  $b\bar{b}$  events tagging on the invariant mass of reconstructed secondary decay vertices. The charge of the underlying b-quark is obtained with an algorithm that takes into account the net charge of the vertex as well as the charge of tracks emanating from the vertex and identified as kaons. This yields (25917 events)  $A_b = 0.9173 \pm 0.0184 \pm 0.0173$ . Taking into account all correlations with earlier results reported in ABE 03F, ABE 02g and ABE 99L, they obtain the quoted overall SLD result.
- <sup>187</sup> ABE 03F obtain an enriched sample of  $b\bar{b}$  events tagging on the invariant mass of a 3-dimensional topologically reconstructed secondary decay. The charge of the underlying b quark is obtained using a self-calibrating track-charge method. For the 1996–1998 data sample they measure  $A_b = 0.906 \pm 0.022 \pm 0.023$ . The value quoted here is obtained combining the above with the result of ABE 98l (1993–1995 data sample).
- <sup>188</sup> ABE 02g tag b and c quarks through their semileptonic decays into electrons and muons. A maximum likelihood fit is performed to extract simultaneously  $A_b$  and  $A_c$ .
- <sup>189</sup> ABE 99L obtain an enriched sample of  $b\bar{b}$  events tagging with an inclusive vertex mass cut. For distinguishing b and  $\bar{b}$  quarks they use the charge of identified  $K^\pm$ .

TRANSVERSE SPIN CORRELATIONS IN  $Z \rightarrow \tau^+ \tau^-$ 

The correlations between the transverse spin components of  $\tau^+ \tau^-$  produced in Z decays may be expressed in terms of the vector and axial-vector couplings:

$$C_{TT} = \frac{|g_A^\tau|^2 - |g_V^\tau|^2}{|g_A^\tau|^2 + |g_V^\tau|^2}$$

$$C_{TN} = -2 \frac{|g_A^\tau| |g_V^\tau|}{|g_A^\tau|^2 + |g_V^\tau|^2} \sin(\Phi_{g_V^\tau} - \Phi_{g_A^\tau})$$

$C_{TT}$  refers to the transverse-transverse (within the collision plane) spin correlation and  $C_{TN}$  refers to the transverse-normal (to the collision plane) spin correlation.

The longitudinal  $\tau$  polarization  $P_\tau$  ( $= -A_\tau$ ) is given by:

$$P_\tau = -2 \frac{|g_A^\tau| |g_V^\tau|}{|g_A^\tau|^2 + |g_V^\tau|^2} \cos(\Phi_{g_V^\tau} - \Phi_{g_A^\tau})$$

Here  $\Phi$  is the phase and the phase difference  $\Phi_{g_V^\tau} - \Phi_{g_A^\tau}$  can be obtained using both the measurements of  $C_{TN}$  and  $P_\tau$ .

$C_{TT}$	VALUE	EVTS	DOCUMENT ID	TECN	COMMENT
<b>1.01 ± 0.12 OUR AVERAGE</b>					
0.87 ± 0.20 ± 0.12	9.1k	ABREU	97G	DLPH	$E_{cm}^{ee} = 91.2$ GeV
1.06 ± 0.13 ± 0.05	120k	BARATE	97D	ALEP	$E_{cm}^{ee} = 91.2$ GeV

$C_{TN}$	VALUE	EVTS	DOCUMENT ID	TECN	COMMENT
<b>0.08 ± 0.13 ± 0.04</b>	120k	190	BARATE	97D	ALEP $E_{cm}^{ee} = 91.2$ GeV

- <sup>190</sup> BARATE 97D combine their value of  $C_{TN}$  with the world average  $P_\tau = -0.140 \pm 0.007$  to obtain  $\tan(\Phi_{g_V^\tau} - \Phi_{g_A^\tau}) = -0.57 \pm 0.97$ .

FORWARD-BACKWARD  $e^+ e^- \rightarrow f\bar{f}$  CHARGE ASYMMETRIES

These asymmetries are experimentally determined by tagging the respective lepton or quark flavor in  $e^+ e^-$  interactions. Details of heavy flavor (c- or b-quark) tagging at LEP are described in the note on “The Z boson” and ref. LEP-SLC 06. The Standard Model predictions for LEP data have been (re)computed using the ZFITTER package (version 6.36) with input parameters  $M_Z = 91.187$  GeV,  $M_{top} = 174.3$  GeV,  $M_{Higgs} = 150$  GeV,  $\alpha_s = 0.119$ ,  $\alpha^{(5)}(M_Z) = 1/128.877$  and the Fermi constant  $G_F = 1.16637 \times 10^{-5}$  GeV<sup>-2</sup> (see the note on “The Z boson” for references). For non-LEP data the Standard Model predictions are as given by the authors of the respective publications.

 $A_{FB}^{(0,e)}$  CHARGE ASYMMETRY IN  $e^+ e^- \rightarrow e^+ e^-$ 

OUR FIT is obtained using the fit procedure and correlations as determined by the LEP Electroweak Working Group (see the note “The Z boson” and ref. LEP-SLC 06). For the Z peak, we report the pole asymmetry defined by  $(3/4)A_e^2$  as determined by the nine-parameter fit to cross-section and lepton forward-backward asymmetry data.

ASYMMETRY (%)	STD. MODEL	$\sqrt{s}$ (GeV)	DOCUMENT ID	TECN
<b>1.45 ± 0.25 OUR FIT</b>				
0.89 ± 0.44	1.57	91.2	191 ABBIENDI	01A OPAL
1.71 ± 0.49	1.57	91.2	ABREU	00F DLPH
1.06 ± 0.58	1.57	91.2	ACCIARRI	00C L3
1.88 ± 0.34	1.57	91.2	192 BARATE	00C ALEP

- <sup>191</sup> ABBIENDI 01A error includes approximately 0.38 due to statistics, 0.16 due to event selection systematics, and 0.18 due to the theoretical uncertainty in t-channel prediction.
- <sup>192</sup> BARATE 00c error includes approximately 0.31 due to statistics, 0.06 due to experimental systematics, and 0.13 due to the theoretical uncertainty in t-channel prediction.

 $A_{FB}^{(0,\mu)}$  CHARGE ASYMMETRY IN  $e^+ e^- \rightarrow \mu^+ \mu^-$ 

OUR FIT is obtained using the fit procedure and correlations as determined by the LEP Electroweak Working Group (see the note “The Z boson” and ref. LEP-SLC 06). For the Z peak, we report the pole asymmetry defined by  $(3/4)A_e A_\mu$  as determined by the nine-parameter fit to cross-section and lepton forward-backward asymmetry data.

ASYMMETRY (%)	STD. MODEL	$\sqrt{s}$ (GeV)	DOCUMENT ID	TECN
<b>1.69 ± 0.13 OUR FIT</b>				
1.59 ± 0.23	1.57	91.2	193 ABBIENDI	01A OPAL
1.65 ± 0.25	1.57	91.2	ABREU	00F DLPH
1.88 ± 0.33	1.57	91.2	ACCIARRI	00C L3
1.71 ± 0.24	1.57	91.2	194 BARATE	00C ALEP

• • • We do not use the following data for averages, fits, limits, etc. • • •

9 ± 30	-1.3	20	195 ABREU	95M	DLPH
7 ± 26	-8.3	40	195 ABREU	95M	DLPH
-11 ± 33	-24.1	57	195 ABREU	95M	DLPH
-62 ± 17	-44.6	69	195 ABREU	95M	DLPH
-56 ± 10	-63.5	79	195 ABREU	95M	DLPH
-13 ± 5	-34.4	87.5	195 ABREU	95M	DLPH
-29.0 ± 5.0 ± 4.8 ± 0.5	-32.1	56.9	196 ABE	90I	VNS
-9.9 ± 1.5 ± 0.5	-9.2	35	HEGNER	90	JADE
0.05 ± 0.22	0.026	91.14	197 ABRAMS	89D	MRK2
-43.4 ± 17.0	-24.9	52.0	198 BACALA	89	AMY
-11.0 ± 16.5	-29.4	55.0	198 BACALA	89	AMY
-30.0 ± 12.4	-31.2	56.0	198 BACALA	89	AMY
-46.2 ± 14.9	-33.0	57.0	198 BACALA	89	AMY
-29 ± 13	-25.9	53.3	ADACHI	88C	TOPZ
+ 5.3 ± 5.0 ± 0.5	-1.2	14.0	ADEVA	88	MRKJ
-10.4 ± 1.3 ± 0.5	-8.6	34.8	ADEVA	88	MRKJ
-12.3 ± 5.3 ± 0.5	-10.7	38.3	ADEVA	88	MRKJ
-15.6 ± 3.0 ± 0.5	-14.9	43.8	ADEVA	88	MRKJ
-1.0 ± 6.0	-1.2	13.9	BRAUNSCH...	88D	TASS
-9.1 ± 2.3 ± 0.5	-8.6	34.5	BRAUNSCH...	88D	TASS
-10.6 ± 2.2 ± 2.3 ± 0.5	-8.9	35.0	BRAUNSCH...	88D	TASS
-17.6 ± 4.4 ± 4.3 ± 0.5	-15.2	43.6	BRAUNSCH...	88D	TASS
-4.8 ± 6.5 ± 1.0	-11.5	39	BEHREND	87C	CELL
-18.8 ± 4.5 ± 1.0	-15.5	44	BEHREND	87C	CELL
+ 2.7 ± 4.9	-1.2	13.9	BARTEL	86C	JADE
-11.1 ± 1.8 ± 1.0	-8.6	34.4	BARTEL	86C	JADE
-17.3 ± 4.8 ± 1.0	-13.7	41.5	BARTEL	86C	JADE
-22.8 ± 5.1 ± 1.0	-16.6	44.8	BARTEL	86C	JADE
-6.3 ± 0.8 ± 0.2	-6.3	29	ASH	85	MAC
-4.9 ± 1.5 ± 0.5	-5.9	29	DERRICK	85	HR5
-7.1 ± 1.7	-5.7	29	LEVI	83	MRK2
-16.1 ± 3.2	-9.2	34.2	BRANDELIK	82C	TASS

- <sup>193</sup> ABBIENDI 01A error is almost entirely on account of statistics.

- <sup>194</sup> BARATE 00c error is almost entirely on account of statistics.

- <sup>195</sup> ABREU 95M perform this measurement using radiative muon-pair events associated with high-energy isolated photons.

- <sup>196</sup> ABE 90I measurements in the range  $50 \leq \sqrt{s} \leq 60.8$  GeV.

- <sup>197</sup> ABRAMS 89D asymmetry includes both  $9 \mu^+ \mu^-$  and  $15 \tau^+ \tau^-$  events.

- <sup>198</sup> BACALA 89 systematic error is about 5%.

 $A_{FB}^{(0,\tau)}$  CHARGE ASYMMETRY IN  $e^+ e^- \rightarrow \tau^+ \tau^-$ 

OUR FIT is obtained using the fit procedure and correlations as determined by the LEP Electroweak Working Group (see the note “The Z boson” and ref. LEP-SLC 06). For the Z peak, we report the pole asymmetry defined by  $(3/4)A_e A_\tau$  as determined by the nine-parameter fit to cross-section and lepton forward-backward asymmetry data.

ASYMMETRY (%)	STD. MODEL	$\sqrt{s}$ (GeV)	DOCUMENT ID	TECN
<b>1.88 ± 0.17 OUR FIT</b>				
1.45 ± 0.30	1.57	91.2	199 ABBIENDI	01A OPAL
2.41 ± 0.37	1.57	91.2	ABREU	00F DLPH
2.60 ± 0.47	1.57	91.2	ACCIARRI	00C L3
1.70 ± 0.28	1.57	91.2	200 BARATE	00C ALEP

• • • We do not use the following data for averages, fits, limits, etc. • • •

-32.8 ± 6.4 ± 6.2 ± 1.5	-32.1	56.9	201 ABE	90I	VNS
-8.1 ± 2.0 ± 0.6	-9.2	35	HEGNER	90	JADE
-18.4 ± 19.2	-24.9	52.0	202 BACALA	89	AMY
-17.7 ± 26.1	-29.4	55.0	202 BACALA	89	AMY
-45.9 ± 16.6	-31.2	56.0	202 BACALA	89	AMY
-49.5 ± 18.0	-33.0	57.0	202 BACALA	89	AMY
-20 ± 14	-25.9	53.3	ADACHI	88C	TOPZ
-10.6 ± 3.1 ± 1.5	-8.5	34.7	ADEVA	88	MRKJ

See key on page 457

## Gauge &amp; Higgs Boson Particle Listings

Z

- 8.5 ± 6.6 ± 1.5	-15.4	43.8	ADEVA	88	MRKJ
- 6.0 ± 2.5 ± 1.0	8.8	34.6	BARTEL	85F	JADE
-11.8 ± 4.6 ± 1.0	14.8	43.0	BARTEL	85F	JADE
- 5.5 ± 1.2 ± 0.5	-0.063	29.0	FERNANDEZ	85	MAC
- 4.2 ± 2.0	0.057	29	LEVI	83	MRK2
-10.3 ± 5.2	-9.2	34.2	BEHREND	82	CELL
- 0.4 ± 6.6	-9.1	34.2	BRANDELIK	82c	TASS

199 ABBIENDI 01A error includes approximately 0.26 due to statistics and 0.14 due to event selection systematics.

200 BARATE 00c error includes approximately 0.26 due to statistics and 0.11 due to experimental systematics.

201 ABE 90i measurements in the range  $50 \leq \sqrt{s} \leq 60.8$  GeV.

202 BACALA 89 systematic error is about 5%.

### $A_{FB}^{(0,l)}$ CHARGE ASYMMETRY IN $e^+e^- \rightarrow \ell^+\ell^-$

For the Z peak, we report the pole asymmetry defined by  $(3/4)A_{FB}^2$  as determined by the five-parameter fit to cross-section and lepton forward-backward asymmetry data assuming lepton universality. For details see the note "The Z boson" and ref. LEP-SLC 06.

ASYMMETRY (%)	STD. MODEL	$\sqrt{s}$ (GeV)	DOCUMENT ID	TECN
<b>1.71 ± 0.10 OUR FIT</b>				
1.45 ± 0.17	1.57	91.2	203 ABBIENDI 01A	OPAL
1.87 ± 0.19	1.57	91.2	ABREU 00F	DLPH
1.92 ± 0.24	1.57	91.2	ACCIARRI 00c	L3
1.73 ± 0.16	1.57	91.2	204 BARATE 00c	ALEP

203 ABBIENDI 01A error includes approximately 0.15 due to statistics, 0.06 due to event selection systematics, and 0.03 due to the theoretical uncertainty in t-channel prediction.

204 BARATE 00c error includes approximately 0.15 due to statistics, 0.04 due to experimental systematics, and 0.02 due to the theoretical uncertainty in t-channel prediction.

### $A_{FB}^{(0,u)}$ CHARGE ASYMMETRY IN $e^+e^- \rightarrow u\bar{u}$

ASYMMETRY (%)	STD. MODEL	$\sqrt{s}$ (GeV)	DOCUMENT ID	TECN
<b>4.0 ± 6.7 ± 2.8</b>	<b>7.2</b>	<b>91.2</b>	205 ACKERSTAFF 97T	OPAL

205 ACKERSTAFF 97T measure the forward-backward asymmetry of various fast hadrons made of light quarks. Then using SU(2) isospin symmetry and flavor independence for down and strange quarks authors solve for the different quark types.

### $A_{FB}^{(0,s)}$ CHARGE ASYMMETRY IN $e^+e^- \rightarrow s\bar{s}$

The s-quark asymmetry is derived from measurements of the forward-backward asymmetry of fast hadrons containing an s quark.

ASYMMETRY (%)	STD. MODEL	$\sqrt{s}$ (GeV)	DOCUMENT ID	TECN
<b>9.8 ± 1.1 OUR AVERAGE</b>				
10.08 ± 1.13 ± 0.40	10.1	91.2	206 ABREU 00b	DLPH
6.8 ± 3.5 ± 1.1	10.1	91.2	207 ACKERSTAFF 97T	OPAL

206 ABREU 00b tag the presence of an s quark requiring a high-momentum-identified charged kaon. The s-quark pole asymmetry is extracted from the charged-kaon asymmetry taking the expected d- and u-quark asymmetries from the Standard Model and using the measured values for the c- and b-quark asymmetries.

207 ACKERSTAFF 97T measure the forward-backward asymmetry of various fast hadrons made of light quarks. Then using SU(2) isospin symmetry and flavor independence for down and strange quarks authors solve for the different quark types. The value reported here corresponds then to the forward-backward asymmetry for "down-type" quarks.

### $A_{FB}^{(0,c)}$ CHARGE ASYMMETRY IN $e^+e^- \rightarrow c\bar{c}$

OUR FIT, which is obtained by a simultaneous fit to several c- and b-quark measurements as explained in the note "The Z boson" and ref. LEP-SLC 06, refers to the Z pole asymmetry. The experimental values, on the other hand, correspond to the measurements carried out at the respective energies.

ASYMMETRY (%)	STD. MODEL	$\sqrt{s}$ (GeV)	DOCUMENT ID	TECN
<b>7.07 ± 0.35 OUR FIT</b>				
6.31 ± 0.93 ± 0.65	6.35	91.26	208 ABDALLAH 04F	DLPH
5.68 ± 0.54 ± 0.39	6.3	91.25	209 ABBIENDI 03P	OPAL
6.45 ± 0.57 ± 0.37	6.10	91.21	210 HEISTER 02H	ALEP
6.59 ± 0.94 ± 0.35	6.2	91.235	211 ABREU 99Y	DLPH
6.3 ± 0.9 ± 0.3	6.1	91.22	212 BARATE 98o	ALEP
6.3 ± 1.2 ± 0.6	6.1	91.22	213 ALEXANDER 97C	OPAL
8.3 ± 3.8 ± 2.7	6.2	91.24	214 ADRIANI 92D	L3
• • • We do not use the following data for averages, fits, limits, etc. • • •				
3.1 ± 3.5 ± 0.5	-3.5	89.43	208 ABDALLAH 04F	DLPH
11.0 ± 2.8 ± 0.7	12.3	92.99	208 ABDALLAH 04F	DLPH
- 6.8 ± 2.5 ± 0.9	-3.0	89.51	209 ABBIENDI 03P	OPAL
14.6 ± 2.0 ± 0.8	12.2	92.95	209 ABBIENDI 03P	OPAL
-12.4 ± 15.9 ± 2.0	-9.6	88.38	210 HEISTER 02H	ALEP
- 2.3 ± 2.6 ± 0.2	-3.8	89.38	210 HEISTER 02H	ALEP
- 0.3 ± 8.3 ± 0.6	0.9	90.21	210 HEISTER 02H	ALEP
10.6 ± 7.7 ± 0.7	9.6	92.05	210 HEISTER 02H	ALEP
11.9 ± 2.1 ± 0.6	12.2	92.94	210 HEISTER 02H	ALEP
12.1 ± 11.0 ± 1.0	14.2	93.90	210 HEISTER 02H	ALEP

- 4.96 ± 3.68 ± 0.53	-3.5	89.434	211 ABREU 99Y	DLPH
-11.80 ± 3.18 ± 0.62	12.3	92.990	211 ABREU 99Y	DLPH
- 1.0 ± 4.3 ± 1.0	-3.9	89.37	212 BARATE 98o	ALEP
-11.0 ± 3.3 ± 0.8	12.3	92.96	212 BARATE 98o	ALEP
3.9 ± 5.1 ± 0.9	-3.4	89.45	213 ALEXANDER 97C	OPAL
15.8 ± 4.1 ± 1.1	12.4	93.00	213 ALEXANDER 97C	OPAL
-12.9 ± 7.8 ± 5.5	-13.6	35	BEHREND 90D	CELL
7.7 ± 13.4 ± 5.0	-22.1	43	BEHREND 90D	CELL
-12.8 ± 4.4 ± 4.1	-13.6	35	ELSEN 90	JADE
-10.9 ± 12.9 ± 4.6	-23.2	44	ELSEN 90	JADE
-14.9 ± 6.7	-13.3	35	OULD-SAADAA 89	JADE

208 ABDALLAH 04F tag b- and c-quarks using semileptonic decays combined with charge flow information from the hemisphere opposite to the lepton. Enriched samples of  $c\bar{c}$  and  $b\bar{b}$  events are obtained using lifetime information.

209 ABBIENDI 03P tag heavy flavors using events with one or two identified leptons. This allows the simultaneous fitting of the b and c quark forward-backward asymmetries as well as the average  $B^0-\bar{B}^0$  mixing.

210 HEISTER 02H measure simultaneously b and c quark forward-backward asymmetries using their semileptonic decays to tag the quark charge. The flavor separation is obtained with a discriminating multivariate analysis.

211 ABREU 99Y tag  $Z \rightarrow b\bar{b}$  and  $Z \rightarrow c\bar{c}$  events with an exclusive reconstruction of several D meson decay modes ( $D^{*+}$ ,  $D^0$ , and  $D^+$  with their charge-conjugate states).

212 BARATE 98o tag  $Z \rightarrow c\bar{c}$  events requiring the presence of high-momentum reconstructed  $D^{*+}$ ,  $D^+$ , or  $D^0$  mesons.

213 ALEXANDER 97C identify the b and c events using a  $D/D^*$  tag.

214 ADRIANI 92D use both electron and muon semileptonic decays.

### $A_{FB}^{(0,b)}$ CHARGE ASYMMETRY IN $e^+e^- \rightarrow b\bar{b}$

OUR FIT, which is obtained by a simultaneous fit to several c- and b-quark measurements as explained in the note "The Z boson" and ref. LEP-SLC 06, refers to the Z pole asymmetry. The experimental values, on the other hand, correspond to the measurements carried out at the respective energies.

ASYMMETRY (%)	STD. MODEL	$\sqrt{s}$ (GeV)	DOCUMENT ID	TECN
<b>9.92 ± 0.16 OUR FIT</b>				
9.58 ± 0.32 ± 0.14	9.68	91.231	215 ABDALLAH 05	DLPH
10.04 ± 0.56 ± 0.25	9.69	91.26	216 ABDALLAH 04F	DLPH
9.72 ± 0.42 ± 0.15	9.67	91.25	217 ABBIENDI 03P	OPAL
9.77 ± 0.36 ± 0.18	9.69	91.26	218 ABBIENDI 02i	OPAL
9.52 ± 0.41 ± 0.17	9.59	91.21	219 HEISTER 02H	ALEP
10.00 ± 0.27 ± 0.11	9.63	91.232	220 HEISTER 01D	ALEP
7.62 ± 1.94 ± 0.85	9.64	91.235	221 ABREU 99Y	DLPH
9.60 ± 0.66 ± 0.33	9.69	91.26	222 ACCIARRI 99D	L3
9.31 ± 1.01 ± 0.55	9.65	91.24	223 ACCIARRI 98U	L3
9.4 ± 2.7 ± 2.2	9.61	91.22	224 ALEXANDER 97C	OPAL

• • • We do not use the following data for averages, fits, limits, etc. • • •

6.37 ± 1.43 ± 0.17	5.8	89.449	215 ABDALLAH 05	DLPH
10.41 ± 1.15 ± 0.24	12.1	92.990	215 ABDALLAH 05	DLPH
6.7 ± 2.2 ± 0.2	5.7	89.43	216 ABDALLAH 04F	DLPH
11.2 ± 1.8 ± 0.2	12.1	92.99	216 ABDALLAH 04F	DLPH
4.7 ± 1.8 ± 0.1	5.9	89.51	217 ABBIENDI 03P	OPAL
10.3 ± 1.5 ± 0.2	12.0	92.95	217 ABBIENDI 03P	OPAL
5.82 ± 1.53 ± 0.12	5.9	89.50	218 ABBIENDI 02i	OPAL
12.21 ± 1.23 ± 0.25	12.0	92.91	218 ABBIENDI 02i	OPAL
-13.1 ± 13.5 ± 1.0	3.2	88.38	219 HEISTER 02H	ALEP
5.5 ± 1.9 ± 0.1	5.6	89.38	219 HEISTER 02H	ALEP
- 0.4 ± 6.7 ± 0.8	7.5	90.21	219 HEISTER 02H	ALEP
11.1 ± 6.4 ± 0.5	11.0	92.05	219 HEISTER 02H	ALEP
10.4 ± 1.5 ± 0.3	12.0	92.94	219 HEISTER 02H	ALEP
13.8 ± 9.3 ± 1.1	12.9	93.90	219 HEISTER 02H	ALEP
4.36 ± 1.19 ± 0.11	5.8	89.472	220 HEISTER 01D	ALEP
11.72 ± 0.97 ± 0.11	12.0	92.950	220 HEISTER 01D	ALEP
5.67 ± 7.56 ± 1.17	5.7	89.434	221 ABREU 99Y	DLPH
8.82 ± 6.33 ± 1.22	12.1	92.990	221 ABREU 99Y	DLPH
6.11 ± 2.93 ± 0.43	5.9	89.50	222 ACCIARRI 99D	L3
13.71 ± 2.40 ± 0.44	12.2	93.10	222 ACCIARRI 99D	L3
4.95 ± 5.23 ± 0.40	5.8	89.45	223 ACCIARRI 98U	L3
11.37 ± 3.99 ± 0.65	12.1	92.99	223 ACCIARRI 98U	L3
- 8.6 ± 10.8 ± 2.9	5.8	89.45	224 ALEXANDER 97C	OPAL
- 2.1 ± 9.0 ± 2.6	12.1	93.00	224 ALEXANDER 97C	OPAL
-71 ± 34 ± 7	-58	58.3	SHIMONAKA 91	TOPZ
-22.2 ± 7.7 ± 3.5	-26.0	35	BEHREND 90D	CELL
-49.1 ± 16.0 ± 5.0	-39.7	43	BEHREND 90D	CELL
-28 ± 11	-23	35	BRAUNSCH... 90	TASS
-16.6 ± 7.7 ± 4.8	-24.3	35	ELSEN 90	JADE
-33.6 ± 22.2 ± 5.2	-39.9	44	ELSEN 90	JADE
3.4 ± 7.0 ± 3.5	-16.0	29.0	BAND 89	MAC
-72 ± 28 ± 13	-56	55.2	SAGAWA 89	AMY

215 ABDALLAH 05 obtain an enriched samples of  $b\bar{b}$  events using lifetime information. The quark (or antiquark) charge is determined with a neural network using the secondary vertex charge, the jet charge and particle identification.

216 ABDALLAH 04F tag b- and c-quarks using semileptonic decays combined with charge flow information from the hemisphere opposite to the lepton. Enriched samples of  $c\bar{c}$  and  $b\bar{b}$  events are obtained using lifetime information.

## Gauge &amp; Higgs Boson Particle Listings

Z

- 217 ABBIENDI 03P tag heavy flavors using events with one or two identified leptons. This allows the simultaneous fitting of the  $b$  and  $c$  quark forward-backward asymmetries as well as the average  $B^0$ - $\bar{B}^0$  mixing.
- 218 ABBIENDI 02i tag  $Z^0 \rightarrow b\bar{b}$  decays using a combination of secondary vertex and lepton tags. The sign of the  $b$ -quark charge is determined using an inclusive tag based on jet, vertex, and kaon charges.
- 219 HEISTER 02H measure simultaneously  $b$  and  $c$  quark forward-backward asymmetries using their semileptonic decays to tag the quark charge. The flavor separation is obtained with a discriminating multivariate analysis.
- 220 HEISTER 01D tag  $Z \rightarrow b\bar{b}$  events using the impact parameters of charged tracks complemented with information from displaced vertices, event shape variables, and lepton identification. The  $b$ -quark direction and charge is determined using the hemisphere charge method along with information from fast kaon tagging and charge estimators of primary and secondary vertices. The change in the quoted value due to variation of  $A_{FB}^c$  and  $R_b$  is given as  $+0.103 (A_{FB}^c - 0.0651) - 0.440 (R_b - 0.21585)$ .
- 221 ABREU 99Y tag  $Z \rightarrow b\bar{b}$  and  $Z \rightarrow c\bar{c}$  events by an exclusive reconstruction of several  $D$  meson decay modes ( $D^{*+}$ ,  $D^0$ , and  $D^+$  with their charge-conjugate states).
- 222 ACCIARRI 99D tag  $Z \rightarrow b\bar{b}$  events using high  $p$  and  $p_T$  leptons. The analysis determines simultaneously a mixing parameter  $\chi_b = 0.1192 \pm 0.0068 \pm 0.0051$  which is used to correct the observed asymmetry.
- 223 ACCIARRI 98u tag  $Z \rightarrow b\bar{b}$  events using lifetime and measure the jet charge using the hemisphere charge.
- 224 ALEXANDER 97C identify the  $b$  and  $c$  events using a  $D/D^*$  tag.

CHARGE ASYMMETRY IN  $e^+e^- \rightarrow q\bar{q}$ 

Summed over five lighter flavors.

Experimental and Standard Model values are somewhat event-selection dependent. Standard Model expectations contain some assumptions on  $B^0$ - $\bar{B}^0$  mixing and on other electroweak parameters.

ASYMMETRY (%)	STD. MODEL	$\sqrt{s}$ (GeV)	DOCUMENT ID	TECN
• • • We do not use the following data for averages, fits, limits, etc. • • •				
$-0.76 \pm 0.12 \pm 0.15$		91.2	225 ABREU 92i	DLPH
$4.0 \pm 0.4 \pm 0.63$	4.0	91.3	226 ACTON 92L	OPAL
$9.1 \pm 1.4 \pm 1.6$	9.0	57.9	ADACHI 91	TOPZ
$-0.84 \pm 0.15 \pm 0.04$		91	DECAMP 91B	ALEP
$8.3 \pm 2.9 \pm 1.9$	8.7	56.6	STUART 90	AMY
$11.4 \pm 2.2 \pm 2.1$	8.7	57.6	ABE 89L	VNS
$6.0 \pm 1.3$	5.0	34.8	GREENSHAW 89	JADE
$8.2 \pm 2.9$	8.5	43.6	GREENSHAW 89	JADE

- 225 ABREU 92i has 0.14 systematic error due to uncertainty of quark fragmentation.
- 226 ACTON 92L use the weight function method on 259k selected  $Z \rightarrow$  hadrons events. The systematic error includes a contribution of 0.2 due to  $B^0$ - $\bar{B}^0$  mixing effect, 0.4 due to Monte Carlo (MC) fragmentation uncertainties and 0.3 due to MC statistics. ACTON 92L derive a value of  $\sin^2 \theta_{eff}^W$  to be  $0.2321 \pm 0.0017 \pm 0.0028$ .

CHARGE ASYMMETRY IN  $p\bar{p} \rightarrow Z \rightarrow e^+e^-$ 

ASYMMETRY (%)	STD. MODEL	$\sqrt{s}$ (GeV)	DOCUMENT ID	TECN
• • • We do not use the following data for averages, fits, limits, etc. • • •				
$5.2 \pm 5.9 \pm 0.4$		91	ABE 91E	CDF

ANOMALOUS  $Z\gamma$ ,  $Z\gamma\gamma$ , AND  $ZZV$  COUPLINGS

Revised March 2012 by M.W. Gr unewald (U. Ghent) and A. Gurtu (King Abdulaziz University).

In on-shell  $Z\gamma$  production, deviations from the Standard Model for the  $Z\gamma\gamma^*$  and  $Z\gamma Z^*$  couplings may be described in terms of 8 parameters,  $h_i^V$  ( $i = 1, 4; V = \gamma, Z$ ) [1]. The parameters  $h_i^\gamma$  describe the  $Z\gamma\gamma^*$  couplings and the parameters  $h_i^Z$  the  $Z\gamma Z^*$  couplings. In this formalism  $h_1^V$  and  $h_2^V$  lead to  $CP$ -violating and  $h_3^V$  and  $h_4^V$  to  $CP$ -conserving effects. All these anomalous contributions to the cross section increase rapidly with center-of-mass energy. In order to ensure unitarity, these parameters are usually described by a form-factor representation,  $h_i^V(s) = h_{i0}^V / (1 + s/\Lambda^2)^n$ , where  $\Lambda$  is the energy scale for the manifestation of a new phenomenon and  $n$  is a sufficiently large power. By convention one uses  $n = 3$  for  $h_{1,3}^V$  and  $n = 4$  for  $h_{2,4}^V$ . Usually limits on  $h_i^V$ 's are put assuming some value of  $\Lambda$ , sometimes  $\infty$ .

In on-shell  $ZZ$  production, deviations from the Standard Model for the  $ZZ\gamma^*$  and  $ZZZ^*$  couplings may be described by

means of four anomalous couplings  $f_i^V$  ( $i = 4, 5; V = \gamma, Z$ ) [2]. As above, the parameters  $f_i^\gamma$  describe the  $ZZ\gamma^*$  couplings and the parameters  $f_i^Z$  the  $ZZZ^*$  couplings. The anomalous couplings  $f_5^V$  lead to violation of  $C$  and  $P$  symmetries while  $f_4^V$  introduces  $CP$  violation. Also here, formfactors depending on a scale  $\Lambda$  are used.

All these couplings  $h_i^V$  and  $f_i^V$  are zero at tree level in the Standard Model; they are measured in  $e^+e^-$ ,  $p\bar{p}$  and  $pp$  collisions at LEP, Tevatron and LHC.

## References

- U. Baur and E.L. Berger Phys. Rev. **D47**, 4889 (1993).
- K. Hagiwara *et al.*, Nucl. Phys. **B282**, 253 (1987).

 $h_i^V$ 

Combining the LEP results properly taking into account the correlations the following 95% CL limits are derived (CERN-PH-EP/2005-051 or hep-ex/0511027):

$$\begin{aligned} -0.13 < h_1^Z < +0.13, & & -0.078 < h_2^Z < +0.071, \\ -0.20 < h_3^Z < +0.07, & & -0.05 < h_4^Z < +0.12, \\ -0.056 < h_1^\gamma < +0.055, & & -0.045 < h_2^\gamma < +0.025, \\ -0.049 < h_3^\gamma < -0.008, & & -0.002 < h_4^\gamma < +0.034. \end{aligned}$$

VALUE	DOCUMENT ID	TECN	COMMENT
• • • We do not use the following data for averages, fits, limits, etc. • • •			
227	AALTONEN 11s	CDF	$E_{cm}^{p\bar{p}} = 1.96$ TeV
228	CHATRCHYAN 11M	CMS	$E_{cm}^{p\bar{p}} = 7$ TeV
229	ABAZOV 09L	D0	$E_{cm}^{p\bar{p}} = 1.96$ TeV
230	ABAZOV 07M	D0	
231	ABDALLAH 07C	DLPH	$E_{cm}^{e\bar{e}} = 183$ – $208$ GeV
232	ACHARD 04H	L3	
233	ABBIENDI, G	OPAL	
234	ABBOTT 98M	D0	
235	ABREU 98K	DLPH	

- 227 AALTONEN 11s study  $Z\gamma$  events in  $p\bar{p}$  interactions at  $\sqrt{s} = 1.96$  TeV with integrated luminosity  $5.1 \text{ fb}^{-1}$  for  $Z \rightarrow e^+e^-/\mu^+\mu^-$  and  $4.9 \text{ fb}^{-1}$  for  $Z \rightarrow \nu\bar{\nu}$ . For the charged lepton case, the two leptons must be of the same flavor with the transverse momentum/energy of one  $> 20$  GeV and the other  $> 10$  GeV. The isolated photon must have  $E_T > 50$  GeV. They observe 91 events with  $87.2 \pm 7.8$  events expected from standard model processes. For the  $\nu\bar{\nu}$  case they require solitary photons with  $E_T > 25$  GeV and missing  $E_T > 25$  GeV and observe 85 events with standard model expectation of  $85.9 \pm 5.6$  events. Taking the form factor  $\Lambda = 1.5$  TeV they derive 95% C.L. limits as  $|h_3^{\gamma, Z}| < 0.022$  and  $|h_4^{\gamma, Z}| < 0.0009$ .
- 228 CHATRCHYAN 11M study  $Z\gamma$  production in  $p\bar{p}$  collisions at  $\sqrt{s} = 7$  TeV using  $36 \text{ pb}^{-1}$   $p\bar{p}$  data, where the  $Z$  decays to  $e^+e^-$  or  $\mu^+\mu^-$ . The total cross sections are measured for photon transverse energy  $E_T^\gamma > 10$  GeV and spatial separation from charged leptons in the plane of pseudo rapidity and azimuthal angle  $\Delta R(\ell, \gamma) > 0.7$  with the dilepton invariant mass requirement of  $M_{\ell\ell} > 50$  GeV. The number of  $e^+e^- \gamma$  and  $\mu^+\mu^- \gamma$  candidates is 81 and 90 with estimated backgrounds of  $20.5 \pm 2.5$  and  $27.3 \pm 3.2$  events respectively. The 95% CL limits for  $Z\gamma\gamma$  couplings are  $-0.05 < h_3^Z < 0.06$  and  $-0.0005 < h_4^Z < 0.0005$ , and for  $Z\gamma\gamma$  couplings are  $-0.07 < h_3^\gamma < 0.07$  and  $-0.0005 < h_4^\gamma < 0.0006$ .
- 229 ABAZOV 09L study  $Z\gamma, Z \rightarrow \nu\bar{\nu}$  production in  $p\bar{p}$  collisions at 1.96 TeV C.M. energy. They select 51 events with a photon of transverse energy  $E_T^\gamma$  larger than 90 GeV, with an expected background of 17 events. Based on the photon  $E_T$  spectrum and including also  $Z$  decays to charged leptons (from ABAZOV 07M), the following 95% CL limits are reported:  $|h_{30}^Z| < 0.033$ ,  $|h_{40}^Z| < 0.0017$ ,  $|h_{30}^\gamma| < 0.033$ ,  $|h_{40}^\gamma| < 0.0017$ .
- 230 ABAZOV 07M use 968  $p\bar{p} \rightarrow e^+e^-/\mu^+\mu^- \gamma X$  candidates, at 1.96 TeV center of mass energy, to tag  $p\bar{p} \rightarrow Z\gamma$  events by requiring  $E_T(\gamma) > 7$  GeV, lepton-gamma separation  $\Delta R_{\ell\gamma} > 0.7$ , and di-lepton invariant mass  $> 30$  GeV. The cross section is in agreement with the SM prediction. Using these  $Z\gamma$  events they obtain 95% C.L. limits on each  $h_i^V$ , keeping all others fixed at their SM values. They report:  $-0.083 < h_{30}^Z < 0.082$ ,  $-0.0053 < h_{40}^Z < 0.0054$ ,  $-0.085 < h_{30}^\gamma < 0.084$ ,  $-0.0053 < h_{40}^\gamma < 0.0054$ , for the form factor scale  $\Lambda = 1.2$  TeV.
- 231 Using data collected at  $\sqrt{s} = 183$ – $208$ , ABDALLAH 07C select 1,877  $e^+e^- \rightarrow Z\gamma$  events with  $Z \rightarrow q\bar{q}$  or  $\nu\bar{\nu}$ , 171  $e^+e^- \rightarrow ZZ$  events with  $Z \rightarrow q\bar{q}$  or lepton pair (except an explicit  $\tau$  pair), and 74  $e^+e^- \rightarrow Z\gamma^*$  events with a  $q\bar{q}\mu^+\mu^-$  or  $q\bar{q}e^+e^-$  signature, to derive 95% CL limits on  $h_i^V$ . Each limit is derived with other parameters set to zero. They report:  $-0.23 < h_1^Z < 0.23$ ,  $-0.30 < h_2^Z < 0.16$ ,  $-0.14 < h_1^\gamma < 0.14$ ,  $-0.049 < h_3^\gamma < 0.044$ .
- 232 ACHARD 04H select 3515  $e^+e^- \rightarrow Z\gamma$  events with  $Z \rightarrow q\bar{q}$  or  $\nu\bar{\nu}$  at  $\sqrt{s} = 189$ – $209$  GeV to derive 95% CL limits on  $h_i^V$ . For deriving each limit the other parameters are fixed at zero. They report:  $-0.153 < h_1^Z < 0.141$ ,  $-0.087 < h_2^Z < 0.079$ ,  $-0.220 <$



- $h_1^Z < 0.112$ ,  $-0.068 < h_4^Z < 0.148$ ,  $-0.057 < h_1^\gamma < 0.057$ ,  $-0.050 < h_2^\gamma < 0.023$ ,  $-0.059 < h_3^\gamma < 0.004$ ,  $-0.004 < h_4^\gamma < 0.042$ .
- 233 ABBIENDI, G 00c study  $e^+e^- \rightarrow Z\gamma$  events (with  $Z \rightarrow q\bar{q}$  and  $Z \rightarrow \nu\bar{\nu}$ ) at 189 GeV to obtain the central values (and 95% CL limits) of these couplings:  $h_1^Z = 0.000 \pm 0.100$  ( $-0.190, 0.190$ ),  $h_2^Z = 0.000 \pm 0.068$  ( $-0.128, 0.128$ ),  $h_3^Z = -0.074^{+0.102}_{-0.103}$  ( $-0.269, 0.119$ ),  $h_4^Z = 0.046 \pm 0.068$  ( $-0.084, 0.175$ ),  $h_1^\gamma = 0.000 \pm 0.061$  ( $-0.115, 0.115$ ),  $h_2^\gamma = 0.000 \pm 0.041$  ( $-0.077, 0.077$ ),  $h_3^\gamma = -0.080^{+0.039}_{-0.041}$  ( $-0.164, -0.006$ ),  $h_4^\gamma = 0.064^{+0.033}_{-0.030}$  ( $+0.007, +0.134$ ). The results are derived assuming that only one coupling at a time is different from zero.
- 234 ABBOTT 98M study  $p\bar{p} \rightarrow Z\gamma + X$ , with  $Z \rightarrow e^+e^-, \mu^+\mu^-, \bar{\nu}\nu$  at 1.8 TeV, to obtain 95% CL limits at  $\Lambda = 750$  GeV:  $|h_{30}^Z| < 0.36$ ,  $|h_{40}^Z| < 0.05$  (keeping  $h_1^Z = 0$ ), and  $|h_{30}^\gamma| < 0.37$ ,  $|h_{40}^\gamma| < 0.05$  (keeping  $h_1^\gamma = 0$ ). Limits on the  $CP$ -violating couplings are  $|h_{20}^Z| < 0.36$ ,  $|h_{20}^\gamma| < 0.05$  (keeping  $h_1^Z = 0$ ), and  $|h_{10}^\gamma| < 0.37$ ,  $|h_{20}^\gamma| < 0.05$  (keeping  $h_1^\gamma = 0$ ).
- 235 ABREU 98k determine a 95% CL upper limit on  $\sigma(e^+e^- \rightarrow \gamma + \text{invisible particles}) < 2.5$  pb using 161 and 172 GeV data. This is used to set 95% CL limits on  $|h_{30}^\gamma| < 0.8$  and  $|h_{30}^Z| < 1.3$ , derived at a scale  $\Lambda = 1$  TeV and with  $n=3$  in the form factor representation.

 $f_i^V$ 

Combining the LEP results properly taking into account the correlations the following 95% CL limits are derived (CERN-PH-EP/2005-051 or hep-ex/0511027):

$$\begin{aligned} -0.30 < f_4^Z < +0.30, & \quad -0.34 < f_5^Z < +0.38, \\ -0.17 < f_4^\gamma < +0.19, & \quad -0.32 < f_5^\gamma < +0.36. \end{aligned}$$

VALUE	DOCUMENT ID	TECN	COMMENT
••• We do not use the following data for averages, fits, limits, etc. •••			
	236 SCHAEEL	09 ALEP	$E_{cm}^{ee} = 192\text{--}209$ GeV
	237 ABAZOV	08k D0	$E_{cm}^{pp} = 1.96$ TeV
	238 ABDALLAH	07c DLPH	$E_{cm}^{ee} = 183\text{--}208$ GeV
	239 ABBIENDI	04c OPAL	
	240 ACHARD	03D L3	
236	Using data collected in the center of mass energy range 192–209 GeV, SCHAEEL 09 select 318 $e^+e^- \rightarrow ZZ$ events with 319.4 expected from the standard model. Using this data they derive the following 95% CL limits: $-0.321 < f_4^Z < 0.318$ , $-0.534 < f_4^\gamma < 0.534$ , $-0.724 < f_5^Z < 0.733$ , $-1.194 < f_5^\gamma < 1.190$ .		
237	ABAZOV 08k search for $ZZ$ and $Z\gamma^*$ events with $1\text{ fb}^{-1}$ $p\bar{p}$ data at $\sqrt{s} = 1.96$ TeV in $(e^+e^-)$ , $(\mu\mu)$ , $(\mu\mu)$ , $(e^+e^-)$ final states requiring the lepton pair masses to be $> 30$ GeV. They observe 1 event, which is consistent with an expected signal of $1.71 \pm 0.15$ events and a background of $0.13 \pm 0.03$ events. From this they derive the following limits, for a form factor ( $\Lambda$ ) value of 1.2 TeV: $-0.28 < f_{40}^Z < 0.28$ , $-0.31 < f_{50}^Z < 0.29$ , $-0.26 < f_{40}^\gamma < 0.26$ , $-0.30 < f_{50}^\gamma < 0.28$ .		
238	Using data collected at $\sqrt{s} = 183\text{--}208$ GeV, ABDALLAH 07c select 171 $e^+e^- \rightarrow ZZ$ events with $Z \rightarrow q\bar{q}$ or lepton pair (except an explicit $\tau$ pair), and 74 $e^+e^- \rightarrow Z\gamma^*$ events with a $q\bar{q}\mu^+\mu^-$ or $q\bar{q}e^+e^-$ signature, to derive 95% CL limits on $f_i^V$ . Each limit is derived with other parameters set to zero. They report: $-0.40 < f_4^Z < 0.42$ , $-0.38 < f_5^Z < 0.62$ , $-0.23 < f_4^\gamma < 0.25$ , $-0.52 < f_5^\gamma < 0.48$ .		
239	ABBIENDI 04c study $ZZ$ production in $e^+e^-$ collisions in the C.M. energy range 190–209 GeV. They select 340 events with an expected background of 180 events. Including the ABBIENDI 00N data at 183 and 189 GeV (118 events with an expected background of 65 events) they report the following 95% CL limits: $-0.45 < f_4^Z < 0.58$ , $-0.94 < f_5^Z < 0.25$ , $-0.32 < f_4^\gamma < 0.33$ , and $-0.71 < f_5^\gamma < 0.59$ .		
240	ACHARD 03D study $Z$ -boson pair production in $e^+e^-$ collisions in the C.M. energy range 200–209 GeV. They select 549 events with an expected background of 432 events. Including the ACCIARRI 99g and ACCIARRI 99o data (183 and 189 GeV respectively, 286 events with an expected background of 241 events) and the 192–202 GeV ACCIARRI 01i results (656 events, expected background of 512 events), they report the following 95% CL limits: $-0.48 \leq f_4^Z \leq 0.46$ , $-0.36 \leq f_5^Z \leq 1.03$ , $-0.28 \leq f_4^\gamma \leq 0.28$ , and $-0.40 \leq f_5^\gamma \leq 0.47$ .		

### ANOMALOUS $W/Z$ QUARTIC COUPLINGS

Revised March 2012 by M.W. Grinewald (U. Ghent) and A. Gurtu (King Abdulaziz University).

The Standard Model quartic couplings,  $WWWW$ ,  $WWZZ$ ,  $WWZ\gamma$ ,  $WW\gamma\gamma$ , and  $ZZ\gamma\gamma$  lead to negligible effects at LEP energies, while they are important at a TeV Linear Collider. Outside the Standard Model framework, possible quartic couplings,  $a_0, a_c, a_n$ , are expressed in terms of the following dimension-6 operators [1,2];

$$\begin{aligned} L_6^0 &= -\frac{e^2}{16\Lambda^2} a_0 F^{\mu\nu} F_{\mu\nu} \vec{W}^\alpha \cdot \vec{W}_\alpha \\ L_6^c &= -\frac{e^2}{16\Lambda^2} a_c F^{\mu\alpha} F_{\mu\beta} \vec{W}^\beta \cdot \vec{W}_\alpha \end{aligned}$$

$$\begin{aligned} L_6^n &= -i\frac{e^2}{16\Lambda^2} a_n \epsilon_{ijk} W_{\mu\alpha}^{(i)} W_\nu^{(j)} W^{(k)\alpha} F^{\mu\nu} \\ \tilde{L}_6^0 &= -\frac{e^2}{16\Lambda^2} \tilde{a}_0 F^{\mu\nu} \tilde{F}_{\mu\nu} \vec{W}^\alpha \cdot \vec{W}_\alpha \\ \tilde{L}_6^n &= -i\frac{e^2}{16\Lambda^2} \tilde{a}_n \epsilon_{ijk} W_{\mu\alpha}^{(i)} W_\nu^{(j)} W^{(k)\alpha} \tilde{F}^{\mu\nu} \end{aligned}$$

where  $F, W$  are photon and  $W$  fields,  $L_6^0$  and  $L_6^c$  conserve  $C$ ,  $P$  separately ( $\tilde{L}_6^0$  conserves only  $C$ ) and generate anomalous  $W^+W^-\gamma\gamma$  and  $ZZ\gamma\gamma$  couplings,  $L_6^n$  violates  $CP$  ( $\tilde{L}_6^n$  violates both  $C$  and  $P$ ) and generates an anomalous  $W^+W^-Z\gamma$  coupling, and  $\Lambda$  is an energy scale for new physics. For the  $ZZ\gamma\gamma$  coupling the  $CP$ -violating term represented by  $L_6^n$  does not contribute. These couplings are assumed to be real and to vanish at tree level in the Standard Model.

Within the same framework as above, a more recent description of the quartic couplings [3] treats the anomalous parts of the  $WW\gamma\gamma$  and  $ZZ\gamma\gamma$  couplings separately leading to two sets parameterized as  $a_0^V/\Lambda^2$  and  $a_c^V/\Lambda^2$ , where  $V = W$  or  $Z$ .

At LEP the processes studied in search of these quartic couplings are  $e^+e^- \rightarrow WW\gamma$ ,  $e^+e^- \rightarrow \gamma\gamma\nu\bar{\nu}$ , and  $e^+e^- \rightarrow Z\gamma\gamma$  and limits are set on the quantities  $a_0^W/\Lambda^2, a_c^W/\Lambda^2, a_n/\Lambda^2$ . The characteristics of the first process depend on all the three couplings whereas those of the latter two depend only on the two  $CP$ -conserving couplings. The sensitive measured variables are the cross sections for these processes as well as the energy and angular distributions of the photon and recoil mass to the photon pair.

### References

- G. Belanger and F. Boudjema, Phys. Lett. **B288**, 201 (1992).
- J.W. Stirling and A. Werthenbach, Eur. Phys. J. **C14**, 103 (2000);  
J.W. Stirling and A. Werthenbach, Phys. Lett. **B466**, 369 (1999);  
A. Denner *et al.*, Eur. Phys. J. **C20**, 201 (2001);  
G. Montagna *et al.*, Phys. Lett. **B515**, 197 (2001).
- G. Belanger *et al.*, Eur. Phys. J. **C13**, 283 (2000).

### $a_0/\Lambda^2, a_c/\Lambda^2$

Combining published and unpublished preliminary LEP results the following 95% CL intervals for the QGCs associated with the  $ZZ\gamma\gamma$  vertex are derived (CERN-PH-EP/2005-051 or hep-ex/0511027):

$$\begin{aligned} -0.008 < a_0^Z/\Lambda^2 < +0.021 \\ -0.029 < a_c^Z/\Lambda^2 < +0.039 \end{aligned}$$

VALUE	DOCUMENT ID	TECN
••• We do not use the following data for averages, fits, limits, etc. •••		
	241 ABBIENDI	04L OPAL
	242 HEISTER	04A ALEP
	243 ACHARD	02G L3
241	ABBIENDI 04L select 20 $e^+e^- \rightarrow \nu\bar{\nu}\gamma\gamma$ acoplanar events in the energy range 180–209 GeV and 176 $e^+e^- \rightarrow q\bar{q}\gamma\gamma$ events in the energy range 130–209 GeV. These samples are used to constrain possible anomalous $W^+W^-\gamma\gamma$ and $ZZ\gamma\gamma$ quartic couplings. Further combining with the $W^+W^-$ sample of ABBIENDI 04B the following one-parameter 95% CL limits are obtained: $-0.007 < a_0^Z/\Lambda^2 < 0.023$ GeV $^{-2}$ , $-0.029 < a_c^Z/\Lambda^2 < 0.029$ GeV $^{-2}$ , $-0.020 < a_0^W/\Lambda^2 < 0.020$ GeV $^{-2}$ , $-0.052 < a_c^W/\Lambda^2 < 0.037$ GeV $^{-2}$ .	
242	In the CM energy range 183 to 209 GeV HEISTER 04A select 30 $e^+e^- \rightarrow \nu\bar{\nu}\gamma\gamma$ events with two acoplanar, high energy and high transverse momentum photons. The photon-photon acoplanarity is required to be $> 5^\circ$ , $E_\gamma/\sqrt{s} > 0.025$ (the more energetic photon having energy $> 0.2\sqrt{s}$ ), $p_{T,\gamma}/E_{\text{beam}} > 0.05$ and $ \cos\theta_\gamma  < 0.94$ . A likelihood fit to the photon energy and recoil missing mass yields the following one-parameter 95% CL limits: $-0.012 < a_0^Z/\Lambda^2 < 0.019$ GeV $^{-2}$ , $-0.041 < a_c^Z/\Lambda^2 < 0.044$ GeV $^{-2}$ , $-0.060 < a_0^W/\Lambda^2 < 0.055$ GeV $^{-2}$ , $-0.099 < a_c^W/\Lambda^2 < 0.093$ GeV $^{-2}$ .	
243	ACHARD 02G study $e^+e^- \rightarrow Z\gamma\gamma \rightarrow q\bar{q}\gamma\gamma$ events using data at center-of-mass energies from 200 to 209 GeV. The photons are required to be isolated, each with energy	



**Higgs Bosons —  $H^0$  and  $H^\pm$ , Searches for****HIGGS BOSONS: THEORY AND SEARCHES**

Updated May 2012 by G. Bernardi (CNRS/IN2P3, LPNHE/U. of Paris VI & VII), M. Carena (Fermi National Accelerator Laboratory and the University of Chicago), and T. Junk (Fermi National Accelerator Laboratory).

- I. Introduction
- II. The Standard Model (SM) Higgs Boson
  - II.1. Indirect Constraints on the SM Higgs Boson
  - II.2. Searches for the SM Higgs Boson at LEP
  - II.3. Searches for the SM Higgs Boson at the Tevatron
  - II.4. SM Higgs Boson Searches at the LHC
  - II.5. Models with a Fourth Generation of SM-Like Fermions
- III. Higgs Bosons in the Minimal Supersymmetric Standard Model (MSSM)
  - III.1. Radiatively-Corrected MSSM Higgs Masses and Couplings
  - III.2. Decay Properties and Production Mechanisms of MSSM Higgs Bosons
  - III.3. Searches for Neutral Higgs Bosons in the CP-Conserving *CPC* Scenario
    - III.3.1. Searches for Neutral MSSM Higgs Bosons at LEP
    - III.3.2. Searches for Neutral MSSM Higgs Bosons at Hadron Colliders
  - III.4. Searches for Charged MSSM Higgs Bosons
  - III.5. Effects of *CP* Violation on the MSSM Higgs Spectrum
  - III.6. Searches for Neutral Higgs Bosons in *CPV* Scenarios
  - III.7. Indirect Constraints on Supersymmetric Higgs Bosons
- IV. Other Model Extensions
- V. Searches for Higgs Bosons Beyond the MSSM
- VI. Outlook
- VII. Addendum

**NOTE:** The 4 July 2012 update on the Higgs search from ATLAS and CMS is described in the Addendum at the end of this review.

**I. Introduction**

Understanding the mechanism that breaks electroweak symmetry and generates the masses of the known elementary particles<sup>1</sup> is one of the most fundamental problems in particle physics. The Higgs mechanism [1] provides a general framework to explain the observed masses of the  $W^\pm$  and  $Z$  gauge bosons by means of charged and neutral Goldstone bosons that are manifested as the longitudinal components of the gauge bosons. These Goldstone bosons are generated by the underlying dynamics of electroweak symmetry breaking (EWSB). However, the fundamental dynamics of the electroweak symmetry breaking are unknown. There are two main classes of

theories proposed in the literature, those with weakly coupled dynamics—such as in the Standard Model (SM) [2]—and those with strongly coupled dynamics; both classes are summarized below.

In the SM, the electroweak interactions are described by a gauge field theory based on the  $SU(2)_L \times U(1)_Y$  symmetry group. The Higgs mechanism posits a self-interacting complex doublet of scalar fields, and renormalizable interactions are arranged such that the neutral component of the scalar doublet acquires a vacuum expectation value  $v \approx 246$  GeV, which sets the scale of EWSB. Three massless Goldstone bosons are generated, which are absorbed to give masses to the  $W^\pm$  and  $Z$  gauge bosons. The remaining component of the complex doublet becomes the Higgs boson—a new fundamental scalar particle. The masses of all fermions are also a consequence of EWSB since the Higgs doublet is postulated to couple to the fermions through Yukawa interactions. If the Higgs boson mass  $m_H$  is below  $\sim 180$  GeV, all fields remain weakly interacting up to the Planck scale,  $M_{\text{Pl}}$ .

The validity of the SM as an effective theory describing physics up to the Planck scale is questionable, however, because of the following “naturalness” argument. All fermion masses and dimensionless couplings are logarithmically sensitive to the scale  $\Lambda$  at which new physics becomes relevant. In contrast, scalar squared masses are quadratically sensitive to  $\Lambda$ . Thus, the observable SM Higgs mass has the following form:

$$m_H^2 = m_{H_0}^2 + \frac{kg^2\Lambda^2}{16\pi^2},$$

where  $m_{H_0}$  is a fundamental parameter of the theory. The second term is a one-loop correction in which  $g$  is an electroweak coupling and  $k$  is a constant, presumably of  $\mathcal{O}(1)$ , that is calculable within the low-energy effective theory. The two contributions arise from independent sources and one would not expect that the observable Higgs boson mass is significantly smaller than either of the two terms. Hence, if the scale of new physics  $\Lambda$  is much larger than the electroweak scale, unnatural cancellations must occur to remove the quadratic dependence of the Higgs boson mass on this large energy scale and to give a Higgs boson mass of order of the electroweak scale, as required from unitarity constraints [3,4], and as preferred by precision measurements of electroweak observables [5]. Most relevantly, recent results from direct Higgs searches at the Tevatron [6] and, in particular, at the LHC [7–10] strongly constrain the SM Higgs boson mass to be in the range 114–129 GeV, in excellent agreement with the indirect predictions from electroweak precision data. Thus, the SM is expected to be embedded in a more fundamental theory which will stabilize the hierarchy between the electroweak scale and the Planck scale in a natural way. A theory of that type would usually predict the onset of new physics at scales of the order of, or just above, the electroweak scale. Theorists strive to construct models of new physics that keep the successful features of the SM while curing its shortcomings, such as the absence of a dark matter candidate or a

<sup>1</sup> In the case of neutrinos, it is possible that the Higgs mechanism plays a role but is not entirely responsible for the generation of their observed masses.

# Gauge & Higgs Boson Particle Listings

## Higgs Bosons — $H^0$ and $H^\pm$

detailed explanation of the observed baryon asymmetry of the universe.

In the weakly-coupled approach to electroweak symmetry breaking, supersymmetric (SUSY) extensions of the SM provide a possible explanation for the stability of the electroweak energy scale in the presence of quantum corrections [11,12]. These theories predict at least five Higgs particles [13]. The properties of the lightest Higgs scalar often resemble those of the SM Higgs boson, with a mass that is predicted to be less than 135 GeV [14] in the simplest supersymmetric model<sup>2</sup>. Additional neutral and charged Higgs bosons are also predicted. Moreover, low-energy supersymmetry with a supersymmetry breaking scale of order 1 TeV allows for grand unification of the electromagnetic, weak and strong gauge interactions in a consistent way, strongly supported by the prediction of the electroweak mixing angle at low energy scales, with an accuracy at the percent level [22,23].

Alternatively new strong interactions near the TeV scale can induce strong breaking of the electroweak symmetry [24]. “Little Higgs” models have been proposed in which the scale of the new strong interactions is pushed up above 10 TeV [25–27], and the lightest Higgs scalar resembles the weakly-coupled SM Higgs boson.

Another approach to electroweak symmetry breaking has been explored in which extra space dimensions beyond the usual  $3 + 1$  dimensional space-time are introduced [28] with characteristic sizes of the fundamental Planck scale of order  $(1 \text{ TeV})^{-1}$ . In such scenarios, the mechanisms for electroweak symmetry breaking are inherently extra-dimensional and the resulting Higgs phenomenology can depart significantly from SM predictions [27,29].

Both in the framework of supersymmetric theories and in the strongly coupled dynamic approach there have been many studies based on effective theory approaches [18,20,21,30,31] that prove useful in exploring departures from the SM Higgs phenomenology in a more model independent way.

Prior to 1989, when the  $e^+e^-$  collider LEP at CERN came into operation, searches were sensitive only to Higgs bosons with masses of a few GeV and below [32]. In the LEP 1 phase, the collider operated at center-of-mass energies close to  $M_Z$ . During the LEP 2 phase, the energy was increased in steps, reaching 209 GeV in the year 2000 before the final shutdown. The combined data of the four LEP experiments, ALEPH, DELPHI, L3, and OPAL, were sensitive to neutral

<sup>2</sup> Larger values of the mass of the lightest Higgs boson, up to about 250 GeV, can be obtained in non-minimal SUSY extensions of the SM [15–21]. However, if the LHC’s indications of a light Higgs boson are confirmed, the main motivation for non-minimal SUSY extensions would be to obtain a Higgs boson mass in the 120–130 GeV mass range without demanding heavy top quark superpartners, and thereby avoid the so-called little hierarchy problem.

Higgs bosons with masses up to about 115 GeV and to charged Higgs bosons with masses up to about 90 GeV [33,34].

The search for the Higgs boson continued at the Tevatron  $p\bar{p}$  collider, which operated at a center-of-mass energy of 1.96 TeV until its shutdown in the Fall of 2011. The two experiments, CDF and DØ, each collected approximately  $10 \text{ fb}^{-1}$  of data with the capability to probe a SM Higgs boson mass in the 90–185 GeV range. The combination of the results from CDF and DØ shows an excess of data events with respect to the background estimation in the mass range  $115 \text{ GeV} < m_H < 135 \text{ GeV}$ . The global significance for such an excess anywhere in the full mass range is approximately 2.2 standard deviations. The excess is concentrated in the  $H \rightarrow b\bar{b}$  channel, although the results in the  $H \rightarrow W^+W^-$  channel are also consistent with the possible presence of a low-mass Higgs boson. Other neutral and charged Higgs particles postulated in most theories beyond the SM are also searched for at the Tevatron. The Tevatron Higgs results are discussed in more detail later in this review. The final results are expected to be available by the end of 2012.

Searches for Higgs bosons are ongoing at the LHC  $pp$  collider. These searches have much higher sensitivity than the Tevatron searches and cover masses up to several hundred GeV. At present both LHC experiments, ATLAS and CMS, have searched for a SM Higgs boson produced mainly through gluon fusion, and decaying dominantly into gauge boson pairs. The initial results are compatible with the presence of a SM-like Higgs boson with a mass in the range 114–129 GeV, with most of the remaining mass values up to at least 500 GeV being excluded at the 95% C.L. by both experiments. Both LHC experiments observe small excesses, predominantly in the  $\gamma\gamma$  and  $ZZ$  modes, which could be compatible with a Higgs boson with a mass near 125 GeV but are not yet conclusive. These results are discussed in more detail later in this review. If a signal is confirmed, the next step is to understand the precise nature of such a particle by scrutinizing the coupling strengths in the different production and decay channels. Searches are also conducted by both LHC collaborations for Higgs bosons produced via vector boson fusion and in association with a  $W$  or a  $Z$  boson. Decays to  $b\bar{b}$  and  $\tau^+\tau^-$  are searched for in addition to the more experimentally distinct boson pair signatures. With additional data, these searches will constrain the production rates and decay branching ratios of the Higgs boson. An exciting time lies ahead in the case of the discovery of a Higgs boson since we would need to understand its nature and the underlying new physics that might be related to it. Beyond a discovery, precision measurements will be crucial to completely understand the mechanism of electroweak symmetry breaking.

## II. The Standard Model (SM) Higgs Boson

In the SM, the Higgs boson mass is given by  $m_H = \sqrt{\lambda/2} v$ , where  $\lambda$  is the Higgs self-coupling parameter and  $v$  is the vacuum expectation value of the Higgs field,  $v = (\sqrt{2}G_F)^{-1/2} \approx$

See key on page 457

## Gauge & Higgs Boson Particle Listings

### Higgs Bosons — $H^0$ and $H^\pm$

246 GeV, fixed by the Fermi coupling  $G_F$ , which is determined with a precision of 0.6 ppm from muon decay measurements [35]. Since  $\lambda$  is presently unknown, the value of the SM Higgs boson mass  $m_H$  cannot be predicted. However, besides the upper bound on the Higgs boson mass from unitarity constraints [3,4], additional theoretical arguments place approximate upper and lower bounds on  $m_H$  [36]. There is an upper bound based on the perturbativity of the theory up to the scale  $\Lambda$  at which the SM breaks down, and a lower bound derived from the stability of the Higgs potential. If  $m_H$  is too large, then the Higgs self-coupling diverges at some scale  $\Lambda$  below the Planck scale. If  $m_H$  is too small, then the Higgs potential develops a second (global) minimum at a large value of the magnitude of the scalar field of order  $\Lambda$ . New physics must enter at a scale  $\Lambda$  or below, so that the global minimum of the theory corresponds to the observed  $SU(2)_L \times U(1)_Y$  broken vacuum with  $v = 246$  GeV. Given a value of  $\Lambda$ , one can compute the minimum and maximum allowed Higgs boson masses. Conversely, the value of  $m_H$  itself can provide an important constraint on the scale up to which the SM remains successful as an effective theory. In particular, a Higgs boson with mass in the range  $130 \text{ GeV} \lesssim m_H \lesssim 180 \text{ GeV}$  would be consistent with an effective SM description that survives all the way to the Planck scale. For smaller Higgs mass values, the stability of our universe prefers new physics at a lower scale. The lower bound on  $m_H$  can be reduced to about 115 GeV [37] if one allows for the electroweak vacuum to be metastable, with a lifetime greater than the age of the universe. The main uncertainties in the stability and perturbativity bounds come from the uncertainties in the value of  $\alpha_s$  and the top quark mass. As can be inferred from Fig. 1 [38], taking these uncertainties into account, a Higgs boson mass of about 125 GeV is close to the boundary of a SM that is consistent up to the Planck scale, and a SM that is unstable with a slow tunneling rate.

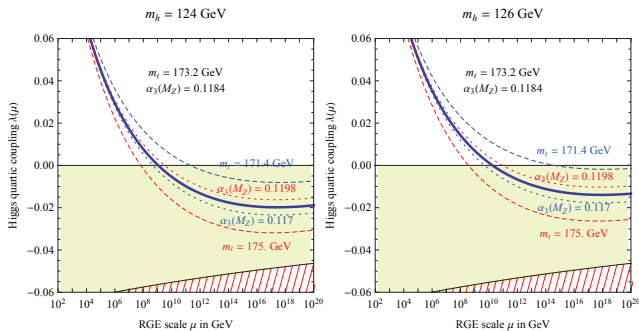


**Figure 1:** Renormalization group evolution of the Higgs self coupling  $\lambda$ , for  $m_H = 124$  GeV (left) and  $m_H = 126$  GeV (right), for the central values of  $m_t$  and  $\alpha_s$  (solid curves), as well as for variations of  $m_t$  (dashed curves) and  $\alpha_s$  (dotted curves). For negative values of  $\lambda$ , the lifetime of the SM vacuum due to quantum tunneling at zero temperature is longer than the age of the universe as long as  $\lambda$  remains above the region shaded in red. From Ref. 38.

The SM Higgs couplings to fundamental fermions are proportional to the fermion masses, and the couplings to bosons are proportional to the squares of the boson masses. In particular, the SM Higgs boson is a  $CP$ -even scalar, and its couplings to gauge bosons, Higgs bosons and fermions are given by:

$$g_{Hf\bar{f}} = \frac{m_f}{v}, \quad g_{HVV} = \frac{2m_V^2}{v}, \quad g_{HHVV} = \frac{2m_V^2}{v^2}$$

$$g_{HHH} = \frac{3m_H^2}{v}, \quad g_{HHHH} = \frac{3m_H^2}{v^2}$$

where  $V = W^\pm$  or  $Z$ . In Higgs boson production and decay processes, the dominant mechanisms involve the coupling of the  $H$  to the  $W^\pm$ ,  $Z$  and/or the third generation quarks and leptons. The Higgs boson's coupling to gluons, is induced at leading order by a one-loop graph in which the  $H$  couples to a virtual  $t\bar{t}$  pair. Likewise, the Higgs boson's coupling to photons is also generated via loops, although in this case the one-loop graph with a virtual  $W^+W^-$  pair provides the dominant contribution [13]. Reviews of the SM Higgs boson's properties and phenomenology, with an emphasis on the impact of loop corrections to the Higgs boson decay rates and cross sections, can be found in Refs. [39–45].

The main Higgs boson production cross sections at an  $e^+e^-$  collider are the Higgs-strahlung process  $e^+e^- \rightarrow ZH$  [4,46], and the  $WW$  fusion process [47]  $e^+e^- \rightarrow \bar{\nu}_e\nu_e W^*W^* \rightarrow \bar{\nu}_e\nu_e H$ . As center-of-mass energy  $\sqrt{s}$  is increased, the cross-section for the Higgs-strahlung process decreases as  $s^{-1}$  and is dominant at low energies, while the cross-section for the  $WW$  fusion process grows as  $\ln(s/m_H^2)$  and dominates at high energies [48,49,50]. The  $ZZ$  fusion mechanism,  $e^+e^- \rightarrow e^+e^- Z^*Z^* \rightarrow e^+e^- H$ , also contributes to Higgs boson production, with a cross-section suppressed by an order of magnitude with respect to that of  $WW$  fusion. The process  $e^+e^- \rightarrow t\bar{t}H$  [51,52] can become relevant for large  $\sqrt{s} \simeq 800$  GeV for SM Higgs masses in the experimentally preferred region. For a more detailed discussion of Higgs production properties at lepton colliders see for example Refs. [44] and [45], and references therein.

At high-energy hadron colliders, the Higgs boson production mechanism with the largest cross section is  $gg \rightarrow H + X$ . This process is known at next-to-next-to-leading order (NNLO) in QCD, in the large top-mass limit, and at NLO in QCD for arbitrary top mass [53]. The NLO QCD corrections approximately double the leading-order prediction, and the NNLO corrections add approximately 50% to the NLO prediction. NLO electroweak corrections range between 0 and 6% of the LO term [54]. Mixed QCD-electroweak corrections  $O(\alpha\alpha_s)$  are computed in Ref. [55]. In addition, soft-gluon contributions to the cross sections have been resummed at next-to-leading logarithmic (NLL), NNLL and partial NNNLL accuracy [56]. Updated predictions for the gluon fusion cross sections at NNLO or through soft-gluon resummation up to next-to-next-to-leading logarithmic accuracy (NNLL), and two-loop electroweak effects can be found in Refs. [55,57]. A better

# Gauge & Higgs Boson Particle Listings

## Higgs Bosons — $H^0$ and $H^\pm$

perturbative convergence is achieved by resumming the enhanced contributions arising from the analytic continuation of the gluon form factor [58]. Updated predictions to compute the gluon fusion cross sections at NNNLL in renormalization group improved perturbation theory and incorporating two-loop electroweak effects can be found in Ref. [59]. Some search strategies look for Higgs boson production in association with jets. In the heavy top quark mass limit, the Higgs boson production cross section in association with one jet is considered in Refs. [60–63] and in association with two jets in Refs. [64,65].

The other relevant Higgs boson production mechanisms at the Tevatron and the LHC are associated production with  $W$  and  $Z$  gauge bosons and vector boson fusion, and at a significantly smaller rate, the associated production with top quark pairs. The cross sections for the associated production processes  $q\bar{q} \rightarrow W^\pm H + X$  and  $q\bar{q} \rightarrow ZH + X$  [66,67,68] are known at NNLO for the QCD corrections and at NLO for the electroweak corrections [69,70]. The residual uncertainty is less than 5%. For the vector boson fusion processes  $qq \rightarrow qqH + X$ , corrections to the production cross section are known at NNLO in QCD and at NLO for the electroweak corrections and the remaining theoretical uncertainties in the inclusive cross section are approximately 2% [71], but are larger if jets are required or vetoed [43]. The cross section for the associated production process  $t\bar{t}H$  has been calculated at NLO in QCD [72], while the bottom fusion Higgs boson production cross section is known at NNLO in the case of five quark flavors [69,73,74]. The cross sections for the production of SM Higgs bosons are summarized in Fig. 2 for  $p\bar{p}$  collisions at the Tevatron, and in Fig. 3 for  $pp$  collisions at  $\sqrt{s} = 7$  TeV at the LHC [75,76]. Ref. [75] also includes cross sections computed at  $\sqrt{s} = 8$  TeV, which are relevant for data collected in 2012.

The branching ratios for the most relevant decay modes of the SM Higgs boson as functions of  $m_H$ , including the most recent theoretical uncertainties, are shown in Fig. 4. The total decay width as function of  $m_H$  is shown in Fig. 5. Details of these calculations can be found in Refs. [40–44]. For Higgs boson masses below 135 GeV, decays to fermion pairs dominate; the decay  $H \rightarrow b\bar{b}$  has the largest branching ratio and the decay  $H \rightarrow \tau^+\tau^-$  is about an order of magnitude smaller. For these low masses, the total decay width is less than 10 MeV. For Higgs boson masses above 135 GeV, the  $W^+W^-$  decay dominates (below the  $W^+W^-$  threshold, one of the  $W$  bosons is virtual) with an important contribution from  $H \rightarrow ZZ$ , and the decay width rises rapidly, reaching about 1 GeV at  $m_H = 200$  GeV and 100 GeV at  $m_H = 500$  GeV. Above the  $t\bar{t}$  threshold, the branching ratio into  $t\bar{t}$  pairs increases rapidly as a function of the Higgs boson mass, reaching a maximum of about 20% at  $m_H \sim 450$  GeV. Higgs boson decays into pairs of gluons, pairs of photons, and  $Z\gamma$  are induced at one loop level. Higgs boson decay into a pair of photons is particularly relevant for the discovery potential of the LHC for a low-mass Higgs boson. In

spite of the small expected signal rate, the reconstructed mass resolution provides a way to separate signal from background, a means to calibrate the background rate with a signal-free sample of events, and a precise measurement of  $m_H$  once a signal is identified.

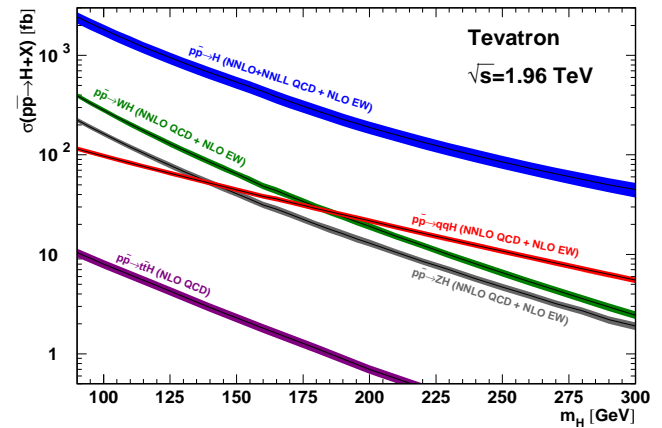


**Figure 2:** SM Higgs boson production cross sections for  $p\bar{p}$  collisions at 1.96 TeV, including theoretical uncertainties [53,70–72].

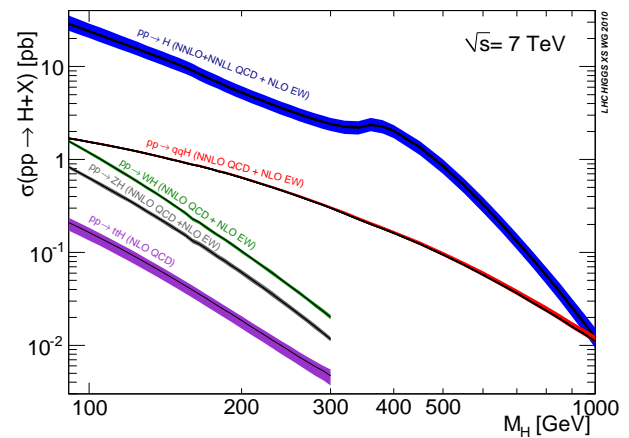


**Figure 3:** SM Higgs boson production cross sections for  $pp$  collisions at 7 TeV, including theoretical uncertainties [76].

### II.1. Indirect Constraints on the SM Higgs Boson

Indirect experimental bounds for the SM Higgs boson mass are obtained from fits to precision measurements of electroweak observables. The Higgs boson contributes to the  $W^\pm$  and  $Z$  vacuum polarization through loop effects, leading to a logarithmic sensitivity of the ratio of the  $W^\pm$  and  $Z$  gauge boson masses on the Higgs boson mass. A global fit to the precision electroweak data accumulated in the last two decades at LEP, SLC, the Tevatron, and elsewhere, gives  $m_H = 94^{+29}_{-24}$  GeV, or

# Gauge & Higgs Boson Particle Listings

## Higgs Bosons — $H^0$ and $H^\pm$

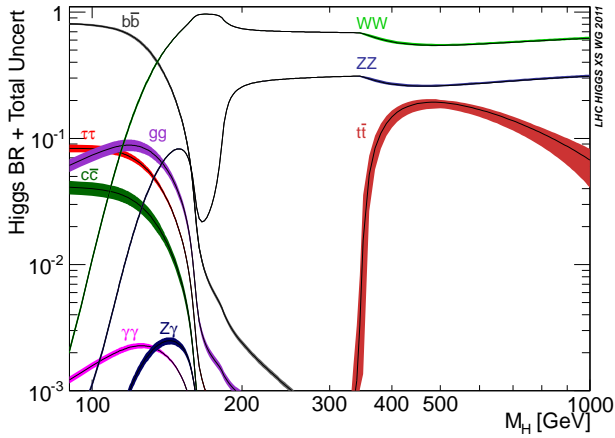


**Figure 4:** Branching ratios for the main decays of the SM Higgs boson, including theoretical uncertainties [40–44].

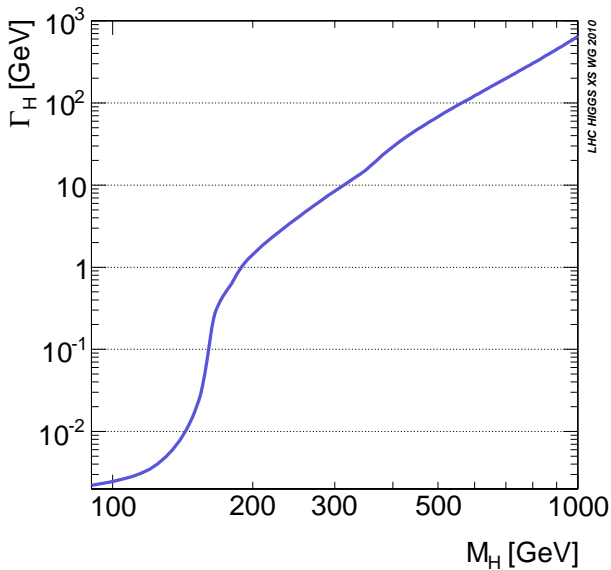


**Figure 5:** The total decay width of the SM Higgs boson, shown as a function of  $m_H$  [76].

$m_H < 152$  GeV at 95% C.L. [5]. The top quark contributes to the  $W^\pm$  boson vacuum polarization through loop effects that depend quadratically on the top mass, which plays an important role in the global fit. A top quark mass of  $173.2 \pm 0.9$  GeV [77] and a  $W^\pm$  boson mass of  $80.385 \pm 0.015$  GeV [5] were used.

### II.2. Searches for the SM Higgs Boson at LEP

The principal mechanism for producing the SM Higgs boson in  $e^+e^-$  collisions at LEP energies is Higgs-strahlung in the  $s$ -channel,  $e^+e^- \rightarrow HZ$ . The  $Z$  boson in the final state is either

virtual (LEP 1), or on mass shell (LEP 2). At LEP energies, SM Higgs boson production via  $W^+W^-$  and  $ZZ$  fusion in the  $t$ -channel has a small cross section. The sensitivity of the LEP searches to the Higgs boson depends on the center-of-mass energy,  $\sqrt{s}$ . For  $m_H < \sqrt{s} - M_Z$ , the cross section is of order 1 pb or more, while for  $m_H > \sqrt{s} - M_Z$ , the cross section is smaller by at least an order of magnitude.

During the LEP 1 phase, the ALEPH, DELPHI, L3 and OPAL collaborations analyzed over 17 million  $Z$  decays and set lower bounds of approximately 65 GeV on the mass of the SM Higgs boson [78]. At LEP 2, substantial data samples were collected at center-of-mass energies up to 209 GeV. Data recorded at each center-of-mass energy were studied independently and the results from the four LEP experiments were then combined. The  $CL_s$  method [79] was used to compute the observed and expected limits on the Higgs boson production cross section as functions of the Higgs boson mass considered, and from that a lower bound on  $m_H$  was derived.

Higgs bosons with mass above  $2m_\tau$  were searched for in four final state topologies: The four-jet topology in which  $H \rightarrow b\bar{b}$  and  $Z \rightarrow q\bar{q}$ ; the final states with tau leptons produced in the processes  $H \rightarrow \tau^+\tau^-$  where  $Z \rightarrow q\bar{q}$ , together with the mode  $H \rightarrow b\bar{b}$  with  $Z \rightarrow \tau^+\tau^-$ ; the missing energy topology produced mainly in the process  $H \rightarrow b\bar{b}$  with  $Z \rightarrow \nu\bar{\nu}$ , and finally the leptonic states  $H \rightarrow b\bar{b}$  with  $Z \rightarrow e^+e^-, \mu^+\mu^-$ . At LEP 1, only the modes with  $Z \rightarrow \ell^+\ell^-$  and  $Z \rightarrow \nu\bar{\nu}$  were used because the backgrounds in the other channels were prohibitive. For the data collected at LEP 2, all decay modes were used.

For very light Higgs bosons, with  $m_H < 2m_\tau$ , the decay modes exploited above are not kinematically allowed, and decays to jets, muon pairs, pion pairs, and lighter particles dominate, depending on  $m_H$ . For very low masses, OPAL’s decay-mode independent search [80] for the Bjorken process  $e^+e^- \rightarrow S^0Z$ , where  $S^0$  denotes a generic neutral scalar particle, provides sensitivity regardless of the branching fractions of the  $S^0$ . This search is based on studies of the recoil mass spectrum in events with  $Z \rightarrow e^+e^-$  and  $Z \rightarrow \mu^+\mu^-$  decays, and on the final states  $Z \rightarrow \nu\bar{\nu}$  and  $S^0 \rightarrow e^+e^-$  or photons. Upper bounds on the  $e^+e^- \rightarrow ZH$  cross section are obtained for scalar masses between 1 KeV and 100 GeV, and are below 0.05 times the SM prediction for  $m_H < 80$  GeV, constraining the coupling of the Higgs boson to the  $Z$ .

The combination of the LEP data yields a 95% C.L. lower bound of 114.4 GeV for the mass of the SM Higgs boson [33]. The median limit one would expect to obtain in a large ensemble of identical experiments with no signal present is 115.3 GeV. An excess of data was seen consistent with a Higgs boson of mass  $m_H \approx 115$  GeV. The significance of this excess is low, however. It is quantified by the background-only  $p$ -value [79], which is the probability to obtain data at least as signal-like as the observed data, assuming a signal is truly absent; a small  $p$ -value indicates data that are inconsistent with the background model but are more consistent with a signal model.



# Gauge & Higgs Boson Particle Listings

## Higgs Bosons — $H^0$ and $H^\pm$

The background-only  $p$ -value for the excess in the LEP data is 9%.

### II.3. Searches for the SM Higgs Boson at the Tevatron

As shown in Fig. 2, at the Tevatron, the most important SM Higgs boson production processes are gluon fusion ( $gg \rightarrow H$ ) and Higgs boson production in association with a vector boson ( $W^\pm H$  or  $ZH$ ). Vector boson fusion (VBF) has a smaller cross section, but some search channels are optimized for it. For  $m_H$  less than about 135 GeV, the most sensitive analyses search for  $W^\pm H$  and  $ZH$  with  $H \rightarrow b\bar{b}$ . The mode  $gg \rightarrow H \rightarrow b\bar{b}$  is overwhelmed by the background from the inclusive production of  $p\bar{p} \rightarrow b\bar{b} + X$  via the strong interaction. The associated production modes  $W^\pm H$  and  $ZH$  allow use of the leptonic  $W$  and  $Z$  decays to purify the signal and reject QCD backgrounds.

The contribution of  $H \rightarrow W^*W$  or  $WW$  is dominant at higher masses,  $m_H > 135$  GeV. Using this decay mode, both the direct ( $gg \rightarrow H$ ) and the associated production ( $p\bar{p} \rightarrow W^\pm H$  or  $ZH$ ) channels are explored, and the results of both Tevatron experiments, CDF and DØ, are combined to maximize the sensitivity to the Higgs boson.

The signal-to-background ratio is much smaller in the Tevatron searches than in the LEP analyses, and the systematic uncertainties on the estimated background rates are typically larger than the signal rates. In order to estimate the background rates in the selected samples more accurately, auxiliary measurements are made in data samples which are expected to be depleted in Higgs boson signal. These auxiliary samples are chosen to maximize the sensitivity to each specific background in turn. Monte Carlo simulations are used to extrapolate these measurements into the Higgs signal regions. The dominant physics backgrounds such as top-pair, diboson,  $W^\pm b\bar{b}$ , and single top production are estimated by Monte Carlo simulations in this way, i.e., after having been tuned or verified by corresponding measurements in dedicated analyses, thereby reducing the uncertainty on the total background estimate. Nearly all Tevatron analyses use multivariate analysis techniques (MVA's) to further separate signals from backgrounds and to provide the final discriminants whose distributions are used to compute limits, best-fit cross sections and uncertainties, and  $p$ -values. Separate MVA's are trained at each  $m_H$  in all the different sub-channels.

Both Tevatron experiments have updated their main search analyses to the full analyzable data sample of approximately  $10 \text{ fb}^{-1}$ . At Higgs boson masses of 150 GeV and below, the searches for associated production,  $p\bar{p} \rightarrow W^\pm H, ZH$ , are performed in different channels, as follows. The  $WH \rightarrow \ell\nu b\bar{b}$  searches [81–85] select events with a charged lepton ( $\ell = e$  or  $\mu$ ), large missing transverse energy, and at least two jets, at least one of which must be  $b$ -tagged. In order to improve the sensitivity of the searches, events with one  $b$ -tag are analyzed separately from those with two, and events with three jets are analyzed separately from those with two jets. Algorithms to identify  $b$  jets provide several levels of purity for each jet, and

this serves as another dimension along which to classify events. The quality and the type of the identified lepton also serves to classify events. An event with an isolated, high- $p_T$  track is analyzed as if that track were a lepton, but such events are collected together in different sub-channels. The signals in such categories come from leptons which the detectors failed to reconstruct as leptons, and hadrons from  $\tau$  lepton decay. The instrumental (“fake-lepton”) backgrounds are higher for these selections, and so samples with well-identified leptons are kept separate from the isolated-track samples.

The  $ZH \rightarrow \nu\bar{\nu} b\bar{b}$  searches [86–89] seek events in which no lepton or high- $p_T$  isolated track is found. These searches also accept signals from  $WH \rightarrow \ell\nu b\bar{b}$  in which the charged lepton is either not identified or falls outside the detector acceptances. Similar  $b$ -tagging categorization is applied to these searches. The  $ZH \rightarrow \ell^+\ell^- b\bar{b}$  searches [90–93] seek leptonic decays of the  $Z$  boson. These events benefit from the absence of neutrinos, and so missing transverse energy can be interpreted as jet energy mismeasurement, and the jet energies are corrected accordingly, improving the dijet mass resolution. CDF searches for associated production and VBF in the all-hadronic mode, in which the  $W$  or the  $Z$  decays hadronically, and the  $H$  decays to  $b\bar{b}$  [94,95].

A cross check of the procedures for searching for the SM Higgs boson in the  $WH, ZH \rightarrow b\bar{b}$  channels, their background estimates, and combination procedures, is provided by measurements of  $WZ + ZZ$  production in  $b$ -tagged final states [96,97], and their combination [98]. In these analyses, the decay  $Z \rightarrow b\bar{b}$  mimics the decay  $H \rightarrow b\bar{b}$ , and  $WW$  production is considered a background. The measured cross section is consistent with the SM expectations, giving confidence in the Higgs boson search procedures.

Both Tevatron experiments also search for  $H \rightarrow \tau^+\tau^-$  in events with one or more associated jets [99–102]. As the di-tau mass resolution is poor due to the presence of unmeasured neutrinos, the  $Z \rightarrow \tau^+\tau^-$  background is large in the absence of the requirement of one or more additional jets, which purifies the sample in associated production and VBF. The process  $gg \rightarrow H$  is considered as well, although the uncertainties on  $gg \rightarrow H + \text{jets}$  are larger than the inclusive uncertainties.

The decay mode  $H \rightarrow \gamma\gamma$  is searched for by both Tevatron collaborations [103–106]. Prompt diphoton production,  $\pi^0 \rightarrow \gamma\gamma$ , and fake photons are the main backgrounds. The backgrounds have a smoothly varying shape as a function of  $m_{\gamma\gamma}$ , while the signal mass resolution is of order 3%. All Higgs boson production mechanisms are considered, but the signal-to-background ratio at the Tevatron is not sufficient for this channel to contribute significantly to the SM search. Nonetheless, the searches for  $H \rightarrow \gamma\gamma$  provide powerful tests of models with enhanced  $\text{BR}(H \rightarrow \gamma\gamma)$ , described later.

Another process searched for at the Tevatron is  $t\bar{t}H$  production with  $H \rightarrow b\bar{b}$  [107,108]. The backgrounds in this channel are low and are dominated by  $t\bar{t}b\bar{b}$ , but the low signal



See key on page 457

## Gauge & Higgs Boson Particle Listings

### Higgs Bosons — $H^0$ and $H^\pm$

production rate and combinatoric ambiguity in assigning jets to the Higgs boson decay reduces the sensitivity.

For Higgs boson masses above 130 GeV, the searches for  $H \rightarrow W^+W^- \rightarrow \ell^+\nu\ell^-\bar{\nu}$  [109–114] are the most sensitive. The candidate mass cannot be fully reconstructed in these events due to the presence of two neutrinos, but the lepton angles are correlated due to the scalar nature of the Higgs boson and the  $V - A W\ell\nu$  coupling. The process  $W^\pm H \rightarrow W^\pm W^+ W^-$  gives rise to like-sign dilepton and trilepton final states which have very low backgrounds [110,115]. CDF also seeks  $H \rightarrow ZZ \rightarrow \ell^+\ell^-\ell^+\ell^-$  [116] where  $\ell = e$  or  $\mu$ . The excellent mass resolution and low backgrounds help the sensitivity of the search, but low decay branching ratio for  $Z \rightarrow \ell^+\ell^-$  reduces the sensitivity.

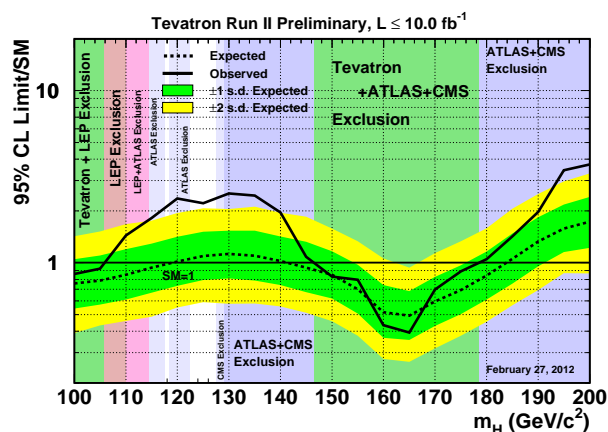


**Figure 6:** Observed and expected 95% C.L. upper limits on the ratios to the SM cross section, as functions of the Higgs boson mass for the combined CDF and D0 analyses [6]. The limits are expressed as a multiple of the SM prediction. The bands indicate the 68% and 95% probability regions where the limits can fluctuate, in the absence of signal. Also shown are the regions excluded by LEP, ATLAS, and CMS.

All of the searches for the SM Higgs boson at the Tevatron are combined together for maximum sensitivity [6,117,118]. The Tevatron combination excludes two ranges in  $m_H$ : between 100 GeV and 106 GeV, and between 147 GeV and 179 GeV. An excess of data is seen in the mass range  $115 \text{ GeV} < m_H < 135 \text{ GeV}$ , as shown in Fig. 6, with a maximum local significance of 2.7 standard deviations ( $\sigma$ ), at  $m_H = 120 \text{ GeV}$ , where the expected local significance for a SM Higgs signal is 2.0  $\sigma$ . When corrected for the look-elsewhere effect (LEE) [119], which accounts for the possibility of selecting the strongest of the several random excess which may happen in the range  $115 \text{ GeV} < m_H < 200 \text{ GeV}$ , the global significance of the

excess is 2.2 standard deviations<sup>3</sup>. The majority of the excess is contributed by the searches for  $H \rightarrow b\bar{b}$ . The best-fit cross section for Higgs boson production, normalized to the SM production rate, and assuming SM decay branching ratios and SM ratios between the production mechanisms, is shown in Fig. 7.

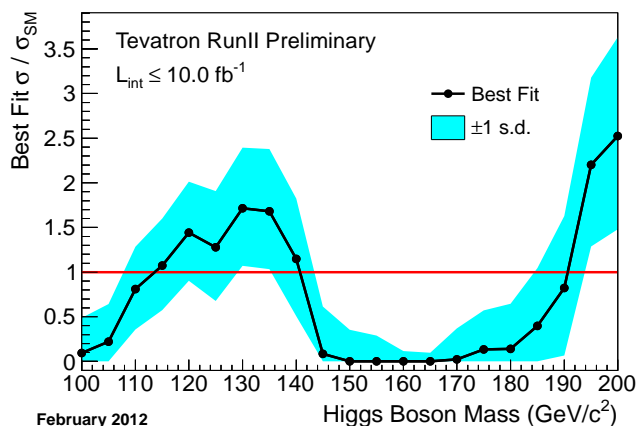


**Figure 7:** Best-fit cross section for the SM Higgs boson from the combined CDF and D0 searches, normalized to the SM production rates, assuming SM decay branching ratios and the SM ratio between the various production mechanisms [6]. The shaded region shows the 68% C.L. interval, as a function of the mass of the Higgs boson considered. In this fit, negative signal cross sections are not considered.

The channels used at the Tevatron for Higgs boson masses below 130 GeV are different from those dominantly used at the LHC, and thus provide complementary information on the couplings of the Higgs boson to gauge bosons and to  $b$  quarks.

#### II.4. SM Higgs Boson Searches at the LHC

At the LHC, the main production processes are the same as those at the Tevatron, but with a different order of importance: gluon fusion ( $gg \rightarrow H$ ), vector boson fusion ( $qqH$  or  $q\bar{q}H$ ) and Higgs boson production in association with a vector boson ( $W^\pm H$  or  $ZH$ ) or with a top-quark pair ( $t\bar{t}H$ ).

The higher center-of-mass energy of 7 TeV (8 TeV in 2012) and the fact that both beams consist of protons has a strong impact on the parton luminosities. The LHC experiments are sensitive to Higgs bosons with much higher masses than the Tevatron experiments. The  $gg$  luminosity is also enhanced at the LHC by the beam energy due to the large gluon PDF at lower parton momentum fraction  $x$  compared to that at higher  $x$ .

A variety of search channels are pursued by the LHC collaborations, ATLAS and CMS, with the channels' relative importances changing due to the branching ratios of the SM Higgs

<sup>3</sup> In this Review, we use the phrase “local significance” to indicate a calculation of the significance not corrected for the LEE.

# Gauge & Higgs Boson Particle Listings

## Higgs Bosons — $H^0$ and $H^\pm$

boson as functions of  $m_H$ . At low masses,  $m_H < 120$  GeV, searches for  $H \rightarrow \gamma\gamma$  provide the highest sensitivity, with searches for  $H \rightarrow b\bar{b}$  and  $H \rightarrow \tau^+\tau^-$  contributing as well. For higher masses,  $120 \text{ GeV} < m_H < 200 \text{ GeV}$ , searches for  $H \rightarrow W^+W^- \rightarrow \ell^+\nu\ell^-\nu$  are the most sensitive, with an important contribution from  $H \rightarrow ZZ \rightarrow \ell^+\ell^-\ell^+\ell^-$  between 120 GeV and 150 GeV. At even higher masses, up to  $m_H = 600$  GeV, the  $H \rightarrow ZZ$  searches are the most sensitive.

Both LHC collaborations seek  $H \rightarrow W^+W^- \rightarrow \ell^+\nu\ell^-\nu$  production [120–122]. This channel provides high sensitivity for Higgs boson masses for which  $\text{BR}(H \rightarrow W^+W^-)$  is large,  $m_H > 135$  GeV. The main SM background, nonresonant  $W^+W^-$  production, is initiated primarily by  $q\bar{q}$  and thus the signal to background ratio benefits at the LHC because of the initial state. The first LHC exclusion of Higgs boson masses was obtained in this search mode. CMS also contributes a search in the mode  $W^\pm H \rightarrow W^\pm W^+W^-$  [123] in the trilepton final state. For ATLAS, the fully leptonic decay mode is supplemented with an  $H \rightarrow W^+W^- \rightarrow \ell\nu jj$  search [124].

At higher masses,  $m_H > 180$  GeV, ATLAS and CMS analyses seeking  $H \rightarrow ZZ$  with  $ZZ \rightarrow \ell^+\ell^-\ell^+\ell^-$  [125,126],  $ZZ \rightarrow \ell^+\ell^-\nu\bar{\nu}$  [127,128],  $ZZ \rightarrow \ell^+\ell^-q\bar{q}$  [129,130], and  $ZZ \rightarrow \ell^+\ell^-\tau^+\tau^-$  [131] become the most sensitive. A small excess of events in the ATLAS  $\ell^+\ell^-\ell^+\ell^-$  channel with reconstructed masses near 125 GeV is seen, with a local significance of  $\approx 2$  sigma. An excess with similar significance is seen in the CMS  $H \rightarrow ZZ \rightarrow 4$  leptons searches at  $\sim 119$  GeV.

ATLAS and CMS seek the process  $H \rightarrow \gamma\gamma$  including the four production mechanisms,  $gg \rightarrow H$ , production in association with a  $W$  or  $Z$  boson, and VBF [132–134]. Events are divided into categories depending on the reconstructed photon type (barrel calorimeter or endcap), and the presence or absence of additional jets. The reconstructed mass resolution of the selected candidates varies between 1% and 3% depending on the event category and detector. ATLAS observes an excess of events with a local significance of  $2.8\sigma$  which is maximized at  $m_H=126.5$  GeV, while CMS observes an excess of events with a local significance of  $2.9\sigma$  which is maximized at  $m_H=124$  GeV. ATLAS computes the global significance, accounting for the probability of a background fluctuation anywhere in the range  $110 \text{ GeV} < m_H < 150 \text{ GeV}$  at least as significant as the observed excess, to be  $1.5\sigma$ . CMS's global significance is  $1.6\sigma$  using the same range of  $m_H$ .

ATLAS and CMS seek Higgs bosons produced in association with a leptonically decaying vector boson and which decay into  $b\bar{b}$  [135,136]. Although these searches benefit from the higher production cross sections at the LHC as compared to the Tevatron, the background cross sections are relatively larger, as a larger fraction of  $W$  and  $Z$  bosons at the LHC are produced with accompanying jets, some of which contain heavy hadrons. The sensitivity of the searches is maximized by tagging jets containing  $B$  hadrons and using MVAs to separate the expected signals from the backgrounds. The achieved sensitivity, in units of the SM production rate, expressed as the 95% exclusion limit

expected in the absence of a signal, varies in the range  $110 \text{ GeV} < m_H < 135 \text{ GeV}$  between 2.6 to 5.1 for ATLAS and between 2.7 to 6.7 for CMS. These results are both with  $4.7 \text{ fb}^{-1}$  of analyzed data. With more data and improved analyses, the LHC will be able to measure the important decay branching ratio to  $b\bar{b}$ , where currently the Tevatron contributes the most.

Both ATLAS and CMS seek SM Higgs boson decays to  $\tau^+\tau^-$  [137–139]. The selected events in these searches are categorized by the number of associated jets, which differentiates signals produced by  $gg \rightarrow H$ , associated production, and VBF from the backgrounds, which are dominated by  $Z \rightarrow \tau^+\tau^-$ . The reconstructed di-tau masses are used as the discriminating variables. If the tau pair has a net transverse boost, then the missing transverse energy can be projected unambiguously on the directions of the two tau leptons, and the reconstructed mass resolution is much better than in the case of little transverse boost, in which case the degree to which the neutrino momenta cancel each other is unknown. With  $4.7 \text{ fb}^{-1}$  of data, ATLAS's expected 95% C.L. limit varies between 3.2 and 7.9 times the SM rate for Higgs bosons with  $100 \text{ GeV} < m_H < 150 \text{ GeV}$ , and with  $4.6 \text{ fb}^{-1}$  of data, CMS's expected limits vary between 3.3 and 5.5 times the SM prediction for  $110 \text{ GeV} < m_H < 145 \text{ GeV}$ . CMS also searches for  $WH \rightarrow W\tau^+\tau^-$  [140] with a 95% C.L. sensitivity between 5 and 15 times the SM prediction in the range  $100 \text{ GeV} < m_H < 140 \text{ GeV}$  using  $4.7 \text{ fb}^{-1}$  of data.

Both ATLAS and CMS have combined their SM Higgs boson searches [7–10]. The most recent combination of ATLAS includes the full suite of channels mentioned above. As shown in Fig. 8, ATLAS excludes at the 95% C.L. the mass ranges  $110.0 \text{ GeV} < m_H < 117.5 \text{ GeV}$ ,  $118.5 \text{ GeV} < m_H < 122.5 \text{ GeV}$ , and  $129 \text{ GeV} < m_H < 539 \text{ GeV}$ , and expects to exclude, in the absence of a signal,  $120 \text{ GeV} < m_H < 555 \text{ GeV}$ . ATLAS's local  $p$ -values [79], computed with the likelihood ratio test statistic, are shown as functions of the tested  $m_H$  in Fig. 9. The local significance is maximal at  $m_H = 126$  GeV, with a value of  $2.9\sigma$ . The global significance is  $1.3\sigma$  when the interval considered for the LEE correction is  $110 \text{ GeV} < m_H < 146 \text{ GeV}$ , and becomes  $0.5\sigma$  for the interval  $110 \text{ GeV} < m_H < 600 \text{ GeV}$ . The best-fit production cross section as a multiple of the SM prediction is shown in Fig. 10. The excesses seen in the  $H \rightarrow \gamma\gamma$  and  $H \rightarrow ZZ \rightarrow \ell^+\ell^-\ell^+\ell^-$  searches are somewhat offset by a more background-like outcome in the  $H \rightarrow W^+W^-$  searches.

The most recent combination of CMS includes the full suite of channels mentioned above. As shown in Fig. 11, CMS excludes at the 95% C.L. the mass range  $127.5 \text{ GeV} < m_H < 600 \text{ GeV}$ , and expects to exclude  $114.5 \text{ GeV} < m_H < 525 \text{ GeV}$  in the absence of a signal. CMS's local  $p$ -values [79], computed using the likelihood ratio test statistic, are shown as functions of the tested  $m_H$  in Fig. 12. The local significance is maximal at  $m_H = 125$  GeV, with a value of  $2.8\sigma$ . The global significance becomes  $2.1\sigma$  ( $0.8\sigma$ ) after correcting for LEE in the range  $110 \text{ GeV} < m_H < 145 \text{ GeV}$  ( $110 \text{ GeV} < m_H < 600 \text{ GeV}$ ). The best-fit production cross section CMS measures as a multiple of the SM prediction is shown in Fig. 13. A signal-like excess

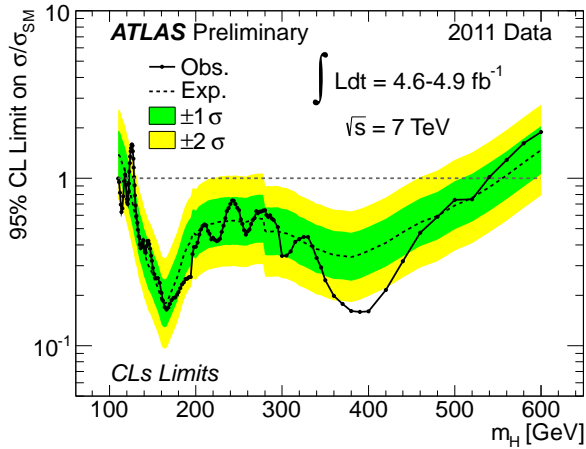


**Figure 8:** Observed and expected 95% C.L. upper limits on the ratios to the SM cross section, as functions of the Higgs boson mass for the combined ATLAS analyses [8].

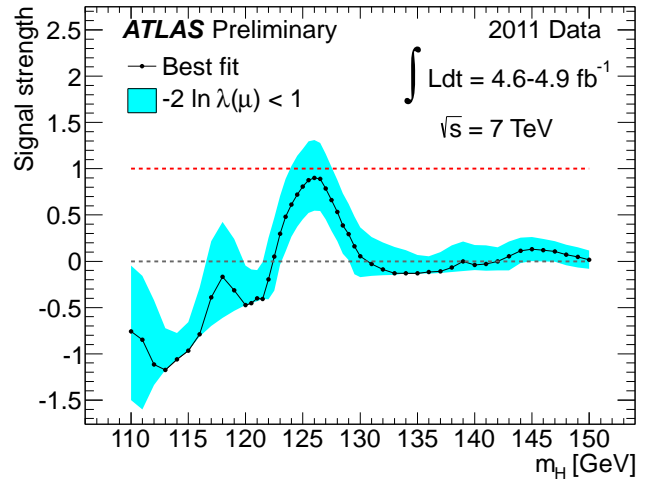


**Figure 10:** ATLAS SM best-fit cross sections [8].

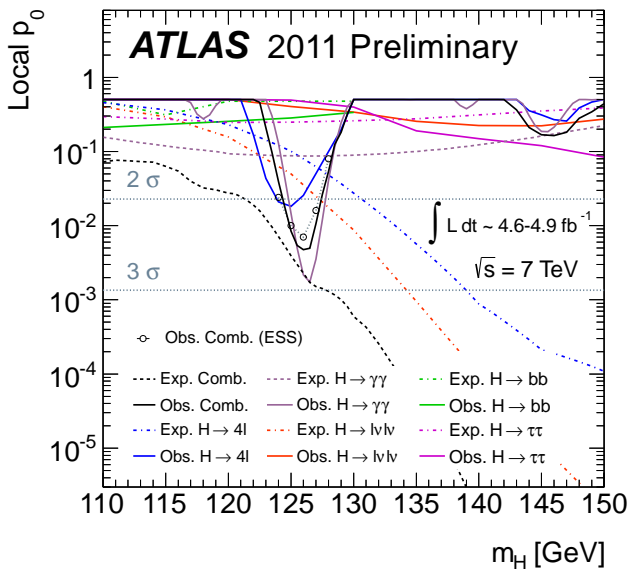


**Figure 9:** Local  $p$ -values for each of ATLAS's SM Higgs boson search channels and the combination [8]. The observed  $p$ -values are shown with solid curves, and the median expected  $p$ -values assuming a signal is present at the SM strength are shown with dashed and dot-dashed curves. Dotted lines indicate the  $2\sigma$  and  $3\sigma$  thresholds. Hollow circles indicate  $p$ -values computed with ensemble tests taking into account energy scale systematic uncertainties (ESS).

is seen in the  $H \rightarrow \gamma\gamma$  and  $H \rightarrow W^+W^-$  searches, but the outcome in the  $H \rightarrow ZZ$  search is less signal-like at  $m_H = 125 \text{ GeV}$ .

In summary, beyond the region excluded by LEP, the region excluded at 95% C.L. by both ATLAS and CMS extends from

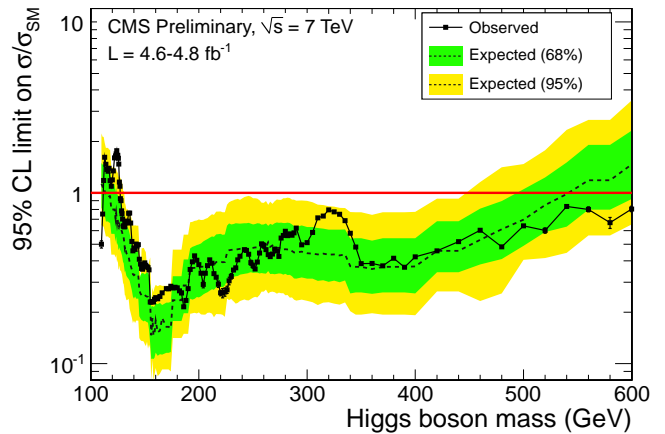


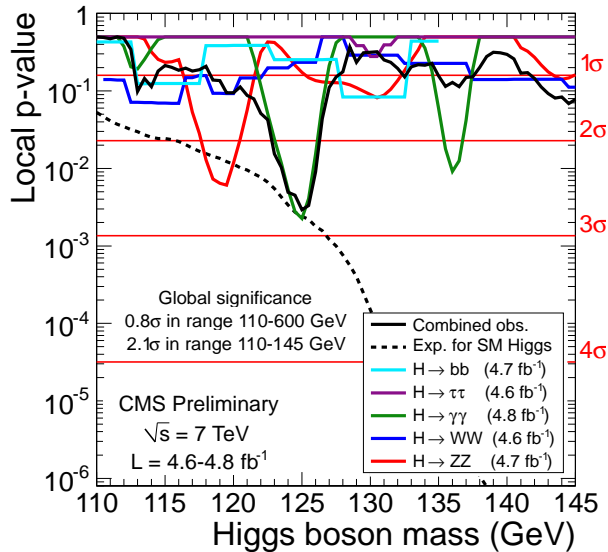
**Figure 11:** Observed and expected 95% C.L. upper limits on the ratios to the SM cross section, as functions of the Higgs boson mass for the combined CMS analyses [10].

129 GeV to 539 GeV. The observed and expected limits from the two LHC collaborations and the Tevatron are listed in Table 1 for the main channels and the combinations searching for the SM Higgs boson with  $m_H = 125 \text{ GeV}$ . The best-fit cross section is close to the SM prediction at the  $m_H$  corresponding to the most significant  $p$ -value for both LHC experiments. The data samples are not yet large enough to make a significant statement about the balance between the individual channels.

If a SM Higgs boson is discovered, its properties will be studied at the LHC. The decay branching ratios, and more generally, the couplings of the Higgs bosons to fermions and gauge bosons will be constrained by the measurements of the cross sections times branching ratios for the processes searched for above.

The mass of the Higgs boson will be measured by each LHC experiment with a precision of  $\sim 0.1\%$ , limited by the energy

## Gauge &amp; Higgs Boson Particle Listings

Higgs Bosons —  $H^0$  and  $H^\pm$ 

**Figure 12:** Local  $p$ -values for each of CMS's SM Higgs boson search channels and the combination [10]. The observed  $p$ -values are shown with solid curves, and the median expected  $p$ -value for the combined search assuming a signal is present at the SM strength is shown with a dashed curve. Horizontal lines indicate the  $1\sigma$ ,  $2\sigma$ ,  $3\sigma$ , and  $4\sigma$  thresholds.

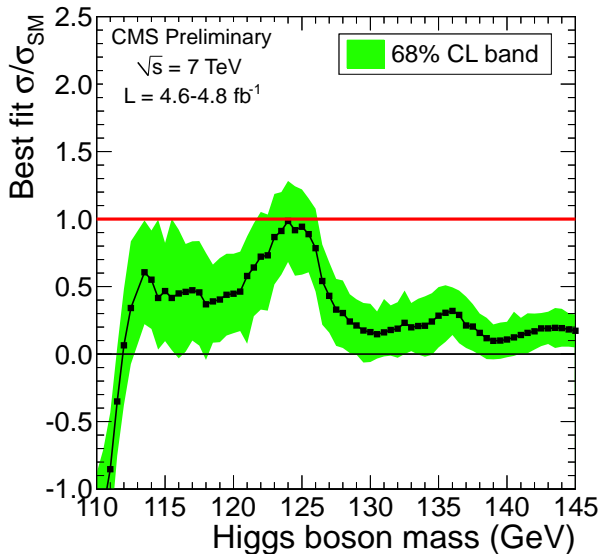


**Figure 13:** CMS SM best-fit cross sections [10].

scale, in the currently allowed low mass range [141,142]. This projection is based on the invariant mass reconstruction from electromagnetic calorimeter objects, using the decays  $H \rightarrow \gamma\gamma$  or  $H \rightarrow ZZ^* \rightarrow 4\ell$ . The precision would be degraded at higher masses because of the larger decay width, but even at  $m_H \sim 700$  GeV a precision of 1% on  $m_H$  is expected to be achievable. The width of the SM Higgs boson may be too narrow to be

**Table 1:** Observed and expected limits at the 95% C.L. normalized to the SM predictions for the main search channels at the Tevatron and the LHC, evaluated for  $m_H = 125$  GeV

Channel	Obs	Exp	Lumi [ $\text{fb}^{-1}$ ]	Ref.
<b>Tevatron</b>				
$H \rightarrow W^+W^-$	2.4	2.2	9.7	[6]
$H \rightarrow b\bar{b}$	3.2	1.4	9.7	[6]
Combined	2.2	1.1	10.0	[6]
<b>ATLAS</b>				
$H \rightarrow \gamma\gamma$ (MVA)	3.5	1.6	4.9	[132]
$H \rightarrow W^+W^- \rightarrow \ell^+\nu\ell^-\bar{\nu}$	1.4	1.2	4.7	[121]
$H \rightarrow ZZ \rightarrow \ell^+\ell^-\ell^+\ell^-$	4.2	2.4	4.8	[125]
Combined	1.5	0.8	4.9	[8]
<b>CMS</b>				
$H \rightarrow \gamma\gamma$ (MVA)	2.9	1.2	4.8	[134]
$H \rightarrow W^+W^- \rightarrow \ell^+\nu\ell^-\bar{\nu}$	1.5	1.1	4.6	[122]
$H \rightarrow ZZ \rightarrow \ell^+\ell^-\ell^+\ell^-$	2.5	1.6	4.7	[126]
Combined	1.6	0.7	4.8	[10]

measured directly. The width could be constrained indirectly using partial width measurements [143,144]. For  $300 < m_H < 700$  GeV, a direct measurement of the decay width of an SM-like Higgs boson could be performed with a precision of about 6%.

The possibilities for measuring other properties of the Higgs boson, such as its spin, its  $CP$  eigenvalue, its couplings to bosons and fermions, and its self-coupling, have been investigated in numerous studies [141,142,145–148]. Given a sufficiently high integrated luminosity ( $300 \text{ fb}^{-1}$ ), most of these properties are expected to be accessible to analysis in the favored mass range  $114 \text{ GeV} < m_H < 129 \text{ GeV}$ . The measurement of Higgs self-couplings, however, may suffer from poor sensitivity at the LHC, although a luminosity upgrade, the so-called Super-LHC, could allow for a more precise measurement. The results of these measurements could either establish the presence of a SM-like Higgs boson or point the way to new physics.

## II.5 Models with a Fourth Generation of SM-Like Fermions

The SM Higgs boson production processes and branching ratios presented above are limited to the case of three generations of quarks and leptons. The existence of a fourth generation of fermions is compatible with present experimental bounds and would have direct consequences on the SM Higgs boson production and decay branching ratios [149], and hence on Higgs boson searches at LEP, the Tevatron, and the LHC [150,151]. Current experimental searches bound the fourth generation quark masses to be above the top quark mass [152]. These additional heavy quarks lead to new contributions in the loop-induced couplings of the Higgs boson to gluons and to photons.

See key on page 457

## Gauge & Higgs Boson Particle Listings

### Higgs Bosons — $H^0$ and $H^\pm$

In particular, they lead to a strong enhancement of the gluon fusion production rate and of the branching ratio of the Higgs boson decay into a pair of gluons. As a result, the branching ratios of Higgs boson decay to  $b\bar{b}$ , tau pairs, and pairs of  $W$  and  $Z$  bosons are reduced, although near  $m_H \sim 2M_W$ , the decay to a pair of  $W$  bosons still nearly saturates the decay width, even with the enhanced gluon decay. Due to a cancellation between the  $W$  and heavy fermion contributions, the photon decay channels may be further suppressed. The enhancement of the gluon fusion production rate makes the search channels using Higgs boson decays into tau leptons and  $W$  and  $Z$  bosons promising for a light Higgs boson. In addition, in the case of a fourth generation Majorana neutrino, exotic signals such as Higgs boson decay into same-sign dileptons may be possible. Interpretations of the experimental searches optimized for a minimal fourth-generation model (SM4) are available from the Tevatron [153] and CMS [10]. CMS excludes the Higgs boson in the SM4 model in the mass range  $120 \text{ GeV} < m_H < 600 \text{ GeV}$  at the 95% C.L.

### III. Higgs Bosons in the Minimal Supersymmetric Standard Model (MSSM)

Electroweak symmetry breaking driven by a weakly-coupled elementary scalar sector requires a mechanism to explain the smallness of the breaking scale compared with the Planck scale [154]. In addition, within supersymmetric extensions of the SM, the supersymmetry-breaking effects, whose origins may lie at energy scales much larger than 1 TeV, can induce a radiative breaking of the electroweak symmetry due to the effects of the large Higgs-top quark Yukawa coupling [155]. In this way, the electroweak symmetry breaking scale is intimately tied to the scale of supersymmetry breaking masses. Supersymmetry provides an explanation for the stability of the hierarchy of scales, provided that the supersymmetry-breaking masses, in particular those related to the stop sector, are at most in the TeV range [154].

A fundamental theory of supersymmetry breaking is unknown at this time. Nevertheless, one can parameterize the low-energy theory in terms of the most general set of soft supersymmetry-breaking renormalizable operators [156]. The Minimal Supersymmetric extension of the Standard Model (MSSM) [12,157] associates a supersymmetric partner to each gauge boson and chiral fermion of the SM, and provides a realistic model of physics at the weak scale. However, even in this minimal model with the most general set of soft supersymmetry-breaking terms, more than 100 new parameters are introduced [158]. Fortunately, only a subset of these parameters impact the Higgs phenomenology through tree-level and quantum effects. Reviews of the properties and phenomenology of the Higgs bosons of the MSSM can be found for example in Refs. [44] and [159].

The MSSM contains the particle spectrum of a two-Higgs-doublet model (2HDM) extension of the SM and the corresponding supersymmetric partners. Two Higgs doublets,  $H_u$

and  $H_d$ , are required to ensure an anomaly-free SUSY extension of the SM and to generate mass for both “up”-type and “down”-type quarks and charged leptons [13]. After the spontaneous breaking of the electroweak symmetry, five physical Higgs particles are left in the spectrum: one charged Higgs pair,  $H^\pm$ , one  $CP$ -odd scalar,  $A$ , and two  $CP$ -even states,  $H$  and  $h$ .

The supersymmetric structure of the theory imposes constraints on the Higgs sector of the model. In particular, the parameters of the Higgs self-interaction are given by the gauge coupling constants. As a result, all Higgs sector parameters at tree level are determined by only two free parameters: the ratio of the  $H_u$  and  $H_d$  vacuum expectation values,  $\tan\beta = v_u/v_d$ , with  $v_u^2 + v_d^2 \approx (246 \text{ GeV})^2$ ; and one Higgs boson mass, conventionally chosen to be  $m_A$ . The other tree-level Higgs boson masses are then given in terms of these parameters

$$m_{H^\pm}^2 = m_A^2 + M_W^2$$

$$m_{H,h}^2 = \frac{1}{2} \left[ m_A^2 + M_Z^2 \pm \sqrt{(m_A^2 + M_Z^2)^2 - 4(M_Z m_A \cos 2\beta)^2} \right]$$

and  $\alpha$  is the angle that diagonalizes the  $CP$ -even Higgs squared-mass matrix. An important consequence of these mass formulae is that the mass of the lightest  $CP$ -even Higgs boson is bounded from above:

$$m_h \leq M_Z |\cos 2\beta|.$$

This contrasts sharply with the SM, in which the Higgs boson mass is bounded from above only by perturbativity and unitarity considerations. In the large  $m_A$  limit, also called the decoupling limit [160], one finds  $m_h^2 \simeq (M_Z \cos 2\beta)^2$  and  $m_A \simeq m_H \simeq m_{H^\pm}$ , up to corrections of  $\mathcal{O}(M_Z^2/m_A)$ . Below the scale  $m_A$ , the Higgs sector of the effective low-energy theory consists only of  $h$ , which behaves as the SM Higgs boson.

The phenomenology of the Higgs sector depends on the couplings of the Higgs bosons to gauge bosons, and fermions. The couplings of the two  $CP$ -even Higgs bosons to  $W^\pm$  and  $Z$  bosons are given in terms of the angles  $\alpha$  and  $\beta$  by

$$g_{hVV} = g_V m_V \sin(\beta - \alpha) \quad g_{HVV} = g_V m_V \cos(\beta - \alpha),$$

where  $g_V \equiv 2m_V/v$ . There are no tree-level couplings of  $A$  or  $H^\pm$  to  $VV$ . The couplings of the  $Z$  boson to two neutral Higgs bosons, which must have opposite  $CP$ -quantum numbers, are given by

$$g_{hAZ} = g_Z \cos(\beta - \alpha)/2 \quad g_{HAZ} = -g_Z \sin(\beta - \alpha)/2.$$

Charged Higgs- $W$  boson couplings to neutral Higgs bosons and four-point couplings of vector bosons and Higgs bosons can be found in Ref. 13.

The tree-level Higgs couplings to fermions obey the following property: the neutral components of one Higgs doublet couple exclusively to down-type fermion pairs while the neutral components of the other doublet couple exclusively to up-type fermion pairs [13,161]. This Higgs-fermion coupling structure defines the Type-II 2HDM [162], and differs from

# Gauge & Higgs Boson Particle Listings

## Higgs Bosons — $H^0$ and $H^\pm$

Type-I 2HDM [163] in which one Higgs field couples to all fermions while the other field is decoupled from them. In the MSSM, fermion masses are generated when both neutral Higgs components acquire vacuum expectation values, and the relations between Yukawa couplings and fermion masses are (in third-generation notation)

$$h_b = \sqrt{2} m_b / v_d = \sqrt{2} m_b / (v \cos \beta)$$

$$h_t = \sqrt{2} m_t / v_u = \sqrt{2} m_t / (v \sin \beta).$$

Similarly, one can define the Yukawa coupling of the Higgs boson to  $\tau$ -leptons (the latter is a down-type fermion).

The couplings of the neutral Higgs bosons to  $f\bar{f}$  relative to the SM value,  $gm_f/2M_W$ , are given by

$$h\bar{b}b: \quad -\sin \alpha / \cos \beta = \sin(\beta - \alpha) - \tan \beta \cos(\beta - \alpha),$$

$$ht\bar{t}: \quad \cos \alpha / \sin \beta = \sin(\beta - \alpha) + \cot \beta \cos(\beta - \alpha),$$

$$H\bar{b}b: \quad \cos \alpha / \cos \beta = \cos(\beta - \alpha) + \tan \beta \sin(\beta - \alpha),$$

$$Ht\bar{t}: \quad \sin \alpha / \sin \beta = \cos(\beta - \alpha) - \cot \beta \sin(\beta - \alpha),$$

$$A\bar{b}b: \quad \gamma_5 \tan \beta, \quad At\bar{t}: \quad \gamma_5 \cot \beta,$$

where the  $\gamma_5$  indicates a pseudoscalar coupling. In each relation above, the factor listed for  $b\bar{b}$  also pertains to  $\tau^+\tau^-$ . The charged Higgs boson couplings to fermion pairs are given by

$$g_{H^-t\bar{b}} = \frac{g}{\sqrt{2}M_W} [m_t \cot \beta P_R + m_b \tan \beta P_L],$$

$$g_{H^- \tau^+ \nu} = \frac{g}{\sqrt{2}M_W} [m_\tau \tan \beta P_L],$$

with  $P_{L,R} = (1 \mp \gamma_5)/2$ .

The Higgs couplings to down-type fermions can be significantly enhanced at large  $\tan \beta$  in the following two cases: (i) If  $m_A \gg M_Z$ , then  $|\cos(\beta - \alpha)| \ll 1$ ,  $m_H \simeq m_A$ , and the  $b\bar{b}H$  and  $b\bar{b}A$  couplings have equal strength and are significantly enhanced by a factor of  $\tan \beta$  relative to the corresponding SM coupling, whereas the  $VVH$  coupling is negligibly small. The values of the  $VVh$  and  $b\bar{b}h$  couplings are equal to the corresponding couplings of the SM Higgs boson. (ii) If  $m_A < M_Z$  and  $\tan \beta \gg 1$ , then  $|\cos(\beta - \alpha)| \approx 1$  and  $m_h \simeq m_A$ . In this case, the  $b\bar{b}h$  and  $b\bar{b}A$  couplings have equal strength and are significantly enhanced by a factor of  $\tan \beta$  relative to the corresponding SM coupling, while the  $VVh$  coupling is negligibly small. In addition, the  $VVH$  coupling is equal in strength to the corresponding SM  $VVH$  coupling and one can refer to  $H$  as a SM-like Higgs boson. The value of the  $b\bar{b}H$  coupling can differ from the corresponding SM coupling and converges to it only for  $m_A \ll M_Z$  for which  $\tan \beta \sin(\beta - \alpha) \rightarrow 0$ . Note that in both cases (i) and (ii) above, only two of the three neutral Higgs bosons have significantly enhanced couplings to  $b\bar{b}$ .

### III.1. Radiatively-Corrected MSSM Higgs Masses and Couplings

Radiative corrections have a significant impact on the values of Higgs boson masses and couplings in the MSSM. Important

contributions come from loops of third generation SM particles as well as their supersymmetric partners. The dominant effects to the Higgs mass arise from the incomplete cancellation between top and scalar-top (stop) loops and at large  $\tan \beta$  also from sbottom and stau loops. The stop, sbottom and stau masses and mixing angles depend on the supersymmetric Higgsino mass parameter  $\mu$  and on the soft-supersymmetry-breaking parameters [12,157]:  $M_Q, M_U, M_D, M_L, M_E$ , and  $A_t, A_b, A_\tau$ . The first three of these are the left-chiral and the two right-chiral top and bottom scalar quark mass parameters. The next two are the left-chiral stau/sneutrino and the right-chiral stau mass parameters, and the last three are the trilinear parameters that enter in the off-diagonal squark/slepton mixing elements:  $X_t \equiv A_t - \mu \cot \beta$  and  $X_{b,\tau} \equiv A_{b,\tau} - \mu \tan \beta$ . The corrections affecting the Higgs boson masses, production, and decay properties depend on all of these parameters in various ways. At the two-loop level, also the masses of the gluino and the electroweak gaugino enter in the calculations. For simplicity, we shall initially assume that  $A_t, A_b, A_\tau, \mu$ , and the gluino and electroweak gaugino masses are real parameters. The impact of complex phases on MSSM parameters, which will induce  $CP$ -violation in the Higgs sector, is addressed below.

Radiative corrections to the Higgs boson masses have been computed using a number of techniques, with a variety of approximations; see Refs. [165–176]. They depend strongly on the top quark mass ( $\sim m_t^4$ ) and the stop mixing parameter  $X_t$ , and there is also a logarithmic dependence on the stop masses. One of the most striking effects is the increase of the upper bound of the light  $CP$ -even Higgs boson mass, as first noted in Refs. [165,166]. The value of  $m_h$  is maximized for large  $m_A \gg M_Z$ , when all other MSSM parameters are fixed. Moreover,  $\tan \beta \gg 1$  also maximizes  $m_h$ , when all other parameters are held fixed. Taking  $m_A$  large (the decoupling limit) and  $\tan \beta \gg 1$ , the value of  $m_h$  can be further maximized at one-loop level for  $X_t \simeq \sqrt{6} M_{\text{SUSY}}$ , where  $M_{\text{SUSY}} \simeq M_Q \simeq M_U \simeq M_D$  is an assumed common value of the soft SUSY-breaking squark mass parameters. This choice of  $X_t$  is called the “maximal-mixing scenario” which will be indicated by  $m_h$ -max. Instead, for  $X_t = 0$ , which is called the “no-mixing scenario,” the value of  $m_h$  has its lowest possible value, for fixed  $m_A$  and all other MSSM parameters. The value of  $m_h$  also depends on the specific value of  $M_{\text{SUSY}}$ , and, for example, raising  $M_{\text{SUSY}}$  from 1 TeV to 2 TeV can increase  $m_h$  by 2–5 GeV. Variation of the value of  $m_t$  by 1 GeV changes the value of  $m_h$  by about the same amount. As mentioned above,  $m_h$  also depends on  $\mu$  and more weakly on the electroweak gaugino mass as well as the gluino mass at the two-loop level. For any given scenario defined by a full set of MSSM parameters, we will denote the maximum value of  $m_h$  by  $m_h^{\text{max}}(\tan \beta)$ , for each value of  $\tan \beta$ . Allowing for the experimental uncertainty on  $m_t$  and for the uncertainty inherent in the theoretical analysis, one finds for  $M_{\text{SUSY}} \lesssim 2$  TeV, large  $m_A$  and  $\tan \beta \gg 1$ ,  $m_h^{\text{max}} = 135$  GeV in the  $m_h$ -max scenario, and  $m_h^{\text{max}} = 122$  GeV in the no-mixing scenario [177,178]. In

See key on page 457

## Gauge & Higgs Boson Particle Listings

### Higgs Bosons — $H^0$ and $H^\pm$

practice, parameter values leading to maximal mixing are not obtained in most models of supersymmetry breaking, so typical upper limits on  $m_h$  will lie between these two extremes [179]. In the large  $\tan\beta$  regime light staus and/or sbottoms with sizable mixing, governed by the  $\mu$  parameter, yield negative radiative corrections to the mass of the lightest Higgs boson, and can lower it by several GeV [173,180]. Hence, if the Higgs boson were to have a mass of about 125 GeV, a sizable mixing in the stop sector would be required [180,181] ( $X_t \geq 1.5M_{\text{SUSY}}$ , or even larger if  $\tan\beta$  is large). The relatively small mass of the lightest neutral scalar boson is a prediction for both the  $CP$ -conserving ( $CPC$ ) and  $CP$ -violating ( $CPV$ ) [182] MSSM scenarios. This is particularly interesting in the light of the intriguing excesses observed at the Tevatron and the LHC and given that masses above 130 GeV are strongly disfavored by LHC data.

Radiative corrections also modify significantly the values of the Higgs boson couplings to fermion pairs and to vector boson pairs. The tree-level Higgs couplings depend strongly on the value of  $\cos(\beta - \alpha)$ . In a first approximation, when radiative corrections of the Higgs squared-mass matrix are computed, the diagonalizing angle  $\alpha$  is shifted from its tree-level value, and hence one may compute a “radiatively-corrected” value for  $\cos(\beta - \alpha)$ . This shift provides one important source of the radiative corrections to the Higgs couplings. In particular, depending on the sign of  $\mu X_t$  and the magnitude of  $X_t/M_{\text{SUSY}}$ , modifications of  $\alpha$  can lead to important variations of the SM-like Higgs boson coupling to bottom quarks and tau leptons [175]. Similar corrections to the mixing angle  $\alpha$  can come for large  $\tan\beta$  from the stau/sbottom sector for sizable  $A_{b,\tau}$  [180]. Additional contributions from the one-loop vertex corrections to tree-level Higgs couplings must also be considered [170–189]. These contributions alter significantly the Higgs-fermion Yukawa couplings at large  $\tan\beta$ , both in the neutral and charged Higgs sector. Moreover, these radiative corrections can modify the basic relationship  $g_{h,H,A\bar{b}b}/g_{h,H,A\tau^+\tau^-} \propto m_b/m_\tau$ , and change the main features of MSSM Higgs phenomenology.

### III.2. Decay Properties and Production Mechanisms of MSSM Higgs Bosons

In the MSSM, neglecting  $CP$ -violating effects, one must consider the decay properties of three neutral Higgs bosons and one charged Higgs pair. In the region of parameter space where  $m_A \gg m_Z$  and the masses of supersymmetric particles are large, the decoupling limit applies, and the decay rates of  $h$  into SM particles are nearly indistinguishable from those of the SM Higgs boson. Hence, the  $h$  boson will decay mainly to fermion pairs, since the mass, less than about 135 GeV, is below the  $W^+W^-$  threshold. The SM-like branching ratios of  $h$  are modified if decays into supersymmetric particles are kinematically allowed [190]. In addition, if light superpartners exist that can couple to photons and/or gluons, then the effective couplings to  $gg$  and  $\gamma\gamma$  could deviate from the corresponding

SM predictions [180,191,192]. In the decoupling limit, the heavier Higgs states,  $H$ ,  $A$  and  $H^\pm$ , are roughly mass degenerate, and their decay branching ratios strongly depend on  $\tan\beta$  as discussed below. The  $AWW$  and  $AZZ$  couplings vanish, and the  $HWW$  and  $HZZ$  couplings are very small. For values of  $m_A \sim \mathcal{O}(M_Z)$ , all Higgs boson masses lie below 200 GeV. In this regime, there is a significant area of the parameter space in which none of the neutral Higgs boson decay properties approximates that of the SM Higgs boson. For  $\tan\beta \gg 1$ , the resulting predictions show marked differences from those for the SM Higgs boson [193]. Significant modifications to the  $b\bar{b}$  and/or the  $\tau^+\tau^-$  decay rates may occur via radiative effects.

After incorporating the leading radiative corrections to Higgs couplings from both QCD and supersymmetry, the following decay features are relevant in the MSSM. The decay modes  $h, H, A \rightarrow b\bar{b}, \tau^+\tau^-$  dominate when  $\tan\beta$  is large for all values of the Higgs boson masses. For small  $\tan\beta$ , these modes are significant for neutral Higgs boson masses below  $2m_t$  (although there are other competing modes in this mass range), whereas the  $t\bar{t}$  decay mode dominates above its kinematic threshold. In contrast to the SM Higgs boson, the vector boson decay modes of  $H$  are strongly suppressed at large  $m_H$  due to the suppressed  $HVV$  couplings in the decoupling limit. For the charged Higgs boson,  $H^+ \rightarrow \tau^+\nu_\tau$  dominates below the  $t\bar{b}$  threshold, while  $H^+ \rightarrow t\bar{b}$  dominates for large values of  $m_{H^\pm}$ . For low values of  $\tan\beta$  ( $\lesssim 1$ ) and low values of the charged Higgs boson mass ( $\lesssim 120$  GeV), the decay mode  $H^+ \rightarrow c\bar{s}$  becomes relevant.

In addition to the decay modes of the neutral Higgs bosons into fermion and gauge boson final states, additional decay channels may be allowed which involve scalars of the extended Higgs sector, *e.g.*,  $h \rightarrow AA$ . Supersymmetric final states from Higgs boson decays into charginos, neutralinos and third-generation squarks and sleptons can be important if they are kinematically allowed [194]. One interesting possibility is a significant branching ratio for the decay of a neutral Higgs boson to the invisible mode  $\tilde{\chi}_1^0\tilde{\chi}_1^0$  (where the lightest neutralino  $\tilde{\chi}_1^0$  is the lightest supersymmetric particle) [195], which poses a challenge at hadron colliders.

The production mechanisms for the SM Higgs boson at  $e^+e^-$  and hadron colliders can also be relevant for the production of the MSSM neutral Higgs bosons. However, one must take into account the possibility of enhanced or suppressed couplings with respect to those of the Standard Model, since these can significantly modify the production cross sections of neutral Higgs bosons. The supersymmetric-QCD corrections due to the exchange of virtual squarks and gluinos may modify the cross sections depending on the values of these supersymmetric particle masses. At both lepton and hadron colliders there are new mechanisms that produce two neutral Higgs bosons, as well as processes that produce charged Higgs bosons singly or in pairs. In the following we summarize the main processes

# Gauge & Higgs Boson Particle Listings

## Higgs Bosons — $H^0$ and $H^\pm$

for MSSM Higgs boson production. For a more detailed discussion and consideration of state-of-the-art calculations, see Refs. [44,75,159].

The main production mechanisms for the neutral MSSM Higgs bosons at  $e^+e^-$  colliders are Higgs-strahlung ( $e^+e^- \rightarrow Zh, ZH$ ), vector boson fusion ( $e^+e^- \rightarrow \nu\bar{\nu}h, \nu\bar{\nu}H$ )—with  $W^+W^-$  fusion about an order of magnitude larger than  $ZZ$  fusion—and  $s$ -channel  $Z$  boson exchange ( $e^+e^- \rightarrow Ah, AH$ ) [196]. For the Higgs-strahlung process, it is possible to reconstruct the mass and momentum of the Higgs boson recoiling against the particles from the  $Z$  boson decay, and hence sensitive searches for Higgs bosons decaying even to invisible final states can be applied.

The main charged Higgs boson production process at  $e^+e^-$  colliders is via  $s$ -channel  $\gamma$  or  $Z$  boson exchange ( $e^+e^- \rightarrow H^+H^-$ ). Charged Higgs bosons can also be produced in top quark decays via  $t \rightarrow b + H^\pm$  if  $m_H^\pm < m_t - m_b$  or via the one-loop process  $e^+e^- \rightarrow W^\pm H^\mp$  [197,198], which allows the production of a charged Higgs boson with  $m_H^\pm > \sqrt{s}/2$ , even when  $H^+H^-$  production is kinematically forbidden. Other single charged Higgs production mechanisms include  $t\bar{b}H^-/\bar{t}bH^+$  production [51],  $\tau^+\nu H^-/\tau^-\bar{\nu}H^+$  production [199], and a variety of processes in which  $H^\pm$  is produced in association with a one or two other gauge and/or Higgs bosons [200].

At hadron colliders, the dominant neutral Higgs production mechanism over the majority of the MSSM parameter space is gluon-gluon fusion, mediated by triangle loops containing heavy top and bottom quarks and the corresponding supersymmetric partners [201]. Higgs boson radiation from bottom quarks becomes important for large  $\tan\beta$ , where at least two of the three neutral Higgs bosons have enhanced couplings to bottom-type fermions [202,203]. A more detailed discussion is presented in Sec. (III.3). The vector boson fusion and Higgs-strahlung production of the  $CP$ -even Higgs bosons as well as the associated production of neutral Higgs bosons with top quark pairs have lower production cross sections by least an order of magnitude with respect to the dominant ones, depending on the precise region of MSSM parameter space.

Charged Higgs bosons can be produced in several different modes at hadron colliders. If  $m_{H^\pm} < m_t - m_b$ , the charged Higgs boson can be produced in decays of the top quark via the decay  $t \rightarrow bH^\pm$ , which would compete with the SM process  $t \rightarrow bW^\pm$ . Relevant QCD and SUSY-QCD corrections to  $\text{BR}(t \rightarrow H^\pm b)$  have been computed [204–207]. For values of  $m_{H^\pm}$  near  $m_t$ , width effects are important. In addition, the full  $2 \rightarrow 3$  processes  $pp/p\bar{p} \rightarrow H^\pm \bar{t}b + X$  and  $pp/p\bar{p} \rightarrow H^\mp \bar{t}b + X$  must be considered. If  $m_{H^\pm} > m_t - m_b$ , then charged Higgs boson production occurs mainly through radiation from a third generation quark. Charged Higgs bosons may also be produced singly in association with a top quark via the  $2 \rightarrow 3$  partonic processes  $gg, q\bar{q} \rightarrow t\bar{b}H^-$  (and the charge conjugate final states). For charged Higgs boson production cross section predictions for the Tevatron and the LHC, see Refs. [12,43,76,208–214]. Charged Higgs bosons can also be

produced via associated production with  $W^\pm$  bosons through  $b\bar{b}$  annihilation and  $gg$ -fusion [215]. They can also be produced in pairs via  $q\bar{q}$  annihilation [216]. The inclusive  $H^+H^-$  cross section is less than the cross section for single charged Higgs associated production [216–218].

### III.3. Searches for Neutral Higgs Bosons in the $CP$ -Conserving ( $CPC$ ) Scenario

Most of the experimental investigations carried out at LEP, the Tevatron, and the LHC, assume  $CP$ -conservation ( $CPC$ ) in the MSSM Higgs sector. In many cases the search results are interpreted in a number of specific benchmark models where a representative set of the relevant SUSY breaking parameters are specified [177].

#### III.3.1. Searches for Neutral MSSM Higgs Bosons at LEP

In  $e^+e^-$  collisions at LEP energies, the main production mechanisms of the neutral MSSM Higgs bosons are the Higgs-strahlung processes  $e^+e^- \rightarrow hZ, HZ$  and the pair production processes  $e^+e^- \rightarrow hA, HA$ , while the fusion processes play a marginal role. Higgs boson decays to  $b\bar{b}$  and  $\tau^+\tau^-$  are used in these searches.

The searches and limits from the four LEP experiments are described in Refs. [219–222]. The combined LEP data did not contain any excess of events which would imply the production of a Higgs boson, and combined limits were derived [34]. For  $m_A \gg M_Z$  the limit on  $m_h$  is nearly that of the SM searches, as  $\sin^2(\beta - \alpha) \approx 1$ . For high values of  $\tan\beta$  and low  $m_A$  ( $m_A \leq m_h^{\text{max}}$ ) the  $e^+e^- \rightarrow hA$  searches become the most important, and the lightest Higgs  $h$  is non SM-like. In this region, the 95% C.L. mass bounds are  $m_h > 92.8$  GeV and  $m_A > 93.4$  GeV. In the  $m_h$ -max. scenario, values of  $\tan\beta$  from 0.7 to 2.0 are excluded taking  $m_t = 174.3$  GeV, while a much larger  $\tan\beta$  region is excluded for other benchmark scenarios such as the no-mixing one.

Neutral Higgs bosons may also be produced by Yukawa processes  $e^+e^- \rightarrow f\bar{f}\phi$ , where the Higgs particle  $\phi \equiv h, H, A$ , is radiated off a massive fermion ( $f \equiv b$  or  $\tau^\pm$ ). These processes can be dominant at low masses, and whenever the  $e^+e^- \rightarrow hZ$  and  $hA$  processes are suppressed. The corresponding ratios of the  $f\bar{f}h$  and  $f\bar{f}A$  couplings to the SM coupling are  $\sin\alpha/\cos\beta$  and  $\tan\beta$ , respectively. The LEP data have been used to search for  $b\bar{b}b\bar{b}, b\bar{b}\tau^+\tau^-$ , and  $\tau^+\tau^-\tau^+\tau^-$  final states [223,224]. Regions of low mass and high enhancement factors are excluded by these searches.

#### III.3.2. Searches for Neutral MSSM Higgs Bosons at Hadron Colliders

Over a large fraction of the MSSM parameter space, one of the  $CP$ -even neutral Higgs bosons ( $h$  or  $H$ ) couples to the vector bosons with SM-like strength and has a mass below 135 GeV. Hence, if the current 95% C.L. exclusion limits for a SM Higgs boson from ATLAS and CMS are interpreted in terms of the SM-like supersymmetric Higgs boson, there is a region of SUSY parameter space beyond that excluded by LEP



See key on page 457

## Gauge & Higgs Boson Particle Listings

### Higgs Bosons — $H^0$ and $H^\pm$

that is strongly disfavored. In particular, the minimal mixing scenario with  $M_{SUSY} \leq 2$  TeV is disfavored considering the LEP and ATLAS data. At the same time, if the excess of events observed in the Higgs boson searches in the diphoton and  $ZZ$  channels are confirmed, this could be interpreted as a SM-like MSSM Higgs boson.

Scenarios with enhanced Higgs boson production cross sections are studied at hadron colliders. The best sensitivity is in the regime with low to moderate  $m_A$  and with large  $\tan\beta$  which enhances the couplings of the Higgs bosons to down-type fermions. The corresponding limits on the Higgs boson production cross section times the branching ratio of the Higgs boson into down-type fermions can be interpreted in MSSM benchmark scenarios [225]. If  $\phi = A, H$  for  $m_A > m_h^{\max}$ , and  $\phi = A, h$  for  $m_A < m_h^{\max}$ , the most promising channels at the Tevatron are  $b\bar{b}\phi, \phi \rightarrow b\bar{b}$  or  $\phi \rightarrow \tau^+\tau^-$ , with three tagged  $b$ -jets or  $b\tau\tau$  in the final state, respectively, and the inclusive  $p\bar{p} \rightarrow \phi \rightarrow \tau^+\tau^-$  process, with contributions from both  $gg \rightarrow \phi$  and  $b\bar{b}\phi$  production. Although Higgs boson production via gluon fusion has a higher cross section than via associated production, it cannot be used to study the  $\phi \rightarrow b\bar{b}$  decay mode since the signal is overwhelmed by QCD background.

The CDF and DØ collaborations have searched for neutral Higgs bosons produced in association with bottom quarks and which decay into  $b\bar{b}$  [226,227], or into  $\tau^+\tau^-$  [228,229]. The most recent searches in the  $b\bar{b}\phi$  channel with  $\phi \rightarrow b\bar{b}$  analyze approximately  $2.6 \text{ fb}^{-1}$  of data (CDF) and  $5.2 \text{ fb}^{-1}$  (DØ), seeking events with at least three  $b$ -tagged jets. The cross section is defined such that at least one  $b$  quark not from  $\phi$  decay is required to have  $p_T > 20$  GeV and  $|\eta| < 5$ . The decay widths of the Higgs bosons are assumed to be much smaller than the experimental resolution. The invariant mass of the two leading jets as well as  $b$ -tagging variables are used to discriminate the signal from the backgrounds. The QCD background rates and shapes are inferred from data control samples, in particular, the sample with two  $b$  tagged jets and a third, untagged jet. Separate signal hypotheses are tested and limits are placed on  $\sigma(p\bar{p} \rightarrow b\bar{b}\phi) \times \text{BR}(\phi \rightarrow b\bar{b})$ . CDF sees a local excess of approximately  $2.5\sigma$  significance in the mass range of 130-160 GeV, but DØ's search is more sensitive and sets stronger limits. The DØ result shown in Fig. 14 displays a  $\approx 2$  sigma local upward fluctuation in the 110 to 125 GeV mass range.

CDF and DØ have also performed searches for inclusive production of Higgs bosons with subsequent decays to  $\tau^+\tau^-$  [230,231,232], although these limits have been superseded by the LHC searches.

In order to interpret the experimental data in terms of MSSM benchmark scenarios, it is necessary to consider carefully the effect of radiative corrections on the production and decay processes. The bounds from the  $b\bar{b}\phi, \phi \rightarrow b\bar{b}$  channel depend strongly on the radiative corrections affecting the relation between the bottom quark mass and the bottom Yukawa

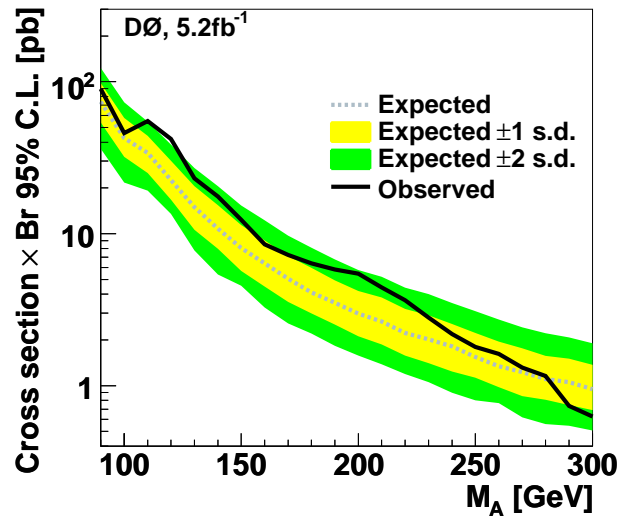


**Figure 14:** The 95% C.L. limits on  $\sigma(p\bar{p} \rightarrow b\bar{b}) \times \text{BR}(\phi \rightarrow b\bar{b})$  from CDF and DØ. The observed limits are indicated with solid lines, and the expected limits are indicated with dashed lines. The limits are to be compared with the sum of signal predictions for Higgs bosons with similar masses.

coupling. In the channels with  $\tau^+\tau^-$  final states, however, compensations occur between large corrections in the Higgs boson production and decay. The total production rates of bottom quarks and  $\tau$  pairs mediated by the production of a  $CP$ -odd Higgs boson in the large  $\tan\beta$  regime are approximately given by

$$\sigma_{b\bar{b}A} \times \text{BR}(A \rightarrow b\bar{b}) \simeq \sigma_{b\bar{b}A}^{\text{SM}} \frac{\tan^2\beta}{(1 + \Delta_b)^2} \frac{9}{(1 + \Delta_b)^2 + 9},$$

and

$$\sigma_{gg \rightarrow A, b\bar{b}A} \times \text{BR}(A \rightarrow \tau^+\tau^-) \simeq \sigma_{gg \rightarrow A, b\bar{b}A}^{\text{SM}} \frac{\tan^2\beta}{(1 + \Delta_b)^2 + 9},$$

where  $\sigma_{b\bar{b}A}^{\text{SM}}$  and  $\sigma_{gg \rightarrow A, b\bar{b}A}^{\text{SM}}$  denote the values of the corresponding SM Higgs boson cross sections for a SM Higgs boson mass equal to  $m_A$ . The function  $\Delta_b$  includes the dominant effects of SUSY radiative corrections for large  $\tan\beta$  [170,175,187,188], and it depends strongly on  $\tan\beta$  and on the SUSY mass parameters. The  $b\bar{b}A$  channel is more sensitive to the value of  $\Delta_b$  through the factor  $1/(1 + \Delta_b)^2$  than the inclusive  $\tau^+\tau^-$  channel, for which this leading dependence on  $\Delta_b$  cancels out. As a consequence, the limits derived from the inclusive  $\tau^+\tau^-$  channel depend less on the precise MSSM scenario chosen than those of the  $b\bar{b}A$  channel.

The production and decay rates of the  $CP$ -even Higgs bosons with  $\tan\beta$ -enhanced couplings to down-type fermions— $H$  (or  $h$ ) for  $m_A$  larger (or smaller) than  $m_h^{\max}$ , respectively—are governed by formulas similar to the ones presented above. At high  $\tan\beta$ , one of the  $CP$ -even Higgs bosons and the  $CP$ -odd Higgs boson are nearly degenerate in mass, enhancing the signal

# Gauge & Higgs Boson Particle Listings

## Higgs Bosons — $H^0$ and $H^\pm$

cross section by roughly a factor of two, without complicating the experimental signature except in a small mass region in which the three neutral MSSM Higgs boson masses are close together and each boson contributes to the total production rate. Detailed discussions of the impact of radiative corrections in these search modes are presented in Refs. [225] and [233].

In Fig. 15, the interpretation is shown for DØ's combination of  $\phi \rightarrow b\bar{b}$  and  $\phi \rightarrow \tau^+\tau^-$  searches [232] in the  $(m_A, \tan\beta)$  plane for the  $m_h$ -max benchmark scenario with  $\mu = 200$  GeV. The neutral Higgs boson searches consider the contribution of both the  $CP$ -odd and the  $CP$ -even neutral Higgs bosons with enhanced couplings to bottom quarks. As explained above, considering other benchmark scenarios will not relevantly change the region of SUSY parameter space that can be explored via the inclusive di-tau searches, but different regions of SUSY parameter space will be probed in the case of the  $b\bar{b}$  searches.

ATLAS and CMS also search for  $\phi \rightarrow \tau^+\tau^-$  in  $pp$  collisions at  $\sqrt{s} = 7$  TeV. ATLAS seeks tau pairs in  $1.06 \text{ fb}^{-1}$  of data [234,235], and CMS's search uses  $4.6 \text{ fb}^{-1}$  of data [138,139]. The searches are performed in categories of the decays of the two tau leptons:  $e\tau_{\text{had}}$ ,  $\mu\tau_{\text{had}}$ ,  $e\mu$ , and  $\mu\mu$ , where  $\tau_{\text{had}}$  denotes a tau lepton which decays to one or more hadrons plus a tau neutrino,  $e$  denotes  $\tau \rightarrow e\nu\nu$ , and  $\mu$  denotes  $\tau \rightarrow \mu\nu\nu$ . The dominant background comes from  $Z \rightarrow \tau^+\tau^-$  decays, although  $t\bar{t}$ ,  $W$ +jets and  $Z$ +jets events contribute as well. Separating events into categories based on the number of  $b$ -tagged jets improves the sensitivity in the MSSM. The  $b\bar{b}$  annihilation process and radiation of a Higgs boson from a  $b$  quark give rise to events in which the Higgs boson is accompanied by a  $b\bar{b}$  pair in the final state, sometimes with only one  $b$  within the detector acceptance. Requiring the presence of one or more  $b$  jets reduces the background from  $Z$ +jets. Data control samples are used to constrain background rates. The rates for jets to be identified as a hadronically decaying tau lepton are measured in dijet samples, and  $W$ +jets samples provide a measurement of the rate of events that, with a fake hadronic tau, can pass the signal selection requirements. Lepton fake rates are measured using samples of unisolated lepton candidates and same-sign lepton candidates. Constraints from ATLAS's and CMS's searches for  $h \rightarrow \tau^+\tau^-$  are also shown in Fig. 15 in the  $m_h$ -max benchmark scenario, with  $\mu = 200$  GeV. The neutral Higgs boson searches consider the contributions of both the  $CP$ -odd and  $CP$ -even neutral Higgs bosons with enhanced couplings to bottom quarks, as they were for the Tevatron results. As explained above, the di-tau inclusive search limits do not significantly change by considering other benchmark scenarios.

In addition to  $\phi \rightarrow \tau^+\tau^-$  at the LHC, studies indicate that with about  $30 \text{ fb}^{-1}$  of data one can search for the non-standard neutral Higgs bosons of the MSSM in the  $b\bar{b}\phi$ ,  $\phi \rightarrow b\bar{b}$  channel with three  $b$ 's in the final state [233]. Due to the dependence of this production and decay mode on the SUSY radiative corrections there is complementarity between the  $3b$  channel and the inclusive tau pair channel in exploring the supersymmetric parameter space.

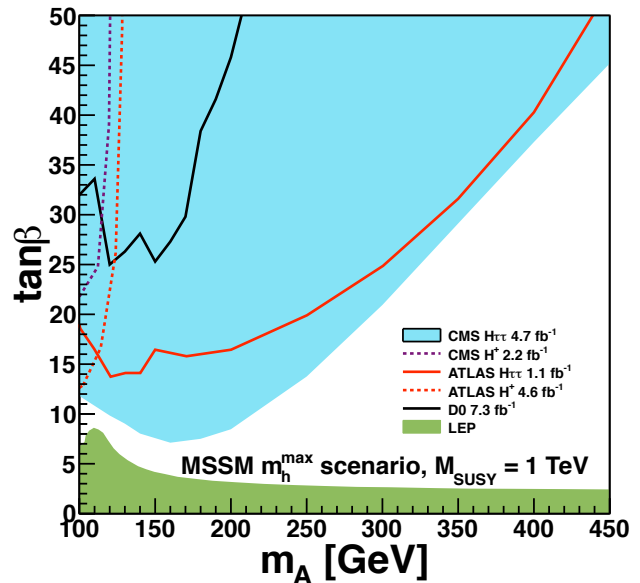


**Figure 15:** The 95% C.L. MSSM exclusion contours  $m_h$ -max benchmark scenario obtained by the ATLAS [234], CMS [138], and DØ [232] collaborations. The LHC collaborations contribute searches for  $H \rightarrow \tau^+\tau^-$  and  $H^\pm \rightarrow \tau\nu_\tau$  while DØ combines  $H \rightarrow \tau^+\tau^-$  with  $H \rightarrow b\bar{b}$  searches for these results. Also shown is the region excluded by LEP searches [34], assuming a top quark mass of 174.3 GeV.

The LHC has the potential to explore a broad range of SUSY parameter space through the search for non-SM-like Higgs bosons. Nevertheless, Fig. 15 shows a broad region with intermediate  $\tan\beta$  and large values of  $m_A$  that is not tested by present neutral or charged Higgs boson searches, and which might be difficult to cover completely via these searches, even with much larger data sets. In this region of parameter space it is possible that only the SM-like Higgs boson can be within the LHC's reach. If a SM-like Higgs boson is discovered, it may be challenging to determine only from the Higgs sector whether there is a supersymmetric extension of the SM in nature.

### III.4. Searches for Charged MSSM Higgs Bosons

Searches for the charged Higgs bosons predicted by 2HDMs have been conducted at LEP, the Tevatron, and the LHC, and the results of these searches have been interpreted in terms of the MSSM. Due to the correlations among Higgs boson masses in the MSSM, the experimental results do not yet significantly constrain the MSSM parameter space beyond what is already obtained from the searches for neutral Higgs bosons. In the near future, however, the LHC experiments will be sensitive to charged Higgs boson decays up to  $\approx 170$  GeV for all values of  $\tan\beta$  [236].

At LEP, searches were performed for pair-produced charged Higgs bosons. In the MSSM and in more general Type-II 2HDMs, for masses which are accessible at LEP energies,

See key on page 457

## Gauge & Higgs Boson Particle Listings

### Higgs Bosons — $H^0$ and $H^\pm$

the decays  $H^+ \rightarrow c\bar{s}$  and  $\tau^+\nu_\tau$  dominate. The final states  $H^+H^- \rightarrow (c\bar{s})(\bar{c}s)$ ,  $(\tau^+\nu_\tau)(\tau^-\bar{\nu}_\tau)$ , and  $(c\bar{s})(\tau^-\bar{\nu}_\tau) + (\bar{c}s)(\tau^+\nu_\tau)$  were considered, and the search results are usually presented as functions of  $\text{BR}(H^+ \rightarrow \tau^+\nu)$ . The sensitivity of the LEP searches was limited to  $m_{H^\pm} < 90$  GeV, due to the background from  $e^+e^- \rightarrow W^+W^-$  [237], and the kinematic limitation on the production cross section. The combined LEP data constrain  $m_{H^\pm} > 78.6$  GeV independently of  $\text{BR}(H^+ \rightarrow \tau^+\nu_\tau)$  [238].

At the Tevatron, the CDF and DØ collaborations have searched for charged Higgs bosons in top quark decays with subsequent decays of the charged Higgs boson to  $\tau\nu$  or to  $c\bar{s}$  [239,240,241]. Assuming  $\text{BR}(H^+ \rightarrow c\bar{s}) = 100\%$ , the limits on  $\text{BR}(t \rightarrow H^+b)$  from CDF and DØ are  $\approx 20\%$  in the mass range  $90 \text{ GeV} < m_{H^+} < 160 \text{ GeV}$ . Assuming  $\text{BR}(H^+ \rightarrow \tau^+\nu_\tau) = 100\%$ , DØ's limits on  $\text{BR}(t \rightarrow H^+b)$  are also  $\approx 20\%$  in the same mass range. These limits are valid in general 2HDMs, and they have also been interpreted in terms of the MSSM in the references.

The ATLAS collaboration has also searched for charged Higgs bosons produced in the decay of top quarks in  $t\bar{t}$  events. ATLAS has searched for the decay  $H^+ \rightarrow \tau^+\nu_\tau$  in three final state topologies: 1) lepton+jets: with  $t\bar{t} \rightarrow \bar{b}WH^+ \rightarrow \bar{b}\bar{b}(q\bar{q}')(\tau_{\text{lep}}\nu)$ , i.e., the  $W$  boson decays hadronically and the tau decays into an electron or a muon, with two neutrinos; 2)  $\tau$  +lepton: with  $t\bar{t} \rightarrow \bar{b}WH^+ \rightarrow \bar{b}\bar{b}(l\nu)(\tau_{\text{had}}\nu)$  i.e., the  $W$  boson decays leptonically (with  $l = e, \mu$ ) and the tau decays hadronically; 3)  $\tau$ +jets:  $t\bar{t} \rightarrow \bar{b}WH^+ \rightarrow \bar{b}\bar{b}(q\bar{q}')(\tau_{\text{had}}\nu)$ , i.e., both the  $W$  boson and the  $\tau$  decay hadronically [242]. Assuming  $\text{BR}(H^+ \rightarrow \tau^+\nu_\tau) = 100\%$ , ATLAS sets upper limits on  $\text{BR}(t \rightarrow H^+b)$  between 5% and 1% for charged Higgs boson masses between 90 GeV to 160 GeV, respectively. These limits are shown in Fig. 16. When interpreted in the context of the  $m_h^{\text{max}}$  scenario of the MSSM, these bounds exclude  $\tan\beta$  values above 20 in this range of charged Higgs boson masses, but also provide sensitivity for  $\tan\beta < 4$  due to the increasing predicted decay rate for  $t \rightarrow H^+b$  at low  $\tan\beta$ . The high- $\tan\beta$  interpretation of this result is shown in Fig. 15. ATLAS has also searched for charged Higgs bosons in top quark decays assuming  $\text{BR}(H^+ \rightarrow c\bar{s}) = 100\%$  [243], and sets limits of  $\approx 20\%$  on  $\text{BR}(t \rightarrow H^+b)$  in the  $90 \text{ GeV} < m_{H^+} < 160 \text{ GeV}$  mass range.

The CMS collaboration has also searched for the charged Higgs boson in the decay products of top quark pairs:  $t\bar{t} \rightarrow H^\pm W^\mp b\bar{b}$  and  $t\bar{t} \rightarrow H^+H^-b\bar{b}$  [244]. Three types of final states with large missing transverse energy and jets originating from  $b$ -quark hadronization have been analyzed: the fully-hadronic channel with a hadronically decaying tau in association with jets, the di-lepton channel with a hadronically decaying tau in association with an electron or muon and the di-lepton channel with an electron-muon pair. Combining the results of these three analyses and assuming  $\text{BR}(H^\pm \rightarrow \tau\nu) = 1$ , the upper limits on  $\text{BR}(t \rightarrow H^+b)$  are less than 2% to 3% depending on the charged Higgs boson mass in the interval 80 GeV

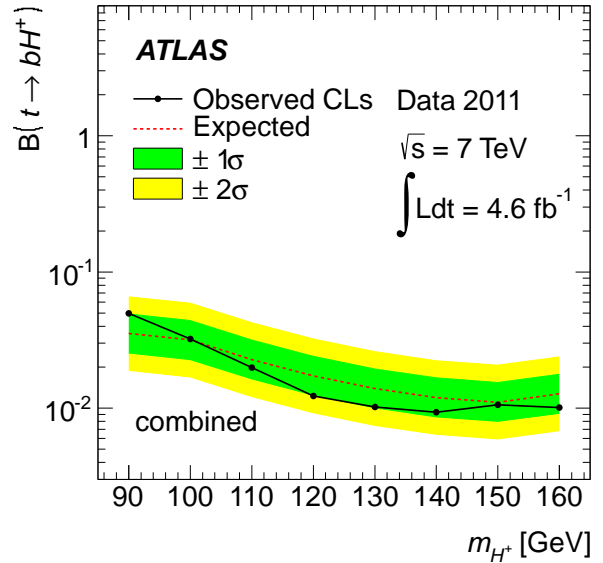


**Figure 16:** 95% C.L. limit on  $\text{BR}(t \rightarrow H^+b)$  assuming  $\text{BR}(H^+ \rightarrow \tau\nu) = 100\%$  from the ATLAS collaboration [242].

$< m_{H^+} < 160$  GeV. The results of this search have been translated into limits in the  $(M_A, \tan\beta)$  plane for the  $m_h$ -max benchmark scenario and are shown in Fig. 15.

### III.5. Effects of CP Violation on the MSSM Higgs Spectrum

In the Standard Model,  $CP$ -violation ( $CPV$ ) is induced by phases in the Yukawa couplings of the quarks to the Higgs field, which results in one non-trivial phase in the CKM mixing matrix. SUSY scenarios with new  $CPV$  phases are theoretically appealing, since additional  $CPV$  beyond that observed in the  $K$ ,  $D$ , and  $B$  meson systems is required to explain the observed cosmic matter-antimatter asymmetry [245,246]. In the MSSM, there are additional sources of  $CPV$  from phases in the various mass parameters. In particular, the gaugino mass parameters ( $M_i$ ,  $i = 1, 2, 3$ ), the Higgsino mass parameter,  $\mu$ , the bilinear Higgs squared-mass parameter,  $m_{12}^2$ , and the trilinear couplings of the squark and slepton fields to the Higgs fields,  $A_f$ , may carry non-trivial phases. The two parameter combinations  $\arg[\mu A_f(m_{12}^2)^*]$  and  $\arg[\mu M_i(m_{12}^2)^*]$  are invariant under phase redefinitions of the MSSM fields [247,248]. Therefore, if one of these quantities is non-zero, there would be new sources of  $CP$ -violation, which affects the MSSM Higgs sector through radiative corrections [182,248–253]. The mixing of the neutral  $CP$ -odd and  $CP$ -even Higgs boson states is no longer forbidden. Hence,  $m_A$  is no longer a physical parameter. However, the charged Higgs boson mass  $m_{H^\pm}$  is still physical and can be used as an input for the computation of the neutral Higgs spectrum of the theory.

For large values of  $m_{H^\pm}$ , corresponding to the decoupling limit, the properties of the lightest neutral Higgs boson state approach those of the SM Higgs boson. That is, for  $m_{H^\pm} \gg M_W$ ,

# Gauge & Higgs Boson Particle Listings

## Higgs Bosons — $H^0$ and $H^\pm$

the lightest neutral Higgs boson is approximately a  $CP$ -even state, with  $CPV$  couplings that are suppressed by terms of  $\mathcal{O}(m_W^2/m_{H^\pm}^2)$ . In particular, the upper bound on the lightest neutral Higgs boson mass, takes the same value as in the  $CP$ -conserving case [248]. Nevertheless, there still can be significant mixing between the two heavier neutral mass eigenstates. For a detailed study of the Higgs boson mass spectrum and parametric dependence of the associated radiative corrections, see Refs. [249,252].

Major variations to the MSSM Higgs phenomenology occur in the presence of explicit  $CPV$  phases. In the  $CPV$  case, vector boson pairs couple to all three neutral Higgs boson mass eigenstates,  $H_i$  ( $i = 1, 2, 3$ ), with couplings

$$g_{H_i VV} = \cos\beta \mathcal{O}_{1i} + \sin\beta \mathcal{O}_{2i}$$

$$g_{H_i H_j Z} = \mathcal{O}_{3i}(\cos\beta \mathcal{O}_{2j} - \sin\beta \mathcal{O}_{1j}) - \mathcal{O}_{3j}(\cos\beta \mathcal{O}_{2i} - \sin\beta \mathcal{O}_{1i})$$

where the  $g_{H_i VV}$  couplings are normalized to the analogous SM coupling and the  $g_{H_i H_j Z}$  have been normalized to  $g_Z^{\text{SM}}/2$ .  $\mathcal{O}_{ij}$  is the orthogonal matrix relating the weak eigenstates to the mass eigenstates. It has non-zero off-diagonal entries mixing the  $CP$ -even and  $CP$ -odd components of the weak eigenstates. The above couplings obey the relations

$$\sum_{i=1}^3 g_{H_i ZZ}^2 = 1 \quad \text{and} \quad g_{H_k ZZ} = \varepsilon_{ijk} g_{H_i H_j Z}$$

where  $\varepsilon_{ijk}$  is the Levi-Civita symbol.

Another consequence of  $CPV$  effects in the scalar sector is that all neutral Higgs bosons can couple to both scalar and pseudoscalar fermion bilinear densities. The couplings of the mass eigenstates  $H_i$  to fermions depend on the loop-corrected fermion Yukawa couplings (similarly to the  $CPC$  case), on  $\tan\beta$  and on the  $\mathcal{O}_{ji}$ . The resulting expressions for the scalar and pseudoscalar components of the neutral Higgs boson mass eigenstates to fermions and the charged Higgs boson to fermions are given in Refs. [249,254].

The production processes of neutral MSSM Higgs bosons in the  $CPV$  scenario are similar to those in the  $CPC$  scenario, except for the fact that in any process, the  $CP$  eigenstates  $h$ ,  $H$ , and  $A$  can be replaced by any of the three neutral Higgs mass eigenstates  $H_i$ . This is the case, since, in the presence of  $CP$  violation, the  $H_i$ 's do not have well-defined  $CP$  quantum numbers. Regarding the decay properties, the lightest mass eigenstate,  $H_1$ , predominantly decays to  $b\bar{b}$  if kinematically allowed, with a smaller fraction decaying to  $\tau^+\tau^-$ , similar to the  $CPC$  case. If kinematically allowed, a SM-like neutral Higgs boson,  $H_2$  or  $H_3$  can decay predominantly to  $H_1 H_1$  leading to many new interesting signals both at lepton and hadron colliders; otherwise it will decay preferentially to  $b\bar{b}$ .

### III.6. Searches for Neutral Higgs Bosons in $CPV$ Scenarios

At LEP, all three neutral Higgs eigenstates could have been produced by Higgs-strahlung,  $e^+e^- \rightarrow H_i Z$ , and in pairs,  $e^+e^- \rightarrow Z^* \rightarrow H_i H_j$ , with  $i \neq j$ . The production rates depend

on the details of the  $CPV$  scenario. Possible cascade decays such as  $H_2$  or  $H_3 \rightarrow H_1 H_1$  can lead to interesting experimental signatures in the Higgs-strahlung processes,  $e^+e^- \rightarrow H_2 Z$  or  $H_3 Z$ , however, the searches in the  $CPV$  MSSM scenario are experimentally more difficult. The cross sections for the Higgs-strahlung and pair production processes are given in Refs [182,248,249,253].

The Higgs boson searches at LEP were interpreted [34] in a  $CPV$  benchmark scenario [182] for which the parameters were chosen so as to maximize the phenomenological differences with respect to the  $CPC$  scenario. Using the most conservative theoretical calculations available at each point in the  $(m_{H_1}, \tan\beta)$  plane, parts of the region  $m_{H_1} < 60$  GeV and  $\tan\beta < 40$  were excluded, and values of  $\tan\beta$  lower than 3 were excluded for all values of  $m_{H_1} < 114$  GeV. The Tevatron  $CP$ -conserving results and projections for MSSM Higgs searches, as well as the existing projections for LHC MSSM  $CP$ -conserving searches have been reinterpreted in the framework of  $CP$ -violating MSSM Higgs in Ref. 255.

### III.7. Indirect Constraints on Supersymmetric Higgs Bosons

Indirect bounds from a global fit to precision measurements of electroweak observables can be derived in terms of MSSM parameters [256] in a way similar to what was done in the SM. Given the MSSM and SM predictions for  $M_W$  as a function of  $m_t$ , and varying the Higgs boson mass and the SUSY spectrum, one finds that the MSSM overlaps with the SM when SUSY masses are large, of  $\mathcal{O}(2$  TeV), and the light SM-like Higgs boson has a mass in the experimentally preferred mass range:  $m_h \hat{=} 114\text{--}129$  GeV. The MSSM Higgs boson mass expectations are compatible with the constraints provided by the measurements of  $m_t$  and  $M_W$  [257]. A global fit for  $m_h$  in the Constrained MSSM, for example, yields  $m_h = 119.1_{-2.9}^{+3.4}$  GeV after including the constraints from LHC data, instead of the pre-LHC value of  $m_h = 111.5_{-1.2}^{+3.5}$  GeV, improving the consistency of the model predictions with the LEP exclusion [258]<sup>4</sup>. These global fit studies show that a SM-like Higgs with mass 125 GeV or larger would start to build up some tension with  $g_\mu - 2$  that may ultimately lead to exclude the CMSSM or other types of constrained SUSY scenarios for which similar results can be obtained.

Improvements in our understanding of  $B$ -physics observables put indirect constraints on MSSM scenarios in regions in which Higgs boson searches at the Tevatron and the LHC are sensitive. In particular,  $\text{BR}(B_s \rightarrow \mu^+\mu^-)$ ,  $\text{BR}(b \rightarrow s\gamma)$ , and  $\text{BR}(B_u \rightarrow \tau\nu)$  play an important role within minimal flavor-violating (MFV) models [259], in which flavor effects proportional to the CKM matrix elements are induced, as in the SM. For example, see Refs. [260–263]. The supersymmetric contributions to these observables come both at the tree- and loop-level, and have a different parametric dependence,

<sup>4</sup> This fit does not include the direct limits on the Higgs boson mass from any collider.

See key on page 457

## Gauge & Higgs Boson Particle Listings

### Higgs Bosons — $H^0$ and $H^\pm$

but share the property that they become significant for large values of  $\tan\beta$ , which is also the regime in which searches for non-standard MSSM Higgs bosons at hadron colliders are the most powerful.

In the SM, the relevant contributions to the rare decay  $B_s \rightarrow \mu^+\mu^-$  come through the  $Z$ -penguin and the  $W^\pm$ -box diagrams [264]. In supersymmetry with large  $\tan\beta$ , there are also significant contributions from Higgs-mediated neutral currents [265–268], which depend on the SUSY spectra, and grow with the sixth power of  $\tan\beta$  and decrease with the fourth power of the  $CP$ -odd Higgs boson mass  $m_A$ . Therefore, the upper limits from the Tevatron and the LHC [269] put strong restrictions on possible flavor-changing neutral currents (FCNC) in the MSSM at large  $\tan\beta$  [270].

Further constraints are obtained from the rare decay  $b \rightarrow s\gamma$ . The SM rate is known up to NNLO corrections [271,272] and is in good agreement with measurements [273]. In the Type-II 2HDM and in the absence of other sources of new physics at the electroweak scale, a bound  $m_{H^\pm} > 295$  GeV has been derived [271]. Although this indirect bound appears much stronger than the results from direct charged Higgs searches, it can be invalidated by new physics contributions, such as those which can be present in the MSSM. In the minimal flavor-violating MSSM, there are new contributions from charged Higgs as well as chargino-stop and gluino-sbottom diagrams. The charged Higgs boson's contribution is enhanced for small values of its mass and can be partially canceled by the chargino and gluino contributions or by higher-order  $\tan\beta$ -enhanced loop effects.

The branching ratio  $B_u \rightarrow \tau\nu$ , measured by the Belle [274,275] and BaBar [276,277] collaborations, also constrains the MSSM. The SM expectation is in slight tension with the latest experimental results [278]. In the MSSM, there is an extra tree-level contribution from the charged Higgs which interferes destructively with the SM contribution, and which increases for small values of the charged Higgs boson mass and large values of  $\tan\beta$  [279]. Charged Higgs effects on  $B \rightarrow D\tau\nu$  decays [280], constrain in an important way the parameter space for small values of the charged Higgs boson mass and large values of  $\tan\beta$ , and exclude a region that is otherwise allowed by values of  $B_u \rightarrow \tau\nu$  [278,281,282]. These two observables are only mildly dependent on the SUSY spectra.

Charged Higgs bosons can play a role in explaining the evidence for CP violation in  $D^0 \rightarrow \pi^+\pi^-$ ,  $K^+K^-$  decays recently presented by LHCb [283] and CDF [284]. In a particular minimal flavor violating 2HDM, tree-level charged Higgs insertions can give large contributions to CP violation in  $D^0$  decays while also being consistent with stringent bounds from  $D^0 - \bar{D}^0$  mixing,  $\text{BR}(b \rightarrow s\gamma)$ , and  $\text{BR}(B_u \rightarrow \tau\nu)$ , as well as direct searches such as  $H \rightarrow \tau^+\tau^-$  [285].

Several studies [260–263,286,287] have shown that, in extended regions of parameter space, the combined  $B$ -physics measurements impose strong constraints on the MSSM models to which Higgs boson searches at the Tevatron and the LHC

are sensitive. Consequently, the observation of a non-SM Higgs boson at the Tevatron or the LHC would point to a rather narrow, well-defined region of MSSM parameter space [260,288] or to something beyond the minimal flavor violation framework.

Another indirect constraint on the Higgs sector comes from the search for dark matter. If dark matter particles are weakly interacting and massive, then particle physics can provide models which predict the correct relic density of the universe. In particular, the lightest supersymmetric particle, typically the lightest neutralino, is an excellent dark matter particle candidate [289]. Within the MSSM, the measured relic density places constraints in the parameter space, which in turn - for specific SUSY low energy spectra- have implications for Higgs searches at colliders, and also for experiments looking for direct evidence of dark matter particles in elastic scattering with atomic nuclei. Large values of  $\tan\beta$  and small  $m_A$  are relevant for the  $b\bar{b}A/H$  and  $A/H \rightarrow \tau^+\tau^-$  searches at the Tevatron and the LHC, and also provide a significant contribution from the  $CP$ -even Higgs  $H$  exchange to the spin-independent cross sections for direct detection experiments such as CDMS or Xenon, for example. Consequently, a signal at colliders would raise prospects for a signal in indirect detection experiments and vice-versa [286,288,290–292]. However, there are theoretical uncertainties in the calculation of dark matter scattering cross sections, and in the precise value of the local dark matter density and velocity distributions, which may dilute these model-dependent correlations.

#### IV. Other Model Extensions

There are many ways to extend the minimal Higgs sector of the Standard Model. In the preceding sections we have considered the phenomenology of the MSSM Higgs sector<sup>5</sup>, which at tree level is a constrained Type-II 2HDM (with restrictions on the Higgs boson masses and couplings). One can consider general Type-II 2HDMs [13,44,162], with no correlations between masses and couplings, or Type-I 2HDMs [163]. The different patterns of Higgs-fermion couplings in each case will lead to different phenomenology. It is also possible to consider models with a SM Higgs boson and one or more additional scalar SU(2) doublets that acquire no vacuum expectation value (vev) and hence play no role in the EWSB mechanism. These models are dubbed Inert Higgs Doublet Models [293]. Due to the lack of vev, the inert Higgs bosons cannot decay into a pair of gauge bosons, and imposing a  $Z_2$  symmetry that prevents them from coupling to the fermions it follows that if the lightest inert Higgs boson is neutral it becomes a good dark matter candidate with interesting associated collider signals.

Other extensions of the Higgs sector can include [15,164] multiple copies of SU(2)<sub>L</sub> doublets, additional Higgs singlets, triplets or more complicated combinations of Higgs multiplets.

<sup>5</sup> In the searches for charged Higgs bosons the results are presented for given branching ratio assumptions within a general 2HDM, and then interpreted in the MSSM.

## Gauge & Higgs Boson Particle Listings

### Higgs Bosons — $H^0$ and $H^\pm$

It is also possible to enlarge the gauge symmetry beyond  $SU(2)_L \times U(1)_Y$  along with the necessary Higgs structure to generate gauge boson and fermion masses. There are two main experimental constraints that govern these extensions: (i) precision measurements which constrain  $\rho = m_W^2 / (m_Z^2 \cos^2 \theta_W)$  to be very close to 1 and (ii) flavor changing neutral current (FCNC) effects. In electroweak models based on the SM gauge group, the tree-level value of  $\rho$  is determined by the Higgs multiplet structure. By suitable choices for the hypercharges, and in some cases the mass splitting between the charged and neutral Higgs sector or the vacuum expectation values of the Higgs fields, it is possible to obtain a richer combination of singlets, doublets, triplets and higher multiplets compatible with precision measurements [294]. Concerning the constraints coming from FCNC effects, the Glashow-Weinberg theorem [295] states that, in the presence of multiple Higgs doublets the tree-level FCNC's mediated by neutral Higgs bosons will be absent if all fermions of a given electric charge couple to no more than one Higgs doublet. The Higgs doublet models Type-I and Type-II are two different ways of satisfying this theorem. The coupling pattern of these two types can be arranged by imposing either a discrete symmetry or, in the case of Type-II, supersymmetry. The resulting phenomenology of extended Higgs sectors can differ significantly from that of the SM Higgs boson.

In supersymmetry, the most studied extensions of the MSSM have a scalar singlet and its supersymmetric partner [296–298]. These models have an extended Higgs sector with two additional neutral scalar states, one  $CP$ -even and one  $CP$ -odd, beyond those present in the MSSM. In these models, the tree-level bound on the lightest Higgs boson, considering arguments of perturbativity of the theory up to the GUT scale, is about 100 GeV. The radiative corrections to the masses are similar to those in the MSSM and yield an upper bound of about 145 GeV for the mass of the lightest neutral  $CP$ -even scalar, for stop masses in the TeV range [16,299]. The couplings of the Higgs bosons to the gauge bosons and fermions are weakened somewhat from mixing with the singlet and this can alter significantly the Higgs phenomenology with respect to the MSSM case.

Another extension of the MSSM which can raise the value of the lightest Higgs boson mass to a few hundred GeV is based on gauge extensions of the MSSM [17,18]. The addition of asymptotically-free gauge interactions naturally yields extra contributions to the quartic Higgs couplings. These extended gauge sector models can be combined with the presence of extra singlets or replace the singlet with a pair of triplets [19].

It is also possible that the MSSM is the low energy effective field theory of a more fundamental SUSY theory that includes additional particles with masses at or somewhat above the TeV range, and that couple significantly to the MSSM Higgs sector. A model-independent analysis of the spectrum and couplings of the MSSM Higgs fields, based on an effective theory of the MSSM degrees of freedom has been studied [18,20,21,300]. In these scenarios the tree-level mass of the lightest  $CP$ -even state

can easily be above the LEP bound of 114 GeV, thus allowing for a relatively light spectrum of superpartners, restricted only by direct searches. The Higgs spectrum and couplings can be significantly modified compared to the MSSM ones, often allowing for interesting new decay modes. It is also possible to moderately enhance the gluon fusion production cross section of the SM-like Higgs with respect to both the Standard Model and the MSSM.

Many non-SUSY solutions to the problem of electroweak symmetry breaking and the hierarchy problem are being developed. For example, Little Higgs models [25–27] propose additional sets of heavy vector-like quarks, gauge bosons, and scalar particles, with masses in the 100 GeV to a few TeV range. The couplings of the new particles are tuned in such a way that the quadratic divergences induced in the SM by the top, gauge-boson and Higgs loops are canceled at the one-loop level. If the Little Higgs mechanism successfully resolves the hierarchy problem, it should be possible to detect some of these new states at the LHC. For reviews of models and phenomenology, and a more complete list of references, see Refs. [301–303].

In Little Higgs models the production and decays of the Higgs boson are modified. For example, when the dominant production mode of the Higgs is through gluon fusion, the contribution of new fermions in the loop diagrams involved in the effective  $\phi gg$  vertex can reduce the production rate. The rate is generally suppressed relative to the SM rate due to the symmetries which protect the Higgs boson mass from quadratic divergences at the one-loop level. As a result, the branching ratio of the Higgs boson to photon pairs can be enhanced in these models [304]. By design, Little Higgs models are valid only up to a scale  $\Lambda \sim 5$ -10 TeV. The new physics which would enter above  $\Lambda$  remains unspecified, and will impact the Higgs sector. In general, it can modify Higgs couplings to third-generation fermions and gauge bosons, though these modifications are suppressed by  $1/\Lambda$  [305].

Distinctive features in the Higgs phenomenology of Little Higgs models may also stem from the fact that loop-level electroweak precision bounds on models with a tree-level custodial symmetry allows for a Higgs boson heavier than the one permitted by precision electroweak fits in the SM. This looser bound follows from a cancellation of the effects on the  $\rho$  parameter of a higher mass Higgs boson and the heavy partner of the top quark. The Higgs boson can have a mass as high as 800-1000 GeV in some Little Higgs models and still be consistent with electroweak precision data [306]. Lastly, the scalar content of a Little Higgs structure is model dependent. There could be two, or even more scalar doublets in a little Higgs model, or even different representations of the electroweak gauge group [26].

Models of extra space dimensions present an alternative way of avoiding the hierarchy problem [28]. New states, known as Kaluza-Klein (KK) excitations, can appear at the TeV scale, where gravity-mediated interactions may become relevant. They share the quantum numbers of the graviton and/or SM particles. In a particular realization of these models, based on



See key on page 457

## Gauge & Higgs Boson Particle Listings

### Higgs Bosons — $H^0$ and $H^\pm$

warped extra dimensions, a light Higgs-like particle, the radion, may appear in the spectrum [307]. The mass of the radion, as well as its possible mixing with the light Higgs boson, depends strongly on the mechanism that stabilizes the extra dimension, and on the curvature-Higgs mixing.

The radion couples to the trace of the energy-momentum tensor of the SM particles, leading to effective interactions with quarks, leptons, and weak gauge bosons which are similar to the ones of the Higgs boson, although they are suppressed by the ratio of the weak scale to the characteristic mass of the new excitations. An important characteristic of the radion is its enhanced coupling to gluons. Therefore, if it is light and mixes with the Higgs boson, it may modify the standard Higgs phenomenology at lepton and hadron colliders. A search for the radion conducted by OPAL at LEP gave negative results [308]. Radion masses below 58 GeV are excluded for the mass eigenstate which becomes the Higgs boson in the no-mixing limit, for all parameters of the Randall-Sundrum model. Most recently there has been a study of the effects of radion-Higgs mixing in Higgs boson searches at the LHC [309].

In models of warped extra dimensions in which the SM particles propagate in the extra dimensions, the KK excitations of the vector-like fermions may be pair-produced at colliders and decay into combinations of two Higgs bosons and jets, or one Higgs boson, a gauge boson, and jets. KK excitations may also be singly-produced. Some of these interesting possible new signatures for SM-like Higgs bosons in association with top or bottom quarks have been studied [27,29]. Most interesting, in models with warped extra dimensions the Kaluza-Klein excitations of the quarks and leptons which can be exchanged as virtual particles in the loops, can significantly change the Higgs production via gluon fusion, as well as its decay into diphotons. These results may depend on the precise localization of the SM-like Higgs in the extra dimension as well as on the precise particle content of the models. There are many studies in the literature that address these issues and compute the effects on the Higgs phenomenology [27,310].

Models of flat extra dimensions, in which SM particles propagate in the extra dimensions, are named Universal Extra Dimensions (UED) [311]. In such models the KK particles affect the Higgs couplings at the 1-loop level. In the minimal UED model, for tree-level masses of the lowest KK particles of order 1 TeV the  $gg \rightarrow h$  production rate is increased by  $\approx 20\%$  while the  $h \rightarrow \gamma\gamma$  decay width is decreased by a factor of  $\lesssim 3\%$  [312].

It is also possible to consider a simple description of models in which electroweak symmetry breaking is triggered by a light composite Higgs, which emerges from a strongly-interacting sector as a pseudo-Goldstone boson, by utilizing an effective low-energy Lagrangian approach [31]. Recent studies of the phenomenology relevant for collider searches can be found in Ref. 313.

The Higgs boson can also be a portal to hidden sectors, in particular, the Higgs boson can decay to the particles of a

low-mass hidden sector; these models are referred to as hidden valley models [314,315]. Since a light Higgs boson is a particle with a narrow width, even modest couplings to new states can give rise to a significant modification of Higgs phenomenology through exotic decays. Simple hidden valley models exist in which the Higgs boson decays to an invisible fundamental particle, which has a long lifetime to decay back to SM particles through small mixings with the SM Higgs boson; Ref. 315 describes an example. The Higgs boson may also decay to a pair of hidden valley “v-quarks,” which subsequently hadronize in the hidden sector, forming “v-mesons.” These mesons often prefer to decay to the heaviest state kinematically available, so that a possible signature is  $h \rightarrow 4b$ . Some of the v-mesons may be stable, implying a mixed missing energy plus heavy flavor final state. In other cases, the v-mesons may decay to leptons, implying the presence of low mass lepton resonances in high  $H_T$  events [316]. Other scenarios have been studied [317] in which Higgs bosons decay predominantly into light hidden sector particles, either directly, or through light SUSY states, and with subsequent cascades that increase the multiplicity of hidden sector particles. In such scenarios, the high multiplicity hidden sector particles, after decaying back into the Standard Model, appear in the detector as clusters of collimated leptons known as lepton jets.

If Higgs bosons are not discovered at the Tevatron or the LHC, other studies might be able to test alternative theories of dynamical electroweak symmetry breaking which do not involve a Higgs particle [318].

#### V. Searches for Higgs Bosons Beyond the MSSM

In extensions of the MSSM with one or more additional scalar singlets, limits have been set at  $e^+e^-$  and hadron colliders. The ALEPH [319] and DELPHI [320] collaborations place constraints on such models. Precise LEP 2 bounds on the Higgs boson masses depend on the couplings of the Higgs bosons to the gauge bosons and such couplings tend to be weakened somewhat from mixing with the singlet(s). At hadron colliders, searches for a light pseudoscalar boson predicted by the NMSSM have been performed by DØ [321], CDF [322], CMS [323], and ATLAS [324]. No significant excesses have been found and limits have been set on these models.

Most of the searches for the processes  $e^+e^- \rightarrow hZ$  and  $hA$ , which have been discussed in the context of the CPC-MSSM, rely on the assumption that the Higgs bosons have a sizable branching ratio to  $b\bar{b}$ . However, for specific parameters of the MSSM [325], the general 2HDM case, or composite models [175,177,326], decays to non- $b\bar{b}$  final states may be significantly enhanced. Flavor-independent hadronically-decaying Higgs boson searches have been performed at LEP which do not require the experimental signature of a  $b$ -jet [327], and a preliminary combination of LEP data has been performed [34,328]. If Higgs bosons are produced at the SM rate and decay only to jets of hadrons, then the 95% C.L. lower limit on the mass of the Higgs boson is 112.9 GeV, independent of the fractions

## Gauge & Higgs Boson Particle Listings

### Higgs Bosons — $H^0$ and $H^\pm$

of gluons and  $b$ ,  $c$ ,  $s$ ,  $u$  and  $d$ -quarks in Higgs boson decay. In conjunction with  $b$ -flavor sensitive searches, large domains of the general Type-II 2HDM parameter space have been excluded [329].

In the Type-I 2HDM, if the  $CP$ -odd neutral Higgs boson  $A$  is light (which is not excluded in the general 2HDM case, nor in some extensions of the MSSM), the decay  $H^\pm \rightarrow W^{\pm*}A$  may be dominant for masses accessible at LEP, a possibility that was investigated by DELPHI [330] and OPAL [331]. CDF's search for this decay chain in top quark decays [322] may also be interpreted in this scenario.

The LEP collaborations searched for Higgs bosons produced in pairs, in association with  $Z$  bosons,  $b$  quarks, and  $\tau$  leptons. The decays considered are  $\phi_{i,j} \rightarrow b\bar{b}, \tau^+\tau^-$ , and  $\phi_j \rightarrow \phi_i\phi_i$ , when kinematically allowed, yielding four- $b$ , four- $b$ +jets, six- $b$  and four- $\tau$  final states as well as mixed modes with  $b$ -quarks and tau leptons. No evidence for a Higgs boson was found [34,224], and mass-dependent coupling limits on a variety of processes, which apply to a large class of models were, set. The limits on the cross sections of Yukawa production of Higgs bosons are typically more than 100 times larger than the SM predictions [224]. Limits on pair-produced Higgs bosons extend up to  $m_{\phi_i} + m_{\phi_j}$  in the range 140- 200 GeV for full-strength production, assuming  $b\bar{b}$  and  $\tau^+\tau^-$  decays. Limits on Higgs-strahlung production with subsequent decay of the Higgs into lighter Higgs pairs exclude Higgs masses of the Higgs produced in association with the  $Z$  up to 114 GeV, if the lighter Higgs bosons decay to  $b\bar{b}$ . Weaker limits are set if the lighter Higgs pair decays to four tau leptons, or to a mixture of tau leptons and  $b$  quarks [34].

Decays of Higgs bosons into invisible (weakly-interacting and neutral) particles may occur in many models<sup>6</sup>. For example, Higgs bosons might decay into pairs of Goldstone bosons or Majorons [332]. In the process  $e^+e^- \rightarrow hZ$ , the mass of the invisible Higgs boson can be inferred from the kinematics of the reconstructed  $Z$  boson by using the beam energy constraint. Results from the LEP experiments can be found in Refs. [219] and [333]. A preliminary combination of LEP data yields a 95% C.L. lower bound of 114.4 GeV for the mass of a Higgs boson, if it is produced with SM production rate, and if it decays exclusively into invisible final states [334].

OPAL's decay-mode independent search for  $e^+e^- \rightarrow S^0Z$  [80] provides sensitivity to arbitrarily-decaying scalar particles, as only the recoiling  $Z$  boson decaying into leptons is required to be reconstructed. The energy and momentum constraints provided by the  $e^+e^-$  collisions allow the  $S^0$ 's four-vector to be reconstructed and limits placed on its production independent of its decay characteristics, allowing sensitivity for very light scalar masses. The limits obtained in this search are less than one-tenth of the SM Higgs-strahlung production rate for

<sup>6</sup> As discussed above, in the MSSM the Higgs can decay into pairs of lightest, stable neutralinos.

1 keV <  $m_{S^0}$  < 19 GeV, and less than the SM Higgs-strahlung rate for  $m_{S^0}$  < 81 GeV.

Hidden-valley models predict a rich phenomenology of new particles, some of which can be long-lived and hadronize with SM particles to form exotic particles which decay at measurable distances in collider experiments. CDF and DØ have searched for pair-produced long-lived particles produced resonantly and which decay to  $b\bar{b}$  pairs, and set limits on Higgs boson production in hidden-valley models [335,336]. The Higgs boson can also be the portal to high multiplicity hidden sector particles that may produce multiple charged leptons in the final state. A search for additional leptons in events containing a leptonically decaying  $W$  or  $Z$  boson by CDF [337] is sensitive to such models and others predicting multi-lepton final states; the results are consistent with SM expectations.

Photonic final states from the processes  $e^+e^- \rightarrow Z/\gamma^* \rightarrow H\gamma$  and from  $H \rightarrow \gamma\gamma$ , could be significantly enhanced, over the SM loop induced effects, in models with anomalous couplings [338]. Searches for the processes  $e^+e^- \rightarrow (H \rightarrow b\bar{b})\gamma$ ,  $(H \rightarrow \gamma\gamma)q\bar{q}$ , and  $(H \rightarrow \gamma\gamma)\gamma$  have been used to set limits on such anomalous couplings [339]. These searches also contribute in the combinations of searches for the standard model Higgs boson, although the small predicted signal rates imply that they contribute less than other channels.

Searches with photonic final states are experimentally very appealing and they have been used to constrain fermiophobic Higgs models, in which the Higgs boson has SM-like properties except that its tree-level couplings to fermions are assumed to be absent or very small. Fermiophobic Higgs models are however quite challenging to construct; they are generally strongly fine-tuned and imply new strong dynamics at low energy scales. A Type-I fermiophobic 2HDM could predict an enhanced  $h_f \rightarrow \gamma\gamma$  branching ratio, where  $h_f$  denotes a fermiophobic Higgs boson. The LEP searches are described in Ref. 340. In a preliminary combination of LEP data [341], a fermiophobic Higgs boson with mass less than 108.2 GeV (95% C.L.) has been excluded. Fermiophobic models would also predict enhanced branching ratios for the decays  $h_f \rightarrow W^*W$  and  $Z^*Z$ , a possibility that has been addressed by L3 [342] and ALEPH [343]. At hadron colliders, the process  $gg \rightarrow h_f$  has a negligible rate in a fermiophobic Higgs model, but the  $Wh_f$ ,  $Zh_f$ , and VBF production cross sections remain close to their SM predictions and the Higgs boson branching ratios to  $\gamma\gamma$ ,  $W^+W^-$ , and  $ZZ$  are enhanced. A search for the SM Higgs boson at a hadron collider can not therefore be re-interpreted as a search in a fermiophobic model, even if a limit is set on the total production cross section times a specific decay branching ratio, due to the different kinematic distributions from the different production modes affecting the signal acceptance. CDF and DØ have re-optimized their  $h_f \rightarrow \gamma\gamma$  searches for the fermiophobic model, and with results based on 9.7 fb<sup>-1</sup> of DØ data [344,345] and 10.0 fb<sup>-1</sup> of CDF data [346,347], combined with  $h_f \rightarrow W^+W^-$  and  $h_f \rightarrow ZZ$  searches extend the exclusion in the fermiophobic Higgs model to 119 GeV [110,348]. Other



production of fermiophobic Higgs bosons, leading to a 3-photons final state, has also been searched for by  $D\bar{O}$  [349].

ATLAS and CMS search for a fermiophobic Higgs boson in  $h_f \rightarrow \gamma\gamma$  searches optimized for the fermiophobic signature [350,351], and CMS combines these with searches for  $h_f \rightarrow W^+W^-$  and  $h_f \rightarrow ZZ$  assuming fermiophobic production and decay [10]. CMS excludes a fermiophobic Higgs boson in the range  $110 \text{ GeV} < m_H < 188 \text{ GeV}$  at the 95% C.L.

Higgs bosons with double electric charge are predicted, for example, by models with additional triplet scalar fields or left-right symmetric models [352]. It has been emphasized that the see-saw mechanism could lead to doubly-charged Higgs bosons with masses which are accessible to current and future colliders [353]. Searches were performed at LEP for the pair-production process  $e^+e^- \rightarrow H^{++}H^{--}$  with four prompt leptons in the final state [354–356]. Lower mass bounds between 95 GeV and 100 GeV were obtained for left-right symmetric models (the exact limits depend on the lepton flavors). Doubly-charged Higgs bosons were also searched for in single production [357]. Furthermore, such particles would modify the Bhabha scattering cross section and forward-backward asymmetry via  $t$ -channel exchange. The absence of a significant deviation from the SM prediction puts constraints on the Yukawa coupling of  $H^{\pm\pm}$  to electrons for Higgs boson masses which reach into the TeV range [356,357].

Searches have also been carried out at the Tevatron for the pair production process  $p\bar{p} \rightarrow H^{++}H^{--}$ . The  $D\bar{O}$  search is performed in the  $\mu^+\mu^+\mu^-\mu^-$  final state [358], while CDF also considers  $e^+e^+e^-e^-$  and  $e^+\mu^+e^-\mu^-$ , and final states with  $\tau$  leptons [359]. A search by CDF for a long-lived  $H^{\pm\pm}$  boson, which would decay outside the detector, is described in [360].

CMS has searched for doubly-charged Higgs bosons which are either pair produced,  $pp \rightarrow H^{++}H^{--}$  or produced in association with a singly-charged Higgs boson via  $s$ -channel  $W^\pm$  exchange,  $pp \rightarrow H^{++}H^-$ , assuming decays of the form  $\ell^+\ell'^-$ , where  $\ell, \ell'$  are combinations of  $e, \mu,$  and  $\tau$  leptons [361]. No significant excess is seen, and limits on the mass of the doubly-charged Higgs boson vary from 165 GeV to 457 GeV, depending on the production and decay mode. ATLAS has searched for doubly charged Higgs bosons in the dimuon decay [362], setting a limit on the mass of 355 GeV assuming a decay branching ratio to dimuons of 100% and coupling to left-handed fermions, and a limit on the mass of 251 GeV assuming coupling to right-handed fermions.

## VI. Outlook

The Tevatron has completed its run and is finalizing its Higgs boson search results with up to  $10 \text{ fb}^{-1}$  of data analyzed. The combination of the preliminary results from CDF and  $D\bar{O}$ 's searches for the SM Higgs boson shows an excess of data events with respect to the background estimation in the mass range  $115 \text{ GeV} < m_H < 135 \text{ GeV}$ , dominated by the  $H \rightarrow b\bar{b}$  channels. The global significance for such an excess anywhere in the full mass range is 2.2 standard deviations.

In 2011, the LHC delivered approximately  $5 \text{ fb}^{-1}$  of  $pp$  collision data at  $\sqrt{s} = 7 \text{ TeV}$ . A variety of searches targeting the SM Higgs boson in the mass range  $100 \text{ GeV} < m_H < 600 \text{ GeV}$  have been performed, excluding all masses except the range between 114 GeV and 129 GeV. Most of the region below 123 GeV is also excluded by the ATLAS experiment but not by other experiments. Within the allowed mass range, both ATLAS and CMS observe independent excesses of events consistent with a SM-like Higgs boson with a mass of  $\approx 125 \text{ GeV}$ , with global significances of  $1.3\sigma$  and  $2.1\sigma$ , respectively. Both experiments observe excesses of data over the corresponding background predictions in searches for Higgs bosons decaying into diphotons and  $Z$  bosons pairs. More data, at  $\sqrt{s} = 8 \text{ TeV}$ , being collected in 2012, are required to understand this excess. The LHC will either exclude the SM Higgs boson or confirm the existence of a SM-like Higgs particle. In the latter case, accurate measurements of the properties of the Higgs particle as well as searches for new particles will be of most relevance.

Searches at the LHC for additional Higgs bosons: charged Higgs bosons, doubly charged Higgs bosons, the neutral Higgs bosons of the MSSM, and other exotic Higgs particles, have yielded results consistent with background expectations and strong limits have been placed in significant regions of parameter space. An upgrade of the center of mass energy to 13–14 TeV is planned for the near future. This upgrade will allow the LHC to explore a wide variety of extended Higgs sectors and search for new particles expected in models beyond the SM. This upgrade will also allow for increased precision of measurements of the properties of a SM-like Higgs boson, if one exists.

A high-energy  $e^+e^-$  linear collider may be built in the future, allowing ultimate high-precision measurements of the properties of Higgs boson(s) and other particles beyond those of the SM. At a  $\mu^+\mu^-$  collider, mass measurements with a precision of a few MeV would be possible, and energy scans may distinguish between signals of Higgs particles nearly degenerate in mass, as predicted in many extended Higgs models.

In the theoretical landscape, numerous models are available with novel approaches to the problem of electroweak symmetry breaking. In the next decade, the LHC's exploration of the multi-TeV energy scale will solidify our understanding of the mechanism of mass generation of the known elementary particles.

## VII. Addendum

Updated July 12, 2012.

On July 4, 2012, the ATLAS and CMS collaborations simultaneously announced observation of a new particle produced in  $pp$  collision data at high energies [363–366]. The data samples used correspond to between 4.6 and  $5.1 \text{ fb}^{-1}$  of collision data collected at  $\sqrt{s} = 7 \text{ TeV}$  in 2011, and between 5.3 and  $5.9 \text{ fb}^{-1}$  of collisions collected at  $\sqrt{s} = 8 \text{ TeV}$  in 2012. The observed decay modes indicate that the new particle is a boson. The evidence is strong that the new particle decays to  $\gamma\gamma$  and  $ZZ$  with rates consistent with those predicted for the Standard

## Gauge & Higgs Boson Particle Listings

### Higgs Bosons — $H^0$ and $H^\pm$

Model (SM) Higgs boson. There are indications that the new particle might also decay to  $W^+W^-$ , and decays to  $b\bar{b}$  and  $\tau^+\tau^-$  are being sought as well.

The ATLAS collaboration has updated its SM Higgs boson searches in the  $H \rightarrow \gamma\gamma$  and  $H \rightarrow ZZ \rightarrow \ell^+\ell^-\ell'^+\ell'^-$  [367] modes with new data collected at  $\sqrt{s} = 8$  TeV and improved analysis techniques applied to both the 7 TeV and 8 TeV data. ATLAS has also finalized its  $\sqrt{s} = 7$  TeV analyses in the  $H \rightarrow ZZ \rightarrow \ell^+\ell^-\nu\bar{\nu}$ ,  $H \rightarrow ZZ \rightarrow \ell^+\ell^-q\bar{q}$ ,  $H \rightarrow W^+W^- \rightarrow \ell^+\nu_\ell\ell'^-\bar{\nu}_{\ell'}$ ,  $H \rightarrow W^+W^- \rightarrow \ell^+\nu_\ell q\bar{q}'$ ,  $H \rightarrow \tau^+\tau^-$ , and  $WH, ZH \rightarrow Wb\bar{b}, Zb\bar{b}$  channels [368], and includes them in its SM Higgs boson combined results [369,364]. ATLAS's  $H \rightarrow \gamma\gamma$  search has been improved with respect to the previous version by separating events with two jets and two photons from other events, which improves the sensitivity for the vector boson fusion (VBF) process, and by improved photon identification and isolation algorithms. ATLAS's  $H \rightarrow ZZ \rightarrow \ell^+\ell^-\ell'^+\ell'^-$  search has been improved with respect to the previous results by re-optimizing the kinematic cuts, improving electron reconstruction and identification efficiency at low  $p_T$ , and improved robustness to pileup events.

The CMS collaboration has updated its SM Higgs boson searches in the  $H \rightarrow \gamma\gamma$ ,  $H \rightarrow ZZ \rightarrow \ell^+\ell^-\ell'^+\ell'^-$ ,  $H \rightarrow ZZ \rightarrow \ell^+\ell^-\nu\bar{\nu}$ ,  $H \rightarrow W^+W^- \rightarrow \ell^+\nu_\ell\ell'^-\bar{\nu}_{\ell'}$ ,  $H \rightarrow b\bar{b}$ , and  $H \rightarrow \tau^+\tau^-$  channels, all of which include 8 TeV data collected in 2012 [370]. The  $t\bar{t}H \rightarrow t\bar{t}b\bar{b}$  [370] search is new and based on 2011 data. The  $H \rightarrow W^+W^- \rightarrow \ell^+\nu_\ell q\bar{q}'$  [370] search is included for the first time in the combination.

CMS's  $H \rightarrow \gamma\gamma$  search has been improved with respect to its earlier version by dividing the diphoton plus two jet category into two, depending on the dijet invariant mass and the jet  $p_T$ , and also by removing jets from pileup collisions. The  $H \rightarrow ZZ \rightarrow \ell^+\ell^-\ell'^+\ell'^-$  search has been improved with respect to its previous version, benefiting from improved lepton identification and isolation algorithms, as well as final state radiation recovery. The discriminant variables used now to separate the expected signal from the backgrounds are two-dimensional, plotting the invariant mass of the four leptons versus a matrix-element-based likelihood discriminant. CMS's  $H \rightarrow W^+W^-$  search combines the results from the multivariate analysis (MVA) for the 7 TeV data with the results of a cut-based analysis on the 8 TeV data sample, which is described in Ref. 372. CMS's  $VH \rightarrow Vb\bar{b}$  (with  $V = W$  or  $Z$ ) search encompasses five channels:  $WH \rightarrow e\nu b\bar{b}$ ,  $WH \rightarrow \mu\nu b\bar{b}$ ,  $ZH \rightarrow e^+e^-b\bar{b}$ ,  $ZH \rightarrow \mu^+\mu^-b\bar{b}$ , and  $ZH \rightarrow \nu\bar{\nu}b\bar{b}$ . CMS's  $H \rightarrow \tau^+\tau^-$  search divides the candidate events by tau lepton decay type and subdivides the samples based on number of jets (0,1) or on VBF type. The 0 and 1 jet categories are also further subdivided according to low or high  $p_T$  of the  $\tau$ .

Each experiment, ATLAS and CMS, separately combine their data to obtain independent results of their searches, computing the significance of the observation, measuring the production rates times the decay branching fractions for each

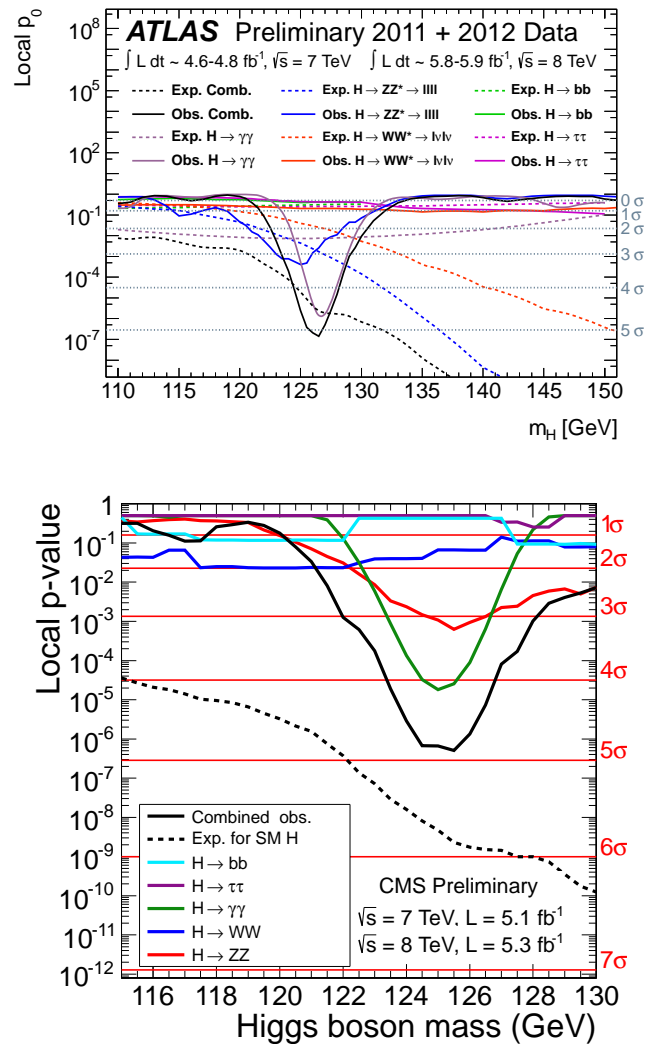


**Figure 17:** Local  $p$ -values for the ATLAS SM Higgs boson search (left), and the CMS SM Higgs boson search (right), separately for each decay mode. The solid lines show the observed  $p$ -values and the dashed lines show the median expected  $p$ -values, assuming a SM Higgs boson is present, computed at each value of  $m_H$  separately.

channel analyzed, and updating the mass and rate exclusions [364,366]. The separate results provide independent confirmations of the observation. The significance is quantified by a  $p$ -value, which is the probability to observe an upward fluctuation of the background which gives a result at least as signal-like as that observed in the data. A  $p$ -value of  $2.87 \times 10^{-7}$  corresponds to a five standard deviation excess over the background prediction. The  $p$ -values are shown for the analysis channels separately for ATLAS and CMS in Fig. 17. ATLAS observes an excess with a local significance of  $5.0\sigma$  at a mass  $m_H = 126.5$  GeV, with an expected significance of  $4.6\sigma$  if a SM Higgs boson were present at such mass value. CMS observes

See key on page 457

## Gauge & Higgs Boson Particle Listings

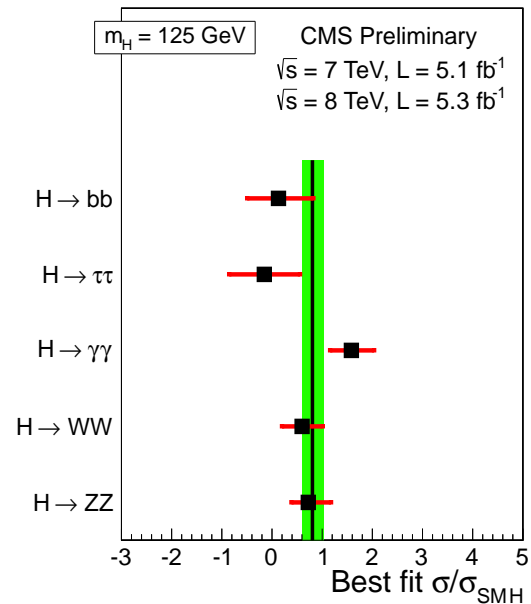
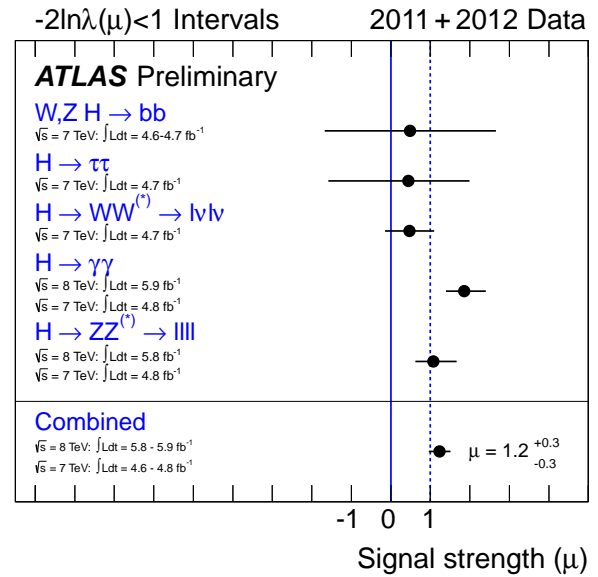
### Higgs Bosons — $H^0$ and $H^\pm$

an excess with a local significance of  $4.9\sigma$  at a mass 125.5 GeV, with an expected significance of  $5.9\sigma$ , and measures the mass of the new boson as  $m_H = 125.3 \pm 0.6$  GeV. Fig. 18 shows the best-fit cross sections times the relevant decay branching fractions for the new particle, normalized to the SM predictions for Higgs boson production and decay, assuming it has a mass of 126.5 GeV (ATLAS), and 125 GeV (CMS). ATLAS's combined signal strength fit, assuming SM ratios for the production and decay modes, is  $\mu = \sigma/\sigma_{\text{SMH}} = 1.2 \pm 0.3$ , and CMS's combined fit is  $\mu = 0.80 \pm 0.22$ . Within the current experimental uncertainties, the measurements are consistent with SM predictions. Both ATLAS and CMS separately exclude SM Higgs bosons with masses outside a narrow range near the local excesses.

The Tevatron collaborations updated their Higgs boson search results on July 2, 2012 [373]. The D0 collaboration has updated its  $VH \rightarrow Vb\bar{b}$  search results by improving the acceptance of the lepton selection, dividing the events into more categories based on the number and quality of  $b$  tags, and improving the MVA treatment [374]. Additional data and analysis improvements also improve the sensitivity of D0's  $H \rightarrow W^+W^-$  searches by 5-10% with respect to the previous result [375]. The CDF Higgs boson searches were updated with the full Run II data set and improved  $b$ -tagging for the Winter 2012 conferences [376]. CDF and D0 combine their results together, and, with the full suite of SM Higgs boson search analyses, see a broad excess in the range  $115 \text{ GeV} < m_H < 135 \text{ GeV}$ , with a global signal significance of  $2.5\sigma$ , and a maximum local significance of  $3.0\sigma$ . Fig. 19 shows the measured cross sections times the relevant decay branching ratios normalized to those expected for a SM Higgs boson at mass  $m_H = 125$  GeV for the combined CDF and D0 searches for  $H \rightarrow W^+W^-$ ,  $H \rightarrow \gamma\gamma$ , and  $VH \rightarrow Vb\bar{b}$  searches. The combined result, assuming SM ratios for the production and decay modes, is  $\mu = 1.4 \pm 0.6$ . In the dominant decay channel,  $VH \rightarrow Vb\bar{b}$ , the global significance is  $2.9\sigma$ , with a maximum local significance of  $3.2\sigma$ . Assuming the existence of a new particle, this provides the first strong indication for its decay into a fermion pair at a rate consistent with the SM prediction for a Higgs boson of such a mass.

In summary, a new particle has been observed at the LHC. Within the experimental uncertainties, it has characteristics consistent with those expected from the Higgs boson predicted by the Standard Model, with a mass near 125 GeV. Tevatron data also are consistent with the production and decay of a SM-like Higgs boson at this mass. However, the present experimental uncertainties still allow for a wide variety of new physics alternatives.

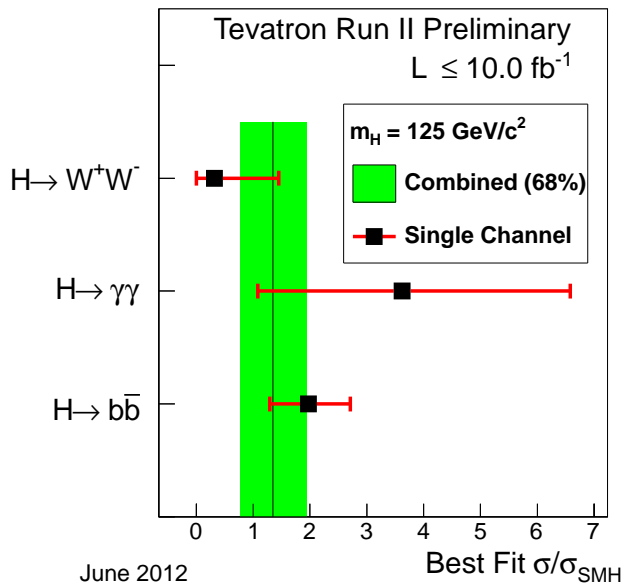
The LHC will continue to run until early 2013, and it is expected to deliver at least  $15 \text{ fb}^{-1}$  more data to both ATLAS and CMS, at  $\sqrt{s} = 8 \text{ TeV}$ . After this run, a shutdown will occur to improve the accelerator components to allow data taking at higher energies. The much larger dataset to be collected will provide the opportunity to make increasingly precise measurements of the properties of the new particle, and



**Figure 18:** Best-fit production cross sections times branching ratios to  $H \rightarrow \gamma\gamma$ ,  $H \rightarrow ZZ$ ,  $H \rightarrow W^+W^-$ ,  $H \rightarrow b\bar{b}$ , and  $H \rightarrow \tau^+\tau^-$ , normalized to the SM predictions for Higgs boson production and decay, assuming it has a mass of 126.5 GeV (ATLAS, left), and 125 GeV (CMS, right). The combined result, assuming SM ratios for the production and decay modes, is shown as a separate point on the ATLAS graph at  $\mu = \sigma/\sigma_{\text{SMH}} = 1.2 \pm 0.3$  and is shown with the shaded band on the CMS graph at  $\mu = 0.80 \pm 0.22$ .

test whether it is the SM Higgs boson or point the way to physics beyond the SM.

## Gauge &amp; Higgs Boson Particle Listings

Higgs Bosons —  $H^0$  and  $H^\pm$ 

**Figure 19:** Best-fit cross sections times branching ratios to  $H \rightarrow W^+W^-$ ,  $H \rightarrow \gamma\gamma$  and  $H \rightarrow b\bar{b}$ , normalized to the SM predictions for Higgs boson production and decay, assuming it has a mass of 125 GeV, for the combined CDF and D0 search results. The combined result, assuming SM ratios for the production and decay modes, is shown with a shaded band, at  $\mu = \sigma/\sigma_{\text{SMH}} = 1.4 \pm 0.6$ .

## References

In order to keep this review up to date, some unpublished results are quoted. LEP results are marked with (\*) in the reference list and can be accessed conveniently from the public web page <http://lepfiggs.web.cern.ch/LEPHIGGS/pdg2008/>. Preliminary results from the CDF Collaboration are marked with (\*\*) and can be obtained from the public web page <http://www-cdf.fnal.gov/physics/physics.html>; those from D0 are marked with (\*\*\*) and can be obtained at <http://www-d0.fnal.gov/Run2Physics/WWW/results.htm>.

1. P.W. Higgs, Phys. Rev. Lett. **13**, 508 (1964); *idem*, Phys. Rev. **145**, 1156 (1966); F. Englert and R. Brout, Phys. Rev. Lett. **13**, 321 (1964); G.S. Guralnik, C.R. Hagen, and T.W. Kibble, Phys. Rev. Lett. **13**, 585 (1964).
2. S.L. Glashow, Nucl. Phys. **20**, 579 (1961); S. Weinberg, Phys. Rev. Lett. **19**, 1264 (1967); A. Salam, *Elementary Particle Theory*, eds.: Svartholm, Almquist, and Wiksell, Stockholm, 1968; S. Glashow, J. Iliopoulos, and L. Maiani, Phys. Rev. **D2**, 1285 (1970).
3. J.M. Cornwall, D.N. Levin, and G. Tiktopoulos, Phys. Rev. Lett. **30**, 1286 (1973); Phys. Rev. **D10**, 1145 (1974); C.H. Llewellyn Smith, Phys. Lett. **B46**, 233 (1973).
4. B.W. Lee, C. Quigg, and H.B. Thacker, Phys. Rev. **D16**, 1519 (1977).

5. LEP Electroweak Working Group, status of March 2012, <http://lepewwg.web.cern.ch/LEPEWWG/>; The ALEPH, CDF, D0, DELPHI, L3, OPAL, SLD Collabs., the LEP Electroweak Working Group, the Tevatron Electroweak Working Group, and the SLD Electroweak and Heavy Flavor groups, LEPEWWG/2009-01 (2009); J. Erler and P. Langacker, *Electroweak Model and Constraints on New Physics*, in this volume.
6. The CDF and D0 Collabs. and the Tevatron New Physics and Higgs Working Group, [arXiv:1203.3774 \[hep-ex\]](https://arxiv.org/abs/1203.3774) (2012).
7. ATLAS Collab., Phys. Lett. **B710**, 49 (2012).
8. ATLAS Collab., “An update to the combined search for the Standard Model Higgs boson with the ATLAS detector at the LHC using up to  $4.9 \text{ fb}^{-1}$  of  $pp$  collision data at  $\sqrt{s} = 7 \text{ TeV}$ ”, ATLAS-CONF-2012-019 (2012).
9. CMS Collab., [arXiv:1202.1488 \[hep-ex\]](https://arxiv.org/abs/1202.1488), submitted to Phys. Lett. B (2012).
10. CMS Collab., “Combination of SM, SM4, FP Higgs boson searches”, CMS-PAS-HIG-12-008 (2012).
11. J. Wess and B. Zumino, Nucl. Phys. **B70**, 39 (1974); *idem*, Phys. Lett. **49B**, 52 (1974); H.P. Nilles, Phys. Rev. **C110**, 1984 (1); S.P. Martin, [arXiv:hep-ph/9709356](https://arxiv.org/abs/hep-ph/9709356) (1997); P. Fayet, Phys. Lett. **B69**, 489 (1977); *ibid.*, **B84**, 421 (1979); *ibid.*, **B86**, 272 (1979); *idem.*, Nucl. Phys. **B101**, 81 (2001).
12. H.E. Haber and G.L. Kane, Phys. Rev. **C117**, 75 (1985).
13. J.F. Gunion *et al.*, *The Higgs Hunter’s Guide*, Addison-Wesley (1990).
14. A detailed discussion and list of references is given in subsection III.
15. E. Accomando, *et al.*, [hep-ph/0608079](https://arxiv.org/abs/hep-ph/0608079).
16. U. Ellwanger and C. Hugonie, Mod. Phys. Lett. **A22**, 1581 (2007).
17. P. Batra *et al.*, JHEP **0402**, 043 (2004); P. Batra *et al.*, JHEP **0406**, 032 (2004).
18. M. Dine, N. Seiberg, and S. Thomas, Phys. Rev. **D76**, 095004 (2007) and refs. therein.
19. J.R. Espinosa and M. Quirós, Phys. Rev. Lett. **81**, 516 (1998).
20. M. Carena *et al.*, Phys. Rev. **D81**, 015001 (2010); W. Altmannshofer *et al.*, Phys. Rev. **D84**, 095027 (2011).
21. I. Antoniadis *et al.*, Nucl. Phys. **B831**, 133 (2010).
22. L.E. Ibáñez and G.G. Ross, Phys. Lett. **B105**, 439 (1981); S. Dimopoulos, S. Raby, and F. Wilczek, Phys. Rev. **D24**, 1681 (1981); M.B. Einhorn and D.R.T. Jones, Nucl. Phys. **B196**, 475 (1982); W.J. Marciano and G. Senjanovic, Phys. Rev. **D25**, 3092 (1982).
23. J. Ellis, S. Kelley and D.V. Nanopoulos, Phys. Lett. **B249**, 441 (1990); P. Langacker and M. Luo, Phys. Rev. **D44**, 817 (1991); U. Amaldi, W. de Boer, and H. Fürstenaun, Phys. Lett. **B260**, 447 (1991); P. Langacker and N. Polonsky, Phys. Rev. **D52**, 3081 (1995); S. Pokorski, *Act. Phys. Pol.* **B30**, 1759 (1999);

See key on page 457

## Gauge & Higgs Boson Particle Listings

### Higgs Bosons — $H^0$ and $H^\pm$

- For a recent review, see R.N. Mohapatra, in *Particle Physics 1999, Proceedings of the ICTP Summer School in Particle Physics*, Trieste, Italy, 21 June–9 July, 1999, edited by G. Senjanovic and A.Yu. Smirnov. (World Scientific, Singapore, 2000) pp. 336–394.
24. S. Weinberg, Phys. Rev. **D13**, 974 (1979); Phys. Rev. **D19**, 1277 (1979);  
L. Susskind, Phys. Rev. **D20**, 2619 (1979);  
E. Farhi and L. Susskind, Phys. Rev. **74**, 277 (1981);  
R.K. Kaul, Rev. Mod. Phys. **55**, 449 (1983);  
C. T. Hill and E. H. Simmons, Phys. Reports **381**, 235 (2003) [E: *ibid.*, **390**, 553 (2004)].
  25. N. Arkani-Hamed, A.G. Cohen, and H. Georgi, Phys. Lett. **B513**, 232 (2001);  
N. Arkani-Hamed *et al.*, JHEP **0207**, 034 (2002);  
N. Arkani-Hamed *et al.*, JHEP **0208**, 020 (2002);  
N. Arkani-Hamed *et al.*, JHEP **0208**, 021 (2002);  
I. Low and A. Vichi, Phys. Rev. **D84**, 045019 (2011);  
A. Azatov and J. Galloway, Phys. Rev. **D85**, 055013 (2012).
  26. I. Low, W. Skiba, and D. Smith, Phys. Rev. **D66**, 072001 (2002).
  27. A. Falkowski, Phys. Rev. **D77**, 055018 (2008).
  28. I. Antoniadis, Phys. Lett. **B246**, 377 (1990);  
N. Arkani-Hamed, S. Dimopoulos, and G.R. Dvali, Phys. Lett. **B429**, 263 (1998);  
L. Randall and R. Sundrum, Phys. Rev. Lett. **83**, 3370 (1999) *idem.*, **84**, 4690 (1999);  
G.F. Giudice *et al.*, Nucl. Phys. **B544**, 3 (1999);  
C. Csáki *et al.*, Phys. Rev. **D63**, 065002 (2001).
  29. J.A. Aguilar-Saavedra, JHEP **0612**, 033 (2006);  
M. Carena *et al.*, Phys. Rev. **D76**, 035006 (2007);  
A.D. Medina, N. R. Shah, and C.E.M. Wagner, Phys. Rev. **D76**, 095010 (2007);  
A. Djouadi and G. Moreau, Phys. Lett. **B660**, 67 (2008);  
H. Davoudiasl, B. Lillie, and T.G. Rizzo, JHEP **0608**, 042 (2006);  
R. Contino, Y. Nomura, and A. Pomarol, Nucl. Phys. **B671**, 148 (2003);  
K. Agashe, R. Contino, and A. Pomarol, Nucl. Phys. **B719**, 165 (2005);  
R. Contino, L. Da Rold, and A. Pomarol, Phys. Rev. **D75**, 055014 (2007).
  30. M. Carena, E. Ponton, and J. Zurita, Phys. Rev. **D82**, 055025 (2010);  
M. Carena, E. Ponton, and J. Zurita, Phys. Rev. **D85**, 035007 (2012).
  31. G.F. Giudice *et al.*, JHEP **0706**, 045 (2007);  
R. Contino *et al.*, JHEP **1005**, 089 (2010);  
J.R. Espinosa, C. Grojean, and M. Mühlleitner, JHEP **1005**, 065 (2010);  
J.R. Espinosa, C. Grojean, and M. Mühlleitner, [arXiv:1202.1286 \[hep-ph\]](https://arxiv.org/abs/1202.1286) (2012);  
G. Panico and A. Wulzer, JHEP **1109**, 135 (2011);  
S. De Curtis, M. Redi, and A. Tesi, JHEP **1204**, 042 (2012);  
R. Contino *et al.*, JHEP **1110**, 081 (2011);  
A. Azatov, R. Contino, and J. Galloway, JHEP **1204**, 127 (2012).
  32. P.J. Franzini and P. Taxil, in *Z physics at LEP 1*, CERN 89-08 (1989).
  33. ALEPH, DELPHI, L3, and OPAL Collabs., The LEP Working Group for Higgs Boson Searches, Phys. Lett. **B565**, 61 (2003).
  34. ALEPH, DELPHI, L3 and OPAL Collabs., The LEP Working Group for Higgs Boson Searches, Eur. Phys. J. **C47**, 547 (2006).
  35. T. van Ritbergen and R. G. Stuart, Phys. Rev. Lett. **82**, 488 (1999);  
T. van Ritbergen and R. G. Stuart, Nucl. Phys. **B564**, 343 (2000);  
M. Steinhauser and T. Seidensticker, Phys. Lett. **B467**, 271 (1999);  
D. M. Webber *et al.*, Phys. Rev. Lett. **106**, 041803 (2011).
  36. N. Cabibbo *et al.*, Nucl. Phys. **B158**, 295 (1979);  
G. Altarelli and G. Isidori, Phys. Lett. **B337**, 141 (1994);  
J.A. Casas, J.R. Espinosa, and M. Quirós, Phys. Lett. **B342**, 171 (1995);  
*idem.*, Phys. Lett. **B382**, 374 (1996);  
T. Hambye and K. Riesselmann, Phys. Rev. **D55**, 7255 (1997).
  37. J.R. Espinosa and M. Quirós, Phys. Lett. **B353**, 257 (1995);  
G. Isidori *et al.*, Nucl. Phys. **B609**, 387 (2001).
  38. J. Elias-Miró *et al.*, Phys. Lett. **B709**, 222 (2012).
  39. B.A. Kniehl, Phys. Rept. **240**, 211 (1994).
  40. A. Denner *et al.*, Eur. Phys. J. **C71**, 1753 (2011);  
A. Djouadi, J. Kalinowski, and M. Spira, Comput. Phys. Commun. **108**, 56 (1998);  
A. Djouadi *et al.*, [arXiv:1003.1643 \[hep-ph\]](https://arxiv.org/abs/1003.1643) (2010);  
A. Bredenstein *et al.*, Phys. Rev. **D74**, 013004 (2006);  
A. Bredenstein *et al.*, JHEP **0702**, 80 (2007);  
S. Actis *et al.*, Nucl. Phys. **B811**, 182 (2009);  
D. Bardin, B. Vilenky, and P. Khristova, Sov. J. Nucl. Phys. **53**, 152 (1991);  
A. Dabelstein and W. Hollik, Z. Phys. **C53**, 507 (1992);  
B.A. Kniehl, Nucl. Phys. **B376**, 3 (1992);  
S.G. Gorishniĭ, A.L. Kataev, and S.A. Larin, Sov. J. Nucl. Phys. **40**, 329 (1984) [Yad. Fiz. **40**, 517 (1984)];  
S.G. Gorishniĭ *et al.*, Phys. Rev. **D43**, 1633 (1991);  
K.G. Chetyrkin, Phys. Lett. **B390**, 309 (1997);  
K.G. Chetyrkin and M. Steinhauser, Phys. Lett. **B408**, 320 (1997);  
E. Braaten and J.P. Leveille, Phys. Rev. **D22**, 715 (1980);  
N. Sakai, Phys. Rev. **D22**, 2220 (1980);  
T. Inami and T. Kubota, Nucl. Phys. **B179**, 171 (1981);  
M. Drees and K. Hikasa, Phys. Lett. **B240**, 455 (1990) [E: **B262** 497 (1991)];  
M. Drees and K. Hikasa, Phys. Rev. **D41**, 1547 (1990);  
R. Harlander and M. Steinhauser, Phys. Rev. **D56**, 3980 (1997);  
A. Ghinculov, Phys. Lett. **B337**, 137 (1994);  
L. Durand, K. Riesselmann, and B.A. Kniehl, Phys. Rev. Lett. **72**, 2534 (1994);  
K. Melnikov and O.I. Yakovlev, Phys. Lett. **B312**, 179 (1993);  
M. Inoue *et al.*, Mod. Phys. Lett. **A9**, 1189 (1994);  
U. Aglietti *et al.*, JHEP **0701**, 021 (2007);  
K.G. Chetyrkin, B.A. Kniehl, and M. Steinhauser, Phys. Rev. Lett. **79**, 353 (1997);  
P.A. Baikov and K.G. Chetyrkin, Phys. Rev. Lett. **97**, 061803 (2006);  
A. Ghinculov, Nucl. Phys. **B455**, 21 (1995);  
A. Frink *et al.*, Phys. Rev. **D54**, 4548 (1996);

## Gauge &amp; Higgs Boson Particle Listings

Higgs Bosons —  $H^0$  and  $H^\pm$ 

- E. Gross *et al.*, Z. Phys. **C63**, 417 (1994); [E: *ibid.*, **C66**, 32 (1995)];  
A.L. Kataev, Sov. Phys. JETP Lett. **66**, 327 (1997) [*Pis'ma Zh. Éksp. Teor. Fiz.* **66** (1997) 308].
41. A. Djouadi, M. Spira, and P.M. Zerwas, Z. Phys. **C70**, 675 (1996).
  42. M. Spira *et al.*, Nucl. Phys. **B453**, 17 (1995).
  43. S. Dittmaier *et al.*, [LHC Higgs Cross Section Working Group], arXiv:1201.3084 [hep-ph] (2012).
  44. M. Carena and H.E. Haber, Prog. in Part. Nucl. Phys. **50**, 152 (2003).
  45. A. Djouadi, Phys. Reports **457**, 1 (2008).
  46. J. Ellis, M.K. Gaillard, and D.V. Nanopoulos, Nucl. Phys. **B106**, 292 (1976);  
B.L. Ioffe and V.A. Khoze. Sov. J. Nucl. Phys. **9**, 50 (1978).
  47. D.R.T. Jones and S. Petcov, Phys. Lett. **B84**, 440 (1979);  
R.N. Cahn and S. Dawson, Phys. Lett. **B136**, 196 (1984);  
G.L. Kane, W.W. Repko, and W.B. Rolnick, Phys. Lett. **B148**, 367 (1984);  
G. Altarelli, B. Mele, and F. Pitolli. Nucl. Phys. **B287**, 205 (1987);  
W. Kilian, M. Krämer, and P.M. Zerwas, Phys. Lett. **B373**, 135 (1996).
  48. B.A. Kniehl, Z. Phys. **C55**, 605 (1992).
  49. J. Fleischer and F. Jegerlehner, Nucl. Phys. **B216**, 469 (1983);  
A. Denner *et al.*, Z. Phys. **C56**, 261 (1992).
  50. B.A. Kniehl, Int. J. Mod. Phys. **A17**, 1457 (2002).
  51. K.J. Gaemers and G.J. Gounaris, Phys. Lett. **B77**, 379 (1978);  
A. Djouadi, J. Kalinowski, and P. M. Zerwas, Z. Phys. **C54**, 255 (1992);  
B.A. Kniehl, F. Madricardo, and M. Steinhauser, Phys. Rev. **D66**, 054016 (2002).
  52. S. Dittmaier *et al.*, Phys. Lett. **B441**, 383 (1998);  
S. Dittmaier *et al.*, Phys. Lett. **B478**, 247 (2000);  
S. Dawson and L. Reina, Phys. Rev. **D59**, 054012 (1999).
  53. A. Djouadi, M. Spira, and P.M. Zerwas, Phys. Rev. **B264**, 440 (1991);  
S. Dawson, Nucl. Phys. **B359**, 283 (1991);  
R.V. Harlander and W.B. Kilgore, Phys. Rev. Lett. **88**, 201801 (2002);  
C. Anastasiou and K. Melnikov, Nucl. Phys. **B646**, 220 (2002);  
V. Ravindran, J. Smith, and W.L. van Neerven, Nucl. Phys. **B665**, 325 (2003).
  54. S. Actis *et al.*, Phys. Lett. **B670**, 12 (2008);  
U. Aglietti *et al.*, Phys. Lett. **B595**, 432 (2004);  
G. Degrossi and F. Maltoni, Phys. Lett. **B600**, 255 (2004).
  55. C. Anastasiou, R. Boughezal, and F. Petriello, JHEP **0904**, 003 (2009).
  56. M. Kramer, E. Laenen, and M. Spira, Nucl. Phys. **B511**, 523 (1998);  
Chetyrkin *et al.*, Nucl. Phys. **B510**, 61 (1998);  
S. Catani *et al.*, JHEP **0307**, 028 (2003);  
S. Moch and A. Vogt, Phys. Lett. **B631**, 48 (2005);  
E. Laenen and L. Magnea, Phys. Lett. **B632**, 270 (2006);  
A. Idilbi *et al.*, Phys. Rev. **D73**, 077501 (2006);  
V. Ravindran, Nucl. Phys. **B764**, 291 (2006).
  57. D. de Florian and M. Grazzini, Phys. Lett. **B674**, 291 (2009).
  58. V. Ahrens *et al.*, Phys. Rev. **D79**, 033013 (2009);  
V. Ahrens *et al.*, Eur. Phys. J. **C62**, 333 (2009).
  59. V. Ahrens *et al.*, Phys. Lett. **B698**, 271 (2011).
  60. C.R. Schmidt, Phys. Lett. **B413**, 391 (1997).
  61. D. de Florian, M. Grazzini, and Z. Kunszt, Phys. Rev. Lett. **82**, 5209 (1999).
  62. Nucl. Phys. **B634**, 247 (2002).
  63. C.J. Glosser and C. R. Schmidt, JHEP **0212**, 016 (2002).
  64. J.M. Campbell, R.K. Ellis, and G. Zanderighi, JHEP **0610**, 028 (2006).
  65. J.M. Campbell, R.K. Ellis, and C. Williams, Phys. Rev. **D81**, 074023 (2010).
  66. S. L. Glashow, D.V. Nanopoulos, and A. Yildiz, Phys. Rev. **D18**, 1724 (1978);  
T. Han and S. Willenbrock, Phys. Lett. **B273**, 167 (1991);  
T. Han, G. Valencia, and S. Willenbrock, Phys. Rev. Lett. **69**, 3274 (1992).
  67. A. Stange, W. Marciano, and S. Willenbrock, Phys. Rev. **D49**, 1354 (1994).
  68. A. Stange, W. Marciano, and S. Willenbrock, Phys. Rev. **D50**, 4491 (1994).
  69. K.A. Assamagan *et al.*, arXiv:hep-ph/0406152 (2004).
  70. O. Brein, A. Djouadi, and R. Harlander, Phys. Lett. **B579**, 149 (2004);  
M.L. Ciccolini, S. Dittmaier, and M. Krämer, Phys. Rev. **D68**, 073003 (2003);  
J. Baglio and A. Djouadi, J. High Energy Phys. **1010**, 064 (2010);  
G. Ferrera, M. Grazzini, and F. Tramontano, Phys. Rev. Lett. **107**, 152003 (2011);  
A. Denner *et al.*, JHEP **1203**, 075 (2012);  
O. Brein *et al.*, Eur. Phys. J. **C72**, 1868 (2012).
  71. T. Figy, S. Palmer, and G. Weiglein, JHEP **1202**, 105 (2012);  
P. Bolzoni *et al.*, Phys. Rev. Lett. **105**, 011801 (2010);  
M. Ciccolini, A. Denner, and S. Dittmaier, Phys. Rev. Lett. **99**, 161803 (2007);  
Ciccolini, A. Denner, and S. Dittmaier, Phys. Rev. **D77**, 103002 (2008);  
T. Han, G. Valencia, and S. Willenbrock, Phys. Rev. Lett. **69**, 3274 (1992);  
E.L. Berger, J. Campbell, Phys. Rev. **D70**, 073011 (2004);  
T. Figy, C. Oleari, and D. Zeppenfeld, Phys. Rev. **D68**, 073005 (2003).
  72. W. Beenakker *et al.*, Phys. Rev. Lett. **87**, 201805 (2001);  
L. Reina and S. Dawson, Phys. Rev. Lett. **87**, 201804 (2001);  
S. Dawson *et al.*, Phys. Rev. **D67**, 071503 (2003);  
W. Beenakker *et al.*, Nucl. Phys. **B653**, 151 (2003).
  73. R.V. Harlander and W.B. Kilgore, Phys. Rev. **D68**, 013001 (2003);  
J. Campbell *et al.*, Phys. Rev. **D67**, 095002 (2003);  
S. Dawson *et al.*, Phys. Rev. Lett. **94**, 031802 (2005);  
S. Dittmaier, M. Krämer, and M. Spira, Phys. Rev. **D70**, 074010 (2004);  
S. Dawson *et al.*, Phys. Rev. **D69**, 074027 (2004).

See key on page 457

## Gauge & Higgs Boson Particle Listings

### Higgs Bosons — $H^0$ and $H^\pm$

74. W.J. Stirling and D.J. Summers, Phys. Lett. **B283**, 411 (1992);  
F. Maltoni *et al.*, Phys. Rev. **D64**, 094023 (2001).
75. For a compilation of theoretical results for SM and MSSM Higgs cross sections at the LHC see:  
<https://twiki.cern.ch/twiki/bin/view/LHCPhysics/CrossSections>.  
For the SM Higgs production via gluon fusion using renormalization group improved predictions see:  
<http://rghiggs.hepforge.org/>.  
The text of this review describes recent updates.
76. S. Dittmaier *et al.*, [LHC Higgs Cross Sections Working Group], arXiv:1101.0593 [hep-ph] (2011).
77. The CDF and DØ Collabs. and the Tevatron Electroweak Working Group, *Combination of the CDF and DØ Results on the Mass of the Top Quark Using up to 5.8 fb<sup>-1</sup> of Data*, arXiv:1107.5255 [hep-ex] (2011).
78. P. Janot, *Searching for Higgs Bosons at LEP 1 and LEP 2, in Perspectives in Higgs Physics II*, World Scientific, ed. G.L. Kane (1998).
79. See the Review on *Statistics* in this volume.
80. OPAL Collab., Eur. Phys. J. **C27**, 311 (2003).
81. CDF Collab., Phys. Rev. **D85**, 052002 (2012).
82. DØ Collab., Phys. Rev. Lett. **102**, 051803 (2009).
83. (\*\*) CDF Collab., CDF Note 10796, “Search for Standard Model Higgs Boson Production in Association with a  $W^\pm$  Boson with 9.45 fb<sup>-1</sup> of CDF Data”, (2012).
84. (\*\*\*) DØ Collab., DØ Note 6309-CONF, “Search for Higgs boson in final states with lepton, missing energy, and at least two jets using b-jet identification in 9.7 fb<sup>-1</sup> of Tevatron data” (2012).
85. (\*\*\*) DØ Collab., DØ Note 5977-CONF, “Search for the standard model Higgs boson in the  $WH \rightarrow \tau\nu b\bar{b}$  channel with 4.0 fb<sup>-1</sup> of  $p\bar{p}$  collisions at  $\sqrt{s} = 1.96$  TeV” (2009).
86. CDF Collab., Phys. Rev. Lett. **104**, 141801 (2010).
87. DØ Collab., Phys. Rev. Lett. **104**, 071801 (2010).
88. (\*\*) CDF Collab., CDF Note 10798, “Search for the SM Higgs boson in the  $\cancel{E}_T + b$ -jets signature with relaxed kinematic cuts in 9.45 fb<sup>-1</sup> of data at CDF” (2012).
89. (\*\*\*) DØ Collab., DØ Note 6299-CONF, “Search for the Standard-Model Higgs Boson in the  $ZH \rightarrow \nu\bar{\nu} b\bar{b}$  Channel in 9.5 fb<sup>-1</sup> of  $p\bar{p}$  Collisions at  $\sqrt{s} = 1.96$  TeV” (2012).
90. CDF Collab., Phys. Rev. **D80**, 071101 (2009);  
CDF Collab., Phys. Rev. Lett. **105**, 251802 (2010).
91. DØ Collab., Phys. Lett. **B655**, 209 (2007).
92. (\*\*) CDF Collab., CDF Note 10799, “A Search for the Standard Model Higgs Boson in the Process  $ZH \rightarrow \ell^+\ell^- b\bar{b}$  Using 9.45 fb<sup>-1</sup> of CDF II Data” (2012).
93. (\*\*\*) DØ Collab., DØ Note 6296-CONF, “Search for  $ZH \rightarrow \ell^+\ell^- b\bar{b}$  production in 9.7 fb<sup>-1</sup> of  $p\bar{p}$  collisions” (2012).
94. CDF Collab., Phys. Rev. **D84**, 052010 (2011).
95. (\*\*) CDF Collab., CDF Note 10792, “A search for the Higgs Boson in the All Hadronic Channel using 9.45 fb<sup>-1</sup> of CDF data” (2012).
96. (\*\*) CDF Collab., CDF Note 10805, “Evidence for  $WZ$  and  $ZZ$  production in final states with  $b$ -tagged jets at CDF” (2012).
97. (\*\*\*) DØ Collab., DØ Note 6260-CONF, “Evidence for  $WZ$  and  $ZZ$  production in final states with  $b$ -tagged jets” (2011).
98. The CDF and DØ Collabs. and the Tevatron New Physics and Higgs Working Group,  
arXiv:1203.3782 [hep-ex] (2012).
99. CDF Collab., arXiv:1201.4880 [hep-ex], submitted to Phys. Rev. Lett (2012).
100. (\*\*) CDF Collab., CDF Note 10625, “Search for the Standard Model Higgs Boson in  $\tau^+\tau^-$ +jets final state with 8.3 fb<sup>-1</sup> of CDF Data” (2012).
101. DØ Collab., Phys. Rev. Lett. **102**, 251801 (2009).
102. (\*\*\*) DØ Collab., DØ Note 6305-CONF, “Search for the standard model Higgs boson in tau lepton pair final states” (2012).
103. CDF Collab., Phys. Rev. Lett. **108**, 011801 (2012).
104. (\*\*) CDF Collab., CDF Note 10737, “Search for a Standard Model Higgs Boson Decaying Into Photons at CDF Using 10.0 fb<sup>-1</sup> of Data” (2012).
105. DØ Collab., Phys. Rev. Lett. **102**, 231801 (2009).
106. (\*\*\*) DØ Collab., DØ Note 6295-CONF, “Search for the Standard Model Higgs Boson in  $\gamma\gamma + X$  final states at DØ using 9.7 fb<sup>-1</sup> data” (2012).
107. (\*\*) CDF Collab., CDF Note 10801, “Search for the Higgs Boson Produced in Association with Top Quarks using 9.4 fb<sup>-1</sup>” (2012).
108. (\*\*) CDF Collab., CDF Note 10582, “Search for SM Higgs boson production in association with  $t\bar{t}$  using no lepton final state” (2011).
109. CDF Collab., Phys. Rev. Lett. **104**, 061803 (2010).
110. (\*\*) CDF Collab., CDF Note 10760, “Search for  $H \rightarrow WW^*$  Production at CDF Using 9.7 fb<sup>-1</sup> Data” (2012).
111. (\*\*) CDF Collab., CDF Note 10781, “Search for  $H \rightarrow WW^*$  Production with Leptons and Hadronic Taus in the Final State Using 9.7 fb<sup>-1</sup>” (2012).
112. DØ Collab., Phys. Rev. Lett. **104**, 061804 (2010).
113. (\*\*\*) DØ Collab., DØ Note 6302-CONF, “Search for Higgs boson production in dilepton plus missing transverse energy final states with 8.6–9.7 fb<sup>-1</sup> of  $p\bar{p}$  collisions at  $\sqrt{s} = 1.96$  TeV” (2012).
114. DØ Collab., Phys. Rev. Lett. **97**, 151804 (2006).
115. (\*\*\*) DØ Collab., DØ Note 5873-CONF, “Search for the Associated Higgs Boson Production with Like Sign Leptons in  $p\bar{p}$  Collisions  $\sqrt{s} = 1.96$  TeV” (2009).
116. (\*\*) CDF Collab., CDF Note 10791, “Search for the SM Higgs in the Four-Lepton Final State” (2012).
117. (\*\*) CDF Collab., CDF Note 10804, “Combination of CDF’s searches for the standard model Higgs boson with up to 10.0 fb<sup>-1</sup> of data” (2012).
118. (\*\*\*) DØ Collab., DØ Note 6304-CONF, “Combined Search for the Standard Model Higgs Boson from the DØ Experiment in up to 9.7 fb<sup>-1</sup> of Data” (2012).
119. L. Lyons, *The Annals of Applied Statistics*, Vol. 2, No. 3, 887 (2008);  
L. Demortier, “P-Values and Nuisance Parameters”, *Proceedings of PHYSTAT 2007*, CERN-2008-001, p. 23 (2008).
120. ATLAS Collab., Phys. Rev. Lett. **108**, 111802 (2012).
121. ATLAS Collab., “Search for the Standard Model Higgs boson in the  $H \rightarrow W^+W^- \rightarrow \ell^+\nu\ell^-\nu$  decay mode with 4.7 fb<sup>-1</sup> of ATLAS data at  $\sqrt{s} = 7$  TeV”, ATLAS-CONF-2012-012 (2012).



## Gauge &amp; Higgs Boson Particle Listings

Higgs Bosons —  $H^0$  and  $H^\pm$ 

122. CMS Collab., “Search for the standard model Higgs boson decaying to a  $W$  pair in the fully leptonic final state in  $pp$  collisions at  $\sqrt{s} = 7$  TeV”, arXiv:1202.1489 [hep-ex], submitted to Phys. Lett. **B** (2012).
123. CMS Collab., “Search for WH to 3 leptons”, CMS-PAS-HIG-11-034 (2012).
124. ATLAS Collab., “Search for the Higgs boson in the  $H \rightarrow W^+W^- \rightarrow \ell\nu jj$  decay channel using  $4.7 \text{ fb}^{-1}$  of  $pp$  collisions at  $\sqrt{s} = 7$  TeV with the ATLAS detector”, ATLAS-CONF-2012-018 (2012).
125. ATLAS Collab., Phys. Lett. **B710**, 383 (2012).
126. CMS Collab., Phys. Rev. Lett. **108**, 111804 (2012).
127. ATLAS Collab., “Search for a Standard Model Higgs in the  $H \rightarrow ZZ \rightarrow \ell^+\ell^-\nu\bar{\nu}$  decay channel with  $4.7 \text{ fb}^{-1}$  with the ATLAS detector”, ATLAS-CONF-2012-016 (2012).
128. CMS Collab., arXiv:1202.3478 [hep-ex], submitted to JHEP (2012).
129. ATLAS Collab., “Search for a Standard Model Higgs in the mass range 200-600 GeV in the channel  $H \rightarrow ZZ \rightarrow \ell^+\ell^-q\bar{q}$  with with the ATLAS detector”, ATLAS-CONF-2012-017 (2012).
130. CMS Collab., arXiv:1202.1416 [hep-ex], submitted to JHEP (2012).
131. CMS Collab., arXiv:1202.3617 [hep-ex], submitted to JHEP (2012).
132. ATLAS Collab., Phys. Rev. Lett. **108**, 111803 (2012).
133. CMS Collab., arXiv:1202.1487 [hep-ex], submitted to Phys. Lett. **B** (2012).
134. CMS Collab., “A search using multivariate techniques for a standard model Higgs boson decaying into two photons”, CMS-PAS-HIG-12-001 (2012).
135. ATLAS Collab., “Search for the Standard Model Higgs boson produced in association with a vector boson and decaying to a  $b$ -quark pair using up to  $4.7 \text{ fb}^{-1}$  of  $pp$  collision data at  $\sqrt{s} = 7$  TeV with the ATLAS detector at the LHC”, ATLAS-CONF-2012-015 (2012).
136. CMS Collab., arXiv:1202.4195 [hep-ex], submitted to Phys. Lett. **B** (2012).
137. ATLAS Collab., “Search for the Standard Model Higgs boson in the  $H \rightarrow \tau^+\tau^-$  decay mode with  $4.7 \text{ fb}^{-1}$  of ATLAS data at 7 TeV”, ATLAS-CONF-2012-014 (2012).
138. CMS Collab., arXiv:1202.4083 [hep-ex], submitted to Phys. Lett. **B** (2012).
139. CMS Collab., “Search for Neutral Higgs Bosons Decaying into Tau Leptons in the Dimuon Channel with CMS in  $pp$  Collisions at 7 TeV”, CMS-PAS-HIG-12-007 (2012).
140. CMS Collab., “Search for WH in Final States with Electrons, Muons, Taus”, CMS-PAS-HIG-12-006 (2012).
141. CMS Collab., J. Phys. **G34**, 995 (2007).
142. V. Buescher and K. Jakobs, Int. J. Mod. Phys. **A20**, 2523 (2005).
143. D. Zeppenfeld *et al.*, Phys. Rev. **D62**, 013009 (2000); D. Zeppenfeld, “Higgs Couplings at the LHC,” in *Proceedings of the APS/DPF/DPB Summer Study on the Future of Particle Physics* (Snowmass 2001), edited by R. Davidson and C. Quigg, SNOWMASS-2001-P123 arXiv:hep-ph/0203123 (2002).
144. M. Dührssen *et al.*, Phys. Rev. **D70**, 113009 (2004).
145. T. Plehn, D.L. Rainwater, and D. Zeppenfeld, Phys. Rev. Lett. **88**, 051801 (2002).
146. V. Hankele *et al.*, Phys. Rev. **D74**, 095001 (2006).
147. C. Ruwiedel, N. Wermes, and M. Schumacher, Eur. Phys. J. **C51**, 385 (2007).
148. M. Klute *et al.*, arXiv:1205.2699 [hep-ph] (2012).
149. A. Denner *et al.*, arXiv:1111.6395 [hep-ph] (2011).
150. G.D. Kribs *et al.*, Phys. Rev. **D76**, 075016 (2007).
151. P. Bechtle *et al.*, Comput. Phys. Commun. **181**, 138 (2010).
152. C.J. Flacco *et al.*, Phys. Rev. Lett. **105**, 111801 (2010).
153. The CDF and DØ Collabs. and the Tevatron New Physics and Higgs Working Group, Phys. Rev. **D82**, 011102 (2010).
154. E. Witten, Nucl. Phys. **B188**, 513 (1981); R.K. Kaul, Phys. Lett. **B19**, 19 (1982); R.K. Kaul, Pramana **19**, 183 (1982); L. Susskind, Phys. Rev. **104**, 181 (1984).
155. L.E. Ibáñez and G.G. Ross, Phys. Lett. **B110**, 215 (1982); L.E. Ibáñez, Phys. Lett. **B118**, 73 (1982); J. Ellis, D.V. Nanopoulos, and K. Tamvakis, Phys. Lett. **B121**, 123 (1983); L. Alvarez-Gaumé, J. Polchinski, and M.B. Wise, Nucl. Phys. **B221**, 495 (1983).
156. S. Dimopoulos and H. Georgi, Nucl. Phys. **B193**, 150 (1981); K. Harada and N. Sakai, Prog. Theor. Phys. **67**, 1877 (1982); K. Inoue *et al.*, Prog. Theor. Phys. **67**, 1889 (1982); L. Girardello and M.T. Grisaru, Nucl. Phys. **B194**, 65 (1982); L.J. Hall and L. Randall, Phys. Rev. Lett. **65**, 2939 (1990); I. Jack and D.R.T. Jones, Phys. Lett. **B457**, 101 (1999).
157. H.E. Haber, *Supersymmetry*, in this volume.
158. S. Dimopoulos and D.W. Sutter, Nucl. Phys. **B452**, 496 (1995); D.W. Sutter, Stanford Ph. D. thesis, hep-ph/9704390 (1997); H.E. Haber, Nucl. Phys. B (Proc. Suppl.) **62A-C** (1998) 469.
159. A. Djouadi, Phys. Reports **459**, 1 (2008).
160. H.E. Haber and Y. Nir, Nucl. Phys. **B335**, 363 (1990); A. Dobado, M. J. Herrero, and S. Penaranda, Eur. Phys. J. **C17**, 487 (2000); J.F. Gunion and H.E. Haber, Phys. Rev. **D67**, 075019 (2003).
161. L.J. Hall and M.B. Wise, Nucl. Phys. **B187**, 397 (1981).
162. T.D. Lee, Phys. Rev. **D8**, 1226 (1973); P. Fayet, Nucl. Phys. **B78**, 14 (1974); R.D. Peccei and H.R. Quinn, Phys. Rev. Lett. **38**, 1440 (1977); P. Fayet and S. Ferrara, Phys. Rept. **32**, 249 (1977); V.D. Barger, J.L. Hewett, and R.J.N. Phillips, Phys. Rev. **D41**, 3421 (1990).
163. S.L. Glashow and S. Weinberg, Phys. Rev. **D15**, 1958 (1977); E.A. Paschos, Phys. Rev. **D15**, 1966 (1977); H. Georgi, Hadronic J. **1**, 1227 (1978); H. Haber, G Kane and T Sterling Nucl. Phys. **B161**, 493 (1979); A. G. Akeroyd, Phys. Lett. **B368**, 89 (1996); A.G. Akeroyd, Nucl. Phys. **B544**, 557 (1999);



See key on page 457

## Gauge &amp; Higgs Boson Particle Listings

Higgs Bosons —  $H^0$  and  $H^\pm$ 

- A. G. Akeroyd, A. Arhrib, and E. Naimi, Eur. Phys. J. **C20**, 51 (2001).
164. V. Barger, H. E. Logan, G. Shaughnessy, Phys. Rev. **D79**, 115018 (2009).
165. Y. Okada, M. Yamaguchi, T. Yanagida, Prog. Theor. Phys. **85**, 1 (1991);  
J. Ellis, G. Ridolfi, F. Zwirner, Phys. Lett. **B257**, 83 (1991).
166. H.E. Haber and R. Hempfling, Phys. Rev. Lett. **66**, 1815 (1991).
167. S.P. Li and M. Sher, Phys. Lett. **B140**, 339 (1984);  
R. Barbieri and M. Frigeni, Phys. Lett. **B258**, 395 (1991);  
M. Drees and M.M. Nojiri, Phys. Rev. **D45**, 2482 (1992);  
J.A. Casas *et al.*, Nucl. Phys. **B436**, 3 (1995) [E: **B439** (1995) 466];  
J. Ellis, G. Ridolfi, and F. Zwirner, Phys. Lett. **B262**, 477 (1991);  
A. Brignole *et al.*, Phys. Lett. **B271**, 123 (1991) [E: **B273** (1991) 550].
168. R.-J. Zhang, Phys. Lett. **B447**, 89 (1999);  
J.R. Espinosa and R.-J. Zhang, JHEP **0003**, 026 (2000);  
J.R. Espinosa and R.-J. Zhang, Nucl. Phys. **B586**, 3 (2000);  
A. Brignole *et al.*, Nucl. Phys. **B631**, 195 (2002), Nucl. Phys. **B643**, 79 (2002);  
A. Dedes, G. Degrassi, and P. Slavich, Nucl. Phys. **B672**, 144 (2003).
169. J.F. Gunion and A. Turski, Phys. Rev. **D39**, 2701 (1989), Phys. Rev. **D40**, 2333 (1989);  
M.S. Berger, Phys. Rev. **D41**, 225 (1990);  
A. Brignole, Phys. Lett. **B277**, 313 (1992), Phys. Lett. **B281**, 284 (1992);  
M.A. Díaz and H.E. Haber, Phys. Rev. **D45**, 4246 (1992);  
P.H. Chankowski, S. Pokorski, and J. Rosiek, Phys. Lett. **B274**, 191 (1992), Nucl. Phys. **B423**, 437 (1994);  
A. Yamada, Phys. Lett. **B263**, 233 (1991), Z. Phys. **C61**, 247 (1994);  
A. Dabelstein, Z. Phys. **C67**, 496 (1995);  
R. Hempfling and A.H. Hoang, Phys. Lett. **B331**, 99 (1994);  
S. Heinemeyer, W. Hollik, and G. Weiglein, Phys. Rev. **D58**, 091701 (1998), Phys. Lett. **B440**, 296 (1998), Eur. Phys. J. **C9**, 343 (1999).
170. D.M. Pierce *et al.*, Nucl. Phys. **B491**, 3 (1997).
171. R. Barbieri, M. Frigeni, and F. Caravaglios, Phys. Lett. **B258**, 167 (1991);  
Y. Okada, M. Yamaguchi, and T. Yanagida, Phys. Lett. **B262**, 45 (1991);  
J.R. Espinosa and M. Quirós, Phys. Lett. **B266**, 389 (1991);  
D.M. Pierce, A. Papadopoulos, and S. Johnson, Phys. Rev. Lett. **68**, 3678 (1992);  
K. Sasaki, M. Carena, and C.E.M. Wagner, Nucl. Phys. **B381**, 66 (1992);  
R. Hempfling, in *Phenomenological Aspects of Supersymmetry*, edited by W. Hollik, R. Rückl, and J. Wess (Springer-Verlag, Berlin, 1992) pp. 260–279;  
J. Kodaira, Y. Yasui, and K. Sasaki, Phys. Rev. **D50**, 7035 (1994);  
H.E. Haber and R. Hempfling, Phys. Rev. **D48**, 4280 (1993);  
M. Carena *et al.*, Phys. Lett. **B355**, 209 (1995).
172. H.E. Haber, R. Hempfling, and A.H. Hoang, Z. Phys. **C75**, 539 (1997);  
M. Carena *et al.*, Nucl. Phys. **B580**, 29 (2000).
173. M. Carena, M. Quirós, and C.E.M. Wagner, Nucl. Phys. **B461**, 407 (1996).
174. S. Martin, Phys. Rev. **D67**, 095012 (2003); Phys. Rev. **D71**, 016012 (2005); Phys. Rev. **D75**, 055005 (2007).
175. M. Carena, S. Mrenna, and C.E.M. Wagner, Phys. Rev. **D60**, 075010 (1999);  
*ibid.*, Phys. Rev. **D62**, 055008 (2000).
176. S. Heinemeyer, W. Hollik, and G. Weiglein, Phys. Lett. **B455**, 179 (1999);  
J.R. Espinosa and I. Navarro, Nucl. Phys. **B615**, 82 (2001);  
G. Degrassi, P. Slavich, and F. Zwirner, Nucl. Phys. **B611**, 403 (2001);  
S. Heinemeyer *et al.*, Eur. Phys. J. **C39**, 465 (2005).
177. M. Carena *et al.*, hep-ph/9912223 (1999); *idem*, Eur. Phys. J. **C26**, 601 (2003).
178. G. Degrassi *et al.*, Eur. Phys. J. **C28**, 133 (2003).
179. S. Heinemeyer *et al.*, J. High Energy Phys. **0808**, 087 (2008).
180. M. Carena *et al.*, JHEP **1203**, 014 (2012).
181. H. Baer, V. Barger, and A. Mustafayev, Phys. Rev. **D85**, 075010 (2012);  
A. Arbey *et al.*, Phys. Lett. **B708**, 162 (2012);  
L.J. Hall, D. Pinner, and J.T. Ruderman, JHEP **1204**, 131 (2012);  
M. Kadastik *et al.*, arXiv:1112.3647 [hep-ph] (2011);  
P. Draper *et al.*, arXiv:1112.3068 [hep-ph] (2011);  
S. Heinemeyer, O. Stal, and G. Weiglein, Phys. Lett. **B710**, 201 (2012).
182. M. Carena *et al.*, Phys. Lett. **B495**, 155 (2000);  
M. Carena *et al.*, Nucl. Phys. **B625**, 345 (2002).
183. A. Dabelstein, Nucl. Phys. **B456**, 25 (1995);  
F. Borzumati *et al.*, Nucl. Phys. **B555**, 53 (1999);  
H. Eberl *et al.*, Phys. Rev. **D62**, 055006 (2000).
184. J.A. Coarasa, R.A. Jiménez, and J. Solà, Phys. Lett. **B389**, 312 (1996);  
R.A. Jiménez and J. Solà, Phys. Lett. **B389**, 53 (1996);  
A. Bartl *et al.*, Phys. Lett. **B378**, 167 (1996).
185. S. Heinemeyer, W. Hollik, and G. Weiglein, Eur. Phys. J. **C16**, 139 (2000).
186. H.E. Haber *et al.*, Phys. Rev. **D63**, 055004 (2001).
187. L. Hall, R. Rattazzi, and U. Sarid, Phys. Rev. **D50**, 7048 (1994);  
R. Hempfling, Phys. Rev. **D49**, 6168 (1994).
188. M. Carena *et al.*, Nucl. Phys. **B426**, 269 (1994).
189. M. Carena *et al.*, Phys. Lett. **B499**, 141 (2001).
190. E. Berger *et al.*, Phys. Rev. **D66**, 095001 (2002).
191. A. Brignole *et al.*, Nucl. Phys. **B643**, 79 (2002); R. Dermisek and I. Low, Phys. Rev. **D77**, 035012 (2008).
192. A. Djouadi, Phys. Lett. **B435**, 101 (1998).
193. E. Boos *et al.*, Phys. Rev. **D66**, 055004 (2002).
194. A. Djouadi, J. Kalinowski, and P.M. Zerwas, Z. Phys. **C57**, 569 (1993);  
H. Baer *et al.*, Phys. Rev. **D47**, 1062 (1993);  
A. Djouadi *et al.*, Phys. Lett. **B376**, 220 (1996);  
A. Djouadi *et al.*, Z. Phys. **C74**, 93 (1997);  
S. Heinemeyer and W. Hollik, Nucl. Phys. **B474**, 32 (1996).

## Gauge &amp; Higgs Boson Particle Listings

Higgs Bosons —  $H^0$  and  $H^\pm$ 

195. J.F. Gunion, Phys. Rev. Lett. **72**, 199 (1994);  
D. Choudhury and D.P. Roy, Phys. Lett. **B322**, 368 (1994);  
O.J. Eboli and D. Zeppenfeld, Phys. Lett. **B495**, 147 (2000);  
B.P. Kersevan, M. Malawski, and E. Richter-Was, Eur. Phys. J. **C29**, 541 (2003).
196. J.F. Gunion *et al.*, Phys. Rev. **D38**, 3444 (1988).
197. S.H. Zhu, hep-ph/9901221 (1999);  
S. Kanemura, Eur. Phys. J. **C17**, 473 (2000);  
A. Arhrib *et al.*, Nucl. Phys. **B581**, 34 (2000).
198. H.E. Logan and S. Su, Phys. Rev. **D66**, 035001 (2002).
199. A. Gutierrez-Rodriguez and O.A. Sampayo, Phys. Rev. **D62**, 055004 (2000);  
A. Gutierrez-Rodriguez, M.A. Hernandez-Ruiz, and O.A. Sampayo, J. Phys. Soc. Jap. **70**, 2300 (2001);  
S. Moretti, EPJdirect **C15**, 1 (2002).
200. S. Kanemura, S. Moretti, and K. Odagiri, JHEP **0102**, 011 (2001).
201. J.F. Gunion and H.E. Haber, Nucl. Phys. **B278**, 449 (1986) [E: **B402**, 567 (1993)];  
S. Dawson, A. Djouadi, and M. Spira, Phys. Rev. Lett. **77**, 16 (1996);  
A. Djouadi *et al.*, Phys. Lett. **B318**, 347 (1993);  
R.V. Harlander and W.B. Kilgore, JHEP **0210**, 017 (2002);  
C. Anastasiou and K. Melnikov, Phys. Rev. **D67**, 037501 (2003);  
J. Guasch, P. Hafziger and M. Spira, Phys. Rev. **D68**, 115001 (2003);  
R.V. Harlander and M. Steinhauser, JHEP **0409**, 066 (2004);  
S. Dawson *et al.*, Mod. Phys. Lett. **A21**, 89 (2006);  
A. Djouadi and M. Spira, Phys. Rev. **D62**, 014004 (2000);  
M. Mühlleitner and M. Spira, Nucl. Phys. **B790**, 1 (2008);  
T. Hahn *et al.*, arXiv:hep-ph/0607308 (2006).
202. D. Dicus *et al.*, Phys. Rev. **D59**, 094016 (1999).
203. C. Balázs, H.-J. He, and C.P. Yuan, Phys. Rev. **D60**, 114001 (1999).
204. J.A. Coarasa *et al.*, Eur. Phys. J. **C2**, 373 (1998).
205. C.S. Li and T.C. Yuan, Phys. Rev. **D42**, 3088 (1990);  
[E: Phys. Rev. **D47**, 2156 (1993)];  
A. Czarnecki and S. Davidson, Phys. Rev. **D47**, 3063 (1993);  
C.S. Li, Y.-S. Wei, and J.-M. Yang, Phys. Lett. **B285**, 137 (1992).
206. J. Guasch, R.A. Jiménez. and J. Solà, Phys. Lett. **B360**, 47 (1995).
207. M. Carena *et al.*, Nucl. Phys. **B577**, 88 (2000).
208. M. Guchait and S. Moretti, JHEP **0201**,001 (2002).
209. R.M. Barnett, H.E. Haber, and D.E. Soper, Nucl. Phys. **B306**, 697 (1988).
210. F. Olness and W.-K. Tung, Nucl. Phys. **B308**, 813 (1988).
211. F. Borzumati, J.-L. Kneur, and N. Polonsky, Phys. Rev. **D60**, 115011 (1999).
212. A. Belyaev *et al.*, JHEP **0206**, 059 (2002).
213. L.G. Jin *et al.*, Eur. Phys. J. **C14**, 91 (2000); Phys. Rev. **D62**, 053008 (2000);  
A. Belyaev *et al.*, Phys. Rev. **D65**, 031701 (2002);  
G. Gao *et al.*, Phys. Rev. **D66**, 015007 (2002).
214. S.-H. Zhu, Phys. Rev. **D67**, 075006 (2005);  
T. Plehn, Phys. Rev. **D67**, 014018 (2003).
215. A.A. Barrientos Bendezú and B.A. Kniehl, Phys. Rev. **D59**, 015009 (1999); Phys. Rev. **D61**, 015009 (2000);  
Phys. Rev. **D63**, 015009 (2001).
216. A.A. Barrientos Bendezú and B.A. Kniehl, Nucl. Phys. **B568**, 305 (2000).
217. A. Krause *et al.*, Nucl. Phys. **B519**, 85 (1998).
218. O. Brein and W. Hollik, Eur. Phys. J. **C13**, 175 (2000).
219. ALEPH Collab., Phys. Lett. **B526**, 191 (2002).
220. DELPHI Collab., Eur. Phys. J. **C32**, 145 (2004).
221. OPAL Collab., Eur. Phys. J. **C37**, 49 (2004).
222. L3 Collab., Phys. Lett. **B545**, 30 (2002).
223. OPAL Collab., Eur. Phys. J. **C23**, 397 (2002).
224. DELPHI Collab., Eur. Phys. J. **C38**, 1 (2004).
225. M. Carena *et al.*, Eur. Phys. J. **C45**, 797 (2006).
226. DØ Collab., Phys. Lett. **B698**, 97 (2011).
227. CDF Collab., Phys. Rev. **D85**, 032005 (2012).
228. DØ Collab., Phys. Rev. Lett. **104**, 151801 (2010);  
DØ Collab., Phys. Rev. Lett. **107**, 121801 (2011).
229. (\*\*\*) DØ Collab., DØ Note 5974-CONF, “Search for neutral Higgs bosons  $\phi b \rightarrow \tau_e \tau_{had} b$  with 3.7 fb<sup>-1</sup> of DØ data” (2011).
230. CDF Collab., Phys. Rev. Lett. **103**, 201801 (2009).
231. DØ Collab., Phys. Rev. Lett. **101**, 071804 (2008);  
DØ Collab., Phys. Lett. **B707**, 323 (2012).
232. DØ Collab., Phys. Lett. **B710**, 569 (2012).
233. M. Carena *et al.*, arXiv:1203.1041 [hep-ph] (2012).
234. ATLAS Collab., “Search for neutral MSSM Higgs bosons decaying to  $\tau^+ \tau^-$  pairs in proton-proton collisions at  $\sqrt{s} = 7$  TeV with the ATLAS detector”, ATLAS-CONF-2011-132 (2011).
235. ATLAS Collab., Phys. Lett. **B705**, 174 (2011).
236. ATLAS Collab., arXiv:0901.0512 [hep-ex] (2009).
237. ALEPH Collab., Phys. Lett. **B543**, 1 (2002);  
DELPHI Collab., Phys. Lett. **B525**, 17 (2002);  
L3 Collab., Phys. Lett. **B575**, 208 (2003);  
OPAL Collab., Eur. Phys. J. **C7**, 407 (1999).
238. (\*) ALEPH, DELPHI, L3 and OPAL Collabs., The LEP Working Group for Higgs Boson Searches, *Search for Charged Higgs Bosons: Preliminary ...*, LHWG-Note/2001-05.
239. DØ Collab., Phys. Rev. Lett. **82**, 4975 (1999);  
*idem*, **88**, 151803 (2002);  
CDF Collab., Phys. Rev. **D62**, 012004 (2000);  
*idem*, Phys. Rev. Lett. **79**, 357 (1997).
240. CDF Collab., Phys. Rev. Lett. **96**, 042003 (2006).
241. DØ Collab., Phys. Lett. **B682**, 278 (2009).
242. ATLAS Collab., arXiv:1204.2760 [hep-ex] (2012).
243. ATLAS Collab., “A Search for a light charged Higgs boson decaying to  $c\bar{s}$  in  $pp$  collisions at  $\sqrt{s} = 7$  TeV with the ATLAS detector”, ATLAS-CONF-2011-094 (2011).
244. CMS Collab., “Search for the light charged Higgs boson in top quark decays in  $pp$  collisions at  $\sqrt{s} = 7$  TeV CMS-PAS-HIG-11-019.
245. A. D. Sakharov, JETP Lett. **5**, 24 (1967).

See key on page 457

## Gauge & Higgs Boson Particle Listings

### Higgs Bosons — $H^0$ and $H^\pm$

246. M. Carena *et al.*, Nucl. Phys. **B599**, 158 (2001).
247. S. Dimopoulos and S. Thomas, Nucl. Phys. **B465**, 23, (1996);  
S. Thomas, Int. J. Mod. Phys. **A13**, 2307 (1998).
248. A. Pilaftsis and C.E.M. Wagner, Nucl. Phys. **B553**, 3 (1999).
249. M. Carena *et al.*, Nucl. Phys. **B586**, 92 (2000).
250. A. Pilaftsis, Phys. Rev. **D58**, 096010 (1998); Phys. Lett. **B435**, 88 (1998);  
K.S. Babu *et al.*, Phys. Rev. **D59**, 016004 (1999).
251. G.L. Kane and L.-T. Wang, Phys. Lett. **B488**, 383 (2000);  
S.Y. Choi, M. Drees and J.S. Lee, Phys. Lett. **B481**, 57 (2000);  
S.Y. Choi and J.S. Lee, Phys. Rev. **D61**, 015003 (2000);  
S.Y. Choi, K. Hagiwara and J.S. Lee, Phys. Rev. **D64**, 032004 (2001); Phys. Lett. **B529**, 212 (2002);  
T. Ibrahim and P. Nath, Phys. Rev. **D63**, 035009 (2001);  
T. Ibrahim, Phys. Rev. **D64**, 035009 (2001);  
S. Heinemeyer, Eur. Phys. J. **C22**, 521 (2001);  
S.W. Ham *et al.*, Phys. Rev. **D68**, 055003 (2003).
252. M. Frank *et al.*, JHEP **0702**, 047 (2007);  
S. Heinemeyer *et al.*, Phys. Lett. **B652**, 300 (2007);  
T. Hahn *et al.*, arXiv:0710.4891 (2007).
253. D.A. Demir, Phys. Rev. **D60**, 055006 (1999);  
S. Y. Choi *et al.*, Phys. Lett. **B481**, 57 (2000).
254. E. Christova *et al.*, Nucl. Phys. **B639**, 263 (2002) [E: Nucl. Phys. **B647**, 359 (2002)].
255. P. Draper, T. Liu, and C.E.M. Wagner, Phys. Rev. **D81**, 015014 (2010).
256. W. de Boer and C. Sander, Phys. Lett. **B585**, 276 (2004);  
S. Heinemeyer *et al.*, JHEP **0608**, 052 (2006);  
A. Djouadi *et al.*, Phys. Rev. Lett. **78**, 3626 (1997);  
A. Djouadi *et al.*, Phys. Rev. **D57**, 4179 (1998);  
S. Heinemeyer and G. Weiglein, JHEP **10** (2002) 072.;  
J. Haestier *et al.*, JHEP **0512**, 027, (2005).;   
S. Heinemeyer, W. Hollik, and G. Weiglein, Phys. Rept. **425**, 265 (2006);  
S. Heinemeyer *et al.*, JHEP **0804**, 039 (2008).
257. O. Buchmueller *et al.*, Phys. Rev. **D81**, 035009 (2010).
258. O. Buchmueller *et al.*, Eur. Phys. J. **C72**, 1878 (2012).
259. G. D'Ambrosio *et al.*, Nucl. Phys. **B645**, 155 (2002).
260. M. Carena, A. Menon, and C.E.M. Wagner, Phys. Rev. **D76**, 035004 (2007);  
P. Draper, T. Liu, and C.E.M. Wagner, Phys. Rev. **D80**, 035025 (2009).
261. J.R. Ellis *et al.*, JHEP **0708**, 083 (2007).
262. E. Lunghi, W. Porod, and O. Vives, Phys. Rev. **D74**, 075003 (2006).
263. M. Carena *et al.*, Phys. Rev. **D74**, 015009 (2006).
264. G. Buchalla, A.J. Buras, and M.E. Lautenbacher, Rev. Mod. Phys. **68**, 1125 (1996).
265. A. Dedes and A. Pilaftsis, Phys. Rev. **D67**, 015012 (2003).
266. A.J. Buras *et al.*, Phys. Lett. **B546**, 96 (2002).
267. A. J. Buras *et al.*, Nucl. Phys. **B659**, 2 (2003).
268. K.S. Babu and C.F. Kolda, Phys. Rev. Lett. **84**, 228 (2000).
269. (\*\*) CDF Collab., “A Search for  $B_{s(d)}^0 \rightarrow \mu^+ \mu^-$  Decays using 9.7 fb<sup>-1</sup> of Data”, CDF Note 10701 (2012);  
CDF Collab., Phys. Rev. Lett. **107**, 191801 (2011);  
LHCb Collab., arXiv:1203.4493 [hep-ex] (2012);  
CMS Collab., “Search for  $B_s \rightarrow \mu^+ \mu^-$  and  $B^0 \rightarrow \mu^+ \mu^-$  decays”, arXiv:1203.3976 (2012). Submitted to JHEP.
270. A. G. Akeroyd, F. Mahmoudi, and D. Martinez Santos, JHEP **1112**, 088 (2011);  
A. Arbey, M. Battaglia, and F. Mahmoudi, Eur. Phys. J. **C72**, 1906 (2012).
271. M. Misiak *et al.*, Phys. Rev. Lett. **98**, 022002 (2007), and refs. therein.
272. T. Becher and M. Neubert, Phys. Rev. Lett. **98**, 022003 (2007).
273. Heavy Flavor Averaging Group (HFAG),  
<http://www.slac.stanford.edu/xorg/hfag/rare/lep-ph09/rad11/btosg.pdf>.
274. Belle Collab., arXiv:0809.3834 [hep-ex] (2008).
275. Belle Collab., Phys. Rev. **D82** 071101 (2010).
276. BaBar Collab., Phys. Rev. D **81**, 051101 (2010).
277. BaBar Collab., arXiv:1008.0104 [hep-ex].
278. M. Bona *et al.* [UTfit Collab.], Phys. Lett. **B687**, 61 (2010), [http://ckmfitter.in2p3.fr/www/html/ckm\\_results.html](http://ckmfitter.in2p3.fr/www/html/ckm_results.html).
279. G. Isidori and P. Paradisi, Phys. Lett. **B639**, 499 (2006).
280. BaBar Collab., Phys. Rev. Lett. **100**, 021801 (2008);  
Belle Collab., arXiv:0910.4301 [hep-ex] (2009).
281. U. Nierste, S. Trine and S. Westhoff, Phys. Rev. **D78**, 015006 (2008).
282. S. Trine, arXiv:0810.3633 [hep-ph] (2008).
283. LHCb Collab., Phys. Rev. Lett. **108**, 111602 (2012).
284. CDF Collab., “Improved Measurement of the Difference between Time Integrated CP Asymmetries in  $D^0 \rightarrow K^+ K^-$  and  $D^0 \rightarrow \pi^+ \pi^-$  Decays at CDF”, CDF Note 10784 (2012).
285. W. Altmannshofer *et al.*, JHEP **1204**, 049 (2012).
286. M. Carena, A. Menon, and C.E.M. Wagner, Phys. Rev. **D79**, 075025 (2009).
287. W. Altmannshofer and D.M. Straub, JHEP **1009**, 078 (2010).
288. J. Ellis *et al.*, Phys. Lett. **B653**, 292 (2007).
289. N. Cabibbo, G.R. Farrar, and L. Maiani, Phys. Lett. **B105**, 155 (1981);  
H. Goldberg, Phys. Rev. Lett. **50**, 1419 (1983);  
J. R. Ellis *et al.*, Nucl. Phys. **B238**, 453 (1984);  
G. Bertone, D. Hooper, and J. Silk, Phys. Reports **405**, 279 (2005).
290. M. Carena, D. Hooper, and A. Vallinotto, Phys. Rev. **D75**, 055010 (2007);  
M. Carena, D. Hooper, and P. Skands, Phys. Rev. Lett. **97**, 051801 (2006).
291. A. Djouadi and Y. Mambrini, JHEP **0612**, 001 (2006).
292. J. Ellis, K.A. Olive, and Y. Santoso, Phys. Rev. **D71**, 095007 (2005).
293. N.G. Deshpande and E. Ma Phys. Rev. **D18**, 2574 (1978);  
R. Barbieri, L.J. Hall, and V. Rychkov Phys. Rev. **D74**, 015007 (2006);  
L. Lopez-Honorez *et al.*, JCAP **0702**, 028 (2007);  
E. Lundstrom, M. Gustafsson, and J. Edjo, Phys. Rev.

## Gauge &amp; Higgs Boson Particle Listings

Higgs Bosons —  $H^0$  and  $H^\pm$ 

- D79, 035013 (2009);  
 E. Dolle *et al.*, Phys. Rev. **D8**, 035003 (2010);  
 X. Miao, S. Su, and B. Thomas, Phys. Rev. **D82**, 035009 (2010);  
 L. Lopez-Honorez and C. Yaguna, JCAP **1101**, 002 (2011).
294. H.E. Haber, *Proceedings of the 1990 Theoretical Advanced Study Institute in Elementary Particle Physics*, edited by M. Cvetič and Paul Langacker (World Scientific, Singapore, 1991) pp. 340–475, and references therein.
295. S. Glashow and S. Weinberg, Phys. Rev. **D15**, 1958 (1977).
296. P. Fayet, Phys. Lett. **B90**, 104 (1975);  
 H.-P. Nilles, M. Srednicki, and D. Wyler, Phys. Lett. **B120**, 346 (1983);  
 J.-M. Frere, D.R.T. Jones, and S. Raby, Nucl. Phys. **B222**, 11 (1983);  
 J.-P. Derendinger and C.A. Savoy, Nucl. Phys. **B237**, 307 (1984);  
 B.R. Greene and P.J. Miron, Phys. Lett. **B168**, 226 (1986);  
 J. Ellis *et al.*, Phys. Lett. **B176**, 403 (1986);  
 L. Durand and J.L. Lopez, Phys. Lett. **B217**, 463 (1989);  
 M. Drees, Int. J. Mod. Phys. **A4**, 3635 (1989);  
 U. Ellwanger, Phys. Lett. **B303**, 271 (1993);  
 U. Ellwanger, M. Rausch de Taubenberg, and C.A. Savoy, Phys. Lett. **B315**, 331 (1993); Z. Phys. **C67**, 665 (1995);  
 Phys. Lett. **B492**, 21 (1997);  
 P.N. Pandita, Phys. Lett. **B318**, 338 (1993); Z. Phys. **C59**, 575 (1993);  
 T. Elliott, S.F. King, and P.L. White, Phys. Lett. **B305**, 71 (1993); Phys. Lett. **B314**, 56 (1993); Phys. Rev. **D49**, 2435 (1994); Phys. Lett. **B351**, 213 (1995);  
 K.S. Babu and S.M. Barr, Phys. Rev. **D49**, R2156 (1994);  
 S.F. King and P.L. White, Phys. Rev. **D52**, 4183 (1995);  
 N. Haba, M. Matsuda, and M. Tanimoto, Phys. Rev. **D54**, 6928 (1996);  
 F. Franke and H. Fraas, Int. J. Mod. Phys. **A12**, 479 (1997);  
 S.W. Ham, S.K. Oh, and H.S. Song, Phys. Rev. **D61**, 055010 (2000);  
 D.A. Demir, E. Ma, and U. Sarkar, J. Phys. **G26**, L117 (2000);  
 R. B. Nevzorov and M. A. Trusov, Phys. Atom. Nucl. **64**, 1299 (2001);  
 U. Ellwanger and C. Hugonie, Eur. Phys. J. **C25**, 297 (2002);  
 U. Ellwanger *et al.*, arXiv:hep-ph/0305109 (2003);  
 D.J. Miller and S. Moretti, arXiv:hep-ph/0403137 (2004).
297. A. Dedes *et al.*, Phys. Rev. **D63**, 055009 (2001);  
 A. Menon, D. Morrissey, and C.E.M. Wagner, Phys. Rev. **D70**, 035005, (2004).
298. R. Dermisek and J.F. Gunion, Phys. Rev. **D76**, 095006 (2007);  
 R. Dermisek and J.F. Gunion, Phys. Rev. **D81**, 075003 (2010);  
 G. Degross and P. Slavich, Nucl. Phys. **B825**, 119 (2010);  
 M. Maniatis, Int. J. Mod. Phys. **A25**, 3505 (2010);  
 U. Ellwanger, G. Espitalier-Noel and C. Hugonie, JHEP **1109**, 105 (2011);  
 U. Ellwanger, JHEP **1203**, 044 (2012);
- J.F. Gunion, Y. Jiang, and S. Kraml, Nucl. Phys. **B710**, 454 (2012);  
 S.F. King, M. Muhlleitner, and R. Nevzorov, Nucl. Phys. **B860**, 207 (2012).
299. J. R. Espinosa and M. Quirós, Phys. Lett. **B279**, 92 (1992).
300. P. Batra and E. Ponton, Phys. Rev. **D79**, 035001 (2009).
301. M. Schmaltz and D. Tucker-Smith, Ann. Rev. Nucl. Part. Sci. **55**, 229 (2005).
302. M. Perelstein, Prog. Part. Nucl. Phys. **58**, 247 (2007).
303. H.C. Cheng, I. Low, and L.T. Wang, Phys. Rev. **D74**, 055001 (2006).
304. C.R. Chen, K. Tobe, and C. P. Yuan, Phys. Lett. **B640**, 263 (2006).
305. G.F. Giudice *et al.*, JHEP **0706**, 045 (2007).
306. J. Hubisz *et al.*, JHEP **0601**, 135 (2006).
307. G. F. Giudice, R. Rattazzi, and J. D. Wells, Nucl. Phys. **B595**, 250 (2001);  
 M. Chaichian *et al.*, Phys. Lett. **B524**, 161 (2002);  
 D. Dominici *et al.*, Acta Phys. Polon. **B33**, 2507 (2002);  
 J. L. Hewett and T. G. Rizzo, JHEP **0308**, 028 (2003).
308. OPAL Collab., Phys. Lett. **B609**, 20 (2005). [E: *ibid.*, **637**, 374 (2006)].
309. B. Grzadkowski and J. F. Gunion, arXiv:1202.5017 [hep-ph] (2012);  
 B. Coleppa, T. Gregoire, and H. Logan, Phys. Rev. **D85**, 055001 (2012).
310. S. Casagrande *et al.*, JHEP **1009**, 014 (2010);  
 A. Azatov, M. Toharia, and L. Zhu, Phys. Rev. **D82**, 056004 (2010);  
 A. Azatov and J. Galloway, Phys. Rev. **D85**, 055013 (2012);  
 F. Goertz, U. Haisch, and M. Neubert, arXiv:1112.5099 [hep-ph] (2012);  
 M. Carena *et al.*, arXiv:1204.0008 [hep-ph] (2012).
311. T. Appelquist, H. -C. Cheng, and B. A. Dobrescu, Phys. Rev. **D64**, 035002 (2001).
312. F.J. Petriello, JHEP **0205**, 003 (2002).
313. A. Azatov *et al.*, arXiv:1204.4817 [hep-ph] (2012);  
 J. R. Espinosa *et al.*, arXiv:1202.3697 [hep-ph] (2012).
314. M. J. Strassler and K. M. Zurek, Phys. Lett. **B651**, 374 (2007).
315. M. J. Strassler and K. M. Zurek, Phys. Lett. **B661**, 263 (2008).
316. T. Han *et al.*, JHEP **0807**, 008 (2008).
317. A. Falkowski *et al.*, JHEP **1005**, 077 (2010);  
 A. Falkowski *et al.*, Phys. Rev. Lett. **105**, 241801 (2010).
318. S. Chivukula *et al.*, *Dynamical Electroweak Symmetry Breaking*, in this volume.
319. S. Schael *et al.*, [ALEPH Collab.], JHEP **1005**, 049 (2010).
320. (\*) DELPHI Collab., Interpretation of the searches for Higgs bosons in the MSSM with an additional scalar singlet, CERN-OPEN-99-438 (1999).
321. DØ Collab., Phys. Rev. Lett. **103**, 061801 (2009).
322. CDF Collab., Phys. Rev. Lett. **107**, 031801 (2011).
323. CMS Collab., “Search for a light pseudoscalar boson in the dimuon channel”, CMS-PAS-HIG-12-004 (2012).

See key on page 457

## Gauge & Higgs Boson Particle Listings

### Higgs Bosons — $H^0$ and $H^\pm$

324. ATLAS Collab., “A Search for Light CP-Odd Higgs Bosons Decaying to  $\mu^+\mu^-$  in ATLAS”, ATLAS-CONF-2011-020 (2012).
325. E.L. Berger *et al.*, Phys. Rev. **D66**, 095001 (2002).
326. W. Loinaz and J. Wells, Phys. Lett. **B445**, 178 (1998); X. Calmet and H. Fritzsch, Phys. Lett. **B496**, 190 (2000).
327. ALEPH Collab., Phys. Lett. **B544**, 25 (2002); DELPHI Collab., Eur. Phys. J. **C44**, 147 (2005); L3 Collab., Phys. Lett. **B583**, 14 (2004); OPAL Collab., Eur. Phys. J. **C18**, 425 (2001).
328. (\*) The LEP Working Group for Higgs Boson Searches, *Flavour Independent Search for Hadronically Decaying Neutral Higgs Bosons at LEP*, LHWG Note 2001-07.
329. OPAL Collab., Eur. Phys. J. **C18**, 425 (2001); DELPHI Collab., Eur. Phys. J. **C38**, 1 (2004).
330. DELPHI Collab., Eur. Phys. J. **C34**, 399 (2004).
331. OPAL Collab., arXiv:0812.0267 [hep-ex] (2008).
332. Y. Chikashige *et al.*, Phys. Lett. **B98**, 265 (1981); A.S. Joshipura and S.D. Rindani, Phys. Rev. Lett. **69**, 3269 (1992); F. de Campos *et al.*, Phys. Rev. **D55**, 1316 (1997).
333. DELPHI Collab., Eur. Phys. J. **C32**, 475 (2004); L3 Collab., Phys. Lett. **B609**, 35 (2005); OPAL Collab., Phys. Lett. **B377**, 273 (1996).
334. (\*) ALEPH, DELPHI, L3 and OPAL Collabs., The LEP Working Group for Higgs Boson Searches, *Search for Invisible Higgs Bosons: Preliminary ...*, LHWG-Note/2001-06.
335. (\*\*) CDF Collab., “Search for heavy metastable particles decaying to quark pairs in  $p\bar{p}$  collisions at  $\sqrt{s} = 1.96$  TeV”, CDF Note 10356 (2010).
336. DØ Collab., Phys. Rev. Lett. **103**, 071801 (2009).
337. (\*\*) CDF Collab., “Search for Anomalous Production of Events with a  $W$  or  $Z$  boson and Additional Leptons”, CDF Note 10526 (2011).
338. A. Abbasabadi *et al.*, Phys. Rev. **D52**, 3919 (1995); K. Hagiwara, R. Szalapski, and D. Zeppenfeld, Phys. Lett. **B318**, 155 (1993); O.J.P. Éboli *et al.*, Phys. Lett. **B434**, 340 (1998).
339. L3 Collab., Phys. Lett. **B589**, 89 (2004).
340. ALEPH Collab., Phys. Lett. **B544**, 16 (2002); DELPHI Collab., Eur. Phys. J. **C35**, 313 (2004); L3 Collab., Phys. Lett. **B534**, 28 (2002); OPAL Collab., Phys. Lett. **B544**, 44 (2002).
341. (\*) ALEPH, DELPHI, L3 and OPAL Collabs., The LEP Working Group for Higgs Boson Searches, *Search for Higgs Bosons Decaying into Photons: Combined ...*, LHWG Note/2002-02.
342. L3 Collab., Phys. Lett. **B568**, 191 (2003).
343. ALEPH Collab., Eur. Phys. J. **C49**, 439 (2007).
344. DØ Collab., Phys. Rev. Lett. **107**, 151801 (2011).
345. (\*\*\*) DØ Collab., DØ Note 6297-CONF, “Search for a Fermiophobic Higgs Boson in the di-photon final state using using 9.7 fb<sup>-1</sup> of DØ data” (2012).
346. CDF Collab., Phys. Rev. Lett. **103**, 061803 (2009).
347. (\*\*) CDF Collab., CDF Note 10731, “Search for a Fermiophobic Higgs Boson in the Di-photon Final State Using 10.0 fb<sup>-1</sup> of CDF Data” (2012).
348. The CDF and DØ Collabs. and the Tevatron New Physics and Higgs Working Group, “Combined CDF and DØ upper limits on Fermiophobic Higgs Boson Production with up to 8.2 fb<sup>-1</sup> of  $p\bar{p}$  data”, arXiv:1109.0576 (2011).
349. (\*\*\*) DØ Collab., DØ Note 5067-CONF, “Search for Fermiophobic Higgs Boson in  $3\gamma + X$  Events” (2007).
350. ATLAS Collab., “Search for a fermiophobic Higgs boson in the diphoton decay channel with 4.9 fb<sup>-1</sup> of ATLAS data at  $\sqrt{s} = 7$  TeV”, ATLAS-CONF-2012-013 (2012).
351. CMS Collab., “Search for the fermiophobic model Higgs boson decaying into two photons”, CMS-PAS-HIG-12-002 (2012).
352. G.B. Gelmini and M. Roncadelli, Phys. Lett. **B99**, 411 (1981); R.N. Mohapatra and J.D. Vergados, Phys. Rev. Lett. **47**, 1713 (1981); V. Barger *et al.*, Phys. Rev. **D26**, 218 (1982).
353. B. Dutta and R.N. Mohapatra, Phys. Rev. **D59**, 015018 (1999); C.S. Aulakh *et al.*, Phys. Rev. **D58**, 115007 (1998); C.S. Aulakh, A. Melfo, and G. Senjanovic, Phys. Rev. **D57**, 4174 (1998).
354. DELPHI Collab., Phys. Lett. **B552**, 127 (2003).
355. OPAL Collab., Phys. Lett. **B295**, 347 (1992); *idem*, **B526**, 221 (2002).
356. L3 Collab., Phys. Lett. **B576**, 18 (2003).
357. OPAL Collab., Phys. Lett. **B577**, 93 (2003).
358. DØ Collab., Phys. Rev. Lett. **93**, 141801 (2004); DØ Collab., Phys. Rev. Lett. **101**, 071803 (2008).
359. CDF Collab., Phys. Rev. Lett. **93**, 221802 (2004); CDF Collab., Phys. Rev. Lett. **101**, 121801 (2008).
360. CDF Collab., Phys. Rev. Lett. **95**, 071801 (2005).
361. CMS Collab., “Inclusive search for doubly charged Higgs in leptonic final states with the 2011 data at 7 TeV”, CMS-PAS-HIG-12-005 (2012).
362. ATLAS Collab., Phys. Rev. **D88**, 032004 (2012).
363. F. Gianotti, on behalf of the ATLAS Collaboration, “Status of Standard Model Higgs Searches in ATLAS”, presentation given July 4, 2012 at CERN.
364. ATLAS Collab., ATLAS-CONF-2012-093 (2012).
365. J. Incandela, on behalf of the CMS Collaboration, “Status of the CMS SM Higgs Search”, presentation given July 4, 2012 at CERN.
366. CMS Collab., CMS-PAS-HIG-12-020 (2012).
367. ATLAS Collab., ATLAS-CONF-2012-091, ATLAS-CONF-2012-092 (2012).
368. ATLAS Collab., arXiv:1205.6744 [hep-ex], submitted to Phys. Lett. B (2012); ATLAS Collab., arXiv:1206.2443 [hep-ex], submitted to Phys. Lett. B (2012); ATLAS Collab., arXiv:1206.0756 [hep-ex], submitted to Phys. Lett. B (2012); ATLAS Collab., arXiv:1206.0756 [hep-ex], submitted to Phys. Lett. B (2012); ATLAS Collab., arXiv:1206.6074 [hep-ex], submitted to Phys. Lett. B (2012); ATLAS Collab., arXiv:1206.5971 [hep-ex], submitted to JHEP (2012); ATLAS Collab., arXiv:1207.0210 [hep-ex], submitted to Phys. Lett. B (2012).
369. ATLAS Collab., arXiv:1207.0319 [hep-ex], submitted to Phys. Rev. D (2012).
370. CMS Collab., CMS-PAS-HIG-12-015, CMS-PAS-HIG-12-016, CMS-PAS-HIG-12-023, CMS-PAS-HIG-12-023,

## Gauge &amp; Higgs Boson Particle Listings

Higgs Bosons —  $H^0$  and  $H^\pm$ 

CMS-PAS-HIG-11-024, CMS-PAS-HIG-12-017, CMS-PAS-HIG-12-003, CMS-PAS-HIG-12-021, CMS-PAS-HIG-12-019, CMS-PAS-HIG-12-018, CMS-PAS-HIG-12-012, CMS-PAS-HIG-12-006, CMS-PAS-HIG-12-025 (2011, 2012).

371. CMS Collab., CMS-PAS-HIG-12-001 (2012).  
 372. CMS Collab., Phys. Lett. B **710**, 91 (2012).  
 373. The CDF and D0 Collaborations and the Tevatron New Physics and Higgs Working Group, arXiv:1207.0449 [hep-ex] (2012).  
 374. D0 Collab., arXiv:1207.0422 [hep-ex] (2012).  
 375. D0 Collab., D0 Note 6302-CONF, (2012).  
 376. CDF Collab., CDF Note 10804, (2012); CDF Collab., arXiv:1207.1707, submitted to Phys. Rev. Lett. (2012).

## CONTENTS:

- Standard Model  $H^0$  (Higgs Boson) Mass Limits  
 –  $H^0$  Direct Search Limits  
 –  $H^0$  Indirect Mass Limits from Electroweak Analysis  
 Mass Limits for Neutral Higgs Bosons in Supersymmetric Models  
 –  $H^0_1$  (Higgs Boson) Mass Limits in Supersymmetric Models  
 –  $A^0$  (Pseudoscalar Higgs Boson) Mass Limits in Supersymmetric Models  
 $H^0$  (Higgs Boson) Mass Limits in Extended Higgs Models  
 $H^\pm$  (Charged Higgs) Mass Limits  
 Mass limits for  $H^{\pm\pm}$  (doubly-charged Higgs boson)  
 – Limits for  $H^{\pm\pm}$  with  $T_3 = \pm 1$   
 – Limits for  $H^{\pm\pm}$  with  $T_3 = 0$

STANDARD MODEL  $H^0$  (Higgs Boson) MASS LIMITS

These limits apply to the Higgs boson of the three-generation Standard Model with the minimal Higgs sector. For a review and a bibliography, see the above review on “Higgs Bosons: Theory and Searches,” where the latest unpublished results are also described.

**Note:** the addendum to the Higgs boson review describes the latest news reported in July 2012 on the discovery of a boson whose properties are consistent with the Standard Model Higgs boson.

 $H^0$  Direct Search Limits

All data that have been superseded by newer results are marked as “not used” or have been removed from this compilation, and are documented in previous editions of this Review of Particle Physics.

VALUE (GeV)	CL%	DOCUMENT ID	TECN	COMMENT
<b>&gt; 115.5 and none 127–600 (CL = 95%) OUR EVALUATION</b>				
none	95	<sup>1</sup> AAD	12E ATLS	$pp \rightarrow H^0 X$
<b>112.9–115.5, 131–236, 251–466</b>				
none 127–600	95	<sup>2</sup> CHATRCHYAN12B	CMS	$pp \rightarrow H^0 X$
none 162–166	95	<sup>3</sup> AALTONEN	10F TEVA	$p\bar{p} \rightarrow H^0 X, H^0 \rightarrow WW^{(*)}$
>114.1	95	<sup>4</sup> ABDALLAH	04 DLPH	$e^+e^- \rightarrow H^0 Z$
>112.7	95	<sup>4</sup> ABBIENDI	03B OPAL	$e^+e^- \rightarrow H^0 Z$
>114.4	95	<sup>4,5</sup> HEISTER	03D LEP	$e^+e^- \rightarrow H^0 Z$
>111.5	95	<sup>4,6</sup> HEISTER	02 ALEP	$e^+e^- \rightarrow H^0 Z$
>112.0	95	<sup>4</sup> ACHARD	01c L3	$e^+e^- \rightarrow H^0 Z$
• • • We do not use the following data for averages, fits, limits, etc. • • •				
none 134–156, 182–233, 256–265, 268–415	95	<sup>7</sup> AAD	12 ATLS	$pp \rightarrow H^0 X, H^0 \rightarrow ZZ$
		<sup>8</sup> AAD	12D ATLS	$pp \rightarrow H^0 X, H^0 \rightarrow ZZ^{(*)}$
none 145–206	95	<sup>9</sup> AAD	12F ATLS	$pp \rightarrow H^0 X, H^0 \rightarrow WW^{(*)}$
none 113–115, 134.5–136	95	<sup>10</sup> AAD	12G ATLS	$pp \rightarrow H^0 X, H^0 \rightarrow \gamma\gamma$
none 129–270	95	<sup>11</sup> AALTONEN	12 CDF	$H^0 \rightarrow \gamma\gamma$
		<sup>12</sup> CHATRCHYAN12C	CMS	$pp \rightarrow H^0 X, H^0 \rightarrow ZZ$
		<sup>13</sup> CHATRCHYAN12D	CMS	$pp \rightarrow H^0 X, H^0 \rightarrow ZZ^{(*)}$
		<sup>14</sup> CHATRCHYAN12E	CMS	$pp \rightarrow H^0 X, H^0 \rightarrow WW^{(*)}$
		<sup>15</sup> CHATRCHYAN12F	CMS	$pp \rightarrow H^0 WX, H^0 ZX$
none 128–132	95	<sup>16</sup> CHATRCHYAN12G	CMS	$pp \rightarrow H^0 X, H^0 \rightarrow \gamma\gamma$
none 134–158, 180–305, 340–465	95	<sup>17</sup> CHATRCHYAN12H	CMS	$pp \rightarrow H^0 X, H^0 \rightarrow ZZ^{(*)}$
none 270–440	95	<sup>18</sup> CHATRCHYAN12I	CMS	$pp \rightarrow H^0 X, H^0 \rightarrow ZZ$
		<sup>19</sup> AAD	11AB ATLS	$pp \rightarrow H^0 X, H^0 \rightarrow WW$
none 191–197, 199–200, 214–224	95	<sup>20</sup> AAD	11T ATLS	$pp \rightarrow H^0 X, H^0 \rightarrow ZZ^{(*)}$
		<sup>21</sup> AAD	11U ATLS	$pp \rightarrow H^0 X, H^0 \rightarrow \gamma\gamma$

none 340–450	95	<sup>22</sup> AAD	11V ATLS	$pp \rightarrow H^0 X, H^0 \rightarrow ZZ$
		<sup>23</sup> AAD	11W ATLS	$pp \rightarrow H^0 X$
		<sup>24</sup> AALTONEN	11AA CDF	$p\bar{p} \rightarrow H^0 WX, H^0 ZX, H^0 q\bar{q}X$
		<sup>25</sup> ABAZOV	11AB D0	$p\bar{p} \rightarrow H^0 WX, H^0 ZX$
		<sup>26</sup> ABAZOV	11G D0	$p\bar{p} \rightarrow H^0 X, H^0 \rightarrow WW^{(*)}$
		<sup>27</sup> ABAZOV	11J D0	$p\bar{p} \rightarrow H^0 WX, H^0 \rightarrow b\bar{b}$
		<sup>28</sup> ABAZOV	11Y D0	$H^0 \rightarrow \gamma\gamma$
		<sup>29</sup> CHATRCHYAN11J	CMS	$pp \rightarrow H^0 X, H^0 \rightarrow WW$
		<sup>30</sup> AALTONEN	10AD CDF	$p\bar{p} \rightarrow H^0 ZX$
		<sup>31</sup> AALTONEN	10G CDF	$p\bar{p} \rightarrow H^0 X, H^0 \rightarrow WW^{(*)}$
		<sup>32</sup> AALTONEN	10J CDF	$p\bar{p} \rightarrow H^0 ZX, H^0 WX$
		<sup>33</sup> AALTONEN	10M TEVA	$p\bar{p} \rightarrow g\bar{g}X \rightarrow H^0 X, H^0 \rightarrow WW^{(*)}$
		<sup>34</sup> ABAZOV	10B D0	$p\bar{p} \rightarrow H^0 X, H^0 \rightarrow WW^{(*)}$
		<sup>35</sup> ABAZOV	10C D0	$p\bar{p} \rightarrow H^0 ZX, H^0 WX$
		<sup>36</sup> ABAZOV	10T D0	$p\bar{p} \rightarrow H^0 ZX$
		<sup>37</sup> AALTONEN	09A CDF	$p\bar{p} \rightarrow H^0 X, H^0 \rightarrow WW^{(*)}$
		<sup>38</sup> AALTONEN	09AG CDF	$p\bar{p} \rightarrow H^0 WX$
		<sup>39</sup> AALTONEN	09AI CDF	$p\bar{p} \rightarrow H^0 WX$
		<sup>40</sup> AALTONEN	09AO CDF	$p\bar{p} \rightarrow H^0 ZX$
		<sup>41</sup> AALTONEN	09AS CDF	$p\bar{p} \rightarrow H^0 WX, H^0 ZX$
		<sup>42</sup> ABAZOV	09C D0	$p\bar{p} \rightarrow H^0 WX$
		<sup>43</sup> ABAZOV	09Q D0	$H^0 \rightarrow \gamma\gamma$
		<sup>44</sup> ABAZOV	09U D0	$H^0 \rightarrow \tau^+\tau^-$
		<sup>45</sup> AALTONEN	08X CDF	$p\bar{p} \rightarrow H^0 ZX, H^0 WX$
		<sup>46</sup> ABAZOV	08AO D0	$p\bar{p} \rightarrow H^0 ZX, H^0 WX$
		<sup>47</sup> ABAZOV	08Y D0	$p\bar{p} \rightarrow H^0 WX$
		<sup>48</sup> ABAZOV	07X D0	$p\bar{p} \rightarrow H^0 ZX$
		<sup>49</sup> ABAZOV	06 D0	$p\bar{p} \rightarrow H^0 X, H^0 \rightarrow WW^*$
		<sup>50</sup> ABAZOV	06O D0	$p\bar{p} \rightarrow H^0 WX, H^0 \rightarrow WW^*$

<sup>1</sup>AAD 12E combine data from AAD 11V, AAD 11AB, AAD 12, AAD 12D, AAD 12F, AAD 12G. The 99% CL exclusion range is 133–230 and 260–437 GeV. An excess of events over background with a local significance of 3.5  $\sigma$  is observed at about  $m_{H^0} = 126$  GeV.

<sup>2</sup>CHATRCHYAN 12B combine CHATRCHYAN 12E, CHATRCHYAN 12F, CHATRCHYAN 12G, CHATRCHYAN 12H, CHATRCHYAN 12I, CHATRCHYAN 12C, CHATRCHYAN 12D, as well as a search in the decay mode  $H^0 \rightarrow \tau\tau$ . The 99% CL exclusion range is 129–525 GeV. An excess of events over background with a local significance of 3.1  $\sigma$  is observed at about  $m_{H^0} = 124$  GeV.

<sup>3</sup>AALTONEN 10F combine searches for  $H^0$  decaying to  $W^+W^-$  in  $p\bar{p}$  collisions at  $E_{cm} = 1.96$  TeV with 4.8 fb $^{-1}$  (CDF) and 5.4 fb $^{-1}$  (D0).

<sup>4</sup>Search for  $e^+e^- \rightarrow H^0 Z$  at  $E_{cm} \leq 209$  GeV in the final states  $H^0 \rightarrow b\bar{b}$  with  $Z \rightarrow \ell\bar{\ell}, \nu\bar{\nu}, q\bar{q}, \tau^+\tau^-$  and  $H^0 \rightarrow \tau^+\tau^-$  with  $Z \rightarrow q\bar{q}$ .

<sup>5</sup>Combination of the results of all LEP experiments.

<sup>6</sup>A 3 $\sigma$  excess of candidate events compatible with  $m_{H^0}$  near 114 GeV is observed in the combined channels  $q\bar{q}q\bar{q}, q\bar{q}\ell\bar{\ell}, q\bar{q}\tau^+\tau^-$ .

<sup>7</sup>AAD 12 search for  $H^0$  production with  $H \rightarrow ZZ \rightarrow \ell^+\ell^-\tau^+\tau^-$  in 1.04 fb $^{-1}$  of  $pp$  collisions at  $E_{cm} = 7$  TeV. A limit on cross section times branching ratio which is (1.7–13) times larger than the expected Standard Model cross section is given for  $m_{H^0} = 200$ –600 GeV at 95% CL. The best limit is at  $m_{H^0} = 360$  GeV.

<sup>8</sup>AAD 12b search for  $H^0$  production with  $H \rightarrow ZZ^{(*)} \rightarrow 4\ell$  in 4.8 fb $^{-1}$  of  $pp$  collisions at  $E_{cm} = 7$  TeV in the mass range  $m_{H^0} = 110$ –600 GeV. An excess of events over background with a local significance of 2.1  $\sigma$  is observed at 125 GeV.

<sup>9</sup>AAD 12f search for  $H^0$  production with  $H \rightarrow WW^{(*)} \rightarrow \ell^+\nu\ell^-\bar{\nu}$  in 2.05 fb $^{-1}$  of  $pp$  collisions at  $E_{cm} = 7$  TeV in the mass range  $m_{H^0} = 110$ –300 GeV.

<sup>10</sup>AAD 12g search for  $H^0$  production with  $H \rightarrow \gamma\gamma$  in 4.9 fb $^{-1}$  of  $pp$  collisions at  $E_{cm} = 7$  TeV in the mass range  $m_{H^0} = 110$ –150 GeV. An excess of events over background with a local significance of 2.8  $\sigma$  is observed at 126.5 GeV.

<sup>11</sup>AALTONEN 12 search for  $H^0 \rightarrow \gamma\gamma$  in 7.0 fb $^{-1}$  of  $p\bar{p}$  collisions at  $E_{cm} = 1.96$  TeV. A limit on cross section times branching ratio which is (8.5–29) times larger than the expected Standard Model cross section is given for  $m_{H^0} = 100$ –150 GeV at 95% CL.

<sup>12</sup>CHATRCHYAN 12c search for  $H^0$  production with  $H \rightarrow ZZ \rightarrow \ell^+\ell^-\tau^+\tau^-$  in 4.7 fb $^{-1}$  of  $pp$  collisions at  $E_{cm} = 7$  TeV. A limit on cross section times branching ratio which is (4–12) times larger than the expected Standard Model cross section is given for  $m_{H^0} = 190$ –600 GeV at 95% CL. The best limit is at  $m_{H^0} = 200$  GeV.

<sup>13</sup>CHATRCHYAN 12d search for  $H^0$  production with  $H \rightarrow ZZ^{(*)} \rightarrow \ell^+\ell^-\tau^+\tau^-$  in 4.6 fb $^{-1}$  of  $pp$  collisions at  $E_{cm} = 7$  TeV. A limit on cross section times branching ratio which corresponds to (1–22) times the expected Standard Model cross section is given for  $m_{H^0} = 130$ –164 GeV, 200–600 GeV at 95% CL. The best limit is at  $m_{H^0} = 230$  GeV. In the Standard Model with an additional generation of heavy quarks and leptons which receive their masses via the Higgs mechanism,  $m_{H^0}$  values in the ranges  $m_{H^0} = 154$ –161 GeV and 200–470 GeV are excluded at 95% CL.

<sup>14</sup>CHATRCHYAN 12e search for  $H^0$  production with  $H \rightarrow WW^{(*)} \rightarrow \ell^+\nu\ell^-\bar{\nu}$  in 4.6 fb $^{-1}$  of  $pp$  collisions at  $E_{cm} = 7$  TeV in the mass range  $m_{H^0} = 110$ –600 GeV.

<sup>15</sup>CHATRCHYAN 12f search for associated  $H^0 W$  and  $H^0 Z$  production followed by  $W \rightarrow \ell\nu, Z \rightarrow \ell^+\ell^-, \nu\bar{\nu}$ , and  $H^0 \rightarrow b\bar{b}$ , in 4.7 fb $^{-1}$  of  $pp$  collisions at  $E_{cm} = 7$  TeV. A limit on cross section times branching ratio which is (3.1–9.0) times larger than the expected Standard Model cross section is given for  $m_{H^0} = 110$ –135 GeV at 95% CL. The best limit is at  $m_{H^0} = 110$  GeV.

<sup>16</sup>CHATRCHYAN 12g search for  $H^0$  production with  $H \rightarrow \gamma\gamma$  in 4.8 fb $^{-1}$  of  $pp$  collisions at  $E_{cm} = 7$  TeV in the mass range  $m_{H^0} = 110$ –150 GeV. An excess of events over background with a local significance of 3.1  $\sigma$  is observed at 124 GeV.

See key on page 457

## Gauge &amp; Higgs Boson Particle Listings

Higgs Bosons —  $H^0$  and  $H^\pm$ 

- 17 CHATRCHYAN 12H search for  $H^0$  production with  $H \rightarrow ZZ^*(*) \rightarrow 4\ell$  in 4.7 fb $^{-1}$  of  $pp$  collisions at  $E_{cm} = 7$  TeV in the mass range  $m_{H^0} = 110$ –600 GeV. Excesses of events over background are observed around 119, 126 and 320 GeV. The region  $m_{H^0} = 114.4$ –134 GeV remains consistent with the expectation for the production of a SM-like Higgs boson.
- 18 CHATRCHYAN 2012I search for  $H^0$  production with  $H \rightarrow ZZ \rightarrow \ell^+ \ell^- \nu \bar{\nu}$  in 4.6 fb $^{-1}$  of  $pp$  collisions at  $E_{cm} = 7$  TeV in the mass range  $m_{H^0} = 250$ –600 GeV.
- 19 AAD 11AB search for  $H^0$  production with  $H \rightarrow W^+ W^- \rightarrow \ell \nu q \bar{q}$  in 1.04 fb $^{-1}$  of  $pp$  collisions at  $E_{cm} = 7$  TeV. A limit on cross section times branching ratio which is (2.7–20) times larger than the expected Standard Model cross section is given for  $m_{H^0} = 240$ –600 GeV at 95% CL. The best limit is at  $m_{H^0} = 400$  GeV.
- 20 AAD 11T search for  $H^0$  production with  $H \rightarrow ZZ^*(*) \rightarrow 4\ell$  in 2.1 fb $^{-1}$  of  $pp$  collisions at  $E_{cm} = 7$  TeV. A limit on cross section times branching ratio which corresponds to (0.8–12) times the expected Standard Model cross section is given for  $m_{H^0} = 120$ –600 GeV at 95% CL. Superseded by AAD 12b.
- 21 AAD 11U search for  $H^0$  production with  $H^0 \rightarrow \gamma\gamma$  in 1.08 fb $^{-1}$  of  $pp$  collisions at  $E_{cm} = 7$  TeV. A limit on cross section times branching ratio which is (2.0–5.8) times larger than the expected Standard Model cross section is given for  $m_{H^0} = 110$ –150 GeV at 95% CL. Superseded by AAD 12c.
- 22 AAD 11V search for  $H^0$  production with  $H \rightarrow ZZ \rightarrow \ell^+ \ell^- \nu \bar{\nu}$  in 1.04 fb $^{-1}$  of  $pp$  collisions at  $E_{cm} = 7$  TeV. A limit on cross section times branching ratio which corresponds to (0.6–6) times the expected Standard Model cross section is given for  $m_{H^0} = 200$ –600 GeV at 95% CL.
- 23 AAD 11W search for Higgs boson production in the decay channels  $\gamma\gamma$ ,  $ZZ^*(*) \rightarrow 4\ell$ ,  $ZZ \rightarrow \ell\ell\nu\nu$ ,  $ZZ \rightarrow \ell\ell q\bar{q}$ ,  $WW^*(*) \rightarrow \ell\ell\nu\nu$ ,  $WW^*(*) \rightarrow \ell\nu q\bar{q}$  in 35–40 pb $^{-1}$  of  $pp$  collisions at  $E_{cm} = 7$  TeV. A limit on cross section times branching ratio which is (2–40) times larger than the expected Standard Model cross section is given for  $m_{H^0} = 110$ –600 GeV at 95% CL. In the Standard Model with an additional generation of heavy quarks and leptons which receive their masses via the Higgs mechanism,  $m_{H^0}$  values between 140 and 185 GeV are excluded at 95% CL. The results for the Standard Model Higgs are superseded by AAD 12e.
- 24 AALTONEN 11AA search in 4.0 fb $^{-1}$  of  $p\bar{p}$  collisions at  $E_{cm} = 1.96$  TeV for associated  $H^0 W$  and  $H^0 Z$  production followed by  $W/Z \rightarrow q\bar{q}$ , and for  $p\bar{p} \rightarrow H^0 q\bar{q} X$  (vector boson fusion), both with  $H^0 \rightarrow b\bar{b}$ . A limit on cross section times branching ratio which is (9–100) times larger than the expected Standard Model cross section is given for  $m_{H^0} = 100$ –150 GeV at 95% CL. The best limit is at  $m_{H^0} = 115$  GeV.
- 25 ABAZOV 11AB search for associated  $H^0 W$  and  $H^0 Z$  production followed by  $H^0 \rightarrow WW^*(*)$  in like-sign dilepton final states using 5.3 fb $^{-1}$  of  $p\bar{p}$  collisions at  $E_{cm} = 1.96$  TeV. A limit on cross section times branching ratio which is (6.4–18) times larger than the expected Standard Model cross section is given for  $m_{H^0} = 115$ –200 GeV at 95% CL. The best limit is for  $m_{H^0} = 135$  and 165 GeV.
- 26 ABAZOV 11c search for  $H^0$  production in 5.4 fb $^{-1}$  of  $p\bar{p}$  collisions at  $E_{cm} = 1.96$  TeV in the decay mode  $H^0 \rightarrow WW^*(*) \rightarrow \ell\nu q\bar{q}$  (and processes with similar final states). A limit on cross section times branching ratio which is (3.9–37) times larger than the expected Standard Model cross section is given for  $m_{H^0} = 115$ –200 GeV at 95% CL. The best limit is at  $m_{H^0} = 160$  GeV.
- 27 ABAZOV 11j search for associated  $H^0 W$  production in 5.3 fb $^{-1}$  of  $p\bar{p}$  collisions at  $E_{cm} = 1.96$  TeV in the final state  $H^0 \rightarrow b\bar{b}$ ,  $W \rightarrow \ell\nu$ . A limit on cross section times branching ratio which is (2.7–30) times larger than the expected Standard Model cross section is given for  $m_{H^0} = 100$ –150 GeV at 95% CL. The limit at  $m_{H^0} = 115$  GeV is 4.5 times larger than the expected Standard Model cross section.
- 28 ABAZOV 11y search for  $H^0 \rightarrow \gamma\gamma$  in 8.2 fb $^{-1}$  of  $p\bar{p}$  collisions at  $E_{cm} = 1.96$  TeV. A limit on cross section times branching ratio which is (10–25) times larger than the expected Standard Model cross section is given for  $m_{H^0} = 100$ –150 GeV at 95% CL.
- 29 CHATRCHYAN 11J search for  $H^0$  production with  $H \rightarrow W^+ W^- \rightarrow \ell\ell\nu\nu$  in 36 pb $^{-1}$  of  $pp$  collisions at  $E_{cm} = 7$  TeV. See their Fig. 6 for a limit on cross section times branching ratio for  $m_{H^0} = 120$ –600 GeV at 95% CL. In the Standard Model with an additional generation of heavy quarks and leptons which receive their masses via the Higgs mechanism,  $m_{H^0}$  values between 144 and 207 GeV are excluded at 95% CL.
- 30 AALTONEN 10AD search for associated  $H^0 Z$  production in 4.1 fb $^{-1}$  of  $p\bar{p}$  collisions at  $E_{cm} = 1.96$  TeV in the decay mode  $H^0 \rightarrow b\bar{b}$ ,  $Z \rightarrow \ell^+ \ell^-$ . A limit  $\sigma \cdot B(H^0 \rightarrow b\bar{b}) < (4.5\text{--}43) \sigma \cdot B_{SM}$  (95% CL) is given for  $m_{H^0} = 100$ –150 GeV. The limit for  $m_{H^0} = 115$  GeV is 5.9 times larger than the expected Standard Model cross section.
- 31 AALTONEN 10G search for  $H^0$  production in 4.8 fb $^{-1}$  of  $p\bar{p}$  collisions at  $E_{cm} = 1.96$  TeV in the decay mode  $H^0 \rightarrow WW^*(*)$ . A limit on  $\sigma(H^0)$  which is (1.3–39) times larger than the expected Standard Model cross section is given for  $m_{H^0} = 110$ –200 GeV at 95% CL. The best limit is obtained for  $m_{H^0} = 165$  GeV.
- 32 AALTONEN 10J search for associated  $H^0 W$  and  $H^0 Z$  production in 2.1 fb $^{-1}$  of  $p\bar{p}$  collisions at  $E_{cm} = 1.96$  TeV in the final state with (b) jets and missing  $p_T$ . A limit  $\sigma < (5.8\text{--}50) \sigma_{SM}$  (95% CL) is given for  $m_{H^0} = 110$ –150 GeV. The limit for  $m_{H^0} = 115$  GeV is 6.9 times larger than the expected Standard Model cross section.
- 33 AALTONEN 10M combine searches for  $H^0$  decaying to  $W^+ W^-$  in  $p\bar{p}$  collisions at  $E_{cm} = 1.96$  TeV with 4.8 fb $^{-1}$  (CDF) and 5.4 fb $^{-1}$  (DØ) and derive limits  $\sigma(p\bar{p} \rightarrow H^0) \cdot B(H^0 \rightarrow W^+ W^-) < (1.75\text{--}0.38)$  pb for  $m_H = 120$ –165 GeV, where  $H^0$  is produced in  $gg$  fusion. In the Standard Model with an additional generation of heavy quarks,  $m_{H^0}$  between 131 and 204 GeV is excluded at 95% CL.
- 34 ABAZOV 10B search for  $H^0$  production in 5.4 fb $^{-1}$  of  $p\bar{p}$  collisions at  $E_{cm} = 1.96$  TeV in the decay mode  $H^0 \rightarrow WW^*(*)$ . A limit on  $\sigma(H^0)$  which is (1.6–21) times larger than the expected Standard Model cross section is given for  $m_{H^0} = 115$ –200 GeV at 95% CL. The best limit is obtained for  $m_{H^0} = 165$  GeV.
- 35 ABAZOV 10C search for associated  $H^0 Z$  and  $H^0 W$  production in 5.2 fb $^{-1}$  of  $p\bar{p}$  collisions at  $E_{cm} = 1.96$  TeV in the final states  $H^0 \rightarrow b\bar{b}$ ,  $Z \rightarrow \nu\bar{\nu}$ , and  $W \rightarrow (\ell)\nu$ , where  $\ell$  is not identified. A limit  $\sigma \cdot B(H^0 \rightarrow b\bar{b}) < (3.4\text{--}38) \sigma \cdot B_{SM}$  (95% CL) is given for  $m_{H^0} = 100$ –150 GeV. The limit for  $m_{H^0} = 115$  GeV is 3.7 times larger than the expected Standard Model cross section.
- 36 ABAZOV 10T search for associated  $H^0 Z$  production in 4.2 fb $^{-1}$  of  $p\bar{p}$  collisions at  $E_{cm} = 1.96$  TeV in the decay mode  $H^0 \rightarrow b\bar{b}$ ,  $Z \rightarrow \ell^+ \ell^-$ . A limit  $\sigma \cdot B(H^0 \rightarrow b\bar{b}) < (3.0\text{--}49) \sigma \cdot B_{SM}$  (95% CL) is given for  $m_{H^0} = 100$ –150 GeV. The limit for  $m_{H^0} = 115$  GeV is 5.9 times larger than the expected Standard Model cross section.
- 37 AALTONEN 09A search for  $H^0$  production in  $p\bar{p}$  collisions at  $E_{cm} = 1.96$  TeV in the decay mode  $H^0 \rightarrow WW^*(*) \rightarrow \ell^+ \ell^- \nu \bar{\nu}$ . A limit on  $\sigma(H^0) \cdot B(H^0 \rightarrow WW^*(*))$  between 0.7 and 2.5 pb (95% CL) is given for  $m_{H^0} = 110$ –200 GeV, which is 1.7–4.5 times larger than the expected Standard Model cross section. The best limit is obtained for  $m_{H^0} = 160$  GeV.
- 38 AALTONEN 09AG search for associated  $H^0 W$  production in 1.9 fb $^{-1}$  of  $p\bar{p}$  collisions at  $E_{cm} = 1.96$  TeV in the decay mode  $H^0 \rightarrow b\bar{b}$ ,  $W \rightarrow \ell\nu$ . A limit on  $\sigma(H^0 W) \cdot B(H^0 \rightarrow b\bar{b})$  (95% CL) is given for  $m_{H^0} = 110$ –150 GeV, which is 7.5–101.9 times larger than the expected Standard Model cross section. The limit for  $m_{H^0} = 115$  GeV is 9.0 times larger than the expected Standard Model cross section. Superseded by AALTONEN 09AI.
- 39 AALTONEN 09AI search for associated  $H^0 W$  production in 2.7 fb $^{-1}$  of  $p\bar{p}$  collisions at  $E_{cm} = 1.96$  TeV in the decay mode  $H^0 \rightarrow b\bar{b}$ ,  $W \rightarrow \ell\nu$ . A limit on  $\sigma(H^0 W) \cdot B(H^0 \rightarrow b\bar{b})$  (95% CL) is given for  $m_{H^0} = 100$ –150 GeV, which is 3.3–75.5 times larger than the expected Standard Model cross section. The limit for  $m_{H^0} = 115$  GeV is 5.6 times larger than the expected Standard Model cross section.
- 40 AALTONEN 09AO search for associated  $H^0 Z$  production in 2.7 fb $^{-1}$  of  $p\bar{p}$  collisions at  $E_{cm} = 1.96$  TeV in the decay mode  $H^0 \rightarrow b\bar{b}$ ,  $Z \rightarrow \ell^+ \ell^-$ . A limit on  $\sigma(H^0 Z) \cdot B(H^0 \rightarrow b\bar{b})$  (95% CL) is given for  $m_{H^0} = 100$ –150 GeV, which is 7.0–71.3 times larger than the expected Standard Model cross section. The limit for  $m_{H^0} = 115$  GeV is 8.2 times larger than the expected Standard Model cross section. Superseded by AALTONEN 10AD.
- 41 AALTONEN 09AS search for associated  $H^0 W$  and  $H^0 Z$  production in 2.0 fb $^{-1}$  of  $p\bar{p}$  collisions at  $E_{cm} = 1.96$  TeV in the decay mode  $H^0 \rightarrow b\bar{b}$ ,  $W/Z \rightarrow q\bar{q}$ . A limit (95% CL) is given for  $m_{H^0} = 100$ –150 GeV, which is 29.4–263 times larger than the expected Standard Model cross section. The limit for  $m_{H^0} = 120$  GeV is 37.5 times larger than the expected Standard Model cross section. Superseded by AALTONEN 11AA.
- 42 ABAZOV 09c search for associated  $H^0 W$  production in 1 fb $^{-1}$  of  $p\bar{p}$  collisions at  $E_{cm} = 1.96$  TeV in the decay mode  $H^0 \rightarrow b\bar{b}$ ,  $W \rightarrow \ell\nu$ . A limit  $\sigma(H^0 W) \cdot B(H^0 \rightarrow b\bar{b}) < (2.1\text{--}0.95)$  pb (95% CL) is given for  $m_{H^0} = 100$ –150 GeV, which is 9.1–84 times larger than the expected Standard Model cross section. Superseded by ABAZOV 11I.
- 43 ABAZOV 09g search for  $H^0 \rightarrow \gamma\gamma$  in 2.7 fb $^{-1}$  of  $p\bar{p}$  collisions at  $E_{cm} = 1.96$  TeV in the mass range  $m_{H^0} = 100$ –150 GeV. A limit (95% CL) is given for  $m_{H^0} = 115$ –130 GeV, which is about 20 times larger than the expected Standard Model cross section. Superseded by ABAZOV 11Y.
- 44 ABAZOV 09u search for  $H^0 \rightarrow \tau^+ \tau^-$  with  $\tau \rightarrow$  hadrons in 1 fb $^{-1}$  of  $p\bar{p}$  collisions at  $E_{cm} = 1.96$  TeV. The production mechanisms include associated  $W/Z+H^0$  production, weak boson fusion, and gluon fusion. A limit (95% CL) is given for  $m_{H^0} = 105$ –145 GeV, which is 20–82 times larger than the expected Standard Model cross section. The limit for  $m_{H^0} = 115$  GeV is 29 times larger than the expected Standard Model cross section.
- 45 AALTONEN 08x search for associated  $H^0 Z$  and  $H^0 W$  production in  $p\bar{p}$  collisions at  $E_{cm} = 1.96$  TeV in the decay mode  $H^0 \rightarrow b\bar{b}$ ,  $Z \rightarrow \nu\bar{\nu}$  and  $W \rightarrow (\ell)\nu$ , where  $\ell$  is not detected. A limit  $\sigma \cdot B(H^0 \rightarrow b\bar{b}) < (4.7\text{--}3.3)$  pb (95% CL) is given for  $m_{H^0} = 110$ –140 GeV, which is 18–66 times larger than the expected Standard Model cross section. Superseded by AALTONEN 10J.
- 46 ABAZOV 08AO search for associated  $H^0 Z$  and  $H^0 W$  production in 0.9 fb $^{-1}$  of  $p\bar{p}$  collisions at  $E_{cm} = 1.96$  TeV in the decay mode  $H^0 \rightarrow b\bar{b}$ ,  $Z \rightarrow \nu\bar{\nu}$  and  $W \rightarrow (\ell)\nu$ , where  $\ell$  is not detected. A limit  $\sigma \cdot B(H^0 \rightarrow b\bar{b}) < (2.6\text{--}2.3)$  pb (95% CL) is given for  $m_{H^0} = 105$ –135 GeV, which is 8.7–34 times larger than the expected Standard Model cross section. Superseded by ABAZOV 10C.
- 47 ABAZOV 08Y search for associated  $H^0 W$  production in  $p\bar{p}$  collisions at  $E_{cm} = 1.96$  TeV in the decay mode  $H^0 \rightarrow b\bar{b}$ ,  $W \rightarrow \ell\nu$ . A limit  $\sigma(H^0 W) \cdot B(H^0 \rightarrow b\bar{b}) < (1.9\text{--}1.6)$  pb (95% CL) is given for  $m_{H^0} = 105$ –145 GeV, which is 10–93 times larger than the expected Standard Model cross section. These results are combined with ABAZOV 06, ABAZOV 06o, ABAZOV 06q, and ABAZOV 07x to give cross section limits for  $m_{H^0} = 100$ –200 GeV which are 6–24 times larger than the Standard Model expectation.
- 48 ABAZOV 07x search for associated  $H^0 Z$  production in  $p\bar{p}$  collisions at  $E_{cm} = 1.96$  TeV in the final state  $Z \rightarrow e^+ e^-$  or  $\mu^+ \mu^-$ ;  $H^0 \rightarrow b\bar{b}$ . A limit  $\sigma(ZH^0) \cdot B(H^0 \rightarrow b\bar{b}) < (4.4\text{--}3.1)$  pb (95% CL) is given for  $m_{H^0} = 105$ –145 GeV, which is more than 40 times larger than the expected Standard Model cross section. Superseded by ABAZOV 10T.
- 49 ABAZOV 06 search for Higgs boson production in  $p\bar{p}$  collisions at  $E_{cm} = 1.96$  TeV with the decay chain  $H^0 \rightarrow WW^* \rightarrow \ell^\pm \ell^\mp \nu \bar{\nu}$ . A limit  $\sigma(H^0) \cdot B(H^0 \rightarrow WW^*) < (5.6\text{--}3.2)$  pb (95% CL) is given for  $m_{H^0} = 120$ –200 GeV, which far exceeds the expected Standard Model cross section.
- 50 ABAZOV 06o search for associated  $H^0 W$  production in  $p\bar{p}$  collisions at  $E_{cm} = 1.96$  TeV with the decay  $H^0 \rightarrow WW^*$ , in the final states  $\ell^\pm \ell^\mp \nu \bar{\nu} X$  where  $\ell = e, \mu$ . A limit  $\sigma(H^0 W) \cdot B(H^0 \rightarrow WW^*) < (3.2\text{--}2.8)$  pb (95% CL) is given for  $m_{H^0} = 115$ –175 GeV, which far exceeds the expected Standard Model cross section.

 **$H^0$  Indirect Mass Limits from Electroweak Analysis**

For limits obtained before the direct measurement of the top quark mass, see the 1996 (Physical Review **D54** 1 (1996)) Edition of this Review. Other studies based on data available prior to 1996 can be found in the 1998 Edition (The European Physical Journal **C3** 1 (1998)) of this Review. For indirect limits obtained from other considerations of theoretical nature, see the Note on “Searches for Higgs Bosons.”

VALUE (GeV)	DOCUMENT ID	TECN
$91^{+31}_{-24}$	51 ERLER	10A RVUE
• • •	We do not use the following data for averages, fits, limits, etc. • • •	
$80^{+30}_{-23}$	52 FLACHER	09 RVUE
$129^{+74}_{-49}$	53 LEP-SLC	06 RVUE

## Gauge &amp; Higgs Boson Particle Listings

Higgs Bosons —  $H^0$  and  $H^\pm$ 

- <sup>51</sup> ERLER 10a makes Standard Model fits to Z and neutral current parameters,  $m_t$ ,  $m_W$  measurements available in 2009 (using also preliminary data). The quoted result is obtained from a fit that does not include the limits from the direct Higgs searches. With direct search data from LEP2 and Tevatron added to the fit, the 90% CL (99% CL) interval is 115–148 (114–197) GeV.
- <sup>52</sup> FLACHER 09 make Standard Model fits to Z and neutral current parameters,  $m_t$ ,  $m_W$ , and  $\Gamma_W$  measurements available in 2008 (using also preliminary data). The  $2\sigma$  ( $3\sigma$ ) interval is 39–155 (26–209) GeV. The quoted results are obtained from a fit that does not include the limit from the direct Higgs searches.
- <sup>53</sup> LEP-SLC 06 make Standard Model fits to Z parameters from LEP/SLC and  $m_t$ ,  $m_W$ , and  $\Gamma_W$  measurements available in 2005 with  $\Delta\alpha_{\text{had}}^{(5)}(m_Z) = 0.02758 \pm 0.00035$ . The 95% CL limit is 285 GeV.

## MASS LIMITS FOR NEUTRAL HIGGS BOSONS IN SUPERSYMMETRIC MODELS

The minimal supersymmetric model has two complex doublets of Higgs bosons. The resulting physical states are two scalars [ $H_1^0$  and  $H_2^0$ ], where we define  $m_{H_1^0} < m_{H_2^0}$ , a pseudoscalar ( $A^0$ ), and a charged Higgs pair ( $H^\pm$ ).  $H_1^0$  and  $H_2^0$  are also called  $h$  and  $H$  in the literature. There are two free parameters in the theory which can be chosen to be  $m_{A^0}$  and  $\tan\beta = v_2/v_1$ , the ratio of vacuum expectation values of the two Higgs doublets. Tree-level Higgs masses are constrained by the model to be  $m_{H_1^0} \leq m_Z$ ,  $m_{H_2^0} \geq m_Z$ ,  $m_{A^0} \geq m_{H_1^0}$ , and  $m_{H^\pm} \geq m_W$ . However, as described in the review on “Searches for Higgs Bosons” in this Volume these relations are violated by radiative corrections.

Unless otherwise noted, the experiments in  $e^+e^-$  collisions search for the processes  $e^+e^- \rightarrow H_1^0 Z^0$  in the channels used for the Standard Model Higgs searches and  $e^+e^- \rightarrow H_1^0 A^0$  in the final states  $b\bar{b}b\bar{b}$  and  $b\bar{b}\tau^+\tau^-$ . In  $p\bar{p}$  collisions the experiments search for a variety of processes, as explicitly specified for each entry. Limits on the  $A^0$  mass arise from these direct searches, as well as from the relations valid in the minimal supersymmetric model between  $m_{A^0}$  and  $m_{H_1^0}$ . As discussed in the review on “Searches for Higgs Bosons” in this Volume, these relations depend, via potentially large radiative corrections, on the mass of the  $t$  quark and on the supersymmetric parameters, in particular those of the stop sector. The limits are weaker for larger  $t$  and  $\tilde{t}$  masses. To include the radiative corrections to the Higgs masses, unless otherwise stated, the listed papers use theoretical predictions incorporating two-loop corrections and examine the two scenarios of no scalar top mixing and the  $m_h^{\text{max}}$  benchmark scenario (which gives rise to the most conservative upper bound on the mass of  $H_1^0$  for given values of  $m_{A^0}$  and  $\tan\beta$ ), see CARENA 99b and CARENA 03.

Limits in the low-mass region of  $H_1^0$ , as well as other by now obsolete limits from different techniques, have been removed from this compilation, and can be found in earlier editions of this Review. Unless otherwise stated, the following results assume no invisible  $H_1^0$  or  $A^0$  decays.

 $H_1^0$  (Higgs Boson) MASS LIMITS in Supersymmetric Models

VALUE (GeV)	CL%	DOCUMENT ID	TECN	COMMENT
>89.7		54 ABDALLAH 08B	DLPH	$E_{\text{cm}} \leq 209$ GeV
>92.8	95	55 SCHAEEL 06B	LEP	$E_{\text{cm}} \leq 209$ GeV
>84.5	95	56,57 ABBIENDI 04M	OPAL	$E_{\text{cm}} \leq 209$ GeV
>86.0	95	56,58 ACHARD 02H	L3	$E_{\text{cm}} \leq 209$ GeV, $\tan\beta > 0.4$
• • • We do not use the following data for averages, fits, limits, etc. • • •				
		59 ABAZOV 12	D0	$p\bar{p} \rightarrow H_{1,2}^0/A^0 + X$ , $H_{1,2}^0/A^0 \rightarrow \tau^+\tau^-$
		60 AAD 11R	ATLS	$p\bar{p} \rightarrow H_{1,2}^0/A^0 + X$ , $H_{1,2}^0/A^0 \rightarrow \tau^+\tau^-$
		61 ABAZOV 11K	D0	$p\bar{p} \rightarrow H_{1,2}^0/A^0 + b + X$ , $H_{1,2}^0/A^0 \rightarrow b\bar{b}$
		62 ABAZOV 11W	D0	$p\bar{p} \rightarrow H_{1,2}^0/A^0 + b + X$ , $H_{1,2}^0/A^0 \rightarrow \tau^+\tau^-$
		63 CHATRCHYAN 11H	CMS	$p\bar{p} \rightarrow H_{1,2}^0/A^0 + X$ , $H_{1,2}^0/A^0 \rightarrow \tau^+\tau^-$
		64 ABAZOV 10D	D0	$p\bar{p} \rightarrow H_{1,2}^0/A^0 + b + X$ , $H_{1,2}^0/A^0 \rightarrow \tau^+\tau^-$
		65 AALTONEN 09AR	CDF	$p\bar{p} \rightarrow H_{1,2}^0/A^0 + X$ , $H_{1,2}^0/A^0 \rightarrow \tau^+\tau^-$
		66 ABAZOV 09F	D0	$p\bar{p} \rightarrow H_{1,2}^0/A^0 + b + X$ , $H_{1,2}^0/A^0 \rightarrow \tau^+\tau^-$
		67 ABAZOV 08AJ	D0	$p\bar{p} \rightarrow H_{1,2}^0/A^0 + b + X$ , $H_{1,2}^0/A^0 \rightarrow b\bar{b}$
		68 ABAZOV 08W	D0	$p\bar{p} \rightarrow H_{1,2}^0/A^0 + X$ , $H_{1,2}^0/A^0 \rightarrow \tau^+\tau^-$
>89.7	95	56,69 ABDALLAH 04	DLPH	$E_{\text{cm}} \leq 209$ GeV, $\tan\beta > 0.4$
		70 ABBIENDI 03G	OPAL	$H_1^0 \rightarrow A^0 A^0$
>89.8	95	56,71 HEISTER 02	ALEP	$E_{\text{cm}} \leq 209$ GeV, $\tan\beta > 0.5$

- <sup>54</sup> ABDALLAH 08B give limits in eight  $CP$ -conserving benchmark scenarios and some  $CP$ -violating scenarios. See paper for excluded regions for each scenario. Supersedes ABDALLAH 04.
- <sup>55</sup> SCHAEEL 06B make a combined analysis of the LEP data. The quoted limit is for the  $m_h^{\text{max}}$  scenario with  $m_t = 174.3$  GeV. In the  $CP$ -violating CPX scenario no lower bound on  $m_{H_1^0}$  can be set at 95% CL. See paper for excluded regions in various scenarios. See Figs. 2–6 and Tabs. 14–21 for limits on  $\sigma(ZH^0) \cdot B(H^0 \rightarrow b\bar{b}, \tau^+\tau^-)$  and  $\sigma(H_1^0 H_2^0) \cdot B(H_1^0 H_2^0 \rightarrow b\bar{b}, \tau^+\tau^-)$ .
- <sup>56</sup> Search for  $e^+e^- \rightarrow H_1^0 A^0$  in the final states  $b\bar{b}b\bar{b}$  and  $b\bar{b}\tau^+\tau^-$ , and  $e^+e^- \rightarrow H_1^0 Z$ . Universal scalar mass of 1 TeV, SU(2) gaugino mass of 200 GeV, and  $\mu = -200$  GeV are assumed, and two-loop radiative corrections incorporated. The limits hold for  $m_t = 175$  GeV, and for the  $m_h^{\text{max}}$  scenario.
- <sup>57</sup> ABBIENDI 04M exclude  $0.7 < \tan\beta < 1.9$ , assuming  $m_t = 174.3$  GeV. Limits for other MSSM benchmark scenarios, as well as for  $CP$  violating cases, are also given.
- <sup>58</sup> ACHARD 02H also search for the final state  $H_1^0 Z \rightarrow 2A^0 q\bar{q}$ ,  $A^0 \rightarrow q\bar{q}$ . In addition, the MSSM parameter set in the “large- $\mu$ ” and “no-mixing” scenarios are examined.
- <sup>59</sup> ABAZOV 12 search for production of a Higgs boson followed by the decay  $H_{1,2}^0/A^0 \rightarrow \tau^+\tau^-$  in 5.4 fb $^{-1}$  of  $p\bar{p}$  collisions at  $E_{\text{cm}} = 1.96$  TeV. See their Fig. 2 for the limit on cross section times branching ratio and Fig. 3 for the excluded region in the MSSM parameter space.
- <sup>60</sup> AAD 11R search for production of a Higgs boson followed by the decay  $H_{1,2}^0/A^0 \rightarrow \tau^+\tau^-$  in 36 pb $^{-1}$  of  $p\bar{p}$  collisions at  $E_{\text{cm}} = 7$  TeV. See their Fig. 3 for the limit on cross section times branching ratio and for the excluded region in the MSSM parameter space.
- <sup>61</sup> ABAZOV 11K search for associated production of a Higgs boson and a  $b$  quark, followed by the decay  $H_{1,2}^0/A^0 \rightarrow b\bar{b}$ , in 5.2 fb $^{-1}$  of  $p\bar{p}$  collisions at  $E_{\text{cm}} = 1.96$  TeV. See their Fig. 5/Table 2 for the limit on cross section times branching ratio and Fig. 6 for the excluded region in the MSSM parameter space for  $\mu = -200$  GeV.
- <sup>62</sup> ABAZOV 11W search for associated production of a Higgs boson and a  $b$  quark, followed by the decay  $H_{1,2}^0/A^0 \rightarrow \tau\tau$ , in 7.3 fb $^{-1}$  of  $p\bar{p}$  collisions at  $E_{\text{cm}} = 1.96$  TeV. See their Fig. 2 for the limit on cross section times branching ratio and for the excluded region in the MSSM parameter space.
- <sup>63</sup> CHATRCHYAN 11H search for production of a Higgs boson followed by the decay  $H_{1,2}^0/A^0 \rightarrow \tau^+\tau^-$  in 36 pb $^{-1}$  of  $p\bar{p}$  collisions at  $E_{\text{cm}} = 7$  TeV. See their Fig. 2 for the limit on cross section times branching ratio and Fig. 3 for the excluded region in the MSSM parameter space.
- <sup>64</sup> ABAZOV 10D search for associated production of a Higgs boson and a  $b$  quark in 2.7 fb $^{-1}$  of  $p\bar{p}$  collisions at  $E_{\text{cm}} = 1.96$  TeV, with the decay  $H_{1,2}^0/A^0 \rightarrow \tau^+\tau^-$ . See their Fig. 1 for the limit on  $\sigma \cdot B(H_{1,2}^0/A^0 \rightarrow \tau^+\tau^-)$  (for different Higgs masses) and for the excluded region in the MSSM parameter space for  $\mu = -200$  GeV. Superseded by ABAZOV 11W.
- <sup>65</sup> AALTONEN 09AR search for Higgs bosons decaying to  $\tau^+\tau^-$  in two doublet models in 1.8 fb $^{-1}$  of  $p\bar{p}$  collisions at  $E_{\text{cm}} = 1.96$  TeV. See their Fig. 2 for the limit on  $\sigma \cdot B(H_{1,2}^0/A^0 \rightarrow \tau^+\tau^-)$  for different Higgs masses, and see their Fig. 3 for the excluded region in the MSSM parameter space.
- <sup>66</sup> ABAZOV 09F search for associated production of a Higgs boson and a  $b$  quark in  $p\bar{p}$  collisions at  $E_{\text{cm}} = 1.96$  TeV with the decay  $H_{1,2}^0/A^0 \rightarrow \tau^+\tau^-$ . See their Fig. 2 for the limit on  $\sigma \cdot B(H_{1,2}^0/A^0 \rightarrow \tau^+\tau^-)$  (for different Higgs masses) and for the excluded region in the MSSM parameter space for  $\mu = \pm 200$  GeV. Superseded by ABAZOV 10D.
- <sup>67</sup> ABAZOV 08AJ search for associated production of a Higgs boson and a  $b$  quark in  $p\bar{p}$  collisions at  $E_{\text{cm}} = 1.96$  TeV with the decay  $H_{1,2}^0/A^0 \rightarrow b\bar{b}$ . See their Tab. 3 for the limit on  $\sigma \cdot B(H_{1,2}^0/A^0 \rightarrow b\bar{b})$  for different Higgs masses, and see their Fig. 3 for the excluded region in the MSSM parameter space for  $\mu = \pm 200$  GeV. Superseded by ABAZOV 11K.
- <sup>68</sup> ABAZOV 08W search for Higgs boson production in  $p\bar{p}$  collisions at  $E_{\text{cm}} = 1.96$  TeV with the decay  $H_{1,2}^0/A^0 \rightarrow \tau^+\tau^-$ . See their Fig. 3 for the limit on  $\sigma \cdot B(H_{1,2}^0/A^0 \rightarrow \tau^+\tau^-)$  for different Higgs masses, and see their Fig. 4 for the excluded region in the MSSM parameter space. Superseded by ABAZOV 12.
- <sup>69</sup> This limit applies also in the no-mixing scenario. Furthermore, ABDALLAH 04 excludes the range  $0.54 < \tan\beta < 2.36$ . The limit improves in the region  $\tan\beta < 6$  (see Fig. 28). Limits for  $\mu = 1$  TeV are given in Fig. 30.
- <sup>70</sup> ABBIENDI 03G search for  $e^+e^- \rightarrow H_1^0 Z$  followed by  $H_1^0 \rightarrow A^0 A^0$ ,  $A^0 \rightarrow c\bar{c}$ ,  $g\bar{g}$ , or  $\tau^+\tau^-$ . In the no-mixing scenario, the region  $m_{H_1^0} = 45\text{--}85$  GeV and  $m_{A^0} = 2\text{--}9.5$  GeV is excluded at 95% CL.
- <sup>71</sup> HEISTER 02 excludes the range  $0.7 < \tan\beta < 2.3$ . A wider range is excluded with different stop mixing assumptions. Updates BARATE 01c.

 $A^0$  (Pseudoscalar Higgs Boson) MASS LIMITS in Supersymmetric Models

VALUE (GeV)	CL%	DOCUMENT ID	TECN	COMMENT
>90.4		72 ABDALLAH 08B	DLPH	$E_{\text{cm}} \leq 209$ GeV
>93.4	95	73 SCHAEEL 06B	LEP	$E_{\text{cm}} \leq 209$ GeV
>85.0	95	74,75 ABBIENDI 04M	OPAL	$E_{\text{cm}} \leq 209$ GeV
>86.5	95	74,76 ACHARD 02H	L3	$E_{\text{cm}} \leq 209$ GeV, $\tan\beta > 0.4$
>90.1	95	74,77 HEISTER 02	ALEP	$E_{\text{cm}} \leq 209$ GeV, $\tan\beta > 0.5$
• • • We do not use the following data for averages, fits, limits, etc. • • •				
		78 ABAZOV 12	D0	$p\bar{p} \rightarrow H_{1,2}^0/A^0 + X$ , $H_{1,2}^0/A^0 \rightarrow \tau^+\tau^-$
		79 AAD 11R	ATLS	$p\bar{p} \rightarrow H_{1,2}^0/A^0 + X$ , $H_{1,2}^0/A^0 \rightarrow \tau^+\tau^-$
		80 ABAZOV 11K	D0	$p\bar{p} \rightarrow H_{1,2}^0/A^0 + b + X$ , $H_{1,2}^0/A^0 \rightarrow b\bar{b}$



81	ABAZOV	11W D0	$p\bar{p} \rightarrow H_{1,2}^0/A^0 + b + X,$ $H_{1,2}^0/A^0 \rightarrow \tau^+\tau^-$
82	CHATRCHYAN11H	CMS	$pp \rightarrow H_{1,2}^0/A^0 + X,$ $H_{1,2}^0/A^0 \rightarrow \tau^+\tau^-$
83	ABAZOV	10D D0	$p\bar{p} \rightarrow H_{1,2}^0/A^0 + b + X,$ $H_{1,2}^0/A^0 \rightarrow \tau^+\tau^-$
84	AALTONEN	09AR CDF	$p\bar{p} \rightarrow H_{1,2}^0/A^0 + X,$ $H_{1,2}^0/A^0 \rightarrow \tau^+\tau^-$
85	ABAZOV	09F D0	$p\bar{p} \rightarrow H_{1,2}^0/A^0 + b + X,$ $H_{1,2}^0/A^0 \rightarrow \tau^+\tau^-$
86	ABAZOV	08AJ D0	$p\bar{p} \rightarrow H_{1,2}^0/A^0 + b + X,$ $H_{1,2}^0/A^0 \rightarrow b\bar{b}$
87	ABAZOV	08W D0	$p\bar{p} \rightarrow H_{1,2}^0/A^0 + X,$ $H_{1,2}^0/A^0 \rightarrow \tau^+\tau^-$
88	ACOSTA	05Q CDF	$p\bar{p} \rightarrow H_{1,2}^0/A^0 + X$
>90.4	95	74,89 ABDALLAH	$E_{\text{cm}} \leq 209$ GeV, $\tan\beta > 0.4$
		90 ABBIENDI	03G OPAL $H_1^0 \rightarrow A^0 A^0$
		91 AKEROYD	02 RVUE

<sup>72</sup> ABDALLAH 08B give limits in eight  $CP$ -conserving benchmark scenarios and some  $CP$ -violating scenarios. See paper for excluded regions for each scenario. Supersedes ABDALLAH 04.  
<sup>73</sup> SCHAEEL 06B make a combined analysis of the LEP data. The quoted limit is for the  $m_h^{\text{max}}$  scenario with  $m_t = 174.3$  GeV. In the  $CP$ -violating CPX scenario no lower bound on  $m_{H_1^0}$  can be set at 95% CL. See paper for excluded regions in various scenarios. See

Figs. 2-6 and Tabs. 14-21 for limits on  $\sigma(ZH^0) \cdot B(H^0 \rightarrow b\bar{b}, \tau^+\tau^-)$  and  $\sigma(H_1^0 H_2^0) \cdot B(H_1^0 H_2^0 \rightarrow b\bar{b}, \tau^+\tau^-)$ .

<sup>74</sup> Search for  $e^+e^- \rightarrow H_1^0 A^0$  in the final states  $b\bar{b}b\bar{b}$  and  $b\bar{b}\tau^+\tau^-$ , and  $e^+e^- \rightarrow H_1^0 Z$ . Universal scalar mass of 1 TeV, SU(2) gaugino mass of 200 GeV, and  $\mu = -200$  GeV are assumed, and two-loop radiative corrections incorporated. The limits hold for  $m_t = 175$  GeV, and for the  $m_h^{\text{max}}$  scenario.

<sup>75</sup> ABBIENDI 04M exclude  $0.7 < \tan\beta < 1.9$ , assuming  $m_t = 174.3$  GeV. Limits for other MSSM benchmark scenarios, as well as for  $CP$  violating cases, are also given.

<sup>76</sup> ACHARD 02H also search for the final state  $H_1^0 Z \rightarrow 2A^0 q\bar{q}, A^0 \rightarrow q\bar{q}$ . In addition, the MSSM parameter set in the “large- $\mu$ ” and “no-mixing” scenarios are examined.

<sup>77</sup> HEISTER 02 excludes the range  $0.7 < \tan\beta < 2.3$ . A wider range is excluded with different stop mixing assumptions. Updates BARATE 01c.

<sup>78</sup> ABAZOV 12 search for production of a Higgs boson followed by the decay  $H_{1,2}^0/A^0 \rightarrow \tau^+\tau^-$  in  $5.4 \text{ fb}^{-1}$  of  $p\bar{p}$  collisions at  $E_{\text{cm}} = 1.96$  TeV. See their Fig. 2 for the limit on cross section times branching ratio and Fig. 3 for the excluded region in the MSSM parameter space.

<sup>79</sup> AAD 11R search for production of a Higgs boson followed by the decay  $H_{1,2}^0/A^0 \rightarrow \tau^+\tau^-$  in  $36 \text{ pb}^{-1}$  of  $pp$  collisions at  $E_{\text{cm}} = 7$  TeV. See their Fig. 3 for the limit on cross section times branching ratio and for the excluded region in the MSSM parameter space.

<sup>80</sup> ABAZOV 11k search for associated production of a Higgs boson and a  $b$  quark, followed by the decay  $H_{1,2}^0/A^0 \rightarrow b\bar{b}$ , in  $5.2 \text{ fb}^{-1}$  of  $p\bar{p}$  collisions at  $E_{\text{cm}} = 1.96$  TeV. See their Fig. 5/ Table 2 for the limit on cross section times branching ratio and Fig. 6 for the excluded region in the MSSM parameter space for  $\mu = -200$  GeV.

<sup>81</sup> ABAZOV 11w search for associated production of a Higgs boson and a  $b$  quark, followed by the decay  $H_{1,2}^0/A^0 \rightarrow \tau\tau$ , in  $7.3 \text{ fb}^{-1}$  of  $p\bar{p}$  collisions at  $E_{\text{cm}} = 1.96$  TeV. See their Fig. 2 for the limit on cross section times branching ratio and for the excluded region in the MSSM parameter space.

<sup>82</sup> CHATRCHYAN 11H search for production of a Higgs boson followed by the decay  $H_{1,2}^0/A^0 \rightarrow \tau^+\tau^-$  in  $36 \text{ pb}^{-1}$  of  $pp$  collisions at  $E_{\text{cm}} = 7$  TeV. See their Fig. 2 for the limit on cross section times branching ratio and Fig. 3 for the excluded region in the MSSM parameter space.

<sup>83</sup> ABAZOV 10D search for associated production of a Higgs boson and a  $b$  quark in  $2.7 \text{ fb}^{-1}$  of  $p\bar{p}$  collisions at  $E_{\text{cm}} = 1.96$  TeV, with the decay  $H_{1,2}^0/A^0 \rightarrow \tau^+\tau^-$ . See their Fig. 1 for the limit on  $\sigma \cdot B(H_{1,2}^0/A^0 \rightarrow \tau^+\tau^-)$  (for different Higgs masses) and for the excluded region in the MSSM parameter space for  $\mu = -200$  GeV. Superseded by ABAZOV 11w.

<sup>84</sup> AALTONEN 09AR search for Higgs bosons decaying to  $\tau^+\tau^-$  in two doublet models in  $1.8 \text{ fb}^{-1}$  of  $p\bar{p}$  collisions at  $E_{\text{cm}} = 1.96$  TeV. See their Fig. 2 for the limit on  $\sigma \cdot B(H_{1,2}^0/A^0 \rightarrow \tau^+\tau^-)$  for different Higgs masses, and see their Fig. 3 for the excluded region in the MSSM parameter space.

<sup>85</sup> ABAZOV 09F search for associated production of a Higgs boson and a  $b$  quark in  $p\bar{p}$  collisions at  $E_{\text{cm}} = 1.96$  TeV with the decay  $H_{1,2}^0/A^0 \rightarrow \tau^+\tau^-$ . See their Fig. 2 for the limit on  $\sigma \cdot B(H_{1,2}^0/A^0 \rightarrow \tau^+\tau^-)$  (for different Higgs masses) and for the excluded region in the MSSM parameter space for  $\mu = \pm 200$  GeV. Superseded by ABAZOV 10D.

<sup>86</sup> ABAZOV 08AJ search for associated production of a Higgs boson and a  $b$  quark in  $p\bar{p}$  collisions at  $E_{\text{cm}} = 1.96$  TeV with the decay  $H_{1,2}^0/A^0 \rightarrow b\bar{b}$ . See their Tab. 3 for the limit on  $\sigma \cdot B(H_{1,2}^0/A^0 \rightarrow b\bar{b})$  for different Higgs masses, and see their Fig. 3 for the excluded region in the MSSM parameter space for  $\mu = \pm 200$  GeV. Superseded by ABAZOV 11k.

<sup>87</sup> ABAZOV 08W search for Higgs boson production in  $p\bar{p}$  collisions at  $E_{\text{cm}} = 1.96$  TeV with the decay  $H_{1,2}^0/A^0 \rightarrow \tau^+\tau^-$ . See their Fig. 3 for the limit on  $\sigma \cdot B(H_{1,2}^0/A^0 \rightarrow \tau^+\tau^-)$  for different Higgs masses, and see their Fig. 4 for the excluded region in the MSSM parameter space. Superseded by ABAZOV 12.

<sup>88</sup> ACOSTA 05Q search for  $H_{1,2}^0/A^0$  production in  $p\bar{p}$  collisions at  $E_{\text{cm}} = 1.8$  TeV with  $H_{1,2}^0/A^0 \rightarrow \tau^+\tau^-$ . At  $m_{A^0} = 100$  GeV, the obtained cross section upper limit is above theoretical expectation.

<sup>89</sup> This limit applies also in the no-mixing scenario. Furthermore, ABDALLAH 04 excludes the range  $0.54 < \tan\beta < 2.36$ . The limit improves in the region  $\tan\beta < 6$  (see Fig. 28). Limits for  $\mu = 1$  TeV are given in Fig. 30.

<sup>90</sup> ABBIENDI 03G search for  $e^+e^- \rightarrow H_1^0 Z$  followed by  $H_1^0 \rightarrow A^0 A^0, A^0 \rightarrow c\bar{c}, gg,$  or  $\tau^+\tau^-$ . In the no-mixing scenario, the region  $m_{H_1^0} = 45-85$  GeV and  $m_{A^0} = 2-9.5$  GeV is excluded at 95% CL.

<sup>91</sup> AKEROYD 02 examine the possibility of a light  $A^0$  with  $\tan\beta < 1$ . Electroweak measurements are found to be inconsistent with such a scenario.

### $H^0$ (Higgs Boson) MASS LIMITS in Extended Higgs Models

This Section covers models which do not fit into either the Standard Model or its simplest minimal Supersymmetric extension (MSSM), leading to anomalous production rates, or nonstandard final states and branching ratios. In particular, this Section covers limits which may apply to generic two-Higgs-doublet models (2HDM), or to special regions of the MSSM parameter space where decays to invisible particles or to photon pairs are dominant (see the Note on ‘Searches for Higgs Bosons’ at the beginning of this Chapter). See the footnotes or the comment lines for details on the nature of the models to which the limits apply.

VALUE (GeV)	CL%	DOCUMENT ID	TECN	COMMENT
• • • We do not use the following data for averages, fits, limits, etc. • • •				
>114	95	92 AALTONEN	12 CDF	$H^0 \rightarrow \gamma\gamma$
		93 AALTONEN	11P CDF	$t \rightarrow bH^\pm, H^\pm \rightarrow W^\pm A^0$
>112.9	95	94 ABAZOV	11Y D0	$H^0 \rightarrow \gamma\gamma$
< $1.0 \times 10^{-10}$	90	95 ABOUZAIID	11A KTEV	$K_L^0 \rightarrow \pi^0 \pi^0 A^0, A^0 \rightarrow \mu^+ \mu^-$
		96 DEL-AMO-SA...	11J BABR	$\Upsilon(1S) \rightarrow A^0 \gamma$
		97 LEES	11H BABR	$\Upsilon(2S, 3S) \rightarrow A^0 \gamma$
>108.2	95	98 ABBIENDI	10 OPAL	invisible $H^0$
		99 ABBIENDI	10 OPAL	$H^0 \rightarrow \tilde{\chi}_1^0 \tilde{\chi}_2^0$
		100 ANDREAS	10 RVUE	
< $2.26 \times 10^{-8}$	90	101 HYUN	10 BELL	$B^0 \rightarrow K^* A^0, A^0 \rightarrow \mu^+ \mu^-$
< $1.73 \times 10^{-8}$	90	101 HYUN	10 BELL	$B^0 \rightarrow \rho A^0, A^0 \rightarrow \mu^+ \mu^-$
		102 SCHAEEL	10 ALEP	$H^0 \rightarrow A^0 A^0$
>106	95	103 AALTONEN	09AB CDF	$H^0 \rightarrow \gamma\gamma$
		104 AALTONEN	09AR CDF	$p\bar{p} \rightarrow H_{1,2}^0/A^0 + X,$ $H_{1,2}^0/A^0 \rightarrow \tau^+\tau^-$
>101	95	105 ABAZOV	09Q D0	$H^0 \rightarrow \gamma\gamma$
		106 ABAZOV	09V D0	$H^0 \rightarrow A^0 A^0$
		107 AUBERT	09P BABR	$\Upsilon(3S) \rightarrow A^0 \gamma$
		108 AUBERT	09Z BABR	$\Upsilon(2S) \rightarrow A^0 \gamma$
		109 AUBERT	09Z BABR	$\Upsilon(3S) \rightarrow A^0 \gamma$
< $2.4 \times 10^{-7}$	90	110 TUNG	09 K391	$K^0 \rightarrow \pi^0 \pi^0 A^0, A^0 \rightarrow \gamma\gamma$
		111 ABAZOV	08U D0	$H^0 \rightarrow \gamma\gamma$
		112 LOVE	08 CLEO	$\Upsilon(1S) \rightarrow A^0 \gamma$
		113 ABBIENDI	07 OPAL	invisible $H^0$ , large width
		114 BESSON	07 CLEO	$\Upsilon(1S) \rightarrow \eta_b \gamma$
>105.8	95	115 SCHAEEL	07 ALEP	$e^+e^- \rightarrow H^0 Z, H^0 \rightarrow$
none 1-55	95	116 ABBIENDI	05A OPAL	$H^0, WW^*$ , Type II model
none 3-63	95	116 ABBIENDI	05A OPAL	$A^0$ , Type II model
>110.6	95	117 ABDALLAH	05D DLPH	$H^0 \rightarrow 2$ jets
>112.3	95	118 ACHARD	05 L3	invisible $H^0$
		119 PARK	05 HYCP	$\Sigma^+ \rightarrow \rho A^0, A^0 \rightarrow \mu^+ \mu^-$
>104	95	120 ABBIENDI	04K OPAL	$H^0 \rightarrow 2$ jets
		121 ABDALLAH	04B DLPH	$H^0 V V$ couplings
>112.1	95	118 ABDALLAH	04B DLPH	Invisible $H^0$
>104.1	95	122,123 ABDALLAH	04L DLPH	$e^+e^- \rightarrow H^0 Z, H^0 \rightarrow \gamma\gamma$
		124 ABDALLAH	04O DLPH	$Z \rightarrow f\bar{f}H$
		125 ABDALLAH	04O DLPH	$e^+e^- \rightarrow H^0 Z, H^0 A^0$
>110.3	95	126 ACHARD	04B L3	$H^0 \rightarrow 2$ jets
		127 ACHARD	04F L3	Anomalous coupling
		128 ABBIENDI	03F OPAL	$e^+e^- \rightarrow H^0 Z, H^0 \rightarrow$ any
		129 ABBIENDI	03G OPAL	$H^0 \rightarrow A^0 A^0$
>107	95	130 ACHARD	03C L3	$H^0 \rightarrow WW^*, Z Z^*, \gamma\gamma$
		131 ABBIENDI	02D OPAL	$e^+e^- \rightarrow b\bar{b}H$
>105.5	95	122,132 ABBIENDI	02F OPAL	$H^0 \rightarrow \gamma\gamma$
>105.4	95	133 ACHARD	02C L3	$H^0 \rightarrow \gamma\gamma$
>114.1	95	118 HEISTER	02 ALEP	Invisible $H^0, E_{\text{cm}} \leq 209$ GeV
>105.4	95	122,134 HEISTER	02L ALEP	$H^0 \rightarrow \gamma\gamma$
>109.1	95	135 HEISTER	02M ALEP	$H^0 \rightarrow 2$ jets or $\tau^+\tau^-$
none 1-44	95	136 ABBIENDI	01E OPAL	$H^0, \text{Type-II model}$
none 12-56	95	136 ABBIENDI	01E OPAL	$A^0, \text{Type-II model}$
> 98	95	137 AFFOLDER	01H CDF	$p\bar{p} \rightarrow H^0 W/Z, H^0 \rightarrow \gamma\gamma$
>106.4	95	118 BARATE	01C ALEP	Invisible $H^0, E_{\text{cm}} \leq 202$ GeV
> 89.2	95	138 ACCIARRI	00M L3	Invisible $H^0$
		139 ACCIARRI	00R L3	$e^+e^- \rightarrow H^0 \gamma$ and/or $H^0 \rightarrow \gamma\gamma$

## Gauge &amp; Higgs Boson Particle Listings

Higgs Bosons —  $H^0$  and  $H^\pm$ 

- |        |     |              |     |      |  |
|--------|-----|--------------|-----|------|--|
|        | 140 | ACCIARRI     | 00R | L3   | $e^+e^- \rightarrow e^+e^-H^0$                                       |
| > 94.9 | 95  | 141 ACCIARRI | 00S | L3   | $e^+e^- \rightarrow H^0Z, H^0 \rightarrow \gamma\gamma$              |
| >100.7 | 95  | 142 BARATE   | 00L | ALEP | $e^+e^- \rightarrow H^0Z, H^0 \rightarrow \gamma\gamma$              |
| > 68.0 | 95  | 143 ABBIENDI | 99E | OPAL | $\tan\beta > 1$  |
| > 96.2 | 95  | 144 ABBIENDI | 99O | OPAL | $e^+e^- \rightarrow H^0Z, H^0 \rightarrow \gamma\gamma$              |
| > 78.5 | 95  | 145 ABBOTT   | 99B | D0   | $p\bar{p} \rightarrow H^0W/Z, H^0 \rightarrow \gamma\gamma$          |
|        |     | 146 ABREU    | 99P | DLPH | $e^+e^- \rightarrow H^0\gamma$ and/or $H^0 \rightarrow \gamma\gamma$ |
|        | 147 | GONZALEZ-G.  | 98B | RVUE | Anomalous coupling   |
|        | 148 | KRAWCZYK     | 97  | RVUE | $(g-2)_\mu$  |
|        | 149 | ALEXANDER    | 96H | OPAL | $Z \rightarrow H^0\gamma$  |
|        | 150 | ABREU        | 95H | DLPH | $Z \rightarrow H^0Z^*, H^0A^0$                                       |
|        | 151 | PICH         | 92  | RVUE | Very light Higgs   |
- 92 AALTONEN 12 search for  $H^0 \rightarrow \gamma\gamma$  in 7.0 fb<sup>-1</sup> of  $p\bar{p}$  collisions at  $E_{\text{cm}} = 1.96$  TeV in the mass range  $m_{H^0} = 100\text{--}150$  GeV. The limit assumes that all fermion Yukawa couplings vanish.
- 93 AALTONEN 11P search in 2.7 fb<sup>-1</sup> of  $p\bar{p}$  collisions at  $E_{\text{cm}} = 1.96$  TeV for the decay chain  $t \rightarrow bH^+, H^+ \rightarrow W^+A^0, A^0 \rightarrow \tau^+\tau^-$  with  $m_{A^0}$  between 4 and 9 GeV. See their Fig. 4 for limits on  $B(t \rightarrow bH^+)$  for  $90 < m_{H^+} < 160$  GeV.
- 94 ABAZOV 11Y search for  $H^0 \rightarrow \gamma\gamma$  in 8.2 fb<sup>-1</sup> of  $p\bar{p}$  collisions at  $E_{\text{cm}} = 1.96$  TeV in the mass range  $m_{H^0} = 100\text{--}150$  GeV. The limit assumes that all fermion Yukawa couplings vanish.
- 95 The limit applies at  $m_{A^0} = 214.3$  MeV, motivated by PARK 05.
- 96 DEL-AMO-SANCHEZ 11J search for the process  $\Upsilon(2S) \rightarrow \Upsilon(1S)\pi^+\pi^- \rightarrow A^0\gamma\pi^+\pi^-$  with  $A^0$  decaying to invisible final states. They give limits on  $B(\Upsilon(1S) \rightarrow A^0\gamma)\cdot B(A^0 \rightarrow \text{invisible})$  in the range  $(1.9\text{--}4.5) \times 10^{-6}$  (90% CL) for  $0 \leq m_{A^0} \leq 8.0$  GeV, and  $(2.7\text{--}37) \times 10^{-6}$  for  $8.0 \leq m_{A^0} \leq 9.2$  GeV.
- 97 LEES 11H search for the process  $\Upsilon(2S, 3S) \rightarrow A^0\gamma$  with  $A^0$  decaying hadronically and give limits on  $B(\Upsilon(2S, 3S) \rightarrow A^0\gamma)\cdot B(A^0 \rightarrow \text{hadrons})$  in the range  $1 \times 10^{-6}\text{--}8 \times 10^{-5}$  (90% CL) for  $0.3 < m_{A^0} < 7$  GeV. The decay rates for  $\Upsilon(2S)$  and  $\Upsilon(3S)$  are assumed to be equal up to the phase space factor.
- 98 ABBIENDI 10 search for  $e^+e^- \rightarrow H^0Z$  with  $H^0$  decaying invisibly. The limit assumes SM production cross section and  $B(H^0 \rightarrow \text{invisible}) = 1$ .
- 99 ABBIENDI 10 search for  $e^+e^- \rightarrow ZH^0$  with the decay chain  $H^0 \rightarrow \tilde{\chi}_1^0\tilde{\chi}_2^0 \rightarrow \tilde{\chi}_1^0 + (\gamma \text{ or } Z^*)$ , when  $\tilde{\chi}_1^0$  and  $\tilde{\chi}_2^0$  are nearly degenerate. For a mass difference of 2 (4) GeV, a lower limit on  $m_{H^0}$  of 108.4 (107.0) GeV (95% CL) is obtained for SM  $ZH^0$  cross section and  $B(H^0 \rightarrow \tilde{\chi}_1^0\tilde{\chi}_2^0) = 1$ .
- 100 ANDREAS 10 analyze various rare decays and find  $m_{A^0} > 210$  MeV or that its couplings to fermions are 4 orders of magnitude below those of the standard Higgs.
- 101 The limit applies at  $m_{A^0} = 214.3$  MeV, motivated by PARK 05. HYUN 10 summarize mass-dependent limits in their Table 1.
- 102 SCHAEEL 10 search for the process  $e^+e^- \rightarrow H^0Z$  followed by the decay chain  $H^0 \rightarrow A^0A^0 \rightarrow \tau^+\tau^-\tau^+\tau^-$  with  $Z \rightarrow \ell^+\ell^-, \nu\bar{\nu}$  at  $E_{\text{cm}} = 183\text{--}209$  GeV. For a  $H^0ZZ$  coupling equal to the SM value,  $B(H^0 \rightarrow A^0A^0) = B(A^0 \rightarrow \tau^+\tau^-) = 1$ , and  $m_{A^0} = 4\text{--}10$  GeV,  $m_{H^0}$  up to 107 GeV is excluded at 95% CL.
- 103 AALTONEN 09AB search for  $H^0 \rightarrow \gamma\gamma$  in 3.0 fb<sup>-1</sup> of  $p\bar{p}$  collisions at  $E_{\text{cm}} = 1.96$  TeV in the mass range  $m_{H^0} = 70\text{--}150$  GeV. Associated  $H^0W, H^0Z$  production and  $WW, ZZ$  fusion are considered. The limit assumes that all fermion Yukawa couplings vanish.
- 104 AALTONEN 09AR search for Higgs bosons decaying to  $\tau^+\tau^-$  in two doublet models in 1.8 fb<sup>-1</sup> of  $p\bar{p}$  collisions at  $E_{\text{cm}} = 1.96$  TeV. See their Fig. 2 for the limit on  $\sigma \cdot B(H_{1,2}^0/A^0 \rightarrow \tau^+\tau^-)$  for different Higgs masses, and see their Fig. 3 for the excluded region in the MSSM parameter space.
- 105 ABAZOV 09Z search for  $H^0 \rightarrow \gamma\gamma$  in 2.7 fb<sup>-1</sup> of  $p\bar{p}$  collisions at  $E_{\text{cm}} = 1.96$  TeV in the mass range  $m_{H^0} = 100\text{--}150$  GeV. The limit assumes that all fermion Yukawa couplings vanish. Superseded by ABAZOV 11Y.
- 106 ABAZOV 09V search for  $H^0$  production followed by the decay chain  $H^0 \rightarrow A^0A^0 \rightarrow \mu^+\mu^-\mu^+\mu^-$  or  $\mu^+\mu^-\tau^+\tau^-$  in 4.2 fb<sup>-1</sup> of  $p\bar{p}$  collisions at  $E_{\text{cm}} = 1.96$  TeV. See their Fig. 3 for limits on  $\sigma(H^0)\cdot B(H^0 \rightarrow A^0A^0)$  for  $m_{A^0} = 3.6\text{--}19$  GeV.
- 107 AUBERT 09P search for the process  $\Upsilon(3S) \rightarrow A^0\gamma$  with  $A^0 \rightarrow \tau^+\tau^-$  for  $4.03 < m_{A^0} < 9.52$  and  $9.61 < m_{A^0} < 10.10$  GeV, and give limits on  $B(\Upsilon(3S) \rightarrow A^0\gamma)\cdot B(A^0 \rightarrow \tau^+\tau^-)$  in the range  $(1.5\text{--}16) \times 10^{-5}$  (90% CL).
- 108 AUBERT 09Z search for the process  $\Upsilon(2S) \rightarrow A^0\gamma$  with  $A^0 \rightarrow \mu^+\mu^-$  for  $0.212 < m_{A^0} < 9.3$  GeV and give limits on  $B(\Upsilon(2S) \rightarrow A^0\gamma)\cdot B(A^0 \rightarrow \mu^+\mu^-)$  in the range  $(0.3\text{--}8) \times 10^{-6}$  (90% CL).
- 109 AUBERT 09Z search for the process  $\Upsilon(3S) \rightarrow A^0\gamma$  with  $A^0 \rightarrow \mu^+\mu^-$  for  $0.212 < m_{A^0} < 9.3$  GeV and give limits on  $B(\Upsilon(3S) \rightarrow A^0\gamma)\cdot B(A^0 \rightarrow \mu^+\mu^-)$  in the range  $(0.3\text{--}5) \times 10^{-6}$  (90% CL).
- 110 The limit applies at  $m_{A^0} = 214.3$  MeV, motivated by PARK 05. TUNG 09 show mass-dependent limits in their Fig. 5.
- 111 ABAZOV 08U search for  $H^0 \rightarrow \gamma\gamma$  in  $p\bar{p}$  collisions at  $E_{\text{cm}} = 1.96$  TeV in the mass range  $m_{H^0} = 70\text{--}150$  GeV. Associated  $H^0W, H^0Z$  production and  $WW, ZZ$  fusion are considered. See their Tab. 1 for the limit on  $\sigma \cdot B(H^0 \rightarrow \gamma\gamma)$ , and see their Fig. 3 for the excluded region in the  $m_{H^0} - B(H^0 \rightarrow \gamma\gamma)$  plane.
- 112 LOVE 08 search for the process  $\Upsilon(1S) \rightarrow A^0\gamma$  with  $A^0 \rightarrow \mu^+\mu^-$  (for  $m_{A^0} < 2m_\tau$ ) and  $A^0 \rightarrow \tau^+\tau^-$ . Limits on  $B(\Upsilon(1S) \rightarrow A^0\gamma) \cdot B(A^0 \rightarrow \ell^+\ell^-)$  in the range  $10^{-6}\text{--}10^{-4}$  (90% CL) are given.
- 113 ABBIENDI 07 search for  $e^+e^- \rightarrow H^0Z$  with  $Z \rightarrow q\bar{q}$  and  $H^0$  decaying to invisible final states. The  $H^0$  width is varied between 1 GeV and 3 TeV. A limit  $\sigma \cdot B(H^0 \rightarrow \text{invisible}) < (0.07\text{--}0.57)$  pb (95% CL) is obtained at  $E_{\text{cm}} = 206$  GeV for  $m_{H^0} = 60\text{--}114$  GeV.
- 114 BESSON 07 give a limit  $B(\Upsilon(1S) \rightarrow \eta_b\gamma) \cdot B(\eta_b \rightarrow \tau^+\tau^-) < 0.27\%$  (95% CL), which constrains a possible  $A^0$  exchange contribution to the  $\eta_b$  decay.
- 115 SCHAEEL 07 search for Higgs bosons in association with a fermion pair and decaying to  $WW^*$ . The limit is from this search and HEISTER 02L for a  $H^0$  with SM production cross section and  $B(H^0 \rightarrow f\bar{f}) = 0$  for all fermions  $f$ .
- 116 ABBIENDI 05A search for  $e^+e^- \rightarrow H_1^0A^0$  in general Type-II two-doublet models, with decays  $H_1^0, A^0 \rightarrow q\bar{q}, gg, \tau^+\tau^-$ , and  $H_1^0 \rightarrow A^0A^0$ .
- 117 ABDALLAH 05D search for  $e^+e^- \rightarrow H^0Z$  and  $H^0A^0$  with  $H^0, A^0$  decaying to two jets of any flavor including  $gg$ . The limit is for SM  $H^0Z$  production cross section with  $B(H^0 \rightarrow jj) = 1$ .
- 118 Search for  $e^+e^- \rightarrow H^0Z$  with  $H^0$  decaying invisibly. The limit assumes SM production cross section and  $B(H^0 \rightarrow \text{invisible}) = 1$ .
- 119 PARK 05 found three candidate events for  $\Sigma^+ \rightarrow p\mu^+\mu^-$  in the HyperCP experiment. Due to a narrow spread in dimuon mass, they hypothesize the events as a possible signal of a new boson. It can be interpreted as a neutral particle with  $m_{A^0} = 214.3 \pm 0.5$  MeV and the branching fraction  $B(\Sigma^+ \rightarrow pA^0) \times B(A^0 \rightarrow \mu^+\mu^-) = (3.1_{-1.9}^{+2.4} \pm 1.5) \times 10^{-8}$ .
- 120 ABBIENDI 04K search for  $e^+e^- \rightarrow H^0Z$  with  $H^0$  decaying to two jets of any flavor including  $gg$ . The limit is for SM production cross section with  $B(H^0 \rightarrow jj) = 1$ .
- 121 ABDALLAH 04 consider the full combined LEP and LEP2 datasets to set limits on the Higgs coupling to  $W$  or  $Z$  bosons, assuming SM decays of the Higgs. Results in Fig. 26.
- 122 Search for associated production of a  $\gamma\gamma$  resonance with a  $Z$  boson, followed by  $Z \rightarrow q\bar{q}, \ell^+\ell^-$ , or  $\nu\bar{\nu}$ , at  $E_{\text{cm}} \leq 209$  GeV. The limit is for a  $H^0$  with SM production cross section and  $B(H^0 \rightarrow f\bar{f}) = 0$  for all fermions  $f$ .
- 123 Updates ABREU 01F.
- 124 ABDALLAH 04o search for  $Z \rightarrow b\bar{b}H^0, b\bar{b}A^0, \tau^+\tau^-H^0$  and  $\tau^+\tau^-A^0$  in the final states  $4b, b\bar{b}\tau^+\tau^-$ , and  $4\tau$ . See paper for limits on Yukawa couplings.
- 125 ABDALLAH 04o search for  $e^+e^- \rightarrow H^0Z$  and  $H^0A^0$ , with  $H^0, A^0$  decaying to  $b\bar{b}, \tau^+\tau^-$ , or  $H^0 \rightarrow A^0A^0$  at  $E_{\text{cm}} = 189\text{--}208$  GeV. See paper for limits on couplings.
- 126 ACHARD 04B search for  $e^+e^- \rightarrow H^0Z$  with  $H^0$  decaying to  $b\bar{b}, c\bar{c}$ , or  $gg$ . The limit is for SM production cross section with  $B(H^0 \rightarrow jj) = 1$ .
- 127 ACHARD 04F search for  $H^0$  with anomalous coupling to gauge boson pairs in the processes  $e^+e^- \rightarrow H^0\gamma, e^+e^-H^0, H^0Z$  with decays  $H^0 \rightarrow f\bar{f}, \gamma\gamma, Z\gamma$ , and  $W^*W$  at  $E_{\text{cm}} = 189\text{--}209$  GeV. See paper for limits.
- 128 ABBIENDI 03F search for  $H^0 \rightarrow$  anything in  $e^+e^- \rightarrow H^0Z$ , using the recoil mass spectrum of  $Z \rightarrow e^+e^-$  or  $\mu^+\mu^-$ . In addition, it searched for  $Z \rightarrow \nu\bar{\nu}$  and  $H^0 \rightarrow e^+e^-$  or photons. Scenarios with large width or continuum  $H^0$  mass distribution are considered. See their Figs. 11–14 for the results.
- 129 ABBIENDI 03G search for  $e^+e^- \rightarrow H_1^0Z$  followed by  $H_1^0 \rightarrow A^0A^0, A^0 \rightarrow c\bar{c}, gg$ , or  $\tau^+\tau^-$  in the region  $m_{H_1^0} = 45\text{--}86$  GeV and  $m_{A^0} = 2\text{--}11$  GeV. See their Fig. 7 for the limits.
- 130 ACHARD 03c search for  $e^+e^- \rightarrow ZH^0$  followed by  $H^0 \rightarrow WW^*$  or  $ZZ^*$  at  $E_{\text{cm}} = 200\text{--}209$  GeV and combine with the ACHARD 02c result. The limit is for a  $H^0$  with SM production cross section and  $B(H^0 \rightarrow f\bar{f}) = 0$  for all  $f$ . For  $B(H^0 \rightarrow WW^*) + B(H^0 \rightarrow ZZ^*) = 1, m_{H^0} > 108.1$  GeV is obtained. See fig. 6 for the limits under different BR assumptions.
- 131 ABBIENDI 02D search for  $Z \rightarrow b\bar{b}H^0$  and  $b\bar{b}A^0$  with  $H_1^0/A^0 \rightarrow \tau^+\tau^-$ , in the range  $4 < m_H < 12$  GeV. See their Fig. 8 for limits on the Yukawa coupling.
- 132 For  $B(H^0 \rightarrow \gamma\gamma) = 1, m_{H^0} > 117$  GeV is obtained.
- 133 ACHARD 02c search for associated production of a  $\gamma\gamma$  resonance with a  $Z$  boson, followed by  $Z \rightarrow q\bar{q}, \ell^+\ell^-$ , or  $\nu\bar{\nu}$ , at  $E_{\text{cm}} \leq 209$  GeV. The limit is for a  $H^0$  with SM production cross section and  $B(H^0 \rightarrow f\bar{f}) = 0$  for all fermions  $f$ . For  $B(H^0 \rightarrow \gamma\gamma) = 1, m_{H^0} > 114$  GeV is obtained.
- 134 For  $B(H^0 \rightarrow \gamma\gamma) = 1, m_{H^0} > 113.1$  GeV is obtained.
- 135 HEISTER 02M search for  $e^+e^- \rightarrow H^0Z$ , assuming that  $H^0$  decays to  $q\bar{q}, gg$ , or  $\tau^+\tau^-$  only. The limit assumes SM production cross section.
- 136 ABBIENDI 01E search for neutral Higgs bosons in general Type-II two-doublet models, at  $E_{\text{cm}} \leq 189$  GeV. In addition to usual final states, the decays  $H_1^0, A^0 \rightarrow q\bar{q}, gg$  are searched for. See their Figs. 15,16 for excluded regions.
- 137 AFFOLDER 01H search for associated production of a  $\gamma\gamma$  resonance and a  $W$  or  $Z$  (tagged by two jets, an isolated lepton, or missing  $E_T$ ). The limit assumes Standard Model values for the production cross section and for the couplings of the  $H^0$  to  $W$  and  $Z$  bosons. See their Fig. 11 for limits with  $B(H^0 \rightarrow \gamma\gamma) < 1$ .
- 138 ACCIARRI 00M search for  $e^+e^- \rightarrow ZH^0$  with  $H^0$  decaying invisibly at  $E_{\text{cm}} = 183\text{--}189$  GeV. The limit assumes SM production cross section and  $B(H^0 \rightarrow \text{invisible}) = 1$ . See their Fig. 6 for limits for smaller branching ratios.
- 139 ACCIARRI 00R search for  $e^+e^- \rightarrow H^0\gamma$  with  $H^0 \rightarrow b\bar{b}, Z\gamma$ , or  $\gamma\gamma$ . See their Fig. 3 for limits on  $\sigma \cdot B$ . Explicit limits within an effective interaction framework are also given, for which the Standard Model Higgs search results are used in addition.
- 140 ACCIARRI 00R search for the two-photon type processes  $e^+e^- \rightarrow e^+e^-H^0$  with  $H^0 \rightarrow b\bar{b}$  or  $\gamma\gamma$ . See their Fig. 4 for limits on  $\Gamma(H^0 \rightarrow \gamma\gamma)\cdot B(H^0 \rightarrow \gamma\gamma \text{ or } b\bar{b})$  for  $m_{H^0} = 70\text{--}170$  GeV.
- 141 ACCIARRI 00s search for associated production of a  $\gamma\gamma$  resonance with a  $q\bar{q}, \nu\bar{\nu}$ , or  $\ell^+\ell^-$  pair in  $e^+e^-$  collisions at  $E_{\text{cm}} = 189$  GeV. The limit is for a  $H^0$  with SM production cross section and  $B(H^0 \rightarrow f\bar{f}) = 0$  for all fermions  $f$ . For  $B(H^0 \rightarrow \gamma\gamma) = 1, m_{H^0} > 98$  GeV is obtained. See their Fig. 5 for limits on  $B(H \rightarrow \gamma\gamma)\cdot\sigma(e^+e^- \rightarrow Hf\bar{f})/\sigma(e^+e^- \rightarrow Hf\bar{f})$  (SM).
- 142 BARATE 00I search for associated production of a  $\gamma\gamma$  resonance with a  $q\bar{q}, \nu\bar{\nu}$ , or  $\ell^+\ell^-$  pair in  $e^+e^-$  collisions at  $E_{\text{cm}} = 88\text{--}202$  GeV. The limit is for a  $H^0$  with SM production cross section and  $B(H^0 \rightarrow f\bar{f}) = 0$  for all fermions  $f$ . For  $B(H^0 \rightarrow \gamma\gamma) = 1, m_{H^0} > 109$  GeV is obtained. See their Fig. 3 for limits on  $B(H \rightarrow \gamma\gamma)\cdot\sigma(e^+e^- \rightarrow Hf\bar{f})/\sigma(e^+e^- \rightarrow Hf\bar{f})$  (SM).

See key on page 457

Gauge & Higgs Boson Particle Listings  
Higgs Bosons —  $H^0$  and  $H^\pm$ 

- 143 ABBIENDI 99E search for  $e^+e^- \rightarrow H^0 A^0$  and  $H^0 Z$  at  $E_{\text{cm}} = 183$  GeV. The limit is with  $m_H = m_A$  in general two Higgs-doublet models. See their Fig. 18 for the exclusion limit in the  $m_H - m_A$  plane. Updates the results of ACKERSTAFF 98S.
- 144 ABBIENDI 99B search for associated production of a  $\gamma\gamma$  resonance with a  $q\bar{q}, \nu\bar{\nu}$ , or  $\ell^+\ell^-$  pair in  $e^+e^-$  collisions at 189 GeV. The limit is for a  $H^0$  with SM production cross section and  $B(H^0 \rightarrow f\bar{f})=0$ , for all fermions  $f$ . See their Fig. 4 for limits on  $\sigma(e^+e^- \rightarrow H^0 Z^0) \times B(H^0 \rightarrow \gamma\gamma) \times B(X^0 \rightarrow f\bar{f})$  for various masses. Updates the results of ACKERSTAFF 98Y.
- 145 ABBOTT 99B search for associated production of a  $\gamma\gamma$  resonance and a dijet pair. The limit assumes Standard Model values for the production cross section and for the couplings of the  $H^0$  to  $W$  and  $Z$  bosons. Limits in the range of  $\sigma(H^0 + Z/W) \cdot B(H^0 \rightarrow \gamma\gamma) = 0.80\text{--}0.34$  pb are obtained in the mass range  $m_{H^0} = 65\text{--}150$  GeV.
- 146 ABREU 99P search for  $e^+e^- \rightarrow H^0\gamma$  with  $H^0 \rightarrow b\bar{b}$  or  $\gamma\gamma$ , and  $e^+e^- \rightarrow H^0 q\bar{q}$  with  $H^0 \rightarrow \gamma\gamma$ . See their Fig. 4 for limits on  $\sigma \times B$ . Explicit limits within an effective interaction framework are also given.
- 147 GONZALEZ-GARCIA 98B use  $D\bar{0}$  limit for  $\gamma\gamma$  events with missing  $E_T$  in  $p\bar{p}$  collisions (ABBOTT 98) to constrain possible  $ZH$  or  $WH$  production followed by unconventional  $H \rightarrow \gamma\gamma$  decay which is induced by higher-dimensional operators. See their Figs. 1 and 2 for limits on the anomalous couplings.
- 148 KRAWCZYK 97 analyse the muon anomalous magnetic moment in a two-doublet Higgs model (with type II Yukawa couplings) assuming no  $H^0 Z$  coupling and obtain  $m_{H^0} \gtrsim 5$  GeV or  $m_{A^0} \gtrsim 5$  GeV for  $\tan\beta > 50$ . Other Higgs bosons are assumed to be much heavier.
- 149 ALEXANDER 96H give  $B(Z \rightarrow H^0\gamma) \times B(H^0 \rightarrow q\bar{q}) < 1.4 \times 10^{-5}$  (95%CL) and  $B(Z \rightarrow H^0\gamma) \times B(H^0 \rightarrow b\bar{b}) < 0.7\text{--}2 \times 10^{-5}$  (95%CL) in the range  $20 < m_{H^0} < 80$  GeV.
- 150 See Fig. 4 of ABREU 95H for the excluded region in the  $m_{H^0} - m_{A^0}$  plane for general two-doublet models. For  $\tan\beta > 1$ , the region  $m_{H^0} + m_{A^0} \lesssim 87$  GeV,  $m_{H^0} < 47$  GeV is excluded at 95% CL.
- 151 PICH 92 analyse  $H^0$  with  $m_{H^0} < 2m_\mu$  in general two-doublet models. Excluded regions in the space of mass-mixing angles from LEP, beam dump, and  $\pi^\pm, \eta$  rare decays are shown in Figs. 3, 4. The considered mass region is not totally excluded.

 **$H^\pm$  (Charged Higgs) MASS LIMITS**

Unless otherwise stated, the limits below assume  $B(H^+ \rightarrow \tau^+\nu) + B(H^+ \rightarrow c\bar{s}) = 1$ , and hold for all values of  $B(H^+ \rightarrow \tau^+\nu_\tau)$ , and assume  $H^+$  weak isospin of  $T_3 = +1/2$ . In the following,  $\tan\beta$  is the ratio of the two vacuum expectation values in two-doublet models (2HDM).

The limits are also applicable to point-like technipions. For a discussion of techniparticles, see the Review of Dynamical Electroweak Symmetry Breaking in this Review.

For limits obtained in hadronic collisions before the observation of the top quark, and based on the top mass values inconsistent with the current measurements, see the 1996 (Physical Review **D54** 1 (1996)) Edition of this Review.

Searches in  $e^+e^-$  collisions at and above the  $Z$  pole have conclusively ruled out the existence of a charged Higgs in the region  $m_{H^\pm} \lesssim 45$  GeV, and are now superseded by the most recent searches in higher energy  $e^+e^-$  collisions at LEP. Results by now obsolete are therefore not included in this compilation, and can be found in the previous Edition (The European Physical Journal **C15** 1 (2000)) of this Review.

In the following, and unless otherwise stated, results from the LEP experiments (ALEPH, DELPHI, L3, and OPAL) are assumed to derive from the study of the  $e^+e^- \rightarrow H^+H^-$  process. Limits from  $b \rightarrow s\gamma$  decays are usually stronger in generic 2HDM models than in Supersymmetric models.

VALUE (GeV)	CL%	DOCUMENT ID	TECN	COMMENT
> 74.4	95	ABDALLAH 04I	DLPH	$E_{\text{cm}} \leq 209$ GeV
> 76.5	95	ACHARD 03E	L3	$E_{\text{cm}} \leq 209$ GeV
> 79.3	95	HEISTER 02P	ALEP	$E_{\text{cm}} \leq 209$ GeV
•••••		We do not use the following data for averages, fits, limits, etc. •••••		
> 316	95	152 AALTONEN 11P	CDF	$t \rightarrow bH^+, H^+ \rightarrow W^+A^0$
		153 DESCHAMPS 10	RVUE	Type II, flavor physics data
		154 AALTONEN 09AJ	CDF	$t \rightarrow bH^+$
		155 ABAZOV 09AC	D0	$t \rightarrow bH^+$
		156 ABAZOV 09AG	D0	$t \rightarrow bH^+$
		157 ABAZOV 09AI	D0	$t \rightarrow bH^+$
		158 ABAZOV 09P	D0	$H^+ \rightarrow t\bar{b}$
> 240	95	159 FLACHER 09	RVUE	Type II, flavor physics data
		160 ABULENCIA 06E	CDF	$t \rightarrow bH^+$
> 92.0	95	ABBIENDI 04	OPAL	$B(\tau\nu) = 1$
> 76.7	95	161 ABDALLAH 04I	DLPH	Type I
		162 ABBIENDI 03	OPAL	$\tau \rightarrow \mu\bar{\nu}_\nu, e\bar{\nu}_\nu$
		163 ABAZOV 02B	D0	$t \rightarrow bH^+, H \rightarrow \tau\nu$
		164 BORZUMATI 02	RVUE	
		165 ABBIENDI 01Q	OPAL	$B \rightarrow \tau\nu_\tau X$
		166 BARATE 01E	ALEP	$B \rightarrow \tau\nu_\tau$
> 315	99	167 GAMBINO 01	RVUE	$b \rightarrow s\gamma$
		168 AFFOLDER 00I	CDF	$t \rightarrow bH^+, H \rightarrow \tau\nu$
> 59.5	95	ABBIENDI 99E	OPAL	$E_{\text{cm}} \leq 183$ GeV
		169 ABBOTT 99E	D0	$t \rightarrow bH^+$
		170 ACKERSTAFF 99D	OPAL	$\tau \rightarrow e\nu\nu, \mu\nu\nu$
		171 ACCIARRI 97F	L3	$B \rightarrow \tau\nu_\tau$
		172 AMMAR 97B	CLEO	$\tau \rightarrow \mu\nu\nu$
		173 COARASA 97	RVUE	$B \rightarrow \tau\nu_\tau X$
		174 GUCHAIT 97	RVUE	$t \rightarrow bH^+, H \rightarrow \tau\nu$
		175 MANGANO 97	RVUE	$B_u(c) \rightarrow \tau\nu_\tau$
		176 STAHL 97	RVUE	$\tau \rightarrow \mu\nu\nu$
> 244	95	177 ALAM 95	CLE2	$b \rightarrow s\gamma$
		178 BUSKULIC 95	ALEP	$b \rightarrow \tau\nu_\tau X$

- 152 AALTONEN 11P search in 2.7 fb<sup>-1</sup> of  $p\bar{p}$  collisions at  $E_{\text{cm}} = 1.96$  TeV for the decay chain  $t \rightarrow bH^+, H^+ \rightarrow W^+A^0, A^0 \rightarrow \tau^+\tau^-$  with  $m_{A^0}$  between 4 and 9 GeV. See their Fig. 4 for limits on  $B(t \rightarrow bH^+)$  for  $90 < m_{H^+} < 160$  GeV.
- 153 DESCHAMPS 10 make Type II two Higgs doublet model fits to weak leptonic and semileptonic decays,  $b \rightarrow s\gamma, B, B_s$  mixings, and  $Z \rightarrow b\bar{b}$ . The limit holds irrespective of  $\tan\beta$ .
- 154 AALTONEN 09AJ search for  $t \rightarrow bH^+, H^+ \rightarrow c\bar{s}$  in  $t\bar{t}$  events in 2.2 fb<sup>-1</sup> of  $p\bar{p}$  collisions at  $E_{\text{cm}} = 1.96$  TeV. Upper limits on  $B(t \rightarrow bH^+)$  between 0.08 and 0.32 (95% CL) are given for  $m_{H^+} = 60\text{--}150$  GeV and  $B(H^+ \rightarrow c\bar{s}) = 1$ .
- 155 ABAZOV 09AC search for  $t \rightarrow bH^+, H^+ \rightarrow \tau^+\nu$  in  $t\bar{t}$  events in 0.9 fb<sup>-1</sup> of  $p\bar{p}$  collisions at  $E_{\text{cm}} = 1.96$  TeV. Upper limits on  $B(t \rightarrow bH^+)$  between 0.19 and 0.25 (95% CL) are given for  $m_{H^+} = 80\text{--}155$  GeV and  $B(H^+ \rightarrow \tau^+\nu) = 1$ . See their Fig. 4 for an excluded region in a MSSM scenario.
- 156 ABAZOV 09AG measure  $t\bar{t}$  cross sections in final states with  $\ell + \text{jets}$  ( $\ell = e, \mu$ ),  $\ell\ell$ , and  $\tau\ell$  in 1 fb<sup>-1</sup> of  $p\bar{p}$  collisions at  $E_{\text{cm}} = 1.96$  TeV, which constrains possible  $t \rightarrow bH^+$  branching fractions. Upper limits (95% CL) on  $B(t \rightarrow bH^+)$  between 0.15 and 0.40 (0.48 and 0.57) are given for  $B(H^+ \rightarrow \tau^+\nu) = 1$  ( $B(H^+ \rightarrow c\bar{s}) = 1$ ) for  $m_{H^+} = 80\text{--}155$  GeV.
- 157 ABAZOV 09AI search for  $t \rightarrow bH^+$  in  $t\bar{t}$  events in 1 fb<sup>-1</sup> of  $p\bar{p}$  collisions at  $E_{\text{cm}} = 1.96$  TeV. Final states with  $\ell + \text{jets}$  ( $\ell = e, \mu$ ),  $\ell\ell$ , and  $\tau\ell$  are examined. Upper limits on  $B(t \rightarrow bH^+)$  (95% CL) between 0.15 and 0.19 (0.19 and 0.22) are given for  $B(H^+ \rightarrow \tau^+\nu) = 1$  ( $B(H^+ \rightarrow c\bar{s}) = 1$ ) for  $m_{H^+} = 80\text{--}155$  GeV. For  $B(H^+ \rightarrow \tau^+\nu) = 1$  also a simultaneous extraction of  $B(t \rightarrow bH^+)$  and the  $t\bar{t}$  cross section is performed, yielding a limit on  $B(t \rightarrow bH^+)$  between 0.12 and 0.26 for  $m_{H^+} = 80\text{--}155$  GeV. See their Figs. 5–8 for excluded regions in several MSSM scenarios.
- 158 ABAZOV 09P search for  $H^+$  production by  $q\bar{q}$  annihilation followed by  $H^+ \rightarrow t\bar{b}$  decay in 0.9 fb<sup>-1</sup> of  $p\bar{p}$  collisions at  $E_{\text{cm}} = 1.96$  TeV. Cross section limits in several two-doublet models are given for  $m_{H^+} = 180\text{--}300$  GeV. A region with  $20 \lesssim \tan\beta \lesssim 70$  is excluded (95% CL) for 180 GeV  $\lesssim m_{H^+} \lesssim 184$  GeV in type-I models.
- 159 FLACHER 09 make Type II two Higgs doublet model fits to weak leptonic and semileptonic decays,  $b \rightarrow s\gamma$ , and  $Z \rightarrow b\bar{b}$ . The limit holds irrespective of  $\tan\beta$ .
- 160 ABULENCIA 06E search for associated  $H^0 W$  production in  $p\bar{p}$  collisions at  $E_{\text{cm}} = 1.96$  TeV. A fit is made for  $t\bar{t}$  production processes in dilepton, lepton + jets, and lepton +  $\tau$  final states, with the decays  $t \rightarrow W^+b$  and  $t \rightarrow H^+\nu$  followed by  $H^+ \rightarrow \tau^+\nu, c\bar{s}, t^*\bar{b}$ , or  $W^+H^0$ . Within the MSSM the search is sensitive to the region  $\tan\beta < 1$  or  $> 30$  in the mass range  $m_{H^+} = 80\text{--}160$  GeV. See Fig. 2 for the excluded region in a certain MSSM scenario.
- 161 ABDALLAH 04I search for  $e^+e^- \rightarrow H^+H^-$  with  $H^\pm$  decaying to  $\tau\nu, c\bar{s}$ , or  $W^*A^0$  in Type-I two-Higgs-doublet models.
- 162 ABBIENDI 03 give a limit  $m_{H^+} > 1.28\tan\beta$  GeV (95%CL) in Type II two-doublet models.
- 163 ABAZOV 02B search for a charged Higgs boson in top decays with  $H^+ \rightarrow \tau^+\nu$  at  $E_{\text{cm}} = 1.8$  TeV. For  $m_{H^+} = 75$  GeV, the region  $\tan\beta > 32.0$  is excluded at 95%CL. The excluded mass region extends to over 140 GeV for  $\tan\beta$  values above 100.
- 164 BORZUMATI 02 point out that the decay modes such as  $b\bar{b}W, A^0 W$ , and supersymmetric ones can have substantial branching fractions in the mass range explored at LEP II and Tevatron.
- 165 ABBIENDI 01Q give a limit  $\tan\beta/m_{H^+} < 0.53$  GeV<sup>-1</sup> (95%CL) in Type II two-doublet models.
- 166 BARATE 01E give a limit  $\tan\beta/m_{H^+} < 0.40$  GeV<sup>-1</sup> (90% CL) in Type II two-doublet models. An independent measurement of  $B \rightarrow \tau\nu_\tau X$  gives  $\tan\beta/m_{H^+} < 0.49$  GeV<sup>-1</sup> (90% CL).
- 167 GAMBINO 01 use the world average data in the summer of 2001  $B(b \rightarrow s\gamma) = (3.23 \pm 0.42) \times 10^{-4}$ . The limit applies for Type-II two-doublet models.
- 168 AFFOLDER 00I search for a charged Higgs boson in top decays with  $H^+ \rightarrow \tau^+\nu$  in  $p\bar{p}$  collisions at  $E_{\text{cm}} = 1.8$  TeV. The excluded mass region extends to over 120 GeV for  $\tan\beta$  values above 100 and  $B(t\nu) = 1$ . If  $B(t \rightarrow bH^+) \gtrsim 0.6$ ,  $m_{H^+}$  up to 160 GeV is excluded. Updates ABE 97L.
- 169 ABBOTT 99E search for a charged Higgs boson in top decays in  $p\bar{p}$  collisions at  $E_{\text{cm}} = 1.8$  TeV, by comparing the observed  $t\bar{t}$  cross section (extracted from the data assuming the dominant decay  $t \rightarrow bW^+$ ) with theoretical expectation. The search is sensitive to regions of the domains  $\tan\beta \lesssim 1, 50 < m_{H^+}(\text{GeV}) \lesssim 120$  and  $\tan\beta \gtrsim 40, 50 < m_{H^+}(\text{GeV}) \lesssim 160$ . See Fig. 3 for the details of the excluded region.
- 170 ACKERSTAFF 99D measure the Michel parameters  $\rho, \xi, \eta$ , and  $\xi\delta$  in leptonic  $\tau$  decays from  $Z \rightarrow \tau\tau$ . Assuming  $e\text{--}\mu$  universality, the limit  $m_{H^+} > 0.97 \tan\beta$  GeV (95%CL) is obtained for two-doublet models in which only one doublet couples to leptons.
- 171 ACCIARRI 97F give a limit  $m_{H^+} > 2.6 \tan\beta$  GeV (90% CL) from their limit on the exclusive  $B \rightarrow \tau\nu_\tau$  branching ratio.
- 172 AMMAR 97B measure the Michel parameter  $\rho$  from  $\tau \rightarrow e\nu\nu$  decays and assumes  $e/\mu$  universality to extract the Michel  $\eta$  parameter from  $\tau \rightarrow \mu\nu\nu$  decays. The measurement is translated to a lower limit on  $m_{H^+}$  in a two-doublet model  $m_{H^+} > 0.97 \tan\beta$  GeV (90% CL).
- 173 COARASA 97 reanalyzed the constraint on the  $(m_{H^\pm}, \tan\beta)$  plane derived from the inclusive  $B \rightarrow \tau\nu_\tau X$  branching ratio in GROSSMAN 95B and BUSKULIC 95. They show that the constraint is quite sensitive to supersymmetric one-loop effects.
- 174 GUCHAIT 97 studies the constraints on  $m_{H^+}$  set by Tevatron data on  $\ell\tau$  final states in  $t\bar{t} \rightarrow (Wb)(Hb), W \rightarrow \ell\nu, H \rightarrow \tau\nu_\tau$ . See Fig. 2 for the excluded region.
- 175 MANGANO 97 reconsiders the limit in ACCIARRI 97F including the effect of the potentially large  $B_c \rightarrow \tau\nu_\tau$  background to  $B_u \rightarrow \tau\nu_\tau$  decays. Stronger limits are obtained.
- 176 STAHL 97 fit  $\tau$  lifetime, leptonic branching ratios, and the Michel parameters and derive limit  $m_{H^+} > 1.5 \tan\beta$  GeV (90% CL) for a two-doublet model. See also STAHL 94.
- 177 ALAM 95 measure the inclusive  $b \rightarrow s\gamma$  branching ratio at  $T(4S)$  and give  $B(b \rightarrow s\gamma) < 4.2 \times 10^{-4}$  (95% CL), which translates to the limit  $m_{H^+} > [244 + 63/(\tan\beta)]^{1.3}$  GeV in the Type II two-doublet model. Light supersymmetric particles can invalidate this bound.
- 178 BUSKULIC 95 give a limit  $m_{H^+} > 1.9 \tan\beta$  GeV (90% CL) for Type-II models from  $b \rightarrow \tau\nu_\tau X$  branching ratio, as proposed in GROSSMAN 94.

# Gauge & Higgs Boson Particle Listings

## Higgs Bosons — $H^0$ and $H^\pm$

### MASS LIMITS for $H^{\pm\pm}$ (doubly-charged Higgs boson)

This section covers searches for a doubly-charged Higgs boson with couplings to lepton pairs. Its weak isospin  $T_3$  is thus restricted to two possibilities depending on lepton chiralities:  $T_3(H^{\pm\pm}) = \pm 1$ , with the coupling  $g_{\ell\ell}$  to  $\ell_L^-\ell_L^-$  and  $\ell_R^+\ell_R^+$  ("left-handed") and  $T_3(H^{\pm\pm}) = 0$ , with the coupling to  $\ell_R^-\ell_R^-$  and  $\ell_L^+\ell_L^+$  ("right-handed"). These Higgs bosons appear in some left-right symmetric models based on the gauge group  $SU(2)_L \times SU(2)_R \times U(1)$ . These two cases are listed separately in the following. Unless noted, one of the lepton flavor combinations is assumed to be dominant in the decay.

### LIMITS for $H^{\pm\pm}$ with $T_3 = \pm 1$

VALUE (GeV)	CL%	DOCUMENT ID	TECN	COMMENT
>128	95	179 ABAZOV	12A D0	$\tau\tau$
>144	95	179 ABAZOV	12A D0	$\mu\tau$
>245	95	180 AALTONEN	11AF CDF	$\mu\mu$
>210	95	180 AALTONEN	11AF CDF	$e\mu$
>225	95	180 AALTONEN	11AF CDF	$ee$
>114	95	181 AALTONEN	08AA CDF	$e\tau$
>112	95	181 AALTONEN	08AA CDF	$\mu\tau$
>168	95	182 ABAZOV	08V D0	$\mu\mu$
> 98.1	95	183 ABDALLAH	03 DLPH	$\tau\tau$
> 99.0	95	184 ABBIENDI	02C OPAL	$\tau\tau$
••• We do not use the following data for averages, fits, limits, etc. •••				
>133	95	185 AKTAS	06A H1	single $H^{\pm\pm}$
>118.4	95	186 ACOSTA	05L CDF	stable
>136	95	187 ABAZOV	04E D0	$\mu\mu$
	95	188 ACOSTA	04G CDF	$\mu\mu$
	95	189 ABBIENDI	03Q OPAL	$E_{cm} \leq 209$ GeV, single $H^{\pm\pm}$
	95	190 GORDEEV	97 SPEC	muonium conversion
	95	191 ASAKA	95 THEO	
> 45.6	95	192 ACTON	92M OPAL	
> 30.4	95	193 ACTON	92M OPAL	
none 6.5–36.6	95	194 SWARTZ	90 MRK2	

- 179 ABAZOV 12A search for  $H^{++}H^{--}$  production in  $7.0 \text{ fb}^{-1}$  of  $p\bar{p}$  collisions at  $E_{cm} = 1.96$  TeV.
- 180 AALTONEN 11AF search for  $H^{++}H^{--}$  production in  $6.1 \text{ fb}^{-1}$  of  $p\bar{p}$  collisions at  $E_{cm} = 1.96$  TeV.
- 181 AALTONEN 08AA search for  $H^{++}H^{--}$  production in  $p\bar{p}$  collisions at  $E_{cm} = 1.96$  TeV. The limit assumes 100% branching ratio to the specified final state.
- 182 ABAZOV 08V search for  $H^{++}H^{--}$  production in  $p\bar{p}$  collisions at  $E_{cm} = 1.96$  TeV. The limit is for  $B(H \rightarrow \mu\mu) = 1$ . The limit is updated in ABAZOV 12A.
- 183 ABDALLAH 03 search for  $H^{++}H^{--}$  pair production either followed by  $H^{++} \rightarrow \tau^+\tau^+$ , or decaying outside the detector.
- 184 ABBIENDI 02c searches for pair production of  $H^{++}H^{--}$ , with  $H^{\pm\pm} \rightarrow \ell^\pm\ell^\pm$  ( $\ell, \ell' = e, \mu, \tau$ ). The limit holds for  $\ell = \ell' = \tau$ , and becomes stronger for other combinations of leptonic final states. To ensure the decay within the detector, the limit only applies for  $g(H\ell\ell) \gtrsim 10^{-7}$ .
- 185 AKTAS 06A search for single  $H^{\pm\pm}$  production in  $ep$  collisions at HERA. Assuming that  $H^{++}$  only couples to  $e^+\mu^+$  with  $g_{e\mu} = 0.3$  (electromagnetic strength), a limit  $m_{H^{++}} > 141$  GeV (95% CL) is derived. For the case where  $H^{++}$  couples to  $e\tau$  only the limit is 112 GeV.
- 186 ACOSTA 05L search for  $H^{++}H^{--}$  pair production in  $p\bar{p}$  collisions. The limit is valid for  $g_{\ell\ell} < 10^{-8}$  so that the Higgs decays outside the detector.
- 187 ABAZOV 04E search for  $H^{++}H^{--}$  pair production in  $H^{\pm\pm} \rightarrow \mu^\pm\mu^\pm$ . The limit is valid for  $g_{\mu\mu} \gtrsim 10^{-7}$ .
- 188 ACOSTA 04G search for  $H^{++}H^{--}$  pair production in  $p\bar{p}$  collisions with muon and electron final states. The limit holds for  $\mu\mu$ . For  $ee$  and  $e\mu$  modes, the limits are 133 and 115 GeV, respectively. The limits are valid for  $g_{\ell\ell} \gtrsim 10^{-5}$ . Superseded by AALTONEN 11AF.
- 189 ABBIENDI 03Q searches for single  $H^{\pm\pm}$  via direct production in  $e^+e^- \rightarrow e^\mp e^\mp H^{\pm\pm}$ , and via  $t$ -channel exchange in  $e^+e^- \rightarrow e^+e^-$ . In the direct case, and assuming  $B(H^{\pm\pm} \rightarrow \ell^\pm\ell^\pm) = 1$ , a 95% CL limit on  $h_{ee} < 0.071$  is set for  $m_{H^{\pm\pm}} < 160$  GeV (see Fig. 6). In the second case, indirect limits on  $h_{ee}$  are set for  $m_{H^{\pm\pm}} < 2$  TeV (see Fig. 8).
- 190 GORDEEV 97 search for muonium-antimuonium conversion and find  $G_{M\bar{M}}/G_F < 0.14$  (90% CL), where  $G_{M\bar{M}}$  is the lepton-flavor violating effective four-fermion coupling. This limit may be converted to  $m_{H^{++}} > 210$  GeV if the Yukawa couplings of  $H^{++}$  to  $ee$  and  $\mu\mu$  are as large as the weak gauge coupling. For similar limits on muonium-antimuonium conversion, see the muon Particle Listings.
- 191 ASAKA 95 point out that  $H^{++}$  decays dominantly to four fermions in a large region of parameter space where the limit of ACTON 92M from the search of dilepton modes does not apply.
- 192 ACTON 92M limit assumes  $H^{\pm\pm} \rightarrow \ell^\pm\ell^\pm$  or  $H^{\pm\pm}$  does not decay in the detector. Thus the region  $g_{\ell\ell} \approx 10^{-7}$  is not excluded.
- 193 ACTON 92M from  $\Delta\Gamma_Z < 40$  MeV.
- 194 SWARTZ 90 assume  $H^{\pm\pm} \rightarrow \ell^\pm\ell^\pm$  (any flavor). The limits are valid for the Higgs-lepton coupling  $g(H\ell\ell) \gtrsim 7.4 \times 10^{-7} [m_H/\text{GeV}]^{1/2}$ . The limits improve somewhat for  $ee$  and  $\mu\mu$  decay modes.

### LIMITS for $H^{\pm\pm}$ with $T_3 = 0$

VALUE (GeV)	CL%	DOCUMENT ID	TECN	COMMENT
>113	95	195 ABAZOV	12A D0	$\mu\tau$
>205	95	196 AALTONEN	11AF CDF	$\mu\mu$
>190	95	196 AALTONEN	11AF CDF	$e\mu$
>205	95	196 AALTONEN	11AF CDF	$ee$
>145	95	197 ABAZOV	08V D0	$\mu\mu$
> 97.3	95	198 ABDALLAH	03 DLPH	$\tau\tau$
> 97.3	95	199 ACHARD	03F L3	$\tau\tau$
> 98.5	95	200 ABBIENDI	02C OPAL	$\tau\tau$
••• We do not use the following data for averages, fits, limits, etc. •••				
>109	95	201 AKTAS	06A H1	single $H^{\pm\pm}$
> 98.2	95	202 ACOSTA	05L CDF	stable
>113	95	203 ABAZOV	04E D0	$\mu\mu$
	95	204 ACOSTA	04G CDF	$\mu\mu$
	95	205 ABBIENDI	03Q OPAL	$E_{cm} \leq 209$ GeV, single $H^{\pm\pm}$
	95	206 GORDEEV	97 SPEC	muonium conversion
> 45.6	95	207 ACTON	92M OPAL	
> 25.5	95	208 ACTON	92M OPAL	
none 7.3–34.3	95	209 SWARTZ	90 MRK2	

- 195 ABAZOV 12A search for  $H^{++}H^{--}$  production in  $7.0 \text{ fb}^{-1}$  of  $p\bar{p}$  collisions at  $E_{cm} = 1.96$  TeV.
- 196 AALTONEN 11AF search for  $H^{++}H^{--}$  production in  $6.1 \text{ fb}^{-1}$  of  $p\bar{p}$  collisions at  $E_{cm} = 1.96$  TeV.
- 197 ABAZOV 08V search for  $H^{++}H^{--}$  production in  $p\bar{p}$  collisions at  $E_{cm} = 1.96$  TeV. The limit is for  $B(H \rightarrow \mu\mu) = 1$ . The limit is updated in ABAZOV 12A.
- 198 ABDALLAH 03 search for  $H^{++}H^{--}$  pair production either followed by  $H^{++} \rightarrow \tau^+\tau^+$ , or decaying outside the detector.
- 199 ACHARD 03F search for  $e^+e^- \rightarrow H^{++}H^{--}$  with  $H^{\pm\pm} \rightarrow \ell^\pm\ell^\pm$ . The limit holds for  $\ell = \ell' = \tau$ , and slightly different limits apply for other flavor combinations. The limit is valid for  $g_{\ell\ell} \gtrsim 10^{-7}$ .
- 200 ABBIENDI 02c searches for pair production of  $H^{++}H^{--}$ , with  $H^{\pm\pm} \rightarrow \ell^\pm\ell^\pm$  ( $\ell, \ell' = e, \mu, \tau$ ). The limit holds for  $\ell = \ell' = \tau$ , and becomes stronger for other combinations of leptonic final states. To ensure the decay within the detector, the limit only applies for  $g(H\ell\ell) \gtrsim 10^{-7}$ .
- 201 AKTAS 06A search for single  $H^{\pm\pm}$  production in  $ep$  collisions at HERA. Assuming that  $H^{++}$  only couples to  $e^+\mu^+$  with  $g_{e\mu} = 0.3$  (electromagnetic strength), a limit  $m_{H^{++}} > 141$  GeV (95% CL) is derived. For the case where  $H^{++}$  couples to  $e\tau$  only the limit is 112 GeV.
- 202 ACOSTA 05L search for  $H^{++}H^{--}$  pair production in  $p\bar{p}$  collisions. The limit is valid for  $g_{\ell\ell} < 10^{-8}$  so that the Higgs decays outside the detector.
- 203 ABAZOV 04E search for  $H^{++}H^{--}$  pair production in  $H^{\pm\pm} \rightarrow \mu^\pm\mu^\pm$ . The limit is valid for  $g_{\mu\mu} \gtrsim 10^{-7}$ .
- 204 ACOSTA 04G search for  $H^{++}H^{--}$  pair production in  $p\bar{p}$  collisions with muon and electron final states. The limit holds for  $\mu\mu$ . Superseded by AALTONEN 11AF.
- 205 ABBIENDI 03Q searches for single  $H^{\pm\pm}$  via direct production in  $e^+e^- \rightarrow e^\mp e^\mp H^{\pm\pm}$ , and via  $t$ -channel exchange in  $e^+e^- \rightarrow e^+e^-$ . In the direct case, and assuming  $B(H^{\pm\pm} \rightarrow \ell^\pm\ell^\pm) = 1$ , a 95% CL limit on  $h_{ee} < 0.071$  is set for  $m_{H^{\pm\pm}} < 160$  GeV (see Fig. 6). In the second case, indirect limits on  $h_{ee}$  are set for  $m_{H^{\pm\pm}} < 2$  TeV (see Fig. 8).
- 206 GORDEEV 97 search for muonium-antimuonium conversion and find  $G_{M\bar{M}}/G_F < 0.14$  (90% CL), where  $G_{M\bar{M}}$  is the lepton-flavor violating effective four-fermion coupling. This limit may be converted to  $m_{H^{++}} > 210$  GeV if the Yukawa couplings of  $H^{++}$  to  $ee$  and  $\mu\mu$  are as large as the weak gauge coupling. For similar limits on muonium-antimuonium conversion, see the muon Particle Listings.
- 207 ACTON 92M limit assumes  $H^{\pm\pm} \rightarrow \ell^\pm\ell^\pm$  or  $H^{\pm\pm}$  does not decay in the detector. Thus the region  $g_{\ell\ell} \approx 10^{-7}$  is not excluded.
- 208 ACTON 92M from  $\Delta\Gamma_Z < 40$  MeV.
- 209 SWARTZ 90 assume  $H^{\pm\pm} \rightarrow \ell^\pm\ell^\pm$  (any flavor). The limits are valid for the Higgs-lepton coupling  $g(H\ell\ell) \gtrsim 7.4 \times 10^{-7} [m_H/\text{GeV}]^{1/2}$ . The limits improve somewhat for  $ee$  and  $\mu\mu$  decay modes.

### $H^0$ and $H^\pm$ REFERENCES

AAD	12	PL B707 27	G. Aad et al.	(ATLAS Collab.)
AAD	12D	PL B710 383	G. Aad et al.	(ATLAS Collab.)
AAD	12E	PL B710 49	G. Aad et al.	(ATLAS Collab.)
AAD	12F	PRL 108 111802	G. Aad et al.	(ATLAS Collab.)
AAD	12G	PRL 108 111803	G. Aad et al.	(ATLAS Collab.)
AALTONEN	12	PRL 108 011801	T. Aaltonen et al.	(CDF Collab.)
ABAZOV	12	PL B707 323	V.M. Abazov et al.	(DO Collab.)
ABAZOV	12A	PRL 108 021801	V.M. Abazov et al.	(DO Collab.)
CHATRCHYAN	12B	PL B710 26	S. Chatrchyan et al.	(CMS Collab.)
CHATRCHYAN	12C	JHEP 1203 081	S. Chatrchyan et al.	(CMS Collab.)
CHATRCHYAN	12D	JHEP 1204 036	S. Chatrchyan et al.	(CMS Collab.)
CHATRCHYAN	12E	PL B710 91	S. Chatrchyan et al.	(CMS Collab.)
CHATRCHYAN	12F	PL B710 284	S. Chatrchyan et al.	(CMS Collab.)
CHATRCHYAN	12G	PL B710 403	S. Chatrchyan et al.	(CMS Collab.)
CHATRCHYAN	12H	PRL 108 111804	S. Chatrchyan et al.	(CMS Collab.)
CHATRCHYAN	12I	JHEP 1203 040	S. Chatrchyan et al.	(CMS Collab.)
AAD	11AB	PRL 107 231801	G. Aad et al.	(ATLAS Collab.)
AAD	11R	PL B705 174	G. Aad et al.	(ATLAS Collab.)
AAD	11T	PL B705 435	G. Aad et al.	(ATLAS Collab.)
AAD	11U	PL B705 452	G. Aad et al.	(ATLAS Collab.)
AAD	11V	PRL 107 221802	G. Aad et al.	(ATLAS Collab.)
AAD	11W	EPJ C71 1728	G. Aad et al.	(ATLAS Collab.)
AALTONEN	11AA	PR D84 052010	T. Aaltonen et al.	(CDF Collab.)
AALTONEN	11AF	PRL 107 181801	T. Aaltonen et al.	(CDF Collab.)
AALTONEN	11P	PRL 107 031801	T. Aaltonen et al.	(CDF Collab.)
ABAZOV	11AB	PR D84 092002	V.M. Abazov et al.	(DO Collab.)
ABAZOV	11G	PRL 106 171802	V.M. Abazov et al.	(DO Collab.)
ABAZOV	11J	PL B698 6	V.M. Abazov et al.	(DO Collab.)
ABAZOV	11K	PL B698 97	V.M. Abazov et al.	(DO Collab.)
ABAZOV	11W	PRL 107 121801	V.M. Abazov et al.	(DO Collab.)

See key on page 457

Gauge & Higgs Boson Particle Listings

Higgs Bosons —  $H^0$  and  $H^\pm$ , Heavy Bosons Other than Higgs Bosons

Table listing various particle experiments and their results, including columns for experiment name, year, publication reference, and collaboration name. Includes a 'Contents' section and a 'W'-BOSON SEARCHES' section.

Heavy Bosons Other Than Higgs Bosons, Searches for

We list here various limits on charged and neutral heavy vector bosons (other than W's and Z's), heavy scalar bosons (other than Higgs bosons), vector or scalar leptoquarks, and axigluons. The latest unpublished results are described in "W' Searches" and "Z' Searches" reviews.

CONTENTS:

- Mass Limits for W' (Heavy Charged Vector Boson Other Than W) in Hadron Collider Experiments
WR (Right-Handed W Boson) Mass Limits
Limit on WL-WR Mixing Angle xi
Mass Limits for Z' (Heavy Neutral Vector Boson Other Than Z)
- Limits for Z'\_SM
- Limits for Z'\_LR
- Limits for Z'\_chi
- Limits for Z'\_nu
- Limits for Z'\_eta
- Limits for other Z'
Indirect Constraints on Kaluza-Klein Gauge Bosons
Mass Limits for Leptoquarks from Pair Production
Mass Limits for Leptoquarks from Single Production
Indirect Limits for Leptoquarks
Mass Limits for Diquarks
Mass Limits for g\_A (axigluon) and Other Color-Octet Gauge Bosons
X^0 (Heavy Boson) Searches in Z Decays
Mass Limits for a Heavy Neutral Boson Coupling to e+e-
Search for X^0 Resonance in e+e- Collisions
Search for X^0 Resonance in ep Collisions
Search for X^0 Resonance in Two-Photon Process
Search for X^0 Resonance in e+e- -> X^0 gamma
Search for X^0 Resonance in Z -> f fbar X^0
Search for X^0 Resonance in p pbar -> W X^0
Heavy Particle Production in Quarkonium Decays

W'-BOSON SEARCHES

Revised May 2012 by G. Brooijmans (Columbia University), M.-C. Chen (UC Irvine) and B.A. Dobrescu (Fermilab).

The W' boson is a hypothetical massive particle of electric charge +/-1 and spin 1, which is predicted in various extensions of the Standard Model.

W' couplings to quarks and leptons. The Lagrangian terms describing couplings of a W'+ boson to fermions are given by

W'^+\_mu / sqrt(2) [ubar\_i (C^R\_{qij} P\_R + C^L\_{qij} P\_L) gamma^mu d\_j + v\_i (C^R\_{l ij} P\_R + C^L\_{l ij} P\_L) gamma^mu e\_j] . (1)

Here u, d, nu and e are the Standard Model fermions in the mass eigenstate basis, i, j = 1, 2, 3 label the fermion generation,

## Gauge & Higgs Boson Particle Listings

### Heavy Bosons Other than Higgs Bosons

and  $P_{R,L} = (1 \pm \gamma_5)/2$ . The coefficients  $C_{qij}^L$ ,  $C_{qij}^R$ ,  $C_{lij}^L$ ,  $C_{lij}^R$  are complex dimensionless parameters. If  $C_{lij}^R \neq 0$ , then the  $i$ th generation includes a right-handed neutrino. Using this notation, the Standard Model  $W$  couplings are  $C_q^L = gV_{\text{CKM}}$ ,  $C_l^L = g$  and  $C_q^R = C_l^R = 0$ .

Unitarity considerations imply that the  $W'$  is a gauge boson associated with a spontaneously-broken gauge symmetry. This is true even when it is a composite particle (*e.g.*, techni- $\rho^\pm$  in technicolor theories [1]) if its mass is much smaller than the compositeness scale, or a Kaluza-Klein mode in theories where the  $W$  boson propagates in extra dimensions [2]. The simplest extension of the electroweak gauge group that includes a  $W'$  boson is  $SU(2)_1 \times SU(2)_2 \times U(1)$ , but larger groups are encountered in some theories. A generic property of these gauge theories is that they also include a  $Z'$  boson; whether the  $W'$  boson can be discovered first depends on theoretical details.

The renormalizable photon- $W'$  coupling is fixed by electromagnetic gauge invariance. By contrast, the  $W'WZ$  and  $W'W'Z$  couplings as well as the  $W'$  boson couplings to  $Z'$  or Higgs bosons are model-dependent.

A tree-level mass mixing may be induced between the electrically-charged gauge bosons. Upon diagonalization of their mass matrix, the  $W - Z$  mass ratio and the couplings of the observed  $W$  boson are shifted from the Standard Model values. Given that these are well measured, the  $W - W'$  mixing angle must be smaller than about  $10^{-2}$ . Similarly, a  $Z - Z'$  mixing is induced in generic theories, leading to even tighter constraints. There are, however, theories in which these mixings are negligible (*e.g.*, due to a new parity [3]), even when the  $W'$  and  $Z'$  masses are below the electroweak scale.

A popular model [4] is based on the “left-right symmetric” gauge group,  $SU(2)_L \times SU(2)_R \times U(1)_{B-L}$ , with the Standard Model fermions that couple to the  $W$  boson transforming as doublets under  $SU(2)_L$ , and the other ones transforming as doublets under  $SU(2)_R$ . In this model the  $W'$  boson couples primarily to the right-handed fermions, and its coupling to left-handed fermions arises solely due to  $W - W'$  mixing. As a result,  $C_q^L$  is proportional to the CKM matrix, and its elements are much smaller than the diagonal elements of  $C_q^R$ .

There are many other models based on the  $SU(2)_1 \times SU(2)_2 \times U(1)$  gauge symmetry. In the “alternate left-right” model [5], all the couplings shown in Eq. (1) vanish, but there are some new fermions such that the  $W'$  boson couples to pairs involving a Standard Model fermion and a new fermion. In the “unified Standard Model” [6], the left-handed quarks are doublets under one  $SU(2)$ , and the left-handed leptons are doublets under a different  $SU(2)$ , leading to a mostly leptophobic  $W'$  boson:  $C_{lij}^L \ll C_{qij}^L$  and  $C_{qij}^R = C_{lij}^R = 0$ . Fermions of different generations may also transform as doublets under different  $SU(2)$  gauge groups [7]. In particular, the couplings to third generation quarks may be enhanced [8].

The  $W'$  couplings to Standard Model fermions may be highly suppressed if the quarks and leptons are singlets under one  $SU(2)$  [9], or if there are some vectorlike fermions that

mix with the Standard Model ones [10]. Gauge groups that embed the electroweak symmetry, such as  $SU(3)_W \times U(1)$  or  $SU(4)_W \times U(1)$ , also include one or more  $W'$  bosons [11].

**Collider searches.** At LEP-II,  $W'$  bosons could have been produced in pairs via their photon and  $Z$  couplings. The production cross section depends only on the  $W'$  mass, and is large enough to rule out  $M_{W'} \leq \sqrt{s}/2 \approx 105$  GeV for most patterns of decay modes.

At hadron colliders,  $W'$  bosons can be detected through resonant pair production of fermions or electroweak bosons. Assuming that the  $W'$  width is much smaller than its mass, the contribution of the  $s$ -channel  $W'$  boson exchange to the total rate for  $pp \rightarrow f\bar{f}'X$ , where  $f$  and  $f'$  are fermions whose electric charges differ by  $\pm 1$ , and  $X$  is any final state, may be approximated by the branching fraction  $B(W' \rightarrow f\bar{f}')$  times the production cross section

$$\sigma(pp \rightarrow W'X) \simeq \frac{\pi}{48s} \sum_{i,j} \left[ (C_{qij}^L)^2 + (C_{qij}^R)^2 \right] w_{ij}(M_{W'}^2/s, M_{W'}). \quad (2)$$

The functions  $w_{ij}$  include the information about proton structure, and are given to leading order in  $\alpha_s$  by

$$w_{ij}(z, \mu) = \int_z^1 \frac{dx}{x} \left[ u_i(x, \mu) \bar{d}_j\left(\frac{z}{x}, \mu\right) + \bar{u}_i(x, \mu) d_j\left(\frac{z}{x}, \mu\right) \right], \quad (3)$$

where  $u_i(x, \mu)$  and  $d_i(x, \mu)$  are the parton distributions inside the proton at the factorization scale  $\mu$  for the up- and down-type quark of the  $i$ th generation, respectively. QCD corrections to  $W'$  production are sizable (they also include quark-gluon initial states), but preserve the above factorization of couplings at next-to-leading order [12].

The most commonly studied  $W'$  signal consists of a high-energy electron or muon and large missing transverse energy, with the transverse mass distribution forming a Jacobian peak with its endpoint at  $M_{W'}$  (see Fig. 1 of Ref. 13). Given that the branching fractions for  $W' \rightarrow e\nu$  and  $W' \rightarrow \mu\nu$  could be very different, these channels should be analyzed separately. Searches in these channels often assume that the left-handed couplings vanish (no interference between  $W$  and  $W'$ ), and that the right-handed neutrino of the first generation is light compared to  $M_{W'}$  and escapes the detector. However, if a  $W'$  boson were discovered and the final state fermions have left-handed helicity, then the effects of  $W - W'$  interference could be observed [14], providing useful information about the  $W'$  couplings.

In the  $e\nu$  channel, the 95% CL limit set by the ATLAS Collaboration [13] with  $1 \text{ fb}^{-1}$  of data on the cross section (at  $\sqrt{s} = 7$  TeV) times branching fraction is shown in Fig. 1. The CMS limit based on  $5 \text{ fb}^{-1}$  of data in this channel [15], for  $M_{W'}$  in the  $0.5 - 3$  TeV range, varies between 70 and 2.6 fb. For  $M_{W'}$  in the  $500 - 600$  GeV range, the strongest limits on  $W'$  couplings are set by CDF [16] with  $5.3 \text{ fb}^{-1}$  (for a comparison, see Fig. 3 of Ref. 13). The limits are much weaker for  $M_{W'}$  in the  $200 - 500$  GeV range because these were obtained using only

## Gauge & Higgs Boson Particle Listings

### Heavy Bosons Other than Higgs Bosons

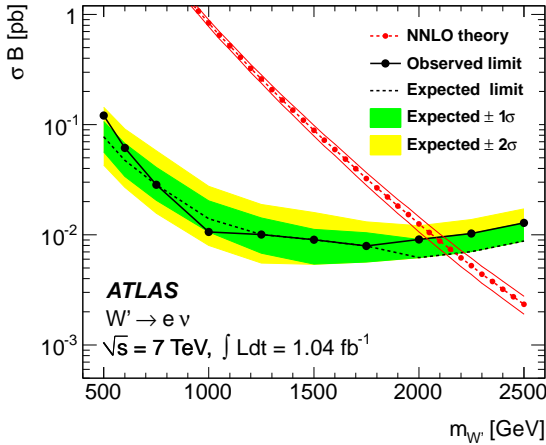


**Figure 1:** 95% CL limit on  $\sigma(pp \rightarrow W'X) \times B(W' \rightarrow e\nu)$  from ATLAS [13]. The theoretical prediction (dash-dotted line) is for  $C_q^R = gV_{CKM}$ ,  $C_l^R = g$ ,  $C_q^L = C_l^L = 0$ .

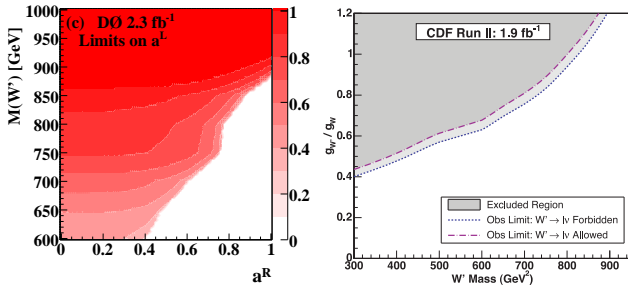


**Figure 2:** 95% CL upper limits on  $W'$  couplings using the  $t\bar{b}$  and  $\bar{t}b$  final states, assuming that the diagonal couplings are generation independent. Left panel: D0 [21] limit on  $C_{q11}^R/g$  as contours in the  $C_{q11}^R/g - M_{W'}$  plane. Right panel: CDF [22] limit on  $C_{q11}^R/g$ .

of Tevatron data [17], while the 105 – 200 GeV range has been even less explored (see the UA1 and UA2 references in Ref. 18).

In the  $\mu\nu$  channel, the most stringent limit in the 0.5 – 3 TeV range, set by CMS [15] with  $5 \text{ fb}^{-1}$ , varies between 39 and 2.7 fb. The ATLAS  $\mu\nu$  limit [13] is higher by about 50% compared to that shown in Fig. 1. For  $M_{W'}$  in the 200 – 500 GeV range there are only weak limits on the  $W'$  couplings from the Tevatron Run I [19]. There are no direct limits on  $W' \rightarrow \mu\nu$  for  $M_{W'}$  in the 105 – 200 GeV range.

Dedicated searches for the  $W' \rightarrow \tau\nu$  decay have not yet been performed, but limits can be derived from some searches in the  $\ell + \cancel{E}_T$  channel as well as from charged-Higgs searches such as  $pp \rightarrow t\bar{b}\tau\nu X$ .

The  $W'$  decay into a lepton and a right-handed neutrino,  $\nu_R$ , may also be followed by the  $\nu_R$  decay through a virtual  $W'$  boson into a lepton and two quark jets. The ATLAS search [20] with  $2.1 \text{ fb}^{-1}$  sets cross-section limits in the  $\ell^+\ell^-jj$  channel decreasing from 20 fb to 3 fb for  $M_{W'}$  in the 1 – 2.7 TeV range.

The  $t\bar{b}$  channel is particularly important because a  $W'$  boson that couples only to right-handed fermions cannot decay to leptons when the right-handed neutrinos are heavier than  $M_{W'}$  (additional motivations are provided by a  $W'$  boson with enhanced couplings to the third generation [8], and by a leptophobic  $W'$  boson). The usual signal consists of a leptonically decaying  $W$  boson and two  $b$ -jets. The upper limits on the  $W'$  couplings to left- and right-handed quarks normalized to the Standard Model  $W$  boson couplings, set by D0 with  $2.3 \text{ fb}^{-1}$  [21] and by CDF with  $1.9 \text{ fb}^{-1}$  [22], respectively, are shown in Fig. 2. LHC searches in this channel have set cross section limits for  $M_{W'}$  in the 0.5 – 2.1 TeV range [23].

For  $M_{W'} \gg m_t$ , one could also use hadronic  $W$  boson decays to search for  $W' \rightarrow t\bar{b}$  with a boosted top quark. If  $W'$  couplings to left-handed quarks are large, then interference effects modify the Standard Model  $s$ -channel single-top production [24].

Searches for dijet resonances may be used to set limits on  $W' \rightarrow q\bar{q}'$  [18]. In the 105 – 200 GeV mass range the limits are rather weak, as they have been set so far only by the UA2 Collaboration; even in the 200 – 700 GeV range only small data sets from the Tevatron and the LHC have been used so far.

In some theories [3], the  $W'$  couplings to Standard Model fermions are suppressed by discrete symmetries.  $W'$  production then occurs in pairs, through a photon or  $Z$  boson. The decay modes are model-dependent and often involve other new particles. The ensuing collider signals arise from cascade decays and typically include missing transverse energy.

A fermiophobic  $W'$  boson which couples to  $WZ$  may be produced at hadron colliders in association with a  $Z$  boson, or via  $WZ$  fusion. This would give rise to  $(WZ)Z$  and  $(WZ)jj$  final states, where the parentheses represent a resonance [25]. The study of these processes is important for understanding the origin of electroweak symmetry-breaking. The D0 [26] and CDF [27] Collaborations have set limits on  $\sigma(pp \rightarrow W'X) \times B(W' \rightarrow WZ)$  for  $M_{W'}$  in the 180 – 1000 GeV range, while searches [28] at the 7 TeV LHC have set cross-section limits for  $M_{W'}$  in the 200 – 1500 GeV range.

**Low-energy constraints.** The properties of  $W'$  bosons are also constrained by measurements of processes at energies much below  $M_{W'}$ . The bounds on  $W - W'$  mixing [18] are mostly due to the change in the properties of the  $W$  boson compared to the Standard Model. Limits on the deviation in the  $ZWW$  coupling provide a leading constraint for fermiophobic  $W'$  bosons [10].

Constraints arising from low-energy effects of  $W'$  exchange are strongly model-dependent. If the  $W'$  couplings to quarks are not suppressed, then box diagrams involving a  $W$  and a  $W'$  boson contribute to neutral meson-mixing. In the case of  $W'$  couplings to right-handed quarks as in the left-right symmetric model, the limit from  $K_L - K_S$  mixing is severe:  $M_{W'} > 2.5 \text{ TeV}$  [29]. However, if no correlation between  $C_{qij}^R$  and  $C_{lij}^R$  is assumed, then the limit on  $M_{W'}$  may be significantly relaxed [30].

# Gauge & Higgs Boson Particle Listings

## Heavy Bosons Other than Higgs Bosons

$W'$  exchange also contributes at tree level to various low-energy processes. In particular, it would impact the measurement of the Fermi constant  $G_F$  in muon decay, which in turn would change the predictions of many other electroweak processes. A recent test of parity violation in polarized muon decay [31] has set limits of about 600 GeV on  $M_{W'}$ , assuming  $W'$  couplings to right-handed leptons as in left-right symmetric models. There are also  $W'$  contributions to the neutron electric dipole moment,  $\beta$  decays, and other processes [18].

If right-handed neutrinos have Majorana masses, then there are tree-level contributions to neutrinoless double-beta decay, and a limit on  $M_{W'}$  versus the  $\nu_R$  mass may be derived [32]. For  $\nu_R$  masses below a few GeV, the  $W'$  boson contributes to leptonic and semileptonic  $B$  meson decays, so that limits may be placed on various combinations of  $W'$  parameters [30]. For  $\nu_R$  masses below  $\sim 30$  MeV, most stringent constraints on  $M_{W'}$  are due to the limits on  $\nu_R$  emission from supernova.

### References

1. M. Bando, T. Kugo, and K. Yamawaki, Phys. Rept. **164**, 217 (1988).
2. H.C. Cheng *et al.*, Phys. Rev. **D64**, 065007 (2001).
3. H.C. Cheng and I. Low, JHEP **0309**, 051 (2003).
4. R.N. Mohapatra and J.C. Pati, Phys. Rev. **D11**, 566 (1975); G. Senjanovic and R.N. Mohapatra, Phys. Rev. **D12**, 1502 (1975).
5. K.S. Babu, X.G. He, and E. Ma, Phys. Rev. **D36**, 878 (1987).
6. H. Georgi, E.E. Jenkins, and E.H. Simmons, Nucl. Phys. **B331**, 541 (1990).
7. See, *e.g.*, X.y. Li and E. Ma, J. Phys. **G19**, 1265 (1993).
8. D.J. Muller and S. Nandi, Phys. Lett. **B383**, 345 (1996); E. Malkawi, T. Tait, and C.P. Yuan, Phys. Lett. **B385**, 304 (1996).
9. A. Donini *et al.*, Nucl. Phys. **B507**, 51 (1997).
10. R.S. Chivukula *et al.*, Phys. Rev. **D74**, 075011 (2006); H.J. He, T. Tait, and C.P. Yuan, Phys. Rev. **D62**, 011702 (2000).
11. F. Pisano and V. Pleitez, Phys. Rev. **D46**, 410 (1992); Phys. Rev. **D51**, 3865 (1995).
12. Z. Sullivan, Phys. Rev. **D66**, 075011 (2002).
13. G. Aad *et al.* [ATLAS Collab.], Phys. Lett. **B705**, 28 (2011).
14. T.G. Rizzo, JHEP **0705**, 037 (2007). E. Boos *et al.*, Phys. Lett. **B655**, 245 (2007).
15. S. Chatrchyan *et al.* [CMS Collaboration], arXiv:1204.4764.
16. T. Aaltonen *et al.* [CDF Collab.], Phys. Rev. **D83**, 031102 (2011).
17. A. Abulencia *et al.* [CDF Collaboration], Phys. Rev. **D75**, 091101 (2007).
18. See the particle listings for  $W'$  in this *Review*.
19. F. Abe *et al.* [CDF Collab.], Phys. Rev. Lett. **84**, 5716 (2000).
20. G. Aad *et al.* [ATLAS Collab.], arXiv:1203.5420 and related plots at [https://atlas.web.cern.ch/Atlas/](https://atlas.web.cern.ch/Atlas/GROUPS/PHYSICS/PAPERS/EXOT-2011-24/) GROUPS/PHYSICS/PAPERS/EXOT-2011-24/;

See also CMS Collab., note CMS-PAS-EXO-11-002, July 2011.

21. V. M. Abazov *et al.* [D0 Collab.], Phys. Lett. **B699**, 145 (2011).
22. T. Aaltonen *et al.* [CDF Collab.], Phys. Rev. Lett. **103**, 041801 (2009).
23. G. Aad *et al.* [ATLAS Collab.], arXiv:1205.1016; CMS Collab., note CMS-PAS-EXO-12-001, April 2012.
24. T.M.P. Tait, C.-P. Yuan, Phys. Rev. **D63**, 014018 (2000).
25. H.J. He *et al.*, Phys. Rev. **D78**, 031701 (2008).
26. V. M. Abazov *et al.* [D0 Collab.], Phys. Rev. Lett. **107**, 011801 (2011).
27. T. Aaltonen *et al.* [CDF Collab.], Phys. Rev. Lett. **104** (2010) 241801.
28. CMS Collab., note CMS-PAS-EXO-11-041, Aug. 2011, updated Mar. 2012: <https://twiki.cern.ch/twiki/bin/view/CMSPublic/PhysicsResultsEXO11041Winter2012>; G. Aad *et al.* [ATLAS Collab.], arXiv:1204.1648.
29. Y. Zhang *et al.*, Phys. Rev. **D76**, 091301 (2007).
30. P. Langacker and S.U. Sankar, Phys. Rev. **D40**, 1569 (1989).
31. J. F. Bueno *et al.* [TWIST Collab.], Phys. Rev. **D84**, 032005 (2011).
32. See Fig. 5 of G. Prezeau, M. Ramsey-Musolf, and P. Vogel, Phys. Rev. **D68**, 034016 (2003).

### MASS LIMITS for $W'$ (Heavy Charged Vector Boson Other Than $W$ ) in Hadron Collider Experiments

Couplings of  $W'$  to quarks and leptons are taken to be identical with those of  $W$ . The following limits are obtained from  $p\bar{p} \rightarrow W'X$  with  $W'$  decaying to the mode indicated in the comments (*e.g.*,  $W' \rightarrow WZ$ ) are assumed to be suppressed. The most recent preliminary results can be found in the " $W'$ -boson searches" review above.

VALUE (GeV)	CL%	DOCUMENT ID	TECN	COMMENT
<b>&gt;2150</b>	95	AAD 11Q	ATLS	$W' \rightarrow e\nu, \mu\nu$
none 180–690	95	<sup>1</sup> ABAZOV 11H	D0	$W' \rightarrow WZ$
> 863	95	<sup>2</sup> ABAZOV 11L	D0	$W' \rightarrow tb$
>1510	95	CHATRCHYAN11Y	CMS	$W' \rightarrow q\bar{q}$
●●● We do not use the following data for averages, fits, limits, etc. ●●●				
>1490	95	AAD 11M	ATLS	$W' \rightarrow e\nu, \mu\nu$
>1120	95	AALTONEN 11C	CDF	$W' \rightarrow e\nu$
>1580	95	CHATRCHYAN11K	CMS	$W' \rightarrow e\nu, \mu\nu$
>1400	95	CHATRCHYAN11K	CMS	$W' \rightarrow \mu\nu$
>1360	95	KHACHATRY.11H	CMS	$W' \rightarrow e\nu$
none 285–516	95	<sup>3</sup> AALTONEN 10N	CDF	$W' \rightarrow WZ$
none 188–520	95	<sup>4</sup> ABAZOV 10A	D0	$W' \rightarrow WZ$
> 800	95	<sup>5</sup> AALTONEN 09AA	CDF	$W' \rightarrow tb$
none 280–840	95	<sup>6</sup> AALTONEN 09AC	CDF	$W' \rightarrow q\bar{q}$
>1000	95	ABAZOV 08C	D0	$W' \rightarrow e\nu$
> 731	95	<sup>7</sup> ABAZOV 08P	D0	$W' \rightarrow tb$
> 788	95	ABULENCIA 07K	CDF	$W' \rightarrow e\nu$
none 200–610	95	<sup>8</sup> ABAZOV 06N	D0	$W' \rightarrow tb$
> 800	95	ABAZOV 04C	D0	$W' \rightarrow q\bar{q}$
225–536	95	<sup>9</sup> ACOSTA 03B	CDF	$W' \rightarrow tb$
none 200–480	95	<sup>10</sup> AFFOLDER 02C	CDF	$W' \rightarrow WZ$
> 786	95	<sup>11</sup> AFFOLDER 01I	CDF	$W' \rightarrow e\nu, \mu\nu$
> 660	95	<sup>12</sup> ABE 00	CDF	$W' \rightarrow \mu\nu$
none 300–420	95	<sup>13</sup> ABE 97G	CDF	$W' \rightarrow q\bar{q}$
> 720	95	<sup>14</sup> ABACHI 96C	D0	$W' \rightarrow e\nu$
> 610	95	<sup>15</sup> ABACHI 95E	D0	$W' \rightarrow e\nu, \tau\nu$
> 652	95	<sup>16</sup> ABE 95M	CDF	$W' \rightarrow e\nu$
none 260–600	95	<sup>17</sup> RIZZO 93	RVUE	$W' \rightarrow q\bar{q}$

<sup>1</sup> The quoted limit is obtained assuming  $W'WZ$  coupling strength is the same as the ordinary  $WWZ$  coupling strength in the Standard Model.

<sup>2</sup> ABAZOV 11L limit is for  $W'$  with SM-like coupling which interferes with the SM  $W$  boson. For  $W'$  with right-handed coupling, the bound becomes  $>885$  GeV ( $>890$  GeV) if  $W'$  decays to both leptons and quarks (only to quarks). If both left- and right-handed couplings present, the limit becomes  $>916$  GeV.

<sup>3</sup> The quoted limit assumes  $g_{W'WZ}/g_{WWZ} = (M_W/M_{W'})^2$ . See their Fig. 4 for limits in mass-coupling plane.

<sup>4</sup> The quoted limit assumes  $g_{W'WZ}/g_{WWZ} = (M_W/M_{W'})^2$ . See their Fig. 3 for limits in mass-coupling plane.



See key on page 457

# Gauge & Higgs Boson Particle Listings

## Heavy Bosons Other than Higgs Bosons

- 5 The AALTONEN 09AA quoted limit is for a right-handed  $W'$  with SM-like coupling allowing  $W' \rightarrow e\nu$  decays.
- 6 AALTONEN 09AC search for new particle decaying to dijets.
- 7 The ABZOV 08P quoted limit is for  $W'$  with SM-like coupling which interferes with the SM  $W$  boson. For  $W'$  with right-handed coupling, the bound becomes  $>739$  GeV ( $>768$  GeV) if  $W'$  decays to both leptons and quarks (only to quarks).
- 8 The ABZOV 06N quoted limit is for  $W'$  with SM-like coupling which interferes with the SM  $W$  boson. For  $W'$  with right-handed coupling,  $M_{W'}$  between 200 and 630 (670) GeV is excluded for  $M_{\nu R} \ll M_{W'}$  ( $M_{\nu R} > M_{W'}$ ).
- 9 The ACOSTA 03B quoted limit is for  $M_{W'} \gg M_{\nu R}$ . For  $M_{W'} < M_{\nu R}$ ,  $M_{W'}$  between 225 and 566 GeV is excluded.
- 10 The quoted limit is obtained assuming  $W'WZ$  coupling strength is the same as the ordinary  $WZ$  coupling strength in the Standard Model. See their Fig. 2 for the limits on the production cross sections as a function of the  $W'$  width.
- 11 AFFOLDER 01I combine a new bound on  $W' \rightarrow e\nu$  of 754 GeV with the bound of ABE 00 on  $W' \rightarrow \mu\nu$  to obtain quoted bound.
- 12 ABE 00 assume that the neutrino from  $W'$  decay is stable and has a mass significantly less than  $m_{W'}$ .
- 13 ABE 97g search for new particle decaying to dijets.
- 14 For bounds on  $W_R$  with nonzero right-handed mass, see Fig. 5 from ABACHI 96c.
- 15 ABACHI 95E assume that the decay  $W' \rightarrow WZ$  is suppressed and that the neutrino from  $W'$  decay is stable and has a mass significantly less than  $m_{W'}$ .
- 16 ABE 95M assume that the decay  $W' \rightarrow WZ$  is suppressed and the (right-handed) neutrino is light, noninteracting, and stable. If  $m_\nu=60$  GeV, for example, the effect on the mass limit is negligible.
- 17 RIZZO 93 analyses CDF limit on possible two-jet resonances. The limit is sensitive to the inclusion of the assumed  $K$  factor.

### $W_R$ (Right-Handed $W$ Boson) MASS LIMITS

Assuming a light right-handed neutrino, except for BEALL 82, LANGACKER 89b, and COLANGELO 91.  $g_R = g_L$  assumed. [Limits in the section MASS LIMITS for  $W'$  below are also valid for  $W_R$  if  $m_{\nu R} \ll m_{W_R}$ .] Some limits assume manifest left-right symmetry, i.e., the equality of left- and right Cabibbo-Kobayashi-Maskawa matrices. For a comprehensive review, see LANGACKER 89b. Limits on the  $W_L$ - $W_R$  mixing angle  $\zeta$  are found in the next section. Values in brackets are from cosmological and astrophysical considerations and assume a light right-handed neutrino.

VALUE (GeV)	CL%	DOCUMENT ID	TECN	COMMENT
<b>&gt; 715</b>	90	18 CZAKON	99 RVUE	Electroweak
• • • We do not use the following data for averages, fits, limits, etc. • • •				
> 245	90	19 WAUTERS	10 CNTR	$^{60}\text{Co}$ $\beta$ decay
> 180	90	20 MELCONIAN	07 CNTR	$^{37}\text{K}$ $\beta^+$ decay
> 290.7	90	21 SCHUMANN	07 CNTR	Polarized neutron decay
[> 3300]	95	22 CYBURT	05 COSM	Nucleosynthesis; light $\nu_R$
> 310	90	23 THOMAS	01 CNTR	$\beta^+$ decay
> 137	95	24 ACKERSTAFF	99D OPAL	$\tau$ decay
> 1400	68	25 BARENBOIM	98 RVUE	Electroweak, $Z$ - $Z'$ mixing
> 549	68	26 BARENBOIM	97 RVUE	$\mu$ decay
> 220	95	27 STAHL	97 RVUE	$\tau$ decay
> 220	90	28 ALLET	96 CNTR	$\beta^+$ decay
> 281	90	29 KUZNETSOV	95 CNTR	Polarized neutron decay
> 282	90	30 KUZNETSOV	94b CNTR	Polarized neutron decay
> 439	90	31 BHATTACH...	93 RVUE	$Z$ - $Z'$ mixing
> 250	90	32 SEVERIJNS	93 CNTR	$\beta^+$ decay
		33 IMAZATO	92 CNTR	$K^+$ decay
> 475	90	34 POLAK	92b RVUE	$\mu$ decay
> 240	90	35 AQUINO	91 RVUE	Neutron decay
> 496	90	36 AQUINO	91 RVUE	Neutron and muon decay
> 700		37 COLANGELO	91 THEO	$m_{K_L^0} - m_{K_S^0}$
> 477	90	37 POLAK	91 RVUE	$\mu$ decay
[none 540-23000]		38 BARBIERI	89b ASTR	SN 1987A; light $\nu_R$
> 300	90	39 LANGACKER	89b RVUE	General
> 160	90	40 BALKE	88 CNTR	$\mu \rightarrow e\nu\bar{\nu}$
> 406	90	41 JODIDIO	86 ELEC	Any $\zeta$
> 482	90	41 JODIDIO	86 ELEC	$\zeta = 0$
> 800		MOHAPATRA	86 RVUE	$SU(2)_L \times SU(2)_R \times U(1)$
> 400	95	42 STOKER	85 ELEC	Any $\zeta$
> 475	95	42 STOKER	85 ELEC	$\zeta < 0.041$
		43 BERGSMA	83 CHRM	$\nu_\mu e \rightarrow \mu\nu e$
> 380	90	44 CARR	83 ELEC	$\mu^+$ decay
> 1600		45 BEALL	82 THEO	$m_{K_L^0} - m_{K_S^0}$

- 18 CZAKON 99 perform a simultaneous fit to charged and neutral sectors.
- 19 WAUTERS 10 limit is from a measurement of the asymmetry parameter of polarized  $^{60}\text{Co}$   $\beta$  decays. The listed limit assumes no mixing.
- 20 MELCONIAN 07 measure the neutrino angular asymmetry in  $\beta^+$ -decays of polarized  $^{37}\text{K}$ , stored in a magneto-optical trap. Result is consistent with SM prediction and does not constrain the  $W_L$ - $W_R$  mixing angle appreciably.
- 21 SCHUMANN 07 limit is from measurements of the asymmetry  $\langle \bar{p}_\nu \cdot \sigma_n \rangle$  in the  $\beta$  decay of polarized neutrons. Zero mixing is assumed.
- 22 CYBURT 05 limit follows by requiring that three light  $\nu_R$ 's decouple when  $T_{dec} > 140$  MeV. For different  $T_{dec}$ , the bound becomes  $M_{W_R} > 3.3 \text{ TeV} (T_{dec} / 140 \text{ MeV})^{3/4}$ .
- 23 THOMAS 01 limit is from measurement of  $\beta^+$  polarization in decay of polarized  $^{12}\text{N}$ . The listed limit assumes no mixing.
- 24 ACKERSTAFF 99D limit is from  $\tau$  decay parameters. Limit increase to 145 GeV for zero mixing.

- 25 BARENBOIM 98 assumes minimal left-right model with Higgs of  $SU(2)_R$  in  $SU(2)_L$  doublet. For Higgs in  $SU(2)_L$  triplet,  $m_{W_R} > 1100$  GeV. Bound calculated from effect of corresponding  $Z_{LR}$  on electroweak data through  $Z$ - $Z_{LR}$  mixing.
- 26 The quoted limit is from  $\mu$  decay parameters. BARENBOIM 97 also evaluate limit from  $K_L$ - $K_S$  mass difference.
- 27 STAHL 97 limit is from fit to  $\tau$ -decay parameters.
- 28 ALLET 96 measured polarization-asymmetry correlation in  $^{12}\text{N}$   $\beta^+$  decay. The listed limit assumes zero  $L$ - $R$  mixing.
- 29 KUZNETSOV 95 limit is from measurements of the asymmetry  $\langle \bar{p}_\nu \cdot \sigma_n \rangle$  in the  $\beta$  decay of polarized neutrons. Zero mixing assumed. See also KUZNETSOV 94b.
- 30 KUZNETSOV 94b limit is from measurements of the asymmetry  $\langle \bar{p}_\nu \cdot \sigma_n \rangle$  in the  $\beta$  decay of polarized neutrons. Zero mixing assumed.
- 31 BHATTACHARYYA 93 uses  $Z$ - $Z'$  mixing limit from LEP '90 data, assuming a specific Higgs sector of  $SU(2)_L \times SU(2)_R \times U(1)$  gauge model. The limit is for  $m_t=200$  GeV and slightly improves for smaller  $m_t$ .
- 32 SEVERIJNS 93 measured polarization-asymmetry correlation in  $^{107}\text{In}$   $\beta^+$  decay. The listed limit assumes zero  $L$ - $R$  mixing. Value quoted here is from SEVERIJNS 94 erratum.
- 33 IMAZATO 92 measure positron asymmetry in  $K^+ \rightarrow \mu^+ \nu_\mu$  decay and obtain  $\xi_{P,\mu} > 0.990$  (90% CL). If  $W_R$  couples to  $u\bar{s}$  with full weak strength ( $V_{us}^R=1$ ), the result corresponds to  $m_{W_R} > 653$  GeV. See their Fig. 4 for  $m_{W_R}$  limits for general  $|V_{us}^R|^2=1-|V_{ud}^R|^2$ .
- 34 POLAK 92b limit is from fit to muon decay parameters and is essentially determined by JODIDIO 86 data assuming  $\zeta=0$ . Supersedes POLAK 91.
- 35 AQUINO 91 limits obtained from neutron lifetime and asymmetries together with unitarity of the CKM matrix. Manifest left-right symmetry assumed. Stronger of the two limits also includes muon decay results.
- 36 COLANGELO 91 limit uses hadronic matrix elements evaluated by QCD sum rule and is less restrictive than BEALL 82 limit which uses vacuum saturation approximation. Manifest left-right symmetry assumed.
- 37 POLAK 91 limit is from fit to muon decay parameters and is essentially determined by JODIDIO 86 data assuming  $\zeta=0$ . Superseded by POLAK 92b.
- 38 BARBIERI 89b limit holds for  $m_{\nu R} \leq 10$  MeV.
- 39 LANGACKER 89b limit is for any  $\nu_R$  mass (either Dirac or Majorana) and for a general class of right-handed quark mixing matrices.
- 40 BALKE 88 limit is for  $m_{\nu e R} = 0$  and  $m_{\nu \mu R} \leq 50$  MeV. Limits come from precise measurements of the muon decay asymmetry as a function of the positron energy.
- 41 JODIDIO 86 is the same TRIUMF experiment as STOKER 85 (and CARR 83); however, it uses a different technique. The results given here are combined results of the two techniques. The technique here involves precise measurement of the end-point  $e^+$  spectrum in the decay of the highly polarized  $\mu^+$ .
- 42 STOKER 85 is same TRIUMF experiment as CARR 83. Here they measure the decay  $e^+$  spectrum asymmetry above 46 MeV/c using a muon-spin-rotation technique. Assumed a light right-handed neutrino. Quoted limits are from combining with CARR 83.
- 43 BERGSMA 83 set limit  $m_{W_2}/m_{W_1} > 1.9$  at CL = 90%.
- 44 CARR 83 is TRIUMF experiment with a highly polarized  $\mu^+$  beam. Looked for deviation from  $V-A$  at the high momentum end of the decay  $e^+$  energy spectrum. Limit from previous world-average muon polarization parameter is  $m_{W_R} > 240$  GeV. Assumes a light right-handed neutrino.
- 45 BEALL 82 limit is obtained assuming that  $W_R$  contribution to  $K_L^0$ - $K_S^0$  mass difference is smaller than the standard one, neglecting the top quark contributions. Manifest left-right symmetry assumed.

### Limit on $W_L$ - $W_R$ Mixing Angle $\zeta$

Lighter mass eigenstate  $W_1 = W_L \cos \zeta - W_R \sin \zeta$ . Light  $\nu_R$  assumed unless noted. Values in brackets are from cosmological and astrophysical considerations.

VALUE	CL%	DOCUMENT ID	TECN	COMMENT
• • • We do not use the following data for averages, fits, limits, etc. • • •				
< 0.022	90	MACDONALD 08	TWST	$\mu \rightarrow e\nu\bar{\nu}$
< 0.12	95	46 ACKERSTAFF 99D	OPAL	$\tau$ decay
< 0.013	90	47 CZAKON	99 RVUE	Electroweak
< 0.0333		48 BARENBOIM	97 RVUE	$\mu$ decay
< 0.04	90	49 MISHRA	92 CCFR	$\nu N$ scattering
-0.0006 to 0.0028	90	50 AQUINO	91 RVUE	
[none 0.00001-0.02]		51 BARBIERI	89b ASTR	SN 1987A
< 0.040	90	52 JODIDIO	86 ELEC	$\mu$ decay
-0.056 to 0.040	90	52 JODIDIO	86 ELEC	$\mu$ decay
46 ACKERSTAFF 99D limit is from $\tau$ decay parameters.				
47 CZAKON 99 perform a simultaneous fit to charged and neutral sectors.				
48 The quoted limit is from $\mu$ decay parameters. BARENBOIM 97 also evaluate limit from $K_L$ - $K_S$ mass difference.				
49 MISHRA 92 limit is from the absence of extra large- $x$ , large- $y$ $\bar{\nu}_\mu N \rightarrow \bar{\nu}_\mu X$ events at Tevatron, assuming left-handed $\nu$ and right-handed $\bar{\nu}$ in the neutrino beam. The result gives $\zeta^2(1-2m_W^2/m_{W_2}^2) < 0.0015$ . The limit is independent of $\nu_R$ mass.				
50 AQUINO 91 limits obtained from neutron lifetime and asymmetries together with unitarity of the CKM matrix. Manifest left-right asymmetry is assumed.				
51 BARBIERI 89b limit holds for $m_{\nu R} \leq 10$ MeV.				
52 First JODIDIO 86 result assumes $m_{W_R} = \infty$ , second is for unconstrained $m_{W_R}$ .				

### $Z'$ -BOSON SEARCHES

Revised May 2012 by G. Brooijmans (Columbia University), M.-C. Chen (UC Irvine), and B.A. Dobrescu (Fermilab).

The  $Z'$  boson is a hypothetical massive, electrically-neutral and color-singlet particle of spin 1. This particle is predicted

# Gauge & Higgs Boson Particle Listings

## Heavy Bosons Other than Higgs Bosons

in many extensions of the Standard Model, and has been the object of extensive phenomenological studies [1].

**$Z'$  boson couplings to quarks and leptons.** The couplings of a  $Z'$  boson to the first-generation fermions are given by

$$Z'_\mu (g_u^L \bar{u}_L \gamma^\mu u_L + g_d^L \bar{d}_L \gamma^\mu d_L + g_u^R \bar{u}_R \gamma^\mu u_R + g_d^R \bar{d}_R \gamma^\mu d_R + g_\nu^L \bar{\nu}_L \gamma^\mu \nu_L + g_e^L \bar{e}_L \gamma^\mu e_L + g_e^R \bar{e}_R \gamma^\mu e_R) , \quad (1)$$

where  $u, d, \nu$  and  $e$  are the quark and lepton fields in the mass eigenstate basis, and the coefficients  $g_u^L, g_d^L, g_u^R, g_d^R, g_\nu^L, g_e^L, g_e^R$  are real dimensionless parameters. If the  $Z'$  couplings to quarks and leptons are generation-independent, then these seven parameters describe the couplings of the  $Z'$  boson to all Standard Model fermions. More generally, however, the  $Z'$  couplings to fermions are generation-dependent, in which case Eq. (1) may be written with generation indices  $i, j = 1, 2, 3$  labeling the quark and lepton fields, and with the seven coefficients promoted to  $3 \times 3$  Hermitian matrices (e.g.,  $g_{eij}^L \bar{e}_L^i \gamma^\mu e_L^j$ , where  $e_L^2$  is the left-handed muon, etc.).

These parameters describing the  $Z'$  boson interactions with quarks and leptons are subject to some theoretical constraints. Quantum field theories that include a heavy spin-1 particle are well behaved at high energies only if that particle is a gauge boson associated with a spontaneously broken gauge symmetry. Quantum effects preserve the gauge symmetry only if the couplings of the gauge boson to fermions satisfy anomaly cancellation conditions. Furthermore, the fermion charges under the new gauge symmetry are constrained by the requirement that the quarks and leptons get masses from gauge-invariant interactions with Higgs doublets or whatever else breaks the electroweak symmetry.

The relation between the couplings displayed in Eq. (1) and the gauge charges  $z_{fi}^L$  and  $z_{fi}^R$  of the fermions  $f = u, d, \nu, e$  involves the unitary  $3 \times 3$  matrices  $V_f^L$  and  $V_f^R$  that transform the gauge eigenstate fermions  $f_L^i$  and  $f_R^i$ , respectively, into the mass eigenstates. In addition, the  $Z'$  couplings are modified if the new gauge boson in the gauge eigenstate basis ( $\tilde{Z}'_\mu$ ) has a kinetic mixing  $(-\chi/2)B^{\mu\nu}\tilde{Z}'_{\mu\nu}$  with the hypercharge gauge boson  $B^\mu$  (due to a dimension-4 or 6 operator, depending on whether the new gauge symmetry is Abelian or not), or a mass mixing  $\delta M^2 \tilde{Z}'^\mu \tilde{Z}'_\mu$  with the linear combination ( $\tilde{Z}_\mu$ ) of neutral bosons which has same couplings as the Standard Model  $Z^0$  [2]. Both the kinetic and mass mixings shift the mass and couplings of the  $Z$  boson, such that the electroweak measurements impose upper limits on  $\chi$  and  $\delta M^2/(M_{Z'}^2 - M_Z^2)$  of the order of  $10^{-3}$  [3]. Keeping only linear terms in these two small quantities, the couplings of the mass-eigenstate  $Z'$  boson are given by

$$g_{fij}^L = g_z V_{fii'}^L z_{f'i'}^L (V_f^L)_{i'j}^\dagger + \frac{e}{c_W} \left( \frac{s_W \chi M_{Z'}^2 + \delta M^2}{2s_W (M_{Z'}^2 - M_Z^2)} \sigma_f^3 - \epsilon Q_f \right) ,$$

$$g_{fij}^R = g_z V_{fii'}^R z_{f'i'}^R (V_f^R)_{i'j}^\dagger - \frac{e}{c_W} \epsilon Q_f , \quad (2)$$

where  $g_z$  is the new gauge coupling,  $Q_f$  is the electric charge of  $f$ ,  $e$  is the electromagnetic gauge coupling,  $s_W$  and  $c_W$  are the

**Table 1:** Examples of generation-independent  $U(1)'$  charges for quarks and leptons. The parameter  $x$  is an arbitrary rational number. Anomaly cancellation requires certain new fermions [4].

fermion	$U(1)_{B-xL}$	$U(1)_{10+x5}$	$U(1)_{d-xu}$	$U(1)_{q+xu}$
$(u_L, d_L)$	1/3	1/3	0	1/3
$u_R$	1/3	-1/3	$-x/3$	$x/3$
$d_R$	1/3	$-x/3$	1/3	$(2-x)/3$
$(\nu_L, e_L)$	$-x$	$x/3$	$(-1+x)/3$	-1
$e_R$	$-x$	-1/3	$x/3$	$-(2+x)/3$

sine and cosine of the weak mixing angle,  $\sigma_f^3 = +1$  for  $f = u, \nu$  and  $\sigma_f^3 = -1$  for  $f = d, e$ , and

$$\epsilon = \frac{\chi (M_{Z'}^2 - c_W^2 M_Z^2) + s_W \delta M^2}{M_{Z'}^2 - M_Z^2} . \quad (3)$$

**$U(1)$  gauge groups.** A simple origin of a  $Z'$  boson is a new  $U(1)'$  gauge symmetry. In that case, the matricial equalities  $z_u^L = z_d^L$  and  $z_\nu^L = z_e^L$  are required by the  $SU(2)_W$  gauge symmetry. Given that the  $U(1)'$  interaction is not asymptotically free, the theory may be well-behaved at high energies (for example, by embedding  $U(1)'$  in a non-Abelian gauge group) only if the  $Z'$  couplings are commensurate numbers, i.e. any ratio of couplings is a rational number. Satisfying the anomaly cancellation conditions (which include an equation cubic in charges) with rational numbers is highly nontrivial, and in general new fermions charged under  $U(1)'$  are necessary.

Consider first the case where the couplings are generation-independent (the  $V_f$  matrices then disappear from Eq. (2)), so that there are five commensurate couplings:  $g_q^L, g_u^R, g_d^R, g_l^L, g_e^R$ . Four sets of charges are displayed in Table 1, each of them spanned by one free parameter,  $x$  [4]. The first set, labelled  $B-xL$ , has charges proportional to the baryon number minus  $x$  times the lepton number. These charges allow all Standard Model Yukawa couplings to a Higgs doublet which is neutral under  $U(1)_{B-xL}$ , so that there is no tree-level  $\tilde{Z}-\tilde{Z}'$  mixing. For  $x=1$  one recovers the  $U(1)_{B-L}$  group, which is non-anomalous in the presence of one ‘‘right-handed neutrino’’ (a chiral fermion that is a singlet under the Standard Model gauge group) per generation. For  $x \neq 1$ , it is necessary to include some fermions that are vector-like (i.e. their mass terms are gauge invariant) with respect to the electroweak gauge group and chiral with respect to  $U(1)_{B-xL}$ . In the particular cases  $x=0$  or  $x \gg 1$  the  $Z'$  is leptophobic or quark-phobic, respectively.

The second set,  $U(1)_{10+x5}$ , has charges that commute with the representations of the  $SU(5)$  grand unified group. Here  $x$  is related to the mixing angle between the two  $U(1)$  bosons encountered in the  $E_6 \rightarrow SU(5) \times U(1) \times U(1)$  symmetry breaking patterns of grand unified theories [1,6]. This set leads to  $\tilde{Z}-\tilde{Z}'$  mass mixing at tree level, such that for a  $Z'$  mass close to the electroweak scale, the measurements at

See key on page 457

## Gauge & Higgs Boson Particle Listings

### Heavy Bosons Other than Higgs Bosons

the  $Z$ -pole require some fine tuning between the charges and VEVs of the two Higgs doublets. Vector-like fermions charged under the electroweak gauge group and also carrying color are required (except for  $x = -3$ ) to make this set anomaly free. The particular cases  $x = -3, 1, -1/2$  are usually labelled  $U(1)_\chi$ ,  $U(1)_\psi$ , and  $U(1)_\eta$ , respectively. Under the third set,  $U(1)_{d-xu}$ , the weak-doublet quarks are neutral, and the ratio of  $u_R$  and  $d_R$  charges is  $-x$ . For  $x = 1$  this is the “right-handed” group  $U(1)_R$ . For  $x = 0$ , the charges are those of the  $E_6$ -inspired  $U(1)_I$  group, which requires new quarks and leptons. Other generation-independent sets of  $U(1)'$  charges are given in [5].

**Table 2:** Lepton-flavor dependent charges under various  $U(1)$  gauge groups. No new fermions other than right-handed neutrinos are required.

fermion	$B - xL_e - yL_\mu$	2+1 leptocratic
$q_{1L}, q_{2L}, q_{3L}$	1/3	1/3
$u_R, c_R, t_R$	1/3	$x/3$
$d_R, s_R, b_R$	1/3	$(2 - x)/3$
$(\nu_L^e, e_L)$	$-x$	$-1 - 2y$
$(\nu_L^\mu, \mu_L)$	$-y$	$-1 + y$
$(\nu_L^\tau, \tau_L)$	$x + y - 3$	$-1 + y$
$e_R$	$-x$	$-(2 + x)/3 - 2y$
$\mu_R$	$-y$	$-(2 + x)/3 + y$
$\tau_R$	$x + y - 3$	$-(2 + x)/3 + y$

In the absence of new fermions charged under the Standard Model group, the most general generation-independent charge assignment is  $U(1)_{q+xu}$ , which is a linear combination of hypercharge and  $B - L$ . Many other anomaly-free solutions exist if generation-dependent charges are allowed. Table 2 shows such solutions that depend on two free parameters,  $x$  and  $y$ , with generation dependence only in the lepton sector, which includes one right-handed neutrino per generation. The charged-lepton masses may be generated by Yukawa couplings to a single Higgs doublet. These are forced to be flavor diagonal by the generation-dependent  $U(1)'$  charges, so that there are no tree-level flavor-changing neutral current (FCNC) processes involving electrically-charged leptons. For the “leptocratic” set, neutrino masses are induced by operators of high dimensionality that may explain their smallness [7].

If the  $SU(2)_W$ -doublet quarks have generation-dependent  $U(1)'$  charges, then the mass eigenstate quarks have flavor off-diagonal couplings to the  $Z'$  boson (see Eq. (1), and note that  $V_u^L (V_d^L)^\dagger$  is the CKM matrix). These are severely constrained by measurements of FCNC processes, which in this case are mediated at tree-level by  $Z'$  boson exchange [8]. The constraints are relaxed if the first and second generation charges are the same, although they are increasingly tightened by the measurements of  $B$  meson properties. If only the  $SU(2)_W$ -singlet quarks have generation-dependent  $U(1)'$  charges, there is more

freedom in adjusting the flavor off-diagonal couplings because the  $V_{u,d}^R$  matrices are not observable in the Standard Model.

The anomaly cancellation conditions for  $U(1)'$  could be relaxed only if at scales above  $\sim 4\pi M_{Z'}/g_z$  there is an axion which has certain dimension-5 couplings to the gauge bosons. However, such a scenario violates unitarity unless the quantum field theory description breaks down at a scale near  $M_{Z'}$  [9].

**Other models.**  $Z'$  bosons may also arise from larger gauge groups. These may be orthogonal to the electroweak group, as in  $SU(2)_W \times U(1)_Y \times SU(2)'$ , or may embed the electroweak group, as in  $SU(3)_W \times U(1)$  [10]. If the larger group is spontaneously broken down to  $SU(2)_W \times U(1)_Y \times U(1)'$  at a scale  $v_\star \gg M_{Z'}/g_z$ , then the above discussion applies up to corrections of order  $M_{Z'}^2/(g_z v_\star)^2$ . For  $v_\star \sim M_{Z'}/g_z$ , additional gauge bosons have masses comparable to  $M_{Z'}$ , including at least a  $W'$  boson [10]. If the larger gauge group breaks together with the electroweak symmetry directly to the electromagnetic  $U(1)_{em}$ , then the left-handed fermion charges are no longer correlated ( $z_u^L \neq z_d^L, z_\nu^L \neq z_e^L$ ) and a  $Z'W^+W^-$  coupling is induced.

If the electroweak gauge bosons propagate in extra dimensions, then their Kaluza-Klein excitations include a series of  $Z'$  boson pairs. Each of these pairs can be associated with a different  $SU(2) \times U(1)$  gauge group in four dimensions. The properties of the Kaluza-Klein particles depend strongly on the extra-dimensional theory [11]. For example, in universal extra dimensions there is a parity that forces all couplings of Eq. (1) to vanish in the case of the lightest Kaluza-Klein bosons, while allowing couplings to pairs of fermions involving a Standard Model one and a heavy vector-like fermion. There are also 4-dimensional gauge theories (*e.g.*, little Higgs with  $T$  parity) with  $Z'$  bosons exhibiting similar properties. By contrast, in a warped extra dimension, the couplings of Eq. (1) may be sizable even when Standard Model fields propagate along the extra dimension.

$Z'$  bosons may also be composite particles. For example, in technicolor theories [12], the techni- $\rho$  is a spin-1 boson that may be interpreted as arising from a spontaneously broken gauge symmetry [13].

**Resonances versus cascade decays.** In the presence of the couplings shown in Eq. (1), the  $Z'$  boson may be produced in the  $s$ -channel at colliders, and would decay to pairs of fermions. The decay width into a pair of electrons is given by

$$\Gamma(Z' \rightarrow e^+e^-) \simeq \left[ (g_e^L)^2 + (g_e^R)^2 \right] \frac{M_{Z'}}{24\pi}, \quad (4)$$

where small corrections from electroweak loops are not included. The decay width into  $q\bar{q}$  is similar, except for an additional color factor of 3, QCD radiative corrections, and fermion mass corrections. Thus, one may compute the  $Z'$  branching fractions in terms of the couplings of Eq. (1). However, other decay channels, such as  $WW$  or a pair of new particles, could have large widths and need to be added to the total decay width.

# Gauge & Higgs Boson Particle Listings

## Heavy Bosons Other than Higgs Bosons

As mentioned above, there are theories in which the  $Z'$  couplings are controlled by a discrete symmetry which does not allow its decay into a pair of Standard Model particles. Typically, such theories involve several new particles, which may be produced only in pairs and undergo cascade decays through  $Z'$  bosons, leading to signals involving some missing (transverse) energy. Given that the cascade decays depend on the properties of new particles other than  $Z'$ , this case is not discussed further here.

**LEP-II limits.** The  $Z'$  contribution to the cross sections for  $e^+e^- \rightarrow f\bar{f}$  proceeds through an  $s$ -channel  $Z'$  exchange (when  $f = e$ , there are also  $t$ - and  $u$ -channel exchanges). For  $M_{Z'} < \sqrt{s}$ , the  $Z'$  appears as an  $f\bar{f}$  resonance in the radiative return process where photon emission tunes the effective center-of-mass energy to  $M_{Z'}$ . The agreement between the LEP-II measurements and the Standard Model predictions implies that either the  $Z'$  couplings are smaller than or of order  $10^{-2}$ , or else  $M_{Z'}$  is above 209 GeV, the maximum energy of LEP-II. In the latter case, the  $Z'$  effects may be approximated up to corrections of order  $s/M_{Z'}^2$ , by the contact interactions

$$\frac{g_z^2}{M_{Z'}^2 - s} [\bar{e}\gamma_\mu (z_e^L P_L + z_e^R P_R) e] [\bar{f}\gamma^\mu (z_f^L P_L + z_f^R P_R) f] \quad , \quad (5)$$

where  $P_{L,R}$  are chirality projection operators, and the relation between  $Z'$  couplings and charges (see Eq. (2) in the limit where the mass and kinetic mixings are neglected) was used assuming generation-independent charges. The four LEP collaborations have set limits on the coefficients of such operators for all possible chiral structures and for various combinations of fermions [14]. Thus, one may derive bounds on  $(M_{Z'}/g_z)|z_e^L z_f^L|^{-1/2}$  and the analogous combinations of  $LR$ ,  $RL$  and  $RR$  charges, which are typically on the order of a few TeV. LEP-II limits were derived in Ref. [4] on the four sets of charges shown in Table 1.

Somewhat stronger bounds could be set on  $M_{Z'}/g_z$  for specific sets of  $Z'$  couplings if the effects of several operators from Eq. (5) are combined. Dedicated analyses by the LEP collaborations have set limits on  $Z'$  bosons for particular values of the gauge coupling (see section 3.5.2 of [14]).

**Searches at hadron colliders.**  $Z'$  bosons with couplings to quarks (see Eq. (1)) may be produced at hadron colliders in the  $s$  channel, and would show up as resonances in the invariant mass distribution of the decay products. The cross section for producing a  $Z'$  boson at the LHC which then decays to some  $f\bar{f}$  final state takes the form

$$\sigma(pp \rightarrow Z'X \rightarrow f\bar{f}X) \simeq \frac{\pi}{48s} \sum_q c_q^f w_q(s, M_{Z'}^2) \quad (6)$$

for flavor-diagonal couplings to quarks. Here we have neglected the interference with the Standard Model contribution to  $f\bar{f}$  production, which is a good approximation for a narrow  $Z'$  resonance. The coefficients

$$c_q^f = \left[ (g_q^L)^2 + (g_q^R)^2 \right] B(Z' \rightarrow f\bar{f}) \quad (7)$$

contain all the dependence on the  $Z'$  couplings, while the functions  $w_q$  include all the information about parton distributions and QCD corrections [4,5]. This factorization holds exactly to NLO, and the deviations from it induced at NNLO are very small. Note that the  $w_u$  and  $w_d$  functions are substantially larger than the  $w_q$  functions for the other quarks. Eq. (6) also applies to the Tevatron, except for changing the  $pp$  initial state to  $p\bar{p}$ , which implies that the  $w_q(s, M_{Z'}^2)$  functions are replaced by some other functions  $\bar{w}_q((1.96 \text{ TeV})^2, M_{Z'}^2)$ .

It is common to present results of  $Z'$  searches as limits on the cross section versus  $M_{Z'}$  (*e.g.*, see Fig. 1). An alternative is to plot exclusion curves for fixed  $M_{Z'}$  values in the  $c_u^f - c_d^f$  planes, allowing a simple derivation of the mass limit within any  $Z'$  model. LHC limits in the  $c_u^\ell - c_d^\ell$  plane ( $\ell = e$  or  $\mu$ ) for different  $M_{Z'}$  are shown in Fig. 2 (for Tevatron limits, see [15]).

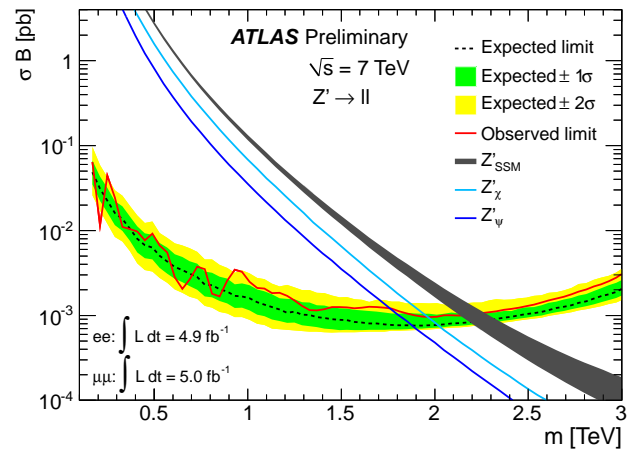


**Figure 1:** Upper limit on  $\sigma(pp \rightarrow Z'X \rightarrow \ell^+\ell^-X)$  with  $\ell = e$  or  $\mu$  as a function of  $M_{Z'}$  [27], assuming equal couplings for electrons and muons. The lines labelled by  $Z'_\psi$  and  $Z'_\chi$  are theoretical predictions for the  $U(1)_{10+x5}$  models in Table 1 with  $x = -3$  and  $x = +1$ , respectively, for  $g_z$  fixed by an  $E_6$  unification condition. The  $Z'_{\text{SSM}}$  line corresponds to  $Z'$  couplings equal to those of the  $Z$  boson.

The observation of a dilepton resonance at the LHC would determine the  $Z'$  mass and width. A measurement of the total cross section would define a band in the  $c_u^\ell - c_d^\ell$  plane. Angular distributions can be used to measure several combinations of  $Z'$  parameters (an example of how angular distributions improve the Tevatron sensitivity is given in [16]). Even though the original quark direction in a  $pp$  collider is unknown, the leptonic forward-backward asymmetry  $A_{\text{FB}}^\ell$  can be extracted from the kinematics of the dilepton system, and is sensitive to parity-violating couplings. A fit to the  $Z'$  rapidity distribution can distinguish between the couplings to up and down quarks. These measurements, combined with off-peak observables, have the potential to differentiate among various  $Z'$  models [17]. For example, the couplings of a  $Z'$  boson with mass below 1.5 TeV

can be well determined with  $100 \text{ fb}^{-1}$  of data at  $\sqrt{s} = 14 \text{ TeV}$ . With this amount of data, the spin of the  $Z'$  boson may be determined for  $M_{Z'} \leq 3 \text{ TeV}$  [18], and the expected sensitivity extends to  $M_{Z'} \sim 5 - 6 \text{ TeV}$  for many models [19].

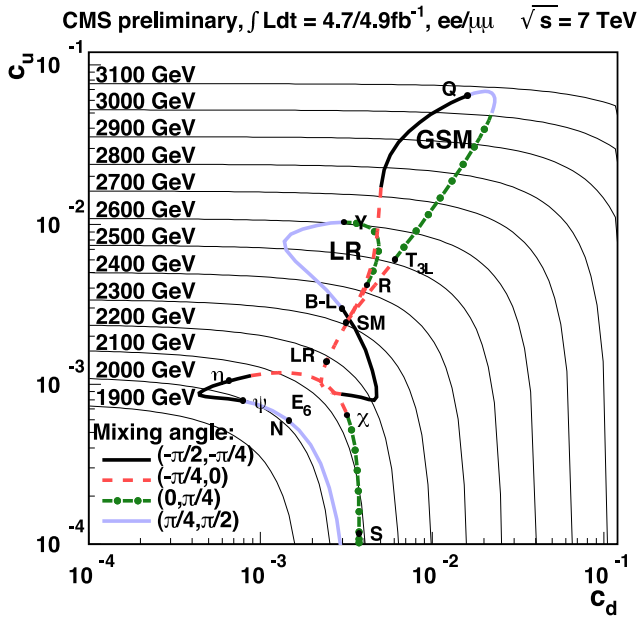


**Figure 2:** CMS results from Ref. 35. Limits in the  $c_d^e - c_d^\mu$  plane ( $\ell = e$  or  $\mu$ ) are shown as thin lines for certain  $M_{Z'}$  values. For specific sets of charges (described in Ref. 5), parametrized by a mixing angle, the mass limit is given by the intersection of the thick and thin lines.

The  $Z'$  decays into  $e^+e^-$  and  $\mu^+\mu^-$  are useful due to relatively good mass resolution and large acceptance. The  $Z'$  decays into  $e\mu$  and  $\tau^+\tau^-$ , along with  $t\bar{t}$ ,  $b\bar{b}$  and  $jj$  which suffer from larger backgrounds, are also important as they probe various combinations of  $Z'$  couplings to fermions.

$Z'$  searches at the Tevatron have been performed by the CDF and DØ Collaborations in the  $e^+e^-$  [20],  $\mu^+\mu^-$  [21],  $e\mu$  [22],  $\tau^+\tau^-$  [23],  $t\bar{t}$  [24],  $jj$  [25] and  $WW$  [26] final states. At the 7 TeV LHC, the ATLAS and CMS Collaborations have searched for  $Z'$  bosons in the  $e^+e^-$  and  $\mu^+\mu^-$  channels [27,28], as well as in the  $e\mu$  [29],  $\tau^+\tau^-$  [30],  $t\bar{t}$  [31] and  $jj$  [32] final states. The  $pp \rightarrow Z'X \rightarrow W^+W^-X$  process may also be explored at the LHC, and is important for disentangling the origin of electroweak symmetry breaking. The  $Z'$  boson may be produced in this process through its couplings to either quarks [33] or  $W$  bosons [34].

**Low-energy constraints.**  $Z'$  boson properties are also constrained by a variety of low-energy experiments [36]. Polarized electron-nucleon scattering and atomic parity violation are sensitive to electron-quark contact interactions, which get contributions from  $Z'$  exchange that can be expressed in terms of the couplings introduced in Eq. (1) and  $M_{Z'}$ . Further corrections to the electron-quark contact interactions are induced in

the presence of  $\tilde{Z} - \tilde{Z}'$  mixing because of the shifts in the  $Z$  couplings to quarks and leptons [2]. Deep-inelastic neutrino-nucleon scattering is similarly affected by  $Z'$  bosons. Other low-energy observables are discussed in [3]. Interestingly, due to the  $\tilde{Z} - \tilde{Z}'$  mixing, the global fit in  $Z'$  models often prefers a higher Higgs mass than in the Standard Model [37]. In some models, the lower limits on  $M_{Z'}$  set by the low energy data are above 1 TeV [3].

Although the LHC data are most constraining for many  $Z'$  models, one should be careful in assessing the relative reach of various experiments given the freedom in  $Z'$  couplings. For example, a  $Z'$  associated with the  $U(1)_{B-xL_e-yL_\mu}$  model (see Table 2) for  $x = 0$  and  $y \gg 1$  couples only to leptons of the second and third generations, with implications for the muon  $g - 2$ , neutrino oscillations or  $\tau$  decays, and would be hard to see in processes involving first-generation fermions. Moreover, the combination of LHC searches and low-energy measurements could allow a precise determination of the  $Z'$  parameters [38].

## References

1. For reviews, see P. Langacker, Rev. Mod. Phys. **81**, 1199 (2009); A. Leike, Phys. Rept. **317**, 143 (1999); J. Hewett and T. Rizzo, Phys. Rept. **183**, 193 (1989).
2. K.S. Babu, C. Kolda, and J. March-Russell, Phys. Rev. **D57**, 6788 (1998); B. Holdom, Phys. Lett. **B259**, 329 (1991).
3. J. Erler *et al.*, JHEP **0908**, 017 (2009).
4. M.S. Carena *et al.*, Phys. Rev. **D70**, 093009 (2004).
5. E. Accomando *et al.* Phys. Rev. **D83**, 075012 (2011).
6. See, *e.g.*, F. Del Aguila, M. Cvetič, and P. Langacker, Phys. Rev. **D52**, 37 (1995).
7. M.-C. Chen, A. de Gouvêa, and B.A. Dobrescu, Phys. Rev. **D75**, 055009 (2007).
8. P. Langacker and M. Plumacher, Phys. Rev. **D62**, 013006 (2000); R.S. Chivukula and E.H. Simmons, Phys. Rev. **D66**, 015006 (2002).
9. L.E. Ibanez and G.G. Ross, Phys. Lett. B **332**, 100 (1994).
10. See the Section on “ $W'$  searches” in this Review.
11. J. Parsons and A. Pomarol, “Extra dimensions” in this Review.
12. R.S. Chivukula, M. Narain, and J. Womersley, “Dynamical electroweak symmetry breaking” in this Review.
13. M. Bando, T. Kugo, and K. Yamawaki, Phys. Rept. **164**, 217 (1988).
14. J. Alcaraz *et al.* [ALEPH, DELPHI, L3, OPAL Collabs., LEP Electroweak Working Group], hep-ex/0612034.
15. A. Abulencia *et al.* [CDF Collab.], Phys. Rev. Lett. **95**, 252001 (2005).
16. A. Abulencia *et al.* [CDF Collab.], Phys. Rev. Lett. **96**, 211801 (2006).
17. F. Petriello and S. Quackenbush, Phys. Rev. **D77**, 115004 (2008).
18. P. Osland *et al.*, Phys. Rev. **D79**, 115021 (2009).
19. G.L. Bayatian *et al.* [CMS Collab.], J. Phys. G **G34**, 995-1579 (2007).
20. V. M. Abazov *et al.* [D0 Collab.], Phys. Lett. **B695**, 88 (2011); T. Aaltonen *et al.* [CDF Collab.], Phys. Rev. Lett. **102**, 031801 (2009).

# Gauge & Higgs Boson Particle Listings

## Heavy Bosons Other than Higgs Bosons

21. CDF Collab., note 10165, May 2010; DØ Collab., note 4577-Conf, Aug. 2004.
22. A. Abulencia *et al.* [CDF Collab.], Phys. Rev. Lett. **96**, 211802 (2006); V. M. Abazov *et al.* [D0 Collab.], Phys. Rev. Lett. **105**, 191802 (2010).
23. D. Acosta *et al.* [CDF Collab.], Phys. Rev. Lett. **95**, 131801 (2005).
24. T. Aaltonen *et al.* [CDF Collab.], Phys. Rev. D **84**, 072004 (2011); V. M. Abazov *et al.* [D0 Collab.], Phys. Rev. D **85**, 051101 (2012).
25. T. Aaltonen *et al.* [CDF Collab.], Phys. Rev. **D79**, 112002 (2009).
26. V. M. Abazov *et al.* [D0 Collab.], Phys. Rev. Lett. **107**, 011801 (2011); T. Aaltonen *et al.* [CDF Collab.], Phys. Rev. Lett. **104**, 241801 (2010).
27. ATLAS Collab., note ATLAS-CONF-2012-007, Mar. 2012.
28. CMS Collab., note CMS-PAS-EXO-11-019, July 2011, updated Mar. 2012: <https://twiki.cern.ch/twiki/bin/view/CMSPublic/PhysicsResultsEXO11019Winter2012>.
29. G. Aad *et al.* [ATLAS Collab.], arXiv:1109.3089.
30. CMS Collab., note CMS-PAS-EXO-10-022, July 2011, updated Mar. 2012: <https://twiki.cern.ch/twiki/bin/view/CMSPublic/PhysicsResultsEXO11031>.
31. ATLAS Collab., note ATLAS-CONF-2012-029, Mar. 2012; note ATLAS-CONF-2011-123, Aug. 2011; S. Chatrchyan *et al.* [CMS Collab.], arXiv:1204.2488; [hep-ex]; CMS Collab., note CMS-PAS-EXO-11-055, Aug. 2011.
32. S. Chatrchyan *et al.* [CMS Collab.], Phys. Lett. B **704**, 123 (2011).
33. A. Alves *et al.*, Phys. Rev. **D80**, 073011 (2009).
34. H. J. He *et al.*, Phys. Rev. **D78**, 031701 (2008).
35. S. Chatrchyan *et al.* [CMS Collab.], JHEP **1105**, 093 (2011), and the Mar. 2012 update in Ref. 28.
36. See, e.g., V.D. Barger *et al.*, Phys. Rev. **D57**, 391 (1998); J. Erler, M.J. Ramsey-Musolf, Prog. Part. Nucl. Phys. **54**, 351 (2005).
37. M. S. Chanowitz, arXiv:0806.0890.
38. Y. Li, F. Petriello, and S. Quackenbush, Phys. Rev. D **80**, 055018 (2009).

### MASS LIMITS for $Z'$ (Heavy Neutral Vector Boson Other Than $Z$ )

#### Limits for $Z'_{SM}$

$Z'_{SM}$  is assumed to have couplings with quarks and leptons which are identical to those of  $Z$ , and decays only to known fermions. The most recent preliminary results can be found in the "Z'-boson searches" review above.

VALUE (GeV)	CL%	DOCUMENT ID	TECN	COMMENT
>1830	95	53 AAD	11AD ATLS	$pp; Z'_{SM} \rightarrow e^+e^-, \mu^+\mu^-$
>1500	95	54 CHEUNG	01B RVUE	Electroweak
>1048	95	55 AAD	11J ATLS	$pp, Z'_{SM} \rightarrow e^+e^-, \mu^+\mu^-$
>1071	95	56 AALTONEN	11i CDF	$p\bar{p}; Z'_{SM} \rightarrow \mu^+\mu^-$
>1023	95	57 ABZOV	11A D0	$p\bar{p}; Z'_{SM} \rightarrow e^+e^-$
>1140	95	58 CHATRCHYAN	11 CMS	$pp, Z'_{SM} \rightarrow e^+e^-, \mu^+\mu^-$
none 247-544	95	59 AALTONEN	10N CDF	$Z' \rightarrow WW$
none 320-740	95	60 AALTONEN	09AC CDF	$Z' \rightarrow q\bar{q}$
> 963	95	57 AALTONEN	09T CDF	$p\bar{p}; Z'_{SM} \rightarrow e^+e^-$
>1030	95	61 AALTONEN	09V CDF	$p\bar{p}; Z'_{SM} \rightarrow \mu^+\mu^-$
>1403	95	62 ERLER	09 RVUE	Electroweak
> 923	95	57 AALTONEN	07H CDF	Repl. by AALTONEN 09T
>1305	95	63 ABDALLAH	06C DLPH	$e^+e^-$
> 850	95	57 ABULENCIA	06L CDF	Repl. by AALTONEN 07H
> 825	95	64 ABULENCIA	05A CDF	$p\bar{p}; Z'_{SM} \rightarrow e^+e^-, \mu^+\mu^-$

> 399	95	65 ACOSTA	05R CDF	$p\bar{p}; Z'_{SM} \rightarrow \tau^+\tau^-$
none 400-640	95	ABAZOV	04C D0	$p\bar{p}; Z'_{SM} \rightarrow q\bar{q}$
>1018	95	66 ABBIENDI	04G OPAL	$e^+e^-$
> 670	95	67 ABZOV	01B D0	$p\bar{p}; Z'_{SM} \rightarrow e^+e^-$
> 710	95	68 ABREU	00s DLPH	$e^+e^-$
> 898	95	69 BARATE	00i ALEP	$e^+e^-$
> 809	95	70 ERLER	99 RVUE	Electroweak
> 690	95	71 ABE	97s CDF	$p\bar{p}; Z'_{SM} \rightarrow e^+e^-, \mu^+\mu^-$
> 490	95	ABACHI	96D D0	$p\bar{p}; Z'_{SM} \rightarrow e^+e^-$
> 398	95	72 VILAIN	94B CHM2	$\nu_\mu e \rightarrow \nu_\mu e$ and $\bar{\nu}_\mu e \rightarrow \bar{\nu}_\mu e$
> 237	90	73 ALITTI	93 UA2	$p\bar{p}; Z'_{SM} \rightarrow q\bar{q}$
none 260-600	95	74 RIZZO	93 RVUE	$p\bar{p}; Z'_{SM} \rightarrow q\bar{q}$
> 426	90	75 ABE	90F VNS	$e^+e^-$
53 AAD 11AD search for resonances decaying to $e^+e^-, \mu^+\mu^-$ in $pp$ collisions at $\sqrt{s} = 7$ TeV.				
54 CHEUNG 01B limit is derived from bounds on contact interactions in a global electroweak analysis.				
55 AAD 11J search for resonances decaying to $e^+e^-$ or $\mu^+\mu^-$ in $pp$ collisions at $\sqrt{s} = 7$ TeV.				
56 AALTONEN 11i search for resonances decaying to $\mu^+\mu^-$ in $p\bar{p}$ collisions at $\sqrt{s} = 1.96$ TeV.				
57 ABZOV 11A, AALTONEN 09T, AALTONEN 07H, and ABULENCIA 06L search for resonances decaying to $e^+e^-$ in $p\bar{p}$ collisions at $\sqrt{s} = 1.96$ TeV.				
58 CHATRCHYAN 11 search for resonances decaying to $e^+e^-$ or $\mu^+\mu^-$ in $pp$ collisions at $\sqrt{s} = 7$ TeV.				
59 The quoted limit assumes $g_{WWZ'}/g_{WWZ} = (M_{W'}/M_Z)^2$ . See their Fig. 4 for limits in mass-coupling plane.				
60 AALTONEN 09AC search for new particle decaying to dijets.				
61 AALTONEN 09V search for resonances decaying to $\mu^+\mu^-$ in $p\bar{p}$ collisions at $\sqrt{s} = 1.96$ TeV.				
62 ERLER 09 give 95% CL limit on the $Z$ - $Z'$ mixing $-0.0026 < \theta < 0.0006$ .				
63 ABDALLAH 06C use data $\sqrt{s} = 130-207$ GeV.				
64 ABULENCIA 05A search for resonances decaying to electron or muon pairs in $p\bar{p}$ collisions at $\sqrt{s} = 1.96$ TeV.				
65 ACOSTA 05R search for resonances decaying to tau lepton pairs in $p\bar{p}$ collisions at $\sqrt{s} = 1.96$ TeV.				
66 ABBIENDI 04G give 95% CL limit on $Z$ - $Z'$ mixing $-0.00422 < \theta < 0.00091$ . $\sqrt{s} = 91$ to 207 GeV.				
67 ABZOV 01B search for resonances in $p\bar{p} \rightarrow e^+e^-$ at $\sqrt{s}=1.8$ TeV. They find $\sigma \cdot B(Z' \rightarrow ee) < 0.06$ pb for $M_{Z'} > 500$ GeV.				
68 ABREU 00s uses LEP data at $\sqrt{s}=90$ to 189 GeV.				
69 BARATE 00i search for deviations in cross section and asymmetries in $e^+e^- \rightarrow$ fermions at $\sqrt{s}=90$ to 183 GeV. Assume $\theta=0$ . Bounds in the mass-mixing plane are shown in their Figure 18.				
70 ERLER 99 give 90%CL limit on the $Z$ - $Z'$ mixing $-0.0041 < \theta < 0.0003$ . $\rho_0=1$ is assumed.				
71 ABE 97s find $\sigma(Z') \times B(e^+e^-, \mu^+\mu^-) < 40$ fb for $M_{Z'} > 600$ GeV at $\sqrt{s}=1.8$ TeV.				
72 VILAIN 94B assume $m_t = 150$ GeV.				
73 ALITTI 93 search for resonances in the two-jet invariant mass. The limit assumes $B(Z' \rightarrow q\bar{q})=0.7$ . See their Fig. 5 for limits in the $m_{Z'}-B(q\bar{q})$ plane.				
74 RIZZO 93 analyses CDF limit on possible two-jet resonances.				
75 ABE 90F use data for $R, R_{\ell\ell}$ , and $A_{\ell\ell}$ . They fix $m_{W'} = 80.49 \pm 0.43 \pm 0.24$ GeV and $m_{Z'} = 91.13 \pm 0.03$ GeV.				

#### Limits for $Z'_{LR}$

$Z'_{LR}$  is the extra neutral boson in left-right symmetric models.  $g_L = g_R$  is assumed unless noted. Values in parentheses assume stronger constraint on the Higgs sector, usually motivated by specific left-right symmetric models (see the Note on the  $W'$ ). Values in brackets are from cosmological and astrophysical considerations and assume a light right-handed neutrino. Direct search bounds assume decays to Standard Model fermions only, unless noted.

VALUE (GeV)	CL%	DOCUMENT ID	TECN	COMMENT
>1162	95	76 DEL-AGUILA	10 RVUE	Electroweak
> 630	95	77 ABE	97s CDF	$p\bar{p}; Z'_{LR} \rightarrow e^+e^-, \mu^+\mu^-$
••• We do not use the following data for averages, fits, limits, etc. •••				
> 998	95	78 ERLER	09 RVUE	Electroweak
> 600	95	SCHAEEL	07A ALEP	$e^+e^-$
> 455	95	79 ABDALLAH	06C DLPH	$e^+e^-$
> 518	95	80 ABBIENDI	04G OPAL	$e^+e^-$
> 860	95	81 CHEUNG	01B RVUE	Electroweak
> 380	95	82 ABREU	00s DLPH	$e^+e^-$
> 436	95	83 BARATE	00i ALEP	Repl. by SCHAEEL 07A
> 550	95	84 CHAY	00 RVUE	Electroweak
		85 ERLER	00 RVUE	Cs
		86 CASALBUONI	99 RVUE	Cs
(> 1205)	90	87 CZAKON	99 RVUE	Electroweak
> 564	95	88 ERLER	99 RVUE	Electroweak
> 1673)	95	89 ERLER	99 RVUE	Electroweak
(> 1700)	68	90 BARENBOIM	98 RVUE	Electroweak
> 244	95	91 CONRAD	98 RVUE	$\nu_\mu N$ scattering
> 253	95	92 VILAIN	94B CHM2	$\nu_\mu e \rightarrow \nu_\mu e$ and $\bar{\nu}_\mu e \rightarrow \bar{\nu}_\mu e$
none 200-600	95	93 RIZZO	93 RVUE	$p\bar{p}; Z'_{LR} \rightarrow q\bar{q}$
[> 2000]		WALKER	91 COSM	Nucleosynthesis; light $\nu_R$
none 200-500		94 GRIFOLS	90 ASTR	SN 1987A; light $\nu_R$
none 350-2400		95 BARBIERI	89B ASTR	SN 1987A; light $\nu_R$

See key on page 457

# Gauge & Higgs Boson Particle Listings

## Heavy Bosons Other than Higgs Bosons

- 76 DEL-AGUILA 10 give 95% CL limit on the  $Z$ - $Z'$  mixing  $-0.0012 < \theta < 0.0004$ .
- 77 ABE 97s find  $\sigma(Z') \times B(e^+e^-, \mu^+\mu^-) < 40$  fb for  $m_{Z'} > 600$  GeV at  $\sqrt{s} = 1.8$  TeV.
- 78 ERLER 09 give 95% CL limit on the  $Z$ - $Z'$  mixing  $-0.0013 < \theta < 0.0006$ .
- 79 ABDALLAH 06c give 95% CL limit  $|\theta| < 0.0028$ . See their Fig. 14 for limit contours in the mass-mixing plane.
- 80 ABBIENDI 04G give 95% CL limit on  $Z$ - $Z'$  mixing  $-0.00098 < \theta < 0.00190$ . See their Fig. 20 for the limit contour in the mass-mixing plane.  $\sqrt{s} = 91$  to 207 GeV.
- 81 CHEUNG 01B limit is derived from bounds on contact interactions in a global electroweak analysis.
- 82 ABREU 00s give 95% CL limit on  $Z$ - $Z'$  mixing  $|\theta| < 0.0018$ . See their Fig. 6 for the limit contour in the mass-mixing plane.  $\sqrt{s} = 90$  to 189 GeV.
- 83 BARATE 00i search for deviations in cross section and asymmetries in  $e^+e^- \rightarrow$  fermions at  $\sqrt{s} = 90$  to 183 GeV. Assume  $\theta = 0$ . Bounds in the mass-mixing plane are shown in their Figure 18.
- 84 CHAY 00 also find  $-0.0003 < \theta < 0.0019$ . For  $g_R$  free,  $m_{Z'} > 430$  GeV.
- 85 ERLER 00 discuss the possibility that a discrepancy between the observed and predicted values of  $Q_W(\text{Cs})$  is due to the exchange of  $Z'$ . The data are better described in a certain class of the  $Z'$  models including  $Z_{LR}$  and  $Z_\chi$ .
- 86 CASALBUONI 99 discuss the discrepancy between the observed and predicted values of  $Q_W(\text{Cs})$ . It is shown that the data are better described in a class of models including the  $Z_{LR}$  model.
- 87 CZAKON 99 perform a simultaneous fit to charged and neutral sectors. Assumes manifest left-right symmetric model. Finds  $|\theta| < 0.0042$ .
- 88 ERLER 99 give 90% CL limit on the  $Z$ - $Z'$  mixing  $-0.0009 < \theta < 0.0017$ .
- 89 ERLER 99 assumes 2 Higgs doublets, transforming as 10 of  $SO(10)$ , embedded in  $E_6$ .
- 90 BARENBOIM 98 also gives 68% CL limits on the  $Z$ - $Z'$  mixing  $-0.0005 < \theta < 0.0033$ . Assumes Higgs sector of minimal left-right model.
- 91 CONRAD 98 limit is from measurements at CCFR, assuming no  $Z$ - $Z'$  mixing.
- 92 VILAIN 94b assume  $m_t = 150$  GeV and  $\theta = 0$ . See Fig. 2 for limit contours in the mass-mixing plane.
- 93 RIZZO 93 analyses CDF limit on possible two-jet resonances.
- 94 GRIFOLS 90 limit holds for  $m_{\nu_R} \lesssim 1$  MeV. A specific Higgs sector is assumed. See also GRIFOLS 90D, RIZZO 91.
- 95 BARBIERI 89b limit holds for  $m_{\nu_R} \leq 10$  MeV. Bounds depend on assumed supernova core temperature.

### Limits for $Z_\chi$

$Z_\chi$  is the extra neutral boson in  $SO(10) \rightarrow SU(5) \times U(1)_\chi$ .  $g_\chi = e/\cos\theta_W$  is assumed unless otherwise stated. We list limits with the assumption  $\rho = 1$  but with no further constraints on the Higgs sector. Values in parentheses assume stronger constraint on the Higgs sector motivated by superstring models. Values in brackets are from cosmological and astrophysical considerations and assume a light right-handed neutrino.

VALUE (GeV)	CL%	DOCUMENT ID	TECN	COMMENT
>1640	95	96 AAD	11AD ATLS	$p\bar{p}; Z'_\chi \rightarrow e^+e^-, \mu^+\mu^-$
>1141	95	97 ERLER	09 RVUE	Electroweak
••• We do not use the following data for averages, fits, limits, etc. •••				
> 900	95	98 AAD	11j ATLS	$p\bar{p}; Z'_\chi \rightarrow e^+e^-, \mu^+\mu^-$
> 930	95	99 AALTONEN	11i CDF	$p\bar{p}; Z'_\chi \rightarrow \mu^+\mu^-$
> 903	95	100 ABAZOV	11A D0	$p\bar{p}; Z'_\chi \rightarrow e^+e^-$
>1022	95	101 DEL-AGUILA	10 RVUE	Electroweak
> 862	95	100 AALTONEN	09T CDF	$p\bar{p}; Z'_\chi \rightarrow e^+e^-$
> 892	95	102 AALTONEN	09V CDF	$p\bar{p}; Z'_\chi \rightarrow \mu^+\mu^-$
> 822	95	100 AALTONEN	07H CDF	Repl. by AALTONEN 09T
> 680	95	SCHAEEL	07A ALEP	$e^+e^-$
> 545	95	103 ABDALLAH	06C DLPH	$e^+e^-$
> 740	95	100 ABULENCIA	06L CDF	Repl. by AALTONEN 07H
> 690	95	104 ABULENCIA	05A CDF	$p\bar{p}; Z'_\chi \rightarrow e^+e^-, \mu^+\mu^-$
> 781	95	105 ABBIENDI	04G OPAL	$e^+e^-$
>2100	95	106 BARGER	03B COSM	Nucleosynthesis; light $\nu_R$
> 680	95	107 CHEUNG	01B RVUE	Electroweak
> 440	95	108 ABREU	00s DLPH	$e^+e^-$
> 533	95	109 BARATE	00i ALEP	Repl. by SCHAEEL 07A
> 554	95	110 CHO	00 RVUE	Electroweak
		111 ERLER	00 RVUE	Cs
		112 ROSNER	00 RVUE	Cs
> 545	95	113 ERLER	99 RVUE	Electroweak
(> 1368)	95	114 ERLER	99 RVUE	Electroweak
> 215	95	115 CONRAD	98 RVUE	$\nu_\mu N$ scattering
> 595	95	116 ABE	97s CDF	$p\bar{p}; Z'_\chi \rightarrow e^+e^-, \mu^+\mu^-$
> 190	95	117 ARIMA	97 VNS	Bhabha scattering
> 262	95	118 VILAIN	94b CHM2	$\nu_\mu e \rightarrow \nu_\mu e; \bar{\nu}_\mu e \rightarrow \bar{\nu}_\mu e$
[>1470]		119 FARAGGI	91 COSM	Nucleosynthesis; light $\nu_R$
> 231	90	120 ABE	90F VNS	$e^+e^-$
[> 1140]		121 GONZALEZ-G..90D	COSM	Nucleosynthesis; light $\nu_R$
[> 2100]		122 GRIFOLS	90 ASTR	SN 1987A; light $\nu_R$

- 96 AAD 11AD search for resonances decaying to  $e^+e^-, \mu^+\mu^-$  in  $p\bar{p}$  collisions at  $\sqrt{s} = 7$  TeV.
- 97 ERLER 09 give 95% CL limit on the  $Z$ - $Z'$  mixing  $-0.0016 < \theta < 0.0006$ .
- 98 AAD 11i search for resonances decaying to  $e^+e^-$  or  $\mu^+\mu^-$  in  $p\bar{p}$  collisions at  $\sqrt{s} = 7$  TeV.
- 99 AALTONEN 11i search for resonances decaying to  $\mu^+\mu^-$  in  $p\bar{p}$  collisions at  $\sqrt{s} = 1.96$  TeV.
- 100 ABAZOV 11A, AALTONEN 09T, AALTONEN 07H, and ABULENCIA 06L search for resonances decaying to  $e^+e^-$  in  $p\bar{p}$  collisions at  $\sqrt{s} = 1.96$  TeV.

- 101 DEL-AGUILA 10 give 95% CL limit on the  $Z$ - $Z'$  mixing  $-0.0011 < \theta < 0.0007$ .
- 102 AALTONEN 09v search for resonances decaying to  $\mu^+\mu^-$  in  $p\bar{p}$  collisions at  $\sqrt{s} = 1.96$  TeV.
- 103 ABDALLAH 06c give 95% CL limit  $|\theta| < 0.0031$ . See their Fig. 14 for limit contours in the mass-mixing plane.
- 104 ABULENCIA 05A search for resonances decaying to electron or muon pairs in  $p\bar{p}$  collisions at  $\sqrt{s} = 1.96$  TeV.
- 105 ABBIENDI 04G give 95% CL limit on  $Z$ - $Z'$  mixing  $-0.00099 < \theta < 0.00194$ . See their Fig. 20 for the limit contour in the mass-mixing plane.  $\sqrt{s} = 91$  to 207 GeV.
- 106 BARGER 03b limit is from the nucleosynthesis bound on the effective number of light neutrino  $\delta N_\nu < 1$ . The quark-hadron transition temperature  $T_C = 150$  MeV is assumed. The limit with  $T_C = 400$  MeV is  $> 4300$  GeV.
- 107 CHEUNG 01B limit is derived from bounds on contact interactions in a global electroweak analysis.
- 108 ABREU 00s give 95% CL limit on  $Z$ - $Z'$  mixing  $|\theta| < 0.0017$ . See their Fig. 6 for the limit contour in the mass-mixing plane.  $\sqrt{s} = 90$  to 189 GeV.
- 109 BARATE 00i search for deviations in cross section and asymmetries in  $e^+e^- \rightarrow$  fermions at  $\sqrt{s} = 90$  to 183 GeV. Assume  $\theta = 0$ . Bounds in the mass-mixing plane are shown in their Figure 18.
- 110 CHO 00 use various electroweak data to constrain  $Z'$  models assuming  $m_H = 100$  GeV. See Fig. 3 for limits in the mass-mixing plane.
- 111 ERLER 00 discuss the possibility that a discrepancy between the observed and predicted values of  $Q_W(\text{Cs})$  is due to the exchange of  $Z'$ . The data are better described in a certain class of the  $Z'$  models including  $Z_{LR}$  and  $Z_\chi$ .
- 112 ROSNER 00 discusses the possibility that a discrepancy between the observed and predicted values of  $Q_W(\text{Cs})$  is due to the exchange of  $Z'$ . The data are better described in a certain class of the  $Z'$  models including  $Z_\chi$ .
- 113 ERLER 99 give 90% CL limit on the  $Z$ - $Z'$  mixing  $-0.0020 < \theta < 0.0015$ .
- 114 ERLER 99 assumes 2 Higgs doublets, transforming as 10 of  $SO(10)$ , embedded in  $E_6$ .
- 115 CONRAD 98 limit is from measurements at CCFR, assuming no  $Z$ - $Z'$  mixing.
- 116 ABE 97s find  $\sigma(Z') \times B(e^+e^-, \mu^+\mu^-) < 40$  fb for  $m_{Z'} > 600$  GeV at  $\sqrt{s} = 1.8$  TeV.
- 117  $Z$ - $Z'$  mixing is assumed to be zero.  $\sqrt{s} = 57.77$  GeV.
- 118 VILAIN 94b assume  $m_t = 150$  GeV and  $\theta = 0$ . See Fig. 2 for limit contours in the mass-mixing plane.
- 119 FARAGGI 91 limit assumes the nucleosynthesis bound on the effective number of neutrinos  $\Delta N_\nu < 0.5$  and is valid for  $m_{\nu_R} < 1$  MeV.
- 120 ABE 90F use data for  $R, R_{\ell\ell}$ , and  $A_{\ell\ell}$ . ABE 90F fix  $m_W = 80.49 \pm 0.43 \pm 0.24$  GeV and  $m_Z = 91.13 \pm 0.03$  GeV.
- 121 Assumes the nucleosynthesis bound on the effective number of light neutrinos ( $\delta N_\nu < 1$ ) and that  $\nu_R$  is light ( $\lesssim 1$  MeV).
- 122 GRIFOLS 90 limit holds for  $m_{\nu_R} \lesssim 1$  MeV. See also GRIFOLS 90D, RIZZO 91.

### Limits for $Z_\psi$

$Z_\psi$  is the extra neutral boson in  $E_6 \rightarrow SO(10) \times U(1)_\psi$ .  $g_\psi = e/\cos\theta_W$  is assumed unless otherwise stated. We list limits with the assumption  $\rho = 1$  but with no further constraints on the Higgs sector. Values in brackets are from cosmological and astrophysical considerations and assume a light right-handed neutrino.

VALUE (GeV)	CL%	DOCUMENT ID	TECN	COMMENT
>1490	95	123 AAD	11AD ATLS	$p\bar{p}; Z'_\psi \rightarrow e^+e^-, \mu^+\mu^-$
> 476	95	124 DEL-AGUILA	10 RVUE	Electroweak
••• We do not use the following data for averages, fits, limits, etc. •••				
> 738	95	125 AAD	11j ATLS	$p\bar{p}; Z'_\psi \rightarrow e^+e^-, \mu^+\mu^-$
> 917	95	126 AALTONEN	11i CDF	$p\bar{p}; Z'_\psi \rightarrow \mu^+\mu^-$
> 891	95	127 ABAZOV	11A D0	$p\bar{p}; Z'_\psi \rightarrow e^+e^-$
> 887	95	128 CHATRCHYAN	11 CMS	$p\bar{p}; Z'_\psi \rightarrow e^+e^-, \mu^+\mu^-$
> 851	95	127 AALTONEN	09T CDF	$p\bar{p}; Z'_\psi \rightarrow e^+e^-$
> 878	95	129 AALTONEN	09V CDF	$p\bar{p}; Z'_\psi \rightarrow \mu^+\mu^-$
> 147	95	130 ERLER	09 RVUE	Electroweak
> 822	95	127 AALTONEN	07H CDF	Repl. by AALTONEN 09T
> 410	95	SCHAEEL	07A ALEP	$e^+e^-$
> 475	95	131 ABDALLAH	06C DLPH	$e^+e^-$
> 725	95	127 ABULENCIA	06L CDF	Repl. by AALTONEN 07H
> 675	95	132 ABULENCIA	05A CDF	$p\bar{p}; Z'_\psi \rightarrow e^+e^-, \mu^+\mu^-$
> 366	95	133 ABBIENDI	04G OPAL	$e^+e^-$
> 600	95	134 BARGER	03B COSM	Nucleosynthesis; light $\nu_R$
> 350	95	135 ABREU	00s DLPH	$e^+e^-$
> 294	95	136 BARATE	00i ALEP	Repl. by SCHAEEL 07A
> 137	95	137 CHO	00 RVUE	Electroweak
> 146	95	138 ERLER	99 RVUE	Electroweak
> 54	95	139 CONRAD	98 RVUE	$\nu_\mu N$ scattering
> 590	95	140 ABE	97s CDF	$p\bar{p}; Z'_\psi \rightarrow e^+e^-, \mu^+\mu^-$
> 135	95	141 VILAIN	94b CHM2	$\nu_\mu e \rightarrow \nu_\mu e; \bar{\nu}_\mu e \rightarrow \bar{\nu}_\mu e$
> 105	90	142 ABE	90F VNS	$e^+e^-$
[> 160]		143 GONZALEZ-G..90D	COSM	Nucleosynthesis; light $\nu_R$
[> 2000]		144 GRIFOLS	90D ASTR	SN 1987A; light $\nu_R$

- 123 AAD 11AD search for resonances decaying to  $e^+e^-, \mu^+\mu^-$  in  $p\bar{p}$  collisions at  $\sqrt{s} = 7$  TeV.
- 124 DEL-AGUILA 10 give 95% CL limit on the  $Z$ - $Z'$  mixing  $-0.0019 < \theta < 0.0007$ .
- 125 AAD 11i search for resonances decaying to  $e^+e^-$  or  $\mu^+\mu^-$  in  $p\bar{p}$  collisions at  $\sqrt{s} = 7$  TeV.
- 126 AALTONEN 11i search for resonances decaying to  $\mu^+\mu^-$  in  $p\bar{p}$  collisions at  $\sqrt{s} = 1.96$  TeV.
- 127 ABAZOV 11A, AALTONEN 09T, AALTONEN 07H, and ABULENCIA 06L search for resonances decaying to  $e^+e^-$  in  $p\bar{p}$  collisions at  $\sqrt{s} = 1.96$  TeV.

# Gauge & Higgs Boson Particle Listings

## Heavy Bosons Other than Higgs Bosons

- 128 CHATRCHYAN 11 search for resonances decaying to  $e^+e^-$  or  $\mu^+\mu^-$  in  $pp$  collisions at  $\sqrt{s} = 7$  TeV.
- 129 AALTONEN 09v search for resonances decaying to  $\mu^+\mu^-$  in  $p\bar{p}$  collisions at  $\sqrt{s} = 1.96$  TeV.
- 130 ERLER 09 give 95% CL limit on the  $Z$ - $Z'$  mixing  $-0.0018 < \theta < 0.0009$ .
- 131 ABDALLAH 06c give 95% CL limit  $|\theta| < 0.0027$ . See their Fig. 14 for limit contours in the mass-mixing plane.
- 132 ABULENCIA 05A search for resonances decaying to electron or muon pairs in  $p\bar{p}$  collisions at  $\sqrt{s} = 1.96$  TeV.
- 133 ABBIENDI 04G give 95% CL limit on  $Z$ - $Z'$  mixing  $-0.00129 < \theta < 0.00258$ . See their Fig. 20 for the limit contour in the mass-mixing plane.  $\sqrt{s} = 91$  to 207 GeV.
- 134 BARGER 03b limit is from the nucleosynthesis bound on the effective number of light neutrino  $\delta N_\nu < 1$ . The quark-hadron transition temperature  $T_C=150$  MeV is assumed. The limit with  $T_C=400$  MeV is  $>1100$  GeV.
- 135 ABREU 00s give 95% CL limit on  $Z$ - $Z'$  mixing  $|\theta| < 0.0018$ . See their Fig. 6 for the limit contour in the mass-mixing plane.  $\sqrt{s}=90$  to 189 GeV.
- 136 BARATE 00i search for deviations in cross section and asymmetries in  $e^+e^- \rightarrow$  fermions at  $\sqrt{s}=90$  to 183 GeV. Assume  $\theta=0$ . Bounds in the mass-mixing plane are shown in their Figure 18.
- 137 CHO 00 use various electroweak data to constrain  $Z'$  models assuming  $m_H=100$  GeV. See Fig. 3 for limits in the mass-mixing plane.
- 138 ERLER 99 give 90% CL limit on the  $Z$ - $Z'$  mixing  $-0.0013 < \theta < 0.0024$ .
- 139 CONRAD 98 limit is from measurements at CCFR, assuming no  $Z$ - $Z'$  mixing.
- 140 ABE 97s find  $\sigma(Z') \times B(e^+e^-, \mu^+\mu^-) < 40$  fb for  $m_{Z'} > 600$  GeV at  $\sqrt{s}=1.8$  TeV.
- 141 VILAIN 94B assume  $m_t = 150$  GeV and  $\theta=0$ . See Fig. 2 for limit contours in the mass-mixing plane.
- 142 ABE 90f use data for  $R$ ,  $R_{\ell\ell}$ , and  $A_{\ell\ell}$ . ABE 90f fix  $m_W = 80.49 \pm 0.43 \pm 0.24$  GeV and  $m_Z = 91.13 \pm 0.03$  GeV.
- 143 Assumes the nucleosynthesis bound on the effective number of light neutrinos ( $\delta N_\nu < 1$ ) and that  $\nu_R$  is light ( $\lesssim 1$  MeV).
- 144 GRIFOLS 90D limit holds for  $m_{\nu_R} \lesssim 1$  MeV. See also RIZZO 91.

### Limits for $Z_\eta$

$Z_\eta$  is the extra neutral boson in  $E_6$  models, corresponding to  $Q_\eta = \sqrt{3/8} Q_\chi - \sqrt{5/8} Q_\psi$ .  $g_\eta = e/\cos\theta_W$  is assumed unless otherwise stated. We list limits with the assumption  $\rho=1$  but with no further constraints on the Higgs sector. Values in parentheses assume stronger constraint on the Higgs sector motivated by superstring models. Values in brackets are from cosmological and astrophysical considerations and assume a light right-handed neutrino.

VALUE (GeV)	CL%	DOCUMENT ID	TECN	COMMENT
>1540	95	145 AAD	11AD ATLS	$pp$ ; $Z'_\eta \rightarrow e^+e^-, \mu^+\mu^-$
> 619	95	146 CHO	00 RVUE	Electroweak
••• We do not use the following data for averages, fits, limits, etc. •••				
> 771	95	147 AAD	11J ATLS	$pp$ ; $Z'_\eta \rightarrow e^+e^-, \mu^+\mu^-$
> 938	95	148 AALTONEN	11i CDF	$p\bar{p}$ ; $Z'_\eta \rightarrow \mu^+\mu^-$
> 923	95	149 ABAZOV	11A D0	$p\bar{p}$ ; $Z'_\eta \rightarrow e^+e^-$
> 488	95	150 DEL-AGUILA	10 RVUE	Electroweak
> 877	95	149 AALTONEN	09T CDF	$p\bar{p}$ ; $Z'_\eta \rightarrow e^+e^-$
> 904	95	151 AALTONEN	09v CDF	$p\bar{p}$ ; $Z'_\eta \rightarrow \mu^+\mu^-$
> 427	95	152 ERLER	09 RVUE	Electroweak
> 891	95	149 AALTONEN	07H CDF	Repl. by AALTONEN 09T
> 350	95	SCHAEEL	07A ALEP	$e^+e^-$
> 360	95	153 ABDALLAH	06c DLPH	$e^+e^-$
> 745	95	149 ABULENCIA	06L CDF	Repl. by AALTONEN 07H
> 720	95	154 ABULENCIA	05A CDF	$p\bar{p}$ ; $Z'_\eta \rightarrow e^+e^-, \mu^+\mu^-$
> 515	95	155 ABBIENDI	04G OPAL	$e^+e^-$
>1600	95	156 BARGER	03B COSM	Nucleosynthesis; light $\nu_R$
> 310	95	157 ABREU	00s DLPH	$e^+e^-$
> 329	95	158 BARATE	00i ALEP	Repl. by SCHAEEL 07A
> 365	95	159 ERLER	99 RVUE	Electroweak
> 87	95	160 CONRAD	98 RVUE	$\nu_\mu N$ scattering
> 620	95	161 ABE	97s CDF	$p\bar{p}$ ; $Z'_\eta \rightarrow e^+e^-, \mu^+\mu^-$
> 100	95	162 VILAIN	94B CHM2	$\nu_\mu e \rightarrow \nu_\mu e; \bar{\nu}_\mu e \rightarrow \bar{\nu}_\mu e$
> 125	90	163 ABE	90f VNS	$e^+e^-$
[> 820]	164	GONZALEZ-G.	90D COSM	Nucleosynthesis; light $\nu_R$
[> 3300]	165	GRIFOLS	90 ASTR	SN 1987A; light $\nu_R$
[> 1040]	164	LOPEZ	90 COSM	Nucleosynthesis; light $\nu_R$

- 145 AAD 11AD search for resonances decaying to  $e^+e^-$ ,  $\mu^+\mu^-$  in  $pp$  collisions at  $\sqrt{s} = 7$  TeV.
- 146 CHO 00 use various electroweak data to constrain  $Z'$  models assuming  $m_H=100$  GeV. See Fig. 3 for limits in the mass-mixing plane.
- 147 AAD 11j search for resonances decaying to  $e^+e^-$  or  $\mu^+\mu^-$  in  $pp$  collisions at  $\sqrt{s} = 7$  TeV.
- 148 AALTONEN 11i search for resonances decaying to  $\mu^+\mu^-$  in  $p\bar{p}$  collisions at  $\sqrt{s} = 1.96$  TeV.
- 149 ABAZOV 11A, AALTONEN 09T, AALTONEN 07H, and ABULENCIA 06L search for resonances decaying to  $e^+e^-$  in  $p\bar{p}$  collisions at  $\sqrt{s} = 1.96$  TeV.
- 150 DEL-AGUILA 10 give 95% CL limit on the  $Z$ - $Z'$  mixing  $-0.0023 < \theta < 0.0027$ .
- 151 AALTONEN 09v search for resonances decaying to  $\mu^+\mu^-$  in  $p\bar{p}$  collisions at  $\sqrt{s} = 1.96$  TeV.
- 152 ERLER 09 give 95% CL limit on the  $Z$ - $Z'$  mixing  $-0.0047 < \theta < 0.0021$ .
- 153 ABDALLAH 06c give 95% CL limit  $|\theta| < 0.0092$ . See their Fig. 14 for limit contours in the mass-mixing plane.
- 154 ABULENCIA 05A search for resonances decaying to electron or muon pairs in  $p\bar{p}$  collisions at  $\sqrt{s} = 1.96$  TeV.

- 155 ABBIENDI 04G give 95% CL limit on  $Z$ - $Z'$  mixing  $-0.00447 < \theta < 0.00331$ . See their Fig. 20 for the limit contour in the mass-mixing plane.  $\sqrt{s} = 91$  to 207 GeV.
- 156 BARGER 03b limit is from the nucleosynthesis bound on the effective number of light neutrino  $\delta N_\nu < 1$ . The quark-hadron transition temperature  $T_C=150$  MeV is assumed. The limit with  $T_C=400$  MeV is  $>3300$  GeV.
- 157 ABREU 00s give 95% CL limit on  $Z$ - $Z'$  mixing  $|\theta| < 0.0024$ . See their Fig. 6 for the limit contour in the mass-mixing plane.  $\sqrt{s}=90$  to 189 GeV.
- 158 BARATE 00i search for deviations in cross section and asymmetries in  $e^+e^- \rightarrow$  fermions at  $\sqrt{s}=90$  to 183 GeV. Assume  $\theta=0$ . Bounds in the mass-mixing plane are shown in their Figure 18.
- 159 ERLER 99 give 90% CL limit on the  $Z$ - $Z'$  mixing  $-0.0062 < \theta < 0.0011$ .
- 160 CONRAD 98 limit is from measurements at CCFR, assuming no  $Z$ - $Z'$  mixing.
- 161 ABE 97s find  $\sigma(Z') \times B(e^+e^-, \mu^+\mu^-) < 40$  fb for  $m_{Z'} > 600$  GeV at  $\sqrt{s}=1.8$  TeV.
- 162 VILAIN 94B assume  $m_t = 150$  GeV and  $\theta=0$ . See Fig. 2 for limit contours in the mass-mixing plane.
- 163 ABE 90f use data for  $R$ ,  $R_{\ell\ell}$ , and  $A_{\ell\ell}$ . ABE 90f fix  $m_W = 80.49 \pm 0.43 \pm 0.24$  GeV and  $m_Z = 91.13 \pm 0.03$  GeV.
- 164 These authors claim that the nucleosynthesis bound on the effective number of light neutrinos ( $\delta N_\nu < 1$ ) constrains  $Z'$  masses if  $\nu_R$  is light ( $\lesssim 1$  MeV).
- 165 GRIFOLS 90 limit holds for  $m_{\nu_R} \lesssim 1$  MeV. See also GRIFOLS 90D, RIZZO 91.

### Limits for other $Z'$

VALUE (GeV)	DOCUMENT ID	TECN	COMMENT
••• We do not use the following data for averages, fits, limits, etc. •••			
166	AAD 11H ATLS	$Z' \rightarrow e\mu$	
167	AAD 11Z ATLS	$Z' \rightarrow e\mu$	
168	AALTONEN 11AD CDF	$Z' \rightarrow t\bar{t}$	
169	AALTONEN 11AE CDF	$Z' \rightarrow t\bar{t}$	
170	CHATRCHYAN 11O CMS	$pp \rightarrow tt$	
171	AALTONEN 08D CDF	$Z' \rightarrow t\bar{t}$	
171	AALTONEN 08Y CDF	$Z' \rightarrow t\bar{t}$	
171	ABAZOV 08AA D0	$Z' \rightarrow t\bar{t}$	
172	ABULENCIA 06M CDF	$Z' \rightarrow e\mu$	
173	ABAZOV 04A D0	Repl. by ABAZOV 08AA	
174	BARGER 03B COSM	Nucleosynthesis; light $\nu_R$	
175	CHO 00	RVUE	$E_6$ -motivated
176	CHO 98	RVUE	$E_6$ -motivated
177	ABE 97G CDF	$Z' \rightarrow \bar{q}q$	

- 166 AAD 11H search for new particle with lepton flavor violating decay in  $pp$  collisions at  $\sqrt{s} = 7$  TeV. See their Fig. 3 for exclusion plot on the production cross section.
- 167 AAD 11Z search for new particle with lepton flavor violating decay in  $pp$  collisions at  $\sqrt{s} = 7$  TeV. See their Fig. 3 for limit on  $\sigma \cdot B$ .
- 168 Search for narrow resonance decaying to  $t\bar{t}$ . See their Fig. 4 for limit on  $\sigma \cdot B$ .
- 169 Search for narrow resonance decaying to  $t\bar{t}$ . See their Fig. 3 for limit on  $\sigma \cdot B$ .
- 170 CHATRCHYAN 11o search for same-sign top production in  $pp$  collisions induced by a hypothetical FCNC  $Z'$  at  $\sqrt{s} = 7$  TeV. See their Fig. 3 for limit in mass-coupling plane.
- 171 Search for narrow resonance decaying to  $t\bar{t}$ . See their Fig. 3 for limit on  $\sigma \cdot B$ .
- 172 ABULENCIA 06M search for new particle with lepton flavor violating decay at  $\sqrt{s} = 1.96$  TeV. See their Fig. 4 for an exclusion plot on a mass-coupling plane.
- 173 Search for narrow resonance decaying to  $t\bar{t}$ . See their Fig. 2 for limit on  $\sigma \cdot B$ .
- 174 BARGER 03b use the nucleosynthesis bound on the effective number of light neutrino  $\delta N_\nu$ . See their Figs. 4-5 for limits in general  $E_6$  motivated models.
- 175 CHO 00 use various electroweak data to constrain  $Z'$  models assuming  $m_H=100$  GeV. See Fig. 2 for limits in general  $E_6$ -motivated models.
- 176 CHO 98 study constraints on four-Fermi contact interactions obtained from low-energy electroweak experiments, assuming no  $Z$ - $Z'$  mixing.
- 177 Search for  $Z'$  decaying to dijets at  $\sqrt{s}=1.8$  TeV. For  $Z'$  with electromagnetic strength coupling, no bound is obtained.

### Indirect Constraints on Kaluza-Klein Gauge Bosons

Bounds on a Kaluza-Klein excitation of the  $Z$  boson or photon in  $d=1$  extra dimension. These bounds can also be interpreted as a lower bound on  $1/R$ , the size of the extra dimension. Unless otherwise stated, bounds assume all fermions live on a single brane and all gauge fields occupy the  $4+d$ -dimensional bulk. See also the section on "Extra Dimensions" in the "Searches" Listings in this Review.

VALUE (TeV)	CL%	DOCUMENT ID	TECN	COMMENT
••• We do not use the following data for averages, fits, limits, etc. •••				
> 4.7		178 MUECK	02 RVUE	Electroweak
> 3.3	95	179 CORNET	00 RVUE	$e\nu q q'$
>5000		180 DELGADO	00 RVUE	$\epsilon_K$
> 2.6	95	181 DELGADO	00 RVUE	Electroweak
> 3.3	95	182 RIZZO	00 RVUE	Electroweak
> 2.9	95	183 MARCIANO	99 RVUE	Electroweak
> 2.5	95	184 MASIP	99 RVUE	Electroweak
> 1.6	90	185 NATH	99 RVUE	Electroweak
> 3.4	95	186 STRUMIA	99 RVUE	Electroweak

- 178 MUECK 02 limit is  $2\sigma$  and is from global electroweak fit ignoring correlations among observables. Higgs is assumed to be confined on the brane and its mass is fixed. For scenarios of bulk Higgs, of brane-SU(2) $_L$ , bulk-U(1) $_Y$ , and of bulk-SU(2) $_L$ , brane-U(1) $_Y$ , the corresponding limits are  $> 4.6$  TeV,  $> 4.3$  TeV and  $> 3.0$  TeV, respectively.
- 179 Bound is derived from limits on  $e\nu q q'$  contact interaction, using data from HERA and the Tevatron.
- 180 Bound holds only if first two generations of quarks lives on separate branes. If quark mixing is not complex, then bound lowers to 400 TeV from  $\Delta m_K$ .
- 181 See Figs. 1 and 2 of DELGADO 00 for several model variations. Special boundary conditions can be found which permit KK states down to 950 GeV and that agree with the



See key on page 457

## Gauge & Higgs Boson Particle Listings

### Heavy Bosons Other than Higgs Bosons

measurement of  $Q_{WW}(Cs)$ . Quoted bound assumes all Higgs bosons confined to brane; placing one Higgs doublet in the bulk lowers bound to 2.3 TeV.

<sup>182</sup> Bound is derived from global electroweak analysis assuming the Higgs field is trapped on the matter brane. If the Higgs propagates in the bulk, the bound increases to 3.8 TeV.

<sup>183</sup> Bound is derived from global electroweak analysis but considering only presence of the KK  $W$  bosons.

<sup>184</sup> Global electroweak analysis used to obtain bound independent of position of Higgs on brane or in bulk.

<sup>185</sup> Bounds from effect of KK states on  $G_F$ ,  $\alpha$ ,  $M_W$ , and  $M_Z$ . Hard cutoff at string scale determined using gauge coupling unification. Limits for  $d=2,3,4$  rise to 3.5, 5.7, and 7.8 TeV.

<sup>186</sup> Bound obtained for Higgs confined to the matter brane with  $m_H=500$  GeV. For Higgs in the bulk, the bound increases to 3.5 TeV.

#### LEPTOQUARKS

Updated May 2012 by S. Rolli (US Department of Energy) and M. Tanabashi (Nagoya Univ.).

Leptoquarks are hypothetical particles carrying both baryon number (B) and lepton number (L). The possible quantum numbers of leptoquark states can be restricted by assuming that their direct interactions with the ordinary SM fermions are dimensionless and invariant under the standard model (SM) gauge group. Table 1 shows the list of all possible quantum numbers with this assumption [1]. The columns of  $SU(3)_C$ ,  $SU(2)_W$ , and  $U(1)_Y$  in Table 1 indicate the QCD representation, the weak isospin representation, and the weak hypercharge, respectively. The spin of a leptoquark state is taken to be 1 (vector leptoquark) or 0 (scalar leptoquark).

**Table 1:** Possible leptoquarks and their quantum numbers.

Spin	$3B+L$	$SU(3)_c$	$SU(2)_W$	$U(1)_Y$	Allowed coupling
0	-2	$\bar{3}$	1	1/3	$\bar{q}_L^c \ell_L$ or $\bar{u}_R^c e_R$
0	-2	$\bar{3}$	1	4/3	$\bar{d}_R^c e_R$
0	-2	$\bar{3}$	3	1/3	$\bar{q}_L^c \ell_L$
1	-2	$\bar{3}$	2	5/6	$\bar{q}_L^c \gamma^\mu e_R$ or $\bar{d}_R^c \gamma^\mu \ell_L$
1	-2	$\bar{3}$	2	-1/6	$\bar{u}_R^c \gamma^\mu \ell_L$
0	0	3	2	7/6	$\bar{q}_L e_R$ or $\bar{u}_R \ell_L$
0	0	3	2	1/6	$\bar{d}_R \ell_L$
1	0	3	1	2/3	$\bar{q}_L \gamma^\mu \ell_L$ or $\bar{d}_R \gamma^\mu e_R$
1	0	3	1	5/3	$\bar{u}_R \gamma^\mu e_R$
1	0	3	3	2/3	$\bar{q}_L \gamma^\mu \ell_L$

If we do not require leptoquark states to couple directly with SM fermions, different assignments of quantum numbers become possible [2,3].

Leptoquark states are expected to exist in various extensions of SM. The Pati-Salam model [4] is an example predicting the existence of a leptoquark state. Vector leptoquark states also exist in grand unification theories based on  $SU(5)$  [5],  $SO(10)$  [6], which includes Pati-Salam color  $SU(4)$ , and larger gauge groups. Scalar quarks in supersymmetric models with R-parity violation may also have leptoquark-type Yukawa couplings. The bounds on the leptoquark states can therefore be applied to constrain R-parity-violating supersymmetric models. Scalar leptoquarks are expected to exist at TeV scale in extended technicolor models [7,8] where leptoquark states appear as the bound states of techni-fermions. Compositeness of quarks

and leptons also provides examples of models which may have light leptoquark states [9].

Bounds on leptoquark states are obtained both directly and indirectly. Direct limits are from their production cross sections at colliders, while indirect limits are calculated from the bounds on the leptoquark-induced four-fermion interactions, which are obtained from low-energy experiments, or from collider experiments below threshold.

If a leptoquark couples to fermions belonging to more than a single generation in the mass eigenbasis of the SM fermions, it can induce four-fermion interactions causing flavor-changing neutral currents and lepton-family-number violations. The quantum number assignment of Table 1 allows several leptoquark states to couple to both left- and right-handed quarks simultaneously. Such leptoquark states are called non-chiral and may cause four-fermion interactions affecting the  $(\pi \rightarrow e\nu)/(\pi \rightarrow \mu\nu)$  ratio [10]. Non-chiral scalar leptoquarks also contribute to the muon anomalous magnetic moment [11,12]. Since indirect limits provide more stringent constraints on these types of leptoquarks, it is often assumed that a leptoquark state couples only to a single generation in a chiral interaction, for which indirect limits become much weaker. Additionally, this assumption gives strong constraints on concrete models of leptoquarks.

Leptoquark states which couple only to left- or right-handed quarks are called chiral leptoquarks. Leptoquark states which couple only to the first (second, third) generation are referred as the first- (second-, third-) generation leptoquarks. Refs. [13,14] give extensive lists of the bounds on the leptoquark-induced four-fermion interactions. For the isoscalar and vector leptoquarks  $S_0$  and  $V_0$ , for example, which couple with the first- (second-) generation left-handed quark, and the first-generation left-handed lepton, the bounds of Ref. 13 read  $\lambda^2 < 0.03 \times (M_{LQ}/300 \text{ GeV})^2$  for  $S_0$ , and  $\lambda^2 < 0.02 \times (M_{LQ}/300 \text{ GeV})^2$  for  $V_0$  ( $\lambda^2 < 5 \times (M_{LQ}/300 \text{ GeV})^2$  for  $S_0$ , and  $\lambda^2 < 3 \times (M_{LQ}/300 \text{ GeV})^2$  for  $V_0$ ) with  $\lambda$  being the leptoquark coupling strength. The  $e^+e^-$  experiments are sensitive to the indirect effects coming from  $t$ - and  $u$ -channel exchanges of leptoquarks in the  $e^+e^- \rightarrow q\bar{q}$  process. The HERA experiments give bounds on the leptoquark-induced four-fermion interaction. For detailed bounds obtained in this way, see the Boson Particle Listings for “Indirect Limits for Leptoquarks” and its references.

Collider experiments provide direct limits on the leptoquark states through limits on the pair- and single-production cross sections. The leading-order cross sections of the parton processes

$$q + \bar{q} \rightarrow LQ + \bar{L}\bar{Q}$$

$$g + g \rightarrow LQ + \bar{L}\bar{Q}$$

$$e + q \rightarrow LQ$$

(1)

# Gauge & Higgs Boson Particle Listings

## Heavy Bosons Other than Higgs Bosons

may be written as [15]

$$\begin{aligned}\hat{\sigma}_{\text{LO}}[q\bar{q} \rightarrow \text{LQ} + \overline{\text{LQ}}] &= \frac{2\alpha_s^2\pi}{27\hat{s}}\beta^3, \\ \hat{\sigma}_{\text{LO}}[gg \rightarrow \text{LQ} + \overline{\text{LQ}}] &= \frac{\alpha_s^2\pi}{96\hat{s}} \\ &\times \left[ \beta(41 - 31\beta^2) + (18\beta^2 - \beta^4 - 17) \log \frac{1+\beta}{1-\beta} \right], \\ \hat{\sigma}_{\text{LO}}[e\bar{q} \rightarrow \text{LQ}] &= \frac{\pi\lambda^2}{4}\delta(\hat{s} - M_{\text{LQ}}^2)\end{aligned}\quad (2)$$

for a scalar leptoquark. Here  $\sqrt{\hat{s}}$  is the invariant energy of the parton subprocess, and  $\beta \equiv \sqrt{1 - 4M_{\text{LQ}}^2/\hat{s}}$ . The leptoquark Yukawa coupling is given by  $\lambda$ . Leptoquarks are also produced singly at hadron colliders through  $g + q \rightarrow \text{LQ} + \ell$  [16], which allows extending to higher masses the collider reach in the leptoquark search [17], depending on the leptoquark Yukawa coupling.

The LHC, Tevatron and LEP experiments search for pair production of the leptoquark states, which arises from the leptoquark gauge interaction. The searches are carried on in signatures including high  $P_T$  leptons,  $E_T$  jets and large missing transverse energy, due to the typical decay of the leptoquark. The gauge couplings of a scalar leptoquark are determined uniquely according to its quantum numbers in Table 1. Since all of the leptoquark states belong to color-triplet representation, the scalar leptoquark pair-production cross section at the Tevatron and LHC can be determined solely as a function of the leptoquark mass without making further assumptions. This is in contrast to the indirect or single-production limits, which give constraints in the leptoquark mass-coupling plane. For the first- and second-generation scalar leptoquark states with decaying branching fraction  $\beta = B(eq) = 1$  and  $\beta = B(\mu q) = 1$ , the CDF and DØ experiments obtain the lower bounds on the leptoquark mass  $> 236$  GeV (first generation, CDF) [18],  $> 299$  GeV (first generation, DØ) [19],  $> 226$  GeV (second generation, CDF) [20], and  $> 316$  GeV (second generation, DØ) [21] at 95% CL. Third generation leptoquark mass bounds come from the DØ experiment [22] which sets a limit at 247 GeV for a charge  $-1/3$  third generation scalar leptoquark, at 95% C.L.

Recent results from the LHC proton-proton collider, running at a center of mass energy of 7 TeV, extend previous Tevatron mass limits for scalar leptoquarks to  $> 384$  GeV (first generation, CMS,  $\beta = 1$ ) [23] and  $> 339$  GeV (first generation, CMS,  $\beta = 0.5$ ) [24];  $> 660$  GeV (first generation, ATLAS,  $\beta = 1$ ) and  $> 607$  GeV (first generation, ATLAS,  $\beta = 0.5$ ) [25];  $> 632$  GeV (second generation, CMS,  $\beta = 1$ ) [26] and  $> 523$  GeV (second generation, CMS,  $\beta = 0.5$ ) [26] and;  $> 685$  GeV (second generation, ATLAS,  $\beta = 1$ ) and  $> 594$  GeV (second generation, ATLAS,  $\beta = 0.5$ ) [27]. All limits at 95% C.L. Finally a new measurement performed by the CMS experiment [28] extends the mass limit to 350 GeV for a charge  $-1/3$  third generation scalar leptoquark, at 95% C.L.

The magnetic-dipole-type and the electric-quadrupole-type interactions of a vector leptoquark are not determined even if we fix its gauge quantum numbers as listed in the Table [29]. The production of vector leptoquarks depends in general on additional assumptions that the leptoquark couplings and their pair-production cross sections are enhanced relative to the scalar leptoquark contributions. At the Tevatron for instance, since the acceptance for vector and scalar leptoquark detection is similar, limits on the vector leptoquark mass will be more stringent (see for example [35,19]). The leptoquark pair-production cross sections in  $e^+e^-$  collisions depend on the leptoquark  $SU(2) \times U(1)$  quantum numbers and Yukawa coupling with electron [30]. The OPAL experiment sets mass bounds on various leptoquark states from the pair-production cross sections [31]. For a second-generation weak-isosinglet weak-hypercharge  $-4/3$  scalar-leptoquark state, for example, the OPAL pair-production bound is  $M_{\text{LQ}} > 100$  GeV/c<sup>2</sup> at 95% C.L. The LEP experiments also searched for the single production of the leptoquark states from the process  $e\gamma \rightarrow \text{LQ} + q$ .

The most stringent searches for the leptoquark single production are performed by the HERA experiments. Since the leptoquark single-production cross section depends on its Yukawa coupling, the leptoquark mass limits from HERA are usually displayed in the mass-coupling plane. For leptoquark Yukawa coupling  $\lambda = 0.1$ , the ZEUS bounds on the first-generation leptoquarks range from 248 to 290 GeV, depending on the leptoquark species [32]. Recently the H1 Collaboration released a comprehensive summary of searches for first generation leptoquarks using the full data sample collected in  $ep$  collisions at HERA (446 pb<sup>-1</sup>). No evidence of production of leptoquarks is observed in final states with a large transverse momentum electron or large missing transverse momentum. For a coupling strength  $\lambda = 0.3$ , first generation leptoquarks with masses up to 800 GeV are excluded at 95% C.L. [34]

Fig. 1 summarizes ATLAS, CMS, DØ, LEP, and H1 limits on two typical first-generation scalar-leptoquark states in the mass-coupling plane [34].

The search for LQ will be continued with more LHC data. Early feasibility studies by the LHC experiments ATLAS [36] and CMS [37] indicate that clear signals can be established for masses up to about  $M(\text{LQ})$  1.3 to 1.4 TeV for first- and second-generation scalar LQ, with a likely final reach 1.5 TeV, for collisions at 14 TeV in the center of mass.

### Reference

1. W. Buchmüller, R. Rückl, and D. Wyler, Phys. Lett. **B191**, 442 (1987).
2. K. S. Babu, C. F. Kolda, and J. March-Russell, Phys. Lett. **B408**, 261 (1997).
3. J. L. Hewett and T. G. Rizzo, Phys. Rev. **D58**, 055005 (1998).
4. J.C. Pati and A. Salam, Phys. Rev. **D10**, 275 (1974).
5. H. Georgi and S.L. Glashow, Phys. Rev. Lett. **32**, 438 (1974).

See key on page 457

## Gauge & Higgs Boson Particle Listings

### Heavy Bosons Other than Higgs Bosons

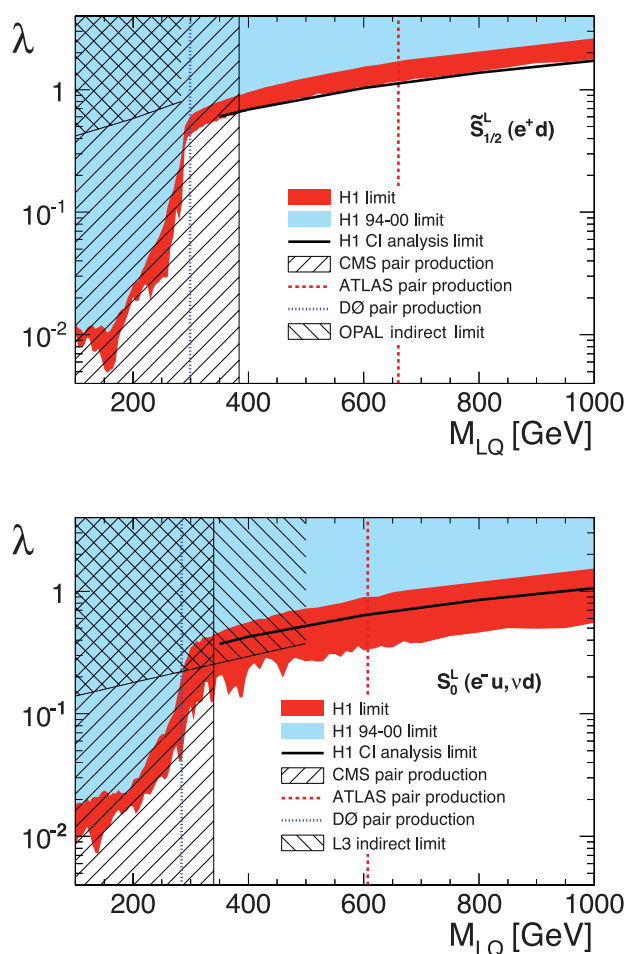


**Figure 1:** Limits on two typical first-generation scalar leptoquark states in the mass-coupling plane. The upper figure is for a weak-isodoublet, weak-hypercharge  $7/6$ ,  $3B + L = 0$  leptoquark state, while the lower figure is for a weak-isosinglet, weak-hypercharge  $-1/3$ ,  $3B + L = 2$  state. Figure adopted from Ref. 34.

6. H. Georgi, AIP Conf. Proc. **23**, 575 (1975);  
H. Fritzsch and P. Minkowski, Ann. Phys. **93**, 193 (1975).
7. For a review, see, E. Farhi and L. Susskind, Phys. Reports **74**, 277 (1981).
8. K. Lane and M. Ramana, Phys. Rev. **D44**, 2678 (1991).
9. See, for example, B. Schrepf and F. Schrepf, Phys. Lett. **153B**, 101 (1985).
10. O. Shanker, Nucl. Phys. **B204**, 375, (1982).
11. U. Mahanta, Eur. Phys. J. **C21**, 171 (2001) [Phys. Lett. **B515**, 111 (2001)].
12. K. Cheung, Phys. Rev. **D64**, 033001 (2001).
13. S. Davidson, D.C. Bailey, and B.A. Campbell, Z. Phys. **C61**, 613 (1994).
14. M. Leurer, Phys. Rev. **D49**, 333 (1994);  
Phys. Rev. **D50**, 536 (1994).
15. T. Plehn *et al.*, Z. Phys. **C74**, 611 (1997);  
M. Kramer *et al.*, Phys. Rev. Lett. **79**, 341 (1997); and references therein.

16. J.L. Hewett and S. Pakvasa, Phys. Rev. **D37**, 3165 (1988);  
O.J.P. Eboli and A.V. Olinto, Phys. Rev. **D38**, 3461 (1988);  
A. Dobado, M.J. Herrero, and C. Muñoz, Phys. Lett. **207B**, 97 (1988);  
V.D. Barger *et al.*, Phys. Lett. **B220**, 464 (1989);  
M. De Montigny and L. Marleau, Phys. Rev. **D40**, 2869 (1989) [Erratum-*ibid.* **D56**, 3156 (1997)].
17. A. Belyaev *et al.*, JHEP **0509**, 005 (2005).
18. D. Acosta *et al.*, [CDF Collab.], Phys. Rev. **D72**, 051107 (2005).
19. V.M. Abazov *et al.*, [DØCollab.], Phys. Lett. **B681**, 224 (2009).
20. A. Abulencia *et al.*, [CDF Collab.], Phys. Rev. **D73**, 051102 (2006).
21. V.M. Abazov *et al.*, [DØCollab.], Phys. Lett. **B671**, 224 (2009).
22. V. Abazov *et al.*, [DØCollab.] Phys. Lett. **B693**, 95 (2010).
23. V. Khachatryan *et al.*, [CMS Collab.], Phys. Rev. Lett. **106**, 201802 (2011).
24. S. Chatrchyan *et al.*, [CMS Collab.], Phys. Lett. **B703**, 246 (2011).
25. G. Aad *et al.*, [ATLAS Collab.] Phys. Lett. **B709**, 158 (2012).
26. V. Khachatryan *et al.*, [CMS Collab.], CMS PAS EXO-11-028 (2011).
27. G. Aad *et al.*, [ATLAS Collab.] arXiv:1203.3172v1.
28. V. Khachatryan *et al.*, [CMS Collab.], CMS PAS EXO-11-030 (2011).
29. J. Blümlein, E. Boos, and A. Kryukov, Z. Phys. **C76**, 137 (1997).
30. J. Blümlein and R. Ruckl, Phys. Lett. **B304**, 337 (1993).
31. G. Abbiendi *et al.*, [OPAL Collab.], Eur. Phys. J. **C31**, 281 (2003).
32. S. Chekanov *et al.*, [ZEUS Collab.], Phys. Rev. **D68**, 052004 (2003).
33. A. Aktas *et al.*, [H1 Collab.], Phys. Lett. **B629**, 9 (2005).
34. F.D. Aaron *et al.*, H1 Collab. arXiv:1107.3716.
35. T. Aalton *et al.*, [CDF Collab.] Phys. Rev. **D77**, 091105 (2008).
36. V.A. Mitsou *et al.*, Czech. J. Phys. **55**, B659-B666, 2005.
37. S. Abdulin and F. Charles, Phys. Lett. **B464**, 223 (1999).

#### MASS LIMITS for Leptoquarks from Pair Production

These limits rely only on the color or electroweak charge of the leptoquark.

VALUE (GeV)	CL%	DOCUMENT ID	TECN	COMMENT
>660	95	187 AAD	12H ATLS	First generation
>422	95	188 AAD	11D ATLS	Second Generation
>247	95	189 ABAZOV	10L D0	Third generation
••• We do not use the following data for averages, fits, limits, etc. •••				
>376	95	190 AAD	11D ATLS	First Generation
>326	95	191 ABAZOV	11V D0	First generation
>339	95	192 CHATRCHYAN	11N CMS	First generation
>384	95	193 KHACHATRY..11D	CMS	First generation
>394	95	194 KHACHATRY..11E	CMS	Second generation
>316	95	195 ABAZOV	09 D0	Second generation
>299	95	196 ABAZOV	09AF D0	First generation
		197 AALTONEN	08P CDF	Third generation
>153	95	198 AALTONEN	08Z CDF	Third generation
>205	95	199 ABAZOV	08AD D0	All generations
>210	95	198 ABAZOV	08AN D0	Third generation
>229	95	200 ABAZOV	07J D0	Third generation
>251	95	201 ABAZOV	06A D0	Superseded by ABAZOV 09
>136	95	202 ABAZOV	06L D0	Superseded by ABAZOV 08AD

# Gauge & Higgs Boson Particle Listings

## Heavy Bosons Other than Higgs Bosons

>226	95	203	ABULENCIA	06T	CDF	Second generation
>256	95	204	ABAZOV	05H	D0	First generation
>117	95	199	ACOSTA	05I	CDF	First generation
>236	95	205	ACOSTA	05P	CDF	First generation
> 99	95	206	ABBIENDI	03R	OPAL	First generation
>100	95	206	ABBIENDI	03R	OPAL	Second generation
> 98	95	206	ABBIENDI	03R	OPAL	Third generation
> 98	95	207	ABAZOV	02	D0	All generations
>225	95	208	ABAZOV	01D	D0	First generation
> 85.8	95	209	ABBIENDI	00M	OPAL	Superseded by ABBIENDI 03R
> 85.5	95	209	ABBIENDI	00M	OPAL	Superseded by ABBIENDI 03R
> 82.7	95	209	ABBIENDI	00M	OPAL	Superseded by ABBIENDI 03R
>200	95	210	ABBOTT	00C	D0	Second generation
>123	95	211	AFFOLDER	00K	CDF	Second generation
>148	95	212	AFFOLDER	00K	CDF	Third generation
>160	95	213	ABBOTT	99J	D0	Second generation
>225	95	214	ABBOTT	98E	D0	First generation
> 94	95	215	ABBOTT	98J	D0	Third generation
>202	95	216	ABE	98S	CDF	Second generation
>242	95	217	GROSS-PILCHER	98		First generation
> 99	95	218	ABE	97F	CDF	Third generation
>213	95	219	ABE	97X	CDF	First generation
> 45.5	95	220,221	ABREU	93J	DLPH	First + second generation
> 44.4	95	222	ADRIANI	93M	L3	First generation
> 44.5	95	222	ADRIANI	93M	L3	Second generation
> 45	95	222	DECAMP	92	ALEP	Third generation
none 8.9-22.6	95	223	KIM	90	AMY	First generation
none 10.2-23.2	95	223	KIM	90	AMY	Second generation
none 5-20.8	95	224	BARTEL	87B	JADE	
none 7-20.5	95	225	BEHREND	86B	CELL	
187	AAD	12H	search for scalar leptoquarks using $e\bar{e}j\bar{j}$ and $e\nu j\bar{j}$ events in $pp$ collisions at $E_{cm} = 7$ TeV. The limit above assumes $B(eq) = 1$ . For $B(eq) = 0.5$ , the limit becomes 607 GeV.			
188	AAD	11d	search for scalar leptoquarks using $\mu\bar{\mu}j\bar{j}$ and $\mu\nu j\bar{j}$ events in $pp$ collisions at $E_{cm} = 7$ TeV. The limit above assumes $B(\mu q) = 1$ . For $B(\mu q) = 0.5$ , the limit becomes 362 GeV.			
189	ABAZOV	10L	search for pair productions of scalar leptoquark state decaying to $\nu b$ in $p\bar{p}$ collisions at $E_{cm} = 1.96$ TeV. The limit above assumes $B(\nu b) = 1$ .			
190	AAD	11d	search for scalar leptoquarks using $e\bar{e}j\bar{j}$ and $e\nu j\bar{j}$ events in $pp$ collisions at $E_{cm} = 7$ TeV. The limit above assumes $B(eq) = 1$ . For $B(eq) = 0.5$ , the limit becomes 319 GeV.			
191	ABAZOV	11v	search for scalar leptoquarks using $e\nu j\bar{j}$ events in $p\bar{p}$ collisions at $E_{cm} = 1.96$ TeV. The limit above assumes $B(eq) = 0.5$ .			
192	CHATRCHYAN	11N	search for scalar leptoquarks using $e\nu j\bar{j}$ events in $pp$ collisions at $E_{cm} = 7$ TeV. The limit above assumes $B(eq) = 0.5$ .			
193	KHACHATRYAN	11D	search for scalar leptoquarks using $e\bar{e}j\bar{j}$ events in $pp$ collisions at $E_{cm} = 7$ TeV. The limit above assumes $B(eq) = 1$ .			
194	KHACHATRYAN	11E	search for scalar leptoquarks using $\mu\bar{\mu}j\bar{j}$ events in $pp$ collisions at $E_{cm} = 7$ TeV. The limit above assumes $B(\mu q) = 1$ .			
195	ABAZOV	09	search for scalar leptoquarks using $\mu\bar{\mu}j\bar{j}$ and $\nu\bar{\nu}j\bar{j}$ events in $p\bar{p}$ collisions at $E_{cm} = 1.96$ TeV. The limit above assumes $B(\mu q) = 1$ . For $B(\mu q) = 0.5$ , the limit becomes 270 GeV.			
196	ABAZOV	09AF	search for scalar leptoquarks using $e\bar{e}j\bar{j}$ and $e\nu j\bar{j}$ events in $p\bar{p}$ collisions at $E_{cm} = 1.96$ TeV. The limit above assumes $B(eq) = 1$ . For $B(eq) = 0.5$ the bound becomes 284 GeV.			
197	AALTONEN	08P	search for vector leptoquarks using $\tau^+\tau^-b\bar{b}$ events in $p\bar{p}$ collisions at $E_{cm} = 1.96$ TeV. Assuming Yang-Mills (minimal) couplings, the mass limit is $>317$ GeV (251 GeV) at 95% CL for $B(\tau b) = 1$ .			
198			Search for pair production of scalar leptoquark state decaying to $\tau b$ in $p\bar{p}$ collisions at $E_{cm} = 1.96$ TeV. The limit above assumes $B(\tau b) = 1$ .			
199			Search for scalar leptoquarks using $\nu\bar{\nu}j\bar{j}$ events in $p\bar{p}$ collisions at $E_{cm} = 1.96$ TeV. The limit above assumes $B(\nu q) = 1$ .			
200	ABAZOV	07I	search for pair productions of scalar leptoquark state decaying to $\nu b$ in $p\bar{p}$ collisions at $E_{cm} = 1.96$ TeV. The limit above assumes $B(\nu b) = 1$ .			
201	ABAZOV	06A	search for scalar leptoquarks using $\mu\bar{\mu}j\bar{j}$ events in $p\bar{p}$ collisions at $E_{cm} = 1.8$ TeV and 1.96 TeV. The limit above assumes $B(\mu q) = 1$ . For $B(\mu q) = 0.5$ , the limit becomes 204 GeV.			
202	ABAZOV	06L	search for scalar leptoquarks using $\nu\bar{\nu}j\bar{j}$ events in $p\bar{p}$ collisions at $E_{cm} = 1.8$ TeV and at 1.96 TeV. The limit above assumes $B(\nu q) = 1$ .			
203	ABULENCIA	06T	search for scalar leptoquarks using $\mu\bar{\mu}j\bar{j}$ , $\mu\nu j\bar{j}$ , and $\nu\bar{\nu}j\bar{j}$ events in $p\bar{p}$ collisions at $E_{cm} = 1.96$ TeV. The quoted limit assumes $B(\mu q) = 1$ . For $B(\mu q) = 0.5$ or 0.1, the bound becomes 208 GeV or 143 GeV, respectively. See their Fig. 4 for the exclusion limit as a function of $B(\mu q)$ .			
204	ABAZOV	05H	search for scalar leptoquarks using $e\bar{e}j\bar{j}$ and $e\nu j\bar{j}$ events in $p\bar{p}$ collisions at $E_{cm} = 1.8$ TeV and 1.96 TeV. The limit above assumes $B(eq) = 1$ . For $B(eq) = 0.5$ the bound becomes 234 GeV.			
205	ACOSTA	05P	search for scalar leptoquarks using $e\bar{e}j\bar{j}$ , $e\nu j\bar{j}$ events in $p\bar{p}$ collisions at $E_{cm} = 1.96$ TeV. The limit above assumes $B(eq) = 1$ . For $B(eq) = 0.5$ and 0.1, the bound becomes 205 GeV and 145 GeV, respectively.			
206	ABBIENDI	03R	search for scalar/vector leptoquarks in $e^+e^-$ collisions at $\sqrt{s} = 189-209$ GeV. The quoted limits are for charge $-4/3$ isospin 0 scalar-leptoquark with $B(\ell q) = 1$ . See their table 12 for other cases.			
207	ABAZOV	02	search for scalar leptoquarks using $\nu\bar{\nu}j\bar{j}$ events in $p\bar{p}$ collisions at $E_{cm} = 1.8$ TeV. The bound holds for all leptoquark generations. Vector leptoquarks are likewise constrained to lie above 200 GeV.			
208	ABAZOV	01D	search for scalar leptoquarks using $e\nu j\bar{j}$ , $e\bar{e}j\bar{j}$ , and $\nu\bar{\nu}j\bar{j}$ events in $p\bar{p}$ collisions at $E_{cm} = 1.8$ TeV. The limit above assumes $B(eq) = 1$ . For $B(eq) = 0.5$ and 0, the bound becomes 204 and 79 GeV, respectively. Bounds for vector leptoquarks are also given. Supersedes ABBOTT 98E.			
209	ABBIENDI	00M	search for scalar/vector leptoquarks in $e^+e^-$ collisions at $\sqrt{s} = 183$ GeV. The quoted limits are for charge $-4/3$ isospin 0 scalar-leptoquarks with $B(\ell q) = 1$ . See their Table 8 and Figs. 6-9 for other cases.			
210	ABBOTT	00C	search for scalar leptoquarks using $\mu\bar{\mu}j\bar{j}$ , $\mu\nu j\bar{j}$ , and $\nu\bar{\nu}j\bar{j}$ events in $p\bar{p}$ collisions at $E_{cm} = 1.8$ TeV. The limit above assumes $B(\mu q) = 1$ . For $B(\mu q) = 0.5$ and 0,			

						the bound becomes 180 and 79 GeV respectively. Bounds for vector leptoquarks are also given.
211	AFFOLDER	00K	search for scalar leptoquark using $\nu\nu c\bar{c}$ events in $p\bar{p}$ collisions at $E_{cm} = 1.8$ TeV. The quoted limit assumes $B(\nu c) = 1$ . Bounds for vector leptoquarks are also given.			
212	AFFOLDER	00K	search for scalar leptoquark using $\nu\nu b\bar{b}$ events in $p\bar{p}$ collisions at $E_{cm} = 1.8$ TeV. The quoted limit assumes $B(\nu b) = 1$ . Bounds for vector leptoquarks are also given.			
213	ABBOTT	99I	search for leptoquarks using $\mu\nu j\bar{j}$ events in $p\bar{p}$ collisions at $E_{cm} = 1.8$ TeV. The quoted limit is for a scalar leptoquark with $B(\mu q) = B(\nu q) = 0.5$ . Limits on vector leptoquarks range from 240 to 290 GeV.			
214	ABBOTT	98E	search for scalar leptoquarks using $e\nu j\bar{j}$ , $e\bar{e}j\bar{j}$ , and $\nu\bar{\nu}j\bar{j}$ events in $p\bar{p}$ collisions at $E_{cm} = 1.8$ TeV. The limit above assumes $B(eq) = 1$ . For $B(eq) = 0.5$ and 0, the bound becomes 204 and 79 GeV, respectively.			
215	ABBOTT	98J	search for charge $-1/3$ third generation scalar and vector leptoquarks in $p\bar{p}$ collisions at $E_{cm} = 1.8$ TeV. The quoted limit is for scalar leptoquark with $B(\nu b) = 1$ .			
216	ABE	98S	search for scalar leptoquarks using $\mu\bar{\mu}j\bar{j}$ events in $p\bar{p}$ collisions at $E_{cm} = 1.8$ TeV. The limit is for $B(\mu q) = 1$ . For $B(\mu q) = B(\nu q) = 0.5$ , the limit is $> 160$ GeV.			
217	GROSS-PILCHER	98	the combined limit of the CDF and DØ Collaborations as determined by a joint CDF/DØ working group and reported in this FNAL Technical Memo. Original data published in ABE 97X and ABBOTT 98E.			
218	ABE	97F	search for third generation scalar and vector leptoquarks in $p\bar{p}$ collisions at $E_{cm} = 1.8$ TeV. The quoted limit is for scalar leptoquark with $B(\tau b) = 1$ .			
219	ABE	97X	search for scalar leptoquarks using $e\bar{e}j\bar{j}$ events in $p\bar{p}$ collisions at $E_{cm} = 1.8$ TeV. The limit is for $B(eq) = 1$ .			
220			Limit is for charge $-1/3$ isospin-0 leptoquark with $B(\ell q) = 2/3$ .			
221			First and second generation leptoquarks are assumed to be degenerate. The limit is slightly lower for each generation.			
222			Limits are for charge $-1/3$ , isospin-0 scalar leptoquarks decaying to $\ell^- q$ or $\nu q$ with any branching ratio. See paper for limits for other charge-isospin assignments of leptoquarks.			
223	KIM	90	assume pair production of charge 2/3 scalar-leptoquark via photon exchange. The decay of the first (second) generation leptoquark is assumed to be any mixture of $d^+e^-$ and $u^+\bar{\nu}$ ( $s\mu^+$ and $c\bar{\nu}$ ). See paper for limits for specific branching ratios.			
224	BARTEL	87B	limit is valid when a pair of charge 2/3 spinless leptoquarks X is produced with point coupling, and when they decay under the constraint $B(X \rightarrow c\bar{\nu}_\mu) + B(X \rightarrow s\mu^+) = 1$ .			
225	BEHREND	86B	assumed that a charge 2/3 spinless leptoquark, $\chi$ , decays either into $s\mu^+$ or $c\bar{\nu}$ : $B(X \rightarrow s\mu^+) + B(X \rightarrow c\bar{\nu}) = 1$ .			

### MASS LIMITS for Leptoquarks from Single Production

These limits depend on the  $q$ - $\ell$ -leptoquark coupling  $g_{LQ}$ . It is often assumed that  $g_{LQ}^2/4\pi = 1/137$ . Limits shown are for a scalar, weak isoscalar, charge  $-1/3$  leptoquark.

VALUE (GeV)	CL %	DOCUMENT ID	TECN	COMMENT
>298	95	226	CHEKANOV 03B	ZEUS First generation
> 73	95	227	ABREU 93J	DLPH Second generation
•••				We do not use the following data for averages, fits, limits, etc. •••
>300	95	228	AARON 11A	H1 Lepton-flavor violation
		229	AARON 11B	H1 First generation
		230	ABAZOV 07E	D0 Second generation
>295	95	231	AKTAS 05B	H1 First generation
		232	CHEKANOV 05A	ZEUS Lepton-flavor violation
>197	95	233	ABBIENDI 02B	OPAL First generation
		234	CHEKANOV 02	ZEUS Repl. by CHEKANOV 05A
>290	95	235	ADLOFF 01C	H1 First generation
>204	95	236	BREITWEG 01	ZEUS First generation
		237	BREITWEG 00E	ZEUS First generation
>161	95	238	ABREU 99G	DLPH First generation
>200	95	239	ADLOFF 99	H1 First generation
		240	DERRICK 97	ZEUS Lepton-flavor violation
>168	95	241	DERRICK 93	ZEUS First generation
226				CHEKANOV 03B limit is for a scalar, weak isoscalar, charge $-1/3$ leptoquark coupled with $e_R$ . See their Figs. 11-12 and Table 5 for limits on states with different quantum numbers.
227				Limit from single production in $Z$ decay. The limit is for a leptoquark coupling of electromagnetic strength and assumes $B(\ell q) = 2/3$ . The limit is 77 GeV if first and second leptoquarks are degenerate.
228				AARON 11A search for various leptoquarks with lepton-flavor violating couplings. See their Figs. 2-3 and Tables 1-4 for detailed limits.
229				The quoted limit is for a scalar, weak isoscalar, charge $-1/3$ leptoquark coupled with $e_R$ . See their Figs. 3-5 for limits on states with different quantum numbers.
230				ABAZOV 07E search for leptoquark single production through $qg$ fusion process in $p\bar{p}$ collisions. See their Fig. 4 for exclusion plot in mass-coupling plane.
231				AKTAS 05B limit is for a scalar, weak isoscalar, charge $-1/3$ leptoquark coupled with $e_R$ . See their Fig. 3 for limits on states with different quantum numbers.
232				CHEKANOV 05 search for various leptoquarks with lepton-flavor violating couplings. See their Figs. 6-10 and Tables 1-8 for detailed limits.
233				For limits on states with different quantum numbers and the limits in the mass-coupling plane, see their Fig. 4 and Fig. 5.
234				CHEKANOV 02 search for various leptoquarks with lepton-flavor violating couplings. See their Figs. 6-7 and Tables 5-6 for detailed limits.
235				For limits on states with different quantum numbers and the limits in the mass-coupling plane, see their Fig. 3.
236				See their Fig. 14 for limits in the mass-coupling plane.
237				BREITWEG 00E search for $F=0$ leptoquarks in $e^+p$ collisions. For limits in mass-coupling plane, see their Fig. 11.
238				ABREU 99G limit obtained from process $e\gamma \rightarrow LQ+q$ . For limits on vector and scalar states with different quantum numbers and the limits in the coupling-mass plane, see their Fig. 4 and Table 2.

See key on page 457

## Gauge & Higgs Boson Particle Listings

### Heavy Bosons Other than Higgs Bosons

- 239 For limits on states with different quantum numbers and the limits in the mass-coupling plane, see their Fig. 13 and Fig. 14. ADLOFF 99 also search for leptoquarks with lepton-flavor violating couplings. ADLOFF 99 supersedes AID 96b.
- 240 DERRICK 97 search for various leptoquarks with lepton-flavor violating couplings. See their Figs. 5–8 and Table 1 for detailed limits.
- 241 DERRICK 93 search for single leptoquark production in  $ep$  collisions with the decay  $eq$  and  $\nu q$ . The limit is for leptoquark coupling of electromagnetic strength and assumes  $B(eq) = B(\nu q) = 1/2$ . The limit for  $B(eq) = 1$  is 176 GeV. For limits on states with different quantum numbers, see their Table 3.

#### Indirect Limits for Leptoquarks

VALUE (TeV)	CL%	DOCUMENT ID	TECN	COMMENT
• • • We do not use the following data for averages, fits, limits, etc. • • •				
> 2.5	95	242 AARON	11c H1	First generation
		243 DORSNER	11 RVUE	scalar, weak singlet, charge 4/3
		244 AKTAS	07A H1	Lepton-flavor violation
> 0.49	95	245 SCHAEEL	07A ALEP	$e^+e^- \rightarrow q\bar{q}$
		246 SMIRNOV	07 RVUE	$K \rightarrow e\mu, B \rightarrow e\tau$
		247 CHEKANOV	05A ZEUS	Lepton-flavor violation
> 1.7	96	248 ADLOFF	03 H1	First generation
> 46	90	249 CHANG	03 BELL	Pati-Salam type
		250 CHEKANOV	02 ZEUS	Repl. by CHEKANOV 05A
> 1.7	95	251 CHEUNG	01B RVUE	First generation
> 0.39	95	252 ACCIARRI	00P L3	$e^+e^- \rightarrow qq$
> 1.5	95	253 ADLOFF	00 H1	First generation
> 0.2	95	254 BARATE	00I ALEP	Repl. by SCHAEEL 07A
		255 BARGER	00 RVUE	Cs
		256 GABRIELLI	00 RVUE	Lepton flavor violation
> 0.74	95	257 ZARNECKI	00 RVUE	$S_1$ leptoquark
		258 ABBIENDI	99 OPAL	
> 19.3	95	259 ABE	98V CDF	$B_s \rightarrow e^\pm \mu^\mp$ , Pati-Salam type
		260 ACCIARRI	98J L3	$e^+e^- \rightarrow q\bar{q}$
		261 ACKERSTAFF	98V OPAL	$e^+e^- \rightarrow q\bar{q}, e^+e^- \rightarrow b\bar{b}$
> 0.76	95	262 DEANDREA	97 RVUE	$\tilde{R}_2$ leptoquark
		263 DERRICK	97 ZEUS	Lepton-flavor violation
		264 GROSSMAN	97 RVUE	$B \rightarrow \tau^+\tau^-(X)$
		265 JADACH	97 RVUE	$e^+e^- \rightarrow q\bar{q}$
>1200		266 KUZNETSOV	95B RVUE	Pati-Salam type
		267 MIZUKOSHI	95 RVUE	Third generation scalar leptoquark
> 0.3	95	268 BHATTACH...	94 RVUE	Spin-0 leptoquark coupled to $\bar{\nu}_R \ell_L$
		269 DAVIDSON	94 RVUE	
> 18		270 KUZNETSOV	94 RVUE	Pati-Salam type
> 0.43	95	271 LEURER	94 RVUE	First generation spin-1 leptoquark
> 0.44	95	271 LEURER	94B RVUE	First generation spin-0 leptoquark
		272 MAHANTA	94 RVUE	$P$ and $T$ violation
> 1		273 SHANKER	82 RVUE	Nonchiral spin-0 leptoquark
> 125		273 SHANKER	82 RVUE	Nonchiral spin-1 leptoquark

- 242 AARON 11c limit is for weak isotriplet spin-0 leptoquark at strong coupling  $\lambda = \sqrt{4\pi}$ . For the limits of leptoquarks with different quantum numbers, see their Table 3. Limits are derived from bounds of  $eq$  contact interactions.
- 243 DORSNER 11 give bounds on scalar, weak singlet, charge 4/3 leptoquark from  $K, B, \tau$  decays, meson mixings,  $L\nu\nu$ ,  $g-2$  and  $Z \rightarrow b\bar{b}$ .
- 244 AKTAS 07A search for lepton-flavor violation in  $ep$  collision. See their Tables 4–7 for limits on lepton-flavor violating four-fermion interactions induced by various leptoquarks.
- 245 SCHAEEL 07A limit is for the weak-isoscalar spin-0 left-handed leptoquark with the coupling of electromagnetic strength. For the limits of leptoquarks with different quantum numbers, see their Table 35.
- 246 SMIRNOV 07 obtains mass limits for the vector and scalar chiral leptoquark states from  $K \rightarrow e\mu, B \rightarrow e\tau$  decays.
- 247 CHEKANOV 05 search for various leptoquarks with lepton-flavor violating couplings. See their Figs. 6–10 and Tables 1–8 for detailed limits.
- 248 ADLOFF 03 limit is for the weak isotriplet spin-0 leptoquark at strong coupling  $\lambda = \sqrt{4\pi}$ . For the limits of leptoquarks with different quantum numbers, see their Table 3. Limits are derived from bounds on  $e^\pm q$  contact interactions.
- 249 The bound is derived from  $B(B^0 \rightarrow e^\pm \mu^\mp) < 1.7 \times 10^{-7}$ .
- 250 CHEKANOV 02 search for lepton-flavor violation in  $ep$  collisions. See their Tables 1–4 for limits on lepton-flavor violating and four-fermion interactions induced by various leptoquarks.
- 251 CHEUNG 01b quoted limit is for a scalar, weak isoscalar, charge  $-1/3$  leptoquark with a coupling of electromagnetic strength. The limit is derived from bounds on contact interactions in a global electroweak analysis. For the limits of leptoquarks with different quantum numbers, see Table 5.
- 252 ACCIARRI 00P limit is for the weak isoscalar spin-0 leptoquark with the coupling of electromagnetic strength. For the limits of leptoquarks with different quantum numbers, see their Table 4.
- 253 ADLOFF 00 limit is for the weak isotriplet spin-0 leptoquark at strong coupling,  $\lambda = \sqrt{4\pi}$ . For the limits of leptoquarks with different quantum numbers, see their Table 2. ADLOFF 00 limits are from the  $Q^2$  spectrum measurement of  $e^+p \rightarrow e^+X$ .
- 254 BARATE 00i search for deviations in cross section and jet-charge asymmetry in  $e^+e^- \rightarrow \bar{q}q$  due to  $t$ -channel exchange of a leptoquark at  $\sqrt{s}=130$  to 183 GeV. Limits for other scalar and vector leptoquarks are also given in their Table 22.
- 255 BARGER 00 explain the deviation of atomic parity violation in cesium atoms from prediction is explained by scalar leptoquark exchange.
- 256 GABRIELLI 00 calculate various process with lepton flavor violation in leptoquark models.
- 257 ZARNECKI 00 limit is derived from data of HERA, LEP, and Tevatron and from various low-energy data including atomic parity violation. Leptoquark coupling with electromagnetic strength is assumed.
- 258 ABBIENDI 99 limits are from  $e^+e^- \rightarrow q\bar{q}$  cross section at 130–136, 161–172, 183 GeV. See their Fig. 8 and Fig. 9 for limits in mass-coupling plane.

- 259 ABE 98v quoted limit is from  $B(B_s \rightarrow e^\pm \mu^\mp) < 8.2 \times 10^{-6}$ . ABE 98v also obtain a similar limit on  $M_{LQ} > 20.4$  TeV from  $B(B_d \rightarrow e^\pm \mu^\mp) < 4.5 \times 10^{-6}$ . Both bounds assume the non-canonical association of the  $b$  quark with electrons or muons under  $SU(4)$ .
- 260 ACCIARRI 98J limit is from  $e^+e^- \rightarrow q\bar{q}$  cross section at  $\sqrt{s}=130$ –172 GeV which can be affected by the  $t$ - and  $u$ -channel exchanges of leptoquarks. See their Fig. 4 and Fig. 5 for limits in the mass-coupling plane.
- 261 ACKERSTAFF 98V limits are from  $e^+e^- \rightarrow q\bar{q}$  and  $e^+e^- \rightarrow b\bar{b}$  cross sections at  $\sqrt{s}=130$ –172 GeV, which can be affected by the  $t$ - and  $u$ -channel exchanges of leptoquarks. See their Fig. 21 and Fig. 22 for limits of leptoquarks in mass-coupling plane.
- 262 DEANDREA 97 limit is for  $\tilde{R}_2$  leptoquark obtained from atomic parity violation (APV). The coupling of leptoquark is assumed to be electromagnetic strength. See Table 2 for limits of the four-fermion interactions induced by various scalar leptoquark exchange. DEANDREA 97 combines APV limit and limits from Tevatron and HERA. See Fig. 1–4 for combined limits of leptoquark in mass-coupling plane.
- 263 DERRICK 97 search for lepton-flavor violation in  $ep$  collision. See their Tables 2–5 for limits on lepton-flavor violating four-fermion interactions induced by various leptoquarks.
- 264 GROSSMAN 97 estimate the upper bounds on the branching fraction  $B \rightarrow \tau^+\tau^-(X)$  from the absence of the  $B$  decay with large missing energy. These bounds can be used to constrain leptoquark induced four-fermion interactions.
- 265 JADACH 97 limit is from  $e^+e^- \rightarrow q\bar{q}$  cross section at  $\sqrt{s}=172.3$  GeV which can be affected by the  $t$ - and  $u$ -channel exchanges of leptoquarks. See their Fig. 1 for limits on vector leptoquarks in mass-coupling plane.
- 266 KUZNETSOV 95B use  $\pi, K, B, \tau$  decays and  $\mu e$  conversion and give a list of bounds on the leptoquark mass and the fermion mixing matrix in the Pati-Salam model. The quoted limit is from  $K_L \rightarrow \mu e$  decay assuming zero mixing.
- 267 MIZUKOSHI 95 calculate the one-loop radiative correction to the  $Z$ -physics parameters in various scalar leptoquark models. See their Fig. 4 for the exclusion plot of third generation leptoquark models in mass-coupling plane.
- 268 BHATTACHARYYA 94 limit is from one-loop radiative correction to the leptonic decay width of the  $Z$ .  $m_H=250$  GeV,  $\alpha_s(m_Z)=0.12$ ,  $m_t=180$  GeV, and the electroweak strength of leptoquark coupling are assumed. For leptoquark coupled to  $\bar{\nu}_L \ell_R, \bar{\mu} \tau$ , and  $\bar{\tau} \nu$ , see Fig. 2 in BHATTACHARYYA 94b erratum and Fig. 3.
- 269 DAVIDSON 94 gives an extensive list of the bounds on leptoquark-induced four-fermion interactions from  $\pi, K, D, B, \mu, \tau$  decays and meson mixings, etc. See Table 15 of DAVIDSON 94 for detail.
- 270 KUZNETSOV 94 gives mixing independent bound of the Pati-Salam leptoquark from the cosmological limit on  $\pi^0 \rightarrow \nu\nu$ .
- 271 LEURER 94, LEURER 94b limits are obtained from atomic parity violation and apply to any chiral leptoquark which couples to the first generation with electromagnetic strength. For a nonchiral leptoquark, universality in  $\pi_{\ell 2}$  decay provides a much more stringent bound.
- 272 MAHANTA 94 gives bounds of  $P$ - and  $T$ -violating scalar-leptoquark couplings from atomic and molecular experiments.
- 273 From  $(\pi \rightarrow e\nu)/(\pi \rightarrow \mu\nu)$  ratio. SHANKER 82 assumes the leptoquark induced four-fermion coupling  $4g^2/M^2$  ( $\bar{\nu}_{eL} u_R$ ) ( $\bar{\nu}_{\mu L} e_R$ ) with  $g=0.004$  for spin-0 leptoquark and  $g^2/M^2$  ( $\bar{\nu}_{eL} \gamma^\mu u_L$ ) ( $\bar{\nu}_{\mu L} \gamma^\mu e_R$ ) with  $g=0.6$  for spin-1 leptoquark.

#### MASS LIMITS for Diquarks

VALUE (GeV)	CL%	DOCUMENT ID	TECN	COMMENT
>3520	95	274 CHATRCHYAN 11Y	CMS	$E_6$ diquark
• • • We do not use the following data for averages, fits, limits, etc. • • •				
none 970–1080, 1450–1600	95	275 KHACHATRY..10	CDF	$E_6$ diquark
none 290–630	95	276 AALTONEN 09AC	CDF	$E_6$ diquark
none 290–420	95	277 ABE	97G CDF	$E_6$ diquark
none 15–31.7	95	278 ABREU	94o DLPH	SUSY $E_6$ diquark
274 CHATRCHYAN 11Y search for new resonance decaying to dijets in $pp$ collisions at $\sqrt{s}=7$ TeV.				
275 KHACHATRYAN 10 search for new resonance decaying to dijets in $pp$ collisions at $\sqrt{s}=7$ TeV.				
276 AALTONEN 09AC search for new narrow resonance decaying to dijets.				
277 ABE 97g search for new particle decaying to dijets.				
278 ABREU 94o limit is from $e^+e^- \rightarrow \bar{c}c$ s. Range extends up to 43 GeV if diquarks are degenerate in mass.				

#### MASS LIMITS for $g_A$ (axigluon) and Other Color-Octet Gauge Bosons

Axigluons are massive color-octet gauge bosons in chiral color models and have axial-vector coupling to quarks with the same coupling strength as gluons.

VALUE (GeV)	CL%	DOCUMENT ID	TECN	COMMENT
>2470	95	279 CHATRCHYAN 11Y	CMS	$pp \rightarrow g_A X, g_A \rightarrow 2$ jets
• • • We do not use the following data for averages, fits, limits, etc. • • •				
none 1470–1520	95	280 AALTONEN 10L	CDF	$p\bar{p} \rightarrow g_A X, g_A \rightarrow t\bar{t}$
none 260–1250	95	281 KHACHATRY..10	CMS	$pp \rightarrow g_A X, g_A \rightarrow 2$ jets
> 910	95	282 AALTONEN 09AC	CDF	$p\bar{p} \rightarrow g_A X, g_A \rightarrow 2$ jets
> 365	95	283 CHOUDHURY 07	RVUE	$p\bar{p} \rightarrow t\bar{t}X$
none 200–980	95	284 DONCHESKI 98	RVUE	$\Gamma(Z \rightarrow \text{hadron})$
none 200–870	95	285 ABE	97G CDF	$p\bar{p} \rightarrow g_A X, g_A \rightarrow 2$ jets
none 240–640	95	286 ABE	95N CDF	$p\bar{p} \rightarrow g_A X, g_A \rightarrow q\bar{q}$
> 50	95	287 ABE	93G CDF	$p\bar{p} \rightarrow g_A X, g_A \rightarrow 2$ jets
none 120–210	95	288 CUYPERS 91	RVUE	$\sigma(e^+e^- \rightarrow \text{hadrons})$
> 29	95	289 ABE	90H CDF	$p\bar{p} \rightarrow g_A X, g_A \rightarrow 2$ jets
none 150–310	95	290 ROBINETT 89	THEO	Partial-wave unitarity
> 20	95	291 ALBAJAR 88B	UA1	$p\bar{p} \rightarrow g_A X, g_A \rightarrow 2$ jets
> 9	95	292 BERGSTROM 88	RVUE	$p\bar{p} \rightarrow T'X$ via $g_A g$
> 25	95	292 CUYPERS 88	RVUE	$T$ decay
		293 DONCHESKI 88B	RVUE	$T$ decay

# Gauge & Higgs Boson Particle Listings

## Heavy Bosons Other than Higgs Bosons

- 279 CHATRCHYAN 11y search for new resonance decaying to dijets in  $pp$  collisions at  $\sqrt{s} = 7$  TeV.
- 280 AALTONEN 10L search for massive color octet non-chiral vector particle decaying into  $t\bar{t}$  pair with mass in the range  $400 \text{ GeV} < M < 800 \text{ GeV}$ . See their Fig. 6 for limit in the mass-coupling plane.
- 281 KHACHATRYAN 10 search for new resonance decaying to dijets in  $pp$  collisions at  $\sqrt{s} = 7$  TeV.
- 282 AALTONEN 09AC search for new narrow resonance decaying to dijets.
- 283 CHOUDHURY 07 limit is from the  $t\bar{t}$  production cross section measured at CDF.
- 284 DONCHESKI 98 compare  $\alpha_S$  derived from low-energy data and that from  $\Gamma(Z \rightarrow \text{hadrons})/\Gamma(Z \rightarrow \text{leptons})$ .
- 285 ABE 97G search for new particle decaying to dijets.
- 286 ABE 95N assume axigluons decaying to quarks in the Standard Model only.
- 287 ABE 93G assume  $\Gamma(g_A) = N\alpha_S m_{g_A}/6$  with  $N = 10$ .
- 288 CUYPERS 91 compare  $\alpha_S$  measured in  $T$  decay and that from  $R$  at PEP/PETRA energies.
- 289 ABE 90H assumes  $\Gamma(g_A) = N\alpha_S m_{g_A}/6$  with  $N = 5$  ( $\Gamma(g_A) = 0.09 m_{g_A}$ ). For  $N = 10$ , the excluded region is reduced to 120–150 GeV.
- 290 ROBINETT 89 result demands partial-wave unitarity of  $J = 0$   $t\bar{t} \rightarrow t\bar{t}$  scattering amplitude and derives a limit  $m_{g_A} > 0.5 m_t$ . Assumes  $m_t > 56 \text{ GeV}$ .
- 291 ALBAJAR 88B result is from the nonobservation of a peak in two-jet invariant mass distribution.  $\Gamma(g_A) < 0.4 m_{g_A}$  assumed. See also BAGGER 88.
- 292 CUYPERS 88 requires  $\Gamma(T \rightarrow g g_A) < \Gamma(T \rightarrow g g g)$ . A similar result is obtained by DONCHESKI 88.
- 293 DONCHESKI 88B requires  $\Gamma(T \rightarrow g q \bar{q})/\Gamma(T \rightarrow g g g) < 0.25$ , where the former decay proceeds via axigluon exchange. A more conservative estimate of  $< 0.5$  leads to  $m_{g_A} > 21 \text{ GeV}$ .

### $X^0$ (Heavy Boson) Searches in Z Decays

Searches for radiative transition of Z to a lighter spin-0 state  $X^0$  decaying to hadrons, a lepton pair, a photon pair, or invisible particles as shown in the comments. The limits are for the product of branching ratios.

VALUE	CL%	DOCUMENT ID	TECN	COMMENT
• • • We do not use the following data for averages, fits, limits, etc. • • •				
		294 BARATE	98U ALEP	$X^0 \rightarrow \ell\bar{\ell}, q\bar{q}, g\bar{g}, \gamma\gamma, \nu\bar{\nu}$
		295 ACCIARRI	97Q L3	$X^0 \rightarrow$ invisible particle(s)
		296 ACTON	93E OPAL	$X^0 \rightarrow \gamma\gamma$
		297 ABREU	92D DLPH	$X^0 \rightarrow$ hadrons
		298 ADRIANI	92F L3	$X^0 \rightarrow$ hadrons
		299 ACTON	91 OPAL	$X^0 \rightarrow$ anything
$< 1.1 \times 10^{-4}$	95	300 ACTON	91B OPAL	$X^0 \rightarrow e^+e^-$
$< 9 \times 10^{-5}$	95	300 ACTON	91B OPAL	$X^0 \rightarrow \mu^+\mu^-$
$< 1.1 \times 10^{-4}$	95	300 ACTON	91B OPAL	$X^0 \rightarrow \tau^+\tau^-$
$< 2.8 \times 10^{-4}$	95	301 ADEVA	91D L3	$X^0 \rightarrow e^+e^-$
$< 2.3 \times 10^{-4}$	95	301 ADEVA	91D L3	$X^0 \rightarrow \mu^+\mu^-$
$< 4.7 \times 10^{-4}$	95	302 ADEVA	91D L3	$X^0 \rightarrow$ hadrons
$< 8 \times 10^{-4}$	95	303 AKRAWY	90J OPAL	$X^0 \rightarrow$ hadrons
294 BARATE 98U obtain limits on $B(Z \rightarrow \gamma X^0)B(X^0 \rightarrow \ell\bar{\ell}, q\bar{q}, g\bar{g}, \gamma\gamma, \nu\bar{\nu})$ . See their Fig. 17.				
295 See Fig. 4 of ACCIARRI 97Q for the upper limit on $B(Z \rightarrow \gamma X^0; E_\gamma > E_{\min})$ as a function of $E_{\min}$ .				
296 ACTON 93E give $\sigma(e^+e^- \rightarrow X^0\gamma) \cdot B(X^0 \rightarrow \gamma\gamma) < 0.4 \text{ pb}$ (95%CL) for $m_{X^0} = 60 \pm 2.5 \text{ GeV}$ . If the process occurs via s-channel $\gamma$ exchange, the limit translates to $\Gamma(X^0) \cdot B(X^0 \rightarrow \gamma\gamma)^2 < 20 \text{ MeV}$ for $m_{X^0} = 60 \pm 1 \text{ GeV}$ .				
297 ABREU 92D give $\sigma_Z \cdot B(Z \rightarrow \gamma X^0) \cdot B(X^0 \rightarrow \text{hadrons}) < (3-10) \text{ pb}$ for $m_{X^0} = 10-78 \text{ GeV}$ . A very similar limit is obtained for spin-1 $X^0$ .				
298 ADRIANI 92F search for isolated $\gamma$ in hadronic Z decays. The limit $\sigma_Z \cdot B(Z \rightarrow \gamma X^0) \cdot B(X^0 \rightarrow \text{hadrons}) < (2-10) \text{ pb}$ (95%CL) is given for $m_{X^0} = 25-85 \text{ GeV}$ .				
299 ACTON 91 searches for $Z \rightarrow Z^* X^0$ , $Z^* \rightarrow e^+e^-, \mu^+\mu^-,$ or $\nu\bar{\nu}$ . Excludes any new scalar $X^0$ with $m_{X^0} < 9.5 \text{ GeV}/c$ if it has the same coupling to $ZZ^*$ as the MSM Higgs boson.				
300 ACTON 91B limits are for $m_{X^0} = 60-85 \text{ GeV}$ .				
301 ADEVA 91D limits are for $m_{X^0} = 30-89 \text{ GeV}$ .				
302 ADEVA 91D limits are for $m_{X^0} = 30-86 \text{ GeV}$ .				
303 AKRAWY 90J give $\Gamma(Z \rightarrow \gamma X^0) \cdot B(X^0 \rightarrow \text{hadrons}) < 1.9 \text{ MeV}$ (95%CL) for $m_{X^0} = 32-80 \text{ GeV}$ . We divide by $\Gamma(Z) = 2.5 \text{ GeV}$ to get product of branching ratios. For nonresonant transitions, the limit is $B(Z \rightarrow \gamma q\bar{q}) < 8.2 \text{ MeV}$ assuming three-body phase space distribution.				

### MASS LIMITS for a Heavy Neutral Boson Coupling to $e^+e^-$

VALUE (GeV)	CL%	DOCUMENT ID	TECN	COMMENT
• • • We do not use the following data for averages, fits, limits, etc. • • •				
none 55–61		304 ODAKA	89 VNS	$\Gamma(X^0 \rightarrow e^+e^-) \cdot B(X^0 \rightarrow \text{had.}) \gtrsim 0.2 \text{ MeV}$
$> 45$	95	305 DERRICK	86 HRS	$\Gamma(X^0 \rightarrow e^+e^-) = 6 \text{ MeV}$
$> 46.6$	95	306 ADEVA	85 MRKJ	$\Gamma(X^0 \rightarrow e^+e^-) = 10 \text{ keV}$
$> 48$	95	306 ADEVA	85 MRKJ	$\Gamma(X^0 \rightarrow e^+e^-) = 4 \text{ MeV}$
		307 BERGER	85B PLUT	
none 39.8–45.5		308 ADEVA	84 MRKJ	$\Gamma(X^0 \rightarrow e^+e^-) = 10 \text{ keV}$
$> 47.8$	95	308 ADEVA	84 MRKJ	$\Gamma(X^0 \rightarrow e^+e^-) = 4 \text{ MeV}$
none 39.8–45.2		308 BEHREND	84C CELL	
$> 47$	95	308 BEHREND	84C CELL	$\Gamma(X^0 \rightarrow e^+e^-) = 4 \text{ MeV}$

- 304 ODAKA 89 looked for a narrow or wide scalar resonance in  $e^+e^- \rightarrow$  hadrons at  $E_{\text{cm}} = 55.0-60.8 \text{ GeV}$ .
- 305 DERRICK 86 found no deviation from the Standard Model Bhabha scattering at  $E_{\text{cm}} = 29 \text{ GeV}$  and set limits on the possible scalar boson  $e^+e^-$  coupling. See their figure 4 for excluded region in the  $\Gamma(X^0 \rightarrow e^+e^-) \cdot m_{X^0}$  plane. Electronic chiral invariance requires a parity doublet of  $X^0$ , in which case the limit applies for  $\Gamma(X^0 \rightarrow e^+e^-) = 3 \text{ MeV}$ .
- 306 ADEVA 85 first limit is from  $2\gamma, \mu^+\mu^-$ , hadrons assuming  $X^0$  is a scalar. Second limit is from  $e^+e^-$  channel.  $E_{\text{cm}} = 40-47 \text{ GeV}$ . Supersedes ADEVA 84.
- 307 BERGER 85B looked for effect of spin-0 boson exchange in  $e^+e^- \rightarrow e^+e^-$  and  $\mu^+\mu^-$  at  $E_{\text{cm}} = 34.7 \text{ GeV}$ . See Fig. 5 for excluded region in the  $m_{X^0} - \Gamma(X^0)$  plane.
- 308 ADEVA 84 and BEHREND 84C have  $E_{\text{cm}} = 39.8-45.5 \text{ GeV}$ . MARK-J searched  $X^0$  in  $e^+e^- \rightarrow$  hadrons,  $2\gamma, \mu^+\mu^-$ ,  $e^+e^-$  and CELLO in the same channels plus  $\tau$  pair. No narrow or broad  $X^0$  is found in the energy range. They also searched for the effect of  $X^0$  with  $m_X > E_{\text{cm}}$ . The second limits are from Bhabha data and for spin-0 singlet. The same limits apply for  $\Gamma(X^0 \rightarrow e^+e^-) = 2 \text{ MeV}$  if  $X^0$  is a spin-0 doublet. The second limit of BEHREND 84C was read off from their figure 2. The original papers also list limits in other channels.

### Search for $X^0$ Resonance in $e^+e^-$ Collisions

The limit is for  $\Gamma(X^0 \rightarrow e^+e^-) \cdot B(X^0 \rightarrow f)$ , where  $f$  is the specified final state. Spin 0 is assumed for  $X^0$ .

VALUE (keV)	CL%	DOCUMENT ID	TECN	COMMENT
• • • We do not use the following data for averages, fits, limits, etc. • • •				
$< 10^3$	95	309 ABE	93C VNS	$\Gamma(ee)$
$< (0.4-10)$	95	310 ABE	93C VNS	$f = \gamma\gamma$
$< (0.3-5)$	95	311,312 ABE	93D TOPZ	$f = \gamma\gamma$
$< (2-12)$	95	311,312 ABE	93D TOPZ	$f =$ hadrons
$< (4-200)$	95	312,313 ABE	93D TOPZ	$f = ee$
$< (0.1-6)$	95	312,313 ABE	93D TOPZ	$f = \mu\mu$
$< (0.5-8)$	90	314 STERNER	93 AMY	$f = \gamma\gamma$
309 Limit is for $\Gamma(X^0 \rightarrow e^+e^-) m_{X^0} = 56-63.5 \text{ GeV}$ for $\Gamma(X^0) = 0.5 \text{ GeV}$ .				
310 Limit is for $m_{X^0} = 56-61.5 \text{ GeV}$ and is valid for $\Gamma(X^0) \ll 100 \text{ MeV}$ . See their Fig. 5 for limits for $\Gamma = 1, 2 \text{ GeV}$ .				
311 Limit is for $m_{X^0} = 57.2-60 \text{ GeV}$ .				
312 Limit is valid for $\Gamma(X^0) \ll 100 \text{ MeV}$ . See paper for limits for $\Gamma = 1 \text{ GeV}$ and those for $J = 2$ resonances.				
313 Limit is for $m_{X^0} = 56.6-60 \text{ GeV}$ .				
314 STERNER 93 limit is for $m_{X^0} = 57-59.6 \text{ GeV}$ and is valid for $\Gamma(X^0) < 100 \text{ MeV}$ . See their Fig. 2 for limits for $\Gamma = 1, 3 \text{ GeV}$ .				

### Search for $X^0$ Resonance in $ep$ Collisions

VALUE	DOCUMENT ID	TECN	COMMENT
• • • We do not use the following data for averages, fits, limits, etc. • • •			
	315 CHEKANOV 02B	ZEUS	$X \rightarrow jj$
315 CHEKANOV 02B search for photoproduction of X decaying into dijets in $ep$ collisions. See their Fig. 5 for the limit on the photoproduction cross section.			

### Search for $X^0$ Resonance in Two-Photon Process

The limit is for  $\Gamma(X^0) \cdot B(X^0 \rightarrow \gamma\gamma)^2$ . Spin 0 is assumed for  $X^0$ .

VALUE (MeV)	CL%	DOCUMENT ID	TECN	COMMENT
• • • We do not use the following data for averages, fits, limits, etc. • • •				
$< 2.6$	95	316 ACTON	93E OPAL	$m_{X^0} = 60 \pm 1 \text{ GeV}$
$< 2.9$	95	BUSKULIC	93F ALEP	$m_{X^0} \sim 60 \text{ GeV}$
316 ACTON 93E limit for a $J = 2$ resonance is $0.8 \text{ MeV}$ .				

### Search for $X^0$ Resonance in $e^+e^- \rightarrow X^0\gamma$

VALUE (GeV)	DOCUMENT ID	TECN	COMMENT
• • • We do not use the following data for averages, fits, limits, etc. • • •			
	317 ABBIENDI	03D OPAL	$X^0 \rightarrow \gamma\gamma$
	318 ABREU	00Z DLPH	$X^0$ decaying invisibly
	319 ADAM	96C DLPH	$X^0$ decaying invisibly
317 ABBIENDI 03D measure the $e^+e^- \rightarrow \gamma\gamma\gamma$ cross section at $\sqrt{s} = 181-209 \text{ GeV}$ . The upper bound on the production cross section, $\sigma(e^+e^- \rightarrow X^0\gamma)$ times the branching ratio for $X^0 \rightarrow \gamma\gamma$ , is less than $0.03 \text{ pb}$ at 95%CL for $X^0$ masses between 20 and 180 GeV. See their Fig. 9b for the limits in the mass-cross section plane.			
318 ABREU 00Z is from the single photon cross section at $\sqrt{s} = 183, 189 \text{ GeV}$ . The production cross section upper limit is less than $0.3 \text{ pb}$ for $X^0$ mass between 40 and 160 GeV. See their Fig. 4 for the limit in mass-cross section plane.			
319 ADAM 96C is from the single photon production cross at $\sqrt{s} = 130, 136 \text{ GeV}$ . The upper bound is less than $3 \text{ pb}$ for $X^0$ masses between 60 and 130 GeV. See their Fig. 5 for the exact bound on the cross section $\sigma(e^+e^- \rightarrow \gamma X^0)$ .			

### Search for $X^0$ Resonance in $Z \rightarrow f\bar{f}X^0$

The limit is for  $B(Z \rightarrow f\bar{f}X^0) \cdot B(X^0 \rightarrow F)$  where  $f$  is a fermion and  $F$  is the specified final state. Spin 0 is assumed for  $X^0$ .

VALUE	CL%	DOCUMENT ID	TECN	COMMENT
• • • We do not use the following data for averages, fits, limits, etc. • • •				



## Gauge &amp; Higgs Boson Particle Listings

Heavy Bosons Other than Higgs Bosons, Axions ( $A^0$ ) and Other Very Light Bosons

ABE	95M	PRL 74 2900	F. Abe <i>et al.</i>	(CDF Collab.)
ABE	95N	PRL 74 3538	F. Abe <i>et al.</i>	(CDF Collab.)
BALEST	95	PR D51 2053	R. Balest <i>et al.</i>	(CLEO Collab.)
KUZNETSOV	95	PRL 75 794	I.A. Kuznetsov <i>et al.</i>	(PNPI, KIAE, HARV+)
KUZNETSOV	95B	PAN 58 2113	A.V. Kuznetsov, N.V. Mikheev	(YARO)
		Translated from YAF 58 2228.		
MIZUKOSHI	95	NP B443 20	J.K. Mizukoshi, O.J.P. Eboli, M.C. Gonzalez-Garcia	(DELPHI Collab.)
ABREU	94O	ZPHY C64 183	P. Abreu <i>et al.</i>	(REHO)
BHATTACH...	94	PL B336 100	G. Bhattacharyya, J. Ellis, K. Sridhar	(CERN)
		Also		
BHATTACH...	94B	PL B338 522 (erratum)	G. Bhattacharyya, J. Ellis, K. Sridhar	(CERN)
DAVIDSON	94	ZPHY C61 613	S. Davidson, D. Bailey, B.A. Campbell	(CFPA+)
KUZNETSOV	94	PL B329 295	A.V. Kuznetsov, N.V. Mikheev	(YARO)
KUZNETSOV	94B	JETPL 60 315	I.A. Kuznetsov <i>et al.</i>	(PNPI, KIAE, HARV+)
		Translated from ZETFP 60 311.		
LEURER	94	PR D50 536	M. Leurer	(REHO)
LEURER	94B	PR D49 333	M. Leurer	(REHO)
		Also		
MAHANTA	94	PL B337 128	U. Mahanta	(MEHTA)
SEVERIJNS	94	PRL 73 611 (erratum)	N. Severijns <i>et al.</i>	(LOUV, WISC, LEUV+)
VILAIN	94B	PL B332 465	P. Vilain <i>et al.</i>	(CHARM II Collab.)
ABE	93C	PL B302 119	K. Abe <i>et al.</i>	(VENUS Collab.)
ABE	93D	PL B304 373	T. Abe <i>et al.</i>	(TOPAZ Collab.)
ABE	93G	PRL 71 2542	F. Abe <i>et al.</i>	(CDF Collab.)
ABREU	93J	PL B316 620	P. Abreu <i>et al.</i>	(DELPHI Collab.)
ACTON	93E	PL B311 391	P.D. Acton <i>et al.</i>	(OPAL Collab.)
ADRIANI	93M	PRPL 236 1	O. Adriani <i>et al.</i>	(L3 Collab.)
ALITI	93	NP B400 3	J. Aliti <i>et al.</i>	(UA2 Collab.)
BHATTACH...	93	PR D47 R3693	G. Bhattacharyya <i>et al.</i>	(CALC, JADA, ICTP+)
BUSKULIC	93F	PL B308 425	D. Buskulic <i>et al.</i>	(ALEPH Collab.)
DERRICK	93	PL B306 173	M. Derrick <i>et al.</i>	(ZEUS Collab.)
RIZZO	93	PR D48 4470	T.G. Rizzo	(ANL)
SEVERIJNS	93	PRL 70 4047	N. Severijns <i>et al.</i>	(LOUV, WISC, LEUV+)
		Also		
STERNER	93	PRL 73 611 (erratum)	N. Severijns <i>et al.</i>	(LOUV, WISC, LEUV+)
ABREU	92D	ZPHY C53 555	K.L. Sterner <i>et al.</i>	(AMY Collab.)
ADRIANI	92F	PL B292 472	P. Abreu <i>et al.</i>	(DELPHI Collab.)
DECAMP	92	PRPL 216 253	O. Adriani <i>et al.</i>	(L3 Collab.)
IMAZATO	92	PRL 69 877	D. Decamp <i>et al.</i>	(ALEPH Collab.)
MISHRA	92	PR D68 3499	J. Imazato <i>et al.</i>	(KEK, INUS, TOKY+)
POLAK	92B	PR D46 3871	S.R. Mishra <i>et al.</i>	(COLU, CHIC, FNAL+)
ACTON	91	PL B268 122	J. Polak, M. Zralek	(SILES)
ACTON	91B	PL B273 338	D.P. Acton <i>et al.</i>	(OPAL Collab.)
ADEVA	91D	PL B262 155	D.P. Acton <i>et al.</i>	(OPAL Collab.)
AQUINO	91	PL B261 280	B. Adeva <i>et al.</i>	(L3 Collab.)
COLANGELO	91	PL B253 154	M. Aquino, A. Fernandez, A. Garcia	(CINV, PUEB)
CUYPERS	91	PL B259 173	P. Colangelo, G. Nardulli	(BARI)
FARAGGI	91	MPL A6 61	F. Cuypers, A.F. Falk, P.H. Frampton	(DURH, HARV+)
POLAK	91	NP B363 385	A.E. Faraggi, D.V. Nanopoulos	(TAMU)
RIZZO	91	PR D44 202	J. Polak, M. Zralek	(SILES)
WALKER	91	APJ 376 51	T.G. Rizzo	(WISC, ISU)
		Also		
ABE	90F	PL B246 297	T.P. Walker <i>et al.</i>	(HSCA, OSU, CHIC+)
ABE	90H	PR D41 1722	K. Abe <i>et al.</i>	(VENUS Collab.)
AKRAWY	90J	PL B246 285	F. Abe <i>et al.</i>	(CDF Collab.)
ANTREASAYAN	90C	PL B251 204	M.Z. Akrawy <i>et al.</i>	(OPAL Collab.)
GONZALEZ-G...	90D	PL B240 163	D. Antreasyan <i>et al.</i>	(Crystal Ball Collab.)
GRIFOLS	90	NP B331 244	M.C. Gonzalez-Garcia, J.W.F. Valle	(VALE)
GRIFOLS	90D	PR D42 3293	J.A. Grifols, E. Masso	(BARC)
KIM	90	PL B240 243	J.A. Grifols, E. Masso, T.G. Rizzo	(BARC, CERN+)
LOPEZ	90	PL B241 392	G.N. Kim <i>et al.</i>	(AMY Collab.)
ALBRECHT	89	ZPHY C42 349	J.L. Lopez, D.V. Nanopoulos	(TAMU)
BARBIERI	89B	PR D39 1229	H. Albrecht <i>et al.</i>	(ARGUS Collab.)
LANGACKER	89B	PR D40 1569	R. Barbieri, R.N. Mohapatra	(PISA, UMID)
ODAKA	89	JPSJ 58 3037	P. Langacker, S. Uma Sankar	(PENN)
ROBINETT	89	PR D39 834	S. Otake <i>et al.</i>	(VENUS Collab.)
ALBAJAR	88B	PL B209 127	R.W. Robinett	(PSU)
BAGGER	88	PR D37 1188	C. Albajar <i>et al.</i>	(UA1 Collab.)
BALKE	88	PR D37 587	J. Bagger, C. Schmidt, S. King	(HARV, BOST)
BERGSTROM	88	PL B212 386	B. Balke <i>et al.</i>	(LBL, UCB, COLO, NWES+)
CUYPERS	88	PRL 60 1237	L. Bergstrom	(STOH)
DONCHESKI	88	PL B206 137	F. Cuypers, P.H. Frampton	(UNCCH)
DONCHESKI	88B	PR D38 412	M.A. Doncheski, H. Grotch, R. Robinett	(PSU)
BARTEL	87B	ZPHY C36 15	M.A. Doncheski, H. Grotch, R.W. Robinett	(PSU)
BEHREND	86B	PL B178 452	W. Bartel <i>et al.</i>	(JADE Collab.)
DERRICK	86	PL 166B 463	H.J. Behrend <i>et al.</i>	(CELLO Collab.)
		Also		
JODIDIO	86	PR D34 1967	M. Derrick <i>et al.</i>	(HRS Collab.)
		Also		
MOHAPATRA	86	PR D34 909	M. Derrick <i>et al.</i>	(HRS Collab.)
ADEVA	85	PL 152B 439	A. Jodidio <i>et al.</i>	(LBL, NWES, TRIU)
BERGER	85B	ZPHY C27 341	A. Jodidio <i>et al.</i>	(LBL, NWES, TRIU)
STOKER	85	PRL 54 1887	R.N. Mohapatra	(UMD)
ADEVA	84	PRL 53 134	B. Adeva <i>et al.</i>	(Mark-J Collab.)
BEHREND	84C	PL 140B 130	C. Berger <i>et al.</i>	(PLUTO Collab.)
BERGSM	83	PL 122B 465	D.P. Stoker <i>et al.</i>	(LBL, NWES, TRIU)
CARR	83	PRL 51 627	B. Adeva <i>et al.</i>	(Mark-J Collab.)
BEALL	82	PRL 48 848	H.J. Behrend <i>et al.</i>	(CELLO Collab.)
SHANKER	82	NP B204 375	F. Bergsm <i>et al.</i>	(CHARM Collab.)
			J. Carr <i>et al.</i>	(LBL, NWES, TRIU)
			G. Beall, M. Bander, A. Soni	(UCI, UCLA)
			O. Shanker	(TRIUM)

Axions ( $A^0$ ) and Other Very Light Bosons, Searches for

## AXIONS AND OTHER SIMILAR PARTICLES

Revised March 2012 by G.G. Raffelt (MPI Physics, Munich) and L.J. Rosenberg (U. of Washington).

## Introduction

In this section, we list coupling-strength and mass limits for light neutral scalar or pseudoscalar bosons that couple weakly to normal matter and radiation. Such bosons may arise from a global spontaneously broken U(1) symmetry, resulting in a massless Nambu-Goldstone (NG) boson. If there is a small explicit symmetry breaking, either already in the Lagrangian or

due to quantum effects such as anomalies, the boson acquires a mass and is called a pseudo-NG boson. Typical examples are axions ( $A^0$ ) [1,2], familons [3] and Majorons [4], associated, respectively, with a spontaneously broken Peccei-Quinn, family and lepton-number symmetry.

A common characteristic among these light bosons  $\phi$  is that their coupling to Standard-Model particles is suppressed by the energy scale that characterizes the symmetry breaking, *i.e.*, the decay constant  $f$ . The interaction Lagrangian is

$$\mathcal{L} = f^{-1} J^\mu \partial_\mu \phi, \quad (1)$$

where  $J^\mu$  is the Noether current of the spontaneously broken global symmetry. If  $f$  is very large, these new particles interact very weakly. Detecting them would provide a window to physics far beyond what can be probed at accelerators.

Axions remain of particular interest because the Peccei-Quinn (PQ) mechanism remains perhaps the most credible scheme to preserve CP in QCD. Moreover, the cold dark matter of the universe may well consist of axions and they are searched for in dedicated experiments with a realistic chance of discovery.

Originally it was assumed that the PQ scale  $f_A$  was related to the electroweak symmetry-breaking scale  $v_{\text{weak}} = (\sqrt{2}G_F)^{-1/2} = 247$  GeV. However, the associated “standard” and “variant” axions were quickly excluded—we refer to the Listings for detailed limits. Here we focus on “invisible axions” with  $f_A \gg v_{\text{weak}}$  as the main possibility.

Axions have a characteristic two-photon vertex, inherited from their mixing with  $\pi^0$  and  $\eta$ . It allows for the main search strategy based on axion-photon conversion in external magnetic fields [5], an effect that also can be of astrophysical interest. While for axions the product “ $A\gamma\gamma$  interaction strength  $\times$  mass” is essentially fixed by the corresponding  $\pi^0$  properties, one may consider more general axion-like particles (ALPs) where the two parameters are independent. Several experiments have recently explored this more general parameter space.

## I. THEORY

## I.1 Peccei-Quinn mechanism and axions

The QCD Lagrangian includes a CP-violating term  $\mathcal{L}_\Theta = \bar{\Theta}(\alpha_s/8\pi) G^{\mu\nu a} \tilde{G}_{\mu\nu}^a$ , where  $-\pi \leq \bar{\Theta} \leq +\pi$  is the effective  $\Theta$  parameter after diagonalizing quark masses,  $G$  is the color field strength tensor, and  $\tilde{G}$  its dual. Limits on the neutron electric dipole moment [6] imply  $|\bar{\Theta}| \lesssim 10^{-10}$  even though  $\bar{\Theta} = \mathcal{O}(1)$  is otherwise completely satisfactory. The spontaneously broken global Peccei-Quinn symmetry  $U(1)_{\text{PQ}}$  was introduced to solve this “strong CP problem” [1], an axion being the pseudo-NG boson of  $U(1)_{\text{PQ}}$  [2]. This symmetry is broken due to the axion’s anomalous triangle coupling to gluons,

$$\mathcal{L} = \left( \bar{\Theta} - \frac{\phi_A}{f_A} \right) \frac{\alpha_s}{8\pi} G^{\mu\nu a} \tilde{G}_{\mu\nu}^a, \quad (2)$$

where  $\phi_A$  is the axion field and  $f_A$  the axion decay constant. Color anomaly factors have been absorbed in the normalization of  $f_A$  which is defined by this Lagrangian. Thus normalized,  $f_A$



See key on page 457

## Gauge & Higgs Boson Particle Listings Axions ( $A^0$ ) and Other Very Light Bosons

is the quantity that enters all low-energy phenomena [7]. Non-perturbative effects induce a potential for  $\phi_A$  whose minimum is at  $\phi_A = \Theta f_A$ , thereby canceling the  $\Theta$  term in the QCD Lagrangian and thus restoring CP symmetry.

The resulting axion mass is given by  $m_A f_A \approx m_\pi f_\pi$  where  $m_\pi = 135$  MeV and  $f_\pi \approx 92$  MeV. In more detail one finds

$$m_A = \frac{z^{1/2}}{1+z} \frac{f_\pi m_\pi}{f_A} = \frac{0.60 \text{ meV}}{f_A/10^{10} \text{ GeV}}, \quad (3)$$

where  $z = m_u/m_d$ . We have used the canonical value  $z = 0.56$  [8], although the range  $z = 0.35\text{--}0.60$  is plausible [9].

Originally one assumed  $f_A \sim v_{\text{weak}}$  [1,2]. Tree-level flavor conservation fixes the axion properties in terms of a single parameter  $\tan\beta$ , the ratio of the vacuum expectation values of two Higgs fields that appear as a minimal ingredient. This “standard axion” is excluded after extensive searches [10]. A narrow peak structure observed in positron spectra from heavy ion collisions [11] suggested an axion-like particle of mass 1.8 MeV that decays into  $e^+e^-$ , but extensive follow-up searches were negative. “Variant axion models” were proposed which keep  $f_A \sim v_{\text{weak}}$  while dropping the constraint of tree-level flavor conservation [12], but these models are also excluded [13].

Axions with  $f_A \gg v_{\text{weak}}$  evade all current experimental limits. One generic class of models invokes “hadronic axions” where new heavy quarks carry  $U(1)_{\text{PQ}}$  charges, leaving ordinary quarks and leptons without tree-level axion couplings. The prototype is the KSVZ model [14], where in addition the heavy quarks are electrically neutral. Another generic class requires at least two Higgs doublets and ordinary quarks and leptons carry PQ charges, the prototype being the DFSZ model [15]. All of these models contain at least one electroweak singlet scalar that acquires a vacuum expectation value and thereby breaks the PQ symmetry. The KSVZ and DFSZ models are frequently used as generic examples, but other models exist where both heavy quarks and Higgs doublets carry PQ charges.

### 1.2 Model-dependent axion couplings

Although the generic axion interactions scale approximately with  $f_\pi/f_A$  from the corresponding  $\pi^0$  couplings, there are non-negligible model-dependent factors and uncertainties. The axion’s two-photon interaction plays a key role for many searches,

$$\mathcal{L}_{A\gamma\gamma} = \frac{G_{A\gamma\gamma}}{4} F_{\mu\nu} \tilde{F}^{\mu\nu} \phi_A = -G_{A\gamma\gamma} \mathbf{E} \cdot \mathbf{B} \phi_A, \quad (4)$$

where  $F$  is the electromagnetic field-strength tensor and  $\tilde{F}$  its dual. The coupling constant is

$$\begin{aligned} G_{A\gamma\gamma} &= \frac{\alpha}{2\pi f_A} \left( \frac{E}{N} - \frac{2}{3} \frac{4+z}{1+z} \right) \\ &= \frac{\alpha}{2\pi} \left( \frac{E}{N} - \frac{2}{3} \frac{4+z}{1+z} \right) \frac{1+z}{z^{1/2}} \frac{m_A}{m_\pi f_\pi}, \end{aligned} \quad (5)$$

where  $E$  and  $N$  are the electromagnetic and color anomalies of the axial current associated with the axion. In grand unified models, and notably for DFSZ [15],  $E/N = 8/3$ , whereas for KSVZ [14]  $E/N = 0$  if the electric charge of the new heavy

quark is taken to vanish. In general, a broad range of  $E/N$  values is possible [16]. The two-photon decay width is

$$\Gamma_{A \rightarrow \gamma\gamma} = \frac{G_{A\gamma\gamma}^2 m_A^3}{64\pi} = 1.1 \times 10^{-24} \text{ s}^{-1} \left( \frac{m_A}{\text{eV}} \right)^5. \quad (6)$$

The second expression uses Eq. (5) with  $z = 0.56$  and  $E/N = 0$ . Axions decay faster than the age of the universe if  $m_A \gtrsim 20$  eV.

The interaction with fermions  $f$  has derivative form and is invariant under a shift  $\phi_A \rightarrow \phi_A + \phi_0$  as behoves a NG boson,

$$\mathcal{L}_{Aff} = \frac{C_f}{2f_A} \bar{\Psi}_f \gamma^\mu \gamma_5 \Psi_f \partial_\mu \phi_A. \quad (7)$$

Here,  $\Psi_f$  is the fermion field,  $m_f$  its mass, and  $C_f$  a model-dependent coefficient. The dimensionless combination  $g_{Aff} \equiv C_f m_f / f_A$  plays the role of a Yukawa coupling and  $\alpha_{Aff} \equiv g_{Aff}^2 / 4\pi$  of a “fine-structure constant.” The often-used pseudoscalar form  $\mathcal{L}_{Aff} = -i(C_f m_f / f_A) \bar{\Psi}_f \gamma_5 \Psi_f \phi_A$  need not be equivalent to the appropriate derivative structure, for example when two NG bosons are attached to one fermion line as in axion emission by nucleon bremsstrahlung [17].

In the DFSZ model [15], the tree-level coupling coefficient to electrons is

$$C_e = \frac{\cos^2 \beta}{3}, \quad (8)$$

where  $\tan\beta$  is the ratio of two Higgs vacuum expectation values that are generic to this and similar models.

For nucleons,  $C_{n,p}$  are related to axial-vector current matrix elements by generalized Goldberger-Treiman relations,

$$\begin{aligned} C_p &= (C_u - \eta)\Delta u + (C_d - \eta z)\Delta d + (C_s - \eta w)\Delta s, \\ C_n &= (C_u - \eta)\Delta d + (C_d - \eta z)\Delta u + (C_s - \eta w)\Delta s. \end{aligned} \quad (9)$$

Here,  $\eta = (1+z+w)^{-1}$  with  $z = m_u/m_d$  and  $w = m_u/m_s \ll z$  and the  $\Delta q$  are given by the axial vector current matrix element  $\Delta q S_\mu = \langle p | \bar{q} \gamma_\mu \gamma_5 q | p \rangle$  with  $S_\mu$  the proton spin.

Neutron beta decay and strong isospin symmetry considerations imply  $\Delta u - \Delta d = F + D = 1.269 \pm 0.003$ , whereas hyperon decays and flavor  $SU(3)$  symmetry imply  $\Delta u + \Delta d - 2\Delta s = 3F - D = 0.586 \pm 0.031$  [19]. The strange-quark contribution is  $\Delta s = -0.08 \pm 0.01_{\text{stat}} \pm 0.05_{\text{sys}}$  from the COMPASS experiment [18], and  $\Delta s = -0.085 \pm 0.008_{\text{exp}} \pm 0.013_{\text{theor}} \pm 0.009_{\text{evol}}$  from HERMES [19], in agreement with each other and with an early estimate of  $\Delta s = -0.11 \pm 0.03$  [20]. We thus adopt  $\Delta u = 0.84 \pm 0.02$ ,  $\Delta d = -0.43 \pm 0.02$  and  $\Delta s = -0.09 \pm 0.02$ , very similar to what was used in the axion literature.

The uncertainty of the axion-nucleon couplings is dominated by the uncertainty  $z = m_u/m_d = 0.35\text{--}0.60$  that we mentioned earlier. For hadronic axions  $C_{u,d,s} = 0$  so that  $-0.51 < C_p < -0.36$  and  $0.10 > C_n > -0.05$ . Therefore it is well possible that  $C_n = 0$  whereas  $C_p$  does not vanish within the plausible  $z$  range. In the DFSZ model,  $C_u = \frac{1}{3} \sin^2 \beta$  and  $C_d = \frac{1}{3} \cos^2 \beta$  and  $C_n$  and  $C_p$  as functions of  $\beta$  and  $z$  do not vanish simultaneously.

The axion-pion interaction is given by the Lagrangian [21]

$$\mathcal{L}_{A\pi} = \frac{C_{A\pi}}{f_\pi f_A} (\pi^0 \pi^+ \partial_\mu \pi^- + \pi^0 \pi^- \partial_\mu \pi^+ - 2\pi^+ \pi^- \partial_\mu \pi^0) \partial_\mu \phi_A, \quad (10)$$

# Gauge & Higgs Boson Particle Listings

## Axions ( $A^0$ ) and Other Very Light Bosons

where  $C_{A\pi} = (1-z)/[3(1+z)]$  in hadronic models. The chiral symmetry-breaking Lagrangian provides an additional term  $\mathcal{L}'_{A\pi} \propto (m_\pi^2/f_\pi f_A)(\pi^0\pi^0 + 2\pi^-\pi^+)\pi^0\phi_A$ . For hadronic axions it vanishes identically, in contrast to the DFSZ model (Roberto Peccei, private communication).

## II. LABORATORY SEARCHES

### II.1 Photon regeneration

Searching for “invisible axions” is extremely challenging. The most promising approaches rely on the axion-two-photon vertex, allowing for axion-photon conversion in external electric or magnetic fields [5]. For the Coulomb field of a charged particle, the conversion is best viewed as a scattering process,  $\gamma + Ze \leftrightarrow Ze + A$ , called Primakoff effect [22]. In the other extreme of a macroscopic field, usually a large-scale  $B$ -field, the momentum transfer is small, the interaction coherent over a large distance, and the conversion is best viewed as an axion-photon oscillation phenomenon in analogy to neutrino flavor oscillations [23].

Photons propagating through a transverse magnetic field, with incident  $\mathbf{E}_\gamma$  and magnet  $\mathbf{B}$  parallel, may convert into axions. For  $m_A^2 L/2\omega \ll 2\pi$ , where  $L$  is the length of the  $B$  field region and  $\omega$  the photon energy, the resultant axion beam is coherent with the incident photon beam and the conversion probability is  $\Pi \sim (1/4)(G_{A\gamma\gamma}BL)^2$ . A practical realization uses a laser beam propagating down the bore of a superconducting dipole magnet (like the bending magnets in high-energy accelerators). If another magnet is in line with the first, but shielded by an optical barrier, then photons may be regenerated from the pure axion beam [24]. The overall probability  $P(\gamma \rightarrow A \rightarrow \gamma) = \Pi^2$ .

The first such experiment utilized two magnets of length  $L = 4.4$  m and  $B = 3.7$  T and found  $G_{A\gamma\gamma} < 6.7 \times 10^{-7}$  GeV $^{-1}$  at 95% CL for  $m_A < 1$  meV [25]. More recently, several such experiments were performed (see Listings), improving the limit to  $G_{A\gamma\gamma} < 0.7 \times 10^{-7}$  GeV $^{-1}$  at 95% CL for  $m_A \lesssim 0.5$  meV [26]. Some of these experiments have also reported limits for scalar bosons where the photon  $\mathbf{E}_\gamma$  must be chosen perpendicular to the magnet  $\mathbf{B}$ .

The concept of resonantly enhanced photon regeneration may open unexplored regions of coupling strength [27]. In this scheme, both the production and detection magnets are within Fabry-Perot optical cavities and actively locked in frequency. The  $\gamma \rightarrow A \rightarrow \gamma$  rate is enhanced by a factor  $2\mathcal{F}\mathcal{F}'/\pi^2$  relative to a single-pass experiment, where  $\mathcal{F}$  and  $\mathcal{F}'$  are the finesses of the two cavities. The resonant enhancement could be of order  $10^{(10-12)}$ , improving the  $G_{A\gamma\gamma}$  sensitivity by  $10^{(2.5-3)}$ .

Another new concept involves axion absorption and emission between electromagnetic fields within a high finesse optical cavity [28]. A signal appears as resonant sidebands on the carrier. This technique could be sensitive in the mass range  $10^{-6}$ – $10^{-4}$  eV and reach the KSVZ line after one year of operation.

### II.2 Photon polarization

An alternative to regenerating the lost photons is to use the beam itself to detect conversion: the polarization of light propagating through a transverse  $B$  field suffers dichroism and birefringence [29]. Dichroism: The  $E_\parallel$  component, but not  $E_\perp$ , is depleted by axion production, causing a small rotation of linearly polarized light. For  $m_A^2 L/2\omega \ll 2\pi$  the effect is independent of  $m_A$ , for heavier axions it oscillates and diminishes as  $m_A$  increases, and it vanishes for  $m_A > \omega$ . Birefringence: This rotation occurs because there is mixing of virtual axions in the  $E_\parallel$  state, but not for  $E_\perp$ . Hence, linearly polarized light will develop elliptical polarization. Higher-order QED also induces vacuum birefringence. A search for these effects was performed on the same dipole magnets in the early experiment above [30]. The dichroic rotation gave a stronger limit than the ellipticity rotation:  $G_{A\gamma\gamma} < 3.6 \times 10^{-7}$  GeV $^{-1}$  at 95% CL for  $m_A < 5 \times 10^{-4}$  eV. The ellipticity limits are better at higher masses, as they fall off smoothly and do not terminate at  $m_A$ .

In 2006 the PVLAS collaboration reported a signature of magnetically induced vacuum dichroism that could be interpreted as the effect of a pseudoscalar with  $m_A = 1$ – $1.5$  meV and  $G_{A\gamma\gamma} = (1.6$ – $5) \times 10^{-6}$  GeV $^{-1}$  [31]. Since then, these findings are attributed to instrumental artifacts [32]. This particle interpretation is also excluded by the above photon regeneration searches that were perhaps inspired by the original PVLAS result.

### II.3 Long-range forces

New bosons would mediate long-range forces, which are severely constrained by “fifth force” experiments [33]. Those looking for new mass-spin couplings provide significant constraints on pseudoscalar bosons [34]. However, they do not yet cover realistic parameters for invisible axion models because they are only sensitive for small  $m_A$ . The corresponding coupling strengths scale with  $f_A^{-1} \approx m_A/m_\pi f_\pi$  and are too small to be detected. Still, these efforts provide constraints on more general low-mass bosons.

## III. AXIONS FROM ASTROPHYSICAL SOURCES

### III.1 Stellar energy-loss limits:

Low-mass weakly-interacting particles (neutrinos, gravitons, axions, baryonic or leptonic gauge bosons, *etc.*) are produced in hot astrophysical plasmas, and can thus transport energy out of stars. The coupling strength of these particles with normal matter and radiation is bounded by the constraint that stellar lifetimes or energy-loss rates not conflict with observation [35–37].

We begin this discussion with our Sun and concentrate on hadronic axions. They are produced predominantly by the Primakoff process  $\gamma + Ze \rightarrow Ze + A$ . Integrating over a standard solar model yields the axion luminosity [51]

$$L_A = G_{10}^2 1.85 \times 10^{-3} L_\odot, \quad (11)$$

See key on page 457

## Gauge & Higgs Boson Particle Listings Axions ( $A^0$ ) and Other Very Light Bosons

where  $G_{10} = G_{A\gamma\gamma} \times 10^{10}$  GeV. The maximum of the spectrum is at 3.0 keV, the average at 4.2 keV, and the number flux at Earth is  $G_{10}^2 3.75 \times 10^{11}$  cm $^{-2}$  s $^{-1}$ . The solar photon luminosity is fixed, so axion losses require enhanced nuclear energy production and thus enhanced neutrino fluxes. The all-flavor measurements by SNO together with a standard solar model imply  $L_A \lesssim 0.10 L_\odot$ , corresponding to  $G_{10} \lesssim 7$  [38], mildly superseding a similar limit from helioseismology [39].

A more restrictive limit derives from globular-cluster (GC) stars that allow for detailed tests of stellar-evolution theory. The stars on the horizontal branch (HB) in the color-magnitude diagram have reached helium burning with a core-averaged energy release of about 80 erg g $^{-1}$  s $^{-1}$ , compared to Primakoff axion losses of  $G_{10}^2 30$  erg g $^{-1}$  s $^{-1}$ . The accelerated consumption of helium reduces the HB lifetime by about 80/(80+30  $G_{10}^2$ ). Number counts of HB stars in 15 GCs compared with the number of red giants (that are not much affected by Primakoff losses) reveal agreement with expectations within 20–40% in any one GC and overall on the 10% level [36]. Therefore, a reasonably conservative limit is

$$G_{A\gamma\gamma} \lesssim 1 \times 10^{-10} \text{ GeV}^{-1}, \quad (12)$$

although a detailed error budget is not available.

We translate this constraint on  $G_{A\gamma\gamma}$  to  $f_A > 2.3 \times 10^7$  GeV ( $m_A < 0.3$  eV), using  $z = 0.56$  and  $E/N = 0$  as in the KSVZ model, and show the excluded range in Figure 1. For the DFSZ model with  $E/N = 8/3$ , the corresponding limits are slightly less restrictive,  $f_A > 0.8 \times 10^7$  GeV ( $m_A < 0.7$  eV). The exact high-mass end of the exclusion range has not been determined. The relevant temperature is around 10 keV and the average photon energy is therefore around 30 keV. The excluded  $m_A$  range thus certainly extends beyond the shown 100 keV.

If axions couple directly to electrons, the dominant emission processes are  $\gamma + e^- \rightarrow e^- + A$  and  $e^- + Ze \rightarrow Ze + e^- + A$ . Moreover, bremsstrahlung is efficient in white dwarfs (WDs), where the Primakoff and Compton processes are suppressed by the large plasma frequency. The enhanced energy losses would delay helium ignition in GC stars, implying  $\alpha_{Aee} \lesssim 0.5 \times 10^{-26}$  [40]. Enhanced WD cooling led to a similar limit from the WD luminosity function [41]. Based on much better data and detailed WD cooling treatment, today it appears that the WD luminosity function fits better with a new energy-loss channel that can be interpreted in terms of axion losses corresponding to  $\alpha_{Aee} \sim 10^{-27}$  [42]. For pulsationally unstable WDs (ZZ Ceti stars), the period decrease  $\dot{P}/P$  is a measure of the cooling speed. A well-studied case is the star G117–B15A, where the measured  $\dot{P}/P$  also implies additional cooling that can be interpreted in terms of similar axion losses [43]. At the moment we prefer to interpret these results as an upper limit  $\alpha_{Aee} \lesssim 10^{-27}$  shown in Figure 1.

Similar constraints derive from the measured duration of the neutrino signal of the supernova SN 1987A. Numerical simulations for a variety of cases, including axions and Kaluza-Klein gravitons, reveal that the energy-loss rate of a nuclear medium

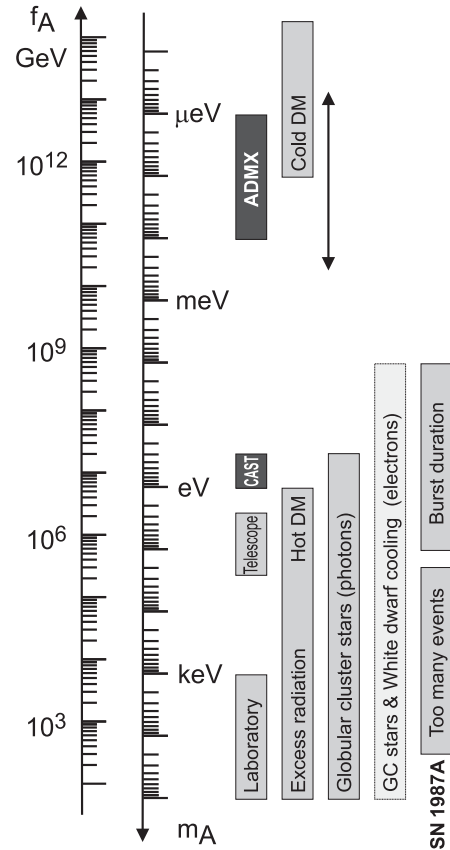


**Figure 1:** Exclusion ranges as described in the text. The dark intervals are the approximate CAST and ADMX search ranges. Limits on coupling strengths are translated into limits on  $m_A$  and  $f_A$  using  $z = 0.56$  and the KSVZ values for the coupling strengths. The “Laboratory” bar is a rough representation of the exclusion range for standard or variant axions. The “GC stars and white-dwarf cooling” range uses the DFSZ model with an axion-electron coupling corresponding to  $\cos^2 \beta = 1/2$ . The Cold Dark Matter exclusion range is particularly uncertain. We show the benchmark case from the misalignment mechanism.

at the density  $3 \times 10^{14}$  g cm $^{-3}$  and temperature 30 MeV should not exceed about  $1 \times 10^{19}$  erg g $^{-1}$  s $^{-1}$  [36]. The energy-loss rate from nucleon bremsstrahlung,  $N + N \rightarrow N + N + A$ , is  $(C_N/2f_A)^2 (T^4/\pi^2 m_N) F$ . Here  $F$  is a numerical factor that represents an integral over the dynamical spin-density structure function because axions couple to the nucleon spin. For realistic conditions, even after considerable effort, one is limited to a heuristic estimate leading to  $F \approx 1$  [37].

The SN 1987A limits are of particular interest for hadronic axions where the bounds on  $\alpha_{Aee}$  are moot. Within uncertainties of  $z = m_u/m_d$  a reasonable choice for the coupling constants is then  $C_p = -0.4$  and  $C_n = 0$ . Using a proton fraction of 0.3,  $F = 1$ , and  $T = 30$  MeV one finds [37]

$$f_A \gtrsim 4 \times 10^8 \text{ GeV} \quad \text{and} \quad m_A \lesssim 16 \text{ meV}. \quad (13)$$

## Gauge & Higgs Boson Particle Listings

### Axions ( $A^0$ ) and Other Very Light Bosons

If axions interact sufficiently strongly they are trapped. Only about three orders of magnitude in  $g_{ANN}$  or  $m_A$  are excluded, a range shown somewhat schematically in Figure 1. For even larger couplings, the axion flux would have been negligible, yet it would have triggered additional events in the detectors, excluding a further range [44]. A possible gap between these two SN 1987A arguments was discussed as the “hadronic axion window” under the assumption that  $G_{A\gamma\gamma}$  was anomalously small [45]. This range is now excluded by hot dark matter bounds (see below).

The very tentative indication for additional WD cooling by axion emission described above is not in conflict with SN 1987A bounds. Still, if the WD interpretation were correct, SNe would lose a large fraction of their energy as axions. This would lead to a diffuse SN axion background (DSAB) in the universe with an energy density comparable to the extra-galactic background light [46]. However, there is no apparent way of detecting it or the axion burst from the next nearby SN.

#### III.2 Searches for solar axions

Instead of using stellar energy losses to derive axion limits, one can also search directly for these fluxes, notably from the Sun. The main focus has been on axion-like particles with a two-photon vertex. They are produced by the Primakoff process with a flux given by Equation 11 and can be detected at Earth with the reverse process in a macroscopic  $B$ -field (“axion helioscope”) [5]. The average energy of solar axions of 4.2 keV implies a photon-axion oscillation length in vacuum of  $2\pi(2\omega/m_A^2) \sim \mathcal{O}(1 \text{ mm})$ , precluding the vacuum mixing from achieving its theoretical maximum in any practical magnet. However, one can endow the photon with an effective mass in a gas,  $m_\gamma = \omega_{\text{plas}}$ , thus matching the axion and photon dispersion relations [47].

An early implementation of these ideas used a conventional dipole magnet, with a conversion volume of variable-pressure gas with a xenon proportional chamber as x-ray detector [48]. The conversion magnet was fixed in orientation and collected data for about 1000 s/day. Axions were excluded for  $G_{A\gamma\gamma} < 3.6 \times 10^{-9} \text{ GeV}^{-1}$  for  $m_A < 0.03 \text{ eV}$ , and  $G_{A\gamma\gamma} < 7.7 \times 10^{-9} \text{ GeV}^{-1}$  for  $0.03 < m_A < 0.11 \text{ eV}$  at 95% CL.

Later, the Tokyo axion helioscope used a superconducting magnet on a tracking mount, viewing the Sun continuously. They reported  $G_{A\gamma\gamma} < 6 \times 10^{-10} \text{ GeV}^{-1}$  for  $m_A < 0.3 \text{ eV}$  [49]. Recently this experiment was recommissioned and a similar limit for masses around 1 eV was reported [50]. These exclusion ranges are shown in Figure 2.

The most recent helioscope CAST (CERN Axion Solar Telescope) uses a decommissioned LHC dipole magnet on a tracking mount. The hardware includes grazing-incidence x-ray optics with solid-state x-ray detectors, as well as a novel x-ray Micromegas position-sensitive gaseous detector. CAST has established a 95% CL limit  $G_{A\gamma\gamma} < 8.8 \times 10^{-11} \text{ GeV}^{-1}$  for  $m_A < 0.02 \text{ eV}$  [51]. To cover larger masses, the magnet bores are filled with a gas at varying pressure. The runs with

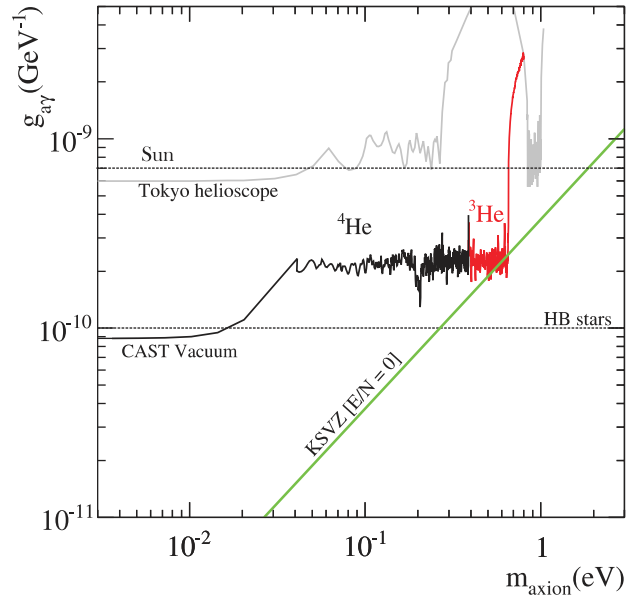


**Figure 2:** Solar exclusion plot for axion-like particles (adapted from [53]). The green solid line corresponds to KSVZ axions.

$^4\text{He}$  cover masses up to about 0.4 eV [52], providing the  $^4\text{He}$  limits shown in Figure 2. To cover yet larger masses to about 1.15 eV,  $^3\text{He}$  was used to achieve a larger pressure at cryogenic temperatures. First limits up to 0.64 eV were recently published [53], allowing CAST to “cross the axion line” for the KSVZ model (Figure 2).

Going to yet larger masses in a helioscope search is not well motivated because of the cosmic hot dark matter bound of  $m_A \lesssim 0.7 \text{ eV}$  (see below). Sensitivity to significantly smaller values of  $G_{A\gamma\gamma}$  can be achieved with a next-generation axion helioscope with a much larger magnetic-field cross section. Realistic design options for this “International Axion Observatory” (IAXO) have been studied in some detail [54].

Other Primakoff searches for solar axions have been carried out using crystal detectors, exploiting the coherent conversion of axions into photons when the axion angle of incidence satisfies a Bragg condition with a crystal plane [55]. However, none of these limits is more restrictive than the one derived from solar neutrinos that was discussed earlier.

Another idea is to look at the Sun with an x-ray satellite when the Earth is in between. Solar axions would convert in the Earth magnetic field on the far side and could be detected [56]. The sensitivity to  $G_{A\gamma\gamma}$  could be comparable to CAST, but only for much smaller  $m_A$ . Deep solar x-ray measurements with existing satellites, using the solar magnetosphere as conversion region, have reported preliminary limits on  $G_{A\gamma\gamma}$  [57].

#### III.3 Conversion of astrophysical photon fluxes

Large-scale  $B$  fields exist in astrophysics that can induce axion-photon oscillations. In practical cases,  $B$  is much smaller than in the laboratory, whereas the conversion region  $L$  is much

See key on page 457

## Gauge & Higgs Boson Particle Listings Axions ( $A^0$ ) and Other Very Light Bosons

larger. Therefore, while the product  $BL$  can be large, realistic sensitivities are usually restricted to very low-mass particles, far away from the “axion line” in a plot like Figure 2.

One example is SN 1987A, which would have emitted a burst of axion-like particles due to the Primakoff production in its core. They would have partially converted into  $\gamma$ -rays in the galactic  $B$ -field. The absence of a  $\gamma$ -ray burst in coincidence with SN 1987A neutrinos provides a limit  $G_{A\gamma\gamma} \lesssim 1 \times 10^{-11} \text{ GeV}^{-1}$  for  $m_A \lesssim 10^{-9} \text{ eV}$  [58], the most restrictive limit for very small  $m_A$ . Axion-like particles from other stars (e.g. magnetic white dwarfs or neutron stars) can be converted to photons, but no tangible new limits or signatures seem to have appeared, except perhaps from solar x-ray observations (see above).

Magnetically induced oscillations between photons and axion-like particles (ALPs) can modify the photon fluxes from distant sources in various ways: (i) Frequency-dependent dimming. (ii) Modified polarization. (iii) Avoiding absorption by propagation in the form of axions. For example, dimming of SNe Ia could influence the interpretation in terms of cosmic acceleration [59], although it has become clear that photon-ALP conversion could only be a subdominant effect [60]. More recently, it appears that the universe could be too transparent to TeV  $\gamma$ -rays that should be absorbed by pair production on the extra-galactic background light [61]. The situation is not conclusive at present, but the possible role of photon-ALP oscillations in TeV  $\gamma$ -ray astronomy is tantalizing [62].

### IV. COSMIC AXIONS

#### IV.1 Cosmic axion populations

In the early universe, axions are produced by processes involving quarks and gluons [63]. After color confinement, the dominant thermalization process is  $\pi + \pi \leftrightarrow \pi + A$  [21]. The resulting axion population would contribute a hot dark matter component in analogy to massive neutrinos. Cosmological precision data provide restrictive constraints on a possible hot dark-matter fraction that translate into  $m_A < 0.7 \text{ eV}$  at the 95% statistical CL [64], but in detail depend on the used data set and assumed cosmological model.

For  $m_A \gtrsim 20 \text{ eV}$ , axions decay fast on a cosmic time scale, removing the axion population while injecting photons. This excess radiation provides additional limits up to very large axion masses [65]. An anomalously small  $G_{A\gamma\gamma}$  provides no loophole because suppressing decays leads to thermal axions overdominating the mass density of the universe.

The main cosmological interest in axions derives from their possible role as cold dark matter (CDM). In addition to thermal processes, axions are abundantly produced by the “misalignment mechanism” [66]. After the breakdown of the PQ symmetry, the axion field relaxes somewhere in the “bottom of the wine bottle” potential. Near the QCD epoch, instanton effects explicitly break the PQ symmetry, the very effect that causes dynamical PQ symmetry restoration. This “tilting of the wine

bottle” drives the axion field toward the CP-conserving minimum, thereby exciting coherent oscillations of the axion field that ultimately represent a condensate of CDM. The cosmic mass density in this homogeneous field mode is [67]

$$\Omega_A h^2 \approx 0.7 \left( \frac{f_A}{10^{12} \text{ GeV}} \right)^{7/6} \left( \frac{\bar{\Theta}_i}{\pi} \right)^2, \quad (14)$$

where  $h$  is the present-day Hubble expansion parameter in units of  $100 \text{ km s}^{-1} \text{ Mpc}^{-1}$ , and  $-\pi \leq \bar{\Theta}_i \leq \pi$  is the initial “misalignment angle” relative to the CP-conserving position. If the PQ symmetry breakdown takes place after inflation,  $\bar{\Theta}_i$  will take on different values in different patches of the universe. The average contribution is [67]

$$\Omega_A h^2 \approx 0.3 \left( \frac{f_A}{10^{12} \text{ GeV}} \right)^{7/6}. \quad (15)$$

Comparing with the measured CDM density of  $\Omega_{\text{CDM}} h^2 \approx 0.13$  implies that axions with  $m_A \approx 10 \text{ } \mu\text{eV}$  provide the dark matter, whereas smaller masses are excluded (Figure 1).

This density sets only a rough scale for the expected  $m_A$ . The mass of CDM axions could be significantly smaller or larger than  $10 \text{ } \mu\text{eV}$ . Apart from the overall particle physics uncertainties, the cosmological sequence of events is crucial. Assuming axions make up CDM, much smaller masses are possible if inflation took place after the PQ transition and the initial value  $\bar{\Theta}_i$  was small (“anthropic axion window” [68]). The oscillating galactic dark matter axion field induces extremely small oscillating nuclear electric dipole moments. Conceivably, these could be measured by extremely tiny energy shifts in cold molecules [69].

Conversely, if the PQ transition took place after inflation, there are additional sources for nonthermal axions, notably the decay of cosmic strings and domain walls. According to Sikivie and collaborators, these populations are comparable to the misalignment contribution [67]. Other groups find a significantly enhanced axion density [70] or rather, a larger  $m_A$  value for axions providing CDM. Moreover, the spatial axion density variations are large at the QCD transition and they are not erased by free streaming. When matter begins to dominate the universe, gravitationally bound “axion mini clusters” form promptly [71]. A significant fraction of CDM axions can reside in these bound objects.

If the reheat temperature after inflation is too small to restore PQ symmetry, the axion field is present during inflation. It is subject to quantum fluctuations, leading to isocurvature fluctuations that are severely constrained [72].

#### IV.2 Telescope searches

The two-photon decay is extremely slow for axions with masses in the CDM regime, but could be detectable for eV masses. The signature would be a quasi-monochromatic emission line from galaxies and galaxy clusters. The expected optical line intensity for DFSZ axions is similar to the continuum night emission. An early search in three rich Abell clusters [73],

## Gauge & Higgs Boson Particle Listings

### Axions ( $A^0$ ) and Other Very Light Bosons

and a recent search in two rich Abell clusters [74], exclude the “Telescope” range in Figure 1 unless the axion-photon coupling is strongly suppressed. Of course, axions in this mass range would anyway provide an excessive hot DM contribution.

Very low-mass axions in halos produce a weak quasi-monochromatic radio line. Virial velocities in undisrupted dwarf galaxies are very low, and the axion decay line would therefore be extremely narrow. A search with the Haystack radio telescope on three nearby dwarf galaxies provided a limit  $G_{A\gamma\gamma} < 1.0 \times 10^{-9} \text{ GeV}^{-1}$  at 96% CL for  $298 < m_A < 363 \mu\text{eV}$  [75]. However, this combination of  $m_A$  and  $G_{A\gamma\gamma}$  does not exclude plausible axion models.

#### IV.3 Microwave cavity experiments

The limits of Figure 1 suggest that axions, if they exist, provide a significant fraction or even perhaps all of the cosmic CDM. In a broad range of the plausible  $m_A$  range for CDM, galactic halo axions may be detected by their resonant conversion into a quasi-monochromatic microwave signal in a high-Q electromagnetic cavity permeated by a strong static  $B$  field [5,76]. The cavity frequency is tunable, and the signal is maximized when the frequency is the total axion energy, rest mass plus kinetic energy, of  $\nu = (m_A/2\pi) [1 + \mathcal{O}(10^{-6})]$ , the width above the rest mass representing the virial distribution in the galaxy. The frequency spectrum may also contain finer structure from axions more recently fallen into the galactic potential and not yet completely virialized [77].

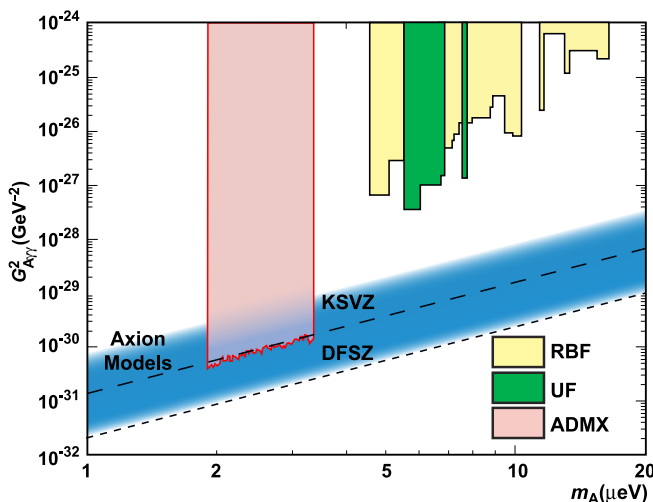


**Figure 3:** Exclusion region reported from the microwave cavity experiments RBF and UF [78] and ADMX [79]. A local dark-matter density of  $450 \text{ MeV cm}^{-3}$  is assumed.

The feasibility of this technique was established in early experiments of relatively small sensitive volume,  $\mathcal{O}(1 \text{ liter})$ , with HFET-based amplifiers, setting limits in the range  $4.5 < m_A < 16.3 \mu\text{eV}$  [78], but lacking by 2–3 orders of magnitude the sensitivity required to detect realistic axions.

Later, ADMX ( $B \sim 8 \text{ T}$ ,  $V \sim 200 \text{ liters}$ ) has achieved sensitivity to KSVZ axions, assuming they saturate the local dark matter density and are well virialized, over the mass range  $1.9\text{--}3.3 \mu\text{eV}$  [79]. Should halo axions have a component not yet virialized, ADMX is sensitive to DFSZ axions [80]. The corresponding 90% CL exclusion regions shown in Figure 3 are normalized to an assumed local CDM density of  $7.5 \times 10^{-25} \text{ g cm}^{-3}$  ( $450 \text{ MeV cm}^{-3}$ ). More recently the ADMX experiment commissioned an upgrade [81] that replaces the microwave HFET amplifiers by near quantum-limited low-noise dc SQUID microwave amplifiers [82], allowing for a significantly improved sensitivity [83]. This apparatus is also sensitive to other hypothetical light bosons over a limited parameter space [84]. Alternatively, a Rydberg atom single-photon detector [85] can in principle evade the standard quantum limit for coherent photon detection.

#### Conclusions

Experimental, astrophysical, and cosmological limits have been refined and indicate that axions, if they exist, very likely have very low mass,  $m_A \lesssim 10 \text{ meV}$ , suggesting that axions are a non-negligible fraction of the cosmic CDM. The upgraded versions of the ADMX experiment will ultimately cover the range  $1\text{--}100 \mu\text{eV}$  with a sensitivity allowing one to detect such axions, unless the local DM density is unexpectedly small or the axion-photon coupling anomalously weak. Other experimental techniques remain of interest to search for axion-like particles, although at present no method besides the DM search is known that could detect realistic axions obeying the astrophysical and cosmological limits, and fulfilling the QCD-implied relationship between mass and coupling strength.

#### References

1. R.D. Peccei and H. Quinn, Phys. Rev. Lett. **38**, 1440 (1977), Phys. Rev. **D16**, 1791 (1977).
2. S. Weinberg, Phys. Rev. Lett. **40**, 223 (1978); F. Wilczek, Phys. Rev. Lett. **40**, 279 (1978).
3. F. Wilczek, Phys. Rev. Lett. **49**, 1549 (1982).
4. Y. Chikashige, R.N. Mohapatra, and R.D. Peccei, Phys. Lett. **98B**, 265 (1981); G.B. Gelmini and M. Roncadelli, Phys. Lett. **99B**, 411 (1981).
5. P. Sikivie, Phys. Rev. Lett. **51**, 1415 (1983) and Erratum *ibid.*, **52**, 695 (1984).
6. C.A. Baker *et al.*, Phys. Rev. Lett. **97**, 131801 (2006).
7. H. Georgi, D.B. Kaplan, and L. Randall, Phys. Lett. **B169**, 73 (1986).
8. H. Leutwyler, Phys. Lett. **B378**, 313 (1996).
9. Mini review on Quark Masses in: C. Amsler *et al.* (Particle Data Group), Phys. Lett. **B667**, 1 (2008).
10. T.W. Donnelly *et al.*, Phys. Rev. **D18**, 1607 (1978); S. Barshay *et al.*, Phys. Rev. Lett. **46**, 1361 (1981); A. Barroso and N.C. Mukhopadhyay, Phys. Lett. **B106**, 91 (1981); R.D. Peccei, in *Proceedings of Neutrino '81*, Honolulu, Hawaii, Vol. 1, p. 149 (1981);

See key on page 457

## Gauge & Higgs Boson Particle Listings Axions ( $A^0$ ) and Other Very Light Bosons

- L.M. Krauss and F. Wilczek, Phys. Lett. **B173**, 189 (1986).
11. J. Schweppe *et al.*, Phys. Rev. Lett. **51**, 2261 (1983);  
T. Cowan *et al.*, Phys. Rev. Lett. **54**, 1761 (1985).
  12. R.D. Peccei, T.T. Wu, and T. Yanagida, Phys. Lett. **B172**, 435 (1986).
  13. W.A. Bardeen, R.D. Peccei, and T. Yanagida, Nucl. Phys. **B279**, 401 (1987).
  14. J.E. Kim, Phys. Rev. Lett. **43**, 103 (1979);  
M.A. Shifman, A.I. Vainshtein, and V.I. Zakharov, Nucl. Phys. **B166**, 493 (1980).
  15. M. Dine, W. Fischler, and M. Srednicki, Phys. Lett. **B104**, 199 (1981);  
A.R. Zhitnitsky, Sov. J. Nucl. Phys. **31**, 260 (1980).
  16. S.L. Cheng, C.Q. Geng, and W.T. Ni, Phys. Rev. **D52**, 3132 (1995).
  17. G. Raffelt and D. Seckel, Phys. Rev. Lett. **60**, 1793 (1988);  
M. Carena and R.D. Peccei, Phys. Rev. **D40**, 652 (1989);  
K. Choi, K. Kang, and J.E. Kim, Phys. Rev. Lett. **62**, 849 (1989).
  18. V.Y. Alexakhin *et al.* (COMPASS Collab.), Phys. Lett. **B647**, 8 (2007).
  19. A. Airapetian *et al.* (HERMES Collab.), Phys. Rev. **D75**, 012007 (2007) and Erratum *ibid.*, **D76**, 039901 (2007).
  20. J.R. Ellis and M. Karliner, in: *The spin structure of the nucleon: International school of nucleon structure* (3–10 August 1995, Erice, Italy), ed. by B. Frois, V.W. Hughes, and N. De Groot (World Scientific, Singapore, 1997) [hep-ph/9601280].
  21. S. Chang and K. Choi, Phys. Lett. **B316**, 51 (1993).
  22. D.A. Dicus *et al.*, Phys. Rev. **D18**, 1829 (1978).
  23. G. Raffelt and L. Stodolsky, Phys. Rev. **D37**, 1237 (1988).
  24. K. van Bibber *et al.*, Phys. Rev. Lett. **59**, 759 (1987).
  25. G. Ruoso *et al.*, Z. Phys. **C56**, 505 (1992);  
R. Cameron *et al.*, Phys. Rev. **D47**, 3707 (1993).
  26. M. Fouche *et al.* (BMV Collab.), Phys. Rev. **D78**, 032013 (2008);  
P. Pagnat *et al.* (OSQAR Collab.), Phys. Rev. **D78**, 092003 (2008);  
A. Chou *et al.* (GammeV T-969 Collab.), Phys. Rev. Lett. **100**, 080402 (2008);  
A. Afanasev *et al.* (LIPSS Collab.), Phys. Rev. Lett. **101**, 120401 (2008);  
K. Ehret *et al.* (ALPS Collab.), Phys. Lett. **B689**, 149 (2010).
  27. F. Hoogeveen and T. Ziegenhagen, Nucl. Phys. **B358**, 3 (1991);  
P. Sikivie, D. Tanner, and K. van Bibber, Phys. Rev. Lett. **98**, 172002 (2007);  
G. Mueller *et al.*, Phys. Rev. **D80**, 072004 (2009).
  28. A. Melissinos, Phys. Rev. Lett. **102**, 202001 (2009).
  29. L. Maiani *et al.*, Phys. Lett. **B175**, 359 (1986).
  30. Y. Semertzidis *et al.*, Phys. Rev. Lett. **64**, 2988 (1990).
  31. E. Zavattini *et al.* (PVLAS Collab.), Phys. Rev. Lett. **96**, 110406 (2006).
  32. E. Zavattini *et al.* (PVLAS Collab.), Phys. Rev. **D77**, 032006 (2008).
  33. E. Fischbach and C. Talmadge, Nature **356**, 207 (1992).
  34. J.E. Moody and F. Wilczek, Phys. Rev. D **30**, 130(1984);  
A.N. Youdin *et al.*, Phys. Rev. Lett. **77**, 2170 (1996);  
Wei-Tou Ni *et al.*, Phys. Rev. Lett. **82**, 2439 (1999);  
D.F. Phillips *et al.*, Phys. Rev. **D63**, 111101 (R)(2001);  
B.R. Heckel *et al.* (Eöt-Wash Collab.), Phys. Rev. Lett. **97**, 021603 (2006);  
S.A. Hoedl *et al.*, Phys. Rev. Lett. **106**, 041801 (2011).
  35. M.S. Turner, Phys. Reports **197**, 67 (1990);  
G.G. Raffelt, Phys. Reports **198**, 1 (1990).
  36. G.G. Raffelt, *Stars as Laboratories for Fundamental Physics*, (Univ. of Chicago Press, Chicago, 1996).
  37. G.G. Raffelt, Lect. Notes Phys. **741**, 51 (2008).
  38. P. Gondolo and G. Raffelt, Phys. Rev. **D79**, 107301 (2009).
  39. H. Schlattl, A. Weiss, and G. Raffelt, Astropart. Phys. **10**, 353 (1999).
  40. G. Raffelt and A. Weiss, Phys. Rev. **D51**, 1495 (1995);  
M. Catelan, J.A. de Freitas Pacheco, and J.E. Horvath, Astrophys. J. **461**, 231 (1996).
  41. G.G. Raffelt, Phys. Lett. **B166**, 402 (1986);  
S.I. Blinnikov and N.V. Dunina-Barkovskaya, Mon. Not. R. Astron. Soc. **266**, 289 (1994).
  42. J. Isern *et al.*, Astrophys. J. Lett. **682**, L109 (2008);  
J. Isern *et al.*, J. Phys. Conf. Ser. **172**, 012005 (2009).
  43. J. Isern *et al.*, Astron. Astrophys. **512**, A86 (2010);  
A.H. Córscico *et al.*, arXiv:1108.3541.
  44. J. Engel, D. Seckel, and A.C. Hayes, Phys. Rev. Lett. **65**, 960 (1990).
  45. T. Moroi and H. Murayama, Phys. Lett. **B440**, 69 (1998).
  46. G.G. Raffelt, J. Redondo, and N. Viaux Maira, Phys. Rev. **D84**, 103008 (2011).
  47. K. van Bibber *et al.*, Phys. Rev. **D39**, 2089 (1989).
  48. D. Lazarus *et al.*, Phys. Rev. Lett. **69**, 2333 (1992).
  49. S. Moriyama *et al.*, Phys. Lett. **B434**, 147 (1998);  
Y. Inoue *et al.*, Phys. Lett. **B536**, 18 (2002).
  50. M. Minowa *et al.*, Phys. Lett. **B668**, 93 (2008).
  51. S. Andriamonje *et al.* (CAST Collab.), JCAP **0704**, 010 (2007).
  52. E. Arik *et al.* (CAST Collab.), JCAP **0902**, 008 (2009).
  53. E. Arik *et al.* (CAST Collab.), Phys. Rev. Lett. **107**, 261302 (2011).
  54. I. Irastorza *et al.*, JCAP **0611**, 013 (2011)..
  55. F.T. Avignone III *et al.*, Phys. Rev. Lett. **81**, 5068 (1998);  
A. Morales *et al.* (COSME Collab.), Astropart. Phys. **16**, 325 (2002);  
R. Bernabei *et al.*, Phys. Lett. **B515**, 6 (2001);  
Z. Ahmed *et al.* (CDMS Collab.), Phys. Rev. Lett. **103**, 141802 (2009).
  56. H. Davoudiasl and P. Huber, Phys. Rev. Lett. **97**, 141302 (2006).
  57. H.S. Hudson *et al.*, arXiv:1201.4607.
  58. J.W. Brockway, E.D. Carlson, and G.G. Raffelt, Phys. Lett. **B383**, 439 (1996);  
J.A. Grifols, E. Massó, and R. Toldrà, Phys. Rev. Lett. **77**, 2372 (1996).
  59. C. Csaki, N. Kaloper, and J. Terning, Phys. Rev. Lett. **88**, 161302 (2002).
  60. A. Mirizzi, G.G. Raffelt, and P.D. Serpico, Lect. Notes Phys. **741**, 115 (2008).
  61. D. Horns and M. Meyer, JCAP **1202**, 033 (2012).
  62. A. De Angelis, G. Galanti, and M. Roncadelli, Phys. Rev. **D84**, 105030 (2011).



# Gauge & Higgs Boson Particle Listings

## Axions ( $A^0$ ) and Other Very Light Bosons

63. M.S. Turner, Phys. Rev. Lett. **59**, 2489 (1987) and Erratum *ibid.*, **60**, 1101 (1988);  
E. Massó, F. Rota, and G. Zsembinszki, Phys. Rev. **D66**, 023004 (2002).
64. A. Melchiorri, O. Mena, and A. Slosar, Phys. Rev. **D76**, 041303 (2007);  
S. Hannestad *et al.*, JCAP **0804**, 019 (2008);  
S. Hannestad *et al.*, JCAP **0810**, 001 (2010).
65. E. Massó and R. Toldra, Phys. Rev. **D55**, 7967 (1997).
66. J. Preskill, M.B. Wise, and F. Wilczek, Phys. Lett. **B120**, 127 (1983);  
L.F. Abbott and P. Sikivie, Phys. Lett. **B120**, 133 (1983);  
M. Dine and W. Fischler, Phys. Lett. **B120**, 137 (1983).
67. P. Sikivie, Lect. Notes Phys. **741**, 19 (2008).
68. M. Tegmark *et al.*, Phys. Rev. **D73**, 023505 (2006);  
K. Mack, JCAP **1107**, 021 (2011).
69. P.W. Graham and S. Rajendran Phys. Rev. **D84**, 055013 (2011).
70. O. Wantz and E.P.S. Shellard Phys. Rev. **D82**, 123508 (2010);  
T. Hiramatsu *et al.*, Phys. Rev. **D83**, 123531 (2011);  
T. Hiramatsu *et al.*, arXiv:1202.5851.
71. E.W. Kolb and I.I. Tkachev, Phys. Rev. Lett. **71**, 3051 (1993), *Astrophys. J.* **460**, L25 (1996);  
K.M. Zurek, C.J. Hogan, and T.R. Quinn, Phys. Rev. **D75**, 043511 (2007).
72. M. Beltrán, J. García-Bellido, and J. Lesgourgues, Phys. Rev. **D75**, 103507 (2007);  
M.P. Hertzberg, M. Tegmark, and F. Wilczek, Phys. Rev. **D78**, 083507 (2008);  
J. Hamann *et al.*, JCAP **0906**, 022 (2009).
73. M. Bershadsky *et al.*, Phys. Rev. Lett. **66**, 1398 (1991);  
M. Ressel, Phys. Rev. **D44**, 3001 (1991).
74. D. Grin *et al.*, Phys. Rev. **D75**, 105018 (2007).
75. B.D. Blout *et al.*, *Astrophys. J.* **546**, 825 (2001).
76. P. Sikivie, Phys. Rev. **D32**, 2988 (1985);  
L. Krauss *et al.*, Phys. Rev. Lett. **55**, 1797 (1985);  
R. Bradley *et al.*, *Rev. Mod. Phys.* **75**, 777 (2003).
77. P. Sikivie and J. Ipser, Phys. Lett. **B291**, 288 (1992);  
P. Sikivie *et al.*, Phys. Rev. Lett. **75**, 2911 (1995).
78. S. DePanfilis *et al.*, Phys. Rev. Lett. **59**, 839 (1987);  
W. Wuensch *et al.*, Phys. Rev. **D40**, 3153 (1989);  
C. Hagmann *et al.*, Phys. Rev. **D42**, 1297 (1990).
79. S. Asztalos *et al.*, Phys. Rev. **D69**, 011101 (2004).
80. L. Duffy *et al.*, Phys. Rev. Lett. **95**, 091304 (2005).
81. S.J. Asztalos *et al.* (ADMX Collab.), arXiv:0910.5914.
82. S.J. Asztalos *et al.*, *Nucl. Instrum. Methods* **A656**, 39 (2011).
83. S.J. Asztalos *et al.*, Phys. Rev. Lett. **104**, 041301 (2010).
84. G. Rybka *et al.*, Phys. Rev. Lett. **105**, 051801 (2010);  
A. Wagner *et al.*, Phys. Rev. Lett. **105**, 171801 (2010).
85. I. Ogawa, S. Matsuki, and K. Yamamoto, Phys. Rev. **D53**, 1740 (1996);  
Y. Kishimoto *et al.*, Phys. Lett. **A303**, 279 (2002);  
M. Tada *et al.*, Phys. Lett. **A303**, 285 (2002);  
T. Haseyama *et al.*, *J. Low Temp. Phys.* **150**, 549 (2008).

>0.2	BARROSO	82	ASTR	Standard Axion
>0.25	<sup>1</sup> RAFFELT	82	ASTR	Standard Axion
>0.2	<sup>2</sup> DICUS	78c	ASTR	Standard Axion
	MIKAELIAN	78	ASTR	Stellar emission
>0.3	<sup>2</sup> SATO	78	ASTR	Standard Axion
>0.2	VYSOTSKII	78	ASTR	Standard Axion

<sup>1</sup> Lower bound from 5.5 MeV  $\gamma$ -ray line from the sun.

<sup>2</sup> Lower bound from requiring the red giants' stellar evolution not be disrupted by axion emission.

### $A^0$ (Axion) and Other Light Boson ( $X^0$ ) Searches in Hadron Decays

Limits are for branching ratios.

VALUE	CL%	DOCUMENT ID	TECN	COMMENT
•••				We do not use the following data for averages, fits, limits, etc. •••
$<7 \times 10^{-10}$	90	<sup>3</sup> ADLER	04 B787	$K^+ \rightarrow \pi^+ X^0$
$<7.3 \times 10^{-11}$	90	<sup>4</sup> ANISIMOVSK..04	B949	$K^+ \rightarrow \pi^+ X^0$
$<4.5 \times 10^{-11}$	90	<sup>5</sup> ADLER	02c B787	$K^+ \rightarrow \pi^+ X^0$
$<4 \times 10^{-5}$	90	<sup>6</sup> ADLER	01 B787	$K^+ \rightarrow \pi^+ \pi^0 A^0$
$<4.9 \times 10^{-5}$	90	AMMAR	01B CLEO	$B^\pm \rightarrow \pi^\pm (K^\pm) X^0$
$<5.3 \times 10^{-5}$	90	AMMAR	01B CLEO	$B^0 \rightarrow K_S^0 X^0$
$<3.3 \times 10^{-5}$	90	<sup>7</sup> ALTEGOER	98 NOMD	$\pi^0 \rightarrow \gamma X^0, m_{X^0} < 120$ MeV
$<5.0 \times 10^{-8}$	90	<sup>8</sup> KITCHING	97 B787	$K^+ \rightarrow \pi^+ X^0 (X^0 \rightarrow \gamma\gamma)$
$<5.2 \times 10^{-10}$	90	<sup>9</sup> ADLER	96 B787	$K^+ \rightarrow \pi^+ X^0$
$<2.8 \times 10^{-4}$	90	<sup>10</sup> AMSLER	96B CBAR	$\pi^0 \rightarrow \gamma X^0, m_{X^0} < 65$ MeV
$<3 \times 10^{-4}$	90	<sup>10</sup> AMSLER	96B CBAR	$\eta \rightarrow \gamma X^0, m_{X^0} = 50-200$ MeV
$<4 \times 10^{-5}$	90	<sup>10</sup> AMSLER	96B CBAR	$\eta' \rightarrow \gamma X^0, m_{X^0} = 50-925$ MeV
$<6 \times 10^{-5}$	90	<sup>10</sup> AMSLER	94B CBAR	$\pi^0 \rightarrow \gamma X^0, m_{X^0} = 65-125$ MeV
$<6 \times 10^{-5}$	90	<sup>10</sup> AMSLER	94B CBAR	$\eta \rightarrow \gamma X^0, m_{X^0} = 200-525$ MeV
$<7 \times 10^{-3}$	90	<sup>11</sup> MEIJERDREES94	CNTR	$\pi^0 \rightarrow \gamma X^0, m_{X^0} = 25$ MeV
$<2 \times 10^{-3}$	90	<sup>11</sup> MEIJERDREES94	CNTR	$\pi^0 \rightarrow \gamma X^0, m_{X^0} = 100$ MeV
$<2 \times 10^{-7}$	90	<sup>12</sup> ATIYA	93B B787	Sup. by ADLER 04
$<3 \times 10^{-13}$	90	<sup>13</sup> NG	93 COSM	$\pi^0 \rightarrow \gamma X^0$
$<1.1 \times 10^{-8}$	90	<sup>14</sup> ALLIEGRO	92 SPEC	$K^+ \rightarrow \pi^+ X^0 (X^0 \rightarrow e^+ e^-)$
$<5 \times 10^{-4}$	90	<sup>15</sup> ATIYA	92 B787	$\pi^0 \rightarrow \gamma X^0$
$<4 \times 10^{-6}$	90	<sup>16</sup> MEIJERDREES92	SPEC	$\pi^0 \rightarrow \gamma X^0, X^0 \rightarrow e^+ e^-, m_{X^0} = 100$ MeV
$<1 \times 10^{-7}$	90	<sup>17</sup> ATIYA	90B B787	Sup. by KITCHING 97
$<1.3 \times 10^{-8}$	90	<sup>18</sup> KORENCHENKO...	87 SPEC	$\pi^+ \rightarrow e^+ \nu A^0 (A^0 \rightarrow e^+ e^-)$
$<1 \times 10^{-9}$	90	<sup>19</sup> EICHLER	86 SPEC	Stopped $\pi^+ \rightarrow e^+ \nu A^0$
$<2 \times 10^{-5}$	90	<sup>20</sup> YAMAZAKI	84 SPEC	For $160 < m < 260$ MeV
$<(1.5-4) \times 10^{-6}$	90	<sup>20</sup> YAMAZAKI	84 SPEC	$K$ decay, $m_{X^0} \ll 100$ MeV
		<sup>21</sup> ASANO	82 CNTR	Stopped $K^+ \rightarrow \pi^+ X^0$
		<sup>22</sup> ASANO	81B CNTR	Stopped $K^+ \rightarrow \pi^+ X^0$
		<sup>23</sup> ZHITNITSKII	79	Heavy axion

<sup>3</sup> This limit applies for a mass near 180 MeV. For other masses in the range  $m_{X^0} = 150-250$  MeV the limit is less restrictive, but still improves ADLER 02c and ATIYA 93b.

<sup>4</sup> ANISIMOVSKY 04 bound is for  $m_{X^0} = 0$ .

<sup>5</sup> ADLER 02c bound is for  $m_{X^0} < 60$  MeV. See Fig. 2 for limits at higher masses.

<sup>6</sup> The quoted limit is for  $m_{X^0} = 0-80$  MeV. See their Fig. 5 for the limit at higher mass. The branching fraction limit assumes pure phase space decay distributions.

<sup>7</sup> ALTEGOER 98 looked for  $X^0$  from  $\pi^0$  decay which penetrate the shielding and convert to  $\pi^0$  in the external Coulomb field of a nucleus.

<sup>8</sup> KITCHING 97 limit is for  $B(K^+ \rightarrow \pi^+ X^0) \cdot B(X^0 \rightarrow \gamma\gamma)$  and applies for  $m_{X^0} \approx 50$  MeV,  $\tau_{X^0} < 10^{-10}$  s. Limits are provided for  $0 < m_{X^0} < 100$  MeV,  $\tau_{X^0} < 10^{-8}$  s.

<sup>9</sup> ADLER 96 looked for a peak in missing-mass distribution. This work is an update of ATIYA 93. The limit is for massless stable  $X^0$  particles and extends to  $m_{X^0} = 80$  MeV at the same level. See paper for dependence on finite lifetime.

<sup>10</sup> AMSLER 94B and AMSLER 96B looked for a peak in missing-mass distribution.

<sup>11</sup> The MEIJERDREES 94 limit is based on inclusive photon spectrum and is independent of  $X^0$  decay modes. It applies to  $\tau(X^0) > 10^{-23}$  sec.

<sup>12</sup> ATIYA 93B looked for a peak in missing mass distribution. The bound applies for stable  $X^0$  of  $m_{X^0} = 150-250$  MeV, and the limit becomes stronger ( $10^{-8}$ ) for  $m_{X^0} = 180-240$  MeV.

<sup>13</sup> NG 93 studied the production of  $X^0$  via  $\gamma\gamma \rightarrow \pi^0 \rightarrow \gamma X^0$  in the early universe at  $T \approx 1$  MeV. The bound on extra neutrinos from nucleosynthesis  $\Delta N_\nu < 0.3$  (WALKER 91) is employed. It applies to  $m_{X^0} \ll 1$  MeV in order to be relativistic down to nucleosynthesis temperature. See paper for heavier  $X^0$ .

<sup>14</sup> ALLIEGRO 92 limit applies for  $m_{X^0} = 150-340$  MeV and is the branching ratio times the decay probability. Limit is  $< 1.5 \times 10^{-8}$  at 99%CL.

<sup>15</sup> ATIYA 92 looked for a peak in missing mass distribution. The limit applies to  $m_{X^0} = 0-130$  MeV in the narrow resonance limit. See paper for the dependence on lifetime. Covariance requires  $X^0$  to be a vector particle.

<sup>16</sup> MEIJERDREES 92 limit applies for  $\tau_{X^0} = 10^{-23}-10^{-11}$  sec. Limits between  $2 \times 10^{-4}$  and  $4 \times 10^{-6}$  are obtained for  $m_{X^0} = 25-120$  MeV. Angular momentum conservation requires that  $X^0$  has spin  $\geq 1$ .

<sup>17</sup> ATIYA 90B limit is for  $B(K^+ \rightarrow \pi^+ X^0) \cdot B(X^0 \rightarrow \gamma\gamma)$  and applies for  $m_{X^0} = 50$  MeV,  $\tau_{X^0} < 10^{-10}$  s. Limits are also provided for  $0 < m_{X^0} < 100$  MeV,  $\tau_{X^0} < 10^{-8}$  s.

<sup>18</sup> KORENCHENKO 87 limit assumes  $m_{A^0} = 1.7$  MeV,  $\tau_{A^0} \lesssim 10^{-12}$  s, and  $B(A^0 \rightarrow e^+ e^-) = 1$ .

### $A^0$ (Axion) MASS LIMITS from Astrophysics and Cosmology

These bounds depend on model-dependent assumptions (i.e. — on a combination of axion parameters).

VALUE (MeV)	DOCUMENT ID	TECN	COMMENT
-------------	-------------	------	---------

••• We do not use the following data for averages, fits, limits, etc. •••



See key on page 457

# Gauge & Higgs Boson Particle Listings

## Axions ( $A^0$ ) and Other Very Light Bosons

- <sup>19</sup>EICHLER 86 looked for  $\pi^+ \rightarrow e^+ \nu A^0$  followed by  $A^0 \rightarrow e^+ e^-$ . Limits on the branching fraction depend on the mass and lifetime of  $A^0$ . The quoted limits are valid when  $\tau(A^0) \gtrsim 3 \times 10^{-10}$  s if the decays are kinematically allowed.
- <sup>20</sup>YAMAZAKI 84 looked for a discrete line in  $K^+ \rightarrow \pi^+ X$ . Sensitive to wide mass range (5–300 MeV), independent of whether X decays promptly or not.
- <sup>21</sup>ASANO 82 at KEK set limits for  $B(K^+ \rightarrow \pi^+ X^0)$  for  $m_{X^0} < 100$  MeV as BR  $< 4 \times 10^{-8}$  for  $\tau(X^0 \rightarrow n\gamma)$ 's  $> 1 \times 10^{-9}$  s, BR  $< 1.4 \times 10^{-6}$  for  $\tau < 1 \times 10^{-9}$  s.
- <sup>22</sup>ASANO 81B is KEK experiment. Set  $B(K^+ \rightarrow \pi^+ X^0) < 3.8 \times 10^{-8}$  at CL = 90%.
- <sup>23</sup>ZHITNITSKII 79 argue that a heavy axion predicted by YANG 78 ( $3 < m < 40$  MeV) contradicts experimental muon anomalous magnetic moments.

### $A^0$ (Axion) Searches in Quarkonium Decays

Decay or transition of quarkonium. Limits are for branching ratio.

VALUE	CL%	DOCUMENT ID	TECN	COMMENT
● ● ● We do not use the following data for averages, fits, limits, etc. ● ● ●				
$< 5 \times 10^{-5}$	90	<sup>24</sup> DRUZHININ 87	ND	$\phi \rightarrow A^0 \gamma (A^0 \rightarrow e^+ e^-)$
$< 2 \times 10^{-3}$	90	<sup>25</sup> DRUZHININ 87	ND	$\phi \rightarrow A^0 \gamma (A^0 \rightarrow \gamma \gamma)$
$< 7 \times 10^{-6}$	90	<sup>26</sup> DRUZHININ 87	ND	$\phi \rightarrow A^0 \gamma (A^0 \rightarrow \text{missing})$
$< 1.4 \times 10^{-5}$	90	<sup>27</sup> EDWARDS 82	CBAL	$J/\psi \rightarrow A^0 \gamma$
<sup>24</sup> The first DRUZHININ 87 limit is valid when $\tau_{A^0}/m_{A^0} < 3 \times 10^{-13}$ s/MeV and $m_{A^0} < 20$ MeV.				
<sup>25</sup> The second DRUZHININ 87 limit is valid when $\tau_{A^0}/m_{A^0} < 5 \times 10^{-13}$ s/MeV and $m_{A^0} < 20$ MeV.				
<sup>26</sup> The third DRUZHININ 87 limit is valid when $\tau_{A^0}/m_{A^0} > 7 \times 10^{-12}$ s/MeV and $m_{A^0} < 200$ MeV.				
<sup>27</sup> EDWARDS 82 looked for $J/\psi \rightarrow \gamma A^0$ decays by looking for events with a single $\gamma$ [of energy $\sim 1/2$ the $J/\psi(1S)$ mass], plus nothing else in the detector. The limit is inconsistent with the axion interpretation of the FAISSNER 81B result.				

### $A^0$ (Axion) Searches in Positronium Decays

Decay or transition of positronium. Limits are for branching ratio.

VALUE	CL%	DOCUMENT ID	TECN	COMMENT
● ● ● We do not use the following data for averages, fits, limits, etc. ● ● ●				
$< 4.4 \times 10^{-5}$	90	<sup>28</sup> BADERT... 02	CNTR	$\alpha\text{-Ps} \rightarrow \gamma X_1 X_2, m_{X_1} + m_{X_2} \leq 900 \text{ keV}$
$< 2 \times 10^{-4}$	90	MAENO 95	CNTR	$\alpha\text{-Ps} \rightarrow A^0 \gamma, m_{A^0} = 850\text{--}1013 \text{ keV}$
$< 3.0 \times 10^{-3}$	90	<sup>29</sup> ASAI 94	CNTR	$\alpha\text{-Ps} \rightarrow A^0 \gamma, m_{A^0} = 30\text{--}500 \text{ keV}$
$< 2.8 \times 10^{-5}$	90	<sup>30</sup> AKOPYAN 91	CNTR	$\alpha\text{-Ps} \rightarrow A^0 \gamma (A^0 \rightarrow \gamma \gamma), m_{A^0} < 30 \text{ keV}$
$< 1.1 \times 10^{-6}$	90	<sup>31</sup> ASAI 91	CNTR	$\alpha\text{-Ps} \rightarrow A^0 \gamma, m_{A^0} < 800 \text{ keV}$
$< 3.8 \times 10^{-4}$	90	GNINENKO 90	CNTR	$\alpha\text{-Ps} \rightarrow A^0 \gamma, m_{A^0} < 30 \text{ keV}$
$< (1\text{--}5) \times 10^{-4}$	95	<sup>32</sup> TSUCHIYAKI 90	CNTR	$\alpha\text{-Ps} \rightarrow A^0 \gamma, m_{A^0} = 300\text{--}900 \text{ keV}$
$< 6.4 \times 10^{-5}$	90	<sup>33</sup> ORITO 89	CNTR	$\alpha\text{-Ps} \rightarrow A^0 \gamma, m_{A^0} < 30 \text{ keV}$
<sup>34</sup> AMALDI 85 CNTR Ortho-positronium				
<sup>35</sup> CARBONI 83 CNTR Ortho-positronium				

- <sup>28</sup>BADERTSCHER 02 looked for a three-body decay of ortho-positronium into a photon and two penetrating (neutral or milli-charged) particles.
- <sup>29</sup>The ASAI 94 limit is based on inclusive photon spectrum and is independent of  $A^0$  decay modes.
- <sup>30</sup>The AKOPYAN 91 limit applies for a short-lived  $A^0$  with  $\tau_{A^0} < 10^{-13}$   $m_{A^0}$  [keV]s.
- <sup>31</sup>ASAI 91 limit translates to  $g_{A^0}^2 e^+ e^- / 4\pi < 1.1 \times 10^{-11}$  (90% CL) for  $m_{A^0} < 800$  keV.
- <sup>32</sup>The TSUCHIYAKI 90 limit is based on inclusive photon spectrum and is independent of  $A^0$  decay modes.
- <sup>33</sup>ORITO 89 limit translates to  $g_{A^0}^2 e^+ e^- / 4\pi < 6.2 \times 10^{-10}$ . Somewhat more sensitive limits are obtained for larger  $m_{A^0}$ :  $B < 7.6 \times 10^{-6}$  at 100 keV.
- <sup>34</sup>AMALDI 85 set limits  $B(A^0 \gamma) / B(\gamma \gamma) < (1\text{--}5) \times 10^{-6}$  for  $m_{A^0} = 900\text{--}100$  keV which are about 1/10 of the CARBONI 83 limits.
- <sup>35</sup>CARBONI 83 looked for ortho-positronium  $\rightarrow A^0 \gamma$ . Set limit for  $A^0$  electron coupling squared,  $g(eeA^0)^2 / (4\pi) < 6 \times 10^{-10}$  for  $m_{A^0}$  from 150–900 keV (CL = 99.7%). This is about 1/10 of the bound from  $g\text{--}2$  experiments.

### $A^0$ (Axion) Search in Photoproduction

VALUE	CL%	DOCUMENT ID	TECN	COMMENT
● ● ● We do not use the following data for averages, fits, limits, etc. ● ● ●				
		<sup>36</sup> BASSOMPIERRE... 95		$m_{A^0} = 1.8 \pm 0.2 \text{ MeV}$
<sup>36</sup> BASSOMPIERRE 95 is an extension of BASSOMPIERRE 93. They looked for a peak in the invariant mass of $e^+ e^-$ pairs in the region $m_{e^+ e^-} = 1.8 \pm 0.2$ MeV. They obtained bounds on the production rate $A^0$ for $\tau(A^0) = 10^{-18}\text{--}10^{-9}$ sec. They also found an excess of events in the range $m_{e^+ e^-} = 2.1\text{--}3.5$ MeV.				

### $A^0$ (Axion) Production in Hadron Collisions

Limits are for  $\sigma(A^0) / \sigma(\pi^0)$ .

VALUE	CL%	EVTS	DOCUMENT ID	TECN	COMMENT
● ● ● We do not use the following data for averages, fits, limits, etc. ● ● ●					

- |                              |     |                              |  |
|------------------------------|-----|------------------------------|--|
| <sup>37</sup> JAIN 07        | 07  | CNTR                         | $A^0 \rightarrow e^+ e^-$                            |
| <sup>38</sup> AHMAD 97       | 97  | SPEC                         | $e^+$ production                                     |
| <sup>39</sup> LEINBERGER 97  | 97  | SPEC                         | $A^0 \rightarrow e^+ e^-$                            |
| <sup>40</sup> GANZ 96        | 96  | SPEC                         | $A^0 \rightarrow e^+ e^-$                            |
| <sup>41</sup> KAMEL 96       | 96  | EMUL                         | $^{32}\text{S}$ emulsion, $A^0 \rightarrow e^+ e^-$  |
| <sup>42</sup> BLUEMLEIN 92   | 92  | BDMP                         | $A^0 N_Z \rightarrow \ell^+ \ell^- N_Z$              |
| <sup>43</sup> MEIJERDREES 92 | 92  | SPEC                         | $\pi^- p \rightarrow n A^0, A^0 \rightarrow e^+ e^-$ |
| <sup>44</sup> BLUEMLEIN 91   | 91  | BDMP                         | $A^0 \rightarrow e^+ e^-, 2\gamma$                   |
| <sup>45</sup> FAISSNER 89    | 89  | OSPK                         | Beam dump, $A^0 \rightarrow e^+ e^-$                 |
| <sup>46</sup> DEBOER 88      | 88  | RVUE                         | $A^0 \rightarrow e^+ e^-$                            |
| <sup>47</sup> EL-NADI 88     | 88  | EMUL                         | $A^0 \rightarrow e^+ e^-$                            |
| <sup>48</sup> FAISSNER 88    | 88  | OSPK                         | Beam dump, $A^0 \rightarrow 2\gamma$                 |
| <sup>49</sup> BADIÉ 86       | 86  | BDMP                         | $A^0 \rightarrow e^+ e^-$                            |
| <sup>50</sup> BERG SMA 85    | 85  | CHRM                         | CERN beam dump                                       |
| <sup>50</sup> BERG SMA 85    | 85  | CHRM                         | CERN beam dump                                       |
| <sup>51</sup> FAISSNER 83    | 83  | OSPK                         | Beam dump, $A^0 \rightarrow 2\gamma$                 |
| <sup>52</sup> FAISSNER 83B   | 83B | RVUE                         | LAMPF beam dump                                      |
| <sup>53</sup> FRANK 83B      | 83B | RVUE                         | LAMPF beam dump                                      |
| <sup>54</sup> HOFFMAN 83     | 83  | CNTR                         | $\pi p \rightarrow n A^0 (A^0 \rightarrow e^+ e^-)$  |
| <sup>55</sup> FETSCHER 82    | 82  | RVUE                         | See FAISSNER 81B                                     |
| <sup>56</sup> FAISSNER 81    | 81  | OSPK                         | CERN PS $\nu$ wideband                               |
| <sup>57</sup> FAISSNER 81B   | 81B | OSPK                         | Beam dump, $A^0 \rightarrow 2\gamma$                 |
| <sup>58</sup> KIM 81         | 81  | OSPK                         | 26 GeV $pN \rightarrow A^0 X$                        |
| <sup>59</sup> FAISSNER 80    | 80  | OSPK                         | Beam dump, $A^0 \rightarrow e^+ e^-$                 |
| $< 1 \times 10^{-8}$         | 90  | <sup>60</sup> JACQUES 80     | HLBC 28 GeV protons                                  |
| $< 1 \times 10^{-14}$        | 90  | <sup>60</sup> JACQUES 80     | HLBC Beam dump                                       |
|                              |     | <sup>61</sup> SOUKAS 80      | CALO 28 GeV $p$ beam dump                            |
|                              |     | <sup>62</sup> BECHIS 79      | CNTR   |
| $< 1 \times 10^{-8}$         | 90  | <sup>63</sup> COTEUS 79      | OSPK Beam dump                                       |
| $< 1 \times 10^{-3}$         | 95  | <sup>64</sup> DISHAW 79      | CALO 400 GeV $pp$                                    |
| $< 1 \times 10^{-8}$         | 90  | ALIBRAN 78                   | HYBR Beam dump                                       |
| $< 6 \times 10^{-9}$         | 95  | ASRATYAN 78B                 | CALO Beam dump                                       |
| $< 1.5 \times 10^{-8}$       | 90  | <sup>65</sup> BELLOTTI 78    | HLBC Beam dump                                       |
| $< 5.4 \times 10^{-14}$      | 90  | <sup>65</sup> BELLOTTI 78    | HLBC $m_{A^0} = 1.5 \text{ MeV}$                     |
| $< 4.1 \times 10^{-9}$       | 90  | <sup>65</sup> BELLOTTI 78    | HLBC $m_{A^0} = 1 \text{ MeV}$                       |
| $< 1 \times 10^{-8}$         | 90  | <sup>66</sup> BOSETTI 78B    | HYBR Beam dump                                       |
|                              |     | <sup>67</sup> DONNELLY 78    |  |
| $< 0.5 \times 10^{-8}$       | 90  | HANSL 78D                    | WIRE Beam dump                                       |
|                              |     | <sup>68</sup> MICELMAC... 78 |  |
|                              |     | <sup>69</sup> VYSOTSII 78    |  |
- <sup>37</sup>JAIN 07 claims evidence for  $A^0 \rightarrow e^+ e^-$  produced in  $^{207}\text{Pb}$  collision on nuclear emulsion (Ag/Br) for  $m(A^0) = 7 \pm 1$  or  $19 \pm 1$  MeV and  $\tau(A^0) \leq 10^{-13}$  s.
- <sup>38</sup>AHMAD 97 reports a result of APEX Collaboration which studied positron production in  $^{238}\text{U} + ^{232}\text{Th}$  and  $^{238}\text{U} + ^{181}\text{Ta}$  collisions, without requiring a coincident electron. No narrow lines were found for  $250 < E_{e^+} < 750$  keV.
- <sup>39</sup>LEINBERGER 97 (ORANGE Collaboration) at GSI looked for a narrow sum-energy  $e^+ e^-$  line at  $\sim 635$  keV in  $^{238}\text{U} + ^{181}\text{Ta}$  collision. Limits on the production probability for a narrow sum-energy  $e^+ e^-$  line are set. See their Table 2.
- <sup>40</sup>GANZ 96 (EPOS II Collaboration) has placed upper bounds on the production cross section of  $e^+ e^-$  pairs from  $^{238}\text{U} + ^{181}\text{Ta}$  and  $^{238}\text{U} + ^{232}\text{Th}$  collisions at GSI. See Table 2 for limits both for back-to-back and isotropic configurations of  $e^+ e^-$  pairs. These limits rule out the existence of peaks in the  $e^+ e^-$  sum-energy distribution, reported by an earlier version of this experiment.
- <sup>41</sup>KAMEL 96 looked for  $e^+ e^-$  pairs from the collision of  $^{32}\text{S}$  (200 GeV/nucleon) and emulsion. No evidence of mass peaks is found in the region of sensitivity  $m_{e^+ e^-} > 2$  MeV.
- <sup>42</sup>BLUEMLEIN 92 is a proton beam dump experiment at Serpukhov with a secondary target to induce Bethe-Heitler production of  $e^+ e^-$  or  $\mu^+ \mu^-$  from the produce  $A^0$ . See Fig. 5 for the excluded region in  $m_{A^0}$ - $x$  plane. For the standard axion,  $0.3 < x < 2.5$  is excluded at 95% CL. If combined with BLUEMLEIN 91,  $0.008 < x < 32$  is excluded.
- <sup>43</sup>MEIJERDREES 92 give  $\Gamma(\pi^- p \rightarrow n A^0) / \Gamma(\pi^- p \rightarrow \text{all}) < 10^{-5}$  (90% CL) for  $m_{A^0} = 100$  MeV,  $\tau_{A^0} = 10^{-11}\text{--}10^{-23}$  sec. Limits ranging from  $2.5 \times 10^{-3}$  to  $10^{-7}$  are given for  $m_{A^0} = 25\text{--}136$  MeV.
- <sup>44</sup>BLUEMLEIN 91 is a proton beam dump experiment at Serpukhov. No candidate event for  $A^0 \rightarrow e^+ e^-, 2\gamma$  are found. Fig. 6 gives the excluded region in  $m_{A^0}$ - $x$  plane ( $x = \tan\beta = v_2/v_1$ ). Standard axion is excluded for  $0.2 < m_{A^0} < 3.2$  MeV for most  $x > 1$ ,  $0.2\text{--}11$  MeV for most  $x < 1$ .
- <sup>45</sup>FAISSNER 89 searched for  $A^0 \rightarrow e^+ e^-$  in a proton beam dump experiment at SIN. No excess of events was observed over the background. A standard axion with mass  $2m_e\text{--}20$  MeV is excluded. Lower limit on  $f_{A^0}$  of  $\sim 10^4$  GeV is given for  $m_{A^0} = 2m_e\text{--}20$  MeV.
- <sup>46</sup>DEBOER 88 reanalyze EL-NADI 88 data and claim evidence for three distinct states with mass  $\sim 1.1, \sim 2.1$ , and  $\sim 9$  MeV, lifetimes  $10^{-16}\text{--}10^{-15}$  s decaying to  $e^+ e^-$  and note the similarity of the data with those of a cosmic-ray experiment by Bristol group (B.M. Anand, Proc. of the Royal Society of London, Section A **A22** 183 (1953)). For a criticism see PERKINS 89, who suggests that the events are compatible with  $\pi^0$  Dalitz decay. DEBOER 89B is a reply which contests the criticism.
- <sup>47</sup>EL-NADI 88 claim the existence of a neutral particle decaying into  $e^+ e^-$  with mass  $1.60 \pm 0.59$  MeV, lifetime  $(0.15 \pm 0.01) \times 10^{-14}$  s, which is produced in heavy ion interactions with emulsion nuclei at  $\sim 4$  GeV/c/nucleon.
- <sup>48</sup>FAISSNER 88 is a proton beam dump experiment at SIN. They found no candidate event for  $A^0 \rightarrow \gamma\gamma$ . A standard axion decaying to  $2\gamma$  is excluded except for a region  $x \approx 1$ . Lower limit on  $f_{A^0}$  of  $10^2\text{--}10^3$  GeV is given for  $m_{A^0} = 0.1\text{--}1$  MeV.

# Gauge & Higgs Boson Particle Listings

## Axions ( $A^0$ ) and Other Very Light Bosons

- <sup>49</sup> BADIÉ 86 did not find long-lived  $A^0$  in 300 GeV  $\pi^-$  Beam Dump Experiment that decays into  $e^+e^-$  in the mass range  $m_{A^0} = (20-200)$  MeV, which excludes the  $A^0$  decay constant  $f(A^0)$  in the interval (60-600) GeV. See their figure 6 for excluded region on  $f(A^0)-m_{A^0}$  plane.
- <sup>50</sup> BERGSMÄ 85 look for  $A^0 \rightarrow 2\gamma, e^+e^-, \mu^+\mu^-$ . First limit above is for  $m_{A^0} = 1$  MeV; second is for 200 MeV. See their figure 4 for excluded region on  $f_{A^0}-m_{A^0}$  plane, where  $f_{A^0}$  is  $A^0$  decay constant. For Peccei-Quinn PECCEI 77  $A^0, m_{A^0} < 180$  keV and  $\tau > 0.037$  s. (CL = 90%). For the axion of FAISSNER 81B at 250 keV, BERGSMÄ 85 expect 15 events but observe zero.
- <sup>51</sup> FAISSNER 83 observed 19  $1-\gamma$  and 12  $2-\gamma$  events where a background of 4.8 and 2.3 respectively is expected. A small-angle peak is observed even if iron wall is set in front of the decay region.
- <sup>52</sup> FAISSNER 83B extrapolate SIN  $\gamma$  signal to LAMPF  $\nu$  experimental condition. Resulting 370  $\gamma$ 's are not at variance with LAMPF upper limit of 450  $\gamma$ 's. Derived from LAMPF limit that  $[d\sigma(A^0)/d\omega \text{ at } 90^\circ] m_{A^0}^2 / \tau_{A^0} < 14 \times 10^{-35} \text{ cm}^2 \text{ sr}^{-1} \text{ MeV ms}^{-1}$ . See comment on FRANK 83B.
- <sup>53</sup> FRANK 83B stress the importance of LAMPF data bins with negative net signal. By statistical analysis say that LAMPF and SIN-A0 are at variance when extrapolation by phase-space model is done. They find LAMPF upper limit is 248 not 450  $\gamma$ 's. See comment on FAISSNER 83B.
- <sup>54</sup> HOFFMAN 83 set CL = 90% limit  $d\sigma/dt B(e^+e^-) < 3.5 \times 10^{-32} \text{ cm}^2/\text{GeV}^2$  for 140  $< m_{A^0} < 160$  MeV. Limit assumes  $\tau(A^0) < 10^{-9}$  s.
- <sup>55</sup> FETSCHER 82 reanalyzes SIN beam-dump data of FAISSNER 81. Claims no evidence for axion since  $2-\gamma$  peak rate remarkably decreases if iron wall is set in front of the decay region.
- <sup>56</sup> FAISSNER 81 see excess  $\mu e$  events. Suggest axion interactions.
- <sup>57</sup> FAISSNER 81B is SIN 590 MeV proton beam dump. Observed  $14.5 \pm 5.0$  events of  $2\gamma$  decay of long-lived neutral penetrating particle with  $m_{2\gamma} \lesssim 1$  MeV. Axion interpretation with  $\eta-A^0$  mixing gives  $m_{A^0} = 250 \pm 25$  keV,  $\tau(2\gamma) = (7.3 \pm 3.7) \times 10^{-3}$  s from above rate. See critical remarks below in comments of FETSCHER 82, FAISSNER 83, FAISSNER 83B, FRANK 83B, and BERGSMÄ 85. Also see in the next subsection ALEKSEEV 82B, CAVAIIGNAC 83, and ANANEV 85.
- <sup>58</sup> KIM 81 analyzed 8 candidates for  $A^0 \rightarrow 2\gamma$  obtained by Aachen-Padova experiment at CERN with 26 GeV protons on Be. Estimated axion mass is about 300 keV and lifetime is  $(0.86 \sim 5.6) \times 10^{-3}$  s depending on models. Faissner (private communication), says axion production underestimated and mass overestimated. Correct value around 200 keV.
- <sup>59</sup> FAISSNER 80 is SIN beam dump experiment with 590 MeV protons looking for  $A^0 \rightarrow e^+e^-$  decay. Assuming  $A^0/\pi^0 = 5.5 \times 10^{-7}$ , obtained decay rate limit  $20/(A^0 \text{ mass}) \text{ MeV/s}$  (CL = 90%), which is about  $10^{-7}$  below theory and interpreted as upper limit to  $m_{A^0} < 2m_{e^-}$ .
- <sup>60</sup> JACQUES 80 is a BNL beam dump experiment. First limit above comes from nonobservation of excess neutral-current-type events  $[\sigma(\text{production})\sigma(\text{interaction}) < 7. \times 10^{-68} \text{ cm}^4, \text{ CL} = 90\%]$ . Second limit is from nonobservation of axion decays into  $2\gamma$ 's or  $e^+e^-$ , and for axion mass a few MeV.
- <sup>61</sup> SOUKAS 80 at BNL observed no excess of neutral-current-type events in beam dump.
- <sup>62</sup> BECHIS 79 looked for the axion production in low energy electron Bremsstrahlung and the subsequent decay into either  $2\gamma$  or  $e^+e^-$ . No signal found. CL = 90% limits for model parameter(s) are given.
- <sup>63</sup> COTEUS 79 is a beam dump experiment at BNL.
- <sup>64</sup> DISHAW 79 is a calorimetric experiment and looks for low energy tail of energy distributions due to energy lost to weakly interacting particles.
- <sup>65</sup> BELLOTTI 78 first value comes from search for  $A^0 \rightarrow e^+e^-$ . Second value comes from search for  $A^0 \rightarrow 2\gamma$ , assuming mass  $< 2m_{e^-}$ . For any mass satisfying this, limit is above value  $\times (\text{mass}^{-4})$ . Third value uses data of PL 60B 401 and quotes  $\sigma(\text{production})\sigma(\text{interaction}) < 10^{-67} \text{ cm}^4$ .
- <sup>66</sup> BOSETTI 78B quotes  $\sigma(\text{production})\sigma(\text{interaction}) < 2. \times 10^{-67} \text{ cm}^4$ .
- <sup>67</sup> DONNELLY 78 examines data from reactor neutrino experiments of REINES 76 and GURR 74 as well as SLAC beam dump experiment. Evidence is negative.
- <sup>68</sup> MICELMACHER 78 finds no evidence of axion existence in reactor experiments of REINES 76 and GURR 74. (See reference under DONNELLY 78 below).
- <sup>69</sup> VYSOTSKI 78 derived lower limit for the axion mass 25 keV from luminosity of the sun and 200 keV from red supergiants.

### $A^0$ (Axion) Searches in Reactor Experiments

VALUE	DOCUMENT ID	TECN	COMMENT
• • • We do not use the following data for averages, fits, limits, etc. • • •			
	70 CHANG 07		Primakoff or Compton
	71 ALTMANN 95	CNTR	Reactor; $A^0 \rightarrow e^+e^-$
	72 KETOV 86	SPEC	Reactor; $A^0 \rightarrow \gamma\gamma$
	73 KOCH 86	SPEC	Reactor; $A^0 \rightarrow \gamma\gamma$
	74 DATAR 82	CNTR	Light water reactor
	75 VUILLEUMIER 81	CNTR	Reactor; $A^0 \rightarrow 2\gamma$
<sup>70</sup> CHANG 07	looked for monochromatic photons from Primakoff or Compton conversion of axions from the Kuo-Sheng reactor due to axion coupling to photon or electron, respectively. The search places model-independent limits on the products $G_{A\gamma\gamma}G_{ANN}$ and $G_{Aee}G_{ANN}$ for $m(A^0)$ less than the MeV range.		
<sup>71</sup> ALTMANN 95	looked for $A^0$ decaying into $e^+e^-$ from the Bugey5 nuclear reactor. They obtain an upper limit on the $A^0$ production rate of $\omega(A^0)/\omega(\gamma) \times B(A^0 \rightarrow e^+e^-) < 10^{-16}$ for $m_{A^0} = 1.5$ MeV at 90% CL. The limit is weaker for heavier $A^0$ . In the case of a standard axion, this limit excludes a mass in the range $2m_e < m_{A^0} < 4.8$ MeV at 90% CL. See Fig. 5 of their paper for exclusion limits of axion-like resonances $Z^0$ in the $(m_{X^0}, f_{X^0})$ plane.		
<sup>72</sup> KETOV 86	searched for $A^0$ at the Rovno nuclear power plant. They found an upper limit on the $A^0$ production probability of $0.8 [100 \text{ keV}/m_{A^0}]^6 \times 10^{-6}$ per fission. In		

- the standard axion model, this corresponds to  $m_{A^0} > 150$  keV. Not valid for  $m_{A^0} \gtrsim 1$  MeV.
- <sup>73</sup> KOCH 86 searched for  $A^0 \rightarrow \gamma\gamma$  at nuclear power reactor Biblis A. They found an upper limit on the  $A^0$  production rate of  $\omega(A^0)/\omega(\gamma(M1)) < 1.5 \times 10^{-10}$  (CL=95%). Standard axion with  $m_{A^0} = 250$  keV gives  $10^{-5}$  for the ratio. Not valid for  $m_{A^0} > 1022$  keV.
- <sup>74</sup> DATAR 82 looked for  $A^0 \rightarrow 2\gamma$  in neutron capture ( $np \rightarrow dA^0$ ) at Tarapur 500 MW reactor. Sensitive to sum of  $l = 0$  and  $l = 1$  amplitudes. With ZEHNDER 81 [ $l = 0 - (l = 1)$ ] result, assert nonexistence of standard  $A^0$ .
- <sup>75</sup> VUILLEUMIER 81 is at Grenoble reactor. Set limit  $m_{A^0} < 280$  keV.

### $A^0$ (Axion) and Other Light Boson ( $X^0$ ) Searches in Nuclear Transitions

Limits are for branching ratio.

VALUE	CL%	DOCUMENT ID	TECN	COMMENT
• • • We do not use the following data for averages, fits, limits, etc. • • •				
$< 8.5 \times 10^{-6}$	90	76 DERBIN 02	CNTR	$125^m\text{Te}$ decay
		77 DEBOER 97c	RVUE	M1 transitions
$< 5.5 \times 10^{-10}$	95	78 TSUNODA 95	CNTR	$^{252}\text{Cf}$ fission, $A^0 \rightarrow e e$
$< 1.2 \times 10^{-6}$	95	79 MINOWA 93	CNTR	$^{139}\text{La}^* \rightarrow ^{139}\text{La} A^0$
$< 2 \times 10^{-4}$	90	80 HICKS 92	CNTR	$^{35}\text{S}$ decay, $A^0 \rightarrow \gamma\gamma$
$< 1.5 \times 10^{-9}$	95	81 ASANUMA 90	CNTR	$^{241}\text{Am}$ decay
$< (0.4-10) \times 10^{-3}$	95	82 DEBOER 90	CNTR	$^8\text{Be}^* \rightarrow ^8\text{Be} A^0$ , $^{16}\text{O}^* \rightarrow ^{16}\text{O} X^0$ , $X^0 \rightarrow e^+e^-$
$< (0.2-1) \times 10^{-3}$	90	83 BINI 89	CNTR	$^{16}\text{O}^* \rightarrow ^{16}\text{O} X^0$ , $X^0 \rightarrow e^+e^-$
		84 AVIGNONE 88	CNTR	$\text{Cu}^* \rightarrow \text{Cu} A^0 (A^0 \rightarrow 2\gamma)$ , $A^0 e^- \rightarrow \gamma e, A^0 Z \rightarrow \gamma Z$
$< 1.5 \times 10^{-4}$	90	85 DATAR 88	CNTR	$^{12}\text{C}^* \rightarrow ^{12}\text{C} A^0$ , $A^0 \rightarrow e^+e^-$
$< 5 \times 10^{-3}$	90	86 DEBOER 88c	CNTR	$^{16}\text{O}^* \rightarrow ^{16}\text{O} X^0$ , $X^0 \rightarrow e^+e^-$
$< 3.4 \times 10^{-5}$	95	87 DOEHNER 88	SPEC	$^2\text{H}^*, A^0 \rightarrow e^+e^-$
$< 4 \times 10^{-4}$	95	88 SAVAGE 88	CNTR	Nuclear decay (isovector)
$< 3 \times 10^{-3}$	95	88 SAVAGE 88	CNTR	Nuclear decay (isoscalar)
$< 10.6 \times 10^{-2}$	90	89 HALLIN 86	SPEC	$^6\text{Li}$ isovector decay
$< 10.8$	90	89 HALLIN 86	SPEC	$^{10}\text{B}$ isoscalar decays
$< 2.2$	90	89 HALLIN 86	SPEC	$^{14}\text{N}$ isoscalar decays
$< 4 \times 10^{-4}$	90	90 SAVAGE 86b	CNTR	$^{14}\text{N}^*$
		91 ANANEV 85	CNTR	$\text{Li}^*, \text{deut}^* A^0 \rightarrow 2\gamma$
		92 CAVAIIGNAC 83	CNTR	$^{97}\text{Nb}^*, \text{deut}^* \text{ transition } A^0 \rightarrow 2\gamma$
		93 ALEKSEEV 82B	CNTR	$\text{Li}^*, \text{deut}^* \text{ transition } A^0 \rightarrow 2\gamma$
		94 LEHMANN 82	CNTR	$\text{Cu}^* \rightarrow \text{Cu} A^0 (A^0 \rightarrow 2\gamma)$
		95 ZEHNDER 82	CNTR	$\text{Li}^*, \text{Nb}^* \text{ decay, } n\text{-capt.}$
		96 ZEHNDER 81	CNTR	$\text{Ba}^* \rightarrow \text{Ba} A^0 (A^0 \rightarrow 2\gamma)$
		97 CALAPRICE 79		Carbon
<sup>76</sup> DERBIN 02	looked for the axion emission in an M1 transition in $^{125m}\text{Te}$ decay. They looked for a possible presence of a shifted energy spectrum in gamma rays due to the undetected axion.			
<sup>77</sup> DEBOER 97c	reanalyzed the existent data on Nuclear M1 transitions and find that a 9 MeV boson decaying into $e^+e^-$ would explain the excess of events with large opening angles. See also DEBOER 01 for follow-up experiments.			
<sup>78</sup> TSUNODA 95	looked for axion emission when $^{252}\text{Cf}$ undergoes a spontaneous fission, with the axion decaying into $e^+e^-$ . The bound is for $m_{A^0} = 40$ MeV. It improves to $2.5 \times 10^{-5}$ for $m_{A^0} = 200$ MeV.			
<sup>79</sup> MINOWA 93	studied chain process, $^{139}\text{Ce} \rightarrow ^{139}\text{La}^*$ by electron capture and M1 transition of $^{139}\text{La}^*$ to the ground state. It does not assume decay modes of $A^0$ . The bound applies for $m_{A^0} < 166$ keV.			
<sup>80</sup> HICKS 92	bound is applicable for $\tau_{X^0} < 4 \times 10^{-11}$ sec.			
<sup>81</sup> The ASANUMA 90	limit is for the branching fraction of $X^0$ emission per $^{241}\text{Am}$ $\alpha$ decay and valid for $\tau_{X^0} < 3 \times 10^{-11}$ s.			
<sup>82</sup> The DEBOER 90	limit is for the branching ratio $^8\text{Be}^* (18.15 \text{ MeV}, 1^+) \rightarrow ^8\text{Be} A^0, A^0 \rightarrow e^+e^-$ for the mass range $m_{A^0} = 4-15$ MeV.			
<sup>83</sup> The BINI 89	limit is for the branching fraction of $^{16}\text{O}^* (6.05 \text{ MeV}, 0^+) \rightarrow ^{16}\text{O} X^0, X^0 \rightarrow e^+e^-$ for $m_X = 1.5-3.1$ MeV. $\tau_{X^0} \lesssim 10^{-11}$ s is assumed. The spin-parity of $X$ is restricted to $0^+$ or $1^-$ .			
<sup>84</sup> AVIGNONE 88	looked for the 1115 keV transition $\text{C}^* \rightarrow \text{Cu} A^0$ , either from $A^0 \rightarrow 2\gamma$ in-flight decay or from the secondary $A^0$ interactions by Compton and by Primakoff processes. Limits for axion parameters are obtained for $m_{A^0} < 1.1$ MeV.			
<sup>85</sup> DATAR 88	rule out light pseudoscalar particle emission through its decay $A^0 \rightarrow e^+e^-$ in the mass range 1.02-2.5 MeV and lifetime range $10^{-13}-10^{-8}$ s. The above limit is for $\tau = 5 \times 10^{-13}$ s and $m = 1.7$ MeV; see the paper for the $\tau$ - $m$ dependence of the limit.			
<sup>86</sup> The limit is for the branching fraction of $^{16}\text{O}^* (6.05 \text{ MeV}, 0^+) \rightarrow ^{16}\text{O} X^0, X^0 \rightarrow e^+e^-$	against internal pair conversion for $m_{X^0} = 1.7$ MeV and $\tau_{X^0} < 10^{-11}$ s. Similar limits are obtained for $m_{X^0} = 1.3-3.2$ MeV. The spin parity of $X^0$ must be either $0^+$ or $1^-$ . The limit at 1.7 MeV is translated into a limit for the $X^0$ -nucleon coupling constant: $g_{X^0 NN}^2/4\pi < 2.3 \times 10^{-9}$ .			
<sup>87</sup> The DOEHNER 88	limit is for $m_{A^0} = 1.7$ MeV, $\tau(A^0) < 10^{-10}$ s. Limits less than $10^{-4}$ are obtained for $m_{A^0} = 1.2-2.2$ MeV.			
<sup>88</sup> SAVAGE 88	looked for $A^0$ that decays into $e^+e^-$ in the decay of the 9.17 MeV $J^P = 2^+$ state in $^{14}\text{N}$ , 17.64 MeV state $J^P = 1^+$ in $^8\text{Be}$ , and the 18.15 MeV state $J^P =$			

See key on page 457

Gauge & Higgs Boson Particle Listings  
Axions ( $A^0$ ) and Other Very Light Bosons

- $1^+$  in  $^8\text{Be}$ . This experiment constrains the isovector coupling of  $A^0$  to hadrons, if  $m_{A^0} = (1.1 \rightarrow 2.2)$  MeV and the isoscalar coupling of  $A^0$  to hadrons, if  $m_{A^0} = (1.1 \rightarrow 2.6)$  MeV. Both limits are valid only if  $\tau(A^0) \lesssim 1 \times 10^{-11}$  s.
- <sup>89</sup>Limits are for  $\Gamma(A^0(1.8 \text{ MeV}))/\Gamma(\pi\text{M}1)$ ; i.e., for 1.8 MeV axion emission normalized to the rate for internal emission of  $e^+e^-$  pairs. Valid for  $\tau_{A^0} < 2 \times 10^{-11}$  s.  $^6\text{Li}$  isovector decay data strongly disfavor PECCEI 86 model I, whereas the  $^{10}\text{B}$  and  $^{14}\text{N}$  isoscalar decay data strongly reject PECCEI 86 model II and III.
- <sup>90</sup>SAVAGE 868 looked for  $A^0$  that decays into  $e^+e^-$  in the decay of the 9.17 MeV  $J^P = 2^+$  state in  $^{14}\text{N}$ . Limit on the branching fraction is valid if  $\tau_{A^0} \lesssim 1 \times 10^{-11}$  s for  $m_{A^0} = (1.1-1.7)$  MeV. This experiment constrains the iso-vector coupling of  $A^0$  to hadrons.
- <sup>91</sup>ANANEV 85 with IBR-2 pulsed reactor exclude standard  $A^0$  at CL = 95% masses below 470 keV ( $\text{Li}^*$  decay) and below  $2m_e$  for deuteron\* decay.
- <sup>92</sup>CAVAIGNAC 83 at Bugey reactor exclude axion at any  $m_{97\text{Nb}^*}$  decay and axion with  $m_{A^0}$  between 275 and 288 keV (deuteron\* decay).
- <sup>93</sup>ALEKSEEV 82 with IBR-2 pulsed reactor exclude standard  $A^0$  at CL = 95% mass-ranges  $m_{A^0} < 400$  keV ( $\text{Li}^*$  decay) and  $330$  keV  $< m_{A^0} < 2.2$  MeV. (deuteron\* decay).
- <sup>94</sup>LEHMANN 82 obtained  $A^0 \rightarrow 2\gamma$  rate  $< 6.2 \times 10^{-5}/\text{s}$  (CL = 95%) excluding  $m_{A^0}$  between 100 and 1000 keV.
- <sup>95</sup>ZEHNDER 82 used Gogsen 2.8GW light-water reactor to check  $A^0$  production. No  $2\gamma$  peak in  $\text{Li}^*$ ,  $\text{Nb}^*$  decay (both single  $p$  transition) nor in  $n$  capture (combined with previous  $\text{Ba}^*$  negative result) rules out standard  $A^0$ . Set limit  $m_{A^0} < 60$  keV for any  $A^0$ .
- <sup>96</sup>ZEHNDER 81 looked for  $\text{Ba}^* \rightarrow A^0\text{Ba}$  transition with  $A^0 \rightarrow 2\gamma$ . Obtained  $2\gamma$  coincidence rate  $< 2.2 \times 10^{-5}/\text{s}$  (CL = 95%) excluding  $m_{A^0} > 160$  keV (or 200 keV depending on Higgs mixing). However, see BARROSO 81.
- <sup>97</sup>CALAPRICE 79 saw no axion emission from excited states of carbon. Sensitive to axion mass between 1 and 15 MeV.

 **$A^0$  (Axion) Limits from Its Electron Coupling**Limits are for  $\tau(A^0 \rightarrow e^+e^-)$ .

VALUE (s)	CL%	DOCUMENT ID	TECN	COMMENT
• • • We do not use the following data for averages, fits, limits, etc. • • •				
none $4 \times 10^{-16}$ - $4.5 \times 10^{-12}$	90	98 BROSS	91 BDMP	$eN \rightarrow eA^0N$ ( $A^0 \rightarrow ee$ )
		99 GUO	90 BDMP	$eN \rightarrow eA^0N$ ( $A^0 \rightarrow ee$ )
		100 BJORKEN	88 CALO	$A \rightarrow e^+e^-$ or $2\gamma$
		101 BLINOV	88 MD1	$ee \rightarrow eeA^0$ ( $A^0 \rightarrow ee$ )
none $1 \times 10^{-14}$ - $1 \times 10^{-10}$	90	102 RIORDAN	87 BDMP	$eN \rightarrow eA^0N$ ( $A^0 \rightarrow ee$ )
none $1 \times 10^{-14}$ - $1 \times 10^{-11}$	90	103 BROWN	86 BDMP	$eN \rightarrow eA^0N$ ( $A^0 \rightarrow ee$ )
none $6 \times 10^{-14}$ - $9 \times 10^{-11}$	95	104 DAVIER	86 BDMP	$eN \rightarrow eA^0N$ ( $A^0 \rightarrow ee$ )
none $3 \times 10^{-13}$ - $1 \times 10^{-7}$	90	105 KONAKA	86 BDMP	$eN \rightarrow eA^0N$ ( $A^0 \rightarrow ee$ )

- <sup>98</sup>The listed BROSS 91 limit is for  $m_{A^0} = 1.14$  MeV.  $B(A^0 \rightarrow e^+e^-) = 1$  assumed. Excluded domain in the  $\tau_{A^0}-m_{A^0}$  plane extends up to  $m_{A^0} \approx 7$  MeV (see Fig. 5). Combining with electron  $g-2$  constraint, axions coupling only to  $e^+e^-$  ruled out for  $m_{A^0} < 4.8$  MeV (90% CL).
- <sup>99</sup>GUO 90 use the same apparatus as BROWN 86 and improve the previous limit in the shorter lifetime region. Combined with  $g-2$  constraint, axions coupling only to  $e^+e^-$  are ruled out for  $m_{A^0} < 2.7$  MeV (90% CL).
- <sup>100</sup>BJORKEN 88 reports limits on axion parameters ( $f_A, m_A, \tau_A$ ) for  $m_{A^0} < 200$  MeV from electron beam-dump experiment with production via Primakoff photoproduction, bremsstrahlung from electrons, and resonant annihilation of positrons on atomic electrons.
- <sup>101</sup>BLINOV 88 assume zero spin,  $m = 1.8$  MeV and lifetime  $< 5 \times 10^{-12}$  s and find  $\Gamma(A^0 \rightarrow \gamma\gamma)B(A^0 \rightarrow e^+e^-) < 2$  eV (CL=90%).
- <sup>102</sup>Assumes  $A^0\gamma\gamma$  coupling is small and hence Primakoff production is small. Their figure 2 shows limits on axions for  $m_{A^0} < 15$  MeV.
- <sup>103</sup>Uses electrons in hadronic showers from an incident 800 GeV proton beam. Limits for  $m_{A^0} < 15$  MeV are shown in their figure 3.
- <sup>104</sup> $m_{A^0} = 1.8$  MeV assumed. The excluded domain in the  $\tau_{A^0}-m_{A^0}$  plane extends up to  $m_{A^0} \approx 14$  MeV, see their figure 4.
- <sup>105</sup>The limits are obtained from their figure 3. Also given is the limit on the  $A^0\gamma\gamma-A^0e^+e^-$  coupling plane by assuming Primakoff production.

**Search for  $A^0$  (Axion) Resonance in Bhabha Scattering**The limit is for  $\Gamma(A^0)B(A^0 \rightarrow e^+e^-)^2$ .

VALUE ( $10^{-3}$ eV)	CL%	DOCUMENT ID	TECN	COMMENT
• • • We do not use the following data for averages, fits, limits, etc. • • •				
$< 1.3$	97	106 HALLIN	92 CNTR	$m_{A^0} = 1.75-1.88$ MeV
none 0.0016-0.47	90	107 HENDERSON	92c CNTR	$m_{A^0} = 1.5-1.86$ MeV
$< 2.0$	90	108 WU	92 CNTR	$m_{A^0} = 1.56-1.86$ MeV
$< 0.013$	95	TSERTOS	91 CNTR	$m_{A^0} = 1.832$ MeV
none 0.19-3.3	95	109 WIDMANN	91 CNTR	$m_{A^0} = 1.78-1.92$ MeV
$< 5$	97	BAUER	90 CNTR	$m_{A^0} = 1.832$ MeV
none 0.09-1.5	95	110 JUDGE	90 CNTR	$m_{A^0} = 1.832$ MeV, elastic

- |            |    |                  |         |                           |
|------------|----|------------------|---------|---------------------------|
| $< 1.9$    | 97 | 111 TSERTOS      | 89 CNTR | $m_{A^0} = 1.82$ MeV      |
| $<(10-40)$ | 97 | 111 TSERTOS      | 89 CNTR | $m_{A^0} = 1.51-1.65$ MeV |
| $<(1-2.5)$ | 97 | 111 TSERTOS      | 89 CNTR | $m_{A^0} = 1.80-1.86$ MeV |
| $< 31$     | 95 | LORENZ           | 88 CNTR | $m_{A^0} = 1.646$ MeV     |
| $< 94$     | 95 | LORENZ           | 88 CNTR | $m_{A^0} = 1.726$ MeV     |
| $< 23$     | 95 | LORENZ           | 88 CNTR | $m_{A^0} = 1.782$ MeV     |
| $< 19$     | 95 | LORENZ           | 88 CNTR | $m_{A^0} = 1.837$ MeV     |
| $< 3.8$    | 97 | 112 TSERTOS      | 88 CNTR | $m_{A^0} = 1.832$ MeV     |
|            |    | 113 VANKLINKEN   | 88 CNTR |                           |
|            |    | 114 MAIER        | 87 CNTR |                           |
| $<2500$    | 90 | MILLS            | 87 CNTR | $m_{A^0} = 1.8$ MeV       |
|            |    | 115 VONWIMMER.87 | CNTR    |                           |
- <sup>106</sup>HALLIN 92 quote limits on lifetime,  $8 \times 10^{-14} - 5 \times 10^{-13}$  sec depending on mass, assuming  $B(A^0 \rightarrow e^+e^-) = 100\%$ . They say that TSERTOS 91 overstated their sensitivity by a factor of 3.
- <sup>107</sup>HENDERSON 92c exclude axion with lifetime  $\tau_{A^0} = 1.4 \times 10^{-12} - 4.0 \times 10^{-10}$  s, assuming  $B(A^0 \rightarrow e^+e^-) = 100\%$ . HENDERSON 92c also exclude a vector boson with  $\tau = 1.4 \times 10^{-12} - 6.0 \times 10^{-10}$  s.
- <sup>108</sup>WU 92 quote limits on lifetime  $> 3.3 \times 10^{-13}$  s assuming  $B(A^0 \rightarrow e^+e^-) = 100\%$ . They say that TSERTOS 89 overestimate the limit by a factor of  $\pi/2$ . WU 92 also quote a bound for vector boson,  $\tau > 8.2 \times 10^{-13}$  s.
- <sup>109</sup>WIDMANN 91 bound applies exclusively to the case  $B(A^0 \rightarrow e^+e^-) = 1$ , since the detection efficiency varies substantially as  $\Gamma(A^0)_{\text{total}}$  changes. See their Fig. 6.
- <sup>110</sup>JUDGE 90 excludes an elastic pseudoscalar  $e^+e^-$  resonance for  $4.5 \times 10^{-13} \text{ s} < \tau(A^0) < 7.5 \times 10^{-12} \text{ s}$  (95% CL) at  $m_{A^0} = 1.832$  MeV. Comparable limits can be set for  $m_{A^0} = 1.776-1.856$  MeV.
- <sup>111</sup>See also TSERTOS 88B in references.
- <sup>112</sup>The upper limit listed in TSERTOS 88 is too large by a factor of 4. See TSERTOS 88B, footnote 3.
- <sup>113</sup>VANKLINKEN 88 looked for relatively long-lived resonance ( $\tau = 10^{-10}-10^{-12}$  s). The sensitivity is not sufficient to exclude such a narrow resonance.
- <sup>114</sup>MAIER 87 obtained limits  $R\Gamma \lesssim 60$  eV (100 eV) at  $m_{A^0} \approx 1.64$  MeV (1.83 MeV) for energy resolution  $\Delta E_{\text{cm}} \approx 3$  keV, where  $R$  is the resonance cross section normalized to that of Bhabha scattering, and  $\Gamma = \Gamma_{ee}^2/\Gamma_{\text{total}}$ . For a discussion implying that  $\Delta E_{\text{cm}} \approx 10$  keV, see TSERTOS 89.
- <sup>115</sup>VONWIMMERSPERG 87 measured Bhabha scattering for  $E_{\text{cm}} = 1.37-1.86$  MeV and found a possible peak at 1.73 with  $\int \sigma dE_{\text{cm}} = 14.5 \pm 6.8$  keV-b. For a comment and a reply, see VANKLINKEN 88B and VONWIMMERSPERG 88. Also see CONNELL 88.

**Search for  $A^0$  (Axion) Resonance in  $e^+e^- \rightarrow \gamma\gamma$** The limit is for  $\Gamma(A^0 \rightarrow e^+e^-)\Gamma(A^0 \rightarrow \gamma\gamma)/\Gamma_{\text{total}}$ 

VALUE ( $10^{-3}$ eV)	CL%	DOCUMENT ID	TECN	COMMENT
• • • We do not use the following data for averages, fits, limits, etc. • • •				
$< 0.18$	95	VO	94 CNTR	$m_{A^0} = 1.1$ MeV
$< 1.5$	95	VO	94 CNTR	$m_{A^0} = 1.4$ MeV
$< 12$	95	VO	94 CNTR	$m_{A^0} = 1.7$ MeV
$< 6.6$	95	116 TRZASKA	91 CNTR	$m_{A^0} = 1.8$ MeV
$< 4.4$	95	WIDMANN	91 CNTR	$m_{A^0} = 1.78-1.92$ MeV
		117 FOX	89 CNTR	
$< 0.11$	95	118 MINOWA	89 CNTR	$m_{A^0} = 1.062$ MeV
$< 33$	97	CONNELL	88 CNTR	$m_{A^0} = 1.580$ MeV
$< 42$	97	CONNELL	88 CNTR	$m_{A^0} = 1.642$ MeV
$< 73$	97	CONNELL	88 CNTR	$m_{A^0} = 1.782$ MeV
$< 79$	97	CONNELL	88 CNTR	$m_{A^0} = 1.832$ MeV

- <sup>116</sup>TRZASKA 91 also give limits in the range  $(6.6-30) \times 10^{-3}$  eV (95%CL) for  $m_{A^0} = 1.6-2.0$  MeV.
- <sup>117</sup>FOX 89 measured positron annihilation with an electron in the source material into two photons and found no signal at 1.062 MeV ( $< 9 \times 10^{-5}$  of two-photon annihilation at rest).
- <sup>118</sup>Similar limits are obtained for  $m_{A^0} = 1.045-1.085$  MeV.

**Search for  $X^0$  (Light Boson) Resonance in  $e^+e^- \rightarrow \gamma\gamma\gamma$** The limit is for  $\Gamma(X^0 \rightarrow e^+e^-)\Gamma(X^0 \rightarrow \gamma\gamma\gamma)/\Gamma_{\text{total}}$ . C invariance forbids spin-0  $X^0$  coupling to both  $e^+e^-$  and  $\gamma\gamma\gamma$ .

VALUE ( $10^{-3}$ eV)	CL%	DOCUMENT ID	TECN	COMMENT
• • • We do not use the following data for averages, fits, limits, etc. • • •				
$< 0.2$	95	119 VO	94 CNTR	$m_{X^0} = 1.1-1.9$ MeV
$< 1.0$	95	120 VO	94 CNTR	$m_{X^0} = 1.1$ MeV
$< 2.5$	95	120 VO	94 CNTR	$m_{X^0} = 1.4$ MeV
$< 120$	95	120 VO	94 CNTR	$m_{X^0} = 1.7$ MeV
$< 3.8$	95	121 SKALSEY	92 CNTR	$m_{X^0} = 1.5$ MeV

- <sup>119</sup>VO 94 looked for  $X^0 \rightarrow \gamma\gamma\gamma$  decaying at rest. The precise limits depend on  $m_{X^0}$ . See Fig. 2(b) in paper.
- <sup>120</sup>VO 94 looked for  $X^0 \rightarrow \gamma\gamma\gamma$  decaying in flight.
- <sup>121</sup>SKALSEY 92 also give limits 4.3 for  $m_{X^0} = 1.54$  and 7.5 for 1.64 MeV. The spin of  $X^0$  is assumed to be one.

# Gauge & Higgs Boson Particle Listings

## Axions ( $A^0$ ) and Other Very Light Bosons

### Light Boson ( $X^0$ ) Search in Nonresonant $e^+e^-$ Annihilation at Rest

Limits are for the ratio of  $n\gamma + X^0$  production relative to  $\gamma\gamma$ .

VALUE (units $10^{-6}$ )	CL%	DOCUMENT ID	TECN	COMMENT
< 4.2	90	122 MITSUI	96	CNTR $\gamma X^0$
< 4	68	123 SKALSEY	95	CNTR $\gamma X^0$
< 40	68	124 SKALSEY	95	RVUE $\gamma X^0$
< 0.18	90	125 ADACHI	94	CNTR $\gamma\gamma X^0, X^0 \rightarrow \gamma\gamma$
< 0.26	90	126 ADACHI	94	CNTR $\gamma\gamma X^0, X^0 \rightarrow \gamma\gamma$
< 0.33	90	127 ADACHI	94	CNTR $\gamma X^0, X^0 \rightarrow \gamma\gamma\gamma$

- • • We do not use the following data for averages, fits, limits, etc. • • •
- 122 MITSUI 96 looked for a monochromatic  $\gamma$ . The bound applies for a vector  $X^0$  with  $C=-1$  and  $m_{X^0} < 200$  keV. They derive an upper bound on  $eeX^0$  coupling and hence on the branching ratio  $B(\rho\text{-Ps} \rightarrow \gamma\gamma X^0) < 6.2 \times 10^{-6}$ . The bounds weaken for heavier  $X^0$ .
- 123 SKALSEY 95 looked for a monochromatic  $\gamma$  without an accompanying  $\gamma$  in  $e^+e^-$  annihilation. The bound applies for scalar and vector  $X^0$  with  $C = -1$  and  $m_{X^0} = 100\text{--}1000$  keV.
- 124 SKALSEY 95 reinterpreted the bound on  $\gamma A^0$  decay of  $\rho$ -Ps by ASA1 91 where 3% of delayed annihilations are not from  $^3S_1$  states. The bound applies for scalar and vector  $X^0$  with  $C = -1$  and  $m_{X^0} = 0\text{--}800$  keV.
- 125 ADACHI 94 looked for a peak in the  $\gamma\gamma$  invariant mass distribution in  $\gamma\gamma\gamma\gamma$  production from  $e^+e^-$  annihilation. The bound applies for  $m_{X^0} = 70\text{--}800$  keV.
- 126 ADACHI 94 looked for a peak in the missing-mass mass distribution in  $\gamma\gamma$  channel, using  $\gamma\gamma\gamma\gamma$  production from  $e^+e^-$  annihilation. The bound applies for  $m_{X^0} < 800$  keV.
- 127 ADACHI 94 looked for a peak in the missing mass distribution in  $\gamma\gamma\gamma$  channel, using  $\gamma\gamma\gamma\gamma$  production from  $e^+e^-$  annihilation. The bound applies for  $m_{X^0} = 200\text{--}900$  keV.

### Searches for Goldstone Bosons ( $X^0$ )

(Including Horizontal Bosons and Majorons.) Limits are for branching ratios.

VALUE	CL%	DOCUMENT ID	TECN	COMMENT
< $3.3 \times 10^{-2}$	95	131 ALBRECHT	90E	ARG $\tau \rightarrow \mu X^0$ , Familon
< $1.8 \times 10^{-2}$	95	131 ALBRECHT	90E	ARG $\tau \rightarrow e X^0$ , Familon
< $6.4 \times 10^{-9}$	90	132 ATIYA	90	B787 $K^+ \rightarrow \pi^+ X^0$ , Familon
< $1.1 \times 10^{-9}$	90	133 BOLTON	88	CBOX $\mu^+ \rightarrow e^+ X^0$ , Familon
		134 CHANDA	88	ASTR Sun, Majoron
		135 CHOI	88	ASTR Majoron, SN 1987A
< $5 \times 10^{-6}$	90	136 PICCIOTTO	88	CNTR $\pi \rightarrow e\nu X^0$ , Majoron
< $1.3 \times 10^{-9}$	90	137 GOLDMAN	87	CNTR $\mu \rightarrow e\gamma X^0$ , Familon
< $3 \times 10^{-4}$	90	138 BRYMAN	86B	RVUE $\mu \rightarrow e X^0$ , Familon
< $1 \times 10^{-10}$	90	139 EICHLER	86	SPEC $\mu^+ \rightarrow e^+ X^0$ , Familon
< $2.6 \times 10^{-6}$	90	140 JODIDIO	86	SPEC $\mu^+ \rightarrow e^+ X^0$ , Familon
		141 BALTRUSAITIS	85	MRK3 $\tau \rightarrow \ell X^0$ , Familon
		142 DICUS	83	COSM $\nu(\text{h}\nu) \rightarrow \nu(\text{light}) X^0$

- • • We do not use the following data for averages, fits, limits, etc. • • •
- 128 LESSA 07 consider decays of the form Meson  $\rightarrow \ell\nu$  Majoron and  $\ell \rightarrow \ell'\nu\pi$  Majoron and use existing data to derive limits on the neutrino-Majoron Yukawa couplings  $g_{\alpha\beta}$  ( $\alpha, \beta = e, \mu, \tau$ ). Their best limits are  $|g_{e\alpha}|^2 < 5.5 \times 10^{-6}$ ,  $|g_{\mu\alpha}|^2 < 4.5 \times 10^{-5}$ ,  $|g_{\tau\alpha}|^2 < 5.5 \times 10^{-2}$  at CL = 90%.
- 129 DIAZ 98 studied models of spontaneously broken lepton number with both singlet and triplet Higgses. They obtain limits on the parameter space from invisible decay  $Z \rightarrow H^0 A^0 \rightarrow X^0 X^0 X^0 X^0$  and  $e^+e^- \rightarrow ZH^0$  with  $H^0 \rightarrow X^0 X^0$ .
- 130 BOBRAKOV 91 searched for anomalous magnetic interactions between polarized electrons expected from the exchange of a massless pseudoscalar boson (arion). A limit  $\chi_e^2 < 2 \times 10^{-4}$  (95% CL) is found for the effective anomalous magneton parametrized as  $\chi_e(G_F/8\pi\sqrt{2})^{1/2}$ .
- 131 ALBRECHT 90E limits are for  $B(\tau \rightarrow \ell X^0)/B(\tau \rightarrow \ell\nu\pi)$ . Valid for  $m_{X^0} < 100$  MeV. The limits rise to 7.1% (for  $\mu$ ), 5.0% (for  $e$ ) for  $m_{X^0} = 500$  MeV.
- 132 ATIYA 90 limit is for  $m_{X^0} = 0$ . The limit  $B < 1 \times 10^{-8}$  holds for  $m_{X^0} < 95$  MeV. For the reduction of the limit due to finite lifetime of  $X^0$ , see their Fig. 3.
- 133 BOLTON 88 limit corresponds to  $F > 3.1 \times 10^9$  GeV, which does not depend on the chirality property of the coupling.
- 134 CHANDA 88 find  $v_T < 10$  MeV for the weak-triplet Higgs vacuum expectation value in Gellmini-Roncadelli model, and  $v_S > 5.8 \times 10^6$  GeV in the singlet Majoron model.
- 135 CHOI 88 used the observed neutrino flux from the supernova SN 1987A to exclude the neutrino Majoron Yukawa coupling  $h$  in the range  $2 \times 10^{-5} < h < 3 \times 10^{-4}$  for the interaction  $L_{\text{int}} = \frac{1}{2} i h \bar{\nu}_\nu \gamma_5 \psi_\nu \phi_X$ . For several families of neutrinos, the limit applies for  $(\Sigma h^2)^{1/4}$ .
- 136 PICCIOTTO 88 limit applies when  $m_{X^0} < 55$  MeV and  $\tau_{X^0} > 2$  ns, and it decreases to  $4 \times 10^{-7}$  at  $m_{X^0} = 125$  MeV, beyond which no limit is obtained.
- 137 GOLDMAN 87 limit corresponds to  $F > 2.9 \times 10^9$  GeV for the family symmetry breaking scale from the Lagrangian  $L_{\text{int}} = (1/F) \bar{\psi}_\mu \gamma^\mu (+a+b\gamma_5) \psi_e \phi_\mu \phi_X$  with  $a^2+b^2 = 1$ . This is not as sensitive as the limit  $F > 9.9 \times 10^9$  GeV derived from the search for  $\mu^+ \rightarrow e^+ X^0$  by JODIDIO 86, but does not depend on the chirality property of the coupling.

- 138 Limits are for  $\Gamma(\mu \rightarrow e X^0)/\Gamma(\mu \rightarrow e\nu\pi)$ . Valid when  $m_{X^0} = 0\text{--}93.4, 98.1\text{--}103.5$  MeV.
- 139 EICHLER 86 looked for  $\mu^+ \rightarrow e^+ X^0$  followed by  $X^0 \rightarrow e^+ e^-$ . Limits on the branching fraction depend on the mass and lifetime of  $X^0$ . The quoted limits are valid when  $\tau_{X^0} \lesssim 3 \times 10^{-10}$  s if the decays are kinematically allowed.
- 140 JODIDIO 86 corresponds to  $F > 9.9 \times 10^9$  GeV for the family symmetry breaking scale with the parity-conserving effective Lagrangian  $L_{\text{int}} = (1/F) \bar{\psi}_\mu \gamma^\mu \psi_e \phi_\mu \phi_X$ .
- 141 BALTRUSAITIS 85 search for light Goldstone boson ( $X^0$ ) of broken U(1). CL = 95% limits are  $B(\tau \rightarrow \mu^+ X^0)/B(\tau \rightarrow \mu^+ \nu\nu) < 0.125$  and  $B(\tau \rightarrow e^+ X^0)/B(\tau \rightarrow e^+ \nu\nu) < 0.04$ . Inferred limit for the symmetry breaking scale is  $m > 3000$  TeV.
- 142 The primordial heavy neutrino must decay into  $\nu$  and familon,  $f_A$ , early so that the red-shifted decay products are below critical density, see their table. In addition,  $K \rightarrow \pi f_A$  and  $\mu \rightarrow e f_A$  are unseen. Combining these excludes  $m_{\text{heavy}\nu}$  between  $5 \times 10^{-5}$  and  $5 \times 10^{-4}$  MeV ( $\mu$  decay) and  $m_{\text{heavy}\nu}$  between  $5 \times 10^{-5}$  and 0.1 MeV ( $K$ -decay).

### Majoron Searches in Neutrinoless Double $\beta$ Decay

Limits are for the half-life of neutrinoless  $\beta\beta$  decay with a Majoron emission.

No experiment currently claims any such evidence. Only the best or comparable limits for each isotope are reported. Also see the reviews ZUBER 98 and FAESSLER 98b.

$t_{1/2}(10^{21} \text{ yr})$	CL%	ISOTOPE	TRANSITION	METHOD	DOCUMENT ID
> 7200	90	128Te	CNTR		143 BERNATOW... 92
• • • We do not use the following data for averages, fits, limits, etc. • • •					
> 16	90	130Te	$0\nu\chi$	NEMO-3	144 ARNOLD 11
> 1.9	90	96Zr	$2\nu\chi$	NEMO-3	145 ARGYRIADES 10
> 1.52	90	150Nd	$0\nu1\chi$	NEMO-3	146 ARGYRIADES 09
> 27	90	100Mo	$0\nu1\chi$	NEMO-3	147 ARNOLD 06
> 15	90	82Se	$0\nu1\chi$	NEMO-3	148 ARNOLD 06
> 14	90	100Mo	$0\nu1\chi$	NEMO-3	149 ARNOLD 04
> 12	90	82Se	$0\nu1\chi$	NEMO-3	150 ARNOLD 04
> 2.2	90	130Te	$0\nu1\chi$	Cryog. det.	151 ARNABOLDI 03
> 0.9	90	130Te	$0\nu2\chi$	Cryog. det.	152 ARNABOLDI 03
> 8	90	116Cd	$0\nu1\chi$	CdWO <sub>4</sub> scint.	153 DANEVICH 03
> 0.8	90	116Cd	$0\nu2\chi$	CdWO <sub>4</sub> scint.	154 DANEVICH 03
> 500	90	136Xe	$0\nu\chi$	Liquid Xe Scint.	155 BERNABEI 02b
> 5.8	90	100Mo	$0\nu\chi$	ELEGANT V	156 FUSHIMI 02
> 0.32	90	100Mo	$0\nu\chi$	Liq. Ar ioniz.	157 ASHITKOV 01
> 0.0035	90	160Gd	$0\nu\chi$	<sup>160</sup> Gd <sub>2</sub> SiO <sub>5</sub> :Ce	158 DANEVICH 01
> 0.013	90	160Gd	$0\nu2\chi$	<sup>160</sup> Gd <sub>2</sub> SiO <sub>5</sub> :Ce	159 DANEVICH 01
> 2.3	90	82Se	$0\nu\chi$	NEMO 2	160 ARNOLD 00
> 0.31	90	96Zr	$0\nu\chi$	NEMO 2	161 ARNOLD 00
> 0.63	90	82Se	$0\nu2\chi$	NEMO 2	162 ARNOLD 00
> 0.063	90	96Zr	$0\nu2\chi$	NEMO 2	162 ARNOLD 00
> 0.16	90	100Mo	$0\nu2\chi$	NEMO 2	162 ARNOLD 00
> 2.4	90	82Se	$0\nu\chi$	NEMO 2	163 ARNOLD 98
> 7.2	90	136Xe	$0\nu2\chi$	TPC	164 LUESCHER 98
> 7.91	90	76Ge		SPEC	165 GUENTHER 96
> 17	90	76Ge		CNTR	BECK 93

- 143 BERNATOWICZ 92 studied double- $\beta$  decays of <sup>128</sup>Te and <sup>130</sup>Te, and found the ratio  $\tau(^{130}\text{Te})/\tau(^{128}\text{Te}) = (3.52 \pm 0.11) \times 10^{-4}$  in agreement with relatively stable theoretical predictions. The bound is based on the requirement that Majoron-emitting decay cannot be larger than the observed double-beta rate of <sup>128</sup>Te of  $(7.7 \pm 0.4) \times 10^{24}$  year. We calculated 90% CL limit as  $(7.7\text{--}1.28 \times 0.4\text{--}7.2) \times 10^{24}$ .
- 144 ARNOLD 11 use the NEMO-3 detector to obtain the reported limit on Majoron emission. It implies that the coupling constant  $g_{\nu\chi} < 0.6\text{--}1.6 \times 10^{-4}$  depending on the nuclear matrix element used. Supersedes ARNABOLDI 03.
- 145 ARGYRIADES 10 use the NEMO-3 tracking detector and <sup>96</sup>Zr to derive the reported limit. No limit for the Majoron electron coupling is given.
- 146 ARGYRIADES 09 use <sup>150</sup>Nd data taken with the NEMO-3 tracking detector. The reported limit corresponds to  $\langle g_{\nu\chi} \rangle < 1.7\text{--}3.0 \times 10^{-4}$  using a range of nuclear matrix elements that include the effect of nuclear deformation.
- 147 ARNOLD 06 use <sup>100</sup>Mo data taken with the NEMO-3 tracking detector. The reported limit corresponds to  $\langle g_{\nu\chi} \rangle < (0.4\text{--}1.8) \times 10^{-4}$  using a range of matrix element calculations. Supersedes ARNOLD 04.
- 148 NEMO-3 tracking calorimeter is used in ARNOLD 06. Reported half-life limit for <sup>82</sup>Se corresponds to  $\langle g_{\nu\chi} \rangle < (0.66\text{--}1.9) \times 10^{-4}$  using a range of matrix element calculations. Supersedes ARNOLD 04.
- 149 ARNOLD 04 use the NEMO-3 tracking detector. The limit corresponds to  $\langle g_{\nu\chi} \rangle < (0.5\text{--}0.9) \times 10^{-4}$  using the matrix elements of SIMKOVIC 99, STOICA 01 and CIVITARESE 03.
- 150 ARNOLD 04 use the NEMO-3 tracking detector. The limit corresponds to  $\langle g_{\nu\chi} \rangle < (0.7\text{--}1.6) \times 10^{-4}$  using the matrix elements of SIMKOVIC 99, STOICA 01 and CIVITARESE 03.
- 151 Supersedes ALESSANDRELLO 00. Array of TeO<sub>2</sub> crystals in high resolution cryogenic calorimeter. Some enriched in <sup>130</sup>Te. Derive  $\langle g_{\nu\chi} \rangle < 17\text{--}33 \times 10^{-5}$  depending on matrix element.
- 152 Supersedes ALESSANDRELLO 00. Cryogenic calorimeter search.
- 153 Limit for the  $0\nu\chi$  decay with Majoron emission of <sup>116</sup>Cd using enriched CdWO<sub>4</sub> scintillators.  $\langle g_{\nu\chi} \rangle < 4.6\text{--}8.1 \times 10^{-5}$  depending on the matrix element. Supersedes DANEVICH 00.
- 154 Limit for the  $0\nu2\chi$  decay of <sup>116</sup>Cd. Supersedes DANEVICH 00.
- 155 BERNABEI 02b obtain limit for  $0\nu\chi$  decay with Majoron emission of <sup>136</sup>Xe using liquid Xe scintillation detector. They derive  $\langle g_{\nu\chi} \rangle < 2.0\text{--}3.0 \times 10^{-5}$  with several nuclear matrix elements.

See key on page 457

Gauge & Higgs Boson Particle Listings  
Axions ( $A^0$ ) and Other Very Light Bosons

- 156 Replaces TANAKA 93. FUSHIMI 02 derive half-life limit for the  $0\nu\chi$  decay by means of tracking calorimeter ELEGANT V. Considering various matrix element calculations, a range of limits for the Majoron-neutrino coupling is given:  $\langle g_{\nu\chi} \rangle < (6.3-360) \times 10^{-5}$ .
- 157 ASHITKOV 01 result for  $0\nu\chi$  of  $^{100}\text{Mo}$  is less stringent than ARNOLD 00.
- 158 DANEVICH 01 obtain limit for the  $0\nu\chi$  decay with Majoron emission of  $^{160}\text{Gd}$  using  $\text{Gd}_2\text{SiO}_5:\text{Ce}$  crystal scintillators.
- 159 DANEVICH 01 obtain limit for the  $0\nu2\chi$  decay with 2 Majoron emission of  $^{160}\text{Gd}$ .
- 160 ARNOLD 00 reports limit for the  $0\nu\chi$  decay with Majoron emission derived from tracking calorimeter NEMO 2. Using  $^{82}\text{Se}$  source:  $\langle g_{\nu\chi} \rangle < 1.6 \times 10^{-4}$ . Matrix element from GUENTHER 96.
- 161 Using  $^{96}\text{Zr}$  source:  $\langle g_{\nu\chi} \rangle < 2.6 \times 10^{-4}$ . Matrix element from ARNOLD 99.
- 162 ARNOLD 00 reports limit for the  $0\nu2\chi$  decay with two Majoron emission derived from tracking calorimeter NEMO 2.
- 163 ARNOLD 98 determine the limit for  $0\nu\chi$  decay with Majoron emission of  $^{82}\text{Se}$  using the NEMO-2 tracking detector. They derive  $\langle g_{\nu\chi} \rangle < 2.3-4.3 \times 10^{-4}$  with several nuclear matrix elements.
- 164 LUESCHER 98 report a limit for the  $0\nu$  decay with Majoron emission of  $^{136}\text{Xe}$  using Xe TPC. This result is more stringent than BARABASH 89. Using the matrix elements of ENGEL 88, they obtain a limit on  $\langle g_{\nu\chi} \rangle$  of  $2.0 \times 10^{-4}$ .
- 165 See Table 1 in GUENTHER 96 for limits on the Majoron coupling in different models.

Invisible  $A^0$  (Axion) MASS LIMITS from Astrophysics and Cosmology

$v_1 = v_2$  is usually assumed ( $v_i$  = vacuum expectation values). For a review of these limits, see RAFFELT 91 and TURNER 90. In the comment lines below, D and K refer to DFSZ and KSVZ axion types, discussed in the above minireview.

VALUE (eV)	CL%	DOCUMENT ID	TECN	COMMENT
• • • We do not use the following data for averages, fits, limits, etc. • • •				
none $0.7-3 \times 10^5$		166 CADAMURO 11	COSM	D abundance
<105	90	167 DERBIN 11A	CNTR	D, solar axion
		168 ANDRIAMON...10	CAST	K, solar axions
< 0.72	95	169 HANNESTAD 10	COSM	K, hot dark matter
		170 ANDRIAMON...09	CAST	K, solar axions
<191	90	171 DERBIN 09A	CNTR	K, solar axions
<334	95	172 KEKEZ 09	HPGE	K, solar axions
< 1.02	95	173 HANNESTAD 08	COSM	K, hot dark matter
< 1.2	95	174 HANNESTAD 07	COSM	K, hot dark matter
< 0.42	95	175 MELCHIORRI 07A	COSM	K, hot dark matter
< 1.05	95	176 HANNESTAD 05A	COSM	K, hot dark matter
3 to 20		177 MOROI 98	COSM	K, hot dark matter
< 0.007		178 BORISOV 97	ASTR	D, neutron star
< 4		179 KACHELRIESS 97	ASTR	D, neutron star cooling
<(0.5-6) $\times 10^{-3}$		180 KEIL 97	ASTR	SN 1987A
< 0.018		181 RAFFELT 95	ASTR	D, red giant
< 0.010		182 ALTHERR 94	ASTR	D, red giants, white dwarfs
		183 CHANG 93	ASTR	K, SN 1987A
< 0.01		WANG 92	ASTR	D, white dwarf
< 0.03		WANG 92c	ASTR	D, C-O burning
none 3-8		184 BERSHADY 91	ASTR	D, K, intergalactic light
< 10		185 KIM 91c	COSM	D, K, mass density of the universe, super-symmetry
		186 RAFFELT 91B	ASTR	D, K, SN 1987A
< 1 $\times 10^{-3}$		187 RESSELL 91	ASTR	K, intergalactic light
none $10^{-3}-3$		BURROWS 90	ASTR	D, K, SN 1987A
		188 ENGEL 90	ASTR	D, K, SN 1987A
< 0.02		189 RAFFELT 90D	ASTR	D, red giant
< 1 $\times 10^{-3}$		190 BURROWS 89	ASTR	D, K, SN 1987A
<(1.4-10) $\times 10^{-3}$		191 ERICSON 89	ASTR	D, K, SN 1987A
< 3.6 $\times 10^{-4}$		192 MAYLE 89	ASTR	D, K, SN 1987A
< 12		CHANDA 88	ASTR	D, Sun
< 1 $\times 10^{-3}$		193 RAFFELT 88B	ASTR	D, K, SN 1987A
		193 RAFFELT 88B	ASTR	red giant
< 0.07		FRIEMAN 87	ASTR	D, red giant
< 0.7		194 RAFFELT 87	ASTR	K, red giant
< 2-5		TURNER 87	COSM	K, thermal production
< 0.01		195 DEARBORN 86	ASTR	D, red giant
< 0.06		RAFFELT 86	ASTR	D, red giant
< 0.7		196 RAFFELT 86	ASTR	K, red giant
< 0.03		RAFFELT 86B	ASTR	D, white dwarf
< 1		197 KAPLAN 85	ASTR	K, red giant
< 0.003-0.02		IWAMOTO 84	ASTR	D, K, neutron star
> 1 $\times 10^{-5}$		ABBOTT 83	COSM	D, K, mass density of the universe
> 1 $\times 10^{-5}$		DINE 83	COSM	D, K, mass density of the universe
< 0.04		ELLIS 83B	ASTR	D, red giant
> 1 $\times 10^{-5}$		PRESKILL 83	COSM	D, K, mass density of the universe
< 0.1		BARROSO 82	ASTR	D, red giant
< 1		198 FUKUGITA 82	ASTR	D, stellar cooling
< 0.07		FUKUGITA 82B	ASTR	D, red giant

- 166 CADAMURO 11 use the deuterium abundance to show that the  $m_{A^0}$  range  $0.7\text{eV} - 300\text{keV}$  is excluded for axions, complementing HANNESTAD 10.
- 167 DERBIN 11A look for solar axions produced by Compton and bremsstrahlung processes, in the resonant excitation of  $^{169}\text{Tm}$ , constraining the axion-electron  $\times$  axion-nucleon couplings.
- 168 ANDRIAMONJE 10 search for solar axions produced from  $^7\text{Li}$  (478 keV) and  $\text{D}(\rho,\gamma)^3\text{He}$  (5.5 MeV) nuclear transitions. They show limits on the axion-photon coupling for two reference values of the axion-nucleon coupling for  $m_A < 100\text{eV}$ .
- 169 This is an update of HANNESTAD 08 including 7 years of WMAP data.
- 170 ANDRIAMONJE 09 look for solar axions produced from the thermally excited 14.4 keV level of  $^{57}\text{Fe}$ . They show limits on the axion-nucleon  $\times$  axion-photon coupling assuming  $m_A < 0.03\text{eV}$ .
- 171 DERBIN 09A look for Primakoff-produced solar axions in the resonant excitation of  $^{169}\text{Tm}$ , constraining the axion-photon  $\times$  axion-nucleon couplings.
- 172 KEKEZ 09 look at axio-electric effect of solar axions in HPGe detectors. The one-loop axion-electron coupling for hadronic axions is used.
- 173 This is an update of HANNESTAD 07 including 5 years of WMAP data.
- 174 This is an update of HANNESTAD 05A with new cosmological data, notably WMAP (3 years) and baryon acoustic oscillations (BAO). Lyman- $\alpha$  data are left out, in contrast to HANNESTAD 05A and MELCHIORRI 07A, because it is argued that systematic errors are large. It uses Bayesian statistics and marginalizes over a possible neutrino hot dark matter component.
- 175 MELCHIORRI 07A is analogous to HANNESTAD 05A, with updated cosmological data, notably WMAP (3 years). Uses Bayesian statistics and marginalizes over a possible neutrino hot dark matter component. Leaving out Lyman- $\alpha$  data, a conservative limit is  $1.4\text{eV}$ .
- 176 HANNESTAD 05A puts an upper limit on the mass of hadronic axion because in this mass range it would have been thermalized and contribute to the hot dark matter component of the universe. The limit is based on the CMB anisotropy from WMAP, SDSS large scale structure, Lyman  $\alpha$ , and the prior Hubble parameter from HST Key Project. A  $\chi^2$  statistic is used. Neutrinos are assumed not to contribute to hot dark matter.
- 177 MOROI 98 points out that a KSVZ axion of this mass range (see CHANG 93) can be a viable hot dark matter of Universe, as long as the model-dependent  $g_{A\gamma}$  is accidentally small enough as originally emphasized by KAPLAN 85; see Fig. 1.
- 178 BORISOV 97 bound is on the axion-electron coupling  $g_{ae} < 1 \times 10^{-13}$  from the photo-production of axions off of magnetic fields in the outer layers of neutron stars.
- 179 KACHELRIESS 97 bound is on the axion-electron coupling  $g_{ae} < 1 \times 10^{-10}$  from the production of axions in strongly magnetized neutron stars. The authors also quote a stronger limit,  $g_{ae} < 9 \times 10^{-13}$  which is strongly dependent on the strength of the magnetic field in white dwarfs.
- 180 KEIL 97 uses new measurements of the axial-vector coupling strength of nucleons, as well as a reanalysis of many-body effects and pion-emission processes in the core of the neutron star, to update limits on the invisible-axion mass.
- 181 RAFFELT 95 reexamined the constraints on axion emission from red giants due to the axion-electron coupling. They improve on DEARBORN 86 by taking into proper account degeneracy effects in the bremsstrahlung rate. The limit comes from requiring the red giant core mass at helium ignition not to exceed its standard value by more than 5% (0.025 solar masses).
- 182 ALTHERR 94 bound is on the axion-electron coupling  $g_{ae} < 1.5 \times 10^{-13}$ , from energy loss via axion emission.
- 183 CHANG 93 updates ENGEL 90 bound with the Kaplan-Manohar ambiguity in  $z=m_\mu/m_d$  (see the Note on the Quark Masses in the Quark Particle Listings). It leaves the window  $f_A=3 \times 10^5-3 \times 10^6\text{GeV}$  open. The constraint from Big-Bang Nucleosynthesis is satisfied in this window as well.
- 184 BERSHADY 91 searched for a line at wave length from 3100-8300  $\text{\AA}$  expected from  $2\gamma$  decays of relic thermal axions in intergalactic light of three rich clusters of galaxies.
- 185 KIM 91c argues that the bound from the mass density of the universe will change drastically for the supersymmetric models due to the entropy production of saxion (scalar component in the axionic chiral multiplet) decay. Note that it is an *upperbound* rather than a lowerbound.
- 186 RAFFELT 91B argue that previous SN 1987A bounds must be relaxed due to corrections to nucleon bremsstrahlung processes.
- 187 RESSELL 91 uses absence of any intracluster line emission to set limit.
- 188 ENGEL 90 rule out  $10^{-10} \lesssim g_{AN} \lesssim 10^{-3}$ , which for a hadronic axion with EMC motivated axion-nucleon couplings corresponds to  $2.5 \times 10^{-3}\text{eV} \lesssim m_{A^0} \lesssim 2.5 \times 10^4\text{eV}$ . The constraint is loose in the middle of the range, i.e. for  $g_{AN} \sim 10^{-6}$ .
- 189 RAFFELT 90D is a re-analysis of DEARBORN 86.
- 190 The region  $m_{A^0} \gtrsim 2\text{eV}$  is also allowed.
- 191 ERICSON 89 considered various nuclear corrections to axion emission in a supernova core, and found a reduction of the previous limit (MAYLE 88) by a large factor.
- 192 MAYLE 89 limit based on naive quark model couplings of axion to nucleons. Limit based on couplings motivated by EMC measurements is 2-4 times weaker. The limit from axion-electron coupling is weak: see HATSUDA 88B.
- 193 RAFFELT 88B derives a limit for the energy generation rate by exotic processes in helium-burning stars  $\epsilon < 100\text{erg g}^{-1}\text{s}^{-1}$ , which gives a firmer basis for the axion limits based on red giant cooling.
- 194 RAFFELT 87 also gives a limit  $g_{A\gamma} < 1 \times 10^{-10}\text{GeV}^{-1}$ .
- 195 DEARBORN 86 also gives a limit  $g_{A\gamma} < 1.4 \times 10^{-11}\text{GeV}^{-1}$ .
- 196 RAFFELT 86 gives a limit  $g_{A\gamma} < 1.1 \times 10^{-10}\text{GeV}^{-1}$  from red giants and  $< 2.4 \times 10^{-9}\text{GeV}^{-1}$  from the sun.
- 197 KAPLAN 85 says  $m_{A^0} < 23\text{eV}$  is allowed for a special choice of model parameters.
- 198 FUKUGITA 82 gives a limit  $g_{A\gamma} < 2.3 \times 10^{-10}\text{GeV}^{-1}$ .

## Search for Relic Invisible Axions

Limits are for  $[G_{A\gamma\gamma}/m_{A^0}]^2\rho_A$  where  $G_{A\gamma\gamma}$  denotes the axion two-photon coupling,

$$L_{\text{int}} = \frac{G_{A\gamma\gamma}}{4}\phi_A F_{\mu\nu}\tilde{F}^{\mu\nu} = G_{A\gamma\gamma}\phi_A \mathbf{E}\cdot\mathbf{B}, \text{ and } \rho_A \text{ is the axion energy density near the earth.}$$

VALUE	CL%	DOCUMENT ID	TECN	COMMENT
-------	-----	-------------	------	---------

• • • We do not use the following data for averages, fits, limits, etc. • • •

# Gauge & Higgs Boson Particle Listings

## Axions ( $A^0$ ) and Other Very Light Bosons

$<3.5 \times 10^{-43}$	199	HOSKINS	11	ADMX	$m_{A^0} = 3.3\text{--}3.69 \times 10^{-6}$ eV
$<2.9 \times 10^{-43}$	90	200 ASZTALOS	10	ADMX	$m_{A^0} = 3.34\text{--}3.53 \times 10^{-6}$ eV
$<1.9 \times 10^{-43}$	97.7	201 DUFFY	06	ADMX	$m_{A^0} = 1.98\text{--}2.17 \times 10^{-6}$ eV
$<5.5 \times 10^{-43}$	90	202 ASZTALOS	04	ADMX	$m_{A^0} = 1.9\text{--}3.3 \times 10^{-6}$ eV
		203 KIM	98	THEO	
$<2 \times 10^{-41}$		204 HAGMANN	90	CNTR	$m_{A^0} = (5.4\text{--}5.9)10^{-6}$ eV
$<1.3 \times 10^{-42}$	95	205 WUENSCH	89	CNTR	$m_{A^0} = (4.5\text{--}10.2)10^{-6}$ eV
$<2 \times 10^{-41}$	95	205 WUENSCH	89	CNTR	$m_{A^0} = (11.3\text{--}16.3)10^{-6}$ eV

199 HOSKINS 11 is analogous to DUFFY 06. See Fig. 4 for the mass-dependent limit in terms of the local density.

200 ASZTALOS 10 used the upgraded detector of ASZTALOS 04 to search for halo axions. See their Fig. 5 for the  $m_{A^0}$  dependence of the limit.

201 DUFFY 06 used the upgraded detector of ASZTALOS 04, while assuming a smaller velocity dispersion than the isothermal model as in Eq. (8) of their paper. See Fig. 10 of their paper on the axion mass dependence of the limit.

202 ASZTALOS 04 looked for a conversion of halo axions to microwave photons in magnetic field. At 90% CL, the KSVZ axion cannot have a local halo density more than  $0.45 \text{ GeV/cm}^3$  in the quoted mass range. See Fig. 7 of their paper on the axion mass dependence of the limit.

203 KIM 98 calculated the axion-to-photon couplings for various axion models and compared them to the HAGMANN 90 bounds. This analysis demonstrates a strong model dependence of  $G_{A\gamma\gamma}$  and hence the bound from relic axion search.

204 HAGMANN 90 experiment is based on the proposal of SIKIVIE 83.

205 WUENSCH 89 looks for condensed axions near the earth that could be converted to photons in the presence of an intense electromagnetic field via the Primakoff effect, following the proposal of SIKIVIE 83. The theoretical prediction with  $[G_{A\gamma\gamma}/m_{A^0}]^2 = 2 \times 10^{-14} \text{ MeV}^{-4}$  (the three generation DFSZ model) and  $\rho_A = 300 \text{ MeV/cm}^3$  that makes up galactic halos gives  $(G_{A\gamma\gamma}/m_{A^0})^2 \rho_A = 4 \times 10^{-44}$ . Note that our definition of  $G_{A\gamma\gamma}$  is  $(1/4\pi)$  smaller than that of WUENSCH 89.

### Invisible $A^0$ (Axion) Limits from Photon Coupling

Limits are for the axion-two-photon coupling  $G_{A\gamma\gamma}$  defined by  $L = G_{A\gamma\gamma}\phi_A^2 \mathbf{E} \cdot \mathbf{B}$ .

For scalars  $S^0$  the limit is on the coupling constant in  $L = G_{S\gamma\gamma}\phi_S(\mathbf{E}^2 - \mathbf{B}^2)$ .

VALUE ( $\text{GeV}^{-1}$ )	CL%	DOCUMENT ID	TECN	COMMENT
$<2.3 \times 10^{-10}$	95	206 ARIK	11	CAST $m_{A^0} = 0.39\text{--}0.64$ eV
$<6.5 \times 10^{-8}$	95	207 EHRET	10	ALPS $m_{A^0} < 0.7$ meV
$<2.4 \times 10^{-9}$	95	208 AHMED	09A	CDMS $m_{A^0} < 100$ eV
$<1.2\text{--}2.8 \times 10^{-10}$	95	209 ARIK	09	CAST $m_{A^0} = 0.02\text{--}0.39$ eV
		210 CHOU	09	Chameleons
		211 GONDOLO	09	ASTR $m_{A^0} < \text{few keV}$
$<7 \times 10^{-10}$		212 AFANA SEV	08	$m_{S^0} < 1$ meV
$<1.3 \times 10^{-6}$	95	213 CHOU	08	$m_{A^0} < 0.5$ meV
$<3.5 \times 10^{-7}$	99.7	214 FOUCHE	08	$m_{A^0} < 1$ meV
$<1.1 \times 10^{-6}$	99.7	215 INOUE	08	$m_{A^0} < 1$ meV
$<5.6\text{--}13.4 \times 10^{-10}$	95	216 ZAVATTINI	08	$m_{A^0} = 0.84\text{--}1.00$ eV
$<5 \times 10^{-7}$		217 ANDRIAMON..07	CAST	$m_{A^0} < 1$ meV
$<8.8 \times 10^{-11}$	95	218 ROBILLIARD	07	$m_{A^0} < 0.02$ eV
$<1.25 \times 10^{-6}$	95	219 ZAVATTINI	06	$m_{A^0} < 1$ meV
$2\text{--}5 \times 10^{-6}$		220 INOUE	02	$m_{A^0} = 1\text{--}1.5$ meV
$<1.1 \times 10^{-9}$	95	221 MORALES	02B	$m_{A^0} = 0.05\text{--}0.27$ eV
$<2.78 \times 10^{-9}$	95	222 BERNABEI	01B	$m_{A^0} < 1$ keV
$<1.7 \times 10^{-9}$	90	223 ASTIER	00B	$m_{A^0} < 100$ eV
$<1.5 \times 10^{-4}$	90	224 MASSO	00	NOMD $m_{A^0} < 40$ eV
		225 AVIGNONE	98	THEO induced $\gamma$ coupling
$<2.7 \times 10^{-9}$	95	226 MORIYAMA	98	SLAX $m_{A^0} < 1$ keV
$<6.0 \times 10^{-10}$	95	227 CAMERON	93	$m_{A^0} < 0.03$ eV
$<3.6 \times 10^{-7}$	95	228 CAMERON	93	$m_{A^0} < 10^{-3}$ eV, optical rotation
		229 LAZARUS	92	$m_{A^0} < 10^{-3}$ eV, photon regeneration
$<3.6 \times 10^{-9}$	99.7	230 RUOSO	92	$m_{A^0} < 0.03$ eV
$<7.7 \times 10^{-9}$	99.7	231 SEMERTZIDIS	90	$m_{A^0} = 0.03\text{--}0.11$ eV
$<1.7 \times 10^{-7}$	99	232 CAMERON	92	$m_{A^0} < 10^{-3}$ eV
$<2.5 \times 10^{-6}$		233 SEMERTZIDIS	90	$m_{A^0} < 7 \times 10^{-4}$ eV

206 ARIK 11 search for solar axions using  $^3\text{He}$  buffer gas in CAST, continuing from the  $^4\text{He}$  version of ARIK 09. See Fig. 2 for the exact mass-dependent limits.

207 ALPS is a photon regeneration experiment. See their Fig. 4 for mass-dependent limits on scalar and pseudoscalar bosons.

208 AHMED 09A is analogous to AVIGNONE 98.

209 ARIK 09 is the  $^4\text{He}$  filling version of the CAST axion helioscope in analogy to INOUE 02 and INOUE 08. See their Fig. 7 for mass-dependent limits.

210 CHOU 09 use the GammeV apparatus in the afterglow mode to search for chameleons, (pseudo)scalar bosons with a mass depending on the environment. For pseudoscalars they exclude at  $3\sigma$  the range  $2.6 \times 10^{-7} \text{ GeV}^{-1} < G_{A\gamma\gamma} < 4.2 \times 10^{-6} \text{ GeV}^{-1}$  for vacuum  $m_{A^0}$  roughly below 6 meV for density scaling index exceeding 0.8.

211 GONDOLO 09 use the all-flavor measured solar neutrino flux to constrain solar interior temperature and thus energy losses.

212 LIPSS photon regeneration experiment, assuming scalar particle  $S^0$ . See Fig. 4 for mass-dependent limits.

213 CHOU 08 perform a variable-baseline photon regeneration experiment. See their Fig. 3 for mass-dependent limits. Excludes the PVLAS result of ZAVATTINI 06.

214 FOUCHE 08 is an update of ROBILLIARD 07. See their Fig. 12 for mass-dependent limits.

215 INOUE 08 is an extension of INOUE 02 to larger axion masses, using the Tokyo axion helioscope. See their Fig. 4 for mass-dependent limits.

216 ZAVATTINI 08 is an upgrade of ZAVATTINI 06, see their Fig. 8 for mass-dependent limits. They now exclude the parameter range where ZAVATTINI 06 had seen a positive signature.

217 ANDRIAMONJE 07 looked for Primakoff conversion of solar axions in 9T superconducting magnet into X-rays. Supersedes ZIOUTAS 05.

218 ROBILLIARD 07 perform a photon regeneration experiment with a pulsed laser and pulsed magnetic field. See their Fig. 4 for mass-dependent limits. Excludes the PVLAS result of ZAVATTINI 06 with a CL exceeding 99.9%.

219 ZAVATTINI 06 propagate a laser beam in a magnetic field and observe dichroism and birefringence effects that could be attributed to an axion-like particle. This result is now excluded by ROBILLIARD 07, ZAVATTINI 08, and CHOU 08.

220 INOUE 02 looked for Primakoff conversion of solar axions in 4T superconducting magnet into X-ray.

221 MORALES 02B looked for the coherent conversion of solar axions to photons via the Primakoff effect in Germanium detector.

222 BERNABEI 01B looked for Primakoff coherent conversion of solar axions into photons via Bragg scattering in NaI crystal in DAMA dark matter detector.

223 ASTIER 00B looked for production of axions from the interaction of high-energy photons with the horn magnetic field and their subsequent re-conversion to photons via the interaction with the NOMAD dipole magnetic field.

224 MASSO 00 studied limits on axion-proton coupling using the induced axion-photon coupling through the proton loop and CAMERON 93 bound on the axion-photon coupling using optical rotation. They obtained the bound  $g_p^2/4\pi < 1.7 \times 10^{-9}$  for the coupling  $g_p \bar{p} \gamma_5 p \phi_A$ .

225 AVIGNONE 98 result is based on the coherent conversion of solar axions to photons via the Primakoff effect in a single crystal germanium detector.

226 Based on the conversion of solar axions to X-rays in a strong laboratory magnetic field.

227 Experiment based on proposal by MAIANI 86.

228 Experiment based on proposal by VANBIBBER 87.

229 LAZARUS 92 experiment is based on proposal found in VANBIBBER 89.

230 RUOSO 92 experiment is based on the proposal by VANBIBBER 87.

231 SEMERTZIDIS 90 experiment is based on the proposal of MAIANI 86. The limit is obtained by taking the noise amplitude as the upper limit. Limits extend to  $m_{A^0} = 4 \times 10^{-3}$  where  $G_{A\gamma\gamma} < 1 \times 10^{-4} \text{ GeV}^{-1}$ .

### Limit on Invisible $A^0$ (Axion) Electron Coupling

The limit is for  $G_{Aee}\partial_\mu\phi_A\bar{e}\gamma^\mu\gamma_5e$  in  $\text{GeV}^{-1}$ , or equivalently, the dipole-dipole

potential  $\frac{G_{Aee}^2}{4\pi}((\sigma_1 \cdot \sigma_2) - 3(\sigma_1 \cdot \mathbf{n})(\sigma_2 \cdot \mathbf{n}))/r^3$  where  $\mathbf{n} = \mathbf{r}/r$ .

VALUE ( $\text{GeV}^{-1}$ )	CL%	DOCUMENT ID	TECN	COMMENT
$<0.02\text{--}1 \times 10^{-7}$	90	232 AALSETH	11	CNTR $m_{A^0} = 0.3\text{--}8$ keV
$<1.4 \times 10^{-9}$	90	233 AHMED	09A	CDMS $m_{A^0} = 2.5$ keV
$<3 \times 10^{-6}$		234 DAVOUDI ASL	09	ASTR Earth cooling
$<5.3 \times 10^{-5}$	66	235 NI	94	Induced magnetism
$<6.7 \times 10^{-5}$	66	236 CHUI	93	Induced magnetism
$<3.6 \times 10^{-4}$	66	237 PAN	92	Torsion pendulum
$<2.7 \times 10^{-5}$	95	238 BOBRAKOV	91	Induced magnetism
$<1.9 \times 10^{-3}$	66	239 WINELAND	91	NMR
$<8.9 \times 10^{-4}$	66	240 RITTER	90	Torsion pendulum
$<6.6 \times 10^{-5}$	95	241 VOROBYOV	88	Induced magnetism

232 AALSETH 11 assume keV-mass pseudoscalars are the local dark matter and constrain the axio-electric effect in the CoGeNT detector. See their Fig. 4 for mass-dependent limits.

233 AHMED 09A is analogous to AALSETH 08, using the CDMS detector. See their Fig. 5 for mass-dependent limits.

234 DAVOUDI ASL 09 use geophysical constraints on Earth cooling by axion emission.

235 These experiments measured induced magnetization of a bulk material by the spin-dependent potential generated from other bulk material with aligned electron spins, where the magnetic field is shielded with superconductor.

236 These experiments used a torsion pendulum to measure the potential between two bulk matter objects where the spins are polarized but without a net magnetic field in either of them.

237 WINELAND 91 looked for an effect of bulk matter with aligned electron spins on atomic hyperfine splitting using nuclear magnetic resonance.

### Invisible $A^0$ (Axion) Limits from Nucleon Coupling

Limits are for the axion mass in eV.

VALUE (eV)	CL%	DOCUMENT ID	TECN	COMMENT
$<145$	95	238 DERBIN	11	CNTR Solar axion
$<1.39 \times 10^4$	90	239 BELL	08A	CNTR Solar axion
		240 BELLINI	08	CNTR Solar axion
		241 ADELBERGER	07	Test of Newton's law
$<1.6 \times 10^4$	90	242 DERBIN	05	CNTR Solar axion
$<400$	95	243 LJUBICIC	04	CNTR Solar axion
$<3.2 \times 10^4$	95	244 KRCMAR	01	CNTR Solar axion

• • • We do not use the following data for averages, fits, limits, etc. • • •





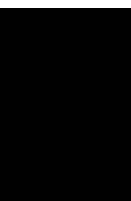


## LEPTONS

$e$ . . . . .	581
$\mu$ . . . . .	582
$\tau$ . . . . .	592
Heavy Charged Lepton Searches . . . . .	621
Neutrino Properties . . . . .	622
Number of Neutrino Types . . . . .	629
Double- $\beta$ Decay . . . . .	631
Neutrino Mixing . . . . .	636
Heavy Neutral Leptons, Searches for . . . . .	647

### Notes in the Lepton Listings

Muon Anomalous Magnetic Moment (rev.) . . . . .	583
Muon Decay Parameters (rev.) . . . . .	587
$\tau$ Branching Fractions (rev.) . . . . .	596
$\tau$ -Lepton Decay Parameters . . . . .	617
Number of Light Neutrino Types from Collider Experiments . . . . .	629
Neutrinoless Double- $\beta$ Decay (rev.) . . . . .	631





See key on page 457

## LEPTONS

e

$$J = \frac{1}{2}$$

## e MASS (atomic mass units u)

The primary determination of an electron's mass comes from measuring the ratio of the mass to that of a nucleus, so that the result is obtained in u (atomic mass units). The conversion factor to MeV is more uncertain than the mass of the electron in u; indeed, the recent improvements in the mass determination are not evident when the result is given in MeV. In this datablock we give the result in u, and in the following datablock in MeV.

VALUE (10 <sup>-6</sup> u)	DOCUMENT ID	TECN	COMMENT
<b>548.5799046 ± 0.0000022</b>	MOHR	12	RVUE 2010 CODATA value
• • • We do not use the following data for averages, fits, limits, etc. • • •			
548.5799043 ± 0.0000023	MOHR	08	RVUE 2006 CODATA value
548.5799045 ± 0.0000024	MOHR	05	RVUE 2002 CODATA value
548.5799092 ± 0.0000004	1 BEIER	02	CNTR Penning trap
548.5799110 ± 0.0000012	MOHR	99	RVUE 1998 CODATA value
548.5799111 ± 0.0000012	2 FARNHAM	95	CNTR Penning trap
548.579903 ± 0.000013	COHEN	87	RVUE 1986 CODATA value

<sup>1</sup> BEIER 02 compares Larmor frequency of the electron bound in a <sup>12</sup>C<sup>5+</sup> ion with the cyclotron frequency of a single trapped <sup>12</sup>C<sup>5+</sup> ion.

<sup>2</sup> FARNHAM 95 compares cyclotron frequency of trapped electrons with that of a single trapped <sup>12</sup>C<sup>6+</sup> ion.

## e MASS

2010 CODATA (MOHR 12) gives the conversion factor from u (atomic mass units, see the above datablock) to MeV as 931.494 061 (21). Earlier values use the then-current conversion factor. The conversion error dominates the uncertainty of the masses given below.

VALUE (MeV)	DOCUMENT ID	TECN	COMMENT
<b>0.510998928 ± 0.00000011</b>	MOHR	12	RVUE 2010 CODATA value
• • • We do not use the following data for averages, fits, limits, etc. • • •			
0.510998910 ± 0.00000013	MOHR	08	RVUE 2006 CODATA value
0.510998918 ± 0.000000044	MOHR	05	RVUE 2002 CODATA value
0.510998901 ± 0.000000020	3.4 BEIER	02	CNTR Penning trap
0.510998902 ± 0.000000021	MOHR	99	RVUE 1998 CODATA value
0.510998903 ± 0.000000020	3.5 FARNHAM	95	CNTR Penning trap
0.510998895 ± 0.000000024	3 COHEN	87	RVUE 1986 CODATA value
0.5110034 ± 0.0000014	COHEN	73	RVUE 1973 CODATA value

<sup>3</sup> Converted to MeV using the 1998 CODATA value of the conversion constant, 931.494013 ± 0.000037 MeV/u.

<sup>4</sup> BEIER 02 compares Larmor frequency of the electron bound in a <sup>12</sup>C<sup>5+</sup> ion with the cyclotron frequency of a single trapped <sup>12</sup>C<sup>5+</sup> ion.

<sup>5</sup> FARNHAM 95 compares cyclotron frequency of trapped electrons with that of a single trapped <sup>12</sup>C<sup>6+</sup> ion.

$$(m_{e^+} - m_{e^-}) / m_{\text{average}}$$

A test of CPT invariance.

VALUE	CL%	DOCUMENT ID	TECN	COMMENT
<b>&lt; 8 × 10<sup>-9</sup></b>	90	6 FEE	93	CNTR Positronium spectroscopy
• • • We do not use the following data for averages, fits, limits, etc. • • •				
< 4 × 10 <sup>-8</sup>	90	CHU	84	CNTR Positronium spectroscopy

<sup>6</sup> FEE 93 value is obtained under the assumption that the positronium Rydberg constant is exactly half the hydrogen one.

$$|q_{e^+} + q_{e^-}|/e$$

A test of CPT invariance. See also similar tests involving the proton.

VALUE	DOCUMENT ID	TECN	COMMENT
<b>&lt; 4 × 10<sup>-8</sup></b>	7 HUGHES	92	RVUE
• • • We do not use the following data for averages, fits, limits, etc. • • •			
< 2 × 10 <sup>-18</sup>	8 SCHAEFER	95	THEO Vacuum polarization
< 1 × 10 <sup>-18</sup>	9 MUELLER	92	THEO Vacuum polarization

<sup>7</sup> HUGHES 92 uses recent measurements of Rydberg-energy and cyclotron-frequency ratios.

<sup>8</sup> SCHAEFER 95 removes model dependency of MUELLER 92.

<sup>9</sup> MUELLER 92 argues that an inequality of the charge magnitudes would, through higher-order vacuum polarization, contribute to the net charge of atoms.

## e MAGNETIC MOMENT ANOMALY

$$\mu_e/\mu_B - 1 = (g-2)/2$$

VALUE (units 10 <sup>-6</sup> )	DOCUMENT ID	TECN	CHG	COMMENT
<b>1159.65218076 ± 0.00000027</b>	MOHR	12	RVUE	2010 CODATA value
• • • We do not use the following data for averages, fits, limits, etc. • • •				
1159.65218073 ± 0.00000028	HANNEKE	08	MRS	Single electron
1159.65218111 ± 0.00000074	10 MOHR	08	RVUE	2006 CODATA value
1159.65218085 ± 0.00000076	11 ODOM	06	MRS	Single electron
1159.6521859 ± 0.0000038	MOHR	05	RVUE	2002 CODATA value
1159.6521869 ± 0.0000041	MOHR	99	RVUE	1998 CODATA value
1159.652193 ± 0.000010	COHEN	87	RVUE	1986 CODATA value
1159.6521884 ± 0.0000043	VANDYCK	87	MRS	Single electron
1159.6521879 ± 0.0000043	VANDYCK	87	MRS	Single positron

<sup>10</sup> MOHR 08 average is dominated by ODOM 06.

<sup>11</sup> Superseded by HANNEKE 08 per private communication with Gerald Gabrielse.

$$(g_+ - g_-) / g_{\text{average}}$$

A test of CPT invariance.

VALUE (units 10 <sup>-12</sup> )	CL%	DOCUMENT ID	TECN	COMMENT
<b>- 0.5 ± 2.1</b>		12 VANDYCK	87	MRS Penning trap
• • • We do not use the following data for averages, fits, limits, etc. • • •				
< 12	95	13 VASSERMAN	87	CNTR Assumes $m_{e^+} = m_{e^-}$
22 ± 64		SCHWINBERG	81	MRS Penning trap

<sup>12</sup> VANDYCK 87 measured  $(g_-/g_+) - 1$  and we converted it.

<sup>13</sup> VASSERMAN 87 measured  $(g_+ - g_-)/(g - 2)$ . We multiplied by  $(g - 2)/g = 1.2 \times 10^{-3}$ .

## e ELECTRIC DIPOLE MOMENT (d)

A nonzero value is forbidden by both T invariance and P invariance.

VALUE (10 <sup>-28</sup> ecm)	CL%	DOCUMENT ID	TECN	COMMENT
<b>&lt; 10.5</b>	90	14 HUDSON	11	NMR YbF molecules
• • • We do not use the following data for averages, fits, limits, etc. • • •				
6.9 ± 7.4		REGAN	02	MRS <sup>205</sup> Tl beams
18 ± 12 ± 10		15 COMMINS	94	MRS <sup>205</sup> Tl beams
- 27 ± 83		15 ABDULLAH	90	MRS <sup>205</sup> Tl beams
- 1400 ± 2400		CHO	89	NMR Tl F molecules
- 150 ± 550 ± 150		MURTHY	89	Cesium, no B field
- 5000 ± 11000		LAMOREAUX	87	NMR <sup>199</sup> Hg
19000 ± 34000	90	SANDARS	75	MRS Thallium
7000 ± 22000	90	PLAYER	70	MRS Xenon
< 30000	90	WEISSKOPF	68	MRS Cesium

<sup>14</sup> HUDSON 11 gives a measurement corresponding to this limit as  $(-2.4 \pm 5.7 \pm 1.5) \times 10^{-28}$  ecm.

<sup>15</sup> ABDULLAH 90, COMMINS 94, and REGAN 02 use the relativistic enhancement of a valence electron's electric dipole moment in a high-Z atom.

e<sup>-</sup> MEAN LIFE / BRANCHING FRACTION

A test of charge conservation. See the "Note on Testing Charge Conservation and the Pauli Exclusion Principle" following this section in our 1992 edition (Physical Review **D45** S1 (1992), p. VI.10).

Most of these experiments are one of three kinds: Attempts to observe (a) the 25.5 keV gamma ray produced in  $e^- \rightarrow \nu_e \gamma$ , (b) the (K) shell x-ray produced when an electron decays without additional energy deposit, e.g.,  $e^- \rightarrow \nu_e \bar{\nu}_e \nu_e$  ("disappearance" experiments), and (c) nuclear de-excitation gamma rays after the electron disappears from an atomic shell and the nucleus is left in an excited state. The last can include both weak boson and photon mediating processes. We use the best  $e^- \rightarrow \nu_e \gamma$  limit for the Summary Tables.

Note that we use the mean life rather than the half life, which is often reported.

e → ν<sub>e</sub>γ and astrophysical limits

VALUE (yr)	CL%	DOCUMENT ID	TECN	COMMENT
<b>&gt; 4.6 × 10<sup>26</sup></b>	90	BACK	02	BORX $e^- \rightarrow \nu \gamma$
• • • We do not use the following data for averages, fits, limits, etc. • • •				
> 1.22 × 10 <sup>26</sup>	68	16 KLAPDOR-K...	07	CNTR $e^- \rightarrow \nu \gamma$
> 3.4 × 10 <sup>26</sup>	68	BELLI	00B	DAMA $e^- \rightarrow \nu \gamma$ , liquid Xe
> 3.7 × 10 <sup>25</sup>	68	AHARONOV	95B	CNTR $e^- \rightarrow \nu \gamma$ , liquid Xe
> 2.35 × 10 <sup>25</sup>	68	BALYSH	93	CNTR $e^- \rightarrow \nu \gamma$ , <sup>76</sup> Ge detector
> 1.5 × 10 <sup>25</sup>	68	AVIGNONE	86	CNTR $e^- \rightarrow \nu \gamma$
> 1 × 10 <sup>39</sup>		17 ORITO	85	ASTR Astrophysical argument
> 3 × 10 <sup>23</sup>	68	BELLOTTI	83B	CNTR $e^- \rightarrow \nu \gamma$

<sup>16</sup> The authors of A. Derbin et al, arXiv:0704.2047v1 argue that this limit is overestimated by at least a factor of 5.

<sup>17</sup> ORITO 85 assumes that electromagnetic forces extend out to large enough distances and that the age of our galaxy is 10<sup>10</sup> years.

## Lepton Particle Listings

 $e, \mu$ 

## Disappearance and nuclear-de-excitation experiments

VALUE (yr)	CL%	DOCUMENT ID	TECN	COMMENT
$>6.4 \times 10^{24}$	68	18 BELLI	99B DAMA	De-excitation of $^{129}\text{Xe}$
••• We do not use the following data for averages, fits, limits, etc. •••				
$>4.2 \times 10^{24}$	68	BELLI	99 DAMA	Iodine L-shell disappearance
$>2.4 \times 10^{23}$	90	19 BELLI	99D DAMA	De-excitation of $^{127}\text{I}$ (in NaI)
$>4.3 \times 10^{23}$	68	AHARONOV	95B CNTR	Ge K-shell disappearance
$>2.7 \times 10^{23}$	68	REUSSER	91 CNTR	Ge K-shell disappearance
$>2 \times 10^{22}$	68	BELLOTTI	83B CNTR	Ge K-shell disappearance
<sup>18</sup> BELLI 99B limit on charge nonconserving $e^-$ capture involving excitation of the 236.1 keV nuclear state of $^{129}\text{Xe}$ ; the 90% CL limit is $3.7 \times 10^{24}$ yr. Less stringent limits for other states are also given.				
<sup>19</sup> BELLI 99D limit on charge nonconserving $e^-$ capture involving excitation of the 57.6 keV nuclear state of $^{127}\text{I}$ . Less stringent limits for the other states and for the state of $^{23}\text{Na}$ are also given.				

## LIMITS ON LEPTON-FLAVOR VIOLATION IN PRODUCTION

Forbidden by lepton family number conservation.

This section was added for the 2008 edition of this Review and is not complete. For a list of further measurements see references in the papers listed below.

 $\sigma(e^+e^- \rightarrow e^+\tau^-) / \sigma(e^+e^- \rightarrow \mu^+\mu^-)$ 

VALUE	CL%	DOCUMENT ID	TECN	COMMENT
$<8.9 \times 10^{-6}$	95	AUBERT	07P BABR	$e^+e^-$ at $E_{\text{cm}} = 10.58$ GeV
••• We do not use the following data for averages, fits, limits, etc. •••				
$<1.8 \times 10^{-3}$	95	GOMEZ-CAD...	91 MRK2	$e^+e^-$ at $E_{\text{cm}} = 29$ GeV

 $\sigma(e^+e^- \rightarrow \mu^+\tau^-) / \sigma(e^+e^- \rightarrow \mu^+\mu^-)$ 

VALUE	CL%	DOCUMENT ID	TECN	COMMENT
$<4.0 \times 10^{-6}$	95	AUBERT	07P BABR	$e^+e^-$ at $E_{\text{cm}} = 10.58$ GeV
••• We do not use the following data for averages, fits, limits, etc. •••				
$<6.1 \times 10^{-3}$	95	GOMEZ-CAD...	91 MRK2	$e^+e^-$ at $E_{\text{cm}} = 29$ GeV

## e REFERENCES

MOHR	12	arXiv:1203.5425	P.J. Mohr, B.N. Taylor, D.B. Newell	(NIST)
HUDSON	11	NAT 473 493	J.J. Hudson et al.	(LOIC)
HANNEKE	08	PRL 100 120801	D. Hanneke, S. Fogwell, G. Gabrielse	(HARV)
MOHR	08	RMP 80 633	P.J. Mohr, B.N. Taylor, D.B. Newell	(NIST)
AUBERT	07P	PR D75 031103R	B. Aubert et al.	(BABAR Collab.)
KLAPDOR-K...	07	PL B644 109	H.V. Klapdor-Kleingrothaus, I.V. Krivosheina, I.V. Titkova	(HARV)
ODOM	06	PRL 97 030801	B. Odom et al.	(NIST)
MOHR	05	RMP 77 1	P.J. Mohr, B.N. Taylor	(NIST)
BACK	02	PL B525 29	H.O. Back et al.	(BOREXINO/SASSO Collab.)
BEIER	02	PRL 88 011603	T. Beier et al.	
REGAN	02	PRL 88 071805	B.C. Regan et al.	
BELLI	00B	PR D61 117301	P. Belli et al.	(DAMA Collab.)
BELLI	99	PL B460 236	P. Belli et al.	(DAMA Collab.)
BELLI	99B	PL B465 315	P. Belli et al.	(DAMA Collab.)
BELLI	99D	PR C60 065501	P. Belli et al.	(DAMA Collab.)
MOHR	99	JPCRD 28 1713	P.J. Mohr, B.N. Taylor	(NIST)
Also		RMP 72 351	P.J. Mohr, B.N. Taylor	(NIST)
AHARONOV	95B	PR D52 3785	Y. Aharonov et al.	(SCUC, PNL, ZARA+)
Also		PL B353 168	Y. Aharonov et al.	(SCUC, PNL, ZARA+)
FARNHAM	95	PRL 75 3598	D.L. Farnham, R.S. van Dyck, P.B. Schwinberg	(WASH)
SCHAEFER	95	PR A51 830	A. Schaefer, J. Reinhardt	(FRAN)
COMMINS	94	PR A50 2960	E.D. Commins et al.	
BALYSH	93	PL B298 278	A. Balysh et al.	(KIAE, MPH, SASSO)
FEE	93	PR A48 192	M.S. Fee et al.	
HUGHES	92	PRL 69 578	R.J. Hughes, B.I. Deutch	(LANL, AARH)
MUELLER	92	PRL 69 3432	B. Muller, M.H. Thoma	(DUKE)
PDG	92	PR D45 51	K. Hikasa et al.	(KEK, LBL, BOST+)
GOMEZ-CAD...	91	PRL 66 1007	J.J. Gomez-Cadenas et al.	(SLAC MARK-2 Collab.)
REUSSER	91	PL B255 143	D. Reusser et al.	(NEUC, CIT, PSI)
ABDULLAH	90	PRL 65 2347	K. Abdullah et al.	(LBL, UCB)
CHO	89	PRL 63 2559	D. Cho, K. Sangster, E.A. Hinds	(YALE)
MURTHY	89	PRL 63 965	S.A. Murthy et al.	(AMHT)
COHEN	87	RMP 59 1121	E.R. Cohen, B.N. Taylor	(RIS C, NBS)
LAMOREAUX	87	PRL 59 2275	S.K. Lamoreaux et al.	(WASH)
VANDYCK	87	PR 59 26	R.S. van Dyck, P.B. Schwinberg, H.G. Dehmelt	(WASH)
VASSERMAN	87	PL B198 302	I.B. Vasserman et al.	(NOVO)
Also		PL B187 172	I.B. Vasserman et al.	(NOVO)
AVIGNONE	86	PR D34 97	F.T. Avignone et al.	(PNL, SCUC)
ORITO	85	PL 54 2457	S. Orito, M. Yoshimura	(TOKY, KEK)
CHU	84	PRL 52 1689	S. Chu, A.P. Mills, J.L. Hall	(BELL, NBS, COLO)
BELLOTTI	83B	PL 124B 435	E. Bellotti et al.	(MILA)
SCHWINBERG	81	PRL 47 1679	P.B. Schwinberg, R.S. van Dyck, H.G. Dehmelt	(WASH)
SANDARS	75	PR A11 473	P.G.H. Sandars, D.M. Sternheimer	(OXF, BNL)
COHEN	73	JPCRD 2 664	E.R. Cohen, B.N. Taylor	(RIS C, NBS)
PLAYER	70	JPB 3 1620	M.A. Player, P.G.H. Sandars	(OXF)
WEISSKOPF	68	PRL 21 1645	M.C. Weisskopf et al.	(BRAN)



$$J = \frac{1}{2}$$

 $\mu$  MASS (atomic mass units u)

The muon's mass is obtained from the muon-electron mass ratio as determined from the measurement of Zeeman transition frequencies in muonium ( $\mu^+e^-$  atom). Since the electron's mass is most accurately known in u, the muon's mass is also most accurately known in u. The conversion factor to MeV has approximately the same relative uncertainty as the mass of the muon in u. In this datablock we give the result in u, and in the following datablock in MeV.

VALUE (u)	DOCUMENT ID	TECN	COMMENT
<b>0.1134289267 ± 0.000000029</b>	MOHR	12 RVUE	2010 CODATA value
••• We do not use the following data for averages, fits, limits, etc. •••			
0.1134289256 ± 0.000000029	MOHR	08 RVUE	2006 CODATA value
0.1134289264 ± 0.000000030	MOHR	05 RVUE	2002 CODATA value
0.1134289168 ± 0.000000034	<sup>1</sup> MOHR	99 RVUE	1998 CODATA value
0.113428913 ± 0.000000017	<sup>2</sup> COHEN	87 RVUE	1986 CODATA value

<sup>1</sup> MOHR 99 make use of other 1998 CODATA entries below.  
<sup>2</sup> COHEN 87 make use of other 1986 CODATA entries below.

 $\mu$  MASS

2010 CODATA (MOHR 12) gives the conversion factor from u (atomic mass units, see the above datablock) to MeV as 931.494 061 (21). Earlier values use the then-current conversion factor. The conversion error contributes significantly to the uncertainty of the masses given below.

VALUE (MeV)	DOCUMENT ID	TECN	CHG	COMMENT
<b>105.6583715 ± 0.0000035</b>	MOHR	12 RVUE		2010 CODATA value
••• We do not use the following data for averages, fits, limits, etc. •••				
105.6583668 ± 0.0000038	MOHR	08 RVUE		2006 CODATA value
105.6583692 ± 0.0000094	MOHR	05 RVUE		2002 CODATA value
105.6583568 ± 0.0000052	MOHR	99 RVUE		1998 CODATA value
105.658353 ± 0.000016	<sup>3</sup> COHEN	87 RVUE		1986 CODATA value
105.658386 ± 0.000044	<sup>4</sup> MARIAM	82 CNTR	+	
105.65836 ± 0.00026	<sup>5</sup> CROWE	72 CNTR		
105.65865 ± 0.00044	<sup>6</sup> CRANE	71 CNTR		

<sup>3</sup> Converted to MeV using the 1998 CODATA value of the conversion constant, 931.494013 ± 0.000037 MeV/u.

<sup>4</sup> MARIAM 82 give  $m_\mu/m_e = 206.768259(62)$ .

<sup>5</sup> CROWE 72 give  $m_\mu/m_e = 206.7682(5)$ .

<sup>6</sup> CRANE 71 give  $m_\mu/m_e = 206.76878(85)$ .

 $\mu$  MEAN LIFE  $\tau$ Measurements with an error  $> 0.001 \times 10^{-6}$  s have been omitted.

VALUE ( $10^{-6}$ s)	DOCUMENT ID	TECN	CHG	COMMENT
<b>2.1969811 ± 0.0000022 OUR AVERAGE</b>				
2.1969803 ± 0.0000022	WEBBER	11 CNTR	+	Surface $\mu^+$ at PSI
2.197083 ± 0.000032 ± 0.000015	BARCZYK	08 CNTR	+	Muons from $\pi^+$ decay at rest
2.197013 ± 0.000021 ± 0.000011	CHITWOOD	07 CNTR	+	Surface $\mu^+$ at PSI
2.197078 ± 0.000073	BARDIN	84 CNTR	+	
2.197025 ± 0.000155	BARDIN	84 CNTR	-	
2.19695 ± 0.000006	GIOVANETTI	84 CNTR	+	
2.19711 ± 0.000008	BALANDIN	74 CNTR	+	
2.1973 ± 0.0003	DUCLOS	73 CNTR	+	

 $\tau_{\mu^+}/\tau_{\mu^-}$  MEAN LIFE RATIO

A test of CPT invariance.

VALUE	DOCUMENT ID	TECN	COMMENT
<b>1.000024 ± 0.000078</b>	BARDIN	84 CNTR	
••• We do not use the following data for averages, fits, limits, etc. •••			
1.0008 ± 0.0010	BAILEY	79 CNTR	Storage ring
1.000 ± 0.001	MEYER	63 CNTR	Mean life $\mu^+/\mu^-$

$$(\tau_{\mu^+} - \tau_{\mu^-}) / \tau_{\text{average}}$$

A test of CPT invariance. Calculated from the mean-life ratio, above.

VALUE	DOCUMENT ID
<b>(2 ± 8) × 10<sup>-5</sup> OUR EVALUATION</b>	

$\mu/p$  MAGNETIC MOMENT RATIO

This ratio is used to obtain a precise value of the muon mass and to reduce experimental muon Larmor frequency measurements to the muon magnetic moment anomaly. Measurements with an error  $> 0.00001$  have been omitted. By convention, the minus sign on this ratio is omitted. CODATA values were fitted using their selection of data, plus other data from multiparameter fits.

VALUE	DOCUMENT ID	TECN	CHG	COMMENT
<b>3.183345137 ± 0.000000085</b>	MOHR	08	RVUE	2006 CODATA value
• • • We do not use the following data for averages, fits, limits, etc. • • •				
3.183345118 ± 0.000000089	MOHR	05	RVUE	2002 CODATA value
3.18334513 ± 0.000000039	LIU	99	CNTR +	HFS in muonium
3.18334539 ± 0.000000010	MOHR	99	RVUE	1998 CODATA value
3.18334547 ± 0.000000047	COHEN	87	RVUE	1986 CODATA value
3.1833441 ± 0.000000017	KLEMPPT	82	CNTR +	Precession strob
3.1833461 ± 0.000000011	MARIAM	82	CNTR +	HFS splitting
3.1833448 ± 0.000000029	CAMANI	78	CNTR +	See KLEMPPT 82
3.1833403 ± 0.000000044	CASPERSON	77	CNTR +	HFS splitting
3.1833402 ± 0.000000072	COHEN	73	RVUE	1973 CODATA value
3.1833467 ± 0.000000082	CROWE	72	CNTR +	Precession phase

## THE MUON ANOMALOUS MAGNETIC MOMENT

Updated July 2011 by A. Hoecker (CERN), and W.J. Marciano (BNL).

The Dirac equation predicts a muon magnetic moment,  $\vec{M} = g_\mu \frac{e}{2m_\mu} \vec{S}$ , with gyromagnetic ratio  $g_\mu = 2$ . Quantum loop effects lead to a small calculable deviation from  $g_\mu = 2$ , parameterized by the anomalous magnetic moment

$$a_\mu \equiv \frac{g_\mu - 2}{2}. \quad (1)$$

That quantity can be accurately measured and, within the Standard Model (SM) framework, precisely predicted. Hence, comparison of experiment and theory tests the SM at its quantum loop level. A deviation in  $a_\mu^{\text{exp}}$  from the SM expectation would signal effects of new physics, with current sensitivity reaching up to mass scales of  $\mathcal{O}(\text{TeV})$  [1,2]. For recent and very thorough muon  $g - 2$  reviews, see Refs. [3,4].

The E821 experiment at Brookhaven National Lab (BNL) studied the precession of  $\mu^+$  and  $\mu^-$  in a constant external magnetic field as they circulated in a confining storage ring. It found [6]<sup>1</sup>

$$\begin{aligned} a_{\mu^+}^{\text{exp}} &= 11\,659\,204(6)(5) \times 10^{-10}, \\ a_{\mu^-}^{\text{exp}} &= 11\,659\,215(8)(3) \times 10^{-10}, \end{aligned} \quad (2)$$

where the first errors are statistical and the second systematic. Assuming CPT invariance and taking into account correlations between systematic errors, one finds for their average [6]

$$a_\mu^{\text{exp}} = 11\,659\,208.9(5.4)(3.3) \times 10^{-10}. \quad (3)$$

These results represent about a factor of 14 improvement over the classic CERN experiments of the 1970's [7]. Improvement of the measurement in Eq. (3) by a factor of four by moving

<sup>1</sup> The original results reported by the experiment have been updated in Eqs. (2) and (3) to the newest value for the absolute muon-to-proton magnetic ratio  $\lambda = 3.183345137(85)$  [5]. The change induced in  $a_\mu^{\text{exp}}$  with respect to the value of  $\lambda = 3.18334539(10)$  used in Ref. 6 amounts to  $+0.92 \times 10^{-10}$ .

the E821 storage ring to Fermilab, and utilizing a cleaner and more intense muon beam has been proposed.

The SM prediction for  $a_\mu^{\text{SM}}$  is generally divided into three parts (see Fig. 1 for representative Feynman diagrams)

$$a_\mu^{\text{SM}} = a_\mu^{\text{QED}} + a_\mu^{\text{EW}} + a_\mu^{\text{Had}}. \quad (4)$$

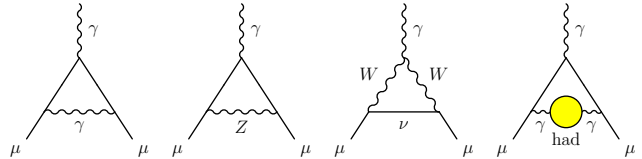


**Figure 1:** Representative diagrams contributing to  $a_\mu^{\text{SM}}$ . From left to right: first order QED (Schwinger term), lowest-order weak, lowest-order hadronic.

The QED part includes all photonic and leptonic ( $e, \mu, \tau$ ) loops starting with the classic  $\alpha/2\pi$  Schwinger contribution. It has been computed through 4 loops and estimated at the 5-loop level [8]

$$\begin{aligned} a_\mu^{\text{QED}} &= \frac{\alpha}{2\pi} + 0.765857410(27) \left(\frac{\alpha}{\pi}\right)^2 + 24.05050964(43) \left(\frac{\alpha}{\pi}\right)^3 \\ &\quad + 130.8055(80) \left(\frac{\alpha}{\pi}\right)^4 + 663(20) \left(\frac{\alpha}{\pi}\right)^5 + \dots \end{aligned} \quad (5)$$

Employing  $\alpha^{-1} = 137.035999084(51)$ , determined [8,9] from the electron  $a_e$  measurement, leads to

$$a_\mu^{\text{QED}} = 116\,584\,718.09(0.15) \times 10^{-11}, \quad (6)$$

where the error results from uncertainties in the coefficients of Eq. (5) and in  $\alpha$ .

Loop contributions involving heavy  $W^\pm, Z$  or Higgs particles are collectively labeled as  $a_\mu^{\text{EW}}$ . They are suppressed by at least a factor of  $\frac{\alpha}{\pi} \frac{m_\mu^2}{M_W^2} \simeq 4 \times 10^{-9}$ . At 1-loop order [10]

$$\begin{aligned} a_\mu^{\text{EW}}[1\text{-loop}] &= \frac{G_\mu m_\mu^2}{8\sqrt{2}\pi^2} \left[ \frac{5}{3} + \frac{1}{3} (1 - 4\sin^2\theta_W)^2 \right. \\ &\quad \left. + \mathcal{O}\left(\frac{m_\mu^2}{M_W^2}\right) + \mathcal{O}\left(\frac{m_\mu^2}{M_H^2}\right) \right], \\ &= 194.8 \times 10^{-11}, \end{aligned} \quad (7)$$

for  $\sin^2\theta_W \equiv 1 - M_W^2/M_Z^2 \simeq 0.223$ , and where  $G_\mu \simeq 1.166 \times 10^{-5} \text{ GeV}^{-2}$  is the Fermi coupling constant. Two-loop corrections are relatively large and negative [11]

$$a_\mu^{\text{EW}}[2\text{-loop}] = -40.7(1.0)(1.8) \times 10^{-11}, \quad (8)$$

where the errors stem from quark triangle loops and the assumed Higgs mass range between 100 and 500 GeV. The 3-loop leading logarithms are negligible [11,12],  $\mathcal{O}(10^{-12})$ , implying in total

$$a_\mu^{\text{EW}} = 154(1)(2) \times 10^{-11}. \quad (9)$$

Hadronic (quark and gluon) loop contributions to  $a_\mu^{\text{SM}}$  give rise to its main theoretical uncertainties. At present, those effects

# Lepton Particle Listings

$\mu$

are not calculable from first principles, but such an approach, at least partially, may become possible as lattice QCD matures. Instead, one currently relies on a dispersion relation approach to evaluate the lowest-order (*i.e.*,  $\mathcal{O}(\alpha^2)$ ) hadronic vacuum polarization contribution  $a_\mu^{\text{Had}}[\text{LO}]$  from corresponding cross section measurements [13]

$$a_\mu^{\text{Had}}[\text{LO}] = \frac{1}{3} \left( \frac{\alpha}{\pi} \right)^2 \int_{m_\pi^2}^{\infty} ds \frac{K(s)}{s} R^{(0)}(s), \quad (10)$$

where  $K(s)$  is a QED kernel function [14], and where  $R^{(0)}(s)$  denotes the ratio of the bare<sup>2</sup> cross section for  $e^+e^-$  annihilation into hadrons to the pointlike muon-pair cross section at center-of-mass energy  $\sqrt{s}$ . The function  $K(s) \sim 1/s$  in Eq. (10) gives a strong weight to the low-energy part of the integral. Hence,  $a_\mu^{\text{Had}}[\text{LO}]$  is dominated by the  $\rho(770)$  resonance.

Currently, the available  $\sigma(e^+e^- \rightarrow \text{hadrons})$  data give a leading-order hadronic vacuum polarization (representative) contribution of [15]

$$a_\mu^{\text{Had}}[\text{LO}] = 6\,923(42)(3) \times 10^{-11}, \quad (11)$$

where the first error is experimental (dominated by systematic uncertainties), and the second due to perturbative QCD, which is used at intermediate and large energies to predict the contribution from the quark-antiquark continuum. New multi-hadron data from the BABAR experiment have increased the constraints on unmeasured exclusive final states and led to a small reduction in the hadronic contribution compared to the 2009 PDG value.

Alternatively, one can use precise vector spectral functions from  $\tau \rightarrow \nu_\tau + \text{hadrons}$  decays [16] that can be related to isovector  $e^+e^- \rightarrow \text{hadrons}$  cross sections by isospin symmetry. Replacing  $e^+e^-$  data in the two-pion and four-pion channels by the corresponding isospin-transformed  $\tau$  data, and applying isospin-violating corrections (from QED and  $m_d - m_u \neq 0$ ), one finds [15]

$$a_\mu^{\text{Had}}[\text{LO}] = 7\,015(42)(19)(3) \times 10^{-11} (\tau), \quad (12)$$

where the first error is experimental, the second estimates the uncertainty in the isospin-breaking corrections applied to the  $\tau$  data, and the third error is due to perturbative QCD. The current discrepancy between the  $e^+e^-$  and  $\tau$ -based determinations of  $a_\mu^{\text{Had}}[\text{LO}]$  has been reduced to  $1.8\sigma$  with respect to earlier evaluations. New  $e^+e^-$  and  $\tau$  data from the  $B$ -factory experiments BABAR and Belle have increased the experimental information. Reevaluated isospin-breaking corrections have also contributed to this improvement [17]. BABAR recently

<sup>2</sup> The bare cross section is defined as the measured cross section corrected for initial-state radiation, electron-vertex loop contributions and vacuum-polarization effects in the photon propagator. However, QED effects in the hadron vertex and final state, as photon radiation, are included.

reported good agreement with the  $\tau$  data in the most important two-pion channel [18]. The remaining discrepancy with the older  $e^+e^-$  and  $\tau$  datasets may be indicative of problems with one or both data sets. It may also suggest the need for additional isospin-violating corrections to the  $\tau$  data.

Higher order,  $\mathcal{O}(\alpha^3)$ , hadronic contributions are obtained from dispersion relations using the same  $e^+e^- \rightarrow \text{hadrons}$  data [16,19,22], giving  $a_\mu^{\text{Had,Disp}}[\text{NLO}] = (-98.4 \pm 0.6) \times 10^{-11}$ , along with model-dependent estimates of the hadronic light-by-light scattering contribution,  $a_\mu^{\text{Had,LBL}}[\text{NLO}]$ , motivated by large- $N_C$  QCD [23–29].<sup>3</sup> Following [27], one finds for the sum of the two terms

$$a_\mu^{\text{Had}}[\text{NLO}] = 7(26) \times 10^{-11}, \quad (13)$$

where the error is dominated by hadronic light-by-light uncertainties.

Adding Eqs. (6), (9), (11) and (13) gives the representative  $e^+e^-$  data based SM prediction

$$a_\mu^{\text{SM}} = 116\,591\,802(2)(42)(26) \times 10^{-11}, \quad (14)$$

where the errors are due to the electroweak, lowest-order hadronic, and higher-order hadronic contributions, respectively. The difference between experiment and theory

$$\Delta a_\mu = a_\mu^{\text{exp}} - a_\mu^{\text{SM}} = 287(63)(49) \times 10^{-11}, \quad (15)$$

(with all errors combined in quadrature) represents an interesting but not yet conclusive discrepancy of 3.6 times the estimated  $1\sigma$  error. All the recent estimates for the hadronic contribution compiled in Fig. 2 exhibit similar discrepancies. Switching to  $\tau$  data reduces the discrepancy to  $2.4\sigma$ , assuming the isospin-violating corrections are under control within the estimated uncertainties.

An alternate interpretation is that  $\Delta a_\mu$  may be a new physics signal with supersymmetric particle loops as the leading candidate explanation. Such a scenario is quite natural, since generically, supersymmetric models predict [1] an additional contribution to  $a_\mu^{\text{SM}}$

$$a_\mu^{\text{SUSY}} \simeq \pm 130 \times 10^{-11} \cdot \left( \frac{100 \text{ GeV}}{m_{\text{SUSY}}} \right)^2 \tan\beta, \quad (16)$$

where  $m_{\text{SUSY}}$  is a representative supersymmetric mass scale, and  $\tan\beta \simeq 3\text{--}40$  is a potential enhancement factor. Supersymmetric particles in the mass range 100–500 GeV could be the source of the deviation  $\Delta a_\mu$ . If so, those particles could be directly observed at the next generation of high energy colliders.

New physics effects [1] other than supersymmetry could also explain a non-vanishing  $\Delta a_\mu$ . A recent popular scenario involves the “dark photon”, a relatively light hypothetical vector boson from the dark matter sector that couples to our world of particle

<sup>3</sup> Some representative recent estimates of the hadronic light-by-light scattering contribution,  $a_\mu^{\text{Had,LBL}}[\text{NLO}]$ , that followed after the sign correction of [25], are:  $105(26) \times 10^{-11}$  [27],  $110(40) \times 10^{-11}$  [23],  $136(25) \times 10^{-11}$  [24].

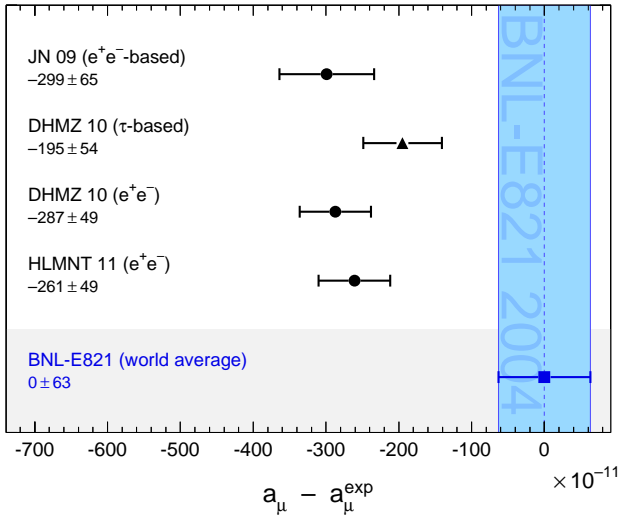


**Figure 2:** Compilation of recently published results for  $a_\mu$  (in units of  $10^{-11}$ ), subtracted by the central value of the experimental average (3). The shaded band indicates the experimental error. The SM predictions are taken from: JN [4], DHMZ [15], and HMNT [19]. Note that the quoted errors do not include the uncertainty on the subtracted experimental value. To obtain for each theory calculation a result equivalent to Eq. (15), the errors from theory and experiment must be added in quadrature.

physics through mixing with the ordinary photon [30,31]. As a result, it couples to ordinary charged particles with strength  $\varepsilon \cdot e$  and gives rise to an additional muon anomalous magnetic moment contribution

$$a_\mu^{\text{dark photon}} = \frac{\alpha}{2\pi} \varepsilon^2 F(m_V/m_\mu), \quad (17)$$

where  $F(x) = \int_0^1 2z(1-z)^2 / [(1-z)^2 + x^2z] dz$ . For values of  $\varepsilon \sim 1-2 \cdot 10^{-3}$  and  $m_V \sim 10-100$  MeV, the dark photon, which was originally motivated by cosmology, can provide a viable solution to the muon  $g-2$  discrepancy. Searches for the dark photon in that mass range are currently underway at Jefferson Lab, USA, and MAMI in Mainz, Germany.

## References

- A. Czarnecki and W.J. Marciano, Phys. Rev. **D64**, 013014 (2001).
- M. Davier and W.J. Marciano, Ann. Rev. Nucl. and Part. Sci. **54**, 115 (2004).
- J. Miller, E. de Rafael, and B. Lee Roberts, Rep. Progress Phys. **70**, 75 (2007).
- F. Jegerlehner and A. Nyffeler, Phys. Reports **477**, 1 (2009).
- P.J. Mohr, B.N. Taylor, and D.B. Newell, CODATA Group, Rev. Mod. Phys. **80**, 633 (2008).
- G.W. Bennett *et al.*, Phys. Rev. Lett. **89**, 101804 (2002); Erratum *ibid.* Phys. Rev. Lett. **89**, 129903 (2002); G.W. Bennett *et al.*, Phys. Rev. Lett. **92**, 161802 (2004); G.W. Bennett *et al.*, Phys. Rev. **D73**, 072003 (2006).
- J. Bailey *et al.*, Nucl. Phys. **B150**, 1 (1979).
- T. Kinoshita and M. Nio, Phys. Rev. **D73**, 013003 (2006); T. Aoyama *et al.*, Phys. Rev. Lett. **99**, 110406 (2007); T. Kinoshita and M. Nio, Phys. Rev. **D70**, 113001 (2004); T. Kinoshita, Nucl. Phys. **B144**, 206 (2005)(Proc. Supp.); T. Kinoshita and M. Nio, Phys. Rev. **D73**, 053007 (2006); A.L. Kataev, arXiv:hep-ph/0602098 (2006); M. Passera, J. Phys. **G31**, 75 (2005).
- G. Gabrielse *et al.*, Phys. Rev. Lett. **97**, 030802 (2006); Erratum *ibid.* Phys. Rev. Lett. **99**, 039902 (2007); D. Hanneke, S. Fogwell, and G. Gabrielse, Phys. Rev. Lett. **100**, 120801 (2008).
- R. Jackiw and S. Weinberg, Phys. Rev. **D5**, 2396 (1972); G. Altarelli *et al.*, Phys. Lett. **B40**, 415 (1972); I. Bars and M. Yoshimura, Phys. Rev. **D6**, 374 (1972); K. Fujikawa, B.W. Lee, and A.I. Sanda, Phys. Rev. **D6**, 2923 (1972).
- A. Czarnecki *et al.*, Phys. Rev. **D67**, 073006 (2003); S. Heinemeyer, D. Stockinger, and G. Weiglein, Nucl. Phys. **B699**, 103 (2004); T. Gribouk and A. Czarnecki, Phys. Rev. **D72**, 053016 (2005); A. Czarnecki, B. Krause, and W.J. Marciano, Phys. Rev. Lett. **76**, 3267 (1996); A. Czarnecki, B. Krause, and W.J. Marciano, Phys. Rev. **D52**, 2619, (1995); S. Peris, M. Perrottet, and E. de Rafael, Phys. Lett. **B355**, 523 (1995); T. Kukkhto *et al.*, Nucl. Phys. **B371**, 567 (1992).
- G. Degrossi and G.F. Giudice, Phys. Rev. **D58**, 053007 (1998).
- C. Bouchiat and L. Michel, J. Phys. Radium **22**, 121 (1961); M. Gourdin and E. de Rafael, Nucl. Phys. **B10**, 667 (1969).
- S.J. Brodsky and E. de Rafael, Phys. Rev. **168**, 1620 (1968).
- M. Davier *et al.*, Eur. Phys. J. **C71**, 1515 (2011).
- R. Alemany *et al.*, Eur. Phys. J. **C2**, 123 (1998).
- M. Davier *et al.*, Eur. Phys. J. **C66**, 127 (2010).
- BABAR Collaboration (B. Aubert *et al.*), Phys. Rev. Lett. **103**, 231801 (2009).
- K. Hagiwara *et al.*, JPHGB **G38**, 085003 (2011).
- M. Davier, Nucl. Phys. (Proc. Suppl.), **B169**, 288 (2007).
- M. Davier *et al.*, Eur. Phys. J. **C31**, 503 (2003); M. Davier *et al.*, Eur. Phys. J. **C27**, 497 (2003).
- B.Krause, Phys. Lett. **B390**, 392 (1997).
- J. Bijnens and J. Prades, Mod. Phys. Lett. **A22**, 767 (2007).
- K. Melnikov and A. Vainshtein, Phys. Rev. **D70**, 113006 (2004).
- M. Knecht and A. Nyffeler, Phys. Rev. **D65**, 073034 (2002); M. Knecht *et al.*, Phys. Rev. Lett. **88**, 071802 (2002).
- J. Bijnens *et al.*, Nucl. Phys. **B626**, 410 (2002).
- J. Prades, E. de Rafael, and A. Vainshtein, arXiv:0901.0306 [hep-ph] (2009).
- J. Hayakawa and T. Kinoshita, Erratum Phys. Rev. **D66**, 019902 (2002).
- E. de Rafael, Phys. Lett. **B322**, 239 (1994).

## Lepton Particle Listings

 $\mu$ 

30. M. Pospelov, Phys. Rev. **D80**, 095002 (2009).  
 31. D. Tucker-Smith and I. Yavin, Phys. Rev. **D83**, 101702 (R)(2011).

 $\mu$  MAGNETIC MOMENT ANOMALY

The parity-violating decay of muons in a storage ring is observed. The difference frequency  $\omega_a$  between the muon spin precession and the orbital angular frequency ( $e/m_\mu c \langle B \rangle$ ) is measured, as is the free proton NMR frequency  $\omega_p$ , thus determining the ratio  $R = \omega_a/\omega_p$ . Given the magnetic moment ratio  $\lambda = \mu_\mu/\mu_p$  (from hyperfine structure in muonium),  $(g-2)/2 = R/(\lambda-R)$ .

$$\mu_\mu/(e\hbar/2m_\mu) - 1 = (g_\mu - 2)/2$$

VALUE (units $10^{-10}$ )	DOCUMENT ID	TECN	CHG	COMMENT
<b>11659208.9 ± 5.4 ± 3.3</b>	<sup>7</sup> BENNETT	06	MUG2	Average $\mu^+$ and $\mu^-$
••• We do not use the following data for averages, fits, limits, etc. •••				
11659208 ± 6	BENNETT	04	MUG2	Average $\mu^+$ and $\mu^-$
11659214 ± 8 ± 3	BENNETT	04	MUG2	Storage ring
11659203 ± 6 ± 5	BENNETT	04	MUG2	Storage ring
11659204 ± 7 ± 5	BENNETT	02	MUG2	Storage ring
11659202 ± 14 ± 6	BROWN	01	MUG2	Storage ring
11659191 ± 59	BROWN	00	MUG2	Storage ring
11659100 ± 110	<sup>8</sup> BAILEY	79	CNTR	Storage ring
11659360 ± 120	<sup>8</sup> BAILEY	79	CNTR	Storage ring
11659230 ± 85	<sup>8</sup> BAILEY	79	CNTR	Storage ring
11620000 ± 5000	CHARPAK	62	CNTR	Storage ring

<sup>7</sup>BENNETT 06 reports  $(g_\mu - 2)/2 = (11659208.0 \pm 5.4 \pm 3.3) \times 10^{-10}$ . We rescaled this value using  $\mu/p$  magnetic moment ratio of 3.183345137(85) from MOHR 08.

<sup>8</sup>BAILEY 79 values recalculated by HUGHES 99 using the COHEN 87  $\mu/p$  magnetic moment. The improved MOHR 99 value does not change the result.

$$(g_{\mu^+} - g_{\mu^-}) / g_{\text{average}}$$

A test of  $CPT$  invariance.

VALUE (units $10^{-8}$ )	DOCUMENT ID	TECN
<b>-0.11 ± 0.12</b>	BENNETT	04 MUG2
••• We do not use the following data for averages, fits, limits, etc. •••		
-2.6 ± 1.6	BAILEY	79 CNTR

 $\mu$  ELECTRIC DIPOLE MOMENT (d)

A nonzero value is forbidden by both  $T$  invariance and  $P$  invariance.

VALUE ( $10^{-19}$ e cm)	DOCUMENT ID	TECN	CHG	COMMENT
<b>-0.1 ± 0.9</b>	<sup>9</sup> BENNETT	09	MUG2	Storage ring
••• We do not use the following data for averages, fits, limits, etc. •••				
-0.1 ± 1.0	BENNETT	09	MUG2	Storage ring
-0.1 ± 0.7	BENNETT	09	MUG2	Storage ring
-3.7 ± 3.4	<sup>10</sup> BAILEY	78	CNTR	Storage ring
8.6 ± 4.5	BAILEY	78	CNTR	Storage ring
0.8 ± 4.3	BAILEY	78	CNTR	Storage ring

<sup>9</sup>This is the combination of the two BENNETT 09 results quoted here separately for  $\mu^+$  and  $\mu^-$ . BENNETT 09 uses the convention  $d = 1/2 \cdot (d_{\mu^-} - d_{\mu^+})$ .

<sup>10</sup>This is the combination of the two BAILEY 78 results quoted here separately for  $\mu^+$  and  $\mu^-$ . BAILEY 78 uses the convention  $d = 1/2 \cdot (d_{\mu^+} - d_{\mu^-})$  and reports  $3.7 \pm 3.4$ . We convert their result to use the same convention as BENNETT 09.

MUON-ELECTRON CHARGE RATIO ANOMALY  $q_{\mu^+}/q_{e^-} + 1$ 

VALUE	DOCUMENT ID	TECN	CHG	COMMENT
<b>(1.1 ± 2.1) × 10<sup>-9</sup></b>	<sup>11</sup> MEYER	00	CNTR	1s-2s muonium interval

<sup>11</sup>MEYER 00 measure the 1s-2s muonium interval, and then interpret the result in terms of muon-electron charge ratio  $q_{\mu^+}/q_{e^-}$ .

 $\mu^-$  DECAY MODES

$\mu^+$  modes are charge conjugates of the modes below.

Mode	Fraction ( $\Gamma_i/\Gamma$ )	Confidence level
$\Gamma_1$ $e^- \bar{\nu}_e \bar{\nu}_\mu$	≈ 100%	
$\Gamma_2$ $e^- \bar{\nu}_e \nu_\mu \gamma$	[a] (1.4 ± 0.4) %	
$\Gamma_3$ $e^- \bar{\nu}_e \nu_\mu e^+ e^-$	[b] (3.4 ± 0.4) × 10 <sup>-5</sup>	

## Lepton Family number (LF) violating modes

$\Gamma_i$	Mode	LF	[c]	%	90%
$\Gamma_4$	$e^- \nu_e \bar{\nu}_\mu$	LF	< 1.2		90%
$\Gamma_5$	$e^- \gamma$	LF	< 2.4	× 10 <sup>-12</sup>	90%
$\Gamma_6$	$e^- e^+ e^-$	LF	< 1.0	× 10 <sup>-12</sup>	90%
$\Gamma_7$	$e^- 2\gamma$	LF	< 7.2	× 10 <sup>-11</sup>	90%

[a] This only includes events with the  $\gamma$  energy > 10 MeV. Since the  $e^- \bar{\nu}_e \nu_\mu$  and  $e^- \bar{\nu}_e \nu_\mu \gamma$  modes cannot be clearly separated, we regard the latter mode as a subset of the former.

[b] See the Particle Listings below for the energy limits used in this measurement.

[c] A test of additive vs. multiplicative lepton family number conservation.

 $\mu^-$  BRANCHING RATIOS

$\Gamma(e^- \bar{\nu}_e \nu_\mu \gamma)/\Gamma_{\text{total}}$	VALUE	DOCUMENT ID	TECN	CHG	COMMENT	$\Gamma_2/\Gamma$
<b>0.014 ± 0.004</b>	7443	<sup>12</sup> BERTL	85	SPEC	+ SINDRUM	
••• We do not use the following data for averages, fits, limits, etc. •••						
0.0033 ± 0.0013	862	BOGART	67	CNTR	$\gamma$ KE > 14.5 MeV	
	27	CRITTENDEN	61	CNTR	$\gamma$ KE > 20 MeV	
		ASHKIN	59	CNTR		

$\Gamma(e^- \bar{\nu}_e \nu_\mu e^+ e^-)/\Gamma_{\text{total}}$	VALUE (units $10^{-5}$ )	DOCUMENT ID	TECN	CHG	COMMENT	$\Gamma_3/\Gamma$
<b>3.4 ± 0.2 ± 0.3</b>	7443	<sup>12</sup> BERTL	85	SPEC	+ SINDRUM	
••• We do not use the following data for averages, fits, limits, etc. •••						
2.2 ± 1.5	7	<sup>13</sup> CRITTENDEN	61	HLBC	+ $E(e^+ e^-) > 10$ MeV	
2	1	<sup>14</sup> GUREVICH	60	EMUL	+	
1.5 ± 1.0	3	<sup>15</sup> LEE	59	HBC	+	

<sup>12</sup>BERTL 85 has transverse momentum cut  $p_T > 17$  MeV/c. Systematic error was increased by us.

<sup>13</sup>CRITTENDEN 61 count only those decays where total energy of either ( $e^+$ ,  $e^-$ ) combination is > 10 MeV.

<sup>14</sup>GUREVICH 60 interpret their event as either virtual or real photon conversion.  $e^+$  and  $e^-$  energies not measured.

<sup>15</sup>In the three LEE 59 events, the sum of energies  $E(e^+) + E(e^-) + E(e^+)$  was 51 MeV, 55 MeV, and 33 MeV.

$\Gamma(e^- \nu_e \bar{\nu}_\mu)/\Gamma_{\text{total}}$	VALUE	CL%	DOCUMENT ID	TECN	CHG	COMMENT	$\Gamma_4/\Gamma$
<b>&lt; 0.012</b>	90	16	FREEDMAN	93	CNTR	+ $\nu$ oscillation search	
••• We do not use the following data for averages, fits, limits, etc. •••							
< 0.018	90		KRAKAUER	91B	CALO	+	
< 0.05	90	17	BERGSMA	83	CALO	$\bar{\nu}_\mu e \rightarrow \mu^- \bar{\nu}_e$	
< 0.09	90		JONKER	80	CALO	See BERGSMA 83	
-0.001 ± 0.061			WILLIS	80	CNTR	+	
0.13 ± 0.15			BLIETSCHAU	78	HLBC	± Avg. of 4 values	
< 0.25	90		EICHTEN	73	HLBC	+	

<sup>16</sup>FREEDMAN 93 limit on  $\bar{\nu}_e$  observation is here interpreted as a limit on lepton family number violation.

<sup>17</sup>BERGSMA 83 gives a limit on the inverse muon decay cross-section ratio  $\sigma(\bar{\nu}_\mu e^- \rightarrow \mu^- \bar{\nu}_e)/\sigma(\nu_\mu e^- \rightarrow \mu^- \nu_e)$ , which is essentially equivalent to  $\Gamma(e^- \nu_e \bar{\nu}_\mu)/\Gamma_{\text{total}}$  for small values like that quoted.

$\Gamma(e^- \gamma)/\Gamma_{\text{total}}$	VALUE (units $10^{-11}$ )	CL%	DOCUMENT ID	TECN	CHG	COMMENT	$\Gamma_5/\Gamma$
<b>&lt; 0.24</b>	90		ADAM	11	SPEC	+ MEG at PSI	
••• We do not use the following data for averages, fits, limits, etc. •••							
< 2.8	90		ADAM	10	SPEC	+ MEG at PSI	
< 1.2	90		AHMED	02	SPEC	+ MEGA	
< 1.2	90		BROOKS	99	SPEC	+ LAMPF	
< 4.9	90		BOLTON	88	CBOX	+ LAMPF	
< 100	90		AZUELOS	83	CNTR	+ TRIUMF	
< 17	90		KININSON	82	SPEC	+ LAMPF	
< 100	90		SCHAAF	80	ELEC	+ SIN	

$\Gamma(e^- e^+ e^-)/\Gamma_{\text{total}}$	VALUE (units $10^{-12}$ )	CL%	DOCUMENT ID	TECN	CHG	COMMENT	$\Gamma_6/\Gamma$
<b>&lt; 1.0</b>	90	18	BELLGARDT	88	SPEC	+ SINDRUM	
••• We do not use the following data for averages, fits, limits, etc. •••							
< 36	90		BARANOV	91	SPEC	+ ARES	
< 35	90		BOLTON	88	CBOX	+ LAMPF	
< 2.4	90	18	BERTL	85	SPEC	+ SINDRUM	
< 160	90	18	BERTL	84	SPEC	+ SINDRUM	
< 130	90	18	BOLTON	84	CNTR	LAMPF	

<sup>18</sup>These experiments assume a constant matrix element.



$\Gamma(e^- 2\gamma)/\Gamma_{\text{total}}$   
Forbidden by lepton family number conservation.

VALUE (units $10^{-11}$ )	CL%	DOCUMENT ID	TECN	CHG	COMMENT
< 7.2	90	BOLTON	88	CBOX +	LAMPF
••• We do not use the following data for averages, fits, limits, etc. •••					
< 840	90	<sup>19</sup> AZUELOS	83	CNTR +	TRIUMF
< 5000	90	<sup>20</sup> BOWMAN	78	CNTR	DEPOMMIER 77 data

<sup>19</sup>AZUELOS 83 uses the phase space distribution of BOWMAN 78.  
<sup>20</sup>BOWMAN 78 assumes an interaction Lagrangian local on the scale of the inverse  $\mu$  mass.

LIMIT ON  $\mu^- \rightarrow e^-$  CONVERSION

Forbidden by lepton family number conservation.

$\sigma(\mu^- 32\text{S} \rightarrow e^- 32\text{S}) / \sigma(\mu^- 32\text{S} \rightarrow \nu_\mu 32\text{P}^*)$

VALUE	CL%	DOCUMENT ID	TECN	COMMENT
< $7 \times 10^{-11}$	90	BADERT...	80	STRC SIN
••• We do not use the following data for averages, fits, limits, etc. •••				
< $4 \times 10^{-10}$	90	BADERT...	77	STRC SIN

$\sigma(\mu^- \text{Cu} \rightarrow e^- \text{Cu}) / \sigma(\mu^- \text{Cu} \rightarrow \text{capture})$

VALUE	CL%	DOCUMENT ID	TECN	COMMENT
< $1.6 \times 10^{-8}$	90	BRYMAN	72	SPEC
••• We do not use the following data for averages, fits, limits, etc. •••				

$\sigma(\mu^- \text{Ti} \rightarrow e^- \text{Ti}) / \sigma(\mu^- \text{Ti} \rightarrow \text{capture})$

VALUE	CL%	DOCUMENT ID	TECN	COMMENT
< $4.3 \times 10^{-12}$	90	<sup>21</sup> DOHMEN	93	SPEC SINDRUM II
••• We do not use the following data for averages, fits, limits, etc. •••				
< $4.6 \times 10^{-12}$	90	AHMAD	88	TPC TRIUMF
< $1.6 \times 10^{-11}$	90	BRYMAN	85	TPC TRIUMF

<sup>21</sup>DOHMEN 93 assumes  $\mu^- \rightarrow e^-$  conversion leaves the nucleus in its ground state, a process enhanced by coherence and expected to dominate.

$\sigma(\mu^- \text{Pb} \rightarrow e^- \text{Pb}) / \sigma(\mu^- \text{Pb} \rightarrow \text{capture})$

VALUE	CL%	DOCUMENT ID	TECN	COMMENT
< $4.6 \times 10^{-11}$	90	HONECKER	96	SPEC SINDRUM II
••• We do not use the following data for averages, fits, limits, etc. •••				
< $4.9 \times 10^{-10}$	90	AHMAD	88	TPC TRIUMF

$\sigma(\mu^- \text{Au} \rightarrow e^- \text{Au}) / \sigma(\mu^- \text{Au} \rightarrow \text{capture})$

VALUE	CL%	DOCUMENT ID	TECN	CHG	COMMENT
< $7 \times 10^{-13}$	90	BERTL	06	SPEC -	SINDRUM II

LIMIT ON  $\mu^- \rightarrow e^+$  CONVERSION

Forbidden by total lepton number conservation.

$\sigma(\mu^- 32\text{S} \rightarrow e^+ 32\text{Si}^*) / \sigma(\mu^- 32\text{S} \rightarrow \nu_\mu 32\text{P}^*)$

VALUE	CL%	DOCUMENT ID	TECN	COMMENT
< $9 \times 10^{-10}$	90	BADERT...	80	STRC SIN
••• We do not use the following data for averages, fits, limits, etc. •••				
< $1.5 \times 10^{-9}$	90	BADERT...	78	STRC SIN

$\sigma(\mu^- 127\text{I} \rightarrow e^+ 127\text{Sb}^*) / \sigma(\mu^- 127\text{I} \rightarrow \text{anything})$

VALUE	CL%	DOCUMENT ID	TECN	COMMENT
< $3 \times 10^{-10}$	90	<sup>22</sup> ABELA	80	CNTR Radiochemical tech.

<sup>22</sup>ABELA 80 is upper limit for  $\mu^- e^+$  conversion leading to particle-stable states of <sup>127</sup>Sb. Limit for total conversion rate is higher by a factor less than 4 (G. Backenstoss, private communication).

$\sigma(\mu^- \text{Cu} \rightarrow e^+ \text{Co}) / \sigma(\mu^- \text{Cu} \rightarrow \nu_\mu \text{Ni})$

VALUE	CL%	DOCUMENT ID	TECN	COMMENT
< $2.6 \times 10^{-8}$	90	BRYMAN	72	SPEC
< $2.2 \times 10^{-7}$	90	CONFORTO	62	OSPK
••• We do not use the following data for averages, fits, limits, etc. •••				

$\sigma(\mu^- \text{Ti} \rightarrow e^+ \text{Ca}) / \sigma(\mu^- \text{Ti} \rightarrow \text{capture})$

VALUE	CL%	EVTS	DOCUMENT ID	TECN	CHG	COMMENT
< $3.6 \times 10^{-11}$	90	1	<sup>23,24</sup> KAULARD	98	SPEC -	SINDRUM II
••• We do not use the following data for averages, fits, limits, etc. •••						
< $1.7 \times 10^{-12}$	90	1	<sup>24,25</sup> KAULARD	98	SPEC -	SINDRUM II
< $4.3 \times 10^{-12}$	90		<sup>25</sup> DOHMEN	93	SPEC	SINDRUM II
< $8.9 \times 10^{-11}$	90		<sup>23</sup> DOHMEN	93	SPEC	SINDRUM II
< $1.7 \times 10^{-10}$	90		<sup>26</sup> AHMAD	88	TPC	TRIUMF

<sup>23</sup>This limit assumes a giant resonance excitation of the daughter Ca nucleus (mean energy and width both 20 MeV).<sup>24</sup>KAULARD 98 obtained these same limits using the unified classical analysis of FELDMAN 98.<sup>25</sup>This limit assumes the daughter Ca nucleus is left in the ground state. However, the probability of this is unknown.<sup>26</sup>Assuming a giant-resonance-excitation model.LIMIT ON MUONIUM  $\rightarrow$  ANTIMUONIUM CONVERSION

Forbidden by lepton family number conservation.

$$R_g = G_C / G_F$$

The effective Lagrangian for the  $\mu^+ e^- \rightarrow \mu^- e^+$  conversion is assumed to be

$$\mathcal{L} = 2^{-1/2} G_C [\bar{\psi}_\mu \gamma_\lambda (1 - \gamma_5) \psi_e] [\bar{\psi}_\mu \gamma_\lambda (1 - \gamma_5) \psi_e] + \text{h.c.}$$

The experimental result is then an upper limit on  $G_C/G_F$ , where  $G_F$  is the Fermi coupling constant.

VALUE	CL%	EVTS	DOCUMENT ID	TECN	CHG	COMMENT
< 0.0030	90	1	<sup>27</sup> WILLMANN	99	SPEC +	$\mu^+$ at 26 GeV/c
••• We do not use the following data for averages, fits, limits, etc. •••						
< 0.14	90	1	<sup>28</sup> GORDEEV	97	SPEC +	JINR phasotron
< 0.018	90	0	<sup>29</sup> ABELA	96	SPEC +	$\mu^+$ at 24 MeV
< 6.9	90		NI	93	CBOX	LAMPF
< 0.16	90		MATTHIAS	91	SPEC	LAMPF
< 0.29	90		HUBER	90B	CNTR	TRIUMF
< 20	95		BEER	86	CNTR	TRIUMF
< 42	95		MARSHALL	82	CNTR	
<sup>27</sup> WILLMANN 99 quote both probability $P_{MM} < 8.3 \times 10^{-11}$ at 90%CL in a 0.1 T field and $R_g = G_C/G_F$ .						
<sup>28</sup> GORDEEV 97 quote limits on both $f = G_{MM}/G_F$ and the probability $W_{MM} < 4.7 \times 10^{-7}$ (90% CL).						
<sup>29</sup> ABELA 96 quote both probability $P_{MM} < 8 \times 10^{-9}$ at 90% CL and $R_g = G_C/G_F$ .						

## MUON DECAY PARAMETERS

Revised January 2012 by W. Fetscher and H.-J. Gerber (ETH Zürich).

**Introduction:** All measurements in direct muon decay,  $\mu^- \rightarrow e^- + 2$  neutrals, and its inverse,  $\nu_\mu + e^- \rightarrow \mu^- + \text{neutral}$ , are successfully described by the “V-A interaction,” which is a particular case of a local, derivative-free, lepton-number-conserving, four-fermion interaction [1]. As shown below, within this framework, the Standard Model assumptions, such as the V-A form and the nature of the neutrals ( $\nu_\mu$  and  $\bar{\nu}_e$ ), and hence the doublet assignments ( $\nu_e e^-$ )<sub>L</sub> and ( $\nu_\mu \mu^-$ )<sub>L</sub>, have been determined from experiments [2,3]. All considerations on muon decay are valid for the leptonic tau decays  $\tau \rightarrow \ell + \nu_\tau + \bar{\nu}_e$  with the replacements  $m_\mu \rightarrow m_\tau$ ,  $m_e \rightarrow m_\ell$ .

**Parameters:** The differential decay probability to obtain an  $e^\pm$  with (reduced) energy between  $x$  and  $x + dx$ , emitted in the direction  $\hat{x}_3$  at an angle between  $\vartheta$  and  $\vartheta + d\vartheta$  with respect to the muon polarization vector  $\mathbf{P}_\mu$ , and with its spin parallel to the arbitrary direction  $\hat{\zeta}$ , neglecting radiative corrections, is given by

$$\frac{d^2\Gamma}{dx d\cos\vartheta} = \frac{m_\mu}{4\pi^3} W_{e\mu}^4 G_F^2 \sqrt{x^2 - x_0^2} \times (F_{\text{IS}}(x) \pm P_\mu \cos\vartheta F_{\text{AS}}(x)) \times [1 + \hat{\zeta} \cdot \mathbf{P}_e(x, \vartheta)] \quad (1)$$

Here,  $W_{e\mu} = \max(E_e) = (m_\mu^2 + m_e^2)/2m_\mu$  is the maximum  $e^\pm$  energy,  $x = E_e/W_{e\mu}$  is the reduced energy,  $x_0 = m_e/W_{e\mu} = 9.67 \times 10^{-3}$ , and  $P_\mu = |\mathbf{P}_\mu|$  is the degree of muon polarization.  $\hat{\zeta}$  is the direction in which a perfect polarization-sensitive electron detector is most sensitive. The isotropic part of the spectrum,  $F_{\text{IS}}(x)$ , the anisotropic part  $F_{\text{AS}}(x)$ , and the electron polarization,  $\mathbf{P}_e(x, \vartheta)$ , may be parametrized by the Michel parameter  $\rho$  [1], by  $\eta$  [4], by  $\xi$  and  $\delta$  [5,6], etc. These are bilinear combinations of the coupling constants  $g_{2\mu}^2$ , which occur in the matrix element (given below).

# Lepton Particle Listings

$\mu$

If the masses of the neutrinos as well as  $x_0^2$  are neglected, the energy and angular distribution of the electron in the rest frame of a muon ( $\mu^\pm$ ) measured by a polarization insensitive detector, is given by

$$\frac{d^2\Gamma}{dx d\cos\vartheta} \sim x^2 \cdot \left\{ 3(1-x) + \frac{2\rho}{3}(4x-3) + 3\eta x_0(1-x)/x \right. \\ \left. \pm P_\mu \cdot \xi \cdot \cos\vartheta \left[ 1-x + \frac{2\delta}{3}(4x-3) \right] \right\}. \quad (2)$$

Here,  $\vartheta$  is the angle between the electron momentum and the muon spin, and  $x \equiv 2E_e/m_\mu$ . For the Standard Model coupling, we obtain  $\rho = \xi\delta = 3/4$ ,  $\xi = 1$ ,  $\eta = 0$  and the differential decay rate is

$$\frac{d^2\Gamma}{dx d\cos\vartheta} = \frac{G_F^2 m_\mu^5}{192\pi^3} [3 - 2x \pm P_\mu \cos\vartheta(2x-1)] x^2. \quad (3)$$

The coefficient in front of the square bracket is the total decay rate.

If only the neutrino masses are neglected, and if the  $e^\pm$  polarization is detected, then the functions in Eq. (1) become

$$F_{\text{IS}}(x) = x(1-x) + \frac{2}{9}\rho(4x^2 - 3x - x_0^2) + \eta \cdot x_0(1-x) \\ F_{\text{AS}}(x) = \frac{1}{3}\xi \sqrt{x^2 - x_0^2} \\ \times [1-x + \frac{2}{3}\delta(4x-3 + (\sqrt{1-x_0^2}-1))] \\ \mathbf{P}_e(x, \vartheta) = P_{T_1} \cdot \hat{\mathbf{x}}_1 + P_{T_2} \cdot \hat{\mathbf{x}}_2 + P_L \cdot \hat{\mathbf{x}}_3. \quad (4)$$

Here  $\hat{\mathbf{x}}_1$ ,  $\hat{\mathbf{x}}_2$ , and  $\hat{\mathbf{x}}_3$  are orthogonal unit vectors defined as follows:

$$\hat{\mathbf{x}}_3 \text{ is along the } e \text{ momentum } \mathbf{p}_e \\ \frac{\hat{\mathbf{x}}_3 \times \mathbf{P}_\mu}{|\hat{\mathbf{x}}_3 \times \mathbf{P}_\mu|} = \hat{\mathbf{x}}_2 \text{ is transverse to } \mathbf{p}_e \text{ and perpendicular} \\ \text{to the "decay plane"} \\ \hat{\mathbf{x}}_2 \times \hat{\mathbf{x}}_3 = \hat{\mathbf{x}}_1 \text{ is transverse to the } \mathbf{p}_e \text{ and in the} \\ \text{"decay plane."}$$

The components of  $\mathbf{P}_e$  then are given by

$$P_{T_1}(x, \vartheta) = P_\mu \sin\vartheta \cdot F_{T_1}(x) / (F_{\text{IS}}(x) \pm P_\mu \cos\vartheta \cdot F_{\text{AS}}(x)) \\ P_{T_2}(x, \vartheta) = P_\mu \sin\vartheta \cdot F_{T_2}(x) / (F_{\text{IS}}(x) \pm P_\mu \cos\vartheta \cdot F_{\text{AS}}(x)) \\ P_L(x, \vartheta) = \left( \pm F_{\text{IP}}(x) + P_\mu \cos\vartheta \right. \\ \left. \times F_{\text{AP}}(x) \right) / (F_{\text{IS}}(x) \pm P_\mu \cos\vartheta \cdot F_{\text{AS}}(x)),$$

where

$$F_{T_1}(x) = \frac{1}{12} \left\{ -2 \left[ \xi'' + 12(\rho - \frac{3}{4}) \right] (1-x)x_0 \right. \\ \left. - 3\eta(x^2 - x_0^2) + \eta''(-3x^2 + 4x - x_0^2) \right\} \\ F_{T_2}(x) = \frac{1}{3} \sqrt{x^2 - x_0^2} \left\{ 3\frac{\alpha'}{A}(1-x) + 2\frac{\beta'}{A}\sqrt{1-x_0^2} \right\} \\ F_{\text{IP}}(x) = \frac{1}{54} \sqrt{x^2 - x_0^2} \left\{ 9\xi' \left( -2x + 2 + \sqrt{1-x_0^2} \right) \right. \\ \left. + 4\xi(\delta - \frac{3}{4})(4x - 4 + \sqrt{1-x_0^2}) \right\} \\ F_{\text{AP}}(x) = \frac{1}{6} \left\{ \xi''(2x^2 - x - x_0^2) + 4(\rho - \frac{3}{4})(4x^2 - 3x - x_0^2) \right. \\ \left. + 2\eta''(1-x)x_0 \right\}. \quad (5)$$

For the experimental values of the parameters  $\rho$ ,  $\xi$ ,  $\xi'$ ,  $\xi''$ ,  $\delta$ ,  $\eta$ ,  $\eta''$ ,  $\alpha/A$ ,  $\beta/A$ ,  $\alpha'/A$ ,  $\beta'/A$ , which are not all independent, see the Data Listings below. Experiments in the past have also been analyzed using the parameters  $a$ ,  $b$ ,  $c$ ,  $a'$ ,  $b'$ ,  $c'$ ,  $\alpha/A$ ,  $\beta/A$ ,  $\alpha'/A$ ,  $\beta'/A$  (and  $\eta = (\alpha - 2\beta)/2A$ ), as defined by Kinoshita and Sirlin [5,6]. They serve as a model-independent summary of all possible measurements on the decay electron (see Listings below). The relations between the two sets of parameters are

$$\rho - \frac{3}{4} = \frac{3}{4}(-a + 2c)/A, \\ \eta = (\alpha - 2\beta)/A, \\ \eta'' = (3\alpha + 2\beta)/A, \\ \delta - \frac{3}{4} = \frac{9}{4} \cdot \frac{(a' - 2c')/A}{1 - [a + 3a' + 4(b + b') + 6c - 14c']/A}, \\ 1 - \xi \frac{\delta}{\rho} = 4 \frac{[(b + b') + 2(c - c')]/A}{1 - (a - 2c)/A}, \\ 1 - \xi' = [(a + a') + 4(b + b') + 6(c + c')]/A, \\ 1 - \xi'' = (-2a + 20c)/A,$$

where

$$A = a + 4b + 6c. \quad (6)$$

The differential decay probability to obtain a *left-handed*  $\nu_e$  with (reduced) energy between  $y$  and  $y + dy$ , neglecting radiative corrections as well as the masses of the electron and of the neutrinos, is given by [7]

$$\frac{d\Gamma}{dy} = \frac{m_\mu^5 G_F^2}{16\pi^3} \cdot Q_L^{\nu_e} \cdot y^2 \left\{ (1-y) - \omega_L \cdot (y - \frac{3}{4}) \right\}. \quad (7)$$

Here,  $y = 2 E_{\nu_e}/m_\mu$ .  $Q_L^{\nu_e}$  and  $\omega_L$  are parameters.  $\omega_L$  is the neutrino analog of the spectral shape parameter  $\rho$  of Michel. Since in the Standard Model,  $Q_L^{\nu_e} = 1$ ,  $\omega_L = 0$ , the measurement of  $d\Gamma/dy$  has allowed a null-test of the Standard Model (see Listings below).

**Matrix element:** All results in direct muon decay (energy spectra of the electron and of the neutrinos, polarizations, and angular distributions), and in inverse muon decay (the reaction cross section) at energies well below  $m_W c^2$ , may be parametrized in terms of amplitudes  $g_{\varepsilon\mu}^{\nu_e}$  and the Fermi coupling constant  $G_F$ , using the matrix element

$$\frac{4G_F}{\sqrt{2}} \sum_{\substack{\gamma=S,V,T \\ \varepsilon,\mu=R,L}} g_{\varepsilon\mu}^{\nu_e} \langle \bar{e}_\varepsilon | \Gamma^\gamma | (\nu_e)_n \rangle \langle (\bar{\nu}_\mu)_m | \Gamma_\gamma | \mu_\mu \rangle. \quad (8)$$

We use the notation of Fetscher *et al.* [2], who in turn use the sign conventions and definitions of Scheck [8]. Here,  $\gamma = S, V, T$  indicates a scalar, vector, or tensor interaction; and  $\varepsilon, \mu = R, L$  indicate a right- or left-handed chirality of the electron or muon. The chiralities  $n$  and  $m$  of the  $\nu_e$  and  $\bar{\nu}_\mu$  are then determined by the values of  $\gamma, \varepsilon$ , and  $\mu$ . The particles are represented by fields of definite chirality [9].

As shown by Langacker and London [10], explicit lepton-number nonconservation still leads to a matrix element equivalent to Eq. (8). They conclude that it is not possible, even in

principle, to test lepton-number conservation in (leptonic) muon decay if the final neutrinos are massless and are not observed.

The ten complex amplitudes  $g_{\varepsilon\mu}^{\tilde{\gamma}}$  ( $g_{RR}^T$  and  $g_{LL}^T$  are identically zero) and  $G_F$  constitute 19 independent (real) parameters to be determined by experiment. The Standard Model interaction corresponds to one single amplitude  $g_{LL}^V$  being unity and all the others being zero.

The (direct) muon decay experiments are compatible with an arbitrary mix of the scalar and vector amplitudes  $g_{LL}^S$  and  $g_{LL}^V$  – in the extreme even with purely scalar  $g_{LL}^S = 2$ ,  $g_{LL}^V = 0$ . The decision in favour of the Standard Model comes from the quantitative observation of inverse muon decay, which would be forbidden for pure  $g_{LL}^S$  [2].

**Experimental determination of V–A:** In order to determine the amplitudes  $g_{\varepsilon\mu}^{\tilde{\gamma}}$  uniquely from experiment, the following set of equations, where the left-hand sides represent experimental results, has to be solved.

$$\begin{aligned} a &= 16(|g_{RL}^V|^2 + |g_{LR}^V|^2) + |g_{RL}^S + 6g_{RL}^T|^2 + |g_{LR}^S + 6g_{LR}^T|^2 \\ a' &= 16(|g_{RL}^V|^2 - |g_{LR}^V|^2) + |g_{RL}^S + 6g_{RL}^T|^2 - |g_{LR}^S + 6g_{LR}^T|^2 \\ \alpha &= 8\text{Re} \left\{ g_{RL}^V(g_{LR}^{S*} + 6g_{LR}^{T*}) + g_{LR}^V(g_{RL}^{S*} + 6g_{RL}^{T*}) \right\} \\ \alpha' &= 8\text{Im} \left\{ g_{LR}^V(g_{RL}^{S*} + 6g_{RL}^{T*}) - g_{RL}^V(g_{LR}^{S*} + 6g_{LR}^{T*}) \right\} \\ b &= 4(|g_{RR}^V|^2 + |g_{LL}^V|^2) + |g_{RR}^S|^2 + |g_{LL}^S|^2 \\ b' &= 4(|g_{RR}^V|^2 - |g_{LL}^V|^2) + |g_{RR}^S|^2 - |g_{LL}^S|^2 \\ \beta &= -4\text{Re} \left\{ g_{RR}^V g_{LL}^{S*} + g_{LL}^V g_{RR}^{S*} \right\} \\ \beta' &= 4\text{Im} \left\{ g_{RR}^V g_{LL}^{S*} - g_{LL}^V g_{RR}^{S*} \right\} \\ c &= \frac{1}{2} \left\{ |g_{RL}^S - 2g_{RL}^T|^2 + |g_{LR}^S - 2g_{LR}^T|^2 \right\} \\ c' &= \frac{1}{2} \left\{ |g_{RL}^S - 2g_{RL}^T|^2 - |g_{LR}^S - 2g_{LR}^T|^2 \right\} \end{aligned}$$

and

$$\begin{aligned} Q_L^{\nu e} &= 1 - \left\{ \frac{1}{4}|g_{LR}^S|^2 + \frac{1}{4}|g_{LL}^S|^2 + |g_{RR}^V|^2 + |g_{RL}^V|^2 + 3|g_{LR}^T|^2 \right\} \\ \omega_L &= \frac{3}{4} \frac{\{|g_{RR}^S|^2 + 4|g_{LR}^V|^2 + |g_{RL}^S + 2g_{RL}^T|^2\}}{|g_{RR}^S|^2 + |g_{RR}^V|^2 + 4|g_{LL}^V|^2 + 4|g_{LR}^V|^2 + 12|g_{RL}^T|^2} \end{aligned}$$

It has been noted earlier by C. Jarlskog [11], that certain experiments observing the decay electron are especially informative if they yield the  $V$ - $A$  values. The complete solution is now found as follows. Fetscher *et al.* [2] introduced four probabilities  $Q_{\varepsilon\mu}(\varepsilon, \mu = R, L)$  for the decay of a  $\mu$ -handed muon into an  $\varepsilon$ -handed electron, and showed that there exist upper bounds on  $Q_{RR}$ ,  $Q_{LR}$ , and  $Q_{RL}$ , and a lower bound on  $Q_{LL}$ . These probabilities are given in terms of the  $g_{\varepsilon\mu}^{\tilde{\gamma}}$ 's by

$$Q_{\varepsilon\mu} = \frac{1}{4}|g_{\varepsilon\mu}^S|^2 + |g_{\varepsilon\mu}^V|^2 + 3(1 - \delta_{\varepsilon\mu})|g_{\varepsilon\mu}^T|^2, \quad (9)$$

where  $\delta_{\varepsilon\mu} = 1$  for  $\varepsilon = \mu$ , and  $\delta_{\varepsilon\mu} = 0$  for  $\varepsilon \neq \mu$ . They are related to the parameters  $a$ ,  $b$ ,  $c$ ,  $a'$ ,  $b'$ , and  $c'$  by

$$\begin{aligned} Q_{RR} &= 2(b + b')/A, \\ Q_{LR} &= [(a - a') + 6(c - c')]/2A, \\ Q_{RL} &= [(a + a') + 6(c + c')]/2A, \\ Q_{LL} &= 2(b - b')/A, \end{aligned} \quad (10)$$

with  $A = 16$ . In the Standard Model,  $Q_{LL} = 1$  and the others are zero.

Since the upper bounds on  $Q_{RR}$ ,  $Q_{LR}$ , and  $Q_{RL}$  are found to be small, and since the helicity of the  $\nu_\mu$  in pion decay is known from experiment [12,13] to very high precision to be  $-1$  [14], the cross section  $S$  of *inverse* muon decay, normalized to the  $V$ - $A$  value, yields [2]

$$|g_{LL}^S|^2 \leq 4(1 - S) \quad (11)$$

and

$$|g_{LL}^V|^2 = S. \quad (12)$$

Thus the Standard Model assumption of a pure  $V$ - $A$  leptonic charged weak interaction of  $e$  and  $\mu$  is derived (within errors) from experiments at energies far below mass of the  $W^\pm$ : Eq. (12) gives a lower limit for  $V$ - $A$ , and Eqs. (9) and (11) give upper limits for the other four-fermion interactions. The existence of such upper limits may also be seen from  $Q_{RR} + Q_{RL} = (1 - \xi')/2$  and  $Q_{RR} + Q_{LR} = \frac{1}{2}(1 + \xi/3 - 16 \xi\delta/9)$ . Table 1 gives the current experimental limits on the magnitudes of the  $g_{\varepsilon\mu}^{\tilde{\gamma}}$ 's. More stringent limits on the six coupling constants  $g_{LR}^V$ ,  $g_{LR}^T$ ,  $g_{LR}^S$ ,  $g_{RL}^V$ ,  $g_{RL}^T$ , and  $g_{RL}^S$  have been derived from upper limits on the neutrino mass [18]. Limits on the ‘‘charge retention’’ coordinates, as used in the older literature (*e.g.*, Ref. 19), are given by Burkard *et al.* [20].

**Table 1.** Coupling constants  $g_{\varepsilon\mu}^{\tilde{\gamma}}$  and some combinations of them. Ninety-percent confidence level experimental limits. The limits on  $|g_{LL}^S|$  and  $|g_{LL}^V|$  are from Ref. 15, and the others from a general analysis of muon decay measurements. Top two rows: Ref. 22, next two rows: Ref. 16, bottom three rows: Ref. 17, last row: Ref. 21. The experimental uncertainty on the muon polarization in pion decay is included. Note that, by definition,  $|g_{\varepsilon\mu}^S| \leq 2$ ,  $|g_{\varepsilon\mu}^V| \leq 1$  and  $|g_{\varepsilon\mu}^T| \leq 1/\sqrt{3}$ .

$ g_{RR}^S  < 0.035$	$ g_{RR}^V  < 0.017$	$ g_{RR}^T  \equiv 0$
$ g_{LR}^S  < 0.050$	$ g_{LR}^V  < 0.023$	$ g_{LR}^T  < 0.015$
$ g_{RL}^S  < 0.412$	$ g_{RL}^V  < 0.104$	$ g_{RL}^T  < 0.103$
$ g_{LL}^S  < 0.550$	$ g_{LL}^V  > 0.960$	$ g_{LL}^T  \equiv 0$
$ g_{LR}^S + 6g_{LR}^T  < 0.143$	$ g_{RL}^S + 6g_{RL}^T  < 0.418$	
$ g_{LR}^S + 2g_{LR}^T  < 0.108$	$ g_{RL}^S + 2g_{RL}^T  < 0.417$	
$ g_{LR}^S - 2g_{LR}^T  < 0.070$	$ g_{RL}^S - 2g_{RL}^T  < 0.418$	
$Q_{RR} + Q_{LR} < 8.2 \times 10^{-4}$		

## References

1. L. Michel, Proc. Phys. Soc. **A63**, 514 (1950).
2. W. Fetscher, H.-J. Gerber, and K.F. Johnson, Phys. Lett. **B173**, 102 (1986).
3. P. Langacker, Comm. Nucl. Part. Phys. **19**, 1 (1989).
4. C. Bouchiat and L. Michel, Phys. Rev. **106**, 170 (1957).
5. T. Kinoshita and A. Sirlin, Phys. Rev. **107**, 593 (1957).
6. T. Kinoshita and A. Sirlin, Phys. Rev. **108**, 844 (1957).
7. W. Fetscher, Phys. Rev. **D49**, 5945 (1994).
8. F. Scheck, in *Electroweak and Strong Interactions* (Springer Verlag, 1996).

# Lepton Particle Listings

$\mu$

9. K. Mursula and F. Scheck, Nucl. Phys. **B253**, 189 (1985).
10. P. Langacker and D. London, Phys. Rev. **D39**, 266 (1989).
11. C. Jarlskog, Nucl. Phys. **75**, 659 (1966).
12. A. Jodidio *et al.*, Phys. Rev. **D34**, 1967 (1986);  
A. Jodidio *et al.*, Phys. Rev. **D37**, 237 (1988).
13. L.Ph. Roesch *et al.*, Helv. Phys. Acta **55**, 74 (1982).
14. W. Fetscher, Phys. Lett. **140B**, 117 (1984).
15. S.R. Mishra *et al.*, Phys. Lett. **B252**, 170 (1990);  
S.R. Mishra, private communication;  
See also P. Vilain *et al.*, Phys. Lett. **B364**, 121 (1995).
16. R.P. MacDonald *et al.*, Phys. Rev. **D78**, 032010 (2008).
17. C.A. Gagliardi, R.E. Tribble, and N.J. Williams, Phys. Rev. **D72**, 073002 (2005).
18. G. Prézeau and A. Kurylov, Phys. Rev. Lett. **95**, 101802 (2005).
19. S.E. Derenzo, Phys. Rev. **181**, 1854 (1969).
20. H. Burkard *et al.*, Phys. Lett. **160B**, 343 (1985).
21. R. Bayes *et al.*, Phys. Rev. Lett. **106**, 041804 (2011).
22. A. Hillairet *et al.*, Phys. Rev. **D85**, 092013 (2012).

••• We do not use the following data for averages, fits, limits, etc. •••

0.75067 ± 0.00030 ± 0.00067		MACDONALD	08	TWST	+	Surface $\mu^+$
0.74964 ± 0.00066 ± 0.00112	6G	GAPONENKO	05	TWST	+	Surface $\mu^+$
		VOSSLER	69			
0.752 ± 0.009	490k	FRYBERGER	68	ASPK	+	25–53 MeV $e^+$
0.782 ± 0.031		KRUGER	61			
0.78 ± 0.05	8354	PLANO	60	HBC	+	Whole spectrum

<sup>39</sup>The quoted systematic error includes a contribution of 0.00006 (added in quadrature) from uncertainties on radiative corrections and on the Michel parameter  $\eta$ .

<sup>40</sup>BALKE 88 uses  $\rho = 0.752 \pm 0.003$ .

<sup>41</sup>VOSSLER 69 has measured the asymmetry below 10 MeV. See comments about radiative corrections in VOSSLER 69.

## [( $\xi$ PARAMETER) × ( $\mu$ LONGITUDINAL POLARIZATION)]

( $V-A$ ) theory predicts  $\xi = 1$ , longitudinal polarization = 1.

VALUE	DOCUMENT ID	TECN	CHG	COMMENT
<b>1.0009 ± 0.0016</b> <b>-0.0007</b> OUR AVERAGE				
1.00084 ± 0.00029 ± 0.00165 -0.00063	BUENO	11	TWST	Surface $\mu^+$ beam
1.0027 ± 0.0079 ± 0.0030	BELTRAMI	87	CNTR	SIN, $\pi$ decay in flight
••• We do not use the following data for averages, fits, limits, etc. •••				
1.0003 ± 0.0006 ± 0.0038	JAMIESON	06	TWST	surface $\mu^+$ beam
1.0013 ± 0.0030 ± 0.0053	42 IMAZATO	92	SPEC	$K^+ \rightarrow \mu^+ \nu_\mu$
0.975 ± 0.015	AKHMANOV	68	EMUL	140 kG
0.975 ± 0.030	GUREVICH	64	EMUL	See AKHMANOV 68
0.903 ± 0.027	43 ALI-ZADE	61	EMUL	27 kG
0.93 ± 0.06	PLANO	60	HBC	8.8 kG
0.97 ± 0.05	BARDON	59	CNTR	Bromoform target

<sup>42</sup>The corresponding 90% confidence limit from IMAZATO 92 is  $|\xi P_\mu| > 0.990$ . This measurement is of  $K^+$  decay, not  $\pi^+$  decay, so we do not include it in an average, nor do we yet set up a separate data block for  $K$  results.

<sup>43</sup>Depolarization by medium not known sufficiently well.

## $\xi \times (\mu$ LONGITUDINAL POLARIZATION) $\times \delta / \rho$

VALUE	CL%	DOCUMENT ID	TECN	CHG	COMMENT
<b>1.00179 ± 0.00156</b> <b>-0.00071</b>		44 BAYES	11	TWST	Surface $\mu^+$ beam
••• We do not use the following data for averages, fits, limits, etc. •••					
>0.99682	90	45 JODIDIO	86	SPEC	TRIUMF
>0.9966	90	46 STOKER	85	SPEC	$\mu$ -spin rotation
>0.9959	90	CARR	83	SPEC	11 kG

<sup>44</sup>BAYES 11 obtains the limit  $> 0.99909$  (90% CL) with the constraint that  $\xi \times (\mu$  LONGITUDINAL POLARIZATION)  $\times \delta / \rho \leq 1.0$ .

<sup>45</sup>JODIDIO 86 includes data from CARR 83 and STOKER 85. The value here is from the erratum.

<sup>46</sup>STOKER 85 find  $(\xi P_\mu \delta / \rho) > 0.9955$  and  $> 0.9966$ , where the first limit is from new  $\mu$  spin-rotation data and the second is from combination with CARR 83 data. In  $V-A$  theory,  $(\delta / \rho) = 1.0$ .

## $\xi'$ = LONGITUDINAL POLARIZATION OF $e^+$

( $V-A$ ) theory predicts the longitudinal polarization =  $\pm 1$  for  $e^\pm$ , respectively. We have flipped the sign for  $e^-$  so our programs can average.

VALUE	EVTS	DOCUMENT ID	TECN	CHG	COMMENT
<b>1.00 ± 0.04</b> OUR AVERAGE					
0.998 ± 0.045	1M	BURKARD	85	CNTR	+ Bhabha + annihil
0.89 ± 0.28	29k	SCHWARTZ	67	OSPK	- Moller scattering
0.94 ± 0.38		BLOOM	64	CNTR	+ Brems. transmiss.
1.04 ± 0.18		DUCLOS	64	CNTR	+ Bhabha scattering
1.05 ± 0.30		BUHLER	63	CNTR	+ Annihilation

## $\xi''$ PARAMETER

VALUE	EVTS	DOCUMENT ID	TECN	CHG	COMMENT
<b>0.65 ± 0.36</b>	326k	47 BURKARD	85	CNTR	+ Bhabha + annihil

<sup>47</sup>BURKARD 85 measure  $(\xi'' - \xi') / \xi$  and  $\xi'$  and set  $\xi = 1$ .

## TRANSVERSE $e^+$ POLARIZATION IN PLANE OF $\mu$ SPIN, $e^+$ MOMENTUM

VALUE (units $10^{-3}$ )	EVTS	DOCUMENT ID	TECN	CHG	COMMENT
<b>7 ± 8</b> OUR AVERAGE					
6.3 ± 7.7 ± 3.4	30M	DANNEBERG	05	CNTR	+ 7–53 MeV $e^+$
16 ± 21 ± 10	5.3M	BURKARD	85B	CNTR	+ Annihil 9–53 MeV

## TRANSVERSE $e^+$ POLARIZATION NORMAL TO PLANE OF $\mu$ SPIN, $e^+$ MOMENTUM

Zero if  $T$  invariance holds.

VALUE (units $10^{-3}$ )	EVTS	DOCUMENT ID	TECN	CHG	COMMENT
<b>-2 ± 8</b> OUR AVERAGE					
-3.7 ± 7.7 ± 3.4	30M	DANNEBERG	05	CNTR	+ 7–53 MeV $e^+$
7 ± 22 ± 7	5.3M	BURKARD	85B	CNTR	+ Annihil 9–53 MeV

## $\alpha/A$

VALUE (units $10^{-3}$ )	EVTS	DOCUMENT ID	TECN	CHG	COMMENT
<b>0.4 ± 4.3</b>		48 BURKARD	85B	FIT	

••• We do not use the following data for averages, fits, limits, etc. •••

15 ± 50 ± 14	5.3M	BURKARD	85B	CNTR	+ 9–53 MeV $e^+$
--------------	------	---------	-----	------	------------------

<sup>48</sup>Global fit to all measured parameters. Correlation coefficients are given in BURKARD 85b.

## $\mu$ DECAY PARAMETERS

### $\rho$ PARAMETER

( $V-A$ ) theory predicts  $\rho = 0.75$ .

VALUE	EVTS	DOCUMENT ID	TECN	CHG	COMMENT
<b>0.74979 ± 0.00026</b> OUR AVERAGE					
0.74977 ± 0.00012 ± 0.00023		30 BAYES	11	TWST	+ Surface $\mu^+$
0.7518 ± 0.0026		DERENZO	69	RVUE	
••• We do not use the following data for averages, fits, limits, etc. •••					
0.75014 ± 0.00017 ± 0.00045		31 MACDONALD	08	TWST	+ Surface $\mu^+$
0.75080 ± 0.00032 ± 0.00100	6G	32 MUSSER	05	TWST	+ Surface $\mu^+$
0.72 ± 0.06 ± 0.08		AMORUSO	04	ICAR	Liquid Ar TPC
0.762 ± 0.008	170k	33 FRYBERGER	68	ASPK	+ 25–53 MeV $e^+$
0.760 ± 0.009	280k	33 SHERWOOD	67	ASPK	+ 25–53 MeV $e^+$
0.7503 ± 0.0026	800k	33 PEOPLES	66	ASPK	+ 20–53 MeV $e^+$

<sup>30</sup>The quoted systematic error includes a contribution of 0.00013 (added in quadrature) from uncertainties on radiative corrections and on the Michel parameter  $\eta$ .

<sup>31</sup>The quoted systematic error includes a contribution of 0.00011 (added in quadrature) from the dependence on the Michel parameter  $\eta$ .

<sup>32</sup>The quoted systematic error includes a contribution of 0.00023 (added in quadrature) from the dependence on the Michel parameter  $\eta$ .

<sup>33</sup> $\eta$  constrained = 0. These values incorporated into a two parameter fit to  $\rho$  and  $\eta$  by DERENZO 69.

### $\eta$ PARAMETER

( $V-A$ ) theory predicts  $\eta = 0$ .

VALUE	EVTS	DOCUMENT ID	TECN	CHG	COMMENT
<b>0.057 ± 0.034</b> OUR AVERAGE					
0.071 ± 0.037 ± 0.005	30M	DANNEBERG	05	CNTR	+ 7–53 MeV $e^+$
0.011 ± 0.081 ± 0.026	5.3M	34 BURKARD	85B	CNTR	+ 9–53 MeV $e^+$
-0.12 ± 0.21	6346	DERENZO	69	HBC	+ 1.6–6.8 MeV $e^+$
••• We do not use the following data for averages, fits, limits, etc. •••					
-0.0021 ± 0.0070 ± 0.0010	30M	35 DANNEBERG	05	CNTR	+ 7–53 MeV $e^+$
-0.012 ± 0.015 ± 0.003	5.3M	35 BURKARD	85B	CNTR	+ 9–53 MeV $e^+$
-0.007 ± 0.013	5.3M	36 BURKARD	85B	FIT	+ 9–53 MeV $e^+$
-0.7 ± 0.5	170k	37 FRYBERGER	68	ASPK	+ 25–53 MeV $e^+$
-0.7 ± 0.6	280k	37 SHERWOOD	67	ASPK	+ 25–53 MeV $e^+$
0.05 ± 0.5	800k	37 PEOPLES	66	ASPK	+ 20–53 MeV $e^+$
-2.0 ± 0.9	9213	38 PLANO	60	HBC	+ Whole spectrum

<sup>34</sup>Previously we used the global fit result from BURKARD 85b in OUR AVERAGE, we now only include their actual measurement.

<sup>35</sup> $\alpha = \alpha' = 0$  assumed.

<sup>36</sup>Global fit to all measured parameters. The fit correlation coefficients are given in BURKARD 85b.

<sup>37</sup> $\rho$  constrained = 0.75.

<sup>38</sup>Two parameter fit to  $\rho$  and  $\eta$ ; PLANO 60 discounts value for  $\eta$ .

### $\delta$ PARAMETER

( $V-A$ ) theory predicts  $\delta = 0.75$ .

VALUE	EVTS	DOCUMENT ID	TECN	CHG	COMMENT
<b>0.75047 ± 0.00034</b> OUR AVERAGE					
0.75049 ± 0.00021 ± 0.00027		39 BAYES	11	TWST	+ Surface $\mu^+$
0.7486 ± 0.0026 ± 0.0028		40 BALKE	88	SPEC	+ Surface $\mu^+$



## Lepton Particle Listings

 $\mu, \tau$ 

NAME	REF	TECN	COMMENT	INSTITUTION
COHEN	73	JPCRD 2 664		(RIS C, NBS)
DUCLOS	73	PL 47B 491		(SACL)
EICHTEN	73	PL 46B 281		(Gargamelle Collab.)
BRYMAN	72	PRL 28 1469		(VPI)
CROWE	72	PR D5 2145		(LBL, WASH)
CRANE	71	PRL 27 474		(YALE)
DERENZO	69	PR 181 1854		(EFI)
VOSSLER	69	NC 63A 423		(EFI)
AKHMANOV	68	SJNP 6 230		(KIAE)
Translated from YAF 6 316.				
FRYBERGER	68	PR 166 1379		(EFI)
BOGART	67	PR 156 1405		(COLU)
SCHWARTZ	67	PR 162 1306		(EFI)
SHERWOOD	67	PR 156 1475		(EFI)
PEOPLES	66	Nevis 147 unpub.		(COLU)
BLOOM	64	PL 8 87		(CERN)
DUCLOS	64	PL 9 62		(CERN)
GUREVICH	64	PL 11 185		(KIAE)
BUHLER	63	PL 7 368		(CERN)
MEYER	63	PR 132 2693		(COLU)
CHARPAK	62	PL 1 16		(CERN)
CONFORTO	62	NC 26 261		(INFN, ROMA, CERN)
ALI-ZADE	61	JETP 13 313		S.A. Ali-Zade, I.I. Gurevich, B.A. Nikolsky
Translated from ZETF 40 452.				
CRITTENDEN	61	PR 121 1823		(WIS C+)
KRUGER	61	UCRL 9322 unpub.		(LRL)
GUREVICH	60	JETP 10 225		(ITEP)
Translated from ZETF 37 318.				
PLANO	60	PR 119 1400		(COLU)
ASHKIN	59	NC 14 1266		(CERN)
BARDON	59	PRL 2 56		(COLU)
LEE	59	PRL 3 55		(COLU)

 $\tau$ 

$$J = \frac{1}{2}$$

$\tau$  discovery paper was PERL 75.  $e^+e^- \rightarrow \tau^+\tau^-$  cross-section threshold behavior and magnitude are consistent with pointlike spin-1/2 Dirac particle. BRANDELIK 78 ruled out pointlike spin-0 or spin-1 particle. FELDMAN 78 ruled out  $J = 3/2$ . KIRKBY 79 also ruled out  $J = \text{integer}$ ,  $J = 3/2$ .

 $\tau$  MASS

VALUE (MeV)	EVTS	DOCUMENT ID	TECN	COMMENT
<b>1776.82 ± 0.16 OUR AVERAGE</b>				
1776.68 ± 0.12 ± 0.41	682k	<sup>1</sup> AUBERT	09AK BABR	423 fb <sup>-1</sup> , $E_{cm}^{ee} = 10.6$ GeV
1776.81 <sup>+0.25</sup> <sub>-0.23</sub> ± 0.15	81	ANASHIN	07 KEDR	6.7 pb <sup>-1</sup> , $E_{cm}^{ee} = 3.54\text{--}3.78$ GeV
1776.61 ± 0.13 ± 0.35		<sup>1</sup> BELOUS	07 BELL	414 fb <sup>-1</sup> , $E_{cm}^{ee} = 10.6$ GeV
1775.1 ± 1.6 ± 1.0	13.3k	<sup>2</sup> ABBIENDI	00A OPAL	1990-1995 LEP runs
1778.2 ± 0.8 ± 1.2		ANASTASSOV	97 CLEO	$E_{cm}^{ee} = 10.6$ GeV
1776.96 <sup>+0.18</sup> <sub>-0.21</sub> ± 0.25 ± 0.17	65	<sup>3</sup> BAI	96 BES	$E_{cm}^{ee} = 3.54\text{--}3.57$ GeV
1776.3 ± 2.4 ± 1.4	11k	<sup>4</sup> ALBRECHT	92M ARG	$E_{cm}^{ee} = 9.4\text{--}10.6$ GeV
1783 <sup>+3</sup> <sub>-4</sub>	692	<sup>5</sup> BACINO	78B DLCO	$E_{cm}^{ee} = 3.1\text{--}7.4$ GeV
••• We do not use the following data for averages, fits, limits, etc. •••				
1777.8 ± 0.7 ± 1.7	35k	<sup>6</sup> BALEST	93 CLEO	Repl. by ANASTASSOV 97
1776.9 <sup>+0.4</sup> <sub>-0.5</sub> ± 0.2	14	<sup>7</sup> BAI	92 BES	Repl. by BAI 96

- AUBERT 09AK and BELOUS 07 fit  $\tau$  pseudomass spectrum in  $\tau \rightarrow \pi^+\pi^-\nu_\tau$  decays. Result assumes  $m_{\nu_\tau} = 0$ .
- ABBIENDI 00A fit  $\tau$  pseudomass spectrum in  $\tau \rightarrow \pi^\pm \leq 2\pi^0 \nu_\tau$  and  $\tau \rightarrow \pi^\pm \pi^+ \pi^- \leq 1\pi^0 \nu_\tau$  decays. Result assumes  $m_{\nu_\tau} = 0$ .
- BAI 96 fit  $\sigma(e^+e^- \rightarrow \tau^+\tau^-)$  at different energies near threshold.
- ALBRECHT 92M fit  $\tau$  pseudomass spectrum in  $\tau^- \rightarrow 2\pi^-\pi^+\nu_\tau$  decays. Result assumes  $m_{\nu_\tau} = 0$ .
- BACINO 78B value comes from  $e^\pm X^\mp$  threshold. Published mass 1782 MeV increased by 1 MeV using the high precision  $\psi(2S)$  mass measurement of ZHOLENTZ 80 to eliminate the absolute SPEAR energy calibration uncertainty.
- BALEST 93 fit spectra of minimum kinematically allowed  $\tau$  mass in events of the type  $e^+e^- \rightarrow \tau^+\tau^- \rightarrow (\pi^+ n\pi^0 \nu_\tau)(\pi^- m\pi^0 \nu_\tau)$ ,  $n \leq 2$ ,  $m \leq 2$ ,  $1 \leq n+m \leq 3$ . If  $m_{\nu_\tau} \neq 0$ , result increases by  $(m_{\nu_\tau}^2/1100)$  MeV.
- BAI 92 fit  $\sigma(e^+e^- \rightarrow \tau^+\tau^-)$  near threshold using  $e\mu$  events.

$$(m_{\tau^+} - m_{\tau^-})/m_{\text{average}}$$

A test of CPT invariance.

VALUE	CL%	DOCUMENT ID	TECN	COMMENT
<b>&lt; 2.8 × 10<sup>-4</sup></b>	90	BELOUS	07 BELL	414 fb <sup>-1</sup> , $E_{cm}^{ee} = 10.6$ GeV
••• We do not use the following data for averages, fits, limits, etc. •••				
< 5.5 × 10 <sup>-4</sup>	90	<sup>1</sup> AUBERT	09AK BABR	423 fb <sup>-1</sup> , $E_{cm}^{ee} = 10.6$ GeV
< 3.0 × 10 <sup>-3</sup>	90	ABBIENDI	00A OPAL	1990-1995 LEP runs
<sup>1</sup> AUBERT 09AK quote both the listed upper limit and $(m_{\tau^+} - m_{\tau^-})/m_{\text{average}} = (-3.4 \pm 1.3 \pm 0.3) \times 10^{-4}$ .				

 $\tau$  MEAN LIFE

VALUE (10 <sup>-15</sup> s)	EVTS	DOCUMENT ID	TECN	COMMENT
<b>290.6 ± 1.0 OUR AVERAGE</b>				
290.9 ± 1.4 ± 1.0		ABDALLAH	04T DLPH	1991-1995 LEP runs
293.2 ± 2.0 ± 1.5		ACCIARRI	00B L3	1991-1995 LEP runs
290.1 ± 1.5 ± 1.1		BARATE	97R ALEP	1989-1994 LEP runs
289.2 ± 1.7 ± 1.2		ALEXANDER	96E OPAL	1990-1994 LEP runs
289.0 ± 2.8 ± 4.0	57.4k	BALEST	96 CLEO	$E_{cm}^{ee} = 10.6$ GeV
••• We do not use the following data for averages, fits, limits, etc. •••				
291.2 ± 2.0 ± 1.2		BARATE	97I ALEP	Repl. by BARATE 97R
291.4 ± 3.0		ABREU	96B DLPH	Repl. by ABDAL-LAH 04T
290.1 ± 4.0	34k	ACCIARRI	96K L3	Repl. by ACCIARRI 00B
297 ± 9 ± 5	1671	ABE	95Y SLD	1992-1993 SLC runs
304 ± 14 ± 7	4100	BATTLE	92 CLEO	$E_{cm}^{ee} = 10.6$ GeV
301 ± 29	3780	KLEINWORT	89 JADE	$E_{cm}^{ee} = 35\text{--}46$ GeV
288 ± 16 ± 17	807	AMIDEI	88 MRK2	$E_{cm}^{ee} = 29$ GeV
306 ± 20 ± 14	695	BRAUNSCH...	88C TASS	$E_{cm}^{ee} = 36$ GeV
299 ± 15 ± 10	1311	ABACHI	87C HRS	$E_{cm}^{ee} = 29$ GeV
295 ± 14 ± 11	5696	ALBRECHT	87P ARG	$E_{cm}^{ee} = 9.3\text{--}10.6$ GeV
309 ± 17 ± 7	3788	BAND	87B MAC	$E_{cm}^{ee} = 29$ GeV
325 ± 14 ± 18	8470	BEBEK	87C CLEO	$E_{cm}^{ee} = 10.5$ GeV
460 ± 190	102	FELDMAN	82 MRK2	$E_{cm}^{ee} = 29$ GeV

 $\tau$  MAGNETIC MOMENT ANOMALY

The  $q^2$  dependence is expected to be small providing no thresholds are nearby.

$$\mu_\tau / (e\hbar/2m_\tau) - 1 = (g_\tau - 2)/2$$

For a theoretical calculation  $[(g_\tau - 2)/2 = 117 721(5) \times 10^{-8}]$ , see EIDELMAN 07.

VALUE	CL%	DOCUMENT ID	TECN	COMMENT
<b>&gt; -0.052 and &lt; 0.013 (CL = 95%) OUR LIMIT</b>				
> -0.052 and < 0.013	95	<sup>1</sup> ABDALLAH	04K DLPH	$e^+e^- \rightarrow e^+e^-\tau^+\tau^-$ at LEP2
••• We do not use the following data for averages, fits, limits, etc. •••				
< 0.107	95	<sup>2</sup> ACHARD	04G L3	$e^+e^- \rightarrow e^+e^-\tau^+\tau^-$ at LEP2
> -0.007 and < 0.005	95	<sup>3</sup> GONZALEZ-S.	00 RVUE	$e^+e^- \rightarrow \tau^+\tau^-$ and $W \rightarrow \tau\nu_\tau$
> -0.052 and < 0.058	95	<sup>4</sup> ACCIARRI	98E L3	1991-1995 LEP runs
> -0.068 and < 0.065	95	<sup>5</sup> ACKERSTAFF	98N OPAL	1990-1995 LEP runs
> -0.004 and < 0.006	95	<sup>6</sup> ESCRIBANO	97 RVUE	$Z \rightarrow \tau^+\tau^-$ at LEP
< 0.01	95	<sup>7</sup> ESCRIBANO	93 RVUE	$Z \rightarrow \tau^+\tau^-$ at LEP
< 0.12	90	GRIFOLS	91 RVUE	$Z \rightarrow \tau\tau\gamma$ at LEP
< 0.023	95	<sup>8</sup> SILVERMAN	83 RVUE	$e^+e^- \rightarrow \tau^+\tau^-$ at PETRA

- ABDALLAH 04K limit is derived from  $e^+e^- \rightarrow e^+e^-\tau^+\tau^-$  total cross-section measurements at  $\sqrt{s}$  between 183 and 208 GeV. In addition to the limits, the authors also quote a value of  $-0.018 \pm 0.017$ .
- ACHARD 04G limit is derived from  $e^+e^- \rightarrow e^+e^-\tau^+\tau^-$  total cross-section measurements at  $\sqrt{s}$  between 189 and 206 GeV, and is on the absolute value of the magnetic moment anomaly.
- GONZALEZ-SPRINGER 00 use data on tau lepton production at LEP1, SLC, and LEP2, and data from colliders and LEP2 to determine limits. Assume imaginary component is zero.
- ACCIARRI 98E use  $Z \rightarrow \tau^+\tau^-\gamma$  events. In addition to the limits, the authors also quote a value of  $0.004 \pm 0.027 \pm 0.023$ .
- ACKERSTAFF 98N use  $Z \rightarrow \tau^+\tau^-\gamma$  events. The limit applies to an average of the form factor for off-shell  $\tau$ 's having  $p^2$  ranging from  $m_\tau^2$  to  $(M_Z - m_\tau)^2$ .
- ESCRIBANO 97 use preliminary experimental results.
- ESCRIBANO 93 limit derived from  $\Gamma(Z \rightarrow \tau^+\tau^-)$ , and is on the absolute value of the magnetic moment anomaly.
- SILVERMAN 83 limit is derived from  $e^+e^- \rightarrow \tau^+\tau^-$  total cross-section measurements for  $q^2$  up to  $(37 \text{ GeV})^2$ .

 $\tau$  ELECTRIC DIPOLE MOMENT ( $d_\tau$ )

A nonzero value is forbidden by both  $T$  invariance and  $P$  invariance.

The  $q^2$  dependence is expected to be small providing no thresholds are nearby.

 $\text{Re}(d_\tau)$ 

VALUE (10 <sup>-16</sup> ecm)	CL%	DOCUMENT ID	TECN	COMMENT
<b>- 0.22 to 0.45</b>	95	<sup>1</sup> INAMI	03 BELL	$E_{cm}^{ee} = 10.6$ GeV
••• We do not use the following data for averages, fits, limits, etc. •••				
< 2.3	90	<sup>2</sup> GROZIN	09A RVUE	From $e$ EDM limit
< 3.7	95	<sup>3</sup> ABDALLAH	04K DLPH	$e^+e^- \rightarrow e^+e^-\tau^+\tau^-$ at LEP2
< 11.4	95	<sup>4</sup> ACHARD	04G L3	$e^+e^- \rightarrow e^+e^-\tau^+\tau^-$ at LEP2
< 4.6	95	<sup>5</sup> ALBRECHT	00 ARG	$E_{cm}^{ee} = 10.4$ GeV
> -3.1 and < 3.1	95	ACCIARRI	98E L3	1991-1995 LEP runs

> -3.8 and < 3.6	95	<sup>6</sup> ACKERSTAFF	98N	OPAL	1990-1995 LEP runs
< 0.11	95	<sup>7,8</sup> ESCRIBANO	97	RVUE	$Z \rightarrow \tau^+ \tau^-$ at LEP
< 0.5	95	<sup>9</sup> ESCRIBANO	93	RVUE	$Z \rightarrow \tau^+ \tau^-$ at LEP
< 7	90	GRIFOLS	91	RVUE	$Z \rightarrow \tau \tau \gamma$ at LEP
< 1.6	90	DELAGUILA	90	RVUE	$e^+ e^- \rightarrow \tau^+ \tau^-$ $E_{cm}^{ee} = 35$ GeV

- INAMI 03 use  $e^+ e^- \rightarrow \tau^+ \tau^-$  events.
- GROZIN 09A calculate the contribution to the electron electric dipole moment from the  $\tau$  electric dipole moment appearing in loops, which is  $\Delta d_e = 6.9 \times 10^{-12} d_\tau$ . Dividing the REGAN 02 upper limit  $|d_e| \leq 1.6 \times 10^{-27}$  e cm at CL=90% by  $6.9 \times 10^{-12}$  gives this limit.
- ABDALLAH 04K limit is derived from  $e^+ e^- \rightarrow e^+ e^- \tau^+ \tau^-$  total cross-section measurements at  $\sqrt{s}$  between 183 and 208 GeV and is on the absolute value of  $d_\tau$ .
- ACHARD 04G limit is derived from  $e^+ e^- \rightarrow e^+ e^- \tau^+ \tau^-$  total cross-section measurements at  $\sqrt{s}$  between 189 and 206 GeV, and is on the absolute value of  $d_\tau$ .
- ALBRECHT 00 use  $e^+ e^- \rightarrow \tau^+ \tau^-$  events. Limit is on the absolute value of  $Re(d_\tau)$ .
- ACKERSTAFF 98N use  $Z \rightarrow \tau^+ \tau^- \gamma$  events. The limit applies to an average of the form factor for off-shell  $\tau$ 's having  $p^2$  ranging from  $m_\tau^2$  to  $(M_Z - m_\tau)^2$ .
- ESCRIBANO 97 derive the relationship  $|d_\tau| = \cot \theta_W |d_\tau^W|$  using effective Lagrangian methods, and use a conference result  $|d_\tau^W| < 5.8 \times 10^{-18}$  e cm at 95% CL (L. Silvestris, ICHEP96) to obtain this result.
- ESCRIBANO 97 use preliminary experimental results.
- ESCRIBANO 93 limit derived from  $\Gamma(Z \rightarrow \tau^+ \tau^-)$ , and is on the absolute value of the electric dipole moment.

**Im( $d_\tau$ )**

VALUE ( $10^{-16}$ e cm)	CL%	DOCUMENT ID	TECN	COMMENT
<b>-0.25 to 0.008</b>	95	<sup>1</sup> INAMI	03	BELL $E_{cm}^{ee} = 10.6$ GeV
• • • We do not use the following data for averages, fits, limits, etc. • • •				
< 1.8	95	<sup>2</sup> ALBRECHT	00	ARG $E_{cm}^{ee} = 10.4$ GeV

<sup>1</sup>INAMI 03 use  $e^+ e^- \rightarrow \tau^+ \tau^-$  events.  
<sup>2</sup>ALBRECHT 00 use  $e^+ e^- \rightarrow \tau^+ \tau^-$  events. Limit is on the absolute value of  $Im(d_\tau)$ .

**$\tau$  WEAK DIPOLE MOMENT ( $d_\tau^W$ )**

A nonzero value is forbidden by CP invariance.  
 The  $q^2$  dependence is expected to be small providing no thresholds are nearby.

**Re( $d_\tau^W$ )**

VALUE ( $10^{-17}$ e cm)	CL%	DOCUMENT ID	TECN	COMMENT
<b>&lt;0.50</b>	95	<sup>1</sup> HEISTER	03F	ALEP 1990-1995 LEP runs
• • • We do not use the following data for averages, fits, limits, etc. • • •				
<3.0	90	<sup>1</sup> ACCIARRI	98c	L3 1991-1995 LEP runs
<0.56	95	<sup>2</sup> ACKERSTAFF	97L	OPAL 1991-1995 LEP runs
<0.78	95	<sup>2</sup> AKERS	95F	OPAL Repl. by ACKERSTAFF 97L
<1.5	95	<sup>2</sup> BUSKULIC	95c	ALEP Repl. by HEISTER 03F
<7.0	95	<sup>2</sup> ACTON	92F	OPAL $Z \rightarrow \tau^+ \tau^-$ at LEP
<3.7	95	<sup>2</sup> BUSKULIC	92J	ALEP Repl. by BUSKULIC 95c

<sup>1</sup>Limit is on the absolute value of the real part of the weak dipole moment.  
<sup>2</sup>Limit is on the absolute value of the real part of the weak dipole moment, and applies for  $q^2 = m_Z^2$ .

**Im( $d_\tau^W$ )**

VALUE ( $10^{-17}$ e cm)	CL%	DOCUMENT ID	TECN	COMMENT
<b>&lt;1.1</b>	95	<sup>1</sup> HEISTER	03F	ALEP 1990-1995 LEP runs
• • • We do not use the following data for averages, fits, limits, etc. • • •				
<1.5	95	<sup>2</sup> ACKERSTAFF	97L	OPAL 1991-1995 LEP runs
<4.5	95	<sup>2</sup> AKERS	95F	OPAL Repl. by ACKERSTAFF 97L

<sup>1</sup>HEISTER 03F limit is on the absolute value of the imaginary part of the weak dipole moment.  
<sup>2</sup>Limit is on the absolute value of the imaginary part of the weak dipole moment, and applies for  $q^2 = m_Z^2$ .

**$\tau$  WEAK ANOMALOUS MAGNETIC DIPOLE MOMENT ( $\alpha_\tau^W$ )**

Electroweak radiative corrections are expected to contribute at the  $10^{-6}$  level. See BERNABEU 95.  
 The  $q^2$  dependence is expected to be small providing no thresholds are nearby.

**Re( $\alpha_\tau^W$ )**

VALUE	CL%	DOCUMENT ID	TECN	COMMENT
<b>&lt;1.1 <math>\times 10^{-3}</math></b>	95	<sup>1</sup> HEISTER	03F	ALEP 1990-1995 LEP runs
• • • We do not use the following data for averages, fits, limits, etc. • • •				
> -0.0024 and < 0.0025	95	<sup>2</sup> GONZALEZ-S.	00	RVUE $e^+ e^- \rightarrow \tau^+ \tau^-$ and $W \rightarrow \tau \nu_\tau$
<4.5 $\times 10^{-3}$	90	<sup>1</sup> ACCIARRI	98c	L3 1991-1995 LEP runs

<sup>1</sup>Limit is on the absolute value of the real part of the weak anomalous magnetic dipole moment.  
<sup>2</sup>GONZALEZ-SPRINGER 00 use data on tau lepton production at LEP1, SLC, and LEP2, and data from colliders and LEP2 to determine limits. Assume imaginary component is zero.

**Im( $\alpha_\tau^W$ )**

VALUE	CL%	DOCUMENT ID	TECN	COMMENT
<b>&lt;2.7 <math>\times 10^{-3}</math></b>	95	<sup>1</sup> HEISTER	03F	ALEP 1990-1995 LEP runs
• • • We do not use the following data for averages, fits, limits, etc. • • •				
<9.9 $\times 10^{-3}$	90	<sup>1</sup> ACCIARRI	98c	L3 1991-1995 LEP runs

<sup>1</sup>Limit is on the absolute value of the imaginary part of the weak anomalous magnetic dipole moment.

**$\tau^-$  DECAY MODES**

$\tau^+$  modes are charge conjugates of the modes below. " $h^\pm$ " stands for  $\pi^\pm$  or  $K^\pm$ . " $l$ " stands for e or  $\mu$ . "Neutrals" stands for  $\gamma$ 's and/or  $\pi^0$ 's.

Mode	Fraction ( $\Gamma_i/\Gamma$ )	Scale factor/ Confidence level
<b>Modes with one charged particle</b>		
$\Gamma_1$ particle $^- \geq 0$ neutrals $\geq 0 K^0 \nu_\tau$ ("1-prong")	(85.35 $\pm$ 0.07) %	S=1.3
$\Gamma_2$ particle $^- \geq 0$ neutrals $\geq 0 K_L^0 \nu_\tau$	(84.71 $\pm$ 0.08) %	S=1.3
$\Gamma_3$ $\mu^- \bar{\nu}_\mu \nu_\tau$	[a] (17.41 $\pm$ 0.04) %	S=1.1
$\Gamma_4$ $\mu^- \bar{\nu}_\mu \nu_\tau \gamma$	[b] (3.6 $\pm$ 0.4) $\times 10^{-3}$	
$\Gamma_5$ $e^- \bar{\nu}_e \nu_\tau$	[a] (17.83 $\pm$ 0.04) %	
$\Gamma_6$ $e^- \bar{\nu}_e \nu_\tau \gamma$	[b] (1.75 $\pm$ 0.18) %	
$\Gamma_7$ $h^- \geq 0 K_L^0 \nu_\tau$	(12.06 $\pm$ 0.06) %	S=1.2
$\Gamma_8$ $h^- \nu_\tau$	(11.53 $\pm$ 0.06) %	S=1.2
$\Gamma_9$ $\pi^- \nu_\tau$	[a] (10.83 $\pm$ 0.06) %	S=1.2
$\Gamma_{10}$ $K^- \nu_\tau$	[a] (7.00 $\pm$ 0.10) $\times 10^{-3}$	S=1.1
$\Gamma_{11}$ $h^- \geq 1$ neutrals $\nu_\tau$	(37.10 $\pm$ 0.10) %	S=1.2
$\Gamma_{12}$ $h^- \geq 1 \pi^0 \nu_\tau$ (ex. $K^0$ )	(36.57 $\pm$ 0.10) %	S=1.2
$\Gamma_{13}$ $h^- \pi^0 \nu_\tau$	(25.95 $\pm$ 0.09) %	S=1.1
$\Gamma_{14}$ $\pi^- \pi^0 \nu_\tau$	[a] (25.52 $\pm$ 0.09) %	S=1.1
$\Gamma_{15}$ $\pi^- \pi^0$ non- $\rho(770) \nu_\tau$	(3.0 $\pm$ 3.2) $\times 10^{-3}$	
$\Gamma_{16}$ $K^- \pi^0 \nu_\tau$	[a] (4.29 $\pm$ 0.15) $\times 10^{-3}$	
$\Gamma_{17}$ $h^- \geq 2 \pi^0 \nu_\tau$	(10.87 $\pm$ 0.11) %	S=1.2
$\Gamma_{18}$ $h^- 2 \pi^0 \nu_\tau$	(9.52 $\pm$ 0.11) %	S=1.1
$\Gamma_{19}$ $h^- 2 \pi^0 \nu_\tau$ (ex. $K^0$ )	(9.36 $\pm$ 0.11) %	S=1.2
$\Gamma_{20}$ $\pi^- 2 \pi^0 \nu_\tau$ (ex. $K^0$ )	[a] (9.30 $\pm$ 0.11) %	S=1.2
$\Gamma_{21}$ $\pi^- 2 \pi^0 \nu_\tau$ (ex. $K^0$ ), scalar	< 9 $\times 10^{-3}$	CL=95%
$\Gamma_{22}$ $\pi^- 2 \pi^0 \nu_\tau$ (ex. $K^0$ ), vector	< 7 $\times 10^{-3}$	CL=95%
$\Gamma_{23}$ $K^- 2 \pi^0 \nu_\tau$ (ex. $K^0$ )	[a] (6.5 $\pm$ 2.3) $\times 10^{-4}$	
$\Gamma_{24}$ $h^- \geq 3 \pi^0 \nu_\tau$	(1.35 $\pm$ 0.07) %	S=1.1
$\Gamma_{25}$ $h^- \geq 3 \pi^0 \nu_\tau$ (ex. $K^0$ )	(1.26 $\pm$ 0.07) %	S=1.1
$\Gamma_{26}$ $h^- 3 \pi^0 \nu_\tau$	(1.19 $\pm$ 0.07) %	
$\Gamma_{27}$ $\pi^- 3 \pi^0 \nu_\tau$ (ex. $K^0$ )	[a] (1.05 $\pm$ 0.07) %	
$\Gamma_{28}$ $K^- 3 \pi^0 \nu_\tau$ (ex. $K^0, \eta$ )	[a] (4.8 $\pm$ 2.2) $\times 10^{-4}$	
$\Gamma_{29}$ $h^- 4 \pi^0 \nu_\tau$ (ex. $K^0$ )	(1.6 $\pm$ 0.4) $\times 10^{-3}$	
$\Gamma_{30}$ $h^- 4 \pi^0 \nu_\tau$ (ex. $K^0, \eta$ )	[a] (1.1 $\pm$ 0.4) $\times 10^{-3}$	
$\Gamma_{31}$ $K^- \geq 0 \pi^0 \geq 0 K^0 \geq 0 \gamma \nu_\tau$	(1.572 $\pm$ 0.033) %	S=1.1
$\Gamma_{32}$ $K^- \geq 1 (\pi^0 \text{ or } K^0 \text{ or } \gamma) \nu_\tau$	(8.72 $\pm$ 0.32) $\times 10^{-3}$	S=1.1
<b>Modes with <math>K^0</math>'s</b>		
$\Gamma_{33}$ $K_S^0$ (particles) $^- \nu_\tau$	(9.2 $\pm$ 0.4) $\times 10^{-3}$	S=1.5
$\Gamma_{34}$ $h^- \bar{K}^0 \nu_\tau$	(1.00 $\pm$ 0.05) %	S=1.8
$\Gamma_{35}$ $\pi^- \bar{K}^0 \nu_\tau$	[a] (8.4 $\pm$ 0.4) $\times 10^{-3}$	S=2.1
$\Gamma_{36}$ $\pi^- \bar{K}^0$ (non- $K^*(892)^-$ ) $\nu_\tau$	(5.4 $\pm$ 2.1) $\times 10^{-4}$	
$\Gamma_{37}$ $K^- K^0 \nu_\tau$	[a] (1.59 $\pm$ 0.16) $\times 10^{-3}$	
$\Gamma_{38}$ $K^- K^0 \geq 0 \pi^0 \nu_\tau$	(3.18 $\pm$ 0.23) $\times 10^{-3}$	
$\Gamma_{39}$ $h^- \bar{K}^0 \pi^0 \nu_\tau$	(5.5 $\pm$ 0.4) $\times 10^{-3}$	
$\Gamma_{40}$ $\pi^- \bar{K}^0 \pi^0 \nu_\tau$	[a] (4.0 $\pm$ 0.4) $\times 10^{-3}$	
$\Gamma_{41}$ $\bar{K}^0 \rho^- \nu_\tau$	(2.2 $\pm$ 0.5) $\times 10^{-3}$	
$\Gamma_{42}$ $K^- K^0 \pi^0 \nu_\tau$	[a] (1.59 $\pm$ 0.20) $\times 10^{-3}$	
$\Gamma_{43}$ $\pi^- \bar{K}^0 \geq 1 \pi^0 \nu_\tau$	(3.2 $\pm$ 1.0) $\times 10^{-3}$	
$\Gamma_{44}$ $\pi^- \bar{K}^0 \pi^0 \pi^0 \nu_\tau$	(2.6 $\pm$ 2.4) $\times 10^{-4}$	
$\Gamma_{45}$ $K^- K^0 \pi^0 \pi^0 \nu_\tau$	< 1.6 $\times 10^{-4}$	CL=95%
$\Gamma_{46}$ $\pi^- K^0 \bar{K}^0 \nu_\tau$	(1.7 $\pm$ 0.4) $\times 10^{-3}$	S=1.7
$\Gamma_{47}$ $\pi^- K_S^0 K_S^0 \nu_\tau$	[a] (2.4 $\pm$ 0.5) $\times 10^{-4}$	
$\Gamma_{48}$ $\pi^- K_S^0 K_L^0 \nu_\tau$	[a] (1.2 $\pm$ 0.4) $\times 10^{-3}$	S=1.7
$\Gamma_{49}$ $\pi^- K^0 \bar{K}^0 \pi^0 \nu_\tau$	(3.1 $\pm$ 2.3) $\times 10^{-4}$	
$\Gamma_{50}$ $\pi^- K^0 K_S^0 \pi^0 \nu_\tau$	< 2.0 $\times 10^{-4}$	CL=95%
$\Gamma_{51}$ $\pi^- K_S^0 K_L^0 \pi^0 \nu_\tau$	(3.1 $\pm$ 1.2) $\times 10^{-4}$	
$\Gamma_{52}$ $K^0 h^+ h^- h^- \geq 0$ neutrals $\nu_\tau$	< 1.7 $\times 10^{-3}$	CL=95%
$\Gamma_{53}$ $K^0 h^+ h^- h^- \nu_\tau$	(2.3 $\pm$ 2.0) $\times 10^{-4}$	

## Lepton Particle Listings

 $\tau$ 

Modes with three charged particles				Miscellaneous other allowed modes			
$\Gamma_{54}$	$h^- h^- h^+ \geq 0$ neutrals $\geq 0 K_L^0 \nu_\tau$	(15.20 $\pm$ 0.08) %	S=1.3	$\Gamma_{105}$	$(5\pi)^- \nu_\tau$	(7.7 $\pm$ 0.5) $\times 10^{-3}$	
$\Gamma_{55}$	$h^- h^- h^+ \geq 0$ neutrals $\nu_\tau$ (ex. $K_S^0 \rightarrow \pi^+ \pi^-$ ) ("3-prong")	(14.57 $\pm$ 0.07) %	S=1.3	$\Gamma_{106}$	$4h^- 3h^+ \geq 0$ neutrals $\nu_\tau$ ("7-prong")	< 3.0 $\times 10^{-7}$	CL=90%
$\Gamma_{56}$	$h^- h^- h^+ \nu_\tau$	(9.80 $\pm$ 0.07) %	S=1.2	$\Gamma_{107}$	$4h^- 3h^+ \nu_\tau$	< 4.3 $\times 10^{-7}$	CL=90%
$\Gamma_{57}$	$h^- h^- h^+ \nu_\tau$ (ex. $K^0$ )	(9.46 $\pm$ 0.06) %	S=1.2	$\Gamma_{108}$	$4h^- 3h^+ \pi^0 \nu_\tau$	< 2.5 $\times 10^{-7}$	CL=90%
$\Gamma_{58}$	$h^- h^- h^+ \nu_\tau$ (ex. $K^0, \omega$ )	(9.42 $\pm$ 0.06) %	S=1.2	$\Gamma_{109}$	$X^- (S=-1) \nu_\tau$	(2.87 $\pm$ 0.07) %	S=1.3
$\Gamma_{59}$	$\pi^- \pi^+ \pi^- \nu_\tau$	(9.31 $\pm$ 0.06) %	S=1.2	$\Gamma_{110}$	$K^*(892)^- \geq 0$ neutrals $\geq 0 K_L^0 \nu_\tau$	(1.42 $\pm$ 0.18) %	S=1.4
$\Gamma_{60}$	$\pi^- \pi^+ \pi^- \nu_\tau$ (ex. $K^0$ )	(9.02 $\pm$ 0.06) %	S=1.1	$\Gamma_{111}$	$K^*(892)^- \nu_\tau$	(1.20 $\pm$ 0.07) %	S=1.8
$\Gamma_{61}$	$\pi^- \pi^+ \pi^- \nu_\tau$ (ex. $K^0$ ), non-axial vector	< 2.4 %	CL=95%	$\Gamma_{112}$	$K^*(892)^- \nu_\tau \rightarrow \pi^- \bar{K}^0 \nu_\tau$	(7.8 $\pm$ 0.5) $\times 10^{-3}$	
$\Gamma_{62}$	$\pi^- \pi^+ \pi^- \nu_\tau$ (ex. $K^0, \omega$ )	[a] (8.99 $\pm$ 0.06) %	S=1.1	$\Gamma_{113}$	$K^*(892)^0 K^- \geq 0$ neutrals $\nu_\tau$	(3.2 $\pm$ 1.4) $\times 10^{-3}$	
$\Gamma_{63}$	$h^- h^- h^+ \geq 1$ neutrals $\nu_\tau$	(5.39 $\pm$ 0.07) %	S=1.2	$\Gamma_{114}$	$K^*(892)^0 K^- \nu_\tau$	(2.1 $\pm$ 0.4) $\times 10^{-3}$	
$\Gamma_{64}$	$h^- h^- h^+ \geq 1 \pi^0 \nu_\tau$ (ex. $K^0$ )	(5.09 $\pm$ 0.06) %	S=1.2	$\Gamma_{115}$	$\bar{K}^*(892)^0 \pi^- \geq 0$ neutrals $\nu_\tau$	(3.8 $\pm$ 1.7) $\times 10^{-3}$	
$\Gamma_{65}$	$h^- h^- h^+ \pi^0 \nu_\tau$	(4.76 $\pm$ 0.06) %	S=1.2	$\Gamma_{116}$	$\bar{K}^*(892)^0 \pi^- \nu_\tau$	(2.2 $\pm$ 0.5) $\times 10^{-3}$	
$\Gamma_{66}$	$h^- h^- h^+ \pi^0 \nu_\tau$ (ex. $K^0$ )	(4.57 $\pm$ 0.06) %	S=1.2	$\Gamma_{117}$	$(\bar{K}^*(892) \pi)^- \nu_\tau \rightarrow \pi^- \bar{K}^0 \pi^0 \nu_\tau$	(1.0 $\pm$ 0.4) $\times 10^{-3}$	
$\Gamma_{67}$	$h^- h^- h^+ \pi^0 \nu_\tau$ (ex. $K^0, \omega$ )	(2.79 $\pm$ 0.08) %	S=1.2	$\Gamma_{118}$	$K_1(1270)^- \nu_\tau$	(4.7 $\pm$ 1.1) $\times 10^{-3}$	
$\Gamma_{68}$	$\pi^- \pi^+ \pi^- \pi^0 \nu_\tau$	(4.62 $\pm$ 0.06) %	S=1.2	$\Gamma_{119}$	$K_1(1400)^- \nu_\tau$	(1.7 $\pm$ 2.6) $\times 10^{-3}$	S=1.7
$\Gamma_{69}$	$\pi^- \pi^+ \pi^- \pi^0 \nu_\tau$ (ex. $K^0$ )	(4.48 $\pm$ 0.06) %	S=1.2	$\Gamma_{120}$	$K^*(1410)^- \nu_\tau$	(1.5 $\pm$ 1.4 / -1.0) $\times 10^{-3}$	
$\Gamma_{70}$	$\pi^- \pi^+ \pi^- \pi^0 \nu_\tau$ (ex. $K^0, \omega$ )	[a] (2.70 $\pm$ 0.08) %	S=1.2	$\Gamma_{121}$	$K_0^*(1430)^- \nu_\tau$	< 5 $\times 10^{-4}$	CL=95%
$\Gamma_{71}$	$h^- \rho^0 \nu_\tau$			$\Gamma_{122}$	$K_2^*(1430)^- \nu_\tau$	< 3 $\times 10^{-3}$	CL=95%
$\Gamma_{72}$	$h^- \rho^+ h^- \nu_\tau$			$\Gamma_{123}$	$a_0(980)^- \geq 0$ neutrals $\nu_\tau$		
$\Gamma_{73}$	$h^- \rho^- h^+ \nu_\tau$			$\Gamma_{124}$	$\eta \pi^- \nu_\tau$	< 9.9 $\times 10^{-5}$	CL=95%
$\Gamma_{74}$	$h^- h^- h^+ \geq 2 \pi^0 \nu_\tau$ (ex. $K^0$ )	(5.21 $\pm$ 0.32) $\times 10^{-3}$		$\Gamma_{125}$	$\eta \pi^- \pi^0 \nu_\tau$	[a] (1.39 $\pm$ 0.10) $\times 10^{-3}$	S=1.4
$\Gamma_{75}$	$h^- h^- h^+ 2 \pi^0 \nu_\tau$	(5.09 $\pm$ 0.32) $\times 10^{-3}$		$\Gamma_{126}$	$\eta \pi^- \pi^0 \pi^0 \nu_\tau$	(1.5 $\pm$ 0.5) $\times 10^{-4}$	
$\Gamma_{76}$	$h^- h^- h^+ 2 \pi^0 \nu_\tau$ (ex. $K^0$ )	(4.98 $\pm$ 0.32) $\times 10^{-3}$		$\Gamma_{127}$	$\eta K^- \nu_\tau$	[a] (1.52 $\pm$ 0.08) $\times 10^{-4}$	
$\Gamma_{77}$	$h^- h^- h^+ 2 \pi^0 \nu_\tau$ (ex. $K^0, \omega, \eta$ )	[a] (1.0 $\pm$ 0.4) $\times 10^{-3}$		$\Gamma_{128}$	$\eta K^*(892)^- \nu_\tau$	(1.38 $\pm$ 0.15) $\times 10^{-4}$	
$\Gamma_{78}$	$h^- h^- h^+ 3 \pi^0 \nu_\tau$	[a] (2.3 $\pm$ 0.6) $\times 10^{-4}$	S=1.2	$\Gamma_{129}$	$\eta K^- \pi^0 \nu_\tau$	(4.8 $\pm$ 1.2) $\times 10^{-5}$	
$\Gamma_{79}$	$K^- h^+ h^- \geq 0$ neutrals $\nu_\tau$	(6.35 $\pm$ 0.24) $\times 10^{-3}$	S=1.5	$\Gamma_{130}$	$\eta K^- \pi^0$ (non- $K^*(892)$ ) $\nu_\tau$	< 3.5 $\times 10^{-5}$	CL=90%
$\Gamma_{80}$	$K^- h^+ \pi^- \nu_\tau$ (ex. $K^0$ )	(4.38 $\pm$ 0.19) $\times 10^{-3}$	S=2.7	$\Gamma_{131}$	$\eta \bar{K}^0 \pi^- \nu_\tau$	(9.3 $\pm$ 1.5) $\times 10^{-5}$	
$\Gamma_{81}$	$K^- h^+ \pi^- \pi^0 \nu_\tau$ (ex. $K^0$ )	(8.7 $\pm$ 1.2) $\times 10^{-4}$	S=1.1	$\Gamma_{132}$	$\eta \bar{K}^0 \pi^- \pi^0 \nu_\tau$	< 5.0 $\times 10^{-5}$	CL=90%
$\Gamma_{82}$	$K^- \pi^+ \pi^- \geq 0$ neutrals $\nu_\tau$	(4.85 $\pm$ 0.21) $\times 10^{-3}$	S=1.4	$\Gamma_{133}$	$\eta K^- K^0 \nu_\tau$	< 9.0 $\times 10^{-6}$	CL=90%
$\Gamma_{83}$	$K^- \pi^+ \pi^- \geq 0 \pi^0 \nu_\tau$ (ex. $K^0$ )	(3.75 $\pm$ 0.19) $\times 10^{-3}$	S=1.5	$\Gamma_{134}$	$\eta \pi^+ \pi^- \pi^- \geq 0$ neutrals $\nu_\tau$	< 3 $\times 10^{-3}$	CL=90%
$\Gamma_{84}$	$K^- \pi^+ \pi^- \nu_\tau$	(3.49 $\pm$ 0.16) $\times 10^{-3}$	S=1.9	$\Gamma_{135}$	$\eta \pi^- \pi^+ \pi^- \nu_\tau$ (ex. $K^0$ )	(1.64 $\pm$ 0.12) $\times 10^{-4}$	
$\Gamma_{85}$	$K^- \pi^+ \pi^- \nu_\tau$ (ex. $K^0$ )	[a] (2.94 $\pm$ 0.15) $\times 10^{-3}$	S=2.2	$\Gamma_{136}$	$\eta a_1(1260)^- \nu_\tau \rightarrow \eta \pi^- \rho^0 \nu_\tau$	< 3.9 $\times 10^{-4}$	CL=90%
$\Gamma_{86}$	$K^- \rho^0 \nu_\tau \rightarrow K^- \pi^+ \pi^- \nu_\tau$	(1.4 $\pm$ 0.5) $\times 10^{-3}$		$\Gamma_{137}$	$\eta \eta \pi^- \nu_\tau$	< 7.4 $\times 10^{-6}$	CL=90%
$\Gamma_{87}$	$K^- \pi^+ \pi^- \pi^0 \nu_\tau$	(1.35 $\pm$ 0.14) $\times 10^{-3}$		$\Gamma_{138}$	$\eta \eta \pi^- \pi^0 \nu_\tau$	< 2.0 $\times 10^{-4}$	CL=95%
$\Gamma_{88}$	$K^- \pi^+ \pi^- \pi^0 \nu_\tau$ (ex. $K^0$ )	(8.1 $\pm$ 1.2) $\times 10^{-4}$		$\Gamma_{139}$	$\eta \eta K^- \nu_\tau$	< 3.0 $\times 10^{-6}$	CL=90%
$\Gamma_{89}$	$K^- \pi^+ \pi^- \pi^0 \nu_\tau$ (ex. $K^0, \eta$ )	[a] (7.8 $\pm$ 1.2) $\times 10^{-4}$		$\Gamma_{140}$	$\eta'(958) \pi^- \nu_\tau$	< 7.2 $\times 10^{-6}$	CL=90%
$\Gamma_{90}$	$K^- \pi^+ \pi^- \pi^0 \nu_\tau$ (ex. $K^0, \omega$ )	(3.7 $\pm$ 0.9) $\times 10^{-4}$		$\Gamma_{141}$	$\eta'(958) \pi^- \pi^0 \nu_\tau$	< 8.0 $\times 10^{-5}$	CL=90%
$\Gamma_{91}$	$K^- \pi^+ K^- \geq 0$ neut. $\nu_\tau$	< 9 $\times 10^{-4}$	CL=95%	$\Gamma_{142}$	$\phi \pi^- \nu_\tau$	(3.4 $\pm$ 0.6) $\times 10^{-5}$	
$\Gamma_{92}$	$K^- K^+ \pi^- \geq 0$ neut. $\nu_\tau$	(1.50 $\pm$ 0.06) $\times 10^{-3}$	S=1.8	$\Gamma_{143}$	$\phi K^- \nu_\tau$	(3.70 $\pm$ 0.33) $\times 10^{-5}$	S=1.3
$\Gamma_{93}$	$K^- K^+ \pi^- \nu_\tau$	[a] (1.44 $\pm$ 0.05) $\times 10^{-3}$	S=1.9	$\Gamma_{144}$	$f_1(1285) \pi^- \nu_\tau$	(3.6 $\pm$ 0.7) $\times 10^{-4}$	
$\Gamma_{94}$	$K^- K^+ \pi^- \pi^0 \nu_\tau$	[a] (6.1 $\pm$ 2.5) $\times 10^{-5}$	S=1.4	$\Gamma_{145}$	$f_1(1285) \pi^- \nu_\tau \rightarrow \eta \pi^- \pi^+ \pi^- \nu_\tau$	(1.11 $\pm$ 0.08) $\times 10^{-4}$	
$\Gamma_{95}$	$K^- K^+ K^- \nu_\tau$	(2.1 $\pm$ 0.8) $\times 10^{-5}$	S=5.4	$\Gamma_{146}$	$\pi(1300)^- \nu_\tau \rightarrow (\rho \pi)^- \nu_\tau \rightarrow (3\pi)^- \nu_\tau$	< 1.0 $\times 10^{-4}$	CL=90%
$\Gamma_{96}$	$K^- K^+ K^- \nu_\tau$ (ex. $\phi$ )	< 2.5 $\times 10^{-6}$	CL=90%	$\Gamma_{147}$	$\pi(1300)^- \nu_\tau \rightarrow ((\pi \pi) S\text{-wave } \pi)^- \nu_\tau \rightarrow (3\pi)^- \nu_\tau$	< 1.9 $\times 10^{-4}$	CL=90%
$\Gamma_{97}$	$K^- K^+ K^- \pi^0 \nu_\tau$	< 4.8 $\times 10^{-6}$	CL=90%	$\Gamma_{148}$	$h^- \omega \geq 0$ neutrals $\nu_\tau$	(2.41 $\pm$ 0.09) %	S=1.2
$\Gamma_{98}$	$\pi^- K^+ \pi^- \geq 0$ neut. $\nu_\tau$	< 2.5 $\times 10^{-3}$	CL=95%	$\Gamma_{149}$	$h^- \omega \nu_\tau$	[a] (2.00 $\pm$ 0.08) %	S=1.3
$\Gamma_{99}$	$e^- e^- e^+ \bar{\nu}_e \nu_\tau$	(2.8 $\pm$ 1.5) $\times 10^{-5}$		$\Gamma_{150}$	$K^- \omega \nu_\tau$	(4.1 $\pm$ 0.9) $\times 10^{-4}$	
$\Gamma_{100}$	$\mu^- e^- e^+ \bar{\nu}_\mu \nu_\tau$	< 3.6 $\times 10^{-5}$	CL=90%	$\Gamma_{151}$	$h^- \omega \pi^0 \nu_\tau$	[a] (4.1 $\pm$ 0.4) $\times 10^{-3}$	
<b>Modes with five charged particles</b>				$\Gamma_{152}$	$h^- \omega 2 \pi^0 \nu_\tau$	(1.4 $\pm$ 0.5) $\times 10^{-4}$	
$\Gamma_{101}$	$3h^- 2h^+ \geq 0$ neutrals $\nu_\tau$ (ex. $K_S^0 \rightarrow \pi^- \pi^+$ ) ("5-prong")	(1.02 $\pm$ 0.04) $\times 10^{-3}$	S=1.1	$\Gamma_{153}$	$h^- 2 \omega \nu_\tau$	< 5.4 $\times 10^{-7}$	CL=90%
$\Gamma_{102}$	$3h^- 2h^+ \nu_\tau$ (ex. $K^0$ )	[a] (8.39 $\pm$ 0.35) $\times 10^{-4}$	S=1.1	$\Gamma_{154}$	$2h^- h^+ \omega \nu_\tau$	(1.20 $\pm$ 0.22) $\times 10^{-4}$	
$\Gamma_{103}$	$3h^- 2h^+ \pi^0 \nu_\tau$ (ex. $K^0$ )	[a] (1.78 $\pm$ 0.27) $\times 10^{-4}$					
$\Gamma_{104}$	$3h^- 2h^+ 2 \pi^0 \nu_\tau$	< 3.4 $\times 10^{-6}$	CL=90%				



Lepton Family number (LF), Lepton number (L), or Baryon number (B) violating modes

L means lepton number violation (e.g. tau minus to e plus pi minus pi minus). Following common usage, LF means lepton family violation and not lepton number violation (e.g. tau minus to e minus pi plus pi minus). B means baryon number violation.

Table with 5 columns: Mode, LF, L, B, CL=90%. Rows include various decay modes like e minus gamma, mu minus gamma, e minus pi 0, etc.

[a] Basis mode for the tau.

[b] See the Particle Listings below for the energy limits used in this measurement.

CONSTRAINED FIT INFORMATION

An overall fit to 66 branching ratios uses 138 measurements and one constraint to determine 31 parameters. The overall fit has a chi squared = 128.9 for 108 degrees of freedom.

The following off-diagonal array elements are the correlation coefficients <delta x\_i delta x\_j> / (delta x\_i delta x\_j), in percent, from the fit to the branching fractions, x\_i = Gamma\_i / Gamma\_Total. The fit constrains the x\_i whose labels appear in this array to sum to one.

Correlation matrix table with rows and columns labeled x\_5, x\_9, x\_10, x\_14, x\_16, x\_20, x\_23, x\_27, x\_28, x\_35, x\_37, x\_40, x\_42, x\_47, x\_48, x\_62, x\_70, x\_77, x\_85, x\_89, x\_93, x\_94, x\_102, x\_103, x\_125, x\_127, x\_149, x\_151, x\_30, x\_35, x\_37, x\_40, x\_42, x\_47, x\_48, x\_62, x\_70, x\_77.

## Lepton Particle Listings

 $\tau$ 

$x_{85}$	0									
$x_{89}$	-1	-2								
$x_{93}$	0	76	-1							
$x_{94}$	0	0	-3	0						
$x_{102}$	0	-2	-1	-2	0					
$x_{103}$	0	-1	0	-1	0	-5				
$x_{125}$	0	0	0	0	0	0	0			
$x_{127}$	0	0	-2	0	0	0	0	0		
$x_{149}$	-1	-2	3	-2	1	-1	-1	0	0	
$x_{151}$	-2	-2	-2	-2	0	1	1	-1	0	-5
	$x_{78}$	$x_{85}$	$x_{89}$	$x_{93}$	$x_{94}$	$x_{102}$	$x_{103}$	$x_{125}$	$x_{127}$	$x_{149}$

 $\tau$  BRANCHING FRACTIONS

Revised April 2012 by K.G. Hayes (Hillsdale College).

Since the previous edition of this *Review*, there have been 7 published papers that have contributed to the  $\tau$  Listings: 4 by the BaBar collaboration and 3 by the Belle collaboration. Four of these papers have provided new upper limits on the branching fractions for neutrinoless  $\tau$ -decay modes. Of the 59 neutrinoless  $\tau$ -decay modes in the  $\tau$  Listings, 17 have had improved limits set. The upper limits have been reduced by factors that range between 1.3 and 43 with the median reduction being a factor of 1.5.

There are now 30 measurements and 13 upper limits from Belle and BaBar on branching fractions of conventional  $\tau$ -decay modes, up from 1 measurement and 3 upper limits in the 2006 edition of this *Review*. Sixteen of these measurements are used in the constrained fit to  $\tau$  branching fractions, and 20 are for  $\tau$ -decay modes for which older non- $B$ -factory measurements exist. For those 20 measurements, the new  $B$ -factory measurements have on average about sixty times the number of events as the most precise earlier measurements, and the statistical uncertainties on the  $B$ -factory measurements are on average about eight times smaller. However, the systematic uncertainties now greatly exceed the statistical uncertainties of all  $B$ -factory branching fraction measurements of major  $\tau$ -decay modes. For example, the average ratio of systematic to statistical uncertainty of the  $B$ -factory measurements of  $\tau$  branching fractions larger than  $10^{-3}$  is 17.6, while the average ratio for branching fractions smaller than  $10^{-4}$  is 0.8. Thus, the total uncertainty on the branching fraction measurements from  $B$ -factories is on average only about 3.4 times smaller than the previous most precise non- $B$ -factory measurements.

**The constrained fit to  $\tau$  branching fractions:** The Lepton Summary Table and the List of  $\tau$ -Decay Modes contain branching fractions for 119 conventional  $\tau$ -decay modes and upper limits on the branching fractions for 31 other conventional  $\tau$ -decay modes. Of the 119 modes with branching fractions, 82 are derived from a constrained fit to  $\tau$  branching fraction data. The goal of the constrained fit is to make optimal use of the experimental data to determine  $\tau$  branching fractions. For example, the branching fractions for the decay mode  $\tau^- \rightarrow \pi^- \pi^+ \pi^- \pi^0 \nu_\tau$  is determined mostly from experimental measurements of the branching fraction for  $\tau^- \rightarrow h^- h^- h^+ \pi^0 \nu_\tau$  and measurements

of exclusive branching fractions for 3-prong modes containing charged kaons and 1  $\pi^0$ .

Branching fractions from the constrained fit are derived from a set of basis modes. The basis modes form an exclusive set whose branching fractions are constrained to sum exactly to one. The set of selected basis modes expands as branching fraction measurements for new  $\tau$ -decay modes are published. The number of basis modes has expanded from 12 in the year 1994 fit to 31 in the 2002 through 2012 fits. The 31 basis modes selected for the 2012 fit are listed in Table 1. See the 1996 edition of this *Review* [1] for a complete description of our notation for naming  $\tau$ -decay modes and the selection of the basis modes. For each edition since the 1996 edition, the changes in the selected basis modes from the previous edition are described in the  $\tau$  Branching Fractions Review. Figure 1 illustrates the basis mode branching fractions from the 2012 fit.

**Table 1:** Basis modes and fit values(%) for the 2012 fit to  $\tau$  branching fraction data.

$e^- \bar{\nu}_e \nu_\tau$	$17.83 \pm 0.04$
$\mu^- \bar{\nu}_\mu \nu_\tau$	$17.41 \pm 0.04$
$\pi^- \nu_\tau$	$10.83 \pm 0.06$
$\pi^- \pi^0 \nu_\tau$	$25.52 \pm 0.09$
$\pi^- 2\pi^0 \nu_\tau$ (ex. $K^0$ )	$9.30 \pm 0.11$
$\pi^- 3\pi^0 \nu_\tau$ (ex. $K^0$ )	$1.05 \pm 0.07$
$h^- 4\pi^0 \nu_\tau$ (ex. $K^0, \eta$ )	$0.11 \pm 0.04$
$K^- \nu_\tau$	$0.700 \pm 0.010$
$K^- \pi^0 \nu_\tau$	$0.429 \pm 0.015$
$K^- 2\pi^0 \nu_\tau$ (ex. $K^0$ )	$0.065 \pm 0.023$
$K^- 3\pi^0 \nu_\tau$ (ex. $K^0, \eta$ )	$0.048 \pm 0.022$
$\pi^- \bar{K}^0 \nu_\tau$	$0.84 \pm 0.04$
$\pi^- \bar{K}^0 \pi^0 \nu_\tau$	$0.40 \pm 0.04$
$\pi^- K_S^0 K_S^0 \nu_\tau$	$0.024 \pm 0.005$
$\pi^- K_S^0 K_L^0 \nu_\tau$	$0.12 \pm 0.04$
$K^- K^0 \nu_\tau$	$0.159 \pm 0.016$
$K^- K^0 \pi^0 \nu_\tau$	$0.159 \pm 0.020$
$\pi^- \pi^+ \pi^- \nu_\tau$ (ex. $K^0, \omega$ )	$8.99 \pm 0.06$
$\pi^- \pi^+ \pi^- \pi^0 \nu_\tau$ (ex. $K^0, \omega$ )	$2.70 \pm 0.08$
$K^- \pi^+ \pi^- \nu_\tau$ (ex. $K^0$ )	$0.294 \pm 0.015$
$K^- \pi^+ \pi^- \pi^0 \nu_\tau$ (ex. $K^0, \eta$ )	$0.078 \pm 0.012$
$K^- K^+ \pi^- \nu_\tau$	$0.144 \pm 0.005$
$K^- K^+ \pi^- \pi^0 \nu_\tau$	$0.0061 \pm 0.0025$
$h^- h^- h^+ 2\pi^0 \nu_\tau$ (ex. $K^0, \omega, \eta$ )	$0.10 \pm 0.04$
$h^- h^- h^+ 3\pi^0 \nu_\tau$	$0.023 \pm 0.006$
$3h^- 2h^+ \nu_\tau$ (ex. $K^0$ )	$0.0839 \pm 0.0035$
$3h^- 2h^+ \pi^0 \nu_\tau$ (ex. $K^0$ )	$0.0178 \pm 0.0027$
$h^- \omega \nu_\tau$	$2.00 \pm 0.08$
$h^- \omega \pi^0 \nu_\tau$	$0.41 \pm 0.04$
$\eta \pi^- \pi^0 \nu_\tau$	$0.139 \pm 0.010$
$\eta K^- \nu_\tau$	$0.0152 \pm 0.0008$

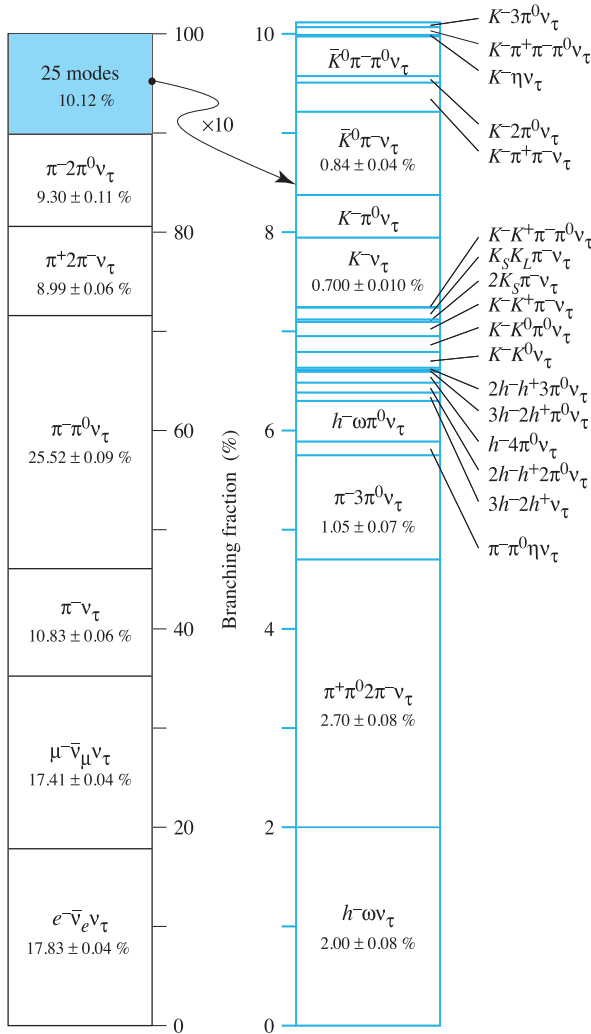


**Figure 1:** Basis mode branching fractions of the  $\tau$ . Six modes account for 90% of the decays, 25 modes account for the last 10%. The list of excluded intermediate states for each basis mode has been suppressed.

In selecting the basis modes, assumptions and choices must be made. For example, we assume the decays  $\tau^- \rightarrow \pi^- K^+ \pi^- \geq 0\pi^0\nu_\tau$  and  $\tau^- \rightarrow \pi^+ K^- K^- \geq 0\pi^0\nu_\tau$  have negligible branching fractions. This is consistent with standard model predictions for  $\tau$  decay, although the experimental limits for these branching fractions are not very stringent. The 95% confidence level upper limits for these branching fractions in the current Listings are  $B(\tau^- \rightarrow \pi^- K^+ \pi^- \geq 0\pi^0\nu_\tau) < 0.25\%$  and  $B(\tau^- \rightarrow \pi^+ K^- K^- \geq 0\pi^0\nu_\tau) < 0.09\%$ , values not so different from measured branching fractions for allowed 3-prong modes containing charged kaons. Although our usual goal is to impose as few theoretical constraints as possible so that the world averages and fit results can be used to test the theoretical constraints (*i.e.*, we do not make use of the theoretical constraint from lepton universality on the ratio of the  $\tau$ -leptonic branching fractions  $B(\tau^- \rightarrow \mu^- \bar{\nu}_\mu \nu_\tau) / B(\tau^- \rightarrow e^- \bar{\nu}_e \nu_\tau) = 0.9726$ ), the

experimental challenge to identify charged prongs in 3-prong  $\tau$  decays is sufficiently difficult that experimenters have been forced to make these assumptions when measuring the branching fractions of the allowed decays. We are constrained by the assumptions made by the experimenters.

There are several  $\tau$ -decay modes with small but well-measured ( $> 2.5$  sigma from zero) branching fractions [2] which cannot be expressed in terms of the selected basis modes and are therefore left out of the fit:

$$\begin{aligned} B(\tau^- \rightarrow \pi^- K_S^0 K_L^0 \pi^0 \nu_\tau) &= (3.1 \pm 1.2) \times 10^{-4} \\ B(\tau^- \rightarrow 2K^- K^+ \nu_\tau) &= (0.21 \pm 0.08) \times 10^{-4} \\ B(\tau^- \rightarrow \eta K^- \pi^0 \nu_\tau) &= (0.48 \pm 0.12) \times 10^{-4} \\ B(\tau^- \rightarrow \eta \bar{K}^0 \pi^- \nu_\tau) &= (0.93 \pm 0.15) \times 10^{-4}. \end{aligned}$$

Certain components of other small but well-measured  $\tau$ -decay modes cannot be expressed in terms of the selected basis modes and therefore are also left out of the fit:

$$\begin{aligned} B(\tau^- \rightarrow \eta \pi^- \pi^0 \pi^0 \nu_\tau) \times \\ B(\eta \rightarrow \gamma\gamma \text{ or } \eta \rightarrow \pi^+ \pi^- \gamma \text{ or } \eta \rightarrow 3\pi^0) &= (1.1 \pm 0.4) \times 10^{-4}, \\ B(\tau^- \rightarrow \eta \pi^- \pi^+ \pi^- \nu_\tau) \times \\ B(\eta \rightarrow \gamma\gamma \text{ or } \eta \rightarrow \pi^+ \pi^- \gamma) &= (0.72 \pm 0.05) \times 10^{-4}, \\ B(\tau^- \rightarrow \phi K^- \nu_\tau) \times \\ B(\phi \rightarrow K_S^0 K_L^0 \text{ or } \phi \rightarrow \eta\gamma) &= (0.13 \pm 0.01) \times 10^{-4}, \\ B(\tau^- \rightarrow f_1(1285) \pi^- \nu_\tau) B(f_1(1285) \rightarrow \rho^0 \gamma) &= (0.20 \pm 0.06) \times 10^{-4}, \\ B(\tau^- \rightarrow h^- \omega \pi^0 \pi^0 \nu_\tau) B(\omega \rightarrow \pi^0 \gamma) &= (0.12 \pm 0.04) \times 10^{-4}, \\ B(\tau^- \rightarrow 2h^- h^+ \omega \nu_\tau) B(\omega \rightarrow \pi^0 \gamma) &= (0.10 \pm 0.02) \times 10^{-4}. \end{aligned}$$

The sum of these excluded branching fractions is  $(0.07 \pm 0.01)\%$ . This is near our goal of 0.1% for the internal consistency of the  $\tau$  Listings for this edition, and thus for simplicity we do not include these small branching fraction decay modes in the basis set.

Beginning with the 2002 edition, the fit algorithm has been improved to allow for correlations between branching fraction measurements used in the fit. If only a few measurements are correlated, the correlation coefficients are listed in the footnote for each measurement. If a large number of measurements are correlated, then the full correlation matrix is listed in the footnote to the measurement that first appears in the  $\tau$  Listings. Footnotes to the other measurements refer to the first measurement. For example, the large correlation matrices for the branching fraction measurements contained in Refs. [3,4] are listed in Footnotes to the  $\Gamma(e^- \bar{\nu}_e \nu_\tau) / \Gamma_{\text{total}}$  and  $\Gamma(h^- \nu_\tau) / \Gamma_{\text{total}}$  measurements respectively. Sometimes experimental papers contain correlation coefficients between measurements using only statistical errors without including systematic errors. We usually cannot make use of these correlation coefficients.

The 2012 constrained fit has a  $\chi^2$  of 128.9 for 108 degrees of freedom, up from 102.9 for 103 degrees of freedom in the 2010 fit. Two basis-mode branching fractions changed by more than  $1.0 \sigma$  from their 2010 values,  $B(\mu^- \bar{\nu}_\mu \nu_\tau)$  and  $B(\pi^- \nu_\tau)$ , due to new measurements by the BaBar Collaboration [5] of  $\tau$ -decay

# Lepton Particle Listings

$\tau$

modes containing one charged prong and no neutral particles other than neutrinos.

### Inconsistencies in the $\tau$ lepton Branching Fraction Data:

Several inconsistencies are known to exist in the branching fraction measurements that are used to determine the  $\tau$ -lepton branching fractions. The sources of the inconsistencies are unknown. The treatment of discrepant data used for fits and averages is described in the introduction of this *Review*. Of the 82 branching fractions that are derived from the constrained fit, 12 (15%) have scale factors that are 1.5 or larger, and the largest is 2.7. Of the 37 branching fractions that are not derived from the constrained fit, 20 make use of only one measurement. Of the 17 averages that make use of more than one measurement, 3 (18%) have scale factors that are 1.5 or larger, and the largest is 5.4. Ideograms for 8 branching fractions are currently displayed in the  $\tau$  Listings.

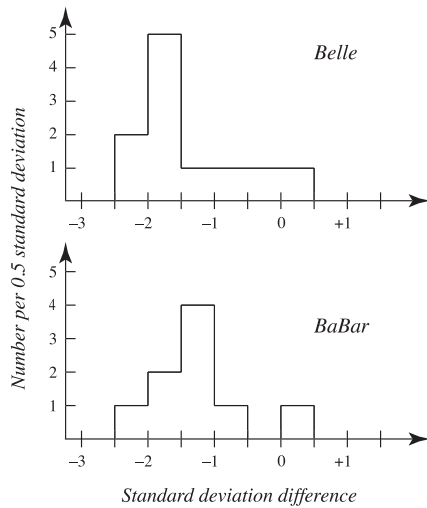


**Figure 2:** Distribution of the normalized difference between the 20  $B$ -factory measurements of conventional  $\tau$ -decay branching fractions and non- $B$ -factory measurements. The Belle and BaBar collaborations have published 11 and 9 measurements respectively.

The  $\tau$  branching fraction measurements by BaBar and Belle tend to be smaller than the non- $B$ -factory measurements. There are 20  $B$ -factory branching fraction measurements of  $\tau$ -decay modes for which older non- $B$ -factory measurements exist. Comparing the  $B$ -factory branching fraction measurements to the earlier non- $B$ -factory measurements reveals a systematic discrepancy between the two sets of measurements. Figure 2 shows a histogram of the normalized difference ( $(B$ -factory value minus non- $B$ -factory value)/estimated uncertainty in the difference) for the 20 measurements. The value used for the non- $B$ -factory measurement is the value listed in the latest edition of this *Review* prior to the first  $B$ -factory measurement for that decay mode. Eighteen of the 20  $B$ -factory branching

fraction measurements are smaller than the non- $B$ -factory values. The average normalized difference between the two sets of measurements is -1.30 (-1.41 for the 11 Belle measurements and -1.24 for the 9 BaBar measurements). The Heavy Flavor Averaging Group (HFAG) analysis of  $\tau$  branching fractions includes a similar comparison of the  $B$ -factory and non- $B$ -factory measurements [6].

Belle and BaBar have each published branching fraction measurements for the six  $\tau$ -decay modes listed in Table 2. The normalized difference between the two measured values is calculated by subtracting the Belle value from the BaBar value and dividing this difference by the quadratic sum of the statistical and systematic errors for each measurement. When a measurement has asymmetric errors, the larger of the two values is used in the quadratic sum. It is apparent from the values in Table 2 that the Belle and BaBar values differ significantly for several of the  $\tau$ -decay modes.

**Table 2:** Comparison of the Belle and Babar branching fraction measurements for the six  $\tau$ -decay modes that both experiments have measured. The normalized difference is the difference between the Belle and BaBar branching fraction values divided by the quadratic sum of the statistical and systematic errors for both measurements.

Mode	BaBar – Belle Normalized Difference ( $\#\sigma$ )
$\pi^- \pi^+ \pi^- \nu_\tau$ (ex. $K^0$ )	+1.4
$K^- \pi^+ \pi^- \nu_\tau$ (ex. $K^0$ )	-2.9
$K^- K^+ \pi^- \nu_\tau$	-2.9
$K^- K^+ K^- \nu_\tau$	-5.4
$\eta K^- \nu_\tau$	-1.0
$\phi K^- \nu_\tau$	-1.3

### Overconsistency of Leptonic Branching Fraction Measurements:

To minimize the effects of older experiments which often have larger systematic errors and sometimes make assumptions that have later been shown to be invalid, we exclude old measurements in decay modes which contain at least several newer data of much higher precision. As a rule, we exclude those experiments with large errors which together would contribute no more than 5% of the weight in the average. This procedure leaves five measurements for  $B_e \equiv B(\tau^- \rightarrow e^- \bar{\nu}_e \nu_\tau)$  and five measurements for  $B_\mu \equiv B(\tau^- \rightarrow \mu^- \bar{\nu}_\mu \nu_\tau)$ . For both  $B_e$  and  $B_\mu$ , the selected measurements are considerably more consistent with each other than should be expected from the quoted errors on the individual measurements. The  $\chi^2$  from the calculation of the average of the selected measurements is 0.34 for  $B_e$  and 0.08 for  $B_\mu$ . Assuming normal errors, the probability of a smaller  $\chi^2$  is 1.3% for  $B_e$  and 0.08% for  $B_\mu$ .

References

1. R.M. Barnett *et al.* (Particle Data Group), *Review of Particle Physics*, Phys. Rev. **D54**, 1 (1996).
2. See the  $\tau$  Listings for references.
3. S. Schael *et al.* (ALEPH Collab.), Phys. Rep. **421**, 191 (2005).
4. J. Abdallah *et al.* (DELPHI Collab.), Eur. Phys. J. **C46**, 1 (2006).
5. B. Aubert *et al.* (BaBar Collab.), Phys. Rev. Lett. **105**, 051602 (2010).
6. S. Banerjee *et al.* (HFAG), <http://arxiv.org/pdf/1101.5138v1.pdf>.

$\tau^-$  BRANCHING RATIOS

$$\Gamma(\text{particle}^- \geq 0 \text{ neutrals} \geq 0K^0 \nu_\tau \text{ ("1-prong")})/\Gamma_{\text{total}} \quad \Gamma_1/\Gamma$$

$$\Gamma_1/\Gamma = (\Gamma_3 + \Gamma_5 + \Gamma_9 + \Gamma_{10} + \Gamma_{14} + \Gamma_{16} + \Gamma_{20} + \Gamma_{23} + \Gamma_{27} + \Gamma_{28} + \Gamma_{30} + \Gamma_{35} + \Gamma_{37} + \Gamma_{40} + \Gamma_{42} + 2\Gamma_{47} + \Gamma_{48} + 0.708\Gamma_{125} + 0.715\Gamma_{127} + 0.09\Gamma_{149} + 0.09\Gamma_{151})/\Gamma$$

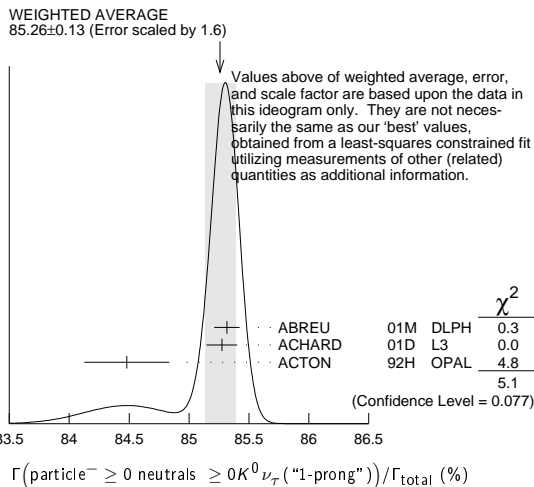
The charged particle here can be  $e$ ,  $\mu$ , or hadron. In many analyses, the sum of the topological branching fractions (1, 3, and 5 prongs) is constrained to be unity. Since the 5-prong fraction is very small, the measured 1-prong and 3-prong fractions are highly correlated and cannot be treated as independent quantities in our overall fit. We arbitrarily choose to use the 3-prong fraction in our fit, and leave the 1-prong fraction out. We do, however, use these 1-prong measurements in our average below. The measurements used only for the average are marked "avg," whereas "f&a" marks a result used for the fit and the average.

VALUE (%)	EVTS	DOCUMENT ID	TECN	COMMENT
<b>85.35 ± 0.07 OUR FIT</b>				Error includes scale factor of 1.3.
<b>85.26 ± 0.13 OUR AVERAGE</b>				Error includes scale factor of 1.6. See the ideogram below.

• • • We use the following data for averages but not for fits. • • •

85.316 ± 0.093 ± 0.049	78k	1 ABREU	01M DLPH	1992–1995 LEP runs
85.274 ± 0.105 ± 0.073		2 ACHARD	01D L3	1992–1995 LEP runs
84.48 ± 0.27 ± 0.23		ACTON	92H OPAL	1990–1991 LEP runs
• • • We do not use the following data for averages, fits, limits, etc. • • •				
85.45 ± 0.69 ± 0.73	± 0.65	DECAMP	92c ALEP	Repl. by SCHAELE 05c

- 1 The correlation coefficients between this measurement and the ABREU 01M measurements of  $B(\tau \rightarrow 3\text{-prong})$  and  $B(\tau \rightarrow 5\text{-prong})$  are  $-0.98$  and  $-0.08$  respectively.
- 2 The correlation coefficients between this measurement and the ACHARD 01D measurements of  $B(\tau \rightarrow 3\text{-prong})$  and  $B(\tau \rightarrow 5\text{-prong})$  are  $-0.978$  and  $-0.082$  respectively.



$$\Gamma(\text{particle}^- \geq 0 \text{ neutrals} \geq 0K^0 \nu_\tau)/\Gamma_{\text{total}} \quad \Gamma_2/\Gamma$$

$$\Gamma_2/\Gamma = (\Gamma_3 + \Gamma_5 + \Gamma_9 + \Gamma_{10} + \Gamma_{14} + \Gamma_{16} + \Gamma_{20} + \Gamma_{23} + \Gamma_{27} + \Gamma_{28} + \Gamma_{30} + 0.6569\Gamma_{35} + 0.6569\Gamma_{37} + 0.6569\Gamma_{40} + 0.6569\Gamma_{42} + 1.0985\Gamma_{47} + 0.3139\Gamma_{48} + 0.708\Gamma_{125} + 0.715\Gamma_{127} + 0.09\Gamma_{149} + 0.09\Gamma_{151})/\Gamma$$

VALUE (%)	EVTS	DOCUMENT ID	TECN	COMMENT
<b>84.71 ± 0.08 OUR FIT</b>				Error includes scale factor of 1.3.
<b>85.1 ± 0.4 OUR AVERAGE</b>				

• • • We use the following data for averages but not for fits. • • •

85.6 ± 0.6 ± 0.3	3300	1 ADEVA	91F L3	$E_{\text{cm}}^{\text{ee}} = 88.3\text{--}94.3 \text{ GeV}$
84.9 ± 0.4 ± 0.3		BEHREND	89B CELL	$E_{\text{cm}}^{\text{ee}} = 14\text{--}47 \text{ GeV}$
84.7 ± 0.8 ± 0.6		2 AIHARA	87B TPC	$E_{\text{cm}}^{\text{ee}} = 29 \text{ GeV}$

• • • We do not use the following data for averages, fits, limits, etc. • • •

86.4 ± 0.3 ± 0.3		ABACHI	89B HRS	$E_{\text{cm}}^{\text{ee}} = 29 \text{ GeV}$
87.1 ± 1.0 ± 0.7		3 BURCHAT	87 MRK2	$E_{\text{cm}}^{\text{ee}} = 29 \text{ GeV}$
87.2 ± 0.5 ± 0.8		SCHMIDKE	86 MRK2	$E_{\text{cm}}^{\text{ee}} = 29 \text{ GeV}$
84.7 ± 1.1 ± 1.6 ± 1.3	169	4 ALTHOFF	85 TASS	$E_{\text{cm}}^{\text{ee}} = 34.5 \text{ GeV}$
86.1 ± 0.5 ± 0.9		BARTEL	85F JADE	$E_{\text{cm}}^{\text{ee}} = 34.6 \text{ GeV}$
87.8 ± 1.3 ± 3.9		5 BERGER	85 PLUT	$E_{\text{cm}}^{\text{ee}} = 34.6 \text{ GeV}$
86.7 ± 0.3 ± 0.6		FERNANDEZ	85 MAC	$E_{\text{cm}}^{\text{ee}} = 29 \text{ GeV}$

- 1 Not independent of ADEVA 91F  $\Gamma(h^- h^+ \geq 0 \text{ neutrals} \geq 0K^0 \nu_\tau)/\Gamma_{\text{total}}$  value.
- 2 Not independent of AIHARA 87B  $\Gamma(\mu^- \bar{\nu}_\mu \nu_\tau)/\Gamma_{\text{total}}$ ,  $\Gamma(e^- \bar{\nu}_e \nu_\tau)/\Gamma_{\text{total}}$ , and  $\Gamma(h^- \geq 0 \text{ neutrals} \geq 0K^0 \nu_\tau)/\Gamma_{\text{total}}$  values.
- 3 Not independent of SCHMIDKE 86 value (also not independent of BURCHAT 87 value for  $\Gamma(h^- h^+ \geq 0 \text{ neutrals} \geq 0K^0 \nu_\tau)/\Gamma_{\text{total}}$ ).
- 4 Not independent of ALTHOFF 85  $\Gamma(\mu^- \bar{\nu}_\mu \nu_\tau)/\Gamma_{\text{total}}$ ,  $\Gamma(e^- \bar{\nu}_e \nu_\tau)/\Gamma_{\text{total}}$ ,  $\Gamma(h^- \geq 0 \text{ neutrals} \geq 0K^0 \nu_\tau)/\Gamma_{\text{total}}$ , and  $\Gamma(h^- h^+ \geq 0 \text{ neutrals} \geq 0K^0 \nu_\tau)/\Gamma_{\text{total}}$  values.
- 5 Not independent of (1-prong +  $0\pi^0$ ) and (1-prong +  $\geq 1\pi^0$ ) values.

$\Gamma(\mu^- \bar{\nu}_\mu \nu_\tau)/\Gamma_{\text{total}}$   $\Gamma_3/\Gamma$   
Data marked "avg" are highly correlated with data appearing elsewhere in the Listings, and are therefore used for the average given below but not in the overall fits. "f&a" marks results used for the fit and the average.

To minimize the effect of experiments with large systematic errors, we exclude experiments which together would contribute 5% of the weight in the average.

VALUE (%)	EVTS	DOCUMENT ID	TECN	COMMENT
<b>17.41 ± 0.04 OUR FIT</b>				Error includes scale factor of 1.1.
<b>17.33 ± 0.05 OUR AVERAGE</b>				

17.319 ± 0.070 ± 0.032	54k	1 SCHAELE	05c ALEP	1991–1995 LEP runs
17.34 ± 0.09 ± 0.06	31.4k	ABBIENDI	03 OPAL	1990–1995 LEP runs
17.342 ± 0.110 ± 0.067	21.5k	2 ACCIARRI	01F L3	1991–1995 LEP runs
17.325 ± 0.095 ± 0.077	27.7k	ABREU	99X DLPH	1991–1995 LEP runs

• • • We use the following data for averages but not for fits. • • •

17.37 ± 0.08 ± 0.18		3 ANASTASSOV	97 CLEO	$E_{\text{cm}}^{\text{ee}} = 10.6 \text{ GeV}$
• • • We do not use the following data for averages, fits, limits, etc. • • •				
17.31 ± 0.11 ± 0.05	20.7k	BUSKULIC	96c ALEP	Repl. by SCHAELE 05c
17.02 ± 0.19 ± 0.24	6586	ABREU	95T DLPH	Repl. by ABREU 99x
17.36 ± 0.27	7941	AKERS	95I OPAL	Repl. by ABBIENDI 03
17.6 ± 0.4 ± 0.4	2148	ADRIANI	93M L3	Repl. by ACCIARRI 01F
17.4 ± 0.3 ± 0.5		4 ALBRECHT	93G ARG	$E_{\text{cm}}^{\text{ee}} = 9.4\text{--}10.6 \text{ GeV}$
17.35 ± 0.41 ± 0.37		DECAMP	92C ALEP	1989–1990 LEP runs
17.7 ± 0.8 ± 0.4	568	BEHREND	90 CELL	$E_{\text{cm}}^{\text{ee}} = 35 \text{ GeV}$
17.4 ± 1.0	2197	ADEVA	88 MRKJ	$E_{\text{cm}}^{\text{ee}} = 14\text{--}16 \text{ GeV}$
17.7 ± 1.2 ± 0.7		AIHARA	87B TPC	$E_{\text{cm}}^{\text{ee}} = 29 \text{ GeV}$
18.3 ± 0.9 ± 0.8		BURCHAT	87 MRK2	$E_{\text{cm}}^{\text{ee}} = 29 \text{ GeV}$
18.6 ± 0.8 ± 0.7	558	5 BARTEL	86D JADE	$E_{\text{cm}}^{\text{ee}} = 34.6 \text{ GeV}$
12.9 ± 1.7 ± 0.7 ± 0.5		ALTHOFF	85 TASS	$E_{\text{cm}}^{\text{ee}} = 34.5 \text{ GeV}$
18.0 ± 0.9 ± 0.5	473	5 ASH	85B MAC	$E_{\text{cm}}^{\text{ee}} = 29 \text{ GeV}$
18.0 ± 1.0 ± 0.6		6 BALTRUSAITIS	85 MRK3	$E_{\text{cm}}^{\text{ee}} = 3.77 \text{ GeV}$
19.4 ± 1.6 ± 1.7	153	BERGER	85 PLUT	$E_{\text{cm}}^{\text{ee}} = 34.6 \text{ GeV}$
17.6 ± 2.6 ± 2.1	47	BEHREND	83c CELL	$E_{\text{cm}}^{\text{ee}} = 34 \text{ GeV}$
17.8 ± 2.0 ± 1.8		BERGER	81B PLUT	$E_{\text{cm}}^{\text{ee}} = 9\text{--}32 \text{ GeV}$

- 1 See footnote to SCHAELE 05c  $\Gamma(\tau^- \rightarrow e^- \bar{\nu}_e \nu_\tau)/\Gamma_{\text{total}}$  measurement for correlations with other measurements.
- 2 The correlation coefficient between this measurement and the ACCIARRI 01F measurement of  $B(\tau^- \rightarrow e^- \bar{\nu}_e \nu_\tau)$  is 0.08.
- 3 The correlation coefficients between this measurement and the ANASTASSOV 97 measurements of  $B(e \bar{\nu}_e \nu_\tau)$ ,  $B(\mu \bar{\nu}_\mu \nu_\tau)/B(e \bar{\nu}_e \nu_\tau)$ ,  $B(h^- \nu_\tau)$ , and  $B(h^- \nu_\tau)/B(e \bar{\nu}_e \nu_\tau)$  are 0.50, 0.58, 0.50, and 0.08 respectively.
- 4 Not independent of ALBRECHT 92D  $\Gamma(\mu^- \bar{\nu}_\mu \nu_\tau)/\Gamma(e^- \bar{\nu}_e \nu_\tau)$  and ALBRECHT 93G  $\Gamma(\mu^- \bar{\nu}_\mu \nu_\tau) \times \Gamma(e^- \bar{\nu}_e \nu_\tau)/\Gamma_{\text{total}}^2$  values.
- 5 Modified using  $B(e^- \bar{\nu}_e \nu_\tau)/B(\text{"1 prong"})$  and  $B(\text{"1 prong"}) = 0.855$ .
- 6 Error correlated with BALTRUSAITIS 85  $e \nu \bar{\nu}$  value.

$$\Gamma(\mu^- \bar{\nu}_\mu \nu_\tau \gamma)/\Gamma_{\text{total}} \quad \Gamma_4/\Gamma$$

VALUE (%)	EVTS	DOCUMENT ID	TECN	COMMENT
<b>0.361 ± 0.016 ± 0.035</b>		1 BERGFELD	00 CLEO	$E_{\text{cm}}^{\text{ee}} = 10.6 \text{ GeV}$

• • • We do not use the following data for averages, fits, limits, etc. • • •

0.30 ± 0.04 ± 0.05	116	2 ALEXANDER	96S OPAL	1991–1994 LEP runs
0.23 ± 0.10	10	3 WU	90 MRK2	$E_{\text{cm}}^{\text{ee}} = 29 \text{ GeV}$

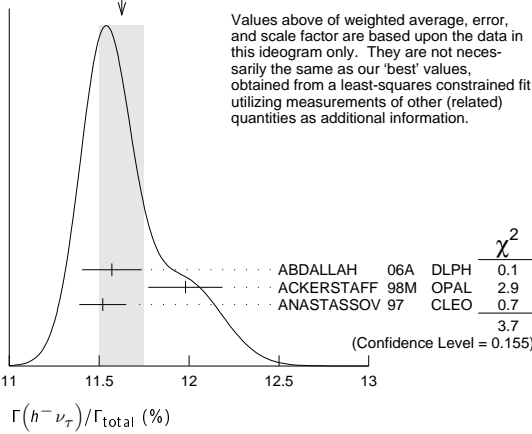
- 1 BERGFELD 00 impose requirements on detected  $\gamma$ 's corresponding to a  $\tau$ -rest-frame energy cutoff  $E_\gamma^* > 10 \text{ MeV}$ . For  $E_\gamma^* > 20 \text{ MeV}$ , they quote  $(3.04 \pm 0.14 \pm 0.30) \times 10^{-3}$ .
- 2 ALEXANDER 96S impose requirements on detected  $\gamma$ 's corresponding to a  $\tau$ -rest-frame energy cutoff  $E_\gamma > 20 \text{ MeV}$ .
- 3 WU 90 reports  $\Gamma(\mu^- \bar{\nu}_\mu \nu_\tau \gamma)/\Gamma(\mu^- \bar{\nu}_\mu \nu_\tau) = 0.013 \pm 0.006$ , which is converted to  $\Gamma(\mu^- \bar{\nu}_\mu \nu_\tau \gamma)/\Gamma_{\text{total}}$  using  $\Gamma(\mu^- \bar{\nu}_\mu \nu_\tau \gamma)/\Gamma_{\text{total}} = 17.35\%$ . Requirements on detected  $\gamma$ 's correspond to a  $\tau$  rest frame energy cutoff  $E_\gamma > 37 \text{ MeV}$ .



(1)	(2)	(3)	(4)	(5)	(6)	(7)	(8)	(9)	(10)
(2)	-34								
(3)	-47	56							
(4)	6	-66	15						
(5)	-6	38	11	-86					
(6)	-7	-8	15	0	-2				
(7)	-2	-1	-5	-3	3	-53			
(8)	-4	-4	-13	-4	-2	-56	75		
(9)	-1	-1	-4	3	-6	26	-78	-16	
(10)	-1	-1	1	0	0	-2	-3	-1	3
(11)	0	0	0	0	0	1	0	-5	5

<sup>2</sup> The correlation coefficients between this measurement and the ANASTASSOV 97 measurements of  $B(\mu\bar{\nu}_\mu\nu_\tau)$ ,  $B(e\bar{\nu}_e\nu_\tau)$ ,  $B(\mu\bar{\nu}_\mu\nu_\tau)/B(e\bar{\nu}_e\nu_\tau)$ , and  $B(h^-\nu_\tau)/B(e\bar{\nu}_e\nu_\tau)$  are 0.50, 0.48, 0.07, and 0.63 respectively.

WEIGHTED AVERAGE  
11.63±0.12 (Error scaled by 1.4)



### $\Gamma(h^-\nu_\tau)/\Gamma(e^-\bar{\nu}_e\nu_\tau)$ $\Gamma_8/\Gamma_5 = (\Gamma_9 + \Gamma_{10})/\Gamma_5$

Data marked "avg" are highly correlated with data appearing elsewhere in the Listings, and are therefore used for the average given below but not in the overall fits. "f&a" marks results used for the fit and the average.

VALUE	EVTS	DOCUMENT ID	TECN	COMMENT
<b>0.647 ± 0.004 OUR FIT</b>				Error includes scale factor of 1.1.
<b>0.640 ± 0.007 OUR AVERAGE</b>				Error includes scale factor of 1.6.
0.6333 ± 0.0014 ± 0.0061	394k	<sup>1</sup> AUBERT 10F BABR	467 fb <sup>-1</sup>	$E_{cm}^{ee} = 10.6$ GeV
0.6484 ± 0.0041 ± 0.0060		<sup>2</sup> ANASTASSOV 97 CLEO		$E_{cm}^{ee} = 10.6$ GeV

<sup>1</sup> Not independent of AUBERT 10F  $\Gamma(\tau^- \rightarrow \pi^-\nu_\tau)/\Gamma(\tau^- \rightarrow e^-\bar{\nu}_e\nu_\tau)$  and  $\Gamma(\tau^- \rightarrow K^-\nu_\tau)/\Gamma(\tau^- \rightarrow e^-\bar{\nu}_e\nu_\tau)$ .

<sup>2</sup> The correlation coefficients between this measurement and the ANASTASSOV 97 measurements of  $B(\mu\bar{\nu}_\mu\nu_\tau)$ ,  $B(e\bar{\nu}_e\nu_\tau)$ ,  $B(\mu\bar{\nu}_\mu\nu_\tau)/B(e\bar{\nu}_e\nu_\tau)$ , and  $B(h^-\nu_\tau)$  are 0.08, -0.39, 0.45, and 0.63 respectively.

### $\Gamma(\pi^-\nu_\tau)/\Gamma_{total}$ $\Gamma_9/\Gamma$

Data marked "avg" are highly correlated with data appearing elsewhere in the Listings, and are therefore used for the average given below but not in the overall fits. "f&a" marks results used for the fit and the average.

VALUE (%)	EVTS	DOCUMENT ID	TECN	COMMENT
<b>10.83 ± 0.06 OUR FIT</b>				Error includes scale factor of 1.2.
<b>10.828 ± 0.070 ± 0.078 f&amp;a</b>	38k	<sup>1</sup> SCHAEEL 05C ALEP		1991-1995 LEP runs
11.06 ± 0.11 ± 0.14		<sup>2</sup> BUSKULIC 96 ALEP		Repl. by SCHAEEL 05C
11.7 ± 0.4 ± 1.8	1138	BLOCKER 82D MRK2		$E_{cm}^{ee} = 3.5-6.7$ GeV

<sup>1</sup> See footnote to SCHAEEL 05C  $\Gamma(\tau^- \rightarrow e^-\bar{\nu}_e\nu_\tau)/\Gamma_{total}$  measurement for correlations with other measurements.

<sup>2</sup> Not independent of BUSKULIC 96  $B(h^-\nu_\tau)$  and  $B(K^-\nu_\tau)$  values.

### $\Gamma(\pi^-\nu_\tau)/\Gamma(e^-\bar{\nu}_e\nu_\tau)$ $\Gamma_9/\Gamma_5$

VALUE	EVTS	DOCUMENT ID	TECN	COMMENT
<b>0.607 ± 0.004 OUR FIT</b>				Error includes scale factor of 1.1.
<b>0.5945 ± 0.0014 ± 0.0061</b>	369k	<sup>1</sup> AUBERT 10F BABR	467 fb <sup>-1</sup>	$E_{cm}^{ee} = 10.6$ GeV

<sup>1</sup> See footnote to AUBERT 10F  $\Gamma(\tau^- \rightarrow \mu^-\bar{\nu}_\mu\nu_\tau)/\Gamma(\tau^- \rightarrow e^-\bar{\nu}_e\nu_\tau)$  for correlations with other measurements.

### $\Gamma(K^-\nu_\tau)/\Gamma_{total}$ $\Gamma_{10}/\Gamma$

VALUE (%)	EVTS	DOCUMENT ID	TECN	COMMENT
<b>0.700 ± 0.010 OUR FIT</b>				Error includes scale factor of 1.1.
<b>0.685 ± 0.023 OUR AVERAGE</b>				
0.658 ± 0.027 ± 0.029		<sup>1</sup> ABBIENDI 01J OPAL		1990-1995 LEP runs
0.696 ± 0.025 ± 0.014	2032	BARATE 99K ALEP		1991-1995 LEP runs
0.85 ± 0.18	27	ABREU 94K DLPH		LEP 1992 Z data
0.66 ± 0.07 ± 0.09	99	BATTLE 94 CLEO		$E_{cm}^{ee} \approx 10.6$ GeV

• • • We do not use the following data for averages, fits, limits, etc. • • •

0.72 ± 0.04 ± 0.04	728	BUSKULIC 96 ALEP		Repl. by BARATE 99k
0.59 ± 0.18	16	MILLS 84 DLCO		$E_{cm}^{ee} = 29$ GeV
1.3 ± 0.5	15	BLOCKER 82B MRK2		$E_{cm}^{ee} = 3.9-6.7$ GeV

<sup>1</sup> The correlation coefficient between this measurement and the ABBIENDI 01J  $B(\tau^- \rightarrow K^-\nu_\tau) \geq 0\pi^0 \geq 0K^0 \geq 0\gamma\nu_\tau$  is 0.60.

### $\Gamma(K^-\nu_\tau)/\Gamma(e^-\bar{\nu}_e\nu_\tau)$ $\Gamma_{10}/\Gamma_5$

VALUE (units 10 <sup>-2</sup> )	EVTS	DOCUMENT ID	TECN	COMMENT
<b>3.93 ± 0.06 OUR FIT</b>				Error includes scale factor of 1.1.
<b>3.882 ± 0.032 ± 0.057</b>	25k	<sup>1</sup> AUBERT 10F BABR	467 fb <sup>-1</sup>	$E_{cm}^{ee} = 10.6$ GeV

<sup>1</sup> See footnote to AUBERT 10F  $\Gamma(\tau^- \rightarrow \mu^-\bar{\nu}_\mu\nu_\tau)/\Gamma(\tau^- \rightarrow e^-\bar{\nu}_e\nu_\tau)$  for correlations with other measurements.

### $\Gamma(K^-\nu_\tau)/\Gamma(\pi^-\nu_\tau)$ $\Gamma_{10}/\Gamma_9$

VALUE (units 10 <sup>-2</sup> )	DOCUMENT ID	TECN	COMMENT
<b>6.46 ± 0.10 OUR FIT</b>			Error includes scale factor of 1.1.

• • • We use the following data for averages but not for fits. • • •

<b>6.531 ± 0.056 ± 0.093</b>	<sup>1</sup> AUBERT 10F BABR	467 fb <sup>-1</sup>	$E_{cm}^{ee} = 10.6$ GeV
------------------------------	------------------------------	----------------------	--------------------------

<sup>1</sup> Not independent of AUBERT 10F  $\Gamma(\tau^- \rightarrow \pi^-\nu_\tau)/\Gamma(\tau^- \rightarrow e^-\bar{\nu}_e\nu_\tau)$  and  $\Gamma(\tau^- \rightarrow K^-\nu_\tau)/\Gamma(\tau^- \rightarrow e^-\bar{\nu}_e\nu_\tau)$ .

### $\Gamma(h^- \geq 1 \text{ neutrals } \nu_\tau)/\Gamma_{total}$ $\Gamma_{11}/\Gamma$

$$\Gamma_{11}/\Gamma = (\Gamma_{14} + \Gamma_{16} + \Gamma_{20} + \Gamma_{23} + \Gamma_{27} + \Gamma_{28} + \Gamma_{30} + 0.157\Gamma_{35} + 0.157\Gamma_{37} + 0.157\Gamma_{40} + 0.157\Gamma_{42} + 0.0985\Gamma_{47} + 0.708\Gamma_{125} + 0.715\Gamma_{127} + 0.09\Gamma_{149} + 0.09\Gamma_{151})/\Gamma$$

VALUE (%)	DOCUMENT ID	TECN	COMMENT
<b>37.10 ± 0.10 OUR FIT</b>			Error includes scale factor of 1.2.

• • • We do not use the following data for averages, fits, limits, etc. • • •

36.14 ± 0.33 ± 0.58	<sup>1</sup> AKERS 94E OPAL		1991-1992 LEP runs
38.4 ± 1.2 ± 1.0	<sup>2</sup> BURCHAT 87 MRK2		$E_{cm}^{ee} = 29$ GeV
42.7 ± 2.0 ± 2.9	BERGER 85 PLUT		$E_{cm}^{ee} = 34.6$ GeV

<sup>1</sup> Not independent of ACKERSTAFF 98M  $B(h^-\pi^0\nu_\tau)$  and  $B(h^- \geq 2\pi^0\nu_\tau)$  values.

<sup>2</sup> BURCHAT 87 quote for  $B(\pi^\pm \geq 1 \text{ neutral } \nu_\tau) = 0.378 \pm 0.012 \pm 0.010$ . We add 0.006 to account for contribution from  $(K^{*-}\nu_\tau)$  which they fixed at BR = 0.013.

### $\Gamma(h^- \geq 1\pi^0\nu_\tau \text{ (ex. } K^0))/\Gamma_{total}$ $\Gamma_{12}/\Gamma = (\Gamma_{14} + \Gamma_{16} + \Gamma_{20} + \Gamma_{23} + \Gamma_{27} + \Gamma_{28} + \Gamma_{30} + 0.325\Gamma_{125} + 0.325\Gamma_{127})/\Gamma$

VALUE (%)	EVTS	DOCUMENT ID	TECN	COMMENT
<b>36.57 ± 0.10 OUR FIT</b>				Error includes scale factor of 1.2.

• • • We use the following data for averages but not for fits. • • •

<b>36.641 ± 0.155 ± 0.127</b>	45k	<sup>1</sup> ABDALLAH 06A DLPH		1992-1995 LEP runs
-------------------------------	-----	--------------------------------	--	--------------------

<sup>1</sup> See footnote to ABDALLAH 06A  $\Gamma(\tau^- \rightarrow h^-\nu_\tau)/\Gamma_{total}$  measurement for correlations with other measurements.

### $\Gamma(h^-\pi^0\nu_\tau)/\Gamma_{total}$ $\Gamma_{13}/\Gamma = (\Gamma_{14} + \Gamma_{16})/\Gamma$

VALUE (%)	EVTS	DOCUMENT ID	TECN	COMMENT
<b>25.95 ± 0.09 OUR FIT</b>				Error includes scale factor of 1.1.
<b>25.73 ± 0.16 OUR AVERAGE</b>				

25.67 ± 0.01 ± 0.39	5.4M	FUJIKAWA 08 BELL		72 fb <sup>-1</sup> $E_{cm}^{ee} = 10.6$ GeV
25.740 ± 0.201 ± 0.138	35k	<sup>1</sup> ABDALLAH 06A DLPH		1992-1995 LEP runs
25.89 ± 0.17 ± 0.29		ACKERSTAFF 98M OPAL		1991-1995 LEP runs
25.05 ± 0.35 ± 0.50	6613	ACCIARRI 95 L3		1992 LEP run
25.87 ± 0.12 ± 0.42	51k	<sup>2</sup> ARTUSO 94 CLEO		$E_{cm}^{ee} = 10.6$ GeV

• • • We do not use the following data for averages, fits, limits, etc. • • •

25.76 ± 0.15 ± 0.13	31k	BUSKULIC 96 ALEP		Repl. by SCHAEEL 05C
25.98 ± 0.36 ± 0.52		<sup>3</sup> AKERS 94E OPAL		Repl. by ACKERSTAFF 98M
22.9 ± 0.8 ± 1.3	283	<sup>4</sup> ABREU 92N DLPH		$E_{cm}^{ee} = 88.2-94.2$ GeV
23.1 ± 0.4 ± 0.9	1249	<sup>5</sup> ALBRECHT 92Q ARG		$E_{cm}^{ee} = 10$ GeV
25.02 ± 0.64 ± 0.88	1849	DECAMP 92C ALEP		1989-1990 LEP runs
22.0 ± 0.8 ± 1.9	779	ANTREASYAN 91 CBAL		$E_{cm}^{ee} = 9.4-10.6$ GeV
22.6 ± 1.5 ± 0.7	1101	BEHREND 90 CELL		$E_{cm}^{ee} = 35$ GeV
23.1 ± 1.9 ± 1.6		BEHREND 84 CELL		$E_{cm}^{ee} = 14,22$ GeV

<sup>1</sup> See footnote to ABDALLAH 06A  $\Gamma(\tau^- \rightarrow h^-\nu_\tau)/\Gamma_{total}$  measurement for correlations with other measurements.

<sup>2</sup> ARTUSO 94 reports the combined result from three independent methods, one of which (23% of the  $\tau^- \rightarrow h^-\pi^0\nu_\tau$ ) is normalized to the inclusive one-prong branching fraction, taken as  $0.854 \pm 0.004$ . Renormalization to the present value causes negligible change.

<sup>3</sup> AKERS 94E quote  $(26.25 \pm 0.36 \pm 0.52) \times 10^{-2}$ ; we subtract 0.27% from their number to correct for  $\tau^- \rightarrow h^-K_L^0\nu_\tau$ .

<sup>4</sup> ABREU 92N with 0.5% added to remove their correction for  $K^*(892)^-$  backgrounds.

<sup>5</sup> ALBRECHT 92Q with 0.5% added to remove their correction for  $\tau^- \rightarrow K^*(892)^-\nu_\tau$  background.

## Lepton Particle Listings

T

 $\Gamma(\pi^- \pi^0 \nu_\tau) / \Gamma_{\text{total}}$   $\Gamma_{14} / \Gamma$ 

Data marked "avg" are highly correlated with data appearing elsewhere in the Listings, and are therefore used for the average given below but not in the overall fits. "f&a" marks results used for the fit and the average.

VALUE (%)	EVTS	DOCUMENT ID	TECN	COMMENT
<b>25.52 ± 0.09 OUR FIT</b>		Error includes scale factor of 1.1.		
<b>25.46 ± 0.12 OUR AVERAGE</b>				
25.471 ± 0.097 ± 0.085	81k	<sup>1</sup> SCHAE L	05c ALEP	1991-1995 LEP runs
• • • We use the following data for averages but not for fits. • • •				
25.36 ± 0.44		<sup>2</sup> ARTUSO	94 CLEO	$E_{\text{cm}}^{ee} = 10.6$ GeV
• • • We do not use the following data for averages, fits, limits, etc. • • •				
25.30 ± 0.15 ± 0.13		<sup>3</sup> BUSKULIC	96 ALEP	Repl. by SCHAE L 05c
21.5 ± 0.4 ± 1.9	4400	<sup>4.5</sup> ALBRECHT	88L ARG	$E_{\text{cm}}^{ee} = 10$ GeV
23.0 ± 1.3 ± 1.7	582	ADLER	87B MRK3	$E_{\text{cm}}^{ee} = 3.77$ GeV
25.8 ± 1.7 ± 2.5		<sup>6</sup> BURCHAT	87 MRK2	$E_{\text{cm}}^{ee} = 29$ GeV
22.3 ± 0.6 ± 1.4	629	<sup>5</sup> YELTON	86 MRK2	$E_{\text{cm}}^{ee} = 29$ GeV

<sup>1</sup> See footnote to SCHAE L 05c  $\Gamma(\tau^- \rightarrow e^- \bar{\nu}_e \nu_\tau) / \Gamma_{\text{total}}$  measurement for correlations with other measurements.

<sup>2</sup> Not independent of ARTUSO 94  $B(h^- \pi^0 \nu_\tau)$  and BATTLE 94  $B(K^- \pi^0 \nu_\tau)$  values.

<sup>3</sup> Not independent of BUSKULIC 96  $B(h^- \pi^0 \nu_\tau)$  and  $B(K^- \pi^0 \nu_\tau)$  values.

<sup>4</sup> The authors divide by  $(\Gamma_3 + \Gamma_5 + \Gamma_{10}) / \Gamma = 0.467$  to obtain this result.

<sup>5</sup> Experiment had no hadron identification. Kaon corrections were made, but insufficient information is given to permit their removal.

<sup>6</sup> BURCHAT 87 value is not independent of YELTON 86 value. Nonresonant decays included.

 $\Gamma(\pi^- \pi^0 \text{non-}\rho(770)\nu_\tau) / \Gamma_{\text{total}}$   $\Gamma_{15} / \Gamma$ 

VALUE (%)	DOCUMENT ID	TECN	COMMENT
<b>0.3 ± 0.1 ± 0.3</b>	<sup>1</sup> BEHREND	84	CELL $E_{\text{cm}}^{ee} = 14.22$ GeV

<sup>1</sup> BEHREND 84 assume a flat nonresonant mass distribution down to the  $\rho(770)$  mass, using events with mass above 1300 to set the level.

 $\Gamma(K^- \pi^0 \nu_\tau) / \Gamma_{\text{total}}$   $\Gamma_{16} / \Gamma$ 

VALUE (%)	EVTS	DOCUMENT ID	TECN	COMMENT
<b>0.429 ± 0.015 OUR FIT</b>		Error includes scale factor of 1.2.		
<b>0.426 ± 0.016 OUR AVERAGE</b>				
0.416 ± 0.003 ± 0.018	78k	AUBERT	07AP BABR	$230 \text{ fb}^{-1}$ $E_{\text{cm}}^{ee} = 10.6$ GeV
0.471 ± 0.059 ± 0.023	360	ABBIENDI	04J OPAL	1991-1995 LEP runs
0.444 ± 0.026 ± 0.024	923	BARATE	99K ALEP	1991-1995 LEP runs
0.51 ± 0.10 ± 0.07	37	BATTLE	94 CLEO	$E_{\text{cm}}^{ee} \approx 10.6$ GeV
• • • We do not use the following data for averages, fits, limits, etc. • • •				
0.52 ± 0.04 ± 0.05	395	BUSKULIC	96 ALEP	Repl. by BARATE 99k

 $\Gamma(h^- \geq 2\pi^0 \nu_\tau) / \Gamma_{\text{total}}$   $\Gamma_{17} / \Gamma$ 

$\Gamma_{17} / \Gamma = (\Gamma_{20} + \Gamma_{23} + \Gamma_{27} + \Gamma_{28} + \Gamma_{30} + 0.157\Gamma_{35} + 0.157\Gamma_{37} + 0.157\Gamma_{40} + 0.157\Gamma_{42} + 0.0985\Gamma_{47} + 0.319\Gamma_{125} + 0.322\Gamma_{127}) / \Gamma$

Data marked "avg" are highly correlated with data appearing elsewhere in the Listings, and are therefore used for the average given below but not in the overall fits. "f&a" marks results used for the fit and the average.

VALUE (%)	EVTS	DOCUMENT ID	TECN	COMMENT
<b>10.87 ± 0.11 OUR FIT</b>		Error includes scale factor of 1.2.		
<b>9.91 ± 0.31 ± 0.27 f&amp;a</b>		ACKERSTAFF	98M OPAL	1991-1995 LEP runs
• • • We do not use the following data for averages, fits, limits, etc. • • •				
9.89 ± 0.34 ± 0.55		<sup>1</sup> AKERS	94E OPAL	Repl. by ACKERSTAFF 98M
14.0 ± 1.2 ± 0.6	938	<sup>2</sup> BEHREND	90 CELL	$E_{\text{cm}}^{ee} = 35$ GeV
12.0 ± 1.4 ± 2.5		<sup>3</sup> BURCHAT	87 MRK2	$E_{\text{cm}}^{ee} = 29$ GeV
13.9 ± 2.0 $\pm_{-2.2}^{+1.9}$		<sup>4</sup> AIHARA	86E TPC	$E_{\text{cm}}^{ee} = 29$ GeV

<sup>1</sup> AKERS 94E not independent of AKERS 94E  $B(h^- \geq \pi^0 \nu_\tau)$  and  $B(h^- \pi^0 \nu_\tau)$  measurements.

<sup>2</sup> No independent of BEHREND 90  $\Gamma(h^- 2\pi^0 \nu_\tau \text{ (exp. } K^0))$  and  $\Gamma(h^- \geq 3\pi^0 \nu_\tau)$ .

<sup>3</sup> Error correlated with BURCHAT 87  $\Gamma(\rho^- \nu_e) / \Gamma(\text{total})$  value.

<sup>4</sup> AIHARA 86E (TPC) quote  $B(2\pi^0 \pi^- \nu_\tau) + 1.6B(3\pi^0 \pi^- \nu_\tau) + 1.1B(\pi^0 \eta \pi^- \nu_\tau)$ .

 $\Gamma(h^- 2\pi^0 \nu_\tau) / \Gamma_{\text{total}}$   $\Gamma_{18} / \Gamma$ 

$\Gamma_{18} / \Gamma = (\Gamma_{20} + \Gamma_{23} + 0.157\Gamma_{35} + 0.157\Gamma_{37}) / \Gamma$

VALUE (%)	EVTS	DOCUMENT ID	TECN	COMMENT
<b>9.52 ± 0.11 OUR FIT</b>		Error includes scale factor of 1.1.		
• • • We do not use the following data for averages, fits, limits, etc. • • •				
9.48 ± 0.13 ± 0.10	12k	<sup>1</sup> BUSKULIC	96 ALEP	Repl. by SCHAE L 05c
<sup>1</sup> BUSKULIC 96 quote $9.29 \pm 0.13 \pm 0.10$ . We add 0.19 to undo their correction for $\tau^- \rightarrow h^- K^0 \nu_\tau$ .				

 $\Gamma(h^- 2\pi^0 \nu_\tau \text{ (ex. } K^0)) / \Gamma_{\text{total}}$   $\Gamma_{19} / \Gamma$ 

$\Gamma_{19} / \Gamma = (\Gamma_{20} + \Gamma_{23}) / \Gamma$

Data marked "avg" are highly correlated with data appearing elsewhere in the Listings, and are therefore used for the average given below but not in the overall fits. f&a marks results used for the fit and the average.

VALUE (%)	EVTS	DOCUMENT ID	TECN	COMMENT
<b>9.36 ± 0.11 OUR FIT</b>		Error includes scale factor of 1.2.		
<b>9.17 ± 0.27 OUR AVERAGE</b>				
9.498 ± 0.320 ± 0.275	9.5k	<sup>1</sup> ABDALLAH	06A DLPH	1992-1995 LEP runs
8.88 ± 0.37 ± 0.42	1060	ACCIARRI	95 L3	1992 LEP run
• • • We use the following data for averages but not for fits. • • •				
8.96 ± 0.16 ± 0.44		<sup>2</sup> PROCARIO	93 CLEO	$E_{\text{cm}}^{ee} \approx 10.6$ GeV
• • • We do not use the following data for averages, fits, limits, etc. • • •				
10.38 ± 0.66 ± 0.82	809	<sup>3</sup> DECAMP	92c ALEP	Repl. by SCHAE L 05c
5.7 ± 0.5 $\pm_{-1.0}^{+1.7}$	133	<sup>4</sup> ANTREASYAN	91 CBAL	$E_{\text{cm}}^{ee} = 9.4-10.6$ GeV
10.0 ± 1.5 ± 1.1	333	<sup>5</sup> BEHREND	90 CELL	$E_{\text{cm}}^{ee} = 35$ GeV
8.7 ± 0.4 ± 1.1	815	<sup>6</sup> BAND	87 MAC	$E_{\text{cm}}^{ee} = 29$ GeV
6.2 ± 0.6 ± 1.2		<sup>7</sup> GAN	87 MRK2	$E_{\text{cm}}^{ee} = 29$ GeV
6.0 ± 3.0 ± 1.8		BEHREND	84 CELL	$E_{\text{cm}}^{ee} = 14.22$ GeV

<sup>1</sup> See footnote to ABDALLAH 06A  $\Gamma(\tau^- \rightarrow h^- \pi^0 \nu_\tau) / \Gamma_{\text{total}}$  measurement for correlations with other measurements.

<sup>2</sup> PROCARIO 93 entry is obtained from  $B(h^- 2\pi^0 \nu_\tau) / B(h^- \pi^0 \nu_\tau)$  using ARTUSO 94 result for  $B(h^- \pi^0 \nu_\tau)$ .

<sup>3</sup> We subtract 0.0015 to account for  $\tau^- \rightarrow K^*(892)^- \nu_\tau$  contribution.

<sup>4</sup> ANTREASYAN 91 subtract 0.001 to account for the  $\tau^- \rightarrow K^*(892)^- \nu_\tau$  contribution.

<sup>5</sup> BEHREND 90 subtract 0.002 to account for the  $\tau^- \rightarrow K^*(892)^- \nu_\tau$  contribution.

<sup>6</sup> BAND 87 assume  $B(\pi^- 3\pi^0 \nu_\tau) = 0.01$  and  $B(\pi^- \pi^0 \eta \nu_\tau) = 0.005$ .

<sup>7</sup> GAN 87 analysis use photon multiplicity distribution.

 $\Gamma(h^- 2\pi^0 \nu_\tau \text{ (ex. } K^0)) / \Gamma(h^- \pi^0 \nu_\tau)$   $\Gamma_{19} / \Gamma_{13}$ 

$\Gamma_{19} / \Gamma_{13} = (\Gamma_{20} + \Gamma_{23}) / (\Gamma_{14} + \Gamma_{16})$

VALUE	DOCUMENT ID	TECN	COMMENT
<b>0.361 ± 0.005 OUR FIT</b>	Error includes scale factor of 1.1.		
<b>0.342 ± 0.006 ± 0.016</b>	<sup>1</sup> PROCARIO	93	CLEO $E_{\text{cm}}^{ee} \approx 10.6$ GeV
<sup>1</sup> PROCARIO 93 quote $0.345 \pm 0.006 \pm 0.016$ after correction for 2 kaon backgrounds assuming $B(K^* \nu_\tau) = 1.42 \pm 0.18\%$ and $B(h^- K^0 \pi^0 \nu_\tau) = 0.48 \pm 0.48\%$ . We multiply by 0.990 ± 0.010 to remove these corrections to $B(h^- \pi^0 \nu_\tau)$ .			

 $\Gamma(\pi^- 2\pi^0 \nu_\tau \text{ (ex. } K^0)) / \Gamma_{\text{total}}$   $\Gamma_{20} / \Gamma$ 

Data marked "avg" are highly correlated with data appearing elsewhere in the Listings, and are therefore used for the average given below but not in the overall fits. "f&a" marks results used for the fit and the average.

VALUE (%)	EVTS	DOCUMENT ID	TECN	COMMENT
<b>9.30 ± 0.11 OUR FIT</b>		Error includes scale factor of 1.2.		
<b>9.239 ± 0.086 ± 0.090 f&amp;a</b>	31k	<sup>1</sup> SCHAE L	05c ALEP	1991-1995 LEP runs
• • • We do not use the following data for averages, fits, limits, etc. • • •				
9.21 ± 0.13 ± 0.11		<sup>2</sup> BUSKULIC	96 ALEP	Repl. by SCHAE L 05c
<sup>1</sup> See footnote to SCHAE L 05c $\Gamma(\tau^- \rightarrow e^- \bar{\nu}_e \nu_\tau) / \Gamma_{\text{total}}$ measurement for correlations with other measurements.				
<sup>2</sup> Not independent of BUSKULIC 96 $B(h^- 2\pi^0 \nu_\tau \text{ (ex. } K^0))$ and $B(K^- 2\pi^0 \nu_\tau \text{ (ex. } K^0))$ values.				

 $\Gamma(\pi^- 2\pi^0 \nu_\tau \text{ (ex. } K^0, \text{ scalar)}) / \Gamma(\pi^- 2\pi^0 \nu_\tau \text{ (ex. } K^0))$   $\Gamma_{21} / \Gamma_{20}$ 

VALUE	CL%	DOCUMENT ID	TECN	COMMENT
<b>&lt;0.094</b>	95	<sup>1</sup> BROWDER	00 CLEO	$4.7 \text{ fb}^{-1}$ $E_{\text{cm}}^{ee} = 10.6$ GeV
<sup>1</sup> Model-independent limit from structure function analysis on contribution to $B(\tau^- \rightarrow \pi^- 2\pi^0 \nu_\tau \text{ (ex. } K^0))$ from scalars.				

 $\Gamma(\pi^- 2\pi^0 \nu_\tau \text{ (ex. } K^0, \text{ vector)}) / \Gamma(\pi^- 2\pi^0 \nu_\tau \text{ (ex. } K^0))$   $\Gamma_{22} / \Gamma_{20}$ 

VALUE	CL%	DOCUMENT ID	TECN	COMMENT
<b>&lt;0.073</b>	95	<sup>1</sup> BROWDER	00 CLEO	$4.7 \text{ fb}^{-1}$ $E_{\text{cm}}^{ee} = 10.6$ GeV
<sup>1</sup> Model-independent limit from structure function analysis on contribution to $B(\tau^- \rightarrow \pi^- 2\pi^0 \nu_\tau \text{ (ex. } K^0))$ from vectors.				

 $\Gamma(K^- 2\pi^0 \nu_\tau \text{ (ex. } K^0)) / \Gamma_{\text{total}}$   $\Gamma_{23} / \Gamma$ 

VALUE (units $10^{-4}$ )	EVTS	DOCUMENT ID	TECN	COMMENT
<b>6.5 ± 2.3 OUR FIT</b>		Error includes scale factor of 1.1.		
<b>5.8 ± 2.4 OUR AVERAGE</b>				
5.6 ± 2.0 ± 1.5	131	BARATE	99k ALEP	1991-1995 LEP runs
9 ± 10 ± 3	3	<sup>1</sup> BATTLE	94 CLEO	$E_{\text{cm}}^{ee} \approx 10.6$ GeV
• • • We do not use the following data for averages, fits, limits, etc. • • •				
8 ± 2 ± 2	59	BUSKULIC	96 ALEP	Repl. by BARATE 99k
<sup>1</sup> BATTLE 94 quote $(14 \pm 10 \pm 3) \times 10^{-4}$ or $< 30 \times 10^{-4}$ at 90% CL. We subtract $(5 \pm 2) \times 10^{-4}$ to account for $\tau^- \rightarrow K^-(K^0 \rightarrow \pi^0 \pi^0) \nu_\tau$ background.				



See key on page 457

## Lepton Particle Listings

T

$$\Gamma(h^- \geq 3\pi^0 \nu_\tau) / \Gamma_{\text{total}} \quad \Gamma_{24} / \Gamma$$

$$\Gamma_{24} / \Gamma = (\Gamma_{27} + \Gamma_{28} + \Gamma_{30} + 0.157\Gamma_{40} + 0.157\Gamma_{42} + 0.0985\Gamma_{47} + 0.319\Gamma_{125} + 0.322\Gamma_{127}) / \Gamma$$

VALUE (%)	EVTS	DOCUMENT ID	TECN	COMMENT
<b>1.35 ± 0.07 OUR FIT</b>				Error includes scale factor of 1.1.
• • •				We do not use the following data for averages, fits, limits, etc. • • •
1.53 ± 0.40 ± 0.46	186	DECAMP	92c	ALEP Repl. by SCHAELE 05c
3.2 ± 1.0 ± 1.0		BEHREND	90	CELL $E_{\text{cm}}^e = 35$ GeV

$$\Gamma(h^- \geq 3\pi^0 \nu_\tau \text{ (ex. } K^0)) / \Gamma_{\text{total}} \quad \Gamma_{25} / \Gamma = (\Gamma_{27} + \Gamma_{28} + \Gamma_{30} + 0.325\Gamma_{125} + 0.325\Gamma_{127}) / \Gamma$$

VALUE (%)	EVTS	DOCUMENT ID	TECN	COMMENT
<b>1.26 ± 0.07 OUR FIT</b>				Error includes scale factor of 1.1.
<b>1.403 ± 0.214 ± 0.224</b>	1.1k	<sup>1</sup> ABDALLAH	06A	DLPH 1992-1995 LEP runs

<sup>1</sup> See footnote to ABDALLAH 06A  $\Gamma(\tau^- \rightarrow h^- \nu_\tau) / \Gamma_{\text{total}}$  measurement for correlations with other measurements.

$$\Gamma(h^- 3\pi^0 \nu_\tau) / \Gamma_{\text{total}} \quad \Gamma_{26} / \Gamma = (\Gamma_{27} + \Gamma_{28} + 0.157\Gamma_{40} + 0.157\Gamma_{42} + 0.322\Gamma_{127}) / \Gamma$$

Data marked "avg" are highly correlated with data appearing elsewhere in the Listings, and are therefore used for the average given below but not in the overall fits. "f&a" marks results used for the fit and the average.

VALUE (%)	EVTS	DOCUMENT ID	TECN	COMMENT
<b>1.19 ± 0.07 OUR FIT</b>				Error includes scale factor of 1.2.
<b>1.21 ± 0.17 OUR AVERAGE</b>				Error includes scale factor of 1.2.
1.70 ± 0.24 ± 0.38	293	ACCIARRI	95	L3 1992 LEP run
• • •				We use the following data for averages but not for fits. • • •
1.15 ± 0.08 ± 0.13		<sup>1</sup> PROCARIO	93	CLEO $E_{\text{cm}}^e \approx 10.6$ GeV
• • •				We do not use the following data for averages, fits, limits, etc. • • •
1.24 ± 0.09 ± 0.11	2.3k	<sup>2</sup> BUSKULIC	96	ALEP Repl. by SCHAELE 05c
0.0 $\begin{smallmatrix} +1.4 & +1.1 \\ -0.1 & -0.1 \end{smallmatrix}$		<sup>3</sup> GAN	87	MRK2 $E_{\text{cm}}^e = 29$ GeV

<sup>1</sup> PROCARIO 93 entry is obtained from  $B(h^- 3\pi^0 \nu_\tau) / B(h^- \pi^0 \nu_\tau)$  using ARTUSO 94 result for  $B(h^- \pi^0 \nu_\tau)$ .

<sup>2</sup> BUSKULIC 96 quote  $B(h^- 3\pi^0 \nu_\tau \text{ (ex. } K^0)) = 1.17 \pm 0.09 \pm 0.11$ . We add 0.07 to remove their correction for  $K^0$  backgrounds.

<sup>3</sup> Highly correlated with GAN 87  $\Gamma(\eta \pi^- \pi^0 \nu_\tau) / \Gamma_{\text{total}}$  value. Authors quote  $B(\pi^\pm 3\pi^0 \nu_\tau) + 0.67B(\pi^\pm \eta \pi^0 \nu_\tau) = 0.047 \pm 0.010 \pm 0.011$ .

$$\Gamma(h^- 3\pi^0 \nu_\tau) / \Gamma(h^- \pi^0 \nu_\tau) \quad \Gamma_{26} / \Gamma_{13} = (\Gamma_{27} + \Gamma_{28} + 0.157\Gamma_{40} + 0.157\Gamma_{42} + 0.322\Gamma_{127}) / (\Gamma_{14} + \Gamma_{16})$$

VALUE	DOCUMENT ID	TECN	COMMENT
<b>0.0459 ± 0.0029 OUR FIT</b>			
<b>0.044 ± 0.003 ± 0.005</b>	<sup>1</sup> PROCARIO	93	CLEO $E_{\text{cm}}^e \approx 10.6$ GeV

<sup>1</sup> PROCARIO 93 quote  $0.041 \pm 0.003 \pm 0.005$  after correction for 2 kaon backgrounds assuming  $B(K^* \nu_\tau) = 1.42 \pm 0.18\%$  and  $B(h^- K^0 \pi^0 \nu_\tau) = 0.48 \pm 0.48\%$ . We add  $0.003 \pm 0.003$  and multiply the sum by  $0.990 \pm 0.010$  to remove these corrections.

$$\Gamma(\pi^- 3\pi^0 \nu_\tau \text{ (ex. } K^0)) / \Gamma_{\text{total}} \quad \Gamma_{27} / \Gamma$$

VALUE (%)	EVTS	DOCUMENT ID	TECN	COMMENT
<b>1.05 ± 0.07 OUR FIT</b>				
<b>0.977 ± 0.069 ± 0.058</b>	6.1k	<sup>1</sup> SCHAELE	05c	ALEP 1991-1995 LEP runs

<sup>1</sup> See footnote to SCHAELE 05c  $\Gamma(\tau^- \rightarrow e^- \bar{\nu}_e \nu_\tau) / \Gamma_{\text{total}}$  measurement for correlations with other measurements.

$$\Gamma(K^- 3\pi^0 \nu_\tau \text{ (ex. } K^0, \eta)) / \Gamma_{\text{total}} \quad \Gamma_{28} / \Gamma$$

VALUE (units $10^{-4}$ )	EVTS	DOCUMENT ID	TECN	COMMENT
<b>4.8 ± 2.2 OUR FIT</b>				
<b>3.7 ± 2.1 ± 1.1</b>	22	BARATE	99k	ALEP 1991-1995 LEP runs

• • • We do not use the following data for averages, fits, limits, etc. • • •

5 ± 13 <sup>1</sup> BUSKULIC 94E ALEP Repl. by BARATE 99k

<sup>1</sup> BUSKULIC 94E quote  $B(K^- \geq 0\pi^0) - [B(K^- \nu_\tau) + B(K^- \pi^0 \nu_\tau) + B(K^- K^0 \nu_\tau) + B(K^- \pi^0 \pi^0 \nu_\tau) + B(K^- \pi^0 K^0 \nu_\tau)] = (5 \pm 13) \times 10^{-4}$  accounting for common systematic errors in BUSKULIC 94E and BUSKULIC 94F measurements of these modes. We assume  $B(K^- \geq 2K^0 \nu_\tau)$  and  $B(K^- \geq 4\pi^0 \nu_\tau)$  are negligible.

$$\Gamma(h^- 4\pi^0 \nu_\tau \text{ (ex. } K^0)) / \Gamma_{\text{total}} \quad \Gamma_{29} / \Gamma = (\Gamma_{30} + 0.319\Gamma_{125}) / \Gamma$$

VALUE (%)	EVTS	DOCUMENT ID	TECN	COMMENT
<b>0.16 ± 0.04 OUR FIT</b>				
<b>0.16 ± 0.05 ± 0.05</b>		<sup>1</sup> PROCARIO	93	CLEO $E_{\text{cm}}^e \approx 10.6$ GeV

• • • We do not use the following data for averages, fits, limits, etc. • • •

0.16 ± 0.04 ± 0.09 <sup>2</sup> BUSKULIC 96 ALEP Repl. by SCHAELE 05c

<sup>1</sup> PROCARIO 93 quotes  $B(h^- 4\pi^0 \nu_\tau) / B(h^- \pi^0 \nu_\tau) = 0.006 \pm 0.002 \pm 0.002$ . We multiply by the ARTUSO 94 result for  $B(h^- \pi^0 \nu_\tau)$  to obtain  $B(h^- 4\pi^0 \nu_\tau)$ . PROCARIO 93 assume  $B(h^- \geq 5\pi^0 \nu_\tau)$  is small and do not correct for it.

<sup>2</sup> BUSKULIC 96 quote result for  $\tau^- \rightarrow h^- \geq 4\pi^0 \nu_\tau$ . We assume  $B(h^- \geq 5\pi^0 \nu_\tau)$  is negligible.

$$\Gamma(h^- 4\pi^0 \nu_\tau \text{ (ex. } K^0, \eta)) / \Gamma_{\text{total}} \quad \Gamma_{30} / \Gamma$$

VALUE (%)	EVTS	DOCUMENT ID	TECN	COMMENT
<b>0.11 ± 0.04 OUR FIT</b>				
<b>0.112 ± 0.037 ± 0.035</b>	957	<sup>1</sup> SCHAELE	05c	ALEP 1991-1995 LEP runs

<sup>1</sup> See footnote to SCHAELE 05c  $\Gamma(\tau^- \rightarrow e^- \bar{\nu}_e \nu_\tau) / \Gamma_{\text{total}}$  measurement for correlations with other measurements.

$$\Gamma(K^- \geq 0\pi^0 \geq 0K^0 \geq 0\gamma \nu_\tau) / \Gamma_{\text{total}} \quad \Gamma_{31} / \Gamma = (\Gamma_{10} + \Gamma_{16} + \Gamma_{23} + \Gamma_{28} + \Gamma_{37} + \Gamma_{42} + 0.715\Gamma_{127}) / \Gamma$$

Data marked "avg" are highly correlated with data appearing elsewhere in the Listings, and are therefore used for the average given below but not in the overall fits. "f&a" marks results used for the fit and the average.

VALUE (%)	EVTS	DOCUMENT ID	TECN	COMMENT
<b>1.572 ± 0.033 OUR FIT</b>				Error includes scale factor of 1.1.
<b>1.53 ± 0.04 OUR AVERAGE</b>				

1.528 ± 0.039 ± 0.040		<sup>1</sup> ABBIENDI	01J	OPAL 1990-1995 LEP runs
1.54 ± 0.24		ABREU	94k	DLPH LEP 1992 Z data
1.70 ± 0.12 ± 0.19	202	<sup>2</sup> BATTLE	94	CLEO $E_{\text{cm}}^e \approx 10.6$ GeV
• • •				We use the following data for averages but not for fits. • • •
1.520 ± 0.040 ± 0.041	4006	<sup>3</sup> BARATE	99k	ALEP 1991-1995 LEP runs
• • •				We do not use the following data for averages, fits, limits, etc. • • •
1.70 ± 0.05 ± 0.06	1610	<sup>4</sup> BUSKULIC	96	ALEP Repl. by BARATE 99k
1.6 ± 0.4 ± 0.2	35	AIHARA	87B	TPC $E_{\text{cm}}^e = 29$ GeV
1.71 ± 0.29	53	MILLS	84	DLCO $E_{\text{cm}}^e = 29$ GeV

<sup>1</sup> The correlation coefficient between this measurement and the ABBIENDI 01J  $B(\tau^- \rightarrow K^- \nu_\tau)$  is 0.60.

<sup>2</sup> BATTLE 94 quote  $1.60 \pm 0.12 \pm 0.19$ . We add  $0.10 \pm 0.02$  to correct for their rejection of  $K_S^0 \rightarrow \pi^+ \pi^-$  decays.

<sup>3</sup> Not independent of BARATE 99k  $B(K^- \nu_\tau)$ ,  $B(K^- \pi^0 \nu_\tau)$ ,  $B(K^- 2\pi^0 \nu_\tau \text{ (ex. } K^0))$ ,  $B(K^- 3\pi^0 \nu_\tau \text{ (ex. } K^0))$ ,  $B(K^- K^0 \nu_\tau)$ , and  $B(K^- K^0 \pi^0 \nu_\tau)$  values.

<sup>4</sup> Not independent of BUSKULIC 96  $B(K^- \nu_\tau)$ ,  $B(K^- \pi^0 \nu_\tau)$ ,  $B(K^- 2\pi^0 \nu_\tau)$ ,  $B(K^- K^0 \nu_\tau)$ , and  $B(K^- K^0 \pi^0 \nu_\tau)$  values.

$$\Gamma(K^- \geq 1(\pi^0 \text{ or } K^0 \text{ or } \gamma) \nu_\tau) / \Gamma_{\text{total}} \quad \Gamma_{32} / \Gamma = (\Gamma_{16} + \Gamma_{23} + \Gamma_{28} + \Gamma_{37} + \Gamma_{42} + 0.715\Gamma_{127}) / \Gamma$$

Data marked "avg" are highly correlated with data appearing elsewhere in the Listings, and are therefore used for the average given below but not in the overall fits. "f&a" marks results used for the fit and the average.

VALUE (%)	EVTS	DOCUMENT ID	TECN	COMMENT
<b>0.872 ± 0.032 OUR FIT</b>				Error includes scale factor of 1.1.
<b>0.86 ± 0.05 OUR AVERAGE</b>				

• • •				We use the following data for averages but not for fits. • • •
0.869 ± 0.031 ± 0.034		<sup>1</sup> ABBIENDI	01J	OPAL 1990-1995 LEP runs
0.69 ± 0.25		<sup>2</sup> ABREU	94k	DLPH LEP 1992 Z data
• • •				We do not use the following data for averages, fits, limits, etc. • • •
1.2 ± 0.5 $\begin{smallmatrix} +0.2 \\ -0.4 \end{smallmatrix}$	9	AIHARA	87B	TPC $E_{\text{cm}}^e = 29$ GeV

<sup>1</sup> Not independent of ABBIENDI 01J  $B(\tau^- \rightarrow K^- \nu_\tau)$  and  $B(\tau^- \rightarrow K^- \geq 0\pi^0 \geq 0K^0 \geq 0\gamma \nu_\tau)$  values.

<sup>2</sup> Not independent of ABREU 94k  $B(K^- \nu_\tau)$  and  $B(K^- \geq 0$  neutrals  $\nu_\tau)$  measurements.

$$\Gamma(K_S^0 \text{ (particles)}^- \nu_\tau) / \Gamma_{\text{total}} \quad \Gamma_{33} / \Gamma = (\frac{1}{2}\Gamma_{35} + \frac{1}{2}\Gamma_{37} + \frac{1}{2}\Gamma_{40} + \frac{1}{2}\Gamma_{42} + \Gamma_{47} + \Gamma_{48}) / \Gamma$$

VALUE (%)	EVTS	DOCUMENT ID	TECN	COMMENT
<b>0.92 ± 0.04 OUR FIT</b>				Error includes scale factor of 1.5.
<b>0.97 ± 0.07 OUR AVERAGE</b>				
0.970 ± 0.058 ± 0.062	929	BARATE	98E	ALEP 1991-1995 LEP runs
0.97 ± 0.09 ± 0.06	141	AKERS	94G	OPAL $E_{\text{cm}}^e = 88-94$ GeV

$$\Gamma(h^- \bar{K}^0 \nu_\tau) / \Gamma_{\text{total}} \quad \Gamma_{34} / \Gamma = (\Gamma_{35} + \Gamma_{37}) / \Gamma$$

Data marked "avg" are highly correlated with data appearing elsewhere in the Listings, and are therefore used for the average given below but not in the overall fits. "f&a" marks results used for the fit and the average.

VALUE (%)	EVTS	DOCUMENT ID	TECN	COMMENT
<b>1.00 ± 0.05 OUR FIT</b>				Error includes scale factor of 1.8.
<b>0.90 ± 0.07 OUR AVERAGE</b>				

• • • We use the following data for averages but not for fits. • • •

1.01 ± 0.11 ± 0.07 <sup>1</sup> BARATE 98E ALEP 1991-1995 LEP runs

<sup>1</sup> Not independent of BARATE 98E  $B(\tau^- \rightarrow \pi^- \bar{K}^0 \nu_\tau)$  and  $B(\tau^- \rightarrow K^- K^0 \nu_\tau)$  values.

## Lepton Particle Listings

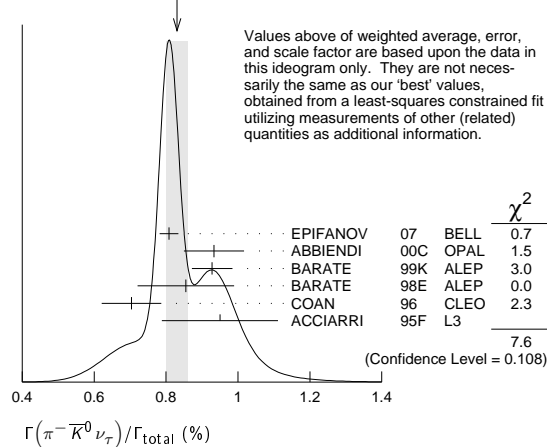
 $\tau$  $\Gamma(\pi^- \bar{K}^0 \nu_\tau) / \Gamma_{\text{total}}$   $\Gamma_{35} / \Gamma$ 

Data marked "avg" are highly correlated with data appearing elsewhere in the Listings, and are therefore used for the average given below but not in the overall fits. "f&a" marks results used for the fit and the average.

VALUE (%)	EVTS	DOCUMENT ID	TECN	COMMENT
<b>0.84 ± 0.04 OUR FIT</b>				Error includes scale factor of 2.1.
<b>0.831 ± 0.030 OUR AVERAGE</b>				Error includes scale factor of 1.4. See the ideogram below.
0.808 ± 0.004 ± 0.026	53k	EPIFANOV 07	BELL	351 fb <sup>-1</sup> $E_{\text{cm}}^{\text{eff}} = 10.6$ GeV
0.933 ± 0.068 ± 0.049	377	ABBIENDI 00c	OPAL	1991-1995 LEP runs
0.928 ± 0.045 ± 0.034	937	<sup>1</sup> BARATE	99k ALEP	1991-1995 LEP runs
0.95 ± 0.15 ± 0.06		<sup>2</sup> ACCIARRI	95F L3	1991-1993 LEP runs
• • • We use the following data for averages but not for fits. • • •				
0.855 ± 0.117 ± 0.066	509	<sup>3</sup> BARATE	98E ALEP	1991-1995 LEP runs
0.704 ± 0.041 ± 0.072		<sup>4</sup> COAN	96 CLEO	$E_{\text{cm}}^{\text{eff}} \approx 10.6$ GeV
• • • We do not use the following data for averages, fits, limits, etc. • • •				
0.79 ± 0.10 ± 0.09	98	<sup>5</sup> BUSKULIC	96 ALEP	Repl. by BARATE 99k

- BARATE 99k measure  $K^0$ 's by detecting  $K_L^0$ 's in their hadron calorimeter.
- ACCIARRI 95F do not identify  $\pi^- / K^-$  and assume  $B(K^- K^0 \nu_\tau) = (0.29 \pm 0.12)\%$ .
- BARATE 98E reconstruct  $K^0$ 's using  $K_S^0 \rightarrow \pi^+ \pi^-$  decays. Not independent of BARATE 98E  $B(K^0 \text{ particles } \nu_\tau)$  value.
- Not independent of COAN 96  $B(h^- K^0 \nu_\tau)$  and  $B(K^- K^0 \nu_\tau)$  measurements.
- BUSKULIC 96 measure  $K^0$ 's by detecting  $K_L^0$ 's in their hadron calorimeter.

WEIGHTED AVERAGE  
0.831 ± 0.030 (Error scaled by 1.4)

 $\Gamma(\pi^- \bar{K}^0 (\text{non-}K^*(892)^- \nu_\tau) / \Gamma_{\text{total}}$   $\Gamma_{36} / \Gamma$ 

VALUE (units 10 <sup>-4</sup> )	CL%	DOCUMENT ID	TECN	COMMENT
<b>5.4 ± 2.1</b>		<sup>1</sup> EPIFANOV 07	BELL	351 fb <sup>-1</sup> $E_{\text{cm}}^{\text{eff}} = 10.6$ GeV

- • • We do not use the following data for averages, fits, limits, etc. • • •
- <17 95 ACCIARRI 95F L3 1991-1993 LEP runs
- EPIFANOV 07 quote  $B(\tau^- \rightarrow K^*(892)^- \nu_\tau) B(K^*(892)^- \rightarrow K_S^0 \pi^-) / B(\tau^- \rightarrow K_S^0 \pi^- \nu_\tau) = 0.933 \pm 0.027$ . We multiply their  $B(\tau^- \rightarrow \bar{K}^0 \pi^- \nu_\tau)$  by  $[1 - (0.933 \pm 0.027)]$  to obtain this result.

 $\Gamma(K^- K^0 \nu_\tau) / \Gamma_{\text{total}}$   $\Gamma_{37} / \Gamma$ 

VALUE (%)	EVTS	DOCUMENT ID	TECN	COMMENT
<b>0.159 ± 0.016 OUR FIT</b>				
<b>0.158 ± 0.017 OUR AVERAGE</b>				
0.162 ± 0.021 ± 0.011	150	<sup>1</sup> BARATE	99k ALEP	1991-1995 LEP runs
0.158 ± 0.042 ± 0.017	46	<sup>2</sup> BARATE	98E ALEP	1991-1995 LEP runs
0.151 ± 0.021 ± 0.022	111	COAN	96 CLEO	$E_{\text{cm}}^{\text{eff}} \approx 10.6$ GeV

- • • We do not use the following data for averages, fits, limits, etc. • • •
- 0.26 ± 0.09 ± 0.02 <sup>3</sup>BUSKULIC 96 ALEP Repl. by BARATE 99k
- BARATE 99k measure  $K^0$ 's by detecting  $K_L^0$ 's in their hadron calorimeter.
  - BARATE 98E reconstruct  $K^0$ 's using  $K_S^0 \rightarrow \pi^+ \pi^-$  decays.
  - BUSKULIC 96 measure  $K^0$ 's by detecting  $K_L^0$ 's in their hadron calorimeter.

 $\Gamma(K^- K^0 \geq 0\pi^0 \nu_\tau) / \Gamma_{\text{total}}$   $\Gamma_{38} / \Gamma = (\Gamma_{37} + \Gamma_{42}) / \Gamma$ 

VALUE (%)	EVTS	DOCUMENT ID	TECN	COMMENT
<b>0.318 ± 0.023 OUR FIT</b>				
<b>0.330 ± 0.055 ± 0.039</b>	124	ABBIENDI 00c	OPAL	1991-1995 LEP runs

 $\Gamma(h^- \bar{K}^0 \pi^0 \nu_\tau) / \Gamma_{\text{total}}$   $\Gamma_{39} / \Gamma = (\Gamma_{40} + \Gamma_{42}) / \Gamma$ 

Data marked "avg" are highly correlated with data appearing elsewhere in the Listings, and are therefore used for the average given below but not in the overall fits. "f&a" marks results used for the fit and the average.

VALUE (%)	EVTS	DOCUMENT ID	TECN	COMMENT
<b>0.55 ± 0.04 OUR FIT</b>				
<b>0.50 ± 0.06 OUR AVERAGE</b>				Error includes scale factor of 1.2.
0.562 ± 0.050 ± 0.048	264	COAN	96 CLEO	$E_{\text{cm}}^{\text{eff}} \approx 10.6$ GeV
• • • We use the following data for averages but not for fits. • • •				
0.446 ± 0.052 ± 0.046	157	<sup>1</sup> BARATE	98E ALEP	1991-1995 LEP runs
<sup>1</sup> Not independent of BARATE 98E $B(\tau^- \rightarrow \pi^- \bar{K}^0 \pi^0 \nu_\tau)$ and $B(\tau^- \rightarrow K^- K^0 \pi^0 \nu_\tau)$ values.				

 $\Gamma(\pi^- \bar{K}^0 \pi^0 \nu_\tau) / \Gamma_{\text{total}}$   $\Gamma_{40} / \Gamma$ 

Data marked "avg" are highly correlated with data appearing elsewhere in the Listings, and are therefore used for the average given below but not in the overall fits. "f&a" marks results used for the fit and the average.

VALUE (%)	EVTS	DOCUMENT ID	TECN	COMMENT
<b>0.40 ± 0.04 OUR FIT</b>				
<b>0.36 ± 0.04 OUR AVERAGE</b>				
0.347 ± 0.053 ± 0.037	299	<sup>1</sup> BARATE	99k ALEP	1991-1995 LEP runs
0.294 ± 0.073 ± 0.037	142	<sup>2</sup> BARATE	98E ALEP	1991-1995 LEP runs
0.41 ± 0.12 ± 0.03		<sup>3</sup> ACCIARRI	95F L3	1991-1993 LEP runs
• • • We use the following data for averages but not for fits. • • •				
0.417 ± 0.058 ± 0.044		<sup>4</sup> COAN	96 CLEO	$E_{\text{cm}}^{\text{eff}} \approx 10.6$ GeV
• • • We do not use the following data for averages, fits, limits, etc. • • •				
0.32 ± 0.11 ± 0.05	23	<sup>5</sup> BUSKULIC	96 ALEP	Repl. by BARATE 99k

- BARATE 99k measure  $K^0$ 's by detecting  $K_L^0$ 's in their hadron calorimeter.
- BARATE 98E reconstruct  $K^0$ 's using  $K_S^0 \rightarrow \pi^+ \pi^-$  decays.
- ACCIARRI 95F do not identify  $\pi^- / K^-$  and assume  $B(K^- K^0 \pi^0 \nu_\tau) = (0.05 \pm 0.05)\%$ .
- Not independent of COAN 96  $B(h^- K^0 \pi^0 \nu_\tau)$  and  $B(K^- K^0 \pi^0 \nu_\tau)$  measurements.
- BUSKULIC 96 measure  $K^0$ 's by detecting  $K_L^0$ 's in their hadron calorimeter.

 $\Gamma(\bar{K}^0 \rho^- \nu_\tau) / \Gamma_{\text{total}}$   $\Gamma_{41} / \Gamma$ 

VALUE (%)	DOCUMENT ID	TECN	COMMENT
<b>0.22 ± 0.05 OUR AVERAGE</b>			
0.250 ± 0.057 ± 0.044	<sup>1</sup> BARATE	99k ALEP	1991-1995 LEP runs
0.188 ± 0.054 ± 0.038	<sup>2</sup> BARATE	98E ALEP	1991-1995 LEP runs

- BARATE 99k measure  $K^0$ 's by detecting  $K_L^0$ 's in hadron calorimeter. They determine the  $\bar{K}^0 \rho^-$  fraction in  $\tau^- \rightarrow \pi^- \bar{K}^0 \pi^0 \nu_\tau$  decays to be  $(0.72 \pm 0.12 \pm 0.10)$  and multiply their  $B(\pi^- \bar{K}^0 \pi^0 \nu_\tau)$  measurement by this fraction to obtain the quoted result.
- BARATE 98E reconstruct  $K^0$ 's using  $K_S^0 \rightarrow \pi^+ \pi^-$  decays. They determine the  $\bar{K}^0 \rho^-$  fraction in  $\tau^- \rightarrow \pi^- \bar{K}^0 \pi^0 \nu_\tau$  decays to be  $(0.64 \pm 0.09 \pm 0.10)$  and multiply their  $B(\pi^- \bar{K}^0 \pi^0 \nu_\tau)$  measurement by this fraction to obtain the quoted result.

 $\Gamma(K^- K^0 \pi^0 \nu_\tau) / \Gamma_{\text{total}}$   $\Gamma_{42} / \Gamma$ 

VALUE (%)	EVTS	DOCUMENT ID	TECN	COMMENT
<b>0.159 ± 0.020 OUR FIT</b>				
<b>0.144 ± 0.023 OUR AVERAGE</b>				
0.143 ± 0.025 ± 0.015	78	<sup>1</sup> BARATE	99k ALEP	1991-1995 LEP runs
0.152 ± 0.076 ± 0.021	15	<sup>2</sup> BARATE	98E ALEP	1991-1995 LEP runs
0.145 ± 0.036 ± 0.020	32	COAN	96 CLEO	$E_{\text{cm}}^{\text{eff}} \approx 10.6$ GeV
• • • We do not use the following data for averages, fits, limits, etc. • • •				
0.10 ± 0.05 ± 0.03	5	<sup>3</sup> BUSKULIC	96 ALEP	Repl. by BARATE 99k

- BARATE 99k measure  $K^0$ 's by detecting  $K_L^0$ 's in their hadron calorimeter.
- BARATE 98E reconstruct  $K^0$ 's using  $K_S^0 \rightarrow \pi^+ \pi^-$  decays.
- BUSKULIC 96 measure  $K^0$ 's by detecting  $K_L^0$ 's in their hadron calorimeter.

 $\Gamma(\pi^- \bar{K}^0 \geq 1\pi^0 \nu_\tau) / \Gamma_{\text{total}}$   $\Gamma_{43} / \Gamma = (\Gamma_{40} + \Gamma_{44}) / \Gamma$ 

VALUE (%)	EVTS	DOCUMENT ID	TECN	COMMENT
<b>0.324 ± 0.074 ± 0.066</b>	148	ABBIENDI 00c	OPAL	1991-1995 LEP runs

 $\Gamma(\pi^- \bar{K}^0 \pi^0 \pi^0 \nu_\tau) / \Gamma_{\text{total}}$   $\Gamma_{44} / \Gamma$ 

VALUE (units 10 <sup>-3</sup> )	CL%	EVTS	DOCUMENT ID	TECN	COMMENT
<b>0.26 ± 0.24</b>			<sup>1</sup> BARATE	99R ALEP	1991-1995 LEP runs
• • • We do not use the following data for averages, fits, limits, etc. • • •					
<0.66		95 17	<sup>2</sup> BARATE	99k ALEP	1991-1995 LEP runs
<0.58 ± 0.33 ± 0.14		5	<sup>3</sup> BARATE	98E ALEP	1991-1995 LEP runs

- BARATE 99R combine the BARATE 98E and BARATE 99k measurements to obtain this value.
- BARATE 99k measure  $K^0$ 's by detecting  $K_L^0$ 's in their hadron calorimeter.
- BARATE 98E reconstruct  $K^0$ 's using  $K_S^0 \rightarrow \pi^+ \pi^-$  decays.

 $\Gamma(K^- K^0 \pi^0 \pi^0 \nu_\tau) / \Gamma_{\text{total}}$   $\Gamma_{45} / \Gamma$ 

VALUE (%)	CL%	DOCUMENT ID	TECN	COMMENT	
<b>&lt;0.16 × 10<sup>-3</sup></b>		95	<sup>1</sup> BARATE	99R ALEP	1991-1995 LEP runs
• • • We do not use the following data for averages, fits, limits, etc. • • •					
<0.18 × 10 <sup>-3</sup>		95	<sup>2</sup> BARATE	99k ALEP	1991-1995 LEP runs
<0.39 × 10 <sup>-3</sup>		95	<sup>3</sup> BARATE	98E ALEP	1991-1995 LEP runs

- BARATE 99R combine the BARATE 98E and BARATE 99k bounds to obtain this value.
- BARATE 99k measure  $K^0$ 's by detecting  $K_L^0$ 's in hadron calorimeter.
- BARATE 98E reconstruct  $K^0$ 's by using  $K_S^0 \rightarrow \pi^+ \pi^-$  decays.

See key on page 457

## Lepton Particle Listings

T

$\Gamma(\pi^- K^0 \bar{K}^0 \nu_\tau)/\Gamma_{\text{total}}$   $\Gamma_{46}/\Gamma = (2\Gamma_{47} + \Gamma_{48})/\Gamma$   
 Data marked "avg" are highly correlated with data appearing elsewhere in the Listings, and are therefore used for the average given below but not in the overall fits. "f&a" marks results used for the fit and the average.

VALUE (%)	EVTS	DOCUMENT ID	TECN	COMMENT
<b>0.17 ± 0.04 OUR FIT</b>				Error includes scale factor of 1.7.
• • •				We use the following data for averages but not for fits. • • •
<b>0.153 ± 0.030 ± 0.016</b>	74	<sup>1</sup> BARATE	98E ALEP	1991–1995 LEP runs
• • •				We do not use the following data for averages, fits, limits, etc. • • •
0.31 ± 0.12 ± 0.04		<sup>2</sup> ACCIARRI	95F L3	1991–1993 LEP runs
		<sup>1</sup> BARATE	98E	obtain this value by adding twice their $B(\pi^- K_S^0 K_L^0 \nu_\tau)$ value to their $B(\pi^- K_S^0 K_L^0 \nu_\tau)$ value.
		<sup>2</sup> ACCIARRI	95F	assume $B(\pi^- K_S^0 K_S^0 \nu) = B(\pi^- K_S^0 K_L^0 \nu) = 1/2 B(\pi^- K_S^0 K_L^0 \nu)$ .

$\Gamma(\pi^- K_S^0 K_L^0 \nu_\tau)/\Gamma_{\text{total}}$   $\Gamma_{47}/\Gamma$   
 Bose-Einstein correlations might make the mixing fraction different than 1/4.

VALUE (units $10^{-4}$ )	EVTS	DOCUMENT ID	TECN	COMMENT
<b>2.4 ± 0.5 OUR FIT</b>				
<b>2.4 ± 0.5 OUR AVERAGE</b>				
2.6 ± 1.0 ± 0.5	6	BARATE	98E ALEP	1991–1995 LEP runs
2.3 ± 0.5 ± 0.3	42	COAN	96 CLEO	$E_{\text{cm}}^{\text{eff}} \approx 10.6$ GeV

$\Gamma(\pi^- K_S^0 K_L^0 \nu_\tau)/\Gamma_{\text{total}}$   $\Gamma_{48}/\Gamma$

VALUE (units $10^{-4}$ )	EVTS	DOCUMENT ID	TECN	COMMENT
<b>12 ± 4 OUR FIT</b>				Error includes scale factor of 1.7.
<b>10.1 ± 2.3 ± 1.3</b>	68	BARATE	98E ALEP	1991–1995 LEP runs

$\Gamma(\pi^- K^0 \bar{K}^0 \pi^0 \nu_\tau)/\Gamma_{\text{total}}$   $\Gamma_{49}/\Gamma$

VALUE	DOCUMENT ID	TECN	COMMENT
<b>(0.31 ± 0.23) × 10<sup>-3</sup></b>	<sup>1</sup> BARATE	99R ALEP	1991–1995 LEP runs
	<sup>1</sup> BARATE	99R	combine
	BARATE	98E	$\Gamma(\pi^- K_S^0 K_S^0 \pi^0 \nu_\tau)/\Gamma_{\text{total}}$ and measurements to obtain this value.

$\Gamma(\pi^- K_S^0 K_S^0 \pi^0 \nu_\tau)/\Gamma_{\text{total}}$   $\Gamma_{50}/\Gamma$

VALUE (units $10^{-4}$ )	CL%	DOCUMENT ID	TECN	COMMENT
<b>&lt;2.0</b>	95	BARATE	98E ALEP	1991–1995 LEP runs

$\Gamma(\pi^- K_S^0 K_L^0 \pi^0 \nu_\tau)/\Gamma_{\text{total}}$   $\Gamma_{51}/\Gamma$

VALUE (units $10^{-4}$ )	EVTS	DOCUMENT ID	TECN	COMMENT
<b>3.1 ± 1.1 ± 0.5</b>	11	BARATE	98E ALEP	1991–1995 LEP runs

$\Gamma(K^0 h^+ h^- h^- \geq 0 \text{ neutrals } \nu_\tau)/\Gamma_{\text{total}}$   $\Gamma_{52}/\Gamma$

VALUE (%)	CL%	DOCUMENT ID	TECN	COMMENT
<b>&lt;0.17</b>	95	TSCHIRHART	88 HRS	$E_{\text{cm}}^{\text{eff}} = 29$ GeV
• • •				We do not use the following data for averages, fits, limits, etc. • • •
<0.27	90	BELTRAMI	85 HRS	$E_{\text{cm}}^{\text{eff}} = 29$ GeV

$\Gamma(K^0 h^+ h^- h^- \nu_\tau)/\Gamma_{\text{total}}$   $\Gamma_{53}/\Gamma$

VALUE (units $10^{-4}$ )	EVTS	DOCUMENT ID	TECN	COMMENT
<b>2.3 ± 1.9 ± 0.7</b>	6	<sup>1</sup> BARATE	98E ALEP	1991–1995 LEP runs
		<sup>1</sup> BARATE	98E	reconstruct $K^0$ 's using $K_S^0 \rightarrow \pi^+ \pi^-$ decays.

$\Gamma(h^- h^- h^+ \geq 0 \text{ neutrals } \geq 0 K^0 \nu_\tau)/\Gamma_{\text{total}}$   $\Gamma_{54}/\Gamma$

VALUE (%)	EVTS	DOCUMENT ID	TECN	COMMENT
<b>15.20 ± 0.08 OUR FIT</b>				Error includes scale factor of 1.3.
<b>14.8 ± 0.4 OUR AVERAGE</b>				
14.4 ± 0.6 ± 0.3		ADEVA	91F L3	$E_{\text{cm}}^{\text{eff}} = 88.3\text{--}94.3$ GeV
15.0 ± 0.4 ± 0.3		BEHREND	89B CELL	$E_{\text{cm}}^{\text{eff}} = 14\text{--}47$ GeV
15.1 ± 0.8 ± 0.6		AIHARA	87B TPC	$E_{\text{cm}}^{\text{eff}} = 29$ GeV
• • •				We do not use the following data for averages, fits, limits, etc. • • •
13.5 ± 0.3 ± 0.3		ABACHI	89B HRS	$E_{\text{cm}}^{\text{eff}} = 29$ GeV
12.8 ± 1.0 ± 0.7		<sup>1</sup> BURCHAT	87 MRK2	$E_{\text{cm}}^{\text{eff}} = 29$ GeV
12.1 ± 0.5 ± 1.2		RUCKSTUHL	86 DLCO	$E_{\text{cm}}^{\text{eff}} = 29$ GeV
12.8 ± 0.5 ± 0.8	1420	SCHMIDKE	86 MRK2	$E_{\text{cm}}^{\text{eff}} = 29$ GeV
15.3 ± 1.1 ± 1.3	367	ALTHOFF	85 TASS	$E_{\text{cm}}^{\text{eff}} = 34.5$ GeV
13.6 ± 0.5 ± 0.8		BARTEL	85F JADE	$E_{\text{cm}}^{\text{eff}} = 34.6$ GeV
12.2 ± 1.3 ± 0.9		<sup>2</sup> BERGER	85 PLUT	$E_{\text{cm}}^{\text{eff}} = 34.6$ GeV
13.3 ± 0.3 ± 0.6		FERNANDEZ	85 MAC	$E_{\text{cm}}^{\text{eff}} = 29$ GeV
24 ± 6	35	BRA NDELIK	80 TASS	$E_{\text{cm}}^{\text{eff}} = 30$ GeV
32 ± 5	692	<sup>3</sup> BACINO	78B DLCO	$E_{\text{cm}}^{\text{eff}} = 3.1\text{--}7.4$ GeV
35 ± 11		<sup>3</sup> BRA NDELIK	78 DASP	Assumes $V\text{--}A$ decay
18 ± 6.5	33	<sup>3</sup> JAROS	78 LGW	$E_{\text{cm}}^{\text{eff}} > 6$ GeV

<sup>1</sup> BURCHAT 87 value is not independent of SCHMIDKE 86 value.  
<sup>2</sup> Not independent of BERGER 85  $\Gamma(\mu^- \bar{\nu}_\mu \nu_\tau)/\Gamma_{\text{total}}$ ,  $\Gamma(e^- \bar{\nu}_e \nu_\tau)/\Gamma_{\text{total}}$ ,  $\Gamma(h^- \geq 1 \text{ neutrals } \nu_\tau)/\Gamma_{\text{total}}$ , and  $\Gamma(h^- \geq 0 K^0 \nu_\tau)/\Gamma_{\text{total}}$ , and therefore not used in the fit.  
<sup>3</sup> Low energy experiments are not in average or fit because the systematic errors in background subtraction are judged to be large.

$\Gamma(h^- h^- h^+ \geq 0 \text{ neutrals } \nu_\tau \text{ (ex. } K_S^0 \rightarrow \pi^+ \pi^- \text{ ("3-prong"))})/\Gamma_{\text{total}}$   $\Gamma_{55}/\Gamma$   
 $\Gamma_{55}/\Gamma = (\Gamma_{62} + \Gamma_{70} + \Gamma_{77} + \Gamma_{78} + \Gamma_{85} + \Gamma_{89} + \Gamma_{93} + \Gamma_{94} + 0.285\Gamma_{125} + 0.285\Gamma_{127} + 0.9101\Gamma_{149} + 0.9101\Gamma_{151})/\Gamma$

Data marked "avg" are highly correlated with data appearing elsewhere in the Listings, and are therefore used for the average given below but not in the overall fits. "f&a" marks results used for the fit and the average.

VALUE (%)	EVTS	DOCUMENT ID	TECN	COMMENT
<b>14.57 ± 0.07 OUR FIT</b>				Error includes scale factor of 1.3.
<b>14.61 ± 0.06 OUR AVERAGE</b>				
14.652 ± 0.067 ± 0.086		<sup>1</sup> ACHARD	01D L3	1992–1995 LEP runs
14.96 ± 0.09 ± 0.22	10.4k	AKERS	95Y OPAL	1991–1994 LEP runs
• • •				We use the following data for averages but not for fits. • • •
14.652 ± 0.067 ± 0.086		SCHAEEL	05C ALEP	1991–1995 LEP runs
14.569 ± 0.093 ± 0.048	23k	<sup>2</sup> ABREU	01M DLPH	1992–1995 LEP runs
14.22 ± 0.10 ± 0.37		<sup>3</sup> BALEST	95C CLEO	$E_{\text{cm}}^{\text{eff}} \approx 10.6$ GeV
• • •				We do not use the following data for averages, fits, limits, etc. • • •
15.26 ± 0.26 ± 0.22		ACTON	92H OPAL	Repl. by AKERS 95Y
13.3 ± 0.3 ± 0.8		<sup>4</sup> ALBRECHT	92D ARG	$E_{\text{cm}}^{\text{eff}} = 9.4\text{--}10.6$ GeV
14.35 +0.40 -0.45 ± 0.24		DECAMP	92C ALEP	1989–1990 LEP runs

<sup>1</sup> The correlation coefficients between this measurement and the ACHARD 01D measurements of  $B(\tau^- \rightarrow \text{"1-prong"})$  and  $B(\tau^- \rightarrow \text{"5-prong"})$  are  $-0.978$  and  $-0.19$  respectively.  
<sup>2</sup> The correlation coefficients between this measurement and the ABREU 01M measurements of  $B(\tau^- \rightarrow \text{1-prong})$  and  $B(\tau^- \rightarrow \text{5-prong})$  are  $-0.98$  and  $-0.08$  respectively.  
<sup>3</sup> Not independent of BALEST 95C  $B(h^- h^- h^+ \pi^0 \nu_\tau)$  and  $B(h^- h^- h^+ \pi^0 \nu_\tau)$  values, and BORTOLETTO 93  $B(h^- h^- h^+ 2\pi^0 \nu_\tau)/B(h^- h^- h^+ \geq 0 \text{ neutrals } \nu_\tau)$  value.  
<sup>4</sup> This ALBRECHT 92D value is not independent of their  $\Gamma(\mu^- \bar{\nu}_\mu \nu_\tau)\Gamma(e^- \bar{\nu}_e \nu_\tau)/\Gamma_{\text{total}}^2$  value.

$\Gamma(h^- h^- h^+ \nu_\tau)/\Gamma_{\text{total}}$   $\Gamma_{56}/\Gamma$   
 $\Gamma_{56}/\Gamma = (0.3431\Gamma_{35} + 0.3431\Gamma_{37} + \Gamma_{62} + \Gamma_{85} + \Gamma_{93} + 0.017\Gamma_{149})/\Gamma$

Data marked "avg" are highly correlated with data appearing elsewhere in the Listings, and are therefore used for the average given below but not in the overall fits. "f&a" marks results used for the fit and the average.

VALUE (%)	EVTS	DOCUMENT ID	TECN	COMMENT
<b>9.80 ± 0.07 OUR FIT</b>				Error includes scale factor of 1.2.
• • •				We use the following data for averages but not for fits. • • •
<b>7.6 ± 0.1 ± 0.5</b>	7.5k	<sup>1</sup> ALBRECHT	96E ARG	$E_{\text{cm}}^{\text{eff}} = 9.4\text{--}10.6$ GeV
• • •				We do not use the following data for averages, fits, limits, etc. • • •
9.92 ± 0.10 ± 0.09	11.2k	<sup>2</sup> BUSKULIC	96 ALEP	Repl. by SCHAEEL 05C
9.49 ± 0.36 ± 0.63		DECAMP	92C ALEP	Repl. by SCHAEEL 05C
8.7 ± 0.7 ± 0.3	694	<sup>3</sup> BEHREND	90 CELL	$E_{\text{cm}}^{\text{eff}} = 35$ GeV
7.0 ± 0.3 ± 0.7	1566	<sup>4</sup> BAND	87 MAC	$E_{\text{cm}}^{\text{eff}} = 29$ GeV
6.7 ± 0.8 ± 0.9		<sup>5</sup> BURCHAT	87 MRK2	$E_{\text{cm}}^{\text{eff}} = 29$ GeV
6.4 ± 0.4 ± 0.9		<sup>6</sup> RUCKSTUHL	86 DLCO	$E_{\text{cm}}^{\text{eff}} = 29$ GeV
7.8 ± 0.5 ± 0.8	890	SCHMIDKE	86 MRK2	$E_{\text{cm}}^{\text{eff}} = 29$ GeV
8.4 ± 0.4 ± 0.7	1255	<sup>6</sup> FERNANDEZ	85 MAC	$E_{\text{cm}}^{\text{eff}} = 29$ GeV
9.7 ± 2.0 ± 1.3		BEHREND	84 CELL	$E_{\text{cm}}^{\text{eff}} = 14.22$ GeV

<sup>1</sup> ALBRECHT 96E not independent of ALBRECHT 93C  $\Gamma(h^- h^- h^+ \nu_\tau \text{ (ex. } K^0) \times \Gamma(\text{particle}^- \geq 0 \text{ neutrals } \geq 0 K^0 \nu_\tau)/\Gamma_{\text{total}}^2$  value.  
<sup>2</sup> BUSKULIC 96 quote  $B(h^- h^- h^+ \nu_\tau \text{ (ex. } K^0)) = 9.50 \pm 0.10 \pm 0.11$ . We add 0.42 to remove their  $K^0$  correction and reduce the systematic error accordingly.  
<sup>3</sup> BEHREND 90 subtract 0.3% to account for the  $\tau^- \rightarrow K^*(892)^- \nu_\tau$  contribution to measured events.  
<sup>4</sup> BAND 87 subtract for charged kaon modes; not independent of FERNANDEZ 85 value.  
<sup>5</sup> BURCHAT 87 value is not independent of SCHMIDKE 86 value.  
<sup>6</sup> Value obtained by multiplying paper's  $R = B(h^- h^- h^+ \nu_\tau)/B(3\text{-prong})$  by  $B(3\text{-prong}) = 0.143$  and subtracting 0.3% for  $K^*(892)$  background.

$\Gamma(h^- h^- h^+ \nu_\tau \text{ (ex. } K^0))/\Gamma_{\text{total}}$   $\Gamma_{57}/\Gamma$   
 $\Gamma_{57}/\Gamma = (\Gamma_{62} + \Gamma_{85} + \Gamma_{93} + 0.017\Gamma_{149})/\Gamma$

Data marked "avg" are highly correlated with data appearing elsewhere in the Listings, and are therefore used for the average given below but not in the overall fits. "f&a" marks results used for the fit and the average.

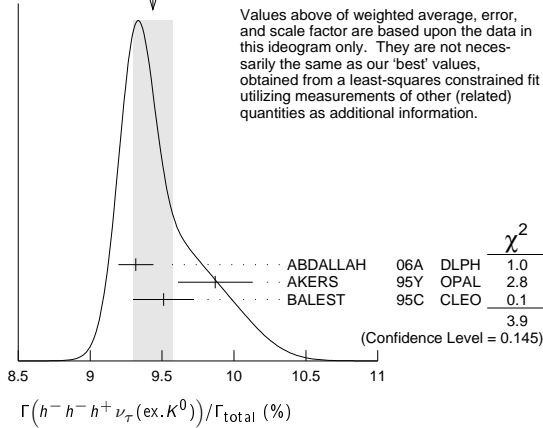
VALUE (%)	EVTS	DOCUMENT ID	TECN	COMMENT
<b>9.46 ± 0.06 OUR FIT</b>				Error includes scale factor of 1.2.
<b>9.44 ± 0.14 OUR AVERAGE</b>				Error includes scale factor of 1.4. See the ideogram below.
9.317 ± 0.090 ± 0.082	12.2k	<sup>1</sup> ABDALLAH	06A DLPH	1992–1995 LEP runs
9.51 ± 0.07 ± 0.20	37.7k	BALEST	95C CLEO	$E_{\text{cm}}^{\text{eff}} \approx 10.6$ GeV
• • •				We use the following data for averages but not for fits. • • •
9.87 ± 0.10 ± 0.24		<sup>2</sup> AKERS	95Y OPAL	1991–1994 LEP runs
• • •				We do not use the following data for averages, fits, limits, etc. • • •
9.50 ± 0.10 ± 0.11	11.2k	<sup>3</sup> BUSKULIC	96 ALEP	Repl. by SCHAEEL 05C

## Lepton Particle Listings

T

- <sup>1</sup> See footnote to ABDALLAH 06A  $\Gamma(\tau^- \rightarrow h^- \nu_\tau)/\Gamma_{\text{total}}$  measurement for correlations with other measurements.  
<sup>2</sup> Not independent of AKERS 95Y  $B(h^- h^- h^+ \geq 0 \text{ neutrals } \nu_\tau \text{ (ex. } K_S^0 \rightarrow \pi^+ \pi^-))$  and  $B(h^- h^- h^+ \nu_\tau \text{ (ex. } K^0))/B(h^- h^- h^+ \geq 0 \text{ neutrals } \nu_\tau \text{ (ex. } K_S^0 \rightarrow \pi^+ \pi^-))$  values.  
<sup>3</sup> Not independent of BUSKULIC 96  $B(h^- h^- h^+ \nu_\tau)$  value.

WEIGHTED AVERAGE  
 $9.44 \pm 0.14$  (Error scaled by 1.4)



Values above of weighted average, error, and scale factor are based upon the data in this ideogram only. They are not necessarily the same as our 'best' values, obtained from a least-squares constrained fit utilizing measurements of other (related) quantities as additional information.

$$\Gamma(h^- h^- h^+ \nu_\tau \text{ (ex. } K^0))/\Gamma(h^- h^- h^+ \geq 0 \text{ neutrals } \nu_\tau \text{ (ex. } K_S^0 \rightarrow \pi^+ \pi^-)) \quad \Gamma_{57}/\Gamma_{55}$$

$$\Gamma_{57}/\Gamma_{55} = (\Gamma_{62} + \Gamma_{85} + \Gamma_{93} + 0.017\Gamma_{149}) / (\Gamma_{62} + \Gamma_{70} + \Gamma_{77} + \Gamma_{78} + \Gamma_{85} + \Gamma_{89} + \Gamma_{93} + \Gamma_{94} + 0.285\Gamma_{125} + 0.285\Gamma_{127} + 0.9101\Gamma_{149} + 0.9101\Gamma_{151})$$

VALUE	DOCUMENT ID	TECN	COMMENT
<b>0.6492 ± 0.0034 OUR FIT</b>			Error includes scale factor of 1.1.
<b>0.660 ± 0.004 ± 0.014</b>	AKERS	95Y	OPAL 1991-1994 LEP runs

$$\Gamma(h^- h^- h^+ \nu_\tau \text{ (ex. } K^0, \omega))/\Gamma_{\text{total}} \quad \Gamma_{58}/\Gamma = (\Gamma_{62} + \Gamma_{85} + \Gamma_{93})/\Gamma$$

VALUE (%)	DOCUMENT ID	TECN	COMMENT
<b>9.42 ± 0.06 OUR FIT</b>			Error includes scale factor of 1.2.

$$\Gamma(\pi^- \pi^+ \pi^- \nu_\tau)/\Gamma_{\text{total}} \quad \Gamma_{59}/\Gamma = (0.3431\Gamma_{35} + \Gamma_{62} + 0.017\Gamma_{149})/\Gamma$$

VALUE (%)	DOCUMENT ID	TECN	COMMENT
<b>9.31 ± 0.06 OUR FIT</b>			Error includes scale factor of 1.2.

$$\Gamma(\pi^- \pi^+ \pi^- \nu_\tau \text{ (ex. } K^0))/\Gamma_{\text{total}} \quad \Gamma_{60}/\Gamma = (\Gamma_{62} + 0.017\Gamma_{149})/\Gamma$$

VALUE (%)	EVTS	DOCUMENT ID	TECN	COMMENT
<b>9.02 ± 0.06 OUR FIT</b>				Error includes scale factor of 1.1.
<b>8.77 ± 0.13 OUR AVERAGE</b>				Error includes scale factor of 1.1.
$8.42 \pm 0.00 \pm 0.26$	8.9M	<sup>1</sup> LEE	10	BELL 666 fb <sup>-1</sup> $E_{\text{cm}}^{\text{ee}} = 10.6$ GeV
$8.83 \pm 0.01 \pm 0.13$	1.6M	<sup>2</sup> AUBERT	08	BABR 342 fb <sup>-1</sup> $E_{\text{cm}}^{\text{ee}} = 10.6$ GeV
$9.13 \pm 0.05 \pm 0.46$	43k	<sup>3</sup> BRIERE	03	CLE3 $E_{\text{cm}}^{\text{ee}} = 10.6$ GeV

<sup>1</sup> Quoted statistical error is 0.003%. Correlation matrix for LEE 10 branching fractions:

- $\Gamma(\tau^- \rightarrow \pi^- \pi^+ \pi^- \nu_\tau \text{ (ex. } K^0))/\Gamma_{\text{total}}$
- $\Gamma(\tau^- \rightarrow K^- \pi^+ \pi^- \nu_\tau \text{ (ex. } K^0))/\Gamma_{\text{total}}$
- $\Gamma(\tau^- \rightarrow K^- K^+ \pi^- \nu_\tau)/\Gamma_{\text{total}}$
- $\Gamma(\tau^- \rightarrow K^- K^+ K^- \nu_\tau)/\Gamma_{\text{total}}$

(1)	(2)	(3)	
(2)	0.175		
(3)	0.049	0.080	
(4)	-0.053	0.035	-0.008

<sup>2</sup> Correlation matrix for AUBERT 08 branching fractions:

- $\Gamma(\tau^- \rightarrow \pi^- \pi^+ \pi^- \nu_\tau \text{ (ex. } K^0))/\Gamma_{\text{total}}$
- $\Gamma(\tau^- \rightarrow K^- \pi^+ \pi^- \nu_\tau \text{ (ex. } K^0))/\Gamma_{\text{total}}$
- $\Gamma(\tau^- \rightarrow K^- K^+ \pi^- \nu_\tau)/\Gamma_{\text{total}}$
- $\Gamma(\tau^- \rightarrow K^- K^+ K^- \nu_\tau)/\Gamma_{\text{total}}$

(1)	(2)	(3)	
(2)	0.544		
(3)	0.390	0.177	
(4)	0.031	0.093	0.087

<sup>3</sup> 47% correlated with BRIERE 03  $\tau^- \rightarrow K^- \pi^+ \pi^- \nu_\tau$  and 71% correlated with  $\tau^- \rightarrow K^- K^+ \pi^- \nu_\tau$  because of a common 5% normalization error.

$$\Gamma(\pi^- \pi^+ \pi^- \nu_\tau \text{ (ex. } K^0, \text{ non-axial vector}))/\Gamma(\pi^- \pi^+ \pi^- \nu_\tau \text{ (ex. } K^0)) \quad \Gamma_{61}/\Gamma_{60} = \Gamma_{61}/(\Gamma_{62} + 0.017\Gamma_{149})$$

VALUE	CL%	DOCUMENT ID	TECN	COMMENT
<b>&lt;0.261</b>	95	<sup>1</sup> ACKERSTAFF	97R	OPAL 1992-1994 LEP runs

<sup>1</sup> Model-independent limit from structure function analysis on contribution to  $B(\tau^- \rightarrow \pi^- \pi^+ \pi^- \nu_\tau \text{ (ex. } K^0))$  from non-axial vectors.

$$\Gamma(\pi^- \pi^+ \pi^- \nu_\tau \text{ (ex. } K^0, \omega))/\Gamma_{\text{total}} \quad \Gamma_{62}/\Gamma$$

VALUE (%)	EVTS	DOCUMENT ID	TECN	COMMENT
<b>9.99 ± 0.06 OUR FIT</b>				Error includes scale factor of 1.1.
<b>9.041 ± 0.060 ± 0.076</b>	29k	<sup>1</sup> SCHAEEL	05c	ALEP 1991-1995 LEP runs

<sup>1</sup> See footnote to SCHAEEL 05c  $\Gamma(\tau^- \rightarrow e^- \bar{\nu}_e \nu_\tau)/\Gamma_{\text{total}}$  measurement for correlations with other measurements.

$$\Gamma(h^- h^- h^+ \geq 1 \text{ neutrals } \nu_\tau)/\Gamma_{\text{total}} \quad \Gamma_{63}/\Gamma$$

$$\Gamma_{63}/\Gamma = (0.3431\Gamma_{40} + 0.3431\Gamma_{42} + 0.4307\Gamma_{47} + 0.6861\Gamma_{48} + \Gamma_{70} + \Gamma_{77} + \Gamma_{78} + \Gamma_{89} + \Gamma_{94} + 0.285\Gamma_{125} + 0.285\Gamma_{127} + 0.888\Gamma_{149} + 0.9101\Gamma_{151})/\Gamma$$

VALUE (%)	EVTS	DOCUMENT ID	TECN	COMMENT
<b>5.39 ± 0.07 OUR FIT</b>				Error includes scale factor of 1.2.
• • •				We do not use the following data for averages, fits, limits, etc. • • •
$5.6 \pm 0.7 \pm 0.3$	352	<sup>1</sup> BEHREND	90	CELL $E_{\text{cm}}^{\text{ee}} = 35$ GeV
$4.2 \pm 0.5 \pm 0.9$	203	<sup>2</sup> ALBRECHT	87L	ARG $E_{\text{cm}}^{\text{ee}} = 10$ GeV
$6.1 \pm 0.8 \pm 0.9$		<sup>3</sup> BURCHAT	87	MRK2 $E_{\text{cm}}^{\text{ee}} = 29$ GeV
$7.6 \pm 0.4 \pm 0.9$		<sup>4,5</sup> RUCKSTUHL	86	DLCO $E_{\text{cm}}^{\text{ee}} = 29$ GeV
$4.7 \pm 0.5 \pm 0.8$	530	<sup>6</sup> SCHMIDKE	86	MRK2 $E_{\text{cm}}^{\text{ee}} = 29$ GeV
$5.6 \pm 0.4 \pm 0.7$		<sup>5</sup> FERNANDEZ	85	MAC $E_{\text{cm}}^{\text{ee}} = 29$ GeV
$6.2 \pm 2.3 \pm 1.7$		BEHREND	84	CELL $E_{\text{cm}}^{\text{ee}} = 14.22$ GeV

<sup>1</sup> BEHREND 90 value is not independent of BEHREND 90  $B(3h^- \nu_\tau \geq 1 \text{ neutrals}) + B(5\text{-prong})$ .

<sup>2</sup> ALBRECHT 87L measure the product of branching ratios  $B(3\pi^+ \pi^0 \nu_\tau) B((e \bar{\nu}_e \text{ or } \mu \bar{\nu}_\mu \text{ or } \pi^0 \text{ or } K^0 \text{ or } \rho) \nu_\tau) = 0.029$  and use the PDG 86 values for the second branching ratio which sum to 0.69 ± 0.03 to get the quoted value.

<sup>3</sup> BURCHAT 87 value is not independent of SCHMIDKE 86 value.

<sup>4</sup> Contributions from kaons and from  $>1\pi^0$  are subtracted. Not independent of (3-prong +  $0\pi^0$ ) and (3-prong +  $\geq 0\pi^0$ ) values.

<sup>5</sup> Value obtained using paper's  $R = B(h^- h^- h^+ \nu_\tau)/B(3\text{-prong})$  and current  $B(3\text{-prong}) = 0.143$ .

<sup>6</sup> Not independent of SCHMIDKE 86  $h^- h^- h^+ \nu_\tau$  and  $h^- h^- h^+ (\geq 0\pi^0) \nu_\tau$  values.

$$\Gamma(h^- h^- h^+ \geq 1\pi^0 \nu_\tau \text{ (ex. } K^0))/\Gamma_{\text{total}} \quad \Gamma_{64}/\Gamma$$

$$\Gamma_{64}/\Gamma = (\Gamma_{70} + \Gamma_{77} + \Gamma_{78} + \Gamma_{89} + \Gamma_{94} + 0.226\Gamma_{125} + 0.226\Gamma_{127} + 0.888\Gamma_{149} + 0.9101\Gamma_{151})/\Gamma$$

Data marked "avg" are highly correlated with data appearing elsewhere in the Listings, and are therefore used for the average given below but not in the overall fits. "f&a" marks results used for the fit and the average.

VALUE (%)	EVTS	DOCUMENT ID	TECN	COMMENT
<b>5.09 ± 0.06 OUR FIT</b>				Error includes scale factor of 1.2.
<b>5.10 ± 0.12 OUR AVERAGE</b>				

• • • We use the following data for averages but not for fits. • • •

$5.106 \pm 0.083 \pm 0.103$	10.1k	<sup>1</sup> ABDALLAH	06A	DLPH 1992-1995 LEP runs
$5.09 \pm 0.10 \pm 0.23$		<sup>2</sup> AKERS	95Y	OPAL 1991-1994 LEP runs

• • • We do not use the following data for averages, fits, limits, etc. • • •

$4.95 \pm 0.29 \pm 0.65$	570	DECAMP	92c	ALEP Repl. by SCHAEEL 05c
--------------------------	-----	--------	-----	---------------------------

<sup>1</sup> See footnote to ABDALLAH 06A  $\Gamma(\tau^- \rightarrow h^- \nu_\tau)/\Gamma_{\text{total}}$  measurement for correlations with other measurements.

<sup>2</sup> Not independent of AKERS 95Y  $B(h^- h^- h^+ \geq 0 \text{ neutrals } \nu_\tau \text{ (ex. } K_S^0 \rightarrow \pi^+ \pi^-))$  and  $B(h^- h^- h^+ \geq 0 \text{ neutrals } \nu_\tau \text{ (ex. } K^0))/B(h^- h^- h^+ \geq 0 \text{ neutrals } \nu_\tau \text{ (ex. } K_S^0 \rightarrow \pi^+ \pi^-))$  values.

$$\Gamma(h^- h^- h^+ \pi^0 \nu_\tau)/\Gamma_{\text{total}} \quad \Gamma_{65}/\Gamma$$

$$\Gamma_{65}/\Gamma = (0.3431\Gamma_{40} + 0.3431\Gamma_{42} + \Gamma_{70} + \Gamma_{89} + \Gamma_{94} + 0.226\Gamma_{127} + 0.888\Gamma_{149} + 0.017\Gamma_{151})/\Gamma$$

VALUE (%)	EVTS	DOCUMENT ID	TECN	COMMENT
<b>4.76 ± 0.06 OUR FIT</b>				Error includes scale factor of 1.2.

• • • We do not use the following data for averages, fits, limits, etc. • • •

$4.45 \pm 0.09 \pm 0.07$	6.1k	<sup>1</sup> BUSKULIC	96	ALEP Repl. by SCHAEEL 05c
--------------------------	------	-----------------------	----	---------------------------

<sup>1</sup> BUSKULIC 96 quote  $B(h^- h^- h^+ \pi^0 \nu_\tau \text{ (ex. } K^0)) = 4.30 \pm 0.09 \pm 0.09$ . We add 0.15 to remove their  $K^0$  correction and reduce the systematic error accordingly.

$$\Gamma(h^- h^- h^+ \pi^0 \nu_\tau \text{ (ex. } K^0, \omega))/\Gamma_{\text{total}} \quad \Gamma_{66}/\Gamma$$

$$\Gamma_{66}/\Gamma = (\Gamma_{70} + \Gamma_{89} + \Gamma_{94} + 0.226\Gamma_{127} + 0.888\Gamma_{149} + 0.017\Gamma_{151})/\Gamma$$

VALUE (%)	EVTS	DOCUMENT ID	TECN	COMMENT
<b>4.57 ± 0.06 OUR FIT</b>				Error includes scale factor of 1.2.
<b>4.45 ± 0.14 OUR AVERAGE</b>				Error includes scale factor of 1.2.
$4.545 \pm 0.106 \pm 0.103$	8.9k	<sup>1</sup> ABDALLAH	06A	DLPH 1992-1995 LEP runs
$4.23 \pm 0.06 \pm 0.22$	7.2k	BALEST	95c	CLEO $E_{\text{cm}}^{\text{ee}} \approx 10.6$ GeV

<sup>1</sup> See footnote to ABDALLAH 06A  $\Gamma(\tau^- \rightarrow h^- \nu_\tau)/\Gamma_{\text{total}}$  measurement for correlations with other measurements.

$$\Gamma(h^- h^- h^+ \pi^0 \nu_\tau \text{ (ex. } K^0, \omega))/\Gamma_{\text{total}} \quad \Gamma_{67}/\Gamma = (\Gamma_{70} + \Gamma_{89} + \Gamma_{94} + 0.226\Gamma_{127})/\Gamma$$

VALUE (%)	DOCUMENT ID	TECN	COMMENT
<b>2.79 ± 0.08 OUR FIT</b>			Error includes scale factor of 1.2.

$$\Gamma(\pi^- \pi^+ \pi^- \pi^0 \nu_\tau)/\Gamma_{\text{total}} \quad \Gamma_{68}/\Gamma = (0.3431\Gamma_{40} + \Gamma_{70} + 0.888\Gamma_{149} + 0.017\Gamma_{151})/\Gamma$$

VALUE (%)	DOCUMENT ID	TECN	COMMENT
<b>4.62 ± 0.06 OUR FIT</b>			Error includes scale factor of 1.2.

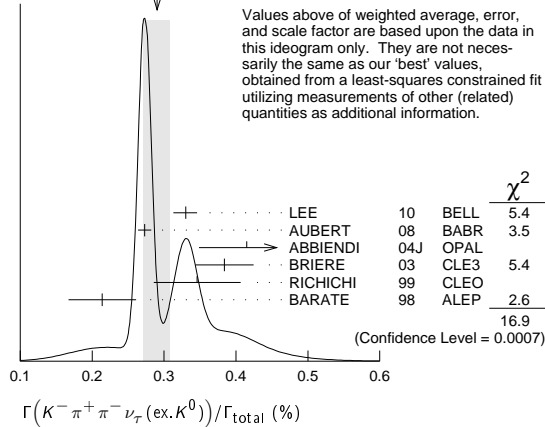


## Lepton Particle Listings

 $\tau$ 

$K^- K^+ \pi^- \nu_\tau / \Gamma(\tau^- \rightarrow \pi^- \pi^+ \pi^- \nu_\tau (\text{ex. } K^0))$  and BALEST 95c  $\Gamma(\tau^- \rightarrow h^- h^- h^+ \nu_\tau (\text{ex. } K^0)) / \Gamma_{\text{total}}$  values.

WEIGHTED AVERAGE  
0.290±0.018 (Error scaled by 2.4)



$\Gamma(K^- \pi^+ \pi^- \nu_\tau (\text{ex. } K^0)) / \Gamma(\pi^- \pi^+ \pi^- \nu_\tau (\text{ex. } K^0))$   
 $\Gamma_{85} / \Gamma_{60} = \Gamma_{85} / (\Gamma_{62} + 0.017 \Gamma_{149})$

VALUE (units  $10^{-2}$ ) EVTS DOCUMENT ID TECN COMMENT  
**3.26±0.17 OUR FIT** Error includes scale factor of 2.3.

• • • We use the following data for averages but not for fits. • • •

**3.92±0.02±0.15** 794k <sup>1</sup>LEE 10 BELL 666 fb<sup>-1</sup>  $E_{\text{cm}}^{\text{ex}} = 10.6$  GeV

<sup>1</sup> Not independent of LEE 10  $\Gamma(\tau^- \rightarrow K^- \pi^+ \pi^- \nu_\tau (\text{ex. } K^0)) / \Gamma_{\text{total}}$  and  $\Gamma(\tau^- \rightarrow \pi^- \pi^+ \pi^- \nu_\tau (\text{ex. } K^0)) / \Gamma_{\text{total}}$  values.

$\Gamma(K^- \rho^0 \nu_\tau \rightarrow K^- \pi^+ \pi^- \nu_\tau) / \Gamma(K^- \pi^+ \pi^- \nu_\tau (\text{ex. } K^0))$   $\Gamma_{86} / \Gamma_{85}$

VALUE DOCUMENT ID TECN COMMENT  
**0.48±0.14±0.10** <sup>1</sup>ASNER 00b CLEO  $E_{\text{cm}}^{\text{ex}} = 10.6$  GeV

• • • We do not use the following data for averages, fits, limits, etc. • • •

0.39±0.14 <sup>2</sup>BARATE 99R ALEP 1991-1995 LEP runs

<sup>1</sup> ASNER 00b assume  $\tau^- \rightarrow K^- \pi^+ \pi^- \nu_\tau (\text{ex. } K^0)$  decays proceed only through  $K\rho$  and  $K^* \pi$  intermediate states. They assume the resonance structure of  $\tau^- \rightarrow K^- \pi^+ \pi^- \nu_\tau (\text{ex. } K^0)$  decays is dominated by  $K_1(1270)^-$  and  $K_1(1400)^-$  resonances, and assume  $B(K_1(1270) \rightarrow K^*(892) \pi) = (16 \pm 5)\%$ ,  $B(K_1(1270) \rightarrow K\rho) = (42 \pm 6)\%$ , and  $B(K_1(1400) \rightarrow K\rho) = 0$ .

<sup>2</sup> BARATE 99R assume  $\tau^- \rightarrow K^- \pi^+ \pi^- \nu_\tau (\text{ex. } K^0)$  decays proceed only through  $K\rho$  and  $K^* \pi$  intermediate states. The quoted error is statistical only.

$\Gamma(K^- \pi^+ \pi^- \pi^0 \nu_\tau) / \Gamma_{\text{total}}$   $\Gamma_{87} / \Gamma = (0.3431 \Gamma_{42} + \Gamma_{89} + 0.226 \Gamma_{127}) / \Gamma$

VALUE (units  $10^{-4}$ ) DOCUMENT ID  
**13.5±1.4 OUR FIT**

$\Gamma(K^- \pi^+ \pi^- \pi^0 \nu_\tau (\text{ex. } K^0)) / \Gamma_{\text{total}}$   $\Gamma_{88} / \Gamma = (\Gamma_{89} + 0.226 \Gamma_{127}) / \Gamma$

Data marked "avg" are highly correlated with data appearing elsewhere in the Listings, and are therefore used for the average given below but not in the overall fits. "f&a" marks results used for the fit and the average.

VALUE (units  $10^{-4}$ ) CL% DOCUMENT ID TECN COMMENT  
**8.1±1.2 OUR FIT**  
**7.3±1.2 OUR AVERAGE**

7.4±0.8±1.1 <sup>1</sup>ARMS 05 CLE3 7.6 fb<sup>-1</sup>,  $E_{\text{cm}}^{\text{ex}} = 10.6$  GeV

6.1±3.9±1.8 BARATE 98 ALEP 1991-1995 LEP runs

• • • We use the following data for averages but not for fits. • • •

7.5±2.6±1.8 <sup>2</sup>RICHICHI 99 CLEO  $E_{\text{cm}}^{\text{ex}} = 10.6$  GeV

• • • We do not use the following data for averages, fits, limits, etc. • • •

<17 95 ABBIENDI 00D OPAL 1990-1995 LEP runs

<sup>1</sup> Not independent of ARMS 05  $\Gamma(\tau^- \rightarrow K^- \pi^+ \pi^- \pi^0 \nu_\tau (\text{ex. } K^0, \omega)) / \Gamma_{\text{total}}$  and  $\Gamma(\tau^- \rightarrow K^- \omega \nu_\tau) / \Gamma_{\text{total}}$  values.

<sup>2</sup> Not independent of RICHICHI 99

$\Gamma(\tau^- \rightarrow K^- h^+ \pi^- \nu_\tau (\text{ex. } K^0)) / \Gamma(\tau^- \rightarrow \pi^- \pi^+ \pi^- \nu_\tau (\text{ex. } K^0))$ ,  $\Gamma(\tau^- \rightarrow K^- K^+ \pi^- \nu_\tau) / \Gamma(\tau^- \rightarrow \pi^- \pi^+ \pi^- \nu_\tau (\text{ex. } K^0))$  and BALEST 95c  $\Gamma(\tau^- \rightarrow h^- h^- h^+ \nu_\tau (\text{ex. } K^0)) / \Gamma_{\text{total}}$  values.

$\Gamma(K^- \pi^+ \pi^- \pi^0 \nu_\tau (\text{ex. } K^0, \eta)) / \Gamma_{\text{total}}$   $\Gamma_{89} / \Gamma$

VALUE (units  $10^{-4}$ ) DOCUMENT ID  
**7.8±1.2 OUR FIT**

$\Gamma(K^- \pi^+ \pi^- \pi^0 \nu_\tau (\text{ex. } K^0, \omega)) / \Gamma_{\text{total}}$   $\Gamma_{90} / \Gamma$

VALUE (units  $10^{-4}$ ) EVTS DOCUMENT ID TECN COMMENT  
**3.7±0.5±0.8** 833 ARMS 05 CLE3 7.6 fb<sup>-1</sup>,  $E_{\text{cm}}^{\text{ex}} = 10.6$  GeV

$\Gamma(K^- \pi^+ K^- \geq 0 \text{ neut. } \nu_\tau) / \Gamma_{\text{total}}$   $\Gamma_{91} / \Gamma$

VALUE (%) CL% DOCUMENT ID TECN COMMENT  
**<0.09** 95 BAUER 94 TPC  $E_{\text{cm}}^{\text{ex}} = 29$  GeV

$\Gamma(K^- K^+ \pi^- \geq 0 \text{ neut. } \nu_\tau) / \Gamma_{\text{total}}$   $\Gamma_{92} / \Gamma = (\Gamma_{93} + \Gamma_{94}) / \Gamma$

Data marked "avg" are highly correlated with data appearing elsewhere in the Listings, and are therefore used for the average given below but not in the overall fits. "f&a" marks results used for the fit and the average.

VALUE (%) EVTS DOCUMENT ID TECN COMMENT  
**0.150±0.006 OUR FIT** Error includes scale factor of 1.8.  
**0.203±0.031 OUR AVERAGE**

0.159±0.053±0.020 ABBIENDI 00D OPAL 1990-1995 LEP runs

0.15 <sup>+0.09</sup>±0.03 <sup>-0.07</sup> 4 <sup>1</sup>BAUER 94 TPC  $E_{\text{cm}}^{\text{ex}} = 29$  GeV

• • • We use the following data for averages but not for fits. • • •

0.238±0.042 <sup>2</sup>BARATE 98 ALEP 1991-1995 LEP runs

<sup>1</sup> We multiply 0.15% by 0.20, the relative systematic error quoted by BAUER 94, to obtain the systematic error.

<sup>2</sup> Not independent of BARATE 98  $\Gamma(\tau^- \rightarrow K^- K^+ \pi^- \nu_\tau) / \Gamma_{\text{total}}$  and  $\Gamma(\tau^- \rightarrow K^- K^+ \pi^- \pi^0 \nu_\tau) / \Gamma_{\text{total}}$  values.

$\Gamma(K^- K^+ \pi^- \nu_\tau) / \Gamma_{\text{total}}$   $\Gamma_{93} / \Gamma$

Data marked "avg" are highly correlated with data appearing elsewhere in the Listings, and are therefore used for the average given below but not in the overall fits. "f&a" marks results used for the fit and the average.

VALUE (units  $10^{-3}$ ) EVTS DOCUMENT ID TECN COMMENT  
**1.44±0.05 OUR FIT** Error includes scale factor of 1.9.  
**1.43±0.07 OUR AVERAGE** Error includes scale factor of 2.4. See the ideogram below.

1.55±0.01±0.06 108k <sup>1</sup>LEE 10 BELL 666 fb<sup>-1</sup>  $E_{\text{cm}}^{\text{ex}} = 10.6$  GeV

1.346±0.010±0.036 18k <sup>2</sup>AUBERT 08 BABR 342 fb<sup>-1</sup>  $E_{\text{cm}}^{\text{ex}} = 10.6$  GeV

1.55±0.06±0.09 932 <sup>3</sup>BRIERE 03 CLE3  $E_{\text{cm}}^{\text{ex}} = 10.6$  GeV

1.63±0.21±0.17 BARATE 98 ALEP 1991-1995 LEP runs

• • • We use the following data for averages but not for fits. • • •

0.87±0.56±0.40 ABBIENDI 00D OPAL 1990-1995 LEP runs

1.45±0.13±0.28 2.3k <sup>4</sup>RICHICHI 99 CLEO  $E_{\text{cm}}^{\text{ex}} = 10.6$  GeV

• • • We do not use the following data for averages, fits, limits, etc. • • •

2.2 <sup>+1.7</sup>±0.5 <sup>-1.1</sup> 9 <sup>5</sup>MILLS 85 DLCO  $E_{\text{cm}}^{\text{ex}} = 29$  GeV

<sup>1</sup> See footnote to LEE 10  $\Gamma(\tau^- \rightarrow \pi^- \pi^+ \pi^- \nu_\tau (\text{ex. } K^0)) / \Gamma_{\text{total}}$  measurement for correlations with other measurements. Not independent of LEE 10  $\Gamma(\tau^- \rightarrow K^- K^+ \pi^- \nu_\tau) / \Gamma(\tau^- \rightarrow \pi^- \pi^+ \pi^- \nu_\tau (\text{ex. } K^0))$  value.

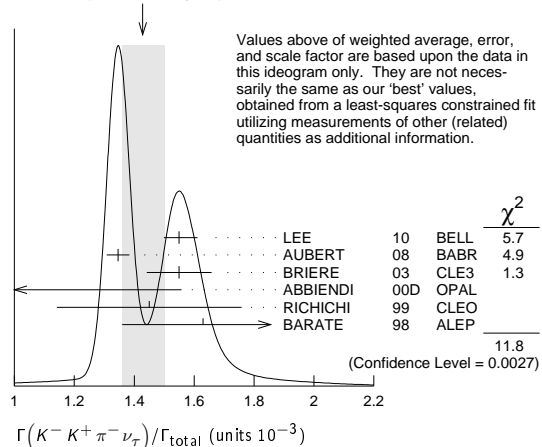
<sup>2</sup> See footnote to AUBERT 08  $\Gamma(\tau^- \rightarrow \pi^- \pi^+ \pi^- \nu_\tau (\text{ex. } K^0)) / \Gamma_{\text{total}}$  measurement for correlations with other measurements.

<sup>3</sup> 71% correlated with BRIERE 03  $\tau^- \rightarrow \pi^- \pi^+ \pi^- \nu_\tau$  and 34% correlated with  $\tau^- \rightarrow K^- \pi^+ \pi^- \nu_\tau$  because of a common 5% normalization error.

<sup>4</sup> Not independent of RICHICHI 99  $\Gamma(\tau^- \rightarrow K^- K^+ \pi^- \nu_\tau) / \Gamma(\tau^- \rightarrow \pi^- \pi^+ \pi^- \nu_\tau (\text{ex. } K^0))$  and BALEST 95c  $\Gamma(\tau^- \rightarrow h^- h^- h^+ \nu_\tau (\text{ex. } K^0)) / \Gamma_{\text{total}}$  values.

<sup>5</sup> Error correlated with MILLS 85  $(K \pi \pi \pi^0 \nu)$  value. We multiply 0.22% by 0.23, the relative systematic error quoted by MILLS 85, to obtain the systematic error.

WEIGHTED AVERAGE  
1.43±0.07 (Error scaled by 2.4)



$\Gamma(K^- K^+ \pi^- \nu_\tau) / \Gamma(\pi^- \pi^+ \pi^- \nu_\tau (\text{ex. } K^0))$   $\Gamma_{93} / \Gamma_{60} = \Gamma_{93} / (\Gamma_{62} + 0.017 \Gamma_{149})$

Data marked "avg" are highly correlated with data appearing elsewhere in the Listings, and are therefore used for the average given below but not in the overall fits. "f&a" marks results used for the fit and the average.

VALUE (%) EVTS DOCUMENT ID TECN COMMENT  
**1.60±0.06 OUR FIT** Error includes scale factor of 1.9.  
**1.83±0.05 OUR AVERAGE**

1.60±0.15±0.30 2.3k RICHICHI 99 CLEO  $E_{\text{cm}}^{\text{ex}} = 10.6$  GeV

• • • We use the following data for averages but not for fits. • • •

1.84±0.01±0.05 108k <sup>1</sup>LEE 10 BELL 666 fb<sup>-1</sup>  $E_{\text{cm}}^{\text{ex}} = 10.6$  GeV

<sup>1</sup> Not independent of LEE 10  $\Gamma(\tau^- \rightarrow K^- K^+ \pi^- \nu_\tau)/\Gamma_{total}$  and  $\Gamma(\tau^- \rightarrow \pi^- \pi^+ \pi^- \nu_\tau(\text{ex. } K^0))/\Gamma_{total}$  values.

$\Gamma(K^- K^+ \pi^- \pi^0 \nu_\tau)/\Gamma_{total}$   $\Gamma_{94}/\Gamma$

Data marked "avg" are highly correlated with data appearing elsewhere in the Listings, and are therefore used for the average given below but not in the overall fits. "f&a" marks results used for the fit and the average.

VALUE (units  $10^{-4}$ ) CL% EVTS DOCUMENT ID TECN COMMENT  
**0.61 ± 0.25 OUR FIT** Error includes scale factor of 1.4.

**0.60 ± 0.18 OUR AVERAGE**  
0.55 ± 0.14 ± 0.12 48 ARMS 05 CLE3 7.6 fb<sup>-1</sup>,  $E_{cm}^{ee} = 10.6$  GeV  
7.5 ± 2.9 ± 1.5 BARATE 98 ALEP 1991-1995 LEP runs

• • • We use the following data for averages but not for fits. • • •  
3.3 ± 1.8 ± 0.7 158 <sup>1</sup>RICHICHI 99 CLEO  $E_{cm}^{ee} = 10.6$  GeV

• • • We do not use the following data for averages, fits, limits, etc. • • •  
<27 95 ABBIENDI 00D OPAL 1990-1995 LEP runs

<sup>1</sup> Not independent of RICHICHI 99  
 $\Gamma(\tau^- \rightarrow K^- K^+ \pi^- \nu_\tau)/\Gamma(\tau^- \rightarrow \pi^- \pi^+ \pi^- \nu_\tau(\text{ex. } K^0))$  and BALEST 95c  $\Gamma(\tau^- \rightarrow h^- h^+ h^+ \nu_\tau(\text{ex. } K^0))/\Gamma_{total}$  values.

$\Gamma(K^- K^+ \pi^- \pi^0 \nu_\tau)/\Gamma(\pi^- \pi^+ \pi^- \pi^0 \nu_\tau(\text{ex. } K^0))$   $\Gamma_{94}/\Gamma_{69} = \Gamma_{94}/(\Gamma_{70} + 0.888\Gamma_{149} + 0.017\Gamma_{151})$

VALUE (%) EVTS DOCUMENT ID TECN COMMENT  
**0.14 ± 0.05 OUR FIT** Error includes scale factor of 1.4.  
**0.79 ± 0.44 ± 0.16** 158 <sup>1</sup>RICHICHI 99 CLEO  $E_{cm}^{ee} = 10.6$  GeV

<sup>1</sup> RICHICHI 99 also quote a 95%CL upper limit of 0.0157 for this measurement.

$\Gamma(K^- K^+ K^- \nu_\tau)/\Gamma_{total}$   $\Gamma_{95}/\Gamma$

VALUE (units  $10^{-5}$ ) CL% EVTS DOCUMENT ID TECN COMMENT  
**2.1 ± 0.8 OUR AVERAGE** Error includes scale factor of 5.4.

3.29 ± 0.17 ± 0.19 3.2k <sup>1</sup>LEE 10 BELL 666 fb<sup>-1</sup>  $E_{cm}^{ee} = 10.6$  GeV  
1.58 ± 0.13 ± 0.20 275 <sup>2</sup>AUBERT 08 BABR 342 fb<sup>-1</sup>  $E_{cm}^{ee} = 10.6$  GeV

• • • We do not use the following data for averages, fits, limits, etc. • • •  
< 3.7 90 BRIERE 03 CLE3  $E_{cm}^{ee} = 10.6$  GeV  
< 19 90 BARATE 98 ALEP 1991-1995 LEP runs

<sup>1</sup> See footnote to LEE 10  $\Gamma(\tau^- \rightarrow \pi^- \pi^+ \pi^- \nu_\tau(\text{ex. } K^0))/\Gamma_{total}$  measurement for correlations with other measurements. Not independent of LEE 10  $\Gamma(\tau^- \rightarrow K^- K^+ K^- \nu_\tau)/\Gamma(\tau^- \rightarrow \pi^- \pi^+ \pi^- \nu_\tau(\text{ex. } K^0))$  value.  
<sup>2</sup> See footnote to AUBERT 08  $\Gamma(\tau^- \rightarrow \pi^- \pi^+ \pi^- \nu_\tau(\text{ex. } K^0))/\Gamma_{total}$  measurement for correlations with other measurements.

$\Gamma(K^- K^+ K^- \nu_\tau)/\Gamma(\pi^- \pi^+ \pi^- \nu_\tau(\text{ex. } K^0))$   $\Gamma_{95}/\Gamma_{60}$

VALUE (units  $10^{-4}$ ) EVTS DOCUMENT ID TECN COMMENT  
• • • We do not use the following data for averages, fits, limits, etc. • • •

3.90 ± 0.02 ± 0.22 3.2k <sup>1</sup>LEE 10 BELL 666 fb<sup>-1</sup>  $E_{cm}^{ee} = 10.6$  GeV

<sup>1</sup> Not independent of LEE 10  $\Gamma(\tau^- \rightarrow K^- K^+ K^- \nu_\tau)/\Gamma_{total}$  and  $\Gamma(\tau^- \rightarrow \pi^- \pi^+ \pi^- \nu_\tau(\text{ex. } K^0))/\Gamma_{total}$  values.

$\Gamma(K^- K^+ K^- \nu_\tau(\text{ex. } \phi))/\Gamma_{total}$   $\Gamma_{96}/\Gamma$

VALUE CL% DOCUMENT ID TECN COMMENT  
**< 2.5 × 10<sup>-6</sup>** 90 AUBERT 08 BABR 342 fb<sup>-1</sup>  $E_{cm}^{ee} = 10.6$  GeV

$\Gamma(K^- K^+ K^- \pi^0 \nu_\tau)/\Gamma_{total}$   $\Gamma_{97}/\Gamma$

VALUE CL% DOCUMENT ID TECN COMMENT  
**< 4.8 × 10<sup>-6</sup>** 90 ARMS 05 CLE3 7.6 fb<sup>-1</sup>,  $E_{cm}^{ee} = 10.6$  GeV

$\Gamma(\pi^- K^+ \pi^- \geq 0 \text{ neut. } \nu_\tau)/\Gamma_{total}$   $\Gamma_{98}/\Gamma$

VALUE (%) CL% DOCUMENT ID TECN COMMENT  
**< 0.25** 95 BAUER 94 TPC  $E_{cm}^{ee} = 29$  GeV

$\Gamma(e^- e^- e^+ \bar{\nu}_e \nu_\tau)/\Gamma_{total}$   $\Gamma_{99}/\Gamma$

VALUE (units  $10^{-5}$ ) EVTS DOCUMENT ID TECN COMMENT  
**2.8 ± 1.4 ± 0.4** 5 ALAM 96 CLEO  $E_{cm}^{ee} = 10.6$  GeV

$\Gamma(\mu^- e^- e^+ \bar{\nu}_\mu \nu_\tau)/\Gamma_{total}$   $\Gamma_{100}/\Gamma$

VALUE (units  $10^{-5}$ ) CL% DOCUMENT ID TECN COMMENT  
**< 3.6** 90 ALAM 96 CLEO  $E_{cm}^{ee} = 10.6$  GeV

$\Gamma(3h^- 2h^+ \geq 0 \text{ neutrals } \nu_\tau(\text{ex. } K_S^0 \rightarrow \pi^- \pi^+)(\text{"5-prong"}))/\Gamma_{total}$   $\Gamma_{101}/\Gamma$

Data marked "avg" are highly correlated with data appearing elsewhere in the Listings, and are therefore used for the average given below but not in the overall fits. "f&a" marks results used for the fit and the average.  $\Gamma_{101}/\Gamma = (\Gamma_{102} + \Gamma_{103})/\Gamma$

VALUE (%) EVTS DOCUMENT ID TECN COMMENT  
**0.102 ± 0.004 OUR FIT** Error includes scale factor of 1.1.  
**0.107 ± 0.007 OUR AVERAGE** Error includes scale factor of 1.1.

0.170 ± 0.022 ± 0.026 <sup>1</sup>ACHARD 01D L3 1992-1995 LEP runs  
0.097 ± 0.005 ± 0.011 419 GIBAUT 94B CLEO  $E_{cm}^{ee} = 10.6$  GeV  
0.102 ± 0.029 13 BYLSMA 87 HRS  $E_{cm}^{ee} = 29$  GeV

• • • We use the following data for averages but not for fits. • • •

0.093 ± 0.009 ± 0.012 SCHAEEL 05c ALEP 1991-1995 LEP runs  
0.115 ± 0.013 ± 0.006 112 <sup>2</sup>ABREU 01M DLPH 1992-1995 LEP runs  
0.119 ± 0.013 ± 0.008 119 <sup>3</sup>ACKERSTAFF 99e OPAL 1991-1995 LEP runs

• • • We do not use the following data for averages, fits, limits, etc. • • •  
0.26 ± 0.06 ± 0.05 ACTON 92H OPAL  $E_{cm}^{ee} = 88.2\text{-}94.2$  GeV

0.10 <sup>+0.05</sup> <sub>-0.04</sub> ± 0.03 DECAMP 92c ALEP 1989-1990 LEP runs

0.16 ± 0.13 ± 0.04 BEHREND 89B CELL  $E_{cm}^{ee} = 14\text{-}47$  GeV

0.3 ± 0.1 ± 0.2 BARTEL 85F JADE  $E_{cm}^{ee} = 34.6$  GeV  
0.13 ± 0.04 10 BELTRAMI 85 HRS Repl. by BYLSMA 87

0.16 ± 0.08 ± 0.04 4 BURCHAT 85 MRK2  $E_{cm}^{ee} = 29$  GeV  
1.0 ± 0.4 10 BEHREND 82 CELL Repl. by BEHREND 89b

<sup>1</sup> The correlation coefficients between this measurement and the ACHARD 01D measurements of  $B(\tau^- \rightarrow \text{"1-prong"})$  and  $B(\tau^- \rightarrow \text{"3-prong"})$  are -0.082 and -0.19 respectively.

<sup>2</sup> The correlation coefficients between this measurement and the ABREU 01M measurements of  $B(\tau^- \rightarrow \text{"1-prong"})$  and  $B(\tau^- \rightarrow \text{"3-prong"})$  are -0.08 and -0.08 respectively.

<sup>3</sup> Not independent of ACKERSTAFF 99e  $B(\tau^- \rightarrow 3h^- 2h^+ \nu_\tau(\text{ex. } K^0))$  and  $B(\tau^- \rightarrow 3h^- 2h^+ \pi^0 \nu_\tau(\text{ex. } K^0))$  measurements.

$\Gamma(3h^- 2h^+ \nu_\tau(\text{ex. } K^0))/\Gamma_{total}$   $\Gamma_{102}/\Gamma$

VALUE (units  $10^{-4}$ ) EVTS DOCUMENT ID TECN COMMENT  
**8.39 ± 0.35 OUR FIT** Error includes scale factor of 1.1.  
**8.32 ± 0.35 OUR AVERAGE**

9.7 ± 1.5 ± 0.5 96 <sup>1</sup>ABDALLAH 06A DLPH 1992-1995 LEP runs  
8.56 ± 0.05 ± 0.42 34k AUBERT,B 05w BABR 232 fb<sup>-1</sup>,  $E_{cm}^{ee} = 10.6$  GeV

7.2 ± 0.9 ± 1.2 165 <sup>2</sup>SCHAEEL 05c ALEP 1991-1995 LEP runs  
9.1 ± 1.4 ± 0.6 97 ACKERSTAFF 99e OPAL 1991-1995 LEP runs

7.7 ± 0.5 ± 0.9 295 GIBAUT 94B CLEO  $E_{cm}^{ee} = 10.6$  GeV  
6.4 ± 2.3 ± 1.0 12 ALBRECHT 88B ARG  $E_{cm}^{ee} = 10$  GeV

5.1 ± 2.0 7 BYLSMA 87 HRS  $E_{cm}^{ee} = 29$  GeV

• • • We do not use the following data for averages, fits, limits, etc. • • •  
8.0 ± 1.1 ± 1.3 58 BUSKULIC 96 ALEP Repl. by SCHAEEL 05c  
6.7 ± 3.0 5 <sup>3</sup>BELTRAMI 85 HRS Repl. by BYLSMA 87

<sup>1</sup> See footnote to ABDALLAH 06A  $\Gamma(\tau^- \rightarrow h^- \nu_\tau)/\Gamma_{total}$  measurement for correlations with other measurements.

<sup>2</sup> See footnote to SCHAEEL 05c  $\Gamma(\tau^- \rightarrow e^- \bar{\nu}_e \nu_\tau)/\Gamma_{total}$  measurement for correlations with other measurements.

<sup>3</sup> The error quoted is statistical only.

$\Gamma(3h^- 2h^+ \pi^0 \nu_\tau(\text{ex. } K^0))/\Gamma_{total}$   $\Gamma_{103}/\Gamma$

VALUE (units  $10^{-4}$ ) EVTS DOCUMENT ID TECN COMMENT  
**1.78 ± 0.27 OUR FIT**  
**1.74 ± 0.27 OUR AVERAGE**

1.6 ± 1.2 ± 0.6 13 <sup>1</sup>ABDALLAH 06A DLPH 1992-1995 LEP runs  
2.1 ± 0.7 ± 0.9 95 <sup>2</sup>SCHAEEL 05c ALEP 1991-1995 LEP runs

1.7 ± 0.2 ± 0.2 231 ANASTASSOV 01 CLEO  $E_{cm}^{ee} = 10.6$  GeV  
2.7 ± 1.8 ± 0.9 23 ACKERSTAFF 99e OPAL 1991-1995 LEP runs

• • • We do not use the following data for averages, fits, limits, etc. • • •  
1.8 ± 0.7 ± 1.2 18 BUSKULIC 96 ALEP Repl. by SCHAEEL 05c  
1.9 ± 0.4 ± 0.4 31 GIBAUT 94B CLEO Repl. by ANASTASSOV 01

5.1 ± 2.2 6 BYLSMA 87 HRS  $E_{cm}^{ee} = 29$  GeV  
6.7 ± 3.0 5 <sup>3</sup>BELTRAMI 85 HRS Repl. by BYLSMA 87

<sup>1</sup> See footnote to ABDALLAH 06A  $\Gamma(\tau^- \rightarrow h^- \nu_\tau)/\Gamma_{total}$  measurement for correlations with other measurements.

<sup>2</sup> SCHAEEL 05c quote  $(1.4 \pm 0.7 \pm 0.9) \times 10^{-4}$ . We add  $0.7 \times 10^{-4}$  to remove their correction for  $\tau^- \rightarrow \eta \pi^- \pi^+ \pi^- \nu_\tau \rightarrow 3\pi^- 2\pi^+ \pi^0 \nu_\tau$  and  $\tau^- \rightarrow K^*(892)^- \eta \nu_\tau \rightarrow 3\pi^- 2\pi^+ \pi^0 \nu_\tau$  decays. See footnote to SCHAEEL 05c  $\Gamma(\tau^- \rightarrow e^- \bar{\nu}_e \nu_\tau)/\Gamma_{total}$  measurement for correlations with other measurements.

<sup>3</sup> The error quoted is statistical only.

$\Gamma(3h^- 2h^+ 2\pi^0 \nu_\tau)/\Gamma_{total}$   $\Gamma_{104}/\Gamma$

VALUE CL% DOCUMENT ID TECN COMMENT  
**< 3.4 × 10<sup>-6</sup>** 90 AUBERT,B 06 BABR 232 fb<sup>-1</sup>  $E_{cm}^{ee} = 10.6$  GeV

• • • We do not use the following data for averages, fits, limits, etc. • • •  
< 1.1 × 10<sup>-4</sup> 90 GIBAUT 94B CLEO  $E_{cm}^{ee} = 10.6$  GeV

$\Gamma((5\pi^-) \nu_\tau)/\Gamma_{total}$   $\Gamma_{105}/\Gamma$

$\Gamma_{105}/\Gamma = (\Gamma_{30} + \Gamma_{47} + \Gamma_{77} + \Gamma_{102} + 0.55\Gamma_{125} + 0.888\Gamma_{151})/\Gamma$

Data marked "avg" are highly correlated with data appearing elsewhere in the Listings, and are therefore used for the average given below but not in the overall fits. "f&a" marks results used for the fit and the average.

VALUE (%) EVTS DOCUMENT ID TECN COMMENT  
**0.77 ± 0.05 OUR FIT**

• • • We use the following data for averages but not for fits. • • •  
**0.61 ± 0.06 ± 0.08** <sup>1</sup>GIBAUT 94B CLEO  $E_{cm}^{ee} = 10.6$  GeV

<sup>1</sup> Not independent of GIBAUT 94B  $B(3h^- 2h^+ \nu_\tau)$ , PROCARIO 93  $B(h^- 4\pi^0 \nu_\tau)$ , and BORTOLETTO 93  $B(2h^- h^+ 2\pi^0 \nu_\tau)/B(\text{"3prong"})$  measurements. Result is corrected for  $\eta$  contributions.

## Lepton Particle Listings

 $\tau$  $\Gamma(4h-3h^+ \geq 0 \text{ neutrals } \nu_\tau \text{ ("7-prong")})/\Gamma_{\text{total}}$   $\Gamma_{106}/\Gamma$ 

VALUE	CL%	DOCUMENT ID	TECN	COMMENT
$<3.0 \times 10^{-7}$	90	AUBERT,B	05F	BABR 232 fb <sup>-1</sup> , $E_{\text{cm}}^{\text{ee}} = 10.6$ GeV
••• We do not use the following data for averages, fits, limits, etc. •••				
$<1.8 \times 10^{-5}$	95	ACKERSTAFF	97J	OPAL 1990-1995 LEP runs
$<2.4 \times 10^{-6}$	90	EDWARDS	97B	CLEO $E_{\text{cm}}^{\text{ee}} = 10.6$ GeV
$<2.9 \times 10^{-4}$	90	BYLSMA	87	HRS $E_{\text{cm}}^{\text{ee}} = 29$ GeV

 $\Gamma(4h-3h^+ \nu_\tau)/\Gamma_{\text{total}}$   $\Gamma_{107}/\Gamma$ 

VALUE	CL%	DOCUMENT ID	TECN	COMMENT
$<4.3 \times 10^{-7}$	90	AUBERT,B	05F	BABR 232 fb <sup>-1</sup> , $E_{\text{cm}}^{\text{ee}} = 10.6$ GeV

 $\Gamma(4h-3h^+ \pi^0 \nu_\tau)/\Gamma_{\text{total}}$   $\Gamma_{108}/\Gamma$ 

VALUE	CL%	DOCUMENT ID	TECN	COMMENT
$<2.5 \times 10^{-7}$	90	AUBERT,B	05F	BABR 232 fb <sup>-1</sup> , $E_{\text{cm}}^{\text{ee}} = 10.6$ GeV

 $\Gamma(X^-(S=-1)\nu_\tau)/\Gamma_{\text{total}}$   $\Gamma_{109}/\Gamma = (\Gamma_{10} + \Gamma_{16} + \Gamma_{23} + \Gamma_{28} + \Gamma_{35} + \Gamma_{40} + \Gamma_{85} + \Gamma_{89} + \Gamma_{127})/\Gamma$ 

Data marked "avg" are highly correlated with data appearing elsewhere in the Listings, and are therefore used for the average given below but not in the overall fits. "f&a" marks results used for the fit and the average.

VALUE (%)	DOCUMENT ID	TECN	COMMENT
<b>2.87 ± 0.07 OUR FIT</b>	Error includes scale factor of 1.3.		

••• We use the following data for averages but not for fits. •••

VALUE (%)	DOCUMENT ID	TECN	COMMENT
<b>2.87 ± 0.12</b>	<sup>1</sup> BARATE	99R	ALEP 1991-1995 LEP runs
<sup>1</sup> BARATE 99R perform a combined analysis of all ALEPH LEP 1 data on $\tau$ branching fraction measurements for decay modes having total strangeness equal to $-1$ .			

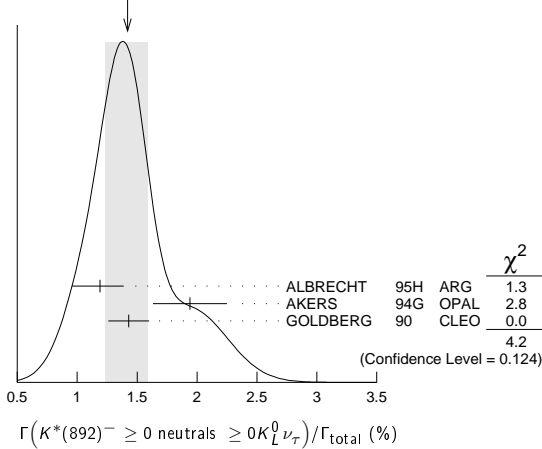
 $\Gamma(K^*(892)^- \geq 0 \text{ neutrals } \geq 0 K_L^0 \nu_\tau)/\Gamma_{\text{total}}$   $\Gamma_{110}/\Gamma$ 

VALUE (%)	EVTS	DOCUMENT ID	TECN	COMMENT
<b>1.42 ± 0.18 OUR AVERAGE</b>	Error includes scale factor of 1.4. See the ideogram below.			
$1.19 \pm 0.15 \pm 0.13$	104	ALBRECHT	95H	ARG $E_{\text{cm}}^{\text{ee}} = 9.4-10.6$ GeV
$1.94 \pm 0.27 \pm 0.15$	74	<sup>1</sup> AKERS	94G	OPAL $E_{\text{cm}}^{\text{ee}} = 88-94$ GeV
$1.43 \pm 0.11 \pm 0.13$	475	<sup>2</sup> GOLDBERG	90	CLEO $E_{\text{cm}}^{\text{ee}} = 9.4-10.9$ GeV

<sup>1</sup> AKERS 94G reject events in which a  $K_S^0$  accompanies the  $K^*(892)^-$ . We do not correct for them.

<sup>2</sup> GOLDBERG 90 estimates that 10% of observed  $K^*(892)$  are accompanied by a  $\pi^0$ .

WEIGHTED AVERAGE  
1.42 ± 0.18 (Error scaled by 1.4)

 $\Gamma(K^*(892)^- \nu_\tau)/\Gamma_{\text{total}}$   $\Gamma_{111}/\Gamma$ 

VALUE (%)	EVTS	DOCUMENT ID	TECN	COMMENT
<b>1.20 ± 0.07 OUR AVERAGE</b>	Error includes scale factor of 1.8. See the ideogram below.			
$1.131 \pm 0.006 \pm 0.051$	49k	<sup>1</sup> EPIFANOV	07	BELL 351 fb <sup>-1</sup> $E_{\text{cm}}^{\text{ee}} = 10.6$ GeV
$1.326 \pm 0.063$		BARATE	99R	ALEP 1991-1995 LEP runs
$1.11 \pm 0.12$		<sup>2</sup> COAN	96	CLEO $E_{\text{cm}}^{\text{ee}} \approx 10.6$ GeV
$1.42 \pm 0.22 \pm 0.09$		<sup>3</sup> ACCIARRI	95F	L3 1991-1993 LEP runs
••• We do not use the following data for averages, fits, limits, etc. •••				
$1.39 \pm 0.09 \pm 0.10$		<sup>4</sup> BUSKULIC	96	ALEP Repl. by BARATE 99R
$1.45 \pm 0.13 \pm 0.11$	273	<sup>5</sup> BUSKULIC	94F	ALEP Repl. by BUSKULIC 96
$1.23 \pm 0.21 \pm 0.11$	54	<sup>6</sup> ALBRECHT	88L	ARG $E_{\text{cm}}^{\text{ee}} = 10$ GeV
$1.9 \pm 0.3 \pm 0.4$	44	<sup>7</sup> TSCHIRHART	88	HRS $E_{\text{cm}}^{\text{ee}} = 29$ GeV
$1.5 \pm 0.4 \pm 0.4$	15	<sup>8</sup> AIHARA	87C	TPC $E_{\text{cm}}^{\text{ee}} = 29$ GeV
$1.3 \pm 0.3 \pm 0.3$	31	YELTON	86	MRK2 $E_{\text{cm}}^{\text{ee}} = 29$ GeV
$1.7 \pm 0.7$	11	DORFAN	81	MRK2 $E_{\text{cm}}^{\text{ee}} = 4.2-6.7$ GeV

<sup>1</sup> EPIFANOV 07 quote  $B(\tau^- \rightarrow K^*(892)^- \nu_\tau) B(K^*(892)^- \rightarrow K_S^0 \pi^-) = (3.77 \pm 0.02(\text{stat}) \pm 0.12(\text{syst}) \pm 0.12(\text{mod})) \times 10^{-3}$ . We add the systematic and model uncertainties in quadrature and divide by  $B(K^*(892)^- \rightarrow K_S^0 \pi^-) = 0.3333$ .

<sup>2</sup> Not independent of COAN 96  $B(\pi^- \bar{K}^0 \nu_\tau)$  and BATTLE 94  $B(K^- \pi^0 \nu_\tau)$  measurements.  $K\pi$  final states are consistent with and assumed to originate from  $K^*(892)^-$  production.

<sup>3</sup> This result is obtained from their  $B(\pi^- \bar{K}^0 \nu_\tau)$  assuming all those decays originate in  $K^*(892)^-$  decays.

<sup>4</sup> Not independent of BUSKULIC 96  $B(\pi^- \bar{K}^0 \nu_\tau)$  and  $B(K^- \pi^0 \nu_\tau)$  measurements.

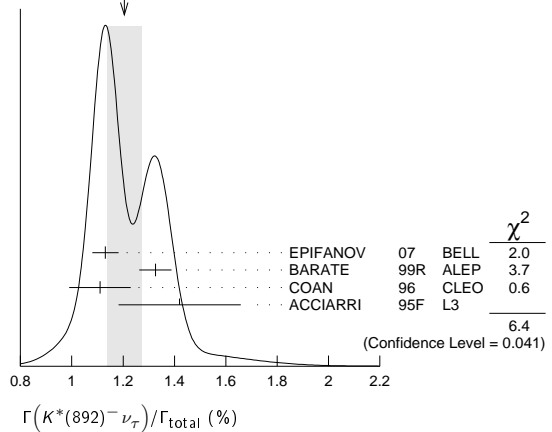
<sup>5</sup> BUSKULIC 94F obtain this result from BUSKULIC 94F  $B(\bar{K}^0 \pi^- \nu_\tau)$  and BUSKULIC 94E  $B(K^- \pi^0 \nu_\tau)$  assuming all of those decays originate in  $K^*(892)^-$  decays.

<sup>6</sup> The authors divide by  $\Gamma_2/\Gamma = 0.865$  to obtain this result.

<sup>7</sup> Not independent of TSCHIRHART 88  $\Gamma(\tau^- \rightarrow h^- \bar{K}^0 \geq 0 \text{ neutrals } \geq 0 K_L^0 \nu_\tau) / \Gamma$ .

<sup>8</sup> Decay  $\pi^-$  identified in this experiment, is assumed in the others.

WEIGHTED AVERAGE  
1.20 ± 0.07 (Error scaled by 1.8)

 $\Gamma(K^*(892)^- \nu_\tau)/\Gamma(\pi^- \pi^0 \nu_\tau)$   $\Gamma_{111}/\Gamma_{14}$ 

VALUE	DOCUMENT ID	TECN	COMMENT
<b>0.075 ± 0.027</b>	<sup>1</sup> ABREU	94K	DLPH LEP 1992 Z data
<sup>1</sup> ABREU 94K quote $B(\tau^- \rightarrow K^*(892)^- \nu_\tau) B(K^*(892)^- \rightarrow K^- \pi^0) / B(\tau^- \rightarrow \rho^- \nu_\tau) = 0.025 \pm 0.009$ . We divide by $B(K^*(892)^- \rightarrow K^- \pi^0) = 0.333$ to obtain this result.			

 $\Gamma(K^*(892)^- \nu_\tau \rightarrow \pi^- \bar{K}^0 \nu_\tau)/\Gamma(\pi^- \bar{K}^0 \nu_\tau)$   $\Gamma_{112}/\Gamma_{35}$ 

VALUE	EVTS	DOCUMENT ID	TECN	COMMENT
<b>0.933 ± 0.027</b>	49k	EPIFANOV	07	BELL 351 fb <sup>-1</sup> $E_{\text{cm}}^{\text{ee}} = 10.6$ GeV

 $\Gamma(K^*(892)^0 K^- \geq 0 \text{ neutrals } \nu_\tau)/\Gamma_{\text{total}}$   $\Gamma_{113}/\Gamma$ 

VALUE (%)	EVTS	DOCUMENT ID	TECN	COMMENT
<b>0.32 ± 0.08 ± 0.12</b>	119	GOLDBERG	90	CLEO $E_{\text{cm}}^{\text{ee}} = 9.4-10.9$ GeV

 $\Gamma(K^*(892)^0 K^- \nu_\tau)/\Gamma_{\text{total}}$   $\Gamma_{114}/\Gamma$ 

VALUE (%)	EVTS	DOCUMENT ID	TECN	COMMENT
<b>0.21 ± 0.04 OUR AVERAGE</b>				
$0.213 \pm 0.048$		<sup>1</sup> BARATE	98	ALEP 1991-1995 LEP runs
$0.20 \pm 0.05 \pm 0.04$	47	ALBRECHT	95H	ARG $E_{\text{cm}}^{\text{ee}} = 9.4-10.6$ GeV

<sup>1</sup> BARATE 98 measure the  $K^- (\rho^0 \rightarrow \pi^+ \pi^-)$  fraction in  $\tau^- \rightarrow K^- \pi^+ \pi^- \nu_\tau$  decays to be  $(35 \pm 11)\%$  and derive this result from their measurement of  $\Gamma(\tau^- \rightarrow K^- \pi^+ \pi^- \nu_\tau) / \Gamma_{\text{total}}$  assuming the intermediate states are all  $K^- \rho$  and  $K^- K^*(892)^0$ .

 $\Gamma(K^*(892)^0 \pi^- \geq 0 \text{ neutrals } \nu_\tau)/\Gamma_{\text{total}}$   $\Gamma_{115}/\Gamma$ 

VALUE (%)	EVTS	DOCUMENT ID	TECN	COMMENT
<b>0.38 ± 0.11 ± 0.13</b>	105	GOLDBERG	90	CLEO $E_{\text{cm}}^{\text{ee}} = 9.4-10.9$ GeV

 $\Gamma(K^*(892)^0 \pi^- \nu_\tau)/\Gamma_{\text{total}}$   $\Gamma_{116}/\Gamma$ 

VALUE (%)	EVTS	DOCUMENT ID	TECN	COMMENT
<b>0.22 ± 0.05 OUR AVERAGE</b>				
$0.209 \pm 0.058$		<sup>1</sup> BARATE	98	ALEP 1991-1995 LEP runs
$0.25 \pm 0.10 \pm 0.05$	27	ALBRECHT	95H	ARG $E_{\text{cm}}^{\text{ee}} = 9.4-10.6$ GeV

<sup>1</sup> BARATE 98 measure the  $K^- K^*(892)^0$  fraction in  $\tau^- \rightarrow K^- K^+ \pi^- \nu_\tau$  decays to be  $(87 \pm 13)\%$  and derive this result from their measurement of  $\Gamma(\tau^- \rightarrow K^- K^+ \pi^- \nu_\tau) / \Gamma_{\text{total}}$ .

 $\Gamma((\bar{K}^*(892) \pi^-) \nu_\tau \rightarrow \pi^- \bar{K}^0 \pi^0 \nu_\tau)/\Gamma_{\text{total}}$   $\Gamma_{117}/\Gamma$ 

VALUE (%)	DOCUMENT ID	TECN	COMMENT
<b>0.10 ± 0.04 OUR AVERAGE</b>			
$0.097 \pm 0.044 \pm 0.036$	<sup>1</sup> BARATE	99K	ALEP 1991-1995 LEP runs
$0.106 \pm 0.037 \pm 0.032$	<sup>2</sup> BARATE	98E	ALEP 1991-1995 LEP runs













## Lepton Particle Listings

T

$\Gamma(e^+K^-K^-)/\Gamma_{\text{total}}$   $\Gamma_{192}/\Gamma$   
Test of lepton number conservation.

VALUE	CL%	DOCUMENT ID	TECN	COMMENT
$<6.0 \times 10^{-8}$	90	MIYAZAKI	10 BELL	$671 \text{ fb}^{-1}$ , $E_{\text{cm}}^{ee}=10.6 \text{ GeV}$
••• We do not use the following data for averages, fits, limits, etc. •••				
$<3.1 \times 10^{-7}$	90	YUSA	06 BELL	$158 \text{ fb}^{-1}$ , $E_{\text{cm}}^{ee}=10.6 \text{ GeV}$
$<1.5 \times 10^{-7}$	90	AUBERT,BE	05D BABR	$221 \text{ fb}^{-1}$ , $E_{\text{cm}}^{ee}=10.6 \text{ GeV}$
$<3.8 \times 10^{-6}$	90	BLISS	98 CLEO	$E_{\text{cm}}^{ee}=10.6 \text{ GeV}$

$\Gamma(\mu^-\pi^+K^-)/\Gamma_{\text{total}}$   $\Gamma_{193}/\Gamma$   
Test of lepton family number conservation.

VALUE	CL%	DOCUMENT ID	TECN	COMMENT
$<1.6 \times 10^{-7}$	90	MIYAZAKI	10 BELL	$671 \text{ fb}^{-1}$ , $E_{\text{cm}}^{ee}=10.6 \text{ GeV}$
••• We do not use the following data for averages, fits, limits, etc. •••				
$<2.7 \times 10^{-7}$	90	YUSA	06 BELL	$158 \text{ fb}^{-1}$ , $E_{\text{cm}}^{ee}=10.6 \text{ GeV}$
$<2.6 \times 10^{-7}$	90	AUBERT,BE	05D BABR	$221 \text{ fb}^{-1}$ , $E_{\text{cm}}^{ee}=10.6 \text{ GeV}$
$<7.5 \times 10^{-6}$	90	BLISS	98 CLEO	$E_{\text{cm}}^{ee}=10.6 \text{ GeV}$
$<8.7 \times 10^{-6}$	90	<sup>1</sup> BARTELT	94 CLEO	Repl. by BLISS 98
$<11 \times 10^{-5}$	90	ALBRECHT	92k ARG	$E_{\text{cm}}^{ee}=10 \text{ GeV}$
$<7.7 \times 10^{-5}$	90	BOWCOCK	90 CLEO	$E_{\text{cm}}^{ee}=10.4\text{-}10.9$
<sup>1</sup> BARTELT 94 assume phase space decays.				

$\Gamma(\mu^-K^+K^-)/\Gamma_{\text{total}}$   $\Gamma_{194}/\Gamma$   
Test of lepton family number conservation.

VALUE	CL%	DOCUMENT ID	TECN	COMMENT
$<1.0 \times 10^{-7}$	90	MIYAZAKI	10 BELL	$671 \text{ fb}^{-1}$ , $E_{\text{cm}}^{ee}=10.6 \text{ GeV}$
••• We do not use the following data for averages, fits, limits, etc. •••				
$<7.3 \times 10^{-7}$	90	YUSA	06 BELL	$158 \text{ fb}^{-1}$ , $E_{\text{cm}}^{ee}=10.6 \text{ GeV}$
$<3.2 \times 10^{-7}$	90	AUBERT,BE	05D BABR	$221 \text{ fb}^{-1}$ , $E_{\text{cm}}^{ee}=10.6 \text{ GeV}$
$<7.4 \times 10^{-6}$	90	BLISS	98 CLEO	$E_{\text{cm}}^{ee}=10.6 \text{ GeV}$
$<1.5 \times 10^{-5}$	90	<sup>1</sup> BARTELT	94 CLEO	Repl. by BLISS 98
$<7.7 \times 10^{-5}$	90	BOWCOCK	90 CLEO	$E_{\text{cm}}^{ee}=10.4\text{-}10.9$
<sup>1</sup> BARTELT 94 assume phase space decays.				

$\Gamma(\mu^+\pi^-K^-)/\Gamma_{\text{total}}$   $\Gamma_{195}/\Gamma$   
Test of lepton number conservation.

VALUE	CL%	DOCUMENT ID	TECN	COMMENT
$<9.4 \times 10^{-8}$	90	MIYAZAKI	10 BELL	$671 \text{ fb}^{-1}$ , $E_{\text{cm}}^{ee}=10.6 \text{ GeV}$
••• We do not use the following data for averages, fits, limits, etc. •••				
$<2.9 \times 10^{-7}$	90	YUSA	06 BELL	$158 \text{ fb}^{-1}$ , $E_{\text{cm}}^{ee}=10.6 \text{ GeV}$
$<2.2 \times 10^{-7}$	90	AUBERT,BE	05D BABR	$221 \text{ fb}^{-1}$ , $E_{\text{cm}}^{ee}=10.6 \text{ GeV}$
$<7.0 \times 10^{-6}$	90	BLISS	98 CLEO	$E_{\text{cm}}^{ee}=10.6 \text{ GeV}$
$<2.0 \times 10^{-5}$	90	<sup>1</sup> BARTELT	94 CLEO	Repl. by BLISS 98
$<5.8 \times 10^{-5}$	90	ALBRECHT	92k ARG	$E_{\text{cm}}^{ee}=10 \text{ GeV}$
$<4.0 \times 10^{-5}$	90	BOWCOCK	90 CLEO	$E_{\text{cm}}^{ee}=10.4\text{-}10.9$
<sup>1</sup> BARTELT 94 assume phase space decays.				

$\Gamma(\mu^-K_S^0K_S^0)/\Gamma_{\text{total}}$   $\Gamma_{196}/\Gamma$

VALUE	CL%	DOCUMENT ID	TECN	COMMENT
$<8.0 \times 10^{-8}$	90	MIYAZAKI	10A BELL	$671 \text{ fb}^{-1}$ , $E_{\text{cm}}^{ee}=10.6 \text{ GeV}$
••• We do not use the following data for averages, fits, limits, etc. •••				
$<3.4 \times 10^{-6}$	90	CHEN	02c CLEO	$E_{\text{cm}}^{ee}=10.6 \text{ GeV}$

$\Gamma(\mu^-K^+K^-)/\Gamma_{\text{total}}$   $\Gamma_{197}/\Gamma$   
Test of lepton family number conservation.

VALUE	CL%	DOCUMENT ID	TECN	COMMENT
$<6.8 \times 10^{-8}$	90	MIYAZAKI	10 BELL	$671 \text{ fb}^{-1}$ , $E_{\text{cm}}^{ee}=10.6 \text{ GeV}$
••• We do not use the following data for averages, fits, limits, etc. •••				
$<8.0 \times 10^{-7}$	90	YUSA	06 BELL	$158 \text{ fb}^{-1}$ , $E_{\text{cm}}^{ee}=10.6 \text{ GeV}$
$<2.5 \times 10^{-7}$	90	AUBERT,BE	05D BABR	$221 \text{ fb}^{-1}$ , $E_{\text{cm}}^{ee}=10.6 \text{ GeV}$
$<15 \times 10^{-6}$	90	BLISS	98 CLEO	$E_{\text{cm}}^{ee}=10.6 \text{ GeV}$

$\Gamma(\mu^+K^-K^-)/\Gamma_{\text{total}}$   $\Gamma_{198}/\Gamma$   
Test of lepton number conservation.

VALUE	CL%	DOCUMENT ID	TECN	COMMENT
$<9.6 \times 10^{-8}$	90	MIYAZAKI	10 BELL	$671 \text{ fb}^{-1}$ , $E_{\text{cm}}^{ee}=10.6 \text{ GeV}$
••• We do not use the following data for averages, fits, limits, etc. •••				
$<4.4 \times 10^{-7}$	90	YUSA	06 BELL	$158 \text{ fb}^{-1}$ , $E_{\text{cm}}^{ee}=10.6 \text{ GeV}$
$<4.8 \times 10^{-7}$	90	AUBERT,BE	05D BABR	$221 \text{ fb}^{-1}$ , $E_{\text{cm}}^{ee}=10.6 \text{ GeV}$
$<6.0 \times 10^{-6}$	90	BLISS	98 CLEO	$E_{\text{cm}}^{ee}=10.6 \text{ GeV}$

$\Gamma(e^-\pi^0\pi^0)/\Gamma_{\text{total}}$   $\Gamma_{199}/\Gamma$   
Test of lepton family number conservation.

VALUE	CL%	DOCUMENT ID	TECN	COMMENT
$<6.5 \times 10^{-6}$	90	BONVICINI	97 CLEO	$E_{\text{cm}}^{ee}=10.6 \text{ GeV}$

$\Gamma(\mu^-\pi^0\pi^0)/\Gamma_{\text{total}}$   $\Gamma_{200}/\Gamma$   
Test of lepton family number conservation.

VALUE	CL%	DOCUMENT ID	TECN	COMMENT
$<14 \times 10^{-6}$	90	BONVICINI	97 CLEO	$E_{\text{cm}}^{ee}=10.6 \text{ GeV}$

$\Gamma(e^-\eta\eta)/\Gamma_{\text{total}}$   $\Gamma_{201}/\Gamma$   
Test of lepton family number conservation.

VALUE	CL%	DOCUMENT ID	TECN	COMMENT
$<35 \times 10^{-6}$	90	BONVICINI	97 CLEO	$E_{\text{cm}}^{ee}=10.6 \text{ GeV}$

$\Gamma(\mu^-\eta\eta)/\Gamma_{\text{total}}$   $\Gamma_{202}/\Gamma$   
Test of lepton family number conservation.

VALUE	CL%	DOCUMENT ID	TECN	COMMENT
$<60 \times 10^{-6}$	90	BONVICINI	97 CLEO	$E_{\text{cm}}^{ee}=10.6 \text{ GeV}$

$\Gamma(e^-\pi^0\eta)/\Gamma_{\text{total}}$   $\Gamma_{203}/\Gamma$   
Test of lepton family number conservation.

VALUE	CL%	DOCUMENT ID	TECN	COMMENT
$<24 \times 10^{-6}$	90	BONVICINI	97 CLEO	$E_{\text{cm}}^{ee}=10.6 \text{ GeV}$

$\Gamma(\mu^-\pi^0\eta)/\Gamma_{\text{total}}$   $\Gamma_{204}/\Gamma$   
Test of lepton family number conservation.

VALUE	CL%	DOCUMENT ID	TECN	COMMENT
$<22 \times 10^{-6}$	90	BONVICINI	97 CLEO	$E_{\text{cm}}^{ee}=10.6 \text{ GeV}$

$\Gamma(\overline{p}\gamma)/\Gamma_{\text{total}}$   $\Gamma_{205}/\Gamma$   
Test of lepton number and baryon number conservation.

VALUE	CL%	DOCUMENT ID	TECN	COMMENT
$<3.5 \times 10^{-6}$	90	GODANG	99 CLEO	$E_{\text{cm}}^{ee}=10.6 \text{ GeV}$
••• We do not use the following data for averages, fits, limits, etc. •••				
$<29 \times 10^{-5}$	90	ALBRECHT	92k ARG	$E_{\text{cm}}^{ee}=10 \text{ GeV}$

$\Gamma(\overline{p}\pi^0)/\Gamma_{\text{total}}$   $\Gamma_{206}/\Gamma$   
Test of lepton number and baryon number conservation.

VALUE	CL%	DOCUMENT ID	TECN	COMMENT
$<15 \times 10^{-6}$	90	GODANG	99 CLEO	$E_{\text{cm}}^{ee}=10.6 \text{ GeV}$
••• We do not use the following data for averages, fits, limits, etc. •••				
$<66 \times 10^{-5}$	90	ALBRECHT	92k ARG	$E_{\text{cm}}^{ee}=10 \text{ GeV}$

$\Gamma(\overline{p}2\pi^0)/\Gamma_{\text{total}}$   $\Gamma_{207}/\Gamma$   
Test of lepton number and baryon number conservation.

VALUE	CL%	DOCUMENT ID	TECN	COMMENT
$<33 \times 10^{-6}$	90	GODANG	99 CLEO	$E_{\text{cm}}^{ee}=10.6 \text{ GeV}$

$\Gamma(\overline{p}\eta)/\Gamma_{\text{total}}$   $\Gamma_{208}/\Gamma$   
Test of lepton number and baryon number conservation.

VALUE	CL%	DOCUMENT ID	TECN	COMMENT
$<8.9 \times 10^{-6}$	90	GODANG	99 CLEO	$E_{\text{cm}}^{ee}=10.6 \text{ GeV}$
••• We do not use the following data for averages, fits, limits, etc. •••				
$<130 \times 10^{-5}$	90	ALBRECHT	92k ARG	$E_{\text{cm}}^{ee}=10 \text{ GeV}$

$\Gamma(\overline{p}\pi^0\eta)/\Gamma_{\text{total}}$   $\Gamma_{209}/\Gamma$   
Test of lepton number and baryon number conservation.

VALUE	CL%	DOCUMENT ID	TECN	COMMENT
$<27 \times 10^{-6}$	90	GODANG	99 CLEO	$E_{\text{cm}}^{ee}=10.6 \text{ GeV}$

$\Gamma(\Lambda\pi^-)/\Gamma_{\text{total}}$   $\Gamma_{210}/\Gamma$   
Test of lepton number and baryon number conservation.

VALUE	CL%	DOCUMENT ID	TECN	COMMENT
$<0.72 \times 10^{-7}$	90	MIYAZAKI	06 BELL	$154 \text{ fb}^{-1}$ , $E_{\text{cm}}^{ee}=10.6 \text{ GeV}$

$\Gamma(\overline{\Lambda}\pi^-)/\Gamma_{\text{total}}$   $\Gamma_{211}/\Gamma$   
Test of lepton number and baryon number conservation.

VALUE	CL%	DOCUMENT ID	TECN	COMMENT
$<1.4 \times 10^{-7}$	90	MIYAZAKI	06 BELL	$154 \text{ fb}^{-1}$ , $E_{\text{cm}}^{ee}=10.6 \text{ GeV}$

$\Gamma(e^-\text{light boson})/\Gamma(e^-\overline{\nu}_e\nu_\tau)$   $\Gamma_{212}/\Gamma_5$   
Test of lepton family number conservation.

VALUE	CL%	DOCUMENT ID	TECN	COMMENT
$<0.015$	95	<sup>1</sup> ALBRECHT	95G ARG	$E_{\text{cm}}^{ee}=9.4\text{-}10.6 \text{ GeV}$
••• We do not use the following data for averages, fits, limits, etc. •••				
$<0.018$	95	<sup>2</sup> ALBRECHT	90E ARG	$E_{\text{cm}}^{ee}=9.4\text{-}10.6 \text{ GeV}$
$<0.040$	95	<sup>3</sup> BALTRUSAIT...85	MRK3	$E_{\text{cm}}^{ee}=3.77 \text{ GeV}$

- <sup>1</sup>ALBRECHT 95G limit holds for bosons with mass  $< 0.4 \text{ GeV}$ . The limit rises to 0.036 for a mass of 1.0 GeV, then falls to 0.006 at the upper mass limit of 1.6 GeV.  
<sup>2</sup>ALBRECHT 90E limit applies for spinless boson with mass  $< 100 \text{ MeV}$ , and rises to 0.050 for mass = 500 MeV.  
<sup>3</sup>BALTRUSAITIS 85 limit applies for spinless boson with mass  $< 100 \text{ MeV}$ .

$\Gamma(\mu^-\text{light boson})/\Gamma(e^-\overline{\nu}_e\nu_\tau)$   $\Gamma_{213}/\Gamma_5$   
Test of lepton family number conservation.

VALUE	CL%	DOCUMENT ID	TECN	COMMENT
$<0.026$	95	<sup>1</sup> ALBRECHT	95G ARG	$E_{\text{cm}}^{ee}=9.4\text{-}10.6 \text{ GeV}$
••• We do not use the following data for averages, fits, limits, etc. •••				
$<0.033$	95	<sup>2</sup> ALBRECHT	90E ARG	$E_{\text{cm}}^{ee}=9.4\text{-}10.6 \text{ GeV}$
$<0.125$	95	<sup>3</sup> BALTRUSAIT...85	MRK3	$E_{\text{cm}}^{ee}=3.77 \text{ GeV}$

- <sup>1</sup>ALBRECHT 95G limit holds for bosons with mass  $< 1.3 \text{ GeV}$ . The limit rises to 0.034 for a mass of 1.4 GeV, then falls to 0.003 at the upper mass limit of 1.6 GeV.  
<sup>2</sup>ALBRECHT 90E limit applies for spinless boson with mass  $< 100 \text{ MeV}$ , and rises to 0.071 for mass = 500 MeV.  
<sup>3</sup>BALTRUSAITIS 85 limit applies for spinless boson with mass  $< 100 \text{ MeV}$ .

**$\tau$ -DECAY PARAMETERS** **$\tau$ -LEPTON DECAY PARAMETERS**

Updated August 2011 by A. Stahl (RWTH Aachen).

The purpose of the measurements of the decay parameters (*i.e.*, Michel parameters) of the  $\tau$  is to determine the structure (spin and chirality) of the current mediating its decays.

**Leptonic Decays:** The Michel parameters are extracted from the energy spectrum of the charged daughter lepton  $\ell = e, \mu$  in the decays  $\tau \rightarrow \ell \nu_\ell \nu_\tau$ . Ignoring radiative corrections, neglecting terms of order  $(m_\ell/m_\tau)^2$  and  $(m_\tau/\sqrt{s})^2$ , and setting the neutrino masses to zero, the spectrum in the laboratory frame reads

$$\frac{d\Gamma}{dx} = \frac{G_{\tau\ell}^2 m_\tau^5}{192 \pi^3} \times \left\{ f_0(x) + \rho f_1(x) + \eta \frac{m_\ell}{m_\tau} f_2(x) - P_\tau [\xi g_1(x) + \xi \delta g_2(x)] \right\}, \quad (1)$$

with

$$\begin{aligned} f_0(x) &= 2 - 6x^2 + 4x^3 \\ f_1(x) &= -\frac{4}{9} + 4x^2 - \frac{32}{9}x^3 \\ f_2(x) &= 12(1-x)^2 \\ g_1(x) &= -\frac{2}{3} + 4x - 6x^2 + \frac{8}{3}x^3 \\ g_2(x) &= \frac{4}{9} - \frac{16}{3}x + 12x^2 - \frac{64}{9}x^3. \end{aligned}$$

The quantity  $x$  is the fractional energy of the daughter lepton  $\ell$ , *i.e.*,  $x = E_\ell/E_{\ell,max} \approx E_\ell/(\sqrt{s}/2)$  and  $P_\tau$  is the polarization of the tau leptons. The integrated decay width is given by

$$\Gamma = \frac{G_{\tau\ell}^2 m_\tau^5}{192 \pi^3} \left( 1 + 4\eta \frac{m_\ell}{m_\tau} \right). \quad (2)$$

The situation is similar to muon decays  $\mu \rightarrow e \nu_e \nu_\mu$ . The generalized matrix element with the couplings  $g_{\varepsilon\mu}^\gamma$  and their relations to the Michel parameters  $\rho, \eta, \xi$ , and  $\delta$  have been described in the “Note on Muon Decay Parameters.” The Standard Model expectations are 3/4, 0, 1, and 3/4, respectively. For more details, see Ref. 1.

**Hadronic Decays:** In the case of hadronic decays  $\tau \rightarrow h \nu_\tau$ , with  $h = \pi, \rho$ , or  $a_1$ , the ansatz is restricted to purely vectorial currents. The matrix element is

$$\frac{G_{\tau h}}{\sqrt{2}} \sum_{\lambda=R,L} g_\lambda \langle \bar{\Psi}_\omega(\nu_\tau) | \gamma^\mu | \Psi_\lambda(\tau) \rangle J_\mu^h \quad (3)$$

with the hadronic current  $J_\mu^h$ . The neutrino chirality  $\omega$  is uniquely determined from  $\lambda$ . The spectrum depends only on a single parameter  $\xi_h$

$$\frac{d^n \Gamma}{dx_1 dx_2 \dots dx_n} = f(\vec{x}) + \xi_h P_\tau g(\vec{x}), \quad (4)$$

with  $f$  and  $g$  being channel-dependent functions of the  $n$  observables  $\vec{x} = (x_1, x_2, \dots, x_n)$  (see Ref. 2). The parameter  $\xi_h$  is related to the couplings through

$$\xi_h = |g_L|^2 - |g_R|^2. \quad (5)$$

$\xi_h$  is the negative of the chirality of the  $\tau$  neutrino in these decays. In the Standard Model,  $\xi_h = 1$ . Also included in the Data Listings for  $\xi_h$  are measurements of the neutrino helicity which coincide with  $\xi_h$ , if the neutrino is massless (ASNER 00, ACKERSTAFF 97R, AKERS 95P, ALBRECHT 93C, and ALBRECHT 90I).

**Combination of Measurements:** The individual measurements are combined, taking into account the correlations between the parameters. In a first fit, universality between the two leptonic decays, and between all hadronic decays, is assumed. A second fit is made without these assumptions. The results of the two fits are provided as OUR FIT in the Data Listings below in the tables whose title includes “(e or mu)” or “(all hadronic modes),” and “(e),” “(mu)” *etc.*, respectively. The measurements show good agreement with the Standard Model. The  $\chi^2$  values with respect to the Standard model predictions are 24.1 for 41 degrees of freedom and 26.8 for 56 degrees of freedom, respectively. The correlations are reduced through this combination to less than 20%, with the exception of  $\rho$  and  $\eta$  which are correlated by +23%, for the fit with universality and by +70% for  $\tau \rightarrow \mu \nu_\mu \nu_\tau$ .

**Table 1:** Coupling constants  $g_{\varepsilon\mu}^\gamma$ . 95% confidence level experimental limits. The limits include the quoted values of  $A_e, A_\mu$ , and  $A_\pi$  and assume  $A_\rho = A_{a_1} = 1$ .

$\tau \rightarrow e \nu_e \nu_\tau$		
$ g_{RR}^S  < 0.70$	$ g_{RR}^V  < 0.17$	$ g_{RR}^T  \equiv 0$
$ g_{LR}^S  < 0.99$	$ g_{LR}^V  < 0.13$	$ g_{LR}^T  < 0.082$
$ g_{RL}^S  < 2.01$	$ g_{RL}^V  < 0.52$	$ g_{RL}^T  < 0.51$
$ g_{LL}^S  < 2.01$	$ g_{LL}^V  < 1.005$	$ g_{LL}^T  \equiv 0$
$\tau \rightarrow \mu \nu_\mu \nu_\tau$		
$ g_{RR}^S  < 0.72$	$ g_{RR}^V  < 0.18$	$ g_{RR}^T  \equiv 0$
$ g_{LR}^S  < 0.95$	$ g_{LR}^V  < 0.12$	$ g_{LR}^T  < 0.079$
$ g_{RL}^S  < 2.01$	$ g_{RL}^V  < 0.52$	$ g_{RL}^T  < 0.51$
$ g_{LL}^S  < 2.01$	$ g_{LL}^V  < 1.005$	$ g_{LL}^T  \equiv 0$
$\tau \rightarrow \pi \nu_\tau$		
$ g_R^V  < 0.15$	$ g_L^V  > 0.992$	
$\tau \rightarrow \rho \nu_\tau$		
$ g_R^V  < 0.10$	$ g_L^V  > 0.995$	
$\tau \rightarrow a_1 \nu_\tau$		
$ g_R^V  < 0.16$	$ g_L^V  > 0.987$	

## Lepton Particle Listings

 $\tau$ 

**Model-independent Analysis:** From the Michel parameters, limits can be derived on the couplings  $g_{e\lambda}^{\kappa}$  without further model assumptions. In the Standard model  $g_{LL}^V = 1$  (leptonic decays), and  $g_L = 1$  (hadronic decays) and all other couplings vanish. First, the partial decay widths have to be compared to the Standard Model predictions to derive limits on the normalization of the couplings  $A_x = G_{\tau x}^2/G_F^2$  with Fermi's constant  $G_F$ :

$$\begin{aligned} A_e &= 1.0029 \pm 0.0046, \\ A_\mu &= 0.981 \pm 0.018, \\ A_\pi &= 1.0020 \pm 0.0073. \end{aligned} \quad (6)$$

Then limits on the couplings (95% CL) can be extracted (see Ref. 3 and Ref. 4). Without the assumption of universality, the limits given in Table 1 are derived.

**Model-dependent Interpretation:** More stringent limits can be derived assuming specific models. For example, in the framework of a two Higgs doublet model, the measurements correspond to a limit of  $m_{H^\pm} > 1.9 \text{ GeV} \times \tan\beta$  on the mass of the charged Higgs boson, or a limit of 253 GeV on the mass of the second  $W$  boson in left-right symmetric models for arbitrary mixing (both 95% CL). See Ref. 4 and Ref. 5.

## Footnotes and References

1. F. Scheck, Phys. Reports **44**, 187 (1978);  
W. Fetscher and H.J. Gerber in *Precision Tests of the Standard Model*, edited by P. Langacker, World Scientific, 1993;  
A. Stahl, *Physics with  $\tau$  Leptons*, Springer Tracts in Modern Physics.
2. M. Davier *et al.*, Phys. Lett. **B306**, 411 (1993).
3. OPAL Collab., K. Ackerstaff *et al.*, Eur. Phys. J. **C8**, 3 (1999).
4. A. Stahl, Nucl. Phys. (Proc. Supp.) **B76**, 173 (1999).
5. M.-T. Dova *et al.*, Phys. Rev. **D58**, 015005 (1998);  
T. Hebbeker and W. Lohmann, Z. Phys. **C74**, 399 (1997);  
A. Pich and J.P. Silva, Phys. Rev. **D52**, 4006 (1995).

 $\rho(e \text{ or } \mu)$  PARAMETER(V-A) theory predicts  $\rho = 0.75$ .

VALUE	EVTS	DOCUMENT ID	TECN	COMMENT
<b>0.745 ± 0.008 OUR FIT</b>				
<b>0.749 ± 0.008 OUR AVERAGE</b>				
0.742 ± 0.014 ± 0.006	81k	HEISTER	01E ALEP	1991-1995 LEP runs
0.775 ± 0.023 ± 0.020	36k	ABREU	00L DLPH	1992-1995 runs
0.781 ± 0.028 ± 0.018	46k	ACKERSTAFF	99D OPAL	1990-1995 LEP runs
0.762 ± 0.035	54k	ACCARRI	98R L3	1991-1995 LEP runs
0.731 ± 0.031		<sup>1</sup> ALBRECHT	98 ARG	$E_{\text{cm}}^{\text{ee}} = 9.5-10.6 \text{ GeV}$
0.72 ± 0.09 ± 0.03		<sup>2</sup> ABE	97o SLD	1993-1995 SLC runs
0.747 ± 0.010 ± 0.006	55k	ALEXANDER	97F CLEO	$E_{\text{cm}}^{\text{ee}} = 10.6 \text{ GeV}$
0.79 ± 0.10 ± 0.10	3732	FORD	87B MAC	$E_{\text{cm}}^{\text{ee}} = 29 \text{ GeV}$
0.71 ± 0.09 ± 0.03	1426	BEHRENDIS	85 CLEO	$e^+e^-$ near $\Upsilon(4S)$
••• We do not use the following data for averages, fits, limits, etc. •••				
0.735 ± 0.013 ± 0.008	31k	AMMAR	97B CLEO	Repl. by ALEXANDER 97F
0.794 ± 0.039 ± 0.031	18k	ACCARRI	96H L3	Repl. by ACCARRI 98R
0.732 ± 0.034 ± 0.020	8.2k	<sup>3</sup> ALBRECHT	95 ARG	$E_{\text{cm}}^{\text{ee}} = 9.5-10.6 \text{ GeV}$
0.738 ± 0.038		<sup>4</sup> ALBRECHT	95C ARG	Repl. by ALBRECHT 98
0.751 ± 0.039 ± 0.022		BUSKULIC	95D ALEP	Repl. by HEISTER 01E
0.742 ± 0.035 ± 0.020	8000	ALBRECHT	90E ARG	$E_{\text{cm}}^{\text{ee}} = 9.4-10.6 \text{ GeV}$

<sup>1</sup> Combined fit to ARGUS tau decay parameter measurements in ALBRECHT 98, ALBRECHT 95C, ALBRECHT 93G, and ALBRECHT 94E. ALBRECHT 98 use tau pair events of the type  $\tau^- \tau^+ \rightarrow (\ell^- \bar{\nu}_\ell \nu_\tau)(\pi^+ \pi^0 \bar{\nu}_\tau)$ , and their charged conjugates.

<sup>2</sup> ABE 97o assume  $\eta = 0$  in their fit. Letting  $\eta$  vary in the fit gives a  $\rho$  value of  $0.69 \pm 0.13 \pm 0.05$ .

<sup>3</sup> Value is from a simultaneous fit for the  $\rho$  and  $\eta$  decay parameters to the lepton energy spectrum. Not independent of ALBRECHT 90E  $\rho(e \text{ or } \mu)$  value which assumes  $\eta = 0$ . Result is strongly correlated with ALBRECHT 95C.

<sup>4</sup> Combined fit to ARGUS tau decay parameter measurements in ALBRECHT 95C, ALBRECHT 93G, and ALBRECHT 94E.

 $\rho(e)$  PARAMETER(V-A) theory predicts  $\rho = 0.75$ .

VALUE	EVTS	DOCUMENT ID	TECN	COMMENT
<b>0.747 ± 0.010 OUR FIT</b>				
<b>0.744 ± 0.010 OUR AVERAGE</b>				
0.747 ± 0.019 ± 0.014	44k	HEISTER	01E ALEP	1991-1995 LEP runs
0.744 ± 0.036 ± 0.037	17k	ABREU	00L DLPH	1992-1995 runs
0.779 ± 0.047 ± 0.029	25k	ACKERSTAFF	99D OPAL	1990-1995 LEP runs
0.68 ± 0.04 ± 0.07		<sup>1</sup> ALBRECHT	98 ARG	$E_{\text{cm}}^{\text{ee}} = 9.5-10.6 \text{ GeV}$
0.71 ± 0.14 ± 0.05		ABE	97o SLD	1993-1995 SLC runs
0.747 ± 0.012 ± 0.004	34k	ALEXANDER	97F CLEO	$E_{\text{cm}}^{\text{ee}} = 10.6 \text{ GeV}$
0.735 ± 0.036 ± 0.020	4.7k	<sup>2</sup> ALBRECHT	95 ARG	$E_{\text{cm}}^{\text{ee}} = 9.5-10.6 \text{ GeV}$
0.79 ± 0.08 ± 0.06	3230	<sup>3</sup> ALBRECHT	93G ARG	$E_{\text{cm}}^{\text{ee}} = 9.4-10.6 \text{ GeV}$
0.64 ± 0.06 ± 0.07	2753	JANSSEN	89 CBAL	$E_{\text{cm}}^{\text{ee}} = 9.4-10.6 \text{ GeV}$
0.62 ± 0.17 ± 0.14	1823	FORD	87B MAC	$E_{\text{cm}}^{\text{ee}} = 29 \text{ GeV}$
0.60 ± 0.13	699	BEHRENDIS	85 CLEO	$e^+e^-$ near $\Upsilon(4S)$
0.72 ± 0.10 ± 0.11	594	BACINO	79B DLCO	$E_{\text{cm}}^{\text{ee}} = 3.5-7.4 \text{ GeV}$
••• We do not use the following data for averages, fits, limits, etc. •••				
0.732 ± 0.014 ± 0.009	19k	AMMAR	97B CLEO	Repl. by ALEXANDER 97F
0.793 ± 0.050 ± 0.025		BUSKULIC	95D ALEP	Repl. by HEISTER 01E
0.747 ± 0.045 ± 0.028	5106	ALBRECHT	90E ARG	Repl. by ALBRECHT 95

<sup>1</sup> ALBRECHT 98 use tau pair events of the type  $\tau^- \tau^+ \rightarrow (\ell^- \bar{\nu}_\ell \nu_\tau)(\pi^+ \pi^0 \bar{\nu}_\tau)$ , and their charged conjugates.

<sup>2</sup> ALBRECHT 95 use tau pair events of the type  $\tau^- \tau^+ \rightarrow (\ell^- \bar{\nu}_\ell \nu_\tau)(h^+ h^- h^+ (\pi^0) \bar{\nu}_\tau)$  and their charged conjugates.

<sup>3</sup> ALBRECHT 93G use tau pair events of the type  $\tau^- \tau^+ \rightarrow (\mu^- \bar{\nu}_\mu \nu_\tau)(e^+ \nu_e \bar{\nu}_\tau)$  and their charged conjugates.

 $\rho(\mu)$  PARAMETER(V-A) theory predicts  $\rho = 0.75$ .

VALUE	EVTS	DOCUMENT ID	TECN	COMMENT
<b>0.763 ± 0.020 OUR FIT</b>				
<b>0.770 ± 0.022 OUR AVERAGE</b>				
0.776 ± 0.045 ± 0.019	46k	HEISTER	01E ALEP	1991-1995 LEP runs
0.999 ± 0.098 ± 0.045	22k	ABREU	00L DLPH	1992-1995 runs
0.777 ± 0.044 ± 0.016	27k	ACKERSTAFF	99D OPAL	1990-1995 LEP runs
0.69 ± 0.06 ± 0.06		<sup>1</sup> ALBRECHT	98 ARG	$E_{\text{cm}}^{\text{ee}} = 9.5-10.6 \text{ GeV}$
0.54 ± 0.28 ± 0.14		ABE	97o SLD	1993-1995 SLC runs
0.750 ± 0.017 ± 0.045	22k	ALEXANDER	97F CLEO	$E_{\text{cm}}^{\text{ee}} = 10.6 \text{ GeV}$
0.76 ± 0.07 ± 0.08	3230	ALBRECHT	93G ARG	$E_{\text{cm}}^{\text{ee}} = 9.4-10.6 \text{ GeV}$
0.734 ± 0.055 ± 0.027	3041	ALBRECHT	90E ARG	$E_{\text{cm}}^{\text{ee}} = 9.4-10.6 \text{ GeV}$
0.89 ± 0.14 ± 0.08	1909	FORD	87B MAC	$E_{\text{cm}}^{\text{ee}} = 29 \text{ GeV}$
0.81 ± 0.13	727	BEHRENDIS	85 CLEO	$e^+e^-$ near $\Upsilon(4S)$
••• We do not use the following data for averages, fits, limits, etc. •••				
0.747 ± 0.048 ± 0.044	13k	AMMAR	97B CLEO	Repl. by ALEXANDER 97F
0.693 ± 0.057 ± 0.028		BUSKULIC	95D ALEP	Repl. by HEISTER 01E

<sup>1</sup> ALBRECHT 98 use tau pair events of the type  $\tau^- \tau^+ \rightarrow (\ell^- \bar{\nu}_\ell \nu_\tau)(\pi^+ \pi^0 \bar{\nu}_\tau)$ , and their charged conjugates.

 $\xi(e \text{ or } \mu)$  PARAMETER(V-A) theory predicts  $\xi = 1$ .

VALUE	EVTS	DOCUMENT ID	TECN	COMMENT
<b>0.985 ± 0.030 OUR FIT</b>				
<b>0.981 ± 0.031 OUR AVERAGE</b>				
0.986 ± 0.068 ± 0.031	81k	HEISTER	01E ALEP	1991-1995 LEP runs
0.929 ± 0.070 ± 0.030	36k	ABREU	00L DLPH	1992-1995 runs
0.98 ± 0.22 ± 0.10	46k	ACKERSTAFF	99D OPAL	1990-1995 LEP runs
0.70 ± 0.16	54k	ACCARRI	98R L3	1991-1995 LEP runs
1.03 ± 0.11		<sup>1</sup> ALBRECHT	98 ARG	$E_{\text{cm}}^{\text{ee}} = 9.5-10.6 \text{ GeV}$
1.05 ± 0.35 ± 0.04		<sup>2</sup> ABE	97o SLD	1993-1995 SLC runs
1.007 ± 0.040 ± 0.015	55k	ALEXANDER	97F CLEO	$E_{\text{cm}}^{\text{ee}} = 10.6 \text{ GeV}$
••• We do not use the following data for averages, fits, limits, etc. •••				
0.94 ± 0.21 ± 0.07	18k	ACCARRI	96H L3	Repl. by ACCARRI 98R
0.97 ± 0.14		<sup>3</sup> ALBRECHT	95C ARG	Repl. by ALBRECHT 98
1.18 ± 0.15 ± 0.16		BUSKULIC	95D ALEP	Repl. by HEISTER 01E
0.90 ± 0.15 ± 0.10	3230	<sup>4</sup> ALBRECHT	93G ARG	$E_{\text{cm}}^{\text{ee}} = 9.4-10.6 \text{ GeV}$

<sup>1</sup> Combined fit to ARGUS tau decay parameter measurements in ALBRECHT 98, ALBRECHT 95C, ALBRECHT 93G, and ALBRECHT 94E. ALBRECHT 98 use tau pair events of the type  $\tau^- \tau^+ \rightarrow (\ell^- \bar{\nu}_\ell \nu_\tau)(\pi^+ \pi^0 \bar{\nu}_\tau)$ , and their charged conjugates.

<sup>2</sup> ABE 97o assume  $\eta = 0$  in their fit. Letting  $\eta$  vary in the fit gives a  $\xi$  value of  $1.02 \pm 0.36 \pm 0.05$ .

<sup>3</sup> Combined fit to ARGUS tau decay parameter measurements in ALBRECHT 95C, ALBRECHT 93G, and ALBRECHT 94E. ALBRECHT 95C use events of the type  $\tau^- \tau^+ \rightarrow (\ell^- \bar{\nu}_\ell \nu_\tau)(h^+ h^- h^+ \bar{\nu}_\tau)$  and their charged conjugates.

<sup>4</sup> ALBRECHT 93G measurement determines  $|\xi|$  for the case  $\xi(e) = \xi(\mu)$ , but the authors point out that other LEP experiments determine the sign to be positive.



$\xi(e)$  PARAMETER

( $V-A$ ) theory predicts  $\xi = 1$ .

Table with columns: VALUE, EVTS, DOCUMENT ID, TECN, COMMENT. Includes sub-sections for OUR FIT and OUR AVERAGE.

••• We do not use the following data for averages, fits, limits, etc. •••
1.03 ± 0.23 ± 0.09 BUSKULIC 95D ALEP Repl. by HEISTER 01E
1 ALBRECHT 98 use tau pair events of the type  $\tau^- \tau^+ \rightarrow (\ell^- \bar{\nu}_\ell \nu_\tau)(\pi^+ \pi^0 \bar{\nu}_\tau)$ , and their charged conjugates.

$\xi(\mu)$  PARAMETER

( $V-A$ ) theory predicts  $\xi = 1$ .

Table with columns: VALUE, EVTS, DOCUMENT ID, TECN, COMMENT. Includes sub-sections for OUR FIT and OUR AVERAGE.

••• We do not use the following data for averages, fits, limits, etc. •••
1.23 ± 0.22 ± 0.10 BUSKULIC 95D ALEP Repl. by HEISTER 01E
1 ALBRECHT 98 use tau pair events of the type  $\tau^- \tau^+ \rightarrow (\ell^- \bar{\nu}_\ell \nu_\tau)(\pi^+ \pi^0 \bar{\nu}_\tau)$ , and their charged conjugates.

$\eta(e \text{ or } \mu)$  PARAMETER

( $V-A$ ) theory predicts  $\eta = 0$ .

Table with columns: VALUE, EVTS, DOCUMENT ID, TECN, COMMENT. Includes sub-sections for OUR FIT and OUR AVERAGE.

••• We do not use the following data for averages, fits, limits, etc. •••
0.25 ± 0.17 ± 0.11 18k ACCIARRI 96H L3 Repl. by ACCIARRI 98R
-0.04 ± 0.15 ± 0.11 BUSKULIC 95D ALEP Repl. by HEISTER 01E

$\eta(\mu)$  PARAMETER

( $V-A$ ) theory predicts  $\eta = 0$ .

Table with columns: VALUE, EVTS, DOCUMENT ID, TECN, COMMENT. Includes sub-sections for OUR FIT and OUR AVERAGE.

••• We do not use the following data for averages, fits, limits, etc. •••
0.10 ± 0.065 ± 0.001 27k 3 ACKERSTAFF 99D OPAL 1990-1995 LEP runs
-0.24 ± 0.23 ± 0.18 BUSKULIC 95D ALEP Repl. by HEISTER 01E
1 Highly correlated (corr. = 0.92) with ABE 97o  $\rho(\mu)$  measurement.
2 Highly correlated (corr. = 0.949) with AMMAR 97B  $\rho(\mu)$  value.
3 ACKERSTAFF 99D result is dominated by a constraint on  $\eta$  from the OPAL measurements of the  $\tau$  lifetime and  $B(\tau^- \rightarrow \mu^- \bar{\nu}_\mu \nu_\tau)$  assuming lepton universality for the total coupling strength.

$(\delta\xi)(e \text{ or } \mu)$  PARAMETER

( $V-A$ ) theory predicts  $(\delta\xi) = 0.75$ .

Table with columns: VALUE, EVTS, DOCUMENT ID, TECN, COMMENT. Includes sub-sections for OUR FIT and OUR AVERAGE.

••• We do not use the following data for averages, fits, limits, etc. •••
0.81 ± 0.14 ± 0.06 18k ACCIARRI 96H L3 Repl. by ACCIARRI 98R
0.65 ± 0.12 3 ALBRECHT 95C ARG Repl. by ALBRECHT 98
0.88 ± 0.11 ± 0.07 BUSKULIC 95D ALEP Repl. by HEISTER 01E

1 Combined fit to ARGUS tau decay parameter measurements in ALBRECHT 98, ALBRECHT 95C, ALBRECHT 93G, and ALBRECHT 94E. ALBRECHT 98 use tau pair events of the type  $\tau^- \tau^+ \rightarrow (\ell^- \bar{\nu}_\ell \nu_\tau)(\pi^+ \pi^0 \bar{\nu}_\tau)$ , and their charged conjugates.

2 ABE 97o assume  $\eta = 0$  in their fit. Letting  $\eta$  vary in the fit gives a  $(\delta\xi)$  value of  $0.87 \pm 0.27 \pm 0.04$ .

3 Combined fit to ARGUS tau decay parameter measurements in ALBRECHT 95C, ALBRECHT 93G, and ALBRECHT 94E. ALBRECHT 95C uses events of the type  $\tau^- \tau^+ \rightarrow (\ell^- \bar{\nu}_\ell \nu_\tau) (h^+ h^- h^+ \bar{\nu}_\tau)$  and their charged conjugates.

$(\delta\xi)(e)$  PARAMETER

( $V-A$ ) theory predicts  $(\delta\xi) = 0.75$ .

Table with columns: VALUE, EVTS, DOCUMENT ID, TECN, COMMENT. Includes sub-sections for OUR FIT and OUR AVERAGE.

••• We do not use the following data for averages, fits, limits, etc. •••
1.11 ± 0.17 ± 0.07 BUSKULIC 95D ALEP Repl. by HEISTER 01E
1 ALBRECHT 98 use tau pair events of the type  $\tau^- \tau^+ \rightarrow (\ell^- \bar{\nu}_\ell \nu_\tau)(\pi^+ \pi^0 \bar{\nu}_\tau)$ , and their charged conjugates.

$(\delta\xi)(\mu)$  PARAMETER

( $V-A$ ) theory predicts  $(\delta\xi) = 0.75$ .

Table with columns: VALUE, EVTS, DOCUMENT ID, TECN, COMMENT. Includes sub-sections for OUR FIT and OUR AVERAGE.

••• We do not use the following data for averages, fits, limits, etc. •••
0.71 ± 0.14 ± 0.06 BUSKULIC 95D ALEP Repl. by HEISTER 01E
1 ALBRECHT 98 use tau pair events of the type  $\tau^- \tau^+ \rightarrow (\ell^- \bar{\nu}_\ell \nu_\tau)(\pi^+ \pi^0 \bar{\nu}_\tau)$ , and their charged conjugates.

$\xi(\pi)$  PARAMETER

( $V-A$ ) theory predicts  $\xi(\pi) = 1$ .

Table with columns: VALUE, EVTS, DOCUMENT ID, TECN, COMMENT. Includes sub-sections for OUR FIT and OUR AVERAGE.

••• We do not use the following data for averages, fits, limits, etc. •••
0.987 ± 0.057 ± 0.027 BUSKULIC 95D ALEP Repl. by HEISTER 01E
0.95 ± 0.11 ± 0.05 1 BUSKULIC 94D ALEP 1990+1991 LEP run
1 Superseded by BUSKULIC 95D.

$\xi(\rho)$  PARAMETER

( $V-A$ ) theory predicts  $\xi(\rho) = 1$ .

Table with columns: VALUE, EVTS, DOCUMENT ID, TECN, COMMENT. Includes sub-sections for OUR FIT and OUR AVERAGE.

••• We do not use the following data for averages, fits, limits, etc. •••
1.045 ± 0.058 ± 0.032 BUSKULIC 95D ALEP Repl. by HEISTER 01E
1.03 ± 0.11 ± 0.05 2 BUSKULIC 94D ALEP 1990+1991 LEP run
1 ALBRECHT 94E measure the square of this quantity and use the sign determined by ALBRECHT 90I to obtain the quoted result.
2 Superseded by BUSKULIC 95D.

$\xi(a_1)$  PARAMETER

( $V-A$ ) theory predicts  $\xi(a_1) = 1$ .

Table with columns: VALUE, EVTS, DOCUMENT ID, TECN, COMMENT. Includes sub-sections for OUR FIT and OUR AVERAGE.

••• We do not use the following data for averages, fits, limits, etc. •••
1.08 +0.46 +0.14 -0.41 -0.25 2.6k 3 AKERS 95P OPAL Repl. by ACKERSTAFF 97R
0.937 ± 0.116 ± 0.064 BUSKULIC 95D ALEP Repl. by HEISTER 01E





# Lepton Particle Listings

## Heavy Charged Lepton Searches, Neutrino Properties

### Charged Long-Lived Heavy Lepton MASS LIMITS

VALUE (GeV)	CL%	EVTS	DOCUMENT ID	TECN	CHG	COMMENT
>102.0	95		ABBIENDI	03L	OPAL	pair produced in $e^+e^-$
> 0.1		0	<sup>16</sup> ANSORGE	73B	HBC	Long-lived
none 0.55-4.5			<sup>17</sup> BUSHNIN	73	CNTR	Long-lived
none 0.2-0.92			<sup>18</sup> BARNA	68	CNTR	Long-lived
none 0.97-1.03			<sup>18</sup> BARNA	68	CNTR	Long-lived

<sup>16</sup> ANSORGE 73B looks for electron pair production and electron-like Bremsstrahlung.  
<sup>17</sup> BUSHNIN 73 is SERPUKHOV 70 GeV  $p$  experiment. Masses assume mean life above  $7 \times 10^{-10}$  and  $3 \times 10^{-8}$  respectively. Calculated from cross section (see "Charged Quasi-Stable Lepton Production Differential Cross Section" below) and 30 GeV muon pair production data.  
<sup>18</sup> BARNA 68 is SLAC photoproduction experiment.

### Doubly-Charged Heavy Lepton MASS LIMITS

VALUE (GeV)	CL%	DOCUMENT ID	TECN	CHG
none 1-9 GeV	90	<sup>19</sup> CLARK	81	SPEC ++

<sup>19</sup> CLARK 81 is FNAL experiment with 209 GeV muons. Bounds apply to  $\mu\mu$  which couples with full weak strength to muon. See also section on "Doubly-Charged Lepton Production Cross Section."

### Doubly-Charged Lepton Production Cross Section ( $\mu N$ Scattering)

VALUE (cm <sup>2</sup> )	EVTS	DOCUMENT ID	TECN	CHG
<6. $\times 10^{-38}$	0	<sup>20</sup> CLARK	81	SPEC ++

<sup>20</sup> CLARK 81 is FNAL experiment with 209 GeV muon. Looked for  $\mu^+ \text{nucleon} \rightarrow \bar{\mu}_P^0 X$ ,  $\bar{\mu}_P^0 \rightarrow \mu^+ \mu^- \bar{\nu}_\mu$  and  $\mu^+ n \rightarrow \mu_P^+ X$ ,  $\mu_P^+ \rightarrow 2\mu^+ \nu_\mu$ . Above limits are for  $\sigma \times BR$  taken from their mass-dependence plot figure 2.

### REFERENCES FOR Heavy Charged Lepton Searches

ABBIENDI	03L	PL B572 8	G. Abbiendi <i>et al.</i>	(OPAL Collab.)
ACHARD	01B	PL B517 75	P. Achard <i>et al.</i>	(L3 Collab.)
ACKERSTAFF	96C	EPJ C1 45	K. Ackerstaff <i>et al.</i>	(OPAL Collab.)
ACCIARRI	96G	PL B377 304	M. Acciari <i>et al.</i>	(L3 Collab.)
ALEXANDER	96P	PL B385 433	G. Alexander <i>et al.</i>	(OPAL Collab.)
BUSKULIC	96S	PL B384 439	D. Buskulic <i>et al.</i>	(ALEPH Collab.)
AHMED	94	PL B340 205	T. Ahmed <i>et al.</i>	(HI Collab.)
KIM	91B	JUMP A6 2583	G.N. Kim <i>et al.</i>	(AMY Collab.)
ADACHI	90C	PL B244 352	I. Adachi <i>et al.</i>	(TOPAZ Collab.)
AKRAWY	90G	PL B240 250	M.Z. Akrawy <i>et al.</i>	(OPAL Collab.)
AKRAWY	90O	PL B252 290	M.Z. Akrawy <i>et al.</i>	(OPAL Collab.)
DECAMP	90F	PL B236 511	D. Decamp <i>et al.</i>	(ALEPH Collab.)
RILES	90	PR D42 1	K. Riles <i>et al.</i>	(Mark II Collab.)
SODERSTROM	90	PRL 64 2980	E. Soderstrom <i>et al.</i>	(Mark II Collab.)
STOKER	89	PR D39 1811	D.P. Stoker <i>et al.</i>	(Mark II Collab.)
ABE	88	PRL 61 915	K. Abe <i>et al.</i>	(VENUS Collab.)
ADACHI	88B	PR D37 1339	I. Adachi <i>et al.</i>	(TOPAZ Collab.)
BEHREND	88C	ZPHY C41 7	H.J. Behrend <i>et al.</i>	(CELLO Collab.)
ALBAJAR	87B	PL B185 241	C. Albajar <i>et al.</i>	(UA1 Collab.)
ADEVA	85	PL 152B 439	B. Adeva <i>et al.</i>	(Mark-J Collab.)
Also		PRPL 109 131	B. Adeva <i>et al.</i>	(Mark-J Collab.)
BARTEL	83	PL 123B 353	W. Bartel <i>et al.</i>	(JADE Collab.)
BERGER	81B	PL 99B 489	C. Berger <i>et al.</i>	(PLUTO Collab.)
BRANDELIK	81	PL 99B 163	R. Brandelik <i>et al.</i>	(TASSO Collab.)
CLARK	81	PRL 46 299	A.R. Clark <i>et al.</i>	(UCB, LBL, FNAL+)
Also		PR D25 2762	W.H. Smith <i>et al.</i>	(LBL, FNAL, PRIM)
AZIMOV	80	JETPL 32 664	Y.I. Azimov, V.A. Khoze	(PMP)
Translated from		ZETFP 32 677		
BARBER	80B	PRL 45 1904	D.P. Barber <i>et al.</i>	(Mark-J Collab.)
BRANDELIK	80	PL 92B 199	R. Brandelik <i>et al.</i>	(TASSO Collab.)
ANSORGE	73B	PR D7 26	R.E. Ansorge <i>et al.</i>	(CAVE)
BUSHNIN	73	NP B58 476	Y.B. Bushnin <i>et al.</i>	(SERP)
Also		PL 42B 136	S.V. Golovkin <i>et al.</i>	(SERP)
ROTHE	69	NP B10 241	K.W. Rothe, A.M. Wolsky	(PENN)
BARNA	68	PR 173 1391	A. Barna <i>et al.</i>	(SLAC, STAN)

### OTHER RELATED PAPERS

PERL	81	SLAC-PUB-2752	M.L. Perl	(SLAC)
Physics in Collision Conference.				

## Neutrino Properties

### INTRODUCTION TO THE NEUTRINO PROPERTIES LISTINGS

Revised August 2011 by P. Vogel (Caltech) and A. Piepke (University of Alabama).

The following Listings concern measurements of various properties of neutrinos. Nearly all of the measurements, all of which so far are limits, actually concern superpositions of

the mass eigenstates  $\nu_i$ , which are in turn related to the weak eigenstates  $\nu_\ell$ , via the neutrino mixing matrix

$$|\nu_\ell\rangle = \sum_i U_{\ell i} |\nu_i\rangle.$$

In the analogous case of quark mixing via the CKM matrix, the smallness of the off-diagonal terms (small mixing angles) permits a "dominant eigenstate" approximation. However, the present results of neutrino oscillation searches show that the mixing matrix contains two large mixing angles. We cannot, therefore, associate any particular state  $|\nu_i\rangle$  with any particular lepton label  $e, \mu$  or  $\tau$ . Nevertheless, neutrinos are produced in weak decays with a definite lepton flavor, and are typically detected by the charged current weak interaction again associated with a specific lepton flavor. Hence, the listings for the neutrino mass that follow are separated into the three associated charged-lepton categories. Other properties (mean lifetime, magnetic moment, charge, and charge radius) are no longer separated this way. If needed, the associated lepton flavor is reported in the footnotes.

Measured quantities (mass-squared, magnetic moments, mean lifetimes, *etc.*) all depend upon the mixing parameters  $|U_{\ell i}|^2$ , but to some extent also on experimental conditions (*e.g.*, on energy resolution). Most of these observables, in particular mass-squared, cannot distinguish between Dirac and Majorana neutrinos, and are unaffected by  $CP$  phases.

Direct neutrino mass measurements are usually based on the analysis of the kinematics of charged particles (leptons, pions) emitted together with neutrinos (flavor states) in various weak decays. The most sensitive neutrino mass measurement to date, involving electron type antineutrinos, is based on fitting the shape of the beta spectrum. The quantity  $\langle m_\beta^2 \rangle = \sum_i |U_{ei}|^2 m_{\nu_i}^2$  is determined or constrained, where the sum is over all mass eigenvalues  $m_{\nu_i}$  that are too close together to be resolved experimentally. If the energy resolution is better than  $\Delta m_{ij}^2 \equiv m_{\nu_i}^2 - m_{\nu_j}^2$ , the corresponding heavier  $m_{\nu_i}$  and mixing parameter could be determined by fitting the resulting spectral anomaly (step or kink).

A limit on  $\langle m_\beta^2 \rangle$  implies an *upper* limit on the *minimum* value  $m_{\min}^2$  of  $m_{\nu_i}^2$ , independent of the mixing parameters  $U_{ei}$ :  $m_{\min}^2 \leq \langle m_\beta^2 \rangle$ . However, if and when the value of  $\langle m_\beta^2 \rangle$  is determined and the study of neutrino oscillations provides us with the values of *all* neutrino mass-squared differences  $\Delta m_{ij}^2 \equiv m_i^2 - m_j^2$  and the mixing parameters  $|U_{ei}|^2$ , then the individual neutrino mass squares  $m_{\nu_j}^2 = \langle m_\beta^2 \rangle - \sum_i |U_{ei}|^2 \Delta m_{ij}^2$  can be determined.

So far solar, reactor, atmospheric and accelerator neutrino oscillation experiments can be consistently described using three active neutrino flavors, i.e. two mass splittings and three mixing angles. However, several experiments with radioactive sources, reactors, and accelerators imply the possible existence of one or more non-interacting neutrino species.

# Lepton Particle Listings

## Neutrino Properties

See key on page 457

Combined three neutrino analyses determine the squared mass differences and two of the mixing angles to within reasonable accuracy. For given  $|\Delta m_{ij}^2|$ , a limit on  $\langle m_\beta^2 \rangle$  from beta decay defines an upper limit on the maximum value  $m_{max}$  of  $m_{\nu_i}$ :  $m_{max}^2 \leq \langle m_\beta^2 \rangle + \sum_{i < j} |\Delta m_{ij}^2|$ . The analysis of the low energy beta decay of tritium, combined with the oscillation results, thus limits all active neutrino masses. Traditionally experimental neutrino mass limits obtained from pion decay  $\pi^+ \rightarrow \mu^+ + \nu_\mu$ , or the shape of the spectrum of decay products of the  $\tau$  lepton, did not distinguish between flavor and mass eigenstates. These results are reported as limits of the  $\mu$  and  $\tau$  based neutrino mass. After the determination of the  $|\Delta m_{ij}^2|$ 's, the corresponding neutrino mass limits are no longer competitive with those derived from low energy beta decays, with the proviso, however, that the oscillation searches, reported below, can be regarded as a reliable source of all  $|\Delta m_{ij}^2|$  values.

The spread of arrival times of the neutrinos from SN1987A, coupled with the measured neutrino energies, provided a time-of-flight limit on a quantity similar to  $\langle m_\beta \rangle \equiv \sqrt{\langle m_\beta^2 \rangle}$ . This statement, clothed in various degrees of sophistication, has been the basis for a very large number of papers. The resulting limits, however, are no longer comparable with the limits from tritium beta decay.

Constraint on the sum of the neutrino masses can be obtained from the analysis of the cosmic microwave background anisotropy, combined with the galaxy redshift surveys and other data. These limits are reported in a separate table (Sum of Neutrino Masses,  $m_{tot}$ ). Discussion concerning the model dependence of this limit is continuing.

### $\overline{\nu}$ MASS (electron based)

Those limits given below are for the square root of  $m_{\nu_e}^{2(\text{eff})} \equiv \sum_i |U_{ei}|^2 m_{\nu_i}^2$ . Limits that come from the kinematics of  ${}^3\text{H}\beta^- \overline{\nu}$  decay are the square roots of the limits for  $m_{\nu_e}^{2(\text{eff})}$ . Obtained from the measurements reported in the Listings for " $\overline{\nu}$  Mass Squared," below.

VALUE (eV)	CL%	DOCUMENT ID	TECN	COMMENT
<b>&lt; 2</b>	<b>OUR EVALUATION</b>			
<b>&lt; 2.05</b>	95	1 ASEEV	11	SPEC ${}^3\text{H}\beta$ decay
••• We do not use the following data for averages, fits, limits, etc. •••				
< 5.8	95	2 PAGLIAROLI	10	ASTR SN1987A
< 2.3	95	3 KRAUS	05	SPEC ${}^3\text{H}\beta$ decay
< 21.7	90	4 ARNABOLDI	03A	BOLO ${}^{187}\text{Re}$ $\beta$ -decay
< 5.7	95	5 LOREDO	02	ASTR SN1987A
< 2.5	95	6 LOBASHEV	99	SPEC ${}^3\text{H}\beta$ decay
< 2.8	95	7 WEINHEIMER	99	SPEC ${}^3\text{H}\beta$ decay
< 4.35	95	8 BELESEV	95	SPEC ${}^3\text{H}\beta$ decay
< 12.4	95	9 CHING	95	SPEC ${}^3\text{H}\beta$ decay
< 92	95	10 HIDDEMANN	95	SPEC ${}^3\text{H}\beta$ decay
15 $\pm$ $\frac{32}{-15}$		HIDDEMANN	95	SPEC ${}^3\text{H}\beta$ decay
< 19.6	95	KERNAN	95	ASTR SN 1987A
< 7.0	95	11 STOEFL	95	SPEC ${}^3\text{H}\beta$ decay
< 7.2	95	12 WEINHEIMER	93	SPEC ${}^3\text{H}\beta$ decay
< 11.7	95	13 HOLZSCHUH	92B	SPEC ${}^3\text{H}\beta$ decay
< 13.1	95	14 KAWAKAMI	91	SPEC ${}^3\text{H}\beta$ decay
< 9.3	95	15 ROBERTSON	91	SPEC ${}^3\text{H}\beta$ decay
< 14	95	AVIGNONE	90	ASTR SN 1987A
< 16		SPERGEL	88	ASTR SN 1987A
17 to 40		16 BORIS	87	SPEC ${}^3\text{H}\beta$ decay

- ASEEV 11 report the analysis of the entire beta endpoint data, taken with the Troitsk integrating electrostatic spectrometer between 1997 and 2002 (some of the earlier runs were rejected), using a windowless gaseous tritium source. The fitted value of  $m_\nu$ , based on the method of Feldman and Cousins, is obtained from the upper limit of the fit for  $m_\nu^2$ . Previous analysis problems were resolved by careful monitoring of the tritium gas column density. Supersedes LOBASHEV 99 and BELESEV 95.
- PAGLIAROLI 10 is critical of the likelihood method used by LOREDO 02.
- KRAUS 05 is a continuation of the work reported in WEINHEIMER 99. This result represents the final analysis of data taken from 1997 to 2001. Various sources of systematic uncertainties have been identified and quantified. The background has been reduced compared to the initial running period. A spectral anomaly at the endpoint, reported in LOBASHEV 99, was not observed.
- ARNABOLDI 03A *et al.* report kinematical neutrino mass limit using  $\beta$ -decay of  ${}^{187}\text{Re}$ . Bolometric  $\text{AgReO}_4$  micro-calorimeters are used. Mass bound is substantially weaker than those derived from tritium  $\beta$ -decays but has different systematic uncertainties.
- LOREDO 02 updates LOREDO 89.
- LOBASHEV 99 report a new measurement which continues the work reported in BELESEV 95. This limit depends on phenomenological fit parameters used to derive their best fit to  $m_\nu^2$ , making unambiguous interpretation difficult. See the footnote under " $\overline{\nu}$  Mass Squared."
- WEINHEIMER 99 presents two analyses which exclude the spectral anomaly and result in an acceptable  $m_\nu^2$ . We report the most conservative limit, but the other is nearly the same. See the footnote under " $\overline{\nu}$  Mass Squared."
- BELESEV 95 (Moscow) use an integral electrostatic spectrometer with adiabatic magnetic collimation and a gaseous tritium source. A fit to a normal Kurie plot above 18300-18350 eV (to avoid a low-energy anomaly) plus a monochromatic line 7-15 eV below the endpoint yields  $m_\nu^2 = -4.1 \pm 10.9 \text{ eV}^2$ , leading to this Bayesian limit.
- CHING 95 quotes results previously given by SUN 93; no experimental details are given. A possible explanation for consistently negative values of  $m_\nu^2$  is given.
- HIDDEMANN 95 (Munich) experiment uses atomic tritium embedded in a metal-dioxide lattice. Bayesian limit calculated from the weighted mean  $m_\nu^2 = 221 \pm 4244 \text{ eV}^2$  from the two runs listed below.
- STOEFL 95 (LLNL) result is the Bayesian limit obtained from the  $m_\nu^2$  errors given below but with  $m_\nu^2$  set equal to 0. The anomalous endpoint accumulation leads to a value of  $m_\nu^2$  which is negative by more than 5 standard deviations.
- WEINHEIMER 93 (Mainz) is a measurement of the endpoint of the tritium  $\beta$  spectrum using an electrostatic spectrometer with a magnetic guiding field. The source is molecular tritium frozen onto an aluminum substrate.
- HOLZSCHUH 92B (Zurich) result is obtained from the measurement  $m_\nu^2 = -24 \pm 48 \pm 61$  ( $1\sigma$  errors), in  $\text{eV}^2$ , using the PDG prescription for conversion to a limit in  $m_\nu$ .
- KAWAKAMI 91 (Tokyo) experiment uses tritium-labeled arachidic acid. This result is the Bayesian limit obtained from the  $m_\nu^2$  limit with the errors combined in quadrature. This was also done in ROBERTSON 91, although the authors report a different procedure.
- ROBERTSON 91 (LANL) experiment uses gaseous molecular tritium. The result is in strong disagreement with the earlier claims by the ITP group [LUBIMOV 80, BORIS 87 (+ BORIS 88 erratum)] that  $m_\nu$  lies between 17 and 40 eV. However, the probability of a positive  $m^2$  is only 3% if statistical and systematic error are combined in quadrature.
- See also comment in BORIS 87B and erratum in BORIS 88.

### $\overline{\nu}$ MASS SQUARED (electron based)

Given troubling systematics which result in improbably negative estimates of  $m_{\nu_e}^{2(\text{eff})} \equiv \sum_i |U_{ei}|^2 m_{\nu_i}^2$ , in many experiments, we use only KRAUS 05 and LOBASHEV 99 for our average.

VALUE (eV <sup>2</sup> )	CL%	DOCUMENT ID	TECN	COMMENT
<b>- 0.6 <math>\pm</math> 1.9</b>	<b>OUR AVERAGE</b>			
- 0.67 $\pm$ 2.53		17 ASEEV	11	SPEC ${}^3\text{H}\beta$ decay
- 0.6 $\pm$ 2.2 $\pm$ 2.1		18 KRAUS	05	SPEC ${}^3\text{H}\beta$ decay
••• We do not use the following data for averages, fits, limits, etc. •••				
- 1.9 $\pm$ 3.4 $\pm$ 2.2		19 LOBASHEV	99	SPEC ${}^3\text{H}\beta$ decay
- 3.7 $\pm$ 5.3 $\pm$ 2.1		20 WEINHEIMER	99	SPEC ${}^3\text{H}\beta$ decay
- 22 $\pm$ 4.8		21 BELESEV	95	SPEC ${}^3\text{H}\beta$ decay
129 $\pm$ 6010		22 HIDDEMANN	95	SPEC ${}^3\text{H}\beta$ decay
313 $\pm$ 5994		22 HIDDEMANN	95	SPEC ${}^3\text{H}\beta$ decay
-130 $\pm$ 20 $\pm$ 15	95	23 STOEFL	95	SPEC ${}^3\text{H}\beta$ decay
- 31 $\pm$ 75 $\pm$ 48		24 SUN	93	SPEC ${}^3\text{H}\beta$ decay
- 39 $\pm$ 34 $\pm$ 15		25 WEINHEIMER	93	SPEC ${}^3\text{H}\beta$ decay
- 24 $\pm$ 48 $\pm$ 61		26 HOLZSCHUH	92B	SPEC ${}^3\text{H}\beta$ decay
- 65 $\pm$ 85 $\pm$ 65		27 KAWAKAMI	91	SPEC ${}^3\text{H}\beta$ decay
-147 $\pm$ 68 $\pm$ 41		28 ROBERTSON	91	SPEC ${}^3\text{H}\beta$ decay
17 ASEEV 11 report the analysis of the entire beta endpoint data, taken with the Troitsk integrating electrostatic spectrometer between 1997 and 2002, using a windowless gaseous tritium source. The analysis does not use the two additional fit parameters (see LOBASHEV 99) for a step-like structure near the endpoint. Using only the runs where the tritium gas column density was carefully monitored the need for such parameters was eliminated. Supersedes LOBASHEV 99 and BELESEV 95.				
18 KRAUS 05 is a continuation of the work reported in WEINHEIMER 99. This result represents the final analysis of data taken from 1997 to 2001. Problems with significantly negative squared neutrino masses, observed in some earlier experiments, have been resolved in this work.				

# Lepton Particle Listings

## Neutrino Properties

- <sup>19</sup>LOBASHEV 99 report a new measurement which continues the work reported in BELESEV 95. The data were corrected for electron trapping effects in the source, eliminating the dependence of the fitted neutrino mass on the fit interval. The analysis assuming a pure beta spectrum yields significantly negative fitted  $m_\nu^2 \approx -(20-10) \text{ eV}^2$ . This problem is attributed to a discrete spectral anomaly of about  $6 \times 10^{-11}$  intensity with a time-dependent energy of 5–15 eV below the endpoint. The data analysis accounts for this anomaly by introducing two extra phenomenological fit parameters resulting in a best fit of  $m_\nu^2 = -1.9 \pm 3.4 \pm 2.2 \text{ eV}^2$  which is used to derive a neutrino mass limit. However, the introduction of phenomenological fit parameters which are correlated with the derived  $m_\nu^2$  limit makes unambiguous interpretation of this result difficult.
- <sup>20</sup>WEINHEIMER 99 is a continuation of the work reported in WEINHEIMER 93. Using a lower temperature of the frozen tritium source eliminated the dewetting of the  $T_2$  film, which introduced a dependence of the fitted neutrino mass on the fit interval in the earlier work. An indication for a spectral anomaly reported in LOBASHEV 99 has been seen, but its time dependence does not agree with LOBASHEV 99. Two analyses, which exclude the spectral anomaly either by choice of the analysis interval or by using a particular data set which does not exhibit the anomaly, result in acceptable  $m_\nu^2$  fits and are used to derive the neutrino mass limit published by the authors. We list the most conservative of the two.
- <sup>21</sup>BELESEV 95 (Moscow) use an integral electrostatic spectrometer with adiabatic magnetic collimation and a gaseous tritium sources. This value comes from a fit to a normal Kurie plot above 18300–18350 eV (to avoid a low-energy anomaly), including the effects of an apparent peak 7–15 eV below the endpoint.
- <sup>22</sup>HIDDEMANN 95 (Munich) experiment uses atomic tritium embedded in a metal-dioxide lattice. They quote measurements from two data sets.
- <sup>23</sup>STOEFL 95 (LLNL) uses a gaseous source of molecular tritium. An anomalous pileup of events at the endpoint leads to the negative value for  $m_\nu^2$ . The authors acknowledge that “the negative value for the best fit of  $m_\nu^2$  has no physical meaning” and discuss possible explanations for this effect.
- <sup>24</sup>SUN 93 uses a tritiated hydrocarbon source. See also CHING 95.
- <sup>25</sup>WEINHEIMER 93 (Mainz) is a measurement of the endpoint of the tritium  $\beta$  spectrum using an electrostatic spectrometer with a magnetic guiding field. The source is molecular tritium frozen onto an aluminum substrate.
- <sup>26</sup>HOLZSCHUH 92B (Zurich) source is a monolayer of tritiated hydrocarbon.
- <sup>27</sup>KAWAKAMI 91 (Tokyo) experiment uses tritium-labeled arachidic acid.
- <sup>28</sup>ROBERTSON 91 (LANL) experiment uses gaseous molecular tritium. The result is in strong disagreement with the earlier claims by the ITEP group [LUBIMOV 80, BORIS 87 (+ BORIS 88 erratum)] that  $m_\nu$  lies between 17 and 40 eV. However, the probability of a positive  $m_\nu^2$  is only 3% if statistical and systematic error are combined in quadrature.

### $\nu$ MASS (electron based)

These are measurement of  $m_\nu$  (in contrast to  $m_{\nu\tau}$  given above). The masses can be different for a Dirac neutrino in the absence of  $CPT$  invariance. The possible distinction between  $\nu$  and  $\bar{\nu}$  properties is usually ignored elsewhere in these Listings.

VALUE (eV)	CL%	DOCUMENT ID	TECN	COMMENT
<460	68	YASUMI	94	CNTR $^{163}\text{Ho}$ decay
<225	95	SPRINGER	87	CNTR $^{163}\text{Ho}$ decay

### $\nu$ MASS (muon based)

Limits given below are for the square root of  $m_{\nu\mu}^{2(\text{eff})} \equiv \sum_i |U_{\mu i}|^2 m_{\nu_i}^2$ .

In some of the COSM papers listed below, the authors did not distinguish between weak and mass eigenstates.

OUR EVALUATION is based on OUR AVERAGE for the  $\pi^\pm$  mass and the ASSAMAGAN 96 value for the muon momentum for the  $\pi^\pm$  decay at rest. The limit is calculated using the unified classical analysis of FELDMAN 98 for a Gaussian distribution near a physical boundary. WARNING: since  $m_{\nu\mu}^{2(\text{eff})}$  is calculated from the differences of large numbers, it and the corresponding limits are extraordinarily sensitive to small changes in the pion mass, the decay muon momentum, and their errors. For example, the limits obtained using JECKELMANN 94, LENZ 98, and the weighted averages are 0.15, 0.29, and 0.19 MeV, respectively.

VALUE (MeV)	CL%	DOCUMENT ID	TECN	COMMENT
<b>&lt;0.19 (CL = 90%) OUR EVALUATION</b>				
<0.17	90	<sup>29</sup> ASSAMAGAN	96	SPEC $m_\nu^2 = -0.016 \pm 0.023$
• • • We do not use the following data for averages, fits, limits, etc. • • •				
<0.15		<sup>30</sup> DOLGOV	95	COSM Nucleosynthesis
<0.48		<sup>31</sup> ENQVIST	93	COSM Nucleosynthesis
<0.3		<sup>32</sup> FULLER	91	COSM Nucleosynthesis
<0.42		<sup>32</sup> LAM	91	COSM Nucleosynthesis
<0.50	90	<sup>33</sup> ANDERHUB	82	SPEC $m_\nu^2 = -0.14 \pm 0.20$
<0.65	90	CLARK	74	ASPK $K_{\mu 3}$ decay

- <sup>29</sup>ASSAMAGAN 96 measurement of  $p_\mu$  from  $\pi^+ \rightarrow \mu^+ \nu$  at rest combined with JECKELMANN 94 Solution B pion mass yields  $m_\nu^2 = -0.016 \pm 0.023$  with corresponding Bayesian limit listed above. If Solution A is used,  $m_\nu^2 = -0.143 \pm 0.024 \text{ MeV}^2$ . Replaces ASSAMAGAN 94.

- <sup>30</sup>DOLGOV 95 removes earlier assumptions (DOLGOV 93) about thermal equilibrium below  $T_{\text{QCD}}$  for wrong-helicity Dirac neutrinos (ENQVIST 93, FULLER 91) to set more stringent limits.
- <sup>31</sup>ENQVIST 93 bases limit on the fact that thermalized wrong-helicity Dirac neutrinos would speed up expansion of early universe, thus reducing the primordial abundance. FULLER 91 exploits the same mechanism but in the older calculation obtains a larger production rate for these states, and hence a lower limit. Neutrino lifetime assumed to exceed nucleosynthesis time,  $\sim 1 \text{ s}$ .
- <sup>32</sup>Assumes neutrino lifetime  $> 1 \text{ s}$ . For Dirac neutrinos only. See also ENQVIST 93.
- <sup>33</sup>ANDERHUB 82 kinematics is insensitive to the pion mass.

### $\nu$ MASS (tau based)

The limits given below are the square roots of limits for  $m_{\nu\tau}^{2(\text{eff})} \equiv \sum_i |U_{\tau i}|^2 m_{\nu_i}^2$ .

In some of the ASTR and COSM papers listed below, the authors did not distinguish between weak and mass eigenstates.

VALUE (MeV)	CL%	EVTS	DOCUMENT ID	TECN	COMMENT
< 18.2	95		<sup>34</sup> BARATE	98F	ALEP 1991–1995 LEP runs
• • • We do not use the following data for averages, fits, limits, etc. • • •					
< 28	95		<sup>35</sup> ATHANAS	00	CLEO $E_{\text{cm}}^{\text{eff}} = 10.6 \text{ GeV}$
< 27.6	95		<sup>36</sup> ACKERSTAFF	98T	OPAL 1990–1995 LEP runs
< 30	95	473	<sup>37</sup> AMMAR	98	CLEO $E_{\text{cm}}^{\text{eff}} = 10.6 \text{ GeV}$
< 60	95		<sup>38</sup> ANASTASSOV	97	CLEO $E_{\text{cm}}^{\text{eff}} = 10.6 \text{ GeV}$
< 0.37 or > 22			<sup>39</sup> FIELDS	97	COSM Nucleosynthesis
< 68	95		<sup>40</sup> SWAIN	97	THEO $m_\tau, \tau_\tau, \tau$ partial widths
< 29.9	95		<sup>41</sup> ALEXANDER	96M	OPAL 1990–1994 LEP runs
< 149			<sup>42</sup> BOTTINO	96	THEO $\pi, \mu, \tau$ leptonic decays
< 1 or > 25			<sup>43</sup> HANNSTAD	96C	COSM Nucleosynthesis
< 71	95		<sup>44</sup> SOBIE	96	THEO $m_\tau, \tau_\tau, B(\tau^- \rightarrow e^- \bar{\nu}_e \nu_\tau)$
< 24	95	25	<sup>45</sup> BUSKULIC	95H	ALEP 1991–1993 LEP runs
< 0.19			<sup>46</sup> DOLGOV	95	COSM Nucleosynthesis
< 3			<sup>47</sup> SIGL	95	ASTR SN 1987A
< 0.4 or > 30			<sup>48</sup> DODELSON	94	COSM Nucleosynthesis
< 0.1 or > 50			<sup>49</sup> KAWASAKI	94	COSM Nucleosynthesis
155–225			<sup>50</sup> PERES	94	THEO $\pi, K, \mu, \tau$ weak decays
< 32.6	95	113	<sup>51</sup> CINABRO	93	CLEO $E_{\text{cm}}^{\text{eff}} \approx 10.6 \text{ GeV}$
< 0.3 or > 35			<sup>52</sup> DOLGOV	93	COSM Nucleosynthesis
< 0.74			<sup>53</sup> ENQVIST	93	COSM Nucleosynthesis
< 31	95	19	<sup>54</sup> ALBRECHT	92M	ARG $E_{\text{cm}}^{\text{eff}} = 9.4\text{--}10.6 \text{ GeV}$
< 0.3			<sup>55</sup> FULLER	91	COSM Nucleosynthesis
< 0.5 or > 25			<sup>56</sup> KOLB	91	COSM Nucleosynthesis
< 0.42			<sup>55</sup> LAM	91	COSM Nucleosynthesis

- <sup>34</sup>BARATE 98F result based on kinematics of  $2939 \tau^- \rightarrow 2\pi^- \pi^+ \nu_\tau$  and  $52 \tau^- \rightarrow 3\pi^- 2\pi^+ (\pi^0) \nu_\tau$  decays. If possible 2.5% excited  $a_1$  decay is included in 3-prong sample analysis, limit increases to 19.2 MeV.
- <sup>35</sup>ATHANAS 00 bound comes from analysis of  $\tau^- \rightarrow \pi^- \pi^+ \pi^- \pi^0 \nu_\tau$  decays.
- <sup>36</sup>ACKERSTAFF 98T use  $\tau^- \rightarrow 5\pi^\pm \nu_\tau$  decays to obtain a limit of 43.2 MeV (95%CL). They combine this with ALEXANDER 96M value using  $\tau^- \rightarrow 3h^\pm \nu_\tau$  decays to obtain quoted limit.
- <sup>37</sup>AMMAR 98 limit comes from analysis of  $\tau^- \rightarrow 3\pi^- 2\pi^+ \nu_\tau$  and  $\tau^- \rightarrow 2\pi^- \pi^+ 2\pi^0 \nu_\tau$  decay modes.
- <sup>38</sup>ANASTASSOV 97 derive limit by comparing their  $m_\tau$  measurement (which depends on  $m_{\nu_\tau}$ ) to BAI 96  $m_\tau$  threshold measurement.
- <sup>39</sup>FIELDS 97 limit for a Dirac neutrino. For a Majorana neutrino the mass region  $< 0.93$  or  $> 31 \text{ MeV}$  is excluded. These bounds assume  $N_\nu < 4$  from nucleosynthesis; a wider excluded region occurs with a smaller  $N_\nu$  upper limit.
- <sup>40</sup>SWAIN 97 derive their limit from the Standard Model relationships between the tau mass, lifetime, branching fractions for  $\tau^- \rightarrow e^- \bar{\nu}_e \nu_\tau, \tau^- \rightarrow \mu^- \bar{\nu}_\mu \nu_\tau, \tau^- \rightarrow \pi^- \nu_\tau$ , and  $\tau^- \rightarrow K^- \nu_\tau$ , and the muon mass and lifetime by assuming lepton universality and using world average values. Limit is reduced to 48 MeV when the CLEO  $\tau$  mass measurement (BALEST 93) is included; see CLEO's more recent  $m_{\nu_\tau}$  limit (ANASTASSOV 97). Consideration of mixing with a fourth generation heavy neutrino yields  $\sin^2 \theta_L < 0.016$  (95%CL).
- <sup>41</sup>ALEXANDER 96M bound comes from analyses of  $\tau^- \rightarrow 3\pi^- 2\pi^+ \nu_\tau$  and  $\tau^- \rightarrow h^- h^+ \nu_\tau$  decays.
- <sup>42</sup>BOTTINO 96 assumes three generations of neutrinos with mixing, finds consistency with massless neutrinos with no mixing based on 1995 data for masses, lifetimes, and leptonic partial widths.
- <sup>43</sup>HANNSTAD 96C limit is on the mass of a Majorana neutrino. This bound assumes  $N_\nu < 4$  from nucleosynthesis. A wider excluded region occurs with a smaller  $N_\nu$  upper limit. This paper is the corrected version of HANNSTAD 96; see the erratum: HANNSTAD 96b.
- <sup>44</sup>SOBIE 96 derive their limit from the Standard Model relationship between the tau mass, lifetime, and leptonic branching fraction, and the muon mass and lifetime, by assuming lepton universality and using world average values.

See key on page 457

## Lepton Particle Listings Neutrino Properties

- <sup>45</sup> BUSKULIC 95H bound comes from a two-dimensional fit of the visible energy and invariant mass distribution of  $\tau \rightarrow 5\pi(\pi^0)\nu_\tau$  decays. Replaced by BARATE 98F.
- <sup>46</sup> DOLGOV 95 removes earlier assumptions (DOLGOV 93) about thermal equilibrium below  $T_{\text{QCD}}$  for wrong-helicity Dirac neutrinos (ENQVIST 93, FULLER 91) to set more stringent limits. DOLGOV 96 argues that a possible window near 20 MeV is excluded.
- <sup>47</sup> SIGL 95 exclude massive Dirac or Majorana neutrinos with lifetimes between  $10^{-3}$  and  $10^8$  seconds if the decay products are predominantly  $\gamma$  or  $e^+e^-$ .
- <sup>48</sup> DODELSON 94 calculate constraints on  $\nu_\tau$  mass and lifetime from nucleosynthesis for 4 generic decay modes. Limits depend strongly on decay mode. Quoted limit is valid for all decay modes of Majorana neutrinos with lifetime greater than about 300s. For Dirac neutrinos limits change to  $< 0.3$  or  $> 33$ .
- <sup>49</sup> KAWASAKI 94 excluded region is for Majorana neutrino with lifetime  $> 1000$ s. Other limits are given as a function of  $\nu_\tau$  lifetime for decays of the type  $\nu_\tau \rightarrow \nu_\mu \phi$  where  $\phi$  is a Nambu-Goldstone boson.
- <sup>50</sup> PERES 94 used PDG 92 values for parameters to obtain a value consistent with mixing. Reexamination by BOTTINO 96 which included radiative corrections and 1995 PDG parameters resulted in two allowed regions,  $m_3 < 70$  MeV and  $140 \text{ MeV} < m_3 < 149$  MeV.
- <sup>51</sup> CINABRO 93 bound comes from analysis of  $\tau^- \rightarrow 3\pi^- 2\pi^+ \nu_\tau$  and  $\tau^- \rightarrow 2\pi^- \pi^+ 2\pi^0 \nu_\tau$  decay modes.
- <sup>52</sup> DOLGOV 93 assumes neutrino lifetime  $> 100$ s. For Majorana neutrinos, the low mass limit is 0.5 MeV. KAWANO 92 points out that these bounds can be overcome for a Dirac neutrino if it possesses a magnetic moment. See also DOLGOV 96.
- <sup>53</sup> ENQVIST 93 bases limit on the fact that thermalized wrong-helicity Dirac neutrinos would speed up expansion of early universe, thus reducing the primordial abundance. FULLER 91 exploits the same mechanism but in the older calculation obtains a larger production rate for these states, and hence a lower limit. Neutrino lifetime assumed to exceed nucleosynthesis time,  $\sim 1$ s.
- <sup>54</sup> ALBRECHT 92M reports measurement of a slightly lower  $\tau$  mass, which has the effect of reducing the  $\nu_\tau$  mass reported in ALBRECHT 88B. Bound is from analysis of  $\tau^- \rightarrow 3\pi^- 2\pi^+ \nu_\tau$  mode.
- <sup>55</sup> Assumes neutrino lifetime  $> 1$ s. For Dirac neutrinos. See also ENQVIST 93.
- <sup>56</sup> KOLB 91 exclusion region is for Dirac neutrino with lifetime  $> 1$ s; other limits are given.

Revised August 2009 by K.A. Olive (University of Minnesota).

The limits on low mass ( $m_\nu \lesssim 1$  MeV) neutrinos apply to  $m_{\text{tot}}$  given by

$$m_{\text{tot}} = \sum_\nu (g_\nu/2)m_\nu,$$

where  $g_\nu$  is the number of spin degrees of freedom for  $\nu$  plus  $\bar{\nu}$ :  $g_\nu = 4$  for neutrinos with Dirac masses;  $g_\nu = 2$  for Majorana neutrinos. Stable neutrinos in this mass range make a contribution to the total energy density of the Universe which is given by

$$\rho_\nu = m_{\text{tot}} n_\nu = m_{\text{tot}} (3/11) n_\gamma,$$

where the factor 3/11 is the ratio of (light) neutrinos to photons. Writing  $\Omega_\nu = \rho_\nu/\rho_c$ , where  $\rho_c$  is the critical energy density of the Universe, and using  $n_\gamma = 412 \text{ cm}^{-3}$ , we have

$$\Omega_\nu h^2 = m_{\text{tot}} / (94 \text{ eV}).$$

While an upper limit to the matter density of  $\Omega_m h^2 < 0.12$  would constrain  $m_{\text{tot}} < 11$  eV, much stronger constraints are obtained from a combination of observations of the CMB and the amplitude of density fluctuations on smaller scales from the clustering of galaxies and the Lyman- $\alpha$  forest. These combine to give an upper limit around 0.5 eV.

### SUM OF THE NEUTRINO MASSES, $m_{\text{tot}}$

(Defined in the above note), of effectively stable neutrinos (i.e., those with mean lives greater than or equal to the age of the universe). These papers assumed Dirac neutrinos. When necessary, we have generalized the results reported so they apply to  $m_{\text{tot}}$ . For other limits, see SZALAY 76, VYSOTSKY 77, BERNSTEIN 81, FREESE 84, SCHRAMM 84, and COWSIK 85.

VALUE (eV)	CL%	DOCUMENT ID	TECN	COMMENT
< 0.81	95	<sup>57</sup> SAITO	11	COSM SDSS

< 0.44	95	<sup>58</sup> HANNESTAD	10	COSM
< 0.6	95	<sup>59</sup> SEKIGUCHI	10	COSM
< 0.28	95	<sup>60</sup> THOMAS	10	COSM
< 1.1		<sup>61</sup> ICHIKI	09	COSM
< 1.3	95	<sup>62</sup> KOMATSU	09	COSM WMAP
< 1.2		<sup>63</sup> TERENO	09	COSM
< 0.33		<sup>64</sup> VIKHLININ	09	COSM
< 0.28		<sup>65</sup> BERNARDIS	08	COSM
< 0.17-2.3		<sup>66</sup> FOGLI	07	COSM
< 0.42	95	<sup>67</sup> KRISTIANSEN	07	COSM
< 0.63-2.2		<sup>68</sup> ZUNCKEL	07	COSM
< 0.24	95	<sup>69</sup> CIRELLI	06	COSM
< 0.62	95	<sup>70</sup> HANNESTAD	06	COSM
< 1.2		<sup>71</sup> SANCHEZ	06	COSM
< 0.17	95	<sup>69</sup> SELJAK	06	COSM
< 2.0	95	<sup>72</sup> ICHIKAWA	05	COSM
< 0.75		<sup>73</sup> BARGER	04	COSM
< 1.0		<sup>74</sup> CROTTY	04	COSM
< 0.7		<sup>75</sup> SPERGEL	03	COSM WMAP
< 0.9		<sup>76</sup> LEWIS	02	COSM
< 4.2		<sup>77</sup> WANG	02	COSM CMB
< 2.7		<sup>78</sup> FUKUGITA	00	COSM
< 5.5		<sup>79</sup> CROFT	99	ASTR Ly $\alpha$ power spec
< 180		SZALAY	74	COSM
< 132		COWSIK	72	COSM
< 280		MARX	72	COSM
< 400		GERSHTEIN	66	COSM

- <sup>57</sup> Constrains the total mass of neutrinos from the Sloan Digital Sky Survey and the five-year WMAP data.
- <sup>58</sup> Constrains the total mass of neutrinos from the 7-year WMAP data including SDSS and HST data. Limit relaxes to 1.19 eV when CMB data is used alone. Supersedes HANNESTAD 06.
- <sup>59</sup> Constrains the total mass of neutrinos from a combination of CMB data, a recent measurement of  $H_0$  (SHOES), and baryon acoustic oscillation data from SDSS.
- <sup>60</sup> Constrains the total mass of neutrinos from SDSS MegaZ LRG DR7 galaxy clustering data combined with CMB, HST, supernovae and baryon acoustic oscillation data. Limit relaxes to 0.47 eV when the equation of state parameter,  $w \neq -1$ .
- <sup>61</sup> Constrains the total mass of neutrinos from weak lensing measurements when combined with CMB. Limit improves to 0.54 eV when supernovae and baryon acoustic oscillation observations are included. Assumes  $\Lambda$ CDM model.
- <sup>62</sup> Constrains the total mass of neutrinos from five-year WMAP data. Limit improves to 0.67 eV when supernovae and baryon acoustic oscillation observations are included. Limits quoted assume the  $\Lambda$ CDM model. Supersedes SPERGEL 07.
- <sup>63</sup> Constrains the total mass of neutrinos from weak lensing measurements when combined with CMB. Limit improves to  $0.03 < \Sigma m_\nu < 0.54$  eV when supernovae and baryon acoustic oscillation observations are included. The slight preference for massive neutrinos at the two-sigma level disappears when systematic errors are taken into account. Assumes  $\Lambda$ CDM model.
- <sup>64</sup> Constrains the total mass of neutrinos from recent Chandra X-ray observations of galaxy clusters when combined with CMB, supernovae, and baryon acoustic oscillation measurements. Assumes flat universe and constant dark-energy equation of state,  $w$ .
- <sup>65</sup> Constrains the total mass of neutrinos from recent CMB and SDDS LRG power spectrum data along with bias mass relations from SDSS, DEEP2, and Lyman-Break Galaxies. It assumes  $\Lambda$ CDM model. Limit degrades to 0.59 eV in a more general  $w$ CDM model.
- <sup>66</sup> Constrains the total mass of neutrinos from neutrino oscillation experiments and cosmological data. The most conservative limit uses only WMAP three-year data, while the most stringent limit includes CMB, large-scale structure, supernova, and Lyman-alpha data.
- <sup>67</sup> Constrains the total mass of neutrinos from recent CMB, large scale structure, SN1a, and baryon acoustic oscillation data. The limit relaxes to 1.75 when WMAP data alone is used with no prior. Paper shows results with several combinations of data sets. Supersedes KRISTIANSEN 06.
- <sup>68</sup> Constrains the total mass of neutrinos from the CMB and the large scale structure data. The most conservative limit is obtained when generic initial conditions are assumed.
- <sup>69</sup> Constrains the total mass of neutrinos from recent CMB, large scale structure, Lyman-alpha forest, and SN1a data.
- <sup>70</sup> Constrains the total mass of neutrinos from recent CMB and large scale structure data. See also GOOBAR 06. Superseded by HANNESTAD 10.
- <sup>71</sup> Constrains the total mass of neutrinos from the CMB and the final 2dF Galaxy Redshift Survey.
- <sup>72</sup> Constrains the total mass of neutrinos from the CMB experiments alone, assuming  $\Lambda$ CDM Universe. FUKUGITA 06 show that this result is unchanged by the 3-year WMAP data.
- <sup>73</sup> Constrains the total mass of neutrinos from the power spectrum of fluctuations derived from the Sloan Digital Sky Survey and the 2dF galaxy redshift survey, WMAP and 27 other CMB experiments and measurements by the HST Key project.
- <sup>74</sup> Constrains the total mass of neutrinos from the power spectrum of fluctuations derived from the Sloan Digital Sky Survey, the 2dF galaxy redshift survey, WMAP and ACBAR. The limit is strengthened to 0.6 eV when measurements by the HST Key project and supernovae data are included.
- <sup>75</sup> Constrains the fractional contribution of neutrinos to the total matter density in the Universe from WMAP data combined with other CMB measurements, the 2dFGRS data, and Lyman  $\alpha$  data. The limit does not noticeably change if the Lyman  $\alpha$  data are not used.
- <sup>76</sup> LEWIS 02 constrains the total mass of neutrinos from the power spectrum of fluctuations derived from the CMB, HST Key project, 2dF galaxy redshift survey, supernovae type Ia, and BBN.

• • • We do not use the following data for averages, fits, limits, etc. • • •

# Lepton Particle Listings

## Neutrino Properties

- <sup>77</sup> WANG 02 constrains the total mass of neutrinos from the power spectrum of fluctuations derived from the CMB and other cosmological data sets such as galaxy clustering and the Lyman  $\alpha$  forest.
- <sup>78</sup> FUKUGITA 00 is a limit on neutrino masses from structure formation. The constraint is based on the clustering scale  $\sigma_8$  and the COBE normalization and leads to a conservative limit of 0.9 eV assuming 3 nearly degenerate neutrinos. The quoted limit is on the sum of the light neutrino masses.
- <sup>79</sup> CROFT 99 result based on the power spectrum of the Ly  $\alpha$  forest. If  $\Omega_{\text{matter}} < 0.5$ , the limit is improved to  $m_\nu < 2.4 (\Omega_{\text{matter}}/0.17-1) \text{ eV}$ .

### Limits on MASSES of Light Stable Right-Handed $\nu$ (with necessarily suppressed interaction strengths)

VALUE (eV)	DOCUMENT ID	TECN	COMMENT
------------	-------------	------	---------

• • • We do not use the following data for averages, fits, limits, etc. • • •

<100-200	80 OLIVE	82 COSM	Dirac $\nu$
<200-2000	80 OLIVE	82 COSM	Majorana $\nu$

<sup>80</sup> Depending on interaction strength  $G_R$  where  $G_R < G_F$ .

### Limits on MASSES of Heavy Stable Right-Handed $\nu$ (with necessarily suppressed interaction strengths)

VALUE (GeV)	DOCUMENT ID	TECN	COMMENT
-------------	-------------	------	---------

• • • We do not use the following data for averages, fits, limits, etc. • • •

> 10	81 OLIVE	82 COSM	$G_R/G_F < 0.1$
>100	81 OLIVE	82 COSM	$G_R/G_F < 0.01$

<sup>81</sup> These results apply to heavy Majorana neutrinos and are summarized by the equation:  $m_\nu > 1.2 \text{ GeV } (G_F/G_R)$ . The bound saturates, and if  $G_R$  is too small no mass range is allowed.

### $\nu$ CHARGE

VALUE (units: electron charge)	CL%	DOCUMENT ID	TECN	COMMENT
--------------------------------	-----	-------------	------	---------

• • • We do not use the following data for averages, fits, limits, etc. • • •

<3.7 $\times 10^{-12}$	90	82 GNINENKO	07 RVUE	Nuclear reactor
<2 $\times 10^{-14}$		83 RAFFELT	99 ASTR	Red giant luminosity
<6 $\times 10^{-14}$		84 RAFFELT	99 ASTR	Solar cooling
<4 $\times 10^{-4}$		85 BABU	94 RVUE	BEBC beam dump
<3 $\times 10^{-4}$		86 DAVIDSON	91 RVUE	SLAC $e^-$ beam dump
<2 $\times 10^{-15}$		87 BARBIELLINI	87 ASTR	SN 1987A
<1 $\times 10^{-13}$		88 BERNSTEIN	63 ASTR	Solar energy losses

<sup>82</sup> GNINENKO 07 use limit on  $\overline{\nu}_e$  magnetic moment from LI 03b to derive this result. The limit is considerably weaker than the limits on the charge of  $\nu_e$  and  $\overline{\nu}_e$  from various astrophysics considerations.

<sup>83</sup> This RAFFELT 99 limit applies to all neutrino flavors which are light enough (<5 keV) to be emitted from globular-cluster red giants.

<sup>84</sup> This RAFFELT 99 limit is derived from the helioseismological limit on a new energy-loss channel of the Sun, and applies to all neutrino flavors which are light enough (<1 keV) to be emitted from the sun.

<sup>85</sup> BABU 94 use COOPER-SARKAR 92 limit on  $\nu$  magnetic moment to derive quoted result. It applies to  $\nu_\tau$ .

<sup>86</sup> DAVIDSON 91 use data from early SLAC electron beam dump experiment to derive charge limit as a function of neutrino mass. It applies to  $\nu_\tau$ .

<sup>87</sup> Exact BARBIELLINI 87 limit depends on assumptions about the intergalactic or galactic magnetic fields and about the direct distance and time through the field. It applies to  $\nu_e$ .

<sup>88</sup> The limit applies to all flavors.

### $\nu$ (MEAN LIFE) / MASS

Measures  $[\sum |U_{\ell j}|^2 \Gamma_j m_j]^{-1}$ , where the sum is over mass eigenstates which cannot be resolved experimentally. Some of the limits constrain the radiative decay and are based on the limit of the corresponding photon flux. Other apply to the decay of a heavier neutrino into the lighter one and a Majoron or other invisible particle. Many of these limits apply to any  $\nu$  within the indicated mass range.

Limits on the radiative decay are either directly based on the limits of the corresponding photon flux, or are derived from the limits on the neutrino magnetic moments. In the later case the transition rate for  $\nu_i \rightarrow \nu_j + \gamma$

is constrained by  $\Gamma_{ij} = \frac{1}{\tau_{ij}} = \frac{(m_i^2 - m_j^2)^3}{m_i^3} \mu_{ij}^2$ , where  $\mu_{ij}$  is the neutrino

transition moment in the mass eigenstates basis. Typically, the limits on lifetime based on the magnetic moments are many orders of magnitude more restrictive than limits based on the nonobservation of photons.

VALUE (s/eV)	CL%	DOCUMENT ID	TECN	COMMENT
--------------	-----	-------------	------	---------

> 15.4	90	89 KRAKAUER	91 CNTR	$\nu_\mu, \overline{\nu}_\mu$ at LAMPF
> 7 $\times 10^9$		90 RAFFELT	85 ASTR	
> 300	90	91 REINES	74 CNTR	$\overline{\nu}_e$

• • • We do not use the following data for averages, fits, limits, etc. • • •

> 10 <sup>5</sup> - 10 <sup>10</sup>	95	92 CECCHINI	11 ASTR	$\nu_2 \rightarrow \nu_1$ radiative decay
	90	93 MIRIZZI	07 CMB	radiative decay
	90	94 MIRIZZI	07 CIB	radiative decay
	95	95 WONG	07 CNTR	Reactor $\overline{\nu}_e$
> 0.11	90	96 XIN	05 CNTR	Reactor $\nu_e$
	97	97 XIN	05 CNTR	Reactor $\nu_e$
> 0.004	90	98 AHARMIM	04 SNO	quasidegen. $\nu$ masses
> 4.4 $\times 10^{-5}$	90	98 AHARMIM	04 SNO	hierarchical $\nu$ masses
$\gtrsim 100$	95	99 CECCHINI	04 ASTR	Radiative decay for $\nu$ mass > 0.01 eV
> 0.067	90	100 EGUCHI	04 KLND	quasidegen. $\nu$ masses
> 1.1 $\times 10^{-3}$	90	100 EGUCHI	04 KLND	hierarchical $\nu$ masses
> 8.7 $\times 10^{-5}$	99	101 BANDYOPA..	03 FIT	nonradiative decay
$\geq 4200$	90	102 DERBIN	02B CNTR	Solar $pp$ and Be $\nu$
> 2.8 $\times 10^{-5}$	99	103 JOSHIPURA	02B FIT	nonradiative decay
	104	104 DOLGOV	99 COSM	
	105	105 BILLER	98 ASTR	$m_\nu = 0.05-1 \text{ eV}$
> 2.8 $\times 10^{15}$	106,107	106,107 BLUDMAN	92 ASTR	$m_\nu < 50 \text{ eV}$
none 10 <sup>-12</sup> - 5 $\times 10^4$	108	108 DODELSON	92 ASTR	$m_\nu = 1-300 \text{ keV}$
< 10 <sup>-12</sup> or > 5 $\times 10^4$	108	108 DODELSON	92 ASTR	$m_\nu = 1-300 \text{ keV}$
	109	109 GRANKE	91 COSM	Decaying $L^0$
> 6.4	90	110 KRAKAUER	91 CNTR	$\nu_e$ at LAMPF
> 1.1 $\times 10^{15}$		111 WALKER	90 ASTR	$m_\nu = 0.03 - \sim 2 \text{ MeV}$
> 6.3 $\times 10^{15}$	107,112	107,112 CHUPP	89 ASTR	$m_\nu < 20 \text{ eV}$
> 1.7 $\times 10^{15}$	107	107 KOLB	89 ASTR	$m_\nu < 20 \text{ eV}$
	113	113 RAFFELT	89 RVUE	$\overline{\nu}$ (Dirac, Majorana)
	114	114 RAFFELT	89B ASTR	
	115	115 VONFEILIT...	88 ASTR	
> 22	68	116 OBERAUER	87	$\overline{\nu}_R$ (Dirac)
> 38	68	116 OBERAUER	87	$\overline{\nu}$ (Majorana)
> 59	68	116 OBERAUER	87	$\overline{\nu}_L$ (Dirac)
> 30	68	KETOV	86 CNTR	$\overline{\nu}$ (Dirac)
> 20	68	KETOV	86 CNTR	$\overline{\nu}$ (Majorana)
	117	117 BINETRUY	84 COSM	$m_\nu \sim 1 \text{ MeV}$
> 0.11	90	118 FRANK	81 CNTR	$\nu \overline{\nu}$ LAMPF
> 2 $\times 10^{21}$		119 STECKER	80 ASTR	$m_\nu = 10-100 \text{ eV}$
> 1.0 $\times 10^{-2}$	90	118 BLIETSCHAU	78 HLBC	$\nu_\mu$ , CERN GGM
> 1.7 $\times 10^{-2}$	90	118 BLIETSCHAU	78 HLBC	$\overline{\nu}_\mu$ , CERN GGM
< 3 $\times 10^{-11}$	120	120 FALK	78 ASTR	$m_\nu < 10 \text{ MeV}$
> 2.2 $\times 10^{-3}$	90	118 BARNES	77 DBC	$\nu$ , ANL 12-ft
	121	121 COWSIK	77 ASTR	
> 3. $\times 10^{-3}$	90	118 BELLOTTI	76 HLBC	$\nu$ , CERN GGM
> 1.3 $\times 10^{-2}$	90	118 BELLOTTI	76 HLBC	$\overline{\nu}$ , CERN GGM

<sup>89</sup> KRAKAUER 91 quotes the limit  $\tau/m_{\nu_1} > (0.75a^2 + 21.65a + 26.3) \text{ s/eV}$ , where  $a$  is a parameter describing the asymmetry in the neutrino decay defined as  $dN_{\nu_1}/d\cos\theta = (1/2)(1 + a\cos\theta)$ . The parameter  $a = 0$  for a Majorana neutrino, but can vary from  $-1$  to  $1$  for a Dirac neutrino. The bound given by the authors is the most conservative (which applies for  $a = -1$ ).

<sup>90</sup> RAFFELT 85 limit on the radiative decay is from solar x- and  $\gamma$ -ray fluxes. Limit depends on  $\nu$  flux from  $pp$ , now established from GALLEX and SAGE to be  $> 0.5$  of expectation.

<sup>91</sup> REINES 74 looked for  $\nu$  of nonzero mass decaying radiatively to a neutral of lesser mass +  $\gamma$ . Used liquid scintillator detector near fission reactor. Finds lab lifetime  $6 \times 10^7 \text{ s}$  or more. Above value of (mean life)/mass assumes average effective neutrino energy of 0.2 MeV. To obtain the limit  $6 \times 10^7 \text{ s}$  REINES 74 assumed that the full  $\overline{\nu}_e$  reactor flux could be responsible for yielding decays with photon energies in the interval 0.1 MeV - 0.5 MeV. This represents some overestimate so their lower limit is an over-estimate of the lab lifetime (VOGEL 84). If so, OBERAUER 87 may be comparable or better.

<sup>92</sup> CECCHINI 11 search for radiative decays of solar neutrinos into visible photons during the 2006 total solar eclipse. The range of (mean life)/mass values corresponds to a range of  $\nu_1$  masses between  $10^{-4}$  and 0.1 eV.

<sup>93</sup> MIRIZZI 07 determine a limit on the neutrino radiative decay from analysis of the maximum allowed distortion of the CMB spectrum as measured by the COBE/FIRAS. For the decay  $\nu_2 \rightarrow \nu_1$  the lifetime limit is  $\lesssim 4 \times 10^{20} \text{ s}$  for  $m_{\text{min}} \lesssim 0.14 \text{ eV}$ . For transition with the  $|\Delta m_{31}|$  mass difference the lifetime limit is  $\sim 2 \times 10^{19} \text{ s}$  for  $m_{\text{min}} \lesssim 0.14 \text{ eV}$  and  $\sim 5 \times 10^{20} \text{ s}$  for  $m_{\text{min}} \gtrsim 0.14 \text{ eV}$ .

<sup>94</sup> MIRIZZI 07 determine a limit on the neutrino radiative decay from analysis of the cosmic infrared background (CIB) using the Spitzer Observatory data. For transition with the  $|\Delta m_{31}|$  mass difference they obtain the lifetime limit  $\sim 10^{20} \text{ s}$  for  $m_{\text{min}} \lesssim 0.14 \text{ eV}$ .

<sup>95</sup> WONG 07 use their limit on the neutrino magnetic moment together with the assumed experimental value of  $\Delta m_{13}^2 \sim 2 \times 10^{-3} \text{ eV}^2$  to obtain  $\tau_{13}/m_1^3 > 3.2 \times 10^{27} \text{ s/eV}^3$  for the radiative decay in the case of the inverted mass hierarchy. Similarly to RAFFELT 89 this limit can be violated if electric and magnetic moments are equal to each other. Analogous, but numerically somewhat different limits are obtained for  $\tau_{23}$  and  $\tau_{21}$ .

<sup>96</sup> XIN 05 search for the  $\gamma$  from radiative decay of  $\nu_e$  produced by the electron capture on  $^{51}\text{Cr}$ . No events were seen and the limit on  $\tau/m_\nu$  was derived. This is a weaker limit on the decay of  $\nu_e$  than KRAKAUER 91.

<sup>97</sup> XIN 05 use their limit on the neutrino magnetic moment of  $\nu_e$  together with the assumed experimental value of  $\Delta m_{13}^2 \sim 2 \times 10^{-3} \text{ eV}^2$  to obtain  $\tau_{13}/m_1^3 > 1 \times 10^{23} \text{ s/eV}^3$  for the radiative decay in the case of the inverted mass hierarchy. Similarly to RAFFELT 89 this limit can be violated if electric and magnetic moments are equal to each other. Analogous, but numerically somewhat different limits are obtained for  $\tau_{23}$  and  $\tau_{21}$ . Again, this limit is specific for  $\nu_e$ .



# Lepton Particle Listings

## Neutrino Properties

See key on page 457

- <sup>98</sup> AHARMIM 04 obtained these results from the solar  $\bar{\nu}_e$  flux limit set by the SNO measurement assuming  $\nu_2$  decay through nonradiative process  $\nu_2 \rightarrow \bar{\nu}_1 X$ , where  $X$  is a Majoron or other invisible particle. Limits are given for the cases of quasidegenerate and hierarchical neutrino masses.
- <sup>99</sup> CECCHINI 04 obtained this bound through the observations performed on the occasion of the 21 June 2001 total solar eclipse, looking for visible photons from radiative decays of solar neutrinos. Limit is a  $\tau/m_{\nu_2}$  in  $\nu_2 \rightarrow \nu_1 \gamma$ . Limit ranges from  $\sim 100$  to  $10^7$  s/eV for  $0.01 < m_{\nu_1} < 0.1$  eV.
- <sup>100</sup> EGUCHI 04 obtained these results from the solar  $\bar{\nu}_e$  flux limit set by the KamLAND measurement assuming  $\nu_2$  decay through nonradiative process  $\nu_2 \rightarrow \bar{\nu}_1 X$ , where  $X$  is a Majoron or other invisible particle. Limits are given for the cases of quasidegenerate and hierarchical neutrino masses.
- <sup>101</sup> The ratio of the lifetime over the mass derived by BANDYOPADHYAY 03 is for  $\nu_2$ . They obtained this result using the following solar-neutrino data: total rates measured in Cl and Ga experiments, the Super-Kamiokande's zenith-angle spectra, and SNO's day and night spectra. They assumed that  $\nu_1$  is the lowest mass, stable or nearly stable neutrino state and  $\nu_2$  decays through nonradiative Majoron emission process,  $\nu_2 \rightarrow \bar{\nu}_1 + J$ , or through nonradiative process with all the final state particles being sterile. The best fit is obtained in the region of the LMA solution.
- <sup>102</sup> DERBIN 02B (also BACK 03B) obtained this bound for the radiative decay from the results of background measurements with Counting Test Facility (the prototype of the Borexino detector). The laboratory gamma spectrum is given as  $dN_\gamma/d\cos\theta = (1/2)(1 + \alpha\cos\theta)$  with  $\alpha=0$  for a Majorana neutrino, and  $\alpha$  varying to  $-1$  to  $1$  for a Dirac neutrino. The listed bound is for the case of  $\alpha=0$ . The most conservative bound  $1.5 \times 10^3$  s eV $^{-1}$  is obtained for the case of  $\alpha=-1$ .
- <sup>103</sup> The ratio of the lifetime over the mass derived by JOSHIPURA 02B is for  $\nu_2$ . They obtained this result from the total rates measured in all solar neutrino experiments. They assumed that  $\nu_1$  is the lowest mass, stable or nearly stable neutrino state and  $\nu_2$  decays through nonradiative process like Majoron emission decay,  $\nu_2 \rightarrow \nu_1' + J$  where  $\nu_1'$  state is sterile. The exact limit depends on the specific solution of the solar neutrino problem. The quoted limit is for the LMA solution.
- <sup>104</sup> DOLGOV 99 places limits in the (Majorana)  $\tau$ -associated  $\nu$  mass-lifetime plane based on nucleosynthesis. Results would be considerably modified if neutrino oscillations exist.
- <sup>105</sup> BILLER 98 use the observed TeV  $\gamma$ -ray spectra to set limits on the mean life of any radiatively decaying neutrino between 0.05 and 1 eV. Curve shows  $\tau_\nu/B_\gamma > 0.15 \times 10^{21}$  s at 0.05 eV,  $> 1.2 \times 10^{21}$  s at 0.17 eV,  $> 3 \times 10^{21}$  s at 1 eV, where  $B_\gamma$  is the branching ratio to photons.
- <sup>106</sup> BLUDMAN 92 sets additional limits by this method for higher mass ranges. Cosmological limits are also obtained.
- <sup>107</sup> Limit on the radiative decay based on nonobservation of  $\gamma$ 's in coincidence with  $\nu$ 's from SN 1987A.
- <sup>108</sup> DODELSON 92 range is for wrong-helicity keV mass Dirac  $\nu$ 's from the core of neutron star in SN 1987A decaying to  $\nu$ 's that would have interacted in KAM2 or IMB detectors.
- <sup>109</sup> GRANEK 91 considers heavy neutrino decays to  $\gamma\nu_L$  and  $3\nu_L$ , where  $m_{\nu_1} < 100$  keV. Lifetime is calculated as a function of heavy neutrino mass, branching ratio into  $\gamma\nu_L$  and  $m_{\nu_L}$ .
- <sup>110</sup> KRAKAUER 91 quotes the limit for  $\nu_e$ ,  $\tau/m_\nu > (0.3a^2 + 9.8a + 15.9)$  s/eV, where  $a$  is a parameter describing the asymmetry in the radiative neutrino decay defined as  $dN_\gamma/d\cos\theta = (1/2)(1 + a\cos\theta)$   $a=0$  for a Majorana neutrino, but can vary from  $-1$  to  $1$  for a Dirac neutrino. The bound given by the authors is the most conservative (which applies for  $a = -1$ ).
- <sup>111</sup> WALKER 90 uses SN 1987A  $\gamma$  flux limits after 289 days.
- <sup>112</sup> CHUPP 89 should be multiplied by a branching ratio (about 1) and a detection efficiency (about 1/4), and pertains to radiative decay of any neutrino to a lighter or sterile neutrino.
- <sup>113</sup> RAFFELT 89 uses KYULDJIEV 84 to obtain  $\tau m^3 > 3 \times 10^{18}$  s eV $^3$  (based on  $\bar{\nu}_e e^-$  cross sections). The bound for the radiative decay is not valid if electric and magnetic transition moments are equal for Dirac neutrinos.
- <sup>114</sup> RAFFELT 89B analyze stellar evolution and exclude the region  $3 \times 10^{12} < \tau m^3 < 3 \times 10^{21}$  s eV $^3$ .
- <sup>115</sup> Model-dependent theoretical analysis of SN 1987A neutrinos. Quoted limit is for  $[\sum_j |U_{ej}|^2 \Gamma_j m_j]^{-1}$ , where  $\ell = \mu, \tau$ . Limit is  $3.3 \times 10^{14}$  s/eV for  $\ell = e$ .
- <sup>116</sup> OBERAUER 87 looks for photons and  $e^+ e^-$  pairs from radiative decays of reactor neutrinos.
- <sup>117</sup> BINETRUY 84 finds  $\tau < 10^8$  s for neutrinos in a radiation-dominated universe.
- <sup>118</sup> These experiments look for  $\nu_k \rightarrow \nu_j \gamma$  or  $\bar{\nu}_k \rightarrow \bar{\nu}_j \gamma$ .
- <sup>119</sup> STECKER 80 limit based on UV background; result given is  $\tau > 4 \times 10^{22}$  s at  $m_\nu = 20$  eV.
- <sup>120</sup> FALK 78 finds lifetime constraints based on supernova energetics.
- <sup>121</sup> COWSIK 77 considers variety of scenarios. For neutrinos produced in the big bang, present limits on optical photon flux require  $\tau > 10^{23}$  s for  $m_\nu \sim 1$  eV. See also COWSIK 79 and GOLDMAN 79.

### $\nu$ MAGNETIC MOMENT

The coupling of neutrinos to an electromagnetic field is characterized by a  $3 \times 3$  matrix  $\lambda$  of the magnetic ( $\mu$ ) and electric ( $d$ ) dipole moments ( $\lambda = \mu - id$ ). For Majorana neutrinos the matrix  $\lambda$  is antisymmetric and only transition moments are allowed, while for Dirac neutrinos  $\lambda$  is a general  $3 \times 3$  matrix. In the standard electroweak theory extended to include neutrino masses (see FUJIKAWA 80)  $\mu_\nu = 3eG_F m_\nu / (8\pi^2 \sqrt{2}) = 3.2 \times 10^{-19} (m_\nu / \text{eV}) \mu_B$ , i.e. it is unobservably small given the known small neutrino masses. In more general models there is no longer a proportionality between neutrino mass and its magnetic moment, even though

only massive neutrinos have nonvanishing magnetic moments without fine tuning.

Laboratory bounds on  $\lambda$  are obtained via elastic  $\nu$ - $e$  scattering, where the scattered neutrino is not observed. The combinations of matrix elements of  $\lambda$  that are constrained by various experiments depend on the initial neutrino flavor and on its propagation between source and detector (e.g., solar  $\nu_e$  and reactor  $\bar{\nu}_e$  do not constrain the same combinations). The listings below therefore identify the initial neutrino flavor.

Other limits, e.g. from various stellar cooling processes, apply to all neutrino flavors. Analogous flavor independent, but weaker, limits are obtained from the analysis of  $e^+ e^- \rightarrow \nu \bar{\nu} \gamma$  collider experiments.

VALUE ( $10^{-10} \mu_B$ )	CL%	DOCUMENT ID	TECN	COMMENT
< 0.32	90	122 BEDA	10 CNTR	Reactor $\bar{\nu}_e$
< 6.8	90	123 AUERBACH	01 LSND	$\nu_e e, \nu_\mu e$ scattering
< 3900	90	124 SCHWIENHO..01	DONU	$\nu_\tau e^- \rightarrow \nu_\tau e^-$
• • • We do not use the following data for averages, fits, limits, etc. • • •				
< 2.2	90	125 DENIZ	10 TEXO	Reactor $\bar{\nu}_e$
< 0.011-0.027		126 KUZNETSOV	09 ASTR	$\nu_L \rightarrow \nu_R$ in SN1987A
< 0.54	90	127 ARPESELLA	08A BORK	Solar $\nu$ spectrum shape
< 0.58	90	128 BEDA	07 CNTR	Reactor $\bar{\nu}_e$
< 0.74	90	129 WONG	07 CNTR	Reactor $\bar{\nu}_e$
< 0.9	90	130 DARAKTCH...	05	Reactor $\bar{\nu}_e$
< 130	90	131 XIN	05 CNTR	Reactor $\nu_e$
< 37	95	132 GRIFOLS	04 FIT	Solar $^8\text{B } \nu$ (SNO NC)
< 3.6	90	133 LIU	04 SKAM	Solar $\nu$ spectrum shape
< 1.1	90	134 LIU	04 SKAM	Solar $\nu$ spectrum shape (LMA region)
< 5.5	90	135 BACK	03B CNTR	Solar $p\bar{p}$ and Be $\nu$
< 1.0	90	136 DARAKTCH...	03	Reactor $\bar{\nu}_e$
< 1.3	90	137 LI	03B CNTR	Reactor $\bar{\nu}_e$
< 2	90	138 GRIMUS	02 FIT	solar + reactor (Majorana $\nu$ )
< 80000	90	139 TANIMOTO	00 RVUE	$e^+ e^- \rightarrow \nu \bar{\nu} \gamma$
< 0.01-0.04		140 AYALA	99 ASTR	$\nu_L \rightarrow \nu_R$ in SN 1987A
< 1.5	90	141 BEACOM	99 SKAM	$\nu$ spectrum shape
< 0.03		142 RAFFELT	99 ASTR	Red giant luminosity
< 4		143 RAFFELT	99 ASTR	Solar cooling
< 44000	90	144 ABREU	97J DLPH	$e^+ e^- \rightarrow \nu \bar{\nu} \gamma$ at LEP
< 33000	90	145 ACCIARRI	97Q L3	$e^+ e^- \rightarrow \nu \bar{\nu} \gamma$ at LEP
< 0.62		146 ELMFORS	97 COSM	Depolarization in early universe plasma
< 27000	95	147 ESCRIBANO	97 RVUE	$\Gamma(Z \rightarrow \nu\nu)$ at LEP
< 30	90	148 VILAIN	95B CHM2	$\nu_\mu e \rightarrow \nu_\mu e$
< 55000	90	149 GOULD	94 RVUE	$e^+ e^- \rightarrow \nu \bar{\nu} \gamma$ at LEP
< 1.9	95	150 DERBIN	93 CNTR	Reactor $\bar{\nu}_e \rightarrow \bar{\nu}_e$
< 5400	90	151 COOPER...	92 BEBC	$\nu_\tau e^- \rightarrow \nu_\tau e^-$
< 2.4	90	152 VIDYAKIN	92 CNTR	Reactor $\bar{\nu}_e \rightarrow \bar{\nu}_e$
< 56000	90	153 DESHPANDE	91 RVUE	$e^+ e^- \rightarrow \nu \bar{\nu} \gamma$
< 100	95	154 DORENBOS..	91 CHRM	$\nu_\mu e \rightarrow \nu_\mu e$
< 8.5	90	155 AHRENS	90 CNTR	$\nu_\mu e \rightarrow \nu_\mu e$
< 10.8	90	156 KRAKAUER	90 CNTR	LAMPF $\nu e \rightarrow \nu e$
< 7.4	90	157 KRAKAUER	90 CNTR	LAMPF ( $\nu_\mu, \bar{\nu}_\mu$ ) $e$ elast.
< 0.02		158 RAFFELT	90 ASTR	Red giant luminosity
< 0.1		159 RAFFELT	89B ASTR	Cooling helium stars
< 40000	90	160 FUKUGITA	88 COSM	Primordial magn. fields
$\leq .3$		161 GROTCHE	88 RVUE	$e^+ e^- \rightarrow \nu \bar{\nu} \gamma$
< 0.11		162 RAFFELT	88B ASTR	He burning stars
< 0.0006		163 FUKUGITA	87 ASTR	Cooling helium stars
		164 NUSSINOV	87 ASTR	Cosmic EM backgrounds
< 0.1-0.2		165 MORGAN	81 COSM	$^4\text{He}$ abundance
< 0.85		166 BEG	78 ASTR	Stellar plasmons
< 0.6		167 SUTHERLAND	76 ASTR	Red giants + degenerate dwarfs
< 81		168 KIM	74 RVUE	$\bar{\nu}_\mu e \rightarrow \bar{\nu}_\mu e$
< 1		169 BERNSTEIN	63 ASTR	Solar cooling
< 14		170 COWAN	57 CNTR	Reactor $\bar{\nu}$

<sup>122</sup> BEDA 10 report  $\bar{\nu}_e e^-$  scattering results, using the Kalinin Nuclear Power Plant and a shielded Ge detector. The recoil electron spectrum is analyzed between 2.9 and 45 keV. Supersedes BEDA 07. This is the most stringent limit on the magnetic moment of reactor  $\bar{\nu}_e$ .

<sup>123</sup> AUERBACH 01 limit is based on the LSND  $\nu_e$  and  $\nu_\mu$  electron scattering measurements. The limit is slightly more stringent than KRAKAUER 90.

<sup>124</sup> SCHWIENHORST 01 quote an experimental sensitivity of  $4.9 \times 10^{-7}$ .

<sup>125</sup> DENIZ 10 observe reactor  $\bar{\nu}_e$  scattering with recoil kinetic energies 3-8 MeV using CsI(Tl) detectors. The observed rate and spectral shape are consistent with the Standard Model prediction, leading to the reported constraint on  $\bar{\nu}_e$  magnetic moment.

<sup>126</sup> KUZNETSOV 09 obtain a limit on the flavor averaged magnetic moment of Dirac neutrinos from the time averaged neutrino signal of SN1987A. Improves and supersedes the analysis of BARBIERI 88 and AYALA 99.

<sup>127</sup> ARPESELLA 08A obtained this limit using the shape of the recoil electron energy spectrum from the Borexino 192 live days of solar neutrino data.

# Lepton Particle Listings

## Neutrino Properties

- 128 BEDA 07 performed search for electromagnetic  $\bar{\nu}_e$ -e scattering at Kalininskaya nuclear reactor. A Ge detector with active and passive shield was used and the electron recoil spectrum between 3.0 and 61.3 keV analyzed. Superseded by BEDA 10.
- 129 WONG 07 performed search for non-standard  $\bar{\nu}_e$ -e scattering at the Kuo-Sheng nuclear reactor. Ge detector equipped with active anti-Compton shield is used. Most stringent laboratory limit on magnetic moment of reactor  $\bar{\nu}_e$ . Supersedes LI 03b.
- 130 DARAKTCHIEVA 05 present the final analysis of the search for non-standard  $\bar{\nu}_e$ -e scattering component at Bugey nuclear reactor. Full kinematical event reconstruction of both the kinetic energy above 700 keV and scattering angle of the recoil electron, by use of TPC. Most stringent laboratory limit on magnetic moment. Supersedes DARAKTCHIEVA 03.
- 131 XIN 05 evaluated the  $\nu_e$  flux at the Kuo-Sheng nuclear reactor and searched for non-standard  $\nu_e$ -e scattering. Ge detector equipped with active anti-Compton shield was used. This laboratory limit on magnetic moment is considerably less stringent than the limits for reactor  $\bar{\nu}_e$ , but is specific to  $\nu_e$ .
- 132 GRIFOLS 04 obtained this bound using the SNO data of the solar  $^8\text{B}$  neutrino flux measured with deuteron breakup. This bound applies to  $\mu_{\text{eff}} = (\mu_{21}^2 + \mu_{22}^2 + \mu_{23}^2)^{1/2}$ .
- 133 LIU 04 obtained this limit using the shape of the recoil electron energy spectrum from the Super-Kamiokande-I 1496 days of solar neutrino data. Neutrinos are assumed to have only diagonal magnetic moments,  $\mu_{\nu 1} = \mu_{\nu 2}$ . This limit corresponds to the oscillation parameters in the vacuum oscillation region.
- 134 LIU 04 obtained this limit using the shape of the recoil electron energy spectrum from the Super-Kamiokande-I 1496 live-day solar neutrino data, by limiting the oscillation parameter region in the LMA region allowed by solar neutrino experiments plus KamLAND.  $\mu_{\nu 1} = \mu_{\nu 2}$  is assumed. In the LMA region, the same limit would be obtained even if neutrinos have off-diagonal magnetic moments.
- 135 BACK 03b obtained this bound from the results of background measurements with Counting Test Facility (the prototype of the Borexino detector). Standard Solar Model flux was assumed. This  $\mu_\nu$  can be different from the reactor  $\mu_\nu$  in certain oscillation scenarios (see BEACOM 99).
- 136 DARAKTCHIEVA 03 searched for non-standard  $\bar{\nu}_e$ -e scattering component at Bugey nuclear reactor. Full kinematical event reconstruction by use of TPC. Superseded by DARAKTCHIEVA 05.
- 137 LI 03b used Ge detector in active shield near nuclear reactor to test for nonstandard  $\bar{\nu}_e$ -e scattering.
- 138 GRIMUS 02 obtain stringent bounds on all Majorana neutrino transition moments from a simultaneous fit of LMA-MSW oscillation parameters and transition moments to global solar neutrino data + reactor data. Using only solar neutrino data, a 90% CL bound of  $6.3 \times 10^{-10} \mu_B$  is obtained.
- 139 TANIMOTO 00 combined  $e^+ e^- \rightarrow \nu \bar{\nu} \gamma$  data from VENUS, TOPAZ, and AMY.
- 140 AYALA 99 improves the limit of BARBIERI 88.
- 141 BEACOM 99 obtain the limit using the shape, but not the absolute magnitude which is affected by oscillations, of the solar neutrino spectrum obtained by Superkamiokande (825 days). This  $\mu_\nu$  can be different from the reactor  $\mu_\nu$  in certain oscillation scenarios.
- 142 RAFFELT 99 is an update of RAFFELT 90. This limit applies to all neutrino flavors which are light enough ( $< 5$  keV) to be emitted from globular-cluster red giants. This limit pertains equally to electric dipole moments and magnetic transition moments, and it applies to both Dirac and Majorana neutrinos.
- 143 RAFFELT 99 is essentially an update of BERNSTEIN 63, but is derived from the helioseismological limit on a new energy-loss channel of the Sun. This limit applies to all neutrino flavors which are light enough ( $< 1$  keV) to be emitted from the Sun. This limit pertains equally to electric dipole and magnetic transition moments, and it applies to both Dirac and Majorana neutrinos.
- 144 ACCIARRI 97Q result applies to both direct and transition magnetic moments and for  $q^2=0$ .
- 145 ELMFORS 97 calculate the rate of depolarization in a plasma for neutrinos with a magnetic moment and use the constraints from a big-bang nucleosynthesis on additional degrees of freedom.
- 146 Applies to absolute value of magnetic moment.
- 147 DERBIN 93 determine the cross section for 0.6–2.0 MeV electron energy as  $(1.28 \pm 0.63) \times \sigma_{\text{weak}}$ . However, the (reactor on - reactor off)/(reactor off) is only  $\sim 1/100$ .
- 148 COOPER-SARKAR 92 assume  $f_{D_S}/f_\pi = 2$  and  $D_S, \bar{D}_S$  production cross section =  $2.6 \mu\text{b}$  to calculate  $\nu$  flux.
- 149 VIDYAKIN 92 limit is from a  $e\bar{\nu}_e$  elastic scattering experiment. No experimental details are given except for the cross section from which this limit is derived. Signal/noise was 1/10. The limit uses  $\sin^2\theta_W = 0.23$  as input.
- 150 DORENBOSCH 91 corrects an incorrect statement in DORENBOSCH 89 that the  $\nu$  magnetic moment is  $< 1 \times 10^{-9}$  at the 95%CL. DORENBOSCH 89 measures both  $\nu_\mu e$  and  $\bar{\nu}_e e$  elastic scattering and assume  $\mu(\nu) = \mu(\bar{\nu})$ .
- 151 KRAKAUER 90 experiment fully reported in ALLEN 93.
- 152 RAFFELT 90 limit applies for a diagonal magnetic moment of a Dirac neutrino, or for a transition magnetic moment of a Majorana neutrino. In the latter case, the same analysis gives  $< 1.4 \times 10^{-12}$ . Limit at 95%CL obtained from  $\delta M_C$ .
- 153 Significant dependence on details of stellar models.
- 154 FUKUGITA 88 find magnetic dipole moments of any two neutrino species are bounded by  $\mu < 10^{-16} [10^{-9} G/B_0]$  where  $B_0$  is the present-day intergalactic field strength.
- 155 GROTCHE 88 combined data from MAC, ASP, CELLO, and Mark J.
- 156 For  $m_\nu = 8-200$  eV. NUSSINOV 87 examines transition magnetic moments for  $\nu_\mu \rightarrow \nu_e$  and obtain  $< 3 \times 10^{-15}$  for  $m_\nu > 16$  eV and  $< 6 \times 10^{-14}$  for  $m_\nu > 4$  eV.
- 157 We obtain above limit from SUTHERLAND 76 using their limit  $f < 1/3$ .
- 158 KIM 74 is a theoretical analysis of  $\bar{\nu}_\mu$  reaction data.

## NEUTRINO CHARGE RADIUS SQUARED

We report limits on the so-called neutrino charge radius squared. While the straight-forward definition of a neutrino charge radius has been proven to be gauge-dependent and, hence, unphysical (LEE 77C), there have been recent attempts to define a physically observable neutrino charge radius (BERNABEU 00, BERNABEU 02). The issue is still controversial (FUJIKAWA 03, BERNABEU 03). A more general interpretation of the experimental results is that they are limits on certain nonstandard contributions to neutrino scattering.

VALUE ( $10^{-32} \text{ cm}^2$ )	CL %	DOCUMENT ID	TECN	COMMENT
-2.1 to 3.3	90	159 DENIZ	10 TEXO	Reactor $\bar{\nu}_e e$
• • • We do not use the following data for averages, fits, limits, etc. • • •				
-0.53 to 0.68	90	160 HIRSCH	03	$\nu_\mu e$ scat.
-8.2 to 9.9	90	161 HIRSCH	03	anomalous $e^+ e^- \rightarrow \nu \bar{\nu} \gamma$
-2.97 to 4.14	90	162 AUERBACH	01 LSND	$\nu_e e \rightarrow \nu_e e$
-0.6 to 0.6	90	VILAIN	95B CHM2	$\nu_\mu e$ elastic scat.
0.9 $\pm$ 2.7		ALLEN	93 CNTR	LAMPF $\nu e \rightarrow \nu e$
< 2.3	95	MOURAO	92 ASTR	HOME/KAM2 $\nu$ rates
< 7.3	90	163 VIDYAKIN	92 CNTR	Reactor $\bar{\nu}_e \rightarrow \bar{\nu}_e$
1.1 $\pm$ 2.3		ALLEN	91 CNTR	Repl. by ALLEN 93
-1.1 $\pm$ 1.0		164 AHRENS	90 CNTR	$\nu_\mu e$ elastic scat.
-0.3 $\pm$ 1.5		164 DORENBOSCH...	89 CHRM	$\nu_\mu e$ elastic scat.
		165 GRIFOLS	89B ASTR	SN 1987A
159 DENIZ 10 observe reactor $\bar{\nu}_e e$ scattering with recoil kinetic energies 3–8 MeV using CsI(Tl) detectors. The observed rate and spectral shape are consistent with the Standard Model prediction, leading to the reported constraint on $\bar{\nu}_e$ charge radius.				
160 Based on analysis of CCFR 98 results. Limit is on $\langle r_V^2 \rangle$ and $\langle r_A^2 \rangle$ . The CHARM II and E734 at BNL results are reanalyzed, and weaker bounds on the charge radius squared than previously published are obtained. The NuTeV result is discussed; when tentatively interpreted as $\nu_\mu$ charge radius it implies $\langle r_V^2 \rangle$ and $\langle r_A^2 \rangle = (4.20 \pm 1.64) \times 10^{-33} \text{ cm}^2$ .				
161 Results of LEP-2 are interpreted as limits on the axial-vector charge radius squared of a Majorana $\nu_\tau$ . Slightly weaker limits for both vector and axial-vector charge radius squared are obtained for the Dirac case, and somewhat weaker limits are obtained from the analysis of lower energy data (LEP-1.5 and TRISTAN).				
162 AUERBACH 01 measure $\nu_e e$ elastic scattering with LSND detector. The cross section agrees with the Standard Model expectation, including the charge and neutral current interference. The 90% CL applies to the range shown.				
163 VIDYAKIN 92 limit is from a $e\bar{\nu}$ elastic scattering experiment. No experimental details are given except for the cross section from which this limit is derived. Signal/noise was 1/10. The limit uses $\sin^2\theta_W = 0.23$ as input.				
164 Result is obtained from reanalysis given in ALLEN 91, followed by our reduction to obtain $1\sigma$ errors.				
165 GRIFOLS 89b sets a limit of $\langle r^2 \rangle < 0.2 \times 10^{-32} \text{ cm}^2$ for right-handed neutrinos.				

## REFERENCES FOR Neutrino Properties

ASEEV	11	PR D84 112003	V.N. Aseev <i>et al.</i>
CECCHINI	11	ASP 34 486	S. Cecchini <i>et al.</i>
SAITO	11	PR D83 043529	S. Saito, M. Takada, A. Taruya
BEDA	10	PNL 7 406	A.G. Beda <i>et al.</i> (GEMMA Collab.)
DENIZ	10	PR D81 072001	M. Deniz <i>et al.</i> (TEXONO Collab.)
HANNESTAD	10	JCAP 1008 001	S. Hannestad <i>et al.</i>
PAGLIAROLI	10	ASP 33 287	G. Pagliaroli, F. Rossi-Torres, E. Vissani (INFN+)
SEKIGUCHI	10	JCAP 1003 015	T. Sekiguchi <i>et al.</i>
THOMAS	10	PRL 105 031301	S.A. Thomas, F.B. Abdalla, O. Lahav (LOUC)
ICHIKI	09	PR D79 023520	K. Ichiki, M. Takada, T. Takahashi
KOMATSU	09	APJS 180 330	E. Komatsu <i>et al.</i>
KUZNETSOV	09	IJMP A24 5977	A.V. Kuznetsov, N.V. Mikheev, A.A. Okrugin (YARO)
TERENO	09	AA 500 657	I. Tereno <i>et al.</i>
VIKHLININ	09	APJ 692 1060	A. Vikhlinin <i>et al.</i>
ARPESELLA	08A	PRL 101 091302	C. Arpesella <i>et al.</i> (Borexino Collab.)
BERNARDIS	08B	PR D78 083535	F. De Bernardis <i>et al.</i>
BEDA	07	PAN 70 1873	A.G. Beda <i>et al.</i>
Translated from YAF 70 1925.			
FOGLI	07	PR D75 053001	G.L. Fogli <i>et al.</i>
GNINENKO	07	PR D75 075014	S.N. Gninenko, N.V. Krasnikov, A. Rubbia
KRISTIANSEN	07	PR D75 083510	J. Kristiansen, O. Elgaroy, H. Dahle
MIRIZZI	07	PR D76 053007	A. Mirizzi, D. Montanino, P.D. Serpico
SPERGEL	07	APJS 170 377	D.N. Spergel <i>et al.</i>
WONG	07	PR D75 012001	H.T. Wong <i>et al.</i> (TEXONO Collab.)
ZUNCKEL	07	JCAP 0708 004	C. Zunckel, P. Ferreira
CIRELLI	06	JCAP 0612 013	M. Cirelli <i>et al.</i>
FUKUGITA	06	PR D74 027302	M. Fukugita <i>et al.</i>
GOOBAR	06	JCAP 0606 019	A. Goobar <i>et al.</i>
HANNESTAD	06	JCAP 0611 016	S. Hannestad, G. Raffelt
KRISTIANSEN	06	PR D74 123005	J. Kristiansen, O. Elgaroy, H. Eriksen
SANCHEZ	06	MNRAS 366 189	A.G. Sanchez <i>et al.</i>
SELJAK	06	JCAP 0610 014	U. Seljak, A. Slosar, P. McDonald
DARAKTCHIEVA	05	PL B615 153	Z. Daraktchieva <i>et al.</i> (MUNU Collab.)
ICHIKAWA	05	PR D71 043001	K. Ichikawa, M. Fukugita, M. Kawasaki (ICRR)
KRAUS	05	EPJ C40 447	Ch. Kraus <i>et al.</i>
XIN	05	PR D72 012006	B. Xin <i>et al.</i> (TEXONO Collab.)
AHARMIM	04	PR D70 093014	B. Aharmim <i>et al.</i> (SNO Collab.)
BARGER	04	PL B595 55	V. Barger, D. Marfatia, A. Tregre
CECCHINI	04	ASP 21 183	S. Cecchini <i>et al.</i> (BGN+)
CROTTY	04	PR D69 123007	P. Crotty, J. Lesgourgues, S. Pastor
EGUCHI	04	PRL 92 071301	K. Eguchi <i>et al.</i> (KamLAND Collab.)
GRIFOLS	04	PL B587 184	J.A. Grifols, E. Masso, S. Mohanty (BARC, AHMED)
LIU	04	PRL 93 021802	D.W. Liu <i>et al.</i> (Super-Kamiokande Collab.)
ARNABOLDI	03A	PRL 91 161802	C. Arnaboldi <i>et al.</i>
BACK	03B	PL B563 35	H.O. Back <i>et al.</i> (Borexino Collab.)
BANDYOPADHYAY	03	PL B555 33	A. Bandyopadhyay, S. Choubey, S. Goswami (SAHA+)
BERNABEU	03	hep-ph/0303202	J. Bernabeu, J. Papavassiliou, J. Vidal
DARAKTCHIEVA	03	PL B564 190	Z. Daraktchieva <i>et al.</i> (MUNU Collab.)
FUJIKAWA	03	hep-ph/0303188	K. Fujikawa, R. Shrock
HIRSCH	03	PR D67 033005	M. Hirsch <i>et al.</i>
LI	03B	PRL 90 131802	H.B. Li <i>et al.</i> (TEXONO Collab.)



# Lepton Particle Listings

## Number of Neutrino Types

much more dependent on the Standard Model, the approach described above is favored.

Before the advent of the SLC and LEP, limits on the number of neutrino generations were placed by experiments at lower-energy  $e^+e^-$  colliders by measuring the cross section of the process  $e^+e^- \rightarrow \nu\bar{\nu}\gamma$ . The ASP, CELLO, MAC, MARK J, and VENUS experiments observed a total of 3.9 events above background [2], leading to a 95% CL limit of  $N_\nu < 4.8$ . This process has a much larger cross section at center-of-mass energies near the  $Z$  mass and has been measured at LEP by the ALEPH, DELPHI, L3, and OPAL experiments [3]. These experiments have observed several thousand such events, and the combined result is  $N_\nu = 3.00 \pm 0.08$ . The same process has also been measured by the LEP experiments at much higher center-of-mass energies, between 130 and 208 GeV, in searches for new physics [4]. Combined with the lower energy data, the result is  $N_\nu = 2.92 \pm 0.05$ .

Experiments at  $p\bar{p}$  colliders also placed limits on  $N_\nu$  by determining the total  $Z$  width from the observed ratio of  $W^\pm \rightarrow \ell^\pm\nu$  to  $Z \rightarrow \ell^+\ell^-$  events [5]. This involved a calculation that assumed Standard Model values for the total  $W$  width and the ratio of  $W$  and  $Z$  leptonic partial widths, and used an estimate of the ratio of  $Z$  to  $W$  production cross sections. Now that the  $Z$  width is very precisely known from the LEP experiments, the approach is now one of those used to determine the  $W$  width.

### References

1. ALEPH, DELPHI, L3, OPAL, and SLD Collaborations, and LEP Electroweak Working Group, and SLD Electroweak Group, and SLD Heavy Flavour Group, Phys. Reports **427**, 257 (2006).
2. VENUS: K. Abe *et al.*, Phys. Lett. **B232**, 431 (1989); ASP: C. Hearty *et al.*, Phys. Rev. **D39**, 3207 (1989); CELLO: H.J. Behrend *et al.*, Phys. Lett. **B215**, 186 (1988); MAC: W.T. Ford *et al.*, Phys. Rev. **D33**, 3472 (1986); MARK J: H. Wu, Ph.D. Thesis, Univ. Hamburg (1986).
3. L3: M. Acciarri *et al.*, Phys. Lett. **B431**, 199 (1998); DELPHI: P. Abreu *et al.*, Z. Phys. **C74**, 577 (1997); OPAL: R. Akers *et al.*, Z. Phys. **C65**, 47 (1995); ALEPH: D. Buskulic *et al.*, Phys. Lett. **B313**, 520 (1993).
4. DELPHI: J. Abdallah *et al.*, Eur. Phys. J. **C38**, 395 (2005); L3: P. Achard *et al.*, Phys. Lett. **B587**, 16 (2004); ALEPH: A. Heister *et al.*, Eur. Phys. J. **C28**, 1 (2003); OPAL: G. Abbiendi *et al.*, Eur. Phys. J. **C18**, 253 (2000).
5. UA1: C. Albajar *et al.*, Phys. Lett. **B198**, 271 (1987); UA2: R. Ansari *et al.*, Phys. Lett. **B186**, 440 (1987).

### Number from $e^+e^-$ Colliders

#### Number of Light $\nu$ Types

VALUE	DOCUMENT ID	TECN
<b>2.9840 ± 0.0082</b>	<sup>1</sup> LEP-SLC	06 RVUE

• • • We do not use the following data for averages, fits, limits, etc. • • •

3.00 ± 0.05	<sup>2</sup> LEP	92 RVUE
-------------	------------------	---------

<sup>1</sup> Combined fit from ALEPH, DELPHI, L3 and OPAL Experiments.

<sup>2</sup> Simultaneous fits to all measured cross section data from all four LEP experiments.

### Number of Light $\nu$ Types from Direct Measurement of Invisible $Z$ Width

In the following, the invisible  $Z$  width is obtained from studies of single-photon events from the reaction  $e^+e^- \rightarrow \nu\bar{\nu}\gamma$ . All are obtained from LEP runs in the  $E_{\text{cm}}^{\text{eff}}$  range 88–209 GeV.

VALUE	DOCUMENT ID	TECN	COMMENT
<b>2.92 ± 0.05 OUR AVERAGE</b>	Error includes scale factor of 1.2.		
2.84 ± 0.10 ± 0.14	ABDALLAH	05B DLPH	$\sqrt{s} = 180\text{--}209$ GeV
2.98 ± 0.05 ± 0.04	ACHARD	04E L3	1990–2000 LEP runs
2.86 ± 0.09	HEISTER	03C ALEP	$\sqrt{s} = 189\text{--}209$ GeV
2.69 ± 0.13 ± 0.11	ABBIENDI,G	00D OPAL	1998 LEP run
2.89 ± 0.32 ± 0.19	ABREU	97J DLPH	1993–1994 LEP runs
3.23 ± 0.16 ± 0.10	AKERS	95C OPAL	1990–1992 LEP runs
2.68 ± 0.20 ± 0.20	BUSKULIC	93L ALEP	1990–1991 LEP runs
• • • We do not use the following data for averages, fits, limits, etc. • • •			
2.84 ± 0.15 ± 0.14	ABREU	00Z DLPH	1997–1998 LEP runs
3.01 ± 0.08	ACCIARRI	99R L3	1991–1998 LEP runs
3.1 ± 0.6 ± 0.1	ADAM	96C DLPH	$\sqrt{s} = 130, 136$ GeV

### Limits from Astrophysics and Cosmology

#### Number of Light $\nu$ Types

("light" means  $<$  about 1 MeV). See also OLIVE 81. For a review of limits based on Nucleosynthesis, Supernovae, and also on terrestrial experiments, see DENEGR1 90. Also see "Big-Bang Nucleosynthesis" in this Review.

VALUE	CL%	DOCUMENT ID	TECN	COMMENT
• • • We do not use the following data for averages, fits, limits, etc. • • •				
$< 4.08$	95	MANGANO	11	BBN
$0.9 < N_\nu < 8.2$		<sup>3</sup> ICHIKAWA	07	COSM
$3 < N_\nu < 7$	95	<sup>4</sup> CIRELLI	06	COSM
$2.7 < N_\nu < 4.6$	95	<sup>5</sup> HANNESTAD	06	COSM
$3.6 < N_\nu < 7.4$	95	<sup>4</sup> SELJAK	06	COSM
$< 4.4$		<sup>6</sup> CYBURT	05	COSM
$< 3.3$		<sup>7</sup> BARGER	03C	COSM
$1.4 < N_\nu < 6.8$		<sup>8</sup> CROTTY	03	COSM
$1.9 < N_\nu < 6.6$		<sup>8</sup> PIERPAOLI	03	COSM
$2 < N_\nu < 4$		LISI	99	BBN
$< 4.3$		OLIVE	99	BBN
$< 4.9$		COPI	97	Cosmology
$< 3.6$		HATA	97B	High D/H quasar abs.
$< 4.0$		OLIVE	97	BBN; high <sup>4</sup> He and <sup>7</sup> Li
$< 4.7$		CARDALL	96B	COSM High D/H quasar abs.
$< 3.9$		FIELDS	96	COSM BBN; high <sup>4</sup> He and <sup>7</sup> Li
$< 4.5$		KERNAN	96	COSM High D/H quasar abs.
$< 3.6$		OLIVE	95	BBN; $\geq 3$ massless $\nu$
$< 3.3$		WALKER	91	Cosmology
$< 3.4$		OLIVE	90	Cosmology
$< 4$		YANG	84	Cosmology
$< 4$		YANG	79	Cosmology
$< 7$		STEIGMAN	77	Cosmology
		PEEBLES	71	Cosmology
$< 16$		<sup>9</sup> SHVARTSMAN	69	Cosmology
		HOYLE	64	Cosmology

<sup>3</sup> Constrains the number of neutrino types from recent CMB and large scale structure data. No priors on other cosmological parameters are used.

<sup>4</sup> Constrains the number of neutrino types from recent CMB, large scale structure, Lyman-alpha forest, and SN1a data. The slight preference for  $N_\nu > 3$  comes mostly from the Lyman-alpha forest data.

<sup>5</sup> Constrains the number of neutrino types from recent CMB and large scale structure data. See also HAMANN 07.

<sup>6</sup> Limit on the number of neutrino types based on <sup>4</sup>He and D/H abundance assuming a baryon density fixed to the WMAP data. Limit relaxes to 4.6 if D/H is not used or to 5.8 if only D/H and the CMB are used. See also CYBURT 01 and CYBURT 03.

<sup>7</sup> Limit on the number of neutrino types based on combination of WMAP data and big-bang nucleosynthesis. The limit from WMAP data alone is 8.3. See also KNELLER 01.  $N_\nu \geq 3$  is assumed to compute the limit.

<sup>8</sup> 95% confidence level range on the number of neutrino flavors from WMAP data combined with other CMB measurements, the 2dGRS data, and HST data.

<sup>9</sup> SHVARTSMAN 69 limit inferred from his equations.

### Number Coupling with Less Than Full Weak Strength

VALUE	DOCUMENT ID	TECN
-------	-------------	------

• • • We do not use the following data for averages, fits, limits, etc. • • •

$< 20$	<sup>10</sup> OLIVE	81C COSM
$< 20$	<sup>10</sup> STEIGMAN	79 COSM

<sup>10</sup> Limit varies with strength of coupling. See also WALKER 91.

## REFERENCES FOR Limits on Number of Neutrino Types

MANGAN0	11	PL B701 296	G. Mangano, P. Serpico
HAMANN	07	JCAP 0708 021	J. Hamann et al.
ICHIKAWA	07	JCAP 0705 007	K. Ichikawa, M. Kawasaki, F. Takahashi
CIRELLI	06	JCAP 0612 013	M. Cirelli et al.
HANNESTAD	06	JCAP 0611 016	S. Hannestad, G. Raffelt
LEP-SLC	06	PRPL 427 257	ALEPH, DELPHI, L3, OPAL, SLD and working groups
SELJAK	06	JCAP 0610 014	U. Seljak, A. Slosar, P. McDonald
ABDALLAH	05B	EPJ C38 395	J. Abdallah et al. (DELPHI Collab.)
CYBURT	05	ASP 23 313	R.H. Cyburt et al.
ACHARD	04E	PL B587 16	P. Achard et al. (L3 Collab.)
BARGER	03C	PL B566 8	V. Barger et al.
CROTTY	03	PR D67 123005	P. Crotty, J. Lesgourgues, S. Pastor
CYBURT	03	PL B567 227	R.H. Cyburt, B.D. Fields, K.A. Olive
HEISTER	03C	EPJ C28 1	A. Heister et al. (ALEPH Collab.)
PIERPAOLI	03	MNRAS 342 L63	E. Pierpaoli
CYBURT	01	ASP 17 87	R.H. Cyburt, B.D. Fields, K.A. Olive
KNELLER	01	PR D64 123506	J.P. Kneller et al.
ABBIENDI.G	00D	EPJ C18 253	G. Abbiendi et al. (OPAL Collab.)
ABREU	00Z	EPJ C17 53	P. Abreu et al. (DELPHI Collab.)
ACCIARRI	99R	PL B470 268	M. Acciarri et al. (L3 Collab.)
LISI	99	PR D59 123520	E. Lisi, S. Sarkar, F.L. Villante
OLIVE	99	ASP 11 403	K.A. Olive, D. Thomas
ABREU	97J	ZPHY C74 577	P. Abreu et al. (DELPHI Collab.)
COPI	97	PR D55 3389	C.J. Copi, D.N. Schramm, M.S. Turner (CHIC)
HATA	97B	PR D55 540	N. Hata et al. (OSU, PENN)
OLIVE	97	ASP 7 27	K.A. Olive, D. Thomas (MINN, FLOR)
ADAM	96C	PL B380 471	W. Adam et al. (DELPHI Collab.)
CARDALL	96B	APJ 472 435	C.Y. Cardall, G.M. Fuller (UCSD)
FIELDS	96	New Ast 1 77	B.D. Fields et al. (NDAM, CERN, MINN+)
KERNAN	96	PR D54 3681	P.S. Kernan, S. Sarkar (CASE, OXFTP)
AKERS	95C	ZPHY C65 47	R. Akers et al. (OPAL Collab.)
OLIVE	95	PL B354 357	K.A. Olive, G. Steigman (MINN, OSU)
BUSKULIC	93L	PL B213 520	D. Buskully et al. (ALEPH Collab.)
LEP	92	PL B276 247	LEP Collabs. (LEP, ALEPH, DELPHI, L3, OPAL)
WALKER	91	APJ 376 51	T.P. Walker et al. (HSCA, OSU, CHIC+)
DENEGRI	90	RMP 62 1	D. Denegri, B. Sadoulet, M. Spiro (CERN, UCB+)
OLIVE	90	PL B236 454	K.A. Olive et al. (MINN, CHIC, OSU+)
YANG	84	APJ 281 493	J. Yang et al. (CHIC, BART)
OLIVE	81	APJ 246 557	K.A. Olive et al. (CHIC, BART)
OLIVE	81C	NP B180 497	K.A. Olive, D.N. Schramm, G. Steigman (EFI+)
STEIGMAN	79	PRL 43 239	G. Steigman, K.A. Olive, D.N. Schramm (BART+)
YANG	79	APJ 227 697	J. Yang et al. (CHIC, YALE, UVA)
STEIGMAN	77	PL 66B 202	G. Steigman, D.N. Schramm, J.E. Gunn (YALE, CHIC+)
PEEBLES	71	Physical Cosmology	P.Z. Peebles (PRIN)
Princeton Univ.	Press (1971)		
SHWARTSMAN	69	JETPL 9 184	V.F. Shwartsman (MOSU)
		Translated from ZETFP 9 315.	
HOYLE	64	NAT 203 1108	F. Hoyle, R.J. Taylor (CAMB)

Double- $\beta$  Decay

OMITTED FROM SUMMARY TABLE

NEUTRINOLESS DOUBLE- $\beta$  DECAY

Revised August 2011 by P. Vogel (Caltech) and A. Piepke (University of Alabama).

Neutrinoless double-beta ( $0\nu\beta\beta$ ) decay would signal violation of total lepton number conservation. The process can be mediated by an exchange of a light Majorana neutrino, or by an exchange of other particles. However, the existence of  $0\nu\beta\beta$ -decay requires Majorana neutrino mass, no matter what the actual mechanism is. As long as only a limit on the lifetime is available, limits on the effective Majorana neutrino mass, on the lepton-number violating right-handed current or other possible mechanisms mediating  $0\nu\beta\beta$ -decay can be obtained, independently of the actual mechanism. These limits are listed in the next three tables, together with a claimed  $0\nu\beta\beta$ -decay signal reported by part of the Heidelberg-Moscow collaboration. A  $6\sigma$  excess of counts at the decay energy is used for a determination of the Majorana neutrino mass. This signal has not yet been independently confirmed. In the following we *assume* that the exchange of light Majorana neutrinos ( $m_{\nu_i} \leq 10$  MeV) contributes dominantly to the decay rate.

Besides a dependence on the phase space ( $G^{0\nu}$ ) and the nuclear matrix element ( $M^{0\nu}$ ), the observable  $0\nu\beta\beta$ -decay rate is proportional to the square of the effective Majorana mass  $\langle m_{\beta\beta} \rangle$ ,  $(T_{1/2}^{0\nu})^{-1} = G^{0\nu} \cdot |M^{0\nu}|^2 \cdot \langle m_{\beta\beta} \rangle^2$ , with  $\langle m_{\beta\beta} \rangle^2 = |\sum_i U_{ei}^2 m_{\nu_i}|^2$ . The sum contains, in general, complex  $CP$ -phases in  $U_{ei}^2$ , *i.e.*, cancellations may occur. For three neutrino flavors, there are

three physical phases for Majorana neutrinos and one for Dirac neutrinos. The two additional Majorana phase differences affect only processes to which lepton-number-changing amplitudes contribute. Given the general  $3 \times 3$  mixing matrix for Majorana neutrinos, one can construct other analogous lepton number violating quantities,  $\langle m_{\ell\ell} \rangle = \sum_i U_{\ell i} U_{\ell' i} m_{\nu_i}$ . However, these are currently much less constrained than  $\langle m_{\beta\beta} \rangle$ .

Nuclear structure calculations are needed to deduce  $\langle m_{\beta\beta} \rangle$  from the decay rate. While  $G^{0\nu}$  can be calculated reliably, the computation of  $M^{0\nu}$  is subject to uncertainty. Comparing different nuclear model evaluations indicates a factor  $\sim 2$  spread in the calculated nuclear matrix elements. The particle physics quantities to be determined are thus nuclear model-dependent, so the half-life measurements are listed first. Where possible, we reference the nuclear matrix elements used in the subsequent analysis. Since rates for the more conventional  $2\nu\beta\beta$  decay serve to calibrate the nuclear theory, results for this process are also given.

Oscillation experiments utilizing atmospheric-, accelerator-, solar-, and reactor-produced neutrinos and anti-neutrinos yield strong evidence that at least some neutrinos are massive. However, these findings shed no light on the mass hierarchy (*i.e.*, on the sign of  $\Delta m_{atm}^2$ ), the absolute neutrino mass values or the properties of neutrinos under  $CPT$ -conjugation (Dirac or Majorana).

All confirmed oscillation experiments can be consistently described using three interacting neutrino species with two mass splittings and three mixing angles. Full three flavor analyses such as *e.g.* [2] yield:  $|\Delta m_{atm}^2| \equiv |m_3^2 - (m_2^2 + m_1^2)/2| = (2.39^{+0.27}_{-0.20}) \times 10^{-3}$  eV<sup>2</sup> and  $\sin^2 \theta_{atm} \equiv \sin^2 \theta_{23} = 0.466^{+0.136}_{-0.100}$  for the parameters observed in atmospheric and accelerator experiments. Oscillations of solar  $\nu_e$  and reactor  $\bar{\nu}_e$  lead to  $\Delta m_{\odot}^2 \equiv m_2^2 - m_1^2 = (7.67^{+0.34}_{-0.36}) \times 10^{-5}$  eV<sup>2</sup> and  $\sin^2 \theta_{\odot} \equiv \sin^2 \theta_{12} = 0.312^{+0.040}_{-0.034}$ . (All errors correspond to 95% CL) The investigation of reactor  $\bar{\nu}_e$  at  $\sim 1$  km baseline, combined with solar neutrino and long baseline reactor experiments, indicates that electron type neutrinos couple only weakly to the third mass eigenstate with  $\sin^2 \theta_{13} < 0.036$ .

Based on the 3-neutrino analysis:  $\langle m_{\beta\beta} \rangle^2 \approx |\cos^2 \theta_{\odot} m_1 + e^{i\Delta\alpha_{21}} \sin^2 \theta_{\odot} m_2 + e^{i\Delta\alpha_{31}} \sin^2 \theta_{13} m_3|^2$ , with  $\Delta\alpha_{21}, \Delta\alpha_{31}$  denoting the physically relevant Majorana  $CP$ -phase differences (possible Dirac phase  $\delta$  is absorbed in these  $\Delta\alpha$ ). Given the present knowledge of the neutrino oscillation parameters one can derive the relation between the effective Majorana mass and the mass of the lightest neutrino, as illustrated in the left panel of Fig. 1. The three mass hierarchies allowed by the oscillation data: normal ( $m_1 < m_2 < m_3$ ), inverted ( $m_3 < m_1 < m_2$ ), and degenerate ( $m_1 \approx m_2 \approx m_3$ ), result in different projections. The width of the innermost hatched bands reflects the uncertainty introduced by the unknown Majorana phases. If the experimental errors of the oscillation parameters are taken into account, then the allowed areas are widened as shown by the outer bands of Fig. 1. Because of the overlap of the

# Lepton Particle Listings

## Double- $\beta$ Decay

different mass scenarios a measurement of  $\langle m_{\beta\beta} \rangle$  in the degenerate or inversely hierarchical ranges would not determine the hierarchy. The middle panel of Fig. 1 depicts the relation of  $\langle m_{\beta\beta} \rangle$  with the summed neutrino mass  $M = m_1 + m_2 + m_3$ , constrained by observational cosmology. The oscillation data thus allow to test whether observed values of  $\langle m_{\beta\beta} \rangle$  and  $M$  are consistent within the 3 neutrino framework. The right hand panel of Fig. 1, finally, shows  $\langle m_{\beta\beta} \rangle$  as a function of the average mass  $\langle m_{\beta} \rangle = [\sum |U_{ei}|^2 m_{\nu_i}^2]^{1/2}$  determined through the analysis of low energy beta decays. The rather large intrinsic width of the  $\beta\beta$ -decay constraint essentially does not allow to positively identify the inverted hierarchy, and thus the sign of  $\Delta m_{atm}^2$ , even in combination with these other observables. Naturally, if the value of  $\langle m_{\beta\beta} \rangle \leq 0.01$  eV is ever established then normal hierarchy becomes the only possible scenario.

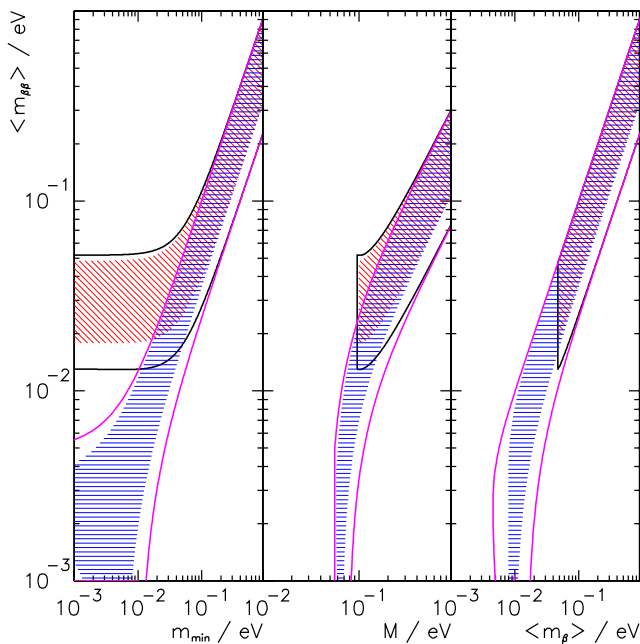


**Figure 1:** The left panel shows the dependence of  $\langle m_{\beta\beta} \rangle$  on the absolute mass of the lightest neutrino  $m_{min}$ . The middle panel shows  $\langle m_{\beta\beta} \rangle$  as a function of the summed neutrino mass  $M$ , while the right panel depicts  $\langle m_{\beta\beta} \rangle$  as a function of the mass  $\langle m_{\beta} \rangle$ . In all panels, the width of the hatched areas is due to the unknown Majorana phases and thus irreducible. The allowed areas given by the solid lines are obtained by taking into account the errors of the oscillation parameters. The two sets of solid lines correspond to the normal and inverted hierarchies. These sets merge into each other for  $\langle m_{\beta\beta} \rangle \geq 0.1$  eV, which corresponds to the degenerate mass pattern.

It should be noted that systematic uncertainties of the nuclear matrix elements are not folded into the mass limits reported by  $\beta\beta$ -decay experiments. Taking this additional uncertainty into account would further widen the projections. The uncertainties in oscillation parameters affect the width of the allowed bands in an asymmetric manner, as shown in Fig. 1. For example, for the degenerate mass pattern ( $\langle m_{\beta\beta} \rangle \geq 0.1$  eV) the upper edge is simply  $\langle m_{\beta\beta} \rangle \sim m$ , where  $m$  is the common mass of the degenerate multiplet, independent of the oscillation parameters, while the lower edge is  $m \cos(2\theta_{\odot})$ . Similar arguments explain the other features of Fig. 1.

If the neutrinoless double-beta decay is observed, it will be possible to fix a *range* of absolute values of the masses  $m_{\nu_i}$ . Unlike the direct neutrino mass measurements, however, a limit on  $\langle m_{\beta\beta} \rangle$  does not allow one to constrain the individual mass values  $m_{\nu_i}$  even when the mass differences  $\Delta m^2$  are known.

Neutrino oscillation data imply, for the first time, the existence of a *lower limit*  $\sim 0.013$  eV for the Majorana neutrino mass for the inverted hierarchy mass pattern while  $\langle m_{\beta\beta} \rangle$  could, by fine tuning, vanish in the case of the normal mass hierarchy. Several new double-beta searches have been proposed to probe the interesting  $\langle m_{\beta\beta} \rangle$  mass range.

If lepton-number-violating right-handed current weak interactions exist, their strength can be characterized by the phenomenological coupling constants  $\eta$  and  $\lambda$  ( $\eta$  describes the coupling between the right-handed lepton current and left-handed quark current while  $\lambda$  describes the coupling when both currents are right-handed). The  $0\nu\beta\beta$  decay rate then depends on  $\langle \eta \rangle = \eta \sum_i U_{ei} V_{ei}$  and  $\langle \lambda \rangle = \lambda \sum_i U_{ei} V_{ei}$  that vanish for massless or unmixed neutrinos ( $V_{\ell j}$  is a matrix analogous to  $U_{\ell j}$  but describing the mixing with the hypothetical right-handed neutrinos). This mechanism of the  $0\nu\beta\beta$  decay could be, in principle, distinguished from the light Majorana neutrino exchange by the observation of the single electron spectra. The limits on  $\langle \eta \rangle$  and  $\langle \lambda \rangle$  are listed in a separate table. The reader is cautioned that a number of earlier experiments did not distinguish between  $\eta$  and  $\lambda$ . In addition, see the section on Majoron searches for additional limits set by these experiments.

### References

1. F. Šimkovic *et al.*, Phys. Rev. **C77**, 045503 (2008).
2. G.L. Fogli *et al.*, Phys. Rev. **D78**, 033010 (2008).

### Half-life Measurements and Limits for Double- $\beta$ Decay

In most cases the transitions  $(Z,A) \rightarrow (Z+2,A) + 2e^- + (0 \text{ or } 2) \bar{\nu}_e$  to the  $0^+$  ground state of the final nucleus are listed. However, we also list transitions that increase the nuclear charge ( $2e^+$ ,  $e^+$ /EC and ECEC) and transitions to excited states of the final nuclei ( $0^+_i$ ,  $2^+$ , and  $2^+_i$ ). In the following Listings, only best or comparable limits or lifetimes for each isotope are reported and only those with  $T_{1/2} > 10^{20}$  years that are relevant for particle physics. For  $2\nu$  decay, which is well established, only measured half-lives are reported.

$t_{1/2}(10^{21} \text{ yr})$	$CL\%$	ISOTOPE	TRANSITION	METHOD	DOCUMENT ID
$2.11 \pm 0.04 \pm 0.21$	68	$^{136}\text{Xe}$	$2\nu$	EXO-200	<sup>1</sup> ACKERMAN 11
$0.7 \pm 0.09 \pm 0.11$	68	$^{130}\text{Te}$	$2\nu$	NEMO-3	<sup>2</sup> ARNOLD 11

••• We do not use the following data for averages, fits, limits, etc. •••



## Lepton Particle Listings

Double- $\beta$  Decay

- <sup>34</sup> Limit on  $0\nu$ -decay to the first excited  $2^+$ -state of daughter nucleus using NEMO-3 tracking calorimeter.
- <sup>35</sup> BARABASH 07 use Ge calorimeter to search for  $\gamma$ -radiation following double electron capture or  $\beta^+$  plus electron capture decays of  $^{74}\text{Ge}$  to the ground state of  $^{74}\text{Ge}$ . This limit is based on the search for the 511 keV annihilation radiation. Various other limits, for the capture from different atomic shells and also to the excited states, are reported in the paper.
- <sup>36</sup> BARABASH 07 use Ge calorimeter to search for  $\gamma$ -radiation following double electron capture decay of  $^{74}\text{Ge}$  into the second excited  $2^+$ -state of  $^{74}\text{Ge}$ . That transition has been considered due to a possible resonance enhancement. The  $2\nu$  mode would be suppressed for this decay by its extremely small phase space factor.
- <sup>37</sup> KLAPDOR-KLEINGROTHAUS 06A present re-analysis of data originally published in KLAPDOR-KLEINGROTHAUS 04A. Modified pulse shape analysis leads the authors to claim improved  $6\sigma$  statistical evidence for observation of  $0\nu$ -decay, compared to  $4.2\sigma$  in KLAPDOR-KLEINGROTHAUS 04A. Analysis of the systematic uncertainty is not presented. Supersedes KLAPDOR-KLEINGROTHAUS 04A.
- <sup>38</sup> Supersedes ARNABOLDI 04. Bolometric  $\text{TeO}_2$  detector array CUORICINO is used for high resolution search for  $0\nu\beta\beta$  decay. The half-life limit is derived from 3.09 kg yr  $^{130}\text{Te}$  exposure.
- <sup>39</sup> NEMO-3 tracking calorimeter containing 6.9 kg of enriched  $^{100}\text{Mo}$  is used in ARNOLD 05A. A limit for  $0\nu\beta\beta$  half-life of  $^{100}\text{Mo}$  is reported. Supersedes ARNOLD 04.
- <sup>40</sup> NEMO-3 tracking calorimeter is used in ARNOLD 05A to place limit on  $0\nu\beta\beta$  half-life of  $^{82}\text{Se}$ . Detector contains 0.93 kg of enriched  $^{82}\text{Se}$ . Supersedes ARNOLD 04.
- <sup>41</sup> ARNOLD 05A use the NEMO-3 tracking calorimeter to determine the  $2\nu\beta\beta$  half-life of  $^{100}\text{Mo}$  with high statistics and low background (389 days of data taking). Supersedes ARNOLD 04.
- <sup>42</sup> ARNOLD 05A use the NEMO-3 tracking detector to determine the  $2\nu\beta\beta$  half-life of  $^{82}\text{Se}$  with high statistics and low background (389 days of data taking). Supersedes ARNOLD 04.
- <sup>43</sup> ARNOLD 04 use the NEMO-3 tracking detector to determine the limit for  $0\nu\beta\beta$  half-life of  $^{82}\text{Se}$ . This represents an improvement, by a factor of  $\sim 10$ , when compared with ELLIOTT 92. It supersedes the limit of ARNOLD 98 for this decay using NEMO-2.
- <sup>44</sup> ARNOLD 04 use the NEMO-3 tracking detector to determine the  $2\nu\beta\beta$  half-life of  $^{100}\text{Mo}$  with high statistics and low background. The half-life is determined assuming the Single State Dominance. It is in agreement with, and more accurate than, previous determinations. Supersedes DASSIE 95 determination of this quantity with NEMO-2.
- <sup>45</sup> BARABASH 04 perform an inclusive measurement of the  $\beta\beta$  decay of  $^{150}\text{Nd}$  into the first excited ( $0^+$ ) state of  $^{150}\text{Sm}$ . Gamma radiation emitted in decay of the excited state is detected.
- <sup>46</sup> Decay into first excited state of daughter nucleus.
- <sup>47</sup> Two neutrino decay into ground state. Relatively large error mainly due to uncertainties in background determination. Reported value is shorter than the geochemical measurements of KIRSTEN 83 and BERNATOWICZ 92 but in agreement with LIN 88 and TAKAOKA 96.
- <sup>48</sup> Supersedes ALESSANDRELLO 00. Array of  $\text{TeO}_2$  crystals in high resolution cryogenic calorimeter. Some enriched in  $^{128}\text{Te}$ . Ground state to ground state decay.
- <sup>49</sup> Calorimetric measurement of  $2\nu$  ground state decay of  $^{116}\text{Cd}$  using enriched  $\text{CdWO}_4$  scintillators. Agrees with EJIRI 95 and ARNOLD 96. Supersedes DANEVICH 00.
- <sup>50</sup> Limit on  $0\nu$  decay of  $^{116}\text{Cd}$  using enriched  $\text{CdWO}_4$  scintillators. Supersedes DANEVICH 00.
- <sup>51</sup> Limit on  $0\nu$  decay of  $^{116}\text{Cd}$  into first excited  $2^+$  state of daughter nucleus using enriched  $\text{CdWO}_4$  scintillators. Supersedes DANEVICH 00.
- <sup>52</sup> Limit on  $0\nu$  decay of  $^{116}\text{Cd}$  into first excited  $0^+$  state of daughter nucleus using enriched  $\text{CdWO}_4$  scintillators. Supersedes DANEVICH 00.
- <sup>53</sup> Limit on  $0\nu$  decay of  $^{116}\text{Cd}$  into second excited  $0^+$  state of daughter nucleus using enriched  $\text{CdWO}_4$  scintillators. Supersedes DANEVICH 00.
- <sup>54</sup> Limit on the  $0\nu$  ground state decay of  $^{186}\text{W}$  using enriched  $\text{CdWO}_4$  scintillators.
- <sup>55</sup> Limit on the  $0\nu$  decay of  $^{186}\text{W}$  to the first excited  $2^+$  state of the daughter nucleus using enriched  $\text{CdWO}_4$  scintillators.
- <sup>56</sup> Results of the Heidelberg-Moscow experiment (KLAPDOR-KLEINGROTHAUS 01 and GUENTHER 97) are reanalyzed using a new simulation of the complete background spectrum. The  $\beta\beta 2\nu$ -decay rate is deduced from a 41.57 kg-y exposure. The result is in agreement and supersedes the above referenced half-lives with similar statistical and systematic errors.
- <sup>57</sup> AALSETH 02b limit is based on 117 mol-yr of data using enriched Ge detectors. Background reduction by means of pulse shape analysis is applied to part of the data set. Reported limit is slightly less restrictive than that in KLAPDOR-KLEINGROTHAUS 01 However, it excludes part of the allowed half-life range reported in KLAPDOR-KLEINGROTHAUS 01B for the same nuclide. The analysis has been criticized in KLAPDOR-KLEINGROTHAUS 04B. The criticism was addressed and disputed in AALSETH 04.
- <sup>58</sup> BERNABEI 02b report a limit for the  $0\nu, 0^+ \rightarrow 0^+$  decay of  $^{134}\text{Xe}$ , present in the source at 17%, by considering the maximum number of events for this mode compatible with the fitted smooth background.
- <sup>59</sup> BERNABEI 02b report a limit for the  $0\nu, 0^+ \rightarrow 0^+$  decay of  $^{136}\text{Xe}$ , by considering the maximum number of events for this mode compatible with the fitted smooth background. The quoted sensitivity is  $450 \times 10^{21}$  yr. The Feldman and Cousins method is used to obtain the quoted limit.
- <sup>60</sup> ASHITKOV 01 result for  $0\nu$  of  $^{100}\text{Mo}$  is less stringent than EJIRI 01.
- <sup>61</sup> DANEVICH 01 place limit on  $0\nu$  decay of  $^{160}\text{Gd}$  using  $\text{Gd}_2\text{SiO}_5:\text{Ce}$  crystal scintillators. The limit is more stringent than KOBAYASHI 95.
- <sup>62</sup> DANEVICH 01 place limits on  $0\nu$  decay of  $^{160}\text{Gd}$  into excited  $2^+$  state of daughter nucleus using  $\text{Gd}_2\text{SiO}_5:\text{Ce}$  crystal scintillators.
- <sup>63</sup> DEBRAECKELEER 01 performed an inclusive measurement of the  $\beta\beta$  decay into the second excited state of the daughter nucleus. A novel coincidence technique counting the de-excitation photons is employed. The result agrees with BARABASH 95.
- <sup>64</sup> KLAPDOR-KLEINGROTHAUS 01 is a continuation of the work published in BAUDIS 99. Isotopically enriched Ge detectors are used in calorimetric measurement. The most stringent bound is derived from the data set in which pulse-shape analysis has been used to reduce background. Exposure time is 35.5 kg y. Supersedes BAUDIS 99 as most stringent result.
- <sup>65</sup> WIESER 01 reports an inclusive geochemical measurement of  $^{96}\text{Zr}$   $\beta\beta$  half life. Their result agrees within  $2\sigma$  with ARNOLD 99 but only marginally, within  $3\sigma$ , with KAWASHIMA 93.
- <sup>66</sup> BRUDANIN 00 determine the  $2\nu$  half-life of  $^{48}\text{Ca}$ . Their value is less accurate than BALTHYSH 96.
- <sup>67</sup> ARNOLD 99 measure directly the  $2\nu$  decay of Zr for the first time, using the NEMO-2 tracking detector and an isotopically enriched source. The lifetime is more accurate than the geochemical result of KAWASHIMA 93.
- <sup>68</sup> ARNOLD 98 measure the  $2\nu$  decay of  $^{82}\text{Se}$  by comparing the spectra in an enriched and natural selenium source using the NEMO-2 tracking detector. The measured half-life is in agreement, perhaps slightly shorter, than ELLIOTT 92.
- <sup>69</sup> ARNOLD 98 determine the limit for  $0\nu$  decay to the excited  $2^+$  state of  $^{82}\text{Se}$  using the NEMO-2 tracking detector.
- <sup>70</sup> ALSTON-GARNJOST 97 report evidence for  $2\nu$  decay of  $^{100}\text{Mo}$ . This decay has been also observed by EJIRI 91, DASSIE 95, and DESILVA 97.
- <sup>71</sup> DESILVA 97 result for  $2\nu$  decay of  $^{100}\text{Mo}$  is in agreement with ALSTON-GARNJOST 97 and DASSIE 95. This measurement has the smallest errors.
- <sup>72</sup> DESILVA 97 result for  $2\nu$  decay of  $^{150}\text{Nd}$  is in marginal agreement with ARTEMEV 93. It has smaller errors.
- <sup>73</sup> ARNOLD 96 measure the  $2\nu$  decay of  $^{116}\text{Cd}$ . This result is in agreement with EJIRI 95, but has smaller errors. Supersedes ARNOLD 95.
- <sup>74</sup> BALTHYSH 96 measure the  $2\nu$  decay of  $^{48}\text{Ca}$ , using a passive source of enriched  $^{48}\text{Ca}$  in a TPC.
- <sup>75</sup> TAKAOKA 96 measure the geochemical half-life of  $^{130}\text{Te}$ . Their value is in disagreement with the quoted values of BERNATOWICZ 92 and KIRSTEN 83; but agrees with several other unquoted determinations, e.g., MANUEL 91.
- <sup>76</sup> BARABASH 95 cannot distinguish  $0\nu$  and  $2\nu$ , but it is inferred indirectly that the  $0\nu$  mode accounts for less than 0.026% of their event sample. They also note that their result disagrees with the previous experiment by the NEMO group (BLUM 92).
- <sup>77</sup> BERNATOWICZ 92 finds  $^{128}\text{Te}/^{130}\text{Te}$  activity ratio from slope of  $^{128}\text{Xe}/^{132}\text{Xe}$  vs  $^{130}\text{Xe}/^{132}\text{Xe}$  ratios during extraction, and normalizes to lead-dated ages for the  $^{130}\text{Te}$  lifetime. The authors state that their results imply that "(a) the double beta decay of  $^{128}\text{Te}$  has been firmly established and its half-life has been determined ... without any ambiguity due to trapped Xe interferences. ... (b) Theoretical calculations ... underestimate the [long half-lives of  $^{128}\text{Te}$   $^{130}\text{Te}$ ] by 1 or 2 orders of magnitude, pointing to a real suppression in the  $2\nu$  decay rate of these isotopes. (c) Despite [this], most  $\beta\beta$ -models predict a ratio of  $2\nu$  decay widths ... in fair agreement with observation." Further details of the experiment are given in BERNATOWICZ 93. Our listed half-life has been revised downward from the published value by the authors, on the basis of reevaluated cosmic-ray  $^{128}\text{Xe}$  production corrections.
- <sup>78</sup> TURKEVICH 91 observes activity in old U sample. The authors compare their results with theoretical calculations. They state "Using the phase-space factors of Boehm and Vogel (BOEHM 87) leads to matrix element values for the  $^{238}\text{U}$  transition in the same range as deduced for  $^{130}\text{Te}$  and  $^{76}\text{Ge}$ . On the other hand, the latest theoretical estimates (STAUDT 90) give an upper limit that is 10 times lower. This large discrepancy implies either a defect in the calculations or the presence of a faster path than the standard two-neutrino mode in this case." See BOEHM 87 and STAUDT 90.
- <sup>79</sup> Result agrees with direct determination of ELLIOTT 92.
- <sup>80</sup> Inclusive half life inferred from mass spectroscopic determination of abundance of  $\beta\beta$ -decay product  $^{130}\text{Te}$  in mineral kirkite (NiTeSe). Systematic uncertainty reflects variations in U-Xe gas-retention-age derived from different uranite samples. Agrees with geochemical determination of TAKAOKA 96 and direct measurement of ARNABOLDI 03. Inconsistent with results of KIRSTEN 83 and BERNATOWICZ 92.
- <sup>81</sup> Ratio of inclusive double beta half lives of  $^{128}\text{Te}$  and  $^{130}\text{Te}$  determined from minerals melonite ( $\text{NiTe}_2$ ) and altaite ( $\text{PbTe}$ ) by means of mass spectroscopic measurement of abundance of  $\beta\beta$ -decay products. As gas-retention-age could not be determined the authors use half life of  $^{130}\text{Te}$  (LIN 88) to infer the half life of  $^{128}\text{Te}$ . No estimate of the systematic uncertainty of this method is given. The directly determined half life ratio agrees with BERNATOWICZ 92. However, the inferred  $^{128}\text{Te}$  half life disagrees with KIRSTEN 83 and BERNATOWICZ 92.
- <sup>82</sup> KIRSTEN 83 reports " $2\sigma$ " error. References are given to earlier determinations of the  $^{130}\text{Te}$  lifetime.

### $\langle m_\nu \rangle$ : The Effective Weighted Sum of Majorana Neutrino Masses Contributing to Neutrinoless Double- $\beta$ Decay

$\langle m_\nu \rangle = |\sum U_{1j}^2 m_\nu|$ , where the sum goes from 1 to  $n$  and where  $n$  = number of neutrino generations, and  $\nu_j$  is a Majorana neutrino. Note that  $U_{ej}^2$ , not  $|U_{ej}|^2$ , occurs in the sum. The possibility of cancellations has been stressed. In the following Listings, only best or comparable limits or lifetimes for each isotope are reported.

VALUE (eV)	CL% ISOTOPE	TRANSITION	METHOD	DOCUMENT ID
• • • We do not use the following data for averages, fits, limits, etc. • • •				
< 0.45-0.93	90 $^{100}\text{Mo}$	$0\nu$	NEMO-3	<sup>83</sup> BARABASH 11A
< 0.89-2.43	90 $^{82}\text{Se}$	$0\nu$	NEMO-3	<sup>84</sup> BARABASH 11A



< 7.2-19.5	90	<sup>96</sup> Zr	0 $\nu$	NEMO-3	85 ARGYRIADES 10
< 4.0-6.8	90	<sup>150</sup> Nd	0 $\nu$	NEMO-3	86 ARGYRIADES 09
< 0.19-0.68	90	<sup>130</sup> Te	0 $\nu$	TeO <sub>2</sub> bolometer	87 ARNABOLDI 08
< 3.5-22	90	<sup>48</sup> Ca	0 $\nu$	CaF <sub>2</sub> scint.	88 UMEHARA 08
< 9.3-60	90	<sup>100</sup> Mo	0 $^+$ $\rightarrow$ 0 $^+$	NEMO-3	89 ARNOLD 07
< 6500	90	<sup>100</sup> Mo	0 $^+$ $\rightarrow$ 2 $^+$	NEMO-3	90 ARNOLD 07
0.32 $\pm$ 0.03	68	<sup>76</sup> Ge	0 $\nu$	Enriched HP Ge	91 KLAPDOR-K... 06A
< 0.2-1.1	90	<sup>130</sup> Te	0 $\nu$	Cryog. det.	92 ARNABOLDI 05
< 0.7-2.8	90	<sup>100</sup> Mo	0 $\nu$	NEMO-3	93 ARNOLD 05A
< 1.7-4.9	90	<sup>82</sup> Se	0 $\nu$	NEMO-3	94 ARNOLD 05A
< 0.37-1.9	90	<sup>130</sup> Te	0 $\nu$	Cryog. det.	95 ARNABOLDI 04
< 0.8-1.2	90	<sup>100</sup> Mo	0 $\nu$	NEMO-3	96 ARNOLD 04
< 1.5-3.1	90	<sup>82</sup> Se	0 $\nu$	NEMO-3	96 ARNOLD 04
0.1-0.9	99.7	<sup>76</sup> Ge	0 $\nu$	Enriched HP Ge	97 KLAPDOR-K... 04A
< 7.2-44.7	90	<sup>48</sup> Ca	0 $\nu$	CaF <sub>2</sub> scint.	98 OGAWA 04
< 1.1-2.6	90	<sup>130</sup> Te	0 $\nu$	Cryog. det.	99 ARNABOLDI 03
< 1.5-1.7	90	<sup>116</sup> Cd	0 $\nu$	<sup>116</sup> CdWO <sub>4</sub> scint.	100 DANEVICH 03
< 0.33-1.35	90		0 $\nu$	Enriched HP Ge	101 AALSETH 02B
< 2.9	90	<sup>136</sup> Xe	0 $\nu$	Liquid Xe Scint.	102 BERNABEI 02D
0.39 $^{+0.17}_{-0.28}$	76	<sup>76</sup> Ge	0 $\nu$	Enriched HP Ge	103 KLAPDOR-K... 02D
< 2.1-4.8	90	<sup>100</sup> Mo	0 $\nu$	ELEGANT V	104 EJIRI 01
< 0.35	90	<sup>76</sup> Ge	0 $\nu$	Enriched HP Ge	105 KLAPDOR-K... 01
< 23	90	<sup>96</sup> Zr	0 $\nu$	NEMO-2	106 ARNOLD 99
< 1.1-1.5		<sup>128</sup> Te	0 $\nu$	Geochem	107 BERNATOW... 92
< 5	68	<sup>82</sup> Se	0 $\nu$	TPC	108 ELLIOTT 92
< 8.3	76	<sup>48</sup> Ca	0 $\nu$	CaF <sub>2</sub> scint.	YOU 91

<sup>83</sup> BARABASH 11A limit is based on NEMO-3 data for <sup>100</sup>Mo. The reported range reflects different nuclear matrix elements. Supersedes ARNOLD 05A and ARNOLD 04.

<sup>84</sup> BARABASH 11A limit is based on NEMO-3 data for <sup>82</sup>Se. The reported range reflects different nuclear matrix elements. Supersedes ARNOLD 05A and ARNOLD 04.

<sup>85</sup> ARGYRIADES 10 use <sup>96</sup>Zr and the NEMO-3 tracking detector to obtain the reported mass limit. The range reflects the fluctuation of the nuclear matrix elements considered.

<sup>86</sup> ARGYRIADES 09 limit is based on data taken with the NEMO-3 detector and <sup>150</sup>Nd. A range of nuclear matrix elements that include the effect of nuclear deformation have been used.

<sup>87</sup> Limit was obtained using high resolution TeO<sub>2</sub> bolometer calorimeter to search for double beta decay of <sup>130</sup>Te. Reported range of limits reflects spread of matrix element calculations used. Supersedes ARNABOLDI 05.

<sup>88</sup> Limit was obtained using CaF<sub>2</sub> scintillation calorimeter to search for double beta decay of <sup>48</sup>Ca. Reported range of limits reflects spread of QRPA and SM matrix element calculations used. Supersedes OGAWA 04.

<sup>89</sup> ARNOLD 07 use NEMO-3 half life limit for 0 $\nu$ -decay of <sup>100</sup>Mo to the first excited 0 $^+$  state of daughter nucleus to obtain neutrino mass limit. The spread reflects the choice of two different nuclear matrix elements. This limit is not competitive when compared to the decay to the ground state.

<sup>90</sup> ARNOLD 07 use NEMO-3 half life limit for 0 $\nu$ -decay of <sup>100</sup>Mo to the first excited 2 $^+$  state of daughter nucleus to obtain neutrino mass limit. This limit is not competitive when compared to the decay to the ground state.

<sup>91</sup> Re-analysis of data originally published in KLAPDOR-KLEINGROTHAUS 04A. Modified pulse shape analysis leads the authors to claim 6 $\sigma$  statistical evidence for observation of 0 $\nu$ -decay. Authors use matrix element of STAUDT 90. Uncertainty of nuclear matrix element is not reflected in stated error. Supersedes KLAPDOR-KLEINGROTHAUS 04A.

<sup>92</sup> Supersedes ARNABOLDI 04. Reported range of limits due to use of different nuclear matrix element calculations.

<sup>93</sup> Mass limits reported in ARNOLD 05A are derived from <sup>100</sup>Mo data, obtained by the NEMO-3 collaboration. The range reflects the spread of matrix element calculations considered in this work. Supersedes ARNOLD 04.

<sup>94</sup> Neutrino mass limits based on <sup>82</sup>Se data utilizing the NEMO-3 detector. The range reported in ARNOLD 05A reflects the spread of matrix element calculations considered in this work. Supersedes ARNOLD 04.

<sup>95</sup> Supersedes ARNABOLDI 03. Reported range of limits due to use of different nuclear matrix element calculations.

<sup>96</sup> ARNOLD 04 limit is based on the nuclear matrix elements of SIMKOVIC 99, STOICA 01 and CIVITARESE 03.

<sup>97</sup> Supersedes KLAPDOR-KLEINGROTHAUS 02D. Event excess at  $\beta\beta$ -decay energy is used to derive Majorana neutrino mass using the nuclear matrix elements of STAUDT 90. The mass range shown is based on the authors evaluation of the uncertainties of the STAUDT 90 matrix element calculation. If this uncertainty is neglected, and only statistical errors are considered, the range in  $\langle m \rangle$  becomes (0.2-0.6) eV at the 3  $\sigma$  level.

<sup>98</sup> Calorimetric CaF<sub>2</sub> scintillator. Range of limits reflects authors' estimate of the uncertainty of the nuclear matrix elements. Replaces YOU 91 as the most stringent limit based on <sup>48</sup>Ca.

<sup>99</sup> Supersedes ALESSANDRELLO 00. Cryogenic calorimeter search. Reported a range reflecting uncertainty in nuclear matrix element calculations.

<sup>100</sup> Limit for  $\langle m_{\nu} \rangle$  is based on the nuclear matrix elements of STAUDT 90 and ARNOLD 96. Supersedes DANEVICH 00.

<sup>101</sup> AALSETH 02B reported range of limits on  $\langle m_{\nu} \rangle$  reflects the spread of theoretical nuclear matrix elements. Excludes part of allowed mass range reported in KLAPDOR-KLEINGROTHAUS 01B.

<sup>102</sup> BERNABEI 02D limit is based on the matrix elements of SIMKOVIC 02. The range of neutrino masses based on a variety of matrix elements is 1.1-2.9 eV.

<sup>103</sup> KLAPDOR-KLEINGROTHAUS 02D is a detailed description of the analysis of the data collected by the Heidelberg-Moscow experiment, previously presented in KLAPDOR-KLEINGROTHAUS 01B. Matrix elements in STAUDT 90 have been used. See the footnote in the preceding table for further details. See also KLAPDOR-KLEINGROTHAUS 02B.

<sup>104</sup> The range of the reported  $\langle m_{\nu} \rangle$  values reflects the spread of the nuclear matrix elements. On axis value assuming  $\langle \lambda \rangle = \langle \eta \rangle = 0$ .

<sup>105</sup> KLAPDOR-KLEINGROTHAUS 01 uses the calculation by STAUDT 90. Using several other models in the literature could worsen the limit up to 1.2eV. This is the most stringent experimental bound on  $m_{\nu}$ . It supersedes BAUDIS 99B.

<sup>106</sup> ARNOLD 99 limit based on the nuclear matrix elements of STAUDT 90.

<sup>107</sup> BERNATOWICZ 92 finds these majorana neutrino mass limits assuming that the measured geochemical decay width is a limit on the 0 $\nu$  decay width. The range is the range found using matrix elements from HAXTON 84, TOMODA 87, and SUHONEN 91. Further details of the experiment are given in BERNATOWICZ 93.

<sup>108</sup> ELLIOTT 92 uses the matrix elements of HAXTON 84.

### Limits on Lepton-Number Violating (V+A) Current Admixture

For reasons given in the discussion at the beginning of this section, we list only results from 1989 and later.  $\langle \lambda \rangle = \lambda \sum U_{ej} V_{ej}$  and  $\langle \eta \rangle = \eta \sum U_{ej} V_{ej}$ , where the sum is over the number of neutrino generations. This sum vanishes for massless or unmixed neutrinos. In the following Listings, only best or comparable limits or lifetimes for each isotope are reported.

$\langle \lambda \rangle$ (10 <sup>-6</sup> )	CL%	$\langle \eta \rangle$ (10 <sup>-8</sup> )	CL%	ISOTOPE	METHOD	DOCUMENT ID
< 120	90			<sup>100</sup> Mo	0 $^+$ $\rightarrow$ 2 $^+$	<sup>109</sup> ARNOLD 07
0.692 $^{+0.058}_{-0.056}$	68	0.305 $^{+0.026}_{-0.025}$	68	<sup>76</sup> Ge	Enriched HPGe	<sup>110</sup> KLAPDOR-K... 06A
< 2.5	90			<sup>100</sup> Mo	0 $\nu$ , NEMO-3	<sup>111</sup> ARNOLD 05A
< 3.8	90			<sup>82</sup> Se	0 $\nu$ , NEMO-3	<sup>112</sup> ARNOLD 05A
< 1.5-2.0	90			<sup>100</sup> Mo	0 $\nu$ , NEMO-3	<sup>113</sup> ARNOLD 04
< 3.2-3.8	90			<sup>82</sup> Se	0 $\nu$ , NEMO-3	<sup>114</sup> ARNOLD 04
< 1.6-2.4	90	< 0.9-5.3	90	<sup>130</sup> Te	Cryog. det.	<sup>115</sup> ARNABOLDI 03
< 2.2	90	< 2.5	90	<sup>116</sup> Cd	<sup>116</sup> CdWO <sub>4</sub> scint.	<sup>116</sup> DANEVICH 03
< 3.2-4.7	90	< 2.4-2.7	90	<sup>100</sup> Mo	ELEGANT V	<sup>117</sup> EJIRI 01
< 1.1	90	< 0.64	90	<sup>76</sup> Ge	Enriched HPGe	<sup>118</sup> GUENTHER 97
< 4.4	90	< 2.3	90	<sup>136</sup> Xe	TPC	<sup>119</sup> VUILLEUMIER 93
		< 5.3		<sup>128</sup> Te	Geochem	<sup>120</sup> BERNATOW... 92

• • • We do not use the following data for averages, fits, limits, etc. • • •

<sup>109</sup> ARNOLD 07 use NEMO-3 half life limit for 0 $\nu$ -decay of <sup>100</sup>Mo to the first excited 2 $^+$  state of daughter nucleus to limit the right-right handed admixture of weak currents  $\langle \lambda \rangle$ . This limit is not competitive when compared to the decay to the ground state.

<sup>110</sup> Re-analysis of data originally published in KLAPDOR-KLEINGROTHAUS 04A. Modified pulse shape analysis leads the authors to claim 6 $\sigma$  statistical evidence for observation of 0 $\nu$ -decay. Authors use matrix element of MUTO 89 to determine  $\langle \lambda \rangle$  and  $\langle \eta \rangle$ . Uncertainty of nuclear matrix element is not reflected in stated errors.

<sup>111</sup> ARNOLD 05A derive limit for  $\langle \lambda \rangle$  based on <sup>100</sup>Mo data collected with NEMO-3 detector. No limit for  $\langle \eta \rangle$  is given. Supersedes ARNOLD 04.

<sup>112</sup> ARNOLD 05A derive limit for  $\langle \lambda \rangle$  based on <sup>82</sup>Se data collected with NEMO-3 detector. No limit for  $\langle \eta \rangle$  is given. Supersedes ARNOLD 04.

<sup>113</sup> ARNOLD 04 use the matrix elements of SUHONEN 94 to obtain a limit for  $\langle \lambda \rangle$ , no limit for  $\langle \eta \rangle$  is given. This limit is more stringent than the limit in EJIRI 01 for the same nucleus.

<sup>114</sup> ARNOLD 04 use the matrix elements of TOMODA 91 and SUHONEN 91 to obtain a limit for  $\langle \lambda \rangle$ , no limit for  $\langle \eta \rangle$  is given.

<sup>115</sup> Supersedes ALESSANDRELLO 00. Cryogenic calorimeter search. Reported a range reflecting uncertainty in nuclear matrix element calculations.

<sup>116</sup> Limits for  $\langle \lambda \rangle$  and  $\langle \eta \rangle$  are based on nuclear matrix elements of STAUDT 90. Supersedes DANEVICH 00.

<sup>117</sup> The range of the reported  $\langle \lambda \rangle$  and  $\langle \eta \rangle$  values reflects the spread of the nuclear matrix elements. On axis value assuming  $\langle m_{\nu} \rangle = 0$  and  $\langle \lambda \rangle = \langle \eta \rangle = 0$ , respectively.

<sup>118</sup> GUENTHER 97 limits use the matrix elements of STAUDT 90. Supersedes BALYSH 95 and BALYSH 92.

<sup>119</sup> VUILLEUMIER 93 uses the matrix elements of MUTO 89. Based on a half-life limit 2.6  $\times$  10<sup>23</sup> y at 90%CL.

<sup>120</sup> BERNATOWICZ 92 takes the measured geochemical decay width as a limit on the 0 $\nu$  width, and uses the SUHONEN 91 coefficients to obtain the least restrictive limit on  $\eta$ . Further details of the experiment are given in BERNATOWICZ 93.

### Double- $\beta$ Decay REFERENCES

ACKERMAN	11	PRL 107 212501	N. Ackerman et al.	(EXO Collab.)
ARNOLD	11	PRL 107 062504	R. Arnold et al.	(NEMO-3 Collab.)
BARABASH	11	PR C83 045503	A.S. Barabash et al.	
BARABASH	11A	PAN 74 312	A.S. Barabash et al.	(NEMO-3 Collab.)
		Translated from YAF 74 330.		
BELLI	11D	JPG 38 115107	P. Belli et al.	(DAMA-INR Collab.)
RUKHADZE	11	NP A852 197	N.I. Rukhadze et al.	(TGV-2 Collab.)
ARGYRIADES	10	NP A847 168	J. Argyriades et al.	(NEMO-3 Collab.)
BELLI	10	NP A846 143	P. Belli et al.	(DAMA-INR Collab.)
ARGYRIADES	09	PR C80 032501	J. Argyriades et al.	(NEMO-3 Collab.)
BELLI	09A	NP A826 256	P. Belli et al.	(DAMA-INR Collab.)
KIDD	09	NP A821 251	M. Kidd et al.	
ARNABOLDI	08	PR C78 035502	C. Arnaboldi et al.	
BELLI	08	PL B56 193	P. Belli et al.	(DAMA-INR Collab.)
BELLI	08B	EPJ A36 167	P. Belli et al.	
UMEHARA	08	PR C78 058501	S. Umebara et al.	
ARNOLD	07	NP A781 209	R. Arnold et al.	(NEMO-3 Collab.)

# Lepton Particle Listings

## Double- $\beta$ Decay, Neutrino Mixing

BARABASH	07	NP A785 371	A.S. Barabash <i>et al.</i>
KLAPDOR-K...	06A	MPL A21 1547	H.V. Klapdor-Kleingrothaus, I.V. Krivosheina
ARNABOLDI	05	PRL 95 142501	C. Arnaboldi <i>et al.</i> (CUORICINO Collab.)
ARNOLD	05A	PRL 95 182302	R. Arnold <i>et al.</i> (NEMO-3 Collab.)
AALSETH	04	PR D70 078302	C.E. Aalseth <i>et al.</i>
ARNABOLDI	04	PL B584 260	C. Arnaboldi <i>et al.</i>
ARNOLD	04	JETPL 80 377	R. Arnold <i>et al.</i> (NEMO3 Detector Collab.)
Translated from ZETFP 80 429			
BARABASH	04	JETPL 79 10	A.S. Barabash <i>et al.</i>
KLAPDOR-K...	04A	PL B586 198	H.V. Klapdor-Kleingrothaus <i>et al.</i>
KLAPDOR-K...	04B	PR D70 078301	H.V. Klapdor-Kleingrothaus, A. Dietz, I.V. Krivosheina
OGAWA	04	NP A730 215	I. Ogawa <i>et al.</i>
ARNABOLDI	03	PL B557 167	C. Arnaboldi <i>et al.</i>
CIVITARESE	03	NP A729 867	O. Civitarese, J. Suhonen
DANEVICH	03	PR C68 035501	F.A. Danevich <i>et al.</i>
DOERR	03	NIM A513 596	C. Doerr, H.V. Klapdor-Kleingrothaus
AALSETH	02B	PR D65 092007	C.E. Aalseth <i>et al.</i> (IGEX Collab.)
BERNABEI	02D	PL B546 23	R. Bernabei <i>et al.</i> (DAMA Collab.)
KLAPDOR-K...	02B	PPNL 110 57	H.V. Klapdor-Kleingrothaus, A. Dietz, I.V. Krivosheina
KLAPDOR-K...	02D	FP 32 1181	H.V. Klapdor-Kleingrothaus, A. Dietz, I.V. Krivosheina
SIMKOVIC	02	hep-ph/0204278	F. Simkovic, P. Domin, A. Faessler
ASHITKOV	01	JETPL 74 529	V.D. Ashitkov <i>et al.</i>
Translated from ZETFP 74 601			
DANEVICH	01	NP A694 375	F.A. Danevich <i>et al.</i>
DEBRAECKEL	01	PRL 86 3510	L. De Braeckeleer <i>et al.</i>
EJRI	01	PR C63 065501	H. Ejri <i>et al.</i>
KLAPDOR-K...	01	EPJ A12 147	H.V. Klapdor-Kleingrothaus <i>et al.</i>
KLAPDOR-K...	01B	MPL A16 2409	H.V. Klapdor-Kleingrothaus <i>et al.</i>
STOICA	01	NP A694 269	S. Stoica, H.V. Klapdor-Kleingrothaus
WIESER	01	PR C64 024308	M.E. Wieser, J.R. De Laeter
ALESSAND...	00	PL B486 13	A. Alessandrello <i>et al.</i>
BRUDANIN	00	PL B495 63	V.B. Brudanin <i>et al.</i> (TGV Collab.)
DANEVICH	00	PR C62 045501	F.A. Danevich <i>et al.</i>
ARNOLD	99	NP A658 299	R. Arnold <i>et al.</i> (NEMO Collab.)
BAUDIS	99	PR D59 022001	L. Baudis <i>et al.</i> (Heidelberg-Moscow Collab.)
BAUDIS	99B	PRL 83 41	L. Baudis <i>et al.</i> (Heidelberg-Moscow Collab.)
SIMKOVIC	99	PR C60 055502	F. Simkovic <i>et al.</i>
ARNOLD	98	NP A636 209	R. Arnold <i>et al.</i> (NEMO-2 Collab.)
ALSTON-...	97	PR C55 474	M. Alston-Garnjost <i>et al.</i> (LBL, MTHO+)
DESILVA	97	PR C56 2451	A. de Silva <i>et al.</i> (UCI)
GUENTHER	97	PR D55 54	M. Gunther <i>et al.</i> (Heidelberg-Moscow Collab.)
ARNOLD	96	ZPHY C72 239	R. Arnold <i>et al.</i> (BCEN, CAEN, JINR+)
BALYSH	96	PRL 77 5186	A. Balysh <i>et al.</i> (KIAE, UCI, CIT)
TAKAOKA	96	PR C53 1557	N. Takaoka, Y. Motomura, K. Nagao
ARNOLD	95	JETPL 61 170	R.G. Arnold <i>et al.</i> (NEMO Collab.)
Translated from ZETFP 61 168			
BALYSH	95	PL B356 450	A. Balysh <i>et al.</i> (Heidelberg-Moscow Collab.)
BARABASH	95	PL B345 408	A.S. Barabash <i>et al.</i> (ITEP, SCUC, PNL+)
DASSIE	95	PR D51 2090	D. Dassie <i>et al.</i> (NEMO Collab.)
EJRI	95	JPSJ 64 339	H. Ejri <i>et al.</i> (OSAK, KIEV)
KOBAYASHI	95	NP A586 457	M. Kobayashi, M. Kobayashi
SUHOENEN	94	PR C49 3055	J. Suhonen, O. Civitarese
ARTEMIEV	93	JETPL 58 262	V.A. Artemiev <i>et al.</i> (ITEP, INRM)
Translated from ZETFP 58 256			
BERNATOW...	93	PR C47 806	T. Bernatowicz <i>et al.</i> (WUSL, TATA)
KAWASHIMA	93	PR C47 R2452	A. Kawashima, K. Takahashi, A. Masuda
VUILLEUMIER	93	PR D48 1009	J.C. Vuilleumier <i>et al.</i> (NEUC, CIT, VILL)
BALYSH	92	PL B283 32	A. Balysh <i>et al.</i> (MPIH, KIAE, SASSO)
BERNATOW...	92	PRL 69 2341	T. Bernatowicz <i>et al.</i> (WUSL, TATA)
BLUM	92	PL B275 506	D. Blum <i>et al.</i> (NEMO Collab.)
ELLIOTT	92	PR C46 1535	S.R. Elliott <i>et al.</i> (UCI)
EJRI	91	PL B258 17	H. Ejri <i>et al.</i> (OSAK)
MANUEL	91	JPG 17 5221	O.K. Manuel <i>et al.</i> (MISSR)
SUHOENEN	91	NP A535 509	J. Suhonen, S.B. Khadikar, A. Faessler
TOMODA	91	RPP 54 53	T. Tomoda
TURKEVICH	91	PRL 67 3211	A. Turkevich, T.E. Economou, G.A. Cowan
YOU	91	PL B265 53	K. You <i>et al.</i> (BHEP, CAST+)
STAUDT	90	EPL 13 31	A. Staudt, K. Muto, H.V. Klapdor-Kleingrothaus
MUTO	89	ZPHY A334 187	K. Muto, E. Bender, H.V. Klapdor
LIN	88	NP A481 477	W.J. Lin <i>et al.</i>
LIN	88B	NP A481 484	W.J. Lin <i>et al.</i>
BOEHM	87	Massive Neutrinos	F. Bohm, P. Vogel (CIT)
Cambridge Univ. Press, Cambridge			
TOMODA	87	PL B199 475	T. Tomoda, A. Faessler (TUBIN)
HAXTON	84	PPNP 12 409	W.C. Haxton, G.J. Stevenson
KIRSTEN	83	PRL 50 474	T. Kirsten, H. Richter, E. Jessberger (MPIH)

## Neutrino Mixing

With the exception of a few possible anomalies such as LSND, current neutrino data can be described within the framework of a  $3 \times 3$  mixing matrix between the flavor eigenstates  $\nu_e$ ,  $\nu_\mu$ , and  $\nu_\tau$  and the mass eigenstates  $\nu_1$ ,  $\nu_2$ , and  $\nu_3$ . (See Eq. (13.79) of the review “Neutrino Mass, Mixing, and Oscillations” by K. Nakamura and S.T. Petcov.) The Listings are divided into the following sections:

**(A) Neutrino fluxes and event ratios:** shows measurements which correspond to various oscillation tests for Accelerator, Reactor, Atmospheric, and Solar neutrino experiments. Typically ratios involve a measurement in a realm sensitive to oscillations compared to one for which no oscillation effect is expected.

**(B) Three neutrino mixing parameters:** shows measurements of  $\sin^2(2\theta_{12})$ ,  $\sin^2(2\theta_{23})$ ,  $\Delta m_{21}^2$ ,  $\Delta m_{32}^2$ , and  $\sin^2(2\theta_{13})$

which are all interpretations of data based on the three neutrino mixing scheme described in the review “Neutrino Mass, Mixing, and Oscillations.” by K. Nakamura and S.T. Petcov. Many parameters have been calculated in the two-neutrino approximation.

**(C) Other neutrino mixing results:** shows measurements and limits for the probability of oscillation for experiments which might be relevant to the LSND oscillation claim. Included are experiments which are sensitive to  $\nu_\mu \rightarrow \nu_e$ ,  $\bar{\nu}_\mu \rightarrow \bar{\nu}_e$ , sterile neutrinos, and CPT tests.

### (A) Neutrino fluxes and event ratios

#### Events (observed/expected) from accelerator $\nu_\mu$ experiments.

Some neutrino oscillation experiments compare the flux in two or more detectors. This is usually quoted as the ratio of the event rate in the far detector to the expected rate based on an extrapolation from the near detector in the absence of oscillations.

VALUE	DOCUMENT ID	TECN	COMMENT
• • •	We do not use the following data for averages, fits, limits, etc. • • •		
$0.71 \pm 0.08$	<sup>1</sup> AHN	06A K2K	K2K to Super-K
$0.64 \pm 0.05$	<sup>2</sup> MICHAEL	06	MINS All charged current events
$0.71 \pm 0.08$ $-0.09$	<sup>3</sup> ALIU	05	K2K KEK to Super-K
$0.70 \pm 0.10$ $-0.11$	<sup>4</sup> AHN	03	K2K KEK to Super-K

<sup>1</sup> Based on the observation of 112 events when  $158.1 \pm 9.2$  were expected without oscillations. Including not only the number of events but also the shape of the energy distribution, the evidence for oscillation is at the level of about  $4.3 \sigma$ . Supersedes ALIU 05.

<sup>2</sup> This ratio is based on the observation of 215 events compared to an expectation of  $336 \pm 14$  without oscillations. See also ADAMSON 08.

<sup>3</sup> This ratio is based on the observation of 107 events at the far detector 250 km away from KEK, and an expectation of  $151 \pm 12$ .

<sup>4</sup> This ratio is based on the observation of 56 events with an expectation of  $80.1 \pm 6.2$ .

#### Events (observed/expected) from reactor $\bar{\nu}_e$ experiments.

The quoted values are the ratios of the measured reactor  $\bar{\nu}_e$  event rate at the quoted distances, and the rate expected without oscillations. The expected rate is based on the experimental data for the most significant reactor fuels ( $^{235}\text{U}$ ,  $^{239}\text{Pu}$ ,  $^{241}\text{Pu}$ ) and on calculations for  $^{238}\text{U}$ .

A recent re-evaluation of the spectral conversion of electron to  $\bar{\nu}_e$  in MUELLER 11 results in an upward shift of the reactor  $\bar{\nu}_e$  spectrum by 3% and, thus, might require revisions to the ratios listed in this table.

VALUE	DOCUMENT ID	TECN	COMMENT
• • •	We do not use the following data for averages, fits, limits, etc. • • •		
$0.944 \pm 0.016 \pm 0.040$	<sup>1</sup> ABE	12	DCHZ Chooz reactors
$0.920 \pm 0.009 \pm 0.014$	<sup>2</sup> AHN	12	RENO Yonggwang reactors
$0.940 \pm 0.011 \pm 0.004$	<sup>3</sup> AN	12	DAYA Daya Bay, Ling Ao, Ling Ao-II reactors
$1.08 \pm 0.21 \pm 0.16$	<sup>4</sup> DENIZ	10	TEXO Kuo-Sheng reactor, 28 m
$0.658 \pm 0.044 \pm 0.047$	<sup>5</sup> ARAKI	05	KLND Japanese react. ~180 km
$0.611 \pm 0.085 \pm 0.041$	<sup>6</sup> EGUCHI	03	KLND Japanese react. ~180 km
$1.01 \pm 0.024 \pm 0.053$	<sup>7</sup> BOEHM	01	Palo Verde react. 0.75–0.89 km
$1.01 \pm 0.028 \pm 0.027$	<sup>8</sup> APOLLONIO	99	CHOZ Chooz reactors 1 km
$0.987 \pm 0.006 \pm 0.037$	<sup>9</sup> GREENWOOD	96	GREENWOOD 96 Savannah River, 18.2 m
$0.988 \pm 0.004 \pm 0.05$	ACHKAR	95	CNTR Bugey reactor, 15 m
$0.994 \pm 0.010 \pm 0.05$	ACHKAR	95	CNTR Bugey reactor, 40 m
$0.915 \pm 0.132 \pm 0.05$	ACHKAR	95	CNTR Bugey reactor, 95 m
$0.987 \pm 0.014 \pm 0.027$	<sup>10</sup> DECLAIS	94	CNTR Bugey reactor, 15 m
$0.985 \pm 0.018 \pm 0.034$	KUVSHINN...	91	CNTR Rovno reactor
$1.05 \pm 0.02 \pm 0.05$	VUILLEUMIER	82	Gösgen reactor
$0.955 \pm 0.035 \pm 0.110$	<sup>11</sup> KWON	81	$\bar{\nu}_e p \rightarrow e^+ n$
$0.89 \pm 0.15$	<sup>11</sup> BOEHM	80	$\bar{\nu}_e p \rightarrow e^+ n$

<sup>1</sup> ABE 12 determine the  $\bar{\nu}_e$  interaction rate in a single detector, located 1050 m from the cores of two reactors. The rate normalization is fixed by the results of the Bugey4 reactor experiment, thus avoiding any dependence on possible very short baseline oscillations.

<sup>2</sup> AHN 12 use two identical detectors, placed at flux weighted distances of 408.56 m and 1433.99 m from six reactor cores, to determine the  $\bar{\nu}_e$  interaction rate ratio.

<sup>3</sup> AN 12 use six identical detectors with three placed near the reactor cores (flux-weighted baselines of 470 m and 576 m) and the remaining three at the far hall (at the flux averaged distance of 1648 m from all six reactor cores) to determine the  $\bar{\nu}_e$  interaction rate ratios.

<sup>4</sup> DENIZ 10 observe reactor  $\bar{\nu}_e e$  scattering with recoil kinetic energies 3–8 MeV using CsI(Tl) detectors. The observed rate is consistent with the Standard Model prediction, leading to a constraint on  $\sin^2\theta_{\nu\bar{\nu}} = 0.251 \pm 0.031(\text{stat}) \pm 0.024(\text{sys})$ .

<sup>5</sup> Updated result of KamLAND, including the data used in EGUCHI 03. Note that the survival probabilities for different periods are not directly comparable because the effective baseline varies with power output of the reactor sources involved, and there were large variations in the reactor power production in Japan in 2003.

<sup>6</sup> EGUCHI 03 observe reactor neutrino disappearance at  $\sim 180$  km baseline to various Japanese nuclear power reactors.

<sup>7</sup> BOEHM 01 search for neutrino oscillations at 0.75 and 0.89 km distance from the Palo Verde reactors.

<sup>8</sup> APOLLONIO 99, APOLLONIO 98 search for neutrino oscillations at 1.1 km fixed distance from Chooz reactors. They use  $\bar{\nu}_e p \rightarrow e^+ n$  in Gd-loaded scintillator target. APOLLONIO 99 supersedes APOLLONIO 98. See also APOLLONIO 03 for detailed description.

<sup>9</sup> GREENWOOD 96 search for neutrino oscillations at 18 m and 24 m from the reactor at Savannah River.

<sup>10</sup> DECLAIS 94 result based on integral measurement of neutrons only. Result is ratio of measured cross section to that expected in standard V-A theory. Replaced by ACHKAR 95.

<sup>11</sup> KWON 81 represents an analysis of a larger set of data from the same experiment as BOEHM 80.

### Atmospheric neutrinos

Neutrinos and antineutrinos produced in the atmosphere induce  $\mu$ -like and  $e$ -like events in underground detectors. The ratio of the numbers of the two kinds of events is defined as  $\mu/e$ . It has the advantage that systematic effects, such as flux uncertainty, tend to cancel, for both experimental and theoretical values of the ratio. The "ratio of the ratios" of experimental to theoretical  $\mu/e$ ,  $R(\mu/e)$ , or that of experimental to theoretical  $\mu/\text{total}$ ,  $R(\mu/\text{total})$  with  $\text{total} = \mu + e$ , is reported below. If the actual value is not unity, the value obtained in a given experiment may depend on the experimental conditions. In addition, the measured "up-down asymmetry" for  $\mu$  ( $N_{\text{up}}(\mu)/N_{\text{down}}(\mu)$ ) or  $e$  ( $N_{\text{up}}(e)/N_{\text{down}}(e)$ ) is reported. The expected "up-down asymmetry" is nearly unity if there is no neutrino oscillation.

### $R(\mu/e) = (\text{Measured Ratio } \mu/e) / (\text{Expected Ratio } \mu/e)$

VALUE	DOCUMENT ID	TECN	COMMENT
-------	-------------	------	---------

• • • We do not use the following data for averages, fits, limits, etc. • • •

$0.658 \pm 0.016 \pm 0.035$	<sup>1</sup> ASHIE	05	SKAM sub-GeV
$0.702 \pm 0.032 \pm 0.101$ -0.030	<sup>2</sup> ASHIE	05	SKAM multi-GeV
$0.69 \pm 0.10 \pm 0.06$	<sup>3</sup> SANCHEZ	03	SOU2 Calorimeter raw data
	<sup>4</sup> FUKUDA	96B	KAMI Water Cherenkov
$1.00 \pm 0.15 \pm 0.08$	<sup>5</sup> DAUM	95	FREJ Calorimeter
$0.60 \pm 0.06 \pm 0.05$ -0.05	<sup>6</sup> FUKUDA	94	KAMI sub-GeV
$0.57 \pm 0.08 \pm 0.07$ -0.07	<sup>7</sup> FUKUDA	94	KAMI multi-GeV
	<sup>8</sup> BECKER-SZ...	92B	IMB Water Cherenkov

<sup>1</sup> ASHIE 05 results are based on an exposure of 92 kton yr during the complete Super-Kamiokande I running period. The analyzed data sample consists of fully-contained single-ring  $e$ -like events with  $0.1 \text{ GeV}/c < p_e$  and  $\mu$ -like events  $0.2 \text{ GeV}/c < p_\mu$ , both having a visible energy  $< 1.33 \text{ GeV}$ . These criteria match the definition used by FUKUDA 94.

<sup>2</sup> ASHIE 05 results are based on an exposure of 92 kton yr during the complete Super-Kamiokande I running period. The analyzed data sample consists of fully-contained single-ring events with visible energy  $> 1.33 \text{ GeV}$  and partially-contained events. All partially-contained events are classified as  $\mu$ -like.

<sup>3</sup> SANCHEZ 03 result is based on an exposure of 5.9 kton yr, and updates ALLISON 99 result. The analyzed data sample consists of fully-contained  $e$ -flavor and  $\mu$ -flavor events having lepton momentum  $> 0.3 \text{ GeV}/c$ .

<sup>4</sup> FUKUDA 96B studied neutron background in the atmospheric neutrino sample observed in the Kamiokande detector. No evidence for the background contamination was found.

<sup>5</sup> DAUM 95 results are based on an exposure of 2.0 kton yr which includes the data used by BERGER 90B. This ratio is for the contained and semicontained events. DAUM 95 also report  $R(\mu/e) = 0.99 \pm 0.13 \pm 0.08$  for the total neutrino induced data sample which includes upward going stopping muons and horizontal muons in addition to the contained and semicontained events.

<sup>6</sup> FUKUDA 94 result is based on an exposure of 7.7 kton yr and updates the HIRATA 92 result. The analyzed data sample consists of fully-contained  $e$ -like events with  $0.1 < p_e < 1.33 \text{ GeV}/c$  and fully-contained  $\mu$ -like events with  $0.2 < p_\mu < 1.5 \text{ GeV}/c$ .

<sup>7</sup> FUKUDA 94 analyzed the data sample consisting of fully contained events with visible energy  $> 1.33 \text{ GeV}$  and partially contained  $\mu$ -like events.

<sup>8</sup> BECKER-SZENDY 92B reports the fraction of nonshowering events (mostly muons from atmospheric neutrinos) as  $0.36 \pm 0.02 \pm 0.02$ , as compared with expected fraction  $0.51 \pm 0.01 \pm 0.05$ . After cutting the energy range to the Kamiokande limits, BEIER 92 finds  $R(\mu/e)$  very close to the Kamiokande value.

### $R(\nu_\mu) = (\text{Measured Flux of } \nu_\mu) / (\text{Expected Flux of } \nu_\mu)$

VALUE	DOCUMENT ID	TECN	COMMENT
-------	-------------	------	---------

• • • We do not use the following data for averages, fits, limits, etc. • • •

$0.84 \pm 0.12$	<sup>1</sup> ADAMSON	06	MINS MINOS atmospheric
$0.72 \pm 0.026 \pm 0.13$	<sup>2</sup> AMBROSIO	01	MCRO upward through-going
$0.57 \pm 0.05 \pm 0.15$	<sup>3</sup> AMBROSIO	00	MCRO upgoing partially contained
$0.71 \pm 0.05 \pm 0.19$	<sup>4</sup> AMBROSIO	00	MCRO downgoing partially contained + upgoing stopping
$0.74 \pm 0.036 \pm 0.046$	<sup>5</sup> AMBROSIO	98	MCRO Streamer tubes
	<sup>6</sup> CASPER	91	IMB Water Cherenkov
	<sup>7</sup> AGLIETTA	89	NUSX
$0.95 \pm 0.22$	<sup>8</sup> BOLIEV	81	Baksan
$0.62 \pm 0.17$	ROUGH	78	Case Western/UCI

<sup>1</sup> ADAMSON 06 uses a measurement of 107 total neutrinos compared to an expected rate of  $127 \pm 13$  without oscillations.

<sup>2</sup> AMBROSIO 01 result is based on the upward through-going muon tracks with  $E_\mu > 1 \text{ GeV}$ . The data came from three different detector configurations, but the statistics is largely dominated by the full detector run, from May 1994 to December 2000. The total live time, normalized to the full detector configuration, is 6.17 years. The first error is the statistical error, the second is the systematic error, dominated by the theoretical error in the predicted flux.

<sup>3</sup> AMBROSIO 00 result is based on the upgoing partially contained event sample. It came from 4.1 live years of data taking with the full detector, from April 1994 to February 1999. The average energy of atmospheric muon neutrinos corresponding to this sample is 4 GeV. The first error is statistical, the second is the systematic error, dominated by the 25% theoretical error in the rate (20% in the flux and 15% in the cross section, added in quadrature). Within statistics, the observed deficit is uniform over the zenith angle.

<sup>4</sup> AMBROSIO 00 result is based on the combined samples of downgoing partially contained events and upgoing stopping events. These two subsamples could not be distinguished due to the lack of timing information. The result came from 4.1 live years of data taking with the full detector, from April 1994 to February 1999. The average energy of atmospheric muon neutrinos corresponding to this sample is 4 GeV. The first error is statistical, the second is the systematic error, dominated by the 25% theoretical error in the rate (20% in the flux and 15% in the cross section, added in quadrature). Within statistics, the observed deficit is uniform over the zenith angle.

<sup>5</sup> AMBROSIO 98 result is for all nadir angles and updates AHLEN 95 result. The lower cutoff on the muon energy is 1 GeV. In addition to the statistical and systematic errors, there is a Monte Carlo flux error (theoretical error) of  $\pm 0.13$ . With a neutrino oscillation hypothesis, the fit either to the flux or zenith distribution independently yields  $\sin^2 2\theta = 1.0$  and  $\Delta(m^2) \sim$  a few times  $10^{-3} \text{ eV}^2$ . However, the fit to the observed zenith distribution gives a maximum probability for  $\chi^2$  of only 5% for the best oscillation hypothesis.

<sup>6</sup> CASPER 91 correlates showering/nonshowering signature of single-ring events with parent atmospheric-neutrino flavor. They find nonshowering ( $\approx \nu_\mu$  induced) fraction is  $0.41 \pm 0.03 \pm 0.02$ , as compared with expected  $0.51 \pm 0.05$  (syst).

<sup>7</sup> AGLIETTA 89 finds no evidence for any anomaly in the neutrino flux. They define  $\rho = (\text{measured number of } \nu_e^{\text{sh}}) / (\text{measured number of } \nu_\mu^{\text{sh}})$ . They report  $\rho(\text{measured}) = \rho(\text{expected}) = 0.96 \pm 0.32$   
-0.28

<sup>8</sup> From this data BOLIEV 81 obtain the limit  $\Delta(m^2) \leq 6 \times 10^{-3} \text{ eV}^2$  for maximal mixing,  $\nu_\mu \leftrightarrow \nu_\mu$  type oscillation.

### $R(\mu/\text{total}) = (\text{Measured Ratio } \mu/\text{total}) / (\text{Expected Ratio } \mu/\text{total})$

VALUE	DOCUMENT ID	TECN	COMMENT
-------	-------------	------	---------

• • • We do not use the following data for averages, fits, limits, etc. • • •

$1.1 \pm 0.07 \pm 0.11$ -0.12	<sup>1</sup> CLARK	97	IMB multi-GeV
----------------------------------	--------------------	----	---------------

<sup>1</sup> CLARK 97 obtained this result by an analysis of fully contained and partially contained events in the IMB water-Cherenkov detector with visible energy  $> 0.95 \text{ GeV}$ .

### $N_{\text{up}}(\mu) / N_{\text{down}}(\mu)$

VALUE	DOCUMENT ID	TECN	COMMENT
-------	-------------	------	---------

• • • We do not use the following data for averages, fits, limits, etc. • • •

$0.551 \pm 0.035 \pm 0.004$ -0.033	<sup>1</sup> ASHIE	05	SKAM multi-GeV
---------------------------------------	--------------------	----	----------------

<sup>1</sup> ASHIE 05 results are based on an exposure of 92 kton yr during the complete Super-Kamiokande I running period. The analyzed data sample consists of fully-contained single-ring  $\mu$ -like events with visible energy  $> 1.33 \text{ GeV}$  and partially-contained events. All partially-contained events are classified as  $\mu$ -like. Upward-going events are those with  $-1 < \cos(\text{zenith angle}) < -0.2$  and downward-going events are those with  $0.2 < \cos(\text{zenith angle}) < 1$ . The  $\mu$ -like up-down ratio for the multi-GeV data deviates from 1 (the expectation for no atmospheric  $\nu_\mu$  oscillations) by more than 12 standard deviations.

### $N_{\text{up}}(e) / N_{\text{down}}(e)$

VALUE	DOCUMENT ID	TECN	COMMENT
-------	-------------	------	---------

• • • We do not use the following data for averages, fits, limits, etc. • • •

$0.961 \pm 0.086 \pm 0.016$ -0.079	<sup>1</sup> ASHIE	05	SKAM multi-GeV
---------------------------------------	--------------------	----	----------------

<sup>1</sup> ASHIE 05 results are based on an exposure of 92 kton yr during the complete Super-Kamiokande I running period. The analyzed data sample consists of fully-contained single-ring  $e$ -like events with visible energy  $> 1.33 \text{ GeV}$ . Upward-going events are those with  $-1 < \cos(\text{zenith angle}) < -0.2$  and downward-going events are those with  $0.2 < \cos(\text{zenith angle}) < 1$ . The  $e$ -like up-down ratio for the multi-GeV data is consistent with 1 (the expectation for no atmospheric  $\nu_e$  oscillations).

# Lepton Particle Listings

## Neutrino Mixing

$R(\text{up/down}; \mu) = (\text{Measured up/down}; \mu) / (\text{Expected up/down}; \mu)$

VALUE	DOCUMENT ID	TECN	COMMENT
-------	-------------	------	---------

• • • We do not use the following data for averages, fits, limits, etc. • • •

$0.62^{+0.19}_{-0.14} \pm 0.02$	1 ADAMSON	06	MINS atmospheric $\nu$ with far detector
---------------------------------	-----------	----	--

<sup>1</sup> ADAMSON 06 result is obtained with the MINOS far detector with an exposure of 4.54 kton yr. The expected ratio is calculated with no neutrino oscillation.

$R(\mu^+/\mu^-) = (\text{Measured } N(\mu^+)/N(\mu^-)) / (\text{Expected } N(\mu^+)/N(\mu^-))$

VALUE	DOCUMENT ID	TECN	COMMENT
-------	-------------	------	---------

• • • We do not use the following data for averages, fits, limits, etc. • • •

$1.39^{+0.35+0.08}_{-0.46-0.14}$	1 ADAMSON	07	MINS Upward and horizontal $\mu$ with far detector
----------------------------------	-----------	----	--

$0.96^{+0.38}_{-0.27} \pm 0.15$	2 ADAMSON	06	MINS atmospheric $\nu$ with far detector
---------------------------------	-----------	----	--

<sup>1</sup> ADAMSON 07 result is obtained with the MINOS far detector in 854.24 live days, based on neutrino-induced upward-going and horizontal muons. This result is consistent with CP T conservation.

<sup>2</sup> ADAMSON 06 result is obtained with the MINOS far detector with an exposure of 4.54 kton yr, based on contained events. The expected ratio is calculated by assuming the same oscillation parameters for neutrinos and antineutrinos.

### Solar neutrinos

Solar neutrinos are produced by thermonuclear fusion reactions in the Sun. Radiochemical experiments measure particular combinations of fluxes from various neutrino-producing reactions, whereas water-Cherenkov experiments mainly measure a flux of neutrinos from decay of <sup>8</sup>B. Solar neutrino fluxes are composed of all active neutrino species,  $\nu_e$ ,  $\nu_\mu$ , and  $\nu_\tau$ . In addition, some other mechanisms may cause antineutrino components in solar neutrino fluxes. Each measurement method is sensitive to a particular component or a combination of components of solar neutrino fluxes. For details, see Section 13.4 of Reviews, Tables, and Plots.

### $\nu_e$ Capture Rates from Radiochemical Experiments

1 SNU (Solar Neutrino Unit) =  $10^{-36}$  captures per atom per second.

VALUE (SNU)	DOCUMENT ID	TECN	COMMENT
-------------	-------------	------	---------

• • • We do not use the following data for averages, fits, limits, etc. • • •

$73.4^{+6.1+3.7}_{-6.0-4.1}$	1 KAETHER	10	GALX reanalysis
------------------------------	-----------	----	-----------------

$67.6 \pm 4.0 \pm 3.2$	2 KAETHER	10	GNO+GALX reanalysis combined
------------------------	-----------	----	------------------------------

$65.4^{+3.1+2.6}_{-3.0-2.8}$	3 ABDURASHI...	09	SAGE <sup>71</sup> Ga $\rightarrow$ <sup>71</sup> Ge
------------------------------	----------------	----	--

$62.9^{+5.5}_{-5.3} \pm 2.5$	4 ALT MANN	05	GNO <sup>71</sup> Ga $\rightarrow$ <sup>71</sup> Ge
------------------------------	------------	----	---

$69.3 \pm 4.1 \pm 3.6$	5 ALT MANN	05	GNO + GALX combined
------------------------	------------	----	---------------------

$77.5 \pm 6.2^{+4.3}_{-4.7}$	6 HAMPEL	99	GALX <sup>71</sup> Ga $\rightarrow$ <sup>71</sup> Ge
------------------------------	----------	----	--

$2.56 \pm 0.16 \pm 0.16$	7 CLEVELAND	98	HOME <sup>37</sup> Cl $\rightarrow$ <sup>37</sup> Ar
--------------------------	-------------	----	--

<sup>1</sup> KAETHER 10 reports the reanalysis results of a complete GALLEX data (GALLEX I+II+III+IV, reported in HAMPEL 99) based on the event selection with a new pulse shape analysis, which provides a better background reduction than the rise time analysis adopted in HAMPEL 99.

<sup>2</sup> Combined result of GALLEX I+II+III+IV reanalysis and GNO I+II+III (ALTMANN 05).

<sup>3</sup> ABDURASHITOV 09 reports a combined analysis of 168 extractions of the SAGE solar neutrino experiment during the period January 1990 through December 2007, and updates the ABDURASHITOV 02 result. The data are consistent with the assumption that the solar neutrino production rate is constant in time. Note that a  $\sim 15\%$  systematic uncertainty in the overall normalization may be added to the ABDURASHITOV 09 result, because calibration experiments for gallium solar neutrino measurements using intense <sup>51</sup>Cr (twice by GALLEX and once by SAGE) and <sup>37</sup>Ar (by SAGE) result in an average ratio of  $0.87 \pm 0.05$  of the observed to calculated rates.

<sup>4</sup> ALT MANN 05 reports the complete result from the GNO solar neutrino experiment (GNO I+II+III), which is the successor project of GALLEX. Experimental technique of GNO is essentially the same as that of GALLEX. The run data cover the period 20 May 1998 through 9 April 2003.

<sup>5</sup> Combined result of GALLEX I+II+III+IV (HAMPEL 99) and GNO I+II+III.

<sup>6</sup> HAMPEL 99 report the combined result for GALLEX I+II+III+IV (65 runs in total), which update the HAMPEL 96 result. The GALLEX IV result (12 runs) is  $118.4 \pm 17.8 \pm 6.6$  SNU. (HAMPEL 99 discuss the consistency of partial results with the mean.) The GALLEX experimental program has been completed with these runs. The total run data cover the period 14 May 1991 through 23 January 1997. A total of 300 <sup>71</sup>Ge events were observed. Note that a  $\sim 15\%$  systematic uncertainty in the overall normalization may be added to the HAMPEL 99 result, because calibration experiments for gallium solar neutrino measurements using intense <sup>51</sup>Cr (twice by GALLEX and once by SAGE) and <sup>37</sup>Ar (by SAGE) result in an average ratio of  $0.87 \pm 0.05$  of the observed to calculated rates.

<sup>7</sup> CLEVELAND 98 is a detailed report of the <sup>37</sup>Cl experiment at the Homestake Mine. The average solar neutrino-induced <sup>37</sup>Ar production rate from 108 runs between 1970 and 1994 updates the DAVIS 89 result.

### $\phi ES$ (<sup>8</sup>B)

<sup>8</sup>B solar-neutrino flux measured via  $\nu e$  elastic scattering. This process is sensitive to all active neutrino flavors, but with reduced sensitivity to  $\nu_\mu$ ,  $\nu_\tau$  due to the cross-section difference,  $\sigma(\nu_{\mu,\tau} e) \sim 0.16\sigma(\nu_e e)$ . If the <sup>8</sup>B solar-neutrino flux involves nonelectron flavor active neutrinos, their contribution to the flux is  $\sim 0.16$  times of  $\nu_e$ .

VALUE ( $10^6 \text{ cm}^{-2} \text{ s}^{-1}$ )	DOCUMENT ID	TECN	COMMENT
---	-------------	------	---------

• • • We do not use the following data for averages, fits, limits, etc. • • •

$2.32 \pm 0.04 \pm 0.05$	1 ABE	11	SKAM SK-III average flux
--------------------------	-------	----	--------------------------

$2.41 \pm 0.05^{+0.16}_{-0.15}$	2 ABE	11	SKAM SK-II average flux
---------------------------------	-------	----	-------------------------

$2.38 \pm 0.02 \pm 0.08$	3 ABE	11	SKAM SK-I average flux
--------------------------	-------	----	------------------------

$2.77 \pm 0.26 \pm 0.32$	4 ABE	11B	KLND average flux
--------------------------	-------	-----	-------------------

$2.4 \pm 0.4 \pm 0.1$	5 BELLINI	10A	BORX average flux
-----------------------	-----------	-----	-------------------

$1.77^{+0.24+0.09}_{-0.21-0.10}$	6 AHARMIM	08	SNO Phase III
----------------------------------	-----------	----	---------------

$2.38 \pm 0.05^{+0.16}_{-0.15}$	7 CRAVENS	08	SKAM average flux
---------------------------------	-----------	----	-------------------

$2.35 \pm 0.02 \pm 0.08$	8 HOSAKA	06	SKAM average flux
--------------------------	----------	----	-------------------

$2.35 \pm 0.22 \pm 0.15$	9 AHARMIM	05A	SNO Salty D <sub>2</sub> O; <sup>8</sup> B shape not constrained
--------------------------	-----------	-----	--

$2.34 \pm 0.23^{+0.15}_{-0.14}$	9 AHARMIM	05A	SNO Salty D <sub>2</sub> O; <sup>8</sup> B shape constrained
---------------------------------	-----------	-----	--

$2.39^{+0.24}_{-0.23} \pm 0.12$	10 AHMAD	02	SNO average flux
---------------------------------	----------	----	------------------

$2.39 \pm 0.34^{+0.16}_{-0.14}$	11 AHMAD	01	SNO average flux
---------------------------------	----------	----	------------------

$2.80 \pm 0.19 \pm 0.33$	12 FUKUDA	96	KAMI average flux
--------------------------	-----------	----	-------------------

$2.70 \pm 0.27$	12 FUKUDA	96	KAMI day flux
-----------------	-----------	----	---------------

$2.87^{+0.27}_{-0.26}$	12 FUKUDA	96	KAMI night flux
------------------------	-----------	----	-----------------

<sup>1</sup> ABE 11 reports the Super-Kamiokande-III results for 548 live days from August 4, 2006 to August 18, 2008. The analysis threshold is 5.0 MeV, but the event sample in the 5.0–6.5 MeV total electron range has a total live time of 298 days.

<sup>2</sup> ABE 11 recalculated the Super-Kamiokande-II results using <sup>8</sup>B spectrum of WINTER 06A.

<sup>3</sup> ABE 11 recalculated the Super-Kamiokande-I results using <sup>8</sup>B spectrum of WINTER 06A.

<sup>4</sup> ABE 11B use a 123 kton-day exposure of the KamLAND liquid scintillation detector to measure the <sup>8</sup>B solar neutrino flux. They utilize  $\nu - e$  elastic scattering above a reconstructed-energy threshold of 5.5 MeV, corresponding to 5 MeV electron recoil energy. 299 electron recoil candidate events are reported, of which  $157 \pm 23.6$  are assigned to background.

<sup>5</sup> BELLINI 10A reports the Borexino result with 3 MeV energy threshold for scattered electrons. The data correspond to 345.3 live days with a target mass of 100 t, between July 15, 2007 and August 23, 2009.

<sup>6</sup> AHARMIM 08 reports the results from SNO Phase III measurement using an array of <sup>3</sup>He proportional counters to measure the rate of NC interactions in heavy water, over the period between November 27, 2004 and November 28, 2006, corresponding to 385.17 live days. A simultaneous fit was made for the number of NC events detected by the proportional counters and the numbers of NC, CC, and ES events detected by the PMTs, where the spectral distributions of the ES and CC events were not constrained to the <sup>8</sup>B shape.

<sup>7</sup> CRAVENS 08 reports the Super-Kamiokande-II results for 791 live days from December 2002 to October 2005. The photocathode coverage of the detector is 19% (reduced from 40% of that of Super-Kamiokande-I due to an accident in 2001). The analysis threshold for the average flux is 7 MeV.

<sup>8</sup> HOSAKA 06 reports the final results for 1496 live days with Super-Kamiokande-I between May 31, 1996 and July 15, 2001, and replace FUKUDA 02 results. The analysis threshold is 5 MeV except for the first 280 live days (6.5 MeV).

<sup>9</sup> AHARMIM 05A measurements were made with dissolved NaCl (0.195% by weight) in heavy water over the period between July 26, 2001 and August 28, 2003, corresponding to 391.4 live days, and update AHMED 04A. The CC, ES, and NC events were statistically separated. In one method, the <sup>8</sup>B energy spectrum was not constrained. In the other method, the constraint of an undistorted <sup>8</sup>B energy spectrum was added for comparison with AHMAD 02 results.

<sup>10</sup> AHMAD 02 reports the <sup>8</sup>B solar-neutrino flux measured via  $\nu e$  elastic scattering above the kinetic energy threshold of 5 MeV. The data correspond to 306.4 live days with SNO between November 2, 1999 and May 28, 2001, and updates AHMAD 01 results.

<sup>11</sup> AHMAD 01 reports the <sup>8</sup>B solar-neutrino flux measured via  $\nu e$  elastic scattering above the kinetic energy threshold of 6.75 MeV. The data correspond to 241 live days with SNO between November 2, 1999 and January 15, 2001.

<sup>12</sup> FUKUDA 96 results are for a total of 2079 live days with Kamiokande II and III from January 1987 through February 1995, covering the entire solar cycle 22, with threshold  $E_e > 9.3$  MeV (first 449 days),  $> 7.5$  MeV (middle 794 days), and  $> 7.0$  MeV (last 836 days). These results update the HIRATA 90 result for the average <sup>8</sup>B solar-neutrino flux and HIRATA 91 result for the day-night variation in the <sup>8</sup>B solar-neutrino flux. The total data sample was also analyzed for short-term variations: within experimental errors, no strong correlation of the solar-neutrino flux with the sunspot numbers was found.

See key on page 457

# Lepton Particle Listings

## Neutrino Mixing

### $\phi_{CC}$ ( $^8\text{B}$ )

$^8\text{B}$  solar-neutrino flux measured with charged-current reaction which is sensitive exclusively to  $\nu_e$ .

VALUE ( $10^6 \text{ cm}^{-2}\text{s}^{-1}$ )	DOCUMENT ID	TECN	COMMENT
• • • We do not use the following data for averages, fits, limits, etc. • • •			
$1.67^{+0.05}_{-0.04} +0.07_{-0.08}$	1 AHARMIM	08 SNO	Phase III
$1.68 \pm 0.06^{+0.08}_{-0.09}$	2 AHARMIM	05A SNO	Salty $\text{D}_2\text{O}$ ; $^8\text{B}$ shape not const.
$1.72 \pm 0.05 \pm 0.11$	2 AHARMIM	05A SNO	Salty $\text{D}_2\text{O}$ ; $^8\text{B}$ shape constrained
$1.76^{+0.06}_{-0.05} \pm 0.09$	3 AHMAD	02 SNO	average flux
$1.75 \pm 0.07^{+0.12}_{-0.11} \pm 0.05$	4 AHMAD	01 SNO	average flux

<sup>1</sup>AHARMIM 08 reports the results from SNO Phase III measurement using an array of  $^3\text{He}$  proportional counters to measure the rate of NC interactions in heavy water, over the period between November 27, 2004 and November 28, 2006, corresponding to 385.17 live days. A simultaneous fit was made for the number of NC events detected by the proportional counters and the numbers of NC, CC, and ES events detected by the PMTs, where the spectral distributions of the ES and CC events were not constrained to the  $^8\text{B}$  shape.

<sup>2</sup>AHARMIM 05A measurements were made with dissolved NaCl (0.195% by weight) in heavy water over the period between July 26, 2001 and August 28, 2003, corresponding to 391.4 live days, and update AHMED 04A. The CC, ES, and NC events were statistically separated. In one method, the  $^8\text{B}$  energy spectrum was not constrained. In the other method, the constraint of an undistorted  $^8\text{B}$  energy spectrum was added for comparison with AHMAD 02 results.

<sup>3</sup>AHMAD 02 reports the SNO result of the  $^8\text{B}$  solar-neutrino flux measured with charged-current reaction on deuterium,  $\nu_e d \rightarrow ppe^-$ , above the kinetic energy threshold of 5 MeV. The data correspond to 306.4 live days with SNO between November 2, 1999 and May 28, 2001, and updates AHMAD 01 results. The complete description of the SNO Phase I data set is given in AHARMIM 07.

<sup>4</sup>AHMAD 01 reports the first SNO result of the  $^8\text{B}$  solar-neutrino flux measured with the charged-current reaction on deuterium,  $\nu_e d \rightarrow ppe^-$ , above the kinetic energy threshold of 6.75 MeV. The data correspond to 241 live days with SNO between November 2, 1999 and January 15, 2001.

### $\phi_{NC}$ ( $^8\text{B}$ )

$^8\text{B}$  solar neutrino flux measured with neutral-current reaction, which is equally sensitive to  $\nu_e$ ,  $\nu_\mu$ , and  $\nu_\tau$ .

VALUE ( $10^6 \text{ cm}^{-2}\text{s}^{-1}$ )	DOCUMENT ID	TECN	COMMENT
• • • We do not use the following data for averages, fits, limits, etc. • • •			
$5.140^{+0.160}_{-0.158} +0.132_{-0.117}$	1 AHARMIM	10 SNO	Phase I+II, low threshold
$5.54^{+0.33}_{-0.31} +0.36_{-0.34}$	2 AHARMIM	08 SNO	Phase III, prop. counter + PMT
$4.94 \pm 0.21^{+0.38}_{-0.34}$	3 AHARMIM	05A SNO	Salty $\text{D}_2\text{O}$ ; $^8\text{B}$ shape not const.
$4.81 \pm 0.19^{+0.28}_{-0.27}$	3 AHARMIM	05A SNO	Salty $\text{D}_2\text{O}$ ; $^8\text{B}$ shape constrained
$5.09^{+0.44}_{-0.43} +0.46_{-0.43}$	4 AHMAD	02 SNO	average flux; $^8\text{B}$ shape const.
$6.42 \pm 1.57^{+0.55}_{-0.58}$	4 AHMAD	02 SNO	average flux; $^8\text{B}$ shape not const.

<sup>1</sup>AHARMIM 10 reports this result from a joint analysis of SNO Phase I+II data with the "effective electron kinetic energy" threshold of 3.5 MeV. This result is obtained with a "binned-histogram unconstrained fit" where binned probability distribution functions of the neutrino signal observables were used without any model constraints on the shape of the neutrino spectrum.

<sup>2</sup>AHARMIM 08 reports the results from SNO Phase III measurement using an array of  $^3\text{He}$  proportional counters to measure the rate of NC interactions in heavy water, over the period between November 27, 2004 and November 28, 2006, corresponding to 385.17 live days. A simultaneous fit was made for the number of NC events detected by the proportional counters and the numbers of NC, CC, and ES events detected by the PMTs, where the spectral distributions of the ES and CC events were not constrained to the  $^8\text{B}$  shape.

<sup>3</sup>AHARMIM 05A measurements were made with dissolved NaCl (0.195% by weight) in heavy water over the period between July 26, 2001 and August 28, 2003, corresponding to 391.4 live days, and update AHMED 04A. The CC, ES, and NC events were statistically separated. In one method, the  $^8\text{B}$  energy spectrum was not constrained. In the other method, the constraint of an undistorted  $^8\text{B}$  energy spectrum was added for comparison with AHMAD 02 results.

<sup>4</sup>AHMAD 02 reports the first SNO result of the  $^8\text{B}$  solar-neutrino flux measured with the neutral-current reaction on deuterium,  $\nu_e d \rightarrow np\nu_e$ , above the neutral-current reaction threshold of 2.2 MeV. The data correspond to 306.4 live days with SNO between November 2, 1999 and May 28, 2001. The complete description of the SNO Phase I data set is given in AHARMIM 07.

### $\phi_{\nu_\mu+\nu_\tau}$ ( $^8\text{B}$ )

Nonelectron-flavor active neutrino component ( $\nu_\mu$  and  $\nu_\tau$ ) in the  $^8\text{B}$  solar-neutrino flux.

VALUE ( $10^6 \text{ cm}^{-2}\text{s}^{-1}$ )	DOCUMENT ID	TECN	COMMENT
• • • We do not use the following data for averages, fits, limits, etc. • • •			

$3.26 \pm 0.25^{+0.40}_{-0.35}$	1 AHARMIM	05A SNO	From $\phi_{NC}$ , $\phi_{CC}$ , and $\phi_{ES}$ ; $^8\text{B}$ shape not const.
$3.09 \pm 0.22^{+0.30}_{-0.27}$	1 AHARMIM	05A SNO	From $\phi_{NC}$ , $\phi_{CC}$ , and $\phi_{ES}$ ; $^8\text{B}$ shape constrained
$3.41 \pm 0.45^{+0.48}_{-0.45}$	2 AHMAD	02 SNO	From $\phi_{NC}$ , $\phi_{CC}$ , and $\phi_{ES}$
$3.69 \pm 1.13$	3 AHMAD	01	Derived from SNO+SuperKam, water Cherenkov

<sup>1</sup>AHARMIM 05A measurements were made with dissolved NaCl (0.195% by weight) in heavy water over the period between July 26, 2001 and August 28, 2003, corresponding to 391.4 live days, and update AHMED 04A. The CC, ES, and NC events were statistically separated. In one method, the  $^8\text{B}$  energy spectrum was not constrained. In the other method, the constraint of an undistorted  $^8\text{B}$  energy spectrum was added for comparison with AHMAD 02 results.

<sup>2</sup>AHMAD 02 deduced the nonelectron-flavor active neutrino component ( $\nu_\mu$  and  $\nu_\tau$ ) in the  $^8\text{B}$  solar-neutrino flux, by combining the charged-current result, the  $\nu_e$  elastic-scattering result and the neutral-current result. The complete description of the SNO Phase I data set is given in AHARMIM 07.

<sup>3</sup>AHMAD 01 deduced the nonelectron-flavor active neutrino component ( $\nu_\mu$  and  $\nu_\tau$ ) in the  $^8\text{B}$  solar-neutrino flux, by combining the SNO charged-current result (AHMAD 01) and the Super-Kamiokande  $\nu_e$  elastic-scattering result (FUKUDA 01).

### Total Flux of Active $^8\text{B}$ Solar Neutrinos

Total flux of active neutrinos ( $\nu_e$ ,  $\nu_\mu$ , and  $\nu_\tau$ ).

VALUE ( $10^6 \text{ cm}^{-2}\text{s}^{-1}$ )	DOCUMENT ID	TECN	COMMENT
• • • We do not use the following data for averages, fits, limits, etc. • • •			
$5.046^{+0.159}_{-0.152} +0.107_{-0.123}$	1 AHARMIM	10 SNO	From $\phi_{NC}$ in Phase III
$5.54^{+0.33}_{-0.31} +0.36_{-0.34}$	2 AHARMIM	08 SNO	$\phi_{NC}$ in Phase III
$4.94 \pm 0.21^{+0.38}_{-0.34}$	3 AHARMIM	05A SNO	From $\phi_{NC}$ ; $^8\text{B}$ shape not const.
$4.81 \pm 0.19^{+0.28}_{-0.27}$	3 AHARMIM	05A SNO	From $\phi_{NC}$ ; $^8\text{B}$ shape constrained
$5.09^{+0.44}_{-0.43} +0.46_{-0.43}$	4 AHMAD	02 SNO	Direct measurement from $\phi_{NC}$
$5.44 \pm 0.99$	5 AHMAD	01	Derived from SNO+SuperKam, water Cherenkov

<sup>1</sup>AHARMIM 10 reports this result from a joint analysis of SNO Phase I+II data with the "effective electron kinetic energy" threshold of 3.5 MeV. This result is obtained with the assumption of unitarity, which relates the NC, CC, and ES rates. The data were fit with the free parameters directly describing the total  $^8\text{B}$  neutrino flux and the energy-dependent  $\nu_e$  survival probability.

<sup>2</sup>AHARMIM 08 reports the results from SNO Phase III measurement using an array of  $^3\text{He}$  proportional counters to measure the rate of NC interactions in heavy water, over the period between November 27, 2004 and November 28, 2006, corresponding to 385.17 live days. A simultaneous fit was made for the number of NC events detected by the proportional counters and the numbers of NC, CC, and ES events detected by the PMTs, where the spectral distributions of the ES and CC events were not constrained to the  $^8\text{B}$  shape.

<sup>3</sup>AHARMIM 05A measurements were made with dissolved NaCl (0.195% by weight) in heavy water over the period between July 26, 2001 and August 28, 2003, corresponding to 391.4 live days, and update AHMED 04A. The CC, ES, and NC events were statistically separated. In one method, the  $^8\text{B}$  energy spectrum was not constrained. In the other method, the constraint of an undistorted  $^8\text{B}$  energy spectrum was added for comparison with AHMAD 02 results.

<sup>4</sup>AHMAD 02 determined the total flux of active  $^8\text{B}$  solar neutrinos by directly measuring the neutral-current reaction,  $\nu_e d \rightarrow np\nu_e$ , which is equally sensitive to  $\nu_e$ ,  $\nu_\mu$ , and  $\nu_\tau$ . The complete description of the SNO Phase I data set is given in AHARMIM 07.

<sup>5</sup>AHMAD 01 deduced the total flux of active  $^8\text{B}$  solar neutrinos by combining the SNO charged-current result (AHMAD 01) and the Super-Kamiokande  $\nu_e$  elastic-scattering result (FUKUDA 01).

### Day-Night Asymmetry ( $^8\text{B}$ )

$$A = (\phi_{\text{night}} - \phi_{\text{day}}) / \phi_{\text{average}}$$

VALUE	DOCUMENT ID	TECN	COMMENT
• • • We do not use the following data for averages, fits, limits, etc. • • •			
$0.063 \pm 0.042 \pm 0.037$	1 CRAVENS	08 SKAM	Based on $\phi_{ES}$
$0.021 \pm 0.020^{+0.012}_{-0.013}$	2 HOSAKA	06 SKAM	Based on $\phi_{ES}$
$0.017 \pm 0.016^{+0.012}_{-0.013}$	3 HOSAKA	06 SKAM	Fitted in the LMA region
$-0.056 \pm 0.074 \pm 0.053$	4 AHARMIM	05A SNO	From salty SNO $\phi_{CC}$
$-0.037 \pm 0.063 \pm 0.032$	4 AHARMIM	05A SNO	From salty SNO $\phi_{CC}$ ; const. of no $\phi_{NC}$ asymmetry
$0.14 \pm 0.063^{+0.015}_{-0.014}$	5 AHMAD	02B SNO	Derived from SNO $\phi_{CC}$
$0.07 \pm 0.049^{+0.013}_{-0.012}$	6 AHMAD	02B SNO	Const. of no $\phi_{NC}$ asymmetry

<sup>1</sup>CRAVENS 08 reports the Super-Kamiokande-II results for 791 live days from December 2002 to October 2005. The photocathode coverage of the detector is 19% (reduced from 40% of that of Super-Kamiokande-I due to an accident in 2001). The analysis threshold for the day and night fluxes is 7.5 MeV.

## Lepton Particle Listings

## Neutrino Mixing

<sup>2</sup>HOSAKA 06 reports the final results for 1496 live days with Super-Kamiokande-I between May 31, 1996 and July 15, 2001, and replace FUKUDA 02 results. The analysis threshold is 5 MeV except for the first 280 live days (6.5 MeV).

<sup>3</sup>This result with reduced statistical uncertainty is obtained by assuming two-neutrino oscillations within the LMA (large mixing angle) region and by fitting the time variation of the solar neutrino flux measured via  $\nu_e$  elastic scattering to the variations expected from neutrino oscillations. For details, see SMY 04. There is an additional small systematic error of  $\pm 0.0004$  coming from uncertainty of oscillation parameters.

<sup>4</sup>AHARMIM 05A measurements were made with dissolved NaCl (0.195% by weight) in heavy water over the period between July 26, 2001 and August 28, 2003, with 176.5 days of the live time recorded during the day and 214.9 days during the night. This result is obtained with the spectral distribution of the CC events not constrained to the  $^8\text{B}$  shape.

<sup>5</sup>AHMAD 02b results are based on the charged-current interactions recorded between November 2, 1999 and May 28, 2001, with the day and night live times of 128.5 and 177.9 days, respectively. The complete description of the SNO Phase I data set is given in AHARMIM 07.

<sup>6</sup>AHMAD 02b results are derived from the charged-current interactions, neutral-current interactions, and  $\nu e$  elastic scattering, with the total flux of active neutrinos constrained to have no asymmetry. The data were recorded between November 2, 1999 and May 28, 2001, with the day and night live times of 128.5 and 177.9 days, respectively. The complete description of the SNO Phase I data set is given in AHARMIM 07.

 $\phi_{ES} (^7\text{Be})$ 

<sup>7</sup>Be solar-neutrino flux measured via  $\nu_e$  elastic scattering. This process is sensitive to all active neutrino flavors, but with reduced sensitivity to  $\nu_\mu, \nu_\tau$  due to the cross-section difference,  $\sigma(\nu_{\mu,\tau} e) \sim 0.2 \sigma(\nu_e e)$ . If the <sup>7</sup>Be solar-neutrino flux involves nonelectron flavor active neutrinos, their contribution to the flux is  $\sim 0.2$  times that of  $\nu_e$ .

VALUE ( $10^9 \text{ cm}^{-2} \text{ s}^{-1}$ )	DOCUMENT ID	TECN	COMMENT
---	-------------	------	---------

• • • We do not use the following data for averages, fits, limits, etc. • • •

3.10 ± 0.15	<sup>1</sup> BELLINI	11A	BORX average flux
-------------	----------------------	-----	-------------------

<sup>1</sup>BELLINI 11A reports the <sup>7</sup>Be solar neutrino flux measured via  $\nu - e$  elastic scattering. The data correspond to 740.7 live days between May 16, 2007 and May 8, 2010, and also correspond to 153.6 ton-year fiducial exposure. BELLINI 11A measured the 862 keV <sup>7</sup>Be solar neutrino flux, which is an 89.6% branch of the <sup>7</sup>Be solar neutrino flux, to be  $(2.78 \pm 0.13) \times 10^9 \text{ cm}^{-2} \text{ s}^{-1}$ . Supersedes ARPESELLA 08A.

 $\phi_{CC}(pp)$ 

pp solar-neutrino flux measured with charged-current reaction which is sensitive exclusively to  $\nu_e$ .

VALUE ( $10^{10} \text{ cm}^{-2} \text{ s}^{-1}$ )	DOCUMENT ID	TECN	COMMENT
--	-------------	------	---------

• • • We do not use the following data for averages, fits, limits, etc. • • •

3.38 ± 0.47	<sup>1</sup> ABDURASHI...	09	FIT Fit existing solar- $\nu$ data
-------------	---------------------------	----	------------------------------------

<sup>1</sup>ABDURASHITOV 09 reports the pp solar-neutrino flux derived from the Ga solar neutrino capture rate by subtracting contributions from  $^8\text{B}$ , <sup>7</sup>Be, pep and CNO solar neutrino fluxes determined by other solar neutrino experiments as well as neutrino oscillation parameters determined from available world neutrino oscillation data.

 $\phi_{ES} (\text{hep})$ 

hep solar-neutrino flux measured via  $\nu e$  elastic scattering. This process is sensitive to all active neutrino flavors, but with reduced sensitivity to  $\nu_\mu, \nu_\tau$  due to the cross-section difference,  $\sigma(\nu_{\mu,\tau} e) \sim 0.16 \sigma(\nu_e e)$ . If the hep solar-neutrino flux involves nonelectron flavor active neutrinos, their contribution to the flux is  $\sim 0.16$  times of  $\nu_e$ .

VALUE ( $10^3 \text{ cm}^{-2} \text{ s}^{-1}$ )	CL%	DOCUMENT ID	TECN	COMMENT
---	-----	-------------	------	---------

• • • We do not use the following data for averages, fits, limits, etc. • • •

<73	90	<sup>1</sup> HOSAKA	06	SKAM
-----	----	---------------------	----	------

<sup>1</sup>HOSAKA 06 result is obtained from the recoil electron energy window of 18–21 MeV, and updates FUKUDA 01 result.

 $\phi_{\overline{\nu}_e} (^8\text{B})$ 

Searches are made for electron antineutrino flux from the Sun. Flux limits listed here are derived relative to the BS05(OP) Standard Solar Model  $^8\text{B}$  solar neutrino flux ( $5.69 \times 10^6 \text{ cm}^{-2} \text{ s}^{-1}$ ), with an assumption that solar  $\overline{\nu}_e$ s follow an unoscillated  $^8\text{B}$  neutrino spectrum.

VALUE (%)	CL%	DOCUMENT ID	TECN	COMMENT
-----------	-----	-------------	------	---------

• • • We do not use the following data for averages, fits, limits, etc. • • •

<0.013	90	BELLINI	11	BORX $E_{\overline{\nu}_e} > 1.8 \text{ MeV}$
<1.9	90	<sup>1</sup> BALATA	06	CNTR $1.8 < E_{\overline{\nu}_e} < 20.0 \text{ MeV}$
<0.72	90	AHARMIM	04	SNO $4.0 < E_{\overline{\nu}_e} < 14.8 \text{ MeV}$
<0.022	90	EGUCHI	04	KLND $8.3 < E_{\overline{\nu}_e} < 14.8 \text{ MeV}$
<0.7	90	GANDO	03	SKAM $8.0 < E_{\overline{\nu}_e} < 20.0 \text{ MeV}$
<1.7	90	AGLIETTA	96	LSD $7 < E_{\overline{\nu}_e} < 17 \text{ MeV}$

<sup>1</sup>BALATA 06 obtained this result from the search for  $\overline{\nu}_e$  interactions with Counting Test Facility (the prototype of the Borexino detector).

## (B) Three-neutrino mixing parameters

## INTRODUCTION TO THREE-NEUTRINO MIXING PARAMETERS LISTINGS

Updated April 2012 by M. Goodman (ANL).

**Introduction and Notation:** With the exception of the LSND anomaly, current accelerator, reactor, solar and atmospheric neutrino data can be described within the framework of a  $3 \times 3$  mixing matrix between the flavor eigenstates  $\nu_e, \nu_\mu$  and  $\nu_\tau$  and mass eigenstates  $\nu_1, \nu_2$  and  $\nu_3$ . (See equation 13.79 of the review “Neutrino Mass, Mixing and Oscillations” by K. Nakamura and S.T. Petcov.) Whether or not this is the ultimately correct framework, it is currently widely used to parametrize neutrino mixing data and to plan new experiments.

The mass differences are called  $\Delta m_{21}^2 \equiv m_2^2 - m_1^2$  and  $\Delta m_{32}^2 \equiv m_3^2 - m_2^2$ . In these listings, we assume

$$\Delta m_{32}^2 \sim \Delta m_{31}^2 \quad (1)$$

although in the future, experiments may be precise enough to measure these separately. The angle are labeled  $\theta_{12}, \theta_{23}$  and  $\theta_{13}$ . The CP violating phase is called  $\delta$ , but that does not yet appear in the listings. The familiar two neutrino form for oscillations is

$$P(\nu_a \rightarrow \nu_b) = \sin^2(2\theta) \sin^2(\Delta m^2 L/4E). \quad (2)$$

Despite the fact that the mixing angles have been measured to be much larger than in the quark sector, the two neutrino form is often a very good approximation and is used in many situations.

The angles appear in the equations below in many forms. They most often appear as  $\sin^2(2\theta)$ . The listings currently use this convention.

**Accelerator neutrino experiments:** Ignoring the small  $\Delta m_{21}^2$  scale, CP violation, and matter effects, the equations for the probability of appearance in an accelerator oscillation experiment are:

$$P(\nu_\mu \rightarrow \nu_\tau) = \sin^2(2\theta_{23}) \cos^4(\theta_{13}) \sin^2(\Delta m_{32}^2 L/4E) \quad (3)$$

$$P(\nu_\mu \rightarrow \nu_e) = \sin^2(2\theta_{13}) \sin^2(\theta_{23}) \sin^2(\Delta m_{32}^2 L/4E) \quad (4)$$

$$P(\nu_e \rightarrow \nu_\mu) = \sin^2(2\theta_{13}) \sin^2(\theta_{23}) \sin^2(\Delta m_{32}^2 L/4E) \quad (5)$$

$$P(\nu_e \rightarrow \nu_\tau) = \sin^2(2\theta_{13}) \cos^2(\theta_{23}) \sin^2(\Delta m_{32}^2 L/4E) \quad (6)$$

For the case of negligible  $\theta_{13}$ , these probabilities vanish except for  $P(\nu_\mu \rightarrow \nu_\tau)$ , which then takes the familiar two-neutrino form.

Current and future long-baseline accelerator experiments are studying non-zero  $\theta_{13}$  through  $P(\nu_\mu \rightarrow \nu_e)$ . Including the CP terms and low mass scale, the equation for neutrino oscillation in vacuum is:

$$P(\nu_\mu \rightarrow \nu_e) = P1 + P2 + P3 + P4$$

$$P1 = \sin^2(\theta_{23}) \sin^2(2\theta_{13}) \sin^2(\Delta m_{32}^2 L/4E)$$

$$P2 = \cos^2(\theta_{23}) \sin^2(2\theta_{13}) \sin^2(\Delta m_{21}^2 L/4E)$$

$$P3 = -/+ J \sin(\delta) \sin(\Delta m_{32}^2 L/4E)$$

$$P4 = J \cos(\delta) \cos(\Delta m_{32}^2 L/4E) \quad (7)$$

See key on page 457

# Lepton Particle Listings

## Neutrino Mixing

where

$$J = \cos(\theta_{13}) \sin(2\theta_{12}) \sin(2\theta_{13}) \sin(2\theta_{23}) \times \sin(\Delta m_{32}^2 L/4E) \sin(\Delta m_{21}^2 L/4E) \quad (8)$$

and the sign in P3 is negative for neutrinos and positive for anti-neutrinos respectively. For most new long-baseline accelerator experiments, P2 can safely be neglected but the other three terms could be comparable. Also, depending on the distance and the mass hierarchy, matter effects will need to be included.

**Reactor neutrino experiments:** Nuclear reactors are prolific sources of  $\bar{\nu}_e$  with an energy near 4 MeV. The oscillation probability can be expressed

$$P(\bar{\nu}_e \rightarrow \bar{\nu}_e) = 1 - \cos^4(\theta_{13}) \sin^2(2\theta_{12}) \sin^2(\Delta m_{21}^2 L/4E) - \cos^2(\theta_{12}) \sin^2(2\theta_{13}) \sin^2(\Delta m_{31}^2 L/4E) - \sin^2(\theta_{12}) \sin^2(2\theta_{13}) \sin^2(\Delta m_{32}^2 L/4E) \quad (9)$$

not using the approximation in Eq. (1). For short distances ( $L < 5$  km) we can ignore the second term on the right and can reimpose approximation Eq. (1). This takes the familiar two neutrino form with  $\theta_{13}$  and  $\Delta m_{32}^2$ :

$$P(\bar{\nu}_e \rightarrow \bar{\nu}_e) = 1 - \sin^2(2\theta_{13}) \sin^2(\Delta m_{32}^2 L/4E). \quad (10)$$

For long distances and small  $\theta_{13}$ , the last two terms in Eq. (9) oscillate rapidly and average to zero for an experiment with finite energy resolution, leading to the familiar two neutrino form but with  $\theta_{12}$  and  $\Delta m_{21}^2$ .

**Solar and Atmospheric neutrino experiments:** Solar neutrino experiments are sensitive to  $\nu_e$  disappearance and have allowed the measurement of  $\theta_{12}$  and  $\Delta m_{21}^2$ . They are also sensitive to  $\theta_{13}$ . We identify  $\Delta m_{\odot}^2 = \Delta m_{21}^2$  and  $\theta_{\odot} = \theta_{12}$ .

Atmospheric neutrino experiments are primarily sensitive to  $\nu_{\mu}$  disappearance through  $\nu_{\mu} \rightarrow \nu_{\tau}$  oscillations, and have allowed the measurement of  $\theta_{23}$  and  $\Delta m_{32}^2$ . We identify  $\Delta m_A^2 = \Delta m_{32}^2$  and  $\theta_A = \theta_{23}$ . Despite the large  $\nu_e$  component of the atmospheric neutrino flux, it is difficult to measure  $\Delta m_{21}^2$  effects. This is because of a cancellation between  $\nu_{\mu} \rightarrow \nu_e$  and  $\nu_e \rightarrow \nu_{\mu}$  together with the fact that the ratio of  $\nu_{\mu}$  and  $\nu_e$  atmospheric fluxes, which arise from sequential  $\pi$  and  $\mu$  decay, is near 2.

**Oscillation Parameter Listings:** In Section (B) we encode the three mixing angles  $\theta_{12}$ ,  $\theta_{23}$ ,  $\theta_{13}$  and two mass squared differences  $\Delta m_{21}^2$  and  $\Delta m_{32}^2$ . Our knowledge of  $\theta_{12}$  and  $\Delta m_{21}^2$  comes from the KamLAND reactor neutrino experiment together with solar neutrino experiments. Our knowledge of  $\theta_{23}$  and  $\Delta m_{32}^2$  comes from atmospheric neutrino experiments and long-baseline accelerator experiments. Results on  $\theta_{13}$  come from reactor antineutrino disappearance experiments. There are also results from long-baseline accelerator experiments looking for  $\nu_e$  appearance. The interpretation of both kinds of results depends on  $\Delta m_{32}^2$ , and the accelerator results also depend on the mass hierarchy,  $\theta_{23}$  and the CP violating phase  $\delta$ .

### $\sin^2(2\theta_{12})$

VALUE	DOCUMENT ID	TECN	COMMENT
$0.857^{+0.023}_{-0.025}$	1 GANDO	11 FIT	KamLAND + solar: $3\nu$
• • • We do not use the following data for averages, fits, limits, etc. • • •			
$0.85 \pm 0.02$	2 ABE	11 FIT	KamLAND + global solar: $2\nu$
$0.84^{+0.03}_{-0.02}$	3 ABE	11 FIT	global solar: $2\nu$
$0.85^{+0.04}_{-0.03}$	4 ABE	11 FIT	KamLAND + global solar: $3\nu$
$0.85^{+0.04}_{-0.05}$	5 ABE	11 FIT	global solar: $3\nu$
$0.861^{+0.022}_{-0.018}$	6 BELLINI	11A FIT	KamLAND + global solar: $2\nu$
$0.869^{+0.024}_{-0.022}$	7 BELLINI	11A FIT	global solar: $2\nu$
$0.846^{+0.064}_{-0.073}$	8 GANDO	11 FIT	KamLAND: $3\nu$
$0.861^{+0.026}_{-0.022}$	9,10 AHARMIM	10 FIT	KamLAND + global solar: $2\nu$
$0.861^{+0.024}_{-0.031}$	9,11 AHARMIM	10 FIT	global solar: $2\nu$
$0.869^{+0.026}_{-0.024}$	9,12 AHARMIM	10 FIT	KamLAND + global solar: $3\nu$
$0.869^{+0.031}_{-0.037}$	9,13 AHARMIM	10 FIT	global solar: $3\nu$
$0.92 \pm 0.05$	14 ABE	08A FIT	KamLAND
$0.87 \pm 0.04$	15 ABE	08A FIT	KamLAND + global fit
$0.87 \pm 0.03$	16 AHARMIM	08 FIT	KamLAND + global solar
$0.85^{+0.04}_{-0.06}$	17 HOSAKA	06 FIT	KamLAND + global solar
$0.85^{+0.06}_{-0.05}$	18 HOSAKA	06 FIT	SKAM+SNO+KamLAND
$0.86^{+0.05}_{-0.07}$	19 HOSAKA	06 FIT	SKAM+SNO
$0.86^{+0.03}_{-0.04}$	20 AHARMIM	05A FIT	KamLAND + global solar
0.75-0.95	21 AHARMIM	05A FIT	global solar
$0.82 \pm 0.05$	22 ARAKI	05 FIT	KamLAND + global solar
$0.82 \pm 0.04$	23 AHMED	04A FIT	KamLAND + global solar
0.71-0.93	24 AHMED	04A FIT	global solar
$0.85^{+0.05}_{-0.07}$	25 SMY	04 FIT	KamLAND + global solar
$0.83^{+0.06}_{-0.08}$	26 SMY	04 FIT	global solar
$0.87^{+0.07}_{-0.08}$	27 SMY	04 FIT	SKAM + SNO
0.62-0.88	28 AHMAD	02B FIT	global solar
0.62-0.95	29 FUKUDA	02 FIT	global solar

<sup>1</sup> GANDO 11 obtain this result with three-neutrino fit using the KamLAND + solar data. Supersedes ABE 08A.

<sup>2</sup> ABE 11 obtained this result by a two-neutrino oscillation analysis using solar neutrino data including Super-Kamiokande, SNO, Borexino (ARPESELLA 08A), Homestake, GALLEX/GNO, SAGE, and KamLAND data. CPT invariance is assumed.

<sup>3</sup> ABE 11 obtained this result by a two-neutrino oscillation analysis using solar neutrino data including Super-Kamiokande, SNO, Borexino (ARPESELLA 08A), Homestake, GALLEX/GNO, and SAGE data.

<sup>4</sup> ABE 11 obtained this result by a three-neutrino oscillation analysis with the value of  $\Delta m_{32}^2$  fixed to  $2.4 \times 10^{-3}$  eV<sup>2</sup>, using solar neutrino data including Super-Kamiokande, SNO, Borexino (ARPESELLA 08A), Homestake, GALLEX/GNO, SAGE, and KamLAND data. The normal neutrino mass hierarchy and CPT invariance are assumed.

<sup>5</sup> ABE 11 obtained this result by a three-neutrino oscillation analysis with the value of  $\Delta m_{32}^2$  fixed to  $2.4 \times 10^{-3}$  eV<sup>2</sup>, using solar neutrino data including Super-Kamiokande, SNO, Borexino (ARPESELLA 08A), Homestake, and GALLEX/GNO data. The normal neutrino mass hierarchy is assumed.

<sup>6</sup> BELLINI 11A obtained this result by a two-neutrino oscillation analysis using KamLAND, Homestake, SAGE, Gallex, GNO, Kamiokande, Super-Kamiokande, SNO, and Borexino (BELLINI 11A) data and the SSM flux prediction in SERENELLI 11 (Astrophysical Journal **743** 24 (2011)) with the exception that the  $^8\text{B}$  flux was left free. CPT invariance is assumed.

<sup>7</sup> BELLINI 11A obtained this result by a two-neutrino oscillation analysis using Homestake, SAGE, Gallex, GNO, Kamiokande, Super-Kamiokande, SNO, and Borexino (BELLINI 11A) data and the SSM flux prediction in SERENELLI 11 (Astrophysical Journal **743** 24 (2011)) with the exception that the  $^8\text{B}$  flux was left free.

<sup>8</sup> GANDO 11 obtain this result with three-neutrino fit using the KamLAND data only. Supersedes ABE 08A.

<sup>9</sup> AHARMIM 10 global solar neutrino data include SNO's low-energy-threshold analysis survival probability day/night curves, SNO Phase III integral rates (AHARMIM 08), CI (CLEVELAND 98), SAGE (ABDURASHITOV 09), Gallex/GNO (HAMPEL 99, ALTMANN 05), Borexino (ARPESELLA 08A), SK-I zenith (HOSAKA 06), and SK-II day/night spectra (CRAVENS 08).

<sup>10</sup> AHARMIM 10 obtained this result by a two-neutrino oscillation analysis using global solar neutrino data and KamLAND data (ABE 08A). CPT invariance is assumed.

<sup>11</sup> AHARMIM 10 obtained this result by a two-neutrino oscillation analysis using global solar neutrino data.

<sup>12</sup> AHARMIM 10 obtained this result by a three-neutrino oscillation analysis with the value of  $\Delta m_{31}^2$  fixed to  $2.3 \times 10^{-3}$  eV<sup>2</sup>, using global solar neutrino data and KamLAND data (ABE 08A). CPT invariance is assumed.

<sup>13</sup> AHARMIM 10 obtained this result by a three-neutrino oscillation analysis with the value of  $\Delta m_{31}^2$  fixed to  $2.3 \times 10^{-3}$  eV<sup>2</sup>, using global solar neutrino data.

# Lepton Particle Listings

## Neutrino Mixing

- <sup>14</sup> ABE 08a obtained this result by a rate + shape + time combined geoneutrino and reactor two-neutrino fit for  $\Delta m_{21}^2$  and  $\tan^2\theta_{12}$ , using KamLAND data only.
- <sup>15</sup> ABE 08a obtained this result by means of a two-neutrino fit using KamLAND, Homestake, SAGE, GALLEX, GNO, SK (zenith angle and E-spectrum), the SNO  $\chi^2$ -map, and solar flux data. *CPT* invariance is assumed.
- <sup>16</sup> The result given by AHARMIM 08 is  $\theta = (34.4^{+1.3}_{-1.2})^\circ$ . This result is obtained by a two-neutrino oscillation analysis using solar neutrino data including those of Borexino (ARPESELLA 08a) and Super-Kamiokande-I (HOSAKA 06), and KamLAND data (ABE 08a). *CPT* invariance is assumed.
- <sup>17</sup> HOSAKA 06 obtained this result by a two-neutrino oscillation analysis using SK  $\nu_e$  data, CC data from other solar neutrino experiments, and KamLAND data (ARAKI 05). *CPT* invariance is assumed.
- <sup>18</sup> HOSAKA 06 obtained this result by a two-neutrino oscillation analysis using the data from Super-Kamiokande, SNO (AHMAD 02 and AHMAD 02b), and KamLAND (ARAKI 05) experiments. *CPT* invariance is assumed.
- <sup>19</sup> HOSAKA 06 obtained this result by a two-neutrino oscillation analysis using the Super-Kamiokande and SNO (AHMAD 02 and AHMAD 02b) solar neutrino data.
- <sup>20</sup> The result given by AHARMIM 05a is  $\theta = (33.9 \pm 1.6)^\circ$ . This result is obtained by a two-neutrino oscillation analysis using SNO pure deuteron and salt phase data, SK  $\nu_e$  data, Cl and Ga CC data, and KamLAND data (ARAKI 05). *CPT* invariance is assumed. AHARMIM 05a also quotes  $\theta = (33.9^{+2.4}_{-2.2})^\circ$  as the error enveloping the 68% CL two-dimensional region. This translates into  $\sin^2 2\theta = 0.86^{+0.05}_{-0.06}$ .
- <sup>21</sup> AHARMIM 05a obtained this result by a two-neutrino oscillation analysis using the data from all solar neutrino experiments. The listed range of the parameter envelops the 95% CL two-dimensional region shown in figure 35a of AHARMIM 05a. AHARMIM 05a also quotes  $\tan^2\theta = 0.45^{+0.09}_{-0.08}$  as the error enveloping the 68% CL two-dimensional region. This translates into  $\sin^2 2\theta = 0.86^{+0.05}_{-0.07}$ .
- <sup>22</sup> ARAKI 05 obtained this result by a two-neutrino oscillation analysis using KamLAND and solar neutrino data. *CPT* invariance is assumed. The  $1\sigma$  error shown here is translated from the number provided by the KamLAND collaboration,  $\tan^2\theta = 0.40^{+0.07}_{-0.07}$ . The corresponding number quoted in ARAKI 05 is  $\tan^2\theta = 0.40^{+0.10}_{-0.07}$  ( $\sin^2 2\theta = 0.82 \pm 0.07$ ), which envelops the 68% CL two-dimensional region.
- <sup>23</sup> The result given by AHMED 04a is  $\theta = (32.5^{+1.7}_{-1.6})^\circ$ . This result is obtained by a two-neutrino oscillation analysis using solar neutrino and KamLAND data (EGUCHI 03). *CPT* invariance is assumed. AHMED 04a also quotes  $\theta = (32.5^{+2.4}_{-2.3})^\circ$  as the error enveloping the 68% CL two-dimensional region. This translates into  $\sin^2 2\theta = 0.82 \pm 0.06$ .
- <sup>24</sup> AHMED 04a obtained this result by a two-neutrino oscillation analysis using the data from all solar neutrino experiments. The listed range of the parameter envelops the 95% CL two-dimensional region shown in Fig. 5(a) of AHMED 04a. The best-fit point is  $\Delta(m^2) = 6.5 \times 10^{-5} \text{ eV}^2$ ,  $\tan^2\theta = 0.40$  ( $\sin^2 2\theta = 0.82$ ).
- <sup>25</sup> The result given by SMY 04 is  $\tan^2\theta = 0.44 \pm 0.08$ . This result is obtained by a two-neutrino oscillation analysis using solar neutrino and KamLAND data (IANNI 03). *CPT* invariance is assumed.
- <sup>26</sup> SMY 04 obtained this result by a two-neutrino oscillation analysis using the data from all solar neutrino experiments. The  $1\sigma$  errors are read from Fig. 6(a) of SMY 04.
- <sup>27</sup> SMY 04 obtained this result by a two-neutrino oscillation analysis using the Super-Kamiokande and SNO (AHMAD 02 and AHMAD 02b) solar neutrino data. The  $1\sigma$  errors are read from Fig. 6(a) of SMY 04.
- <sup>28</sup> AHMAD 02b obtained this result by a two-neutrino oscillation analysis using the data from all solar neutrino experiments. The listed range of the parameter envelops the 95% CL two-dimensional region shown in Fig. 4(b) of AHMAD 02b. The best fit point is  $\Delta(m^2) = 5.0 \times 10^{-5} \text{ eV}^2$  and  $\tan\theta = 0.34$  ( $\sin^2 2\theta = 0.76$ ).
- <sup>29</sup> FUKUDA 02 obtained this result by a two-neutrino oscillation analysis using the data from all solar neutrino experiments. The listed range of the parameter envelops the 95% CL two-dimensional region shown in Fig. 4 of FUKUDA 02. The best fit point is  $\Delta(m^2) = 6.9 \times 10^{-5} \text{ eV}^2$  and  $\tan^2\theta = 0.38$  ( $\sin^2 2\theta = 0.80$ ).

### $\Delta m_{21}^2$

VALUE ( $10^{-5} \text{ eV}^2$ )	DOCUMENT ID	TECN	COMMENT
<b><math>7.50^{+0.19}_{-0.20}</math></b>	1 GANDO	11	FIT KamLAND + solar: $3\nu$
• • • We do not use the following data for averages, fits, limits, etc. • • •			
$7.6 \pm 0.2$	2 ABE	11	FIT KamLAND + global solar: $2\nu$
$6.2^{+1.1}_{-1.9}$	3 ABE	11	FIT global solar: $2\nu$
$7.7 \pm 0.3$	4 ABE	11	FIT KamLAND + global solar: $3\nu$
$6.0^{+2.2}_{-2.5}$	5 ABE	11	FIT global solar: $3\nu$
$7.50^{+0.16}_{-0.24}$	6 BELLINI	11A	FIT KamLAND + global solar: $2\nu$
$5.2^{+1.5}_{-0.9}$	7 BELLINI	11A	FIT global solar: $2\nu$
$7.49 \pm 0.20$	8 GANDO	11	FIT KamLAND: $3\nu$
$7.59^{+0.20}_{-0.21}$	9,10 AHARMIM	10	FIT KamLAND + global solar: $2\nu$
$5.89^{+2.13}_{-2.16}$	9,11 AHARMIM	10	FIT global solar: $2\nu$
$7.59 \pm 0.21$	9,12 AHARMIM	10	FIT KamLAND + global solar: $3\nu$

$6.31^{+2.49}_{-2.58}$	9,13 AHARMIM	10	FIT global solar: $3\nu$
$7.58^{+0.14}_{-0.13} \pm 0.15$	14 ABE	08A	FIT KamLAND
$7.59 \pm 0.21$	15 ABE	08A	FIT KamLAND + global solar
$7.59^{+0.19}_{-0.21}$	16 AHARMIM	08	FIT KamLAND + global solar
$8.0 \pm 0.3$	17 HOSAKA	06	FIT KamLAND + global solar
$8.0 \pm 0.3$	18 HOSAKA	06	FIT SKAM+SNO+KamLAND
$6.3^{+3.7}_{-1.5}$	19 HOSAKA	06	FIT SKAM+SNO
5–12	20 HOSAKA	06	FIT SKAM day/night in the LMA region
$8.0^{+0.4}_{-0.3}$	21 AHARMIM	05A	FIT KamLAND + global solar LMA
3.3–14.4	22 AHARMIM	05A	FIT global solar
$7.9^{+0.4}_{-0.3}$	23 ARAKI	05	FIT KamLAND + global solar
$7.1^{+1.0}_{-0.3}$	24 AHMED	04A	FIT KamLAND + global solar
3.2–13.7	25 AHMED	04A	FIT global solar
$7.1^{+0.6}_{-0.5}$	26 SMY	04	FIT KamLAND + global solar
$6.0^{+1.7}_{-1.6}$	27 SMY	04	FIT global solar
$6.0^{+2.5}_{-1.6}$	28 SMY	04	FIT SKAM + SNO
2.8–12.0	29 AHMAD	02B	FIT global solar
3.2–19.1	30 FUKUDA	02	FIT global solar

- <sup>1</sup> GANDO 11 obtain this result with three-neutrino fit using the KamLAND + solar data. Supersedes ABE 08a.
- <sup>2</sup> ABE 11 obtained this result by a two-neutrino oscillation analysis using solar neutrino data including Super-Kamiokande, SNO, Borexino (ARPESELLA 08a), Homestake, GALLEX/GNO, SAGE, and KamLAND data. *CPT* invariance is assumed.
- <sup>3</sup> ABE 11 obtained this result by a two-neutrino oscillation analysis using solar neutrino data including Super-Kamiokande, SNO, Borexino (ARPESELLA 08a), Homestake, GALLEX/GNO, and SAGE data.
- <sup>4</sup> ABE 11 obtained this result by a three-neutrino oscillation analysis with the value of  $\Delta m_{21}^2$  fixed to  $2.4 \times 10^{-3} \text{ eV}^2$ , using solar neutrino data including Super-Kamiokande, SNO, Borexino (ARPESELLA 08a), Homestake, GALLEX/GNO, SAGE, and KamLAND data. The normal neutrino mass hierarchy and *CPT* invariance are assumed.
- <sup>5</sup> ABE 11 obtained this result by a three-neutrino oscillation analysis with the value of  $\Delta m_{21}^2$  fixed to  $2.4 \times 10^{-3} \text{ eV}^2$ , using solar neutrino data including Super-Kamiokande, SNO, Borexino (ARPESELLA 08a), Homestake, and GALLEX/GNO data. The normal neutrino mass hierarchy is assumed.
- <sup>6</sup> BELLINI 11a obtained this result by a two-neutrino oscillation analysis using KamLAND, Homestake, SAGE, Gallex, GNO, Kamiokande, Super-Kamiokande, SNO, and Borexino (BELLINI 11a) data and the SSM flux prediction in SERENELLI 11 (Astrophysical Journal **743** 24 (2011)) with the exception that the  $^8\text{B}$  flux was left free. *CPT* invariance is assumed.
- <sup>7</sup> BELLINI 11a obtained this result by a two-neutrino oscillation analysis using Homestake, SAGE, Gallex, GNO, Kamiokande, Super-Kamiokande, SNO, and Borexino (BELLINI 11a) data and the SSM flux prediction in SERENELLI 11 (Astrophysical Journal **743** 24 (2011)) with the exception that the  $^8\text{B}$  flux was left free.
- <sup>8</sup> GANDO 11 obtain this result with three-neutrino fit using the KamLAND data only. Supersedes ABE 08a.
- <sup>9</sup> AHARMIM 10 global solar neutrino data include SNO's low-energy-threshold analysis survival probability day/night curves, SNO Phase III integral rates (AHARMIM 08), Cl (CLEVELAND 98), SAGE (ABDURASHITOV 09), Gallex/GNO (HAMPEL 99, ALTMANN 05), Borexino (ARPESELLA 08a), SK-I zenith (HOSAKA 06), and SK-II day/night spectra (CRAVENS 08).
- <sup>10</sup> AHARMIM 10 obtained this result by a two-neutrino oscillation analysis using global solar neutrino data and KamLAND data (ABE 08a). *CPT* invariance is assumed.
- <sup>11</sup> AHARMIM 10 obtained this result by a two-neutrino oscillation analysis using global solar neutrino data.
- <sup>12</sup> AHARMIM 10 obtained this result by a three-neutrino oscillation analysis with the value of  $\Delta m_{31}^2$  fixed to  $2.3 \times 10^{-3} \text{ eV}^2$ , using global solar neutrino data and KamLAND data (ABE 08a). *CPT* invariance is assumed.
- <sup>13</sup> AHARMIM 10 obtained this result by a three-neutrino oscillation analysis with the value of  $\Delta m_{31}^2$  fixed to  $2.3 \times 10^{-3} \text{ eV}^2$ , using global solar neutrino data.
- <sup>14</sup> ABE 08a obtained this result by a rate + shape + time combined geoneutrino and reactor two-neutrino fit for  $\Delta m_{21}^2$  and  $\tan^2\theta_{12}$ , using KamLAND data only.
- <sup>15</sup> ABE 08a obtained this result by means of a two-neutrino fit using KamLAND, Homestake, SAGE, GALLEX, GNO, SK (zenith angle and E-spectrum), the SNO  $\chi^2$ -map, and solar flux data. *CPT* invariance is assumed.
- <sup>16</sup> AHARMIM 08 obtained this result by a two-neutrino oscillation analysis using all solar neutrino data including those of Borexino (ARPESELLA 08a) and Super-Kamiokande-I (HOSAKA 06), and KamLAND data (ABE 08a). *CPT* invariance is assumed.
- <sup>17</sup> HOSAKA 06 obtained this result by a two-neutrino oscillation analysis using solar neutrino and KamLAND data (ARAKI 05). *CPT* invariance is assumed.
- <sup>18</sup> HOSAKA 06 obtained this result by a two-neutrino oscillation analysis using the data from Super-Kamiokande, SNO (AHMAD 02 and AHMAD 02b), and KamLAND (ARAKI 05) experiments. *CPT* invariance is assumed.
- <sup>19</sup> HOSAKA 06 obtained this result by a two-neutrino oscillation analysis using the Super-Kamiokande and SNO (AHMAD 02 and AHMAD 02b) solar neutrino data.
- <sup>20</sup> HOSAKA 06 obtained this result from the consistency between the observed and expected day-night flux asymmetry amplitude. The listed 68% CL range is derived from the  $1\sigma$  boundary of the amplitude fit to the data. Oscillation parameters are constrained to be in the LMA region. The mixing angle is fixed at  $\tan^2\theta = 0.44$  because the fit depends only very weakly on it.



# Lepton Particle Listings

## Neutrino Mixing

See key on page 457

- 21 AHARMIM 05A obtained this result by a two-neutrino oscillation analysis using solar neutrino and KamLAND data (ARAKI 05).  $CPT$  invariance is assumed. AHARMIM 05A also quotes  $\Delta(m^2) = (8.0^{+0.6}_{-0.4}) \times 10^{-5} \text{ eV}^2$  as the error enveloping the 68% CL two-dimensional region.
- 22 AHARMIM 05A obtained this result by a two-neutrino oscillation analysis using the data from all solar neutrino experiments. The listed range of the parameter envelops the 95% CL two-dimensional region shown in figure 35a of AHARMIM 05A. AHARMIM 05A also quotes  $\Delta(m^2) = (6.5^{+4.4}_{-2.3}) \times 10^{-5} \text{ eV}^2$  as the error enveloping the 68% CL two-dimensional region.
- 23 ARAKI 05 obtained this result by a two-neutrino oscillation analysis using KamLAND and solar neutrino data.  $CPT$  invariance is assumed. The  $1\sigma$  error shown here is provided by the KamLAND collaboration. The error quoted in ARAKI 05,  $\Delta(m^2) = (7.9^{+0.6}_{-0.5}) \times 10^{-5}$ , envelops the 68% CL two-dimensional region.
- 24 AHMED 04A obtained this result by a two-neutrino oscillation analysis using solar neutrino and KamLAND data (EGUCHI 03).  $CPT$  invariance is assumed. AHMED 04A also quotes  $\Delta(m^2) = (7.1^{+1.2}_{-0.6}) \times 10^{-5} \text{ eV}^2$  as the error enveloping the 68% CL two-dimensional region.
- 25 AHMED 04A obtained this result by a two-neutrino oscillation analysis using the data from all solar neutrino experiments. The listed range of the parameter envelops the 95% CL two-dimensional region shown in Fig. 5(a) of AHMED 04A. The best-fit point is  $\Delta(m^2) = 6.5 \times 10^{-5} \text{ eV}^2$ ,  $\tan^2\theta = 0.40$  ( $\sin^2 2\theta = 0.82$ ).
- 26 SMY 04 obtained this result by a two-neutrino oscillation analysis using solar neutrino and KamLAND data (IANNI 03).  $CPT$  invariance is assumed.
- 27 SMY 04 obtained this result by a two-neutrino oscillation analysis using the data from all solar neutrino experiments. The  $1\sigma$  errors are read from Fig. 6(a) of SMY 04.
- 28 SMY 04 obtained this result by a two-neutrino oscillation analysis using the Super-Kamiokande and SNO (AHMAD 02 and AHMAD 02B) solar neutrino data. The  $1\sigma$  errors are read from Fig. 6(a) of SMY 04.
- 29 AHMAD 02B obtained this result by a two-neutrino oscillation analysis using the data from all solar neutrino experiments. The listed range of the parameter envelops the 95% CL two-dimensional region shown in Fig. 4(b) of AHMAD 02B. The best fit point is  $\Delta(m^2) = 5.0 \times 10^{-5} \text{ eV}^2$  and  $\tan\theta = 0.34$  ( $\sin^2 2\theta = 0.76$ ).
- 30 FUKUDA 02 obtained this result by a two-neutrino oscillation analysis using the data from all solar neutrino experiments. The listed range of the parameter envelops the 95% CL two-dimensional region shown in Fig. 4 of FUKUDA 02. The best fit point is  $\Delta(m^2) = 6.9 \times 10^{-5} \text{ eV}^2$  and  $\tan^2\theta = 0.38$  ( $\sin^2 2\theta = 0.80$ ).

### $\sin^2(2\theta_{23})$

The ranges below correspond to the projection onto the  $\sin^2(2\theta_{23})$  axis of the 90% CL contours in the  $\sin^2(2\theta_{23}) - \Delta m_{32}^2$  plane presented by the authors. The values are reported with one standard deviation uncertainty.

VALUE	DOCUMENT ID	TECN	COMMENT
<b>&gt;0.95</b>	1 ABE	11c SKAM	Super-Kamiokande
••• We do not use the following data for averages, fits, limits, etc. •••			
>0.90	ADAMSON	11 MINS	$2\nu$ oscillation; maximal mixing
0.86 $^{+0.11}_{-0.12}$	2 ADAMSON	11b MINS	$\bar{\nu}$ beam
>0.965	3 WENDELL	10 SKAM	$3\nu$ oscillation with solar terms; $\theta_{13}=0$
>0.95	4 WENDELL	10 SKAM	$3\nu$ oscillation; normal mass hierarchy
>0.93	5 WENDELL	10 SKAM	$3\nu$ oscillation; inverted mass hierarchy
>0.85	ADAMSON	08A MINS	MINOS
>0.2	6 ADAMSON	06 MINS	atmospheric $\nu$ with far detector
>0.59	7 AHN	06A K2K	KEK to Super-K
>0.7	8 MICHAEL	06 MINS	MINOS
>0.58	9 ALIU	05 K2K	KEK to Super-K
>0.6	10 ALLISON	05 SOU2	
>0.92	11 ASHIE	05 SKAM	Super-Kamiokande
>0.80	12 AMBROSIO	04 MCRO	MACRO
>0.90	13 ASHIE	04 SKAM	L/E distribution
>0.30	14 AHN	03 K2K	KEK to Super-K
>0.45	15 AMBROSIO	03 MCRO	MACRO
>0.77	16 AMBROSIO	03 MCRO	MACRO
>0.50	17 SANCHEZ	03 SOU2	Soudan-2 Atmospheric
>0.80	18 AMBROSIO	01 MCRO	upward $\mu$
>0.82	19 AMBROSIO	01 MCRO	upward $\mu$
>0.45	20 FUKUDA	99c SKAM	upward $\mu$
>0.70	21 FUKUDA	99d SKAM	upward $\mu$
>0.30	22 FUKUDA	99d SKAM	stop $\mu$ / through
>0.82	23 FUKUDA	98c SKAM	Super-Kamiokande
>0.30	24 HATAKEYAMA	98 KAMI	Kamiokande
>0.73	25 HATAKEYAMA	98 KAMI	Kamiokande
>0.65	26 FUKUDA	94 KAMI	Kamiokande

- 1 ABE 11c obtained this result by a two-neutrino oscillation analysis using the Super-Kamiokande-I+II+III atmospheric neutrino data. ABE 11c also reported results under a two-neutrino disappearance model with separate mixing parameters between  $\nu$  and  $\bar{\nu}$ , and obtained  $\sin^2 2\theta > 0.93$  for  $\nu$  and  $\sin^2 2\theta > 0.83$  for  $\bar{\nu}$  at 90% C.L.
- 2 ADAMSON 11b obtained this result by a two-neutrino oscillation analysis of antineutrinos in an antineutrino enhanced beam with  $1.71 \times 10^{20}$  protons on target. This results is consistent with the neutrino measurements of ADAMSON 11 at 2% C.L.
- 3 WENDELL 10 obtained this result ( $\sin^2 \theta_{23} = 0.407\text{--}0.583$ ) by a three-neutrino oscillation analysis using the Super-Kamiokande-I+II+III atmospheric neutrino data, assuming  $\theta_{13} = 0$  but including the solar oscillation parameters  $\Delta m_{21}^2$  and  $\sin^2 \theta_{12}$  in the fit.

- 4 WENDELL 10 obtained this result ( $\sin^2 \theta_{23} = 0.43\text{--}0.61$ ) by a three-neutrino oscillation analysis with one mass scale dominance ( $\Delta m_{21}^2 = 0$ ) using the Super-Kamiokande-I+II+III atmospheric neutrino data, and updates the HOSAKA 06A result.
- 5 WENDELL 10 obtained this result ( $\sin^2 \theta_{23} = 0.44\text{--}0.63$ ) by a three-neutrino oscillation analysis with one mass scale dominance ( $\Delta m_{21}^2 = 0$ ) using the Super-Kamiokande-I+II+III atmospheric neutrino data, and updates the HOSAKA 06A result.
- 6 ADAMSON 06 obtained this result by a two-neutrino oscillation analysis of the L/E distribution using 4.54 kton yr atmospheric neutrino data with the MINOS far detector.
- 7 Supercedes ALIU 05.
- 8 MICHAEL 06 best fit is for maximal mixing. See also ADAMSON 08.
- 9 The best fit is for maximal mixing.
- 10 ALLISON 05 result is based upon atmospheric neutrino interactions including upward-stopping muons, with an exposure of 5.9 kton yr. From a two-flavor oscillation analysis the best-fit point is  $\Delta m^2 = 0.0017 \text{ eV}^2$  and  $\sin^2(2\theta) = 0.97$ .
- 11 ASHIE 05 obtained this result by a two-neutrino oscillation analysis using 92 kton yr atmospheric neutrino data from the complete Super-Kamiokande I running period.
- 12 AMBROSIO 04 obtained this result, without using the absolute normalization of the neutrino flux, by combining the angular distribution of upward through-going muon tracks with  $E_\mu > 1 \text{ GeV}$ ,  $N_{low}$  and  $N_{high}$ , and the numbers of InDown + UpStop and InUp events. Here,  $N_{low}$  and  $N_{high}$  are the number of events with reconstructed neutrino energies  $< 30 \text{ GeV}$  and  $> 130 \text{ GeV}$ , respectively. InDown and InUp represent events with downward and upward-going tracks starting inside the detector due to neutrino interactions, while UpStop represents entering upward-going tracks which stop in the detector. The best fit is for maximal mixing.
- 13 ASHIE 04 obtained this result from the L(flight length)/E(estimated neutrino energy) distribution of  $\nu_\mu$  disappearance probability, using the Super-Kamiokande-I 1489 live-day atmospheric neutrino data.
- 14 There are several islands of allowed region from this K2K analysis, extending to high values of  $\Delta m^2$ . We only include the one that overlaps atmospheric neutrino analyses. The best fit is for maximal mixing.
- 15 AMBROSIO 03 obtained this result on the basis of the ratio  $R = N_{low}/N_{high}$ , where  $N_{low}$  and  $N_{high}$  are the number of upward through-going muon events with reconstructed neutrino energy  $< 30 \text{ GeV}$  and  $> 130 \text{ GeV}$ , respectively. The data came from the full detector run started in 1994. The method of FELDMAN 98 is used to obtain the limits.
- 16 AMBROSIO 03 obtained this result by using the ratio R and the angular distribution of the upward through-going muons. R is given in the previous note and the angular distribution is reported in AMBROSIO 01. The method of FELDMAN 98 is used to obtain the limits. The best fit is to maximal mixing.
- 17 SANCHEZ 03 is based on an exposure of 5.9 kton yr. The result is obtained using a likelihood analysis of the neutrino L/E distribution for a selection  $\mu$  flavor sample while the e-flavor sample provides flux normalization. The method of FELDMAN 98 is used to obtain the allowed region. The best fit is  $\sin^2(2\theta) = 0.97$ .
- 18 AMBROSIO 01 result is based on the angular distribution of upward through-going muon tracks with  $E_\mu > 1 \text{ GeV}$ . The data came from three different detector configurations, but the statistics is largely dominated by the full detector run, from May 1994 to December 2000. The total live time, normalized to the full detector configuration is 6.17 years. The best fit is obtained outside the physical region. The method of FELDMAN 98 is used to obtain the limits. The best fit is for maximal mixing.
- 19 AMBROSIO 01 result is based on the angular distribution and normalization of upward through-going muon tracks with  $E_\mu > 1 \text{ GeV}$ . See the previous footnote.
- 20 FUKUDA 99c obtained this result from a total of 537 live days of upward through-going muon data in Super-Kamiokande between April 1996 to January 1998. With a threshold of  $E_\mu > 1.6 \text{ GeV}$ , the observed flux is  $(1.74 \pm 0.07 \pm 0.02) \times 10^{-13} \text{ cm}^{-2}\text{s}^{-1}\text{sr}^{-1}$ . The best fit is  $\sin^2(2\theta) = 0.95$ .
- 21 FUKUDA 99d obtained this result from a simultaneous fitting to zenith angle distributions of upward-stopping and through-going muons. The flux of upward-stopping muons of minimum energy of 1.6 GeV measured between April 1996 and January 1998 is  $(0.39 \pm 0.04 \pm 0.02) \times 10^{-13} \text{ cm}^{-2}\text{s}^{-1}\text{sr}^{-1}$ . This is compared to the expected flux of  $(0.73 \pm 0.16 \text{ (theoretical error)}) \times 10^{-13} \text{ cm}^{-2}\text{s}^{-1}\text{sr}^{-1}$ . The best fit is to maximal mixing.
- 22 FUKUDA 99d obtained this result from the zenith dependence of the upward-stopping/through-going flux ratio. The best fit is to maximal mixing.
- 23 FUKUDA 98c obtained this result by an analysis of 33.0 kton yr atmospheric neutrino data. The best fit is for maximal mixing.
- 24 HATAKEYAMA 98 obtained this result from a total of 2456 live days of upward-going muon data in Kamiokande between December 1985 and May 1995. With a threshold of  $E_\mu > 1.6 \text{ GeV}$ , the observed flux of upward through-going muons is  $(1.94 \pm 0.10 \pm 0.07) \times 10^{-13} \text{ cm}^{-2}\text{s}^{-1}\text{sr}^{-1}$ . This is compared to the expected flux of  $(2.46 \pm 0.54 \text{ (theoretical error)}) \times 10^{-13} \text{ cm}^{-2}\text{s}^{-1}\text{sr}^{-1}$ . The best fit is for maximal mixing.
- 25 HATAKEYAMA 98 obtained this result from a combined analysis of Kamiokande contained events (FUKUDA 94) and upward going muon events. The best fit is  $\sin^2(2\theta) = 0.95$ .
- 26 FUKUDA 94 obtained the result by a combined analysis of sub- and multi-GeV atmospheric neutrino events in Kamiokande. The best fit is for maximal mixing.

### $\Delta m_{32}^2$

The sign of  $\Delta m_{32}^2$  is not known at this time. Only the absolute value is quoted below. Unless otherwise specified, the ranges below correspond to the projection onto the  $\Delta m_{32}^2$  axis of the 90% CL contours in the  $\sin^2(2\theta_{23}) - \Delta m_{32}^2$  plane presented by the authors. The values are reported with one standard deviation uncertainty.

VALUE ( $10^{-3} \text{ eV}^2$ )	DOCUMENT ID	TECN	COMMENT
<b><math>2.32^{+0.12}_{-0.06}</math></b>	ADAMSON	11 MINS	$2\nu$ oscillation; maximal mixing

# Lepton Particle Listings

## Neutrino Mixing

• • • We do not use the following data for averages, fits, limits, etc. • • •

1.3 - 4.0	<sup>1</sup> ABE	11c	SKAM	atmospheric $\bar{\nu}$
$3.36^{+0.46}_{-0.40}$	<sup>2</sup> ADAMSON	11b	MINS	$\bar{\nu}$ beam
<3.37	<sup>3</sup> ADAMSON	11c	MINS	MINOS
1.9 - 2.6	<sup>4</sup> WENDELL	10	SKAM	$3\nu$ osc.; normal mass hierarchy
1.7 - 2.7	<sup>4</sup> WENDELL	10	SKAM	$3\nu$ osc.; inverted mass hierarchy
$2.43 \pm 0.13$	ADAMSON	08a	MINS	MINOS
0.07-50	<sup>5</sup> ADAMSON	06	MINS	atmospheric $\nu$ with far detector
1.9-4.0	<sup>6,7</sup> AHN	06a	K2K	KEK to Super-K
2.2-3.8	<sup>8</sup> MICHAEL	06	MINS	MINOS
1.9-3.6	<sup>6</sup> ALIU	05	K2K	KEK to Super-K
0.3-12	<sup>9</sup> ALLISON	05	SOU2	
1.5-3.4	<sup>10</sup> ASHIE	05	SKAM	atmospheric neutrino
0.6-8.0	<sup>11</sup> AMBROSIO	04	MCR0	MACRO
1.9 to 3.0	<sup>12</sup> ASHIE	04	SKAM	L/E distribution
1.5-3.9	<sup>13</sup> AHN	03	K2K	KEK to Super-K
0.25-9.0	<sup>14</sup> AMBROSIO	03	MCR0	MACRO
0.6-7.0	<sup>15</sup> AMBROSIO	03	MCR0	MACRO
0.15-15	<sup>16</sup> SANCHEZ	03	SOU2	Soudan-2 Atmospheric
0.6-15	<sup>17</sup> AMBROSIO	01	MCR0	upward $\mu$
1.0-6.0	<sup>18</sup> AMBROSIO	01	MCR0	upward $\mu$
1.0-50	<sup>19</sup> FUKUDA	99c	SKAM	upward $\mu$
1.5-15.0	<sup>20</sup> FUKUDA	99d	SKAM	upward $\mu$
0.7-18	<sup>21</sup> FUKUDA	99d	SKAM	stop $\mu$ / through
0.5-6.0	<sup>22</sup> FUKUDA	98c	SKAM	Super-Kamiokande
0.55-50	<sup>23</sup> HATAKEYAMA	98	KAMI	Kamiokande
4-23	<sup>24</sup> HATAKEYAMA	98	KAMI	Kamiokande
5-25	<sup>25</sup> FUKUDA	94	KAMI	Kamiokande

<sup>1</sup> ABE 11c obtained this result by a two-neutrino oscillation analysis with separate mixing parameters between neutrinos and antineutrinos, using the Super-Kamiokande-I+II+III atmospheric neutrino data. The corresponding 90% CL neutrino oscillation parameter range obtained from this analysis is  $\Delta m^2 = 1.7\text{--}3.0 \times 10^{-3} \text{ eV}^2$ .

<sup>2</sup> ADAMSON 11b obtained this result by a two-neutrino oscillation analysis of antineutrinos in an antineutrino enhanced beam with  $1.71 \times 10^{20}$  protons on target. This result is consistent with the neutrino measurements of ADAMSON 11 at 2% C.L.

<sup>3</sup> ADAMSON 11c obtains this result based on a study of antineutrinos in a neutrino beam and assumes maximal mixing in the two-flavor approximation.

<sup>4</sup> WENDELL 10 obtained this result by a three-neutrino oscillation analysis with one mass scale dominance ( $\Delta m_{21}^2 = 0$ ) using the Super-Kamiokande-I+II+III atmospheric neutrino data, and updates the HOSAKA 06a result.

<sup>5</sup> ADAMSON 06 obtained this result by a two-neutrino oscillation analysis of the L/E distribution using 4.54 kton yr atmospheric neutrino data with the MINOS far detector.

<sup>6</sup> The best fit in the physical region is for  $\Delta m^2 = 2.8 \times 10^{-3} \text{ eV}^2$ .

<sup>7</sup> Supersedes ALIU 05.

<sup>8</sup> MICHAEL 06 best fit is  $2.74 \times 10^{-3} \text{ eV}^2$ . See also ADAMSON 08.

<sup>9</sup> ALLISON 05 result is based on an atmospheric neutrino observation with an exposure of 5.9 kton yr. From a two-flavor oscillation analysis the best-fit point is  $\Delta m^2 = 0.0017 \text{ eV}^2$  and  $\sin^2 2\theta = 0.97$ .

<sup>10</sup> ASHIE 05 obtained this result by a two-neutrino oscillation analysis using 92 kton yr atmospheric neutrino data from the complete Super-Kamiokande-I running period. The best fit is for  $\Delta m^2 = 2.1 \times 10^{-3} \text{ eV}^2$ .

<sup>11</sup> AMBROSIO 04 obtained this result, without using the absolute normalization of the neutrino flux, by combining the angular distribution of upward through-going muon tracks with  $E_\mu > 1 \text{ GeV}$ ,  $N_{low}$ , and  $N_{high}$ , and the numbers of InDown + UpStop and InUp events. Here,  $N_{low}$  and  $N_{high}$  are the number of events with reconstructed neutrino energies  $< 30 \text{ GeV}$  and  $> 130 \text{ GeV}$ , respectively. InDown and InUp represent events with downward and upward-going tracks starting inside the detector due to neutrino interactions, while UpStop represents entering upward-going tracks which stop in the detector. The best fit is for  $\Delta m^2 = 2.3 \times 10^{-3} \text{ eV}^2$ .

<sup>12</sup> ASHIE 04 obtained this result from the L(flight length)/E(estimated neutrino energy) distribution of  $\nu_\mu$  disappearance probability, using the Super-Kamiokande-I 1489 live-day atmospheric neutrino data. The best fit is for  $\Delta m^2 = 2.4 \times 10^{-3} \text{ eV}^2$ .

<sup>13</sup> There are several islands of allowed region from this K2K analysis, extending to high values of  $\Delta m^2$ . We only include the one that overlaps atmospheric neutrino analyses. The best fit is for  $\Delta m^2 = 2.8 \times 10^{-3} \text{ eV}^2$ .

<sup>14</sup> AMBROSIO 03 obtained this result on the basis of the ratio  $R = N_{low}/N_{high}$ , where  $N_{low}$  and  $N_{high}$  are the number of upward through-going muon events with reconstructed neutrino energy  $< 30 \text{ GeV}$  and  $> 130 \text{ GeV}$ , respectively. The data came from the full detector run started in 1994. The method of FELDMAN 98 is used to obtain the limits. The best fit is for  $\Delta m^2 = 2.5 \times 10^{-3} \text{ eV}^2$ .

<sup>15</sup> AMBROSIO 03 obtained this result by using the ratio R and the angular distribution of the upward through-going muons. R is given in the previous note and the angular distribution is reported in AMBROSIO 01. The method of FELDMAN 98 is used to obtain the limits. The best fit is for  $\Delta m^2 = 2.5 \times 10^{-3} \text{ eV}^2$ .

<sup>16</sup> SANCHEZ 03 is based on an exposure of 5.9 kton yr. The result is obtained using a likelihood analysis of the neutrino L/E distribution for a selection  $\mu$  flavor sample while the e-flavor sample provides flux normalization. The method of FELDMAN 98 is used to obtain the allowed region. The best fit is for  $\Delta m^2 = 5.2 \times 10^{-3} \text{ eV}^2$ .

<sup>17</sup> AMBROSIO 01 result is based on the angular distribution of upward through-going muon tracks with  $E_\mu > 1 \text{ GeV}$ . The data came from three different detector configurations, but the statistics is largely dominated by the full detector run, from May 1994 to December 2000. The total live time, normalized to the full detector configuration is 6.17 years. The best fit is obtained outside the physical region. The method of FELDMAN 98 is used to obtain the limits.

<sup>18</sup> AMBROSIO 01 result is based on the angular distribution and normalization of upward through-going muon tracks with  $E_\mu > 1 \text{ GeV}$ . See the previous footnote.

<sup>19</sup> FUKUDA 99c obtained this result from a total of 537 live days of upward through-going muon data in Super-Kamiokande between April 1996 to January 1998. With a threshold of  $E_\mu > 1.6 \text{ GeV}$ , the observed flux is  $(1.74 \pm 0.07 \pm 0.02) \times 10^{-13} \text{ cm}^{-2}\text{s}^{-1}\text{sr}^{-1}$ . The best fit is for  $\Delta m^2 = 5.9 \times 10^{-3} \text{ eV}^2$ .

<sup>20</sup> FUKUDA 99d obtained this result from a simultaneous fitting to zenith angle distributions of upward-stopping and through-going muons. The flux of upward-stopping muons of minimum energy of 1.6 GeV measured between April 1996 and January 1998 is  $(0.39 \pm 0.04 \pm 0.02) \times 10^{-13} \text{ cm}^{-2}\text{s}^{-1}\text{sr}^{-1}$ . This is compared to the expected flux of  $(0.73 \pm 0.16 \text{ (theoretical error)}) \times 10^{-13} \text{ cm}^{-2}\text{s}^{-1}\text{sr}^{-1}$ . The best fit is for  $\Delta m^2 = 3.9 \times 10^{-3} \text{ eV}^2$ .

<sup>21</sup> FUKUDA 99d obtained this result from the zenith dependence of the upward-stopping/through-going flux ratio. The best fit is for  $\Delta m^2 = 3.1 \times 10^{-3} \text{ eV}^2$ .

<sup>22</sup> FUKUDA 98c obtained this result by an analysis of 33.0 kton yr atmospheric neutrino data. The best fit is for  $\Delta m^2 = 2.2 \times 10^{-3} \text{ eV}^2$ .

<sup>23</sup> HATAKEYAMA 98 obtained this result from a total of 2456 live days of upward-going muon data in Kamiokande between December 1985 and May 1995. With a threshold of  $E_\mu > 1.6 \text{ GeV}$ , the observed flux of upward through-going muons is  $(1.94 \pm 0.10^{+0.07}_{-0.06}) \times 10^{-13} \text{ cm}^{-2}\text{s}^{-1}\text{sr}^{-1}$ . This is compared to the expected flux of  $(2.46 \pm 0.54 \text{ (theoretical error)}) \times 10^{-13} \text{ cm}^{-2}\text{s}^{-1}\text{sr}^{-1}$ . The best fit is for  $\Delta m^2 = 2.2 \times 10^{-3} \text{ eV}^2$ .

<sup>24</sup> HATAKEYAMA 98 obtained this result from a combined analysis of Kamiokande contained events (FUKUDA 94) and upward going muon events. The best fit is for  $\Delta m^2 = 13 \times 10^{-3} \text{ eV}^2$ .

<sup>25</sup> FUKUDA 94 obtained the result by a combined analysis of sub- and multi-GeV atmospheric neutrino events in Kamiokande. The best fit is for  $\Delta m^2 = 16 \times 10^{-3} \text{ eV}^2$ .

### $\sin^2(2\theta_{13})$

At present time direct measurements of  $\sin^2(2\theta_{13})$  are derived from the reactor  $\bar{\nu}_e$  disappearance at distances corresponding to the  $\Delta m_{32}^2$  value, i.e.  $L \sim 1 \text{ km}$ . Alternatively, limits can also be obtained from the analysis of the solar neutrino data and accelerator-based  $\nu_\mu \rightarrow \nu_e$  experiments.

VALUE	CL%	DOCUMENT ID	TECN	COMMENT
<b>0.098 ± 0.013 OUR AVERAGE</b>				
$0.086 \pm 0.041 \pm 0.030$		<sup>1</sup> ABE	12	DCHZ Chooz reactors
$0.113 \pm 0.013 \pm 0.019$		<sup>2</sup> AHN	12	RENO Yonggwang reactors
$0.092 \pm 0.016 \pm 0.005$		<sup>3</sup> AN	12	DAYA Daya Bay, Ling Ao, Ling Ao-II reactors
• • • We do not use the following data for averages, fits, limits, etc. • • •				
$0.098^{+0.067}_{-0.062}$	68	<sup>4</sup> ABE	11	FIT KamLAND + global solar
< 0.23	95	<sup>5</sup> ABE	11	FIT Global solar
0.05 - 0.21	68	<sup>6</sup> ABE	11A	T2K Normal mass hierarchy
0.06 - 0.25	68	<sup>7</sup> ABE	11A	T2K Inverted mass hierarchy
0.01 - 0.09	68	<sup>8</sup> ADAMSON	11D	MINS Normal mass hierarchy
0.03 - 0.15	68	<sup>9</sup> ADAMSON	11D	MINS Inverted mass hierarchy
$0.08 \pm 0.03$	68	<sup>10</sup> FOGLI	11	FIT Global neutrino data
$0.078 \pm 0.062$	68	<sup>11</sup> GANDO	11	FIT KamLAND + solar: $3\nu$
$0.124 \pm 0.133$	68	<sup>12</sup> GANDO	11	FIT KamLAND: $3\nu$
$0.03^{+0.09}_{-0.07}$	90	<sup>13</sup> ADAMSON	10A	MINS Normal mass hierarchy
$0.06^{+0.14}_{-0.06}$	90	<sup>14</sup> ADAMSON	10A	MINS Inverted mass hierarchy
$0.08^{+0.08}_{-0.07}$	15,16	AHARMIM	10	FIT KamLAND + global solar: $3\nu$
< 0.30	95,17	AHARMIM	10	FIT global solar: $3\nu$
< 0.15	90	<sup>18</sup> WENDELL	10	SKAM $3\nu$ osc.; normal $m$ hierarchy
< 0.33	90	<sup>18</sup> WENDELL	10	SKAM $3\nu$ osc.; inverted $m$ hierarchy
$0.11^{+0.11}_{-0.08}$		<sup>19</sup> ADAMSON	09	MINS Normal mass hierarchy
$0.18^{+0.15}_{-0.11}$		<sup>20</sup> ADAMSON	09	MINS Inverted mass hierarchy
$0.06 \pm 0.04$		<sup>21</sup> FOGLI	08	FIT Global neutrino data
$0.08 \pm 0.07$		<sup>22</sup> FOGLI	08	FIT Solar + KamLAND data
$0.05 \pm 0.05$		<sup>23</sup> FOGLI	08	FIT Atmospheric+LBL+CHOOZ
< 0.36	90	<sup>24</sup> YAMAMOTO	06	K2K Accelerator experiment
< 0.48	90	<sup>25</sup> AHN	04	K2K Accelerator experiment
< 0.36	90	<sup>26</sup> BOEHM	01	Palo Verde react.
< 0.45	90	<sup>27</sup> BOEHM	00	Palo Verde react.
< 0.15	90	<sup>28</sup> APOLLONIO	99	CHOZ Reactor Experiment

<sup>1</sup> ABE 12 determine the  $\bar{\nu}_e$  interaction rate in a single detector, located 1050 m from the cores of two reactors. The rate normalization is fixed by the results of the Bugey4 reactor experiment, thus avoiding any dependence on possible very short baseline oscillations. The value of  $\Delta m_{31}^2 = 2.4 \times 10^{-3} \text{ eV}^2$  is used in the analysis.

<sup>2</sup> AHN 12 use two identical detectors, placed at flux weighted distances of 408.56 m and 1433.99 m from six reactor cores, to determine the mixing angle  $\theta_{13}$ . This rate-only analysis excludes the no-oscillation hypothesis at 4.9 standard deviations. The value of  $\Delta m_{31}^2 = (2.32^{+0.12}_{-0.08}) \times 10^{-3} \text{ eV}^2$  was assumed in the analysis.

- <sup>3</sup> AN 12 use six identical detectors with three placed near the reactor cores (flux-weighted baselines of 470 m and 576 m) and the remaining three at the far hall (at the flux averaged distance of 1648 m from all six reactor cores) to determine the mixing angle  $\theta_{13}$  using the  $\bar{\nu}_e$  observed interaction rate ratios. This rate-only analysis excludes the no-oscillation hypothesis at 5.2 standard deviations. The value of  $\Delta m_{31}^2 = (2.32 \pm_{-0.08}^{+0.12}) \times 10^{-3} \text{ eV}^2$  was assumed in the analysis.
- <sup>4</sup> ABE 11 obtained this result by a three-neutrino oscillation analysis with the value of  $\Delta m_{32}^2$  fixed to  $2.4 \times 10^{-3} \text{ eV}^2$ , using solar neutrino data including Super-Kamiokande, SNO, Borexino (ARPESELLA 08a), Homestake, GALLEX/GNO, SAGE, and KamLAND data. This result implies an upper bound of  $\sin^2 \theta_{13} < 0.059$  (95% CL) or  $\sin^2 2\theta_{13} < 0.22$  (95% CL). The normal neutrino mass hierarchy and CPT invariance are assumed.
- <sup>5</sup> ABE 11 obtained this result by a three-neutrino oscillation analysis with the value of  $\Delta m_{32}^2$  fixed to  $2.4 \times 10^{-3} \text{ eV}^2$ , using solar neutrino data including Super-Kamiokande, SNO, Borexino (ARPESELLA 08a), Homestake, and GALLEX/GNO data. The normal neutrino mass hierarchy is assumed.
- <sup>6</sup> The quoted limit is for  $\Delta m_{32}^2 = 2.4 \times 10^{-3} \text{ eV}^2$ ,  $\theta_{23} = \pi/2$ ,  $\delta = 0$ , and the normal mass hierarchy. For other values of  $\delta$ , the 68% region spans from 0.04 to 0.25, and the 90% region from 0.02 to 0.32.
- <sup>7</sup> The quoted limit is for  $\Delta m_{32}^2 = 2.4 \times 10^{-3} \text{ eV}^2$ ,  $\theta_{23} = \pi/2$ ,  $\delta = 0$ , and the inverted mass hierarchy. For other values of  $\delta$ , the 68% region spans from 0.04 to 0.30, and the 90% region from 0.02 to 0.39.
- <sup>8</sup> The quoted limit is for  $\Delta m_{32}^2 = 2.32 \times 10^{-3} \text{ eV}^2$ ,  $\theta_{23} = \pi/2$ ,  $\delta = 0$ , and the normal mass hierarchy. For other values of  $\delta$ , the 68% region spans from 0.02 to 0.12, and the 90% region from 0 to 0.16.
- <sup>9</sup> The quoted limit is for  $\Delta m_{32}^2 = 2.32 \times 10^{-3} \text{ eV}^2$ ,  $\theta_{23} = \pi/2$ ,  $\delta = 0$ , and the inverted mass hierarchy. For other values of  $\delta$ , the 68% region spans from 0.02 to 0.16, and the 90% region from 0 to 0.21.
- <sup>10</sup> FOGLE 11 obtained this result from an analysis using the atmospheric, accelerator long baseline, CHOOZ, solar, and KamLAND data. Recently, MUELLER 11 suggested an average increase of about 3.5% in normalization of the reactor  $\bar{\nu}_e$  fluxes, and using these fluxes, the fitted result becomes  $0.10 \pm 0.03$ .
- <sup>11</sup> GANDO 11 report  $\sin^2 \theta_{13} = 0.020 \pm 0.016$ . This result was obtained with three-neutrino fit using the KamLAND + solar data.
- <sup>12</sup> GANDO 11 report  $\sin^2 \theta_{13} = 0.032 \pm 0.037$ . This result was obtained with three-neutrino fit using the KamLAND data only.
- <sup>13</sup> This result corresponds to the limit of  $< 0.12$  at 90% CL for  $\Delta m_{32}^2 = 2.43 \times 10^{-3} \text{ eV}^2$ ,  $\theta_{23} = \pi/2$ , and  $\delta = 0$ . For other values of  $\delta$ , the 90% CL region spans from 0 to 0.16.
- <sup>14</sup> This result corresponds to the limit of  $< 0.20$  at 90% CL for  $\Delta m_{32}^2 = 2.43 \times 10^{-3} \text{ eV}^2$ ,  $\theta_{23} = \pi/2$ , and  $\delta = 0$ . For other values of  $\delta$ , the 90% CL region spans from 0 to 0.21.
- <sup>15</sup> AHARMIM 10 global solar neutrino data include SNO's low-energy-threshold analysis survival probability day/night curves, SNO Phase III integral rates (AHARMIM 08), CL (CLEVELAND 98), SAGE (ABDURASHITOV 09), Gallex/GNO (HAMPEL 99, ALTMANN 05), Borexino (ARPESELLA 08a), SK-I zenith (HOSAKA 06), and SK-II day/night spectra (CRAVENS 08).
- <sup>16</sup> AHARMIM 10 obtained this result by a three-neutrino oscillation analysis with the value of  $\Delta m_{31}^2$  fixed to  $2.3 \times 10^{-3} \text{ eV}^2$ , using global solar neutrino data and KamLAND data (ABE 08a). CPT invariance is assumed. This result implies an upper bound of  $\sin^2 \theta_{13} < 0.057$  (95% CL) or  $\sin^2 2\theta_{13} < 0.22$  (95% CL).
- <sup>17</sup> AHARMIM 10 obtained this result by a three-neutrino oscillation analysis with the value of  $\Delta m_{31}^2$  fixed to  $2.3 \times 10^{-3} \text{ eV}^2$ , using global solar neutrino data.
- <sup>18</sup> WENDELL 10 obtained this result by a three-neutrino oscillation analysis with one mass scale dominance ( $\Delta m_{21}^2 = 0$ ) using the Super-Kamiokande-I+II+III atmospheric neutrino data, and updates the HOSAKA 06a result.
- <sup>19</sup> The quoted limit is for  $\Delta m_{32}^2 = 2.43 \times 10^{-3} \text{ eV}^2$ ,  $\theta_{23} = \pi/2$ , and  $\delta = 0$ . For other values of  $\delta$ , the 68% CL region spans from 0.02 to 0.26.
- <sup>20</sup> The quoted limit is for  $\Delta m_{32}^2 = 2.43 \times 10^{-3} \text{ eV}^2$ ,  $\theta_{23} = \pi/2$ , and  $\delta = 0$ . For other values of  $\delta$ , the 68% CL region spans from 0.04 to 0.34.
- <sup>21</sup> FOGLE 08 obtained this result from a global analysis of all neutrino oscillation data, that is, solar + KamLAND + atmospheric + accelerator long baseline + CHOOZ.
- <sup>22</sup> FOGLE 08 obtained this result from an analysis using the solar and KamLAND neutrino oscillation data.
- <sup>23</sup> FOGLE 08 obtained this result from an analysis using the atmospheric, accelerator long baseline, and CHOOZ neutrino oscillation data.
- <sup>24</sup> YAMAMOTO 06 searched for  $\nu_\mu \rightarrow \nu_e$  appearance. Assumes  $2 \sin^2(2\theta_{\mu e}) = \sin^2(2\theta_{13})$ . The quoted limit is for  $\Delta m_{32}^2 = 1.9 \times 10^{-3} \text{ eV}^2$ . That value of  $\Delta m_{32}^2$  is the one- $\sigma$  low value for AHN 06a. For the AHN 06a best fit value of  $2.8 \times 10^{-3} \text{ eV}^2$ , the  $\sin^2(2\theta_{13})$  limit is  $< 0.26$ . Supersedes AHN 04.
- <sup>25</sup> AHN 04 searched for  $\nu_\mu \rightarrow \nu_e$  appearance. Assuming  $2 \sin^2(2\theta_{\mu e}) = \sin^2(2\theta_{13})$ , a limit on  $\sin^2(2\theta_{\mu e})$  is converted to a limit on  $\sin^2(2\theta_{13})$ . The quoted limit is for  $\Delta m_{32}^2 = 1.9 \times 10^{-3} \text{ eV}^2$ . That value of  $\Delta m_{32}^2$  is the one- $\sigma$  low value for ALIU 05. For the ALIU 05 best fit value of  $2.8 \times 10^{-3} \text{ eV}^2$ , the  $\sin^2(2\theta_{13})$  limit is  $< 0.30$ .
- <sup>26</sup> The quoted limit is for  $\Delta m_{32}^2 = 1.9 \times 10^{-3} \text{ eV}^2$ . That value of  $\Delta m_{32}^2$  is the 1- $\sigma$  low value for ALIU 05. For the ALIU 05 best fit value of  $2.8 \times 10^{-3} \text{ eV}^2$ , the  $\sin^2 2\theta_{13}$  limit is  $< 0.19$ . In this range, the  $\theta_{13}$  limit is larger for lower values of  $\Delta m_{32}^2$ , and smaller for higher values of  $\Delta m_{32}^2$ .
- <sup>27</sup> The quoted limit is for  $\Delta m_{32}^2 = 1.9 \times 10^{-3} \text{ eV}^2$ . That value of  $\Delta m_{32}^2$  is the 1- $\sigma$  low value for ALIU 05. For the ALIU 05 best fit value of  $2.8 \times 10^{-3} \text{ eV}^2$ , the  $\sin^2 2\theta_{13}$  limit is  $< 0.23$ .
- <sup>28</sup> The quoted limit is for  $\Delta m_{32}^2 = 2.43 \times 10^{-3} \text{ eV}^2$ . That value of  $\Delta m_{32}^2$  is the central value for ADAMSON 08. For the ADAMSON 08 1- $\sigma$  low value of  $2.30 \times 10^{-3} \text{ eV}^2$ , the  $\sin^2 2\theta_{13}$  limit is  $< 0.16$ . See also APOLLONIO 03 for a detailed description of the experiment.

## (C) Other neutrino mixing results

The LSND collaboration reported in AGUILAR 01 a signal which is consistent with  $\bar{\nu}_\mu \rightarrow \bar{\nu}_e$  oscillations. In a three neutrino framework, this would be a measurement of  $\theta_{12}$  and  $\Delta m_{21}^2$ . This does not appear to be consistent with the interpretation of other neutrino data. The MiniBooNE experiment, reported in AGUILAR-AREVALO 07, does a two-neutrino analysis which, assuming CPT conservation, rules out AGUILAR 01. The following listings include results which might be relevant towards understanding these observations. They include searches for  $\nu_\mu \rightarrow \nu_e$ ,  $\bar{\nu}_\mu \rightarrow \bar{\nu}_e$ , sterile neutrino oscillations, and CPT violation.

 $\Delta(m^2)$  for  $\sin^2(2\theta) = 1$  ( $\nu_\mu \rightarrow \nu_e$ )

VALUE (eV <sup>2</sup> )	CL%	DOCUMENT ID	TECN	COMMENT
• • • We do not use the following data for averages, fits, limits, etc. • • •				
<0.034	90	AGUILAR-AR...07	MBOO	MiniBooNE
<0.0008	90	AHN 04	K2K	Water Cherenkov
<0.4	90	ASTIER 03	NOMD	CERN SPS
<2.4	90	AVVAKUMOV 02	NTEV	NUTEV FNAL
		1 AGUILAR 01	LSND	$\nu_\mu \rightarrow \nu_e$ osc.prob.
0.03 to 0.3	95	2 ATHANASSO...98	LSND	$\nu_\mu \rightarrow \nu_e$
<2.3	90	3 LOVERRE 96	CHARM/CDHS	
<0.9	90	VILAIN 94c	CHM2	CERN SPS
<0.09	90	ANGELINI 86	HLBC	BEBC CERN PS

<sup>1</sup> AGUILAR 01 is the final analysis of the LSND full data set. Search is made for the  $\nu_\mu \rightarrow \nu_e$  oscillations using  $\nu_\mu$  from  $\pi^+$  decay in flight by observing beam-on electron events from  $\nu_e C \rightarrow e^- X$ . Present analysis results in  $8.1 \pm 12.2 \pm 1.7$  excess events in the  $60 < E_e < 200$  MeV energy range, corresponding to oscillation probability of  $0.10 \pm 0.16 \pm 0.04\%$ . This is consistent, though less significant, with the previous result of ATHANASSOPOULOS 98, which it supersedes. The present analysis uses selection criteria developed for the decay at rest region, and is less effective in removing the background above 60 MeV than ATHANASSOPOULOS 98.

<sup>2</sup> ATHANASSOPOULOS 98 is a search for the  $\nu_\mu \rightarrow \nu_e$  oscillations using  $\nu_\mu$  from  $\pi^+$  decay in flight. The 40 observed beam-on electron events are consistent with  $\nu_e C \rightarrow e^- X$ ; the expected background is  $21.9 \pm 2.1$ . Authors interpret this excess as evidence for an oscillation signal corresponding to oscillations with probability  $(0.26 \pm 0.10 \pm 0.05)\%$ . Although the significance is only  $2.3\sigma$ , this measurement is an important and consistent cross check of ATHANASSOPOULOS 96 who reported evidence for  $\bar{\nu}_\mu \rightarrow \bar{\nu}_e$  oscillations from  $\mu^+$  decay at rest. See also ATHANASSOPOULOS 98b.

<sup>3</sup> LOVERRE 96 uses the charged-current to neutral-current ratio from the combined CHARM (ALLABY 86) and CDHS (ABRAMOWICZ 86) data from 1986.

 $\sin^2(2\theta)$  for "Large"  $\Delta(m^2)$  ( $\nu_\mu \rightarrow \nu_e$ )

VALUE (units $10^{-3}$ )	CL%	DOCUMENT ID	TECN	COMMENT
• • • We do not use the following data for averages, fits, limits, etc. • • •				
< 1.8	90	1 AGUILAR-AR...07	MBOO	MiniBooNE
<110	90	2 AHN 04	K2K	Water Cherenkov
< 1.4	90	ASTIER 03	NOMD	CERN SPS
< 1.6	90	AVVAKUMOV 02	NTEV	NUTEV FNAL
		3 AGUILAR 01	LSND	$\nu_\mu \rightarrow \nu_e$ osc.prob.
0.5 to 30	95	4 ATHANASSO...98	LSND	$\nu_\mu \rightarrow \nu_e$
< 3.0	90	5 LOVERRE 96	CHARM/CDHS	
< 9.4	90	VILAIN 94c	CHM2	CERN SPS
< 5.6	90	6 VILAIN 94c	CHM2	CERN SPS

<sup>1</sup> The limit is  $\sin^2 2\theta < 0.9 \times 10^{-3}$  at  $\Delta m^2 = 2 \text{ eV}^2$ . That value of  $\Delta m^2$  corresponds to the smallest mixing angle consistent with the reported signal from LSND in AGUILAR 01.

<sup>2</sup> The limit becomes  $\sin^2 2\theta < 0.15$  at  $\Delta m^2 = 2.8 \times 10^{-3} \text{ eV}^2$ , the best-fit value of the  $\nu_\mu$  disappearance analysis in K2K.

<sup>3</sup> AGUILAR 01 is the final analysis of the LSND full data set of the search for the  $\nu_\mu \rightarrow \nu_e$  oscillations. See footnote in preceding table for further details.

<sup>4</sup> ATHANASSOPOULOS 98 report  $(0.26 \pm 0.10 \pm 0.05)\%$  for the oscillation probability; the value of  $\sin^2 2\theta$  for large  $\Delta m^2$  is deduced from this probability. See footnote in preceding table for further details, and see the paper for a plot showing allowed regions. If effect is due to oscillation, it is most likely to be intermediate  $\sin^2 2\theta$  and  $\Delta m^2$ . See also ATHANASSOPOULOS 98b.

<sup>5</sup> LOVERRE 96 uses the charged-current to neutral-current ratio from the combined CHARM (ALLABY 86) and CDHS (ABRAMOWICZ 86) data from 1986.

<sup>6</sup> VILAIN 94c limit derived by combining the  $\nu_\mu$  and  $\bar{\nu}_\mu$  data assuming CP conservation.

 $\Delta(m^2)$  for  $\sin^2(2\theta) = 1$  ( $\bar{\nu}_\mu \rightarrow \bar{\nu}_e$ )

VALUE (eV <sup>2</sup> )	CL%	DOCUMENT ID	TECN	COMMENT
• • • We do not use the following data for averages, fits, limits, etc. • • •				
0.03-0.09	90	1 AGUILAR-AR...10	MBOO	$E_\nu > 475$ MeV
0.03-0.07	90	2 AGUILAR-AR...10	MBOO	$E_\nu > 200$ MeV
<0.06	90	AGUILAR-AR...09b	MBOO	MiniBooNE
<0.055	90	3 ARMBRUSTER02	KAR2	Liquid Sci. calor.
<2.6	90	AVVAKUMOV 02	NTEV	NUTEV FNAL
0.03-0.05		4 AGUILAR 01	LSND	LAMPF

## Lepton Particle Listings

## Neutrino Mixing

0.05–0.08	90	5	ATHANASSO...96	LSND	LAMPF
0.048–0.090	80	6	ATHANASSO...95		
<0.07	90	7	HILL 95		
<0.9	90		VILAIN 94c	CHM2	CERN SP5
<0.14	90	8	FREEDMAN 93	CNTR	LAMPF

<sup>1</sup> This value is for a two neutrino oscillation analysis for excess antineutrino events with  $E_\nu > 475$  MeV. The best fit is at 0.07. The allowed region is consistent with LSND reported by AGUILAR 01. Supersedes AGUILAR-AREVALO 09B.

<sup>2</sup> This value is for a two neutrino oscillation analysis for excess antineutrino events with  $E_\nu > 200$  MeV with subtraction of the expected 12 events low energy excess seen in the neutrino component of the beam. The best fit value is 0.007 for  $\Delta(m^2) = 4.4$  eV<sup>2</sup>.

<sup>3</sup> ARMBRUSTER 02 is the final analysis of the KARMEN 2 data for 17.7 m distance from the ISIS stopped pion and muon neutrino source. It is a search for  $\bar{\nu}_e$ , detected by the inverse  $\beta$ -decay reaction on protons and <sup>12</sup>C. 15 candidate events are observed, and 15.8 ± 0.5 background events are expected, hence no oscillation signal is detected. The results exclude large regions of the parameter area favored by the LSND experiment.

<sup>4</sup> AGUILAR 01 is the final analysis of the LSND full data set. It is a search for  $\bar{\nu}_e$  30 m from LAMPF beam stop. Neutrinos originate mainly from  $\pi^+$  decay at rest.  $\bar{\nu}_e$  are detected through  $\bar{\nu}_e p \rightarrow e^+ n$  ( $20 < E_{e^+} < 60$  MeV) in delayed coincidence with  $np \rightarrow d\gamma$ . Authors observe 87.9 ± 22.4 ± 6.0 total excess events. The observation is attributed to  $\bar{\nu}_\mu \rightarrow \bar{\nu}_e$  oscillations with the oscillation probability of 0.264 ± 0.067 ± 0.045%, consistent with the previously published result. Taking into account all constraints, the most favored allowed region of oscillation parameters is a band of  $\Delta(m^2)$  from 0.2–2.0 eV<sup>2</sup>. Supersedes ATHANASSOPOULOS 95, ATHANASSOPOULOS 96, and ATHANASSOPOULOS 98.

<sup>5</sup> ATHANASSOPOULOS 96 is a search for  $\bar{\nu}_e$  30 m from LAMPF beam stop. Neutrinos originate mainly from  $\pi^+$  decay at rest.  $\bar{\nu}_e$  could come from either  $\bar{\nu}_\mu \rightarrow \bar{\nu}_e$  or  $\nu_e \rightarrow \bar{\nu}_e$ ; our entry assumes the first interpretation. They are detected through  $\bar{\nu}_e p \rightarrow e^+ n$  ( $20$  MeV  $< E_{e^+} < 60$  MeV) in delayed coincidence with  $np \rightarrow d\gamma$ . Authors observe 51 ± 20 ± 8 total excess events over an estimated background 12.5 ± 2.9. ATHANASSOPOULOS 96B is a shorter version of this paper.

<sup>6</sup> ATHANASSOPOULOS 95 error corresponds to the 1.6 $\sigma$  band in the plot. The expected background is 2.7 ± 0.4 events. Corresponds to an oscillation probability of (0.34 ± 0.20 ± 0.18 ± 0.07)%. For a different interpretation, see HILL 95. Replaced by ATHANASSOPOULOS 96.

<sup>7</sup> HILL 95 is a report by one member of the LSND Collaboration, reporting a different conclusion from the analysis of the data of this experiment (see ATHANASSOPOULOS 95). Contrary to the rest of the LSND Collaboration, Hill finds no evidence for the neutrino oscillation  $\bar{\nu}_\mu \rightarrow \bar{\nu}_e$  and obtains only upper limits.

<sup>8</sup> FREEDMAN 93 is a search at LAMPF for  $\bar{\nu}_e$  generated from any of the three neutrino types  $\nu_\mu, \bar{\nu}_\mu$ , and  $\nu_e$  which come from the beam stop. The  $\bar{\nu}_e$ 's would be detected by the reaction  $\bar{\nu}_e p \rightarrow e^+ n$ . FREEDMAN 93 replaces DURKIN 88.

 **$\sin^2(2\theta)$  for "Large"  $\Delta(m^2)$  ( $\bar{\nu}_\mu \rightarrow \bar{\nu}_e$ )**

VALUE (units 10 <sup>-3</sup> )	CL%	DOCUMENT ID	TECN	COMMENT
0.4–9.0	99	1	AGUILAR-AR...10	MBOO $E_\nu > 475$ MeV
0.4–9.0	99	2	AGUILAR-AR...10	MBOO $E_\nu > 200$ MeV
<3.3	90	3	AGUILAR-AR...09B	MBOO MiniBooNE
<1.7	90	4	ARMBRUSTER02	KAR2 Liquid Sci. calor.
<1.1	90		AVVAKUMOV 02	NTEV NUTEV FNAL
5.3 ± 1.3 ± 9.0		5	AGUILAR 01	LSND LAMPF
6.2 ± 2.4 ± 1.0		6	ATHANASSO...96	LSND LAMPF
3–12	80	7	ATHANASSO...95	
<6	90	8	HILL 95	

<sup>1</sup> This value is for a two neutrino oscillation analysis for excess antineutrino events with  $E_\nu > 475$  MeV. At 90% CL there is no solution at high  $\Delta(m^2)$ . The best fit is at maximal mixing. The allowed region is consistent with LSND reported by AGUILAR 01. Supersedes AGUILAR-AREVALO 09B.

<sup>2</sup> This value is for a two neutrino oscillation analysis for excess antineutrino events with  $E_\nu > 200$  MeV with subtraction of the expected 12 events low energy excess seen in the neutrino component of the beam. At 90% CL there is no solution at high  $\Delta(m^2)$ . The best fit value is 0.007 for  $\Delta(m^2) = 4.4$  eV<sup>2</sup>.

<sup>3</sup> This result is inconclusive with respect to small amplitude mixing suggested by LSND.

<sup>4</sup> ARMBRUSTER 02 is the final analysis of the KARMEN 2 data. See footnote in preceding table for further details, and the paper for the exclusion plot.

<sup>5</sup> AGUILAR 01 is the final analysis of the LSND full data set. The deduced oscillation probability is 0.264 ± 0.067 ± 0.045%; the value of  $\sin^2 2\theta$  for large  $\Delta(m^2)$  is twice this probability (although these values are excluded by other constraints). See footnote in preceding table for further details, and the paper for a plot showing allowed regions. Supersedes ATHANASSOPOULOS 95, ATHANASSOPOULOS 96, and ATHANASSOPOULOS 98.

<sup>6</sup> ATHANASSOPOULOS 96 reports (0.31 ± 0.12 ± 0.05)% for the oscillation probability; the value of  $\sin^2 2\theta$  for large  $\Delta(m^2)$  should be twice this probability. See footnote in preceding table for further details, and see the paper for a plot showing allowed regions.

<sup>7</sup> ATHANASSOPOULOS 95 error corresponds to the 1.6 $\sigma$  band in the plot. The expected background is 2.7 ± 0.4 events. Corresponds to an oscillation probability of (0.34 ± 0.20 ± 0.18 ± 0.07)%. For a different interpretation, see HILL 95. Replaced by ATHANASSOPOULOS 96.

<sup>8</sup> HILL 95 is a report by one member of the LSND Collaboration, reporting a different conclusion from the analysis of the data of this experiment (see ATHANASSOPOULOS 95). Contrary to the rest of the LSND Collaboration, Hill finds no evidence for the neutrino oscillation  $\bar{\nu}_\mu \rightarrow \bar{\nu}_e$  and obtains only upper limits.

 **$\Delta(m^2)$  for  $\sin^2(2\theta) = 1$  ( $\nu_\mu(\bar{\nu}_\mu) \rightarrow \nu_e(\bar{\nu}_e)$ )**

VALUE (eV <sup>2</sup> )	CL%	DOCUMENT ID	TECN	COMMENT
<0.075	90	BORODOV... 92	CNTR	BNL E776

• • • We do not use the following data for averages, fits, limits, etc. • • •

<1.6 90 <sup>1</sup> ROMOSAN 97 CCFR FNAL

<sup>1</sup> ROMOSAN 97 uses wideband beam with a 0.5 km decay region.

 **$\sin^2(2\theta)$  for "Large"  $\Delta(m^2)$  ( $\nu_\mu(\bar{\nu}_\mu) \rightarrow \nu_e(\bar{\nu}_e)$ )**

VALUE (units 10 <sup>-3</sup> )	CL%	DOCUMENT ID	TECN	COMMENT
<1.8	90	1	ROMOSAN 97	CCFR FNAL

• • • We do not use the following data for averages, fits, limits, etc. • • •

<3.8 90 <sup>2</sup> MCFARLAND 95 CCFR FNAL

<3 90 BORODOV... 92 CNTR BNL E776

<sup>1</sup> ROMOSAN 97 uses wideband beam with a 0.5 km decay region.

<sup>2</sup> MCFARLAND 95 state that "This result is the most stringent to date for 250 <  $\Delta(m^2)$  < 450 eV<sup>2</sup> and also excludes at 90%CL much of the high  $\Delta(m^2)$  region favored by the recent LSND observation." See ATHANASSOPOULOS 95 and ATHANASSOPOULOS 96.

 **$\Delta(m^2)$  for  $\sin^2(2\theta) = 1$  ( $\bar{\nu}_e \not\rightarrow \bar{\nu}_e$ )**

VALUE (eV <sup>2</sup> )	CL%	DOCUMENT ID	TECN	COMMENT
<0.01	90	1	ACHKAR 95	CNTR Bugey reactor

• • • We do not use the following data for averages, fits, limits, etc. • • •

<sup>1</sup> ACHKAR 95 bound is for  $L=15, 40,$  and 95 m.

 **$\sin^2(2\theta)$  for "Large"  $\Delta(m^2)$  ( $\bar{\nu}_e \not\rightarrow \bar{\nu}_e$ )**

VALUE	CL%	DOCUMENT ID	TECN	COMMENT
<0.02	90	1	ACHKAR 95	CNTR For $\Delta(m^2) = 0.6$ eV <sup>2</sup>

• • • We do not use the following data for averages, fits, limits, etc. • • •

<sup>1</sup> ACHKAR 95 bound is from data for  $L=15, 40,$  and 95 m distance from the Bugey reactor.

**Sterile neutrino limits from atmospheric neutrino studies** **$\Delta(m^2)$  for  $\sin^2(2\theta) = 1$  ( $\nu_\mu \rightarrow \nu_s$ )**

$\nu_s$  means  $\nu_\tau$  or any sterile (noninteracting)  $\nu$ .

VALUE (10 <sup>-5</sup> eV <sup>2</sup> )	CL%	DOCUMENT ID	TECN	COMMENT
<3000 (or <550)	90	1	OYAMA 89	KAMI Water Cherenkov
<4.2 (or >54).	90		BIONTA 88	IMB Flux has $\nu_\mu, \bar{\nu}_\mu, \nu_e,$ and $\bar{\nu}_e$

• • • We do not use the following data for averages, fits, limits, etc. • • •

<3000 (or <550) 90 <sup>1</sup> OYAMA 89 KAMI Water Cherenkov

<4.2 (or >54). 90 BIONTA 88 IMB Flux has  $\nu_\mu, \bar{\nu}_\mu, \nu_e,$  and  $\bar{\nu}_e$

<sup>1</sup> OYAMA 89 gives a range of limits, depending on assumptions in their analysis. They argue that the region  $\Delta(m^2) = (100-1000) \times 10^{-5}$  eV<sup>2</sup> is not ruled out by any data for large mixing.

**Search for  $\nu_\mu \rightarrow \nu_s$** 

VALUE	DOCUMENT ID	TECN	COMMENT
• • • We do not use the following data for averages, fits, limits, etc. • • •			

• • • We do not use the following data for averages, fits, limits, etc. • • •

<sup>1</sup> AMBROSIO 01 MCRO matter effects

<sup>2</sup> FUKUDA 00 SKAM neutral currents + matter effects

<sup>1</sup> AMBROSIO 01 tested the pure 2-flavor  $\nu_\mu \rightarrow \nu_s$  hypothesis using matter effects which change the shape of the zenith-angle distribution of upward through-going muons. With maximum mixing and  $\Delta(m^2)$  around 0.0024 eV<sup>2</sup>, the  $\nu_\mu \rightarrow \nu_s$  oscillation is disfavored with 99% confidence level with respect to the  $\nu_\mu \rightarrow \nu_\tau$  hypothesis.

<sup>2</sup> FUKUDA 00 tested the pure 2-flavor  $\nu_\mu \rightarrow \nu_s$  hypothesis using three complementary atmospheric-neutrino data samples. With this hypothesis, zenith-angle distributions are expected to show characteristic behavior due to neutral currents and matter effects. In the  $\Delta(m^2)$  and  $\sin^2 2\theta$  region preferred by the Super-Kamiokande data, the  $\nu_\mu \rightarrow \nu_s$  hypothesis is rejected at the 99% confidence level, while the  $\nu_\mu \rightarrow \nu_\tau$  hypothesis consistently fits all of the data sample.

**CPT tests** **$\langle \Delta m_{21}^2 - \Delta \bar{m}_{21}^2 \rangle$** 

VALUE (10 <sup>-4</sup> eV <sup>2</sup> )	CL%	DOCUMENT ID	TECN	COMMENT
<1.1	99.7	1	DEGOUVEA 05	FIT solar vs. reactor

• • • We do not use the following data for averages, fits, limits, etc. • • •

<1.1 99.7 <sup>1</sup> DEGOUVEA 05 FIT solar vs. reactor

<sup>1</sup> DEGOUVEA 05 obtained this bound at the 3 $\sigma$  CL from the KamLAND (ARAKI 05) and solar neutrino data.

See key on page 457

Lepton Particle Listings  
Neutrino Mixing, Heavy Neutral Leptons, Searches for

REFERENCES FOR Neutrino Mixing

Table listing neutrino mixing references with columns for author names, publication details (PRL, PR, EPJ, etc.), and collaboration names (e.g., RENO, Daya Bay, KamLAND).

Table listing heavy neutral lepton searches with columns for author names, publication details (PR, PL, PRL, etc.), and collaboration names (e.g., IMB, KAM2, PENN).

Heavy Neutral Leptons, Searches for

(A) Heavy Neutral Leptons

Stable Neutral Heavy Lepton MASS LIMITS

Note that LEP results in combination with REUSSER 91 exclude a fourth stable neutrino with m < 2400 GeV.

Table of mass limits for stable neutral heavy leptons, including columns for VALUE (GeV), CL%, DOCUMENT ID, TECN, and COMMENT.

1 ADEVA 90s limits for the heavy neutrino apply if the mixing with the charged leptons satisfies |U1j|^2 + |U2j|^2 + |U3j|^2 > 6.2 x 10^-8 at mL0 = 20 GeV and > 5.1 x 10^-10 for mL0 = 40 GeV.

Heavy Neutral Lepton MASS LIMITS

Limits apply only to heavy lepton type given in comment at right of data Listings.

See the "Quark and Lepton Compositeness, Searches for" Listings for limits on radiatively decaying excited neutral leptons, i.e. nu\* -> nu gamma.

Table of mass limits for heavy neutral leptons, including columns for VALUE (GeV), CL%, DOCUMENT ID, TECN, and COMMENT.

• • • We do not use the following data for averages, fits, limits, etc. • • •

Table of mass limits for heavy neutral leptons, including columns for VALUE (GeV), CL%, DOCUMENT ID, TECN, and COMMENT.

2 BUSKULIC 96s requires the decay length of the heavy lepton to be < 1 cm, limiting the square of the mixing angle |Uej|^2 to 10^-10.

3 BUSKULIC 96s limit for mixing with tau. Mass is > 63.6 GeV for mixing with e or mu.

4 BUSKULIC 96s limit for mixing with tau. Mass is > 55.2 GeV for mixing with e or mu.

Astrophysical Limits on Neutrino MASS for m\_nu > 1 GeV

Table of astrophysical limits on neutrino mass, including columns for VALUE (GeV), CL%, DOCUMENT ID, TECN, and COMMENT.

• • • We do not use the following data for averages, fits, limits, etc. • • •

# Lepton Particle Listings

## Heavy Neutral Leptons, Searches for

none 60–115	5	FARGION	95	ASTR	Dirac
none 9.2–2000	6	GARCIA	95	COSM	Nucleosynthesis
none 26–4700	6	BECK	94	COSM	Dirac
none 6 – hundreds	7,8	MORI	92B	KAM2	Dirac neutrino
none 24 – hundreds	7,8	MORI	92B	KAM2	Majorana neutrino
none 10–2400	90	REUSSER	91	CNTR	HPGe search
none 3–100	90	SATO	91	KAM2	Kamiokande II
none 12–1400	10	ENQVIST	89	COSM	
none 4–16	90	6,7	OLIVE	88	COSM Dirac $\nu$
none 4–35	90	OLIVE	88	COSM	Majorana $\nu$
>4.2 to 4.7		SREDNICKI	88	COSM	Dirac $\nu$
>5.3 to 7.4		SREDNICKI	88	COSM	Majorana $\nu$
none 20–1000	95	6	AHLEN	87	COSM Dirac $\nu$
>4.1		GRIEST	87	COSM	Dirac $\nu$

< 4–20	90	700–3500	38mK	Trap	15	TRINCZEK	03
< 9–116	95	1–0.1	187Re	cryog.	16	GALEAZZI	01
< 1	95	10–90	35S	Mag spect	17	HOLZSCHUH	00
< 4	95	14–17	241Pu	Electrostatic spec	18	DRAGOUN	99
< 1	95	4–30	63Ni	Mag spect	19	HOLZSCHUH	99
< 10–40	90	370–640	37Ar	EC ion recoil	20	HINDI	98
< 10	95	1	3H	SPEC	21	HIDDEMANN	95
< 6	95	2	3H	SPEC	21	HIDDEMANN	95
< 2	95	3	3H	SPEC	21	HIDDEMANN	95
< 0.7	99	16.3–16.6	3H	Prop chamber	22	KALBFLEISCH	93
< 2	95	13–40	35S	Si(Li)	23	MORTARA	93
< 0.73	95	17	63Ni	Mag spect		OHSHIMA	93
< 1.0	95	10–24	63Ni	Mag spect		KAWAKAMI	92
< 0.9–2.5	90	1200–6800	20F	beta spectrum	24	DEUTSCH	90
< 8	90	80	35S	Mag spect	25	APALIKOV	85
< 1.5	90	60	35S	Mag spect		APALIKOV	85
< 3.0	90	5–50		Mag spect		MARKEY	85
< 0.62	90	48		Si(Li)		OHI	85
< 0.90	90	30		Si(Li)		OHI	85
< 4	90	140	64Cu	Mag spect	26	SCHRECK...	83
< 8	90	440	64Cu	Mag spect	26	SCHRECK...	83
< 100	90	0.1–3000		THEO	27	SHROCK	80
< 0.1	68	80		THEO	28	SHROCK	80

<sup>5</sup> FARGION 95 bound is sensitive to assumed  $\nu$  concentration in the Galaxy. See also KONOPLICH 94.  
<sup>6</sup> These results assume that neutrinos make up dark matter in the galactic halo.  
<sup>7</sup> Limits based on annihilations in the sun and are due to an absence of high energy neutrinos detected in underground experiments.  
<sup>8</sup> MORI 92B results assume that neutrinos make up dark matter in the galactic halo. Limits based on annihilations in earth are also given.  
<sup>9</sup> REUSSER 91 uses existing  $\beta\beta$  detector (see FISHER 89) to search for CDM Dirac neutrinos.  
<sup>10</sup> ENQVIST 89 argue that there is no cosmological upper bound on heavy neutrinos.

<sup>15</sup> TRINCZEK 03 is a search for admixture of heavy neutrino to  $\nu_e$ , in contrast to  $\bar{\nu}_e$  used in many other searches. Full kinematic reconstruction of the neutrino momentum by use of a magneto optical trap.

### (B) Other Bounds from Nuclear and Particle Decays

#### Limits on $|U_{ex}|^2$ as Function of $m_{\nu_x}$

#### Peak and kink search tests

Limits on  $|U_{ex}|^2$  as function of  $m_{\nu_j}$

VALUE	CL%	DOCUMENT ID	TECN	COMMENT
<1 $\times 10^{-7}$	90	11 BRITTON	92B CNTR	50 MeV $< m_{\nu_x} < 130$ MeV

• • • We do not use the following data for averages, fits, limits, etc. • • •

<5 $\times 10^{-6}$	90	DELEENER...	91	$m_{\nu_x} = 20$ MeV
<5 $\times 10^{-7}$	90	DELEENER...	91	$m_{\nu_x} = 40$ MeV
<3 $\times 10^{-7}$	90	DELEENER...	91	$m_{\nu_x} = 60$ MeV
<1 $\times 10^{-6}$	90	DELEENER...	91	$m_{\nu_x} = 80$ MeV
<1 $\times 10^{-6}$	90	DELEENER...	91	$m_{\nu_x} = 100$ MeV
<5 $\times 10^{-7}$	90	AZUELOS	86 CNTR	$m_{\nu_x} = 60$ MeV
<2 $\times 10^{-7}$	90	AZUELOS	86 CNTR	$m_{\nu_x} = 80$ MeV
<3 $\times 10^{-7}$	90	AZUELOS	86 CNTR	$m_{\nu_x} = 100$ MeV
<1 $\times 10^{-6}$	90	AZUELOS	86 CNTR	$m_{\nu_x} = 120$ MeV
<2 $\times 10^{-7}$	90	AZUELOS	86 CNTR	$m_{\nu_x} = 130$ MeV
<1 $\times 10^{-4}$	90	12 BRYMAN	83B CNTR	$m_{\nu_x} = 5$ MeV
<1.5 $\times 10^{-6}$	90	BRYMAN	83B CNTR	$m_{\nu_x} = 53$ MeV
<1 $\times 10^{-5}$	90	BRYMAN	83B CNTR	$m_{\nu_x} = 70$ MeV
<1 $\times 10^{-4}$	90	BRYMAN	83B CNTR	$m_{\nu_x} = 130$ MeV
<1 $\times 10^{-4}$	68	13 SHROCK	81 THEO	$m_{\nu_x} = 10$ MeV
<5 $\times 10^{-6}$	68	13 SHROCK	81 THEO	$m_{\nu_x} = 60$ MeV
<1 $\times 10^{-5}$	68	14 SHROCK	80 THEO	$m_{\nu_x} = 80$ MeV
<3 $\times 10^{-6}$	68	14 SHROCK	80 THEO	$m_{\nu_x} = 160$ MeV

<sup>11</sup> BRITTON 92B is from a search for additional peaks in the  $e^+$  spectrum from  $\pi^+ \rightarrow e^+ \nu_e$  decay at TRIUMF. See also BRITTON 92.  
<sup>12</sup> BRYMAN 83B obtain upper limits from both direct peak search and analysis of  $B(\pi \rightarrow e\nu)/B(\pi \rightarrow \mu\nu)$ . Latter limits are not listed, except for this entry (i.e. — we list the most stringent limits for given mass).  
<sup>13</sup> Analysis of  $(\pi^+ \rightarrow e^+ \nu_e)/(\pi^+ \rightarrow \mu^+ \nu_\mu)$  and  $(K^+ \rightarrow e^+ \nu_e)/(K^+ \rightarrow \mu^+ \nu_\mu)$  decay ratios.  
<sup>14</sup> Analysis of  $(K^+ \rightarrow e^+ \nu_e)$  spectrum.

#### Kink search in nuclear $\beta$ decay

High-sensitivity follow-up experiments show that indications for a neutrino with mass 17 keV (Simpson, Hime, and others) were not valid. Accordingly, we no longer list the experiments by these authors and some others which made positive claims of 17 keV neutrino emission. Complete listings are given in the 1994 edition (Physical Review D50 1173 (1994)) and in the 1998 edition (The European Physical Journal C3 1 (1998)). We list below only the best limits on  $|U_{ex}|^2$  for each  $m_{\nu_x}$ . See WIETFELDT 96 for a comprehensive review.

VALUE (units $10^{-3}$ )	CL%	$m_{\nu_j}$ (keV)	ISOTOPE	METHOD	DOCUMENT ID
--------------------------	-----	-------------------	---------	--------	-------------

• • • We do not use the following data for averages, fits, limits, etc. • • •

<sup>16</sup> GALEAZZI 01 use an cryogenic microcalorimeter to search for mass 50–1000 eV neutrino admixtures using the <sup>187</sup>Re beta spectrum with 2.4 keV endpoint. They derive limits for the admixture of heavy neutrinos, ranging from  $9 \times 10^{-3}$  for mass 1 keV to 0.116 for mass 100 eV. This is a significant improvement with respect to HIDDEMANN 95, especially for masses below  $\sim 500$  MeV, where the limit is about a factor of  $\sim 2$  higher.

<sup>17</sup> HOLZSCHUH 00 use an iron-free  $\beta$  spectrometer to measure the <sup>35</sup>S  $\beta$  decay spectrum. An analysis of the spectrum in the energy range 56–173 keV is used to derive limits for the admixture of heavy neutrinos. This extends the range of neutrino masses explored in HOLZSCHUH 99.

<sup>18</sup> DRAGOUN 99 analyze the  $\beta$  decay spectrum of <sup>241</sup>Pu in the energy range 0.2–9.2 keV to derive limits for the admixture of heavy neutrinos. It is not competitive with HOLZSCHUH 99.

<sup>19</sup> HOLZSCHUH 99 use an iron-free  $\beta$  spectrometer to measure the <sup>63</sup>Ni  $\beta$  decay spectrum. An analysis of the spectrum in the energy range 33–67.8 keV is used to derive limits for the admixture of heavy neutrinos.

<sup>20</sup> HINDI 98 obtain a limit on heavy neutrino admixture from EC decay of <sup>37</sup>Ar by measuring the time-of-flight distribution of the recoiling ions in coincidence with x-rays or Auger electrons. The authors report upper limit for  $|U_{ex}|^2$  of  $\approx 3\%$  for  $m_{\nu_x} = 500$  keV, 1% for  $m_{\nu_x} = 550$  keV, 2% for  $m_{\nu_x} = 600$  keV, and 4% for  $m_{\nu_x} = 650$  keV. Their reported limits for  $m_{\nu_x} \leq 450$  keV are inferior to the limits of SCHRECKENBACH 83.

<sup>21</sup> In the beta spectrum from tritium  $\beta$  decay nonvanishing or mixed  $m_{\nu_1}$  state in the mass region 0.01–4 keV. For  $m_{\nu_x} < 1$  keV, their upper limit on  $|U_{ex}|^2$  becomes less

<sup>22</sup> KALBFLEISCH 93 extends the 17 keV neutrino search of BAHRAN 92, using an improved proportional chamber to which a small amount of <sup>3</sup>H is added. Systematics are significantly reduced, allowing for an improved upper limit. The authors give a 99% confidence limit on  $|U_{ex}|^2$  as a function of  $m_{\nu_x}$  in the range from 13.5 keV to 17.5 keV. See also the related papers BAHRAN 93, BAHRAN 93b, and BAHRAN 95 on theoretical aspects of beta spectra and fitting methods for heavy neutrinos.

<sup>23</sup> MORTARA 93 limit is from study using a high-resolution solid-state detector with a superconducting solenoid. The authors note that “The sensitivity to neutrino mass is verified by measurement with a mixed source of <sup>35</sup>S and <sup>14</sup>C, which artificially produces a distortion in the beta spectrum similar to that expected from the massive neutrino.”

<sup>24</sup> DEUTSCH 90 search for emission of heavy  $\bar{\nu}_e$  in super-allowed beta decay of <sup>20</sup>F by spectral analysis of the electrons.

<sup>25</sup> This limit was taken from the figure 3 of APALIKOV 85; the text gives a more restrictive limit of  $1.7 \times 10^{-3}$  at CL = 90%.

<sup>26</sup> SCHRECKENBACH 83 is a combined measurement of the  $\beta^+$  and  $\beta^-$  spectrum.

<sup>27</sup> SHROCK 80 was a retroactive analysis of data on several superallowed  $\beta$  decays to search for kinks in the Kurie plot.

<sup>28</sup> Application of test to search for kinks in  $\beta$  decay Kurie plots.

#### Searches for Decays of Massive $\nu$

Limits on  $|U_{ex}|^2$  as function of  $m_{\nu_x}$

VALUE	CL%	DOCUMENT ID	TECN	COMMENT
-------	-----	-------------	------	---------

• • • We do not use the following data for averages, fits, limits, etc. • • •

<1.6 $\times 10^{-4}$	90	29 BACK	03A CNTR	$m_{\nu_x} = 4$ MeV
<4.5 $\times 10^{-5}$	90	29 BACK	03A CNTR	$m_{\nu_x} = 7$ MeV
<3.8 $\times 10^{-5}$	90	29 BACK	03A CNTR	$m_{\nu_x} = 10$ MeV
<1.5 $\times 10^{-3}$	95	ACHARD	01 L3	$m_{\nu_x} = 80$ GeV
<2 $\times 10^{-2}$	95	ACHARD	01 L3	$m_{\nu_x} = 175$ GeV
<0.3	95	ACHARD	01 L3	$m_{\nu_x} = 200$ GeV
<4 $\times 10^{-3}$	95	ACCIARRI	99k L3	$m_{\nu_x} = 80$ GeV
<5 $\times 10^{-2}$	95	ACCIARRI	99k L3	$m_{\nu_x} = 175$ GeV
<2 $\times 10^{-5}$	95	30 ABREU	97i DLPH	$m_{\nu_x} = 6$ GeV

See key on page 457

Lepton Particle Listings
Heavy Neutral Leptons, Searches for

Table listing neutrino mass limits and searches for various experiments including ABREU, HAGNER, BARANOV, ADEVA, BURCHAT, DEKAMP, AKERLOF, BERNARDI, OBERAUER, BADIER, DORENBOS, COOPER, BERGSMA, and GRONAU.

Table listing neutrino mass limits and searches for experiments including ASSAMAGAN, BRYMAN, ARMBRUSTER, BILGER, DAUM, MINEHART, HAYANO, and ABELA.

29BACK 03A searched for heavy neutrinos emitted from 8B decay in the Sun using the decay nu\_h -> nu\_e e+ e- in the Counting Test Facility...

30ABREU 97l long-lived nu\_x analysis. Short-lived analysis extends limit to lower masses with decreasing sensitivity except at 3.5 GeV, where the limit is the same as at 6 GeV.

31HAGNER 95 obtain limits on heavy neutrino admixture from the decay nu\_h -> nu\_e e+ e- at a nuclear reactor for the nu\_h mass range 2-9 MeV.

32BARANOV 93 is a search for neutrino decays into e+ e- nu\_e using a beam dump experiment at the 70 GeV Serpukhov proton synchrotron. The limits are not as good as those achieved earlier by BERGSMA 83 and BERNARDI 86, BERNARDI 88.

33BURCHAT 90 includes the analyses reported in JUNG 90, ABRAMS 89c, and WENDT 87.

34OBERAUER 87 bounds from search for nu -> nu' ee decay mode using reactor (anti)neutrinos.

35COOPER-SARKAR 85 also give limits based on model-dependent assumptions for nu\_tau flux. We do not list these. Note that for this bound to be nontrivial, x is not equal to 3, i.e. nu\_x cannot be the dominant mass eigenstate in nu\_tau since m\_nu\_3 < 70 MeV (ALBRECHT 85i). Also, of course, x is not equal to 1 or 2, so a fourth generation would be required for this bound to be nontrivial.

36BERGSMA 83b also quote limits on |U\_e3|^2 where the index 3 refers to the mass eigenstate dominantly coupled to the tau. Those limits were based on assumptions about the D\_s mass and D\_s -> tau nu\_tau branching ratio which are no longer valid. See COOPER-SARKAR 85.

Limits on Coupling of mu to nu\_x as Function of m\_nu\_x

Peak search test

Table with columns: VALUE, CL%, DOCUMENT ID, TECN, COMMENT. Lists peak search results for experiments like ASTIER, DAUM, FORMAGGIO, and ASSAMAGAN.

37ASTIER 02 search for anomalous pion decay into a 33.9 MeV neutral particle. No evidence was found and the sensitivity to the branching ratio B(pi -> mu X) B(X -> nu e+ e-) is as low as 3.7 x 10^-15, depending on the X lifetime.

38DAUM 00 search for anomalous pion decay into a 33.9 MeV neutral particle that might be responsible for the time-distribution anomaly observed by the KARMEN Collaboration.

39FORMAGGIO 00 search for anomalous pion decay into a 33.9 MeV neutral particle Q0 that might be responsible for the time-distribution anomaly observed by the KARMEN Collaboration. In the E815 (NuTeV) experiment at Fermilab no evidence was found, with sensitivity for the pion branching ratio B(pi -> mu Q0) B(Q0 -> visible) as low as 10^-13.

40ASSAMAGAN 98 obtain a limit on heavy neutrino admixture from pi+ decay essentially at rest, by measuring with good resolution the momentum distribution of the muons. However, the search uses an ad hoc shape correction. The authors report upper limit for |U\_mu x|^2 of 0.22 for m\_nu = 0.53 MeV, 0.029 for m\_nu = 0.75 MeV, and 0.016 for m\_nu = 1.0 MeV at 90%CL.

41BRYMAN 96 search for massive unconventional neutrinos of mass m\_nu\_x in pi+ decay.

42ARMBRUSTER 95 study the reactions 12C(nu\_e, e-) 12N and 12C(nu\_mu, e-) 12C\* induced by neutrinos from pi+ and mu+ decay at the ISIS neutron spallation source at the Rutherford-Appleton laboratory. An anomaly in the time distribution can be interpreted as the decay pi+ -> mu+ nu\_x, where nu\_x is a neutral weakly interacting particle with mass approx 33.9 MeV and spin 1/2. The lower limit to the branching ratio is a function of the lifetime of the new massive neutral particle, and reaches a minimum of a few x 10^-16 for tau\_x ~ 5 s.

43From experiments of pi+ and pi- decay in flight at PSI, to check the claim of the KARMEN Collaboration quoted above (ARMBRUSTER 95).

44pi+ -> mu+ nu\_mu peak search experiment.

45K+ -> mu+ nu\_mu peak search experiment.

Peak search test

Limits on |U\_mu x|^2 as function of m\_nu\_x

Table with columns: VALUE, CL%, DOCUMENT ID, TECN, COMMENT. Lists peak search results for experiments like BRYMAN, ASANO, CALAPRICE, SHROCK, and THEO.

46BRYMAN 96 search for massive unconventional neutrinos of mass m\_nu\_x in pi+ decay. They interpret the result as an upper limit for the admixture of a heavy sterile or otherwise

47K+ -> mu+ nu\_mu peak search experiment.

48Analysis of experiment on K+ -> mu+ nu\_mu nu\_x anti-nu\_x decay.

49pi+ -> mu+ nu\_mu peak search experiment.

50Analysis of magnetic spectrometer experiment, bubble chamber experiment, and emulsion experiment on pi+ -> mu+ nu\_mu decay.





See key on page 457

# Lepton Particle Listings

## Heavy Neutral Leptons, Searches for

ABREU	92B	PL B274 230	P. Abreu <i>et al.</i>	(DELPHI Collab.)	MISHRA	87	PRL 59 1397	S.R. Mishra <i>et al.</i>	(COLU, CIT, FNAL+)
BAHRAN	92	PL B291 336	M.Y. Bahrán, G.R. Kalbfleisch	(OKLA)	OBERAUER	87	PL B198 113	L.F. Oberauer, F. von Feilitzsch, R.L. Mossbauer	
BRITTON	92	PRL 68 3000	D.I. Britton <i>et al.</i>	(TRIUM, CARL)	WENDT	87	PRL 58 1810	C. Wendt <i>et al.</i>	(Mark II Collab.)
Also		PR D49 28	D.I. Britton <i>et al.</i>	(TRIUM, CARL)	AZUELOS	86	PRL 56 2241	G. Azuelos <i>et al.</i>	(TRIUM, CNRC)
BRITTON	92B	PR D46 R885	D.I. Britton <i>et al.</i>	(TRIUM, CARL)	BADIER	86	ZPHY C31 21	J. Badier <i>et al.</i>	(NA3 Collab.)
KAWAKAMI	92	PL B287 45	H. Kawakami <i>et al.</i>	(INUS, KEK, SCUC+)	BERNARDI	86	PL 166B 479	G. Bernardi <i>et al.</i>	(CURIN, INFN, CDEF+)
MORI	92B	PL B289 463	M. Mori <i>et al.</i>	(KAM2 Collab.)	DORENBOS...	86	PL 166B 473	J. Dorenbosch <i>et al.</i>	(CHARM Collab.)
ALEXANDER	91F	ZPHY C52 175	G. Alexander <i>et al.</i>	(OPAL Collab.)	ALBRECHT	85I	PL 163B 404	H. Albrecht <i>et al.</i>	(ARGUS Collab.)
DELEENER...	91	PR D43 3611	N. de Leener-Rosier <i>et al.</i>	(LOUV, ZURH+)	APALIKOV	85	JETPL 42 289	A.M. Apalikov <i>et al.</i>	(ITEP)
REUSSER	91	PL B255 143	D. Reusser <i>et al.</i>	(NEUC, CIT, PSI)			Translated from ZETFP 42 233.		
SATO	91	PR D44 2220	N. Sato <i>et al.</i>	(Kamiokande Collab.)	COOPER...	85	PL 160B 207	A.M. Cooper-Sarkar <i>et al.</i>	(CERN, LOIC+)
ADEVA	90S	PL B251 321	B. Adeva <i>et al.</i>	(L3 Collab.)	MARKEY	85	PR C32 2215	J. Markey, F. Boehm	(CIT)
BURCHAT	90	PR D41 3542	P.R. Burchat <i>et al.</i>	(Mark II Collab.)	OH	85	PL 160B 322	T. Oh <i>et al.</i>	(TOKY, INUS, KEK)
DECAMP	90F	PL B236 511	D. Decamp <i>et al.</i>	(ALEPH Collab.)	MINIHART	84	PRL 52 804	R.C. Minehart <i>et al.</i>	(UVA, SIN)
DEUTSCH	90	NP A518 149	J. Deutsch, M. Lebrun, R. Prieels		BERGSM	83	PL 122B 465	F. Bergsma <i>et al.</i>	(CHARM Collab.)
JUNG	90	PRL 64 1091	C. Jung <i>et al.</i>	(Mark II Collab.)	BERGSM	83B	PL 128B 361	F. Bergsma <i>et al.</i>	(CHARM Collab.)
ABRAMS	89C	PRL 63 2447	G.S. Abrams <i>et al.</i>	(Mark II Collab.)	BRYMAN	83B	PRL 50 1546	D.A. Bryman <i>et al.</i>	(TRIUM, CNRC)
ENQVIST	89	NP B317 647	K. Enqvist, K. Kainulainen, J. Maalampi	(HELS)	DEUTSCH	83	PR D27 1644	J.P. Deutsch, M. Lebrun, R. Prieels	(LOUV)
FISHER	89	PL B218 257	P.H. Fisher <i>et al.</i>	(CIT, NEUC, PSI)	GRONAU	83	PR D28 2762	M. Gronau	(HAIF)
AKERLOF	88	PR D37 577	C.W. Akerlof <i>et al.</i>	(HRS Collab.)	SCHRECK...	83	PL 129B 265	K. Schreckenbach <i>et al.</i>	(ISNG, ILLG)
BERNARDI	88	PL B203 332	G. Bernardi <i>et al.</i>	(PARIN, CERN, INFN+)	HAYANO	82	PRL 49 1305	R.S. Hayano <i>et al.</i>	(TOKY, KEK, TSUK)
CALDWELL	88	PRL 61 510	D.O. Caldwell <i>et al.</i>	(UCSB, UCB, LBL)	ABELA	81	PL 105B 263	R. Abela <i>et al.</i>	(SIN)
OLIVE	88	PL B205 553	K.A. Olive, M. Srednicki	(MINN, UCSB)	ASANO	81	PL 104B 84	Y. Asano <i>et al.</i>	(KEK, TOKY, INUS, OSAK)
SREDNICKI	88	NP B310 693	M. Srednicki, R. Watkins, K.A. Olive	(MINN, UCSB)	CALAPRICE	81	PL 106B 175	F.P. Calaprice <i>et al.</i>	(PRIN, IND)
AHLEN	87	PL B195 603	S.P. Ahlen <i>et al.</i>	(BOST, SCUC, HARV+)	SHROCK	81	PR D24 1232	R.E. Shrock	(STON)
DAUM	87	PR D36 2624	M. Daum <i>et al.</i>	(SIN, UVA)	SHROCK	81B	PR D24 1275	R.E. Shrock	(STON)
GRIEST	87	NP B283 681	K. Griest, D. Seckel	(UCSC, CERN)	SHROCK	80	PL 96B 159	R.E. Shrock	(STON)
Also		NP B296 1034 (erratum)	K. Griest, D. Seckel	(UCSC, CERN)					

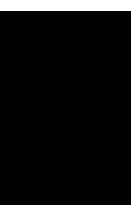


## QUARKS

<i>u</i> . . . . .	662
<i>d</i> . . . . .	662
<i>s</i> . . . . .	662
<i>c</i> . . . . .	666
<i>b</i> . . . . .	667
<i>t</i> . . . . .	668
<i>b'</i> (Fourth Generation) Quark . . . . .	687
<i>t'</i> (Fourth Generation) Quark . . . . .	688
Free Quark Searches . . . . .	688

## Notes in the Quark Listings

Quark Masses (rev.) . . . . .	655
The Top Quark (rev.) . . . . .	668
Free Quark Searches . . . . .	688





# QUARKS

## QUARK MASSES

Updated Jan 2012 by A.V. Manohar (University of California, San Diego) and C.T. Sachrajda (University of Southampton).

### A. Introduction

This note discusses some of the theoretical issues relevant for the determination of quark masses, which are fundamental parameters of the Standard Model of particle physics. Unlike the leptons, quarks are confined inside hadrons and are not observed as physical particles. Quark masses therefore cannot be measured directly, but must be determined indirectly through their influence on hadronic properties. Although one often speaks loosely of quark masses as one would of the mass of the electron or muon, any quantitative statement about the value of a quark mass must make careful reference to the particular theoretical framework that is used to define it. It is important to keep this *scheme dependence* in mind when using the quark mass values tabulated in the data listings.

Historically, the first determinations of quark masses were performed using quark models. The resulting masses only make sense in the limited context of a particular quark model, and cannot be related to the quark mass parameters of the Standard Model. In order to discuss quark masses at a fundamental level, definitions based on quantum field theory be used, and the purpose of this note is to discuss these definitions and the corresponding determinations of the values of the masses.

### B. Mass parameters and the QCD Lagrangian

The QCD [1] Lagrangian for  $N_F$  quark flavors is

$$\mathcal{L} = \sum_{k=1}^{N_F} \bar{q}_k (i\mathcal{D} - m_k) q_k - \frac{1}{4} G_{\mu\nu} G^{\mu\nu}, \quad (1)$$

where  $\mathcal{D} = (\partial_\mu - igA_\mu) \gamma^\mu$  is the gauge covariant derivative,  $A_\mu$  is the gluon field,  $G_{\mu\nu}$  is the gluon field strength,  $m_k$  is the mass parameter of the  $k^{\text{th}}$  quark, and  $q_k$  is the quark Dirac field. After renormalization, the QCD Lagrangian Eq. (1) gives finite values for physical quantities, such as scattering amplitudes. Renormalization is a procedure that invokes a subtraction scheme to render the amplitudes finite, and requires the introduction of a dimensionful scale parameter  $\mu$ . The mass parameters in the QCD Lagrangian Eq. (1) depend on the renormalization scheme used to define the theory, and also on the scale parameter  $\mu$ . The most commonly used renormalization scheme for QCD perturbation theory is the  $\overline{\text{MS}}$  scheme.

The QCD Lagrangian has a chiral symmetry in the limit that the quark masses vanish. This symmetry is spontaneously broken by dynamical chiral symmetry breaking, and explicitly broken by the quark masses. The nonperturbative scale of dynamical chiral symmetry breaking,  $\Lambda_\chi$ , is around 1 GeV [2]. It is conventional to call quarks heavy if  $m > \Lambda_\chi$ , so that explicit

chiral symmetry breaking dominates ( $c$ ,  $b$ , and  $t$  quarks are heavy), and light if  $m < \Lambda_\chi$ , so that spontaneous chiral symmetry breaking dominates ( $u$ ,  $d$  and  $s$  quarks are light). The determination of light- and heavy-quark masses is considered separately in sections D and E below.

At high energies or short distances, nonperturbative effects, such as chiral symmetry breaking, become small and one can, in principle, determine quark masses by analyzing mass-dependent effects using QCD perturbation theory. Such computations are conventionally performed using the  $\overline{\text{MS}}$  scheme at a scale  $\mu \gg \Lambda_\chi$ , and give the  $\overline{\text{MS}}$  “running” mass  $\overline{m}(\mu)$ . We use the  $\overline{\text{MS}}$  scheme when reporting quark masses; one can readily convert these values into other schemes using perturbation theory.

The  $\mu$  dependence of  $\overline{m}(\mu)$  at short distances can be calculated using the renormalization group equation,

$$\mu^2 \frac{d\overline{m}(\mu)}{d\mu^2} = -\gamma(\overline{\alpha}_s(\mu)) \overline{m}(\mu), \quad (2)$$

where  $\gamma$  is the anomalous dimension which is now known to four-loop order in perturbation theory [3,4].  $\overline{\alpha}_s$  is the coupling constant in the  $\overline{\text{MS}}$  scheme. Defining the expansion coefficients  $\gamma_r$  by

$$\gamma(\overline{\alpha}_s) \equiv \sum_{r=1}^{\infty} \gamma_r \left( \frac{\overline{\alpha}_s}{4\pi} \right)^r,$$

the first four coefficients are given by

$$\begin{aligned} \gamma_1 &= 4, \\ \gamma_2 &= \frac{202}{3} - \frac{20N_L}{9}, \\ \gamma_3 &= 1249 + \left( -\frac{2216}{27} - \frac{160}{3}\zeta(3) \right) N_L - \frac{140}{81} N_L^2, \\ \gamma_4 &= \frac{4603055}{162} + \frac{135680}{27}\zeta(3) - 8800\zeta(5) \\ &\quad + \left( -\frac{91723}{27} - \frac{34192}{9}\zeta(3) + 880\zeta(4) + \frac{18400}{9}\zeta(5) \right) N_L \\ &\quad + \left( \frac{5242}{243} + \frac{800}{9}\zeta(3) - \frac{160}{3}\zeta(4) \right) N_L^2 \\ &\quad + \left( -\frac{332}{243} + \frac{64}{27}\zeta(3) \right) N_L^3, \end{aligned}$$

where  $N_L$  is the number of active light quark flavors at the scale  $\mu$ , i.e. flavors with masses  $< \mu$ , and  $\zeta$  is the Riemann zeta function ( $\zeta(3) \simeq 1.2020569$ ,  $\zeta(4) \simeq 1.0823232$ , and  $\zeta(5) \simeq 1.0369278$ ). In addition, as the renormalization scale crosses quark mass thresholds one needs to match the scale dependence of  $m$  below and above the threshold. There are finite threshold corrections; the necessary formulae can be found in Ref. [5].

The quark masses for light quarks discussed so far are often referred to as current quark masses. Nonrelativistic quark models use constituent quark masses, which are of order 350 MeV for the  $u$  and  $d$  quarks. Constituent quark masses

# Quark Particle Listings

## Quarks

model the effects of dynamical chiral symmetry breaking, and are not related to the quark mass parameters  $m_k$  of the QCD Lagrangian Eq. (1). Constituent masses are only defined in the context of a particular hadronic model.

### C. Lattice Gauge Theory

The use of the lattice simulations for *ab initio* determinations of the fundamental parameters of QCD, including the coupling constant and quark masses (except for the top-quark mass) is a very active area of research (see the review on Lattice Quantum Chromodynamics in this *Review*). Here we only briefly recall those features which are required for the determination of quark masses. In order to determine the lattice spacing ( $a$ , i.e. the distance between neighboring points of the lattice) and quark masses, one computes a convenient and appropriate set of physical quantities (frequently chosen to be a set of hadronic masses) for a variety of input values of the quark masses. The true (physical) values of the quark masses are those which correctly reproduce the set of physical quantities being used for the calibration.

The values of the quark masses obtained directly in lattice simulations are bare quark masses, corresponding to a particular discretization of QCD and with the lattice spacing as the ultraviolet cut-off. In order for these results to be useful in phenomenological applications, it is necessary to relate them to renormalized masses defined in some standard renormalization scheme such as  $\overline{\text{MS}}$ . Provided that both the ultraviolet cut-off  $a^{-1}$  and the renormalization scale are much greater than  $\Lambda_{\text{QCD}}$ , the bare and renormalized masses can be related in perturbation theory. However, in order to avoid uncertainties due to the unknown higher-order coefficients in lattice perturbation theory, most results obtained recently use *non-perturbative renormalization* to relate the bare masses to those defined in renormalization schemes which can be simulated directly in lattice QCD (e.g. those obtained from quark and gluon Green functions at specified momenta in the Landau gauge [50] or those defined using finite-volume techniques and the Schrödinger functional [51]). The conversion to the  $\overline{\text{MS}}$  scheme (which cannot be simulated) is then performed using continuum perturbation theory.

The determination of quark masses using lattice simulations is well established and the current emphasis is on the reduction and control of the systematic uncertainties. With improved algorithms and access to more powerful computing resources, the precision of the results has improved immensely in recent years. Particularly pleasing is the observation that results obtained using different formulations of lattice QCD, with different systematic uncertainties, give results which are largely consistent with each other. This gives us broad confidence in the estimates of the systematic errors. As the precision of the results approaches the percent level, more attention will now have to be given to sources of systematic uncertainty which have only been studied in a limited way up to now. In particular most current simulations are performed with degenerate  $u$

and  $d$  quarks and without including electromagnetic effects. Vacuum polarisation effects are included with  $N_f = 2 + 1$  or  $N_f = 2$  flavors of sea quarks, although simulations with charm sea quarks are now beginning. In earlier *reviews*, results were presented from simulations in which vacuum polarization effects were completely neglected (this is the so-called *quenched* approximation), leading to systematic uncertainties which could not be estimated reliably. It is no longer necessary to include quenched results in compilations of quark masses.

### D. Light quarks

In this section we review the determination of the masses of the light quarks  $u$ ,  $d$  and  $s$  from lattice simulations and then discuss the consequences of the approximate chiral symmetry.

**Lattice Gauge Theory:** The most reliable determinations of the strange quark mass  $m_s$  and of the average of the up and down quark masses  $m_{ud} = (m_u + m_d)/2$  are obtained from lattice simulations. As explained in section C above, the simulations are performed with degenerate up and down quarks ( $m_u = m_d$ ) and so it is the average which is obtained directly from the computations. Below we discuss attempts to derive  $m_u$  and  $m_d$  separately using lattice results in combination with other techniques, but here we briefly present our estimate of the current status of the latest lattice results. Based largely on references [19–26], which have among the most reliable estimates of the systematic errors, our summary is

$$\overline{m}_s = (93.5 \pm 2.5) \text{ MeV}, \quad \overline{m}_{ud} = (3.40 \pm 0.25) \text{ MeV} \quad (3)$$

and

$$\frac{\overline{m}_s}{\overline{m}_{ud}} = 27.5 \pm 0.3. \quad (4)$$

The masses are given in the  $\overline{\text{MS}}$  scheme at a renormalization scale of 2 GeV. Because the errors are dominated by systematics, these results are not simply the combinations of all the results in quadrature, but include a judgement of the remaining uncertainties. Since the different collaborations use different formulations of lattice QCD, the (relatively small) variations of the results between the groups provides important information about the reliability of the estimates.

Current lattice simulations are performed in the isospin symmetry limit, i.e. with the masses of the up and down quarks equal,  $m_u = m_d \equiv m_{ud}$  and, apart from Refs. [31,32], electromagnetic effects are not included in the simulation. It is the average of the physical up and down quark masses which is determined directly. In order to estimate  $m_u$  and  $m_d$  separately, further experimental and theoretical inputs have to be included. Recent studies which combine lattice data with studies of isospin breaking effects using chiral perturbation theory and phenomenology include those by the MILC [20,27] and BMW [22,23] collaborations and by the Flavianet Lattice Averaging Group [32]. Based on these results we summarise the current status as

$$\frac{\overline{m}_u}{\overline{m}_d} = 0.46(5), \quad \overline{m}_u = 2.15(15) \text{ MeV}, \quad \overline{m}_d = 4.70(20) \text{ MeV}. \quad (5)$$

Again the masses are given in the  $\overline{\text{MS}}$  scheme at a renormalization scale of 2 GeV. Of particular importance is the fact that  $m_u \neq 0$  since there would have been no strong  $CP$  problem had  $m_u$  been equal to zero.

The quark mass ranges for the light quarks given in the listings combine the lattice and continuum values and use the PDG method for determining errors given in the introductory notes.

**Chiral Perturbation Theory:** For light quarks, one can use the techniques of chiral perturbation theory [6–8] to extract quark mass ratios. The mass term for light quarks in the QCD Lagrangian is

$$\overline{\Psi}M\Psi = \overline{\Psi}_L M \Psi_R + \overline{\Psi}_R M^\dagger \Psi_L, \quad (6)$$

where  $M$  is the light quark mass matrix,

$$M = \begin{pmatrix} m_u & 0 & 0 \\ 0 & m_d & 0 \\ 0 & 0 & m_s \end{pmatrix}, \quad (7)$$

$\Psi = (u, d, s)$ , and  $L$  and  $R$  are the left- and right-chiral components of  $\Psi$  given by  $\Psi_{L,R} = P_{L,R}\Psi$ ,  $P_L = (1 - \gamma_5)/2$ ,  $P_R = (1 + \gamma_5)/2$ . The mass term is the only term in the QCD Lagrangian that mixes left- and right-handed quarks. In the limit  $M \rightarrow 0$ , there is an independent  $SU(3) \times U(1)$  flavor symmetry for the left- and right-handed quarks. The vector  $U(1)$  symmetry is baryon number; the axial  $U(1)$  symmetry of the classical theory is broken in the quantum theory due to the anomaly. The remaining  $G_\chi = SU(3)_L \times SU(3)_R$  chiral symmetry of the QCD Lagrangian is spontaneously broken to  $SU(3)_V$ , which, in the limit  $M \rightarrow 0$ , leads to eight massless Goldstone bosons, the  $\pi$ 's,  $K$ 's, and  $\eta$ .

The symmetry  $G_\chi$  is only an approximate symmetry, since it is explicitly broken by the quark mass matrix  $M$ . The Goldstone bosons acquire masses which can be computed in a systematic expansion in  $M$ , in terms of low-energy constants, which are unknown nonperturbative parameters of the effective theory, and are not fixed by the symmetries. One treats the quark mass matrix  $M$  as an external field that transforms under  $G_\chi$  as  $M \rightarrow LMR^\dagger$ , where  $\Psi_L \rightarrow L\Psi_L$  and  $\Psi_R \rightarrow R\Psi_R$  are the  $SU(3)_L$  and  $SU(3)_R$  transformations, and writes down the most general Lagrangian invariant under  $G_\chi$ . Then one sets  $M$  to its given constant value Eq. (7), which implements the symmetry breaking. To first order in  $M$  one finds that [9]

$$\begin{aligned} m_{\pi^0}^2 &= B(m_u + m_d), \\ m_{\pi^\pm}^2 &= B(m_u + m_d) + \Delta_{\text{em}}, \\ m_{K^0}^2 &= m_{\overline{K}^0}^2 = B(m_d + m_s), \\ m_{K^\pm}^2 &= B(m_u + m_s) + \Delta_{\text{em}}, \\ m_\eta^2 &= \frac{1}{3}B(m_u + m_d + 4m_s), \end{aligned} \quad (8)$$

with two unknown constants  $B$  and  $\Delta_{\text{em}}$ , the electromagnetic mass difference. From Eq. (8), one can determine the quark mass ratios [9]

$$\begin{aligned} \frac{m_u}{m_d} &= \frac{2m_{\pi^0}^2 - m_{\pi^\pm}^2 + m_{K^+}^2 - m_{K^0}^2}{m_{K^0}^2 - m_{K^+}^2 + m_{\pi^+}^2} = 0.56, \\ \frac{m_s}{m_d} &= \frac{m_{K^0}^2 + m_{K^+}^2 - m_{\pi^+}^2}{m_{K^0}^2 + m_{\pi^+}^2 - m_{K^+}^2} = 20.2, \end{aligned} \quad (9)$$

to lowest order in chiral perturbation theory, with an error which will be estimated below. Since the mass ratios extracted using chiral perturbation theory use the symmetry transformation property of  $M$  under the chiral symmetry  $G_\chi$ , it is important to use a renormalization scheme for QCD that does not change this transformation law. Any mass independent subtraction scheme such as  $\overline{\text{MS}}$  is suitable. The ratios of quark masses are scale independent in such a scheme, and Eq. (9) can be taken to be the ratio of  $\overline{\text{MS}}$  masses. Chiral perturbation theory cannot determine the overall scale of the quark masses, since it uses only the symmetry properties of  $M$ , and any multiple of  $M$  has the same  $G_\chi$  transformation law as  $M$ .

Chiral perturbation theory is a systematic expansion in powers of the light quark masses. The typical expansion parameter is  $m_K^2/\Lambda_\chi^2 \sim 0.25$  if one uses  $SU(3)$  chiral symmetry, and  $m_\pi^2/\Lambda_\chi^2 \sim 0.02$  if instead one uses  $SU(2)$  chiral symmetry. Electromagnetic effects at the few percent level also break  $SU(2)$  and  $SU(3)$  symmetry. The mass formulæ Eq. (8) were derived using  $SU(3)$  chiral symmetry, and are expected to have approximately a 25% uncertainty due to second order corrections. This estimate of the uncertainty is consistent with the lattice results found in Eq. (3) and Eq. (4).

There is a subtlety which arises when one tries to determine quark mass ratios at second order in chiral perturbation theory. The second order quark mass term [10]

$$\left(M^\dagger\right)^{-1} \det M^\dagger \quad (10)$$

(which can be generated by instantons) transforms in the same way under  $G_\chi$  as  $M$ . Chiral perturbation theory cannot distinguish between  $M$  and  $\left(M^\dagger\right)^{-1} \det M^\dagger$ ; one can make the replacement  $M \rightarrow M(\lambda) = M + \lambda M \left(M^\dagger M\right)^{-1} \det M^\dagger$  in the chiral Lagrangian,

$$\begin{aligned} M(\lambda) &= \text{diag}(m_u(\lambda), m_d(\lambda), m_s(\lambda)) \\ &= \text{diag}(m_u + \lambda m_d m_s, m_d + \lambda m_u m_s, m_s + \lambda m_u m_d), \end{aligned} \quad (11)$$

and leave all observables unchanged.

The combination

$$\left(\frac{m_u}{m_d}\right)^2 + \frac{1}{Q^2} \left(\frac{m_s}{m_d}\right)^2 = 1 \quad (12)$$

where

$$Q^2 = \frac{m_s^2 - \hat{m}^2}{m_d^2 - m_u^2}, \quad \hat{m} = \frac{1}{2}(m_u + m_d),$$

# Quark Particle Listings

## Quarks

is insensitive to the transformation in Eq. (11). Eq. (12) gives an ellipse in the  $m_u/m_d - m_s/m_d$  plane. The ellipse is well-determined by chiral perturbation theory, but the exact location on the ellipse, and the absolute normalization of the quark masses, has larger uncertainties.  $Q$  is determined to be in the range 21–25 from  $\eta \rightarrow 3\pi$  decay and the electromagnetic contribution to the  $K^+ - K^0$  and  $\pi^+ - \pi^0$  mass differences [11].

The absolute normalization of the quark masses cannot be determined using chiral perturbation theory. Other methods, such as lattice simulations discussed above or spectral function sum rules [12,13] for hadronic correlation functions, which we review next are necessary.

**Sum Rules:** Sum rule methods have been used extensively to determine quark masses and for illustration we briefly discuss here their application to hadronic  $\tau$  decays [14]. Other applications involve very similar techniques.

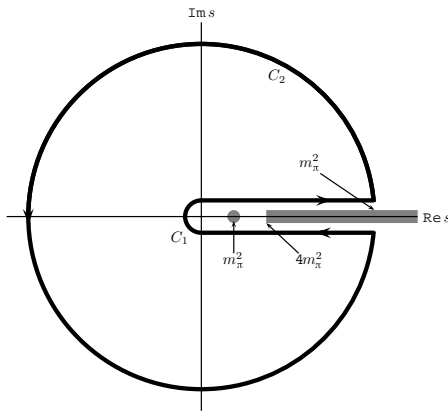


**Figure 1:** The analytic structure of  $\Pi(s)$  in the complex  $s$ -plane. The contours  $C_1$  and  $C_2$  are the integration contours discussed in the text.

The experimentally measured quantity is  $R_\tau$ ,

$$\frac{dR_\tau}{ds} = \frac{d\Gamma/ds(\tau^- \rightarrow \text{hadrons} + \nu_\tau(\gamma))}{\Gamma(\tau^- \rightarrow e^- \bar{\nu}_e \nu_\tau(\gamma))} \quad (13)$$

the hadronic invariant mass spectrum in semihadronic  $\tau$  decay, normalized to the leptonic  $\tau$  decay rate. It is useful to define  $q$  as the total momentum of the hadronic final state, so  $s = q^2$  is the hadronic invariant mass. The total hadronic  $\tau$  decay rate  $R_\tau$  is then given by integrating  $dR_\tau/ds$  over the kinematically allowed range  $0 \leq s \leq M_\tau^2$ .

$R_\tau$  can be written as

$$R_\tau = 12\pi \int_0^{M_\tau^2} \frac{ds}{M_\tau^2} \left(1 - \frac{s}{M_\tau^2}\right)^2 \times \left[ \left(1 + 2\frac{s}{M_\tau^2}\right) \text{Im} \Pi^T(s) + \text{Im} \Pi^L(s) \right] \quad (14)$$

where  $s = q^2$ , and the hadronic spectral functions  $\Pi^{L,T}$  are defined from the time-ordered correlation function of two weak

currents is the time-ordered correlator of the weak interaction current ( $j^\mu(x)$  and  $j^\nu(0)$ ) by

$$\Pi^{\mu\nu}(q) = i \int d^4x e^{iq \cdot x} \langle 0 | T \left( j^\mu(x) j^\nu(0)^\dagger \right) | 0 \rangle, \quad (15)$$

$$\Pi^{\mu\nu}(q) = (-g^{\mu\nu} + q^\mu q^\nu) \Pi^T(s) + q^\mu q^\nu \Pi^L(s), \quad (16)$$

and the decomposition Eq. (16) is the most general possible structure consistent with Lorentz invariance.

By the optical theorem, the imaginary part of  $\Pi^{\mu\nu}$  is proportional to the total cross-section for the current to produce all possible states. A detailed analysis including the phase space factors leads to Eq. (14). The spectral functions  $\Pi^{L,T}(s)$  are analytic in the complex  $s$  plane, with singularities along the real axis. There is an isolated pole at  $s = m_\pi^2$ , and single- and multi-particle singularities for  $s \geq 4m_\pi^2$ , the two-particle threshold. The discontinuity along the real axis is  $\Pi^{L,T}(s + i0^+) - \Pi^{L,T}(s - i0^+) = 2i \text{Im} \Pi^{L,T}(s)$ . As a result, Eq. (14) can be rewritten with the replacement  $\text{Im} \Pi^{L,T}(s) \rightarrow -i\Pi^{L,T}(s)/2$ , and the integration being over the contour  $C_1$ . Finally, the contour  $C_1$  can be deformed to  $C_2$  without crossing any singularities, and so leaving the integral unchanged. One can derive a series of sum rules analogous to Eq. (14) by weighting the differential  $\tau$  hadronic decay rate by different powers of the hadronic invariant mass,

$$R_\tau^{kl} = \int_0^{M_\tau^2} ds \left(1 - \frac{s}{M_\tau^2}\right)^k \left(\frac{s}{M_\tau^2}\right)^l \frac{dR_\tau}{ds} \quad (17)$$

where  $dR_\tau/ds$  is the hadronic invariant mass distribution in  $\tau$  decay normalized to the leptonic decay rate. This leads to the final form of the sum rule(s),

$$R_\tau^{kl} = -6\pi i \int_{C_2} \frac{ds}{M_\tau^2} \left(1 - \frac{s}{M_\tau^2}\right)^{2+k} \left(\frac{s}{M_\tau^2}\right)^l \times \left[ \left(1 + 2\frac{s}{M_\tau^2}\right) \Pi^T(s) + \Pi^L(s) \right]. \quad (18)$$

The manipulations so far are completely rigorous and exact, relying only on the general analytic structure of quantum field theory. The left-hand side of the sum rule Eq. (18) is obtained from experiment. The right hand-side can be computed for  $s$  far away from any physical cuts using the operator product expansion (OPE) for the time-ordered product of currents in Eq. (15), and QCD perturbation theory. The OPE is an expansion for the time-ordered product Eq. (15) in a series of local operators, and is an expansion about the  $q \rightarrow \infty$  limit. It gives  $\Pi(s)$  as an expansion in powers of  $\alpha_s(s)$  and  $\Lambda_{\text{QCD}}^2/s$ , and is valid when  $s$  is far (in units of  $\Lambda_{\text{QCD}}^2$ ) from any singularities in the complex  $s$ -plane.

The OPE gives  $\Pi(s)$  as a series in  $\alpha_s$ , quark masses, and various non-perturbative vacuum matrix element. By computing  $\Pi(s)$  theoretically, and comparing with the experimental values of  $R_\tau^{kl}$ , one determines various parameters such as  $\alpha_s$  and the quark masses. The theoretical uncertainties in using Eq. (18) arise from neglected higher order corrections (both



perturbative and non-perturbative), and because the OPE is no longer valid near the real axis, where  $\Pi$  has singularities. The contribution of neglected higher order corrections can be estimated as for any other perturbative computation. The error due to the failure of the OPE is more difficult to estimate. In Eq. (18), the OPE fails on the endpoints of  $C_2$  that touch the real axis at  $s = M_\tau^2$ . The weight factor  $(1 - s/M_\tau^2)$  in Eq. (18) vanishes at this point, so the importance of the endpoint can be reduced by choosing larger values of  $k$ .

### E. Heavy quarks

For heavy-quark physics one can exploit the fact that  $m_Q \gg \Lambda_{\text{QCD}}$  to construct effective theories ( $m_Q$  is the mass of the heavy quark  $Q$ ). The masses and decay rates of hadrons containing a single heavy quark, such as the  $B$  and  $D$  mesons can be determined using the heavy quark effective theory (HQET) [33]. The theoretical calculations involve radiative corrections computed in perturbation theory with an expansion in  $\alpha_s(m_Q)$  and non-perturbative corrections with an expansion in powers of  $\Lambda_{\text{QCD}}/m_Q$ . Due to the asymptotic nature of the QCD perturbation series, the two kinds of corrections are intimately related; an example of this are renormalon effects in the perturbative expansion which are associated with non-perturbative corrections.

Systems containing two heavy quarks such as the  $\Upsilon$  or  $J/\Psi$  are treated using non-relativistic QCD (NRQCD) [34]. The typical momentum and energy transfers in these systems are  $\alpha_s m_Q$ , and  $\alpha_s^2 m_Q$ , respectively, so these bound states are sensitive to scales much smaller than  $m_Q$ . However, smeared observables, such as the cross-section for  $e^+e^- \rightarrow \bar{b}b$  averaged over some range of  $s$  that includes several bound state energy levels, are better behaved and only sensitive to scales near  $m_Q$ . For this reason, most determinations of the  $c, b$  quark masses using perturbative calculations compare smeared observables with experiment [35–37].

There are many continuum extractions of the  $c$  and  $b$  quark masses, some with quoted errors of 10 MeV or smaller. There are systematic effects of comparable size, which are typically not included in these error estimates. Reference [30], for example, shows that even though the error estimate of  $m_c$  using the rapid convergence of the  $\alpha_s$  perturbation series is only a few MeV, the central value of  $m_c$  can differ by a much larger amount depending on which algorithm (all of which are formally equally good) is used to determine  $m_c$  from the data. This leads to a systematic error from perturbation theory of around 20 MeV for the  $c$  quark and 25 MeV for the  $b$  quark. Electromagnetic effects, which also are important at this precision, are often not included. For this reason, we inflate the errors on the continuum extractions of  $m_c$  and  $m_b$ . The average values of  $m_c$  and  $m_b$  from continuum determinations are (see Sec. G for the 1S scheme)

$$\overline{m}_c(\overline{m}_c) = (1.275 \pm 0.025) \text{ GeV}$$

$$\overline{m}_b(\overline{m}_b) = (4.18 \pm 0.03) \text{ GeV}, \quad m_b^{1S} = (4.65 \pm 0.03) \text{ GeV}.$$

Lattice simulations of QCD lead to discretization errors which are powers of  $m_Q a$  (modulated by logarithms); the power depends on the formulation of lattice QCD being used and in most cases is quadratic. Clearly these errors can be reduced by performing simulations at smaller lattice spacings, but also by using *improved* discretizations of the theory. Recently, with more powerful computing resources, better algorithms and techniques, it has become possible to perform simulations in the charm quark region and beyond, also decreasing the extrapolation which has to be performed to reach the  $b$ -quark. A novel approach proposed in [52] has been to compare the lattice results for moments of correlation functions of  $c\bar{c}$  quark-bilinear operators to perturbative calculations of the same quantities at 4-loop order. In this way both the strong coupling constant and the charm quark mass can be determined with remarkably small errors; in particular  $\overline{m}_c(\overline{m}_c) = 1.273(6) \text{ GeV}$  [26]. This lattice determination also uses the perturbative expression for the current-current correlator, and so has the perturbation theory systematic error discussed above.

Traditionally, the main approach to controlling the discretization errors in lattice studies of heavy quark physics is to perform simulations of the effective theories such as HQET and NRQCD. This remains an important technique, both in its own right and in providing additional information for extrapolations from lower masses to the bottom region. Using effective theories,  $m_b$  is obtained from what is essentially a computation of the difference of  $M_{H_b} - m_b$ , where  $M_{H_b}$  is the mass of a hadron  $H_b$  containing a  $b$ -quark. The relative error on  $m_b$  is therefore much smaller than that for  $M_{H_b} - m_b$ , and this is the reason for the small errors quoted in section G. The principal systematic errors are the matching of the effective theories to QCD and the presence of power divergences in  $a^{-1}$  in the  $1/m_b$  corrections which have to be subtracted numerically. The use of HQET or NRQCD is less precise for the charm quark, but in this case, as mentioned above, direct QCD simulations have recently become possible.

### F. Pole Mass

For an observable particle such as the electron, the position of the pole in the propagator is the definition of its mass. In QCD this definition of the quark mass is known as the pole mass. It is known that the on-shell quark propagator has no infrared divergences in perturbation theory [40,41], so this provides a perturbative definition of the quark mass. The pole mass cannot be used to arbitrarily high accuracy because of nonperturbative infrared effects in QCD. The full quark propagator has no pole because the quarks are confined, so that the pole mass cannot be defined outside of perturbation theory. The relation between the pole mass  $m_Q$  and the  $\overline{\text{MS}}$  mass  $\overline{m}_Q$  is known to three loops [42,43,44,45]

$$m_Q = \overline{m}_Q(\overline{m}_Q) \left\{ 1 + \frac{4\overline{\alpha}_s(\overline{m}_Q)}{3\pi} + \left[ -1.0414 \sum_k \left( 1 - \frac{4\overline{m}_{Qk}}{3\overline{m}_Q} \right) + 13.4434 \right] \left[ \frac{\overline{\alpha}_s(\overline{m}_Q)}{\pi} \right]^2 \right.$$

# Quark Particle Listings

## Quarks

$$+ [0.6527N_L^2 - 26.655N_L + 190.595] \left[ \frac{\bar{\alpha}_s(\bar{m}_Q)}{\pi} \right]^3 \}, \quad (19)$$

where  $\bar{\alpha}_s(\mu)$  is the strong interaction coupling constants in the  $\overline{\text{MS}}$  scheme, and the sum over  $k$  extends over the  $N_L$  flavors  $Q_k$  lighter than  $Q$ . The complete mass dependence of the  $\alpha_s^2$  term can be found in [42]; the mass dependence of the  $\alpha_s^3$  term is not known. For the  $b$ -quark, Eq. (19) reads

$$m_b = \bar{m}_b(\bar{m}_b) [1 + 0.09 + 0.05 + 0.03], \quad (20)$$

where the contributions from the different orders in  $\alpha_s$  are shown explicitly. The two and three loop corrections are comparable in size and have the same sign as the one loop term. This is a signal of the asymptotic nature of the perturbation series [there is a renormalon in the pole mass]. Such a badly behaved perturbation expansion can be avoided by directly extracting the  $\overline{\text{MS}}$  mass from data without extracting the pole mass as an intermediate step.

### G. Numerical values and caveats

The quark masses in the particle data listings have been obtained by using a wide variety of methods. Each method involves its own set of approximations and uncertainties. In most cases, the errors are an estimate of the size of neglected higher-order corrections or other uncertainties. The expansion parameters for some of the approximations are not very small (for example, they are  $m_K^2/\Lambda_\chi^2 \sim 0.25$  for the chiral expansion and  $\Lambda_{\text{QCD}}/m_b \sim 0.1$  for the heavy-quark expansion), so an unexpectedly large coefficient in a neglected higher-order term could significantly alter the results. It is also important to note that the quark mass values can be significantly different in the different schemes.

The heavy quark masses obtained using HQET, QCD sum rules, or lattice gauge theory are consistent with each other if they are all converted into the same scheme and scale. We have specified all masses in the  $\overline{\text{MS}}$  scheme. For light quarks, the renormalization scale has been chosen to be  $\mu = 2 \text{ GeV}$ . The light quark masses at 1 GeV are significantly different from those at 2 GeV,  $\bar{m}(1 \text{ GeV})/\bar{m}(2 \text{ GeV}) \sim 1.35$ . It is conventional to choose the renormalization scale equal to the quark mass for a heavy quark, so we have quoted  $\bar{m}_Q(\mu)$  at  $\mu = \bar{m}_Q$  for the  $c$  and  $b$  quarks. Recent analyses of inclusive  $B$  meson decays have shown that recently proposed mass definitions lead to a better behaved perturbation series than for the  $\overline{\text{MS}}$  mass, and hence to more accurate mass values. We have chosen to also give values for one of these, the  $b$  quark mass in the 1S-scheme [46,47]. Other schemes that have been proposed are the PS-scheme [48] and the kinetic scheme [49].

If necessary, we have converted values in the original papers to our chosen scheme using two-loop formulæ. It is important to realized that our conversions introduce significant additional errors. In converting to the  $\overline{\text{MS}}$   $b$ -quark mass, for example, the three-loop conversions from the 1S and pole masses give values about 40 MeV and 135 MeV lower than the two-loop

conversions. The uncertainty in  $\alpha_s(M_Z) = 0.1187(20)$  gives an uncertainty of  $\pm 20 \text{ MeV}$  and  $\pm 35 \text{ MeV}$  respectively in the same conversions. We have not added these additional errors when we do our conversions. The  $\alpha_s$  value in the conversion is correlated with the  $\alpha_s$  value used in determining the quark mass, so the conversion error is not a simple additional error on the quark mass.

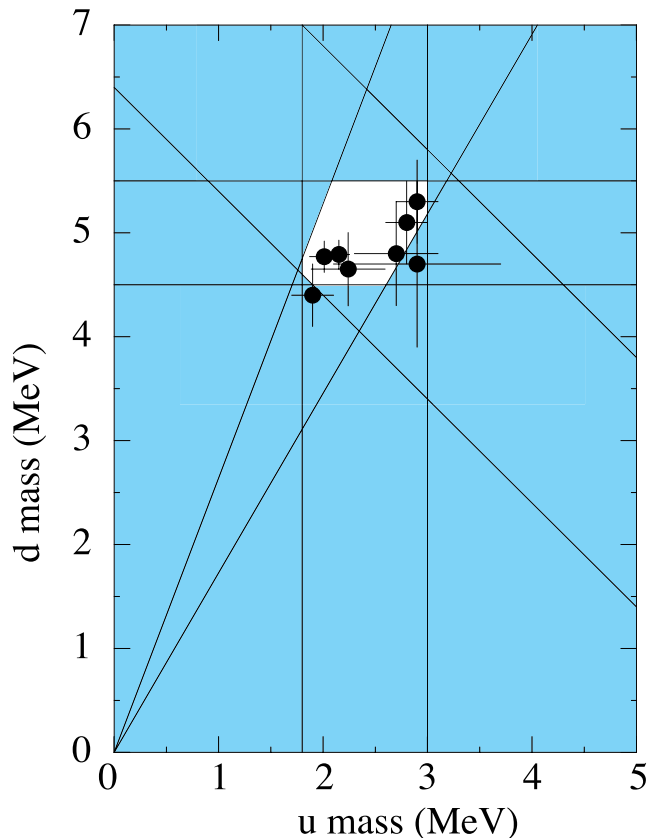


**Figure 2:** The allowed region (shown in white) for up quark and down quark masses. This region was determined in part from papers reporting values for  $m_u$  and  $m_d$  (data points shown) and in part from analysis of the allowed ranges of other mass parameters (see Fig. 3). The parameter  $(m_u + m_d)/2$  yields the two downward-sloping lines, while  $m_u/m_d$  yields the two rising lines originating at  $(0,0)$ .

See key on page 457

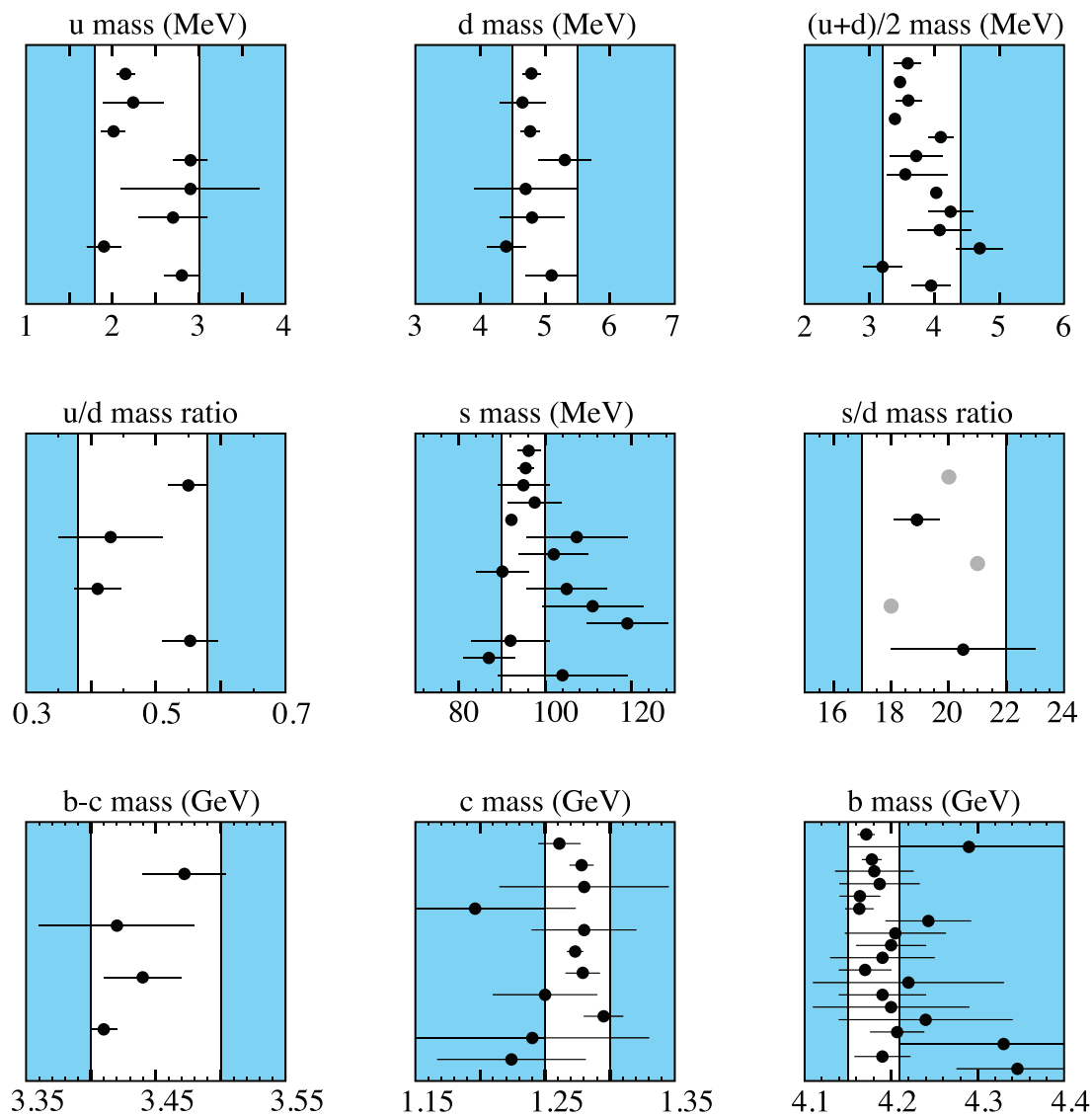


**Figure 3.** The values of each quark mass parameter taken from the Data Listings. The points are in chronological order with the more recent measurements at the top. Points from papers reporting no error bars are colored grey. The shaded regions indicate values excluded by our evaluations; some regions were determined in part through examination of Fig. 2.

# Quark Particle Listings

## Quarks, $u$ , $d$ , $s$ , Light Quarks ( $u$ , $d$ , $s$ )

### References

1. See the review of QCD in this volume..
2. A.V. Manohar and H. Georgi, Nucl. Phys. **B234**, 189 (1984).
3. K.G. Chetyrkin, Phys. Lett. **B404**, 161 (1997).
4. J.A.M. Vermaseren, S.A. Larin, and T. van Ritbergen, Phys. Lett. **B405**, 327 (1997).
5. K.G. Chetyrkin, B.A. Kniehl, and M. Steinhauser, Nucl. Phys. **B510**, 61 (1998).
6. S. Weinberg, Physica **96A**, 327 (1979).
7. J. Gasser and H. Leutwyler, Ann. Phys. **158**, 142 (184).
8. For a review, see A. Pich, Rept. Prog. Phys. **58**, 563 (1995).
9. S. Weinberg, Trans. N.Y. Acad. Sci. **38**, 185 (1977).
10. D.B. Kaplan and A.V. Manohar, Phys. Rev. Lett. **56**, 2004 (1986).
11. H. Leutwyler, Phys. Lett. **B374**, 163 (1996).
12. S. Weinberg, Phys. Rev. Lett. **18**, 507 (1967)..
13. M.A. Shifman, A.I. Vainshtein, and V.I. Zakharov, Nucl. Phys. **B147**, 385 (1979).
14. E. Braaten, S. Narison, and A. Pich, Nucl. Phys. **B373**, 581 (1992).
15. C. Bernard *et al.*, PoS **LAT2007** (2007) 090.
16. A. Bazavov *et al.*, arXiv:0903.3598 [hep-lat].
17. C. Aubin *et al.* [HPQCD Collab.], Phys. Rev. **D70**, 031504 (2004).
18. C. Aubin *et al.* [MILC Collab.], Phys. Rev. D **70** (2004) 114501.
19. B. Blossier *et al.* [ETM Collab.], Phys. Rev. **D82** (2010) 114513.
20. A. Bazavov *et al.* [MILC Collab.], PoS **CD09** (2009) 007.
21. A. Bazavov *et al.*, PoS **LATTICE2010** (2010) 083.
22. S. Durr *et al.*, Phys. Lett. **B701** (2011) 265-268.
23. S. Durr *et al.*, JHEP **1108** (2011) 148.
24. Y. Aoki *et al.* [RBC and UKQCD Collabs.], Phys. Rev. **D83** (2011) 074508.
25. C.T.H. Davies *et al.*, Phys. Rev. Lett. **104** (2010) 132003.
26. C. McNeile *et al.*, Phys. Rev. **D82** (2010) 034512.
27. C. Aubin *et al.* [MILC Collab.], Nucl. Phys. Proc. Suppl. **140** (2005) 231.
28. C. Aubin *et al.* [MILC Collab.], Phys. Rev. D **70** (2004) 114501.
29. G. Colangelo *et al.*, Eur. Phys. J. C **71** (2011) 1695.
30. B. Dehnadi *et al.*, arXiv:1102.2264 [hep-ph].
31. T. Blum *et al.*, Phys. Rev. D **76** (2007) 114508.
32. G. Colangelo *et al.*, Eur. Phys. J. C **71** (2011) 1695; A. Ali Khan *et al.* [CP-PACS Collab.], Phys. Rev. D **65** (2002) 054505; [Erratum-ibid. D **67** (2003) 059901].
33. N. Isgur and M.B. Wise, Phys. Lett. **B232**, 113 (1989), *ibid.* **B237**, 527 (1990).
34. G.T. Bodwin, E. Braaten, and G.P. Lepage, Phys. Rev. **D51**, 1125 (1995).
35. A.H. Hoang, Phys. Rev. **D61**, 034005 (2000).
36. K. Melnikov and A. Yelkhovsky, Phys. Rev. **D59**, 114009 (1999).
37. M. Beneke and A. Signer, Phys. Lett. **B471**, 233 (1999).
38. A.X. El-Khadra, A.S. Kronfeld, and P.B. Mackenzie, Phys. Rev. **D55**, 3933 (1997).
39. S. Aoki, Y. Kuramashi, and S.i. Tominaga, Prog. Theor. Phys. **109**, 383 (2003).
40. R. Tarrach, Nucl. Phys. **B183**, 384 (1981).
41. A. Kronfeld, Phys. Rev. **D58**, 051501 (1998).
42. N. Gray *et al.*, Z. Phys. **C48**, 673 (1990).
43. D.J. Broadhurst, N. Gray, and K. Schilcher, Z. Phys. **C52**, 111 (1991).
44. K.G. Chetyrkin and M. Steinhauser, Phys. Rev. Lett. **83**, 4001 (1999).
45. K. Melnikov and T. van Ritbergen, Phys. Lett. **B482**, 99 (2000).
46. A.H. Hoang, Z. Ligeti, A.V. Manohar, Phys. Rev. Lett. **82**, 277 (1999).
47. A.H. Hoang, Z. Ligeti, A.V. Manohar, Phys. Rev. **D59**, 074017 (1999).
48. M. Beneke, Phys. Lett. **B434**, 115 (1998).
49. P. Gambino and N. Uraltsev, Eur. Phys. J. **C34**, 181 (2004).
50. G. Martinelli *et al.*, Nucl. Phys. B **445** (1995) 81.
51. K. Jansen *et al.*, Phys. Lett. B **372** (1996) 275.
52. I. Allison *et al.* [HPQCD Collab.], Phys. Rev. D **78** (2008) 054513.

**u**

$$I(J^P) = \frac{1}{2}(\frac{1}{2}^+)$$

$$\text{Mass } m = 2.3_{-0.5}^{+0.7} \text{ MeV} \quad \text{Charge} = \frac{2}{3} e \quad I_z = +\frac{1}{2}$$

$$m_u/m_d = 0.38\text{--}0.58$$

**d**

$$I(J^P) = \frac{1}{2}(\frac{1}{2}^+)$$

$$\text{Mass } m = 4.8_{-0.3}^{+0.7} \text{ MeV} \quad \text{Charge} = -\frac{1}{3} e \quad I_z = -\frac{1}{2}$$

$$m_s/m_d = 17\text{--}22$$

$$\bar{m} = (m_u + m_d)/2 = 3.2\text{--}4.4 \text{ MeV}$$

**s**

$$I(J^P) = 0(\frac{1}{2}^+)$$

$$\text{Mass } m = 95 \pm 5 \text{ MeV} \quad \text{Charge} = -\frac{1}{3} e \quad \text{Strangeness} = -1$$

$$(m_s - (m_u + m_d)/2)/(m_d - m_u) = 27 \pm 1$$

## LIGHT QUARKS ( $u$ , $d$ , $s$ )

OMITTED FROM SUMMARY TABLE

### u-QUARK MASS

The  $u$ -,  $d$ -, and  $s$ -quark masses are estimates of so-called "current-quark masses," in a mass-independent subtraction scheme such as  $\overline{\text{MS}}$ . The ratios  $m_u/m_d$  and  $m_s/m_d$  are extracted from pion and kaon masses using chiral symmetry. The estimates of  $d$  and  $u$  masses are not without controversy and remain under active investigation. Within the literature there are even suggestions that the  $u$  quark could be essentially massless. The  $s$ -quark mass is estimated from SU(3) splittings in hadron masses.

We have normalized the  $\overline{\text{MS}}$  masses at a renormalization scale of  $\mu = 2$  GeV. Results quoted in the literature at  $\mu = 1$  GeV have been rescaled by dividing by 1.35. The values of "Our Evaluation" were determined in part via Figures 1 and 2.

VALUE (MeV)	DOCUMENT ID	TECN	COMMENT
<b>2.3 <math>\pm</math> 0.7 <math>\pm</math> 0.5 OUR EVALUATION</b>	See the ideogram below.		
2.15 $\pm$ 0.03 $\pm$ 0.10	<sup>1</sup> DURR	11	LATT $\overline{\text{MS}}$ scheme
2.24 $\pm$ 0.10 $\pm$ 0.34	<sup>2</sup> BLUM	10	LATT $\overline{\text{MS}}$ scheme
2.01 $\pm$ 0.14	<sup>3</sup> MCNEILE	10	LATT $\overline{\text{MS}}$ scheme
2.9 $\pm$ 0.2	<sup>4</sup> DOMINGUEZ	09	THEO $\overline{\text{MS}}$ scheme
2.9 $\pm$ 0.8	<sup>5</sup> DEANDREA	08	THEO $\overline{\text{MS}}$ scheme
2.7 $\pm$ 0.4	<sup>6</sup> JAMIN	06	THEO $\overline{\text{MS}}$ scheme
1.9 $\pm$ 0.2	<sup>7</sup> MASON	06	LATT $\overline{\text{MS}}$ scheme
2.8 $\pm$ 0.2	<sup>8</sup> NARISON	06	THEO $\overline{\text{MS}}$ scheme

# Quark Particle Listings

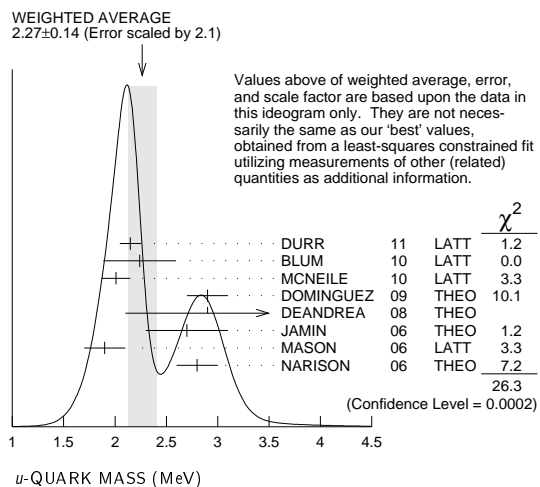
## Light Quarks (*u, d, s*)

See key on page 457

••• We do not use the following data for averages, fits, limits, etc. •••

2.01 ± 0.14	<sup>3</sup> DAVIES	10	LATT	$\overline{MS}$ scheme
3.02 ± 0.33	<sup>9</sup> BLUM	07	LATT	$\overline{MS}$ scheme
1.7 ± 0.3	<sup>10</sup> AUBIN	04A	LATT	$\overline{MS}$ scheme

- <sup>1</sup> DURR 11 determine quark mass from a lattice computation of the meson spectrum using  $N_f = 2 + 1$  dynamical flavors. The lattice simulations were done at the physical quark mass, so that extrapolation in the quark mass was not needed. The individual  $m_u, m_d$  values are obtained using the lattice determination of the average mass  $m_{ud}$ , and isospin violation in  $\eta \rightarrow 3\pi$ .
- <sup>2</sup> BLUM 10 determines light quark masses using a QCD plus QED lattice computation of the electromagnetic mass splittings of the low-lying hadrons. The lattice simulations use 2+1 dynamical quark flavors.
- <sup>3</sup> DAVIES 10 and MCNEILE 10 determine  $\overline{m}_c(\mu)/\overline{m}_s(\mu) = 11.85 \pm 0.16$  using a lattice computation with  $N_f = 2 + 1$  dynamical fermions of the pseudoscalar meson masses. Mass  $m_u$  is obtained from this using the value of  $m_c$  from ALLISON 08 or MCNEILE 10 and the BAZAVOV 10 values for the light quark mass ratios,  $m_s/\overline{m}$  and  $m_u/m_d$ .
- <sup>4</sup> DOMINGUEZ 09 use QCD finite energy sum rules for the two-point function of the divergence of the axial vector current computed to order  $\alpha_s^4$ .
- <sup>5</sup> DEANDREA 08 determine  $m_u - m_d$  from  $\eta \rightarrow 3\pi^0$ , and combine with the PDG 06 lattice average value of  $m_u + m_d = 7.6 \pm 1.6$  to determine  $m_u$  and  $m_d$ .
- <sup>6</sup> JAMIN 06 determine  $m_u(2 \text{ GeV})$  by combining the value of  $m_s$  obtained from the spectral function for the scalar  $K\pi$  form factor with other determinations of the quark mass ratios.
- <sup>7</sup> MASON 06 extract light quark masses from a lattice simulation using staggered fermions with an improved action, and three dynamical light quark flavors with degenerate  $u$  and  $d$  quarks. Perturbative corrections were included at NNLO order. The quark masses  $m_u$  and  $m_d$  were determined from their  $(m_u + m_d)/2$  measurement and AUBIN 04A  $m_u/m_d$  value.
- <sup>8</sup> NARISON 06 uses sum rules for  $e^+e^- \rightarrow \text{hadrons}$  to order  $\alpha_s^3$  to determine  $m_s$  combined with other determinations of the quark mass ratios.
- <sup>9</sup> BLUM 07 determine quark masses from the pseudoscalar meson masses using a QED plus QCD lattice computation with two dynamical quark flavors.
- <sup>10</sup> AUBIN 04A employ a partially quenched lattice calculation of the pseudoscalar meson masses.



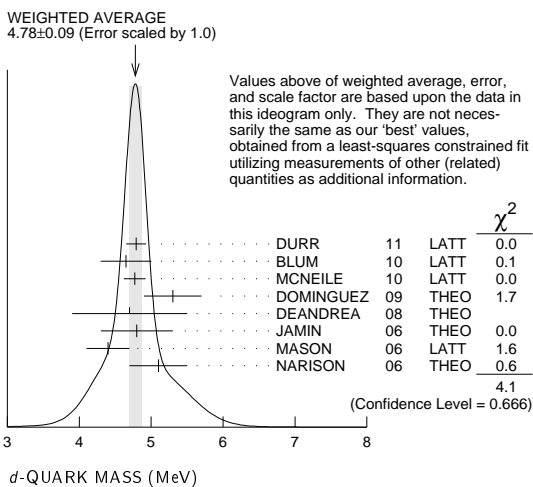
### d-QUARK MASS

See the comment for the *u* quark above.

We have normalized the  $\overline{MS}$  masses at a renormalization scale of  $\mu = 2$  GeV. Results quoted in the literature at  $\mu = 1$  GeV have been rescaled by dividing by 1.35. The values of "Our Evaluation" were determined in part via Figures 1 and 2.

VALUE (MeV)	DOCUMENT ID	TECN	COMMENT
<b>4.8 ± 0.7</b>	<b>OUR EVALUATION</b>		See the ideogram below.
4.79 ± 0.07 ± 0.12	<sup>11</sup> DURR	11	LATT $\overline{MS}$ scheme
4.65 ± 0.15 ± 0.32	<sup>12</sup> BLUM	10	LATT $\overline{MS}$ scheme
4.77 ± 0.15	<sup>13</sup> MCNEILE	10	LATT $\overline{MS}$ scheme
5.3 ± 0.4	<sup>14</sup> DOMINGUEZ	09	THEO $\overline{MS}$ scheme
4.7 ± 0.8	<sup>15</sup> DEANDREA	08	THEO $\overline{MS}$ scheme
4.8 ± 0.5	<sup>16</sup> JAMIN	06	THEO $\overline{MS}$ scheme
4.4 ± 0.3	<sup>17</sup> MASON	06	LATT $\overline{MS}$ scheme
5.1 ± 0.4	<sup>18</sup> NARISON	06	THEO $\overline{MS}$ scheme
••• We do not use the following data for averages, fits, limits, etc. •••			
4.79 ± 0.16	<sup>13</sup> DAVIES	10	LATT $\overline{MS}$ scheme
5.49 ± 0.39	<sup>19</sup> BLUM	07	LATT $\overline{MS}$ scheme
3.9 ± 0.5	<sup>20</sup> AUBIN	04A	LATT $\overline{MS}$ scheme

- <sup>11</sup> DURR 11 determine quark mass from a lattice computation of the meson spectrum using  $N_f = 2 + 1$  dynamical flavors. The lattice simulations were done at the physical quark mass, so that extrapolation in the quark mass was not needed. The individual  $m_u, m_d$  values are obtained using the lattice determination of the average mass  $m_{ud}$ , and isospin violation in  $\eta \rightarrow 3\pi$ .
- <sup>12</sup> BLUM 10 determines light quark masses using a QCD plus QED lattice computation of the electromagnetic mass splittings of the low-lying hadrons. The lattice simulations use 2+1 dynamical quark flavors.
- <sup>13</sup> DAVIES 10 and MCNEILE 10 determine  $\overline{m}_c(\mu)/\overline{m}_s(\mu) = 11.85 \pm 0.16$  using a lattice computation with  $N_f = 2 + 1$  dynamical fermions of the pseudoscalar meson masses. Mass  $m_d$  is obtained from this using the value of  $m_c$  from ALLISON 08 or MCNEILE 10 and the BAZAVOV 10 values for the light quark mass ratios,  $m_s/\overline{m}$  and  $m_u/m_d$ .
- <sup>14</sup> DOMINGUEZ 09 use QCD finite energy sum rules for the two-point function of the divergence of the axial vector current computed to order  $\alpha_s^4$ .
- <sup>15</sup> DEANDREA 08 determine  $m_u - m_d$  from  $\eta \rightarrow 3\pi^0$ , and combine with the PDG 06 lattice average value of  $m_u + m_d = 7.6 \pm 1.6$  to determine  $m_u$  and  $m_d$ .
- <sup>16</sup> JAMIN 06 determine  $m_d(2 \text{ GeV})$  by combining the value of  $m_s$  obtained from the spectral function for the scalar  $K\pi$  form factor with other determinations of the quark mass ratios.
- <sup>17</sup> MASON 06 extract light quark masses from a lattice simulation using staggered fermions with an improved action, and three dynamical light quark flavors with degenerate  $u$  and  $d$  quarks. Perturbative corrections were included at NNLO order. The quark masses  $m_u$  and  $m_d$  were determined from their  $(m_u + m_d)/2$  measurement and AUBIN 04A  $m_u/m_d$  value.
- <sup>18</sup> NARISON 06 uses sum rules for  $e^+e^- \rightarrow \text{hadrons}$  to order  $\alpha_s^3$  to determine  $m_s$  combined with other determinations of the quark mass ratios.
- <sup>19</sup> BLUM 07 determine quark masses from the pseudoscalar meson masses using a QED plus QCD lattice computation with two dynamical quark flavors.
- <sup>20</sup> AUBIN 04A perform three flavor dynamical lattice calculation of pseudoscalar meson masses, with continuum estimate of electromagnetic effects in the kaon masses, and one-loop perturbative renormalization constant.



$$\overline{m} = (m_u + m_d)/2$$

See the comments for the *u* quark above.

We have normalized the  $\overline{MS}$  masses at a renormalization scale of  $\mu = 2$  GeV. Results quoted in the literature at  $\mu = 1$  GeV have been rescaled by dividing by 1.35. The values of "Our Evaluation" were determined in part via Figures 1 and 2.

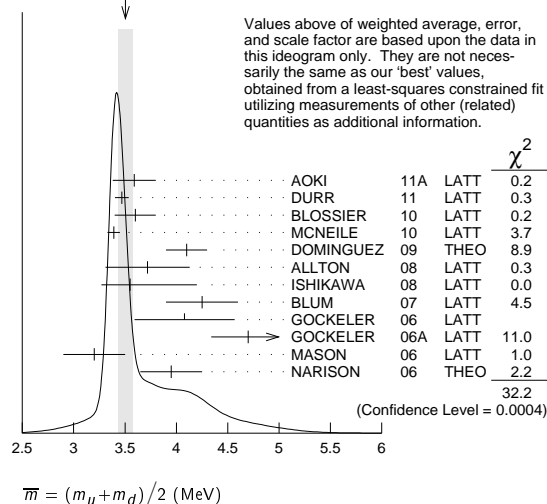
VALUE (MeV)	DOCUMENT ID	TECN	COMMENT
<b>3.2-4.4 OUR EVALUATION</b>	See the ideogram below.		
3.59 ± 0.21	<sup>21</sup> AOKI	11A	LATT $\overline{MS}$ scheme
3.469 ± 0.047 ± 0.048	<sup>22</sup> DURR	11	LATT $\overline{MS}$ scheme
3.6 ± 0.2	<sup>23</sup> BLOSSIER	10	LATT $\overline{MS}$ scheme
3.39 ± 0.06	<sup>24</sup> MCNEILE	10	LATT $\overline{MS}$ scheme
4.1 ± 0.2	<sup>25</sup> DOMINGUEZ	09	THEO $\overline{MS}$ scheme
3.72 ± 0.41	<sup>26</sup> ALLTON	08	LATT $\overline{MS}$ scheme
3.55 + 0.65 - 0.28	<sup>27</sup> ISHIKAWA	08	LATT $\overline{MS}$ scheme
4.25 ± 0.35	<sup>28</sup> BLUM	07	LATT $\overline{MS}$ scheme
4.08 ± 0.25 ± 0.42	<sup>29</sup> GOCKELER	06	LATT $\overline{MS}$ scheme
4.7 ± 0.2 ± 0.3	<sup>30</sup> GOCKELER	06A	LATT $\overline{MS}$ scheme
3.2 ± 0.3	<sup>31</sup> MASON	06	LATT $\overline{MS}$ scheme
3.95 ± 0.3	<sup>32</sup> NARISON	06	THEO $\overline{MS}$ scheme
••• We do not use the following data for averages, fits, limits, etc. •••			
3.40 ± 0.07	<sup>24</sup> DAVIES	10	LATT $\overline{MS}$ scheme
3.85 ± 0.12 ± 0.4	<sup>33</sup> BLOSSIER	08	LATT $\overline{MS}$ scheme
≥ 4.85 ± 0.20	<sup>34</sup> DOMINGUEZ	..08B	THEO $\overline{MS}$ scheme
4.026 ± 0.048	<sup>35</sup> NAKAMURA	08	LATT $\overline{MS}$ scheme
2.8 ± 0.3	<sup>36</sup> AUBIN	04	LATT $\overline{MS}$ scheme
4.29 ± 0.14 ± 0.65	<sup>37</sup> AOKI	03	LATT $\overline{MS}$ scheme
3.223 ± 0.3	<sup>38</sup> AOKI	03B	LATT $\overline{MS}$ scheme
4.4 ± 0.1 ± 0.4	<sup>39</sup> BECIREVIC	03	LATT $\overline{MS}$ scheme
4.1 ± 0.3 ± 1.0	<sup>40</sup> CHIU	03	LATT $\overline{MS}$ scheme

# Quark Particle Listings

## Light Quarks ( $u, d, s$ )

- 21 AOKI 11A determine quark masses from a lattice computation of the hadron spectrum using  $N_f = 2 + 1$  dynamical flavors of domain wall fermions.
- 22 DURR 11 determine quark mass from a lattice computation of the meson spectrum using  $N_f = 2 + 1$  dynamical flavors. The lattice simulations were done at the physical quark mass, so that extrapolation in the quark mass was not needed.
- 23 BLOSSIER 10 determines quark masses from a computation of the hadron spectrum using  $N_f=2$  dynamical twisted-mass Wilson fermions.
- 24 DAVIES 10 and MCNEILE 10 determine  $\overline{m}_C(\mu)/\overline{m}_S(\mu) = 11.85 \pm 0.16$  using a lattice computation with  $N_f = 2 + 1$  dynamical fermions of the pseudoscalar meson masses. Mass  $\overline{m}$  is obtained from this using the value of  $m_C$  from ALLISON 08 or MCNEILE 10 and the BAZAVOV 10 values for the light quark mass ratio,  $m_S/\overline{m}$ .
- 25 DOMINGUEZ 09 use QCD finite energy sum rules for the two-point function of the divergence of the axial vector current computed to order  $\alpha_s^4$ .
- 26 ALLTON 08 use a lattice computation of the  $\pi, K$ , and  $\Omega$  masses with 2+1 dynamical flavors of domain wall quarks, and non-perturbative renormalization.
- 27 ISHIKAWA 08 use a lattice computation of the light meson spectrum with 2+1 dynamical flavors of  $\mathcal{O}(a)$  improved Wilson quarks, and one-loop perturbative renormalization.
- 28 BLUM 07 determine quark masses from the pseudoscalar meson masses using a QED plus QCD lattice computation with two dynamical quark flavors.
- 29 GOCKELER 06 use an unquenched lattice computation of the axial Ward Identity with  $N_f = 2$  dynamical light quark flavors, and non-perturbative renormalization, to obtain  $\overline{m}(2 \text{ GeV}) = 4.08 \pm 0.25 \pm 0.19 \pm 0.23 \text{ MeV}$ , where the first error is statistical, the second and third are systematic due to the fit range and force scale uncertainties, respectively. We have combined the systematic errors linearly.
- 30 GOCKELER 06A use an unquenched lattice computation of the pseudoscalar meson masses with  $N_f = 2$  dynamical light quark flavors, and non-perturbative renormalization.
- 31 MASON 06 extract light quark masses from a lattice simulation using staggered fermions with an improved action, and three dynamical light quark flavors with degenerate  $u$  and  $d$  quarks. Perturbative corrections were included at NNLO order.
- 32 NARISON 06 uses sum rules for  $e^+e^- \rightarrow$  hadrons to order  $\alpha_s^3$  to determine  $m_S$  combined with other determinations of the quark mass ratios.
- 33 BLOSSIER 08 use a lattice computation of pseudoscalar meson masses and decay constants with 2 dynamical flavors and non-perturbative renormalization.
- 34 DOMINGUEZ-CLARIMON 08B obtain an inequality from sum rules for the scalar two-point correlator.
- 35 NAKAMURA 08 do a lattice computation using quenched domain wall fermions and non-perturbative renormalization.
- 36 AUBIN 04 perform three flavor dynamical lattice calculation of pseudoscalar meson masses, with one-loop perturbative renormalization constant.
- 37 AOKI 03 uses quenched lattice simulation of the meson and baryon masses with degenerate light quarks. The extrapolations are done using quenched chiral perturbation theory.
- 38 The errors given in AOKI 03b were  $+0.046$   
 $-0.069$ . We changed them to  $\pm 0.3$  for calculating the overall best values. AOKI 03b uses lattice simulation of the meson and baryon masses with two dynamical light quarks. Simulations are performed using the  $\mathcal{O}(a)$  improved Wilson action.
- 39 BECIREVIC 03 perform quenched lattice computation using the vector and axial Ward identities. Uses  $\mathcal{O}(a)$  improved Wilson action and nonperturbative renormalization.
- 40 CHIU 03 determines quark masses from the pion and kaon masses using a lattice simulation with a chiral fermion action in quenched approximation.

WEIGHTED AVERAGE  
3.51±0.07 (Error scaled by 1.8)

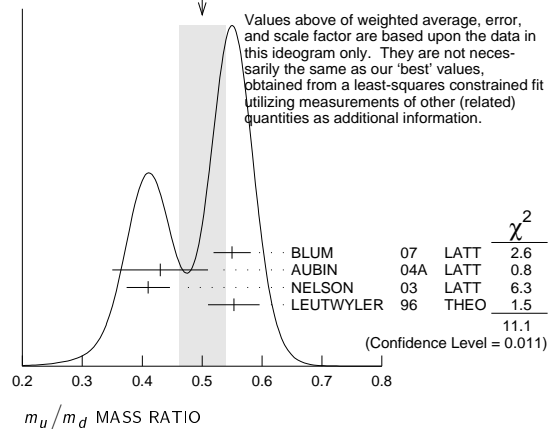


$m_u/m_d$  MASS RATIO

VALUE	DOCUMENT ID	TECN	COMMENT
<b>0.38–0.58 OUR EVALUATION</b>	See the ideogram below.		
0.550±0.031	41 BLUM	07 LATT	
0.43±0.08	42 AUBIN	04A LATT	
0.410±0.036	43 NELSON	03 LATT	
0.553±0.043	44 LEUTWYLER	96 THEO	Compilation

- 41 BLUM 07 determine quark masses from the pseudoscalar meson masses using a QED plus QCD lattice computation with two dynamical quark flavors.
- 42 AUBIN 04A perform three flavor dynamical lattice calculation of pseudoscalar meson masses, with continuum estimate of electromagnetic effects in the kaon masses.
- 43 NELSON 03 computes coefficients in the order  $p^4$  chiral Lagrangian using a lattice calculation with three dynamical flavors. The ratio  $m_u/m_d$  is obtained by combining this with the chiral perturbation theory computation of the meson masses to order  $p^4$ .
- 44 LEUTWYLER 96 uses a combined fit to  $\eta \rightarrow 3\pi$  and  $\psi' \rightarrow J/\psi(\pi, \eta)$  decay rates, and the electromagnetic mass differences of the  $\pi$  and  $K$ .

WEIGHTED AVERAGE  
0.50±0.04 (Error scaled by 1.9)



### s-QUARK MASS

See the comment for the  $u$  quark above.

We have normalized the  $\overline{MS}$  masses at a renormalization scale of  $\mu = 2 \text{ GeV}$ . Results quoted in the literature at  $\mu = 1 \text{ GeV}$  have been rescaled by dividing by 1.35.

VALUE (MeV)	DOCUMENT ID	TECN	COMMENT
<b>95 ± 5 OUR EVALUATION</b>	See the ideogram below.		
96.2 ± 2.7	45 AOKI	11A LATT	$\overline{MS}$ scheme
95.5 ± 1.1 ± 1.5	46 DURR	11 LATT	$\overline{MS}$ scheme
95 ± 6	47 BLOSSIER	10 LATT	$\overline{MS}$ scheme
97.6 ± 2.9 ± 5.5	48 BLUM	10 LATT	$\overline{MS}$ scheme
92.2 ± 1.3	49 MCNEILE	10 LATT	$\overline{MS}$ scheme
107.3 ± 11.7	50 ALLTON	08 LATT	$\overline{MS}$ scheme
102 ± 8	51 DOMINGUEZ	08A THEO	$\overline{MS}$ scheme
90.1 +17.2 - 6.1	52 ISHIKAWA	08 LATT	$\overline{MS}$ scheme
105 ± 6 ± 7	53 CHETYRKIN	06 THEO	$\overline{MS}$ scheme
111 ± 6 ± 10	54 GOCKELER	06 LATT	$\overline{MS}$ scheme
119 ± 5 ± 8	55 GOCKELER	06A LATT	$\overline{MS}$ scheme
92 ± 9	56 JAMIN	06 THEO	$\overline{MS}$ scheme
87 ± 6	57 MASON	06 LATT	$\overline{MS}$ scheme
104 ± 15	58 NARISON	06 THEO	$\overline{MS}$ scheme
••• We do not use the following data for averages, fits, limits, etc. •••			
92.4 ± 1.5	49 DAVIES	10 LATT	$\overline{MS}$ scheme
105 ± 3 ± 9	59 BLOSSIER	08 LATT	$\overline{MS}$ scheme
105.6 ± 1.2	60 NAKAMURA	08 LATT	$\overline{MS}$ scheme
119.5 ± 9.3	61 BLUM	07 LATT	$\overline{MS}$ scheme
≥ 71 ± 4, ≤ 151 ± 14	62 NARISON	06 THEO	$\overline{MS}$ scheme
96 + 5 +16 - 3 -18	63 BAIKOV	05 THEO	$\overline{MS}$ scheme
81 ± 22	64 GAMIZ	05 THEO	$\overline{MS}$ scheme
125 ± 28	65 GORBUNOV	05 THEO	$\overline{MS}$ scheme
93 ± 32	66 NARISON	05 THEO	$\overline{MS}$ scheme
76 ± 8	67 AUBIN	04 LATT	$\overline{MS}$ scheme
116 ± 6 ± 0.65	68 AOKI	03 LATT	$\overline{MS}$ scheme
84.5 +12 - 1.7	69 AOKI	03B LATT	$\overline{MS}$ scheme
106 ± 2 ± 8	70 BECIREVIC	03 LATT	$\overline{MS}$ scheme
92 ± 9 ± 16	71 CHIU	03 LATT	$\overline{MS}$ scheme
117 ± 17	72 GAMIZ	03 THEO	$\overline{MS}$ scheme
103 ± 17	73 GAMIZ	03 THEO	$\overline{MS}$ scheme

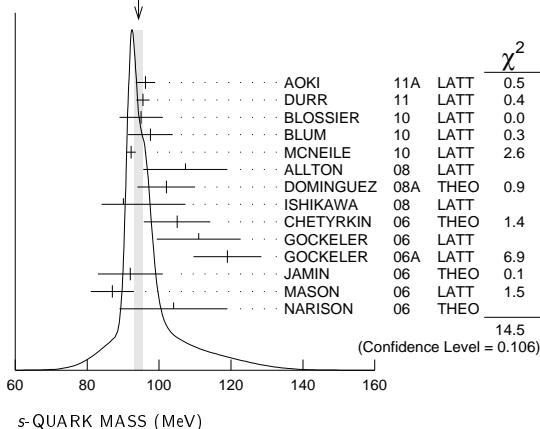
- 45 AOKI 11A determine quark masses from a lattice computation of the hadron spectrum using  $N_f = 2 + 1$  dynamical flavors of domain wall fermions.
- 46 DURR 11 determine quark mass from a lattice computation of the meson spectrum using  $N_f = 2 + 1$  dynamical flavors. The lattice simulations were done at the physical quark mass, so that extrapolation in the quark mass was not needed.
- 47 BLOSSIER 10 determines quark masses from a computation of the hadron spectrum using  $N_f=2$  dynamical twisted-mass Wilson fermions.
- 48 BLUM 10 determines light quark masses using a QCD plus QED lattice computation of the electromagnetic mass splittings of the low-lying hadrons. The lattice simulations use 2+1 dynamical quark flavors.

# Quark Particle Listings

## Light Quarks ( $u, d, s$ )

- <sup>49</sup> DAVIES 10 and MCNEILE 10 determine  $\overline{m}_c(\mu)/\overline{m}_s(\mu) = 11.85 \pm 0.16$  using a lattice computation with  $N_f = 2 + 1$  dynamical fermions of the pseudoscalar meson masses. Mass  $m_s$  is obtained from this using the value of  $m_c$  from ALLISON 08 or MCNEILE 10.
- <sup>50</sup> ALLTON 08 use a lattice computation of the  $\pi$ ,  $K$ , and  $\Omega$  masses with 2+1 dynamical flavors of domain wall quarks, and non-perturbative renormalization.
- <sup>51</sup> DOMINGUEZ 08A make determination from QCD finite energy sum rules for the pseudoscalar two-point function computed to order  $\alpha_s^4$ .
- <sup>52</sup> ISHIKAWA 08 use a lattice computation of the light meson spectrum with 2+1 dynamical flavors of  $\mathcal{O}(a)$  improved Wilson quarks, and one-loop perturbative renormalization.
- <sup>53</sup> CHETYRKIN 06 use QCD sum rules in the pseudoscalar channel to order  $\alpha_s^4$ .
- <sup>54</sup> GOCKELER 06 use an unquenched lattice computation of the axial Ward Identity with  $N_f = 2$  dynamical light quark flavors, and non-perturbative renormalization, to obtain  $\overline{m}_s(2 \text{ GeV}) = 111 \pm 6 \pm 4 \pm 6 \text{ MeV}$ , where the first error is statistical, the second and third are systematic due to the fit range and force scale uncertainties, respectively. We have combined the systematic errors linearly.
- <sup>55</sup> GOCKELER 06A use an unquenched lattice computation of the pseudoscalar meson masses with  $N_f = 2$  dynamical light quark flavors, and non-perturbative renormalization.
- <sup>56</sup> JAMIN 06 determine  $\overline{m}_s(2 \text{ GeV})$  from the spectral function for the scalar  $K\pi$  form factor.
- <sup>57</sup> MASON 06 extract light quark masses from a lattice simulation using staggered fermions with an improved action, and three dynamical light quark flavors with degenerate  $u$  and  $d$  quarks. Perturbative corrections were included at NNLO order.
- <sup>58</sup> NARISON 06 uses sum rules for  $e^+e^- \rightarrow$  hadrons to order  $\alpha_s^3$ .
- <sup>59</sup> BLOSSIER 08 use a lattice computation of pseudoscalar meson masses and decay constants with 2 dynamical flavors and non-perturbative renormalization.
- <sup>60</sup> NAKAMURA 08 do a lattice computation using quenched domain wall fermions and non-perturbative renormalization.
- <sup>61</sup> BLUM 07 determine quark masses from the pseudoscalar meson masses using a QED plus QCD lattice computation with two dynamical quark flavors.
- <sup>62</sup> NARISON 06 obtains the quoted range from positivity of the spectral functions.
- <sup>63</sup> BAIKOV 05 determines  $\overline{m}_s(M_\tau) = 100^{+5}_{-3} +^{17}_{-19}$  from sum rules using the strange spectral function in  $\tau$  decay. The computations were done to order  $\alpha_s^3$ , with an estimate of the  $\alpha_s^4$  terms. We have converted the result to  $\mu = 2 \text{ GeV}$ .
- <sup>64</sup> GAMIZ 05 determines  $\overline{m}_s(2 \text{ GeV})$  from sum rules using the strange spectral function in  $\tau$  decay. The computations were done to order  $\alpha_s^2$ , with an estimate of the  $\alpha_s^3$  terms.
- <sup>65</sup> GORBUNOV 05 use hadronic tau decays to  $N^3\text{LO}$ , including power corrections.
- <sup>66</sup> NARISON 05 determines  $\overline{m}_s(2 \text{ GeV})$  from sum rules using the strange spectral function in  $\tau$  decay. The computations were done to order  $\alpha_s^3$ .
- <sup>67</sup> AUBIN 04 perform three flavor dynamical lattice calculation of pseudoscalar meson masses, with one-loop perturbative renormalization constant.
- <sup>68</sup> AOKI 03 uses quenched lattice simulation of the meson and baryon masses with degenerate light quarks. The extrapolations are done using quenched chiral perturbation theory. Determines  $m_s = 113.8 \pm 2.3^{+5.8}_{-2.9}$  using  $K$  mass as input and  $m_s = 142.3 \pm 5.8^{+22}_{-0}$  using  $\phi$  mass as input. We have performed a weighted average of these values.
- <sup>69</sup> AOKI 03B uses lattice simulation of the meson and baryon masses with two dynamical light quarks. Simulations are performed using the  $\mathcal{O}(a)$  improved Wilson action.
- <sup>70</sup> BECIREVIC 03 perform quenched lattice computation using the vector and axial Ward identities. Uses  $\mathcal{O}(a)$  improved Wilson action and nonperturbative renormalization. They also quote  $\overline{m}/m_s = 24.3 \pm 0.2 \pm 0.6$ .
- <sup>71</sup> CHIU 03 determines quark masses from the pion and kaon masses using a lattice simulation with a chiral fermion action in quenched approximation.
- <sup>72</sup> GAMIZ 03 determines  $m_s$  from SU(3) breaking in the  $\tau$  hadronic width. The value of  $V_{us}$  is chosen to satisfy CKM unitarity.
- <sup>73</sup> GAMIZ 03 determines  $m_s$  from SU(3) breaking in the  $\tau$  hadronic width. The value of  $V_{us}$  is taken from the PDG.

WEIGHTED AVERAGE  
94.3±1.2 (Error scaled by 1.3)



s-QUARK MASS (MeV)

### OTHER LIGHT QUARK MASS RATIOS

#### $m_s/m_d$ MASS RATIO

VALUE	DOCUMENT ID	TECN	COMMENT
<b>17-22 OUR EVALUATION</b>			
••• We do not use the following data for averages, fits, limits, etc. •••			
20.0	<sup>74</sup> GAO	97	THEO
18.9±0.8	<sup>75</sup> LEUTWYLER	96	THEO Compilation
21	<sup>76</sup> DONOGHUE	92	THEO
18	<sup>77</sup> GERARD	90	THEO
18 to 23	<sup>78</sup> LEUTWYLER	90B	THEO

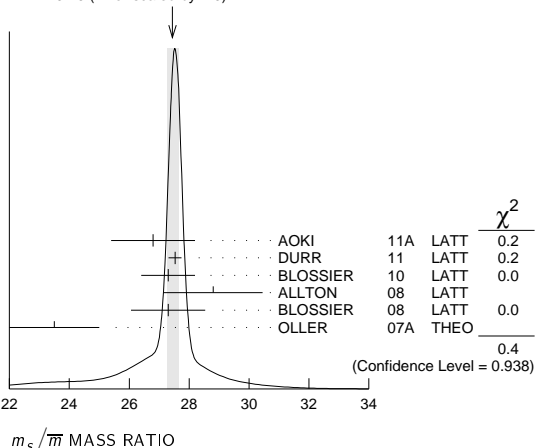
- <sup>74</sup> GAO 97 uses electromagnetic mass splittings of light mesons.
- <sup>75</sup> LEUTWYLER 96 uses a combined fit to  $\eta \rightarrow 3\pi$  and  $\psi' \rightarrow J/\psi(\pi, \eta)$  decay rates, and the electromagnetic mass differences of the  $\pi$  and  $K$ .
- <sup>76</sup> DONOGHUE 92 result is from a combined analysis of meson masses,  $\eta \rightarrow 3\pi$  using second-order chiral perturbation theory including nonanalytic terms, and  $(\psi(2S) \rightarrow J/\psi(1S)\pi)/(\psi(2S) \rightarrow J/\psi(1S)\eta)$ .
- <sup>77</sup> GERARD 90 uses large  $N$  and  $\eta$ - $\eta'$  mixing.
- <sup>78</sup> LEUTWYLER 90B determines quark mass ratios using second-order chiral perturbation theory for the meson and baryon masses, including nonanalytic corrections. Also uses Weinberg sum rules to determine  $L_7$ .

#### $m_s/\overline{m}$ MASS RATIO

VALUE	DOCUMENT ID	TECN
<b>27 ±1 OUR EVALUATION</b>		
See the ideogram below.		
26.8 ±1.4	<sup>79</sup> AOKI	11A LATT
27.53±0.20±0.08	<sup>80</sup> DURR	11 LATT
27.3 ±0.9	<sup>81</sup> BLOSSIER	10 LATT
28.8 ±1.65	<sup>82</sup> ALLTON	08 LATT
27.3 ±0.3 ±1.2	<sup>83</sup> BLOSSIER	08 LATT
23.5 ±1.5	<sup>84</sup> OLLER	07A THEO
27.4 ±0.4	<sup>85</sup> AUBIN	04 LATT

- We do not use the following data for averages, fits, limits, etc. •••
- <sup>79</sup> AOKI 11A determine quark masses from a lattice computation of the hadron spectrum using  $N_f = 2 + 1$  dynamical flavors of domain wall fermions.
- <sup>80</sup> DURR 11 determine quark mass from a lattice computation of the meson spectrum using  $N_f = 2 + 1$  dynamical flavors. The lattice simulations were done at the physical quark mass, so that extrapolation in the quark mass was not needed.
- <sup>81</sup> BLOSSIER 10 determines quark masses from a computation of the hadron spectrum using  $N_f=2$  dynamical twisted-mass Wilson fermions.
- <sup>82</sup> ALLTON 08 use a lattice computation of the  $\pi$ ,  $K$ , and  $\Omega$  masses with 2+1 dynamical flavors of domain wall quarks, and non-perturbative renormalization.
- <sup>83</sup> BLOSSIER 08 use a lattice computation of pseudoscalar meson masses and decay constants with 2 dynamical flavors and non-perturbative renormalization.
- <sup>84</sup> OLLER 07A use unitarized chiral perturbation theory to order  $p^4$ .
- <sup>85</sup> Three flavor dynamical lattice calculation of pseudoscalar meson masses.

WEIGHTED AVERAGE  
27.44±0.20 (Error scaled by 1.0)



$m_s/\overline{m}$  MASS RATIO

#### Q MASS RATIO

$Q \equiv \sqrt{(m_s^2 - \overline{m}^2)/(m_d^2 - m_u^2)}$ ;  $\overline{m} \equiv (m_u + m_d)/2$

VALUE	DOCUMENT ID	TECN
••• We do not use the following data for averages, fits, limits, etc. •••		
22.8±0.4	<sup>86</sup> MARTEMYA...	05 THEO
22.7±0.8	<sup>87</sup> ANISOVICH	96 THEO

- <sup>86</sup> MARTEMYANOV 05 determine  $Q$  from  $\eta \rightarrow 3\pi$  decay.
- <sup>87</sup> ANISOVICH 96 find  $Q$  from  $\eta \rightarrow \pi^+\pi^-\pi^0$  decay using dispersion relations and chiral perturbation theory.

# Quark Particle Listings

## Light Quarks ( $u, d, s, c$ )

### LIGHT QUARKS ( $u, d, s$ ) REFERENCES

AOKI	11A	PR D83 074508	Y. Aoki et al. (RBC-UKQCD Collab.)
DURR	11	PL B701 265	S. Durr et al. (BMW Collab.)
BAZANOV	10	RMP 82 1349	A. Bazanov et al. (MILC Collab.)
BLOSSIER	10	PR D82 114513	B. Blossier et al. (ETM Collab.)
BLUM	10	PR D82 094508	T. Blum et al.
DAVIES	10	PRL 104 132003	C.T.H. Davies et al. (HPQCD Collab.)
MCNEILE	10	PR D82 034512	C. McNeile et al. (HPQCD Collab.)
DOMINGUEZ	09	PR D79 014009	C.A. Dominguez et al.
ALLISON	08	PR D78 054513	I. Allison et al. (HPQCD Collab.)
ALLTON	08	PR D78 114509	C. Allton et al. (RBC and UKQCD Collab.)
BLOSSIER	08	JHEP 0804 020	B. Blossier et al. (ETM Collab.)
DEANDREA	08	PR D78 034032	A. Deandrea, A. Nehme, P. Talavera
DOMINGUEZ	08A	JHEP 0805 020	C.A. Dominguez et al.
DOMINGUEZ...	08B	PL B660 49	A. Dominguez-Clarimon, E. de Rafael, J. Taron
ISHIKAWA	08	PR D78 011502R	T. Ishikawa et al. (CP-PACS and JLQCD Collab.)
NAKAMURA	08	PR D78 034502	Y. Nakamura et al. (CP-PACS Collab.)
BLUM	07	PR D76 114508	T. Blum et al. (RBC Collab.)
OLLER	07A	EPJ A34 371	J.A. Oller, L. Roca
CHETYRKIN	06	EPJ C46 721	K.G. Chetyrkin, A. Khodjamirian
GOCKELER	06	PR D73 054508	M. Gockeler et al. (QCDSF, UKQCD Collabs)
GOCKELER	06A	PL B639 307	M. Gockeler et al. (QCDSF, UKQCD Collabs)
JAMIN	06	PR D74 074009	M. Jamin, J.A. Oller, A. Pich
MASON	06	PR D73 114501	Q. Mason et al. (HPQCD Collab.)
NARISON	06	PR D74 034013	S. Narison
PDG	06	JPG 33 1	W.-M. Yao et al. (PDG Collab.)
BAIKOV	05	PRL 95 012003	P.A. Baikov, K.G. Chetyrkin, J.H. Kuhn
GAMIZ	05	PRL 94 011803	E. Gamiz et al.
GORBUNOV	05	PR D71 013002	D.S. Gorbunov, A.A. Pivovarov
MARTEMYA...	05	PR D71 017501	B.V. Martemyanov, V.S. Sopov
NARISON	05	PL B626 101	S. Narison
AUBIN	04	PR D70 031504R	C. Aubin et al. (HPQCD, MILC, UKQCD Collabs.)
AUBIN	04A	PR D70 114501	C. Aubin et al. (MILC Collab.)
AOKI	03	PR D67 034503	S. Aoki et al. (CP-PACS Collab.)
AOKI	03B	PR D68 054502	S. Aoki et al. (CP-PACS Collab.)
BECHIREVIC	03	PL B558 69	D. Becirevic, V. Lubitz, C. Tarantino
CHIU	03	NP B673 217	T.-W. Chiu, T.-H. Hsieh
GAMIZ	03	JHEP 0301 060	E. Gamiz et al.
NELSON	03	PRL 90 021601	D. Nelson, G.T. Fleming, G.W. Kilcup
GAO	97	PR D56 4115	D.-N. Gao, B.A. Li, M.-L. Yan
ANISOVICH	96	PL B375 335	A.V. Anisovich, H. Leutwyler
LEUTWYLER	96	PL B378 313	H. Leutwyler
DONOGHUE	92	PRL 69 3444	J.F. Donoghue, B.R. Holstein, D. Wyler
GERARD	90	MPL A5 391	J.M. Gerard (MPlM)
LEUTWYLER	90B	NP B337 108	H. Leutwyler (BERN)



$$I(J^P) = 0(\frac{1}{2}^+)$$

$$\text{Charge} = \frac{2}{3} e \quad \text{Charm} = +1$$

### c-QUARK MASS

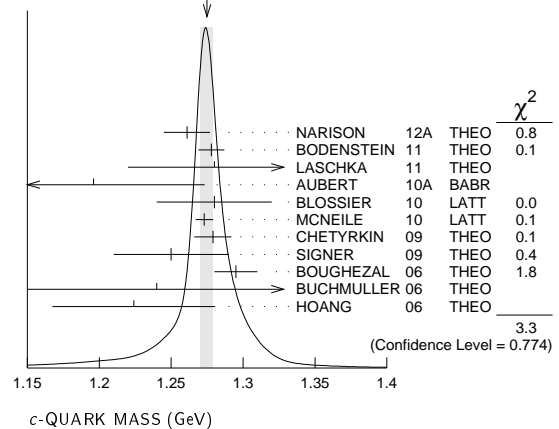
The  $c$ -quark mass corresponds to the "running" mass  $m_c(\mu = m_c)$  in the  $\overline{\text{MS}}$  scheme. We have converted masses in other schemes to the  $\overline{\text{MS}}$  scheme using two-loop QCD perturbation theory with  $\alpha_s(\mu = m_c) = 0.38 \pm 0.03$ . The value  $1.275 \pm 0.025$  GeV for the  $\overline{\text{MS}}$  mass corresponds to  $1.67 \pm 0.07$  GeV for the pole mass (see the "Note on Quark Masses").

VALUE (GeV)	DOCUMENT ID	TECN	COMMENT
<b>1.275 ± 0.025 OUR EVALUATION</b>	See the ideogram below.		
1.261 ± 0.016	1	NARISON 12A	THEO $\overline{\text{MS}}$ scheme
1.278 ± 0.009	2	BODENSTEIN 11	THEO $\overline{\text{MS}}$ scheme
1.28 ± 0.07 -0.06	3	LASCHKA 11	THEO $\overline{\text{MS}}$ scheme
1.196 ± 0.059 ± 0.050	4	AUBERT 10A	BABR $\overline{\text{MS}}$ scheme
1.28 ± 0.04	5	BLOSSIER 10	LATT $\overline{\text{MS}}$ scheme
1.273 ± 0.006	6	MCNEILE 10	LATT $\overline{\text{MS}}$ scheme
1.279 ± 0.013	7	CHETYRKIN 09	THEO $\overline{\text{MS}}$ scheme
1.25 ± 0.04	8	SIGNER 09	THEO $\overline{\text{MS}}$ scheme
1.295 ± 0.015	9	BOUGHEZAL 06	THEO $\overline{\text{MS}}$ scheme
1.24 ± 0.09	10	BUCHMULLER 06	THEO $\overline{\text{MS}}$ scheme
1.224 ± 0.017 ± 0.054	11	HOANG 06	THEO $\overline{\text{MS}}$ scheme
••• We do not use the following data for averages, fits, limits, etc. •••			
1.299 ± 0.026	12	BODENSTEIN 10	THEO $\overline{\text{MS}}$ scheme
1.261 ± 0.018	13	NARISON 10	THEO $\overline{\text{MS}}$ scheme
1.268 ± 0.009	14	ALLISON 08	LATT $\overline{\text{MS}}$ scheme
1.286 ± 0.013	15	KUHN 07	THEO $\overline{\text{MS}}$ scheme
1.33 ± 0.10	16	AUBERT 04x	THEO $\overline{\text{MS}}$ scheme
1.29 ± 0.07	17	HOANG 04	THEO $\overline{\text{MS}}$ scheme
1.319 ± 0.028	18	DEDIVITIIS 03	LATT $\overline{\text{MS}}$ scheme
1.19 ± 0.11	19	EIDEMULLER 03	THEO $\overline{\text{MS}}$ scheme
1.289 ± 0.043	20	ERLER 03	THEO $\overline{\text{MS}}$ scheme
1.26 ± 0.02	21	ZYABLYUK 03	THEO $\overline{\text{MS}}$ scheme

- NARISON 12A determines  $m_c$  using sum rules for the vector current correlator to order  $\alpha_s^3$ , including the effect of gluon condensates up to dimension eight.
- BODENSTEIN 11 determine  $\overline{m}_c(3 \text{ GeV}) = 0.987 \pm 0.009$  GeV and  $\overline{m}_c(\overline{m}_c) = 1.278 \pm 0.009$  GeV using QCD sum rules for the charm quark vector current correlator.
- LASCHKA 11 determine the  $c$  mass from the charmonium spectrum. The theoretical computation uses the heavy  $Q\overline{Q}$  potential to order  $1/m_Q$  obtained by matching the short-distance perturbative result onto lattice QCD result at larger scales.
- AUBERT 10A determine the  $b$ - and  $c$ -quark masses from a fit to the inclusive decay spectra in semileptonic  $B$  decays in the kinetic scheme (and convert it to the  $\overline{\text{MS}}$  scheme).
- BLOSSIER 10 determines quark masses from a computation of the hadron spectrum using  $N_f=2$  dynamical twisted-mass Wilson fermions.
- MCNEILE 10 determines  $m_c$  by comparing four-loop perturbative results for the pseudoscalar current to lattice simulations with  $N_f = 2+1$  sea-quarks by the HPQCD collaboration.

- CHETYRKIN 09 determine  $m_c$  and  $m_b$  from the  $e^+e^- \rightarrow Q\overline{Q}$  cross-section and sum rules, using a four-loop computation of the heavy quark vacuum polarization. They also determine  $m_c(3 \text{ GeV}) = 0.986 \pm 0.013$  GeV.
- SIGNER 09 determines the  $c$ -quark mass using non-relativistic sum rules to analyze the  $e^+e^- \rightarrow c\overline{c}$  cross-section near threshold. Also determine the PS mass  $m_{PS}(\mu_F = 0.7 \text{ GeV}) = 1.50 \pm 0.04$  GeV.
- BOUGHEZAL 06 result comes from the first moment of the hadronic production cross-section to order  $\alpha_s^3$ .
- BUCHMULLER 06 determine  $m_b$  and  $m_c$  by a global fit to inclusive  $B$  decay spectra.
- HOANG 06 determines  $\overline{m}_c(\overline{m}_c)$  from a global fit to inclusive  $B$  decay data. The  $B$  decay distributions were computed to order  $\alpha_s^2\beta_0$ , and the conversion between different  $m_c$  mass schemes to order  $\alpha_s^3$ .
- BODENSTEIN 10 determines  $\overline{m}_c(3 \text{ GeV}) = 1.008 \pm 0.026$  GeV using finite energy sum rules for the vector current correlator. The authors have converted this to  $\overline{m}_c(\overline{m}_c)$  using  $\alpha_s(M_Z) = 0.1189 \pm 0.0020$ .
- NARISON 10 determines  $m_c$  from ratios of moments of vector current correlators computed to order  $\alpha_s^3$  and including the dimension-six gluon condensate.
- ALLISON 08 determine  $m_c$  by comparing four-loop perturbative results for the pseudoscalar current correlator to lattice simulations by the HPQCD collaboration. The result has been updated in MCNEILE 10.
- KUHN 07 determine  $\overline{m}_c(\mu = 3 \text{ GeV}) = 0.986 \pm 0.013$  GeV and  $\overline{m}_c(\overline{m}_c)$  from a four-loop sum-rule computation of the cross-section for  $e^+e^- \rightarrow$  hadrons in the charm threshold region.
- AUBERT 04x obtain  $m_c$  from a fit to the hadron mass and lepton energy distributions in semileptonic  $B$  decay. The paper quotes values in the kinetic scheme. The  $\overline{\text{MS}}$  value has been provided by the BABAR collaboration.
- HOANG 04 determines  $\overline{m}_c(\overline{m}_c)$  from moments at order  $\alpha_s^2$  of the charm production cross-section in  $e^+e^-$  annihilation.
- DEDIVITIIS 03 use a quenched lattice computation of heavy-heavy and heavy-light meson masses.
- EIDEMULLER 03 determines  $m_b$  and  $m_c$  using QCD sum rules.
- ERLER 03 determines  $m_b$  and  $m_c$  using QCD sum rules. Includes recent BES data.
- ZYABLYUK 03 determines  $m_c$  by using QCD sum rules in the pseudoscalar channel and comparing with the  $\eta_c$  mass.

WEIGHTED AVERAGE  
1.275±0.004 (Error scaled by 1.0)



### $m_b - m_c$ QUARK MASS DIFFERENCE

VALUE (GeV)	DOCUMENT ID	TECN
<b>3.45 ± 0.05 OUR EVALUATION</b>		

••• We do not use the following data for averages, fits, limits, etc. •••

3.472 ± 0.032	22	AUBERT 10A	BABR
3.42 ± 0.06	23	ABDALLAH 06B	DLPH
3.44 ± 0.03	24	AUBERT 04x	BABR
3.41 ± 0.01	24	BAUER 04	THEO

22 AUBERT 10A determine the  $b$ - and  $c$ -quark masses from a fit to the inclusive decay spectra in semileptonic  $B$  decays in the kinetic scheme.

23 ABDALLAH 06B determine  $m_b - m_c$  from moments of the hadron invariant mass and lepton energy spectra in semileptonic inclusive  $B$  decays.

24 Determine  $m_b - m_c$  from a global fit to inclusive  $B$  decay spectra.

### c-QUARK REFERENCES

NARISON 12A	PL B706 412	S. Narison	(MONP)
BODENSTEIN 11	PR D83 074014	S. Bodenstein et al.	
LASCHKA 11	PR D83 094002	A. Laschka, N. Kaiser, W. Weise	
AUBERT 10A	PR D81 032003	B. Aubert et al.	(BABAR Collab.)
BLOSSIER 10	PR D82 114513	B. Blossier et al.	(ETM Collab.)
BODENSTEIN 10	PR D82 114013	S. Bodenstein et al.	
MCNEILE 10	PR D82 034512	C. McNeile et al.	(HPQCD Collab.)
NARISON 10	PL B693 559	S. Narison	(MONP)
Also	PL B705 544 (errata.)	S. Narison	(MONP)
CHETYRKIN 09	PR D80 074010	K.G. Chetyrkin et al.	(KARL, BNL)
SIGNER 09	PL B672 333	A. Signer	(DURH)
ALLISON 08	PR D78 054513	I. Allison et al.	(HPQCD Collab.)
KUHN 07	NP B778 192	J.H. Kuhn, M. Steinhauser, C. Sturm	



See key on page 457

ABDALLAH 06B	EPJ C45 35	J. Abdallah et al.	(DELPHI Collab.)
BOUGHEZAL 06	PR D74 074006	R. Boughezal, M. Czakon, T. Schutzmeier	
BUCHMULLER 06	PR D73 073008	O.L. Buchmuller, H.U. Flaecher	
HOANG 06	PL B633 526	A.H. Hoang, A.V. Manohar	
AUBERT 04X	PRL 93 011803	B. Aubert et al.	(BABAR Collab.)
BAUER 04	PR D70 094017	C. Bauer et al.	
HOANG 04	PL B594 127	A.H. Hoang, M. Jamin	
DEDIVITIIS 03	NP B475 309	G.M. de Divitiis et al.	
EIDEMULLER 03	PR D67 113002	M. Eidemuller	
ERLER 03	PL B558 125	J. Erler, M. Luo	
ZYABLYUK 03	JHEP 0301 081	K.N. Zybalyuk	(ITEP)

**b**

$$I(J^P) = 0(\frac{1}{2}^+)$$

$$\text{Charge} = -\frac{1}{3} e \quad \text{Bottom} = -1$$

**b-QUARK MASS**

The first value is the “running mass”  $\overline{m}_b(\mu = \overline{m}_b)$  in the  $\overline{MS}$  scheme, and the second value is the 1S mass, which is half the mass of the  $\Upsilon(1S)$  in perturbation theory. For a review of different quark mass definitions and their properties, see EL-KHADRA 02. The 1S mass is better suited for use in analyzing  $B$  decays than the  $\overline{MS}$  mass because it gives a stable perturbative expansion. We have converted masses in other schemes to the  $\overline{MS}$  mass and 1S mass using two-loop QCD perturbation theory with  $\alpha_s(\mu = \overline{m}_b) = 0.223 \pm 0.008$ . The values  $4.18 \pm 0.03$  GeV for the  $\overline{MS}$  mass and  $4.65 \pm 0.03$  GeV for the 1S mass correspond to  $4.78 \pm 0.06$  GeV for the pole mass, using the two-loop conversion formula. A discussion of masses in different schemes can be found in the “Note on Quark Masses.”

$\overline{MS}$ MASS (GeV)	1S MASS (GeV)	DOCUMENT ID	TECN
<b>4.18 ± 0.03</b>	<b>OUR EVALUATION</b>	of $\overline{MS}$ Mass. See the ideogram below.	
<b>4.65 ± 0.03</b>	<b>OUR EVALUATION</b>	of 1S Mass. See the ideogram below.	
4.171 ± 0.009	4.642 ± 0.010	1 BODENSTEIN 12	THEO
4.29 ± 0.14	4.77 ± 0.16	2 DIMOPOUL... 12	LATT
4.177 ± 0.011	4.649 ± 0.012	3 NARISON 12	THEO
4.18 ± 0.05	4.65 ± 0.06	4 LASCHKA 11	THEO
4.186 ± 0.044 ± 0.015	4.659 ± 0.050 ± 0.017	5 AUBERT 10A	BABR
4.164 ± 0.023	4.635 ± 0.026	6 MCNEILE 10	LATT
4.163 ± 0.016	4.633 ± 0.018	7 CHETYRKIN 09	THEO
5.26 ± 1.2	5.85 ± 1.3	8 ABDALLAH 08D	DLPH
4.243 ± 0.049	4.723 ± 0.055	9 SCHWANDA 08	BELL
4.19 ± 0.40	4.66 ± 0.45	10 ABDALLAH 06D	DLPH
4.205 ± 0.058	4.68 ± 0.06	11 BOUGHEZAL 06	THEO
4.20 ± 0.04	4.67 ± 0.04	12 BUCHMULLER 06	THEO
4.19 ± 0.06	4.66 ± 0.07	13 PINEDA 06	THEO
4.17 ± 0.03	4.68 ± 0.03	14 BAUER 04	THEO
4.22 ± 0.11	4.72 ± 0.12	15,16 HOANG 04	THEO
4.19 ± 0.05	4.66 ± 0.05	17 BORDES 03	THEO
4.20 ± 0.09	4.67 ± 0.10	18 CORCELLA 03	THEO
4.24 ± 0.10	4.72 ± 0.11	19 EIDEMULLER 03	THEO
4.207 ± 0.031	4.682 ± 0.035	20 ERLER 03	THEO
4.33 ± 0.06 ± 0.10	4.82 ± 0.07 ± 0.11	21 MAHMOOD 03	CLEO
4.190 ± 0.032	4.663 ± 0.036	22 BRAMBILLA 02	THEO
4.346 ± 0.070	4.837 ± 0.078	23 PENIN 02	THEO
• • • We do not use the following data for averages, fits, limits, etc. • • •			
4.212 ± 0.032	4.688 ± 0.036	24 NARISON 12	THEO
4.171 ± 0.014	4.642 ± 0.016	25 NARISON 12A	THEO
4.173 ± 0.010	4.645 ± 0.011	26 NARISON 10	THEO
4.42 ± 0.06 ± 0.08	4.92 ± 0.07 ± 0.09	27 GUAZZINI 08	LATT
4.347 ± 0.048 ± 0.08	4.838 ± 0.053 ± 0.09	28 DELLA-MOR... 07	LATT
4.164 ± 0.025	4.635 ± 0.028	29 KUHN 07	THEO
4.4 ± 0.3	4.9 ± 0.3	15,30 GRAY 05	LATT
4.22 ± 0.06	4.72 ± 0.07	31 AUBERT 04X	THEO
4.25 ± 0.11	4.76 ± 0.12	15,32 MCNEILE 04	LATT
4.22 ± 0.09	4.74 ± 0.10	33 BAUER 03	THEO
4.33 ± 0.10	4.84 ± 0.11	15,34 DEDIVITIIS 03	LATT

1 BODENSTEIN 12 determine  $m_b$  using sum rules for the vector current correlator and the  $e^+e^- \rightarrow Q\overline{Q}$  total cross-section. We have converted  $\overline{m}_b(\overline{m}_b)$  to the 1S scheme.

2 DIMOPOULOS 12 determine quark masses from a lattice computation using  $N_f = 2$  dynamical flavors of twisted mass fermions. We have converted  $\overline{m}_b(\overline{m}_b)$  to the 1S scheme.

3 Determines  $m_b$  to order  $\alpha_s^3$ , including the effect of gluon condensates up to dimension eight combining the methods of NARISON 12 and NARISON 12A. We have converted  $\overline{m}_b(\overline{m}_b)$  to the 1S scheme.

4 LASCHKA 11 determine the  $b$  mass from the charmonium spectrum. The theoretical computation uses the heavy  $Q\overline{Q}$  potential to order  $1/m_Q$  obtained by matching the short-distance perturbative result onto lattice QCD result at larger scales. We have converted  $\overline{m}_b(\overline{m}_b)$  to the 1S scheme.

5 AUBERT 10A determine the  $b$ - and  $c$ -quark masses from a fit to the inclusive decay spectra in semileptonic  $B$  decays in the kinetic scheme (and convert it to the  $\overline{MS}$  scheme). We have converted this to the 1S scheme.

6 MCNEILE 10 determines  $m_b$  by comparing four-loop perturbative results for the pseudoscalar current to lattice simulations with  $N_f = 2+1$  sea-quarks by the HPQCD collaboration. We have converted  $\overline{m}_b(\overline{m}_b)$  to the 1S scheme.

7 CHETYRKIN 09 determine  $m_c$  and  $m_b$  from the  $e^+e^- \rightarrow Q\overline{Q}$  cross-section and sum rules, using a four-loop computation of the heavy quark vacuum polarization. We have converted their  $m_b$  to the 1S scheme.

8 ABDALLAH 08D determine  $\overline{m}_b(M_Z) = 3.76 \pm 1.0$  GeV from a leading order study of four-jet rates at LEP. We have converted this to  $\overline{m}_b(\overline{m}_b)$  and  $m_b^{1S}$ .

9 SCHWANDA 08 measure moments of the inclusive photon spectrum in  $B \rightarrow X_S \gamma$  decay to determine  $m_b^{1S}$ . We have converted this to  $\overline{MS}$  scheme.

10 ABDALLAH 06D determine  $m_b(M_Z) = 2.85 \pm 0.32$  GeV from  $Z$ -decay three-jet events containing a  $b$ -quark. We have converted this to  $\overline{m}_b(\overline{m}_b)$  and  $m_b^{1S}$ .

11 BOUGHEZAL 06  $\overline{MS}$  scheme result comes from the first moment of the hadronic production cross-section to order  $\alpha_s^3$ . We have converted it to the 1S scheme.

12 BUCHMULLER 06 determine  $m_b$  and  $m_c$  by a global fit to inclusive  $B$  decay spectra. We have converted this to the 1S scheme.

13 PINEDA 06  $\overline{MS}$  scheme result comes from a partial NNLL evaluation (complete at NNLO) of sum rules of the bottom production cross-section in  $e^+e^-$  annihilation. We have converted it to the 1S scheme.

14 BAUER 04 determine  $m_b$ ,  $m_c$  and  $m_b - m_c$  by a global fit to inclusive  $B$  decay spectra. We have converted  $m_b$  to the 1S scheme.

16 HOANG 04 determine  $\overline{m}_b(\overline{m}_b)$  from moments at order  $\alpha_s^2$  of the bottom production cross-section in  $e^+e^-$  annihilation.

17 BORDES 03 determines  $m_b$  using QCD finite energy sum rules to order  $\alpha_s^2$ .

18 CORCELLA 03 determines  $\overline{m}_b$  using sum rules computed to order  $\alpha_s^2$ . Includes charm quark mass effects.

19 EIDEMULLER 03 determines  $\overline{m}_b$  and  $\overline{m}_c$  using QCD sum rules.

20 ERLER 03 determines  $\overline{m}_b$  and  $\overline{m}_c$  using QCD sum rules. Includes recent BES data.

21 MAHMOOD 03 determines  $m_b^{1S}$  by a fit to the lepton energy moments in  $B \rightarrow X_c \ell \nu_\ell$  decay. The theoretical expressions used are of order  $1/m^3$  and  $\alpha_s^2 \beta_0$ . We have converted their result to the  $\overline{MS}$  scheme.

22 BRAMBILLA 02 determine  $\overline{m}_b(\overline{m}_b)$  from a computation of the  $\Upsilon(1S)$  mass to order  $\alpha_s^4$ , including finite  $m_c$  corrections. We have converted this to the 1S scheme.

23 PENIN 02 determines  $\overline{m}_b$  from the spectrum of the  $\Upsilon$  system.

24 NARISON 12 determines  $m_b$  using exponential sum rules for the vector current correlator to order  $\alpha_s^3$ , including the effect of gluon condensates up to dimension eight. We have converted  $\overline{m}_b(\overline{m}_b)$  to the 1S scheme.

25 NARISON 12A determines  $m_b$  using sum rules for the vector current correlator to order  $\alpha_s^3$ , including the effect of gluon condensates up to dimension eight. We have converted  $\overline{m}_b(\overline{m}_b)$  to the 1S scheme.

26 NARISON 10 determines  $m_b$  from ratios of moments of vector current correlators computed to order  $\alpha_s^3$  and including the dimension-six gluon condensate. These values are taken from the erratum to that reference.

27 GUAZZINI 08 determine  $\overline{m}_b(\overline{m}_b)$  from a quenched lattice simulation of heavy meson masses. The  $\pm 0.08$  is an estimate of the quenching error. We have converted these values to the 1S scheme.

28 DELLA-MORTE 07 determine  $\overline{m}_b(\overline{m}_b)$  from a computation of the spin-averaged  $B$  meson mass using quenched lattice HQET at order  $1/m$ . The  $\pm 0.08$  is an estimate of the quenching error.

29 KUHN 07 determine  $\overline{m}_b(\mu = 10 \text{ GeV}) = 3.609 \pm 0.025$  GeV and  $\overline{m}_b(\overline{m}_b)$  from a four-loop sum-rule computation of the cross-section for  $e^+e^- \rightarrow$  hadrons in the bottom threshold region. We have converted this to the 1S scheme.

30 GRAY 05 determines  $\overline{m}_b(\overline{m}_b)$  from a lattice computation of the  $\Upsilon$  spectrum. The simulations have 2+1 dynamical light flavors. The  $b$  quark is implemented using NRQCD.

31 AUBERT 04x obtain  $m_b$  from a fit to the hadron mass and lepton energy distributions in semileptonic  $B$  decay. The paper quotes values in the kinetic scheme. The  $\overline{MS}$  value has been provided by the BABAR collaboration, and we have converted this to the 1S scheme.

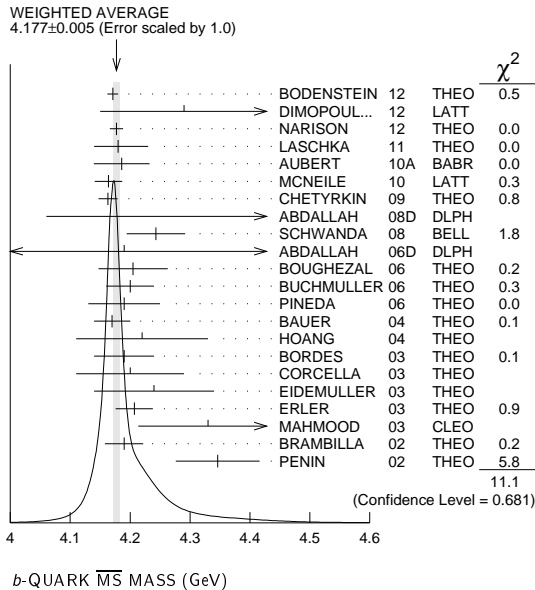
32 MCNEILE 04 use lattice QCD with dynamical light quarks and a static heavy quark to compute the masses of heavy-light mesons.

33 BAUER 03 determine the  $b$  quark mass by a global fit to  $B$  decay observables. The experimental data includes lepton energy and hadron invariant mass moments in semileptonic  $B \rightarrow X_c \ell \nu_\ell$  decay, and the inclusive photon spectrum in  $B \rightarrow X_S \gamma$  decay. The theoretical expressions used are of order  $1/m^3$ , and  $\alpha_s^2 \beta_0$ .

34 DEDIVITIIS 03 use a quenched lattice computation of heavy-heavy and heavy-light meson masses.

# Quark Particle Listings

*b, t*



b-QUARK  $\overline{MS}$  MASS (GeV)

## b-QUARK REFERENCES

BODENSTEIN	12	PR D85 034003	S. Bodenstein <i>et al.</i>	
DIMOPOUL...	12	JHEP 1201 046	P. Dimopoulos <i>et al.</i>	(ETM Collab.)
NARISON	12	PL B707 259	S. Narison	(MONP)
NARISON	12A	PL B706 412	S. Narison	(MONP)
LASCHKA	11	PR D83 094002	A. Laschka, N. Kaiser, W. Weise	
AUBERT	10A	PR D81 032003	B. Aubert <i>et al.</i>	(BABAR Collab.)
MCNEILE	10	PR D82 034512	C. McNeile <i>et al.</i>	(HPQCD Collab.)
NARISON	10	PL B693 959	S. Narison	(MONP)
Also		PL B705 544 (errata.)	S. Narison	(MONP)
CHETYRKIN	09	PR D80 074010	K.G. Chetyrkin <i>et al.</i>	(KARL, BNL)
ABDALLAH	08D	EPJ C95 525	J. Abdallah <i>et al.</i>	(DELPHI Collab.)
GUAZZINI	08	JHEP 0801 076	D. Guazzini, R. Sommer, N. Tantalo	
SCHWANDA	08	PR D78 032016	C. Schwanda <i>et al.</i>	(BELLE Collab.)
DELLA-MOR...	07	JHEP 0701 007	M. Della Morte <i>et al.</i>	
KUHN	07	NP B778 192	J.H. Kuhn, M. Steinhauser, C. Sturm	
ABDALLAH	06D	EPJ C46 569	J. Abdallah <i>et al.</i>	(DELPHI Collab.)
BOUGHEZAL	06	PR D74 074006	R. Boughezal, M. Czakon, T. Schutzmeier	
BUCHMULLER	06	PR D73 073008	O.L. Buchmuller, H.U. Flaecher	
PINEDA	06	PR D73 111501R	A. Pineda, A. Signer	
GRAY	05	PR D72 094507	A. Gray <i>et al.</i>	(HPQCD, UKQCD Collab.)
AUBERT	04X	PRL 93 011803	B. Aubert <i>et al.</i>	(BABAR Collab.)
BAUER	04	PR D70 094017	C. Bauer <i>et al.</i>	
HOANG	04	PL B594 127	A.H. Hoang, M. Jamin	
MCNEILE	04	PL B600 77	C. McNeile, C. Michael, G. Thompson	(UKQCD Collab.)
BAUER	03	PR D67 054012	C.W. Bauer <i>et al.</i>	
BORDES	03	PL B562 81	J. Bordes, J. Penarrocha, K. Schilcher	
CORCELLA	03	PL B554 133	G. Corcella, A.H. Hoang	
DEDIVITIIS	03	NP B675 309	G.M. de Divitiis <i>et al.</i>	
EIDEMULLER	03	PR D67 113002	M. Eidemuller	
ERLER	03	PL B558 125	J. Erler, M. Luo	
MAHMOOD	03	PR D67 072001	A.H. Mahmood <i>et al.</i>	(CLEO Collab.)
BRAMBILLA	02	PR D65 034001	N. Brambilla, Y. Sumino, A. Vairo	
EL-KHADRA	02	ARNPS 92 201	A.X. El-Khadra, M. Luke	
PENIN	02	PL B538 335	A. Penin, M. Steinhauser	

**t**

$$I(J^P) = 0(\frac{1}{2}^+)$$

$$\text{Charge} = \frac{2}{3} e \quad \text{Top} = +1$$

## THE TOP QUARK

Updated December 2011 by T.M. Liss (Univ. Illinois) and A. Quadt (Univ. Göttingen).

**A. Introduction:** The top quark is the  $Q = 2/3$ ,  $T_3 = +1/2$  member of the weak-isospin doublet containing the bottom quark (see the review on the “Electroweak Model and Constraints on New Physics” for more information). This note summarizes the properties of the top quark (mass, production cross section, decay branching ratios, *etc.*), and provides a discussion of the experimental and theoretical issues involved in their determination

### B. Top quark production at the Tevatron and LHC:

In hadron collisions, top quarks are produced dominantly in pairs through the QCD processes  $q\bar{q} \rightarrow t\bar{t}$  and  $gg \rightarrow t\bar{t}$ . In  $p\bar{p}$

collisions at the Tevatron with  $\sqrt{s} = 1.96$  TeV the most recent calculations are at NLO with next-to-leading-log soft gluon resummation [1], and at approximate next-to-next-to-leading order (NNLO) [2]. Cacciari *et al.* give a production cross section of 7.93 pb for  $m_t = 172.5$  GeV/ $c^2$  with MRST2006nnlo PDFs. Over the range  $150$  GeV/ $c^2 \leq m_t \leq 190$  GeV/ $c^2$  the calculated cross section changes by approximately 0.24 pb/(GeV/ $c^2$ ) for  $m_t$  greater or less than 172.5 GeV/ $c^2$ . An approximate NNLO calculation by Kidonakis and Vogt yields a production cross section of 7.68 pb for  $m_t = 172.5$  GeV/ $c^2$  using MRST2006nnlo, with nearly the same mass-dependence. The difference in the central value obtained using different PDFs is typically a few tenths of a pb or less. Langenfeld *et al.* [3], in an approximate NNLO calculation find 7.04 pb for  $m_t = 173$  GeV/ $c^2$  using MSTW2008nnlo. The uncertainties on these calculations, due to the choice of scale, which is set at  $\mu = m_t$ , are typically 0.5 pb or less. In  $pp$  collisions at the LHC with  $\sqrt{s} = 7$  TeV, Langenfeld *et al.* calculate an approximate NNLO production cross section of 161 pb for  $m_t = 172.5$  GeV/ $c^2$  using CTEQ6.6 with an uncertainty of less than 10%. Approximately 85% of the production cross section at the Tevatron is from  $q\bar{q}$  annihilation, with the remainder from gluon-gluon fusion [4], while at LHC energies about 90% of the production is from the latter process at  $\sqrt{s} = 14$  TeV ( $\approx 80\%$  at  $\sqrt{s} = 7$  TeV). The resulting theoretical prediction of the top quark cross-section at the LHC is  $\sigma_{t\bar{t}} = 165_{-16}^{+11}$  pb, assuming a top quark mass of 172.5 GeV/ $c^2$  [5].

Somewhat smaller cross sections are expected from electroweak single top production mechanisms, namely from  $q\bar{q}' \rightarrow t\bar{b}$  [6] and  $qb \rightarrow q't$  [7], mediated by virtual  $s$ -channel and  $t$ -channel W bosons, respectively. At the Tevatron, the production cross sections of top and antitop are identical, while at the LHC they are not. Approximate NNLO cross sections for  $t$ -channel single top quark production are calculated for  $m_t = 173$  GeV/ $c^2$  to be 1.04 pb in  $p\bar{p}$  collisions at  $\sqrt{s} = 1.96$  TeV and 41.7 pb in  $pp$  collisions at  $\sqrt{s} = 7$  TeV [8]. For the  $s$ -channel, these calculations yield 0.52 pb for the Tevatron, and 3.2 pb for  $\sqrt{s} = 7$  TeV LHC [9]. The corresponding single *anti*-top-quark cross sections at the LHC are 22.5 pb and 1.4 pb for  $t$ - and  $s$ -channel, respectively, at  $\sqrt{s} = 7$  TeV. At LHC energies, the production of a single top quark in association with a  $W^-$  boson, through  $bg \rightarrow W^-t$ , becomes relevant. At  $\sqrt{s} = 7$  TeV, an approximate NNLO calculation using the MSTW2008 PDF gives 8.1 pb [10]. The production cross section for single *anti*-top quarks in this channel ( $W^+t$ ) is the same as for single top quarks.

The cross sections for single top production are proportional to  $|V_{tb}|^2$ , and no assumption is needed on the number of quark families or on the unitarity of the CKM matrix in extracting  $|V_{tb}|$ . Separate measurements of the  $s$ - and  $t$ -channel processes provide sensitivity to physics beyond the Standard Model (SM) [11].

The identification of top quarks in the electroweak single-top channel is much more difficult than in the QCD  $t\bar{t}$  channel,

due to a less distinctive signature and significantly larger backgrounds.

In top decay, the  $Ws$  and  $Wd$  final states are expected to be suppressed relative to  $Wb$  by the square of the CKM matrix elements  $V_{ts}$  and  $V_{td}$ . Assuming unitarity of the three-generation CKM matrix, these matrix element values are estimated to be less than 0.043 and 0.014, respectively, implying a value of  $V_{tb} > 0.999$  (see the review “The CKM Quark-Mixing Matrix” for more information). With a mass above the  $Wb$  threshold, and  $V_{tb}$  close to unity, the decay width of the top quark is expected to be dominated by the two-body channel  $t \rightarrow Wb$ . Neglecting terms of order  $m_b^2/m_t^2$ ,  $\alpha_s^2$ , and  $(\alpha_s/\pi)M_W^2/m_t^2$ , the width predicted in the Standard Model (SM) at NLO is [12]:

$$\Gamma_t = \frac{G_F m_t^3}{8\pi\sqrt{2}} \left(1 - \frac{M_W^2}{m_t^2}\right)^2 \left(1 + 2\frac{M_W^2}{m_t^2}\right) \left[1 - \frac{2\alpha_s}{3\pi} \left(\frac{2\pi^2}{3} - \frac{5}{2}\right)\right], \quad (1)$$

where  $m_t$  refers to the top quark pole mass. The width for a value of  $m_t = 171$  GeV/ $c^2$ , close to the world average, is 1.29 GeV/ $c^2$  (we use  $\alpha_s(M_Z) = 0.118$ ) and increases with mass. With its correspondingly short lifetime of  $\approx 0.5 \times 10^{-24}$  s, the top quark is expected to decay before top-flavored hadrons or  $t\bar{t}$ -quarkonium-bound states can form [13]. The order  $\alpha_s^2$  QCD corrections to  $\Gamma_t$  are also available [14], thereby improving the overall theoretical accuracy to better than 1%.

The final states for the leading pair-production process can be divided into three classes:

- A.  $t\bar{t} \rightarrow W^+ b W^- \bar{b} \rightarrow q \bar{q}' b q'' \bar{q}''' \bar{b}$ , (45.7%)
- B.  $t\bar{t} \rightarrow W^+ b W^- \bar{b} \rightarrow q \bar{q}' b \ell^- \bar{\nu}_\ell \bar{b} + \ell^+ \nu_\ell b q'' \bar{q}''' \bar{b}$ , (43.8%)
- C.  $t\bar{t} \rightarrow W^+ b W^- \bar{b} \rightarrow \bar{\ell} \nu_\ell b \ell' \bar{\nu}_{\ell'}$ . (10.5%)

The quarks in the final state evolve into jets of hadrons. A, B, and C are referred to as the all-jets, lepton+jets ( $\ell$ +jets), and dilepton ( $\ell\ell$ ) channels, respectively. Their relative contributions, including hadronic corrections, are given in parentheses assuming lepton universality. While  $\ell$  in the above processes refers to  $e$ ,  $\mu$ , or  $\tau$ , most of the results to date rely on the  $e$  and  $\mu$  channels. Therefore, in what follows, we will use  $\ell$  to refer to  $e$  or  $\mu$ , unless otherwise noted.

The initial and final-state quarks can radiate gluons that can be detected as additional jets. The number of jets reconstructed in the detectors depends on the decay kinematics, as well as on the algorithm for reconstructing jets used by the analysis. The transverse momenta of neutrinos are reconstructed from the imbalance in transverse momentum measured in each event (missing  $p_T$ , which is here also missing  $E_T$ ).

NLO Monte Carlo programs are available for the  $t\bar{t}$  production processes [15]. Theoretical estimates of the background processes ( $W$  or  $Z$  bosons+jets and dibosons+jets) using leading order (LO) calculations have large uncertainties. While this limitation affects estimates of the overall production rates, it is believed that the LO determination of event kinematics, and of the fraction of  $W$ +multi-jet events that contain  $b$ - or  $c$ -quarks, are relatively accurate [16]. Comparison to CDF and DØ data,

however, indicates the  $b$ - and  $c$ -quark fractions to be underestimated by the LO generators and hence does not seem to support the theoretical expectations.

**C. Top quark measurements:** Since the discovery of the top quark, direct measurements of  $t\bar{t}$  production have been made at three center-of-mass energies, providing stringent tests of QCD. The first measurements were made in Run I at the Tevatron at  $\sqrt{s} = 1.8$  TeV. In Run II at the Tevatron relatively precise measurements were made at  $\sqrt{s} = 1.96$  TeV. Finally, beginning in 2010 measurements have been made at the LHC at  $\sqrt{s} = 7$  TeV.

Production of single top quarks through electroweak production mechanisms has now been measured with good precision at the Tevatron at  $\sqrt{s} = 1.96$  TeV, and at the LHC at  $\sqrt{s} = 7$  TeV. Recent measurements are beginning to separate the  $s$ - and  $t$ -channel production cross sections, and at the LHC, the  $Wt$  mechanism as well, though only  $t$ -channel is well measured to date. The measurements allow an extraction of the CKM matrix element  $V_{tb}$ .

The top quark mass is now measured at the 0.6% level, by far the most precisely measured quark mass. Together with the  $W$  boson mass measurement, this places strong constraints on the mass of the Standard Model Higgs boson.

With more than 5 fb $^{-1}$  of Tevatron data analyzed as of this writing, and 1 – 2 fb $^{-1}$  of LHC data, many properties of the top quark are now being measured with precision. These include properties related to the production mechanism, such as  $t\bar{t}$  spin correlations, forward-backward or charge asymmetries, and differential production cross sections, as well as properties related to the  $t - W - b$  decay vertex, such as the helicity of the  $W$  bosons from the top decay. In addition, many searches for physics beyond the Standard Model are being performed with increasing reach in both production and decay channels.

In the following sections we review the current status of measurements of the characteristics of the top quark.

### C.1 Top quark production

**C.1.1  $t\bar{t}$  production** Fig. 1 summarizes the  $t\bar{t}$  production cross-section measurements from both the Tevatron and LHC. The most recent measurement from DØ [17], combining the measurements from the dilepton and lepton plus jets final states in 5.4 fb $^{-1}$ , is 7.56 $^{+0.63}_{-0.56}$  pb. From CDF the most precise measurement made recently [18] is in 4.6 fb $^{-1}$  and is a combination of dilepton, lepton plus jets, and all-hadronic final-state measurements, yielding 7.50 ± 0.48 pb. Both of these measurements assume a top mass of 172.5 GeV/ $c^2$ . The dependence of the cross section measurements on the value chosen for the mass is less than that of the theory calculations because it only affects the determination of the acceptance. In some analyses also the shape of topological variables might be modified. At LHC energies, ATLAS [19] combines measurements in the lepton plus jets and dilepton final states with 0.7 fb $^{-1}$  to find 176 ± 14 pb, whereas a more recent analysis of that dataset in the lepton

# Quark Particle Listings

## $t$

plus jets channel without  $b$ -tagging yields the most precise result of  $179 \pm 12$  pb [20] and a measurement in the all-jets channels using  $1.02 \text{ fb}^{-1}$  yields  $167 \pm 80$  pb [21]. CMS [22] uses  $0.8 - 1.1 \text{ fb}^{-1}$  in the lepton plus jets channel and measures  $164 \pm 14$  pb. In the all-hadronic channel they use  $1.1 \text{ fb}^{-1}$  for a cut-based event selection combined with a kinematic fit and obtain  $136 \pm 45$  pb [23]. These should be compared to the theoretical calculations that yield  $7.9 - 6.7$  pb for top masses from  $170$  to  $175 \text{ GeV}/c^2$  respectively [1] at  $\sqrt{s} = 1.96 \text{ TeV}$  and  $\sigma_{t\bar{t}} = 165_{-16}^{+11}$  pb, assuming  $m_t = 172.5 \text{ GeV}/c^2$  at  $\sqrt{s} = 7 \text{ TeV}$  at the LHC [5] (see Listings).

Most of these measurements assume a  $t \rightarrow Wb$  branching ratio of 100%. CDF and DØ have made direct measurements of the  $t \rightarrow Wb$  branching ratio [24]. Comparing the number of events with 0, 1 and 2 tagged  $b$  jets in the lepton+jets channel, and also in the dilepton channel, using the known  $b$ -tagging efficiency, the ratio  $R = B(t \rightarrow Wb) / \sum_{q=d,s,b} B(t \rightarrow Wq)$  can be extracted. In  $5.4 \text{ fb}^{-1}$  of data, DØ measures  $R = 0.90 \pm 0.04$ ,  $2.5\sigma$  from unity. A significant deviation of  $R$  from unity would imply either non-SM top decay (for example a flavor-changing neutral-current decay), or a fourth generation of quarks.

CDF also performs measurements of the  $t\bar{t}$  production cross section normalized to the  $Z$  production cross section in order to reduce the impact of the luminosity uncertainty.

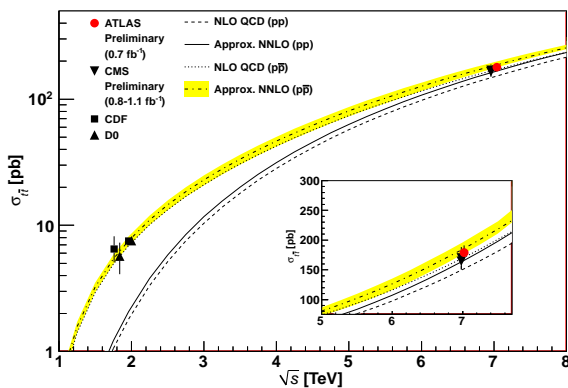


**Figure 1:** Measured and predicted  $t\bar{t}$  production cross sections from Tevatron energies in  $p\bar{p}$  collisions to LHC energies in  $pp$  collisions. Tevatron data points at  $\sqrt{s} = 1.8 \text{ TeV}$  are from Refs. [25] and [26]. Those at  $\sqrt{s} = 1.96 \text{ TeV}$  are from Refs. [17] and [18]. The ATLAS and CMS data points are from Refs. [20] and [22], respectively. Theory curves are generated using HATHOR [5] with input from Ref. [27] for the NLO curves and Ref. [2] for the approximate NNLO curves. Figure adapted from Ref. [19].

In Fig. 1, one sees the importance of  $p\bar{p}$  at Tevatron energies where the valence antiquarks in the antiprotons contribute to the dominant  $q\bar{q}$  production mechanism. At LHC energies the dominant production mode is gluon-gluon fusion and the  $pp$ - $p\bar{p}$  difference nearly disappears. The excellent agreement of these measurements with the theory calculations is a strong validation of QCD and the soft-gluon resummation techniques employed in

the calculations. The measurements are not yet precise enough to distinguish between the NLO and approximate NNLO calculations including their respective PDF uncertainties.

**C.1.2 Single-top production** Single-top quark production was first observed in 2009 by DØ [28] and CDF [29,30] at the Tevatron. The production cross section at the Tevatron is roughly half that of the  $t\bar{t}$  cross section, but the final state with a single  $W$ -boson and typically two jets is less distinct than that for  $t\bar{t}$  and much more difficult to distinguish from the background of  $W$ +jets and other sources. A recent review of the first observation and the techniques used to extract the signal from the backgrounds can be found in [31].

The dominant production at the Tevatron is through  $s$ -channel and  $t$ -channel  $W$ -boson exchange. Associated production with a  $W$ -boson ( $Wt$  production) has a cross section that is too small to observe at the Tevatron. The  $t$ -channel process includes  $qb \rightarrow q't$  and  $qg \rightarrow q't\bar{b}$ , while the  $s$ -channel process is  $q\bar{q}' \rightarrow t\bar{b}$ . The  $s$ - and  $t$ -channel productions can be separated kinematically. This is of particular interest because potential physics beyond the Standard Model, such as fourth-generation quarks, heavy  $W$  and  $Z$  bosons, or flavor-changing-neutral-currents [11], would affect the  $s$ - and  $t$ -channels differently. However, the separation is difficult and initial observations and measurements at the Tevatron by both experiments were of combined  $s + t$ -channel production. The two experiments combined their measurements for maximum precision with a resulting  $s+t$  channel production cross section of  $2.76_{-0.47}^{+0.58}$  pb [32]. The measured value assumes a top quark mass of  $170 \text{ GeV}/c^2$ . The mass dependence of the result comes both from the acceptance dependence and from the  $t\bar{t}$  background evaluation. Also the shape of discriminating topological variables is sensitive to  $m_t$ . It is therefore not necessarily a simple linear dependence but amounts to only a few tenths of picobarns over the range  $170 - 175 \text{ GeV}/c^2$ . The measured value agrees well with the theoretical calculation at  $m_t = 173 \text{ GeV}/c^2$  of  $\sigma_{s+t} = 3.12$  pb (including both top and anti-top production) [8,9].

Both experiments have done separate measurements of the  $s$ - and  $t$ -channel cross sections by reoptimizing the analysis for one or both of the channels separately. In a simultaneous measurement of  $s$ - and  $t$ -channel cross sections, CDF measures  $\sigma_s = 1.8_{-0.5}^{+0.7}$  pb and  $\sigma_t = 0.8_{-0.4}^{+0.4}$  pb, respectively, in  $3.2 \text{ fb}^{-1}$  of data [30], while DØ measures  $2.7_{-0.6}^{+0.7}$  pb and  $0.7_{-0.4}^{+0.4}$  pb, respectively in  $5.4 \text{ fb}^{-1}$  of integrated luminosity [33]. In a separate analysis, optimized for the  $s$ -channel alone, CDF measures  $1.49_{-0.75}^{+0.92}$  pb in  $3.2 \text{ fb}^{-1}$  of data [34].

Recently, DØ has measured the  $t$ -channel production cross section separately in  $5.4 \text{ fb}^{-1}$  of data [35] using a variety of advanced analysis techniques similar to those described in [31]. These take advantage of kinematic differences in such things as the leading  $b$ -tagged jet  $p_T$ , centrality of jets, lepton charge times  $\eta$  of the jets, and the scalar sum of the energy of the final state objects. The  $s$ -channel production is considered a background and integrated over the full measured  $s$ -channel

plane. The  $p\bar{p} \rightarrow tqb + X$  cross section is measured to be  $2.90 \pm 0.59$  pb, assuming a top quark mass of  $172.5 \text{ GeV}/c^2$ . This is in good agreement with the theoretical value at this mass of  $2.08 \pm 0.13$  pb [8]. It should be noted that the theory citations here list cross sections for  $t$  or  $\bar{t}$  alone, whereas the experiments measure the sum. At the Tevatron these cross sections are equal. The theory values quoted here already include this factor of two.

At the LHC the  $t$ -channel cross section is expected to be more than three times as large as  $s$ -channel and  $Wt$  production, combined. Both ATLAS and CMS have measured single top production cross sections at  $\sqrt{s} = 7 \text{ TeV}$  in  $pp$  collisions. In the measurement of the  $t$ -channel cross section, both experiments treat  $s$ -channel and  $Wt$  production as backgrounds. ATLAS uses a counting experiment in  $0.7 \text{ fb}^{-1}$  and combines  $W + 2$  and 3 jet data to measure  $\sigma_t = 90^{+32}_{-22}$  pb [36]. In  $36 \text{ pb}^{-1}$  of data, CMS uses a boosted decision tree and kinematic observables to separate signal from background, and combines the two measurements to find  $\sigma_t = 83.6 \pm 30.0$  pb [37]. The experimental uncertainties are still too large for a precision test, but the measurements are consistent with the theoretical expectation of  $64.2^{+1.8}_{-1.1}$  pb at  $m_t = 173 \text{ GeV}/c^2$  [8]. This theoretical value is the sum of the  $t$  and  $\bar{t}$  production cross sections, which individually are  $41.7$  pb and  $22.5$  pb, respectively, at  $\sqrt{s} = 7 \text{ TeV}$ .

The  $s$ -channel production cross section is expected to be only  $4.6 \pm 0.3$  pb for  $m_t = 173 \text{ GeV}/c^2$  at  $\sqrt{s} = 7 \text{ TeV}$  [9], and has not yet been observed at LHC. The  $Wt$  process has also not yet been observed, but appears a bit closer and has a theoretical cross section of  $15.6 \pm 1.2$  pb [10]. This is of interest because it probes the  $W - t - b$  vertex in a different kinematic region than  $s$ - and  $t$ -channel production, and because of its similarity to the associated production of a charged-Higgs boson and a top quark. The signal is difficult to extract because of its similarity to the  $t\bar{t}$  signature. Similarly, it is difficult to uniquely define because at NLO a subset of diagrams have the same final state as  $t\bar{t}$  and the two interfere [38]. The cross section is calculated using the *diagram removal* technique [39] to define the signal process. In the diagram removal technique the interfering diagrams are removed, at the amplitude level, from the signal definition (an alternate technique, *diagram subtraction* removes these diagrams at the cross-section level and yields similar results). These techniques work provided the selection cuts are defined such that the interference effects are small, which is usually the case.

At ATLAS, a search is performed in  $0.7 \text{ fb}^{-1}$  using dilepton decays of the two putative  $W$  bosons in the final state and selecting events with exactly one high- $p_T$  jet and large missing  $E_T$  [40]. No significant signal is observed yet, and the background-only hypothesis is rejected at only the  $1.2\sigma$  level. Interpreted as a signal, the measured cross section is  $14 \pm 11$  pb. At CMS a recent result has been released using  $2.7 \text{ fb}^{-1}$  of data. CMS also uses the dilepton channel and selects events with at least one high- $p_T$  jet and large missing  $E_T$  [41]. The

CMS analysis requires exactly one  $b$ -tagged jet, which helps to distinguish the signal from non-top backgrounds and from  $t\bar{t}$  production. The observed data are inconsistent with the background-only hypothesis at the  $2.7\sigma$  level. If interpreted as a signal, the measured cross section is  $22^{+9}_{-7}$  pb, consistent with the theoretical expectation.

The CKM matrix element  $V_{tb}$  is extracted from the measured cross sections using the ratio to the theoretical values, which assume  $V_{tb} = 1.0$ . The extracted value therefore depends on the theoretical cross section. The results, including limits at the 95% C.L., are summarized in Table 1.

**Table 1:** Measurements and 95% C.L. limits of  $|V_{tb}|$  from single-top results.

$ V_{tb} $	Source	$\int \mathcal{L} dt \text{ (fb}^{-1}\text{)}$	Ref.
$ V_{tb}  = 0.88 \pm 0.07$	DØ+CDF Run II	2.3-3.2	[32]
$ V_{tb}  > 0.77$	DØ+CDF Run II	2.3-3.2	[32]
$ V_{tb}  = 1.02^{+0.10}_{-0.11}$	DØ	5.4	[33]
$ V_{tb}  = 1.14 \pm 0.22$	CMS	0.036	[37]
$ V_{tb}  > 0.62$	CMS	0.036	[37]

### C.1.3 Top Quark Forward-Backward & Charge Asymmetry:

NLO calculations predict a small forward-backward asymmetry in  $t\bar{t}$  production at the Tevatron of ( $\approx 5.0 \pm 1.5$ )% [42]. The asymmetry arises from an interference between the Born and box diagrams for  $t\bar{t}$  production and between diagrams with initial- and final-state gluon radiation. Both CDF and DØ have measured asymmetry values in excess of the SM prediction, fueling speculation about exotic production mechanisms (see, for example, [43] and references therein). The first measurement of this asymmetry by DØ in  $0.9 \text{ fb}^{-1}$  [44] found an asymmetry at the detector level of  $(12 \pm 8)\%$ . The first CDF measurement in  $1.9 \text{ fb}^{-1}$  [45] yielded  $(24 \pm 14)\%$  at parton level. Both values were higher, though statistically consistent with the small SM expectation. With the addition of more data, the uncertainties have been reduced, but the measured asymmetries remain in excess of the SM expectation. The most recent measurement from DØ in  $5.4 \text{ fb}^{-1}$  finds an asymmetry, corrected for detector acceptance and resolution, of  $(19.6 \pm 6.5)\%$  [46]. From CDF, the most recent measurement combines results in the lepton+jets and dilepton channels, using up to  $5.3 \text{ fb}^{-1}$ , and finds  $(20.1 \pm 6.7)\%$  [47]. CDF has recently reported a mass-dependent asymmetry [48], with a larger asymmetry at large  $t\bar{t}$  invariant mass. DØ does not see any significant increase at large mass [46].

At LHC, where the dominant  $t\bar{t}$  production mechanism is the charge-symmetric gluon-gluon fusion, the measurement is more difficult. For the sub-dominant  $q\bar{q}$  production mechanism, the symmetric  $pp$  collision does not define a forward and backward direction. Instead, the charge asymmetry is defined

# Quark Particle Listings

## *t*

in terms of a positive versus a negative  $t - \bar{t}$  rapidity difference. Both CMS [49] and ATLAS [50] have made preliminary measurements of the charge asymmetry in almost  $1 \text{ fb}^{-1}$ . The uncertainties are still too large for a precision test, but both measurements are consistent with the very small asymmetry expected at the LHC while also not being inconsistent with the larger asymmetry observed at the Tevatron.

### C.2 Top Quark Properties

**C.2.1 Top Quark Mass Measurements:** The most precisely studied property of the top quark is its mass. The top mass has been measured in the lepton+jets, the dilepton, and the all-jets channel by both CDF and DØ. At the LHC, both CMS and ATLAS have made measurements in the lepton+jets channel, CMS also in the dilepton channel. The latest results are summarized in Table 2. The lepton+jets channel yields the most precise single measurements because of good signal to background (in particular after b-tagging) and the presence of only a single neutrino in the final state. The momentum of a single neutrino can be reconstructed (up to a quadratic ambiguity) via the missing  $E_T$  measurement and the constraint that the lepton and neutrino momenta reconstruct to the known  $W$  boson mass.

A large number of techniques have now been applied to measuring the top mass. The original ‘template method’ [51], in which Monte Carlo templates of reconstructed mass distributions are fit to data, has evolved into a precision tool in the lepton+jets channel, where the systematic uncertainty due to the jet energy scale uncertainty is controlled by a simultaneous, *in situ*, fit to the  $W \rightarrow jj$  hypothesis [52]. The latest measurements with this technique, which is now also used in the all-jets channel, are from ATLAS and CDF. In  $0.7 \text{ fb}^{-1}$  of data in the lepton+jets channel, ATLAS already achieves a total uncertainty of better than 2%, with a statistical component of close to 0.5% [53]. The measurement from CDF with  $5.6 \text{ fb}^{-1}$  [54] achieves a precision of better than 1% in the lepton+jets channel and is combined with a measurement in the dilepton channel yielding a precision of about 0.8%.

The template method is complemented by the ‘matrix element’ method. This method was first applied by the DØ Collaboration [55], and is similar to a technique originally suggested by Kondo *et al.* [56] and Dalitz and Goldstein [57]. In the matrix element method a probability for each event is calculated as a function of the top mass, using a LO matrix element for the production and decay of  $t\bar{t}$  pairs. The *in situ* calibration of dijet pairs to the  $W \rightarrow jj$  hypothesis is now also used with the matrix element technique to constrain the jet energy scale uncertainty. The latest measurement with this technique is from DØ in the lepton+jets channel with  $3.6 \text{ fb}^{-1}$  yielding an uncertainty of about 0.9% [58].

CMS has measured the top mass at LHC using an ‘ideogram’ method, first used by DØ [59], in which a constrained fit is performed and an event-by-event likelihood for signal or background is calculated taking into account all jet-parton

assignments. In the lepton+jets channel at CMS, the measurement has a precision of 2% in just  $0.036 \text{ fb}^{-1}$ . The precision is slightly improved by a combination with a measurement in the dilepton channel.

In the dilepton channel, the signal to background is typically very good, but reconstruction of the mass is non-trivial because there are two neutrinos in the final state, yielding a kinematically unconstrained system. A variety of techniques have been developed to handle this. Recently, an analytic solution to the problem has been proposed [60], but this has not yet been used in the mass measurement. The most precise measurements in the dilepton channel come from the application of the matrix element technique, in which an integration is performed over the unmeasured neutrino energies. A detailed description of the use of the matrix element technique in the dilepton channel is given in [61]. The most recent measurement in the dilepton channel by DØ uses  $5.4 \text{ fb}^{-1}$  of data and has a precision of better than 2% [62].

Several other techniques also yield precise measurements in the dilepton channel. In the neutrino weighting technique a weight is assigned by assuming a top mass value and applying energy-momentum conservation to the top decay, resulting in up to four possible pairs of solutions for the neutrino and anti-neutrino momenta. The missing  $E_T$  calculated in this way is then compared to the observed missing  $E_T$  to assign a weight [63]. Another recent measurement in the dilepton channel uses the Dalitz and Goldstein technique [64]. The precision of these techniques approaches that of the matrix element technique, but the measurements to date have used only  $2 \text{ fb}^{-1}$  of data.

In the all-jets channel there is no ambiguity due to neutrino momenta, but the signal to background is significantly poorer due to the severe QCD multijets background. The emphasis therefore has been on background modeling, and reduction through event selection. The most recent measurement in the all-jets channel, by CDF in  $5.8 \text{ fb}^{-1}$  [65], uses a template method for reconstruction and achieves a precision of almost 1%.

A recent measurement from CDF in  $5.7 \text{ fb}^{-1}$  uses a neural net to select events with a missing  $E_T$  plus jets signature [66]. A modified template method is used to extract the top mass, and a precision of about 1.5% is achieved.

The dominant systematic uncertainty in these methods is the understanding of the jet energy scale, and so several techniques have been developed that have little sensitivity to the jet energy scale uncertainty. These include the measurement of the top mass using the following techniques: Fitting of the lepton  $p_T$  spectrum of candidate events [67]; Fitting of the transverse decay length of the  $b$ -jet ( $L_{xy}$ ) [68]; Fitting the invariant mass of a lepton from the  $W$ -decay and a muon from the semileptonic  $b$  decay [69].

Several measurements have now been made in which the top mass is extracted from the measured cross section using the theoretical relationship between the mass and the production

cross section. This allows an extraction of both the pole and  $\overline{\text{MS}}$  mass [70]. The direct measurements of the top mass, such as those shown in Table 2, are generally assumed to be measurements of the pole mass. Strictly speaking, the mass measured in these direct measurements is the mass used in the Monte Carlo generators, but the relation between the Monte Carlo generator mass and the pole mass is uncertain at the level of 1 GeV [71], which is now comparable to the measurement uncertainty.

**Table 2:** Measurements of top quark mass from Tevatron and LHC.  $\int \mathcal{L} dt$  is given in  $\text{fb}^{-1}$ . The results shown are mostly preliminary (not yet submitted for publication as of December 2011); for a complete set of published results see the Listings. Statistical uncertainties are listed first, followed by systematic uncertainties.

$m_t$ (GeV/ $c^2$ )	Source	$\int \mathcal{L} dt$	Ref.	Channel
$175.1 \pm 0.8 \pm 1.3$	DØ	Run I+II $\leq 5.4$	[72]	$\ell$ +jets + $\ell\ell$
$172.5 \pm 1.4 \pm 1.5$	CDF Run II	5.8	[65]	All jets
$172.3 \pm 2.4 \pm 1.0$	CDF Run II	5.7	[66]	Missing $E_T$ +jets
$172.3 \pm 3.4 \pm 2.1$	CDF Run II	2.0	[64]	$\ell\ell$
$172.7 \pm 9.3 \pm 3.7$	CDF Run II	2.2	[73]	$\tau$ +jets
$172.7 \pm 0.6 \pm 0.9$	CDF Run I+II	$\leq 5.8$	[74]	Multiple channels
$173.4 \pm 1.9 \pm 2.7$	CMS	0.036	[75]	$\ell$ +jets + $\ell\ell$
$175.9 \pm 0.9 \pm 2.7$	ATLAS	0.70	[53]	$\ell$ +jets
$173.5 \pm 0.6 \pm 0.8^*$	CDF,DØ CMS			publ. results, PDG best
$173.2 \pm 0.6 \pm 0.8^{**}$	CDF,DØ (I+II)	$\leq 5.8$	[76]	publ. or prelim. results

\* PDG uses this result as its best value. It is a combination of published measurements. See Listings for more details.

\*\*The TEVEWWG world average is a combination of published Run I and preliminary or pub. Run-II meas., yielding a  $\chi^2$  of 8.3 for 11 deg. of freedom.

Current global fits performed within the SM or its minimal supersymmetric extension, in which the top-mass measurements play a crucial role, provide indications for a relatively light Higgs (see “ $H^0$  Indirect Mass Limits” in the Particle Listings of this *Review* for more information). Such fits, including  $Z$ -pole data [77] and direct measurements of the mass and width of the  $W$ -boson, yield a pole top mass  $m_t = 179_{-9}^{+12}$  GeV/ $c^2$  [78]. A fit including additional electroweak precision data (see the review “Electroweak Model and Constraints on New Physics” in this *Review*) yields  $m_t = 177.5_{-7.8}^{+9.4}$  GeV/ $c^2$ . Both indirect evaluations are in good agreement with the direct top quark mass measurements. A review of top quark mass measurements can be found in reference [79].

**C.2.2 Top Quark Spin Correlations and Width:** One of the unique features of the top quark is that it typically decays before its spin can be depolarized by the strong interaction.

Thus the top quark polarisation is directly observable via the angular distribution of its decay products. Hence, it is possible to define and measure observables sensitive to the top quark spin and its production mechanism. Although the top and antitop quarks are produced in strong interactions essentially unpolarized in hadron collisions, the spins of  $t$  and  $\bar{t}$  are correlated. For QCD processes, the  $t\bar{t}$  system is dominantly produced in a  $^3S_1$  state with parallel spins for  $q\bar{q}$  annihilation or in a  $^1S_0$  state with antiparallel spins for gluon-gluon fusion. Hence, the situation at the Tevatron and at the LHC are complementary. The sensitivity to top spin is greatest when the top quark daughters are down-type fermions (charged leptons or  $d$ -type quarks), in which case the joint angular distribution is [80–82]

$$\frac{1}{\sigma} \frac{d^2\sigma}{d(\cos\theta_+)d(\cos\theta_-)} = \frac{1 + \kappa \cdot \cos\theta_+ \cdot \cos\theta_-}{4}, \quad (2)$$

where  $\theta_+$  and  $\theta_-$  are the angles of the daughters in the top rest frames with respect to a particular spin quantization axis. The maximum value for  $\kappa$ , 0.782 at NLO at the Tevatron [83], is found in the off-diagonal basis [80] while at the LHC the value at NLO is 0.326 in the helicity basis [83]. The spin correlation could be modified by a new production mechanism such as  $Z'$  bosons, Kaluza-Klein gluons or the Higgs boson.

CDF uses 5.1  $\text{fb}^{-1}$  in the dilepton channel to measure the correlation coefficient in the beam axis [84]. They use the expected distributions of  $(\cos\theta_+, \cos\theta_-)$  and  $(\cos\theta_b, \cos\theta_{\bar{b}})$  of the charged leptons or the  $b$ -quarks in the  $t\bar{t}$  signal and background templates to calculate a likelihood of observed reconstructed distributions as a function of assumed  $\kappa$ . They determine the 68% confidence interval for the correlation coefficient  $\kappa$  as  $-0.52 < \kappa < 0.61$  or  $\kappa = 0.04 \pm 0.56$  assuming  $m_t = 172.5$  GeV/ $c^2$ .

CDF also analyzes lepton+jets events in 5.3  $\text{fb}^{-1}$  [85] assuming  $m_t = 172.5$  GeV/ $c^2$ . They form three separate templates - the same-spin template, the opposite-spin template, and the background template for the 2-dimensional distributions in  $\cos(\theta_l)\cos(\theta_d)$  vs.  $\cos(\theta_l)\cos(\theta_b)$ . The fit to the data in the helicity basis returns an opposite helicity fraction of  $F_{OH} = 0.74 \pm 0.24(\text{stat}) \pm 0.11(\text{syst})$ . Converting this to the spin correlation coefficient yields  $\kappa_{\text{helicity}} = 0.48 \pm 0.48(\text{stat}) \pm 0.22(\text{syst})$ . In the beamline basis, they find an opposite spin fraction of  $F_{OS} = 0.86 \pm 0.32(\text{stat}) \pm 0.13(\text{syst})$  which can be converted into a correlation coefficient of  $\kappa_{\text{beam}} = 0.72 \pm 0.64(\text{stat}) \pm 0.26(\text{syst})$ .

DØ performs a measurement of the ratio  $f$  of events with correlated  $t$  and  $\bar{t}$  spins to the total number of  $t\bar{t}$  events in 5.3  $\text{fb}^{-1}$  in the 1+jets channel using a matrix element technique [86]. From 729 events they obtain  $f_{\text{meas}} = 1.15_{-0.43}^{+0.42}$  (stat + syst) and can exclude values of  $f < 0.420$  at the 95% C.L. In the dilepton channel [87], they also use a matrix element method and can exclude the hypothesis that the spins of the  $t\bar{t}$  are uncorrelated at the 97.7% C.L.. The combination [86] yields  $f_{\text{meas}} = 0.85 \pm 0.29$  (stat + syst) and a  $t\bar{t}$  production cross section which is in good agreement with the SM prediction

# Quark Particle Listings

*t*

and previous measurements. For an expected fraction of  $f = 1$ , they can exclude  $f < 0.481$  at the 95% C.L. For the observed value of  $f_{meas} = 0.85$ , they can exclude  $f < 0.344(0.052)$  at the 95(99.7)% C.L. The observed fraction  $f_{meas}$  translates to a measured asymmetry value of  $A_{meas} = 0.66 \pm 0.23$  (stat + syst). They therefore obtain first evidence of SM spin correlation at 3.1 standard deviations.

Using  $5.4 \text{ fb}^{-1}$  of data,  $D\mathcal{O}$  measures the correlation in the dilepton channel also from the angles of the two leptons in the  $t$  and  $\bar{t}$  rest frames, yielding a correlation strength  $C = 0.10 \pm 0.45$  [88], in agreement with the NLO QCD prediction, but also in agreement with the no correlation hypothesis.

The ATLAS collaboration has performed a study of spin correlation in  $t\bar{t}$  production at  $\sqrt{s} = 7 \text{ TeV}$  using  $0.70 \text{ fb}^{-1}$  of data. Candidate events are selected in the dilepton topology with large missing transverse energy and at least two jets. The difference in azimuthal angle between the two charged leptons is compared to the expected distributions in the Standard Model, and to the case where the top quarks are produced with uncorrelated spin. Using the helicity basis as the quantisation axis, the strength of the spin correlation between the top and antitop quark is measured to be  $A_{helicity} = 0.34^{+0.15}_{-0.11}$  [89], which is in agreement with the NLO Standard Model prediction.

Related to the measurement of top-spin correlations, which requires a top lifetime less than the hadronization timescale, is the measurement of the top width. The top width is expected to be of order  $1 \text{ GeV}/c^2$  (Eq. 1). The sensitivity of current experiments does not approach this level in direct measurements.

CDF presents a measurement of the top quark width in the lepton+jets decay channel of  $t\bar{t}$  events from a data sample corresponding to  $4.3 \text{ fb}^{-1}$  of integrated luminosity, yielding 756 events. The top quark mass and the mass of the hadronically decaying  $W$  boson that comes from the top quark decay are reconstructed for each event and compared with templates of different top quark widths ( $\Gamma_t$ ) and deviations from nominal jet energy scale ( $\Delta JES$ ) to perform a simultaneous fit for both parameters, where  $\Delta JES$  is used for the in situ calibration of the jet energy scale. By applying a Feldman-Cousins approach, they establish an upper limit at 95% C.L. of  $\Gamma_t < 7.6 \text{ GeV}$  and a two-sided 68% C.L. interval of  $0.3 \text{ GeV} < \Gamma_t < 4.4 \text{ GeV}$  [90], consistent with the Standard Model prediction.

$D\mathcal{O}$  extracts the total width of the top quark from the partial decay width  $\Gamma(t \rightarrow Wb)$  and the branching fraction  $B(t \rightarrow Wb)$ .  $\Gamma(t \rightarrow Wb)$  is obtained from the measured  $t$ -channel cross section for single top quark production in  $2.3 \text{ fb}^{-1}$ , and  $B(t \rightarrow Wb)$  is extracted from a measurement of the ratio  $R = B(t \rightarrow Wb)/B(t \rightarrow Wq)$  in  $t\bar{t}$  events in lepton+jets channels with 0, 1 and 2 b-tags in  $1 \text{ fb}^{-1}$  of integrated luminosity. Assuming  $B(t \rightarrow Wq) = 1$ , where  $q$  includes any kinematically accessible quark, the result is:  $\Gamma_t = 1.99^{+0.69}_{-0.55} \text{ GeV}$  which translates to a top quark lifetime of  $\tau_t = (3.3^{+1.3}_{-0.9}) \times 10^{-25} \text{ s}$ . Assuming a high mass fourth generation  $b'$  quark and unitarity of the four-generation quark-mixing matrix, they set the first upper limit on  $|V_{tb'}| < 0.63$  at 95% C.L. [91].

**C.2.3  $W$  Boson Helicity in Top Quark Decay:** The Standard Model dictates that the top quark has the same vector-minus-axial-vector ( $V - A$ ) charged-current weak interactions  $\left(-i\frac{g}{\sqrt{2}}V_{tb}\gamma^\mu\frac{1}{2}(1-\gamma_5)\right)$  as all the other fermions. In the SM, the fraction of top quark decays to longitudinally polarized  $W$  bosons is similar to its Yukawa coupling and hence enhanced with respect to the weak coupling. It is expected to be [92]  $\mathcal{F}_0^{\text{SM}} \approx x/(1+x)$ ,  $x = m_t^2/2M_W^2$  ( $\mathcal{F}_0^{\text{SM}} \sim 70\%$  for  $m_t = 175 \text{ GeV}/c^2$ ). Fractions of left-handed, right-handed, or longitudinal  $W$  bosons are denoted as  $\mathcal{F}_-$ ,  $\mathcal{F}_+$ , and  $\mathcal{F}_0$  respectively. In the SM,  $\mathcal{F}_-$  is expected to be  $\approx 30\%$  and  $\mathcal{F}_+ \approx 0\%$ .

The Tevatron and the LHC experiments use various techniques to measure the helicity of the  $W$  boson in top quark decays, in both the lepton+jets events and dilepton channels.

The first method uses a kinematic fit, similar to that used in the lepton+jets mass analyses, but with the top quark mass constrained to a fixed value, to improve the reconstruction of final-state observables, and render the under-constrained dilepton channel solvable. The distribution of the helicity angle ( $\cos\theta^*$ ) between the lepton and the  $b$  quark in the  $W$  rest frame provides the most direct measure of the  $W$  helicity. In a simplified version of this approach, the  $\cos\theta^*$  distribution is reduced to a forward-backward asymmetry.

The second method ( $p_T^\ell$ ) uses the different lepton  $p_T$  spectra from longitudinally or transversely polarized  $W$ -decays to determine the relative contributions.

A third method uses the invariant mass of the lepton and the  $b$ -quark in top decays ( $M_{l\bar{b}}^2$ ) as an observable, which is directly related to  $\cos\theta^*$ .

At the LHC, top quark pairs in the dilepton channels are reconstructed by solving a set of six independent kinematic equations on the missing transverse energy in  $x$ - and in  $y$ -direction, two  $W$ -masses, and the two top/antitop quark masses. In addition, the two jets with the largest  $p_T$  in the event are interpreted as  $b$ -jets. The pairing of the jets to the charged leptons is based on the minimisation of the sum of invariant masses  $m_{min}$ . Simulations show that this criterion gives the correct pairing in 68% of the events.

Finally, the Matrix Element method (ME) has also been used, in which a likelihood is formed from a product of event probabilities calculated from the ME for a given set of measured kinematic variables and assumed  $W$ -helicity fractions. The results of recent CDF,  $D\mathcal{O}$  and ATLAS analyses are summarized in Table 3.

The datasets are now large enough to allow for a simultaneous fit of  $\mathcal{F}_0$  and  $\mathcal{F}_+$ , which we denote by ‘2-param’ in the table. Results with either  $\mathcal{F}_0$  or  $\mathcal{F}_+$  fixed at its SM value are denoted ‘1-param’. For the simultaneous fits the correlation coefficient between the two values is about  $-0.8$  for both experiments. A complete set of published results can be found in the Listings. All results are in agreement with the SM expectation.



**Table 3:** Measurement and 95% C.L. upper limits of the  $W$  helicity in top quark decays. Most results listed are preliminary and not yet submitted for publication, as of December 2011. A full set of published results is given in the Listings.

$W$ Helicity	Source	$\int \mathcal{L} dt$ ( $\text{fb}^{-1}$ )	Ref.	Method
$\mathcal{F}_0 = 0.71 \pm 0.20$	CDF Run II	5.3	[93]	$\cos \theta^*$ 2-param
$\mathcal{F}_0 = 0.59 \pm 0.11$	CDF Run II	5.3	[93]	$\cos \theta^*$ 1-param
$\mathcal{F}_0 = 0.65 \pm 0.19$	CDF Run II	1.9	[94]	$\cos \theta^*$ 2-param
$\mathcal{F}_0 = 0.59 \pm 0.12$	CDF Run II	1.9	[94]	$\cos \theta^*$ 1-param
$\mathcal{F}_0 = 0.67 \pm 0.13$	DØ Run II	5.4	[95]	$\cos \theta^*$ 2-param
$\mathcal{F}_0 = 0.73 \pm 0.08$	CDF+DØ Run II	5.4	[96]	$\cos \theta^*$ 2-param
$\mathcal{F}_0 = 0.69 \pm 0.06$	CDF+DØ Run II	5.4	[96]	$\cos \theta^*$ 1-param
$\mathcal{F}_0 = 0.57 \pm 0.11$	ATLAS	0.7	[97]	$\cos \theta^*$ 3-param
$\mathcal{F}_0 = 0.75 \pm 0.08$	ATLAS	0.7	[97]	$\cos \theta^*$ , $m_{min}$ 2-par
$\mathcal{F}_+ = -0.07 \pm 0.10$	CDF Run II	5.3	[93]	$\cos \theta^*$ 2-param
$\mathcal{F}_+ = -0.07 \pm 0.05$	CDF Run II	5.3	[93]	$\cos \theta^*$ 1-param
$\mathcal{F}_+ = -0.03 \pm 0.08$	CDF Run II	1.9	[94]	$\cos \theta^*$ 2-param
$\mathcal{F}_+ = -0.04 \pm 0.05$	CDF Run II	1.9	[94]	$\cos \theta^*$ 1-param
$\mathcal{F}_+ = 0.02 \pm 0.05$	DØ Run II	5.4	[95]	$\cos \theta^*$ 2-param
$\mathcal{F}_+ = -0.04 \pm 0.05$	CDF+DØ Run II	5.4	[96]	$\cos \theta^*$ 2-param
$\mathcal{F}_+ = -0.01 \pm 0.04$	CDF+DØ Run II	5.4	[96]	$\cos \theta^*$ 1-param
$\mathcal{F}_+ = 0.09 \pm 0.09$	ATLAS	0.7	[97]	$\cos \theta^*$ 3-param

**C.2.4 Top Quark Electric Charge:** The top quark is the only quark whose electric charge has not been measured through production at threshold in  $e^+e^-$  collisions. Furthermore, it is the only quark whose electromagnetic coupling has not been observed and studied until recently. Since the CDF and DØ analyses on top quark production did not associate the  $b$ ,  $\bar{b}$ , and  $W^\pm$  uniquely to the top or antitop, decays such as  $t \rightarrow W^+\bar{b}, \bar{t} \rightarrow W^-b$  were not excluded. A charge 4/3 quark of this kind is consistent with current electroweak precision data. The  $Z \rightarrow \ell^+\ell^-$  and  $Z \rightarrow b\bar{b}$  data, in particular the discrepancy between  $A_{LR}$  from SLC at SLAC and  $A_{FB}^{0,b}$  of  $b$ -quarks and  $A_{FB}^{0,\ell}$  of leptons from LEP at CERN, can be fitted with a top quark of mass  $m_t = 270 \text{ GeV}/c^2$ , provided that the right-handed  $b$  quark mixes with the isospin +1/2 component of an exotic doublet of charge  $-1/3$  and  $-4/3$  quarks,  $(Q_1, Q_4)_R$  [98,99].

DØ studies the top quark charge in double-tagged lepton+jets events, CDF does it in single-tagged lepton+jets and dilepton events. Assuming the top and antitop quarks have equal but opposite electric charge, then reconstructing the charge of the  $b$ -quark through jet charge discrimination techniques, the  $|Q_{top}| = 4/3$  and  $|Q_{top}| = 2/3$  scenarios can be differentiated. For the exotic model of Chang *et al.* [99] with a top quark charge  $|Q_{top}| = 4/3$ , DØ excludes the exotic model at 91.2% C.L.% [100] using  $370 \text{ pb}^{-1}$ , while CDF excludes the model at 99% C.L. [101] in  $5.6 \text{ fb}^{-1}$ . Both results indicate that the observed particle is indeed consistent with being a SM  $|Q_{top}| = 2/3$  quark. In  $0.70 \text{ fb}^{-1}$ , ATLAS performed a similar

analysis, reconstructing the  $b$ -quark charge either via a jet-charge technique or via the lepton charge in soft muon decays in combination with a kinematic likelihood fit. They exclude the exotic scenario at more than  $5 \sigma$  [102].

The electromagnetic or the weak coupling of the top quark can be probed directly by investigating  $t\bar{t}$  events with an additional gauge boson, like  $t\bar{t}\gamma$  and  $t\bar{t}Z$  events. Top quark pair events with additional photons in the final state are directly sensitive to the  $t\bar{t}\gamma$  vertex.

CDF performs a search for events containing a lepton, a photon, significant missing transverse momentum, and a jet identified as containing a  $b$ -quark and at least three jets and large total transverse energy in  $1.9 \text{ fb}^{-1}$ . They find 16  $t\bar{t}\gamma$  events with an expectation from SM sources of  $11.2_{-2.1}^{+2.3}$  events which they translate into a measurement of the  $t\bar{t}\gamma$  cross section measurement of  $0.15 \pm 0.08 \text{ pb}$  [103]. Recently, CDF repeated this measurement with  $6.0 \text{ fb}^{-1}$  and reported evidence for the observation of  $t\bar{t}\gamma$  production with a cross section  $\sigma_{t\bar{t}\gamma} = 0.18 \pm 0.08 \text{ pb}$  and a ratio of  $\sigma_{t\bar{t}\gamma}/\sigma_{t\bar{t}} = 0.024 \pm 0.009$  [104].

ATLAS performed a first measurement of the  $t\bar{t}\gamma$  cross section in pp collisions at  $\sqrt{s} = 7 \text{ TeV}$  using  $1.04 \text{ fb}^{-1}$  of data. Events are selected that contain a large transverse momentum electron or muon and a large transverse momentum photon, yielding 52 and 70 events in the electron and muon samples, respectively. The resulting cross section times branching ratio into the single lepton and dilepton channels for  $t\bar{t}\gamma$  production with a photon with transverse momentum above 8 GeV is  $\sigma(t\bar{t}\gamma) = 2.0 \pm 0.5(\text{stat.}) \pm 0.7(\text{syst.}) \pm 0.1(\text{lumi.}) \text{ pb}$  [105], which is consistent with theoretical calculations. A real test, however, of the vector and axial vector couplings in  $t\bar{t}\gamma$  events or searches for possible tensor couplings of top quarks to photons will only be feasible with an integrated luminosity of several  $\text{fb}^{-1}$  in the future.

### C.3 Searches for Non-Standard Model Top Quark Production & Decay:

Motivated by the large mass of the top quark, several models suggest that the top quark plays a role in the dynamics of electroweak symmetry breaking. One example is topcolor [106], where a large top quark mass can be generated through the formation of a dynamic  $t\bar{t}$  condensate,  $X$ , which is formed by a new strong gauge force coupling preferentially to the third generation. Another example is topcolor-assisted technicolor [107], predicting a heavy  $Z'$  boson that couples preferentially to the third generation of quarks with cross sections expected to be visible at the Tevatron and the LHC. CDF, DØ ATLAS, and CMS have searched for  $t\bar{t}$  production via intermediate, narrow-width, heavy-vector bosons  $X$  in the lepton+jets, the dilepton or the all-jets channels.

CDF has searched for resonant production of  $t\bar{t}$  pairs in  $4.8 \text{ fb}^{-1}$  of data in the lepton+jets channel. A matrix element reconstruction technique is used; for each event a probability density function (pdf) of the  $t\bar{t}$  candidate invariant mass is sampled. These pdfs are used to construct a likelihood function, whereby the cross section for resonant  $t\bar{t}$  production is

# Quark Particle Listings

*t*

estimated, given a hypothetical resonance mass and width. The data indicate no evidence of resonant production of  $t\bar{t}$  pairs. A benchmark model of leptophobic  $Z \rightarrow t\bar{t}$  is excluded with  $m_{Z'} < 900$  GeV at 95% C.L. [108]. A similar analysis has been performed in the all-jets channel using  $2.8 \text{ fb}^{-1}$  of data [109]. In the absence of any evidence for top-antitop quark resonant production upper limits on the production cross section times branching ratio for a specific topcolor assisted technicolor model with width of  $\Gamma_{Z'} = 0.012M_{Z'}$  are set. Within this model, they exclude  $Z'$  bosons with masses below 805 GeV at the 95% C.L.

DØ has searched for narrow  $t\bar{t}$  resonances that decay into a lepton+jets final state based on  $5.3 \text{ fb}^{-1}$ . They place upper limits on the production cross section times branching fraction to  $t\bar{t}$  in comparison to the prediction for a leptophobic topcolor  $Z'$  boson. They exclude such a resonance at the 95% C.L. for masses below 835 GeV at width  $\Gamma_{Z'} = 0.012M_{Z'}$  [110]. This limit turns out to be independent of couplings of the  $t\bar{t}$  resonance (pure vector, pure axial-vector, or Standard Model Z-like) and is valid for any narrow resonance decaying 100% to a  $t\bar{t}$  final state.

ATLAS has performed a search for  $t\bar{t}$  resonances in the lepton+jets final states using  $0.2 \text{ fb}^{-1}$  of data at  $\sqrt{s} = 7$  TeV. No evidence for a resonance is found. Using the reconstructed  $t\bar{t}$  mass spectrum, limits are set on the production cross-section times branching ratio to  $t\bar{t}$  for narrow and wide resonances. For narrow  $Z'$  models, the observed 95% C.L. limits range from approximately 38 pb to 3.2 pb for masses going from  $m_{Z'} = 500$  GeV to  $m_{Z'} = 1300$  GeV [111]. In Randall-Sundrum models, Kaluza-Klein gluons with masses below 650 GeV are excluded at 95% C.L. Using  $1.04 \text{ fb}^{-1}$  of data in the dilepton channel, they have not observed any significant excess and place upper limits at the 95% C.L. on the cross section times branching ratio of the resonance decaying to  $t\bar{t}$  pairs as a function of the resonance pole mass. A lower mass limit of 0.84 TeV is set for the case of a Kaluza Klein gluon resonance in the Randall-Sundrum Model [112].

CMS performs a search for massive neutral bosons decaying via a top-antitop quark pair. The analysis is based on  $36 \text{ pb}^{-1}$  of data. From a combined analysis of the muon plus jets and electron plus jets decay modes no significant signal is observed, and upper limits on the production cross section as a function of the boson mass are reported [113]. They also perform a search for narrow heavy resonances decaying to top quark pairs in the  $\mu$ -+jets channel using  $1.1 \text{ fb}^{-1}$  and set sub-picobarn limits at 95% C.L. on  $\sigma(pp \rightarrow Z' \rightarrow t\bar{t})$  for invariant  $Z'$  masses above  $1.35 \text{ TeV}/c^2$  [114]. Using  $0.9 \text{ fb}^{-1}$ , they search in the all-hadronic channel for sufficiently heavy resonances with decay products partially or fully merged into one jet. They set sub-picobarn limits on  $\sigma_{Z'} \times B(Z' \rightarrow t\bar{t})$  at 95% C.L. for  $Z'$  heavier than  $1.1 \text{ TeV}/c^2$  [115].

Both CDF and DØ have searched for non-SM top decays [116–121], particularly those expected in supersymmetric models, such as  $t \rightarrow H^+b$ , followed by  $H^+ \rightarrow \tau^+\nu$  or  $c\bar{s}$ . The  $t \rightarrow H^+b$  branching ratio has a minimum at

$\tan\beta = \sqrt{m_t/m_b} \simeq 6$ , and is large in the region of either  $\tan\beta \ll 6$  or  $\tan\beta \gg 6$ . In the former range,  $H^+ \rightarrow c\bar{s}$  is dominant, while  $H^+ \rightarrow \tau^+\nu$  dominates in the latter range. These studies are based either on direct searches for these final states, or on top “disappearance.” In the standard lepton+jets or dilepton cross-section analyses, any charged-Higgs decays are not detected as efficiently as  $t \rightarrow W^\pm b$ , primarily because the selection criteria are optimized for the standard decays, and because of the absence of energetic isolated leptons in Higgs decays. A significant  $t \rightarrow H^+b$  contribution would give rise to measured  $t\bar{t}$  cross sections that would be lower than the prediction from the SM (assuming that non-SM contributions to  $t\bar{t}$  production are negligible), and the measured cross-section ratio  $\sigma_{t\bar{t}}^{\ell+jets}/\sigma_{t\bar{t}}^{\ell\ell}$  would differ from unity.

In Run II, CDF has searched for charged-Higgs production in dilepton, lepton+jets, and lepton+hadronic tau final states, considering possible  $H^\pm$  decays to  $c\bar{s}$ ,  $\tau\nu$ ,  $t^*b$ , or  $W^+h^0$ , in addition to the SM decay  $t \rightarrow W^+b$  [118,119]. Depending on the top and Higgs-decay branching ratios, which are scanned in a particular 2-Higgs doublet benchmark model, the number of expected events in these decay channels can show an excess or deficit when compared to SM expectations. A model-independent interpretation yields a limit of  $B(t \rightarrow H^\pm b) < 0.91$  at 95% C.L. for  $m_{H^\pm} \approx 100$  GeV, and  $B(t \rightarrow H^\pm b) < 0.4$  in the tauonic model with  $B(H^\pm \rightarrow \tau\nu) = 100\%$ . In a more recent search, the dijet invariant mass in lepton+jets events has been used in  $2.2 \text{ fb}^{-1}$  to search for a charged Higgs decaying to  $c\bar{s}$  with mass above the  $W$  boson mass. The absence of a signal leads to a 95% C.L. limit of  $B(t \rightarrow H^\pm b) \times B(H^\pm \rightarrow c\bar{s}) < 0.1$  to 0.3 for masses between 90 and 150 GeV/ $c^2$  [119].

In  $1 \text{ fb}^{-1}$  of integrated luminosity, the DØ collaboration has used the  $t\bar{t}$  dilepton and lepton+jets events, including  $\tau$  lepton channels, to search for evidence of charged-Higgs decays into  $\tau$  leptons via the ratio of events with  $\tau$  leptons to those with  $e$  and  $\mu$  [120], global fits [121] and topological searches [122]. They exclude regions of  $B(t \rightarrow H^\pm b)$  as a function of Higgs mass, ranging from  $B(t \rightarrow H^\pm b) > 0.12$  at low mass to  $B(t \rightarrow H^\pm b) > 0.2$  at high mass. In a companion analysis they look for evidence of leptophobic charged Higgs production in top decays in which the Higgs decays purely hadronically, leading to a suppression of the measured  $t\bar{t}$  rate in all leptonic channels. They exclude  $B(t \rightarrow H^\pm b) > 0.2$  for charged-Higgs masses between 80 and 155 GeV/ $c^2$ .

DØ combines measurements of the top quark pair production cross section in the  $\ell$ +jets,  $\ell\ell$ , and  $\tau\ell$  final states (where  $\ell$  is an electron or muon) in  $1 \text{ fb}^{-1}$  of data, yielding  $\sigma_{t\bar{t}} = 8.18_{-0.87}^{+0.98}$  pb for  $m_t = 170$  GeV, or based on QCD predictions extract a top quark mass consistent with the world average. In addition, they measure the cross section ratios to be  $\sigma_{ll}/\sigma_{lj} = 0.86_{-0.17}^{+0.19}(\text{stat} + \text{syst})$  and  $\sigma_{\tau\ell}/\sigma_{ll} = 0.97_{-0.29}^{+0.32}(\text{stat} + \text{syst})$ . Based on this, they set upper limits on the branching fractions  $B(t \rightarrow H^+b \rightarrow \tau^+\nu b)$  and  $B(t \rightarrow H^+b \rightarrow c\bar{s}b)$  as a function of the charged Higgs boson mass [123].

See key on page 457

In  $35 \text{ pb}^{-1}$ , ATLAS searches for the decay  $H^+ \rightarrow c\bar{s}$  in the lepton+jets channel by investigation of the invariant  $jj$ -mass spectrum. The observed limits are within one standard deviation of the expected limits and range from  $B = 0.25$  to  $0.14$  for  $m_{H^\pm} = 90$  to  $130 \text{ GeV}/c^2$  [124]. In  $1.03 \text{ fb}^{-1}$  ATLAS searches for  $t\bar{t} \rightarrow \tau(\rightarrow \text{hadrons}) + \text{jets}$ . They set a 95% C.L. limit on the production of branching ratios  $B(t \rightarrow bH^\pm) \times B(H^\pm \rightarrow \tau\nu)$  of  $0.03$  to  $0.10$  for  $H^\pm$  masses in the range  $90 \text{ GeV}/c^2 < m_{H^\pm} < 160 \text{ GeV}/c^2$  [125]. A similar analysis with  $\tau$  decaying to leptons in  $1.03 \text{ fb}^{-1}$ , assuming  $B(H^\pm \rightarrow \tau\nu) = 1$ , this leads to 95% C.L. upper limits on the branching fraction  $B(t \rightarrow bH^\pm)$  between  $5.2\%$  and  $14.1\%$  for  $H^\pm$  masses in the range  $90 \text{ GeV}/c^2 < m_{H^\pm} < 160 \text{ GeV}/c^2$  [126].

The ATLAS collaboration has also searched for FCNC processes in  $0.7 \text{ fb}^{-1}$  of  $t\bar{t}$  events with one top quark decaying through FCNC ( $t \rightarrow qZ$ ) and the other through the Standard Model dominant mode ( $t \rightarrow bW$ ). Only the decays of the  $Z$  boson to charged leptons and leptonic  $W$  boson decays were considered as signal, leading to a final state topology characterised by the presence of three isolated leptons, at least two jets and missing transverse energy from the undetected neutrino. No evidence for an FCNC signal was found. An upper limit on the  $t \rightarrow qZ$  branching ratio of  $B(t \rightarrow qZ) < 1.1\%$  is set at the 95% confidence level, compatible with the expected limit, assuming no FCNC decay, of  $B(t \rightarrow qZ) < 1.3\%$  [127].

More details, and the results of these studies for the exclusion in the  $m_{H^\pm}, \tan\beta$  plane, can be found in the review ‘‘Higgs Bosons: Theory and Searches’’ and in the ‘‘ $H^+$  Mass Limits’’ section of the Higgs Particle Listings of the current edition.

Using up to  $2.7 \text{ fb}^{-1}$  of data, DØ has measured the  $Wtb$  coupling form factors by combining information from the  $W$  boson helicity in top quark decays in  $t\bar{t}$  events and single-top quark production, allowing to place limits on the left-handed and right-handed vector and tensor couplings [128–130].

In  $2.3 \text{ fb}^{-1}$ , DØ excludes the production of  $W'$  bosons with masses below  $863 \text{ GeV}/c^2$  for a  $W'$  boson with Standard Model-like couplings, below  $885 \text{ GeV}/c^2$  for a  $W'$  boson with right-handed couplings that is allowed to decay to both leptons and quarks, and below  $890 \text{ GeV}/c^2$  for a  $W'$  boson with right-handed couplings that is only allowed to decay to quarks [131]. CDF has recently released  $W'$  limits also using the single-top analysis [132]. In  $1.9 \text{ fb}^{-1}$  of Run-II data, a  $W'$  with Standard Model couplings is searched for in the  $t\bar{b}$  decay mode. Masses below  $800 \text{ GeV}/c^2$  are excluded, assuming that any right-handed neutrino is lighter than the  $W'$ , and below  $825 \text{ GeV}/c^2$  if the right-handed neutrino is heavier than the  $W'$ .

CDF reported a search for flavor-changing neutral-current (FCNC) decays of the top quark  $t \rightarrow q\gamma$  and  $t \rightarrow qZ$  in the Run-I data [133], and recently with enhanced sensitivity in Run II [134]. The SM predicts such small rates that any observation would be a sign of new physics. CDF assumes that one top decays via FCNC, while the other decays via  $Wb$ . The Run-I analysis included a  $t \rightarrow q\gamma$  search in which two signatures are examined, depending on whether the  $W$  decays leptonically

or hadronically. For leptonic  $W$  decay, the signature is  $\gamma\ell$  and missing  $E_T$  and two or more jets, while for hadronic  $W$  decay, it is  $\gamma + \geq 4$  jets. In either case, one of the jets must have a secondary vertex  $b$  tag. One event is observed ( $\mu\gamma$ ) with an expected background of less than half an event, giving an upper limit on the top branching ratio of  $B(t \rightarrow q\gamma) < 3.2\%$  at 95% C.L. In the search for  $t \rightarrow qZ$ , CDF considers  $Z \rightarrow \mu\mu$  or  $ee$  and  $W \rightarrow qq'$ , giving a  $Z + \text{four jets}$  signature. A Run-II dataset of  $1.9 \text{ fb}^{-1}$  is found consistent with background expectations and a 95% C.L. on the  $t \rightarrow qZ$  branching fraction of  $< 3.7\%$  (for  $m_t = 175 \text{ GeV}/c^2$ ) is set [134]. By comparison to the number expected from the theoretical production cross section, CDF has used the observed number of double  $b$ -tagged lepton+jets candidate events to place limits on a variety of decay modes, ranging from  $B(t \rightarrow Zc) < 13\%$  to  $B(t \rightarrow \text{invisible}) < 9\%$  [135].

In  $4.1 \text{ fb}^{-1}$ , DØ performs a search for events with  $t\bar{t} \rightarrow \ell'\nu\ell\bar{\ell} + \text{jets}$  ( $\ell, \ell' = e, \mu$ ) and extracts limits on the branching ratio  $B(t \rightarrow Zq)(q = u, c \text{ quarks}) < 3.2\%$  at 95% C.L. [136]. DØ performs also in single-top event candidates with an additional jet searches for flavor changing neutral currents via quark-gluon couplings, using  $2.3 \text{ fb}^{-1}$ . They find consistency between background expectation and observed data and set cross section limits at the 95% C.L. of  $\sigma_{tgc} < 0.20 \text{ pb}$  and  $\sigma_{tgc} < 0.27 \text{ pb}$  which corresponds to limits on the top quark decay branching fractions of  $B(t \rightarrow gu) < 2.0 \cdot 10^{-4}$  and  $B(t \rightarrow gc) < 3.9 \cdot 10^{-3}$  [137].

Constraints on FCNC couplings of the top quark can also be obtained from searches for anomalous single-top production in  $e^+e^-$  collisions, via the process  $e^+e^- \rightarrow \gamma, Z^* \rightarrow t\bar{q}$  and its charge-conjugate ( $q = u, c$ ), or in  $e^\pm p$  collisions, via the process  $e^\pm u \rightarrow e^\pm t$ . For a leptonic  $W$  decay, the topology is at least a high- $p_T$  lepton, a high- $p_T$  jet and missing  $E_T$ , while for a hadronic  $W$ -decay, the topology is three high- $p_T$  jets. Limits on the cross section for this reaction have been obtained by the LEP collaborations [138] in  $e^+e^-$  collisions, and by H1 [139] and ZEUS [140] in  $e^\pm p$  collisions. When interpreted in terms of branching ratios in top decay [141,142], the LEP limits lead to typical 95% C.L. upper bounds of  $B(t \rightarrow qZ) < 0.137$ . Assuming no coupling to the  $Z$  boson, the 95% C.L. limits on the anomalous FCNC coupling  $\kappa_\gamma < 0.13$  and  $< 0.27$  by ZEUS and H1, respectively, are stronger than the CDF limit of  $\kappa_\gamma < 0.42$ , and improve over LEP sensitivity in that domain. The H1 limit is slightly weaker than the ZEUS limit due to an observed excess of five-candidate events over an expected background of  $3.2 \pm 0.4$ . If this excess is attributed to FCNC top quark production, this leads to a total cross section of  $\sigma(ep \rightarrow e + t + X, \sqrt{s} = 319 \text{ GeV}) < 0.25 \text{ pb}$  [139,143].

## References

CDF note references can be retrieved from [www-cdf.fnal.gov/physics/new/top/top.html](http://www-cdf.fnal.gov/physics/new/top/top.html), and DØ note references from [www-d0.fnal.gov/Run2Physics/WWW/documents/Run2Results.htm](http://www-d0.fnal.gov/Run2Physics/WWW/documents/Run2Results.htm) and ATLAS note references from <https://twiki.cern.ch/twiki/bin/view/AtlasPublic/>

## Quark Particle Listings

*t*

TopPublicResults and CMS note references from  
<https://twiki.cern.ch/twiki/bin/view/CMSPublic/PhysicsResultsTOP>.

1. M. Cacciari *et al.*, J. High Energy Phys.0809, 127 (2008); N. Kidonakis and R. Vogt, Phys. Rev. **D78**, 074005 (2008); S. Moch and P. Uwer, Nucl. Phys. (Proc. Supp.) **B183**, 75 (2008).
2. S. Moch and P. Uwer, Phys. Rev. **D78**, 034003 (2008); M. Beneke *et al.* Phys. Lett. **B690**, 483 (2010); M. Beneke, P. Falgari, S. Klein and C. Schwinn, Nucl. Phys. **B855**, 695 (2012); V. Ahrens, M. Neubert, B. D. Pecjak, A. Ferroglia and L. L. Yang, Phys. Lett. **B703**, 135 (2011); M. Cacciari, M. Czakon, M. L. Mangano, A. Mitov and P. Nason, arXiv:1111.5869 [hep-ph] (2011).
3. U. Langenfeld, S. Moch, and P. Uwer, Phys. Rev. **D80**, 054009 (2009); U. Langenfeld, S. Moch, and P. Uwer, arXiv:0907.2527 [hep-ph] (2009).
4. M. Cacciari *et al.*, Sov. Phys. JETP **04**, 068 (2004).
5. M. Aliev *et al.* Comp. Phys. Comm. **182**, 10341046 (2011).
6. S. Cortese and R. Petronzio, Phys. Lett. **B253**, 494 (1991).
7. S. Willenbrock and D. Dicus, Phys. Rev. **D34**, 155 (1986).
8. N. Kidonakis, Phys. Rev. **D83**, 091503 (2011).
9. N. Kidonakis, Phys. Rev. **D81**, 054028 (2010).
10. N. Kidonakis, Phys. Rev. **D82**, 054018 (2010).
11. T. Tait and C.-P. Yuan. Phys. Rev. **D63**, 014018 (2001).
12. M. Jezabek and J.H. Kühn, Nucl. Phys. **B314**, 1 (1989).
13. I.I.Y. Bigi *et al.*, Phys. Lett. **B181**, 157 (1986).
14. A. Czarnecki and K. Melnikov, Nucl. Phys. **B544**, 520 (1999); K.G. Chetyrkin *et al.*, Phys. Rev. **D60**, 114015 (1999).
15. S. Frixione and B. Webber, hep-ph/0402116; S. Frixione and B. Webber, J. High Energy Phys.06, 029 (2002); S. Frixione, P. Nason and B. Webber, J. High Energy Phys.08,007 (2003); S. Frixione, P. Nason and G. Ridolfi, hep-ph/07073088.
16. J.M. Campbell and R.K. Ellis, Phys. Rev. **D62**, 114012 (2000), Phys. Rev. **D65**, 113007 (2002); J.M. Campbell and J. Huston, Phys. Rev. **D70**, 094021 (2004); J. Campbell and M. Mangano, Ann. Rev. Nucl. and Part. Sci. **61**, 311 (2011).
17. V.M. Abazov *et al.* (DØ Collab.), Phys. Lett. **B704**, 403 (2011).
18. T. Aaltonen *et al.* (CDF Collab.), CDF conference note 9913 (2009).
19. ATLAS Collab., ATLAS-CONF-2011-108.
20. ATLAS Collab., ATLAS-CONF-2011-121.
21. ATLAS Collab., ATLAS-CONF-2011-140.
22. CMS Collab., CMS-PAS-TOP-11-003.
23. CMS Collab., CMS-PAS-TOP-11-007.
24. V.M. Abazov *et al.* (DØ Collab.) Phys. Rev. Lett. **107**, 121802, (2011); D. Acosta *et al.* (CDF Collab.) Phys. Rev. Lett. **95**, 102002, (2005).
25. V.M. Abazov *et al.* (DØ Collab.), Phys. Rev. **D67**, 012004 (2003).
26. T. Affolder *et al.* (CDF Collab.), Phys. Rev. **D64**, 032002 (2001).
27. M. Czakon and A. Mitov, Nucl. Phys. **B824**, 111 (2010).
28. V.M. Abazov *et al.* (DØ Collab.), Phys. Rev. Lett. **103**, 092001 (2009); V.M. Abazov *et al.* (DØ Collab.), Phys. Rev. **D78**, 12005 (2008); V.M. Abazov *et al.* (DØ Collab.), Phys. Rev. Lett. **98**, 181802 (2007).
29. T. Aaltonen *et al.* (CDF Collab.), Phys. Rev. Lett. **103**, 092002 (2009); T. Aaltonen *et al.* (CDF Collab.), Phys. Rev. **D81**, 072003 (2010).
30. T. Aaltonen *et al.* (CDF Collab.), Phys. Rev. **D82**, 112005 (2010).
31. A. Heinson and T. Junk, Ann. Rev. Nucl. Part. Sci. **61**, 171 (2011).
32. Tevatron Electroweak Working Group, arXiv:0908.2171v1 [hep-ex].
33. V.A. Abazov *et al.* (DØ Collab.), Phys. Rev. **D84**, 112001 (2001).
34. CDF Collab., CDF conference note 9712 (2009).
35. V.M. Abazov *et al.* (DØ Collab.), Phys. Lett. **B705**, 313 (2011).
36. ATLAS Collab., ATLAS-CONF-2011-101.
37. CMS Collab., Phys. Rev. Lett. **107**, 091802 (2011).
38. C.D. White *et al.*, J. High Energy Phys.11, 74 (2009).
39. S. Frixione *et al.*, J. High Energy Phys.07, 29 (2008).
40. ATLAS Collab., ATLAS-CONF-2011-104.
41. CMS Collab., CMS-PAS-TOP-11-022.
42. O. Antunano, J.H. Kühn and G. Rodrigo, Phys. Rev. **D77**, 014003 (2008); M.T. Bowen, S. Ellis and D. Rainwater, Phys. Rev. **D73**, 014008 (2006); S. Dittmaier, P. Uwer and S. Weinzierl, Phys. Rev. Lett. **98**, 262002 (2007); L.G. Almeida, G. Sterman, and W. Vogelsang, Phys. Rev. **D78**, 014008 (2008).
43. S. Jung, H. Murayama, A. Pierce, J.D. Wells, Phys. Rev. **D81**, 015004 (2010).
44. V.M. Abazov *et al.* (DØ Collab.), Phys. Rev. Lett. **100**, 142002 (2008).
45. T. Aaltonen *et al.* (CDF Collab.), Phys. Rev. Lett. **101**, 202001 (2008).
46. V.M. Abazov *et al.* (DØ Collab.), Phys. Rev. **D84**, 112005 (2011).
47. CDF Collab., CDF conference note 10584 (2011).
48. T. Aaltonen, *et al.* (CDF Collab.), Phys. Rev. **D83**, 112003 (2011).
49. CMS Collab., CMS-PAS-TOP-11-014.
50. ATLAS Collab., ATLAS-CONF-2011-106.
51. F. Abe *et al.* (CDF Collab.), Phys. Rev. **D50**, 2966 (1994).
52. A. Abulencia *et al.* (CDF Collab.), Phys. Rev. **D73**, 032003 (2006).
53. ATLAS Collab., ATLAS-CONF-2011-120.
54. T. Aaltonen *et al.* (CDF Collab.), Phys. Rev. **D83**, 111101 (R)(2011).
55. V.M. Abazov *et al.* (DØ Collab.), Nature, **429**, 638 (2004).
56. K. Kondo *et al.* J. Phys. Soc. Jpn. **G62**, 1177 (1993).
57. R.H. Dalitz and G.R. Goldstein, Phys. Rev. **D45**, 1531 (1992); Phys. Lett. **B287**, 225 (1992); Proc. Royal Soc. London **A445**, 2803 (1999).
58. V.M. Abazov *et al.* (DØ Collab.), Phys. Rev. **D84**, 032004 (2011).

See key on page 457

- 
59. V.M. Abazov *et al.* (DØ Collab.), Phys. Rev. **D75**, 092001 (2007).
60. L. Sonnenschein, Phys. Rev. **D73**, 054015 (2006).
61. A. Abulencia *et al.* (CDF Collab.), Phys. Rev. **D74**, 032009 (2006).
62. V.M. Abazov *et al.* (DØ Collab.), Phys. Rev. Lett. **107**, 082004 (2011).
63. B. Abbot *et al.* (DØ Collab.), Phys. Rev. **D60**, 052001 (1999); F. Abe *et al.* (CDF Collab.), Phys. Rev. Lett. **82**, 271 (1999).
64. CDF Collab., CDF conference note 10635 (2011).
65. CDF Collab., CDF conference note 10456 (2011), [arXiv:1112.4891](#).
66. T.Aaltonen *et al.* (CDF Collab.), Phys. Rev. Lett. **107**, 232002 (2011).
67. T.Aaltonen *et al.* (CDF Collab.), Phys. Lett. **B698**, 371 (2011).
68. T. Aaltonen *et al.* (CDF Collab.), Phys. Rev. **D81**, 032002, (2010).
69. T. Aaltonen *et al.* (CDF Collab.), Phys. Rev. **D80**, 051104, (2009).
70. V.M. Abazov *et al.* (DØ Collab.) Phys. Rev. Lett. **100**, 192004, (2008); V.M. Abazov *et al.* (DØ Collab.) Phys. Lett. **B703**, 422, (2011); ATLAS Collab., ATLAS-CONF-2011-054; CMS Collab., CMS-PAS-TOP-11-008; U.Langefeld, S.Moch, P.Uwer, Phys. Rev. **D80**, 054009 (2009).
71. A.H. Hoang and J.W. Stewart, Nucl. Phys. Proc. Suppl. **185**, 220 (2008).
72. DØ Collab., DØ conference note 6189 (2011).
73. CDF Collab., CDF conference note 10562 (2011).
74. CDF Collab., CDF conference note 10444 (2011).
75. CMS Collab., CMS-PAS-TOP-10-009.
76. The Tevatron Electroweak Working Group, For the CDF and DØ Collaborations, [arXiv:1107.5255v3](#).
77. ALEPH, DELPHI, L3, OPAL, SLD and Working Groups, Phys. Reports **427**, 257 (2006).
78. The LEP Collaborations: ALEPH, DELPHI, L3, OPAL, SLD, CDF, and DØ Collaborations, and the LEP, Tevatron and SLD Electroweak Working Groups, [arXiv:1012.2367v2](#).
79. A. B. Galtieri, F. Margaroli, I. Volobouev, Rept. on Prog. in Phys. **75**, 056201 (2012).
80. G. Mahlon and S. Parke, Phys. Rev. **D53**, 4886 (1996); G. Mahlon and S. Parke, Phys. Lett. **B411**, 173 (1997).
81. G.R. Goldstein, in *Spin 96: Proceedings of the 12th International Symposium on High Energy Spin Physics*, Amsterdam, 1996, ed. C.W. Jager (World Scientific, Singapore, 1997), p. 328.
82. T. Stelzer and S. Willenbrock, Phys. Lett. **B374**, 169 (1996).
83. W. Bernreuther *et al.* Nucl. Phys. **B690**, 81 (2004).
84. CDF Collab., CDF conference note 10719 (2011).
85. CDF Collab., CDF conference note 10211 (2010).
86. V.M. Abazov *et al.* (DØ Collab.) [arXiv:1110.4194](#), to be published in Phys. Rev. Lett.
87. V.M. Abazov *et al.* (DØ Collab.), Phys. Rev. Lett. **107**, 032001 (2011).
88. V.M. Abazov *et al.* (DØ Collab.), Phys. Lett. **B702**, 16 (2011).
89. ATLAS Collab., ATLAS-CONF-2011-117.
90. T. Aaltonen *et al.* (CDF Collab.) Phys. Rev. Lett. **105**, 232003 (2010).
91. V.M. Abazov *et al.* (DØ Collab.) Phys. Rev. Lett. **106**, 02201 (2011).
92. G.L. Kane, G.A. Ladinsky, and C.P. Yuan, Phys. Rev. **D45**, 124 (1992).
93. CDF Collab., CDF conference note 10543 (2011).
94. CDF Collab., CDF conference note 9215 (2007).
95. V.M. Abazov *et al.* (DØ Collab.), Phys. Rev. **D83**, 032009 (2011).
96. CDF Collab., CDF conference note 10622 (2011); DØ Collab., DØ conference note 6231 (2011).
97. ATLAS Collab., ATLAS-CONF-2011-122.
98. D. Choudhury, T.M.P. Tait, and C.E.M. Wagner, Phys. Rev. **D65**, 053002 (2002).
99. D. Chang, W.F. Chang, and E. Ma, Phys. Rev. **D59**, 091503 (1999), Phys. Rev. **D61**, 037301 (2000).
100. V.M. Abazov *et al.* (DØ Collab.), Phys. Rev. Lett. **98**, 041801 (2007).
101. CDF Collab., CDF conference note 10460 (2011).
102. ATLAS Collab., ATLAS-CONF-2011-141.
103. T. Aaltonen *et al.* (CDF Collab.), Phys. Rev. **D80**, 011102 (2009).
104. T. Aaltonen *et al.* (CDF Collab.), Phys. Rev. **D84**, 031104 (2011).
105. ATLAS Collab., ATLAS-CONF-2011-153.
106. C.T. Hill, Phys. Lett. **B266**, 419 (1991).
107. C.T. Hill, Phys. Lett. **B345**, 483 (1995).
108. T. Aaltonen (CDF Collab.), Phys. Rev. **D84**, 072004 (2011).
109. T. Aaltonen (CDF Collab.), Phys. Rev. **D84**, 072003 (2011).
110. DØ Collab., FERMILAB-PUB-05/9-E, submitted to Phys. Rev. Lett.
111. ATLAS Collab., ATLAS-CONF-2011-087.
112. ATLAS Collab., ATLAS-CONF-2011-123.
113. CMS Collab., CMS-PAS-TOP-10-007.
114. CMS Collab., CMS-PAS-EXO-11-055.
115. CMS Collab., CMS-PAS-EXO-11-0006.
116. F. Abe *et al.* (CDF Collab.), Phys. Rev. Lett. **79**, 357 (1997); T. Affolder *et al.* (CDF Collab.), Phys. Rev. **D62**, 012004 (2000).
117. B. Abbott *et al.* (DØ Collab.), Phys. Rev. Lett. **82**, 4975 (1999); V.M. Abazov *et al.* (DØ Collab.), Phys. Rev. Lett. **88**, 151803 (2002).
118. A. Abulencia *et al.* (CDF Collab.), Phys. Rev. Lett. **96**, 042003 (2006).
119. T. Aaltonen *et al.* (CDF Collab.), Phys. Rev. Lett. **103**, 101803 (2009).
120. V.M. Abazov *et al.* (DØ Collab.), Phys. Rev. **D80**, 071102 (2009).
121. V.M. Abazov *et al.* (DØ Collab.), Phys. Lett. **B682**, 278 (2009).

## Quark Particle Listings

*t*

122. V.M. Abazov *et al.* (DØ Collab.), Phys. Rev. **D80**, 051107 (2009).
123. V.M. Abazov *et al.* (DØ Collab.), Phys. Rev. **D80**, 071102 (2009).
124. ATLAS Collab., ATLAS-CONF-2011-094.
125. ATLAS Collab., ATLAS-CONF-2011-138.
126. ATLAS Collab., ATLAS-CONF-2011-151.
127. ATLAS Collab., ATLAS-CONF-2011-154.
128. V.M. Abazov *et al.* (DØ Collab.), Phys. Rev. Lett. **102**, 092002 (2009).
129. V.M. Abazov *et al.* (DØ Collab.), DØ conference note 5838 (2009).
130. V.M. Abazov *et al.* (DØ Collab.), arXiv:1110.4592, submitted to Phys.Lett.B.
131. V.M. Abazov *et al.* (DØ Collab.), Phys. Lett. **B699**, 145 (2011).
132. T. Aaltonen *et al.* (CDF Collab.), Phys. Rev. Lett. **103**, 041801 (2009).
133. F. Abe *et al.* (CDF Collab.), Phys. Rev. Lett. **80**, 2525 (1998).
134. T. Aaltonen *et al.* (CDF Collab.), Phys. Rev. Lett. **101**, 192002 (2009).
135. CDF Collab., CDF conference note 9496 (2008).
136. V.M. Abazov *et al.* (DØ Collab.), Phys. Lett. **B701**, 313 (2011).
137. V.M. Abazov *et al.* (DØ Collab.), Phys. Lett. **B693**, 81 (2010).
138. A. Heister *et al.* (ALEPH Collab.), Phys. Lett. **B543**, 173 (2002); J. Abdallah *et al.* (DELPHI Collab.), Phys. Lett. **B590**, 21 (2004); P. Achard *et al.* (L3 Collab.), Phys. Lett. **B549**, 290 (2002); G. Abbiendi *et al.* (OPAL Collab.), Phys. Lett. **B521**, 181 (2001).
139. F.D. Aaron *et al.* (H1 Collab.), Phys. Lett. **B678**, 450 (2009).
140. H. Abramowicz *et al.* (ZEUS Collab.), arXiv:1111.3901, submitted to Phys. Lett. B.
141. M. Beneke *et al.*, hep-ph/0003033, in *Proceedings of 1999 CERN Workshop on Standard Model Physics (and more) at the LHC*, G. Altarelli and M.L. Mangano eds.
142. V.F. Obraztsov, S.R. Slabospitsky, and O.P. Yushchenko, Phys. Lett. **B426**, 393 (1998).
143. T. Carli, D. Dannheim, and L. Bellagamba, Mod. Phys. Lett. **A19**, 1881 (2004).

**t-QUARK MASS**

We first list the direct measurements of the top quark mass which employ the event kinematics and then list the measurements which extract a top quark mass from the measured  $t\bar{t}$  cross-section using theory calculations. A discussion of the definition of the top quark mass in these measurements can be found in the review "The Top Quark."

OUR EVALUATION of  $173.5 \pm 0.6 \pm 0.8$  GeV is an average of published top mass measurements from Tevatron Run-I (1992–1996) and Run-II (2001–present) and of the LHC. The Tevatron average ( $173.4 \pm 0.6 \pm 0.8$  GeV) was provided by the Tevatron Electroweak Working Group (TEVEWWG). It takes correlated uncertainties into account and has a  $\chi^2$  of 8.5 for 11 degrees of freedom. We include in OUR EVALUATION the measurement from CHATRCHYAN 11F assuming uncorrelated systematic uncertainties. The average would be  $173.4 \pm 0.6 \pm 0.8$  GeV if we assumed fully correlated systematics between the Tevatron average and CHATRCHYAN 11F.

For earlier search limits see PDG 96, Physical Review **D54** 1 (1996). We no longer include a compilation of indirect top mass determinations from Standard Model Electroweak fits in the Listings (our last compilation can be found in the Listings of the 2007 partial update). For a discussion of current results see the reviews "The Top Quark" and "Electroweak Model and Constraints on New Physics."

**t-Quark Mass (Direct Measurements)**

The following measurements extract a  $t$ -quark mass from the kinematics of  $t\bar{t}$  events. They are sensitive to the top quark mass used in the MC generator that is usually interpreted as the pole mass, but the theoretical uncertainty in this interpretation is hard to quantify. See the review "The Top Quark" and references therein for more information.

VALUE (GeV)	DOCUMENT ID	TECN	COMMENT
<b>173.5 ± 0.6 ± 0.8</b>	<b>OUR EVALUATION</b>		See comments in the header above.
172.3 ± 2.4 ± 1.0	<sup>1</sup> AALTONEN	11AK CDF	$E_T + \geq 4$ jets ( $\geq 1$ $b$ -tag)
172.1 ± 1.1 ± 0.9	<sup>2</sup> AALTONEN	11E CDF	$\ell +$ jets and dilepton
174.94 ± 0.83 ± 1.24	<sup>3</sup> ABZOV	11P D0	$\ell + E_T + 4$ jets ( $\geq 1$ $b$ -tag)
174.0 ± 1.8 ± 2.4	<sup>4</sup> ABZOV	11R D0	dilepton + $E_T + \geq 2$ jets
175.5 ± 4.6 ± 4.6	<sup>5</sup> CHATRCHYAN	11F CMS	dilepton + $E_T +$ jets
173.0 ± 1.2	<sup>6</sup> AALTONEN	10AE CDF	$\ell + E_T + 4$ jets ( $\geq 1$ $b$ -tag), ME method
170.7 ± 6.3 ± 2.6	<sup>7</sup> AALTONEN	10D CDF	$\ell + E_T + 4$ jets ( $b$ -tag)
174.8 ± 2.4 ± 1.2 - 1.0	<sup>8</sup> AALTONEN	10E CDF	$\geq 6$ jets, vtx $b$ -tag
180.1 ± 3.6 ± 3.9	<sup>9,10</sup> ABZOV	04G D0	lepton + jets
176.1 ± 5.1 ± 5.3	<sup>11</sup> AFFOLDER	01 CDF	lepton + jets
167.4 ± 10.3 ± 4.8	<sup>12,13</sup> ABE	99B CDF	dilepton
168.4 ± 12.3 ± 3.6	<sup>10</sup> ABBOTT	98D D0	dilepton
186 ± 10 ± 5.7	<sup>12,14</sup> ABE	97R CDF	6 or more jets
• • • We do not use the following data for averages, fits, limits, etc. • • •			
172.4 ± 1.4 ± 1.3	<sup>15</sup> AALTONEN	11AC CDF	$\ell + E_T + 4$ jets ( $\geq 1$ $b$ -tag)
176.9 ± 8.0 ± 2.7	<sup>16</sup> AALTONEN	11T CDF	$\ell + E_T + 4$ jets ( $\geq 1$ $b$ -tag), $p_T(\ell)$ shape
169.3 ± 2.7 ± 3.2	<sup>17</sup> AALTONEN	10C CDF	dilepton + $b$ -tag (MT2+NWA)
180.5 ± 12.0 ± 3.6	<sup>18</sup> AALTONEN	09AK CDF	$\ell + E_T +$ jets (soft $\mu$ $b$ -tag)
172.7 ± 1.8 ± 1.2	<sup>19</sup> AALTONEN	09J CDF	$\ell + E_T + 4$ jets ( $b$ -tag)
171.1 ± 3.7 ± 2.1	<sup>20</sup> AALTONEN	09K CDF	6 jets, vtx $b$ -tag
171.9 ± 1.7 ± 1.1	<sup>21</sup> AALTONEN	09L CDF	$\ell +$ jets, $\ell\ell +$ jets
171.2 ± 2.7 ± 2.9	<sup>22</sup> AALTONEN	09O CDF	dilepton
165.5 ± 3.4 ± 3.3	<sup>23</sup> AALTONEN	09X CDF	$\ell\ell + E_T$ ( $\nu\phi$ weighting)
174.7 ± 4.4 ± 2.0	<sup>24</sup> ABZOV	09AH D0	dilepton + $b$ -tag ( $\nu$ WT+MWT)
170.7 ± 4.2 ± 3.9	<sup>25,26</sup> AALTONEN	08C CDF	dilepton, $\sigma_{t\bar{t}}$ constrained
171.5 ± 1.8 ± 1.1	<sup>27</sup> ABZOV	08AH D0	$\ell + E_T + 4$ jets
177.1 ± 4.9 ± 4.7	<sup>28,29</sup> AALTONEN	07 CDF	6 jets with $\geq 1$ $b$ vtx
172.3 ± 10.8 ± 9.6	<sup>30</sup> AALTONEN	07B CDF	$\geq 4$ jets ( $b$ -tag)
174.0 ± 2.2 ± 4.8	<sup>31</sup> AALTONEN	07D CDF	$\geq 6$ jets, vtx $b$ -tag
170.8 ± 2.2 ± 1.4	<sup>32,33</sup> AALTONEN	07I CDF	lepton + jets ( $b$ -tag)
173.7 ± 4.4 ± 2.1 ± 2.0	<sup>29,34</sup> ABZOV	07F D0	lepton + jets
176.2 ± 9.2 ± 3.9	<sup>35</sup> ABZOV	07W D0	dilepton (MWT)
179.5 ± 7.4 ± 5.6	<sup>35</sup> ABZOV	07W D0	dilepton ( $\nu$ WT)
164.5 ± 3.9 ± 3.9	<sup>33,36</sup> ABULENCIA	07D CDF	dilepton
180.7 ± 15.5 ± 13.4	<sup>37</sup> ABULENCIA	07J CDF	lepton + jets
170.3 ± 4.1 ± 1.2 ± 4.5 ± 1.8	<sup>33,38</sup> ABZOV	06U D0	lepton + jets ( $b$ -tag)
173.2 ± 2.6 ± 2.4 ± 3.2	<sup>39,40</sup> ABULENCIA	06D CDF	lepton + jets
173.5 ± 3.7 ± 3.6 ± 1.3	<sup>26,39</sup> ABULENCIA	06D CDF	lepton + jets
165.2 ± 6.1 ± 3.4	<sup>33,41</sup> ABULENCIA	06G CDF	dilepton
170.1 ± 6.0 ± 4.1	<sup>26,42</sup> ABULENCIA	06V CDF	dilepton
178.5 ± 13.7 ± 7.7	<sup>43,44</sup> ABZOV	05 D0	6 or more jets
176.1 ± 6.6	<sup>45</sup> AFFOLDER	01 CDF	dilepton, lepton+jets, all-jets
172.1 ± 5.2 ± 4.9	<sup>46</sup> ABBOTT	99G D0	di-lepton, lepton+jets
176.0 ± 6.5	<sup>13,47</sup> ABE	99B CDF	dilepton, lepton+jets, all-jets
173.3 ± 5.6 ± 5.5	<sup>10,48</sup> ABBOTT	98F D0	lepton + jets
175.9 ± 4.8 ± 5.3	<sup>12,49</sup> ABE	98E CDF	lepton + jets
161 ± 17 ± 10	<sup>12</sup> ABE	98F CDF	dilepton
172.1 ± 5.2 ± 4.9	<sup>50</sup> BHAT	98B RVUE	dilepton and lepton+jets
173.8 ± 5.0	<sup>51</sup> BHAT	98B RVUE	dilepton, lepton+jets, all-jets
173.3 ± 5.6 ± 6.2	<sup>10</sup> ABACHI	97E D0	lepton + jets
199 ± 19 ± 21	ABACHI	95 D0	lepton + jets
176 ± 8 ± 10	ABE	95F CDF	lepton + $b$ -jet
174 ± 10 ± 13 ± 12	ABE	94E CDF	lepton + $b$ -jet

**t-Quark  $\overline{MS}$  Mass from Cross-Section Measurements**

The top quark  $\overline{MS}$  or pole mass can be extracted from a measurement of  $\sigma(t\bar{t})$  by using theory calculations. We quote below the  $\overline{MS}$  mass. See the review "The Top Quark" and references therein for more information.

VALUE (GeV)	DOCUMENT ID	TECN	COMMENT
<b>160.0 + 4.8 - 4.3</b>	<sup>52</sup> ABZOV	11S D0	$\sigma(t\bar{t}) +$ theory
• • • We do not use the following data for averages, fits, limits, etc. • • •			
	<sup>53</sup> ABZOV	09AG D0	cross sects, theory + exp
	<sup>54</sup> ABZOV	09R D0	cross sects, theory + exp

- 1 Based on  $5.7 \text{ fb}^{-1}$  in  $p\bar{p}$  collisions at  $\sqrt{s} = 1.96 \text{ TeV}$ . Events with an identified charged lepton or small  $E_T$  are rejected from the event sample, so that the measurement is statistically independent from those in the  $\ell + \text{jets}$  and all hadronic channels while being sensitive to those events with a  $\tau$  lepton in the final state. Supersedes AALTONEN 07B.
- 2 Based on  $5.6 \text{ fb}^{-1}$  in  $p\bar{p}$  collisions at  $\sqrt{s} = 1.96 \text{ TeV}$ . Employs a multi-dimensional template likelihood technique where the lepton plus jets (one or two  $b$ -tags) channel gives  $172.2 \pm 1.2 \pm 0.9 \text{ GeV}$  while the dilepton channel yields  $170.3 \pm 2.0 \pm 3.1 \text{ GeV}$ . The results are combined. OUR EVALUATION includes the measurement in the dilepton channel only.
- 3 Based on  $3.6 \text{ fb}^{-1}$  in  $p\bar{p}$  collisions at  $\sqrt{s} = 1.96 \text{ TeV}$ . ABZOV 11P reports  $174.94 \pm 0.83 \pm 0.78 \pm 0.96 \text{ GeV}$ , where the first uncertainty is from statistics, the second from JES, and the last from other systematic uncertainties. We combine the JES and systematic uncertainties. A matrix-element method is used where the JES uncertainty is constrained by the  $W$  mass. ABZOV 11P describes a measurement based on  $2.6 \text{ fb}^{-1}$  that is combined with ABZOV 08AH, which employs an independent  $1 \text{ fb}^{-1}$  of data.
- 4 Based on a matrix-element method which employs  $5.4 \text{ fb}^{-1}$  in  $p\bar{p}$  collisions at  $\sqrt{s} = 1.96 \text{ TeV}$ .
- 5 Based on  $36 \text{ pb}^{-1}$  of  $pp$  collisions at  $\sqrt{s} = 7 \text{ TeV}$ . A Kinematic Method using  $b$ -tagging and an analytical Matrix Weighting Technique give consistent results and are combined.
- 6 Based on  $5.6 \text{ fb}^{-1}$  in  $p\bar{p}$  collisions at  $\sqrt{s} = 1.96 \text{ TeV}$ . The likelihood calculated using a matrix element method gives  $m_t = 173.0 \pm 0.7(\text{stat}) \pm 0.6(\text{JES}) \pm 0.9(\text{syst}) \text{ GeV}$ , for a total uncertainty of  $1.2 \text{ GeV}$ .
- 7 Based on  $1.9 \text{ fb}^{-1}$  in  $p\bar{p}$  collisions at  $\sqrt{s} = 1.96 \text{ TeV}$ . The result is from the measurement using the transverse decay length of  $b$ -hadrons and that using the transverse momentum of the  $W$  decay muons, which are both insensitive to the JES (jet energy scale) uncertainty. OUR EVALUATION uses only the measurement exploiting the decay length significance which yields  $166.9^{+9.5}_{-8.5}(\text{stat}) \pm 2.9(\text{syst}) \text{ GeV}$ . The measurement that uses the lepton transverse momentum is excluded from the average because of a statistical correlation with other samples.
- 8 Based on  $2.9 \text{ fb}^{-1}$  in  $p\bar{p}$  collisions at  $\sqrt{s} = 1.96 \text{ TeV}$ . The first error is from statistics and JES uncertainty, and the latter is from the other systematics. Neural-network-based kinematical selection of 6 highest  $E_T$  jets with a vtx  $b$ -tag is used to distinguish signal from background.
- 9 Obtained by re-analysis of the lepton + jets candidate events that led to ABBOTT 98F. It is based upon the maximum likelihood method which makes use of the leading order matrix elements.
- 10 Based on  $125 \pm 7 \text{ pb}^{-1}$  of data at  $\sqrt{s} = 1.8 \text{ TeV}$ .
- 11 Based on  $\sim 106 \text{ pb}^{-1}$  of data at  $\sqrt{s} = 1.8 \text{ TeV}$ .
- 12 Based on  $109 \pm 7 \text{ pb}^{-1}$  of data at  $\sqrt{s} = 1.8 \text{ TeV}$ .
- 13 See AFFOLDER 01 for details of systematic error re-evaluation.
- 14 Based on the first observation of all hadronic decays of  $t\bar{t}$  pairs. Single  $b$ -quark tagging with jet-shape variable constraints was used to select signal enriched multi-jet events. The updated systematic error is listed. See AFFOLDER 01, appendix C.
- 15 Based on  $3.2 \text{ fb}^{-1}$  in  $p\bar{p}$  collisions at  $\sqrt{s} = 1.96 \text{ TeV}$ . The first error is from statistics and JES combined, and the latter is from the other systematic uncertainties. The result is obtained using an unbinned maximum likelihood method where the top quark mass and the JES are measured simultaneously, with  $\Delta_{JES} = 0.3 \pm 0.3(\text{stat})$ .
- 16 Uses a likelihood fit of the lepton  $p_T$  distribution based on  $2.7 \text{ fb}^{-1}$  in  $p\bar{p}$  collisions at  $\sqrt{s} = 1.96 \text{ TeV}$ .
- 17 Based on  $3.4 \text{ fb}^{-1}$  in  $p\bar{p}$  collisions at  $\sqrt{s} = 1.96 \text{ TeV}$ . The result is obtained by combining the MT2 variable method and the NWA (Neutrino Weighting Algorithm). The MT2 method alone gives  $m_t = 168.0^{+4.8}_{-4.0}(\text{stat}) \pm 2.9(\text{syst}) \text{ GeV}$  with smaller systematic error due to small JES uncertainty.
- 18 Based on  $2 \text{ fb}^{-1}$  of data at  $\sqrt{s} = 1.96 \text{ TeV}$ . The top mass is obtained from the measurement of the invariant mass of the lepton ( $e$  or  $\mu$ ) from  $W$  decays and the soft  $\mu$  in  $b$ -jet. The result is insensitive to jet energy scaling.
- 19 Based on  $1.9 \text{ fb}^{-1}$  of data at  $\sqrt{s} = 1.96 \text{ TeV}$ . The first error is from statistics and jet energy scale uncertainty, and the latter is from the other systematics. Matrix element method with effective propagators.
- 20 Based on  $943 \text{ pb}^{-1}$  of data at  $\sqrt{s} = 1.96 \text{ TeV}$ . The first error is from statistical and jet-energy-scale uncertainties, and the latter is from other systematics. AALTONEN 09k selected 6 jet events with one or more vertex  $b$ -tags and used the tree-level matrix element to construct template models of signal and background.
- 21 Based on  $1.9 \text{ fb}^{-1}$  of data at  $\sqrt{s} = 1.96 \text{ TeV}$ . The first error is from statistical and jet-energy-scale (JES) uncertainties, and the second is from other systematics. Events with lepton + jets and those with dilepton + jets were simultaneously fit to constrain  $m_t$  and JES. Lepton + jets data only give  $m_t = 171.8^{+5.3}_{-5.1} \text{ GeV}$ .
- 22 Based on  $2 \text{ fb}^{-1}$  of data at  $\sqrt{s} = 1.96 \text{ TeV}$ . Matrix Element method. Optimal selection criteria for candidate events with two high  $p_T$  leptons, high  $E_T$ , and two or more jets with and without  $b$ -tag are obtained by neural network with neuroevolution technique to minimize the statistical error of  $m_t$ .
- 23 Based on  $2.9 \text{ fb}^{-1}$  of data at  $\sqrt{s} = 1.96 \text{ TeV}$ . Mass  $m_t$  is estimated from the likelihood for the eight-fold kinematical solutions in the plane of the azimuthal angles of the two neutrino momenta.
- 24 Based on  $1 \text{ fb}^{-1}$  of data at  $\sqrt{s} = 1.96 \text{ TeV}$ . Events with two identified leptons, and those with one lepton plus one isolated track and a  $b$ -tag were used to constrain  $m_t$ . The result is a combination of the  $\nu$ WT ( $\nu$  Weighting Technique) result of  $176.2 \pm 4.8 \pm 2.1 \text{ GeV}$  and the MWT (Matrix-element Weighting Technique) result of  $173.2 \pm 4.9 \pm 2.0 \text{ GeV}$ .
- 25 Reports measurement of  $170.7^{+4.2}_{-3.9} \pm 2.6 \pm 2.4 \text{ GeV}$  based on  $1.2 \text{ fb}^{-1}$  of data at  $\sqrt{s} = 1.96 \text{ TeV}$ . The last error is due to the theoretical uncertainty on  $\sigma_{t\bar{t}}$ . Without the cross-section constraint a top mass of  $169.7^{+5.2}_{-4.9} \pm 3.1 \text{ GeV}$  is obtained.
- 26 Template method.
- 27 Result is based on  $1 \text{ fb}^{-1}$  of data at  $\sqrt{s} = 1.96 \text{ TeV}$ . The first error is from statistics and jet energy scale uncertainty, and the latter is from the other systematics.
- 28 Based on  $310 \text{ pb}^{-1}$  of data at  $\sqrt{s} = 1.96 \text{ TeV}$ .
- 29 Ideogram method.
- 30 Based on  $311 \text{ pb}^{-1}$  of data at  $\sqrt{s} = 1.96 \text{ TeV}$ . Events with 4 or more jets with  $E_T > 15 \text{ GeV}$ , significant missing  $E_T$ , and secondary vertex  $b$ -tag are used in the fit. About 44% of the signal acceptance is from  $\tau\nu + 4$  jets. Events with identified  $e$  or  $\mu$  are vetoed to provide a statistically independent measurement.
- 31 Based on  $1.02 \text{ fb}^{-1}$  of data at  $\sqrt{s} = 1.96 \text{ TeV}$ .
- 32 Based on  $955 \text{ pb}^{-1}$  of data at  $\sqrt{s} = 1.96 \text{ TeV}$ .  $m_t$  and JES (Jet Energy Scale) are fitted simultaneously, and the first error contains the JES contribution of  $1.5 \text{ GeV}$ .
- 33 Matrix element method.
- 34 Based on  $425 \text{ pb}^{-1}$  of data at  $\sqrt{s} = 1.96 \text{ TeV}$ . The first error is a combination of statistics and JES (Jet Energy Scale) uncertainty, which has been measured simultaneously to give  $JES = 0.989 \pm 0.029(\text{stat})$ .
- 35 Based on  $370 \text{ pb}^{-1}$  of data at  $\sqrt{s} = 1.96 \text{ TeV}$ . Combined result of MWT (Matrix-element Weighting Technique) and  $\nu$ WT ( $\nu$  Weighting Technique) analyses is  $178.1 \pm 6.7 \pm 4.8 \text{ GeV}$ .
- 36 Based on  $1.0 \text{ fb}^{-1}$  of data at  $\sqrt{s} = 1.96 \text{ TeV}$ . ABULENCIA 07D improves the matrix element description by including the effects of initial-state radiation.
- 37 Based on  $695 \text{ pb}^{-1}$  of data at  $\sqrt{s} = 1.96 \text{ TeV}$ . The transverse decay length of the  $b$  hadron is used to determine  $m_t$ , and the result is free from the JES (jet energy scale) uncertainty.
- 38 Based on  $\sim 400 \text{ pb}^{-1}$  of data at  $\sqrt{s} = 1.96 \text{ TeV}$ . The first error includes statistical and systematic jet energy scale uncertainties, the second error is from the other systematics. The result is obtained with the  $b$ -tagging information. The result without  $b$ -tagging is  $169.2^{+5.0+1.5}_{-7.4-1.4} \text{ GeV}$ . Superseded by ABZOV 08AH.
- 39 Based on  $318 \text{ pb}^{-1}$  of data at  $\sqrt{s} = 1.96 \text{ TeV}$ .
- 40 Dynamical likelihood method.
- 41 Based on  $340 \text{ pb}^{-1}$  of data at  $\sqrt{s} = 1.96 \text{ TeV}$ .
- 42 Based on  $360 \text{ pb}^{-1}$  of data at  $\sqrt{s} = 1.96 \text{ TeV}$ .
- 43 Based on  $110.2 \pm 5.8 \text{ pb}^{-1}$  at  $\sqrt{s} = 1.8 \text{ TeV}$ .
- 44 Based on the all hadronic decays of  $t\bar{t}$  pairs. Single  $b$ -quark tagging via the decay chain  $b \rightarrow c \rightarrow \mu$  was used to select signal enriched multijet events. The result was obtained by the maximum likelihood method after bias correction.
- 45 Obtained by combining the measurements in the lepton + jets [AFFOLDER 01], all-jets [ABE 97r, ABE 99b], and dilepton [ABE 99b] decay topologies.
- 46 Obtained by combining the D0 result  $m_t(\text{GeV}) = 168.4 \pm 12.3 \pm 3.6$  from 6 di-lepton events (see also ABBOTT 98D) and  $m_t(\text{GeV}) = 173.3 \pm 5.6 \pm 5.5$  from lepton+jet events (ABBOTT 98F).
- 47 Obtained by combining the CDF results of  $m_t(\text{GeV}) = 167.4 \pm 10.3 \pm 4.8$  from 8 dilepton events,  $m_t(\text{GeV}) = 175.9 \pm 4.8 \pm 5.3$  from lepton+jet events (ABE 98e), and  $m_t(\text{GeV}) = 186.0 \pm 10.0 \pm 5.7$  from all-jet events (ABE 97r). The systematic errors in the latter two measurements are changed in this paper.
- 48 See ABZOV 04g.
- 49 The updated systematic error is listed. See AFFOLDER 01, appendix C.
- 50 Obtained by combining the D0 results of  $m_t(\text{GeV}) = 168.4 \pm 12.3 \pm 3.6$  from 6 dilepton events and  $m_t(\text{GeV}) = 173.3 \pm 5.6 \pm 5.5$  from 77 lepton+jet events.
- 51 Obtained by combining the D0 results from dilepton and lepton+jet events, and the CDF results (ABE 99b) from dilepton, lepton+jet events, and all-jet events.
- 52 Based on  $5.3 \text{ fb}^{-1}$  in  $p\bar{p}$  collisions at  $\sqrt{s} = 1.96 \text{ TeV}$ . ABZOV 11s uses the measured  $t\bar{t}$  production cross section of  $8.13^{+1.02}_{-0.90} \text{ pb}$  [ABZOV 11e] in the lepton plus jets channel to obtain the top quark  $\overline{MS}$  mass by using an approximate NNLO computation (MOCH 08, LANGENFELD 09). The corresponding top quark pole mass is  $167.5^{+5.4}_{-4.9} \text{ GeV}$ . A different theory calculation (AHRENS 10, AHRENS 10a) is also used and yields  $m_t^{\overline{MS}} = 154.5^{+5.0}_{-4.3} \text{ GeV}$ .
- 53 Based on  $1 \text{ fb}^{-1}$  of data at  $\sqrt{s} = 1.96 \text{ TeV}$ . Uses the  $\ell + \text{jets}$ ,  $\ell\ell$ , and  $\ell\tau + \text{jets}$  channels. ABZOV 09AG extract the pole mass of the top quark using two different calculations that yield  $169.1^{+5.9}_{-5.2} \text{ GeV}$  (MOCH 08, LANGENFELD 09) and  $168.2^{+5.9}_{-5.4} \text{ GeV}$  (KIDONAKIS 08).
- 54 Based on  $1 \text{ fb}^{-1}$  of data at  $\sqrt{s} = 1.96 \text{ TeV}$ . Uses the  $\ell\ell$  and  $\ell\tau + \text{jets}$  channels. ABZOV 09R extract the pole mass of the top quark using two different calculations that yield  $173.3^{+9.8}_{-8.6} \text{ GeV}$  (MOCH 08, LANGENFELD 09) and  $171.5^{+9.9}_{-8.8} \text{ GeV}$  (CACIARI 08).

 $m_t - m_{\bar{t}}$ 

Test of  $CPT$  conservation. OUR AVERAGE assumes that the systematic uncertainties are uncorrelated.

VALUE (GeV)	DOCUMENT ID	TECN	COMMENT
<b><math>-1.4 \pm 2.0</math> OUR AVERAGE</b>	Error includes scale factor of 1.6.		
$-3.3 \pm 1.4 \pm 1.0$	1 AALTONEN	11K CDF	$\ell + E_T + 4$ jets
$0.8 \pm 1.8 \pm 0.5$	2 ABZOV	11T D0	$\ell + E_T + 4$ jets ( $\geq 1$ $b$ -tag)
$3.8 \pm 3.4 \pm 1.2$	3 ABZOV	09AA D0	$\ell + E_T + 4$ jets ( $\geq 1$ $b$ -tag)
• • • We do not use the following data for averages, fits, limits, etc. • • •			
	1	Based on a template likelihood technique which employs $5.6 \text{ fb}^{-1}$ in $p\bar{p}$ collisions at $\sqrt{s} = 1.96 \text{ TeV}$ .	
	2	Based on a matrix-element method which employs $3.6 \text{ fb}^{-1}$ in $p\bar{p}$ collisions at $\sqrt{s} = 1.96 \text{ TeV}$ .	
	3	Based on $1 \text{ fb}^{-1}$ of data in $p\bar{p}$ collisions at $\sqrt{s} = 1.96 \text{ TeV}$ .	

## t-quark DECAY WIDTH

VALUE (GeV)	CL%	DOCUMENT ID	TECN	COMMENT
<b><math>1.99 \pm 0.69</math> <math>-0.55</math></b>		1 ABZOV	11B D0	$\Gamma(t \rightarrow Wb)/B(t \rightarrow Wb)$
• • • We do not use the following data for averages, fits, limits, etc. • • •				
$> 1.21$	95	1 ABZOV	11B D0	$\Gamma(t \rightarrow Wb)$
$< 7.6$	95	2 AALTONEN	10AC CDF	$\ell + \text{jets}$ , direct
$< 13.1$	95	3 AALTONEN	09M CDF	$m_t(\text{rec})$ distribution

## Quark Particle Listings

t

- <sup>1</sup> Based on  $2.3 \text{ fb}^{-1}$  in  $p\bar{p}$  collisions at  $\sqrt{s} = 1.96 \text{ TeV}$ . ABAZOV 11B extracted  $\Gamma_t$  from the partial width  $\Gamma(t \rightarrow Wb) = 1.92^{+0.58}_{-0.51} \text{ GeV}$  measured using the  $t$ -channel single top production cross section, and the branching fraction  $\text{br}(t \rightarrow Wb) = 0.962^{+0.068}_{-0.066}(\text{stat}) \pm 0.064_{-0.052}(\text{syst})$ . The  $\Gamma(t \rightarrow Wb)$  measurement gives the 95% CL lowerbound of  $\Gamma(t \rightarrow Wb)$  and hence that of  $\Gamma_t$ .
- <sup>2</sup> Results are based on  $4.3 \text{ fb}^{-1}$  of data in  $p\bar{p}$  collisions at  $\sqrt{s} = 1.96 \text{ TeV}$ . The top quark mass and the hadronically decaying  $W$  boson mass are reconstructed for each candidate events and compared with templates of different top quark width. The two sided 68% CL interval is  $0.3 \text{ GeV} < \Gamma_t < 4.4 \text{ GeV}$  for  $m_t = 172.5 \text{ GeV}$ .
- <sup>3</sup> Based on  $955 \text{ pb}^{-1}$  of  $p\bar{p}$  collision data at  $\sqrt{s} = 1.96 \text{ TeV}$ . AALTONEN 09M selected  $t\bar{T}$  candidate events for the  $\ell + E_T + \text{jets}$  channel with one or two  $b$ -tags, and examine the decay width dependence of the reconstructed  $m_t$  distribution. The result is for  $m_t = 175 \text{ GeV}$ , whereas the upper limit is lower for smaller  $m_t$ .

## t DECAY MODES

Mode	Fraction ( $\Gamma_i/\Gamma$ )	Confidence level
$\Gamma_1$ $Wq (q = b, s, d)$		
$\Gamma_2$ $Wb$		
$\Gamma_3$ $\ell\nu_\ell \text{ anything}$	[a,b] $(9.4 \pm 2.4) \%$	
$\Gamma_4$ $\tau\nu_\tau b$		
$\Gamma_5$ $\gamma q (q=u, c)$	[c] $< 5.9 \times 10^{-3}$	95%
<b><math>\Delta T = 1</math> weak neutral current (<math>T_1</math>) modes</b>		
$\Gamma_6$ $Zq (q=u, c)$	$T_1$ [d] $< 3.2 \%$	95%

- [a]  $\ell$  means  $e$  or  $\mu$  decay mode, not the sum over them.  
 [b] Assumes lepton universality and  $W$ -decay acceptance.  
 [c] This limit is for  $\Gamma(t \rightarrow \gamma q)/\Gamma(t \rightarrow Wb)$ .  
 [d] This limit is for  $\Gamma(t \rightarrow Zq)/\Gamma(t \rightarrow Wb)$ .

## t BRANCHING RATIOS

$\Gamma(Wb)/\Gamma(Wq (q=b, s, d))$	$\Gamma_2/\Gamma_1$
OUR AVERAGE assumes that the systematic uncertainties are uncorrelated.	
VALUE	DOCUMENT ID TECN COMMENT
<b>0.91 ± 0.04 OUR AVERAGE</b>	
$0.90 \pm 0.04$	<sup>1</sup> ABAZOV 11X D0
$1.12^{+0.21+0.17}_{-0.19-0.13}$	<sup>2</sup> ACOSTA 05A CDF
• • • We do not use the following data for averages, fits, limits, etc. • • •	
$0.97^{+0.09}_{-0.08}$	<sup>3</sup> ABAZOV 08M D0 $\ell + n$ jets with 0,1,2 $b$ -tag
$1.03^{+0.19}_{-0.17}$	<sup>4</sup> ABAZOV 06K D0
$0.94^{+0.26+0.17}_{-0.21-0.12}$	<sup>5</sup> AFFOLDER 01C CDF

- <sup>1</sup> Based on  $5.4 \text{ fb}^{-1}$  of data. The error is statistical and systematic combined. The result is a combination of  $0.95 \pm 0.07$  from  $\ell + \text{jets}$  channel and  $0.86 \pm 0.05$  from  $\ell\ell$  channel.  $|V_{tb}| = 0.95 \pm 0.02$  follows from the result by assuming unitarity of the  $3 \times 3$  CKM matrix.
- <sup>2</sup> ACOSTA 05A result is from the analysis of lepton + jets and di-lepton + jets final states of  $t\bar{T}$  candidate events with  $\sim 162 \text{ pb}^{-1}$  of data at  $\sqrt{s} = 1.96 \text{ TeV}$ . The first error is statistical and the second systematic. It gives  $R > 0.61$ , or  $|V_{tb}| > 0.78$  at 95% CL.
- <sup>3</sup> Result is based on  $0.9 \text{ fb}^{-1}$  of data. The 95% CL lower bound  $R > 0.79$  gives  $|V_{tb}| > 0.89$  (95% CL).
- <sup>4</sup> ABAZOV 06K result is from the analysis of  $t\bar{T} \rightarrow \ell\nu + \geq 3$  jets with 230  $\text{pb}^{-1}$  of data at  $\sqrt{s} = 1.96 \text{ TeV}$ . It gives  $R > 0.61$  and  $|V_{tb}| > 0.78$  at 95% CL. Superseded by ABAZOV 08M.
- <sup>5</sup> AFFOLDER 01C measures the top-quark decay width ratio  $R = \Gamma(Wb)/\Gamma(Wq)$ , where  $q$  is a  $d, s,$  or  $b$  quark, by using the number of events with multiple  $b$ tags. The first error is statistical and the second systematic. A numerical integration of the likelihood function gives  $R > 0.61$  (0.56) at 90% (95%) CL. By assuming three generation unitarity,  $|V_{tb}| = 0.97^{+0.16}_{-0.12}$  or  $|V_{tb}| > 0.78$  (0.75) at 90% (95%) CL is obtained. The result is based on  $109 \text{ pb}^{-1}$  of data at  $\sqrt{s} = 1.8 \text{ TeV}$ .

$\Gamma(\ell\nu_\ell \text{ anything})/\Gamma_{\text{total}}$	$\Gamma_3/\Gamma$
VALUE	DOCUMENT ID TECN COMMENT
<b>0.094 ± 0.024</b>	
	<sup>1</sup> ABE 98X CDF

- <sup>1</sup>  $\ell$  means  $e$  or  $\mu$  decay mode, not the sum. Assumes lepton universality and  $W$ -decay acceptance.

$\Gamma(\tau\nu_\tau b)/\Gamma_{\text{total}}$	$\Gamma_4/\Gamma$
VALUE	DOCUMENT ID TECN COMMENT
• • • We do not use the following data for averages, fits, limits, etc. • • •	
	<sup>1</sup> ABULENCIA 06R CDF $\ell\tau + \text{jets}$
	<sup>2</sup> ABE 97V CDF $\ell\tau + \text{jets}$

- <sup>1</sup> ABULENCIA 06R looked for  $t\bar{T} \rightarrow (\ell\nu_\ell)(\tau\nu_\tau)b\bar{b}$  events in  $194 \text{ pb}^{-1}$  of  $p\bar{p}$  collisions at  $\sqrt{s} = 1.96 \text{ TeV}$ . 2 events are found where  $1.00 \pm 0.17$  signal and  $1.29 \pm 0.25$  background events are expected, giving a 95% CL upper bound for the partial width ratio  $\Gamma(t \rightarrow \tau\nu q)/\Gamma_{SM}(t \rightarrow \tau\nu q) < 5.2$ .
- <sup>2</sup> ABE 97V searched for  $t\bar{T} \rightarrow (\ell\nu_\ell)(\tau\nu_\tau)b\bar{b}$  events in  $109 \text{ pb}^{-1}$  of  $p\bar{p}$  collisions at  $\sqrt{s} = 1.8 \text{ TeV}$ . They observed 4 candidate events where one expects  $\sim 1$  signal and  $\sim 2$  background events. Three of the four observed events have jets identified as  $b$  candidates.

$\Gamma(\gamma q (q=u, c))/\Gamma_{\text{total}}$	$\Gamma_5/\Gamma$
VALUE	DOCUMENT ID TECN COMMENT
$< 0.0064$	<sup>1</sup> AARON 09A H1 $t \rightarrow \gamma u$
<b>&lt; 0.0059</b>	<sup>2</sup> CHEKANOV 03 ZEUS $B(t \rightarrow \gamma u)$
• • • We do not use the following data for averages, fits, limits, etc. • • •	
$< 0.0465$	<sup>3</sup> ABDALLAH 04C DLPH $B(\gamma c \text{ or } \gamma u)$
$< 0.0132$	<sup>4</sup> AKTAS 04 H1 $B(t \rightarrow \gamma u)$
$< 0.041$	<sup>5</sup> ACHARD 02J L3 $B(t \rightarrow \gamma c \text{ or } \gamma u)$
$< 0.032$	<sup>6</sup> ABE 98G CDF $t\bar{T} \rightarrow (Wb)(\gamma c \text{ or } \gamma u)$

- <sup>1</sup> AARON 09A looked for single top production via FCNC in  $e^\pm p$  collisions at HERA with  $474 \text{ pb}^{-1}$ . The upper bound of the cross section gives the bound on the FCNC coupling  $\kappa_{t u \gamma}/\Lambda < 1.03 \text{ TeV}^{-1}$ , which corresponds to the result for  $m_t = 175 \text{ GeV}$ .
- <sup>2</sup> CHEKANOV 03 looked for single top production via FCNC in the reaction  $e^\pm p \rightarrow e^\pm (t \text{ or } \bar{T}) X$  in  $130.1 \text{ pb}^{-1}$  of data at  $\sqrt{s} = 300\text{--}318 \text{ GeV}$ . No evidence for top production and its decay into  $bW$  was found. The result is obtained for  $m_t = 175 \text{ GeV}$  when  $B(\gamma c) = B(Zq) = 0$ , where  $q$  is a  $u$  or  $c$  quark. Bounds on the effective  $t\text{--}u\text{--}\gamma$  and  $t\text{--}u\text{--}Z$  couplings are found in their Fig. 4. The conversion to the constraint listed is from private communication, E. Gallo, January 2004.
- <sup>3</sup> ABDALLAH 04C looked for single top production via FCNC in the reaction  $e^+ e^- \rightarrow \bar{T}c$  or  $\bar{T}u$  in  $541 \text{ pb}^{-1}$  of data at  $\sqrt{s} = 189\text{--}208 \text{ GeV}$ . No deviation from the SM is found, which leads to the bound on  $B(t \rightarrow \gamma q)$ , where  $q$  is a  $u$  or  $c$  quark, for  $m_t = 175 \text{ GeV}$  when  $B(t \rightarrow Zq) = 0$  is assumed. The conversion to the listed bound is from private communication, O. Yushchenko, April 2005. The bounds on the effective  $t\text{--}q\text{--}\gamma$  and  $t\text{--}q\text{--}Z$  couplings are given in their Fig. 7 and Table 4, for  $m_t = 170\text{--}180 \text{ GeV}$ , where most conservative bounds are found by choosing the chiral couplings to maximize the negative interference between the virtual  $\gamma$  and  $Z$  exchange amplitudes.
- <sup>4</sup> AKTAS 04 looked for single top production via FCNC in  $e^\pm$  collisions at HERA with  $118.3 \text{ pb}^{-1}$ , and found 5 events in the  $e$  or  $\mu$  channels. By assuming that they are due to statistical fluctuation, the upper bound on the  $t u \gamma$  coupling  $\kappa_{t u \gamma} < 0.27$  (95% CL) is obtained. The conversion to the partial width limit, when  $B(\gamma c) = B(Zu) = B(Zc) = 0$ , is from private communication, E. Perez, May 2005.
- <sup>5</sup> ACHARD 02J looked for single top production via FCNC in the reaction  $e^+ e^- \rightarrow \bar{T}c$  or  $\bar{T}u$  in  $634 \text{ pb}^{-1}$  of data at  $\sqrt{s} = 189\text{--}209 \text{ GeV}$ . No deviation from the SM is found, which leads to a bound on the top-quark decay branching fraction  $B(\gamma q)$ , where  $q$  is a  $u$  or  $c$  quark. The bound assumes  $B(Zq) = 0$  and is for  $m_t = 175 \text{ GeV}$ ; bounds for  $m_t = 170 \text{ GeV}$  and  $180 \text{ GeV}$  and  $B(Zq) \neq 0$  are given in Fig. 5 and Table 7.
- <sup>6</sup> ABE 98G looked for  $t\bar{T}$  events where one  $t$  decays into  $q\gamma$  while the other decays into  $bW$ . The quoted bound is for  $\Gamma(\gamma q)/\Gamma(Wb)$ .

$\Gamma(Zq (q=u, c))/\Gamma_{\text{total}}$	$\Gamma_6/\Gamma$
Test for $\Delta T = 1$ weak neutral current. Allowed by higher-order electroweak interaction.	
VALUE	DOCUMENT ID TECN COMMENT

<b>&lt; 0.032</b>	<sup>1</sup> ABAZOV 11M D0 $t \rightarrow Zq (q = u, c)$
$< 0.037$	<sup>2</sup> AALTONEN 08AD CDF $t \rightarrow Zq (q = u, c)$
$< 0.159$	<sup>3</sup> ABDALLAH 04C DLPH $e^+ e^- \rightarrow \bar{T}c$ or $\bar{T}u$
$< 0.137$	<sup>4</sup> ACHARD 02J L3 $e^+ e^- \rightarrow \bar{T}c$ or $\bar{T}u$
$< 0.14$	<sup>5</sup> HEISTER 02Q ALEP $e^+ e^- \rightarrow \bar{T}c$ or $\bar{T}u$
$< 0.137$	<sup>6</sup> ABBIENDI 01T OPAL $e^+ e^- \rightarrow \bar{T}c$ or $\bar{T}u$
• • • We do not use the following data for averages, fits, limits, etc. • • •	
$< 0.083$	<sup>7</sup> AALTONEN 09AL CDF $t \rightarrow Zq (q=c)$
$< 0.17$	<sup>8</sup> BARATE 00S ALEP $e^+ e^- \rightarrow \bar{T}c$ or $\bar{T}u$
$< 0.33$	<sup>9</sup> ABE 98G CDF $t\bar{T} \rightarrow (Wb)(Zc \text{ or } Zu)$

- <sup>1</sup> Based on  $4.1 \text{ fb}^{-1}$  of data. ABAZOV 11M searched for FCNC decays of the top quark in  $t\bar{T} \rightarrow \ell^+ \ell^- \ell^\pm u + \text{jets}$  ( $\ell, \ell' = e, \mu$ ) final states, and absence of the signal gives the bound.
- <sup>2</sup> Result is based on  $1.9 \text{ fb}^{-1}$  of data at  $\sqrt{s} = 1.96 \text{ TeV}$ .  $t\bar{T} \rightarrow WbZq$  or  $ZqZq$  processes have been looked for in  $Z + \geq 4$  jet events with and without  $b$ -tag. No signal leads to the bound  $B(t \rightarrow Zq) < 0.037$  (0.041) for  $m_t = 175$  (170) GeV.
- <sup>3</sup> ABDALLAH 04C looked for single top production via FCNC in the reaction  $e^+ e^- \rightarrow \bar{T}c$  or  $\bar{T}u$  in  $541 \text{ pb}^{-1}$  of data at  $\sqrt{s} = 189\text{--}208 \text{ GeV}$ . No deviation from the SM is found, which leads to the bound on  $B(t \rightarrow Zq)$ , where  $q$  is a  $u$  or  $c$  quark, for  $m_t = 175 \text{ GeV}$  when  $B(t \rightarrow \gamma q) = 0$  is assumed. The conversion to the listed bound is from private communication, O. Yushchenko, April 2005. The bounds on the effective  $t\text{--}q\text{--}\gamma$  and  $t\text{--}q\text{--}Z$  couplings are given in their Fig. 7 and Table 4, for  $m_t = 170\text{--}180 \text{ GeV}$ , where most conservative bounds are found by choosing the chiral couplings to maximize the negative interference between the virtual  $\gamma$  and  $Z$  exchange amplitudes.
- <sup>4</sup> ACHARD 02J looked for single top production via FCNC in the reaction  $e^+ e^- \rightarrow \bar{T}c$  or  $\bar{T}u$  in  $634 \text{ pb}^{-1}$  of data at  $\sqrt{s} = 189\text{--}209 \text{ GeV}$ . No deviation from the SM is found, which leads to a bound on the top-quark decay branching fraction  $B(Zq)$ , where  $q$  is a  $u$  or  $c$  quark. The bound assumes  $B(\gamma q) = 0$  and is for  $m_t = 175 \text{ GeV}$ ; bounds for  $m_t = 170 \text{ GeV}$  and  $180 \text{ GeV}$  and  $B(\gamma q) \neq 0$  are given in Fig. 5 and Table 7. Table 6 gives constraints on  $t\text{--}c\text{--}e\text{--}e$  four-fermi contact interactions.
- <sup>5</sup> HEISTER 02Q looked for single top production via FCNC in the reaction  $e^+ e^- \rightarrow \bar{T}c$  or  $\bar{T}u$  in  $214 \text{ pb}^{-1}$  of data at  $\sqrt{s} = 204\text{--}209 \text{ GeV}$ . No deviation from the SM is found, which leads to a bound on the branching fraction  $B(Zq)$ , where  $q$  is a  $u$  or  $c$  quark. The bound assumes  $B(\gamma q) = 0$  and is for  $m_t = 174 \text{ GeV}$ . Bounds on the effective  $t\text{--}(c \text{ or } u)\text{--}\gamma$  and  $t\text{--}(c \text{ or } u)\text{--}Z$  couplings are given in their Fig. 2.
- <sup>6</sup> ABBIENDI 01T looked for single top production via FCNC in the reaction  $e^+ e^- \rightarrow \bar{T}c$  or  $\bar{T}u$  in  $600 \text{ pb}^{-1}$  of data at  $\sqrt{s} = 189\text{--}209 \text{ GeV}$ . No deviation from the SM is found, which leads to bounds on the branching fractions  $B(Zq)$  and  $B(\gamma q)$ , where  $q$  is a  $u$  or  $c$  quark. The result is obtained for  $m_t = 174 \text{ GeV}$ . The upper bound becomes 9.7% (20.6%) for  $m_t = 169$  (179) GeV. Bounds on the effective  $t\text{--}(c \text{ or } u)\text{--}\gamma$  and  $t\text{--}(c \text{ or } u)\text{--}Z$  couplings are given in their Fig. 4.
- <sup>7</sup> Based on  $p\bar{p}$  data of  $1.52 \text{ fb}^{-1}$ . AALTONEN 09AL compared  $t\bar{T} \rightarrow WbWb \rightarrow \ell\nu bjjb$  and  $t\bar{T} \rightarrow ZcWb \rightarrow \ell\ell cjjb$  decay chains, and absence of the latter signal gives the bound. The result is for 100% longitudinally polarized  $Z$  boson and the theoretical  $t\bar{T}$  production cross section. The results for different  $Z$  polarizations and those without the cross section assumption are given in their Table XI.
- <sup>8</sup> BARATE 00S looked for single top production via FCNC in the reaction  $e^+ e^- \rightarrow \bar{T}c$  or  $\bar{T}u$  in  $411 \text{ pb}^{-1}$  of data at c.m. energies between 189 and 202 GeV. No deviation from





# Quark Particle Listings

*t*

• • • We do not use the following data for averages, fits, limits, etc. • • •

0.98±0.63		<sup>3</sup> ABAZOV	11AA D0	s-channel
2.90±0.59		<sup>3</sup> ABAZOV	11AA D0	t-channel
1.8 <sup>+0.7</sup> <sub>-0.5</sub>		<sup>4</sup> AALTONEN	10AB CDF	s-channel
0.8 ±0.4		<sup>4</sup> AALTONEN	10AB CDF	t-channel
4.9 <sup>+2.5</sup> <sub>-2.2</sub>		<sup>5</sup> AALTONEN	10U CDF	$E_T$ + jets decay
3.14 <sup>+0.94</sup> <sub>-0.80</sub>		<sup>6</sup> ABAZOV	10 D0	t-channel
1.05±0.81		<sup>6</sup> ABAZOV	10 D0	s-channel
< 7.3	95	<sup>7</sup> ABAZOV	10J D0	$\tau$ + jets decay
3.94±0.88		<sup>8</sup> ABAZOV	09Z D0	s- + t-channel
2.2 <sup>+0.7</sup> <sub>-0.6</sub>		<sup>9</sup> AALTONEN	08AH CDF	s- + t-channel
4.7 ±1.3		<sup>10</sup> ABAZOV	08I D0	s- + t-channel
4.9 ±1.4		<sup>11</sup> ABAZOV	07H D0	s- + t-channel
< 6.4	95	<sup>12</sup> ABAZOV	05P D0	$p\bar{p} \rightarrow tb + X$
< 5.0	95	<sup>12</sup> ABAZOV	05P D0	$p\bar{p} \rightarrow tqb + X$
<10.1	95	<sup>13</sup> ACOSTA	05N CDF	$p\bar{p} \rightarrow tqb + X$
<13.6	95	<sup>13</sup> ACOSTA	05N CDF	$p\bar{p} \rightarrow tb + X$
<17.8	95	<sup>13</sup> ACOSTA	05N CDF	$p\bar{p} \rightarrow tb + X, tqb + X$

<sup>1</sup> Based on 5.4 fb<sup>-1</sup> of data and for  $m_t = 172.5$  GeV. The error is statistical + systematic combined. Results for other  $m_t$  values are given in Table III of ABAZOV 11AD. The result is obtained by assuming the SM ratio between  $tb$  (s-channel) and  $tqb$  (t-channel) productions, and gives  $|V_{tb}|^2 = 1.02 \pm 0.10$ , or  $|V_{tb}| > 0.79$  at 95% CL for a flat prior within  $0 < |V_{tb}|^2 < 1$ .

<sup>2</sup> Based on 3.2 fb<sup>-1</sup> of data. Events with isolated  $\ell$  +  $E_T$  + jets with at least one  $b$ -tag are analyzed and s- and t-channel single top events are selected by using the likelihood function, matrix element, neural-network, boosted decision tree, likelihood function optimized for s-channel process, and neural-network based analysis of events with  $E_T$  that has sensitivity for  $W \rightarrow \tau\nu$  decays. The result is for  $m_t = 175$  GeV, and the mean value decreases by 0.02 pb/GeV for smaller  $m_t$ . The signal has 5.0 sigma significance. The result gives  $|V_{tb}| = 0.91 \pm 0.11$  (stat+syst)  $\pm 0.07$  (theory), or  $|V_{tb}| > 0.71$  at 95% CL.

<sup>3</sup> Based on 5.4 fb<sup>-1</sup> of data. The error is statistical + systematic combined. The results are for  $m_t = 172.5$  GeV. Results for other  $m_t$  values are given in Table 2 of ABAZOV 11AA.

<sup>4</sup> Based on 3.2 fb<sup>-1</sup> of data. For combined s- + t-channel result see AALTONEN 09AT.

<sup>5</sup> Result is based on 2.1 fb<sup>-1</sup> of data. Events with large missing  $E_T$  and jets with at least one  $b$ -jet without identified electron or muon are selected. Result is obtained when observed 2.1  $\sigma$  excess over the background originates from the signal for  $m_t = 175$  GeV, giving  $|V_{tb}| = 1.24 \pm 0.34$ <sub>-0.29</sub>  $\pm 0.07$ (theory).

<sup>6</sup> Result is based on 2.3 fb<sup>-1</sup> of data. Events with isolated  $\ell$  +  $E_T$  + 2, 3, 4 jets with one or two  $b$ -tags are selected. The analysis assumes  $m_t = 170$  GeV.

<sup>7</sup> Result is based on 4.8 fb<sup>-1</sup> of data. Events with an isolated reconstructed tau lepton, missing  $E_T$  + 2, 3 jets with one or two  $b$ -tags are selected. When combined with ABAZOV 09Z result for  $e + \mu$  channels, the s- and t-channels combined cross section is  $3.84 \pm 0.89$ <sub>-0.83</sub> pb.

<sup>8</sup> Based on 2.3 fb<sup>-1</sup> of data. Events with isolated  $\ell$  +  $E_T$  +  $\geq 2$  jets with 1 or 2  $b$ -tags are analyzed and s- and t-channel single top events are selected by using boosted decision tree, Bayesian neural networks and the matrix element method. The signal has 5.0 sigma significance. The result gives  $|V_{tb}| = 1.07 \pm 0.12$ , or  $|V_{tb}| > 0.78$  at 95% CL. The analysis assumes  $m_t = 170$  GeV.

<sup>9</sup> Result is based on 2.2 fb<sup>-1</sup> of data. Events with isolated  $\ell$  +  $E_T$  + 2, 3 jets with at least one  $b$ -tag are selected, and s- and t-channel single top events are selected by using likelihood, matrix element, and neural network discriminants. The result can be interpreted as  $|V_{tb}| = 0.88 \pm 0.13$ (stat + syst)  $\pm 0.07$ (theory), and  $|V_{tb}| > 0.66$  (95% CL) under the  $|V_{tb}| < 1$  constraint.

<sup>10</sup> Result is based on 0.9 fb<sup>-1</sup> of data. Events with isolated  $\ell$  +  $E_T$  + 2, 3, 4 jets with one or two  $b$ -vertex-tag are selected, and contributions from  $W$  + jets,  $t\bar{t}$ , s- and t-channel single top events are identified by using boosted decision trees, Bayesian neural networks, and matrix element analysis. The result can be interpreted as the measurement of the CKM matrix element  $|V_{tb}| = 1.31 \pm 0.25$ <sub>-0.21</sub>, or  $|V_{tb}| > 0.68$  (95% CL) under the  $|V_{tb}| < 1$  constraint.

<sup>11</sup> Result is based on 0.9 fb<sup>-1</sup> of data. This result constrains  $V_{tb}$  to  $0.68 < |V_{tb}| \leq 1$  at 95% CL.

<sup>12</sup> ABAZOV 05P bounds single top-quark production from either the s-channel  $W$ -exchange process,  $q'\bar{q} \rightarrow t\bar{b}$ , or the t-channel  $W$ -exchange process,  $q'g \rightarrow qt\bar{b}$ , based on  $\sim 230$  pb<sup>-1</sup> of data.

<sup>13</sup> ACOSTA 05N bounds single top-quark production from the t-channel  $W$ -exchange process ( $q'g \rightarrow qt\bar{b}$ ), the s-channel  $W$ -exchange process ( $q'\bar{q} \rightarrow t\bar{b}$ ), and from the combined cross section of t- and s-channel. Based on  $\sim 162$  pb<sup>-1</sup> of data.

## Single t-Quark Production Cross Section in pp Collisions at $\sqrt{s} = 7$ TeV

Direct probe of the  $tbW$  coupling and possible new physics at  $\sqrt{s} = 7$  TeV.

VALUE (pb)	DOCUMENT ID	TECN	COMMENT
<b>83.6±29.8±3.3</b>	<sup>1</sup> CHATRCHYAN11R	CMS	t-channel

<sup>1</sup> Based on 36 pb<sup>-1</sup> of data. The first error is statistical + systematic combined, the second is luminosity. The result gives  $|V_{tb}| = 1.114 \pm 0.22$ (exp)  $\pm 0.02$ (th) from the ratio  $\sigma(\text{exp})/\sigma(\text{th})$ , where  $\sigma(\text{th})$  is the SM prediction for  $|V_{tb}| = 1$ . The 95% CL lower bound of  $|V_{tb}| > 0.62$  (0.68) is found from the 2D (BDT) analysis under the constraint  $0 < |V_{tb}|^2 < 1$ .

## Single t-Quark Production Cross Section in ep Collisions

VALUE (pb)	CL%	DOCUMENT ID	TECN	COMMENT
<0.25	95	<sup>1</sup> AARON	09A H1	$e^\pm p \rightarrow e^\pm tX$
<0.55	95	<sup>2</sup> AKTAS	04 H1	$e^\pm p \rightarrow e^\pm tX$
<0.225	95	<sup>3</sup> CHEKANOV	03 ZEUS	$e^\pm p \rightarrow e^\pm tX$

<sup>1</sup> AARON 09A looked for single top production via FCNC in  $e^\pm p$  collisions at HERA with 474 pb<sup>-1</sup> of data at  $\sqrt{s} = 301$ -319 GeV. The result supersedes that of AKTAS 04.

<sup>2</sup> AKTAS 04 looked for single top production via FCNC in  $e^\pm$  collisions at HERA with 118.3 pb<sup>-1</sup>, and found 5 events in the  $e$  or  $\mu$  channels while  $1.31 \pm 0.22$  events are expected from the Standard Model background. No excess was found for the hadronic channel. The observed cross section of  $\sigma(ep \rightarrow etX) = 0.29 \pm 0.15$ <sub>-0.14</sub> pb at  $\sqrt{s} = 319$  GeV gives the quoted upper bound if the observed events are due to statistical fluctuation.

<sup>3</sup> CHEKANOV 03 looked in 130.1 pb<sup>-1</sup> of data at  $\sqrt{s} = 301$  and 318 GeV. The limit is for  $\sqrt{s} = 318$  GeV and assumes  $m_t = 175$  GeV.

## t $\bar{t}$ production cross section in pp collisions at $\sqrt{s} = 1.8$ TeV

Only the final combined  $t\bar{t}$  production cross sections obtained from Tevatron Run I by the CDF and D0 experiments are quoted below.

VALUE (pb)	DOCUMENT ID	TECN	COMMENT
5.69±1.21±1.04	<sup>1</sup> ABAZOV	03A D0	Combined Run I data
6.5 <sup>+1.7</sup> <sub>-1.4</sub>	<sup>2</sup> AFOLDER	01A CDF	Combined Run I data

<sup>1</sup> Combined result from 110 pb<sup>-1</sup> of Tevatron Run I data. Assume  $m_t = 172.1$  GeV.

<sup>2</sup> Combined result from 105 pb<sup>-1</sup> of Tevatron Run I data. Assume  $m_t = 175$  GeV.

## t $\bar{t}$ production cross section in p $\bar{p}$ collisions at $\sqrt{s} = 1.96$ TeV

Unless otherwise noted the first quoted error is from statistics, the second from systematic uncertainties, and the third from luminosity. If only two errors are quoted the luminosity is included in the systematic uncertainties.

VALUE (pb)	DOCUMENT ID	TECN	COMMENT
• • • We do not use the following data for averages, fits, limits, etc. • • •			
8.5 ±0.6 ±0.7	<sup>1</sup> AALTONEN	11D CDF	$\ell + E_T$ + jets ( $\geq 1b$ -tag)
7.64±0.57±0.45	<sup>2</sup> AALTONEN	11W CDF	$\ell + E_T$ + jets ( $\geq 1b$ -tag)
7.99±0.55±0.76±0.46	<sup>3</sup> AALTONEN	11Y CDF	$E_T + \geq 4$ jets (0,1,2 $b$ -tag)
7.78 <sup>+0.77</sup> <sub>-0.64</sub>	<sup>4</sup> ABAZOV	11E D0	$\ell + E_T + \geq 2$ jets
7.56 <sup>+0.63</sup> <sub>-0.56</sub>	<sup>5</sup> ABAZOV	11Z D0	Combination
6.27±0.73±0.63±0.39	<sup>6</sup> AALTONEN	10AA CDF	$\ell\ell + E_T + \geq 2$ jets
7.2 ±0.5 ±1.0 ±0.4	<sup>7</sup> AALTONEN	10E CDF	$\geq 6$ jets, vtx $b$ -tag
7.8 ±2.4 ±1.6 ±0.5	<sup>8</sup> AALTONEN	10V CDF	$\ell + \geq 3$ jets, soft- $b$ -tag
7.70±0.52	<sup>9</sup> AALTONEN	10W CDF	$\ell + E_T + \geq 3$ jets + $b$ -tag, norm. to $\sigma(Z \rightarrow \ell\ell)_{TH}$
6.9 ±2.0	<sup>10</sup> ABAZOV	10I D0	$\geq 6$ jets with 2 $b$ -tags
6.9 ±1.2 <sup>+0.8</sup> <sub>-0.7</sub> ±0.4	<sup>11</sup> ABAZOV	10Q D0	$\tau_h$ + jets
9.6 ±1.2 <sup>+0.6</sup> <sub>-0.5</sub> ±0.6	<sup>12</sup> AALTONEN	09AD CDF	$\ell\ell + E_T$ / vtx $b$ -tag
9.1 ±1.1 <sup>+1.0</sup> <sub>-0.9</sub> ±0.6	<sup>13</sup> AALTONEN	09H CDF	$\ell + \geq 3$ jets + $E_T$ / soft $\mu$ $b$ -tag
8.18 <sup>+0.98</sup> <sub>-0.87</sub>	<sup>14</sup> ABAZOV	09AG D0	$\ell +$ jets, $\ell\ell$ and $\ell\tau$ + jets
7.5 ±1.0 <sup>+0.7</sup> <sub>-0.6</sub> <sup>+0.6</sup> <sub>-0.5</sub>	<sup>15</sup> ABAZOV	09R D0	$\ell\ell$ and $\ell\tau$ + jets
8.18 <sup>+0.90</sup> <sub>-0.84</sub> ±0.50	<sup>16</sup> ABAZOV	08M D0	$\ell + n$ jets with 0,1,2 $b$ -tag
7.62±0.85	<sup>17</sup> ABAZOV	08N D0	$\ell + n$ jets + $b$ -tag or kinematics
8.5 <sup>+2.7</sup> <sub>-2.2</sub>	<sup>18</sup> ABULENCIA	08 CDF	$t^+ \ell^-$ ( $\ell = e, \mu$ )
8.3 ±1.0 <sup>+2.0</sup> <sub>-1.5</sub> ±0.5	<sup>19</sup> AALTONEN	07D CDF	$\geq 6$ jets, vtx $b$ -tag
7.4 ±1.4 ±1.0	<sup>20</sup> ABAZOV	07O D0	$\ell\ell +$ jets, vtx $b$ -tag
4.5 <sup>+2.0</sup> <sub>-1.9</sub> <sup>+1.4</sup> <sub>-1.1</sub> ±0.3	<sup>21</sup> ABAZOV	07P D0	$\geq 6$ jets, vtx $b$ -tag
6.4 <sup>+1.3</sup> <sub>-1.2</sub> ±0.7 ±0.4	<sup>22</sup> ABAZOV	07R D0	$\ell + \geq 4$ jets
6.6 ±0.9 ±0.4	<sup>23</sup> ABAZOV	06X D0	$\ell +$ jets, vtx $b$ -tag
8.7 ±0.9 <sup>+1.1</sup> <sub>-0.9</sub>	<sup>24</sup> ABULENCIA	06Z CDF	$\ell +$ jets, vtx $b$ -tag
5.8 ±1.2 <sup>+0.9</sup> <sub>-0.7</sub>	<sup>25</sup> ABULENCIA,A	06c CDF	missing $E_T$ + jets, vtx $b$ -tag
7.5 ±2.1 <sup>+3.3</sup> <sub>-2.2</sub> <sup>+0.5</sup> <sub>-0.4</sub>	<sup>26</sup> ABULENCIA,A	06E CDF	6-8 jets, $b$ -tag
8.9 ±1.0 <sup>+1.1</sup> <sub>-1.0</sub>	<sup>27</sup> ABULENCIA,A	06F CDF	$\ell + \geq 3$ jets, $b$ -tag
8.6 <sup>+1.6</sup> <sub>-1.5</sub> ±0.6	<sup>28</sup> ABAZOV	05Q D0	$\ell + n$ jets
8.6 <sup>+3.2</sup> <sub>-2.7</sub> ±1.1 ±0.6	<sup>29</sup> ABAZOV	05R D0	di-lepton + $n$ jets
6.7 <sup>+1.4</sup> <sub>-1.3</sub> <sup>+1.6</sup> <sub>-1.1</sub> ±0.4	<sup>30</sup> ABAZOV	05X D0	$\ell +$ jets / kinematics
5.3 ±3.3 <sup>+1.3</sup> <sub>-1.0</sub>	<sup>31</sup> ACOSTA	05S CDF	$\ell +$ jets / soft $\mu$ $b$ -tag
6.6 ±1.1 ±1.5	<sup>32</sup> ACOSTA	05T CDF	$\ell +$ jets / kinematics
6.0 <sup>+1.5</sup> <sub>-1.6</sub> <sup>+1.2</sup> <sub>-1.3</sub>	<sup>33</sup> ACOSTA	05U CDF	$\ell +$ jets/kinematics + vtx $b$ -tag
5.6 <sup>+1.2</sup> <sub>-1.1</sub> <sup>+0.9</sup> <sub>-0.6</sub>	<sup>34</sup> ACOSTA	05V CDF	$\ell + n$ jets
7.0 <sup>+2.4</sup> <sub>-2.1</sub> <sup>+1.6</sup> <sub>-1.1</sub> ±0.4	<sup>35</sup> ACOSTA	04I CDF	di-lepton + jets + missing ET

- <sup>1</sup> Based on  $1.12 \text{ fb}^{-1}$  and assumes  $m_t = 175 \text{ GeV}$ , where the cross section changes by  $\pm 0.1 \text{ pb}$  for every  $\mp 1 \text{ GeV}$  shift in  $m_t$ . AALTONEN 11D fits simultaneously the  $t\bar{t}$  production cross section and the  $b$ -tagging efficiency and find improvements in both measurements.
- <sup>2</sup> Based on  $2.7 \text{ fb}^{-1}$ . The first error is from statistics and systematics, the second is from luminosity. The result is for  $m_t = 175 \text{ GeV}$ . AALTONEN 11W fits simultaneously a jet flavor discriminator between  $b$ -,  $c$ -, and light-quarks, and find significant reduction in the systematic error.
- <sup>3</sup> Based on  $2.2 \text{ fb}^{-1}$ . The result is for  $m_t = 172.5 \text{ GeV}$ . AALTONEN 11Y selects multi-jet events with large  $E_{Tj}$ , and vetoes identified electrons and muons.
- <sup>4</sup> Based on  $5.3 \text{ fb}^{-1}$ . The error is statistical + systematic + luminosity combined. The result is for  $m_t = 172.5 \text{ GeV}$ . The results for other  $m_t$  values are given in Table XII and eq.(10) of ABZOV 11E.
- <sup>5</sup> Combination of a dilepton measurement presented in ABZOV 11Z (based on  $5.4 \text{ fb}^{-1}$ ), which yields  $7.36^{+0.90}_{-0.79}$  (stat+syst) pb, and the lepton + jets measurement of ABZOV 11E. The result is for  $m_t = 172.5 \text{ GeV}$ . The results for other  $m_t$  values is given by eq.(5) of ABZOV 11A.
- <sup>6</sup> Based on  $2.8 \text{ fb}^{-1}$ . The result is for  $m_t = 175 \text{ GeV}$ .
- <sup>7</sup> Based on  $2.9 \text{ fb}^{-1}$ . Result is obtained from the fraction of signal events in the top quark mass measurement in the all hadronic decay channel.
- <sup>8</sup> Based on  $1.7 \text{ fb}^{-1}$ . The result is for  $m_t = 175 \text{ GeV}$ . AALTONEN 10V uses soft electrons from  $b$ -hadron decays to suppress  $W$ +jets background events.
- <sup>9</sup> Based on  $4.6 \text{ fb}^{-1}$ . The result is for  $m_t = 172.5 \text{ GeV}$ . The ratio  $\sigma(t\bar{t} \rightarrow \ell + \text{jets}) / \sigma(Z/\gamma^* \rightarrow \ell\ell)$  is measured and then multiplied by the theoretical  $Z/\gamma^* \rightarrow \ell\ell$  cross section of  $\sigma(Z/\gamma^* \rightarrow \ell\ell) = 251.3 \pm 5.0 \text{ pb}$ , which is free from the luminosity error.
- <sup>10</sup> Based on  $1 \text{ fb}^{-1}$ . The result is for  $m_t = 175 \text{ GeV}$ .  $7.9 \pm 2.3 \text{ pb}$  is found for  $m_t = 170 \text{ GeV}$ . ABZOV 10I uses a likelihood discriminant to separate signal from background, where the background model was created from lower jet-multiplicity data.
- <sup>11</sup> Based on  $1 \text{ fb}^{-1}$ . The result is for  $m_t = 170 \text{ GeV}$ . For  $m_t = 175 \text{ GeV}$ , the result is  $6.3^{+1.2}_{-1.1}(\text{stat}) \pm 0.7(\text{syst}) \pm 0.4(\text{lumi}) \text{ pb}$ . Cross section of  $t\bar{t}$  production has been measured in the  $t\bar{t} \rightarrow \tau_h$  + jets topology, where  $\tau_h$  denotes hadronically decaying  $\tau$  leptons. The result for the cross section times the branching ratio is  $\sigma(t\bar{t}) \cdot B(t\bar{t} \rightarrow \tau_h + \text{jets}) = 0.60^{+0.19}_{-0.17} \pm 0.23^{+0.15}_{-0.14} \pm 0.04 \text{ pb}$  for  $m_t = 170 \text{ GeV}$ .
- <sup>12</sup> Based on  $1.1 \text{ fb}^{-1}$ . The result is for  $B(W \rightarrow \ell\nu) = 10.8\%$  and  $m_t = 175 \text{ GeV}$ ; the mean value is  $9.8$  for  $m_t = 172.5 \text{ GeV}$  and  $10.1$  for  $m_t = 170 \text{ GeV}$ . AALTONEN 09AD used high  $p_{Tj}$   $e$  or  $\mu$  with an isolated track to select  $t\bar{t}$  decays into dileptons including  $\ell = \tau$ . The result is based on the candidate event samples with and without vertex  $b$ -tag.
- <sup>13</sup> Based on  $2 \text{ fb}^{-1}$ . The result is for  $m_t = 175 \text{ GeV}$ ; the mean value is 3% higher for  $m_t = 170 \text{ GeV}$  and 4% lower for  $m_t = 180 \text{ GeV}$ .
- <sup>14</sup> Result is based on  $1 \text{ fb}^{-1}$  of data. The result is for  $m_t = 170 \text{ GeV}$ , and the mean value decreases with increasing  $m_t$ ; see their Fig. 2. The result is obtained after combining  $\ell + \text{jets}$ ,  $\ell\ell$ , and  $\ell\tau$  final states, and the ratios of the extracted cross sections are  $R^{\ell\ell/\ell j} = 0.86^{+0.19}_{-0.17}$  and  $R^{\ell\tau/\ell\ell - \ell j} = 0.97^{+0.32}_{-0.29}$ , consistent with the SM expectation of  $R = 1$ . This leads to the upper bound of  $B(t \rightarrow bH^+)$  as a function of  $m_{H^+}$ . Results are shown in their Fig. 1 for  $B(H^+ \rightarrow \tau\nu) = 1$  and  $B(H^+ \rightarrow c\bar{s}) = 1$  cases. Comparison of the  $m_t$  dependence of the extracted cross section and a partial NNLO prediction gives  $m_t = 169.1^{+5.9}_{-5.2} \text{ GeV}$ .
- <sup>15</sup> Result is based on  $1 \text{ fb}^{-1}$  of data. The result is for  $m_t = 170 \text{ GeV}$ , and the mean value changes by  $-0.07 [m_t(\text{GeV}) - 170] \text{ pb}$  near the reference  $m_t$  value. Comparison of the  $m_t$  dependence of the extracted cross section and a partial NNLO QCD prediction gives  $m_t = 171.5^{+9.9}_{-8.8} \text{ GeV}$ . The  $\ell\tau$  channel alone gives  $7.6^{+4.9+3.5+1.4}_{-4.3-3.4-0.9} \text{ pb}$  and the  $\ell\ell$  channel gives  $7.5^{+1.2+0.7+0.7}_{-1.1-0.6-0.5} \text{ pb}$ .
- <sup>16</sup> Result is based on  $0.9 \text{ fb}^{-1}$  of data. The first error is from stat + syst, while the latter error is from luminosity. The result is for  $m_t = 175 \text{ GeV}$ , and the mean value changes by  $-0.09 \text{ pb} [m_t(\text{GeV}) - 175]$ .
- <sup>17</sup> Result is based on  $0.9 \text{ fb}^{-1}$  of data. The cross section is obtained from the  $\ell + \geq 3$  jet event rates with 1 or 2  $b$ -tag, and also from the kinematical likelihood analysis of the  $\ell + 3, 4$  jet events. The result is for  $m_t = 172.6 \text{ GeV}$ , and its  $m_t$  dependence shown in Fig. 3 leads to the constraint  $m_t = 170 \pm 7 \text{ GeV}$  when compared to the SM prediction.
- <sup>18</sup> Result is based on  $360 \text{ pb}^{-1}$  of data. Events with high  $p_{Tj}$  oppositely charged dileptons  $\ell^+ \ell^-$  ( $\ell = e, \mu$ ) are used to obtain cross sections for  $t\bar{t}$ ,  $W^+W^-$ , and  $Z \rightarrow \tau^+\tau^-$  production processes simultaneously. The other cross sections are given in Table IV.
- <sup>19</sup> Based on  $1.02 \text{ fb}^{-1}$  of data. Result is for  $m_t = 175 \text{ GeV}$ . Secondary vertex  $b$ -tag and neural network selections are used to achieve a signal-to-background ratio of about 1/2.
- <sup>20</sup> Based on  $425 \text{ pb}^{-1}$  of data. Result is for  $m_t = 175 \text{ GeV}$ . For  $m_t = 170.9 \text{ GeV}$ ,  $7.8 \pm 1.8(\text{stat} + \text{syst}) \text{ pb}$  is obtained.
- <sup>21</sup> Based on  $405 \pm 25 \text{ pb}^{-1}$  of data. Result is for  $m_t = 175 \text{ GeV}$ . The last error is for luminosity. Secondary vertex  $b$ -tag and neural network are used to separate the signal events from the background.
- <sup>22</sup> Based on  $425 \text{ pb}^{-1}$  of data. Assumes  $m_t = 175 \text{ GeV}$ .
- <sup>23</sup> Based on  $\sim 425 \text{ pb}^{-1}$ . Assuming  $m_t = 175 \text{ GeV}$ . The first error is combined statistical and systematic, the second one is luminosity.
- <sup>24</sup> Based on  $\sim 318 \text{ pb}^{-1}$ . Assuming  $m_t = 178 \text{ GeV}$ . The cross section changes by  $\pm 0.08 \text{ pb}$  for each  $\mp 1 \text{ GeV}$  change in the assumed  $m_t$ . Result is for at least one  $b$ -tag. For at least two  $b$ -tagged jets,  $t\bar{t}$  signal of significance greater than  $5\sigma$  is found, and the cross section is  $10.1^{+1.6+2.0}_{-1.4-1.3} \text{ pb}$  for  $m_t = 178 \text{ GeV}$ .
- <sup>25</sup> Based on  $\sim 311 \text{ pb}^{-1}$ . Assuming  $m_t = 178 \text{ GeV}$ . For  $m_t = 175 \text{ GeV}$ , the result is  $6.0 \pm 1.2^{+0.9}_{-0.7}$ . This is the first CDF measurement without lepton identification, and hence it has sensitivity to the  $W \rightarrow \tau\nu$  mode.
- <sup>26</sup> ABULENCIA, A 06E measures the  $t\bar{t}$  production cross section in the all hadronic decay mode by selecting events with 6 to 8 jets and at least one  $b$ -jet.  $S/B = 1/5$  has been achieved. Based on  $311 \text{ pb}^{-1}$ . Assuming  $m_t = 178 \text{ GeV}$ .
- <sup>27</sup> Based on  $\sim 318 \text{ pb}^{-1}$ . Assuming  $m_t = 178 \text{ GeV}$ . Result is for at least one  $b$ -tag. For at least two  $b$ -tagged jets, the cross section is  $11.1^{+2.3+2.5}_{-1.9-1.9} \text{ pb}$ .
- <sup>28</sup> ABZOV 05Q measures the top-quark pair production cross section with  $\sim 230 \text{ pb}^{-1}$  of data, based on the analysis of  $W$  plus  $n$ -jet events where  $W$  decays into  $e$  or  $\mu$

plus neutrino, and at least one of the jets is  $b$ -jet like. The first error is statistical and systematic, and the second accounts for the luminosity uncertainty. The result assumes  $m_t = 175 \text{ GeV}$ ; the mean value changes by  $(175 - m_t(\text{GeV})) \times 0.06 \text{ pb}$  in the mass range 160 to 190 GeV.

<sup>29</sup> ABZOV 05R measures the top-quark pair production cross section with  $224\text{--}243 \text{ pb}^{-1}$  of data, based on the analysis of events with two charged leptons in the final state. The result assumes  $m_t = 175 \text{ GeV}$ ; the mean value changes by  $(175 - m_t(\text{GeV})) \times 0.08 \text{ pb}$  in the mass range 160 to 190 GeV.

<sup>30</sup> Based on  $230 \text{ pb}^{-1}$ . Assuming  $m_t = 175 \text{ GeV}$ .

<sup>31</sup> Based on  $194 \text{ pb}^{-1}$ . Assuming  $m_t = 175 \text{ GeV}$ .

<sup>32</sup> Based on  $194 \pm 11 \text{ pb}^{-1}$ . Assuming  $m_t = 175 \text{ GeV}$ .

<sup>33</sup> Based on  $162 \pm 10 \text{ pb}^{-1}$ . Assuming  $m_t = 175 \text{ GeV}$ .

<sup>34</sup> ACOSTA 05V measures the top-quark pair production cross section with  $\sim 162 \text{ pb}^{-1}$  data, based on the analysis of  $W$  plus  $n$ -jet events where  $W$  decays into  $e$  or  $\mu$  plus neutrino, and at least one of the jets is  $b$ -jet like. Assumes  $m_t = 175 \text{ GeV}$ .

<sup>35</sup> ACOSTA 04I measures the top-quark pair production cross section with  $197 \pm 12 \text{ pb}^{-1}$  data, based on the analysis of events with two charged leptons in the final state. Assumes  $m_t = 175 \text{ GeV}$ .

### Ratio of the production cross sections of $t\bar{t}\gamma$ to $t\bar{t}$ at $\sqrt{s} = 1.96 \text{ TeV}$

VALUE	DOCUMENT ID	TECN	COMMENT
$0.024 \pm 0.009$	<sup>1</sup> AALTONEN 11Z CDF		$E_{Tj}(\gamma) > 10 \text{ GeV}$ , $ \eta(\gamma)  < 1.0$

• • • We do not use the following data for averages, fits, limits, etc. • • •

<sup>1</sup> Based on  $6.0 \text{ fb}^{-1}$  of data. The error is statistical and systematic combined. Events with lepton +  $E_{Tj} + \geq 3$  jets ( $\geq 1b$ ) and without central, high  $E_{Tj}$  photon are measured. The result is consistent with the SM prediction of  $0.024 \pm 0.005$ . The absolute production cross section is measured to be  $0.18 \pm 0.08 \text{ fb}$ . The statistical significance is 3.0 standard deviations.

### $t\bar{t}$ production cross section in $p\bar{p}$ collisions at $\sqrt{s} = 7 \text{ TeV}$

Unless otherwise noted the first quoted error is from statistics, the second from systematic uncertainties, and the third from luminosity. If only two errors are quoted the luminosity is included in the systematic uncertainties.

VALUE (pb)	DOCUMENT ID	TECN	COMMENT
$177 \pm 20 \pm 14 \pm 7$	<sup>1</sup> AAD 12B ATLAS		$\ell\ell + E_{Tj} + \geq 2j$
$145 \pm 31^{+42}_{-27}$	<sup>2</sup> AAD 11A ATLAS		$\ell + E_{Tj} + \geq 4j$ , $\ell\ell + E_{Tj} + \geq 2j$
$173^{+39}_{-32} \pm 7$	<sup>3</sup> CHATRCHYAN11AA CMS		$\ell + E_{Tj} + \geq 3$ jets
$168 \pm 18 \pm 14 \pm 7$	<sup>4</sup> CHATRCHYAN11F CMS		$\ell\ell + E_{Tj} + \text{jets}$
$154 \pm 17 \pm 6$	<sup>5</sup> CHATRCHYAN11Z CMS		Combination
$194 \pm 72 \pm 24 \pm 21$	<sup>6</sup> KHACHATRY...11A CMS		$\ell\ell + E_{Tj} + \geq 2$ jets

<sup>1</sup> Based on  $35 \text{ pb}^{-1}$  of data for an assumed top quark mass of  $m_t = 172.5 \text{ GeV}$ .

<sup>2</sup> Based on  $2.9 \text{ pb}^{-1}$  of data. The result for single lepton channels is  $142 \pm 34^{+50}_{-31} \text{ pb}$ , while for the dilepton channels is  $151^{+78+37}_{-62-24} \text{ pb}$ .

<sup>3</sup> Result is based on  $36 \text{ pb}^{-1}$  of data. The first uncertainty corresponds to the statistical and systematic uncertainties, and the second corresponds to the luminosity.

<sup>4</sup> Based on  $36 \text{ pb}^{-1}$  of data. The ratio of  $t\bar{t}$  and  $Z/\gamma^*$  cross sections is measured as  $\sigma(pp \rightarrow t\bar{t})/\sigma(pp \rightarrow Z/\gamma^* \rightarrow e^+e^-/\mu^+\mu^-) = 0.175 \pm 0.018(\text{stat}) \pm 0.015(\text{syst})$  for  $60 < m_{\ell\ell} < 120 \text{ GeV}$ , for which they use an NNLO prediction for the denominator cross section of  $972 \pm 42 \text{ pb}$ .

<sup>5</sup> Result is based on  $36 \text{ pb}^{-1}$  of data. The first error is from statistical and systematic uncertainties, and the second from luminosity. This is a combination of a measurement in the dilepton channel (CHATRCHYAN 11F) and the measurement in the  $\ell + \text{jets}$  channel (CHATRCHYAN 11Z) which yields  $150 \pm 9 \pm 17 \pm 6 \text{ pb}$ .

<sup>6</sup> Result is based on  $3.1 \pm 0.3 \text{ pb}^{-1}$  of data.

### $g\bar{g} \rightarrow t\bar{t}$ fraction in $p\bar{p}$ collisions at $\sqrt{s} = 1.96 \text{ TeV}$

VALUE	CL%	DOCUMENT ID	TECN	COMMENT
$0.07 \pm 0.14 \pm 0.07$		<sup>1</sup> AALTONEN 08AG CDF		low $p_{Tj}$ number of tracks
$< 0.33$	68	<sup>2</sup> AALTONEN 09F CDF		$t\bar{t}$ correlations

• • • We do not use the following data for averages, fits, limits, etc. • • •

<sup>1</sup> Result is based on  $0.96 \text{ fb}^{-1}$  of data. The contribution of the subprocesses  $g\bar{g} \rightarrow t\bar{t}$  and  $q\bar{q} \rightarrow t\bar{t}$  is distinguished by using the difference between quark and gluon initiated jets in the number of small  $p_{Tj}$  ( $0.3 \text{ GeV} < p_{Tj} < 3 \text{ GeV}$ ) charged particles in the central region ( $|\eta| < 1.1$ ).

<sup>2</sup> Based on  $955 \text{ pb}^{-1}$ . AALTONEN 09F used differences in the  $t\bar{t}$  production angular distribution and polarization correlation to discriminate between  $g\bar{g} \rightarrow t\bar{t}$  and  $q\bar{q} \rightarrow t\bar{t}$  subprocesses. The combination with the result of AALTONEN 08AG gives  $0.07^{+0.15}_{-0.07}$ .

### $A_{FB}$ of $t\bar{t}$ in $p\bar{p}$ collisions at $\sqrt{s} = 1.96 \text{ TeV}$

VALUE (%)	DOCUMENT ID	TECN	COMMENT
$-11.6 \pm 15.3$	<sup>1</sup> AALTONEN 11F CDF		$m_{t\bar{t}} < 450 \text{ GeV}$
$47.5 \pm 11.4$	<sup>1</sup> AALTONEN 11F CDF		$m_{t\bar{t}} > 450 \text{ GeV}$
$19.6 \pm 6.5$	<sup>2</sup> ABZOV 11AH D0		$\ell + E_{Tj} + \geq 4$ jets ( $\geq 1b$ -tag)
$17 \pm 8$	<sup>3</sup> AALTONEN 08AB CDF		$p\bar{p}$ frame
$24 \pm 14$	<sup>3</sup> AALTONEN 08AB CDF		$t\bar{t}$ frame
$12 \pm 8 \pm 1$	<sup>4</sup> ABZOV 08L D0		$\ell + E_{Tj} + \geq 4$ jets

• • • We do not use the following data for averages, fits, limits, etc. • • •



See key on page 457

# Quark Particle Listings

## $b'$ (Fourth Generation) Quark

### $b'$ (4<sup>th</sup> Generation) Quark, Searches for

#### $b'$ -quark/hadron mass limits in $p\bar{p}$ and $pp$ collisions

VALUE (GeV)	CL%	DOCUMENT ID	TECN	COMMENT
>372	95	1 AALTONEN 11J	CDF	$b' \rightarrow tW$
>361	95	2 CHATRCHYAN11L	CMS	$b' \rightarrow tW$
>190	95	3 ABAZOV 08X	D0	$c\tau = 200\text{mm}$
>268	95	4,5 AALTONEN 07C	CDF	$B(b' \rightarrow bZ) = 1$ assumed
>190	95	6 ACOSTA 03	CDF	quasi-stable $b'$
>128	95	7 ABACHI 95F	D0	$\ell\ell + \text{jets}, \ell + \text{jets}$
• • • We do not use the following data for averages, fits, limits, etc. • • •				
>338	95	8 AALTONEN 10H	CDF	$b' \rightarrow tW$
>380-430	95	9 FLACCO 10	RVUE	$m_{b'} > m_{t'}$
>199	95	10 AFFOLDER 00	CDF	NC: $b' \rightarrow bZ$
>148	95	11 ABE 98N	CDF	NC: $b' \rightarrow bZ + \text{decay vertex}$
>96	95	12 ABACHI 97D	D0	NC: $b' \rightarrow b\gamma$
>75	95	13 MUKHOPAD.. 93	RVUE	NC: $b' \rightarrow b\ell\ell$
>85	95	14 ABE 92	CDF	CC: $\ell\ell$
>72	95	15 ABE 90B	CDF	CC: $e + \mu$
>54	95	16 AKESSON 90	UA2	CC: $e + \text{jets} + \text{missing } E_T$
>43	95	17 ALBAJAR 90B	UA1	CC: $\mu + \text{jets}$
>34	95	18 ALBAJAR 88	UA1	CC: $e$ or $\mu + \text{jets}$

- 1 Based on  $4.8 \text{ fb}^{-1}$  of data in  $p\bar{p}$  collisions at 1.96 TeV. AALTONEN 11J looked for events with  $\ell + \cancel{E}_T + \geq 5j$  ( $\geq 1 b$  or  $c$ ). No signal is observed and the bound  $\sigma(b' \bar{b}')$  < 30 fb for  $m_{b'} > 375 \text{ GeV}$  is found for  $B(b' \rightarrow tW) = 1$ .
- 2 Based on  $34 \text{ pb}^{-1}$  of data in  $pp$  collisions at 7 TeV. CHATRCHYAN 11L looked for multi-jet events with trileptons or same-sign dileptons. No excess above the SM background excludes  $m_{b'}$  between 255 and 361 GeV at 95% CL for  $B(b' \rightarrow tW) = 1$ .
- 3 Result is based on  $1.1 \text{ fb}^{-1}$  of data. No signal is found for the search of long-lived particles which decay into final states with two electrons or photons, and upper bound on the cross section times branching fraction is obtained for  $2 < c\tau < 7000 \text{ mm}$ ; see Fig. 3. 95% CL excluded region of  $b'$  lifetime and mass is shown in Fig. 4.
- 4 Result is based on  $1.06 \text{ fb}^{-1}$  of data. No excess from the SM  $Z + \text{jet}$  events is found when  $Z$  decays into  $e\bar{e}$  or  $\mu\bar{\mu}$ . The  $m_{b'}$  bound is found by comparing the resulting upper bound on  $\sigma(b' \bar{b}')$   $[1 - (1 - B(b' \rightarrow bZ))^2]$  and the LO estimate of the  $b'$  pair production cross section shown in Fig. 38 of the article.
- 5 HUANG 08 reexamined the  $b'$  mass lower bound of 268 GeV obtained in AALTONEN 07C that assumes  $B(b' \rightarrow bZ) = 1$ , which does not hold for  $m_{b'} > 255 \text{ GeV}$ . The lower mass bound is given in the plane of  $\sin^2(\theta_{tb'})$  and  $m_{b'}$ .
- 6 ACOSTA 03 looked for long-lived fourth generation quarks in the data sample of  $90 \text{ pb}^{-1}$  of  $\sqrt{s} = 1.8 \text{ TeV}$   $p\bar{p}$  collisions by using the muon-like penetration and anomalously high ionization energy loss signature. The corresponding lower mass bound for the charge (2/3)e quark ( $t'$ ) is 220 GeV. The  $t'$  bound is higher than the  $b'$  bound because  $t'$  is more likely to produce charged hadrons than  $b'$ . The 95% CL upper bounds for the production cross sections are given in their Fig. 3.
- 7 ABACHI 95F bound on the top-quark also applies to  $b'$  and  $t'$  quarks that decay predominantly into  $W$ . See FROGGATT 97.
- 8 Based on  $2.7 \text{ fb}^{-1}$  of data in  $p\bar{p}$  collisions at  $\sqrt{s} = 1.96 \text{ TeV}$ . AALTONEN 10H looked for pair production of heavy quarks which decay into  $tW^-$  or  $tW^+$ , in events with same sign dileptons ( $e$  or  $\mu$ ), several jets and large missing  $E_T$ . The result is obtained for  $b'$  which decays into  $tW^-$ . For the charge 5/3 quark ( $T_{5/3}$ ) which decays into  $tW^+$ ,  $m_{T_{5/3}} > 365 \text{ GeV}$  (95% CL) is found when it has the charge  $-1/3$  partner  $B$  of the same mass.
- 9 FLACCO 10 result is obtained from AALTONEN 10H result of  $m_{b'} > 338 \text{ GeV}$ , by relaxing the condition  $B(b' \rightarrow tW) = 100\%$  when  $m_{b'} > m_{t'}$ .
- 10 AFFOLDER 00 looked for  $b'$  that decays into  $b+Z$ . The signal searched for is  $bbZ$  events where one  $Z$  decays into  $e^+e^-$  or  $\mu^+\mu^-$  and the other  $Z$  decays hadronically. The bound assumes  $B(b' \rightarrow bZ) = 100\%$ . Between 100 GeV and 199 GeV, the 95%CL upper bound on  $\sigma(b' \rightarrow \bar{b}') \times B^2(b' \rightarrow bZ)$  is also given (see their Fig. 2).
- 11 ABE 98N looked for  $Z \rightarrow e^+e^-$  decays with displaced vertices. Quoted limit assumes  $B(b' \rightarrow bZ) = 1$  and  $c\tau_{b'} = 1 \text{ cm}$ . The limit is lower than  $m_Z + m_b$  ( $\sim 96 \text{ GeV}$ ) if  $c\tau > 22 \text{ cm}$  or  $c\tau < 0.009 \text{ cm}$ . See their Fig. 4.
- 12 ABACHI 97D searched for  $b'$  that decays mainly via FCNC. They obtained 95%CL upper bounds on  $B(b' \bar{b}') \rightarrow \gamma + 3 \text{ jets}$  and  $B(b' \bar{b}') \rightarrow 2\gamma + 2 \text{ jets}$ , which can be interpreted as the lower mass bound  $m_{b'} > m_Z + m_b$ .
- 13 MUKHOPADHYAYA 93 analyze CDF dilepton data of ABE 92G in terms of a new quark decaying via flavor-changing neutral current. The above limit assumes  $B(b' \rightarrow b\ell^+\ell^-) = 1\%$ . For an exotic quark decaying only via virtual  $Z$  [ $B(b\ell^+\ell^-) = 3\%$ ], the limit is 85 GeV.
- 14 ABE 92 dilepton analysis limit of  $>85 \text{ GeV}$  at  $\text{CL} = 95\%$  also applies to  $b'$  quarks, as discussed in ABE 90B.
- 15 ABE 90B exclude the region 28-72 GeV.
- 16 AKESSON 90 searched for events having an electron with  $p_T > 12 \text{ GeV}$ , missing momentum  $> 15 \text{ GeV}$ , and a jet with  $E_T > 10 \text{ GeV}$ ,  $|\eta| < 2.2$ , and excluded  $m_{b'}$  between 30 and 69 GeV.
- 17 For the reduction of the limit due to non-charged-current decay modes, see Fig. 19 of ALBAJAR 90B.
- 18 ALBAJAR 88 study events at  $E_{\text{cm}} = 546$  and  $630 \text{ GeV}$  with a muon or isolated electron, accompanied by one or more jets and find agreement with Monte Carlo predictions for the production of charm and bottom, without the need for a new quark. The lower mass limit is obtained by using a conservative estimate for the  $b' \bar{b}'$  production cross section and by assuming that it cannot be produced in  $W$  decays. The value quoted here is revised using the full  $O(\alpha_s^3)$  cross section of ALTARELLI 88.

#### $b'$ mass limits from single production in $p\bar{p}$ and $pp$ collisions

VALUE (GeV)	CL%	DOCUMENT ID	TECN	COMMENT
>693	95	19 ABAZOV 11F	D0	$qu \rightarrow q'b' \rightarrow q'(Wu)$ $\bar{\kappa}_{ub'}=1, B(b' \rightarrow Wu)=1$
>430	95	19 ABAZOV 11F	D0	$qd \rightarrow qb' \rightarrow q(Zd)$ $\bar{\kappa}_{db'}=\sqrt{2}, B(b' \rightarrow Zd)=1$

19 Based on  $5.4 \text{ fb}^{-1}$  of data in  $p\bar{p}$  collisions at 1.96 TeV. ABAZOV 11F looked for single production of  $b'$  via the  $W$  or  $Z$  coupling to the first generation up or down quarks, respectively. Model independent cross section limits for the single production processes  $p\bar{p} \rightarrow b'q \rightarrow W u q$ , and  $p\bar{p} \rightarrow b'q \rightarrow Z d q$  are given in Figs. 3 and 4, respectively, and the mass limits are obtained for the model of ATRE 09 with degenerate bi-doublets of vector-like quarks.

#### MASS LIMITS for $b'$ (4<sup>th</sup> Generation) Quark or Hadron in $e^+e^-$ Collisions

Search for hadrons containing a fourth-generation  $-1/3$  quark denoted  $b'$ .

The last column specifies the assumption for the decay mode ( $CC$  denotes the conventional charged-current decay) and the event signature which is looked for.

VALUE (GeV)	CL%	DOCUMENT ID	TECN	COMMENT
>46.0	95	20 DECAMP 90F	ALEP	any decay
• • • We do not use the following data for averages, fits, limits, etc. • • •				
none 96-103	95	21 ABDALLAH 07	DLPH	$b' \rightarrow bZ, cW$
>44.7	95	22 ADRIANI 93G	L3	Quarkonium
>45	95	ADRIANI 93M	L3	$\Gamma(Z)$
none 19.4-28.2	95	ABREU 91F	DLPH	$\Gamma(Z)$
>45.0	95	ABREU 90D	VNS	Any decay; event shape
>44.5	95	23 ABREU 90D	DLPH	$B(C C) = 1$ ; event shape
>40.5	95	24 ABREU 90D	DLPH	$b' \rightarrow cH^-, H^- \rightarrow \bar{c}s, \tau^- \nu$
>28.3	95	ADACHI 90	TOPZ	$\Gamma(Z \rightarrow \text{hadrons})$ $\gamma$ or 4 jets
>41.4	95	25 AKRAWY 90B	OPAL	Any decay; acoplanarity
>45.2	95	25 AKRAWY 90B	OPAL	$B(C C) = 1$ ; acoplanarity
>46	95	26 AKRAWY 90J	OPAL	$b' \rightarrow \gamma + \text{any}$
>27.5	95	27 ABE 89E	VNS	$B(C C) = 1; \mu, e$
none 11.4-27.3	95	28 ABE 89G	VNS	$B(b' \rightarrow b\gamma) > 10\%$ ; isolated $\gamma$
>44.7	95	29 ABRAMS 89C	MRK2	$B(C C) = 100\%$ ; isol. track
>42.7	95	29 ABRAMS 89C	MRK2	$B(bg) = 100\%$ ; event shape
>42.0	95	29 ABRAMS 89C	MRK2	Any decay; event shape
>28.4	95	30,31 ADACHI 89C	TOPZ	$B(C C) = 1; \mu$
>28.8	95	32 ENO 89	AMY	$B(C C) \geq 90\%; \mu, e$
>27.2	95	32,33 ENO 89	AMY	Any decay; event shape
>29.0	95	32 ENO 89	AMY	$B(b' \rightarrow bg) \gtrsim 85\%$ ; event shape
>24.4	95	34 IGARASHI 88	AMY	$\mu, e$
>23.8	95	35 SAGAWA 88	AMY	event shape
>22.7	95	36 ADEVA 86	MRKJ	$\mu$
>21	95	37 ALTHOFF 84C	TASS	$R$ , event shape
>19	95	38 ALTHOFF 84I	TASS	Aplanarity

- 20 DECAMP 90F looked for isolated charged particles, for isolated photons, and for four-jet final states. The modes  $b' \rightarrow bg$  for  $B(b' \rightarrow bg) > 65\%$   $b' \rightarrow b\gamma$  for  $B(b' \rightarrow b\gamma) > 5\%$  are excluded. Charged Higgs decay were not discussed.
- 21 ABDALLAH 07 searched for  $b'$  pair production at  $E_{\text{cm}} = 196-209 \text{ GeV}$ , with  $420 \text{ pb}^{-1}$ . No signal leads to the 95% CL upper limits on  $B(b' \rightarrow bZ)$  and  $B(b' \rightarrow cW)$  for  $m_{b'} = 96$  to  $103 \text{ GeV}$ .
- 22 ADRIANI 93G search for vector quarkonium states near  $Z$  and give limit on quarkonium- $Z$  mixing parameter  $\delta m^2 < (10-30) \text{ GeV}^2$  (95%CL) for the mass 88-94.5 GeV. Using Richardson potential, a  $1S(b' \bar{b}')$  state is excluded for the mass range 87.7-94.7 GeV. This range depends on the potential choice.
- 23 ABREU 90D assumed  $m_{H^-} < m_{b'} - 3 \text{ GeV}$ .
- 24 Superseded by ABREU 91F.
- 25 AKRAWY 90B search was restricted to data near the  $Z$  peak at  $E_{\text{cm}} = 91.26 \text{ GeV}$  at LEP. The excluded region is between 23.6 and 41.4 GeV if no  $H^+$  decays exist. For charged Higgs decays the excluded regions are between  $(m_{H^+} + 1.5 \text{ GeV})$  and  $45.5 \text{ GeV}$ .
- 26 AKRAWY 90J search for isolated photons in hadronic  $Z$  decay and derive  $B(Z \rightarrow b' \bar{b}') \cdot B(b' \rightarrow \gamma X) / B(Z \rightarrow \text{hadrons}) < 2.2 \times 10^{-3}$ . Mass limit assumes  $B(b' \rightarrow \gamma X) > 10\%$ .
- 27 ABE 89E search at  $E_{\text{cm}} = 56-57 \text{ GeV}$  at TRISTAN for multihadron events with a spherical shape (using thrust and acoplanarity) or containing isolated leptons.
- 28 ABE 89G search was at  $E_{\text{cm}} = 55-60.8 \text{ GeV}$  at TRISTAN.
- 29 If the photonic decay mode is large ( $B(b' \rightarrow b\gamma) > 25\%$ ), the ABRAMS 89C limit is 45.4 GeV. The limit for Higgs decay ( $b' \rightarrow cH^-, H^- \rightarrow \bar{c}s$ ) is 45.2 GeV.
- 30 ADACHI 89C search was at  $E_{\text{cm}} = 56.5-60.8 \text{ GeV}$  at TRISTAN using multi-hadron events accompanying muons.
- 31 ADACHI 89C also gives limits for any mixture of  $CC$  and  $bg$  decays.
- 32 ENO 89 search at  $E_{\text{cm}} = 50-60.8 \text{ GeV}$  at TRISTAN.
- 33 ENO 89 considers arbitrary mixture of the charged current,  $bg$ , and  $b\gamma$  decays.
- 34 IGARASHI 88 searches for leptons in low-thrust events and gives  $\Delta R(b') < 0.26$  (95% CL) assuming charged current decay, which translates to  $m_{b'} > 24.4 \text{ GeV}$ .

# Quark Particle Listings

## $b'$ (Fourth Generation) Quark, $t'$ (Fourth Generation) Quark, Free Quark Searches

- <sup>35</sup> SAGAWA 88 set limit  $\sigma(\text{top}) < 6.1$  pb at CL=95% for top-flavored hadron production from event shape analyses at  $E_{\text{cm}} = 52$  GeV. By using the quark parton model cross-section formula near threshold, the above limit leads to lower mass bounds of 23.8 GeV for charge  $-1/3$  quarks.
- <sup>36</sup> ADEVA 86 give 95%CL upper bound on an excess of the normalized cross section,  $\Delta R$ , as a function of the minimum c.m. energy (see their figure 3). Production of a pair of  $1/3$  charge quarks is excluded up to  $E_{\text{cm}} = 45.4$  GeV.
- <sup>37</sup> ALTHOFF 84c narrow state search sets limit  $\Gamma(e^+e^-)B(\text{hadrons}) < 2.4$  keV CL = 95% and heavy charge  $1/3$  quark pair production  $m > 21$  GeV, CL = 95%.
- <sup>38</sup> ALTHOFF 84i exclude heavy quark pair production for  $7 < m < 19$  GeV ( $1/3$  charge) using aplanarity distributions (CL = 95%).

- <sup>7</sup> HUANG 08 reexamined the  $t'$  mass lower bound of 256 GeV obtained in AALTONEN 08h that assumes  $B(b' \rightarrow qZ) = 1$  for  $q = u, c$  which does not hold when  $m_{b'} < m_{t'} - m_W$  or the mixing  $\sin^2(\theta_{bt'})$  is so tiny that the decay occurs outside of the vertex detector. Fig. 1 gives that lower bound on  $m_{t'}$  in the plane of  $\sin^2(\theta_{bt'})$  and  $m_{b'}$ .

### $t'$ mass limits from single production in $p\bar{p}$ and $pp$ collisions

VALUE (GeV)	CL%	DOCUMENT ID	TECN	COMMENT
>403	95	<sup>8</sup> ABAZOV	11F D0	$q\bar{d} \rightarrow q't' \rightarrow q'(Wd)$ $\bar{\kappa}_{d t'}=1, B(t' \rightarrow Wd)=1$
>551	95	<sup>8</sup> ABAZOV	11F D0	$qu \rightarrow q't' \rightarrow q(Zu)$ $\bar{\kappa}_{u t'}=\sqrt{2}, B(t' \rightarrow Zu)=1$

- <sup>8</sup> Based on  $5.4 \text{ fb}^{-1}$  of data in ppbar collisions at 1.96 TeV. ABAZOV 11F looked for single production of  $t'$  via the Z or E coupling to the first generation up or down quarks, respectively. Model independent cross section limits for the single production processes  $p\bar{p} \rightarrow t'q \rightarrow (Wd)q$ , and  $p\bar{p} \rightarrow t'q \rightarrow (Zd)q$  are given in FIGS. 3 and 4, respectively, and the mass limits are obtained for the model of ATRE 09 with degenerate bi-doublets of vector-like quarks.

### REFERENCES FOR Searches for (Fourth Generation) $b'$ Quark

AALTONEN 11J	PRL 106 141803	T. Aaltonen et al.	(CDF Collab.)
ABAZOV 11F	PRL 106 081801	V.M. Abazov et al.	(D0 Collab.)
CHATRCHYAN 11L	PL B701 204	S. Chatrchyan et al.	(CMS Collab.)
AALTONEN 10H	PRL 104 091801	T. Aaltonen et al.	(CDF Collab.)
FLACCO 10	PRL 105 111801	C.J. Flacco et al.	(UCI, HAIF)
ATRE 09	PR D79 054018	A. Atre et al.	
ABAZOV 08X	PRL 101 111802	V.M. Abazov et al.	(D0 Collab.)
HUANG 08	PR D77 037302	P.Q. Hung, M. Sher	(UVA, WILL)
AALTONEN 07C	PR D76 072006	T. Aaltonen et al.	(CDF Collab.)
ABDALLAH 07	EPJ C50 507	J. Abdallah et al.	(DELPHI Collab.)
ACOSTA 03	PRL 90 131801	D. Acosta et al.	(CDF Collab.)
AFFOLDER 00	PRL 84 835	A. Affolder et al.	(CDF Collab.)
ABE 98N	PR D58 051102	F. Abe et al.	(CDF Collab.)
ABACHI 97D	PRL 78 3818	S. Abachi et al.	(D0 Collab.)
FROGGATT 97	ZPHY C73 333	C.D. Froggatt, D.J. Smith, H.B. Nielsen	(GLAS+)
ABACHI 95F	PR D52 4877	S. Abachi et al.	(D0 Collab.)
ADRIANI 93G	PL B313 326	O. Adriani et al.	(L3 Collab.)
ADRIANI 93M	PRPL 236 1	O. Adriani et al.	(L3 Collab.)
MUKHOPAD... 93	PR D48 2105	B. Mukhopadhyaya, D.P. Roy	(TATA)
ABE 92	PRL 68 447	F. Abe et al.	(CDF Collab.)
Also			
ABE 92G	PR D45 3921	F. Abe et al.	(CDF Collab.)
ABREU 91F	NP B367 511	P. Abreu et al.	(DELPHI Collab.)
ABE 90B	PRL 64 147	F. Abe et al.	(CDF Collab.)
ABE 90D	PL B234 382	K. Abe et al.	(VENUS Collab.)
ABREU 90D	PL B242 536	P. Abreu et al.	(DELPHI Collab.)
ADACHI 90	PL B234 197	I. Adachi et al.	(TOPAZ Collab.)
AKESSON 90	ZPHY C46 179	T. Akesson et al.	(UA2 Collab.)
AKRAWY 90B	PL B236 364	M.Z. Akrawy et al.	(OPAL Collab.)
AKRAWY 90J	PL B246 285	M.Z. Akrawy et al.	(OPAL Collab.)
ALBAJAR 90B	ZPHY C48 1	C. Albajar et al.	(UA1 Collab.)
DECAMP 90F	PL B236 511	D. Decamp et al.	(ALEPH Collab.)
ABE 89E	PR D39 3524	K. Abe et al.	(VENUS Collab.)
ABE 89G	PRL 63 1776	K. Abe et al.	(VENUS Collab.)
ABRAMS 89C	PRL 63 2447	G.S. Abrams et al.	(Mark II Collab.)
ADACHI 89C	PL B229 427	I. Adachi et al.	(TOPAZ Collab.)
ENO 89	PRL 63 1910	S. Eno et al.	(AMY Collab.)
ALBAJAR 88	ZPHY C37 505	C. Albajar et al.	(UA1 Collab.)
ALTARELLI 88	NP B308 724	G. Altarelli et al.	(CERN, ROMA, ETH)
IGARASHI 88	PRL 60 2359	S. Igarashi et al.	(AMY Collab.)
SAGAWA 88	PRL 60 93	H. Sagawa et al.	(AMY Collab.)
ADEVA 86	PR D34 681	M. Adeva et al.	(Mark-J Collab.)
ALTHOFF 84C	PL 138B 441	M. Althoff et al.	(TASSO Collab.)
ALTHOFF 84I	ZPHY C22 307	M. Althoff et al.	(TASSO Collab.)

### REFERENCES FOR Searches for (Fourth Generation) $t'$ Quark

AAD 12C	PRL 108 041805	G. Aad et al.	(ATLAS Collab.)
AALTONEN 11AH	PRL 107 191803	T. Aaltonen et al.	(CDF Collab.)
AALTONEN 11AL	PRL 107 261801	T. Aaltonen et al.	(CDF Collab.)
AALTONEN 11O	PRL 106 191801	T. Aaltonen et al.	(CDF Collab.)
ABAZOV 11F	PRL 106 081801	V.M. Abazov et al.	(D0 Collab.)
ABAZOV 11Q	PRL 107 082001	V.M. Abazov et al.	(D0 Collab.)
ATRE 09	PR D79 054018	A. Atre et al.	
AALTONEN 08H	PRL 100 161803	T. Aaltonen et al.	(CDF Collab.)
HUANG 08	PR D77 037302	P.Q. Hung, M. Sher	(UVA, WILL)

## Free Quark Searches

### FREE QUARK SEARCHES

The basis for much of the theory of particle scattering and hadron spectroscopy is the construction of the hadrons from a set of fractionally charged constituents (quarks). A central but unproven hypothesis of this theory, Quantum Chromodynamics, is that quarks cannot be observed as free particles but are confined to mesons and baryons.

Experiments show that it is at best difficult to “unglue” quarks. Accelerator searches at increasing energies have produced no evidence for free quarks, while only a few cosmic-ray and matter searches have produced uncorroborated events.

This compilation is only a guide to the literature, since the quoted experimental limits are often only indicative. Reviews can be found in Refs. 1–4.

### References

1. M.L. Perl, E.R. Lee, and D. Lomba, Mod. Phys. Lett. **A19**, 2595 (2004).
2. P.F. Smith, Ann. Rev. Nucl. and Part. Sci. **39**, 73 (1989).
3. L. Lyons, Phys. Reports **129**, 225 (1985).
4. M. Marinelli and G. Morpurgo, Phys. Reports **85**, 161 (1982).

## $t'$ ( $4^{\text{th}}$ Generation) Quark, Searches for

### $t'$ -quark/hadron mass limits in $p\bar{p}$ and $pp$ collisions

VALUE (GeV)	CL%	DOCUMENT ID	TECN	COMMENT
>420	95	<sup>1</sup> AAD	12C ATLS	$t' \rightarrow tX$ ( $m_X < 140$ GeV)
>358	95	<sup>2</sup> AALTONEN	11AL CDF	$t' \rightarrow Wb$
>340	95	<sup>2</sup> AALTONEN	11AL CDF	$t' \rightarrow Wq$ ( $q=d,s,b$ )
•••				••• We do not use the following data for averages, fits, limits, etc. •••
>400	95	<sup>3</sup> AALTONEN	11AH CDF	$t' \rightarrow tX$ ( $m_X < 70$ GeV)
>360	95	<sup>4</sup> AALTONEN	11o CDF	$t' \rightarrow tX$ ( $m_X < 100$ GeV)
>285	95	<sup>5</sup> ABAZOV	11Q D0	$t' \rightarrow Wq$ ( $q=d,s,b$ )
>256	95	<sup>6,7</sup> AALTONEN	08H CDF	$t' \rightarrow Wq$

- <sup>1</sup> Based on  $1.04 \text{ fb}^{-1}$  of data in pp collisions at 7 TeV. AAD 12c looked for  $t'\bar{t}'$  production followed by  $t'$  decaying into a top quark and X, an invisible particle, in a final state with an isolated high- $P_T$  lepton, four or more jets, and a large missing transverse energy. No excess over the SM  $t\bar{t}$  production gives the upper limit on  $t'\bar{t}'$  production cross section as a function of  $m_{t'}$  and  $m_X$ . The result is obtained for  $B(t' \rightarrow tW) = 1$ .
- <sup>2</sup> Based on  $5.6 \text{ fb}^{-1}$  of data in ppbar collisions at 1.96 TeV. AALTONEN 11AL looked for  $\ell + \geq 4j$  events and set upper limits on  $\sigma(t'\bar{t}')$  as functions of  $m_{t'}$ .
- <sup>3</sup> Based on  $5.7 \text{ fb}^{-1}$  of data in pp collisions at 1.96 TeV. AALTONEN 11AH looked for  $t'\bar{t}'$  production followed by  $t'$  decaying into a top quark and X, an invisible particle, in the all hadronic decay mode of  $t\bar{t}$ . No excess over the SM  $t\bar{t}$  production gives the upper limit on  $t'\bar{t}'$  production cross section as a function of  $m_{t'}$  and  $m_X$ . The result is obtained for  $B(t' \rightarrow tX) = 1$ .
- <sup>4</sup> Based on  $4.8 \text{ fb}^{-1}$  of data in pp collisions at 1.96 TeV. AALTONEN 11o looked for  $t'\bar{t}'$  production signal when  $t'$  decays into a top quark and X, an invisible particle, in  $\ell + \cancel{E}_T + j$  channel. No excess over the SM  $t\bar{t}$  production gives the upper limit on  $t'\bar{t}'$  production cross section as a function of  $m_{t'}$  and  $m_X$ . The result is obtained for  $B(t' \rightarrow tX) = 1$ .
- <sup>5</sup> Based on  $5.3 \text{ fb}^{-1}$  of data in pp collisions at 1.96 TeV. ABAZOV 11Q looked for  $\ell + \cancel{E}_T + \geq 4j$  events and set upper limits on  $\sigma(t'\bar{t}')$  as functions of  $m_{t'}$ .
- <sup>6</sup> Searches for pair production of a new heavy top-like quark  $t'$  decaying to a W boson and another quark by fitting the observed spectrum of total transverse energy and reconstructed  $t'$  mass in the lepton + jets events.

### Quark Production Cross Section — Accelerator Searches

X-SECT (cm <sup>2</sup> )	CHG (e/3)	MASS (GeV)	ENERGY (GeV)	BEAM	EVTS	DOCUMENT ID	TECN
<1.3E-36	$\pm 2$	45-84	130-172	$e^+e^-$	0	ABREU 97D	DLPH
<2.E-35	+2	250	1800	$p\bar{p}$	0	<sup>1</sup> ABE 92J	CDF
<1.E-35	+4	250	1800	$p\bar{p}$	0	<sup>1</sup> ABE 92J	CDF
<3.8E-28			14.5A	<sup>28</sup> Si-pb	0	<sup>2</sup> HE 91	PLAS
<3.2E-28			14.5A	<sup>28</sup> Si-Cu	0	<sup>2</sup> HE 91	PLAS
<1.E-40	$\pm 1,2$	<10		$\rho, \nu, \bar{\nu}$	0	BERGSM 84B	CHRM
<1.E-36	$\pm 1,2$	<9	200	$\mu$	0	AUBERT 83C	SPEC
<2.E-10	$\pm 2,4$	1-3	200	$p$	0	<sup>3</sup> BUSSIÈRE 80	CNTR
<5.E-38	+1,2	>5	300	$p$	0	<sup>4,5</sup> STEVENSON 79	CNTR
<1.E-33	$\pm 1$	<20	52	$pp$	0	BASILE 78	SPEC
<9.E-39	$\pm 1,2$	<6	400	$p$	0	<sup>4</sup> ANTREASVAN 77	SPEC
<8.E-35	+1,2	<20	52	$pp$	0	<sup>6</sup> FABJAN 75	CNTR
<5.E-38	-1,2	4-9	200	$p$	0	NASH 74	CNTR
<1.E-32	+2,4	4-24	52	$pp$	0	ALPER 73	SPEC



Quark Particle Listings
Free Quark Searches

Table listing experimental searches for quarks. Columns include quark flavor (e.g., <1.E-10), sensitivity (e.g., +1,2), cross-section (e.g., 2.8 \*), target material (e.g., COX), detector/experiment (e.g., ELEC), and references (e.g., 72). Includes searches for levitated niobium, hydrogen/mass spec, water+/ion beam, etc.

32 95% CL limit for fractional charge particles with 0.18e <= |Q\_residual| <= 0.82e in total of 70.1 mg of silicone oil.
33 95% CL limit for particles with fractional charge |Q\_residual| > 0.16e in total of 17.4 mg of silicone oil.

34 Also set limits for Q = +/- e/6.
35 Note that in PHILLIPS 88 these authors report a subtle magnetic effect which could account for the apparent fractional charges.
36 Limit inferred by JONES 77b.

REFERENCES FOR Free Quark Searches. Table listing authors (LEE, AMBROSIO, HALYO, etc.), journal abbreviations (PR, PL, NP, etc.), volume/page numbers, and full publication titles.

Quark Density — Matter Searches

Table with columns: QUARKS/NUCLEON, CHG (e/3), MASS (GeV), MATERIAL/METHOD, EVTS, DOCUMENT ID. Lists searches for quark density in various materials like silicone oil, water, etc., with associated experimental parameters and references.

Continuation of the Quark Density — Matter Searches table, listing further experimental searches and references for quark density measurements in various media.



# Quark Particle Listings

## Free Quark Searches

See key on page 457

SCHIFFER	78	PR D17 2241	J.P. Schiffer <i>et al.</i>	(CHIC, ANL)	FUKUSHIMA	69	PR 178 2058	Y. Fukushima <i>et al.</i>	(TOKY)
YOCK	78	PR D18 641	P.C.M. Yock	(AUCK)	MCCUSKER	69	PR 23 658	C.B.A. McCusker, I. Cairns	(SYDN)
ANTREASYAN	77	PRL 39 513	D. Antreasyan <i>et al.</i>	(EFI, PRIN)	BELLAMY	68	PR 166 1391	E.H. Bellamy <i>et al.</i>	(STAN, SLAC)
BASILE	77	NC 40A 41	M. Basile <i>et al.</i>	(CERN, BGNA)	BJORNBOE	68	NC B53 241	J. Bjoernboe <i>et al.</i>	(BOHR, TATA, BERN+)
BLAND	77	PRL 39 369	R.W. Bland <i>et al.</i>	(SFSU)	BRAGINSKY	68	JETP 27 51	V.B. Braginsky <i>et al.</i>	(MOSU)
GALLINARO	77	PRL 38 1255	G. Gallinaro, M. Marinelli, G. Morpurgo	(GENO)	BRIATORE	68	Translated from ZETF 54 91	L. Briatore <i>et al.</i>	(TORI, CERN, BGNA)
JONES	77B	RMP 49 717	L.W. Jones	(S TAN)	FRANZINI	68	PRL 21 1013	P. Franzini, S. Shulman	(COLU)
LARUE	77	PRL 38 1011	G.S. Larue, W.M. Fairbank, A.F. Hebard	(LBL)	GARMIRE	68	PR 166 1280	G. Garmire, C. Leong, V. Sreekantan	(MIT)
MULLER	77	SCI 196 521	R.A. Muller <i>et al.</i>	(LBL)	HANAYAMA	68	CJP 46 5734	Y. Hanayama <i>et al.</i>	(OSAK)
OGOROD...	77	JETP 45 857	D.D. Ogorodnikov, I.M. Samoilov, A.M. Solntsev		KASHA	68	PR 172 1297	H. Kasha, R.J. Stefanski	(BNL, YALE)
BALDIN	76	SJNP 22 264	B.Y. Baldin <i>et al.</i>	(JINR)	KASHA	68B	PRL 20 217	H. Kasha <i>et al.</i>	(BNL, YALE)
		Translated from ZETF 72 1633.			KASHA	68C	CJP 46 5730	H. Kasha <i>et al.</i>	(BNL, YALE)
		Translated from YAF 22 512.			RANK	68	PR 176 1635	D. Rank	(MICH)
BRIATORE	76	NC 31A 553	L. Briatore <i>et al.</i>	(LCGT, FRAS, FREIB)	BARTON	67	PRSL 90 87	J.C. Barton	(NPOL)
STEVENS	76	PR D14 716	C.M. Stevens, J.P. Schiffer, W. Chupka	(ANL)	BATHOW	67	PL 25B 163	G. Bathow <i>et al.</i>	(DESY)
ALBROW	75	NP B97 189	M.G. Albrow <i>et al.</i>	(CERN, DARE, FOH+)	BUHLER	67	NC 49A 209	A. Buhler-Broglin <i>et al.</i>	(CERN, BGNA)
FABIAN	75	NP B101 349	C.W. Fabjan <i>et al.</i>	(CERN, MPIM)	BUHLER	67B	NC 51A 837	A. Buhler-Broglin <i>et al.</i>	(CERN, BGNA+)
HAZEN	75	NP B95 189	W.E. Hazen <i>et al.</i>	(MICH, LEED)	FOSS	67	PL 25B 166	J. Foss <i>et al.</i>	(MIT)
JOVANOV...	75	PL 56B 105	J.V. Jovanovich <i>et al.</i>	(MANI, AACH, CERN+)	GOMEZ	67	PRL 18 1022	R. Gomez <i>et al.</i>	(CIT)
KRISOR	75	NC 27A 132	K. Krisor	(AACH3)	KASHA	67	PR 154 1263	H. Kasha <i>et al.</i>	(BNL, YALE)
CLARK	74B	PR D10 2721	A.F. Clark <i>et al.</i>	(LLL)	STOVER	67	PR 164 1599	R.W. Stover, T.J. Moran, J.W. Trischka	(SYRA)
GALIK	74	PR D9 1856	R.S. Galik <i>et al.</i>	(SLAC, FNAL)	BARTON	66	PL 21 360	J.C. Barton, C.T. Stockel	(NPOL)
KIFUNE	74	JPS J 36 629	T. Kifune <i>et al.</i>	(TOKY, KEK)	BENNETT	66	PRL 17 1196	W.R. Bennett	(YALE)
NASH	74	PRL 32 858	T. Nash <i>et al.</i>	(FNAL, CORN, NYU)	BUHLER	66	NC 45A 520	A. Buhler-Broglin <i>et al.</i>	(CERN, BGNA+)
ALPER	73	PL 46B 245	B. Alper <i>et al.</i>	(CERN, LVP, LUND, BOHR+)	CHUPKA	66	PRL 17 60	W.A. Chupka, J.P. Schiffer, C.M. Stevens	(ANL)
ASHTON	73	JPA 6 577	F. Ashton <i>et al.</i>	(DURH)	GALLINARO	66	PL 23 609	G. Gallinaro, G. Morpurgo	(GENO)
HICKS	73B	NC 14A 65	R.B. Hicks, R.W. Flint, S. Standil	(MANI)	KASHA	66	PR 150 1140	H. Kasha, L.B. Leipuner, R.K. Adair	(BNL, YALE)
LEIPUNER	73	PRL 31 1226	L.B. Leipuner <i>et al.</i>	(BNL, YALE)	LAMB	66	PRL 17 1068	R.C. Lamb <i>et al.</i>	(ANL)
BEAUCHAMP	72	PR D6 1211	W.T. Beauchamp <i>et al.</i>	(ARIZ)	DELISE	65	PR 140B 458	D.A. de Lise, T. Bowen	(ARIZ)
BOHM	72B	PRL 28 326	A. Bohm <i>et al.</i>	(AACH)	DORFAN	65	PRL 14 999	D.E. Dorfman <i>et al.</i>	(COLU)
BOTT	72	PL 40B 693	M. Bott-Bodenhausen <i>et al.</i>	(CERN, MPIM)	FRANZINI	65B	PRL 14 196	P. Franzini <i>et al.</i>	(BNL, COLU)
COX	72	PR D6 1203	A.J. Cox <i>et al.</i>	(ARIZ)	MASSAM	65	NC 40A 589	T. Massam, T. Muller, A. Zichichi	(CERN)
CROUCH	72	PR D5 2667	M.F. Crouch, K. Mori, G.R. Smith	(CASE)	BINGHAM	64	PL 9 201	H.H. Bingham <i>et al.</i>	(CERN, EPOL)
DARDO	72	NC 9A 319	M. Dardo <i>et al.</i>	(TORI)	BLUM	64	PRL 13 353A	W. Blum <i>et al.</i>	(CERN)
EVANS	72	PRSE A70 143	G.R. Evans <i>et al.</i>	(EDIN, LEED)	BOWEN	64	PRL 13 728	T. Bowen <i>et al.</i>	(ARIZ)
TONWAR	72	JPA 5 569	S.C. Tonwar, S. Naranan, B.V. Sreekantan	(TATA)	HAGOPIAN	64	PRL 13 280	V. Hagopian <i>et al.</i>	(PENN, BNL)
ANTIPOV	71	NP B29 374	Y.M. Antipov <i>et al.</i>	(SERP)	LEIPUNER	64	PRL 12 423	L.B. Leipuner <i>et al.</i>	(BNL, YALE)
CHIN	71	NC 2A 419	S. Chin <i>et al.</i>	(OSAK)	MORRISON	64	PL 9 199	D.R.O. Morrison	(CERN)
CLARK	71B	PRL 27 51	A.F. Clark <i>et al.</i>	(LLL, LBL)	SUNYAR	64	PR 136 B1157	A.W. Sunyar, A.Z. Schwarzschild, P.I. Connors	(BNL)
HAZEN	71	PRL 26 682	W.E. Hazen	(MICH)	HILLAS	59	NAT 184 B92	A.M. Hillas, T.E. Cranshaw	(AERE)
BOSIA	70	NC 66A 167	G.F. Bosia, L. Briatore	(TORI)	MILLIKAN	10	Phil Mag 19 209	R.A. Millikan	(CHIC)
CHU	70	PRL 24 917	W.T. Chu <i>et al.</i>	(OSU, ROSE, KANS)					
Also		PRL 25 550	W.W.M. Allison <i>et al.</i>	(ANL)					
ELBERT	70	NP B20 217	J.W. Elbert <i>et al.</i>	(WIS C)					
FAISSNER	70B	PRL 24 1357	H. Faissner <i>et al.</i>	(AACH3)					
KRIDER	70	PR D1 835	E.P. Krider, T. Bowen, R.M. Kalbach	(ARIZ)					
MORPURGO	70	NIM 79 95	G. Morpurgo, G. Gallinaro, G. Palmieri	(GENO)					
ALLABY	69B	NC 64A 75	J.V. Allaby <i>et al.</i>	(CERN)					
ANTIPOV	69	PL 29B 245	Y.M. Antipov <i>et al.</i>	(SERP)	LYONS	85	PRPL C129 225	L. Lyons	(OXF)
ANTIPOV	69B	PL 30B 576	Y.M. Antipov <i>et al.</i>	(SERP)	MARINELLI	82	PRPL 85 161	M. Marinelli, G. Morpurgo	(GENO)
CAIRNS	69	PR 186 1394	I. Cairns <i>et al.</i>	(SYDN)					
COOK	69	PR 188 2092	D.D. Cook <i>et al.</i>	(ILL)					

### OTHER RELATED PAPERS

LYONS	85	PRPL C129 225	L. Lyons	(OXF)
Review				
MARINELLI	82	PRPL 85 161	M. Marinelli, G. Morpurgo	(GENO)
Review				



**LIGHT UNFLAVORED MESONS ( $S = C = B = 0$ )**

- $\pi^\pm$  . . . . . 695
- $\pi^0$  . . . . . 699
- $\eta$  . . . . . 701
- $f_0(500)$  . . . . . 706
- $\rho(770)$  . . . . . 715
- $\omega(782)$  . . . . . 721
- $\eta'(958)$  . . . . . 726
- $f_0(980)$  . . . . . 731
- $a_0(980)$  . . . . . 734
- $\phi(1020)$  . . . . . 735
- $h_1(1170)$  . . . . . 741
- $b_1(1235)$  . . . . . 742
- $a_1(1260)$  . . . . . 743
- $f_2(1270)$  . . . . . 745
- $f_1(1285)$  . . . . . 748
- $\eta(1295)$  . . . . . 751
- $\pi(1300)$  . . . . . 751
- $a_2(1320)$  . . . . . 752
- $f_0(1370)$  . . . . . 755
- $h_1(1380)$  . . . . . 758
- $\pi_1(1400)$  . . . . . 758
- $\eta(1405)$  . . . . . 759
- $f_1(1420)$  . . . . . 763
- $\omega(1420)$  . . . . . 765
- $f_2(1430)$  . . . . . 766
- $a_0(1450)$  . . . . . 766
- $\rho(1450)$  . . . . . 767
- $\eta(1475)$  . . . . . 769
- $f_0(1500)$  . . . . . 770
- $f_1(1510)$  . . . . . 773
- $f_2'(1525)$  . . . . . 774
- $f_2(1565)$  . . . . . 776
- $\rho(1570)$  . . . . . 777
- $h_1(1595)$  . . . . . 778
- $\pi_1(1600)$  . . . . . 778
- $a_1(1640)$  . . . . . 779
- $f_2(1640)$  . . . . . 779
- $\eta_2(1645)$  . . . . . 780
- $\omega(1650)$  . . . . . 780
- $\omega_3(1670)$  . . . . . 781
- $\pi_2(1670)$  . . . . . 781
- $\phi(1680)$  . . . . . 783
- $\rho_3(1690)$  . . . . . 784
- $\rho(1700)$  . . . . . 788
- $a_2(1700)$  . . . . . 792
- $f_0(1710)$  . . . . . 793
- $\eta(1760)$  . . . . . 795
- $\pi(1800)$  . . . . . 795
- $f_2(1810)$  . . . . . 797
- $X(1835)$  . . . . . 798
- $\phi_3(1850)$  . . . . . 798
- $\eta_2(1870)$  . . . . . 798
- $\pi_2(1880)$  . . . . . 799
- $\rho(1900)$  . . . . . 799
- $f_2(1910)$  . . . . . 800
- $f_2(1950)$  . . . . . 801
- $\rho_3(1990)$  . . . . . 802

• Indicates the particle is in the Meson Summary Table

- $f_2(2010)$  . . . . . 802
- $f_0(2020)$  . . . . . 802
- $a_4(2040)$  . . . . . 803
- $f_4(2050)$  . . . . . 804
- $\pi_2(2100)$  . . . . . 805
- $f_0(2100)$  . . . . . 806
- $f_2(2150)$  . . . . . 806
- $\rho(2150)$  . . . . . 807
- $\phi(2170)$  . . . . . 808
- $f_0(2200)$  . . . . . 809
- $f_J(2220)$  . . . . . 809
- $\eta(2225)$  . . . . . 810
- $\rho_3(2250)$  . . . . . 810
- $f_2(2300)$  . . . . . 811
- $f_4(2300)$  . . . . . 811
- $f_0(2330)$  . . . . . 812
- $f_2(2340)$  . . . . . 812
- $\rho_5(2350)$  . . . . . 813
- $a_6(2450)$  . . . . . 813
- $f_6(2510)$  . . . . . 814

**OTHER LIGHT UNFLAVORED ( $S = C = B = 0$ )**

- Further States . . . . . 815

**STRANGE MESONS ( $S = \pm 1, C = B = 0$ )**

- $K^\pm$  . . . . . 820
- $K^0$  . . . . . 839
- $K_S^0$  . . . . . 842
- $K_L^0$  . . . . . 846
- $K_0^*(800)$  . . . . . 868
- $K^*(892)$  . . . . . 869
- $K_1(1270)$  . . . . . 872
- $K_1(1400)$  . . . . . 873
- $K^*(1410)$  . . . . . 874
- $K_0^*(1430)$  . . . . . 874
- $K_2^*(1430)$  . . . . . 875
- $K(1460)$  . . . . . 877
- $K_2(1580)$  . . . . . 878
- $K(1630)$  . . . . . 878
- $K_1(1650)$  . . . . . 878
- $K^*(1680)$  . . . . . 878
- $K_2(1770)$  . . . . . 879
- $K_3^*(1780)$  . . . . . 880
- $K_2(1820)$  . . . . . 881
- $K(1830)$  . . . . . 881
- $K_0^*(1950)$  . . . . . 881
- $K_2^*(1980)$  . . . . . 882
- $K_4^*(2045)$  . . . . . 882
- $K_2(2250)$  . . . . . 883
- $K_3(2320)$  . . . . . 883
- $K_5^*(2380)$  . . . . . 883
- $K_4(2500)$  . . . . . 883
- $K(3100)$  . . . . . 884

**CHARMED MESONS ( $C = \pm 1$ )**

- $D^\pm$  . . . . . 885
- $D^0$  . . . . . 903
- $D^*(2007)^0$  . . . . . 933
- $D^*(2010)^\pm$  . . . . . 934
- $D_0^*(2400)^0$  . . . . . 935

(continued on the next page)

$D_0^*(2400)^\pm$	935
• $D_1(2420)^0$	936
$D_1(2420)^\pm$	937
$D_1(2430)^0$	937
• $D_2^*(2460)^0$	937
• $D_2^*(2460)^\pm$	939
$D(2550)^0$	939
$D(2600)$	940
$D^*(2640)^\pm$	940
$D(2750)$	940

### CHARMED, STRANGE MESONS ( $C = S = \pm 1$ )

• $D_s^\pm$	941
• $D_s^{*\pm}$	957
• $D_{s0}^*(2317)^\pm$	957
• $D_{s1}(2460)^\pm$	958
• $D_{s1}(2536)^\pm$	960
• $D_{s2}(2573)$	961
$D_{s1}^*(2700)^\pm$	961
$D_{sJ}^*(2860)^\pm$	962
$D_{sJ}(3040)^\pm$	962

### BOTTOM MESONS ( $B = \pm 1$ )

$B$ -particle organization	963
• $B^\pm$	974
• $B^0$	1020
• $B^\pm/B^0$ ADMIXTURE	1087
• $B^\pm/B^0/B_s^0/b$ -baryon ADMIXTURE	1104
$V_{cb}$ and $V_{ub}$ CKM Matrix Elements	1111
• $B^*$	1126
$B_J^*(5732)$	1126
• $B_1(5721)^0$	1126
• $B_2^*(5747)^0$	1127

### BOTTOM, STRANGE MESONS ( $B = \pm 1, S = \mp 1$ )

• $B_s^0$	1128
• $B_s^*$	1138
• $B_{s1}(5830)^0$	1138
• $B_{s2}^*(5840)^0$	1138
$B_{sJ}^*(5850)$	1138

### BOTTOM, CHARMED MESONS ( $B = C = \pm 1$ )

• $B_c^\pm$	1139
-------------	------

### $c\bar{c}$ MESONS

Charmonium system	1146
• $\eta_c(1S)$	1146
• $J/\psi(1S)$	1151
• $\chi_{c0}(1P)$	1168
• $\chi_{c1}(1P)$	1176
• $h_c(1P)$	1182
• $\chi_{c2}(1P)$	1183
• $\eta_c(2S)$	1191
• $\psi(2S)$	1192
• $\psi(3770)$	1205
• $X(3872)$	1210
• $X(3915)$	1212
$\chi_{c2}(2P)$	1212
$X(3940)$	1213
• $\psi(4040)$	1213

• Indicates the particle is in the Meson Summary Table

$X(4050)^\pm$	1215
$X(4140)$	1215
• $\psi(4160)$	1215
$X(4160)$	1217
$X(4250)^\pm$	1217
• $X(4260)$	1218
$X(4350)$	1220
$X(4360)$	1220
• $\psi(4415)$	1220
$X(4430)^\pm$	1222
$X(4660)$	1222

### $b\bar{b}$ MESONS

Bottomonium system	1223
$\eta_b(1S)$	1224
• $\Upsilon(1S)$	1224
• $\chi_{b0}(1P)$	1228
• $\chi_{b1}(1P)$	1229
• $h_b(1P)$	1231
• $\chi_{b2}(1P)$	1231
• $\Upsilon(2S)$	1232
$\Upsilon(1D)$	1235
• $\chi_{b0}(2P)$	1235
• $\chi_{b1}(2P)$	1237
$h_b(2P)$	1239
• $\chi_{b2}(2P)$	1239
• $\Upsilon(3S)$	1241
$\chi_b(3P)$	1244
• $\Upsilon(4S)$	1244
$X(10610)^\pm$	1246
$X(10650)^\pm$	1247
• $\Upsilon(10860)$	1247
• $\Upsilon(11020)$	1249

### Notes in the Meson Listings

Form Factors for Radiative Pion & Kaon Decays	696
Note on Scalar Mesons (rev.)	706
The $\rho(770)$ (rev.)	715
The $\eta(1405)$ , $\eta(1475)$ , $f_1(1420)$ , and $f_1(1510)$ (rev.)	759
The $\rho(1450)$ and the $\rho(1700)$ (rev.)	788
The Charged Kaon Mass	820
Rare Kaon Decays (rev.)	822
Dalitz Plot Parameters for $K \rightarrow 3\pi$ Decays	832
$K_{\ell 3}^\pm$ and $K_{\ell 3}^0$ Form Factors (rev.)	833
$CPT$ Invariance Tests in Neutral Kaon Decay (rev.)	839
$CP$ Violation in $K_S \rightarrow 3\pi$	845
$V_{ud}$ , $V_{us}$ , Cabibbo Angle, and CKM Unitarity (rev.)	852
$CP$ -Violation in $K_L$ Decays (rev.)	859
Dalitz-Plot Analysis Formalism (rev.)	889
Review of Charm Dalitz-Plot Analyses	893
$D^0$ - $\bar{D}^0$ Mixing (rev.)	903
$D_s^+$ Branching Fractions	943
Decay Constants of Charged Pseudoscalar Mesons (rev.)	945
Production and Decay of $b$ -flavored Hadrons (rev.)	963
Polarization in $B$ Decays (rev.)	1060
$B^0$ - $\bar{B}^0$ Mixing (rev.)	1066
Determination of $V_{cb}$ and $V_{ub}$ (rev.)	1111
Heavy Quarkonium Spectroscopy	1139
Branching Ratios of $\psi(2S)$ and $\chi_{c0,1,2}$ (rev.)	1168

See key on page 457

## LIGHT UNFLAVORED MESONS ( $S = C = B = 0$ )

For  $l = 1$  ( $\pi, b, \rho, a$ ):  $u\bar{d}, (u\bar{u}-d\bar{d})/\sqrt{2}, d\bar{u}$ ;  
for  $l = 0$  ( $\eta, \eta', h, h', \omega, \phi, f, f'$ ):  $c_1(u\bar{u} + d\bar{d}) + c_2(s\bar{s})$

 $\pi^\pm$ 

$$I^G(J^P) = 1^-(0^-)$$

We have omitted some results that have been superseded by later experiments. The omitted results may be found in our 1988 edition Physics Letters **B204** 1 (1988).

### $\pi^\pm$ MASS

The most accurate charged pion mass measurements are based upon x-ray wavelength measurements for transitions in  $\pi^-$ -mesonic atoms. The observed line is the blend of three components, corresponding to different K-shell occupancies. JECKELMANN 94 revisits the occupancy question, with the conclusion that two sets of occupancy ratios, resulting in two different pion masses (Solutions A and B), are equally probable. We choose the higher Solution B since only this solution is consistent with a positive mass-squared for the muon neutrino, given the precise muon momentum measurements now available (DAUM 91, ASSAMAGAN 94, and ASSAMAGAN 96) for the decay of pions at rest. Earlier mass determinations with  $\pi^-$ -mesonic atoms may have used incorrect K-shell screening corrections.

Measurements with an error of  $> 0.005$  MeV have been omitted from this Listing.

VALUE (MeV)	DOCUMENT ID	TECN	CHG	COMMENT	
<b>139.57018 ± 0.00035 OUR FIT</b>	Error includes scale factor of 1.2.				
<b>139.57018 ± 0.00035 OUR AVERAGE</b>	Error includes scale factor of 1.2.				
139.57071 ± 0.00053	<sup>1</sup> LENZ	98	CNTR	— pionic N2-atoms gas target	
139.56995 ± 0.00035	<sup>2</sup> JECKELMANN 94	CNTR	—	$\pi^-$ atom, Soln. B	
• • • We do not use the following data for averages, fits, limits, etc. • • •					
139.57022 ± 0.00014	<sup>3</sup> ASSAMAGAN 96	SPEC	+	$\pi^+ \rightarrow \mu^+ \nu_\mu$	
139.56782 ± 0.00037	<sup>4</sup> JECKELMANN 94	CNTR	—	$\pi^-$ atom, Soln. A	
139.56996 ± 0.00067	<sup>5</sup> DAUM	91	SPEC	+	$\pi^+ \rightarrow \mu^+ \nu$
139.56752 ± 0.00037	<sup>6</sup> JECKELMANN 86b	CNTR	—	Mesonic atoms	
139.5704 ± 0.0011	<sup>5</sup> ABELA	84	SPEC	+	See DAUM 91
139.5664 ± 0.0009	<sup>7</sup> LU	80	CNTR	—	Mesonic atoms
139.5686 ± 0.0020	CARTER	76	CNTR	—	Mesonic atoms
139.5660 ± 0.0024	<sup>7,8</sup> MARUSHEN..	76	CNTR	—	Mesonic atoms

<sup>1</sup> LENZ 98 result does not suffer K-electron configuration uncertainties as does JECKELMANN 94.

<sup>2</sup> JECKELMANN 94 Solution B (dominant 2-electron K-shell occupancy), chosen for consistency with positive  $m_{\nu_\mu}^2$ .

<sup>3</sup> ASSAMAGAN 96 measures the  $\mu^+$  momentum  $p_\mu$  in  $\pi^+ \rightarrow \mu^+ \nu_\mu$  decay at rest to be  $29.79200 \pm 0.00011$  MeV/c. Combined with the  $\mu^+$  mass and the assumption  $m_{\nu_\mu} = 0$ , this gives the  $\pi^+$  mass above; if  $m_{\nu_\mu} > 0$ ,  $m_{\pi^+}$  given above is a lower limit.

Combined instead with  $m_\mu$  and (assuming *CPT*) the  $\pi^-$  mass of JECKELMANN 94,  $p_\mu$  gives an upper limit on  $m_{\nu_\mu}$  (see the  $\nu_\mu$ ).

<sup>4</sup> JECKELMANN 94 Solution A (small 2-electron K-shell occupancy) in combination with either the DAUM 91 or ASSAMAGAN 94 pion decay muon momentum measurement yields a significantly negative  $m_{\nu_\mu}^2$ . It is accordingly not used in our fits.

<sup>5</sup> The DAUM 91 value includes the ABELA 84 result. The value is based on a measurement of the  $\mu^+$  momentum for  $\pi^+$  decay at rest,  $p_\mu = 29.79179 \pm 0.00053$  MeV, uses  $m_\mu = 105.658389 \pm 0.000034$  MeV, and assumes that  $m_{\nu_\mu} = 0$ . The last assumption means that in fact the value is a lower limit.

<sup>6</sup> JECKELMANN 86b gives  $m_\pi/m_e = 273.12677(71)$ . We use  $m_e = 0.51099906(15)$  MeV from COHEN 87. The authors note that two solutions for the probability distribution of K-shell occupancy fit equally well, and use other data to choose the lower of the two possible  $\pi^\pm$  masses.

<sup>7</sup> These values are scaled with a new wavelength-energy conversion factor  $\lambda E = 1.23984244(37) \times 10^{-6}$  eV m from COHEN 87. The LU 80 screening correction relies upon a theoretical calculation of inner-shell refilling rates.

<sup>8</sup> This MARUSHENKO 76 value used at the authors' request to use the accepted set of calibration  $\gamma$  energies. Error increased from 0.0017 MeV to include QED calculation error of 0.0017 MeV (12 ppm).

$$m_{\pi^+} - m_{\mu^+}$$

Measurements with an error  $> 0.05$  MeV have been omitted from this Listing.

VALUE (MeV)	EVTS	DOCUMENT ID	TECN	CHG	COMMENT	
• • • We do not use the following data for averages, fits, limits, etc. • • •						
33.91157 ± 0.00067	<sup>9</sup>	DAUM	91	SPEC	+	$\pi^+ \rightarrow \mu^+ \nu$
33.9111 ± 0.0011		ABELA	84	SPEC	—	See DAUM 91
33.925 ± 0.025		BOOTH	70	CNTR	+	Magnetic spect.
33.881 ± 0.035	145	HYMAN	67	HEBC	+	$K^-$ He

<sup>9</sup> The DAUM 91 value assumes that  $m_{\nu_\mu} = 0$  and uses our  $m_\mu = 105.658389 \pm 0.000034$  MeV.

$$(m_{\pi^+} - m_{\pi^-}) / m_{\text{average}}$$

A test of *CPT* invariance.

VALUE (units $10^{-4}$ )	DOCUMENT ID	TECN
<b>2 ± 5</b>	AYRES	71 CNTR

### $\pi^\pm$ MEAN LIFE

Measurements with an error  $> 0.02 \times 10^{-8}$  s have been omitted.

VALUE ( $10^{-8}$ s)	DOCUMENT ID	TECN	CHG	COMMENT	
<b>2.6033 ± 0.0005 OUR AVERAGE</b>	Error includes scale factor of 1.2.				
2.60361 ± 0.00052	<sup>10</sup> KOPTEV	95	SPEC	+	Surface $\mu^+$ 's
2.60231 ± 0.00050 ± 0.00084	NUMAO	95	SPEC	+	Surface $\mu^+$ 's
2.609 ± 0.008	DUNAITSEV	73	CNTR	+	
2.602 ± 0.004	AYRES	71	CNTR	±	
2.604 ± 0.005	NORDBERG	67	CNTR	+	
2.602 ± 0.004	ECKHAUSE	65	CNTR	+	
• • • We do not use the following data for averages, fits, limits, etc. • • •					
2.640 ± 0.008	<sup>11</sup> KINSEY	66	CNTR	+	

<sup>10</sup> KOPTEV 95 combines the statistical and systematic errors; the statistical error dominates.

<sup>11</sup> Systematic errors in the calibration of this experiment are discussed by NORDBERG 67.

$$(\tau_{\pi^+} - \tau_{\pi^-}) / \tau_{\text{average}}$$

A test of *CPT* invariance.

VALUE (units $10^{-4}$ )	DOCUMENT ID	TECN
<b>5.5 ± 7.1</b>	AYRES	71 CNTR
• • • We do not use the following data for averages, fits, limits, etc. • • •		
-14 ± 29	PETRUKHIN	68 CNTR
40 ± 70	BARDON	66 CNTR
23 ± 40	<sup>12</sup> LOBKOWICZ	66 CNTR
<sup>12</sup> This is the most conservative value given by LOBKOWICZ 66.		

### $\pi^+$ DECAY MODES

$\pi^-$  modes are charge conjugates of the modes below.

For decay limits to particles which are not established, see the section on Searches for Axions and Other Very Light Bosons.

Mode	Fraction ( $\Gamma_i/\Gamma$ )	Confidence level
$\Gamma_1$ $\mu^+ \nu_\mu$	[a] (99.98770 ± 0.00004) %	
$\Gamma_2$ $\mu^+ \nu_\mu \gamma$	[b] ( 2.00 ± 0.25 ) × $10^{-4}$	
$\Gamma_3$ $e^+ \nu_e$	[a] ( 1.230 ± 0.004 ) × $10^{-4}$	
$\Gamma_4$ $e^+ \nu_e \pi^0 \gamma$	[b] ( 7.39 ± 0.05 ) × $10^{-7}$	
$\Gamma_5$ $e^+ \nu_e \pi^0$	( 1.036 ± 0.006 ) × $10^{-8}$	
$\Gamma_6$ $e^+ \nu_e e^+ e^-$	( 3.2 ± 0.5 ) × $10^{-9}$	
$\Gamma_7$ $e^+ \nu_e \nu \bar{\nu}$	< 5	× $10^{-6}$ 90%
<b>Lepton Family number (LF) or Lepton number (L) violating modes</b>		
$\Gamma_8$ $\mu^+ \bar{\nu}_e$	L [c] < 1.5	× $10^{-3}$ 90%
$\Gamma_9$ $\mu^+ \nu_e$	LF [c] < 8.0	× $10^{-3}$ 90%
$\Gamma_{10}$ $\mu^- e^+ e^+ \nu$	LF < 1.6	× $10^{-6}$ 90%

[a] Measurements of  $\Gamma(e^+ \nu_e)/\Gamma(\mu^+ \nu_\mu)$  always include decays with  $\gamma$ 's, and measurements of  $\Gamma(e^+ \nu_e \gamma)$  and  $\Gamma(\mu^+ \nu_\mu \gamma)$  never include low-energy  $\gamma$ 's. Therefore, since no clean separation is possible, we consider the modes with  $\gamma$ 's to be subreactions of the modes without them, and let  $[\Gamma(e^+ \nu_e) + \Gamma(\mu^+ \nu_\mu)]/\Gamma_{\text{total}} = 100\%$ .

[b] See the Particle Listings below for the energy limits used in this measurement; low-energy  $\gamma$ 's are not included.

[c] Derived from an analysis of neutrino-oscillation experiments.

### $\pi^+$ BRANCHING RATIOS

$\Gamma(e^+ \nu_e)/\Gamma_{\text{total}}$  See note [a] in the list of  $\pi^+$  decay modes just above, and see also the next block of data. See also the note on "Decay Constants of Charged Pseudoscalar Mesons" in the  $D_s^\pm$  Listings.

VALUE (units $10^{-4}$ )	DOCUMENT ID
<b>1.230 ± 0.004 OUR EVALUATION</b>	

## Meson Particle Listings

 $\pi^\pm$ 

$$\frac{\Gamma(e^+\nu_e) + \Gamma(e^+\nu_e\gamma)}{\Gamma(\mu^+\nu_\mu) + \Gamma(\mu^+\nu_\mu\gamma)} \quad (\Gamma_3 + \Gamma_4) / (\Gamma_1 + \Gamma_2)$$

See note [a] in the list of  $\pi^\pm$  decay modes above. See NUMAO 92 for a discussion of  $e\text{-}\mu$  universality. See also the note on "Decay Constants of Charged Pseudoscalar Mesons" in the  $D_s^\pm$  Listings.

VALUE (units $10^{-4}$ )	EVTS	DOCUMENT ID	TECN	CHG	COMMENT
<b>1.230 ± 0.004 OUR AVERAGE</b>					
1.2346 ± 0.0035 ± 0.0036	120k	CZAPEK	93	CALO	Stopping $\pi^+$
1.2265 ± 0.0034 ± 0.0044	190k	BRITTON	92	CNTR	Stopping $\pi^+$
1.218 ± 0.014	32k	BRYMAN	86	CNTR	Stopping $\pi^+$
• • • We do not use the following data for averages, fits, limits, etc. • • •					
1.273 ± 0.028	11k	<sup>13</sup> DICAPUA	64	CNTR	
1.21 ± 0.07		ANDERSON	60	SPEC	
<sup>13</sup> DICAPUA 64 has been updated using the current mean life.					

$$\Gamma(\mu^+\nu_\mu\gamma) / \Gamma_{\text{total}} \quad \Gamma_2 / \Gamma$$

Note that measurements here do not cover the full kinematic range.

VALUE (units $10^{-4}$ )	EVTS	DOCUMENT ID	TECN	CHG	COMMENT
<b>2.0 ± 0.24 ± 0.08</b>		<sup>14</sup> BRESSI	98	CALO	+ Stopping $\pi^+$
• • • We do not use the following data for averages, fits, limits, etc. • • •					
1.24 ± 0.25	26	CASTAGNOLI	58	EMUL	$KE_\mu < 3.38$ MeV
<sup>14</sup> BRESSI 98 result is given for $E_\gamma > 1$ MeV only. Result agrees with QED expectation, $2.283 \times 10^{-4}$ and does not confirm discrepancy of earlier experiment CASTAGNOLI 58.					

$$\Gamma(e^+\nu_e\gamma) / \Gamma_{\text{total}} \quad \Gamma_4 / \Gamma$$

The very different values reflect the very different kinematic ranges covered (bigger range, bigger value). And none of them covers the whole kinematic range.

VALUE (units $10^{-3}$ )	EVTS	DOCUMENT ID	TECN	CHG	COMMENT
<b>73.86 ± 0.54</b>		<sup>15</sup> BYCHKOV	09	PIBE	$e^+\nu\gamma$ at rest
• • • We do not use the following data for averages, fits, limits, etc. • • •					
16.1 ± 2.3		<sup>16</sup> BOLOTOV	90b	SPEC	17 GeV $\pi^- \rightarrow e^- \bar{\nu}_e \gamma$
5.6 ± 0.7	226	<sup>17</sup> STETZ	78	SPEC	$P_e > 56$ MeV/c
3.0	143	DEPOMMIER	63b	CNTR	(KE) $_{e^+\gamma} > 48$ MeV
<sup>15</sup> This BYCHKOV 09 value is for $E_\gamma > 10$ MeV and $\Theta_{e^+\gamma} > 40^\circ$ .					
<sup>16</sup> BOLOTOV 90b is for $E_\gamma > 21$ MeV, $E_e > 70 - 0.8E_\gamma$ .					
<sup>17</sup> STETZ 78 is for an $e^- \gamma$ opening angle $> 132^\circ$ . Obtains 3.7 when using same cutoffs as DEPOMMIER 63b.					

$$\Gamma(e^+\nu_e\pi^0) / \Gamma_{\text{total}} \quad \Gamma_5 / \Gamma$$

VALUE (units $10^{-8}$ )	EVTS	DOCUMENT ID	TECN	CHG	COMMENT
<b>1.036 ± 0.006 OUR AVERAGE</b>					
1.036 ± 0.006	64k <sup>18,19</sup>	POCANIC	04	PIBE	+ $\pi$ decay at rest
1.026 ± 0.039	1224	<sup>20</sup> MCFARLANE	85	CNTR	+ Decay in flight
1.00 $\pm 0.08$ -0.10	332	DEPOMMIER	68	CNTR	+
1.07 ± 0.21	38	<sup>21</sup> BACASTOW	65	OSPK	+
1.10 ± 0.26		<sup>21</sup> BERTRAM	65	OSPK	+
1.1 ± 0.2	43	<sup>21</sup> DUNAITSEV	65	CNTR	+
0.97 ± 0.20	36	<sup>21</sup> BARTLETT	64	OSPK	+
• • • We do not use the following data for averages, fits, limits, etc. • • •					
1.15 ± 0.22	52	<sup>21</sup> DEPOMMIER	63	CNTR	+ See DEPOMMIER 68
<sup>18</sup> POCANIC 04 normalizes to $e^+\nu_e$ decays, using the PDG 2004 value $B(\pi^+ \rightarrow e^+\nu_e) = (1.230 \pm 0.004) \times 10^{-4}$ . We add their statistical $(0.004 \times 10^{-8})$ , systematic $(0.004 \times 10^{-8})$ and systematic error due to the uncertainty of $B(\pi^+ \rightarrow e^+\nu_e)$ $(0.003 \times 10^{-8})$ in quadrature.					
<sup>19</sup> This result can be used to calculate $V_{ud}$ from pion beta decay: $V_{ud}^{PIBETA} = 0.9728 \pm 0.0030$ .					
<sup>20</sup> MCFARLANE 85 combines a measured rate $(0.394 \pm 0.015)$ /s with 1982 PDG mean life.					
<sup>21</sup> DEPOMMIER 68 says the result of DEPOMMIER 63 is at least 10% too large because of a systematic error in the $\pi^0$ detection efficiency, and that this may be true of all the previous measurements (also V. Soergel, private communication, 1972).					

$$\Gamma(e^+\nu_e e^+) / \Gamma(\mu^+\nu_\mu) \quad \Gamma_6 / \Gamma_1$$

VALUE (units $10^{-3}$ )	CL%	EVTS	DOCUMENT ID	TECN	COMMENT
<b>3.2 ± 0.5 ± 0.2</b>		98	EGLI	89	SPEC Uses $R_{PCAC} = 0.068 \pm 0.004$
• • • We do not use the following data for averages, fits, limits, etc. • • •					
0.46 ± 0.16 ± 0.07		7	<sup>22</sup> BARANOV	92	SPEC Stopped $\pi^+$
< 4.8	90		KORENCHEN...	76b	SPEC
< 34	90		KORENCHEN...	71	OSPK
<sup>22</sup> This measurement by BARANOV 92 is of the structure-dependent part of the decay. The value depends on values assumed for ratios of form factors.					

$$\Gamma(e^+\nu_e\bar{\nu}) / \Gamma_{\text{total}} \quad \Gamma_7 / \Gamma$$

VALUE (units $10^{-6}$ )	CL%	DOCUMENT ID	TECN	
<b>&lt; 5</b>	90	PICCIOTTO	88	SPEC

$$\Gamma(\mu^+\bar{\nu}_e) / \Gamma_{\text{total}} \quad \Gamma_8 / \Gamma$$

Forbidden by total lepton number conservation. See the note on "Decay Constants of Charged Pseudoscalar Mesons" in the  $D_s^\pm$  Listings.

VALUE (units $10^{-3}$ )	CL%	DOCUMENT ID	TECN	COMMENT
<b>&lt; 1.5</b>	90	<sup>23</sup> COOPER	82	HLBC Wideband $\nu$ beam
<sup>23</sup> COOPER 82 limit on $\bar{\nu}_e$ observation is here interpreted as a limit on lepton number violation.				

$$\Gamma(\mu^+\nu_e) / \Gamma_{\text{total}} \quad \Gamma_9 / \Gamma$$

Forbidden by lepton family number conservation.

VALUE (units $10^{-3}$ )	CL%	DOCUMENT ID	TECN	COMMENT
<b>&lt; 8.0</b>	90	<sup>24</sup> COOPER	82	HLBC Wideband $\nu$ beam
<sup>24</sup> COOPER 82 limit on $\nu_e$ observation is here interpreted as a limit on lepton family number violation.				

$$\Gamma(\mu^- e^+ e^+) / \Gamma_{\text{total}} \quad \Gamma_{10} / \Gamma$$

Forbidden by lepton family number conservation.

VALUE (units $10^{-6}$ )	CL%	DOCUMENT ID	TECN	CHG
<b>&lt; 1.6</b>	90	BARANOV	91b	SPEC +
• • • We do not use the following data for averages, fits, limits, etc. • • •				
< 7.7	90	KORENCHEN...	87	SPEC +

 $\pi^\pm$  — POLARIZATION OF EMITTED  $\mu^\pm$ 

$$\pi^\pm \rightarrow \mu^\pm \nu$$

Tests the Lorentz structure of leptonic charged weak interactions.

VALUE	CL%	DOCUMENT ID	TECN	CHG	COMMENT
• • • We do not use the following data for averages, fits, limits, etc. • • •					
< (-0.9959)	90	<sup>25</sup> FETSCHER	84	RVUE	+
-0.99 ± 0.16		<sup>26</sup> ABELA	83	SPEC	- $\mu$ X-rays
<sup>25</sup> FETSCHER 84 uses only the measurement of CARR 83.					
<sup>26</sup> Sign of measurement reversed in ABELA 83 to compare with $\mu^\pm$ measurements.					

## FORM FACTORS FOR RADIATIVE PION AND KAON DECAYS

Updated August 2009 by W. Bertl (Paul Scherrer Inst.)

The radiative decays,  $\pi^\pm \rightarrow l^\pm \nu \gamma$  and  $K^\pm \rightarrow l^\pm \nu \gamma$ , with  $l$  standing for an  $e$  or a  $\mu$ , and  $\gamma$  for a real or virtual photon ( $e^+e^-$  pair), provide a powerful tool to investigate the hadronic structure of pions and kaons. The structure-dependent part  $SD_i$  of the amplitude describes the emission of photons from virtual hadronic states, and is parametrized in terms of form factors  $F_i$ , with  $i = V, A$  (vector, axial vector), in the standard description [1,2]. Exotic, non-standard contributions like  $i = T, S$  (tensor, scalar) have also been considered, and we shall discuss them below. Apart from the SD terms, the decay amplitude depends also on Inner Bremsstrahlung IB from the weak decay  $\pi^\pm(K^\pm) \rightarrow l^\pm \nu$  accompanied by the photon radiated from the external charged particles. Naturally, experiments try to optimize their kinematics so as to minimize the "trivial" IB part of the amplitude.

The SD amplitude in its standard form is given as

$$M(SD_V) = \frac{-eG_F V_{qq'}}{\sqrt{2}m_P} \epsilon^\mu \ell^\nu F_V^P \epsilon_{\mu\nu\sigma\tau} k^\sigma q^\tau \quad (1)$$

$$M(SD_A) = \frac{-ieG_F V_{qq'}}{\sqrt{2}m_P} \epsilon^\mu \ell^\nu \{F_A^P [(qk - k^2)g_{\mu\nu} - q_\mu k_\nu] + R^P k^2 g_{\mu\nu}\}, \quad (2)$$

which contains an additional axial form factor  $R^P$  which only can be accessed if the photon remains virtual.  $V_{qq'}$  is the Cabibbo-Kobayashi-Maskawa mixing-matrix element;  $\epsilon^\mu$  is the polarization vector of the photon (or the effective vertex,  $\epsilon^\mu = (e/k^2)\bar{u}(p_-)\gamma^\mu v(p_+)$ , of the  $e^+e^-$  pair);  $\ell^\nu = \bar{u}(p_\nu)\gamma^\nu(1 - \gamma_5)v(p_l)$  is the lepton-neutrino current;  $q$  and  $k$  are the meson

and photon four-momenta ( $k = p_+ + p_-$  for virtual photons); and  $P$  stands for  $\pi$  or  $K$ .

The pion vector form factor,  $F_V^\pi$ , is related via CVC (Conserved Vector Current) to the  $\pi^0 \rightarrow \gamma\gamma$  decay width by  $|F_V^\pi| = (1/\alpha)\sqrt{2\Gamma_{\pi^0 \rightarrow \gamma\gamma}/\pi m_{\pi^0}}$  [3]. The resulting value,  $F_V^\pi(0) = 0.0259(9)$ , has been confirmed by calculations based on chiral perturbation theory ( $\chi PT$ ) [4], and by two experiments given in the Listings below. A recent experiment by the PIBETA collaboration [5] obtained an  $F_V$  that is in excellent agreement with the CVC hypothesis. It also measured the slope parameter  $a$  in  $F_V^\pi(s) = F_V^\pi(0)(1 + a \cdot s)$ , where  $s = (1 - 2E_\gamma/m_\pi)$ , and  $E_\gamma$  is the gamma energy in the pion rest frame:  $a = 0.095 \pm 0.058$ . A functional dependence on  $s$  is expected for all form factors. It becomes non-negligible in the case of  $F_V^\pi(s)$  when a wide range of photon momenta is recorded; proper treatment in the analysis of  $K$  decays is mandatory.

The form factor,  $R^P$ , can be related to the electromagnetic radius,  $r_P$ , of the meson [2]:  $R^P = \frac{1}{3}m_P f_P \langle r_P^2 \rangle$  using PCAC (Partial Conserved Axial vector Current;  $f_P$  is the meson decay constant). In lowest order  $\chi PT$ , the ratio  $F_A/F_V$  is related to the pion electric polarizability  $\alpha_E = [\alpha/(8\pi^2 m_\pi f_\pi^2)] \times F_A/F_V$  [6]. The calculation of the other form factors,  $F_A^\pi, F_V^K$ , and  $F_A^K$ , is model-dependent [1,2,4].

For decay processes where the photon is real, the partial decay width can be written in analytical form as a sum of IB, SD, and IB/SD interference terms INT [1,4]:

$$\begin{aligned} \frac{d^2\Gamma_{P \rightarrow \ell\nu\gamma}}{dx dy} &= \frac{d^2(\Gamma_{\text{IB}} + \Gamma_{\text{SD}} + \Gamma_{\text{INT}})}{dx dy} \\ &= \frac{\alpha}{2\pi} \Gamma_{P \rightarrow \ell\nu} \frac{1}{(1-r)^2} \left\{ \text{IB}(x, y) \right. \\ &+ \frac{1}{r} \left( \frac{m_P}{2f_P} \right)^2 \left[ (F_V + F_A)^2 \text{SD}^+(x, y) + (F_V - F_A)^2 \text{SD}^-(x, y) \right] \\ &\left. + \frac{m_P}{f_P} \left[ (F_V + F_A) \text{S}_{\text{INT}}^+(x, y) + (F_V - F_A) \text{S}_{\text{INT}}^-(x, y) \right] \right\}. \quad (3) \end{aligned}$$

Here

$$\begin{aligned} \text{IB}(x, y) &= \left[ \frac{1-y+r}{x^2(x+y-1-r)} \right] \\ &\left[ x^2 + 2(1-x)(1-r) - \frac{2xr(1-r)}{x+y-1-r} \right] \\ \text{SD}^+(x, y) &= (x+y-1-r) \left[ (x+y-1)(1-x) - r \right] \\ \text{SD}^-(x, y) &= (1-y+r) \left[ (1-x)(1-y) + r \right] \\ \text{S}_{\text{INT}}^+(x, y) &= \left[ \frac{1-y+r}{x(x+y-1-r)} \right] \left[ (1-x)(1-x-y) + r \right] \\ \text{S}_{\text{INT}}^-(x, y) &= \left[ \frac{1-y+r}{x(x+y-1-r)} \right] \left[ x^2 - (1-x)(1-x-y) - r \right] \end{aligned} \quad (4)$$

where  $x = 2E_\gamma/m_P$ ,  $y = 2E_\ell/m_P$ , and  $r = (m_\ell/m_P)^2$ . Recently, formulas (3) and (4) have been extended to describe polarized distributions in radiative meson and muon decays [7].

The ‘‘helicity’’ factor  $r$  is responsible for the enhancement of the SD over the IB amplitude in the decays  $\pi^\pm \rightarrow e^\pm \nu \gamma$ , while  $\pi^\pm \rightarrow \mu^\pm \nu \gamma$  is dominated by IB. Interference terms are important for the decay  $K^\pm \rightarrow \mu^\pm \nu \gamma$  [8], but contribute only a few percent correction to pion decays. However, they provide the basis for determining the signs of  $F_V$  and  $F_A$ . Radiative corrections to the decay  $\pi^+ \rightarrow e^+ \nu \gamma$  have to be taken into account in the analysis of the precision experiments. They make up to 4% corrections in the total decay rate [9]. In  $\pi^\pm \rightarrow e^\pm \nu e^+ e^-$  and  $K^\pm \rightarrow \ell^\pm \nu e^+ e^-$  decays, all three form factors,  $F_V^P, F_A^P$ , and  $R^P$ , can be determined [10,11].

We give the experimental  $\pi^\pm$  form factors  $F_V^\pi, F_A^\pi$ , and  $R^\pi$  in the Listings below. In the  $K^\pm$  Listings, we give the extracted sum  $F_A^K + F_V^K$  and difference  $F_A^K - F_V^K$ , as well as  $F_V^K, F_A^K$  and  $R^K$ .

Several searches for the exotic form factors  $F_T^K, F_T^K$  (tensor), and  $F_S^K$  (scalar) have been pursued in the past, some of them claiming non-zero results [12,13]. In particular,  $F_T^K$  has been brought into focus by experimental as well as theoretical work. It was shown that a tensor contribution could destructively interfere with the inner bremsstrahlung amplitude, leading to a substantial reduction of the branching ratio as compared with standard V–A calculations [14]. In addition, a tensor contribution as large as  $F_T = -(5.6 \pm 1.7) \times 10^{-3}$  could not be completely ruled out by constraints from other measurements [15]. New high-statistics data from the PIBETA collaboration have been re-analyzed together with an additional data set optimized for low backgrounds in the radiative pion decay. In particular, lower beam rates have been used in order to reduce the accidental background, thereby making the treatment of systematic uncertainties easier and more reliable. The PIBETA analysis now restricts  $F_T$  to the range  $-5.2 \times 10^{-4} < F_T < 4.0 \times 10^{-4}$  at a 90% confidence limit [5]. This result is in excellent agreement with the most recent theoretical work [4].

Precision measurements of radiative pion and kaon decays are effective tools to study QCD in the non-perturbative region. The structure-dependent form factors have direct relations to (renormalized) coupling constants of chiral perturbation theories. Therefore, they are of interest beyond the scope of radiative decays. On the other hand, the interest in searching for new physics manifesting in exotic form factors  $F_T$  or  $F_S$  has weakened over the last years mainly for two reasons: (i) on the experimental side, the lack of results confirming the non-zero findings; (ii) on the theoretical side, numerical uncertainties are still too large to allow a clear distinction of exotic and standard contributions at the currently required level. Likely this will change in the future, but meanwhile other processes such as  $\pi^+ \rightarrow e^+ \nu$  seem to be better suited to search for new physics at the precision frontier, because of the very accurate and reliable theoretical predictions and the more straightforward experimental analysis.

## Meson Particle Listings

 $\pi^\pm$ 

## References

- D.A. Bryman *et al.*, Phys. Reports **88**, 151 (1982). See our note on "Decay Constants of Charged Pseudoscalar Mesons" elsewhere in this *Review*;  
S.G. Brown and S.A. Bludman, Phys. Rev. **136**, B1160 (1964);  
P. DeBaenst and J. Pestieau, Nuovo Cim. **A53**, 137 (1968).
- W.T. Chu *et al.*, Phys. Rev. **166**, 1577 (1968);  
D.Yu. Bardin and E.A. Ivanov, Sov. J. Part. Nucl. **7**, 286 (1976);  
A. Kersch and F. Scheck, Nucl. Phys. **B263**, 475 (1986).
- V.G. Vaks and B.L. Ioffe, Nuovo Cim. **10**, 342 (1958);  
V.F. Muller, Z. Phys. **173**, 438 (1963).
- C.Q. Geng, I-Lin Ho, and T.H. Wu, Nucl. Phys. **B684**, 281 (2004);  
J. Bijnens and P. Talavera, Nucl. Phys. **B489**, 387 (1997);  
V. Mateu and J. Portoles, Eur. Phys. J. **C52**, 325 (2007);  
R. Unterdorfer, H. Pichl, Eur. Phys. J. **C55**, 273 (2008).
- D. Počanić *et al.*, Phys. Rev. Lett. **93**, 181803 (2004);  
E. Frlež *et al.*, Phys. Rev. Lett. **93**, 181804 (2004);  
M. Bychkov *et al.*, Phys. Rev. Lett. **103**, 051802 (2009).
- J.F. Donoghue and B.R. Holstein, Phys. Rev. **D40**, 2378 (1989).
- E. Gabrielli and L. Trentadue, Nucl. Phys. **B792**, 48 (2008).
- S. Adler *et al.*, Phys. Rev. Lett. **85**, 2256 (2000).
- Yu.M. Bystritsky, E.A. Kuraev, and E.P. Velicheva, Phys. Rev. **D69**, 114004 (2004);  
R. Unterdorfer and H. Pichl have treated radiative corrections of the structure terms to lowest order within  $\chi PT$  for the first time. See the reference under [4].
- S. Egli *et al.*, Phys. Lett. **B175**, 97 (1986).
- A.A. Poblaguev *et al.*, Phys. Rev. Lett. **89**, 061803 (2002).
- V.N. Bolotov *et al.*, Phys. Lett. **B243**, 308 (1990).
- S.A. Akimenko *et al.*, Phys. Lett. **B259**, 225 (1991).
- A.A. Poblaguev, Phys. Lett. **B238**, 108 (1990);  
V.M. Belyaev and I.I. Kogan, Phys. Lett. **B280**, 238 (1992);  
A.V. Chernyshev *et al.*, Mod. Phys. Lett. **A12**, 1669 (1997);  
A.A. Poblaguev, Phys. Rev. **D68**, 054020 (2003);  
M.V. Chizhov, Phys. Part. Nucl. Lett. **2**, 193 (2005).
- P. Herzceg, Phys. Rev. **D49**, 247 (1994).

 $\pi^\pm$  FORM FACTORS $F_V$ , VECTOR FORM FACTOR

VALUE	EVTS	DOCUMENT ID	TECN	COMMENT
<b>0.0254 ± 0.0017 OUR AVERAGE</b>				
0.0258 ± 0.0017	65k	27 BYCHKOV	09 PIBE	$e^+ \nu \gamma$ at rest
0.014 ± 0.009		28 BOLOTOV	90B SPEC	17 GeV $\pi^- \rightarrow e^- \bar{\nu}_e \gamma$
0.023 ± 0.015 0.013	98	EGLI	89 SPEC	$\pi^+ \rightarrow e^+ \nu_e e^+ e^-$

<sup>27</sup>The BYCHKOV 09  $F_A$  and  $F_V$  results are highly (anti-)correlated:  $F_A + 1.0286 F_V = 0.03853 \pm 0.00014$ .

<sup>28</sup>BOLOTOV 90B only determines the absolute value.

 $F_A$ , AXIAL-VECTOR FORM FACTOR

VALUE	EVTS	DOCUMENT ID	TECN	COMMENT
<b>0.0119 ± 0.0001</b>	65k 29,30	BYCHKOV	09 PIBE	$e^+ \nu \gamma$ at rest
• • • We do not use the following data for averages, fits, limits, etc. • • •				
0.0115 ± 0.0004	41k 29,31	FRLEZ	04 PIBE	$\pi^+ \rightarrow e^+ \nu \gamma$ at rest
0.0106 ± 0.0060	29,32	BOLOTOV	90B SPEC	17 GeV $\pi^- \rightarrow e^- \bar{\nu}_e \gamma$
0.021 ± 0.011 0.013	98	EGLI	89 SPEC	$\pi^+ \rightarrow e^+ \nu_e e^+ e^-$
0.0135 ± 0.0016	29,32	BAY	86 SPEC	$\pi^+ \rightarrow e^+ \nu \gamma$
0.006 ± 0.003	29,32	PIILONEN	86 SPEC	$\pi^+ \rightarrow e^+ \nu \gamma$
0.011 ± 0.003	29,32,33	STETZ	78 SPEC	$\pi^+ \rightarrow e^+ \nu \gamma$

<sup>29</sup>These values come from fixing the vector form factor at the CVC prediction,  $F_V = 0.0259 \pm 0.0005$ .

<sup>30</sup>When  $F_V$  is released, the BYCHKOV 09  $F_A$  is  $0.0117 \pm 0.0017$ , and  $F_A$  and  $F_V$  results are highly (anti-)correlated:  $F_A + 1.0286 F_V = 0.03853 \pm 0.00014$ .

<sup>31</sup>The sign of  $\gamma = F_A / F_V$  is determined to be positive.

<sup>32</sup>Only the absolute value of  $F_A$  is determined.

<sup>33</sup>The result of STETZ 78 has a two-fold ambiguity. We take the solution compatible with later determinations.

VECTOR FORM FACTOR SLOPE PARAMETER  $a$ 

This is  $a$  in  $F_V(q^2) = F_V(0)(1 + a q^2)$

VALUE	EVTS	DOCUMENT ID	TECN	COMMENT
<b>0.10 ± 0.06</b>	65k	BYCHKOV	09 PIBE	$e^+ \nu \gamma$ at rest

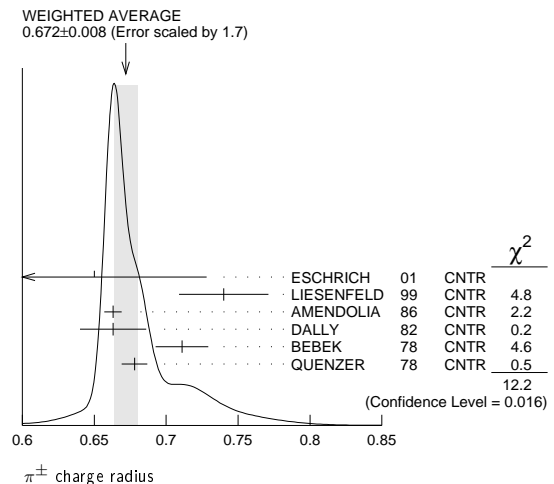
 $R$ , SECOND AXIAL-VECTOR FORM FACTOR

VALUE	EVTS	DOCUMENT ID	TECN	COMMENT
<b>0.059 ± 0.009 -0.008</b>	98	EGLI	89 SPEC	$\pi^+ \rightarrow e^+ \nu_e e^+ e^-$

 $\pi^\pm$  CHARGE RADIUS

VALUE (fm)	DOCUMENT ID	TECN	COMMENT
<b>0.672 ± 0.008 OUR AVERAGE</b>	Error includes scale factor of 1.7. See the ideogram below.		
0.65 ± 0.05 ± 0.06	ESCHRICH	01 CNTR	$\pi e \rightarrow \pi e$
0.740 ± 0.031	LIESENFELD	99 CNTR	$e p \rightarrow e \pi^+ n$
0.663 ± 0.006	AMENDOLIA	86 CNTR	$\pi e \rightarrow \pi e$
0.663 ± 0.023	DALLY	82 CNTR	$\pi e \rightarrow \pi e$
0.711 ± 0.009 ± 0.016	BEBEK	78 CNTR	$e N \rightarrow e \pi N$
0.678 ± 0.004 ± 0.008	QUENZER	78 CNTR	$e^+ e^- \rightarrow \pi^+ \pi^-$
• • • We do not use the following data for averages, fits, limits, etc. • • •			
0.661 ± 0.012	<sup>34</sup> BIJNENS	98 CNTR	$\chi PT$ extraction
0.660 ± 0.024	AMENDOLIA	84 CNTR	$\pi e \rightarrow \pi e$
0.78 + 0.09 - 0.10	ADYLOV	77 CNTR	$\pi e \rightarrow \pi e$
0.74 + 0.11 - 0.13	BARDIN	77 CNTR	$e p \rightarrow e \pi^+ n$
0.56 ± 0.04	DALLY	77 CNTR	$\pi e \rightarrow \pi e$

<sup>34</sup>BIJNENS 98 fits existing data.

 $\pi^\pm$  REFERENCES

We have omitted some papers that have been superseded by later experiments. The omitted papers may be found in our 1988 edition Physics Letters **B204** 1 (1988).

BYCHKOV	09	PRL 103 051802	M. Bychkov <i>et al.</i>	(PSI PIBETA Collab.)
FRLEZ	04	PRL 93 181804	E. Frlež <i>et al.</i>	(PSI PIBETA Collab.)
POČANIĆ	04	PRL 93 181803	D. Počanić <i>et al.</i>	(PSI PIBETA Collab.)
ESCHRICH	01	PL B522 233	I. Eschrich <i>et al.</i>	(FNAL SELEX Collab.)
LIESENFELD	99	PL B468 20	A. Liesenfeld <i>et al.</i>	
BIJNENS	98	JHEP 9805 014	J. Bijnens <i>et al.</i>	
BRESSI	98	NP B513 555	G. Bressi <i>et al.</i>	
LENZ	98	PL B416 50	S. Lenz <i>et al.</i>	
ASSAMAGAN	96	PR D53 6065	K.A. Assamagan <i>et al.</i>	(PSI, ZURI, VILL+)
KOPEV	95	JETPL 61 877	V.P. Koptev <i>et al.</i>	(PNPI)
NUMAO	95	Translated from ZETFP 61 865.	T. Numao <i>et al.</i>	(TRIUM, BRCO)
ASSAMAGAN	94	PL B335 231	K.A. Assamagan <i>et al.</i>	(PSI, ZURI, VILL+)
JECKELMANN	94	PL B335 326	B. Jecckelmann, P.F.A. Goudsmit, H.J. Leisi	(WABRN+)
CZAPEK	93	PRL 70 17	G. Czapek <i>et al.</i>	(BERN, VILL)
BARANOV	92	SJNP 55 1644	V.A. Baranov <i>et al.</i>	(JINR)
		Translated from YAF 55 2940.		
BRITTON	92	PRL 68 3000	D.I. Britton <i>et al.</i>	(TRIUM, CARL)
		Also PR D43 28	D.I. Britton <i>et al.</i>	(TRIUM, CARL)
NUMAO	92	MPL A7 3357	T. Numao	(TRIUM)
BARANOV	91B	SJNP 54 790	V.A. Baranov <i>et al.</i>	(JINR)
		Translated from YAF 54 1298.		



See key on page 457

## Meson Particle Listings

$\pi^\pm, \pi^0$

DAUM	91	PL B265 425	M. Daum <i>et al.</i>	(VILL)
BOLOTOV	90B	PL B243 308	V.N. Bolotov <i>et al.</i>	(INRM)
EGLI	89	PL B222 533	S. Egli <i>et al.</i>	(SINDRUM Collab.)
Also		PL B175 97	S. Egli <i>et al.</i>	(AACH3, ETH, SIN, ZURI)
PDG	88	PL B204 1	G.P. Yost <i>et al.</i>	(LBL+)
PICCIOTTO	88	PR D37 1131	C.E. Picciotto <i>et al.</i>	(TRIU, CNRC)
COHEN	87	RMP 59 1121	E.R. Cohen, B.N. Taylor	(RISC, NBS)
KORENCHENKO...	87	SJNP 46 192	S.M. Korenchenko <i>et al.</i>	(JINR)
Translated from YAF 46 313:				
AMENDOLIA	86	NP B277 168	S.R. Amendolia <i>et al.</i>	(CERN NA7 Collab.)
BAY	86	PL B174 445	A. Bay <i>et al.</i>	(LAUS, ZURI)
BRYMAN	86	PR D33 1211	D.A. Bryman <i>et al.</i>	(TRIU, CNRC)
Also		PRL 50 7	D.A. Bryman <i>et al.</i>	(TRIU, CNRC)
JECKELMANN	86B	NP A457 709	B. Jeckelmann <i>et al.</i>	(ETH, FRIB)
Also		PRL 56 1444	B. Jeckelmann <i>et al.</i>	(ETH, FRIB)
PILONEN	86	PRL 57 1402	L.E. Pilonen <i>et al.</i>	(LANL, TEMP, CHIC)
MCFARLANE	85	PR D32 547	W.K. McFarlane <i>et al.</i>	(TEMP, LANL)
ABELA	84	PL 146B 431	R. Abela <i>et al.</i>	(SIN)
Also		PL 74B 126	M. Daum <i>et al.</i>	(SIN)
Also		PR D20 2692	M. Daum <i>et al.</i>	(SIN)
AMENDOLIA	84	PL 146B 116	S.R. Amendolia <i>et al.</i>	(CERN NA7 Collab.)
FETSCHER	84	PL 140B 117	W. Fetscher	(ETH)
ABELA	83	NP A395 413	R. Abela <i>et al.</i>	(BASL, KARLK, KARLE)
CARR	83	PRL 51 627	J. Carr <i>et al.</i>	(LBL, NWES, TRIU)
COOPER	82	PL 112B 97	A.M. Cooper <i>et al.</i>	(RL)
DALLY	82	PRL 48 375	E.B. Dally <i>et al.</i>	
LU	80	PRL 45 1066	D.C. Lu <i>et al.</i>	(YALE, COLU, JHU)
BEBEK	78	PR D17 1693	C.J. Bebek <i>et al.</i>	
QUENZER	78	PL 74B 512	A. Quenner <i>et al.</i>	(LALO)
STETZ	78	NP B138 285	A.W. Stetz <i>et al.</i>	(LBL, UCLA)
ADYLOV	77	NP B128 461	G.T. Adylov <i>et al.</i>	
BARDIN	77	NP B120 45	G. Bardin <i>et al.</i>	
DALLY	77	PRL 39 1176	E.B. Dally <i>et al.</i>	
CARTER	76	PRL 37 1380	A.L. Carter <i>et al.</i>	(CARL, CNRC, CHIC+)
KORENCHENKO...	76B	JETP 44 35	S.M. Korenchenko <i>et al.</i>	(JINR)
Translated from ZETF 71 69:				
MARUSHENKO...	76	JETPL 23 72	V.I. Marushenko <i>et al.</i>	(PNPI)
Also		Translated from ZETFP 23 80:		
Private Comm.		R.E. Shafer		(FNAL)
Also		Private Comm.	A. Smirnov	(PNPI)
DUNAITSEV	73	SJNP 16 292	A.F. Dunaitsev <i>et al.</i>	(SERP)
Translated from YAF 16 524:				
AYRES	71	PR D3 1051	D.S. Ayres <i>et al.</i>	(LRL, UCSB)
Also		PR 157 1288	D.S. Ayres <i>et al.</i>	(LRL)
Also		PRL 21 261	D.S. Ayres <i>et al.</i>	(LRL, UCSB)
Also		Thesis UCRL 18369	D.S. Ayres	(LRL)
Also		PRL 23 1267	A.J. Greenberg <i>et al.</i>	(LRL, UCSB)
KORENCHENKO...	71	SJNP 13 189	S.M. Korenchenko <i>et al.</i>	(JINR)
Translated from YAF 13 339:				
BOOTH	70	PL 32B 723	P.S.L. Booth <i>et al.</i>	(LIVP)
DEPOMMIER	68	NP B4 189	P. Depommier <i>et al.</i>	(CERN)
PETRUKHIN	68	JINR P1 3862	V.I. Petrukhin <i>et al.</i>	(JINR)
HYMAN	67	PL 25B 376	L.G. Hyman <i>et al.</i>	(ANL, CMU, NWES)
NORDBERG	67	PL 24B 594	M.E. Nordberg, F. Lobkowicz, R.L. Burman	(ROCH)
BARDON	66	PRL 16 775	M. Bardon <i>et al.</i>	(COLU)
KINSEY	66	PR 144 1132	K.F. Kinsey, F. Lobkowicz, M.E. Nordberg	(ROCH)
LOBKOWICZ	66	PRL 17 548	F. Lobkowicz <i>et al.</i>	(ROCH, BNL)
BACASTOW	65	PR 139 B407	R.B. Bacastow <i>et al.</i>	(LRL, SLAC)
BERTRAM	65	PR 139 B617	W.K. Bertram <i>et al.</i>	(MICH, CMU)
DUNAITSEV	65	JETP 20 58	A.F. Dunaitsev <i>et al.</i>	(JINR)
Translated from ZETF 47 84:				
ECKHAUSE	65	PL 19 348	M. Eckhause <i>et al.</i>	(WILL)
BARTLETT	64	PR 136 B1452	D. Bartlett <i>et al.</i>	(COLU)
DIAPUA	64	PR 133 B1333	M. di Capua <i>et al.</i>	(COLU)
Also		Private Comm.	L. Pondrom	(WISC)
DEPOMMIER	63	PL 5 61	P. Depommier <i>et al.</i>	(CERN)
DEPOMMIER	63B	PL 7 285	P. Depommier <i>et al.</i>	(CERN)
ANDERSON	60	PR 119 2050	H.L. Anderson <i>et al.</i>	(EFI)
CASTAGNOLI	58	PR 112 1779	C. Castagnoli, M. Muchnik	(ROMA)

the time. More information on the  $\pi^0$  lifetime can be found in BERNSTEIN 11.

VALUE ( $10^{-17}$ s)	EVTS	DOCUMENT ID	TECN	COMMENT
<b>8.52±0.18 OUR AVERAGE</b>		Error includes scale factor of 1.2.		
8.32±0.15±0.18		<sup>1</sup> LARIN	11	PRMX Primakoff effect
8.5 ± 1.1		<sup>2</sup> BYCHKOV	09	PIBE $\pi^+ \rightarrow e^+ \nu \gamma$ at rest
8.4 ± 0.5 ± 0.5	1182	<sup>3</sup> WILLIAMS	88	CBAL $e^+ e^- \rightarrow e^+ e^- \pi^0$
8.97±0.22±0.17		ATHERTON	85	CNTR Direct measurement
8.2 ± 0.4		<sup>4</sup> BROWMAN	74	CNTR Primakoff effect
••• We do not use the following data for averages, fits, limits, etc. •••				
5.6 ± 0.6		BELLETTINI	70	CNTR Primakoff effect
9 ± 0.68		KRYSHKIN	70	CNTR Primakoff effect
7.3 ± 1.1		BELLETTINI	65B	CNTR Primakoff effect

- <sup>1</sup>LARIN 11 reported  $\Gamma(\pi^0 \rightarrow \gamma\gamma) = 7.82 \pm 0.14 \pm 0.17$  eV which we converted to mean life  $\tau = \hbar/\Gamma(\text{total})$ .
- <sup>2</sup>BYCHKOV 09 obtains this using the conserved-vector-current relation between the vector form factor  $F_V$  and the  $\pi^0$  lifetime.
- <sup>3</sup>WILLIAMS 88 gives  $\Gamma(\gamma\gamma) = 7.7 \pm 0.5 \pm 0.5$  eV. We give here  $\tau = \hbar/\Gamma(\text{total})$ .
- <sup>4</sup>BROWMAN 74 gives a  $\pi^0$  width  $\Gamma = 8.02 \pm 0.42$  eV. The mean life is  $\hbar/\Gamma$ .

 $\pi^0$  DECAY MODES

For decay limits to particles which are not established, see the appropriate Search sections ( $A^0$  (axion) and Other Light Boson ( $X^0$ ) Searches, etc.).

Mode	Fraction ( $\Gamma_i/\Gamma$ )	Scale factor / Confidence level
$\Gamma_1$ $2\gamma$	(98.823±0.034) %	S=1.5
$\Gamma_2$ $e^+ e^- \gamma$	( 1.174±0.035) %	S=1.5
$\Gamma_3$ $\gamma$ positronium	( 1.82 ± 0.29 ) × 10 <sup>-9</sup>	
$\Gamma_4$ $e^+ e^- e^- e^-$	( 3.34 ± 0.16 ) × 10 <sup>-5</sup>	
$\Gamma_5$ $e^+ e^-$	( 6.46 ± 0.33 ) × 10 <sup>-8</sup>	
$\Gamma_6$ $4\gamma$	< 2	× 10 <sup>-8</sup> CL=90%
$\Gamma_7$ $\nu\bar{\nu}$	[a] < 2.7	× 10 <sup>-7</sup> CL=90%
$\Gamma_8$ $\nu_e \bar{\nu}_e$	< 1.7	× 10 <sup>-6</sup> CL=90%
$\Gamma_9$ $\nu_\mu \bar{\nu}_\mu$	< 1.6	× 10 <sup>-6</sup> CL=90%
$\Gamma_{10}$ $\nu_\tau \bar{\nu}_\tau$	< 2.1	× 10 <sup>-6</sup> CL=90%
$\Gamma_{11}$ $\gamma\nu\bar{\nu}$	< 6	× 10 <sup>-4</sup> CL=90%

## Charge conjugation (C) or Lepton Family number (LF) violating modes

$\Gamma_{12}$ $3\gamma$	C	< 3.1	× 10 <sup>-8</sup>	CL=90%
$\Gamma_{13}$ $\mu^+ e^-$	LF	< 3.8	× 10 <sup>-10</sup>	CL=90%
$\Gamma_{14}$ $\mu^- e^+$	LF	< 3.4	× 10 <sup>-9</sup>	CL=90%
$\Gamma_{15}$ $\mu^+ e^- + \mu^- e^+$	LF	< 3.6	× 10 <sup>-10</sup>	CL=90%

[a] Astrophysical and cosmological arguments give limits of order 10<sup>-13</sup>; see the Particle Listings below.

## CONSTRAINED FIT INFORMATION

An overall fit to 2 branching ratios uses 6 measurements and one constraint to determine 3 parameters. The overall fit has a  $\chi^2 = 4.6$  for 4 degrees of freedom.

The following *off-diagonal* array elements are the correlation coefficients  $\langle \delta x_i \delta x_j \rangle / (\delta x_i \delta x_j)$ , in percent, from the fit to the branching fractions,  $x_i \equiv \Gamma_i/\Gamma_{\text{total}}$ . The fit constrains the  $x_i$  whose labels appear in this array to sum to one.

$$\begin{array}{c|cc} x_2 & -100 & \\ \hline & 0 & -1 \\ \hline x_4 & & x_2 \end{array}$$

 $\pi^0$  BRANCHING RATIOS

VALUE (%)	EVTS	DOCUMENT ID	TECN	COMMENT	$\Gamma_2/\Gamma_1$	
<b>1.188±0.035 OUR FIT</b>		Error includes scale factor of 1.5.				
<b>1.188±0.034 OUR AVERAGE</b>		Error includes scale factor of 1.4. See the ideogram below.				
1.140±0.024±0.033	12.5k	<sup>5</sup> BEDDALL	08	ALEP $e^+ e^- \rightarrow Z \rightarrow$ hadrons		
1.25 ± 0.04		SCHARDT	81	SPEC $\pi^- p \rightarrow n \pi^0$		
1.166±0.047	3071	<sup>6</sup> SAMIOS	61	HBC $\pi^- p \rightarrow n \pi^0$		
1.17 ± 0.15	27	BUDAGOV	60	HBC		
••• We do not use the following data for averages, fits, limits, etc. •••						
1.196		JOSEPH	60	THEO QED calculation		



$$I^G(J^{PC}) = 1^-(0^{-+})$$

We have omitted some results that have been superseded by later experiments. The omitted results may be found in our 1988 edition Physics Letters **B204** 1 (1988).

 $\pi^0$  MASS

The value is calculated from  $m_{\pi^\pm}$  and  $(m_{\pi^\pm} - m_{\pi^0})$ . See also the notes under the  $\pi^\pm$  Mass Listings.

VALUE (MeV)	DOCUMENT ID
<b>134.9766±0.0006 OUR FIT</b>	Error includes scale factor of 1.1.

$$m_{\pi^\pm} - m_{\pi^0}$$

Measurements with an error > 0.01 MeV have been omitted.

VALUE (MeV)	DOCUMENT ID	TECN	COMMENT
<b>4.5936 ± 0.0005 OUR FIT</b>			
<b>4.5936 ± 0.0005 OUR AVERAGE</b>			
4.59364 ± 0.00048	CRAWFORD	91	CNTR $\pi^- p \rightarrow \pi^0 n, n$ TOF
4.930 ± 0.0013	CRAWFORD	86	CNTR $\pi^- p \rightarrow \pi^0 n, n$ TOF
••• We do not use the following data for averages, fits, limits, etc. •••			
4.59366 ± 0.00048	CRAWFORD	88B	CNTR See CRAWFORD 91
4.6034 ± 0.0052	VASILEVSKY	66	CNTR
4.6056 ± 0.0055	CZIRR	63	CNTR

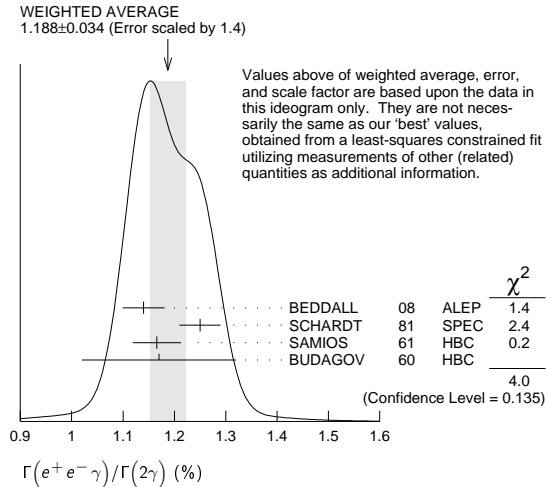
 $\pi^0$  MEAN LIFE

Most experiments measure the  $\pi^0$  width which we convert to a lifetime. ATHERTON 85 is the only direct measurement of the  $\pi^0$  lifetime. Our average based only on indirect measurement yields  $(8.30 \pm 0.19) \times 10^{-17}$  s. The two Primakoff measurements from 1970 have been excluded from our average because they suffered model-related systematics unknown at

# Meson Particle Listings

$\pi^0$

<sup>5</sup> This BEDDALL 08 value is obtained from ALEPH archived data.  
<sup>6</sup> SAMIOS 61 value uses a Panofsky ratio = 1.62.



## Γ(γpositronium)/Γ(2γ) Γ<sub>3</sub>/Γ<sub>1</sub>

VALUE (units 10 <sup>-9</sup> )	EVTS	DOCUMENT ID	TECN	COMMENT
<b>1.84 ± 0.29</b>	277	AFANASYEV 90	CNTR	p C 70 GeV

## Γ(e<sup>+</sup>e<sup>+</sup>e<sup>-</sup>e<sup>-</sup>)/Γ(2γ) Γ<sub>4</sub>/Γ<sub>1</sub>

VALUE (units 10 <sup>-5</sup> )	EVTS	DOCUMENT ID	TECN	COMMENT
<b>3.38 ± 0.16 OUR FIT</b>				
<b>3.38 ± 0.16 OUR AVERAGE</b>				
3.46 ± 0.19	30.5k	<sup>7</sup> ABOUZAIID 08D	KTEV	$K_L^0 \rightarrow \pi^0 \pi^0 \pi_{DD}^0$
3.18 ± 0.30	146	<sup>8</sup> SAMIOS 62B	HBC	

<sup>7</sup> This ABOUZAIID 08D value includes all radiative final states. The error includes both statistical and systematic errors. The correlation between the Dalitz-pair planes gives a direct measurement of the  $\pi^0$  parity. The  $\pi^0 2\gamma^*$  form factor is measured and limits are placed on a scalar contribution to the decay.  
<sup>8</sup> SAMIOS 62B value uses a Panofsky ratio = 1.62.

## Γ(e<sup>+</sup>e<sup>-</sup>)/Γ<sub>total</sub> Γ<sub>5</sub>/Γ

Experimental results are listed; branching ratios corrected for radiative effects are given in the footnotes. BERMAN 60 found  $B(\pi^0 \rightarrow e^+e^-) \geq 4.69 \times 10^{-8}$  via an exact QED calculation.

VALUE (units 10 <sup>-8</sup> )	EVTS	DOCUMENT ID	TECN	CHG	COMMENT
<b>6.44 ± 0.33 OUR AVERAGE</b>					
6.44 ± 0.25 ± 0.22	794	<sup>9</sup> ABOUZAIID 07	KTEV		$K_L^0 \rightarrow 3\pi^0$ in flight
6.9 ± 2.3 ± 0.6	21	<sup>10</sup> DESHPANDE 93	SPEC		$K^+ \rightarrow \pi^+\pi^0$
7.6 $^{+2.9}_{-2.8}$ ± 0.5	8	<sup>11</sup> MCFARLAND 93	SPEC		$K_L^0 \rightarrow 3\pi^0$ in flight

••• We do not use the following data for averages, fits, limits, etc. •••  
 6.09 ± 0.40 ± 0.24 275 <sup>12</sup> ALAVI-HARATI 99c SPEC 0 Repl. by ABOUZAIID 07  
<sup>9</sup> ABOUZAIID 07 result is for  $m_{e^+e^-}/m_{\pi^0} > 0.95$ . With radiative corrections the result becomes  $(7.48 \pm 0.29 \pm 0.25) \times 10^{-8}$ .  
<sup>10</sup> The DESHPANDE 93 result with bremsstrahlung radiative corrections is  $(8.0 \pm 2.6 \pm 0.6) \times 10^{-8}$ .  
<sup>11</sup> The MCFARLAND 93 result is for  $B[\pi^0 \rightarrow e^+e^-, (m_{e^+e^-}/m_{\pi^0})^2 > 0.95]$ . With radiative corrections it becomes  $(8.8^{+4.5}_{-3.2} \pm 0.6) \times 10^{-8}$ .  
<sup>12</sup> ALAVI-HARATI 99c quote result for  $B[\pi^0 \rightarrow e^+e^-, (m_{e^+e^-}/m_{\pi^0})^2 > 0.95]$  to minimize radiative contributions from  $\pi^0 \rightarrow e^+e^-\gamma$ . After radiative corrections they obtain  $(7.04 \pm 0.46 \pm 0.28) \times 10^{-8}$ .

## Γ(e<sup>+</sup>e<sup>-</sup>)/Γ(2γ) Γ<sub>5</sub>/Γ<sub>1</sub>

VALUE (units 10 <sup>-7</sup> )	CL%	EVTS	DOCUMENT ID	TECN	COMMENT
<b>••• We do not use the following data for averages, fits, limits, etc. •••</b>					
<1.3	90		NIEBUHR 89	SPEC	$\pi^- p \rightarrow \pi^0 n$ at rest
<5.3	90		ZEPHAT 87	SPEC	$\pi^- p \rightarrow \pi^0 n$ 0.3 GeV/c
1.7 ± 0.6 ± 0.3		59	FRANK 83	SPEC	$\pi^- p \rightarrow n\pi^0$
1.8 ± 0.6		58	MISCHKE 82	SPEC	See FRANK 83
2.23 $^{+2.40}_{-1.10}$		90	8 FISCHER 78B	SPRK	$K^+ \rightarrow \pi^+\pi^0$

## Γ(4γ)/Γ<sub>total</sub> Γ<sub>6</sub>/Γ

VALUE (units 10 <sup>-8</sup> )	CL%	EVTS	DOCUMENT ID	TECN	COMMENT
<b>&lt; 2</b>	90		MCDONOUGH 88	CBOX	$\pi^- p$ at rest
••• We do not use the following data for averages, fits, limits, etc. •••					
<160	90		BOLOTOV 86c	CALO	
<440	90	0	AUERBACH 80	CNTR	

## Γ(νν̄)/Γ<sub>total</sub> Γ<sub>7</sub>/Γ

The astrophysical and cosmological limits are many orders of magnitude lower, but we use the best laboratory limit for the Summary Tables.

VALUE (units 10 <sup>-6</sup> )	CL%	EVTS	DOCUMENT ID	TECN	COMMENT
<b>&lt; 0.27</b>	90		<sup>13</sup> ARTAMONOV 05A	B949	$K^+ \rightarrow \pi^+\pi^0$
••• We do not use the following data for averages, fits, limits, etc. •••					
< 0.83	90		<sup>13</sup> ATIYA 91	B787	$K^+ \rightarrow \pi^+\nu\nu'$
< 2.9 × 10 <sup>-7</sup>			<sup>14</sup> LAM 91	91	Cosmological limit
< 3.2 × 10 <sup>-7</sup>			<sup>15</sup> NATALE 91	91	SN 1987A
< 6.5	90		DORENBOS... 88	CHRM	Beam dump, prompt ν
<24	90	0	<sup>13</sup> HERCZEG 81	RVUE	$K^+ \rightarrow \pi^+\nu\nu'$

## Γ(ν<sub>e</sub>ν̄<sub>e</sub>)/Γ<sub>total</sub> Γ<sub>8</sub>/Γ

VALUE (units 10 <sup>-6</sup> )	CL%	DOCUMENT ID	TECN	COMMENT
<b>&lt;1.7</b>	90	DORENBOS... 88	CHRM	Beam dump, prompt ν
••• We do not use the following data for averages, fits, limits, etc. •••				
<3.1	90	<sup>16</sup> HOFFMAN 88	RVUE	Beam dump, prompt ν
<sup>16</sup> HOFFMAN 88				analyzes data from a 400-GeV BEBC beam-dump experiment.

## Γ(ν<sub>μ</sub>ν̄<sub>μ</sub>)/Γ<sub>total</sub> Γ<sub>9</sub>/Γ

VALUE (units 10 <sup>-6</sup> )	CL%	EVTS	DOCUMENT ID	TECN	COMMENT
<b>&lt;1.6</b>	90	8.7	AUERBACH 04	LSND	800 MeV p on Cu
<3.1	90		<sup>17</sup> HOFFMAN 88	RVUE	Beam dump, prompt ν
••• We do not use the following data for averages, fits, limits, etc. •••					
<7.8	90		DORENBOS... 88	CHRM	Beam dump, prompt ν
<sup>17</sup> HOFFMAN 88					analyzes data from a 400-GeV BEBC beam-dump experiment.

## Γ(ν<sub>τ</sub>ν̄<sub>τ</sub>)/Γ<sub>total</sub> Γ<sub>10</sub>/Γ

VALUE (units 10 <sup>-6</sup> )	CL%	DOCUMENT ID	TECN	COMMENT
<b>&lt;2.1</b>	90	<sup>18</sup> HOFFMAN 88	RVUE	Beam dump, prompt ν
••• We do not use the following data for averages, fits, limits, etc. •••				
<4.1	90	DORENBOS... 88	CHRM	Beam dump, prompt ν
<sup>18</sup> HOFFMAN 88				analyzes data from a 400-GeV BEBC beam-dump experiment.

## Γ(γνν̄)/Γ<sub>total</sub> Γ<sub>11</sub>/Γ

Standard Model prediction is  $6 \times 10^{-18}$ .

VALUE	CL%	DOCUMENT ID	TECN	COMMENT
<b>&lt;6 × 10<sup>-4</sup></b>	90	ATIYA 92	CNTR	$K^+ \rightarrow \gamma\nu\pi^+$

## Γ(3γ)/Γ<sub>total</sub> Γ<sub>12</sub>/Γ

Forbidden by C invariance.

VALUE (units 10 <sup>-8</sup> )	CL%	EVTS	DOCUMENT ID	TECN	COMMENT
<b>&lt; 3.1</b>	90		MCDONOUGH 88	CBOX	$\pi^- p$ at rest
••• We do not use the following data for averages, fits, limits, etc. •••					
< 38	90	0	HIGHLAND 80	CNTR	
<150	90	0	AUERBACH 78	CNTR	
<490	90	0	<sup>19</sup> DUCLOS 65	CNTR	
<490	90		<sup>19</sup> KUTIN 65	CNTR	

<sup>19</sup> These experiments give  $B(3\gamma/2\gamma) < 5.0 \times 10^{-6}$ .

## Γ(μ<sup>+</sup>e<sup>-</sup>)/Γ<sub>total</sub> Γ<sub>13</sub>/Γ

Forbidden by lepton family number conservation.

VALUE (units 10 <sup>-9</sup> )	CL%	EVTS	DOCUMENT ID	TECN	COMMENT
<b>&lt; 0.38</b>	90	0	APPEL 00	SPEC	$K^+ \rightarrow \pi^+\mu^+e^-$
••• We do not use the following data for averages, fits, limits, etc. •••					
<16	90		LEE 90	SPEC	$K^+ \rightarrow \pi^+\mu^+e^-$
<78	90		CAMPAGNARI 88	SPEC	See LEE 90

## Γ(μ<sup>-</sup>e<sup>+</sup>)/Γ<sub>total</sub> Γ<sub>14</sub>/Γ

Forbidden by lepton family number conservation.

VALUE (units 10 <sup>-9</sup> )	CL%	EVTS	DOCUMENT ID	TECN	COMMENT
<b>&lt;3.4</b>	90	0	APPEL 00B	B865	$K^+ \rightarrow \pi^+e^+\mu^-$

## Γ(μ<sup>+</sup>e<sup>-</sup> + Γ(μ<sup>-</sup>e<sup>+</sup>))/Γ<sub>total</sub> Γ<sub>15</sub>/Γ

Forbidden by lepton family number conservation.

VALUE (units 10 <sup>-9</sup> )	CL%	DOCUMENT ID	TECN	COMMENT
<b>&lt; 0.36</b>	90	ABOUZAIID 08c	KTEV	$K_L^0 \rightarrow 2\pi^0\mu^\pm e^\mp$
••• We do not use the following data for averages, fits, limits, etc. •••				
< 17.2	90	KROLAK 94	E799	$\ln K_L^0 \rightarrow 3\pi^0$
<140		HERCZEG 84	RVUE	$K^+ \rightarrow \pi^+\mu e$
< 2 × 10 <sup>-6</sup>		HERCZEG 84	THEO	$\mu^- \rightarrow e^-$ conversion
< 70	90	BRYMAN 82	RVUE	$K^+ \rightarrow \pi^+\mu e$



## Meson Particle Listings

 $\eta$ 

Charge conjugation (C), Parity (P),  
Charge conjugation  $\times$  Parity (CP), or  
Lepton Family number (LF) violating modes

$\Gamma_{23}$	$\pi^0\gamma$	C	< 9	$\times 10^{-5}$	CL=90%
$\Gamma_{24}$	$\pi^+\pi^-$	P,CP	< 1.3	$\times 10^{-5}$	CL=90%
$\Gamma_{25}$	$2\pi^0$	P,CP	< 3.5	$\times 10^{-4}$	CL=90%
$\Gamma_{26}$	$2\pi^0\gamma$	C	< 5	$\times 10^{-4}$	CL=90%
$\Gamma_{27}$	$3\pi^0\gamma$	C	< 6	$\times 10^{-5}$	CL=90%
$\Gamma_{28}$	$3\gamma$	C	< 1.6	$\times 10^{-5}$	CL=90%
$\Gamma_{29}$	$4\pi^0$	P,CP	< 6.9	$\times 10^{-7}$	CL=90%
$\Gamma_{30}$	$\pi^0 e^+ e^-$	C	[a] < 4	$\times 10^{-5}$	CL=90%
$\Gamma_{31}$	$\pi^0 \mu^+ \mu^-$	C	[a] < 5	$\times 10^{-6}$	CL=90%
$\Gamma_{32}$	$\mu^+ e^- + \mu^- e^+$	LF	< 6	$\times 10^{-6}$	CL=90%

[a] C parity forbids this to occur as a single-photon process.

## CONSTRAINED FIT INFORMATION

An overall fit to a decay rate and 19 branching ratios uses 49 measurements and one constraint to determine 9 parameters. The overall fit has a  $\chi^2 = 56.4$  for 41 degrees of freedom.

The following *off-diagonal* array elements are the correlation coefficients  $\langle \delta x_i \delta x_j \rangle / (\delta x_i \delta x_j)$ , in percent, from the fit to the branching fractions,  $x_i \equiv \Gamma_i / \Gamma_{\text{total}}$ . The fit constrains the  $x_i$  whose labels appear in this array to sum to one.

$x_3$	26								
$x_4$	-1	-1							
$x_9$	-66	-73	-1						
$x_{10}$	-44	-46	0	12					
$x_{11}$	-5	-5	0	-6	-3				
$x_{12}$	0	0	0	-1	0	0			
$x_{16}$	0	0	0	0	0	0	0		
$\Gamma$	-10	-2	0	6	4	1	0	0	
	$x_2$	$x_3$	$x_4$	$x_9$	$x_{10}$	$x_{11}$	$x_{12}$	$x_{16}$	

Mode	Rate (keV)	Scale factor	
$\Gamma_2$	$2\gamma$	$0.510 \pm 0.026$	
$\Gamma_3$	$3\pi^0$	$0.423 \pm 0.022$	
$\Gamma_4$	$\pi^0 2\gamma$	$(3.5 \pm 0.7) \times 10^{-4}$	
$\Gamma_9$	$\pi^+ \pi^- \pi^0$	$0.295 \pm 0.016$	
$\Gamma_{10}$	$\pi^+ \pi^- \gamma$	$0.060 \pm 0.004$	1.2
$\Gamma_{11}$	$e^+ e^- \gamma$	$0.0089 \pm 0.0007$	1.1
$\Gamma_{12}$	$\mu^+ \mu^- \gamma$	$(4.0 \pm 0.6) \times 10^{-4}$	
$\Gamma_{16}$	$\pi^+ \pi^- e^+ e^- (\gamma)$	$(3.48 \pm 0.23) \times 10^{-4}$	

 $\eta$  DECAY RATES $\Gamma(2\gamma)$  $\Gamma_2$ 

See the table immediately above giving the fitted decay rates. Following the advice of NEFKENS 02, we have removed the Primakoff-effect measurement from the average. See also the "Note on the Decay Width  $\Gamma(\eta \rightarrow \gamma\gamma)$ ," in our 1994 edition, Phys. Rev. D50, 1 August 1994, Part I, p. 1451, for a discussion of the various measurements.

VALUE (keV)	EVTS	DOCUMENT ID	TECN	COMMENT
<b>0.510 <math>\pm</math> 0.026 OUR FIT</b>				
<b>0.510 <math>\pm</math> 0.026 OUR AVERAGE</b>				
0.51 $\pm$ 0.12 $\pm$ 0.05	36	BARU	90 MD1	$e^+ e^- \rightarrow e^+ e^- \eta$
0.490 $\pm$ 0.010 $\pm$ 0.048	2287	ROE	90 ASP	$e^+ e^- \rightarrow e^+ e^- \eta$
0.514 $\pm$ 0.017 $\pm$ 0.035	1295	WILLIAMS	88 CBAL	$e^+ e^- \rightarrow e^+ e^- \eta$
0.53 $\pm$ 0.04 $\pm$ 0.04		BARTEL	85E JADE	$e^+ e^- \rightarrow e^+ e^- \eta$
••• We do not use the following data for averages, fits, limits, etc. •••				
0.476 $\pm$ 0.062		<sup>2</sup> RODRIGUES	08 CNTR	Reanalysis
0.64 $\pm$ 0.14 $\pm$ 0.13		AIHARA	86 TPC	$e^+ e^- \rightarrow e^+ e^- \eta$
0.56 $\pm$ 0.16	56	WEINSTEIN	83 CBAL	$e^+ e^- \rightarrow e^+ e^- \eta$
0.324 $\pm$ 0.046		BROWMAN	74B CNTR	Primakoff effect
1.00 $\pm$ 0.22		<sup>3</sup> BEMPORAD	67 CNTR	Primakoff effect

<sup>2</sup>RODRIGUES 08 uses a more sophisticated calculation for the inelastic background due to incoherent photoproduction to reanalyze the  $\eta$  photoproduction data on Be and Cu at 9 GeV from BROWMAN 74B. This brings the value of  $\Gamma(\eta \rightarrow 2\gamma)$  in line with direct measurements of the width. The error here is only statistical.

<sup>3</sup>BEMPORAD 67 gives  $\Gamma(2\gamma) = 1.21 \pm 0.26$  keV assuming  $\Gamma(2\gamma)/\Gamma(\text{total}) = 0.314$ . Bemporad private communication gives  $\Gamma(2\gamma)^2/\Gamma(\text{total}) = 0.380 \pm 0.083$ . We evaluate this using  $\Gamma(2\gamma)/\Gamma(\text{total}) = 0.38 \pm 0.01$ . Not included in average because the uncertainty resulting from the separation of the coulomb and nuclear amplitudes has apparently been underestimated.

 $\eta$  BRANCHING RATIOS

## Neutral modes

$\Gamma(\text{neutral modes})/\Gamma_{\text{total}}$	VALUE	EVTS	DOCUMENT ID	TECN	COMMENT
<b>0.7191 <math>\pm</math> 0.0034 OUR FIT</b>					Error includes scale factor of 1.2.
<b>0.705 <math>\pm</math> 0.008</b>	16k	BASILE	71D CNTR	MM spectrometer	••• We do not use the following data for averages, fits, limits, etc. •••
0.79 $\pm$ 0.08		BUNIATOV	67 OSPK		

 $\Gamma(2\gamma)/\Gamma_{\text{total}}$  $\Gamma_2/\Gamma$ 

VALUE (units $10^{-2}$ )	EVTS	DOCUMENT ID	TECN	COMMENT
<b>39.31 <math>\pm</math> 0.20 OUR FIT</b>				Error includes scale factor of 1.1.
<b>39.49 <math>\pm</math> 0.17 <math>\pm</math> 0.30</b>	65k	ABEGG	96 SPEC	$p d \rightarrow {}^3\text{He} \eta$
••• We do not use the following data for averages, fits, limits, etc. •••				
38.45 $\pm$ 0.40 $\pm$ 0.36	14k	<sup>4</sup> LOPEZ	07 CLEO	$\psi(2S) \rightarrow J/\psi \eta$

<sup>4</sup>Not independent of other results listed for LOPEZ 07. Assuming decays of  $\eta \rightarrow \gamma\gamma$ ,  $3\pi^0$ ,  $\pi^+ \pi^- \pi^0$ ,  $\pi^+ \pi^- \gamma$ , and  $e^+ e^- \gamma$  account for all  $\eta$  decays within a contribution of 0.3% to the systematic error.

 $\Gamma(2\gamma)/\Gamma(\text{neutral modes})$  $\Gamma_2/\Gamma_1 = \Gamma_2/(\Gamma_2 + \Gamma_3 + \Gamma_4)$ 

VALUE	EVTS	DOCUMENT ID	TECN	COMMENT
<b>0.5467 <math>\pm</math> 0.0019 OUR FIT</b>				
<b>0.548 <math>\pm</math> 0.023 OUR AVERAGE</b>				Error includes scale factor of 1.5.
0.535 $\pm$ 0.018		BUTTRAM	70 OSPK	
0.59 $\pm$ 0.033		BUNIATOV	67 OSPK	
••• We do not use the following data for averages, fits, limits, etc. •••				
0.52 $\pm$ 0.09	88	ABROSIMOV	80 HLBC	
0.60 $\pm$ 0.14	113	KENDALL	74 OSPK	
0.57 $\pm$ 0.09		STRUGALSKI	71 HLBC	
0.579 $\pm$ 0.052		FELDMAN	67 OSPK	
0.416 $\pm$ 0.044		DIGIUGNO	66 CNTR	Error doubled
0.44 $\pm$ 0.07		GRUNHAUS	66 OSPK	
0.39 $\pm$ 0.06	5	JONES	66 CNTR	

<sup>5</sup>This result from combining cross sections from two different experiments.

 $\Gamma(3\pi^0)/\Gamma_{\text{total}}$  $\Gamma_3/\Gamma$ 

VALUE (units $10^{-2}$ )	EVTS	DOCUMENT ID	TECN	COMMENT
<b>32.57 <math>\pm</math> 0.23 OUR FIT</b>				Error includes scale factor of 1.1.
••• We do not use the following data for averages, fits, limits, etc. •••				
34.03 $\pm$ 0.56 $\pm$ 0.49	1821	<sup>6</sup> LOPEZ	07 CLEO	$\psi(2S) \rightarrow J/\psi \eta$

<sup>6</sup>Not independent of other results listed for LOPEZ 07. Assuming decays of  $\eta \rightarrow \gamma\gamma$ ,  $3\pi^0$ ,  $\pi^+ \pi^- \pi^0$ ,  $\pi^+ \pi^- \gamma$ , and  $e^+ e^- \gamma$  account for all  $\eta$  decays within a contribution of 0.3% to the systematic error.

 $\Gamma(3\pi^0)/\Gamma(\text{neutral modes})$  $\Gamma_3/\Gamma_1 = \Gamma_3/(\Gamma_2 + \Gamma_3 + \Gamma_4)$ 

VALUE	EVTS	DOCUMENT ID	TECN	COMMENT
<b>0.4529 <math>\pm</math> 0.0019 OUR FIT</b>				
<b>0.439 <math>\pm</math> 0.024</b>		BUTTRAM	70 OSPK	
••• We do not use the following data for averages, fits, limits, etc. •••				
0.44 $\pm$ 0.08	75	ABROSIMOV	80 HLBC	
0.32 $\pm$ 0.09		STRUGALSKI	71 HLBC	
0.41 $\pm$ 0.033		BUNIATOV	67 OSPK	Not indep. of $\Gamma(2\gamma)/\Gamma(\text{neutral modes})$
0.177 $\pm$ 0.035		FELDMAN	67 OSPK	
0.209 $\pm$ 0.054		DIGIUGNO	66 CNTR	Error doubled
0.29 $\pm$ 0.10		GRUNHAUS	66 OSPK	

 $\Gamma(3\pi^0)/\Gamma(2\gamma)$  $\Gamma_3/\Gamma_2$ 

VALUE	EVTS	DOCUMENT ID	TECN	COMMENT
<b>0.829 <math>\pm</math> 0.006 OUR FIT</b>				
<b>0.829 <math>\pm</math> 0.007 OUR AVERAGE</b>				
0.884 $\pm$ 0.022 $\pm$ 0.019	1821	LOPEZ	07 CLEO	$\psi(2S) \rightarrow J/\psi \eta$
0.817 $\pm$ 0.012 $\pm$ 0.032	17.4k	<sup>7</sup> AKHMETSHIN	05 CMD2	$e^+ e^- \rightarrow \phi \rightarrow \eta\gamma$
0.826 $\pm$ 0.024		ACHASOV	00D SND	$e^+ e^- \rightarrow \phi \rightarrow \eta\gamma$
0.832 $\pm$ 0.005 $\pm$ 0.012		KRUSCHE	95D SPEC	$\gamma p \rightarrow \eta p$ , threshold
0.841 $\pm$ 0.034		AMSLER	93 CBAR	$\bar{p} p \rightarrow \pi^+ \pi^- \eta$ at rest
0.822 $\pm$ 0.009		ALDE	84 GAM2	
••• We do not use the following data for averages, fits, limits, etc. •••				
0.796 $\pm$ 0.016 $\pm$ 0.016		ACHASOV	00 SND	See ACHASOV 00D
0.91 $\pm$ 0.14		COX	70B HBC	
0.75 $\pm$ 0.09		DEVONS	70 OSPK	
0.88 $\pm$ 0.16		BALTAY	67D DBC	
1.1 $\pm$ 0.2		CENCE	67 OSPK	
1.25 $\pm$ 0.39		BACCI	63 CNTR	Inverse BR reported

<sup>7</sup>Uses result from AKHMETSHIN 01b.

$\Gamma(\pi^0 2\gamma)/\Gamma_{total}$   $\Gamma_4/\Gamma$   
Early results are summarized in the review by LANDSBERG 85.

VALUE (units $10^{-4}$ )	CL%	EVTS	DOCUMENT ID	TECN	COMMENT
<b>2.7 ± 0.5 OUR FIT</b>					Error includes scale factor of 1.1.
<b>2.21 ± 0.24 ± 0.47</b>		≈ 500	<sup>8</sup> PRAKHOV 08	CRYB	$\pi^- \rho \rightarrow \eta n \approx$ threshold
• • •					We do not use the following data for averages, fits, limits, etc. • • •
3.5 ± 0.7 ± 0.6		1.6k	<sup>9,10</sup> PRAKHOV 05	CRYB	See PRAKHOV 08
<8.4	90	7	ACHASOV 01D	SND	$e^+ e^- \rightarrow \phi \rightarrow \eta \gamma$
<30	90	0	DAVYDOV 81	GAM2	$\pi^- \rho \rightarrow \eta n$

<sup>8</sup> PRAKHOV 08 is a reanalysis of the data of PRAKHOV 05, using for the first time the invariant-mass spectrum of the two photons.  
<sup>9</sup> Normalized using  $\Gamma(\eta \rightarrow 2\gamma)/\Gamma = 0.3943 \pm 0.0026$ .  
<sup>10</sup> This measurement and the independent analysis of the same data by KNECHT 04 both imply a lower value of  $\Gamma(\pi^0 2\gamma)$  than the one obtained by ALDE 84 from  $\Gamma(\pi^0 2\gamma)/\Gamma(2\gamma)$ .

$\Gamma(\pi^0 2\gamma)/\Gamma(2\gamma)$   $\Gamma_4/\Gamma_2$

VALUE (units $10^{-3}$ )	EVTS	DOCUMENT ID	TECN	CHG	COMMENT
<b>0.69 ± 0.13 OUR FIT</b>					Error includes scale factor of 1.1.
<b>1.8 ± 0.4</b>		ALDE 84	GAM2	0	
• • •					We do not use the following data for averages, fits, limits, etc. • • •
2.5 ± 0.6	70	BINON 82	GAM2		See ALDE 84

$\Gamma(\pi^0 2\gamma)/\Gamma(3\pi^0)$   $\Gamma_4/\Gamma_3$

VALUE (units $10^{-4}$ )	EVTS	DOCUMENT ID	TECN	COMMENT
<b>8.3 ± 1.6 OUR FIT</b>				Error includes scale factor of 1.1.
• • •				We do not use the following data for averages, fits, limits, etc. • • •
8.3 ± 2.8 ± 1.4		<sup>11</sup> KNECHT 04	CRYB	$\pi^- \rho \rightarrow n \eta$

<sup>11</sup> Independent analysis of same data as PRAKHOV 05.

$\Gamma(2\pi^0 2\gamma)/\Gamma_{total}$   $\Gamma_5/\Gamma$

VALUE	CL%	DOCUMENT ID	TECN	COMMENT
<b>&lt;1.2 × 10<sup>-3</sup></b>	90	<sup>12</sup> NEFKENS 05A	CRYB	$p(720 \text{ MeV}/c) \pi^- \rightarrow n \eta$
• • •				We do not use the following data for averages, fits, limits, etc. • • •
<4.0 × 10 <sup>-3</sup>	90	BLIK 07	GAM4	$\pi^- \rho \rightarrow \eta n$

<sup>12</sup> Measurement is done in limited  $\gamma\gamma$  energy range.

$\Gamma(4\gamma)/\Gamma_{total}$   $\Gamma_6/\Gamma$

VALUE	CL%	DOCUMENT ID	TECN	COMMENT
<b>&lt;2.8 × 10<sup>-4</sup></b>	90	BLIK 07	GAM4	$\pi^- \rho \rightarrow \eta n$

$\Gamma(\text{invisible})/\Gamma(2\gamma)$   $\Gamma_7/\Gamma_2$

VALUE	CL%	DOCUMENT ID	TECN	COMMENT
<b>&lt;1.65 × 10<sup>-3</sup></b>	90	<sup>13</sup> ABLIKIM 06Q	BES2	$J/\psi \rightarrow \phi \eta$

<sup>13</sup> Based on 58M  $J/\psi$  decays.

Charged modes

$\Gamma(\pi^+ \pi^- \pi^0)/\Gamma_{total}$   $\Gamma_9/\Gamma$

VALUE (units $10^{-2}$ )	EVTS	DOCUMENT ID	TECN	COMMENT
<b>22.74 ± 0.28 OUR FIT</b>				Error includes scale factor of 1.2.
• • •				We do not use the following data for averages, fits, limits, etc. • • •
22.60 ± 0.35 ± 0.29	3915	<sup>14</sup> LOPEZ 07	CLEO	$\psi(2S) \rightarrow J/\psi \eta$

<sup>14</sup> Not independent of other results listed for LOPEZ 07. Assuming decays of  $\eta \rightarrow \gamma\gamma$ ,  $3\pi^0$ ,  $\pi^+ \pi^- \pi^0$ ,  $\pi^+ \pi^- \gamma$ , and  $e^+ e^- \gamma$  account for all  $\eta$  decays within a contribution of 0.3% to the systematic error.

$\Gamma(\text{neutral modes})/\Gamma(\pi^+ \pi^- \pi^0)$   $\Gamma_1/\Gamma_9 = (\Gamma_2 + \Gamma_3 + \Gamma_4)/\Gamma_9$

VALUE	EVTS	DOCUMENT ID	TECN	COMMENT
<b>3.16 ± 0.05 OUR FIT</b>				Error includes scale factor of 1.2.
<b>3.26 ± 0.30 OUR AVERAGE</b>				
2.54 ± 1.89	74	KENDALL 74	OSPK	
3.4 ± 1.1	29	AGUILAR...	72B	HBC
2.83 ± 0.80	70	<sup>15</sup> BLOODWO...	72B	HBC
3.6 ± 0.6	244	FLATTE 67B	HBC	
2.89 ± 0.56		ALFF...	66	HBC
3.6 ± 0.8	50	KRAEMER 64	DBC	
3.8 ± 1.1		PAULI 64	DBC	

<sup>15</sup> Error increased from published value 0.5 by Bloodworth (private communication).

$\Gamma(2\gamma)/\Gamma(\pi^+ \pi^- \pi^0)$   $\Gamma_2/\Gamma_9$

VALUE	EVTS	DOCUMENT ID	TECN	COMMENT
<b>1.728 ± 0.028 OUR FIT</b>				Error includes scale factor of 1.2.
<b>1.70 ± 0.04 OUR AVERAGE</b>				
1.704 ± 0.032 ± 0.026	3915	<sup>16</sup> LOPEZ 07	CLEO	$\psi(2S) \rightarrow J/\psi \eta$
1.61 ± 0.14		ABLIKIM 06E	BES2	$e^+ e^- \rightarrow J/\psi \rightarrow \eta \gamma$
1.78 ± 0.10 ± 0.13	1077	AMSLER 95	CBAR	$\bar{p} p \rightarrow \pi^+ \pi^- \eta$ at rest
1.72 ± 0.25	401	BAGLIN 69	HLBC	
1.61 ± 0.39		FOSTER 65	HBC	

<sup>16</sup> LOPEZ 07 reports  $\Gamma(\eta \rightarrow \pi^+ \pi^- \pi^0) / \Gamma(\eta \rightarrow 2\gamma) = \Gamma_9/\Gamma_2 = 0.587 \pm 0.011 \pm 0.009$ .

$\Gamma(3\pi^0)/\Gamma(\pi^+ \pi^- \pi^0)$   $\Gamma_3/\Gamma_9$

VALUE	EVTS	DOCUMENT ID	TECN	COMMENT
<b>1.432 ± 0.026 OUR FIT</b>				Error includes scale factor of 1.2.
<b>1.48 ± 0.05 OUR AVERAGE</b>				
1.46 ± 0.03 ± 0.09		ACHASOV 06A	SND	$e^+ e^- \rightarrow \eta \gamma$
1.52 ± 0.04 ± 0.08	23k	<sup>17</sup> AKHMETSHIN 01B	CMD2	$e^+ e^- \rightarrow \phi \rightarrow \eta \gamma$
1.44 ± 0.09 ± 0.10	1627	AMSLER 95	CBAR	$\bar{p} p \rightarrow \pi^+ \pi^- \eta$ at rest
1.50 <sup>+0.15</sup> <sub>-0.29</sub>	199	BAGLIN 69	HLBC	
1.47 <sup>+0.20</sup> <sub>-0.17</sub>		BULLOCK 68	HLBC	
• • •				We do not use the following data for averages, fits, limits, etc. • • •
1.3 ± 0.4		BAGLIN 67B	HLBC	
0.90 ± 0.24		FOSTER 65	HBC	
2.0 ± 1.0		FOELSCHKE 64	HBC	
0.83 ± 0.32		CRAWFORD 63	HBC	

<sup>17</sup> AKHMETSHIN 01B uses results from AKHMETSHIN 99F.

$\Gamma(\pi^+ \pi^- \pi^0)/[\Gamma(2\gamma) + \Gamma(3\pi^0)]$   $\Gamma_9/(\Gamma_2 + \Gamma_3)$

VALUE	EVTS	DOCUMENT ID	TECN	COMMENT
<b>0.316 ± 0.005 OUR FIT</b>				Error includes scale factor of 1.2.
<b>0.304 ± 0.012</b>		ACHASOV 00B	SND	$e^+ e^- \rightarrow \phi \rightarrow \eta \gamma$
• • •				We do not use the following data for averages, fits, limits, etc. • • •
0.3141 ± 0.0081 ± 0.0058		ACHASOV 00B	SND	See ACHASOV 00D

$\Gamma(\pi^+ \pi^- \gamma)/\Gamma_{total}$   $\Gamma_{10}/\Gamma$

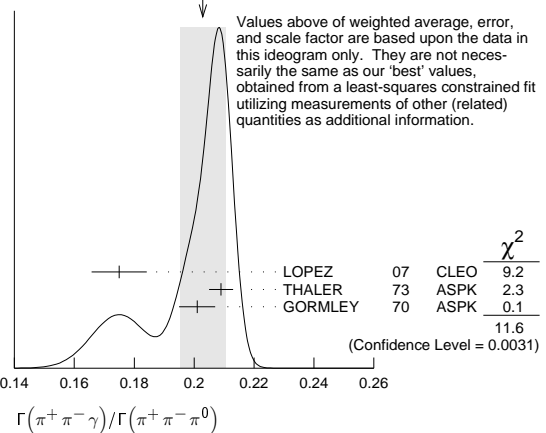
VALUE (units $10^{-2}$ )	EVTS	DOCUMENT ID	TECN	COMMENT
<b>4.60 ± 0.16 OUR FIT</b>				Error includes scale factor of 2.0.
• • •				We do not use the following data for averages, fits, limits, etc. • • •
3.96 ± 0.14 ± 0.14	859	<sup>18</sup> LOPEZ 07	CLEO	$\psi(2S) \rightarrow J/\psi \eta$

<sup>18</sup> Not independent of other results listed for LOPEZ 07. Assuming decays of  $\eta \rightarrow \gamma\gamma$ ,  $3\pi^0$ ,  $\pi^+ \pi^- \pi^0$ ,  $\pi^+ \pi^- \gamma$ , and  $e^+ e^- \gamma$  account for all  $\eta$  decays within a contribution of 0.3% to the systematic error.

$\Gamma(\pi^+ \pi^- \gamma)/\Gamma(\pi^+ \pi^- \pi^0)$   $\Gamma_{10}/\Gamma_9$

VALUE	EVTS	DOCUMENT ID	TECN	COMMENT
<b>0.202 ± 0.007 OUR FIT</b>				Error includes scale factor of 2.3.
<b>0.203 ± 0.008 OUR AVERAGE</b>				Error includes scale factor of 2.4. See the ideogram below.
0.175 ± 0.007 ± 0.006	859	LOPEZ 07	CLEO	$\psi(2S) \rightarrow J/\psi \eta$
0.209 ± 0.004	18k	THALER 73	ASPK	
0.201 ± 0.006	7250	GORMLEY 70	ASPK	
• • •				We do not use the following data for averages, fits, limits, etc. • • •
0.28 ± 0.04		BALTAY 67B	DBC	
0.25 ± 0.035		LITCHFIELD 67	DBC	
0.30 ± 0.06		CRAWFORD 66	HBC	
0.196 ± 0.041		FOSTER 65C	HBC	

WEIGHTED AVERAGE  
0.203±0.008 (Error scaled by 2.4)



$\Gamma(e^+ e^- \gamma)/\Gamma_{total}$   $\Gamma_{11}/\Gamma$

VALUE (units $10^{-3}$ )	EVTS	DOCUMENT ID	TECN	COMMENT
<b>6.9 ± 0.4 OUR FIT</b>				Error includes scale factor of 1.2.
<b>6.7 ± 0.5 OUR AVERAGE</b>				Error includes scale factor of 1.2.
6.6 ± 0.4 ± 0.4	1345	BERGHAUSER 11	SPEC	$\gamma p \rightarrow p \eta$
7.8 ± 0.5 ± 0.8	435 ± 31	BERLOWSKI 08	WASA	$pd \rightarrow ^3\text{He} \eta$
5.15 ± 0.62 ± 0.74	283	ACHASOV 01B	SND	$e^+ e^- \rightarrow \phi \rightarrow \eta \gamma$
7.10 ± 0.64 ± 0.46	323	AKHMETSHIN 01	CMD2	$e^+ e^- \rightarrow \phi \rightarrow \eta \gamma$
• • •				We do not use the following data for averages, fits, limits, etc. • • •
9.4 ± 0.7 ± 0.5	172	<sup>19</sup> LOPEZ 07	CLEO	$\psi(2S) \rightarrow J/\psi \eta$

<sup>19</sup> Not independent of other results listed for LOPEZ 07. Assuming decays of  $\eta \rightarrow \gamma\gamma$ ,  $3\pi^0$ ,  $\pi^+ \pi^- \pi^0$ ,  $\pi^+ \pi^- \gamma$ , and  $e^+ e^- \gamma$  account for all  $\eta$  decays within a contribution of 0.3% to the systematic error.



$\Gamma(3\gamma)/\Gamma(3\pi^0)$ 

VALUE	CL%	DOCUMENT ID	TECN	COMMENT
$<4.9 \times 10^{-5}$	90	ALOISIO	04	KLOE $\phi \rightarrow \eta\gamma$

 $\Gamma_{28}/\Gamma_3$  $\Gamma(4\pi^0)/\Gamma_{\text{total}}$ 

Forbidden by  $P$  and  $CP$  invariance.

VALUE	CL%	DOCUMENT ID	TECN	COMMENT
$< 6.9 \times 10^{-7}$	90	PRAKHOV	00	CRYB $\pi^- p \rightarrow n\eta$ , 720 MeV/c
$< 200 \times 10^{-7}$	90	BLIK	07	GAM4 $\pi^- p \rightarrow \eta n$

 $\Gamma_{29}/\Gamma$  $\Gamma(\pi^0 e^+ e^-)/\Gamma_{\text{total}}$ 

$C$  parity forbids this to occur as a single-photon process.

VALUE	CL%	DOCUMENT ID	TECN	COMMENT
$< 1.6 \times 10^{-4}$	90	MARTYNOV	76	HLBC
$< 8.4 \times 10^{-4}$	90	BAZIN	68	DBC
$< 70 \times 10^{-4}$		RITTENBERG	65	HBC

 $\Gamma_{30}/\Gamma$  $\Gamma(\pi^0 e^+ e^-)/\Gamma(\pi^+ \pi^- \pi^0)$ 

$C$  parity forbids this to occur as a single-photon process.

VALUE	CL%	EVTS	DOCUMENT ID	TECN	COMMENT
$< 1.9 \times 10^{-4}$	90		JANE	75	OSPK
$< 42 \times 10^{-4}$	90		BAGLIN	67	HLBC
$< 16 \times 10^{-4}$	90	0	BILLING	67	HLBC
$< 77 \times 10^{-4}$	0		FOSTER	65B	HBC
$< 110 \times 10^{-4}$			PRICE	65	HBC

 $\Gamma_{30}/\Gamma_9$  $\Gamma(\pi^0 \mu^+ \mu^-)/\Gamma_{\text{total}}$ 

$C$  parity forbids this to occur as a single-photon process.

VALUE	CL%	DOCUMENT ID	TECN	COMMENT
$< 5 \times 10^{-6}$	90	DZHELADIN	81	SPEC $\pi^- p \rightarrow \eta n$
$< 500 \times 10^{-6}$		WEHMANN	68	OSPK

 $\Gamma_{31}/\Gamma$  $[\Gamma(\mu^+ e^-) + \Gamma(\mu^- e^+)]/\Gamma_{\text{total}}$ 

Forbidden by lepton family number conservation.

VALUE	CL%	DOCUMENT ID	TECN	COMMENT
$< 6 \times 10^{-6}$	90	WHITE	96	SPEC $p d \rightarrow \eta^3 \text{He}$

 $\Gamma_{32}/\Gamma$  $\eta$  C-NONCONSERVING DECAY PARAMETERS $\pi^+ \pi^- \pi^0$  LEFT-RIGHT ASYMMETRY PARAMETER

Measurements with an error  $> 1.0 \times 10^{-2}$  have been omitted.

VALUE (units $10^{-2}$ )	EVTS	DOCUMENT ID	TECN	COMMENT
<b><math>0.09^{+0.11}_{-0.12}</math> OUR AVERAGE</b>				
$+0.09 \pm 0.10^{+0.09}_{-0.14}$	1.34M	AMBROSINO	08D	KLOE
$0.28 \pm 0.26$	165k	JANE	74	OSPK
$-0.05 \pm 0.22$	220k	LAYTER	72	ASPK
$1.5 \pm 0.5$	37k	25 GORMLEY	68c	ASPK

• • • We do not use the following data for averages, fits, limits, etc. • • •

<sup>25</sup> The GORMLEY 68c asymmetry is probably due to unmeasured ( $\mathbf{E} \times \mathbf{B}$ ) spark chamber effects. New experiments with ( $\mathbf{E} \times \mathbf{B}$ ) controls don't observe an asymmetry.

 $\pi^+ \pi^- \pi^0$  SEXTANT ASYMMETRY PARAMETER

Measurements with an error  $> 2.0 \times 10^{-2}$  have been omitted.

VALUE (units $10^{-2}$ )	EVTS	DOCUMENT ID	TECN	COMMENT
<b><math>0.12^{+0.10}_{-0.11}</math> OUR AVERAGE</b>				
$+0.08 \pm 0.10^{+0.08}_{-0.13}$	1.34M	AMBROSINO	08D	KLOE
$0.20 \pm 0.25$	165k	JANE	74	OSPK
$0.10 \pm 0.22$	220k	LAYTER	72	ASPK
$0.5 \pm 0.5$	37k	GORMLEY	68c	WIRE

 $\pi^+ \pi^- \pi^0$  QUADRANT ASYMMETRY PARAMETER

VALUE (units $10^{-2}$ )	EVTS	DOCUMENT ID	TECN	COMMENT
<b><math>-0.09 \pm 0.09</math> OUR AVERAGE</b>				
$-0.05 \pm 0.10^{+0.03}_{-0.05}$	1.34M	AMBROSINO	08D	KLOE
$-0.30 \pm 0.25$	165k	JANE	74	OSPK
$-0.07 \pm 0.22$	220k	LAYTER	72	ASPK

 $\pi^+ \pi^- \gamma$  LEFT-RIGHT ASYMMETRY PARAMETER

Measurements with an error  $> 2.0 \times 10^{-2}$  have been omitted.

VALUE (units $10^{-2}$ )	EVTS	DOCUMENT ID	TECN	COMMENT
<b><math>0.9 \pm 0.4</math> OUR AVERAGE</b>				
$1.2 \pm 0.6$	35k	JANE	74B	OSPK
$0.5 \pm 0.6$	36k	THALER	72	ASPK
$1.22 \pm 1.56$	7257	GORMLEY	70	ASPK

 $\pi^+ \pi^- \gamma$  PARAMETER  $\beta$  ( $D$ -wave)

Sensitive to a  $D$ -wave contribution:  $dN/d\cos\theta = \sin^2\theta (1 + \beta \cos^2\theta)$ .

VALUE	EVTS	DOCUMENT ID	TECN	COMMENT
<b><math>-0.02 \pm 0.07</math> OUR AVERAGE</b>				Error includes scale factor of 1.3.
$0.11 \pm 0.11$	35k	JANE	74B	OSPK
$-0.060 \pm 0.065$	7250	GORMLEY	70	WIRE
$0.12 \pm 0.06$	26	THALER	72	ASPK

• • • We do not use the following data for averages, fits, limits, etc. • • •

<sup>26</sup> The authors don't believe this indicates  $D$ -wave because the dependence of  $\beta$  on the  $\gamma$  energy is inconsistent with the theoretical prediction. A  $\cos^2\theta$  dependence can also come from  $P$ - and  $F$ -wave interference.

 $\eta$  CP-NONCONSERVING DECAY PARAMETER $\pi^+ \pi^- e^+ e^-$  DECAY-PLANE ASYMMETRY PARAMETER  $A_\phi$ 

In the  $\eta$  rest frame, the total momentum of the  $e^+ e^-$  pair is equal and opposite to that of the  $\pi^+ \pi^-$  pair. Let  $\hat{z}$  be the unit vector along the momentum of the  $e^+ e^-$  pair; let  $\hat{n}_{ee}$  and  $\hat{n}_{\pi\pi}$  be the unit vectors normal to the  $e^+ e^-$  and  $\pi^+ \pi^-$  planes; and let  $\phi$  be the angle between the two normals. Then

$$\sin\phi \cos\phi = [(\hat{n}_{ee} \times \hat{n}_{\pi\pi}) \cdot \hat{z}] (\hat{n}_{ee} \cdot \hat{n}_{\pi\pi}),$$

and

$$A_\phi \equiv \frac{N_{\sin\phi \cos\phi > 0} - N_{\sin\phi \cos\phi < 0}}{N_{\sin\phi \cos\phi > 0} + N_{\sin\phi \cos\phi < 0}}.$$

VALUE (units $10^{-2}$ )	EVTS	DOCUMENT ID	TECN	COMMENT
<b><math>-0.6 \pm 2.5 \pm 1.8</math></b>	1555 $\pm$ 52	AMBROSINO	09B	KLOE $e^+ e^- \rightarrow \phi \rightarrow \eta\gamma$

ENERGY DEPENDENCE OF  $\eta \rightarrow 3\pi^0$  DALITZ PLOTSPARAMETERS FOR  $\eta \rightarrow \pi^+ \pi^- \pi^0$ 

See the "Note on  $\eta$  Decay Parameters" in our 1994 edition, Phys. Rev. **D50**, 1 August 1994, Part I, p. 1454. The following experiments fit to one or more of the coefficients  $a, b, c, d$ , or  $e$  for  $|\text{matrix element}|^2 = 1 + ay + by^2 + cx + dx^2 + exy$ .

VALUE	EVTS	DOCUMENT ID	TECN	COMMENT
1.34M		AMBROSINO	08D	KLOE
3230	27	ABELE	98D	CBAR $\bar{p}p \rightarrow \pi^0 \pi^0 \eta$ at rest
1077	28	AMSLER	95	CBAR $\bar{p}p \rightarrow \pi^+ \pi^- \eta$ at rest
81k		LAYTER	73	ASPK
220k		LAYTER	72	ASPK
1138		CARPENTER	70	HBC
349		DANBURG	70	DBC
7250		GORMLEY	70	WIRE
526		BAGLIN	69	HLBC
7170		CNOPS	68	OSPK
37k		GORMLEY	68c	WIRE
1300		CLPWY	66	HBC
705		LARRIBE	66	HBC

<sup>27</sup> ABELE 98D obtains  $a = -1.22 \pm 0.07$  and  $b = 0.22 \pm 0.11$  when  $c$  (our  $d$ ) is fixed at 0.06.

<sup>28</sup> AMSLER 95 fits to  $(1+ay+by^2)$  and obtains  $a = -0.94 \pm 0.15$  and  $b = 0.11 \pm 0.27$ .

 $\alpha$  PARAMETER FOR  $\eta \rightarrow 3\pi^0$ 

See the "Note on  $\eta$  Decay Parameters" in our 1994 edition, Phys. Rev. **D50**, 1 August 1994, Part I, p. 1454. The value here is of  $\alpha$  in  $|\text{matrix element}|^2 = 1 + 2\alpha z$ .

VALUE	EVTS	DOCUMENT ID	TECN	COMMENT
<b><math>-0.0315 \pm 0.0015</math> OUR AVERAGE</b>				
$-0.0301 \pm 0.0035^{+0.0022}_{-0.0035}$	512k	AMBROSINO	10A	KLOE $e^+ e^- \rightarrow \phi \rightarrow \eta\gamma$
$-0.027 \pm 0.008 \pm 0.005$	120k	29 ADOLPH	09	WASA $pp \rightarrow pp\eta$
$-0.0322 \pm 0.0012 \pm 0.0022$	3M	30 PRAKHOV	09	CRYB $\gamma p \rightarrow p\eta$
$-0.032 \pm 0.002 \pm 0.002$	1.8M	30 UNVERZAGT	09	CRYB $\gamma p \rightarrow p\eta$
$-0.026 \pm 0.010 \pm 0.010$	75k	BASHKANOV	07	WASA $pp \rightarrow pp\eta$
$-0.010 \pm 0.021 \pm 0.010$	12k	ACHASOV	01c	SND $e^+ e^- \rightarrow \phi \rightarrow \eta\gamma$
$-0.031 \pm 0.004$	1M	TIPPENS	01	CRYB $\pi^- p \rightarrow n\eta$ , 720 MeV
$-0.052 \pm 0.017 \pm 0.010$	98k	ABELE	98c	CBAR $\bar{p}p \rightarrow 5\pi^0$
$-0.022 \pm 0.023$	50k	ALDE	84	GAM2
$-0.038 \pm 0.003^{+0.012}_{-0.008}$	1.34M	31 AMBROSINO	08D	KLOE
$-0.32 \pm 0.37$	192	BAGLIN	70	HLBC

<sup>29</sup> This ADOLPH 09 result is independent of the BASHKANOV 07 result.

<sup>30</sup> The PRAKHOV 09 and UNVERZAGT 09 results are independent.

<sup>31</sup> This AMBROSINO 08D value is an indirect result using  $\eta \rightarrow \pi^+ \pi^0 \pi^-$  events and a rescattering matrix that mixes isospin decay amplitudes.

Meson Particle Listings

$\eta, f_0(500)$

$\eta$  REFERENCES

AGAKISHIEV 12A EPJ A48 64 G. Agakishiev et al. (HADES Collab.)

ABLIKIM 11G PR D84 032006 M. Ablikim et al. (BES-III Collab.)

AMBROSINO 11B PL B702 324 F. Ambrosino et al. (KLOE Collab.)

BERGHAUSER 11 PL B701 562 H. Berghauser et al. (GIES, UCLA, GUTE)

AMBROSINO 10A PL B694 16 F. Ambrosino et al. (KLOE Collab.)

ADOLPH 09 PL B677 24 C. Adolph et al. (WASA at COSY Collab.)

AMBROSINO 09B PL B675 283 F. Ambrosino et al. (KLOE Collab.)

PRAKHOV 09 PR C79 035204 S. Prakhov et al. (MAMI-C Crystal Ball Collab.)

UNVERZAGT 09 EPJ A39 169 M. Unverzagt et al. (MAMI-B Crystal Ball Collab.)

AMBROSINO 08D JHEP 0805 006 F. Ambrosino et al. (DAPHNE KLOE Collab.)

BERLOWSKI 08 PR D77 032004 M. Berlowski et al. (CELSIUS/WASA Collab.)

PRAKHOV 08 PR D73 052008 S. Prakhov et al. (BNL Crystal Ball Collab.)

RODRIGUES 08 PRL 101 012301 T.F. Rodrigues et al. (USP, FESP, UNESP+)

AMBROSINO 07B JHEP 0712 073 F. Ambrosino et al. (KLOE Collab.)

BARGHOLTZ 07 PL B644 299 Chr. Bargholtz et al. (CELSIUS/WASA Collab.)

BASHKANOV 07 PR C76 048201 M. Bashkanov et al. (CELSIUS/WASA Collab.)

BLIK 07 PAN 70 693 A.M. Blik et al. (GAMS Collab.)

LOPEZ 07 PRL 99 122001 A. Lopez et al. (CLEO Collab.)

MILLER 07 PRL 99 122002 D.H. Miller et al. (CLEO Collab.)

ABLIKIM 06E PR D73 052008 M. Ablikim et al. (BES Collab.)

ABLIKIM 06Q PRL 97 202002 M. Ablikim et al. (BES Collab.)

ACHASOV 06A PR D74 014016 M.N. Achasov et al. (SND Collab.)

ABDEL-BARY 05 PL B619 281 M. Abdel-Bary et al. (GEM Collab.)

AKHMETSHIN 05 PL B605 26 R.R. Akhmetshin et al. (Novosibirsk CMD-2 Collab.)

AMBROSINO 05A PL B606 276 F. Ambrosino et al. (KLOE Collab.)

NEFKENS 05 PRL 94 041601 B.M.K. Nefkens et al. (BNL Crystal Ball Collab.)

NEFKENS 05A PR C72 035212 B.M.K. Nefkens et al. (BNL Crystal Ball Collab.)

PRAKHOV 05 PR C72 025201 S. Prakhov et al. (BNL Crystal Ball Collab.)

ALOISIO 04 PL B591 49 A. Aloisio et al. (KLOE Collab.)

KNECHT 04 PL B589 14 N. Knecht et al. (CERN NA48 Collab.)

LAI 02 PL B533 196 A. Lai et al. (UCLA)

NEFKENS 02 PS T99 114 B.M.K. Nefkens, J.W. Price (Novosibirsk SND Collab.)

ACHASOV 01B PL B504 275 M.N. Achasov et al. (Novosibirsk SND Collab.)

ACHASOV 01C JETPL 73 451 M.N. Achasov et al. (Novosibirsk SND Collab.)

ACHASOV 01D NP B600 3 M.N. Achasov et al. (Novosibirsk SND Collab.)

AKHMETSHIN 01 PL B501 191 R.R. Akhmetshin et al. (Novosibirsk CMD-2 Collab.)

AKHMETSHIN 01B PL B509 217 R.R. Akhmetshin et al. (Novosibirsk CMD-2 Collab.)

TIPPENS 01 PRL 87 192001 W.B. Tippens et al. (BNL Crystal Ball Collab.)

ACHASOV 00 EPJ C12 25 M.N. Achasov et al. (Novosibirsk SND Collab.)

ACHASOV 00B JETP 90 17 M.N. Achasov et al. (Novosibirsk SND Collab.)

ACHASOV 00D JETPL 72 282 M.N. Achasov et al. (Novosibirsk SND Collab.)

PRAKHOV 00 PRL 84 4802 S. Prakhov et al. (BNL Crystal Ball Collab.)

AKHMETSHIN 99B PL B462 371 R.R. Akhmetshin et al. (Novosibirsk CMD-2 Collab.)

AKHMETSHIN 99C PL B462 380 R.R. Akhmetshin et al. (Novosibirsk CMD-2 Collab.)

AKHMETSHIN 99F PL B460 242 R.R. Akhmetshin et al. (Novosibirsk CMD-2 Collab.)

ABELE 98 PL B417 193 A. Abele et al. (Crystal Barrel Collab.)

ABELE 98D PL B417 197 A. Abele et al. (Crystal Barrel Collab.)

ACHASOV 98 PL B425 388 M.N. Achasov et al. (Novosibirsk SND Collab.)

AKHMETSHIN 97C PL B415 452 R.R. Akhmetshin et al. (Novosibirsk CMD-2 Collab.)

BROWDER 97B PR D56 5359 T.E. Browder et al. (CLEO Collab.)

ABEGG 96 PR D53 11 R. Abegg et al. (Saturne SPES2 Collab.)

WHITE 96 PR D53 6658 D.B. White et al. (Saturne SPES2 Collab.)

AMSLER 95 PL B346 203 C. AMSler et al. (Crystal Barrel Collab.)

KRUSCHE 95D ZPHY A351 237 B. Krusche et al. (TAPS + A2 Collab.)

ABEGG 94 PR D50 92 R. Abegg et al. (Saturne SPES2 Collab.)

AMSLER 93 ZPHY C58 175 C. AMSler et al. (Crystal Barrel Collab.)

KESSLER 93 PRL 70 892 R.S. Kessler et al. (Saturne SPES2 Collab.)

PLOUIN 92 PL B276 526 F. Plouin et al. (Saturne SPES4 Collab.)

BARU 90 ZPHY C48 581 S.E. Baru et al. (MD-1 Collab.)

ROE 90 PR D41 17 N.A. Roe et al. (ASP Collab.)

WILLIAMS 88 PR D38 1365 D.A. Williams et al. (Crystal Ball Collab.)

AIHARA 86 PR D33 844 H. Aihara et al. (TPC-2 Collab.)

BARTEL 85E PL 160B 421 W. Bartel et al. (JADE Collab.)

LANDSBERG 85 PRPL 128 301 L.G. Landsberg (SERP)

ALDE 84 ZPHY C25 225 D.M. Alde et al. (SERP, BELG, LAPP)

WEINSTEIN 83 PR D28 2896 A.J. Weinstein et al. (Crystal Ball Collab.)

BINON 82 SJNP 36 391 F.G. Binon et al. (SERP, BELG, LAPP+)

DAVYDOV 81 LNC 32 45 V.A. Davydov et al. (SERP, BELG, LAPP+)

DZHELJADIN 81 SJNP 33 825 V.A. Davydov et al. (SERP)

R.I. Dzheyladin et al. (SERP)

SJNP 33 822 R.I. Dzheyladin et al. (SERP)

Translated from YAF 33 1534 R.I. Dzheyladin et al. (SERP)

Translated from YAF 33 1529 R.I. Dzheyladin et al. (SERP)

ABROSIMOV 80 SJNP 31 195 A.T. Abrosimov et al. (JINR)

DZHELJADIN 80 PL 94B 548 R.I. Dzheyladin et al. (SERP)

SJNP 32 516 R.I. Dzheyladin et al. (SERP)

Translated from YAF 32 998 R.I. Dzheyladin et al. (SERP)

DZHELJADIN 80B PL 97B 471 R.I. Dzheyladin et al. (SERP)

SJNP 32 518 R.I. Dzheyladin et al. (SERP)

Translated from YAF 32 1002 R.I. Dzheyladin et al. (SERP)

BUSHNIN 78 PL 79B 147 Y.B. Bushnin et al. (SERP)

SJNP 28 775 Y.B. Bushnin et al. (SERP)

Translated from YAF 28 1507 Y.B. Bushnin et al. (SERP)

MARTYNOV 76 SJNP 23 48 A.S. Martynov et al. (JINR)

JANE 75 PL 59B 99 M.R. Jane et al. (RHEL, LOWC)

JANE 75B PL 59B 103 M.R. Jane et al. (RHEL, LOWC)

Also PL 73B 503 M.R. Jane (RHEL, LOWC)

Erratum in private communication.

BROWMAN 74B PRL 32 1047 A. Brownman et al. (CORN, BING)

DAVIES 74 NC 24A 324 J.D. Davies, J.G. Guy, R.K.P. Zia (BIRM, RHEL+)

DUANE 74 PRL 32 425 A. Duane et al. (LOIC, SHMP)

JANE 74 PL 48B 260 M.R. Jane et al. (RHEL, LOWC, SUSS)

JANE 74 PL 48B 265 M.R. Jane et al. (RHEL, LOWC, SUSS)

KENDALL 74 NC 21A 387 B.N. Kendall et al. (BROW, BARI, MIT)

LAYTER 73 PR D7 2565 J.G. Layter et al. (COLU)

THALER 73 PR D7 2569 J.J. Thaler et al. (COLU)

AGUILAR... 72B PR D6 29 M. Aguilar-Benitez et al. (BNL)

BLOODWORTH... 72B NP B39 525 I.J. Bloodworth et al. (TNTO)

LAYTER 72 PRL 29 316 J.G. Layter et al. (COLU)

THALER 72 PRL 29 313 J.J. Thaler et al. (COLU)

THALER 71D NC 3A 796 M. Basile et al. (CERN, BGNA, STRB)

BASILE 71D NC 3A 796 M. Basile et al. (CERN, BGNA, STRB)

STRUGALSKI 71 NP B27 429 Z.S. Strugalski et al. (JINR)

BAGLIN 70 NP B22 66 C. Baglin et al. (EPOL, MADR, STRB)

BUTTRAM 70 PRL 25 1358 M.T. Buttram, M.N. Kreisler, R.E. Mische (PRIN)

CARPENTER 70 PR D1 1303 D.W. Carpenter et al. (DUKE)

COX 70B PRL 24 534 B. Cox, L. Fortney, J.P. Golson (DUKE)

DANBURG 70 PR D2 2564 J.S. Danburg et al. (LRL)

DEVONS 70 PR D1 1936 S. Devons et al. (COLU, SYRA)

GORMLEY 70 PR D2 501 M. Gormley et al. (COLU, BNL)

Also Thesis Nevis 181 M. Gormley (COLU)

BAGLIN 69 PL 29B 445 C. Baglin et al. (EPOL, UCB, MADR, STRB)

Also NP B22 66 C. Baglin et al. (EPOL, MADR, STRB)

HYAMS 69 PL 29B 128 B.D. Hyams et al. (CERN, MPIM)

ARNOLD 68 PL 27B 466 R.G. Arnold et al. (STRB, MADR, EPOL+)

BAZIN 68 PRL 20 895 M.J. Bazin et al. (PRIN, UKI)

BULLOCK 68 PL 27B 402 F.W. Bullock et al. (LOUC)

CNOPS 68 PRL 21 1609 A.M. Cnops et al. (BNL, ORNL, UCND+)

GORMLEY 68C PRL 21 402 M. Gormley et al. (COLU, BNL)

WEHMANN 68 PRL 20 748 A.W. Wehmann et al. (HARV, CASE, SLAC+)

BAGLIN 67 PL 24B 637 C. Baglin et al. (EPOL, UCB)

BAGLIN 67B BAPS 12 567 C. Baglin et al. (EPOL, UCB)

BALTAY 67B PRL 19 1498 C. Baltay et al. (COLU, STON)

BALTAY 67D PRL 19 1495 C. Baltay et al. (COLU, BRAN)

TEMPORAD 67 PL 25B 380 C. Temporad et al. (PISA, SCONN)

Also Private Comm. I. Lon

BILLING 67 PL 25B 435 K.D. Billing et al. (LOUC, OXF)

BUNIATOV 67 PL 25B 560 S.A. Bunyatov et al. (CERN, KARL)

CENCE 67 PRL 19 1393 R.J. Cence et al. (HAWA, LRL)

ESTEN 67 PL 24B 115 M.J. Esten et al. (LOUC, OXF)

FELDMAN 67 PRL 18 868 M. Feldman et al. (PENN)

FLATTE 67 PRL 18 976 S.M. Flatte et al. (LRL)

FLATTE 67B PR 163 1441 S.M. Flatte, C.G. Wohl (LRL)

LITCHFELD 67 PL 24B 486 P.J. Litichfeld et al. (RHEL, SAFL)

PRICE 67 PRL 18 1207 L.R. Price, F.S. Crawford (RHL)

ALFF... 66 PR 145 1072 C. Alf-Steinberger et al. (COLU, RUTG)

CLPWY 66 PR 149 1044 C. Baltay (SCUC, LRL, PURD, WISC, YALE)

CRAWFORD 66 PRL 16 333 F.S. Crawford, L.R. Price (LRL)

DIGUONO 66 PRL 16 767 G. di Guigno et al. (NAPL, TRST, FRAS)

GRUNHAUS 66 Thesis J. Grunhaus (COLU)

JAMES 66 PR 142 896 F.E. James, H.L. Kraybill (YALE, BNL)

JONES 66 PL 23 597 W.G. Jones et al. (LOIC, RHEL)

LARRIERE 66 PL 23 600 A. LARRIERE et al. (SAFL, RHEL)

FOSTER 65 PR 138 B652 M. Foster, M. Good, M. Meer (WISC)

FOSTER 65C Thesis M. Foster (WISC)

PRICE 65 PRL 15 123 L.R. Price, F.S. Crawford (LRL)

RITTENBERG 65 PRL 15 556 A. Rittenberg, G.R. Kalbfleisch (LRL, BNL)

FOELSCH 64 PR 134 B1138 H.W.J. Foelsche, H.L. Kraybill (YALE)

KRAEMER 64 PR 136 B496 R.W. Kraemer et al. (JHU, NWES, WOOD)

PAULI 64 PL 13 351 E. Pauli, A. Muller (SAFL)

BACCI 63 PRL 11 37 C. Bacci et al. (ROMA, FRAS)

CRAWFORD 63 PRL 10 546 F.S. Crawford, L.J. Lloyd, E.C. Fowler (LRL+)

Also PRL 16 907 F.S. Crawford, L.J. Lloyd, E.C. Fowler (LRL+)

ALFF... 62 PRL 9 322 C. Alf-Steinberger et al. (COLU, RUTG)

BASTIEN 62 PRL 8 114 P.L. Bastien et al. (LRL)

PICKUP 62 PRL 8 329 E. Pickup, D.K. Robinson, E.O. Salant (CNR-C)

$f_0(500)$  or  $\sigma$   
was  $f_0(600)$

$$I^G(J^{PC}) = 0^+(0^{++})$$

NOTE ON SCALAR MESONS BELOW 2 GEV

Released September 2011 by C. Amsler (University of Zurich), S. Eidelman (Budker Institute of Nuclear Physics, Novosibirsk), T. Gutsche (University of Tübingen), C. Hanhart (Forschungszentrum Jülich), S. Spanier (University of Tennessee), and N.A. Törnqvist (University of Helsinki)

**I. Introduction:** In contrast to the vector and tensor mesons, the identification of the scalar mesons is a long-standing puzzle. Scalar resonances are difficult to resolve because some of them have large decay widths which cause a strong overlap between resonances and background. In addition, several decay channels sometimes open up within a short mass interval (e.g. at the  $K\bar{K}$  and  $\eta\eta$  thresholds), producing cusps in the line shapes of the near-by resonances. Furthermore, one expects non- $q\bar{q}$  scalar objects, such as glueballs and multiquark states in the mass range below 2 GeV (for reviews see, e.g., Refs. [1-4]) .

Scalars are produced, for example, in  $\pi N$  scattering on polarized/unpolarized targets,  $p\bar{p}$  annihilation, central hadronic production,  $J/\Psi$ ,  $B^-$ ,  $D^-$  and  $K^-$ -meson decays,  $\gamma\gamma$  formation, and  $\phi$  radiative decays. Especially for the lightest scalar mesons simple parameterizations fail and more advanced theory tools are necessary to extract the resonance parameters from data. In the analyses available in the literature fundamental properties of the amplitudes such as unitarity, analyticity, Lorentz invariance, chiral and flavor symmetry are implemented at different levels of rigor. Especially, chiral symmetry implies the appearance of zeros close to the threshold in elastic  $S$ -wave scattering amplitudes involving soft pions [5,6], which may be shifted or removed in associated production processes [7]. The methods employed are the  $K$ -matrix formalism, the  $N/D$ -method, the



Dalitz Tuan ansatz, unitarized quark models with coupled channels, effective chiral field theories and the linear sigma model, *etc.* Dynamics near the lowest two-body thresholds in some analyses are described by crossed channel ( $t$ ,  $u$ ) meson exchange or with an effective range parameterization instead of, or in addition to, resonant features in the  $s$ -channel. Recent dispersion theoretical approaches made it possible to accurately pin down the location of resonance poles for the low lying states [8–11].

The mass and width of a resonance are found from the position of the nearest pole in the process amplitude ( $T$ -matrix or  $S$ -matrix) at an unphysical sheet of the complex energy plane, traditionally labeled as

$$\sqrt{s_{\text{Pole}}} = M - i\Gamma/2.$$

It is important to note that the Breit-Wigner parameterization agrees with this pole position only for narrow and well-separated resonances, far away from the opening of decay channels.

In this note, we discuss the light scalars below 2 GeV organized in the listings under the entries ( $I = 1/2$ )  $K_0^*(800)$  (or  $\kappa$ , currently omitted from the summary table),  $K_0^*(1430)$ , ( $I = 1$ )  $a_0(980)$ ,  $a_0(1450)$ , and ( $I = 0$ )  $f_0(500)$  (or  $\sigma$ ),  $f_0(980)$ ,  $f_0(1370)$ ,  $f_0(1500)$ , and  $f_0(1710)$ . This list is minimal and does not necessarily exhaust the list of actual resonances. The ( $I = 2$ )  $\pi\pi$  and ( $I = 3/2$ )  $K\pi$  phase shifts do not exhibit any resonant behavior. See also our notes in previous issues for further comments on, *e.g.*, scattering lengths and older papers.

**II. The  $I = 1/2$  States:** The  $K_0^*(1430)$  [12] is perhaps the least controversial of the light scalar mesons. The  $K\pi$   $S$ -wave scattering has two possible isospin channels,  $I = 1/2$  and  $I = 3/2$ . The  $I = 3/2$  wave is elastic and repulsive up to 1.7 GeV [13] and contains no known resonances. The  $I = 1/2$   $K\pi$  phase shift, measured from about 100 MeV above threshold in  $Kp$  production, rises smoothly, passes  $90^\circ$  at 1350 MeV, and continues to rise to about  $170^\circ$  at 1600 MeV. The first important inelastic threshold is  $K\eta'(958)$ . In the inelastic region the continuation of the amplitude is uncertain since the partial-wave decomposition has several solutions. The data are extrapolated towards the  $K\pi$  threshold using effective range type formulas [12,14] or chiral perturbation predictions [15,16]. From analyses using unitarized amplitudes there is agreement on the presence of a resonance pole around 1410 MeV having a width of about 300 MeV. With reduced model dependence, Ref. 17 finds a larger width of 500 MeV.

Similar to the situation for the  $f_0(500)$ , discussed in the next section, the presence and properties of the light  $K_0^*(800)$  (or  $\kappa$ ) meson in the 700-900 MeV region are difficult to establish since it appears to have a very large width ( $\Gamma \approx 500$  MeV) and resides close to the  $K\pi$  threshold. Hadronic  $D$ -meson decays provide additional data points in the vicinity of the  $K\pi$  threshold - experimental results from E791, *e.g.*, Ref. [18,19], FOCUS [17,20], CLEO [21], and BaBar [22] are discussed in the *Review of Charm Dalitz Plot Analyses*. Precision information

from semileptonic  $D$  decays avoiding theoretically ambiguous three-body final state interactions is not available. BES II [23] (re-analyzed in [24]) finds a  $K_0^*(800)$ -like structure in  $J/\psi$  decays to  $\bar{K}^{*0}(892)K^+\pi^-$  where  $K_0^*(800)$  recoils against the  $K^*(892)$ . Also clean with respect to final state interaction is the decay  $\tau^- \rightarrow K_S^0\pi^-\nu_\tau$  studied by Belle [25], with  $K_0^*(800)$  parameters fixed to Ref. 23.

Some authors find a  $K_0^*(800)$  pole in their phenomenological analysis (see, *e.g.*, [21,26–36]), while others do not need to include it in their fits (see, *e.g.*, [16,22,37–39]). Similarly to the case of the  $f_0(500)$  discussed below, all works including constraints from chiral symmetry at low energies naturally seem to find a light  $K_0^*(800)$  below 800 MeV, see, *e.g.*, [40–44]. In these works the  $K_0^*(800)$ ,  $f_0(500)$ ,  $f_0(980)$  and  $a_0(980)$  appear to form a nonet [41,42]. Additional evidence for this assignment is presented in Ref. 11, where the couplings of the nine states to  $\bar{q}q$  sources were compared. The same low lying scalar nonet was also found earlier in the unitarized quark model of Ref. 43. The analysis of Ref. 45 is based on the Roy-Steiner equations, which include analyticity and crossing symmetry. It establishes the existence of a light  $K_0^*(800)$  pole in the  $K\pi \rightarrow K\pi$  amplitude on the second sheet.

**III. The  $I = 1$  States:** Two isovector states are known, the established  $a_0(980)$  and the  $a_0(1450)$ . Independent of any model, the  $K\bar{K}$  component in the  $a_0(980)$  wave function must be large: it lies just below the opening of the  $K\bar{K}$  channel to which it strongly couples [14,46]. This generates an important cusp-like behavior in the resonant amplitude. Hence, its mass and width parameters are strongly distorted. To reveal its true coupling constants, a coupled channel model with energy-dependent widths and mass shift contributions is necessary. All listed  $a_0(980)$  measurements agree on a mass position value near 980 MeV, but the width takes values between 50 and 100 MeV, mostly due to the different models. For example, the analysis of the  $p\bar{p}$ -annihilation data [14] using a unitary  $K$ -matrix description finds a width as determined from the  $T$ -matrix pole of  $92 \pm 8$  MeV, while the observed width of the peak in the  $\pi\eta$  mass spectrum is about 45 MeV.

The relative coupling  $K\bar{K}/\pi\eta$  is determined indirectly from  $f_1(1285)$  [47–49] or  $\eta(1410)$  decays [50–52], from the line shape observed in the  $\pi\eta$  decay mode [54–57], or from the coupled-channel analysis of the  $\pi\pi\eta$  and  $K\bar{K}\pi$  final states of  $p\bar{p}$  annihilation at rest [14].

The  $a_0(1450)$  is seen in  $p\bar{p}$  annihilation experiments with stopped and higher momenta antiprotons, with a mass of about 1450 MeV or close to the  $a_2(1320)$  meson which is typically a dominant feature. A contribution from  $a_0(1450)$  is also found in the analysis of the  $D^\pm \rightarrow K^+K^-\pi^\pm$  decay [58]. The broad structure at about 1300 MeV observed in  $\pi N \rightarrow K\bar{K}N$  reactions [59] needs still further confirmation in its existence and isospin assignment.

**IV. The  $I = 0$  States:** The  $I = 0$ ,  $J^{PC} = 0^{++}$  sector is the most complex one, both experimentally and theoretically. The

## Meson Particle Listings

 $f_0(500)$ 

data have been obtained from  $\pi\pi$ ,  $K\bar{K}$ ,  $\eta\eta$ ,  $4\pi$ , and  $\eta\eta'(958)$  systems produced in  $S$ -wave. Analyses based on several different production processes conclude that probably four poles are needed in the mass range from  $\pi\pi$  threshold to about 1600 MeV. The claimed isoscalar resonances are found under separate entries  $f_0(500)$  (or  $\sigma$ ),  $f_0(980)$ ,  $f_0(1370)$ , and  $f_0(1500)$ .

For discussions of the  $\pi\pi$   $S$  wave below the  $K\bar{K}$  threshold and on the long history of the  $f_0(500)$ , which was suggested in linear sigma models more than 50 years ago, see our reviews in previous editions and the conference proceedings [60].

Information on the  $\pi\pi$   $S$ -wave phase shift  $\delta_J^I = \delta_0^0$  was already extracted many years ago from  $\pi N$  scattering [61–63], and near threshold from the  $K_{e4}$ -decay [64]. The kaon decays were later revisited leading to consistent data, however, with very much improved statistics [65,66]. The reported  $\pi\pi \rightarrow K\bar{K}$  cross sections [67–70] have large uncertainties. The  $\pi N$  data have been analyzed in combination with high-statistics data (see entries labeled as RVUE for re-analyses of the data). The  $2\pi^0$  invariant mass spectra of the  $p\bar{p}$  annihilation at rest [71–73] and the central collision [74] do not show a distinct resonance structure below 900 MeV, but these data are consistently described with the standard solution for  $\pi N$  data [62,75], which allows for the existence of the broad  $f_0(500)$ . An enhancement is observed in the  $\pi^+\pi^-$  invariant mass near threshold in the decays  $D^+ \rightarrow \pi^+\pi^-\pi^+$  [76–103] and  $J/\psi \rightarrow \omega\pi^+\pi^-$  [79,100], and in  $\psi(2S) \rightarrow J/\psi\pi^+\pi^-$  with very limited phase space [81,82].

The precise  $f_0(500)$  (or  $\sigma$ ) pole is difficult to establish because of its large width, and because it can certainly not be modeled by a naive Breit-Wigner resonance. For the same reason a splitting in background and resonance contributions is not possible in a model-independent way. The  $\pi\pi$  scattering amplitude shows an unusual energy dependence due to the presence of a zero in the unphysical regime close to the threshold [5–6], required by chiral symmetry, and possibly due to crossed channel exchanges, the  $f_0(1370)$ , and other dynamical features. However, most of the analyses listed under  $f_0(500)$  agree on a pole position near  $(500 - i250)$  MeV. In particular, analyses of  $\pi\pi$  data that include unitarity,  $\pi\pi$  threshold behavior, strongly constrained by the  $K_{e4}$  data, and the chiral symmetry constraints from Adler zeroes and/or scattering lengths find a light  $f_0(500)$ , see, *e.g.*, [83,84].

Precise pole positions with an uncertainty of less than 20 MeV (see our table for  $T$ -matrix pole) were extracted by use of Roy equations, which are twice subtracted dispersion relations derived from crossing symmetry and analyticity. In Ref. [9] the subtraction constants were fixed to the  $S$ -wave scattering lengths  $a_0^0$  and  $a_2^0$  derived from matching Roy equations and two-loop chiral perturbation theory [8]. The only additional relevant input to fix the  $f_0(500)$  pole turned out to be the  $\pi\pi$ -wave phase shifts at 800 MeV. The analysis was improved further in Ref. 11. Alternatively, in Ref. 10 only data was used as input inside Roy equations. In that reference also once-subtracted Roy-like equations, called GKPY equations,

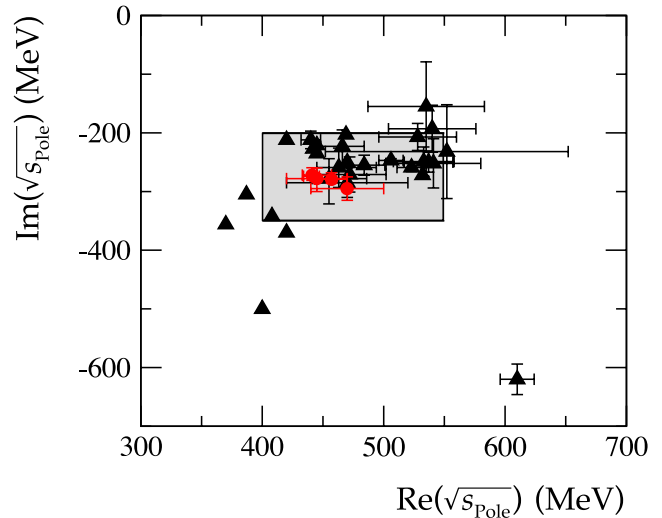


**Figure 1:** Location of the  $f_0(500)$  (or  $\sigma$ ) poles in the complex energy plane. Circles denote the recent analyses based on Roy(-like) dispersion relations [8–11], while all other analyses are denoted by triangles. The corresponding references are given in the listing.

were used, since the extrapolation into the complex plane based on the twice subtracted equations leads to larger uncertainties mainly due to the limited experimental information on the isospin 2  $\pi\pi$  scattering length. All these extractions find consistent results. Using analyticity and unitarity only to describe data from  $K_{2\pi}$  and  $K_{e4}$  decays, Ref. 85 finds consistent values for pole position and scattering length  $a_0^0$ . The importance of the  $\pi\pi$  scattering data for fixing the  $f_0(500)$  pole is nicely illustrated by comparing analyses of  $\bar{p}p \rightarrow 3\pi^0$  omitting [71,86] or including [72,87] information on  $\pi\pi$  scattering: while the former analyses find an extremely broad structure above 1 GeV, the latter find  $f_0(500)$  masses of the order of 400 MeV.

As a result of the sensitivity of the extracted  $f_0(500)$  pole position on the high accuracy low energy  $\pi\pi$  scattering data [65,66], the currently quoted range of pole positions for the  $f_0(500)$ , namely

$$\sqrt{s_{\text{Pole}}} = (400 - 550) - i(200 - 350) \text{ MeV} ,$$

in the listing was fixed including only those analyses consistent with these data, Refs. [29,32,41,43,44,53,56,72], [81–85] and [88–103] as well as the advanced dispersion analyses [8–11]. The pole positions from those references are compared to the range of poles positions quoted above in Fig. 1. Note that this range is labeled as ‘our estimate’ — it is not an average over the quoted analyses but is chosen to include the bulk of the analyses consistent with the mentioned criteria. An averaging procedure is not justified, since the analyses use overlapping or identical data sets.

One might also take the more radical point of view and just average the most advanced dispersive analyses, Refs. [8–11],

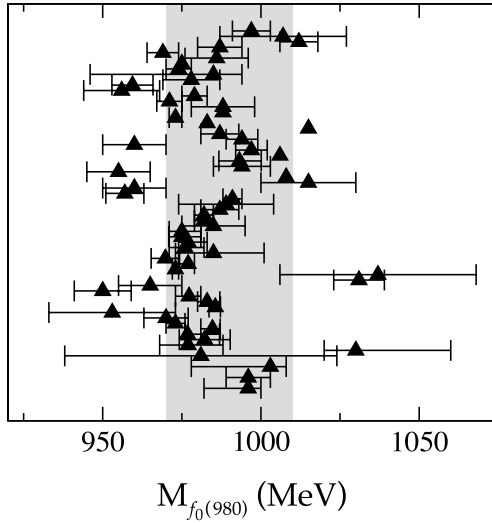


**Figure 2:** Values of the  $f_0(980)$  masses as they appear in the listing compared to the currently quoted mass estimate. The newest references appear at the bottom, the oldest on the top. The corresponding references are given in the listing.

shown as solid dots in Fig. 1, for they provide a determination of the pole positions with minimal bias. This procedure leads to the much more restricted range of  $f_0(500)$  parameters

$$\sqrt{s_{\text{Pole}}^\sigma} = (446 \pm 6) - i(276 \pm 5) \text{ MeV} .$$

Due to the large strong width of the  $f_0(500)$  an extraction of its two-photon width directly from data is not possible. Thus, the values for  $\Gamma(\gamma\gamma)$  quoted in the literature as well as the listing are based on the expression in the narrow width approximation [104]  $\Gamma(\gamma\gamma) \simeq \alpha^2 |g_\gamma|^2 / (4\text{Re}(\sqrt{s_{\text{Pole}}^\sigma}))$  where  $g_\gamma$  is derived from the residue at the  $f_0(500)$  pole to two photons and  $\alpha$  denotes the electromagnetic fine structure constant. The explicit form of the expression may vary between different authors due to different definitions of the coupling constant, however, the expression given for  $\Gamma(\gamma\gamma)$  is free of ambiguities. According to Refs. [105,106], the data for  $f_0(500) \rightarrow \gamma\gamma$  are consistent with what is expected for a two-step process of  $\gamma\gamma \rightarrow \pi^+\pi^-$  via pion exchange in the  $t$ - and  $u$ -channel, followed by a final state interaction  $\pi^+\pi^- \rightarrow \pi^0\pi^0$ . The same conclusion is drawn in Ref. 107 where the bulk part of the  $f_0(500) \rightarrow \gamma\gamma$  decay width is dominated by re-scattering. Therefore, it might be difficult to learn anything new about the nature of the  $f_0(500)$  from its  $\gamma\gamma$  coupling. For the most recent work on  $\gamma\gamma \rightarrow \pi\pi$ , see Refs. [108,109]. There are theoretical indications (e.g., [110–113]) that the  $f_0(500)$  pole behaves differently from a  $q\bar{q}$ -state – see next section for details.

The  $f_0(980)$  overlaps strongly with the background represented mainly by the  $f_0(500)$  and the  $f_0(1370)$ . This can lead to a dip in the  $\pi\pi$  spectrum at the  $K\bar{K}$  threshold. It changes from a dip into a peak structure in the  $\pi^0\pi^0$  invariant mass

spectrum of the reaction  $\pi^-p \rightarrow \pi^0\pi^0n$  [114], with increasing four-momentum transfer to the  $\pi^0\pi^0$  system, which means increasing the  $a_1$ -exchange contribution in the amplitude, while the  $\pi$ -exchange decreases. The  $f_0(500)$  and the  $f_0(980)$  are also observed in data for radiative decays ( $\phi \rightarrow f_0\gamma$ ) from SND [115,116], CMD2 [117], and KLOE [118,119]. Recently a dispersive analysis was used to simultaneously pin down the pole parameters of both the  $f_0(500)$  and the  $f_0(980)$  [10]; the uncertainty in the pole position quoted for the latter state is of the order of 10 MeV, only (see lowest point in Fig. 2). Compared to the 2010 issue of the *Review of Particle Physics*, in this issue we extended the allowed range of  $f_0(980)$  masses to include the mass value derived in Ref. 10. We now quote for the mass

$$M_{f_0(980)} = 990 \pm 20 \text{ MeV} .$$

As in case of the  $f_0(500)$  (or  $\sigma$ ), this range is not an average, but is labeled as 'our estimate'. A comparison of the mass values in the listing and the allocated range is shown in Fig. 2.

Analyses of  $\gamma\gamma \rightarrow \pi\pi$  data [120–122] underline the importance of the  $K\bar{K}$  coupling of  $f_0(980)$ , while the resulting two-photon width of the  $f_0(980)$  cannot be determined precisely [123].

**The  $f_0$ 's above 1 GeV.** A meson resonance that is very well studied experimentally, is the  $f_0(1500)$  seen by the Crystal Barrel experiment in five decay modes:  $\pi\pi$ ,  $K\bar{K}$ ,  $\eta\eta$ ,  $\eta\eta'(958)$ , and  $4\pi$  [14,72,73]. Due to its interference with the  $f_0(1370)$  (and  $f_0(1710)$ ), the peak attributed to  $f_0(1500)$  can appear shifted in invariant mass spectra. Therefore, the application of simple Breit-Wigner forms arrive at slightly different resonance masses for  $f_0(1500)$ . Analyses of central-production data of the likewise five decay modes Refs. [124,125] agree on the description of the  $S$ -wave with the one above. The  $p\bar{p}$ ,  $p\bar{n}/n\bar{p}$  measurements [126–128,73] show a single enhancement at 1400 MeV in the invariant  $4\pi$  mass spectra, which is resolved into  $f_0(1370)$  and  $f_0(1500)$  [129,130]. The data on  $4\pi$  from central production [131] require both resonances, too, but disagree on the relative content of  $\rho\rho$  and  $f_0(500)f_0(500)$  in  $4\pi$ . All investigations agree that the  $4\pi$  decay mode represents about half of the  $f_0(1500)$  decay width and is dominant for  $f_0(1370)$ .

The determination of the  $\pi\pi$  coupling of  $f_0(1370)$  is aggravated by the strong overlap with the broad  $f_0(500)$  and  $f_0(1500)$ . Since it does not show up prominently in the  $2\pi$  spectra, its mass and width are difficult to determine. Multi-channel analyses of hadronically produced two- and three-body final states agree on a mass between 1300 MeV and 1400 MeV and a narrow  $f_0(1500)$ , but arrive at a somewhat smaller width for  $f_0(1370)$ .

Both Belle and BaBar have observed scalars in  $B$  and  $D$  meson decays. They observe broad or narrow structures between 1 and 1.6 GeV in  $K^+K^-$  and  $\pi^+\pi^-$  decays [132–136] (see also [137]). It could be a result of interference of several resonances in this mass range, but lack of statistics prevents an

# Meson Particle Listings

## $f_0(500)$

unambiguous identification of this effect. In  $\gamma\gamma$  collisions the observation of scalars was reported in Refs. [121,138–196].

**V. Interpretation of the scalars below 1 GeV:** In the literature, many suggestions are discussed, such as conventional  $q\bar{q}$  mesons,  $q\bar{q}q\bar{q}$  or meson-meson bound states. In addition one expects a scalar glueball in this mass range. In reality, there can be superpositions of these components, and one often depends on models to determine the dominant one. Although we have seen progress in recent years, this question remains open. Here, we mention some of the present conclusions.

The  $f_0(980)$  and  $a_0(980)$  are often interpreted as multiquark states [140–144] or  $K\bar{K}$  bound states [145]. The insight into their internal structure using two-photon widths [116,146–152] is not conclusive. The  $f_0(980)$  appears as a peak structure in  $J/\psi \rightarrow \phi\pi^+\pi^-$  and in  $D_s$  decays without  $f_0(500)$  background, while being nearly invisible in  $J/\psi \rightarrow \omega\pi^+\pi^-$ . Based on that observation it is suggested that  $f_0(980)$  has a large  $s\bar{s}$  component, which according to Ref. 153 is surrounded by a virtual  $K\bar{K}$  cloud (see also Ref. 154). Data on radiative decays ( $\phi \rightarrow f_0\gamma$  and  $\phi \rightarrow a_0\gamma$ ) from SND, CMD2, and KLOE (see above) are consistent with a prominent role of kaon loops. This observation is interpreted as evidence for a compact four-quark [155] or a molecular [160,156] nature of these states. Details of this controversy are given in the comments [157,158]; see also Ref. 159. It remains quite possible that the states  $f_0(980)$  and  $a_0(980)$ , together with the  $f_0(500)$  and the  $K_0^*(800)$ , form a new low-mass state nonet of predominantly four-quark states, where at larger distances the quarks recombine into a pair of pseudoscalar mesons creating a meson cloud (see *e.g.*, Ref. 161). Different QCD sum rule studies [162–166] do not agree on a tetraquark configuration for the same particle group.

Models that start directly from chiral Lagrangians, either in non-linear [44,28,83,160] or in linear [167–172] realization, predict the existence of the  $f_0(500)$  meson near 500 MeV. Here the  $f_0(500)$ ,  $a_0(980)$ ,  $f_0(980)$ , and  $K_0^*(800)$  (in some models the  $K_0^*(1430)$ ) would form a nonet (not necessarily  $q\bar{q}$ ). In the linear sigma models the lightest pseudoscalars appear as their chiral partners. In these models the light  $f_0(500)$  is often referred to as the "Higgs boson of strong interactions", since here the  $f_0(500)$  plays a role similar to the Higgs particle in electro-weak symmetry breaking: within the linear sigma models it is important for the mechanism of chiral symmetry breaking, which generates most of the proton mass, and what is referred to as the constituent quark mass.

In the non-linear approaches of Ref. 28 [83], the above resonances together with the low lying vector states are generated starting from chiral perturbation theory predictions near the first open channel, and then by extending the predictions to the resonance regions using unitarity and analyticity.

Ref. 167 uses a framework with explicit resonances that are unitarized and coupled to the light pseudo-scalars in a chirally invariant way. Evidence for a non- $q\bar{q}$  nature of the lightest scalar resonances is derived from their mixing scheme. To

identify the nature of the resonances generated from scattering equations, in Ref. 175 the large  $N_c$  behavior of the poles was studied, with the conclusion that, while the light vector states behave consistent with what is predicted for  $q\bar{q}$  states, the light scalars behave very differently. This finding provides strong support for a non- $q\bar{q}$  nature of the light scalar resonances. Note, the more refined study of Ref. 110 found, in case of the  $f_0(500)$ , in addition to a dominant non- $q\bar{q}$  nature, indications for a subdominant  $q\bar{q}$  component located around 1 GeV. A model-independent method to identify hadronic molecules goes back to a proposal by Weinberg [176], shown to be equivalent to the pole counting arguments of Ref. 177 [178] in Ref. 179. The formalism allows one to extract the amount of molecular component in the wave function from the effective coupling constant of a physical state to a nearby continuum channel. It can be applied to near threshold states only and provided strong evidence that the  $f_0(980)$  is a  $\bar{K}K$  molecule, while the situation turned out to be less clear for the  $a_0(980)$  (see also Refs. [152,150]). Further insights into  $a_0(980)$  and  $f_0(980)$  are expected from their mixing [180]. The corresponding signal predicted in Refs. [181,182] was recently observed at BES III [183].

In the unitarized quark model with coupled  $q\bar{q}$  and meson-meson channels, the light scalars can be understood as additional manifestations of bare  $q\bar{q}$  confinement states, strongly mass shifted from the 1.3 - 1.5 GeV region and very distorted due to the strong  $^3P_0$  coupling to  $S$ -wave two-meson decay channels [173–184]. Thus, in these models the light scalar nonet comprising the  $f_0(500)$ ,  $f_0(980)$ ,  $K_0^*(800)$ , and  $a_0(980)$ , as well as the nonet consisting of the  $f_0(1370)$ ,  $f_0(1500)$  (or  $f_0(1710)$ ),  $K_0^*(1430)$ , and  $a_0(1450)$ , respectively, are two manifestations of the same bare input states (see also Ref. 185).

Other models with different groupings of the observed resonances exist and may, *e.g.*, be found in earlier versions of this review.

**VI. Interpretation of the  $f_0$ 's above 1 GeV:** The  $f_0(1370)$  and  $f_0(1500)$  decay mostly into pions ( $2\pi$  and  $4\pi$ ) while the  $f_0(1710)$  decays mainly into  $K\bar{K}$  final states. The  $K\bar{K}$  decay branching ratio of the  $f_0(1500)$  is small [124,186].

If one uses the naive quark model, it is natural to assume that the  $f_0(1370)$ ,  $a_0(1450)$ , and the  $K_0^*(1430)$  are in the same SU(3) flavor nonet, being the  $(u\bar{u} + d\bar{d})$ ,  $u\bar{d}$  and  $u\bar{s}$  states, probably mixing with the light scalars [187], while the  $f_0(1710)$  is the  $s\bar{s}$  state. Indeed, the production of  $f_0(1710)$  (and  $f_2'(1525)$ ) is observed in  $p\bar{p}$  annihilation [188] but the rate is suppressed compared to  $f_0(1500)$  (respectively,  $f_2(1270)$ ), as would be expected from the OZI rule for  $s\bar{s}$  states. The  $f_0(1500)$  would also qualify as  $(u\bar{u} + d\bar{d})$  state, although it is very narrow compared to the other states and too light to be the first radial excitation.

However, in  $\gamma\gamma$  collisions leading to  $K_S^0 K_S^0$  [189] a spin 0 signal is observed at the  $f_0(1710)$  mass (together with a dominant spin 2 component), while the  $f_0(1500)$  is not observed

See key on page 457

in  $\gamma\gamma \rightarrow K\bar{K}$  nor  $\pi^+\pi^-$  [190]. In  $\gamma\gamma$  collisions leading to  $\pi^0\pi^0$  Ref. 138 reports the observation of a scalar around 1470 MeV albeit with large uncertainties on the mass and  $\gamma\gamma$  couplings. This state could be the  $f_0(1370)$  or the  $f_0(1500)$ . The upper limit from  $\pi^+\pi^-$  [190] excludes a large  $n\bar{n}$  (here  $n$  stands for the two lightest quarks) content for the  $f_0(1500)$  and hence points to a mainly  $s\bar{s}$  state [191]. This appears to contradict the small  $K\bar{K}$  decay branching ratio of the  $f_0(1500)$  and makes a  $q\bar{q}$  assignment difficult for this state. Hence the  $f_0(1500)$  could be mainly glue due the absence of a  $2\gamma$ -coupling, while the  $f_0(1710)$  coupling to  $2\gamma$  would be compatible with an  $s\bar{s}$  state. However, the  $2\gamma$ -couplings are sensitive to glue mixing with  $q\bar{q}$  [192].

Note that an isovector scalar, possibly the  $a_0(1450)$  (albeit at a lower mass of 1317 MeV) is observed in  $\gamma\gamma$  collisions leading to  $\eta\pi^0$  [193]. The state interferes destructively with the non-resonant background, but its  $\gamma\gamma$  coupling is comparable to that of the  $a_2(1320)$ , in accord with simple predictions (see, *e.g.*, Ref. 191).

The small width of  $f_0(1500)$ , and its enhanced production at low transverse momentum transfer in central collisions [197–199] also favor  $f_0(1500)$  to be non- $q\bar{q}$ . In the mixing scheme of Ref. 192, which uses central production data from WA102 and the recent hadronic  $J/\psi$  decay data from BES [200,201], glue is shared between  $f_0(1370)$ ,  $f_0(1500)$  and  $f_0(1710)$ . The  $f_0(1370)$  is mainly  $n\bar{n}$ , the  $f_0(1500)$  mainly glue and the  $f_0(1710)$  dominantly  $s\bar{s}$ . This agrees with previous analyses [202,203].

However, alternative schemes have been proposed (*e.g.*, in Ref. 204 [205]; for a review see, *e.g.*, Ref. 1). In particular, for a scalar glueball, the two-gluon coupling to  $n\bar{n}$  appears to be suppressed by chiral symmetry [206] and therefore the  $K\bar{K}$  decay could be enhanced. This mechanism would imply that the  $f_0(1710)$  can possibly be interpreted as an unmixed glueball [207]. In Ref. 208, a large  $K^+K^-$  scalar signal reported by Belle in  $B$  decays into  $KK\bar{K}$  [209], compatible with the  $f_0(1500)$ , is explained as due to constructive interference with a broad glueball background. However, the Belle data are inconsistent with the BaBar measurements which show instead a broad scalar at this mass for  $B$  decays into both  $K^\pm K^\pm K^\mp$  [135] and  $K^+K^-\pi^0$  [210].

Whether the  $f_0(1500)$  is observed in 'gluon rich' radiative  $J/\psi$  decays is debatable [211] because of the limited amount of data - more data for this and the  $\gamma\gamma$  mode are needed.

In Ref. 212  $f_0(1370)$  and  $f_0(1710)$  (together with  $f_2(1270)$  and  $f'_2(1525)$ ) were interpreted as bound systems of two vector mesons. This picture could be tested in radiative  $J/\psi$  decays [213] as well as radiative decays of the states themselves [214].

## References

1. C. Amsler and N.A. Tornqvist, Phys. Reports **389**, 61 (2004).
2. D.V. Bugg, Phys. Reports **397**, 257 (2004).
3. F.E. Close and N.A. Tornqvist, J. Phys. **G28**, R249 (2002).
4. E. Klempt and A. Zaitsev, Phys. Reports **454**, 1 (2007).
5. J.L. Adler, Phys. Rev. **137**, B1022 (1965).
6. J.L. Adler, Phys. Rev. **139**, B1638 (1965).
7. J. A. Oller, Phys. Rev. **D71**, 054030 (2005).
8. G. Colangelo, J. Gasser, and H. Leutwyler, Nucl. Phys. **B603**, 125 (2001).
9. I. Caprini, G. Colangelo, and H. Leutwyler, Phys. Rev. Lett. **96**, 132001 (2006).
10. R. Garcia-Martin *et al.*, Phys. Rev. Lett. **107**, 072001 (2011).
11. B. Moussallam, Eur. Phys. J. **C71**, 1814 (2011).
12. D. Aston *et al.*, Nucl. Phys. **B296**, 493 (1988).
13. P.G. Estabrooks *et al.*, Nucl. Phys. **B133**, 490 (1978).
14. A. Abele *et al.*, Phys. Rev. **D57**, 3860 (1998).
15. V. Bernard, N. Kaiser, and U.-G. Meißner, Phys. Rev. **D43**, 2757 (1991).
16. S.N. Cherry and M.R. Pennington, Nucl. Phys. **A688**, 823 (2001).
17. J.M. Link *et al.*, Phys. Lett. **B648**, 156 (2007).
18. E.M. Aitala *et al.*, Phys. Rev. Lett. **89**, 121801 (2002).
19. E.M. Aitala *et al.*, Phys. Rev. **D73**, 032004 (2006).
20. J.M. Link *et al.*, Phys. Lett. **B525**, 205 (2002).
21. C. Cawlfeld *et al.*, Phys. Rev. **D74**, 031108R (2006).
22. B. Aubert *et al.*, Phys. Rev. **D76**, 011102R (2007).
23. M. Ablikim *et al.*, Phys. Lett. **B633**, 681 (2006).
24. F.K. Guo *et al.*, Nucl. Phys. **A773**, 78 (2006).
25. D. Epifanov *et al.*, Phys. Lett. **B654**, 65 (2007).
26. A.V. Anisovich and A.V. Sarantsev, Phys. Lett. **B413**, 137 (1997).
27. R. Delbourgo *et al.*, Int. J. Mod. Phys. **A13**, 657 (1998).
28. J.A. Oller *et al.*, Phys. Rev. **D60**, 099906E (1999).
29. J.A. Oller and E. Oset, Phys. Rev. **D60**, 074023 (1999).
30. C.M. Shakin and H. Wang, Phys. Rev. **D63**, 014019 (2001).
31. M.D. Scadron *et al.*, Nucl. Phys. **A724**, 391 (2003).
32. D.V. Bugg, Phys. Lett. **B572**, 1 (2003).
33. M. Ishida, Prog. Theor. Phys. Supp. **149**, 190 (2003).
34. H.Q. Zheng *et al.*, Nucl. Phys. **A733**, 235 (2004).
35. Z.Y. Zhou and H.Q. Zheng, Nucl. Phys. **A775**, 212 (2006).
36. J.M. Link *et al.*, Phys. Lett. **B653**, 1 (2007).
37. S. Kopp *et al.*, Phys. Rev. **D63**, 092001 (2001).
38. J.M. Link *et al.*, Phys. Lett. **B535**, 43 (2002).
39. J.M. Link *et al.*, Phys. Lett. **B621**, 72 (2005).
40. M. Jamin *et al.*, Nucl. Phys. **B587**, 331 (2000).
41. D. Black, Phys. Rev. **D64**, 014031 (2001).
42. J. A. Oller, Nucl. Phys. **A727**, 353 (2003).
43. E. Van Beveren *et al.*, Z. Phys. **C30**, 615 (1986).
44. J.R. Pelaez, Mod. Phys. Lett. **A19**, 2879 (2004).
45. S. Descotes-Genon and B. Moussallam, Eur. Phys. J. **C48**, 553 (2006).
46. M. Bargiotti *et al.*, Eur. Phys. J. **C26**, 371 (2003).
47. D. Barberis *et al.*, Phys. Lett. **B440**, 225 (1998).
48. M.J. Corden *et al.*, Nucl. Phys. **B144**, 253 (1978).

## Meson Particle Listings

 $f_0(500)$ 

- 
49. C. Defoix *et al.*, Nucl. Phys. **B44**, 125 (1972).  
50. Z. Bai *et al.*, Phys. Rev. Lett. **65**, 2507 (1990).  
51. T. Bolton *et al.*, Phys. Rev. Lett. **69**, 1328 (1992).  
52. C. Amsler *et al.*, Phys. Lett. **B353**, 571 (1995).  
53. N.A. Tornqvist and M. Roos, Phys. Rev. Lett. **76**, 1575 (1996).  
54. S.M. Flatte, Phys. Lett. **63B**, 224 (1976).  
55. C. Amsler *et al.*, Phys. Lett. **B333**, 277 (1994).  
56. G. Janssen *et al.*, Phys. Rev. **D52**, 2690 (1995).  
57. D.V. Bugg, Phys. Rev. **D78**, 074023 (2008).  
58. P. Rubin *et al.*, Phys. Rev. **D78**, 072003 (2008).  
59. A.D. Martin and E.N. Ozmutlu, Nucl. Phys. **B158**, 520 (1979).  
60. S. Ishida *et al.*, *KEK-Proceedings 2000-4*.  
61. S. D. Protopopescu *et al.*, Phys. Rev. **D7**, 1279 (1973).  
62. G. Grayer *et al.*, Nucl. Phys. **B75**, 189 (1974).  
63. H. Becker *et al.*, Nucl. Phys. **B151**, 46 (1979).  
64. L. Rosselet *et al.*, Phys. Rev. **D15**, 574 (1977).  
65. S. Pislak *et al.*, Phys. Rev. Lett. **87**, 221801 (2001).  
66. J.R. Batley *et al.*, Eur. Phys. J. **C70**, 635 (2010).  
67. W. Wetzel *et al.*, Nucl. Phys. **B115**, 208 (1976).  
68. V.A. Polychronakos *et al.*, Phys. Rev. **D19**, 1317 (1979).  
69. D. Cohen *et al.*, Phys. Rev. **D22**, 2595 (1980).  
70. A. Etkin *et al.*, Phys. Rev. **D25**, 1786 (1982).  
71. C. Amsler *et al.*, Phys. Lett. **B342**, 433 (1995).  
72. C. Amsler *et al.*, Phys. Lett. **B355**, 425 (1995).  
73. A. Abele *et al.*, Phys. Lett. **B380**, 453 (1996).  
74. D.M. Alde *et al.*, Phys. Lett. **B397**, 250 (1997).  
75. R. Kaminski, L. Lesniak, and K. Rybicki, Z. Phys. **C74**, 79 (1997).  
76. E.M. Aitala *et al.*, Phys. Rev. Lett. **86**, 770 (2001).  
77. J.M. Link *et al.*, Phys. Lett. **B585**, 200 (2004).  
78. G. Bonvicini *et al.*, Phys. Rev. **D76**, 012001 (2007).  
79. J.E. Augustin and G. Cosme, Nucl. Phys. **B320**, 1 (1989).  
80. M. Ablikim *et al.*, Phys. Lett. **B598**, 149 (2004).  
81. A. Gallegos *et al.*, Phys. Rev. **D69**, 074033 (2004).  
82. M. Ablikim *et al.*, Phys. Lett. **B645**, 19 (2007).  
83. A. Dobado and J.R. Pelaez, Phys. Rev. **D56**, 3057 (1997).  
84. I. Caprini, Phys. Rev. **D77**, 114019 (2008).  
85. R. Garcia-Martin, J.R. Pelaez, and F.J. Yndurain, Phys. Rev. **D76**, 074034 (2007).  
86. V.V. Anisovich *et al.*, Sov. Phys. Usp. **41**, 419 (1998).  
87. V.V. Anisovich, Int. Jour. of Mod. Phys. A **21**, 3615 (2006).  
88. B.S. Zou and D.V. Bugg, Phys. Rev. **D48**, R3948 (1993).  
89. B.S. Zou and D.V. Bugg, Phys. Rev. **D50**, 3145 (1994).  
90. N.N. Achasov and G.N. Shestakov, Phys. Rev. **D49**, 5779 (1994).  
91. M.P. Locher *et al.*, Eur. Phys. J. **C4**, 317 (1998).  
92. J.A. Oller and E. Oset, Nucl. Phys. **A652**, 407 (1999).  
93. T. Hannah, Phys. Rev. **D60**, 017502 (1999).  
94. R. Kaminski *et al.*, Phys. Rev. **D50**, 3145 (1994).  
95. R. Kaminski *et al.*, Phys. Lett. **B413**, 130 (1997).  
96. R. Kaminski *et al.*, Eur. Phys. J. **C9**, 141 (1999).  
97. M. Ishida *et al.*, Prog. Theor. Phys. **104**, 203 (2000).  
98. Y.S. Surovtsev *et al.*, Phys. Rev. **D61**, 054024 (2001).  
99. M. Ishida *et al.*, Phys. Lett. **B518**, 47 (2001).  
100. M. Ablikim *et al.*, Phys. Lett. **B598**, 149 (2004).  
101. Z.Y. Zhou *et al.*, JHEP **0502**, 043 (2005).  
102. D.V. Bugg *et al.*, J. Phys. **G34**, 151 (2007).  
103. G. Bonvicini *et al.*, Phys. Rev. **D76**, 012001 (2007).  
104. D. Morgan and M. R. Pennington, Z. Phys. **C48**, 623 (1990).  
105. M.R. Pennington, Phys. Rev. Lett. **97**, 011601 (2006).  
106. M.R. Pennington, Mod. Phys. Lett. **A22**, 1439 (2007).  
107. G. Mennessier, S. Narison, and W. Ochs, Phys. Lett. **B665**, 205 (2008).  
108. R. Garcia-Martin and B. Moussallam, Eur. Phys. J. **C70**, 155 (2010).  
109. M. Hoferichter *et al.*, Eur. Phys. J. **C71**, 1743 (2011).  
110. J.R. Pelaez and G. Rios, Phys. Rev. Lett. **97**, 242002 (2006).  
111. H.-X. Chen, A. Hosaka, and S.-L. Zhu, Phys. Lett. **B650**, 369 (2007).  
112. F. Giacosa, Phys. Rev. **D75**, 054007 (2007).  
113. L. Maiani *et al.*, Eur. Phys. J. **C50**, 609 (2007).  
114. N.N. Achasov and G.N. Shestakov, Phys. Rev. **D58**, 054011 (1998).  
115. N.N. Achasov *et al.*, Phys. Lett. **B479**, 53 (2000).  
116. N.N. Achasov *et al.*, Phys. Lett. **B485**, 349 (2000).  
117. R.R. Akhmetshin *et al.*, Phys. Lett. **B462**, 371 (1999).  
118. A. Aloisio *et al.*, Phys. Lett. **B536**, 209 (2002).  
119. F. Ambrosino *et al.*, Eur. Phys. J. **C49**, 473 (2007).  
120. M. Boggione and M.R. Pennington, Eur. Phys. J. **C9**, 11 (1999).  
121. T. Mori *et al.*, Phys. Rev. **D75**, 051101R (2007).  
122. N.N. Achasov and G.N. Shestakov, Phys. Rev. **D77**, 074020 (2008).  
123. M.R. Pennington *et al.*, Eur. Phys. J. **C56**, 1 (2008).  
124. D. Barberis *et al.*, Phys. Lett. **B462**, 462 (1999).  
125. D. Barberis *et al.*, Phys. Lett. **B479**, 59 (2000).  
126. M. Gaspero, Nucl. Phys. **A562**, 407 (1993).  
127. A. Adamo *et al.*, Nucl. Phys. **A558**, 13C (1993).  
128. C. Amsler *et al.*, Phys. Lett. **B322**, 431 (1994).  
129. A. Abele *et al.*, Eur. Phys. J. **C19**, 667 (2001).  
130. A. Abele *et al.*, Eur. Phys. J. **C21**, 261 (2001).  
131. D. Barberis *et al.*, Phys. Lett. **B471**, 440 (2000).  
132. A. Garmash *et al.*, Phys. Rev. **D65**, 092005 (2002).  
133. A. Garmash *et al.*, Phys. Rev. Lett. **96**, 251803 (2006).  
134. A. Garmash *et al.*, Phys. Rev. **D75**, 012006 (2007).  
135. B. Aubert *et al.*, Phys. Rev. **D74**, 032003 (2006).  
136. B. Aubert *et al.*, Phys. Rev. Lett. **99**, 221801 (2007).  
137. E. Klempt, M. Matveev, A.V. Sarantsev, Eur. Phys. J. **C55**, 39 (2008).  
138. S. Uehara *et al.*, Phys. Rev. **D78**, 052004 (2008).  
139. S. Uehara *et al.*, Phys. Rev. **D80**, 032001 (2009).  
140. R. Jaffe, Phys. Rev. **D15**, 267,281 (1977).  
141. M. Alford and R.L. Jaffe, Nucl. Phys. **B578**, 367 (2000).  
142. L. Maiani *et al.*, Phys. Rev. Lett. **93**, 212002 (2004).

See key on page 457

143. L. Maiani, A.D. Polosa, and V. Riquer, Phys. Lett. **B651**, 129 (2007).
144. G. 'tHooft *et al.*, Phys. Lett. **B662**, 424 (2008).
145. J. Weinstein and N. Isgur, Phys. Rev. **D41**, 2236 (1990).
146. T. Barnes, Phys. Lett. **B165**, 434 (1985).
147. Z.P. Li *et al.*, Phys. Rev. **D43**, 2161 (1991).
148. R. Delbourgo, D. Lui, and M. Scadron, Phys. Lett. **B446**, 332 (1999).
149. J.L. Lucio and M. Napsuciale, Phys. Lett. **B454**, 365 (1999).
150. C. Hanhart *et al.*, Phys. Rev. **D75**, 074015 (2007).
151. R.H. Lemmer, Phys. Lett. **B650**, 152 (2007).
152. T. Branz, T. Gutsche, and V. Lyubovitskij, Eur. Phys. J. **A37**, 303 (2008).
153. A. Deandrea *et al.*, Phys. Lett. **B502**, 79 (2001).
154. K.M. Ecklund *et al.*, Phys. Rev. **D80**, 052009 (2010).
155. N. N. Achasov, V. N. Ivanchenko, Nucl. Phys. **B315**, 465 (1989).
156. Y. S. Kalashnikova *et al.*, Eur. Phys. J. **A24**, 437 (2005).
157. Y. S. Kalashnikova *et al.*, Phys. Rev. **D78**, 058501 (2008).
158. N. N. Achasov and A. V. Kiselev, Phys. Rev. **D78**, 058502 (2008).
159. M. Boglione and M.R. Pennington, Eur. Phys. J. **C30**, 503 (2003).
160. J.A. Oller *et al.*, Nucl. Phys. **A714**, 161 (2003).
161. F. Giacosa and G. Pagliara, Phys. Rev. **C76**, 065204 (2007).
162. S. Narison, Nucl. Phys. **B96**, 244 (2001).
163. H.J. Lee, Eur. Phys. J. **A30**, 423 (2006).
164. H.X. Chen, A. Hosaka, and S.L. Zhu, Phys. Rev. **D76**, 094025 (2007).
165. J. Sugiyama *et al.*, Phys. Rev. **D76**, 114010 (2007).
166. T. Kojo and D. Jido, Phys. Rev. **D78**, 114005 (2008).
167. D. Black *et al.*, Phys. Rev. **D59**, 074026 (1999).
168. M. Scadron, Eur. Phys. J. **C6**, 141 (1999).
169. M. Ishida, Prog. Theor. Phys. **101**, 661 (1999).
170. N. Tornqvist, Eur. Phys. J. **C11**, 359 (1999).
171. M. Napsuciale and S. Rodriguez, Phys. Lett. **B603**, 195 (2004).
172. M. Napsuciale and S. Rodriguez, Phys. Rev. **D70**, 094043 (2004).
173. N.A. Tornqvist, Z. Phys. **C68**, 647 (1995).
174. E. Van Beveren and G. Rupp, Eur. Phys. J. **C10**, 469 (1999).
175. J. R. Pelaez, Phys. Rev. Lett. **92**, 102001 (2004).
176. S. Weinberg, Phys. Rev. **130**, 776 (1963).
177. D. Morgan, Nucl. Phys. **A543**, 632 (1992).
178. N. Tornqvist, Phys. Rev. **D51**, 5312 (1995).
179. V. Baru *et al.*, Phys. Lett. **B586**, 53 (2004).
180. N. N. Achasov *et al.*, Phys. Lett. **B88**, 367 (1979).
181. J. -J. Wu *et al.*, Phys. Rev. D **75**, 114012 (2007).
182. C. Hanhart *et al.*, Phys. Rev. **D76**, 074028 (2007).
183. M. Ablikim *et al.*, Phys. Rev. D **83**, 032003 (2011).
184. E. Van Beveren, Eur. Phys. J. **C22**, 493 (2001).
185. M. Boglione and M.R. Pennington, Phys. Rev. **D65**, 114010 (2002).
186. A. Abele *et al.*, Phys. Lett. **B385**, 425 (1996).
187. D. Black *et al.*, Phys. Rev. **D61**, 074001 (2000).
188. C. Amsler *et al.*, Phys. Lett. **B639**, 165 (2006).
189. M. Acciarri *et al.*, Phys. Lett. **B501**, 173 (2001).
190. R. Barate *et al.*, Phys. Lett. **B472**, 189 (2000).
191. C. Amsler, Phys. Lett. **B541**, 22 (2002).
192. F.E. Close and Q. Zhao, Phys. Rev. **D71**, 094022 (2005).
193. S. Uehara *et al.*, Phys. Rev. **D80**, 032001 (2009).
194. H. Nakazawa *et al.*, Phys. Lett. **B615**, 39 (2005).
195. K. Abe *et al.*, Eur. Phys. J. **C32**, 323 (2004).
196. W.T. Chen *et al.*, Phys. Lett. **B651**, 15 (2007).
197. F.E. Close *et al.*, Phys. Lett. **B397**, 333 (1997).
198. F.E. Close, Phys. Lett. **B419**, 387 (1998).
199. A. Kirk, Phys. Lett. **B489**, 29 (2000).
200. M. Ablikim *et al.*, Phys. Lett. **B603**, 138 (2004).
201. M. Ablikim *et al.*, Phys. Lett. **B607**, 243 (2005).
202. C. Amsler and F.E. Close, Phys. Rev. **D53**, 295 (1996).
203. F.E. Close and A. Kirk, Eur. Phys. J. **C21**, 531 (2001).
204. P. Minkowski and W. Ochs, Eur. Phys. J. **C9**, 283 (1999).
205. W. Lee and D. Weingarten, Phys. Rev. **D61**, 014015 (2000).
206. M. Chanowitz, Phys. Rev. Lett. **95**, 172001 (2005).
207. M. Albaladejo and J.A. Oller, Phys. Rev. Lett. **101**, 252002 (2008).
208. P. Minkowski, W. Ochs, Eur. Phys. J. **C39**, 71 (2005).
209. A. Garmash *et al.*, Phys. Rev. **D71**, 092003 (2005).
210. B. Aubert *et al.*, Phys. Rev. Lett. **99**, 161802 (2007).
211. M. Ablikim *et al.*, Phys. Lett. **B642**, 441 (2006).
212. R. Molina *et al.*, Phys. Rev. **D78**, 114018 (2008).
213. L. S. Geng *et al.*, Eur. Phys. J. **A44**, 305 (2010).
214. T. Branz *et al.*, Phys. Rev. **D81**, 054037 (2010).

 $f_0(500)$  T-MATRIX POLE  $\sqrt{s}$ Note that  $\Gamma \approx 2 \text{ Im}(\sqrt{s_{\text{pole}}})$ .

VALUE (MeV)	DOCUMENT ID	TECN	COMMENT
<b>(400–550)–i(200–350) OUR ESTIMATE</b>			
• • • We do not use the following data for averages, fits, limits, etc. • • •			
$(445 \pm 25) - i(278 \pm \frac{22}{18})$	1,2	GARCIA-MAR..11	RVUE Compilation
$(457 \pm \frac{14}{13}) - i(279 \pm \frac{11}{7})$	1,3	GARCIA-MAR..11	RVUE Compilation
$(442 \pm \frac{5}{8}) - i(274 \pm \frac{6}{5})$	4	MOUSSALLAM11	RVUE Compilation
$(452 \pm 13) - i(259 \pm 16)$	5	MENNESSIER 10	RVUE Compilation
$(448 \pm 43) - i(266 \pm 43)$	6	MENNESSIER 10	RVUE Compilation
$(455 \pm 6 \pm \frac{31}{13}) - i(278 \pm 6 \pm \frac{34}{43})$	7	CAPRINI 08	RVUE Compilation
$(463 \pm 6 \pm \frac{31}{17}) - i(259 \pm 6 \pm \frac{33}{34})$	8	CAPRINI 08	RVUE Compilation
$(552 \pm \frac{84}{106}) - i(232 \pm \frac{81}{72})$	9	ABLIKIM 07A	BES2 $\psi(2S) \rightarrow \pi^+ \pi^- J/\psi$
$(466 \pm 18) - i(223 \pm 28)$	10	BONVICINI 07	CLEO $D^+ \rightarrow \pi^+ \pi^- \pi^+$
$(472 \pm 30) - i(271 \pm 30)$	11	BUGG 07A	RVUE Compilation
$(484 \pm 17) - i(255 \pm 10)$		GARCIA-MAR..07	RVUE Compilation
$(430) - i(325)$	12	ANISOVICH 06	RVUE Compilation
$(441 \pm \frac{16}{8}) - i(272 \pm \frac{9}{12.5})$	13	CAPRINI 06	RVUE $\pi\pi \rightarrow \pi\pi$
$(470 \pm 50) - i(285 \pm 25)$	14	ZHOU 05	RVUE
$(541 \pm 39) - i(252 \pm 42)$	15	ABLIKIM 04A	BES2 $J/\psi \rightarrow \omega \pi^+ \pi^-$
$(528 \pm 32) - i(207 \pm 23)$	16	GALLEGOS 04	RVUE Compilation
$(440 \pm 8) - i(212 \pm 15)$	17	PELAEZ 04A	RVUE $\pi\pi \rightarrow \pi\pi$
$(533 \pm 25) - i(249 \pm 25)$	18	BUGG 03	RVUE
517 – i240		BLACK 01	RVUE $\pi^0 \pi^0 \rightarrow \pi^0 \pi^0$
$(470 \pm 30) - i(295 \pm 20)$	13	COLANGELO 01	RVUE $\pi\pi \rightarrow \pi\pi$
$(535 \pm \frac{48}{36}) - i(155 \pm \frac{76}{53})$	19	ISHIDA 01	$\Upsilon(3S) \rightarrow \Upsilon \pi\pi$
$610 \pm 14 - i620 \pm 26$	20	SUROVTSEV 01	RVUE $\pi\pi \rightarrow \pi\pi, K\bar{K}$
$(540 \pm \frac{36}{29}) - i(193 \pm \frac{32}{40})$		ISHIDA 00B	$\rho\bar{\rho} \rightarrow \pi^0 \pi^0 \pi^0$
445 – i235		HANNAH 99	RVUE $\pi$ scalar form factor

## Meson Particle Listings

 $f_0(500)$ 

(523 ± 12) - i(259 ± 7)	KAMINSKI	99	RVUE	$\pi\pi \rightarrow \pi\pi, K\bar{K}, \sigma\sigma$
442 - i 227	OLLER	99	RVUE	$\pi\pi \rightarrow \pi\pi, K\bar{K}$
469 - i203	OLLER	99B	RVUE	$\pi\pi \rightarrow \pi\pi, K\bar{K}$
445 - i221	OLLER	99C	RVUE	$\pi\pi \rightarrow \pi\pi, K\bar{K}, \eta\eta$
(1530 <sup>+</sup> <sub>-250</sub> ) <sup>90</sup> - i(560 ± 40)	ANISOVICH	98B	RVUE	Compilation
420 - i 212	LOCHER	98	RVUE	$\pi\pi \rightarrow \pi\pi, K\bar{K}$
440 - i245	21 DOBADO	97	RVUE	Compilation
(602 ± 26) - i(196 ± 27)	22 ISHIDA	97		$\pi\pi \rightarrow \pi\pi$
(537 ± 20) - i(250 ± 17)	23 KAMINSKI	97B	RVUE	$\pi\pi \rightarrow \pi\pi, K\bar{K}, 4\pi$
470 - i250	24,25 TORNQVIST	96	RVUE	$\pi\pi \rightarrow \pi\pi, K\bar{K}, K\pi, \eta\eta$
387 - i305	25,26 JANSSEN	95	RVUE	$\pi\pi \rightarrow \pi\pi, K\bar{K}$
420 - i370	27 ACHASOV	94	RVUE	$\pi\pi \rightarrow \pi\pi$
(506 ± 10) - i(247 ± 3)	KAMINSKI	94	RVUE	$\pi\pi \rightarrow \pi\pi, K\bar{K}$
370 - i356	28 ZOU	94B	RVUE	$\pi\pi \rightarrow \pi\pi, K\bar{K}$
408 - i342	25,28 ZOU	93	RVUE	$\pi\pi \rightarrow \pi\pi, K\bar{K}$
470 - i208	29 VANBEVEREN	86	RVUE	$\pi\pi \rightarrow \pi\pi, K\bar{K}, \eta\eta, \dots$
(750 ± 50) - i(450 ± 50)	30 ESTABROOKS	79	RVUE	$\pi\pi \rightarrow \pi\pi, K\bar{K}$
(660 ± 100) - i(320 ± 70)	PROTOPOP...	73	HBC	$\pi\pi \rightarrow \pi\pi, K\bar{K}$
650 - i370	31 BASDEVANT	72	RVUE	$\pi\pi \rightarrow \pi\pi$

- 1 Uses the  $K_{e4}$  data of BATLEY 10c and the  $\pi N \rightarrow \pi\pi N$  data of HYAMS 73, GRAYER 74, and PROTOPOESCU 73.
- 2 Analytic continuation using Roy equations.
- 3 Analytic continuation using GKPY equations.
- 4 Using Roy equations.
- 5 Average of three variants of the analytic K-matrix model. Uses the  $K_{e4}$  data of BATLEY 08a and the  $\pi N \rightarrow \pi\pi N$  data of HYAMS 73 and GRAYER 74.
- 6 Average of the analyses of three data sets in the K-matrix model. Uses the data of BATLEY 08a, HYAMS 73, and GRAYER 74, partially of COHEN 80 or ETKIN 82b.
- 7 From the  $K_{e4}$  data of BATLEY 08a and  $\pi N \rightarrow \pi\pi N$  data of HYAMS 73.
- 8 From the  $K_{e4}$  data of BATLEY 08a and  $\pi N \rightarrow \pi\pi N$  data of PROTOPOESCU 73, GRAYER 74, and ESTABROOKS 74.
- 9 From a mean of three different  $f_0(500)$  parametrizations. Uses 40k events.
- 10 From an isobar model using 2.6k events.
- 11 Reanalysis of ABLIKIM 04a, PISLAK 01, and HYAMS 73 data.
- 12 Using the N/D method.
- 13 From the solution of the Roy equation (ROY 71) for the isoscalar S-wave and using a phase-shift analysis of HYAMS 73 and PROTOPOESCU 73 data.
- 14 Reanalysis of the data from PROTOPOESCU 73, ESTABROOKS 74, GRAYER 74, ROSSELET 77, PISLAK 03, and AKHMETSHIN 04.
- 15 From a mean of six different analyses and  $f_0(500)$  parametrizations.
- 16 Using data on  $\psi(2S) \rightarrow J/\psi\pi\pi$  from BAI 00e and on  $\Upsilon(nS) \rightarrow \Upsilon(mS)\pi\pi$  from BUTLER 94b and ALEXANDER 98.
- 17 Reanalysis of data from PROTOPOESCU 73, ESTABROOKS 74, GRAYER 74, and COHEN 80 in the unitarized ChPT model.
- 18 From a combined analysis of HYAMS 73, AUGUSTIN 89, AITALA 01b, and PISLAK 01.
- 19 A similar analysis (KOMADA 01) finds  $(580^{+79}_{-30}) - i(190^{+107}_{-49})$  MeV.
- 20 Coupled channel reanalysis of BATON 70, BENSINGER 71, BAILLON 72, HYAMS 73, HYAMS 75, ROSSELET 77, COHEN 80, and ETKIN 82b using the uniformizing variable.
- 21 Using the inverse amplitude method and data of ESTABROOKS 73, GRAYER 74, and PROTOPOESCU 73.
- 22 Reanalysis of data from HYAMS 73, GRAYER 74, SRINIVASAN 75, and ROSSELET 77 using the interfering amplitude method.
- 23 Average and spread of 4 variants ("up" and "down") of KAMINSKI 97B 3-channel model.
- 24 Uses data from BEIER 72b, OCHS 73, HYAMS 73, GRAYER 74, ROSSELET 77, CASON 83, ASTON 88, and ARMSTRONG 91b. Coupled channel analysis with flavor symmetry and all light two-pseudoscalars systems.
- 25 Demonstrates explicitly that  $f_0(500)$  and  $f_0(1370)$  are two different poles.
- 26 Analysis of data from FALVARD 88.
- 27 Analysis of data from OCHS 73, ESTABROOKS 75, ROSSELET 77, and MUKHIN 80.
- 28 Analysis of data from OCHS 73, GRAYER 74, and ROSSELET 77.
- 29 Coupled-channel analysis using data from PROTOPOESCU 73, HYAMS 73, HYAMS 75, GRAYER 74, ESTABROOKS 74, ESTABROOKS 75, FROGGATT 77, CORDEN 79, BISWAS 81.
- 30 Analysis of data from APEL 73, GRAYER 74, CASON 76, PAWLICKI 77. Includes spread and errors of 4 solutions.
- 31 Analysis of data from BATON 70, BENSINGER 71, COLTON 71, BAILLON 72, PROTOPOESCU 73, and WALKER 67.

 $f_0(500)$  BREIT-WIGNER MASS OR K-MATRIX POLE PARAMETERS

VALUE (MeV)	DOCUMENT ID	TECN	COMMENT
<b>(400-550) OUR ESTIMATE</b>			
513 ± 32	32 MURAMATSU 02	CLEO	$e^+e^- \approx 10$ GeV
478 <sup>+</sup> <sub>-23</sub> ± 17	AITALA	01B E791	$D^+ \rightarrow \pi^-\pi^+\pi^+$
563 <sup>+</sup> <sub>-29</sub>	33 ISHIDA	01	$\Upsilon(3S) \rightarrow \Upsilon\pi\pi$
555	34 ASNER	00 CLE2	$\tau^- \rightarrow \pi^-\pi^0\pi^0\nu_\tau$
540 ± 36	ISHIDA	00B	$p\bar{p} \rightarrow \pi^0\pi^0\pi^0$
750 ± 4	ALEKSEEV	99 SPEC	$1.78 \pi^-\rho_{\text{polar}} \rightarrow \pi^-\pi^+n$
744 ± 5	ALEKSEEV	98 SPEC	$1.78 \pi^-\rho_{\text{polar}} \rightarrow \pi^-\pi^+n$
759 ± 5	35 TROYAN	98	$5.2 n\rho \rightarrow n\rho\pi^+\pi^-$

780 ± 30	ALDE	97	GAM2	450 $p\rho \rightarrow p\rho\pi^0\pi^0$
585 ± 20	36 ISHIDA	97		$\pi\pi \rightarrow \pi\pi$
761 ± 12	37 SVEC	96	RVUE	6-17 $\pi N_{\text{polar}} \rightarrow \pi^+\pi^-N$
~ 860	38,39 TORNQVIST	96	RVUE	$\pi\pi \rightarrow \pi\pi, K\bar{K}, K\pi, \eta\pi$
1165 ± 50	40,41 ANISOVICH	95	RVUE	$\pi^-p \rightarrow \pi^0\pi^0n,$ $\bar{p}p \rightarrow \pi^0\pi^0\pi^0, \pi^0\pi^0\eta,$ $\pi^0\eta\eta$
~ 1000	42 ACHASOV	94	RVUE	$\pi\pi \rightarrow \pi\pi$
414 ± 20	37 AUGUSTIN	89	DM2	

32 Statistical uncertainty only.

33 A similar analysis (KOMADA 01) finds  $526^{+48}_{-37}$  MeV.

34 From the best fit of the Dalitz plot.

35  $6\sigma$  effect, no PWA.

36 Reanalysis of data from HYAMS 73, GRAYER 74, SRINIVASAN 75, and ROSSELET 77 using the interfering amplitude method.

37 Breit-Wigner fit to S-wave intensity measured in  $\pi N \rightarrow \pi^-\pi^+N$  on polarized targets. The fit does not include  $f_0(980)$ .

38 Uses data from ASTON 88, OCHS 73, HYAMS 73, ARMSTRONG 91b, GRAYER 74, CASON 83, ROSSELET 77, and BEIER 72b. Coupled channel analysis with flavor symmetry and all light two-pseudoscalars systems.

39 Also observed by ASNER 00 in  $\tau^- \rightarrow \pi^-\pi^0\pi^0\nu_\tau$  decays.40 Uses  $\pi^0\pi^0$  data from ANISOVICH 94, AMSLER 94d, and ALDE 95b,  $\pi^+\pi^-$  data from OCHS 73, GRAYER 74 and ROSSELET 77, and  $\eta\eta$  data from ANISOVICH 94.41 The pole is on Sheet III. Demonstrates explicitly that  $f_0(500)$  and  $f_0(1370)$  are two different poles.

42 Analysis of data from OCHS 73, ESTABROOKS 75, ROSSELET 77, and MUKHIN 80.

 $f_0(500)$  BREIT-WIGNER WIDTH

VALUE (MeV)	DOCUMENT ID	TECN	COMMENT	
<b>(400-700) OUR ESTIMATE</b>				
• • • We do not use the following data for averages, fits, limits, etc. • • •				
335 ± 67	43 MURAMATSU 02	CLEO	$e^+e^- \approx 10$ GeV	
324 <sup>+</sup> <sub>-40</sub> ± 21	AITALA	01B E791	$D^+ \rightarrow \pi^-\pi^+\pi^+$	
372 <sup>+</sup> <sub>-95</sub>	44 ISHIDA	01	$\Upsilon(3S) \rightarrow \Upsilon\pi\pi$	
540	45 ASNER	00 CLE2	$\tau^- \rightarrow \pi^-\pi^0\pi^0\nu_\tau$	
372 ± 80	ISHIDA	00B	$p\bar{p} \rightarrow \pi^0\pi^0\pi^0$	
119 ± 13	ALEKSEEV	99 SPEC	$1.78 \pi^-\rho_{\text{polar}} \rightarrow \pi^-\pi^+n$	
77 ± 22	ALEKSEEV	98 SPEC	$1.78 \pi^-\rho_{\text{polar}} \rightarrow \pi^-\pi^+n$	
35 ± 12	46 TROYAN	98	$5.2 n\rho \rightarrow n\rho\pi^+\pi^-$	
780 ± 60	ALDE	97	GAM2	450 $p\rho \rightarrow p\rho\pi^0\pi^0$
385 ± 70	47 ISHIDA	97		$\pi\pi \rightarrow \pi\pi$
290 ± 54	48 SVEC	96	RVUE	6-17 $\pi N_{\text{polar}} \rightarrow \pi^+\pi^-N$
~ 880	49,50 TORNQVIST	96	RVUE	$\pi\pi \rightarrow \pi\pi, K\bar{K}, K\pi, \eta\pi$
460 ± 40	51,52 ANISOVICH	95	RVUE	$\pi^-p \rightarrow \pi^0\pi^0n,$ $\bar{p}p \rightarrow \pi^0\pi^0\pi^0, \pi^0\pi^0\eta,$ $\pi^0\eta\eta$
~ 3200	53 ACHASOV	94	RVUE	$\pi\pi \rightarrow \pi\pi$
494 ± 58	48 AUGUSTIN	89	DM2	

43 Statistical uncertainty only.

44 A similar analysis (KOMADA 01) finds  $301^{+145}_{-100}$  MeV.

45 From the best fit of the Dalitz plot.

46  $6\sigma$  effect, no PWA.

47 Reanalysis of data from HYAMS 73, GRAYER 74, SRINIVASAN 75, and ROSSELET 77 using the interfering amplitude method.

48 Breit-Wigner fit to S-wave intensity measured in  $\pi N \rightarrow \pi^-\pi^+N$  on polarized targets. The fit does not include  $f_0(980)$ .

49 Uses data from ASTON 88, OCHS 73, HYAMS 73, ARMSTRONG 91b, GRAYER 74, CASON 83, ROSSELET 77, and BEIER 72b. Coupled channel analysis with flavor symmetry and all light two-pseudoscalars systems.

50 Also observed by ASNER 00 in  $\tau^- \rightarrow \pi^-\pi^0\pi^0\nu_\tau$  decays.51 Uses  $\pi^0\pi^0$  data from ANISOVICH 94, AMSLER 94d, and ALDE 95b,  $\pi^+\pi^-$  data from OCHS 73, GRAYER 74 and ROSSELET 77, and  $\eta\eta$  data from ANISOVICH 94.52 The pole is on Sheet III. Demonstrates explicitly that  $f_0(500)$  and  $f_0(1370)$  are two different poles.

53 Analysis of data from OCHS 73, ESTABROOKS 75, ROSSELET 77, and MUKHIN 80.

 $f_0(500)$  DECAY MODES

Mode	Fraction ( $\Gamma_i/\Gamma$ )
$\Gamma_1$ $\pi\pi$	dominant
$\Gamma_2$ $\gamma\gamma$	seen





## Meson Particle Listings

 $\rho(770)$ 

two-pion mass spectrum in  $\tau$  decays, and the  $e^+e^- \rightarrow \pi^+\pi^-$  cross section, gave indications of discrepancies between the overall normalization:  $\tau$  data are about 3% higher than  $e^+e^-$  data [7,9]. A detailed analysis using such two-pion mass spectra from  $\tau$  decays measured by OPAL [10], CLEO [7], and ALEPH [11,12], as well as recent pion form factor measurements in  $e^+e^-$  annihilation by CMD-2 [13,14], showed that the discrepancy can be as high as 10% above the  $\rho$  meson [15,16]. This discrepancy remains after recent measurements of the two-pion cross section in  $e^+e^-$  annihilation at KLOE [17,18] and SND [19,20]. This effect is not accounted for by isospin breaking [21–24], but the accuracy of its calculation may be overestimated [25,26].

This problem seems to be solved after a recent analysis in [27] which showed that after correcting the  $\tau$  data for the missing  $\rho - \gamma$  mixing contribution, besides the other known isospin symmetry violating corrections, the  $\pi\pi$  I=1 part of the hadronic vacuum polarization contribution to the muon  $g - 2$  is fully compatible between  $\tau$  based and  $e^+e^-$  based evaluations including more recent BaBar [28] and KLOE [29] data. Further proof of the consistency of the data on  $\tau$  decays to two pions and  $e^+e^-$  annihilation is given by the global fit of the whole set of the  $\rho$ ,  $\omega$ , and  $\phi$  decays, taking into account mixing effects in the hidden local symmetry model [30].

## References

- J. Pisut and M. Roos, Nucl. Phys. **B6**, 325 (1968).
- G.D. Lafferty, Z. Phys. **C60**, 659 (1993).
- A. Abele *et al.*, Phys. Lett. **B402**, 195 (1997).
- M. Benayoun *et al.*, Eur. Phys. J. **C31**, 525 (2003).
- R. Barate *et al.*, Z. Phys. **C76**, 15 (1997).
- L.M. Barkov *et al.*, Nucl. Phys. **B256**, 365 (1985).
- S. Anderson *et al.*, Phys. Rev. **D61**, 112002 (2000).
- M. Fujikawa *et al.*, Phys. Rev. **D78**, 072006 (2008).
- S. Eidelman and V. Ivanchenko, Nucl. Phys. (Proc. Supp.) **B76**, 319 (1999).
- K. Akerstaff *et al.*, Eur. Phys. J. **C7**, 571 (1999).
- M. Davier *et al.*, Nucl. Phys. (Proc. Supp.) **B123**, 47 (2003).
- S. Schael *et al.*, Phys. Reports **421**, 191 (2005).
- R.R. Akhmetshin *et al.*, Phys. Lett. **B527**, 161 (2002).
- R.R. Akhmetshin *et al.*, Phys. Lett. **B578**, 285 (2004).
- M. Davier *et al.*, Eur. Phys. J. **C27**, 497 (2003).
- M. Davier *et al.*, Eur. Phys. J. **C31**, 503 (2003).
- A. Aloisio *et al.*, Phys. Lett. **B606**, 12 (2005).
- F. Ambrosino *et al.*, Phys. Lett. **B670**, 285 (2009).
- M.N. Achasov *et al.*, Sov. Phys. JETP **101**, 1053 (2005).
- M.N. Achasov *et al.*, Sov. Phys. JETP **103**, 380 (2006).
- R. Alemany *et al.*, Eur. Phys. J. **C2**, 123 (1998).
- H. Czyz and J.J. Kuhn, Eur. Phys. J. **C18**, 497 (2001).
- V. Cirigliano *et al.*, Phys. Lett. **B513**, 361 (2001).
- V. Cirigliano *et al.*, Eur. Phys. J. **C23**, 121 (2002).
- K. Maltman and C.E. Wolfe, Phys. Rev. **D73**, 013004 (2006).

- C.E. Wolfe and K. Maltman, Phys. Rev. **D80**, 114024 (2009).
- F. Jegerlehner and R. Szafron, Eur. Phys. J. **C71**, 1632 (2011).
- B. Aubert *et al.*, Phys. Rev. Lett. **103**, 231801 (2009).
- F. Ambrosino *et al.*, Phys. Lett. **B700**, 102 (2011).
- M. Benayoun *et al.*, Eur. Phys. J. **C72**, 1848 (2012).

 $\rho(770)$  MASS

We no longer list S-wave Breit-Wigner fits, or data with high combinatorial background.

NEUTRAL ONLY,  $e^+e^-$ 

VALUE (MeV)	EVTS	DOCUMENT ID	TECN	COMMENT
<b>775.49 ± 0.34 OUR AVERAGE</b>				
775.97 ± 0.46 ± 0.70	900k	1 AKHMETSHIN 07		$e^+e^- \rightarrow \pi^+\pi^-$
774.6 ± 0.4 ± 0.5	800k	2,3 ACHASOV 06	SND	$e^+e^- \rightarrow \pi^+\pi^-$
775.65 ± 0.64 ± 0.50	114k	4,5 AKHMETSHIN 04	CMD2	$e^+e^- \rightarrow \pi^+\pi^-$
775.9 ± 0.5 ± 0.5	1.98M	6 ALOISIO 03	KLOE	$1.02 e^+e^- \rightarrow \pi^+\pi^-$
775.8 ± 0.9 ± 2.0	500k	6 ACHASOV 02	SND	$1.02 e^+e^- \rightarrow \pi^+\pi^-$
775.9 ± 1.1		7 BARKOV 85	OLYA	$e^+e^- \rightarrow \pi^+\pi^-$
• • • We do not use the following data for averages, fits, limits, etc. • • •				
775.8 ± 0.5 ± 0.3	1.98M	8 ALOISIO 03	KLOE	$1.02 e^+e^- \rightarrow \pi^+\pi^-$
775.9 ± 0.6 ± 0.5	1.98M	9 ALOISIO 03	KLOE	$1.02 e^+e^- \rightarrow \pi^+\pi^-$
775.0 ± 0.6 ± 1.1	500k	10 ACHASOV 02	SND	$1.02 e^+e^- \rightarrow \pi^+\pi^-$
775.1 ± 0.7 ± 5.3		11 BENAYOUN 98	RVUE	$e^+e^- \rightarrow \pi^+\pi^-$ , $\mu^+\mu^-$
770.5 ± 1.9 ± 5.1		12 GARDNER 98	RVUE	0.28–0.92 $e^+e^- \rightarrow \pi^+\pi^-$
764.1 ± 0.7		13 O'CONNELL 97	RVUE	$e^+e^- \rightarrow \pi^+\pi^-$
757.5 ± 1.5		14 BERNICHA 94	RVUE	$e^+e^- \rightarrow \pi^+\pi^-$
768 ± 1		15 GESHKEN... 89	RVUE	$e^+e^- \rightarrow \pi^+\pi^-$

CHARGED ONLY,  $\tau$  DECAYS and  $e^+e^-$ 

VALUE (MeV)	EVTS	DOCUMENT ID	TECN	CHG	COMMENT
<b>775.11 ± 0.34 OUR AVERAGE</b>					
774.6 ± 0.2 ± 0.5	5.4M	16,17 FUJIKAWA 08	BELL	±	$\tau^- \rightarrow \pi^- \pi^0 \nu_\tau$
775.5 ± 0.7		17,18 SCHAEF 05c	ALEP		$\tau^- \rightarrow \pi^- \pi^0 \nu_\tau$
775.5 ± 0.5 ± 0.4	1.98M	6 ALOISIO 03	KLOE		$1.02 e^+e^- \rightarrow \pi^+\pi^-$
775.1 ± 1.1 ± 0.5	87k	19,20 ANDERSON 00A	CLE2		$\tau^- \rightarrow \pi^- \pi^0 \nu_\tau$
• • • We do not use the following data for averages, fits, limits, etc. • • •					
774.8 ± 0.6 ± 0.4	1.98M	9 ALOISIO 03	KLOE	–	$1.02 e^+e^- \rightarrow \pi^+\pi^-$
776.3 ± 0.6 ± 0.7	1.98M	9 ALOISIO 03	KLOE	+	$1.02 e^+e^- \rightarrow \pi^+\pi^-$
773.9 ± 2.0 ± 0.3 ± 1.0		21 SANZ-CILLERCO3	RVUE		$\tau^- \rightarrow \pi^- \pi^0 \nu_\tau$
774.5 ± 0.7 ± 1.5	500k	6 ACHASOV 02	SND	±	$1.02 e^+e^- \rightarrow \pi^+\pi^-$
775.1 ± 0.5		22 PICH 01	RVUE		$\tau^- \rightarrow \pi^- \pi^0 \nu_\tau$

## MIXED CHARGES, OTHER REACTIONS

VALUE (MeV)	EVTS	DOCUMENT ID	TECN	CHG	COMMENT
<b>763.0 ± 0.3 ± 1.2</b>	600k	23 ABELE 99E	CBAR	0±	0.0 $\bar{p}p \rightarrow \pi^+\pi^-\pi^0$

## CHARGED ONLY, HADROPRODUCED

VALUE (MeV)	EVTS	DOCUMENT ID	TECN	CHG	COMMENT
<b>766.5 ± 1.1 OUR AVERAGE</b>					
763.7 ± 3.2		ABELE 97	CBAR		$\bar{p}n \rightarrow \pi^- \pi^0 \pi^0$
768 ± 9		AGUILAR... 91	EHS		400 $pp$
767 ± 3	2935	24 CAPRARO 87	SPEC	–	200 $\pi^- \text{Cu} \rightarrow \pi^- \pi^0 \text{Cu}$
761 ± 5	967	24 CAPRARO 87	SPEC	–	200 $\pi^- \text{Pb} \rightarrow \pi^- \pi^0 \text{Pb}$
771 ± 4		HUSTON 86	SPEC	+	202 $\pi^+ \text{A} \rightarrow \pi^+ \pi^0 \text{A}$
766 ± 7	6500	25 BYERLY 73	OSPK	–	5 $\pi^- p$
766.8 ± 1.5	9650	26 PISUT 68	RVUE	–	1.7–3.2 $\pi^- p, t < 10$
767 ± 6	900	24 EISNER 67	HBC	–	4.2 $\pi^- p, t < 10$

## NEUTRAL ONLY, PHOTOPRODUCED

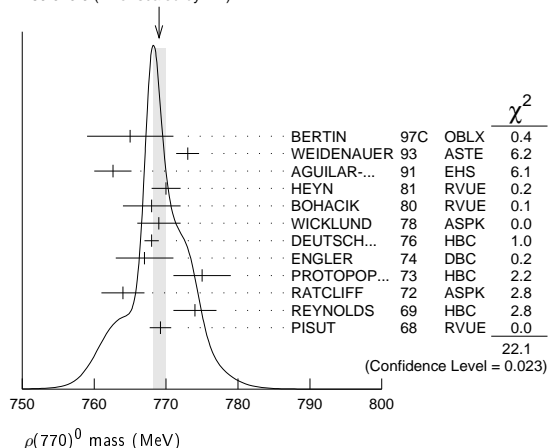
VALUE (MeV)	EVTS	DOCUMENT ID	TECN	CHG	COMMENT
<b>768.5 ± 1.1 OUR AVERAGE</b>					
770 ± 2 ± 1	79k	27 BREITWEG 98B	ZEUS	0	50–100 $\gamma p$
767.6 ± 2.7		BARTALUCCI 78	CNTR	0	$\gamma p \rightarrow e^+e^- p$
775 ± 5		GLADDING 73	CNTR	0	2.9–4.7 $\gamma p$
767 ± 4	1930	BALLAM 72	HBC	0	2.8 $\gamma p$

See key on page 457

770 ± 4	2430	BALLAM	72	HBC	0	4.7 $\gamma p$
765 ± 10		ALVENSLEB...	70	CNTR	0	$\gamma A$ , $t < 0.01$
767.7 ± 1.9	140k	BIGGS	70	CNTR	0	$< 4.1 \gamma C \rightarrow \pi^+ \pi^- C$
765 ± 5	4000	ASBURY	67B	CNTR	0	$\gamma + Pb$
••• We do not use the following data for averages, fits, limits, etc. •••						
771 ± 2	79k	<sup>28</sup> BREITWEG	98B	ZEUS	0	50–100 $\gamma p$

## NEUTRAL ONLY, OTHER REACTIONS

VALUE (MeV)	EVTs	DOCUMENT ID	TECN	CHG	COMMENT
<b>769.0 ± 0.9 OUR AVERAGE</b>					Error includes scale factor of 1.4. See the ideogram below.
765 ± 6		BERTIN 97C	OBLX		0.0 $\bar{p} p \rightarrow \pi^+ \pi^- \pi^0$
773 ± 1.6		WEIDENAUER 93	ASTE		$\bar{p} p \rightarrow \pi^+ \pi^- \omega$
762.6 ± 2.6		AGUILAR-... 91	EHS		400 $p p$
770 ± 2		<sup>29</sup> HEYN 81	RVUE		Pion form factor
768 ± 4		<sup>30,31</sup> BOHACIK 80	RVUE	0	
769 ± 3		<sup>25</sup> WICKLUND 78	ASPK	0	3,4,6 $\pi^\pm N$
768 ± 1	76000	DEUTSCH... 76	HBC	0	16 $\pi^+ p$
767 ± 4	4100	ENGLER 74	DBC	0	6 $\pi^+ n \rightarrow \pi^+ \pi^- p$
775 ± 4	32000	<sup>30</sup> PROTOPOP... 73	HBC	0	7.1 $\pi^+ p$ , $t < 0.4$
764 ± 3	6800	RATCLIFF 72	ASPK	0	15 $\pi^- p$ , $t < 0.3$
774 ± 3	1700	REYNOLDS 69	HBC	0	2.26 $\pi^- p$
769.2 ± 1.5	13300	<sup>32</sup> PISUT 68	RVUE	0	1.7–3.2 $\pi^- p$ , $t < 10$
••• We do not use the following data for averages, fits, limits, etc. •••					
773.5 ± 2.5		<sup>33</sup> COLANGELO 01	RVUE		$\pi \pi \rightarrow \pi \pi$
762.3 ± 0.5 ± 1.2	600k	<sup>34</sup> ABELE 99E	CBAR	0	0.0 $\bar{p} p \rightarrow \pi^+ \pi^- \pi^0$
777 ± 2	4943	<sup>35</sup> ADAMS 97	E665		470 $\mu p \rightarrow \mu X B$
770 ± 2		<sup>36</sup> BOGOLYUB... 97	MIRA		32 $\bar{p} p \rightarrow \pi^+ \pi^- X$
768 ± 8		<sup>36</sup> BOGOLYUB... 97	MIRA		32 $p p \rightarrow \pi^+ \pi^- X$
761.1 ± 2.9		DUBNICKA 89	RVUE		$\pi$ form factor
777.4 ± 2.0		<sup>37</sup> CHABAUD 83	ASPK	0	17 $\pi^- p$ polarized
769.5 ± 0.7		<sup>30,31</sup> LANG 79	RVUE	0	
770 ± 9		<sup>31</sup> ESTABROOKS 74	RVUE	0	17 $\pi^- p \rightarrow \pi^+ \pi^- n$
773.5 ± 1.7	11200	<sup>24</sup> JACOBS 72	HBC	0	2.8 $\pi^- p$
775 ± 3	2250	HYAMS 68	OSPK	0	11.2 $\pi^- p$

WEIGHTED AVERAGE  
769.0 ± 0.9 (Error scaled by 1.4)

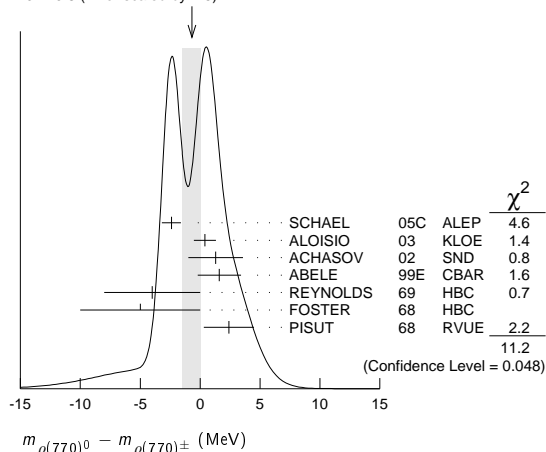
- 1 A combined fit of AKHMETSHIN 07, AULCHENKO 06, and AULCHENKO 05.
- 2 Supersedes ACHASOV 05A.
- 3 A fit of the SND data from 400 to 1000 MeV using parameters of the  $\rho(1450)$  and  $\rho(1700)$  from a fit of the data of BARKOV 85, BISELLO 89 and ANDERSON 00A.
- 4 Using the GOUNARIS 68 parametrization with the complex phase of the  $\rho$ - $\omega$  interference.
- 5 Update of AKHMETSHIN 02.
- 6 Assuming  $m_{\rho^+} = m_{\rho^-}$ ,  $\Gamma_{\rho^+} = \Gamma_{\rho^-}$ .
- 7 From the GOUNARIS 68 parametrization of the pion form factor.
- 8 Assuming  $m_{\rho^+} = m_{\rho^-} = m_{\rho^0}$ ,  $\Gamma_{\rho^+} = \Gamma_{\rho^-} = \Gamma_{\rho^0}$ .
- 9 Without limitations on masses and widths.
- 10 Assuming  $m_{\rho^0} = m_{\rho^\pm}$ ,  $g_{\rho^0 \pi \pi} = g_{\rho^\pm \pi \pi}$ .
- 11 Using the data of BARKOV 85 in the hidden local symmetry model.
- 12 From the fit to  $e^+ e^- \rightarrow \pi^+ \pi^-$  data from the compilations of HEYN 81 and BARKOV 85, including the GOUNARIS 68 parametrization of the pion form factor.
- 13 A fit of BARKOV 85 data assuming the direct  $\omega \pi \pi$  coupling.
- 14 Applying the S-matrix formalism to the BARKOV 85 data.
- 15 Includes BARKOV 85 data. Model-dependent width definition.
- 16  $|F_\pi(0)|^2$  fixed to 1.
- 17 From the GOUNARIS 68 parametrization of the pion form factor.
- 18 The error combines statistical and systematic uncertainties. Supersedes BARATE 97M.
- 19  $\rho(1700)$  mass and width fixed at 1700 MeV and 235 MeV respectively.
- 20 From the GOUNARIS 68 parametrization of the pion form factor. The second error is a model error taking into account different parametrizations of the pion form factor.
- 21 Using the data of BARATE 97M and the effective chiral Lagrangian.
- 22 From a fit of the model-independent parameterization of the pion form factor to the data of BARATE 97M.

- 23 Assuming the equality of  $\rho^+$  and  $\rho^-$  masses and widths.
- 24 Mass errors enlarged by us to  $\Gamma/\sqrt{N}$ ; see the note with the  $K^*(892)$  mass.
- 25 Phase shift analysis. Systematic errors added corresponding to spread of different fits.
- 26 From fit of 3-parameter relativistic P-wave Breit-Wigner to total mass distribution. Includes BATON 68, MILLER 67B, ALFF-STEINBERGER 66, HAGOPIAN 66, HAGOPIAN 66B, JACOBS 66B, JAMES 66, WEST 66, BLIEDEN 65 and CARMONY 64.
- 27 From the parametrization according to SOEDING 66.
- 28 From the parametrization according to ROSS 66.
- 29 HEYN 81 includes all spacelike and timelike  $F_\pi$  values until 1978.
- 30 From pole extrapolation.
- 31 From phase shift analysis of GRAYER 74 data.
- 32 Includes MALAMUD 69, ARMENISE 68, BACON 67, HUWE 67, MILLER 67B, ALFF-STEINBERGER 66, HAGOPIAN 66, HAGOPIAN 66B, JACOBS 66B, JAMES 66, WEST 66, GOLDBABER 64, ABOLINS 63.
- 33 Breit-Wigner mass from a phase-shift analysis of HYAMS 73 and PROTOPODESCU 73 data.
- 34 Using relativistic Breit-Wigner and taking into account  $\rho$ - $\omega$  interference.
- 35 Systematic errors not evaluated.
- 36 Systematic effects not studied.
- 37 From fit of 3-parameter relativistic Breit-Wigner to helicity-zero part of P-wave intensity. CHABAUD 83 includes data of GRAYER 74.

 $m_{\rho(770)^0} - m_{\rho(770)^\pm}$ 

VALUE (MeV)	EVTs	DOCUMENT ID	TECN	CHG	COMMENT
<b>-0.7 ± 0.8 OUR AVERAGE</b>					Error includes scale factor of 1.5. See the ideogram below.
-2.4 ± 0.8		<sup>38</sup> SCHAELE 05c	ALEP		$\tau^- \rightarrow \pi^- \pi^0 \nu_\tau$
0.4 ± 0.7 ± 0.6	1.98M	<sup>39</sup> ALOISIO 03	KLOE		1.02 $e^+ e^- \rightarrow \pi^+ \pi^- \pi^0$
1.3 ± 1.1 ± 2.0	500k	<sup>39</sup> ACHASOV 02	SND		1.02 $e^+ e^- \rightarrow \pi^+ \pi^- \pi^0$
1.6 ± 0.6 ± 1.7	600k	ABELE 99E	CBAR	0 ±	0.0 $\bar{p} p \rightarrow \pi^+ \pi^- \pi^0$
-4 ± 4	3000	<sup>40</sup> REYNOLDS 69	HBC	-0	2.26 $\pi^- p$
-5 ± 5	3600	<sup>40</sup> FOSTER 68	HBC	± 0	0.0 $\bar{p} p$
2.4 ± 2.1	22950	<sup>41</sup> PISUT 68	RVUE		$\pi N \rightarrow \rho N$

- 38 From the combined fit of the  $\tau^-$  data from ANDERSON 00A and SCHAELE 05c and  $e^+ e^-$  data from the compilation of BARKOV 85, AKHMETSHIN 04, and ALOISIO 05. Supersedes BARATE 97M.
- 39 Assuming  $m_{\rho^+} = m_{\rho^-}$ ,  $\Gamma_{\rho^+} = \Gamma_{\rho^-}$ .
- 40 From quoted masses of charged and neutral modes.
- 41 Includes MALAMUD 69, ARMENISE 68, BATON 68, BACON 67, HUWE 67, MILLER 67B, ALFF-STEINBERGER 66, HAGOPIAN 66, HAGOPIAN 66B, JACOBS 66B, JAMES 66, WEST 66, BLIEDEN 65, CARMONY 64, GOLDBABER 64, ABOLINS 63.

WEIGHTED AVERAGE  
-0.7 ± 0.8 (Error scaled by 1.5) $m_{\rho(770)^+} - m_{\rho(770)^-}$ 

VALUE (MeV)	EVTs	DOCUMENT ID	TECN	COMMENT
••• We do not use the following data for averages, fits, limits, etc. •••				
1.5 ± 0.8 ± 0.7	1.98M	<sup>42</sup> ALOISIO 03	KLOE	1.02 $e^+ e^- \rightarrow \pi^+ \pi^- \pi^0$
42 Without limitations on masses and widths.				

 $\rho(770)$  RANGE PARAMETER

The range parameter  $R$  enters an energy-dependent correction to the width, of the form  $(1 + q^2 R^2) / (1 + q^2 R^2)$ , where  $q$  is the momentum of one of the pions in the  $\pi\pi$  rest system. At resonance,  $q = q_r$ .

VALUE (GeV <sup>-1</sup> )	DOCUMENT ID	TECN	CHG	COMMENT
<b>5.3 ± 0.9</b> <b>-0.7</b>	CHABAUD 83	ASPK	0	17 $\pi^- p$ polarized

# Meson Particle Listings

## $\rho(770)$

### $\rho(770)$ WIDTH

We no longer list S-wave Breit-Wigner fits, or data with high combinatorial background.

#### NEUTRAL ONLY, $e^+e^-$

VALUE (MeV)	EVTS	DOCUMENT ID	TECN	CHG	COMMENT
<b>146.2 ± 0.7 OUR AVERAGE</b> Error includes scale factor of 1.1.					
145.98 ± 0.75 ± 0.50	900k	43 AKHMETSHIN 07			$e^+e^- \rightarrow \pi^+\pi^-$
146.1 ± 0.8 ± 1.5	800k	44,45 ACHASOV 06	SND		$e^+e^- \rightarrow \pi^+\pi^-$
143.85 ± 1.33 ± 0.80	114k	46,47 AKHMETSHIN 04	CMD2		$e^+e^- \rightarrow \pi^+\pi^-$
147.3 ± 1.5 ± 0.7	1.98M	48 ALOISIO 03	KLOE		$1.02 e^+e^- \rightarrow \pi^+\pi^- \pi^0$
151.1 ± 2.6 ± 3.0	500k	48 ACHASOV 02	SND	0	$1.02 e^+e^- \rightarrow \pi^+\pi^- \pi^0$
150.5 ± 3.0		49 BARKOV 85	OLYA	0	$e^+e^- \rightarrow \pi^+\pi^-$
••• We do not use the following data for averages, fits, limits, etc. •••					
143.9 ± 1.3 ± 1.1	1.98M	50 ALOISIO 03	KLOE		$1.02 e^+e^- \rightarrow \pi^+\pi^- \pi^0$
147.4 ± 1.5 ± 0.7	1.98M	51 ALOISIO 03	KLOE		$1.02 e^+e^- \rightarrow \pi^+\pi^- \pi^0$
149.8 ± 2.2 ± 2.0	500k	52 ACHASOV 02	SND		$1.02 e^+e^- \rightarrow \pi^+\pi^- \pi^0$
147.9 ± 1.5 ± 7.5		53 BENAYOUN 98	RVUE		$e^+e^- \rightarrow \pi^+\pi^- \mu^+\mu^-$
153.5 ± 1.3 ± 4.6		54 GARDNER 98	RVUE		$0.28-0.92 e^+e^- \rightarrow \pi^+\pi^- \mu^+\mu^-$
145.0 ± 1.7		55 O'CONNELL 97	RVUE		$e^+e^- \rightarrow \pi^+\pi^-$
142.5 ± 3.5		56 BERNICHA 94	RVUE		$e^+e^- \rightarrow \pi^+\pi^-$
138 ± 1		57 GESKEN... 89	RVUE		$e^+e^- \rightarrow \pi^+\pi^-$

#### CHARGED ONLY, $\tau$ DECAYS and $e^+e^-$

VALUE (MeV)	EVTS	DOCUMENT ID	TECN	CHG	COMMENT
<b>149.1 ± 0.8 OUR FIT</b>					
<b>149.1 ± 0.8 OUR AVERAGE</b>					
148.1 ± 0.4 ± 1.7	5.4M	58,59 FUJIKAWA 08	BELL	±	$\tau^- \rightarrow \pi^- \pi^0 \nu_\tau$
149.0 ± 1.2		59,60 SCHAEEL 05c	ALEP		$\tau^- \rightarrow \pi^- \pi^0 \nu_\tau$
149.4 ± 2.3 ± 2.0	500k	48 ACHASOV 02	SND	±	$1.02 e^+e^- \rightarrow \pi^+\pi^- \pi^0$
150.4 ± 1.4 ± 1.4	87k	61,62 ANDERSON 00a	CLE2		$\tau^- \rightarrow \pi^- \pi^0 \nu_\tau$
••• We do not use the following data for averages, fits, limits, etc. •••					
143.7 ± 1.3 ± 1.2	1.98M	48 ALOISIO 03	KLOE	±	$1.02 e^+e^- \rightarrow \pi^+\pi^- \pi^0$
142.9 ± 1.3 ± 1.4	1.98M	51 ALOISIO 03	KLOE	-	$1.02 e^+e^- \rightarrow \pi^+\pi^- \pi^0$
144.7 ± 1.4 ± 1.2	1.98M	51 ALOISIO 03	KLOE	+	$1.02 e^+e^- \rightarrow \pi^+\pi^- \pi^0$
150.2 ± 2.0 ± 0.7		63 SANZ-CILLERO3	RVUE		$\tau^- \rightarrow \pi^- \pi^0 \nu_\tau$
150.9 ± 2.2 ± 2.0	500k	52 ACHASOV 02	SND		$1.02 e^+e^- \rightarrow \pi^+\pi^- \pi^0$

#### MIXED CHARGES, OTHER REACTIONS

VALUE (MeV)	EVTS	DOCUMENT ID	TECN	CHG	COMMENT
<b>149.5 ± 1.3</b>	600k	64 ABELE 99E	CBAR	0±	$0.0 \bar{p}p \rightarrow \pi^+\pi^- \pi^0$

#### CHARGED ONLY, HADROPRODUCED

VALUE (MeV)	EVTS	DOCUMENT ID	TECN	CHG	COMMENT
<b>150.2 ± 2.4 OUR FIT</b>					
<b>150.2 ± 2.4 OUR AVERAGE</b>					
152.8 ± 4.3		ABELE 97	CBAR		$\bar{p}n \rightarrow \pi^- \pi^0 \pi^0$
155 ± 11	2935	65 CAPRARO 87	SPEC	-	$200 \pi^- \text{Cu} \rightarrow \pi^- \pi^0 \text{Cu}$
154 ± 20	967	65 CAPRARO 87	SPEC	-	$200 \pi^- \text{Pb} \rightarrow \pi^- \pi^0 \text{Pb}$
150 ± 5		HUSTON 86	SPEC	+	$202 \pi^+ \text{A} \rightarrow \pi^+ \pi^0 \text{A}$
146 ± 12	6500	66 BYERLY 73	OSPK	-	$5 \pi^- p$
148.2 ± 4.1	9650	67 PISUT 68	RVUE	-	$1.7-3.2 \pi^- p, t < 10$
146 ± 13	900	EISNER 67	HBC	-	$4.2 \pi^- p, t < 10$

#### NEUTRAL ONLY, PHOTOPRODUCED

VALUE (MeV)	EVTS	DOCUMENT ID	TECN	CHG	COMMENT
<b>150.7 ± 2.9 OUR AVERAGE</b>					
146 ± 3 ± 13	79k	68 BREITWEG 98B	ZEUS	0	50-100 $\gamma p$
150.9 ± 3.0		BARTALUCCI 78	CNTR	0	$\gamma p \rightarrow e^+e^- p$
••• We do not use the following data for averages, fits, limits, etc. •••					
138 ± 3	79k	69 BREITWEG 98B	ZEUS	0	50-100 $\gamma p$
147 ± 11		GLADDING 73	CNTR	0	2.9-4.7 $\gamma p$
155 ± 12	2430	BALLAM 72	HBC	0	4.7 $\gamma p$
145 ± 13	1930	BALLAM 72	HBC	0	2.8 $\gamma p$
140 ± 5		ALVENSLEB... 70	CNTR	0	$\gamma A, t < 0.01$
146.1 ± 2.9	140k	BIGGS 70	CNTR	0	$< 4.1 \gamma C \rightarrow \pi^+\pi^- C$
160 ± 10		LANZEROTTI 68	CNTR	0	$\gamma p$
130 ± 5	4000	ASBURY 67B	CNTR	0	$\gamma + Pb$

#### NEUTRAL ONLY, OTHER REACTIONS

VALUE (MeV)	EVTS	DOCUMENT ID	TECN	CHG	COMMENT
<b>150.9 ± 1.7 OUR AVERAGE</b> Error includes scale factor of 1.1.					
122 ± 20		BERTIN 97c	OBLX		$0.0 \bar{p}p \rightarrow \pi^+\pi^- \pi^0$
145.7 ± 5.3		WEIDENAUER 93	ASTE		$\bar{p}p \rightarrow \pi^+\pi^- \omega$
144.9 ± 3.7		DUBNICKA 89	RVUE		$\pi$ form factor
148 ± 6		70,71 BOHACIK 80	RVUE	0	
152 ± 9		66 WICKLUND 78	ASPK	0	$3.4, 6 \pi^\pm p N$
154 ± 2	76000	DEUTSCH... 76	HBC	0	$16 \pi^+ p$
157 ± 8	6800	RATCLIFF 72	ASPK	0	$15 \pi^- p, t < 0.3$
143 ± 8	1700	REYNOLDS 69	HBC	0	$2.26 \pi^- p$
••• We do not use the following data for averages, fits, limits, etc. •••					
147.0 ± 2.5	600k	72 ABELE 99E	CBAR	0	$0.0 \bar{p}p \rightarrow \pi^+\pi^- \pi^0$
146 ± 3	4943	73 ADAMS 97	E665		$470 \mu p \rightarrow \mu XB$
160.0 ± 4.1		74 CHABAUD 83	ASPK	0	$17 \pi^- p$ polarized
155 ± 1		75 HEYN 81	RVUE	0	$\pi$ form factor
148.0 ± 1.3		70,71 LANG 79	RVUE	0	
146 ± 14	4100	ENGLER 74	DBC	0	$6 \pi^+ n \rightarrow \pi^+\pi^- p$
143 ± 13		71 ESTABROOKS 74	RVUE	0	$17 \pi^- p \rightarrow \pi^+\pi^- n$
160 ± 10	32000	70 PROTOPOP... 73	HBC	0	$7.1 \pi^+ p, t < 0.4$
145 ± 12	2250	65 HYAMS 68	OSPK	0	$11.2 \pi^- p$
163 ± 15	13300	76 PISUT 68	RVUE	0	$1.7-3.2 \pi^- p, t < 10$

43 A combined fit of AKHMETSHIN 07, AULCHENKO 06, and AULCHENKO 05.  
 44 Supersedes ACHASOV 05A.  
 45 A fit of the SND data from 400 to 1000 MeV using parameters of the  $\rho(1450)$  and  $\rho(1700)$  from a fit of the data of BARKOV 85, BISELLO 89 and ANDERSON 00A.  
 46 Using the GOUNARIS 68 parametrization with the complex phase of the  $\rho\omega$  interference.  
 47 From a fit in the energy range 0.61 to 0.96 GeV. Update of AKHMETSHIN 02.  
 48 Assuming  $m_{\rho^+} = m_{\rho^-}, \Gamma_{\rho^+} = \Gamma_{\rho^-}$ .  
 49 From the GOUNARIS 68 parametrization of the pion form factor.  
 50 Assuming  $m_{\rho^+} = m_{\rho^-} = m_{\rho^0}, \Gamma_{\rho^+} = \Gamma_{\rho^-} = \Gamma_{\rho^0}$ .  
 51 Without limitations on masses and widths.  
 52 Assuming  $m_{\rho^0} = m_{\rho^\pm}, g_{\rho^0} \pi\pi = g_{\rho^\pm} \pi\pi$ .  
 53 Using the data of BARKOV 85 in the hidden local symmetry model.  
 54 From the fit to  $e^+e^- \rightarrow \pi^+\pi^-$  data from the compilations of HEYN 81 and BARKOV 85, including the GOUNARIS 68 parametrization of the pion form factor.  
 55 A fit of BARKOV 85 data assuming the direct  $\omega\pi\pi$  coupling.  
 56 Applying the S-matrix formalism to the BARKOV 85 data.  
 57 Includes BARKOV 85 data. Model-dependent width definition.  
 58  $|F_\pi(0)|^2$  fixed to 1.  
 59 From the GOUNARIS 68 parametrization of the pion form factor.  
 60 The error combines statistical and systematic uncertainties. Supersedes BARATE 97M.  
 61  $\rho(1700)$  mass and width fixed at 1700 MeV and 235 MeV respectively.  
 62 From the GOUNARIS 68 parametrization of the pion form factor. The second error is a model error taking into account different parametrizations of the pion form factor.  
 63 Using the data of BARATE 97M and the effective chiral Lagrangian.  
 64 Assuming the equality of  $\rho^+$  and  $\rho^-$  masses and widths.  
 65 Width errors enlarged by us to  $4\Gamma/\sqrt{N}$ ; see the note with the  $K^*(892)$  mass.  
 66 Phase shift analysis. Systematic errors added corresponding to spread of different fits.  
 67 From fit of 3-parameter relativistic P-wave Breit-Wigner to total mass distribution. Includes BATON 68, MILLER 67B, ALFF-STEINBERGER 66, HAGOPIAN 66, HAGOPIAN 66B, JACOBS 66B, JAMES 66, WEST 66, BLIEDEN 65 and CARMONY 64.  
 68 From the parametrization according to SOEDING 66.  
 69 From the parametrization according to ROSS 66.  
 70 From pole extrapolation.  
 71 From phase shift analysis of GRAYER 74 data.  
 72 Using relativistic Breit-Wigner and taking into account  $\rho\omega$  interference.  
 73 Systematic errors not evaluated.  
 74 From fit of 3-parameter relativistic Breit-Wigner to helicity-zero part of P-wave intensity. CHABAUD 83 includes data of GRAYER 74.  
 75 HEYN 81 includes all spacelike and timelike  $F_\pi$  values until 1978.  
 76 Includes MALAMUD 69, ARMENISE 68, BACON 67, HUWE 67, MILLER 67B, ALFF-STEINBERGER 66, HAGOPIAN 66, HAGOPIAN 66B, JACOBS 66B, JAMES 66, WEST 66, GOLDHABER 64, ABOLINS 63.

#### $\Gamma_{\rho(770)^0} - \Gamma_{\rho(770)^\pm}$

VALUE	EVTS	DOCUMENT ID	TECN	COMMENT
<b>0.3 ± 1.3 OUR AVERAGE</b> Error includes scale factor of 1.4.				
-0.2 ± 1.0		77 SCHAEEL 05c	ALEP	$\tau^- \rightarrow \pi^- \pi^0 \nu_\tau$
3.6 ± 1.8 ± 1.7	1.98M	78 ALOISIO 03	KLOE	$1.02 e^+e^- \rightarrow \pi^+\pi^- \pi^0$

#### $\Gamma_{\rho(770)^+} - \Gamma_{\rho(770)^-}$

VALUE	EVTS	DOCUMENT ID	TECN	COMMENT
<b>1.8 ± 2.0 ± 0.5</b>				
1.98M	79	ALOISIO 03	KLOE	$1.02 e^+e^- \rightarrow \pi^+\pi^- \pi^0$
77 From the combined fit of the $\tau^-$ data from ANDERSON 00a and SCHAEEL 05c and $e^+e^-$ data from the compilation of BARKOV 85, AKHMETSHIN 04, and ALOISIO 05. Supersedes BARATE 97M. 78 Assuming $m_{\rho^+} = m_{\rho^-}, \Gamma_{\rho^+} = \Gamma_{\rho^-}$ . 79 Without limitations on masses and widths.				

$\rho(770)$  DECAY MODES

Mode	Fraction ( $\Gamma_i/\Gamma$ )	Scale factor/ Confidence level
$\Gamma_1$ $\pi\pi$	$\sim 100$	%
<b><math>\rho(770)^\pm</math> decays</b>		
$\Gamma_2$ $\pi^\pm\pi^0$	$\sim 100$	%
$\Gamma_3$ $\pi^\pm\gamma$	$(4.5 \pm 0.5)$	$\times 10^{-4}$ S=2.2
$\Gamma_4$ $\pi^\pm\eta$	$< 6$	$\times 10^{-3}$ CL=84%
$\Gamma_5$ $\pi^\pm\pi^+\pi^-\pi^0$	$< 2.0$	$\times 10^{-3}$ CL=84%
<b><math>\rho(770)^0</math> decays</b>		
$\Gamma_6$ $\pi^+\pi^-$	$\sim 100$	%
$\Gamma_7$ $\pi^+\pi^-\gamma$	$(9.9 \pm 1.6)$	$\times 10^{-3}$
$\Gamma_8$ $\pi^0\gamma$	$(6.0 \pm 0.8)$	$\times 10^{-4}$
$\Gamma_9$ $\eta\gamma$	$(3.00 \pm 0.20)$	$\times 10^{-4}$
$\Gamma_{10}$ $\pi^0\pi^0\gamma$	$(4.5 \pm 0.8)$	$\times 10^{-5}$
$\Gamma_{11}$ $\mu^+\mu^-$	[a]	$(4.55 \pm 0.28)$ $\times 10^{-5}$
$\Gamma_{12}$ $e^+e^-$	[a]	$(4.72 \pm 0.05)$ $\times 10^{-5}$
$\Gamma_{13}$ $\pi^+\pi^-\pi^0$	$(1.01^{+0.54}_{-0.36} \pm 0.34)$	$\times 10^{-4}$
$\Gamma_{14}$ $\pi^+\pi^-\pi^+\pi^-$	$(1.8 \pm 0.9)$	$\times 10^{-5}$
$\Gamma_{15}$ $\pi^+\pi^-\pi^0\pi^0$	$(1.6 \pm 0.8)$	$\times 10^{-5}$
$\Gamma_{16}$ $\pi^0e^+e^-$	$< 1.2$	$\times 10^{-5}$ CL=90%
$\Gamma_{17}$ $\eta e^+e^-$		

[a] The  $\omega\rho$  interference is then due to  $\omega\rho$  mixing only, and is expected to be small. If  $e\mu$  universality holds,  $\Gamma(\rho^0 \rightarrow \mu^+\mu^-) = \Gamma(\rho^0 \rightarrow e^+e^-) \times 0.99785$ .

## CONSTRAINED FIT INFORMATION

An overall fit to the total width and a partial width uses 10 measurements and one constraint to determine 3 parameters. The overall fit has a  $\chi^2 = 10.7$  for 8 degrees of freedom.

The following *off-diagonal* array elements are the correlation coefficients  $\langle \delta p_i \delta p_j \rangle / (\delta p_i \delta p_j)$ , in percent, from the fit to parameters  $p_i$ , including the branching fractions,  $x_i \equiv \Gamma_i/\Gamma_{\text{total}}$ . The fit constrains the  $x_i$  whose labels appear in this array to sum to one.

$x_3$	-100	
$\Gamma$	15	-15
	$x_2$	$x_3$

Mode	Rate (MeV)	Scale factor
$\Gamma_2$ $\pi^\pm\pi^0$	$150.2 \pm 2.4$	
$\Gamma_3$ $\pi^\pm\gamma$	$0.068 \pm 0.007$	2.3

## CONSTRAINED FIT INFORMATION

An overall fit to the total width, a partial width, and 7 branching ratios uses 21 measurements and one constraint to determine 9 parameters. The overall fit has a  $\chi^2 = 6.0$  for 13 degrees of freedom.

The following *off-diagonal* array elements are the correlation coefficients  $\langle \delta p_i \delta p_j \rangle / (\delta p_i \delta p_j)$ , in percent, from the fit to parameters  $p_i$ , including the branching fractions,  $x_i \equiv \Gamma_i/\Gamma_{\text{total}}$ . The fit constrains the  $x_i$  whose labels appear in this array to sum to one.

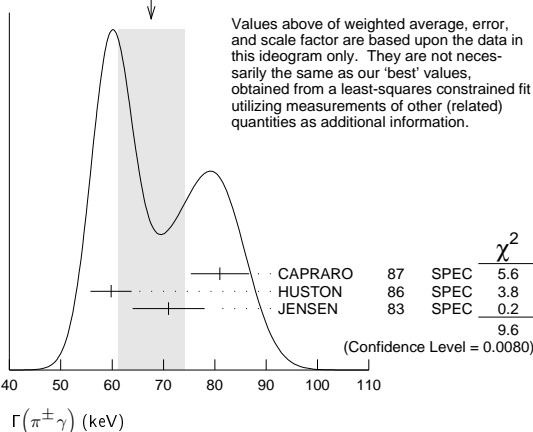
$x_7$	-100							
$x_8$	-5	0						
$x_9$	-1	0	1					
$x_{10}$	-1	0	0	0				
$x_{11}$	2	-3	0	0	0			
$x_{12}$	0	0	-8	-9	0	0		
$x_{14}$	-1	0	0	0	0	0		
$\Gamma$	0	0	4	5	0	-54		
	$x_6$	$x_7$	$x_8$	$x_9$	$x_{10}$	$x_{11}$	$x_{12}$	$x_{14}$

Mode	Rate (MeV)
$\Gamma_6$ $\pi^+\pi^-$	$147.5 \pm 0.9$
$\Gamma_7$ $\pi^+\pi^-\gamma$	$1.48 \pm 0.24$
$\Gamma_8$ $\pi^0\gamma$	$0.089 \pm 0.012$
$\Gamma_9$ $\eta\gamma$	$0.0447 \pm 0.0031$
$\Gamma_{10}$ $\pi^0\pi^0\gamma$	$0.0066 \pm 0.0012$
$\Gamma_{11}$ $\mu^+\mu^-$	[a] $0.0068 \pm 0.0004$
$\Gamma_{12}$ $e^+e^-$	[a] $0.00704 \pm 0.00006$
$\Gamma_{14}$ $\pi^+\pi^-\pi^+\pi^-$	$0.0027 \pm 0.0014$

 $\rho(770)$  PARTIAL WIDTHS $\Gamma(\pi^\pm\gamma)$ 

VALUE (keV)	DOCUMENT ID	TECN	CHG	COMMENT
<b>68 ± 7 OUR FIT</b>				Error includes scale factor of 2.3.
<b>68 ± 7 OUR AVERAGE</b>				Error includes scale factor of 2.2. See the ideogram below.
81 ± 4 ± 4	CAPRARO	87	SPEC	- 200 $\pi^-A \rightarrow \pi^- \pi^0 A$
59.8 ± 4.0	HUSTON	86	SPEC	+ 202 $\pi^+A \rightarrow \pi^+ \pi^0 A$
71 ± 7	JENSEN	83	SPEC	- 156-260 $\pi^-A \rightarrow \pi^- \pi^0 A$

WEIGHTED AVERAGE  
68±7 (Error scaled by 2.2)

 $\Gamma(e^+e^-)$ 

VALUE (keV)	EVTS	DOCUMENT ID	TECN	COMMENT
<b>7.04 ± 0.06 OUR FIT</b>				
<b>7.04 ± 0.06 OUR AVERAGE</b>				
7.048 ± 0.057 ± 0.050	900k	80 AKHMETSHIN 07		$e^+e^- \rightarrow \pi^+\pi^-$
7.06 ± 0.11 ± 0.05	114k	81,82 AKHMETSHIN 04	CMD2	$e^+e^- \rightarrow \pi^+\pi^-$
6.77 ± 0.10 ± 0.30		BARKOV 85	OLYA	$e^+e^- \rightarrow \pi^+\pi^-$
• • • We do not use the following data for averages, fits, limits, etc. • • •				
7.12 ± 0.02 ± 0.11	800k	83 ACHASOV 06	SND	$e^+e^- \rightarrow \pi^+\pi^-$
6.3 ± 0.1		84 BENAYOUN 98	RVUE	$e^+e^- \rightarrow \pi^+\pi^-, \mu^+\mu^-$

 $\Gamma(\pi^0\gamma)$ 

VALUE (keV)	EVTS	DOCUMENT ID	TECN	COMMENT
• • • We do not use the following data for averages, fits, limits, etc. • • •				
77 ± 17 ± 11	36500	85 ACHASOV 03	SND	0.60-0.97 $e^+e^- \rightarrow \pi^0\gamma$
121 ± 31		DOLINSKY 89	ND	$e^+e^- \rightarrow \pi^0\gamma$

 $\Gamma(\eta\gamma)$ 

VALUE (keV)	DOCUMENT ID	TECN	COMMENT
• • • We do not use the following data for averages, fits, limits, etc. • • •			
62 ± 17	86 DOLINSKY 89	ND	$e^+e^- \rightarrow \eta\gamma$

 $\Gamma(\pi^+\pi^-\pi^+\pi^-)$ 

VALUE (keV)	EVTS	DOCUMENT ID	TECN	COMMENT
• • • We do not use the following data for averages, fits, limits, etc. • • •				
2.8 ± 1.4 ± 0.5	153	AKHMETSHIN 00	CMD2	0.6-0.97 $e^+e^- \rightarrow \pi^+\pi^-\pi^+\pi^-$

<sup>80</sup>A combined fit of AKHMETSHIN 07, AULCHENKO 06, and AULCHENKO 05.  
<sup>81</sup>Using the GOUNARIS 68 parametrization with the complex phase of the  $\rho\omega$  interference.  
<sup>82</sup>From a fit in the energy range 0.61 to 0.96 GeV. Update of AKHMETSHIN 02.  
<sup>83</sup>Supersedes ACHASOV 05A.  
<sup>84</sup>Using the data of BARKOV 85 in the hidden local symmetry model.  
<sup>85</sup>Using  $\Gamma_{\text{total}} = 147.9 \pm 1.3$  MeV and  $B(\rho \rightarrow \pi^0\gamma)$  from ACHASOV 03.  
<sup>86</sup>Solution corresponding to constructive  $\omega\rho$  interference.

# Meson Particle Listings

## $\rho(770)$

$\rho(770) \Gamma(e^+e^-)\Gamma(\pi)\Gamma^2(\text{total})$

$\Gamma(e^+e^-)/\Gamma_{\text{total}} \times \Gamma(\pi^+\pi^-)/\Gamma_{\text{total}}$   $\Gamma_{12}/\Gamma \times \Gamma_6/\Gamma$

VALUE (units 10 <sup>-5</sup> )	EVTS	DOCUMENT ID	TECN	COMMENT
<b>4.876 ± 0.023 ± 0.064</b>	800k	87,88 ACHASOV	06	SND e <sup>+</sup> e <sup>-</sup> → π <sup>+</sup> π <sup>-</sup>
4.72 ± 0.02	89	BENAYOUN	10	RVUE 0.4-1.05 e <sup>+</sup> e <sup>-</sup>

87 Supersedes ACHASOV 05A.

88 A fit of the SND data from 400 to 1000 MeV using parameters of the  $\rho(1450)$  and  $\rho(1700)$  from a fit of the data of BARKOV 85, BISELLO 89 and ANDERSON 00A.

89 A simultaneous fit of e<sup>+</sup>e<sup>-</sup> → π<sup>+</sup>π<sup>-</sup>, π<sup>+</sup>π<sup>-</sup>π<sup>0</sup>, π<sup>0</sup>γ, ηγ data.

$\Gamma(e^+e^-)/\Gamma_{\text{total}} \times \Gamma(\eta\gamma)/\Gamma_{\text{total}}$   $\Gamma_{12}/\Gamma \times \Gamma_9/\Gamma$

VALUE (units 10 <sup>-8</sup> )	EVTS	DOCUMENT ID	TECN	COMMENT
<b>1.42 ± 0.10 OUR FIT</b>				
<b>1.45 ± 0.12 OUR AVERAGE</b>				
1.32 ± 0.14 ± 0.08	33k	90 ACHASOV	07B	SND 0.6-1.38 e <sup>+</sup> e <sup>-</sup> → ηγ
1.50 ± 0.65 ± 0.09	17.4k	91 AKHMETSHIN	05	CMD2 0.60-1.38 e <sup>+</sup> e <sup>-</sup> → ηγ
1.61 ± 0.20 ± 0.11	23k	92,93 AKHMETSHIN	01B	CMD2 e <sup>+</sup> e <sup>-</sup> → ηγ
1.85 ± 0.49	94	DOLINSKY	89	ND e <sup>+</sup> e <sup>-</sup> → ηγ
1.05 ± 0.02	95	BENAYOUN	10	RVUE 0.4-1.05 e <sup>+</sup> e <sup>-</sup>

90 From a combined fit of σ(e<sup>+</sup>e<sup>-</sup> → ηγ) with η → 3π<sup>0</sup> and η → π<sup>+</sup>π<sup>-</sup>π<sup>0</sup>, and fixing B(η → 3π<sup>0</sup>) / B(η → π<sup>+</sup>π<sup>-</sup>π<sup>0</sup>) = 1.44 ± 0.04. Recalculated by us from the cross section at the peak. Supersedes ACHASOV 00D and ACHASOV 06A.

91 From the η → 2γ decay and using B(η → γγ) = 39.43 ± 0.26%.

92 From the η → 3π<sup>0</sup> decay and using B(η → 3π<sup>0</sup>) = (32.24 ± 0.29) × 10<sup>-2</sup>.

93 The combined fit from 600 to 1380 MeV taking into account  $\rho(770)$ , ω(782), φ(1020), and  $\rho(1450)$  (mass and width fixed at 1450 MeV and 310 MeV respectively).

94 Recalculated by us from the cross section in the peak.

95 A simultaneous fit of e<sup>+</sup>e<sup>-</sup> → π<sup>+</sup>π<sup>-</sup>, π<sup>+</sup>π<sup>-</sup>π<sup>0</sup>, π<sup>0</sup>γ, ηγ data.

$\Gamma(e^+e^-)/\Gamma_{\text{total}} \times \Gamma(\pi^0\gamma)/\Gamma_{\text{total}}$   $\Gamma_{12}/\Gamma \times \Gamma_8/\Gamma$

VALUE (units 10 <sup>-8</sup> )	EVTS	DOCUMENT ID	TECN	COMMENT
<b>2.8 ± 0.4 OUR FIT</b>				
<b>2.8 ± 0.4 OUR AVERAGE</b>				
2.90 <sup>+0.60</sup> <sub>-0.55</sub> ± 0.18	18680	AKHMETSHIN	05	CMD2 0.60-1.38 e <sup>+</sup> e <sup>-</sup> → π <sup>0</sup> γ
2.37 ± 0.53 ± 0.33	36500	96 ACHASOV	03	SND 0.60-0.97 e <sup>+</sup> e <sup>-</sup> → π <sup>0</sup> γ
3.61 ± 0.74 ± 0.49	10625	97 DOLINSKY	89	ND e <sup>+</sup> e <sup>-</sup> → π <sup>0</sup> γ
1.875 ± 0.026	98	BENAYOUN	10	RVUE 0.4-1.05 e <sup>+</sup> e <sup>-</sup>

96 Using σ<sub>φ → π<sup>0</sup>γ</sub> from ACHASOV 00 and m<sub>ρ</sub> = 775.97 MeV in the model with the energy-independent phase of ρ-ω interference equal to (-10.2 ± 7.0)<sup>o</sup>.

97 Recalculated by us from the cross section in the peak.

98 A simultaneous fit of e<sup>+</sup>e<sup>-</sup> → π<sup>+</sup>π<sup>-</sup>, π<sup>+</sup>π<sup>-</sup>π<sup>0</sup>, π<sup>0</sup>γ, ηγ data.

$\Gamma(e^+e^-)/\Gamma_{\text{total}} \times \Gamma(\pi^+\pi^-\pi^0)/\Gamma_{\text{total}}$   $\Gamma_{12}/\Gamma \times \Gamma_{13}/\Gamma$

VALUE (units 10 <sup>-9</sup> )	EVTS	DOCUMENT ID	TECN	COMMENT
0.903 ± 0.076	99	BENAYOUN	10	RVUE 0.4-1.05 e <sup>+</sup> e <sup>-</sup>
4.58 <sup>+2.46</sup> <sub>-1.64</sub> ± 1.56	1.2M	100 ACHASOV	03D	RVUE 0.44-2.00 e <sup>+</sup> e <sup>-</sup> → π <sup>+</sup> π <sup>-</sup> π <sup>0</sup>

99 A simultaneous fit of e<sup>+</sup>e<sup>-</sup> → π<sup>+</sup>π<sup>-</sup>, π<sup>+</sup>π<sup>-</sup>π<sup>0</sup>, π<sup>0</sup>γ, ηγ data.

100 Statistical significance is less than 3σ.

### $\rho(770)$ BRANCHING RATIOS

$\Gamma(\pi^\pm\eta)/\Gamma(\pi\pi)$   $\Gamma_4/\Gamma_1$

VALUE (units 10 <sup>-4</sup> )	CL%	DOCUMENT ID	TECN	CHG	COMMENT
<60	84	FERBEL	66	HBC	± π <sup>±</sup> p above 2.5

$\Gamma(\pi^\pm\pi^+\pi^-\pi^0)/\Gamma(\pi\pi)$   $\Gamma_5/\Gamma_1$

VALUE (units 10 <sup>-4</sup> )	CL%	DOCUMENT ID	TECN	CHG	COMMENT
<20	84	FERBEL	66	HBC	± π <sup>±</sup> p above 2.5
35 ± 40		JAMES	66	HBC	+ 2.1 π <sup>±</sup> p

••• We do not use the following data for averages, fits, limits, etc. •••

$\Gamma(\mu^+\mu^-)/\Gamma(\pi^+\pi^-)$   $\Gamma_{11}/\Gamma_6$

VALUE (units 10 <sup>-5</sup> )	DOCUMENT ID	TECN	COMMENT
<b>4.60 ± 0.28 OUR FIT</b>			
<b>4.6 ± 0.2 ± 0.2</b>			
6.2 ± 1.6	101 ROTHWELL	69	CNTR Photoproduction
5.6 ± 1.5	102 WEHMANN	69	OSPK 12 π <sup>-</sup> C, Fe
9.7 <sup>+3.1</sup> <sub>-3.3</sub>	103 HYAMS	67	OSPK 11 π <sup>-</sup> Li, H

••• We do not use the following data for averages, fits, limits, etc. •••

$\Gamma(e^+e^-)/\Gamma(\pi\pi)$   $\Gamma_{12}/\Gamma_1$

VALUE (units 10 <sup>-4</sup> )	DOCUMENT ID	TECN	COMMENT	
0.40 ± 0.05	104	BENAKSAS	72	OSPK e <sup>+</sup> e <sup>-</sup> → π <sup>+</sup> π <sup>-</sup>

••• We do not use the following data for averages, fits, limits, etc. •••

$\Gamma(\eta\gamma)/\Gamma_{\text{total}}$   $\Gamma_9/\Gamma$

VALUE (units 10 <sup>-4</sup> )	EVTS	DOCUMENT ID	TECN	CHG	COMMENT
<b>3.00 ± 0.21 OUR FIT</b>					
<b>2.90 ± 0.32 OUR AVERAGE</b>					
2.79 ± 0.34 ± 0.03	33k	105 ACHASOV	07B	SND	0.6-1.38 e <sup>+</sup> e <sup>-</sup> → ηγ
3.6 ± 0.9	106	ANDREWS	77	CNTR	0 6.7-10 γCu
3.21 ± 1.39 ± 0.20	17.4k	107,108 AKHMETSHIN	05	CMD2	0.60-1.38 e <sup>+</sup> e <sup>-</sup> → ηγ
3.39 ± 0.42 ± 0.23	106,109,110	AKHMETSHIN	01B	CMD2	e <sup>+</sup> e <sup>-</sup> → ηγ
1.9 <sup>+0.6</sup> <sub>-0.8</sub>	111	BENAYOUN	96	RVUE	0.54-1.04 e <sup>+</sup> e <sup>-</sup> → ηγ
4.0 ± 1.1	106,108	DOLINSKY	89	ND	e <sup>+</sup> e <sup>-</sup> → ηγ

$\Gamma(\pi^+\pi^-\pi^+\pi^-)/\Gamma_{\text{total}}$   $\Gamma_{14}/\Gamma$

VALUE (units 10 <sup>-5</sup> )	CL%	EVTS	DOCUMENT ID	TECN	COMMENT
<b>1.8 ± 0.9 OUR FIT</b>					
<b>1.8 ± 0.9 ± 0.3</b>		153	AKHMETSHIN	00	CMD2 0.6-0.97 e <sup>+</sup> e <sup>-</sup> → π <sup>+</sup> π <sup>-</sup> π <sup>+</sup> π <sup>-</sup>
<20	90	KURDADZE	88	OLYA	e <sup>+</sup> e <sup>-</sup> → π <sup>+</sup> π <sup>-</sup> π <sup>+</sup> π <sup>-</sup>

••• We do not use the following data for averages, fits, limits, etc. •••

$\Gamma(\pi^+\pi^-\pi^+\pi^-)/\Gamma(\pi\pi)$   $\Gamma_{14}/\Gamma_1$

VALUE (units 10 <sup>-4</sup> )	CL%	DOCUMENT ID	TECN	CHG	COMMENT
<15	90	ERBE	69	HBC	0 2.5-5.8 γp
<20		CHUNG	68	HBC	0 3.2, 4.2 π <sup>-</sup> p
<20	90	HUSON	68	HLBC	0 16.0 π <sup>-</sup> p
<80		JAMES	66	HBC	0 2.1 π <sup>±</sup> p

••• We do not use the following data for averages, fits, limits, etc. •••

$\Gamma(\pi^+\pi^-\pi^0)/\Gamma_{\text{total}}$   $\Gamma_{13}/\Gamma$

VALUE (units 10 <sup>-4</sup> )	CL%	EVTS	DOCUMENT ID	TECN	COMMENT
1.01 <sup>+0.54</sup> <sub>-0.36</sub> ± 0.34	1.2M	112	ACHASOV	03D	RVUE 0.44-2.00 e <sup>+</sup> e <sup>-</sup> → π <sup>+</sup> π <sup>-</sup> π <sup>0</sup>
<1.2	90	VASSERMAN	88B	ND	e <sup>+</sup> e <sup>-</sup> → π <sup>+</sup> π <sup>-</sup> π <sup>0</sup>

••• We do not use the following data for averages, fits, limits, etc. •••

$\Gamma(\pi^+\pi^-\pi^0)/\Gamma(\pi\pi)$   $\Gamma_{13}/\Gamma_1$

VALUE	CL%	DOCUMENT ID	TECN	CHG	COMMENT
~0.01		BRAMON	86	RVUE	0 J/ψ → ωπ <sup>0</sup>
<0.01	84	113 ABRAMS	71	HBC	0 3.7 π <sup>±</sup> p

••• We do not use the following data for averages, fits, limits, etc. •••

$\Gamma(\pi^+\pi^-\pi^0\pi^0)/\Gamma_{\text{total}}$   $\Gamma_{15}/\Gamma$

VALUE (units 10 <sup>-5</sup> )	CL%	DOCUMENT ID	TECN	COMMENT	
<b>1.60 ± 0.74 ± 0.18</b>		114	ACHASOV	09A	SND e <sup>+</sup> e <sup>-</sup> → π <sup>+</sup> π <sup>-</sup> π <sup>0</sup> π <sup>0</sup>
< 4	90	AULCHENKO	87C	ND	e <sup>+</sup> e <sup>-</sup> → π <sup>+</sup> π <sup>-</sup> π <sup>0</sup> π <sup>0</sup>
<20	90	KURDADZE	86	OLYA	e <sup>+</sup> e <sup>-</sup> → π <sup>+</sup> π <sup>-</sup> π <sup>0</sup> π <sup>0</sup>

••• We do not use the following data for averages, fits, limits, etc. •••

$\Gamma(\pi^+\pi^-\gamma)/\Gamma_{\text{total}}$   $\Gamma_7/\Gamma$

VALUE	CL%	DOCUMENT ID	TECN	COMMENT	
<b>0.0099 ± 0.0016 OUR FIT</b>					
<b>0.0099 ± 0.0016</b>		115	DOLINSKY	91	ND e <sup>+</sup> e <sup>-</sup> → π <sup>+</sup> π <sup>-</sup> γ
0.0111 ± 0.0014		116	VASSERMAN	88	ND e <sup>+</sup> e <sup>-</sup> → π <sup>+</sup> π <sup>-</sup> γ
<0.005	90	117	VASSERMAN	88	ND e <sup>+</sup> e <sup>-</sup> → π <sup>+</sup> π <sup>-</sup> γ

••• We do not use the following data for averages, fits, limits, etc. •••

$\Gamma(\pi^0\gamma)/\Gamma_{\text{total}}$   $\Gamma_8/\Gamma$

VALUE (units 10 <sup>-4</sup> )	EVTS	DOCUMENT ID	TECN	COMMENT	
6.21 <sup>+1.28</sup> <sub>-1.18</sub> ± 0.39	18680	118,119	AKHMETSHIN	05	CMD2 0.60-1.38 e <sup>+</sup> e <sup>-</sup> → π <sup>0</sup> γ
5.22 ± 1.17 ± 0.75	36500	99,120	ACHASOV	03	SND 0.60-0.97 e <sup>+</sup> e <sup>-</sup> → π <sup>0</sup> γ
6.8 ± 1.7	121	BENAYOUN	96	RVUE	0.54-1.04 e <sup>+</sup> e <sup>-</sup> → π <sup>0</sup> γ
7.9 ± 2.0	119	DOLINSKY	89	ND	e <sup>+</sup> e <sup>-</sup> → π <sup>0</sup> γ

$\Gamma(\pi^0e^+e^-)/\Gamma_{\text{total}}$   $\Gamma_{16}/\Gamma$

VALUE (units 10 <sup>-5</sup> )	CL%	DOCUMENT ID	TECN	COMMENT
<1.2	90	ACHASOV	08	SND 0.36-0.97 e <sup>+</sup> e <sup>-</sup> → π <sup>0</sup> e <sup>+</sup> e <sup>-</sup>
<1.6		AKHMETSHIN	05A	CMD2 0.72-0.84 e <sup>+</sup> e <sup>-</sup>

••• We do not use the following data for averages, fits, limits, etc. •••



# Meson Particle Listings

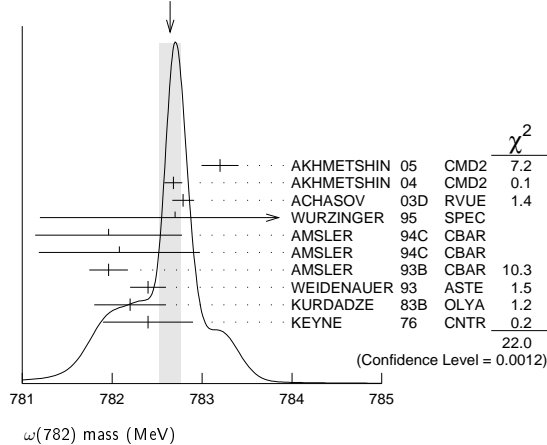
## $\omega(782)$

••• We do not use the following data for averages, fits, limits, etc. •••

781.78 ± 0.10		6 BARKOV	87	CMD	$e^+e^- \rightarrow \pi^+\pi^-\pi^0$
783.3 ± 0.4	433	CORDIER	80	DM1	$e^+e^- \rightarrow \pi^+\pi^-\pi^0$
782.5 ± 0.8	33260	ROOS	80	RVUE	0.0-3.6 $\bar{p}p$
782.6 ± 0.8	3000	BENKHEIRI	79	OMEG	9-12 $\pi^\pm p$
781.8 ± 0.6	1430	COOPER	78B	HBC	0.7-0.8 $\bar{p}p \rightarrow 5\pi$
782.7 ± 0.9	535	VANAPEL...	78	HBC	7.2 $\bar{p}p \rightarrow \bar{p}\rho\omega$
783.5 ± 0.8	2100	GESSAROLI	77	HBC	11 $\pi^-p \rightarrow \omega n$
782.5 ± 0.8	418	AGUILAR-...	72B	HBC	3.9,4.6 $K^-p$
783.4 ± 1.0	248	BIZZARRI	71	HBC	0.0 $p\bar{p} \rightarrow K^+K^-\omega$
781.0 ± 0.6	510	BIZZARRI	71	HBC	0.0 $p\bar{p} \rightarrow K_1^+K_1^-\omega$
783.7 ± 1.0	3583	7 COYNE	71	HBC	3.7 $\pi^+p \rightarrow \rho\pi^+\pi^+\pi^-\pi^0$
784.1 ± 1.2	750	ABRAMOVI...	70	HBC	3.9 $\pi^-p$
783.2 ± 1.6		8 BIGGS	70B	CNTR	<4.1 $\gamma C \rightarrow \pi^+\pi^-C$
782.4 ± 0.5	2400	BIZZARRI	69	HBC	0.0 $\bar{p}p$

- Update of AKHMETSHIN 00c.
- From the combined fit of ANTONELLI 92, ACHASOV 01E, ACHASOV 02E, and ACHASOV 03D data on the  $\pi^+\pi^-\pi^0$  and ANTONELLI 92 on the  $\omega\pi^+\pi^-$  final states. Supersedes ACHASOV 99E and ACHASOV 02E.
- From the  $\eta \rightarrow \gamma\gamma$  decay.
- From the  $\eta \rightarrow 3\pi^0$  decay.
- Observed by threshold-crossing technique. Mass resolution = 4.8 MeV FWHM.
- Systematic uncertainties underestimated.
- From best-resolution sample of COYNE 71.
- From  $\omega$ - $\rho$  interference in the  $\pi^+\pi^-$  mass spectrum assuming  $\omega$  width 12.6 MeV.

WEIGHTED AVERAGE  
782.65±0.12 (Error scaled by 1.9)



### $\omega(782)$ WIDTH

VALUE (MeV)	EVTS	DOCUMENT ID	TECN	COMMENT
<b>8.49 ± 0.08 OUR AVERAGE</b>				
8.68 ± 0.23 ± 0.10	11200	9 AKHMETSHIN 04	CMD2	$e^+e^- \rightarrow \pi^+\pi^-\pi^0$
8.68 ± 0.04 ± 0.15	1.2M	10 ACHASOV 03D	RVUE	0.44-2.00 $e^+e^- \rightarrow \pi^+\pi^-\pi^0$
8.2 ± 0.3	19500	WURZINGER 95	SPEC	1.33 $pd \rightarrow {}^3\text{He}\omega$
8.4 ± 0.1		11 AULCHENKO 87	ND	$e^+e^- \rightarrow \pi^+\pi^-\pi^0$
8.30 ± 0.40		BARKOV 87	CMD	$e^+e^- \rightarrow \pi^+\pi^-\pi^0$
9.8 ± 0.9	1488	KURDADZE 83B	OLYA	$e^+e^- \rightarrow \pi^+\pi^-\pi^0$
9.0 ± 0.8	433	CORDIER 80	DM1	$e^+e^- \rightarrow \pi^+\pi^-\pi^0$
9.1 ± 0.8	451	BENAKSAS 72B	OSPK	$e^+e^- \rightarrow \pi^+\pi^-\pi^0$
••• We do not use the following data for averages, fits, limits, etc. •••				
12 ± 2	1430	COOPER 78B	HBC	0.7-0.8 $\bar{p}p \rightarrow 5\pi$
9.4 ± 2.5	2100	GESSAROLI 77	HBC	11 $\pi^-p \rightarrow \omega n$
10.22 ± 0.43	20000	12 KEYNE 76	CNTR	$\pi^-p \rightarrow \omega n$
13.3 ± 2	418	AGUILAR-... 72B	HBC	3.9,4.6 $K^-p$
10.5 ± 1.5		BORENSTEIN 72	HBC	2.18 $K^-p$
7.70 ± 0.9 ± 1.15	940	BROWN 72	MMS	2.5 $\pi^-p \rightarrow n\text{MM}$
10.3 ± 1.4	510	BIZZARRI 71	HBC	0.0 $p\bar{p} \rightarrow K_1^+K_1^-\omega$
12.8 ± 3.0	248	BIZZARRI 71	HBC	0.0 $p\bar{p} \rightarrow K^+K^-\omega$
9.5 ± 1.0	3583	COYNE 71	HBC	3.7 $\pi^+p \rightarrow \rho\pi^+\pi^+\pi^-\pi^0$

- Update of AKHMETSHIN 00c.
- From the combined fit of ANTONELLI 92, ACHASOV 01E, ACHASOV 02E, and ACHASOV 03D data on the  $\pi^+\pi^-\pi^0$  and ANTONELLI 92 on the  $\omega\pi^+\pi^-$  final states. Supersedes ACHASOV 99E and ACHASOV 02E.
- Relativistic Breit-Wigner includes radiative corrections.
- Observed by threshold-crossing technique. Mass resolution = 4.8 MeV FWHM.

### $\omega(782)$ DECAY MODES

Mode	Fraction ( $\Gamma_i/\Gamma$ )	Scale factor/Confidence level
$\Gamma_1$ $\pi^+\pi^-\pi^0$	(89.2 ± 0.7) %	
$\Gamma_2$ $\pi^0\gamma$	( 8.28 ± 0.28) %	S=2.1
$\Gamma_3$ $\pi^+\pi^-$	( 1.53 <sup>+0.11</sup> <sub>-0.13</sub> ) %	S=1.2
$\Gamma_4$ neutrals (excluding $\pi^0\gamma$ )	( 8 <sup>+8</sup> <sub>-5</sub> ) × 10 <sup>-3</sup>	S=1.1
$\Gamma_5$ $\eta\gamma$	( 4.6 ± 0.4) × 10 <sup>-4</sup>	S=1.1
$\Gamma_6$ $\pi^0 e^+e^-$	( 7.7 ± 0.6) × 10 <sup>-4</sup>	
$\Gamma_7$ $\pi^0 \mu^+\mu^-$	( 1.3 ± 0.4) × 10 <sup>-4</sup>	S=2.1
$\Gamma_8$ $\eta e^+e^-$		
$\Gamma_9$ $e^+e^-$	( 7.28 ± 0.14) × 10 <sup>-5</sup>	S=1.3
$\Gamma_{10}$ $\pi^+\pi^-\pi^0\pi^0$	< 2 × 10 <sup>-4</sup>	CL=90%
$\Gamma_{11}$ $\pi^+\pi^-\gamma$	< 3.6 × 10 <sup>-3</sup>	CL=95%
$\Gamma_{12}$ $\pi^+\pi^-\pi^+\pi^-$	< 1 × 10 <sup>-3</sup>	CL=90%
$\Gamma_{13}$ $\pi^0\pi^0\gamma$	( 6.6 ± 1.1) × 10 <sup>-5</sup>	
$\Gamma_{14}$ $\eta\pi^0\gamma$	< 3.3 × 10 <sup>-5</sup>	CL=90%
$\Gamma_{15}$ $\mu^+\mu^-$	( 9.0 ± 3.1) × 10 <sup>-5</sup>	
$\Gamma_{16}$ $3\gamma$	< 1.9 × 10 <sup>-4</sup>	CL=95%

### Charge conjugation (C) violating modes

Mode	C	Value	CL=90%
$\Gamma_{17}$ $\eta\pi^0$	C	< 2.1 × 10 <sup>-4</sup>	CL=90%
$\Gamma_{18}$ $2\pi^0$	C	< 2.1 × 10 <sup>-4</sup>	CL=90%
$\Gamma_{19}$ $3\pi^0$	C	< 2.3 × 10 <sup>-4</sup>	CL=90%

### CONSTRAINED FIT INFORMATION

An overall fit to 15 branching ratios uses 51 measurements and one constraint to determine 10 parameters. The overall fit has a  $\chi^2 = 51.8$  for 42 degrees of freedom.

The following *off-diagonal* array elements are the correlation coefficients  $\langle \delta x_i \delta x_j \rangle / (\delta x_i \delta x_j)$ , in percent, from the fit to the branching fractions,  $x_i \equiv \Gamma_i / \Gamma_{\text{total}}$ . The fit constrains the  $x_i$  whose labels appear in this array to sum to one.

$x_2$	22								
$x_3$	-18	-4							
$x_4$	-92	-56	1						
$x_5$	7	7	-1	-9					
$x_6$	-1	0	0	0	0				
$x_7$	-1	0	0	0	0	0			
$x_9$	-38	-33	7	44	-21	0	0		
$x_{13}$	1	4	0	-2	0	0	0	-1	
$x_{15}$	0	0	0	0	0	0	0	0	0
	$x_1$	$x_2$	$x_3$	$x_4$	$x_5$	$x_6$	$x_7$	$x_9$	$x_{13}$

### $\omega(782)$ PARTIAL WIDTHS

VALUE (keV)	EVTS	DOCUMENT ID	TECN	COMMENT	$\Gamma_2$
••• We do not use the following data for averages, fits, limits, etc. •••					
788 ± 12 ± 27	36500	13 ACHASOV 03	SND	0.60-0.97 $e^+e^- \rightarrow \pi^0\gamma$	
764 ± 51	10625	DOLINSKY 89	ND	$e^+e^- \rightarrow \pi^0\gamma$	
				13 Using $\Gamma_\omega = 8.44 \pm 0.09$ MeV and $B(\omega \rightarrow \pi^0\gamma)$ from ACHASOV 03.	

VALUE (keV)	DOCUMENT ID	TECN	COMMENT	$\Gamma_5$
••• We do not use the following data for averages, fits, limits, etc. •••				
6.1 ± 2.5	14 DOLINSKY 89	ND	$e^+e^- \rightarrow \eta\gamma$	
			14 Using $\Gamma_\omega = 8.4 \pm 0.1$ MeV and $B(\omega \rightarrow \eta\gamma)$ from DOLINSKY 89.	

VALUE (keV)	EVTS	DOCUMENT ID	TECN	COMMENT	$\Gamma_9$
<b>0.60 ± 0.02 OUR EVALUATION</b>					
••• We do not use the following data for averages, fits, limits, etc. •••					
0.591 ± 0.015	11200	15,16 AKHMETSHIN 04	CMD2	$e^+e^- \rightarrow \pi^+\pi^-\pi^0$	
0.653 ± 0.003 ± 0.021	1.2M	17 ACHASOV 03D	RVUE	0.44-2.00 $e^+e^- \rightarrow \pi^+\pi^-\pi^0$	
0.600 ± 0.031	10625	DOLINSKY 89	ND	$e^+e^- \rightarrow \pi^0\gamma$	
				15 Using $B(\omega \rightarrow \pi^+\pi^-\pi^0) = 0.891 \pm 0.007$ and $\Gamma_{\text{total}} = 8.44 \pm 0.09$ MeV.	
				16 Update of AKHMETSHIN 00c.	
				17 Using ACHASOV 03, ACHASOV 03D and $B(\omega \rightarrow \pi^+\pi^-) = (1.70 \pm 0.28)\%$ .	



See key on page 457

## Meson Particle Listings

 $\omega(782)$ 

$\omega(782) \Gamma(e^+e^-)\Gamma(l)/\Gamma^2(\text{total})$				
$\Gamma(e^+e^-)/\Gamma_{\text{total}} \times \Gamma(\pi^+\pi^-\pi^0)/\Gamma_{\text{total}}$	$\Gamma_9/\Gamma \times \Gamma_1/\Gamma$			
VALUE (units $10^{-5}$ )	EVTS	DOCUMENT ID	TECN	COMMENT
<b>6.49±0.11 OUR FIT</b>	Error includes scale factor of 1.3.			
<b>6.38±0.10 OUR AVERAGE</b>	Error includes scale factor of 1.1.			
6.24±0.11±0.08	11.2k	18 AKHMETSHIN 04	CMD2	$e^+e^- \rightarrow \pi^+\pi^-\pi^0$
6.70±0.06±0.27		AUBERT,B	04N	BABR 10.6 $e^+e^- \rightarrow \pi^+\pi^-\pi^0\gamma$
6.74±0.04±0.24	1.2M	19,20 ACHASOV	03D	RVUE 0.44-2.00 $e^+e^- \rightarrow \pi^+\pi^-\pi^0$
6.37±0.35		19 DOLINSKY	89	ND $e^+e^- \rightarrow \pi^+\pi^-\pi^0$
6.45±0.24		19 BARKOV	87	CMD $e^+e^- \rightarrow \pi^+\pi^-\pi^0$
5.79±0.42	1488	19 KURDADZE	83B	OLYA $e^+e^- \rightarrow \pi^+\pi^-\pi^0$
5.89±0.54	433	19 CORDIER	80	DM1 $e^+e^- \rightarrow \pi^+\pi^-\pi^0$
7.54±0.84	451	19 BENAJSAS	72B	OSPK $e^+e^- \rightarrow \pi^+\pi^-\pi^0$
• • • We do not use the following data for averages, fits, limits, etc. • • •				
6.20±0.13		21 BENAYOUN	10	RVUE 0.4-1.05 $e^+e^-$

<sup>18</sup>Update of AKHMETSHIN 00c.  
<sup>19</sup>Recalculated by us from the cross section in the peak.  
<sup>20</sup>From the combined fit of ANTONELLI 92, ACHASOV 01E, ACHASOV 02E, and ACHASOV 03d data on the  $\pi^+\pi^-\pi^0$  and ANTONELLI 92 on the  $\omega\pi^+\pi^-$  final states. Supersedes ACHASOV 99E and ACHASOV 02E.  
<sup>21</sup>A simultaneous fit of  $e^+e^- \rightarrow \pi^+\pi^-, \pi^+\pi^-\pi^0, \pi^0\gamma, \eta\gamma$  data.

$\Gamma(e^+e^-)/\Gamma_{\text{total}} \times \Gamma(\pi^0\gamma)/\Gamma_{\text{total}}$				
$\Gamma_9/\Gamma \times \Gamma_2/\Gamma$				
VALUE (units $10^{-6}$ )	EVTS	DOCUMENT ID	TECN	COMMENT
<b>6.02±0.20 OUR FIT</b>	Error includes scale factor of 1.9.			
<b>6.45±0.17 OUR AVERAGE</b>				
6.47±0.14±0.39	18680	AKHMETSHIN 05	CMD2	0.60-1.38 $e^+e^- \rightarrow \pi^0\gamma$
6.50±0.11±0.20	36500	22 ACHASOV	03	SND 0.60-0.97 $e^+e^- \rightarrow \pi^0\gamma$
6.34±0.21±0.21	10625	23 DOLINSKY	89	ND $e^+e^- \rightarrow \pi^0\gamma$
• • • We do not use the following data for averages, fits, limits, etc. • • •				
6.80±0.13		24 BENAYOUN	10	RVUE 0.4-1.05 $e^+e^-$
<sup>22</sup> Using $\sigma_{\phi \rightarrow \pi^0\gamma}$ from ACHASOV 00 and $m_{\omega} = 782.57$ MeV in the model with the energy-independent phase of $\rho$ - $\omega$ interference equal to $(-10.2 \pm 7.0)^\circ$ .				
<sup>23</sup> Recalculated by us from the cross section in the peak.				
<sup>24</sup> A simultaneous fit of $e^+e^- \rightarrow \pi^+\pi^-, \pi^+\pi^-\pi^0, \pi^0\gamma, \eta\gamma$ data.				

$\Gamma(e^+e^-)/\Gamma_{\text{total}} \times \Gamma(\pi^+\pi^-)/\Gamma_{\text{total}}$				
$\Gamma_9/\Gamma \times \Gamma_3/\Gamma$				
VALUE (units $10^{-6}$ )	EVTS	DOCUMENT ID	TECN	COMMENT
<b>1.225±0.058±0.041</b>	800k	25 ACHASOV	06	SND $e^+e^- \rightarrow \pi^+\pi^-$
• • • We do not use the following data for averages, fits, limits, etc. • • •				
1.146±0.057		26 BENAYOUN	10	RVUE 0.4-1.05 $e^+e^-$
<sup>25</sup> Supersedes ACHASOV 05A.				
<sup>26</sup> A simultaneous fit of $e^+e^- \rightarrow \pi^+\pi^-, \pi^+\pi^-\pi^0, \pi^0\gamma, \eta\gamma$ data.				

$\Gamma(e^+e^-)/\Gamma_{\text{total}} \times \Gamma(\eta\gamma)/\Gamma_{\text{total}}$				
$\Gamma_9/\Gamma \times \Gamma_5/\Gamma$				
VALUE (units $10^{-8}$ )	EVTS	DOCUMENT ID	TECN	COMMENT
<b>3.32±0.28 OUR FIT</b>	Error includes scale factor of 1.1.			
<b>3.18±0.28 OUR AVERAGE</b>				
3.10±0.31±0.11	33k	27 ACHASOV	07B	SND 0.6-1.38 $e^+e^- \rightarrow \eta\gamma$
3.17 $^{+1.85}_{-1.31}$ ±0.21	17.4k	28 AKHMETSHIN 05	CMD2	0.60-1.38 $e^+e^- \rightarrow \eta\gamma$
3.41±0.52±0.21	23k	29,30 AKHMETSHIN 01B	CMD2	$e^+e^- \rightarrow \eta\gamma$
• • • We do not use the following data for averages, fits, limits, etc. • • •				
4.50±0.10		31 BENAYOUN	10	RVUE 0.4-1.05 $e^+e^-$
<sup>27</sup> From a combined fit of $\sigma(e^+e^- \rightarrow \eta\gamma)$ with $\eta \rightarrow 3\pi^0$ and $\eta \rightarrow \pi^+\pi^-\pi^0$ , and fixing $B(\eta \rightarrow 3\pi^0) / B(\eta \rightarrow \pi^+\pi^-\pi^0) = 1.44 \pm 0.04$ . Recalculated by us from the cross section at the peak. Supersedes ACHASOV 00D and ACHASOV 06A.				
<sup>28</sup> From the $\eta \rightarrow 2\gamma$ decay and using $B(\eta \rightarrow \gamma\gamma) = 39.43 \pm 0.26\%$ .				
<sup>29</sup> From the $\eta \rightarrow 3\pi^0$ decay and using $B(\eta \rightarrow 3\pi^0) = (32.24 \pm 0.29) \times 10^{-2}$ .				
<sup>30</sup> The combined fit from 600 to 1380 MeV taking into account $\rho(770), \omega(782), \phi(1020)$ , and $\rho(1450)$ (mass and width fixed at 1450 MeV and 310 MeV respectively).				
<sup>31</sup> A simultaneous fit of $e^+e^- \rightarrow \pi^+\pi^-, \pi^+\pi^-\pi^0, \pi^0\gamma, \eta\gamma$ data.				

 $\omega(782)$  BRANCHING RATIOS

$\Gamma(\pi^+\pi^-\pi^0)/\Gamma_{\text{total}}$	$\Gamma_1/\Gamma$			
VALUE	EVTS	DOCUMENT ID	TECN	COMMENT
• • • We do not use the following data for averages, fits, limits, etc. • • •				
0.9024±0.0019		32 AMBROSINO	08G	KLOE 1.0-1.03 $e^+e^- \rightarrow \pi^+\pi^-\pi^0, 2\pi^0\gamma$
0.8965±0.0016±0.0048	1.2M	33,34 ACHASOV	03D	RVUE 0.44-2.00 $e^+e^- \rightarrow \pi^+\pi^-\pi^0$
0.880 ±0.020 ±0.032	11200	34,35 AKHMETSHIN 00C	CMD2	$e^+e^- \rightarrow \pi^+\pi^-\pi^0$
0.8942±0.0062		34 DOLINSKY	89	ND $e^+e^- \rightarrow \pi^+\pi^-\pi^0$
<sup>32</sup> Not independent of $\Gamma(\pi^0\gamma) / \Gamma(\pi^+\pi^-\pi^0)$ from AMBROSINO 08G.				
<sup>33</sup> Using ACHASOV 03, ACHASOV 03D and $B(\omega \rightarrow \pi^+\pi^-) = (1.70 \pm 0.28)\%$ .				
<sup>34</sup> Not independent of the corresponding $\Gamma(e^+e^-) \times \Gamma(\pi^+\pi^-\pi^0)/\Gamma_{\text{total}}^2$ .				
<sup>35</sup> Using $\Gamma(e^+e^-) = 0.60 \pm 0.02$ keV.				

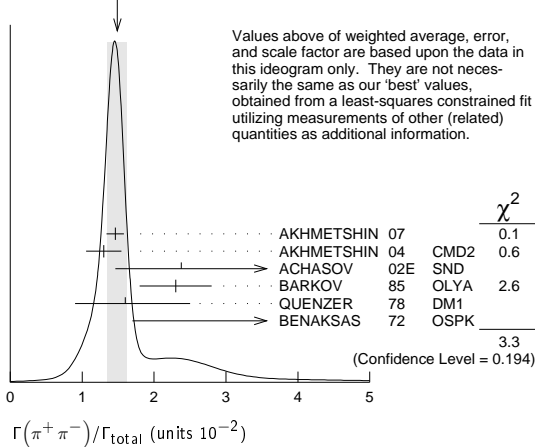
$\Gamma(\pi^0\gamma)/\Gamma_{\text{total}}$	$\Gamma_2/\Gamma$			
VALUE (units $10^{-2}$ )	EVTS	DOCUMENT ID	TECN	COMMENT
• • • We do not use the following data for averages, fits, limits, etc. • • •				
8.09±0.14		36 AMBROSINO	08G	KLOE $e^+e^- \rightarrow \pi^+\pi^-\pi^0, 2\pi^0\gamma$
9.06±0.20±0.57	18680	37,38 AKHMETSHIN 05	CMD2	0.60-1.38 $e^+e^- \rightarrow \pi^0\gamma$
9.34±0.15±0.31	36500	38 ACHASOV	03	SND 0.60-0.97 $e^+e^- \rightarrow \pi^0\gamma$
8.65±0.16±0.42	1.2M	39,40 ACHASOV	03D	RVUE 0.44-2.00 $e^+e^- \rightarrow \pi^+\pi^-\pi^0$
8.39±0.24	9975	41 BENAYOUN	96	RVUE $e^+e^- \rightarrow \pi^0\gamma$
8.88±0.62	10625	38 DOLINSKY	89	ND $e^+e^- \rightarrow \pi^0\gamma$
<sup>36</sup> Not independent of $\Gamma(\pi^0\gamma) / \Gamma(\pi^+\pi^-\pi^0)$ from AMBROSINO 08G.				
<sup>37</sup> Using $B(\omega \rightarrow e^+e^-) = (7.14 \pm 0.13) \times 10^{-5}$ .				
<sup>38</sup> Not independent of the corresponding $\Gamma(e^+e^-) \times \Gamma(\pi^0\gamma)/\Gamma_{\text{total}}^2$ .				
<sup>39</sup> Using ACHASOV 03, ACHASOV 03D and $B(\omega \rightarrow \pi^+\pi^-) = (1.70 \pm 0.28)\%$ .				
<sup>40</sup> Not independent of the corresponding $\Gamma(e^+e^-) \times \Gamma(\pi^+\pi^-\pi^0)/\Gamma_{\text{total}}^2$ .				
<sup>41</sup> Reanalysis of DRUZHININ 84, DOLINSKY 89, DOLINSKY 91 taking into account the triangle anomaly contributions.				

$\Gamma(\pi^0\gamma)/\Gamma(\pi^+\pi^-\pi^0)$	$\Gamma_2/\Gamma_1$			
VALUE (units $10^{-2}$ )	EVTS	DOCUMENT ID	TECN	COMMENT
<b>9.28±0.31 OUR FIT</b>	Error includes scale factor of 2.3.			
<b>9.05±0.27 OUR AVERAGE</b>	Error includes scale factor of 1.8.			
8.97±0.16		AMBROSINO	08G	KLOE $e^+e^- \rightarrow \pi^+\pi^-\pi^0, 2\pi^0\gamma$
9.94±0.36±0.38		42 AULCHENKO	00A	SND $e^+e^- \rightarrow \pi^+\pi^-\pi^0, 2\pi^0\gamma$
8.4 ±1.3		KEYNE	76	CNTR $\pi^-\rho \rightarrow \omega\eta$
10.9 ±2.5		BENAJSAS	72C	OSPK $e^+e^- \rightarrow \pi^0\gamma$
8.1 ±2.0		BALDIN	71	HLBC 2.9 $\pi^+\pi^0$
13 ±4		JACQUET	69B	HLBC 2.05 $\pi^+\pi^0 \rightarrow \pi^+\pi^0$
• • • We do not use the following data for averages, fits, limits, etc. • • •				
9.7 ±0.2 ±0.5	43,44	ACHASOV	03D	RVUE 0.44-2.00 $e^+e^- \rightarrow \pi^+\pi^-\pi^0$
9.9 ±0.7		43 DOLINSKY	89	ND $e^+e^- \rightarrow \pi^0\gamma$
<sup>42</sup> From $\sigma_{\phi \rightarrow \pi^0\gamma} / \sigma_{\phi \rightarrow \pi^+\pi^-\pi^0} / \sigma_{\phi \rightarrow \pi^+\pi^-\pi^0}^2$ with a phase-space correction factor of 1/1.023.				
<sup>43</sup> Not independent of the corresponding $\Gamma(e^+e^-) \times \Gamma(\pi^0\gamma)/\Gamma_{\text{total}}^2$ .				
<sup>44</sup> Using ACHASOV 03. Based on 1.2M events.				

$\Gamma(\pi^+\pi^-)/\Gamma_{\text{total}}$	$\Gamma_3/\Gamma$			
VALUE (units $10^{-2}$ )	EVTS	DOCUMENT ID	TECN	COMMENT
See also $\Gamma(\pi^+\pi^-)/\Gamma(\pi^+\pi^-\pi^0)$ .				
<b>1.53<math>^{+0.11}_{-0.13}</math> OUR FIT</b>	Error includes scale factor of 1.2.			
<b>1.49±0.13 OUR AVERAGE</b>	Error includes scale factor of 1.3. See the ideogram below.			
1.46±0.12±0.02	900k	45 AKHMETSHIN 07		$e^+e^- \rightarrow \pi^+\pi^-$
1.30±0.24±0.05	11.2k	46 AKHMETSHIN 04	CMD2	$e^+e^- \rightarrow \pi^+\pi^-$
2.38 $^{+1.77}_{-0.90}$ ±0.18	5.4k	47 ACHASOV	02E	SND 1.1-1.38 $e^+e^- \rightarrow \pi^+\pi^-$
2.3 ±0.5		BARKOV	85	OLYA $e^+e^- \rightarrow \pi^+\pi^-$
1.6 $^{+0.9}_{-0.7}$		QUENZER	78	DM1 $e^+e^- \rightarrow \pi^+\pi^-$
3.6 ±1.9		BENAJSAS	72	OSPK $e^+e^- \rightarrow \pi^+\pi^-$
• • • We do not use the following data for averages, fits, limits, etc. • • •				
1.75±0.11	4.5M	48 ACHASOV	05A	SND $e^+e^- \rightarrow \pi^+\pi^-$
2.01±0.29		49 BENAYOUN	03	RVUE $e^+e^- \rightarrow \pi^+\pi^-$
1.9 ±0.3		50 GARDNER	99	RVUE $e^+e^- \rightarrow \pi^+\pi^-$
2.3 ±0.4		51 BENAYOUN	98	RVUE $e^+e^- \rightarrow \pi^+\pi^-, \mu^+\mu^-$
1.0 ±0.11		52 WICKLUND	78	ASPK 3,4,6 $\pi^{\pm}\pi^{\mp}$
1.22±0.30		ALVENSLEB...	71C	CNTR Photoproduction
1.3 $^{+1.2}_{-0.9}$		MOFFEIT	71	HBC 2.8,4.7 $\gamma\rho$
0.80±0.28±0.20		53 BIGGS	70B	CNTR 4.2 $\gamma$ C $\rightarrow \pi^+\pi^-$ C

<sup>45</sup>A combined fit of AKHMETSHIN 07, AULCHENKO 06, and AULCHENKO 08.  
<sup>46</sup>Update of AKHMETSHIN 02.  
<sup>47</sup>From the  $m_{\pi^+\pi^-}$  spectrum taking into account the interference of the  $\rho\pi$  and  $\omega\pi$  amplitudes.  
<sup>48</sup>Using  $\Gamma(\omega \rightarrow e^+e^-)$  from the 2004 Edition of this Review (PDG 04).  
<sup>49</sup>Using the data of AKHMETSHIN 02 in the hidden local symmetry model.  
<sup>50</sup>Using the data of BARKOV 85.  
<sup>51</sup>Using the data of BARKOV 85 in the hidden local symmetry model.  
<sup>52</sup>From a model-dependent analysis assuming complete coherence.  
<sup>53</sup>Re-evaluated under  $\Gamma(\pi^+\pi^-)/\Gamma(\pi^+\pi^-\pi^0)$  by BEHREND 71 using more accurate  $\omega \rightarrow \rho$  photoproduction cross-section ratio.

## Meson Particle Listings

 $\omega(782)$ WEIGHTED AVERAGE  
1.49±0.13 (Error scaled by 1.3)

Values above of weighted average, error, and scale factor are based upon the data in this ideogram only. They are not necessarily the same as our 'best' values, obtained from a least-squares constrained fit utilizing measurements of other (related) quantities as additional information.

 $\Gamma(\pi^+\pi^-)/\Gamma(\pi^+\pi^-\pi^0)$   $\Gamma_3/\Gamma_1$ 

See also  $\Gamma(\pi^+\pi^-)/\Gamma_{total}$ .

VALUE	EVTS	DOCUMENT ID	TECN	COMMENT
<b>0.0172±0.0014 OUR FIT</b>				Error includes scale factor of 1.2.
<b>0.026 ±0.005 OUR AVERAGE</b>				
0.021 +0.028		54,55	RATCLIFF 72	ASPK 15 $\pi^-p \rightarrow n2\pi$
-0.009				
0.028 ±0.006		54	BEHREND 71	ASPK Photoproduction
0.022 +0.009		56	ROOS 70	RVUE
-0.01				

<sup>54</sup>The fitted width of these data is 160 MeV in agreement with present average, thus the  $\omega$  contribution is overestimated. Assuming  $\rho$  width 145 MeV.

<sup>55</sup>Significant interference effect observed. NB of  $\omega \rightarrow 3\pi$  comes from an extrapolation.

<sup>56</sup>ROOS 70 combines ABRAMOVICH 70 and BIZZARRI 70.

 $\Gamma(\pi^+\pi^-)/\Gamma(\pi^0\gamma)$   $\Gamma_3/\Gamma_2$ 

VALUE	EVTS	DOCUMENT ID	TECN	COMMENT
<b>0.20±0.04</b>	1.98M	57	ALOISIO 03	KLOE 1.02 $e^+e^- \rightarrow \pi^+\pi^-\pi^0$

<sup>57</sup>Using the data of ALOISIO 02D.

 $\Gamma(\text{neutrals})/\Gamma_{total}$   $(\Gamma_2+\Gamma_4)/\Gamma$ 

VALUE	EVTS	DOCUMENT ID	TECN	COMMENT
<b>0.091±0.006 OUR FIT</b>				
<b>0.081±0.011 OUR AVERAGE</b>				
0.075±0.025		BIZZARRI 71	HBC	0.0 $\rho\bar{p}$
0.079±0.019		DEINET 69B	OSPK	1.5 $\pi^-p$
0.084±0.015		BOLLINI 68C	CNTR	2.1 $\pi^-p$
••• We do not use the following data for averages, fits, limits, etc. •••				
0.073±0.018	42	BASILE 72B	CNTR	1.67 $\pi^-p$

 $\Gamma(\text{neutrals})/\Gamma(\pi^+\pi^-\pi^0)$   $(\Gamma_2+\Gamma_4)/\Gamma_1$ 

VALUE	EVTS	DOCUMENT ID	TECN	COMMENT
<b>0.102±0.008 OUR FIT</b>				
<b>0.103±0.011 OUR AVERAGE</b>				
-0.010				
0.15 ±0.04	46	AGUILAR...	72B HBC	3.9,4.6 $K^-p$
0.10 ±0.03	19	BARASH 67B	HBC	0.0 $\bar{p}p$
0.134±0.026	850	DIGIUGNO 66B	CNTR	1.4 $\pi^-p$
0.097±0.016	348	FLATTE 66	HBC	1.4 - 1.7 $K^-p \rightarrow \Lambda MM$
0.06 +0.05		JAMES 66	HBC	2.1 $\pi^+p$
-0.02				
0.08 ±0.03	35	KRAEMER 64	DBC	1.2 $\pi^+d$
••• We do not use the following data for averages, fits, limits, etc. •••				
0.11 ±0.02	20	BUSCHBECK 63	HBC	1.5 $K^-p$

 $\Gamma(\pi^0\gamma)/\Gamma(\text{neutrals})$   $\Gamma_2/(\Gamma_2+\Gamma_4)$ 

VALUE	CL%	DOCUMENT ID	TECN	COMMENT
••• We do not use the following data for averages, fits, limits, etc. •••				
0.78±0.07		58	DAKIN 72	OSPK 1.4 $\pi^-p \rightarrow nMM$
>0.81	90	DEINET 69B	OSPK	

<sup>58</sup>Error statistical only. Authors obtain good fit also assuming  $\pi^0\gamma$  as the only neutral decay.

 $\Gamma(\text{neutrals})/\Gamma(\text{charged particles})$   $(\Gamma_2+\Gamma_4)/(\Gamma_1+\Gamma_3)$ 

VALUE	DOCUMENT ID	TECN	COMMENT
<b>0.100±0.008 OUR FIT</b>			
<b>0.124±0.021</b>	FELDMAN 67C	OSPK	1.2 $\pi^-p$

 $\Gamma(\eta\gamma)/\Gamma_{total}$   $\Gamma_5/\Gamma$ 

VALUE (units $10^{-4}$ )	EVTS	DOCUMENT ID	TECN	COMMENT
<b>4.6 ±0.4 OUR FIT</b>				Error includes scale factor of 1.1.
<b>6.3 ±1.3 OUR AVERAGE</b>				Error includes scale factor of 1.2.
6.6 ±1.7		59	ABELE 97E	CBAR 0.0 $\bar{p}p \rightarrow 5\gamma$
8.3 ±2.1			ALDE 93	GAM2 38 $\pi^-p \rightarrow \omega n$
3.0 +2.5		60	ANDREWS 77	CNTR 6.7-10 $\gamma Cu$
-1.8				
••• We do not use the following data for averages, fits, limits, etc. •••				
4.3 ±0.5 ±0.1	33k	61	ACHASOV 07B	SND 0.6-1.38 $e^+e^- \rightarrow \eta\gamma$
4.44 +2.59	17.4k	62,63	AKHMETSHIN 05	CMD2 0.60-1.38 $e^+e^- \rightarrow \eta\gamma$
-1.83 ±0.28				
5.10±0.72±0.34	23k	64	AKHMETSHIN 01B	CMD2 $e^+e^- \rightarrow \eta\gamma$
0.7 to 5.5		65	CASE 00	CBAR 0.0 $\rho\bar{p} \rightarrow \eta\eta\gamma$
6.56 +2.41	3525	60,66	BENAYOUN 96	RVUE $e^+e^- \rightarrow \eta\gamma$
-2.55				
7.3 ±2.9		60,62	DOLINSKY 89	ND $e^+e^- \rightarrow \eta\gamma$

<sup>59</sup>No flat  $\eta\eta\gamma$  background assumed.

<sup>60</sup>Solution corresponding to constructive  $\omega\rho$  interference.

<sup>61</sup>ACHASOV 07B reports  $[\Gamma(\omega(782) \rightarrow \eta\gamma)/\Gamma_{total}] \times [B(\omega(782) \rightarrow e^+e^-)] = (3.10 \pm 0.31 \pm 0.11) \times 10^{-8}$  which we divide by our best value  $B(\omega(782) \rightarrow e^+e^-) = (7.28 \pm 0.14) \times 10^{-5}$ . Our first error is their experiment's error and our second error is the systematic error from using our best value. Supersedes ACHASOV 00D and ACHASOV 06A.

<sup>62</sup>Not independent of the corresponding  $\Gamma(e^+e^-) \times \Gamma(\eta\gamma)/\Gamma_{total}^2$ .

<sup>63</sup>Using  $B(\omega \rightarrow e^+e^-) = (7.14 \pm 0.13) \times 10^{-5}$  and  $B(\eta \rightarrow \gamma\gamma) = 39.43 \pm 0.26\%$ .

<sup>64</sup>Using  $B(\omega \rightarrow e^+e^-) = (7.07 \pm 0.19) \times 10^{-5}$  and using  $B(\eta \rightarrow 3\pi^0) = (32.24 \pm 0.29) \times 10^{-2}$ . Solution corresponding to constructive  $\omega\rho$  interference. The combined fit from 600 to 1380 MeV taking into account  $\rho(770)$ ,  $\omega(782)$ ,  $\phi(1020)$ , and  $\rho(1450)$  (mass and width fixed at 1450 MeV and 310 MeV respectively). Not independent of the corresponding  $\Gamma(e^+e^-) \times \Gamma(\eta\gamma)/\Gamma_{total}^2$ .

<sup>65</sup>Depending on the degree of coherence with the flat  $\eta\eta\gamma$  background and using  $B(\omega \rightarrow \pi^0\gamma) = (8.5 \pm 0.5) \times 10^{-2}$ .

<sup>66</sup>Reanalysis of DRUZHININ 84, DOLINSKY 89, DOLINSKY 91 taking into account the triangle anomaly contributions.

 $\Gamma(\eta\gamma)/\Gamma(\pi^0\gamma)$   $\Gamma_5/\Gamma_2$ 

VALUE	DOCUMENT ID	TECN	COMMENT
••• We do not use the following data for averages, fits, limits, etc. •••			
0.0098±0.0024	67	ALDE 93	GAM2 38 $\pi^-p \rightarrow \omega n$
0.0082±0.0033	68	DOLINSKY 89	ND $e^+e^- \rightarrow \eta\gamma$
0.010 ±0.045		APEL 72B	OSPK 4-8 $\pi^-p \rightarrow n3\gamma$

<sup>67</sup>Model independent determination.

<sup>68</sup>Solution corresponding to constructive  $\omega\rho$  interference.

 $\Gamma(\pi^0 e^+ e^-)/\Gamma_{total}$   $\Gamma_6/\Gamma$ 

VALUE (units $10^{-4}$ )	EVTS	DOCUMENT ID	TECN	COMMENT
<b>7.7 ±0.6 OUR FIT</b>				
<b>7.7 ±0.6 OUR AVERAGE</b>				
7.61 ±0.53 ±0.64		ACHASOV 08	SND	0.36-0.97 $e^+e^- \rightarrow \pi^0 e^+ e^-$
8.19±0.71±0.62		AKHMETSHIN 05A	CMD2	0.72-0.84 $e^+e^-$
5.9 ±1.9	43	DOLINSKY 88	ND	$e^+e^- \rightarrow \pi^0 e^+ e^-$

 $\Gamma(\pi^0 \mu^+ \mu^-)/\Gamma_{total}$   $\Gamma_7/\Gamma$ 

VALUE (units $10^{-4}$ )	EVTS	DOCUMENT ID	TECN	COMMENT
<b>1.3 ±0.4 OUR FIT</b>				Error includes scale factor of 2.1.
<b>1.3 ±0.4 OUR AVERAGE</b>				Error includes scale factor of 2.1.
1.72±0.25±0.14	3k	ARNALDI 09	NA60	158A In-In collisions
0.96±0.23		DZHELJADIN 81B	CNTR	25-33 $\pi^-p \rightarrow \omega n$

 $\Gamma(\eta e^+ e^-)/\Gamma_{total}$   $\Gamma_8/\Gamma$ 

VALUE (units $10^{-5}$ )	DOCUMENT ID	TECN	COMMENT
••• We do not use the following data for averages, fits, limits, etc. •••			
<1.1	AKHMETSHIN 05A	CMD2	0.72-0.84 $e^+e^-$

 $\Gamma(e^+e^-)/\Gamma_{total}$   $\Gamma_9/\Gamma$ 

VALUE (units $10^{-4}$ )	EVTS	DOCUMENT ID	TECN	COMMENT
<b>0.728±0.014 OUR FIT</b>				Error includes scale factor of 1.3.
••• We do not use the following data for averages, fits, limits, etc. •••				
0.700±0.016	11200	69,70	AKHMETSHIN 04	CMD2 $e^+e^- \rightarrow \pi^+\pi^-\pi^0$
0.752±0.004±0.024	1.2M	70,71	ACHASOV 03D	RVUE 0.44-2.00 $e^+e^- \rightarrow \pi^+\pi^-\pi^0$
0.714±0.036		70	DOLINSKY 89	ND $e^+e^- \rightarrow \pi^+\pi^-\pi^0$
0.72 ±0.03		70	BARKOV 87	CMD $e^+e^- \rightarrow \pi^+\pi^-\pi^0$
0.64 ±0.04	1488	70	KURDADZE 83B	OLYA $e^+e^- \rightarrow \pi^+\pi^-\pi^0$
0.675±0.069	433	70	CORDIER 80	DM1 $e^+e^- \rightarrow \pi^+\pi^-\pi^0$
0.83 ±0.10	451	70	BENAKSAS 72B	OSPK $e^+e^- \rightarrow \pi^+\pi^-\pi^0$
0.77 ±0.06		72	AUGUSTIN 69D	OSPK $e^+e^- \rightarrow \pi^+\pi^-\pi^0$
0.65 ±0.13	33	73	ASTVACAT...	68 OSPK Assume SU(3)+mixing

<sup>69</sup>Using  $B(\omega \rightarrow \pi^+\pi^-\pi^0) = 0.891 \pm 0.007$ . Update of AKHMETSHIN 00c.

<sup>70</sup>Not independent of the corresponding  $\Gamma(e^+e^-) \times \Gamma(\pi^+\pi^-\pi^0)/\Gamma_{total}^2$ .

<sup>71</sup>Using ACHASOV 03, ACHASOV 03D and  $B(\omega \rightarrow \pi^+\pi^-) = (1.70 \pm 0.28)\%$ .

<sup>72</sup>Rescaled by us to correspond to  $\omega$  width 8.4 MeV. Systematic errors underestimated.

<sup>73</sup>Not resolved from  $\rho$  decay. Error statistical only.

$\Gamma(\pi^+\pi^-\pi^0\pi^0)/\Gamma_{\text{total}}$   $\Gamma_{10}/\Gamma$ 

VALUE (units $10^{-4}$ )	CL%	DOCUMENT ID	TECN	COMMENT
< 2	90	ACHASOV 09A	SND	$e^+e^- \rightarrow \pi^+\pi^-\pi^0\pi^0$
••• We do not use the following data for averages, fits, limits, etc. •••				
<200	90	KURDADZE 86	OLYA	$e^+e^- \rightarrow \pi^+\pi^-\pi^0\pi^0$

 $\Gamma(\pi^+\pi^-\gamma)/\Gamma_{\text{total}}$   $\Gamma_{11}/\Gamma$ 

VALUE	CL%	DOCUMENT ID	TECN	COMMENT
<0.0036	95	WEIDENAUER 90	ASTE	$p\bar{p} \rightarrow \pi^+\pi^-\pi^+\pi^- \gamma$
••• We do not use the following data for averages, fits, limits, etc. •••				
<0.004	95	BITYUKOV 88B	SPEC	$32 \pi^- p \rightarrow \pi^+\pi^-\gamma X$

 $\Gamma(\pi^+\pi^-\gamma)/\Gamma(\pi^+\pi^-\pi^0)$   $\Gamma_{11}/\Gamma_1$ 

VALUE	CL%	DOCUMENT ID	TECN	COMMENT
••• We do not use the following data for averages, fits, limits, etc. •••				
<0.066	90	KALBFLEISCH 75	HBC	$2.18 K^- p \rightarrow \Lambda \pi^+\pi^- \gamma$
<0.05	90	FLATTE 66	HBC	$1.2 - 1.7 K^- p \rightarrow \Lambda \pi^+\pi^- \gamma$

 $\Gamma(\pi^+\pi^-\pi^+\pi^-)/\Gamma_{\text{total}}$   $\Gamma_{12}/\Gamma$ 

VALUE	CL%	DOCUMENT ID	TECN	COMMENT
<1 × 10 <sup>-3</sup>	90	KURDADZE 88	OLYA	$e^+e^- \rightarrow \pi^+\pi^-\pi^+\pi^-$

 $\Gamma(\pi^0\pi^0\gamma)/\Gamma_{\text{total}}$   $\Gamma_{13}/\Gamma$ 

VALUE (units $10^{-5}$ )	EVTS	DOCUMENT ID	TECN	COMMENT
<b>6.6 ± 1.1 OUR FIT</b>				
<b>6.5 ± 1.2 OUR AVERAGE</b>				
6.4 <sup>+2.4</sup> <sub>-2.0</sub> ± 0.8	190	<sup>74</sup> AKHMETSHIN 04B	CMD2	$0.6 - 0.97 e^+e^- \rightarrow \pi^0\pi^0\gamma$
6.6 <sup>+1.4</sup> <sub>-1.3</sub> ± 0.6	295	ACHASOV 02F	SND	$0.36 - 0.97 e^+e^- \rightarrow \pi^0\pi^0\gamma$
••• We do not use the following data for averages, fits, limits, etc. •••				
11.8 <sup>+2.1</sup> <sub>-1.9</sub> ± 1.4	190	<sup>75</sup> AKHMETSHIN 04B	CMD2	$0.6 - 0.97 e^+e^- \rightarrow \pi^0\pi^0\gamma$
7.8 ± 2.7 ± 2.0	63	<sup>74,76</sup> ACHASOV 00G	SND	$e^+e^- \rightarrow \pi^0\pi^0\gamma$
12.7 ± 2.3 ± 2.5	63	<sup>75,76</sup> ACHASOV 00G	SND	$e^+e^- \rightarrow \pi^0\pi^0\gamma$
<sup>74</sup> In the model assuming the $\rho \rightarrow \pi^0\pi^0\gamma$ decay via the $\omega\pi$ and $f_0(500)\gamma$ mechanisms.				
<sup>75</sup> In the model assuming the $\rho \rightarrow \pi^0\pi^0\gamma$ decay via the $\omega\pi$ mechanism only.				
<sup>76</sup> Superseded by ACHASOV 02F.				

 $\Gamma(\pi^0\pi^0\gamma)/\Gamma(\pi^+\pi^-\pi^0)$   $\Gamma_{13}/\Gamma_1$ 

VALUE	CL%	DOCUMENT ID	TECN	COMMENT
<0.00045	90	DOLINSKY 89	ND	$e^+e^- \rightarrow \pi^0\pi^0\gamma$
••• We do not use the following data for averages, fits, limits, etc. •••				
<0.08	95	JACQUET 69B	HLBC	$2.05 \pi^+ p \rightarrow \pi^+ p \omega$

 $\Gamma(\pi^0\pi^0\gamma)/\Gamma(\pi^0\gamma)$   $\Gamma_{13}/\Gamma_2$ 

VALUE (units $10^{-4}$ )	CL%	EVTS	DOCUMENT ID	TECN	COMMENT
<b>8.0 ± 1.3 OUR FIT</b>					
<b>8.5 ± 2.9</b>					
40 ± 14		40 ± 14	ALDE 94B	GAM2	$38\pi^- p \rightarrow \pi^0\pi^0\gamma n$
••• We do not use the following data for averages, fits, limits, etc. •••					
< 50	90		DOLINSKY 89	ND	$e^+e^- \rightarrow \pi^0\pi^0\gamma$
<1800	95		KEYNE 76	CNTR	$\pi^- p \rightarrow \omega n$
<1500	90		BENAKSAS 72C	OSPK	$e^+e^-$
<1400			BALDIN 71	HLBC	$2.9 \pi^+ p$
<1000	90		BARMIN 64	HLBC	$1.3 - 2.8 \pi^- p$

 $\Gamma(\pi^0\pi^0\gamma)/\Gamma(\text{neutrals})$   $\Gamma_{13}/(\Gamma_2+\Gamma_4)$ 

VALUE	CL%	DOCUMENT ID	TECN	COMMENT
••• We do not use the following data for averages, fits, limits, etc. •••				
0.22 ± 0.07		<sup>77</sup> DAKIN 72	OSPK	$1.4 \pi^- p \rightarrow nMM$
<0.19	90	DEINET 69B	OSPK	
<sup>77</sup> See $\Gamma(\pi^0\gamma)/\Gamma(\text{neutrals})$ .				

 $\Gamma(\eta\pi^0\gamma)/\Gamma_{\text{total}}$   $\Gamma_{14}/\Gamma$ 

VALUE (units $10^{-5}$ )	CL%	DOCUMENT ID	TECN	COMMENT
<3.3	90	AKHMETSHIN 04B	CMD2	$0.6 - 0.97 e^+e^- \rightarrow \eta\pi^0\gamma$

 $\Gamma(\mu^+\mu^-)/\Gamma_{\text{total}}$   $\Gamma_{15}/\Gamma$ 

VALUE (units $10^{-5}$ )	EVTS	DOCUMENT ID	TECN	COMMENT
<b>9.0 ± 3.1 OUR FIT</b>				
9.0 ± 2.9 ± 1.1	18	HEISTER 02C	ALEP	$Z \rightarrow \mu^+\mu^- + X$

 $\Gamma(\mu^+\mu^-)/\Gamma(\pi^+\pi^-\pi^0)$   $\Gamma_{15}/\Gamma_1$ 

VALUE (units $10^{-3}$ )	CL%	DOCUMENT ID	TECN	COMMENT
<0.2	90	WILSON 69	OSPK	$12 \pi^- C \rightarrow Fe$
••• We do not use the following data for averages, fits, limits, etc. •••				
<1.7	74	FLATTE 66	HBC	$1.2 - 1.7 K^- p \rightarrow \Lambda \mu^+\mu^-$
<1.2		BARBARO... 65	HBC	$2.7 K^- p$

 $\Gamma(\pi^0\mu^+\mu^-)/\Gamma(\mu^+\mu^-)$   $\Gamma_7/\Gamma_{15}$ 

VALUE	EVTS	DOCUMENT ID	TECN	COMMENT
••• We do not use the following data for averages, fits, limits, etc. •••				
1.2 ± 0.6	30	<sup>78</sup> DZHELYADIN 79	CNTR	25-33 $\pi^- p$
<sup>78</sup> Superseded by DZHELYADIN 81B result above.				

 $\Gamma(3\gamma)/\Gamma_{\text{total}}$   $\Gamma_{16}/\Gamma$ 

VALUE (units $10^{-4}$ )	CL%	DOCUMENT ID	TECN	COMMENT
<1.9	95	<sup>79</sup> ABELE 97E	CBAR	$0.0 \bar{p} p \rightarrow 5\gamma$
••• We do not use the following data for averages, fits, limits, etc. •••				
<2	90	<sup>79</sup> PROKOSHKIN 95	GAM2	$38 \pi^- p \rightarrow 3\gamma n$
<sup>79</sup> From direct $3\gamma$ decay search.				

 $\Gamma(\eta\pi^0)/\Gamma_{\text{total}}$   $\Gamma_{17}/\Gamma$ 

VALUE	CL%	DOCUMENT ID	TECN	COMMENT
Violates C conservation.				
••• We do not use the following data for averages, fits, limits, etc. •••				
<0.001	90	ALDE 94B	GAM2	$38\pi^- p \rightarrow \eta\pi^0 n$

 $[\Gamma(\eta\gamma) + \Gamma(\eta\pi^0)]/\Gamma(\pi^+\pi^-\pi^0)$   $(\Gamma_5+\Gamma_{17})/\Gamma_1$ 

VALUE	CL%	DOCUMENT ID	TECN	COMMENT
<0.016	90	<sup>80</sup> FLATTE 66	HBC	$1.2 - 1.7 K^- p \rightarrow \Lambda \pi^+\pi^- MM$
••• We do not use the following data for averages, fits, limits, etc. •••				
<0.045	95	JACQUET 69B	HLBC	$2.05 \pi^+ p \rightarrow \pi^+ p \omega$
<sup>80</sup> Restated by us using $B(\eta \rightarrow \text{charged modes}) = 29.2\%$ .				

 $\Gamma(\eta\pi^0)/\Gamma(\pi^0\gamma)$   $\Gamma_{17}/\Gamma_2$ 

VALUE (units $10^{-3}$ )	CL%	DOCUMENT ID	TECN	COMMENT
<2.6	90	<sup>81</sup> STAROSTIN 09	CRYM	$\gamma p \rightarrow \eta\pi^0 p$
<sup>81</sup> STAROSTIN 09 reports $[\Gamma(\omega(782) \rightarrow \eta\pi^0)/\Gamma(\omega(782) \rightarrow \pi^0\gamma)] \times [B(\eta \rightarrow 2\gamma)] < 1.01 \times 10^{-3}$ which we divide by our best value $B(\eta \rightarrow 2\gamma) = 39.31 \times 10^{-2}$ .				

 $\Gamma(2\pi^0)/\Gamma(\pi^0\gamma)$   $\Gamma_{18}/\Gamma_2$ 

VALUE (units $10^{-3}$ )	CL%	DOCUMENT ID	TECN	COMMENT
<2.59	90	STAROSTIN 09	CRYM	$\gamma p \rightarrow 2\pi^0 p$

 $\Gamma(3\pi^0)/\Gamma_{\text{total}}$   $\Gamma_{19}/\Gamma$ 

VALUE	CL%	DOCUMENT ID	TECN	COMMENT
Violates C conservation.				
••• We do not use the following data for averages, fits, limits, etc. •••				
<3 × 10 <sup>-4</sup>	90	PROKOSHKIN 95	GAM2	$38 \pi^- p \rightarrow 3\pi^0 n$

 $\Gamma(3\pi^0)/\Gamma(\pi^0\gamma)$   $\Gamma_{19}/\Gamma_2$ 

VALUE (units $10^{-3}$ )	CL%	DOCUMENT ID	TECN	COMMENT
<2.72	90	STAROSTIN 09	CRYM	$\gamma p \rightarrow 3\pi^0 p$

 $\Gamma(3\pi^0)/\Gamma(\pi^+\pi^-\pi^0)$   $\Gamma_{19}/\Gamma_1$ 

VALUE	CL%	DOCUMENT ID	COMMENT
Violates C conservation.			
••• We do not use the following data for averages, fits, limits, etc. •••			
<0.009	90	BARBERIS 01	450 $p p \rightarrow p_f 3\pi^0 p_s$

PARAMETER  $\Lambda$  IN  $\omega \rightarrow \pi^0\mu^+\mu^-$  DECAY

In the pole approximation the electromagnetic transition form factor for a resonance of mass  $M$  is given by the expression:

$$|F|^2 = (1 - M^2/\Lambda^2)^{-2},$$

where for the parameter  $\Lambda$  vector dominance predicts  $\Lambda = M_p \approx 0.770$  GeV. The ARNALDI 09 measurement is in obvious conflict with this expectation. Note that for  $\eta \rightarrow \mu^+\mu^-\gamma$  decay ARNALDI 09 and DZHELYADIN 80 obtain the value of  $\Lambda$  consistent with vector dominance.

VALUE (GeV)	EVTS	DOCUMENT ID	TECN	COMMENT
<b>0.668 ± 0.009 ± 0.003</b>	3k	ARNALDI 09	NA60	158A In-In collisions
••• We do not use the following data for averages, fits, limits, etc. •••				
0.65 ± 0.03		DZHELYADIN 81B	CNTR	25-33 $\pi^- p \rightarrow \omega n$

 $\omega(782)$  REFERENCES

BENAYOUN 10	EPJ C65 211	M. Benayoun et al.		
ACHASOV 09A	JETP 109 379	M.N. Achasov et al.		(SND Collab.)
	Translated from ZETF 136 442.			
ARNALDI 09	PL B677 260	R. Arnaldi et al.		(NA60 Collab.)
STAROSTIN 09	PR C79 045201	A. Starostin et al.		(Crystal Ball Collab. at MAMI)
ACHASOV 08	JETP 107 61	M.N. Achasov et al.		(SND Collab.)
	Translated from ZETF 134 80.			
AMBROSINO 08B	PL B669 223	F. Ambrosino et al.		(KLOE Collab.)
ACHASOV 07G	PR D76 077101	M.N. Achasov et al.		(SND Collab.)
AKHMETSHIN 07	PL B648 28	R. Akhmetshin et al.		(Novosibirsk CMD-2 Collab.)
ACHASOV 06	JETP 103 380	M.N. Achasov et al.		(Novosibirsk SND Collab.)
	Translated from ZETF 130 437.			
ACHASOV 06A	PR D74 014016	M.N. Achasov et al.		(SND Collab.)
AULCHENKO 06A	JETPL 84 413	V.M. Aulchenko et al.		(Novosibirsk CMD-2 Collab.)
	Translated from ZETFP 84 491.			
ACHASOV 05A	JETP 101 1053	M.N. Achasov et al.		(Novosibirsk SND Collab.)
	Translated from ZETF 128 1201.			



## CONSTRAINED FIT INFORMATION

An overall fit to the total width, a partial width, 2 combinations of partial widths obtained from integrated cross section, and 13 branching ratios uses 40 measurements and one constraint to determine 9 parameters. The overall fit has a  $\chi^2 = 31.5$  for 32 degrees of freedom.

The following *off-diagonal* array elements are the correlation coefficients  $\langle \delta p_i \delta p_j \rangle / (\delta p_i \delta p_j)$ , in percent, from the fit to parameters  $p_i$ , including the branching fractions,  $x_i \equiv \Gamma_i / \Gamma_{\text{total}}$ . The fit constrains the  $x_i$  whose labels appear in this array to sum to one.

$x_2$	1									
$x_3$	-76	-57								
$x_4$	-20	-24	6							
$x_5$	-31	-26	35	0						
$x_6$	-23	-17	28	1	10					
$x_9$	-1	-5	-7	-3	-4	-2				
$x_{17}$	-4	-6	-5	-2	-3	-2	-1			
$\Gamma$	26	5	-21	4	-72	-6	4	3		
	$x_1$	$x_2$	$x_3$	$x_4$	$x_5$	$x_6$	$x_9$	$x_{17}$		
Mode									Rate (MeV)	
$\Gamma_1$	$\pi^+ \pi^- \eta$								0.086 ± 0.004	
$\Gamma_2$	$\rho^0 \gamma$ (including non-resonant $\pi^+ \pi^- \gamma$ )								0.0583 ± 0.0028	
$\Gamma_3$	$\pi^0 \pi^0 \eta$								0.0430 ± 0.0022	
$\Gamma_4$	$\omega \gamma$								0.0055 ± 0.0005	
$\Gamma_5$	$\gamma \gamma$								0.00434 ± 0.00013	
$\Gamma_6$	$3\pi^0$								(3.3 ± 0.5) × 10 <sup>-4</sup>	
$\Gamma_9$	$\pi^+ \pi^- \pi^0$								(7.2 +2.2 -1.9) × 10 <sup>-4</sup>	
$\Gamma_{17}$	$\pi^+ \pi^- e^+ e^-$								(4.8 +2.6 -1.9) × 10 <sup>-4</sup>	

 $\eta'(958)$  PARTIAL WIDTHS

$\Gamma(\gamma\gamma)$					$\Gamma_5$
VALUE (keV)	EVTS	DOCUMENT ID	TECN	COMMENT	
<b>4.34 ± 0.19 OUR FIT</b>					
<b>4.28 ± 0.19 OUR AVERAGE</b>					
4.17 ± 0.10 ± 0.27	2000	<sup>4</sup> ACCIARRI	98Q L3	$e^+ e^- \rightarrow e^+ e^- \pi^+ \pi^- \gamma$	
4.53 ± 0.29 ± 0.51	266	KARCH	92 CBAL	$e^+ e^- \rightarrow e^+ e^- \eta \pi^0 \pi^0$	
3.61 ± 0.13 ± 0.48		<sup>5</sup> BEHREND	91 CELL	$e^+ e^- \rightarrow e^+ e^- \eta'(958)$	
4.6 ± 1.1 ± 0.6	23	BARU	90 MD1	$e^+ e^- \rightarrow e^+ e^- \pi^+ \pi^- \gamma$	
4.57 ± 0.25 ± 0.44		BUTLER	90 MRK2	$e^+ e^- \rightarrow e^+ e^- \eta'(958)$	
5.08 ± 0.24 ± 0.71	547	<sup>6</sup> ROE	90 ASP	$e^+ e^- \rightarrow e^+ e^- 2\gamma$	
3.8 ± 0.7 ± 0.6	34	AIHARA	88c TPC	$e^+ e^- \rightarrow e^+ e^- \eta \pi^+ \pi^-$	
4.9 ± 0.5 ± 0.5	136	<sup>7</sup> WILLIAMS	88 CBAL	$e^+ e^- \rightarrow e^+ e^- 2\gamma$	
<b>••• We do not use the following data for averages, fits, limits, etc. •••</b>					
4.7 ± 0.6 ± 0.9	143	<sup>8</sup> GIDAL	87 MRK2	$e^+ e^- \rightarrow e^+ e^- \eta \pi^+ \pi^-$	
4.0 ± 0.9		<sup>9</sup> BARTEL	85E JADE	$e^+ e^- \rightarrow e^+ e^- 2\gamma$	

<sup>4</sup> No non-resonant  $\pi^+ \pi^-$  contribution found.

<sup>5</sup> Reevaluated by us using  $B(\eta' \rightarrow \rho(770)\gamma) = (30.2 \pm 1.3)\%$ .

<sup>6</sup> Reevaluated by us using  $B(\eta' \rightarrow \gamma\gamma) = (2.11 \pm 0.13)\%$ .

<sup>7</sup> Reevaluated by us using  $B(\eta' \rightarrow \gamma\gamma) = (2.11 \pm 0.13)\%$ .

<sup>8</sup> Superseded by BUTLER 90.

<sup>9</sup> Systematic error not evaluated.

 $\eta'(958) \Gamma(i)\Gamma(\gamma\gamma)/\Gamma(\text{total})$ 

This combination of a partial width with the partial width into  $\gamma\gamma$  and with the total width is obtained from the integrated cross section into channel(i) in the  $\gamma\gamma$  annihilation.

$\Gamma(\gamma\gamma) \times \Gamma(\rho^0 \gamma$ (including non-resonant $\pi^+ \pi^- \gamma$ ))/ $\Gamma_{\text{total}}$				$\Gamma_5 \Gamma_2 / \Gamma$	
VALUE (keV)	EVTS	DOCUMENT ID	TECN	COMMENT	
<b>1.27 ± 0.04 OUR FIT</b>					
<b>1.26 ± 0.07 OUR AVERAGE</b>					
1.09 ± 0.04 ± 0.13		BEHREND	91 CELL	$e^+ e^- \rightarrow e^+ e^- \rho(770)^0 \gamma$	
1.35 ± 0.09 ± 0.21		AIHARA	87 TPC	$e^+ e^- \rightarrow e^+ e^- \rho\gamma$	
1.13 ± 0.04 ± 0.13	867	ALBRECHT	87B ARG	$e^+ e^- \rightarrow e^+ e^- \rho\gamma$	
1.53 ± 0.09 ± 0.21		ALTHOFF	84E TASS	$e^+ e^- \rightarrow e^+ e^- \rho\gamma$	
1.14 ± 0.08 ± 0.11	243	BERGER	84B PLUT	$e^+ e^- \rightarrow e^+ e^- \rho\gamma$	
1.73 ± 0.34 ± 0.35	95	JENNI	83 MRK2	$e^+ e^- \rightarrow e^+ e^- \rho\gamma$	
1.49 ± 0.13 ± 0.027	213	BARTEL	82B JADE	$e^+ e^- \rightarrow e^+ e^- \rho\gamma$	
<b>••• We do not use the following data for averages, fits, limits, etc. •••</b>					
1.85 ± 0.31 ± 0.24	43	BEHREND	83B CELL	$e^+ e^- \rightarrow e^+ e^- \rho\gamma$	

 $\Gamma(\gamma\gamma) \times \Gamma(\pi^0 \pi^0 \eta) / \Gamma_{\text{total}}$ 

VALUE (keV)	DOCUMENT ID	TECN	COMMENT	$\Gamma_5 \Gamma_3 / \Gamma$
<b>0.94 ± 0.05 OUR FIT</b>				
<b>0.92 ± 0.06 ± 0.11</b>				
0.95 ± 0.05 ± 0.08	<sup>10</sup> KARCH	92 CBAL	$e^+ e^- \rightarrow e^+ e^- \eta \pi^0 \pi^0$	
<b>••• We do not use the following data for averages, fits, limits, etc. •••</b>				
1.00 ± 0.08 ± 0.10	<sup>11</sup> KARCH	90 CBAL	$e^+ e^- \rightarrow e^+ e^- \eta \pi^0 \pi^0$	
	<sup>11,12</sup> ANTREASYAN	87 CBAL	$e^+ e^- \rightarrow e^+ e^- \eta \pi^0 \pi^0$	
<sup>10</sup> Reevaluated by us using $B(\eta \rightarrow \gamma\gamma) = (39.21 \pm 0.34)\%$ . Supersedes ANTREASYAN 87 and KARCH 90.				
<sup>11</sup> Superseded by KARCH 92.				
<sup>12</sup> Using $BR(\eta \rightarrow 2\gamma) = (38.9 \pm 0.5)\%$ .				

 $\eta'(958) \rightarrow \eta \pi \pi$  DECAY PARAMETERS

$$|\text{MATRIX ELEMENT}|^2 = |1 + \alpha Y|^2 + CX + DX^2$$

$X$  and  $Y$  are Dalitz variables;  $\alpha$  is complex and  $C$ , and  $D$  are real-valued. Parameters  $C$  and  $D$  are not necessarily equal to  $c$  and  $d$ , respectively, in the generalized parameterization following this one. May be different for  $\eta'(958) \rightarrow \eta \pi^+ \pi^-$  and  $\eta'(958) \rightarrow \eta \pi^0 \pi^0$  decays. Because of different initial assumptions and strong correlations of the parameters we do not average the parameters in the section below.

 $Re(\alpha)$  decay parameter

VALUE	EVTS	DOCUMENT ID	TECN	COMMENT
<b>••• We do not use the following data for averages, fits, limits, etc. •••</b>				
-0.033 ± 0.005 ± 0.003	44k	<sup>13</sup> ABLIKIM	11 BES3	$J/\psi \rightarrow \gamma \eta \pi^+ \pi^-$
-0.072 ± 0.012 ± 0.006	7k	<sup>14</sup> AMELIN	05A VES	$28 \pi^- A \rightarrow \eta \pi^+ \pi^- \pi^- A^*$
-0.021 ± 0.018 ± 0.017	6.7k	<sup>15</sup> BRIERE	00 CLEO	$10.6 e^+ e^- \rightarrow \eta \pi^+ \pi^- X$
-0.058 ± 0.013 ± 0.003	5.4k	<sup>16</sup> ALDE	86 GAM2	$38 \pi^- \rho \rightarrow n \eta \pi^0 \pi^0$
-0.08 ± 0.03		<sup>16,17</sup> KALBFLEISCH	74 RVUE	$\eta' \rightarrow \eta \pi^+ \pi^-$
<sup>13</sup> See ABLIKIM 11 for the full correlation matrix.				
<sup>14</sup> Superseded by DOROFEEV 07, which found this parameterization unacceptable. See below.				
<sup>15</sup> Assuming $\text{Im}(\alpha) = 0$ , $C = 0$ , and $D = 0$ .				
<sup>16</sup> Assuming $C = 0$ .				
<sup>17</sup> From the data of DAUBER 64, RITTENBERG 69, AGUILAR-BENITEZ 72B, JACOBS 73, and DANBURG 73.				

 $Im(\alpha)$  decay parameter

VALUE	EVTS	DOCUMENT ID	TECN	COMMENT
<b>••• We do not use the following data for averages, fits, limits, etc. •••</b>				
0.000 ± 0.049 ± 0.001	44k	<sup>18</sup> ABLIKIM	11 BES3	$J/\psi \rightarrow \gamma \eta \pi^+ \pi^-$
0.0 ± 0.1 ± 0.0	7k	<sup>19</sup> AMELIN	05A VES	$28 \pi^- A \rightarrow \eta \pi^+ \pi^- \pi^- A^*$
-0.00 ± 0.13 ± 0.00	5.4k	<sup>20</sup> ALDE	86 GAM2	$38 \pi^- \rho \rightarrow n \eta \pi^0 \pi^0$
0.0 ± 0.3		<sup>20,21</sup> KALBFLEISCH	74 RVUE	$\eta' \rightarrow \eta \pi^+ \pi^-$
<sup>18</sup> See ABLIKIM 11 for the full correlation matrix.				
<sup>19</sup> Superseded by DOROFEEV 07, which found this parameterization unacceptable. See below.				
<sup>20</sup> Assuming $C = 0$ .				
<sup>21</sup> From the data of DAUBER 64, RITTENBERG 69, AGUILAR-BENITEZ 72B, JACOBS 73, and DANBURG 73.				

 $C$  decay parameter

VALUE	EVTS	DOCUMENT ID	TECN	COMMENT
<b>••• We do not use the following data for averages, fits, limits, etc. •••</b>				
+0.018 ± 0.009 ± 0.003	44k	<sup>22</sup> ABLIKIM	11 BES3	$J/\psi \rightarrow \gamma \eta \pi^+ \pi^-$
0.020 ± 0.018 ± 0.004	7k	<sup>23</sup> AMELIN	05A VES	$28 \pi^- A \rightarrow \eta \pi^+ \pi^- \pi^- A^*$
<sup>22</sup> See ABLIKIM 11 for the full correlation matrix.				
<sup>23</sup> Superseded by DOROFEEV 07, which found this parameterization unacceptable. See below.				

 $D$  decay parameter

VALUE	EVTS	DOCUMENT ID	TECN	COMMENT
<b>••• We do not use the following data for averages, fits, limits, etc. •••</b>				
-0.059 ± 0.012 ± 0.004	44k	<sup>24</sup> ABLIKIM	11 BES3	$J/\psi \rightarrow \gamma \eta \pi^+ \pi^-$
-0.066 ± 0.030 ± 0.015	7k	<sup>25</sup> AMELIN	05A VES	$28 \pi^- A \rightarrow \eta \pi^+ \pi^- \pi^- A^*$
0.00 ± 0.03 ± 0.00	5.4k	<sup>26</sup> ALDE	86 GAM2	$38 \pi^- \rho \rightarrow n \eta \pi^0 \pi^0$
0		<sup>26,27</sup> KALBFLEISCH	74 RVUE	$\eta' \rightarrow \eta \pi^+ \pi^-$
<sup>24</sup> See ABLIKIM 11 for the full correlation matrix.				
<sup>25</sup> Superseded by DOROFEEV 07, which found this parameterization unacceptable. See below.				
<sup>26</sup> Assuming $C = 0$ .				
<sup>27</sup> From the data of DAUBER 64, RITTENBERG 69, AGUILAR-BENITEZ 72B, JACOBS 73, and DANBURG 73.				

## Meson Particle Listings

 $\eta'(958)$  $\eta'(958) \rightarrow \eta\pi\pi$  DECAY PARAMETERS

$$|\text{MATRIX ELEMENT}|^2 \propto 1 + aY + bY^2 + cX + dX^2$$

X and Y are Dalitz variables and a, b, c, and d are real-valued parameters. May be different for  $\eta'(958) \rightarrow \eta\pi^+\pi^-$  and  $\eta'(958) \rightarrow \eta\pi^0\pi^0$  decays. We do not average measurements in the section below because parameter values from each experiment are strongly correlated.

**a decay parameter**

VALUE	EVTS	DOCUMENT ID	TECN	COMMENT
••• We do not use the following data for averages, fits, limits, etc. •••				
$-0.047 \pm 0.011 \pm 0.003$	44k	<sup>28</sup> ABLIKIM	11	BES3 $J/\psi \rightarrow \gamma\eta\pi^+\pi^-$
$-0.066 \pm 0.016 \pm 0.003$	15k	<sup>29</sup> BLIK	09	GAM4 $32.5 \pi^- p \rightarrow \eta' n$
$-0.127 \pm 0.016 \pm 0.008$	20k	<sup>30</sup> DOROFEEV	07	VES $27 \pi^- p \rightarrow \eta' n$ , $\pi^- A \rightarrow \eta' \pi^- A^*$

<sup>28</sup> See ABLIKIM 11 for the full correlation matrix.  
<sup>29</sup> From  $\eta' \rightarrow \eta\pi^0\pi^0$  decay.  
<sup>30</sup> From  $\eta' \rightarrow \eta\pi^+\pi^-$  decay.

**b decay parameter**

VALUE	EVTS	DOCUMENT ID	TECN	COMMENT
••• We do not use the following data for averages, fits, limits, etc. •••				
$-0.069 \pm 0.019 \pm 0.009$	44k	<sup>31</sup> ABLIKIM	11	BES3 $J/\psi \rightarrow \gamma\eta\pi^+\pi^-$
$-0.063 \pm 0.028 \pm 0.004$	15k	<sup>32</sup> BLIK	09	GAM4 $32.5 \pi^- p \rightarrow \eta' n$
$-0.106 \pm 0.028 \pm 0.014$	20k	<sup>33</sup> DOROFEEV	07	VES $27 \pi^- p \rightarrow \eta' n$ , $\pi^- A \rightarrow \eta' \pi^- A^*$

<sup>31</sup> See ABLIKIM 11 for the full correlation matrix.  
<sup>32</sup> From  $\eta' \rightarrow \eta\pi^0\pi^0$  decay.  
<sup>33</sup> From  $\eta' \rightarrow \eta\pi^+\pi^-$  decay.

**c decay parameter**

VALUE	EVTS	DOCUMENT ID	TECN	COMMENT
••• We do not use the following data for averages, fits, limits, etc. •••				
$+0.019 \pm 0.011 \pm 0.003$	44k	<sup>34</sup> ABLIKIM	11	BES3 $J/\psi \rightarrow \gamma\eta\pi^+\pi^-$
$-0.107 \pm 0.096 \pm 0.003$	15k	<sup>35</sup> BLIK	09	GAM4 $32.5 \pi^- p \rightarrow \eta' n$
$0.015 \pm 0.011 \pm 0.014$	20k	<sup>36</sup> DOROFEEV	07	VES $27 \pi^- p \rightarrow \eta' n$ , $\pi^- A \rightarrow \eta' \pi^- A^*$

<sup>34</sup> See ABLIKIM 11 for the full correlation matrix.  
<sup>35</sup> From  $\eta' \rightarrow \eta\pi^0\pi^0$  decay.  
<sup>36</sup> From  $\eta' \rightarrow \eta\pi^+\pi^-$  decay.

**d decay parameter**

VALUE	EVTS	DOCUMENT ID	TECN	COMMENT
••• We do not use the following data for averages, fits, limits, etc. •••				
$-0.073 \pm 0.012 \pm 0.003$	44k	<sup>37</sup> ABLIKIM	11	BES3 $J/\psi \rightarrow \gamma\eta\pi^+\pi^-$
$0.018 \pm 0.078 \pm 0.006$	15k	<sup>38</sup> BLIK	09	GAM4 $32.5 \pi^- p \rightarrow \eta' n$
$-0.082 \pm 0.017 \pm 0.008$	20k	<sup>39</sup> DOROFEEV	07	VES $27 \pi^- p \rightarrow \eta' n$ , $\pi^- A \rightarrow \eta' \pi^- A^*$

<sup>37</sup> See ABLIKIM 11 for the full correlation matrix.  
<sup>38</sup> From  $\eta' \rightarrow \eta\pi^0\pi^0$  decay. If  $c \equiv 0$  from Bose-Einstein symmetry,  $d = -0.067 \pm 0.020 \pm 0.003$ .  
<sup>39</sup> From  $\eta' \rightarrow \eta\pi^+\pi^-$  decay.

 $\eta'(958)$   $\beta$  PARAMETER

$$|\text{MATRIX ELEMENT}|^2 = (1 + 2\beta Z)$$

See the "Note on  $\eta$  Decay Parameters" in our 1994 edition Physical Review D50 1173 (1994), p. 1454.

 **$\beta$  decay parameter**

VALUE	EVTS	DOCUMENT ID	TECN	COMMENT
<b><math>-0.46 \pm 0.22</math> OUR AVERAGE</b>	Error	includes scale factor of 1.4.		
$-0.59 \pm 0.18$	235	BLIK	08	GAMS $32 \pi^- p \rightarrow \eta' n$
$-0.1 \pm 0.3$		ALDE	87B	GAM2 $38 \pi^- p \rightarrow n3\pi^0$

 $\eta'(958)$  BRANCHING RATIOS

$\Gamma(\pi^+\pi^-\eta)/\Gamma_{\text{total}}$					$\Gamma_1/\Gamma$	
VALUE	EVTS	DOCUMENT ID	TECN	COMMENT		
<b><math>0.434 \pm 0.007</math> OUR FIT</b>						
••• We do not use the following data for averages, fits, limits, etc. •••						
$0.424 \pm 0.011 \pm 0.004$	1.2k	<sup>40</sup> PEDLAR	09	CLEO $J/\psi \rightarrow \gamma\eta'$		

<sup>40</sup> Not independent of other  $\eta'$  branching fractions and ratios in PEDLAR 09.

$\Gamma(\pi^+\pi^-\eta(\text{charged decay}))/\Gamma_{\text{total}}$					$0.286\Gamma_1/\Gamma$	
VALUE	EVTS	DOCUMENT ID	TECN	COMMENT		
<b><math>0.1240 \pm 0.0020</math> OUR FIT</b>						
••• We do not use the following data for averages, fits, limits, etc. •••						
$0.123 \pm 0.014$	107	RITTENBERG	69	HBC $1.7\text{--}2.7 K^- p$		
$0.10 \pm 0.04$	10	LONDON	66	HBC $2.24 K^- p \rightarrow \Lambda\pi^+\pi^-\pi^0$		
$0.07 \pm 0.04$	7	BADIER	65B	HBC $3 K^- p$		

$\Gamma(\pi^+\pi^-\eta(\text{neutral decay}))/\Gamma_{\text{total}}$					$0.714\Gamma_1/\Gamma$	
VALUE	EVTS	DOCUMENT ID	TECN	COMMENT		
<b><math>0.310 \pm 0.005</math> OUR FIT</b>						
••• We do not use the following data for averages, fits, limits, etc. •••						
$0.314 \pm 0.026$	281	RITTENBERG	69	HBC $1.7\text{--}2.7 K^- p$		

$\Gamma(\rho^0\gamma(\text{including non-resonant } \pi^+\pi^-\gamma))/\Gamma_{\text{total}}$					$\Gamma_2/\Gamma$	
VALUE	EVTS	DOCUMENT ID	TECN	COMMENT		
<b><math>0.293 \pm 0.006</math> OUR FIT</b>						
••• We do not use the following data for averages, fits, limits, etc. •••						
$0.287 \pm 0.007 \pm 0.004$	0.2k	<sup>41</sup> PEDLAR	09	CLEO $J/\psi \rightarrow \gamma\eta'$		
$0.329 \pm 0.033$	298	RITTENBERG	69	HBC $1.7\text{--}2.7 K^- p$		
$0.2 \pm 0.1$	20	LONDON	66	HBC $2.24 K^- p \rightarrow \Lambda\pi^+\pi^-\gamma$		
$0.34 \pm 0.09$	35	BADIER	65B	HBC $3 K^- p$		

<sup>41</sup> Not independent of other  $\eta'$  branching fractions and ratios in PEDLAR 09.

$\Gamma(\rho^0\gamma(\text{including non-resonant } \pi^+\pi^-\gamma))/\Gamma(\pi^+\pi^-\eta)$					$\Gamma_2/\Gamma_1$
VALUE	DOCUMENT ID	TECN	COMMENT		
<b><math>0.676 \pm 0.017</math> OUR FIT</b>					
<b><math>0.683 \pm 0.020</math> OUR AVERAGE</b>					
$0.677 \pm 0.024 \pm 0.011$	PEDLAR	09	CLE3 $J/\psi \rightarrow \eta'\gamma$		
$0.69 \pm 0.03$	ABLIKIM	06E	BES2 $J/\psi \rightarrow \eta'\gamma$		

$\Gamma(\rho^0\gamma(\text{including non-resonant } \pi^+\pi^-\gamma))/\Gamma(\pi^+\pi^-\eta(\text{neutral decay}))$					$\Gamma_2/0.714\Gamma_1$
VALUE	EVTS	DOCUMENT ID	TECN	COMMENT	
<b><math>0.947 \pm 0.024</math> OUR FIT</b>					
<b><math>0.97 \pm 0.09</math> OUR AVERAGE</b>					
$0.70 \pm 0.22$		AMSLER	04B	CBAR $0 \bar{p} p \rightarrow \pi^+\pi^-\eta$	
$1.07 \pm 0.17$		BELADIDZE	92C	VES $36 \pi^- \text{Be} \rightarrow \pi^- \eta' \eta \text{Be}$	
$0.92 \pm 0.14$	473	DANBURG	73	HBC $2.2 K^- p \rightarrow \Lambda X^0$	
$1.11 \pm 0.18$	192	JACOBS	73	HBC $2.9 K^- p \rightarrow \Lambda X^0$	

$\Gamma(\pi^0\pi^0\eta)/\Gamma_{\text{total}}$					$\Gamma_3/\Gamma$
VALUE	EVTS	DOCUMENT ID	TECN	COMMENT	
<b><math>0.216 \pm 0.008</math> OUR FIT</b>					
••• We do not use the following data for averages, fits, limits, etc. •••					
$0.235 \pm 0.013 \pm 0.004$	3.2k	<sup>42</sup> PEDLAR	09	CLEO $J/\psi \rightarrow \gamma\eta'$	

<sup>42</sup> Not independent of other  $\eta'$  branching fractions and ratios in PEDLAR 09.

$\Gamma(\pi^0\pi^0\eta(3\pi^0 \text{ decay}))/\Gamma_{\text{total}}$					$0.321\Gamma_3/\Gamma$
VALUE	EVTS	DOCUMENT ID	TECN	COMMENT	
<b><math>0.0694 \pm 0.0026</math> OUR FIT</b>					
••• We do not use the following data for averages, fits, limits, etc. •••					
$0.11 \pm 0.06$	4	BENSINGER	70	DBC $2.2 \pi^+ d$	

$\Gamma(\pi^0\pi^0\eta)/\Gamma(\pi^+\pi^-\eta)$					$\Gamma_3/\Gamma_1$
VALUE	DOCUMENT ID	TECN	COMMENT		
<b><math>0.498 \pm 0.025</math> OUR FIT</b>					
<b><math>0.555 \pm 0.043 \pm 0.013</math></b>	PEDLAR	09	CLE3 $J/\psi \rightarrow \eta'\gamma$		

$\Gamma(\rho^0\gamma(\text{including non-resonant } \pi^+\pi^-\gamma))/\Gamma(\pi\pi\eta)$					$\Gamma_2/(\Gamma_1+\Gamma_3)$
VALUE	DOCUMENT ID	TECN	COMMENT		
<b><math>0.451 \pm 0.012</math> OUR FIT</b>					
<b><math>0.43 \pm 0.02 \pm 0.02</math></b>	BARBERIS	98C	OMEG $450 p p \rightarrow p_f \eta' p_s$		
••• We do not use the following data for averages, fits, limits, etc. •••					
$0.31 \pm 0.15$	DAVIS	68	HBC $5.5 K^- p$		

$\Gamma(\omega\gamma)/\Gamma_{\text{total}}$					$\Gamma_4/\Gamma$
VALUE	EVTS	DOCUMENT ID	TECN	COMMENT	
<b><math>0.0275 \pm 0.0022</math> OUR FIT</b>					
••• We do not use the following data for averages, fits, limits, etc. •••					
$0.0234 \pm 0.0030 \pm 0.0004$	70	<sup>43</sup> PEDLAR	09	CLEO $J/\psi \rightarrow \gamma\eta'$	

<sup>43</sup> Not independent of other  $\eta'$  branching fractions and ratios in PEDLAR 09.

$\Gamma(\omega\gamma)/\Gamma(\pi^+\pi^-\eta)$					$\Gamma_4/\Gamma_1$
VALUE	EVTS	DOCUMENT ID	TECN	COMMENT	
<b><math>0.063 \pm 0.005</math> OUR FIT</b>					
<b><math>0.055 \pm 0.007 \pm 0.001</math></b>	PEDLAR	09	CLE3 $J/\psi \rightarrow \eta'\gamma$		
••• We do not use the following data for averages, fits, limits, etc. •••					
$0.068 \pm 0.013$	68	ZANFINO	77	ASP $8.4 \pi^- p$	

$\Gamma(\omega\gamma)/\Gamma(\pi^0\pi^0\eta)$					$\Gamma_4/\Gamma_3$
VALUE	DOCUMENT ID	TECN	COMMENT		
<b><math>0.127 \pm 0.011</math> OUR FIT</b>					
<b><math>0.147 \pm 0.016</math></b>	ALDE	87B	GAM2 $38 \pi^- p \rightarrow n4\gamma$		

$\Gamma(\rho^0\gamma(\text{including non-resonant } \pi^+\pi^-\gamma))/[\Gamma(\pi^+\pi^-\eta) + \Gamma(\pi^0\pi^0\eta) + \Gamma(\omega\gamma)]$					$\Gamma_2/(\Gamma_1+\Gamma_3+\Gamma_4)$
VALUE	DOCUMENT ID	TECN	COMMENT		
<b><math>0.433 \pm 0.012</math> OUR FIT</b>					
••• We do not use the following data for averages, fits, limits, etc. •••					
$0.25 \pm 0.14$	DAUBER	64	HBC $1.95 K^- p$		

$$[\Gamma(\pi^0\pi^0\eta(\text{charged decay})) + \Gamma(\omega(\text{charged decay})\gamma)]/\Gamma_{\text{total}} \quad (0.286\Gamma_3 + 0.89\Gamma_4)/\Gamma$$

VALUE	EVTS	DOCUMENT ID	TECN	COMMENT
<b>0.0863 ± 0.0032 OUR FIT</b>				
• • • We do not use the following data for averages, fits, limits, etc. • • •				
0.045 ± 0.029	42	RITTENBERG 69	HBC	1.7-2.7 $K^-p$

$$\Gamma(\pi^+\pi^-\text{ neutrals})/\Gamma_{\text{total}} \quad (0.714\Gamma_1 + 0.286\Gamma_3 + 0.89\Gamma_4)/\Gamma$$

VALUE	EVTS	DOCUMENT ID	TECN	COMMENT
<b>0.396 ± 0.004 OUR FIT</b>				
• • • We do not use the following data for averages, fits, limits, etc. • • •				
0.4 ± 0.1	39	LONDON 66	HBC	2.24 $K^-p \rightarrow \Lambda\pi^+\pi^-\text{ neutrals}$
0.35 ± 0.06	33	BADIER 65B	HBC	3 $K^-p$

$$\Gamma(\gamma\gamma)/\Gamma_{\text{total}} \quad \Gamma_5/\Gamma$$

VALUE (units $10^{-2}$ )	EVTS	DOCUMENT ID	TECN	COMMENT
<b>2.18 ± 0.08 OUR FIT</b>				
<b>2.00 ± 0.15 OUR AVERAGE</b>				
1.98 <sup>+0.31</sup> <sub>-0.27</sub> ± 0.07	114	44 WICHT 08	BELL	$B^\pm \rightarrow K^\pm\gamma\gamma$
2.00 ± 0.18		45 STANTON 80	SPEC	8.45 $\pi^-p \rightarrow n\pi^+\pi^-2\gamma$
• • • We do not use the following data for averages, fits, limits, etc. • • •				
2.25 ± 0.16 ± 0.03	0.3k	46 PEDLAR 09	CLEO	$J/\psi \rightarrow \gamma\eta'$
1.8 ± 0.2	6000	47 APEL 79	NICE	15-40 $\pi^-p \rightarrow n2\gamma$
2.5 ± 0.7		DUANE 74	MMS	$\pi^-p \rightarrow n\text{MM}$
1.71 ± 0.33	68	DALPIAZ 72	CNTR	1.6 $\pi^-p \rightarrow nX^0$
2.0 <sup>+0.8</sup> <sub>-0.6</sub>	31	HARVEY 71	OSPK	3.65 $\pi^-p \rightarrow nX^0$

44 WICHT 08 reports  $[\Gamma(\eta'(958) \rightarrow \gamma\gamma)/\Gamma_{\text{total}}] \times [B(B^\pm \rightarrow \eta'K^\pm)] = (1.40^{+0.16+0.15}_{-0.15-0.12}) \times 10^{-6}$  which we divide by our best value  $B(B^\pm \rightarrow \eta'K^\pm) = (7.06 \pm 0.25) \times 10^{-5}$ . Our first error is their experiment's error and our second error is the systematic error from using our best value.

45 Includes APEL 79 result.  
46 Not independent of other  $\eta'$  branching fractions and ratios in PEDLAR 09.  
47 Data is included in STANTON 80 evaluation.

$$\Gamma(\gamma\gamma)/\Gamma(\pi^+\pi^-\eta) \quad \Gamma_5/\Gamma_1$$

VALUE	DOCUMENT ID	TECN	COMMENT
<b>0.0503 ± 0.0022 OUR FIT</b>			
<b>0.053 ± 0.004 ± 0.001</b>	PEDLAR 09	CLE3	$J/\psi \rightarrow \eta'\gamma$

$$\Gamma(\gamma\gamma)/\Gamma(\rho^0\gamma(\text{including non-resonant } \pi^+\pi^-\gamma)) \quad \Gamma_5/\Gamma_2$$

VALUE	DOCUMENT ID	TECN	COMMENT
<b>0.0744 ± 0.0033 OUR FIT</b>			
<b>0.080 ± 0.008</b>	ABLIKIM 06E	BES2	$J/\psi \rightarrow \eta'\gamma$

$$\Gamma(\gamma\gamma)/\Gamma(\pi^0\pi^0\eta) \quad \Gamma_5/\Gamma_3$$

VALUE	DOCUMENT ID	TECN	COMMENT
<b>0.101 ± 0.004 OUR FIT</b>			
<b>0.105 ± 0.010 OUR AVERAGE</b>			Error includes scale factor of 1.9.
0.091 ± 0.009	AMSLER 93	CBAR	0.0 $\bar{p}p$
0.112 ± 0.002 ± 0.006	ALDE 87B	GAM2	38 $\pi^-p \rightarrow n2\gamma$

$$\Gamma(\gamma\gamma)/\Gamma(\pi^0\pi^0\eta(\text{neutral decay})) \quad \Gamma_5/0.714\Gamma_3$$

VALUE	EVTS	DOCUMENT ID	TECN	COMMENT
<b>0.141 ± 0.006 OUR FIT</b>				
• • • We do not use the following data for averages, fits, limits, etc. • • •				
0.188 ± 0.058	16	APEL 72	OSPK	3.8 $\pi^-p \rightarrow nX^0$

$$\Gamma(\text{neutrals})/\Gamma_{\text{total}} \quad (0.714\Gamma_3 + 0.09\Gamma_4 + \Gamma_5)/\Gamma$$

VALUE	EVTS	DOCUMENT ID	TECN	COMMENT
<b>0.179 ± 0.006 OUR FIT</b>				
• • • We do not use the following data for averages, fits, limits, etc. • • •				
0.185 ± 0.022	535	BASILE 71	CNTR	1.6 $\pi^-p \rightarrow nX^0$
0.189 ± 0.026	123	RITTENBERG 69	HBC	1.7-2.7 $K^-p$

$$\Gamma(3\pi^0)/\Gamma(\pi^0\pi^0\eta) \quad \Gamma_6/\Gamma_3$$

VALUE (units $10^{-4}$ )	EVTS	DOCUMENT ID	TECN	COMMENT
<b>78 ± 10 OUR FIT</b>				
<b>78 ± 10 OUR AVERAGE</b>				
86 ± 19	235	BLIK 08	GAMS	32 $\pi^-p \rightarrow \eta'n$
74 ± 15		ALDE 87B	GAM2	38 $\pi^-p \rightarrow n6\gamma$
75 ± 18		BINON 84	GAM2	30-40 $\pi^-p \rightarrow n6\gamma$

$$\Gamma(\mu^+\mu^-\gamma)/\Gamma(\gamma\gamma) \quad \Gamma_7/\Gamma_5$$

VALUE (units $10^{-3}$ )	EVTS	DOCUMENT ID	TECN	COMMENT
<b>4.9 ± 1.2</b>	33	VIKTOROV 80	CNTR	25,33 $\pi^-p \rightarrow 2\mu\gamma$

$$\Gamma(\pi^+\pi^-\mu^+\mu^-)/\Gamma_{\text{total}} \quad \Gamma_8/\Gamma$$

VALUE (units $10^{-4}$ )	CL%	DOCUMENT ID	TECN	COMMENT
<b>&lt; 2.4</b>	90	48 NAIK 09	CLEO	$J/\psi \rightarrow \gamma\eta'$
• • • We do not use the following data for averages, fits, limits, etc. • • •				
48 Not independent of measured value of $\Gamma_8/\Gamma_1$ from NAIK 09.				

$$\Gamma(\pi^+\pi^-\mu^+\mu^-)/\Gamma(\pi^+\pi^-\eta) \quad \Gamma_8/\Gamma_1$$

VALUE (units $10^{-3}$ )	CL%	DOCUMENT ID	TECN	COMMENT
<b>&lt; 0.5</b>	90	49 NAIK 09	CLEO	$J/\psi \rightarrow \gamma\eta'$
49 NAIK 09 reports $[\Gamma(\eta'(958) \rightarrow \pi^+\pi^-\mu^+\mu^-)/\Gamma(\eta'(958) \rightarrow \pi^+\pi^-\eta)] / [B(\eta \rightarrow 2\gamma)] < 1.3 \times 10^{-3}$ which we multiply by our best value $B(\eta \rightarrow 2\gamma) = 39.31 \times 10^{-2}$ .				

$$\Gamma(\pi^+\pi^-\pi^0)/\Gamma_{\text{total}} \quad \Gamma_9/\Gamma$$

VALUE (units $10^{-2}$ )	CL%	DOCUMENT ID	TECN	COMMENT
<b>0.36 ± 0.11 ± 0.09 OUR FIT</b>				
• • • We do not use the following data for averages, fits, limits, etc. • • •				
0.37 <sup>+0.11</sup> <sub>-0.09</sub> ± 0.04		50 NAIK 09	CLEO	$J/\psi \rightarrow \gamma\eta'$
< 9	95	DANBURG 73	HBC	2.2 $K^-p \rightarrow \Lambda X^0$
< 5	90	RITTENBERG 69	HBC	1.7-2.7 $K^-p$

$$\Gamma(\pi^+\pi^-\pi^0)/\Gamma(\pi^+\pi^-\eta) \quad \Gamma_9/\Gamma_1$$

VALUE (units $10^{-3}$ )	EVTS	DOCUMENT ID	TECN	COMMENT
<b>8.3<sup>+2.5</sup><sub>-2.1</sub> OUR FIT</b>				
<b>8.26 ± 2.49 ± 0.04</b>	20	51 NAIK 09	CLEO	$J/\psi \rightarrow \gamma\eta'$

51 NAIK 09 reports  $[\Gamma(\eta'(958) \rightarrow \pi^+\pi^-\pi^0)/\Gamma(\eta'(958) \rightarrow \pi^+\pi^-\eta)] / [B(\eta \rightarrow 2\gamma)] = (21^{+6}_{-5} \pm 2) \times 10^{-3}$  which we multiply by our best value  $B(\eta \rightarrow 2\gamma) = (39.31 \pm 0.20) \times 10^{-2}$ . Our first error is their experiment's error and our second error is the systematic error from using our best value.

$$\Gamma(\pi^0\rho^0)/\Gamma_{\text{total}} \quad \Gamma_{10}/\Gamma$$

VALUE	CL%	DOCUMENT ID	TECN	COMMENT
<b>&lt; 0.04</b>	90	RITTENBERG 65	HBC	2.7 $K^-p$

$$\Gamma(2(\pi^+\pi^-))/\Gamma_{\text{total}} \quad \Gamma_{11}/\Gamma$$

VALUE (units $10^{-4}$ )	CL%	DOCUMENT ID	TECN	COMMENT
<b>&lt; 2.4</b>	90	52 NAIK 09	CLEO	$J/\psi \rightarrow \gamma\eta'$
< 100	90	RITTENBERG 69	HBC	1.7-2.7 $K^-p$
52 Not independent of measured value of $\Gamma_{11}/\Gamma_1$ from NAIK 09.				

$$\Gamma(2(\pi^+\pi^-))/\Gamma(\pi^+\pi^-\eta) \quad \Gamma_{11}/\Gamma_1$$

VALUE (units $10^{-3}$ )	CL%	DOCUMENT ID	TECN	COMMENT
<b>&lt; 0.6</b>	90	53 NAIK 09	CLEO	$J/\psi \rightarrow \gamma\eta'$
53 NAIK 09 reports $[\Gamma(\eta'(958) \rightarrow 2(\pi^+\pi^-))/\Gamma(\eta'(958) \rightarrow \pi^+\pi^-\eta)] / [B(\eta \rightarrow 2\gamma)] < 1.4 \times 10^{-3}$ which we multiply by our best value $B(\eta \rightarrow 2\gamma) = 39.31 \times 10^{-2}$ .				

$$\Gamma(\pi^+\pi^-\pi^0)/\Gamma_{\text{total}} \quad \Gamma_{12}/\Gamma$$

VALUE (units $10^{-4}$ )	CL%	DOCUMENT ID	TECN	COMMENT
<b>&lt; 27</b>	90	54 NAIK 09	CLEO	$J/\psi \rightarrow \gamma\eta'$
54 Not independent of measured value of $\Gamma_{12}/\Gamma_1$ from NAIK 09.				

$$\Gamma(\pi^+\pi^-\pi^0)/\Gamma(\pi^+\pi^-\eta) \quad \Gamma_{12}/\Gamma_1$$

VALUE (units $10^{-3}$ )	CL%	DOCUMENT ID	TECN	COMMENT
<b>&lt; 6</b>	90	55 NAIK 09	CLEO	$J/\psi \rightarrow \gamma\eta'$
55 NAIK 09 reports $[\Gamma(\eta'(958) \rightarrow \pi^+\pi^-\pi^0)/\Gamma(\eta'(958) \rightarrow \pi^+\pi^-\eta)] / [B(\eta \rightarrow 2\gamma)] < 15 \times 10^{-3}$ which we multiply by our best value $B(\eta \rightarrow 2\gamma) = 39.31 \times 10^{-2}$ .				

$$\Gamma(2(\pi^+\pi^-)\text{ neutrals})/\Gamma_{\text{total}} \quad \Gamma_{13}/\Gamma$$

VALUE	CL%	DOCUMENT ID	TECN	COMMENT
<b>&lt; 0.01</b>	95	DANBURG 73	HBC	2.2 $K^-p \rightarrow \Lambda X^0$
• • • We do not use the following data for averages, fits, limits, etc. • • •				
< 0.01	90	RITTENBERG 69	HBC	1.7-2.7 $K^-p$

$$\Gamma(2(\pi^+\pi^-)\pi^0)/\Gamma_{\text{total}} \quad \Gamma_{14}/\Gamma$$

VALUE	CL%	DOCUMENT ID	TECN	COMMENT
<b>&lt; 0.002</b>	90	56 NAIK 09	CLEO	$J/\psi \rightarrow \gamma\eta'$
< 0.01	90	RITTENBERG 69	HBC	1.7-2.7 $K^-p$
56 Not independent of measured value of $\Gamma_{14}/\Gamma_1$ from NAIK 09.				

$$\Gamma(2(\pi^+\pi^-)\pi^0)/\Gamma(\pi^+\pi^-\eta) \quad \Gamma_{14}/\Gamma_1$$

VALUE (units $10^{-3}$ )	CL%	DOCUMENT ID	TECN	COMMENT
<b>&lt; 4</b>	90	57 NAIK 09	CLEO	$J/\psi \rightarrow \gamma\eta'$
57 NAIK 09 reports $[\Gamma(\eta'(958) \rightarrow 2(\pi^+\pi^-)\pi^0)/\Gamma(\eta'(958) \rightarrow \pi^+\pi^-\eta)] / [B(\eta \rightarrow 2\gamma)] < 11 \times 10^{-3}$ which we multiply by our best value $B(\eta \rightarrow 2\gamma) = 39.31 \times 10^{-2}$ .				

## Meson Particle Listings

 $\eta'(958)$ 

$\Gamma(2(\pi^+\pi^-)2\pi^0)/\Gamma_{\text{total}}$					$\Gamma_{15}/\Gamma$
VALUE	CL%	DOCUMENT ID	TECN	COMMENT	
<0.01	95	KALBFLEISCH 64B	HBC	$K^-\rho \rightarrow \Lambda 2(\pi^+\pi^-)+MM$	
••• We do not use the following data for averages, fits, limits, etc. •••					
<0.01	90	LONDON	66	HBC	Compilation

$\Gamma(3(\pi^+\pi^-))/\Gamma_{\text{total}}$					$\Gamma_{16}/\Gamma$
VALUE (units $10^{-3}$ )	CL%	DOCUMENT ID	TECN	COMMENT	
••• We do not use the following data for averages, fits, limits, etc. •••					
<0.53	90	58 NAIK	09	CLEO	$J/\psi \rightarrow \gamma\eta'$
<5	95	KALBFLEISCH 64B	HBC	$K^-\rho \rightarrow \Lambda 2(\pi^+\pi^-)$	
58 Not independent of measured value of $\Gamma_{16}/\Gamma_1$ from NAIK 09.					

$\Gamma(3(\pi^+\pi^-))/\Gamma(\pi^+\pi^-)$					$\Gamma_{16}/\Gamma_1$
VALUE (units $10^{-3}$ )	CL%	DOCUMENT ID	TECN	COMMENT	
<1.2	90	59 NAIK	09	CLEO	$J/\psi \rightarrow \gamma\eta'$
59 NAIK 09 reports $[\Gamma(\eta'(958) \rightarrow 3(\pi^+\pi^-))/\Gamma(\eta'(958) \rightarrow \pi^+\pi^-)] / [B(\eta \rightarrow 2\gamma)] < 3.0 \times 10^{-3}$ which we multiply by our best value $B(\eta \rightarrow 2\gamma) = 39.31 \times 10^{-2}$ .					

$\Gamma(\pi^+\pi^-e^+e^-)/\Gamma_{\text{total}}$					$\Gamma_{17}/\Gamma$
VALUE (units $10^{-3}$ )	CL%	DOCUMENT ID	TECN	COMMENT	
<b><math>2.4 \pm 1.3</math></b>		<b>OUR FIT</b>			
••• We do not use the following data for averages, fits, limits, etc. •••					
$2.5 \pm 1.2$	$-0.9 \pm 0.5$	60 NAIK	09	CLEO	$J/\psi \rightarrow \gamma\eta'$
<6	90	RITTENBERG 65	HBC	2.7 $K^-\rho$	
60 Not independent of measured value of $\Gamma_{17}/\Gamma_1$ from NAIK 09.					

$\Gamma(\pi^+\pi^-e^+e^-)/\Gamma(\pi^+\pi^-)$					$\Gamma_{17}/\Gamma_1$
VALUE (units $10^{-3}$ )	EVTS	DOCUMENT ID	TECN	COMMENT	
<b><math>5.6 \pm 3.0</math></b>		<b>OUR FIT</b>			
<b><math>5.50 \pm 2.99 \pm 0.03</math></b>	8	61 NAIK	09	CLEO	$J/\psi \rightarrow \gamma\eta'$
61 NAIK 09 reports $[\Gamma(\eta'(958) \rightarrow \pi^+\pi^-e^+e^-)/\Gamma(\eta'(958) \rightarrow \pi^+\pi^-)] / [B(\eta \rightarrow 2\gamma)] = (14 \pm 7 \pm 3) \times 10^{-3}$ which we multiply by our best value $B(\eta \rightarrow 2\gamma) = (39.31 \pm 0.20) \times 10^{-2}$ . Our first error is their experiment's error and our second error is the systematic error from using our best value.					

$\Gamma(\gamma e^+e^-)/\Gamma_{\text{total}}$					$\Gamma_{18}/\Gamma$
VALUE (units $10^{-3}$ )	CL%	DOCUMENT ID	TECN	COMMENT	
<0.9	90	BRIERE 00	CLEO	10.6 $e^+e^-$	

$\Gamma(\pi^0\gamma\gamma)/\Gamma(\pi^0\pi^0\eta)$					$\Gamma_{19}/\Gamma_3$
VALUE (units $10^{-4}$ )	CL%	DOCUMENT ID	TECN	COMMENT	
<37	90	ALDE 87B	GAM2	$38 \pi^-\rho \rightarrow n4\gamma$	

$\Gamma(4\pi^0)/\Gamma(\pi^0\pi^0\eta)$					$\Gamma_{20}/\Gamma_3$
VALUE (units $10^{-4}$ )	CL%	DOCUMENT ID	TECN	COMMENT	
<23	90	ALDE 87B	GAM2	$38 \pi^-\rho \rightarrow n8\gamma$	

$\Gamma(e^+e^-)/\Gamma_{\text{total}}$					$\Gamma_{21}/\Gamma$
VALUE (units $10^{-7}$ )	CL%	DOCUMENT ID	TECN	COMMENT	
<2.1	90	VOROBYEV 88	ND	$e^+e^- \rightarrow \pi^+\pi^-\eta$	

$\Gamma(\text{invisible})/\Gamma_{\text{total}}$					$\Gamma_{22}/\Gamma$
VALUE (units $10^{-4}$ )	CL%	DOCUMENT ID	TECN	COMMENT	
••• We do not use the following data for averages, fits, limits, etc. •••					
<9.5	90	62 NAIK	09	CLEO	$J/\psi \rightarrow \gamma\eta'$
62 Not independent of measured value of $\Gamma_{22}/\Gamma_1$ from NAIK 09.					

$\Gamma(\text{invisible})/\Gamma(\gamma\gamma)$					$\Gamma_{22}/\Gamma_5$
VALUE (units $10^{-2}$ )	CL%	DOCUMENT ID	TECN	COMMENT	
••• We do not use the following data for averages, fits, limits, etc. •••					
<6.69	90	ABLIKIM 06Q	BES	$J/\psi \rightarrow \phi\eta'$	

$\Gamma(\text{invisible})/\Gamma(\pi^+\pi^-\eta)$					$\Gamma_{22}/\Gamma_1$
VALUE (units $10^{-3}$ )	CL%	DOCUMENT ID	TECN	COMMENT	
<2.1	90	63 NAIK	09	CLEO	$J/\psi \rightarrow \gamma\eta'$
63 NAIK 09 reports $[\Gamma(\eta'(958) \rightarrow \text{invisible})/\Gamma(\eta'(958) \rightarrow \pi^+\pi^-\eta)] / [B(\eta \rightarrow 2\gamma)] < 5.4 \times 10^{-3}$ which we multiply by our best value $B(\eta \rightarrow 2\gamma) = 39.31 \times 10^{-2}$ .					

$\Gamma(\pi^+\pi^-)/\Gamma_{\text{total}}$					$\Gamma_{23}/\Gamma$
VALUE (units $10^{-4}$ )	CL%	DOCUMENT ID	TECN	COMMENT	
< 0.6	90	64 ABLIKIM 11G	BES3	$J/\psi \rightarrow \gamma\pi^+\pi^-$	
••• We do not use the following data for averages, fits, limits, etc. •••					
< 29	90	65 MORI 07A	BELL	$\gamma\gamma \rightarrow \pi^+\pi^-$	
< 3.3	90	66 MORI 07A	BELL	$\gamma\gamma \rightarrow \pi^+\pi^-$	
<200	95	DANBURG 73	HBC	2.2 $K^-\rho \rightarrow \Lambda X^0$	
<200	90	RITTENBERG 69	HBC	1.7-2.7 $K^-\rho$	
64 ABLIKIM 11G reports $[\Gamma(\eta'(958) \rightarrow \pi^+\pi^-)/\Gamma_{\text{total}}] \times [B(J/\psi(1S) \rightarrow \gamma\eta'(958))] < 2.84 \times 10^{-7}$ which we divide by our best value $B(J/\psi(1S) \rightarrow \gamma\eta'(958)) = 5.16 \times 10^{-3}$ .					
65 Taking into account interference with the $\gamma\gamma \rightarrow \pi^+\pi^-$ continuum.					
66 Without interference with the $\gamma\gamma \rightarrow \pi^+\pi^-$ continuum.					

$\Gamma(\pi^0\pi^0)/\Gamma_{\text{total}}$					$\Gamma_{24}/\Gamma$
VALUE	CL%	DOCUMENT ID	TECN	COMMENT	
< $4 \times 10^{-4}$	90	67 ABLIKIM 11G	BES3	$J/\psi \rightarrow \gamma\pi^0\pi^0$	
67 ABLIKIM 11G reports $[\Gamma(\eta'(958) \rightarrow \pi^+\pi^-)/\Gamma_{\text{total}}] \times [B(J/\psi(1S) \rightarrow \gamma\eta'(958))] < 2.84 \times 10^{-7}$ which we divide by our best value $B(J/\psi(1S) \rightarrow \gamma\eta'(958)) = 5.16 \times 10^{-3}$ .					

$\Gamma(\pi^0\pi^0)/\Gamma(\pi^0\pi^0\eta)$					$\Gamma_{24}/\Gamma_3$
VALUE (units $10^{-4}$ )	CL%	DOCUMENT ID	TECN	COMMENT	
<45	90	ALDE 87B	GAM2	$38 \pi^-\rho \rightarrow n4\gamma$	

$\Gamma(\pi^0e^+e^-)/\Gamma_{\text{total}}$					$\Gamma_{25}/\Gamma$
VALUE (units $10^{-3}$ )	CL%	DOCUMENT ID	TECN	COMMENT	
< 1.4	90	BRIERE 00	CLEO	10.6 $e^+e^-$	
••• We do not use the following data for averages, fits, limits, etc. •••					
<13	90	RITTENBERG 65	HBC	2.7 $K^-\rho$	

$\Gamma(\eta e^+e^-)/\Gamma_{\text{total}}$					$\Gamma_{26}/\Gamma$
VALUE (units $10^{-3}$ )	CL%	DOCUMENT ID	TECN	COMMENT	
< 2.4	90	BRIERE 00	CLEO	10.6 $e^+e^-$	
••• We do not use the following data for averages, fits, limits, etc. •••					
<11	90	RITTENBERG 65	HBC	2.7 $K^-\rho$	

$\Gamma(3\gamma)/\Gamma(\pi^0\pi^0\eta)$					$\Gamma_{27}/\Gamma_3$
VALUE (units $10^{-4}$ )	CL%	DOCUMENT ID	TECN	COMMENT	
<4.6	90	ALDE 87B	GAM2	$38 \pi^-\rho \rightarrow n3\gamma$	

$\Gamma(\mu^+\mu^-)/\Gamma_{\text{total}}$					$\Gamma_{28}/\Gamma$
VALUE (units $10^{-5}$ )	CL%	DOCUMENT ID	TECN	COMMENT	
<6.0	90	DZHELADIN 81	CNTR	$30 \pi^-\rho \rightarrow \eta' n$	

$\Gamma(\mu^+\mu^-\eta)/\Gamma_{\text{total}}$					$\Gamma_{29}/\Gamma$
VALUE (units $10^{-5}$ )	CL%	DOCUMENT ID	TECN	COMMENT	
<1.5	90	DZHELADIN 81	CNTR	$30 \pi^-\rho \rightarrow \eta' n$	

$\Gamma(e\mu)/\Gamma_{\text{total}}$					$\Gamma_{30}/\Gamma$
VALUE (units $10^{-4}$ )	CL%	DOCUMENT ID	TECN	COMMENT	
<4.7	90	BRIERE 00	CLEO	10.6 $e^+e^-$	

 $\eta'(958)$  C-NONCONSERVING DECAY PARAMETER

See the note on  $\eta$  decay parameters in the Stable Particle Particle Listings for definition of this parameter.

DECAY ASYMMETRY PARAMETER FOR  $\pi^+\pi^-\gamma$ 

VALUE	EVTS	DOCUMENT ID	TECN	COMMENT
<b><math>-0.03 \pm 0.04</math></b>		<b>OUR AVERAGE</b>		
$-0.019 \pm 0.056$		AIHARA 87	TPC	$2\gamma \rightarrow \pi^+\pi^-\gamma$
$-0.069 \pm 0.078$	295	GRIGORIAN 75	STRC	2.1 $\pi^-\rho$
$0.00 \pm 0.10$	103	KALBFLEISCH 75	HBC	2.18 $K^-\rho \rightarrow \Lambda\pi^+\pi^-\gamma$
••• We do not use the following data for averages, fits, limits, etc. •••				
$0.07 \pm 0.08$	152	RITTENBERG 65	HBC	2.1-2.7 $K^-\rho$

 $\eta'(958)$  REFERENCES

ABLIKIM 11	PR D83 012003	M. Ablikim et al.	(BES III Collab.)
ABLIKIM 11G	PR D84 032006	M. Ablikim et al.	(BES-III Collab.)
CZERWINSKI 10	PRL 105 122001	E. Czerwinski et al.	(COSY-11 Collab.)
BLIK 09	PAN 72 231	A.M. Blük et al.	(IHEP (Protvino))
	Translated from YAF 72 258.		
NAIK 09	PRL 102 061801	P. Naik et al.	(CLEO Collab.)
PEDLAR 09	PR D79 111101	T.K. Pedlar et al.	(CLEO Collab.)
BLIK 08	PAN 71 2124	A. Blük et al.	(GAMS-4π Collab.)
	Translated from YAF 71 2161.		
LIBBY 08	PRL 101 182002	J. Libby et al.	(CLEO Collab.)
WICHT 08	PL B652 323	J. Wicht et al.	(BELLE Collab.)
DOROFFEV 07	PL B651 22	V. Dorofeev et al.	(VES Collab.)
MORI 07A	JPSJ 76 074102	T. Mori et al.	(BELLE Collab.)
ABLIKIM 06E	PR D73 052008	M. Ablikim et al.	(BES Collab.)
ABLIKIM 06Q	PRL 97 202002	M. Ablikim et al.	(BES Collab.)
AMELIN 05A	PAN 68 372	D.V. Amelin et al.	(VES Collab.)
	Translated from YAF 68 401.		





## Meson Particle Listings

 $f_0(980)$ 

- <sup>18</sup> K-matrix pole from combined analysis of  $\pi^- p \rightarrow \pi^0 \pi^0 n$ ,  $\pi^- p \rightarrow K \bar{K} n$ ,  $\pi^+ \pi^- \rightarrow \pi^+ \pi^-$ ,  $\bar{p} p \rightarrow \pi^0 \pi^0 \pi^0$ ,  $\pi^0 \eta \eta$ ,  $\pi^0 \pi^0 \eta$ ,  $\pi^+ \pi^- \pi^0$ ,  $K^+ K^- \pi^0$ ,  $K_S^0 K_S^0 \pi^0$ ,  $K^+ K_S^0 \pi^-$  at rest,  $\bar{p} n \rightarrow \pi^- \pi^- \pi^+$ ,  $K_S^0 K^- \pi^0$ ,  $K_S^0 K_S^0 \pi^-$  at rest.
- <sup>19</sup> From the negative interference with the  $f_0(500)$  meson of AITALA 01B using the ACHASOV 89 parameterization for the  $f_0(980)$ , a Breit-Wigner for the  $f_0(500)$ , and ACHASOV 01F for the  $\rho\pi$  contribution.
- <sup>20</sup> Coupled-channel Breit-Wigner, couplings  $g_{\pi\pi}=0.09 \pm 0.01 \pm 0.01$ ,  $g_K=0.02 \pm 0.04 \pm 0.03$ .
- <sup>21</sup> Supersedes ACHASOV 98i. Using the model of ACHASOV 89.
- <sup>22</sup> Supersedes ACHASOV 98i.
- <sup>23</sup> In the "narrow resonance" approximation.
- <sup>24</sup> Assuming  $\Gamma(f_0) = 40$  MeV.
- <sup>25</sup> From a narrow pole fit taking into account  $f_0(980)$  and  $f_0(1200)$  intermediate mechanisms.
- <sup>26</sup> From the combined fit of the photon spectra in the reactions  $e^+ e^- \rightarrow \pi^+ \pi^- \gamma$ ,  $\pi^0 \pi^0 \gamma$ .
- <sup>27</sup> Supersedes BARBERIS 99 and BARBERIS 99b
- <sup>28</sup> T-matrix pole.
- <sup>29</sup> From invariant mass fit.
- <sup>30</sup> On sheet II in a 2 pole solution. The other pole is found on sheet III at (1039–93i) MeV.
- <sup>31</sup> On sheet II in a 2 pole solution. The other pole is found on sheet III at (963–29i) MeV.
- <sup>32</sup> Reanalysis of data from HYAMS 73, GRAYER 74, SRINIVASAN 75, and ROSSELET 77 using the interfering amplitude method.
- <sup>33</sup> At high  $|t|$ .
- <sup>34</sup> At low  $|t|$ .
- <sup>35</sup> On sheet II in a 4-pole solution, the other poles are found on sheet III at (953–55i) MeV and on sheet IV at (938–35i) MeV.
- <sup>36</sup> Combined fit of ALDE 95B, ANISOVICH 94, AMSLER 94D.
- <sup>37</sup> On sheet II in a 2 pole solution. The other pole is found on sheet III at (996–103i) MeV.
- <sup>38</sup> From sheet II pole position.
- <sup>39</sup> On sheet II in a 2 pole solution. The other pole is found on sheet III at (797–185i) MeV and can be interpreted as a shadow pole.
- <sup>40</sup> On sheet II in a 2 pole solution. The other pole is found on sheet III at (978–28i) MeV.
- <sup>41</sup> From coupled channel analysis.
- <sup>42</sup> Coupled channel analysis with finite width corrections.
- <sup>43</sup> Included in AGUILAR-BENITEZ 78 fit.

 $f_0(980)$  WIDTH

Width determination very model dependent. Peak width in  $\pi\pi$  is about 50 MeV, but decay width can be much larger.

VALUE (MeV)	EVS	DOCUMENT ID	TECN	COMMENT
<b>40 to 100 OUR ESTIMATE</b>				
• • • We do not use the following data for averages, fits, limits, etc. • • •				
42 $\pm$ 20 16	44,45	GARCIA-MAR.11	RVUE	Compilation
50 $\pm$ 20 12	45,46	GARCIA-MAR.11	RVUE	Compilation
48 $\pm$ 22 6	47	MOUSSALLAM11	RVUE	Compilation
36 $\pm$ 22	48	MENNESSIER 10	RVUE	Compilation
70 $\pm$ 20 32	49	ANISOVICH 09	RVUE	0.0 $\bar{p} p$ , $\pi N$
91 $\pm$ 30 22 $\pm$ 3	44	50 ECKLUND 09	CLEO	4.17 $e^+ e^- \rightarrow D_S^- D_S^{*+} + c.c.$
66.9 $\pm$ 2.2 $\pm$ 17.6 12.5	51	UEHARA 08A	BELL	10.6 $e^+ e^- \rightarrow \pi^0 \pi^0$
65 $\pm$ 13	262 $\pm$ 30	52 AUBERT	07AK BABR	10.6 $e^+ e^- \rightarrow \phi \pi^+ \pi^- \gamma$
81 $\pm$ 21	54 $\pm$ 9	52 AUBERT	07AK BABR	10.6 $e^+ e^- \rightarrow \phi \pi^0 \pi^0 \gamma$
51.3 $\pm$ 20.8 $\pm$ 13.2 17.7 – 3.8	53	MORI 07	BELL	10.6 $e^+ e^- \rightarrow e^+ e^- \pi^+ \pi^-$
61 $\pm$ 9 $\pm$ 14 8	2584	54 GARMASH 05	BELL	$B^+ \rightarrow K^+ \pi^+ \pi^-$
64 $\pm$ 16	55	ANISOVICH 03	RVUE	
121 $\pm$ 23		TIKHOMIROV 03	SPEC	$40.0 \frac{\pi^- C}{K_S^0 K_S^0 K_L^0 X}$
$\sim$ 70	56	BRAMON 02	RVUE	1.02 $e^+ e^- \rightarrow \pi^0 \pi^0 \gamma$
44 $\pm$ 2 $\pm$ 2	848	57 AITALA 01A	E791	$D^+ \rightarrow \pi^- \pi^+ \pi^+$
201 $\pm$ 28	419	58 ACHASOV 00H	SND	$e^+ e^- \rightarrow \pi^0 \pi^0 \gamma$
122 $\pm$ 13	419, 59, 60	ACHASOV 00H	SND	$e^+ e^- \rightarrow \pi^0 \pi^0 \gamma$
56 $\pm$ 20	61	AKHMETSHIN 99C	CMD2	$e^+ e^- \rightarrow \pi^0 \pi^0 \gamma$
65 $\pm$ 20		BARBERIS 99	OMEG	450 $pp \rightarrow p_S p_f K^+ K^-$
80 $\pm$ 10		BARBERIS 99B	OMEG	450 $pp \rightarrow p_S p_f \pi^+ \pi^-$
80 $\pm$ 10		BARBERIS 99C	OMEG	450 $pp \rightarrow p_S p_f \pi^0 \pi^0$
48 $\pm$ 12 $\pm$ 8	62	BARBERIS 99D	OMEG	450 $pp \rightarrow K^+ K^-$ , $\pi^+ \pi^-$
65 $\pm$ 25		BELLAZZINI 99	GAM4	450 $pp \rightarrow pp \pi^0 \pi^0$
71 $\pm$ 14	63	KAMINSKI 99	RVUE	$\pi\pi \rightarrow \pi\pi, K \bar{K}, \sigma\sigma$
$\sim$ 28	63	OLLER 99	RVUE	$\pi\pi \rightarrow \pi\pi, K \bar{K}$
$\sim$ 25		OLLER 99B	RVUE	$\pi\pi \rightarrow \pi\pi, K \bar{K}$
$\sim$ 14	63	OLLER 99C	RVUE	$\pi\pi \rightarrow \pi\pi, K \bar{K}, \eta\eta$
70 $\pm$ 20		ALDE 98	GAM4	
86 $\pm$ 16	63	ANISOVICH 98B	RVUE	Compilation

54	64	LOCHER 98	RVUE	$\pi\pi \rightarrow \pi\pi, K \bar{K}$
69 $\pm$ 15	65	ALDE 97	GAM2	450 $pp \rightarrow pp \pi^0 \pi^0$
38 $\pm$ 20	66	BERTIN 97C	OBLX	0.0 $\bar{p} p \rightarrow \pi^+ \pi^- \pi^0$
$\sim$ 100	67	ISHIDA 96	RVUE	$\pi\pi \rightarrow \pi\pi, K \bar{K}$
34		TORNQVIST 96	RVUE	$\pi\pi \rightarrow \pi\pi, K \bar{K}, K\pi, \eta\pi$
48 $\pm$ 10	3k	68 ALDE 95B	GAM2	38 $\pi^- p \rightarrow \pi^0 \pi^0 n$
95 $\pm$ 20	10k	69 ALDE 95B	GAM2	38 $\pi^- p \rightarrow \pi^0 \pi^0 n$
26 $\pm$ 10		AMSLER 95B	CBAR	0.0 $\bar{p} p \rightarrow 3\pi^0$
$\sim$ 112		70 AMSLER 95D	CBAR	0.0 $\bar{p} p \rightarrow \pi^0 \pi^0 \pi^0$ , $\pi^0 \eta \eta$ , $\pi^0 \pi^0 \eta$
80 $\pm$ 12		71 ANISOVICH 95	RVUE	
30		JANSSEN 95	RVUE	$\pi\pi \rightarrow \pi\pi, K \bar{K}$
74		72 BUGG 94	RVUE	$\bar{p} p \rightarrow \eta 2\pi^0$
29 $\pm$ 2		73 KAMINSKI 94	RVUE	$\pi\pi \rightarrow \pi\pi, K \bar{K}$
46		74 ZOU 94B	RVUE	
48 $\pm$ 12		75 MORGAN 93	RVUE	$\pi\pi(K \bar{K}) \rightarrow \pi\pi(K \bar{K}), J/\psi \rightarrow \phi\pi\pi(K \bar{K}), D_S \rightarrow \pi(\pi\pi)$
37.4 $\pm$ 10.6	65	AGUILAR-... 91	EHS	400 $pp$
72 $\pm$ 8	76	ARMSTRONG 91	OMEG	300 $pp \rightarrow pp\pi\pi$ , $ppK \bar{K}$
110 $\pm$ 30		BREAKSTONE 90	SFM	$pp \rightarrow pp\pi^+ \pi^-$
29 $\pm$ 13	65	ABACHI 86B	HRS	$e^+ e^- \rightarrow \pi^+ \pi^- X$
120 $\pm$ 281 $\pm$ 20		ETKIN 82B	MPS	23 $\pi^- p \rightarrow n 2K_S^0$
28 $\pm$ 10	76	GIDAL 81	MRK2	$J/\psi \rightarrow \pi^+ \pi^- X$
70 $\pm$ 300	77	ACHASOV 80	RVUE	
100 $\pm$ 80	78	AGUILAR-... 78	HBC	0.7 $\bar{p} p \rightarrow K_S^0 K_S^0$
30 $\pm$ 8	76	LEEPER 77	ASPK	2–2.4 $\pi^- p \rightarrow \pi^+ \pi^- n$ , $K^+ K^- n$
48 $\pm$ 14	76	BINNIE 73	CNTR	$\pi^- p \rightarrow nMM$
32 $\pm$ 10	79	GRAYER 73	ASPK	17 $\pi^- p \rightarrow \pi^+ \pi^- n$
30 $\pm$ 10	79	HYAMS 73	ASPK	17 $\pi^- p \rightarrow \pi^+ \pi^- n$
54 $\pm$ 16	79	PROTOPOP... 73	HBC	7 $\pi^+ p \rightarrow \pi^+ p \pi^+ \pi^-$

- <sup>44</sup> Analytic continuation using Roy equations. Uses the  $K_{e4}$  data of BATLEY 10c and the  $\pi N \rightarrow \pi\pi N$  data of HYAMS 73, GRAYER 74, and PROTOPODESCU 73.
- <sup>45</sup> Quoted number refers to twice imaginary part of pole position.
- <sup>46</sup> Analytic continuation using GPKY equations. Uses the  $K_{e4}$  data of BATLEY 10c and the  $\pi N \rightarrow \pi\pi N$  data of HYAMS 73, GRAYER 74, and PROTOPODESCU 73.
- <sup>47</sup> Pole position. Used Roy equations.
- <sup>48</sup> Average of the analyses of three data sets in the K-matrix model. Uses the data of BATLEY 08A, HYAMS 73, and GRAYER 74, partially of COHEN 80 or ETKIN 82B.
- <sup>49</sup> On sheet II in a 2-pole solution. The other pole is found on sheet III at (850–100i) MeV
- <sup>50</sup> Using a relativistic Breit-Wigner function and taking into account the finite  $D_S$  mass.
- <sup>51</sup> Breit-Wigner  $\pi\pi$  width. Using finite width corrections according to FLATTE 76 and ACHASOV 05, and the ratio  $g_{f_0}^2 K K / g_{f_0}^2 \pi\pi = 0$ .
- <sup>52</sup> Systematic errors not estimated.
- <sup>53</sup> Breit-Wigner  $\pi\pi$  width. Using finite width corrections according to FLATTE 76 and ACHASOV 05, and the ratio  $g_{f_0}^2 K K / g_{f_0}^2 \pi\pi = 4.21 \pm 0.25 \pm 0.21$  from ABLIKIM 05.
- <sup>54</sup> Breit-Wigner, solution 1, PWA ambiguous.
- <sup>55</sup> K-matrix pole from combined analysis of  $\pi^- p \rightarrow \pi^0 \pi^0 n$ ,  $\pi^- p \rightarrow K \bar{K} n$ ,  $\pi^+ \pi^- \rightarrow \pi^+ \pi^-$ ,  $\bar{p} p \rightarrow \pi^0 \pi^0 \pi^0$ ,  $\pi^0 \eta \eta$ ,  $\pi^0 \pi^0 \eta$ ,  $\pi^+ \pi^- \pi^0$ ,  $K^+ K^- \pi^0$ ,  $K_S^0 K_S^0 \pi^0$ ,  $K^+ K_S^0 \pi^-$  at rest,  $\bar{p} n \rightarrow \pi^- \pi^- \pi^+$ ,  $K_S^0 K^- \pi^0$ ,  $K_S^0 K_S^0 \pi^-$  at rest.
- <sup>56</sup> Using the data of AKHMETSHIN 99C, ACHASOV 00H, and ALOISIO 02D.
- <sup>57</sup> Breit-Wigner width.
- <sup>58</sup> Supersedes ACHASOV 98i. Using the model of ACHASOV 89.
- <sup>59</sup> Supersedes ACHASOV 98i.
- <sup>60</sup> In the "narrow resonance" approximation.
- <sup>61</sup> From the combined fit of the photon spectra in the reactions  $e^+ e^- \rightarrow \pi^+ \pi^- \gamma$ ,  $\pi^0 \pi^0 \gamma$ .
- <sup>62</sup> Supersedes BARBERIS 99 and BARBERIS 99b
- <sup>63</sup> T-matrix pole.
- <sup>64</sup> On sheet II in a 2 pole solution. The other pole is found on sheet III at (1039–93i) MeV.
- <sup>65</sup> From invariant mass fit.
- <sup>66</sup> On sheet II in a 2 pole solution. The other pole is found on sheet III at (963–29i) MeV.
- <sup>67</sup> Reanalysis of data from HYAMS 73, GRAYER 74, SRINIVASAN 75, and ROSSELET 77 using the interfering amplitude method.
- <sup>68</sup> At high  $|t|$ .
- <sup>69</sup> At low  $|t|$ .
- <sup>70</sup> On sheet II in a 4-pole solution, the other poles are found on sheet III at (953–55i) MeV and on sheet IV at (938–35i) MeV.
- <sup>71</sup> Combined fit of ALDE 95B, ANISOVICH 94,
- <sup>72</sup> On sheet II in a 2 pole solution. The other pole is found on sheet III at (996–103i) MeV.
- <sup>73</sup> From sheet II pole position.
- <sup>74</sup> On sheet II in a 2 pole solution. The other pole is found on sheet III at (797–185i) MeV and can be interpreted as a shadow pole.
- <sup>75</sup> On sheet II in a 2 pole solution. The other pole is found on sheet III at (978–28i) MeV.
- <sup>76</sup> From coupled channel analysis.
- <sup>77</sup> Coupled channel analysis with finite width corrections.
- <sup>78</sup> From coupled channel fit to the HYAMS 73 and PROTOPODESCU 73 data. With a simultaneous fit to the  $\pi\pi$  phase-shifts, inelasticity and to the  $K_S^0 K_S^0$  invariant mass.
- <sup>79</sup> Included in AGUILAR-BENITEZ 78 fit.

f<sub>0</sub>(980) DECAY MODES

f<sub>0</sub>(980) REFERENCES

Table with 3 columns: Mode, Fraction (Γ<sub>j</sub>/Γ), and Decay Modes. Includes entries for ππ, K-K̄, γγ, and e<sup>+</sup>e<sup>-</sup>.

Extensive list of references for f<sub>0</sub>(980) from various experiments and publications, including authors like Garcia-Marín, Mennessier, and Batley, and collaboration names like BABAR, CLEO, and Belle.

f<sub>0</sub>(980) PARTIAL WIDTHS

Table with 5 columns: Γ(γγ), VALUE (keV), DOCUMENT ID, TECN, COMMENT, and Γ<sub>3</sub>.

OUR AVERAGE

Main table of partial widths for f<sub>0</sub>(980) decays, listing values in keV and associated document IDs and technical notes.

80 Using finite width corrections according to FLATTE 76 and ACHASOV 05, and the ratio g<sub>2</sub><sup>2</sup> K K / g<sub>0</sub><sup>2</sup> π π = 0.

81 Using finite width corrections according to FLATTE 76 and ACHASOV 05, and the ratio g<sub>2</sub><sup>2</sup> K K / g<sub>0</sub><sup>2</sup> π π = 4.21 ± 0.25 ± 0.21 from ABLIKIM 05.

82 Supersedes MORGAN 90.

83 OEST 90 quote systematic errors +0.08, -0.18. We use ±0.18. Observed 60 events.

84 Uses an analytic K-matrix model. Compilation.

85 Using dispersion integral with phase input from Roy equations and data from MARSISKE 90, BOYER 90, BEHREND 92, UEHARA 08a, and MORI 07.

86 Solution A (preferred solution based on χ<sup>2</sup>-analysis).

87 Dispersion theory based amplitude analysis of BOYER 90, MARSISKE 90, BEHREND 92, and MORI 07.

88 Solution B (worse than solution A; still acceptable when systematic uncertainties are included).

89 From analysis allowing arbitrary background unconstrained by unitarity.

90 Data included in MORGAN 90, BOGLIONE 99 analyses.

91 From amplitude analysis of BOYER 90 and MARSISKE 90, data corresponds to resonance parameters m = 989 MeV, Γ = 61 MeV.

Γ(e<sup>+</sup>e<sup>-</sup>)

Table with 5 columns: VALUE (eV), CL%, DOCUMENT ID, TECN, COMMENT. Shows a value of <math>8.4</math> for document ID VOROBYEV 88.

f<sub>0</sub>(980) BRANCHING RATIOS

Table with 5 columns: Γ(ππ) / [Γ(ππ) + Γ(K-K̄)], VALUE, EVTS, DOCUMENT ID, TECN, COMMENT, and Γ<sub>1</sub> / (Γ<sub>1</sub> + Γ<sub>2</sub>).

••• We do not use the following data for averages, fits, limits, etc. •••

Main table of branching ratios for f<sub>0</sub>(980), listing ratios and associated document IDs and technical notes.

92 Recalculated by us using Γ(K<sup>+</sup>K<sup>-</sup>) / Γ(π<sup>+</sup>π<sup>-</sup>) = 0.69 ± 0.32 from AUBERT 06a and isospin relations.

93 Using data from ABLIKIM 04g.

94 From a combined K-matrix analysis of Crystal Barrel (0, pπ̄ → π<sup>0</sup>π<sup>0</sup>π<sup>0</sup>, π<sup>0</sup>ηη, π<sup>0</sup>π<sup>0</sup>η), GAMS (πρ → π<sup>0</sup>π<sup>0</sup>n, ηηη, ηη'n), and BNL (πρ → K-K̄n) data.

95 Measure ππ elasticity assuming two resonances coupled to the ππ and K-K̄ channels only.

## Meson Particle Listings

 $a_0(980)$  $a_0(980)$ 

$$J^{PC} = 1^-(0^{++})$$

See our minireview on scalar mesons under  $f_0(500)$ . (See the index for the page number.)

 $a_0(980)$  MASS

VALUE (MeV) DOCUMENT ID  
**980 ± 20 OUR ESTIMATE** Mass determination very model dependent

 $\eta\pi$  FINAL STATE ONLY

VALUE (MeV)	EVTS	DOCUMENT ID	TECN	CHG	COMMENT
• • •					We do not use the following data for averages, fits, limits, etc. • • •
982.5 ± 1.6 ± 1.1	16.9k	<sup>1</sup> AMBROSINO	09F	KLOE	1.02 $e^+e^- \rightarrow \eta\pi^0\gamma$
986 ± 4		ANISOVICH	09	RVUE	0.0 $\bar{p}p, \pi N$
982.3 ± 0.6 ± 3.1 -0.7 -4.7		<sup>2</sup> UEHARA	09A	BELL	$\gamma\gamma \rightarrow \pi^0\eta$
987.4 ± 1.0 ± 3.0		<sup>3,4</sup> BUGG	08A	RVUE 0	$\bar{p}p \rightarrow \pi^0\pi^0\eta$
989.1 ± 1.0 ± 3.0		<sup>4,5</sup> BUGG	08A	RVUE 0	$\bar{p}p \rightarrow \pi^0\pi^0\eta$
985 ± 4 ± 6	318	ACHARD	02B	L3	183-209 $e^+e^- \rightarrow e^+e^-\eta\pi^+\pi^-$
995 ± 5.2 -10	36	<sup>6</sup> ACHASOV	00F	SND	$e^+e^- \rightarrow \eta\pi^0\gamma$
994 ± 3.3 -8	36	<sup>7</sup> ACHASOV	00F	SND	$e^+e^- \rightarrow \eta\pi^0\gamma$
975 ± 7		BARBERIS	00H		450 $pp \rightarrow \rho_f\eta\pi^0\rho_S$
988 ± 8		BARBERIS	00H		450 $pp \rightarrow \Delta_f^{++}\eta\pi^-\rho_S$
~ 1055		<sup>8</sup> OLLER	99	RVUE	$\eta\pi, K\bar{K}$
~ 1009.2		<sup>8</sup> OLLER	99B	RVUE	$\pi\pi \rightarrow \pi\pi, K\bar{K}$
993.1 ± 2.1		<sup>9</sup> TEIGE	99	B852	18.3 $\pi^-\rho \rightarrow \eta\pi^+\pi^-n$
988 ± 6		<sup>8</sup> ANISOVICH	98B	RVUE	Compilation
987		TORNQVIST	96	RVUE	$\pi\pi \rightarrow \pi\pi, K\bar{K}, K\pi, \eta\pi$
991		JANSSEN	95	RVUE	$\eta\pi \rightarrow \eta\pi, K\bar{K}, K\pi, \eta\pi$
984.45 ± 1.23 ± 0.34		AMSLER	94C	CBAR	0.0 $\bar{p}p \rightarrow \omega\eta\pi^0$
982 ± 2		<sup>10</sup> AMSLER	92	CBAR	0.0 $\bar{p}p \rightarrow \eta\eta\pi^0$
984 ± 4	1040	<sup>10</sup> ARMSTRONG	91B	OMEG ±	300 $pp \rightarrow \rho\rho\eta\pi^+\pi^-$
976 ± 6		ATKINSON	84E	OMEG ±	25-55 $\gamma\rho \rightarrow \eta\pi n$
986 ± 3	500	<sup>11</sup> EVANGELIS...	81	OMEG ±	12 $\pi^-\rho \rightarrow \eta\pi^+\pi^-\pi^-\rho$
990 ± 7	145	<sup>11</sup> GURTU	79	HBC ±	4.2 $K^-\rho \rightarrow \Lambda\eta 2\pi$
980 ± 11	47	CONFORTO	78	OSPK -	4.5 $\pi^-\rho \rightarrow \rho X^-$
978 ± 16	50	CORDEN	78	OMEG ±	12-15 $\pi^-\rho \rightarrow n\eta 2\pi$
977 ± 7		GRASSLER	77	HBC -	16 $\pi^+\rho \rightarrow \rho\eta 3\pi$
989 ± 4	70	WELLS	75	HBC -	3.1-6 $K^-\rho \rightarrow \Lambda\eta 2\pi$
972 ± 10	150	DEFOIX	72	HBC ±	0.7 $\bar{p}p \rightarrow 7\pi$
970 ± 15	20	BARNES	69C	HBC -	4-5 $K^-\rho \rightarrow \Lambda\eta 2\pi$
980 ± 10		CAMPBELL	69	DBC ±	2.7 $\pi^+d$
980 ± 10	15	MILLER	69B	HBC -	4.5 $K^-N \rightarrow \eta\pi\Lambda$
980 ± 10	30	AMMAR	68	HBC ±	5.5 $K^-\rho \rightarrow \Lambda\eta 2\pi$

<sup>1</sup> Using the model of ACHASOV 89 and ACHASOV 03B.

<sup>2</sup> From a fit with the S-wave amplitude including two interfering Breit-Wigners plus a background term.

<sup>3</sup> Parameterizes couplings to  $\bar{K}K, \pi\eta,$  and  $\pi\eta'$ .

<sup>4</sup> Using AMSLER 94D and ABELE 98.

<sup>5</sup> From the T-matrix pole on sheet II.

<sup>6</sup> Using the model of ACHASOV 89. Supersedes ACHASOV 98B.

<sup>7</sup> Using the model of JAFFE 77. Supersedes ACHASOV 98B.

<sup>8</sup> T-matrix pole.

<sup>9</sup> Breit-Wigner fit, average between  $a_0^+$  and  $a_0^0$ . The fit favors a slightly heavier  $a_0^+$ .

<sup>10</sup> From a single Breit-Wigner fit.

<sup>11</sup> From  $f_1(1285)$  decay.

 $K\bar{K}$  ONLY

VALUE (MeV)	EVTS	DOCUMENT ID	TECN	CHG	COMMENT
• • •					We do not use the following data for averages, fits, limits, etc. • • •
~ 1053		<sup>12</sup> OLLER	99C	RVUE	$\pi\pi \rightarrow \pi\pi, K\bar{K}$
982 ± 3		<sup>13</sup> ABELE	98	CBAR	0.0 $\bar{p}p \rightarrow K_L^0 K^\pm \pi^\mp$
975 ± 15		BERTIN	98B	OBLX ±	0.0 $\bar{p}p \rightarrow K^\pm K_S \pi^\mp$
976 ± 6	316	DEBILLY	80	HBC ±	1.2-2 $\bar{p}p \rightarrow f_1(1285)\omega$
1016 ± 10	100	<sup>14</sup> ASTIER	67	HBC ±	0.0 $\bar{p}p$
1003.3 ± 7.0	143	<sup>15</sup> ROSENFELD	65	RVUE ±	

<sup>12</sup> T-matrix pole.

<sup>13</sup> T-matrix pole on sheet II, the pole on sheet III is at 1006-i49 MeV.

<sup>14</sup> ASTIER 67 includes data of BARLOW 67, CONFORTO 67, ARMENTEROS 65.

<sup>15</sup> Plus systematic errors.

 $a_0(980)$  WIDTH

VALUE (MeV) EVTS DOCUMENT ID TECN CHG COMMENT  
**50 to 100 OUR ESTIMATE** Width determination very model dependent. Peak width in  $\eta\pi$  is about 60 MeV, but decay width can be much larger.

• • • We do not use the following data for averages, fits, limits, etc. • • •

75.6 ± 1.6 +17.4 -10.0		<sup>16</sup> UEHARA	09A	BELL	$\gamma\gamma \rightarrow \pi^0\eta$
80.2 ± 3.8 ± 5.4		<sup>17</sup> BUGG	08A	RVUE 0	$\bar{p}p \rightarrow \pi^0\pi^0\eta$
50 ± 13 ± 4	318	ACHARD	02B	L3	183-209 $e^+e^- \rightarrow e^+e^-\eta\pi^+\pi^-$
72 ± 16		BARBERIS	00H		450 $pp \rightarrow \rho_f\eta\pi^0\rho_S$
61 ± 19		BARBERIS	00H		450 $pp \rightarrow \Delta_f^{++}\eta\pi^-\rho_S$
~ 42		<sup>18</sup> OLLER	99	RVUE	$\eta\pi, K\bar{K}$
~ 112		<sup>18</sup> OLLER	99B	RVUE	$\pi\pi \rightarrow \eta\pi, K\bar{K}$
71 ± 7		TEIGE	99	B852	18.3 $\pi^-\rho \rightarrow \eta\pi^+\pi^-n$
92 ± 20		<sup>18</sup> ANISOVICH	98B	RVUE	Compilation
65 ± 10		<sup>19</sup> BERTIN	98B	OBLX ±	0.0 $\bar{p}p \rightarrow K^\pm K_S \pi^\mp$
~ 100		TORNQVIST	96	RVUE	$\pi\pi \rightarrow \pi\pi, K\bar{K}, K\pi, \eta\pi$
202		JANSSEN	95	RVUE	$\eta\pi \rightarrow \eta\pi, K\bar{K}, K\pi, \eta\pi$
54.12 ± 0.34 ± 0.12		AMSLER	94C	CBAR	0.0 $\bar{p}p \rightarrow \omega\eta\pi^0$
54 ± 10		<sup>20</sup> AMSLER	92	CBAR	0.0 $\bar{p}p \rightarrow \eta\eta\pi^0$
95 ± 14	1040	<sup>20</sup> ARMSTRONG	91B	OMEG ±	300 $pp \rightarrow \rho\rho\eta\pi^+\pi^-$
62 ± 15	500	<sup>21</sup> EVANGELIS...	81	OMEG ±	12 $\pi^-\rho \rightarrow \eta\pi^+\pi^-\pi^-\rho$
60 ± 20	145	<sup>21</sup> GURTU	79	HBC ±	4.2 $K^-\rho \rightarrow \Lambda\eta 2\pi$
60 +50 -30	47	CONFORTO	78	OSPK -	4.5 $\pi^-\rho \rightarrow \rho X^-$
86.0 +60.0 -50.0	50	CORDEN	78	OMEG ±	12-15 $\pi^-\rho \rightarrow n\eta 2\pi$
44 ± 22		GRASSLER	77	HBC -	16 $\pi^+\rho \rightarrow \rho\eta 3\pi$
80 to 300		<sup>22</sup> FLATTE	76	RVUE -	4.2 $K^-\rho \rightarrow \Lambda\eta 2\pi$
16.0 +25.0 -16.0	70	WELLS	75	HBC -	3.1-6 $K^-\rho \rightarrow \Lambda\eta 2\pi$
30 ± 5	150	DEFOIX	72	HBC ±	0.7 $\bar{p}p \rightarrow 7\pi$
40 ± 15		CAMPBELL	69	DBC ±	2.7 $\pi^+d$
60 ± 30	15	MILLER	69B	HBC -	4.5 $K^-N \rightarrow \eta\pi\Lambda$
80 ± 30	30	AMMAR	68	HBC ±	5.5 $K^-\rho \rightarrow \Lambda\eta 2\pi$

 $K\bar{K}$  ONLY

VALUE (MeV)	EVTS	DOCUMENT ID	TECN	CHG	COMMENT
<b>92 ± 8</b>		<sup>23</sup> ABELE	98	CBAR	0.0 $\bar{p}p \rightarrow K_L^0 K^\pm \pi^\mp$

• • • We do not use the following data for averages, fits, limits, etc. • • •

~ 24		<sup>24</sup> OLLER	99C	RVUE	$\pi\pi \rightarrow \pi\pi, K\bar{K}$
~ 25	100	<sup>25</sup> ASTIER	67	HBC ±	
57 ± 13	143	<sup>26</sup> ROSENFELD	65	RVUE ±	

<sup>23</sup> T-matrix pole on sheet II, the pole on sheet III is at 1006-i49 MeV.

<sup>24</sup> T-matrix pole.

<sup>25</sup> ASTIER 67 includes data of BARLOW 67, CONFORTO 67, ARMENTEROS 65.

<sup>26</sup> Plus systematic errors.

 $a_0(980)$  DECAY MODES

Mode	Fraction ( $\Gamma_i/\Gamma$ )
$\Gamma_1$ $\eta\pi$	dominant
$\Gamma_2$ $K\bar{K}$	seen
$\Gamma_3$ $\rho\pi$	
$\Gamma_4$ $\gamma\gamma$	seen
$\Gamma_5$ $e^+e^-$	

 $a_0(980)$  PARTIAL WIDTHS $\Gamma(\gamma\gamma)$ 

VALUE (keV)	DOCUMENT ID	TECN	
• • •			We do not use the following data for averages, fits, limits, etc. • • •
0.30 ± 0.10	<sup>27</sup> AMSLER	98	RVUE

• • • We do not use the following data for averages, fits, limits, etc. • • •

<sup>27</sup> Using  $\Gamma_{\gamma\gamma} B(a_0(980) \rightarrow \eta\pi) = 0.24 \pm 0.08$  keV.

 $\Gamma_4$



# Meson Particle Listings

## $\phi(1020)$

4.3 ± 0.6		12	CORDIER	80	DM1	$e^+e^- \rightarrow \pi^+\pi^-\pi^0$
4.36 ± 0.29	3681	12	BUKIN	78c	OLYA	$e^+e^- \rightarrow \text{hadrons}$
4.4 ± 0.6	984	12	BESCH	74	CNTR	$2\gamma\rho \rightarrow \rho K^+K^-$
4.67 ± 0.72	681	12	BALAKIN	71	OSPK	$e^+e^- \rightarrow \text{hadrons}$
4.09 ± 0.29			BIZOT	70	OSPK	$e^+e^- \rightarrow \text{hadrons}$
• • • We do not use the following data for averages, fits, limits, etc. • • •						
4.24 ± 0.02 ± 0.03	542k	13	AKHMETSHIN	08	CMD2	$1.02 e^+e^- \rightarrow K^+K^-$
4.28 ± 0.13	12540	14	AUBERT,B	05J	BABR	$D^0 \rightarrow \bar{K}^0 K^+ K^-$
4.45 ± 0.06	271k		DIJKSTRA	86	SPEC	$100 \pi^- \text{Be}$
3.6 ± 0.8	337	12	COOPER	78B	HBC	$0.7-0.8 \bar{p}p \rightarrow K_S^0 K_L^0 \pi^+\pi^-$
4.5 ± 0.50	1300	12,14	AKERLOF	77	SPEC	$400 \rho A \rightarrow K^+K^-X$
4.5 ± 0.8	500	12,14	AYRES	74	ASPK	$3-6 \pi^- p \rightarrow K^+K^-n, K^-p \rightarrow K^+K^-A/\Sigma^0$
3.81 ± 0.37			COSME	74B	OSPK	$e^+e^- \rightarrow K_L^0 K_S^0$
3.8 ± 0.7	454	12	BORENSTEIN	72	HBC	$2.18 K^-p \rightarrow K\bar{K}n$

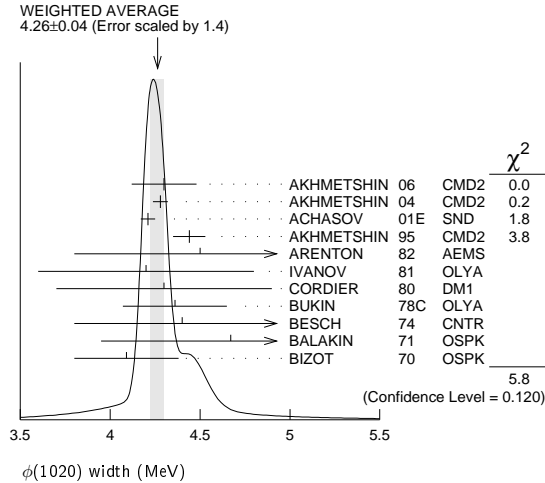
<sup>10</sup>Update of AKHMETSHIN 99d

<sup>11</sup>From the combined fit assuming that the total  $\phi(1020)$  production cross section is saturated by those of  $K^+K^-$ ,  $K_S K_L$ ,  $\pi^+\pi^-\pi^0$ , and  $\eta\gamma$  decays modes and using ACHASOV 00b for the  $\eta\gamma$  decay mode.

<sup>12</sup>Width errors enlarged by us to  $4\Gamma/\sqrt{N}$ ; see the note with the  $K^*(892)$  mass.

<sup>13</sup>Strongly correlated with AKHMETSHIN 04.

<sup>14</sup>Systematic errors not evaluated.



### $\phi(1020)$ DECAY MODES

Mode	Fraction ( $\Gamma_i/\Gamma$ )	Scale factor/ Confidence level
$\Gamma_1 K^+K^-$	(48.9 ± 0.5) %	S=1.1
$\Gamma_2 K_L^0 K_S^0$	(34.2 ± 0.4) %	S=1.1
$\Gamma_3 \rho\pi + \pi^+\pi^-\pi^0$	(15.32 ± 0.32) %	S=1.1
$\Gamma_4 \rho\pi$		
$\Gamma_5 \pi^+\pi^-\pi^0$		
$\Gamma_6 \eta\gamma$	( 1.309 ± 0.024) %	S=1.2
$\Gamma_7 \pi^0\gamma$	( 1.27 ± 0.06 ) × 10 <sup>-3</sup>	
$\Gamma_8 \ell^+\ell^-$	—	
$\Gamma_9 e^+e^-$	( 2.954 ± 0.030 ) × 10 <sup>-4</sup>	S=1.1
$\Gamma_{10} \mu^+\mu^-$	( 2.87 ± 0.19 ) × 10 <sup>-4</sup>	
$\Gamma_{11} \eta e^+e^-$	( 1.15 ± 0.10 ) × 10 <sup>-4</sup>	
$\Gamma_{12} \pi^+\pi^-$	( 7.4 ± 1.3 ) × 10 <sup>-5</sup>	
$\Gamma_{13} \omega\pi^0$	( 4.7 ± 0.5 ) × 10 <sup>-5</sup>	
$\Gamma_{14} \omega\gamma$	< 5 %	CL=84%
$\Gamma_{15} \rho\gamma$	< 1.2 × 10 <sup>-5</sup>	CL=90%
$\Gamma_{16} \pi^+\pi^-\gamma$	( 4.1 ± 1.3 ) × 10 <sup>-5</sup>	
$\Gamma_{17} f_0(980)\gamma$	( 3.22 ± 0.19 ) × 10 <sup>-4</sup>	S=1.1
$\Gamma_{18} \pi^0\pi^0\gamma$	( 1.13 ± 0.06 ) × 10 <sup>-4</sup>	
$\Gamma_{19} \pi^+\pi^-\pi^+\pi^-$	( 4.0 <sup>+2.8</sup> / <sub>-2.2</sub> ) × 10 <sup>-6</sup>	
$\Gamma_{20} \pi^+\pi^+\pi^-\pi^-\pi^0$	< 4.6 × 10 <sup>-6</sup>	CL=90%
$\Gamma_{21} \pi^0 e^+e^-$	( 1.12 ± 0.28 ) × 10 <sup>-5</sup>	
$\Gamma_{22} \pi^0 \eta\gamma$	( 7.27 ± 0.30 ) × 10 <sup>-5</sup>	S=1.5
$\Gamma_{23} a_0(980)\gamma$	( 7.6 ± 0.6 ) × 10 <sup>-5</sup>	
$\Gamma_{24} K^0 \bar{K}^0 \gamma$	< 1.9 × 10 <sup>-8</sup>	CL=90%
$\Gamma_{25} \eta'(958)\gamma$	( 6.25 ± 0.21 ) × 10 <sup>-5</sup>	
$\Gamma_{26} \eta\pi^0\pi^0\gamma$	< 2 × 10 <sup>-5</sup>	CL=90%

$\Gamma_{27} \mu^+\mu^-\gamma$	( 1.4 ± 0.5 ) × 10 <sup>-5</sup>	
$\Gamma_{28} \rho\gamma\gamma$	< 1.2 × 10 <sup>-4</sup>	CL=90%
$\Gamma_{29} \eta\pi^+\pi^-$	< 1.8 × 10 <sup>-5</sup>	CL=90%
$\Gamma_{30} \eta\mu^+\mu^-$	< 9.4 × 10 <sup>-6</sup>	CL=90%

### Lepton Family number (LF) violating modes

$\Gamma_{31} e^\pm \mu^\mp$	LF < 2	× 10 <sup>-6</sup> CL=90%
-----------------------------	--------	---------------------------

### CONSTRAINED FIT INFORMATION

An overall fit to 30 branching ratios uses 79 measurements and one constraint to determine 14 parameters. The overall fit has a  $\chi^2 = 57.4$  for 66 degrees of freedom.

The following *off-diagonal* array elements are the correlation coefficients  $\langle \delta x_i \delta x_j \rangle / (\delta x_i \delta x_j)$ , in percent, from the fit to the branching fractions,  $x_i \equiv \Gamma_i/\Gamma_{\text{total}}$ . The fit constrains the  $x_i$  whose labels appear in this array to sum to one.

$x_2$	-72																			
$x_3$	-53	-21																		
$x_6$	-13	7	2																	
$x_7$	-5	3	1	5																
$x_9$	30	-25	-10	-32	-15															
$x_{10}$	-4	3	1	3	2	-11														
$x_{12}$	-2	1	0	2	1	-5	1													
$x_{13}$	-2	2	1	2	1	-7	1	0												
$x_{17}$	0	0	0	0	0	0	0	0	0											
$x_{18}$	-6	4	2	17	3	-17	2	1	1	0										
$x_{19}$	0	0	0	0	0	-1	0	0	0	0										
$x_{23}$	0	0	0	0	0	0	0	0	0	0										
$x_{25}$	-4	2	1	32	2	-10	1	1	1	0										
		$x_1$	$x_2$	$x_3$	$x_6$	$x_7$	$x_9$	$x_{10}$	$x_{12}$	$x_{13}$	$x_{17}$									
$x_{19}$	0																			
$x_{23}$	0	0																		
$x_{25}$	5	0	0																	
		$x_{18}$	$x_{19}$	$x_{23}$																

### $\phi(1020)$ PARTIAL WIDTHS

$\Gamma(\eta\gamma)$	VALUE (keV)	DOCUMENT ID	TECN	COMMENT	$\Gamma_6$
----------------------	-------------	-------------	------	---------	------------

• • • We do not use the following data for averages, fits, limits, etc. • • •

58.9 ± 0.5 ± 2.4	ACHASOV	00	SND	$e^+e^- \rightarrow \eta\gamma$
------------------	---------	----	-----	---------------------------------

$\Gamma(\pi^0\gamma)$	VALUE (keV)	DOCUMENT ID	TECN	COMMENT	$\Gamma_7$
-----------------------	-------------	-------------	------	---------	------------

• • • We do not use the following data for averages, fits, limits, etc. • • •

5.40 ± 0.16 <sup>+0.43</sup> / <sub>-0.40</sub>	ACHASOV	00	SND	$e^+e^- \rightarrow \pi^0\gamma$
---	---------	----	-----	----------------------------------

$\Gamma(\ell^+\ell^-)$	VALUE (keV)	DOCUMENT ID	TECN	COMMENT	$\Gamma_8$
------------------------	-------------	-------------	------	---------	------------

• • • We do not use the following data for averages, fits, limits, etc. • • •

1.320 ± 0.017 ± 0.015	15	AMBROSINO	05	KLOE	$1.02 e^+e^- \rightarrow \mu^+\mu^-$
-----------------------	----	-----------	----	------	--------------------------------------

$\Gamma(e^+e^-)$	VALUE (keV)	DOCUMENT ID	TECN	COMMENT	$\Gamma_9$
------------------	-------------	-------------	------	---------	------------

**1.27 ± 0.04 OUR EVALUATION**

**1.251 ± 0.021 OUR AVERAGE** Error includes scale factor of 1.1.

1.235 ± 0.006 ± 0.022	16	AKHMETSHIN	11	CMD2	$1.02 e^+e^- \rightarrow \phi$
-----------------------	----	------------	----	------	--------------------------------

1.32 ± 0.05 ± 0.03	17	AMBROSINO	05	KLOE	$1.02 e^+e^- \rightarrow e^+e^-$
--------------------	----	-----------	----	------	----------------------------------

1.28 ± 0.05		AKHMETSHIN	95	CMD2	$1.02 e^+e^- \rightarrow \phi$
-------------	--	------------	----	------	--------------------------------

$(\Gamma(e^+e^-) \times \Gamma(\mu^+\mu^-))^{1/2}$	VALUE (keV)	DOCUMENT ID	TECN	COMMENT	$(\Gamma_9\Gamma_{10})^{1/2}$
--	-------------	-------------	------	---------	-------------------------------

**1.320 ± 0.018 ± 0.017**

<sup>15</sup>Weighted average of  $\Gamma_{ee}$  and  $\sqrt{\Gamma_{ee}\Gamma_{\mu\mu}}$  from AMBROSINO 05 assuming lepton universality.

<sup>16</sup>Combined analysis of the CMD-2 data on  $\phi \rightarrow K^+K^-$ ,  $K_S^0 K_L^0$ ,  $\pi^+\pi^-\pi^0$ ,  $\eta\gamma$  assuming that the sum of their branching fractions is 0.99741 ± 0.00007.

<sup>17</sup>From forward-backward asymmetry and using  $\Gamma_{\text{total}} = 4.26 \pm 0.05$  MeV from the 2004 edition of this Review.

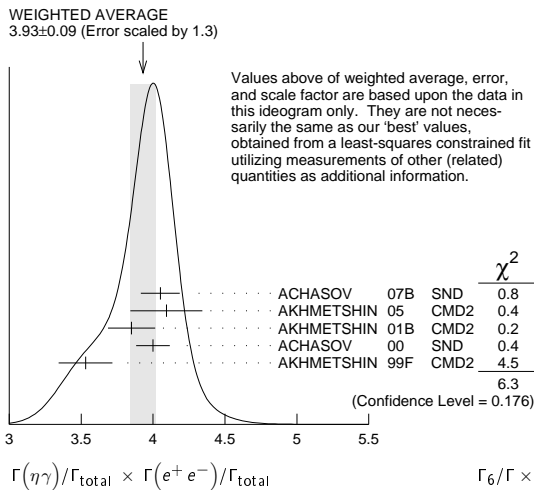
$\phi(1020) \Gamma(\eta)\Gamma(e^+e^-)/\Gamma^2(\text{total})$

$\Gamma(K^+K^-)/\Gamma_{\text{total}} \times \Gamma(e^+e^-)/\Gamma_{\text{total}}$					$\Gamma_1/\Gamma \times \Gamma_9/\Gamma$
VALUE (units $10^{-5}$ )	EVTS	DOCUMENT ID	TECN	COMMENT	
<b>14.46 ± 0.23 OUR FIT</b>				Error includes scale factor of 1.1.	
<b>14.24 ± 0.30 OUR AVERAGE</b>					
14.27 ± 0.05 ± 0.31	542k	AKHMETSHIN 08	CMD2	1.02 $e^+e^- \rightarrow K^+K^-$	
13.93 ± 0.14 ± 0.99	1000k	18 ACHASOV	01E	SND $e^+e^- \rightarrow K^+K^-, K_S^0 K_L^0, \pi^+\pi^-\pi^0$	

$\Gamma(K_L^0 K_S^0)/\Gamma_{\text{total}} \times \Gamma(e^+e^-)/\Gamma_{\text{total}}$					$\Gamma_2/\Gamma \times \Gamma_9/\Gamma$
VALUE (units $10^{-5}$ )	EVTS	DOCUMENT ID	TECN	COMMENT	
<b>10.10 ± 0.13 OUR FIT</b>					
<b>10.06 ± 0.16 OUR AVERAGE</b>					
10.01 ± 0.04 ± 0.17	272k	19 AKHMETSHIN 04	CMD2	$e^+e^- \rightarrow K_L^0 K_S^0$	
10.27 ± 0.07 ± 0.34	500k	18 ACHASOV	01E	SND $e^+e^- \rightarrow K^+K^-, K_S^0 K_L^0, \pi^+\pi^-\pi^0$	

$[\Gamma(\rho\pi) + \Gamma(\pi^+\pi^-\pi^0)]/\Gamma_{\text{total}} \times \Gamma(e^+e^-)/\Gamma_{\text{total}}$					$\Gamma_3/\Gamma \times \Gamma_9/\Gamma$
VALUE (units $10^{-5}$ )	EVTS	DOCUMENT ID	TECN	COMMENT	
<b>4.53 ± 0.10 OUR FIT</b>				Error includes scale factor of 1.1.	
<b>4.46 ± 0.12 OUR AVERAGE</b>					
4.51 ± 0.16 ± 0.11	105k	AKHMETSHIN 06	CMD2	0.98-1.06 $e^+e^- \rightarrow \pi^+\pi^-\pi^0$	
4.30 ± 0.08 ± 0.21		AUBERT,B	04N	BABR 10.6 $e^+e^- \rightarrow \pi^+\pi^-\pi^0\gamma$	
4.665 ± 0.042 ± 0.261	400k	18 ACHASOV	01E	SND $e^+e^- \rightarrow K^+K^-, K_S^0 K_L^0, \pi^+\pi^-\pi^0$	
4.35 ± 0.27 ± 0.08	11169	20 AKHMETSHIN 98	CMD2	$e^+e^- \rightarrow \pi^+\pi^-\pi^0$	
• • • We do not use the following data for averages, fits, limits, etc. • • •					
4.38 ± 0.12		BENAYOUN 10	RVUE	0.4-1.05 $e^+e^-$	

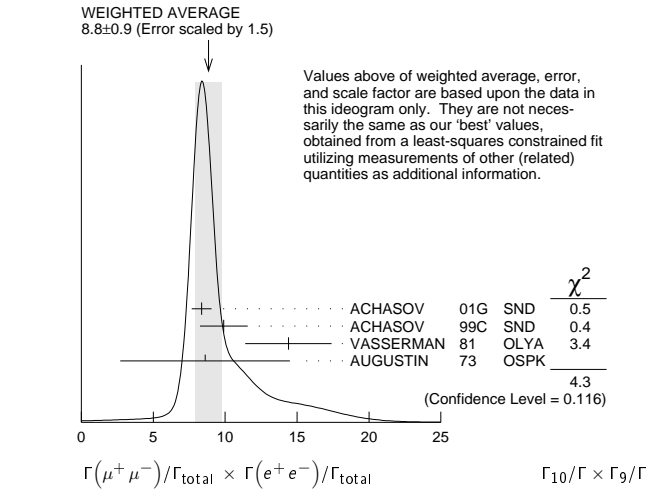
$\Gamma(\eta\gamma)/\Gamma_{\text{total}} \times \Gamma(e^+e^-)/\Gamma_{\text{total}}$					$\Gamma_6/\Gamma \times \Gamma_9/\Gamma$
VALUE (units $10^{-6}$ )	EVTS	DOCUMENT ID	TECN	COMMENT	
<b>3.87 ± 0.07 OUR FIT</b>				Error includes scale factor of 1.2.	
<b>3.93 ± 0.09 OUR AVERAGE</b>				Error includes scale factor of 1.3. See the ideogram below.	
4.050 ± 0.067 ± 0.118	33k	21 ACHASOV	07B	SND 0.6-1.38 $e^+e^- \rightarrow \eta\gamma$	
4.093 <sup>+0.040</sup> <sub>-0.043</sub> ± 0.247	17.4k	22 AKHMETSHIN 05	CMD2	0.60-1.38 $e^+e^- \rightarrow \eta\gamma$	
3.850 ± 0.041 ± 0.159	23k	23,24 AKHMETSHIN 01B	CMD2	$e^+e^- \rightarrow \eta\gamma$	
4.00 ± 0.04 ± 0.11		25 ACHASOV 00	SND	$e^+e^- \rightarrow \eta\gamma$	
3.53 ± 0.08 ± 0.17	2200	26,27 AKHMETSHIN 99F	CMD2	$e^+e^- \rightarrow \eta\gamma$	
• • • We do not use the following data for averages, fits, limits, etc. • • •					
4.19 ± 0.06		28 BENAYOUN 10	RVUE	0.4-1.05 $e^+e^-$	



$\Gamma(\pi^0\gamma)/\Gamma_{\text{total}} \times \Gamma(e^+e^-)/\Gamma_{\text{total}}$					$\Gamma_7/\Gamma \times \Gamma_9/\Gamma$
VALUE (units $10^{-7}$ )	EVTS	DOCUMENT ID	TECN	COMMENT	
<b>3.74 ± 0.18 OUR FIT</b>					
<b>3.71 ± 0.21 OUR AVERAGE</b>					
3.75 ± 0.11 ± 0.29	18680	AKHMETSHIN 05	CMD2	0.60-1.38 $e^+e^- \rightarrow \pi^0\gamma$	
3.67 ± 0.10 <sup>+0.27</sup> <sub>-0.25</sub>		29 ACHASOV 00	SND	$e^+e^- \rightarrow \pi^0\gamma$	
• • • We do not use the following data for averages, fits, limits, etc. • • •					
4.29 ± 0.11		28 BENAYOUN 10	RVUE	0.4-1.05 $e^+e^-$	

$\Gamma(\mu^+\mu^-)/\Gamma_{\text{total}} \times \Gamma(e^+e^-)/\Gamma_{\text{total}}$   $\Gamma_{10}/\Gamma \times \Gamma_9/\Gamma$

VALUE (units $10^{-8}$ )	DOCUMENT ID	TECN	COMMENT
<b>8.5<sup>+0.5</sup><sub>-0.6</sub> OUR FIT</b>			
<b>8.8 ± 0.9 OUR AVERAGE</b>			Error includes scale factor of 1.5. See the ideogram below.
8.36 ± 0.59 ± 0.37	ACHASOV 01G	SND	$e^+e^- \rightarrow \mu^+\mu^-$
9.9 ± 1.4 ± 0.9	26 ACHASOV 99C	SND	$e^+e^- \rightarrow \mu^+\mu^-$
14.4 ± 3.0	20 VASSERMAN 81	OLYA	$e^+e^- \rightarrow \mu^+\mu^-$
8.6 ± 0.9	20 AUGUSTIN 73	OSPK	$e^+e^- \rightarrow \mu^+\mu^-$



$\Gamma(\pi^+\pi^-)/\Gamma_{\text{total}} \times \Gamma(e^+e^-)/\Gamma_{\text{total}}$					$\Gamma_{12}/\Gamma \times \Gamma_9/\Gamma$
VALUE (units $10^{-8}$ )	DOCUMENT ID	TECN	COMMENT		
<b>2.2 ± 0.4 OUR FIT</b>					
<b>2.2 ± 0.4 OUR AVERAGE</b>					
2.1 ± 0.3 ± 0.3	26 ACHASOV 00c	SND	$e^+e^- \rightarrow \pi^+\pi^-$		
1.95 <sup>+1.15</sup> <sub>-0.87</sub>	20 GOLUBEV 86	ND	$e^+e^- \rightarrow \pi^+\pi^-$		
6.01 <sup>+3.19</sup> <sub>-2.51</sub>	20 VASSERMAN 81	OLYA	$e^+e^- \rightarrow \pi^+\pi^-$		

$\Gamma(\omega\pi^0)/\Gamma_{\text{total}} \times \Gamma(e^+e^-)/\Gamma_{\text{total}}$					$\Gamma_{13}/\Gamma \times \Gamma_9/\Gamma$
VALUE (units $10^{-8}$ )	DOCUMENT ID	TECN	COMMENT		
<b>1.40 ± 0.15 OUR FIT</b>					
<b>1.37 ± 0.17 ± 0.01</b>	30,31 AMBROSINO 08G	KLOE	$e^+e^- \rightarrow \pi^+\pi^-\pi^0, 2\pi^0\gamma$		

$\Gamma(\pi^0\pi^0\gamma)/\Gamma_{\text{total}} \times \Gamma(e^+e^-)/\Gamma_{\text{total}}$					$\Gamma_{18}/\Gamma \times \Gamma_9/\Gamma$
VALUE (units $10^{-8}$ )	DOCUMENT ID	TECN	COMMENT		
<b>3.34 ± 0.17 OUR FIT</b>					
<b>3.33<sup>+0.04</sup><sub>-0.09</sub> ± 0.20</b>	32 AMBROSINO 07	KLOE	$e^+e^- \rightarrow \pi^0\pi^0\gamma$		

$\Gamma(\pi^+\pi^-\pi^+\pi^-)/\Gamma_{\text{total}} \times \Gamma(e^+e^-)/\Gamma_{\text{total}}$					$\Gamma_{19}/\Gamma \times \Gamma_9/\Gamma$
VALUE (units $10^{-9}$ )	EVTS	DOCUMENT ID	TECN	COMMENT	
<b>1.2<sup>+0.8</sup><sub>-0.7</sub> OUR FIT</b>					
<b>1.17 ± 0.52 ± 0.64</b>	3285	26 AKHMETSHIN 00E	CMD2	$e^+e^- \rightarrow \pi^+\pi^-\pi^+\pi^-$	

18 From the combined fit assuming that the total  $\phi(1020)$  production cross section is saturated by those of  $K^+K^-$ ,  $K_S^0 K_L^0$ ,  $\pi^+\pi^-\pi^0$ , and  $\eta\gamma$  decays modes and using ACHASOV 00b for the  $\eta\gamma$  decay mode.

19 Update of AKHMETSHIN 99d

20 Recalculated by us from the cross section in the peak.

21 From a combined fit of  $\sigma(e^+e^- \rightarrow \eta\gamma)$  with  $\eta \rightarrow 3\pi^0$  and  $\eta \rightarrow \pi^+\pi^-\pi^0$ , and fixing  $B(\eta \rightarrow 3\pi^0) / B(\eta \rightarrow \pi^+\pi^-\pi^0) = 1.44 \pm 0.04$ . Recalculated by us from the cross section at the peak. Supersedes ACHASOV 00D and ACHASOV 06A.

22 From the  $\eta \rightarrow 2\gamma$  decay and using  $B(\eta \rightarrow \gamma\gamma) = 39.43 \pm 0.26\%$ .

23 From the  $\eta \rightarrow 3\pi^0$  decay and using  $B(\eta \rightarrow 3\pi^0) = (32.24 \pm 0.29) \times 10^{-2}$ .

24 The combined fit from 600 to 1380 MeV taking into account  $\rho(770)$ ,  $\omega(782)$ ,  $\phi(1020)$ , and  $\rho(1450)$  (mass and width fixed at 1450 MeV and 310 MeV respectively).

25 From the  $\eta \rightarrow 2\gamma$  decay and using  $B(\eta \rightarrow 2\gamma) = (39.21 \pm 0.34) \times 10^{-2}$ .

26 Recalculated by the authors from the cross section in the peak.

27 From the  $\eta \rightarrow \pi^+\pi^-\pi^0$  decay and using  $B(\eta \rightarrow \pi^+\pi^-\pi^0) = (23.1 \pm 0.5) \times 10^{-2}$ .

28 A simultaneous fit of  $e^+e^- \rightarrow \pi^+\pi^-, \pi^+\pi^-\pi^0, \pi^0\gamma, \eta\gamma$  data.

29 From the  $\pi^0 \rightarrow 2\gamma$  decay and using  $B(\pi^0 \rightarrow 2\gamma) = (98.798 \pm 0.032) \times 10^{-2}$ .

30 Recalculated by the authors from the cross section at the peak.

31 AMBROSINO 08G reports  $[\Gamma(\phi(1020) \rightarrow \omega\pi^0)/\Gamma_{\text{total}} \times \Gamma(\phi(1020) \rightarrow e^+e^-)/\Gamma_{\text{total}}] \times [B(\omega(782) \rightarrow \pi^+\pi^-\pi^0)] = (1.22 \pm 0.13 \pm 0.08) \times 10^{-8}$  which we divide by our best value  $B(\omega(782) \rightarrow \pi^+\pi^-\pi^0) = (89.2 \pm 0.7) \times 10^{-2}$ . Our first error is their experiment's error and our second error is the systematic error from using our best value.

32 Calculated by the authors from the cross section at the peak.





$\Gamma(\pi^+\pi^-)/\Gamma_{total}$   $\Gamma_{12}/\Gamma$

Table with columns: VALUE (units 10^-4), CL%, DOCUMENT ID, TECN, COMMENT. Contains data points for various experiments like ACHASOV, GOLUBEV, VASSERMAN, BUKIN, ALVENSLEB...

$\Gamma(\omega\pi^0)/\Gamma_{total}$   $\Gamma_{13}/\Gamma$

Table with columns: VALUE (units 10^-5), DOCUMENT ID, TECN, COMMENT. Contains data points for AULCHENKO, AMBROSINO, ACHASOV.

$\Gamma(\omega\gamma)/\Gamma_{total}$   $\Gamma_{14}/\Gamma$

Table with columns: VALUE, CL%, DOCUMENT ID, TECN, COMMENT. Contains data point for LINDSEY.

$\Gamma(\rho\gamma)/\Gamma_{total}$   $\Gamma_{15}/\Gamma$

Table with columns: VALUE (units 10^-4), CL%, DOCUMENT ID, TECN, COMMENT. Contains data points for AKHMETSHIN, AKHMETSHIN, LINDSEY.

$\Gamma(\pi^+\pi^-\gamma)/\Gamma_{total}$   $\Gamma_{16}/\Gamma$

Table with columns: VALUE (units 10^-4), CL%, EVTS, DOCUMENT ID, TECN, COMMENT. Contains data points for AKHMETSHIN, KALBFLEISCH, COSME, LINDSEY.

$\Gamma(f_0(980)\gamma)/\Gamma_{total}$   $\Gamma_{17}/\Gamma$

Table with columns: VALUE (units 10^-4), CL%, EVTS, DOCUMENT ID, TECN, COMMENT. Includes 'OUR FIT' and 'OUR AVERAGE' values. Contains data points for AMBROSINO, AKHMETSHIN, ALOISIO, ACHASOV.

$\Gamma(f_0(980)\gamma)/\Gamma(\eta\gamma)$   $\Gamma_{17}/\Gamma_6$

Table with columns: VALUE (units 10^-2), EVTS, DOCUMENT ID, TECN, COMMENT. Contains data point for ACHASOV.

$\Gamma(\pi^0\pi^0\gamma)/\Gamma_{total}$   $\Gamma_{18}/\Gamma$

Table with columns: VALUE (units 10^-4), CL%, EVTS, DOCUMENT ID, TECN, COMMENT. Contains data points for AMBROSINO, AKHMETSHIN, ALOISIO, ACHASOV, DRUZHININ.

$\Gamma(\pi^0\pi^0\gamma)/\Gamma(\eta\gamma)$   $\Gamma_{18}/\Gamma_6$

Table with columns: VALUE (units 10^-2), EVTS, DOCUMENT ID, TECN, COMMENT. Includes 'OUR FIT' and 'OUR AVERAGE' values. Contains data points for ACHASOV.

$\Gamma(\pi^+\pi^-\pi^+\pi^-)/\Gamma_{total}$   $\Gamma_{19}/\Gamma$

Table with columns: VALUE (units 10^-6), CL%, EVTS, DOCUMENT ID, TECN, COMMENT. Contains data points for AKHMETSHIN, CORDIER.

$\Gamma(\pi^+\pi^+\pi^-\pi^0)/\Gamma_{total}$   $\Gamma_{20}/\Gamma$

Table with columns: VALUE (units 10^-6), CL%, DOCUMENT ID, TECN, COMMENT. Contains data points for AKHMETSHIN, BARKOV.

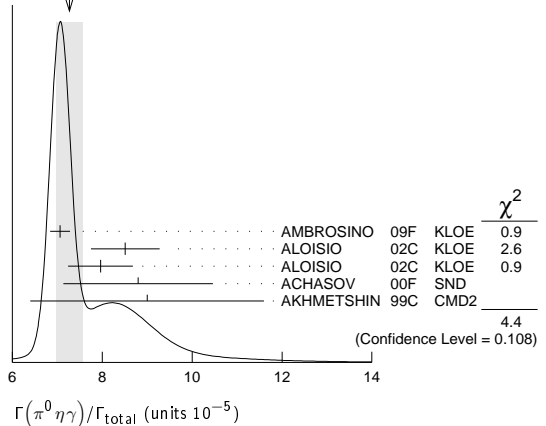
$\Gamma(\pi^0e^+e^-)/\Gamma_{total}$   $\Gamma_{21}/\Gamma$

Table with columns: VALUE (units 10^-5), CL%, EVTS, DOCUMENT ID, TECN, COMMENT. Includes 'OUR AVERAGE' value. Contains data points for ACHASOV, AKHMETSHIN, DOLINSKY.

$\Gamma(\pi^0\eta\gamma)/\Gamma_{total}$   $\Gamma_{22}/\Gamma$

Table with columns: VALUE (units 10^-5), CL%, EVTS, DOCUMENT ID, TECN, COMMENT. Includes 'OUR AVERAGE' value. Contains data points for AMBROSINO, ALOISIO, ACHASOV, DOLINSKY.

WEIGHTED AVERAGE  $7.27 \pm 0.30$  (Error scaled by 1.5)



$\Gamma(a_0(980)\gamma)/\Gamma_{total}$   $\Gamma_{23}/\Gamma$

Table with columns: VALUE (units 10^-5), CL%, EVTS, DOCUMENT ID, TECN, COMMENT. Includes 'OUR FIT' and 'OUR AVERAGE' values. Contains data points for ALOISIO, ACHASOV, GOKALP, DOLINSKY.

$\Gamma(f_0(980)\gamma)/\Gamma(a_0(980)\gamma)$   $\Gamma_{17}/\Gamma_{23}$

Table with columns: VALUE, DOCUMENT ID, TECN, COMMENT. Contains data point for ALOISIO.

$\Gamma(K^0\bar{K}^0\gamma)/\Gamma_{total}$   $\Gamma_{24}/\Gamma$

Table with columns: VALUE, CL%, DOCUMENT ID, TECN, COMMENT. Contains data point for AMBROSINO.



See key on page 457

Meson Particle Listings
phi(1020), h1(1170)

- 99 Averaging AULCHENKO 03b with AULCHENKO 99.
100 Using B(phi -> eta gamma) = (1.297 +/- 0.033)%.
101 Using the value B(phi -> eta gamma) = (1.26 +/- 0.06) x 10^-2.
102 Using B(phi -> K\_L^0 K\_S^0) = (33.8 +/- 0.6)%.
103 Averaging AKHMETSHIN 00b with AKHMETSHIN 00f.
104 Using the value B(eta' -> eta pi+ pi-) = (43.7 +/- 1.5) x 10^-2 and B(eta -> gamma gamma) = (39.25 +/- 0.31) x 10^-2.
105 Using various branching ratios of K\_S^0, K\_L^0, eta, eta' from the 2000 edition (The European Physical Journal C15 1 (2000)) of this Review.
106 From the decay mode eta' -> eta pi+ pi-, eta -> gamma gamma.
107 Superseded by AKHMETSHIN 00b.
108 For E\_gamma > 20 MeV.

Lepton Family number (LF) violating modes

Table with 5 columns: VALUE, CL%, DOCUMENT ID, TECN, COMMENT. Row 1: < 2 x 10^-6, 90, ACHASOV, 10A, SND, e+ e- -> e+ mu+ mu-.

pi+ pi- pi0 / rho pi AMPLITUDE RATIO a1 IN DECAY OF phi -> pi+ pi- pi0

Table with 5 columns: VALUE (units 10^-2), CL%, EVTS, DOCUMENT ID, TECN, COMMENT. Row 1: 10.1 +/- 4.4 +/- 1.7, 80k, 109, AKHMETSHIN 06, CMD2, 1.017-1.021 e+ e- -> pi+ pi- pi0.

- • • We do not use the following data for averages, fits, limits, etc. • • •
-6 < a1 < 6, 500k, 111, ACHASOV, 02, SND, e+ e- -> pi+ pi- pi0
-16 < a1 < 11, 90, 9.8k, 109,112, AKHMETSHIN 98, CMD2, e+ e- -> pi+ pi- gamma gamma
109 Dalitz plot analysis taking into account interference between the contact and rho pi amplitudes.
110 From a fit without limitations on charged and neutral rho masses and widths.
111 Recalculated by us to match the notations of AKHMETSHIN 98.
112 Assuming zero phase for the contact term.

phi(1020) REFERENCES

List of references for phi(1020) decays, including authors like AKHMETSHIN, ACHASOV, BENAYOUN, AMBROSINO, AULCHENKO, FLOREZ-BAEZ, etc., and their respective document IDs and techniques.

List of references for h1(1170) decays, including authors like ACHASOV, ARMSTRONG, ATKINSON, BEBEK, DAVENPORT, DIJKSTRA, FRAME, GOLUBEV, ALBRECHT, DRUZHININ, etc., and their respective document IDs and techniques.

h1(1170)

I^G(J^PC) = 0^-(1^+ -)

h1(1170) MASS

Table with 5 columns: VALUE (MeV), DOCUMENT ID, TECN, CHG, COMMENT. Row 1: 1168 +/- 4, ANDO, 92, SPEC, 8 pi- p -> pi+ pi- pi0 n.

h1(1170) WIDTH

Table with 5 columns: VALUE (MeV), DOCUMENT ID, TECN, CHG, COMMENT. Row 1: 360 +/- 40 OUR ESTIMATE, followed by a note: • • • We do not use the following data for averages, fits, limits, etc. • • •

# Meson Particle Listings

## $h_1(1170)$ , $b_1(1235)$

345 ± 6	ANDO	92	SPEC	$8 \pi^- p \rightarrow \pi^+ \pi^- \pi^0 n$
375 ± 6 ± 34	<sup>3</sup> ANDO	92	SPEC	$8 \pi^- p \rightarrow \pi^+ \pi^- \pi^0 n$
320 ± 50	<sup>4</sup> DANKOWY...	81	SPEC	$8 \pi p \rightarrow 3 \pi n$

<sup>3</sup> Average and spread of values using 2 variants of the model of BOWLER 75.  
<sup>4</sup> Uses the model of BOWLER 75.

### $h_1(1170)$ DECAY MODES

Mode	Fraction ( $\Gamma_i/\Gamma$ )
$\Gamma_1$ $\rho\pi$	seen

### $h_1(1170)$ BRANCHING RATIOS

$\Gamma(\rho\pi)/\Gamma_{total}$	DOCUMENT ID	TECN	COMMENT	$\Gamma_1/\Gamma$
• • • We do not use the following data for averages, fits, limits, etc. • • •				
seen	ANDO	92	SPEC	$8 \pi^- p \rightarrow \pi^+ \pi^- \pi^0 n$
seen	ATKINSON	84	OMEG	$20-70 \gamma p \rightarrow \pi^+ \pi^- \pi^0 p$
seen	DANKOWY...	81	SPEC	$8 \pi p \rightarrow 3 \pi n$

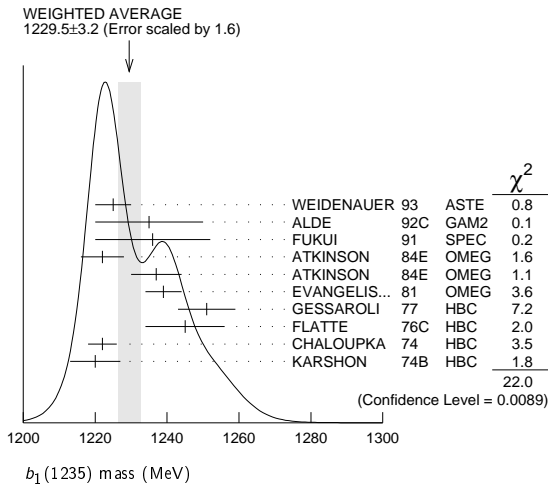
### $h_1(1170)$ REFERENCES

ANDO	92	PL B291 496	A. Ando <i>et al.</i>	(KEK, KYOT, NIRS, SAGA+)
ATKINSON	84	NP B231 15	M. Atkinson <i>et al.</i>	(BONN, CERN, GLAS+)
DANKOWY...	81	PRL 46 580	J.A. Dankowycz <i>et al.</i>	(TNT0, BNL, CARL+)
BOWLER	75	NP B97 227	M.G. Bowler <i>et al.</i>	(OXFPT, DARE)

$b_1(1235)$ 
 $J^{PC} = 1^+(1^+ -)$

### $b_1(1235)$ MASS

VALUE (MeV)	EVTS	DOCUMENT ID	TECN	CHG	COMMENT
<b>1229.5 ± 3.2 OUR AVERAGE</b>					Error includes scale factor of 1.6. See the ideogram below.
1225 ± 5		WEIDENAUER 93	ASTE		$\bar{p}p \rightarrow 2\pi^+ 2\pi^- \pi^0$
1235 ± 15		ALDE 92C	GAM2		38,100 $\pi^- p \rightarrow \omega \pi^0 n$
1236 ± 16		FUKUI 91	SPEC		8.95 $\pi^- p \rightarrow \omega \pi^0 n$
1222 ± 6		ATKINSON 84E	OMEG ±		25-55 $\gamma p \rightarrow \omega \pi X$
1237 ± 7		ATKINSON 84E	OMEG 0		25-55 $\gamma p \rightarrow \omega \pi X$
1239 ± 5		EVANGELIS... 81	OMEG -		12 $\pi^- p \rightarrow \omega \pi p$
1251 ± 8	450	GESSAROLI 77	HBC -		11 $\pi^- p \rightarrow \pi^- \omega p$
1245 ± 11	890	FLATTE 76C	HBC -		4.2 $K^- p \rightarrow \pi^- \omega \Sigma^+$
1222 ± 4	1400	CHALOUKKA 74	HBC -		3.9 $\pi^- p$
1220 ± 7	600	KARSHON 74B	HBC +		4.9 $\pi^+ p$
• • • We do not use the following data for averages, fits, limits, etc. • • •					
1190 ± 10		AUGUSTIN 89	DM2 ±		$e^+ e^- \rightarrow 5\pi$
1213 ± 5		ATKINSON 84C	OMEG 0		20-70 $\gamma p$
1271 ± 11		COLLICK 84	SPEC +		200 $\pi^+ Z \rightarrow Z \pi \omega$



### $b_1(1235)$ WIDTH

VALUE (MeV)	EVTS	DOCUMENT ID	TECN	CHG	COMMENT
<b>142 ± 9 OUR AVERAGE</b>					Error includes scale factor of 1.2.
113 ± 12		WEIDENAUER 93	ASTE		$\bar{p}p \rightarrow 2\pi^+ 2\pi^- \pi^0$
160 ± 30		ALDE 92C	GAM2		38,100 $\pi^- p \rightarrow \omega \pi^0 n$
151 ± 31		FUKUI 91	SPEC		8.95 $\pi^- p \rightarrow \omega \pi^0 n$
170 ± 15		EVANGELIS... 81	OMEG -		12 $\pi^- p \rightarrow \omega \pi p$

170 ± 50	225	BALTAY	78B	HBC +	15 $\pi^+ p \rightarrow p 4\pi$
155 ± 32	450	GESSAROLI 77	HBC -		11 $\pi^- p \rightarrow \pi^- \omega p$
182 ± 45	890	FLATTE 76C	HBC -		4.2 $K^- p \rightarrow \pi^- \omega \Sigma^+$
135 ± 20	1400	CHALOUKKA 74	HBC -		3.9 $\pi^- p$
156 ± 22	600	KARSHON 74B	HBC +		4.9 $\pi^+ p$
• • • We do not use the following data for averages, fits, limits, etc. • • •					
210 ± 19		AUGUSTIN 89	DM2 ±		$e^+ e^- \rightarrow 5\pi$
231 ± 14		ATKINSON 84C	OMEG 0		20-70 $\gamma p$
232 ± 29		COLLICK 84	SPEC +		200 $\pi^+ Z \rightarrow Z \pi \omega$

### $b_1(1235)$ DECAY MODES

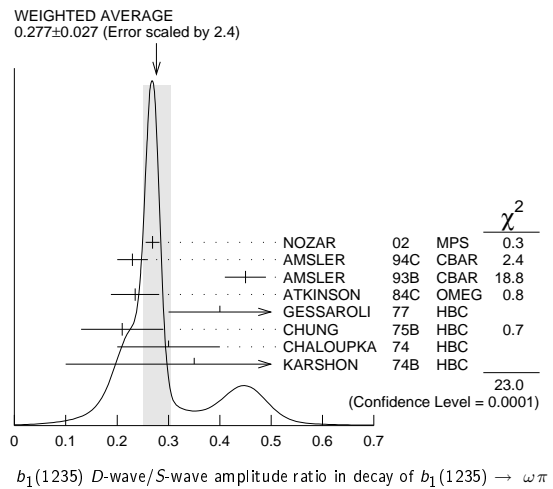
Mode	Fraction ( $\Gamma_i/\Gamma$ )	Confidence level
$\Gamma_1$ $\omega\pi$	dominant	
$\Gamma_2$ $\pi^\pm \gamma$	(1.6 ± 0.4) × 10 <sup>-3</sup>	
$\Gamma_3$ $\eta\rho$	seen	
$\Gamma_4$ $\pi^+ \pi^+ \pi^- \pi^0$	< 50	% 84%
$\Gamma_5$ $K^*(892)^\pm K^\mp$	seen	
$\Gamma_6$ $(K\bar{K})^\pm \pi^0$	< 8	% 90%
$\Gamma_7$ $K_S^0 K_L^0 \pi^\pm$	< 6	% 90%
$\Gamma_8$ $K_S^0 K_S^0 \pi^\pm$	< 2	% 90%
$\Gamma_9$ $\phi\pi$	< 1.5	% 84%

### $b_1(1235)$ PARTIAL WIDTHS

$\Gamma(\pi^\pm \gamma)$	DOCUMENT ID	TECN	CHG	COMMENT
<b>230 ± 60</b>	COLLICK 84	SPEC	+	200 $\pi^+ Z \rightarrow Z \pi \omega$

### $b_1(1235)$ D-wave/S-wave AMPLITUDE RATIO IN DECAY OF $b_1(1235) \rightarrow \omega\pi$

VALUE	EVTS	DOCUMENT ID	TECN	CHG	COMMENT
<b>0.277 ± 0.027 OUR AVERAGE</b>					Error includes scale factor of 2.4. See the ideogram below.
0.269 ± 0.009 ± 0.010		NOZAR 02	MPS -		18 $\pi^- p \rightarrow \omega \pi^- p$
0.23 ± 0.03		AMSLER 94C	CBAR		0.0 $\bar{p}p \rightarrow \omega \eta \pi^0$
0.45 ± 0.04		AMSLER 93B	CBAR		0.0 $\bar{p}p \rightarrow \omega \pi^0 \pi^0$
0.235 ± 0.047		ATKINSON 84C	OMEG		20-70 $\gamma p$
0.4 ± 0.1		GESSAROLI 77	HBC -		11 $\pi^- p \rightarrow \pi^- \omega p$
-0.1					
0.21 ± 0.08		CHUNG 75B	HBC +		7.1 $\pi^+ p$
0.3 ± 0.1		CHALOUKKA 74	HBC -		3.9-7.5 $\pi^- \pi^0 p$
0.35 ± 0.25	600	KARSHON 74B	HBC +		4.9 $\pi^+ p$



### $b_1(1235)$ D-wave/S-wave AMPLITUDE PHASE DIFFERENCE IN DECAY OF $b_1(1235) \rightarrow \omega\pi$

VALUE (°)	DOCUMENT ID	TECN	CHG	COMMENT
<b>10.5 ± 2.4 ± 3.9</b>	NOZAR 02	MPS	-	18 $\pi^- p \rightarrow \omega \pi^- p$

### $b_1(1235)$ BRANCHING RATIOS

$\Gamma(\eta\rho)/\Gamma(\omega\pi)$	DOCUMENT ID	TECN	COMMENT	$\Gamma_3/\Gamma_1$
<b>&lt; 0.10</b>	ATKINSON 84D	OMEG	20-70 $\gamma p$	

See key on page 457

Meson Particle Listings

b<sub>1</sub>(1235), a<sub>1</sub>(1260)

Table with 5 columns: VALUE, DOCUMENT ID, TECN, CHG, COMMENT. Rows include decay widths for pi+ pi+ pi- pi0, K\*(892) +/- Kmp, ((K Kbar) +/- pi0), K\_S^0 K\_L^0 pi0, phi pi, and phi pi pi.

b<sub>1</sub>(1235) REFERENCES

Table with 4 columns: AUTHOR, YEAR, JOURNAL, COLLAB. Lists references for the b<sub>1</sub>(1235) meson.

a<sub>1</sub>(1260)

I^G(JPC) = 1^-(1++)

See also our review under the a<sub>1</sub>(1260) in PDG 06, Journal of Physics, G 33 1 (2006).

a<sub>1</sub>(1260) MASS

Table with 5 columns: VALUE (MeV), EVTS, DOCUMENT ID, TECN, COMMENT. Lists mass measurements for the a<sub>1</sub>(1260) meson.

Table with 5 columns: VALUE (MeV), EVTS, DOCUMENT ID, TECN, COMMENT. Lists measurements for the a<sub>1</sub>(1260) width.

a<sub>1</sub>(1260) WIDTH

Table with 5 columns: VALUE (MeV), EVTS, DOCUMENT ID, TECN, COMMENT. Lists measurements for the a<sub>1</sub>(1260) width.

## Meson Particle Listings

 $a_1(1260)$ 

- 27 Includes the effect of a possible  $a_1^+$  state.  
 28 Uses the model of FEINDT 90.  
 29 Supersedes AKERS 95P.  
 30 Average and spread of values using 2 variants of the model of BOWLER 75.  
 31 Reanalysis of RUCKSTUHL 86.  
 32 Reanalysis of SCHMIDKE 86.  
 33 Reanalysis of ALBRECHT 86B.  
 34 From a combined reanalysis of ALBRECHT 86B, SCHMIDKE 86, and RUCKSTUHL 86.  
 35 From a combined reanalysis of ALBRECHT 86B and DAUM 81B.  
 36 Uses the model of BOWLER 75.  
 37 Produced in  $K^-$  backward scattering.

 $a_1(1260)$  DECAY MODES

Mode	Fraction ( $\Gamma_i/\Gamma$ )
$\Gamma_1$ $\pi^+\pi^-\pi^0$	
$\Gamma_2$ $\pi^0\pi^0\pi^0$	
$\Gamma_3$ $(\rho\pi)S$ -wave	seen
$\Gamma_4$ $(\rho\pi)D$ -wave	seen
$\Gamma_5$ $(\rho(1450)\pi)S$ -wave	seen
$\Gamma_6$ $(\rho(1450)\pi)D$ -wave	seen
$\Gamma_7$ $\sigma\pi$	seen
$\Gamma_8$ $f_0(980)\pi$	not seen
$\Gamma_9$ $f_0(1370)\pi$	seen
$\Gamma_{10}$ $f_2(1270)\pi$	seen
$\Gamma_{11}$ $K\bar{K}^*(892) + c.c.$	seen
$\Gamma_{12}$ $\pi\gamma$	seen

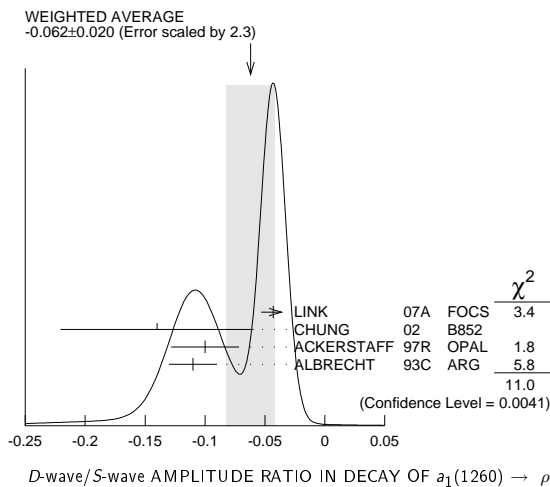
 $a_1(1260)$  PARTIAL WIDTHS

$\Gamma(\pi\gamma)$	$\Gamma_{12}$		
VALUE (keV)	DOCUMENT ID	TECN	COMMENT
<b>640 ± 246</b>	ZIELINSKI	84c	SPEC 200 $\pi^+Z \rightarrow Z3\pi$

D-wave/S-wave AMPLITUDE RATIO IN DECAY OF  $a_1(1260) \rightarrow \rho\pi$ 

VALUE	DOCUMENT ID	TECN	COMMENT
<b>-0.062 ± 0.020 OUR AVERAGE</b>	Error includes scale factor of 2.3. See the ideogram below.		
-0.043 ± 0.009 ± 0.005	LINK	07A	FOCS $D^0 \rightarrow \pi^-\pi^+\pi^-\pi^+$
-0.14 ± 0.04 ± 0.07	38 CHUNG	02	B852 $18.3 \pi^-p \rightarrow \pi^+\pi^-\pi^-\rho$
-0.10 ± 0.02 ± 0.02	39,40 ACKERSTAFF	97R	OPAL $E_{cm}^{pp} = 88-94, \tau \rightarrow 3\pi\nu$
-0.11 ± 0.02	39 ALBRECHT	93C	ARG $\tau^+ \rightarrow \pi^+\pi^+\pi^-\nu$

- 38 Deck-type background not subtracted.  
 39 Uses the model of ISGUR 89.  
 40 Supersedes AKERS 95P.

 $a_1(1260)$  BRANCHING RATIOS

$\Gamma((\rho\pi)S\text{-wave})/\Gamma_{\text{total}}$	$\Gamma_3/\Gamma$		
VALUE (units $10^{-2}$ )	EVTS	DOCUMENT ID	TECN COMMENT
60.19	37k	41 ASNER	00 CLE2 $10.6 e^+e^- \rightarrow \tau^+\tau^-$ , $\tau^- \rightarrow \pi^-\pi^0\pi^0\nu_\tau$

$\Gamma((\rho\pi)D\text{-wave})/\Gamma_{\text{total}}$	$\Gamma_4/\Gamma$		
VALUE (units $10^{-2}$ )	EVTS	DOCUMENT ID	TECN COMMENT
1.30 ± 0.60 ± 0.22	37k	41 ASNER	00 CLE2 $10.6 e^+e^- \rightarrow \tau^+\tau^-$ , $\tau^- \rightarrow \pi^-\pi^0\pi^0\nu_\tau$

$\Gamma((\rho(1450)\pi)S\text{-wave})/\Gamma_{\text{total}}$	$\Gamma_5/\Gamma$		
VALUE (units $10^{-2}$ )	EVTS	DOCUMENT ID	TECN COMMENT
0.56 ± 0.84 ± 0.32	37k	41,42 ASNER	00 CLE2 $10.6 e^+e^- \rightarrow \tau^+\tau^-$ , $\tau^- \rightarrow \pi^-\pi^0\pi^0\nu_\tau$

$\Gamma((\rho(1450)\pi)D\text{-wave})/\Gamma_{\text{total}}$	$\Gamma_6/\Gamma$		
VALUE (units $10^{-2}$ )	EVTS	DOCUMENT ID	TECN COMMENT
2.04 ± 1.20 ± 0.28	37k	41,42 ASNER	00 CLE2 $10.6 e^+e^- \rightarrow \tau^+\tau^-$ , $\tau^- \rightarrow \pi^-\pi^0\pi^0\nu_\tau$

$\Gamma(\sigma\pi)/\Gamma_{\text{total}}$	$\Gamma_7/\Gamma$		
VALUE (units $10^{-2}$ )	EVTS	DOCUMENT ID	TECN COMMENT
18.76 ± 4.29 ± 1.48	37k	41,43 ASNER	00 CLE2 $10.6 e^+e^- \rightarrow \tau^+\tau^-$ , $\tau^- \rightarrow \pi^-\pi^0\pi^0\nu_\tau$

$\Gamma(f_0(980)\pi)/\Gamma_{\text{total}}$	$\Gamma_8/\Gamma$		
VALUE (units $10^{-2}$ )	EVTS	DOCUMENT ID	TECN COMMENT
not seen	37k	ASNER	00 CLE2 $10.6 e^+e^- \rightarrow \tau^+\tau^-$ , $\tau^- \rightarrow \pi^-\pi^0\pi^0\nu_\tau$

$\Gamma(f_0(1370)\pi)/\Gamma_{\text{total}}$	$\Gamma_9/\Gamma$		
VALUE (units $10^{-2}$ )	EVTS	DOCUMENT ID	TECN COMMENT
7.40 ± 2.71 ± 1.26	37k	41,44 ASNER	00 CLE2 $10.6 e^+e^- \rightarrow \tau^+\tau^-$ , $\tau^- \rightarrow \pi^-\pi^0\pi^0\nu_\tau$

$\Gamma(f_2(1270)\pi)/\Gamma_{\text{total}}$	$\Gamma_{10}/\Gamma$		
VALUE (units $10^{-2}$ )	EVTS	DOCUMENT ID	TECN COMMENT
1.19 ± 0.49 ± 0.17	37k	41,45 ASNER	00 CLE2 $10.6 e^+e^- \rightarrow \tau^+\tau^-$ , $\tau^- \rightarrow \pi^-\pi^0\pi^0\nu_\tau$

$\Gamma(K\bar{K}^*(892) + c.c.)/\Gamma_{\text{total}}$	$\Gamma_{11}/\Gamma$		
VALUE (units $10^{-2}$ )	EVTS	DOCUMENT ID	TECN COMMENT
2.2 ± 0.5	2255	46 COAN	04 CLEO $\tau^- \rightarrow K^-\pi^-K^+\nu_\tau$
8 to 15	205	47 DRUTSKOY	02 BELL $B \rightarrow D^{(*)}K^-K^{*0}$
3.3 ± 0.5 ± 0.1	37k	48 ASNER	00 CLE2 $10.6 e^+e^- \rightarrow \tau^+\tau^-$ , $\tau^- \rightarrow \pi^-\pi^0\pi^0\nu_\tau$
2.6 ± 0.3	49	BARATE	99R ALEP $\tau \rightarrow K\bar{K}\pi\nu_\tau$

$\Gamma(\sigma\pi)/\Gamma((\rho\pi)S\text{-wave})$	$\Gamma_7/\Gamma_3$		
VALUE	EVTS	DOCUMENT ID	TECN COMMENT
0.06 ± 0.05	90k	SALVINI	04 OBLX $\bar{p}p \rightarrow 2\pi^+2\pi^-$
~0.3	28k	AKHMETSHIN	99E CMD2 $1.05-1.38 e^+e^- \rightarrow \pi^+\pi^-\pi^+\pi^-$
0.003 ± 0.003	50	LONGACRE	82 RVUE

$\Gamma(\pi^0\pi^0\pi^0)/\Gamma(\pi^+\pi^-\pi^0)$	$\Gamma_2/\Gamma_1$		
VALUE	CL%	DOCUMENT ID	COMMENT
<0.008	90	51 BARBERIS	01 450 $p\bar{p} \rightarrow p_f 3\pi^0 p_s$

- 41 From a fit to the Dalitz plot.  
 42 Assuming for  $\rho(1450)$  mass and width of 1370 and 386 MeV respectively.  
 43 Assuming for  $\sigma$  mass and width of 860 and 880 MeV respectively.  
 44 Assuming for  $f_0(1370)$  mass and width of 1186 and 350 MeV respectively.  
 45 Assuming for  $f_2(1270)$  mass and width of 1275 and 185 MeV respectively.  
 46 Using structure functions from KUHN 92 and DECKER 93A and B ( $\tau^- \rightarrow K^-\pi^-K^+\nu_\tau$ ) = (0.155 ± 0.006 ± 0.009)% from BRIERE 03.  
 47 From a comparison to ALAM 94 assuming purely resonant production of the  $K^-K^{*0}$  system.  
 48 From a fit to the  $3\pi$  mass spectrum including the  $K\bar{K}^*(892)$  threshold.  
 49 Assuming  $a_1(1260)$  dominance and taking  $B(\tau^- \rightarrow a_1(1260)\nu_\tau)$  from BUSKULIC 96.  
 50 Uses multichannel Aitchison-Bowler model (BOWLER 75). Uses data from GAVILLET 77, DAUM 80, and DANKOWYCH 81.  
 51 Inconsistent with observations of  $\sigma\pi$ ,  $f_0(1370)\pi$ , and  $f_2(1270)\pi$  decay modes.

## Meson Particle Listings

 $a_1(1260)$ ,  $f_2(1270)$ 

See key on page 457

 $a_1(1260)$  REFERENCES

ALEKSEEV	10	PRL 104 241803	M.G. Alekseev <i>et al.</i>	(COMPASS Collab.)
AUBERT	07AU	PR D74 092005	B. Aubert <i>et al.</i>	(BABAR Collab.)
LINK	07A	PR D75 052003	J.M. Link <i>et al.</i>	(FNAL FOCUS Collab.)
PDG	06	JPG 33 1	W.-M. Yao <i>et al.</i>	(PDG Collab.)
COAN	04	PRL 92 232001	T.E. Coan <i>et al.</i>	(CLEO Collab.)
GOMEZ-DUM...	04	PR D69 073002	D. Gomez Dumm, A. Pich, J. Portoles	
SALVINI	04	EPJ C35 21	P. Salvini <i>et al.</i>	(OBELIX Collab.)
BRIERE	03	PRL 90 181802	R. A. Briere <i>et al.</i>	(CLEO Collab.)
CHUNG	02	PR D65 072001	S.U. Chung <i>et al.</i>	(BNL E852 Collab.)
DRUTSKOY	02	PL B542 171	A. Drutskoy <i>et al.</i>	(BELLE Collab.)
BARBERIS	01	PL B507 14	D. Barberis <i>et al.</i>	
ASNER	00	PR D61 012002	D.M. Asner <i>et al.</i>	(CLEO Collab.)
AKHMETSHTSHIN	99E	PL B466 392	R.R. Akhmetshin <i>et al.</i>	(Novosibirsk CMD-2 Collab.)
BARATE	99R	EPJ C11 599	R. Barate <i>et al.</i>	(ALEPH Collab.)
BONDAR	99	PL B466 403	A.E. Bondar <i>et al.</i>	(Novosibirsk CMD-2 Collab.)
ABREU	98G	PL B426 411	P. Abreu <i>et al.</i>	(DELPHI Collab.)
BARATE	98R	EPJ C4 409	R. Barate <i>et al.</i>	(ALEPH Collab.)
BARBERIS	98B	PL B422 399	D. Barberis <i>et al.</i>	(WA 102 Collab.)
ACKERSTAFF	97R	ZPHY C75 593	K. Ackerstaff <i>et al.</i>	(OPAL Collab.)
BUSKULIC	96	ZPHY C70 579	D. Buskulic <i>et al.</i>	(ALEPH Collab.)
AKERS	95P	ZPHY C67 45	R. Akers <i>et al.</i>	(OPAL Collab.)
ALAM	94	PR D50 43	M.S. Alam <i>et al.</i>	(CLEO Collab.)
ALBRECHT	93C	ZPHY C58 61	H. Albrecht <i>et al.</i>	(ARGUS Collab.)
DECKER	93A	ZPHY C58 445	R. Decker <i>et al.</i>	
ANDO	92	PL B291 496	A. Ando <i>et al.</i>	(KEK, KYOT, NIRS, SAGA+)
KUHN	92	ZPHY C56 661	J.H. Kuhn, E. Mirkes	
IVANOV	91	ZPHY C49 563	Y.P. Ivanov, A.A. Osipov, M.K. Volkov	(JINR)
ARMSTRONG	90	ZPHY C48 213	T.A. Armstrong, M. Benayoun, W. Busch	(WA76 Coll.)
FEINDT	90	ZPHY C48 681	M. Feindt	(HAMB)
KUHN	90	ZPHY C48 445	J.H. Kuhn <i>et al.</i>	(MPIM)
ISGUR	89	PR D39 1357	N. Isgur, C. Morningstar, C. Reader	(TNTO)
BOWLER	88	PL B209 99	M.G. Bowler	(OXF)
BAND	87	PL B198 297	H.R. Band <i>et al.</i>	(MAC Collab.)
TORNOQUIST	87	ZPHY C36 695	N.A. Tornqvist	(HELS)
ALBRECHT	86B	ZPHY C33 7	H. Albrecht <i>et al.</i>	(ARGUS Collab.)
RUCKSTUHL	86	PRL 56 2132	W. Ruckstuhl <i>et al.</i>	(DELCO Collab.)
SCHMIDKE	86	PRL 57 527	W.B. Schmidke <i>et al.</i>	(Mark II Collab.)
BELLINI	85	SJNP 41 781	D. Bellini <i>et al.</i>	
		Translated from YAF 41 1223.		
ZIELINSKI	84C	PRL 52 1195	M. Zielinski <i>et al.</i>	(ROCH, MINN, FNAL)
LONGACRE	82	PR D28 82	R.S. Longacre	(BNL)
DANKOWYCH...	81	PRL 46 580	J.A. Dankowych <i>et al.</i>	(TNTO, BNL, CARL+)
DAUM	81B	NP B182 269	C. Daum <i>et al.</i>	(AMST, CERN, CRAC, MPIM+)
DAUM	80	PL 89B 281	C. Daum <i>et al.</i>	(AMST, CERN, CRAC, MPIM+)
GAUILLET	77	PL 69B 119	P. Gavillet <i>et al.</i>	(AMST, CERN, NIJ+)
BOWLER	75	NP B97 227	M.G. Bowler <i>et al.</i>	(OXFTP, DARE)

 $f_2(1270)$ 

$$J^G(J^{PC}) = 0^+(2^{++})$$

 $f_2(1270)$  MASS

VALUE (MeV)	EVTs	DOCUMENT ID	TECN	COMMENT
<b>1275.1 ± 1.2 OUR AVERAGE</b>		Error includes scale factor of 1.1.		
1262 ± 1/2 ± 8		ABLIKIM	06v	BES2 $e^+e^- \rightarrow J/\psi \rightarrow \gamma\pi^+\pi^-$
1275 ± 15		ABLIKIM	05	BES2 $J/\psi \rightarrow \phi\pi^+\pi^-$
1283 ± 5		ALDE	98	GAM4 $100\pi^-p \rightarrow \pi^0\pi^0n$
1278 ± 5		1 BERTIN	97c	OBLX $0.0\bar{p}p \rightarrow \pi^+\pi^-\pi^0$
1272 ± 8	200k	PROKOSHKIN	94	GAM2 $38\pi^-p \rightarrow \pi^0\pi^0n$
1269.7 ± 5.2	5730	AUGUSTIN	89	DM2 $e^+e^- \rightarrow 5\pi$
1283 ± 8	400	2 ALDE	98	GAM4 $100\pi^-p \rightarrow 4\pi^0n$
1274 ± 5		2 AUGUSTIN	87	DM2 $J/\psi \rightarrow \gamma\pi^+\pi^-$
1283 ± 6		3 LONGACRE	86	MPS $22\pi^-p \rightarrow n2K_S^0$
1276 ± 7		COURAU	84	DLCO $e^+e^- \rightarrow e^+e^-\pi^+\pi^-$
1273.3 ± 2.3		4 CHABAUD	83	ASPK $17\pi^-p$ polarized
1280 ± 4		5 CASON	82	STRC $8\pi^+p \rightarrow \Delta^{++}\pi^0\pi^0$
1281 ± 7	11600	GIDAL	81	MRK2 $J/\psi$ decay
1282 ± 5		6 CORDEN	79	OMEG $12-15\pi^-p \rightarrow n2\pi$
1269 ± 4	10k	APEL	75	NICE $40\pi^-p \rightarrow n2\pi^0$
1272 ± 4	4600	ENGLER	74	DBC $6\pi^+n \rightarrow \pi^+\pi^-p$
1277 ± 4	5300	FLATTE	71	HBC $7.0\pi^+p$
1275 ± 8		2 STUNTEBECK	70	HBC $8\pi^-p, 5.4\pi^+d$
1273 ± 8		BOESEBECK	68	HBC $8\pi^+p$
● ● ● We do not use the following data for averages, fits, limits, etc. ● ● ●				
1270 ± 8		7 ANISOVICH	09	RVUE $0.0\bar{p}p, \pi N$
1277 ± 6	870	8 SCHEGELSKY	06A	RVUE $\gamma\gamma \rightarrow K_S^0 K_S^0$
1251 ± 10		TIKHOMIROV	03	SPEC $40.0\pi^-C \rightarrow K_S^0 K_S^0 K_L^0 X$
1260 ± 10		9 ALDE	97	GAM2 $450pp \rightarrow pp\pi^0\pi^0$
1278 ± 6		9 GRYGOREV	96	SPEC $40\pi^-N \rightarrow K_S^0 K_S^0 X$
1262 ± 11		AGUILAR...	91	EHS $400pp$
1275 ± 10		AKER	91	CBAR $0.0\bar{p}p \rightarrow 3\pi^0$
1220 ± 10		BREAKSTONE	90	SFM $pp \rightarrow pp\pi^+\pi^-$
1288 ± 12		ABACHI	86B	HRS $e^+e^- \rightarrow \pi^+\pi^-X$
1284 ± 30	3k	BINON	83	GAM2 $38\pi^-p \rightarrow n2\eta$
1280 ± 20	3k	APEL	82	CNTR $25\pi^-p \rightarrow n2\pi^0$
1284 ± 10	16000	DEUTSCH...	76	HBC $16\pi^+p$
1258 ± 10	600	TAKAHASHI	72	HBC $8\pi^-p \rightarrow n2\pi$
1275 ± 13		ARMENISE	70	HBC $9\pi^+n \rightarrow p\pi^+\pi^-$
1261 ± 5	1960	2 ARMENISE	68	DBC $5.1\pi^+n \rightarrow p\pi^+MM^-$
1270 ± 10	360	2 ARMENISE	68	DBC $5.1\pi^+n \rightarrow p\pi^0MM$
1268 ± 6		10 JOHNSON	68	HBC $3.7-4.2\pi^-p$

- T-matrix pole.
- Mass errors enlarged by us to  $\Gamma/\sqrt{N}$ ; see the note with the  $K^*(892)$  mass.
- From a partial-wave analysis of data using a K-matrix formalism with 5 poles.
- From an energy-independent partial-wave analysis.
- From an amplitude analysis of the reaction  $\pi^+\pi^- \rightarrow 2\pi^0$ .
- From an amplitude analysis of  $\pi^+\pi^- \rightarrow \pi^+\pi^-$  scattering data.
- 4-poles, 5-channel K matrix fit.
- From analysis of L3 data at 91 and 183–209 GeV.
- Systematic uncertainties not estimated.
- JOHNSON 68 includes BONDAR 63, LEE 64, DERADO 65, EISNER 67.

 $f_2(1270)$  WIDTH

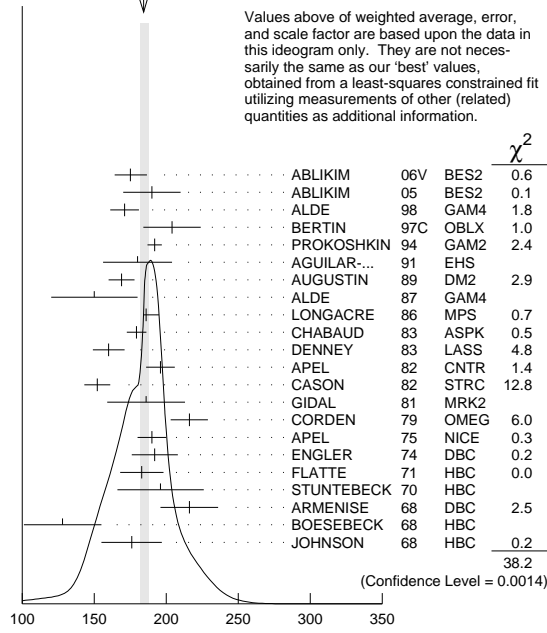
VALUE (MeV)	EVTs	DOCUMENT ID	TECN	COMMENT
<b>185.1 ± 2.9 OUR FIT</b>		Error includes scale factor of 1.5.		
<b>184.2 ± 4.0 OUR AVERAGE</b>		Error includes scale factor of 1.5. See the ideogram below.		
175 ± 6 ± 10		ABLIKIM	06v	BES2 $e^+e^- \rightarrow J/\psi \rightarrow \gamma\pi^+\pi^-$
190 ± 20		ABLIKIM	05	BES2 $J/\psi \rightarrow \phi\pi^+\pi^-$
171 ± 10		ALDE	98	GAM4 $100\pi^-p \rightarrow \pi^0\pi^0n$
204 ± 20		11 BERTIN	97c	OBLX $0.0\bar{p}p \rightarrow \pi^+\pi^-\pi^0$
192 ± 5	200k	PROKOSHKIN	94	GAM2 $38\pi^-p \rightarrow \pi^0\pi^0n$
180 ± 24		AGUILAR...	91	EHS $400pp$
169 ± 9	5730	12 AUGUSTIN	89	DM2 $e^+e^- \rightarrow 5\pi$
150 ± 30	400	12 ALDE	87	GAM4 $100\pi^-p \rightarrow 4\pi^0n$
186 ± 9		13 LONGACRE	86	MPS $22\pi^-p \rightarrow n2K_S^0$
179.2 ± 6.9 ± 6.6		14 CHABAUD	83	ASPK $17\pi^-p$ polarized
160 ± 11		DENNEY	83	LASS $10\pi^+N$
196 ± 10	3k	APEL	82	CNTR $25\pi^-p \rightarrow n2\pi^0$
152 ± 9		15 CASON	82	STRC $8\pi^+p \rightarrow \Delta^{++}\pi^0\pi^0$
186 ± 27	11600	GIDAL	81	MRK2 $J/\psi$ decay
216 ± 13		16 CORDEN	79	OMEG $12-15\pi^-p \rightarrow n2\pi$
190 ± 10	10k	APEL	75	NICE $40\pi^-p \rightarrow n2\pi^0$
192 ± 16	4600	ENGLER	74	DBC $6\pi^+n \rightarrow \pi^+\pi^-p$
183 ± 15	5300	FLATTE	71	HBC $7\pi^+p \rightarrow \Delta^{++}\pi^0$
196 ± 30		12 STUNTEBECK	70	HBC $8\pi^-p, 5.4\pi^+d$
216 ± 20	1960	12 ARMENISE	68	DBC $5.1\pi^+n \rightarrow p\pi^+MM^-$
128 ± 27		12 BOESEBECK	68	HBC $8\pi^+p$
176 ± 21		12.17 JOHNSON	68	HBC $3.7-4.2\pi^-p$
● ● ● We do not use the following data for averages, fits, limits, etc. ● ● ●				
194 ± 36		18 ANISOVICH	09	RVUE $0.0\bar{p}p, \pi N$
195 ± 15	870	19 SCHEGELSKY	06A	RVUE $\gamma\gamma \rightarrow K_S^0 K_S^0$
121 ± 26		TIKHOMIROV	03	SPEC $40.0\pi^-C \rightarrow K_S^0 K_S^0 K_L^0 X$
187 ± 20		20 ALDE	97	GAM2 $450pp \rightarrow pp\pi^0\pi^0$
184 ± 10		20 GRYGOREV	96	SPEC $40\pi^-N \rightarrow K_S^0 K_S^0 X$
200 ± 10		AKER	91	CBAR $0.0\bar{p}p \rightarrow 3\pi^0$
240 ± 40	3k	BINON	83	GAM2 $38\pi^-p \rightarrow n2\eta$
187 ± 30	650	12 ANTIPOV	77	CIBS $25\pi^-p \rightarrow p3\pi$
225 ± 38	16000	DEUTSCH...	76	HBC $16\pi^+p$
166 ± 28	600	12 TAKAHASHI	72	HBC $8\pi^-p \rightarrow n2\pi$
173 ± 53		12 ARMENISE	70	HBC $9\pi^+n \rightarrow p\pi^+\pi^-$

- T-matrix pole.
- Width errors enlarged by us to  $4\Gamma/\sqrt{N}$ ; see the note with the  $K^*(892)$  mass.
- From a partial-wave analysis of data using a K-matrix formalism with 5 poles.
- From an energy-independent partial-wave analysis.
- From an amplitude analysis of the reaction  $\pi^+\pi^- \rightarrow 2\pi^0$ .
- From an amplitude analysis of  $\pi^+\pi^- \rightarrow \pi^+\pi^-$  scattering data.
- JOHNSON 68 includes BONDAR 63, LEE 64, DERADO 65, EISNER 67.
- 4-poles, 5-channel K matrix fit.
- From analysis of L3 data at 91 and 183–209 GeV.
- Systematic uncertainties not estimated.

# Meson Particle Listings

## $f_2(1270)$

WEIGHTED AVERAGE  
184.2±4.0-2.4 (Error scaled by 1.5)



Values above of weighted average, error, and scale factor are based upon the data in this ideogram only. They are not necessarily the same as our 'best' values, obtained from a least-squares constrained fit utilizing measurements of other (related) quantities as additional information.

$f_2(1270)$  width (MeV)

### $f_2(1270)$ DECAY MODES

Mode	Fraction ( $\Gamma_i/\Gamma$ )	Scale factor/ Confidence level
$\Gamma_1$ $\pi\pi$	$(84.8 \pm 2.4) \%$	S=1.2
$\Gamma_2$ $\pi^+\pi^-2\pi^0$	$(7.1 \pm 1.4) \%$	S=1.3
$\Gamma_3$ $K\bar{K}$	$(4.6 \pm 0.4) \%$	S=2.8
$\Gamma_4$ $2\pi^+2\pi^-$	$(2.8 \pm 0.4) \%$	S=1.2
$\Gamma_5$ $\eta\eta$	$(4.0 \pm 0.8) \times 10^{-3}$	S=2.1
$\Gamma_6$ $4\pi^0$	$(3.0 \pm 1.0) \times 10^{-3}$	
$\Gamma_7$ $\gamma\gamma$	$(1.64 \pm 0.19) \times 10^{-5}$	S=1.9
$\Gamma_8$ $\eta\pi\pi$	$< 8 \times 10^{-3}$	CL=95%
$\Gamma_9$ $K^0K^-\pi^+ + c.c.$	$< 3.4 \times 10^{-3}$	CL=95%
$\Gamma_{10}$ $e^+e^-$	$< 6 \times 10^{-10}$	CL=90%

### CONSTRAINED FIT INFORMATION

An overall fit to the total width, 4 partial widths, a combination of partial widths obtained from integrated cross sections, and 6 branching ratios uses 44 measurements and one constraint to determine 8 parameters. The overall fit has a  $\chi^2 = 81.8$  for 37 degrees of freedom.

The following off-diagonal array elements are the correlation coefficients  $\langle \delta p_i \delta p_j \rangle / (\delta p_i \delta p_j)$ , in percent, from the fit to parameters  $p_i$ , including the branching fractions,  $x_i \equiv \Gamma_i/\Gamma_{\text{total}}$ . The fit constrains the  $x_i$  whose labels appear in this array to sum to one.

$x_2$	-91						
$x_3$	11	-39					
$x_4$	10	-37	1				
$x_5$	1	-6	0	0			
$x_6$	0	-7	0	0	0		
$x_7$	8	-5	-6	1	0	0	
$\Gamma$	-78	71	-11	-8	-1	0	-11
	$x_1$	$x_2$	$x_3$	$x_4$	$x_5$	$x_6$	$x_7$

Mode	Rate (MeV)	Scale factor
$\Gamma_1$ $\pi\pi$	156.9 ± 4.0 -1.2	
$\Gamma_2$ $\pi^+\pi^-2\pi^0$	13.2 ± 2.8 -5.0	1.3
$\Gamma_3$ $K\bar{K}$	8.5 ± 0.8	2.9
$\Gamma_4$ $2\pi^+2\pi^-$	5.2 ± 0.7	1.2

$\Gamma_5$ $\eta\eta$	0.74 ± 0.14	2.1
$\Gamma_6$ $4\pi^0$	0.55 ± 0.18	
$\Gamma_7$ $\gamma\gamma$	0.00303 ± 0.00035	1.9

### $f_2(1270)$ PARTIAL WIDTHS

$\Gamma(\pi\pi)$	VALUE (MeV)	EVTS	DOCUMENT ID	TECN	COMMENT	$\Gamma_1$
	<b>156.9 ± 4.0</b>					
	<b>-1.2</b>					
	<b>OUR FIT</b>					

	<b>157.0 ± 6.0</b>		21 LONGACRE 86	MPS	22 $\pi^-p \rightarrow n2K_S^0$	
•••					We do not use the following data for averages, fits, limits, etc. •••	
	152 ± 8	870	22 SCHEGELSKY 06A	RVUE	$\gamma\gamma \rightarrow K_S^0 K_S^0$	

$\Gamma(K\bar{K})$	VALUE (MeV)	EVTS	DOCUMENT ID	TECN	COMMENT	$\Gamma_3$
	<b>8.5 ± 0.8</b>					
	<b>OUR FIT</b>				Error includes scale factor of 2.9.	

	<b>9.0 ± 0.7</b>		21 LONGACRE 86	MPS	22 $\pi^-p \rightarrow n2K_S^0$	
•••					We do not use the following data for averages, fits, limits, etc. •••	
	7.5 ± 2.0	870	22 SCHEGELSKY 06A	RVUE	$\gamma\gamma \rightarrow K_S^0 K_S^0$	

$\Gamma(\eta\eta)$	VALUE (MeV)	EVTS	DOCUMENT ID	TECN	COMMENT	$\Gamma_5$
	<b>0.74 ± 0.14</b>					
	<b>OUR FIT</b>				Error includes scale factor of 2.1.	

	<b>1.0 ± 0.1</b>		21 LONGACRE 86	MPS	22 $\pi^-p \rightarrow n2K_S^0$	
•••					We do not use the following data for averages, fits, limits, etc. •••	
	1.8 ± 0.4	870	22 SCHEGELSKY 06A	RVUE	$\gamma\gamma \rightarrow K_S^0 K_S^0$	

$\Gamma(\gamma\gamma)$	VALUE (keV)	EVTS	DOCUMENT ID	TECN	COMMENT	$\Gamma_7$
	<b>3.03 ± 0.35</b>					
	<b>OUR FIT</b>				Error includes scale factor of 1.9.	

	<b>3.14 ± 0.20</b>		23,24 PENNINGTON 08	RVUE	Compilation	
•••					We do not use the following data for averages, fits, limits, etc. •••	
	3.82 ± 0.30		24,25 PENNINGTON 08	RVUE	Compilation	

	2.55 ± 0.15	870	22 SCHEGELSKY 06A	RVUE	$\gamma\gamma \rightarrow K_S^0 K_S^0$	
	2.84 ± 0.35		BOGLIONE 99	RVUE	$\gamma\gamma \rightarrow \pi^+\pi^-, \pi^0\pi^0$	
	2.93 ± 0.23 ± 0.32		26 YABUKI 95	VNS		

	2.58 ± 0.13 ± 0.36		27 BEHREND 92	CELL	$e^+e^- \rightarrow e^+e^-\pi^+\pi^-$	
	3.10 ± 0.35 ± 0.35		28 BLINOV 92	MD1	$e^+e^- \rightarrow e^+e^-\pi^+\pi^-$	
	2.27 ± 0.47 ± 0.11		ADACHI 90	TOPZ	$e^+e^- \rightarrow e^+e^-\pi^+\pi^-$	

	3.15 ± 0.04 ± 0.39		BOYER 90	MRK2	$e^+e^- \rightarrow e^+e^-\pi^+\pi^-$	
	3.19 ± 0.16 ± 0.29		MARSISKE 90	CBAL	$e^+e^- \rightarrow e^+e^-\pi^0\pi^0$	
	2.35 ± 0.65		29 MORGAN 90	RVUE	$\gamma\gamma \rightarrow \pi^+\pi^-, \pi^0\pi^0$	

	3.19 ± 0.09 ± 0.22	2177	OEST 90	JADE	$e^+e^- \rightarrow e^+e^-\pi^0\pi^0$	
	3.2 ± 0.1 ± 0.4		30 AIHARA 86B	TPC	$e^+e^- \rightarrow e^+e^-\pi^+\pi^-$	
	2.5 ± 0.1 ± 0.5		84B CELL	$e^+e^- \rightarrow e^+e^-\pi^+\pi^-$		

	2.85 ± 0.25 ± 0.5		31 BERGER 84	PLUT	$e^+e^- \rightarrow e^+e^-2\pi$	
	2.70 ± 0.05 ± 0.20		COURAU 84	DLCO	$e^+e^- \rightarrow e^+e^-\pi^+\pi^-$	
	2.52 ± 0.13 ± 0.38		32 SMITH 84C	MRK2	$e^+e^- \rightarrow e^+e^-\pi^+\pi^-$	

	2.7 ± 0.2 ± 0.6		EDWARDS 82F	CBAL	$e^+e^- \rightarrow e^+e^-2\pi^0$	
	2.9 ± 0.6 ± 0.6		33 EDWARDS 82F	CBAL	$e^+e^- \rightarrow e^+e^-2\pi^0$	
	3.2 ± 0.2 ± 0.6		BRANDELIK 81B	TASS	$e^+e^- \rightarrow e^+e^-\pi^+\pi^-$	

	3.6 ± 0.3 ± 0.5		81 MRK2	$e^+e^- \rightarrow e^+e^-\pi^+\pi^-$		
	2.3 ± 0.8		34 BERGER 80B	PLUT	$e^+e^-$	

$\Gamma(e^+e^-)$	VALUE (eV)	CL%	DOCUMENT ID	TECN	COMMENT	$\Gamma_{10}$
	<b>&lt;0.11</b>	90	ACHASOV 00K	SND	$e^+e^- \rightarrow \pi^0\pi^0$	
•••					We do not use the following data for averages, fits, limits, etc. •••	
	<1.7	90	VOROBYEV 88	ND	$e^+e^- \rightarrow \pi^0\pi^0$	

21 From a partial-wave analysis of data using a K-matrix formalism with 5 poles.  
 22 From analysis of L3 data at 91 and 183-209 GeV and using SU(3) relations.  
 23 Solution A (preferred solution based on  $\chi^2$ -analysis).  
 24 Dispersion theory based amplitude analysis of BOYER 90, MARSISKE 90, BEHREND 92, and MORI 07.  
 25 Solution B (worse than solution A; still acceptable when systematic uncertainties are included).  
 26 With a narrow scalar state around 1220 MeV.  
 27 Using a unitarized model with a 300 - 500 keV wide scalar at 1100 MeV.  
 28 Using the unitarized model of LYTH 85.  
 29 Error includes spread of different solutions. Data of MARK2 and CRYSTAL BALL used in the analysis. Authors report strong correlations with  $\gamma\gamma$  width of  $f_0(1370)$ :  $\Gamma(f_2) + 1/4 \Gamma(f_0) = 3.6 \pm 0.3$  KeV.  
 30 Radiative corrections modify the partial widths; for instance the COURAU 84 value becomes  $2.66 \pm 0.21$  in the calculation of LANDRO 86.  
 31 Using the MENNESSIER 83 model.  
 32 Superseded by BOYER 90.  
 33 If helicity = 2 assumption is not made.  
 34 Using mass, width and  $B(f_2(1270) \rightarrow 2\pi)$  from PDG 78.





# Meson Particle Listings

## $f_2(1270)$ , $f_1(1285)$

CHABAUD	83	NP B223 1	V. Chabaud et al. (CERN, CRAC, MPIM)
DENNEY	83	PR D28 2726	D.L. Denney et al. (IOWA, MICH)
MENNESSIER	83	ZPHY C16 241	G. Mennessier (MONP)
APEL	82	NP B201 197	W.D. Apel et al. (KARLK, KARLE, PISA, SERP+)
CASON	82	PRL 48 1316	N.M. Cason et al. (NDAM, ANL)
EDWARDS	82F	PL 110B 82	C. Edwards et al. (CIT, HARV, PRIN+)
ETKIN	82B	PR D25 1786	A. Etkin et al. (BNL, CUNY, TUFTS, VAND)
BRANDELIC	81B	ZPHY C10 117	R. Brandelic et al. (TASSO Collab.)
CHABAUD	81	APP B12 575	V. Chabaud et al. (CERN, CRAC, MPIM)
GIDAL	81	PL 107B 153	G. Gidal et al. (SLAC, LBL)
ROUSSARIE	81	PL 105B 304	A. Roussarie et al. (SLAC, LBL)
BERGER	80B	PL 94B 254	C. Berger et al. (PLUTO Collab.)
COSTA...	80	NP B175 402	G. Costa de Beauregard et al. (BARI, BONN+)
LOVERRE	80	ZPHY C6 187	P.F. Loverre et al. (CERN, CDEF, MADR+)
CORDEN	79	NP B157 250	M.J. Corden et al. (BIRM, RHEL, TELA+)
MARTIN	79	NP B158 520	A.D. Martin, E.N. Ozmutlu
POLYCHRO...	79	PR D19 1317	V.A. Polychronakos et al. (NDAM, ANL)
PDG	78	PL 75B 1	C. Bricsman et al.
ANTIPOV	77	NP B119 45	Y.M. Antipov et al. (SERP, GEVA)
PAWLICKI	77	PR D15 3196	A.J. Pawlicki et al. (ANL)
DEUTSCH...	76	NP B103 426	M. Deuschmann et al. (AACH3, BERL, BONN+)
APEL	75	PL 57B 398	W.D. Apel et al. (KARLK, KARLE, PISA, SERP+)
EMMS	75D	NP B96 155	M.J. Emms et al. (BIRM, DURH, RHEL)
EISENBERG	74	PL 52B 239	Y. Eisenberg et al. (REHO)
ENGLER	74	PR D10 2070	A. Engler et al. (CERN, CASE)
LOUIE	74	PL 48B 385	J. Louie et al. (SACL, CERN)
ANDERSON	73	PRL 31 562	J.C. Anderson et al. (CMU, CASE)
TAKAHASHI	72	PR D6 1266	K. Takahashi et al. (TOHOK, PENN, NDAM+)
BEAUPRE	71	NP B28 77	J.V. Beaupre et al. (AACH, BERL, CERN)
FLATTE	71	PL 34B 551	S.M. Flatté et al. (LBL)
ARMENISE	70	LNC 4 199	N. Armenise et al. (BARI, BGNA, FIRZ)
OH	70	PR D1 2494	B.Y. Oh et al. (WISC, TUNO) JP
STUNTEBECK	70	PL 32B 391	P.H. Stuntebeck et al. (NDAM)
ADERHOLZ	69	NP B11 259	M. Aderholz et al. (AACH3, BERL, CERN+)
ARMENISE	68	NC 54A 999	N. Armenise et al. (BARI, BGNA, FIRZ+)
ASCOLI	68D	PRL 21 1712	G. Ascoli et al. (ILL)
BOESEBECK	68	NP B4 501	K. Boesebeck et al. (AACH, BERL, CERN)
JOHNSON	68	PR 176 1651	P.B. Johnson et al. (NDAM, PURD, SLAC)
EISNER	67	PR 164 1699	R.L. Eisner et al. (PURD)
DERADO	65	PRL 14 872	I. Derado et al. (NDAM)
LEE	64	PRL 12 342	Y.Y. Lee et al. (MICH)
BONDAR	63	PL 5 153	L. Bondar et al. (AACH, BIRM, BONN, DESY+)

1281 ± 1	ARMSTRONG	89E	OMEG	300	$pp \rightarrow pp2(\pi^+ \pi^-)$	
1279 ± 6 ± 10	16	BECKER	87	MRK3	$e^+ e^- \rightarrow \phi K \bar{K} \pi$	
1286 ± 9	GIDAL	87	MRK2	$e^+ e^- \rightarrow e^+ e^- \eta \pi^+ \pi^-$		
1287 ± 5	353	BITYUKOV	84B	SPEC	$32 \pi^- p \rightarrow K^+ K^- \pi^0 n$	
~ 1279	5	TORNQVIST	82B	RVUE		
1275 ± 6	31	BROMBERG	80	SPEC	$100 \pi^- p \rightarrow K \bar{K} \pi X$	
1288 ± 9	200	GURTU	79	HBC	$4.2 K^- p \rightarrow n \eta 2\pi$	
~ 1275.0	46	6	STANTON	79	CNTR	$8.5 \pi^- p \rightarrow n 2 \gamma 2\pi$
1271 ± 10	34	CORDEN	78	OMEG	$12-15 \pi^- p \rightarrow K^+ K^- \pi n$	
1295 ± 12	85	CORDEN	78	OMEG	$12-15 \pi^- p \rightarrow n 5\pi$	
1292 ± 10	150	DEFOIX	72	HBC	$0.7 \bar{p} p \rightarrow 7\pi$	
1280 ± 3	500	7	THUN	72	MMS	$13.4 \pi^- p$
1303 ± 8	BARDADIN...	71	HBC	$8 \pi^+ p \rightarrow p 6\pi$		
1283 ± 6	BOESEBECK	71	HBC	$16.0 \pi p \rightarrow p 5\pi$		
1270 ± 10	CAMPBELL	69	DBC	$2.7 \pi^+ d$		
1285 ± 7	LORSTAD	69	HBC	$0.7 \bar{p} p, 4,5\text{-body}$		
1290 ± 7	D'ANDLAW	68	HBC	$1.2 \bar{p} p, 5-6 \text{ body}$		

- The selected process is  $J/\psi \rightarrow \omega a_0(980) \pi$ .
- Supersedes ABATZIS 94, ARMSTRONG 89E.
- From partial wave analysis of  $K^+ \bar{K}^0 \pi^-$  system.
- No systematic error given.
- From a unitarized quark-model calculation.
- From phase shift analysis of  $\eta \pi^+ \pi^-$  system.
- Seen in the missing mass spectrum.

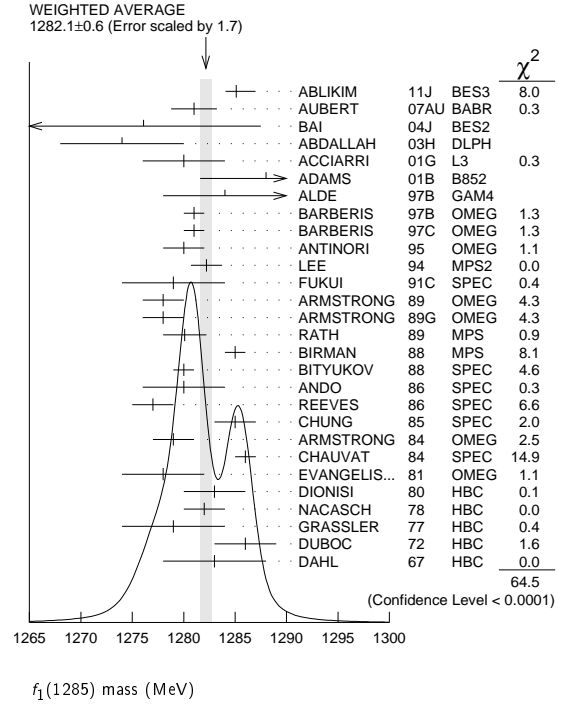
### $f_1(1285)$

$$I^G(JPC) = 0^+(1^{++})$$

### $f_1(1285)$ MASS

VALUE (MeV)	EVTS	DOCUMENT ID	TECN	COMMENT	
<b>1282.1 ± 0.6</b>	<b>OUR AVERAGE</b>			Error includes scale factor of 1.7. See the ideogram below.	
1285.1 ± 1.0 ± 1.6	0.3	1	ABLIKIM 11J BES3	$J/\psi \rightarrow \omega(\eta \pi^+ \pi^-)$	
1281 ± 2 ± 1			AUBERT 07AU BABR	$10.6 e^+ e^- \rightarrow f_1(1285) \pi^+ \pi^- \gamma$	
1276.1 ± 8.1 ± 8.0	203		BAI 04J BES2	$J/\psi \rightarrow \gamma \gamma \pi^+ \pi^-$	
1274 ± 6	237		ABDALLAH 03H DLPH	$91.2 e^+ e^- \rightarrow K_S^0 K_{\pm}^0 \pi^{\mp} + X$	
1280 ± 4			ACCIIARRI 01G L3		
1288 ± 4 ± 5	20k		ADAMS 01B B852	$18 \text{ GeV } \pi^- p \rightarrow K^+ K^- \pi^0 n$	
1284 ± 6	1400		ALDE 97B GAM4	$100 \pi^- p \rightarrow \eta \pi^0 \pi^0 n$	
1281 ± 1			BARBERIS 97B OMEG	$450 pp \rightarrow pp2(\pi^+ \pi^-)$	
1281 ± 1			BARBERIS 97C OMEG	$450 pp \rightarrow pp K_S^0 K_{\pm}^0 \pi^{\mp}$	
1280 ± 2			2	ANTINORI 95 OMEG	$300,450 pp \rightarrow pp2(\pi^+ \pi^-)$
1282.2 ± 1.5			LEE 94 MPS2	$18 \pi^- p \rightarrow K^+ \bar{K}^0 2\pi^- p$	
1279 ± 5			FUKUI 91C SPEC	$8.95 \pi^- p \rightarrow \eta \pi^+ \pi^- n$	
1278 ± 2	140		ARMSTRONG 89 OMEG	$300 pp \rightarrow K \bar{K} \pi pp$	
1278 ± 2			ARMSTRONG 89G OMEG	$85 \pi^+ p \rightarrow 4\pi \pi p, pp \rightarrow 4\pi pp$	
1280.1 ± 2.1	60		RATH 89 MPS	$21.4 \pi^- p \rightarrow K_S^0 K_S^0 \pi^0 n$	
1285 ± 1	4750		3	BIRMAN 88 MPS	$8 \pi^- p \rightarrow K^+ \bar{K}^0 \pi^- n$
1280 ± 1	504		BITYUKOV 88 SPEC	$32.5 \pi^- p \rightarrow K^+ K^- \pi^0 n$	
1280 ± 4			ANDO 86 SPEC	$8 \pi^- p \rightarrow \eta \pi^+ \pi^- n$	
1277 ± 2	420		REEVES 86 SPEC	$6.6 p \bar{p} \rightarrow K K \pi X$	
1285 ± 2			CHUNG 85 SPEC	$8 \pi^- p \rightarrow N K \bar{K} \pi$	
1279 ± 2	604		ARMSTRONG 84 OMEG	$85 \pi^+ p \rightarrow K \bar{K} \pi \pi p, pp \rightarrow K \bar{K} \pi pp$	
1286 ± 1			CHAUVAT 84 SPEC	ISR 31.5 $pp$	
1278 ± 4			EVANGELIS... 81 OMEG	$12 \pi^- p \rightarrow \eta \pi^+ \pi^- \pi^- p$	
1283 ± 3	103		DIONISI 80 HBC	$4 \pi^- p \rightarrow K \bar{K} \pi n$	
1282 ± 2	320		NACASCH 78 HBC	$0.7, 0.76 \bar{p} p \rightarrow K \bar{K} 3\pi$	
1279 ± 5	210		GRASSLER 77 HBC	$16 \pi^+ p$	
1286 ± 3	180		DUBOC 72 HBC	$1.2 \bar{p} p \rightarrow 2K4\pi$	
1283 ± 5			DAHL 67 HBC	$1.6-4.2 \pi^- p$	
1281.9 ± 0.5			4	SOSA 99 SPEC	$pp \rightarrow p_{\text{slow}}(K_S^0 K^+ \pi^-) p_{\text{fast}}$
1282.8 ± 0.6			4	SOSA 99 SPEC	$pp \rightarrow p_{\text{slow}}(K_S^0 K^- \pi^+) p_{\text{fast}}$
1270 ± 10			AMELIN 95 VES	$37 \pi^- N \rightarrow \pi^- \pi^+ \pi^- \gamma N$	
1280 ± 2			ABATZIS 94 OMEG	$450 pp \rightarrow pp2(\pi^+ \pi^-)$	
1282 ± 4			ARMSTRONG 93C E760	$\bar{p} p \rightarrow \pi^0 \eta \eta \rightarrow 6\gamma$	
1270 ± 6 ± 10			ARMSTRONG 92C OMEG	$300 pp \rightarrow pp \pi^+ \pi^- \gamma$	

• • • We do not use the following data for averages, fits, limits, etc. • • •



### $f_1(1285)$ WIDTH

Only experiments giving width error less than 20 MeV are kept for averaging.

VALUE (MeV)	EVTS	DOCUMENT ID	TECN	COMMENT	
<b>24.2 ± 1.1</b>	<b>OUR AVERAGE</b>			Error includes scale factor of 1.3. See the ideogram below.	
22.0 ± 3.1 ± 2.0	1.5	8	ABLIKIM 11J BES3	$J/\psi \rightarrow \omega(\eta \pi^+ \pi^-)$	
35 ± 6 ± 4			AUBERT 07AU BABR	$10.6 e^+ e^- \rightarrow f_1(1285) \pi^+ \pi^- \gamma$	
40.0 ± 8.6 ± 9.3	203		BAI 04J BES2	$J/\psi \rightarrow \gamma \gamma \pi^+ \pi^-$	
29 ± 12	237		ABDALLAH 03H DLPH	$91.2 e^+ e^- \rightarrow K_S^0 K_{\pm}^0 \pi^{\mp} + X$	
45 ± 9 ± 7	20k		ADAMS 01B B852	$18 \text{ GeV } \pi^- p \rightarrow K^+ K^- \pi^0 n$	
55 ± 18	1400		ALDE 97B GAM4	$100 \pi^- p \rightarrow \eta \pi^0 \pi^0 n$	
24 ± 3			BARBERIS 97B OMEG	$450 pp \rightarrow pp2(\pi^+ \pi^-)$	
20 ± 2			BARBERIS 97C OMEG	$450 pp \rightarrow pp K_S^0 K_{\pm}^0 \pi^{\mp}$	
36 ± 5			9	ANTINORI 95 OMEG	$300,450 pp \rightarrow pp2(\pi^+ \pi^-)$
29.0 ± 4.1			LEE 94 MPS2	$18 \pi^- p \rightarrow K^+ \bar{K}^0 2\pi^- p$	

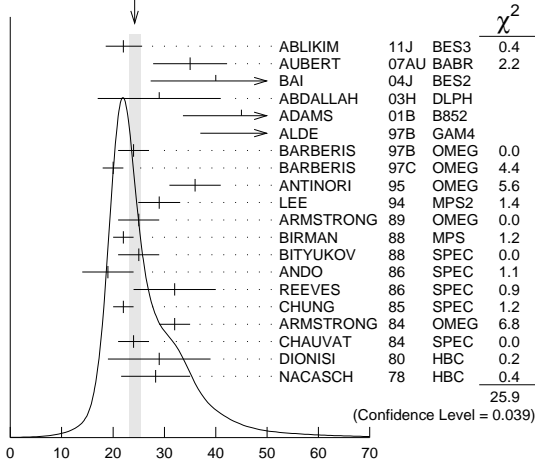
25 ± 4	140	ARMSTRONG 89	OMEG	300	$pp \rightarrow K\bar{K}\pi pp$
22 ± 2	4750	<sup>10</sup> BIRMAN 88	MPS	8	$\pi^- p \rightarrow K^+ \bar{K}^0 \pi^- n$
25 ± 4	504	BITYUKOV 88	SPEC	32.5	$\pi^- p \rightarrow K^+ K^- \pi^0 n$
19 ± 5		ANDO 86	SPEC	8	$\pi^- p \rightarrow \eta \pi^+ \pi^- n$
32 ± 8	420	REEVES 86	SPEC	6.6	$\rho \bar{p} \rightarrow K K \pi X$
22 ± 2		CHUNG 85	SPEC	8	$\pi^- p \rightarrow N K \bar{K} \pi$
32 ± 3	604	ARMSTRONG 84	OMEG	85	$\pi^+ p \rightarrow K \bar{K} \pi \pi p$ , $\rho p \rightarrow K \bar{K} \pi \rho p$
24 ± 3		CHAUVAT 84	SPEC	ISR 31.5	$\rho p$
29 ± 10	103	DIONISI 80	HBC	4	$\pi^- p \rightarrow K \bar{K} \pi n$
28.3 ± 6.7	320	NACASCH 78	HBC	0.7, 0.76	$\bar{p} p \rightarrow K \bar{K} 3\pi$

••• We do not use the following data for averages, fits, limits, etc. •••

18.2 ± 1.2		<sup>11</sup> SOSA 99	SPEC	$\rho p \rightarrow \rho_{slow} (K_S^0 K^+ \pi^-)$	
19.4 ± 1.5		<sup>11</sup> SOSA 99	SPEC	$\rho p \rightarrow \rho_{slow} (K_S^0 K^- \pi^+)$	
40 ± 5		ABATZIS 94	OMEG	450	$pp \rightarrow pp 2(\pi^+ \pi^-)$
31 ± 5		ARMSTRONG 89E	OMEG	300	$pp \rightarrow pp 2(\pi^+ \pi^-)$
41 ± 12		ARMSTRONG 89G	OMEG	85	$\pi^+ p \rightarrow 4\pi \pi p$ , $\rho p \rightarrow 4\pi \pi p$
17.9 ± 10.9	60	RATH 89	MPS	21.4	$\pi^- p \rightarrow K_S^0 K_S^0 \pi^0 n$
14 <sup>+20</sup> <sub>-14</sub> ± 10	16	BECKER 87	MRK3		$e^+ e^- \rightarrow \phi K \bar{K} \pi$
26 ± 12		EVANGELIS... 81	OMEG	12	$\pi^- p \rightarrow \eta \pi^+ \pi^- \pi^- p$
25 ± 15	200	GURTU 79	HBC	4.2	$K^- p \rightarrow n \eta 2\pi$
~10		<sup>12</sup> STANTON 79	CNTR	8.5	$\pi^- p \rightarrow n 2\gamma 2\pi$
24 ± 18	210	GRASSLER 77	HBC	16	$\pi^+ p$
28 ± 5	150	<sup>13</sup> DEFOIX 72	HBC	0.7	$\bar{p} p \rightarrow 7\pi$
46 ± 9	180	<sup>13</sup> DUBOC 72	HBC	1.2	$\bar{p} p \rightarrow 2K 4\pi$
37 ± 5	500	<sup>14</sup> THUN 72	MMS	13.4	$\pi^- p$
10 ± 10		BOESEBECK 71	HBC	16.0	$\pi p \rightarrow p 5\pi$
30 ± 15		CAMPBELL 69	DBC	2.7	$\pi^+ d$
60 ± 15		<sup>13</sup> LORSTAD 69	HBC	0.7	$\bar{p} p$ , 4,5-body
35 ± 10		<sup>13</sup> DAHL 67	HBC	1.6-4.2	$\pi^- p$

<sup>8</sup>The selected process is  $J/\psi \rightarrow \omega a_0(980)\pi$ .  
<sup>9</sup>Supersedes ABATZIS 94, ARMSTRONG 89E.  
<sup>10</sup>From partial wave analysis of  $K^+ \bar{K}^0 \pi^-$  system.  
<sup>11</sup>No systematic error given.  
<sup>12</sup>From phase shift analysis of  $\eta \pi^+ \pi^-$  system.  
<sup>13</sup>Resolution is not unfolded.  
<sup>14</sup>Seen in the missing mass spectrum.

WEIGHTED AVERAGE  
24.2 ± 1.1 (Error scaled by 1.3)



$f_1(1285)$  width (MeV)

$f_1(1285)$  DECAY MODES

Mode	Fraction ( $\Gamma_i/\Gamma$ )	Scale factor/ Confidence level
$\Gamma_1$ $4\pi$	$(33.1^{+2.1}_{-1.8})\%$	S=1.3
$\Gamma_2$ $\pi^0 \pi^0 \pi^+ \pi^-$	$(22.0^{+1.4}_{-1.2})\%$	S=1.3
$\Gamma_3$ $2\pi^+ 2\pi^-$	$(11.0^{+0.7}_{-0.6})\%$	S=1.3
$\Gamma_4$ $\rho^0 \pi^+ \pi^-$	$(11.0^{+0.7}_{-0.6})\%$	S=1.3
$\Gamma_5$ $\rho^0 \rho^0$	seen	
$\Gamma_6$ $4\pi^0$	$< 7 \times 10^{-4}$	CL=90%
$\Gamma_7$ $\eta \pi^+ \pi^-$	$(35 \pm 15)\%$	
$\Gamma_8$ $\eta \pi \pi$	$(52.4^{+1.9}_{-2.2})\%$	S=1.2

$\Gamma_9$	$a_0(980)\pi$ [ignoring $a_0(980) \rightarrow K\bar{K}$ ]	$(36 \pm 7)\%$	
$\Gamma_{10}$	$\eta \pi \pi$ [excluding $a_0(980)\pi$ ]	$(16 \pm 7)\%$	
$\Gamma_{11}$	$K \bar{K} \pi$	$(9.0 \pm 0.4)\%$	S=1.1
$\Gamma_{12}$	$K \bar{K}^*(892)$	not seen	
$\Gamma_{13}$	$\pi^+ \pi^- \pi^0$	$(3.0 \pm 0.9) \times 10^{-3}$	
$\Gamma_{14}$	$\rho^\pm \pi^\mp$	$< 3.1 \times 10^{-3}$	CL=95%
$\Gamma_{15}$	$\gamma \rho^0$	$(5.5 \pm 1.3)\%$	S=2.8
$\Gamma_{16}$	$\phi \gamma$	$(7.4 \pm 2.6) \times 10^{-4}$	
$\Gamma_{17}$	$\gamma \gamma^*$		
$\Gamma_{18}$	$\gamma \gamma$		

CONSTRAINED FIT INFORMATION

An overall fit to 7 branching ratios uses 16 measurements and one constraint to determine 5 parameters. The overall fit has a  $\chi^2 = 24.7$  for 12 degrees of freedom.

The following off-diagonal array elements are the correlation coefficients  $\langle \delta x_i \delta x_j \rangle / (\delta x_i \delta x_j)$ , in percent, from the fit to the branching fractions,  $x_i \equiv \Gamma_i / \Gamma_{total}$ . The fit constrains the  $x_i$  whose labels appear in this array to sum to one.

$x_9$	-17			
$x_{10}$	-8	-95		
$x_{11}$	46	-9	-4	
$x_{15}$	-36	-4	-2	-34
	$x_1$	$x_9$	$x_{10}$	$x_{11}$

$f_1(1285) \Gamma(i)\Gamma(\gamma\gamma)/\Gamma(total)$

$\Gamma(\eta\pi\pi) \times \Gamma(\gamma\gamma)/\Gamma_{total}$	$\Gamma_8 \Gamma_{18}/\Gamma = (\Gamma_9 + \Gamma_{10})\Gamma_{18}/\Gamma$			
VALUE (keV)	CL%	DOCUMENT ID	TECN	COMMENT
<b>&lt;0.62</b>	95	GIDAL	87	MRK2 $e^+ e^- \rightarrow e^+ e^- \eta \pi^+ \pi^-$
$\Gamma(\eta\pi\pi) \times \Gamma(\gamma\gamma^*)/\Gamma_{total}$	$\Gamma_8 \Gamma_{17}/\Gamma = (\Gamma_9 + \Gamma_{10})\Gamma_{17}/\Gamma$			
VALUE (keV)	EVTS	DOCUMENT ID	TECN	COMMENT
<b>1.4 ± 0.4 OUR AVERAGE</b>				Error includes scale factor of 1.4.
1.18 ± 0.25 ± 0.20	26	<sup>15,16</sup> AIHARA	88B	TPC $e^+ e^- \rightarrow e^+ e^- \eta \pi^+ \pi^-$
2.30 ± 0.61 ± 0.42		<sup>15,17</sup> GIDAL	87	MRK2 $e^+ e^- \rightarrow e^+ e^- \eta \pi^+ \pi^-$
••• We do not use the following data for averages, fits, limits, etc. •••				
1.8 ± 0.3 ± 0.3	420	<sup>18</sup> ACHARD	02B L3	183-209 $e^+ e^- \rightarrow e^+ e^- \eta \pi^+ \pi^-$

<sup>15</sup> Assuming a  $\rho$ -pole form factor.  
<sup>16</sup> Published value multiplied by  $\eta \pi \pi$  branching ratio 0.49.  
<sup>17</sup> Published value divided by 2 and multiplied by the  $\eta \pi \pi$  branching ratio 0.49.  
<sup>18</sup> Published value multiplied by the  $\eta \pi \pi$  branching ratio 0.52.

$f_1(1285)$  BRANCHING RATIOS

$\Gamma(K\bar{K}\pi)/\Gamma(4\pi)$	$\Gamma_{11}/\Gamma_1$		
VALUE	DOCUMENT ID	TECN	COMMENT
<b>0.271 ± 0.016 OUR FIT</b>			Error includes scale factor of 1.3.
<b>0.271 ± 0.016 OUR AVERAGE</b>			Error includes scale factor of 1.2.
0.265 ± 0.014	<sup>19</sup> BARBERIS	97C	OMEG 450 $pp \rightarrow pp K_S^0 K^\pm \pi^\mp$
0.28 ± 0.05	<sup>20</sup> ARMSTRONG 89E	OMEG 300	$pp \rightarrow pp f_1(1285)$
0.37 ± 0.03 ± 0.05	<sup>21</sup> ARMSTRONG 89G	OMEG 85	$\pi p \rightarrow 4\pi X$
<sup>19</sup> Using $2(\pi^+ \pi^-)$ data from BARBERIS 97B. <sup>20</sup> Assuming $\rho \pi \pi$ and $a_0(980)\pi$ intermediate states. <sup>21</sup> $4\pi$ consistent with being entirely $\rho \pi \pi$ .			

$\Gamma(\pi^0 \pi^+ \pi^-)/\Gamma_{total}$	$\Gamma_2/\Gamma = \frac{2}{3}\Gamma_1/\Gamma$
VALUE	DOCUMENT ID
<b>0.220 ± 0.014</b>	
<b>-0.012 OUR FIT</b>	
	Error includes scale factor of 1.3.

$\Gamma(2\pi^+ 2\pi^-)/\Gamma_{total}$	$\Gamma_3/\Gamma = \frac{1}{3}\Gamma_1/\Gamma$
VALUE	DOCUMENT ID
<b>0.110 ± 0.007</b>	
<b>-0.006 OUR FIT</b>	
	Error includes scale factor of 1.3.

$\Gamma(\rho^0 \pi^+ \pi^-)/\Gamma_{total}$	$\Gamma_4/\Gamma = \frac{1}{3}\Gamma_1/\Gamma$
VALUE	DOCUMENT ID
<b>0.110 ± 0.007</b>	
<b>-0.006 OUR FIT</b>	
	Error includes scale factor of 1.3.

$\Gamma(\rho^0 \pi^+ \pi^-)/\Gamma(2\pi^+ 2\pi^-)$	$\Gamma_4/\Gamma_3$		
VALUE	DOCUMENT ID	TECN	COMMENT
1.0 ± 0.4	GRASSLER	77 HBC	16 GeV $\pi^\pm p$

••• We do not use the following data for averages, fits, limits, etc. •••

## Meson Particle Listings

 $f_1(1285)$ 

$\Gamma(\rho^0 \rho^0)/\Gamma_{\text{total}}$   $\Gamma_5/\Gamma$   
 VALUE DOCUMENT ID COMMENT

• • • We do not use the following data for averages, fits, limits, etc. • • •  
 seen BARBERIS 00c 450  $p\rho \rightarrow p_f 4\pi_S$

$\Gamma(4\pi^0)/\Gamma_{\text{total}}$   $\Gamma_6/\Gamma$   
 VALUE (units  $10^{-4}$ ) CL% DOCUMENT ID TECN COMMENT  
 <7 90 ALDE 87 GAM4 100  $\pi^- p \rightarrow 4\pi^0 n$

$\Gamma(\pi^+ \pi^- \pi^0)/\Gamma(\eta \pi^+ \pi^-)$   $\Gamma_{13}/\Gamma_7$   
 VALUE (%) EVTS DOCUMENT ID TECN COMMENT  
 $0.86 \pm 0.16 \pm 0.20$  2.3k 22 DOROFEEV 11 VES  $\pi^- N \rightarrow \pi^- f_1(1285) N$   
 22 Value obtained selecting the region corresponding to  $f_0(980)$  in the  $\pi^+ \pi^-$  mass spectrum.

$\Gamma(\eta \pi \pi)/\Gamma_{\text{total}}$   $\Gamma_8/\Gamma = (\Gamma_9 + \Gamma_{10})/\Gamma$   
 VALUE DOCUMENT ID COMMENT  
 $0.524 \pm 0.019$  OUR FIT Error includes scale factor of 1.2.  
 $-0.022$

$\Gamma(4\pi)/\Gamma(\eta \pi \pi)$   $\Gamma_1/\Gamma_8 = \Gamma_1/(\Gamma_9 + \Gamma_{10})$   
 VALUE DOCUMENT ID TECN COMMENT  
 $0.63 \pm 0.06$  OUR FIT Error includes scale factor of 1.2.  
 $0.41 \pm 0.14$  OUR AVERAGE

0.37  $\pm$  0.11  $\pm$  0.11 BOLTON 92 MRK3  $J/\psi \rightarrow \gamma f_1(1285)$   
 0.64  $\pm$  0.40 GURTU 79 HBC 4.2  $K^- p$   
 • • • We do not use the following data for averages, fits, limits, etc. • • •  
 0.93  $\pm$  0.30 23 GRASSLER 77 HBC 16  $\pi^\mp p$   
 23 Assuming  $\rho\pi\pi$  and  $a_0(980)\pi$  intermediate states.

$\Gamma(a_0(980)\pi [\text{ignoring } a_0(980) \rightarrow K\bar{K}])/ \Gamma(\eta \pi \pi)$   $\Gamma_9/\Gamma_8 = \Gamma_9/(\Gamma_9 + \Gamma_{10})$   
 VALUE CL% EVTS DOCUMENT ID TECN COMMENT  
 $0.69 \pm 0.13$  OUR FIT  
 $0.69 \pm 0.12$  OUR AVERAGE

0.72  $\pm$  0.15 GURTU 79 HBC 4.2  $K^- p$   
 0.6  $\pm$  0.3 CORDEN 78 OMEG 12-15  $\pi^- p$   
 -0.2  
 • • • We do not use the following data for averages, fits, limits, etc. • • •  
 >0.69 95 318 ACHARD 02b L3 183-209  $e^+ e^- \rightarrow e^+ e^- \eta \pi^+ \pi^-$   
 0.28  $\pm$  0.07 1400 ALDE 97b GAM4 100  $\pi^- p \rightarrow \eta \pi^0 \pi^0 n$   
 1.0  $\pm$  0.3 GRASSLER 77 HBC 16  $\pi^\mp p$

$\Gamma(K\bar{K}\pi)/\Gamma(\eta \pi \pi)$   $\Gamma_{11}/\Gamma_8 = \Gamma_{11}/(\Gamma_9 + \Gamma_{10})$   
 VALUE DOCUMENT ID TECN COMMENT  
 $0.171 \pm 0.013$  OUR FIT Error includes scale factor of 1.1.  
 $0.170 \pm 0.012$  OUR AVERAGE

0.166  $\pm$  0.01  $\pm$  0.008 BARBERIS 98c OMEG 450  $p\rho \rightarrow p_f f_1(1285) p_S$   
 0.42  $\pm$  0.15 GURTU 79 HBC 4.2  $K^- p$   
 0.5  $\pm$  0.2 24 CORDEN 78 OMEG 12-15  $\pi^- p$   
 0.20  $\pm$  0.08 25 DEFOIX 72 HBC 0.7  $\bar{p}p \rightarrow 7\pi$   
 0.16  $\pm$  0.08 CAMPBELL 69 DBC 2.7  $\pi^+ d$   
 24 CORDEN 78 assumes low-mass  $\eta\pi\pi$  region is dominantly  $1^{++}$ . See BARBERIS 98c and MANAK 00a for discussion.  
 25  $K\bar{K}$  system characterized by the  $l = 1$  threshold enhancement. (See under  $a_0(980)$ ).

$\Gamma(K\bar{K}^*(892))/\Gamma_{\text{total}}$   $\Gamma_{12}/\Gamma$   
 VALUE DOCUMENT ID TECN COMMENT  
 not seen NACASCH 78 HBC 0.7, 0.76  $\bar{p}p \rightarrow K\bar{K}3\pi$

• • • We do not use the following data for averages, fits, limits, etc. • • •  
 seen 26 ACHARD 07 L3 183-209  $e^+ e^- \rightarrow e^+ e^- K_S^0 K^\pm \pi^\mp$   
 26 A clear signal of  $19.8 \pm 4.4$  events observed at high  $Q^2$ .

$\Gamma(\pi^+ \pi^- \pi^0)/\Gamma_{\text{total}}$   $\Gamma_{13}/\Gamma$   
 VALUE (%) EVTS DOCUMENT ID TECN COMMENT  
 $0.30 \pm 0.055 \pm 0.074$  2.3k 27 DOROFEEV 11 VES  $\pi^- N \rightarrow \pi^- f_1(1285) N$

27 Value obtained selecting the region corresponding to  $f_0(980)$  in the  $\pi^+ \pi^-$  mass spectrum. The systematic error includes the uncertainty on the partial width  $f_1 \rightarrow \eta\pi\pi$  obtained from PDG 10 data.

$\Gamma(\rho^\pm \pi^\mp)/\Gamma_{\text{total}}$   $\Gamma_{14}/\Gamma$   
 VALUE CL% DOCUMENT ID TECN COMMENT  
 <0.31 95 DOROFEEV 11 VES  $\pi^- N \rightarrow \pi^- f_1(1285) N$

$\Gamma(\gamma \rho^0)/\Gamma_{\text{total}}$   $\Gamma_{15}/\Gamma$   
 VALUE (units  $10^{-2}$ ) CL% DOCUMENT ID TECN COMMENT  
 $5.5 \pm 1.3$  OUR FIT Error includes scale factor of 2.8.  
 $2.8 \pm 0.7 \pm 0.6$  AMELIN 95 VES 37  $\pi^- N \rightarrow \pi^- \pi^+ \pi^- \gamma N$

• • • We do not use the following data for averages, fits, limits, etc. • • •  
 <5 95 BITYUKOV 91b SPEC 32  $\pi^- p \rightarrow \pi^+ \pi^- \gamma n$

$\Gamma(\gamma \rho^0)/\Gamma(2\pi^+ 2\pi^-)$   $\Gamma_{15}/\Gamma_3 = \Gamma_{15}/\frac{1}{3}\Gamma_1$   
 VALUE DOCUMENT ID TECN COMMENT  
 $0.50 \pm 0.13$  OUR FIT Error includes scale factor of 2.5.  
 $0.45 \pm 0.18$  28 COFFMAN 90 MRK3  $J/\psi \rightarrow \gamma \gamma \pi^+ \pi^-$

28 Using  $B(J/\psi \rightarrow \gamma f_1(1285) \rightarrow \gamma \gamma \rho^0) = 0.25 \times 10^{-4}$  and  $B(J/\psi \rightarrow \gamma f_1(1285) \rightarrow \gamma 2\pi^+ 2\pi^-) = 0.55 \times 10^{-4}$  given by MIR 88.

$\Gamma(\eta \pi \pi)/\Gamma(\gamma \rho^0)$   $\Gamma_8/\Gamma_{15} = (\Gamma_9 + \Gamma_{10})/\Gamma_{15}$   
 VALUE DOCUMENT ID TECN COMMENT  
 $9.5 \pm 2.0$  OUR FIT Error includes scale factor of 2.5.  
 $7.9 \pm 0.9$  OUR AVERAGE

10.0  $\pm$  1.0  $\pm$  2.0 BARBERIS 98c OMEG 450  $p\rho \rightarrow p_f f_1(1285) p_S$   
 7.5  $\pm$  1.0 29 ARMSTRONG 92c OMEG 300  $p\rho \rightarrow p\rho \pi^+ \pi^- \gamma, p\rho \eta \pi^+ \pi^-$   
 29 Published value multiplied by 1.5.

$\Gamma(\gamma \rho^0)/\Gamma(K\bar{K}\pi)$   $\Gamma_{15}/\Gamma_{11}$   
 VALUE CL% DOCUMENT ID TECN COMMENT  
 • • • We do not use the following data for averages, fits, limits, etc. • • •

>0.035 90 30 COFFMAN 90 MRK3  $J/\psi \rightarrow \gamma \gamma \pi^+ \pi^-$   
 30 Using  $B(J/\psi \rightarrow \gamma f_1(1285) \rightarrow \gamma \gamma \rho^0) = 0.25 \times 10^{-4}$  and  $B(J/\psi \rightarrow \gamma f_1(1285) \rightarrow \gamma K\bar{K}\pi) < 0.72 \times 10^{-3}$ .

$\Gamma(\phi \gamma)/\Gamma(K\bar{K}\pi)$   $\Gamma_{16}/\Gamma_{11}$   
 VALUE (units  $10^{-2}$ ) CL% EVTS DOCUMENT ID TECN COMMENT  
 $0.82 \pm 0.21 \pm 0.20$  19 BITYUKOV 88 SPEC 32.5  $\pi^- p \rightarrow K^+ K^- \pi^0 n$

• • • We do not use the following data for averages, fits, limits, etc. • • •  
 <0.50 95 BARBERIS 98c OMEG 450  $p\rho \rightarrow p_f f_1(1285) p_S$   
 <0.93 95 AMELIN 95 VES 37  $\pi^- N \rightarrow \pi^- \pi^+ \pi^- \gamma N$

 $f_1(1285)$  REFERENCES

ABLIKIM	11J	PRL 107 182001	M. Ablikim <i>et al.</i>	(BES III Collab.)
DOROFEEV	11	EPJ A47 68	V. Dorofeev <i>et al.</i>	(SERP, MIP)T
PDG	10	JPG 37 075021	K. Nakamura <i>et al.</i>	(PDG Collab.)
ACHARD	07	JHEP 0703 018	P. Achard <i>et al.</i>	(L3 Collab.)
AUBERT	07AU	PR D76 092005	B. Aubert <i>et al.</i>	(BABAR Collab.)
BAI	04J	PL B594 47	J.Z. Bai <i>et al.</i>	(BES Collab.)
ABDALLAH	03H	PL B569 129	J. Abdallah <i>et al.</i>	(DELPHI Collab.)
ACHARD	02B	PL B526 269	P. Achard <i>et al.</i>	(L3 Collab.)
ACCIARRI	01B	PL B501 1	M. Acciarri <i>et al.</i>	(L3 Collab.)
ADAMS	01G	PL B516 264	G.S. Adams <i>et al.</i>	(BNL E852 Collab.)
BARBERIS	00C	PL B471 440	D. Barberis <i>et al.</i>	(WA 102 Collab.)
MANAK	00A	PR D62 012003	J.J. Manak <i>et al.</i>	(BNL E852 Collab.)
SOSA	99	PRL 83 913	M. Sosa <i>et al.</i>	
BARBERIS	98C	PL B440 225	D. Barberis <i>et al.</i>	(WA 102 Collab.)
ALDE	97B	PAN 60 386	D. Alde <i>et al.</i>	(GAMS Collab.)
BARBERIS	97B	PL B413 217	D. Barberis <i>et al.</i>	(WA 102 Collab.)
BARBERIS	97C	PL B413 225	D. Barberis <i>et al.</i>	(WA 102 Collab.)
AMELIN	95	ZPHY C66 71	D.V. Amelin <i>et al.</i>	(VES Collab.)
ANTINORI	95	PL B353 589	F. Antinori <i>et al.</i>	(ATHU, BARI, BIRM+)
ABATZIS	94	PL B324 509	S. Abatzis <i>et al.</i>	(ATHU, BARI, BIRM+)
LEE	94	PL B323 227	J.H. Lee <i>et al.</i>	(BNL, IND, KYUN, MASD+)
ARMSTRONG	93C	PL B307 394	T.A. Armstrong <i>et al.</i>	(FNAL, FERR, GENO+)
ARMSTRONG	92C	ZPHY C54 371	T.A. Armstrong <i>et al.</i>	(ATHU, BARI, BIRM+)
BOLTON	92C	PL B278 495	T. Bolton <i>et al.</i>	(Mark III Collab.)
BITYUKOV	91B	SJNP 54 318	S.I. Bityukov <i>et al.</i>	(SERP)
FUKUI	91C	PL B267 293	S. Fukui <i>et al.</i>	(SUGI, NAGO, KEK, KYOT+)
COFFMAN	90	PR D41 1410	D.M. Coffman <i>et al.</i>	(Mark III Collab.)
ARMSTRONG	89	PL B221 216	T.A. Armstrong <i>et al.</i>	(CERN, CDF, BIRM+)
ARMSTRONG	89E	PL B228 536	T.A. Armstrong, M. Benayoun	(ATHU, BARI, BIRM+)
ARMSTRONG	89G	ZPHY C43 55	T.A. Armstrong <i>et al.</i>	(CERN, BIRM, BARI+)
RATH	89	PR D40 693	M.G. Rath <i>et al.</i>	(NDAM, BRAN, BNL, CUNY+)
AIHARA	88B	PL B209 107	H. Aihara <i>et al.</i>	(TPC-2 $\gamma$ Collab.)
BIRMAN	88	PRL 61 1557	A. Birman <i>et al.</i>	(BNL, FSU, IND, MASD)JP
BITYUKOV	88	PL B203 327	S.I. Bityukov <i>et al.</i>	(SERP)
MIR	88	Photon-Photon 88, 126	R. Mir	(Mark III Collab.)
ALDE	87	PL B198 286	D.M. Alde <i>et al.</i>	(LANL, BRUX, SERP, LAPP)
BECKER	87	PRL 59 186	J.J. Becker <i>et al.</i>	(Mark III Collab.)
GIDAL	87	PRL 59 2012	G. Gidal <i>et al.</i>	(LBL, SLAC, HARV)
ANDO	86	PRL 57 1296	A. Ando <i>et al.</i>	(KEK, KYOT, NIRS, SAGA+)
REEVES	86	PR D34 1960	D.F. Reeves <i>et al.</i>	(FLOR, BNL, IND+)
CHUNG	85	PRL 55 779	S.U. Chung <i>et al.</i>	(BNL, FLOR, IND+)
ARMSTRONG	84	PL 146B 273	T.A. Armstrong <i>et al.</i>	(ATHU, BARI, BIRM+)
BITYUKOV	84B	PL 144B 133	S.I. Bityukov <i>et al.</i>	(SERP)
CHAUVAT	84	PL 148B 382	P. Chauvat <i>et al.</i>	(CERN, CLER, UCLA+)
TORQVIST	82B	NP B203 268	N.A. Torqvist	(HELS)
EVANGELISTA	81	NP B178 197	C. Evangelista <i>et al.</i>	(BARI, BONN, CERN+)
BROMBERG	80	PR D22 1513	M. Bromberg <i>et al.</i>	(CIT, FNAL, ILLC+)
DIONIISI	80	NP B169 1	C. Dionisi <i>et al.</i>	(CERN, MADR, CDF+)
GURTU	79	NP B151 181	A. Gurtu <i>et al.</i>	(CERN, ZEEM, NIJM, OXF)
STANTON	79	PRL 42 346	N.R. Stanton <i>et al.</i>	(OSU, CARL, MCGI+)
CORDEN	78	NP B144 253	M.J. Corden <i>et al.</i>	(BIRM, RHEL, TELA+)
NACASCH	78	NP B135 203	R. Nacasch <i>et al.</i>	(PARIS, MADR, CERN)
GRASSLER	77	NP B121 189	H. Grassler <i>et al.</i>	(AACH3, BERL, BONN+)
DEFOIX	72	NP B44 125	C. Defoix <i>et al.</i>	(CDFE, CERN)
DUBOC	72	NP B46 429	J. Duboc <i>et al.</i>	(PARIS, LIVP)
THUN	72	PRL 28 1733	R. Thun <i>et al.</i>	(STON, NEAS)
BARDADIN-...	71	PR D4 2711	M. Bardadin-Otwinowska <i>et al.</i>	(WARSA)
BOESEBECK	71	PL 34B 659	K. Boesebeck	(AACH, BERL, BONN, CERN, CRA+)
CAMPBELL	69	PRL 22 1204	J.H. Campbell <i>et al.</i>	(PURD)
LORSTAD	69	NP B14 63	B. Lorstad <i>et al.</i>	(CDFE, CERN)JP
d'ANDLAU	68	NP B5 693	C. d'Andlau <i>et al.</i>	(CDFE, CERN, IRAD+)
DAHL	67	PR 163 1377	O.I. Dahl <i>et al.</i>	(LRL)IJP

See key on page 457

Meson Particle Listings

$\eta(1295)$ ,  $\pi(1300)$

$\eta(1295)$

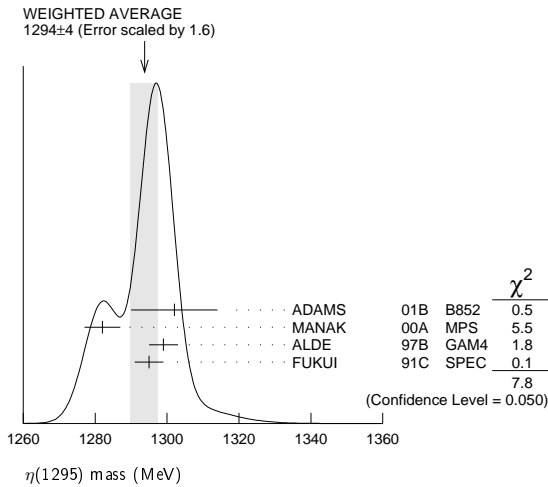
$I^G(J^{PC}) = 0^+(0^{-+})$

See also the mini-review under  $\eta(1405)$

$\eta(1295)$  MASS

VALUE (MeV)	EVTS	DOCUMENT ID	TECN	COMMENT
<b>1294 ± 4 OUR AVERAGE</b>	Error includes scale factor of 1.6. See the ideogram below.			
1302 ± 9 ± 8	20k	ADAMS	01B B852	18 GeV $\pi^- p \rightarrow K^+ K^- \pi^0 n$
1282 ± 5	9082	MANAK	00A MPS	18 $\pi^- p \rightarrow \eta \pi^+ \pi^- n$
1299 ± 4	2100	ALDE	97B GAM4	100 $\pi^- p \rightarrow \eta \pi^0 \pi^0 n$
1295 ± 4		FUKUI	91C SPEC	8.95 $\pi^- p \rightarrow \eta \pi^+ \pi^- n$

- • • We do not use the following data for averages, fits, limits, etc. • • •
- 1264 ± 8     1 AUGUSTIN    90    DM2     $J/\psi \rightarrow \gamma \eta \pi^+ \pi^-$
- ~ 1275     STANTON            79    CNTR     $8.4 \pi^- p \rightarrow n \eta 2\pi$



1 PWA analysis of AUGUSTIN 92 assigns  $0^{-+}$  quantum numbers to this state rather than  $1^{++}$  as before.

$\eta(1295)$  WIDTH

VALUE (MeV)	EVTS	DOCUMENT ID	TECN	COMMENT
<b>55 ± 5 OUR AVERAGE</b>				
57 ± 23 ± 21	20k	ADAMS	01B B852	18 GeV $\pi^- p \rightarrow K^+ K^- \pi^0 n$
66 ± 13	9082	MANAK	00A MPS	18 $\pi^- p \rightarrow \eta \pi^+ \pi^- n$
53 ± 6		FUKUI	91C SPEC	8.95 $\pi^- p \rightarrow \eta \pi^+ \pi^- n$

- • • We do not use the following data for averages, fits, limits, etc. • • •
  - < 40     2100     ALDE     97B    GAM4    100  $\pi^- p \rightarrow \eta \pi^0 \pi^0 n$
  - 44 ± 20     2 AUGUSTIN    90    DM2     $J/\psi \rightarrow \gamma \eta \pi^+ \pi^-$
  - ~ 70     STANTON            79    CNTR     $8.4 \pi^- p \rightarrow n \eta 2\pi$
- 2 PWA analysis of AUGUSTIN 92 assigns  $0^{-+}$  quantum numbers to this state rather than  $1^{++}$  as before.

$\eta(1295)$  DECAY MODES

Mode	Fraction ( $\Gamma_i/\Gamma$ )
$\Gamma_1 \eta \pi^+ \pi^-$	seen
$\Gamma_2 a_0(980) \pi$	seen
$\Gamma_3 \gamma \gamma$	
$\Gamma_4 \eta \pi^0 \pi^0$	seen
$\Gamma_5 \eta(\pi\pi)S\text{-wave}$	seen
$\Gamma_6 \sigma \eta$	
$\Gamma_7 K \bar{K} \pi$	

$\eta(1295) \Gamma(i)\Gamma(\gamma\gamma)/\Gamma(\text{total})$

VALUE (keV)	CL%	DOCUMENT ID	TECN	COMMENT
<b>&lt; 0.066</b>	95	ACCIARRI	01G L3	183-202 $e^+ e^- \rightarrow e^+ e^- \eta \pi^+ \pi^-$
• • • We do not use the following data for averages, fits, limits, etc. • • •				
< 0.6	90	AIHARA	88C TPC	$e^+ e^- \rightarrow e^+ e^- \eta \pi^+ \pi^-$
< 0.3		ANTREASIAN	87 CBAL	$e^+ e^- \rightarrow e^+ e^- \eta \pi \pi$

$\Gamma(K\bar{K}\pi) \times \Gamma(\gamma\gamma)/\Gamma_{\text{total}}$

VALUE (keV)	CL%	DOCUMENT ID	TECN	COMMENT
• • • We do not use the following data for averages, fits, limits, etc. • • •				
< 0.014	90	3,4 AHOHE	05 CLE2	10.6 $e^+ e^- \rightarrow e^+ e^- K_S^0 K^\pm \pi^\mp$

- 3 Using  $\eta(1295)$  mass and width 1294 MeV and 55 MeV, respectively.
- 4 Assuming three-body phase-space decay to  $K_S^0 K^\pm \pi^\mp$ .

$\eta(1295)$  BRANCHING RATIOS

$\Gamma(a_0(980)\pi)/\Gamma_{\text{total}}$	DOCUMENT ID	TECN	COMMENT
• • • We do not use the following data for averages, fits, limits, etc. • • •			
not seen	BERTIN	97 OBLX	0.0 $\bar{p} p \rightarrow K^\pm(K^0)\pi^\mp\pi^+\pi^-$
seen	BIRMAN	88 MPS	8 $\pi^- p \rightarrow K^+ \bar{K}^0 \pi^- n$
large	ANDO	86 SPEC	8 $\pi^- p \rightarrow \eta \pi^+ \pi^- n$
large	STANTON	79 CNTR	8.4 $\pi^- p \rightarrow n \eta 2\pi$

$\Gamma(a_0(980)\pi)/\Gamma(\eta\pi^0\pi^0)$

VALUE	DOCUMENT ID	TECN	COMMENT
<b>0.65 ± 0.10</b>	5 ALDE	97B GAM4	100 $\pi^- p \rightarrow \eta \pi^0 \pi^0 n$

5 Assuming that  $a_0(980)$  decays only to  $\eta\pi$ .

$\Gamma(\eta(\pi\pi)S\text{-wave})/\Gamma(\eta\pi^0\pi^0)$

VALUE	DOCUMENT ID	TECN	COMMENT
<b>0.35 ± 0.10</b>	ALDE	97B GAM4	100 $\pi^- p \rightarrow \eta \pi^0 \pi^0 n$

$\Gamma(a_0(980)\pi)/\Gamma(\sigma\eta)$

VALUE	EVTS	DOCUMENT ID	TECN	COMMENT
<b>0.48 ± 0.22</b>	9082	MANAK	00A MPS	18 $\pi^- p \rightarrow \eta \pi^+ \pi^- n$

$\eta(1295)$  REFERENCES

AHOHE 05 PR D71 072001 R. Ahohe et al. (CLEO Collab.)  
 ACCIARRI 01G PL B501 1 M. Acciari et al. (L3 Collab.)  
 ADAMS 01B PL B516 264 G.S. Adams et al. (BNL E852 Collab.)  
 MANAK 00A PR D62 012003 J.J. Manak et al. (BNL E852 Collab.)  
 ALDE 97B PAN 60 386 D. Alde et al. (GAMS Collab.)  
 Translated from YAF 60 458.  
 BERTIN 97 PL B400 226 A. Bertin et al. (OBELIX Collab.)  
 AUGUSTIN 92 PR D46 1951 J.E. Augustin, G. Cosme (DM2 Collab.)  
 FUKUI 91C PL B267 293 S. Fukui et al. (SUGI, NAGO, KEK, KYOT+)  
 AUGUSTIN 90 PR D42 10 J.E. Augustin et al. (DM2 Collab.)  
 AIHARA 88C PR D38 1 H. Aihara et al. (TPC-2 Collab.)  
 BIRMAN 88 PRL 61 1557 A. Birman et al. (BNL FSU, IND, MASD)JP  
 ANTREASIAN 87 PR D36 2633 D. Antreasian et al. (Crystal Ball Collab.)  
 ANDO 86 PRL 57 1296 A. Ando et al. (KEK, KYOT, NIRS, SAGA+IJP  
 STANTON 79 PRL 42 346 N.R. Stanton et al. (OSU, CARL, MCGI+JP)

$\pi(1300)$

$I^G(J^{PC}) = 1^-(0^{-+})$

$\pi(1300)$  MASS

VALUE (MeV)	EVTS	DOCUMENT ID	TECN	COMMENT
<b>1300 ± 100 OUR ESTIMATE</b>				

- • • We do not use the following data for averages, fits, limits, etc. • • •
- 1345 ± 8 ± 10    18k    1 SCHEGELSKY    06    RVUE     $\gamma \gamma \rightarrow \pi^+ \pi^- \pi^0$
- 1200 ± 40    90k    SALVINI    04    OBLX     $\bar{p} p \rightarrow 2\pi^+ 2\pi^-$
- 1343 ± 15 ± 24    CHUNG    02    B852    18.3  $\pi^- p \rightarrow \pi^+ \pi^- \pi^- p$
- 1375 ± 40    ABELE    01    CBAR    0.0  $\bar{p} d \rightarrow \pi^- 4\pi^0 p$
- 1275 ± 15    BERTIN    97D    OBLX    0.05  $\bar{p} p \rightarrow 2\pi^+ 2\pi^-$
- ~ 1114    ABELE    96    CBAR    0.0  $\bar{p} p \rightarrow 5\pi^0$
- 1190 ± 30    ZIELINSKI    84    SPEC    200  $\pi^+ Z \rightarrow Z 3\pi$
- 1240 ± 30    BELLINI    82    SPEC    40  $\pi^- A \rightarrow A 3\pi$
- 1273 ± 50    2 AARON    81    RVUE
- 1342 ± 20    BONESINI    81    OMEG    12  $\pi^- p \rightarrow p 3\pi$
- ~ 1400    DAUM    81B    SPEC    63,94  $\pi^- p$

- 1 From analysis of L3 data at 183-209 GeV.
- 2 Uses multichannel Aitchison-Bowler model (BOWLER 75). Uses data from DAUM 80 and DANKOWYCH 81.

$\pi(1300)$  WIDTH

VALUE (MeV)	EVTS	DOCUMENT ID	TECN	COMMENT
<b>200 to 600 OUR ESTIMATE</b>				

- • • We do not use the following data for averages, fits, limits, etc. • • •
- 260 ± 20 ± 30    18k    3 SCHEGELSKY    06    RVUE     $\gamma \gamma \rightarrow \pi^+ \pi^- \pi^0$
- 470 ± 120    90k    SALVINI    04    OBLX     $\bar{p} p \rightarrow 2\pi^+ 2\pi^-$
- 449 ± 39 ± 47    CHUNG    02    B852    18.3  $\pi^- p \rightarrow \pi^+ \pi^- \pi^- p$
- 268 ± 50    ABELE    01    CBAR    0.0  $\bar{p} d \rightarrow \pi^- 4\pi^0 p$
- 218 ± 100    BERTIN    97D    OBLX    0.05  $\bar{p} p \rightarrow 2\pi^+ 2\pi^-$
- ~ 340    ABELE    96    CBAR    0.0  $\bar{p} p \rightarrow 5\pi^0$

## Meson Particle Listings

 $\pi(1300)$ ,  $a_2(1320)$ 

440 ± 80	ZIELINSKI	84	SPEC	200 $\pi^+ Z \rightarrow Z 3\pi$
360 ± 120	BELLINI	82	SPEC	40 $\pi^- A \rightarrow A 3\pi$
580 ± 100	<sup>4</sup> AARON	81	RVUE	
220 ± 70	BONESINI	81	OMEG	12 $\pi^- p \rightarrow p 3\pi$
~ 600	DAUM	81B	SPEC	63,94 $\pi^- p$

<sup>3</sup>From analysis of L3 data at 183–209 GeV.<sup>4</sup>Uses multichannel Aitchison-Bowler model (BOWLER 75). Uses data from DAUM 80 and DANKOWYCH 81. $\pi(1300)$  DECAY MODES

Mode	Fraction ( $\Gamma_i/\Gamma$ )
$\Gamma_1$ $\rho\pi$	seen
$\Gamma_2$ $\pi(\pi\pi)S$ -wave	seen
$\Gamma_3$ $\gamma\gamma$	

 $\pi(1300)$   $\Gamma(i)\Gamma(\gamma\gamma)/\Gamma(\text{total})$ 

VALUE (keV)	CL%	DOCUMENT ID	TECN	COMMENT	$\Gamma_1\Gamma_3/\Gamma$
<0.085	90	ACCIARRI 97T	L3	$e^+e^- \rightarrow e^+e^-\pi^+\pi^-\pi^0$	
<0.8	95	<sup>5</sup> SCHEGELSKY 06	RVUE	$\gamma\gamma \rightarrow \pi^+\pi^-\pi^0$	
<0.54	90	ALBRECHT 97B	ARG	$e^+e^- \rightarrow e^+e^-\pi^+\pi^-\pi^0$	

<sup>5</sup>From analysis of L3 data at 183–209 GeV. $\pi(1300)$  BRANCHING RATIOS

$\Gamma(\pi(\pi\pi)S\text{-wave})/\Gamma(\rho\pi)$	CL%	EVTS	DOCUMENT ID	TECN	COMMENT	$\Gamma_2/\Gamma_1$
2.2 ± 0.4		90k	SALVINI 04	OBLX	$\bar{p}p \rightarrow 2\pi^+2\pi^-$	
seen			CHUNG 02	B852	18.3 $\pi^- p \rightarrow \pi^+2\pi^-\pi^0$	
<0.15	90		ABELE 01	CBAR	0.0 $\bar{p}d \rightarrow \pi^-4\pi^0p$	
2.12			<sup>6</sup> AARON 81	RVUE		

<sup>6</sup>Uses multichannel Aitchison-Bowler model (BOWLER 75). Uses data from DAUM 80 and DANKOWYCH 81. $\pi(1300)$  REFERENCES

SCHEGELSKY 06	EPJ A27 199	V.A. Schegelsky et al.	(OBELIX Collab.)
SALVINI 04	EPJ C35 21	P. Salvini et al.	(BNL E852 Collab.)
CHUNG 02	PR D65 072001	S.U. Chung et al.	(BNL E852 Collab.)
ABELE 01	EPJ C19 667	A. Abele et al.	(Crystal Barrel Collab.)
ACCIARRI 97T	PL B413 147	M. Acciari et al.	(L3 Collab.)
ALBRECHT 97B	ZPHY C74 469	H. Albrecht et al.	(ARGUS Collab.)
BERTINI 97D	PL B414 220	A. Bertini et al.	(OBELIX Collab.)
ABELE 96	PL B380 453	A. Abele et al.	(Crystal Barrel Collab.)
ZIELINSKI 84	PR D30 1855	M. Zielinski et al.	(ROCH, MINN, FNAL)
BELLINI 82	PRL 48 1697	G. Bellini et al.	(MILA, BGN, JINR)
AARON 81	PR D24 1207	R.A. Aaron, R.S. Longacre	(NEAS, BNL)
BONESINI 81	PL 103B 75	M. Bonesini et al.	(MILA, BGN, JINR)
DANKOWYCH... 81	PRL 46 580	J.A. Dankowycz et al.	(TNT0, BNL, CARL+)
DAUM 81B	NP B182 269	C. Daum et al.	(AMST, CERN, CRAC, MPIM+)
DAUM 80	PL 89B 281	C. Daum et al.	(AMST, CERN, CRAC, MPIM+)
BOWLER 75	NP B97 227	M.G. Bowler et al.	(OXFTP, DARE)

 $a_2(1320)$ 

$$I^G(J^{PC}) = 1^-(2^{++})$$

 $a_2(1320)$  MASS

VALUE (MeV)	DOCUMENT ID
<b>1318.3 ± 0.5 ± 0.6 OUR AVERAGE</b>	Includes data from the 4 datablocks that follow this one. Error includes scale factor of 1.2.

3 $\pi$  MODE

VALUE (MeV)	EVTS	DOCUMENT ID	TECN	CHG	COMMENT
The data in this block is included in the average printed for a previous datablock.					

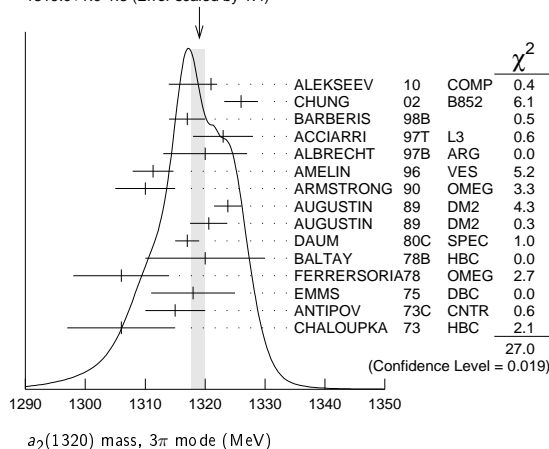
**1319.0 ± 1.0 ± 1.3 OUR AVERAGE** Error includes scale factor of 1.4. See the ideogram below.

1321 ± 1 ± 0/-7	420k	ALEKSEEV 10	COMP	190 $\pi^- Pb \rightarrow \pi^-\pi^+\pi^+ Pb'$
1326 ± 2 ± 2		CHUNG 02	B852	18.3 $\pi^- p \rightarrow \pi^+\pi^-\pi^- p$
1317 ± 3		BARBERIS 98B		450 $pp \rightarrow \rho f \pi^+\pi^-\pi^0 p_S$
1323 ± 4 ± 3		ACCIARRI 97T	L3	$e^+e^- \rightarrow e^+\pi^-\pi^+\pi^-\pi^0$
1320 ± 7		ALBRECHT 97B	ARG	$e^+e^- \rightarrow e^+\pi^-\pi^+\pi^-\pi^0$
1311.3 ± 1.6 ± 3.0	72.4k	AMELIN 96	VES	36 $\pi^- p \rightarrow \pi^+\pi^-\pi^0 n$
1310 ± 5		ARMSTRONG 90	OMEG	300.0 $pp \rightarrow \rho\rho\pi^+\pi^-\pi^0$

1323.8 ± 2.3	4022	AUGUSTIN 89	DM2	±	$J/\psi \rightarrow \rho^\pm a_2^\mp$
1320.6 ± 3.1	3562	AUGUSTIN 89	DM2	0	$J/\psi \rightarrow \rho^0 a_2^0$
1317 ± 2	25k	<sup>1</sup> DAUM 80C	SPEC	-	63,94 $\pi^- p \rightarrow 3\pi\rho$
1320 ± 10	1097	<sup>1</sup> BALTAY 78B	HBC	+0	15 $\pi^+ p \rightarrow p 4\pi$
1306 ± 8		FERRERSORIA 78	OMEG	-	9 $\pi^- p \rightarrow p 3\pi$
1318 ± 7	1.6k	<sup>1</sup> EMMS 75	DBC	0	4 $\pi^+ n \rightarrow p(3\pi)^0$
1315 ± 5		<sup>1</sup> ANTIPOV 73c	CNTR	-	25,40 $\pi^- p \rightarrow \rho\eta\pi^-$

1306 ± 9 1580 CHALOUKPA 73 HBC - 3.9  $\pi^- p$   
 ●●● We do not use the following data for averages, fits, limits, etc. ●●●

1300 ± 2 ± 4	18k	<sup>2</sup> SCHEGELSKY 06	RVUE	0	$\gamma\gamma \rightarrow \pi^+\pi^-\pi^0$
1305 ± 14		CONDO 93	SHF		$\gamma p \rightarrow \eta\pi^+\pi^-\pi^-$
1310 ± 2		<sup>1</sup> EVANGELIS... 81	OMEG	-	12 $\pi^- p \rightarrow 3\pi\rho$
1343 ± 11	490	BALTAY 78B	HBC	0	15 $\pi^+ p \rightarrow \Delta 3\pi$
1309 ± 5	5k	BINNIE 71	MMS	-	$\pi^- p$ near $a_2$ threshold
1299 ± 6	28k	BOWEN 71	MMS	-	5 $\pi^- p$
1300 ± 6	24k	BOWEN 71	MMS	+	5 $\pi^+ p$
1309 ± 4	17k	BOWEN 71	MMS	-	7 $\pi^- p$
1306 ± 4	941	ALSTON... 70	HBC	+	7.0 $\pi^+ p \rightarrow 3\pi\rho$

<sup>1</sup>From a fit to  $J^P = 2^+$   $\rho\pi$  partial wave.<sup>2</sup>From analysis of L3 data at 183–209 GeV.WEIGHTED AVERAGE  
1319.0 ± 1.0 - 1.3 (Error scaled by 1.4) $K\bar{K}$  MODE

VALUE (MeV)	EVTS	DOCUMENT ID	TECN	CHG	COMMENT
The data in this block is included in the average printed for a previous datablock.					

## 1318.1 ± 0.7 OUR AVERAGE

1319 ± 5	4700	<sup>3,4</sup> CLELAND 82B	SPEC	+	50 $\pi^+ p \rightarrow K_S^0 K^+ p$
1324 ± 6	5200	<sup>3,4</sup> CLELAND 82B	SPEC	-	50 $\pi^- p \rightarrow K_S^0 K^- p$
1320 ± 2	4000	CHABAUD 80	SPEC	-	17 $\pi^- A \rightarrow K_S^0 K^- A$
1312 ± 4	11000	CHABAUD 78	SPEC	-	9.8 $\pi^- p \rightarrow K^- K_S^0 p$
1316 ± 2	4730	CHABAUD 78	SPEC	-	18.8 $\pi^- p \rightarrow K^- K_S^0 p$
1318 ± 1		<sup>3,5</sup> MARTIN 78D	SPEC	-	10 $\pi^- p \rightarrow K_S^0 K^- p$
1320 ± 2	2724	MARGULIE 76	SPEC	-	23 $\pi^- p \rightarrow K^- K_S^0 p$
1313 ± 4	730	FOLEY 72	CNTR	-	20.3 $\pi^- p \rightarrow K^- K_S^0 p$
1319 ± 3	1500	<sup>5</sup> GRAY 71	ASPK	-	17.2 $\pi^- p \rightarrow K^- K_S^0 p$

●●● We do not use the following data for averages, fits, limits, etc. ●●●

1304 ± 10	870	<sup>6</sup> SCHEGELSKY 06A	RVUE	0	$\gamma\gamma \rightarrow K_S^0 K_S^0$
1330 ± 11	1000	<sup>3,4</sup> CLELAND 82B	SPEC	+	30 $\pi^+ p \rightarrow K_S^0 K^+ p$
1324 ± 5	350	HYAMS 78	ASPK	+	12.7 $\pi^+ p \rightarrow K^+ K_S^0 p$

<sup>3</sup>From a fit to  $J^P = 2^+$  partial wave.<sup>4</sup>Number of events evaluated by us.<sup>5</sup>Systematic error in mass scale subtracted.<sup>6</sup>From analysis of L3 data at 91 and 183–209 GeV. $\eta\pi$  MODE

VALUE (MeV)	EVTS	DOCUMENT ID	TECN	CHG	COMMENT
The data in this block is included in the average printed for a previous datablock.					

## 1317.7 ± 1.4 OUR AVERAGE

1308 ± 9		BARBERIS 00H			450 $pp \rightarrow p f \eta \pi^0 p_S$
1316 ± 9		BARBERIS 00H			450 $pp \rightarrow \Delta_f^+ \eta \pi^- p_S$
1317 ± 1 ± 2		THOMPSON 97	MPS		18 $\pi^- p \rightarrow \eta \pi^- p$
1315 ± 5 ± 2		<sup>7</sup> AMSLER 94D	CBAR		0.0 $\bar{p}p \rightarrow \pi^0 \pi^0 \eta$
1325.1 ± 5.1		AOYAGI 93	BKEI		$\pi^- p \rightarrow \eta \pi^- p$
1317.7 ± 1.4 ± 2.0		BELADIDZE 93	VES		37 $\pi^- N \rightarrow \eta \pi^- N$
1323 ± 8	1000	<sup>8</sup> KEY 73	OSPK	-	6 $\pi^- p \rightarrow p \pi^- \eta$

See key on page 457

## Meson Particle Listings

 $a_2(1320)$ 

••• We do not use the following data for averages, fits, limits, etc. •••

1309 ± 4		ANISOVICH	09	RVUE		$\bar{p}p, \pi N$
1324 ± 5		ARMSTRONG	93c	E760	0	$\bar{p}p \rightarrow \pi^0 \eta \eta \rightarrow 6\gamma$
1336.2 ± 1.7	2561	DELFOSSÉ	81	SPEC	+	$\pi^\pm p \rightarrow \rho \pi^\pm \eta$
1330.7 ± 2.4	1653	DELFOSSÉ	81	SPEC	-	$\pi^\pm p \rightarrow \rho \pi^\pm \eta$
1324 ± 8	6200	8,9 CONFORTO	73	OSPK	-	$6 \pi^- p \rightarrow \rho \text{MM}^-$

<sup>7</sup> The systematic error of 2 MeV corresponds to the spread of solutions.<sup>8</sup> Error includes 5 MeV systematic mass-scale error.<sup>9</sup> Missing mass with enriched MMS =  $\eta \pi^-$ ,  $\eta = 2\gamma$ . $\eta/\pi$  MODE

VALUE (MeV)	DOCUMENT ID	TECN	CHG	COMMENT
The data in this block is included in the average printed for a previous datablock.				

**1322 ± 7 OUR AVERAGE**

1318 ± 8 $^{+3}_{-5}$	IVANOV	01	B852	$18 \pi^- p \rightarrow \eta' \pi^- p$
1327.0 ± 10.7	BELADIDZE	93	VES	$37 \pi^- N \rightarrow \eta' \pi^- N$

 $a_2(1320)$  WIDTH**3π MODE**

VALUE (MeV)	EVTs	DOCUMENT ID	TECN	CHG	COMMENT
<b>105.0 <math>^{+1.6}_{-1.9}</math> OUR AVERAGE</b>					
110 ± 2 $^{+2}_{-15}$	420k	ALEKSEEV	10	COMP	$190 \pi^- P b \rightarrow \pi^- \pi^- \pi^+ P b'$
108 ± 3 ± 15		CHUNG	02	B852	$18.3 \pi^- p \rightarrow \pi^\pm \pi^- \pi^- p$
120 ± 10		BARBERIS	98B		$450 \rho p \rightarrow \rho_f \pi^+ \pi^- \pi^0 \rho_S$
105 ± 10 ± 11		ACCIARRI	97T	L3	$e^+ e^- \rightarrow e^+ e^- \pi^+ \pi^- \pi^0$
120 ± 10		ALBRECHT	97B	ARG	$e^+ e^- \rightarrow e^+ e^- \pi^+ \pi^- \pi^0$
103.0 ± 6.0 ± 3.3	72.4k	AMELIN	96	VES	$36 \pi^- p \rightarrow \pi^\pm \pi^- \pi^0 n$
120 ± 10		ARMSTRONG	90	OMEG 0	$300.0 \rho p \rightarrow \rho p \pi^+ \pi^- \pi^0$
107.0 ± 9.7	4022	AUGUSTIN	89	DM2 ±	$J/\psi \rightarrow \rho^\pm a_2^\mp$
118.5 ± 12.5	3562	AUGUSTIN	89	DM2 0	$J/\psi \rightarrow \rho^0 a_2^0$
97 ± 5		10 EVANGELIS...	81	OMEG -	$12 \pi^- p \rightarrow 3\pi p$
96 ± 9	25k	10 DAUM	80c	SPEC -	$63,94 \pi^- p \rightarrow 3\pi p$
110 ± 15	1097	10 BALTAY	78B	HBC +0	$15 \pi^+ p \rightarrow p 4\pi$
112 ± 18	1.6k	10 EMMS	75	DBC 0	$4 \pi^+ n \rightarrow \rho(3\pi)^0$
122 ± 14	1.2k	10,11 WAGNER	75	HBC 0	$7 \pi^+ p \rightarrow \Delta^{++}(3\pi)^0$
115 ± 15		10 ANTIPOV	73c	CNTR -	$25,40 \pi^- p \rightarrow \rho \eta \pi^-$
99 ± 15	1580	CHALOUKKA	73	HBC -	$3,9 \pi^- p$
105 ± 5	28k	BOWEN	71	MMS -	$5 \pi^- p$
99 ± 5	24k	BOWEN	71	MMS +	$5 \pi^+ p$
103 ± 5	17k	BOWEN	71	MMS -	$7 \pi^- p$

••• We do not use the following data for averages, fits, limits, etc. •••

117 ± 6 ± 20	18k	12 SCHEGELSKY	06	RVUE 0	$\gamma \gamma \rightarrow \pi^+ \pi^- \pi^0$
120 ± 40		CONDO	93	SHF	$\gamma p \rightarrow \eta \pi^+ \pi^+ \pi^-$
115 ± 14	490	BALTAY	78B	HBC 0	$15 \pi^+ p \rightarrow \Delta 3\pi$
72 ± 16	5k	BINNIE	71	MMS -	$\pi^- p$ near $a_2$ thresh- old
79 ± 12	941	ALSTON...	70	HBC +	$7,0 \pi^+ p \rightarrow 3\pi p$

<sup>10</sup> From a fit to  $J^P = 2^+ \rho \pi$  partial wave.<sup>11</sup> Width errors enlarged by us to  $4\Gamma/\sqrt{N}$ ; see the note with the  $K^*(892)$  mass.<sup>12</sup> From analysis of L3 data at 183–209 GeV. $K\bar{K}$  AND  $\eta\pi$  MODES

VALUE (MeV)	DOCUMENT ID
<b>107 ± 5 OUR ESTIMATE</b>	
<b>110.4 ± 1.7 OUR AVERAGE</b> Includes data from the 2 datablocks that follow this one.	

 $K\bar{K}$  MODE

VALUE (MeV)	EVTs	DOCUMENT ID	TECN	CHG	COMMENT
The data in this block is included in the average printed for a previous datablock.					

**109.8 ± 2.4 OUR AVERAGE**

112 ± 20	4700	13,14 CLELAND	82B	SPEC +	$50 \pi^+ p \rightarrow K_S^0 K^+ p$
120 ± 25	5200	13,14 CLELAND	82B	SPEC -	$50 \pi^- p \rightarrow K_S^0 K^- p$
106 ± 4	4000	CHABAUD	80	SPEC -	$17 \pi^- A \rightarrow K_S^0 K^- A$
126 ± 11	11000	CHABAUD	78	SPEC -	$9,8 \pi^- p \rightarrow K^- K_S^0 p$
101 ± 8	4730	CHABAUD	78	SPEC -	$18,8 \pi^- p \rightarrow K^- K_S^0 p$
113 ± 4		13,15 MARTIN	78D	SPEC -	$10 \pi^- p \rightarrow K_S^0 K^- p$
105 ± 8	2724	15 MARGULIE	76	SPEC -	$23 \pi^- p \rightarrow K^- K_S^0 p$
113 ± 19	730	FOLEY	72	CNTR -	$20,3 \pi^- p \rightarrow K^- K_S^0 p$
123 ± 13	1500	15 GRAYER	71	ASPK -	$17,2 \pi^- p \rightarrow K^- K_S^0 p$

••• We do not use the following data for averages, fits, limits, etc. •••

120 ± 15	870	16 SCHEGELSKY	06A	RVUE 0	$\gamma \gamma \rightarrow K_S^0 K_S^0$
121 ± 5.1	1000	13,14 CLELAND	82B	SPEC +	$30 \pi^+ p \rightarrow K_S^0 K^+ p$
110 ± 18	350	HYAMS	78	ASPK +	$12,7 \pi^+ p \rightarrow K^+ K_S^0 p$

<sup>13</sup> From a fit to  $J^P = 2^+$  partial wave.<sup>14</sup> Number of events evaluated by us.<sup>15</sup> Width errors enlarged by us to  $4\Gamma/\sqrt{N}$ ; see the note with the  $K^*(892)$  mass.<sup>16</sup> From analysis of L3 data at 91 and 183–209 GeV. $\eta\pi$  MODE

VALUE (MeV)	EVTs	DOCUMENT ID	TECN	CHG	COMMENT
The data in this block is included in the average printed for a previous datablock.					

**111.1 ± 2.4 OUR AVERAGE**

115 ± 20		BARBERIS	00H		$450 \rho p \rightarrow \rho_f \eta \pi^0 \rho_S$
112 ± 14		BARBERIS	00H		$450 \rho p \rightarrow \Delta_f^+ \eta \pi^- \rho_S$
112 ± 3 ± 2		17 AMSLER	94D	CBAR	$0,0 \bar{p} p \rightarrow \pi^0 \pi^0 \eta$
103 ± 6 ± 3		BELADIDZE	93	VES	$37 \pi^- N \rightarrow \eta \pi^- N$
112.2 ± 5.7	2561	DELFOSSÉ	81	SPEC +	$\pi^\pm p \rightarrow \rho \pi^\pm \eta$
116.6 ± 7.7	1653	DELFOSSÉ	81	SPEC -	$\pi^\pm p \rightarrow \rho \pi^\pm \eta$
108 ± 9	1000	KEY	73	OSPK -	$6 \pi^- p \rightarrow \rho \pi^- \eta$

••• We do not use the following data for averages, fits, limits, etc. •••

110 ± 4		ANISOVICH	09	RVUE	$\bar{p}p, \pi N$
127 ± 2 ± 2		18 THOMPSON	97	MPs	$18 \pi^- p \rightarrow \eta \pi^- p$
118 ± 10		ARMSTRONG	93c	E760	$0 \bar{p} p \rightarrow \pi^0 \eta \eta \rightarrow 6\gamma$
104 ± 9	6200	19 CONFORTO	73	OSPK -	$6 \pi^- p \rightarrow \rho \text{MM}^-$

<sup>17</sup> The systematic error of 2 MeV corresponds to the spread of solutions.<sup>18</sup> Resolution is not unfolded.<sup>19</sup> Missing mass with enriched MMS =  $\eta \pi^-$ ,  $\eta = 2\gamma$ . $\eta/\pi$  MODE

VALUE (MeV)	DOCUMENT ID	TECN	CHG	COMMENT
<b>119 ± 25 OUR AVERAGE</b>				
140 ± 35 ± 20	IVANOV	01	B852	$18 \pi^- p \rightarrow \eta' \pi^- p$
106 ± 32	BELADIDZE	93	VES	$37 \pi^- N \rightarrow \eta' \pi^- N$

 $a_2(1320)$  DECAY MODES

Mode	Fraction ( $\Gamma_i/\Gamma$ )	Scale factor/ Confidence level
$\Gamma_1$ $3\pi$	(70.1 ± 2.7) %	S=1.2
$\Gamma_2$ $\rho(770)\pi$		
$\Gamma_3$ $f_2(1270)\pi$		
$\Gamma_4$ $\rho(1450)\pi$		
$\Gamma_5$ $\eta\pi$	(14.5 ± 1.2) %	
$\Gamma_6$ $\omega\pi\pi$	(10.6 ± 3.2) %	S=1.3
$\Gamma_7$ $K\bar{K}$	(4.9 ± 0.8) %	
$\Gamma_8$ $\eta'(958)\pi$	(5.3 ± 0.9) × 10 <sup>-3</sup>	
$\Gamma_9$ $\pi^\pm \gamma$	(2.68 ± 0.31) × 10 <sup>-3</sup>	
$\Gamma_{10}$ $\gamma\gamma$	(9.4 ± 0.7) × 10 <sup>-6</sup>	
$\Gamma_{11}$ $e^+ e^-$	< 5 × 10 <sup>-9</sup>	CL=90%

## CONSTRAINED FIT INFORMATION

An overall fit to 5 branching ratios uses 18 measurements and one constraint to determine 4 parameters. The overall fit has a  $\chi^2 = 9.3$  for 15 degrees of freedom.

The following *off-diagonal* array elements are the correlation coefficients  $\langle \delta x_i \delta x_j \rangle / (\delta x_i \delta x_j)$ , in percent, from the fit to the branching fractions,  $x_i \equiv \Gamma_i/\Gamma_{\text{total}}$ . The fit constrains the  $x_i$  whose labels appear in this array to sum to one.

$x_5$	10		
$x_6$	-89	-46	
$x_7$	-1	-2	-24
	$x_1$	$x_5$	$x_6$

 $a_2(1320)$  PARTIAL WIDTHS

VALUE (MeV)	EVTs	DOCUMENT ID	TECN	CHG	COMMENT
<b>119 ± 25 OUR AVERAGE</b>					
18.5 ± 3.0	870	20 SCHEGELSKY	06A	RVUE 0	$\gamma \gamma \rightarrow K_S^0 K_S^0$

••• We do not use the following data for averages, fits, limits, etc. •••

18.5 ± 3.0	870	20 SCHEGELSKY	06A	RVUE 0	$\gamma \gamma \rightarrow K_S^0 K_S^0$
------------	-----	---------------	-----	--------	---

<sup>20</sup> From analysis of L3 data at 91 and 183–209 GeV, using  $\Gamma(a_2(1320) \rightarrow \gamma\gamma) = 0.91$  keV and SU(3) relations.

# Meson Particle Listings

## $a_2(1320)$

### $\Gamma(K\bar{K})$ $\Gamma_7$

VALUE (MeV)	EVTS	DOCUMENT ID	TECN	CHG	COMMENT
$7.0^{+2.0}_{-1.5}$	870	21 SCHEGELSKY 06A	RVUE	0	$\gamma\gamma \rightarrow K_S^0 K_S^0$
••• We do not use the following data for averages, fits, limits, etc. •••					
<sup>21</sup> From analysis of L3 data at 91 and 183–209 GeV, using $\Gamma(a_2(1320) \rightarrow \gamma\gamma) = 0.91$ keV and SU(3) relations.					

### $\Gamma(\pi^+\gamma)$ $\Gamma_9$

VALUE (keV)	EVTS	DOCUMENT ID	TECN	CHG	COMMENT
<b><math>287 \pm 30</math> OUR AVERAGE</b>					
$284 \pm 25 \pm 25$	7100	MOLCHANOV 01	SELX		$600 \pi^- A \rightarrow \pi^+ \pi^- \pi^- A$
$295 \pm 60$		CIHANGIR 82	SPEC	+	$200 \pi^+ A$
••• We do not use the following data for averages, fits, limits, etc. •••					
$461 \pm 110$		<sup>22</sup> MAY 77	SPEC	±	$9.7 \gamma A$
<sup>22</sup> Assuming one-pion exchange.					

### $\Gamma(\gamma\gamma)$ $\Gamma_{10}$

VALUE (keV)	EVTS	DOCUMENT ID	TECN	CHG	COMMENT
<b><math>1.00 \pm 0.06</math> OUR AVERAGE</b>					
$0.98 \pm 0.05 \pm 0.09$		ACCIARRI 97T	L3		$e^+e^- \rightarrow e^+e^- \pi^+ \pi^- \pi^0$
$0.96 \pm 0.03 \pm 0.13$		ALBRECHT 97B	ARG		$e^+e^- \rightarrow e^+e^- \pi^+ \pi^- \pi^0$
$1.26 \pm 0.26 \pm 0.18$	36	BARU 90	MD1		$e^+e^- \rightarrow e^+e^- \pi^+ \pi^- \pi^0$
$1.00 \pm 0.07 \pm 0.15$	415	BEHREND 90C	CELL	0	$e^+e^- \rightarrow e^+e^- \pi^+ \pi^- \pi^0$
$1.03 \pm 0.13 \pm 0.21$		BUTLER 90	MRK2		$e^+e^- \rightarrow e^+e^- \pi^+ \pi^- \pi^0$
$1.01 \pm 0.14 \pm 0.22$	85	OEST 90	JADE		$e^+e^- \rightarrow e^+e^- \pi^0 \eta$
$0.90 \pm 0.27 \pm 0.15$	56	<sup>23</sup> ALTHOFF 86	TASS	0	$e^+e^- \rightarrow e^+e^- 3\pi$
$1.14 \pm 0.20 \pm 0.26$		<sup>24</sup> ANTREASIAN 86	CBAL	0	$e^+e^- \rightarrow e^+e^- \pi^0 \eta$
$1.06 \pm 0.18 \pm 0.19$		BERGER 84C	PLUT	0	$e^+e^- \rightarrow e^+e^- 3\pi$
••• We do not use the following data for averages, fits, limits, etc. •••					
$0.81 \pm 0.19 \pm 0.42$	35	<sup>23</sup> BEHREND 83B	CELL	0	$e^+e^- \rightarrow e^+e^- 3\pi$
$0.77 \pm 0.18 \pm 0.27$	22	<sup>24</sup> EDWARDS 82F	CBAL	0	$e^+e^- \rightarrow e^+e^- \pi^0 \eta$
<sup>23</sup> From $\rho\pi$ decay mode. <sup>24</sup> From $\eta\pi^0$ decay mode.					

### $\Gamma(e^+e^-)$ $\Gamma_{11}$

VALUE (eV)	CL%	DOCUMENT ID	TECN	COMMENT
<b>&lt; 0.56</b>	90	ACHASOV 00K	SND	$e^+e^- \rightarrow \pi^0 \pi^0$
••• We do not use the following data for averages, fits, limits, etc. •••				
<25	90	VOROBYEV 88	ND	$e^+e^- \rightarrow \pi^0 \eta$

### $a_2(1320) \Gamma(i)\Gamma(\gamma\gamma)/\Gamma(\text{total})$

### $\Gamma(3\pi) \times \Gamma(\gamma\gamma)/\Gamma_{\text{total}}$ $\Gamma_1 \Gamma_{10}/\Gamma$

VALUE (keV)	EVTS	DOCUMENT ID	TECN	COMMENT
••• We do not use the following data for averages, fits, limits, etc. •••				
$0.65 \pm 0.02 \pm 0.02$	18k	<sup>25</sup> SCHEGELSKY 06	RVUE	$\gamma\gamma \rightarrow \pi^+ \pi^- \pi^0$
<sup>25</sup> From analysis of L3 data at 183–209 GeV.				

### $\Gamma(\eta\pi) \times \Gamma(\gamma\gamma)/\Gamma_{\text{total}}$ $\Gamma_5 \Gamma_{10}/\Gamma$

VALUE (keV)	DOCUMENT ID	TECN	COMMENT
••• We do not use the following data for averages, fits, limits, etc. •••			
$0.145^{+0.097}_{-0.034}$	<sup>26</sup> UEHARA 09A	BELL	$e^+e^- \rightarrow e^+e^- \eta \pi^0$
<sup>26</sup> From the $D_2$ -wave. The fraction of the $D_0$ -wave is $3.4^{+2.3}_{-1.1}\%$ .			

### $\Gamma(K\bar{K}) \times \Gamma(\gamma\gamma)/\Gamma_{\text{total}}$ $\Gamma_7 \Gamma_{10}/\Gamma$

VALUE (keV)	DOCUMENT ID	TECN	COMMENT
••• We do not use the following data for averages, fits, limits, etc. •••			
<b><math>0.126 \pm 0.007 \pm 0.028</math></b>	<sup>27</sup> ALBRECHT 90G	ARG	$e^+e^- \rightarrow e^+e^- K^+ K^-$
••• We do not use the following data for averages, fits, limits, etc. •••			
$0.081 \pm 0.006 \pm 0.027$	<sup>28</sup> ALBRECHT 90G	ARG	$e^+e^- \rightarrow e^+e^- K^+ K^-$
<sup>27</sup> Using an incoherent background. <sup>28</sup> Using a coherent background.			

### $a_2(1320)$ BRANCHING RATIOS

### $[\Gamma(\rho(1270)\pi) + \Gamma(\rho(1450)\pi)]/\Gamma(\rho(770)\pi)$ $(\Gamma_3 + \Gamma_4)/\Gamma_2$

VALUE	CL%	DOCUMENT ID	TECN	CHG	COMMENT
<b>&lt;0.12</b>	90	ABRAMOVI... 70B	HBC	-	$3.93 \pi^- p$

### $\Gamma(\eta\pi)/\Gamma(3\pi)$ $\Gamma_6/\Gamma_1$

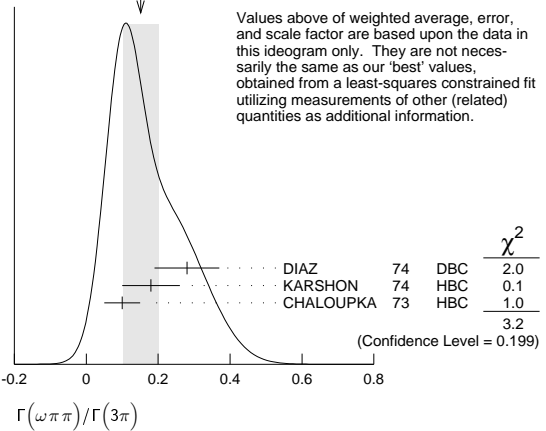
VALUE	EVTS	DOCUMENT ID	TECN	CHG	COMMENT
<b><math>0.207 \pm 0.018</math> OUR FIT</b> <b><math>0.213 \pm 0.020</math> OUR AVERAGE</b>					
$0.18 \pm 0.05$		FORINO 76	HBC		$11 \pi^- p$
$0.22 \pm 0.05$	52	ANTIPOV 73	CNTR	-	$40 \pi^- p$
$0.211 \pm 0.044$	149	CHALOUPKA 73	HBC	-	$3.9 \pi^- p$
$0.246 \pm 0.042$	167	ALSTON-... 71	HBC	+	$7.0 \pi^+ p$
$0.25 \pm 0.09$	15	BOECKMANN 70	HBC	+	$5.0 \pi^+ p$
$0.23 \pm 0.08$	22	ASCOLI 68	HBC	-	$5 \pi^- p$
$0.12 \pm 0.08$		CHUNG 68	HBC	-	$3.2 \pi^- p$
$0.22 \pm 0.09$		CONTE 67	HBC	-	$11.0 \pi^- p$

### $\Gamma(\omega\pi\pi)/\Gamma(3\pi)$ $\Gamma_6/\Gamma_1$

VALUE	EVTS	DOCUMENT ID	TECN	CHG	COMMENT
<b><math>0.15 \pm 0.05</math> OUR FIT</b> Error includes scale factor of 1.3. <b><math>0.15 \pm 0.05</math> OUR AVERAGE</b> Error includes scale factor of 1.3. See the ideogram below.					
$0.28 \pm 0.09$	60	DIAZ 74	DBC	0	$6 \pi^+ n$
$0.18 \pm 0.08$		<sup>29</sup> KARSHON 74	HBC		Avg. of above two
$0.10 \pm 0.05$	279	CHALOUPKA 73	HBC	-	$3.9 \pi^- p$
••• We do not use the following data for averages, fits, limits, etc. •••					
$0.29 \pm 0.08$	140	<sup>29</sup> KARSHON 74	HBC	0	$4.9 \pi^+ p$
$0.10 \pm 0.04$	60	<sup>29</sup> KARSHON 74	HBC	+	$4.9 \pi^+ p$
$0.19 \pm 0.08$		DEFOIX 73	HBC	0	$0.7 \bar{p} p$

<sup>29</sup> KARSHON 74 suggest an additional  $l = 0$  state strongly coupled to  $\omega\pi\pi$  which could explain discrepancies in branching ratios and masses. We use a central value and a systematic spread.

WEIGHTED AVERAGE  
 $0.15 \pm 0.05$  (Error scaled by 1.3)



### $\Gamma(K\bar{K})/\Gamma(3\pi)$ $\Gamma_7/\Gamma_1$

VALUE	EVTS	DOCUMENT ID	TECN	CHG	COMMENT
<b><math>0.070 \pm 0.012</math> OUR FIT</b> <b><math>0.078 \pm 0.017</math></b>					
••• We do not use the following data for averages, fits, limits, etc. •••					
$0.011 \pm 0.003$	30	BERTIN 98B	OBLX		$0.0 \bar{p} p \rightarrow K^\pm K_S \pi^\mp$
$0.056 \pm 0.014$	50	<sup>31</sup> CHALOUPKA 73	HBC	-	$3.9 \pi^- p$
$0.097 \pm 0.018$	113	<sup>31</sup> ALSTON-... 71	HBC	+	$7.0 \pi^+ p$
$0.06 \pm 0.03$		<sup>31</sup> ABRAMOVI... 70B	HBC	-	$3.93 \pi^- p$
$0.054 \pm 0.022$		<sup>31</sup> CHUNG 68	HBC	-	$3.2 \pi^- p$
<sup>30</sup> Using $4\pi$ data from BERTIN 97D. <sup>31</sup> Included in CHABAUD 78 review.					

### $\Gamma(K\bar{K})/\Gamma(\eta\pi)$ $\Gamma_7/\Gamma_5$

VALUE	DOCUMENT ID	TECN	COMMENT
••• We do not use the following data for averages, fits, limits, etc. •••			
$0.08 \pm 0.02$	<sup>32</sup> BERTIN 98B	OBLX	$0.0 \bar{p} p \rightarrow K^\pm K_S \pi^\mp$
<sup>32</sup> Using $\eta\pi\pi$ data from AMSLER 94D.			

### $\Gamma(\eta\pi)/[\Gamma(3\pi) + \Gamma(\eta\pi) + \Gamma(K\bar{K})]$ $\Gamma_5/(\Gamma_1 + \Gamma_5 + \Gamma_7)$

VALUE	EVTS	DOCUMENT ID	TECN	CHG	COMMENT
<b><math>0.162 \pm 0.012</math> OUR FIT</b> <b><math>0.140 \pm 0.028</math> OUR AVERAGE</b>					
$0.13 \pm 0.04$		ESPIGAT 72	HBC	±	$0.0 \bar{p} p$
$0.15 \pm 0.04$	34	BARNHAM 71	HBC	+	$3.7 \pi^+ p$



$a_2(1320), f_0(1370)$

$\Gamma(K\bar{K})/[\Gamma(3\pi) + \Gamma(\eta\pi) + \Gamma(K\bar{K})]$		$\Gamma_7/(\Gamma_1 + \Gamma_5 + \Gamma_7)$				
VALUE	EVTS	DOCUMENT ID	TECN	CHG	COMMENT	
<b>0.054 ± 0.009 OUR FIT</b>						
<b>0.048 ± 0.012 OUR AVERAGE</b>						
0.05 ± 0.02		TOET 73	HBC	+	5 $\pi^+ \rho$	
0.09 ± 0.04		TOET 73	HBC	0	5 $\pi^+ \rho$	
0.03 ± 0.02	8	DAMERI 72	HBC	-	11 $\pi^- \rho$	
0.06 ± 0.03	17	BARNHAM 71	HBC	+	3.7 $\pi^+ \rho$	
••• We do not use the following data for averages, fits, limits, etc. •••						
0.020 ± 0.004		33 ESPIGAT 72	HBC	±	0.0 $\bar{p} \rho$	
33 Not averaged because of discrepancy between masses from $K\bar{K}$ and $\rho \pi$ modes.						

$\Gamma(\eta'(958)\pi)/\Gamma_{\text{total}}$		$\Gamma_8/\Gamma$				
VALUE	CL%	DOCUMENT ID	TECN	CHG	COMMENT	
••• We do not use the following data for averages, fits, limits, etc. •••						
<0.006	95	ALDE 92B	GAM2		38,100 $\pi^- \rho \rightarrow \eta' \pi^0 n$	
<0.02	97	BARNHAM 71	HBC	+	3.7 $\pi^+ \rho$	
0.004 ± 0.004		BOESEBECK 68	HBC	+	8 $\pi^+ \rho$	

$\Gamma(\eta'(958)\pi)/\Gamma(3\pi)$		$\Gamma_8/\Gamma_1$				
VALUE	CL%	DOCUMENT ID	TECN	CHG	COMMENT	
••• We do not use the following data for averages, fits, limits, etc. •••						
<0.011	90	EISENSTEIN 73	HBC	-	5 $\pi^- \rho$	
<0.04		ALSTON... 71	HBC	+	7.0 $\pi^+ \rho$	
0.04 $\begin{matrix} +0.03 \\ -0.04 \end{matrix}$		BOECKMANN 70	HBC	0	5.0 $\pi^+ \rho$	

$\Gamma(\eta'(958)\pi)/\Gamma(\eta\pi)$		$\Gamma_8/\Gamma_5$				
VALUE	CL%	DOCUMENT ID	TECN	CHG	COMMENT	
<b>0.037 ± 0.006 OUR AVERAGE</b>						
0.032 ± 0.009		ABELE 97C	CBAR		0.0 $\bar{p} \rho \rightarrow \pi^0 \pi^0 \eta'$	
0.047 ± 0.010 ± 0.004		34 BELADIDZE 93	VES		37 $\pi^- N \rightarrow a_2^- N$	
0.034 ± 0.008 ± 0.005		BELADIDZE 92	VES		36 $\pi^- C \rightarrow a_2^- C$	
34 Using $B(\eta' \rightarrow \pi^+ \pi^- \eta) = 0.441$ , $B(\eta \rightarrow \gamma \gamma) = 0.389$ and $B(\eta \rightarrow \pi^+ \pi^- \pi^0) = 0.236$ .						

$\Gamma(\pi^\pm \gamma)/\Gamma_{\text{total}}$		$\Gamma_9/\Gamma$				
VALUE	CL%	DOCUMENT ID	TECN	CHG	COMMENT	
••• We do not use the following data for averages, fits, limits, etc. •••						
0.005 $\begin{matrix} +0.005 \\ -0.003 \end{matrix}$		35 EISENBERG 72	HBC		4,3,5,25,7,5 $\gamma \rho$	
35 Pion-exchange model used in this estimation.						

$\Gamma(e^+ e^-)/\Gamma_{\text{total}}$		$\Gamma_{11}/\Gamma$				
VALUE (units $10^{-3}$ )	CL%	DOCUMENT ID	TECN	CHG	COMMENT	
••• We do not use the following data for averages, fits, limits, etc. •••						
<6	90	ACHASOV 00K	SND		$e^+ e^- \rightarrow \pi^0 \pi^0$	

$a_2(1320)$  REFERENCES

ALEKSEEV 10 PRL 104 241803 M.G. Alekseev et al. (COMPASS Collab.)

ANISOVICH 09 JUMP A24 2481 V.V. Anisovich, A.V. Sarantsev

UEHARA 09A PR D80 032001 S. Uehara et al. (BELLE Collab.)

SCHEGELSKY 06 EPJ A27 199 V.A. Schegelsky et al.

SCHEGELSKY 06A EPJ A27 207 V.A. Schegelsky et al. (BNL E852 Collab.)

CHUNG 02 PR D65 072001 S.I. Chung et al. (BNL E852 Collab.)

IVANOY 01 PRL 86 3977 E.I. Ivanov et al. (FNAL SELEX Collab.)

MOLCHANOV 01 PL B521 171 V.V. Molchanov et al. (FNAL SLEX Collab.)

ACHASOV 00K PL B492 8 M.N. Achasov et al. (Novosibirsk SND Collab.)

BARBERIS 00H PL B488 225 D. Barberis et al. (WA 102 Collab.)

BARBERIS 98B PL B422 399 D. Barberis et al. (WA 102 Collab.)

BERTIN 98B PL B434 180 A. Bertin et al. (OBELIX Collab.)

ABELE 97C PL B404 179 A. Abele et al. (Crystal Barrel Collab.)

ACCIARRI 97T PL B413 147 M. Acciari et al. (L3 Collab.)

ALBRECHT 97B ZPHY C74 469 H. Albrecht et al. (ARGUS Collab.)

THOMPSON 97 PRL 79 1630 D.R. Thompson et al. (BNL E852 Collab.)

AMELIN 96 ZPHY C70 71 G.V. Amelin et al. (SERP, TBL Collab.)

AMSLER 94D PL B333 277 C. Amstutz et al. (Crystal Barrel Collab.)

AOYAGI 93 PL B314 246 H. Aoyagi et al. (BKEI Collab.)

ARMSTRONG 93C PL B307 394 T.A. Armstrong et al. (FNAL, FERR, GENO+) (YES Collab.)

BELADIDZE 93 PL B313 276 G.M. Beladidze et al. (YES Collab.)

CONDO 93 PR D48 3045 G.T. Condo et al. (SLAC Hybrid Collab.)

ALDE 92B ZPHY C54 549 D.M. Alde et al. (SERP, BELG, LANS, LAPP+) (YES Collab.)

BELADIDZE 92 ZPHY C54 235 G.M. Beladidze et al. (YES Collab.)

ALBRECHT 90G ZPHY C48 183 H. Albrecht et al. (ARGUS Collab.)

ARMSTRONG 90 ZPHY C48 213 T.A. Armstrong, M. Benayoun, W. Beusch (WA76 Coll.)

BARU 90 ZPHY C48 581 S.E. Baru et al. (MD-1 Collab.)

BEHREND 90C ZPHY C46 583 H.J. Behrend et al. (CELLO Collab.)

BUTTLER 90 PR D42 1368 F. Butler et al. (Mark II Collab.)

OEST 90 ZPHY C47 343 T. Oest et al. (JADE Collab.)

AUGUSTIN 89 NP B320 1 J.E. Augustin, G. Cosme (DM2 Collab.)

VOROBIEV 88 SJNP 48 273 P.V. Vorobiey et al. (NOVO)

Translated from YAF 48 436.

ALTHOFF 86 ZPHY C31 537 M. Althoff et al. (TASSO Collab.)

ANTREAS-YAN 86 PR D33 1847 D. Antreasyan et al. (Crystal Ball Collab.)

BERGER 84C PL 149B 427 C. Berger et al. (PLUTO Collab.)

BEHREND 83B PL 125B 518 (erratum) H.J. Behrend et al. (CELLO Collab.)

CIRIANGIR 82 PL 117B 123 S. Ciriangir et al. (FNAL, MINN, ROCH) (DURH, GEVA, LAUS+) (CIT, HARV, PRIN+) (GEVA, LAUS)

CLELAND 82B NP B208 228 W.E. Cleland et al. (DURH, GEVA, LAUS+) (CIT, HARV, PRIN+) (GEVA, LAUS)

EDWARDS 82F PL 110B 82 C. Edwards et al. (BARI, BONN, CERN+) (CERN, MPIM, AMST)

DELFOSE 81 NP B183 349 A. Delfosse et al. (CERN, MPIM, AMST)

EVANGELISTA 81 NP B178 197 C. Evangelista et al. (CERN, MPIM, AMST)

CHABAUD 80 NP B175 189 V. Chabaud et al. (CERN, MPIM, AMST)

DAUM 80C PL 89B 276 C. Daum et al. (AMST, CERN, CRAC, MPIM+) JP

BALTAY 78B PR D17 62 C. Baltay et al. (COLU, BING)

CHABAUD 78 NP B145 349 V. Chabaud et al. (CERN, MPIM)

FERRERSORIA 78 PL 74B 287 A. Ferrer Soria et al. (ORSAY, CERN, CDEF+)

HYAMS 78 NP B146 303 B.D. Hyams et al. (CERN, MPIM, ATEN)

MARTIN 78D PL 74B 417 A.D. Martin et al. (DURH, GEVA) JP

MAY 77 PR D16 1983 E.N. May et al. (ROCH, CORN)

FORINO 76 NC 35A 465 A. Forino et al. (BGNA, FIRZ, GENO, MILA+)

MARGULIE 76 PR D14 667 M. Margulies et al. (BNL, CUNY)

EMMS 75 PL 58B 117 M.J. Emms et al. (BIRM, DURH, RHEL) JP

WAGNER 75 PL 58B 201 F. Wagner, M. Tabak, D.M. Chew (LBL JP)

DIAZ 74 PRL 32 260 J. Diaz et al. (CASE, CMU)

KARSHON 74 PRL 32 852 U. Karshon et al. (REHO)

ANTIPOV 73 NP B63 175 Y.M. Antipov et al. (CERN, SERP) JP

ANTIPOV 73C NP B63 153 Y.M. Antipov et al. (CERN, SERP) JP

CHALOUKPA 73 PL 44B 211 V. Chaloupka et al. (CERN)

CONFORTO 73 PL 45B 154 G. Conforto et al. (EFI, FNAL, TINTO+)

DEFOIX 73 PL 43B 141 C. Defoix et al. (CDEF)

EISENSTEIN 73 PR D7 278 L. Eisenstein et al. (ILL)

KEY 73 PRL 30 503 A.W. Key et al. (TINTO, EFI, FNAL, WISC)

TOET 72 NP B83 248 D.Z. Toet et al. (NIM, BONN, DURH, TORI)

DAMERI 72 NC 9A 1 M. Dameri et al. (GENO, MILA, SAQL)

EISENBERG 72 PR D5 15 Y. Eisenberg et al. (REHO, SLAC, TELA)

ESPIGAT 72 NP B36 93 P. Espigat et al. (CERN, CDEF)

FOLEY 72 PR D6 747 K.J. Foley et al. (BNL, CUNY)

ALSTON... 71 PL 34B 156 M. Alston-Garnjost et al. (LRL)

BARNHAM 71 PRL 26 1494 K.W.J. Barnham et al. (LBL)

BINNIE 71 PL 36B 257 D.M. Binnie et al. (LOIC, SHMP)

BOWEN 71 PRL 26 1663 D.R. Bowen et al. (NEAS, STON)

GRAYEY 71 PL 34B 333 G. Grayey et al. (CERN, MPIM)

ABRAMOVI... 70B NP B23 466 M. Abramovitch et al. (CERN) JP

ALSTON... 70 PL 33B 607 M. Alston-Garnjost et al. (LRL)

BOECKMANN 70 NP B16 221 K. Boeckmann et al. (BONN, DURH, NIM+) (ILL) JP

ASCOLI 68 PRL 20 1321 G. Ascoli et al. (ILL) JP

BOESEBECK 68 NP B4 501 K. Boesebeck et al. (AACH, BERL, CERN)

CHUNG 68 PR 165 1491 S.U. Chung et al. (SACL)

CONTE 67 NC 51A 175 F. Conte et al. (GENO, HAMB, MILA, SAQL)

$f_0(1370)$

$I^G(J^{PC}) = 0^+(0^+ +)$

See also the mini-reviews on scalar mesons under  $f_0(500)$  (see the index for the page number) and on non- $q\bar{q}$  candidates in PDG 06, Journal of Physics, G 33 1 (2006).

$f_0(1370)$  T-MATRIX POLE POSITION

Note that  $\Gamma \approx 2 \text{Im}(\sqrt{s_{\text{pole}}})$ .

VALUE (MeV)	DOCUMENT ID	TECN	COMMENT
<b>(1200–1500)–i(150–250) OUR ESTIMATE</b>			
••• We do not use the following data for averages, fits, limits, etc. •••			
(1290 ± 50)–i(170 ± 40)	1 ANISOVICH	09 RVUE	0.0 $\bar{p} \rho, \pi N$
(1373 ± 15)–i(137 ± 10)	2 BARGIOTTI	03 OBLX	$\bar{p} \rho$
(1302 ± 17)–i(166 ± 18)	3 BARBERIS	00C	450 $\bar{p} \rho \rightarrow p_f 4 \pi p_s$
(1312 ± 25 ± 10)–i(109 ± 22 ± 15)	BARBERIS	99D	OMEG 450 $\bar{p} \rho \rightarrow K^+ K^-, \pi^+ \pi^-$
(1406 ± 19)–i(80 ± 6)	4 KAMINSKI	99 RVUE	$\pi \pi \rightarrow \pi \pi, K\bar{K}, \sigma \sigma$
(1300 ± 20)–i(120 ± 20)	ANISOVICH	98B	RVUE Compilation
(1290 ± 15)–i(145 ± 15)	BARBERIS	97B	OMEG 450 $\bar{p} \rho \rightarrow p \rho 2(\pi^+ \pi^-)$
(1548 ± 40)–i(560 ± 40)	BERTIN	97C	OBLX 0.0 $\bar{p} \rho \rightarrow \pi^+ \pi^- \pi^0$
(1380 ± 40)–i(180 ± 25)	ABELE	96B	CBAR 0.0 $\bar{p} \rho \rightarrow \pi^0 K_L^0 K_L^0$
(1300 ± 15)–i(115 ± 8)	BUGG	96	RVUE
(1330 ± 50)–i(150 ± 40)	5 AMSLER	95B	CBAR $\bar{p} \rho \rightarrow 3 \pi^0$
(1360 ± 35)–i(150–300)	5 AMSLER	95C	CBAR $\bar{p} \rho \rightarrow \pi^0 \eta \eta$
(1390 ± 30)–i(190 ± 40)	6 AMSLER	95D	CBAR $\bar{p} \rho \rightarrow 3 \pi^0, \pi^0 \eta \eta, \pi^0 \pi^0 \eta$
1346 – i249	7,8 JANSSEN	95	RVUE $\pi \pi \rightarrow \pi \pi, K\bar{K}$
1214 – i168	8,9 TORNVQVIST	95	RVUE $\pi \pi \rightarrow \pi \pi, K\bar{K}, K \pi, \eta \pi$
1364 – i139	AMSLER	94D	CBAR $\bar{p} \rho \rightarrow \pi^0 \pi^0 \eta$
(1365 ± 20)–i(134 ± 35)	ANISOVICH	94	CBAR $\bar{p} \rho \rightarrow 3 \pi^0, \pi^0 \eta \eta$
(1340 ± 40)–i(127 ± 30, –20)	10 BUGG	94	RVUE $\bar{p} \rho \rightarrow 3 \pi^0, \eta \eta \pi^0, \eta \pi^0 \pi^0$
(1430 ± 5)–i(73 ± 13)	11 KAMINSKI	94	RVUE $\pi \pi \rightarrow \pi \pi, K\bar{K}$
1420 – i220	12 AU	87	RVUE $\pi \pi \rightarrow \pi \pi, K\bar{K}$

1 Another pole is found at  $(1510 \pm 130) - i(800^{+100}_{-150})$  MeV.

2 Coupled channel analysis of  $\pi^+ \pi^- \pi^0, K^+ K^- \pi^0$ , and  $K^\pm K_S^0 \pi^\mp$ .

3 Average between  $\pi^+ \pi^- \pi^0$  and  $2(\pi^+ \pi^-)$ .

4 T-matrix pole on sheet ---.

5 Supersedes ANISOVICH 94.

6 Coupled-channel analysis of  $\bar{p} \rho \rightarrow 3 \pi^0, \pi^0 \eta \eta$ , and  $\pi^0 \pi^0 \eta$  on sheet IV. Demonstrates explicitly that  $f_0(500)$  and  $f_0(1370)$  are two different poles.

7 Analysis of data from FALVARD 88.

8 The pole is on Sheet III. Demonstrates explicitly that  $f_0(500)$  and  $f_0(1370)$  are two different poles.

9 Uses data from BEIER 72B, OCHS 73, HYAMS 73, GRAYEY 74, ROSSELET 77, CASON 83, ASTON 88, and ARMSTRONG 91B. Coupled channel analysis with flavor symmetry and all light two-pseudoscalars systems.

10 Reanalysis of ANISOVICH 94 data.

11 T-matrix pole on sheet III.

12 Analysis of data from OCHS 73, GRAYEY 74, BECKER 79, and CASON 83.

## Meson Particle Listings

 $f_0(1370)$  $f_0(1370)$  BREIT-WIGNER MASS OR K-MATRIX POLE PARAMETER

VALUE (MeV)	DOCUMENT ID	TECN	COMMENT
<b>1200 to 1500 OUR ESTIMATE</b>			
<b><math>\pi\pi</math> MODE</b>			
VALUE (MeV)	EVTS	DOCUMENT ID	TECN COMMENT
••• We do not use the following data for averages, fits, limits, etc. •••			
1400 ± 40		13 AUBERT 09L BABR	$B^\pm \rightarrow \pi^\pm \pi^\pm \pi^\mp$
1470 <sup>+6+72</sup> <sub>-7-255</sub>		14 UEHARA 08A BELL	10.6 $e^+e^- \rightarrow e^+e^-\pi^0\pi^0$
1259 ± 55	2.6k	BONVICINI 07 CLEO	$D^+ \rightarrow \pi^-\pi^+\pi^+$
1309 ± 1 ± 15		15 BUGG 07A RVUE	0.0 $p\bar{p} \rightarrow 3\pi^0$
1449 ± 13	4286	16 GARMASH 06 BELL	$B^+ \rightarrow K^+\pi^+\pi^-$
1350 ± 50		ABLIKIM 05 BES2	$J/\psi \rightarrow \phi\pi^+\pi^-$
1265 ± 30 <sup>+20</sup> <sub>-35</sub>		ABLIKIM 05Q BES2	$\psi(2S) \rightarrow \gamma\pi^+\pi^-K^+K^-$
1434 ± 18 ± 9	848	AITALA 01A E791	$D_s^+ \rightarrow \pi^-\pi^+\pi^+$
1308 ± 10		BARBERIS 99B OMEG	450 $pp \rightarrow p_S p_f \pi^+\pi^-$
1315 ± 50		BELLAZZINI 99 GAM4	450 $pp \rightarrow p p \pi^0 \pi^0$
1315 ± 30		ALDE 98 GAM4	100 $\pi^-\pi^- \rightarrow \pi^0 \pi^0 n$
1280 ± 55		BERTIN 98 OBLX	0.05-0.405 $\bar{p}p \rightarrow \pi^+\pi^+\pi^-$
1186	17,18	TORNQVIST 95 RVUE	$\pi\pi \rightarrow \pi\pi, K\bar{K}, K\pi, \eta\pi$
1472 ± 12		ARMSTRONG 91 OMEG	300 $pp \rightarrow p p \pi\pi, p p K\bar{K}$
1275 ± 20		BREAKSTONE 90 SFM	62 $pp \rightarrow p p \pi^+\pi^-$
1420 ± 20		AKESSON 86 SPEC	63 $pp \rightarrow p p \pi^+\pi^-$
1256		FROGGATT 77 RVUE	$\pi^+\pi^-$ channel
13			Breit-Wigner mass.
14			Breit-Wigner mass. May also be the $f_0(1500)$ .
15			Reanalysis of ABELE 96c data.
16			Also observed by GARMASH 07 in $B^0 \rightarrow K_S^0 \pi^+ \pi^-$ decays. Supersedes GARMASH 05.
17			Uses data from BEIER 72b, OCHS 73, HYAMS 73, GRAYER 74, ROSSELET 77, CASON 83, ASTON 88, and ARMSTRONG 91b. Coupled channel analysis with flavor symmetry and all light two-pseudoscalars systems.
18			Also observed by ASNER 00 in $\tau^- \rightarrow \pi^-\pi^0\pi^0\nu_\tau$ decays

VALUE (MeV)	DOCUMENT ID	TECN	COMMENT
••• We do not use the following data for averages, fits, limits, etc. •••			
1440 ± 6		VLADIMIRSK...06 SPEC	40 $\pi^-\pi^- \rightarrow K_S^0 K_S^0 n$
1391 ± 10		TIKHOMIROV 03 SPEC	40.0 $\pi^-\pi^- \rightarrow K_S^0 K_S^0 K_L^0 X$
1440 ± 50		BOLONKIN 88 SPEC	40 $\pi^-\pi^- \rightarrow K_S^0 K_S^0 n$
1463 ± 9		ETKIN 82B MPS	23 $\pi^-\pi^- \rightarrow n 2K_S^0$
1425 ± 15		WICKLUND 80 SPEC	6 $\pi N \rightarrow K^+ K^- N$
~ 1300		POLYCHRO... 79 STRC	7 $\pi^-\pi^- \rightarrow n 2K_S^0$

VALUE (MeV)	EVTS	DOCUMENT ID	TECN	COMMENT
••• We do not use the following data for averages, fits, limits, etc. •••				
1395 ± 40		ABELE 01 CBAR	0.0 $\bar{p}d \rightarrow \pi^- 4\pi^0 p$	
1374 ± 38		AMSLER 94 CBAR	0.0 $\bar{p}p \rightarrow \pi^+\pi^- 3\pi^0$	
1345 ± 12		ADAMO 93 OBLX	$\bar{p}p \rightarrow 3\pi^+ 2\pi^-$	
1386 ± 30		GASPERO 93 DBC	0.0 $\bar{p}n \rightarrow 2\pi^+ 3\pi^-$	
~ 1410	5751	19 BETTINI 66 DBC	0.0 $\bar{p}n \rightarrow 2\pi^+ 3\pi^-$	
19			$\rho\rho$ dominant.	

VALUE (MeV)	DOCUMENT ID	TECN	COMMENT
••• We do not use the following data for averages, fits, limits, etc. •••			
1262 <sup>+51+82</sup> <sub>-78-103</sub>	20 UEHARA 10A BELL	10.6 $e^+e^- \rightarrow e^+e^-\eta\eta$	
1430	AMSLER 92 CBAR	0.0 $\bar{p}p \rightarrow \pi^0\eta\eta$	
1220 ± 40	ALDE 86D GAM4	100 $\pi^-\pi^- \rightarrow n 2\eta$	
20			Breit-Wigner mass. May also be the $f_0(1500)$ .

VALUE (MeV)	DOCUMENT ID	TECN	COMMENT
••• We do not use the following data for averages, fits, limits, etc. •••			
1306 ± 20	21 ANISOVICH 03 RVUE		
21			K-matrix pole from combined analysis of $\pi^-\pi^- \rightarrow \pi^0\pi^0 n, \pi^-\pi^- \rightarrow K\bar{K}n, \pi^+\pi^- \rightarrow \pi^+\pi^-, \bar{p}p \rightarrow \pi^0\pi^0\pi^0, \pi^0\eta\eta, \pi^0\pi^0\eta, \pi^+\pi^-\pi^0, K^+K^-\pi^0, K_S^0 K_S^0 \pi^0, K^+K_S^0 \pi^-$ at rest, $\bar{p}n \rightarrow \pi^-\pi^-\pi^+, K_S^0 K^-\pi^0, K_S^0 K_S^0 \pi^-$ at rest.

 $f_0(1370)$  BREIT-WIGNER WIDTH

VALUE (MeV)	DOCUMENT ID
<b>200 to 500 OUR ESTIMATE</b>	

VALUE (MeV)	EVTS	DOCUMENT ID	TECN	COMMENT
••• We do not use the following data for averages, fits, limits, etc. •••				
300 ± 80		22 AUBERT 09L BABR	BABR	$B^\pm \rightarrow \pi^\pm \pi^\pm \pi^\mp$
90 <sup>+2+50</sup> <sub>-1-22</sub>		23 UEHARA 08A BELL	BELL	10.6 $e^+e^- \rightarrow e^+e^-\pi^0\pi^0$
298 ± 21	2.6k	BONVICINI 07 CLEO	CLEO	$D^+ \rightarrow \pi^-\pi^+\pi^+$
126 ± 25	4286	24 GARMASH 06 BELL	BELL	$B^+ \rightarrow K^+\pi^+\pi^-$
265 ± 40		ABLIKIM 05 BES2	BES2	$J/\psi \rightarrow \phi\pi^+\pi^-$
350 ± 100 <sup>+105</sup> <sub>-60</sub>		ABLIKIM 05Q BES2	BES2	$\psi(2S) \rightarrow \gamma\pi^+\pi^-K^+K^-$
173 ± 32 ± 6	848	AITALA 01A E791	E791	$D_s^+ \rightarrow \pi^-\pi^+\pi^+$
222 ± 20		BARBERIS 99B OMEG	OMEG	450 $pp \rightarrow p_S p_f \pi^+\pi^-$
255 ± 60		BELLAZZINI 99 GAM4	GAM4	450 $pp \rightarrow p p \pi^0 \pi^0$
190 ± 50		ALDE 98 GAM4	GAM4	100 $\pi^-\pi^- \rightarrow \pi^0 \pi^0 n$
323 ± 13		BERTIN 98 OBLX	OBLX	0.05-0.405 $\bar{p}p \rightarrow \pi^+\pi^+\pi^-$
350	25,26	TORNQVIST 95 RVUE	RVUE	$\pi\pi \rightarrow \pi\pi, K\bar{K}, K\pi, \eta\pi$
195 ± 33		ARMSTRONG 91 OMEG	OMEG	300 $pp \rightarrow p p \pi\pi, p p K\bar{K}$
285 ± 60		BREAKSTONE 90 SFM	SFM	62 $pp \rightarrow p p \pi^+\pi^-$
460 ± 50		AKESSON 86 SPEC	SPEC	63 $pp \rightarrow p p \pi^+\pi^-$
~ 400		27 FROGGATT 77 RVUE	RVUE	$\pi^+\pi^-$ channel
22				The systematic errors are not reported.
23				Breit-Wigner width. May also be the $f_0(1500)$ .
24				Also observed by GARMASH 07 in $B^0 \rightarrow K_S^0 \pi^+ \pi^-$ decays. Supersedes GARMASH 05.
25				Uses data from BEIER 72b, OCHS 73, HYAMS 73, GRAYER 74, ROSSELET 77, CASON 83, ASTON 88, and ARMSTRONG 91b. Coupled channel analysis with flavor symmetry and all light two-pseudoscalars systems.
26				Also observed by ASNER 00 in $\tau^- \rightarrow \pi^-\pi^0\pi^0\nu_\tau$ decays
27				Width defined as distance between 45 and 135° phase shift.

VALUE (MeV)	DOCUMENT ID	TECN	COMMENT
••• We do not use the following data for averages, fits, limits, etc. •••			
121 ± 15	VLADIMIRSK...06 SPEC	40 $\pi^-\pi^- \rightarrow K_S^0 K_S^0 n$	
55 ± 26	TIKHOMIROV 03 SPEC	40.0 $\pi^-\pi^- \rightarrow K_S^0 K_S^0 K_L^0 X$	
250 ± 80	BOLONKIN 88 SPEC	40 $\pi^-\pi^- \rightarrow K_S^0 K_S^0 n$	
118 <sup>+138</sup> <sub>-16</sub>	ETKIN 82B MPS	23 $\pi^-\pi^- \rightarrow n 2K_S^0$	
160 ± 30	WICKLUND 80 SPEC	6 $\pi N \rightarrow K^+ K^- N$	
~ 1500	POLYCHRO... 79 STRC	7 $\pi^-\pi^- \rightarrow n 2K_S^0$	

VALUE (MeV)	EVTS	DOCUMENT ID	TECN	COMMENT
••• We do not use the following data for averages, fits, limits, etc. •••				
275 ± 55		ABELE 01 CBAR	0.0 $\bar{p}d \rightarrow \pi^- 4\pi^0 p$	
375 ± 61		AMSLER 94 CBAR	0.0 $\bar{p}p \rightarrow \pi^+\pi^- 3\pi^0$	
398 ± 26		ADAMO 93 OBLX	$\bar{p}p \rightarrow 3\pi^+ 2\pi^-$	
310 ± 50		GASPERO 93 DBC	0.0 $\bar{p}n \rightarrow 2\pi^+ 3\pi^-$	
~ 900	5751	28 BETTINI 66 DBC	0.0 $\bar{p}n \rightarrow 2\pi^+ 3\pi^-$	
28			$\rho\rho$ dominant.	

VALUE (MeV)	DOCUMENT ID	TECN	COMMENT
••• We do not use the following data for averages, fits, limits, etc. •••			
484 <sup>+246+246</sup> <sub>-170-263</sub>	29 UEHARA 10A BELL	10.6 $e^+e^- \rightarrow e^+e^-\eta\eta$	
250	AMSLER 92 CBAR	0.0 $\bar{p}p \rightarrow \pi^0\eta\eta$	
320 ± 40	ALDE 86D GAM4	100 $\pi^-\pi^- \rightarrow n 2\eta$	
29			Breit-Wigner width. May also be the $f_0(1500)$ .

VALUE (MeV)	DOCUMENT ID	TECN	COMMENT
••• We do not use the following data for averages, fits, limits, etc. •••			
147 <sup>+30</sup> <sub>-50</sub>	30 ANISOVICH 03 RVUE		
30			K-matrix pole from combined analysis of $\pi^-\pi^- \rightarrow \pi^0\pi^0 n, \pi^-\pi^- \rightarrow K\bar{K}n, \pi^+\pi^- \rightarrow \pi^+\pi^-, \bar{p}p \rightarrow \pi^0\pi^0\pi^0, \pi^0\eta\eta, \pi^0\pi^0\eta, \pi^+\pi^-\pi^0, K^+K^-\pi^0, K_S^0 K_S^0 \pi^0, K^+K_S^0 \pi^-$ at rest, $\bar{p}n \rightarrow \pi^-\pi^-\pi^+, K_S^0 K^-\pi^0, K_S^0 K_S^0 \pi^-$ at rest.

 $f_0(1370)$  DECAY MODES

Mode	Fraction ( $\Gamma_i/\Gamma$ )
$\Gamma_1$ $\pi\pi$	seen
$\Gamma_2$ $4\pi$	seen
$\Gamma_3$ $4\pi^0$	seen
$\Gamma_4$ $2\pi^+ 2\pi^-$	seen
$\Gamma_5$ $\pi^+\pi^-\pi^0$	seen
$\Gamma_6$ $\rho\rho$	dominant
$\Gamma_7$ $2(\pi\pi)$ S-wave	seen
$\Gamma_8$ $\pi(1300)\pi$	seen

$\Gamma_9$	$a_1(1260)\pi$	seen
$\Gamma_{10}$	$\eta\eta$	seen
$\Gamma_{11}$	$K\bar{K}$	seen
$\Gamma_{12}$	$K\bar{K}n\pi$	not seen
$\Gamma_{13}$	$6\pi$	not seen
$\Gamma_{14}$	$\omega\omega$	not seen
$\Gamma_{15}$	$\gamma\gamma$	seen
$\Gamma_{16}$	$e^+e^-$	not seen

 $f_0(1370)$  PARTIAL WIDTHS

$\Gamma(\gamma\gamma)$	$\Gamma_{15}$
See $\gamma\gamma$ widths under $f_0(500)$ and MORGAN 90.	

$\Gamma(e^+e^-)$	$\Gamma_{16}$				
VALUE (eV)	CL%	DOCUMENT ID	TECN	COMMENT	
<20	90	VOROBYEV	88	ND	$e^+e^- \rightarrow \pi^0\pi^0$

 $f_0(1370)$   $\Gamma(i)\Gamma(\gamma\gamma)/\Gamma(\text{total})$ 

$\Gamma(\eta\eta) \times \Gamma(\gamma\gamma)/\Gamma_{\text{total}}$	$\Gamma_{10}\Gamma_{15}/\Gamma$			
VALUE (eV)	DOCUMENT ID	TECN	COMMENT	
$121^{+133+169}_{-53-106}$	<sup>31</sup> UEHARA	10A	BELL	10.6 $e^+e^- \rightarrow e^+e^-\eta\eta$
••• We do not use the following data for averages, fits, limits, etc. •••				
<sup>31</sup> Including interference with the $f'_2(1525)$ (parameters fixed to the values from the 2008 edition of this review, PDG 08) and $f_2(1270)$ . May also be the $f_0(1500)$ .				

 $f_0(1370)$  BRANCHING RATIOS

$\Gamma(\pi\pi)/\Gamma_{\text{total}}$	$\Gamma_1/\Gamma$			
VALUE	DOCUMENT ID	TECN	COMMENT	
••• We do not use the following data for averages, fits, limits, etc. •••				
0.26±0.09	BUGG	96	RVUE	
<0.15	<sup>32</sup> AMSLER	94	CBAR	$\bar{p}p \rightarrow \pi^+\pi^-3\pi^0$
<0.06	GASPERO	93	DBC	0.0 $\bar{p}n \rightarrow \text{hadrons}$
<sup>32</sup> Using AMSLER 95B ( $3\pi^0$ ).				

$\Gamma(4\pi)/\Gamma_{\text{total}}$	$\Gamma_2/\Gamma = (\Gamma_3+\Gamma_4+\Gamma_5)/\Gamma$			
VALUE	DOCUMENT ID	TECN	COMMENT	
••• We do not use the following data for averages, fits, limits, etc. •••				
>0.72	GASPERO	93	DBC	0.0 $\bar{p}n \rightarrow \text{hadrons}$

$\Gamma(4\pi^0)/\Gamma(4\pi)$	$\Gamma_3/\Gamma_2$			
VALUE	DOCUMENT ID	TECN	COMMENT	
••• We do not use the following data for averages, fits, limits, etc. •••				
seen	ABELE	96	CBAR	0.0 $\bar{p}p \rightarrow 5\pi^0$
0.068±0.005	<sup>33</sup> GASPERO	93	DBC	0.0 $\bar{p}n \rightarrow \text{hadrons}$
<sup>33</sup> Model-dependent evaluation.				

$\Gamma(2\pi^+2\pi^-)/\Gamma(4\pi)$	$\Gamma_4/\Gamma_2 = \Gamma_4/(\Gamma_3+\Gamma_4+\Gamma_5)$			
VALUE	DOCUMENT ID	TECN	COMMENT	
••• We do not use the following data for averages, fits, limits, etc. •••				
0.420±0.014	<sup>34</sup> GASPERO	93	DBC	0.0 $\bar{p}n \rightarrow 2\pi^+3\pi^-$
<sup>34</sup> Model-dependent evaluation.				

$\Gamma(\pi^+ \pi^- 2\pi^0)/\Gamma(4\pi)$	$\Gamma_5/\Gamma_2 = \Gamma_5/(\Gamma_3+\Gamma_4+\Gamma_5)$			
VALUE	DOCUMENT ID	TECN	COMMENT	
••• We do not use the following data for averages, fits, limits, etc. •••				
0.512±0.019	<sup>35</sup> GASPERO	93	DBC	0.0 $\bar{p}n \rightarrow \text{hadrons}$
<sup>35</sup> Model-dependent evaluation.				

$\Gamma(\rho\rho)/\Gamma(4\pi)$	$\Gamma_6/\Gamma_2$			
VALUE	DOCUMENT ID	TECN	COMMENT	
••• We do not use the following data for averages, fits, limits, etc. •••				
0.26±0.07	ABELE	01B	CBAR	0.0 $\bar{p}d \rightarrow 5\pi p$

$\Gamma(2(\pi\pi)s\text{-wave})/\Gamma(\pi\pi)$	$\Gamma_7/\Gamma_1$			
VALUE	DOCUMENT ID	TECN	COMMENT	
••• We do not use the following data for averages, fits, limits, etc. •••				
5.6±2.6	<sup>36</sup> ABELE	01	CBAR	0.0 $\bar{p}d \rightarrow \pi^-4\pi^0 p$
<sup>36</sup> From the combined data of ABELE 96 and ABELE 96c.				

$\Gamma(2(\pi\pi)s\text{-wave})/\Gamma(4\pi)$	$\Gamma_7/\Gamma_2$			
VALUE	DOCUMENT ID	TECN	COMMENT	
••• We do not use the following data for averages, fits, limits, etc. •••				
0.51±0.09	ABELE	01B	CBAR	0.0 $\bar{p}d \rightarrow 5\pi p$

$\Gamma(\rho\rho)/\Gamma(2(\pi\pi)s\text{-wave})$	$\Gamma_6/\Gamma_7$			
VALUE	DOCUMENT ID	TECN	COMMENT	
••• We do not use the following data for averages, fits, limits, etc. •••				
large	BARBERIS	00c	450 $p\bar{p} \rightarrow p_f 4\pi p_s$	
1.6 ± 0.2	AMSLER	94	CBAR	$\bar{p}p \rightarrow \pi^+\pi^-3\pi^0$
~0.65	GASPERO	93	DBC	0.0 $\bar{p}n \rightarrow \text{hadrons}$

$\Gamma(\pi(1300)\pi)/\Gamma(4\pi)$	$\Gamma_8/\Gamma_2$			
VALUE	DOCUMENT ID	TECN	COMMENT	
••• We do not use the following data for averages, fits, limits, etc. •••				
0.17±0.06	ABELE	01B	CBAR	0.0 $\bar{p}d \rightarrow 5\pi p$

$\Gamma(a_1(1260)\pi)/\Gamma(4\pi)$	$\Gamma_9/\Gamma_2$			
VALUE	DOCUMENT ID	TECN	COMMENT	
••• We do not use the following data for averages, fits, limits, etc. •••				
0.06±0.02	ABELE	01B	CBAR	0.0 $\bar{p}d \rightarrow 5\pi p$

$\Gamma(\eta\eta)/\Gamma(4\pi)$	$\Gamma_{10}/\Gamma_2 = \Gamma_{10}/(\Gamma_3+\Gamma_4+\Gamma_5)$			
VALUE	DOCUMENT ID	TECN	COMMENT	
••• We do not use the following data for averages, fits, limits, etc. •••				
(28 ± 11) × 10 <sup>-3</sup>	<sup>37</sup> ANISOVICH	02D	SPEC	Combined fit
(4.7 ± 2.0) × 10 <sup>-3</sup>	BARBERIS	00E		450 $p\bar{p} \rightarrow p_f \eta \eta p_s$
<sup>37</sup> From a combined K-matrix analysis of Crystal Barrel (0. $p\bar{p} \rightarrow \pi^0\pi^0\pi^0, \pi^0\eta\eta, \pi^0\pi^0\eta$ ), GAMS ( $\pi\rho \rightarrow \pi^0\pi^0n, \eta\eta n, \eta\eta'n$ ), and BNL ( $\pi\rho \rightarrow K\bar{K}n$ ) data.				

$\Gamma(K\bar{K})/\Gamma_{\text{total}}$	$\Gamma_{11}/\Gamma$		
VALUE	DOCUMENT ID	TECN	COMMENT
••• We do not use the following data for averages, fits, limits, etc. •••			
0.35±0.13	BUGG	96	RVUE

$\Gamma(K\bar{K}n\pi)/\Gamma(\pi\pi)$	$\Gamma_{11}/\Gamma_1$			
VALUE	DOCUMENT ID	TECN	COMMENT	
••• We do not use the following data for averages, fits, limits, etc. •••				
0.08±0.08	ABLIKIM	05	BES2	$J/\psi \rightarrow \phi\pi^+\pi^-, \phi K^+K^-$
0.91±0.20	<sup>38</sup> BARGIOTTI	03	OBLX	$\bar{p}p$
0.12±0.06	<sup>39</sup> ANISOVICH	02D	SPEC	Combined fit
0.46±0.15±0.11	BARBERIS	99D	OMEG	450 $p\bar{p} \rightarrow K^+K^-\pi^+, \pi^+\pi^-$
<sup>38</sup> Coupled channel analysis of $\pi^+\pi^-\pi^0, K^+K^-\pi^0$ , and $K^\pm K_S^0 \pi^\mp$ .				
<sup>39</sup> From a combined K-matrix analysis of Crystal Barrel (0. $p\bar{p} \rightarrow \pi^0\pi^0\pi^0, \pi^0\eta\eta, \pi^0\pi^0\eta$ ), GAMS ( $\pi\rho \rightarrow \pi^0\pi^0n, \eta\eta n, \eta\eta'n$ ), and BNL ( $\pi\rho \rightarrow K\bar{K}n$ ) data.				

$\Gamma(K\bar{K}n\pi)/\Gamma_{\text{total}}$	$\Gamma_{12}/\Gamma$			
VALUE	DOCUMENT ID	TECN	COMMENT	
••• We do not use the following data for averages, fits, limits, etc. •••				
<0.03	GASPERO	93	DBC	0.0 $\bar{p}n \rightarrow \text{hadrons}$

$\Gamma(6\pi)/\Gamma_{\text{total}}$	$\Gamma_{13}/\Gamma$			
VALUE	DOCUMENT ID	TECN	COMMENT	
••• We do not use the following data for averages, fits, limits, etc. •••				
<0.22	GASPERO	93	DBC	0.0 $\bar{p}n \rightarrow \text{hadrons}$

$\Gamma(\omega\omega)/\Gamma_{\text{total}}$	$\Gamma_{14}/\Gamma$			
VALUE	DOCUMENT ID	TECN	COMMENT	
••• We do not use the following data for averages, fits, limits, etc. •••				
<0.13	GASPERO	93	DBC	0.0 $\bar{p}n \rightarrow \text{hadrons}$

 $f_0(1370)$  REFERENCES

UEHARA	10A	PR D82 114031	S. Uehara et al.	(BELLE Collab.)
ANISOVICH	09	IJMP A24 2481	V.V. Anisovich, A.V. Sarantsev	
AUBERT	09L	PR D79 072006	B. Aubert et al.	(BABAR Collab.)
PDG	08	PL B667 1	C. Amisler et al.	(PDG Collab.)
UEHARA	08A	PR D78 052004	S. Uehara et al.	(BELLE Collab.)
BONVICINI	07	PR D75 012001	G. Bonvicini et al.	(CLEO Collab.)
BUGG	07A	JPG 34 151	D.V. Bugg et al.	
GARMASH	07	PR D75 012006	A. Garmash et al.	(BELLE Collab.)
GARMASH	06	PRL 96 251803	A. Garmash et al.	(BELLE Collab.)
PDG	06	JPG 33 1	W.-M. Yao et al.	(PDG Collab.)
VLADIMIRSKY...	06	PAN 69 493	V.V. Vladimirov et al.	(ITEP, Moscow)
Translated from YAF 69 515.				
ABLIKIM	05	PL B607 243	M. Ablikim et al.	(BES Collab.)
ABLIKIM	05Q	PR D72 092002	M. Ablikim et al.	(BES Collab.)
GARMASH	05	PR D71 092003	A. Garmash et al.	(BELLE Collab.)
ANISOVICH	03	EPJ A16 229	V.V. Anisovich et al.	
BARGIOTTI	03	EPJ C26 371	M. Bargiotti et al.	
TIKHOMIROV	03	PAN 66 828	G.D. Tikhomirov et al.	(OBELIX Collab.)
Translated from YAF 66 860.				
ANISOVICH	02D	PAN 65 1545	V.V. Anisovich et al.	
Translated from YAF 65 1583.				
ABELE	01	EPJ C19 667	A. Abele et al.	(Crystal Barrel Collab.)
ABELE	01B	EPJ C21 261	A. Abele et al.	(Crystal Barrel Collab.)
AITALA	01A	PRL 86 765	E.M. Aitala et al.	(FNAL E791 Collab.)
ASNER	00	PR D61 012002	D.M. Asner et al.	(CLEO Collab.)
BARBERIS	00C	PL B471 440	D. Barberis et al.	(WA 102 Collab.)
BARBERIS	00E	PL B479 59	D. Barberis et al.	(WA 102 Collab.)
BARBERIS	99B	PL B453 316	D. Barberis et al.	(Omega Expt.)
BARBERIS	99D	PL B462 462	D. Barberis et al.	(Omega Expt.)
BELLAZZINI	99	PL B467 296	R. Bellazzini et al.	
KAMINSKI	99	EPJ C9 141	R. Kaminski, L. Lesniak, B. Loiseau	(CRAC, PARIN)
ALDE	98	EPJ A3 361	D. Alde et al.	(GAM4 Collab.)
Also				
PAN 62 405				
Translated from YAF 62 446.				

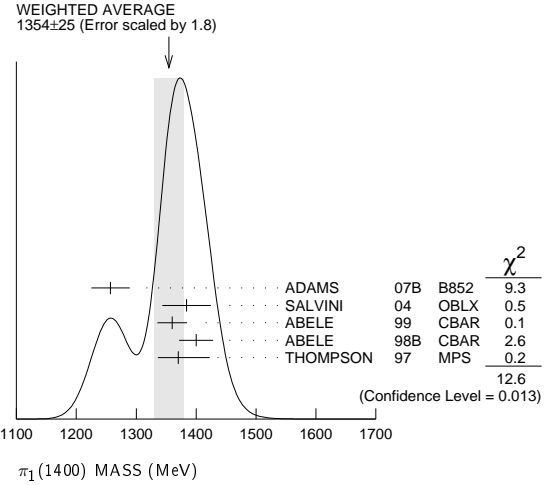
# Meson Particle Listings

## $f_0(1370)$ , $h_1(1380)$ , $\pi_1(1400)$

ANISOVICH	98B	SPU 41 419	V.V. Anisovich et al.	
		Translated from UFN 168 481.		
BERTIN	98	PR D57 55	A. Bertin et al.	(OBELIX Collab.)
BARBERIS	97B	PL B413 217	D. Barberis et al.	(WA 102 Collab.)
BERTIN	97C	PL B408 476	A. Bertin et al.	(OBELIX Collab.)
ABELE	96	PL B380 453	A. Abele et al.	(Crystal Barrel Collab.)
ABELE	96B	PL B385 425	A. Abele et al.	(Crystal Barrel Collab.)
ABELE	96C	NP A609 562	A. Abele et al.	(Crystal Barrel Collab.)
BUGG	96	NP B471 59	D.V. Bugg, A.V. Sarantsev, B.S. Zou	(LOQM, PNPI)
AMSLER	95B	PL B342 433	C. Amstler et al.	(Crystal Barrel Collab.)
AMSLER	95C	PL B353 571	C. Amstler et al.	(Crystal Barrel Collab.)
AMSLER	95D	PL B355 425	C. Amstler et al.	(Crystal Barrel Collab.)
JANSEN	95	PR D52 2690	G. Janssen et al.	(STON, ADLJ, JULI)
TORNQVIST	95	ZPHY C68 647	N.A. Tornqvist	(HELS)
AMSLER	94	PL B322 431	C. Amstler et al.	(Crystal Barrel Collab.) JPC
AMSLER	94D	PL B333 277	C. Amstler et al.	(Crystal Barrel Collab.)
ANISOVICH	94	PL B323 233	V.V. Anisovich et al.	(Crystal Barrel Collab.) JPC
BUGG	94	PR D50 4412	D.V. Bugg et al.	(LOQM)
KAMINSKI	94	PR D50 3145	R. Kaminski, L. Lesniak, J.P. Maillet	(CRAC+)
ADAMO	93	NP A558 13C	A. Adamo et al.	(OBELIX Collab.) JPC
GASPERO	93	NP A562 407	M. Gaspero	(ROMA1) JPC
AMSLER	92	PL B291 347	C. Amstler et al.	(Crystal Barrel Collab.)
ARMSTRONG	91	ZPHY C51 351	T.A. Armstrong et al.	(ATHU, BARI, BIRM+)
ARMSTRONG	91B	ZPHY C52 389	T.A. Armstrong et al.	(ATHU, BARI, BIRM+)
BREAKSTONE	90	ZPHY C48 569	A.M. Breakstone et al.	(ISU, BGN, CERN+)
MORGAN	90	ZPHY C48 623	D. Morgan, M.R. Pennington	(RAL, DURH)
ASTON	88	NP B296 493	D. Aston et al.	(SLAC, NAGO, CINC, INUS)
BOLONKIN	88	NP B309 426	B.V. Bolonkin et al.	(ITEP, SERP)
FALVARD	88	PR D38 2706	A. Falvard et al.	(CLER, FRAS, LALO+)
VOROBYEV	88	SJNP 46 273	P.V. Vorobyev et al.	(NOVO)
		Translated from YAF 48 436.		
AU	87	PR D35 1633	K.L. Au, D. Morgan, M.R. Pennington	(DURH, RAL)
AKESSON	86	NP B264 154	T. Akesson et al.	(Axial Field Spec. Collab.)
ALDE	86D	NP B269 485	D.M. Alde et al.	(BELG, LAPP, SERP, CERN+)
CASON	83	PR D28 1586	N.M. Cason et al.	(NDAM, ANL)
ETKIN	82B	PR D25 1786	A. Etkin et al.	(BNL, CUNY, TUFTS, VAND)
WICKLUND	80	PRL 45 1469	A.B. Wicklund et al.	(ANL)
BECKER	79	NP B151 46	H. Becker et al.	(MPIM, CERN, ZEEM, CRAC)
POLYCHRO...	79	PR D19 1317	V.A. Polychronakos et al.	(NDAM, ANL)
FROGGATT	77	NP B129 89	C.D. Froggatt, J.L. Petersen	(GLAS, NORD)
ROSSELET	77	PR D15 574	L. Rosselet et al.	(GEVA, SACL)
GRAYR	74	NP B75 189	G. Grayer et al.	(CERN, MPIM)
HYAMS	73	NP B64 134	B.D. Hyams et al.	(CERN, MPIM)
OCHS	73	Thesis	W. Ochs	(MPIM, MUNI)
BEIER	72B	PRL 29 511	E.W. Beier et al.	(PENN)
BETTINI	66	NC 42A 695	A. Bettini et al.	(PADO, PISA)

1323.1 ± 4.6 <sup>2</sup> AOYAGI 93 BKEI  $\pi^- p \rightarrow \eta \pi^- p$   
 1406 ± 20 <sup>3</sup> ALDE 88B GAM4 0 100  $\pi^- p \rightarrow \eta \pi^0 n$

- <sup>1</sup> Natural parity exchange, questioned by DZIERBA 03.
- <sup>2</sup> Unnatural parity exchange.
- <sup>3</sup> Seen in the  $P_0$ -wave intensity of the  $\eta \pi^0$  system, unnatural parity exchange.



### $h_1(1380)$

$$I^G(J^{PC}) = ?^-(1^{+-})$$

OMITTED FROM SUMMARY TABLE

Seen in partial-wave analysis of the  $K \bar{K} \pi$  system. Needs confirmation.

#### $h_1(1380)$ MASS

VALUE (MeV)	DOCUMENT ID	TECN	COMMENT
<b>1386 ± 19 OUR AVERAGE</b>			
1440 ± 60	ABELE 97H	CBAR	$\bar{p} p \rightarrow K_L^0 K_S^0 \pi^0 \pi^0$
1380 ± 20	ASTON 88C	LASS 11	$K^- p \rightarrow K_S^0 K^\pm \pi^\mp \Lambda$

#### $h_1(1380)$ WIDTH

VALUE (MeV)	DOCUMENT ID	TECN	COMMENT
<b>91 ± 30 OUR AVERAGE</b>			Error includes scale factor of 1.1.
170 ± 80	ABELE 97H	CBAR	$\bar{p} p \rightarrow K_L^0 K_S^0 \pi^0 \pi^0$
80 ± 30	ASTON 88C	LASS 11	$K^- p \rightarrow K_S^0 K^\pm \pi^\mp \Lambda$

#### $h_1(1380)$ DECAY MODES

Mode	DOCUMENT ID	TECN	COMMENT
$\Gamma_1$ $K \bar{K}^*(892) + c.c.$			

#### $h_1(1380)$ REFERENCES

ABELE	97H	PL B415 280	A. Abele et al.	(Crystal Barrel Collab.)
ASTON	88C	PL B201 573	D. Aston et al.	(SLAC, NAGO, CINC, INUS)

### $\pi_1(1400)$

$$I^G(J^{PC}) = 1^-(1^{-+})$$

See also the mini-review under non- $q\bar{q}$  candidates in PDG 06, Journal of Physics, G 33 1 (2006).

#### $\pi_1(1400)$ MASS

VALUE (MeV)	EVTs	DOCUMENT ID	TECN	CHG	COMMENT
<b>1354 ± 25 OUR AVERAGE</b>					Error includes scale factor of 1.8. See the ideogram below.
1257 ± 20 ± 25	23.5k	ADAMS 07b	B852		$18 \pi^- p \rightarrow \eta \pi^0 n$
1384 ± 20 ± 35	90k	SALVINI 04	OBLX		$\bar{p} p \rightarrow 2\pi^+ 2\pi^-$
1360 ± 25		ABELE 99	CBAR		$0.0 \bar{p} p \rightarrow \pi^0 \pi^0 \eta$
1400 ± 20 ± 20		ABELE 98b	CBAR		$0.0 \bar{p} n \rightarrow \pi^- \pi^0 \eta$
1370 ± 16 ± 30		<sup>1</sup> THOMPSON 97	MPS		$18 \pi^- p \rightarrow \eta \pi^- p$

- • • We do not use the following data for averages, fits, limits, etc. • • •

#### $\pi_1(1400)$ WIDTH

VALUE (MeV)	EVTs	DOCUMENT ID	TECN	CHG	COMMENT
<b>330 ± 35 OUR AVERAGE</b>					
354 ± 64 ± 58	23.5k	ADAMS 07b	B852		$18 \pi^- p \rightarrow \eta \pi^0 n$
378 ± 50 ± 50	90k	SALVINI 04	OBLX		$\bar{p} p \rightarrow 2\pi^+ 2\pi^-$
220 ± 90		ABELE 99	CBAR		$0.0 \bar{p} p \rightarrow \pi^0 \pi^0 \eta$
310 ± 50 ± 50		ABELE 98b	CBAR		$0.0 \bar{p} n \rightarrow \pi^- \pi^0 \eta$
385 ± 40 ± 65		<sup>4</sup> THOMPSON 97	MPS		$18 \pi^- p \rightarrow \eta \pi^- p$

- • • We do not use the following data for averages, fits, limits, etc. • • •

143.2 ± 12.5 <sup>5</sup> AOYAGI 93 BKEI  $\pi^- p \rightarrow \eta \pi^- p$   
 180 ± 20 <sup>6</sup> ALDE 88B GAM4 0 100  $\pi^- p \rightarrow \eta \pi^0 n$

- <sup>4</sup> Resolution is not unfolded, natural parity exchange, questioned by DZIERBA 03.
- <sup>5</sup> Unnatural parity exchange.
- <sup>6</sup> Seen in the  $P_0$ -wave intensity of the  $\eta \pi^0$  system, unnatural parity exchange.

#### $\pi_1(1400)$ DECAY MODES

Mode	Fraction ( $\Gamma_i/\Gamma$ )
$\Gamma_1$ $\eta \pi^0$	seen
$\Gamma_2$ $\eta \pi^-$	seen
$\Gamma_3$ $\eta' \pi$	

#### $\pi_1(1400)$ BRANCHING RATIOS

$\Gamma(\eta \pi^0)/\Gamma_{total}$	DOCUMENT ID	TECN	CHG	COMMENT	$\Gamma_1/\Gamma$
not seen	PROKOSHKIN 95b	GAM4		$100 \pi^- p \rightarrow \eta \pi^0 n$	
not seen	<sup>7</sup> BUGG 94	RVUE		$\bar{p} p \rightarrow \eta 2\pi^0$	
not seen	<sup>8</sup> APEL 81	NICE 0		$40 \pi^- p \rightarrow \eta \pi^0 n$	

- <sup>7</sup> Using Crystal Barrel data.
- <sup>8</sup> A general fit allowing S, D, and P waves (including  $m=0$ ) is not done because of limited statistics.

$\Gamma(\eta \pi^-)/\Gamma_{total}$	DOCUMENT ID	TECN	COMMENT	$\Gamma_2/\Gamma$
possibly seen	BELADIDZE 93	VES	$37\pi^- N \rightarrow \eta \pi^- N$	

$\Gamma(\eta' \pi)/\Gamma(\eta \pi^0)$	CL%	DOCUMENT ID	TECN	COMMENT	$\Gamma_3/\Gamma_1$
<0.80	95	BOUTEMEUR 90	GAM4	$100 \pi^- p \rightarrow 4\eta n$	

- • • We do not use the following data for averages, fits, limits, etc. • • •

$\pi_1(1400)$  REFERENCES

ADAMS	07B	PL B657 27	G.S. Adams <i>et al.</i>	(BNL E852 Collab.)
PDG	06	JPG 33 1	W.-M. Yao <i>et al.</i>	(PDG Collab.)
SALVINI	04	EPI C35 21	P. Salvini <i>et al.</i>	(OBELIX Collab.)
DZIERBA	03	PR D67 094015	A.R. Dzierba <i>et al.</i>	
ABELE	99	PL B446 349	A. Abele <i>et al.</i>	(Crystal Barrel Collab.)
ABELE	98B	PL B423 175	A. Abele <i>et al.</i>	(Crystal Barrel Collab.)
THOMPSON	97	PRL 79 1630	D.R. Thompson <i>et al.</i>	(BNL E852 Collab.)
PROKOSHKIN	95B	PAN 58 606	Y.D. Prokoshkin, S.A. Sadovsky	(SERP)
		Translated from YAF 58 662.		
BUGG	94	PR D50 4412	D.V. Bugg <i>et al.</i>	(LOQM)
AOYAGI	93	PL B314 246	H. Aoyagi <i>et al.</i>	(BKEI Collab.)
BELADIDZE	93	PL B313 276	G.M. Beladidze <i>et al.</i>	(VES Collab.)
BOUTEMEUR	90	Hadron 89 Conf. p 119	M. BoutemEUR, M. Poulet	(SERP, BELG, LANL+)
ALDE	88B	PL B205 397	D.M. Alde <i>et al.</i>	(SERP, BELG, LANL, LAPP)
APEL	81	NP B193 269	W.D. Apel <i>et al.</i>	(SERP, CERN)

 $\eta(1405)$ 

$$J^{PC} = 0^+(0^-)$$

THE  $\eta(1405)$ ,  $\eta(1475)$ ,  $f_1(1420)$ , AND  $f_1(1510)$ 

Revised February 2012 by C. Amsler (Zürich) and A. Masoni (INFN Cagliari).

The first observation of the  $\eta(1440)$  was made in  $p\bar{p}$  annihilation at rest into  $\eta(1440)\pi^+\pi^-$ ,  $\eta(1440) \rightarrow K\bar{K}\pi$  [1]. This state was reported to decay through  $a_0(980)\pi$  and  $K^*(892)\bar{K}$  with roughly equal contributions. The  $\eta(1440)$  was also observed in radiative  $J/\psi(1S)$  decay into  $K\bar{K}\pi$  [2–4] and  $\gamma\rho$  [5]. There is evidence for the existence of two pseudoscalars in this mass region, the  $\eta(1405)$  and  $\eta(1475)$ . The former decays mainly through  $a_0(980)\pi$  (or direct  $K\bar{K}\pi$ ) and the latter mainly to  $K^*(892)\bar{K}$ .

The simultaneous observation of two pseudoscalars is reported in three production mechanisms:  $\pi^-p$  [6,7]; radiative  $J/\psi(1S)$  decay [8,9]; and  $p\bar{p}$  annihilation at rest [10–13]. All of them give values for the masses, widths, and decay modes in reasonable agreement. However, Ref. [9] favors a state decaying into  $K^*(892)\bar{K}$  at a lower mass than the state decaying into  $a_0(980)\pi$ . In  $J/\psi(1S)$  radiative decay, the  $\eta(1405)$  decays into  $K\bar{K}\pi$  through  $a_0(980)\pi$ , and hence a signal is also expected in the  $\eta\pi\pi$  mass spectrum. This was indeed observed by MARK III in  $\eta\pi^+\pi^-$  [14], which reports a mass of 1400 MeV, in line with the existence of the  $\eta(1405)$  decaying into  $a_0(980)\pi$ .

BES [15] reports an enhancement in  $K^+K^-\pi^0$  around 1.44 GeV in  $J/\psi(1S)$  decay, recoiling against an  $\omega$  (but not a  $\phi$ ) without resolving the presence of two states nor performing a spin-parity analysis, due to low statistics. This state could also be the  $f_1(1420)$  (see below). On the other hand, BES observes  $\eta(1405) \rightarrow \eta\pi\pi$  in  $J/\psi(1S)$  decay, recoiling against an  $\omega$  [16].

The  $\eta(1405)$  is also observed in  $p\bar{p}$  annihilation at rest into  $\eta\pi^+\pi^-\pi^0\pi^0$ , where it decays into  $\eta\pi\pi$  [17]. The intermediate  $a_0(980)\pi$  accounts for roughly half of the  $\eta\pi\pi$  signal, in agreement with MARK III [14] and DM2 [4].

However, the issue remains controversial as to whether two pseudoscalar mesons really exist. According to Ref. [18] the splitting of a single state could be due to nodes in the decay amplitudes which differ in  $\eta\pi\pi$  and  $K^*(892)\bar{K}$ . Based on the isospin violating decay  $J/\psi(1S) \rightarrow \gamma 3\pi$  observed by BES [19] the splitting could also be due to a triangular singularity mixing  $\eta\pi\pi$  and  $K^*(892)\bar{K}$  [20].

The  $\eta(1295)$  has been observed by four  $\pi^-p$  experiments [7,21–23], and evidence is reported in  $p\bar{p}$  annihilation [24–26].

In  $J/\psi(1S)$  radiative decay, an  $\eta(1295)$  signal is evident in the  $0^{-+} \eta\pi\pi$  wave of the DM2 data [9]. Also BaBar [27] reports evidence for a signal around 1295 MeV in  $B$  decays into  $\eta\pi\pi K$ . However, the existence of the  $\eta(1295)$  is questioned in Refs. [18] and [28]. The authors claim a single pseudoscalar meson in the 1400 MeV region. This conclusion is based on properties of the wave functions in the  ${}^3P_0$  model (and on an unpublished analysis of the annihilation  $p\bar{p} \rightarrow 4\pi\eta$ ). The pseudoscalar signal around 1400 MeV is then attributed to the first radial excitation of the  $\eta$ .

Assuming establishment of the  $\eta(1295)$ , the  $\eta(1475)$  could be the first radial excitation of the  $\eta'$ , with the  $\eta(1295)$  being the first radial excitation of the  $\eta$ . Ideal mixing, suggested by the  $\eta(1295)$  and  $\pi(1300)$  mass degeneracy, would then imply that the second isoscalar in the nonet is mainly  $s\bar{s}$ , and hence couples to  $K^*\bar{K}$ , in agreement with properties of the  $\eta(1475)$ . Also, its width matches the expected width for the radially excited  $s\bar{s}$  state [29,30]. A study of radial excitations of pseudoscalar mesons [31] favors the  $s\bar{s}$  interpretation of the  $\eta(1475)$ . However, due to the strong kinematical suppression the data are not sufficient to exclude a sizeable  $s\bar{s}$  admixture also in the  $\eta(1405)$ .

The  $K\bar{K}\pi$  and  $\eta\pi\pi$  channels were studied in  $\gamma\gamma$  collisions by L3 [32]. The analysis led to a clear  $\eta(1475)$  signal in  $K\bar{K}\pi$ , decaying into  $K^*\bar{K}$ , very well identified in the untagged data sample, where contamination from spin 1 resonances is not allowed. At the same time, L3 [32] did not observe the  $\eta(1405)$ , neither in  $K\bar{K}\pi$  nor in  $\eta\pi\pi$ . The observation of the  $\eta(1475)$ , combined with the absence of an  $\eta(1405)$  signal, strengthens the two-resonances hypothesis. Since gluonium production is presumably suppressed in  $\gamma\gamma$  collisions, the L3 results [32] suggest that  $\eta(1405)$  has a large gluonic content (see also Refs. [33] and [34]).

The L3 result is somewhat in disagreement with that of CLEO-II, which did not observe any pseudoscalar signal in  $\gamma\gamma \rightarrow \eta(1475) \rightarrow K_S^0 K^\pm \pi^\mp$  [35]. However, more data are required. Moreover, after the CLEO-II result, L3 performed a further analysis with full statistics [36], confirming their previous evidence for the  $\eta(1475)$ . The CLEO upper limit [35] for  $\Gamma_{\gamma\gamma}(\eta(1475))$ , and the L3 results [36], are consistent with the world average for the  $\eta(1475)$  width.

BaBar [27] also reports the  $\eta(1475)$  in  $B$  decays into  $K\bar{K}^*$  recoiling against a  $K$ , but upper limits only are given for the  $\eta(1405)$ . As mentioned above, in  $B$  decays into  $\eta\pi\pi K$  the  $\eta(1295) \rightarrow \eta\pi\pi$  is observed while only upper limits are given for the  $\eta(1405)$ . The  $f_1(1420)$  (and the  $f_1(1285)$ ) are not seen.

The gluonium interpretation for the  $\eta(1405)$  is not favored by lattice gauge theories which predict the  $0^{-+}$  state above 2 GeV [37,38] (see also the article on the “Quark model” in this issue of the Review). However, the  $\eta(1405)$  is an excellent candidate for the  $0^{-+}$  glueball in the fluxtube model [39]. In this model, the  $0^{++} f_0(1500)$  glueball is also naturally related to a  $0^{-+}$  glueball with mass degeneracy broken in QCD. Also, Ref. 40 shows that the pseudoscalar glueball could lie at a lower

# Meson Particle Listings

## $\eta(1405)$

mass than predicted from lattice calculation. In this model the  $\eta(1405)$  appears as the natural glueball candidate (see also Refs. [41] and [42]). A detailed review of the experimental situation is available in Ref. 43.

Let us now deal with  $1^{++}$  isoscalars. The  $f_1(1420)$ , decaying into  $K^*\bar{K}$ , was first reported in  $\pi^-p$  reactions at 4 GeV/c [44]. However, later analyses found that the 1400–1500 MeV region was far more complex [45–47]. A reanalysis of the MARK III data in radiative  $J/\psi(1S)$  decay into  $K\bar{K}\pi$  [8] shows the  $f_1(1420)$  decaying into  $K^*\bar{K}$ . Also, a  $C=+1$  state is observed in tagged  $\gamma\gamma$  collisions (*e.g.*, Ref. 48).

In  $\pi^-p \rightarrow \eta\pi\pi n$  charge-exchange reactions at 8–9 GeV/c the  $\eta\pi\pi$  mass spectrum is dominated by the  $\eta(1440)$  and  $\eta(1295)$  [21,49], and at 100 GeV/c Ref. 22 reports the  $\eta(1295)$  and  $\eta(1440)$  decaying into  $\eta\pi^0\pi^0$  with a weak  $f_1(1285)$  signal, and no evidence for the  $f_1(1420)$ .

Axial ( $1^{++}$ ) mesons are not observed in  $\bar{p}p$  annihilation at rest in liquid hydrogen, which proceeds dominantly through  $S$ -wave annihilation. However, in gaseous hydrogen,  $P$ -wave annihilation is enhanced and, indeed, Ref. 11 reports  $f_1(1420)$  decaying into  $K^*\bar{K}$ . The  $f_1(1420)$ , decaying into  $K\bar{K}\pi$ , is also seen in  $pp$  central production, together with the  $f_1(1285)$ . The latter decays via  $a_0(980)\pi$ , and the former only via  $K^*\bar{K}$ , while the  $\eta(1440)$  is absent [50,51]. The  $K_S K_S \pi^0$  decay mode of the  $f_1(1420)$  establishes unambiguously  $C=+1$ . On the other hand, there is no evidence for any state decaying into  $\eta\pi\pi$  around 1400 MeV, and hence the  $\eta\pi\pi$  mode of the  $f_1(1420)$  must be suppressed [52].

We now turn to the experimental evidence for the  $f_1(1510)$ . Two states, the  $f_1(1420)$  and  $f_1(1510)$ , decaying into  $K^*\bar{K}$ , compete for the  $s\bar{s}$  assignment in the  $1^{++}$  nonet. The  $f_1(1510)$  was seen in  $K^-p \rightarrow \Lambda K\bar{K}\pi$  at 4 GeV/c [53], and at 11 GeV/c [54]. Evidence is also reported in  $\pi^-p$  at 8 GeV/c, based on the phase motion of the  $1^{++} K^*\bar{K}$  wave [47]. A somewhat broader  $1^{++}$  signal is also observed in  $J/\psi(1S) \rightarrow \gamma\eta\pi^+\pi^-$  [55] as well as a small signal in  $J/\psi(1S) \rightarrow \gamma\eta'\pi^+\pi^-$ , attributed to the  $f_1(1510)$  [56].

The absence of  $f_1(1420)$  in  $K^-p$  [54] argues against the  $f_1(1420)$  being the  $s\bar{s}$  member of the  $1^{++}$  nonet. However, the  $f_1(1420)$  was reported in  $K^-p$  but not in  $\pi^-p$  [57], while two experiments do not observe the  $f_1(1510)$  in  $K^-p$  [57,58]. The latter is also not seen in central collisions [51], or  $\gamma\gamma$  collisions [59], although, surprisingly for an  $s\bar{s}$  state, a signal is reported in  $4\pi$  decays [60]. These facts lead to the conclusion that  $f_1(1510)$  is not well established [61].

Assigning the  $f_1(1420)$  to the  $1^{++}$  nonet, one finds a nonet mixing angle of  $\sim 50^\circ$  [61]. However, arguments favoring the  $f_1(1420)$  being a hybrid  $q\bar{q}g$  meson, or a four-quark state, were put forward in Refs. [62] and [63], respectively, while Ref. 64 argued for a molecular state formed by the  $\pi$  orbiting in a  $P$ -wave around an  $S$ -wave  $K\bar{K}$  state.

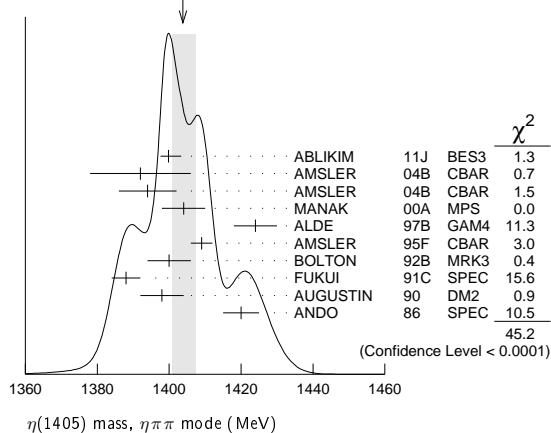
Summarizing, there is convincing evidence for the  $f_1(1420)$  decaying into  $K^*\bar{K}$ , and for two pseudoscalars (possibly one dynamically split into two) in the  $\eta(1440)$  region, the  $\eta(1405)$

and  $\eta(1475)$ , decaying into  $a_0(980)\pi$  and  $K^*\bar{K}$ , respectively. The  $f_1(1510)$  is not well established.

### References

1. P.H. Baillon *et al.*, Nuovo Cimento **50A**, 393 (1967).
2. D.L. Scharre *et al.*, Phys. Lett. **97B**, 329 (1980).
3. C. Edwards *et al.*, Phys. Rev. Lett. **49**, 259 (1982).
4. J.E. Augustin *et al.*, Phys. Rev. **D42**, 10 (1990).
5. J.Z. Bai *et al.*, Phys. Lett. **B594**, 47 (2004).
6. M.G. Rath *et al.*, Phys. Rev. **D40**, 693 (1989).
7. T. Adams *et al.*, Phys. Rev. Lett. **87**, 041801 (2001).
8. J.Z. Bai *et al.*, Phys. Rev. Lett. **65**, 2507 (1990).
9. J.E. Augustin and G. Cosme, Phys. Rev. **D46**, 1951 (1992).
10. A. Bertin *et al.*, Phys. Lett. **B361**, 187 (1995).
11. A. Bertin *et al.*, Phys. Lett. **B400**, 226 (1997).
12. C. Cicalo *et al.*, Phys. Lett. **B462**, 453 (1999).
13. F. Nichitiu *et al.*, Phys. Lett. **B545**, 261 (2002).
14. T. Bolton *et al.*, Phys. Rev. Lett. **69**, 1328 (1992).
15. M. Ablikim *et al.*, Phys. Rev. **D77**, 032005 (2008).
16. M. Ablikim *et al.*, Phys. Rev. Lett. **107**, 182001 (2011).
17. C. Amsler *et al.*, Phys. Lett. **B358**, 389 (1995).
18. E. Klempt and A. Zaitsev, Phys. Reports **454**, 1 (2007).
19. M. Ablikim *et al.*, preprint arXiv: 1201.2737v1 [hep-ex] 2012.
20. Jia-Jun Wu *et al.*, preprint arXiv: 1108.3772v2 [hep-ph] 2012.
21. S. Fukui *et al.*, Phys. Lett. **B267**, 293 (1991).
22. D. Alde *et al.*, Phys. Atom. Nucl. **60**, 386 (1997).
23. J.J. Manak *et al.*, Phys. Rev. **D62**, 012003 (2000).
24. A.V. Anisovich *et al.*, Nucl. Phys. **A690**, 567 (2001).
25. A. Abele *et al.*, Phys. Rev. **D57**, 3860 (1998).
26. C. Amsler *et al.*, Eur. Phys. J. **C33**, 23 (2004).
27. B. Aubert *et al.*, Phys. Rev. Lett. **101**, 091801 (2008).
28. E. Klempt, Int. J. Mod. Phys. **A21**, 739 (2006).
29. F. Close *et al.*, Phys. Lett. **B397**, 333 (1997).
30. T. Barnes *et al.*, Phys. Rev. **D55**, 4157 (1997).
31. T. Gutsche *et al.*, Phys. Rev. **D79**, 014036 (2009).
32. M. Acciarri *et al.*, Phys. Lett. **B501**, 1 (2001).
33. F. Close *et al.*, Phys. Rev. **D55**, 5749 (1997).
34. D.M. Li *et al.*, Eur. Phys. J. **C28**, 335 (2003).
35. R. Ahohe *et al.*, Phys. Rev. **D71**, 072001 (2005).
36. P. Achard *et al.*, JHEP **0703**, 018 (2007).
37. G.S. Bali *et al.*, Phys. Lett. **B309**, 378 (1993).
38. C. Morningstar and M. Peardon, Phys. Rev. **D60**, 034509 (1999).
39. L. Faddeev *et al.*, Phys. Rev. **D70**, 114033 (2004).
40. H.-Y. Cheng *et al.*, Phys. Rev. **D79**, 014024 (2009).
41. G. Li *et al.*, J. Phys. G: Nucl. Part. Phys. **35**, 055002 (2008).
42. T. Gutsche *et al.*, Phys. Rev. **D80**, 014014 (2009).
43. A. Masoni, C. Cicalo, and G.L. Usai, J. Phys. **G32**, R293 (2006).
44. C. Dionisi *et al.*, Nucl. Phys. **B169**, 1 (1980).
45. S.U. Chung *et al.*, Phys. Rev. Lett. **55**, 779 (1985).

46. D.F. Reeves *et al.*, Phys. Rev. **D34**, 1960 (1986).  
 47. A. Birman *et al.*, Phys. Rev. Lett. **61**, 1557 (1988).  
 48. H.J. Behrend *et al.*, Z. Phys. **C42**, 367 (1989).  
 49. A. Ando *et al.*, Phys. Rev. Lett. **57**, 1296 (1986).  
 50. T.A. Armstrong *et al.*, Phys. Lett. **B221**, 216 (1989).  
 51. D. Barberis *et al.*, Phys. Lett. **B413**, 225 (1997).  
 52. T.A. Armstrong *et al.*, Z. Phys. **C52**, 389 (1991).  
 53. P. Gavillet *et al.*, Z. Phys. **C16**, 119 (1982).  
 54. D. Aston *et al.*, Phys. Lett. **B201**, 573 (1988).  
 55. J.Z. Bai *et al.*, Phys. Lett. **B446**, 356 (1999).  
 56. M. Ablikim *et al.*, Phys. Rev. Lett. **106**, (2011) 072002.  
 57. S. Bitjukov *et al.*, Sov. J. Nucl. Phys. **39**, 738 (1984).  
 58. E. King *et al.*, Nucl. Phys. (Proc. Supp.) **B21**, 11 (1991).  
 59. H. Aihara *et al.*, Phys. Rev. **D38**, 1 (1988).  
 60. D.A. Bauer *et al.*, Phys. Rev. **D48**, 3976 (1993).  
 61. F.E. Close and A. Kirk, Z. Phys. **C76**, 469 (1997).  
 62. S. Ishida *et al.*, Prog. Theor. Phys. **82**, 119 (1989).  
 63. D.O. Caldwell, *Hadron 89 Conf.*, p. 127.  
 64. R.S. Longacre, Phys. Rev. **D42**, 874 (1990).

WEIGHTED AVERAGE  
1403.8±3.4-3.0 (Error scaled by 2.2) $\eta(1405)$  mass,  $\eta\pi\pi$  mode (MeV) **$K\bar{K}\pi$  MODE ( $a_0(980)\pi$  or direct  $K\bar{K}\pi$ )**

VALUE (MeV)	EVTS	DOCUMENT ID	TECN	COMMENT
-------------	------	-------------	------	---------

The data in this block is included in the average printed for a previous datablock.

**1413.9 ± 1.7 OUR AVERAGE** Error includes scale factor of 1.1.

1413 ± 14	3651	<sup>4</sup> NICHITIU	02	OBLX
1416 ± 4 ± 2	20k	ADAMS	01B B852	18 GeV $\pi^- p \rightarrow K^+ K^- \pi^0 n$
1405 ± 5		<sup>5</sup> CICALO	99	OBLX $0 \bar{p} p \rightarrow K^\pm K_S^0 \pi^\mp \pi^+ \pi^-$
1407 ± 5		<sup>5</sup> BERTIN	97	OBLX $0 \bar{p} p \rightarrow K^\pm (K^0) \pi^\mp \pi^+ \pi^-$
1416 ± 2		<sup>5</sup> BERTIN	95	OBLX $0 \bar{p} p \rightarrow K\bar{K}\pi\pi$
1416 ± 8 <sup>+7</sup> / <sub>-5</sub>	700	<sup>6</sup> BAI	90c	MRK3 $J/\psi \rightarrow \gamma K_S^0 K^\pm \pi^\mp$
1413 ± 5		<sup>6</sup> RATH	89	MPS $21.4 \pi^- p \rightarrow n K_S^0 K_S^0 \pi^0$
1459 ± 5		<sup>7</sup> AUGUSTIN	92	DM2 $J/\psi \rightarrow \gamma K\bar{K}\pi$

••• We do not use the following data for averages, fits, limits, etc. •••

 **$\pi\pi\gamma$  MODE**

VALUE (MeV)	EVTS	DOCUMENT ID	TECN	COMMENT
-------------	------	-------------	------	---------

<b>1390 ± 12</b>	235 ± 91	AMSLER	04B CBAR	$0 \bar{p} p \rightarrow \pi^+ \pi^- \pi^+ \pi^- \gamma$
•••	•••	•••	•••	•••
1424 ± 10 ± 11	547	BAI	04J BES2	$J/\psi \rightarrow \gamma \gamma \pi^+ \pi^-$
1401 ± 18		<sup>8,9</sup> AUGUSTIN	90	DM2 $J/\psi \rightarrow \pi^+ \pi^- \gamma \gamma$
1432 ± 8		<sup>9</sup> COFFMAN	90	MRK3 $J/\psi \rightarrow \pi^+ \pi^- 2\gamma$

 **$4\pi$  MODE**

VALUE (MeV)	EVTS	DOCUMENT ID	TECN	COMMENT
-------------	------	-------------	------	---------

•••	•••	•••	•••	•••
1420 ± 20		BUGG	95	MRK3 $J/\psi \rightarrow \gamma \pi^+ \pi^- \pi^+ \pi^-$
1489 ± 12	3270	<sup>10</sup> BISELLO	89B	DM2 $J/\psi \rightarrow 4\pi\gamma$

 **$K\bar{K}\pi$  MODE (unresolved)**

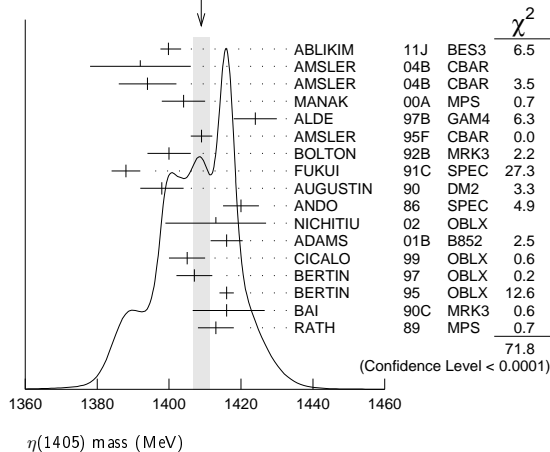
VALUE (MeV)	EVTS	DOCUMENT ID	TECN	COMMENT
-------------	------	-------------	------	---------

•••	•••	•••	•••	•••
1437.6 ± 3.2	249 ± 35	<sup>11,12</sup> ABLIKIM	08E	BES2 $J/\psi \rightarrow \omega K_S^0 K^+ \pi^- + c.c.$
1445.9 ± 5.7	62 ± 18	<sup>11,12</sup> ABLIKIM	08E	BES2 $J/\psi \rightarrow \omega K^+ K^- \pi^0$
1442 ± 10	410	<sup>11</sup> BAI	98C	BES $J/\psi \rightarrow \gamma K^+ K^- \pi^0$
1445 ± 8	693	<sup>11</sup> AUGUSTIN	90	DM2 $J/\psi \rightarrow \gamma K_S^0 K^\pm \pi^\mp$
1433 ± 8	296	<sup>11</sup> AUGUSTIN	90	DM2 $J/\psi \rightarrow \gamma K^+ K^- \pi^0$
1413 ± 8	500	<sup>11</sup> DUCH	89	ASTE $\bar{p} p \rightarrow \pi^+ \pi^- K^\pm \pi^\mp K^0$
1453 ± 7	170	<sup>11</sup> RATH	89	MPS $21.4 \pi^- p \rightarrow K_S^0 K_S^0 \pi^0 n$
1419 ± 1	8800	<sup>11</sup> BIRMAN	88	MPS $8 \pi^- p \rightarrow K^+ \bar{K}^0 \pi^- n$
1424 ± 3	620	<sup>11</sup> REEVES	86	SPEC $6.6 p\bar{p} \rightarrow K^+ \bar{K}^0 \pi^+ n$
1421 ± 2		<sup>11</sup> CHUNG	85	SPEC $8 \pi^- p \rightarrow K\bar{K}\pi n$
1440 <sup>+20</sup> / <sub>-15</sub>	174	<sup>11</sup> EDWARDS	82E	CBAL $J/\psi \rightarrow \gamma K^+ K^- \pi^0$
1440 <sup>+10</sup> / <sub>-15</sub>		<sup>11</sup> SCHARRE	80	MRK2 $J/\psi \rightarrow \gamma K_S^0 K^\pm \pi^\mp$
1425 ± 7	800	<sup>11,13</sup> BAILLON	67	HBC $0 \bar{p} p \rightarrow K\bar{K}\pi\pi$

- The selected process is  $J/\psi \rightarrow \omega a_0(980)\pi$ .
- From fit to the  $a_0(980)\pi 0^- +$  partial wave.
- Best fit with a single Breit Wigner.
- Decaying dominantly directly to  $K^+ K^- \pi^0$ .
- Decaying into  $(K\bar{K})_S \pi$ ,  $(K\pi)_S \bar{K}$ , and  $a_0(980)\pi$ .
- From fit to the  $a_0(980)\pi 0^- +$  partial wave. Cannot rule out a  $a_0(980)\pi 1^+ +$  partial wave.
- Excluded from averaging because averaging would be meaningless.
- Best fit with a single Breit Wigner.
- This peak in the  $\gamma\rho$  channel may not be related to the  $\eta(1405)$ .
- Estimated by us from various fits.
- These experiments identify only one pseudoscalar in the 1400–1500 range. Data could also refer to  $\eta(1475)$ .
- Systematic uncertainty not evaluated.
- From best fit of  $0^- +$  partial wave, 50%  $K^*(892)K$ , 50%  $a_0(980)\pi$ .

 **$\eta(1405)$  MASS**

VALUE (MeV)	DOCUMENT ID
-------------	-------------

**1408.9 ± 2.4 OUR AVERAGE** Includes data from the 2 datablocks that follow this one. Error includes scale factor of 2.3. See the ideogram below.WEIGHTED AVERAGE  
1408.9±2.4 (Error scaled by 2.3) $\eta(1405)$  mass (MeV) **$\eta\pi\pi$  MODE**

VALUE (MeV)	EVTS	DOCUMENT ID	TECN	COMMENT
-------------	------	-------------	------	---------

The data in this block is included in the average printed for a previous datablock.

**1403.8 <sup>+3.4</sup>/<sub>-3.0</sub> OUR AVERAGE** Error includes scale factor of 2.2. See the ideogram below.

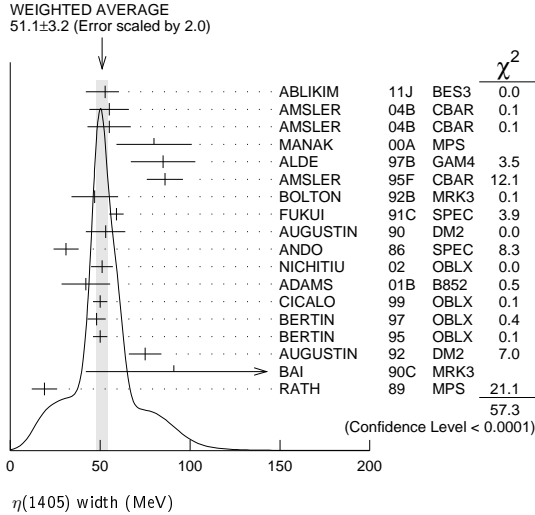
1399.8 ± 2.2 <sup>+2.8</sup> / <sub>-0.1</sub>		<sup>1</sup> ABLIKIM	11J BES3	$J/\psi \rightarrow \omega(\eta)\pi^+\pi^-$
1392 ± 14	900 ± 375	AMSLER	04B CBAR	$0 \bar{p} p \rightarrow \pi^+ \pi^- \pi^+ \pi^- \eta$
1394 ± 8	6.6 ± 2.0k	AMSLER	04B CBAR	$0 \bar{p} p \rightarrow \pi^+ \pi^- \pi^0 \pi^0 \eta$
1404 ± 6	9082	MANAK	00A MPS	$18 \pi^- p \rightarrow \eta\pi^+\pi^- n$
1424 ± 6	2200	ALDE	97B GAM4	$100 \pi^- p \rightarrow \eta\pi^0 \pi^0 n$
1409 ± 3		AMSLER	95F CBAR	$0 \bar{p} p \rightarrow \pi^+ \pi^- \pi^0 \pi^0 \eta$
1400 ± 6		<sup>2</sup> BOLTON	92B MRK3	$J/\psi \rightarrow \gamma\eta\pi^+\pi^-$
1388 ± 4		FUKUI	91C SPEC	$8.95 \pi^- p \rightarrow \eta\pi^+\pi^- n$
1398 ± 6	261	<sup>3</sup> AUGUSTIN	90 DM2	$J/\psi \rightarrow \gamma\eta\pi^+\pi^-$
1420 ± 5		ANDO	86 SPEC	$8 \pi^- p \rightarrow \eta\pi^+\pi^- n$
•••	•••	•••	•••	•••
1385 ± 7		BAI	99 BES	$J/\psi \rightarrow \gamma\eta\pi^+\pi^-$

# Meson Particle Listings

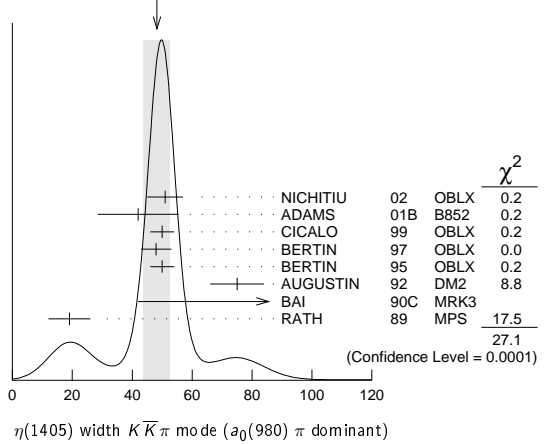
## $\eta(1405)$

### $\eta(1405)$ WIDTH

**51.1 ± 3.2 OUR AVERAGE** Includes data from the 2 datablocks that follow this one. Error includes scale factor of 2.0. See the ideogram below.



### WEIGHTED AVERAGE



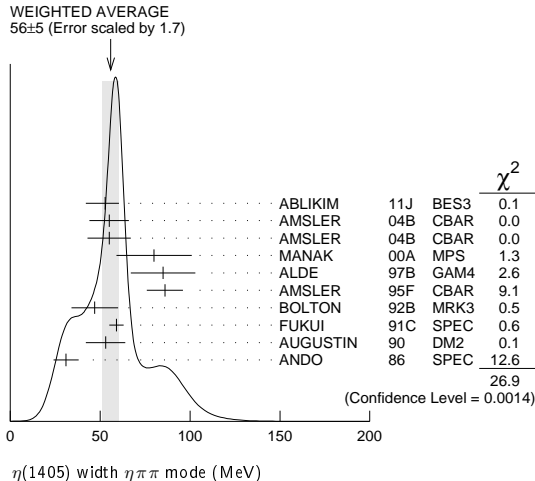
$\eta(1405)$  width  $K\bar{K}\pi$  mode ( $a_0(980)\pi$  dominant)

### $\eta\pi\pi$ MODE

The data in this block is included in the average printed for a previous datablock.

**56 ± 5 OUR AVERAGE** Error includes scale factor of 1.7. See the ideogram below.

VALUE (MeV)	EVTs	DOCUMENT ID	TECN	COMMENT
52.8 ± 7.6 <sup>+0.1</sup> <sub>-7.6</sub>	14	ABLIKIM 11J BES3		$J/\psi \rightarrow \omega(\eta\pi^+\pi^-)$
55 ± 11	900 ± 375	AMSLER 04B CBAR		$0\bar{p}p \rightarrow \pi^+\pi^-\pi^+\pi^- \eta$
55 ± 12	6.6 ± 2.0k	AMSLER 04B CBAR		$0\bar{p}p \rightarrow \pi^+\pi^-\pi^0\pi^0\gamma$
80 ± 21	9082	MANAK 00A MPS		$18\pi^-\rho \rightarrow \eta\pi^+\pi^-n$
85 ± 18	2200	ALDE 97B GAM4		$100\pi^-\rho \rightarrow \eta\pi^0\pi^0n$
86 ± 10		AMSLER 95F CBAR		$0\bar{p}p \rightarrow \pi^+\pi^-\pi^0\pi^0\eta$
47 ± 13		BOLTON 92B MRK3		$J/\psi \rightarrow \gamma\eta\pi^+\pi^-$
59 ± 4		FUKUI 91C SPEC		$8.95\pi^-\rho \rightarrow \eta\pi^+\pi^-n$
53 ± 11		AUGUSTIN 90 DM2		$J/\psi \rightarrow \gamma\eta\pi^+\pi^-$
31 ± 7		ANDO 86 SPEC		$8\pi^-\rho \rightarrow \eta\pi^+\pi^-n$



### $\pi\pi\gamma$ MODE

VALUE (MeV)	EVTs	DOCUMENT ID	TECN	COMMENT
<b>64 ± 18</b>	235 ± 91	AMSLER 04B CBAR		$0\bar{p}p \rightarrow \pi^+\pi^-\pi^+\pi^-\gamma$
• • • We do not use the following data for averages, fits, limits, etc. • • •				
101.0 ± 8.8 ± 8.8	547	BAI 04J BES2		$J/\psi \rightarrow \gamma\gamma\pi^+\pi^-$
174 ± 44		AUGUSTIN 90 DM2		$J/\psi \rightarrow \pi^+\pi^-\gamma\gamma$
90 ± 26		COFFMAN 90 MRK3		$J/\psi \rightarrow \pi^+\pi^-\gamma$

### 4 $\pi$ MODE

VALUE (MeV)	EVTs	DOCUMENT ID	TECN	COMMENT
160 ± 30		BUGG 95 MRK3		$J/\psi \rightarrow \gamma\pi^+\pi^-\pi^+\pi^-$
144 ± 13	3270	BISELLO 89B DM2		$J/\psi \rightarrow 4\pi\gamma$

### $K\bar{K}\pi$ MODE (unresolved)

VALUE (MeV)	EVTs	DOCUMENT ID	TECN	COMMENT
• • • We do not use the following data for averages, fits, limits, etc. • • •				
48.9 ± 9.0	249 ± 35	22,23 ABLIKIM 08E BES2		$J/\psi \rightarrow \omega K_S^0 K^+\pi^- + c.c.$
34.2 ± 18.5	62 ± 18	22,23 ABLIKIM 08E BES2		$J/\psi \rightarrow \omega K^+ K^- \pi^0$
93 ± 14	296	22 AUGUSTIN 90 DM2		$J/\psi \rightarrow \gamma K^+ K^- \pi^0$
105 ± 10	693	22 AUGUSTIN 90 DM2		$J/\psi \rightarrow \gamma K_S^0 K^\pm \pi^\mp$
62 ± 16	500	22 DUCH 89 ASTE		$\bar{p}p \rightarrow K\bar{K}\pi\pi\pi$
100 ± 11	170	22 RATH 89 MPS		$21.4\pi^-\rho \rightarrow K_S^0 K_S^0 \pi^0 n$
66 ± 2	8800	22 BIRMAN 88 MPS		$8\pi^-\rho \rightarrow K^+ \bar{K}^0 \pi^- n$
60 ± 10	620	22 REEVES 86 SPEC		$6.6\bar{p}p \rightarrow K K \pi X$
60 ± 10		22 CHUNG 85 SPEC		$8\pi^-\rho \rightarrow K\bar{K}\pi n$
55 <sup>+20</sup> <sub>-30</sub>	174	22 EDWARDS 82E CBAL		$J/\psi \rightarrow \gamma K^+ K^- \pi^0$
50 <sup>+30</sup> <sub>-20</sub>		22 SCHARRE 80 MRK2		$J/\psi \rightarrow \gamma K_S^0 K^\pm \pi^\mp$
80 ± 10	800	22,24 BAILLON 67 HBC		$0.0\bar{p}p \rightarrow K\bar{K}\pi\pi\pi$

- The selected process is  $J/\psi \rightarrow \omega a_0(980)\pi$ .
- From fit to the  $a_0(980)\pi 0^-+$  partial wave.
- From  $\eta\pi^+\pi^-$  mass distribution - mainly  $a_0(980)\pi$  - no spin-parity determination available.
- Decaying dominantly directly to  $K^+K^-\pi^0$ .
- Decaying into  $(K\bar{K})_S\pi, (K\pi)_S\bar{K},$  and  $a_0(980)\pi$ .
- From fit to the  $a_0(980)\pi 0^-+$  partial wave, but  $a_0(980)\pi 1^++$  cannot be excluded.
- This peak in the  $\gamma\rho$  channel may not be related to the  $\eta(1405)$ .
- Estimated by us from various fits.
- These experiments identify only one pseudoscalar in the 1400–1500 range. Data could also refer to  $\eta(1475)$ .
- Systematic uncertainty not evaluated.
- From best fit to  $0^-+$  partial wave, 50%  $K^*(892)K, 50\% a_0(980)\pi$ .

### $K\bar{K}\pi$ MODE ( $a_0(980)\pi$ or direct $K\bar{K}\pi$ )

The data in this block is included in the average printed for a previous datablock.

**48 ± 4 OUR AVERAGE** Error includes scale factor of 2.1. See the ideogram below.

VALUE (MeV)	EVTs	DOCUMENT ID	TECN	COMMENT
51 ± 6	3651	17 NICHITIU 02 OBLX		
42 ± 10 ± 9	20k	ADAMS 01B B852		$18\text{ GeV } \pi^-\rho \rightarrow K^+K^-\pi^0 n$
50 ± 4		CICALO 99 OBLX		$0\bar{p}p \rightarrow K^\pm K_S^0 \pi^\mp \pi^+\pi^-$
48 ± 5		BERTIN 97 OBLX		$0.0\bar{p}p \rightarrow K^\pm(K^0)\pi^\mp \pi^+\pi^-$
50 ± 4		BERTIN 95 OBLX		$0\bar{p}p \rightarrow K\bar{K}\pi\pi\pi$
75 ± 9		AUGUSTIN 92 DM2		$J/\psi \rightarrow \gamma K\bar{K}\pi$
91 <sup>+67</sup> <sub>-31-38</sub>		BAI 90C MRK3		$J/\psi \rightarrow \gamma K_S^0 K^\pm \pi^\mp$
19 ± 7		RATH 89 MPS		$21.4\pi^-\rho \rightarrow n K_S^0 K_S^0 \pi^0$

### $\eta(1405)$ DECAY MODES

Mode	Fraction ( $\Gamma_i/\Gamma$ )	Confidence level
$\Gamma_1$ $K\bar{K}\pi$	seen	
$\Gamma_2$ $\eta\pi\pi$	seen	
$\Gamma_3$ $a_0(980)\pi$	seen	
$\Gamma_4$ $\eta(\pi\pi)_S\text{-wave}$	seen	
$\Gamma_5$ $f_0(980)\eta$	seen	
$\Gamma_6$ $4\pi$	seen	
$\Gamma_7$ $\rho\rho$	<5% %	99.85%
$\Gamma_8$ $\gamma\gamma$		
$\Gamma_9$ $\rho^0\gamma$	seen	
$\Gamma_{10}$ $\phi\gamma$		
$\Gamma_{11}$ $K^*(892)K$	seen	



See key on page 457

Meson Particle Listings  
 $\eta(1405)$ ,  $f_1(1420)$ 

$\eta(1405) \Gamma(i)\Gamma(\gamma\gamma)/\Gamma(\text{total})$					
$\Gamma(K\bar{K}\pi) \times \Gamma(\gamma\gamma)/\Gamma(\text{total})$					$\Gamma_1/\Gamma_8/\Gamma$
VALUE (keV)	CL%	DOCUMENT ID	TECN	COMMENT	
••• We do not use the following data for averages, fits, limits, etc. •••					
<0.035	90	25,26 AHOHE	05	CLE2	$10.6 e^+e^- \rightarrow e^+e^- K_S^0 K^\pm \pi^\mp$
$\Gamma(\eta\pi\pi) \times \Gamma(\gamma\gamma)/\Gamma(\text{total})$					$\Gamma_2/\Gamma_8/\Gamma$
VALUE (keV)	CL%	DOCUMENT ID	TECN	COMMENT	
<0.095	95	ACCIARRI	01G	L3	$183\text{--}202 e^+e^- \rightarrow e^+e^- \eta\pi^+\pi^-$
$\Gamma(\rho^0\gamma) \times \Gamma(\gamma\gamma)/\Gamma(\text{total})$					$\Gamma_9/\Gamma_8/\Gamma$
VALUE (keV)	CL%	DOCUMENT ID	TECN	COMMENT	
••• We do not use the following data for averages, fits, limits, etc. •••					
<1.5	95	ALTHOFF	84E	TASS	$e^+e^- \rightarrow e^+\pi^+\pi^-\gamma$
25 Using $\eta(1405)$ mass and width 1410 MeV and 51 MeV, respectively.					
26 Assuming three-body phase-space decay to $K_S^0 K^\pm \pi^\mp$ .					

 $\eta(1405)$  BRANCHING RATIOS

$\Gamma(\eta\pi\pi)/\Gamma(K\bar{K}\pi)$						$\Gamma_2/\Gamma_1$
VALUE	CL%	DOCUMENT ID	TECN	COMMENT		
••• We do not use the following data for averages, fits, limits, etc. •••						
$1.09 \pm 0.48$		27 AMSLER	04B	CBAR	$0 \bar{p}p \rightarrow \pi^+\pi^-\pi^+\pi^-\eta$	
<0.5	90	EDWARDS	83B	CBAL	$J/\psi \rightarrow \eta\pi\pi\gamma$	
<1.1	90	SCHARRE	80	MRK2	$J/\psi \rightarrow \eta\pi\pi\gamma$	
<1.5	95	FOSTER	68B	HBC	$0.0 \bar{p}p$	
$\Gamma(\rho^0\gamma)/\Gamma(\eta\pi\pi)$						$\Gamma_9/\Gamma_2$
VALUE	DOCUMENT ID	TECN	COMMENT			
$0.111 \pm 0.064$	AMSLER	04B	CBAR	$0 \bar{p}p$		
$\Gamma(a_0(980)\pi)/\Gamma(K\bar{K}\pi)$						$\Gamma_3/\Gamma_1$
VALUE	EVTS	DOCUMENT ID	TECN	COMMENT		
••• We do not use the following data for averages, fits, limits, etc. •••						
$\sim 0.15$		28 BERTIN	95	OBLX	$0 \bar{p}p \rightarrow K\bar{K}\pi\pi\pi$	
$\sim 0.8$	500	28 DUCH	89	ASTE	$\bar{p}p \rightarrow \pi^+\pi^-K^\pm\pi^\mp K^0$	
$\sim 0.75$		28 REEVES	86	SPEC	$6.6 \bar{p}p \rightarrow K K\pi X$	
$\Gamma(a_0(980)\pi)/\Gamma(\eta\pi\pi)$						$\Gamma_3/\Gamma_2$
VALUE	EVTS	DOCUMENT ID	TECN	COMMENT		
••• We do not use the following data for averages, fits, limits, etc. •••						
$0.29 \pm 0.10$		ABELE	98E	CBAR	$0 \bar{p}p \rightarrow \eta\pi^0\pi^0\pi^0$	
$0.19 \pm 0.04$	2200	29 ALDE	97B	GAM4	$100 \pi^-\rho \rightarrow \eta\pi^+\pi^-\eta$	
$0.56 \pm 0.04 \pm 0.03$		29 AMSLER	95F	CBAR	$0 \bar{p}p \rightarrow \pi^+\pi^-\pi^0\pi^0\eta$	
$\Gamma(a_0(980)\pi)/\Gamma(\eta(\pi\pi)s\text{-wave})$						$\Gamma_3/\Gamma_4$
VALUE	EVTS	DOCUMENT ID	TECN	COMMENT		
••• We do not use the following data for averages, fits, limits, etc. •••						
$0.91 \pm 0.12$		ANISOVICH	01	SPEC	$0.0 \bar{p}p \rightarrow \eta\pi^+\pi^-\pi^+\pi^-$	
$0.15 \pm 0.04$	9082	30 MANAK	00A	MPS	$18 \pi^-\rho \rightarrow \eta\pi^+\pi^-\eta$	
$0.70 \pm 0.12 \pm 0.20$		31 BAI	99	BES	$J/\psi \rightarrow \gamma\eta\pi^+\pi^-$	
$\Gamma(\rho^0\gamma)/\Gamma(K\bar{K}\pi)$						$\Gamma_9/\Gamma_1$
VALUE	DOCUMENT ID	TECN	COMMENT			
$0.0152 \pm 0.0038$	32	COFFMAN	90	MRK3	$J/\psi \rightarrow \gamma\gamma\pi^+\pi^-$	
$\Gamma(\eta(\pi\pi)s\text{-wave})/\Gamma(\eta\pi\pi)$						$\Gamma_4/\Gamma_2$
VALUE	EVTS	DOCUMENT ID	TECN	COMMENT		
••• We do not use the following data for averages, fits, limits, etc. •••						
$0.81 \pm 0.04$	2200	ALDE	97B	GAM4	$100 \pi^-\rho \rightarrow \eta\pi^0\pi^0 n$	
$\Gamma(f_0(980)\eta)/\Gamma(\eta\pi\pi)$						$\Gamma_5/\Gamma_2$
VALUE	DOCUMENT ID	TECN	COMMENT			
••• We do not use the following data for averages, fits, limits, etc. •••						
$0.32 \pm 0.07$	33	ANISOVICH	00	SPEC	$0.9\text{--}1.2 \bar{p}p \rightarrow \eta 3\pi^0$	
$\Gamma(\rho\rho)/\Gamma(\text{total})$						$\Gamma_7/\Gamma$
VALUE	CL%	DOCUMENT ID	TECN	COMMENT		
<0.58	99.85	27,34	AMSLER	04B	CBAR	$0 \bar{p}p$
$\Gamma(K^*(892)K)/\Gamma(a_0(980)\pi)$						$\Gamma_{11}/\Gamma_3$
VALUE	DOCUMENT ID	TECN	COMMENT			
••• We do not use the following data for averages, fits, limits, etc. •••						
$0.084 \pm 0.024$	30	ADAMS	01B	B852	$18 \text{ GeV } \pi^-\rho \rightarrow K^+K^-\pi^0 n$	

$\Gamma(\phi\gamma)/\Gamma(\rho^0\gamma)$						$\Gamma_{10}/\Gamma_9$
VALUE	CL%	DOCUMENT ID	TECN	COMMENT		
••• We do not use the following data for averages, fits, limits, etc. •••						
<0.77	95	35 BAI	04J	BES2	$J/\psi \rightarrow \gamma\gamma K^+K^-$	
27 Using the data of BAILLON 67 on $\bar{p}p \rightarrow K\bar{K}\pi$ .						
28 Assuming that the $a_0(980)$ decays only into $K\bar{K}$ .						
29 Assuming that the $a_0(980)$ decays only into $\eta\pi$ .						
30 Statistical error only.						
31 Assuming that the $a_0(980)$ decays only into $\eta\pi$ .						
32 Using $B(J/\psi \rightarrow \gamma\eta(1405) \rightarrow \gamma K\bar{K}\pi) = 4.2 \times 10^{-3}$ and $B(J/\psi \rightarrow \gamma\eta(1405) \rightarrow \gamma\gamma\rho^0) = 6.4 \times 10^{-5}$ and assuming that the $\rho^0$ signal does not come from the $f_1(1420)$ .						
33 Using preliminary Crystal Barrel data.						
34 Assuming that the $\eta(1405)$ decays are saturated by the $\pi\pi\eta$ , $K\bar{K}\pi$ and $\rho\rho$ modes.						
35 Calculated by us from $B(J/\psi \rightarrow \eta(1405)\gamma \rightarrow \phi\gamma\gamma) < 0.82 \times 10^{-4}$ and $B(J/\psi \rightarrow \eta(1405)\gamma \rightarrow \rho^0\gamma\gamma) = (1.07 \pm 0.17 \pm 0.11) \times 10^{-4}$ .						

 $\eta(1405)$  REFERENCES

ABLIKIM	11J	PRL 107 182001	M. Ablikim et al.	(BES III Collab.)
ABLIKIM	08E	PR D77 032005	M. Ablikim et al.	(BES Collab.)
AHOHE	05	PR D71 072001	R. Ahohe et al.	(CLEO Collab.)
AMSLER	04B	EPJ C33 23	C. Amisler et al.	(Crystal Barrel Collab.)
BAI	04J	PL B594 47	J.Z. Bai et al.	(BES Collab.)
NICHITIU	02	PL B545 261	F. Nichitiu et al.	(OBELIX Collab.)
ACCIARRI	01G	PL B501 1	M. Acciari et al.	(L3 Collab.)
ADAMS	01B	PL B516 264	G.S. Adams et al.	(BNL E852 Collab.)
ANISOVICH	01	NP A690 567	A.V. Anisovich et al.	
ANISOVICH	00	PL B472 168	A.V. Anisovich et al.	
MANAK	00A	PR D52 012003	J.J. Manak et al.	(BNL E852 Collab.)
BAI	99	PL B446 356	J.Z. Bai et al.	(BES Collab.)
CICALO	99	PL B462 453	C. Cicalo et al.	(OBELIX Collab.)
ABELE	98E	NP B514 45	A. Abele et al.	(Crystal Barrel Collab.)
BAI	98C	PL B440 217	J.Z. Bai et al.	(BES Collab.)
ALDE	97B	PAN 60 386	D. Alde et al.	(GAMS Collab.)
BERTIN	97	PL B400 226	A. Bertin et al.	(OBELIX Collab.)
AMSLER	95F	PL B358 389	C. Amisler et al.	(Crystal Barrel Collab.)
BERTIN	95	PL B361 187	A. Bertin et al.	(OBELIX Collab.)
BUGG	95	PL B353 378	D.V. Bugg et al.	(LOQM, PNP, WASH)
AUGUSTIN	92	PR D46 1951	J.E. Augustin, G. Cosme	(DM2 Collab.)
BOLTON	92B	PRL 69 1328	T. Bolton et al.	(Mark III Collab.)
FUKUI	91C	PL B267 293	S. Fukui et al.	(SUGI, NAGO, KEK, KYOT+)
AUGUSTIN	90	PR D42 10	J.E. Augustin et al.	(DM2 Collab.)
BAI	90C	PRL 65 2507	Z. Bai et al.	(Mark III Collab.)
COFFMAN	90	PR D41 1410	D.M. Coffman et al.	(Mark III Collab.)
BISELLO	89B	PR D39 701	G. Busetto et al.	(DM2 Collab.)
DUCH	89	ZPHY C45 223	K.D. Duch et al.	(ASTERIX Collab.)
RATH	89	PR D40 632	M.G. Rath et al.	(NDAM, BRAN, BNL, CUNY+)
BIRMAN	88	PRL 61 1557	A. Birman et al.	(BNL, FSU, IND, MASD) JP
ANDO	86	PRL 57 1296	A. Ando et al.	(KEK, KYOT, NIRS, SAGA+) IJP
REEVES	86	PR D34 1960	D.F. Reeves et al.	(FLOR, BNL, IND+) IJP
CHUNG	85	PRL 55 779	S.U. Chung et al.	(BNL, FLOR, IND+) IJP
ALTHOFF	84E	PL 147B 487	M. Althoff et al.	(TASSO Collab.)
EDWARDS	83B	PRL 51 859	C. Edwards et al.	(CIT, HARV, PRIN+)
EDWARDS	82E	PRL 49 259	C. Edwards et al.	(CIT, HARV, PRIN+)
Also		PRL 50 219	C. Edwards et al.	(CIT, HARV, PRIN+)
SCHARRE	80	PL 97B 329	D.L. Scharre et al.	(SLAC, LBL)
FOSTER	68B	NP B8 174	M. Foster et al.	(CERN, CDEF)
BAILLON	67	NC 50A 393	P.H. Baillon et al.	(CERN, CDEF, IRAD)

 $f_1(1420)$ 

$$I^G(J^{PC}) = 0^+(1^+ +)$$

See the minireview under  $\eta(1405)$ . $f_1(1420)$  MASS

VALUE (MeV)	EVTS	DOCUMENT ID	TECN	COMMENT
<b>1426.4 ± 0.9 OUR AVERAGE</b>		Error includes scale factor of 1.1.		
$1434 \pm 5 \pm 5$	133	1	ACHARD	07 L3 $183\text{--}209 e^+e^- \rightarrow e^+e^- K_S^0 K^\pm \pi^\mp$
$1426 \pm 6$	711		ABDALLAH	03H DLPH $91.2 e^+e^- \rightarrow K_S^0 K^\pm \pi^\mp + X$
$1420 \pm 14$	3651		NICHITIU	02 OBLX
$1428 \pm 4 \pm 2$	20k		ADAMS	01B B852 $18 \text{ GeV } \pi^-\rho \rightarrow K^+K^-\pi^0 n$
$1426 \pm 1$			BARBERIS	97C OMEG $450 \bar{p}p \rightarrow \bar{p}p K_S^0 K^\pm \pi^\mp$
$1425 \pm 8$			BERTIN	97 OBLX $0.0 \bar{p}p \rightarrow K^\pm(K^0)\pi^\mp\pi^+\pi^-$
$1435 \pm 9$			PROKOSHKIN	97B GAM4 $100 \pi^-\rho \rightarrow \eta\pi^0\pi^0 n$
$1430 \pm 4$			2	ARMSTRONG 92E OMEG $85,300 \pi^+\rho, \bar{p}p \rightarrow \pi^+\rho, \bar{p}p(K\bar{K}\pi)$
$1462 \pm 20$			3	AUGUSTIN 92 DM2 $J/\psi \rightarrow \gamma K\bar{K}\pi$
$1443 \pm 7 \pm 3$	1100		BAI	90C MRK3 $J/\psi \rightarrow \gamma K_S^0 K^\pm \pi^\mp$
$1425 \pm 10$	17		BEHREND	89 CELL $\gamma\gamma \rightarrow K_S^0 K^\pm \pi^\mp$
$1442 \pm 5 \pm 10$	111		BECKER	87 MRK3 $e^+e^-, \omega K\bar{K}\pi$
$1423 \pm 4$			GIDAL	87B MRK2 $e^+e^- \rightarrow e^+e^- K\bar{K}\pi$
$1417 \pm 13$	13		AIHARA	86C TPC $e^+e^- \rightarrow e^+e^- K\bar{K}\pi$
$1422 \pm 3$			CHAUVAT	84 SPEC ISR 31.5 $\bar{p}p$
$1440 \pm 10$			4	BROMBERG 80 SPEC $100 \pi^-\rho \rightarrow K\bar{K}\pi X$
$1426 \pm 6$	221		DIONISI	80 HBC $4 \pi^-\rho \rightarrow K\bar{K}\pi n$
$1420 \pm 20$			DAHL	67 HBC $1.6\text{--}4.2 \pi^-\rho$

## Meson Particle Listings

 $f_1(1420)$ 

• • • We do not use the following data for averages, fits, limits, etc. • • •

$1430.8 \pm 0.9$	5	SOSA	99	SPEC	$pp \rightarrow p_{\text{slow}} (K_S^0 K^+ \pi^-) p_{\text{fast}}$
$1433.4 \pm 0.8$	5	SOSA	99	SPEC	$pp \rightarrow p_{\text{slow}} (K_S^0 K^- \pi^+) p_{\text{fast}}$
$1429 \pm 3$	389	ARMSTRONG	89	OMEG	$300 pp \rightarrow K \bar{K} \pi p p$
$1425 \pm 2$	1520	ARMSTRONG	84	OMEG	$85 \pi^+ p, pp \rightarrow (\pi^+, \rho)(K \bar{K} \pi) p$
$\sim 1420$		BITYUKOV	84	SPEC	$32 K^- p \rightarrow K^+ K^- \pi^0 \gamma$

- 1 From a fit with a width fixed at 55 MeV.  
 2 This result supersedes ARMSTRONG 84, ARMSTRONG 89.  
 3 From fit to the  $K^*(892) K 1^{++}$  partial wave.  
 4 Mass error increased to account for  $a_0(980)$  mass cut uncertainties.  
 5 No systematic error given.

 $f_1(1420)$  WIDTH

VALUE (MeV)	EVTS	DOCUMENT ID	TECN	COMMENT
<b><math>54.9 \pm 2.6</math> OUR AVERAGE</b>				
$51 \pm 14$	711	ABDALLAH	03H DLPH	$91.2 e^+ e^- \rightarrow K_S^0 K^\pm \pi^\mp + X$
$61 \pm 8$	3651	NICHITIU	02 OBLX	
$38 \pm 9 \pm 6$	20k	ADAMS	01B B852	$18 \text{ GeV } \pi^- p \rightarrow K^+ K^- \pi^0 n$
$58 \pm 4$		BARBERIS	97C OMEG	$450 pp \rightarrow pp K_S^0 K^\pm \pi^\mp$
$45 \pm 10$		BERTIN	97 OBLX	$0.0 \bar{p} p \rightarrow K^\pm (K^0) \pi^\mp \pi^+ \pi^-$
$90 \pm 25$		PROKOSHKIN	97B GAM4	$100 \pi^- p \rightarrow \eta \pi^0 \pi^0 n$
$58 \pm 10$		6 ARMSTRONG	92E OMEG	$85,300 \pi^+ p, pp \rightarrow \pi^+ p, pp (K \bar{K} \pi)$
$129 \pm 41$		7 AUGUSTIN	92 DM2	$J/\psi \rightarrow \gamma K \bar{K} \pi$
$68 \pm 29 \pm 18 \pm 8 \pm 9$	1100	BAI	90C MRK3	$J/\psi \rightarrow \gamma K_S^0 K^\pm \pi^\mp$
$42 \pm 22$	17	BEHREND	89 CELL	$\gamma \gamma \rightarrow K_S^0 K^\pm \pi^\mp$
$40 \pm 17 \pm 13 \pm 5$	111	BECKER	87 MRK3	$e^+ e^- \rightarrow \omega K \bar{K} \pi$
$35 \pm 47 \pm 20$	13	AIHARA	86C TPC	$e^+ e^- \rightarrow e^+ e^- K \bar{K} \pi$
$47 \pm 10$		CHAUVAT	84 SPEC	ISR 31.5 $pp$
$62 \pm 14$		BROMBERG	80 SPEC	$100 \pi^- p \rightarrow K \bar{K} \pi X$
$40 \pm 15$	221	DIONISI	80 HBC	$4 \pi^- p \rightarrow K \bar{K} \pi n$
$60 \pm 20$		DAHL	67 HBC	$1.6-4.2 \pi^- p$
$68.7 \pm 2.9$		8 SOSA	99 SPEC	$pp \rightarrow p_{\text{slow}} (K_S^0 K^+ \pi^-) p_{\text{fast}}$
$58.8 \pm 3.3$		8 SOSA	99 SPEC	$pp \rightarrow p_{\text{slow}} (K_S^0 K^- \pi^+) p_{\text{fast}}$
$58 \pm 8$	389	ARMSTRONG	89 OMEG	$300 pp \rightarrow K \bar{K} \pi p p$
$62 \pm 5$	1520	ARMSTRONG	84 OMEG	$85 \pi^+ p, pp \rightarrow (\pi^+, \rho)(K \bar{K} \pi) p$
$\sim 50$		BITYUKOV	84 SPEC	$32 K^- p \rightarrow K^+ K^- \pi^0 \gamma$

- 6 This result supersedes ARMSTRONG 84, ARMSTRONG 89.  
 7 From fit to the  $K^*(892) K 1^{++}$  partial wave.  
 8 No systematic error given.

 $f_1(1420)$  DECAY MODES

Mode	Fraction ( $\Gamma_i/\Gamma$ )
$\Gamma_1$ $K \bar{K} \pi$	dominant
$\Gamma_2$ $K \bar{K}^*(892) + \text{c.c.}$	dominant
$\Gamma_3$ $\eta \pi \pi$	possibly seen
$\Gamma_4$ $a_0(980) \pi$	
$\Gamma_5$ $\pi \pi \rho$	
$\Gamma_6$ $4\pi$	
$\Gamma_7$ $\rho^0 \gamma$	
$\Gamma_8$ $\phi \gamma$	seen

 $f_1(1420)$   $\Gamma(i)\Gamma(\gamma\gamma)/\Gamma(\text{total})$ 

VALUE (keV)	CL%	EVTS	DOCUMENT ID	TECN	COMMENT
<b><math>1.9 \pm 0.4</math> OUR AVERAGE</b>					
$3.2 \pm 0.6 \pm 0.7$		133	9,10 ACHARD	07 L3	$183-209 e^+ e^- \rightarrow e^+ e^- K_S^0 K^\pm \pi^\mp$
$3.0 \pm 0.9 \pm 0.7$			11,12 BEHREND	89 CELL	$e^+ e^- \rightarrow e^+ e^- K_S^0 K \pi$
$2.3 \pm 1.0 \pm 0.8$			HILL	89 JADE	$e^+ e^- \rightarrow e^+ e^- K^\pm K_S^0 \pi^\mp$
$1.3 \pm 0.5 \pm 0.3$			AIHARA	88B TPC	$e^+ e^- \rightarrow e^+ e^- K^\pm K_S^0 \pi^\mp$
$1.6 \pm 0.7 \pm 0.3$			11,13 GIDAL	87B MRK2	$e^+ e^- \rightarrow e^+ e^- K \bar{K} \pi$

- • • We do not use the following data for averages, fits, limits, etc. • • •

<8.0	95	JENNI	83	MRK2	$e^+ e^- \rightarrow e^+ e^- K \bar{K} \pi$
					9 From a fit with a width fixed at 55 MeV.
					10 The form factor parameter from the fit is $926 \pm 78$ MeV.
					11 Assume a $\rho$ -pole form factor.
					12 A $\phi$ -pole form factor gives considerably smaller widths.
					13 Published value divided by 2.

 $f_1(1420)$  BRANCHING RATIOS

$\Gamma(K \bar{K}^*(892) + \text{c.c.})/\Gamma(K \bar{K} \pi)$	$\Gamma_2/\Gamma_1$		
VALUE	DOCUMENT ID	TECN	COMMENT
• • • We do not use the following data for averages, fits, limits, etc. • • •			
$0.76 \pm 0.06$	BROMBERG	80 SPEC	$100 \pi^- p \rightarrow K \bar{K} \pi X$
$0.86 \pm 0.12$	DIONISI	80 HBC	$4 \pi^- p \rightarrow K \bar{K} \pi n$

$\Gamma(\pi \pi \rho)/\Gamma(K \bar{K} \pi)$	$\Gamma_5/\Gamma_1$			
VALUE	CL%	DOCUMENT ID	TECN	COMMENT
• • • We do not use the following data for averages, fits, limits, etc. • • •				
<0.3	95	CORDEN	78 OMEG	$12-15 \pi^- p$
<2.0		DAHL	67 HBC	$1.6-4.2 \pi^- p$

$\Gamma(\eta \pi \pi)/\Gamma(K \bar{K} \pi)$	$\Gamma_3/\Gamma_1$			
VALUE	CL%	DOCUMENT ID	TECN	COMMENT
• • • We do not use the following data for averages, fits, limits, etc. • • •				
<0.1	95	ARMSTRONG	91B OMEG	$300 pp \rightarrow pp \eta \pi^+ \pi^-$
• • • We do not use the following data for averages, fits, limits, etc. • • •				
$1.35 \pm 0.75$		KOPKE	89 MRK3	$J/\psi \rightarrow \omega \eta \pi \pi (K \bar{K} \pi)$
<0.6	90	GIDAL	87 MRK2	$e^+ e^- \rightarrow e^+ e^- \eta \pi^+ \pi^-$
<0.5	95	CORDEN	78 OMEG	$12-15 \pi^- p$
$1.5 \pm 0.8$		DEFOIX	72 HBC	$0.7 \bar{p} p$

$\Gamma(a_0(980)\pi)/\Gamma(\eta \pi \pi)$	$\Gamma_4/\Gamma_3$			
VALUE	CL%	DOCUMENT ID	TECN	COMMENT
>0.1	90	PROKOSHKIN	97B GAM4	$100 \pi^- p \rightarrow \eta \pi^0 \pi^0 n$
• • • We do not use the following data for averages, fits, limits, etc. • • •				
not seen in either mode		ANDO	86 SPEC	$8 \pi^- p$
not seen in either mode		CORDEN	78 OMEG	$12-15 \pi^- p$
$0.4 \pm 0.2$		DEFOIX	72 HBC	$0.7 \bar{p} p \rightarrow 7\pi$

$\Gamma(4\pi)/\Gamma(K \bar{K}^*(892) + \text{c.c.})$	$\Gamma_6/\Gamma_2$			
VALUE	CL%	DOCUMENT ID	TECN	COMMENT
• • • We do not use the following data for averages, fits, limits, etc. • • •				
<0.90	95	DIONISI	80 HBC	$4 \pi^- p$

$\Gamma(K \bar{K} \pi)/[\Gamma(K \bar{K}^*(892) + \text{c.c.}) + \Gamma(a_0(980)\pi)]$	$\Gamma_1/(\Gamma_2 + \Gamma_4)$			
VALUE	DOCUMENT ID	TECN	COMMENT	
• • • We do not use the following data for averages, fits, limits, etc. • • •				
$0.65 \pm 0.27$	14	DIONISI	80 HBC	$4 \pi^- p$
				14 Calculated using $\Gamma(K \bar{K})/\Gamma(\eta \pi) = 0.24 \pm 0.07$ for $a_0(980)$ fractions.

$\Gamma(a_0(980)\pi)/\Gamma(K \bar{K}^*(892) + \text{c.c.})$	$\Gamma_4/\Gamma_2$			
VALUE	CL%	DOCUMENT ID	TECN	COMMENT
<b><math>0.04 \pm 0.01 \pm 0.01</math></b>		BARBERIS	98C OMEG	$450 pp \rightarrow p f_1(1420) p_S$
• • • We do not use the following data for averages, fits, limits, etc. • • •				
<0.04	68	ARMSTRONG	84 OMEG	$85 \pi^+ p$

$\Gamma(4\pi)/\Gamma(K \bar{K} \pi)$	$\Gamma_6/\Gamma_1$			
VALUE	CL%	DOCUMENT ID	TECN	COMMENT
<0.62	95	ARMSTRONG	89G OMEG	$85 \pi p \rightarrow 4\pi X$

$\Gamma(\rho^0 \gamma)/\Gamma_{\text{total}}$	$\Gamma_7/\Gamma$			
VALUE	CL%	DOCUMENT ID	TECN	COMMENT
<0.08	95	15 ARMSTRONG	92C SPEC	$300 pp \rightarrow pp \pi^+ \pi^- \gamma$
				15 Using the data on the $\bar{K} K \pi$ mode from ARMSTRONG 89.

$\Gamma(\rho^0 \gamma)/\Gamma(K \bar{K} \pi)$	$\Gamma_7/\Gamma_1$			
VALUE	CL%	DOCUMENT ID	TECN	COMMENT
<0.02	95	BARBERIS	98C OMEG	$450 pp \rightarrow p f_1(1420) p_S$

$\Gamma(\phi \gamma)/\Gamma(K \bar{K} \pi)$	$\Gamma_8/\Gamma_1$		
VALUE	DOCUMENT ID	TECN	COMMENT
<b><math>0.003 \pm 0.001 \pm 0.001</math></b>	BARBERIS	98C OMEG	$450 pp \rightarrow p f_1(1420) p_S$

# Meson Particle Listings

## $f_1(1420), \omega(1420)$

### $f_1(1420)$ REFERENCES

ACHARD 07	JHEP 0703 018	P. Achard et al.	(L3 Collab.)
ABDALLAH 05H	PL B569 129	J. Abdallah et al.	(DELPHI Collab.)
NICHTIUI 02	PL B545 261	F. Nichtiui et al.	(OBELIX Collab.)
ADAMS 01B	PL B516 264	G.S. Adams et al.	(BNL E852 Collab.)
SOSA 99	PRL 83 913	M. Sosa et al.	
BARBERIS 98C	PL B440 225	D. Barberis et al.	(WA 102 Collab.)
BARBERIS 97C	PL B413 225	D. Barberis et al.	(WA 102 Collab.)
BERTIN 97	PL B400 226	A. Bertin et al.	(OBELIX Collab.)
PROKOSHKIN 97B	SPD 42 298	Yu.D. Prokoshkin, S.A. Sadovsky	
Translated from DANS 354 751.			
ARMSTRONG 92C	ZPHY C54 371	T.A. Armstrong et al.	(ATHU, BARI, BIRM+)
ARMSTRONG 92E	ZPHY C56 29	T.A. Armstrong et al.	(ATHU, BARI, BIRM+)
AUGUSTIN 92	PR D46 1951	J.E. Augustin, G. Cosme	(DM2 Collab.)
ARMSTRONG 91B	ZPHY C52 389	T.A. Armstrong et al.	(ATHU, BARI, BIRM+)
BAI 90C	PRL 65 2507	Z. Bai et al.	(Mark III Collab.)
ARMSTRONG 89	PL B221 216	T.A. Armstrong et al.	(CERN, CDEF, BIRM+)
ARMSTRONG 89G	ZPHY C43 55	T.A. Armstrong et al.	(CERN, BIRM, BARI+)
BEHREND 89	ZPHY C42 367	H.J. Behrend et al.	(CELLO Collab.)
HILL 89	ZPHY C42 355	P. Hill et al.	(JADE Collab.)
KOPKE 89	PRPL 174 67	L. Kopke et al.	(CERN)
AIHARA 88B	PL B209 107	H. Aihara et al.	(TPC-2 $\gamma$ Collab.)
BECKER 87	PRL 59 186	J.J. Becker et al.	(Mark III Collab.)
GIDAL 87	PRL 59 2012	G. Gidal et al.	(LBL, SLAC, HARV)
GIDAL 87B	PRL 59 2016	G. Gidal et al.	(LBL, SLAC, HARV)
AIHARA 86C	PRL 57 2500	H. Aihara et al.	(TPC-2 $\gamma$ Collab.)
ANDO 86	PRL 57 1296	A. Ando et al.	(KEK, KYOT, NIRS, SAGA+)
ARMSTRONG 84	PL 146B 273	T.A. Armstrong et al.	(ATHU, BARI, BIRM+)
BITYUKOV 84	SJNP 39 735	S. Bitjukov et al.	(SERP)
Translated from YAF 39 1165.			
CHAUVAT 84	PL 148B 382	P. Chauvat et al.	(CERN, CLER, UCLA+)
JENNI 83	PR D27 1031	P. Jenni et al.	(SLAC, LBL)
BROMBERG 80	PR D22 1513	C.M. Bromberg et al.	(CIT, FNAL, ILLC+)
DIONISI 80	NP B169 1	C. Dionisi et al.	(CERN, MADR, CDEF+)
CORDEN 78	NP B144 253	M.J. Corden et al.	(BIRM, RHEL, TELA+)
DEFOIX 72	NP B44 125	C. Defoix et al.	(CDEF, CERN)
DAHL 67	PR 163 1377	O.L. Dahl et al.	(LRL)IUP
Also	PRL 14 1074	D.H. Miller et al.	(LRL, UCB)

- <sup>9</sup>From the combined fit of ANTONELLI 92, ACHASOV 01E, ACHASOV 02E, and ACHASOV 03D data on the  $\pi^+\pi^-\pi^0$  and ANTONELLI 92 on the  $\omega\pi^+\pi^-$  final states. Supersedes ACHASOV 99E and ACHASOV 02E.
- <sup>10</sup>Using results of CORDIER 81 and preliminary data of DOLINSKY 91 and ANTONELLI 92.
- <sup>11</sup>Using the data of AKHMETSHIN 00D and ANTONELLI 92. The  $\rho\pi$  dominance for the energy dependence of the  $\omega(1420)$  and  $\omega(1650)$  width assumed.
- <sup>12</sup>From a fit to two Breit-Wigner functions and using the data of DOLINSKY 91 and ANTONELLI 92.
- <sup>13</sup>From a fit to two Breit-Wigner functions interfering between them and with the  $\omega,\phi$  tails with fixed (+,-,+,-) phases.

### $\omega(1420)$ DECAY MODES

Mode	Fraction ( $\Gamma_i/\Gamma$ )
$\Gamma_1$ $\rho\pi$	dominant
$\Gamma_2$ $\omega\pi\pi$	seen
$\Gamma_3$ $b_1(1235)\pi$	seen
$\Gamma_4$ $e^+e^-$	seen
$\Gamma_5$ $\pi^0\gamma$	

### $\omega(1420)$ $\Gamma(i)\Gamma(e^+e^-)/\Gamma^2(\text{total})$

$\Gamma(\rho\pi)/\Gamma_{\text{total}} \times \Gamma(e^+e^-)/\Gamma_{\text{total}}$	$\Gamma_1/\Gamma \times \Gamma_4/\Gamma$
VALUE (units $10^{-6}$ )	EVTS DOCUMENT ID TECN COMMENT
0.82 $\pm$ 0.05 $\pm$ 0.06	AUBERT,B 04N BABR 10.6 $e^+e^- \rightarrow \pi^+\pi^-\pi^0\gamma$
0.65 $\pm$ 0.13 $\pm$ 0.21	1.2M <sup>14,15</sup> ACHASOV 03D RVUE 0.44-2.00 $e^+e^- \rightarrow \pi^+\pi^-\pi^0$
0.625 $\pm$ 0.160	16,17 CLEGG 94 RVUE
0.466 $\pm$ 0.178	18,19 ANTONELLI 92 DM2 1.34-2.4 $e^+e^- \rightarrow \rho\pi$

- <sup>14</sup>Calculated by us from the cross section at the peak.
- <sup>15</sup>From the combined fit of ANTONELLI 92, ACHASOV 01E, ACHASOV 02E, and ACHASOV 03D data on the  $\pi^+\pi^-\pi^0$  and ANTONELLI 92 on the  $\omega\pi^+\pi^-$  final states. Supersedes ACHASOV 99E and ACHASOV 02E.
- <sup>16</sup>From a fit to two Breit-Wigner functions and using the data of DOLINSKY 91 and ANTONELLI 92.
- <sup>17</sup>From the partial and leptonic width given by the authors.
- <sup>18</sup>From a fit to two Breit-Wigner functions interfering between them and with the  $\omega,\phi$  tails with fixed (+,-,+,-) phases.
- <sup>19</sup>From the product of the leptonic width and partial branching ratio given by the authors.

$\Gamma(\omega\pi\pi)/\Gamma_{\text{total}} \times \Gamma(e^+e^-)/\Gamma_{\text{total}}$	$\Gamma_2/\Gamma \times \Gamma_4/\Gamma$
VALUE (units $10^{-8}$ )	EVTS DOCUMENT ID TECN COMMENT
19.7 $\pm$ 5.7	AUBERT 07AU BABR 10.6 $e^+e^- \rightarrow \omega\pi^+\pi^-$
1.9 $\pm$ 1.9	20 AKHMETSHIN 00D CMD2 1.2-2.4 $e^+e^- \rightarrow \omega\pi^+\pi^-$

- <sup>20</sup>Using the data of AKHMETSHIN 00D and ANTONELLI 92. The  $\rho\pi$  dominance for the energy dependence of the  $\omega(1420)$  and  $\omega(1650)$  width assumed.

$\Gamma(\pi^0\gamma)/\Gamma_{\text{total}} \times \Gamma(e^+e^-)/\Gamma_{\text{total}}$	$\Gamma_5/\Gamma \times \Gamma_4/\Gamma$
VALUE (units $10^{-8}$ )	EVTS DOCUMENT ID TECN COMMENT
2.03 $\pm$ 0.70	21 AKHMETSHIN 05 CMD2 0.60-1.38 $e^+e^- \rightarrow \pi^0\gamma$
-0.75	

- <sup>21</sup>Using 1420 MeV and 220 MeV for the  $\omega(1420)$  mass and width.

### $\omega(1420)$ BRANCHING RATIOS

$\Gamma(\omega\pi\pi)/\Gamma_{\text{total}}$	$\Gamma_2/\Gamma$
VALUE	EVTS DOCUMENT ID TECN COMMENT
0.301 $\pm$ 0.029	22 HENNER 02 RVUE 1.2-2.0 $e^+e^- \rightarrow \rho\pi, \omega\pi\pi$
possibly seen	AKHMETSHIN 00D CMD2 $e^+e^- \rightarrow \omega\pi^+\pi^-$

$\Gamma(\omega\pi\pi)/\Gamma(b_1(1235)\pi)$	$\Gamma_2/\Gamma_3$
VALUE	EVTS DOCUMENT ID TECN COMMENT
0.60 $\pm$ 0.16	5095 ANISOVICH 00H SPEC 0.0 $\rho\bar{p} \rightarrow \omega\pi^0\pi^0\pi^0$

$\Gamma(\rho\pi)/\Gamma_{\text{total}}$	$\Gamma_1/\Gamma$
VALUE	EVTS DOCUMENT ID TECN COMMENT
0.699 $\pm$ 0.029	22 HENNER 02 RVUE 1.2-2.0 $e^+e^- \rightarrow \rho\pi, \omega\pi\pi$

$\Gamma(e^+e^-)/\Gamma_{\text{total}}$	$\Gamma_4/\Gamma$
VALUE (units $10^{-7}$ )	EVTS DOCUMENT ID TECN COMMENT
$\sim$ 6.6	1.2M <sup>23,24</sup> ACHASOV 03D RVUE 0.44-2.00 $e^+e^- \rightarrow \pi^+\pi^-\pi^0$
23 $\pm$ 1	22 HENNER 02 RVUE 1.2-2.0 $e^+e^- \rightarrow \rho\pi, \omega\pi\pi$

- <sup>22</sup>Assuming that the  $\omega(1420)$  decays into  $\rho\pi$  and  $\omega\pi\pi$  only.
- <sup>23</sup>Calculated by us from the cross section at the peak.
- <sup>24</sup>Assuming that the  $\omega(1420)$  decays into  $\rho\pi$  only.

$\omega(1420)$

$$I^G(J^{PC}) = 0^-(1^{--})$$

### $\omega(1420)$ MASS

VALUE (MeV)	EVTS	DOCUMENT ID	TECN	COMMENT
<b>(1400-1450) OUR ESTIMATE</b>				
1382 $\pm$ 23 $\pm$ 70		AUBERT 07AU BABR 10.6 $e^+e^- \rightarrow \omega\pi^+\pi^-\gamma$		
1350 $\pm$ 20 $\pm$ 20		AUBERT,B 04N BABR 10.6 $e^+e^- \rightarrow \pi^+\pi^-\pi^0\gamma$		
1400 $\pm$ 50 $\pm$ 130	1.2M	<sup>1</sup> ACHASOV 03D RVUE 0.44-2.00 $e^+e^- \rightarrow \pi^+\pi^-\pi^0$		
1450 $\pm$ 10		<sup>2</sup> HENNER 02 RVUE 1.2-2.0 $e^+e^- \rightarrow \rho\pi, \omega\pi\pi$		
1373 $\pm$ 70	177	<sup>3</sup> AKHMETSHIN 00D CMD2 1.2-1.38 $e^+e^- \rightarrow \omega\pi^+\pi^-$		
1370 $\pm$ 25	5095	ANISOVICH 00H SPEC 0.0 $\rho\bar{p} \rightarrow \omega\pi^0\pi^0\pi^0$		
1400 $\pm$ 100		<sup>4</sup> ACHASOV 98H RVUE $e^+e^- \rightarrow \pi^+\pi^-\pi^0$		
$\sim$ 1400		<sup>5</sup> ACHASOV 98H RVUE $e^+e^- \rightarrow \omega\pi^+\pi^-$		
$\sim$ 1460		<sup>6</sup> ACHASOV 98H RVUE $e^+e^- \rightarrow K^+K^-$		
1440 $\pm$ 70		<sup>7</sup> CLEGG 94 RVUE		
1419 $\pm$ 31	315	<sup>8</sup> ANTONELLI 92 DM2 1.34-2.4 $e^+e^- \rightarrow \rho\pi$		

- <sup>1</sup>From the combined fit of ANTONELLI 92, ACHASOV 01E, ACHASOV 02E, and ACHASOV 03D data on the  $\pi^+\pi^-\pi^0$  and ANTONELLI 92 on the  $\omega\pi^+\pi^-$  final states. Supersedes ACHASOV 99E and ACHASOV 02E.
- <sup>2</sup>Using results of CORDIER 81 and preliminary data of DOLINSKY 91 and ANTONELLI 92.
- <sup>3</sup>Using the data of AKHMETSHIN 00D and ANTONELLI 92. The  $\rho\pi$  dominance for the energy dependence of the  $\omega(1420)$  and  $\omega(1650)$  width assumed.
- <sup>4</sup>Using data from BARKOV 87, DOLINSKY 91, and ANTONELLI 92.
- <sup>5</sup>Using the data from ANTONELLI 92.
- <sup>6</sup>Using the data from IVANOV 81 and BISELLO 88b.
- <sup>7</sup>From a fit to two Breit-Wigner functions and using the data of DOLINSKY 91 and ANTONELLI 92.
- <sup>8</sup>From a fit to two Breit-Wigner functions interfering between them and with the  $\omega,\phi$  tails with fixed (+,-,+,-) phases.

### $\omega(1420)$ WIDTH

VALUE (MeV)	EVTS	DOCUMENT ID	TECN	COMMENT
<b>(180-250) OUR ESTIMATE</b>				
130 $\pm$ 50 $\pm$ 100		AUBERT 07AU BABR 10.6 $e^+e^- \rightarrow \omega\pi^+\pi^-\gamma$		
450 $\pm$ 70 $\pm$ 70		AUBERT,B 04N BABR 10.6 $e^+e^- \rightarrow \pi^+\pi^-\pi^0\gamma$		
870 $\pm$ 500	1.2M	<sup>9</sup> ACHASOV 03D RVUE 0.44-2.00 $e^+e^- \rightarrow \pi^+\pi^-\pi^0$		
-300 $\pm$ 450				
199 $\pm$ 15		<sup>10</sup> HENNER 02 RVUE 1.2-2.0 $e^+e^- \rightarrow \rho\pi, \omega\pi\pi$		
188 $\pm$ 45	177	<sup>11</sup> AKHMETSHIN 00D CMD2 1.2-1.38 $e^+e^- \rightarrow \omega\pi^+\pi^-$		
360 $\pm$ 100	5095	ANISOVICH 00H SPEC 0.0 $\rho\bar{p} \rightarrow \omega\pi^0\pi^0\pi^0$		
-60				
240 $\pm$ 70		<sup>12</sup> CLEGG 94 RVUE		
174 $\pm$ 59	315	<sup>13</sup> ANTONELLI 92 DM2 1.34-2.4 $e^+e^- \rightarrow \rho\pi$		

# Meson Particle Listings

## $\omega(1420)$ , $f_2(1430)$ , $a_0(1450)$

### $\omega(1420)$ REFERENCES

AUBERT	07AU	PR D76 092005	B. Aubert <i>et al.</i>	(BABAR Collab.)
AKHMETS SHIN	05	PL B605 26	R.R. Akhmetshin <i>et al.</i>	(Novosibirsk CMD-2 Collab.)
AUBERT B	04N	PR D70 072004	B. Aubert <i>et al.</i>	(BABAR Collab.)
ACHASOV	03D	PR D68 052006	M.N. Achasov <i>et al.</i>	(Novosibirsk SND Collab.)
ACHASOV	02E	PR D66 032001	M.N. Achasov <i>et al.</i>	(Novosibirsk SND Collab.)
HENNER	02	EPJ C26 3	V.K. Henner <i>et al.</i>	
ACHASOV	01E	PR D63 072002	M.N. Achasov <i>et al.</i>	(Novosibirsk SND Collab.)
AKHMETS SHIN	00D	PL B489 125	R.R. Akhmetshin <i>et al.</i>	(Novosibirsk CMD-2 Collab.)
ANISOVICH	00H	PL B485 341	A.V. Anisovich <i>et al.</i>	
ACHASOV	99E	PL B462 365	M.N. Achasov <i>et al.</i>	(Novosibirsk SND Collab.)
ACHASOV	98H	PR D57 4334	N.N. Achasov, A.A. Kozhevnikov	
CLEGG	94	ZPHY C62 455	A.B. Clegg, A. Donnachie	(LANC, MCHS)
ANTONELLI	92	ZPHY C56 15	A. Antonelli <i>et al.</i>	(DM2 Collab.)
DOLINSKY	91	PRPL 202 99	S.I. Dolinsky <i>et al.</i>	(NOVO)
BISELLO	88B	ZPHY C39 13	D. Bisello <i>et al.</i>	(PADO, CLER, FRAS+)
BARKOV	87	JETPL 46 164	L.M. Barkov <i>et al.</i>	(NOVO)
		Translated from ZETFP 46 132.		
CORDIER	81	PL 106B 155	A. Cordier <i>et al.</i>	(ORSAY)
IVANOV	81	PL 107B 297	P.M. Ivanov <i>et al.</i>	(NOVO)

### $f_2(1430)$

$$I^G(J^{PC}) = 0^+(2^{++})$$

OMITTED FROM SUMMARY TABLE

This entry lists nearby peaks observed in the  $D$  wave of the  $K\bar{K}$  and  $\pi^+\pi^-$  systems. Needs confirmation.

### $f_2(1430)$ MASS

VALUE (MeV)	DOCUMENT ID	TECN	COMMENT
<b><math>\approx 1430</math> OUR ESTIMATE</b>			
• • • We do not use the following data for averages, fits, limits, etc. • • •			
1453 ± 4	<sup>1</sup> VLADIMIRSK..01	SPEC	$40 \pi^- p \rightarrow K_S^0 K_S^0 n$
1421 ± 5	AUGUSTIN 87	DM2	$J/\psi \rightarrow \gamma \pi^+ \pi^-$
1480 ± 50	AKESSON 86	SPEC	$pp \rightarrow pp \pi^+ \pi^-$
1436 $^{+26}_{-16}$	DAUM 84	CNTR	$17-18 \pi^- p \rightarrow K^+ K^- n$
1412 ± 3	DAUM 84	CNTR	$63 \pi^- p \rightarrow K_S^0 K_S^0 n, K^+ K^- n$
1439 $^{+5}_{-6}$	<sup>2</sup> BEUSCH 67	OSPK	$5,7,12 \pi^- p \rightarrow K_S^0 K_S^0 n$
<sup>1</sup> $J^{PC} = 0^{++}$ or $2^{++}$ .			
<sup>2</sup> Not seen by WETZEL 76.			

### $f_2(1430)$ WIDTH

VALUE (MeV)	DOCUMENT ID	TECN	COMMENT
• • • We do not use the following data for averages, fits, limits, etc. • • •			
13 ± 5	<sup>3</sup> VLADIMIRSK..01	SPEC	$40 \pi^- p \rightarrow K_S^0 K_S^0 n$
30 ± 9	AUGUSTIN 87	DM2	$J/\psi \rightarrow \gamma \pi^+ \pi^-$
150 ± 50	AKESSON 86	SPEC	$pp \rightarrow pp \pi^+ \pi^-$
81 $^{+56}_{-29}$	DAUM 84	CNTR	$17-18 \pi^- p \rightarrow K^+ K^- n$
14 ± 6	DAUM 84	CNTR	$63 \pi^- p \rightarrow K_S^0 K_S^0 n, K^+ K^- n$
43 $^{+17}_{-18}$	<sup>4</sup> BEUSCH 67	OSPK	$5,7,12 \pi^- p \rightarrow K_S^0 K_S^0 n$
<sup>3</sup> $J^{PC} = 0^{++}$ or $2^{++}$ .			
<sup>4</sup> Not seen by WETZEL 76.			

### $f_2(1430)$ DECAY MODES

Mode	
$\Gamma_1$	$K\bar{K}$
$\Gamma_2$	$\pi\pi$

### $f_2(1430)$ REFERENCES

VLADIMIRSK..01	PAN 64 1895	V.V. Vladimirov <i>et al.</i>	
	Translated from YAF 64 1975.		
AUGUSTIN 87	ZPHY C36 369	J.E. Augustin <i>et al.</i>	(LALO, CLER, FRAS+)
AKESSON 86	NP B264 154	T. Akesson <i>et al.</i>	(Axial Field Spec. Collab.)
DAUM 84	ZPHY C23 339	C. Daum <i>et al.</i>	(AMST, CERN, CRAC, MPIM+JP)
WETZEL 76	NP B115 208	W. Wetzel <i>et al.</i>	(ETH, CERN, LOIC)
BEUSCH 67	PL 25B 357	W. Beusch <i>et al.</i>	(ETH, CERN)

### $a_0(1450)$

$$I^G(J^{PC}) = 1^-(0^{++})$$

See minireview on scalar mesons under  $f_0(500)$ .

### $a_0(1450)$ MASS

VALUE (MeV)	EVTS	DOCUMENT ID	TECN	COMMENT
<b>1474 ± 19 OUR AVERAGE</b>				
1480 ± 30		ABELE 98	CBAR	$0.0 \bar{p}p \rightarrow K^0 K^\pm \pi^\mp$
1470 ± 25		<sup>1</sup> AMSLER 95D	CBAR	$0.0 \bar{p}p \rightarrow \pi^0 \pi^0 \pi^0, \pi^0 \eta, \pi^0 \pi^0 \eta$

• • • We do not use the following data for averages, fits, limits, etc. • • •

1515 ± 30		<sup>2</sup> ANISOVICH 09	RVUE	$0.0 \bar{p}p, \pi N$
1316.8 $^{+0.7+24.7}_{-1.0-4.6}$		<sup>3</sup> UEHARA 09A	BELL	$\gamma\gamma \rightarrow \pi^0 \eta$
1432 ± 13 ± 25		<sup>4</sup> BUGG 08A	RVUE	$\bar{p}p$
1477 ± 10	80k	<sup>5</sup> UMAN 06	E835	$5.2 \bar{p}p \rightarrow \eta \eta \pi^0$
1441 ± 40	35280	<sup>2</sup> BAKER 03	SPEC	$\bar{p}p \rightarrow \omega \pi^+ \pi^- \pi^0$
1303 ± 16		<sup>6</sup> BARGIOTTI 03	OBLX	$\bar{p}p$
1296 ± 10		<sup>7</sup> AMSLER 02	CBAR	$0.9 \bar{p}p \rightarrow \pi^0 \pi^0 \eta$
1565 ± 30		<sup>7</sup> ANISOVICH 98B	RVUE	Compilation
1290 ± 10		<sup>8</sup> BERTIN 98B	OBLX	$0.0 \bar{p}p \rightarrow K^\pm K_S^0 \pi^\mp$
1450 ± 40		AMSLER 94D	CBAR	$0.0 \bar{p}p \rightarrow \pi^0 \pi^0 \eta$
1410 ± 25		ETKIN 82C	MPS	$23 \pi^- p \rightarrow n 2 K_S^0$
~ 1300		MARTIN 78	SPEC	$10 K^\pm p \rightarrow K_S^0 \pi p$
1255 ± 5		<sup>9</sup> CASON 76		

<sup>1</sup>Coupled-channel analysis of AMSLER 95B, AMSLER 95c, and AMSLER 94D.

<sup>2</sup>From the pole position.

<sup>3</sup>May be a different state.

<sup>4</sup>Using data from AMSLER 94d, ABELE 98, and BAKER 03. Supersedes BUGG 94.

<sup>5</sup>Statistical error only.

<sup>6</sup>Coupled channel analysis of  $\pi^+ \pi^- \pi^0, K^+ K^- \pi^0$ , and  $K^\pm K_S^0 \pi^\mp$ .

<sup>7</sup>T-matrix pole.

<sup>8</sup>Not confirmed by BUGG 08a.

<sup>9</sup>Isospin 0 not excluded.

### $a_0(1450)$ WIDTH

VALUE (MeV)	EVTS	DOCUMENT ID	TECN	COMMENT
<b>265 ± 13 OUR AVERAGE</b>				
265 ± 15		ABELE 98	CBAR	$0.0 \bar{p}p \rightarrow K^0 K^\pm \pi^\mp$
265 ± 30		<sup>10</sup> AMSLER 95D	CBAR	$0.0 \bar{p}p \rightarrow \pi^0 \pi^0 \pi^0, \pi^0 \eta, \pi^0 \pi^0 \eta$
• • • We do not use the following data for averages, fits, limits, etc. • • •				
230 ± 36		<sup>11</sup> ANISOVICH 09	RVUE	$0.0 \bar{p}p, \pi N$
65.0 $^{+2.1+99.1}_{-5.4-32.6}$		<sup>12</sup> UEHARA 09A	BELL	$\gamma\gamma \rightarrow \pi^0 \eta$
196 ± 10 ± 10		<sup>13</sup> BUGG 08A	RVUE	$\bar{p}p$
267 ± 11	80k	<sup>14</sup> UMAN 06	E835	$5.2 \bar{p}p \rightarrow \eta \eta \pi^0$
110 ± 14	35280	<sup>11</sup> BAKER 03	SPEC	$\bar{p}p \rightarrow \omega \pi^+ \pi^- \pi^0$
92 ± 16		<sup>15</sup> BARGIOTTI 03	OBLX	$\bar{p}p$
81 ± 21		<sup>16</sup> AMSLER 02	CBAR	$0.9 \bar{p}p \rightarrow \pi^0 \pi^0 \eta$
292 ± 40		<sup>16</sup> ANISOVICH 98B	RVUE	Compilation
80 ± 5		<sup>17</sup> BERTIN 98B	OBLX	$0.0 \bar{p}p \rightarrow K^\pm K_S^0 \pi^\mp$
270 ± 40		AMSLER 94D	CBAR	$0.0 \bar{p}p \rightarrow \pi^0 \pi^0 \eta$
230 ± 30		ETKIN 82C	MPS	$23 \pi^- p \rightarrow n 2 K_S^0$
~ 250		MARTIN 78	SPEC	$10 K^\pm p \rightarrow K_S^0 \pi p$
79 ± 10		<sup>18</sup> CASON 76		

<sup>10</sup>Coupled-channel analysis of AMSLER 95B, AMSLER 95c, and AMSLER 94D.

<sup>11</sup>From the pole position.

<sup>12</sup>May be a different state.

<sup>13</sup>Using data from AMSLER 94d, ABELE 98, and BAKER 03. Supersedes BUGG 94.

<sup>14</sup>Statistical error only.

<sup>15</sup>Coupled channel analysis of  $\pi^+ \pi^- \pi^0, K^+ K^- \pi^0$ , and  $K^\pm K_S^0 \pi^\mp$ .

<sup>16</sup>T-matrix pole.

<sup>17</sup>Not confirmed by BUGG 08a.

<sup>18</sup>Isospin 0 not excluded.

### $a_0(1450)$ DECAY MODES

Mode	Fraction ( $\Gamma_i/\Gamma$ )
$\Gamma_1$	$\pi\eta$ seen
$\Gamma_2$	$\pi\eta'(958)$ seen
$\Gamma_3$	$K\bar{K}$ seen
$\Gamma_4$	$\omega\pi\pi$ seen
$\Gamma_5$	$a_0(980)\pi\pi$ seen
$\Gamma_6$	$\gamma\gamma$ seen

### $a_0(1450)$ $\Gamma(i)\Gamma(\gamma\gamma)/\Gamma(\text{total})$

$\Gamma(\pi\eta) \times \Gamma(\gamma\gamma)/\Gamma_{\text{total}}$	VALUE (eV)	DOCUMENT ID	TECN	COMMENT	$\Gamma_1\Gamma_6/\Gamma$
---	------------	-------------	------	---------	---------------------------

• • • We do not use the following data for averages, fits, limits, etc. • • •

432 $\pm 6$ $^{+1073}_{-256}$		<sup>19</sup> UEHARA 09A	BELL	$\gamma\gamma \rightarrow \pi^0 \eta$	
-------------------------------	--	--------------------------	------	---------------------------------------	--

<sup>19</sup>May be a different state.

## Meson Particle Listings

 $a_0(1450)$ ,  $\rho(1450)$  $a_0(1450)$  BRANCHING RATIOS $\Gamma(\pi\eta(958))/\Gamma(\pi\eta)$   $\Gamma_2/\Gamma_1$ 

VALUE	DOCUMENT ID	TECN	COMMENT
$0.35 \pm 0.16$	<sup>20</sup> ABELE	98	CBAR $0.0 \bar{p}p \rightarrow K_L^0 K^\pm \pi^\mp$

• • • We do not use the following data for averages, fits, limits, etc. • • •

0.43 ± 0.19 ABELE 97c CBAR  $0.0 \bar{p}p \rightarrow \pi^0 \pi^0 \eta'$ <sup>20</sup> Using  $\pi^0 \eta$  from AMSLER 94D. $\Gamma(K\bar{K})/\Gamma(\pi\eta)$   $\Gamma_3/\Gamma_1$ 

VALUE	DOCUMENT ID	TECN	COMMENT
$0.88 \pm 0.23$	<sup>21</sup> ABELE	98	CBAR $0.0 \bar{p}p \rightarrow K_L^0 K^\pm \pi^\mp$

<sup>21</sup> Using  $\pi^0 \eta$  from AMSLER 94D. $\Gamma(\omega\pi\pi)/\Gamma(\pi\eta)$   $\Gamma_4/\Gamma_1$ 

VALUE	EVTS	DOCUMENT ID	TECN	COMMENT
$10.7 \pm 2.3$	35280	<sup>22</sup> BAKER	03	SPEC $\bar{p}p \rightarrow \omega\pi^+\pi^-\pi^0$

• • • We do not use the following data for averages, fits, limits, etc. • • •

<sup>22</sup> Using results on  $\bar{p}p \rightarrow a_0(1450)^0 \pi^0$ ,  $a_0(1450) \rightarrow \eta\pi^0$  from ABELE 96C and assuming the  $\omega\rho$  mechanism for the  $\omega\pi\pi$  state. $\Gamma(a_0(980)\pi\pi)/\Gamma_{\text{total}}$   $\Gamma_5/\Gamma$ 

VALUE	DOCUMENT ID	TECN	COMMENT
seen	BUGG	08A	RVUE $\bar{p}p$

 $\Gamma(a_0(980)\pi\pi)/\Gamma(\pi\eta)$   $\Gamma_5/\Gamma_1$ 

VALUE	DOCUMENT ID	TECN	CHG	COMMENT
$\leq 4.3$	ANISOVICH	01	RVUE	0 $\bar{p}p \rightarrow \eta 2\pi^+ 2\pi^-$

• • • We do not use the following data for averages, fits, limits, etc. • • •

seen  $\gamma\gamma \rightarrow \pi^0 \eta$  $\Gamma(\gamma\gamma)/\Gamma_{\text{total}}$   $\Gamma_6/\Gamma$ 

VALUE	DOCUMENT ID	TECN	COMMENT
seen	<sup>23</sup> UEHARA	09A	BELL

<sup>23</sup> May be a different state. $a_0(1450)$  REFERENCES

ANISOVICH	09	IJMP A24 2481	V.V. Anisovich, A.V. Sarantsev
UEHARA	09A	PR D50 032001	S. Uehara et al.
BUGG	08A	PR D78 074023	D.V. Bugg
UMAN	06	PR D73 052009	I. Uman et al.
BAKER	03	PL B563 140	C.A. Baker et al.
BARGIOTTI	03	EPJ C26 371	M. Bargiotti et al.
AMSLER	02	EPJ C23 29	C. Amisler et al.
ANISOVICH	01	NP A690 567	A.V. Anisovich et al.
ABELE	98	PR D57 3860	A. Abele et al.
ANISOVICH	98B	SPU 41 419	V.V. Anisovich et al.
BERTIN	98B	PL B434 180	A. Bertin et al.
ABELE	97C	PL B404 179	A. Abele et al.
ABELE	96C	NP A609 562	A. Abele et al.
AMSLER	95B	PL B342 433	C. Amisler et al.
AMSLER	95C	PL B353 571	C. Amisler et al.
AMSLER	95D	PL B355 425	C. Amisler et al.
AMSLER	94D	PL B333 277	C. Amisler et al.
BUGG	94	PR D50 4412	D.V. Bugg et al.
ETKIN	82C	PR D25 2446	A. Etkin et al.
MARTIN	78	NP B134 392	A.D. Martin et al.
CASON	76	PRL 36 1485	N.M. Cason et al.

 $\rho(1450)$ 

$$J^G(J^PC) = 1^+(1^{--})$$

See our mini-review under the  $\rho(1700)$ . $\rho(1450)$  MASS

VALUE (MeV)	DOCUMENT ID
$1465 \pm 25$ OUR ESTIMATE	This is only an educated guess; the error given is larger than the error on the average of the published values.

 $\eta\rho^0$  MODE

VALUE (MeV)	DOCUMENT ID	TECN	COMMENT
1497 ± 14	<sup>1</sup> AKHMETSHIN 01B	CMD2	$e^+e^- \rightarrow \eta\gamma$
1421 ± 15	<sup>2</sup> AKHMETSHIN 00D	CMD2	$e^+e^- \rightarrow \eta\pi^+\pi^-$
1470 ± 20	ANTONELLI 88	DM2	$e^+e^- \rightarrow \eta\pi^+\pi^-$
1446 ± 10	FUKUI 88	SPEC	$8.95 \pi^-p \rightarrow \eta\pi^+\pi^-\pi^-$

• • • We do not use the following data for averages, fits, limits, etc. • • •

<sup>1</sup> Using the data of AKHMETSHIN 01B on  $e^+e^- \rightarrow \eta\gamma$ , AKHMETSHIN 00D and ANTONELLI 88 on  $e^+e^- \rightarrow \eta\pi^+\pi^-$ .<sup>2</sup> Using the data of ANTONELLI 88, DOLINSKY 91, and AKHMETSHIN 00D. The energy-independent width of the  $\rho(1450)$  and  $\rho(1700)$  mesons assumed. $\omega\pi$  MODE

VALUE (MeV)	EVTS	DOCUMENT ID	TECN	COMMENT
$1582 \pm 17 \pm 25$	2382	<sup>3</sup> AKHMETSHIN 03B	CMD2	$e^+e^- \rightarrow \pi^0 \pi^0 \gamma$
$1349 \pm 25 \pm 10$	341	<sup>4</sup> ALEXANDER 01B	CLE2	$B \rightarrow D^{(*)} \omega\pi^-$
1523 ± 10		<sup>5</sup> EDWARDS 00A	CLE2	$\tau^- \rightarrow \omega\pi^- \nu_\tau$
1463 ± 25		<sup>6</sup> CLEGG 94	RVUE	
1250		<sup>7</sup> ASTON 80c	OMEG	$20\text{--}70 \gamma p \rightarrow \omega\pi^0 p$
1290 ± 40		<sup>7</sup> BARBER 80c	SPEC	$3\text{--}5 \gamma p \rightarrow \omega\pi^0 p$

<sup>3</sup> Using the data of AKHMETSHIN 03B and BISELLO 91B assuming the  $\omega\pi^0$  and  $\pi^+\pi^-$  mass dependence of the total width.  $\rho(1700)$  mass and width fixed at 1700 MeV and 240 MeV, respectively.<sup>4</sup> Using Breit-Wigner parameterization of the  $\rho(1450)$  and assuming the  $\omega\pi^-$  mass dependence of the total width.<sup>5</sup> Mass-independent width parameterization.  $\rho(1700)$  mass and width fixed at 1700 MeV and 235 MeV respectively.<sup>6</sup> Using data from BISELLO 91B, DOLINSKY 86 and ALBRECHT 87L.<sup>7</sup> Not separated from  $b_1(1235)$ , not pure  $J^P = 1^-$  effect.4 $\pi$  MODE

VALUE (MeV)	DOCUMENT ID	TECN	COMMENT
1435 ± 40	ABELE 01B	CBAR	$0.0 \bar{p}n \rightarrow 2\pi^- 2\pi^0 \pi^+$
1350 ± 50	ACHASOV 97	RVUE	$e^+e^- \rightarrow 2(\pi^+\pi^-)$
1449 ± 4	<sup>8</sup> ARMSTRONG 89E	OMEG	$300 \rho p \rightarrow \rho p 2(\pi^+\pi^-)$

• • • We do not use the following data for averages, fits, limits, etc. • • •

<sup>8</sup> Not clear whether this observation has  $l=1$  or 0. $\pi\pi$  MODE

VALUE (MeV)	EVTS	DOCUMENT ID	TECN	COMMENT
$1446 \pm 7 \pm 28$	5.4 M	<sup>9,10</sup> FUJIKAWA 08	BELL	$\tau^- \rightarrow \pi^- \pi^0 \nu_\tau$
1328 ± 15		<sup>11</sup> SCHAEEL 05c	ALEP	$\tau^- \rightarrow \pi^- \pi^0 \nu_\tau$
1406 ± 15	87k	<sup>9,12</sup> ANDERSON 00A	CLE2	$\tau^- \rightarrow \pi^- \pi^0 \nu_\tau$
$\sim 1368$		<sup>13</sup> ABELE 99c	CBAR	$0.0 \bar{p}d \rightarrow \pi^+\pi^-\pi^-p$
1348 ± 33		BERTIN 98	OBLX	$0.05\text{--}0.405 \bar{p}p \rightarrow 2\pi^+\pi^-$
1411 ± 14		<sup>14</sup> ABELE 97	CBAR	$\bar{p}n \rightarrow \pi^- \pi^0 \pi^0$
1370 $\pm 90$ -70		ACHASOV 97	RVUE	$e^+e^- \rightarrow \pi^+\pi^-$
1359 ± 40		<sup>12</sup> BERTIN 97c	OBLX	$0.0 \bar{p}p \rightarrow \pi^+\pi^-\pi^0$
1282 ± 37		BERTIN 97D	OBLX	$0.05 \bar{p}p \rightarrow 2\pi^+ 2\pi^-$
1424 ± 25		BISELLO 89	DM2	$e^+e^- \rightarrow \pi^+\pi^-$
1265.5 ± 75.3		DUBNICKA 89	RVUE	$e^+e^- \rightarrow \pi^+\pi^-$
1292 ± 17		<sup>15</sup> KURDADZE 83	OLYA	$0.64\text{--}1.4 e^+e^- \rightarrow \pi^+\pi^-$

<sup>9</sup> From the GOUNARIS 68 parametrization of the pion form factor.<sup>10</sup>  $|F_\pi(0)|^2$  fixed to 1.<sup>11</sup> From the combined fit of the  $\tau^-$  data from ANDERSON 00A and SCHAEEL 05c and  $e^+e^-$  data from the compilation of BARKOV 85, AKHMETSHIN 04, and ALLOISIO 05.  $\rho(1700)$  mass and width fixed at 1713 MeV and 235 MeV, respectively. Supersedes BARATE 97M.<sup>12</sup>  $\rho(1700)$  mass and width fixed at 1700 MeV and 235 MeV, respectively.<sup>13</sup>  $\rho(1700)$  mass and width fixed at 1780 MeV and 275 MeV respectively.<sup>14</sup> T-matrix pole.<sup>15</sup> Using for  $\rho(1700)$  mass and width 1600 ± 20 and 300 ± 10 MeV respectively. $K\bar{K}$  MODE

VALUE (MeV)	EVTS	DOCUMENT ID	TECN	CHG	COMMENT
$1422.8 \pm 6.5$	27k	<sup>16</sup> ABELE 99D	CBAR	$\pm$	$0.0 \bar{p}p \rightarrow K^+ K^- \pi^0$

• • • We do not use the following data for averages, fits, limits, etc. • • •

<sup>16</sup> K-matrix pole. Isospin not determined, could be  $\omega(1420)$ . $K\bar{K}^*(892) + c.c.$  MODE

VALUE (MeV)	DOCUMENT ID	TECN	COMMENT
$1505 \pm 19 \pm 7$	AUBERT 08s	BABR	$10.6 e^+e^- \rightarrow K\bar{K}^*(892)\gamma$

 $\rho(1450)$  WIDTH

VALUE (MeV)	DOCUMENT ID
$400 \pm 60$ OUR ESTIMATE	This is only an educated guess; the error given is larger than the error on the average of the published values.

 $\eta\rho^0$  MODE

VALUE (MeV)	DOCUMENT ID	TECN	COMMENT
226 ± 44	<sup>17</sup> AKHMETSHIN 01B	CMD2	$e^+e^- \rightarrow \eta\gamma$
211 ± 31	<sup>18</sup> AKHMETSHIN 00D	CMD2	$e^+e^- \rightarrow \eta\pi^+\pi^-$
230 ± 30	ANTONELLI 88	DM2	$e^+e^- \rightarrow \eta\pi^+\pi^-$
60 ± 15	FUKUI 88	SPEC	$8.95 \pi^-p \rightarrow \eta\pi^+\pi^-\pi^-$

• • • We do not use the following data for averages, fits, limits, etc. • • •

<sup>17</sup> Using the data of AKHMETSHIN 01B on  $e^+e^- \rightarrow \eta\gamma$ , AKHMETSHIN 00D and ANTONELLI 88 on  $e^+e^- \rightarrow \eta\pi^+\pi^-$ .<sup>18</sup> Using the data of ANTONELLI 88, DOLINSKY 91, and AKHMETSHIN 00D. The energy-independent width of the  $\rho(1450)$  and  $\rho(1700)$  mesons assumed.

## Meson Particle Listings

 $\rho(1450)$  $\omega\pi$  MODE

VALUE (MeV)	EVTS	DOCUMENT ID	TECN	COMMENT
429 ± 42 ± 10	2382	19 AKHMETSHIN 03B	CMD2	$e^+e^- \rightarrow \pi^0\pi^0\gamma$
547 ± 86 <sup>+46</sup> <sub>-45</sub>	341	20 ALEXANDER 01B	CLE2	$B \rightarrow D^{(*)}\omega\pi^-$
400 ± 35		21 EDWARDS 00A	CLE2	$\tau^- \rightarrow \omega\pi^-\nu_\tau$
311 ± 62		22 CLEGG 94	RVUE	
300		23 ASTON 80C	OMEG	20-70 $\gamma\rho \rightarrow \omega\pi^0\rho$
320 ± 100		23 BARBER 80C	SPEC	3-5 $\gamma\rho \rightarrow \omega\pi^0\rho$

<sup>19</sup>Using the data of AKHMETSHIN 03B and BISELLO 91B assuming the  $\omega\pi^0$  and  $\pi^+\pi^-$  mass dependence of the total width.  $\rho(1700)$  mass and width fixed at 1700 MeV and 240 MeV, respectively.

<sup>20</sup>Using Breit-Wigner parameterization of the  $\rho(1450)$  and assuming the  $\omega\pi^-$  mass dependence for the total width.

<sup>21</sup>Mass-independent width parameterization.  $\rho(1700)$  mass and width fixed at 1700 MeV and 235 MeV respectively.

<sup>22</sup>Using data from BISELLO 91B, DOLINSKY 86 and ALBRECHT 87L.

<sup>23</sup>Not separated from  $b_1(1235)$ , not pure  $J^P = 1^-$  effect.

4 $\pi$  MODE

VALUE (MeV)	DOCUMENT ID	TECN	COMMENT
325 ± 100	ABELE 01B	CBAR	0.0 $\bar{p}n \rightarrow 2\pi^- 2\pi^0\pi^+$

 $\pi\pi$  MODE

VALUE (MeV)	EVTS	DOCUMENT ID	TECN	COMMENT
434 ± 16 ± 60	5.4M	24,25 FUJIKAWA 08	BELL	$\tau^- \rightarrow \pi^-\pi^0\nu_\tau$
468 ± 41		26 SCHAEEL 05C	ALEP	$\tau^- \rightarrow \pi^-\pi^0\nu_\tau$
455 ± 41	87k	24,27 ANDERSON 00A	CLE2	$\tau^- \rightarrow \pi^-\pi^0\nu_\tau$
~ 374		28 ABELE 99C	CBAR	0.0 $\bar{p}d \rightarrow \pi^+\pi^-\pi^-\rho$
~ 275 ± 10		BERTIN 98	OBLX	0.05-0.405 $\bar{p}p \rightarrow \pi^+\pi^+\pi^-$
343 ± 20		29 ABELE 97	CBAR	$\bar{p}n \rightarrow \pi^-\pi^0\pi^0$
310 ± 40		27 BERTIN 97C	OBLX	0.0 $\bar{p}p \rightarrow \pi^+\pi^-\pi^0$
236 ± 36		BERTIN 97D	OBLX	0.05 $\bar{p}p \rightarrow 2\pi^+ 2\pi^-$
269 ± 31		BISELLO 89	DM2	$e^+e^- \rightarrow \pi^+\pi^-$
391 ± 70		DUBNICKA 89	RVUE	$e^+e^- \rightarrow \pi^+\pi^-$
218 ± 46		30 KURDADZE 83	OLYA	0.64-1.4 $e^+e^- \rightarrow \pi^+\pi^-$

<sup>24</sup>From the GOUNARIS 68 parametrization of the pion form factor.

<sup>25</sup> $|F_\pi(0)|^2$  fixed to 1.

<sup>26</sup>From the combined fit of the  $\tau^-$  data from ANDERSON 00A and SCHAEEL 05C and  $e^+e^-$  data from the compilation of BARKOV 85, AKHMETSHIN 04, and AL OISIO 05.  $\rho(1700)$  mass and width fixed at 1713 MeV and 235 MeV, respectively. Supersedes BARATE 97M.

<sup>27</sup> $\rho(1700)$  mass and width fixed at 1700 MeV and 235 MeV, respectively.

<sup>28</sup> $\rho(1700)$  mass and width fixed at 1780 MeV and 275 MeV respectively.

<sup>29</sup>T-matrix pole.

<sup>30</sup>Using for  $\rho(1700)$  mass and width 1600 ± 20 and 300 ± 10 MeV respectively.

 $K\bar{K}$  MODE

VALUE (MeV)	EVTS	DOCUMENT ID	TECN	CHG	COMMENT
146.5 ± 10.5	27k	31 ABELE 99D	CBAR	±	0.0 $\bar{p}p \rightarrow K^+K^-\pi^0$

<sup>31</sup>K-matrix pole. Isospin not determined, could be  $\omega(1420)$ .

 $K\bar{K}^*(892) + c.c.$  MODE

VALUE (MeV)	DOCUMENT ID	TECN	COMMENT
418 ± 25 ± 4	AUBERT 08s	BABR	10.6 $e^+e^- \rightarrow K\bar{K}^*(892)\gamma$

 $\rho(1450)$  DECAY MODES

Mode	Fraction ( $\Gamma_i/\Gamma$ )
$\Gamma_1$ $\pi\pi$	seen
$\Gamma_2$ $4\pi$	seen
$\Gamma_3$ $\omega\pi$	
$\Gamma_4$ $a_1(1260)\pi$	
$\Gamma_5$ $h_1(1170)\pi$	
$\Gamma_6$ $\pi(1300)\pi$	
$\Gamma_7$ $\rho\rho$	
$\Gamma_8$ $\rho(\pi\pi)$ s-wave	
$\Gamma_9$ $e^+e^-$	seen
$\Gamma_{10}$ $\eta\rho$	possibly seen
$\Gamma_{11}$ $a_2(1320)\pi$	not seen
$\Gamma_{12}$ $K\bar{K}$	not seen
$\Gamma_{13}$ $K\bar{K}^*(892) + c.c.$	possibly seen
$\Gamma_{14}$ $\eta\gamma$	possibly seen
$\Gamma_{15}$ $f_0(500)\gamma$	not seen
$\Gamma_{16}$ $f_0(980)\gamma$	not seen
$\Gamma_{17}$ $f_0(1370)\gamma$	not seen
$\Gamma_{18}$ $f_2(1270)\gamma$	not seen

 $\rho(1450)$   $\Gamma(i)\Gamma(e^+e^-)/\Gamma(\text{total})$ 

VALUE (keV)	DOCUMENT ID	TECN	COMMENT	$\Gamma_1/\Gamma_9$
0.12	32 DIEKMANN 88	RVUE	$e^+e^- \rightarrow \pi^+\pi^-$	
0.027 <sup>+0.015</sup> <sub>-0.010</sub>	33 KURDADZE 83	OLYA	0.64-1.4 $e^+e^- \rightarrow \pi^+\pi^-$	

• • • We do not use the following data for averages, fits, limits, etc. • • •

 $\Gamma(\eta\rho) \times \Gamma(e^+e^-)/\Gamma(\text{total})$ 

VALUE (eV)	DOCUMENT ID	TECN	COMMENT	$\Gamma_{10}/\Gamma_9$
74 ± 20	34 AKHMETSHIN 00D	CMD2	$e^+e^- \rightarrow \eta\pi^+\pi^-$	
91 ± 19	ANTONELLI 88	DM2	$e^+e^- \rightarrow \eta\pi^+\pi^-$	

 $\Gamma(\eta\gamma) \times \Gamma(e^+e^-)/\Gamma(\text{total})$ 

VALUE (eV)	DOCUMENT ID	TECN	COMMENT	$\Gamma_{14}/\Gamma_9$
<16.4	35 AKHMETSHIN 05	CMD2	0.60-1.38 $e^+e^- \rightarrow \eta\gamma$	
2.2 ± 0.5 ± 0.3	36 AKHMETSHIN 01B	CMD2	$e^+e^- \rightarrow \eta\gamma$	

 $\Gamma(K\bar{K}^*(892) + c.c.) \times \Gamma(e^+e^-)/\Gamma(\text{total})$ 

VALUE (eV)	DOCUMENT ID	TECN	COMMENT	$\Gamma_{13}/\Gamma_9$
127 ± 15 ± 6	AUBERT 08s	BABR	10.6 $e^+e^- \rightarrow K\bar{K}^*(892)\gamma$	

<sup>32</sup>Using total width = 235 MeV.

<sup>33</sup>Using for  $\rho(1700)$  mass and width 1600 ± 20 and 300 ± 10 MeV respectively.

<sup>34</sup>Using the data of ANTONELLI 88, DOLINSKY 91, and AKHMETSHIN 00D. The energy-independent width of the  $\rho(1450)$  and  $\rho(1700)$  mesons assumed.

<sup>35</sup>From  $2\gamma$  decay mode of  $\eta$  using 1465 MeV and 310 MeV for the  $\rho(1450)$  mass and width. Recalculated by us.

<sup>36</sup>Using the data of AKHMETSHIN 01B on  $e^+e^- \rightarrow \eta\gamma$ , AKHMETSHIN 00D and ANTONELLI 88 on  $e^+e^- \rightarrow \eta\pi^+\pi^-$ . Recalculated by us using width of 226 MeV.

 $\rho(1450)$   $\Gamma(i)/\Gamma(\text{total}) \times \Gamma(e^+e^-)/\Gamma(\text{total})$ 

VALUE (units $10^{-3}$ )	CL%	DOCUMENT ID	TECN	COMMENT	$\Gamma_{15}/\Gamma \times \Gamma_9/\Gamma$
<4.0	90	ACHASOV 11	SND	$e^+e^- \rightarrow \pi^0\pi^0\gamma$	

VALUE (units $10^{-3}$ )	CL%	DOCUMENT ID	TECN	COMMENT	$\Gamma_{16}/\Gamma \times \Gamma_9/\Gamma$
<2.6	90	ACHASOV 11	SND	$e^+e^- \rightarrow \pi^0\pi^0\gamma$	

VALUE (units $10^{-3}$ )	CL%	DOCUMENT ID	TECN	COMMENT	$\Gamma_{17}/\Gamma \times \Gamma_9/\Gamma$
<3.5	90	ACHASOV 11	SND	$e^+e^- \rightarrow \pi^0\pi^0\gamma$	

VALUE (units $10^{-3}$ )	CL%	DOCUMENT ID	TECN	COMMENT	$\Gamma_{18}/\Gamma \times \Gamma_9/\Gamma$
<0.8	90	37 ACHASOV 11	SND	$e^+e^- \rightarrow \pi^0\pi^0\gamma$	

<sup>37</sup>Using Breit-Wigner parametrization of the  $\rho(1450)$  with mass and width of 1465 MeV and 400 MeV, respectively.

 $\rho(1450)$  BRANCHING RATIOS

VALUE	DOCUMENT ID	TECN	COMMENT	$\Gamma_1/\Gamma_2$
0.37 ± 0.10	38,39 ABELE 01B	CBAR	0.0 $\bar{p}n \rightarrow 5\pi$	

 $\Gamma(\omega\pi)/\Gamma(\text{total})$ 

VALUE	DOCUMENT ID	TECN	COMMENT	$\Gamma_3/\Gamma$
~ 0.21	CLEGG 94	RVUE		

 $\Gamma(\pi\pi)/\Gamma(\omega\pi)$ 

VALUE	DOCUMENT ID	TECN	COMMENT	$\Gamma_1/\Gamma_3$
~ 0.32	CLEGG 94	RVUE		

 $\Gamma(\omega\pi)/\Gamma(4\pi)$ 

VALUE	DOCUMENT ID	TECN	COMMENT	$\Gamma_3/\Gamma_2$
<0.14	CLEGG 88	RVUE		

 $\Gamma(a_1(1260)\pi)/\Gamma(4\pi)$ 

VALUE	DOCUMENT ID	TECN	COMMENT	$\Gamma_4/\Gamma_2$
0.27 ± 0.08	38 ABELE 01B	CBAR	0.0 $\bar{p}n \rightarrow 5\pi$	

See key on page 457

# Meson Particle Listings

## $\rho(1450), \eta(1475)$

### $\Gamma(h_1(1170)\pi)/\Gamma(4\pi)$ $\Gamma_5/\Gamma_2$

VALUE	DOCUMENT ID	TECN	COMMENT
0.08±0.04	<sup>38</sup> ABELE	01B	CBAR 0.0 $\bar{p}n \rightarrow 5\pi$

### $\Gamma(\pi(1300)\pi)/\Gamma(4\pi)$ $\Gamma_6/\Gamma_2$

VALUE	DOCUMENT ID	TECN	COMMENT
0.37±0.13	<sup>38</sup> ABELE	01B	CBAR 0.0 $\bar{p}n \rightarrow 5\pi$

### $\Gamma(\rho\rho)/\Gamma(4\pi)$ $\Gamma_7/\Gamma_2$

VALUE	DOCUMENT ID	TECN	COMMENT
0.11±0.05	<sup>38</sup> ABELE	01B	CBAR 0.0 $\bar{p}n \rightarrow 5\pi$

### $\Gamma(\rho(\pi\pi)_{s\text{-wave}})/\Gamma(4\pi)$ $\Gamma_8/\Gamma_2$

VALUE	DOCUMENT ID	TECN	COMMENT
0.17±0.09	<sup>38</sup> ABELE	01B	CBAR 0.0 $\bar{p}n \rightarrow 5\pi$

### $\Gamma(\eta\rho)/\Gamma_{\text{total}}$ $\Gamma_{10}/\Gamma_3$

VALUE	DOCUMENT ID	TECN	COMMENT
<0.04	DONNACHIE	87B	RVUE

### $\Gamma(\eta\rho)/\Gamma(\omega\pi)$ $\Gamma_{10}/\Gamma_3$

VALUE	DOCUMENT ID	TECN	COMMENT
~0.24	<sup>40</sup> DONNACHIE	91	RVUE
>2	FUKUI	91	SPEC 8.95 $\pi^- \rho \rightarrow \omega \pi^0 n$

### $\Gamma(a_2(1320)\pi)/\Gamma_{\text{total}}$ $\Gamma_{11}/\Gamma$

VALUE	DOCUMENT ID	TECN	COMMENT
not seen	AMELIN	00	VES 37 $\pi^- \rho \rightarrow \eta \pi^+ \pi^- n$

### $\Gamma(K\bar{K})/\Gamma(\omega\pi)$ $\Gamma_{12}/\Gamma_3$

VALUE	DOCUMENT ID	TECN	COMMENT
<0.08	<sup>40</sup> DONNACHIE	91	RVUE

### $\Gamma(K\bar{K}^*(892) + c.c.)/\Gamma_{\text{total}}$ $\Gamma_{13}/\Gamma$

VALUE	DOCUMENT ID	TECN	COMMENT
possibly seen	COAN	04	CLEO $\tau^- \rightarrow K^- \pi^- K^+ \nu_\tau$

<sup>38</sup>  $\omega\pi$  not included.  
<sup>39</sup> Using ABELE 97.  
<sup>40</sup> Using data from BISELLO 91B, DOLINSKY 86 and ALBRECHT 87L.

### $\rho(1450)$ REFERENCES

ACHASOV	11	JETP 113 75	M.N. Achasov et al. (SND Collab.)
AUBERT	08S	Translated from ZETF 140, 87	(BABAR Collab.)
FUJIKAWA	08	PR D78 072006	M. Fujikawa et al. (BELLE Collab.)
AKHMETSHIN	05	PL B605 26	R.R. Akhmetshin et al. (Novosibirsk CMD-2 Collab.)
ALOISIO	05	PL B606 12	A. Aloisio et al. (KLOE Collab.)
SCHAEL	05C	PRPL 421 191	S. Schael et al. (ALEPH Collab.)
AKHMETSHIN	04	PL B578 285	R.R. Akhmetshin et al. (Novosibirsk CMD-2 Collab.)
COAN	04	PRL 92 232001	T.E. Coan et al. (CLEO Collab.)
AKHMETSHIN	03B	PL B562 173	R.R. Akhmetshin et al. (Novosibirsk CMD-2 Collab.)
ABELE	01B	EPJ C21 261	A. Abele et al. (Crystal Barrel Collab.)
AKHMETSHIN	01B	PL B509 217	R.R. Akhmetshin et al. (Novosibirsk CMD-2 Collab.)
ALEXANDER	01B	PR D64 092001	J.P. Alexander et al. (CLEO Collab.)
AKHMETSHIN	00D	PL B489 125	R.R. Akhmetshin et al. (Novosibirsk CMD-2 Collab.)
AMELIN	00	NP A668 83	D. Amelin et al. (VES Collab.)
ANDERSON	00A	PR D61 112002	S. Anderson et al. (CLEO Collab.)
EDWARDS	00A	PR D61 072003	K.W. Edwards et al. (CLEO Collab.)
ABELE	99C	PL B450 275	A. Abele et al. (Crystal Barrel Collab.)
ABELE	99D	PL B468 178	A. Abele et al. (Crystal Barrel Collab.)
BERTIN	98	PR D57 55	A. Bertin et al. (OBELIX Collab.)
ABELE	97	PL B391 191	A. Abele et al. (Crystal Barrel Collab.)
ACHASOV	97	PR D55 2663	M.N. Achasov et al. (NOVM)
BARATE	97M	ZPHY C76 15	R. Barate et al. (ALEPH Collab.)
BERTIN	97C	PL B408 476	A. Bertin et al. (OBELIX Collab.)
BERTIN	97D	PL B414 220	A. Bertin et al. (OBELIX Collab.)
CLEGG	94	ZPHY C62 455	A.B. Clegg, A. Donnachie (LANC, MCHS)
BISELLO	91B	NPBPS B21 111	D. Bisello (DM2 Collab.)
DOLINSKY	91	PRPL 202 99	S.I. Dolinsky et al. (NOVO)
DONNACHIE	91	ZPHY C51 689	A. Donnachie, A.B. Clegg (MCHS, LANC)
FUKUI	91	PL B257 241	S. Fukui et al. (SUGI, NAGO, KEK, KYOT+)
ARMSTRONG	89E	PL B228 536	T.A. Armstrong, M. Benayoun (ATHU, BARI, BIRM+)
BISELLO	89	PL B220 321	D. Bisello et al. (DM2 Collab.)
DUBNICKA	89	JPG 15 1349	S. Dubnicka et al. (JINR, SLOV)
ANTONELLI	88	PL B212 133	A. Antonelli et al. (DM2 Collab.)
CLEGG	88	ZPHY C40 313	A.B. Clegg, A. Donnachie (MCHS, LANC)
DIEKMANN	88	PRPL 159 99	B. Diekmann (BONN)
FUKUI	88	PL B202 441	S. Fukui et al. (SUGI, NAGO, KEK, KYOT+)
ALBRECHT	87L	PL B185 223	H. Albrecht et al. (ARGUS Collab.)
DONNACHIE	87B	ZPHY C34 257	A. Donnachie, A.B. Clegg (MCHS, LANC)
DOLINSKY	86	PL B174 453	S.I. Dolinsky et al. (NOVO)
BARKOV	85	NP B256 365	L.M. Barkov et al. (NOVO)
KURDADZE	83	JETPL 37 733	L.M. Kurdadze et al. (NOVO)
ASTON	80C	Translated from ZETFP 37 613	D. Aston (BONN, CERN, EPOL, GLAS, LANCA+)
BARBER	80C	PL 32B 211	D.P. Barber et al. (DARE, LANC, SHEF)
GOUNARIS	68	PRL 21 244	G.J. Gounaris, J.J. Sakurai

### $\eta(1475)$

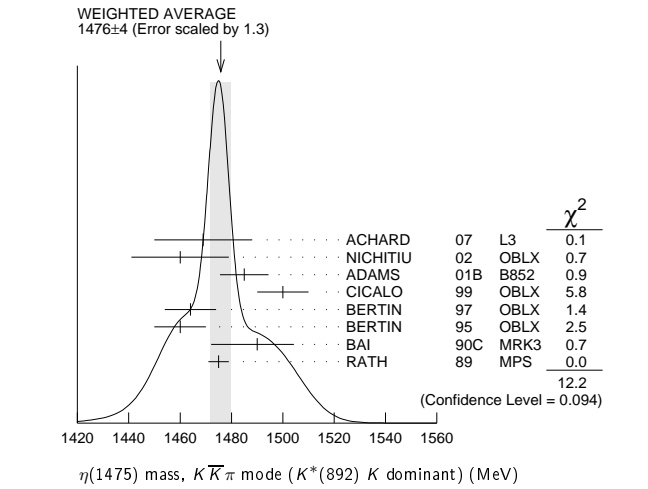
$$J^{PC} = 0^+(0^-+)$$

See also the  $\eta(1405)$ .

### $\eta(1475)$ MASS

#### $K\bar{K}\pi$ MODE ( $K^*(892)$ $K$ dominant)

VALUE (MeV)	EVTs	DOCUMENT ID	TECN	COMMENT
<b>1476±4 OUR AVERAGE</b>				Error includes scale factor of 1.3. See the ideogram below.
1469±14±13	74	ACHARD	07 L3	183-209 $e^+e^- \rightarrow e^+e^- K_S^0 K^\pm \pi^\mp$
1460±19	3651	NICHITIU	02 OBLX	
1485±8±5	20k	ADAMS	01B B852	18 GeV $\pi^- \rho \rightarrow K^+ K^- \pi^0 n$
1500±10		CICALO	99 OBLX	0 $\bar{p}p \rightarrow K^\pm K_S^0 \pi^\mp \pi^+ \pi^-$
1464±10		BERTIN	97 OBLX	0 $\bar{p}p \rightarrow K^\pm (K^0) \pi^\mp \pi^+ \pi^-$
1460±10		BERTIN	95 OBLX	0 $\bar{p}p \rightarrow K \bar{K} \pi \pi$
1490 <sup>+14+3</sup> <sub>-8-16</sub>	1100	BAI	90C MRK3	$J/\psi \rightarrow \gamma K_S^0 K^\pm \pi^\mp$
1475±4		RATH	89 MPS	21.4 $\pi^- \rho \rightarrow n K_S^0 K_S^0 \pi^0$
1421±14		AUGUSTIN	92 DM2	$J/\psi \rightarrow \gamma K \bar{K} \pi$



### $\eta(1475)$ WIDTH

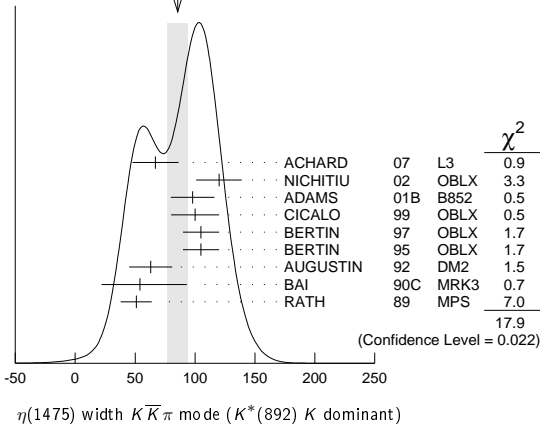
#### $K\bar{K}\pi$ MODE ( $K^*(892)$ $K$ dominant)

VALUE (MeV)	EVTs	DOCUMENT ID	TECN	COMMENT
<b>85±9 OUR AVERAGE</b>				Error includes scale factor of 1.5. See the ideogram below.
67±18±7	74	ACHARD	07 L3	183-209 $e^+e^- \rightarrow e^+e^- K_S^0 K^\pm \pi^\mp$
120±19	3651	NICHITIU	02 OBLX	
98±18±3	20k	ADAMS	01B B852	18 GeV $\pi^- \rho \rightarrow K^+ K^- \pi^0 n$
100±20		CICALO	99 OBLX	0 $\bar{p}p \rightarrow K^\pm K_S^0 \pi^\mp \pi^+ \pi^-$
105±15		BERTIN	97 OBLX	0.0 $\bar{p}p \rightarrow K^\pm (K^0) \pi^\mp \pi^+ \pi^-$
105±15		BERTIN	95 OBLX	0 $\bar{p}p \rightarrow K \bar{K} \pi \pi$
63±18		AUGUSTIN	92 DM2	$J/\psi \rightarrow \gamma K \bar{K} \pi$
54+37+13 -21-24		BAI	90C MRK3	$J/\psi \rightarrow \gamma K_S^0 K^\pm \pi^\mp$
51±13		RATH	89 MPS	21.4 $\pi^- \rho \rightarrow n K_S^0 K_S^0 \pi^0$

# Meson Particle Listings

## $\eta(1475)$ , $f_0(1500)$

WEIGHTED AVERAGE  
85±9 (Error scaled by 1.5)



### $\eta(1475)$ DECAY MODES

Mode	Fraction ( $\Gamma_i/\Gamma$ )
$\Gamma_1$ $K\bar{K}\pi$	dominant
$\Gamma_2$ $K\bar{K}^*(892) + c.c.$	seen
$\Gamma_3$ $a_0(980)\pi$	seen
$\Gamma_4$ $\gamma\gamma$	seen

### $\eta(1475)$ $\Gamma(i)\Gamma(\gamma\gamma)/\Gamma(\text{total})$

VALUE (keV)	CL%	EVTS	DOCUMENT ID	TECN	COMMENT	$\Gamma_1\Gamma_4/\Gamma$
<b>0.23±0.05±0.05</b>		74	1 ACHARD	07 L3	183-209 $e^+e^- \rightarrow e^+e^-K_S^0 K^\pm \pi^\mp$	

- • • We do not use the following data for averages, fits, limits, etc. • • •
- < 0.089 90 2,3 AHOHE 05 CLE2 10.6  $e^+e^- \rightarrow e^+e^-K_S^0 K^\pm \pi^\mp$
- <sup>1</sup> Supersedes ACCIARRI 01G. Compatible with  $K^*K$  decay. Using  $B(K_S^0 \rightarrow \pi^+\pi^-) = 0.6895$ .
- <sup>2</sup> Using  $\eta(1475)$  mass of 1481 MeV and width of 48 MeV. The upper limit increases to 0.140 keV if the world average value, 87 MeV, of the width is used.
- <sup>3</sup> Assuming three-body phase-space decay to  $K_S^0 K^\pm \pi^\mp$ .

### $\eta(1475)$ BRANCHING RATIOS

VALUE	DOCUMENT ID	TECN	COMMENT	$\Gamma_2/\Gamma_1$
$\Gamma(K\bar{K}^*(892) + c.c.)/\Gamma(K\bar{K}\pi)$				
0.50±0.10	4 BAILLON	67 HBC	0.0 $\bar{p}p \rightarrow K\bar{K}\pi\pi$	

VALUE	CL%	DOCUMENT ID	TECN	COMMENT	$\Gamma_2/(\Gamma_2+\Gamma_3)$
$\Gamma(K\bar{K}^*(892) + c.c.) / [\Gamma(K\bar{K}^*(892) + c.c.) + \Gamma(a_0(980)\pi)]$					
<0.25	90	EDWARDS	82E CBAL	$J/\psi \rightarrow K^+K^-\pi^0\gamma$	

<sup>4</sup> Data could also refer to  $\eta(1405)$ .

### $\eta(1475)$ REFERENCES

ACHARD	07	JHEP 0703 018	P. Achard et al.	(L3 Collab.)
AHOHE	05	PR D71 072001	R. Ahohe et al.	(CLEO Collab.)
NICHTIU	02	PL B545 261	F. Nichtiu et al.	(OBELX Collab.)
ACCIARRI	01G	PL B501 1	M. Acciarrì et al.	(L3 Collab.)
ADAMS	01B	PL B516 264	G.S. Adams et al.	(BNL E852 Collab.)
CICALO	99	PL B462 453	C. Cicalo et al.	(OBELIX Collab.)
BERTIN	97	PL B400 226	A. Bertin et al.	(OBELIX Collab.)
BERTIN	95	PL B361 187	A. Bertin et al.	(OBELIX Collab.)
AUGUSTIN	92	PR D46 1951	J.E. Augustin, G. Cosme	(DM2 Collab.)
BAI	90C	PRL 65 2507	Z. Bai et al.	(Mark III Collab.)
RATH	89	PR D40 693	M.G. Rath et al.	(NDAM, BRAN, BNL, CUNY+)
EDWARDS	82E	PRL 49 259	C. Edwards et al.	(CIT, HARV, FRIV+)
BAILLON	67	NC 50A 393	P.H. Baillon et al.	(CERN, CDEF, IRAD)

## $f_0(1500)$

$$J^G(PC) = 0^+(0^+ +)$$

See also the mini-reviews on scalar mesons under  $f_0(500)$  (see the index for the page number) and on non- $q\bar{q}$  candidates in PDG 06, Journal of Physics, G **33** 1 (2006).

### $f_0(1500)$ MASS

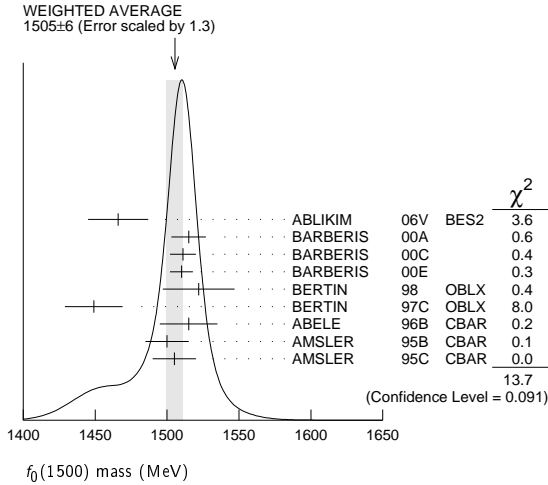
VALUE (MeV)	EVTS	DOCUMENT ID	TECN	COMMENT
<b>1505 ± 6 OUR AVERAGE</b>				Error includes scale factor of 1.3. See the ideogram below.
1466 ± 6 ± 20		ABLIKIM	06v BES2	$e^+e^- \rightarrow J/\psi \rightarrow \gamma\pi^+\pi^-$
1515 ± 12		<sup>1</sup> BARBERIS	00A	450 $pp \rightarrow p_f \eta \eta p_S$
1511 ± 9		<sup>1,2</sup> BARBERIS	00c	450 $pp \rightarrow p_f 4\pi p_S$
1510 ± 8		<sup>1</sup> BARBERIS	00E	450 $pp \rightarrow p_f \eta \eta p_S$
1522 ± 25		BERTIN	98 OBLX	0.05-0.405 $\bar{p}p \rightarrow \pi^+\pi^-\pi^0$
1449 ± 20		<sup>1</sup> BERTIN	97c OBLX	0.0 $\bar{p}p \rightarrow \pi^+\pi^-\pi^0$
1515 ± 20		ABELE	96B CBAR	0.0 $\bar{p}p \rightarrow \pi^0 K^0_L K^0_L$
1500 ± 15		<sup>3</sup> AMSLER	95B CBAR	0.0 $\bar{p}p \rightarrow 3\pi^0$
1505 ± 15		<sup>4</sup> AMSLER	95c CBAR	0.0 $\bar{p}p \rightarrow \eta\eta\pi^0$

- • • We do not use the following data for averages, fits, limits, etc. • • •
- 1486 ± 10 <sup>1</sup> ANISOVICH 09 RVUE 0.0  $\bar{p}p, \pi N$
- 1470 ± 60 568 <sup>5</sup> KLEMP T E791  $D_S^+ \rightarrow \pi^-\pi^+\pi^+$
- 1470  $^{+6}_{-7} \text{ } ^{+72}_{-255}$  <sup>6</sup> UEHARA 08A BELL 10.6  $e^+e^- \rightarrow e^+e^-\pi^0\pi^0$
- 1495 ± 4 AMSLER 06 CBAR 0.9  $\bar{p}p \rightarrow K^+K^-\pi^0$
- 1539 ± 20 9.9k AUBERT 06O BABR  $B^+ \rightarrow K^+K^+K^-$
- 1473 ± 5 80k <sup>7,8</sup> UMAN 06 E835 5.2  $\bar{p}p \rightarrow \eta\eta\pi^0$
- 1478 ± 6 VLADIMIRSK...06 SPEC 40  $\pi^-\pi^0 \rightarrow K_S^0 K_S^0 n$
- 1493 ± 7 <sup>7</sup> BINON 05 GAMS 33  $\pi^-\pi^0 \rightarrow \eta\eta n$
- 1524 ± 14 1400 <sup>9</sup> GARMASH 05 BELL  $B^+ \rightarrow K^+K^+K^-$
- 1489  $^{+8}_{-4}$  <sup>10</sup> ANISOVICH 03 RVUE
- 1490 ± 30 <sup>7</sup> ABELE 01 CBAR 0.0  $\bar{p}d \rightarrow \pi^-4\pi^0 p$
- 1497 ± 10 <sup>7</sup> BARBERIS 99 OMEG 450  $pp \rightarrow p_S p_f K^+K^-$
- 1502 ± 10 <sup>7</sup> BARBERIS 99B OMEG 450  $pp \rightarrow p_S p_f \pi^+\pi^-$
- 1502 ± 12 ± 10 <sup>11</sup> BARBERIS 99D OMEG 450  $pp \rightarrow K^+K^-, \pi^+\pi^-$
- 1530 ± 45 <sup>7</sup> BELLAZZINI 99 GAM4 450  $pp \rightarrow pp\pi^0\pi^0$
- 1505 ± 18 <sup>7</sup> FRENCH 99 300  $pp \rightarrow p_f(K^+K^-)p_S$
- 1447 ± 27 <sup>12</sup> KAMINSKI 99 RVUE  $\pi\pi \rightarrow \pi\pi, K\bar{K}, \sigma\sigma$
- 1580 ± 80 <sup>7</sup> ALDE 98 GAM4 100  $\pi^-\pi^0 \rightarrow \pi^0\pi^0 n$
- 1499 ± 8 <sup>1</sup> ANISOVICH 98B RVUE Compilation
- ~ 1520 REYES 98 SPEC 800  $pp \rightarrow p_S p_f K_S^0 K_S^0$
- 1510 ± 20 <sup>1</sup> BARBERIS 97B OMEG 450  $pp \rightarrow pp2(\pi^+\pi^-)$
- ~ 1475 FRABETTI 97D E687  $D_S^\pm \rightarrow \pi^\mp \pi^\pm \pi^\pm$
- ~ 1505 ABELE 96 CBAR 0.0  $\bar{p}p \rightarrow 5\pi^0$
- 1500 ± 8 <sup>1</sup> ABELE 96C RVUE Compilation
- 1460 ± 20 120 <sup>7</sup> AMELIN 96B VES 37  $\pi^-A \rightarrow \eta\eta\pi^-A$
- 1500 ± 8 BUGG 96 RVUE
- 1500 ± 10 <sup>13</sup> AMSLER 95D CBAR 0.0  $\bar{p}p \rightarrow \pi^0\pi^0\pi^0, \pi^0\eta\eta, \pi^0\pi^0\eta$
- 1445 ± 5 <sup>14</sup> ANTINORI 95 OMEG 300,450  $pp \rightarrow pp2(\pi^+\pi^-)$
- 1497 ± 30 <sup>7</sup> ANTINORI 95 OMEG 300,450  $pp \rightarrow pp\pi^+\pi^-$
- ~ 1505 BUGG 95 MRK3  $J/\psi \rightarrow \gamma\pi^+\pi^-\pi^+\pi^-$
- 1446 ± 5 <sup>7</sup> ABATZIS 94 OMEG 450  $pp \rightarrow pp2(\pi^+\pi^-)$
- 1545 ± 25 <sup>7</sup> AMSLER 94E CBAR 0.0  $\bar{p}p \rightarrow \pi^0\eta\eta'$
- 1520 ± 25 <sup>1,15</sup> ANISOVICH 94 CBAR 0.0  $\bar{p}p \rightarrow 3\pi^0, \pi^0\eta\eta$
- 1505 ± 20 <sup>1,16</sup> BUGG 94 RVUE  $\bar{p}p \rightarrow 3\pi^0, \eta\eta\pi^0, \eta\pi^0\pi^0$
- 1560 ± 25 <sup>7</sup> AMSLER 92 CBAR 0.0  $\bar{p}p \rightarrow \pi^0\eta\eta$
- 1550 ± 45 ± 30 <sup>7</sup> BELADIDZE 92C VES 36  $\pi^-Be \rightarrow \pi^-\eta\eta Be$
- 1449 ± 4 <sup>7</sup> ARMSTRONG 89E OMEG 300  $pp \rightarrow pp2(\pi^+\pi^-)$
- 1610 ± 20 <sup>7</sup> ALDE 88 GAM4 300  $\pi^-N \rightarrow \pi^-N2\eta$
- ~ 1525 ASTON 88D LASS 11  $K^-p \rightarrow K_S^0 K_S^0 \Lambda$
- 1570 ± 20 600 <sup>7</sup> ALDE 87 GAM4 100  $\pi^-\pi^0 \rightarrow 4\pi^0 n$
- 1575 ± 45 <sup>17</sup> ALDE 86D GAM4 100  $\pi^-\pi^0 \rightarrow 2\eta n$
- 1568 ± 33 <sup>7</sup> BINON 84C GAM2 38  $\pi^-\pi^0 \rightarrow \eta\eta' n$
- 1592 ± 25 <sup>7</sup> BINON 83C GAM2 38  $\pi^-\pi^0 \rightarrow 2\eta n$
- 1525 ± 5 <sup>7</sup> GRAY 83 DBC 0.0  $\bar{p}N \rightarrow 3\pi$

- T-matrix pole.
- Average between  $\pi^+\pi^-\pi^0$  and  $2(\pi^+\pi^-)$ .
- T-matrix pole, supersedes ANISOVICH 94.
- T-matrix pole, supersedes ANISOVICH 94 and AMSLER 92.
- Reanalysis of AITALA 01A data. This state could also be  $f_0(1370)$ .
- Breit-Wigner mass. May also be the  $f_0(1370)$ .
- Breit-Wigner mass.
- Statistical error only.
- Breit-Wigner, solution 1, PWA ambiguous.
- K-matrix pole from combined analysis of  $\pi^-\pi^0 \rightarrow \pi^0\pi^0 n, \pi^-\pi^0 \rightarrow K\bar{K}n, \pi^+\pi^-\pi^0 \rightarrow \pi^+\pi^-, \bar{p}p \rightarrow \pi^0\pi^0\pi^0, \pi^0\eta\eta, \pi^0\pi^0\eta, \pi^+\pi^-\pi^0, K^+K^-\pi^0, K_S^0 K_S^0 \pi^0, K^+K_S^0 \pi^-$  at rest,  $\bar{p}n \rightarrow \pi^-\pi^-\pi^+, K_S^0 K^-\pi^0, K_S^0 K_S^0 \pi^-$  at rest.
- Supersedes BARBERIS 99 and BARBERIS 99B.
- T-matrix pole on sheet -- +.



- 13 T-matrix pole. Coupled-channel analysis of AMSLER 95B, AMSLER 95C, and AMSLER 94D.
- 14 Supersedes ABATZIS 94, ARMSTRONG 89E. Breit-Wigner mass.
- 15 From a simultaneous analysis of the annihilations  $\bar{p}p \rightarrow 3\pi^0, \pi^0\eta\eta$ .
- 16 Reanalysis of ANISOVICH 94 data.
- 17 From central value and spread of two solutions. Breit-Wigner mass.



**$f_0(1500)$  WIDTH**

VALUE (MeV)	EVTS	DOCUMENT ID	TECN	COMMENT
<b>109 ± 7</b>	<b>OUR AVERAGE</b>			
108 ± 11	14 ± 25	ABLIKIM	06V BES2	$e^+e^- \rightarrow J/\psi \rightarrow \gamma\pi^+\pi^-$
110 ± 24		18 BARBERIS	00A	$450 pp \rightarrow p_f\eta\eta p_S$
102 ± 18		18,19 BARBERIS	00C	$450 pp \rightarrow p_f 4\pi p_S$
110 ± 16		18 BARBERIS	00E	$450 pp \rightarrow p_f\eta\eta p_S$
108 ± 33		BERTIN	98 OBLX	$0.05-0.405 \bar{p}p \rightarrow \pi^+\pi^+\pi^-$
114 ± 30		18 BERTIN	97C OBLX	$0.0 \bar{p}p \rightarrow \pi^+\pi^-\pi^0$
105 ± 15		ABELE	96B CBAR	$0.0 \bar{p}p \rightarrow \pi^0 K_L^0 K_L^0$
120 ± 25		20 AMSLER	95B CBAR	$0.0 \bar{p}p \rightarrow 3\pi^0$
120 ± 30		21 AMSLER	95C CBAR	$0.0 \bar{p}p \rightarrow \eta\eta\pi^0$
• • • We do not use the following data for averages, fits, limits, etc. • • •				
114 ± 10		18 ANISOVICH	09 RVUE	$0.0 \bar{p}p, \pi N$
90 ± 1	2 + 50 / 1 - 22	22 UEHARA	08A BELL	$10.6 e^+e^- \rightarrow e^+e^-\pi^0\pi^0$
121 ± 8		AMSLER	06 CBAR	$0.9 \bar{p}p \rightarrow K^+K^-\pi^0$
257 ± 33	9.9k	AUBERT	06O BABR	$B^+ \rightarrow K^+K^+K^-$
108 ± 9	80k	23,24 UMAN	06 E835	$5.2 \bar{p}p \rightarrow \eta\eta\pi^0$
119 ± 10		VLADIMIRSK...	06 SPEC	$40 \pi^-\pi^- \rightarrow K_S^0 K_S^0 n$
90 ± 15		23 BINON	05 GAMS	$33 \pi^-\pi^- \rightarrow \eta\eta n$
136 ± 23	1400	25 GARMASH	05 BELL	$B^+ \rightarrow K^+K^+K^-$
102 ± 10		26 ANISOVICH	03 RVUE	
140 ± 40		23 ABELE	01 CBAR	$0.0 \bar{p}d \rightarrow \pi^- 4\pi^0 p$
104 ± 25		23 BARBERIS	99 OMEG	$450 pp \rightarrow p_S p_f K^+ K^-$
131 ± 15		23 BARBERIS	99B OMEG	$450 pp \rightarrow p_S p_f \pi^+\pi^-$
98 ± 18 ± 16		27 BARBERIS	99D OMEG	$450 pp \rightarrow K^+K^-, \pi^+\pi^-$
160 ± 50		23 BELLAZZINI	99 GAM4	$450 pp \rightarrow p p \pi^0 \pi^0$
100 ± 33		23 FRENCH	99	$300 pp \rightarrow p_f(K^+K^-)p_S$
108 ± 46		28 KAMINSKI	99 RVUE	$\pi\pi \rightarrow \pi\pi, K\bar{K}, \sigma\sigma$
280 ± 100		23 ALDE	98 GAM4	$100 \pi^-\pi^- \rightarrow \pi^0\pi^0 n$
130 ± 20		18 ANISOVICH	98B RVUE	Compilation
120 ± 35		18 BARBERIS	97B OMEG	$450 pp \rightarrow p p 2(\pi^+\pi^-)$
~ 100		FRABETTI	97D E687	$D_s^\pm \rightarrow \pi^\mp \pi^\pm \pi^\pm$
~ 169		ABELE	96 CBAR	$0.0 \bar{p}p \rightarrow 5\pi^0$
100 ± 30	120	23 AMELIN	96B VES	$37 \pi^- A \rightarrow \eta\eta\pi^- A$
132 ± 15		BUGG	96 RVUE	
154 ± 30		29 AMSLER	95D CBAR	$0.0 \bar{p}p \rightarrow \pi^0\pi^0\pi^0, \pi^0\eta\eta, \pi^0\pi^0\eta$
65 ± 10		30 ANTINORI	95 OMEG	$300,450 pp \rightarrow p p 2(\pi^+\pi^-)$
199 ± 30		23 ANTINORI	95 OMEG	$300,450 pp \rightarrow p p \pi^+\pi^-$
56 ± 12		23 ABATZIS	94 OMEG	$450 pp \rightarrow p p 2(\pi^+\pi^-)$
100 ± 40		23 AMSLER	94E CBAR	$0.0 \bar{p}p \rightarrow \pi^0\eta\eta'$
148 ± 20		18,31 ANISOVICH	94 CBAR	$0.0 \bar{p}p \rightarrow 3\pi^0, \pi^0\eta\eta$
150 ± 25		18,32 BUGG	94 RVUE	$\bar{p}p \rightarrow 3\pi^0, \eta\eta\pi^0, \eta\pi^0\pi^0$
245 ± 50		23 AMSLER	92 CBAR	$0.0 \bar{p}p \rightarrow \pi^0\eta\eta$
153 ± 67 ± 50		23 BELADIDZE	92C VES	$36 \pi^- Be \rightarrow \pi^- \eta' \eta Be$
78 ± 18		23 ARMSTRONG	89E OMEG	$300 pp \rightarrow p p 2(\pi^+\pi^-)$
170 ± 40		23 ALDE	88 GAM4	$300 \pi^- N \rightarrow \pi^- N 2\eta$
150 ± 20	600	23 ALDE	87 GAM4	$100 \pi^-\pi^- \rightarrow 4\pi^0 n$

- 265 ± 65
- 260 ± 60
- 210 ± 40
- 101 ± 13
- 33 ALDE
- 23 BINON
- 23 BINON
- 23 GRAY
- 86D GAM4
- 84C GAM2
- 83 GAM2
- 83 DBC
- 100  $\pi^-\pi^- \rightarrow 2\eta n$
- 38  $\pi^-\pi^- \rightarrow \eta\eta' n$
- 38  $\pi^-\pi^- \rightarrow 2\eta n$
- 0.0  $\bar{p}N \rightarrow 3\pi$
- 18 T-matrix pole.
- 19 Average between  $\pi^+\pi^- 2\pi^0$  and  $2(\pi^+\pi^-)$ .
- 20 T-matrix pole, supersedes ANISOVICH 94.
- 21 T-matrix pole, supersedes ANISOVICH 94 and AMSLER 92.
- 22 Breit-Wigner width. May also be the  $f_0(1370)$ .
- 23 Breit-Wigner width.
- 24 Statistical error only.
- 25 Breit-Wigner, solution 1, PWA ambiguous.
- 26 K-matrix pole from combined analysis of  $\pi^-\pi^- \rightarrow \pi^0\pi^0 n, \pi^-\pi^- \rightarrow K\bar{K}n, \pi^+\pi^- \rightarrow \pi^+\pi^-, \bar{p}p \rightarrow \pi^0\pi^0\pi^0, \pi^0\eta\eta, \pi^0\pi^0\eta, \pi^+\pi^-\pi^0, K^+K^-\pi^0, K_S^0 K_S^0 \pi^0, K^+ K_S^0 \pi^-$  at rest,  $\bar{p}n \rightarrow \pi^-\pi^-\pi^+, K_S^0 K^-\pi^0, K_S^0 K_S^0 \pi^-$  at rest.
- 27 Supersedes BARBERIS 99 and BARBERIS 99B.
- 28 T-matrix pole on sheet -- +.
- 29 T-matrix pole. Coupled-channel analysis of AMSLER 95B, AMSLER 95C, and AMSLER 94D.
- 30 Supersedes ABATZIS 94, ARMSTRONG 89E. Breit-Wigner mass.
- 31 From a simultaneous analysis of the annihilations  $\bar{p}p \rightarrow 3\pi^0, \pi^0\eta\eta$ .
- 32 Reanalysis of ANISOVICH 94 data.
- 33 From central value and spread of two solutions. Breit-Wigner mass.

**$f_0(1500)$  DECAY MODES**

Mode	Fraction ( $\Gamma_i/\Gamma$ )	Scale factor
$\Gamma_1$ $\pi\pi$	(34.9 ± 2.3) %	1.2
$\Gamma_2$ $\pi^+\pi^-$	seen	
$\Gamma_3$ $2\pi^0$	seen	
$\Gamma_4$ $4\pi$	(49.5 ± 3.3) %	1.2
$\Gamma_5$ $4\pi^0$	seen	
$\Gamma_6$ $2\pi^+ 2\pi^-$	seen	
$\Gamma_7$ $2(\pi\pi)$ s-wave	seen	
$\Gamma_8$ $\rho\rho$	seen	
$\Gamma_9$ $\pi(1300)\pi$	seen	
$\Gamma_{10}$ $a_1(1260)\pi$	seen	
$\Gamma_{11}$ $\eta\eta$	( 5.1 ± 0.9) %	1.4
$\Gamma_{12}$ $\eta\eta'(958)$	( 1.9 ± 0.8) %	1.7
$\Gamma_{13}$ $K\bar{K}$	( 8.6 ± 1.0) %	1.1
$\Gamma_{14}$ $\gamma\gamma$	not seen	

**CONSTRAINED FIT INFORMATION**

An overall fit to 6 branching ratios uses 10 measurements and one constraint to determine 5 parameters. The overall fit has a  $\chi^2 = 11.4$  for 6 degrees of freedom.

The following *off-diagonal* array elements are the correlation coefficients  $\langle \delta x_i \delta x_j \rangle / (\delta x_i \delta x_j)$ , in percent, from the fit to the branching fractions,  $x_i \equiv \Gamma_i / \Gamma_{\text{total}}$ . The fit constrains the  $x_i$  whose labels appear in this array to sum to one.

$x_4$	-83			
$x_{11}$	11	-52		
$x_{12}$	-5	-31	29	
$x_{13}$	39	-67	33	6
	$x_1$	$x_4$	$x_{11}$	$x_{12}$

**$f_0(1500)$   $\Gamma(i)\Gamma(\gamma\gamma)/\Gamma(\text{total})$**

VALUE (eV)	CL%	DOCUMENT ID	TECN	COMMENT	$\Gamma_{14}/\Gamma$
• • • We do not use the following data for averages, fits, limits, etc. • • •					
33 ± 12 + 1809 / 6 - 21		34 UEHARA	08A BELL	$10.6 e^+e^- \rightarrow e^+e^-\pi^0\pi^0$	
not seen		ACCIARRI	01H L3	$\gamma\gamma \rightarrow K_S^0 K_S^0, E_{\text{cm}}^{ee} = 91, 183-209 \text{ GeV}$	
<460	95	BARATE	00E ALEP	$\gamma\gamma \rightarrow \pi^+\pi^-$	
34 May also be the $f_0(1370)$ . Multiplied by us by 3 to obtain the $\pi\pi$ value.					

**$f_0(1500)$  BRANCHING RATIOS**

$\Gamma(\pi\pi)/\Gamma_{\text{total}}$	DOCUMENT ID	TECN	$\Gamma_1/\Gamma$
0.454 ± 0.104	BUGG	96 RVUE	
• • • We do not use the following data for averages, fits, limits, etc. • • •			

## Meson Particle Listings

 $f_0(1500)$  $\Gamma(\pi^+\pi^-)/\Gamma_{\text{total}}$   $\Gamma_2/\Gamma$ 

VALUE	DOCUMENT ID	TECN	COMMENT
seen	BERTIN	98	OBLX 0.05-0.405 $\pi p \rightarrow \pi^+\pi^+\pi^-$
possibly seen	FRABETTI	97D E687	$D_S^\pm \rightarrow \pi^\mp \pi^\pm \pi^\pm$

 $\Gamma(4\pi)/\Gamma(\pi\pi)$   $\Gamma_4/\Gamma_1$ 

VALUE	DOCUMENT ID	TECN	COMMENT
<b>1.42±0.18 OUR FIT</b>			Error includes scale factor of 1.2.
<b>1.42±0.18 OUR AVERAGE</b>			Error includes scale factor of 1.2.
1.37±0.16	BARBERIS	00D	450 $pp \rightarrow p_f 4\pi p_S$
2.1 ± 0.6	<sup>35</sup> AMSLER	98	RVUE
• • • We do not use the following data for averages, fits, limits, etc. • • •			
2.1 ± 0.2	<sup>36</sup> ANISOVICH	02D	SPEC Combined fit
3.4 ± 0.8	<sup>35</sup> ABELE	96	CBAR 0.0 $\bar{p}p \rightarrow 5\pi^0$

 $\Gamma(2(\pi\pi)S\text{-wave})/\Gamma(\pi\pi)$   $\Gamma_7/\Gamma_1$ 

VALUE	DOCUMENT ID	TECN	COMMENT
• • • We do not use the following data for averages, fits, limits, etc. • • •			
0.42±0.26	<sup>37</sup> ABELE	01	CBAR 0.0 $\bar{p}d \rightarrow \pi^- 4\pi^0 p$

 $\Gamma(2(\pi\pi)S\text{-wave})/\Gamma(4\pi)$   $\Gamma_7/\Gamma_4$ 

VALUE	DOCUMENT ID	TECN	COMMENT
• • • We do not use the following data for averages, fits, limits, etc. • • •			
0.26±0.07	ABELE	01B	CBAR 0.0 $\bar{p}d \rightarrow 5\pi p$

 $\Gamma(\rho\rho)/\Gamma(4\pi)$   $\Gamma_8/\Gamma_4$ 

VALUE	DOCUMENT ID	TECN	COMMENT
• • • We do not use the following data for averages, fits, limits, etc. • • •			
0.13±0.08	ABELE	01B	CBAR 0.0 $\bar{p}d \rightarrow 5\pi p$

 $\Gamma(\rho\rho)/\Gamma(2(\pi\pi)S\text{-wave})$   $\Gamma_8/\Gamma_7$ 

VALUE	DOCUMENT ID	COMMENT
• • • We do not use the following data for averages, fits, limits, etc. • • •		
3.3±0.5	BARBERIS	00C 450 $pp \rightarrow p_f \pi^+ \pi^- 2\pi^0 p_S$
2.6±0.4	BARBERIS	00C 450 $pp \rightarrow p_f 2(\pi^+ \pi^-) p_S$

 $\Gamma(\pi(1300)\pi)/\Gamma(4\pi)$   $\Gamma_9/\Gamma_4$ 

VALUE	DOCUMENT ID	TECN	COMMENT
• • • We do not use the following data for averages, fits, limits, etc. • • •			
0.50±0.25	ABELE	01B	CBAR 0.0 $\bar{p}d \rightarrow 5\pi p$

 $\Gamma(a_1(1260)\pi)/\Gamma(4\pi)$   $\Gamma_{10}/\Gamma_4$ 

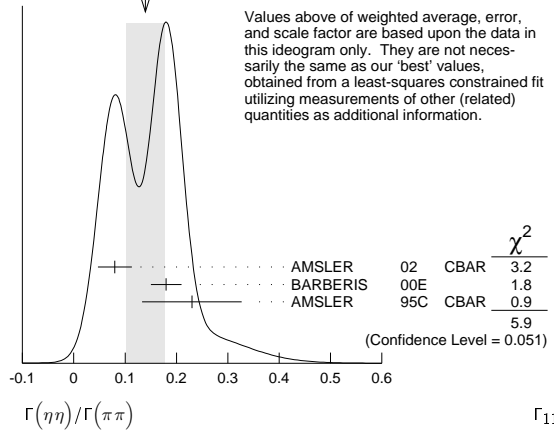
VALUE	DOCUMENT ID	TECN	COMMENT
• • • We do not use the following data for averages, fits, limits, etc. • • •			
0.12±0.05	ABELE	01B	CBAR 0.0 $\bar{p}d \rightarrow 5\pi p$

 $\Gamma(\eta\eta)/\Gamma_{\text{total}}$   $\Gamma_{11}/\Gamma$ 

VALUE	DOCUMENT ID	TECN	COMMENT
• • • We do not use the following data for averages, fits, limits, etc. • • •			
large	ALDE	88	GAM4 300 $\pi^- N \rightarrow \eta\eta\pi^- N$
large	BINON	83	GAM2 38 $\pi^- p \rightarrow 2\eta n$

 $\Gamma(\eta\eta)/\Gamma(\pi\pi)$   $\Gamma_{11}/\Gamma_1$ 

VALUE	DOCUMENT ID	TECN	COMMENT
<b>0.145±0.027 OUR FIT</b>			Error includes scale factor of 1.5.
<b>0.14 ± 0.04 OUR AVERAGE</b>			Error includes scale factor of 1.7. See the ideogram below.
0.080±0.033	AMSLER	02	CBAR 0.9 $\bar{p}p \rightarrow \pi^0 \eta\eta, \pi^0 \pi^0 \pi^0$
0.18 ± 0.03	BARBERIS	00E	450 $pp \rightarrow p_f \eta\eta p_S$
0.230±0.097	<sup>38</sup> AMSLER	95C	CBAR 0.0 $\bar{p}p \rightarrow \eta\eta\pi^0$
• • • We do not use the following data for averages, fits, limits, etc. • • •			
0.11 ± 0.03	<sup>36</sup> ANISOVICH	02D	SPEC Combined fit
0.078±0.013	<sup>39</sup> ABELE	96C	RVUE Compilation
0.157±0.060	<sup>40</sup> AMSLER	95D	CBAR 0.0 $\bar{p}p \rightarrow \pi^0 \pi^0 \pi^0, \pi^0 \eta\eta, \pi^0 \pi^0 \eta$

WEIGHTED AVERAGE  
0.14±0.04 (Error scaled by 1.7) $\Gamma(4\pi^0)/\Gamma(\eta\eta)$   $\Gamma_5/\Gamma_{11}$ 

VALUE	DOCUMENT ID	TECN	COMMENT
• • • We do not use the following data for averages, fits, limits, etc. • • •			
0.8±0.3	ALDE	87	GAM4 100 $\pi^- p \rightarrow 4\pi^0 n$

 $\Gamma(\eta\eta'(958))/\Gamma(\pi\pi)$   $\Gamma_{12}/\Gamma_1$ 

VALUE	DOCUMENT ID	TECN	COMMENT
<b>0.055±0.024 OUR FIT</b>			Error includes scale factor of 1.8.
<b>0.095±0.026</b>			
• • • We do not use the following data for averages, fits, limits, etc. • • •			
0.005±0.003	<sup>36</sup> ANISOVICH	02D	SPEC Combined fit

 $\Gamma(\eta\eta'(958))/\Gamma(\eta\eta)$   $\Gamma_{12}/\Gamma_{11}$ 

VALUE	DOCUMENT ID	TECN	COMMENT
<b>0.38±0.16 OUR FIT</b>			Error includes scale factor of 1.9.
<b>0.29±0.10</b>			
• • • We do not use the following data for averages, fits, limits, etc. • • •			
0.05±0.03	<sup>36</sup> ANISOVICH	02D	SPEC Combined fit
0.84±0.23	ABELE	96C	RVUE Compilation
2.7 ± 0.8	BINON	84C	GAM2 38 $\pi^- p \rightarrow \eta\eta' n$

 $\Gamma(K\bar{K})/\Gamma_{\text{total}}$   $\Gamma_{13}/\Gamma$ 

VALUE	DOCUMENT ID	TECN
• • • We do not use the following data for averages, fits, limits, etc. • • •		
0.044±0.021	BUGG	96

 $\Gamma(K\bar{K})/\Gamma(\pi\pi)$   $\Gamma_{13}/\Gamma_1$ 

VALUE	DOCUMENT ID	TECN	COMMENT
<b>0.246±0.026 OUR FIT</b>			
<b>0.241±0.028 OUR AVERAGE</b>			
0.25 ± 0.03	<sup>42</sup> BARGIOTTI	03	OBLX $\bar{p}p$
0.19 ± 0.07	<sup>43</sup> ABELE	98	CBAR 0.0 $\bar{p}p \rightarrow K_L^0 K_S^\pm \pi^\mp$
• • • We do not use the following data for averages, fits, limits, etc. • • •			
0.16 ± 0.05	<sup>36</sup> ANISOVICH	02D	SPEC Combined fit
0.33 ± 0.03 ± 0.07	BARBERIS	99D	OMEG 450 $pp \rightarrow K^+ K^-, \pi^+ \pi^-$
0.20 ± 0.08	<sup>44</sup> ABELE	96B	CBAR 0.0 $\bar{p}p \rightarrow \pi^0 K_L^0 K_L^0$

 $\Gamma(K\bar{K})/\Gamma(\eta\eta)$   $\Gamma_{13}/\Gamma_{11}$ 

VALUE	CL%	DOCUMENT ID	TECN	COMMENT
<b>1.69±0.33 OUR FIT</b>				Error includes scale factor of 1.4.
<b>1.85±0.41</b>				
• • • We do not use the following data for averages, fits, limits, etc. • • •				
1.5 ± 0.6		<sup>36</sup> ANISOVICH	02D	SPEC Combined fit
<0.4	90	<sup>45</sup> PROKOSHKIN	91	GAM4 300 $\pi^- p \rightarrow \pi^- \rho \eta\eta$
<0.6		<sup>46</sup> BINON	83	GAM2 38 $\pi^- p \rightarrow 2\eta n$

<sup>35</sup> Excluding  $\rho\rho$  contribution to  $4\pi$ .<sup>36</sup> From a combined K-matrix analysis of Crystal Barrel (0.  $\bar{p}p \rightarrow \pi^0 \pi^0 \pi^0, \pi^0 \eta\eta, \pi^0 \pi^0 \eta$ ), GAMS ( $\pi p \rightarrow \pi^0 \pi^0 n, \eta\eta n, \eta\eta' n$ ), and BNL ( $\pi p \rightarrow K\bar{K} n$ ) data.<sup>37</sup> From the combined data of ABELE 96 and ABELE 96C.<sup>38</sup> Using AMSLER 95B (3 $\pi^0$ ).<sup>39</sup>  $2\pi$  width determined to be 60 ± 12 MeV.<sup>40</sup> Coupled-channel analysis of AMSLER 95B, AMSLER 95C, and AMSLER 94D.<sup>41</sup> Using AMSLER 94E ( $\eta\eta' \pi^0$ ).<sup>42</sup> Coupled channel analysis of  $\pi^+ \pi^- \pi^0, K^+ K^- \pi^0$ , and  $K^\pm K_S^0 \pi^\mp$ .<sup>43</sup> Using  $\pi^0 \pi^0$  from AMSLER 95B.<sup>44</sup> Using AMSLER 95B (3 $\pi^0$ ), AMSLER 94C (2 $\pi^0 \eta$ ) and SU(3).<sup>45</sup> Combining results of GAM4 with those of WA76 on  $K\bar{K}$  central production.<sup>46</sup> Using ETKIN 82B and COHEN 80.

See key on page 457

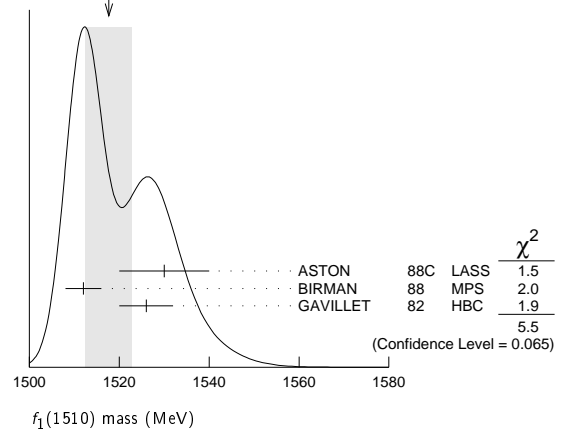
# Meson Particle Listings

## $f_0(1500)$ , $f_1(1510)$

### $f_0(1500)$ REFERENCES

ANISOVICH	09	JMP A04 2481	V.V. Anisovich, A.V. Sarantsev	
KLEMPF	08	EPJ C55 39	E. Klimoi, M. Matveev, A.V. Sarantsev	(BONN+)
UEHARA	08A	PR D78 052004	S. Uehara et al.	(BELLE Collab.)
ABLIKIM	06V	PL B642 441	M. Ablikim et al.	(BES Collab.)
AMSLER	06	PL B639 165	C. Amisler et al.	(CBAR Collab.)
AUBERT	06O	PR D74 032003	B. Aubert et al.	(BABAR Collab.)
PDG	06	JPG 33 1	W.-M. Yao et al.	(PDG Collab.)
UMAN	06	PR D73 052009	I. Uman et al.	(FNAL E835)
VLADIMIRSK...	06	PAN 69 493	V.V. Vladimirov et al.	(ITEP, Moscow)
		Translated from YAF 69 515	F. Binon et al.	
BINON	05	PAN 68 960	F. Binon et al.	
		Translated from YAF 68 998	A. Garmash et al.	(BELLE Collab.)
GARMASH	05	PR D71 092003	A. Garmash et al.	(BELLE Collab.)
ANISOVICH	03	EPJ A16 229	V.V. Anisovich et al.	
BARGIOTTI	03	EPJ C26 371	M. Bargiotti et al.	(OBELIX Collab.)
AMSLER	02	EPJ C23 29	C. Amisler et al.	
ANISOVICH	02D	PAN 65 1545	V.V. Anisovich et al.	
		Translated from YAF 65 1583	A. Abele et al.	(Crystal Barrel Collab.)
ABELE	01	EPJ C19 667	A. Abele et al.	(Crystal Barrel Collab.)
ABELE	01B	EPJ C21 261	A. Abele et al.	(Crystal Barrel Collab.)
ACCIARRI	01H	PL B501 173	M. Acciarri et al.	(L3 Collab.)
AITALA	01A	PRL 86 765	E.M. Aitala et al.	(FNAL E791 Collab.)
BARATE	00E	PL B472 189	R. Barate et al.	(ALEPH Collab.)
BARBERIS	00A	PL B471 429	D. Barberis et al.	(WA 102 Collab.)
BARBERIS	00C	PL B471 440	D. Barberis et al.	(WA 102 Collab.)
BARBERIS	00D	PL B474 423	D. Barberis et al.	(WA 102 Collab.)
BARBERIS	00E	PL B479 59	D. Barberis et al.	(WA 102 Collab.)
BARBERIS	99	PL B453 305	D. Barberis et al.	(Omega Expt.)
BARBERIS	99B	PL B453 316	D. Barberis et al.	(Omega Expt.)
BARBERIS	99D	PL B462 462	D. Barberis et al.	(Omega Expt.)
BELLAZZINI	99	PL B467 296	R. Bellazzini et al.	
FRENCH	99	PL B460 213	B. French et al.	(WA76 Collab.)
KAMINSKI	99	EPJ C9 141	R. Kaminski, L. Lesniak, B. Loiseau	(CRAC, PARIN)
ABELE	98	PR D57 3860	A. Abele et al.	(Crystal Barrel Collab.)
ALDE	98	EPJ A3 361	D. Alde et al.	(GAM4 Collab.)
		Also PAN 62 405	D. Alde et al.	(GAMS Collab.)
		Translated from YAF 62 446	C. Amisler	
AMSLER	98	RMP 70 1293	C. Amisler	
ANISOVICH	98B	SPI 41 419	V.V. Anisovich et al.	
		Translated from UFN 168 481	A. Bertin et al.	(OBELIX Collab.)
BERTIN	98	PR D57 55	A. Bertin et al.	(OBELIX Collab.)
REYES	98	PRL 81 4079	M.A. Reyes et al.	
BARBERIS	97B	PL B413 217	D. Barberis et al.	(WA 102 Collab.)
BERTIN	97C	PL B408 476	A. Bertin et al.	(OBELIX Collab.)
FRABETTI	97D	PL B407 79	P.L. Frabetti et al.	(FNAL E687 Collab.)
ABELE	96	PL B380 453	A. Abele et al.	(Crystal Barrel Collab.)
ABELE	96B	PL B385 425	A. Abele et al.	(Crystal Barrel Collab.)
ABELE	96C	NP A609 562	A. Abele et al.	(Crystal Barrel Collab.)
AMELIN	96B	PAN 59 976	D.V. Amelin et al.	(SERP, TBIL)
		Translated from YAF 59 1021	D.V. Bugg, A.V. Sarantsev, B.S. Zou	(LOQM, PNPI)
BUGG	96	NP B471 59	D.V. Bugg et al.	(Crystal Barrel Collab.)
AMSLER	95B	PL B342 433	C. Amisler et al.	(Crystal Barrel Collab.)
AMSLER	95C	PL B353 571	C. Amisler et al.	(Crystal Barrel Collab.)
AMSLER	95D	PL B355 425	C. Amisler et al.	(Crystal Barrel Collab.)
ANTINORI	95	PL B353 589	F. Antinori et al.	(ATHU, BARI, BIRM+)
BUGG	95	PL B353 378	D.V. Bugg et al.	(LOQM, PNPI, WASH)
ABATZIS	94	PL B324 509	S. Abatzis et al.	(ATHU, BARI, BIRM+)
AMSLER	94C	PL B327 425	C. Amisler et al.	(Crystal Barrel Collab.)
AMSLER	94D	PL B333 277	C. Amisler et al.	(Crystal Barrel Collab.)
AMSLER	94E	PL B340 259	C. Amisler et al.	(Crystal Barrel Collab.)
ANISOVICH	94	PL B323 233	V.V. Anisovich et al.	(Crystal Barrel Collab.)
BUGG	94	PR D50 4412	D.V. Bugg et al.	(LOQM)
AMSLER	92	PL B291 347	C. Amisler et al.	(Crystal Barrel Collab.)
BELADIDZE	92C	SJNP 55 1535	G.M. Beladidze, S.I. Bityukov, G.V. Borisov	(SERP+)
		Translated from YAF 55 2748	V.D. Prokoshkin	(GAM2, GAM4 Collab.)
PROKOSHKIN	91	SPD 36 155	V.D. Prokoshkin	(GAM2, GAM4 Collab.)
		Translated from DANS 316 900	T.A. Armstrong, M. Benayoun	(ATHU, BARI, BIRM+)
ARMSTRONG	89E	PL B228 536	T.A. Armstrong, M. Benayoun	(SERP, BELG, LANL, LAPP+)
ALDE	88	PL B201 160	D.M. Alde et al.	(SLAC, NAGO, CINC, INUS)
ASTON	88D	NP B301 525	D. Aston et al.	(LANL, BRUX, SERP, LAPP)
ALDE	87	PL B198 286	D.M. Alde et al.	(BELG, LAPP, SERP, CERN+)
ALDE	86D	NP B269 485	D.M. Alde et al.	(BELG, LAPP, SERP+)
BINON	84C	NC 80A 363	F.G. Binon et al.	(BELG, LAPP, SERP+)
BINON	83	NC 78A 313	F.G. Binon et al.	(BELG, LAPP, SERP+)
		Also SJNP 38 561	F.G. Binon et al.	(BELG, LAPP, SERP+)
		Translated from YAF 38 934	L. Gray et al.	(SYRA)
GRAY	83	PR D27 307	L. Gray et al.	(SYRA)
ETKIN	82B	PR D25 1786	A. Etkin et al.	(BNL, CUNY, TUFTS, VAND)
COHEN	80	PR D22 2595	D. Cohen et al.	(ANL)

WEIGHTED AVERAGE  
1518±5 (Error scaled by 1.7)

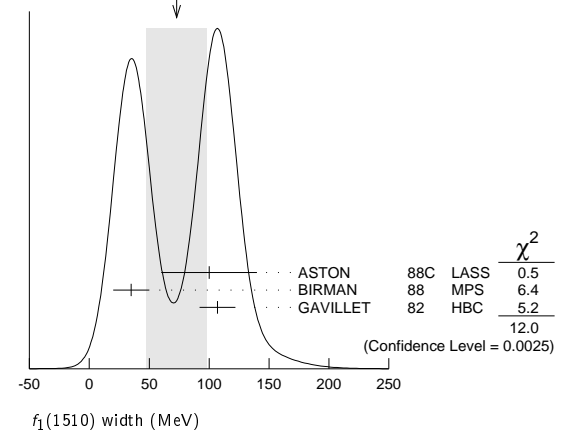


### $f_1(1510)$ WIDTH

VALUE (MeV)	EVTS	DOCUMENT ID	TECN	COMMENT
<b>73±25 OUR AVERAGE</b>		Error includes scale factor of 2.5. See the ideogram below.		
100±40		ASTON	88C LASS	11 $K^-p \rightarrow K_S^0 K^\pm \pi^\mp \Lambda$
35±15	600	<sup>3</sup> BIRMAN	88 MPS	8 $\pi^-p \rightarrow K^+ K^0 \pi^- n$
107±15	271	GAVILLET	82 HBC	4.2 $K^-p \rightarrow \Lambda K K \pi$

<sup>3</sup>From partial wave analysis of  $K^+ \bar{K}^0 \pi^-$  state.

WEIGHTED AVERAGE  
73±25 (Error scaled by 2.5)



## $f_1(1510)$

$$J^{PC} = 0^+(1^{++})$$

OMITTED FROM SUMMARY TABLE  
See the minireview under  $\eta(1405)$ .

### $f_1(1510)$ MASS

VALUE (MeV)	EVTS	DOCUMENT ID	TECN	COMMENT
<b>1518±5 OUR AVERAGE</b>		Error includes scale factor of 1.7. See the ideogram below.		
1530±10		ASTON	88C LASS	11 $K^-p \rightarrow K_S^0 K^\pm \pi^\mp \Lambda$
1512±4	600	<sup>1</sup> BIRMAN	88 MPS	8 $\pi^-p \rightarrow K^+ K^0 \pi^- n$
1526±6	271	GAVILLET	82 HBC	4.2 $K^-p \rightarrow \Lambda K K \pi$
~ 1525		<sup>2</sup> BAUER	93B	$\gamma \gamma^* \rightarrow \pi^+ \pi^- \pi^0 \pi^0$

• • • We do not use the following data for averages, fits, limits, etc. • • •  
<sup>1</sup> From partial wave analysis of  $K^+ \bar{K}^0 \pi^-$  state.  
<sup>2</sup> Not seen by AIHARA 88C in the  $K_S^0 K^\pm \pi^\mp$  final state.

### $f_1(1510)$ DECAY MODES

Mode	Fraction ( $\Gamma_i/\Gamma$ )
$\Gamma_1$ $K \bar{K}^*(892) + c.c.$	seen
$\Gamma_2$ $\pi^+ \pi^- \eta'$	seen

### $f_1(1510)$ BRANCHING RATIOS

$\Gamma(\pi^+ \pi^- \eta')/\Gamma_{total}$	$\Gamma_2/\Gamma$
seen	seen

### $f_1(1510)$ REFERENCES

ABLIKIM	11C PRL 106 072002	M. Ablikim et al.	(BES III Collab.)
BAUER	93B PR D48 3976	D.A. Bauer et al.	(SLAC)
AIHARA	88C PR D38 1	H. Aihara et al.	(TPC-2 $\gamma$ Collab.)
ASTON	88C PL B201 573	D. Aston et al.	(SLAC, NAGO, CINC, INUS, JIP)
BIRMAN	88 PRL 61 1557	A. Birman et al.	(BNL, FSU, IND, MASD, JIP)
GAVILLET	82 ZPHY C16 119	P. Gavillet et al.	(CERN, CDEF, PADO+)

## Meson Particle Listings

 $f'_2(1525)$  $f'_2(1525)$ 

$$I^G(J^{PC}) = 0^+(2^{++})$$

 $f'_2(1525)$  MASS

VALUE (MeV) DOCUMENT ID  
**1525 ± 5 OUR ESTIMATE** This is only an educated guess; the error given is larger than the error on the average of the published values.

## PRODUCED BY PION BEAM

VALUE (MeV)	EVTS	DOCUMENT ID	TECN	COMMENT
••• We do not use the following data for averages, fits, limits, etc. •••				
1521 ± 13		TIKHOMIROV 03	SPEC	40.0 $\pi^- C \rightarrow K_S^0 K_S^0 K_L^0 X$
1547 <sup>+10</sup> <sub>-2</sub>		<sup>1</sup> LONGACRE 86	MPS	22 $\pi^- p \rightarrow K_S^0 K_S^0 n$
1496 <sup>+9</sup> <sub>-8</sub>		<sup>2</sup> CHABAUD 81	ASPK	6 $\pi^- p \rightarrow K^+ K^- n$
1497 <sup>+8</sup> <sub>-9</sub>		CHABAUD 81	ASPK	18.4 $\pi^- p \rightarrow K^+ K^- n$
1492 ± 29		GORLICH 80	ASPK	17 $\pi^- p$ polarized $\rightarrow K^+ K^- n$
1502 ± 25		<sup>3</sup> CORDEN 79	OMEG	12-15 $\pi^- p \rightarrow \pi^+ \pi^- n$
1480	14	CRENNELL 66	HBC	6.0 $\pi^- p \rightarrow K_S^0 K_S^0 n$

PRODUCED BY  $K^\pm$  BEAM

VALUE (MeV)	EVTS	DOCUMENT ID	TECN	COMMENT
<b>1523.4 ± 1.3 OUR AVERAGE</b> Includes data from the datablock that follows this one. Error includes scale factor of 1.1.				
1526.8 ± 4.3		ASTON 88D	LASS	11 $K^- p \rightarrow K_S^0 K_S^0 \Lambda$
1504 ± 12		BOLONKIN 86	SPEC	40 $K^- p \rightarrow K_S^0 K_S^0 Y$
1529 ± 3		ARMSTRONG 83B	OMEG	18.5 $K^- p \rightarrow K^- K^+ \Lambda$
1521 ± 6	650	AGUILAR... 81B	HBC	4.2 $K^- p \rightarrow \Lambda K^+ K^-$
1521 ± 3	572	ALHARRAN 81	HBC	8.25 $K^- p \rightarrow \Lambda K \bar{K}$
1522 ± 6	123	BARREIRO 77	HBC	4.15 $K^- p \rightarrow \Lambda K_S^0 K_S^0$
1528 ± 7	166	EVANGELIS... 77	OMEG	10 $K^- p \rightarrow K^+ K^- (\Lambda, \Sigma)$
1527 ± 3	120	BRANDENB... 76C	ASPK	13 $K^- p \rightarrow K^+ K^- (\Lambda, \Sigma)$
1519 ± 7	100	AGUILAR... 72B	HBC	3.9, 4.6 $K^- p \rightarrow K \bar{K} (\Lambda, \Sigma)$
••• We do not use the following data for averages, fits, limits, etc. •••				
1514 ± 8	61	BINON 07	GAMS	32.5 $K^- p \rightarrow \eta \eta (\Lambda / \Sigma^0)$
1513 ± 10		<sup>4</sup> BARKOV 99	SPEC	40 $K^- p \rightarrow K_S^0 K_S^0 y$

PRODUCED IN  $e^+ e^-$  ANNIHILATION

VALUE (MeV)	EVTS	DOCUMENT ID	TECN	COMMENT
The data in this block is included in the average printed for a previous datablock.				
<b>1520.7 ± 2.0 OUR AVERAGE</b>				
1521 ± 5		ABLIKIM 05	BES2	$J/\psi \rightarrow \phi K^+ K^-$
1518 ± 1 ± 3		ABE 04	BELL	10.6 $e^+ e^- \rightarrow e^+ e^- K^+ K^-$
1519 ± 2 <sup>+15</sup> <sub>-5</sub>		BAI 03G	BES	$J/\psi \rightarrow \gamma K \bar{K}$
1523 ± 6	331	<sup>5</sup> ACCIARRI 01H	L3	91, 183-209 $e^+ e^- \rightarrow e^+ e^- K_S^0 K_S^0$
1535 ± 5 ± 4		ABREU 96C	DLPH	$Z^0 \rightarrow K^+ K^- + X$
1516 ± 5 <sup>+9</sup> <sub>-15</sub>		BAI 96C	BES	$J/\psi \rightarrow \gamma K^+ K^-$
1531.6 ± 10.0		AUGUSTIN 88	DM2	$J/\psi \rightarrow \gamma K^+ K^-$
1515 ± 5		<sup>6</sup> FALVARD 88	DM2	$J/\psi \rightarrow \phi K^+ K^-$
1525 ± 10 ± 10		BALTRUSAIT... 87	MRK3	$J/\psi \rightarrow \gamma K^+ K^-$
••• We do not use the following data for averages, fits, limits, etc. •••				
1523 ± 5	870	<sup>7</sup> SCHEGELSKY 06A	RVUE	$\gamma \gamma \rightarrow K_S^0 K_S^0$
1496 ± 2		<sup>8</sup> FALVARD 88	DM2	$J/\psi \rightarrow \phi K^+ K^-$

PRODUCED IN  $\bar{p}p$  ANNIHILATION

VALUE (MeV)	EVTS	DOCUMENT ID	TECN	COMMENT
••• We do not use the following data for averages, fits, limits, etc. •••				
1530 ± 12		<sup>9</sup> ANISOVICH 09	RVUE	0.0 $\bar{p}p, \pi N$
1513 ± 4		AMSLER 06	CBAR	0.9 $\bar{p}p \rightarrow K^+ K^- \pi^0$
1508 ± 9		<sup>10</sup> AMSLER 02	CBAR	0.9 $\bar{p}p \rightarrow \pi^0 \eta \eta, \pi^0 \pi^0 \pi^0$

## CENTRAL PRODUCTION

VALUE (MeV)	DOCUMENT ID	TECN	COMMENT
<b>1515 ± 15</b>	BARBERIS 99	OMEG	450 $pp \rightarrow p_S p_f K^+ K^-$

PRODUCED IN  $ep$  COLLISIONS

VALUE (MeV)	EVTS	DOCUMENT ID	TECN	COMMENT
••• We do not use the following data for averages, fits, limits, etc. •••				
<b>1512 ± 3<sup>+1.4</sup><sub>-0.5</sub></b>		<sup>11</sup> CHEKANOV 08	ZEUS	$ep \rightarrow K_S^0 K_S^0 X$
1537 <sup>+9</sup> <sub>-8</sub>		84 <sup>12</sup> CHEKANOV 04	ZEUS	$ep \rightarrow K_S^0 K_S^0 X$

- From a partial-wave analysis of data using a K-matrix formalism with 5 poles.
- CHABAUD 81 is a reanalysis of PAWLICKI 77 data.
- From an amplitude analysis where the  $f'_2(1525)$  width and elasticity are in complete disagreement with the values obtained from  $K \bar{K}$  channel, making the solution dubious.
- Systematic errors not estimated.
- Supersedes ACCIARRI 95J.
- From an analysis ignoring interference with  $f_0(1710)$ .
- From analysis of L3 data at 91 and 183-209 GeV.
- From an analysis including interference with  $f_0(1710)$ .
- 4-poles, 5-channel K matrix fit.
- T-matrix pole.
- In the SU(3) based model with a specific interference pattern of the  $f_2(1270)$ ,  $a_2^0(1320)$ , and  $f'_2(1525)$  mesons incoherently added to the  $f_0(1710)$  and non-resonant background.
- Systematic errors not estimated.

 $f'_2(1525)$  WIDTH

VALUE (MeV)	DOCUMENT ID	COMMENT
<b>73 ± 6<sup>5</sup> OUR FIT</b>		
<b>76 ± 10</b>	PDG 90	For fitting

## PRODUCED BY PION BEAM

VALUE (MeV)	EVTS	DOCUMENT ID	TECN	COMMENT
••• We do not use the following data for averages, fits, limits, etc. •••				
102 ± 4.2		TIKHOMIROV 03	SPEC	40.0 $\pi^- C \rightarrow K_S^0 K_S^0 K_L^0 X$
108 <sup>+5</sup> <sub>-2</sub>		<sup>13</sup> LONGACRE 86	MPS	22 $\pi^- p \rightarrow K_S^0 K_S^0 n$
69 <sup>+22</sup> <sub>-16</sub>		<sup>14</sup> CHABAUD 81	ASPK	6 $\pi^- p \rightarrow K^+ K^- n$
137 <sup>+23</sup> <sub>-21</sub>		CHABAUD 81	ASPK	18.4 $\pi^- p \rightarrow K^+ K^- n$
150 <sup>+83</sup> <sub>-50</sub>		GORLICH 80	ASPK	17 $\pi^- p$ polarized $\rightarrow K^+ K^- n$
165 ± 4.2		<sup>15</sup> CORDEN 79	OMEG	12-15 $\pi^- p \rightarrow \pi^+ \pi^- n$
92 <sup>+39</sup> <sub>-22</sub>		<sup>16</sup> POLYCHRO... 79	STRC	7 $\pi^- p \rightarrow n K_S^0 K_S^0$

PRODUCED BY  $K^\pm$  BEAM

VALUE (MeV)	EVTS	DOCUMENT ID	TECN	COMMENT
<b>80.2 ± 2.6 OUR AVERAGE</b> Includes data from the datablock that follows this one.				
90 ± 12		ASTON 88D	LASS	11 $K^- p \rightarrow K_S^0 K_S^0 \Lambda$
73 ± 18		BOLONKIN 86	SPEC	40 $K^- p \rightarrow K_S^0 K_S^0 Y$
83 ± 15		ARMSTRONG 83B	OMEG	18.5 $K^- p \rightarrow K^- K^+ \Lambda$
85 ± 16	650	AGUILAR... 81B	HBC	4.2 $K^- p \rightarrow \Lambda K^+ K^-$
80 <sup>+14</sup> <sub>-11</sub>	572	ALHARRAN 81	HBC	8.25 $K^- p \rightarrow \Lambda K \bar{K}$
72 ± 25	166	EVANGELIS... 77	OMEG	10 $K^- p \rightarrow K^+ K^- (\Lambda, \Sigma)$
69 ± 22	100	AGUILAR... 72B	HBC	3.9, 4.6 $K^- p \rightarrow K \bar{K} (\Lambda, \Sigma)$
••• We do not use the following data for averages, fits, limits, etc. •••				
92 <sup>+25</sup> <sub>-16</sub>	61	BINON 07	GAMS	32.5 $K^- p \rightarrow \eta \eta (\Lambda / \Sigma^0)$
75 ± 20		<sup>17</sup> BARKOV 99	SPEC	40 $K^- p \rightarrow K_S^0 K_S^0 y$
62 <sup>+19</sup> <sub>-14</sub>	123	BARREIRO 77	HBC	4.15 $K^- p \rightarrow \Lambda K_S^0 K_S^0$
61 ± 8	120	BRANDENB... 76C	ASPK	13 $K^- p \rightarrow K^+ K^- (\Lambda, \Sigma)$

PRODUCED IN  $e^+ e^-$  ANNIHILATION

VALUE (MeV)	EVTS	DOCUMENT ID	TECN	COMMENT
The data in this block is included in the average printed for a previous datablock.				
<b>79.9 ± 3.3 OUR AVERAGE</b> Error includes scale factor of 1.1.				
77 ± 15		ABLIKIM 05	BES2	$J/\psi \rightarrow \phi K^+ K^-$
82 ± 2 ± 3		ABE 04	BELL	10.6 $e^+ e^- \rightarrow e^+ e^- K^+ K^-$
75 ± 4 <sup>+15</sup> <sub>-5</sub>		BAI 03G	BES	$J/\psi \rightarrow \gamma K \bar{K}$
100 ± 15	331	<sup>18</sup> ACCIARRI 01H	L3	91, 183-209 $e^+ e^- \rightarrow e^+ e^- K_S^0 K_S^0$
60 ± 20 ± 19		ABREU 96C	DLPH	$Z^0 \rightarrow K^+ K^- + X$
60 ± 23 <sup>+13</sup> <sub>-20</sub>		BAI 96C	BES	$J/\psi \rightarrow \gamma K^+ K^-$
103 ± 30		AUGUSTIN 88	DM2	$J/\psi \rightarrow \gamma K^+ K^-$
62 ± 10		<sup>19</sup> FALVARD 88	DM2	$J/\psi \rightarrow \phi K^+ K^-$
85 ± 35		BALTRUSAIT... 87	MRK3	$J/\psi \rightarrow \gamma K^+ K^-$
••• We do not use the following data for averages, fits, limits, etc. •••				
104 ± 10	870	<sup>20</sup> SCHEGELSKY 06A	RVUE	$\gamma \gamma \rightarrow K_S^0 K_S^0$
100 ± 3		<sup>21</sup> FALVARD 88	DM2	$J/\psi \rightarrow \phi K^+ K^-$

PRODUCED IN  $\bar{p}p$  ANNIHILATION

VALUE (MeV)	EVTS	DOCUMENT ID	TECN	COMMENT
••• We do not use the following data for averages, fits, limits, etc. •••				
<b>79 ± 8</b>		<sup>22</sup> AMSLER 02	CBAR	0.9 $\bar{p}p \rightarrow \pi^0 \eta \eta, \pi^0 \pi^0 \pi^0$
128 ± 20		<sup>23</sup> ANISOVICH 09	RVUE	0.0 $\bar{p}p, \pi N$
76 ± 6		AMSLER 06	CBAR	0.9 $\bar{p}p \rightarrow K^+ K^- \pi^0$

## CENTRAL PRODUCTION

VALUE (MeV)	DOCUMENT ID	TECN	COMMENT
$70 \pm 25$	BARBERIS 99	OMEG	450 $pp \rightarrow p_S p_f K^+ K^-$

PRODUCED IN  $ep$  COLLISIONS

VALUE (MeV)	EVTS	DOCUMENT ID	TECN	COMMENT
$83 \pm 9^{+5}_{-4}$		24 CHEKANOV 08	ZEUS	$ep \rightarrow K_S^0 K_S^0 X$

• • • We do not use the following data for averages, fits, limits, etc. • • •

$50^{+34}_{-22}$	84	25 CHEKANOV 04	ZEUS	$ep \rightarrow K_S^0 K_S^0 X$
------------------	----	----------------	------	--------------------------------

- <sup>13</sup> From a partial-wave analysis of data using a K-matrix formalism with 5 poles.  
<sup>14</sup> CHABAUD 81 is a reanalysis of PAWLICKI 77 data.  
<sup>15</sup> From an amplitude analysis where the  $f_2'(1525)$  width and elasticity are in complete disagreement with the values obtained from  $K\bar{K}$  channel, making the solution dubious.  
<sup>16</sup> From a fit to the  $D$  with  $f_2(1270)$ - $f_2'(1525)$  interference. Mass fixed at 1516 MeV.  
<sup>17</sup> Systematic errors not estimated.  
<sup>18</sup> Supersedes ACCIARRI 95J.  
<sup>19</sup> From an analysis ignoring interference with  $f_0(1710)$ .  
<sup>20</sup> From analysis of L3 data at 91 and 183-209 GeV.  
<sup>21</sup> From an analysis including interference with  $f_0(1710)$ .  
<sup>22</sup> T-matrix pole.  
<sup>23</sup> 4-poles, 5-channel K matrix fit.  
<sup>24</sup> In the SU(3) based model with a specific interference pattern of the  $f_2(1270)$ ,  $a_2^0(1320)$ , and  $f_2'(1525)$  mesons incoherently added to the  $f_0(1710)$  and non-resonant background.  
<sup>25</sup> Systematic errors not estimated.

 $f_2'(1525)$  DECAY MODES

Mode	Fraction ( $\Gamma_i/\Gamma$ )
$\Gamma_1$ $K\bar{K}$	(88.7 $\pm$ 2.2) %
$\Gamma_2$ $\eta\eta$	(10.4 $\pm$ 2.2) %
$\Gamma_3$ $\pi\pi$	( 8.2 $\pm$ 1.5 ) $\times 10^{-3}$
$\Gamma_4$ $K\bar{K}^*(892) + c.c.$	
$\Gamma_5$ $\pi K\bar{K}$	
$\Gamma_6$ $\pi\pi\eta$	
$\Gamma_7$ $\pi^+\pi^+\pi^-\pi^-$	
$\Gamma_8$ $\gamma\gamma$	( 1.11 $\pm$ 0.14 ) $\times 10^{-6}$

## CONSTRAINED FIT INFORMATION

An overall fit to the total width, 2 partial widths, a combination of partial widths obtained from integrated cross sections, and 3 branching ratios uses 16 measurements and one constraint to determine 5 parameters. The overall fit has a  $\chi^2 = 14.0$  for 12 degrees of freedom.

The following *off-diagonal* array elements are the correlation coefficients  $\langle \delta p_i \delta p_j \rangle / (\delta p_i \delta p_j)$ , in percent, from the fit to parameters  $p_i$ , including the branching fractions,  $x_i \equiv \Gamma_i/\Gamma_{\text{total}}$ . The fit constrains the  $x_i$  whose labels appear in this array to sum to one.

$x_2$	-100			
$x_3$	-6	-1		
$x_8$	-6	6	1	
$\Gamma$	-23	23	-1	-55
	$x_1$	$x_2$	$x_3$	$x_8$

Mode	Rate (MeV)
$\Gamma_1$ $K\bar{K}$	65 $^{+5}_{-4}$
$\Gamma_2$ $\eta\eta$	7.6 $\pm$ 1.8
$\Gamma_3$ $\pi\pi$	0.60 $\pm$ 0.12
$\Gamma_8$ $\gamma\gamma$	( 8.1 $\pm$ 0.9 ) $\times 10^{-5}$

 $f_2'(1525)$  PARTIAL WIDTHS

$\Gamma(K\bar{K})$	DOCUMENT ID	TECN	COMMENT	$\Gamma_1$
--------------------	-------------	------	---------	------------

$65^{+5}_{-4}$  OUR FIT

$63^{+6}_{-5}$	26	LONGACRE 86	MPS	22 $\pi^- p \rightarrow K_S^0 K_S^0 n$
----------------	----	-------------	-----	--

$\Gamma(\eta\eta)$	DOCUMENT ID	TECN	COMMENT	$\Gamma_2$
--------------------	-------------	------	---------	------------

$7.6 \pm 1.8$  OUR FIT

• • • We do not use the following data for averages, fits, limits, etc. • • •

5.0 $\pm$ 0.8	870	27 SCHEGELSKY 06A	RVUE	$\gamma\gamma \rightarrow K_S^0 K_S^0$
24 $^{+3}_{-1}$	26	LONGACRE 86	MPS	22 $\pi^- p \rightarrow K_S^0 K_S^0 n$

 $\Gamma(\pi\pi)$   $\Gamma_3$ 

VALUE (MeV)	EVTS	DOCUMENT ID	TECN	COMMENT
-------------	------	-------------	------	---------

$0.60 \pm 0.12$  OUR FIT

1.4 $^{+1.0}_{-0.5}$		26	LONGACRE 86	MPS 22 $\pi^- p \rightarrow K_S^0 K_S^0 n$
----------------------	--	----	-------------	--

• • • We do not use the following data for averages, fits, limits, etc. • • •

0.2 $^{+1.0}_{-0.2}$	870	27	SCHEGELSKY 06A	RVUE $\gamma\gamma \rightarrow K_S^0 K_S^0$
----------------------	-----	----	----------------	---

 $\Gamma(\gamma\gamma)$   $\Gamma_8$ 

VALUE (keV)	EVTS	DOCUMENT ID	TECN	COMMENT
-------------	------	-------------	------	---------

$0.081 \pm 0.009$  OUR FIT

• • • We do not use the following data for averages, fits, limits, etc. • • •

0.13 $\pm$ 0.03	870	27	SCHEGELSKY 06A	RVUE $\gamma\gamma \rightarrow K_S^0 K_S^0$
-----------------	-----	----	----------------	---

- <sup>26</sup> From a partial-wave analysis of data using a K-matrix formalism with 5 poles.  
<sup>27</sup> From analysis of L3 data at 91 and 183-209 GeV, using  $\Gamma(f_2'(1525) \rightarrow K\bar{K}) = 68$  MeV and SU(3) relations.

 $f_2'(1525)$   $\Gamma(\eta)\Gamma(\gamma\gamma)/\Gamma(\text{total})$ 

$\Gamma(K\bar{K}) \times \Gamma(\gamma\gamma)/\Gamma_{\text{total}}$	DOCUMENT ID	TECN	COMMENT	$\Gamma_1\Gamma_8/\Gamma$
--	-------------	------	---------	---------------------------

$0.072 \pm 0.007$  OUR FIT

$0.072 \pm 0.007$  OUR AVERAGE

0.0564 $\pm$ 0.0048 $\pm$ 0.0116	ABE	04	BELL	10.6 $e^+e^- \rightarrow e^+e^- K^+K^-$
0.076 $\pm$ 0.006 $\pm$ 0.011	331	28	ACCIARRI 01H	L3 $e^+e^- \rightarrow e^+e^- K_S^0 K_S^0$
0.067 $\pm$ 0.008 $\pm$ 0.015	29	ALBRECHT 90G	ARG	$e^+e^- \rightarrow e^+e^- K^+K^-$
0.11 $^{+0.03}_{-0.02}$ $\pm$ 0.02	89C	BEHREND	CELL	$e^+e^- \rightarrow e^+e^- K_S^0 K_S^0$
0.10 $^{+0.04}_{-0.03}$ $^{+0.03}_{-0.02}$	88	BERGER	PLUT	$e^+e^- \rightarrow e^+e^- K_S^0 K_S^0$
0.12 $\pm$ 0.07 $\pm$ 0.04	29	AIHARA 86B	TPC	$e^+e^- \rightarrow e^+e^- K^+K^-$
0.11 $\pm$ 0.02 $\pm$ 0.04	29	ALTHOFF 83	TASS	$e^+e^- \rightarrow e^+e^- K\bar{K}$

• • • We do not use the following data for averages, fits, limits, etc. • • •

0.0314  $\pm$  0.0050  $\pm$  0.0077

<sup>30</sup> ALBRECHT 90G ARG  $e^+e^- \rightarrow e^+e^- K^+K^-$

<sup>28</sup> Supersedes ACCIARRI 95J. From analysis of L3 data at 91 and 183-209 GeV.

<sup>29</sup> Using an incoherent background.

<sup>30</sup> Using a coherent background.

 $f_2'(1525)$  BRANCHING RATIOS

$\Gamma(\eta\eta)/\Gamma_{\text{total}}$	DOCUMENT ID	TECN	COMMENT	$\Gamma_2/\Gamma$
--	-------------	------	---------	-------------------

• • • We do not use the following data for averages, fits, limits, etc. • • •

seen

0.10 $\pm$ 0.03	31	PROKOSHKIN 91A	GAM4	300 $\pi^- p \rightarrow \pi^- \rho\eta\eta$
-----------------	----	----------------	------	--

<sup>31</sup> Combining results of GAM4 with those of WA76 on  $K\bar{K}$  central production and results of CBAL, MRK3 and DM2 on  $J/\psi \rightarrow \gamma\eta\eta$ .

$\Gamma(\eta\eta)/\Gamma(K\bar{K})$	CL%	EVTS	DOCUMENT ID	TECN	COMMENT	$\Gamma_2/\Gamma_1$
-------------------------------------	-----	------	-------------	------	---------	---------------------

$0.118 \pm 0.028$  OUR FIT

$0.119 \pm 0.028$  OUR AVERAGE

0.119 $\pm$ 0.015 $\pm$ 0.036	61	32	BINON 07	GAMS 32.5	$K^- p \rightarrow \eta\eta(\Lambda/\Sigma^0)$	
-------------------------------	----	----	----------	-----------	--	--

0.11  $\pm$  0.04

<sup>33</sup> PROKOSHKIN 91 GAM4 300  $\pi^- p \rightarrow \pi^- \rho\eta\eta$

• • • We do not use the following data for averages, fits, limits, etc. • • •

< 0.14

90 BARBERIS 00E 450  $pp \rightarrow p_f \eta\eta p_S$

< 0.50

67 HBC 4.6, 5.0  $K^- p$

<sup>32</sup> Using the compilation of the cross sections for  $f_2'(1525)$  production in  $K^- p$  collisions from ASTON 88D.

<sup>33</sup> Combining results of GAM4 with those of WA76 on  $K\bar{K}$  central production and results of CBAL, MRK3 and DM2 on  $J/\psi \rightarrow \gamma\eta\eta$ .

$\Gamma(\pi\pi)/\Gamma_{\text{total}}$	CL%	EVTS	DOCUMENT ID	TECN	COMMENT	$\Gamma_3/\Gamma$
--	-----	------	-------------	------	---------	-------------------

$0.0082 \pm 0.0016$  OUR FIT

$0.0075 \pm 0.0016$  OUR AVERAGE

0.007  $\pm$  0.002

80 COSTA... OMEG 10  $\pi^- p \rightarrow K^+ K^- n$

0.027  $^{+0.071}_{-0.013}$

34 GORLICH 80 ASPK 17, 18  $\pi^- p$

0.0075  $\pm$  0.0025

34, 35 MARTIN 79 RVUE

• • • We do not use the following data for averages, fits, limits, etc. • • •

< 0.06

95 AGUILAR... 81B HBC 4.2  $K^- p \rightarrow \Lambda K^+ K^-$

0.19  $\pm$  0.03

79 OMEG 12-15  $\pi^- p \rightarrow \pi^+ \pi^- n$

< 0.045

95 BARREIRO 77 HBC 4.15  $K^- p \rightarrow \Lambda K_S^0 K_S^0$

0.012  $\pm$  0.004

34 PAWLICKI 77 SPEC 6  $\pi N \rightarrow K^+ K^- N$

< 0.063

90 BRANDENB... 76C ASPK 13  $K^- p \rightarrow K^+ K^- (\Lambda, \Sigma)$

< 0.0086

34 BEUSCH 75B OSPK 8.9  $\pi^- p \rightarrow K^0 \bar{K}^0 n$

<sup>34</sup> Assuming that the  $f_2'(1525)$  is produced by an one-pion exchange production mechanism.

<sup>35</sup> MARTIN 79 uses the PAWLICKI 77 data with different input value of the  $f_2'(1525) \rightarrow K\bar{K}$  branching ratio.

# Meson Particle Listings

## $f_2'(1525), f_2(1565)$

$\Gamma(\pi\pi)/\Gamma(K\bar{K})$				$\Gamma_3/\Gamma_1$
VALUE	DOCUMENT ID	TECN	COMMENT	
<b>0.0092 ± 0.0018 OUR FIT</b>				
<b>0.075 ± 0.035</b>	AUGUSTIN	87	DM2	$J/\psi \rightarrow \gamma\pi^+\pi^-$

$[\Gamma(K\bar{K}^*(892) + c.c.) + \Gamma(\pi K\bar{K})]/\Gamma(K\bar{K})$				$(\Gamma_4 + \Gamma_5)/\Gamma_1$
VALUE	CL%	DOCUMENT ID	TECN	COMMENT
••• We do not use the following data for averages, fits, limits, etc. •••				
<0.35	95	AGUILAR-...	72B	HBC
<0.4	67	AMMAR	67	HBC

$\Gamma(\pi\pi\eta)/\Gamma(K\bar{K})$				$\Gamma_6/\Gamma_1$
VALUE	CL%	DOCUMENT ID	TECN	COMMENT
••• We do not use the following data for averages, fits, limits, etc. •••				
<0.41	95	AGUILAR-...	72B	HBC
<0.3	67	AMMAR	67	HBC

$\Gamma(\pi^+\pi^+\pi^-\pi^-)/\Gamma(K\bar{K})$				$\Gamma_7/\Gamma_1$
VALUE	CL%	DOCUMENT ID	TECN	COMMENT
••• We do not use the following data for averages, fits, limits, etc. •••				
<0.32	95	AGUILAR-...	72B	HBC

••• We do not use the following data for averages, fits, limits, etc. •••

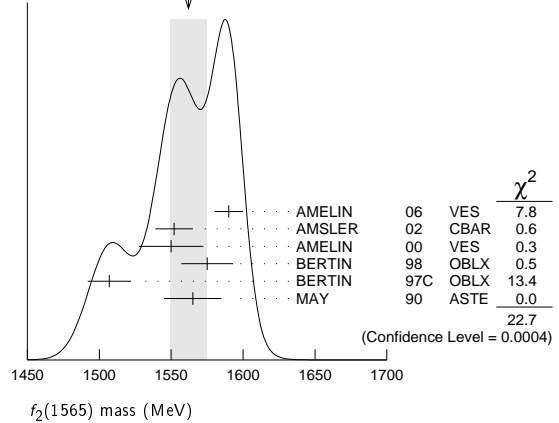
1560 ± 15	<sup>3</sup> ANISOVICH	09	RVUE	0.0 $\bar{p}p, \pi N$
1598 ± 11 ± 9	BAKER	99B	SPEC	0.0 $\bar{p}p \rightarrow \omega\omega\pi^0$
1534 ± 20	<sup>4</sup> ABELE	96C	RVUE	Compilation
~ 1552	<sup>5</sup> AMSLER	95D	CBAR	0.0 $\bar{p}p \rightarrow \pi^0\pi^0\pi^0, \pi^0\eta\eta, \pi^0\pi^0\eta$
1598 ± 72	BALOSHIN	95	SPEC	40 $\pi^-C \rightarrow K_S^0 K_S^0 X$
1566 <sup>+80</sup> <sub>-50</sub>	<sup>6</sup> ANISOVICH	94	CBAR	0.0 $\bar{p}p \rightarrow 3\pi^0, \eta\eta\pi^0$
1502 ± 9	ADAMO	93	OBLX	$\bar{p}p \rightarrow \pi^+\pi^+\pi^-$
1488 ± 10	<sup>7</sup> ARMSTRONG	93C	E760	$\bar{p}p \rightarrow \pi^0\eta\eta \rightarrow 6\gamma$
1508 ± 10	<sup>7</sup> ARMSTRONG	93D	E760	$\bar{p}p \rightarrow 3\pi^0 \rightarrow 6\gamma$
1525 ± 10	<sup>7</sup> ARMSTRONG	93D	E760	$\bar{p}p \rightarrow \eta\pi^0\pi^0 \rightarrow 6\gamma$
~ 1504	<sup>8</sup> WEIDENAUER	93	ASTE	0.0 $\bar{p}N \rightarrow 3\pi^- 2\pi^+$
1540 ± 15	<sup>7</sup> ADAMO	92	OBLX	$\bar{p}p \rightarrow \pi^+\pi^+\pi^-$
1515 ± 10	<sup>9</sup> AKER	91	CBAR	0.0 $\bar{p}p \rightarrow 3\pi^0$
1477 ± 5	BRIDGES	86c	DBC	0.0 $\bar{p}N \rightarrow 3\pi^- 2\pi^+$

<sup>1</sup> Supersedes the  $\omega\omega$  state of BELADIDZE 92b earlier assigned to the  $f_2(1640)$ .  
<sup>2</sup> T-matrix pole.  
<sup>3</sup> On sheet II in a two-pole solution.  
<sup>4</sup> T-matrix pole, large coupling to  $\rho\rho$  and  $\omega\omega$ , could be  $f_2(1640)$ .  
<sup>5</sup> Coupled-channel analysis of AMSLER 95B, AMSLER 95C, and AMSLER 94D.  
<sup>6</sup> From a simultaneous analysis of the annihilations  $\bar{p}p \rightarrow 3\pi^0, \pi^0\eta\eta$  including AKER 91 data.  
<sup>7</sup>  $J^P$  not determined, could be partly  $f_0(1500)$ .  
<sup>8</sup>  $J^P$  not determined.  
<sup>9</sup> Superseded by AMSLER 95B.

### $f_2'(1525)$ REFERENCES

UEHARA	10A	PR D82 114031	S. Uehara et al.	(BELLE Collab.)
ANISOVICH	09	IJMP A24 2481	V.V. Anisovich, A.V. Sarantsev	(ZEUS Collab.)
CHEKANOV	08	PRL 101 112003	S. Chekanov et al.	(GAMS Collab.)
BINON	07	PAN 70 1713	F. Binon et al.	(CBAR Collab.)
AMSLER	06	PL B639 165	C. Amisler et al.	(BES Collab.)
SCHEGELSKY	06A	EPJ A27 207	V.A. Schegelsky et al.	(BELLE Collab.)
ABLIKIM	05	PL B607 243	M. Ablikim et al.	(ZEUS Collab.)
ABE	04	EPJ C32 323	K. Abe et al.	(BELLE Collab.)
CHEKANOV	04	PL B578 33	S. Chekanov et al.	(ZEUS Collab.)
BAI	03G	PR D68 052003	J.Z. Bai et al.	(BES Collab.)
TIKHOMIROV	03	PAN 66 828	G.D. Tikhomirov et al.	(BES Collab.)
AMSLER	02	EPJ C23 29	C. Amisler et al.	(L3 Collab.)
ACCIARRI	01H	PL B501 173	M. Acciari et al.	(WA 102 Collab.)
BARBERIS	00E	PL B479 59	D. Barberis et al.	(Omega Expt.)
BARBERIS	99	PL B453 305	D. Barberis et al.	(Omega Expt.)
BARKOV	99	JETPL 70 248	B.P. Barkov et al.	(DELPHI Collab.)
ABREU	96C	PL B379 309	P. Abreu et al.	(BES Collab.)
ACCIARRI	95J	PL B363 118	M. Acciari et al.	(L3 Collab.)
PROKOSHKIN	91	SPD 36 155	Y.D. Prokoshkin	(GAM2, GAM4 Collab.)
ALBRECHT	90G	ZPHY C48 183	H. Albrecht et al.	(ARGUS Collab.)
BEHREND	89C	ZPHY C43 91	J.J. Behrend et al.	(IFIC, BOST, CIT+)
ASTON	88D	NP B301 525	D. Aston et al.	(SLAC, NAGO, CINC, INUS)
AUGUSTIN	88	PRL 60 2238	J.E. Augustin et al.	(DM2 Collab.)
BERGER	88	ZPHY C37 329	A. Berger et al.	(PLUTO Collab.)
FALVARD	88	PR D38 2706	A. Falvard et al.	(CLER, FRAS, LALO+)
AUGUSTIN	87	ZPHY C36 369	J.E. Augustin et al.	(LALO, CLER, FRAS+)
BALTRUSAITIS	87	PR D35 2077	R.M. Baltrusaitis et al.	(Mark III Collab.)
AIHARA	86B	PRL 57 404	H. Aihara et al.	(TPC-2 $\gamma$ Collab.)
BOLONKIN	86	SJNP 43 776	B.V. Bolonkin et al.	(ITEP) JP
LONGACRE	86	PL B177 223	R.S. Longacre et al.	(BNL, BRAN, CUNY+)
ALTHOFF	83	PL 121B 216	M. Althoff et al.	(TASSO Collab.)
ARMSTRONG	35B	NP B224 193	T.A. Armstrong et al.	(BARI, BIRM, CERN+)
AGUILAR...	81B	ZPHY C9 313	M. Aguilar-Benitez et al.	(CERN, CDEF+)
ALHARRAN	81	NP B191 26	S. Al-Harran et al.	(BIRM, CERN, GLAS+)
CHABAUD	81	APP B12 575	V. Chabaud et al.	(CERN, CRAC, MPIM)
COSTA...	80	NP B175 402	G. Costa de Beauregard et al.	(BARI, BONN+)
GORLICH	80	NP B174 16	L. Gorlich et al.	(CRAC, MPIM, CERN+)
CORDEN	79	NP B157 250	M.J. Corden et al.	(BIRM, RHEL, TELA+)
MARTIN	79	NP B158 520	A.D. Martin, E.N. Ozmutlu	(DURH)
POLYCHRO...	79	PR D19 1317	V.A. Polychronakos et al.	(NDAM, ANL)
BARREIRO	77	NP B121 237	F. Barreiro et al.	(CERN, AMST, NIJM+)
EVANGELISTA	77	NP B127 384	C. Evangelista et al.	(BARI, BONN, CERN+)
PAWLICKI	77	PR D15 3196	A.J. Pawlicki et al.	(ANL) JJP
BRANDENB...	76C	NP B104 413	G.W. Brandenburg et al.	(SLAC)
BEUSCH	75B	PL 60B 101	M. Beusch et al.	(CERN, ETH)
AGUILAR...	72B	PR D6 29	M. Aguilar-Benitez et al.	(BNL)
AMMAR	67	PRL 19 1071	R. Ammar et al.	(NWES, ANL) JP
BARNES	67	PRL 19 964	V.E. Barnes et al.	(BNL, SYRA) JJP
CRENNELL	66	PRL 16 1025	D.J. Crennell et al.	(BNL) I

WEIGHTED AVERAGE  
1562 ± 13 (Error scaled by 2.1)



### $f_2(1565)$ WIDTH

VALUE (MeV)	DOCUMENT ID	TECN	COMMENT
<b>134 ± 8 OUR AVERAGE</b>			
140 ± 11	<sup>10</sup> AMELIN	06	VES
113 ± 23	<sup>11</sup> AMSLER	02	CBAR
130 ± 20 ± 40	AMELIN	00	VES
119 ± 24	BERTIN	98	OBLX
130 ± 20	BERTIN	97C	OBLX
170 ± 40	MAY	90	ASTE
••• We do not use the following data for averages, fits, limits, etc. •••			
280 ± 40	<sup>12</sup> ANISOVICH	09	RVUE
180 ± 60	<sup>13</sup> ABELE	96C	RVUE
~ 142	<sup>14</sup> AMSLER	95D	CBAR
263 ± 101	BALOSHIN	95	SPEC
166 <sup>+80</sup> <sub>-20</sub>	<sup>15</sup> ANISOVICH	94	CBAR
130 ± 10	<sup>16</sup> ADAMO	93	OBLX
148 ± 27	<sup>17</sup> ARMSTRONG	93C	E760
103 ± 15	<sup>17</sup> ARMSTRONG	93D	E760
111 ± 10	<sup>17</sup> ARMSTRONG	93D	E760
~ 206	<sup>18</sup> WEIDENAUER	93	ASTE
132 ± 37	<sup>17</sup> ADAMO	92	OBLX
120 ± 10	<sup>19</sup> AKER	91	CBAR
116 ± 9	BRIDGES	86c	DBC

<sup>10</sup> Supersedes the  $\omega\omega$  state of BELADIDZE 92b earlier assigned to the  $f_2(1640)$ .  
<sup>11</sup> T-matrix pole.  
<sup>12</sup> On sheet II in a two-pole solution.  
<sup>13</sup> T-matrix pole, large coupling to  $\rho\rho$  and  $\omega\omega$ , could be  $f_2(1640)$ .  
<sup>14</sup> Coupled-channel analysis of AMSLER 95B, AMSLER 95C, and AMSLER 94D.  
<sup>15</sup> From a simultaneous analysis of the annihilations  $\bar{p}p \rightarrow 3\pi^0, \pi^0\eta\eta$  including AKER 91 data.

## $f_2(1565)$

$$I^G(J^{PC}) = 0^+(2^{++})$$

OMITTED FROM SUMMARY TABLE

Seen mostly in antinucleon-nucleon annihilation. Needs confirmation in other channels.

### $f_2(1565)$ MASS

VALUE (MeV)	DOCUMENT ID	TECN	COMMENT
<b>1562 ± 13 OUR AVERAGE</b>	Error includes scale factor of 2.1. See the ideogram below.		
1590 ± 10	<sup>1</sup> AMELIN	06	VES
1552 ± 13	<sup>2</sup> AMSLER	02	CBAR
1550 ± 10 ± 20	AMELIN	00	VES
1575 ± 18	BERTIN	98	OBLX
1507 ± 15	<sup>2</sup> BERTIN	97C	OBLX
1565 ± 20	MAY	90	ASTE

See key on page 457

## Meson Particle Listings

 $f_2(1565), \rho(1570)$ 

- <sup>16</sup> Supersedes ADAMO 92.  
<sup>17</sup>  $J^P$  not determined, could be partly  $f_0(1500)$ .  
<sup>18</sup>  $J^P$  not determined.  
<sup>19</sup> Superseded by AMSLER 95B.

 $f_2(1565)$  REFERENCES

ANISOVICH	09	IJMP A24 2481	V.V. Anisovich, A.V. Sarantsev	
AMELIN	06	PAN 69 590	D.V. Amelin et al.	(VES Collab.)
		Translated from YAF 69 715		
SCHEGELSKY	06A	EPJ A27 207	V.A. Schegelsky et al.	
AMSLER	02	EPJ C23 29	C. Amisler et al.	
AMELIN	00	NP A668 83	D. Amelin et al.	(VES Collab.)
BAKER	99B	PL B467 147	C.A. Baker et al.	
BERTIN	98	PR D57 55	A. Bertin et al.	(OBELIX Collab.)
BERTIN	97C	PL B408 476	A. Bertin et al.	(OBELIX Collab.)
ABELE	96C	NP A509 562	A. Abele et al.	(Crystal Barrel Collab.)
AMSLER	95B	PL B342 433	C. Amisler et al.	(Crystal Barrel Collab.)
AMSLER	95C	PL B353 571	C. Amisler et al.	(Crystal Barrel Collab.)
AMSLER	95D	PL B355 425	C. Amisler et al.	(Crystal Barrel Collab.)
BALOSHIN	95	PAN 58 46	O.N. Baloshin et al.	(ITFP)
		Translated from YAF 58 50.		
AMSLER	94D	PL B333 277	C. Amisler et al.	(Crystal Barrel Collab.)
ANISOVICH	94	PL B323 233	V.V. Anisovich et al.	(Crystal Barrel Collab.)
ANISOVICH	94B	PR D50 1972	V.V. Anisovich et al.	(LOQM)
ADAMO	93	NP A558 13C	A. Adamo et al.	(OBELIX Collab.)
ARMSTRONG	93C	PL B307 394	T.A. Armstrong et al.	(FNAL, FERR, GENO+)
ARMSTRONG	93D	PL B307 399	T.A. Armstrong et al.	(FNAL, FERR, GENO+)
WEIDENAUER	93	ZPHY C59 387	P. Weidenaueer et al.	(ASTERIX Collab.)
ADAMO	92	PL B287 368	A. Adamo et al.	(OBELIX Collab.)
BELADIDZE	92B	ZPHY C54 367	G.M. Beladidze et al.	(VES Collab.)
AKER	91	PL B260 249	E. Aker et al.	(Crystal Barrel Collab.)
MAY	90	ZPHY C46 203	B. May et al.	(ASTERIX Collab.)
MAY	89	PL B225 450	B. May et al.	(ASTERIX Collab.)
BRIDGES	86B	PRL 56 215	D.L. Bridges et al.	(SYRA, CASE)
BRIDGES	86C	PRL 57 1534	D.L. Bridges et al.	(SYRA)

 $f_2(1565)$  DECAY MODES

Mode	Fraction ( $\Gamma_i/\Gamma$ )
$\Gamma_1$ $\pi\pi$	seen
$\Gamma_2$ $\pi^+\pi^-$	seen
$\Gamma_3$ $\pi^0\pi^0$	seen
$\Gamma_4$ $\rho^0\rho^0$	seen
$\Gamma_5$ $2\pi^+2\pi^-$	seen
$\Gamma_6$ $\eta\eta$	seen
$\Gamma_7$ $a_2(1320)\pi$	
$\Gamma_8$ $\omega\omega$	seen
$\Gamma_9$ $K\bar{K}$	
$\Gamma_{10}$ $\gamma\gamma$	

 $f_2(1565)$  PARTIAL WIDTHS $\Gamma(\eta\eta)$   $\Gamma_6$ 

VALUE (MeV)	EVTS	DOCUMENT ID	TECN	COMMENT
1.2±0.3	870	<sup>20</sup> SCHEGELSKY 06A	RVUE	$\gamma\gamma \rightarrow K_S^0 K_S^0$

• • • We do not use the following data for averages, fits, limits, etc. • • •

 $\Gamma(K\bar{K})$   $\Gamma_9$ 

VALUE (MeV)	EVTS	DOCUMENT ID	TECN	COMMENT
2.0±1.0	870	<sup>20</sup> SCHEGELSKY 06A	RVUE	$\gamma\gamma \rightarrow K_S^0 K_S^0$

• • • We do not use the following data for averages, fits, limits, etc. • • •

 $\Gamma(\gamma\gamma)$   $\Gamma_{10}$ 

VALUE (keV)	EVTS	DOCUMENT ID	TECN	COMMENT
0.70±0.14	870	<sup>20</sup> SCHEGELSKY 06A	RVUE	$\gamma\gamma \rightarrow K_S^0 K_S^0$

• • • We do not use the following data for averages, fits, limits, etc. • • •

<sup>20</sup> From analysis of L3 data at 91 and 183–209 GeV, using  $f_2(1565)$  mass of 1570 MeV, width of 160 MeV,  $\Gamma(\pi\pi) = 25$  MeV, and SU(3) relations.

 $f_2(1565)$  BRANCHING RATIOS $\Gamma(\pi\pi)/\Gamma_{\text{total}}$   $\Gamma_1/\Gamma$ 

VALUE	DOCUMENT ID	TECN	COMMENT
seen	BAKER 99B	SPEC	$0 \bar{p}p \rightarrow \omega\omega\pi^0$

• • • We do not use the following data for averages, fits, limits, etc. • • •

 $\Gamma(\pi^+\pi^-)/\Gamma_{\text{total}}$   $\Gamma_2/\Gamma$ 

VALUE	DOCUMENT ID	TECN	COMMENT
seen	BERTIN 98	OBLX	$0.05-0.405 \bar{p}p \rightarrow \pi^+\pi^-\pi^0$

• • • We do not use the following data for averages, fits, limits, etc. • • •

not seen	<sup>21</sup> ANISOVICH 94B	RVUE	$\bar{p}p \rightarrow \pi^+\pi^-\pi^0$
seen	MAY 89	ASTE	$\bar{p}p \rightarrow \pi^+\pi^-\pi^0$

<sup>21</sup> ANISOVICH 94B is from a reanalysis of MAY 90.

 $\Gamma(\pi^0\pi^0)/\Gamma_{\text{total}}$   $\Gamma_3/\Gamma$ 

VALUE	DOCUMENT ID	TECN	COMMENT
seen	AMSLER 95B	CBAR	$0.0 \bar{p}p \rightarrow 3\pi^0$

 $\Gamma(\pi^+\pi^-)/\Gamma(\rho^0\rho^0)$   $\Gamma_2/\Gamma_4$ 

VALUE	DOCUMENT ID	TECN	COMMENT
0.042±0.013	BRIDGES 86B	DBC	$\bar{p}N \rightarrow 3\pi^-2\pi^+$

• • • We do not use the following data for averages, fits, limits, etc. • • •

 $\Gamma(\eta\eta)/\Gamma(\pi^0\pi^0)$   $\Gamma_6/\Gamma_3$ 

VALUE	DOCUMENT ID	TECN	COMMENT
0.024±0.005±0.012	<sup>22</sup> ARMSTRONG 93C	E760	$\bar{p}p \rightarrow \pi^0\eta\eta \rightarrow 6\gamma$

• • • We do not use the following data for averages, fits, limits, etc. • • •

<sup>22</sup>  $J^P$  not determined, could be partly  $f_0(1500)$ .

 $\Gamma(\omega\omega)/\Gamma_{\text{total}}$   $\Gamma_8/\Gamma$ 

VALUE	DOCUMENT ID	TECN	COMMENT
seen	BAKER 99B	SPEC	$0 \bar{p}p \rightarrow \omega\omega\pi^0$

• • • We do not use the following data for averages, fits, limits, etc. • • •

 $\rho(1570)$ 

$$J^{PC} = 1^+(1^-)$$

OMITTED FROM SUMMARY TABLE

May be an OZI-violating decay mode of  $\rho(1700)$ . See our mini-review under the  $\rho(1700)$ .

 $\rho(1570)$  MASS

VALUE (MeV)	EVTS	DOCUMENT ID	TECN	COMMENT
<b>1570±36±62</b>	54	<sup>1</sup> AUBERT 08s	BABR	$10.6 e^+e^- \rightarrow \phi\pi^0\gamma$
1480±40		<sup>2</sup> BITYUKOV 87	SPEC	$32.5 \pi^-p \rightarrow \phi\pi^0n$

• • • We do not use the following data for averages, fits, limits, etc. • • •

<sup>1</sup> From the fit with two resonances.  
<sup>2</sup> Systematic errors not estimated.

 $\rho(1570)$  WIDTH

VALUE (MeV)	EVTS	DOCUMENT ID	TECN	COMMENT
<b>144±75±43</b>	54	<sup>3</sup> AUBERT 08s	BABR	$10.6 e^+e^- \rightarrow \phi\pi^0\gamma$
130±60		<sup>4</sup> BITYUKOV 87	SPEC	$32.5 \pi^-p \rightarrow \phi\pi^0n$

• • • We do not use the following data for averages, fits, limits, etc. • • •

<sup>3</sup> From the fit with two resonances.  
<sup>4</sup> Systematic errors not estimated.

 $\rho(1570)$  DECAY MODES

Mode	Fraction ( $\Gamma_i/\Gamma$ )
$\Gamma_1$ $e^+e^-$	
$\Gamma_2$ $\phi\pi$	not seen
$\Gamma_3$ $\omega\pi$	

 $\rho(1570) \Gamma(i)\Gamma(e^+e^-)/\Gamma_{\text{total}}$  $\Gamma(\phi\pi) \times \Gamma(e^+e^-)/\Gamma_{\text{total}}$   $\Gamma_2\Gamma_1/\Gamma$ 

VALUE (eV)	CL%	EVTS	DOCUMENT ID	TECN	COMMENT
<b>3.5±0.9±0.3</b>		54	<sup>5</sup> AUBERT 08s	BABR	$10.6 e^+e^- \rightarrow \phi\pi^0\gamma$
<70	90		<sup>6</sup> AULCHENKO 87B	ND	$e^+e^- \rightarrow K_S^0 K_L^0 \pi^0$

• • • We do not use the following data for averages, fits, limits, etc. • • •

<sup>5</sup> From the fit with two resonances.  
<sup>6</sup> Using mass and width of BITYUKOV 87.

 $\rho(1570)$  BRANCHING RATIOS $\Gamma(\phi\pi)/\Gamma_{\text{total}}$   $\Gamma_2/\Gamma$ 

VALUE	DOCUMENT ID	TECN	COMMENT
not seen	ABELE 97H	CBAR	$\bar{p}p \rightarrow K_L^0 K_S^0 \pi^0 \pi^0$
<0.01	<sup>7</sup> DONNACHIE 91	RVUE	

• • • We do not use the following data for averages, fits, limits, etc. • • •

<sup>7</sup> Using data from BISELLO 91B, DOLINSKY 86, and ALBRECHT 87L.

 $\Gamma(\phi\pi)/\Gamma(\omega\pi)$   $\Gamma_2/\Gamma_3$ 

VALUE	CL%	DOCUMENT ID	TECN	COMMENT
>0.5	95	BITYUKOV 87	SPEC	$32.5 \pi^-p \rightarrow \phi\pi^0n$

• • • We do not use the following data for averages, fits, limits, etc. • • •

# Meson Particle Listings

## $\rho(1570)$ , $h_1(1595)$ , $\pi_1(1600)$

### $\rho(1570)$ REFERENCES

AUBERT	085	PR D77 092002	B. Aubert et al.	(BABAR Collab.)
ABELE	97H	PL B415 200	A. Abele et al.	(Crystal Barrel Collab.)
BISELLO	91B	NPBPS B21 111	D. Bisello	(DM2 Collab.)
DONNACHIE	91	ZPHY C51 689	A. Donnachie, A.B. Clegg	(MCHS, LANC)
ALBRECHT	87L	PL B185 223	H. Albrecht et al.	(ARGUS Collab.)
AULCHENKO	87B	JETPL 45 145	V.M. Aulchenko et al.	(NOVO)
		Translated from ZETFP 45 118.		
BITYUKOV	87	PL B188 383	S.I. Bityukov et al.	(SERP)
DOLINSKY	86	PL B174 453	S.I. Dolinsky et al.	(NOVO)

### $h_1(1595)$

$$I^G(J^{PC}) = 0^-(1^{+-})$$

OMITTED FROM SUMMARY TABLE

Seen in a partial-wave analysis of the  $\omega\eta$  system produced in the reaction  $\pi^- p \rightarrow \omega\eta n$  at 18 GeV/c.

### $h_1(1595)$ MASS

VALUE (MeV)	DOCUMENT ID	TECN	COMMENT
$1594 \pm 15^{+10}_{-60}$	EUGENIO	01	SPEC 18 $\pi^- p \rightarrow \omega\eta n$

### $h_1(1595)$ WIDTH

VALUE (MeV)	DOCUMENT ID	TECN	COMMENT
$384 \pm 60^{+70}_{-100}$	EUGENIO	01	SPEC 18 $\pi^- p \rightarrow \omega\eta n$

### $h_1(1595)$ DECAY MODES

Mode	Fraction ( $\Gamma_i/\Gamma$ )
$\Gamma_1$ $\omega\eta$	seen

### $h_1(1595)$ REFERENCES

EUGENIO	01	PL B497 190	P. Eugenio et al.
---------	----	-------------	-------------------

### $\pi_1(1600)$

$$I^G(J^{PC}) = 1^-(1^{-+})$$

### $\pi_1(1600)$ MASS

VALUE (MeV)	EVTS	DOCUMENT ID	TECN	COMMENT
$1662 \pm 8^{+9}_{-9}$ OUR AVERAGE				
$1660 \pm 10^{+0}_{-64}$	420k	ALEKSEEV	10	COMP 190 $\pi^- Pb \rightarrow \pi^- \pi^- \pi^+ Pb'$
$1664 \pm 8 \pm 10$	145k	<sup>1</sup> LU	05	B852 18 $\pi^- p \rightarrow \omega\pi^- \pi^0 p$
$1709 \pm 24 \pm 41$	69k	<sup>2</sup> KUHN	04	B852 18 $\pi^- p \rightarrow \eta\pi^+ \pi^- \pi^- p$
$1597 \pm 10^{+45}_{-10}$		<sup>2</sup> IVANOV	01	B852 18 $\pi^- p \rightarrow \eta' \pi^- p$
• • • We do not use the following data for averages, fits, limits, etc. • • •				
$1593 \pm 8^{+29}_{-47}$		<sup>2,3</sup> ADAMS	98B	B852 18.3 $\pi^- p \rightarrow \pi^+ \pi^- \pi^- p$

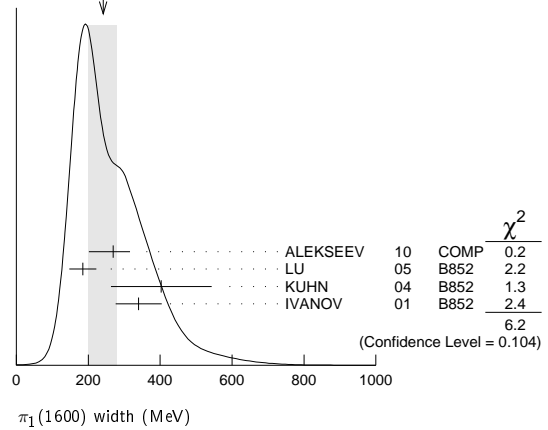
<sup>1</sup> May be a different state: natural and unnatural parity exchanges.  
<sup>2</sup> Natural parity exchange.  
<sup>3</sup> Superseded by DZIERBA 06 excluding this state in a more refined PWA analysis, with 2.6 M events of  $\pi^- p \rightarrow \pi^- \pi^- \pi^+ p$  and 3 M events of  $\pi^- p \rightarrow \pi^- \pi^0 \pi^0 p$  of E852 data.

### $\pi_1(1600)$ WIDTH

VALUE (MeV)	EVTS	DOCUMENT ID	TECN	COMMENT
$241 \pm 40$ OUR AVERAGE				Error includes scale factor of 1.4. See the ideogram below.
$269 \pm 21^{+42}_{-64}$	420k	ALEKSEEV	10	COMP 190 $\pi^- Pb \rightarrow \pi^- \pi^- \pi^+ Pb'$
$185 \pm 25 \pm 28$	145k	<sup>4</sup> LU	05	B852 18 $\pi^- p \rightarrow \omega\pi^- \pi^0 p$
$403 \pm 80 \pm 115$	69k	<sup>5</sup> KUHN	04	B852 18 $\pi^- p \rightarrow \eta\pi^+ \pi^- \pi^- p$
$340 \pm 40 \pm 50$		<sup>5</sup> IVANOV	01	B852 18 $\pi^- p \rightarrow \eta' \pi^- p$
• • • We do not use the following data for averages, fits, limits, etc. • • •				
$168 \pm 20^{+150}_{-12}$		<sup>5,6</sup> ADAMS	98B	B852 18.3 $\pi^- p \rightarrow \pi^+ \pi^- \pi^- p$

<sup>4</sup> May be a different state: natural and unnatural parity exchanges.  
<sup>5</sup> Natural parity exchange.  
<sup>6</sup> Superseded by DZIERBA 06 excluding this state in a more refined PWA analysis, with 2.6 M events of  $\pi^- p \rightarrow \pi^- \pi^- \pi^+ p$  and 3 M events of  $\pi^- p \rightarrow \pi^- \pi^0 \pi^0 p$  of E852 data.

WEIGHTED AVERAGE  
241±40 (Error scaled by 1.4)



### $\pi_1(1600)$ DECAY MODES

Mode	Fraction ( $\Gamma_i/\Gamma$ )
$\Gamma_1$ $\pi\pi\pi$	not seen
$\Gamma_2$ $\rho^0\pi^-$	not seen
$\Gamma_3$ $f_2(1270)\pi^-$	not seen
$\Gamma_4$ $b_1(1235)\pi$	seen
$\Gamma_5$ $\eta'(958)\pi^-$	seen
$\Gamma_6$ $f_1(1285)\pi$	seen

### $\pi_1(1600)$ BRANCHING RATIOS

$\Gamma(\rho^0\pi^-)/\Gamma_{total}$	DOCUMENT ID	TECN	COMMENT	$\Gamma_2/\Gamma$
not seen	NOZAR	09	CLAS $\gamma p \rightarrow 2\pi^+ \pi^- n$	
not seen	<sup>7</sup> DZIERBA	06	B852 18 $\pi^- p$	

<sup>7</sup> From the PWA analysis of 2.6 M  $\pi^- p \rightarrow \pi^- \pi^- \pi^+ p$  and 3 M events of  $\pi^- p \rightarrow \pi^- \pi^0 \pi^0 p$  of E852 data. Supersedes ADAMS 98B.

$\Gamma(f_2(1270)\pi^-)/\Gamma_{total}$	DOCUMENT ID	TECN	COMMENT	$\Gamma_3/\Gamma$
not seen	<sup>8</sup> DZIERBA	06	B852 18 $\pi^- p$	

<sup>8</sup> From the PWA analysis of 2.6 M  $\pi^- p \rightarrow \pi^- \pi^- \pi^+ p$  and 3 M events of  $\pi^- p \rightarrow \pi^- \pi^0 \pi^0 p$  of E852 data. Supersedes CHUNG 02.

$\Gamma(b_1(1235)\pi)/\Gamma_{total}$	EVTS	DOCUMENT ID	TECN	COMMENT	$\Gamma_4/\Gamma$
seen	35280	<sup>9</sup> BAKER	03	SPEC $\bar{p}p \rightarrow \omega\pi^+ \pi^- \pi^0$	

• • • We do not use the following data for averages, fits, limits, etc. • • •  
 seen 145k LU 05 B852 18  $\pi^- p \rightarrow \omega\pi^- \pi^0 p$   
<sup>9</sup>  $B((b_1\pi)_{D-wave})/B((b_1\pi)_{S-wave}) = 0.3 \pm 0.1$ .

$\Gamma(\eta'(958)\pi^-)/\Gamma_{total}$	DOCUMENT ID	TECN	COMMENT	$\Gamma_5/\Gamma$
seen	IVANOV	01	B852 18 $\pi^- p \rightarrow \eta' \pi^- p$	

$\Gamma(f_1(1285)\pi)/\Gamma(\eta'(958)\pi^-)$	EVTS	DOCUMENT ID	TECN	COMMENT	$\Gamma_6/\Gamma_5$
$3.80 \pm 0.78$	69k	<sup>10</sup> KUHN	04	B852 18 $\pi^- p \rightarrow \eta\pi^+ \pi^- \pi^- p$	

<sup>10</sup> Using  $\eta'(958)\pi$  data from IVANOV 01.

### $\pi_1(1600)$ REFERENCES

ALEKSEEV	10	PRL 104 241803	M.G. Alekseev et al.	(COMPASS Collab.)
NOZAR	09	PRL 102 102002	M. Nozar et al.	(CLAS Collab.)
DZIERBA	06	PR D73 072001	A.R. Dzierba et al.	(BNL E852 Collab.)
LU	05	PRL 94 032002	M. Lu et al.	(BNL E852 Collab.)
KUHN	04	PL B595 109	J. Kuhn et al.	(BNL E852 Collab.)
BAKER	03	PL B563 140	C.A. Baker et al.	(BNL E852 Collab.)
CHUNG	02	PR D65 072001	S.U. Chung et al.	(BNL E852 Collab.)
IVANOV	01	PRL 86 3977	E.I. Ivanov et al.	(BNL E852 Collab.)
ADAMS	98B	PRL 81 5760	G.S. Adams et al.	(BNL E852 Collab.)



See key on page 457

Meson Particle Listings

$a_1(1640)$ ,  $f_2(1640)$

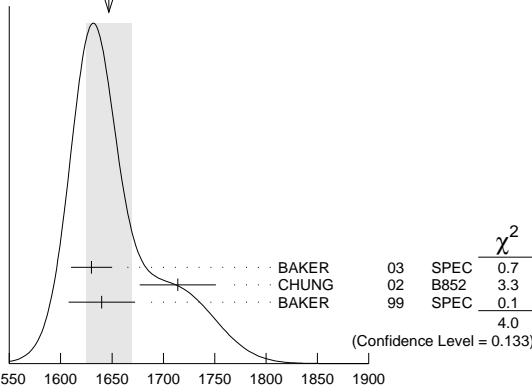
**$a_1(1640)$**   $I^G(J^{PC}) = 1^-(1^{++})$

OMITTED FROM SUMMARY TABLE  
 Seen in the amplitude analysis of the  $3\pi^0$  system produced in  $\bar{p}p \rightarrow 4\pi^0$ . Possibly seen in the study of the hadronic structure in decay  $\tau \rightarrow 3\pi\nu_\tau$  (ABREU 98G and ASNER 00). Needs confirmation.

**$a_1(1640)$  MASS**

VALUE (MeV)	EVTS	DOCUMENT ID	TECN	COMMENT
<b>1647±22 OUR AVERAGE</b>		Error includes scale factor of 1.4. See the ideogram below.		
1630±20	35280	<sup>1</sup> BAKER	03	SPEC $\bar{p}p \rightarrow \omega\pi^+\pi^-\pi^0$
1714±9±36		CHUNG	02	B852 $18.3\pi^-p \rightarrow \pi^+\pi^-\pi^-p$
1640±12±30		BAKER	99	SPEC $1.94\bar{p}p \rightarrow 4\pi^0$
••• We do not use the following data for averages, fits, limits, etc. •••				
1670±90		BELLINI	85	SPEC $40\pi^-A \rightarrow \pi^-\pi^+\pi^-A$

WEIGHTED AVERAGE  
1647±22 (Error scaled by 1.4)



<sup>1</sup> Using the  $a_1(1260)$  mass and width results of BOWLER 88.

**$a_1(1640)$  WIDTH**

VALUE (MeV)	EVTS	DOCUMENT ID	TECN	COMMENT
<b>254±27 OUR AVERAGE</b>		Error includes scale factor of 1.1.		
225±30	35280	<sup>2</sup> BAKER	03	SPEC $\bar{p}p \rightarrow \omega\pi^+\pi^-\pi^0$
308±37±62		CHUNG	02	B852 $18.3\pi^-p \rightarrow \pi^+\pi^-\pi^-p$
300±22±40		BAKER	99	SPEC $1.94\bar{p}p \rightarrow 4\pi^0$
••• We do not use the following data for averages, fits, limits, etc. •••				
300±100		BELLINI	85	SPEC $40\pi^-A \rightarrow \pi^-\pi^+\pi^-A$

<sup>2</sup> Using the  $a_1(1260)$  mass and width results of BOWLER 88.

**$a_1(1640)$  DECAY MODES**

Mode	Fraction ( $\Gamma_i/\Gamma$ )
$\Gamma_1$ $\pi\pi\pi$	seen
$\Gamma_2$ $f_2(1270)\pi$	seen
$\Gamma_3$ $\sigma\pi$	seen
$\Gamma_4$ $\rho\pi S$ -wave	seen
$\Gamma_5$ $\rho\pi D$ -wave	seen
$\Gamma_6$ $\omega\pi\pi$	seen
$\Gamma_7$ $f_1(1285)\pi$	seen
$\Gamma_8$ $a_1(1260)\eta$	not seen

**$a_1(1640)$  BRANCHING RATIOS**

$\Gamma(f_2(1270)\pi)/\Gamma(\sigma\pi)$	$\Gamma_2/\Gamma_3$
0.24±0.07	
	BAKER 99 SPEC $1.94\bar{p}p \rightarrow 4\pi^0$

$\Gamma(\rho\pi D$ -wave)/ $\Gamma_{total}$	$\Gamma_5/\Gamma$
seen	
	CHUNG 02 B852 $18.3\pi^-p \rightarrow \pi^+\pi^-\pi^-p$
	AMELIN 95B VES $36\pi^-A \rightarrow \pi^+\pi^-\pi^-A$

$\Gamma(\omega\pi\pi)/\Gamma_{total}$	$\Gamma_6/\Gamma$
seen	
	35280 <sup>3</sup> BAKER 03 SPEC $\bar{p}p \rightarrow \omega\pi^+\pi^-\pi^0$

$\Gamma(f_1(1285)\pi)/\Gamma_{total}$	$\Gamma_7/\Gamma$
not seen	
seen	KUHN 04 B852 $18\pi^-p \rightarrow \eta\pi^+\pi^-\pi^-p$
	LEE 94 MPS2 $18\pi^-p \rightarrow K^+\bar{K}^0\pi^-\pi^-p$

$\Gamma(a_1(1260)\eta)/\Gamma_{total}$	$\Gamma_8/\Gamma$
not seen	
	KUHN 04 B852 $18\pi^-p \rightarrow \eta\pi^+\pi^-\pi^-p$

<sup>3</sup> Assuming the  $\omega\rho$  mechanism for the  $\omega\pi\pi$  state.

**$a_1(1640)$  REFERENCES**

KUHN 04	PL B595 109	J. Kuhn et al.	(BNL E852 Collab.)
BAKER 03	PL B563 140	C.A. Baker et al.	
CHUNG 02	PR D65 072001	S.U. Chung et al.	(BNL E852 Collab.)
ASNER 00	PR D61 012002	D.M. Asner et al.	(CLEO Collab.)
BAKER 99	PL B449 114	C.A. Baker et al.	
ABREU 98G	PL B426 411	P. Abreu et al.	(DELPHI Collab.)
AMELIN 95B	PL B356 595	D.V. Amelin et al.	(SERP, TBL)
LEE 94	PL B323 227	J.H. Lee et al.	(BNL, IND, KYUN, MASD+)
BOWLER 88	PL B209 99	M.G. Bowler	(OXF)
BELLINI 85	SJNP 41 781	D. Bellini et al.	

Translated from YAF 41 1223.

**$f_2(1640)$**

$I^G(J^{PC}) = 0^+(2^{++})$

OMITTED FROM SUMMARY TABLE

**$f_2(1640)$  MASS**

VALUE (MeV)	DOCUMENT ID	TECN	COMMENT
<b>1639±6 OUR AVERAGE</b>	Error includes scale factor of 1.2.		
1620±16	BUGG 95	MRK3	$J/\psi \rightarrow \gamma\pi^+\pi^-\pi^+\pi^-$
1647±7	ADAMO 92	OBLX	$\bar{\pi}p \rightarrow 3\pi^+2\pi^-$
1635±7	ALDE 90	GAM2	$38\pi^-p \rightarrow \omega\omega n$
••• We do not use the following data for averages, fits, limits, etc. •••			
1640±5	AMSLER 06	CBAR	$0.9\bar{p}p \rightarrow K^+K^-\pi^0$
1659±6	VLADIMIRSK..06	SPEC	$40\pi^-p \rightarrow K_S^0 K_S^0 n$
1643±7	<sup>1</sup> ALDE 89B	GAM2	$38\pi^-p \rightarrow \omega\omega n$

<sup>1</sup> Superseded by ALDE 90.

**$f_2(1640)$  WIDTH**

VALUE (MeV)	CL%	DOCUMENT ID	TECN	COMMENT
<b>99<sup>+60</sup><sub>-40</sub> OUR AVERAGE</b>		Error includes scale factor of 2.9.		
140 <sup>+60</sup> <sub>-20</sub>		BUGG 95	MRK3	$J/\psi \rightarrow \gamma\pi^+\pi^-\pi^+\pi^-$
58±20		ADAMO 92	OBLX	$\bar{\pi}p \rightarrow 3\pi^+2\pi^-$
••• We do not use the following data for averages, fits, limits, etc. •••				
44±9		AMSLER 06	CBAR	$0.9\bar{p}p \rightarrow K^+K^-\pi^0$
152±18		VLADIMIRSK..06	SPEC	$40\pi^-p \rightarrow K_S^0 K_S^0 n$
< 70	90	ALDE 90	GAM2	$38\pi^-p \rightarrow \omega\omega n$

**$f_2(1640)$  DECAY MODES**

Mode	Fraction ( $\Gamma_i/\Gamma$ )
$\Gamma_1$ $\omega\omega$	seen
$\Gamma_2$ $4\pi$	seen
$\Gamma_3$ $K\bar{K}$	seen

**$f_2(1640)$  BRANCHING RATIOS**

$\Gamma(K\bar{K})/\Gamma_{total}$	$\Gamma_3/\Gamma$
seen	
	AMSLER 06 CBAR $0.9\bar{p}p \rightarrow K^+K^-\pi^0$

**$f_2(1640)$  REFERENCES**

AMSLER 06	PL B639 165	C. Amsler et al.	(CBAR Collab.)
VLADIMIRSK..06	PAN 69 493	N.V. Vladimirov et al.	(ITEP, Moscow)
BUGG 95	PL B353 378	D.V. Bugg et al.	(LOQM, PNPI, WASH)JP
ADAMO 92	PL B287 368	A. Adamo et al.	(OBELIX Collab.)
ALDE 90	PL B241 600	D.M. Alde et al.	(SERP, BELG, LANL, LAPP+)
ALDE 89B	PL B216 451	D.M. Alde et al.	(SERP, BELG, LANL, LAPP+)IGJPC

## Meson Particle Listings

 $\eta_2(1645), \omega(1650)$  $\eta_2(1645)$ 

$$J^G(J^{PC}) = 0^+(2^-)$$

 $\eta_2(1645)$  MASS

VALUE (MeV)	DOCUMENT ID	TECN	CHG	COMMENT
<b>1617 ± 5 OUR AVERAGE</b>				
1613 ± 8	BARBERIS 00b			450 $pp \rightarrow \rho_f \eta \pi^+ \pi^- \rho_S$
1617 ± 8	BARBERIS 00c			450 $pp \rightarrow \rho_f 4\pi \rho_S$
1620 ± 20	BARBERIS 97b	OMEG		450 $pp \rightarrow \rho p 2(\pi^+ \pi^-)$
1645 ± 14 ± 15	ADOMEIT 96	CBAR 0		1.94 $\bar{p}p \rightarrow \eta 3\pi^0$
• • • We do not use the following data for averages, fits, limits, etc. • • •				
1645 ± 6 ± 20	ANISOVICH 00e	SPEC		0.9-1.94 $\bar{p}p \rightarrow \eta 3\pi^0$

 $\eta_2(1645)$  WIDTH

VALUE (MeV)	DOCUMENT ID	TECN	CHG	COMMENT
<b>181 ± 11 OUR AVERAGE</b>				
185 ± 17	BARBERIS 00b			450 $pp \rightarrow \rho_f \eta \pi^+ \pi^- \rho_S$
177 ± 18	BARBERIS 00c			450 $pp \rightarrow \rho_f 4\pi \rho_S$
180 ± 25	BARBERIS 97b	OMEG		450 $pp \rightarrow \rho p 2(\pi^+ \pi^-)$
180 <sup>+40</sup> <sub>-21</sub> ± 25	ADOMEIT 96	CBAR 0		1.94 $\bar{p}p \rightarrow \eta 3\pi^0$
• • • We do not use the following data for averages, fits, limits, etc. • • •				
200 ± 25	ANISOVICH 00e	SPEC		0.9-1.94 $\bar{p}p \rightarrow \eta 3\pi^0$

 $\eta_2(1645)$  DECAY MODES

Mode	Fraction ( $\Gamma_i/\Gamma$ )
$\Gamma_1$ $a_2(1320)\pi$	seen
$\Gamma_2$ $K\bar{K}\pi$	seen
$\Gamma_3$ $K^*\bar{K}$	seen
$\Gamma_4$ $\eta\pi^+\pi^-$	seen
$\Gamma_5$ $a_0(980)\pi$	seen
$\Gamma_6$ $f_2(1270)\eta$	not seen

 $\eta_2(1645)$  BRANCHING RATIOS

$\Gamma(K\bar{K}\pi)/\Gamma(a_2(1320)\pi)$	DOCUMENT ID	TECN	COMMENT	$\Gamma_2/\Gamma_1$
<b>0.07 ± 0.03</b>	1 BARBERIS 97c	OMEG	450 $pp \rightarrow \rho p K\bar{K}\pi$	
• • • We do not use the following data for averages, fits, limits, etc. • • •				
			Using $2(\pi^+\pi^-)$ data from BARBERIS 97b.	

$\Gamma(a_2(1320)\pi)/\Gamma(a_0(980)\pi)$	DOCUMENT ID	TECN	COMMENT	$\Gamma_1/\Gamma_5$
<b>13.1 ± 2.3 OUR AVERAGE</b>				
13.5 ± 4.6	2 ANISOVICH 11	SPEC	0.9-1.94 $\rho\bar{p}$	
13.0 ± 2.7	BARBERIS 00b		450 $pp \rightarrow \rho_f \eta \pi^+ \pi^- \rho_S$	
• • • We do not use the following data for averages, fits, limits, etc. • • •				
			Reanalysis of ADOMEIT 96 and ANISOVICH 00e.	

$\Gamma(f_2(1270)\eta)/\Gamma_{\text{total}}$	DOCUMENT ID	COMMENT	$\Gamma_6/\Gamma$
• • • We do not use the following data for averages, fits, limits, etc. • • •			
not seen	BARBERIS 00b	450 $pp \rightarrow \rho_f \eta \pi^+ \pi^- \rho_S$	

 $\eta_2(1645)$  REFERENCES

ANISOVICH 11	EPJ C71 1511	A.V. Anisovich et al.	(LOQM, RAL, PNPI)
ANISOVICH 00e	PL B477 19	A.V. Anisovich et al.	
BARBERIS 00b	PL B471 435	D. Barberis et al.	(WA 102 Collab.)
BARBERIS 00c	PL B471 440	D. Barberis et al.	(WA 102 Collab.)
BARBERIS 97b	PL B413 217	D. Barberis et al.	(WA 102 Collab.)
BARBERIS 97c	PL B413 225	D. Barberis et al.	(WA 102 Collab.)
ADOMEIT 96	ZPHY C71 227	J. Adomeit et al.	(Crystal Barrel Collab.)

 $\omega(1650)$ 

$$J^G(J^{PC}) = 0^-(1^-)$$

 $\omega(1650)$  MASS

VALUE (MeV)	EVTS	DOCUMENT ID	TECN	COMMENT
<b>1670 ± 30 OUR ESTIMATE</b>				
• • • We do not use the following data for averages, fits, limits, etc. • • •				
1667 ± 13 ± 6		AUBERT 07Au BABR		10.6 $e^+e^- \rightarrow \omega\pi^+\pi^-\gamma$
1645 ± 8	13	AUBERT 06d BABR		10.6 $e^+e^- \rightarrow \omega\eta\gamma$
1660 ± 10 ± 2		AUBERT,B 04N BABR		10.6 $e^+e^- \rightarrow \pi^+\pi^-\pi^0\gamma$
1770 ± 50 ± 60	1.2M	1 ACHASOV 03d RVUE		0.44-2.00 $e^+e^- \rightarrow \pi^+\pi^-\pi^0$
1619 ± 5		2 HENNER 02 RVUE		1.2-2.0 $e^+e^- \rightarrow \rho\pi, \omega\pi\pi$
1700 ± 20		EUGENIO 01 SPEC		18 $\pi^-\rho \rightarrow \omega\eta\eta$
1705 ± 26	612	3 AKHMETSHIN 00d CMD2		$e^+e^- \rightarrow \omega\pi^+\pi^-$
1820 <sup>+190</sup> <sub>-150</sub>		4 ACHASOV 98H RVUE		$e^+e^- \rightarrow \pi^+\pi^-\pi^0$

1840 <sup>+100</sup> <sub>-70</sub>		5 ACHASOV 98H RVUE		$e^+e^- \rightarrow \omega\pi^+\pi^-$
1780 <sup>+170</sup> <sub>-300</sub>		6 ACHASOV 98H RVUE		$e^+e^- \rightarrow K^+K^-$
~ 2100		7 ACHASOV 98H RVUE		$e^+e^- \rightarrow K_S^0 K^\pm\pi^\mp$
1606 ± 9		8 CLEGG 94 RVUE		
1662 ± 13	750	9 ANTONELLI 92 DM2		1.34-2.4 $e^+e^- \rightarrow \rho\pi, \omega\pi\pi$
1670 ± 20		ATKINSON 83B OMEG		20-70 $\gamma\rho \rightarrow 3\pi X$
1657 ± 13		CORDIER 81 DM1		$e^+e^- \rightarrow \omega 2\pi$
1679 ± 34	21	ESPOSITO 80 FRAM		$e^+e^- \rightarrow 3\pi$
1652 ± 17		COSME 79 OSPK		$e^+e^- \rightarrow 3\pi$

- 1 From the combined fit of ANTONELLI 92, ACHASOV 01e, ACHASOV 02e, and ACHASOV 03d data on the  $\pi^+\pi^-\pi^0$  and ANTONELLI 92 on the  $\omega\pi^+\pi^-$  final states. Supersedes ACHASOV 99e and ACHASOV 02e.
- 2 Using results of CORDIER 81 and preliminary data of DOLINSKY 91 and ANTONELLI 92.
- 3 Using the data of AKHMETSHIN 00d and ANTONELLI 92. The  $\rho\pi$  dominance for the energy dependence of the  $\omega(1420)$  and  $\omega(1650)$  width assumed.
- 4 Using data from BARKOV 87, DOLINSKY 91, and ANTONELLI 92.
- 5 Using the data from ANTONELLI 92.
- 6 Using the data from IVANOV 81 and BISELLO 88b.
- 7 Using the data from BISELLO 91c.
- 8 From a fit to two Breit-Wigner functions and using the data of DOLINSKY 91 and ANTONELLI 92.
- 9 From the combined fit of the  $\rho\pi$  and  $\omega\pi\pi$  final states.

 $\omega(1650)$  WIDTH

VALUE (MeV)	EVTS	DOCUMENT ID	TECN	COMMENT
<b>315 ± 35 OUR ESTIMATE</b>				
• • • We do not use the following data for averages, fits, limits, etc. • • •				
222 ± 25 ± 20		AUBERT 07Au BABR		10.6 $e^+e^- \rightarrow \omega\pi^+\pi^-\gamma$
114 ± 14	13	AUBERT 06d BABR		10.6 $e^+e^- \rightarrow \omega\eta\gamma$
230 ± 30 ± 20		AUBERT,B 04N BABR		10.6 $e^+e^- \rightarrow \pi^+\pi^-\pi^0\gamma$
490 <sup>+200</sup> <sub>-150</sub> ± 130	1.2M	10 ACHASOV 03d RVUE		0.44-2.00 $e^+e^- \rightarrow \pi^+\pi^-\pi^0$
250 ± 14		11 HENNER 02 RVUE		1.2-2.0 $e^+e^- \rightarrow \rho\pi, \omega\pi\pi$
250 ± 50		EUGENIO 01 SPEC		18 $\pi^-\rho \rightarrow \omega\eta\eta$
370 ± 25	612	12 AKHMETSHIN 00d CMD2		$e^+e^- \rightarrow \omega\pi^+\pi^-$
113 ± 20		13 CLEGG 94 RVUE		
280 ± 24	750	14 ANTONELLI 92 DM2		1.34-2.4 $e^+e^- \rightarrow \rho\pi, \omega\pi\pi$
160 ± 20		ATKINSON 83B OMEG		20-70 $\gamma\rho \rightarrow 3\pi X$
136 ± 46		CORDIER 81 DM1		$e^+e^- \rightarrow \omega 2\pi$
99 ± 49	21	ESPOSITO 80 FRAM		$e^+e^- \rightarrow 3\pi$
42 ± 17		COSME 79 OSPK		$e^+e^- \rightarrow 3\pi$

- 10 From the combined fit of ANTONELLI 92, ACHASOV 01e, ACHASOV 02e, and ACHASOV 03d data on the  $\pi^+\pi^-\pi^0$  and ANTONELLI 92 on the  $\omega\pi^+\pi^-$  final states. Supersedes ACHASOV 99e and ACHASOV 02e.
- 11 Using results of CORDIER 81 and preliminary data of DOLINSKY 91 and ANTONELLI 92.
- 12 Using the data of AKHMETSHIN 00d and ANTONELLI 92. The  $\rho\pi$  dominance for the energy dependence of the  $\omega(1420)$  and  $\omega(1650)$  width assumed.
- 13 From a fit to two Breit-Wigner functions and using the data of DOLINSKY 91 and ANTONELLI 92.
- 14 From the combined fit of the  $\rho\pi$  and  $\omega\pi\pi$  final states.

 $\omega(1650)$  DECAY MODES

Mode	Fraction ( $\Gamma_i/\Gamma$ )
$\Gamma_1$ $\rho\pi$	seen
$\Gamma_2$ $\omega\pi\pi$	seen
$\Gamma_3$ $\omega\eta$	seen
$\Gamma_4$ $e^+e^-$	seen

 $\omega(1650)$   $\Gamma_1\Gamma(e^+e^-)/\Gamma^2(\text{total})$ 

$\Gamma(\rho\pi)/\Gamma_{\text{total}} \times \Gamma(e^+e^-)/\Gamma_{\text{total}}$	$\Gamma_1/\Gamma \times \Gamma_4/\Gamma$			
VALUE (units $10^{-6}$ )	EVTS	DOCUMENT ID	TECN	COMMENT
• • • We do not use the following data for averages, fits, limits, etc. • • •				
1.3 ± 0.1 ± 0.1		AUBERT,B 04N BABR		10.6 $e^+e^- \rightarrow \pi^+\pi^-\pi^0\gamma$
1.2 <sup>+0.4</sup> <sub>-0.1</sub> ± 0.8	1.2M	15,16 ACHASOV 03d RVUE		0.44-2.00 $e^+e^- \rightarrow \pi^+\pi^-\pi^0$
0.921 ± 0.230		17,18 CLEGG 94 RVUE		
0.479 ± 0.050	750	19,20 ANTONELLI 92 DM2		1.34-2.4 $e^+e^- \rightarrow \rho\pi, \omega\pi\pi$

$\Gamma(\omega\pi\pi)/\Gamma_{\text{total}} \times \Gamma(e^+e^-)/\Gamma_{\text{total}}$	$\Gamma_2/\Gamma \times \Gamma_4/\Gamma$			
VALUE (units $10^{-7}$ )	EVTS	DOCUMENT ID	TECN	COMMENT
• • • We do not use the following data for averages, fits, limits, etc. • • •				
7.0 ± 0.5		AUBERT 07Au BABR		10.6 $e^+e^- \rightarrow \omega\pi^+\pi^-\gamma$
4.1 ± 0.9 ± 1.3	1.2M	15,16 ACHASOV 03d RVUE		0.44-2.00 $e^+e^- \rightarrow \pi^+\pi^-\pi^0$
5.40 ± 0.95		21 AKHMETSHIN 00d CMD2		1.2-1.38 $e^+e^- \rightarrow \omega\pi^+\pi^-$
3.18 ± 0.80		17,18 CLEGG 94 RVUE		
6.07 ± 0.61	750	19,20 ANTONELLI 92 DM2		1.34-2.4 $e^+e^- \rightarrow \rho\pi, \omega\pi\pi$

# Meson Particle Listings

## $\omega(1650), \omega_3(1670), \pi_2(1670)$

$\Gamma(\omega\pi)/\Gamma_{\text{total}} \times \Gamma(e^+e^-)/\Gamma_{\text{total}}$					$\Gamma_3/\Gamma \times \Gamma_4/\Gamma$
VALUE (units $10^{-6}$ )	CL%	EVTS	DOCUMENT ID	TECN	COMMENT
••• We do not use the following data for averages, fits, limits, etc. •••					
0.57±0.06		13	AUBERT	06D BABR	10.6 $e^+e^- \rightarrow \omega\eta\gamma$
<6	90		22 AKHMETSHIN	03B CMD2	$e^+e^- \rightarrow \eta\pi^0\gamma$
<sup>15</sup> Calculated by us from the cross section at the peak. <sup>16</sup> From the combined fit of ANTONELLI 92, ACHASOV 01E, ACHASOV 02E, and ACHASOV 03D data on the $\pi^+\pi^-\pi^0$ and ANTONELLI 92 on the $\omega\pi^+\pi^-$ final states. Supersedes ACHASOV 99E and ACHASOV 02E. <sup>17</sup> From a fit to two Breit-Wigner functions and using the data of DOLINSKY 91 and ANTONELLI 92. <sup>18</sup> From the partial and leptonic width given by the authors. <sup>19</sup> From the combined fit of the $\rho\pi$ and $\omega\pi\pi$ final states. <sup>20</sup> From the product of the leptonic width and partial branching ratio given by the authors. <sup>21</sup> Using the data of AKHMETSHIN 00D and ANTONELLI 92. The $\rho\pi$ dominance for the energy dependence of the $\omega(1420)$ and $\omega(1650)$ width assumed. <sup>22</sup> $\omega(1650)$ mass and width fixed at 1700 MeV and 250 MeV, respectively.					

 **$\omega(1650)$  BRANCHING RATIOS**

$\Gamma(\omega\pi\pi)/\Gamma_{\text{total}}$					$\Gamma_2/\Gamma$
VALUE	EVTS	DOCUMENT ID	TECN	COMMENT	
••• We do not use the following data for averages, fits, limits, etc. •••					
~0.35	1.2M	23 ACHASOV	03D RVUE	0.44–2.00 $e^+e^- \rightarrow \pi^+\pi^-\pi^0$	
0.620±0.014		24 HENNER	02 RVUE	1.2–2.0 $e^+e^- \rightarrow \rho\pi, \omega\pi\pi$	
$\Gamma(\rho\pi)/\Gamma_{\text{total}}$					
~0.65	1.2M	23 ACHASOV	03D RVUE	0.44–2.00 $e^+e^- \rightarrow \pi^+\pi^-\pi^0$	
0.380±0.014		24 HENNER	02 RVUE	1.2–2.0 $e^+e^- \rightarrow \rho\pi, \omega\pi\pi$	

$\Gamma(e^+e^-)/\Gamma_{\text{total}}$					$\Gamma_4/\Gamma$
VALUE (units $10^{-7}$ )	EVTS	DOCUMENT ID	TECN	COMMENT	
••• We do not use the following data for averages, fits, limits, etc. •••					
~18	1.2M	24,25 ACHASOV	03D RVUE	0.44–2.00 $e^+e^- \rightarrow \pi^+\pi^-\pi^0$	
32±1		24 HENNER	02 RVUE	1.2–2.0 $e^+e^- \rightarrow \rho\pi, \omega\pi\pi$	
<sup>23</sup> From the combined fit of ANTONELLI 92, ACHASOV 01E, ACHASOV 02E, and ACHASOV 03D data on the $\pi^+\pi^-\pi^0$ and ANTONELLI 92 on the $\omega\pi^+\pi^-$ final states. Supersedes ACHASOV 99E and ACHASOV 02E. <sup>24</sup> Assuming that the $\omega(1650)$ decays into $\rho\pi$ and $\omega\pi\pi$ only. <sup>25</sup> Calculated by us from the cross section at the peak.					

 **$\omega(1650)$  REFERENCES**

AUBERT	07AU	PR D76 092005	B. Aubert <i>et al.</i>	(BABAR Collab.)
AUBERT	06D	PR D73 052003	B. Aubert <i>et al.</i>	(BABAR Collab.)
AUBERT	04N	PR D70 072004	B. Aubert <i>et al.</i>	(BABAR Collab.)
ACHASOV	03D	PR D68 052006	M.N. Achasov <i>et al.</i>	(Novosibirsk SND Collab.)
AKHMETSHIN	03B	PL B562 173	R.R. Akhmetshin <i>et al.</i>	(Novosibirsk CMD-2 Collab.)
ACHASOV	02E	PR D66 032001	M.N. Achasov <i>et al.</i>	(Novosibirsk SND Collab.)
HENNER	02	EPJ C26 3	V.K. Henner <i>et al.</i>	(Novosibirsk SND Collab.)
ACHASOV	01E	PR D63 072002	M.N. Achasov <i>et al.</i>	(Novosibirsk SND Collab.)
EUGENIO	01	PL B497 190	P. Eugenio <i>et al.</i>	(Novosibirsk SND Collab.)
AKHMETSHIN	00D	PL B489 125	R.R. Akhmetshin <i>et al.</i>	(Novosibirsk CMD-2 Collab.)
ACHASOV	99E	PL B462 365	M.N. Achasov <i>et al.</i>	(Novosibirsk SND Collab.)
ACHASOV	98H	PR D57 4334	N.N. Achasov, A.A. Kozhevnikov	(Novosibirsk SND Collab.)
CLEGG	94	ZPHY C62 455	A.B. Clegg, A. Donnachie	(LANC, MCHS)
ANTONELLI	92	ZPHY C56 15	A. Antonelli <i>et al.</i>	(DM2 Collab.)
BISELLO	91C	ZPHY C52 227	D. Bisello <i>et al.</i>	(DM2 Collab.)
DOLINSKY	91	PRPL 202 99	S.I. Dolinsky <i>et al.</i>	(NOVO)
BISELLO	85B	ZPHY C39 13	D. Bisello <i>et al.</i>	(PADO, CLER, FRAS+)
BARKOV	87	JETPL 46 164	L.M. Barkov <i>et al.</i>	(NOVO)
Translated from ZETFP 46 132.				
ATKINSON	83B	PL 127B 132	M. Atkinson <i>et al.</i>	(BONN, CERN, GLAS+)
CORDIER	81	PL 106B 155	A. Cordier <i>et al.</i>	(ORSAY)
IVANOV	81	PL 107B 297	P.M. Ivanov <i>et al.</i>	(NOVO)
ESPOSITO	80	LNC 28 195	B. Esposito <i>et al.</i>	(FRAS, NAPL, PADO+)
COSME	79	NP B152 215	G. Cosme <i>et al.</i>	(IPN)

 $\omega_3(1670)$ 

$$I^G(J^{PC}) = 0^-(3^{--})$$

 **$\omega_3(1670)$  MASS**

VALUE (MeV)	EVTS	DOCUMENT ID	TECN	COMMENT
<b>1667 ± 4 OUR AVERAGE</b>				
1665.3 ± 5.2 ± 4.5	23400	AMELIN	96 VES	36 $\pi^-p \rightarrow \pi^+\pi^-\pi^0n$
1685 ± 20	60	1,2 BAUBILLIER	79 HBC	8.2 $K^-p \rightarrow \Delta^+3\pi$
1673 ± 12	430	BALTAY	78E HBC	15 $\pi^+p \rightarrow \Delta^+3\pi$
1650 ± 12		CORDEN	78B OMEG	8–12 $\pi^-p \rightarrow N3\pi$
1669 ± 11	600	2 WAGNER	75 HBC	7 $\pi^+p \rightarrow \Delta^+3\pi$
1678 ± 14	500	DIAZ	74 DBC	6 $\pi^+n \rightarrow \rho^+3\pi^0$
1660 ± 13	200	DIAZ	74 DBC	6 $\pi^+n \rightarrow \rho\omega\pi^0\pi^0$
1679 ± 17	200	MATTHEWS	71D DBC	7.0 $\pi^+n \rightarrow \rho^+3\pi^0$
1670 ± 20		KENYON	69 DBC	8 $\pi^+n \rightarrow \rho^+3\pi^0$

••• We do not use the following data for averages, fits, limits, etc. •••					
~1700	110	1 CERRADA	77B HBC	4.2 $K^-p \rightarrow \Lambda 3\pi$	
1695 ± 20		BARNES	69B HBC	4.6 $K^-p \rightarrow \omega 2\pi X$	
1636 ± 20		ARMENISE	68B DBC	5.1 $\pi^+n \rightarrow \rho^+3\pi^0$	
<sup>1</sup> Phase rotation seen for $J^P = 3^- \rho\pi$ wave. <sup>2</sup> From a fit to $I(J^P) = 0(3^-) \rho\pi$ partial wave.					

 **$\omega_3(1670)$  WIDTH**

VALUE (MeV)	EVTS	DOCUMENT ID	TECN	COMMENT
<b>168±10 OUR AVERAGE</b>				
149±19±7	23400	AMELIN	96 VES	36 $\pi^-p \rightarrow \pi^+\pi^-\pi^0n$
160±80	60	3 BAUBILLIER	79 HBC	8.2 $K^-p$ backward
173±16	430	4,5 BALTAY	78E HBC	15 $\pi^+p \rightarrow \Delta^+3\pi$
253±39		CORDEN	78B OMEG	8–12 $\pi^-p \rightarrow N3\pi$
173±28	600	3,5 WAGNER	75 HBC	7 $\pi^+p \rightarrow \Delta^+3\pi$
167±40	500	DIAZ	74 DBC	6 $\pi^+n \rightarrow \rho^+3\pi^0$
122±39	200	DIAZ	74 DBC	6 $\pi^+n \rightarrow \rho\omega\pi^0\pi^0$
155±40	200	3 MATTHEWS	71D DBC	7.0 $\pi^+n \rightarrow \rho^+3\pi^0$
••• We do not use the following data for averages, fits, limits, etc. •••				
90±20		BARNES	69B HBC	4.6 $K^-p \rightarrow \omega 2\pi$
100±40		KENYON	69 DBC	8 $\pi^+n \rightarrow \rho^+3\pi^0$
112±60		ARMENISE	68B DBC	5.1 $\pi^+n \rightarrow \rho^+3\pi^0$
<sup>3</sup> Width errors enlarged by us to $4\Gamma/\sqrt{N}$ ; see the note with the $K^*(892)$ mass. <sup>4</sup> Phase rotation seen for $J^P = 3^- \rho\pi$ wave. <sup>5</sup> From a fit to $I(J^P) = 0(3^-) \rho\pi$ partial wave.				

 **$\omega_3(1670)$  DECAY MODES**

Mode	Fraction ( $\Gamma_i/\Gamma$ )
$\Gamma_1$ $\rho\pi$	seen
$\Gamma_2$ $\omega\pi\pi$	seen
$\Gamma_3$ $b_1(1235)\pi$	possibly seen

 **$\omega_3(1670)$  BRANCHING RATIOS**

$\Gamma(\omega\pi\pi)/\Gamma(\rho\pi)$					$\Gamma_2/\Gamma_1$
VALUE	EVTS	DOCUMENT ID	TECN	COMMENT	
••• We do not use the following data for averages, fits, limits, etc. •••					
0.71±0.27	100	DIAZ	74 DBC	6 $\pi^+n \rightarrow \rho^+3\pi^0$	

$\Gamma(b_1(1235)\pi)/\Gamma(\rho\pi)$					$\Gamma_3/\Gamma_1$
VALUE	EVTS	DOCUMENT ID	TECN	COMMENT	
possibly seen					
		DIAZ	74 DBC	6 $\pi^+n \rightarrow \rho^+3\pi^0$	

$\Gamma(b_1(1235)\pi)/\Gamma(\omega\pi\pi)$					$\Gamma_3/\Gamma_2$
VALUE	CL%	DOCUMENT ID	TECN	COMMENT	
••• We do not use the following data for averages, fits, limits, etc. •••					
>0.75	68	BAUBILLIER	79 HBC	8.2 $K^-p$ backward	

 **$\omega_3(1670)$  REFERENCES**

AMELIN	96	ZPHY C70 71	D.V. Amelin <i>et al.</i>	(SERP, TBIL)
BAUBILLIER	79	PL 89B 131	M. Baubillier <i>et al.</i>	(BIRM, CERN, GLAS+)
BALTAY	78E	PRL 40 87	C. Baltay, C.V. Cautis, M. Katelkar	(COLU)JP
CORDEN	78B	NP B138 235	M.J. Corden <i>et al.</i>	(BIRM, RHEL, TELA+)
CERRADA	77B	NP B126 241	M. Cerrada <i>et al.</i>	(AMST, CERN, NIJ+)
WAGNER	75	PL 58B 201	F. Wagner, M. Tabak, D.M. Chew	(LBL)JP
DIAZ	74	PRL 32 260	J. Diaz <i>et al.</i>	(CASE, CMU)
MATTHEWS	71D	PR D3 2561	J.A.J. Matthews <i>et al.</i>	(TNT, WISC)
BARNES	69B	PRL 23 142	V.E. Barnes <i>et al.</i>	(BNL)
KENYON	69	PRL 23 146	I.R. Kenyon <i>et al.</i>	(BNL, UCND, ORNL)
ARMENISE	68B	PL 26B 336	N. Armenise <i>et al.</i>	(BARI, BGNA, FIRZ+)

 $\pi_2(1670)$ 

$$I^G(J^{PC}) = 1^-(2^{-+})$$

 **$\pi_2(1670)$  MASS**

VALUE (MeV)	EVTS	DOCUMENT ID	TECN	CHG	COMMENT
<b>1672.2 ± 3.0 OUR AVERAGE</b>					
1658 ± 3 ± 24	420k	ALEKSEEV	10 COMP		190 $\pi^-Pb \rightarrow \pi^+\pi^-\pi^+Pb'$
1749 ± 10 ± 100	145k	LU	05 B852		18 $\pi^-p \rightarrow \omega\pi^-\pi^0\rho$
1676 ± 3 ± 8		1 CHUNG	02 B852		18.3 $\pi^-p \rightarrow \pi^+\pi^-\pi^-\pi^0\rho$
1685 ± 10 ± 30		2 BARBERIS	01		450 $\rho\rho \rightarrow p_f 3\pi^0 p_s$
1687 ± 9 ± 15		AMELIN	99 VES		37 $\pi^-A \rightarrow \omega\pi^-\pi^0A^*$
1669 ± 4		BARBERIS	98B		450 $\rho\rho \rightarrow p_f\rho p_s$

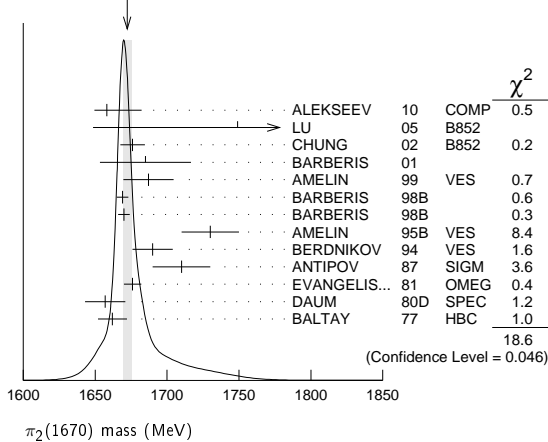
# Meson Particle Listings

## $\pi_2(1670)$

1670 ± 4		BARBERIS	98B		450 $pp \rightarrow p_f f_2(1270) \pi p_s$
1730 ± 20		<sup>3</sup> AMELIN	95B	VES	$36 \pi^- A \rightarrow \pi^+ \pi^- \pi^- A$
1690 ± 14		<sup>4</sup> BERDNIKOV	94	VES	$37 \pi^- A \rightarrow K^+ K^- \pi^- A$
1710 ± 20	700	ANTIPOV	87	SIGM	$50 \pi^- Cu \rightarrow \mu^+ \mu^- \pi^- Cu$
1676 ± 6		<sup>4</sup> EVANGELIS...	81	OMEG	$12 \pi^- p \rightarrow 3\pi p$
1657 ± 14		<sup>4,5</sup> DAUM	80D	SPEC	$63-94 \pi p \rightarrow 3\pi X$
1662 ± 10	2000	<sup>4</sup> BALTAY	77	HBC	$15 \pi^+ p \rightarrow \rho 3\pi$

- • • We do not use the following data for averages, fits, limits, etc. • • •
- 1742 ± 31 ± 49 ANTREASIAN 90 CBAL  $e^+ e^- \rightarrow e^+ e^- \pi^0 \pi^0 \pi^0$
- 1624 ± 21 <sup>1</sup> BELLINI 85 SPEC  $40 \pi^- A \rightarrow \pi^- \pi^+ \pi^- A$
- 1622 ± 35 <sup>6</sup> BELLINI 85 SPEC  $40 \pi^- A \rightarrow \pi^- \pi^+ \pi^- A$
- 1693 ± 28 <sup>7</sup> BELLINI 85 SPEC  $40 \pi^- A \rightarrow \pi^- \pi^+ \pi^- A$
- 1710 ± 20 <sup>8</sup> DAUM 81B SPEC  $63,94 \pi^- p$
- 1660 ± 10 <sup>4</sup> ASCOLI 73 HBC  $5-25 \pi^- p \rightarrow \rho \pi_2$

WEIGHTED AVERAGE  
1672.2±3.0 (Error scaled by 1.4)



### $\pi_2(1670)$ WIDTH

VALUE (MeV)	EVTS	DOCUMENT ID	TECN	CHG	COMMENT
<b>260 ± 9</b>	<b>22</b>	<b>9 OUR AVERAGE</b>			Error includes scale factor of 1.2.
271 ± 9 ± 24	420k	ALEKSEEV	10	COMP	$190 \pi^- Pb \rightarrow \pi^- \pi^- \pi^+ Pb'$
408 ± 60 ± 250	145k	LU	05	B852	$18 \pi^- p \rightarrow \omega \pi^- \pi^0 p$
254 ± 3 ± 31		<sup>9</sup> CHUNG	02	B852	$18.3 \pi^- p \rightarrow \pi^+ \pi^- \pi^- p$
265 ± 30 ± 40		<sup>10</sup> BARBERIS	01		$450 pp \rightarrow p_f 3\pi^0 p_s$
168 ± 43 ± 53		AMELIN	99	VES	$37 \pi^- A \rightarrow \omega \pi^- \pi^0 A^*$
268 ± 15		BARBERIS	98B		$450 pp \rightarrow p_f \rho \pi p_s$
256 ± 15		BARBERIS	98B		$450 pp \rightarrow p_f f_2(1270) \pi p_s$
310 ± 20		<sup>11</sup> AMELIN	95B	VES	$36 \pi^- A \rightarrow \pi^+ \pi^- \pi^- A$
190 ± 50		<sup>12</sup> BERDNIKOV	94	VES	$37 \pi^- A \rightarrow K^+ K^- \pi^- A$
170 ± 80	700	ANTIPOV	87	SIGM	$50 \pi^- Cu \rightarrow \mu^+ \mu^- \pi^- Cu$
260 ± 20		<sup>12</sup> EVANGELIS...	81	OMEG	$12 \pi^- p \rightarrow 3\pi p$
219 ± 20		<sup>12,13</sup> DAUM	80D	SPEC	$63-94 \pi p \rightarrow 3\pi X$
285 ± 60	2000	<sup>12</sup> BALTAY	77	HBC	$15 \pi^+ p \rightarrow \rho 3\pi$
• • • We do not use the following data for averages, fits, limits, etc. • • •					
236 ± 49 ± 36		ANTREASIAN	90	CBAL	$e^+ e^- \rightarrow e^+ e^- \pi^0 \pi^0 \pi^0$
304 ± 22		<sup>9</sup> BELLINI	85	SPEC	$40 \pi^- A \rightarrow \pi^- \pi^+ \pi^- A$
404 ± 108		<sup>14</sup> BELLINI	85	SPEC	$40 \pi^- A \rightarrow \pi^- \pi^+ \pi^- A$
330 ± 90		<sup>15</sup> BELLINI	85	SPEC	$40 \pi^- A \rightarrow \pi^- \pi^+ \pi^- A$
312 ± 50		<sup>16</sup> DAUM	81B	SPEC	$63,94 \pi^- p$
270 ± 60		<sup>12</sup> ASCOLI	73	HBC	$5-25 \pi^- p \rightarrow \rho \pi_2$

- <sup>9</sup> From  $f_2(1270) \pi$  decay.
- <sup>10</sup> From a fit to the invariant mass distribution.
- <sup>11</sup> From a fit to  $J^PC = 2^-+ f_2(1270) \pi, f_0(1370) \pi$  waves.
- <sup>12</sup> From a fit to  $J^P = 2^- f_2(1270) \pi$  partial wave.
- <sup>13</sup> Clear phase rotation seen in  $2^-S, 2^-P, 2^-D$  waves. We quote central value and spread of single-resonance fits to three channels.
- <sup>14</sup> From  $\rho \pi$  decay.
- <sup>15</sup> From  $\sigma \pi$  decay.
- <sup>16</sup> From a two-resonance fit to four  $2^-0^+$  waves. This should not be averaged with all the single resonance fits.

### $\pi_2(1670)$ DECAY MODES

Mode	Fraction ( $\Gamma_i/\Gamma$ )	Confidence level
$\Gamma_1$ $3\pi$	(95.8±1.4) %	
$\Gamma_2$ $\pi^+ \pi^- \pi^0$		
$\Gamma_3$ $\pi^0 \pi^0 \pi^0$		
$\Gamma_4$ $f_2(1270) \pi$	(56.3±3.2) %	
$\Gamma_5$ $\rho \pi$	(31 ± 4) %	
$\Gamma_6$ $\sigma \pi$	(10.9±3.4) %	
$\Gamma_7$ $(\pi\pi) s$ -wave	( 8.7±3.4) %	
$\Gamma_8$ $K \bar{K}^*(892) + c.c.$	( 4.2±1.4) %	
$\Gamma_9$ $\omega \rho$	( 2.7±1.1) %	
$\Gamma_{10}$ $\gamma \gamma$	< 2.8 × 10 <sup>-7</sup>	90%
$\Gamma_{11}$ $\eta \pi$		
$\Gamma_{12}$ $\pi^\pm 2\pi^+ 2\pi^-$		
$\Gamma_{13}$ $\rho(1450) \pi$	< 3.6 × 10 <sup>-3</sup>	97.7%
$\Gamma_{14}$ $b_1(1235) \pi$	< 1.9 × 10 <sup>-3</sup>	97.7%
$\Gamma_{15}$ $\eta 3\pi$		
$\Gamma_{16}$ $f_1(1285) \pi$	possibly seen	
$\Gamma_{17}$ $a_2(1320) \pi$	not seen	

### CONSTRAINED FIT INFORMATION

An overall fit to 4 branching ratios uses 6 measurements and one constraint to determine 4 parameters. The overall fit has a  $\chi^2 = 1.9$  for 3 degrees of freedom.

The following off-diagonal array elements are the correlation coefficients  $\langle \delta x_i \delta x_j \rangle / (\delta x_i \delta x_j)$ , in percent, from the fit to the branching fractions,  $x_i \equiv \Gamma_i/\Gamma_{total}$ . The fit constrains the  $x_i$  whose labels appear in this array to sum to one.

$x_5$	-53		
$x_7$	-29	-59	
$x_8$	-8	-21	-9
	$x_4$	$x_5$	$x_7$

### $\pi_2(1670)$ PARTIAL WIDTHS

$\Gamma(\gamma\gamma)$	VALUE (keV)	CL%	DOCUMENT ID	TECN	CHG	COMMENT
	<0.072	90	17 ACCIARRI	97T	L3	$e^+ e^- \rightarrow e^+ e^- \pi^+ \pi^- \pi^0$
• • • We do not use the following data for averages, fits, limits, etc. • • •						
	<0.19	90	17 ALBRECHT	97B	ARG	$e^+ e^- \rightarrow e^+ e^- \pi^+ \pi^- \pi^0$
	1.41 ± 0.23 ± 0.28		ANTREASIAN	90	CBAL	0 $e^+ e^- \rightarrow \pi^+ \pi^- \pi^0 \pi^0$
	0.8 ± 0.3 ± 0.12		<sup>18</sup> BEHREND	90c	CELL	0 $e^+ e^- \rightarrow \pi^+ \pi^- \pi^0 \pi^0$
	1.3 ± 0.3 ± 0.2		<sup>19</sup> BEHREND	90c	CELL	0 $e^+ e^- \rightarrow \pi^+ \pi^- \pi^0 \pi^0$
<sup>17</sup> Decaying into $f_2(1270) \pi$ and $\rho \pi$ .						
<sup>18</sup> Constructive interference between $f_2(1270) \pi, \rho \pi$ and background.						
<sup>19</sup> Incoherent Ansatz.						

### $\pi_2(1670)$ $\Gamma(i)\Gamma(\gamma\gamma)/\Gamma(\text{total})$

$\Gamma(\pi^+ \pi^- \pi^0) \times \Gamma(\gamma\gamma)/\Gamma_{total}$	VALUE (keV)	CL%	DOCUMENT ID	TECN	COMMENT
	<0.1	95	20 SCHEGELSKY	06	RVUE $\gamma \gamma \rightarrow \pi^+ \pi^- \pi^0$
<sup>20</sup> From analysis of L3 data at 183–209 GeV.					

### $\pi_2(1670)$ BRANCHING RATIOS

$\Gamma(3\pi)/\Gamma_{total}$	VALUE	DOCUMENT ID
	<b>0.958 ± 0.014 OUR FIT</b>	
$\Gamma(\pi^0 \pi^0 \pi^0)/\Gamma(\pi^+ \pi^- \pi^0)$	VALUE	DOCUMENT ID
	<b>0.29 ± 0.03 ± 0.05</b>	<sup>21</sup> BARBERIS 01 450 $pp \rightarrow p_f 3\pi^0 p_s$

$$\Gamma_1/\Gamma = (\Gamma_4 + \Gamma_5 + \Gamma_7)/\Gamma$$

$$\Gamma_3/\Gamma_2$$

See key on page 457

# Meson Particle Listings

## $\pi_2(1670), \phi(1680)$

### $\Gamma(\rho\pi)/0.565\Gamma(f_2(1270)\pi)$

(With  $f_2(1270) \rightarrow \pi^+\pi^-$ )

VALUE	DOCUMENT ID	TECN	COMMENT
<b>0.97 ± 0.09 OUR AVERAGE</b>	Error includes scale factor of 1.9.		
0.76 ± 0.07 ± 0.10	CHUNG 02 B852		18.3 $\pi^- p \rightarrow \pi^+\pi^-\pi^- p$
1.01 ± 0.05	BARBERIS 98B		450 $pp \rightarrow p_f \pi^+\pi^-\pi^0 p_S$

### $\Gamma(\sigma\pi)/\Gamma(f_2(1270)\pi)$

**0.19 ± 0.06 OUR AVERAGE**

VALUE	DOCUMENT ID	TECN	COMMENT
0.17 ± 0.02 ± 0.07	CHUNG 02 B852		18.3 $\pi^- p \rightarrow \pi^+\pi^-\pi^- p$
0.24 ± 0.10	22,23 BAKER 99 SPEC		1.94 $\bar{p}p \rightarrow 4\pi^0$

### $\frac{1}{2}\Gamma(\rho\pi)/\Gamma(\pi^\pm\pi^+\pi^-)$

**0.29 ± 0.05 OUR FIT**

VALUE	DOCUMENT ID	TECN	CHG	COMMENT
<b>0.29 ± 0.05</b>	24 DAUM 81B	SPEC		63.94 $\pi^- p$

• • • We do not use the following data for averages, fits, limits, etc. • • •

< 0.3	BARTSCH 68 HBC	+		8 $\pi^+ p \rightarrow 3\pi p$
-------	----------------	---	--	--------------------------------

### $0.565\Gamma(f_2(1270)\pi)/\Gamma(\pi^\pm\pi^+\pi^-)$

(With  $f_2(1270) \rightarrow \pi^+\pi^-$ )

VALUE	DOCUMENT ID	TECN	CHG	COMMENT
<b>0.604 ± 0.035 OUR FIT</b>	Error includes scale factor of 1.3.			
<b>0.60 ± 0.05 OUR AVERAGE</b>	24 DAUM 81B	SPEC		63.94 $\pi^- p$
0.61 ± 0.04	ARMENISE 69 DBC	+		5.1 $\pi^+ d \rightarrow d 3\pi$
0.76 ± 0.24 ± 0.34	BALTAY 68 HBC	+		7-8.5 $\pi^+ p$
0.35 ± 0.20	BARTSCH 68 HBC	+		8 $\pi^+ p \rightarrow 3\pi p$
0.59	BARTSCH 68 HBC	+		8 $\pi^+ p \rightarrow 3\pi p$

• • • We do not use the following data for averages, fits, limits, etc. • • •

### $0.624\Gamma((\pi\pi)S\text{-wave})/\Gamma(\pi^\pm\pi^+\pi^-)$

(With  $(\pi\pi)_{S\text{-wave}} \rightarrow \pi^+\pi^-$ )

VALUE	DOCUMENT ID	TECN	CHG	COMMENT
<b>0.10 ± 0.04 OUR FIT</b>	24 DAUM 81B	SPEC		63.94 $\pi^- p$
<b>0.10 ± 0.05</b>				

### $\Gamma(K\bar{K}^*(892) + c.c.)/\Gamma(f_2(1270)\pi)$

VALUE	DOCUMENT ID	TECN	CHG	COMMENT
<b>0.075 ± 0.025 OUR FIT</b>	25 ARMSTRONG 82B	OMEG	-	16 $\pi^- p \rightarrow K^+ K^- \pi^- p$
<b>0.075 ± 0.025</b>				

### $\Gamma(\omega\rho)/\Gamma_{\text{total}}$

VALUE	DOCUMENT ID	TECN	COMMENT
<b>0.027 ± 0.004 ± 0.010</b>	26 AMELIN 99 VES		37 $\pi^- A \rightarrow \omega \pi^+ \pi^- A^*$

### $\Gamma(\eta\pi)/\Gamma(\pi^\pm\pi^+\pi^-)$

(All  $\eta$  decays.)

VALUE	DOCUMENT ID	TECN	CHG	COMMENT
<b>&lt; 0.09</b>	BALTAY 68 HBC	+		7-8.5 $\pi^+ p$

• • • We do not use the following data for averages, fits, limits, etc. • • •

< 0.10	CRENNELL 70 HBC	-		6 $\pi^- p \rightarrow f_2 \pi^- N$
--------	-----------------	---	--	-------------------------------------

### $\Gamma(\pi^\pm 2\pi^+ 2\pi^-)/\Gamma(\pi^\pm\pi^+\pi^-)$

VALUE	DOCUMENT ID	TECN	CHG	COMMENT
<b>&lt; 0.10</b>	CRENNELL 70 HBC	-		6 $\pi^- p \rightarrow f_2 \pi^- N$
< 0.1	BALTAY 68 HBC	+		7,8.5 $\pi^+ p$

### $\Gamma(\rho(1450)\pi)/\Gamma_{\text{total}}$

VALUE	CL%	DOCUMENT ID	TECN	COMMENT
<b>&lt; 0.0036</b>	97.7	AMELIN 99 VES		37 $\pi^- A \rightarrow \omega \pi^+ \pi^- A^*$

### $\Gamma(b_1(1235)\pi)/\Gamma_{\text{total}}$

VALUE	CL%	DOCUMENT ID	TECN	COMMENT
<b>&lt; 0.0019</b>	97.7	AMELIN 99 VES		37 $\pi^- A \rightarrow \omega \pi^+ \pi^- A^*$

### $\Gamma(f_1(1285)\pi)/\Gamma_{\text{total}}$

VALUE	EVTS	DOCUMENT ID	TECN	COMMENT
possibly seen	69k	KUHN 04 B852		18 $\pi^- p \rightarrow \eta \pi^+ \pi^- \pi^- p$

### $\Gamma(a_2(1320)\pi)/\Gamma_{\text{total}}$

VALUE	EVTS	DOCUMENT ID	TECN	COMMENT
not seen	69k	KUHN 04 B852		18 $\pi^- p \rightarrow \eta \pi^+ \pi^- \pi^- p$

### D-wave/S-wave RATIO FOR $\pi_2(1670) \rightarrow f_2(1270)\pi$

VALUE	DOCUMENT ID	TECN	COMMENT
<b>-0.18 ± 0.06</b>	22 BAKER 99 SPEC		1.94 $\bar{p}p \rightarrow 4\pi^0$
0.22 ± 0.10	24 DAUM 81B	SPEC	63.94 $\pi^- p$

• • • We do not use the following data for averages, fits, limits, etc. • • •

### F-wave/P-wave RATIO FOR $\pi_2(1670) \rightarrow \rho\pi$

VALUE	DOCUMENT ID	TECN	COMMENT
<b>-0.72 ± 0.07 ± 0.14</b>	CHUNG 02 B852		18.3 $\pi^- p \rightarrow \pi^+\pi^-\pi^- p$

21 Using BARBERIS 98b.  
22 Using preliminary CBAR data.  
23 With the  $\sigma\pi$  in  $L=2$  and the  $f_2(1270)\pi$  in  $L=0$ .  
24 From a two-resonance fit to four  $2^-0^+$  waves.  
25 From a partial-wave analysis of  $K^+ K^- \pi^-$  system.  
26 Normalized to the  $B(\pi_2(1670) \rightarrow f_2\pi)$ .

### $\pi_2(1670)$ REFERENCES

ALEKSEEV 10 PRL 104 241803	M.G. Alekseev et al.	(COMPASS Collab.)
SCHEGELSKY 06 EPJ A27 199	V.A. Schegelsky et al.	
LU 05 PRL 94 032002	M. Lu et al.	(BNL E852 Collab.)
KUHN 04 PL B595 109	J. Kuhn et al.	(BNL E852 Collab.)
CHUNG 02 PR D65 072001	S.U. Chung et al.	(SERP, TBL)
BARBERIS 01 PL B507 14	D. Barberis et al.	(BNL E852 Collab.)
AMELIN 99 PAN 62 445	D.V. Amelin et al.	(VES Collab.)
BAKER 99 PL B449 114	C.A. Baker et al.	
BARBERIS 98B PL B422 399	D. Barberis et al.	(WA 102 Collab.)
ACCIARRI 97T PL B413 147	M. Acciarri et al.	(L3 Collab.)
ALBRECHT 97B ZPHY C74 469	H. Albrecht et al.	(ARGUS Collab.)
AMELIN 95B PL B356 595	D.V. Amelin et al.	(SERP, TBL)
BERDNIKOV 94 PL B337 219	E.B. Berdnikov et al.	(SERP, TBL)
ANTREASIAN 90 ZPHY C48 561	D. Antreasian et al.	(Crystal Ball Collab.)
BEHREND 90C ZPHY C46 583	H.J. Behrend et al.	(CELLO Collab.)
ANTIPOV 87 EPL 4 403	Y.M. Antipov et al.	(SERP, JINR, INRM+)
BELLINI 85 SNJP 41 781	D. Bellini et al.	
ARMSTRONG 82B NP B202 1	T.A. Armstrong, B. Baccari	(AACH3, BARI, BONN+)
DAUM 81B NP B182 269	C. Daum et al.	(AMST, CERN, CRAC, MPIM+)
EVANGELIS... 81 NP B178 197	C. Evangelista et al.	(BARI, BONN, CERN+)
Also NP B186 594	C. Evangelista	
DAUM 80D PL B98 285	C. Daum et al.	(AMST, CERN, CRAC, MPIM+)
BALTAY 77 PRL 39 591	C. Baltay, C.V. Cautis, M. Katelkar	(COLU) JP
ASCOLI 73 PR D7 669	G. Ascoli (ILL, TNTO, GENO, HAMB, MILA+)	JP
CRENNELL 70 PRL 24 781	D.J. Crennell et al.	(BNL)
ARMENISE 69 LNC 2 501	N. Armenise et al.	(BARI, BGNA, FIRZ)
BALTAY 68 PRL 20 887	C. Baltay et al.	(COLU, ROCH, RUTG, YALE)
BARTSCH 68 NP B7 345	J. Bartsch et al.	(AACH, BERL, CERN) JP

## $\phi(1680)$

$$J^{PC} = 0^{-}(1^{-}-)$$

### $\phi(1680)$ MASS

### e<sup>+</sup>e<sup>-</sup> PRODUCTION

VALUE (MeV)	EVTS	DOCUMENT ID	TECN	COMMENT
<b>1680 ± 20 OUR ESTIMATE</b>				
1689 ± 7 ± 10	4.8k	1 SHEN 09 BELL	09 BELL	10.6 e <sup>+</sup> e <sup>-</sup> → K <sup>+</sup> K <sup>-</sup> π <sup>+</sup> π <sup>-</sup> η
1709 ± 20 ± 43		2 AUBERT 08s BABR	08s BABR	10.6 e <sup>+</sup> e <sup>-</sup> → hadrons
1623 ± 20	948	3 AKHMESHIN 03 CMD2	03 CMD2	1.05-1.38 e <sup>+</sup> e <sup>-</sup> → K <sub>S</sub> <sup>0</sup> K <sub>S</sub> <sup>0</sup>
~ 1500		4 ACHASOV 98H RVUE	98H RVUE	e <sup>+</sup> e <sup>-</sup> → π <sup>+</sup> π <sup>-</sup> π <sup>0</sup> , ωπ <sup>+</sup> π <sup>-</sup> , K <sup>+</sup> K <sup>-</sup>
~ 1900		5 ACHASOV 98H RVUE	98H RVUE	e <sup>+</sup> e <sup>-</sup> → K <sub>S</sub> <sup>0</sup> K <sub>S</sub> <sup>0</sup> π <sup>+</sup> π <sup>-</sup>
1700 ± 20		6 CLEGG 94 RVUE	94 RVUE	e <sup>+</sup> e <sup>-</sup> → K <sup>+</sup> K <sup>-</sup> , K <sub>S</sub> <sup>0</sup> K <sub>S</sub> <sup>0</sup> ππ
1657 ± 27	367	BISELLO 91c DM2	91c DM2	e <sup>+</sup> e <sup>-</sup> → K <sub>S</sub> <sup>0</sup> K <sub>S</sub> <sup>0</sup> π <sup>+</sup> π <sup>-</sup>
1655 ± 17		7 BISELLO 88B DM2	88B DM2	e <sup>+</sup> e <sup>-</sup> → K <sup>+</sup> K <sup>-</sup>
1680 ± 10		8 BUON 82 DM1	82 DM1	e <sup>+</sup> e <sup>-</sup> → hadrons
1677 ± 12		9 MANE 82 DM1	82 DM1	e <sup>+</sup> e <sup>-</sup> → K <sub>S</sub> <sup>0</sup> K <sub>S</sub> <sup>0</sup> ππ

1 From a fit with two incoherent Breit-Wigners.  
2 From the simultaneous fit to the  $K\bar{K}^*(892) + c.c.$  and  $\phi\eta$  data from AUBERT 08s using the results of AUBERT 07AK.  
3 From the combined fit of AKHMESHIN 03 and MANE 81 also including  $\rho$ ,  $\omega$ , and  $\phi$ . Neither isospin nor flavor structure known.  
4 Using data from IVANOV 81, BARKOV 87, BISELLO 88b, DOLINSKY 91, and ANTONELLI 92.  
5 Using the data from BISELLO 91c.  
6 Using BISELLO 88b and MANE 82 data.  
7 From global fit including  $\rho$ ,  $\omega$ ,  $\phi$  and  $\rho(1700)$  assume mass 1570 MeV and width 510 MeV for  $\rho$  radial excitation.  
8 From global fit of  $\rho$ ,  $\omega$ ,  $\phi$  and their radial excitations to channels  $\omega\pi^+\pi^-$ ,  $K^+K^-$ ,  $K_S^0 K_S^0$ ,  $K_S^0 K^\pm\pi^\mp$ . Assume mass 1570 MeV and width 510 MeV for  $\rho$  radial excitations, mass 1570 and width 500 MeV for  $\omega$  radial excitation.  
9 Fit to one channel only, neglecting interference with  $\omega$ ,  $\rho(1700)$ .

### PHOTOPRODUCTION

VALUE (MeV)	DOCUMENT ID	TECN	COMMENT
1753 ± 3	10 LINK 02k FOCS	02k FOCS	20-160 $\gamma p \rightarrow K^+ K^- p$
1726 ± 22	10 BUSENITZ 89 TFS	89 TFS	$\gamma p \rightarrow K^+ K^- X$
1760 ± 20	10 ATKINSON 85c OMEG	85c OMEG	20-70 $\gamma p \rightarrow K\bar{K} X$
1690 ± 10	10 ASTON 81F OMEG	81F OMEG	25-70 $\gamma p \rightarrow K^+ K^- X$

10 We list here a state decaying into  $K^+ K^-$  possibly different from  $\phi(1680)$ .

### $\rho\rho$ ANNIHILATION

VALUE (MeV)	DOCUMENT ID	TECN	COMMENT
1700 ± 8	11 AMSLER 06 CBAR	06 CBAR	0.9 $\bar{p}p \rightarrow K^+ K^- \pi^0$

11 Could also be  $\rho(1700)$ .

# Meson Particle Listings

## $\phi(1680)$ , $\rho_3(1690)$

### $\phi(1680)$ WIDTH

#### $e^+e^-$ PRODUCTION

VALUE (MeV)	EVTs	DOCUMENT ID	TECN	COMMENT
<b>150±50 OUR ESTIMATE</b>				This is only an educated guess; the error given is larger than the error on the average of the published values.
••• We do not use the following data for averages, fits, limits, etc. •••				
211±14±19	4.8k	12 SHEN	09 BELL	10.6 $e^+e^- \rightarrow K^+K^-\pi^+\pi^-\gamma$
322±77±160		13 AUBERT	08s BABR	10.6 $e^+e^- \rightarrow$ hadrons
139±60	948	14 AKHMETSHIN	03 CMD2	1.05-1.38 $e^+e^- \rightarrow K_S^0 K_S^0$
300±60		15 CLEGG	94 RVUE	$e^+e^- \rightarrow K^+K^-, K_S^0 K_S^0$
146±55	367	BISELLO	91c DM2	$e^+e^- \rightarrow K_S^0 K_S^0 \pi^+ \pi^-$
207±45		16 BISELLO	88B DM2	$e^+e^- \rightarrow K^+K^-$
185±22		17 BUON	82 DM1	$e^+e^- \rightarrow$ hadrons
102±36		18 MANE	82 DM1	$e^+e^- \rightarrow K_S^0 K_S^0$

- <sup>12</sup> From a fit with two incoherent Breit-Wigners.
- <sup>13</sup> From the simultaneous fit to the  $K\bar{K}^*(892) + c.c.$  and  $\phi\eta$  data from AUBERT 08s using the results of AUBERT 07AK.
- <sup>14</sup> From the combined fit of AKHMETSHIN 03 and MANE 81 also including  $\rho, \omega$ , and  $\phi$ . Neither isospin nor flavor structure known.
- <sup>15</sup> Using BISELLO 88B and MANE 82 data.
- <sup>16</sup> From global fit including  $\rho, \omega, \phi$  and  $\rho(1700)$
- <sup>17</sup> From global fit of  $\rho, \omega, \phi$  and their radial excitations to channels  $\omega\pi^+\pi^-, K^+K^-, K_S^0 K_S^0, K_S^0 K_S^0 \pi^+ \pi^-$ . Assume mass 1570 MeV and width 510 MeV for  $\rho$  radial excitations, mass 1570 and width 500 MeV for  $\omega$  radial excitation.
- <sup>18</sup> Fit to one channel only, neglecting interference with  $\omega, \rho(1700)$ .

#### PHOTOPRODUCTION

VALUE (MeV)	DOCUMENT ID	TECN	COMMENT
••• We do not use the following data for averages, fits, limits, etc. •••			
122±63	19 LINK	02k FOCUS	20-160 $\gamma p \rightarrow K^+K^-\rho$
121±47	19 BUSENITZ	89 TPS	$\gamma p \rightarrow K^+K^-X$
80±40	19 ATKINSON	85c OMEG	20-70 $\gamma p \rightarrow K\bar{K}X$
100±40	19 ASTON	81F OMEG	25-70 $\gamma p \rightarrow K^+K^-X$

<sup>19</sup> We list here a state decaying into  $K^+K^-$  possibly different from  $\phi(1680)$ .

#### $p\bar{p}$ ANNIHILATION

VALUE (MeV)	DOCUMENT ID	TECN	COMMENT
••• We do not use the following data for averages, fits, limits, etc. •••			
143±24	20 AMSLER	06 CBAR	0.9 $p\bar{p} \rightarrow K^+K^-\pi^0$

<sup>20</sup> Could also be  $\rho(1700)$ .

### $\phi(1680)$ DECAY MODES

Mode	Fraction ( $\Gamma_i/\Gamma$ )
$\Gamma_1$ $K\bar{K}^*(892) + c.c.$	dominant
$\Gamma_2$ $K_S^0 K_S^0$	seen
$\Gamma_3$ $K\bar{K}$	seen
$\Gamma_4$ $K_L^0 K_S^0$	
$\Gamma_5$ $e^+e^-$	seen
$\Gamma_6$ $\omega\pi\pi$	not seen
$\Gamma_7$ $\phi\pi\pi$	
$\Gamma_8$ $K^+K^-\pi^+\pi^-$	seen
$\Gamma_9$ $\phi\eta$	
$\Gamma_{10}$ $K^+K^-\pi^0$	

### $\phi(1680)$ $\Gamma(i)\Gamma(e^+e^-)/\Gamma^2(\text{total})$

This combination of a branching ratio into channel (i) and branching ratio into  $e^+e^-$  is directly measured and obtained from the cross section at the peak. We list only data that have not been used to determine the branching ratio into (i) or  $e^+e^-$ .

$\Gamma(K_S^0 K_S^0)/\Gamma_{\text{total}} \times \Gamma(e^+e^-)/\Gamma_{\text{total}}$	$\Gamma_4/\Gamma \times \Gamma_5/\Gamma$
••• We do not use the following data for averages, fits, limits, etc. •••	
0.131±0.059	948

<sup>21</sup> From the combined fit of AKHMETSHIN 03 and MANE 81 also including  $\rho, \omega$ , and  $\phi$ . Neither isospin nor flavor structure known. Recalculated by us.

$\Gamma(K\bar{K}^*(892) + c.c.)/\Gamma_{\text{total}} \times \Gamma(e^+e^-)/\Gamma_{\text{total}}$	$\Gamma_1/\Gamma \times \Gamma_5/\Gamma$
••• We do not use the following data for averages, fits, limits, etc. •••	
1.15±0.16±0.01	22 AUBERT

<sup>22</sup> From the simultaneous fit to the  $K\bar{K}^*(892) + c.c.$  and  $\phi\eta$  data from AUBERT 08s using the results of AUBERT 07AK.

<sup>23</sup> Recalculated by us with the published value of  $B(K\bar{K}^*(892) + c.c.) \times \Gamma(e^+e^-)$ .

### $\Gamma(\phi\pi\pi)/\Gamma_{\text{total}} \times \Gamma(e^+e^-)/\Gamma_{\text{total}}$

VALUE (units $10^{-7}$ )	EVTs	DOCUMENT ID	TECN	COMMENT
••• We do not use the following data for averages, fits, limits, etc. •••				
1.86±0.14±0.21	4.8k	24 SHEN	09 BELL	10.6 $e^+e^- \rightarrow K^+K^-\pi^+\pi^-\gamma$

<sup>24</sup> Multiplied by 3/2 to take into account the  $\phi\pi^0\pi^0$  mode. Using  $B(\phi \rightarrow K^+K^-) = (49.2 \pm 0.6)\%$ .

### $\Gamma(\phi\eta)/\Gamma_{\text{total}} \times \Gamma(e^+e^-)/\Gamma_{\text{total}}$

VALUE (units $10^{-6}$ )	DOCUMENT ID	TECN	COMMENT
••• We do not use the following data for averages, fits, limits, etc. •••			
0.43±0.10±0.09	25 AUBERT	08s BABR	10.6 $e^+e^- \rightarrow \phi\eta\gamma$

<sup>25</sup> From the simultaneous fit to the  $K\bar{K}^*(892) + c.c.$  and  $\phi\eta$  data from AUBERT 08s using the results of AUBERT 07AK.

### $\phi(1680)$ BRANCHING RATIOS

$\Gamma(K\bar{K}^*(892) + c.c.)/\Gamma(K_S^0 K_S^0)$	$\Gamma_1/\Gamma_2$
••• We do not use the following data for averages, fits, limits, etc. •••	
dominant	MANE

$\Gamma(K\bar{K})/\Gamma(K\bar{K}^*(892) + c.c.)$	$\Gamma_3/\Gamma_1$
••• We do not use the following data for averages, fits, limits, etc. •••	
0.07±0.01	BUON

$\Gamma(\omega\pi\pi)/\Gamma(K\bar{K}^*(892) + c.c.)$	$\Gamma_6/\Gamma_1$
••• We do not use the following data for averages, fits, limits, etc. •••	
<0.10	BUON

$\Gamma(\phi\eta)/\Gamma(K\bar{K}^*(892) + c.c.)$	$\Gamma_9/\Gamma_1$
••• We do not use the following data for averages, fits, limits, etc. •••	
≈ 0.37	26 AUBERT

<sup>26</sup> From the fit including data from AUBERT 07AK.

### $\phi(1680)$ REFERENCES

SHEN	09	PR D80 031101R	C.P. Shen <i>et al.</i>	(BELLE Collab.)
AUBERT	08s	PR D77 092002	B. Aubert <i>et al.</i>	(BABAR Collab.)
AUBERT	07AK	PR D76 012008	B. Aubert <i>et al.</i>	(BABAR Collab.)
AMSLER	06	PL B639 165	C. Amshar <i>et al.</i>	(CBAR Collab.)
AKHMETSHIN	03	PL B551 27	R.R. Akhmetshin <i>et al.</i>	(Novosibirsk CMD-2 Collab.)
		Also		
		PAN 65 1222	E.V. Anashkin, V.M. Aulchenko, R.R. Akhmetshin	
		Translated from YAF 65 1255.		
LINK	02k	PL B545 50	J.M. Link <i>et al.</i>	(FNAL FOCUS Collab.)
ACHASOV	98H	PR D57 4334	N.N. Achasov, A.A. Kozhevnikov	
CLEGG	94	ZPHY C62 455	A.B. Clegg, A. Donnachie	(LANC, MCHS)
ANTONELLI	92	ZPHY C56 15	A. Antonelli <i>et al.</i>	(DM2 Collab.)
BISELLO	91c	ZPHY C52 227	D. Bisello <i>et al.</i>	(DM2 Collab.)
DOLINSKY	91	PRPL 202 99	S.I. Dolinsky <i>et al.</i>	(NOVO)
BUSENITZ	89	PR D40 1	J.K. Busenitz <i>et al.</i>	(ILL, FNAL)
BISELLO	88B	ZPHY C39 13	D. Bisello <i>et al.</i>	(PADO, CLER, FRAS-)
BARKOV	87	JETPL 46 164	L.M. Barkov <i>et al.</i>	(NOVO)
		Translated from ZETFP 46 132.		
ATKINSON	85c	ZPHY C27 233	M. Atkinson <i>et al.</i>	(BONN, CERN, GLAS-)
BUON	82	PL 118B 221	J. Buon <i>et al.</i>	(LALO, MONP)
MANE	82	PL 112B 178	F. Mane <i>et al.</i>	(LALO)
ASTON	81F	PL 104B 231	D. Aston	(BONN, CERN, EPOL, GLAS, LANC+)
IVANOV	81	PL 107B 297	P.M. Ivanov <i>et al.</i>	(NOVO)
MANE	81	PL 99B 261	F. Mane <i>et al.</i>	(ORSAY)

## $\rho_3(1690)$

$$I^G(J^{PC}) = 1^+(3^{--})$$

### $\rho_3(1690)$ MASS

VALUE (MeV)	DOCUMENT ID
<b>1688.8±2.1 OUR AVERAGE</b>	Includes data from the 5 datablocks that follow this one.

2 $\pi$ MODE	VALUE (MeV)	EVTs	DOCUMENT ID	TECN	CHG	COMMENT
						The data in this block is included in the average printed for a previous datablock.

1686±4 OUR AVERAGE	VALUE (MeV)	EVTs	DOCUMENT ID	TECN	CHG	COMMENT	
1677±14			EVANGELIS..	81	OMEG	—	12 $\pi^-p \rightarrow 2\pi\rho$
1679±11	476		BALTAY	78B	HBC	0	15 $\pi^+p \rightarrow \pi^+\pi^-n$
1678±12	175	1	ANTIPOV	77	CIBS	0	25 $\pi^-p \rightarrow p3\pi$
1690±7	600	1	ENGLER	74	DBC	0	6 $\pi^+n \rightarrow \pi^+\pi^-p$
1693±8		2	GRAYEY	74	ASP	0	17 $\pi^-p \rightarrow \pi^+\pi^-n$
1678±12			MATTHEWS	71c	DBC	0	7 $\pi^+N$

See key on page 457

## Meson Particle Listings

 $\rho_3(1690)$ 

• • • We do not use the following data for averages, fits, limits, etc. • • •

1734 ± 10		<sup>3</sup> CORDEN	79	OMEG		12-15 $\pi^- p \rightarrow n2\pi$
1692 ± 12		<sup>2,4</sup> ESTABROOKS	75	RVUE		17 $\pi^- p \rightarrow \pi^+ \pi^- n$
1737 ± 23		ARMENISE	70	DBC	0	9 $\pi^+ N$
1650 ± 35	122	BARTSCH	70B	HBC	+	8 $\pi^+ p \rightarrow N2\pi$
1687 ± 21		STUNTEBECK	70	HDBC	0	8 $\pi^- p, 5.4 \pi^+ d$
1683 ± 13		ARMENISE	68	DBC	0	5.1 $\pi^+ d$
1670 ± 30		GOLDBERG	65	HBC	0	6 $\pi^+ d, 8 \pi^- p$

<sup>1</sup> Mass errors enlarged by us to  $\Gamma/\sqrt{N}$ ; see the note with the  $K^*(892)$  mass.<sup>2</sup> Uses same data as HYAMS 75.<sup>3</sup> From a phase shift solution containing a  $f_2'(1525)$  width two times larger than the  $K\bar{K}$  result.<sup>4</sup> From phase-shift analysis. Error takes account of spread of different phase-shift solutions. **$K\bar{K}$  AND  $K\bar{K}\pi$  MODES**

VALUE (MeV)	EVTS	DOCUMENT ID	TECN	CHG	COMMENT
The data in this block is included in the average printed for a previous datablock.					

**1696 ± 4 OUR AVERAGE**

1699 ± 5		ALPER	80	CNTR	0	62 $\pi^- p \rightarrow K^+ K^- n$
1698 ± 12	6k	<sup>5,6</sup> MARTIN	78D	SPEC		10 $\pi p \rightarrow K_S^0 K^- p$
1692 ± 6		BLUM	75	ASPK	0	18.4 $\pi^- p \rightarrow nK^+ K^-$
1690 ± 16		ADERHOLZ	69	HBC	+	8 $\pi^+ p \rightarrow K\bar{K}\pi$
1694 ± 8		<sup>7</sup> COSTA...	80	OMEG		10 $\pi^- p \rightarrow K^+ K^- n$

<sup>5</sup> From a fit to  $J^P = 3^-$  partial wave.<sup>6</sup> Systematic error on mass scale subtracted.<sup>7</sup> They cannot distinguish between  $\rho_3(1690)$  and  $\omega_3(1670)$ . **$(4\pi)^\pm$  MODE**

VALUE (MeV)	EVTS	DOCUMENT ID	TECN	CHG	COMMENT
The data in this block is included in the average printed for a previous datablock.					

**1686 ± 5 OUR AVERAGE** Error includes scale factor of 1.1.

1694 ± 6		<sup>8</sup> EVANGELIS...	81	OMEG	-	12 $\pi^- p \rightarrow p4\pi$
1665 ± 15	177	BALTAY	78B	HBC	+	15 $\pi^+ p \rightarrow p4\pi$
1670 ± 10		THOMPSON	74	HBC	+	13 $\pi^+ p$
1687 ± 20		CASON	73	HBC	-	8,18.5 $\pi^- p$
1685 ± 14		<sup>9</sup> CASON	73	HBC	-	8,18.5 $\pi^- p$
1680 ± 40	144	BARTSCH	70B	HBC	+	8 $\pi^+ p \rightarrow N4\pi$
1689 ± 20	102	<sup>9</sup> BARTSCH	70B	HBC	+	8 $\pi^+ p \rightarrow N2\rho$
1705 ± 21		CASO	70	HBC	-	11.2 $\pi^- p \rightarrow n\rho2\pi$

• • • We do not use the following data for averages, fits, limits, etc. • • •

1718 ± 10		<sup>10</sup> EVANGELIS...	81	OMEG	-	12 $\pi^- p \rightarrow p4\pi$
1673 ± 9		<sup>11</sup> EVANGELIS...	81	OMEG	-	12 $\pi^- p \rightarrow p4\pi$
1733 ± 9	66	<sup>9</sup> KLIGER	74	HBC	-	4.5 $\pi^- p \rightarrow p4\pi$
1630 ± 15		HOLMES	72	HBC	+	10-12 $K^+ p$
1720 ± 15		BALTAY	68	HBC	+	7, 8.5 $\pi^+ p$

<sup>8</sup> From  $\rho^- \rho^0$  mode, not independent of the other two EVANGELISTA 81 entries.<sup>9</sup> From  $\rho^\pm \rho^0$  mode.<sup>10</sup> From  $a_2(1320)^- \pi^0$  mode, not independent of the other two EVANGELISTA 81 entries.<sup>11</sup> From  $a_2(1320)^0 \pi^-$  mode, not independent of the other two EVANGELISTA 81 entries. **$\omega\pi$  MODE**

VALUE (MeV)	DOCUMENT ID	TECN	CHG	COMMENT
The data in this block is included in the average printed for a previous datablock.				

**1681 ± 7 OUR AVERAGE**

1670 ± 25		<sup>12</sup> ALDE	95	GAM2		38 $\pi^- p \rightarrow \omega\pi^0 n$
1690 ± 15		EVANGELIS...	81	OMEG	-	12 $\pi^- p \rightarrow \omega\pi p$
1666 ± 14		GESSAROLI	77	HBC		11 $\pi^- p \rightarrow \omega\pi p$
1686 ± 9		THOMPSON	74	HBC	+	13 $\pi^+ p$
1654 ± 24		BARNHAM	70	HBC	+	10 $K^+ p \rightarrow \omega\pi X$

<sup>12</sup> Supersedes ALDE 92c. **$\eta\pi^+ \pi^-$  MODE**(For difficulties with MMS experiments, see the  $a_2(1320)$  mini-review in the 1973 edition.)

VALUE (MeV)	DOCUMENT ID	TECN	CHG	COMMENT
The data in this block is included in the average printed for a previous datablock.				

**1682 ± 12 OUR AVERAGE**

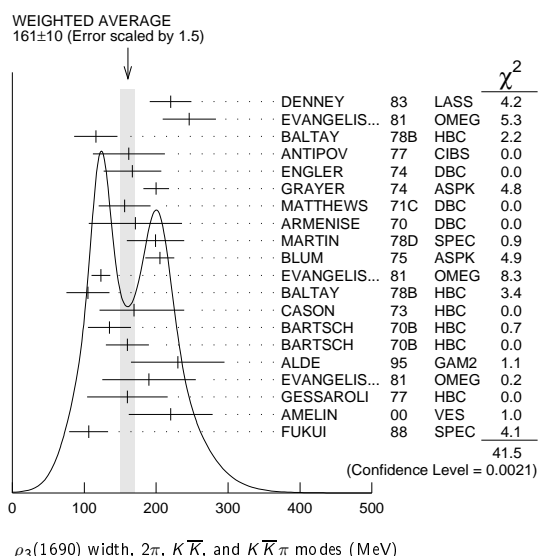
1685 ± 10 ± 20		AMELIN	00	VES		37 $\pi^- p \rightarrow \eta\pi^+ \pi^- n$
1680 ± 15		FUKUI	88	SPEC	0	8.95 $\pi^- p \rightarrow \eta\pi^+ \pi^- n$

• • • We do not use the following data for averages, fits, limits, etc. • • •

1700 ± 47		<sup>13</sup> ANDERSON	69	MMS	-	16 $\pi^- p$ backward
1632 ± 15		<sup>13,14</sup> FOCACCI	66	MMS	-	7-12 $\pi^- p \rightarrow \rho MM$
1700 ± 15		<sup>13,14</sup> FOCACCI	66	MMS	-	7-12 $\pi^- p \rightarrow \rho MM$
1748 ± 15		<sup>13,14</sup> FOCACCI	66	MMS	-	7-12 $\pi^- p \rightarrow \rho MM$

<sup>13</sup> Seen in 2.5-3 GeV/c  $\bar{p}p$ .  $2\pi^+ 2\pi^-$ , with 0, 1, 2  $\pi^+ \pi^-$  pairs in  $\rho$  band not seen by OREN 74 (2.3 GeV/c  $\bar{p}p$ ) with more statistics. (Jan. 1976)<sup>14</sup> Not seen by BOWEN 72. **$\rho_3(1690)$  WIDTH****2 $\pi$ ,  $K\bar{K}$ , AND  $K\bar{K}\pi$  MODES**

VALUE (MeV) DOCUMENT ID  
**161 ± 10 OUR AVERAGE** Includes data from the 5 datablocks that follow this one. Error includes scale factor of 1.5. See the ideogram below.

**2 $\pi$  MODE**

VALUE (MeV) EVTS DOCUMENT ID TECN CHG COMMENT  
 The data in this block is included in the average printed for a previous datablock.

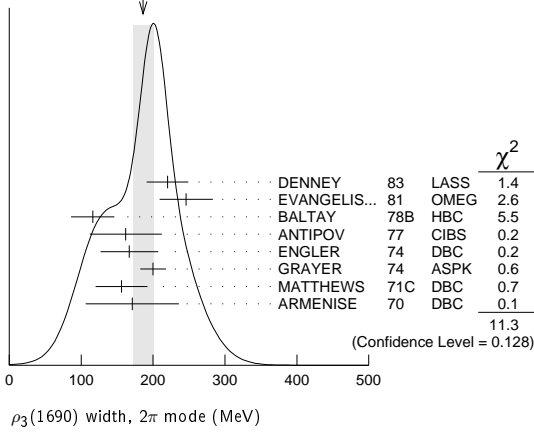
<b>186 ± 14 OUR AVERAGE</b>	Error includes scale factor of 1.3. See the ideogram below.
220 ± 29	DENNEY 83 LASS 10 $\pi^+ N$
246 ± 37	EVANGELIS... 81 OMEG - 12 $\pi^- p \rightarrow 2\pi p$
116 ± 30	476 BALTAY 78B HBC 0 15 $\pi^+ p \rightarrow \pi^+ \pi^- n$
162 ± 50	175 <sup>15</sup> ANTIPOV 77 CIBS 0 25 $\pi^- p \rightarrow p3\pi$
167 ± 40	600 ENGLER 74 DBC 0 6 $\pi^+ n \rightarrow \pi^+ \pi^- p$
200 ± 18	<sup>16</sup> GRAYER 74 ASPK 0 17 $\pi^- p \rightarrow \pi^+ \pi^- n$
156 ± 36	MATTHEWS 71C DBC 0 7 $\pi^+ N$
171 ± 65	ARMENISE 70 DBC 0 9 $\pi^+ d$
322 ± 35	<sup>17</sup> CORDEN 79 OMEG 12-15 $\pi^- p \rightarrow n2\pi$
240 ± 30	<sup>16,18</sup> ESTABROOKS 75 RVUE 17 $\pi^- p \rightarrow \pi^+ \pi^- n$
180 ± 30	122 BARTSCH 70B HBC + 8 $\pi^+ p \rightarrow N2\pi$
267 + 72 - 46	STUNTEBECK 70 HDBC 0 8 $\pi^- p, 5.4 \pi^+ d$
188 ± 49	ARMENISE 68 DBC 0 5.1 $\pi^+ d$
180 ± 40	GOLDBERG 65 HBC 0 6 $\pi^+ d, 8 \pi^- p$

<sup>15</sup> Width errors enlarged by us to  $4\Gamma/\sqrt{N}$ ; see the note with the  $K^*(892)$  mass.<sup>16</sup> Uses same data as HYAMS 75 and BECKER 79.<sup>17</sup> From a phase shift solution containing a  $f_2'(1525)$  width two times larger than the  $K\bar{K}$  result.<sup>18</sup> From phase-shift analysis. Error takes account of spread of different phase-shift solutions.

# Meson Particle Listings

## $\rho_3(1690)$

WEIGHTED AVERAGE  
186±14 (Error scaled by 1.3)



### $K\bar{K}$ AND $K\bar{K}\pi$ MODES

VALUE (MeV)	EVTS	DOCUMENT ID	TECN	CHG	COMMENT
-------------	------	-------------	------	-----	---------

The data in this block is included in the average printed for a previous datablock.

#### 204±18 OUR AVERAGE

199±40	6000	19 MARTIN	78D	SPEC	$10 \pi p \rightarrow K_S^0 K^- p$
205±20		BLUM	75	ASPK 0	$18.4 \pi^- p \rightarrow n K^+ K^-$
219±4		ALPER	80	CNTR 0	$62 \pi^- p \rightarrow K^+ K^- n$
186±11		20 COSTA...	80	OMEG	$10 \pi^- p \rightarrow K^+ K^- n$
112±60		ADERHOLZ	69	HBC +	$8 \pi^+ p \rightarrow K \bar{K} \pi$

••• We do not use the following data for averages, fits, limits, etc. •••  
<sup>19</sup> From a fit to  $J^P = 3^-$  partial wave.  
<sup>20</sup> They cannot distinguish between  $\rho_3(1690)$  and  $\omega_3(1670)$ .

### $(4\pi)^\pm$ MODE

VALUE (MeV)	EVTS	DOCUMENT ID	TECN	CHG	COMMENT
-------------	------	-------------	------	-----	---------

The data in this block is included in the average printed for a previous datablock.

#### 129±10 OUR AVERAGE

123±13		21 EVANGELIS...	81	OMEG -	$12 \pi^- p \rightarrow p 4\pi$
105±30	177	BALTAY	78B	HBC +	$15 \pi^+ p \rightarrow p 4\pi$
169±70 -48		CASON	73	HBC -	$8,18.5 \pi^- p$
135±30	144	BARTSCH	70B	HBC +	$8 \pi^+ p \rightarrow N 4\pi$
160±30	102	BARTSCH	70B	HBC +	$8 \pi^+ p \rightarrow N 2\rho$
230±28		22 EVANGELIS...	81	OMEG -	$12 \pi^- p \rightarrow p 4\pi$
184±33		23 EVANGELIS...	81	OMEG -	$12 \pi^- p \rightarrow p 4\pi$
150	66	24 KLIGER	74	HBC -	$4.5 \pi^- p \rightarrow p 4\pi$
106±25		THOMPSON	74	HBC +	$13 \pi^+ p$
125±83 -35		24 CASON	73	HBC -	$8,18.5 \pi^- p$
130±30		HOLMES	72	HBC +	$10-12 K^+ p$
180±30	90	24 BARTSCH	70B	HBC +	$8 \pi^+ p \rightarrow N a_2 \pi$
100±35		BALTAY	68	HBC +	$7, 8.5 \pi^+ p$

••• We do not use the following data for averages, fits, limits, etc. •••  
<sup>21</sup> From  $\rho^- \rho^0$  mode, not independent of the other two EVANGELISTA 81 entries.  
<sup>22</sup> From  $a_2(1320)^- \pi^0$  mode, not independent of the other two EVANGELISTA 81 entries.  
<sup>23</sup> From  $a_2(1320)^0 \pi^-$  mode, not independent of the other two EVANGELISTA 81 entries.  
<sup>24</sup> From  $\rho^\pm \rho^0$  mode.

### $\omega\pi$ MODE

VALUE (MeV)	DOCUMENT ID	TECN	CHG	COMMENT
-------------	-------------	------	-----	---------

The data in this block is included in the average printed for a previous datablock.

#### 190±40 OUR AVERAGE

230±65	25 ALDE	95	GAM2	$38 \pi^- p \rightarrow \omega \pi^0 n$
190±65	EVANGELIS...	81	OMEG -	$12 \pi^- p \rightarrow \omega \pi p$
160±56	GESSAROLI	77	HBC	$11 \pi^- p \rightarrow \omega \pi p$
89±25	THOMPSON	74	HBC +	$13 \pi^+ p$
130±73 -43	BARNHAM	70	HBC +	$10 K^+ p \rightarrow \omega \pi X$

••• We do not use the following data for averages, fits, limits, etc. •••  
<sup>25</sup> Supersedes ALDE 92c.

### $\eta\pi^+\pi^-$ MODE

(For difficulties with MMS experiments, see the  $a_2(1320)$  mini-review in the 1973 edition.)

VALUE (MeV)	DOCUMENT ID	TECN	CHG	COMMENT
-------------	-------------	------	-----	---------

The data in this block is included in the average printed for a previous datablock.

126±40 OUR AVERAGE				Error includes scale factor of 1.8.
220±30±50	AMELIN	00	VES	$37 \pi^- p \rightarrow \eta \pi^+ \pi^- n$
106±27	FUKUI	88	SPEC 0	$8.95 \pi^- p \rightarrow \eta \pi^+ \pi^- n$

••• We do not use the following data for averages, fits, limits, etc. •••  
 195 26 ANDERSON 69 MMS -  $16 \pi^- p$  backward  
 < 21 26,27 FOCACCI 66 MMS -  $7-12 \pi^- p \rightarrow \rho MM$   
 < 30 26,27 FOCACCI 66 MMS -  $7-12 \pi^- p \rightarrow \rho MM$   
 < 38 26,27 FOCACCI 66 MMS -  $7-12 \pi^- p \rightarrow \rho MM$

<sup>26</sup> Seen in 2.5-3 GeV/c  $\bar{p}p$ .  $2\pi^+ 2\pi^-$ , with 0, 1, 2  $\pi^+ \pi^-$  pairs in  $\rho^0$  band not seen by OREN 74 (2.3 GeV/c  $\bar{p}p$ ) with more statistics. (Jan. 1979)  
<sup>27</sup> Not seen by BOWEN 72.

### $\rho_3(1690)$ DECAY MODES

Mode	Fraction ( $\Gamma_i/\Gamma$ )	Scale factor
$\Gamma_1$ $4\pi$	(71.1 ± 1.9) %	
$\Gamma_2$ $\pi^\pm \pi^+ \pi^- \pi^0$	(67 ± 22) %	
$\Gamma_3$ $\omega\pi$	(16 ± 6) %	
$\Gamma_4$ $\pi\pi$	(23.6 ± 1.3) %	
$\Gamma_5$ $K\bar{K}\pi$	(3.8 ± 1.2) %	
$\Gamma_6$ $K\bar{K}$	(1.58 ± 0.26) %	1.2
$\Gamma_7$ $\eta\pi^+\pi^-$	seen	
$\Gamma_8$ $\rho(770)\eta$	seen	
$\Gamma_9$ $\pi\pi\rho$	seen	
$\Gamma_{10}$ $a_2(1320)\pi$	seen	
$\Gamma_{11}$ $\rho\rho$	seen	
$\Gamma_{12}$ $\phi\pi$		
$\Gamma_{13}$ $\eta\pi$		
$\Gamma_{14}$ $\pi^\pm 2\pi^+ 2\pi^- \pi^0$	Excluding $2\rho$ and $a_2(1320)\pi$ .	

### CONSTRAINED FIT INFORMATION

An overall fit to 5 branching ratios uses 10 measurements and one constraint to determine 4 parameters. The overall fit has a  $\chi^2 = 14.7$  for 7 degrees of freedom.

The following off-diagonal array elements are the correlation coefficients  $\langle \delta x_i \delta x_j \rangle / (\delta x_i \delta x_j)$ , in percent, from the fit to the branching fractions,  $x_i \equiv \Gamma_i / \Gamma_{\text{total}}$ . The fit constrains the  $x_i$  whose labels appear in this array to sum to one.

$x_4$	-77		
$x_5$	-74	17	
$x_6$	-15	2	0
	$x_1$	$x_4$	$x_5$

### $\rho_3(1690)$ BRANCHING RATIOS

$\Gamma(\pi\pi)/\Gamma_{\text{total}}$	DOCUMENT ID	TECN	CHG	COMMENT	$\Gamma_4/\Gamma$
0.236±0.013 OUR FIT					
0.243±0.013 OUR AVERAGE					
0.259±0.018 -0.019	BECKER	79	ASPK 0	$17 \pi^- p$ polarized	
0.23 ± 0.02	CORDEN	79	OMEG	$12-15 \pi^- p \rightarrow n 2\pi$	
0.22 ± 0.04	28 MATTHEWS	71C	HDBC 0	$7 \pi^+ n \rightarrow \pi^- p$	
0.245 ± 0.006	29 ESTABROOKS	75	RVUE	$17 \pi^- p \rightarrow \pi^+ \pi^- n$	

••• We do not use the following data for averages, fits, limits, etc. •••  
<sup>28</sup> One-pion-exchange model used in this estimation.  
<sup>29</sup> From phase-shift analysis of HYAMS 75 data.

### $\Gamma(\pi\pi)/\Gamma(\pi^\pm \pi^+ \pi^- \pi^0)$

VALUE	DOCUMENT ID	TECN	CHG	COMMENT	$\Gamma_4/\Gamma_2$
0.35 ± 0.11	CASON	73	HBC -	$8,18.5 \pi^- p$	
< 0.2	HOLMES	72	HBC +	$10-12 K^+ p$	
< 0.12	BALLAM	71B	HBC -	$16 \pi^- p$	



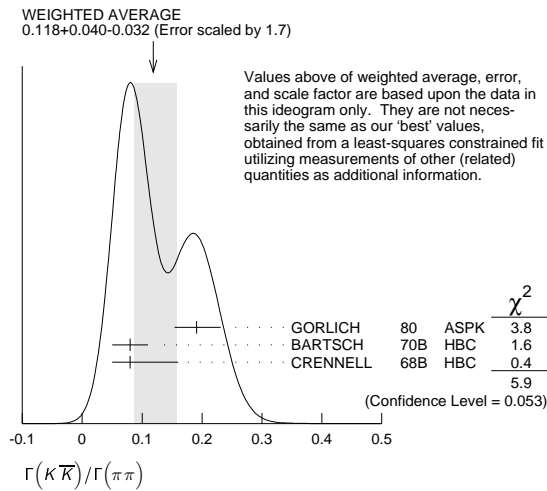
See key on page 457

## Meson Particle Listings

 $\rho_3(1690)$ 

$\Gamma(\pi\pi)/\Gamma(4\pi)$				$\Gamma_4/\Gamma_1$	
VALUE	DOCUMENT ID	TECN	CHG	COMMENT	
<b>0.332 ± 0.026 OUR FIT</b>	Error includes scale factor of 1.1.				
0.30 ± 0.10	BALTAY	78B	HBC	0	15 $\pi^+ \rho \rightarrow \rho 4\pi$

$\Gamma(K\bar{K})/\Gamma(\pi\pi)$				$\Gamma_6/\Gamma_4$	
VALUE	DOCUMENT ID	TECN	CHG	COMMENT	
<b>0.067 ± 0.011 OUR FIT</b>	Error includes scale factor of 1.2.				
<b>0.118 ± 0.040</b>	Error includes scale factor of 1.7. See the ideogram below.				
0.191 ± 0.040	GORLICH	80	ASPK	0	17,18 $\pi^- \rho$ polarized
0.08 ± 0.03	BARTSCH	70B	HBC	+	8 $\pi^+ \rho$
0.08 ± 0.08	CRENNELL	68B	HBC		6.0 $\pi^- \rho$



$\Gamma(K\bar{K}\pi)/\Gamma(\pi\pi)$				$\Gamma_5/\Gamma_4$	
VALUE	DOCUMENT ID	TECN	CHG	COMMENT	
<b>0.16 ± 0.05 OUR FIT</b>					
0.16 ± 0.05	30 BARTSCH	70B	HBC	+	8 $\pi^+ \rho$
30 Increased by us to correspond to $B(\rho_3(1690) \rightarrow \pi\pi) = 0.24$ .					

$[\Gamma(\pi\rho\rho) + \Gamma(a_2(1320)\pi) + \Gamma(\rho)]/\Gamma(\pi^+\pi^-\pi^0)$				$(\Gamma_9 + \Gamma_{10} + \Gamma_{11})/\Gamma_2$	
VALUE	DOCUMENT ID	TECN	CHG	COMMENT	
<b>0.94 ± 0.09 OUR AVERAGE</b>					
0.96 ± 0.21	BALTAY	78B	HBC	+	15 $\pi^+ \rho \rightarrow \rho 4\pi$
0.88 ± 0.15	BALLAM	71B	HBC	-	16 $\pi^- \rho$
1 ± 0.15	BARTSCH	70B	HBC	+	8 $\pi^+ \rho$
consistent with 1	CASO	68	HBC	-	11 $\pi^- \rho$

$\Gamma(\rho\rho)/\Gamma(\pi^+\pi^-\pi^0)$				$\Gamma_{11}/\Gamma_2$		
VALUE	EVTS	DOCUMENT ID	TECN	CHG	COMMENT	
• • • We do not use the following data for averages, fits, limits, etc. • • •						
0.12 ± 0.11		BALTAY	78B	HBC	+	15 $\pi^+ \rho \rightarrow \rho 4\pi$
0.56	66	KLIGER	74	HBC	-	4.5 $\pi^- \rho \rightarrow \rho 4\pi$
0.13 ± 0.09		31 THOMPSON	74	HBC	+	13 $\pi^+ \rho$
0.7 ± 0.15		BARTSCH	70B	HBC	+	8 $\pi^+ \rho$
31 $\rho\rho$ and $a_2(1320)\pi$ modes are indistinguishable.						

$\Gamma(\rho\rho)/[\Gamma(\pi\rho\rho) + \Gamma(a_2(1320)\pi) + \Gamma(\rho\rho)]$				$\Gamma_{11}/(\Gamma_9 + \Gamma_{10} + \Gamma_{11})$		
VALUE	DOCUMENT ID	TECN	CHG	COMMENT		
• • • We do not use the following data for averages, fits, limits, etc. • • •						
0.48 ± 0.16		CASO	68	HBC	-	11 $\pi^- \rho$

$\Gamma(a_2(1320)\pi)/\Gamma(\pi^+\pi^-\pi^0)$				$\Gamma_{10}/\Gamma_2$		
VALUE	DOCUMENT ID	TECN	CHG	COMMENT		
• • • We do not use the following data for averages, fits, limits, etc. • • •						
0.66 ± 0.08		BALTAY	78B	HBC	+	15 $\pi^+ \rho \rightarrow \rho 4\pi$
0.36 ± 0.14	32	THOMPSON	74	HBC	+	13 $\pi^+ \rho$
not seen		CASO	73	HBC	-	8, 18.5 $\pi^- \rho$
0.6 ± 0.15		BARTSCH	70B	HBC	+	8 $\pi^+ \rho$
0.6		BALTAY	68	HBC	+	7, 8.5 $\pi^+ \rho$
32 $\rho\rho$ and $a_2(1320)\pi$ modes are indistinguishable.						

$\Gamma(\omega\pi)/\Gamma(\pi^+\pi^-\pi^0)$				$\Gamma_3/\Gamma_2$		
VALUE	CL%	DOCUMENT ID	TECN	CHG	COMMENT	
<b>0.23 ± 0.05 OUR AVERAGE</b>	Error includes scale factor of 1.2.					
0.33 ± 0.07		THOMPSON	74	HBC	+	13 $\pi^+ \rho$
0.12 ± 0.07		BALLAM	71B	HBC	-	16 $\pi^- \rho$
0.25 ± 0.10		BALTAY	68	HBC	+	7, 8.5 $\pi^+ \rho$
0.25 ± 0.10		JOHNSTON	68	HBC	-	7.0 $\pi^- \rho$
• • • We do not use the following data for averages, fits, limits, etc. • • •						
< 0.11	95	BALTAY	78B	HBC	+	15 $\pi^+ \rho \rightarrow \rho 4\pi$
< 0.09		KLIGER	74	HBC	-	4.5 $\pi^- \rho \rightarrow \rho 4\pi$

$\Gamma(\phi\pi)/\Gamma(\pi^+\pi^-\pi^0)$				$\Gamma_{12}/\Gamma_2$		
VALUE	DOCUMENT ID	TECN	CHG	COMMENT		
• • • We do not use the following data for averages, fits, limits, etc. • • •						
< 0.11		BALTAY	68	HBC	+	7, 8.5 $\pi^+ \rho$

$\Gamma(\pi^+2\pi^+2\pi^-\pi^0)/\Gamma(\pi^+\pi^-\pi^0)$				$\Gamma_{14}/\Gamma_2$		
VALUE	DOCUMENT ID	TECN	CHG	COMMENT		
• • • We do not use the following data for averages, fits, limits, etc. • • •						
< 0.15		BALTAY	68	HBC	+	7, 8.5 $\pi^+ \rho$

$\Gamma(\eta\pi)/\Gamma(\pi^+\pi^-\pi^0)$				$\Gamma_{13}/\Gamma_2$		
VALUE	DOCUMENT ID	TECN	CHG	COMMENT		
• • • We do not use the following data for averages, fits, limits, etc. • • •						
< 0.02		THOMPSON	74	HBC	+	13 $\pi^+ \rho$

$\Gamma(K\bar{K})/\Gamma_{total}$				$\Gamma_6/\Gamma$	
VALUE	DOCUMENT ID	TECN	CHG	COMMENT	
<b>0.0158 ± 0.0026 OUR FIT</b>	Error includes scale factor of 1.2.				
<b>0.0130 ± 0.0024 OUR AVERAGE</b>					
0.013 ± 0.003	COSTA...	80	OMEG	0	10 $\pi^- \rho \rightarrow K^+ K^- \pi$
0.013 ± 0.004	33 MARTIN	78B	SPEC	-	10 $\pi \rho \rightarrow K_S^0 K^- \rho$
33 From $(\Gamma_4 \Gamma_6)^{1/2} = 0.056 \pm 0.034$ assuming $B(\rho_3(1690) \rightarrow \pi\pi) = 0.24$ .					

$\Gamma(\omega\pi)/[\Gamma(\omega\pi) + \Gamma(\rho\rho)]$				$\Gamma_3/(\Gamma_3 + \Gamma_{11})$		
VALUE	DOCUMENT ID	TECN	CHG	COMMENT		
• • • We do not use the following data for averages, fits, limits, etc. • • •						
0.22 ± 0.08		CASON	73	HBC	-	8, 18.5 $\pi^- \rho$

$\Gamma(\eta\pi^+\pi^-)/\Gamma_{total}$				$\Gamma_7/\Gamma$
VALUE	DOCUMENT ID	TECN	COMMENT	
seen				
	FUKUI	88	SPEC	8.95 $\pi^- \rho \rightarrow \eta \pi^+ \pi^-$

$\Gamma(a_2(1320)\pi)/\Gamma(\rho(770)\eta)$				$\Gamma_{10}/\Gamma_8$
VALUE	DOCUMENT ID	TECN	COMMENT	
<b>5.5 ± 2.0</b>	AMELIN	00	VES	37 $\pi^- \rho \rightarrow \eta \pi^+ \pi^-$

 $\rho_3(1690)$  REFERENCES

AMELIN	00	NP A668 83	D. Amelin et al.	(VES Collab.)
ALDE	95	ZPHY C66 379	D.M. Alde et al.	(GAMS Collab.) JP
ALDE	92C	ZPHY C64 553	D.M. Alde et al.	(BELG, SERP, KEK, LANL+)
FUKUI	88	PL B202 441	S. Fukui et al.	(SUGI, NAGO, KEK, KYOT+)
DENNEY	83	PR D28 2726	D.L. Denney et al.	(IOWA, MICH)
EVANGELIS...	81	NP B178 197	C. Evangelista et al.	(BARI, BONN, CERN+)
ALPER	80	PL 94B 422	B. Alper et al.	(AMST, CERN, CRAC, MPIM+)
COSTA...	80	NP B175 402	G. Costa de Beauregard et al.	(BARI, BONN+)
GORLICH	80	NP B174 16	L. Gorlich et al.	(CRAC, MPIM, CERN+)
BECKER	79	NP B151 46	H. Becker et al.	(MPIM, CERN, ZEEM, CRAC)
CORDEN	79	NP B157 250	M.J. Corden et al.	(BIRM, RHEL, TELA+ JP)
BALTAY	78B	PR D17 62	C. Baltay et al.	(COLU, BING)
MARTIN	78B	NP B140 158	A.D. Martin et al.	(DURH, GEVA)
MARTIN	78D	PL 74B 417	A.D. Martin et al.	(DURH, GEVA)
ANTIPOV	77	NP B119 45	Y.M. Antipov et al.	(SERP, GEVA)
GESSAROLI	77	NP B126 382	R. Gessaroli et al.	(BGNA, FIRZ, GENO+)
BLUM	75	PL 57B 403	W. Blum et al.	(CERN, MPIM) JP
ESTABROOKS	75	NP B95 322	P.G. Estabrooks, A.D. Martin	(DURH)
HYAMS	75	NP B100 205	B.D. Hyams et al.	(CERN, MPIM)
ENGLER	74	PR D10 2070	A. Engler et al.	(CMU, CASE)
GRAYER	74	NP B75 189	G. Grayer et al.	(CERN, MPIM)
KLIGER	74	SJNP 19 428	G.K. Kliger et al.	(ITEP)
Translated from YAF 19 839.				
OREN	74	NP B71 189	Y. Oren et al.	(ANL, OXF)
THOMPSON	74	NP B69 220	G. Thompson et al.	(PURD)
CASON	73	PR D7 1971	N.M. Cason et al.	(NDAM)
BOWEN	72	PRL 29 890	D.R. Bowen et al.	(NEAS, STON)
HOLMES	72	PR D6 3336	R. Holmes et al.	(ROCH)
BALLAM	71B	PR D3 2606	J. Ballam et al.	(SLAC)
MATTHEWS	71C	NP B33 1	J.A.J. Matthews et al.	(TNTO, WISC) JP
ARMENISE	70	LNC 4 199	N. Armenise et al.	(BARI, BGNA, FIRZ)
BARNHAM	70	PRL 24 1083	K.W.J. Barnham et al.	(KIRM)
BARTSCH	70B	NP B22 109	J. Bartsch et al.	(AACH, BERL, CERN)
CASO	70	LNC 3 707	C. Caso et al.	(GENO, HAMB, MILA, SACL)
STUNTEBECK	70	PL 32B 391	P.H. Stuntebeck et al.	(NDAM)
ADERHOLZ	69	NP B11 259	M. Aderholz et al.	(AACH3, BERL, CERN+)
ANDERSON	69	PRL 22 1390	E.W. Anderson et al.	(BNL, CMU)
ARMENISE	68	NC 54A 999	N. Armenise et al.	(BARI, BGNA, FIRZ+)
BALTAY	68	PRL 20 887	C. Baltay et al.	(COLU, ROCH, RUTG, YALE) I
CASO	68	NC 54A 983	C. Caso et al.	(GENO, HAMB, MILA, SACL)
CRENNELL	68B	PL 28B 136	D.J. Crennell et al.	(BNL)
JOHNSTON	68	PRL 20 1414	T.F. Johnston et al.	(TNTO, WISC) JP
FOCACCI	66	PRL 17 890	M.N. Focacci et al.	(CERN)
GOLDBERG	65	PL 17 354	M. Goldberg et al.	(CERN, EPOL, ORSAY+)

## Meson Particle Listings

 $\rho(1700)$  $\rho(1700)$ 

$$J^{PC} = 1^+(1^{--})$$

THE  $\rho(1450)$  AND THE  $\rho(1700)$ 

Updated May 2010 by S. Eidelman (Novosibirsk) and G. Veneziani (Frascati).

In our 1988 edition, we replaced the  $\rho(1600)$  entry with two new ones, the  $\rho(1450)$  and the  $\rho(1700)$ , because there was emerging evidence that the 1600-MeV region actually contains two  $\rho$ -like resonances. Erkal [1] had pointed out this possibility with a theoretical analysis on the consistency of  $2\pi$  and  $4\pi$  electromagnetic form factors and the  $\pi\pi$  scattering length. Donnachie [2], with a full analysis of data on the  $2\pi$  and  $4\pi$  final states in  $e^+e^-$  annihilation and photoproduction reactions, had also argued that in order to obtain a consistent picture, two resonances were necessary. The existence of  $\rho(1450)$  was supported by the analysis of  $\eta\rho^0$  mass spectra obtained in photoproduction and  $e^+e^-$  annihilation [3], as well as that of  $e^+e^- \rightarrow \omega\pi$  [4].

The analysis of [2] was further extended by [5,6] to include new data on  $4\pi$ -systems produced in  $e^+e^-$  annihilation, and in  $\tau$ -decays ( $\tau$  decays to  $4\pi$ , and  $e^+e^-$  annihilation to  $4\pi$  can be related by the Conserved Vector Current assumption). These systems were successfully analyzed using interfering contributions from two  $\rho$ -like states, and from the tail of the  $\rho(770)$  decaying into two-body states. While specific conclusions on  $\rho(1450) \rightarrow 4\pi$  were obtained, little could be said about the  $\rho(1700)$ .

Independent evidence for two  $1^-$  states is provided by [7] in  $4\pi$  electroproduction at  $\langle Q^2 \rangle = 1$  (GeV/c)<sup>2</sup>, and by [8] in a high-statistics sample of the  $\eta\pi\pi$  system in  $\pi^-p$  charge exchange.

This scenario with two overlapping resonances is supported by other data. Bisello [9] measured the pion form factor in the interval 1.35–2.4 GeV, and observed a deep minimum around 1.6 GeV. The best fit was obtained with the hypothesis of  $\rho$ -like resonances at 1420 and 1770 MeV, with widths of about 250 MeV. Antonelli [10] found that the  $e^+e^- \rightarrow \eta\pi^+\pi^-$  cross section is better fitted with two fully interfering Breit-Wigners, with parameters in fair agreement with those of [2] and [9]. These results can be considered as a confirmation of the  $\rho(1450)$ .

Decisive evidence for the  $\pi\pi$  decay mode of both  $\rho(1450)$  and  $\rho(1700)$  comes from  $\bar{p}p$  annihilation at rest [11]. It has been shown that these resonances also possess a  $K\bar{K}$  decay mode [12–14]. High-statistics studies of the decays  $\tau \rightarrow \pi\pi\nu_\tau$  [15,16], and  $\tau \rightarrow 4\pi\nu_\tau$  [17] also require the  $\rho(1450)$ , but are not sensitive to the  $\rho(1700)$ , because it is too close to the  $\tau$  mass. A recent very-high-statistics study of the  $\tau \rightarrow \pi\pi\nu_\tau$  decay performed at Belle [18] reports the first observation of both  $\rho(1450)$  and  $\rho(1700)$  in  $\tau$  decays.

The structure of these  $\rho$  states is not yet completely clear. Barnes [19] and Close [20] claim that  $\rho(1450)$  has a mass consistent with radial  $2S$ , but its decays show characteristics of hybrids, and suggest that this state may be a  $2S$ -hybrid

mixture. Donnachie [21] argues that hybrid states could have a  $4\pi$  decay mode dominated by the  $a_1\pi$ . Such behavior has been observed by [22] in  $e^+e^- \rightarrow 4\pi$  in the energy range 1.05–1.38 GeV, and by [17] in  $\tau \rightarrow 4\pi$  decays. Alexander [23] observes the  $\rho(1450) \rightarrow \omega\pi$  decay mode in  $B$ -meson decays, however, does not find  $\rho(1700) \rightarrow \omega\pi^0$ . A similar conclusion is made by [24], who studied the process  $e^+e^- \rightarrow \omega\pi^0$ . Various decay modes of the  $\rho(1450)$  and  $\rho(1700)$  are observed in  $\bar{p}n$  and  $\bar{p}p$  annihilation [25,26], but no definite conclusions can be drawn. More data should be collected to clarify the nature of the  $\rho$  states, particularly in the energy range above 1.6 GeV.

We now list under a separate entry the  $\rho(1570)$ , the  $\phi\pi$  state with  $J^{PC} = 1^{--}$  earlier observed by [27] (referred to as  $C(1480)$ ) and recently confirmed by [28]. While [29] shows that it may be a threshold effect, [5] and [30] suggest two independent vector states with this decay mode. The  $C(1480)$  has not been seen in the  $\bar{p}p$  [31] and  $e^+e^-$  [32,33] experiments. However, the sensitivity of the two latter is an order of magnitude lower than that of [28]. Note that [28] can not exclude that their observation is due to an OZI-suppressed decay mode of the  $\rho(1700)$ .

Several observations on the  $\omega\pi$  system in the 1200-MeV region [34–40] may be interpreted in terms of either  $J^P = 1^- \rho(770) \rightarrow \omega\pi$  production [41], or  $J^P = 1^+ b_1(1235)$  production [39,40]. We argue that no special entry for a  $\rho(1250)$  is needed. The LASS amplitude analysis [42] showing evidence for  $\rho(1270)$  is preliminary and needs confirmation. For completeness, the relevant observations are listed under the  $\rho(1450)$ .

Recently [43] reported a very broad  $1^{--}$  resonance-like  $K^+K^-$  state in  $J/\psi \rightarrow K^+K^-\pi^0$  decays. Its pole position corresponds to mass of 1576 MeV and width of 818 MeV. [44–46] suggest its exotic structure (molecular or multiquark), while [47] and [48] explain it by the interference between the  $\rho(1450)$  and  $\rho(1700)$ . We quote [43] as  $X(1575)$  in the section “Further States.”

Evidence for  $\rho$ -like mesons decaying into  $6\pi$  states was first noted by [49] in the analysis of  $6\pi$  mass spectra from  $e^+e^-$  annihilation [50,51] and diffractive photoproduction [52]. Clegg [49] argued that two states at about 2.1 and 1.8 GeV exist: while the former is a candidate for the  $\rho(2150)$ , the latter could be a manifestation of the  $\rho(1700)$  distorted by threshold effects. BaBar reported observations of the new decay modes of the  $\rho(2150)$  in the channels  $\eta'(958)\pi^+\pi^-$  and  $f_1(1285)\pi^+\pi^-$  [53]. The relativistic quark model [54] predicts the  $2^3D_1$  state with  $J^{PC} = 1^{--}$  at 2.15 GeV which can be identified with the  $\rho(2150)$ .

The E687 Collaboration at Fermilab reported an observation of a narrow-dip structure at 1.9 GeV in the  $3\pi^+3\pi^-$  diffractive photoproduction [55]. A similar effect of the dip in the cross section of  $e^+e^- \rightarrow 6\pi$  around 1.9 GeV has been earlier reported by DM2 [51], where  $6\pi$  included both  $3\pi^+3\pi^-$  and  $2\pi^+2\pi^-\pi^0$ . Later the dip in the  $R$  value (the total cross section of  $e^+e^- \rightarrow$  hadrons divided by the cross section of  $e^+e^- \rightarrow \mu^+\mu^-$ ) was

See key on page 457

observed by [56], again around 1.9 GeV. This energy is close to the  $N\bar{N}$  threshold, which hints at the possible relation between the dip and  $N\bar{N}$ , *e.g.*, the frequently discussed narrow  $N\bar{N}$  resonance or just a threshold effect. Such behaviour is also characteristic of exotic objects like vector  $q\bar{q}$  hybrids. Note that [57] failed to find this state in the reaction  $\bar{n}p \rightarrow 3\pi^+2\pi^-\pi^0$ . A reanalysis of the E687 data by [58] shows that a dip may arise due to interference of a narrow object with a broad  $\rho(1700)$  independently of the nature of the former. BaBar studied the processes  $e^+e^- \rightarrow 3\pi^+3\pi^-$  and  $e^+e^- \rightarrow 2\pi^+2\pi^-2\pi^0$  using the radiative return, and observed a structure around 1.9 GeV in both final states [59]. The data are not well described by a single Breit-Wigner state, and a good fit is achieved while taking into account the interference of such a structure with a Jacob-Slansky amplitude for continuum. The mass of this state obtained by BaBar is consistent with [56] and [55], but the width is substantially larger. Recently [28] observed a structure at 1.9 GeV in the radiative return to the  $\phi\pi$  final state, with a much smaller width of  $48 \pm 17$  MeV consistent with that of [56,58]. We list these observations under a separate particle  $\rho(1900)$ , which needs confirmation.

## References

1. C. Erkal, Z. Phys. **C31**, 615 (1986).
2. A. Donnachie and H. Mirzaie, Z. Phys. **C33**, 407 (1987).
3. A. Donnachie and A.B. Clegg, Z. Phys. **C34**, 257 (1987).
4. A. Donnachie and A.B. Clegg, Z. Phys. **C51**, 689 (1991).
5. A.B. Clegg and A. Donnachie, Z. Phys. **C40**, 313 (1988).
6. A.B. Clegg and A. Donnachie, Z. Phys. **C62**, 455 (1994).
7. T.J. Killian *et al.*, Phys. Rev. **D21**, 3005 (1980).
8. S. Fukui *et al.*, Phys. Lett. **B202**, 441 (1988).
9. D. Bisello *et al.*, Phys. Lett. **B220**, 321 (1989).
10. A. Antonelli *et al.*, Phys. Lett. **B212**, 133 (1988).
11. A. Abele *et al.*, Phys. Lett. **B391**, 191 (1997).
12. A. Abele *et al.*, Phys. Rev. **D57**, 3860 (1998).
13. A. Bertin *et al.*, Phys. Lett. **B434**, 180 (1998).
14. A. Abele *et al.*, Phys. Lett. **B468**, 178 (1999).
15. R. Barate *et al.*, Z. Phys. **C76**, 15 (1997).
16. S. Anderson, Phys. Rev. **D61**, 112002 (2000).
17. K.W. Edwards *et al.*, Phys. Rev. **D61**, 072003 (2000).
18. M. Fujikawa *et al.*, Phys. Rev. **D78**, 072006 (2008).
19. T. Barnes *et al.*, Phys. Rev. **D55**, 4157 (1997).
20. F.E. Close *et al.*, Phys. Rev. **D56**, 1584 (1997).
21. A. Donnachie and Yu.S. Katashnikova, Phys. Rev. **D60**, 114011 (1999).
22. R.R. Akhmetshin *et al.*, Phys. Lett. **B466**, 392 (1999).
23. J.P. Alexander *et al.*, Phys. Rev. **D64**, 092001 (2001).
24. R.R. Akhmetshin *et al.*, Phys. Lett. **B562**, 173 (2003).
25. A. Abele *et al.*, Eur. Phys. J. **C21**, 261 (2001).
26. M. Bargiotti *et al.*, Phys. Lett. **B561**, 233 (2003).
27. S.I. Bitukov *et al.*, Phys. Lett. **B188**, 383 (1987).
28. B. Aubert *et al.*, Phys. Rev. **D77**, 092002 (2008).
29. N.N. Achasov and G.N. Shestakov, Phys. Atom. Nucl. **59**, 1262 (1996).
30. L.G. Landsberg, Sov. J. Nucl. Phys. **55**, 1051 (1992).

31. A. Abele *et al.*, Phys. Lett. **B415**, 280 (1997).
32. V.M. Aulchenko *et al.*, Sov. Phys. JETP Lett. **45**, 145 (1987).
33. D. Bisello *et al.*, Z. Phys. **C52**, 227 (1991).
34. P. Frenkiel *et al.*, Nucl. Phys. **B47**, 61 (1972).
35. G. Cosme *et al.*, Phys. Lett. **B63**, 352 (1976).
36. D.P. Barber *et al.*, Z. Phys. **C4**, 169 (1980).
37. D. Aston, Phys. Lett. **B92**, 211 (1980).
38. M. Atkinson *et al.*, Nucl. Phys. **B243**, 1 (1984).
39. J.E. Brau *et al.*, Phys. Rev. **D37**, 2379 (1988).
40. C. Amsler *et al.*, Phys. Lett. **B311**, 362 (1993).
41. J. Layssac and F.M. Renard, Nuovo Cimento **6A**, 134 (1971).
42. D. Aston *et al.*, Nucl. Phys. (Proc. Supp.) **B21**, 105 (1991).
43. M. Ablikim *et al.*, Phys. Rev. Lett. **97**, 142002 (2006).
44. G.-J. Ding and M.-L. Yan, Phys. Lett. **B643**, 33 (2006).
45. F.K. Guo *et al.*, Nucl. Phys. **A773**, 78 (2006).
46. A. Zhang *et al.*, Phys. Rev. **D76**, 036004 (2007).
47. B.A. Li, Phys. Rev. **D76**, 094016 (2007).
48. X. Liu *et al.*, Phys. Rev. **D75**, 074017 (2007).
49. A.B. Clegg and A. Donnachie, Z. Phys. **C45**, 677 (1990).
50. D. Bisello *et al.*, Phys. Lett. **107B**, 145 (1981).
51. A. Castro *et al.*, LAL-88-58(1988).
52. M. Atkinson *et al.*, Z. Phys. **C29**, 333 (1985).
53. B. Aubert *et al.*, Phys. Rev. **D76**, 092005 (2007).
54. S. Godfrey and N. Isgur, Phys. Rev. **D32**, 189 (1985).
55. P.L. Frabetti *et al.*, Phys. Lett. **B514**, 240 (2001).
56. A. Antonelli *et al.*, Phys. Lett. **B365**, 427 (1996).
57. M. Agnello *et al.*, Phys. Lett. **B527**, 39 (2002).
58. P.L. Frabetti *et al.*, Phys. Lett. **B578**, 290 (2004).
59. B. Aubert *et al.*, Phys. Rev. **D73**, 052003 (2006).

## $\rho(1700)$ MASS

### $\eta\rho^0$ AND $\pi^+\pi^-$ MODES

VALUE (MeV)	DOCUMENT ID
$1720 \pm 20$ OUR ESTIMATE	

### $\eta\rho^0$ MODE

VALUE (MeV)	DOCUMENT ID	TECN	COMMENT
The data in this block is included in the average printed for a previous datablock.			

••• We do not use the following data for averages, fits, limits, etc. •••

$1740 \pm 20$	ANTONELLI	88	DM2	$e^+e^- \rightarrow \eta\pi^+\pi^-$
$1701 \pm 15$	FUKUI	88	SPEC	$8.95 \pi^-p \rightarrow \eta\pi^+\pi^-n$

<sup>1</sup> Assuming  $\rho^+ f_0(1370)$  decay mode interferes with  $a_1(1260)^+\pi$  background. From a two Breit-Wigner fit.

### $\pi\pi$ MODE

VALUE (MeV)	EVTS	DOCUMENT ID	TECN	COMMENT
The data in this block is included in the average printed for a previous datablock.				

••• We do not use the following data for averages, fits, limits, etc. •••

$1728 \pm 17 \pm 89$	5.4M	2,3 FUJIKAWA	08	BELL	$\tau^- \rightarrow \pi^-\pi^0\nu_\tau$
$1780 \pm 37 \pm 29$		4 ABELE	97	CBAR	$\bar{p}n \rightarrow \pi^-\pi^0\pi^0$
$1719 \pm 15$		4 BERTIN	97c	OBLX	$0.0 \bar{p}p \rightarrow \pi^+\pi^-\pi^0$
$1730 \pm 30$		CLEGG	94	RVUE	$e^+e^- \rightarrow \pi^+\pi^-$
$1768 \pm 21$		BISELLO	89	DM2	$e^+e^- \rightarrow \pi^+\pi^-$
$1745.7 \pm 91.9$		DUBNICKA	89	RVUE	$e^+e^- \rightarrow \pi^+\pi^-$
$1546 \pm 26$		GESHKEN...	89	RVUE	
1650		5 ERKAL	85	RVUE	$20-70 \gamma\rho \rightarrow \gamma\pi$
$1550 \pm 70$		ABE	84B	HYBR	$20 \gamma\rho \rightarrow \pi^+\pi^-\pi^0$
$1590 \pm 20$		6 ASTON	80	OMEG	$20-70 \gamma\rho \rightarrow \rho 2\pi$
$1600 \pm 10$		7 ATIYA	79B	SPEC	$50 \gamma C \rightarrow C 2\pi$
$1598 \pm 24 \pm 22$		BECKER	79	ASPK	$17 \pi^-p$ polarized
$1659 \pm 25$		5 LANG	79	RVUE	
1575		5 MARTIN	78c	RVUE	$17 \pi^-p \rightarrow \pi^+\pi^-n$
$1610 \pm 30$		5 FROGGATT	77	RVUE	$17 \pi^-p \rightarrow \pi^+\pi^-n$
$1590 \pm 20$		8 HYAMS	73	ASPK	$17 \pi^-p \rightarrow \pi^+\pi^-n$

# Meson Particle Listings

## $\rho(1700)$

- <sup>2</sup>  $|F_\pi(0)|^2$  fixed to 1.
- <sup>3</sup> From the GOUNARIS 68 parametrization of the pion form factor.
- <sup>4</sup> T-matrix pole.
- <sup>5</sup> From phase shift analysis of HYAMS 73 data.
- <sup>6</sup> Simple relativistic Breit-Wigner fit with constant width.
- <sup>7</sup> An additional 40 MeV uncertainty in both the mass and width is present due to the choice of the background shape.
- <sup>8</sup> Included in BECKER 79 analysis.

### $\pi\omega$ MODE

VALUE (MeV)	DOCUMENT ID	TECN	COMMENT
● ● ● We do not use the following data for averages, fits, limits, etc. ● ● ●			
1550 to 1620	<sup>9</sup> ACHASOV	00i	SND $e^+e^- \rightarrow \pi^0\pi^0\gamma$
1580 to 1710	<sup>10</sup> ACHASOV	00i	SND $e^+e^- \rightarrow \pi^0\pi^0\gamma$
1710±90	ACHASOV	97	RVUE $e^+e^- \rightarrow \omega\pi^0$

<sup>9</sup> Taking into account both  $\rho(1450)$  and  $\rho(1700)$  contributions. Using the data of ACHASOV 00i on  $e^+e^- \rightarrow \omega\pi^0$  and of EDWARDS 00A on  $\tau^- \rightarrow \omega\pi^-\nu_\tau$ .  $\rho(1450)$  mass and width fixed at 1400 MeV and 500 MeV respectively.

<sup>10</sup> Taking into account the  $\rho(1700)$  contribution only. Using the data of ACHASOV 00i on  $e^+e^- \rightarrow \omega\pi^0$  and of EDWARDS 00A on  $\tau^- \rightarrow \omega\pi^-\nu_\tau$ .

### $K\bar{K}$ MODE

VALUE (MeV)	EVTs	DOCUMENT ID	TECN	CHG	COMMENT
● ● ● We do not use the following data for averages, fits, limits, etc. ● ● ●					
1740.8±22.2	27k	<sup>11</sup> ABELE	99D	CBAR ±	0.0 $\bar{p}p \rightarrow K^+K^-\pi^0$
1582 ±36	1600	CLELAND	82B	SPEC ±	50 $\pi p \rightarrow K_S^0 K^\pm p$

<sup>11</sup> K-matrix pole. Isospin not determined, could be  $\omega(1650)$  or  $\phi(1680)$ .

### $2(\pi^+\pi^-)$ MODE

VALUE (MeV)	EVTs	DOCUMENT ID	TECN	COMMENT
● ● ● We do not use the following data for averages, fits, limits, etc. ● ● ●				
1851 $\pm$ $\frac{27}{24}$		ACHASOV	97	RVUE $e^+e^- \rightarrow 2(\pi^+\pi^-)$
1570 ± 20		<sup>12</sup> CORDIER	82	DM1 $e^+e^- \rightarrow 2(\pi^+\pi^-)$
1520 ± 30		<sup>13</sup> ASTON	81E	OMEG 20-70 $\gamma p \rightarrow p4\pi$
1654 ± 25		<sup>14</sup> DIBIANCA	81	DBC $\pi^+ d \rightarrow pp2(\pi^+\pi^-)$
1666 ± 39		<sup>12</sup> BACCI	80	FRAG $e^+e^- \rightarrow 2(\pi^+\pi^-)$
1780	34	KILLIAN	80	SPEC 11 $e^- p \rightarrow 2(\pi^+\pi^-)$
1500		<sup>15</sup> ATIYA	79B	SPEC 50 $\gamma C \rightarrow C4\pi^\pm$
1570 ± 60	65	<sup>16</sup> ALEXANDER	75	HBC 7.5 $\gamma p \rightarrow p4\pi$
1550 ± 60		<sup>13</sup> CONVERSI	74	OSPK $e^+e^- \rightarrow 2(\pi^+\pi^-)$
1550 ± 50	160	SCHACHT	74	STRC 5.5-9 $\gamma p \rightarrow p4\pi$
1450 ± 100	340	SCHACHT	74	STRC 9-18 $\gamma p \rightarrow p4\pi$
1430 ± 50	400	BINGHAM	72B	HBC 9.3 $\gamma p \rightarrow p4\pi$

<sup>12</sup> Simple relativistic Breit-Wigner fit with model dependent width.  
<sup>13</sup> Simple relativistic Breit-Wigner fit with constant width.  
<sup>14</sup> One peak fit result.  
<sup>15</sup> Parameters roughly estimated, not from a fit.  
<sup>16</sup> Skew mass distribution compensated by Ross-Stodolsky factor.

### $\pi^+\pi^-\pi^0\pi^0$ MODE

VALUE (MeV)	DOCUMENT ID	TECN	COMMENT
● ● ● We do not use the following data for averages, fits, limits, etc. ● ● ●			
1660±30	ATKINSON	85B	OMEG 20-70 $\gamma p$

### $3(\pi^+\pi^-)$ AND $2(\pi^+\pi^-\pi^0)$ MODES

VALUE (MeV)	DOCUMENT ID	TECN	COMMENT
● ● ● We do not use the following data for averages, fits, limits, etc. ● ● ●			
1730±34	<sup>17</sup> FRABETTI	04	E687 $\gamma p \rightarrow 3\pi^+3\pi^-p$
1783±15	CLEGG	90	RVUE $e^+e^- \rightarrow 3(\pi^+\pi^-)2(\pi^+\pi^-\pi^0)$

<sup>17</sup> From a fit with two resonances with the JACOB 72 continuum.

### $\rho(1700)$ WIDTH

### $\eta\rho^0$ AND $\pi^+\pi^-$ MODES

VALUE (MeV)	DOCUMENT ID	TECN	COMMENT
<b>250±100 OUR ESTIMATE</b>			

### $\eta\rho^0$ MODE

VALUE (MeV)	DOCUMENT ID	TECN	COMMENT
The data in this block is included in the average printed for a previous datablock.			

- ● ● We do not use the following data for averages, fits, limits, etc. ● ● ●
  - 150±30 ANTONELLI 88 DM2  $e^+e^- \rightarrow \eta\pi^+\pi^-$
  - 282±44 <sup>18</sup> FUKUI 88 SPEC 8.95  $\pi^- p \rightarrow \eta\pi^+\pi^- n$
- <sup>18</sup> Assuming  $\rho^+\rho^0(1370)$  decay mode interferes with  $a_1(1260)^+\pi$  background. From a two Breit-Wigner fit.

### $\pi\pi$ MODE

VALUE (MeV)	EVTs	DOCUMENT ID	TECN	COMMENT
The data in this block is included in the average printed for a previous datablock.				
● ● ● We do not use the following data for averages, fits, limits, etc. ● ● ●				
164 ± 21 $\frac{+89}{-26}$	5.4M	<sup>19,20</sup> FUJIKAWA	08	BELL $\tau^- \rightarrow \pi^-\pi^0\nu_\tau$
275 ± 45		<sup>21</sup> ABELE	97	CBAR $\bar{p}n \rightarrow \pi^-\pi^0\pi^0$
310 ± 40		BERTIN	97C	OBLX 0.0 $\bar{p}p \rightarrow \pi^+\pi^-\pi^0$
400 ± 100		CLEGG	94	RVUE $e^+e^- \rightarrow \pi^+\pi^-$
224 ± 22		BISELLO	89	DM2 $e^+e^- \rightarrow \pi^+\pi^-$
242.5±163.0		DUBNICKA	89	RVUE $e^+e^- \rightarrow \pi^+\pi^-$
620 ± 60		GESHKEN...	89	RVUE
<315		<sup>22</sup> ERKAL	85	RVUE 20-70 $\gamma p \rightarrow \gamma\pi$
280 $\pm$ $\frac{30}{80}$		ABE	84B	HYBR 20 $\gamma p \rightarrow \pi^+\pi^-p$
230 ± 80		<sup>23</sup> ASTON	80B	OMEG 20-70 $\gamma p \rightarrow p2\pi$
283 ± 14		<sup>24</sup> ATIYA	79B	SPEC 50 $\gamma C \rightarrow C2\pi$
175 $\pm$ $\frac{98}{-53}$		BECKER	79	ASPK 17 $\pi^- p$ polarized
232 ± 34		<sup>22</sup> LANG	79	RVUE
340		<sup>22</sup> MARTIN	78C	RVUE 17 $\pi^- p \rightarrow \pi^+\pi^- n$
300 ± 100		<sup>22</sup> FROGGATT	77	RVUE 17 $\pi^- p \rightarrow \pi^+\pi^- n$
180 ± 50		<sup>25</sup> HYAMS	73	ASPK 17 $\pi^- p \rightarrow \pi^+\pi^- n$

- <sup>19</sup>  $|F_\pi(0)|^2$  fixed to 1.
- <sup>20</sup> From the GOUNARIS 68 parametrization of the pion form factor.
- <sup>21</sup> T-matrix pole.
- <sup>22</sup> From phase shift analysis of HYAMS 73 data.
- <sup>23</sup> Simple relativistic Breit-Wigner fit with constant width.
- <sup>24</sup> An additional 40 MeV uncertainty in both the mass and width is present due to the choice of the background shape.
- <sup>25</sup> Included in BECKER 79 analysis.

### $K\bar{K}$ MODE

VALUE (MeV)	EVTs	DOCUMENT ID	TECN	CHG	COMMENT
● ● ● We do not use the following data for averages, fits, limits, etc. ● ● ●					
187.2± 26.7	27k	<sup>26</sup> ABELE	99D	CBAR ±	0.0 $\bar{p}p \rightarrow K^+K^-\pi^0$
265 ± 120	1600	CLELAND	82B	SPEC ±	50 $\pi p \rightarrow K_S^0 K^\pm p$

<sup>26</sup> K-matrix pole. Isospin not determined, could be  $\omega(1650)$  or  $\phi(1680)$ .

### $2(\pi^+\pi^-)$ MODE

VALUE (MeV)	EVTs	DOCUMENT ID	TECN	COMMENT
● ● ● We do not use the following data for averages, fits, limits, etc. ● ● ●				
510 ± 40		<sup>27</sup> CORDIER	82	DM1 $e^+e^- \rightarrow 2(\pi^+\pi^-)$
400 ± 50		<sup>28</sup> ASTON	81E	OMEG 20-70 $\gamma p \rightarrow p4\pi$
400±146		<sup>29</sup> DIBIANCA	81	DBC $\pi^+ d \rightarrow pp2(\pi^+\pi^-)$
700±160		<sup>27</sup> BACCI	80	FRAG $e^+e^- \rightarrow 2(\pi^+\pi^-)$
100	34	KILLIAN	80	SPEC 11 $e^- p \rightarrow 2(\pi^+\pi^-)$
600		<sup>30</sup> ATIYA	79B	SPEC 50 $\gamma C \rightarrow C4\pi^\pm$
340±160	65	<sup>31</sup> ALEXANDER	75	HBC 7.5 $\gamma p \rightarrow p4\pi$
360±100		<sup>28</sup> CONVERSI	74	OSPK $e^+e^- \rightarrow 2(\pi^+\pi^-)$
400±120	160	<sup>32</sup> SCHACHT	74	STRC 5.5-9 $\gamma p \rightarrow p4\pi$
850±200	340	<sup>32</sup> SCHACHT	74	STRC 9-18 $\gamma p \rightarrow p4\pi$
650±100	400	BINGHAM	72B	HBC 9.3 $\gamma p \rightarrow p4\pi$

<sup>27</sup> Simple relativistic Breit-Wigner fit with model-dependent width.  
<sup>28</sup> Simple relativistic Breit-Wigner fit with constant width.  
<sup>29</sup> One peak fit result.  
<sup>30</sup> Parameters roughly estimated, not from a fit.  
<sup>31</sup> Skew mass distribution compensated by Ross-Stodolsky factor.  
<sup>32</sup> Width errors enlarged by us to  $4\Gamma/\sqrt{N}$ ; see the note with the  $K^*(892)$  mass.

- <sup>27</sup> Simple relativistic Breit-Wigner fit with model-dependent width.
- <sup>28</sup> Simple relativistic Breit-Wigner fit with constant width.
- <sup>29</sup> One peak fit result.
- <sup>30</sup> Parameters roughly estimated, not from a fit.
- <sup>31</sup> Skew mass distribution compensated by Ross-Stodolsky factor.
- <sup>32</sup> Width errors enlarged by us to  $4\Gamma/\sqrt{N}$ ; see the note with the  $K^*(892)$  mass.

### $\pi^+\pi^-\pi^0\pi^0$ MODE

VALUE (MeV)	DOCUMENT ID	TECN	COMMENT
● ● ● We do not use the following data for averages, fits, limits, etc. ● ● ●			
300±50	ATKINSON	85B	OMEG 20-70 $\gamma p$

### $\omega\pi^0$ MODE

VALUE (MeV)	DOCUMENT ID	TECN	COMMENT
● ● ● We do not use the following data for averages, fits, limits, etc. ● ● ●			
350 to 580	<sup>33</sup> ACHASOV	00i	SND $e^+e^- \rightarrow \pi^0\pi^0\gamma$
490 to 1040	<sup>34</sup> ACHASOV	00i	SND $e^+e^- \rightarrow \pi^0\pi^0\gamma$

- <sup>33</sup> Taking into account both  $\rho(1450)$  and  $\rho(1700)$  contributions. Using the data of ACHASOV 00i on  $e^+e^- \rightarrow \omega\pi^0$  and of EDWARDS 00A on  $\tau^- \rightarrow \omega\pi^-\nu_\tau$ .  $\rho(1450)$  mass and width fixed at 1400 MeV and 500 MeV respectively.
- <sup>34</sup> Taking into account the  $\rho(1700)$  contribution only. Using the data of ACHASOV 00i on  $e^+e^- \rightarrow \omega\pi^0$  and of EDWARDS 00A on  $\tau^- \rightarrow \omega\pi^-\nu_\tau$ .

### $3(\pi^+\pi^-)$ AND $2(\pi^+\pi^-\pi^0)$ MODES

VALUE (MeV)	DOCUMENT ID	TECN	COMMENT
● ● ● We do not use the following data for averages, fits, limits, etc. ● ● ●			
315±100	<sup>35</sup> FRABETTI	04	E687 $\gamma p \rightarrow 3\pi^+3\pi^-p$
285 ± 20	CLEGG	90	RVUE $e^+e^- \rightarrow 3(\pi^+\pi^-)2(\pi^+\pi^-\pi^0)$

<sup>35</sup> From a fit with two resonances with the JACOB 72 continuum.

$\rho(1700)$  DECAY MODES

Mode	Fraction ( $\Gamma_i/\Gamma$ )
$\Gamma_1$ $4\pi$	
$\Gamma_2$ $2(\pi^+\pi^-)$	large
$\Gamma_3$ $\rho\pi\pi$	dominant
$\Gamma_4$ $\rho^0\pi^+\pi^-$	large
$\Gamma_5$ $\rho^0\pi^0\pi^0$	
$\Gamma_6$ $\rho^\pm\pi^\mp\pi^0$	large
$\Gamma_7$ $a_1(1260)\pi$	seen
$\Gamma_8$ $h_1(1170)\pi$	seen
$\Gamma_9$ $\pi(1300)\pi$	seen
$\Gamma_{10}$ $\rho\rho$	seen
$\Gamma_{11}$ $\pi^+\pi^-$	seen
$\Gamma_{12}$ $\pi\pi$	seen
$\Gamma_{13}$ $K\bar{K}^*(892) + c.c.$	seen
$\Gamma_{14}$ $\eta\rho$	seen
$\Gamma_{15}$ $a_2(1320)\pi$	not seen
$\Gamma_{16}$ $KK$	seen
$\Gamma_{17}$ $e^+e^-$	seen
$\Gamma_{18}$ $\pi^0\omega$	seen

 $\rho(1700)$   $\Gamma(i)\Gamma(e^+e^-)/\Gamma(\text{total})$ 

This combination of a partial width with the partial width into  $e^+e^-$  and with the total width is obtained from the cross-section into channel  $i$  in  $e^+e^-$  annihilation.

 $\Gamma(2(\pi^+\pi^-)) \times \Gamma(e^+e^-)/\Gamma_{\text{total}}$   $\Gamma_2\Gamma_{17}/\Gamma$ 

VALUE (keV)	DOCUMENT ID	TECN	COMMENT
••• We do not use the following data for averages, fits, limits, etc. •••			
2.6 ± 0.2	DEL COURT	81B	DM1 $e^+e^- \rightarrow 2(\pi^+\pi^-)$
2.83 ± 0.42	BACCI	80	FRAG $e^+e^- \rightarrow 2(\pi^+\pi^-)$

 $\Gamma(\pi^+\pi^-) \times \Gamma(e^+e^-)/\Gamma_{\text{total}}$   $\Gamma_{11}\Gamma_{17}/\Gamma$ 

VALUE (keV)	DOCUMENT ID	TECN	COMMENT
••• We do not use the following data for averages, fits, limits, etc. •••			
0.13	<sup>36</sup> DIEKMAN	88	RVUE $e^+e^- \rightarrow \pi^+\pi^-$
0.029 <sup>+0.016</sup> <sub>-0.012</sub>	KURDADZE	83	OLYA 0.64–1.4 $e^+e^- \rightarrow \pi^+\pi^-$
<sup>36</sup> Using total width = 220 MeV.			

 $\Gamma(K\bar{K}^*(892) + c.c.) \times \Gamma(e^+e^-)/\Gamma_{\text{total}}$   $\Gamma_{13}\Gamma_{17}/\Gamma$ 

VALUE (keV)	DOCUMENT ID	TECN	COMMENT
••• We do not use the following data for averages, fits, limits, etc. •••			
0.305 ± 0.071	<sup>37</sup> BIZOT	80	DM1 $e^+e^-$
<sup>37</sup> Model dependent.			

 $\Gamma(\eta\rho) \times \Gamma(e^+e^-)/\Gamma_{\text{total}}$   $\Gamma_{14}\Gamma_{17}/\Gamma$ 

VALUE (eV)	DOCUMENT ID	TECN	COMMENT
••• We do not use the following data for averages, fits, limits, etc. •••			
7 ± 3	ANTONELLI	88	DM2 $e^+e^- \rightarrow \eta\pi^+\pi^-$

 $\Gamma(K\bar{K}) \times \Gamma(e^+e^-)/\Gamma_{\text{total}}$   $\Gamma_{16}\Gamma_{17}/\Gamma$ 

VALUE (keV)	DOCUMENT ID	TECN	COMMENT
••• We do not use the following data for averages, fits, limits, etc. •••			
0.035 ± 0.029	<sup>38</sup> BIZOT	80	DM1 $e^+e^-$
<sup>38</sup> Model dependent.			

 $\Gamma(\rho\pi\pi) \times \Gamma(e^+e^-)/\Gamma_{\text{total}}$   $\Gamma_3\Gamma_{17}/\Gamma$ 

VALUE (keV)	DOCUMENT ID	TECN	COMMENT
••• We do not use the following data for averages, fits, limits, etc. •••			
3.510 ± 0.090	<sup>39</sup> BIZOT	80	DM1 $e^+e^-$
<sup>39</sup> Model dependent.			

 $\rho(1700)$  BRANCHING RATIOS $\Gamma(\rho\pi\pi)/\Gamma(4\pi)$   $\Gamma_3/\Gamma_1$ 

VALUE	DOCUMENT ID	TECN	COMMENT
••• We do not use the following data for averages, fits, limits, etc. •••			
0.28 ± 0.06	<sup>40</sup> ABELE	01B	CBAR 0.0 $\bar{p}n \rightarrow 5\pi$
<sup>40</sup> $\omega\pi$ not included.			

 $\Gamma(\rho^0\pi^+\pi^-)/\Gamma(2(\pi^+\pi^-))$   $\Gamma_4/\Gamma_2$ 

VALUE	EVTS	DOCUMENT ID	TECN	COMMENT
••• We do not use the following data for averages, fits, limits, etc. •••				
~1.0		DEL COURT	81B	DM1 $e^+e^- \rightarrow 2(\pi^+\pi^-)$
0.7 ± 0.1	500	SCHACHT	74	STRC 5.5–18 $\gamma p \rightarrow p4\pi$
0.80		<sup>41</sup> BINGHAM	72B	HBC 9.3 $\gamma p \rightarrow p4\pi$

<sup>41</sup>The  $\pi\pi$  system is in S-wave.

 $\Gamma(\rho^0\pi^0\pi^0)/\Gamma(\rho^\pm\pi^\mp\pi^0)$   $\Gamma_5/\Gamma_6$ 

VALUE	DOCUMENT ID	TECN	CHG	COMMENT
••• We do not use the following data for averages, fits, limits, etc. •••				
<0.10	ATKINSON	85B	OMEG	20–70 $\gamma p$
<0.15	ATKINSON	82	OMEG 0	20–70 $\gamma p \rightarrow p4\pi$

 $\Gamma(a_1(1260)\pi)/\Gamma(4\pi)$   $\Gamma_7/\Gamma_1$ 

VALUE	DOCUMENT ID	TECN	COMMENT
••• We do not use the following data for averages, fits, limits, etc. •••			
0.16 ± 0.05	<sup>42</sup> ABELE	01B	CBAR 0.0 $\bar{p}n \rightarrow 5\pi$
<sup>42</sup> $\omega\pi$ not included.			

 $\Gamma(h_1(1170)\pi)/\Gamma(4\pi)$   $\Gamma_8/\Gamma_1$ 

VALUE	DOCUMENT ID	TECN	COMMENT
••• We do not use the following data for averages, fits, limits, etc. •••			
0.17 ± 0.06	<sup>43</sup> ABELE	01B	CBAR 0.0 $\bar{p}n \rightarrow 5\pi$
<sup>43</sup> $\omega\pi$ not included.			

 $\Gamma(\pi(1300)\pi)/\Gamma(4\pi)$   $\Gamma_9/\Gamma_1$ 

VALUE	DOCUMENT ID	TECN	COMMENT
••• We do not use the following data for averages, fits, limits, etc. •••			
0.30 ± 0.10	<sup>44</sup> ABELE	01B	CBAR 0.0 $\bar{p}n \rightarrow 5\pi$
<sup>44</sup> $\omega\pi$ not included.			

 $\Gamma(\rho\rho)/\Gamma(4\pi)$   $\Gamma_{10}/\Gamma_1$ 

VALUE	DOCUMENT ID	TECN	COMMENT
••• We do not use the following data for averages, fits, limits, etc. •••			
0.09 ± 0.03	<sup>45</sup> ABELE	01B	CBAR 0.0 $\bar{p}n \rightarrow 5\pi$
<sup>45</sup> $\omega\pi$ not included.			

 $\Gamma(\pi^+\pi^-)/\Gamma_{\text{total}}$   $\Gamma_{11}/\Gamma$ 

VALUE	DOCUMENT ID	TECN	COMMENT
••• We do not use the following data for averages, fits, limits, etc. •••			
0.287 <sup>+0.043</sup> <sub>-0.042</sub>	BECKER	79	ASPK 17 $\pi^- p$ polarized
0.15 to 0.30	<sup>46</sup> MARTIN	78C	RVUE 17 $\pi^- p \rightarrow \pi^+\pi^- n$
<0.20	<sup>47</sup> COSTA...	77B	RVUE $e^+e^- \rightarrow 2\pi, 4\pi$
0.30 ± 0.05	<sup>46</sup> FROGGATT	77	RVUE 17 $\pi^- p \rightarrow \pi^+\pi^- n$
<0.15	<sup>48</sup> EISENBERG	73	HBC 5 $\pi^+ p \rightarrow \Delta^{++} 2\pi$
0.25 ± 0.05	<sup>49</sup> HYAMS	73	ASPK 17 $\pi^- p \rightarrow \pi^+\pi^- n$
<sup>46</sup> From phase shift analysis of HYAMS 73 data.			
<sup>47</sup> Estimate using unitarity, time reversal invariance, Breit-Wigner.			
<sup>48</sup> Estimated using one-pion-exchange model.			
<sup>49</sup> Included in BECKER 79 analysis.			

 $\Gamma(\pi^+\pi^-)/\Gamma(2(\pi^+\pi^-))$   $\Gamma_{11}/\Gamma_2$ 

VALUE	DOCUMENT ID	TECN	COMMENT
••• We do not use the following data for averages, fits, limits, etc. •••			
0.13 ± 0.05	ASTON	80	OMEG 20–70 $\gamma p \rightarrow p2\pi$
<0.14	<sup>50</sup> DAVIER	73	STRC 6–18 $\gamma p \rightarrow p4\pi$
<0.2	<sup>51</sup> BINGHAM	72B	HBC 9.3 $\gamma p \rightarrow p2\pi$
<sup>50</sup> Upper limit is estimate.			
<sup>51</sup> 2 $\sigma$ upper limit.			

 $\Gamma(\pi\pi)/\Gamma(4\pi)$   $\Gamma_{12}/\Gamma_1$ 

VALUE	DOCUMENT ID	TECN	COMMENT
••• We do not use the following data for averages, fits, limits, etc. •••			
0.16 ± 0.04	<sup>52,53</sup> ABELE	01B	CBAR 0.0 $\bar{p}n \rightarrow 5\pi$
<sup>52</sup> Using ABELE 97.			
<sup>53</sup> $\omega\pi$ not included.			

 $\Gamma(K\bar{K}^*(892) + c.c.)/\Gamma_{\text{total}}$   $\Gamma_{13}/\Gamma$ 

VALUE	DOCUMENT ID	TECN	COMMENT
••• We do not use the following data for averages, fits, limits, etc. •••			
possibly seen	COAN	04	CLEO $\tau^- \rightarrow K^-\pi^- K^+\nu_\tau$

 $\Gamma(K\bar{K}^*(892) + c.c.)/\Gamma(2(\pi^+\pi^-))$   $\Gamma_{13}/\Gamma_2$ 

VALUE	DOCUMENT ID	TECN	COMMENT
••• We do not use the following data for averages, fits, limits, etc. •••			
0.15 ± 0.03	<sup>54</sup> DEL COURT	81B	DM1 $e^+e^- \rightarrow \bar{K} K \pi$
<sup>54</sup> Assuming $\rho(1700)$ and $\omega$ radial excitations to be degenerate in mass.			

 $\Gamma(\eta\rho)/\Gamma_{\text{total}}$   $\Gamma_{14}/\Gamma$ 

VALUE	CL%	DOCUMENT ID	TECN	COMMENT
••• We do not use the following data for averages, fits, limits, etc. •••				
possibly seen		AKHMETSHIN	00D	CMD2 $e^+e^- \rightarrow \eta\pi^+\pi^-$
<0.04		DONNACHIE	87B	RVUE
<0.02	58	ATKINSON	86B	OMEG 20–70 $\gamma p$

# Meson Particle Listings

## $\rho(1700)$ , $a_2(1700)$

### $\Gamma(\eta\rho)/\Gamma(2\pi^+\pi^-)$ $\Gamma_{14}/\Gamma_2$

VALUE	DOCUMENT ID	TECN	COMMENT
0.123±0.027	DEL COURT 82	DM1	$e^+e^- \rightarrow \pi^+\pi^-MM$
~0.1	ASTON 80	OMEG	20-70 $\gamma\rho$

### $\Gamma(\pi^+\pi^- \text{ neutrals})/\Gamma(2\pi^+\pi^-)$ $(\Gamma_5+\Gamma_6+0.714\Gamma_{14})/\Gamma_2$

VALUE	DOCUMENT ID	TECN	COMMENT
2.6±0.4	<sup>55</sup> BALLAM 74	HBC	9.3 $\gamma\rho$

<sup>55</sup> Upper limit. Background not subtracted.

### $\Gamma(a_2(1320)\pi)/\Gamma_{\text{total}}$ $\Gamma_{15}/\Gamma$

VALUE	DOCUMENT ID	TECN	COMMENT
not seen	AMELIN 00	VES	37 $\pi^-p \rightarrow \eta\pi^+\pi^-n$

### $\Gamma(K\bar{K})/\Gamma(2\pi^+\pi^-)$ $\Gamma_{16}/\Gamma_2$

VALUE	CL%	DOCUMENT ID	TECN	CHG	COMMENT
0.015±0.010		<sup>56</sup> DEL COURT 81B	DM1		$e^+e^- \rightarrow \bar{K}K$
<0.04	95	BINGHAM 72B	HBC	0	9.3 $\gamma\rho$

<sup>56</sup> Assuming  $\rho(1700)$  and  $\omega$  radial excitations to be degenerate in mass.

### $\Gamma(K\bar{K}^*)/\Gamma(K\bar{K}^*(892)+c.c.)$ $\Gamma_{16}/\Gamma_{13}$

VALUE	DOCUMENT ID	TECN	COMMENT
0.052±0.026	BUON 82	DM1	$e^+e^- \rightarrow \text{hadrons}$

### $\Gamma(\pi^0\omega)/\Gamma_{\text{total}}$ $\Gamma_{18}/\Gamma$

VALUE	EVTs	DOCUMENT ID	TECN	COMMENT
not seen	2382	AKHMETSHIN 03B	CMD2	$e^+e^- \rightarrow \pi^0\pi^0\gamma$
seen		ACHASOV 97	RVUE	$e^+e^- \rightarrow \omega\pi^0$

### $\rho(1700)$ REFERENCES

FUJIKAWA 08 PR D78 072006	M. Fujikawa et al. (BELLE Collab.)
COAN 04 PRL 92 232001	T.E. Coan et al. (CLEO Collab.)
FRABETTI 04 PL B578 290	P.L. Frabetti et al. (FNAL E687 Collab.)
AKHMETSHIN 03B PL B562 173	R.R. Akhmetshin et al. (Novosibirsk CMD-2 Collab.)
ABELE 01B EPJ C21 261	A. Abele et al. (Crystal Barrel Collab.)
ACHASOV 001 PL B486 29	M.N. Achasov et al. (Novosibirsk SND Collab.)
AKHMETSHIN 00D PL B489 125	R.R. Akhmetshin et al. (Novosibirsk CMD-2 Collab.)
AMELIN 00 NP A668 83	D. Amelin et al. (VES Collab.)
EDWARDS 00A PR D61 072003	K.W. Edwards et al. (CLEO Collab.)
ABELE 99D PL B468 178	A. Abele et al. (Crystal Barrel Collab.)
ABELE 97 PL B391 191	A. Abele et al. (Crystal Barrel Collab.)
ACHASOV 97 PR D55 2663	N.N. Achasov et al. (NOVM)
BERTIN 97C PL B408 476	A. Bertin et al. (OBELIX Collab.)
CLEGG 94 ZPHY C62 455	A.B. Clegg, A. Donnachie (LANC, MCHS)
CLEGG 90 ZPHY C45 677	A.B. Clegg, A. Donnachie (LANC, MCHS)
BISELLO 89 PL B220 321	D. Bisello et al. (DM2 Collab.)
DUBNICKA 89 JPG 15 1349	S. Dubnicka et al. (JINR, SLOV)
GESHKENBEIN 89 ZPHY C45 351	B.V. Geshkenbein (ITEP)
ANTONELLI 88 PL B212 133	A. Antonelli et al. (DM2 Collab.)
DIEKMANN 88 PRPL 159 99	B. Diekmann (BOHN)
FUKUI 88 PL B202 441	S. Fukui et al. (SUGI, NAGO, KEK, KYOT+)
DONNACHIE 87B ZPHY C34 257	A. Donnachie, A.B. Clegg (MCHS, LANC)
ATKINSON 86B ZPHY C30 531	M. Atkinson et al. (BONN, CERN, GLAS+)
ATKINSON 85B ZPHY C26 499	M. Atkinson et al. (BONN, CERN, GLAS+)
ERKAL 85 ZPHY C29 485	C. Erkal, M.G. Olsson (WIS C)
ABE 84B PRL 53 751	K. Abe et al.
KURDADZE 83 JETPL 37 733	L.M. Kurdadze et al. (NOVO)
Translated from ZETFP 37 613.	
ATKINSON 82 PL 108B 55	M. Atkinson et al. (BONN, CERN, GLAS+)
BUON 82 PL 118B 221	J. Buon et al. (LALO, MONP)
CLELAND 82B NP B208 228	W.E. Cleland et al. (DURH, GEVA, LAUS+)
CORDIER 82 PL 109B 129	A. Cordier et al. (LALO)
DEL COURT 82 PL 113B 93	B. Delcourt et al. (LALO)
ASTON 81E NP B189 15	D. Aston (BONN, CERN, EPOL, GLAS, LAN C+)
DEL COURT 81B Bonn Conf. 205	B. Delcourt (ORSAY)
Also	PL 109B 129
DIBIANCA 81 PR D23 595	F.A. di Bianca et al. (CASE, CMU)
ASTON 80 PL 92B 215	D. Aston (BONN, CERN, EPOL, GLAS, LAN C+)
BACCI 80 PL 95B 139	C. Bacci et al. (ROMA, FRAS)
BIZOT 80 Madison Conf. 546	J.C. Bizot et al. (LALO, MONP)
KILLIAN 80 PR D21 3005	T.J. Killian et al. (CORN)
ATYA 79B PRL 43 1691	M.S. Atiya et al. (COLU, ILL, FNAL)
BECKER 79 NP B151 46	H. Becker et al. (MPIM, CERN, ZEEM, CRAC)
LANG 79 PR D19 956	C.B. Lang, A. Mas-Parada (GRAZ)
MARTIN 78C ANP 114 1	A.D. Martin, M.R. Pennington (CERN)
COSTA... 77B PL 71B 345	B. Costa de Beauregard, B. Pire, T.N. Truong (EPOL)
FROGGATT 77 NP B129 89	C.D. Froggatt, J.L. Petersen (GLAS, NORD)
ALEXANDER 75 PL 57B 487	G. Alexander et al. (TELA)
BALLAM 74 NP B76 375	J. Ballam et al. (SLAC, LBL, MPIM)
CONVERSI 74 PL 52B 493	M. Conversi et al. (ROMA, FRAS)
SCHACHT 74 NP B81 205	P. Schacht et al. (MPIM)
DAVIER 73 NP B58 31	M. Davier et al. (SLAC)
EISENBERG 73 PL 43B 149	Y. Eisenberg et al. (REHO)
HYAMS 73 NP B64 134	B.D. Hyams et al. (CERN, MPIM)
BINGHAM 72B PL 41B 635	H.H. Bingham et al. (LBL, UCB, SLAC)IGJP
JACOB 72 PR D5 1847	M. Jacob, R. Slansky
GOUNARIS 68 PRL 21 244	G.J. Gounaris, J.J. Sakurai

## $a_2(1700)$

$$I^G(J^{PC}) = 1^-(2^{++})$$

OMITTED FROM SUMMARY TABLE

### $a_2(1700)$ MASS

VALUE (MeV)	EVTs	DOCUMENT ID	TECN	CHG	COMMENT
<b>1732±16 OUR AVERAGE</b> Error includes scale factor of 1.9.					
1737±5±7		ABE 04	BELL		10.6 $e^+e^- \rightarrow e^+e^-K^+K^-$
1698±44	1	AMSLER 02	CBAR		0.9 $\bar{p}p \rightarrow \pi^0\eta\eta$
1660±40		ABELE 99B	CBAR		1.94 $\bar{p}p \rightarrow \pi^0\eta\eta$
• • • We do not use the following data for averages, fits, limits, etc. • • •					
1675±25		ANISOVICH 09	RVUE		0.0 $\bar{p}p, \pi N$
1722±9±15	18k	<sup>2</sup> SCHEGELSKY 06	RVUE	0	$\gamma\gamma \rightarrow \pi^+\pi^-\pi^0$
1702±7	80k	<sup>3</sup> UMAN 06	E835		5.2 $\bar{p}p \rightarrow \eta\eta\pi^0$
1721±13±44	145k	LU 05	B852		1.8 $\pi^-p \rightarrow \omega\pi^-\pi^0\rho$
1767±14	221	<sup>4</sup> ACCIARRI 01H	L3		$\gamma\gamma \rightarrow K_S^0 K_S^0, E_{cm}^{ee} = 91, 183-209 \text{ GeV}$
~1775		<sup>5</sup> GRYGOREV 99	SPEC		4.0 $\pi^-p \rightarrow K_S^0 K_S^0 n$
1752±21±4		ACCIARRI 97T	L3		$\gamma\gamma \rightarrow \pi^+\pi^-\pi^0$

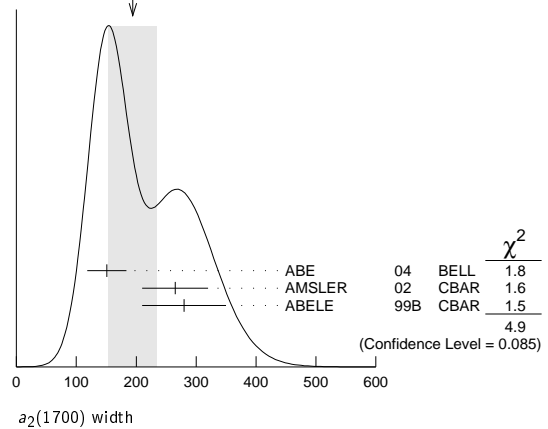
<sup>1</sup> T-matrix pole.  
<sup>2</sup> From analysis of L3 data at 183-209 GeV.  
<sup>3</sup> Statistical error only.  
<sup>4</sup> Spin 2 dominant, isospin not determined, could also be  $I=1$ .  
<sup>5</sup> Possibly two  $J^P = 2^+$  resonances with isospins 0 and 1.

### $a_2(1700)$ WIDTH

VALUE (MeV)	EVTs	DOCUMENT ID	TECN	CHG	COMMENT
<b>194±40 OUR AVERAGE</b> Error includes scale factor of 1.6. See the ideogram below.					
151±22±24		ABE 04	BELL		10.6 $e^+e^- \rightarrow e^+e^-K^+K^-$
265±55	6	AMSLER 02	CBAR		0.9 $\bar{p}p \rightarrow \pi^0\eta\eta$
280±70		ABELE 99B	CBAR		1.94 $\bar{p}p \rightarrow \pi^0\eta\eta$
• • • We do not use the following data for averages, fits, limits, etc. • • •					
270 <sup>+</sup> <sub>-20</sub>		ANISOVICH 09	RVUE		0.0 $\bar{p}p, \pi N$
336±20±20	18k	<sup>7</sup> SCHEGELSKY 06	RVUE	0	$\gamma\gamma \rightarrow \pi^+\pi^-\pi^0$
417±19	80k	<sup>8</sup> UMAN 06	E835		5.2 $\bar{p}p \rightarrow \eta\eta\pi^0$
279±49±66	145k	LU 05	B852		1.8 $\pi^-p \rightarrow \omega\pi^-\pi^0\rho$
187±60	221	<sup>9</sup> ACCIARRI 01H	L3		$\gamma\gamma \rightarrow K_S^0 K_S^0, E_{cm}^{ee} = 91, 183-209 \text{ GeV}$
150±110±34		ACCIARRI 97T	L3		$\gamma\gamma \rightarrow \pi^+\pi^-\pi^0$

<sup>6</sup> T-matrix pole.  
<sup>7</sup> From analysis of L3 data at 183-209 GeV.  
<sup>8</sup> Statistical error only.  
<sup>9</sup> Spin 2 dominant, isospin not determined, could also be  $I=1$ .

WEIGHTED AVERAGE  
194±40 (Error scaled by 1.6)



### $a_2(1700)$ DECAY MODES

Mode	Fraction ( $\Gamma_i/\Gamma$ )
$\Gamma_1$ $\eta\pi$	seen
$\Gamma_2$ $\gamma\gamma$	
$\Gamma_3$ $\rho\pi$	
$\Gamma_4$ $f_2(1270)\pi$	
$\Gamma_5$ $K\bar{K}$	seen
$\Gamma_6$ $\omega\pi^-\pi^0$	seen
$\Gamma_7$ $\omega\rho$	seen

$a_2(1700)$ ,  $f_0(1710)$

$a_2(1700)$  PARTIAL WIDTHS

Table with 5 columns: VALUE (MeV), EVTS, DOCUMENT ID, TECN, COMMENT. Header:  $\Gamma(\eta\pi)$   $\Gamma_1$

••• We do not use the following data for averages, fits, limits, etc. •••
9.5±2.0 870 10 SCHEGELSKY 06A RVUE  $\gamma\gamma \rightarrow K_S^0 K_S^0$

Table with 5 columns: VALUE (keV), EVTS, DOCUMENT ID, TECN, COMMENT. Header:  $\Gamma(\gamma\gamma)$   $\Gamma_2$

••• We do not use the following data for averages, fits, limits, etc. •••
0.30±0.05 870 10 SCHEGELSKY 06A RVUE  $\gamma\gamma \rightarrow K_S^0 K_S^0$

Table with 5 columns: VALUE (MeV), EVTS, DOCUMENT ID, TECN, COMMENT. Header:  $\Gamma(K\bar{K})$   $\Gamma_5$

••• We do not use the following data for averages, fits, limits, etc. •••
5.0±3.0 870 10 SCHEGELSKY 06A RVUE  $\gamma\gamma \rightarrow K_S^0 K_S^0$

10 From analysis of L3 data at 91 and 183–209 GeV, using  $a_2(1700)$  mass of 1730 MeV and width of 340 MeV, and SU(3) relations.

$a_2(1700)$   $\Gamma(i)\Gamma(\gamma\gamma)/\Gamma(\text{total})$

Table with 5 columns: VALUE (keV), EVTS, DOCUMENT ID, TECN, COMMENT. Header:  $[\Gamma(\rho\pi) + \Gamma(f_2(1270)\pi)] \times \Gamma(\gamma\gamma)/\Gamma_{\text{total}}$   $(\Gamma_3 + \Gamma_4)\Gamma_2/\Gamma$

••• We do not use the following data for averages, fits, limits, etc. •••
0.29±0.04±0.02 ACCIARRI 97T L3  $\gamma\gamma \rightarrow \pi^+\pi^-\pi^0$

••• We do not use the following data for averages, fits, limits, etc. •••
0.37 $^{+0.12}_{-0.08}$ ±0.10 18k 11 SCHEGELSKY 06 RVUE  $\gamma\gamma \rightarrow \pi^+\pi^-\pi^0$

Table with 5 columns: VALUE (eV), DOCUMENT ID, TECN, COMMENT. Header:  $\Gamma(K\bar{K}) \times \Gamma(\gamma\gamma)/\Gamma_{\text{total}}$   $\Gamma_5\Gamma_2/\Gamma$

••• We do not use the following data for averages, fits, limits, etc. •••
20.6± 4.2± 4.6 12 ABE 04 BELL 10.6 e<sup>+</sup>e<sup>-</sup> → e<sup>+</sup>e<sup>-</sup>K<sup>+</sup>K<sup>-</sup>

49 ±11 ±13 13 ACCIARRI 01H L3  $\gamma\gamma \rightarrow K_S^0 K_S^0, E_{\text{cm}}^{\text{ee}} = 91, 183\text{--}209 \text{ GeV}$

11 From analysis of L3 data at 183–209 GeV.
12 Assuming spin 2.
13 Spin 2 dominant, isospin not determined, could also be I=1.

$a_2(1700)$  BRANCHING RATIOS

Table with 5 columns: VALUE, EVTS, DOCUMENT ID, TECN, COMMENT. Header:  $\Gamma(\rho\pi)/\Gamma(f_2(1270)\pi)$   $\Gamma_3/\Gamma_4$

••• We do not use the following data for averages, fits, limits, etc. •••
3.4±0.4±0.1 18k 14 SCHEGELSKY 06 RVUE  $\gamma\gamma \rightarrow \pi^+\pi^-\pi^0$

14 From analysis of L3 data at 183–209 GeV.

$a_2(1700)$  REFERENCES

Table with 5 columns: AUTHOR, YEAR, DOCUMENT ID, TECN, COMMENT. Lists references for various experiments and collaborations.

$f_0(1710)$   $I^G(J^{PC}) = 0^+(0^{++})$

See our mini-review in the 2004 edition of this Review, Physics Letters B592 1 (2004). See also the mini-review on scalar mesons under  $f_0(500)$  (see the index for the page number).

$f_0(1710)$  MASS

Table with 5 columns: VALUE (MeV), EVTS, DOCUMENT ID, TECN, COMMENT. Header: 1720±6 OUR AVERAGE

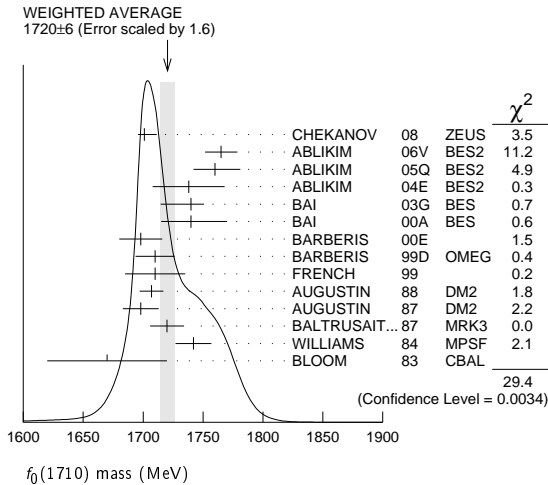
Table with 5 columns: VALUE (MeV), EVTS, DOCUMENT ID, TECN, COMMENT. Lists mass measurements from various experiments.

Table with 5 columns: VALUE, EVTS, DOCUMENT ID, TECN, COMMENT. Lists various meson production and decay channels with associated references.

- 1 In the SU(3) based model with a specific interference pattern of the  $f_2(1270)$ ,  $a_2^0(1320)$ , and  $f_2'(1525)$  mesons incoherently added to the  $f_0(1710)$  and non-resonant background.
2 This state may be different from  $f_0(1710)$ , see CLOSE 05.
3  $J^P = 0^+$ .
4 T-matrix pole.
5 Supersedes BARBERIS 99 and BARBERIS 99b.
6  $J^P = 0^+$ , supersedes by ARMSTRONG 89D.
7 No  $J^{PC}$  determination.
8  $J^P = 2^+$ .
9 Breit-Wigner mass.
10 Systematic errors not estimated.
11 K-matrix pole, assuming  $J^P = 0^+$ , from combined analysis of  $\pi^-\rho \rightarrow \pi^0\pi^0 n$ ,  $\pi^-\rho \rightarrow K\bar{K} n$ ,  $\pi^+\pi^- \rightarrow \pi^+\pi^-$ ,  $\bar{p}p \rightarrow \pi^0\pi^0\pi^0$ ,  $\pi^0\eta\eta$ ,  $\pi^0\pi^0\eta$ ,  $\pi^+\pi^-\pi^0$ ,  $K^+K^-\pi^0$ ,  $K_S^0 K_S^0\pi^0$ ,  $K^+K_S^0\pi^-$  at rest,  $\bar{p}n \rightarrow \pi^-\pi^-\pi^+$ ,  $K_S^0 K^- \pi^0$ ,  $K_S^0 K_S^0\pi^-$  at rest.
12 Decaying to  $f_0(1370)\pi\pi$ .
13  $J^P = 0^+$ .
14 Not seen by AMSLER 02.
15 T-matrix pole, assuming  $J^P = 0^+$ .
16 No  $J^{PC}$  determination.
17 No  $J^{PC}$  determination, width not determined.
18 From a fit to the  $0^+$  partial wave.
19 ALDE 92d combines all the GAMS-2000 data.
20  $J^P = 2^+$ , superseded by FRENCH 99.
21 From an analysis ignoring interference with  $f_2'(1525)$ .
22 From an analysis including interference with  $f_2'(1525)$ .
23 Superseded by ALDE 92d.
24 Uses MRK3 data. From a partial-wave analysis of data using a K-matrix formalism with 5 poles, but assuming spin 2. Fit with constrained inelasticity.
25  $J^P = 2^+$  preferred.
26 From fit neglecting nearby  $f_2'(1525)$ . Replaced by BLOOM 83.
27 Superseded by LONGACRE 86.

# Meson Particle Listings

## $f_0(1710)$



### $f_0(1710)$ WIDTH

VALUE (MeV)	EVTs	DOCUMENT ID	TECN	COMMENT
<b>135 ± 8</b>	<b>OUR AVERAGE</b>	Error includes scale factor of 1.1.		
100 ± 24	+7 -22	4k 28 CHEKANOV 08 ZEUS	$e p \rightarrow K_S^0 K_S^0 X$	
145 ± 8	±69	ABLIKIM 06V BES2	$e^+ e^- \rightarrow J/\psi \rightarrow \gamma \pi^+ \pi^-$	
125 ± 25	+10 -15	29 ABLIKIM 05Q BES2	$\psi(2S) \rightarrow \gamma \pi^+ \pi^- K^+ K^-$	
125 ± 20		ABLIKIM 04E BES2	$J/\psi \rightarrow \omega K^+ K^-$	
166 ± 5	+15 -10	30 BAI 03G BES	$J/\psi \rightarrow \gamma K^+ K^-$	
120 ± 50	-40	30 BAI 00A BES	$J/\psi \rightarrow \gamma (\pi^+ \pi^- \pi^+ \pi^-)$	
120 ± 26		31 BARBERIS 00E	$450 pp \rightarrow p_f \eta \eta p_S$	
126 ± 16	±18	32 BARBERIS 99D OMEG	$450 pp \rightarrow K^+ K^-, \pi^+ \pi^-$	
105 ± 34		33 FRENCH 99	$300 pp \rightarrow p_f (K^+ K^-) p_S$	
166.4 ± 33.2		34 AUGUSTIN 88 DM2	$J/\psi \rightarrow \gamma K^+ K^-, K_S^0 K_S^0$	
136 ± 28		34 AUGUSTIN 87 DM2	$J/\psi \rightarrow \gamma \pi^+ \pi^-$	
130 ± 20		35 BALTRUSAIT... 87 MRK3	$J/\psi \rightarrow \gamma K^+ K^-$	
57 ± 38		36 WILLIAMS 84 MP SF	$200 \pi^- N \rightarrow 2K_S^0 X$	
160 ± 80		BLOOM 83 CBAL	$J/\psi \rightarrow \gamma 2\eta$	
•••		We do not use the following data for averages, fits, limits, etc. •••		
148 ± 40	-30	AMSLER 06 CBAR	$1.64 \bar{p} p \rightarrow K^+ K^- \pi^0$	
188 ± 13		80k 29,37 UMAN 06 E835	$5.2 \bar{p} p \rightarrow \eta \eta \pi^0$	
250 ± 30		VLADIMIRSK... 05 SPEC	$40 \pi^- p \rightarrow K_S^0 K_S^0 n$	
270 ± 60	-30	38 ABLIKIM 05 BES2	$J/\psi \rightarrow \phi \pi^+ \pi^-$	
260 ± 50		29 BINON 05 GAMS	$33 \pi^- p \rightarrow \eta \eta n$	
38 ± 20	-14	74 37 CHEKANOV 04 ZEUS	$e p \rightarrow K_S^0 K_S^0 X$	
144 ± 30		39,40 ANISOVICH 03 RVUE		
320 ± 50	-20	40,41 ANISOVICH 03 RVUE		
102 ± 26		TIKHOIROV 03 SPEC	$40.0 \pi^- C \rightarrow K_S^0 K_S^0 K_L^0 X$	
267 ± 44		3651 30,42 NICHITIU 02 OBLX		
220 ± 40		43,44 ANISOVICH 99B SPEC	$0.6-1.2 p \bar{p} \rightarrow \eta \eta \pi^0$	
100 ± 25		30 BARBERIS 99 OMEG	$450 pp \rightarrow p_S p_f K^+ K^-$	
160 ± 30		30 BARBERIS 99B OMEG	$450 pp \rightarrow p_S p_f \pi^+ \pi^-$	
250 ± 140		45 ANISOVICH 98B RVUE	Compilation	
30 ± 7		57 46 BARKOV 98	$\pi^- p \rightarrow K_S^0 K_S^0 n$	
103 ± 18	+30 -11	35 BAI 96C BES	$J/\psi \rightarrow \gamma K^+ K^-$	
85 ± 24	+22 -19	30 BAI 96C BES	$J/\psi \rightarrow \gamma K^+ K^-$	
56 ± 19		BALOSHIN 95 SPEC	$40 \pi^- C \rightarrow K_S^0 K_S^0 X$	
160 ± 40		47 BUGG 95 MRK3	$J/\psi \rightarrow \gamma \pi^+ \pi^- \pi^+ \pi^-$	
160 ± 60	-20	35 BUGG 95 MRK3	$J/\psi \rightarrow \gamma \pi^+ \pi^- \pi^+ \pi^-$	
264 ± 25		34 ARMSTRONG 93C E760	$\bar{p} p \rightarrow \pi^0 \eta \eta \rightarrow 6\gamma$	
200 to 300		BREAKSTONE 93 SFM	$pp \rightarrow pp \pi^+ \pi^- \pi^+ \pi^-$	
< 80 90% CL		48 ALDE 92D GAM2	$38 \pi^- p \rightarrow \eta \eta N^*$	
181 ± 30		49 ARMSTRONG 89D OMEG	$300 pp \rightarrow pp K^+ K^-$	
104 ± 30		49 ARMSTRONG 89D OMEG	$300 pp \rightarrow pp K_S^0 K_S^0$	
30 ± 20		35 BOLONKIN 88 SPEC	$40 \pi^- p \rightarrow K_S^0 K_S^0 n$	
350 ± 150		30 BOLONKIN 88 SPEC	$40 \pi^- p \rightarrow K_S^0 K_S^0 n$	
148 ± 17		50 FALVARD 88 DM2	$J/\psi \rightarrow \phi K^+ K^-, K_S^0 K_S^0$	
184 ± 6		51 FALVARD 88 DM2	$J/\psi \rightarrow \phi K^+ K^-, K_S^0 K_S^0$	
122 ± 74	-15	52 LONGACRE 86 RVUE	$22 \pi^- p \rightarrow n 2K_S^0$	
200 ± 100		BURKE 82 MRK2	$J/\psi \rightarrow \gamma 2\rho$	

- 220  $+100$   
 $-70$  53,54 EDWARDS 82D CBAL  $J/\psi \rightarrow \gamma 2\eta$
- 200  $+156$   
 $-9$  55 ETKIN 82B MPS  $23 \pi^- p \rightarrow n 2K_S^0$
- 28 In the SU(3) based model with a specific interference pattern of the  $f_2(1270)$ ,  $a_2^0(1320)$ , and  $f_2'(1525)$  mesons incoherently added to the  $f_0(1710)$  and non-resonant background.
- 29 Breit-Wigner width.
- 30  $J^P = 0^+$ .
- 31 T-matrix pole.
- 32 Supersedes BARBERIS 99 and BARBERIS 99b.
- 33  $J^P = 0^+$ , superseded by ARMSTRONG 89D.
- 34 No  $J^{PC}$  determination.
- 35  $J^P = 2^+$ .
- 36 No  $J^{PC}$  determination.
- 37 Systematic errors not estimated.
- 38 This state may be different from  $f_0(1710)$ , see CLOSE 05.
- 39 (Solution I)
- 40 K-matrix pole, assuming  $J^P = 0^+$ , from combined analysis of  $\pi^- p \rightarrow \pi^0 \pi^0 n$ ,  $\pi^- p \rightarrow K^+ K^- n$ ,  $\pi^+ \pi^- \rightarrow \pi^+ \pi^-$ ,  $\bar{p} p \rightarrow \pi^0 \pi^0 \pi^0$ ,  $\pi^0 \eta \eta$ ,  $\pi^0 \pi^0 \eta$ ,  $\pi^+ \pi^- \pi^0$ ,  $K^+ K^- \pi^0$ ,  $K_S^0 K_S^0 \pi^0$ ,  $K^+ K_S^0 \pi^-$  at rest,  $\bar{p} n \rightarrow \pi^- \pi^- \pi^+$ ,  $K_S^0 K^- \pi^0$ ,  $K_S^0 K_S^0 \pi^-$  at rest.
- 41 (Solution I)
- 42 Decaying to  $f_0(1370) \pi \pi$ .
- 43  $J^P = 0^+$ .
- 44 Not seen by AMSLER 02.
- 45 T-matrix pole, assuming  $J^P = 0^+$
- 46 No  $J^{PC}$  determination.
- 47 From a fit to the  $0^+$  partial wave.
- 48 ALDE 92D combines all the GAMS-2000 data.
- 49  $J^P = 2^+$ , ( $0^+$  excluded).
- 50 From an analysis ignoring interference with  $f_2'(1525)$ .
- 51 From an analysis including interference with  $f_2'(1525)$ .
- 52 Uses MRK3 data. From a partial-wave analysis of data using a K-matrix formalism with 5 poles, but assuming spin 2. Fit with constrained inelasticity.
- 53  $J^P = 2^+$  preferred.
- 54 From fit neglecting nearby  $f_2'(1525)$ . Replaced by BLOOM 83.
- 55 From an amplitude analysis of the  $K_S^0 K_S^0$  system, superseded by LONGACRE 86.

### $f_0(1710)$ DECAY MODES

Mode	Fraction ( $\Gamma_i/\Gamma$ )
$\Gamma_1$ $K^+ K^-$	seen
$\Gamma_2$ $\eta \eta$	seen
$\Gamma_3$ $\pi \pi$	seen
$\Gamma_4$ $\gamma \gamma$	
$\Gamma_5$ $\omega \omega$	seen

### $f_0(1710)$ $\Gamma(\eta\eta)/\Gamma(\text{total})$

VALUE (eV)	CL%	DOCUMENT ID	TECN	COMMENT	$\Gamma_1 \Gamma_4 / \Gamma$
<b>&lt;110</b>	95	56 BEHREND 89c	CELL	$\gamma \gamma \rightarrow K_S^0 K_S^0$	
•••		We do not use the following data for averages, fits, limits, etc. •••			
<480	95	ALBRECHT 90G	ARG	$\gamma \gamma \rightarrow K^+ K^-$	
<280	95	56 ALTHOFF 85B	TASS	$\gamma \gamma \rightarrow K^+ K^- \pi$	
56		Assuming helicity 2.			

VALUE (keV)	CL%	DOCUMENT ID	TECN	COMMENT	$\Gamma_3 \Gamma_4 / \Gamma$
<b>&lt;0.82</b>	95	57 BARATE 00E	ALEP	$\gamma \gamma \rightarrow \pi^+ \pi^-$	
57		Assuming spin 0.			

### $f_0(1710)$ BRANCHING RATIOS

VALUE	DOCUMENT ID	TECN	COMMENT	$\Gamma_1/\Gamma$
•••		We do not use the following data for averages, fits, limits, etc. •••		
0.36 ± 0.12	ALBALADEJO 08	RVUE		
0.38 $^{+0.09}$ $-0.19$	58,59 LONGACRE 86	MPS	$22 \pi^- p \rightarrow n 2K_S^0$	
$\Gamma(\eta\eta)/\Gamma_{\text{total}}$				$\Gamma_2/\Gamma$
VALUE	DOCUMENT ID	TECN	COMMENT	
•••		We do not use the following data for averages, fits, limits, etc. •••		
0.22 ± 0.12	ALBALADEJO 08	RVUE		
0.18 $^{+0.03}$ $-0.13$	58,59 LONGACRE 86	RVUE		
$\Gamma(\pi\pi)/\Gamma_{\text{total}}$				$\Gamma_3/\Gamma$
VALUE	DOCUMENT ID	TECN	COMMENT	
•••		We do not use the following data for averages, fits, limits, etc. •••		
not seen	AMSLER 02	CBAR	$0.9 \bar{p} p \rightarrow \pi^0 \eta \eta, \pi^0 \pi^0 \pi^0$	
0.039 $^{+0.002}$ $-0.024$	58,59 LONGACRE 86	RVUE		



See key on page 457

Meson Particle Listings  
 $f_0(1710), \eta(1760), \pi(1800)$  $\Gamma(\pi\pi)/\Gamma(K\bar{K})$   $\Gamma_3/\Gamma_1$ 

VALUE	CL%	DOCUMENT ID	TECN	COMMENT
$0.41 \pm 0.11$ $-0.17$		ABLIKIM	06v BES2	$e^+e^- \rightarrow J/\psi \rightarrow \gamma\pi^+\pi^-$
• • • We do not use the following data for averages, fits, limits, etc. • • •				
0.32±0.14		ALBALADEJO	08 RVUE	
< 0.11	95	<sup>60</sup> ABLIKIM	04E BES2	$J/\psi \rightarrow \omega K^+K^-$
$5.8 \pm 9.1$ $-5.5$		<sup>61</sup> ANISOVICH	02D SPEC	Combined fit
0.2 ± 0.024 ± 0.036		BARBERIS	99D OMEG	450 $\rho\rho \rightarrow K^+K^-, \pi^+\pi^-$
0.39±0.14		ARMSTRONG	91 OMEG	300 $\rho\rho \rightarrow \rho\rho\pi\pi, \rho\rho K\bar{K}$

 $\Gamma(\eta\eta)/\Gamma(K\bar{K})$   $\Gamma_2/\Gamma_1$ 

VALUE	CL%	DOCUMENT ID	TECN	COMMENT
$0.48 \pm 0.15$		BARBERIS	00E	450 $\rho\rho \rightarrow \rho_f\eta\eta\rho_s$
• • • We do not use the following data for averages, fits, limits, etc. • • •				
$0.46 \pm 0.70$ $-0.38$		<sup>61</sup> ANISOVICH	02D SPEC	Combined fit
< 0.02	90	<sup>62</sup> PROKOSHKIN	91 GA24	300 $\pi^-\rho \rightarrow \pi^-\rho\eta\eta$

 $\Gamma(\omega\omega)/\Gamma_{\text{total}}$   $\Gamma_5/\Gamma$ 

VALUE	EVTS	DOCUMENT ID	TECN	COMMENT
seen	180	ABLIKIM	06H BES	$J/\psi \rightarrow \gamma\omega\omega$

<sup>58</sup> From a partial-wave analysis of data using a K-matrix formalism with 5 poles, but assuming spin 2.<sup>59</sup> Fit with constrained inelasticity.<sup>60</sup> Using data from ABLIKIM 04A.<sup>61</sup> From a combined K-matrix analysis of Crystal Barrel ( $0. \rho\bar{\rho} \rightarrow \pi^0\pi^0\pi^0, \pi^0\eta\eta, \pi^0\pi^0\eta$ ), GAMS ( $\pi\rho \rightarrow \pi^0\pi^0n, \eta\eta n, \eta\eta'n$ ), and BNL ( $\pi\rho \rightarrow K\bar{K}n$ ) data.<sup>62</sup> Combining results of GAM4 with those of ARMSTRONG 89D. $f_0(1710)$  REFERENCES

ALBALADEJO	08	PRL 101 252002	M. Albaladejo, J.A. Oller	
CHEKANOV	08	PRL 101 112003	S. Chekanov et al.	(ZEUS Collab.)
ABLIKIM	06H	PR D73 112007	M. Ablikim et al.	(BES Collab.)
ABLIKIM	06V	PL B642 441	M. Ablikim et al.	(BES Collab.)
AMSLER	06	PL B639 165	C. Amisler et al.	(CBAR Collab.)
UMAN	06	PR D73 052009	I. Uman et al.	(FNAL E835)
VLADIMIRSK...	06	PAN 69 493	V.V. Vladimirov et al.	(ITEP, Moscow)
ABLIKIM	05	PL B607 243	M. Ablikim et al.	(BES Collab.)
ABLIKIM	05Q	PR D72 092002	M. Ablikim et al.	(BES Collab.)
BINON	05	PAN 68 960	F. Binon et al.	
CLOSE	05	PR D71 094022	F.E. Close, Q. Zhao	
ABLIKIM	04A	PL B598 149	M. Ablikim et al.	(BES Collab.)
ABLIKIM	04E	PL B603 138	M. Ablikim et al.	(BES Collab.)
CHEKANOV	04	PL B578 33	S. Chekanov et al.	(ZEUS Collab.)
PDG	04	PL B592 1	S. Eidelman et al.	(PDG Collab.)
ANISOVICH	03	EPJ A16 229	V.V. Anisovich et al.	(BES Collab.)
BAI	03G	PR D68 052003	J.Z. Bai et al.	
TIKHOMIROV	03	PAN 66 828	G.D. Tikhomirov et al.	
AMSLER	02	EPJ C23 29	C. Amisler et al.	
ANISOVICH	02D	PAN 65 1545	V.V. Anisovich et al.	
NICHITIU	02	PL B545 261	F. Nichitiu et al.	(OBELIX Collab.)
BAI	00A	PL B472 207	J.Z. Bai et al.	(BES Collab.)
BARATE	00E	PL B472 189	R. Barate et al.	(ALEPH Collab.)
BARBERIS	00E	PL B479 59	D. Barberis et al.	(WA 102 Collab.)
ANISOVICH	99B	PL B449 154	A.V. Anisovich et al.	
BARBERIS	99	PL B453 305	D. Barberis et al.	(Omega Expt.)
BARBERIS	99B	PL B453 316	D. Barberis et al.	(Omega Expt.)
BARBERIS	99D	PL B462 462	D. Barberis et al.	(Omega Expt.)
FRENCH	99	PL B460 213	B. French et al.	(WA76 Collab.)
ANISOVICH	98B	SPU 41 419	V.V. Anisovich et al.	
BAI	98H	PRL 81 1179	J.Z. Bai et al.	(BES Collab.)
BARKOV	98	JETPL 68 764	B.P. Barkov et al.	
ABREU	96C	PL B379 309	P. Abreu et al.	(DELPHI Collab.)
BAI	96C	PRL 77 3959	J.Z. Bai et al.	(BES Collab.)
BALOSHIN	95	PAN 58 46	O.N. Baloshin et al.	(ITEP)
BUGG	95	PL B353 378	D.V. Bugg et al.	(LOQM, PNPI, WASH)
ARMSTRONG	93C	PL B307 394	T.A. Armstrong et al.	(FNAL, FERR, GENO+)
BREAKSTONE	93	ZPHY C58 251	A.M. Breakstone et al.	(IOWA, CERN, DORT+)
ALDE	92D	PL B284 457	D.M. Alde et al.	(GAM2 Collab.)
		SJNP 54 451	D.M. Alde et al.	(GAM2 Collab.)
ARMSTRONG	91	ZPHY C51 351	T.A. Armstrong et al.	(ATHU, BARI, BIRM+)
PROKOSHKIN	91	SPD 36 155	Y.D. Prokoshkin	(GAM2, GAM4 Collab.)
ALBRECHT	90G	ZPHY C48 183	H. Albrecht et al.	(ARGUS Collab.)
ARMSTRONG	89D	PL B227 186	T.A. Armstrong, M. Benayoun	(ATHU, BARI, BIRM+)
BEHREND	89C	ZPHY C43 91	H.J. Behrend et al.	(CELLO Collab.)
AUGUSTIN	88	PRL 60 2238	J.E. Augustin et al.	(DM2 Collab.)
BOLONKIN	88	NP B309 426	B.V. Bolonkin et al.	(ITEP, SERP)
FALVARD	88	PR D38 2706	A. Falvard et al.	(CLER, FRAS, LALO+)
AUGUSTIN	87	ZPHY C36 369	J.E. Augustin et al.	(LALO, CLER, FRAS+)
BALTRUSAITIS	87	PR D35 2077	R.M. Baltrusaitis et al.	(Mark III Collab.)
ALDE	86C	PL B182 105	D.M. Alde et al.	(SERP, BELG, LANL, LAPP)
LONGACRE	86	PL B177 223	R.S. Longacre et al.	(BNL, BRAN, CUNY+)
ALTHOFF	85B	ZPHY C29 189	M. Althoff et al.	(TASSO Collab.)
WILLIAMS	84	PR D30 877	E.G.H. Williams et al.	(VAND, NDAM, TUFTS+)
BLOOM	83	ARNS 33 143	E.D. Bloom, C. Peck	(SLAC, CIT)
BURKE	82	PRL 49 632	D.L. Burke et al.	(LBL, SLAC)
EDWARDS	82D	PRL 48 458	C. Edwards et al.	(CIT, HARV, PRIN+)
ETKIN	82B	PR D25 1786	A. Etkin et al.	(BNL, CUNY, TUFTS, VAND)
ETKIN	82C	PR D25 2446	A. Etkin et al.	(BNL, CUNY, TUFTS, VAND)

 $\eta(1760)$ 

$I^G(J^{PC}) = 0^+(0^{-+})$

OMITTED FROM SUMMARY TABLE

Seen by DM2 in the  $\rho\rho$  system (BISELLO 89B). Structure in this region has been reported before in the same system (BALTRUSAITIS 86B) and in the  $\omega\omega$  system (BALTRUSAITIS 85C, BISELLO 87). $\eta(1760)$  MASS

VALUE (MeV)	EVTS	DOCUMENT ID	TECN	COMMENT
<b>1756± 9 OUR AVERAGE</b>				
1744±10±15	1045	<sup>1</sup> ABLIKIM	06H BES	$J/\psi \rightarrow \gamma\omega\omega$
1760±11	320	<sup>2</sup> BISELLO	89B DM2	$J/\psi \rightarrow 4\pi\gamma$

<sup>1</sup> From a partial wave analysis including  $\eta(1760)$ ,  $f_0(1710)$ ,  $f_2(1640)$ , and  $f_2(1910)$ .<sup>2</sup> Estimated by us from various fits. $\eta(1760)$  WIDTH

VALUE (MeV)	EVTS	DOCUMENT ID	TECN	COMMENT
<b>96±70 OUR AVERAGE</b>				Error includes scale factor of 5.1.
$244 \pm 24$ $-21 \pm 25$	1045	<sup>3</sup> ABLIKIM	06H BES	$J/\psi \rightarrow \gamma\omega\omega$
60±16	320	<sup>4</sup> BISELLO	89B DM2	$J/\psi \rightarrow 4\pi\gamma$

<sup>3</sup> From a partial wave analysis including  $\eta(1760)$ ,  $f_0(1710)$ ,  $f_2(1640)$ , and  $f_2(1910)$ .<sup>4</sup> Estimated by us from various fits. $\eta(1760)$  REFERENCES

ABLIKIM	06H	PR D73 112007	M. Ablikim et al.	(BES Collab.)
BISELLO	89B	PR D39 701	G. Busetto et al.	(DM2 Collab.)
BISELLO	87	PL B192 239	D. Bisello et al.	(PADO, CLER, FRAS+)
BALTRUSAITIS...	86B	PR D33 1222	R.M. Baltrusaitis et al.	(Mark III Collab.)
BALTRUSAITIS...	85C	PRL 55 1723	R.M. Baltrusaitis et al.	(CIT, UCS C+)

 $\pi(1800)$ 

$I^G(J^{PC}) = 1^-(0^{-+})$

See also minireview under non- $q\bar{q}$  candidates in PDG 06, Journal of Physics, G **33** 1 (2006). $\pi(1800)$  MASS

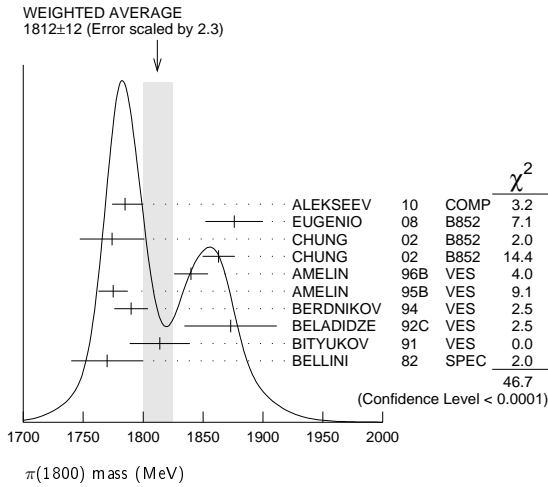
VALUE (MeV)	EVTS	DOCUMENT ID	TECN	CHG	COMMENT
<b>1812±12 OUR AVERAGE</b>					Error includes scale factor of 2.3. See the ideogram below.
$1785 \pm 9 \pm 12$ $-6$	420k	ALEKSEEV	10 COMP		$190 \pi^- Pb \rightarrow \pi^- \pi^+ \pi^+ Pb'$
1876±18±16	4k	<sup>1</sup> EUGENIO	08 B852	-	$18 \pi^- p \rightarrow \eta\eta\pi^- p$
1774±18±20		<sup>2</sup> CHUNG	02 B852		$18.3 \pi^- p \rightarrow \pi^+ \pi^- \pi^- p$
1863± 9±10		<sup>3</sup> CHUNG	02 B852		$18.3 \pi^- p \rightarrow \pi^+ \pi^- \pi^- p$
1840±10±10	1200	AMELIN	96B VES	-	$37 \pi^- A \rightarrow \eta\eta\pi^- A$
1775± 7±10		<sup>4</sup> AMELIN	95B VES	-	$36 \pi^- A \rightarrow \pi^+ \pi^- \pi^- A$
1790±14		<sup>5</sup> BERDNIKOV	94 VES	-	$37 \pi^- A \rightarrow K^+ K^- \pi^- A$
1873±33±20		BELADIDZE	92C VES	-	$36 \pi^- Be \rightarrow \pi^- \eta' \eta Be$
1814±10±23 426±57		BITYUKOV	91 VES	-	$36 \pi^- C \rightarrow \pi^- \eta\eta C$
1770±30	1100	BELLINI	82 SPEC	-	$40 \pi^- A \rightarrow 3\pi A$

• • • We do not use the following data for averages, fits, limits, etc. • • •

1737± 5±15 AMELIN 99 VES  $37 \pi^- A \rightarrow \omega\pi^-\pi^0 A^*$ <sup>1</sup> From a single-pole fit.<sup>2</sup> In the  $f_0(980)\pi$  wave.<sup>3</sup> In the  $f_0(500)\pi$  wave.<sup>4</sup> From a fit to  $J^{PC} = 0^{-+} f_0(980)\pi, f_0(1370)\pi$  waves.<sup>5</sup> From a fit to  $J^{PC} = 0^{-+} K_0^*(1430)K^-, f_0(980)\pi^-$  waves.

# Meson Particle Listings

## $\pi(1800)$



### $\pi(1800)$ WIDTH

VALUE (MeV)	EVTs	DOCUMENT ID	TECN	CHG	COMMENT
<b>208±12 OUR AVERAGE</b>					
208±22 <sup>+21</sup> <sub>-37</sub>	420k	ALEKSEEV	10	COMP	190 $\pi^- Pb \rightarrow \pi^- \pi^- \pi^+ Pb'$
221±26±38	4k	<sup>6</sup> EUGENIO	08	B852	- 18 $\pi^- p \rightarrow \eta \eta \pi^- p$
223±48±50		<sup>7</sup> CHUNG	02	B852	18.3 $\pi^- p \rightarrow \pi^+ \pi^- \pi^- p$
191±21±20		<sup>8</sup> CHUNG	02	B852	18.3 $\pi^- p \rightarrow \pi^+ \pi^- \pi^- p$
210±30±30	1200	AMELIN	96B	VES	- 37 $\pi^- A \rightarrow \eta \eta \pi^- A$
190±15±15		<sup>9</sup> AMELIN	95B	VES	- 36 $\pi^- A \rightarrow \pi^+ \pi^- \pi^- A$
210±70		<sup>10</sup> BERDNIKOV	94	VES	- 37 $\pi^- A \rightarrow K^+ K^- \pi^- A$
225±35±20		BELADIDZE	92C	VES	- 36 $\pi^- Be \rightarrow \pi^- \eta' \eta Be$
205±18±32	426 ± 57	BITYUKOV	91	VES	- 36 $\pi^- C \rightarrow \pi^- \eta \eta C$
310±50	1100	BELLINI	82	SPEC	- 40 $\pi^- A \rightarrow 3\pi A$
• • • We do not use the following data for averages, fits, limits, etc. • • •					
259±19±6		AMELIN	99	VES	37 $\pi^- A \rightarrow \omega \pi^- \pi^0 A^*$

<sup>6</sup> From a single-pole fit.  
<sup>7</sup> In the  $f_0(980) \pi$  wave.  
<sup>8</sup> In the  $f_0(500) \pi$  wave.  
<sup>9</sup> From a fit to  $J^{PC} = 0^{-+} f_0(980) \pi, f_0(1370) \pi$  waves.  
<sup>10</sup> From a fit to  $J^{PC} = 0^{-+} K_0^*(1430) K^-$  and  $f_0(980) \pi^-$  waves.

### $\pi(1800)$ DECAY MODES

Mode	Fraction ( $\Gamma_i/\Gamma$ )
$\Gamma_1$ $\pi^+ \pi^- \pi^-$	seen
$\Gamma_2$ $f_0(500) \pi^-$	seen
$\Gamma_3$ $f_0(980) \pi^-$	seen
$\Gamma_4$ $f_0(1370) \pi^-$	seen
$\Gamma_5$ $f_0(1500) \pi^-$	not seen
$\Gamma_6$ $\rho \pi^-$	not seen
$\Gamma_7$ $\eta \eta \pi^-$	seen
$\Gamma_8$ $a_0(980) \eta$	seen
$\Gamma_9$ $a_2(1320) \eta$	not seen
$\Gamma_{10}$ $f_2(1270) \pi$	not seen
$\Gamma_{11}$ $f_0(1370) \pi^-$	not seen
$\Gamma_{12}$ $f_0(1500) \pi^-$	seen
$\Gamma_{13}$ $\eta \eta' (958) \pi^-$	seen
$\Gamma_{14}$ $K_0^*(1430) K^-$	seen
$\Gamma_{15}$ $K^*(892) K^-$	not seen

### $\pi(1800)$ BRANCHING RATIOS

$\Gamma(f_0(980) \pi^-) / \Gamma(f_0(500) \pi^-)$		$\Gamma_3 / \Gamma_2$		
VALUE	DOCUMENT ID	TECN	COMMENT	
<b>0.44±0.08±0.38</b>	<sup>11</sup> CHUNG	02	B852 18.3 $\pi^- p \rightarrow \pi^+ \pi^- \pi^- p$	
$\Gamma(f_0(980) \pi^-) / \Gamma(f_0(1370) \pi^-)$		$\Gamma_3 / \Gamma_4$		
VALUE	DOCUMENT ID	TECN	CHG	COMMENT
• • • We do not use the following data for averages, fits, limits, etc. • • •				
1.7±1.3	<sup>12</sup> AMELIN	95B	VES	- 36 $\pi^- A \rightarrow \pi^+ \pi^- \pi^- A$

$\Gamma(f_0(1370) \pi^-) / \Gamma_{total}$		$\Gamma_4 / \Gamma$		
VALUE	DOCUMENT ID	TECN	CHG	COMMENT
seen	BELLINI	82	SPEC	- 40 $\pi^- A \rightarrow 3\pi A$

$\Gamma(f_0(1500) \pi^-) / \Gamma_{total}$		$\Gamma_5 / \Gamma$	
VALUE	DOCUMENT ID	TECN	COMMENT
not seen	CHUNG	02	B852 18.3 $\pi^- p \rightarrow \pi^+ \pi^- \pi^- p$

$\Gamma(\rho \pi^-) / \Gamma_{total}$		$\Gamma_6 / \Gamma$		
VALUE	DOCUMENT ID	TECN	CHG	COMMENT
not seen	BELLINI	82	SPEC	- 40 $\pi^- A \rightarrow 3\pi A$

$\Gamma(\rho \pi^-) / \Gamma(f_0(980) \pi^-)$		$\Gamma_6 / \Gamma_3$			
VALUE	CL%	DOCUMENT ID	TECN	CHG	COMMENT
• • • We do not use the following data for averages, fits, limits, etc. • • •					
<0.25		CHUNG	02	B852	18.3 $\pi^- p \rightarrow \pi^+ \pi^- \pi^- p$
<0.14	90	AMELIN	95B	VES	- 36 $\pi^- A \rightarrow \pi^+ \pi^- \pi^- A$

$\Gamma(\eta \eta \pi^-) / \Gamma(\pi^+ \pi^- \pi^-)$		$\Gamma_7 / \Gamma_1$			
VALUE	EVTs	DOCUMENT ID	TECN	CHG	COMMENT
• • • We do not use the following data for averages, fits, limits, etc. • • •					
0.5±0.1	1200	<sup>12</sup> AMELIN	96B	VES	- 37 $\pi^- A \rightarrow \eta \eta \pi^- A$

$\Gamma(a_2(1320) \eta) / \Gamma_{total}$		$\Gamma_9 / \Gamma$	
VALUE	DOCUMENT ID	TECN	COMMENT
not seen	EUGENIO	08	B852 18 $\pi^- p \rightarrow \eta \eta \pi^- p$

$\Gamma(f_2(1270) \pi) / \Gamma_{total}$		$\Gamma_{10} / \Gamma$	
VALUE	DOCUMENT ID	TECN	COMMENT
not seen	EUGENIO	08	B852 18 $\pi^- p \rightarrow \eta \eta \pi^- p$

$\Gamma(f_0(1370) \pi^-) / \Gamma_{total}$		$\Gamma_{11} / \Gamma$	
VALUE	DOCUMENT ID	TECN	COMMENT
not seen	EUGENIO	08	B852 18 $\pi^- p \rightarrow \eta \eta \pi^- p$

$\Gamma(f_0(1500) \pi^-) / \Gamma(a_0(980) \eta)$		$\Gamma_{12} / \Gamma_8$			
VALUE	EVTs	DOCUMENT ID	TECN	CHG	COMMENT
• • • We do not use the following data for averages, fits, limits, etc. • • •					
0.48 ± 0.17	4k	<sup>12,13</sup> EUGENIO	08	B852	- 18 $\pi^- p \rightarrow \eta \eta \pi^- p$
0.030 <sup>+0.014</sup> <sub>-0.011</sub>		<sup>12</sup> ANISOVICH	01B	SPEC	0 0.6-1.94 $p \bar{p} \rightarrow \eta \eta \pi^0 \pi^0$
0.08 ± 0.03	1200	<sup>12,14</sup> AMELIN	96B	VES	- 37 $\pi^- A \rightarrow \eta \eta \pi^- A$

$\Gamma(\eta \eta' (958) \pi^-) / \Gamma(\eta \eta \pi^-)$		$\Gamma_{13} / \Gamma_7$			
VALUE	EVTs	DOCUMENT ID	TECN	CHG	COMMENT
• • • We do not use the following data for averages, fits, limits, etc. • • •					
0.29±0.07		<sup>12</sup> BELADIDZE	92c	VES	- 36 $\pi^- Be \rightarrow \pi^- \eta' \eta Be$
0.3 ± 0.1	426 ± 57	<sup>12</sup> BITYUKOV	91	VES	- 36 $\pi^- C \rightarrow \pi^- \eta \eta C$

$\Gamma(K_0^*(1430) K^-) / \Gamma_{total}$		$\Gamma_{14} / \Gamma$		
VALUE	DOCUMENT ID	TECN	CHG	COMMENT
seen	BERDNIKOV	94	VES	- 37 $\pi^- A \rightarrow K^+ K^- \pi^- A$

$\Gamma(K^*(892) K^-) / \Gamma_{total}$		$\Gamma_{15} / \Gamma$		
VALUE	DOCUMENT ID	TECN	CHG	COMMENT
not seen	BERDNIKOV	94	VES	- 37 $\pi^- A \rightarrow K^+ K^- \pi^- A$

<sup>11</sup> Assuming that  $f_0(980)$  decays only to  $\pi \pi$ .  
<sup>12</sup> Systematic errors not estimated.  
<sup>13</sup> From a single-pole fit.  
<sup>14</sup> Assuming that  $f_0(1500)$  decays only to  $\eta \eta$  and  $a_0(980)$  decays only to  $\eta \pi$ .

### $\pi(1800)$ REFERENCES

ALEKSEEV	10	PRL 104 241803	M.G. Alekseev et al.	(COMPASS Collab.)
EUGENIO	08	PL B660 466	P. Eugenio et al.	(BNL E852 Collab.)
PDG	06	JPG 33 1	W.-M. Yao et al.	(PDG Collab.)
CHUNG	02	PR D55 072001	S.U. Chung et al.	(BNL E852 Collab.)
ANISOVICH	01B	PL B500 222	A.V. Anisovich et al.	
AMELIN	99	PAN 62 445	D.V. Amelin et al.	(VES Collab.)
		Translated from YAF 62 487.		
AMELIN	96B	PAN 59 976	D.V. Amelin et al.	(SERP, TBIL)IGJPC
		Translated from YAF 59 1021.		
AMELIN	95B	PL B356 595	D.V. Amelin et al.	(SERP, TBIL)
BERDNIKOV	94	PL B337 219	E.B. Berdnikov et al.	(SERP, TBIL)
BELADIDZE	92C	SJNP 55 1535	G.M. Beladidze, S.I. Bityukov, G.V. Borisov	(SERP+)
		Translated from YAF 55 2748.		
BITYUKOV	91	PL B268 137	S.I. Bityukov et al.	(SERP, TBIL)
BELLINI	82	PRL 48 1697	G. Bellini et al.	(MILA, BGNA, JINR)

$f_2(1810)$ 

$$I^G(J^{PC}) = 0^+(2^{++})$$

OMITTED FROM SUMMARY TABLE  
Needs confirmation.

 $f_2(1810)$  MASS

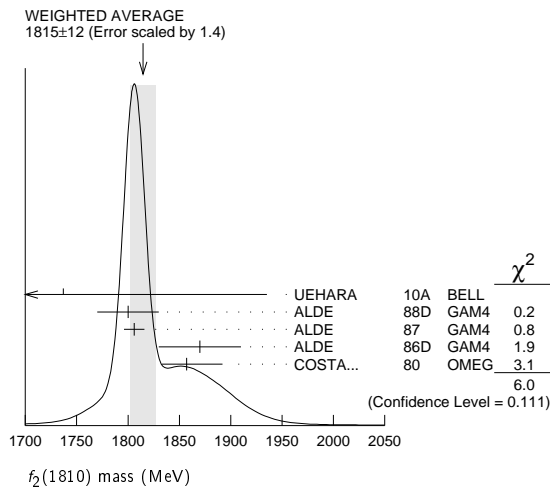
VALUE (MeV)	EVTs	DOCUMENT ID	TECN	COMMENT
<b>1815 ± 12 OUR AVERAGE</b>		Error includes scale factor of 1.4. See the ideogram below.		
1737 ± 9 <sup>+198</sup> <sub>-65</sub>		1 UEHARA	10A BELL	10.6 e <sup>+</sup> e <sup>-</sup> → e <sup>+</sup> e <sup>-</sup> ηη
1800 ± 30	40	ALDE	88D GAM4	300 π <sup>-</sup> p → π <sup>-</sup> p4π <sup>0</sup>
1806 ± 10	1600	ALDE	87 GAM4	100 π <sup>-</sup> p → 4π <sup>0</sup> n
1870 ± 40		2 ALDE	86D GAM4	100 π <sup>-</sup> p → ηηn
1857 ± 35 <sub>-24</sub>		3 COSTA...	80 OMEG	10 π <sup>-</sup> p → K <sup>+</sup> K <sup>-</sup> n
• • • We do not use the following data for averages, fits, limits, etc. • • •				
1858 ± 18 <sub>-71</sub>		4 LONGACRE	86 RVUE	Compilation
1799 ± 15		5 CASON	82 STRC	8 π <sup>+</sup> p → Δ <sup>++</sup> π <sup>0</sup> π <sup>0</sup>

1 Breit-Wigner mass.

2 Seen in only one solution.

3 Error increased by spread of two solutions. Included in LONGACRE 86 global analysis.

4 From a partial-wave analysis of data using a K-matrix formalism with 5 poles. Includes compilation of several other experiments.

5 From an amplitude analysis of the reaction π<sup>+</sup>π<sup>-</sup> → 2π<sup>0</sup>. The resonance in the 2π<sup>0</sup> final state is not confirmed by PROKOSHKIN 97. $f_2(1810)$  WIDTH

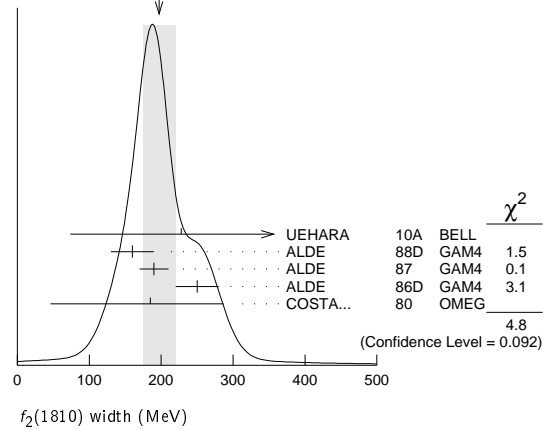
VALUE (MeV)	EVTs	DOCUMENT ID	TECN	COMMENT
<b>197 ± 22 OUR AVERAGE</b>		Error includes scale factor of 1.5. See the ideogram below.		
228 <sup>+21+234</sup> <sub>-20-153</sub>		6 UEHARA	10A BELL	10.6 e <sup>+</sup> e <sup>-</sup> → e <sup>+</sup> e <sup>-</sup> ηη
160 ± 30	40	ALDE	88D GAM4	300 π <sup>-</sup> p → π <sup>-</sup> p4π <sup>0</sup>
190 ± 20	1600	ALDE	87 GAM4	100 π <sup>-</sup> p → 4π <sup>0</sup> n
250 ± 30		7 ALDE	86D GAM4	100 π <sup>-</sup> p → ηηn
185 ± 102 <sub>-139</sub>		8 COSTA...	80 OMEG	10 π <sup>-</sup> p → K <sup>+</sup> K <sup>-</sup> n
• • • We do not use the following data for averages, fits, limits, etc. • • •				
388 ± 15 <sub>-21</sub>		9 LONGACRE	86 RVUE	Compilation
280 ± 42 <sub>-35</sub>		10 CASON	82 STRC	8 π <sup>+</sup> p → Δ <sup>++</sup> π <sup>0</sup> π <sup>0</sup>

6 Breit-Wigner width.

7 Seen in only one solution.

8 Error increased by spread of two solutions. Included in LONGACRE 86 global analysis.

9 From a partial-wave analysis of data using a K-matrix formalism with 5 poles. Includes compilation of several other experiments.

10 From an amplitude analysis of the reaction π<sup>+</sup>π<sup>-</sup> → 2π<sup>0</sup>. The resonance in the 2π<sup>0</sup> final state is not confirmed by PROKOSHKIN 97.WEIGHTED AVERAGE  
197 ± 22 (Error scaled by 1.5) $f_2(1810)$  DECAY MODES

Mode	Fraction ( $\Gamma_i/\Gamma$ )
$\Gamma_1$ ππ	
$\Gamma_2$ ηη	
$\Gamma_3$ 4π <sup>0</sup>	seen
$\Gamma_4$ K <sup>+</sup> K <sup>-</sup>	
$\Gamma_5$ γγ	seen

 $f_2(1810)$   $\Gamma(i)\Gamma(\gamma\gamma)/\Gamma(\text{total})$ 

VALUE (eV)	DOCUMENT ID	TECN	COMMENT	$\Gamma_2\Gamma_5/\Gamma$
<b>5.2 ± 0.9 + 37.3</b> <b>-0.8 - 4.5</b>	11 UEHARA	10A BELL	10.6 e <sup>+</sup> e <sup>-</sup> → e <sup>+</sup> e <sup>-</sup> ηη	

11 Including interference with the  $f_2'(1525)$  (parameters fixed to the values from the 2008 edition of this review, PDG 08) and  $f_2(1270)$ . May also be the  $f_0(1500)$ . $f_2(1810)$  BRANCHING RATIOS

$\Gamma(\pi\pi)/\Gamma_{\text{total}}$	DOCUMENT ID	TECN	COMMENT	$\Gamma_1/\Gamma$
• • • We do not use the following data for averages, fits, limits, etc. • • •				
not seen	AMSLER 02	CBAR	0.9 $\bar{p}p \rightarrow \pi^0\eta\eta, \pi^0\pi^0\pi^0$	
not seen	PROKOSHKIN 97	GAM2	38 π <sup>-</sup> p → π <sup>0</sup> π <sup>0</sup> n	
0.21 <sup>+0.02</sup> <sub>-0.03</sub>	12 LONGACRE	86 RVUE	Compilation	
0.44 ± 0.03	13 CASON	82 STRC	8 π <sup>+</sup> p → Δ <sup>++</sup> π <sup>0</sup> π <sup>0</sup>	

12 From a partial-wave analysis of data using a K-matrix formalism with 5 poles. Includes compilation of several other experiments.

13 Included in LONGACRE 86 global analysis.

$\Gamma(\eta\eta)/\Gamma_{\text{total}}$	DOCUMENT ID	TECN	COMMENT	$\Gamma_2/\Gamma$
• • • We do not use the following data for averages, fits, limits, etc. • • •				
0.008 <sup>+0.028</sup> <sub>-0.003</sub>	14 LONGACRE	86 RVUE	Compilation	

14 From a partial-wave analysis of data using a K-matrix formalism with 5 poles. Includes compilation of several other experiments.

$\Gamma(\pi\pi)/\Gamma(4\pi^0)$	DOCUMENT ID	TECN	COMMENT	$\Gamma_1/\Gamma_3$
• • • We do not use the following data for averages, fits, limits, etc. • • •				
< 0.75	ALDE	87 GAM4	100 π <sup>-</sup> p → 4π <sup>0</sup> n	

$\Gamma(4\pi^0)/\Gamma(\eta\eta)$	DOCUMENT ID	TECN	COMMENT	$\Gamma_3/\Gamma_2$
• • • We do not use the following data for averages, fits, limits, etc. • • •				
0.8 ± 0.3	ALDE	87 GAM4	100 π <sup>-</sup> p → 4π <sup>0</sup> n	

$\Gamma(K^+K^-)/\Gamma_{\text{total}}$	DOCUMENT ID	TECN	COMMENT	$\Gamma_4/\Gamma$
• • • We do not use the following data for averages, fits, limits, etc. • • •				
0.003 ± 0.019 <sub>-0.002</sub>	15 LONGACRE	86 RVUE	Compilation	
seen	COSTA...	80 OMEG	10 π <sup>-</sup> p → K <sup>+</sup> K <sup>-</sup> n	

15 From a partial-wave analysis of data using a K-matrix formalism with 5 poles. Includes compilation of several other experiments.

## Meson Particle Listings

 $f_2(1810)$ ,  $X(1835)$ ,  $\phi_3(1850)$ ,  $\eta_2(1870)$  $f_2(1810)$  REFERENCES

UEHARA	10A	PR D92 114031	S. Uehara et al.	(BELLE Collab.)
PDG	08	PL B667 1	C. Amisler et al.	(PDG Collab.)
AMSLER	02	EPL C23 29	C. Amisler et al.	
PROKOSHKIN	97	SPD 42 117	Y.D. Prokoshkin et al.	(SERP)
		Translated from DANS 353 323.		
ALDE	88D	SJNP 47 810	D.M. Alde et al.	(SERP, BELG, LANL, LAPP+)
		Translated from YAF 47 1273.		
ALDE	87	PL B198 286	D.M. Alde et al.	(LANL, BRUX, SERP, LAPP)
ALDE	86D	NP B369 485	D.M. Alde et al.	(BELG, LAPP, SERP, CERN+)
LONGACRE	86	PL B177 223	R.S. Longacre et al.	(BNL, BRAN, CUNY+)
CASON	82	PRL 48 1316	N.M. Cason et al.	(NDAM, ANL)
COSTA...	80	NP B175 402	G. Costa de Beauregard et al.	(BARI, BONN+)

 $X(1835)$ 

$$I^G(J^{PC}) = ?^?(? - +)$$

OMITTED FROM SUMMARY TABLE

Could be a superposition of several states.

 $X(1835)$  MASS

VALUE (MeV)	EVTS	DOCUMENT ID	TECN	COMMENT
<b>1835.7 ± 3.0 ± 5.6</b> <b>3.2 2.1</b>	<b>4265</b>	<b>1</b> ABLIKIM	<b>11c</b> BES3	$J/\psi \rightarrow \gamma\pi^+\pi^-\eta'$
1833.7 ± 6.1 ± 2.7	264	ABLIKIM	05R BES2	$J/\psi \rightarrow \gamma\pi^+\pi^-\eta'$
• • • We do not use the following data for averages, fits, limits, etc. • • •				
1877.3 ± 6.3 ± 3.4 -12 -7		<b>2</b> ABLIKIM	<b>11j</b> BES3	$J/\psi \rightarrow \omega(\eta\pi^+\pi^-)$
1837 +10 +9 -12 -7	231	3,4 ALEXANDER	10 CLEO	$J/\psi \rightarrow \gamma\rho\bar{p}$
1831 ± 7		4,5 ABLIKIM	05R BES2	$J/\psi \rightarrow \gamma\rho\bar{p}$
1859 +3 +5 -10 -25		<b>4</b> BAI	<b>03F</b> BES2	$J/\psi \rightarrow \gamma\rho\bar{p}$

<sup>1</sup> From a fit of the  $\pi^+\pi^-\eta'$  mass distribution to a combination of  $\gamma f_1(1510)$ ,  $\gamma X(1835)$ , and two unconfirmed states  $\gamma X(2120)$ , and  $\gamma X(2370)$ , for  $M(p\bar{p}) < 2.8$  GeV, and accounting for backgrounds from non- $\eta'$  events and  $J/\psi \rightarrow \pi^0\pi^+\pi^-\eta'$ .

<sup>2</sup> The selected process is  $J/\psi \rightarrow \omega a_0(980)\pi$ . This state may be due also to  $\eta_2(1870)$  or to a combination of  $X(1835)$  and  $\eta_2(1870)$ .

<sup>3</sup> From a fit of the  $p\bar{p}$  mass distribution to a combination of  $\gamma X(1835)$ ,  $\gamma R$  with  $M(R) = 2100$  MeV and  $\Gamma(R) = 160$  MeV, and  $\gamma\rho\bar{p}$  phase space, for  $M(p\bar{p}) < 2.85$  GeV.

<sup>4</sup> Evidence for a threshold enhancement in the  $p\bar{p}$  mass spectrum was also reported by ABE 02K, AUBERT,B 05L, and WANG 05A in  $B^+ \rightarrow p\bar{p}K^+$ , WANG 05A in  $B^0 \rightarrow p\bar{p}K_S^0$ , ABE 02W in  $\bar{B}^0 \rightarrow p\bar{p}D^0$ , and WEI 08 in  $B^+ \rightarrow p\bar{p}\pi^+$  decays. Not seen by ATHAR 06 in  $\Upsilon(1S) \rightarrow p\bar{p}\gamma$ .

<sup>5</sup> From the fit including final state interaction effects in isospin 0 S-wave according to SIBIRTSEV 05A. Systematic errors not estimated.

 $X(1835)$  WIDTH

VALUE (MeV)	CL%	EVTS	DOCUMENT ID	TECN	COMMENT
<b>99 ± 50</b>	<b>OUR AVERAGE</b>				Error includes scale factor of 2.8.
190 ± 9 +38 -36		4265	<b>6</b> ABLIKIM	<b>11c</b> BES3	$J/\psi \rightarrow \gamma\pi^+\pi^-\eta'$
67.7 ± 20.3 ± 7.7		264	ABLIKIM	05R BES2	$J/\psi \rightarrow \gamma\pi^+\pi^-\eta'$
• • • We do not use the following data for averages, fits, limits, etc. • • •					
57 ± 12 +19 -4			<b>7</b> ABLIKIM	<b>11j</b> BES3	$J/\psi \rightarrow \omega(\eta\pi^+\pi^-)$
0 +44 -0		231	8,9 ALEXANDER	10 CLEO	$J/\psi \rightarrow \gamma\rho\bar{p}$
< 153	90		9,10 ABLIKIM	05R BES2	$J/\psi \rightarrow \gamma\rho\bar{p}$
< 30			<b>9</b> BAI	<b>03F</b> BES2	$J/\psi \rightarrow \gamma\rho\bar{p}$

<sup>6</sup> From a fit of the  $\pi^+\pi^-\eta'$  mass distribution to a combination of  $\gamma f_1(1510)$ ,  $\gamma X(1835)$ , and two unconfirmed states  $\gamma X(2120)$ , and  $\gamma X(2370)$ , for  $M(p\bar{p}) < 2.8$  GeV, and accounting for backgrounds from non- $\eta'$  events and  $J/\psi \rightarrow \pi^0\pi^+\pi^-\eta'$ .

<sup>7</sup> The selected process is  $J/\psi \rightarrow \omega a_0(980)\pi$ . This state may be due also to  $\eta_2(1870)$  or to a combination of  $X(1835)$  and  $\eta_2(1870)$ .

<sup>8</sup> From a fit of the  $p\bar{p}$  mass distribution to a combination of  $\gamma X(1835)$ ,  $\gamma R$  with  $M(R) = 2100$  MeV and  $\Gamma(R) = 160$  MeV, and  $\gamma\rho\bar{p}$  phase space, for  $M(p\bar{p}) < 2.85$  GeV.

<sup>9</sup> Evidence for a threshold enhancement in the  $p\bar{p}$  mass spectrum was also reported by ABE 02K, AUBERT,B 05L, and WANG 05A in  $B^+ \rightarrow p\bar{p}K^+$ , WANG 05A in  $B^0 \rightarrow p\bar{p}K_S^0$ , ABE 02W in  $\bar{B}^0 \rightarrow p\bar{p}D^0$ , and WEI 08 in  $B^+ \rightarrow p\bar{p}\pi^+$  decays. Not seen by ATHAR 06 in  $\Upsilon(1S) \rightarrow p\bar{p}\gamma$ .

<sup>10</sup> From the fit including final state interaction effects in isospin 0 S-wave according to SIBIRTSEV 05A. Systematic errors not estimated.

 $X(1835)$  DECAY MODES

Mode	Fraction ( $\Gamma_i/\Gamma$ )
$\Gamma_1$ $p\bar{p}$	seen
$\Gamma_2$ $\pi^+\pi^-\eta'$	seen

 $X(1835)$  BRANCHING RATIOS

$\Gamma(p\bar{p})/\Gamma(\pi^+\pi^-\eta')$	DOCUMENT ID	TECN	COMMENT	$\Gamma_1/\Gamma_2$
0.333	ABLIKIM	05R BES2	$J/\psi \rightarrow \gamma\pi^+\pi^-\eta'$	

• • • We do not use the following data for averages, fits, limits, etc. • • •

 $X(1835)$  REFERENCES

ABLIKIM	11C	PRL 106 072002	M. Ablikim et al.	(BES III Collab.)
ABLIKIM	11J	PRL 107 162001	M. Ablikim et al.	(BES III Collab.)
ALEXANDER	10	PR D82 092002	J.P. Alexander et al.	(CLEO Collab.)
WEI	08	PL B659 80	J.-T. Wei et al.	(BELLE Collab.)
ATHAR	06	PR D73 032001	S.B. Athar et al.	(CLEO Collab.)
ABLIKIM	05R	PRL 95 262001	M. Ablikim et al.	(BES Collab.)
AUBERT,B	05L	PR D72 051101R	B. Aubert et al.	(BABAR Collab.)
SIBIRTSEV	05A	PR D71 054010	A. Sibirtsev, J. Haidenbauer	
WANG	05A	PL B617 141	M.-Z. Wang et al.	(BELLE Collab.)
BAI	03F	PRL 91 022001	J.Z. Bai et al.	(BES II Collab.)
ABE	02K	PRL 88 181803	K. Abe et al.	(BELLE Collab.)
ABE	02W	PRL 89 151802	K. Abe et al.	(BELLE Collab.)

 $\phi_3(1850)$ 

$$I^G(J^{PC}) = 0^-(3^{--})$$

 $\phi_3(1850)$  MASS

VALUE (MeV)	EVTS	DOCUMENT ID	TECN	COMMENT
<b>1854 ± 7</b>	<b>OUR AVERAGE</b>			
1855 ± 10		ASTON	88E LASS	$11 K^-p \rightarrow K^-K^+\Lambda$ , $K_S^0 K^\pm\pi^\mp\Lambda$
1870 +30 -20	430	ARMSTRONG	82 OMEG	$18.5 K^-p \rightarrow$ $K^-K^+\Lambda$
1850 ± 10	123	ALHARRAN	81B HBC	$8.25 K^-p \rightarrow K\bar{K}\Lambda$

 $\phi_3(1850)$  WIDTH

VALUE (MeV)	EVTS	DOCUMENT ID	TECN	COMMENT
<b>87 +28</b> <b>-23</b>	<b>OUR AVERAGE</b>			Error includes scale factor of 1.2.
64 ± 31		ASTON	88E LASS	$11 K^-p \rightarrow K^-K^+\Lambda$ , $K_S^0 K^\pm\pi^\mp\Lambda$
160 +90 -50	430	ARMSTRONG	82 OMEG	$18.5 K^-p \rightarrow$ $K^-K^+\Lambda$
80 +40 -30	123	ALHARRAN	81B HBC	$8.25 K^-p \rightarrow K\bar{K}\Lambda$

 $\phi_3(1850)$  DECAY MODES

Mode	Fraction ( $\Gamma_i/\Gamma$ )
$\Gamma_1$ $K\bar{K}$	seen
$\Gamma_2$ $K\bar{K}^*(892) + c.c.$	seen

 $\phi_3(1850)$  BRANCHING RATIOS

$\Gamma(K\bar{K}^*(892) + c.c.)/\Gamma(K\bar{K})$	DOCUMENT ID	TECN	COMMENT	$\Gamma_2/\Gamma_1$
<b>0.55 ± 0.85</b> <b>-0.45</b>	ASTON	88E LASS	$11 K^-p \rightarrow K^-K^+\Lambda$ , $K_S^0 K^\pm\pi^\mp\Lambda$	
0.8 ± 0.4	ALHARRAN	81B HBC	$8.25 K^-p \rightarrow K\bar{K}\pi\Lambda$	

• • • We do not use the following data for averages, fits, limits, etc. • • •

 $\phi_3(1850)$  REFERENCES

ASTON	88E	PL B208 324	D. Aston et al.	(SLAC, NAGO, CINC, INUS)IGJPC
ARMSTRONG	82	PL 110B 77	T.A. Armstrong et al.	(BARI, BIRM, CERN+)JP
ALHARRAN	81B	PL 101B 357	S. AlHarran et al.	(BIRM, CERN, GLAS+)

 $\eta_2(1870)$ 

$$I^G(J^{PC}) = 0^+(2^{--})$$

OMITTED FROM SUMMARY TABLE

Needs confirmation.

 $\eta_2(1870)$  MASS

VALUE (MeV)	EVTS	DOCUMENT ID	TECN	COMMENT
<b>1842 ± 8</b>	<b>OUR AVERAGE</b>			
1835 ± 12		BARBERIS	00B	$450 p\bar{p} \rightarrow p_f\eta\pi^+\pi^-\rho_S$
1844 ± 13		BARBERIS	00C	$450 p\bar{p} \rightarrow p_f4\pi\rho_S$
1840 ± 25		BARBERIS	97B OMEG	$450 p\bar{p} \rightarrow p\rho2(\pi^+\pi^-)$
1875 ± 20 ± 35		ADOMEIT	96 CBAR	$1.94 p\bar{p} \rightarrow \eta3\pi^0$
1881 ± 32 ± 40	26	KARCH	92 CBAL	$e^+e^- \rightarrow e^+e^-\eta\pi^0\pi^0$

• • • We do not use the following data for averages, fits, limits, etc. • • •

See key on page 457

Meson Particle Listings  
 $\eta_2(1870)$ ,  $\pi_2(1880)$ ,  $\rho(1900)$ 

1860 ± 5 ± 15	ANISOVICH	00E	SPEC	0.9-1.94	$\bar{p}p \rightarrow \eta_2 3\pi^0$
1840 ± 15	BAI	99	BES		$J/\psi \rightarrow \gamma \eta \pi^+ \pi^-$

 $\eta_2(1870)$  WIDTH

VALUE (MeV)	EVTS	DOCUMENT ID	TECN	CHG	COMMENT
<b>225 ± 14 OUR AVERAGE</b>					
235 ± 22		BARBERIS	00B		450 $pp \rightarrow \rho_f \eta \pi^+ \pi^- \rho_S$
228 ± 23		BARBERIS	00C		450 $pp \rightarrow \rho_f 4\pi \rho_S$
200 ± 40		BARBERIS	97B	OMEG	450 $pp \rightarrow \rho \rho 2(\pi^+ \pi^-)$
200 ± 25 ± 45		ADOMEIT	96	CBAR	1.94 $\bar{p}p \rightarrow \eta_2 3\pi^0$
221 ± 92 ± 44	26	KARCH	92	CBAL	$e^+ e^- \rightarrow e^+ e^- \eta \pi^0 \pi^0$
• • • We do not use the following data for averages, fits, limits, etc. • • •					
250 ± 25 <sup>+50</sup> <sub>-35</sub>		ANISOVICH	00E	SPEC	0.9-1.94 $\bar{p}p \rightarrow \eta_2 3\pi^0$
170 ± 40		BAI	99	BES	$J/\psi \rightarrow \gamma \eta \pi^+ \pi^-$

 $\eta_2(1870)$  DECAY MODES

Mode	Fraction ( $\Gamma_i/\Gamma$ )
$\Gamma_1$ $\eta \pi \pi$	
$\Gamma_2$ $a_2(1320) \pi$	
$\Gamma_3$ $f_2(1270) \eta$	
$\Gamma_4$ $a_0(980) \pi$	
$\Gamma_5$ $\gamma \gamma$	seen

 $\eta_2(1870)$  BRANCHING RATIOS

VALUE	DOCUMENT ID	TECN	CHG	COMMENT	$\Gamma_2/\Gamma_3$
<b>1.7 ± 0.4 OUR AVERAGE</b>					
1.60 ± 0.40	<sup>1</sup> ANISOVICH	11	SPEC	0.9-1.94 $\bar{p}\bar{p}$	
20.4 ± 6.6	BARBERIS	00B		450 $pp \rightarrow \rho_f \eta \pi^+ \pi^- \rho_S$	
4.1 ± 2.3	ADOMEIT	96	CBAR	1.94 $\bar{p}p \rightarrow \eta_2 3\pi^0$	
<sup>1</sup> Reanalysis of ADOMEIT 96 and ANISOVICH 00E.					

VALUE	DOCUMENT ID	TECN	CHG	COMMENT	$\Gamma_2/\Gamma_4$
<b>32.6 ± 12.6</b>					
	BARBERIS	00B		450 $pp \rightarrow \rho_f \eta \pi^+ \pi^- \rho_S$	

VALUE	DOCUMENT ID	TECN	CHG	COMMENT	$\Gamma_4/\Gamma_3$
<b>0.48 ± 0.45</b>					
	<sup>2</sup> ANISOVICH	11	SPEC	0.9-1.94 $\bar{p}\bar{p}$	
<sup>2</sup> Reanalysis of ADOMEIT 96 and ANISOVICH 00E.					

VALUE	DOCUMENT ID	TECN	CHG	COMMENT	$\Gamma_5/\Gamma$
<b>seen</b>					
	KARCH	92	CBAL	$e^+ e^- \rightarrow e^+ e^- \eta \pi^0 \pi^0$	

 $\eta_2(1870)$  REFERENCES

ANISOVICH	11	EPJ C71	1511	A.V. Anisovich et al.	(LOQM, RAL, PNPI)
ANISOVICH	00E	PL B477	19	A.V. Anisovich et al.	
BARBERIS	00B	PL B471	435	D. Barberis et al.	(WA 102 Collab.)
BARBERIS	00C	PL B471	440	D. Barberis et al.	(WA 102 Collab.)
BAI	99	PL B446	356	J.Z. Bai et al.	(BES Collab.)
BARBERIS	97B	PL B413	217	D. Barberis et al.	(WA 102 Collab.)
ADOMEIT	96	ZPHY C71	227	J. Adomeit et al.	(Crystal Barrel Collab.)
KARCH	92	ZPHY C54	33	K. Karch et al.	(Crystal Ball Collab.)

 $\pi_2(1880)$ 

$$I^G(J^{PC}) = 1^-(2^-+)$$

 $\pi(1880)$  MASS

VALUE (MeV)	EVTS	DOCUMENT ID	TECN	CHG	COMMENT
<b>1895 ± 16 OUR AVERAGE</b>					
1929 ± 24 ± 18	4k	EUGENIO	08	B852	- 18 $\pi^- p \rightarrow \eta \eta \pi^- p$
1876 ± 11 ± 67	145k	LU	05	B852	- 18 $\pi^- p \rightarrow \omega \pi^- \pi^0 p$
2003 ± 88 ± 148	69k	KUHN	04	B852	- 18 $\pi^- p \rightarrow \eta \pi^+ \pi^- \pi^- p$
1880 ± 20		ANISOVICH	01B	SPEC	0 0.6-1.94 $\bar{p}p \rightarrow \eta \eta \pi^0 \pi^0$

 $\pi(1880)$  WIDTH

VALUE (MeV)	EVTS	DOCUMENT ID	TECN	CHG	COMMENT
<b>235 ± 34 OUR AVERAGE</b>					
323 ± 87 ± 43	4k	EUGENIO	08	B852	- 18 $\pi^- p \rightarrow \eta \eta \pi^- p$
146 ± 17 ± 62	145k	LU	05	B852	- 18 $\pi^- p \rightarrow \omega \pi^- \pi^0 p$
306 ± 132 ± 121	69k	KUHN	04	B852	- 18 $\pi^- p \rightarrow \eta \pi^+ \pi^- \pi^- p$
255 ± 45		ANISOVICH	01B	SPEC	0 0.6-1.94 $\bar{p}p \rightarrow \eta \eta \pi^0 \pi^0$

 $\pi_2(1880)$  DECAY MODES

Mode	Fraction ( $\Gamma_i/\Gamma$ )
$\Gamma_1$ $\eta \eta \pi^-$	
$\Gamma_2$ $a_0(980) \eta$	
$\Gamma_3$ $a_2(1320) \eta$	
$\Gamma_4$ $f_0(1500) \pi$	
$\Gamma_5$ $f_1(1285) \pi$	
$\Gamma_6$ $\omega \pi^- \pi^0$	

 $\Gamma(a_2(1320)\eta)/\Gamma(f_1(1285)\pi)$   $\Gamma_3/\Gamma_5$ 

VALUE	EVTS	DOCUMENT ID	TECN	CHG	COMMENT
• • • We do not use the following data for averages, fits, limits, etc. • • •					
22.7 ± 7.3	69k	KUHN	04	B852	- 18 $\pi^- p \rightarrow \eta \pi^+ \pi^- \pi^- p$

 $\Gamma(f_0(1500)\pi)/\Gamma(a_0(980)\eta)$   $\Gamma_4/\Gamma_2$ 

VALUE	DOCUMENT ID	TECN	CHG	COMMENT
• • • We do not use the following data for averages, fits, limits, etc. • • •				
0.28 <sup>+0.20</sup> <sub>-0.15</sub>	<sup>1</sup> ANISOVICH	01B	SPEC	0 0.6-1.94 $\bar{p}p \rightarrow \eta \eta \pi^0 \pi^0$
<sup>1</sup> Systematic errors not estimated.				

 $\pi_2(1880)$  REFERENCES

EUGENIO	08	PL B660	466	P. Eugenio et al.	(BNL E852 Collab.)
LU	05	PRL 94	032002	M. Lu et al.	(BNL E852 Collab.)
KUHN	04	PL B595	109	J. Kuhn et al.	(BNL E852 Collab.)
ANISOVICH	01B	PL B500	222	A.V. Anisovich et al.	

 $\rho(1900)$ 

$$I^G(J^{PC}) = 1^+(1^-)$$

OMITTED FROM SUMMARY TABLE  
See our mini-review under the  $\rho(1700)$ . $\rho(1900)$  MASS

VALUE (MeV)	EVTS	DOCUMENT ID	TECN	CHG	COMMENT
• • • We do not use the following data for averages, fits, limits, etc. • • •					
1909 ± 17 ± 25	54	<sup>1</sup> AUBERT	08s	BABR	10.6 $e^+ e^- \rightarrow \phi \pi^0 \gamma$
1880 ± 30		AUBERT	06D	BABR	10.6 $e^+ e^- \rightarrow 3\pi^+ 3\pi^- \gamma$
1860 ± 20		AUBERT	06D	BABR	10.6 $e^+ e^- \rightarrow 2(\pi^+ \pi^- \pi^0) \gamma$
1910 ± 10		<sup>2,3</sup> FRABETTI	04	E687	$\gamma p \rightarrow 3\pi^+ 3\pi^- p$
1870 ± 10		ANTONELLI	96	SPEC	$e^+ e^- \rightarrow$ hadrons
<sup>1</sup> From the fit with two resonances.					
<sup>2</sup> From a fit with two resonances with the JACOB 72 continuum.					
<sup>3</sup> Supersedes FRABETTI 01.					

 $\rho(1900)$  WIDTH

VALUE (MeV)	EVTS	DOCUMENT ID	TECN	CHG	COMMENT
• • • We do not use the following data for averages, fits, limits, etc. • • •					
48 ± 17 ± 2	54	<sup>4</sup> AUBERT	08s	BABR	10.6 $e^+ e^- \rightarrow \phi \pi^0 \gamma$
130 ± 30		AUBERT	06D	BABR	10.6 $e^+ e^- \rightarrow 3\pi^+ 3\pi^- \gamma$
160 ± 20		AUBERT	06D	BABR	10.6 $e^+ e^- \rightarrow 2(\pi^+ \pi^- \pi^0) \gamma$
37 ± 13		<sup>5,6</sup> FRABETTI	04	E687	$\gamma p \rightarrow 3\pi^+ 3\pi^- p$
10 ± 5		ANTONELLI	96	SPEC	$e^+ e^- \rightarrow$ hadrons
<sup>4</sup> From the fit with two resonances.					
<sup>5</sup> From a fit with two resonances with the JACOB 72 continuum.					
<sup>6</sup> Supersedes FRABETTI 01.					

 $\rho(1900) \Gamma(i)\Gamma(e^+ e^-)/\Gamma^2(\text{total})$ 

VALUE (units 10 <sup>-8</sup> )	EVTS	DOCUMENT ID	TECN	CHG	COMMENT
• • • We do not use the following data for averages, fits, limits, etc. • • •					
4.2 ± 1.2 ± 0.8	54	<sup>7</sup> AUBERT	08s	BABR	10.6 $e^+ e^- \rightarrow \phi \pi^0 \gamma$
<sup>7</sup> From the fit with two resonances.					

 $\rho(1900)$  DECAY MODES

Mode	Fraction ( $\Gamma_i/\Gamma$ )
$\Gamma_1$ $6\pi$	seen
$\Gamma_2$ $3\pi^+ 3\pi^-$	seen
$\Gamma_3$ $2\pi^+ 2\pi^- 2\pi^0$	
$\Gamma_4$ $\phi \pi$	
$\Gamma_5$ hadrons	seen
$\Gamma_6$ $e^+ e^-$	seen
$\Gamma_7$ $\bar{N} N$	not seen

# Meson Particle Listings

## $\rho(1900)$ , $f_2(1910)$

### $\rho(1900)$ BRANCHING RATIOS

$\Gamma(6\pi)/\Gamma_{total}$	DOCUMENT ID	TECN	COMMENT	$\Gamma_1/\Gamma$
not seen	AGNELLO 02	OBLX	$\pi\rho \rightarrow 3\pi^+ 2\pi^- \pi^0$	
seen	FRABETTI 01	E687	$\gamma\rho \rightarrow 3\pi^+ 3\pi^- p$	
seen	ANTONELLI 96	SPEC	$e^+ e^- \rightarrow$ hadrons	

### $\rho(1900)$ REFERENCES

AUBERT 08S	PR D77 092002	B. Aubert <i>et al.</i>	(BABAR Collab.)
AUBERT 06D	PR D73 052003	B. Aubert <i>et al.</i>	(BABAR Collab.)
FRABETTI 04	PL B578 290	P.L. Frabetti <i>et al.</i>	(FNAL E687 Collab.)
AGNELLO 02	PL B527 39	M. Agnello <i>et al.</i>	(OBELIX Collab.)
FRABETTI 01	PL B514 240	P.L. Frabetti <i>et al.</i>	(FNAL E687 Collab.)
ANTONELLI 96	PL B365 427	A. Antonelli <i>et al.</i>	(FENICE Collab.)
JACOB 72	PR D5 1847	M. Jacob, R. Slansky	

## $f_2(1910)$

$$J^G(J^{PC}) = 0^+(2^{++})$$

OMITTED FROM SUMMARY TABLE

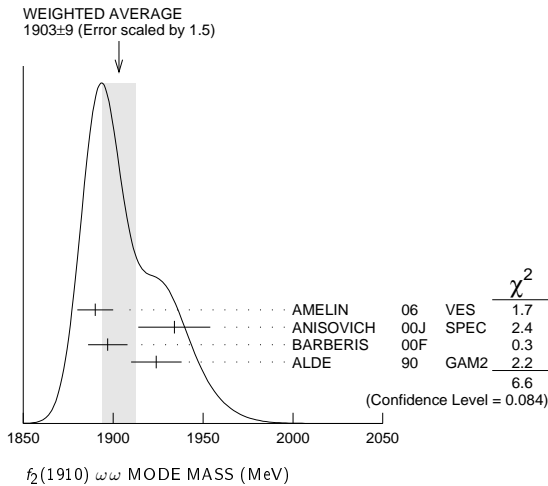
We list here three different peaks with close masses and widths seen in the mass distributions of  $\omega\omega$ ,  $\eta\eta'$ , and  $K^+K^-$  final states. ALDE 91B argues that they are of different nature.

### $f_2(1910)$ MASS

#### $f_2(1910)$ $\omega\omega$ MODE

VALUE (MeV)	DOCUMENT ID	TECN	COMMENT
<b>1903 ± 9 OUR AVERAGE</b>	Error includes scale factor of 1.5. See the ideogram below.		
1890 ± 10	1 AMELIN 06	VES	36 $\pi^- p \rightarrow \omega\omega n$
1934 ± 20	ANISOVICH 00J	SPEC	
1897 ± 11	BARBERIS 00F		450 $pp \rightarrow p_f \omega p_S$
1924 ± 14	ALDE 90	GAM2	38 $\pi^- p \rightarrow \omega\omega n$

<sup>1</sup> Supersedes BELADIDZE 92b.



#### $f_2(1910)$ $\eta\eta'$ MODE

VALUE (MeV)	DOCUMENT ID	TECN	COMMENT
<b>1934 ± 16</b>	2 BARBERIS 00A 450 $pp \rightarrow p_f \eta\eta' p_S$		
1911 ± 10	ALDE 91B	GAM2	38 $\pi^- p \rightarrow \eta\eta' n$

<sup>2</sup> Also compatible with  $J^{PC}=1^-+$ .

#### $f_2(1910)$ $K^+K^-$ MODE

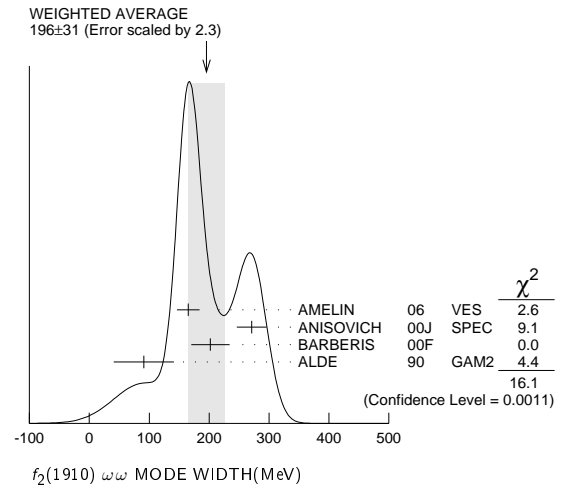
VALUE (MeV)	DOCUMENT ID	TECN	COMMENT
1941 ± 18	AMSLER 06	CBAR	1.64 $\bar{p}p \rightarrow K^+K^-\pi^0$

### $f_2(1910)$ WIDTH

#### $f_2(1910)$ $\omega\omega$ MODE

VALUE (MeV)	DOCUMENT ID	TECN	COMMENT
<b>196 ± 31 OUR AVERAGE</b>	Error includes scale factor of 2.3. See the ideogram below.		
165 ± 19	3 AMELIN 06	VES	36 $\pi^- p \rightarrow \omega\omega n$
271 ± 25	ANISOVICH 00J	SPEC	
202 ± 32	BARBERIS 00F		450 $pp \rightarrow p_f \omega p_S$
91 ± 50	ALDE 90	GAM2	38 $\pi^- p \rightarrow \omega\omega n$

<sup>3</sup> Supersedes BELADIDZE 92b.



#### $f_2(1910)$ $\eta\eta'$ MODE

VALUE (MeV)	DOCUMENT ID	TECN	COMMENT
<b>141 ± 41</b>	4 BARBERIS 00A 450 $pp \rightarrow p_f \eta\eta' p_S$		
90 ± 35	ALDE 91B	GAM2	38 $\pi^- p \rightarrow \eta\eta' n$

<sup>4</sup> Also compatible with  $J^{PC}=1^-+$ .

#### $f_2(1910)$ $K^+K^-$ MODE

VALUE (MeV)	DOCUMENT ID	TECN	COMMENT
120 ± 40	AMSLER 06	CBAR	1.64 $\bar{p}p \rightarrow K^+K^-\pi^0$

### $f_2(1910)$ DECAY MODES

Mode	Fraction ( $\Gamma_i/\Gamma$ )
$\Gamma_1$ $\pi^0\pi^0$	
$\Gamma_2$ $K^+K^-$	seen
$\Gamma_3$ $K_S^0 K_S^0$	
$\Gamma_4$ $\eta\eta$	seen
$\Gamma_5$ $\omega\omega$	seen
$\Gamma_6$ $\eta\eta'$	seen
$\Gamma_7$ $\eta'\eta'$	
$\Gamma_8$ $\rho\rho$	seen
$\Gamma_9$ $a_2(1320)\pi$	seen
$\Gamma_{10}$ $f_2(1270)\eta$	seen

### $f_2(1910)$ BRANCHING RATIOS

$\Gamma(K^+K^-)/\Gamma_{total}$	DOCUMENT ID	TECN	COMMENT	$\Gamma_2/\Gamma$
seen	AMSLER 06	CBAR	1.64 $\bar{p}p \rightarrow K^+K^-\pi^0$	

$\Gamma(\pi^0\pi^0)/\Gamma(\eta\eta')$	DOCUMENT ID	TECN	COMMENT	$\Gamma_1/\Gamma_6$
<0.1	ALDE 89	GAM2	38 $\pi^- p \rightarrow \eta\eta' n$	

$\Gamma(K_S^0 K_S^0)/\Gamma(\eta\eta')$	DOCUMENT ID	TECN	COMMENT	$\Gamma_3/\Gamma_6$
<0.066	90	BALOSHIN 86	SPEC 40 $\pi p \rightarrow K_S^0 K_S^0 n$	

$\Gamma(\eta\eta)/\Gamma(\eta\eta')$	DOCUMENT ID	TECN	COMMENT	$\Gamma_4/\Gamma_6$
<0.05	90	ALDE 91B	GAM2 38 $\pi^- p \rightarrow \eta\eta' n$	

$\Gamma(\omega\omega)/\Gamma(\eta\eta')$	DOCUMENT ID	COMMENT	$\Gamma_5/\Gamma_6$
2.6 ± 0.6	BARBERIS 00F	450 $pp \rightarrow p_f \omega p_S$	

See key on page 457

# Meson Particle Listings

## $f_2(1910), f_2(1950)$

$\Gamma(\eta'\eta')/\Gamma_{total}$	DOCUMENT ID	TECN	COMMENT	$\Gamma_7/\Gamma$
••• We do not use the following data for averages, fits, limits, etc. •••				
probably not seen	BARBERIS	00A	450 $pp \rightarrow \rho_f \eta' \eta' \rho_S$	
possibly seen	BELADIDZE	92D	VES 37 $\pi^- p \rightarrow \eta' \eta' n$	

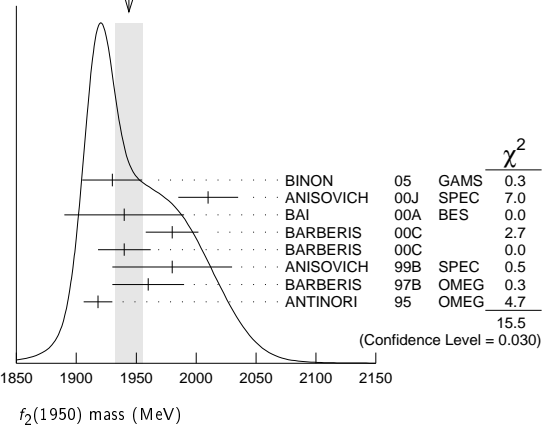
$\Gamma(\rho\rho)/\Gamma(\omega\omega)$	DOCUMENT ID	TECN	COMMENT	$\Gamma_8/\Gamma_5$
••• We do not use the following data for averages, fits, limits, etc. •••				
2.6 ± 0.4	BARBERIS	00F	450 $pp \rightarrow \rho_f \omega \omega \rho_S$	

$\Gamma(f_2(1270)\eta)/\Gamma(a_2(1320)\pi)$	DOCUMENT ID	TECN	COMMENT	$\Gamma_{10}/\Gamma_9$
0.09 ± 0.05	5 ANISOVICH	11	SPEC 0.9-1.94 $p\bar{p}$	

<sup>5</sup> Reanalysis of ADOMEIT 96 and ANISOVICH 00e.

WEIGHTED AVERAGE  
1944±12 (Error scaled by 1.5)



### $f_2(1910)$ REFERENCES

Author	Year	Document ID	TECN	COMMENT
ANISOVICH	11	EPJ C71 1511		A.V. Anisovich et al. (LOQM, RAL, PNPI)
AMELIN	06	PAN 69 690		D.V. Amelin et al. (VES Collab.)
AMSLER	06	PL B639 165		C. Amstler et al. (CBAR Collab.)
ANISOVICH	00E	PL B477 19		A.V. Anisovich et al.
ANISOVICH	00J	PL B491 47		A.V. Anisovich et al.
BARBERIS	00A	PL B471 429		D. Barberis et al. (WA 102 Collab.)
BARBERIS	00F	PL B484 198		D. Barberis et al. (WA 102 Collab.)
ADOMEIT	96	ZPHY C71 227		J. Adomeit et al. (Crystal Barrel Collab.)
BELADIDZE	92B	ZPHY C54 367		G.M. Beladidze et al. (VES Collab.)
BELADIDZE	92D	ZPHY C57 13		G.M. Beladidze et al. (VES Collab.)
ALDE	91B	SJNP 54 455		D.M. Alde et al. (SERP, BELG, LANL, LAPP+)
ALDE	90	PL B276 375		D.M. Alde et al. (BELG, SERP, KEK, LANL+)
ALDE	89	PL B241 600		D.M. Alde et al. (SERP, BELG, LANL, LAPP+)
ALDE	89	PL B216 447		D.M. Alde et al. (SERP, BELG, LANL, LAPP+)
ALDE	89	SJNP 48 1035		D.M. Alde et al. (BELG, SERP, LANL, LAPP)
BALOSHIN	86	SJNP 43 959		O.N. Baloshin et al. (ITEP)
		Translated from YAF 43 1487.		

### $f_2(1950)$

$$J^{PC} = 0^+(2^{++})$$

### $f_2(1950)$ MASS

VALUE (MeV)	DOCUMENT ID	TECN	COMMENT
<b>1944 ± 12 OUR AVERAGE</b>	Error includes scale factor of 1.5. See the ideogram below.		
1930 ± 25	1 BINON	05	GAMS 33 $\pi^- p \rightarrow \eta \eta n$
2010 ± 25	ANISOVICH	00J	SPEC
1940 ± 50	BAI	00A	BES $J/\psi \rightarrow \gamma(\pi^+ \pi^- \pi^+ \pi^-)$
1980 ± 22	2 BARBERIS	00c	450 $pp \rightarrow pp4\pi$
1940 ± 22	3 BARBERIS	00c	450 $pp \rightarrow pp2\pi2\pi^0$
1980 ± 50	ANISOVICH	99B	SPEC 1.35-1.94 $p\bar{p} \rightarrow \eta \eta \pi^0$
1960 ± 30	BARBERIS	97B	OMEG 450 $pp \rightarrow pp2(\pi^+ \pi^-)$
1918 ± 12	ANTINORI	95	OMEG 300,450 $pp \rightarrow pp2(\pi^+ \pi^-)$
••• We do not use the following data for averages, fits, limits, etc. •••			
2038 <sup>+13+12</sup> <sub>-11-73</sub>	4 UEHARA	09	BELL 10.6 $e^+ e^- \rightarrow e^+ e^- \pi^0 \pi^0$
1980 ± 2 ± 14	ABE	04	BELL 10.6 $e^+ e^- \rightarrow e^+ e^- K^+ K^-$
1867 ± 46	5 AMSLER	02	CBAR 0.9 $\bar{p}p \rightarrow \pi^0 \eta \eta, \pi^0 \pi^0 \pi^0$
~ 1990	6 OAKDEN	94	RVUE 0.36-1.55 $\bar{p}p \rightarrow \pi \pi$
1950 ± 15	7 ASTON	91	LASS 11 $K^- p \rightarrow \Lambda K \bar{K} \pi \pi$

- 1 First solution, PWA is ambiguous.
- 2 Decaying into  $\pi^+ \pi^- 2\pi^0$ .
- 3 Decaying into  $2(\pi^+ \pi^-)$ .
- 4 Taking into account  $f_4(2050)$ .
- 5 T-matrix pole.
- 6 From solution B of amplitude analysis of data on  $\bar{p}p \rightarrow \pi \pi$ . See however KLOET 96 who fit  $\pi^+ \pi^-$  only and find waves only up to  $J = 3$  to be important but not significantly resonant.
- 7 Cannot determine spin to be 2.

### $f_2(1950)$ WIDTH

VALUE (MeV)	DOCUMENT ID	TECN	COMMENT
<b>472 ± 18 OUR AVERAGE</b>			
450 ± 50	8 BINON	05	GAMS 33 $\pi^- p \rightarrow \eta \eta n$
495 ± 35	ANISOVICH	00J	SPEC
380 <sup>+120</sup> <sub>-90</sub>	BAI	00A	BES $J/\psi \rightarrow \gamma(\pi^+ \pi^- \pi^+ \pi^-)$
520 ± 50	9 BARBERIS	00c	450 $pp \rightarrow pp4\pi$
485 ± 55	10 BARBERIS	00c	450 $pp \rightarrow pp4\pi$
500 ± 100	ANISOVICH	99B	SPEC 1.35-1.94 $p\bar{p} \rightarrow \eta \eta \pi^0$
460 ± 40	BARBERIS	97B	OMEG 450 $pp \rightarrow pp2(\pi^+ \pi^-)$
390 ± 60	ANTINORI	95	OMEG 300,450 $pp \rightarrow pp2(\pi^+ \pi^-)$
••• We do not use the following data for averages, fits, limits, etc. •••			
441 <sup>+27+28</sup> <sub>-25-192</sub>	11 UEHARA	09	BELL 10.6 $e^+ e^- \rightarrow e^+ e^- \pi^0 \pi^0$
297 ± 12 ± 6	ABE	04	BELL 10.6 $e^+ e^- \rightarrow e^+ e^- K^+ K^-$
385 ± 58	12 AMSLER	02	CBAR 0.9 $\bar{p}p \rightarrow \pi^0 \eta \eta, \pi^0 \pi^0 \pi^0$
~ 100	13 OAKDEN	94	RVUE 0.36-1.55 $\bar{p}p \rightarrow \pi \pi$
250 ± 50	14 ASTON	91	LASS 11 $K^- p \rightarrow \Lambda K \bar{K} \pi \pi$

8 First solution, PWA is ambiguous.  
9 Decaying into  $\pi^+ \pi^- 2\pi^0$ .  
10 Decaying into  $2(\pi^+ \pi^-)$ .  
11 Taking into account  $f_4(2050)$ .  
12 T-matrix pole.  
13 From solution B of amplitude analysis of data on  $\bar{p}p \rightarrow \pi \pi$ . See however KLOET 96 who fit  $\pi^+ \pi^-$  only and find waves only up to  $J = 3$  to be important but not significantly resonant.  
14 Cannot determine spin to be 2.

### $f_2(1950)$ DECAY MODES

Mode	Fraction ( $\Gamma_i/\Gamma$ )
$\Gamma_1$ $K^*(892) \bar{K}^*(892)$	seen
$\Gamma_2$ $\pi \pi$	
$\Gamma_3$ $\pi^+ \pi^-$	seen
$\Gamma_4$ $\pi^0 \pi^0$	seen
$\Gamma_5$ $4\pi$	seen
$\Gamma_6$ $\pi^+ \pi^- \pi^+ \pi^-$	
$\Gamma_7$ $a_2(1320)\pi$	
$\Gamma_8$ $f_2(1270)\pi\pi$	
$\Gamma_9$ $\eta\eta$	seen
$\Gamma_{10}$ $K\bar{K}$	seen
$\Gamma_{11}$ $\gamma\gamma$	seen
$\Gamma_{12}$ $\rho\bar{\rho}$	seen

### $f_2(1950)$ $\Gamma(i)\Gamma(\gamma\gamma)/\Gamma(total)$

$\Gamma(K\bar{K}) \times \Gamma(\gamma\gamma)/\Gamma_{total}$	DOCUMENT ID	TECN	COMMENT	$\Gamma_{10}\Gamma_{11}/\Gamma$
••• We do not use the following data for averages, fits, limits, etc. •••				
122 ± 4 ± 26	15 ABE	04	BELL 10.6 $e^+ e^- \rightarrow e^+ e^- K^+ K^-$	

<sup>15</sup> Assuming spin 2.

# Meson Particle Listings

## $f_2(1950)$ , $\rho_3(1990)$ , $f_2(2010)$ , $f_0(2020)$

$\Gamma(\pi\pi) \times \Gamma(\gamma\gamma)/\Gamma_{total}$   $\Gamma_2\Gamma_{11}/\Gamma$   
VALUE DOCUMENT ID TECN COMMENT

• • • We do not use the following data for averages, fits, limits, etc. • • •  
 $162^{+69}_{-42} - 1137_{-204}$  <sup>16</sup> UEHARA 09 BELL 10.6  $e^+e^- \rightarrow e^+e^-\pi^0\pi^0$   
<sup>16</sup> Taking into account  $f_4(2050)$ .

### $f_2(1950)$ BRANCHING RATIOS

$\Gamma(K^*(892)\bar{K}^*(892))/\Gamma_{total}$   $\Gamma_1/\Gamma$   
VALUE DOCUMENT ID TECN CHG COMMENT

seen ASTON 91 LASS 0 11  $K^-p \rightarrow \Lambda K \bar{K} \pi \pi$

$\Gamma(\rho_2(1320)\pi)/\Gamma_{total}$   $\Gamma_7/\Gamma$   
VALUE DOCUMENT ID TECN COMMENT

• • • We do not use the following data for averages, fits, limits, etc. • • •  
 not seen BARBERIS 00B 450  $pp \rightarrow p_f \eta \pi^+ \pi^- p_S$   
 not seen BARBERIS 00C 450  $pp \rightarrow p_f 4\pi p_S$   
 possibly seen BARBERIS 97B OMEG 450  $pp \rightarrow pp 2(\pi^+ \pi^-)$

$\Gamma(\eta\eta)/\Gamma(4\pi)$   $\Gamma_9/\Gamma_5$   
VALUE CL% DOCUMENT ID COMMENT

• • • We do not use the following data for averages, fits, limits, etc. • • •  
 $<5.0 \times 10^{-3}$  90 BARBERIS 00E 450  $pp \rightarrow p_f \eta \eta p_S$

$\Gamma(\eta\eta)/\Gamma(\pi^+\pi^-)$   $\Gamma_9/\Gamma_3$   
VALUE DOCUMENT ID TECN COMMENT

$0.14 \pm 0.05$  AMSLER 02 CBAR 0.9  $\bar{p}p \rightarrow \pi^0 \eta \eta, \pi^0 \pi^0 \pi^0$

$\Gamma(p\bar{p})/\Gamma_{total}$   $\Gamma_{12}/\Gamma$   
VALUE EVTS DOCUMENT ID TECN COMMENT

seen 111 ALEXANDER 10 CLEO  $\psi(2S) \rightarrow \gamma p\bar{p}$

### $f_2(1950)$ REFERENCES

ALEXANDER 10	PR D82 092002	J.P. Alexander et al.	(CLEO Collab.)
UEHARA 09	PR D79 052009	S. Uehara et al.	(BELLE Collab.)
BINON 05	PAN 68 960	F. Binon et al.	
	Translated from YAF 68 998.		
ABE 04	EPJ C32 323	K. Abe et al.	(BELLE Collab.)
AMSLER 02	EPJ C23 29	C. Amisler et al.	
ANISOVICH 00J	PL B491 47	A.V. Anisovich et al.	
BAI 00A	PL B472 207	J.Z. Bai et al.	(BES Collab.)
BARBERIS 00B	PL B471 435	D. Barberis et al.	(WA 102 Collab.)
BARBERIS 00C	PL B471 440	D. Barberis et al.	(WA 102 Collab.)
BARBERIS 00E	PL B479 59	D. Barberis et al.	(WA 102 Collab.)
ANISOVICH 99B	PL B449 154	A.V. Anisovich et al.	
BARBERIS 97B	PL B413 217	D. Barberis et al.	(WA 102 Collab.)
KLOET 96	PR D53 6120	W.M. Kloet, F. Myhrer	(RUTG, NORD)
ANTINORI 95	PL B353 589	F. Antinori et al.	(ATHU, BARI, BIRM+)JP
OAKDEN 94	NP A574 731	M.N. Oakden, M.R. Pennington	(DURH)
ASTON 91	NPBPS B21 5	D. Aston et al.	(LASS Collab.)

## $\rho_3(1990)$

$$I^G(J^{PC}) = 1^+(3^{--})$$

OMITTED FROM SUMMARY TABLE

### $\rho_3(1990)$ MASS

VALUE (MeV) DOCUMENT ID TECN COMMENT

• • • We do not use the following data for averages, fits, limits, etc. • • •  
 $1982 \pm 14$  <sup>1</sup> ANISOVICH 02 SPEC 0.6-1.9  $p\bar{p} \rightarrow \omega \pi^0, \omega \eta \pi^0, \pi^+ \pi^-$   
 $\sim 2007$  HASAN 94 RVUE  $\bar{p}p \rightarrow \pi \pi$   
<sup>1</sup> From the combined analysis of ANISOVICH 00J, ANISOVICH 01D, ANISOVICH 01E, and ANISOVICH 02.

### $\rho_3(1990)$ WIDTH

VALUE (MeV) DOCUMENT ID TECN COMMENT

• • • We do not use the following data for averages, fits, limits, etc. • • •  
 $188 \pm 24$  <sup>2</sup> ANISOVICH 02 SPEC 0.6-1.9  $p\bar{p} \rightarrow \omega \pi^0, \omega \eta \pi^0, \pi^+ \pi^-$   
 $\sim 287$  HASAN 94 RVUE  $\bar{p}p \rightarrow \pi \pi$   
<sup>2</sup> From the combined analysis of ANISOVICH 00J, ANISOVICH 01D, ANISOVICH 01E, and ANISOVICH 02.

### $\rho_3(1990)$ REFERENCES

ANISOVICH 02	PL B542 8	A.V. Anisovich et al.	
ANISOVICH 01D	PL B508 6	A.V. Anisovich et al.	
ANISOVICH 01E	PL B513 281	A.V. Anisovich et al.	
ANISOVICH 00J	PL B491 47	A.V. Anisovich et al.	
HASAN 94	PL B334 215	A. Hasan, D.V. Bugg	(LOQM)

## $f_2(2010)$

$$I^G(J^{PC}) = 0^+(2^{++})$$

### $f_2(2010)$ MASS

VALUE (MeV) DOCUMENT ID TECN COMMENT

$2011^{+62}_{-76}$  <sup>1</sup> ETKIN 88 MPS 22  $\pi^- p \rightarrow \phi \phi n$   
 • • • We do not use the following data for averages, fits, limits, etc. • • •  
 $2005 \pm 12$  VLADIMIRSK..06 SPEC 40  $\pi^- p \rightarrow K_S^0 K_S^0 n$   
 $1980 \pm 20$  <sup>2</sup> BOLONKIN 88 SPEC 40  $\pi^- p \rightarrow K_S^0 K_S^0 n$   
 $2050^{+90}_{-50}$  ETKIN 85 MPS 22  $\pi^- p \rightarrow 2\phi n$   
 $2120^{+20}_{-120}$  LINDENBAUM 84 RVUE  
 $2160 \pm 50$  ETKIN 82 MPS 22  $\pi^- p \rightarrow 2\phi n$

<sup>1</sup> Includes data of ETKIN 85. The percentage of the resonance going into  $\phi \phi 2^+ + S_2, D_2$ , and  $D_0$  is  $98^{+3}_-1, 0^{+1}_-0$ , and  $2^{+2}_-1$ , respectively.  
<sup>2</sup> Statistically very weak, only 1.4 s.d.

### $f_2(2010)$ WIDTH

VALUE (MeV) DOCUMENT ID TECN COMMENT

$202^{+67}_{-62}$  <sup>3</sup> ETKIN 88 MPS 22  $\pi^- p \rightarrow \phi \phi n$   
 • • • We do not use the following data for averages, fits, limits, etc. • • •  
 $209 \pm 32$  VLADIMIRSK..06 SPEC 40  $\pi^- p \rightarrow K_S^0 K_S^0 n$   
 $145 \pm 50$  <sup>4</sup> BOLONKIN 88 SPEC 40  $\pi^- p \rightarrow K_S^0 K_S^0 n$   
 $200^{+160}_{-50}$  ETKIN 85 MPS 22  $\pi^- p \rightarrow 2\phi n$   
 $300^{+150}_{-50}$  LINDENBAUM 84 RVUE  
 $310 \pm 70$  ETKIN 82 MPS 22  $\pi^- p \rightarrow 2\phi n$

<sup>3</sup> Includes data of ETKIN 85.  
<sup>4</sup> Statistically very weak, only 1.4 s.d.

### $f_2(2010)$ DECAY MODES

Mode	Fraction ( $\Gamma_i/\Gamma$ )
$\Gamma_1 \phi\phi$	seen
$\Gamma_2 K\bar{K}$	seen

### $f_2(2010)$ BRANCHING RATIOS

$\Gamma(K\bar{K})/\Gamma_{total}$   $\Gamma_2/\Gamma$   
VALUE DOCUMENT ID TECN COMMENT

seen VLADIMIRSK..06 SPEC 40  $\pi^- p \rightarrow K_S^0 K_S^0 n$

### $f_2(2010)$ REFERENCES

VLADIMIRSK..06	PAN 69 493	V.V. Vladimirov et al.	(ITEP, Moscow)
	Translated from YAF 69 515.		
BOLONKIN 88	NP B309 426	B.V. Bolonkin et al.	(ITEP, SERP)
ETKIN 88	PL B201 568	A. Etkin et al.	(BNL, CUNY)
ETKIN 85	PL 165B 217	A. Etkin et al.	(BNL, CUNY)
LINDENBAUM 84	CNPP 13 285	S.J. Lindenbaum	(CUNY)
ETKIN 82	PRL 49 1620	A. Etkin et al.	(BNL, CUNY)
	Also Brighton Conf. 351	S.J. Lindenbaum	(BNL, CUNY)

## $f_0(2020)$

$$I^G(J^{PC}) = 0^+(0^{++})$$

OMITTED FROM SUMMARY TABLE

Needs confirmation.

### $f_0(2020)$ MASS

VALUE (MeV) EVTS DOCUMENT ID TECN COMMENT

$1992 \pm 16$  <sup>1,2</sup> BARBERIS 00c 450  $pp \rightarrow p_f 4\pi p_S$   
 • • • We do not use the following data for averages, fits, limits, etc. • • •  
 $2037 \pm 8$  80k <sup>3</sup> UMAN 06 E835 5.2  $\bar{p}p \rightarrow \eta \eta \pi^0$   
 $2040 \pm 38$  ANISOVICH 00J SPEC  
 $2010 \pm 60$  ALDE 98 GAM4 100  $\pi^- p \rightarrow \pi^0 \pi^0 n$   
 $2020 \pm 35$  BARBERIS 97B OMEG 450  $pp \rightarrow pp 2(\pi^+ \pi^-)$

<sup>1</sup> Average between  $\pi^+ \pi^- 2\pi^0$  and  $2(\pi^+ \pi^-)$ .  
<sup>2</sup> T-matrix pole.  
<sup>3</sup> Statistical error only.

### $f_0(2020)$ WIDTH

VALUE (MeV) EVTS DOCUMENT ID TECN COMMENT

$442 \pm 60$  <sup>4,5</sup> BARBERIS 00c 450  $pp \rightarrow p_f 4\pi p_S$



See key on page 457

# Meson Particle Listings

## $f_0(2020), a_4(2040)$

••• We do not use the following data for averages, fits, limits, etc. •••

296 ± 17	80k	6 UMAN	06	E835	5.2 $\bar{p}p \rightarrow \eta\eta\pi^0$
405 ± 40		ANISOVICH	00J	SPEC	
240 ± 100		ALDE	98	GAM4	100 $\pi^- p \rightarrow \pi^0 \pi^0 n$
410 ± 50		BARBERIS	97B	OMEG	450 $p\bar{p} \rightarrow p\rho 2(\pi^+\pi^-)$

<sup>4</sup> Average between  $\pi^+\pi^-2\pi^0$  and  $2(\pi^+\pi^-)$ .  
<sup>5</sup> T-matrix pole.  
<sup>6</sup> Statistical error only.

350 ± 100 <sup>+70</sup> <sub>-50</sub>		IVANOV	01	B852	18 $\pi^- p \rightarrow \eta' \pi^- p$
324 ± 26 ± 75		<sup>9</sup> AMELIN	99	VES	37 $\pi^- A \rightarrow \omega \pi^- \pi^0 A^*$
370 ± 80		<sup>10</sup> DONSKOV	96	GAM2 0	38 $\pi^- p \rightarrow \eta \pi^0 n$
380 ± 150		<sup>11</sup> CLELAND	82B	SPEC ±	50 $\pi p \rightarrow K_S^0 K^\pm p$
510 ± 200		<sup>12</sup> CORDEN	78c	OMEG 0	15 $\pi^- p \rightarrow 3\pi n$

••• We do not use the following data for averages, fits, limits, etc. •••

401 ± 16	80k	<sup>13</sup> UMAN	06	E835	5.2 $\bar{p}p \rightarrow \eta\eta\pi^0$
166 ± 43		<sup>14</sup> BALDI	78	SPEC -	10 $\pi^- p \rightarrow \rho K_S^0 K^-$

<sup>8</sup> From the combined analysis of ANISOVICH 99C, ANISOVICH 99E, and ANISOVICH 01F.  
<sup>9</sup> May be a different state.  
<sup>10</sup> From a simultaneous fit to the  $G_+$  and  $G_0$  wave intensities.  
<sup>11</sup> From an amplitude analysis.  
<sup>12</sup>  $J^P = 4^+$  is favored, though  $J^P = 2^+$  cannot be excluded.  
<sup>13</sup> Statistical error only.  
<sup>14</sup> From a fit to the  $Y_8^0$  moment. Limited by phase space.

### $f_0(2020)$ DECAY MODES

Mode	Fraction ( $\Gamma_i/\Gamma$ )
$\Gamma_1$ $\rho\pi\pi$	seen
$\Gamma_2$ $\pi^0\pi^0$	seen
$\Gamma_3$ $\rho\rho$	seen
$\Gamma_4$ $\omega\omega$	seen
$\Gamma_5$ $\eta\eta$	seen

### $f_0(2020)$ BRANCHING RATIOS

$\Gamma(\rho\rho)/\Gamma(\omega\omega)$	DOCUMENT ID	TECN	CHG	COMMENT	$\Gamma_3/\Gamma_4$
~ 3	BARBERIS	00F	450	$p\bar{p} \rightarrow \rho_f \omega \rho_s$	

$\Gamma(\eta\eta)/\Gamma_{total}$	DOCUMENT ID	TECN	CHG	COMMENT	$\Gamma_5/\Gamma$
seen	UMAN	06	E835	5.2 $\bar{p}p \rightarrow \eta\eta\pi^0$	

### $f_0(2020)$ REFERENCES

UMAN	06	PR D73 052009	I. Uman et al.	(FNAL E835)
ANISOVICH	00J	PL B491 47	A.V. Anisovich et al.	
BARBERIS	00C	PL B471 440	D. Barberis et al.	(WA 102 Collab.)
BARBERIS	00F	PL B484 198	D. Barberis et al.	(WA 102 Collab.)
ALDE	98	EPJ A3 361	D. Alde et al.	(GAM4 Collab.)
Also		PAN 62 405	D. Alde et al.	(GAMS Collab.)
BARBERIS	97B	Translated from YAF 62 446. PL B413 217	D. Barberis et al.	(WA 102 Collab.)

$a_4(2040)$

$$I^G(J^{PC}) = 1^-(4^{++})$$

### $a_4(2040)$ MASS

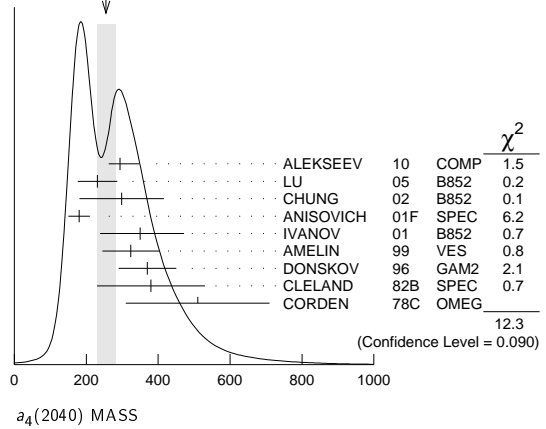
VALUE (MeV)	EVTS	DOCUMENT ID	TECN	CHG	COMMENT
<b>1996 ± 10<sup>+10</sup></b>	<b>OUR AVERAGE</b>	Error includes scale factor of 1.1.			
1885 ± 13 <sup>+50</sup> <sub>-2</sub>	420k	ALEKSEEV	10	COMP	190 $\pi^- Pb \rightarrow \pi^- \pi^- \pi^+ Pb'$
1985 ± 10 ± 13	145k	LU	05	B852	18 $\pi^- p \rightarrow \omega \pi^- \pi^0 p$
1996 ± 25 ± 43		CHUNG	02	B852	18.3 $\pi^- p \rightarrow 3\pi p$
2005 ± 25 <sup>+25</sup> <sub>-45</sub>		<sup>1</sup> ANISOVICH	01F	SPEC	2.0 $\bar{p}p \rightarrow 3\pi^0, \pi^0\eta, \pi^0\eta'$
2000 ± 40 ± 60 <sup>+60</sup> <sub>-20</sub>		IVANOV	01	B852	18 $\pi^- p \rightarrow \eta' \pi^- p$
1944 ± 8 ± 50		<sup>2</sup> AMELIN	99	VES	37 $\pi^- A \rightarrow \omega \pi^- \pi^0 A^*$
2010 ± 20		<sup>3</sup> DONSKOV	96	GAM2 0	38 $\pi^- p \rightarrow \eta \pi^0 n$
2040 ± 30		<sup>4</sup> CLELAND	82B	SPEC ±	50 $\pi p \rightarrow K_S^0 K^\pm p$
2030 ± 50		<sup>5</sup> CORDEN	78c	OMEG 0	15 $\pi^- p \rightarrow 3\pi n$
••• We do not use the following data for averages, fits, limits, etc. •••					
2004 ± 6	80k	<sup>6</sup> UMAN	06	E835	5.2 $\bar{p}p \rightarrow \eta\eta\pi^0$
1903 ± 10		<sup>7</sup> BALDI	78	SPEC -	10 $\pi^- p \rightarrow \rho K_S^0 K^-$

<sup>1</sup> From the combined analysis of ANISOVICH 99C, ANISOVICH 99E, and ANISOVICH 01F.  
<sup>2</sup> May be a different state.  
<sup>3</sup> From a simultaneous fit to the  $G_+$  and  $G_0$  wave intensities.  
<sup>4</sup> From an amplitude analysis.  
<sup>5</sup>  $J^P = 4^+$  is favored, though  $J^P = 2^+$  cannot be excluded.  
<sup>6</sup> Statistical error only.  
<sup>7</sup> From a fit to the  $Y_8^0$  moment. Limited by phase space.

### $a_4(2040)$ WIDTH

VALUE (MeV)	EVTS	DOCUMENT ID	TECN	CHG	COMMENT
<b>255 ± 28<sup>+28</sup></b>	<b>OUR AVERAGE</b>	Error includes scale factor of 1.3. See the ideogram below.			
294 ± 25 ± 46 <sup>+46</sup> <sub>-19</sub>	420k	ALEKSEEV	10	COMP	190 $\pi^- Pb \rightarrow \pi^- \pi^- \pi^+ Pb'$
231 ± 30 ± 46	145k	LU	05	B852	18 $\pi^- p \rightarrow \omega \pi^- \pi^0 p$
298 ± 81 ± 85		CHUNG	02	B852	18.3 $\pi^- p \rightarrow 3\pi p$
180 ± 30		<sup>8</sup> ANISOVICH	01F	SPEC	2.0 $\bar{p}p \rightarrow 3\pi^0, \pi^0\eta, \pi^0\eta'$

WEIGHTED AVERAGE  
255±28-24 (Error scaled by 1.3)



### $a_4(2040)$ DECAY MODES

Mode	Fraction ( $\Gamma_i/\Gamma$ )
$\Gamma_1$ $K\bar{K}$	seen
$\Gamma_2$ $\pi^+\pi^-\pi^0$	seen
$\Gamma_3$ $\rho\pi$	seen
$\Gamma_4$ $f_2(1270)\pi$	seen
$\Gamma_5$ $\omega\pi^-\pi^0$	seen
$\Gamma_6$ $\omega\rho$	seen
$\Gamma_7$ $\eta\pi^0$	seen
$\Gamma_8$ $\eta'(958)\pi$	seen

### $a_4(2040)$ BRANCHING RATIOS

$\Gamma(K\bar{K})/\Gamma_{total}$	DOCUMENT ID	TECN	CHG	COMMENT	$\Gamma_1/\Gamma$
seen	BALDI	78	SPEC ±	10 $\pi^- p \rightarrow K_S^0 K^- p$	

$\Gamma(\pi^+\pi^-\pi^0)/\Gamma_{total}$	DOCUMENT ID	TECN	CHG	COMMENT	$\Gamma_2/\Gamma$
seen	CORDEN	78c	OMEG 0	15 $\pi^- p \rightarrow 3\pi n$	

$\Gamma(\rho\pi)/\Gamma(f_2(1270)\pi)$	DOCUMENT ID	TECN	CHG	COMMENT	$\Gamma_3/\Gamma_4$
<b>1.1 ± 0.2 ± 0.2</b>	CHUNG	02	B852	18.3 $\pi^- p \rightarrow 3\pi p$	

$\Gamma(\eta\pi^0)/\Gamma_{total}$	DOCUMENT ID	TECN	CHG	COMMENT	$\Gamma_7/\Gamma$
seen	DONSKOV	96	GAM2 0	38 $\pi^- p \rightarrow \eta \pi^0 n$	

$\Gamma(\omega\rho)/\Gamma_{total}$	EVTS	DOCUMENT ID	TECN	COMMENT	$\Gamma_6/\Gamma$
seen	145k	LU	05	B852	18 $\pi^- p \rightarrow \omega \pi^- \pi^0 p$

## Meson Particle Listings

 $a_4(2040)$ ,  $f_4(2050)$  $a_4(2040)$  REFERENCES

ALEKSEEV	10	PRL 104 241803	M.G. Alekseev et al.	(COMPASS Collab.)
UMAN	06	PR D73 052009	I. Uman et al.	(FNAL E835)
LU	05	PRL 94 032002	M. Lu et al.	(BNL E852 Collab.)
CHUNG	02	PR D65 072001	S.U. Chung et al.	(BNL E852 Collab.)
ANISOVICH	01F	PL B517 261	A.V. Anisovich et al.	
IVANOV	01	PRL 86 3977	E.I. Ivanov et al.	(BNL E852 Collab.)
AMELIN	99	PAN 62 445	D.V. Amelin et al.	(VES Collab.)
		Translated from YAF 62 487.		
ANISOVICH	99C	PL B452 173	A.V. Anisovich et al.	
ANISOVICH	99E	PL B452 187	A.V. Anisovich et al.	
DONSKOV	96	PAN 59 382	S.V. Donskov et al.	(GAMS Collab.)IGJPC
		Translated from YAF 59 1027.		
CLELAND	82B	NP B208 228	W.E. Cleland et al.	(DURH, GEVA, LAUS+)
BALDI	78	PL 74B 413	R. Baldi et al.	(GEVA)JP
CORDEN	78C	NP B136 77	M.J. Corden et al.	(BIRM, RHEL, TELA+)JP

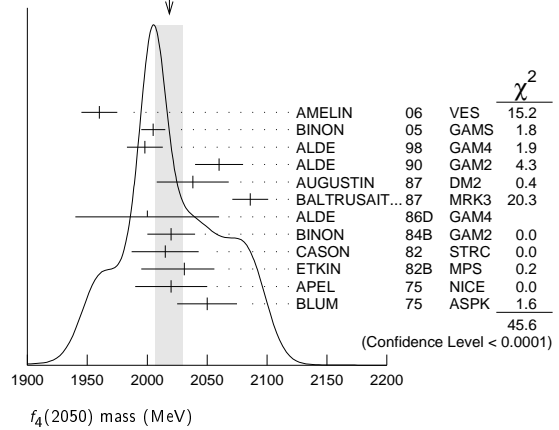
 $f_4(2050)$ 

$$I^G(J^{PC}) = 0^+(4^{++})$$

 $f_4(2050)$  MASS

VALUE (MeV)	EVTs	DOCUMENT ID	TECN	COMMENT
<b>2018±11 OUR AVERAGE</b>		Error includes scale factor of 2.1. See the ideogram below.		
1960±15		AMELIN	06 VES	$36 \pi^- p \rightarrow \omega \omega n$
2005±10	1	BINON	05 GAMS	$33 \pi^- p \rightarrow \eta \eta n$
1998±15		ALDE	98 GAM4	$100 \pi^- p \rightarrow \pi^0 \pi^0 n$
2060±20		ALDE	90 GAM2	$38 \pi^- p \rightarrow \omega \omega n$
2038±30		AUGUSTIN	87 DM2	$J/\psi \rightarrow \gamma \pi^+ \pi^-$
2086±15		BALTRUSAIT..	87 MRK3	$J/\psi \rightarrow \gamma \pi^+ \pi^-$
2000±60		ALDE	86D GAM4	$100 \pi^- p \rightarrow n 2 \eta$
2020±20	40k	2 BINON	84B GAM2	$38 \pi^- p \rightarrow n 2 \pi^0$
2015±28	3	CASON	82 STRC	$8 \pi^+ p \rightarrow \Delta^{++} \pi^0 \pi^0$
2031 <sup>+25</sup> <sub>-36</sub>		ETKIN	82B MPS	$23 \pi^- p \rightarrow n 2 K_S^0$
2020±30	700	APEL	75 NICE	$40 \pi^- p \rightarrow n 2 \pi^0$
2050±25		BLUM	75 ASPK	$18.4 \pi^- p \rightarrow n K^+ K^-$
• • • We do not use the following data for averages, fits, limits, etc. • • •				
1966±25	4	ANISOVICH	09 RVUE	$0.0 \bar{p} p, \pi N$
1885 <sup>+14+218</sup> <sub>-13-25</sub>	5	UEHARA	09 BELL	$10.6 e^+ e^- \rightarrow e^+ e^- \pi^0 \pi^0$
2018±6		ANISOVICH	00j SPEC	$2.0 \bar{p} p \rightarrow \eta \pi^0 \pi^0, \pi^0 \pi^0,$ $\eta \eta, \eta \eta', \pi \pi$
~ 2000	6	MARTIN	98 RVUE	$N \bar{N} \rightarrow \pi \pi$
~ 2010	7	MARTIN	97 RVUE	$N \bar{N} \rightarrow \pi \pi$
~ 2040	8	OAKDEN	94 RVUE	$0.36-1.55 \bar{p} p \rightarrow \pi \pi$
~ 1990	9	OAKDEN	94 RVUE	$0.36-1.55 \bar{p} p \rightarrow \pi \pi$
1978±5	10	ALPER	80 CNTR	$62 \pi^- p \rightarrow K^+ K^- n$
2040±10	10	ROZANSKA	80 SPRK	$18 \pi^- p \rightarrow \rho \bar{p} n$
1935±13	10	CORDEN	79 OMEG	$12-15 \pi^- p \rightarrow n 2 \pi$
1988±7		EVANGELIS...	79B OMEG	$10 \pi^- p \rightarrow K^+ K^- n$
1922±14	11	ANTIPOV	77 CIBS	$25 \pi^- p \rightarrow \rho 3 \pi$

- 1 From the first PWA solution.
- 2 From a partial-wave analysis of the data.
- 3 From an amplitude analysis of the reaction  $\pi^+ \pi^- \rightarrow 2 \pi^0$ .
- 4 K matrix pole.
- 5 Taking into account the  $f_2(1950)$ . Helicity-2 production favored.
- 6 Energy-dependent analysis.
- 7 Single energy analysis.
- 8 From solution A of amplitude analysis of data on  $\bar{p} p \rightarrow \pi \pi$ . See however KLOET 96 who fit  $\pi^+ \pi^-$  only and find waves only up to  $J = 3$  to be important but not significantly resonant.
- 9 From solution B of amplitude analysis of data on  $\bar{p} p \rightarrow \pi \pi$ . See however KLOET 96 who fit  $\pi^+ \pi^-$  only and find waves only up to  $J = 3$  to be important but not significantly resonant.
- 10  $I(J^P) = 0(4^+)$  from amplitude analysis assuming one-pion exchange.
- 11 Width errors enlarged by us to  $4\Gamma/\sqrt{N}$ ; see the note with the  $K^*(892)$  mass.

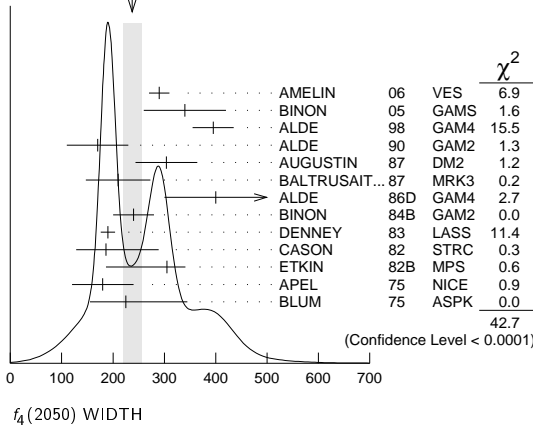
WEIGHTED AVERAGE  
2018±11 (Error scaled by 2.1) $f_4(2050)$  WIDTH

VALUE (MeV)	EVTs	DOCUMENT ID	TECN	COMMENT
<b>237±18 OUR AVERAGE</b>		Error includes scale factor of 1.9. See the ideogram below.		
290±20		AMELIN	06 VES	$36 \pi^- p \rightarrow \omega \omega n$
340±80	12	BINON	05 GAMS	$33 \pi^- p \rightarrow \eta \eta n$
395±40		ALDE	98 GAM4	$100 \pi^- p \rightarrow \pi^0 \pi^0 n$
170±60		ALDE	90 GAM2	$38 \pi^- p \rightarrow \omega \omega n$
304±60		AUGUSTIN	87 DM2	$J/\psi \rightarrow \gamma \pi^+ \pi^-$
210±63		BALTRUSAIT..	87 MRK3	$J/\psi \rightarrow \gamma \pi^+ \pi^-$
400±100		ALDE	86D GAM4	$100 \pi^- p \rightarrow n 2 \eta$
240±40	40k	13 BINON	84B GAM2	$38 \pi^- p \rightarrow n 2 \pi^0$
190±14		DENNEY	83 LASS	$10 \pi^+ n / \pi^+ p$
186 <sup>+103</sup> <sub>-58</sub>	14	CASON	82 STRC	$8 \pi^+ p \rightarrow \Delta^{++} \pi^0 \pi^0$
305 <sup>+36</sup> <sub>-119</sub>		ETKIN	82B MPS	$23 \pi^- p \rightarrow n 2 K_S^0$
180±60	700	APEL	75 NICE	$40 \pi^- p \rightarrow n 2 \pi^0$
225 <sup>+120</sup> <sub>-70</sub>		BLUM	75 ASPK	$18.4 \pi^- p \rightarrow n K^+ K^-$
• • • We do not use the following data for averages, fits, limits, etc. • • •				
260±40	15	ANISOVICH	09 RVUE	$0.0 \bar{p} p, \pi N$
453±20 <sup>+31</sup> <sub>-129</sub>	16	UEHARA	09 BELL	$10.6 e^+ e^- \rightarrow e^+ e^- \pi^0 \pi^0$
182±7		ANISOVICH	00j SPEC	$2.0 \bar{p} p \rightarrow \eta \pi^0 \pi^0, \pi^0 \pi^0,$ $\eta \eta, \eta \eta', \pi \pi$
~ 170	17	MARTIN	98 RVUE	$N \bar{N} \rightarrow \pi \pi$
~ 200	18	MARTIN	97 RVUE	$N \bar{N} \rightarrow \pi \pi$
~ 60	19	OAKDEN	94 RVUE	$0.36-1.55 \bar{p} p \rightarrow \pi \pi$
~ 80	20	OAKDEN	94 RVUE	$0.36-1.55 \bar{p} p \rightarrow \pi \pi$
243±16	21	ALPER	80 CNTR	$62 \pi^- p \rightarrow K^+ K^- n$
140±15	21	ROZANSKA	80 SPRK	$18 \pi^- p \rightarrow \rho \bar{p} n$
263±57	21	CORDEN	79 OMEG	$12-15 \pi^- p \rightarrow n 2 \pi$
100±28		EVANGELIS...	79B OMEG	$10 \pi^- p \rightarrow K^+ K^- n$
107±56	22	ANTIPOV	77 CIBS	$25 \pi^- p \rightarrow \rho 3 \pi$

- 12 From the first PWA solution.
- 13 From a partial-wave analysis of the data.
- 14 From an amplitude analysis of the reaction  $\pi^+ \pi^- \rightarrow 2 \pi^0$ .
- 15 K matrix pole.
- 16 Taking into account the  $f_2(1950)$ . Helicity-2 production favored.
- 17 Energy-dependent analysis.
- 18 Single energy analysis.
- 19 From solution A of amplitude analysis of data on  $\bar{p} p \rightarrow \pi \pi$ . See however KLOET 96 who fit  $\pi^+ \pi^-$  only and find waves only up to  $J = 3$  to be important but not significantly resonant.
- 20 From solution B of amplitude analysis of data on  $\bar{p} p \rightarrow \pi \pi$ . See however KLOET 96 who fit  $\pi^+ \pi^-$  only and find waves only up to  $J = 3$  to be important but not significantly resonant.
- 21  $I(J^P) = 0(4^+)$  from amplitude analysis assuming one-pion exchange.
- 22 Width errors enlarged by us to  $4\Gamma/\sqrt{N}$ ; see the note with the  $K^*(892)$  mass.

See key on page 457

## Meson Particle Listings

 $f_4(2050), \pi_2(2100)$ WEIGHTED AVERAGE  
237±18 (Error scaled by 1.9) $f_4(2050)$  DECAY MODES

Mode	Fraction ( $\Gamma_i/\Gamma$ )
$\Gamma_1$ $\omega\omega$	seen
$\Gamma_2$ $\pi\pi$	(17.0±1.5) %
$\Gamma_3$ $K\bar{K}$	( 6.8 <sup>+3.4</sup> -1.8 ) × 10 <sup>-3</sup>
$\Gamma_4$ $\eta\eta$	( 2.1±0.8 ) × 10 <sup>-3</sup>
$\Gamma_5$ $4\pi^0$	< 1.2 %
$\Gamma_6$ $\gamma\gamma$	
$\Gamma_7$ $a_2(1320)\pi$	seen

 $f_4(2050)$   $\Gamma(i)\Gamma(\gamma\gamma)/\Gamma(\text{total})$ 

Mode	CL%	DOCUMENT ID	TECN	COMMENT	$\Gamma_3\Gamma_6/\Gamma$
$\Gamma(K\bar{K}) \times \Gamma(\gamma\gamma)/\Gamma_{\text{total}}$					
••• We do not use the following data for averages, fits, limits, etc. •••					
<0.29	95	ALTHOFF	85B	TASS $\gamma\gamma \rightarrow K\bar{K}\pi$	

Mode	CL%	EVTS	DOCUMENT ID	TECN	COMMENT	$\Gamma_2\Gamma_6/\Gamma$
$\Gamma(\pi\pi) \times \Gamma(\gamma\gamma)/\Gamma_{\text{total}}$						
••• We do not use the following data for averages, fits, limits, etc. •••						
23.1 <sup>+3.6</sup> -3.3 -70.5		23	UEHARA	09	BELL 10.6 e <sup>+</sup> e <sup>-</sup> → π <sup>0</sup> π <sup>0</sup>	
<1100	95	13 ± 4	OEST	90	JADE e <sup>+</sup> e <sup>-</sup> → π <sup>0</sup> π <sup>0</sup>	
23 Taking into account the $f_2(1950)$ . Helicity-2 production favored.						

 $f_4(2050)$  BRANCHING RATIOS

Mode	DOCUMENT ID	TECN	COMMENT	$\Gamma_1/\Gamma$
$\Gamma(\omega\omega)/\Gamma_{\text{total}}$				
seen	AMELIN	06	VES 36 π <sup>-</sup> p → ωωn	
••• We do not use the following data for averages, fits, limits, etc. •••				
not seen	BARBERIS	00F	450 pp → p <sub>f</sub> ωp <sub>s</sub>	

Mode	DOCUMENT ID	TECN	COMMENT	$\Gamma_1/\Gamma_2$
$\Gamma(\omega\omega)/\Gamma(\pi\pi)$				
1.5 ± 0.3	ALDE	90	GAM2 38 π <sup>-</sup> p → ωωn	

Mode	DOCUMENT ID	TECN	COMMENT	$\Gamma_2/\Gamma$
$\Gamma(\pi\pi)/\Gamma_{\text{total}}$				
0.170 ± 0.015 OUR AVERAGE				
0.18 ± 0.03	24	BINON	83C GAM2 38 π <sup>-</sup> p → n4γ	
0.16 ± 0.03	24	CASON	82 STRC 8 π <sup>+</sup> p → Δ <sup>+</sup> π <sup>0</sup> π <sup>0</sup>	
0.17 ± 0.02	24	CORDEN	79 OMEG 12-15 π <sup>-</sup> p → n2π	
24 Assuming one pion exchange.				

Mode	DOCUMENT ID	TECN	COMMENT	$\Gamma_3/\Gamma_2$
$\Gamma(K\bar{K})/\Gamma(\pi\pi)$				
0.04 <sup>+0.02</sup> -0.01	ETKIN	82B	MPS 23 π <sup>-</sup> p → n2K <sub>S</sub> <sup>0</sup>	

Mode	DOCUMENT ID	TECN	COMMENT	$\Gamma_4/\Gamma$
$\Gamma(\eta\eta)/\Gamma_{\text{total}}$				
2.1 ± 0.8	ALDE	86D	GAM4 100 π <sup>-</sup> p → n4γ	

Mode	DOCUMENT ID	TECN	COMMENT	$\Gamma_5/\Gamma$
$\Gamma(4\pi^0)/\Gamma_{\text{total}}$				
<0.012	ALDE	87	GAM4 100 π <sup>-</sup> p → 4π <sup>0</sup> n	

Mode	DOCUMENT ID	TECN	COMMENT	$\Gamma_7/\Gamma$
$\Gamma(a_2(1320)\pi)/\Gamma_{\text{total}}$				
seen	AMELIN	00	VES 37 π <sup>-</sup> p → ηπ <sup>+</sup> π <sup>-</sup> n	

 $f_4(2050)$  REFERENCES

ANISOVICH	09	IJMP A24 2481	V.V. Anisovich, A.V. Sarantsev	
UEHARA	09	PR D79 052009	S. Uehara et al.	(BELLE Collab.)
AMELIN	06	PAN 69 690	D.V. Amelin et al.	(VES Collab.)
		Translated from YAF 69 715		
BINON	05	PAN 68 960	F. Binon et al.	
		Translated from YAF 68 998		
AMELIN	00J	NP A668 83	D. Amelin et al.	(VES Collab.)
ANISOVICH	00J	PL B491 47	A.V. Anisovich et al.	
BARBERIS	00F	PL B484 198	D. Barberis et al.	(WA 102 Collab.)
ALDE	98	EPJ A3 361	D. Alde et al.	(GAM4 Collab.)
		PAN 62 405	D. Alde et al.	(GAMS Collab.)
		Translated from YAF 62 446		
MARTIN	98	PR C57 3492	B.R. Martin et al.	
MARTIN	97	PR C56 1114	B.R. Martin, G.C. Oades	(LOUC, AARH)
KLOET	96	PR D53 6120	W.M. Kloet, F. Myhrer	(RUTG, NORD)
OAKDEN	94	NP A574 731	M.N. Oakden, M.R. Pennington	(DURH)
ALDE	90	PL B241 600	D.M. Alde et al.	(SERP, BELG, LANL, LAPP+)
OEST	90	ZPHY C47 343	T. Oest et al.	(JADE Collab.)
ALDE	87	PL B198 286	D.M. Alde et al.	(LANL, BRUX, SERP, LAPP)
AUGUSTIN	87	ZPHY C36 369	J.E. Augustin et al.	(LALO, CLER, FRAS+)
BALTRUSAIT...	87	PR D35 2077	R.M. Baltrusaitis et al.	(Mark III Collab.)
ALDE	86D	NP B269 485	D.M. Alde et al.	(BELG, LAPP, SERP, CERN+)
ALTHOFF	85B	ZPHY C29 189	M. Althoff et al.	(TASSO Collab.)
BINON	84B	LNC 39 41	F.G. Binon et al.	(SERP, BELG, LAPP)
BINON	83C	SJNP 38 723	F.G. Binon et al.	(SERP, BRUX+)
		Translated from YAF 38 1199		
DENNEY	83	PR D28 2726	D.L. Denney et al.	(IOWA, MICH)
CASON	82	PRL 48 1316	N.M. Cason et al.	(NDAM, ANL)
ETKIN	82B	PR D25 1786	A. Etkin et al.	(BNL, CUNY, TUFTS, VAND)
ALPER	80	PL 94B 422	B. Alper et al.	(AMST, CERN, CRAC, MPIM+)
ROZANSKA	80	NP B162 505	M. Rozanska et al.	(MPIM, CERN)
CORDEN	79	NP B157 250	M.J. Corden et al.	(BIRM, RHEL, TELA+JP)
EVANGELIS...	79B	NP B154 381	C. Evangelista et al.	(BARI, BONN, CERN+)
ANTIPOV	77	NP B119 45	Y.M. Antipov et al.	(SERP, GEVA)
APEL	75	PL 57B 398	W.D. Apel et al.	(KARLK, KARLE, PISA, SERP+JP)
BLUM	75	PL 57B 403	W. Blum et al.	(CERN, MPIM)JP

 $\pi_2(2100)$ 

$$I^G(J^{PC}) = 1^-(2^{-+})$$

OMITTED FROM SUMMARY TABLE  
Needs confirmation. $\pi_2(2100)$  MASS

Mode	DOCUMENT ID	TECN	COMMENT
$2090 \pm 29$ OUR AVERAGE			
2090 ± 30	1	AMELIN	95B VES 36 π <sup>-</sup> A → π <sup>+</sup> π <sup>-</sup> π <sup>-</sup> A
2100 ± 150	2	DAUM	81B CNTR 63,94 π <sup>-</sup> p → 3πX
1 From a fit to $J^{PC} = 2^{-+}$ $f_2(1270)\pi, (\pi\pi)_S\pi$ waves.			
2 From a two-resonance fit to four 2 <sup>-</sup> 0 <sup>+</sup> waves.			

 $\pi_2(2100)$  WIDTH

Mode	DOCUMENT ID	TECN	COMMENT
$625 \pm 50$ OUR AVERAGE			Error includes scale factor of 1.2.
520 ± 100	3	AMELIN	95B VES 36 π <sup>-</sup> A → π <sup>+</sup> π <sup>-</sup> π <sup>-</sup> A
651 ± 50	4	DAUM	81B CNTR 63,94 π <sup>-</sup> p → 3πX
3 From a fit to $J^{PC} = 2^{-+}$ $f_2(1270)\pi, (\pi\pi)_S\pi$ waves.			
4 From a two-resonance fit to four 2 <sup>-</sup> 0 <sup>+</sup> waves.			

 $\pi_2(2100)$  DECAY MODES

Mode	Fraction ( $\Gamma_i/\Gamma$ )
$\Gamma_1$ 3π	seen
$\Gamma_2$ ρπ	seen
$\Gamma_3$ $f_2(1270)\pi$	seen
$\Gamma_4$ $(\pi\pi)_S\pi$	seen

 $\pi_2(2100)$  BRANCHING RATIOS

Mode	DOCUMENT ID	TECN	COMMENT	$\Gamma_2/\Gamma_1$
$\Gamma(\rho\pi)/\Gamma(3\pi)$				
0.19 ± 0.05	5	DAUM	81B CNTR 63,94 π <sup>-</sup> p	

Mode	DOCUMENT ID	TECN	COMMENT	$\Gamma_3/\Gamma_1$
$\Gamma(f_2(1270)\pi)/\Gamma(3\pi)$				
0.36 ± 0.09	5	DAUM	81B CNTR 63,94 π <sup>-</sup> p	

Mode	DOCUMENT ID	TECN	COMMENT	$\Gamma_4/\Gamma_1$
$\Gamma((\pi\pi)_S\pi)/\Gamma(3\pi)$				
0.45 ± 0.07	5	DAUM	81B CNTR 63,94 π <sup>-</sup> p	

## Meson Particle Listings

 $\pi_2(2100)$ ,  $f_0(2100)$ ,  $f_2(2150)$ **D-wave/S-wave RATIO FOR  $\pi_2(2100) \rightarrow f_2(1270)\pi$** 

VALUE	DOCUMENT ID	TECN	COMMENT
<b>0.39±0.23</b>	<sup>5</sup> DAUM	81B	CNTR 63,94 $\pi^- p$

<sup>5</sup> From a two-resonance fit to four  $2^{-0+}$  waves.

 **$\pi_2(2100)$  REFERENCES**

AMELIN	95B	PL B356 595	D.V. Amelin et al.	(SERP; TBIL)
DAUM	81B	NP B182 269	C. Daum et al.	(AMST, CERN, CRAC, MPIM+)

 **$f_0(2100)$** 

$$I^G(J^{PC}) = 0^+(0^{++})$$

OMITTED FROM SUMMARY TABLE  
Needs confirmation.

 **$f_0(2100)$  MASS**

VALUE (MeV)	EVTS	DOCUMENT ID	TECN	COMMENT
<b>2103±8 OUR AVERAGE</b>				
2102±13		<sup>1</sup> ANISOVICH	00J	SPEC 2.0 $\bar{p}p \rightarrow \eta\pi^0\pi^0, \pi^0\pi^0,$ $\eta\eta, \eta\eta', \pi^+\pi^-$

2090±30		BAI	00A	BES $J/\psi \rightarrow \gamma(\pi^+\pi^-\pi^+\pi^-)$
2105±10		ANISOVICH	99K	SPEC 0.6-1.94 $\bar{p}p \rightarrow \eta\eta, \eta\eta'$

• • • We do not use the following data for averages, fits, limits, etc. • • •

2105±8	80k	<sup>2</sup> UMAN	06	E835 5.2 $\bar{p}p \rightarrow \eta\eta\pi^0$
~2104		BUGG	95	$J/\psi \rightarrow \gamma\pi^+\pi^-\pi^+\pi^-$
~2122		HASAN	94	RVUE $\bar{p}p \rightarrow \pi\pi$

<sup>1</sup> Includes the data of ANISOVICH 00B indicating to exotic decay pattern.

<sup>2</sup> Statistical error only.

 **$f_0(2100)$  WIDTH**

VALUE (MeV)	EVTS	DOCUMENT ID	TECN	COMMENT
<b>209±19 OUR AVERAGE</b>				
211±29		<sup>3</sup> ANISOVICH	00J	SPEC 2.0 $\bar{p}p \rightarrow \eta\pi^0\pi^0, \pi^0\pi^0,$ $\eta\eta, \eta\eta', \pi^+\pi^-$

330±100		BAI	00A	BES $J/\psi \rightarrow \gamma(\pi^+\pi^-\pi^+\pi^-)$
200±25		ANISOVICH	99K	SPEC 0.6-1.94 $\bar{p}p \rightarrow \eta\eta, \eta\eta'$

• • • We do not use the following data for averages, fits, limits, etc. • • •

236±14	80k	<sup>4</sup> UMAN	06	E835 5.2 $\bar{p}p \rightarrow \eta\eta\pi^0$
~203		BUGG	95	$J/\psi \rightarrow \gamma\pi^+\pi^-\pi^+\pi^-$
~273		HASAN	94	RVUE $\bar{p}p \rightarrow \pi\pi$

<sup>3</sup> Includes the data of ANISOVICH 00B indicating to exotic decay pattern.

<sup>4</sup> Statistical error only.

 **$f_0(2100)$  REFERENCES**

UMAN	06	PR D73 052009	I. Uman et al.	(FNAL E835)
ANISOVICH	00B	NP A662 319	A.V. Anisovich et al.	
ANISOVICH	00J	PL B491 47	A.V. Anisovich et al.	
BAI	00A	PL B472 207	J.Z. Bai et al.	(BES Collab.)
ANISOVICH	99K	PL B468 309	A.V. Anisovich et al.	
BUGG	95	PL B353 378	D.V. Bugg et al.	(LOQM, PNPI, WASH)
HASAN	94	PL B334 215	A. Hasan, D.V. Bugg	(LOQM)

 **$f_2(2150)$** 

$$I^G(J^{PC}) = 0^+(2^{++})$$

OMITTED FROM SUMMARY TABLE  
This entry was previously called  $T_0$ .

 **$f_2(2150)$  MASS** **$f_2(2150)$  MASS, COMBINED MODES (MeV)**

VALUE (MeV)	EVTS	DOCUMENT ID	TECN	COMMENT
<b>2157±12 OUR AVERAGE</b>				Includes data from the 2 datablocks that follow this one.

• • • We do not use the following data for averages, fits, limits, etc. • • •

2170±6	80k	<sup>1</sup> UMAN	06	E835 5.2 $\bar{p}p \rightarrow \eta\eta\pi^0$
--------	-----	-------------------	----	---

<sup>1</sup> Statistical error only.

 **$\eta\eta$  MODE**

VALUE (MeV)	DOCUMENT ID	TECN	COMMENT
The data in this block is included in the average printed for a previous datablock.			

**2157±12 OUR AVERAGE**

2151±16		BARBERIS	00E	450 $pp \rightarrow p_f\eta\eta p_S$
2175±20		PROKOSHKIN	95D	GAM4 300 $\pi^- N \rightarrow \pi^- N 2\eta,$ 450 $pp \rightarrow p p 2\eta$
2130±35		SINGOVSKI	94	GAM4 450 $pp \rightarrow p p 2\eta$

• • • We do not use the following data for averages, fits, limits, etc. • • •

2140±30		<sup>2</sup> ABELE	99B	CBAR
2104±20		<sup>3</sup> ARMSTRONG	93C	E760 $\bar{p}p \rightarrow \pi^0\eta\eta \rightarrow 6\gamma$

<sup>2</sup> Spin not determined.

<sup>3</sup> No  $J^{PC}$  determination.

 **$\eta\pi\pi$  MODE**

VALUE (MeV)	DOCUMENT ID	TECN	CHG	COMMENT
The data in this block is included in the average printed for a previous datablock.				

• • • We do not use the following data for averages, fits, limits, etc. • • •

2135±20±45		<sup>4</sup> ADOMEIT	96	CBAR 0 1.94 $\bar{p}p \rightarrow \eta 3\pi^0$
------------	--	----------------------	----	--

<sup>4</sup> ANISOVICH 00E recommends to withdraw ADOMEIT 96 that assumed a single  $J^P = 2^+$  resonance.

 **$\bar{p}p \rightarrow \pi\pi$** 

VALUE (MeV)	DOCUMENT ID	TECN	COMMENT
-------------	-------------	------	---------

• • • We do not use the following data for averages, fits, limits, etc. • • •

~2090		<sup>5</sup> OAKDEN	94	RVUE 0.36-1.55 $\bar{p}p \rightarrow \pi\pi$
~2120		<sup>6</sup> OAKDEN	94	RVUE 0.36-1.55 $\bar{p}p \rightarrow \pi\pi$
~2170		<sup>7</sup> MARTIN	80B	RVUE
~2150		<sup>7</sup> MARTIN	80C	RVUE
~2150		<sup>8</sup> DULUDE	78B	OSPK 1-2 $\bar{p}p \rightarrow \pi^0\pi^0$

<sup>5</sup> OAKDEN 94 makes an amplitude analysis of LEAR data on  $\bar{p}p \rightarrow \pi\pi$  using a method based on Barrelet zeros. This is solution A. The amplitude analysis of HASAN 94 includes earlier data as well, and assume that the data can be parametrized in terms of towers of nearly degenerate resonances on the leading Regge trajectory. See also KLOET 96 and MARTIN 97 who make related analyses.

<sup>6</sup> From solution B of amplitude analysis of data on  $\bar{p}p \rightarrow \pi\pi$ .

<sup>7</sup>  $I(J^P) = 0(2^+)$  from simultaneous analysis of  $p\bar{p} \rightarrow \pi^-\pi^+$  and  $\pi^0\pi^0$ .

<sup>8</sup>  $I^G(J^P) = 0^+(2^+)$  from partial-wave amplitude analysis.

**S-CHANNEL  $\bar{p}p, \bar{N}N$  or  $K\bar{K}$** 

VALUE (MeV)	DOCUMENT ID	TECN	CHG	COMMENT
-------------	-------------	------	-----	---------

• • • We do not use the following data for averages, fits, limits, etc. • • •

2139± <sup>8</sup> <sub>9</sub>		<sup>9</sup> EVANGELIS...	97	SPEC 0.6-2.4 $\bar{p}p \rightarrow K_S^0 K_S^0$
~2190		<sup>9</sup> CUTTS	78B	CNTR 0.97-3 $\bar{p}p \rightarrow \bar{N}N$
2155±15		<sup>9,10</sup> COUPLAND	77	CNTR 0 0.7-2.4 $\bar{p}p \rightarrow \bar{p}p$
2193±2		<sup>9,11</sup> ALSPECTOR	73	CNTR $\bar{p}p$ S channel

<sup>9</sup> Isospins 0 and 1 not separated.

<sup>10</sup> From a fit to the total elastic cross section.

<sup>11</sup> Referred to as  $T$  or  $T$  region by ALSPECTOR 73.

 **$K\bar{K}$  MODE**

VALUE (MeV)	DOCUMENT ID	TECN	COMMENT
-------------	-------------	------	---------

• • • We do not use the following data for averages, fits, limits, etc. • • •

2200±13		VLADIMIRSK...	06	SPEC 40 $\pi^- p \rightarrow K_S^0 K_S^0 n$
2150±20		ABLIKIM	04E	BES2 $J/\psi \rightarrow \omega K^+ K^-$
2130±35		BARBERIS	99	OMEG 450 $pp \rightarrow p_S p_f K^+ K^-$

 **$f_2(2150)$  WIDTH** **$f_2(2150)$  WIDTH, COMBINED MODES (MeV)**

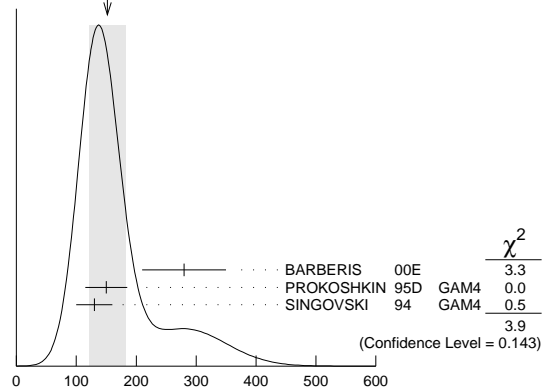
VALUE (MeV)	EVTS	DOCUMENT ID	TECN	COMMENT
<b>152±30 OUR AVERAGE</b>				Includes data from the 2 datablocks that follow this one. Error includes scale factor of 1.4. See the ideogram below.

• • • We do not use the following data for averages, fits, limits, etc. • • •

182±11	80k	<sup>12</sup> UMAN	06	E835 5.2 $\bar{p}p \rightarrow \eta\eta\pi^0$
--------	-----	--------------------	----	---

<sup>12</sup> Statistical error only.

WEIGHTED AVERAGE  
152±30 (Error scaled by 1.4)



$f_2(2150)$  WIDTH, COMBINED MODES (MeV)

See key on page 457

## Meson Particle Listings

 $f_2(2150), \rho(2150)$  $\eta\eta$  MODE

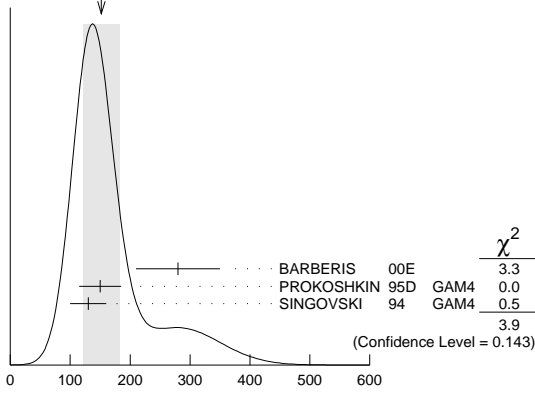
VALUE (MeV)	DOCUMENT ID	TECN	COMMENT
The data in this block is included in the average printed for a previous datablock.			

**152±30 OUR AVERAGE** Error includes scale factor of 1.4. See the ideogram below.

280±70	BARBERIS	00E	450 $pp \rightarrow \rho_f \eta \eta p_S$
150±35	PROKOSHKIN	95D	GAM4 300 $\pi^- N \rightarrow \pi^- N 2\eta$ , 450 $pp \rightarrow \rho p 2\eta$
130±30	SINGOVSKI	94	GAM4 450 $pp \rightarrow \rho p 2\eta$
•••	We do not use the following data for averages, fits, limits, etc. •••		
310±50	<sup>13</sup> ABELE	99B	CBAR
203±10	<sup>14</sup> ARMSTRONG	93C	E760 $\bar{p}p \rightarrow \pi^0 \eta \eta \rightarrow 6\gamma$

<sup>13</sup> Spin not determined.  
<sup>14</sup> No  $J^{PC}$  determination.

WEIGHTED AVERAGE  
152±30 (Error scaled by 1.4)



$f_2(2150)$  WIDTH,  $\eta\eta$  MODE (MeV)

 $\eta\pi\pi$  MODE

VALUE (MeV)	DOCUMENT ID	TECN	CHG	COMMENT
The data in this block is included in the average printed for a previous datablock.				

••• We do not use the following data for averages, fits, limits, etc. •••

250±25±45	<sup>15</sup> ADOMEIT	96	CBAR	0	1.94 $\bar{p}p \rightarrow \eta 3\pi^0$
<sup>15</sup> ANISOVICH 00E recommends to withdraw ADOMEIT 96 that assumed a single $J^P = 2^+$ resonance.					

 $\bar{p}p \rightarrow \pi\pi$ 

VALUE (MeV)	DOCUMENT ID	TECN	COMMENT
<b>250 OUR ESTIMATE</b>			

••• We do not use the following data for averages, fits, limits, etc. •••

~ 70	<sup>16</sup> OAKDEN	94	RVUE	0.36–1.55 $\bar{p}p \rightarrow \pi\pi$	
~ 250	<sup>17</sup> MARTIN	80B	RVUE		
~ 250	<sup>17</sup> MARTIN	80C	RVUE		
~ 250	<sup>18</sup> DULUDE	78B	OSPK	1–2 $\bar{p}p \rightarrow \pi^0 \pi^0$	
<sup>16</sup> See however KLOET 96 who fit $\pi^+ \pi^-$ only and find waves only up to $J = 3$ to be important but not significantly resonant.					
<sup>17</sup> $I(J^P) = 0(2^+)$ from simultaneous analysis of $p\bar{p} \rightarrow \pi^- \pi^+ + \pi^0 \pi^0$ .					
<sup>18</sup> $I^G(J^P) = 0^+(2^+)$ from partial-wave amplitude analysis.					

S-CHANNEL  $\bar{p}p, \bar{N}N$  or  $\bar{K}K$ 

VALUE (MeV)	DOCUMENT ID	TECN	CHG	COMMENT
••• We do not use the following data for averages, fits, limits, etc. •••				

56+31 -16	<sup>19</sup> EVANGELIS...	97	SPEC	0.6–2.4 $\bar{p}p \rightarrow K_S^0 K_S^0$	
135±75	<sup>20,21</sup> COUPLAND	77	CNTR	0	0.7–2.4 $\bar{p}p \rightarrow \bar{p}p$
98±8	<sup>21</sup> ALSPECTOR	73	CNTR		$\bar{p}p$ S channel

<sup>19</sup> Isospin 0 and 2 not separated.  
<sup>20</sup> From a fit to the total elastic cross section.  
<sup>21</sup> Isospins 0 and 1 not separated.

 $K\bar{K}$  MODE

VALUE (MeV)	DOCUMENT ID	TECN	COMMENT
••• We do not use the following data for averages, fits, limits, etc. •••			

91±62	VLADIMIRSK...	06	SPEC	40 $\pi^- p \rightarrow K_S^0 K_S^0 n$
150±30	ABLIKIM	04E	BES2	$J/\psi \rightarrow \omega K^+ K^-$
270±50	BARBERIS	99	OMEG	450 $pp \rightarrow p_S \rho_f K^+ K^-$

 $f_2(2150)$  DECAY MODES

Mode	Fraction ( $\Gamma_i/\Gamma$ )
$\Gamma_1$ $\pi\pi$	
$\Gamma_2$ $\eta\eta$	seen
$\Gamma_3$ $K\bar{K}$	seen
$\Gamma_4$ $f_2(1270)\eta$	seen
$\Gamma_5$ $a_2(1320)\pi$	seen
$\Gamma_6$ $\rho\bar{\rho}$	seen

 $f_2(2150)$  BRANCHING RATIOS

$\Gamma(K\bar{K})/\Gamma(\eta\eta)$	VALUE	CL%	DOCUMENT ID	TECN	COMMENT	$\Gamma_3/\Gamma_2$
	<b>1.28±0.23</b>		BARBERIS	00E	450 $pp \rightarrow \rho_f \eta \eta p_S$	
••• We do not use the following data for averages, fits, limits, etc. •••						
	<0.1	95	<sup>22</sup> PROKOSHKIN	95D	GAM4 300 $\pi^- N \rightarrow \pi^- N 2\eta$ , 450 $pp \rightarrow \rho p 2\eta$	

<sup>22</sup> Using data from ARMSTRONG 89D.

$\Gamma(\pi\pi)/\Gamma(\eta\eta)$	VALUE	CL%	DOCUMENT ID	TECN	COMMENT	$\Gamma_1/\Gamma_2$
	<0.33	95	<sup>23</sup> PROKOSHKIN	95D	GAM4 300 $\pi^- N \rightarrow \pi^- N 2\eta$ , 450 $pp \rightarrow \rho p 2\eta$	

<sup>23</sup> Derived from a  $\pi^0 \pi^0/\eta\eta$  limit.

$\Gamma(f_2(1270)\eta)/\Gamma(a_2(1320)\pi)$	VALUE	CL%	DOCUMENT ID	TECN	COMMENT	$\Gamma_4/\Gamma_5$
	<b>0.79±0.11</b>		<sup>24</sup> ADOMEIT	96	CBAR 1.94 $\bar{p}p \rightarrow \eta 3\pi^0$	

<sup>24</sup> Using  $B(a_2(1320) \rightarrow \eta\pi) = 0.145$

$\Gamma(\rho\bar{\rho})/\Gamma_{total}$	VALUE	EVTS	DOCUMENT ID	TECN	COMMENT	$\Gamma_6/\Gamma$
seen		73	ALEXANDER	10	CLEO $\psi(2S) \rightarrow \gamma\rho\bar{\rho}$	

 $f_2(2150)$  REFERENCES

ALEXANDER	10	PR D82 092002	J.P. Alexander et al.	(CLEO Collab.)
UMAN	06	PR D73 052009	I. Uman et al.	(FNAL E835)
VLADIMIRSK...	06	PAN 69 4 93	V.V. Vladimirov et al.	(ITEP, Moscow)
ABLIKIM	04E	PL B603 138	M. Ablikim et al.	(BES Collab.)
ANISOVICH	00E	PL B477 19	A.V. Anisovich et al.	
BARBERIS	00E	PL B479 59	D. Barberis et al.	(WA 102 Collab.)
ABELE	99B	EPJ C8 67	A. Abele et al.	(Crystal Barrel Collab.)
BARBERIS	99	PL B453 305	D. Barberis et al.	(Omega Expt.)
EVANGELIS...	97	PR D56 3803	C. Evangelista et al.	(LEAR Collab.)
MARTIN	97	PR C56 1114	B.R. Martin, G.C. Oades	(LOUC, AARH)
ADOMEIT	96	ZPHY C71 227	J. Adomeit et al.	(Crystal Barrel Collab.)
KLOET	96	PR D53 6120	W.M. Kloet, F. Myhrer	(RUTG, NORD)
PROKOSHKIN	95D	SPD 40 4 95	Y.D. Prokoshkin	(SERP)IGJPC
		Translated from	DANS 344 4 95	
HASAN	94	PL B334 215	A. Hasan, D.V. Bugg	(LOQM)
OAKDEN	94	NP A574 731	M.N. Oakden, M.R. Pennington	(DURH)
SINGOVSKI	94	NC 107A 1911	A.V. Singovsky	(SERP)
ARMSTRONG	93C	PL B307 394	T.A. Armstrong et al.	(FNAL, FERR, GENO+)
ARMSTRONG	89D	PL B227 186	T.A. Armstrong, M. Benayoun	(ATHU, BARI, BIRM+)
MARTIN	80B	NP B176 355	B.R. Martin, D. Morgan	(LOUC, RHEL)JP
MARTIN	80C	NP B169 216	A.D. Martin, M.R. Pennington	(DURH)JP
CUTTS	78B	PL D17 16	D. Cutts et al.	(STON, WISC)
DULUDE	78B	PL 79B 335	R.S. Dulude et al.	(BROW, MIT, BARI)JP
COUPLAND	77	PL 71B 460	M. Coupland et al.	(LOQM, RHEL)
ALSPECTOR	73	PRL 30 511	J. Alspector et al.	(RUTG, UPNJ)

 $\rho(2150)$ 

$$I^G(J^{PC}) = 1^+(1^{--})$$

OMITTED FROM SUMMARY TABLE

This entry was previously called  $T_1(2190)$ . See our mini-review under the  $\rho(1700)$ .

 $\rho(2150)$  MASS $e^+e^-$  PRODUCED

VALUE (MeV)	DOCUMENT ID	TECN	COMMENT
<b>2149±17 OUR AVERAGE</b> Includes data from the datablock that follows this one.			

2150±40±50	AUBERT	07AU	BABR 10.6 $e^+e^- \rightarrow f_1(1285)\pi^+\pi^-\gamma$
2153±37	BIAGINI	91	RVUE $e^+e^- \rightarrow \pi^+\pi^-, K^+K^-$
2110±50	<sup>1</sup> CLEGG	90	RVUE $e^+e^- \rightarrow 3(\pi^+\pi^-), 2(\pi^+\pi^-\pi^0)$

••• We do not use the following data for averages, fits, limits, etc. •••

1990±80	AUBERT	07AU	BABR 10.6 $e^+e^- \rightarrow \eta'\pi^+\pi^-\gamma$
---------	--------	------	--

 $\bar{p}p \rightarrow \pi\pi$ 

VALUE (MeV)	DOCUMENT ID	TECN	COMMENT
••• We do not use the following data for averages, fits, limits, etc. •••			

~ 2191	HASAN	94	RVUE $\bar{p}p \rightarrow \pi\pi$
~ 2070	<sup>2</sup> OAKDEN	94	RVUE 0.36–1.55 $\bar{p}p \rightarrow \pi\pi$
~ 2170	<sup>3</sup> MARTIN	80B	RVUE
~ 2100	<sup>3</sup> MARTIN	80C	RVUE

# Meson Particle Listings

## $\rho(2150), \phi(2170)$

### S-CHANNEL $\bar{N}N$

VALUE (MeV)	DOCUMENT ID	TECN	COMMENT
••• We do not use the following data for averages, fits, limits, etc. •••			
2110±35	<sup>4</sup> ANISOVICH	02	SPEC 0.6–1.9 $p\bar{p} \rightarrow \omega\pi^0, \omega\eta\pi^0, \pi^+\pi^-$
~ 2190	<sup>5</sup> CUTTS	78B	CNTR 0.97–3 $\bar{p}p \rightarrow \bar{N}N$
2155±15	<sup>5,6</sup> COUPLAND	77	CNTR 0.7–2.4 $\bar{p}p \rightarrow \bar{p}p$
2193±2	<sup>5,7</sup> ALSPECTOR	73	CNTR $\bar{p}p$ S channel
2190±10	<sup>8</sup> ABRAMS	70	CNTR S channel $\bar{p}N$

### $\pi^-p \rightarrow \omega\pi^0n$

VALUE (MeV)	DOCUMENT ID	TECN	COMMENT
The data in this block is included in the average printed for a previous datablock.			

### 2155±21 OUR AVERAGE

2140±30	ALDE	95	GAM2 38 $\pi^-p \rightarrow \omega\pi^0n$
2170±30	ALDE	92c	GAM4 100 $\pi^-p \rightarrow \omega\pi^0n$

- Includes ATKINSON 85.
- See however KLOET 96 who fit  $\pi^+\pi^-$  only and find waves only up to  $J = 3$  to be important but not significantly resonant.
- $I(J^P) = 1(1^-)$  from simultaneous analysis of  $p\bar{p} \rightarrow \pi^-\pi^+$  and  $\pi^0\pi^0$ .
- From the combined analysis of ANISOVICH 00J, ANISOVICH 01D, ANISOVICH 01E, and ANISOVICH 02.
- Isospins 0 and 1 not separated.
- From a fit to the total elastic cross section.
- Referred to as T or T region by ALSPECTOR 73.
- Seen as bump in  $l = 1$  state. See also COOPER 68. PEASLEE 75 confirm  $\bar{p}p$  results of ABRAMS 70, no narrow structure.

### $\rho(2150)$ WIDTH

#### $e^+e^-$ PRODUCED

VALUE (MeV)	DOCUMENT ID	TECN	COMMENT
<b>359±40 OUR AVERAGE</b> Includes data from the datablock that follows this one.			
350±40±50	AUBERT	07AU BABR	10.6 $e^+e^- \rightarrow f_1(1285)\pi^+\pi^-\gamma$
389±79	BIAGINI	91 RVUE	$e^+e^- \rightarrow \pi^+\pi^-, K^+K^-$
410±100	<sup>9</sup> CLEGG	90 RVUE	$e^+e^- \rightarrow 3(\pi^+\pi^-), 2(\pi^+\pi^-\pi^0)$
••• We do not use the following data for averages, fits, limits, etc. •••			
310±140	AUBERT	07AU BABR	10.6 $e^+e^- \rightarrow \eta'\pi^+\pi^-\gamma$

### $\bar{p}p \rightarrow \pi\pi$

VALUE (MeV)	DOCUMENT ID	TECN	COMMENT
••• We do not use the following data for averages, fits, limits, etc. •••			
~ 296	HASAN	94 RVUE	$\bar{p}p \rightarrow \pi\pi$
~ 40	<sup>10</sup> OAKDEN	94 RVUE	0.36–1.55 $\bar{p}p \rightarrow \pi\pi$
~ 250	<sup>11</sup> MARTIN	80B RVUE	
~ 200	<sup>11</sup> MARTIN	80c RVUE	

### S-CHANNEL $\bar{N}N$

VALUE (MeV)	DOCUMENT ID	TECN	COMMENT
••• We do not use the following data for averages, fits, limits, etc. •••			
230±50	<sup>12</sup> ANISOVICH	02	SPEC 0.6–1.9 $p\bar{p} \rightarrow \omega\pi^0, \omega\eta\pi^0, \pi^+\pi^-$
135±75	<sup>13,14</sup> COUPLAND	77	CNTR 0.7–2.4 $\bar{p}p \rightarrow \bar{p}p$
98±8	<sup>14</sup> ALSPECTOR	73	CNTR $\bar{p}p$ S channel
~ 85	<sup>15</sup> ABRAMS	70	CNTR S channel $\bar{p}N$

### $\pi^-p \rightarrow \omega\pi^0n$

VALUE (MeV)	DOCUMENT ID	TECN	COMMENT
The data in this block is included in the average printed for a previous datablock.			

<b>320±70</b>	ALDE	95	GAM2 38 $\pi^-p \rightarrow \omega\pi^0n$
••• We do not use the following data for averages, fits, limits, etc. •••			
~ 300	ALDE	92c	GAM4 100 $\pi^-p \rightarrow \omega\pi^0n$

- Includes ATKINSON 85.
- See however KLOET 96 who fit  $\pi^+\pi^-$  only and find waves only up to  $J = 3$  to be important but not significantly resonant.
- $I(J^P) = 1(1^-)$  from simultaneous analysis of  $p\bar{p} \rightarrow \pi^-\pi^+$  and  $\pi^0\pi^0$ .
- From the combined analysis of ANISOVICH 00J, ANISOVICH 01D, ANISOVICH 01E, and ANISOVICH 02.
- From a fit to the total elastic cross section.
- Isospins 0 and 1 not separated.
- Seen as bump in  $l = 1$  state. See also COOPER 68. PEASLEE 75 confirm  $\bar{p}p$  results of ABRAMS 70, no narrow structure.

### $\rho(2150)$ DECAY MODES

Mode	Fraction ( $\Gamma_i/\Gamma$ )
$\Gamma_1$ $e^+e^-$	
$\Gamma_2$ $\pi^+\pi^-$	seen
$\Gamma_3$ $K^+K^-$	seen
$\Gamma_4$ $3(\pi^+\pi^-)$	seen
$\Gamma_5$ $2(\pi^+\pi^-\pi^0)$	seen
$\Gamma_6$ $\eta'\pi^+\pi^-$	seen
$\Gamma_7$ $f_1(1285)\pi^+\pi^-$	seen
$\Gamma_8$ $\omega\pi^0$	seen
$\Gamma_9$ $\omega\pi^0\eta$	seen
$\Gamma_{10}$ $p\bar{p}$	

### $\rho(2150) \Gamma(i)\Gamma(e^+e^-)/\Gamma^2(\text{total})$

$$\Gamma(f_1(1285)\pi^+\pi^-)/\Gamma_{\text{total}} \times \Gamma(e^+e^-)/\Gamma_{\text{total}} \quad \Gamma_7/\Gamma \times \Gamma_1/\Gamma$$

VALUE (units 10 <sup>-7</sup> )	DOCUMENT ID	TECN	COMMENT
<b>3.1±0.6±0.5</b>	<sup>16</sup> AUBERT	07AU BABR	10.6 $e^+e^- \rightarrow f_1(1285)\pi^+\pi^-\gamma$
<sup>16</sup> Calculated by us from the reported value of cross section at the peak.			

$$\Gamma(\eta'\pi^+\pi^-)/\Gamma_{\text{total}} \times \Gamma(e^+e^-)/\Gamma_{\text{total}} \quad \Gamma_6/\Gamma \times \Gamma_1/\Gamma$$

VALUE (units 10 <sup>-8</sup> )	DOCUMENT ID	TECN	COMMENT
••• We do not use the following data for averages, fits, limits, etc. •••			
4.9±1.9	<sup>17</sup> AUBERT	07AU BABR	10.6 $e^+e^- \rightarrow \eta'\pi^+\pi^-\gamma$
<sup>17</sup> Calculated by us from the reported value of cross section at the peak.			

### $\rho(2150)$ REFERENCES

AUBERT	07AU	PR D76 092005	B. Aubert et al.	(BABAR Collab.)
ANISOVICH	02	PL B542 8	A.V. Anisovich et al.	
ANISOVICH	01D	PL B508 6	A.V. Anisovich et al.	
ANISOVICH	01E	PL B513 281	A.V. Anisovich et al.	
ANISOVICH	00J	PL B491 47	A.V. Anisovich et al.	
KLOET	96	PR D53 6120	W.M. Kloet, F. Myhrer	(RUTG, NORD)
ALDE	95	ZPHY C66 379	D.M. Alde et al.	(GAMS Collab.) JP
HASAN	94	PL B334 215	A. Hasan, D.V. Bugg	(LOQM)
OAKDEN	94	NP A574 731	M.N. Oakden, M.R. Pennington	(DURH)
ALDE	92C	ZPHY C54 553	D.M. Alde et al.	(BELG, SERP, KEK, LANL+)
BIAGINI	91	NC 104A 363	M.E. Biagini et al.	(FRAS, PRAG)
CLEGG	90	ZPHY C45 677	A.B. Clegg, A. Donnachie	(LANC, MCHS)
ATKINSON	85	ZPHY C29 333	M. Atkinson et al.	(BONN, CERN, GLAS+)
MARTIN	80B	NP B176 355	B.R. Martin, D. Morgan	(LOUC, RHEL) JP
MARTIN	80C	NP B169 216	A.D. Martin, M.R. Pennington	(DURH) JP
CUTTS	78B	PR D17 16	D. Cutts et al.	(STON, WISC)
COUPLAND	77	PL 71B 460	M. Coupland et al.	(LOQM, RHEL)
PEASLEE	75	PL 57B 109	D.C. Peaslee et al.	(CANB, BARI, BROW+)
ALSPECTOR	73	PRL 30 511	J. Alspector et al.	(RUTG, UPNJ)
ABRAMS	70	PR D1 1917	R.J. Abrams et al.	(BNL)
COOPER	68	PRL 20 1059	W.A. Cooper et al.	(ANL)

### $\phi(2170)$

$$I(G^{JPC}) = 0^-(1^{--})$$

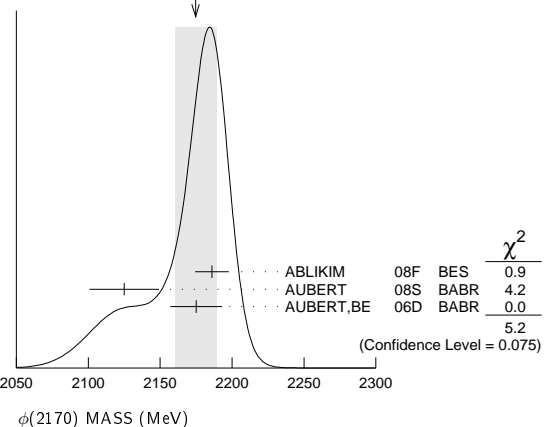
Observed by AUBERT, BE 06D in the initial-state radiation process  $e^+e^- \rightarrow \phi f_0(980)\gamma$ .

### $\phi(2170)$ MASS

VALUE (MeV)	EVTs	DOCUMENT ID	TECN	COMMENT
<b>2175±15 OUR AVERAGE</b> Error includes scale factor of 1.6. See the ideogram below.				
2186±10±6	52	ABLIKIM	08F BES	$J/\psi \rightarrow \eta\phi f_0(980)$
2125±22±10	483	AUBERT	08S BABR	10.6 $e^+e^- \rightarrow \phi\eta\gamma$
2175±10±15	201	<sup>1</sup> AUBERT, BE 06D	BABR	10.6 $e^+e^- \rightarrow K^+K^-\pi\pi\gamma$
••• We do not use the following data for averages, fits, limits, etc. •••				
2079±13 <sup>+79</sup> <sub>-28</sub>	4.8k	<sup>2</sup> SHEN	09 BELL	10.6 $e^+e^- \rightarrow K^+K^-\pi^+\pi^-\gamma$
2192±14	116±95	<sup>3</sup> AUBERT	07AK BABR	10.6 $e^+e^- \rightarrow K^+K^-\pi^+\pi^-\gamma$
2169±20	149±36	<sup>3</sup> AUBERT	07AK BABR	10.6 $e^+e^- \rightarrow K^+K^-\pi^0\pi^0\gamma$

- From the  $\phi f_0(980)$  component.
- From a fit with two incoherent Breit-Wigners.
- From the  $K^+K^-\phi_0(980)$  component.

WEIGHTED AVERAGE  
2175±15 (Error scaled by 1.6)



### $\phi(2170)$ WIDTH

VALUE (MeV)	EVTs	DOCUMENT ID	TECN	COMMENT
<b>61±18 OUR AVERAGE</b>				
65±23±17	52	ABLIKIM	08F BES	$J/\psi \rightarrow \eta\phi f_0(980)$
61±50±13	483	AUBERT	08S BABR	10.6 $e^+e^- \rightarrow \phi\eta\gamma$
58±16±20	201	<sup>4</sup> AUBERT, BE 06D	BABR	10.6 $e^+e^- \rightarrow K^+K^-\pi\pi\gamma$

See key on page 457

# Meson Particle Listings

## $\phi(2170)$ , $f_0(2200)$ , $f_J(2220)$

••• We do not use the following data for averages, fits, limits, etc. •••

192±23 <sup>+25</sup> <sub>-61</sub>	4.8k	<sup>5</sup> SHEN	09	BELL	10.6 e <sup>+</sup> e <sup>-</sup> → K <sup>+</sup> K <sup>-</sup> π <sup>+</sup> π <sup>-</sup> γ
71±21	116 ± 95	<sup>6</sup> AUBERT	07AK	BABR	10.6 e <sup>+</sup> e <sup>-</sup> → K <sup>+</sup> K <sup>-</sup> π <sup>+</sup> π <sup>-</sup> γ
102±27	149 ± 36	<sup>6</sup> AUBERT	07AK	BABR	10.6 e <sup>+</sup> e <sup>-</sup> → K <sup>+</sup> K <sup>-</sup> π <sup>0</sup> π <sup>0</sup> γ

<sup>4</sup> From the  $\phi f_0(980)$  component.<sup>5</sup> From a fit with two incoherent Breit-Wigners.<sup>6</sup> From the K<sup>+</sup>K<sup>-</sup>f<sub>0</sub>(980) component. **$\phi(2170)$  DECAY MODES**

Mode	Fraction ( $\Gamma_i/\Gamma$ )
$\Gamma_1$ e <sup>+</sup> e <sup>-</sup>	seen
$\Gamma_2$ $\phi\eta$	
$\Gamma_3$ $\phi\pi\pi$	
$\Gamma_4$ $\phi f_0(980)$	seen
$\Gamma_5$ K <sup>+</sup> K <sup>-</sup> π <sup>+</sup> π <sup>-</sup>	
$\Gamma_6$ K <sup>+</sup> K <sup>-</sup> f <sub>0</sub> (980) → K <sup>+</sup> K <sup>-</sup> π <sup>+</sup> π <sup>-</sup>	seen
$\Gamma_7$ K <sup>+</sup> K <sup>-</sup> π <sup>0</sup> π <sup>0</sup>	
$\Gamma_8$ K <sup>+</sup> K <sup>-</sup> f <sub>0</sub> (980) → K <sup>+</sup> K <sup>-</sup> π <sup>0</sup> π <sup>0</sup>	seen
$\Gamma_9$ K <sup>*</sup> 0 K <sup>±</sup> π <sup>∓</sup>	not seen
$\Gamma_{10}$ K <sup>*</sup> (892) <sup>0</sup> K <sup>*</sup> (892) <sup>0</sup>	not seen

 **$\phi(2170)$   $\Gamma(i)\Gamma(e^+e^-)/\Gamma(\text{total})$** 

$\Gamma(\phi\eta) \times \Gamma(e^+e^-)/\Gamma_{\text{total}}$	$\Gamma_2\Gamma_1/\Gamma$			
VALUE (eV)	EVTS	DOCUMENT ID	TECN	COMMENT

••• We do not use the following data for averages, fits, limits, etc. •••

1.7±0.7±1.3	483	AUBERT	08s	BABR	10.6 e <sup>+</sup> e <sup>-</sup> → $\phi\eta\gamma$
-------------	-----	--------	-----	------	---

$\Gamma(\phi f_0(980)) \times \Gamma(e^+e^-)/\Gamma_{\text{total}}$	$\Gamma_4\Gamma_1/\Gamma$			
VALUE (eV)	EVTS	DOCUMENT ID	TECN	COMMENT

2.5±0.8±0.4	201	<sup>7</sup> AUBERT,BE	06d	BABR	10.6 e <sup>+</sup> e <sup>-</sup> → K <sup>+</sup> K <sup>-</sup> ππγ
-------------	-----	------------------------	-----	------	--

<sup>7</sup> From the  $\phi f_0(980)$  component. **$\phi(2170)$   $\Gamma(i)\Gamma(e^+e^-)/\Gamma^2(\text{total})$** 

$\Gamma(\phi\pi\pi)/\Gamma_{\text{total}} \times \Gamma(e^+e^-)/\Gamma_{\text{total}}$	$\Gamma_3/\Gamma \times \Gamma_1/\Gamma$			
VALUE (units 10 <sup>-7</sup> )	EVTS	DOCUMENT ID	TECN	COMMENT

••• We do not use the following data for averages, fits, limits, etc. •••

1.65±0.15±0.18	4.8k	<sup>8</sup> SHEN	09	BELL	10.6 e <sup>+</sup> e <sup>-</sup> → K <sup>+</sup> K <sup>-</sup> π <sup>+</sup> π <sup>-</sup> γ
----------------	------	-------------------	----	------	--

<sup>8</sup> Multiplied by 3/2 to take into account the  $\phi\pi^0\pi^0$  mode. Using B( $\phi \rightarrow K^+K^-$ ) = (49.2 ± 0.6)%. **$\phi(2170)$  BRANCHING RATIOS**

$\Gamma(K^+K^-f_0(980) \rightarrow K^+K^-\pi^+\pi^-)/\Gamma_{\text{total}}$	$\Gamma_6/\Gamma$		
VALUE	DOCUMENT ID	TECN	COMMENT

seen	AUBERT	07AK	BABR	10.6 e <sup>+</sup> e <sup>-</sup> → K <sup>+</sup> K <sup>-</sup> π <sup>+</sup> π <sup>-</sup> γ
------	--------	------	------	--

$\Gamma(K^+K^-f_0(980) \rightarrow K^+K^-\pi^0\pi^0)/\Gamma_{\text{total}}$	$\Gamma_8/\Gamma$		
VALUE	DOCUMENT ID	TECN	COMMENT

seen	AUBERT	07AK	BABR	10.6 e <sup>+</sup> e <sup>-</sup> → K <sup>+</sup> K <sup>-</sup> π <sup>0</sup> π <sup>0</sup> γ
------	--------	------	------	--

$\Gamma(K^*0 K^{\pm}\pi^{\mp})/\Gamma_{\text{total}}$	$\Gamma_9/\Gamma$		
VALUE	DOCUMENT ID	TECN	COMMENT

not seen	AUBERT	07AK	BABR	10.6 GeV e <sup>+</sup> e <sup>-</sup>
----------	--------	------	------	--

$\Gamma(K^*(892)^0 \bar{K}^*(892)^0)/\Gamma_{\text{total}}$	$\Gamma_{10}/\Gamma$		
VALUE	DOCUMENT ID	TECN	COMMENT

not seen	ABLIKIM	10C	BES2	J/ψ → ηK <sup>+</sup> π <sup>-</sup> K <sup>-</sup> π <sup>+</sup>
----------	---------	-----	------	--

 **$\phi(2170)$  REFERENCES**

ABLIKIM	10C	PL B685 27	M. Ablikim et al.	(BES II Collab.)
SHEN	09	PR D80 031101R	C.P. Shen et al.	(BELLE Collab.)
ABLIKIM	08F	PRL 100 102003	M. Ablikim et al.	(BES Collab.)
AUBERT	08S	PR D77 092002	B. Aubert et al.	(BABAR Collab.)
AUBERT	07AK	PR D76 012008	B. Aubert et al.	(BABAR Collab.)
AUBERT,BE	06D	PR D74 091103R	B. Aubert et al.	(BABAR Collab.)

 **$f_0(2200)$** 

$$J^G(J^{PC}) = 0^+(0^{++})$$

OMITTED FROM SUMMARY TABLE

Seen in K<sub>S</sub><sup>0</sup>K<sub>S</sub><sup>0</sup> (AUGUSTIN 88), K<sup>+</sup>K<sup>-</sup> (ABLIKIM 05Q) and ηη (BINON 05) system. Not seen in T(1S) radiative decays (BARU 89). **$f_0(2200)$  MASS**

VALUE (MeV)	DOCUMENT ID	TECN	COMMENT
<b>2189±13 OUR AVERAGE</b>			
2170±20 <sup>+10</sup> <sub>-15</sub>	ABLIKIM	05Q	BES2 $\psi(2S) \rightarrow \gamma\pi^+\pi^-K^+K^-$
2210±50	<sup>1</sup> BINON	05	GAMS 33 $\pi^-p \rightarrow \eta\eta n$
2197±17	<sup>2</sup> AUGUSTIN	88	DM2 J/ψ → γK <sub>S</sub> <sup>0</sup> K <sub>S</sub> <sup>0</sup>

••• We do not use the following data for averages, fits, limits, etc. •••

~2122	HASAN	94	RVUE $\bar{p}p \rightarrow \pi\pi$
-------	-------	----	------------------------------------

~2321	HASAN	94	RVUE $\bar{p}p \rightarrow \pi\pi$
-------	-------	----	------------------------------------

<sup>1</sup> First solution, PWA is ambiguous.<sup>2</sup> Cannot determine spin to be 0. **$f_0(2200)$  WIDTH**

VALUE (MeV)	DOCUMENT ID	TECN	COMMENT
<b>238±50 OUR AVERAGE</b>			Error includes scale factor of 1.2.
220±60 <sup>+40</sup> <sub>-45</sub>	ABLIKIM	05Q	BES2 $\psi(2S) \rightarrow \gamma\pi^+\pi^-K^+K^-$
380±90	<sup>3</sup> BINON	05	GAMS 33 $\pi^-p \rightarrow \eta\eta n$
201±51	<sup>4</sup> AUGUSTIN	88	DM2 J/ψ → γK <sub>S</sub> <sup>0</sup> K <sub>S</sub> <sup>0</sup>

••• We do not use the following data for averages, fits, limits, etc. •••

~273	HASAN	94	RVUE $\bar{p}p \rightarrow \pi\pi$
------	-------	----	------------------------------------

~223	HASAN	94	RVUE $\bar{p}p \rightarrow \pi\pi$
------	-------	----	------------------------------------

<sup>3</sup> First solution, PWA is ambiguous.<sup>4</sup> Cannot determine spin to be 0. **$f_0(2200)$  REFERENCES**

ABLIKIM	05Q	PR D72 092002	M. Ablikim et al.	(BES Collab.)
BINON	05	PAN 68 960	F. Binon et al.	
		Translated from YAF 68 998.		
HASAN	94	PL B334 215	A. Hasan, D.V. Bugg	(LOQM)
BARU	89	ZPHY C42 505	S.E. Baru et al.	(NOVO)
AUGUSTIN	88	PRL 60 2238	J.E. Augustin et al.	(DM2 Collab.)

 **$f_J(2220)$** 

$$J^G(J^{PC}) = 0^+(2^{++} \text{ or } 4^{++})$$

OMITTED FROM SUMMARY TABLE

Needs confirmation. See our mini-review in the 2004 edition of this Review, PDG 04.

 **$f_J(2220)$  MASS**

VALUE (MeV)	EVTS	DOCUMENT ID	TECN	COMMENT
<b>2231.1 ± 3.5 OUR AVERAGE</b>				
2235 ± 4 ± 6	74	BAI	96B	BES e <sup>+</sup> e <sup>-</sup> → J/ψ → γπ <sup>+</sup> π <sup>-</sup>
2230 ± 6 <sup>+7</sup> <sub>-7</sub>	±16	46	BAI	96B BES e <sup>+</sup> e <sup>-</sup> → J/ψ → γK <sup>+</sup> K <sup>-</sup>
2232 ± 8 <sup>+7</sup> <sub>-7</sub>	±15	23	BAI	96B BES e <sup>+</sup> e <sup>-</sup> → J/ψ → γK <sub>S</sub> <sup>0</sup> K <sub>S</sub> <sup>0</sup>
2235 ± 4 ± 5	32	BAI	96B	BES e <sup>+</sup> e <sup>-</sup> → J/ψ → γρ $\bar{\rho}$
2209 ± 17 <sup>+17</sup> <sub>-15</sub>	±10	ASTON	88F	LASS 11 K <sup>-</sup> p → K <sup>+</sup> K <sup>-</sup> Λ
2230 ± 20		BOLONKIN	88	SPEC 40 π <sup>-</sup> p → K <sub>S</sub> <sup>0</sup> K <sub>S</sub> <sup>0</sup> n
2220 ± 10	41	<sup>1</sup> ALDE	86B	GA24 38-100 πp → nηη'
2230 ± 6 ± 14	93	BALTRUSAIT..86D	MRK3	e <sup>+</sup> e <sup>-</sup> → γK <sup>+</sup> K <sup>-</sup>
2232 ± 7 ± 7	23	BALTRUSAIT..86D	MRK3	e <sup>+</sup> e <sup>-</sup> → γK <sub>S</sub> <sup>0</sup> K <sub>S</sub> <sup>0</sup>
2223.9 ± 2.5		<sup>2</sup> VLADIMIRSK..08	SPEC	40 π <sup>-</sup> p → K <sub>S</sub> <sup>0</sup> K <sub>S</sub> <sup>0</sup> n + mπ <sup>0</sup>
2246 ± 36		BAI	98H	BES J/ψ → γπ <sup>0</sup> π <sup>0</sup>

<sup>1</sup> ALDE 86B uses data from both the GAMS-2000 and GAMS-4000 detectors.<sup>2</sup> J<sup>PC</sup> = 2<sup>++</sup>. Systematic uncertainties not evaluated **$f_J(2220)$  WIDTH**

VALUE (MeV)	CL%	EVTS	DOCUMENT ID	TECN	COMMENT
<b>23 ± 8 OUR AVERAGE</b>					
19 ± 13 <sup>+11</sup> <sub>-11</sub>		74	BAI	96B	BES e <sup>+</sup> e <sup>-</sup> → J/ψ → γπ <sup>+</sup> π <sup>-</sup>
20 ± 20 <sup>+15</sup> <sub>-15</sub>		46	BAI	96B	BES e <sup>+</sup> e <sup>-</sup> → J/ψ → γK <sup>+</sup> K <sup>-</sup>
20 ± 25 <sup>+16</sup> <sub>-16</sub>		23	BAI	96B	BES e <sup>+</sup> e <sup>-</sup> → J/ψ → γK <sub>S</sub> <sup>0</sup> K <sub>S</sub> <sup>0</sup>

# Meson Particle Listings

## $f_J(2220)$ , $\eta(2225)$ , $\rho_3(2250)$

$15^{+12}_{-9} \pm 9$	32	BAI	96B	BES	$e^+e^- \rightarrow J/\psi \rightarrow \gamma p \bar{p}$
$60^{+107}_{-57}$		ASTON	88F	LASS	$11 K^- p \rightarrow K^+ K^- \Lambda$
$80 \pm 30$		BOLONKIN	88	SPEC	$40 \pi^- p \rightarrow K_S^0 K_S^0 n$
$26^{+20}_{-16} \pm 17$	93	BALTRUSAIT...86D	MRK3		$e^+e^- \rightarrow \gamma K^+ K^-$
$18^{+23}_{-15} \pm 10$	23	BALTRUSAIT...86D	MRK3		$e^+e^- \rightarrow \gamma K_S^0 K_S^0$
$8.6 \pm 2.5$		<sup>3</sup> VLADIMIRSK...08	SPEC		$40 \pi^- p \rightarrow K_S^0 K_S^0 n + m\pi^0$
$<80$	90	ALDE	87C	GAM2	$38 \pi^- p \rightarrow \eta' \eta n$

<sup>3</sup>  $J^{PC} = 2^+ +$ . Systematic uncertainties not evaluated

### $f_J(2220)$ DECAY MODES

Mode	Fraction ( $\Gamma_i/\Gamma$ )
$\Gamma_1$ $\pi\pi$	seen
$\Gamma_2$ $\pi^+\pi^-$	seen
$\Gamma_3$ $K\bar{K}$	seen
$\Gamma_4$ $p\bar{p}$	
$\Gamma_5$ $\gamma\gamma$	not seen
$\Gamma_6$ $\eta\eta'(958)$	seen
$\Gamma_7$ $\phi\phi$	not seen
$\Gamma_8$ $\eta\eta$	not seen

### $f_J(2220)$ $\Gamma(i)\Gamma(\gamma\gamma)/\Gamma(\text{total})$

$\Gamma(K\bar{K}) \times \Gamma(\gamma\gamma)/\Gamma_{\text{total}}$	CL%	DOCUMENT ID	TECN	COMMENT	$\Gamma_3\Gamma_5/\Gamma$
$< 1.4$	95	<sup>4</sup> ACCIARRI	01H	L3	$\gamma\gamma \rightarrow K_S^0 K_S^0, E_{\text{cm}}^{\text{th}} = 91, 183-209 \text{ GeV}$
$< 5.6$	95	<sup>4</sup> GODANG	97	CLE2	$\gamma\gamma \rightarrow K_S^0 K_S^0$
$< 86$	95	<sup>4</sup> ALBRECHT	90G	ARG	$\gamma\gamma \rightarrow K^+ K^-$
$< 1000$	95	<sup>5</sup> ALTHOFF	85B	TASS	$\gamma\gamma, K\bar{K}\pi$

••• We do not use the following data for averages, fits, limits, etc. •••

$\Gamma(\pi\pi) \times \Gamma(\gamma\gamma)/\Gamma_{\text{total}}$	CL%	DOCUMENT ID	TECN	COMMENT	$\Gamma_1\Gamma_5/\Gamma$
$< 2.5$	95	ALAM	98C	CLE2	$\gamma\gamma \rightarrow \pi^+\pi^-$

<sup>4</sup> Assuming  $J^P = 2^+$ .  
<sup>5</sup> True for  $J^P = 0^+$  and  $J^P = 2^+$ .

### $f_J(2220)$ $\Gamma(i)\Gamma(p\bar{p})/\Gamma^2(\text{total})$

$\Gamma(p\bar{p})/\Gamma_{\text{total}} \times \Gamma(\pi\pi)/\Gamma_{\text{total}}$	CL%	DOCUMENT ID	TECN	COMMENT	$\Gamma_4/\Gamma \times \Gamma_1/\Gamma$
$< 18$	95	<sup>6</sup> AMSLER	01	CBAR	$1.4-1.5 p\bar{p} \rightarrow \pi^0\pi^0$
$< (11-42)$	99	<sup>7</sup> HASAN	96	SPEC	$1.35-1.55 p\bar{p} \rightarrow \pi^+\pi^-$

••• We do not use the following data for averages, fits, limits, etc. •••

$\Gamma(p\bar{p})/\Gamma_{\text{total}} \times \Gamma(\phi\phi)/\Gamma_{\text{total}}$	CL%	DOCUMENT ID	TECN	COMMENT	$\Gamma_4/\Gamma \times \Gamma_7/\Gamma$
$< 6$	95	<sup>8</sup> EVANGELIS...	98	SPEC	$1.1-2.0 p\bar{p} \rightarrow \phi\phi$

$\Gamma(p\bar{p})/\Gamma_{\text{total}} \times \Gamma(\eta\eta)/\Gamma_{\text{total}}$	CL%	DOCUMENT ID	TECN	COMMENT	$\Gamma_4/\Gamma \times \Gamma_8/\Gamma$
$< 4$	95	<sup>6</sup> AMSLER	01	CBAR	$1.4-1.5 p\bar{p} \rightarrow \eta\eta$

<sup>6</sup> For  $J^P = 2^+$  in the mass range 2222-2240 MeV and the total width between 10 and 20 MeV.  
<sup>7</sup> For  $J^P = 2^+$  and  $J^P = 4^+$  in the mass range 2220-2245 MeV and the total width of 15 MeV.  
<sup>8</sup> For  $J^P = 2^+$ , the mass of 2235 MeV and the total width of 15 MeV.

### $f_J(2220)$ BRANCHING RATIOS

$\Gamma(p\bar{p})/\Gamma_{\text{total}}$	CL%	DOCUMENT ID	TECN	COMMENT	$\Gamma_4/\Gamma$
not seen		<sup>9</sup> AUBERT	07AV	BABR	$B \rightarrow p\bar{p}K^{(*)}$
not seen		WANG	05A	BELL	$B^+ \rightarrow \bar{p}pK^+$
$< 3.0$	95	<sup>10</sup> EVANGELIS...	97	SPEC	$1.96-2.40 p\bar{p} \rightarrow K_S^0 K_S^0$
$< 1.1$	99.7	<sup>11</sup> BARNES	93	SPEC	$1.3-1.57 p\bar{p} \rightarrow K_S^0 K_S^0$
$< 2.6$	99.7	<sup>11</sup> BARDIN	87	CNTR	$1.3-1.5 p\bar{p} \rightarrow K^+ K^-$
$< 3.6$	99.7	<sup>11</sup> SCULLI	87	CNTR	$1.29-1.55 p\bar{p} \rightarrow K^+ K^-$

<sup>9</sup> Assuming  $\Gamma < 30 \text{ MeV}$ .  
<sup>10</sup> Assuming  $\Gamma \sim 20 \text{ MeV}$ ,  $J^P = 2^+$  and  $B(f_J(2220) \rightarrow K\bar{K}) = 100\%$ .  
<sup>11</sup> Assuming  $\Gamma = 30-35 \text{ MeV}$ ,  $J^P = 2^+$  and  $B(f_J(2220) \rightarrow K\bar{K}) = 100\%$ .

$\Gamma(\pi\pi)/\Gamma(K\bar{K})$	DOCUMENT ID	TECN	COMMENT	$\Gamma_1/\Gamma_3$
$1.0 \pm 0.5$	BAI	96B	BES	$e^+e^- \rightarrow J/\psi \rightarrow \gamma 2\pi, K\bar{K}$

$\Gamma(p\bar{p})/\Gamma(K\bar{K})$	DOCUMENT ID	TECN	COMMENT	$\Gamma_4/\Gamma_3$
$0.17 \pm 0.09$	BAI	96B	BES	$e^+e^- \rightarrow J/\psi \rightarrow \gamma p\bar{p}, K\bar{K}$

### $f_J(2220)$ REFERENCES

VLADIMIRSK... 08	PAN 71 2129	V.V. Vladimirov <i>et al.</i>	(ITEP)
AUBERT 07AV	PR D76 092004	B. Aubert <i>et al.</i>	(BABAR Collab.)
WANG 05A	PL B617 141	M.-Z. Wang <i>et al.</i>	(BELLE Collab.)
PDG 04	PL B592 1	S. Edelman <i>et al.</i>	(PDG Collab.)
ACCIARRI 01H	PL B501 173	M. Acciarri <i>et al.</i>	(L3 Collab.)
AMSLER 01	PL B520 175	C. Amisler <i>et al.</i>	(Crystal Barrel Collab.)
ALAM 98C	PRL 81 3328	M.S. Alam <i>et al.</i>	(CLEO Collab.)
BAI 98H	PRL 81 1179	J.Z. Bai <i>et al.</i>	(BES Collab.)
EVANGELIS... 98	PR D57 5370	C. Evangelista <i>et al.</i>	(JETSET Collab.)
EVANGELIS... 97	PR D56 3803	C. Evangelista <i>et al.</i>	(LEAR Collab.)
GODANG 97	PRL 79 3829	R. Godang <i>et al.</i>	(CLEO Collab.)
BAI 96B	PRL 76 3502	J.Z. Bai <i>et al.</i>	(BES Collab.)
HASAN 96	PL B388 376	A. Hasan, D.V. Bugg	(BRUN, LOQM)
BARNES 93	PL B309 469	P.D. Barnes <i>et al.</i>	(PS185 Collab.)
ALBRECHT 90G	ZPHY C48 183	H. Albrecht <i>et al.</i>	(ARGUS Collab.)
ASTON 88F	PL B215 199	D. Aston <i>et al.</i>	(SLAC, NAGO, CIN, INUS) JP
BOLONKIN 88	NP B309 426	B.V. Bolonkin <i>et al.</i>	(ITEP, SERP)
ALDE 87C	SJNP 45 255	D. Alde <i>et al.</i>	
BARDIN 87	PL B195 292	G. Bardin <i>et al.</i>	(SACL, FERR, CERN, PADO+)
SCULLI 87	PRL 58 1715	J. Sculli <i>et al.</i>	(NYU, BNL)
ALDE 86B	PL B177 120	D.M. Alde <i>et al.</i>	(SERP, BELG, LANL, LAPP)
BALTRUSAIT...86D	PRL 56 107	R.M. Baltrusaitis	(CIT, UCSC, ILL, SLA+)
ALTHOFF 85B	ZPHY C29 189	M. Althoff <i>et al.</i>	(TASSO Collab.)

### OTHER RELATED PAPERS

DEL-AMO-SA...100	PRL 105 172001	P. del Amo Sanchez <i>et al.</i>	(BABAR Collab.)
------------------	----------------	----------------------------------	-----------------

## $\eta(2225)$

$$I^G(J^{PC}) = 0^+(0^-)$$

OMITTED FROM SUMMARY TABLE

Seen in  $J/\psi \rightarrow \gamma\phi$ . Possibly seen in  $B \rightarrow \phi\phi K$  by LEES 11A.

### $\eta(2225)$ MASS

VALUE (MeV)	EVTS	DOCUMENT ID	TECN	COMMENT	
$2226 \pm 16$	OUR AVERAGE				
$2240^{+30}_{-20} \pm 30$	196 $\pm$ 19	ABLIKIM	08i	BES	$J/\psi \rightarrow \gamma K^+ K^- K_S^0 K_L^0$
$2230 \pm 25 \pm 15$		BAI	90B	MRK3	$J/\psi \rightarrow \gamma K^+ K^- K^+ K^-$
$2214 \pm 20 \pm 13$		BAI	90B	MRK3	$J/\psi \rightarrow \gamma K^+ K^- K_S^0 K_L^0$
$\sim 2220$		BISELLO	86B	DM2	$J/\psi \rightarrow \gamma K^+ K^- K^+ K^-$

••• We do not use the following data for averages, fits, limits, etc. •••

### $\eta(2225)$ WIDTH

VALUE (MeV)	EVTS	DOCUMENT ID	TECN	COMMENT	
$185^{+70}_{-40}$	OUR AVERAGE				
$190 \pm 30^{+60}_{-40}$	196 $\pm$ 19	ABLIKIM	08i	BES	$J/\psi \rightarrow \gamma K^+ K^- K_S^0 K_L^0$
$150^{+300}_{-60} \pm 60$		BAI	90B	MRK3	$J/\psi \rightarrow \gamma K^+ K^- K^+ K^-$
$\sim 80$		BISELLO	86B	DM2	$J/\psi \rightarrow \gamma K^+ K^- K^+ K^-$

••• We do not use the following data for averages, fits, limits, etc. •••

### $\eta(2225)$ REFERENCES

LEES 11A	PR D84 012001	J.P. Lees <i>et al.</i>	(BABAR Collab.)
ABLIKIM 08i	PL B662 330	M. Ablikim <i>et al.</i>	(BES Collab.)
BAI 90B	PRL 65 1309	Z. Bai <i>et al.</i>	(Mark III Collab.)
BISELLO 86B	PL B179 294	D. Bisello <i>et al.</i>	(DM2 Collab.)

## $\rho_3(2250)$

$$I^G(J^{PC}) = 1^+(3^-)$$

OMITTED FROM SUMMARY TABLE

Contains results mostly from formation experiments. For further production experiments see the Further States entry. See also  $\rho(2150)$ ,  $f_2(2150)$ ,  $f_4(2300)$ ,  $\rho_5(2350)$ .



See key on page 457

## Meson Particle Listings

 $\rho_3(2250)$ ,  $f_2(2300)$ ,  $f_4(2300)$  $\rho_3(2250)$  MASS $\bar{p}p \rightarrow \pi\pi \text{ or } K\bar{K}$ 

VALUE (MeV)	DOCUMENT ID	TECN	CHG	COMMENT
••• We do not use the following data for averages, fits, limits, etc. •••				
~ 2232	HASAN 94	RVUE		$\bar{p}p \rightarrow \pi\pi$
~ 2090	1 OAKDEN 94	RVUE		$0.36\text{--}1.55 \bar{p}p \rightarrow \pi\pi$
~ 2250	2 MARTIN 80B	RVUE		
~ 2300	2 MARTIN 80C	RVUE		
~ 2140	3 CARTER 78B	CNTR 0		$0.7\text{--}2.4 \bar{p}p \rightarrow K^- K^+$
~ 2150	4 CARTER 77	CNTR 0		$0.7\text{--}2.4 \bar{p}p \rightarrow \pi\pi$

<sup>1</sup> See however KLOET 96 who fit  $\pi^+\pi^-$  only and find waves only up to  $J = 3$  to be important but not significantly resonant.

<sup>2</sup>  $I(J^P) = 1(3^-)$  from simultaneous analysis of  $p\bar{p} \rightarrow \pi^-\pi^+$  and  $\pi^0\pi^0$ .

<sup>3</sup>  $I = 0, 1, J^P = 3^-$  from Barrelet-zero analysis.

<sup>4</sup>  $I(J^P) = 1(3^-)$  from amplitude analysis.

S-CHANNEL  $\bar{N}N$ 

VALUE (MeV)	DOCUMENT ID	TECN	CHG	COMMENT
••• We do not use the following data for averages, fits, limits, etc. •••				
$2260 \pm 20$	5 ANISOVICH 02	SPEC		$0.6\text{--}1.9 p\bar{p} \rightarrow \omega\pi^0, \omega\eta\pi^0, \pi^+\pi^-$
~ 2190	6 CUTTS 78B	CNTR		$0.97\text{--}3 \bar{p}p \rightarrow \bar{N}N$
$2155 \pm 15$	6,7 COUPLAND 77	CNTR 0		$0.7\text{--}2.4 \bar{p}p \rightarrow \bar{p}p$
$2193 \pm 2$	6,8 ALSPECTOR 73	CNTR		$\bar{p}p$ S channel
$2190 \pm 10$	9 ABRAMS 70	CNTR		S channel $\bar{p}N$

<sup>5</sup> From the combined analysis of ANISOVICH 00J, ANISOVICH 01D, ANISOVICH 01E, and ANISOVICH 02.

<sup>6</sup> Isospins 0 and 1 not separated.

<sup>7</sup> From a fit to the total elastic cross section.

<sup>8</sup> Referred to as T or T region by ALSPECTOR 73.

<sup>9</sup> Seen as bump in  $I = 1$  state. See also COOPER 68. PEASLEE 75 confirm  $\bar{p}p$  results of ABRAMS 70, no narrow structure.

 $\pi^-p \rightarrow \eta\pi\pi$ 

VALUE (MeV)	DOCUMENT ID	TECN	COMMENT
••• We do not use the following data for averages, fits, limits, etc. •••			
$2290 \pm 20 \pm 30$	AMELIN 00	VES	37 $\pi^-p \rightarrow \eta\pi^+\pi^-n$

 $\rho_3(2250)$  WIDTH $\bar{p}p \rightarrow \pi\pi \text{ or } K\bar{K}$ 

VALUE (MeV)	DOCUMENT ID	TECN	CHG	COMMENT
••• We do not use the following data for averages, fits, limits, etc. •••				
~ 220	HASAN 94	RVUE		$\bar{p}p \rightarrow \pi\pi$
~ 60	10 OAKDEN 94	RVUE		$0.36\text{--}1.55 \bar{p}p \rightarrow \pi\pi$
~ 250	11 MARTIN 80B	RVUE		
~ 200	11 MARTIN 80C	RVUE		
~ 150	12 CARTER 78B	CNTR 0		$0.7\text{--}2.4 \bar{p}p \rightarrow K^- K^+$
~ 200	13 CARTER 77	CNTR 0		$0.7\text{--}2.4 \bar{p}p \rightarrow \pi\pi$

<sup>10</sup> See however KLOET 96 who fit  $\pi^+\pi^-$  only and find waves only up to  $J = 3$  to be important but not significantly resonant.

<sup>11</sup>  $I(J^P) = 1(3^-)$  from simultaneous analysis of  $p\bar{p} \rightarrow \pi^-\pi^+$  and  $\pi^0\pi^0$ .

<sup>12</sup>  $I = 0, 1, J^P = 3^-$  from Barrelet-zero analysis.

<sup>13</sup>  $I(J^P) = 1(3^-)$  from amplitude analysis.

S-CHANNEL  $\bar{N}N$ 

VALUE (MeV)	DOCUMENT ID	TECN	CHG	COMMENT
••• We do not use the following data for averages, fits, limits, etc. •••				
$160 \pm 25$	14 ANISOVICH 02	SPEC		$0.6\text{--}1.9 p\bar{p} \rightarrow \omega\pi^0, \omega\eta\pi^0, \pi^+\pi^-$
$135 \pm 75$	15,16 COUPLAND 77	CNTR 0		$0.7\text{--}2.4 \bar{p}p \rightarrow \bar{p}p$
$98 \pm 8$	16 ALSPECTOR 73	CNTR		$\bar{p}p$ S channel
~ 85	17 ABRAMS 70	CNTR		S channel $\bar{p}N$

<sup>14</sup> From the combined analysis of ANISOVICH 00J, ANISOVICH 01D, ANISOVICH 01E, and ANISOVICH 02.

<sup>15</sup> From a fit to the total elastic cross section.

<sup>16</sup> Isospins 0 and 1 not separated.

<sup>17</sup> Seen as bump in  $I = 1$  state. See also COOPER 68. PEASLEE 75 confirm  $\bar{p}p$  results of ABRAMS 70, no narrow structure.

 $\pi^-p \rightarrow \eta\pi\pi$ 

VALUE (MeV)	DOCUMENT ID	TECN	COMMENT
••• We do not use the following data for averages, fits, limits, etc. •••			
$230 \pm 50 \pm 80$	AMELIN 00	VES	37 $\pi^-p \rightarrow \eta\pi^+\pi^-n$

 $\rho_3(2250)$  REFERENCES

ANISOVICH 02	PL B542 8	A.V. Anisovich <i>et al.</i>	
ANISOVICH 01D	PL B508 6	A.V. Anisovich <i>et al.</i>	
ANISOVICH 01E	PL B513 281	A.V. Anisovich <i>et al.</i>	
AMELIN 00	NP A668 83	D. Amelin <i>et al.</i>	(VES Collab.)
ANISOVICH 00J	PL B491 47	A.V. Anisovich <i>et al.</i>	
KLOET 96	PR D53 6120	W.M. Kloet, F. Myhrer	(RUTG, NORD)
HASAN 94	PL B334 215	A. Hasan, D.V. Bugg	(LOQM)
OAKDEN 94	NP A574 731	M.N. Oakden, M.R. Pennington	(DURH)
MARTIN 80B	NP B176 355	B.R. Martin, D. Morgan	(LOUC, RHEL) JP
MARTIN 80C	NP B169 216	A.D. Martin, M.R. Pennington	(DURH) JP
CARTER 78B	NP B141 467	A.A. Carter	(LOQM)
CUTTS 78B	PR D17 16	D. Cutts <i>et al.</i>	(STON, WISC)
CARTER 77	PL 67B 117	A.A. Carter <i>et al.</i>	(LOQM, RHEL) JP
COUPLAND 77	PL 71B 460	M. Coupland <i>et al.</i>	(LOQM, RHEL)
PEASLEE 75	PL 57B 189	D.C. Peaslee <i>et al.</i>	(CANB, BARI, BROW+)
ALSPECTOR 73	PRL 30 511	J. Alspector <i>et al.</i>	(RUTG, UPNJ)
ABRAMS 70	PR D1 1917	R.J. Abrams <i>et al.</i>	(BNL)
COOPER 68	PRL 20 1059	W.A. Cooper <i>et al.</i>	(ANL)

 $f_2(2300)$ 

$$I^G(J^{PC}) = 0^+(2^{++})$$

 $f_2(2300)$  MASS

VALUE (MeV)	DOCUMENT ID	TECN	COMMENT
••• We do not use the following data for averages, fits, limits, etc. •••			
$2297 \pm 28$	1 ETKIN 88	MPS	$22 \pi^-p \rightarrow \phi\phi n$
$2270 \pm 12$	VLADIMIRSK...06	SPEC	$40 \pi^-p \rightarrow K_S^0 K_S^0 n$
$2327 \pm 9 \pm 6$	ABE 04	BELL	$10.6 e^+e^- \rightarrow e^+e^- K^+ K^-$
$2231 \pm 10$	BOOTH 86	OMEG	$85 \pi^-Be \rightarrow 2\phi Be$
$2220 \pm 90$	LINDENBAUM 84	RVUE	
$2320 \pm 20$	ETKIN 82	MPS	$22 \pi^-p \rightarrow 2\phi n$

<sup>1</sup> Includes data of ETKIN 85. The percentage of the resonance going into  $\phi\phi 2^+ + S_2, D_2,$  and  $D_0$  is  $6 \pm 15, 25 \pm 18,$  and  $69 \pm 16$ , respectively.

 $f_2(2300)$  WIDTH

VALUE (MeV)	DOCUMENT ID	TECN	COMMENT
••• We do not use the following data for averages, fits, limits, etc. •••			
$149 \pm 41$	2 ETKIN 88	MPS	$22 \pi^-p \rightarrow \phi\phi n$
$90 \pm 29$	VLADIMIRSK...06	SPEC	$40 \pi^-p \rightarrow K_S^0 K_S^0 n$
$275 \pm 36 \pm 20$	ABE 04	BELL	$10.6 e^+e^- \rightarrow e^+e^- K^+ K^-$
$133 \pm 50$	BOOTH 86	OMEG	$85 \pi^-Be \rightarrow 2\phi Be$
$200 \pm 50$	LINDENBAUM 84	RVUE	
$220 \pm 70$	ETKIN 82	MPS	$22 \pi^-p \rightarrow 2\phi n$

<sup>2</sup> Includes data of ETKIN 85.

 $f_2(2300)$  DECAY MODES

Mode	Fraction ( $\Gamma_i/\Gamma$ )
$\Gamma_1 \phi\phi$	seen
$\Gamma_2 K\bar{K}$	seen
$\Gamma_3 \gamma\gamma$	seen

 $f_2(2300)$   $\Gamma(i)\Gamma(\gamma\gamma)/\Gamma(\text{total})$ 

VALUE (eV)	DOCUMENT ID	TECN	COMMENT	$\Gamma_2\Gamma_3/\Gamma$
••• We do not use the following data for averages, fits, limits, etc. •••				
$44 \pm 6 \pm 12$	3 ABE 04	BELL	$10.6 e^+e^- \rightarrow e^+e^- K^+ K^-$	

<sup>3</sup> Assuming spin 2.

 $f_2(2300)$  REFERENCES

VLADIMIRSK... 06	PAN 69 493	V.V. Vladimirov <i>et al.</i>	(ITEP, Moscow)
ABE 04	EPJ C32 323	K. Abe <i>et al.</i>	(BELLE Collab.)
ETKIN 88	PL B201 568	A. Etkin <i>et al.</i>	(BNL, CUNY)
BOOTH 86	NP B273 677	P.S.L. Booth <i>et al.</i>	(LIVP, GLAS, CERN)
ETKIN 85	PL 165B 217	A. Etkin <i>et al.</i>	(BNL, CUNY)
LINDENBAUM 84	CNPP 13 285	S.J. Lindenbaum	(CUNY)
ETKIN 82	PRL 49 1620	A. Etkin <i>et al.</i>	(BNL, CUNY)

 $f_4(2300)$ 

$$I^G(J^{PC}) = 0^+(4^{++})$$

OMITTED FROM SUMMARY TABLE

This entry was previously called  $U_0(2350)$ . Contains results mostly from formation experiments. For further production experiments see the Further States entry. See also  $\rho(2150)$ ,  $f_2(2150)$ ,  $\rho_3(2250)$ ,  $\rho_5(2350)$ .

## Meson Particle Listings

 $f_4(2300)$ ,  $f_0(2330)$ ,  $f_2(2340)$  $f_4(2300)$  MASS $\bar{p}p \rightarrow \pi\pi \text{ or } \bar{K}K$ 

VALUE (MeV)	DOCUMENT ID	TECN	COMMENT
••• We do not use the following data for averages, fits, limits, etc. •••			
~ 2314	HASAN	94	RVUE $\bar{p}p \rightarrow \pi\pi$
~ 2300	1 MARTIN	80B	RVUE
~ 2300	1 MARTIN	80C	RVUE
~ 2340	2 CARTER	78B	CNTR 0.7-2.4 $\bar{p}p \rightarrow \pi^- K^+$
~ 2330	DULUDE	78B	OSPK 1-2 $\bar{p}p \rightarrow \pi^0 \pi^0$
~ 2310	3 CARTER	77	CNTR 0.7-2.4 $\bar{p}p \rightarrow \pi\pi$
<sup>1</sup> $I(J^P) = 0(4^+)$ from simultaneous analysis of $p\bar{p} \rightarrow \pi^- \pi^+$ and $\pi^0 \pi^0$ .			
<sup>2</sup> $I(J^P) = 0(4^+)$ from Barrelet-zero analysis.			
<sup>3</sup> $I(J^P) = 0(4^+)$ from amplitude analysis.			

S-CHANNEL  $\bar{p}p$  or  $\bar{N}N$ 

VALUE (MeV)	DOCUMENT ID	TECN	COMMENT
••• We do not use the following data for averages, fits, limits, etc. •••			
2283 ± 17	4 ANISOVICH	00J	SPEC
~ 2380	5 CUTTS	78B	CNTR 0.97-3 $\bar{p}p \rightarrow \bar{N}N$
2345 ± 15	5,6 COUPLAND	77	CNTR 0.7-2.4 $\bar{p}p \rightarrow \bar{p}p$
2359 ± 2	5,7 ALSPECTOR	73	CNTR $\bar{p}p$ S channel
2375 ± 10	ABRAMS	70	CNTR S channel $\bar{N}N$
<sup>4</sup> From the combined analysis of ANISOVICH 99C and ANISOVICH 99F on $\bar{p}p \rightarrow \eta\pi^0 \pi^0$ , $\pi^0 \pi^0$ , $\eta\eta$ , $\eta\eta'$ , $\pi^+ \pi^-$ .			
<sup>5</sup> Isospins 0 and 1 not separated.			
<sup>6</sup> From a fit to the total elastic cross section.			
<sup>7</sup> Referred to as U or U region by ALSPECTOR 73.			

 $\pi^- p \rightarrow \eta\pi\pi n$ 

VALUE (MeV)	DOCUMENT ID	TECN	COMMENT
••• We do not use the following data for averages, fits, limits, etc. •••			
2330 ± 20 ± 40	AMELIN	00	VES 37 $\pi^- p \rightarrow \eta\pi^+ \pi^- n$

 $p\bar{p}$  CENTRAL PRODUCTION

VALUE (MeV)	DOCUMENT ID	COMMENT
<b>2320 ± 60 OUR ESTIMATE</b>		
••• We do not use the following data for averages, fits, limits, etc. •••		
2332 ± 15	BARBERIS	00F 450 $p\bar{p} \rightarrow p_f \omega p_S$

 $f_4(2300)$  WIDTH $\bar{p}p \rightarrow \pi\pi \text{ or } \bar{K}K$ 

VALUE (MeV)	DOCUMENT ID	TECN	COMMENT
••• We do not use the following data for averages, fits, limits, etc. •••			
~ 278	HASAN	94	RVUE $\bar{p}p \rightarrow \pi\pi$
~ 200	8 MARTIN	80C	RVUE
~ 150	9 CARTER	78B	CNTR 0.7-2.4 $\bar{p}p \rightarrow K^- K^+$
~ 210	10 CARTER	77	CNTR 0.7-2.4 $\bar{p}p \rightarrow \pi\pi$
<sup>8</sup> $I(J^P) = 0(4^+)$ from simultaneous analysis of $p\bar{p} \rightarrow \pi^- \pi^+$ and $\pi^0 \pi^0$ .			
<sup>9</sup> $I(J^P) = 0(4^+)$ from Barrelet-zero analysis.			
<sup>10</sup> $I(J^P) = 0(4^+)$ from amplitude analysis.			

S-CHANNEL  $\bar{p}p$  or  $\bar{N}N$ 

VALUE (MeV)	DOCUMENT ID	TECN	COMMENT
••• We do not use the following data for averages, fits, limits, etc. •••			
310 ± 25	11 ANISOVICH	00J	SPEC
135 ± 150 - 65	12,13 COUPLAND	77	CNTR 0.7-2.4 $\bar{p}p \rightarrow \bar{p}p$
165 ± 18 - 8	13 ALSPECTOR	73	CNTR $\bar{p}p$ S channel
~ 190	ABRAMS	70	CNTR S channel $\bar{N}N$
<sup>11</sup> From the combined analysis of ANISOVICH 99C and ANISOVICH 99F on $\bar{p}p \rightarrow \eta\pi^0 \pi^0$ , $\pi^0 \pi^0$ , $\eta\eta$ , $\eta\eta'$ , $\pi^+ \pi^-$ .			
<sup>12</sup> From a fit to the total elastic cross section.			
<sup>13</sup> Isospins 0 and 1 not separated.			

 $\pi^- p \rightarrow \eta\pi\pi n$ 

VALUE (MeV)	DOCUMENT ID	TECN	COMMENT
••• We do not use the following data for averages, fits, limits, etc. •••			
235 ± 50 ± 40	AMELIN	00	VES 37 $\pi^- p \rightarrow \eta\pi^+ \pi^- n$

 $p\bar{p}$  CENTRAL PRODUCTION

VALUE (MeV)	DOCUMENT ID	COMMENT
<b>250 ± 80 OUR ESTIMATE</b>		
••• We do not use the following data for averages, fits, limits, etc. •••		
260 ± 57	BARBERIS	00F 450 $p\bar{p} \rightarrow p_f \omega p_S$

 $f_4(2300)$  DECAY MODES

Mode	Fraction ( $\Gamma_i/\Gamma$ )
$\Gamma_1$ $\rho\rho$	seen
$\Gamma_2$ $\omega\omega$	seen
$\Gamma_3$ $\eta\pi\pi$	seen
$\Gamma_4$ $\pi\pi$	seen
$\Gamma_5$ $K\bar{K}$	seen
$\Gamma_6$ $N\bar{N}$	seen

 $f_4(2300)$  BRANCHING RATIOS

$\Gamma(\rho\rho)/\Gamma(\omega\omega)$	DOCUMENT ID	COMMENT	$\Gamma_1/\Gamma_2$
••• We do not use the following data for averages, fits, limits, etc. •••			
2.8 ± 0.5	BARBERIS	00F 450 $p\bar{p} \rightarrow p_f \omega p_S$	

 $f_4(2300)$  REFERENCES

AMELIN	00	NP A668 83	D. Amelin et al.	(VES Collab.)
ANISOVICH	00J	PL B491 47	A.V. Anisovich et al.	
BARBERIS	00F	PL B484 198	D. Barberis et al.	(WA 102 Collab.)
ANISOVICH	99C	PL B452 173	A.V. Anisovich et al.	
ANISOVICH	99F	NP A651 253	A.V. Anisovich et al.	
HASAN	94	PL B334 215	A. Hasan, D.V. Bugg	(LOQM)
MARTIN	80B	NP B176 355	B.R. Martin, D. Morgan	(LOUC, RHEL) JP
MARTIN	80C	NP B169 216	A.D. Martin, M.R. Pennington	(DURH) JP
CARTER	78B	NP B341 467	A.A. Carter	(LOQM)
CUTTS	78B	PR D17 16	D. Cutts et al.	(STON, WISC)
DULUDE	78B	PL 79B 335	R.S. Dulude et al.	(BROW, MIT, BARI) JP
CARTER	77	PL 67B 117	A.A. Carter et al.	(LOQM, RHEL) JP
COUPLAND	77	PL 71B 460	M. Coupland et al.	(LOQM, RHEL)
ALSPECTOR	73	PRL 30 511	J. Alspector et al.	(RUTG, UPNJ)
ABRAMS	70	PR D1 1917	R.J. Abrams et al.	(BNL)

 $f_0(2330)$ 

$$I^G(J^{PC}) = 0^+(0^{++})$$

OMITTED FROM SUMMARY TABLE

 $f_0(2330)$  MASS

VALUE (MeV)	DOCUMENT ID	TECN	COMMENT
••• We do not use the following data for averages, fits, limits, etc. •••			
2314 ± 25	1 BUGG	04A	RVUE
2337 ± 14	ANISOVICH	00J	SPEC 2.0 $\bar{p}p \rightarrow \pi\pi, \eta\eta$
~ 2321	HASAN	94	RVUE $\bar{p}p \rightarrow \pi\pi$
<sup>1</sup> Partial wave analysis of the data on $p\bar{p} \rightarrow \bar{\Lambda}\Lambda$ from BARNES 00.			

 $f_0(2330)$  WIDTH

VALUE (MeV)	DOCUMENT ID	TECN	COMMENT
••• We do not use the following data for averages, fits, limits, etc. •••			
144 ± 20	2 BUGG	04A	RVUE
217 ± 33	ANISOVICH	00J	SPEC 2.0 $\bar{p}p \rightarrow \pi\pi, \eta\eta$
~ 223	HASAN	94	RVUE $\bar{p}p \rightarrow \pi\pi$
<sup>2</sup> Partial wave analysis of the data on $p\bar{p} \rightarrow \bar{\Lambda}\Lambda$ from BARNES 00.			

 $f_0(2330)$  REFERENCES

BUGG	04A	EPJ C36 161	D.V. Bugg	
ANISOVICH	00J	PL B491 47	A.V. Anisovich et al.	
BARNES	00	PR C62 055203	P.D. Barnes et al.	
HASAN	94	PL B334 215	A. Hasan, D.V. Bugg	(LOQM)

 $f_2(2340)$ 

$$I^G(J^{PC}) = 0^+(2^{++})$$

 $f_2(2340)$  MASS

VALUE (MeV)	EVTS	DOCUMENT ID	TECN	COMMENT
••• We do not use the following data for averages, fits, limits, etc. •••				
2339 ± 55		1 ETKIN	88	MPS 22 $\pi^- p \rightarrow \phi\phi n$
2350 ± 7	80k	2 UMAN	06	E835 5.2 $\bar{p}p \rightarrow \eta\eta\pi^0$
2392 ± 10		BOOTH	86	OMEG 85 $\pi^- \text{Be} \rightarrow 2\phi\text{Be}$
2360 ± 20		LINDENBAUM	84	RVUE
<sup>1</sup> Includes data of ETKIN 85. The percentage of the resonance going into $\phi\phi 2^+ + S_2$ , $D_2$ , and $D_0$ is $37 \pm 19$ , $4 \pm 12$ , and $59 \pm 21$ , respectively.				
<sup>2</sup> Statistical error only.				

 $f_2(2340)$  WIDTH

VALUE (MeV)	EVTS	DOCUMENT ID	TECN	COMMENT
319 ± 81 - 69		3 ETKIN	88	MPS 22 $\pi^- p \rightarrow \phi\phi n$

See key on page 457

Meson Particle Listings  
 $f_2(2340)$ ,  $\rho_5(2350)$ ,  $a_6(2450)$ 

• • • We do not use the following data for averages, fits, limits, etc. • • •

218 ± 16	80k	<sup>4</sup> UMAN	06	E835	5.2	$\bar{p}p \rightarrow \eta\eta\pi^0$
198 ± 50		BOOTH	86	OMEG	85	$\pi^- p \rightarrow 2\phi\text{Be}$
150 <sup>+150</sup> <sub>-50</sub>		LINDENBAUM	84	RVUE		

<sup>3</sup> Includes data of ETKIN 85.<sup>4</sup> Statistical error only. $f_2(2340)$  DECAY MODES

Mode	Fraction ( $\Gamma_i/\Gamma$ )
$\Gamma_1$ $\phi\phi$	seen
$\Gamma_2$ $\eta\eta$	seen

 $f_2(2340)$  BRANCHING RATIOS

$\Gamma(\eta\eta)/\Gamma_{\text{total}}$	DOCUMENT ID	TECN	CHG	COMMENT	$\Gamma_2/\Gamma$
seen	UMAN	06	E835	5.2 $\bar{p}p \rightarrow \eta\eta\pi^0$	

 $f_2(2340)$  REFERENCES

UMAN	06	PR D73 052009	I. Uman <i>et al.</i>	(FNAL E835)
ETKIN	88	PL B201 568	A. Etkin <i>et al.</i>	(BNL, CUNY)
BOOTH	86	NP B273 677	P.S.L. Booth <i>et al.</i>	(LIVP, GLAS, CERN)
ETKIN	85	PL 165B 217	A. Etkin <i>et al.</i>	(BNL, CUNY)
LINDENBAUM	84	CNPP 13 285	S.J. Lindenbaum	(CUNY)

 $\rho_5(2350)$ 

$$I^G(J^{PC}) = 1^+(5^{--})$$

OMITTED FROM SUMMARY TABLE

This entry was previously called  $U_1(2400)$ . See also  $\rho(2150)$ ,  $f_2(2150)$ ,  $\rho_3(2250)$ ,  $f_4(2300)$ . $\rho_5(2350)$  MASS

$\pi^- p \rightarrow \omega\pi^0 n$	DOCUMENT ID	TECN	CHG	COMMENT
VALUE (MeV)				
2330 ± 35	ALDE	95	GAM2	38 $\pi^- p \rightarrow \omega\pi^0 n$

VALUE (MeV)	DOCUMENT ID	TECN	CHG	COMMENT
-------------	-------------	------	-----	---------

• • • We do not use the following data for averages, fits, limits, etc. • • •

~ 2303	HASAN	94	RVUE	$\bar{p}p \rightarrow \pi\pi$
~ 2300	<sup>1</sup> MARTIN	80B	RVUE	
~ 2250	<sup>1</sup> MARTIN	80C	RVUE	
~ 2500	<sup>2</sup> CARTER	78B	CNTR	0 0.7-2.4 $\bar{p}p \rightarrow K^- K^+$
~ 2480	<sup>3</sup> CARTER	77	CNTR	0 0.7-2.4 $\bar{p}p \rightarrow \pi\pi$

S-CHANNEL  $\bar{N}N$ 

VALUE (MeV)	DOCUMENT ID	TECN	CHG	COMMENT
-------------	-------------	------	-----	---------

• • • We do not use the following data for averages, fits, limits, etc. • • •

2300 ± 45	<sup>4</sup> ANISOVICH	02	SPEC	0.6-1.9 $\rho\bar{p} \rightarrow \omega\pi^0, \omega\eta\pi^0, \pi^+\pi^-$
2295 ± 30	ANISOVICH	00J	SPEC	
~ 2380	<sup>5</sup> CUTTS	78B	CNTR	0.97-3 $\bar{p}p \rightarrow \bar{N}N$
2345 ± 15	<sup>5,6</sup> COUPLAND	77	CNTR	0 0.7-2.4 $\bar{p}p \rightarrow \bar{p}p$
2359 ± 2	<sup>5,7</sup> ALSPECTOR	73	CNTR	$\bar{p}p$ S channel
2350 ± 10	<sup>8</sup> ABRAMS	70	CNTR	S channel $\bar{N}N$
2360 ± 25	<sup>9</sup> OH	70B	HDDB	-0 $\bar{p}(p\eta), K^* K 2\pi$

 $\pi^- p \rightarrow K^+ K^- n$ 

VALUE (MeV)	DOCUMENT ID	TECN	CHG	COMMENT
-------------	-------------	------	-----	---------

• • • We do not use the following data for averages, fits, limits, etc. • • •

2307 ± 6	ALPER	80	CNTR	0 62 $\pi^- p \rightarrow K^+ K^- n$
----------	-------	----	------	--------------------------------------

<sup>1</sup>  $I(J^P) = 1(5^-)$  from simultaneous analysis of  $p\bar{p} \rightarrow \pi^- \pi^+$  and  $\pi^0 \pi^0$ .<sup>2</sup>  $I = 0(1); J^P = 5^-$  from Barrelet-zero analysis.<sup>3</sup>  $I(J^P) = 1(5^-)$  from amplitude analysis.<sup>4</sup> From the combined analysis of ANISOVICH 00J, ANISOVICH 01D, ANISOVICH 01E, and ANISOVICH 02.<sup>5</sup> Isospins 0 and 1 not separated.<sup>6</sup> From a fit to the total elastic cross section.<sup>7</sup> Referred to as U or U region by ALSPECTOR 73.<sup>8</sup> For  $l = 1 \bar{N}N$ .<sup>9</sup> No evidence for this bump seen in the  $\bar{p}p$  data of CHAPMAN 71B. Narrow state not confirmed by OH 73 with more data. $\rho_5(2350)$  WIDTH $\pi^- p \rightarrow \omega\pi^0 n$ 

VALUE (MeV)	DOCUMENT ID	TECN	CHG	COMMENT
400 ± 100	ALDE	95	GAM2	38 $\pi^- p \rightarrow \omega\pi^0 n$

 $\bar{p}p \rightarrow \pi\pi \alpha \bar{K}K$ 

VALUE (MeV)	DOCUMENT ID	TECN	CHG	COMMENT
-------------	-------------	------	-----	---------

• • • We do not use the following data for averages, fits, limits, etc. • • •

~ 169	HASAN	94	RVUE	$\bar{p}p \rightarrow \pi\pi$
~ 250	<sup>10</sup> MARTIN	80B	RVUE	
~ 300	<sup>10</sup> MARTIN	80C	RVUE	
~ 150	<sup>11</sup> CARTER	78B	CNTR	0 0.7-2.4 $\bar{p}p \rightarrow K^- K^+$
~ 210	<sup>12</sup> CARTER	77	CNTR	0 0.7-2.4 $\bar{p}p \rightarrow \pi\pi$

S-CHANNEL  $\bar{N}N$ 

VALUE (MeV)	DOCUMENT ID	TECN	CHG	COMMENT
-------------	-------------	------	-----	---------

• • • We do not use the following data for averages, fits, limits, etc. • • •

260 ± 75	<sup>13</sup> ANISOVICH	02	SPEC	0.6-1.9 $\rho\bar{p} \rightarrow \omega\pi^0, \omega\eta\pi^0, \pi^+\pi^-$
235 <sup>+65</sup> <sub>-40</sub>	ANISOVICH	00J	SPEC	
135 ± 150	<sup>14,15</sup> COUPLAND	77	CNTR	0 0.7-2.4 $\bar{p}p \rightarrow \bar{p}p$
165 ± 18	<sup>15</sup> ALSPECTOR	73	CNTR	$\bar{p}p$ S channel
< 60	<sup>16</sup> OH	70B	HDDB	-0 $\bar{p}(p\eta), K^* K 2\pi$
~ 140	ABRAMS	67C	CNTR	S channel $\bar{N}N$

 $\pi^- p \rightarrow K^+ K^- n$ 

VALUE (MeV)	DOCUMENT ID	TECN	CHG	COMMENT
-------------	-------------	------	-----	---------

• • • We do not use the following data for averages, fits, limits, etc. • • •

245 ± 20	ALPER	80	CNTR	0 62 $\pi^- p \rightarrow K^+ K^- n$
<sup>10</sup> $I(J^P) = 1(5^-)$ from simultaneous analysis of $p\bar{p} \rightarrow \pi^- \pi^+$ and $\pi^0 \pi^0$ .				
<sup>11</sup> $I = 0(1); J^P = 5^-$ from Barrelet-zero analysis.				
<sup>12</sup> $I(J^P) = 1(5^-)$ from amplitude analysis.				
<sup>13</sup> From the combined analysis of ANISOVICH 00J, ANISOVICH 01D, ANISOVICH 01E, and ANISOVICH 02.				
<sup>14</sup> From a fit to the total elastic cross section.				
<sup>15</sup> Isospins 0 and 1 not separated.				
<sup>16</sup> No evidence for this bump seen in the $\bar{p}p$ data of CHAPMAN 71B. Narrow state not confirmed by OH 73 with more data.				

 $\rho_5(2350)$  REFERENCES

ANISOVICH	02	PL B542 8	A.V. Anisovich <i>et al.</i>	
ANISOVICH	01D	PL B508 6	A.V. Anisovich <i>et al.</i>	
ANISOVICH	01E	PL B513 281	A.V. Anisovich <i>et al.</i>	
ANISOVICH	00J	PL B491 47	A.V. Anisovich <i>et al.</i>	
ALDE	95	ZPHY C66 379	D.M. Alde <i>et al.</i>	(GAMS Collab.)JP
HASAN	94	PL B334 215	A. Hasan, D.V. Bugg	(LOQM)
ALPER	80	PL 94B 422	B. Alper <i>et al.</i>	(AMST, CERN, CRAC, MPIM+)
MARTIN	80B	NP B176 355	B.R. Martin, D. Morgan	(LOQC, RHEL)JP
MARTIN	80C	NP B169 216	A.D. Martin, M.R. Pennington	(DURH)JP
CARTER	78B	NP B141 467	A.A. Carter	(LOQM)
CUTTS	78B	PR D17 16	D. Cutts <i>et al.</i>	(STON, WISC)
CARTER	77	PL 67B 117	A.A. Carter <i>et al.</i>	(LOQM, RHEL)JP
COUPLAND	77	PL 71B 460	M. Coupland <i>et al.</i>	(LOQM, RHEL)
ALSPECTOR	73	PL 30 511	J. Alspector <i>et al.</i>	(RUTG, UPNJ)
OH	73	NP B51 57	B.Y. Oh <i>et al.</i>	(MSU)
CHAPMAN	71B	PR D4 1275	J.W. Chapman <i>et al.</i>	(MICH)
ABRAMS	70	PR D1 1917	R.J. Abrams <i>et al.</i>	(BNL)
OH	70B	PRL 24 1257	B.Y. Oh <i>et al.</i>	(MSU)
ABRAMS	67C	PRL 18 1209	R.J. Abrams <i>et al.</i>	(BNL)

 $a_6(2450)$ 

$$I^G(J^{PC}) = 1^-(6^{++})$$

OMITTED FROM SUMMARY TABLE

Needs confirmation.

 $a_6(2450)$  MASS

VALUE (MeV)	DOCUMENT ID	TECN	CHG	COMMENT
2450 ± 130	<sup>1</sup> CLELAND	82B	SPEC	± 50 $\pi p \rightarrow K_S^0 K^\pm p$

<sup>1</sup> From an amplitude analysis. $a_6(2450)$  WIDTH

VALUE (MeV)	DOCUMENT ID	TECN	CHG	COMMENT
400 ± 250	<sup>2</sup> CLELAND	82B	SPEC	± 50 $\pi p \rightarrow K_S^0 K^\pm p$

<sup>2</sup> From an amplitude analysis.

# Meson Particle Listings

## $a_6(2450)$ , $f_6(2510)$

### $a_6(2450)$ DECAY MODES

Mode
$\Gamma_1$ $K\bar{K}$

### $a_6(2450)$ REFERENCES

CLELAND 82B NP B208 228 W.E. Cleland *et al.* (DURH, GEVA, LAUS+)

## $f_6(2510)$

$$J^G(J^{PC}) = 0^+(6^{++})$$

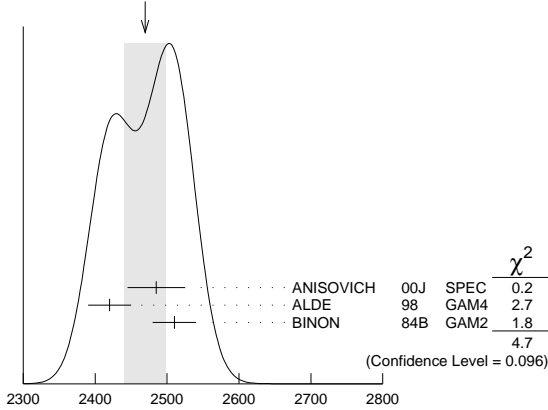
OMITTED FROM SUMMARY TABLE  
Needs confirmation.

### $f_6(2510)$ MASS

VALUE (MeV)	DOCUMENT ID	TECN	COMMENT
<b>2469 ± 29 OUR AVERAGE</b>	Error includes scale factor of 1.5. See the ideogram below.		
2485 ± 40	<sup>1</sup> ANISOVICH 00J	SPEC	1.92-2.41 $p\bar{p}$
2420 ± 30	ALDE 98	GAM4	100 $\pi^- p \rightarrow \pi^0 \pi^0 n$
2510 ± 30	BINON 84B	GAM2	38 $\pi^- p \rightarrow n 2\pi^0$

<sup>1</sup> From the combined analysis of ANISOVICH 99c, ANISOVICH 99f, ANISOVICH 99j, ANISOVICH 99k, and ANISOVICH 00b.

WEIGHTED AVERAGE  
2469 ± 29 (Error scaled by 1.5)



$f_6(2510)$  MASS (MeV)

### $f_6(2510)$ WIDTH

VALUE (MeV)	DOCUMENT ID	TECN	COMMENT
<b>283 ± 40 OUR AVERAGE</b>	Error includes scale factor of 1.1.		
410 ± 90	<sup>2</sup> ANISOVICH 00J	SPEC	1.92-2.41 $p\bar{p}$
270 ± 60	ALDE 98	GAM4	100 $\pi^- p \rightarrow \pi^0 \pi^0 n$
240 ± 60	BINON 84B	GAM2	38 $\pi^- p \rightarrow n 2\pi^0$

<sup>2</sup> From the combined analysis of ANISOVICH 99c, ANISOVICH 99f, ANISOVICH 99j, ANISOVICH 99k, and ANISOVICH 00b.

### $f_6(2510)$ DECAY MODES

Mode	Fraction ( $\Gamma_i/\Gamma$ )
$\Gamma_1$ $\pi\pi$	(6.0 ± 1.0) %

### $f_6(2510)$ BRANCHING RATIOS

$\Gamma(\pi\pi)/\Gamma_{total}$	DOCUMENT ID	TECN	COMMENT	$\Gamma_1/\Gamma$
<b>0.06 ± 0.01</b>	<sup>3</sup> BINON 83c	GAM2	38 $\pi^- p \rightarrow n 4\gamma$	

<sup>3</sup> Assuming one pion exchange and using data of BOLOTOV 74.

### $f_6(2510)$ REFERENCES

ANISOVICH 00B	NP A662 319	A.V. Anisovich <i>et al.</i>	
ANISOVICH 00J	PL B491 47	A.V. Anisovich <i>et al.</i>	
ANISOVICH 99C	PL B452 173	A.V. Anisovich <i>et al.</i>	
ANISOVICH 99F	NP A651 253	A.V. Anisovich <i>et al.</i>	
ANISOVICH 99J	PL B471 271	A.V. Anisovich <i>et al.</i>	
ANISOVICH 99K	PL B468 309	A.V. Anisovich <i>et al.</i>	
ALDE 98	EPJ A3 361	D. Alde <i>et al.</i>	(GAM4 Collab.)
Also	PAN 62 405	D. Alde <i>et al.</i>	(GAMS Collab.)
	Translated from YAF 62 446.		
BINON 84B	LNC 39 41	F.G. Binon <i>et al.</i>	(SERP, BELG, LAPP) JP
BINON 83C	SJNP 38 723	F.G. Binon <i>et al.</i>	(SERP, BRUX+)
	Translated from YAF 38 1199.		
BOLOTOV 74	PL 52B 489	V.N. Bolotov <i>et al.</i>	(SERP)

## OTHER LIGHT MESONS

## Further States

OMITTED FROM SUMMARY TABLE

This section contains states observed by a single group or states poorly established that thus need confirmation.

QUANTUM NUMBERS, MASSES, WIDTHS, AND BRANCHING RATIOS

<b>X(360)</b> $I^G(J^{PC}) = ??(??^+)$					
MASS (MeV)	WIDTH (MeV)	EVTs	DOCUMENT ID	TECN	COMMENT
360 ± 7 ± 9	64 ± 18	2.3k	<sup>1</sup> ABRAAMYAN 09	CNTR	2.75 dC → $\gamma\gamma X$
<sup>1</sup> Not seen in $pC \rightarrow \gamma\gamma X$ at 5.5 GeV/c.					

<b>X(1070)</b> $I^G(J^{PC}) = ??(0^{++})$					
MASS (MeV)	WIDTH (MeV)	DOCUMENT ID	COMMENT		
1072 ± 1	3.5 ± 0.5	<sup>2</sup> VLADIMIRSK...08	40 $\pi^- p \rightarrow K_S^0 K_S^0 n + m\pi^0$		
<sup>2</sup> Supersedes GRIGOR'EV 05.					

<b>X(1110)</b> $I^G(J^{PC}) = 0^+(\text{even}^{++})$					
MASS (MeV)	WIDTH (MeV)	DOCUMENT ID	TECN	COMMENT	
1107 ± 4	111 ± 8 ± 15	DAFTARI 87	DBC	0. $\bar{p}n \rightarrow \rho^- \pi^+ \pi^-$	

<b><math>\eta_2(1200-1600)</math></b> $I^G(J^{PC}) = 0^+(0^{++})$					
MASS (MeV)	WIDTH (MeV)	DOCUMENT ID	TECN	COMMENT	
1323 ± 8	237 ± 20	VLADIMIRSK...06	SPEC	40 $\pi^- p \rightarrow K_S^0 K_S^0 n$	
1480 <sup>+100</sup> <sub>-150</sub>	1030 <sup>+80</sup> <sub>-170</sub>	<sup>3</sup> ANISOVICH 03	SPEC		
1530 <sup>+90</sup> <sub>-250</sub>	560 ± 40	<sup>4</sup> ANISOVICH 03	SPEC		
<sup>3</sup> K-matrix pole from combined analysis of $\pi^- p \rightarrow \pi^0 \pi^0 n$ , $\pi^- p \rightarrow K \bar{K} n$ , $\pi^+ \pi^- \rightarrow \pi^+ \pi^-$ , $\bar{p}p \rightarrow \pi^0 \pi^0 \pi^0$ , $\pi^0 \eta$ , $\pi^0 \pi^0 \eta$ , $\pi^+ \pi^- \pi^0$ , $K^+ K^- \pi^0$ , $K_S^0 K_S^0 \pi^0$ , $K^+ K_S^0 \pi^-$ at rest, $\bar{p}n \rightarrow \pi^- \pi^- \pi^+$ , $K_S^0 K^- \pi^0$ , $K_S^0 K_S^0 \pi^-$ at rest.					
<sup>4</sup> K-matrix pole from combined analysis of $\pi^- p \rightarrow \pi^0 \pi^0 n$ , $\pi^- p \rightarrow K \bar{K} n$ , $\bar{p}p \rightarrow \pi^0 \pi^0 \pi^0$ , $\pi^0 \eta$ , $\pi^0 \pi^0 \eta$ at rest.					

<b>X(1420)</b> $I^G(J^{PC}) = 2^+(0^{++})$					
MASS (MeV)	WIDTH (MeV)	DOCUMENT ID	TECN	COMMENT	
1420 ± 20	160 ± 10	FILIPPI 00	OBLX	0 $\bar{p}p \rightarrow \pi^+ \pi^+ \pi^-$	

<b>X(1545)</b> $I^G(J^{PC}) = ??(??^{++})$					
MASS (MeV)	WIDTH (MeV)	DOCUMENT ID	COMMENT		
1545 ± 3	6.0 ± 2.5	<sup>5</sup> VLADIMIRSK...08	40 $\pi^- p \rightarrow K_S^0 K_S^0 n + m\pi^0$		
<sup>5</sup> Supersedes VLADIMIRSKII 00.					

<b>X(1575)</b> $I^G(J^{PC}) = ??(1^{--})$					
MASS (MeV)	WIDTH (MeV)	DOCUMENT ID	TECN	COMMENT	
1576 <sup>+49+98</sup> <sub>-55-91</sub>	818 <sup>+22+64</sup> <sub>-23-133</sub>	<sup>6</sup> ABLIKIM 06s	BES	$J/\psi \rightarrow K^+ K^- \pi^0$	
<sup>6</sup> A broad peak observed at $K^+ K^-$ invariant mass. Mass and width above are its pole position. The observed branching ratio is $B(J/\psi \rightarrow X \pi^0) B(X \rightarrow K^+ K^-) = (8.5 \pm 0.6^{+2.7}_{-3.6}) \times 10^{-4}$ .					

<b>X(1600)</b> $I^G(J^{PC}) = 2^+(2^{++})$					
MASS (MeV)	WIDTH (MeV)	DOCUMENT ID	TECN	COMMENT	
1600 ± 100	400 ± 200	<sup>7</sup> ALBRECHT 91F ARG	10.2 $e^+ e^- \rightarrow e^+ e^- 2(\pi^+ \pi^-)$		
<sup>7</sup> Our estimate.					

<b>X(1650)</b> $I^G(J^{PC}) = 0^-(??^-)$					
MASS (MeV)	WIDTH (MeV)	EVTs	DOCUMENT ID	TECN	COMMENT
1652 ± 7	<50	100	PROKOSHKIN 96	GAM2	32,38 $\pi p \rightarrow \omega \eta n$

<b>X(1730)</b> $I^G(J^{PC}) = ??(??^{++})$					
MASS (MeV)	WIDTH (MeV)	EVTs	DOCUMENT ID	TECN	COMMENT
1731.0 ± 1.2 ± 2.0	3.2 ± 0.8 ± 1.3	58	VLADIMIRSK...07	SPEC	40 $\pi^- p \rightarrow K_S^0 K_S^0 X$

<b>X(1750)</b> $I^G(J^{PC}) = ??(1^{--})$					
MASS (MeV)	WIDTH (MeV)	DOCUMENT ID	TECN	COMMENT	
1753.5 ± 1.5 ± 2.3	122.2 ± 6.2 ± 8.0	LINK 02k	FOCS	20-160 $\gamma p \rightarrow K^+ K^- p$	

**B(X(1750) →  $\bar{K}^*(892)^0 K^0 \rightarrow K^\pm \pi^\mp K_S^0$ )/B(X(1750) →  $K^+ K^-$ )**

VALUE	CL%	DOCUMENT ID	TECN
<0.065	90	LINK	02k FOCS

**B(X(1750) →  $\bar{K}^*(892)^\pm K^\mp \rightarrow K^\pm \pi^\mp K_S^0$ )/B(X(1750) →  $K^+ K^-$ )**

VALUE	CL%	DOCUMENT ID	TECN
<0.183	90	LINK	02k FOCS

<b><math>\phi_2(1750)</math></b> $I^G(J^{PC}) = 0^+(2^{++})$					
MASS (MeV)	WIDTH (MeV)	EVTs	DOCUMENT ID	TECN	COMMENT
1755 ± 10	67 ± 12	870	<sup>8</sup> SCHEGELSKY 06A	RVUE	$\gamma\gamma \rightarrow K_S^0 K_S^0$

<b><math>\Gamma(K \bar{K})</math></b>					
VALUE (MeV)	EVTs	DOCUMENT ID	TECN	COMMENT	
17 ± 5	870	<sup>9</sup> SCHEGELSKY 06A	RVUE	$\gamma\gamma \rightarrow K_S^0 K_S^0$	

<b><math>\Gamma(\gamma\gamma)</math></b>					
VALUE (keV)	EVTs	DOCUMENT ID	TECN	COMMENT	
0.13 ± 0.04	870	<sup>9</sup> SCHEGELSKY 06A	RVUE	$\gamma\gamma \rightarrow K_S^0 K_S^0$	

<b><math>\Gamma(\pi\pi)</math></b>					
VALUE (MeV)	EVTs	DOCUMENT ID	TECN	COMMENT	
1.3 ± 1.0	870	<sup>9</sup> SCHEGELSKY 06A	RVUE	$\gamma\gamma \rightarrow K_S^0 K_S^0$	

<b><math>\Gamma(\eta\eta)</math></b>					
VALUE (MeV)	EVTs	DOCUMENT ID	TECN	COMMENT	
2.0 ± 0.5	870	<sup>9</sup> SCHEGELSKY 06A	RVUE	$\gamma\gamma \rightarrow K_S^0 K_S^0$	

<sup>8</sup> From analysis of L3 data at 91 and 183-209 GeV.<sup>9</sup> From analysis of L3 data at 91 and 183-209 GeV and using SU(3) relations.

<b>X(1775)</b> $I^G(J^{PC}) = 1^-(?^{-+})$					
MASS (MeV)	WIDTH (MeV)	DOCUMENT ID	TECN	COMMENT	
1763 ± 20	192 ± 60	CONDO 91	SHF	$\gamma p \rightarrow (p\pi^+)(\pi^+ \pi^- \pi^-)$	
1787 ± 18	118 ± 60	CONDO 91	SHF	$\gamma p \rightarrow n\pi^+ \pi^+ \pi^-$	

<b>X(1812)</b> $I^G(J^{PC}) = ??(??^{++})$					
MASS (MeV)	WIDTH (MeV)	DOCUMENT ID	TECN	COMMENT	
1812 <sup>+19</sup> <sub>-26</sub> ± 18	105 ± 20 ± 28	<sup>10</sup> ABLIKIM 06j	BES2	$J/\psi \rightarrow \gamma\omega\phi$	

<sup>10</sup> Favors  $J^{PC} = 0^{++}$ . Not seen by LIU 09 in  $B^\pm \rightarrow K^\pm \omega\phi$ .

<b>X(1850 - 3100)</b> $I^G(J^{PC}) = ??(1^{--})$					
$\Gamma(e^+e^-)B(X \rightarrow \text{hadrons})$ (eV)	CL%	DOCUMENT ID	TECN	COMMENT	
<120	90	<sup>11</sup> ANASHIN 11	KEDR	$e^+ e^- \rightarrow \text{hadrons}$	
<sup>11</sup> This limit is center-of-mass energy dependent. We quote the most stringent one.					

<b>X(1855)</b> $I^G(J^{PC}) = ??(??^{??})$					
MASS (MeV)	WIDTH (MeV)	DOCUMENT ID	TECN	COMMENT	
1856.6 ± 5	20 ± 5	BRIDGES 86D	SPEC	0. $\bar{p}d \rightarrow \pi\pi N$	

<b>X(1870)</b> $I^G(J^{PC}) = ??(2^{??})$					
MASS (MeV)	WIDTH (MeV)	DOCUMENT ID	TECN	COMMENT	
1870 ± 40	250 ± 30	ALDE 86D	GAM4	100 $\pi^- p \rightarrow 2\eta X$	

<b><math>a_3(1875)</math></b> $I^G(J^{PC}) = 1^-(3^{++})$					
MASS (MeV)	WIDTH (MeV)	DOCUMENT ID	TECN	COMMENT	
1874 ± 43 ± 96	385 ± 121 ± 114	CHUNG 02	B852	18.3 $\pi^- p \rightarrow \pi^+ \pi^- \pi^- p$	

**B( $a_3(1875) \rightarrow f_2(1270)\pi$ )/B( $a_3(1875) \rightarrow \rho\pi$ )**

VALUE	DOCUMENT ID	TECN	COMMENT
0.8 ± 0.2	<sup>12</sup> CHUNG 02	B852	18.3 $\pi^- p \rightarrow \pi^+ \pi^- \pi^- p$
<sup>12</sup> Using the observable fractions of 50.0% $\rho\pi$ , 56.5% $f_2\pi$ , and 11.8% $\rho_3\pi$ .			

**B( $a_3(1875) \rightarrow \rho_3(1690)\pi$ )/B( $a_3(1875) \rightarrow \rho\pi$ )**

VALUE	DOCUMENT ID	TECN	COMMENT
0.9 ± 0.3	<sup>13</sup> CHUNG 02	B852	18.3 $\pi^- p \rightarrow \pi^+ \pi^- \pi^- p$
<sup>13</sup> Using the observable fractions of 50.0% $\rho\pi$ , 56.5% $f_2\pi$ , and 11.8% $\rho_3\pi$ .			

<b><math>a_1(1930)</math></b> $I^G(J^{PC}) = 1^-(1^{++})$					
MASS (MeV)	WIDTH (MeV)	DOCUMENT ID	TECN	COMMENT	
1930 <sup>+30</sup> <sub>-70</sub>	155 ± 45	ANISOVICH 01F	SPEC	2.0 $\bar{p}p \rightarrow 3\pi^0, \pi^0 \eta, \pi^0 \eta'$	

## Meson Particle Listings

## Further States

<b>X(1935)</b> $I^G(J^{PC}) = 1^+(1^{-?})$					
MASS (MeV)	WIDTH (MeV)	DOCUMENT ID	TECN	COMMENT	
1935 ± 20	215 ± 30	EVANGELIS...	79	OMEG	10,16 $\pi^- p \rightarrow \bar{p} p n$

<b><math>\rho_2(1940)</math></b> $I^G(J^{PC}) = 1^+(2^{- -})$					
MASS (MeV)	WIDTH (MeV)	DOCUMENT ID	TECN	COMMENT	
1940 ± 40	155 ± 40	14 ANISOVICH	02	SPEC	0.6-1.9 $p\bar{p} \rightarrow \omega\pi^0, \omega\eta\pi^0, \pi^+\pi^-$

<sup>14</sup>From the combined analysis of ANISOVICH 00J, ANISOVICH 01D, ANISOVICH 01E, and ANISOVICH 02.

<b><math>\omega_3(1945)</math></b> $I^G(J^{PC}) = 0^-(3^{- -})$					
MASS (MeV)	WIDTH (MeV)	DOCUMENT ID	TECN	COMMENT	
1945 ± 20	115 ± 22	15 ANISOVICH	02B	SPEC	0.6-1.9 $p\bar{p} \rightarrow \omega\eta, \omega\pi^0\pi^0$

<sup>15</sup>From the combined analysis of ANISOVICH 00B, ANISOVICH 01C, and ANISOVICH 02B.

<b><math>a_2(1950)</math></b> $I^G(J^{PC}) = 1^-(2^{+ +})$					
MASS (MeV)	WIDTH (MeV)	DOCUMENT ID	TECN	COMMENT	
1950 ± $\begin{smallmatrix} 30 \\ -70 \end{smallmatrix}$	180 ± $\begin{smallmatrix} 30 \\ -70 \end{smallmatrix}$	16 ANISOVICH	01F	SPEC	1.96-2.41 $\bar{p}p$

<sup>16</sup>From the combined analysis of ANISOVICH 99C, ANISOVICH 99E, and ANISOVICH 01F.

<b><math>\omega(1960)</math></b> $I^G(J^{PC}) = 0^-(1^{- -})$					
MASS (MeV)	WIDTH (MeV)	DOCUMENT ID	TECN	COMMENT	
1960 ± 25	195 ± 60	17 ANISOVICH	02B	SPEC	0.6-1.9 $p\bar{p} \rightarrow \omega\eta, \omega\pi^0\pi^0$

<sup>17</sup>From the combined analysis of ANISOVICH 00D, ANISOVICH 01C, and ANISOVICH 02B.

<b><math>b_1(1960)</math></b> $I^G(J^{PC}) = 1^+(1^{+ -})$					
MASS (MeV)	WIDTH (MeV)	DOCUMENT ID	TECN	COMMENT	
1960 ± 35	230 ± 50	18 ANISOVICH	02	SPEC	0.6-1.9 $p\bar{p} \rightarrow \omega\pi^0, \omega\eta\pi^0, \pi^+\pi^-$

<sup>18</sup>From the combined analysis of ANISOVICH 00J, ANISOVICH 01D, ANISOVICH 01E, and ANISOVICH 02.

<b><math>h_1(1965)</math></b> $I^G(J^{PC}) = 0^-(1^{+ -})$					
MASS (MeV)	WIDTH (MeV)	DOCUMENT ID	TECN	COMMENT	
1965 ± 45	345 ± 75	19 ANISOVICH	02B	SPEC	0.6-1.9 $p\bar{p} \rightarrow \omega\eta, \omega\pi^0\pi^0$

<sup>19</sup>From the combined analysis of ANISOVICH 00D, ANISOVICH 01C, and ANISOVICH 02B.

<b><math>f_1(1970)</math></b> $I^G(J^{PC}) = 0^+(1^{+ +})$					
MASS (MeV)	WIDTH (MeV)	DOCUMENT ID	TECN	COMMENT	
1971 ± 15	240 ± 45	ANISOVICH	00J	SPEC	

<b>X(1970)</b> $I^G(J^{PC}) = ?^?(?^{??})$					
MASS (MeV)	WIDTH (MeV)	DOCUMENT ID	TECN	COMMENT	
1970 ± 10	40 ± 20	CHLIAPNIK...	80	HBC	32 $K^+ p \rightarrow 2K_S^0 2\pi X$

<b>X(1975)</b> $I^G(J^{PC}) = ?^?(?^{??})$					
MASS (MeV)	WIDTH (MeV)	EVTS	DOCUMENT ID	TECN	COMMENT
1973 ± 15	80	30	CASO	70	HBC 11.2 $\pi^- p \rightarrow \rho 2\pi$

<b><math>\omega_2(1975)</math></b> $I^G(J^{PC}) = 0^-(2^{- -})$					
MASS (MeV)	WIDTH (MeV)	DOCUMENT ID	TECN	COMMENT	
1975 ± 20	175 ± 25	20 ANISOVICH	02B	SPEC	0.6-1.9 $p\bar{p} \rightarrow \omega\eta, \omega\pi^0\pi^0$

<sup>20</sup>From the combined analysis of ANISOVICH 00D, ANISOVICH 01C, and ANISOVICH 02B.

<b><math>a_2(1990)</math></b> $I^G(J^{PC}) = 1^-(2^{+ +})$					
MASS (MeV)	WIDTH (MeV)	EVTS	DOCUMENT ID	TECN	COMMENT
2050 ± 10 ± 40	190 ± 22 ± 100	18k	21 SCHEGELSKY	06	RVUE $\gamma\gamma \rightarrow \pi^+\pi^-\pi^0$
2003 ± 10 ± 19	249 ± 23 ± 32		LU	05	B852 18 $\pi^- p \rightarrow \omega\pi^+\pi^0\pi^0$

<sup>21</sup>From analysis of L3 data at 183-209 GeV.

<b><math>\Gamma(\gamma\gamma) \Gamma(\pi^+\pi^-\pi^0) / \Gamma(\text{total})</math></b>					
VALUE (keV)	EVTS	DOCUMENT ID	TECN	COMMENT	
0.11 ± 0.04 ± 0.05	18k	22 SCHEGELSKY	06	RVUE	$\gamma\gamma \rightarrow \pi^+\pi^-\pi^0$

<sup>22</sup>From analysis of L3 data at 183-209 GeV.

<b><math>\rho(2000)</math></b> $I^G(J^{PC}) = 1^+(1^{- -})$					
MASS (MeV)	WIDTH (MeV)	DOCUMENT ID	TECN	COMMENT	
2000 ± 30	260 ± 45	23 BUGG	04c	RVUE	Compilation
~ 1988	~ 244	HASAN	94	RVUE	$\bar{p}p \rightarrow \pi\pi$

<sup>23</sup>From the combined analysis of ANISOVICH 00J, ANISOVICH 01D, ANISOVICH 01E, and ANISOVICH 02.

<b><math>f_2(2000)</math></b> $I^G(J^{PC}) = 0^+(2^{+ +})$					
MASS (MeV)	WIDTH (MeV)	DOCUMENT ID	TECN	COMMENT	
2001 ± 10	312 ± 32	ANISOVICH	00J	SPEC	
~ 1996	~ 134	HASAN	94	RVUE	$\bar{p}p \rightarrow \pi\pi$

<b>X(2000)</b> $I^G(J^{PC}) = 1^-(?^{?+})$					
MASS (MeV)	WIDTH (MeV)	DOCUMENT ID	TECN	CHG	COMMENT
1964 ± 35	225 ± 50	24 ARMSTRONG	93D	E760	$\bar{p}p \rightarrow 3\pi^0 \rightarrow 6\gamma$
~ 2100	~ 500	24 ANTIPOV	77	CIBS	- 25 $\pi^- p \rightarrow \rho\pi^- \rho_3$
2214 ± 15	355 ± 21	25 BALTAY	77	HBC	0 15 $\pi^- p \rightarrow \Delta^{++} 3\pi$
2080 ± 40	340 ± 80	KALELKAR	75	HBC	+ 15 $\pi^+ p \rightarrow \rho\pi^+ \rho_3$

<sup>24</sup>Cannot determine spin to be 3.

<sup>25</sup>BALTAY 77 favors  $J^P = ,3^+$ .

<b>X(2000)</b> $I^G(J^{PC}) = ?^?(4^{+ +})$					
MASS (MeV)	WIDTH (MeV)	DOCUMENT ID	TECN	COMMENT	
1998 ± 3 ± 5	<15	VLADIMIRSK..03	SPEC		$\pi^- p \rightarrow K_S^0 K_S^0 M M$

<b><math>\pi_2(2005)</math></b> $I^G(J^{PC}) = 1^-(2^{- +})$					
MASS (MeV)	WIDTH (MeV)	EVTS	DOCUMENT ID	TECN	COMMENT
1974 ± 14 ± 83	341 ± 61 ± 139	145k	LU	05	B852 18 $\pi^- p \rightarrow \omega\pi^-\pi^0 p$
2005 ± 15	200 ± 40		ANISOVICH	01F	SPEC 2.0 $\bar{p}p \rightarrow 3\pi^0, \pi^0\eta, \pi^0\eta'$

<b><math>\eta(2010)</math></b> $I^G(J^{PC}) = 0^+(0^{- +})$					
MASS (MeV)	WIDTH (MeV)	DOCUMENT ID	TECN	COMMENT	
2010 ± $\begin{smallmatrix} 35 \\ -60 \end{smallmatrix}$	270 ± 60	ANISOVICH	00J	SPEC	

<b><math>\pi_1(2015)</math></b> $I^G(J^{PC}) = 1^-(1^{- +})$					
MASS (MeV)	WIDTH (MeV)	EVTS	DOCUMENT ID	TECN	COMMENT
2014 ± 20 ± 16	230 ± 32 ± 73	145k	LU	05	B852 18 $\pi^- p \rightarrow \omega\pi^-\pi^0 p$
2001 ± 30 ± 92	333 ± 52 ± 49	69k	KUHN	04	B852 18 $\pi^- p \rightarrow \eta\pi^+\pi^-\pi^- p$

<b><math>a_0(2020)</math></b> $I^G(J^{PC}) = 1^-(0^{+ +})$					
MASS (MeV)	WIDTH (MeV)	DOCUMENT ID	TECN	COMMENT	
2025 ± 30	330 ± 75	ANISOVICH	99C	SPEC	

<b>X(2020)</b> $I^G(J^{PC}) = ?^?(?^{??})$					
MASS (MeV)	WIDTH (MeV)	DOCUMENT ID	TECN	COMMENT	
2015 ± 3	10 ± 4	FERRER	99	RVUE	$\pi p \rightarrow \rho p \bar{p} \pi(\pi)$

<b><math>h_3(2025)</math></b> $I^G(J^{PC}) = 0^-(3^{+ -})$					
MASS (MeV)	WIDTH (MeV)	DOCUMENT ID	TECN	COMMENT	
2025 ± 20	145 ± 30	26 ANISOVICH	02B	SPEC	0.6-1.9 $p\bar{p} \rightarrow \omega\eta, \omega\pi^0\pi^0$

<sup>26</sup>From the combined analysis of ANISOVICH 00D, ANISOVICH 01C, and ANISOVICH 02B.

<b><math>b_3(2030)</math></b> $I^G(J^{PC}) = 1^+(3^{+ -})$					
MASS (MeV)	WIDTH (MeV)	DOCUMENT ID	TECN	COMMENT	
2032 ± 12	117 ± 11	27 ANISOVICH	02	SPEC	0.6-1.9 $p\bar{p} \rightarrow \omega\pi^0, \omega\eta\pi^0, \pi^+\pi^-$

<sup>27</sup>From the combined analysis of ANISOVICH 00J, ANISOVICH 01D, ANISOVICH 01E, and ANISOVICH 02.

<b><math>a_2(2030)</math></b> $I^G(J^{PC}) = 1^-(2^{+ +})$					
MASS (MeV)	WIDTH (MeV)	DOCUMENT ID	TECN	COMMENT	
2030 ± 20	205 ± 30	28 ANISOVICH	01F	SPEC	1.96-2.41 $\bar{p}p$

<sup>28</sup> From the combined analysis of ANISOVICH 99c, ANISOVICH 99e, and ANISOVICH 01f.

<b><math>a_3(2030)</math> <math>I^G(J^{PC}) = 1^-(3^{++})</math></b>					
MASS (MeV)	WIDTH (MeV)	DOCUMENT ID	TECN	COMMENT	
2031 ± 12	150 ± 18	29 ANISOVICH	01F	SPEC	1.96–2.41 $\bar{p}p$

<sup>29</sup> From the combined analysis of ANISOVICH 99c, ANISOVICH 99e, and ANISOVICH 01f.

<b><math>\eta_2(2030)</math> <math>I^G(J^{PC}) = 0^+(2^{-+})</math></b>					
MASS (MeV)	WIDTH (MeV)	DOCUMENT ID	TECN	COMMENT	
2030 ± 5 ± 15	205 ± 10 ± 15	ANISOVICH	00E	SPEC	

<b><math>B(a_2\pi)_{L=0}/B(a_2\pi)_{L=2}</math></b>					
VALUE	DOCUMENT ID	TECN	COMMENT		
0.05 ± 0.03	30 ANISOVICH	11	SPEC	0.9–1.94 $p\bar{p}$	

<sup>30</sup> Reanalysis of ADOMEIT 96 and ANISOVICH 00e.

<b><math>B(a_0\pi)/B(a_2\pi)_{L=2}</math></b>					
VALUE	DOCUMENT ID	TECN	COMMENT		
0.10 ± 0.08	31 ANISOVICH	11	SPEC	0.9–1.94 $p\bar{p}$	

<sup>31</sup> Reanalysis of ADOMEIT 96 and ANISOVICH 00e.

<b><math>B(f_2\eta)/B(a_2\pi)_{L=2}</math></b>					
VALUE	DOCUMENT ID	TECN	COMMENT		
0.13 ± 0.06	32 ANISOVICH	11	SPEC	0.9–1.94 $p\bar{p}$	

<sup>32</sup> Reanalysis of ADOMEIT 96 and ANISOVICH 00e.

<b><math>f_3(2050)</math> <math>I^G(J^{PC}) = 0^+(3^{++})</math></b>					
MASS (MeV)	WIDTH (MeV)	DOCUMENT ID	TECN	COMMENT	
2048 ± 8	213 ± 34	ANISOVICH	00J	SPEC	2.0 $p\bar{p} \rightarrow \eta\pi^0\pi^0$

<b><math>f_0(2060)</math> <math>I^G(J^{PC}) = 0^+(0^{++})</math></b>					
MASS (MeV)	WIDTH (MeV)	DOCUMENT ID	TECN	COMMENT	
~ 2050	~ 120	33 OAKDEN	94	RVUE	0.36–1.55 $\bar{p}p \rightarrow \pi\pi$
~ 2060	~ 50	33 OAKDEN	94	RVUE	0.36–1.55 $\bar{p}p \rightarrow \pi\pi$

<sup>33</sup> See SEMENOV 99 and KLOET 96.

<b><math>\pi(2070)</math> <math>I^G(J^{PC}) = 1^-(0^{-+})</math></b>					
MASS (MeV)	WIDTH (MeV)	DOCUMENT ID	TECN	COMMENT	
2070 ± 35	310 <sup>+100</sup> <sub>-50</sub>	ANISOVICH	01F	SPEC	2.0 $\bar{p}p \rightarrow 3\pi^0, \pi^0\eta, \pi^0\eta'$

<b><math>X(2075)</math> <math>I^G(J^{PC}) = ?^?(???)</math></b>					
MASS (MeV)	WIDTH (MeV)	DOCUMENT ID	TECN	COMMENT	
2075 ± 12 ± 5	90 ± 35 ± 9	34 ABLIKIM	04J	BES2	$J/\psi \rightarrow K^- p\bar{\Lambda}$

<sup>34</sup> From a fit in the region  $M_{p\bar{\Lambda}} - M_p - M_{\Lambda} < 150$  MeV. S-wave in the  $p\bar{\Lambda}$  system preferred. A similar near-threshold enhancement in the  $p\bar{\Lambda}$  system is observed in  $B^+ \rightarrow p\bar{\Lambda}D^0$  by CHEN 11f.

<b><math>X(2080)</math> <math>I^G(J^{PC}) = ?^?(???)</math></b>					
MASS (MeV)	WIDTH (MeV)	DOCUMENT ID	TECN	COMMENT	
2080 ± 10	110 ± 20	KREYMER	80	STRC	13 $\pi^- d \rightarrow p\bar{p}n(n_s)$

<b><math>X(2080)</math> <math>I^G(J^{PC}) = ?^?(3^{-?})</math></b>					
MASS (MeV)	WIDTH (MeV)	DOCUMENT ID	TECN	COMMENT	
2080 ± 10	190 ± 15	ROZANSKA	80	SPRK	18 $\pi^- p \rightarrow p\bar{p}n$

<b><math>a_1(2095)</math> <math>I^G(J^{PC}) = 1^-(1^{++})</math></b>					
MASS (MeV)	WIDTH (MeV)	EVTS	DOCUMENT ID	TECN	COMMENT
2096 ± 17 ± 121	451 ± 41 ± 81	69k	KUHN	04	B852 18 $\pi^- p \rightarrow \eta\pi^+\pi^-\pi^-p$

<b><math>B(a_1(2095) \rightarrow f_1(1285)\pi) / B(a_1(2095) \rightarrow a_1(1260))</math></b>					
VALUE	EVTS	DOCUMENT ID	TECN	COMMENT	
3.18 ± 0.64	69k	KUHN	04	B852	18 $\pi^- p \rightarrow \eta\pi^+\pi^-\pi^-p$

<b><math>\eta(2100)</math> <math>I^G(J^{PC}) = 0^+(0^{-+})</math></b>					
MASS (MeV)	WIDTH (MeV)	EVTS	DOCUMENT ID	TECN	COMMENT
2103 ± 50	187 ± 75	586	35 BISELLO	89B	DM2 $J/\psi \rightarrow 4\pi\gamma$

<sup>35</sup> ASTON 81B sees no peak, has 850 events in Ajinenko+Barth bins. ARESTOV 80 sees no peak.

<b><math>X(2100)</math> <math>I^G(J^{PC}) = ?^?(0^{??})</math></b>					
MASS (MeV)	WIDTH (MeV)	DOCUMENT ID	TECN	COMMENT	
2100 ± 40	250 ± 40	ALDE	86D	GAM4	100 $\pi^- p \rightarrow 2\eta X$

<b><math>X(2110)</math> <math>I^G(J^{PC}) = 1^+(3^{-?})</math></b>					
MASS (MeV)	WIDTH (MeV)	DOCUMENT ID	TECN	COMMENT	
2110 ± 10	330 ± 20	EVANGELIS...	79	OMEG	10,16 $\pi^- p \rightarrow \bar{p}pn$

<b><math>f_2(2140)</math> <math>I^G(J^{PC}) = 0^+(2^{++})</math></b>					
MASS (MeV)	WIDTH (MeV)	EVTS	DOCUMENT ID	TECN	COMMENT
2141 ± 12	49 ± 28	389	GREEN	86	MPSF 400 $pA \rightarrow 4KX$

<b><math>X(2150)</math> <math>I^G(J^{PC}) = ?^?(2^{+?})</math></b>					
MASS (MeV)	WIDTH (MeV)	DOCUMENT ID	TECN	COMMENT	
2150 ± 10	260 ± 10	ROZANSKA	80	SPRK	18 $\pi^- p \rightarrow p\bar{p}n$

<b><math>a_2(2175)</math> <math>I^G(J^{PC}) = 1^-(2^{++})</math></b>					
MASS (MeV)	WIDTH (MeV)	DOCUMENT ID	TECN	COMMENT	
2175 ± 40	310 <sup>+90</sup> <sub>-45</sub>	ANISOVICH	01F	SPEC	2.0 $\bar{p}p \rightarrow 3\pi^0, \pi^0\eta, \pi^0\eta'$

<b><math>\eta(2190)</math> <math>I^G(J^{PC}) = 0^+(0^{-+})</math></b>					
MASS (MeV)	WIDTH (MeV)	DOCUMENT ID	TECN	COMMENT	
2190 ± 50	850 ± 100	BUGG	99	BES	

<b><math>\omega_2(2195)</math> <math>I^G(J^{PC}) = 0^-(2^{--})</math></b>					
MASS (MeV)	WIDTH (MeV)	DOCUMENT ID	TECN	COMMENT	
2195 ± 30	225 ± 40	36 ANISOVICH	02B	SPEC	0.6–1.9 $p\bar{p} \rightarrow \omega\eta, \omega\pi^0\pi^0$

<sup>36</sup> From the combined analysis of ANISOVICH 00d, ANISOVICH 01c, and ANISOVICH 02b.

<b><math>\omega(2205)</math> <math>I^G(J^{PC}) = 0^-(1^{-+})</math></b>					
MASS (MeV)	WIDTH (MeV)	DOCUMENT ID	TECN	COMMENT	
2205 ± 30	350 ± 90	37 ANISOVICH	02B	SPEC	0.6–1.9 $p\bar{p} \rightarrow \omega\eta, \omega\pi^0\pi^0$

<sup>37</sup> From the combined analysis of ANISOVICH 00d, ANISOVICH 01c, and ANISOVICH 02b.

<b><math>X(2210)</math> <math>I^G(J^{PC}) = ?^?(???)</math></b>					
MASS (MeV)	WIDTH (MeV)	DOCUMENT ID	TECN	COMMENT	
2210 <sup>+79</sup> <sub>-21</sub>	203 <sup>+437</sup> <sub>-87</sub>	EVANGELIS...	79B	OMEG	10 $\pi^- p \rightarrow K^+ K^- n$

<b><math>X(2210)</math> <math>I^G(J^{PC}) = ?^?(???)</math></b>					
MASS (MeV)	WIDTH (MeV)	DOCUMENT ID	TECN	COMMENT	
2207 ± 22	130	CASO	70	HBC	11.2 $\pi^- p$

<b><math>h_1(2215)</math> <math>I^G(J^{PC}) = 0^-(1^{+-})</math></b>					
MASS (MeV)	WIDTH (MeV)	DOCUMENT ID	TECN	COMMENT	
2215 ± 40	325 ± 55	38 ANISOVICH	02B	SPEC	0.6–1.9 $p\bar{p} \rightarrow \omega\eta, \omega\pi^0\pi^0$

<sup>38</sup> From the combined analysis of ANISOVICH 00d, ANISOVICH 01c, and ANISOVICH 02b.

<b><math>\rho_2(2225)</math> <math>I^G(J^{PC}) = 1^+(2^{--})</math></b>					
MASS (MeV)	WIDTH (MeV)	DOCUMENT ID	TECN	COMMENT	
2225 ± 35	335 <sup>+100</sup> <sub>-50</sub>	39 ANISOVICH	02	SPEC	0.6–1.9 $p\bar{p} \rightarrow \omega\pi^0, \omega\eta\pi^0, \pi^+\pi^-$

<sup>39</sup> From the combined analysis of ANISOVICH 00j, ANISOVICH 01d, ANISOVICH 01e, and ANISOVICH 02.

<b><math>\rho_4(2230)</math> <math>I^G(J^{PC}) = 1^+(4^{-+})</math></b>					
MASS (MeV)	WIDTH (MeV)	DOCUMENT ID	TECN	COMMENT	
2230 ± 25	210 ± 30	40 ANISOVICH	02	SPEC	0.6–1.9 $p\bar{p} \rightarrow \omega\pi^0, \omega\eta\pi^0, \pi^+\pi^-$

<sup>40</sup> From the combined analysis of ANISOVICH 00j, ANISOVICH 01d, ANISOVICH 01e, and ANISOVICH 02.

<b><math>b_1(2240)</math> <math>I^G(J^{PC}) = 1^+(1^{+-})</math></b>					
MASS (MeV)	WIDTH (MeV)	DOCUMENT ID	TECN	COMMENT	
2240 ± 35	320 ± 85	41 ANISOVICH	02	SPEC	0.6–1.9 $p\bar{p} \rightarrow \omega\pi^0, \omega\eta\pi^0, \pi^+\pi^-$

## Meson Particle Listings

## Further States

<sup>41</sup> From the combined analysis of ANISOVICH 00J, ANISOVICH 01D, ANISOVICH 01E, and ANISOVICH 02.

$f_2(2240) \quad I^G(J^{PC}) = 0^+(2^+ +)$					
MASS (MeV)	WIDTH (MeV)	DOCUMENT ID	TECN	COMMENT	
$2240 \pm 15$	$241 \pm 30$	<sup>42</sup> ANISOVICH 00J	SPEC	1.92–2.41 $\rho\bar{p}$	
• • • We do not use the following data for averages, fits, limits, etc. • • •					
$\sim 2226$	$\sim 226$	HASAN 94	RVUE	$\rho\bar{p} \rightarrow \pi\pi$	

<sup>42</sup> From the combined analysis of ANISOVICH 99c, ANISOVICH 99f, ANISOVICH 99j, ANISOVICH 99k, and ANISOVICH 00b. See also ANISOVICH 12.

$b_3(2245) \quad I^G(J^{PC}) = 1^+(3^+ -)$					
MASS (MeV)	WIDTH (MeV)	DOCUMENT ID	TECN	COMMENT	
$2245 \pm 50$	$320 \pm 70$	<sup>43</sup> BUGG 04c	RVUE		

<sup>43</sup> From the combined analysis of ANISOVICH 00J, ANISOVICH 01D, ANISOVICH 01E, and ANISOVICH 02.

$\eta_2(2250) \quad I^G(J^{PC}) = 0^+(2^- +)$					
MASS (MeV)	WIDTH (MeV)	DOCUMENT ID	TECN	COMMENT	
$2248 \pm 20$	$280 \pm 20$	ANISOVICH 00i	SPEC		
$2267 \pm 14$	$290 \pm 50$	ANISOVICH 00j	SPEC		

$\pi_4(2250) \quad I^G(J^{PC}) = 1^-(4^- +)$					
MASS (MeV)	WIDTH (MeV)	DOCUMENT ID	TECN	COMMENT	
$2250 \pm 15$	$215 \pm 25$	ANISOVICH 01f	SPEC	2.0 $\bar{p}p \rightarrow 3\pi^0, \pi^0\eta, \pi^0\eta'$	

$\omega_4(2250) \quad I^G(J^{PC}) = 0^-(4^- -)$					
MASS (MeV)	WIDTH (MeV)	DOCUMENT ID	TECN	COMMENT	
$2250 \pm 30$	$150 \pm 50$	<sup>44</sup> ANISOVICH 02b	SPEC	0.6–1.9 $\rho\bar{p} \rightarrow \omega\eta, \omega\pi^0\pi^0$	

<sup>44</sup> From the combined analysis of ANISOVICH 00b, ANISOVICH 01c, and ANISOVICH 02b.

$\omega_5(2250) \quad I^G(J^{PC}) = 0^-(5^- -)$					
MASS (MeV)	WIDTH (MeV)	DOCUMENT ID	TECN	COMMENT	
$2250 \pm 70$	$320 \pm 95$	<sup>45</sup> BUGG 04	RVUE		

<sup>45</sup> From the combined analysis of ANISOVICH 00b, ANISOVICH 01c, and ANISOVICH 02b.

$\omega_3(2255) \quad I^G(J^{PC}) = 0^-(3^- -)$					
MASS (MeV)	WIDTH (MeV)	DOCUMENT ID	TECN	COMMENT	
$2255 \pm 15$	$175 \pm 30$	<sup>46</sup> ANISOVICH 02b	SPEC	0.6–1.9 $\rho\bar{p} \rightarrow \omega\eta, \omega\pi^0\pi^0$	

<sup>46</sup> From the combined analysis of ANISOVICH 00b, ANISOVICH 01c, and ANISOVICH 02b.

$a_4(2255) \quad I^G(J^{PC}) = 1^-(4^+ +)$					
MASS (MeV)	WIDTH (MeV)	DOCUMENT ID	TECN	COMMENT	
<b>2237 ± 5 OUR AVERAGE</b>					
$2237 \pm 5$	$291 \pm 12$	UMAN 06	E835	5.2 $\bar{p}p \rightarrow \eta\eta\pi^0$	
$2255 \pm 40$	$330_{-50}^{+110}$	<sup>47</sup> ANISOVICH 01f	SPEC	1.96–2.41 $\bar{p}p$	

<sup>47</sup> From the combined analysis of ANISOVICH 99c, ANISOVICH 99e, and ANISOVICH 01f.

$a_2(2255) \quad I^G(J^{PC}) = 1^-(2^+ +)$					
MASS (MeV)	WIDTH (MeV)	DOCUMENT ID	TECN	COMMENT	
$2255 \pm 20$	$230 \pm 15$	<sup>48</sup> ANISOVICH 01g	SPEC	1.96–2.41 $\bar{p}p$	

<sup>48</sup> From the combined analysis of ANISOVICH 99c, ANISOVICH 99e, ANISOVICH 01f, and ANISOVICH 01g.

$X(2260) \quad I^G(J^{PC}) = 0^+(4^+ ?)$					
MASS (MeV)	WIDTH (MeV)	DOCUMENT ID	TECN	COMMENT	
$2260 \pm 20$	$400 \pm 100$	EVANGELIS... 79	OMEG	10,16 $\pi^-p \rightarrow \bar{p}pn$	

$\rho(2270) \quad I^G(J^{PC}) = 1^+(1^- -)$					
MASS (MeV)	WIDTH (MeV)	DOCUMENT ID	TECN	COMMENT	
$2265 \pm 40$	$325 \pm 80$	<sup>49</sup> ANISOVICH 02	SPEC	0.6–1.9 $\rho\bar{p} \rightarrow \omega\pi^0, \omega\eta\pi^0, \pi^+\pi^-$	
$2280 \pm 50$	$440 \pm 110$	ATKINSON 85	OMEG	20–70 $\gamma p \rightarrow p\omega\pi^+\pi^-\pi^0$	

<sup>49</sup> From the combined analysis of ANISOVICH 00J, ANISOVICH 01D, ANISOVICH 01E, and ANISOVICH 02.

$a_1(2270) \quad I^G(J^{PC}) = 1^-(1^+ +)$					
MASS (MeV)	WIDTH (MeV)	DOCUMENT ID	TECN	COMMENT	
$2270_{-40}^{+55}$	$305_{-40}^{+70}$	ANISOVICH 01f	SPEC	2.0 $\bar{p}p \rightarrow 3\pi^0, \pi^0\eta, \pi^0\eta'$	

$h_3(2275) \quad I^G(J^{PC}) = 0^-(3^+ -)$					
MASS (MeV)	WIDTH (MeV)	DOCUMENT ID	TECN	COMMENT	
$2275 \pm 25$	$190 \pm 45$	<sup>50</sup> ANISOVICH 02b	SPEC	0.6–1.9 $\rho\bar{p} \rightarrow \omega\eta, \omega\pi^0\pi^0$	

<sup>50</sup> From the combined analysis of ANISOVICH 00b, ANISOVICH 01c, and ANISOVICH 02b.

$a_3(2275) \quad I^G(J^{PC}) = 1^-(3^+ +)$					
MASS (MeV)	WIDTH (MeV)	DOCUMENT ID	TECN	COMMENT	
$2275 \pm 35$	$350_{-50}^{+100}$	<sup>51</sup> ANISOVICH 01g	SPEC	1.96–2.41 $\bar{p}p$	

<sup>51</sup> From the combined analysis of ANISOVICH 99c, ANISOVICH 99e, ANISOVICH 01f, and ANISOVICH 01g.

$\pi_2(2285) \quad I^G(J^{PC}) = 1^-(2^- +)$					
MASS (MeV)	WIDTH (MeV)	DOCUMENT ID	TECN	COMMENT	
$2285 \pm 20 \pm 25$	$250 \pm 20 \pm 25$	<sup>52</sup> ANISOVICH 11	SPEC	0.9–1.94 $\rho\bar{p}$	

<sup>52</sup> Reanalysis of ADOMEIT 96 and ANISOVICH 00e.

$\omega_3(2285) \quad I^G(J^{PC}) = 0^-(3^- -)$					
MASS (MeV)	WIDTH (MeV)	DOCUMENT ID	TECN	COMMENT	
$2278 \pm 28$	$224 \pm 50$	<sup>53</sup> BUGG 04a	RVUE		
$2285 \pm 60$	$230 \pm 40$	<sup>54</sup> ANISOVICH 02b	SPEC	0.6–1.9 $\rho\bar{p} \rightarrow \omega\eta, \omega\pi^0\pi^0$	

<sup>53</sup> Partial wave analysis of the data on  $\rho\bar{p} \rightarrow \bar{\Lambda}\Lambda$  from BARNES 00.

<sup>54</sup> From the combined analysis of ANISOVICH 00b, ANISOVICH 01c, and ANISOVICH 02b.

$\omega(2290) \quad I^G(J^{PC}) = 0^-(1^- -)$					
MASS (MeV)	WIDTH (MeV)	DOCUMENT ID	TECN	COMMENT	
$2290 \pm 20$	$275 \pm 35$	<sup>55</sup> BUGG 04a	RVUE		

<sup>55</sup> Partial wave analysis of the data on  $\rho\bar{p} \rightarrow \bar{\Lambda}\Lambda$  from BARNES 00.

$f_2(2295) \quad I^G(J^{PC}) = 0^+(2^+ +)$					
MASS (MeV)	WIDTH (MeV)	DOCUMENT ID	TECN	COMMENT	
$2293 \pm 13$	$216 \pm 37$	<sup>56</sup> ANISOVICH 00j	SPEC	1.92–2.41 $\rho\bar{p}$	

<sup>56</sup> From the combined analysis of ANISOVICH 99c, ANISOVICH 99f, ANISOVICH 99j, ANISOVICH 99k, and ANISOVICH 00b. See also ANISOVICH 12.

$f_3(2300) \quad I^G(J^{PC}) = 0^+(3^+ +)$					
MASS (MeV)	WIDTH (MeV)	DOCUMENT ID	TECN	COMMENT	
$2334 \pm 25$	$200 \pm 20$	<sup>57</sup> BUGG 04a	RVUE		

<sup>57</sup> Partial wave analysis of the data on  $\rho\bar{p} \rightarrow \bar{\Lambda}\Lambda$  from BARNES 00.

$f_1(2310) \quad I^G(J^{PC}) = 0^+(1^+ +)$					
MASS (MeV)	WIDTH (MeV)	DOCUMENT ID	TECN	COMMENT	
$2310 \pm 60$	$255 \pm 70$	ANISOVICH 00j	SPEC		

$\eta(2320) \quad I^G(J^{PC}) = 0^+(0^- +)$					
MASS (MeV)	WIDTH (MeV)	DOCUMENT ID	TECN	COMMENT	
$2320 \pm 15$	$230 \pm 35$	<sup>58</sup> ANISOVICH 00m	SPEC		

<sup>58</sup> From the combined analysis of  $\bar{p}p \rightarrow \eta\eta\eta$  from ANISOVICH 00m and  $\bar{p}p \rightarrow \eta\pi^0\pi^0$  from ANISOVICH 00j.

$\eta_4(2330) \quad I^G(J^{PC}) = 0^+(4^- +)$					
MASS (MeV)	WIDTH (MeV)	DOCUMENT ID	TECN	COMMENT	
$2328 \pm 38$	$240 \pm 90$	ANISOVICH 00j	SPEC	2.0 $\rho\bar{p} \rightarrow \eta\pi^0\pi^0$	

$\omega(2330) \quad I^G(J^{PC}) = 0^-(1^- -)$					
MASS (MeV)	WIDTH (MeV)	DOCUMENT ID	TECN	COMMENT	
$2330 \pm 30$	$435 \pm 75$	ATKINSON 88	OMEG	25–50 $\gamma p \rightarrow \rho^\pm\rho^0\pi^\mp$	

$X(2340) \quad I^G(J^{PC}) = ?^?(?^?)$					
MASS (MeV)	WIDTH (MeV)	EVTS	DOCUMENT ID	TECN	COMMENT
$2340 \pm 20$	$180 \pm 60$	126	<sup>59</sup> BALTAY 75	HBC	$15\pi^+p \rightarrow p5\pi$

<sup>59</sup> Dominant decay into  $\rho^0\rho^0\pi^+$ . BALTAY 78 finds confirmation in  $2\pi^+\pi^-2\pi^0$  events which contain  $\rho^+\rho^0\pi^0$  and  $2\rho^+\pi^-$ .

$\pi(2360) \quad I^G(J^{PC}) = 1^-(0^- +)$					
MASS (MeV)	WIDTH (MeV)	DOCUMENT ID	TECN	COMMENT	
$2360 \pm 25$	$300_{-50}^{+100}$	ANISOVICH 01f	SPEC	2.0 $\bar{p}p \rightarrow 3\pi^0, \pi^0\eta, \pi^0\eta'$	

$X(2360) \quad I^G(J^{PC}) = ?^?(4^+ ?)$					
MASS (MeV)	WIDTH (MeV)	DOCUMENT ID	TECN	COMMENT	
$2360 \pm 10$	$430 \pm 30$	ROZANSKA 80	SPRK	18 $\pi^-p \rightarrow \rho\bar{p}n$	



See key on page 457

Meson Particle Listings  
Further States

<b>X(2440)</b> $I^G(J^{PC}) = ?^?(5^{-?})$					
MASS (MeV)	WIDTH (MeV)	DOCUMENT ID	TECN	COMMENT	
2440 ± 10	310 ± 20	ROZANSKA	80	SPRK	18 $\pi^- p \rightarrow \rho \bar{p} n$

<b>X(2632)</b> $I^G(J^{PC}) = ?^?(???)$					
MASS (MeV)	WIDTH (MeV)	DOCUMENT ID	TECN	COMMENT	
2635.2 ± 3.3		<sup>60</sup> EVDOKIMOV	04	SELX	X(2632) → $D_s^+ \eta$
2631.6 ± 2.1	< 17	<sup>61</sup> EVDOKIMOV	04	SELX	X(2632) → $D_s^0 K^+$

<sup>60</sup>From a mass difference to  $D_s^+$  of 666.9 ± 3.3 MeV.<sup>61</sup>From a mass difference to  $D_s^0$  of 767.0 ± 2.0 MeV.**B(X(2632) → D<sup>0</sup>K<sup>+</sup>)/B(X(2632) → D<sub>s</sub><sup>+</sup>η)**

VALUE	DOCUMENT ID	TECN
0.14 ± 0.06	<sup>62</sup> EVDOKIMOV 04	SELX

<sup>62</sup>Possible interpretation of this decay pattern is discussed by YASUI 07.

<b>X(2680)</b> $I^G(J^{PC}) = ?^?(???)$					
MASS (MeV)	WIDTH (MeV)	DOCUMENT ID	TECN	COMMENT	
2676 ± 27	150	CASO	70	HBC	11.2 $\pi^- p \rightarrow \rho^- \pi^+ \pi^- p$

<b>X(2710)</b> $I^G(J^{PC}) = ?^?(6^{++})$					
MASS (MeV)	WIDTH (MeV)	DOCUMENT ID	TECN	COMMENT	
2710 ± 20	170 ± 40	ROZANSKA	80	SPRK	18 $\pi^- p \rightarrow \rho \bar{p} n$

<b>X(2750)</b> $I^G(J^{PC}) = ?^?(7^{-?})$					
MASS (MeV)	WIDTH (MeV)	DOCUMENT ID	TECN	COMMENT	
2747 ± 32	195 ± 75	DENNEY	83	LASS	10 $\pi^+ p \rightarrow K^+ K^- \pi^+ p$

<b>ϕ<sub>2</sub>(3100)</b> $I^G(J^{PC}) = 0^+(6^{++})$					
MASS (MeV)	WIDTH (MeV)	DOCUMENT ID	TECN	COMMENT	
3100 ± 100	700 ± 130	BINON	05	GAMS	33 $\pi^- p \rightarrow \eta \eta n$

<b>X(3250)</b> $I^G(J^{PC}) = ?^?(???)$ 3-Body Decays					
MASS (MeV)	WIDTH (MeV)	DOCUMENT ID	TECN	COMMENT	
3250 ± 8 ± 20	45 ± 18	ALEEV	93	BIS2	X(3250) → $\Lambda \bar{p} K^+$
3265 ± 7 ± 20	40 ± 18	ALEEV	93	BIS2	X(3250) → $\bar{\Lambda} p K^-$

<b>X(3250)</b> $I^G(J^{PC}) = ?^?(???)$ 4-Body Decays					
MASS (MeV)	WIDTH (MeV)	DOCUMENT ID	TECN	COMMENT	
3245 ± 8 ± 20	25 ± 11	ALEEV	93	BIS2	X(3250) → $\Lambda \bar{p} K^+ \pi^\pm$
3250 ± 9 ± 20	50 ± 20	ALEEV	93	BIS2	X(3250) → $\bar{\Lambda} p K^- \pi^\mp$
3270 ± 8 ± 20	25 ± 11	ALEEV	93	BIS2	X(3250) → $K_S^0 \rho \bar{p} K^\pm$

<b>X(3350)</b> $I^G(J^{PC}) = ?^?(???)$					
MASS (MeV)	WIDTH (MeV)	EVTS	DOCUMENT ID	TECN	COMMENT
3350 $^{+10}_{-20}$ ± 20	70 $^{+40}_{-30}$ ± 40	50 ± 10	<sup>63</sup> GABYSHEV 06a	BELL	$B^- \rightarrow \Lambda_c^+ \bar{p} \pi^-$

<sup>63</sup>A similar enhancement in the  $\Lambda_c^+ \bar{p}$  final state is also reported by BABAR collaboration in AUBERT 10h.

## REFERENCES for Further States

ANISOVICH	12	PR D85 014001	A.V. Anisovich et al.	
ANASHIN	11	PL B703 543	V.V. Anashin et al.	(KEDR Collab.)
ANISOVICH	11	EPJ C71 1511	A.V. Anisovich et al.	(LOQM, RAL, PNPI)
CHEN	11F	PR D84 071501	P. Chen et al.	(BELLE Collab.)
AUBERT	10H	PR D82 031102R	B. AUBERT et al.	(BABAR Collab.)
ABRAAMYAN	09	PR C80 034001	Kh.U. Abraamyan et al.	
LIU	09	PR D79 071102R	C. Liu et al.	(BELLE Collab.)
VLADIMIRSK...	08	PAN 71 2129	V.V. Vladimirov et al.	(ITEP)
		Translated from YAF 71 2166.		
VLADIMIRSK...	07	PAN 70 1706	V. Vladimirov et al.	
		Translated from YAF 70 1751.		
YASUI	07	PR D76 034009	S. Yasui, M. Oka	
ABLIKIM	06J	PRL 96 162002	M. Ablikim et al.	(BES Collab.)
ABLIKIM	06J	PRL 97 142002	M. Ablikim et al.	(BES Collab.)
GABYSHEV	06A	PRL 97 242001	N. Gabyshev et al.	(BELLE Collab.)
SCHEGELSKY	06A	EPJ A27 159	V.A. Schegelsky et al.	
SCHEGELSKY	06A	EPJ A27 207	V.A. Schegelsky et al.	
UMAN	06	PR D73 052009	I. Uman et al.	(FNAL E835)
VLADIMIRSK...	06	PAN 69 493	V.V. Vladimirov et al.	(ITEP, Moscow)
		Translated from YAF 69 515.		
BINON	05	PAN 68 960	F. Binon et al.	
		Translated from YAF 68 998.		
GRIGOR'EV	05	PAN 68 1271	V.K. Grigor'ev et al.	(ITEP)
		Translated from YAF 68 1324.		
LU	05	PRL 94 032002	M. Lu et al.	(BNL E852 Collab.)
ABLIKIM	04J	PRL 93 112002	M. Ablikim et al.	(BES Collab.)
BUGG	04	PL B595 556 (erratum)	D.V. Bugg	
BUGG	04A	EPJ C36 161	D.V. Bugg	
BUGG	04C	PRPL 397 257	D.V. Bugg	
EVDOKIMOV	04	PRL 93 242001	A.V. Evdokimov et al.	(SELEX Collab.)
KUHN	04	PL B595 109	J. Kuhn et al.	(BNL E852 Collab.)
ANISOVICH	03	EPJ A16 229	V.V. Anisovich et al.	
VLADIMIRSK...	03	PAN 66 700	V.V. Vladimirov et al.	
		Translated from YAF 66 729.		
ANISOVICH	02	PL B542 8	A.V. Anisovich et al.	
ANISOVICH	02B	PL B542 19	A.V. Anisovich et al.	
CHUNG	02	PR D65 072001	S.U. Chung et al.	(BNL E852 Collab.)
LINK	02K	PL B545 50	J.M. Link et al.	(FNAL FOCUS Collab.)
ANISOVICH	01C	PL B507 23	A.V. Anisovich et al.	
ANISOVICH	01D	PL B508 6	A.V. Anisovich et al.	
ANISOVICH	01E	PL B513 281	A.V. Anisovich et al.	
ANISOVICH	01F	PL B517 261	A.V. Anisovich et al.	
ANISOVICH	01G	PL B517 273	A.V. Anisovich et al.	
ANISOVICH	00B	NP A662 319	A.V. Anisovich et al.	
ANISOVICH	00D	PL B476 15	A.V. Anisovich et al.	
ANISOVICH	00E	PL B477 19	A.V. Anisovich et al.	
ANISOVICH	00J	PL B491 40	A.V. Anisovich et al.	
ANISOVICH	00J	PL B491 47	A.V. Anisovich et al.	
ANISOVICH	00M	PL B496 145	A.V. Anisovich et al.	
BARNES	00	PR C62 055203	P.D. Barnes et al.	(OBELIX Experiment)
FILIPPI	00	PL B495 284	A. Filippi et al.	
VLADIMIRSKII	00	JETPL 72 486	V.V. Vladimirov et al.	
		Translated from ZETFP 72 698.		
ANISOVICH	99C	PL B452 173	A.V. Anisovich et al.	
ANISOVICH	99E	PL B452 187	A.V. Anisovich et al.	
ANISOVICH	99F	NP A651 253	A.V. Anisovich et al.	
ANISOVICH	99J	PL B471 271	A.V. Anisovich et al.	
ANISOVICH	99K	PL B468 309	A.V. Anisovich et al.	
BUGG	99	PL B458 511	D.V. Bugg et al.	
FERRER	99	EPJ C10 249	A. Ferrer et al.	
SEMENOV	99	SPU 42 847	S.V. Semenov	
		Translated from UFN 42 937.		
ADOMEIT	96	ZPHY C71 227	J. Adomeit et al.	(Crystal Barrel Collab.)
KLOET	96	PR D53 6120	W.M. Kloet, F. Myhrer	(RUTG, NORD)
PROKOSHKIN	96	SPD 41 247	Y.D. Prokoshkin, V.D. Samoilenko	(SERP)
		Translated from DANS 348 481.		
HASAN	94	PL B334 215	A. Hasan, D.V. Bugg	(LOQM)
OAKDEN	94	NP A574 731	M.N. Oakden, M.R. Pennington	(DURH)
ALEEV	93	PAN 56 1358	A.N. Aleev et al.	(BIS-2 Collab.)
		Translated from YAF 56 100.		
ARMSTRONG	93D	PL B307 399	T.A. Armstrong et al.	(FNAL, FERR, GENO+)
ALBRECHT	91F	ZPHY C50 1	H. Albrecht et al.	(ARGUS Collab.)
CONDO	91	PR D43 2787	G.T. Condo et al.	(SLAC Hybrid Collab.)
BISELLO	89B	PR D39 701	G. Busetto et al.	(DM2 Collab.)
ATKINSON	88	ZPHY C38 535	M. Atkinson et al.	(BONN, CERN, GLAS+)
DAFTAR	87	PRL 58 859	I.K. Diftari et al.	(SYRA)
ALDE	86D	NP B269 485	D.M. Alde et al.	(BELG, LAPP, SERP, CERN+)
BRIDGES	86D	PL B180 313	D.L. Bridges et al.	(SYRA, BNL, CASE+)
GREEN	86	PRL 56 1639	D.R. Green et al.	(FNAL, ARIZ, FSU+)
ATKINSON	85	ZPHY C29 333	M. Atkinson et al.	(BONN, CERN, GLAS+)
DENNEY	83	PR D28 2726	D.L. Denney et al.	(IOWA, MICH)
ASTON	81B	NP B189 205	D. Aston et al.	(BONN, CERN, EPOL, GLAS+)
ARESTOV	80	IHEP 80-165	Y.I. Arestov et al.	(SERP)
CHLIAPNIK...	80	ZPHY C3 285	P.V. Chliapnikov et al.	(SERP, BRUX, MONS)
KREYMER	80	PR D22 36	A.E. Kreymer et al.	(IND, PURD, SLAC+)
ROZANSKA	80	NP B162 505	M. Rozanska et al.	(MPIM, CERN)
EVANGELIS...	79	NP B153 253	C. Evangelista et al.	(BARI, BONN, CERN+)
EVANGELIS...	79B	NP B154 381	C. Evangelista et al.	(BARI, BONN, CERN+)
BALTAY	78	PR D17 52	C. Baltay et al.	(COLU, BING)
ANTIPOV	77	NP B119 45	Y.M. Antipov et al.	(SERP, GEVA)
BALTAY	77	PRL 39 591	C. Baltay, C.V. Cuttis, M. Katalikar	(COLU)
BALTAY	75	PRL 35 891	C. Baltay et al.	(COLU, BING)
KALELKAR	75	Thesis Nevis 207	M.S. Kalelkar	(COLU)
CASO	70	LCN 3 707	C. Caso et al.	(GENO, HAMB, MILA, SAEL)

## Meson Particle Listings

 $K^\pm$ 

**STRANGE MESONS**  
**( $S = \pm 1, C = B = 0$ )**

$K^+ = u\bar{s}, K^0 = d\bar{s}, \bar{K}^0 = \bar{d}s, K^- = \bar{u}s,$  similarly for  $K^{*s}$

 $K^\pm$  $I(J^P) = \frac{1}{2}(0^-)$ **THE CHARGED KAON MASS**

Revised 1994 by T.G. Trippe (LBNL).

The average of the six charged kaon mass measurements which we use in the Particle Listings is

$$m_{K^\pm} = 493.677 \pm 0.013 \text{ MeV } (S = 2.4), \quad (1)$$

where the error has been increased by the scale factor  $S$ . The large scale factor indicates a serious disagreement between different input data. The average before scaling the error is

$$m_{K^\pm} = 493.677 \pm 0.005 \text{ MeV}, \quad (2)$$

$$\chi^2 = 22.9 \text{ for } 5 \text{ D.F.}, \text{ Prob.} = 0.04\%,$$

where the high  $\chi^2$  and correspondingly low  $\chi^2$  probability further quantify the disagreement.

The main disagreement is between the two most recent and precise results,

$$m_{K^\pm} = 493.696 \pm 0.007 \text{ MeV} \quad \text{DENISOV 91}$$

$$m_{K^\pm} = 493.636 \pm 0.011 \text{ MeV } (S = 1.5) \quad \text{GALL 88}$$

$$\text{Average} = 493.679 \pm 0.006 \text{ MeV}$$

$$\chi^2 = 21.2 \text{ for } 1 \text{ D.F.}, \text{ Prob.} = 0.0004\%, \quad (3)$$

both of which are measurements of x-ray energies from kaonic atoms. Comparing the average in Eq. (3) with the overall average in Eq. (2), it is clear that DENISOV 91 and GALL 88 dominate the overall average, and that their disagreement is responsible for most of the high  $\chi^2$ .

The GALL 88 measurement was made using four different kaonic atom transitions,  $K^- \text{Pb } (9 \rightarrow 8)$ ,  $K^- \text{Pb } (11 \rightarrow 10)$ ,  $K^- \text{W } (9 \rightarrow 8)$ , and  $K^- \text{W } (11 \rightarrow 10)$ . The  $m_{K^\pm}$  values they obtain from each of these transitions is shown in the Particle Listings and in Fig. 1. Their  $K^- \text{Pb } (9 \rightarrow 8)$   $m_{K^\pm}$  is below and somewhat inconsistent with their other three transitions. The average of their four measurements is

$$m_{K^\pm} = 493.636 \pm 0.007, \quad (4)$$

$$\chi^2 = 7.0 \text{ for } 3 \text{ D.F.}, \text{ Prob.} = 7.2\%.$$

This is a low but acceptable  $\chi^2$  probability so, to be conservative, GALL 88 scaled up the error on their average by  $S=1.5$  to obtain their published error  $\pm 0.011$  shown in Eq. (3) above and used in the Particle Listings average.

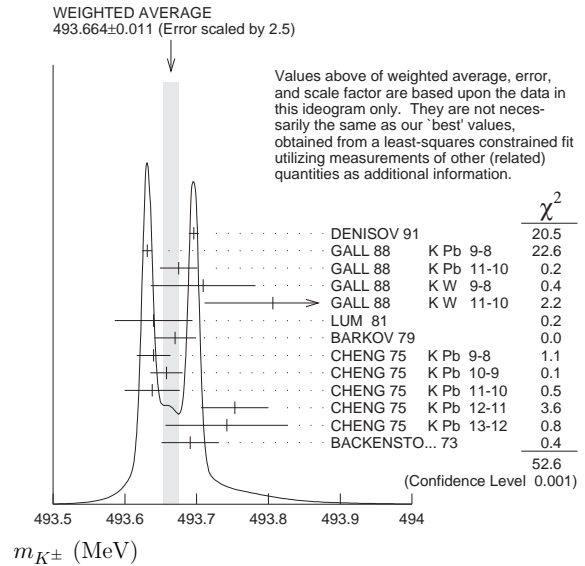


**Figure 1:** Ideogram of  $m_{K^\pm}$  mass measurements. GALL 88 and CHENG 75 measurements are shown separately for each transition they measured.

The ideogram in Fig. 1 shows that the DENISOV 91 measurement and the GALL 88  $K^- \text{Pb } (9 \rightarrow 8)$  measurement yield two well-separated peaks. One might suspect the GALL 88  $K^- \text{Pb } (9 \rightarrow 8)$  measurement since it is responsible both for the internal inconsistency in the GALL 88 measurements and the disagreement with DENISOV 91.

To see if the disagreement could result from a systematic problem with the  $K^- \text{Pb } (9 \rightarrow 8)$  transition, we have separated the CHENG 75 data, which also used  $K^- \text{Pb}$ , into its separate transitions. Figure 1 shows that the CHENG 75 and GALL 88  $K^- \text{Pb } (9 \rightarrow 8)$  values are consistent, suggesting the possibility of a common effect such as contaminant nuclear  $\gamma$  rays near the  $K^- \text{Pb } (9 \rightarrow 8)$  transition energy, although the CHENG 75 errors are too large to make a strong conclusion. The average of all 13 measurements has a  $\chi^2$  of 52.6 as shown in Fig. 1 and the first line of Table 1, yielding an unacceptable  $\chi^2$  probability of 0.00005%. The second line of Table 1 excludes both the GALL 88 and CHENG 75 measurements of the  $K^- \text{Pb } (9 \rightarrow 8)$  transition and yields a  $\chi^2$  probability of 43%. The third [fourth] line of Table 1 excludes only the GALL 88  $K^- \text{Pb } (9 \rightarrow 8)$  [DENISOV 91] measurement and yields a  $\chi^2$  probability of 20% [8.6%]. Table 1 shows that removing both measurements of the  $K^- \text{Pb } (9 \rightarrow 8)$  transition produces the most consistent set of data, but that excluding only the GALL 88  $K^- \text{Pb } (9 \rightarrow 8)$  transition or DENISOV 91 also produces acceptable probabilities.

**Table 1:**  $m_{K^\pm}$  averages for some combinations of Fig. 1 data.

$m_{K^\pm}$ (MeV)	$\chi^2$	D.F.	Prob. (%)	Measurements used
$493.664 \pm 0.004$	52.6	12	0.00005	all 13 measurements
$493.690 \pm 0.006$	10.1	10	43	no $K^-$ Pb(9→8)
$493.687 \pm 0.006$	14.6	11	20	no GALL 88 $K^-$ Pb(9→8)
$493.642 \pm 0.006$	17.8	11	8.6	no DENISOV 91

Yu.M. Ivanov, representing DENISOV 91, has estimated corrections needed for the older experiments because of improved  $^{192}\text{Ir}$  and  $^{198}\text{Au}$  calibration  $\gamma$ -ray energies. He estimates that CHENG 75 and BACKENSTOSS 73  $m_{K^\pm}$  values could be raised by about 15 keV and 22 keV, respectively. With these estimated corrections, Table 1 becomes Table 2. The last line of Table 2 shows that if such corrections are assumed, then GALL 88  $K^-$  Pb (9 → 8) is inconsistent with the rest of the data even when DENISOV 91 is excluded. Yu.M. Ivanov warns that these are rough estimates. Accordingly, we do not use Table 2 to reject the GALL 88  $K^-$  Pb (9 → 8) transition, but we note that a future reanalysis of the CHENG 75 data could be useful because it might provide supporting evidence for such a rejection.

**Table 2:**  $m_{K^\pm}$  averages for some combinations of Fig. 1 data after raising CHENG 75 and BACKENSTOSS 73 values by 0.015 and 0.022 MeV respectively.

$m_{K^\pm}$ (MeV)	$\chi^2$	D.F.	Prob. (%)	Measurements used
$493.666 \pm 0.004$	53.9	12	0.00003	all 13 measurements
$493.693 \pm 0.006$	9.0	10	53	no $K^-$ Pb(9→8)
$493.690 \pm 0.006$	11.5	11	40	no GALL 88 $K^-$ Pb(9→8)
$493.645 \pm 0.006$	23.0	11	1.8	no DENISOV 91

The GALL 88 measurement uses a Ge semiconductor spectrometer which has a resolution of about 1 keV, so they run the risk of some contaminant nuclear  $\gamma$  rays. Studies of  $\gamma$  rays following stopped  $\pi^-$  and  $\Sigma^-$  absorption in nuclei (unpublished) do not show any evidence for contaminants according to GALL 88 spokesperson, B.L. Roberts. The DENISOV 91 measurement uses a crystal diffraction spectrometer with a resolution of 6.3 eV for radiation at 22.1 keV to measure the 4f-3d transition in  $K^-$   $^{12}\text{C}$ . The high resolution and the light nucleus reduce the probability for overlap by contaminant  $\gamma$  rays, compared with the measurement of GALL 88. The DENISOV 91 measurement is supported by their high-precision measurement of the 4d-2p transition energy in  $\pi^-$   $^{12}\text{C}$ , which is good agreement with the calculated energy.

While we suspect that the GALL 88  $K^-$  Pb (9 → 8) measurements could be the problem, we are unable to find clear grounds for rejecting it. Therefore, we retain their measurement in the average and accept the large scale factor until further information can be obtained from new measurements and/or from reanalysis of GALL 88 and CHENG 75 data.

We thank B.L. Roberts (Boston Univ.) and Yu.M. Ivanov (Petersburg Nuclear Physics Inst.) for their extensive help in understanding this problem.

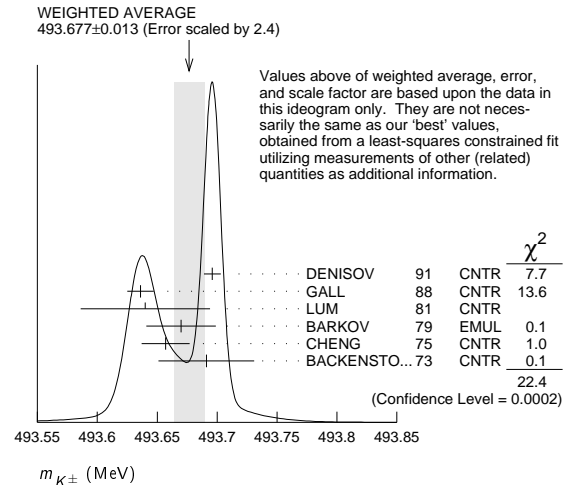
 **$K^\pm$  MASS**

VALUE (MeV)	DOCUMENT ID	TECN	CHG	COMMENT
<b><math>493.677 \pm 0.016</math> OUR FIT</b>	Error includes scale factor of 2.8.			
<b><math>493.677 \pm 0.013</math> OUR AVERAGE</b>	Error includes scale factor of 2.4. See the ideogram below.			
$493.696 \pm 0.007$	<sup>1</sup> DENISOV	91	CNTR	— Kaonic atoms
$493.636 \pm 0.011$	<sup>2</sup> GALL	88	CNTR	— Kaonic atoms
$493.640 \pm 0.054$	LUM	81	CNTR	— Kaonic atoms
$493.670 \pm 0.029$	BARKOV	79	EMUL	± $e^+ e^- \rightarrow K^+ K^-$
$493.657 \pm 0.020$	<sup>2</sup> CHENG	75	CNTR	— Kaonic atoms
$493.691 \pm 0.040$	BACKENSTO...73	CNTR	—	Kaonic atoms
• • • We do not use the following data for averages, fits, limits, etc. • • •				
$493.631 \pm 0.007$	GALL	88	CNTR	— $K^-$ Pb (9 → 8)
$493.675 \pm 0.026$	GALL	88	CNTR	— $K^-$ Pb (11 → 10)
$493.709 \pm 0.073$	GALL	88	CNTR	— $K^-$ W (9 → 8)
$493.806 \pm 0.095$	GALL	88	CNTR	— $K^-$ W (11 → 10)
$493.640 \pm 0.022 \pm 0.008$	<sup>3</sup> CHENG	75	CNTR	— $K^-$ Pb (9 → 8)
$493.658 \pm 0.019 \pm 0.012$	<sup>3</sup> CHENG	75	CNTR	— $K^-$ Pb (10 → 9)
$493.638 \pm 0.035 \pm 0.016$	<sup>3</sup> CHENG	75	CNTR	— $K^-$ Pb (11 → 10)
$493.753 \pm 0.042 \pm 0.021$	<sup>3</sup> CHENG	75	CNTR	— $K^-$ Pb (12 → 11)
$493.742 \pm 0.081 \pm 0.027$	<sup>3</sup> CHENG	75	CNTR	— $K^-$ Pb (13 → 12)

<sup>1</sup> Error increased from 0.0059 based on the error analysis in IVANOV 92.

<sup>2</sup> This value is the authors' combination of all of the separate transitions listed for this paper.

<sup>3</sup> The CHENG 75 values for separate transitions were calculated from their Table 7 transition energies. The first error includes a 20% systematic error in the noncircular contaminant shift. The second error is due to a  $\pm 5$  eV uncertainty in the theoretical transition energies.

 **$m_{K^+} - m_{K^-}$** 

Test of CPT.

VALUE (MeV)	EVTS	DOCUMENT ID	TECN	CHG
<b><math>-0.032 \pm 0.090</math></b>	1.5M	<sup>4</sup> FORD	72	ASPK ±

<sup>4</sup> FORD 72 uses  $m_{\pi^+} - m_{\pi^-} = +28 \pm 70$  keV.

 **$K^\pm$  MEAN LIFE**

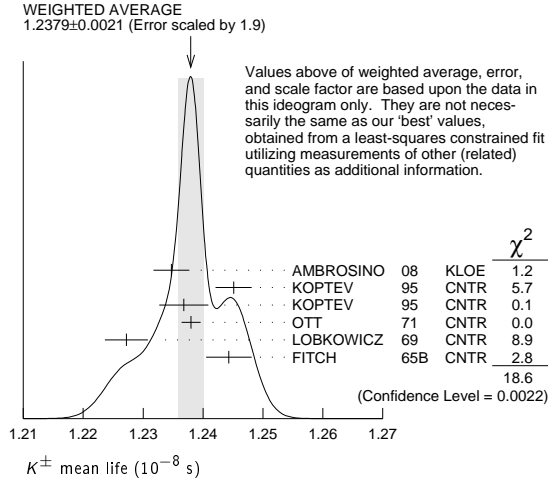
VALUE ( $10^{-8}$ s)	EVTS	DOCUMENT ID	TECN	CHG	COMMENT
<b><math>1.2380 \pm 0.0021</math> OUR FIT</b>	Error includes scale factor of 1.9.				
<b><math>1.2379 \pm 0.0021</math> OUR AVERAGE</b>	Error includes scale factor of 1.9. See the ideogram below.				
$1.2347 \pm 0.0030$	15M	<sup>5</sup> AMBROSINO	08	KLOE	± $\phi \rightarrow K^+ K^-$
$1.2451 \pm 0.0030$	250k	KOPTEV	95	CNTR	K at rest, U target
$1.2368 \pm 0.0041$	150k	KOPTEV	95	CNTR	K at rest, Cu target
$1.2380 \pm 0.0016$	3M	OTT	71	CNTR	+ K at rest
$1.2272 \pm 0.0036$		LOBKOWICZ	69	CNTR	+ K in flight
$1.2443 \pm 0.0038$		FITCH	65B	CNTR	+ K at rest
• • • We do not use the following data for averages, fits, limits, etc. • • •					
$1.2415 \pm 0.0024$	400k	<sup>6</sup> KOPTEV	95	CNTR	K at rest
$1.221 \pm 0.011$		FORD	67	CNTR	±
$1.231 \pm 0.011$		BOYARSKI	62	CNTR	±

## Meson Particle Listings

 $K^\pm$ 

<sup>5</sup> Result obtained by averaging the decay length and decay time analyses taking correlations into account.

<sup>6</sup> KOPTEV 95 report this weighted average of their U-target and Cu-target results, where they have weighted by  $1/\sigma$  rather than  $1/\sigma^2$ .



$$\frac{(\tau_{K^+} - \tau_{K^-})}{\tau_{\text{average}}}$$

This quantity is a measure of  $CPT$  invariance in weak interactions.

VALUE (%)	DOCUMENT ID	TECN
<b>0.10 ± 0.09 OUR AVERAGE</b>	Error includes scale factor of 1.2.	
-0.4 ± 0.4	AMBROSINO 08	KLOE
0.090 ± 0.078	LOBKOWICZ 69	CNTR
0.47 ± 0.30	FORD 67	CNTR

## RARE KAON DECAYS

Revised November 2011 by L. Littenberg (BNL) and G. Valencia (Iowa State University).

**A. Introduction:** There are several useful reviews on rare kaon decays and related topics [1–15]. Activity in rare kaon decays can be divided roughly into four categories:

1. Searches for explicit violations of the Standard Model
2. Measurements of Standard Model parameters
3. Searches for  $CP$  violation
4. Studies of strong interactions at low energy.

The paradigm of Category 1 is the lepton flavor violating decay  $K_L \rightarrow \mu e$ . Category 2 includes processes such as  $K^+ \rightarrow \pi^+ \nu \bar{\nu}$ , which is sensitive to  $|V_{td}|$ . Much of the interest in Category 3 is focused on the decays  $K_L \rightarrow \pi^0 \ell^+ \ell^-$ , where  $\ell \equiv e, \mu, \nu$ . Category 4 includes reactions like  $K^+ \rightarrow \pi^+ \ell^+ \ell^-$  which constitute a testing ground for the ideas of chiral perturbation theory. Category 4 also includes  $K_L \rightarrow \pi^0 \gamma \gamma$  and  $K_L \rightarrow \ell^+ \ell^- \gamma$ . The former is important in understanding a  $CP$ -conserving contribution to  $K_L \rightarrow \pi^0 \ell^+ \ell^-$ , whereas the latter could shed light on long distance contributions to  $K_L \rightarrow \mu^+ \mu^-$ .

The interplay between Categories 2-4 can be illustrated in Fig. 1. The modes  $K \rightarrow \pi \nu \bar{\nu}$  are the cleanest ones theoretically. They can provide accurate determinations of certain CKM parameters (shown in the figure). In combination with alternate determinations of these parameters, they also constrain new interactions. The modes  $K_L \rightarrow \pi^0 e^+ e^-$ ,  $K_L \rightarrow \pi^0 \mu^+ \mu^-$  and  $K_L \rightarrow \mu^+ \mu^-$  are also sensitive to CKM parameters. However, they suffer from a series of hadronic uncertainties that can be addressed, at least in part, through a systematic study of the additional modes indicated in the figure.

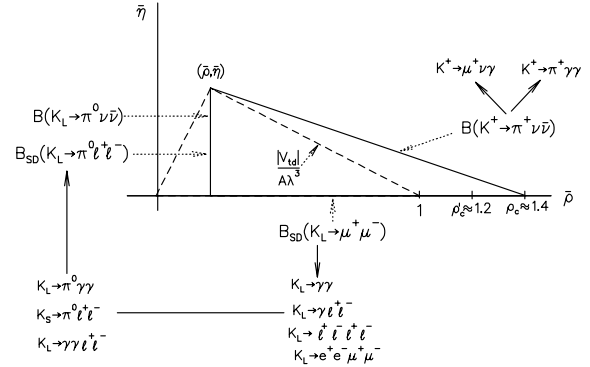


**Figure 1:** Role of rare kaon decays in determining the unitarity triangle. The solid arrows point to auxiliary modes needed to interpret the main results, or potential backgrounds to them.

**B. Explicit violations of the Standard Model:** Much activity has focussed on searches for lepton flavor violation (LFV). This is motivated by the fact that many extensions of the minimal Standard Model violate lepton flavor and by the potential to access very high energy scales. For example, the tree-level exchange of a LFV vector boson of mass  $M_X$  that couples to left-handed fermions with electroweak strength and without mixing angles yields  $B(K_L \rightarrow \mu e) = 4.7 \times 10^{-12} (148 \text{ TeV}/M_X)^4$  [4]. This simple dimensional analysis may be used to read from Table 1 that the reaction  $K_L \rightarrow \mu e$  is already probing scales of over 100 TeV. Table 1 summarizes the present experimental situation vis a vis LFV. The decays  $K_L \rightarrow \mu^\pm e^\mp$  and  $K^+ \rightarrow \pi^+ e^\mp \mu^\pm$  (or  $K_L \rightarrow \pi^0 e^\mp \mu^\pm$ ) provide complementary information on potential family number violating interactions, since the former is sensitive to parity-odd couplings and the latter is sensitive to parity-even couplings. Limits on certain lepton-number violating kaon decays also exist, some recent ones being those of Refs. [16–18]. Related searches in  $\mu$  and  $\tau$  processes are discussed in our section “Tests of Conservation Laws.”

**Table 1:** Searches for lepton flavor violation in  $K$  decay

Mode	90% CL		
	upper limit	Exp't	Yr./Ref.
$K^+ \rightarrow \pi^+ e^- \mu^+$	$1.2 \times 10^{-11}$	BNL-865	2005/Ref. 19
$K^+ \rightarrow \pi^+ e^+ \mu^-$	$5.2 \times 10^{-10}$	BNL-865	2000/Ref. 16
$K_L \rightarrow \mu e$	$4.7 \times 10^{-12}$	BNL-871	1998/Ref. 20
$K_L \rightarrow \pi^0 e \mu$	$7.6 \times 10^{-11}$	KTeV	2008/Ref. 21
$K_L \rightarrow \pi^0 \mu e$	$1.7 \times 10^{-10}$	KTeV	2008/Ref. 21

Physics beyond the SM is also pursued through the search for  $K^+ \rightarrow \pi^+ X^0$ , where  $X^0$  is a new light particle. The searches cover both long-lived particles (*e.g.*, hyperphoton, axion, familon, *etc.*), and short lived ones that decay to muon, electron or photon pairs. The 90% CL upper limit on  $K^+ \rightarrow \pi^+ X^0$  is  $7.3 \times 10^{-11}$  [22]. Recent new bounds for a short lived

pseudoscalar  $X^0$  decaying to muons or photons are  $B(K_L \rightarrow \pi^0 \pi^0 \mu^+ \mu^-) < 1 \times 10^{-10}$  [23] and  $B(K_L \rightarrow \pi^0 \pi^0 \gamma \gamma) < 2.4 \times 10^{-7}$  [24].

### C. Measurements of Standard Model parameters:

In the SM, the decay  $K^+ \rightarrow \pi^+ \nu \bar{\nu}$  is dominated by one-loop diagrams with top-quark intermediate states and long-distance contributions are known to be quite small [2,25]. This permits a precise calculation of this rate in terms of SM parameters. Studies of this process are thus motivated by the possibility of detecting non-SM physics when comparing with the results of global fits [28,29].

BNL-787 observed two candidate events [30,31] in the clean high  $\pi^+$  momentum and one event [32] in the low-momentum region. The successor experiment BNL-949 observed one more in the high-momentum region [22] and three more in the low-momentum region [33] yielding a branching ratio of  $(1.73_{-1.05}^{+1.15}) \times 10^{-10}$  [34]. A new experiment, NA62, with a sensitivity goal of  $\sim 10^{-12}$ /event was proposed [35] at CERN in 2005. It has been approved and is scheduled to run with a partial detector in autumn 2012. In the future, this mode may provide grounds for precision tests of flavor dynamics [36]. The branching ratio can be written in a compact form that exhibits the different ingredients that go into the calculation [37],

$$B(K^+ \rightarrow \pi^+ \nu \bar{\nu}(\gamma)) = \kappa_+(1 + \Delta_{\text{EM}}) \left[ \left( \frac{\text{Im}(V_{ts}^* V_{td})}{\lambda^5} X_t \right)^2 + \left( \frac{\text{Re}(V_{cs}^* V_{cd})}{\lambda} (P_c + \delta P_{c,u}) + \frac{\text{Re}(V_{ts}^* V_{td})}{\lambda^5} X_t \right)^2 \right]. \quad (1)$$

The parameters in Eq. (1) incorporate the *a priori* unknown hadronic matrix element in terms of the very well-measured  $K_{e3}$  rate [2] in  $\kappa_+$ ; long distance QED corrections in  $\Delta_{\text{EM}}$  [27]; the Inami-Lim function for the short distance top-quark contribution [38] including NLO QCD corrections [39] and the two-loop electroweak correction [37], all in  $X_t$ ; and the charm-quark contributions due to short distance effects including NNLO QCD corrections [40] and NLO electroweak corrections via  $P_c$  [41], as well as certain long distance effects via  $\delta P_{c,u}$  [26]. An interesting approximate way to cast this result in terms of the CKM parameters  $\lambda$ ,  $V_{cb}$ ,  $\bar{\rho}$  and  $\bar{\eta}$  (see our Section on “The Cabibbo-Kobayashi-Maskawa mixing matrix”) [11] is:

$$B(K^+ \rightarrow \pi^+ \nu \bar{\nu}) \approx 1.6 \times 10^{-5} |V_{cb}|^4 [\sigma \bar{\eta}^2 + (\rho_c - \bar{\rho})^2], \quad (2)$$

where  $\rho_c \approx 1.45$  and  $\sigma \equiv 1/(1 - \frac{1}{2}\lambda^2)^2$ . Thus,  $B(K^+ \rightarrow \pi^+ \nu \bar{\nu})$  determines an ellipse in the  $\bar{\rho}$ ,  $\bar{\eta}$  plane with center  $(\rho_c, 0)$  and semiaxes  $\approx \frac{1}{|V_{cb}|^2} \sqrt{\frac{B(K^+ \rightarrow \pi^+ \nu \bar{\nu})}{1.6 \times 10^{-5}}}$  and  $\frac{1}{\sigma |V_{cb}|^2} \sqrt{\frac{B(K^+ \rightarrow \pi^+ \nu \bar{\nu})}{1.6 \times 10^{-5}}}$ . The latest numerical study leads to a predicted branching ratio  $(7.81_{-0.71}^{+0.80} \pm 0.29) \times 10^{-11}$  [37], near the lower end of the measurement of BNL-787 and 949.

Modes with an extra pion,  $K \rightarrow \pi \pi \nu \bar{\nu}$ , could also be used in the extraction of CKM parameters as they are also dominated by short distance contributions [42]. However, they occur at much lower rates with branching ratios of order  $10^{-13}$ , and the current best bound from E391a is  $B(K_L \rightarrow \pi^0 \pi^0 \nu \bar{\nu}) <$

$8.1 \times 10^{-7}$  at 90% c.l. [43]. There is also an older bound of  $B(K^+ \rightarrow \pi^+ \pi^0 \nu \bar{\nu}) < 4.3 \times 10^{-5}$  at 90% c.l. [44] from BNL E787.

The decay  $K_L \rightarrow \mu^+ \mu^-$  also has a short distance contribution sensitive to the CKM parameter  $\bar{\rho}$ , given by [11]:

$$B_{\text{SD}}(K_L \rightarrow \mu^+ \mu^-) \approx 2.7 \times 10^{-4} |V_{cb}|^4 (\rho'_c - \bar{\rho})^2 \quad (3)$$

where  $\rho'_c$  depends on the charm quark mass and is approximately 1.2. This decay, however, is dominated by a long-distance contribution from a two-photon intermediate state. The absorptive (imaginary) part of the long-distance component is determined by the measured rate for  $K_L \rightarrow \gamma \gamma$  to be  $B_{\text{abs}}(K_L \rightarrow \mu^+ \mu^-) = (6.64 \pm 0.07) \times 10^{-9}$ ; and it almost completely saturates the observed rate  $B(K_L \rightarrow \mu^+ \mu^-) = (6.84 \pm 0.11) \times 10^{-9}$  [45]. The difference between the observed rate and the absorptive component can be attributed to the (coherent) sum of the short-distance amplitude and the real part of the long-distance amplitude. The latter cannot be derived directly from experiment [46], but can be estimated with certain assumptions [47,48]. The decay  $K_L \rightarrow e^+ e^-$  is completely dominated by long distance physics and is easier to estimate. The result,  $B(K_L \rightarrow e^+ e^-) \sim 9 \times 10^{-12}$  [46,49], is in good agreement with the BNL-871 measurement,  $(8.7_{-4.1}^{+5.7}) \times 10^{-12}$  [50].

**D. Searches for direct CP violation:** The mode  $K_L \rightarrow \pi^0 \nu \bar{\nu}$  is dominantly *CP*-violating and free of hadronic uncertainties [2,51,52]. In the Standard Model, this mode is dominated by an intermediate top-quark state and does not suffer from the small uncertainty associated with the charm-quark intermediate state that affects the mode  $K^+ \rightarrow \pi^+ \nu \bar{\nu}$ . The branching ratio is given by Ref. 11:

$$B(K_L \rightarrow \pi^0 \nu \bar{\nu}) = \kappa_L \left( \frac{\text{Im}(V_{ts}^* V_{td})}{\lambda^5} X_t \right)^2 \approx 7.6 \times 10^{-5} |V_{cb}|^4 \bar{\eta}^2. \quad (4)$$

The hadronic matrix element can be related to that measured in  $K_{e3}$  decay and is parameterized in  $\kappa_L$ . The latest numerical evaluation leads to a predicted branching ratio  $(2.43_{-0.37}^{+0.40} \pm 0.06) \times 10^{-11}$  [37]. The 90% CL bound on  $K^+ \rightarrow \pi^+ \nu \bar{\nu}$  provides a nearly model-independent bound  $B(K_L \rightarrow \pi^0 \nu \bar{\nu}) < 1.46 \times 10^{-9}$  [53]. KEK-391a, which took data in 2004 and 2005, has published a 90% CL upper bound of  $B(K_L \rightarrow \pi^0 \nu \bar{\nu}) \leq 2.6 \times 10^{-8}$  [54]. The KOTO experiment, whose initial goal is to reach the  $10^{-11}$ /event level, is in the final stages of construction at J-PARC [55].

There has been much theoretical work on possible contributions to rare *K* decays beyond the SM. A comprehensive discussion of these can be found in Refs. [14] and [56].

The decay  $K_L \rightarrow \pi^0 e^+ e^-$  also has sensitivity to the CKM parameter  $\eta$  through its *CP*-violating component. There are both direct and indirect *CP*-violating amplitudes which can interfere. The direct *CP*-violating amplitude is short distance dominated and has been calculated in detail within the SM [8]. The indirect *CP*-violating amplitude can be inferred from a

# Meson Particle Listings

## $K^\pm$

measurement of  $K_S \rightarrow \pi^0 e^+ e^-$ . The complete  $CP$ -violating contribution to the rate can be written as [57,58]:

$$B_{\text{CPV}} \approx 10^{-12} \left[ 15.7 |a_S|^2 \pm 1.4 \left( \frac{|V_{cb}|^2 \bar{\eta}}{10^{-4}} \right) |a_S| + 0.12 \left( \frac{|V_{cb}|^2 \bar{\eta}}{10^{-4}} \right)^2 \right] \quad (5)$$

where the three terms correspond to the indirect  $CP$  violation, the interference, and the direct  $CP$  violation respectively. The parameter  $a_S$  has been extracted by NA48 from a measurement of the decay  $K_S \rightarrow \pi^0 e^+ e^-$  with the result  $|a_S| = 1.06_{-0.21}^{+0.26} \pm 0.07$  [59], as well as from a measurement of the decay  $K_S \rightarrow \pi^0 \mu^+ \mu^-$  with the result  $|a_S| = 1.54_{-0.32}^{+0.40} \pm 0.06$  [60]. With current constraints on the CKM parameters, and assuming a positive sign for the interference term [58,61], this implies that  $B_{\text{CPV}}(K_L \rightarrow \pi^0 e^+ e^-) \approx (3.1 \pm 0.9) \times 10^{-11}$ , and that the indirect  $CP$  violation is larger than the direct  $CP$  violation. The complete  $CP$  violating amplitude for the related mode  $K_L \rightarrow \pi^0 \mu^+ \mu^-$  is predicted to be  $B_{\text{CPV}}(K_L \rightarrow \pi^0 \mu^+ \mu^-) \approx (1.4 \pm 0.5) \times 10^{-11}$  [62,15].

$K_L \rightarrow \pi^0 \gamma \gamma$  also has a  $CP$ -conserving component dominated by a two-photon intermediate state. This component can be decomposed into an absorptive and a dispersive part. The absorptive part can be extracted from the measurement of the low  $m_{\gamma\gamma}$  region of the  $K_L \rightarrow \pi^0 \gamma \gamma$  spectrum. The rate and the shape of the distribution  $d\Gamma/dm_{\gamma\gamma}$  in  $K_L \rightarrow \pi^0 \gamma \gamma$  are well described in chiral perturbation theory in terms of three (*a priori*) unknown parameters [63,64].

Both KTeV and NA48 have studied the mode  $K_L \rightarrow \pi^0 \gamma \gamma$ , reporting similar results. KTeV finds  $B(K_L \rightarrow \pi^0 \gamma \gamma) = (1.29 \pm 0.03_{\text{stat}} \pm 0.05_{\text{sys}}) \times 10^{-6}$  [65], while NA48 finds  $B(K_L \rightarrow \pi^0 \gamma \gamma) = (1.36 \pm 0.03_{\text{stat}} \pm 0.03_{\text{sys}} \pm 0.03_{\text{norm}}) \times 10^{-6}$  [66]. Both experiments are consistent with a negligible rate in the low  $m_{\gamma\gamma}$  region, suggesting a very small  $CP$ -conserving component  $B_{\text{CP}}(K_L \rightarrow \pi^0 e^+ e^-) \sim \mathcal{O}(10^{-13})$  [58,64,66]. There remains some model dependence in the estimate of the dispersive part of the  $CP$ -conserving  $K_L \rightarrow \pi^0 e^+ e^-$  [58].

The related process,  $K_L \rightarrow \pi^0 \gamma e^+ e^-$ , is potentially an additional background in some region of phase space [67]. This process has been observed with a branching ratio of  $(1.62 \pm 0.14_{\text{stat}} \pm 0.09_{\text{sys}}) \times 10^{-8}$  [68].

The decay  $K_L \rightarrow \gamma \gamma e^+ e^-$  constitutes the dominant background to  $K_L \rightarrow \pi^0 e^+ e^-$ . It was first observed by BNL-845 [69], and subsequently confirmed with a much larger sample by FNAL-799 [70]. It has been estimated that this background will enter at about the  $10^{-10}$  level [71,72], comparable to or larger than the signal level. Because of this, the observation of  $K_L \rightarrow \pi^0 e^+ e^-$  at the SM level will depend on background subtraction with good statistics. Possible alternative strategies are discussed in Ref. 58 and references cited therein.

The 90% CL upper bound for the process  $K_L \rightarrow \pi^0 e^+ e^-$  is  $2.8 \times 10^{-10}$  [72]. For the closely related muonic process, the published upper bound is  $B(K_L \rightarrow \pi^0 \mu^+ \mu^-) \leq 3.8 \times 10^{-10}$  [73], compared with the SM prediction of  $(1.5 \pm 0.3) \times 10^{-11}$  [62]

(assuming positive interference between the direct- and indirect- $CP$  violating components).

A study of  $K_L \rightarrow \pi^0 \mu^+ \mu^-$  has indicated that it might be possible to extract the direct  $CP$ -violating contribution by a joint study of the Dalitz plot variables and the components of the  $\mu^+$  polarization [74]. The latter tends to be quite substantial so that large statistics may not be necessary.

Combined information from the two  $K_L \rightarrow \pi^0 \ell^+ \ell^-$  modes complements the  $K \rightarrow \pi \nu \bar{\nu}$  measurements in constraining physics beyond the SM [75].

### **E. Other long distance dominated modes:**

The decays  $K^+ \rightarrow \pi^+ \ell^+ \ell^-$  ( $\ell = e$  or  $\mu$ ) have received considerable attention. The rate and spectrum have been measured for both the electron and muon modes [76,77,18]. Ref. 57 has proposed a parametrization inspired by chiral perturbation theory, which provides a successful description of data but indicates the presence of large corrections beyond leading order. More work is needed to fully understand the origin of these large corrections.

Much information has been recorded by KTeV and NA48 on the rates and spectrum for the Dalitz pair conversion modes  $K_L \rightarrow \ell^+ \ell^- \gamma$  [78,79], and  $K_L \rightarrow \ell^+ \ell^- \ell'^+ \ell'^-$  for  $\ell, \ell' = e$  or  $\mu$  [17,80–82]. All these results are used to test hadronic models and could further our understanding of the long distance component in  $K_L \rightarrow \mu^+ \mu^-$ .

### References

1. D. Bryman, Int. J. Mod. Phys. **A4**, 79 (1989).
2. J. Hagelin and L. Littenberg, Prog. in Part. Nucl. Phys. **23**, 1 (1989).
3. L. Littenberg and G. Valencia, Ann. Rev. Nucl. and Part. Sci. **43**, 729 (1993).
4. J. Ritchie and S. Wojcicki, Rev. Mod. Phys. **65**, 1149 (1993).
5. B. Winstein and L. Wolfenstein, Rev. Mod. Phys. **65**, 1113 (1993).
6. G. D'Ambrosio *et al.*, *Radiative Non-Leptonic Kaon Decays*, in The DAΦNE Physics Handbook (second edition), eds. L. Maiani, G. Panzeri, and N. Paver (Frascati), Vol. I, 265 (1995).
7. A. Pich, Rept. on Prog. in Phys. **58**, 563 (1995).
8. G. Buchalla, A.J. Buras, and M.E. Lautenbacher, Rev. Mod. Phys. **68**, 1125 (1996).
9. G. D'Ambrosio and G. Isidori, Int. J. Mod. Phys. **A13**, 1 (1996).
10. P. Buchholz and B. Renk, Prog. in Part. Nucl. Phys. **39**, 253 (1997).
11. A.J. Buras and R. Fleischer, TUM-HEP-275-97, hep-ph/9704376, *Heavy Flavours II*, World Scientific, eds. A.J. Buras and M. Lindner (1997), 65–238.
12. A.J. Buras, TUM-HEP-349-99, Lectures given at Lake Louise Winter Institute: Electroweak Physics, Lake Louise, Alberta, Canada, 14–20 Feb. 1999.
13. A.R. Barker and S.H. Kettell, Ann. Rev. Nucl. and Part. Sci. **50**, 249 (2000).
14. A.J. Buras, F. Schwab, and S. Uhlig, Rev. Mod. Phys. **80**, 965 (2008).

See key on page 457

- 
15. V. Cirigliano *et al.*, “Kaon Decays in the Standard Model,” [arXiv:1107.6001 [hep-ph]].
  16. R. Appel *et al.*, Phys. Rev. Lett. **85**, 2877 (2000).
  17. A. Alavi-Harati *et al.*, Phys. Rev. Lett. **90**, 141801 (2003).
  18. J.R. Batley *et al.*, Phys. Lett. **B697**, 107 (2011).
  19. A. Sher *et al.*, Phys. Rev. **D72**, 012005 (2005).
  20. D. Ambrose *et al.*, Phys. Rev. Lett. **81**, 5734 (1998).
  21. E. Abouzaid *et al.*, Phys. Rev. Lett. **100**, 131803 (2008).
  22. V.V. Anisimovsky *et al.*, Phys. Rev. Lett. **93**, 031801 (2004).
  23. E. Abouzaid *et al.*, [arXiv:1105.4800 [hep-ex]] see also, D.G. Phillips II, “Search for the Rare Decay  $K_L \rightarrow \pi^0 \pi^0 \mu^+ \mu^-$ ,” University of Virginia thesis, May 2009.
  24. Y.C. Tung *et al.*, Phys. Rev. Lett. **102**, 051802 (2009).
  25. M. Lu and M.B. Wise, Phys. Lett. **B324**, 461 (1994); A.F. Falk, A. Lewandowski, and A.A. Petrov, Phys. Lett. **B505**, 107 (2001).
  26. G. Isidori, F. Mescia, and C. Smith, Nucl. Phys. **B718**, 319 (2005); A.F. Falk, A. Lewandowski, and A.A. Petrov, Phys. Lett. **B505**, 107 (2001).
  27. F. Mescia and C. Smith, Phys. Rev. **D76**, 034017 (2007).
  28. CKMfitter Group (J. Charles *et al.*), Phys. Rev. **D84**, 1 (2011), [arXiv:1106.4041[hep-ph]], updated results and plots available at: <http://ckmfitter.in2p3.fr>.
  29. M. Bona *et al.*, [UTfit Collaboration] “Model-independent constraints on Delta F=2 operators and the scale of New Physics,” arXiv:0707.0636 [hep-ph].
  30. S. Adler *et al.*, Phys. Rev. Lett. **88**, 041803 (2002).
  31. S. Adler *et al.*, Phys. Rev. Lett. **84**, 3768 (2000).
  32. S. Adler *et al.*, Phys. Lett. **B537**, 237 (2002).
  33. A.V. Artamonov *et al.*, Phys. Rev. Lett. **101**, 191802 (2008).
  34. A.V. Artamonov *et al.*, Phys. Rev. **D79**, 092004 (2009).
  35. G. Anelli *et al.*, CERN-SPSC-2005-013, 11 June 2005.
  36. G. D’Ambrosio and G. Isidori, Phys. Lett. **B530**, 108 (2002).
  37. J. Brod, M. Gorbahn, and E. Stamou, Phys. Rev. **D83**, 034030 (2011).
  38. T. Inami and C.S. Lim, Prog. Theor. Phys. **65**, 297 (1981); Erratum Prog. Theor. Phys. **65**, 172 (1981).
  39. G. Buchalla and A.J. Buras, Nucl. Phys. **B548**, 309 (1999); M. Misiak and J. Urban, Phys. Lett. **B451**, 161 (1999).
  40. A.J. Buras *et al.*, Phys. Rev. Lett. **95**, 261805 (2005); A.J. Buras *et al.*, JHEP **0611**, 002 (2006).
  41. J. Brod and M. Gorbahn, Phys. Rev. **D78**, 034006 (2008).
  42. L. Littenberg and G. Valencia, Phys. Lett. **B385**, 379 (1996); C.-W. Chiang and F.J. Gilman, Phys. Rev. **D62**, 094026 (2000); C.Q. Geng, I.J. Hsu, and Y.C. Lin, Phys. Rev. **D50**, 5744 (1994).
  43. R. Ogata, *et al.*, arXiv:1106.3404(2011).
  44. S. Adler, *et al.*, Phys. Rev. **D63**, 032004 (2001).
  45. D. Ambrose *et al.*, Phys. Rev. Lett. **84**, 1389 (2000).
  46. G. Valencia, Nucl. Phys. **B517**, 339 (1998).
  47. G. D’Ambrosio, G. Isidori, and J. Portoles, Phys. Lett. **B423**, 385 (1998).
  48. G. Isidori and R. Unterdorfer, JHEP **0401**, 009 (2004).
  49. D. Gomez-Dumm and A. Pich, Phys. Rev. Lett. **80**, 4633 (1998).
  50. D. Ambrose *et al.*, Phys. Rev. Lett. **81**, 4309 (1998).
  51. L. Littenberg, Phys. Rev. **D39**, 3322 (1989).
  52. G. Buchalla and G. Isidori, Phys. Lett. **B440**, 170 (1998).
  53. Y. Grossman and Y. Nir, Phys. Lett. **B398**, 163 (1997).
  54. J.K. Ahn *et al.*, Phys. Rev. **D81**, 072004 (2010).
  55. J. Comfort *et al.*, “Proposal for  $K_L^0 \rightarrow \pi^0 \nu \bar{\nu}$  Experiment at J-Parc,” J-PARC Proposal 14 (2006).
  56. D. Bryman *et al.*, Int. J. Mod. Phys. **A21**, 487 (2006).
  57. G. D’Ambrosio *et al.*, JHEP **9808**, 004 (1998); C.O. Dib, I. Dumietz, and F.J. Gilman, Phys. Rev. **D39**, 2639 (1989).
  58. G. Buchalla, G. D’Ambrosio, and G. Isidori, Nucl. Phys. **B672**, 387 (2003).
  59. J.R. Batley *et al.*, Phys. Lett. **B576**, 43 (2003).
  60. J.R. Batley *et al.*, Phys. Lett. **B599**, 197 (2004).
  61. S. Friot, D. Greynat, and E. de Rafael, Phys. Lett. **B595**, 301 (2004).
  62. G. Isidori, C. Smith, and R. Unterdorfer, Eur. Phys. J. **C36**, 57 (2004).
  63. G. Ecker, A. Pich, and E. de Rafael, Phys. Lett. **237B**, 481 (1990); L. Cappiello, G. D’Ambrosio, and M. Miragliuolo, Phys. Lett. **B298**, 423 (1993); A. Cohen, G. Ecker, and A. Pich, Phys. Lett. **B304**, 347 (1993).
  64. F. Gabbiani and G. Valencia, Phys. Rev. **D66**, 074006 (2002).
  65. E. Abouzaid *et al.*, Phys. Rev. **D77**, 112004 (2008).
  66. A. Lai *et al.*, Phys. Lett. **B536**, 229 (2002).
  67. J. Donoghue and F. Gabbiani, Phys. Rev. **D56**, 1605 (1997).
  68. E. Abouzaid *et al.*, Phys. Rev. **D76**, 052001 (2007).
  69. W.M. Morse *et al.*, Phys. Rev. **D45**, 36 (1992).
  70. A. Alavi-Harati *et al.*, Phys. Rev. **D64**, 012003 (2001).
  71. H.B. Greenlee, Phys. Rev. **D42**, 3724 (1990).
  72. A. Alavi-Harati *et al.*, Phys. Rev. Lett. **93**, 021805 (2004).
  73. A. Alavi-Harati *et al.*, Phys. Rev. Lett. **84**, 5279 (2000).
  74. M.V. Diwan, H. Ma, and T.L. Trueman, Phys. Rev. **D65**, 054020 (2002).
  75. F. Mescia, C. Smith, and S. Trine, JHEP **0608**, 088 (2006).
  76. R. Appel *et al.*, Phys. Rev. Lett. **83**, 4482 (1999); J.R. Batley *et al.*, Phys. Lett. **B677**, 246 (2009).
  77. S.C. Adler *et al.*, Phys. Rev. Lett. **79**, 4756 (1997); R. Appel *et al.*, Phys. Rev. Lett. **84**, 2580 (2000); H.K. Park *et al.*, Phys. Rev. Lett. **88**, 111801 (2002).
  78. A. Alavi-Harati *et al.*, Phys. Rev. Lett. **87**, 071801 (2001).
  79. A. Abouzaid *et al.*, Phys. Rev. Lett. **99**, 051804 (2007).
  80. J.R. LaDue “Understanding Dalitz Decays of the  $K_L$  in particular the decays of  $K_L \rightarrow e^+ e^- \gamma$  and  $K_L \rightarrow e^+ e^- e^+ e^-$ ” University of Colorado Thesis, May 2003. The preliminary result for  $K_L \rightarrow e^+ e^- \gamma$  in this thesis has been superseded by the final result in [79].
  81. A. Alavi-Harati *et al.*, Phys. Rev. Lett. **86**, 5425 (2001).
  82. V. Fanti *et al.*, Phys. Lett. **B458**, 458 (1999).
-

## Meson Particle Listings

 $K^\pm$  **$K^\pm$  DECAY MODES** $K^-$  modes are charge conjugates of the modes below.

Mode	Fraction ( $\Gamma_i/\Gamma$ )	Scale factor/ Confidence level
<b>Leptonic and semileptonic modes</b>		
$\Gamma_1$ $e^+ \nu_e$	$(1.581 \pm 0.008) \times 10^{-5}$	
$\Gamma_2$ $\mu^+ \nu_\mu$	$(63.55 \pm 0.11) \%$	S=1.2
$\Gamma_3$ $\pi^0 e^+ \nu_e$	$(5.07 \pm 0.04) \%$	S=2.1
Called $K_{e3}^+$ .		
$\Gamma_4$ $\pi^0 \mu^+ \nu_\mu$	$(3.353 \pm 0.034) \%$	S=1.8
Called $K_{\mu 3}^+$ .		
$\Gamma_5$ $\pi^0 \pi^0 e^+ \nu_e$	$(2.2 \pm 0.4) \times 10^{-5}$	
$\Gamma_6$ $\pi^+ \pi^- e^+ \nu_e$	$(4.09 \pm 0.10) \times 10^{-5}$	
$\Gamma_7$ $\pi^+ \pi^- \mu^+ \nu_\mu$	$(1.4 \pm 0.9) \times 10^{-5}$	
$\Gamma_8$ $\pi^0 \pi^0 \pi^0 e^+ \nu_e$	$< 3.5 \times 10^{-6}$	CL=90%
<b>Hadronic modes</b>		
$\Gamma_9$ $\pi^+ \pi^0$	$(20.66 \pm 0.08) \%$	S=1.2
$\Gamma_{10}$ $\pi^+ \pi^0 \pi^0$	$(1.761 \pm 0.022) \%$	S=1.1
$\Gamma_{11}$ $\pi^+ \pi^+ \pi^-$	$(5.59 \pm 0.04) \%$	S=1.3
<b>Leptonic and semileptonic modes with photons</b>		
$\Gamma_{12}$ $\mu^+ \nu_\mu \gamma$	[a,b] $(6.2 \pm 0.8) \times 10^{-3}$	
$\Gamma_{13}$ $\mu^+ \nu_\mu \gamma (SD^+)$	[c,d] $(1.33 \pm 0.22) \times 10^{-5}$	
$\Gamma_{14}$ $\mu^+ \nu_\mu \gamma (SD^+ INT)$	[c,d] $< 2.7 \times 10^{-5}$	CL=90%
$\Gamma_{15}$ $\mu^+ \nu_\mu \gamma (SD^- + SD^- INT)$	[c,d] $< 2.6 \times 10^{-4}$	CL=90%
$\Gamma_{16}$ $e^+ \nu_e \gamma$	$(9.4 \pm 0.4) \times 10^{-6}$	
$\Gamma_{17}$ $\pi^0 e^+ \nu_e \gamma$	[a,b] $(2.56 \pm 0.16) \times 10^{-4}$	
$\Gamma_{18}$ $\pi^0 e^+ \nu_e \gamma (SD)$	[c,d] $< 5.3 \times 10^{-5}$	CL=90%
$\Gamma_{19}$ $\pi^0 \mu^+ \nu_\mu \gamma$	[a,b] $(1.25 \pm 0.25) \times 10^{-5}$	
$\Gamma_{20}$ $\pi^0 \pi^0 e^+ \nu_e \gamma$	$< 5 \times 10^{-6}$	CL=90%
<b>Hadronic modes with photons or <math>\ell\bar{\ell}</math> pairs</b>		
$\Gamma_{21}$ $\pi^+ \pi^0 \gamma (INT)$	$(-4.2 \pm 0.9) \times 10^{-6}$	
$\Gamma_{22}$ $\pi^+ \pi^0 \gamma (DE)$	[a,e] $(6.0 \pm 0.4) \times 10^{-6}$	
$\Gamma_{23}$ $\pi^+ \pi^0 \pi^0 \gamma$	[a,b] $(7.6 \pm 3.0) \times 10^{-6}$	
$\Gamma_{24}$ $\pi^+ \pi^+ \pi^- \gamma$	[a,b] $(1.04 \pm 0.31) \times 10^{-4}$	
$\Gamma_{25}$ $\pi^+ \gamma \gamma$	[a] $(1.10 \pm 0.32) \times 10^{-6}$	
$\Gamma_{26}$ $\pi^+ 3\gamma$	[a] $< 1.0 \times 10^{-4}$	CL=90%
$\Gamma_{27}$ $\pi^+ e^+ e^- \gamma$	$(1.19 \pm 0.13) \times 10^{-8}$	
<b>Leptonic modes with <math>\ell\bar{\ell}</math> pairs</b>		
$\Gamma_{28}$ $e^+ \nu_e \nu\bar{\nu}$	$< 6 \times 10^{-5}$	CL=90%
$\Gamma_{29}$ $\mu^+ \nu_\mu \nu\bar{\nu}$	$< 6.0 \times 10^{-6}$	CL=90%
$\Gamma_{30}$ $e^+ \nu_e e^+ e^-$	$(2.48 \pm 0.20) \times 10^{-8}$	
$\Gamma_{31}$ $\mu^+ \nu_\mu e^+ e^-$	$(7.06 \pm 0.31) \times 10^{-8}$	
$\Gamma_{32}$ $e^+ \nu_e \mu^+ \mu^-$	$(1.7 \pm 0.5) \times 10^{-8}$	
$\Gamma_{33}$ $\mu^+ \nu_\mu \mu^+ \mu^-$	$< 4.1 \times 10^{-7}$	CL=90%
<b>Lepton Family number (LF), Lepton number (L), <math>\Delta S = \Delta Q</math> (SQ) violating modes, or <math>\Delta S = 1</math> weak neutral current (SI) modes</b>		
$\Gamma_{34}$ $\pi^+ \pi^+ e^- \bar{\nu}_e$	SQ $< 1.2 \times 10^{-8}$	CL=90%
$\Gamma_{35}$ $\pi^+ \pi^+ \mu^- \bar{\nu}_\mu$	SQ $< 3.0 \times 10^{-6}$	CL=95%
$\Gamma_{36}$ $\pi^+ e^+ e^-$	SI $(3.00 \pm 0.09) \times 10^{-7}$	
$\Gamma_{37}$ $\pi^+ \mu^+ \mu^-$	SI $(9.4 \pm 0.6) \times 10^{-8}$	S=2.6
$\Gamma_{38}$ $\pi^+ \nu\bar{\nu}$	SI $(1.7 \pm 1.1) \times 10^{-10}$	
$\Gamma_{39}$ $\pi^+ \pi^0 \nu\bar{\nu}$	SI $< 4.3 \times 10^{-5}$	CL=90%
$\Gamma_{40}$ $\mu^- \nu e^+ e^+$	LF $< 2.0 \times 10^{-8}$	CL=90%
$\Gamma_{41}$ $\mu^+ \nu_e$	LF [f] $< 4 \times 10^{-3}$	CL=90%
$\Gamma_{42}$ $\pi^+ \mu^+ e^-$	LF $< 1.3 \times 10^{-11}$	CL=90%
$\Gamma_{43}$ $\pi^+ \mu^- e^+$	LF $< 5.2 \times 10^{-10}$	CL=90%
$\Gamma_{44}$ $\pi^- \mu^+ e^+$	L $< 5.0 \times 10^{-10}$	CL=90%
$\Gamma_{45}$ $\pi^- e^+ e^+$	L $< 6.4 \times 10^{-10}$	CL=90%
$\Gamma_{46}$ $\pi^- \mu^+ \mu^+$	L [f] $< 1.1 \times 10^{-9}$	CL=90%
$\Gamma_{47}$ $\mu^+ \bar{\nu}_e$	L [f] $< 3.3 \times 10^{-3}$	CL=90%
$\Gamma_{48}$ $\pi^0 e^+ \bar{\nu}_e$	L $< 3 \times 10^{-3}$	CL=90%
$\Gamma_{49}$ $\pi^+ \gamma$	[g] $< 2.3 \times 10^{-9}$	CL=90%

[a] See the Particle Listings below for the energy limits used in this measurement.

[b] Most of this radiative mode, the low-momentum  $\gamma$  part, is also included in the parent mode listed without  $\gamma$ 's.

[c] Structure-dependent part.

[d] See the "Note on  $\pi^\pm \rightarrow \ell^\pm \nu \gamma$  and  $K^\pm \rightarrow \ell^\pm \nu \gamma$  Form Factors" in the  $\pi^\pm$  Particle Listings for definitions and details.

[e] Direct-emission branching fraction.

[f] Derived from an analysis of neutrino-oscillation experiments.

[g] Violates angular-momentum conservation.

**CONSTRAINED FIT INFORMATION**

An overall fit to the mean life, a decay rate, and 13 branching ratios uses 32 measurements and one constraint to determine 8 parameters. The overall fit has a  $\chi^2 = 51.8$  for 25 degrees of freedom.

The following *off-diagonal* array elements are the correlation coefficients  $\langle \delta p_i \delta p_j \rangle / (\delta p_i \delta p_j)$ , in percent, from the fit to parameters  $p_i$ , including the branching fractions,  $x_i \equiv \Gamma_i / \Gamma_{\text{total}}$ . The fit constrains the  $x_i$  whose labels appear in this array to sum to one.

$x_3$	-64						
$x_4$	-62	90					
$x_5$	-3	4	3				
$x_9$	-65	1	-1	0			
$x_{10}$	-13	-6	-6	0	-6		
$x_{11}$	-21	-9	-9	0	-10	3	
$\Gamma$	5	2	2	0	2	-1	-24
	$x_2$	$x_3$	$x_4$	$x_5$	$x_9$	$x_{10}$	$x_{11}$

Mode	Rate ( $10^8 \text{ s}^{-1}$ )	Scale factor
$\Gamma_2$ $\mu^+ \nu_\mu$	$0.5133 \pm 0.0013$	1.5
$\Gamma_3$ $\pi^0 e^+ \nu_e$	$0.0410 \pm 0.0004$	2.1
Called $K_{e3}^+$ .		
$\Gamma_4$ $\pi^0 \mu^+ \nu_\mu$	$0.02708 \pm 0.00028$	1.9
Called $K_{\mu 3}^+$ .		
$\Gamma_5$ $\pi^0 \pi^0 e^+ \nu_e$	$(1.77 \pm_{-0.30}^{+0.35}) \times 10^{-5}$	
$\Gamma_9$ $\pi^+ \pi^0$	$0.1669 \pm 0.0007$	1.3
$\Gamma_{10}$ $\pi^+ \pi^0 \pi^0$	$0.01423 \pm 0.00018$	1.1
$\Gamma_{11}$ $\pi^+ \pi^+ \pi^-$	$0.04518 \pm 0.00029$	1.2

 **$K^\pm$  DECAY RATES** **$\Gamma(\mu^+ \nu_\mu)$** 

VALUE ( $10^6 \text{ s}^{-1}$ ) DOCUMENT ID TECN CHG  
**51.33 ± 0.13 OUR FIT** Error includes scale factor of 1.5.

• • • We do not use the following data for averages, fits, limits, etc. • • •  
 51.2 ± 0.8 FORD 67 CNTR ±

 **$\Gamma(\pi^+ \pi^+ \pi^-)$** 

VALUE ( $10^6 \text{ s}^{-1}$ ) EVTS DOCUMENT ID TECN CHG  
**4.518 ± 0.029 OUR FIT** Error includes scale factor of 1.2.

4.511 ± 0.024 7 FORD 70 ASPK  
 • • • We do not use the following data for averages, fits, limits, etc. • • •  
 4.529 ± 0.032 3.2M 7 FORD 70 ASPK  
 4.496 ± 0.030 7 FORD 67 CNTR ±

<sup>7</sup> First FORD 70 value is second FORD 70 combined with FORD 67.

 **$(\Gamma(K^+) - \Gamma(K^-)) / \Gamma(K)$**  **$K^\pm \rightarrow \mu^\pm \nu_\mu$  RATE DIFFERENCE/AVERAGE**

Test of *CPT* conservation.

VALUE (%) DOCUMENT ID TECN  
**-0.54 ± 0.41** FORD 67 CNTR

 **$K^\pm \rightarrow \pi^\pm \pi^+ \pi^-$  RATE DIFFERENCE/AVERAGE**

Test of *CP* conservation.

VALUE (%) EVTS DOCUMENT ID TECN CHG  
**0.08 ± 0.12** 8 FORD 70 ASPK

• • • We do not use the following data for averages, fits, limits, etc. • • •  
 -0.02 ± 0.16 9 SMITH 73 ASPK ±  
 0.10 ± 0.14 3.2M 8 FORD 70 ASPK  
 -0.50 ± 0.90 FLETCHER 67 OSPK  
 -0.04 ± 0.21 8 FORD 67 CNTR

<sup>8</sup> First FORD 70 value is second FORD 70 combined with FORD 67.

<sup>9</sup> SMITH 73 value of  $K^\pm \rightarrow \pi^\pm \pi^+ \pi^-$  rate difference is derived from SMITH 73 value of  $K^\pm \rightarrow \pi^\pm 2\pi^0$  rate difference.





## Meson Particle Listings

 $K^\pm$ 

$[\Gamma(\pi^0 \mu^+ \nu_\mu) + \Gamma(\pi^+ \pi^0)]/\Gamma_{\text{total}}$  ( $\Gamma_4 + \Gamma_9$ )/ $\Gamma$   
We combine these two modes for experiments measuring them in xenon bubble chamber because of difficulties of separating them there.

VALUE (units $10^{-2}$ )	EVTS	DOCUMENT ID	TECN	CHG
<b>24.02 ± 0.08 OUR FIT</b>				
Error includes scale factor of 1.2.				
• • • We do not use the following data for averages, fits, limits, etc. • • •				
25.4 ± 0.9	886	SHAKLEE 64	HLBC +	
23.4 ± 1.1		ROE 61	HLBC +	

$\Gamma(\pi^0 \mu^+ \nu_\mu)/\Gamma(\pi^+ \pi^0)$   $\Gamma_4/\Gamma_9$   
VALUE (units  $10^{-2}$ ) EVTS DOCUMENT ID TECN CHG  
**0.1637 ± 0.0006 ± 0.0003** 77k BATLEY 07A NA48 ±

$\Gamma(\pi^0 \mu^+ \nu_\mu)/\Gamma(\pi^+ \pi^+ \pi^-)$   $\Gamma_4/\Gamma_{11}$   
VALUE (units  $10^{-2}$ ) EVTS DOCUMENT ID TECN CHG COMMENT  
**0.599 ± 0.007 OUR FIT** Error includes scale factor of 1.6.  
• • • We do not use the following data for averages, fits, limits, etc. • • •

0.503 ± 0.019	1505	28 HAIDT 71	HLBC +	
0.510 ± 0.017	1505	28 EICHTEN 68	HLBC +	
0.63 ± 0.07	2845	29 BISI 65B	BC + HBC+HLBC	

<sup>28</sup> HAIDT 71 is a reanalysis of EICHTEN 68. Not included in average because of large discrepancy in  $\Gamma(\pi^0 \mu^+ \nu)/\Gamma(\pi^0 e^+ \nu)$  with more precise results.  
<sup>29</sup> Error enlarged for background problems. See GAILLARD 70.

$\Gamma(\pi^0 \pi^0 e^+ \nu_e)/\Gamma_{\text{total}}$   $\Gamma_5/\Gamma$   
VALUE (units  $10^{-5}$ ) EVTS DOCUMENT ID TECN CHG  
**2.2 ± 0.4 OUR FIT**  
**2.54 ± 0.89** 10 BARMIN 88B HLBC +

$\Gamma(\pi^0 \pi^0 e^+ \nu_e)/\Gamma(\pi^0 e^+ \nu_e)$   $\Gamma_5/\Gamma_3$   
VALUE (units  $10^{-4}$ ) EVTS DOCUMENT ID TECN CHG  
**4.3<sup>+0.9</sup><sub>-0.7</sub> OUR FIT**  
**4.1<sup>+1.0</sup><sub>-0.7</sub> OUR AVERAGE**

4.2 <sup>+1.0</sup> <sub>-0.9</sub>	25	BOLOTOV 86B	CALO -	
3.8 <sup>+5.0</sup> <sub>-1.2</sub>	2	LJUNG 73	HLBC +	

$\Gamma(\pi^+ \pi^- e^+ \nu_e)/\Gamma(\pi^+ \pi^+ \pi^-)$   $\Gamma_6/\Gamma_{11}$   
VALUE (units  $10^{-4}$ ) EVTS DOCUMENT ID TECN CHG  
**7.31 ± 0.16 OUR AVERAGE**

7.35 ± 0.01 ± 0.19	388k	30 PISLAK 01	B865	
7.21 ± 0.32	30k	ROSSELET 77	SPEC +	
• • • We do not use the following data for averages, fits, limits, etc. • • •				
7.36 ± 0.68	500	BOURQUIN 71	ASPK	
7.0 ± 0.9	106	SCHWEINB... 71	HLBC +	
5.83 ± 0.63	269	ELY 69	HLBC +	

<sup>30</sup> PISLAK 01 reports  $\Gamma(\pi^+ \pi^- e^+ \nu_e)/\Gamma_{\text{total}} = (4.109 \pm 0.008 \pm 0.110) \times 10^{-5}$  using the PDG 00 value  $\Gamma(\pi^+ \pi^+ \pi^-)/\Gamma_{\text{total}} = (5.59 \pm 0.05) \times 10^{-2}$ . We divide by the PDG value and unfold its error from the systematic error. PISLAK 03 and PISLAK 10a give additional details on the branching ratio measurement and give improved errors on the S-wave  $\pi\pi$  scattering length:  $a_0^0 = 0.235 \pm 0.013$  and  $a_0^2 = -0.0410 \pm 0.0027$ .

$\Gamma(\pi^+ \pi^- \mu^+ \nu_\mu)/\Gamma_{\text{total}}$   $\Gamma_7/\Gamma$   
VALUE (units  $10^{-5}$ ) EVTS DOCUMENT ID TECN CHG  
• • • We do not use the following data for averages, fits, limits, etc. • • •

0.77 <sup>+0.54</sup> <sub>-0.50</sub>	1	CLINE 65	FBC +	
--	---	----------	-------	--

$\Gamma(\pi^+ \pi^- \mu^+ \nu_\mu)/\Gamma(\pi^+ \pi^+ \pi^-)$   $\Gamma_7/\Gamma_{11}$   
VALUE (units  $10^{-4}$ ) EVTS DOCUMENT ID TECN CHG  
**2.57 ± 1.55** 7 BISI 67 DBC +  
• • • We do not use the following data for averages, fits, limits, etc. • • •  
~ 2.5 1 GREINER 64 EMUL +

$\Gamma(\pi^0 \pi^0 \pi^0 e^+ \nu_e)/\Gamma_{\text{total}}$   $\Gamma_8/\Gamma$   
VALUE (units  $10^{-6}$ ) CL% EVTS DOCUMENT ID TECN CHG  
**<3.5** 90 0 BOLOTOV 88 SPEC -  
• • • We do not use the following data for averages, fits, limits, etc. • • •  
<9 90 0 BARMIN 92 XEBC +

## Hadronic modes

$\Gamma(\pi^+ \pi^0)/\Gamma_{\text{total}}$   $\Gamma_9/\Gamma$   
VALUE (units  $10^{-2}$ ) EVTS DOCUMENT ID TECN CHG COMMENT  
**20.66 ± 0.08 OUR FIT** Error includes scale factor of 1.2.  
**20.70 ± 0.16 OUR AVERAGE** Error includes scale factor of 1.8.

20.65 ± 0.05 ± 0.08	1.4M	31 AMBROSINO 08E	KLOE +	$\phi \rightarrow K^+ K^-$
21.18 ± 0.28	16k	CHIANG 72	OSPK +	1.84 GeV/c $K^+$
• • • We do not use the following data for averages, fits, limits, etc. • • •				
21.0 ± 0.6		CALLAHAN 65	HLBC	See $\Gamma_9/\Gamma_{11}$

<sup>31</sup> Fully inclusive of final-state radiation. The branching ratio is evaluated using  $K^+$  lifetime,  $\tau = 12.385$  ns.

$\Gamma(\pi^+ \pi^0)/\Gamma(\pi^+ \pi^+ \pi^-)$   $\Gamma_9/\Gamma_{11}$   
VALUE EVTS DOCUMENT ID TECN CHG  
**3.694 ± 0.029 OUR FIT** Error includes scale factor of 1.2.  
• • • We do not use the following data for averages, fits, limits, etc. • • •  
3.96 ± 0.15 1045 CALLAHAN 66 FBC +

$\Gamma(\pi^+ \pi^0)/\Gamma(\mu^+ \nu_\mu)$   $\Gamma_9/\Gamma_2$   
VALUE EVTS DOCUMENT ID TECN CHG COMMENT  
**0.3252 ± 0.0016 OUR FIT** Error includes scale factor of 1.2.  
**0.3325 ± 0.0032 OUR AVERAGE**

0.3329 ± 0.0047 ± 0.0010	45k	USHER 92	SPEC +	$p\bar{p}$ at rest
0.3355 ± 0.0057		32 WEISSENBE... 76	SPEC +	
0.3277 ± 0.0065	4517	33 AUERBACH 67	OSPK +	
• • • We do not use the following data for averages, fits, limits, etc. • • •				
0.328 ± 0.005	25k	32 WEISSENBE... 74	STRC +	
0.305 ± 0.018	1600	ZELLER 69	ASPK +	
32 WEISSENBERG 76 revises WEISSENBERG 74.				
33 AUERBACH 67 changed from 0.3253 ± 0.0065. See comment with ratio $\Gamma(\pi^0 \mu^+ \nu_\mu)/\Gamma(\mu^+ \nu_\mu)$ .				

$\Gamma(\pi^+ \pi^0 \pi^0)/\Gamma_{\text{total}}$   $\Gamma_{10}/\Gamma$   
VALUE (units  $10^{-2}$ ) EVTS DOCUMENT ID TECN CHG COMMENT  
**1.761 ± 0.022 OUR FIT** Error includes scale factor of 1.1.  
**1.775 ± 0.028 OUR AVERAGE** Error includes scale factor of 1.2.

1.763 ± 0.013 ± 0.022		ALOISIO 04A	KLOE ±	
1.84 ± 0.06	1307	CHIANG 72	OSPK +	1.84 GeV/c $K^+$
• • • We do not use the following data for averages, fits, limits, etc. • • •				
1.53 ± 0.11	198	34 PANDOULAS 70	EMUL +	
1.8 ± 0.2	108	SHAKLEE 64	HLBC +	
1.7 ± 0.2		ROE 61	HLBC +	
1.5 ± 0.2		35 TAYLOR 59	EMUL +	

<sup>34</sup> Includes events of TAYLOR 59.  
<sup>35</sup> Earlier experiments not averaged.

$\Gamma(\pi^+ \pi^0 \pi^0)/\Gamma(\pi^+ \pi^0)$   $\Gamma_{10}/\Gamma_9$   
VALUE EVTS DOCUMENT ID TECN CHG COMMENT  
**0.0852 ± 0.0011 OUR FIT** Error includes scale factor of 1.1.  
• • • We do not use the following data for averages, fits, limits, etc. • • •  
0.081 ± 0.005 574 36 LUCAS 73B HBC - Dalitz pairs only  
<sup>36</sup> LUCAS 73B gives  $N(\pi 2\pi^0) = 574 \pm 5.9\%$ ,  $N(2\pi) = 3564 \pm 3.1\%$ . We quote  $0.5N(\pi 2\pi^0)/N(2\pi)$  where 0.5 is because only Dalitz pair  $\pi^0$ 's were used.

$\Gamma(\pi^+ \pi^0 \pi^0)/\Gamma(\pi^+ \pi^+ \pi^-)$   $\Gamma_{10}/\Gamma_{11}$   
VALUE EVTS DOCUMENT ID TECN CHG COMMENT  
**0.315 ± 0.004 OUR FIT** Error includes scale factor of 1.1.  
**0.303 ± 0.009** 2027 BISI 65 BC + HBC+HLBC  
• • • We do not use the following data for averages, fits, limits, etc. • • •  
0.393 ± 0.099 17 YOUNG 65 EMUL +

$\Gamma(\pi^+ \pi^+ \pi^-)/\Gamma_{\text{total}}$   $\Gamma_{11}/\Gamma$   
VALUE (units  $10^{-2}$ ) EVTS DOCUMENT ID TECN CHG COMMENT  
**5.59 ± 0.04 OUR FIT** Error includes scale factor of 1.3.  
• • • We do not use the following data for averages, fits, limits, etc. • • •  
5.56 ± 0.20 2330 37 CHIANG 72 OSPK + 1.84 GeV/c  $K^+$   
5.34 ± 0.21 693 38 PANDOULAS 70 EMUL +  
5.71 ± 0.15 DEMARCO 65 HBC  
6.0 ± 0.4 44 YOUNG 65 EMUL +  
5.54 ± 0.12 2332 CALLAHAN 64 HLBC +  
5.1 ± 0.2 540 SHAKLEE 64 HLBC +  
5.7 ± 0.3 ROE 61 HLBC +  
<sup>37</sup> Value is not independent of CHIANG 72  $\Gamma(\mu^+ \nu_\mu)/\Gamma_{\text{total}}$ ,  $\Gamma(\pi^+ \pi^0)/\Gamma_{\text{total}}$ ,  $\Gamma(\pi^+ \pi^0 \pi^0)/\Gamma_{\text{total}}$ ,  $\Gamma(\pi^0 \mu^+ \nu_\mu)/\Gamma_{\text{total}}$ , and  $\Gamma(\pi^0 e^+ \nu_e)/\Gamma_{\text{total}}$ .  
<sup>38</sup> Includes events of TAYLOR 59.

## Leptonic and semileptonic modes with photons

$\Gamma(\mu^+ \nu_\mu \gamma)/\Gamma_{\text{total}}$   $\Gamma_{12}/\Gamma$   
VALUE (units  $10^{-3}$ ) EVTS DOCUMENT ID TECN CHG COMMENT  
**6.2 ± 0.8 OUR AVERAGE**

6.6 ± 1.5	39,40	DEMIDOV 90	XEBC	$P(\mu) < 231.5$ MeV/c
6.0 ± 0.9		BARMIN 88	HLBC +	$P(\mu) < 231.5$ MeV/c
• • • We do not use the following data for averages, fits, limits, etc. • • •				
3.5 ± 0.8	40,41	DEMIDOV 90	XEBC	$E(\gamma) > 20$ MeV
3.2 ± 0.5	57	42 BARMIN 88	HLBC +	$E(\gamma) > 20$ MeV
5.4 ± 0.3		43 AKIBA 85	SPEC	$P(\mu) < 231.5$ MeV/c

<sup>39</sup>  $P(\mu)$  cut given in DEMIDOV 90 paper, 235.1 MeV/c, is a misprint according to authors (private communication).  
<sup>40</sup> DEMIDOV 90 quotes only inner bremsstrahlung (IB) part.  
<sup>41</sup> Not independent of above DEMIDOV 90 value. Cuts differ.  
<sup>42</sup> Not independent of above BARMIN 88 value. Cuts differ.  
<sup>43</sup> Assumes  $\mu$ -e universality and uses constraints from  $K \rightarrow e\nu\gamma$ .

$\Gamma(\mu^+ \nu_\mu \gamma(SD^+))/\Gamma_{total}$   $\Gamma_{13}/\Gamma$ 

Structure-dependent part with  $+\gamma$  helicity ( $SD^+$  term). See the "Note on  $\pi^\pm \rightarrow \ell^\pm \nu_\ell \gamma$  and  $K^\pm \rightarrow \ell^\pm \nu_\ell \gamma$  Form Factors" in the  $\pi^\pm$  section of the Particle Data Listings above.

VALUE (units $10^{-5}$ )	CL%	EVTS	DOCUMENT ID	TECN
<b>1.33 ± 0.12 ± 0.18</b>		25 88	44 ADLER	00B B787

• • • We do not use the following data for averages, fits, limits, etc. • • •

<3.0	90		AKIBA	85 SPEC
------	----	--	-------	---------

44 ADLER 00B obtains the branching ratio by extrapolating the measurement in the kinematic region  $E_\mu > 137$  MeV,  $E_\gamma > 90$  MeV to the full  $SD^+$  phase-space. Also reports  $|F_V + F_A| = 0.165 \pm 0.007 \pm 0.011$  and  $-0.04 < F_V - F_A < 0.24$  at 90% CL.

 $\Gamma(\mu^+ \nu_\mu \gamma(SD^+INT))/\Gamma_{total}$   $\Gamma_{14}/\Gamma$ 

Interference term between internal Bremsstrahlung and  $SD^+$  term. See the "Note on  $\pi^\pm \rightarrow \ell^\pm \nu_\ell \gamma$  and  $K^\pm \rightarrow \ell^\pm \nu_\ell \gamma$  Form Factors" in the  $\pi^\pm$  section of the Particle Data Listings above.

VALUE (units $10^{-5}$ )	CL%	DOCUMENT ID	TECN
<b>&lt;2.7</b>	90	AKIBA	85 SPEC

 $\Gamma(\mu^+ \nu_\mu \gamma(SD^- + SD^-INT))/\Gamma_{total}$   $\Gamma_{15}/\Gamma$ 

Sum of structure-dependent part with  $-\gamma$  helicity ( $SD^-$  term) and interference term between internal Bremsstrahlung and  $SD^-$  term. See the "Note on  $\pi^\pm \rightarrow \ell^\pm \nu_\ell \gamma$  and  $K^\pm \rightarrow \ell^\pm \nu_\ell \gamma$  Form Factors" in the  $\pi^\pm$  section of the Particle Data Listings above.

VALUE (units $10^{-4}$ )	CL%	DOCUMENT ID	TECN
<b>&lt;2.6</b>	90	45 AKIBA	85 SPEC

45 Assumes  $\mu$ -e universality and uses constraints from  $K \rightarrow e \nu \gamma$ .

 $\Gamma(e^+ \nu_e \gamma)/\Gamma(\mu^+ \nu_\mu)$   $\Gamma_{16}/\Gamma_2$ 

VALUE (units $10^{-5}$ )	EVTS	DOCUMENT ID	TECN	CHG	COMMENT
<b>1.483 ± 0.066 ± 0.013</b>	1.4K	46 AMBROSINO	09E KLOE	±	$E_\gamma$ in 10–250 MeV, $p_e > 200$ MeV/c

46 AMBROSINO 09E measured the differential width  $dR_\gamma/dE_\gamma = (1/\Gamma(K \rightarrow \mu \nu)) (d\Gamma(K \rightarrow e \nu \gamma)/dE_\gamma)$ . Result obtained by integrating the differential width over  $E_\gamma$  from 10 to 250 MeV.

 $\Gamma(\pi^0 e^+ \nu_e \gamma)/\Gamma(\pi^0 e^+ \nu_e)$   $\Gamma_{17}/\Gamma_3$ 

VALUE (units $10^{-2}$ )	EVTS	DOCUMENT ID	TECN	CHG	COMMENT
<b>0.505 ± 0.032 OUR AVERAGE</b>		Error includes scale factor of 1.3. See the ideogram below.			

0.47 ± 0.02 ± 0.03 4476 47 AKIMENKO 07 ISTR -  $E_\gamma > 10$  MeV,  $0.6 < \cos(\theta_{e\gamma}) < 0.9$

0.46 ± 0.08 82 48 BARMIN 91 XEBC  $E_\gamma > 10$  MeV,  $0.6 < \cos(\theta_{e\gamma}) < 0.9$

0.56 ± 0.04 192 49 BOLOTOV 86B CALO -  $E_\gamma > 10$  MeV

• • • We do not use the following data for averages, fits, limits, etc. • • •

1.81 ± 0.03 ± 0.07 4476 47 AKIMENKO 07 ISTR -  $E_\gamma > 10$  MeV,  $\theta_{e\gamma} > 10^\circ$

0.63 ± 0.02 ± 0.03 4476 47 AKIMENKO 07 ISTR -  $E_\gamma > 30$  MeV,  $\theta_{e\gamma} > 20^\circ$

1.51 ± 0.25 82 48 BARMIN 91 XEBC  $E_\gamma > 10$  MeV,  $\cos(\theta_{e\gamma}) < 0.98$

0.48 ± 0.20 16 50 LJUNG 73 HLBC +  $E_\gamma > 30$  MeV

0.22  $^{+0.15}_{-0.10}$  50 LJUNG 73 HLBC +  $E_\gamma > 30$  MeV

0.76 ± 0.28 13 51 ROMANO 71 HLBC  $E_\gamma > 10$  MeV

0.53 ± 0.22 51 ROMANO 71 HLBC +  $E_\gamma > 30$  MeV

1.2 ± 0.8 BELLOTTI 67 HLBC  $E_\gamma > 30$  MeV

47 AKIMENKO 07 provides values for three kinematic regions. For averaging, we use value with  $E_\gamma > 10$  MeV and  $0.6 < \cos(\theta_{e\gamma}) < 0.9$ .

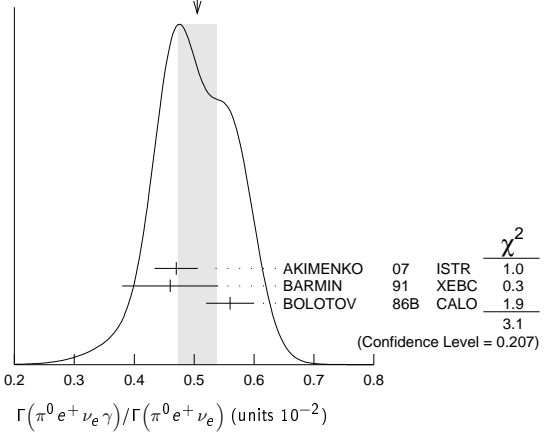
48 BARMIN 91 quotes branching ratio  $\Gamma(K \rightarrow e \pi^0 \nu_\ell \gamma)/\Gamma_{all}$ . The measured normalization is  $[\Gamma(K \rightarrow e \pi^0 \nu) + \Gamma(K \rightarrow \pi^+ \pi^+ \pi^-)]$ . For comparison with other experiments we used  $\Gamma(K \rightarrow e \pi^0 \nu)/\Gamma_{all} = 0.0482$  to calculate the values quoted here.

49  $\cos(\theta_{e\gamma})$  between 0.6 and 0.9.

50 First LJUNG 73 value is for  $\cos(\theta_{e\gamma}) < 0.9$ , second value is for  $\cos(\theta_{e\gamma})$  between 0.6 and 0.9 for comparison with ROMANO 71.

51 Both ROMANO 71 values are for  $\cos(\theta_{e\gamma})$  between 0.6 and 0.9. Second value is for comparison with second LJUNG 73 value. We use lowest  $E_\gamma$  cut for Summary Table value. See ROMANO 71 for  $E_\gamma$  dependence.

WEIGHTED AVERAGE  
0.505 ± 0.032 (Error scaled by 1.3)

 $\Gamma(\pi^0 e^+ \nu_e \gamma(SD))/\Gamma_{total}$   $\Gamma_{18}/\Gamma$ 

Structure-dependent part.

VALUE (units $10^{-5}$ )	CL%	DOCUMENT ID	TECN	CHG
<b>&lt;5.3</b>	90	BOLOTOV	86B CALO	-

 $\Gamma(\pi^0 \mu^+ \nu_\mu \gamma)/\Gamma_{total}$   $\Gamma_{19}/\Gamma$ 

VALUE (units $10^{-5}$ )	CL%	EVTS	DOCUMENT ID	TECN	CHG	COMMENT
<b>1.25 ± 0.25 OUR AVERAGE</b>						

1.10 ± 0.32 ± 0.05 23 52 ADLER 10 B787 30  $< E_\gamma < 60$  MeV

1.46 ± 0.22 ± 0.32 153 53 TCHIKILEV 07 ISTR - 30  $< E_\gamma < 60$  MeV

• • • We do not use the following data for averages, fits, limits, etc. • • •

2.4 ± 0.5 ± 0.6 125 SHIMIZU 06 K470 +  $E_\gamma > 30$  MeV;

$\theta_{\mu\gamma} > 20^\circ$

<6.1 90 0 LJUNG 73 HLBC +  $E_\gamma > 30$  MeV

52 Value obtained from  $B(K^+ \rightarrow \pi^0 \mu^+ \nu_\mu \gamma) = (2.51 \pm 0.74 \pm 0.12) \times 10^{-5}$  obtained in the kinematic region  $E_\gamma > 20$  MeV, and then theoretical  $K_{\mu 3\gamma}$  spectrum has been used. Also  $B(K^+ \rightarrow \pi^0 \mu^+ \nu_\mu \gamma) = (1.58 \pm 0.46 \pm 0.08) \times 10^{-5}$ , for  $E_\gamma > 30$  MeV and  $\theta_{\mu\gamma} > 20^\circ$ , was determined.

53 Obtained from measuring  $B(K_{\mu 3\gamma})/B(K_{\mu 3})$  and using PDG 02 value  $B(K_{\mu 3}) = 3.27\%$ .  $B(K_{\mu 3\gamma}) = (8.82 \pm 0.94 \pm 0.86) \times 10^{-5}$  is obtained for  $5 \text{ MeV} < E_\gamma < 30 \text{ MeV}$ .

 $\Gamma(\pi^0 \pi^0 e^+ \nu_e \gamma)/\Gamma_{total}$   $\Gamma_{20}/\Gamma$ 

VALUE (units $10^{-6}$ )	CL%	EVTS	DOCUMENT ID	TECN	CHG	COMMENT
<b>&lt;5</b>	90	0	BARMIN	92 XEBC	+	$E_\gamma > 10$ MeV

## Hadronic modes with photons

 $\Gamma(\pi^+ \pi^0 \gamma(INT))/\Gamma_{total}$   $\Gamma_{21}/\Gamma$ 

The  $K^+ \rightarrow \pi^+ \pi^0 \gamma$  differential decay rate can be described in terms of  $T_{\pi^+}$ , the charged pion kinetic energy, and  $W^2 = (P_K \cdot P_\gamma) (P_{\pi^+} \cdot P_\gamma) / (m_K m_{\pi^+})^2$ ; then we can write  $d^2\Gamma(K^+ \rightarrow \pi^+ \pi^0 \gamma) / (dT_{\pi^+} dW^2) = d^2\Gamma(K^+ \rightarrow \pi^+ \pi^0 \gamma)_{IB} / (dT_{\pi^+} dW^2) [1 + 2 \cos(\pm\phi + \delta_1^1 - \delta_0^2) m_\pi^2 m_K^2 W^2 X_E + m_K^4 m_\pi^4 (X_E^2 + X_M^2) W^4]$ . The IB differential and total branching ratios are expressed in terms of the non-radiative experimental width  $\Gamma(K^+ \rightarrow \pi^+ \pi^0)$  by Low's theorem. Using PDG 10  $B(K^+ \rightarrow \pi^+ \pi^0) = 0.2066 \pm 0.0008$ , one obtains respectively  $B(K^+ \rightarrow \pi^+ \pi^0 \gamma)_{IB} (55 < T_{\pi^+} < 90 \text{ MeV}) = 2.55 \times 10^{-4}$  and  $B(K^+ \rightarrow \pi^+ \pi^0 \gamma)_{IB} (0 < T_{\pi^+} < 80 \text{ MeV}) = 1.80 \times 10^{-4}$ . Fitting respectively the piece proportional to  $W^2$  and the piece proportional to  $W^4$ , the interference contribution (INT), proportional to  $X_E$ , and the direct contribution (DE) proportional to  $X_E^2 + X_M^2$  are extracted.

VALUE (units $10^{-6}$ )	EVTS	DOCUMENT ID	TECN	CHG	COMMENT
<b>-4.24 ± 0.63 ± 0.70</b>	600k	54 BATLEY	10A NA48	±	$T_{\pi^+}$ 0–80 MeV

54 The cut on the photon energy implies  $W^2 > 0.2$ . BATLEY 10A obtains the INT and DE fractional branchings with respect to IB from a simultaneous kinematical fit of INT and DE and then we use the PDG 10 value for  $B(K^+ \rightarrow \pi^+ \pi^0) = 20.66 \pm 0.08$  to determine the IB. The INT and DE correlation coefficients  $-0.83$ . Assuming a constant electric amplitude,  $X_E$ , this INT value implies  $X_E = -24 \pm 6 \text{ GeV}^{-4}$ .

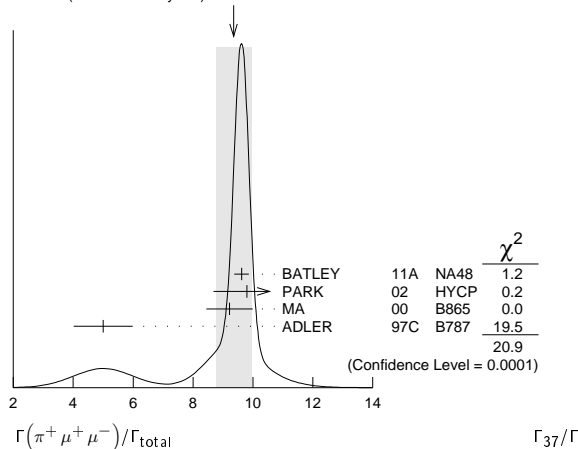
 $\Gamma(\pi^+ \pi^0 \gamma(DE))/\Gamma_{total}$   $\Gamma_{22}/\Gamma$ 

Direct emission (DE) part of  $\Gamma(\pi^+ \pi^0 \gamma)/\Gamma_{total}$ , assuming that interference (INT) component is zero.

VALUE (units $10^{-6}$ )	EVTS	DOCUMENT ID	TECN	CHG	COMMENT
<b>5.99 ± 0.27 ± 0.25</b>	600k	55 BATLEY	10A NA48	±	$T_{\pi^+}$ 0–80 MeV



See key on page 457

WEIGHTED AVERAGE  
9.4±0.6 (Error scaled by 2.6)

$\Gamma(\pi^+ \nu \bar{\nu})/\Gamma_{\text{total}}$   $\Gamma_{38}/\Gamma$   
 Test for  $\Delta S = 1$  weak neutral current. Allowed by higher-order electroweak interactions. Branching ratio values are extrapolated from the momentum or energy regions shown in the comments assuming Standard Model phase space except for those labeled "Scalar" or "Tensor" to indicate the assumed non-Standard-Model interaction.

VALUE (units $10^{-9}$ )	CL%	EVTS	DOCUMENT ID	TECN	CHG	COMMENT
<b>0.173<sup>+0.115</sup><sub>-0.105</sub></b>	7	70	ARTAMONOV 08	B949	+	140 < P <sub>π</sub> < 199 MeV, 211 < P <sub>π</sub> < 229 MeV
••• We do not use the following data for averages, fits, limits, etc. •••						
0.789 <sup>+0.926</sup> <sub>-0.510</sub>	3	71	ARTAMONOV 08	B949	+	140 < P <sub>π</sub> < 199 MeV
< 2.2	90	1	72 ADLER	04 B787	+	211 < P <sub>π</sub> < 229 MeV
< 2.7	90		ADLER	04 B787	+	Scalar
< 1.8	90		ADLER	04 B787	+	Tensor
0.147 <sup>+0.130</sup> <sub>-0.089</sub>	3	73	ANISIMOVSK...04	B949	+	211 < P <sub>π</sub> < 229 MeV
0.157 <sup>+0.175</sup> <sub>-0.082</sub>	2		ADLER	02 B787	+	P <sub>π</sub> > 211 MeV/c
< 4.2	90	1	ADLER	02c B787	+	140 < P <sub>π</sub> < 195 MeV
< 4.7	90		74 ADLER	02c B787	+	Scalar
< 2.5	90		74 ADLER	02c B787	+	Tensor
0.15 <sup>+0.34</sup> <sub>-0.12</sub>	1		ADLER	00 B787		In ADLER 02
0.42 <sup>+0.97</sup> <sub>-0.35</sub>	1		ADLER	97 B787		
< 2.4	90		ADLER	96 B787		
< 7.5	90		ATIYA	93 B787	+	T(π) 115-127 MeV
< 5.2	90		75 ATIYA	93 B787	+	
< 17	90	0	ATIYA	93B B787	+	T(π) 60-100 MeV
< 34	90		ATIYA	90 B787	+	
< 140	90		ASANO	81B CNTR	+	T(π) 116-127 MeV

<sup>70</sup> Value obtained combining ANISIMOVSKY 04, ADLER 04, and the present ARTAMONOV 08 results.

<sup>71</sup> Observed 3 events with an estimated background of 0.93 ± 0.17<sup>+0.32</sup><sub>-0.24</sub>. Signal-to-background ratio for each of these 3 events is 0.20, 0.42, and 0.47.

<sup>72</sup> Value obtained combining the previous result ADLER 02c with 1 event and the present result with 0 events to obtain an expected background 1.22 ± 0.24 events and 1 event observed.

<sup>73</sup> Value obtained combining the previous E787 result ADLER 02 with 2 events and the present E949 with 1 event. The additional event has a signal-to-background ratio 0.9. Superseded by ARTAMONOV 08.

<sup>74</sup> Superseded by ADLER 04.

<sup>75</sup> Combining ATIYA 93 and ATIYA 93B results. Superseded by ADLER 96.

$\Gamma(\pi^+ \pi^0 \nu \bar{\nu})/\Gamma_{\text{total}}$   $\Gamma_{39}/\Gamma$   
 Test for  $\Delta S = 1$  weak neutral current. Allowed by higher-order electroweak interactions.

VALUE (units $10^{-5}$ )	CL%	DOCUMENT ID	TECN
<b>&lt; 4.3</b>	90	76 ADLER 01	SPEC

<sup>76</sup> Search region defined by 90 MeV < P<sub>π<sup>+</sup></sub> < 188 MeV/c and 135 MeV < E<sub>π<sup>0</sup></sub> < 180 MeV.

$\Gamma(\mu^- \nu e^+ e^-)/\Gamma(\pi^+ \pi^- e^+ \nu_e)$   $\Gamma_{40}/\Gamma_6$   
 Test of lepton family number conservation.

VALUE (units $10^{-3}$ )	CL%	EVTS	DOCUMENT ID	TECN	CHG
<b>&lt; 0.5</b>	90	0	77 DIAMANT-...	76	SPEC +

<sup>77</sup> DIAMANT-BERGER 76 quotes this result times our 1975 π<sup>+</sup>π<sup>-</sup>eν BR ratio.

$\Gamma(\mu^+ \nu_e)/\Gamma_{\text{total}}$   $\Gamma_{41}/\Gamma$   
 Forbidden by lepton family number conservation.

VALUE	CL%	EVTS	DOCUMENT ID	TECN	COMMENT
<b>&lt; 0.004</b>	90	0	78 LYONS 81	HLBC	200 GeV K <sup>+</sup> narrow band ν beam

••• We do not use the following data for averages, fits, limits, etc. •••

< 0.012	90		78 COOPER	82 HLBC	Wideband ν beam
---------	----	--	-----------	---------	-----------------

<sup>78</sup> COOPER 82 and LYONS 81 limits on ν<sub>e</sub> observation are here interpreted as limits on lepton family number violation in the absence of mixing.

$\Gamma(\pi^+ \mu^+ e^-)/\Gamma_{\text{total}}$   $\Gamma_{42}/\Gamma$   
 Test of lepton family number conservation.

VALUE (units $10^{-10}$ )	CL%	DOCUMENT ID	TECN	CHG
<b>&lt; 0.13</b>	90	79 SHER 05	RVUE	+

••• We do not use the following data for averages, fits, limits, etc. •••

< 0.21	90	SHER	05	B865 +
< 0.39	90	APPEL	00	B865 +
< 2.1	90	LEE	90	SPEC +

<sup>79</sup> This result combines SHER 05 1998 data, APPEL 00 1996 data, and data from BERGMAN 97 and PISLAK 97 theses, all from BNL-E865, with LEE 90 BNL-E777 data.

$\Gamma(\pi^+ \mu^- e^+)/\Gamma_{\text{total}}$   $\Gamma_{43}/\Gamma$   
 Test of lepton family number conservation.

VALUE (units $10^{-10}$ )	CL%	EVTS	DOCUMENT ID	TECN	CHG
<b>&lt; 5.2</b>	90	0	APPEL	00B	B865 +

••• We do not use the following data for averages, fits, limits, etc. •••

< 70	90	0	80 DIAMANT-...	76	SPEC +
------	----	---	----------------	----	--------

<sup>80</sup> Measurement actually applies to the sum of the π<sup>+</sup>μ<sup>-</sup>e<sup>+</sup> and π<sup>-</sup>μ<sup>+</sup>e<sup>+</sup> modes.

$\Gamma(\pi^- \mu^+ e^+)/\Gamma_{\text{total}}$   $\Gamma_{44}/\Gamma$   
 Test of total lepton number conservation.

VALUE (units $10^{-10}$ )	CL%	EVTS	DOCUMENT ID	TECN	CHG
<b>&lt; 5.0</b>	90	0	APPEL	00B	B865 +

••• We do not use the following data for averages, fits, limits, etc. •••

< 70	90	0	81 DIAMANT-...	76	SPEC +
------	----	---	----------------	----	--------

<sup>81</sup> Measurement actually applies to the sum of the π<sup>+</sup>μ<sup>-</sup>e<sup>+</sup> and π<sup>-</sup>μ<sup>+</sup>e<sup>+</sup> modes.

$\Gamma(\pi^- e^+ e^+)/\Gamma_{\text{total}}$   $\Gamma_{45}/\Gamma$   
 Test of total lepton number conservation.

VALUE	CL%	EVTS	DOCUMENT ID	TECN	CHG
<b>&lt; 6.4 × 10<sup>-10</sup></b>	90	0	APPEL	00B	B865 +

••• We do not use the following data for averages, fits, limits, etc. •••

< 9.2 × 10 <sup>-9</sup>	90	0	DIAMANT-...	76	SPEC +
< 1.5 × 10 <sup>-5</sup>			CHANG	68	HBC -

$\Gamma(\pi^- \mu^+ \mu^+)/\Gamma_{\text{total}}$   $\Gamma_{46}/\Gamma$   
 Forbidden by total lepton number conservation.

VALUE	CL%	DOCUMENT ID	TECN	CHG
<b>&lt; 1.1 × 10<sup>-9</sup></b>	90	BATLEY 11A NA48		±

••• We do not use the following data for averages, fits, limits, etc. •••

< 3.0 × 10 <sup>-9</sup>	90	APPEL	00B	B865 +
< 1.5 × 10 <sup>-4</sup>	90	82 LITTENBERG	92	HBC

<sup>82</sup> LITTENBERG 92 is from retroactive data analysis of CHANG 68 bubble chamber data.

$\Gamma(\mu^+ \bar{\nu}_e)/\Gamma_{\text{total}}$   $\Gamma_{47}/\Gamma$   
 Forbidden by total lepton number conservation.

VALUE (units $10^{-3}$ )	CL%	DOCUMENT ID	TECN	COMMENT
<b>&lt; 3.3</b>	90	83 COOPER 82	HLBC	Wideband ν beam

<sup>83</sup> COOPER 82 limit on ν<sub>e</sub> observation is here interpreted as a limit on lepton number violation in the absence of mixing.

$\Gamma(\pi^0 e^+ \bar{\nu}_e)/\Gamma_{\text{total}}$   $\Gamma_{48}/\Gamma$   
 Forbidden by total lepton number conservation.

VALUE	CL%	DOCUMENT ID	TECN	COMMENT
<b>&lt; 0.003</b>	90	84 COOPER 82	HLBC	Wideband ν beam

<sup>84</sup> COOPER 82 limit on ν<sub>e</sub> observation is here interpreted as a limit on lepton number violation in the absence of mixing.

$\Gamma(\pi^+ \gamma)/\Gamma_{\text{total}}$   $\Gamma_{49}/\Gamma$   
 Violates angular momentum conservation and gauge invariance. Current interest in this decay is as a search for non-commutative space-time effects as discussed in ARTAMONOV 05 and for exotic physics such as a vacuum expectation value of a new vector field, non-local Superstring effects, or departures from Lorentz invariance, as discussed in ADLER 02b.

VALUE (units $10^{-3}$ )	CL%	DOCUMENT ID	TECN	CHG
<b>&lt; 2.3</b>	90	ARTA MONOV 05	B949	+

••• We do not use the following data for averages, fits, limits, etc. •••

< 360	90	ADLER	02B	B787 +
< 1400	90	ASANO	82	CNTR +
< 4000	90	85 KLEMS	71	OSPK +

<sup>85</sup> Test of model of Selleri, Nuovo Cimento **60A** 291 (1969).

K<sup>+</sup> LONGITUDINAL POLARIZATION OF EMITTED μ<sup>+</sup>

VALUE	CL%	DOCUMENT ID	TECN	CHG	COMMENT
<b>&lt; -0.990</b>	90	86 AOKI 94	SPEC	+	

••• We do not use the following data for averages, fits, limits, etc. •••

< -0.990	90	IMAZATO	92	SPEC +	Repl. by AOKI 94
-0.970 ± 0.047		87 YAMANAKA	86	SPEC +	
-1.0 ± 0.1		87 CUTTS	69	SPRK +	
-0.96 ± 0.12		87 COOMBES	57	CNTR +	

## Meson Particle Listings

 $K^\pm$ 

<sup>86</sup>AOKI 94 measures  $\xi P_\mu = -0.9996 \pm 0.0030 \pm 0.0048$ . The above limit is obtained by summing the statistical and systematic errors in quadrature, normalizing to the physically significant region ( $|\xi P_\mu| < 1$ ) and assuming that  $\xi=1$ , its maximum value.

<sup>87</sup>Assumes  $\xi=1$ .

DALITZ PLOT PARAMETERS FOR  $K \rightarrow 3\pi$  DECAYS

Revised 1999 by T.G. Trippe (LBNL).

The Dalitz plot distribution for  $K^\pm \rightarrow \pi^\pm \pi^\pm \pi^\mp$ ,  $K^\pm \rightarrow \pi^0 \pi^0 \pi^\pm$ , and  $K_L^0 \rightarrow \pi^+ \pi^- \pi^0$  can be parameterized by a series expansion such as that introduced by Weinberg [1]. We use the form

$$\begin{aligned} |M|^2 \propto & 1 + g \frac{(s_3 - s_0)}{m_{\pi^+}^2} + h \left[ \frac{s_3 - s_0}{m_{\pi^+}^2} \right]^2 \\ & + j \frac{(s_2 - s_1)}{m_{\pi^+}^2} + k \left[ \frac{s_2 - s_1}{m_{\pi^+}^2} \right]^2 \\ & + f \frac{(s_2 - s_1)(s_3 - s_0)}{m_{\pi^+}^2 m_{\pi^+}^2} + \dots, \end{aligned} \quad (1)$$

where  $m_{\pi^+}^2$  has been introduced to make the coefficients  $g$ ,  $h$ ,  $j$ , and  $k$  dimensionless, and

$$s_i = (P_K - P_i)^2 = (m_K - m_i)^2 - 2m_K T_i, \quad i = 1, 2, 3,$$

$$s_0 = \frac{1}{3} \sum_i s_i = \frac{1}{3} (m_K^2 + m_1^2 + m_2^2 + m_3^2).$$

Here the  $P_i$  are four-vectors,  $m_i$  and  $T_i$  are the mass and kinetic energy of the  $i^{\text{th}}$  pion, and the index 3 is used for the odd pion.

The coefficient  $g$  is a measure of the slope in the variable  $s_3$  (or  $T_3$ ) of the Dalitz plot, while  $h$  and  $k$  measure the quadratic dependence on  $s_3$  and  $(s_2 - s_1)$ , respectively. The coefficient  $j$  is related to the asymmetry of the plot and must be zero if  $CP$  invariance holds. Note also that if  $CP$  is good,  $g$ ,  $h$ , and  $k$  must be the same for  $K^+ \rightarrow \pi^+ \pi^+ \pi^-$  as for  $K^- \rightarrow \pi^- \pi^- \pi^+$ .

Since different experiments use different forms for  $|M|^2$ , in order to compare the experiments we have converted to  $g$ ,  $h$ ,  $j$ , and  $k$  whatever coefficients have been measured. Where such conversions have been done, the measured coefficient  $a_y$ ,  $a_t$ ,  $a_u$ , or  $a_v$  is given in the comment at the right. For definitions of these coefficients, details of this conversion, and discussion of the data, see the April 1982 version of this note [2].

## References

1. S. Weinberg, Phys. Rev. Lett. **4**, 87 (1960).
2. Particle Data Group, Phys. Lett. **111B**, 69 (1982).

ENERGY DEPENDENCE OF  $K^\pm$  DALITZ PLOT

$$|\text{matrix element}|^2 = 1 + gu + hu^2 + kv^2$$

where  $u = (s_3 - s_0) / m_\pi^2$  and  $v = (s_2 - s_1) / m_\pi^2$

LINEAR COEFFICIENT  $g$  FOR  $K^\pm \rightarrow \pi^\pm \pi^0 \pi^\mp$ 

Some experiments use Dalitz variables  $x$  and  $y$ . In the comments we give  $a_y =$  coefficient of  $y$  term. See note above on "Dalitz Plot Parameters for  $K \rightarrow 3\pi$  Decays." For discussion of the conversion of  $a_y$  to  $g$ , see the earlier version of the same note in the Review published in Physics Letters **111B** 70 (1982).

VALUE	EVTS	DOCUMENT ID	TECN	CHG	COMMENT
<b>-0.21134 ± 0.00017</b>	471M	<sup>88</sup> BATLEY	07B	NA48	±

••• We do not use the following data for averages, fits, limits, etc. •••

-0.2221 ± 0.0065	225k	DEVAUX	77	SPEC	+	$a_y = .2814 \pm .0082$
-0.199 ± 0.008	81k	<sup>89</sup> LUCAS	73	HBC	-	$a_y = 0.252 \pm 0.011$
-0.2157 ± 0.0028	750k	FORD	72	ASPK	+	$a_y = .2734 \pm .0035$
-0.2186 ± 0.0028	750k	FORD	72	ASPK	-	$a_y = .2770 \pm .0035$
-0.200 ± 0.009	39819	<sup>90</sup> HOFFMASTER	72	HLBC	+	
-0.196 ± 0.012	17898	<sup>91</sup> GRAUMAN	70	HLBC	+	$a_y = 0.228 \pm 0.030$
-0.193 ± 0.010	50919	MAST	69	HBC	-	$a_y = 0.244 \pm 0.013$
-0.218 ± 0.016	9994	<sup>92</sup> BUTLER	68	HBC	+	$a_y = 0.277 \pm 0.020$
-0.190 ± 0.023	5778	<sup>92,93</sup> MOSCOSO	68	HBC	-	$a_y = 0.242 \pm 0.029$
-0.22 ± 0.024	5428	<sup>92,93</sup> ZINCHENKO	67	HBC	+	$a_y = 0.28 \pm 0.03$
-0.220 ± 0.035	1347	<sup>94</sup> FERRO-LUZZI	61	HBC	-	$a_y = 0.28 \pm 0.045$

<sup>88</sup>Final state strong interaction and radiative corrections not included in the fit.

<sup>89</sup>Quadratic dependence is required by  $K_L^0$  experiments.

<sup>90</sup>HOFFMASTER 72 includes GRAUMAN 70 data.

<sup>91</sup>Emulsion data added — all events included by HOFFMASTER 72.

<sup>92</sup>Experiments with large errors not included in average.

<sup>93</sup>Also includes DBC events.

<sup>94</sup>No radiative corrections included.

QUADRATIC COEFFICIENT  $h$  FOR  $K^\pm \rightarrow \pi^\pm \pi^+ \pi^-$ 

VALUE (units $10^{-2}$ )	EVTS	DOCUMENT ID	TECN	CHG
--------------------------	------	-------------	------	-----

**1.848 ± 0.040** 471M <sup>95</sup>BATLEY 07B NA48 ±

••• We do not use the following data for averages, fits, limits, etc. •••

-0.06 ± 1.43	225k	DEVAUX	77	SPEC	+
1.87 ± 0.62	750k	FORD	72	ASPK	+
1.25 ± 0.62	750k	FORD	72	ASPK	-
-0.9 ± 1.4	39819	HOFFMASTER	72	HLBC	+
-0.1 ± 1.2	50919	MAST	69	HBC	-

<sup>95</sup>Final state strong interaction and radiative corrections not included in the fit.

QUADRATIC COEFFICIENT  $k$  FOR  $K^\pm \rightarrow \pi^\pm \pi^+ \pi^-$ 

VALUE (units $10^{-3}$ )	EVTS	DOCUMENT ID	TECN	CHG
--------------------------	------	-------------	------	-----

**-4.63 ± 0.14** 471M <sup>96</sup>BATLEY 07B NA48 ±

••• We do not use the following data for averages, fits, limits, etc. •••

-20.5 ± 3.9	225k	DEVAUX	77	SPEC	+
-7.5 ± 1.9	750k	FORD	72	ASPK	+
-8.3 ± 1.9	750k	FORD	72	ASPK	-
-10.5 ± 4.5	39819	HOFFMASTER	72	HLBC	+
-14 ± 12	50919	MAST	69	HBC	-

<sup>96</sup>Final state strong interaction and radiative corrections not included in the fit.

 $(g_+ - g_-) / (g_+ + g_-)$  FOR  $K^\pm \rightarrow \pi^\pm \pi^+ \pi^-$ 

This is a  $CP$  violating asymmetry between linear coefficients  $g_\pm$  for  $K^+ \rightarrow \pi^+ \pi^+ \pi^-$  decay and  $g_-$  for  $K^- \rightarrow \pi^- \pi^+ \pi^-$  decay.

VALUE (units $10^{-4}$ )	EVTS	DOCUMENT ID	TECN
--------------------------	------	-------------	------

**-1.5 ± 1.5 ± 1.6** 3.1G <sup>97</sup>BATLEY 07E NA48 ±

••• We do not use the following data for averages, fits, limits, etc. •••

1.7 ± 2.1 ± 2.0	1.7G	<sup>98</sup> BATLEY	06 NA48
-70.0 ± 53	3.2M	FORD	70 ASPK

<sup>97</sup>BATLEY 07E includes data from BATLEY 06. Uses quadratic parametrization and value  $g_+ + g_- = 2g$  from BATLEY 07B. This measurement neglects any possible charge asymmetries in higher order slope parameters  $h$  or  $k$ .

<sup>98</sup>This measurement neglects any possible charge asymmetries in higher order slope parameters  $h$  or  $k$ .

LINEAR COEFFICIENT  $g$  FOR  $K^\pm \rightarrow \pi^\pm \pi^0 \pi^\mp$ 

Unless otherwise stated, all experiments include terms quadratic in  $(s_3 - s_0) / m_{\pi^+}^2$ . See note above on "Dalitz Plot Parameters for  $K \rightarrow 3\pi$  Decays."

See BATUSOV 98 for a discussion of the discrepancy between their result and others, especially BOLOTOV 86. At this time we have no way to resolve the discrepancy so we depend on the large scale factor as a warning.

VALUE	EVTS	DOCUMENT ID	TECN	CHG	COMMENT
-------	------	-------------	------	-----	---------

**0.626 ± 0.007 OUR AVERAGE**

0.6259 ± 0.0043 ± 0.0093 493k AKOPDZHAN.05B TNF ±

0.627 ± 0.004 ± 0.010 252k <sup>99,100</sup>AJINENKO 03B ISTR -

••• We do not use the following data for averages, fits, limits, etc. •••

0.736 ± 0.014 ± 0.012	33k	BATUSOV	98	SPEC	+
0.582 ± 0.021	43k	BOLOTOV	86	CALO	-
0.670 ± 0.054	3263	BRAUN	76B	HLBC	+
0.630 ± 0.038	5635	SHEAFF	75	HLBC	+
0.510 ± 0.060	27k	SMITH	75	WIRE	+
0.67 ± 0.06	1365	AUBERT	72	HLBC	+
0.544 ± 0.048	4048	DAVISON	69	HLBC	+

<sup>99</sup>Measured using in-flight decays of the 25 GeV negative secondary beam.

<sup>100</sup>They form new world averages  $g_- = (0.617 \pm 0.018)$  and  $g_+ = (0.684 \pm 0.033)$  which give  $\Delta g_{\pi^0} = 0.051 \pm 0.028$ .

**QUADRATIC COEFFICIENT  $h$  FOR  $K^\pm \rightarrow \pi^\pm \pi^0 \pi^0$** 

VALUE	EVTS	DOCUMENT ID	TECN	CHG	COMMENT
<b>0.052 ± 0.008 OUR AVERAGE</b>					
0.0551 ± 0.0044 ± 0.0086	493k	AKOPDZHAN..05B	TNF	±	
0.046 ± 0.004 ± 0.012	252k	101 AJINENKO	03B ISTR	–	
• • • We do not use the following data for averages, fits, limits, etc. • • •					
0.128 ± 0.015 ± 0.024	33k	BATUSOV	98 SPEC	+	
0.037 ± 0.024	43k	BOLOTOV	86 CALO	–	
0.152 ± 0.082	3263	BRAUN	76B HLBC	+	
0.041 ± 0.030	5635	SHEAFF	75 HLBC	+	
0.009 ± 0.040	27k	SMITH	75 WIRE	+	
–0.01 ± 0.08	1365	AUBERT	72 HLBC	+	
0.026 ± 0.050	4048	DAVISON	69 HLBC	+	Also emulsion

<sup>101</sup> Measured using in-flight decays of the 25 GeV negative secondary beam.

**QUADRATIC COEFFICIENT  $k$  FOR  $K^\pm \rightarrow \pi^\pm \pi^0 \pi^0$** 

VALUE	EVTS	DOCUMENT ID	TECN	CHG	COMMENT
<b>0.0054 ± 0.0035 OUR AVERAGE</b>					
0.0082 ± 0.0011 ± 0.0014	493k	AKOPDZHAN..05B	TNF	±	Error includes scale factor of 2.5.
0.001 ± 0.001 ± 0.002	252k	102 AJINENKO	03B ISTR	–	
• • • We do not use the following data for averages, fits, limits, etc. • • •					
0.0197 ± 0.0045 ± 0.0029	33k	BATUSOV	98 SPEC	+	

<sup>102</sup> Measured using in-flight decays of the 25 GeV negative secondary beam.

 **$(g_+ - g_-) / (g_+ + g_-)$  FOR  $K^\pm \rightarrow \pi^\pm \pi^0 \pi^0$** 

A nonzero value for this quantity indicates CP violation.

VALUE (units $10^{-4}$ )	EVTS	DOCUMENT ID	TECN	CHG	COMMENT
<b>1.8 ± 1.8 OUR AVERAGE</b>					
1.8 ± 1.7 ± 0.6	91.3M	103 BATLEY	07E NA48		
2 ± 18 ± 5	619k	104 AKOPDZHAN..05	TNF		
• • • We do not use the following data for averages, fits, limits, etc. • • •					
1.8 ± 2.2 ± 1.3	47M	105 BATLEY	06A NA48		

<sup>103</sup> BATLEY 07E includes data from BATLEY 06A. Uses quadratic parametrization and PDG 06 value  $g = 0.626 \pm 0.007$  to obtain  $g_+ - g_- = (2.2 \pm 2.1 \pm 0.7) \times 10^{-4}$ . Neglects any possible charge asymmetries in higher order slope parameters  $h$  or  $k$ .

<sup>104</sup> Asymmetry obtained assuming that  $g_+ + g_- = 2 \times 0.652$  (PDG 02) and that asymmetries in  $h$  and  $k$  are zero.

<sup>105</sup> Linear and quadratic slopes from PDG 04 are used. Any possible charge asymmetries in higher order slope parameters  $h$  or  $k$  are neglected.

**ALTERNATIVE PARAMETRIZATIONS OF  $K^\pm \rightarrow \pi^\pm \pi^0 \pi^0$  DALITZ PLOT**

The following functional form for the matrix element suggested by  $\pi\pi$  rescattering in  $K^+ \rightarrow \pi^+ \pi^+ \pi^- \rightarrow \pi^+ \pi^0 \pi^0$  is used for this fit (CABIBBO 04A, CABIBBO 05): Matrix element =  $M_0 + M_1$  where  $M_0 = 1 + (1/2)g_0 u + (1/2)h' u^2 + (1/2)k_0 v^2$  with  $u = (s_3 - s_0)/(m_{\pi^+})^2$ ,  $v = (s_2 - s_1)/(m_{\pi^+})^2$  and where  $M_1$  takes into account the non-analytic piece due to  $\pi\pi$  rescattering amplitudes  $a_0$  and  $a_2$ ; The parameters  $g_0$  and  $h'$  are related to the parameters  $g$  and  $h$  of the matrix element squared given in the previous section by the approximations  $g_0 \sim g^{PDG}$  and  $h' \sim h^{PDG} - (g/2)^2$  and  $k_0 \sim k^{PDG}$ .

In addition, we also consider the effective field theory framework of COLANGELO 06A and BISSEGGER 09 to extract  $g_{BB}$  and  $h'_{BB}$ .

**LINEAR COEFFICIENT  $g_0$  FOR  $K^\pm \rightarrow \pi^\pm \pi^0 \pi^0$** 

VALUE	EVTS	DOCUMENT ID	TECN	CHG	COMMENT
<b>0.6525 ± 0.0009 ± 0.0033</b>	60M	106 BATLEY	09A NA48	±	
• • • We do not use the following data for averages, fits, limits, etc. • • •					
0.645 ± 0.004 ± 0.009	23M	107 BATLEY	06B NA48	±	

<sup>106</sup> This fit is obtained with the CABIBBO 05 matrix element in the  $2\pi^0$  invariant mass squared range  $0.074094 < m_{2\pi^0}^2 < 0.104244$  GeV<sup>2</sup>. Electromagnetic corrections and CHPT constraints for  $\pi\pi$  phase shifts ( $a_0$  and  $a_2$ ) have been used. Also measured ( $a_0 - a_2$ )  $m_{\pi^+} = 0.2646 \pm 0.0021 \pm 0.0023$ , where  $k_0$  was kept fixed in the fit at  $-0.0099$ .

<sup>107</sup> Superseded by BATLEY 09A. This fit is obtained with the CABIBBO 05 matrix element in the  $2\pi^0$  invariant mass squared range  $0.074$  GeV<sup>2</sup>  $< m_{2\pi^0}^2 < 0.097$  GeV<sup>2</sup>, assuming  $k = 0$  (no term proportional to  $(s_2 - s_1)^2$ ) and excluding the kinematic region around the cusp ( $m_{2\pi^0}^2 = (2m_{\pi^+})^2 \pm 0.000525$  GeV<sup>2</sup>). Also  $\pi\pi$  phase shifts  $a_0$  and  $a_2$  are measured: ( $a_0 - a_2$ )  $m_{\pi^+} = 0.268 \pm 0.010 \pm 0.004 \pm 0.013$ (external) and  $a_2 m_{\pi^+} = -0.041 \pm 0.022 \pm 0.014$ .

**QUADRATIC COEFFICIENT  $h'$  FOR  $K^\pm \rightarrow \pi^\pm \pi^0 \pi^0$** 

VALUE	EVTS	DOCUMENT ID	TECN	CHG	COMMENT
<b>–0.0433 ± 0.0008 ± 0.0026</b>	60M	108 BATLEY	09A NA48	±	
• • • We do not use the following data for averages, fits, limits, etc. • • •					
–0.047 ± 0.012 ± 0.011	23M	109 BATLEY	06B NA48	±	

<sup>108</sup> This fit is obtained with the CABIBBO 05 matrix element in the  $2\pi^0$  invariant mass squared range  $0.074094 < m_{2\pi^0}^2 < 0.104244$  GeV<sup>2</sup>. Electromagnetic corrections and CHPT constraints for  $\pi\pi$  phase shifts ( $a_0$  and  $a_2$ ) have been used. Also measured ( $a_0 - a_2$ )  $m_{\pi^+} = 0.2646 \pm 0.0021 \pm 0.0023$ , where  $k_0$  was kept fixed in the fit at  $-0.0099$ .

<sup>109</sup> Superseded by BATLEY 09A. This fit is obtained with the CABIBBO 05 matrix element in the  $2\pi^0$  invariant mass squared range  $0.074$  GeV<sup>2</sup>  $< m_{2\pi^0}^2 < 0.097$  GeV<sup>2</sup>, assuming  $k = 0$  (no term proportional to  $(s_2 - s_1)^2$ ) and excluding the kinematic region around the cusp ( $m_{2\pi^0}^2 = (2m_{\pi^+})^2 \pm 0.000525$  GeV<sup>2</sup>). Also  $\pi\pi$  phase shifts  $a_0$  and  $a_2$  are measured: ( $a_0 - a_2$ )  $m_{\pi^+} = 0.268 \pm 0.010 \pm 0.004 \pm 0.013$ (external) and  $a_2 m_{\pi^+} = -0.041 \pm 0.022 \pm 0.014$ .

**QUADRATIC COEFFICIENT  $k_0$  FOR  $K^\pm \rightarrow \pi^\pm \pi^0 \pi^0$** 

VALUE	EVTS	DOCUMENT ID	TECN	CHG	COMMENT
<b>0.0095 ± 0.00017 ± 0.00048</b>	60M	110 BATLEY	09A NA48	±	

<sup>110</sup> Assumed  $a_2 m_{\pi^+} = -0.0044$  in the fit.

**LINEAR COEFFICIENT  $g_{BB}$  FOR  $K^\pm \rightarrow \pi^\pm \pi^0 \pi^0$** 

VALUE	EVTS	DOCUMENT ID	TECN	CHG	COMMENT
<b>0.6219 ± 0.0009 ± 0.0033</b>	60M	111 BATLEY	09A NA48	±	

<sup>111</sup> This fit is obtained using parametrizations of COLANGELO 06A and BISSEGGER 09 in the  $2\pi^0$  invariant mass squared range  $0.074094 < m_{2\pi^0}^2 < 0.104244$  GeV<sup>2</sup>. Electromagnetic corrections and CHPT constraints for  $\pi\pi$  phase shifts ( $a_0$  and  $a_2$ ) have been used. Also measured ( $a_0 - a_2$ )  $m_{\pi^+} = 0.2633 \pm 0.0024 \pm 0.0024$ , where  $k_0$  was kept fixed in the fit at 0.0085.

**QUADRATIC COEFFICIENT  $h'_{BB}$  FOR  $K^\pm \rightarrow \pi^\pm \pi^0 \pi^0$** 

VALUE	EVTS	DOCUMENT ID	TECN	CHG	COMMENT
<b>–0.0520 ± 0.0009 ± 0.0026</b>	60M	112 BATLEY	09A NA48	±	

<sup>112</sup> This fit is obtained using parametrizations of COLANGELO 06A and BISSEGGER 09 in the  $2\pi^0$  invariant mass squared range  $0.074094 < m_{2\pi^0}^2 < 0.104244$  GeV<sup>2</sup>. Electromagnetic corrections and CHPT constraints for  $\pi\pi$  phase shifts ( $a_0$  and  $a_2$ ) have been used. Also measured ( $a_0 - a_2$ )  $m_{\pi^+} = 0.2633 \pm 0.0024 \pm 0.0024$ , where  $k_0$  was kept fixed in the fit at 0.0085.

 **$K_{\ell 3}$  AND  $K_{\ell 3}^0$  FORM FACTORS**

Updated March 2012 by T.G. Trippe (LBNL) and C.-J. Lin (LBNL).

Assuming that only the vector current contributes to  $K \rightarrow \pi \ell \nu$  decays, we write the matrix element as

$$M \propto f_+(t) [(P_K + P_\pi)_\mu \bar{\ell} \gamma_\mu (1 + \gamma_5) \nu] + f_-(t) [m_\ell \bar{\ell} (1 + \gamma_5) \nu], \quad (1)$$

where  $P_K$  and  $P_\pi$  are the four-momenta of the  $K$  and  $\pi$  mesons,  $m_\ell$  is the lepton mass, and  $f_+$  and  $f_-$  are dimensionless form factors which can depend only on  $t = (P_K - P_\pi)^2$ , the square of the four-momentum transfer to the leptons. If time-reversal invariance holds,  $f_+$  and  $f_-$  are relatively real.  $K_{\mu 3}$  experiments, discussed immediately below, measure  $f_+$  and  $f_-$ , while  $K_{e 3}$  experiments, discussed further below, are sensitive only to  $f_+$  because the small electron mass makes the  $f_-$  term negligible.

**$K_{\mu 3}$  Experiments.** Analyses of  $K_{\mu 3}$  data frequently assume a linear dependence of  $f_+$  and  $f_-$  on  $t$ , i.e.,

$$f_\pm(t) = f_\pm(0) [1 + \lambda_\pm (t/m_{\pi^+}^2)]. \quad (2)$$

Most  $K_{\mu 3}$  data are adequately described by Eq. (2) for  $f_+$  and a constant  $f_-$  (i.e.,  $\lambda_- = 0$ ).

There are two equivalent parametrizations commonly used in these analyses:

**(1)  $\lambda_+$ ,  $\xi(0)$  parametrization.** Older analyses of  $K_{\mu 3}$  data often introduce the ratio of the two form factors

$$\xi(t) = f_-(t)/f_+(t). \quad (3)$$

# Meson Particle Listings

## $K^\pm$

The  $K_{\mu 3}$  decay distribution is then described by the two parameters  $\lambda_+$  and  $\xi(0)$  (assuming time reversal invariance and  $\lambda_- = 0$ ).

(2)  $\lambda_+, \lambda_0$  parametrization. More recent  $K_{\mu 3}$  analyses have parametrized in terms of the form factors  $f_+$  and  $f_0$ , which are associated with vector and scalar exchange, respectively, to the lepton pair.  $f_0$  is related to  $f_+$  and  $f_-$  by

$$f_0(t) = f_+(t) + [t/(m_K^2 - m_\pi^2)] f_-(t). \quad (4)$$

Here  $f_0(0)$  must equal  $f_+(0)$  unless  $f_-(t)$  diverges at  $t = 0$ . The earlier assumption that  $f_+$  is linear in  $t$  and  $f_-$  is constant leads to  $f_0$  linear in  $t$ :

$$f_0(t) = f_0(0) [1 + \lambda_0(t/m_{\pi^+}^2)]. \quad (5)$$

With the assumption that  $f_0(0) = f_+(0)$ , the two parametrizations,  $(\lambda_+, \xi(0))$  and  $(\lambda_+, \lambda_0)$  are equivalent as long as correlation information is retained.  $(\lambda_+, \lambda_0)$  correlations tend to be less strong than  $(\lambda_+, \xi(0))$  correlations.

Since the 2006 edition of the *Review* [4], we no longer quote results in the  $(\lambda_+, \xi(0))$  parametrization. We have removed many older low statistics results from the Listings. See the 2004 version of this note [5] for these older results, and the 1982 version [6] for additional discussion of the  $K_{\mu 3}^0$  parameters, correlations, and conversion between parametrizations.

**Quadratic Parametrization.** More recent high-statistics experiments have included a quadratic term in the expansion of  $f_+(t)$ ,

$$f_+(t) = f_+(0) \left[ 1 + \lambda'_+(t/m_{\pi^+}^2) + \frac{\lambda''_+}{2}(t/m_{\pi^+}^2)^2 \right]. \quad (6)$$

If there is a non-vanishing quadratic term, then  $\lambda_+$  of Eq. (2) represents the average slope, which is then different from  $\lambda'_+$ . Our convention is to include the factor  $\frac{1}{2}$  in the quadratic term, and to use  $m_{\pi^+}$  even for  $K_{e3}^+$  and  $K_{\mu 3}^+$  decays. We have converted other's parametrizations to match our conventions, as noted in the beginning of the “ $K_{e3}^\pm$  and  $K_{e3}^0$  Form Factors” sections of the Listings.

**Pole Parametrization.** The pole model describes the  $t$ -dependence of  $f_+(t)$  and  $f_0(t)$  in terms of the exchange of the lightest vector and scalar  $K^*$  mesons with masses  $M_v$  and  $M_s$ , respectively:

$$f_+(t) = f_+(0) \left[ \frac{M_v^2}{M_v^2 - t} \right], \quad f_0(t) = f_0(0) \left[ \frac{M_s^2}{M_s^2 - t} \right]. \quad (7)$$

**Dispersive Parametrization** [7,8]. This approach uses dispersive techniques and the known low-energy  $K$ - $\pi$  phases to parametrize the vector and scalar form factors:

$$f_+(t) = f_+(0) \exp \left[ \frac{t}{m_\pi^2} (\Lambda_+ + H(t)) \right]; \quad (8)$$

$$f_0(t) = f_+(0) \exp \left[ \frac{t}{(m_K^2 - m_\pi^2)} (\ln[C] - G(t)) \right], \quad (9)$$

where  $\Lambda_+$  is the slope of the vector form factor, and  $\ln[C] = \ln[f_0(m_K^2 - m_\pi^2)]$  is the logarithm of the scalar form factor at

the Callan-Treiman point. The functions  $H(t)$  and  $G(t)$  are dispersive integrals.

**$K_{e3}$  Experiments:** Analysis of  $K_{e3}$  data is simpler than that of  $K_{\mu 3}$  because the second term of the matrix element assuming a pure vector current [Eq. (1) above] can be neglected. Here  $f_+$  can be assumed to be linear in  $t$ , in which case the linear coefficient  $\lambda_+$  of Eq. (2) is determined, or quadratic, in which case the linear coefficient  $\lambda'_+$  and quadratic coefficient  $\lambda''_+$  of Eq. (6) are determined.

If we remove the assumption of a pure vector current, then the matrix element for the decay, in addition to the terms in Eq. (1), would contain

$$+2m_K f_S \bar{\ell}(1 + \gamma_5)\nu + (2f_T/m_K)(P_K)_\lambda(P_\pi)_\mu \bar{\ell}\sigma_{\lambda\mu}(1 + \gamma_5)\nu, \quad (10)$$

where  $f_S$  is the scalar form factor, and  $f_T$  is the tensor form factor. In the case of the  $K_{e3}$  decays where the  $f_-$  term can be neglected, experiments have yielded limits on  $|f_S/f_+|$  and  $|f_T/f_+|$ .

**Fits for  $K_{e3}$  Form Factors.** For  $K_{e3}$  data, we determine best values for the three parametrizations: linear ( $\lambda_+$ ), quadratic ( $\lambda'_+, \lambda''_+$ ) and pole ( $M_v$ ). For  $K_{\mu 3}$  data, we determine best values for the three parametrizations: linear ( $\lambda_+, \lambda_0$ ), quadratic ( $\lambda'_+, \lambda''_+, \lambda_0$ ) and pole ( $M_v, M_s$ ). We then assume  $\mu - e$  universality so that we can combine  $K_{e3}$  and  $K_{\mu 3}$  data, and again determine best values for the three parametrizations: linear ( $\lambda_+, \lambda_0$ ), quadratic ( $\lambda'_+, \lambda''_+, \lambda_0$ ), and pole ( $M_v, M_s$ ). When there is more than one parameter, fits are done including input correlations. Simple averages suffice in the two  $K_{e3}$  cases where there is only one parameter: linear ( $\lambda_+$ ) and pole ( $M_v$ ).

Both KTeV and KLOE see an improvement in the quality of their fits relative to linear fits when a quadratic term is introduced, as well as when the pole parametrization is used. The quadratic parametrization has the disadvantage that the quadratic parameter  $\lambda''_+$  is highly correlated with the linear parameter  $\lambda'_+$ , in the neighborhood of 95%, and that neither parameter is very well determined. The pole fit has the same number of parameters as the linear fit, but yields slightly better fit probabilities, so that it would be advisable for all experiments to include the pole parametrization as one of their choices [9].

The “Kaon Particle Listings” show the results with and without assuming  $\mu$ - $e$  universality. The “Meson Summary Tables” show all of the results assuming  $\mu$ - $e$  universality, but most results not assuming  $\mu$ - $e$  universality are given only in the Listings.

## References

1. L.M. Chounet, J.M. Gaillard, and M.K. Gaillard, *Phys. Reports* **4C**, 199 (1972).
2. H.W. Fearing, E. Fischbach, and J. Smith, *Phys. Rev.* **D2**, 542 (1970).
3. N. Cabibbo and A. Maksymowicz, *Phys. Lett.* **9**, 352 (1964).
4. W.-M. Yao *et al.*, Particle Data Group, *J. Phys.* **G33**, 1 (2006).



- S. Eidleman *et al.*, Particle Data Group, Phys. Lett. **B592**, 1 (2004).
- M. Roos *et al.*, Particle Data Group, Phys. Lett. **111B**, 73 (1982).
- V. Bernard *et al.*, Phys. Lett. **B638**, 48 (2006).
- A. Lai *et al.*, Phys. Lett. **B647**, 341 (2007), and references therein.
- We thank P. Franzini (Rome U. and Frascati) for useful discussions on this point.

 **$K_{e3}^\pm$  FORM FACTORS**

In the form factor comments, the following symbols are used.

$f_+$  and  $f_-$  are form factors for the vector matrix element.

$f_S$  and  $f_T$  refer to the scalar and tensor term.

$$f_0 = f_+ + f_- t / (m_{K^+}^2 - m_{\pi^0}^2).$$

$t =$  momentum transfer to the  $\pi$ .

$\lambda_+$  and  $\lambda_0$  are the linear expansion coefficients of  $f_+$  and  $f_0$ :

$$f_+(t) = f_+(0) (1 + \lambda_+ t / m_{\pi^+}^2)$$

For quadratic expansion

$$f_+(t) = f_+(0) (1 + \lambda'_+ t / m_{\pi^+}^2 + \frac{\lambda''_+}{2} t^2 / m_{\pi^+}^4)$$

as used by KTeV. If there is a non-vanishing quadratic term, then  $\lambda_+$  represents an average slope, which is then different from  $\lambda'_+$ .

NA48 and ISTRA quadratic expansion coefficients are converted with

$$\lambda'_+{}^{PDG} = \lambda_+{}^{NA48} \text{ and } \lambda''_+{}^{PDG} = 2 \lambda'_+{}^{NA48}$$

$$\lambda'_+{}^{PDG} = (\frac{m_{\pi^+}}{m_{\pi^0}})^2 \lambda_+{}^{ISTRA} \text{ and}$$

$$\lambda''_+{}^{PDG} = 2 (\frac{m_{\pi^+}}{m_{\pi^0}})^4 \lambda''_+{}^{ISTRA}$$

ISTRA linear expansion coefficients are converted with

$$\lambda_+{}^{PDG} = (\frac{m_{\pi^+}}{m_{\pi^0}})^2 \lambda_+{}^{ISTRA} \text{ and } \lambda_0{}^{PDG} = (\frac{m_{\pi^+}}{m_{\pi^0}})^2 \lambda_0{}^{ISTRA}$$

The pole parametrization is

$$f_+(t) = f_+(0) (\frac{M_V^2}{M_V^2 - t})$$

$$f_0(t) = f_0(0) (\frac{M_S^2}{M_S^2 - t})$$

where  $M_V$  and  $M_S$  are the vector and scalar pole masses.

The following abbreviations are used:

DP = Dalitz plot analysis.

PI =  $\pi$  spectrum analysis.

MU =  $\mu$  spectrum analysis.

POL =  $\mu$  polarization analysis.

BR =  $K_{e3}^\pm / K_{e3}^\pm$  branching ratio analysis.

E = positron or electron spectrum analysis.

RC = radiative corrections.

 **$\lambda_+$  (LINEAR ENERGY DEPENDENCE OF  $f_+$  IN  $K_{e3}^\pm$  DECAY)**

These results are for a linear expansion only. See the next section for fits including a quadratic term. For radiative correction of the  $K_{e3}^\pm$  Dalitz plot, see GINSBERG 67, BECHERRAWY 70, CIRIGLIANO 02, CIRIGLIANO 04, and ANDRE 07. Results labeled OUR FIT are discussed in the review " $K_{e3}^\pm$  and  $K_{e3}^0$  Form Factors" above. For earlier, lower statistics results, see the 2004 edition of this review, Physics Letters **B592** 1 (2004).

VALUE (units $10^{-2}$ )	EVTS	DOCUMENT ID	TECN	CHG	COMMENT
<b>2.97 ± 0.05 OUR FIT</b>		Assuming $\mu$ -e universality			
<b>2.98 ± 0.05 OUR AVERAGE</b>					
3.044 ± 0.083 ± 0.074	1.1M	AKOPDZANOV 09	TNF	±	
2.966 ± 0.050 ± 0.034	919k	113 YUSHCHENKO 04B	ISTR	- DP	
2.78 ± 0.26 ± 0.30	41k	SHIMIZU 00	SPEC	+ DP	
2.84 ± 0.27 ± 0.20	32k	114 AKIMENKO 91	SPEC	PI, no RC	
2.9 ± 0.4	62k	115 BOLOTOV 88	SPEC	PI, no RC	
••• We do not use the following data for averages, fits, limits, etc. •••					
3.06 ± 0.09 ± 0.06	550k	113,116 AJINENKO 03c	ISTR	- DP	
2.93 ± 0.15 ± 0.2	130k	116 AJINENKO 02	SPEC	DP	

<sup>113</sup>Rescaled to agree with our conventions as noted above.

<sup>114</sup>AKIMENKO 91 state that radiative corrections would raise  $\lambda_+$  by 0.0013.

<sup>115</sup>BOLOTOV 88 state radiative corrections of GINSBERG 67 would raise  $\lambda_+$  by 0.002.

<sup>116</sup>Superseded by YUSHCHENKO 04B.

 **$\lambda_+$  (LINEAR ENERGY DEPENDENCE OF  $f_+$  IN  $K_{\mu 3}^\pm$  DECAY)**

Results labeled OUR FIT are discussed in the review " $K_{e3}^\pm$  and  $K_{e3}^0$  Form Factors" above. For earlier, lower statistics results, see the 2004 edition of this review, Physics Letters **B592** 1 (2004).

VALUE (units $10^{-2}$ )	EVTS	DOCUMENT ID	TECN	CHG	COMMENT
<b>2.97 ± 0.05 OUR FIT</b>		Assuming $\mu$ -e universality			
<b>2.96 ± 0.17 OUR FIT</b>		Not assuming $\mu$ -e universality			
2.96 ± 0.14 ± 0.10	540k	117 YUSHCHENKO04	ISTR	- DP	
••• We do not use the following data for averages, fits, limits, etc. •••					
3.21 ± 0.45	112k	118 AJINENKO 03	ISTR	- DP	
<sup>117</sup> Rescaled to agree with our conventions as noted above.					
<sup>118</sup> Superseded by YUSHCHENKO 04.					

 **$\lambda_0$  (LINEAR ENERGY DEPENDENCE OF  $f_0$  IN  $K_{e3}^\pm$  DECAY)**

Results labeled OUR FIT are discussed in the review " $K_{e3}^\pm$  and  $K_{e3}^0$  Form Factors" above. For earlier, lower statistics results, see the 2004 edition of this review, Physics Letters **B592** 1 (2004).

VALUE (units $10^{-2}$ )	$d\lambda_0/d\lambda_+$	EVTS	DOCUMENT ID	TECN	CHG	COMMENT
<b>1.95 ± 0.12 OUR FIT</b>			Assuming $\mu$ -e universality			
<b>1.96 ± 0.13 OUR FIT</b>			Not assuming $\mu$ -e universality			
+1.96 ± 0.12 ± 0.06	-0.348	540k	119 YUSHCHENKO04	ISTR	- DP	
••• We do not use the following data for averages, fits, limits, etc. •••						
+2.09 ± 0.45	-0.46	112k	120 AJINENKO 03	ISTR	- DP	
+1.9 ± 0.64	24k	121 HORIE 01	SPEC	+ BR		
+1.9 ± 1.0	+0.03	55k	122 HEINTZE 77	SPEC	+ BR	
<sup>119</sup> Rescaled to agree with our conventions as noted above.						
<sup>120</sup> Superseded by YUSHCHENKO 04.						
<sup>121</sup> HORIE 01 assumes $\mu$ -e universality in $K_{e3}^\pm$ decay and uses SHIMIZU 00 value $\lambda = 0.0278 \pm 0.0040$ from $K_{e3}^\pm$ decay.						
<sup>122</sup> HEINTZE 77 uses $\lambda_+ = 0.029 \pm 0.003$ . $d\lambda_0/d\lambda_+$ estimated by us.						

 **$\lambda'_+$  (LINEAR  $K_{e3}^\pm$  FORM FACTOR FROM QUADRATIC FIT)**

VALUE (units $10^{-2}$ )	EVTS	DOCUMENT ID	TECN	CHG	COMMENT
<b>2.485 ± 0.163 ± 0.034</b>	919k	123,124 YUSHCHENKO04B	ISTR	- DP	
••• We do not use the following data for averages, fits, limits, etc. •••					
3.07 ± 0.21	550k	123,125 AJINENKO 03c	ISTR	- DP	
<sup>123</sup> Rescaled to agree with our conventions as noted above.					
<sup>124</sup> YUSHCHENKO 04B $\lambda'_+$ and $\lambda''_+$ are strongly correlated with coefficient $\rho(\lambda'_+, \lambda''_+) = -0.95$ .					
<sup>125</sup> Superseded by YUSHCHENKO 04B.					

 **$\lambda''_+$  (QUADRATIC  $K_{e3}^\pm$  FORM FACTOR)**

VALUE (units $10^{-2}$ )	EVTS	DOCUMENT ID	TECN	CHG	COMMENT
<b>0.192 ± 0.062 ± 0.071</b>	919k	126,127 YUSHCHENKO04B	ISTR	- DP	
••• We do not use the following data for averages, fits, limits, etc. •••					
-0.5 ± 0.7 ± 1.5	550k	126,128 AJINENKO 03c	ISTR	- DP	
<sup>126</sup> Rescaled to agree with our conventions as noted above.					
<sup>127</sup> YUSHCHENKO 04B $\lambda'_+$ and $\lambda''_+$ are strongly correlated with coefficient $\rho(\lambda'_+, \lambda''_+) = -0.95$ .					
<sup>128</sup> Superseded by YUSHCHENKO 04B.					

 **$|f_S/f_+|$  FOR  $K_{e3}^\pm$  DECAY**

Ratio of scalar to  $f_+$  couplings.

VALUE (units $10^{-2}$ )	CL%	EVTS	DOCUMENT ID	TECN	CHG	COMMENT
<b>-0.3 ± 0.8</b>			<b>OUR AVERAGE</b>			
-0.37 ± 0.66 ± 0.41		919k	YUSHCHENKO04B	ISTR	-	$\lambda'_+, \lambda''_+, f_S$ fit
0.2 ± 2.6 ± 1.4		41k	SHIMIZU 00	SPEC	+	$\lambda_+, f_S, f_T$ fit
••• We do not use the following data for averages, fits, limits, etc. •••						
0.2 ± 2.0 ± 0.3		550k	129 AJINENKO 03c	ISTR	-	$\lambda_+, f_S, f_T$ fit
-1.9 ± 2.5 ± 1.6		130k	129 AJINENKO 02	SPEC		$\lambda_+, f_S$ fit
7.0 ± 1.6 ± 1.6		32k	AKIMENKO 91	SPEC		$\lambda_+, f_S, f_T, \phi$ fit
0 ± 10		2827	130 BRAUN 75	HLBC	+	
< 13		4017	CHIANG 72	OSPK	+	
14 ± 3 ± 4		2707	130 STEINER 71	HLBC	+	$\lambda_+, f_S, f_T, \phi$ fit
< 23		90	BOTTERILL 68c	ASPK		
< 18		90	BELLOTTI 67b	HLBC		
< 30		95	KALMUS 67	HLBC	+	
<sup>129</sup> Superseded by YUSHCHENKO 04B.						
<sup>130</sup> Statistical errors only.						

 **$|f_T/f_+|$  FOR  $K_{e3}^\pm$  DECAY**

Ratio of tensor to  $f_+$  couplings.

VALUE (units $10^{-2}$ )	CL%	EVTS	DOCUMENT ID	TECN	CHG	COMMENT
<b>-1.2 ± 2.3 OUR AVERAGE</b>						
-1.2 ± 2.1 ± 1.1		919k	YUSHCHENKO04B	ISTR	-	$\lambda'_+, \lambda''_+, f_T$ fit
1 ± 14 ± 9		41k	SHIMIZU 00	SPEC	+	$\lambda_+, f_S, f_T$ fit

## Meson Particle Listings

 $K^\pm$ 

• • • We do not use the following data for averages, fits, limits, etc. • • •

$2.1^{+0.6}_{-0.5} \pm 2.6$	550k	131	AJINENKO	03c	ISTR	-	$\lambda_+$ , $f_S$ , $f_T$ fit
$-4.5^{+6.0}_{-5.7}$	130k	131	AJINENKO	02	SPEC		$\lambda_+$ , $f_T$ fit
$53^{+9}_{-10} \pm 10$	32k		AKIMENKO	91	SPEC		$\lambda_+$ , $f_S$ , $f_T$ , $\phi$ fit
$7 \pm 37$	2827	132	BRAUN	75	HLBC	+	
$< 75$	90	4017	CHIANG	72	OSPK	+	
$24^{+16}_{-14}$	2707	132	STEINER	71	HLBC	+	$\lambda_+$ , $f_S$ , $f_T$ , $\phi$ fit
$< 58$	90		BOTTERILL	68c	ASPK		
$< 58$	90		BELLOTTI	67b	HLBC		
$< 110$	95		KALMUS	67	HLBC	+	

<sup>131</sup> Superseded by YUSHCHENKO 04b.

<sup>132</sup> Statistical errors only.

 $f_S/f_+$  FOR  $K_{\mu 3}^\pm$  DECAY

Ratio of scalar to  $f_+$  couplings.

VALUE (units $10^{-2}$ )	EVTS	DOCUMENT ID	TECN	CHG	COMMENT
<b><math>0.17 \pm 0.14 \pm 0.54</math></b>	540k	133	YUSHCHENKO04	ISTR	- DP
• • • We do not use the following data for averages, fits, limits, etc. • • •					
$0.4 \pm 0.5 \pm 0.5$	112k	134	AJINENKO	03	ISTR - DP

<sup>133</sup> The second error is the theoretical error from the uncertainty in the chiral perturbation theory prediction for  $\lambda_0$ ,  $\pm 0.0053$ , combined in quadrature with the systematic error  $\pm 0.0009$ .

<sup>134</sup> The second error is the theoretical error from the uncertainty in the chiral perturbation theory prediction for  $\lambda_0$ . Superseded by YUSHCHENKO 04.

 $f_T/f_+$  FOR  $K_{\mu 3}^\pm$  DECAY

Ratio of tensor to  $f_+$  couplings.

VALUE (units $10^{-2}$ )	EVTS	DOCUMENT ID	TECN	CHG	COMMENT
<b><math>-0.07 \pm 0.71 \pm 0.20</math></b>	540k	YUSHCHENKO04	ISTR	-	DP
• • • We do not use the following data for averages, fits, limits, etc. • • •					
$-2.1 \pm 2.8 \pm 1.4$	112k	135	AJINENKO	03	ISTR - DP
$2 \pm 12$	1585		BRAUN	75	HLBC

<sup>135</sup> The second error is the theoretical error from the uncertainty in the chiral perturbation theory prediction for  $\lambda_0$ . Superseded by YUSHCHENKO 04.

 $K_{\mu 4}^\pm$  FORM FACTORS

Based on the parametrizations of AMOROS 99, the  $K_{\mu 4}^\pm$  form factors can be expressed as

$$F_S = f_S + f'_S q^2 + f''_S q^4 + f'_e S_e / 4m_\pi^2$$

$$F_P = f_P + f'_P q^2$$

$$G_P = g_P + g'_P q^2$$

$$H_P = h_P + h'_P q^2$$

where  $q^2 = (S_\pi / 4m_\pi^2) - 1$ ,  $S_\pi$  is the invariant mass squared of the dipion, and  $S_e$  is the invariant mass squared of the dilepton.

 $f'_S$  FOR  $K^\pm \rightarrow \pi^+ \pi^- e^\pm \nu$  DECAY

VALUE	EVTS	DOCUMENT ID	TECN	CHG
<b><math>5.75 \pm 0.02 \pm 0.08</math></b>	400k	136	PISLAK	03 B865 +

<sup>136</sup> Radiative corrections included. Using Roy equations and not including isospin breaking, PISLAK 03 obtains the following  $\pi\pi$  scattering lengths  $a_0^0 = 0.228 \pm 0.012 \pm 0.004^{+0.012}_{-0.016}$  (theor.) and  $a_0^2 = -0.0365 \pm 0.0023 \pm 0.0008^{+0.0031}_{-0.0026}$  (theor.).

 $f''_S/f_S$  FOR  $K^\pm \rightarrow \pi^+ \pi^- e^\pm \nu$  DECAY

VALUE (units $10^{-2}$ )	EVTS	DOCUMENT ID	TECN	CHG
<b><math>15.2 \pm 0.7 \pm 0.5</math></b>	1.13M	137	BATLEY	10c NA48 ±

• • • We do not use the following data for averages, fits, limits, etc. • • •

$17.2 \pm 0.9 \pm 0.6$  670k 138 BATLEY 08a NA48 ±

<sup>137</sup> Radiative corrections included. Using Roy equations and including isospin breaking, BATLEY 10c obtains the following scattering lengths  $a_0^0 = 0.2220 \pm 0.0128 \pm 0.0050 \pm 0.0037$  (theor.),  $a_0^2 = -0.0432 \pm 0.0086 \pm 0.0034 \pm 0.0028$  (theor.). The correlation with  $f''_S/f_S = -0.954$  and with  $f'_e/f_S = 0.080$ . Supersedes BATLEY 08a.

<sup>138</sup> Radiative corrections included. Using Roy equations and not including isospin breaking, BATLEY 08a obtains the following  $\pi\pi$  scattering length  $a_0^0 = 0.233 \pm 0.016 \pm 0.007$   $a_0^2 = -0.0471 \pm 0.011 \pm 0.004$ .

 $f''_S/f_S$  FOR  $K^\pm \rightarrow \pi^+ \pi^- e^\pm \nu$  DECAY

VALUE (units $10^{-2}$ )	EVTS	DOCUMENT ID	TECN	CHG
<b><math>-7.3 \pm 0.7 \pm 0.6</math></b>	1.13M	139	BATLEY	10c NA48 ±

• • • We do not use the following data for averages, fits, limits, etc. • • •

$-9.0 \pm 0.9 \pm 0.7$  670k 140 BATLEY 08a NA48 ±

<sup>139</sup> Radiative corrections included. Using Roy equations and including isospin breaking, BATLEY 10c obtains the following scattering lengths  $a_0^0 = 0.2220 \pm 0.0128 \pm 0.0050 \pm 0.0037$  (theor.),  $a_0^2 = -0.0432 \pm 0.0086 \pm 0.0034 \pm 0.0028$  (theor.). The correlation with  $f'_e/f_S = -0.954$  and with  $f'_S/f_S = 0.019$ . Supersedes BATLEY 08a.

<sup>140</sup> Radiative corrections included. Using Roy equations and not including isospin breaking, BATLEY 08a obtains the following  $\pi\pi$  scattering length  $a_0^0 = 0.233 \pm 0.016 \pm 0.007$   $a_0^2 = -0.0471 \pm 0.011 \pm 0.004$ .

 $f'_e/f_S$  FOR  $K^\pm \rightarrow \pi^+ \pi^- e^\pm \nu$  DECAY

VALUE (units $10^{-2}$ )	EVTS	DOCUMENT ID	TECN	CHG
--------------------------	------	-------------	------	-----

**$6.8 \pm 0.6 \pm 0.7$**  1.13M 141 BATLEY 10c NA48 ±

• • • We do not use the following data for averages, fits, limits, etc. • • •

$8.1 \pm 0.8 \pm 0.9$  670k 142 BATLEY 08a NA48 ±

<sup>141</sup> Radiative corrections included. Using Roy equations and including isospin breaking, BATLEY 10c obtains the following scattering lengths  $a_0^0 = 0.2220 \pm 0.0128 \pm 0.0050 \pm 0.0037$  (theor.),  $a_0^2 = -0.0432 \pm 0.0086 \pm 0.0034 \pm 0.0028$  (theor.). The correlation with  $f'_S/f_S = 0.080$  and with  $f''_S/f_S = 0.019$ . Supersedes BATLEY 08a.

<sup>142</sup> Radiative corrections included. Using Roy equations and not including isospin breaking, BATLEY 08a obtains the following  $\pi\pi$  scattering length  $a_0^0 = 0.233 \pm 0.016 \pm 0.007$   $a_0^2 = -0.0471 \pm 0.011 \pm 0.004$ .

 $f_P/f_S$  FOR  $K^\pm \rightarrow \pi^+ \pi^- e^\pm \nu$  DECAY

VALUE (units $10^{-2}$ )	EVTS	DOCUMENT ID	TECN	CHG
--------------------------	------	-------------	------	-----

**$-4.8 \pm 0.3 \pm 0.4$**  1.13M 143 BATLEY 10c NA48 ±

• • • We do not use the following data for averages, fits, limits, etc. • • •

$-4.8 \pm 0.4 \pm 0.4$  670k 144 BATLEY 08a NA48 ±

<sup>143</sup> Radiative corrections included. Using Roy equations and including isospin breaking, BATLEY 10c obtains the following scattering lengths  $a_0^0 = 0.2220 \pm 0.0128 \pm 0.0050 \pm 0.0037$  (theor.),  $a_0^2 = -0.0432 \pm 0.0086 \pm 0.0034 \pm 0.0028$  (theor.). Supersedes BATLEY 08a.

<sup>144</sup> Radiative corrections included. Using Roy equations and not including isospin breaking, BATLEY 08a obtains the following  $\pi\pi$  scattering length  $a_0^0 = 0.233 \pm 0.016 \pm 0.007$   $a_0^2 = -0.0471 \pm 0.011 \pm 0.004$ .

 $g_P/f_S$  FOR  $K^\pm \rightarrow \pi^+ \pi^- e^\pm \nu$  DECAY

VALUE (units $10^{-2}$ )	EVTS	DOCUMENT ID	TECN	CHG
--------------------------	------	-------------	------	-----

**$86.8 \pm 1.0 \pm 1.0$**  1.13M 145 BATLEY 10c NA48 ±

• • • We do not use the following data for averages, fits, limits, etc. • • •

$87.3 \pm 1.3 \pm 1.2$  670k 146 BATLEY 08a NA48 ±

$80.9 \pm 0.9 \pm 1.2$  400k 147 PISLAK 03 B865 ±

<sup>145</sup> Radiative corrections included. Using Roy equations and including isospin breaking, BATLEY 10c obtains the following scattering lengths  $a_0^0 = 0.2220 \pm 0.0128 \pm 0.0050 \pm 0.0037$  (theor.),  $a_0^2 = -0.0432 \pm 0.0086 \pm 0.0034 \pm 0.0028$  (theor.). Supersedes BATLEY 08a. The correlation with  $g'_P/f_S = -0.914$ . Supersedes BATLEY 08a.

<sup>146</sup> Radiative corrections included. Using Roy equations and not including isospin breaking, BATLEY 08a obtains the following  $\pi\pi$  scattering length  $a_0^0 = 0.233 \pm 0.016 \pm 0.007$   $a_0^2 = -0.0471 \pm 0.011 \pm 0.004$ .

<sup>147</sup> Radiative corrections included. Using Roy equations PISLAK 03 obtains the following scattering lengths  $a_0^0 = 0.203 \pm 0.033 \pm 0.004$ ,  $a_0^2 = -0.055 \pm 0.023 \pm 0.003$ .

 $g'_P/f_S$  FOR  $K^\pm \rightarrow \pi^+ \pi^- e^\pm \nu$  DECAY

VALUE (units $10^{-2}$ )	EVTS	DOCUMENT ID	TECN	CHG
--------------------------	------	-------------	------	-----

**$8.9 \pm 1.7 \pm 1.3$**  1.13M 148 BATLEY 10c NA48 ±

• • • We do not use the following data for averages, fits, limits, etc. • • •

$8.1 \pm 2.2 \pm 1.5$  670k 149 BATLEY 08a NA48 ±

$12.0 \pm 1.9 \pm 0.7$  400k 150 PISLAK 03 B865 ±

<sup>148</sup> Radiative corrections included. Using Roy equations and including isospin breaking, BATLEY 10c obtains the following scattering lengths  $a_0^0 = 0.2220 \pm 0.0128 \pm 0.0050 \pm 0.0037$  (theor.),  $a_0^2 = -0.0432 \pm 0.0086 \pm 0.0034 \pm 0.0028$  (theor.). The correlation with  $g_P/f_S = -0.914$ . Supersedes BATLEY 08a.

<sup>149</sup> Radiative corrections included. Using Roy equations and not including isospin breaking, BATLEY 08a obtains the following  $\pi\pi$  scattering length  $a_0^0 = 0.233 \pm 0.016 \pm 0.007$   $a_0^2 = -0.0471 \pm 0.011 \pm 0.004$ .

<sup>150</sup> Radiative corrections included. Using Roy equations PISLAK 03 obtains the following scattering lengths  $a_0^0 = 0.203 \pm 0.033 \pm 0.004$ ,  $a_0^2 = -0.055 \pm 0.023 \pm 0.003$ .

 $h_P/f_S$  FOR  $K^\pm \rightarrow \pi^+ \pi^- e^\pm \nu$  DECAY

VALUE (units $10^{-2}$ )	EVTS	DOCUMENT ID	TECN	CHG
--------------------------	------	-------------	------	-----

**$-39.8 \pm 1.5 \pm 0.8$**  1.13M 151 BATLEY 10c NA48 ±

• • • We do not use the following data for averages, fits, limits, etc. • • •

$-41.1 \pm 1.9 \pm 0.8$  670k 152 BATLEY 08a NA48 ±

$-51.3 \pm 3.3 \pm 3.5$  400k 153 PISLAK 03 B865 ±

- <sup>151</sup> Radiative corrections included. Using Roy equations and including isospin breaking, BATLEY 10C obtains the following scattering lengths  $a_0^0 = 0.2220 \pm 0.0128 \pm 0.0050 \pm 0.0037$  (theor.),  $a_0^2 = -0.0432 \pm 0.0086 \pm 0.0034 \pm 0.0028$  (theor.). Supersedes BATLEY 08A.
- <sup>152</sup> Radiative corrections included. Using Roy equations and not including isospin breaking, BATLEY 08A obtains the following  $\pi\pi$  scattering length  $a_0^0 = 0.233 \pm 0.016 \pm 0.007$ ,  $a_0^2 = -0.0471 \pm 0.011 \pm 0.004$ .
- <sup>153</sup> Radiative corrections included. Using Roy equations PISLAK 03 obtains the following scattering lengths  $a_0^0 = 0.203 \pm 0.033 \pm 0.004$ ,  $a_0^2 = -0.055 \pm 0.023 \pm 0.003$ .

**DECAY FORM FACTOR FOR  $K^\pm \rightarrow \pi^0 \pi^0 e^\pm \nu$** 

Given in BOLOTOV 86B, BARMIN 88B, and SHIMIZU 04.

 **$K^\pm \rightarrow \ell^\pm \nu \gamma$  FORM FACTORS**

For definitions of the axial-vector  $F_A$  and vector  $F_V$  form factor, see the "Note on  $\pi^\pm \rightarrow \ell^\pm \nu \gamma$  and  $K^\pm \rightarrow \ell^\pm \nu \gamma$  Form Factors" in the  $\pi^\pm$  section. In the kaon literature, often different definitions  $a_K = F_A/m_K$  and  $v_K = F_V/m_K$  are used.

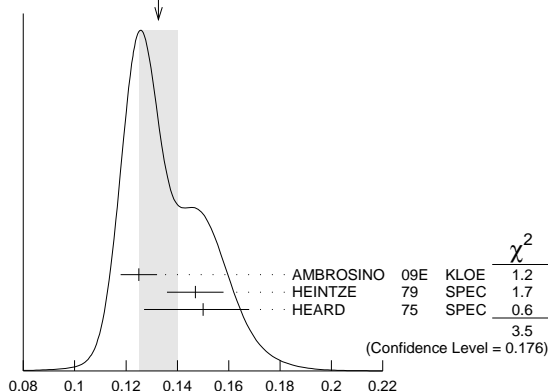
 **$F_A + F_V$ , SUM OF AXIAL-VECTOR AND VECTOR FORM FACTOR FOR  $K \rightarrow e\nu\gamma$** 

VALUE	EVTS	DOCUMENT ID	TECN	COMMENT
<b>0.133 ± 0.008 OUR AVERAGE</b>				Error includes scale factor of 1.3. See the ideogram below.
0.125 ± 0.007 ± 0.001	1.4K	<sup>154</sup> AMBROSINO 09E	KLOE	$E_\gamma$ in 10–250 MeV, $p_e > 200$ MeV/c
0.147 ± 0.011	51	<sup>155</sup> HEINTZE 79	SPEC	
0.150 ± 0.018 – 0.023	56	<sup>156</sup> HEARD 75	SPEC	

<sup>154</sup> Vector form factor fitted with a linear function,  $V(x) = F_V(1 + \lambda(1-x))$ ,  $x = 2E_\gamma/m_K$ . The fitted value of  $\lambda = 0.38 \pm 0.20 \pm 0.02$  with a correlation of  $-0.93$  between  $(F_V + F_A)$  and  $\lambda$ .

<sup>155</sup> HEINTZE 79 quotes absolute value of  $|F_A + F_V| \sin\theta_C$ . We use  $\sin\theta_C = V_{US} = 0.2205$ .

<sup>156</sup> HEARD 75 quotes absolute value of  $|F_A + F_V| \sin\theta_C$ . We use  $\sin\theta_C = V_{US} = 0.2205$ .

WEIGHTED AVERAGE  
0.133 ± 0.008 (Error scaled by 1.3) **$F_A + F_V$ , SUM OF AXIAL-VECTOR AND VECTOR FORM FACTOR FOR  $K \rightarrow e\nu\gamma$**  **$F_A + F_V$ , SUM OF AXIAL-VECTOR AND VECTOR FORM FACTOR FOR  $K \rightarrow \mu\nu\gamma$** 

VALUE	CL%	EVTS	DOCUMENT ID	TECN	CHG
<b>0.165 ± 0.007 ± 0.011</b>		2588	<sup>157</sup> ADLER 00B	B787	+
– 1.2 to 1.1	90		DEMIDOV 90	XEBC	
< 0.23	90		<sup>157</sup> AKIBA 85	SPEC	

<sup>157</sup> Quotes absolute value. Sign not determined. **$F_A - F_V$ , DIFFERENCE OF AXIAL-VECTOR AND VECTOR FORM FACTOR FOR  $K \rightarrow e\nu\gamma$** 

VALUE	EVTS	DOCUMENT ID	TECN
<b>&lt; 0.49</b>	90	<sup>158</sup> HEINTZE 79	SPEC

<sup>158</sup> HEINTZE 79 quotes  $|F_A - F_V| < \sqrt{11} |F_A + F_V|$ . **$F_A - F_V$ , DIFFERENCE OF AXIAL-VECTOR AND VECTOR FORM FACTOR FOR  $K \rightarrow \mu\nu\gamma$** 

VALUE	CL%	EVTS	DOCUMENT ID	TECN	CHG
<b>– 0.24 to 0.04</b>	90	2588	ADLER 00B	B787	+
– 2.2 to 0.6	90		DEMIDOV 90	XEBC	
– 2.5 to 0.3	90		AKIBA 85	SPEC	

 **$K^\pm$  CHARGE RADIUS**

VALUE (fm)	DOCUMENT ID	COMMENT
<b>0.560 ± 0.031 OUR AVERAGE</b>		
0.580 ± 0.040	AMENDOLIA 86B	$Ke \rightarrow Ke$
0.530 ± 0.050	DALLY 80	$Ke \rightarrow Ke$
• • • We do not use the following data for averages, fits, limits, etc. • • •		
0.620 ± 0.037	BLATNIK 79	VMD + dispersion relations

**CP VIOLATION TESTS IN  $K^+$  AND  $K^-$  DECAYS**

$$\Delta(K_{\pi e e}^\pm) = \frac{\Gamma(K_{\pi e e}^+) - \Gamma(K_{\pi e e}^-)}{\Gamma(K_{\pi e e}^+) + \Gamma(K_{\pi e e}^-)}$$

VALUE (units $10^{-2}$ )	DOCUMENT ID	TECN
<b>– 2.2 ± 1.5 ± 0.6</b>	<sup>159</sup> BATLEY 09	NA48

<sup>159</sup> This implies an upper limit of  $2.1 \times 10^{-2}$  at 90% CL.

$$\Delta(K_{\pi \mu \mu}^\pm) = \frac{\Gamma(K_{\pi \mu \mu}^+) - \Gamma(K_{\pi \mu \mu}^-)}{\Gamma(K_{\pi \mu \mu}^+) + \Gamma(K_{\pi \mu \mu}^-)}$$

VALUE	DOCUMENT ID	TECN
<b>0.010 ± 0.023 OUR AVERAGE</b>		
0.011 ± 0.023	<sup>160</sup> BATLEY 11A	NA48
– 0.02 ± 0.11 ± 0.04	PARK 02	HYCP

<sup>160</sup> This corresponds to the asymmetry upper limit of  $< 2.9 \times 10^{-2}$  at 90% CL.

$$\Delta(K_{\pi \pi \gamma}^\pm) = \frac{\Gamma(K_{\pi \pi \gamma}^+) - \Gamma(K_{\pi \pi \gamma}^-)}{\Gamma(K_{\pi \pi \gamma}^+) + \Gamma(K_{\pi \pi \gamma}^-)}$$

VALUE (units $10^{-3}$ )	EVTS	DOCUMENT ID	TECN
<b>0.0 ± 1.0 ± 0.6</b>	1M	<sup>161</sup> BATLEY 10A	NA48

<sup>161</sup> This value implies the upper bound for this asymmetry  $1.5 \times 10^{-3}$  at 90% CL.**FORWARD-BACKWARD ASYMMETRY IN  $K^\pm$  DECAYS**

$$A_{FB}(K_{\pi \mu \mu}^\pm) = \frac{\Gamma(\cos(\theta_{K\mu}) > 0) - \Gamma(\cos(\theta_{K\mu}) < 0)}{\Gamma(\cos(\theta_{K\mu}) > 0) + \Gamma(\cos(\theta_{K\mu}) < 0)}$$

VALUE	CL%	DOCUMENT ID	TECN
<b>&lt; 2.3 × 10<sup>–2</sup></b>	90	<sup>162</sup> BATLEY 11A	NA48

<sup>162</sup> BATLEY 11A gives a corresponding value of the asymmetry  $A_{FB} = (-2.4 \pm 1.8) \times 10^{-2}$ .**T VIOLATION TESTS IN  $K^+$  AND  $K^-$  DECAYS** **$P_T$  in  $K^+ \rightarrow \pi^0 \mu^+ \nu_\mu$** 

T-violating muon polarization. Sensitive to new sources of CP violation beyond the Standard Model.

VALUE (units $10^{-3}$ )	EVTS	DOCUMENT ID	TECN	CHG
<b>– 1.7 ± 2.3 ± 1.1</b>	<sup>163</sup> ABE 04F	K246	+	

• • • We do not use the following data for averages, fits, limits, etc. • • •

– 4.2 ± 4.9 ± 0.9      3.9M      ABE      99S      K246      +

<sup>163</sup> Includes three sets of data: 96–97 (ABE 99S), 98, and 99–00 totaling about three times the ABE 99S data sample. Corresponds to  $P_T < 5.0 \times 10^{-3}$  at 90% CL. **$P_T$  in  $K^+ \rightarrow \mu^+ \nu_\mu \gamma$** 

T-violating muon polarization. Sensitive to new sources of CP violation beyond the Standard Model.

VALUE (units $10^{-2}$ )	EVTS	DOCUMENT ID	TECN	CHG
<b>– 0.64 ± 1.85 ± 0.10</b>	114k	<sup>164</sup> ANISIMOVSK..03	K246	+

<sup>164</sup> Muons stopped and polarization measured from decay to positrons. **$\text{Im}(\xi)$  in  $K^+ \rightarrow \pi^0 \mu^+ \nu_\mu$  DECAY (from transverse  $\mu$  pol.)**

Test of T reversal invariance.

VALUE	EVTS	DOCUMENT ID	TECN	CHG	COMMENT
<b>– 0.006 ± 0.008 OUR AVERAGE</b>					
– 0.0053 ± 0.0071 ± 0.0036	<sup>165</sup> ABE	04F	K246	+	
– 0.016 ± 0.025	20M	CAMPBELL 81	CNTR	+	Pol.

• • • We do not use the following data for averages, fits, limits, etc. • • •

– 0.013 ± 0.016 ± 0.003      3.9M      ABE      99S      CNTR      +       $P_T$   $K^+$  at rest<sup>165</sup> Includes three sets of data: 96–97 (ABE 99S), 98, and 99–00 totaling about three times the ABE 99S data sample. Corresponds to  $\text{Im}(\xi) < 0.016$  at 90% CL. **$K^\pm$  REFERENCES**

BATLEY 11A	PL B697 107	J.R. Batley et al.	(CERN NA48/2 Collab.)
LAZZERONI 11	PL B698 105	C. Lazzeroni et al.	(CERN NA62 Collab.)
ADLER 10	PR D81 092001	S. Adler et al.	(BNL E787 Collab.)
BATLEY 10A	EPJ C68 75	J.R. Batley et al.	(CERN NA48/2 Collab.)
BATLEY 10C	EPJ C70 635	J.R. Batley et al.	(CERN NA48/2 Collab.)
PDG 10	JPG 37 075021	K. Nakamura et al.	(PDG Collab.)
PISLAK 10A	PRL 105 019901E	S. Pislak et al.	(BNL E865 Collab.)
AKOPDZANOV 09	PAN 71 2074	G.A. Akopdzanov et al.	(IHEP)

Translated from YAF 71 2108.



See key on page 457

# Meson Particle Listings

$K^\pm, K^0$

BISI	65B	PR 139 B1068	V. Bisi <i>et al.</i>	(TORI)
CALLAHAN	65	PRL 15 129	A. Callahan, D. Cline	(WIS C)
CLINE	65	PL 15 293	D. Cline, W.F. Fy	(WIS C)
DEMARCO	65	PR 140B 1430	A. de Marco, C. Grosso, G. Rinaudo	(TORI, CERN)
FITCH	65B	PR 140B 1088	V.L. Fitch, C.A. Quarles, H.C. Wilkins	(PRIN+)
STAMER	65	PR 138 B440	P. Stamer <i>et al.</i>	(STEV)
YOUNG	65	Thesis UCRL 16362	P.S. Young	(LRL)
Also		PR 156 1464	P.S. Young, W.Z. Osborne, W.H. Barkas	(LRL)
BORREANI	64	PL 12 123	G. Borreani, G. Rinaudo, A.E. Wertrouck	(TORI)
CALLAHAN	64	PR 136 B1463	A. Callahan, R. March, R. Stark	(WIS C)
GREINER	64	PRL 13 284	D.E. Greiner, W.Z. Osborne, W.H. Barkas	(LRL)
SHAKLEE	64	PR 136 B1423	F.S. Shaklee <i>et al.</i>	(MICH)
BOYARSKI	62	PR 128 2398	A.M. Boyarski <i>et al.</i>	(MIT)
FERRO-LUZZI	61	NC 22 1087	M. Ferro-Luzzi <i>et al.</i>	(LRL)
ROE	61	PRL 7 346	B.P. Roe <i>et al.</i>	(MICH, LRL)
TAYLOR	59	PR 114 359	S. Taylor <i>et al.</i>	(COLU)
COOMBES	57	PR 108 1348	C.A. Coombes <i>et al.</i>	(LBL)

### OTHER RELATED PAPERS

LITTENBERG	93	ARNPS 43 729	L.S. Littenberg, G. Valencia	(BNL, FNAL)
Rare and Radiative Kaon Decays				
RITCHIE	93	RMP 65 1149	J.L. Ritchie, S.G. Wojcicki	
"Rare K Decays"				
BATTISTON	92	PRPL 214 293	R. Battiston <i>et al.</i>	(PGIA, CERN, TRSTT)
Status and Perspectives of K Decay Physics				
BRYMAN	89	IJMP A4 79	D.A. Bryman	(TRIU)
"Rare Kaon Decays"				
CHOUNET	72	PRPL 4C 199	L.M. Chounet, J.M. Gaillard, M.K. Gaillard	(ORSAY+)
FEARING	70	PR D2 542	H.W. Fearing, E. Fischbach, J. Smith	(STON, BOHR)
HAIDT	69B	PL 29B 696	D. Haidt <i>et al.</i>	(AACH, BARI, CERN, EPOL+)
CRONIN	68B	Vienna Conf. 241	J.W. Cronin	(PRIN)
Rapporteur talk.				
WILLIS	67	Heidelberg Conf. 273	W.J. Willis	(YALE)
Rapporteur talk.				
CABIBBO	66	Berkeley Conf. 33	N. Cabibbo	(CERN)
ADAIR	64	PL 12 67	R.K. Adair, L.B. Leipuner	(YALE, BNL)
CABIBBO	64	PL 9 352	N. Cabibbo, A. Maksymowicz	(CERN)
Also		PL 11 360	N. Cabibbo, A. Maksymowicz	(CERN)
Also		PL 14 72	N. Cabibbo, A. Maksymowicz	(CERN)
BIRGE	63	PRL 11 35	R.W. Birge <i>et al.</i>	(LRL, WIS C, BARI)
BLOCK	62B	CERN Conf. 371	M.M. Block, L. Lendinara, L. Monari	(NWES, BGNA)
BRENE	61	NP 22 553	N. Brene, L. Egardt, B. Qvist	(NORD)

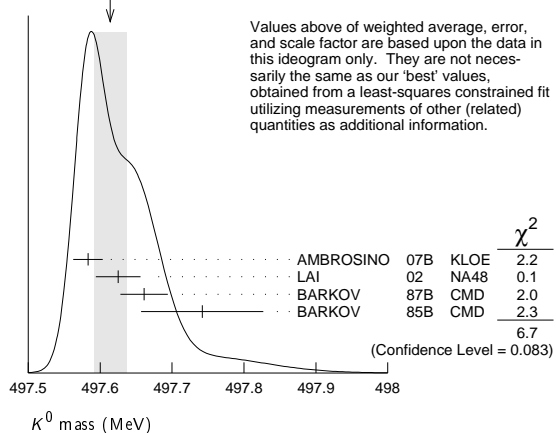


$$I(J^P) = \frac{1}{2}(0^-)$$

### $K^0$ MASS

VALUE (MeV)	EVTS	DOCUMENT ID	TECN	COMMENT
<b>497.614 ± 0.024 OUR FIT</b>				Error includes scale factor of 1.6.
<b>497.614 ± 0.022 OUR AVERAGE</b>				Error includes scale factor of 1.5. See the ideogram below.
497.583 ± 0.005 ± 0.020	35k	AMBROSINO 07B	KLOE	$e^+e^- \rightarrow K_L^0 K_S^0$
497.625 ± 0.001 ± 0.031	655k	LAI 02	NA48	$K_L^0$ beam
497.661 ± 0.033	3713	BARKOV 87B	CMD	$e^+e^- \rightarrow K_L^0 K_S^0$
497.742 ± 0.085	780	BARKOV 85B	CMD	$e^+e^- \rightarrow K_L^0 K_S^0$
• • • We do not use the following data for averages, fits, limits, etc. • • •				
497.44 ± 0.50		FITCH 67	OSPK	
498.9 ± 0.5	4500	BALTAY 66	HBC	$K^0$ from $\bar{p}p$
497.44 ± 0.33	2223	KIM 65B	HBC	$K^0$ from $\bar{p}p$
498.1 ± 0.4		CHRISTENS... 64	OSPK	

WEIGHTED AVERAGE  
497.614 ± 0.022 (Error scaled by 1.5)



$$m_{K^0} - m_{K^\pm}$$

VALUE (MeV)	EVTS	DOCUMENT ID	TECN	CHG	COMMENT
<b>3.937 ± 0.028 OUR FIT</b>					Error includes scale factor of 1.8.
• • • We do not use the following data for averages, fits, limits, etc. • • •					

3.95 ± 0.21	417	HILL 68B	DBC	+	$K^+d \rightarrow K^0 p p$
3.90 ± 0.25	9	BURNSTEIN 65	HBC	-	
3.71 ± 0.35	7	KIM 65B	HBC	-	$K^-p \rightarrow n \bar{K}^0$
5.4 ± 1.1		CRAWFORD 59	HBC	+	
3.9 ± 0.6		ROSENFELD 59	HBC	-	

### $K^0$ MEAN SQUARE CHARGE RADIUS

VALUE (fm <sup>2</sup> )	EVTS	DOCUMENT ID	TECN	COMMENT
<b>-0.077 ± 0.010 OUR AVERAGE</b>				
-0.077 ± 0.007 ± 0.011	5037	ABOUZAID 06	KTEV	$K_L^0 \rightarrow \pi^+ \pi^- e^+ e^-$
-0.090 ± 0.021		LAI 03C	NA48	$K_L^0 \rightarrow \pi^+ \pi^- e^+ e^-$
-0.054 ± 0.026		MOLZON 78		$K_S$ regen. by electrons
• • • We do not use the following data for averages, fits, limits, etc. • • •				
-0.087 ± 0.046		BLATNIK 79		VMD + dispersion relations
-0.050 ± 0.130		FOETH 69B		$K_S$ regen. by electrons

### T-VIOLATION PARAMETER IN $K^0$ - $\bar{K}^0$ MIXING

The asymmetry  $A_T = \frac{\Gamma(\bar{K}^0 \rightarrow K^0) - \Gamma(K^0 \rightarrow \bar{K}^0)}{\Gamma(\bar{K}^0 \rightarrow K^0) + \Gamma(K^0 \rightarrow \bar{K}^0)}$  must vanish if  $T$  invariance holds.

### ASYMMETRY $A_T$ IN $K^0$ - $\bar{K}^0$ MIXING

VALUE (units 10 <sup>-3</sup> )	EVTS	DOCUMENT ID	TECN
<b>6.6 ± 1.3 ± 1.0</b>	640k	ANGELOPO... 98E	CPLR

<sup>1</sup>ANGELOPOULOS 98E measures the asymmetry  $A_T = \frac{\Gamma(\bar{K}^0_{t=0} \rightarrow e^+ \pi^- \nu_{t=\tau}) - \Gamma(K^0_{t=0} \rightarrow e^- \pi^+ \bar{\nu}_{t=\tau})}{\Gamma(\bar{K}^0_{t=0} \rightarrow e^+ \pi^- \nu_{t=\tau}) + \Gamma(K^0_{t=0} \rightarrow e^- \pi^+ \bar{\nu}_{t=\tau})}$  as a function of the neutral-kaon eigentime  $\tau$ . The initial strangeness of the neutral kaon is tagged by the charge of the accompanying charged kaon in the reactions  $p\bar{p} \rightarrow K^- \pi^+ K^0$  and  $p\bar{p} \rightarrow K^+ \pi^- \bar{K}^0$ . The strangeness at the time of the decay is tagged by the lepton charge. The reported result is the average value of  $A_T$  over the interval  $1\tau_S < \tau < 20\tau_S$ . From this value of  $A_T$  ANGELOPOULOS 01B, assuming  $CPT$  invariance in the  $e\pi\nu$  decay amplitude, determine the  $T$ -violating as  $\Delta S = \Delta S$  conserving parameter (for its definition, see Review below)  $4\text{Re}(\epsilon) = (6.2 \pm 1.4 \pm 1.0) \times 10^{-3}$ .

### CPT INVARIANCE TESTS IN NEUTRAL KAON DECAY

Updated April 2012 by M. Antonelli (LNF-INFN, Frascati) and G. D'Ambrosio (INFN Sezione di Napoli).

$CPT$  theorem is based on three assumptions: quantum field theory, locality, and Lorentz invariance, and thus it is a fundamental probe of our basic understanding of particle physics. Strangeness oscillation in  $K^0 - \bar{K}^0$  system, described by the equation

$$i \frac{d}{dt} \begin{bmatrix} K^0 \\ \bar{K}^0 \end{bmatrix} = [M - i\Gamma/2] \begin{bmatrix} K^0 \\ \bar{K}^0 \end{bmatrix},$$

where  $M$  and  $\Gamma$  are hermitian matrices (see PDG review [1], references [2,3], and KLOE paper [4] for notations and previous literature), allows a very accurate test of  $CPT$  symmetry; indeed since  $CPT$  requires  $M_{11} = M_{22}$  and  $\Gamma_{11} = \Gamma_{22}$ , the mass and width eigenstates,  $K_{S,L}$ , have a  $CPT$ -violating piece,  $\delta$ , in addition to the usual  $CPT$ -conserving parameter  $\epsilon$ :

$$K_{S,L} = \frac{1}{\sqrt{2(1+|\epsilon_{S,L}|^2)}} \left[ (1 + \epsilon_{S,L}) K^0 + (1 - \epsilon_{S,L}) \bar{K}^0 \right]$$

$$\epsilon_{S,L} = \frac{-i\Im(M_{12}) - \frac{1}{2}\Im(\Gamma_{12}) \mp \frac{1}{2} \left[ M_{11} - M_{22} - \frac{i}{2}(\Gamma_{11} - \Gamma_{22}) \right]}{m_L - m_S + i(\Gamma_S - \Gamma_L)/2}$$

$$\equiv \epsilon \pm \delta. \tag{1}$$

Using the phase convention  $\Im(\Gamma_{12}) = 0$ , we determine the phase of  $\epsilon$  to be  $\varphi_{SW} \equiv \arctan \frac{2(m_L - m_S)}{\Gamma_S - \Gamma_L}$ . Imposing unitarity to an arbitrary combination of  $K^0$  and  $\bar{K}^0$  wave functions, we obtain the Bell-Steinberger relation [5] connecting  $CP$  and

# Meson Particle Listings

## $K^0$

$CPT$  violation in the mass matrix to  $CP$  and  $CPT$  violation in the decay; in fact, neglecting  $\mathcal{O}(\epsilon)$  corrections to the coefficient of the  $CPT$ -violating parameter,  $\delta$ , we can write [4]

$$\left[ \frac{\Gamma_S + \Gamma_L}{\Gamma_S - \Gamma_L} + i \tan \phi_{\text{SW}} \right] \left[ \frac{\Re(\epsilon)}{1 + |\epsilon|^2} - i \Im(\delta) \right] = \frac{1}{\Gamma_S - \Gamma_L} \sum_f A_L(f) A_S^*(f), \quad (2)$$

where  $A_{L,S}(f) \equiv A(K_{L,S} \rightarrow f)$ . We stress that this relation is phase-convention-independent. The advantage of the neutral kaon system is that only a few decay modes give significant contributions to the r.h.s. in Eq. (2); in fact, defining for the hadronic modes

$$\alpha_i \equiv \frac{1}{\Gamma_S} \langle \mathcal{A}_L(i) \mathcal{A}_S^*(i) \rangle = \eta_i \mathcal{B}(K_S \rightarrow i),$$

$$i = \pi^0 \pi^0, \pi^+ \pi^- (\gamma), 3\pi^0, \pi^0 \pi^+ \pi^- (\gamma), \quad (3)$$

the recent data from CPLEAR, KLOE, KTeV, and NA48 have led to the following determinations (the analysis described in Ref. 4 has been updated by using the recent measurements of  $K_L$  branching ratios from KTeV [6,7], NA48 [8,9], and the results described in the  $CP$  violation in  $K_L$  decays minireview)

$$\alpha_{\pi^+ \pi^-} = ((1.112 \pm 0.010) + i(1.061 \pm 0.010)) \times 10^{-3},$$

$$\alpha_{\pi^0 \pi^0} = ((0.493 \pm 0.005) + i(0.471 \pm 0.005)) \times 10^{-3},$$

$$\alpha_{\pi^+ \pi^- \pi^0} = ((0 \pm 2) + i(0 \pm 2)) \times 10^{-6},$$

$$|\alpha_{\pi^0 \pi^0 \pi^0}| < 7 \times 10^{-6} \quad \text{at 95\% CL.} \quad (4)$$

The semileptonic contribution to the right-handed side of Eq. (2) requires the determination of several observables: we define [2,3]

$$\mathcal{A}(K^0 \rightarrow \pi^- l^+ \nu) = \mathcal{A}_0(1 - y),$$

$$\mathcal{A}(K^0 \rightarrow \pi^+ l^- \nu) = \mathcal{A}_0^*(1 + y^*)(x_+ - x_-)^*,$$

$$\mathcal{A}(\bar{K}^0 \rightarrow \pi^+ l^- \nu) = \mathcal{A}_0^*(1 + y^*),$$

$$\mathcal{A}(\bar{K}^0 \rightarrow \pi^- l^+ \nu) = \mathcal{A}_0(1 - y)(x_+ + x_-), \quad (5)$$

where  $x_+$  ( $x_-$ ) describes the violation of the  $\Delta S = \Delta Q$  rule in  $CPT$ -conserving (violating) decay amplitudes, and  $y$  parametrizes  $CPT$  violation for  $\Delta S = \Delta Q$  transitions. Taking advantage of their tagged  $K^0(\bar{K}^0)$  beams, CPLEAR has measured  $\Im(x_+)$ ,  $\Re(x_-)$ ,  $\Im(\delta)$ , and  $\Re(\delta)$  [11]. These determinations have been improved in Ref. 4 by including the information  $A_S - A_L = 4[\Re(\delta) + \Re(x_-)]$ , where  $A_{L,S}$  are the  $K_L$  and  $K_S$  semileptonic charge asymmetries, respectively, from the PDG [12] and KLOE [13]. Here we are also including the  $T$ -violating asymmetry measurement from CPLEAR [14].

**Table 1:** Values, errors, and correlation coefficients for  $\Re(\delta)$ ,  $\Im(\delta)$ ,  $\Re(x_-)$ ,  $\Im(x_+)$ , and  $A_S + A_L$  obtained from a combined fit, including KLOE [4] and CPLEAR [14].

	value	Correlations coefficients			
$\Re(\delta)$	$(3.0 \pm 2.3) \times 10^{-4}$	1			
$\Im(\delta)$	$(-0.66 \pm 0.65) \times 10^{-2}$	-0.21	1		
$\Re(x_-)$	$(-0.30 \pm 0.21) \times 10^{-2}$	-0.21	-0.60	1	
$\Im(x_+)$	$(0.02 \pm 0.22) \times 10^{-2}$	-0.38	-0.14	0.47	1
$A_S + A_L$	$(-0.40 \pm 0.83) \times 10^{-2}$	-0.10	-0.63	0.99	0.43

The value  $A_S + A_L$  in Table 1 can be directly included in the semileptonic contributions to the Bell Steinberger relations in Eq. (2)

$$\sum_{\pi l \nu} \langle \mathcal{A}_L(\pi l \nu) \mathcal{A}_S^*(\pi l \nu) \rangle$$

$$= 2\Gamma(K_L \rightarrow \pi l \nu)(\Re(\epsilon) - \Re(y) - i(\Im(x_+) + \Im(\delta)))$$

$$= 2\Gamma(K_L \rightarrow \pi l \nu)((A_S + A_L)/4 - i(\Im(x_+) + \Im(\delta))). \quad (6)$$

Defining

$$\alpha_{\pi l \nu} \equiv \frac{1}{\Gamma_S} \sum_{\pi l \nu} \langle \mathcal{A}_L(\pi l \nu) \mathcal{A}_S^*(\pi l \nu) \rangle + 2i \frac{\tau_{K_S}}{\tau_{K_L}} \mathcal{B}(K_L \rightarrow \pi l \nu) \Im(\delta), \quad (7)$$

we find:

$$\alpha_{\pi l \nu} = ((-0.2 \pm 0.5) + i(0.1 \pm 0.5)) \times 10^{-5}.$$

Inserting the values of the  $\alpha$  parameters into Eq. (2), we find

$$\Re(\epsilon) = (161.1 \pm 0.5) \times 10^{-5},$$

$$\Im(\delta) = (-0.7 \pm 1.4) \times 10^{-5}. \quad (8)$$

The complete information on Eq. (8) is given in Table 2.

**Table 2:** Summary of results: values, errors, and correlation coefficients for  $\Re(\epsilon)$ ,  $\Im(\delta)$ ,  $\Re(\delta)$ , and  $\Re(x_-)$ .

	value	Correlations coefficients			
$\Re(\epsilon)$	$(161.1 \pm 0.5) \times 10^{-5}$	+1			
$\Im(\delta)$	$(-0.7 \pm 1.4) \times 10^{-5}$	+0.09	1		
$\Re(\delta)$	$(2.4 \pm 2.3) \times 10^{-4}$	+0.08	-0.12	1	
$\Re(x_-)$	$(-4.1 \pm 1.7) \times 10^{-3}$	+0.14	0.22	-0.43	1

Now the agreement with  $CPT$  conservation,  $\Im(\delta) = \Re(\delta) = \Re(x_-) = 0$ , is at 18% C.L.

The allowed region in the  $\Re(\epsilon) - \Im(\delta)$  plane at 68% CL and 95% C.L. is shown in the top panel of Fig. 1.

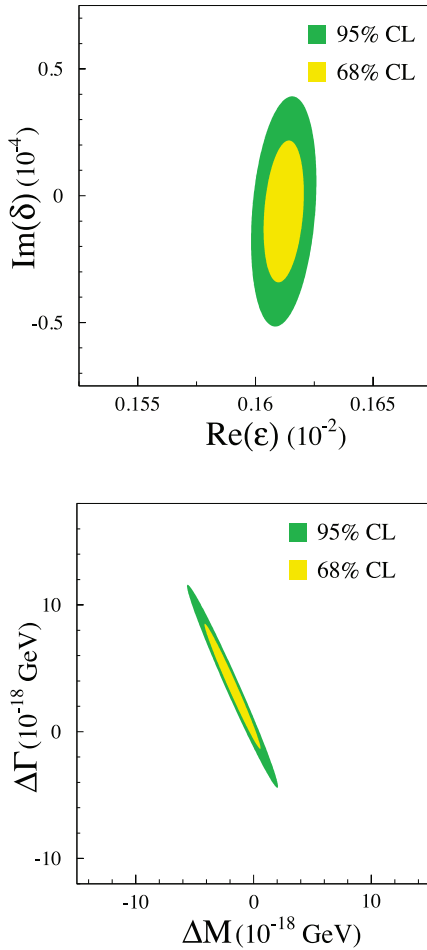


**Figure 1:** Top: allowed region at 68% and 95% C.L. in the  $\Re(\epsilon)$ ,  $\Im(\delta)$  plane. Bottom: allowed region at 68% and 95% C.L. in the  $\Delta M$ ,  $\Delta\Gamma$  plane.

The process giving the largest contribution to the size of the allowed region is  $K_L \rightarrow \pi^+\pi^-$ , through the uncertainty on  $\phi_{+-}$ .

The limits on  $\Im(\delta)$  and  $\Re(\delta)$  can be used to constrain the  $K^0 - \bar{K}^0$  mass and width difference

$$\delta = \frac{i(m_{K^0} - m_{\bar{K}^0}) + \frac{1}{2}(\Gamma_{K^0} - \Gamma_{\bar{K}^0})}{\Gamma_S - \Gamma_L} \cos \phi_{SW} e^{i\phi_{SW}} [1 + \mathcal{O}(\epsilon)].$$

The allowed region in the  $\Delta M = (m_{K^0} - m_{\bar{K}^0})$ ,  $\Delta\Gamma = (\Gamma_{K^0} - \Gamma_{\bar{K}^0})$  plane is shown in the bottom panel of Fig. 1. As a result, we improve on the previous limits (see for instance, P. Bloch in Ref. 12) and in the limit  $\Gamma_{K^0} - \Gamma_{\bar{K}^0} = 0$  we obtain

$$-4.0 \times 10^{-19} \text{ GeV} < m_{K^0} - m_{\bar{K}^0} < 4.0 \times 10^{-19} \text{ GeV} \quad \text{at } 95\% \text{ C.L.}$$

## References

1. See the “*CP* Violation in Meson Decays,” in this *Review*.
2. L. Maiani, “*CP* And *CPT* Violation in Neutral Kaon Decays,” L. Maiani, G. Pancheri, and N. Paver, *The Second Daphne Physics Handbook*, Vol. 1, 2.
3. G. D’Ambrosio, G. Isidori, and A. Pugliese, “*CP* and *CPT* measurements at DAΦNE,” L. Maiani, G. Pancheri, and N. Paver, *The Second Daphne Physics Handbook*, Vol. 1, 2.
4. F. Ambrosino *et al.*, [KLOE Collab.], *JHEP* **0612**, 011 (2006) [[arXiv:hep-ex/0610034](#)].
5. J. S. Bell and J. Steinberger, In Wolfenstein, L. (ed.): *CP violation*, 42-57. (In *Oxford International Symposium Conference on Elementary Particles*, September 1965, 195-208, 221-222). (See Book Index).
6. T. Alexopoulos *et al.*, [KTeV Collab.], *Phys. Rev.* **D70**, 092006 (1998).
7. E. Abouzaid *et al.* [KTeV Collab.], *Phys. Rev.* **D83**, 092001 (2011).
8. A. Lai *et al.*, [NA48 Collab.], *Phys. Lett.* **B645**, 26 (2007); A. Lai *et al.*, [NA48 Collab.], *Phys. Lett.* **B602**, 41 (2004).
9. We thank G. Isidori and M. Palutan for their contribution to the original analysis [4] performed with KLOE data.
10. A. Angelopoulos *et al.*, [CPLEAR Collab.], *Phys. Reports* **374**, 165 (2003).
11. A. Angelopoulos *et al.*, [CPLEAR Collab.], *Phys. Lett.* **B444**, 52 (1998).
12. W. M. Yao *et al.*, [Particle Data Group], *J. Phys.* **G33**, 1 (2006).
13. F. Ambrosino *et al.*, [KLOE Collab.], *Phys. Lett.* **B636**, 173 (2006) [[arXiv:hep-ex/0601026](#)].
14. P. Bloch, M. Fidecaro, private communication of the data in a finer binning format; A. Angelopoulos *et al.*, [CPLEAR Collab.], *Phys. Lett.* **B444**, 43 (1998).
15. We thank M. Palutan for the collaboration in this analysis.

## CP-VIOLATION PARAMETERS

### Re(ε)

VALUE (units  $10^{-3}$ )

**1.596 ± 0.013**

• • • We do not use the following data for averages, fits, limits, etc. • • •

1.664 ± 0.010

DOCUMENT ID

<sup>2</sup> AMBROSINO 06H KLOE

<sup>3</sup> LAI 05A NA48

<sup>2</sup> AMBROSINO 06H uses Bell-Steinberger relations with the following measurements:  $B(K_L^0 \rightarrow \pi^+\pi^-)$  in AMBROSINO 06F,  $B(K_S^0 \rightarrow \pi^0\pi^0\pi^0)$  in AMBROSINO 05B, the  $K_S^0$ -semileptonic charge asymmetry in AMBROSINO 06E, and  $K^0$ -semileptonic results in ANGELOPOULOS 98F.

<sup>3</sup> LAI 05A values are obtained through unitarity (Bell-Steinberger relations), improving determination of  $\eta_{000}$  and combining other data from PDG 04 and APOSTOLAKIS 99B.

## CPT-VIOLATION PARAMETERS

In  $K^0 - \bar{K}^0$  mixing, if *CP*-violating interactions include a *T* conserving part then

$$|K_S\rangle = [|K_1\rangle + (\epsilon + \delta)|K_2\rangle] / \sqrt{1 + |\epsilon + \delta|^2}$$

$$|K_L\rangle = [|K_2\rangle + (\epsilon - \delta)|K_1\rangle] / \sqrt{1 + |\epsilon - \delta|^2}$$

where

$$|K_1\rangle = [|K^0\rangle + |\bar{K}^0\rangle] / \sqrt{2}$$

$$|K_2\rangle = [|K^0\rangle - |\bar{K}^0\rangle] / \sqrt{2}$$

and

$$|\bar{K}^0\rangle = CP|K^0\rangle.$$

The parameter  $\delta$  specifies the *CPT*-violating part.

## Meson Particle Listings

 $K^0, K_S^0$ 

Estimates of  $\delta$  are given below assuming the validity of the  $\Delta S = \Delta Q$  rule. See also THOMSON 95 for a test of  $CPT$ -symmetry conservation in  $K^0$  decays using the Bell-Steinberger relation.

**REAL PART OF  $\delta$** 

A nonzero value violates  $CPT$  invariance.

VALUE (units $10^{-4}$ )	EVTS	DOCUMENT ID	TECN	COMMENT
$2.51 \pm 2.25$		<sup>4</sup> ABOUZAID 11	KTEV	
••• We do not use the following data for averages, fits, limits, etc. •••				
$2.3 \pm 2.7$		<sup>5</sup> AMBROSINO 06H	KLOE	
$2.4 \pm 2.8$		<sup>6</sup> APOSTOLA... 99B	RVUE	
$2.9 \pm 2.6 \pm 0.6$	1.3M	<sup>7</sup> ANGELOPO... 98F	CPLR	
$180 \pm 200$	6481	<sup>8</sup> DEMIDOV 95		$K_{L3}$ reanalysis

- <sup>4</sup> ABOUZAID 11 uses Bell-Steinberger relations.  
<sup>5</sup> AMBROSINO 06H uses Bell-Steinberger relations with the following measurements:  $B(K_L^0 \rightarrow \pi^+ \pi^-)$  in AMBROSINO 06F,  $B(K_S^0 \rightarrow \pi^0 \pi^0 \pi^0)$  in AMBROSINO 05B, the  $K_S^0$ -semileptonic charge asymmetry in AMBROSINO 06E, and  $K^0$ -semileptonic results in ANGELOPOULOS 98F.  
<sup>6</sup> APOSTOLAKIS 99B assumes only unitarity and combines CPLEAR and other results.  
<sup>7</sup> ANGELOPOULOS 98F use  $\Delta S = \Delta Q$ . If  $\Delta S = \Delta Q$  is not assumed, they find  $\text{Re}(\delta) = (3.0 \pm 3.3 \pm 0.6) \times 10^{-4}$ .  
<sup>8</sup> DEMIDOV 95 reanalyzes data from HART 73 and NIEBERGALL 74.

**IMAGINARY PART OF  $\delta$** 

A nonzero value violates  $CPT$  invariance.

VALUE (units $10^{-5}$ )	EVTS	DOCUMENT ID	TECN	COMMENT
$-1.5 \pm 1.6$		<sup>9</sup> ABOUZAID 11	KTEV	
••• We do not use the following data for averages, fits, limits, etc. •••				
$0.4 \pm 2.1$		<sup>10</sup> AMBROSINO 06H	KLOE	
$0.2 \pm 2.0$		<sup>11</sup> LAI	05A NA48	
$2.4 \pm 5.0$		<sup>12</sup> APOSTOLA... 99B	RVUE	
$-90 \pm 290 \pm 100$	1.3M	<sup>13</sup> ANGELOPO... 98F	CPLR	
$2100 \pm 3700$	6481	<sup>14</sup> DEMIDOV 95		$K_{L3}$ reanalysis

- <sup>9</sup> ABOUZAID 11 uses Bell-Steinberger relations.  
<sup>10</sup> AMBROSINO 06H uses Bell-Steinberger relations with the following measurements:  $B(K_L^0 \rightarrow \pi^+ \pi^-)$  in AMBROSINO 06F,  $B(K_S^0 \rightarrow \pi^0 \pi^0 \pi^0)$  in AMBROSINO 05B, the  $K_S^0$ -semileptonic charge asymmetry in AMBROSINO 06E, and  $K^0$ -semileptonic results in ANGELOPOULOS 98F.  
<sup>11</sup> LAI 05A values are obtained through unitarity (Bell-Steinberger relations), improving determination of  $\eta_{000}$  and combining other data from PDG 04 and APOSTOLAKIS 99B.  
<sup>12</sup> APOSTOLAKIS 99B assumes only unitarity and combines CPLEAR and other results.  
<sup>13</sup> If  $\Delta S = \Delta Q$  is not assumed, ANGELOPOULOS 98F find  $\text{Im}(\delta) = (-15 \pm 23 \pm 3) \times 10^{-3}$ .  
<sup>14</sup> DEMIDOV 95 reanalyzes data from HART 73 and NIEBERGALL 74.

**Re( $\eta$ )**

A non-zero value would violate  $CPT$  invariance in  $\Delta S = \Delta Q$  amplitude. Re( $\eta$ ) is the following combination of  $K_{L3}$  decay amplitudes:

$$\text{Re}(\eta) = \text{Re} \left( \frac{A(K^0 \rightarrow e^- \pi^+ \bar{\nu}_e)^* - A(K^0 \rightarrow e^+ \pi^- \nu_e)}{A(K^0 \rightarrow e^- \pi^+ \bar{\nu}_e)^* + A(K^0 \rightarrow e^+ \pi^- \nu_e)} \right)$$

VALUE (units $10^{-3}$ )	EVTS	DOCUMENT ID	TECN	COMMENT
$0.4 \pm 2.5$	13k	<sup>15</sup> AMBROSINO 06E	KLOE	
••• We do not use the following data for averages, fits, limits, etc. •••				
$0.3 \pm 3.1$		<sup>16</sup> APOSTOLA... 99B	CPLR	
<sup>15</sup> They use the PDG 04 for the $K^0$ semileptonic charge asymmetry and PDG 04 (CP review, $CPT$ NOT ASSUMED) for Re( $\epsilon$ ). <sup>16</sup> Constrained by Bell-Steinberger (or unitarity) relation.				

**Re( $x_{\pm}$ )**

A non-zero value would violate  $CPT$  invariance in decay amplitudes with  $\Delta S \neq \Delta Q$ .  $x_{\pm}$ , used here to define Re( $x_{\pm}$ ), and  $x_{\pm}$ , used below in the  $\Delta S = \Delta Q$  section are the following combinations of  $K_{L3}$  decay amplitudes:

$$x_{\pm} = \frac{1}{2} \left( \frac{A(K^0 \rightarrow \pi^- e^+ \nu_e)}{A(K^0 \rightarrow \pi^- e^+ \nu_e)} \pm \frac{A(K^0 \rightarrow \pi^+ e^- \bar{\nu}_e)^*}{A(K^0 \rightarrow \pi^+ e^- \bar{\nu}_e)^*} \right)$$

VALUE (units $10^{-3}$ )	EVTS	DOCUMENT ID	TECN	COMMENT
$-2.9 \pm 2.0$		<sup>17</sup> AMBROSINO 06H	KLOE	
••• We do not use the following data for averages, fits, limits, etc. •••				
$-0.8 \pm 2.5$	13k	<sup>18</sup> AMBROSINO 06E	KLOE	
$-0.5 \pm 3.0$		<sup>19</sup> APOSTOLA... 99B	CPLR	Strangeness tagged
$2 \pm 13 \pm 3$	650k	ANGELOPO... 98F	CPLR	Strangeness tagged

- <sup>17</sup> AMBROSINO 06H uses Bell-Steinberger relations with the following measurements:  $B(K_L^0 \rightarrow \pi^+ \pi^-)$  in AMBROSINO 06F,  $B(K_S^0 \rightarrow \pi^0 \pi^0 \pi^0)$  in AMBROSINO 05B, the  $K_S^0$ -semileptonic charge asymmetry in AMBROSINO 06E, and  $K^0$ -semileptonic results in ANGELOPOULOS 98F.  
<sup>18</sup> Uses PDG 04 for the  $K_L^0$  semileptonic charge asymmetry and Re( $\delta$ ) from CPLEAR, ANGELOPOULOS 98F.  
<sup>19</sup> Constrained by Bell-Steinberger (or unitarity) relation.

$$|m_{K^0} - m_{\bar{K}^0}| / m_{\text{average}}$$

A test of  $CPT$  invariance. "Our Evaluation" is described in the "Tests of Conservation Laws" section. It assumes  $CPT$  invariance in the decay and neglects some contributions from decay channels other than  $\pi\pi$ .

VALUE	CL%	DOCUMENT ID	TECN	COMMENT
$< 6 \times 10^{-19}$	90	PDG	12	
••• We do not use the following data for averages, fits, limits, etc. •••				
$(-3 \pm 4) \times 10^{-18}$		<sup>20</sup> ANGELOPO... 99B	RVUE	

<sup>20</sup> ANGELOPOULOS 99B assumes only unitarity and combines CPLEAR and other results.

$$(\Gamma_{K^0} - \Gamma_{\bar{K}^0}) / m_{\text{average}}$$

A test of  $CPT$  invariance.

VALUE	DOCUMENT ID	TECN
$(7.8 \pm 8.4) \times 10^{-18}$	<sup>21</sup> ANGELOPO... 99B	RVUE
<sup>21</sup> ANGELOPOULOS 99B assumes only unitarity and combines CPLEAR with other results. Correlated with $(m_{K^0} - m_{\bar{K}^0}) / m_{\text{average}}$ with a correlation coefficient of $-0.95$ .		

**TESTS OF  $\Delta S = \Delta Q$  RULE****Re( $x_{\pm}$ )**

A non-zero value would violate the  $\Delta S = \Delta Q$  rule in  $CPT$  conserving transitions.  $x_{\pm}$  is defined above in the Re( $x_{\pm}$ ) section.

VALUE (units $10^{-3}$ )	EVTS	DOCUMENT ID	TECN
$-0.9 \pm 3.0$		<b>OUR AVERAGE</b>	
$-2 \pm 10$		<sup>22</sup> BATLEY	07D NA48
$-0.5 \pm 3.6$	13k	<sup>23</sup> AMBROSINO 06E	KLOE
$-1.8 \pm 6.1$		<sup>24</sup> ANGELOPO... 98D	CPLR

- <sup>22</sup> Result obtained from the measurement  $\Gamma(K_S^0 \rightarrow \pi e \nu) / \Gamma(K_L^0 \rightarrow \pi e \nu) = 0.993 \pm 0.34$ , neglecting possible  $CPT$  non-invariance and using PDG 06 values of  $B(K_L^0 \rightarrow \pi e \nu) = 0.4053 \pm 0.0015$ ,  $\tau_L = (5.114 \pm 0.021) \times 10^{-8}$  s and  $\tau_S = (0.8958 \pm 0.0005) \times 10^{-10}$  s.  
<sup>23</sup> Re( $x_{\pm}$ ) can be shown to be equal to the following combination of rates:

$$\text{Re}(x_{\pm}) = \frac{1}{2} \frac{\Gamma(K_S^0 \rightarrow \pi e \nu) - \Gamma(K_L^0 \rightarrow \pi e \nu)}{\Gamma(K_S^0 \rightarrow \pi e \nu) + \Gamma(K_L^0 \rightarrow \pi e \nu)}$$

which is valid up to first order in terms violating  $CPT$  and/or the  $\Delta S = \Delta Q$  rule.

<sup>24</sup> Obtained neglecting  $CPT$  violating amplitudes.

 **$K^0$  REFERENCES**

PDG	12	PR D86 010001	J. Beringer et al.	(PDG Collab.)
ABOUZAID	11	PR D83 032001	E. Abouzaid et al.	(FNAL KTeV Collab.)
AMBROSINO	07B	JHEP 0712 073	F. Ambrosino et al.	(KLOE Collab.)
BATLEY	07D	PL B653 145	J.R. Batley et al.	(CERN NA48 Collab.)
ABOUZAID	06	PRL 96 101801	E. Abouzaid et al.	(KTeV Collab.)
AMBROSINO	06F	PL B636 173	F. Ambrosino et al.	(KLOE Collab.)
AMBROSINO	06F	PL B638 140	F. Ambrosino et al.	(KLOE Collab.)
AMBROSINO	06H	JHEP 0612 011	F. Ambrosino et al.	(KLOE Collab.)
PDG	06	JPG 33 1	W.-M. Yao et al.	(PDG Collab.)
AMBROSINO	05B	PL B619 61	F. Ambrosino et al.	(KLOE Collab.)
LAI	05A	PL B610 165	A. Lai et al.	(CERN NA48 Collab.)
PDG	04	PL B592 1	S. Edelman et al.	(PDG Collab.)
LAI	03C	EPJ C30 33	A. Lai et al.	(CERN NA48 Collab.)
LAI	02	PL B533 196	A. Lai et al.	(CERN NA48 Collab.)
ANGELOPO... 01B	EPJ C22 55	A. Angelopoulos et al.	(CLEAR Collab.)	
ANGELOPO... 99B	PL B471 332	A. Angelopoulos et al.	(CLEAR Collab.)	
APOSTOLA... 99B	PL B456 297	A. Apostolakis et al.	(CLEAR Collab.)	
ANGELOPO... 98D	PL B444 38	A. Angelopoulos et al.	(CLEAR Collab.)	
Also	EPJ C22 55	A. Angelopoulos et al.	(CLEAR Collab.)	
ANGELOPO... 98E	PL B444 43	A. Angelopoulos et al.	(CLEAR Collab.)	
ANGELOPO... 98F	PL B444 52	A. Angelopoulos et al.	(CLEAR Collab.)	
Also	EPJ C22 55	A. Angelopoulos et al.	(CLEAR Collab.)	
DEMIDOV	95	PAN 58 968	V. Demidov, K. Gusev, E. Shabalina	(ITEP)
From YAF	58	1041		
THOMSON	95	PR D51 1412	G.B. Thomson, Y. Zou	(RUTG)
BARKOV	87B	SJNP 46 630	L.M. Barkov et al.	(NOVO)
		Translated from YAF 46 1088.		
BARKOV	85B	JETPL 42 138	L.M. Barkov et al.	(NOVO)
		Translated from ZETFP 42 113.		
BLATNIK	79	LNC 24 39	S. Blatnik, J. Stahov, C.B. Lang	(TUZL, GRAZ)
MOLZON	78	PRL 41 1213	W.R. Molzon et al.	(EP1+)
NIEBERGALL	74	PL 49B 103	F. Niebergall et al.	(CERN, ORSAY, VIEN)
HART	73	NP B66 317	J.C. Hart et al.	(CAVE, RHEL)
FOETH	69B	PL 30B 276	H. Foeth et al.	(AACH, CERN, TORI)
HILL	68B	PR 168 1534	D.G. Hill et al.	(BNL, CMU)
FITCH	67	PR 164 1711	V.L. Fitch et al.	(PRIN)
BALTAY	65	PR 142 932	C. Baltay et al.	(YALE, BNL)
BURNSTEIN	66	PR 138 B895	R.A. Burnstein, H.A. Rubin	(UMD)
KIM	65B	PR 140B 1334	J.K. Kim, L. Kirsch, D. Miller	(COLU)
CHRISTENS... 64	PRL 13 138	J.H. Christenson et al.	(PRIN)	
CRAWFORD	59	PRL 2 112	F.S. Crawford et al.	(LRL)
ROSENFELD	59	PRL 2 110	A.H. Rosenfeld, F.T. Solmitz, R.D. Tripp	(LRL)



$$|J^P| = \frac{1}{2}(0^-)$$

 **$K_S^0$  MEAN LIFE**

For earlier measurements, beginning with BOLDT 58B, see our 1986 edition, Physics Letters **170B** 130 (1986).

OUR FIT is described in the note on "CP violation in  $K_L$  decays" in the  $K^0$  Particle Listings. The result labeled "OUR FIT Assuming  $CPT$ " ["OUR FIT Not assuming  $CPT$ "] includes all measurements except those with the comment "Not assuming  $CPT$ " ["Assuming  $CPT$ "]. Measurements with neither comment do not assume  $CPT$  and enter both fits.

VALUE ( $10^{-10}$ s)	EVTS	DOCUMENT ID	TECN	COMMENT
$0.8954 \pm 0.0004$		<b>OUR FIT</b> Error includes scale factor of 1.1. Assuming $CPT$		
$0.89564 \pm 0.00033$		<b>OUR FIT</b> Not assuming $CPT$		
$0.89589 \pm 0.00070$		<sup>1,2</sup> ABOUZAID	11	KTEV Not assuming $CPT$
$0.89623 \pm 0.00047$		<sup>1,3</sup> ABOUZAID	11	KTEV Assuming $CPT$



0.89562 ± 0.00029 ± 0.00043	20M	<sup>4</sup> AMBROSINO	11	KLOE	Not assuming <i>CPT</i>
0.89598 ± 0.00048 ± 0.00051	16M	LAI	02c	NA48	
0.8971 ± 0.0021		BERTANZA	97	NA31	
0.8941 ± 0.0014 ± 0.0009		SCHWINGEN...	95	E773	Assuming <i>CPT</i>
0.8929 ± 0.0016		GIBBONS	93	E731	Assuming <i>CPT</i>
• • • We do not use the following data for averages, fits, limits, etc. • • •					
0.8965 ± 0.0007		<sup>5</sup> ALAVI-HARATI	03	KTEV	Assuming <i>CPT</i>
0.8958 ± 0.0013		<sup>6</sup> ALAVI-HARATI	03	KTEV	Not assuming <i>CPT</i>
0.8920 ± 0.0044	214k	GROSSMAN	87	SPEC	
0.905 ± 0.007		<sup>7</sup> ARONSON	82b	SPEC	
0.881 ± 0.009	26k	ARONSON	76	SPEC	
0.8926 ± 0.0032 ± 0.0002		<sup>8</sup> CARITHERS	75	SPEC	
0.8937 ± 0.0048	6M	GEWENIGER	74b	ASP K	
0.8958 ± 0.0045	50k	<sup>9</sup> SKJEGGEST...	72	HBC	
0.856 ± 0.008	19994	<sup>10</sup> DONALD	68b	HBC	
0.872 ± 0.009	20000	<sup>9,10</sup> HILL	68	DBC	

<sup>1</sup> The two ABOUZAID 11 values use the same full KTeV dataset from 1996, 1997, and 1999. The first enters the "assuming *CPT*" fit and the second enters the "not assuming *CPT*" fit.

<sup>2</sup> ABOUZAID 11 fit has  $\Delta m$ ,  $\tau_S$ ,  $\phi_\epsilon$ ,  $\text{Re}(\epsilon'/\epsilon)$ , and  $\text{Im}(\epsilon'/\epsilon)$  as free parameters. See  $\text{Im}(\epsilon'/\epsilon)$  in the " $K_L^0$  CP violation" section for correlation information.

<sup>3</sup> ABOUZAID 11 fit has  $\Delta m$  and  $\tau_S$  free but constrains  $\phi_\epsilon$  to the Superweak value, i.e. assumes *CPT*. This  $\tau_S$  value is correlated with their  $\Delta m = m_{K_L^0} - m_{K_S^0}$  measurement in the  $K_L^0$  listings. The correlation coefficient  $\rho(\tau_S, \Delta m) = -0.670$ .

<sup>4</sup> Fit to the proper time distribution.

<sup>5</sup> This ALAVI-HARATI 03 fit has  $\Delta m$  and  $\tau_S$  free but constrains  $\phi_{+-}$  to the Superweak value, i.e. assumes *CPT*. This  $\tau_S$  value is correlated with their  $\Delta m = m_{K_L^0} - m_{K_S^0}$  measurement in the  $K_L^0$  listings. The correlation coefficient  $\rho(\tau_S, \Delta m) = -0.396$ . Superseded by ABOUZAID 11.

<sup>6</sup> This ALAVI-HARATI 03 fit has  $\Delta m$ ,  $\phi_{+-}$ , and  $\tau_{K_S^0}$  free. See  $\phi_{+-}$  in the " $K_L^0$  CP violation" section for correlation information. Superseded by ABOUZAID 11.

<sup>7</sup> ARONSON 82 find that  $K_S^0$  mean life may depend on the kaon energy.

<sup>8</sup> CARITHERS 75 measures the  $\Delta m$  dependence of the total decay rate (inverse mean life) to be  $\Gamma(K_S^0) = [(1.122 \pm 0.004) + 0.16(\Delta m - 0.5348)/\Delta m] 10^{10}/s$ , or, in terms of mean life, CARITHERS 75 measures  $\tau_S = (0.8913 \pm 0.0032) - 0.238 [\Delta m - 0.5348] (10^{-10} s)$ . We have adjusted the measurement to use our best values of  $(\Delta m = 0.5293 \pm 0.0009) (10^{10} \text{ h s}^{-1})$ . Our first error is their experiment's error and our second error is the systematic error from using our best values.

<sup>9</sup> HILL 68 has been changed by the authors from the published value  $(0.865 \pm 0.009)$  because of a correction in the shift due to  $\eta_{+-}$ . SKJEGGESTAD 72 and HILL 68 give detailed discussions of systematics encountered in this type of experiment.

<sup>10</sup> Pre-1971 experiments are excluded from the average because of disagreement with later more precise experiments.

 $K_S^0$  DECAY MODES

Mode	Fraction ( $\Gamma_i/\Gamma$ )	Scale factor/ Confidence level
<b>Hadronic modes</b>		
$\Gamma_1$ $\pi^0 \pi^0$	(30.69 ± 0.05) %	
$\Gamma_2$ $\pi^+ \pi^-$	(69.20 ± 0.05) %	
$\Gamma_3$ $\pi^+ \pi^- \pi^0$	( 3.5 $\pm$ 1.1 / -0.9 ) × 10 <sup>-7</sup>	
<b>Modes with photons or <math>\ell\bar{\ell}</math> pairs</b>		
$\Gamma_4$ $\pi^+ \pi^- \gamma$	[a,b] ( 1.79 ± 0.05 ) × 10 <sup>-3</sup>	
$\Gamma_5$ $\pi^+ \pi^- e^+ e^-$	( 4.79 ± 0.15 ) × 10 <sup>-5</sup>	
$\Gamma_6$ $\pi^0 \gamma \gamma$	[a] ( 4.9 ± 1.8 ) × 10 <sup>-8</sup>	
$\Gamma_7$ $\gamma \gamma$	( 2.63 ± 0.17 ) × 10 <sup>-6</sup>	S=3.0
<b>Semileptonic modes</b>		
$\Gamma_8$ $\pi^\pm e^\mp \nu_e$	[c] ( 7.04 ± 0.08 ) × 10 <sup>-4</sup>	
$\Gamma_9$ $\pi^\pm \mu^\mp \nu_\mu$	[c,d] ( 4.69 ± 0.05 ) × 10 <sup>-4</sup>	
<b>CP violating (CP) and <math>\Delta S = 1</math> weak neutral current (SI) modes</b>		
$\Gamma_{10}$ $3\pi^0$	CP < 1.2 × 10 <sup>-7</sup>	CL=90%
$\Gamma_{11}$ $\mu^+ \mu^-$	SI < 3.2 × 10 <sup>-7</sup>	CL=90%
$\Gamma_{12}$ $e^+ e^-$	SI < 9 × 10 <sup>-9</sup>	CL=90%
$\Gamma_{13}$ $\pi^0 e^+ e^-$	SI [a] ( 3.0 $\pm$ 1.5 / -1.2 ) × 10 <sup>-9</sup>	
$\Gamma_{14}$ $\pi^0 \mu^+ \mu^-$	SI ( 2.9 $\pm$ 1.5 / -1.2 ) × 10 <sup>-9</sup>	

[a] See the Particle Listings below for the energy limits used in this measurement.

[b] Most of this radiative mode, the low-momentum  $\gamma$  part, is also included in the parent mode listed without  $\gamma$ 's.

[c] The value is for the sum of the charge states or particle/antiparticle states indicated.

[d] Not a measurement. Calculated as  $0.666 \cdot B(\pi^\pm e^\mp \nu_e)$ .

## CONSTRAINED FIT INFORMATION

An overall fit to 4 branching ratios uses 5 measurements and one constraint to determine 4 parameters. The overall fit has a  $\chi^2 = 0.1$  for 2 degrees of freedom.

The following *off-diagonal* array elements are the correlation coefficients  $\langle \delta x_i \delta x_j \rangle / (\delta x_i \delta x_j)$ , in percent, from the fit to the branching fractions,  $x_i \equiv \Gamma_i / \Gamma_{\text{total}}$ . The fit constrains the  $x_i$  whose labels appear in this array to sum to one.

$x_2$	-100		
$x_8$	-6	3	
$x_9$	-6	3	100
	$x_1$	$x_2$	$x_8$

 $K_S^0$  DECAY RATES

$\Gamma(\pi^\pm e^\mp \nu_e)$   $\Gamma_8$

VALUE (10 <sup>6</sup> s <sup>-1</sup> )	EVTS	DOCUMENT ID	TECN	COMMENT
• • • We do not use the following data for averages, fits, limits, etc. • • •				
8.1 ± 1.6	75	<sup>11</sup> AKHMETSHIN 99	CMD2	Tagged $K_S^0 \rightarrow \pi e \nu_e$ using $\phi \rightarrow K_L^0 K_S^0$
7.50 ± 0.08		<sup>12</sup> PDG	98	
seen		BURGUN	72	HBC $K^+ p \rightarrow K^0 p \pi^+$
9.3 ± 2.5		AUBERT	65	HLBC $\Delta S = \Delta Q$ , CP cons. not assumed

<sup>11</sup> AKHMETSHIN 99 is from a measured branching ratio  $B(K_S^0 \rightarrow \pi e \nu_e) = (7.2 \pm 1.4) \times 10^{-4}$  and  $\tau_{K_S^0} = (0.8934 \pm 0.0008) \times 10^{-10}$  s. Not independent of measured branching ratio.

<sup>12</sup> PDG 98 from  $K_L^0$  measurements, assuming that  $\Delta S = \Delta Q$  in  $K^0$  decay so that  $\Gamma(K_S^0 \rightarrow \pi^\pm e^\mp \nu_e) = \Gamma(K_L^0 \rightarrow \pi^\pm e^\mp \nu_e)$ .

$\Gamma(\pi^\pm \mu^\mp \nu_\mu)$   $\Gamma_9$

VALUE (10 <sup>6</sup> s <sup>-1</sup> )	DOCUMENT ID
• • • We do not use the following data for averages, fits, limits, etc. • • •	
5.25 ± 0.07	<sup>13</sup> PDG 98
<sup>13</sup> PDG 98 from $K_L^0$ measurements, assuming that $\Delta S = \Delta Q$ in $K^0$ decay so that $\Gamma(K_S^0 \rightarrow \pi^\pm \mu^\mp \nu_\mu) = \Gamma(K_L^0 \rightarrow \pi^\pm \mu^\mp \nu_\mu)$ .	

 $K_S^0$  BRANCHING RATIOS

## Hadronic modes

$\Gamma(\pi^0 \pi^0) / \Gamma_{\text{total}}$	$\Gamma_1 / \Gamma$
0.3069 ± 0.0005 OUR FIT	
• • • We do not use the following data for averages, fits, limits, etc. • • •	
0.335 ± 0.014	1066 BROWN 63 HLBC
0.288 ± 0.021	198 CHRETIEN 63 HLBC
0.30 ± 0.035	BROWN 61 HLBC

$\Gamma(\pi^+ \pi^-) / \Gamma_{\text{total}}$   $\Gamma_2 / \Gamma$

VALUE	EVTS	DOCUMENT ID	TECN	COMMENT
• • • We do not use the following data for averages, fits, limits, etc. • • •				
0.670 ± 0.010	3447	DOYLE 69	HBC	$\pi^- p \rightarrow \Lambda K^0$

$\Gamma(\pi^+ \pi^-) / \Gamma(\pi^0 \pi^0)$   $\Gamma_2 / \Gamma_1$

VALUE	EVTS	DOCUMENT ID	TECN	COMMENT
• • • We do not use the following data for averages, fits, limits, etc. • • •				
2.255 ± 0.0012 ± 0.0054		<sup>15</sup> AMBROSINO 06c	KLOE	
2.236 ± 0.003 ± 0.015	766k	<sup>15</sup> ALOISIO 02b	KLOE	
2.11 ± 0.09	1315	EVERHART 76	WIRE	$\pi^- p \rightarrow \Lambda K^0$
2.169 ± 0.094	16k	COWELL 74	OSPK	$\pi^- p \rightarrow \Lambda K^0$
2.16 ± 0.08	4799	HILL 73	DBC	$K^+ d \rightarrow K^0 p p$
2.22 ± 0.10	3068	HBC 72	HBC	$K^+ p \rightarrow \pi^+ p K^0$
2.22 ± 0.08	6380	MORSE 72b	DBC	$K^+ n \rightarrow K^0 p$
2.10 ± 0.11	701	<sup>17</sup> NAGY 72	HLBC	$K^+ n \rightarrow K^0 p$
2.22 ± 0.095	6150	<sup>18</sup> BALTAY 71	HBC	$K p \rightarrow K^0 \text{ neutrals}$
2.282 ± 0.043	7944	<sup>19</sup> MOFFETT 70	OSPK	$K^+ n \rightarrow K^0 p$
2.12 ± 0.17	267	<sup>17</sup> BOZOKI 69	HLBC	
2.285 ± 0.055	3016	<sup>19</sup> GOBBI 69	OSPK	$K^+ n \rightarrow K^0 p$
2.10 ± 0.06	3700	MORFIN 69	HLBC	$K^+ n \rightarrow K^0 p$

<sup>14</sup> This result combines AMBROSINO 06c KLOE 2001-02 data with ALOISIO 02b KLOE 2000 data.  $K_S^0 \rightarrow \pi^+ \pi^-$  fully inclusive.

<sup>15</sup> Includes radiative decays  $\pi^+ \pi^- \gamma$ .

<sup>16</sup> The directly measured quantity is  $K_S^0 \rightarrow \pi^+ \pi^- / \text{all } K^0 = 0.345 \pm 0.005$ .

<sup>17</sup> NAGY 72 is a final result which includes BOZOKI 69.

<sup>18</sup> The directly measured quantity is  $K_S^0 \rightarrow \pi^+ \pi^- / \text{all } \bar{K}^0 = 0.345 \pm 0.005$ .

<sup>19</sup> MOFFETT 70 is a final result which includes GOBBI 69.

## Meson Particle Listings

 $K_S^0$ 

$\Gamma(\pi^+\pi^-\pi^0)/\Gamma_{\text{total}}$   $\Gamma_3/\Gamma$

VALUE (units  $10^{-7}$ ) EVTS DOCUMENT ID TECN COMMENT

**$3.5 \pm 0.5$  OUR AVERAGE**

4.7<sup>+2.2+1.7</sup><sub>-1.7-1.5</sub> 20 BATLEY 05 NA48  
 2.5<sup>+1.3+0.5</sup><sub>-1.0-0.6</sub> 500k 21 ADLER 97B CPLR  
 4.8<sup>+2.2</sup><sub>-1.6</sub>±1.1 22 ZOU 96 E621

••• We do not use the following data for averages, fits, limits, etc. •••

4.1<sup>+2.5+0.5</sup><sub>-1.9-0.6</sub> 23 ADLER 96E CPLR Sup. by ADLER 97B  
 3.9<sup>+5.4+0.9</sup><sub>-1.8-0.7</sub> 24 THOMSON 94 E621 Sup. by ZOU 96

20 BATLEY 05 is obtained by measuring the interference parameters in  $K_S, K_L \rightarrow \pi^+\pi^-\pi^0$ .  $\text{Re}(\lambda) = 0.038 \pm 0.008 \pm 0.006$  and  $\text{Im}(\lambda) = -0.013 \pm 0.005 \pm 0.004$ ; the correlation coeff. between  $\text{Re}(\lambda)$  and  $\text{Im}(\lambda)$  is 0.66 (statistical only).

21 ADLER 97B find the CP-conserving parameters  $\text{Re}(\lambda) = (28 \pm 7 \pm 3) \times 10^{-3}$ ,  $\text{Im}(\lambda) = (-10 \pm 8 \pm 2) \times 10^{-3}$ . They estimate  $B(K_S^0 \rightarrow \pi^+\pi^-\pi^0)$  from  $\text{Re}(\lambda)$  and the  $K_L^0$  decay parameters. See also ANGELOPOULOS 98c.

22 ZOU 96 is from the the measured quantities  $|\rho_{+-0}| = 0.039 \pm 0.009 \pm 0.005$  and  $\phi_\rho = (-9 \pm 18)^\circ$ .

23 ADLER 96E is from the measured quantities  $\text{Re}(\lambda) = 0.036 \pm 0.010 \pm 0.002$  and  $\text{Im}(\lambda) = -0.003$  consistent with zero. Note that the quantity  $\lambda$  is the same as  $\rho_{+-0}$  used in other footnotes.

24 THOMSON 94 calculates this branching ratio from their measurements  $|\rho_{+-0}| = 0.035 \pm 0.019 \pm 0.004$  and  $\phi_\rho = (-59 \pm 48)^\circ$  where  $|\rho_{+-0}| e^{i\phi_\rho} = A(K_S^0 \rightarrow \pi^+\pi^-\pi^0, I=2)/A(K_L^0 \rightarrow \pi^+\pi^-\pi^0)$ .

Modes with photons or  $\ell\bar{\ell}$  pairs

$\Gamma(\pi^+\pi^-\gamma)/\Gamma(\pi^+\pi^-)$   $\Gamma_4/\Gamma_2$

VALUE (units  $10^{-3}$ ) EVTS DOCUMENT ID TECN COMMENT

**$2.59 \pm 0.08$  OUR AVERAGE**

2.56±0.09 1286 RAMBERG 93 E731  $p_\gamma > 50$  MeV/c  
 2.68±0.15 25 TAUREG 76 SPEC  $p_\gamma > 50$  MeV/c

••• We do not use the following data for averages, fits, limits, etc. •••

7.10±0.22 3723 RAMBERG 93 E731  $p_\gamma > 20$  MeV/c  
 3.0 ± 0.6 29 BOBISUT 74 HLBC  $p_\gamma > 40$  MeV/c  
 2.8 ± 0.6 27 BURGUN 73 HBC  $p_\gamma > 50$  MeV/c

25 TAUREG 76 find direct emission contribution  $< 0.06$ , CL = 90%.

26 BOBISUT 74 not included in average because  $p_\gamma$  cut differs. Estimates direct emission contribution to be 0.5 or less, CL = 95%.

27 BURGUN 73 estimates that direct emission contribution is  $0.3 \pm 0.6$ .

$\Gamma(\pi^+\pi^-e^+e^-)/\Gamma_{\text{total}}$   $\Gamma_5/\Gamma$

VALUE (units  $10^{-5}$ ) EVTS DOCUMENT ID TECN COMMENT

**$4.79 \pm 0.15$  OUR AVERAGE**

4.83±0.11±0.14 23k 28 BATLEY 11 NA48 2002 data  
 4.69±0.30 676 29 LAI 03C NA48 1998+1999 data

••• We do not use the following data for averages, fits, limits, etc. •••

4.71±0.23±0.22 620 29,30 LAI 03C NA48 1999 data  
 4.5 ± 0.7 ± 0.4 56 LAI 00B NA48 1998 data

28 BATLEY 11 reports  $[\Gamma(K_S^0 \rightarrow \pi^+\pi^-e^+e^-)/\Gamma_{\text{total}}] / [B(K_L^0 \rightarrow \pi^+\pi^-\pi^0)] / [B(\pi^0 \rightarrow e^+e^-\gamma)] = (3.28 \pm 0.06 \pm 0.04) \times 10^{-2}$  which we multiply by our best values  $B(K_L^0 \rightarrow \pi^+\pi^-\pi^0) = (12.54 \pm 0.05) \times 10^{-2}$ ,  $B(\pi^0 \rightarrow e^+e^-\gamma) = (1.174 \pm 0.035) \times 10^{-2}$ . Our first error is their experiment's error and our second error is the systematic error from using our best values. Also a limit on the absolute value of the interference between bremsstrahlung and E1 transition is given:  $< 4 \times 10^{-7}$  at 90% CL.

29 Uses normalization  $\text{BR}(K_L \rightarrow \pi^+\pi^-\pi^0) \cdot \text{BR}(\pi^0 \rightarrow e^+e^-) = (1.505 \pm 0.047) \times 10^{-3}$  from our 2000 Edition.

30 Second error is  $0.16(\text{syst}) \pm 0.15(\text{norm})$  combined in quadrature.

$\Gamma(\pi^0\gamma\gamma)/\Gamma_{\text{total}}$   $\Gamma_6/\Gamma$

VALUE (units  $10^{-8}$ ) CL% EVTS DOCUMENT ID TECN COMMENT

**$4.9 \pm 1.6 \pm 0.9$**  17 31 LAI 04 NA48  $m_{\gamma\gamma}^2/m_K^2 > 0.2$

••• We do not use the following data for averages, fits, limits, etc. •••

<33 90 LAI 03B NA48  $m_{\gamma\gamma}^2/m_K^2 > 0.2$

31 Spectrum also measured and found consistent with the one generated by a constant matrix element.

$\Gamma(\gamma\gamma)/\Gamma_{\text{total}}$   $\Gamma_7/\Gamma$

VALUE (units  $10^{-6}$ ) CL% EVTS DOCUMENT ID TECN COMMENT

**$2.63 \pm 0.17$  OUR AVERAGE** Error includes scale factor of 3.0.

2.26 ± 0.12 ± 0.06 711 32 AMBROSINO 08c KLOE  $\phi \rightarrow K_S^0 K_L^0$

2.713±0.063±0.005 7.5k 33 LAI 03 NA48

••• We do not use the following data for averages, fits, limits, etc. •••

2.58 ± 0.36 ± 0.22 149 LAI 00 NA48

2.2 ± 1.1 16 34 BARR 95B NA31

2.4 ± 0.9 35 BARR 95B NA31

< 13 90 BALATS 89 SPEC

2.4 ± 1.2 19 BURKHARDT 87 NA31

<133 90 BARMIN 86B XEBC

32 AMBROSINO 08c reports  $(2.26 \pm 0.12 \pm 0.06) \times 10^{-6}$  from a measurement of  $[\Gamma(K_S^0 \rightarrow \gamma\gamma)/\Gamma_{\text{total}}] \times [B(K_S^0 \rightarrow \pi^0\pi^0)]$  assuming  $B(K_S^0 \rightarrow \pi^0\pi^0) = (30.69 \pm 0.05) \times 10^{-2}$ .

33 LAI 03 reports  $[\Gamma(K_S^0 \rightarrow \gamma\gamma)/\Gamma_{\text{total}}] / [B(K_S^0 \rightarrow \pi^0\pi^0)] = (8.84 \pm 0.18 \pm 0.10) \times 10^{-6}$  which we multiply by our best value  $B(K_S^0 \rightarrow \pi^0\pi^0) = (30.69 \pm 0.05) \times 10^{-2}$ . Our first error is their experiment's error and our second error is the systematic error from using our best value.

34 BARR 95B result is calculated using  $B(K_L \rightarrow \gamma\gamma) = (5.86 \pm 0.17) \times 10^{-4}$ .

35 BARR 95B quotes this as the combined BARR 95B + BURKHARDT 87 result after rescaling BURKHARDT 87 to use same branching ratios and lifetimes as BARR 95B.

## Semileptonic modes

$\Gamma(\pi^\pm e^\mp \nu_e)/\Gamma_{\text{total}}$   $\Gamma_8/\Gamma$

VALUE (units  $10^{-4}$ ) EVTS DOCUMENT ID TECN COMMENT

**$7.04 \pm 0.08$  OUR FIT**

**$7.04 \pm 0.08$  OUR AVERAGE**

7.046±0.18±0.16 36 BATLEY 07D NA48  $K^0(\bar{K}^0)(t) \rightarrow \pi e \nu$

6.91 ± 0.34 ± 0.15 624 37 ALOISIO 02 KLOE Tagged  $K_S^0$  using  $\phi \rightarrow K_L^0 K_S^0$

••• We use the following data for averages but not for fits. •••

7.05 ± 0.09 13k 38 AMBROSINO 06E KLOE Not fitted

••• We do not use the following data for averages, fits, limits, etc. •••

7.2 ± 1.4 75 AKHMETSHIN 99 CMD2 Tagged  $K_S^0$  using  $\phi \rightarrow K_L^0 K_S^0$

36 Reconstructed from  $K^0(\bar{K}^0)(t) \rightarrow \pi e \nu$  distributions using PDG values of  $B(K_L^0 \rightarrow \pi e \nu) = 0.4053 \pm 0.0015$ ,  $\tau_L = (5.114 \pm 0.021) \times 10^{-8}$  s and  $\tau_S = (0.8958 \pm 0.0005) \times 10^{-10}$  s.

37 Uses the PDG 00 value for  $B(K_S^0 \rightarrow \pi^+\pi^-)$ .

38 Obtained by imposing  $\Sigma_i B(K_S^0 \rightarrow i) = 1$ , where  $i$  runs over all the four branching ratios  $\pi^+\pi^-$ ,  $\pi^0\pi^0$ ,  $\pi e \nu$ , and  $\pi \mu \nu$ . Input value of  $B(K_S^0 \rightarrow \pi^+\pi^-) / B(K_S^0 \rightarrow \pi^0\pi^0)$  from AMBROSINO 06c is used. To derive  $\Gamma(K_S^0 \rightarrow \pi^+\mu\nu) / \Gamma(K_S^0 \rightarrow \pi^+e\nu)$ , lepton universality is assumed, radiative corrections from ANDRE 07 are used, and phase space integrals are taken from KTeV, ALEXOPOULOS 04A. This branching fraction enters our fit via their  $\Gamma(\pi^\pm e^\mp \nu_e) / \Gamma(\pi^+\pi^-)$  branching ratio measurement.

$\Gamma(\pi^\pm \mu^\mp \nu_\mu)/\Gamma_{\text{total}}$   $\Gamma_9/\Gamma$

The PDG 06 value below has not been measured but is computed to be 0.666 times the  $K_S \rightarrow \pi^\pm e^\mp \nu_e$  branching fraction. It is included in the fit that constrains the four branching ratios  $\pi^+\pi^-$ ,  $\pi^0\pi^0$ ,  $\pi e \nu$ , and  $\pi \mu \nu$  to sum to 1. This treatment, used by AMBROSINO 06E, is preferable to our previous practice of constraining the  $\pi^+\pi^-$  and  $\pi^0\pi^0$  modes to sum to 1. The 0.666 factor is obtained from AMBROSINO 06E and assumes lepton universality, radiative corrections from ANDRE 07, and phase space integrals from KTeV, ALEXOPOULOS 04A.

VALUE (units  $10^{-4}$ ) DOCUMENT ID COMMENT

**$4.69 \pm 0.06$  OUR FIT**

**$4.691 \pm 0.001 \pm 0.056$**  39 PDG 06 calculated from  $\pi^\pm e^\mp \nu_e$

39 The PDG 06 value is computed to be  $B_{\text{PDG06}}(\pi\mu\nu) = 0.666 B_{\text{FIT}}(\pi e\nu)$ . The first error specifies the arbitrarily small error,  $0.001 \times 10^{-4}$ , on  $B_{\text{PDG06}}(\pi\mu\nu)$  for fixed  $B_{\text{FIT}}(\pi e\nu)$ . The second error is that due to the uncertainty in  $B_{\text{FIT}}(\pi e\nu)$ .

$\Gamma(\pi^\pm e^\mp \nu_e)/\Gamma(\pi^+\pi^-)$   $\Gamma_8/\Gamma_2$

VALUE (units  $10^{-4}$ ) EVTS DOCUMENT ID TECN

**$10.18 \pm 0.12$  OUR FIT**

**$10.19 \pm 0.11 \pm 0.07$**  13k AMBROSINO 06E KLOE

CP violating (CP) and  $\Delta S = 1$  weak neutral current (S1) modes

$\Gamma(3\pi^0)/\Gamma_{\text{total}}$   $\Gamma_{10}/\Gamma$   
Violates CP conservation.

VALUE (units  $10^{-7}$ ) CL% EVTS DOCUMENT ID TECN

< 1.2 90 37.8M AMBROSINO 05B KLOE

••• We do not use the following data for averages, fits, limits, etc. •••

< 7.4 90 4.9M 40 LAI 05A NA48

<140 90 7M ACHASOV 99B SND

<190 90 17300 41 ANGELOPO... 98B CPLR

<370 90 BARMIN 83 HLBC

40 LAI 05A value is obtained from their bound on  $|\eta_{000}|$  (not assuming CPT) and  $B(K_L^0 \rightarrow 3\pi^0) = 0.211 \pm 0.003$ , and PDG 04 values for  $K_L^0$  and  $K_S^0$  lifetimes. If CPT is assumed then  $B(K_S^0 \rightarrow 3\pi^0)_{\text{CPT}} < 2.3 \times 10^{-7}$  at 90% CL

41 ANGELOPOULOS 98B is from  $\text{Im}(\eta_{000}) = -0.05 \pm 0.12 \pm 0.05$ , assuming  $\text{Re}(\eta_{000}) = \text{Re}(\epsilon) = 1.635 \times 10^{-3}$  and using the value  $B(K_L^0 \rightarrow \pi^0\pi^0\pi^0) = 0.2112 \pm 0.0027$ .

See key on page 457

## Meson Particle Listings

 $K_S^0$ 

$\Gamma(\mu^+ \mu^-)/\Gamma_{\text{total}}$   $\Gamma_{11}/\Gamma$   
 Test for  $\Delta S = 1$  weak neutral current. Allowed by first-order weak interaction combined with electromagnetic interaction.

VALUE (units $10^{-5}$ )	CL%	DOCUMENT ID	TECN
<b>&lt;0.032</b>	90	GJESDAL 73	ASPK
• • • We do not use the following data for averages, fits, limits, etc. • • •			
<0.7	90	HYAMS 69B	OSPK

$\Gamma(e^+ e^-)/\Gamma_{\text{total}}$   $\Gamma_{12}/\Gamma$   
 Test for  $\Delta S = 1$  weak neutral current. Allowed by first-order weak interaction combined with electromagnetic interaction.

VALUE (units $10^{-7}$ )	CL%	DOCUMENT ID	TECN	COMMENT
<b>&lt; 0.09</b>	90	42 AMBROSINO 09A	KLOE	$e^+ e^- \rightarrow \phi \rightarrow K_S^0 K_L^0$
• • • We do not use the following data for averages, fits, limits, etc. • • •				
< 1.4	90	ANGELOPO... 97	CPLR	
< 28	90	BLICK 94	CNTR	Hyperon facility
<100	90	BARMIN 86	XEBC	

<sup>42</sup>AMBROSINO 09A reports  $< 0.09 \times 10^{-7}$  from a measurement of  $[\Gamma(K_S^0 \rightarrow e^+ e^-)/\Gamma_{\text{total}}] / [B(K_S^0 \rightarrow \pi^+ \pi^-)]$  assuming  $B(K_S^0 \rightarrow \pi^+ \pi^-) = (69.20 \pm 0.05) \times 10^{-2}$ .

$\Gamma(\pi^0 e^+ e^-)/\Gamma_{\text{total}}$   $\Gamma_{13}/\Gamma$   
 Test for  $\Delta S = 1$  weak neutral current. Allowed by first-order weak interaction combined with electromagnetic interaction.

VALUE (units $10^{-9}$ )	CL%	EVTS	DOCUMENT ID	TECN	COMMENT
<b><math>3.0^{+1.5}_{-1.2} \pm 0.2</math></b>	7	43	BATLEY 03	NA48	$m_{ee} > 0.165$ GeV
• • • We do not use the following data for averages, fits, limits, etc. • • •					
< 140	90		LAI 01	NA48	
< 1100	90	0	BARR 93B	NA31	
<45000	90		GIBBONS 88	E731	

<sup>43</sup>BATLEY 03 extrapolate also to the full kinematical region using a constant form factor and a vector matrix element. The resulting branching ratio is  $(5.8^{+2.9}_{-2.4}) \times 10^{-9}$ .

$\Gamma(\pi^0 \mu^+ \mu^-)/\Gamma_{\text{total}}$   $\Gamma_{14}/\Gamma$   
 Test for  $\Delta S = 1$  weak neutral current. Allowed by first-order weak interaction combined with electromagnetic interaction.

VALUE (units $10^{-9}$ )	EVTS	DOCUMENT ID	TECN	COMMENT
<b><math>2.9^{+1.5}_{-0.2} \pm 0.2</math></b>	6	44	BATLEY 04A	NA48 NA48/1 $K_S^0$ beam
<sup>44</sup> Background estimate is $0.22^{+0.18}_{-0.11}$ events. Branching ratio assumes a vector matrix element and unit form factor.				

 $K_S^0$  FORM FACTORS

For discussion, see note on  $K_{e3}$  form factors in the  $K^\pm$  section of the Particle Listings above. Because the semileptonic branching fraction is smaller in  $K_S^0$  than  $K_L^0$  by the ratio of the mean lives, the  $K_S^0$  semileptonic form factor has so far been measured only in the  $K_{e3}$  mode using the linear expansion  $f_+(t) = f_+(0) (1 + \lambda_+ t / m_{\pi^\pm}^2)$ , which gives the vector form factor  $f_+(t)$  relative to its value at  $t = 0$ .

 $\lambda_+$  (LINEAR ENERGY DEPENDENCE OF  $f_+$  IN  $K_{e3}^0$  DECAY)

VALUE (units $10^{-2}$ )	EVTS	DOCUMENT ID	TECN
<b><math>3.39 \pm 0.41</math></b>	15k	AMBROSINO 06E	KLOE

CP VIOLATION IN  $K_S \rightarrow 3\pi$ 

Written 1996 by T. Nakada (Paul Scherrer Institute) and L. Wolfenstein (Carnegie-Mellon University).

The possible final states for the decay  $K^0 \rightarrow \pi^+ \pi^- \pi^0$  have isospin  $I = 0, 1, 2$ , and  $3$ . The  $I = 0$  and  $I = 2$  states have  $CP = +1$  and  $K_S$  can decay into them without violating  $CP$  symmetry, but they are expected to be strongly suppressed by centrifugal barrier effects. The  $I = 1$  and  $I = 3$  states, which have no centrifugal barrier, have  $CP = -1$  so that the  $K_S$  decay to these requires  $CP$  violation.

In order to see  $CP$  violation in  $K_S \rightarrow \pi^+ \pi^- \pi^0$ , it is necessary to observe the interference between  $K_S$  and  $K_L$  decay, which determines the amplitude ratio

$$\eta_{+-0} = \frac{A(K_S \rightarrow \pi^+ \pi^- \pi^0)}{A(K_L \rightarrow \pi^+ \pi^- \pi^0)}. \quad (1)$$

If  $\eta_{+-0}$  is obtained from an integration over the whole Dalitz plot, there is no contribution from the  $I = 0$  and  $I = 2$  final

states and a nonzero value of  $\eta_{+-0}$  is entirely due to  $CP$  violation.

Only  $I = 1$  and  $I = 3$  states, which are  $CP = -1$ , are allowed for  $K^0 \rightarrow \pi^0 \pi^0 \pi^0$  decays and the decay of  $K_S$  into  $3\pi^0$  is an unambiguous sign of  $CP$  violation. Similarly to  $\eta_{+-0}$ ,  $\eta_{000}$  is defined as

$$\eta_{000} = \frac{A(K_S \rightarrow \pi^0 \pi^0 \pi^0)}{A(K_L \rightarrow \pi^0 \pi^0 \pi^0)}. \quad (2)$$

If one assumes that  $CPT$  invariance holds and that there are no transitions to  $I = 3$  (or to nonsymmetric  $I = 1$  states), it can be shown that

$$\begin{aligned} \eta_{+-0} &= \eta_{000} \\ &= \epsilon + i \frac{\text{Im } a_1}{\text{Re } a_1}. \end{aligned} \quad (3)$$

With the Wu-Yang phase convention,  $a_1$  is the weak decay amplitude for  $K^0$  into  $I = 1$  final states;  $\epsilon$  is determined from  $CP$  violation in  $K_L \rightarrow 2\pi$  decays. The real parts of  $\eta_{+-0}$  and  $\eta_{000}$  are equal to  $\text{Re}(\epsilon)$ . Since currently-known upper limits on  $|\eta_{+-0}|$  and  $|\eta_{000}|$  are much larger than  $|\epsilon|$ , they can be interpreted as upper limits on  $\text{Im}(\eta_{+-0})$  and  $\text{Im}(\eta_{000})$  and so as limits on the  $CP$ -violating phase of the decay amplitude  $a_1$ .

CP-VIOLATION PARAMETERS IN  $K_S^0$  DECAY

$A_S = [\Gamma(K_S^0 \rightarrow \pi^- e^+ \nu_e) - \Gamma(K_S^0 \rightarrow \pi^+ e^- \bar{\nu}_e)] / \text{SUM}$   
 Such asymmetry violates  $CP$ . If  $CPT$  is assumed then  $A_S = 2 \text{Re}(\epsilon)$ .

VALUE (units $10^{-3}$ )	EVTS	DOCUMENT ID	TECN
<b><math>1.5 \pm 9.6 \pm 2.9</math></b>	13k	AMBROSINO 06E	KLOE

PARAMETERS FOR  $K_S^0 \rightarrow 3\pi$  DECAY

$\text{Im}(\eta_{+-0})^2 = \Gamma(K_S^0 \rightarrow \pi^+ \pi^- \pi^0, CP\text{-violating}) / \Gamma(K_L^0 \rightarrow \pi^+ \pi^- \pi^0)$   
 $CPT$  assumed valid (i.e.  $\text{Re}(\eta_{+-0}) \simeq 0$ ).

VALUE	CL%	EVTS	DOCUMENT ID	TECN
• • • We do not use the following data for averages, fits, limits, etc. • • •				
<0.23	90	601	45 BARMIN 85	HLBC
<0.12	90	384	METCALF 72	ASPK

<sup>45</sup>BARMIN 85 find  $\text{Re}(\eta_{+-0}) = (0.05 \pm 0.17)$  and  $\text{Im}(\eta_{+-0}) = (0.15 \pm 0.33)$ . Includes events of BALDO-CEOLIN 75.

$\text{Im}(\eta_{+-0}) = \text{Im}(A(K_S^0 \rightarrow \pi^+ \pi^- \pi^0, CP\text{-violating}) / A(K_L^0 \rightarrow \pi^+ \pi^- \pi^0))$

VALUE	EVTS	DOCUMENT ID	TECN	COMMENT
<b><math>-0.002 \pm 0.009 \pm 0.001</math></b>	500k	46 ADLER 97B	CPLR	

• • • We do not use the following data for averages, fits, limits, etc. • • •

$-0.002 \pm 0.018 \pm 0.003$	137k	47 ADLER 96D	CPLR	Sup. by ADLER 97B
$-0.015 \pm 0.017 \pm 0.025$	272k	48 ZOU 94	SPEC	

<sup>46</sup>ADLER 97B also find  $\text{Re}(\eta_{+-0}) = -0.002 \pm 0.007^{+0.004}_{-0.001}$ . See also ANGELOPOULOS 98c.

<sup>47</sup>The ADLER 96D fit also yields  $\text{Re}(\eta_{+-0}) = 0.006 \pm 0.013 \pm 0.001$  with a correlation +0.66 between real and imaginary parts. Their results correspond to  $|\eta_{+-0}| < 0.037$  with 90% CL.

<sup>48</sup>ZOU 94 use theoretical constraint  $\text{Re}(\eta_{+-0}) = \text{Re}(\epsilon) = 0.0016$ . Without this constraint they find  $\text{Im}(\eta_{+-0}) = 0.019 \pm 0.061$  and  $\text{Re}(\eta_{+-0}) = 0.019 \pm 0.027$ .

$\text{Im}(\eta_{000})^2 = \Gamma(K_S^0 \rightarrow 3\pi^0) / \Gamma(K_L^0 \rightarrow 3\pi^0)$

$CPT$  assumed valid (i.e.  $\text{Re}(\eta_{000}) \simeq 0$ ). This limit determines branching ratio  $\Gamma(3\pi^0)/\Gamma_{\text{total}}$  above.

VALUE	CL%	EVTS	DOCUMENT ID	TECN	COMMENT
• • • We do not use the following data for averages, fits, limits, etc. • • •					
<0.1	90	632	49 BARMIN 83	HLBC	
<0.28	90	50	GJESDAL 74B	SPEC	Indirect meas.

<sup>49</sup>BARMIN 83 find  $\text{Re}(\eta_{000}) = (-0.08 \pm 0.18)$  and  $\text{Im}(\eta_{000}) = (-0.05 \pm 0.27)$ . Assuming  $CPT$  invariance they obtain the limit quoted above.

<sup>50</sup>GJESDAL 74B uses  $K_{2\pi}$ ,  $K_{\mu 3}$ , and  $K_{e3}$  decay results, unitarity, and  $CPT$ . Calculates  $|\langle \eta_{000} \rangle| = 0.26 \pm 0.20$ . We convert to upper limit.



See key on page 457

- <sup>1</sup> The two ABOUZAID 11 values use the same data. The first enters the "assuming  $CPT$ " fit and the second enters the "not assuming  $CPT$ " fit.
- <sup>2</sup> ABOUZAID 11 fit has  $\Delta m$ ,  $\tau_S$ ,  $\phi_\epsilon$ ,  $\text{Re}(\epsilon'/\epsilon)$ , and  $\text{Im}(\epsilon'/\epsilon)$  as free parameters. See  $\text{Im}(\epsilon'/\epsilon)$  in the " $K_L^0$  CP violation" section for correlation information.
- <sup>3</sup> ABOUZAID 11 fit has  $\Delta m$  and  $\tau_S$  free but constrains  $\phi_\epsilon$  to the Superweak value, i.e. assumes  $CP T$ . See " $K_L^0$  Mean Life" section for correlation information.
- <sup>4</sup> Fits  $\Delta m$  and  $\phi_{+-}$  simultaneously. GIBBONS 93c systematic error is from B. Winstein via private communication. 20–160 GeV  $K$  beams.
- <sup>5</sup> GIBBONS 93 value assume  $\phi_{+-} = \phi_{00} = \phi_{SW} = (43.7 \pm 0.2)^\circ$ , i.e. assumes  $CP T$ . 20–160 GeV  $K$  beams.
- <sup>6</sup> These two experiments have a common systematic error due to the uncertainty in the momentum scale, as pointed out in WAHL 89.
- <sup>7</sup> GJESDAL 74 uses charge asymmetry in  $K_{S3}^0$  decays.
- <sup>8</sup> ALAVI-HARATI 03 fit  $\Delta m$  and  $\tau_{K_S^0}$  simultaneously.  $\phi_{+-}$  is constrained to the Superweak value, i.e.  $CP T$  is assumed. See " $K_L^0$  Mean Life" section for correlation information. Superseded by ABOUZAID 11.
- <sup>9</sup> ALAVI-HARATI 03 fit  $\Delta m$ ,  $\phi_{+-}$ , and  $\tau_{K_S}$  simultaneously. See  $\phi_{+-}$  in the " $K_L$  CP violation" section for correlation information. Superseded by ABOUZAID 11.
- <sup>10</sup> ANGELOPOULOS 01 uses strong interactions strangeness tagging at two different times.
- <sup>11</sup> Uses  $K_{e3}^0$  and  $K_{\mu 3}^0$  strangeness tagging at production and decay. Assumes  $CP T$  conservation on  $\Delta S = -\Delta Q$  transitions.
- <sup>12</sup> ADLER 96c is the result of a fit which includes nearly the same data as entered into the "OUR FIT" value above.
- <sup>13</sup> ARONSON 82 find that  $\Delta m$  may depend on the kaon energy
- <sup>14</sup> ARONSON 70 and CARNEGIE 71 use  $K_S^0$  mean life =  $(0.862 \pm 0.006) \times 10^{-10}$  s. We have not attempted to adjust these values for the subsequent change in the  $K_S^0$  mean life or in  $\eta_{+-}$ .

 $K_L^0$  MEAN LIFE

VALUE ( $10^{-8}$ s)	EVTS	DOCUMENT ID	TECN	COMMENT		
<b>5.116 ± 0.021 OUR FIT</b>	Error	includes scale factor of 1.1.				
<b>5.099 ± 0.021 OUR AVERAGE</b>						
5.072 ± 0.011 ± 0.035	13M	1 AMBROSINO 06	KLOE	$\sum_i B_i = 1$		
5.092 ± 0.017 ± 0.025	15M	AMBROSINO 05c	KLOE			
5.154 ± 0.044	0.4M	VOSBURGH 72	CNTR			
• • •		We do not use the following data for averages, fits, limits, etc. • • •				
5.15 ± 0.14		DEVLIN 67	CNTR			
<sup>1</sup> AMBROSINO 06 uses $\phi \rightarrow K_L K_S$ with $K_L$ tagged by $K_S \rightarrow \pi^+ \pi^-$ . The four major $K_L$ BR's are measured, the small remainder ( $\pi^+ \pi^-, \pi^0 \pi^0, \gamma \gamma$ ) is taken from PDG 04. This KLOE $K_L$ lifetime is obtained by imposing $\sum_i B_i = 1$ . The correlation matrix among the four measured $K_L$ BR's and this $K_L$ lifetime is						
	$K_{e3}$	$K_{\mu 3}$	$3\pi^0$	$\pi^+ \pi^- \pi^0$	$\tau_{K_L}$	
	$K_{e3}$	1	-0.25	-0.56	-0.07	0.25
	$K_{\mu 3}$		1	-0.43	-0.20	0.33
	$3\pi^0$			1	-0.39	-0.21
	$\pi^+ \pi^- \pi^0$				1	-0.39
	$\tau_{K_L}$					1

These correlations are taken into account in our fit. The average of this KLOE mean life measurement and the independent KLOE measurement in AMBROSINO 05c is  $(5.084 \pm 0.023) \times 10^{-8}$  s.

 $K_L^0$  DECAY MODES

Mode	Fraction ( $\Gamma_i/\Gamma$ )	Scale factor/ Confidence level
<b>Semileptonic modes</b>		
$\Gamma_1$ $\pi^\pm e^\mp \nu_e$ Called $K_{e3}^0$ .	[a] (40.55 ± 0.11) %	S=1.7
$\Gamma_2$ $\pi^\pm \mu^\mp \nu_\mu$ Called $K_{\mu 3}^0$ .	[a] (27.04 ± 0.07) %	S=1.1
$\Gamma_3$ $(\pi \mu \text{atom}) \nu$	(1.05 ± 0.11) × 10 <sup>-7</sup>	
$\Gamma_4$ $\pi^0 \pi^\pm e^\mp \nu$	[a] (5.20 ± 0.11) × 10 <sup>-5</sup>	
$\Gamma_5$ $\pi^\pm e^\mp \nu e^+ e^-$	[a] (1.26 ± 0.04) × 10 <sup>-5</sup>	
<b>Hadronic modes, including Charge conjugation × Parity Violating (CPV) modes</b>		
$\Gamma_6$ $3\pi^0$	(19.52 ± 0.12) %	S=1.6
$\Gamma_7$ $\pi^+ \pi^- \pi^0$	(12.54 ± 0.05) %	
$\Gamma_8$ $\pi^+ \pi^-$	CPV [b] (1.967 ± 0.010) × 10 <sup>-3</sup>	S=1.5
$\Gamma_9$ $\pi^0 \pi^0$	CPV (8.64 ± 0.06) × 10 <sup>-4</sup>	S=1.8
<b>Semileptonic modes with photons</b>		
$\Gamma_{10}$ $\pi^\pm e^\mp \nu_e \gamma$	[a,c,d] (3.79 ± 0.06) × 10 <sup>-3</sup>	
$\Gamma_{11}$ $\pi^\pm \mu^\mp \nu_\mu \gamma$	(5.65 ± 0.23) × 10 <sup>-4</sup>	
<b>Hadronic modes with photons or <math>\ell\bar{\ell}</math> pairs</b>		
$\Gamma_{12}$ $\pi^0 \pi^0 \gamma$	< 2.43 × 10 <sup>-7</sup>	CL=90%
$\Gamma_{13}$ $\pi^+ \pi^- \gamma$	[c,d] (4.15 ± 0.15) × 10 <sup>-5</sup>	S=2.8
$\Gamma_{14}$ $\pi^+ \pi^- \gamma$ (DE)	(2.84 ± 0.11) × 10 <sup>-5</sup>	S=2.0
$\Gamma_{15}$ $\pi^0 2\gamma$	[c] (1.273 ± 0.033) × 10 <sup>-6</sup>	
$\Gamma_{16}$ $\pi^0 \gamma e^+ e^-$	(1.62 ± 0.17) × 10 <sup>-8</sup>	

Other modes with photons or  $\ell\bar{\ell}$  pairs

$\Gamma_{17}$ $2\gamma$	(5.47 ± 0.04) × 10 <sup>-4</sup>	S=1.1
$\Gamma_{18}$ $3\gamma$	< 7.4 × 10 <sup>-8</sup>	CL=90%
$\Gamma_{19}$ $e^+ e^- \gamma$	(9.4 ± 0.4) × 10 <sup>-6</sup>	S=2.0
$\Gamma_{20}$ $\mu^+ \mu^- \gamma$	(3.59 ± 0.11) × 10 <sup>-7</sup>	S=1.3
$\Gamma_{21}$ $e^+ e^- \gamma \gamma$	[c] (5.95 ± 0.33) × 10 <sup>-7</sup>	
$\Gamma_{22}$ $\mu^+ \mu^- \gamma \gamma$	[c] (1.0 ± 0.6) × 10 <sup>-8</sup>	

Charge conjugation × Parity (CP) or Lepton Family number (LF) violating modes, or  $\Delta S = 1$  weak neutral current (SI) modes

$\Gamma_{23}$ $\mu^+ \mu^-$	SI (6.84 ± 0.11) × 10 <sup>-9</sup>	
$\Gamma_{24}$ $e^+ e^-$	SI (9 ± 6) × 10 <sup>-12</sup>	
$\Gamma_{25}$ $\pi^+ \pi^- e^+ e^-$	SI [c] (3.11 ± 0.19) × 10 <sup>-7</sup>	
$\Gamma_{26}$ $\pi^0 \pi^0 e^+ e^-$	SI < 6.6 × 10 <sup>-9</sup>	CL=90%
$\Gamma_{27}$ $\pi^0 \pi^0 \mu^+ \mu^-$	SI < 9.2 × 10 <sup>-11</sup>	CL=90%
$\Gamma_{28}$ $\mu^+ \mu^- e^+ e^-$	SI (2.69 ± 0.27) × 10 <sup>-9</sup>	
$\Gamma_{29}$ $e^+ e^- e^+ e^-$	SI (3.56 ± 0.21) × 10 <sup>-8</sup>	
$\Gamma_{30}$ $\pi^0 \mu^+ \mu^-$	CP,SI [e] < 3.8 × 10 <sup>-10</sup>	CL=90%
$\Gamma_{31}$ $\pi^0 e^+ e^-$	CP,SI [e] < 2.8 × 10 <sup>-10</sup>	CL=90%
$\Gamma_{32}$ $\pi^0 \nu \bar{\nu}$	CP,SI [f] < 2.6 × 10 <sup>-8</sup>	CL=90%
$\Gamma_{33}$ $\pi^0 \pi^0 \nu \bar{\nu}$	SI < 8.1 × 10 <sup>-7</sup>	CL=90%
$\Gamma_{34}$ $e^\pm \mu^\mp$	LF [a] < 4.7 × 10 <sup>-12</sup>	CL=90%
$\Gamma_{35}$ $e^\pm e^\pm \mu^\mp \mu^\mp$	LF [a] < 4.12 × 10 <sup>-11</sup>	CL=90%
$\Gamma_{36}$ $\pi^0 \mu^\pm e^\mp$	LF [a] < 7.6 × 10 <sup>-11</sup>	CL=90%
$\Gamma_{37}$ $\pi^0 \pi^0 \mu^\pm e^\mp$	LF < 1.7 × 10 <sup>-10</sup>	CL=90%

[a] The value is for the sum of the charge states or particle/antiparticle states indicated.

[b] This mode includes gammas from inner bremsstrahlung but not the direct emission mode  $K_L^0 \rightarrow \pi^+ \pi^- \gamma$  (DE).

[c] See the Particle Listings below for the energy limits used in this measurement.

[d] Most of this radiative mode, the low-momentum  $\gamma$  part, is also included in the parent mode listed without  $\gamma$ 's.

[e] Allowed by higher-order electroweak interactions.

[f] Violates  $CP$  in leading order. Test of direct  $CP$  violation since the indirect  $CP$ -violating and  $CP$ -conserving contributions are expected to be suppressed.

## CONSTRAINED FIT INFORMATION

An overall fit to the mean life and 15 branching ratios uses 27 measurements and one constraint to determine 11 parameters. The overall fit has a  $\chi^2 = 37.4$  for 17 degrees of freedom.

The following *off-diagonal* array elements are the correlation coefficients  $\langle \delta p_i \delta p_j \rangle / (\delta p_i \delta p_j)$ , in percent, from the fit to parameters  $p_i$ , including the branching fractions,  $x_i \equiv \Gamma_i / \Gamma_{\text{total}}$ . The fit constrains the  $x_i$  whose labels appear in this array to sum to one.

$x_2$	-21									
$x_6$	-77	-29								
$x_7$	-15	-20	-18							
$x_8$	53	-11	-47	4						
$x_9$	30	-23	-11	-12	64					
$x_{13}$	6	-1	-6	0	12	8				
$x_{14}$	6	-1	-6	0	11	7	93			
$x_{17}$	-46	-22	64	-14	-21	8	-3	-3		
$x_{19}$	-5	-2	7	-1	-3	-1	0	0	4	
$\Gamma$	-27	-9	24	15	-13	-6	-2	-2	15	2
	$x_1$	$x_2$	$x_6$	$x_7$	$x_8$	$x_9$	$x_{13}$	$x_{14}$	$x_{17}$	$x_{19}$

Mode	Rate ( $10^8 \text{ s}^{-1}$ )	Scale factor
$\Gamma_1$ $\pi^\pm e^\mp \nu_e$ Called $K_{e3}^0$ .	[a] 0.07927 ± 0.00034	1.1
$\Gamma_2$ $\pi^\pm \mu^\mp \nu_\mu$ Called $K_{\mu 3}^0$ .	[a] 0.05286 ± 0.00025	1.1

## Meson Particle Listings

 $K_L^0$ 

$\Gamma_6$	$3\pi^0$	$0.03815 \pm 0.00030$	1.5
$\Gamma_7$	$\pi^+\pi^-\pi^0$	$0.02451 \pm 0.00015$	
$\Gamma_8$	$\pi^+\pi^-$	$[b](3.844 \pm 0.023) \times 10^{-4}$	1.2
$\Gamma_9$	$\pi^0\pi^0$	$(1.690 \pm 0.013) \times 10^{-4}$	1.4
$\Gamma_{13}$	$\pi^+\pi^-\gamma$	$[c,d](8.11 \pm 0.29) \times 10^{-6}$	2.7
$\Gamma_{14}$	$\pi^+\pi^-\gamma(\text{DE})$	$(5.55 \pm 0.21) \times 10^{-6}$	2.0
$\Gamma_{17}$	$2\gamma$	$(1.069 \pm 0.010) \times 10^{-4}$	1.2
$\Gamma_{19}$	$e^+e^-\gamma$	$(1.84 \pm 0.08) \times 10^{-6}$	1.9

 $K_L^0$  DECAY RATES

$\Gamma(\pi^+\pi^-\pi^0)$		$\Gamma_7$		
VALUE ( $10^6 \text{ s}^{-1}$ )	EVTS	DOCUMENT ID	TECN	COMMENT
<b><math>2.451 \pm 0.015</math> OUR FIT</b>				
••• We do not use the following data for averages, fits, limits, etc. •••				
$2.32^{+0.13}_{-0.15}$	192	BALDO...	75 HLBC	Assumes CP
$2.35 \pm 0.20$	180	<sup>1</sup> JAMES	72 HBC	Assumes CP
$2.71 \pm 0.28$	99	CHO	71 DBC	Assumes CP
$2.5 \pm 0.3$	98	<sup>1</sup> JAMES	71 HBC	Assumes CP
$2.12 \pm 0.33$	50	MEISNER	71 HBC	Assumes CP
$2.20 \pm 0.35$	53	WEBBER	70 HBC	Assumes CP
$2.62^{+0.28}_{-0.27}$	136	BEHR	66 HLBC	Assumes CP
$3.26 \pm 0.77$	18	ANDERSON	65 HBC	
$1.4 \pm 0.4$	14	FRANZINI	65 HBC	

<sup>1</sup> JAMES 72 is a final measurement and includes JAMES 71.

$\Gamma(\pi^+e^-\nu_e)$		$\Gamma_1$		
VALUE ( $10^6 \text{ s}^{-1}$ )	EVTS	DOCUMENT ID	TECN	COMMENT
<b><math>7.927 \pm 0.034</math> OUR FIT</b>				Error includes scale factor of 1.1.
••• We do not use the following data for averages, fits, limits, etc. •••				
$7.81 \pm 0.56$	620	CHAN	71 HBC	
$7.52^{+0.85}_{-0.72}$		AUBERT	65 HLBC	$\Delta S = \Delta Q$ , CP assumed

$\Gamma(\pi^+e^-\nu_e) + \Gamma(\pi^+\mu^-\nu_\mu)$		$(\Gamma_1 + \Gamma_2)$		
VALUE ( $10^6 \text{ s}^{-1}$ )	EVTS	DOCUMENT ID	TECN	COMMENT
<b><math>13.21 \pm 0.05</math> OUR FIT</b>				
••• We do not use the following data for averages, fits, limits, etc. •••				
$12.4 \pm 0.7$	410	<sup>1</sup> BURGUN	72 HBC	$K^+p \rightarrow K^0p\pi^+$
$8.47 \pm 1.69$	126	<sup>1</sup> MANN	72 HBC	$K^-\rho \rightarrow \pi^0 K^0$
$13.1 \pm 1.3$	252	<sup>1</sup> WEBBER	71 HBC	$K^-\rho \rightarrow \pi^0 K^0$
$11.6 \pm 0.9$	393	<sup>1,2</sup> CHO	70 DBC	$K^+n \rightarrow K^0p$
$10.3 \pm 0.8$	335	<sup>2</sup> HILL	67 DBC	$K^+n \rightarrow K^0p$
$9.85^{+1.15}_{-1.05}$	109	<sup>1</sup> FRANZINI	65 HBC	

<sup>1</sup> Assumes  $\Delta S = \Delta Q$  rule.<sup>2</sup> CHO 70 includes events of HILL 67. $K_L^0$  BRANCHING RATIOS

## Semileptonic modes

$\Gamma(\pi^+e^-\nu_e)/\Gamma_{\text{total}}$		$\Gamma_1/\Gamma$		
VALUE	EVTS	DOCUMENT ID	TECN	COMMENT
<b><math>0.4055 \pm 0.0011</math> OUR FIT</b>				Error includes scale factor of 1.7.
<b><math>0.4047 \pm 0.0028</math> OUR AVERAGE</b>				Error includes scale factor of 3.1.
$0.4007 \pm 0.0005 \pm 0.0015$	13M	<sup>1</sup> AMBROSINO 06	KLOE	Not fitted
$0.4067 \pm 0.0011$		<sup>2</sup> ALEXOPOU... 04	KTEV	Not fitted

<sup>1</sup> There are correlations between these five KLOE measurements:  $B(K_L \rightarrow \pi e \nu)$ ,  $B(K_L \rightarrow \pi \mu \nu)$ ,  $B(K_L \rightarrow 3\pi^0)$ ,  $B(K_L \rightarrow \pi^+\pi^-\pi^0)$ , and  $\tau_{K_L}$  measured in AMBROSINO 06. See the footnote for the  $\tau_{K_L}$  measurement for the correlation matrix.<sup>2</sup> ALEXOPOULOS 04 constrains  $\sum_i B_i = 0.9993$  for the six major  $K_L$  branching fractions. The correlations among these branching fractions are taken into account in our fit. The correlation matrix is

	$K_{e3}$	$K_{\mu 3}$	$3\pi^0$	$\pi^+\pi^-\pi^0$	$\pi^+\pi^-$	$\pi^0\pi^0$
$K_{e3}$	1					
$K_{\mu 3}$	0.15	1				
$3\pi^0$	-0.77	-0.62	1			
$\pi^+\pi^-\pi^0$	0.18	0.08	-0.54	1		
$\pi^+\pi^-$	0.28	0.22	-0.48	0.49	1	
$\pi^0\pi^0$	-0.72	-0.54	0.89	-0.46	-0.39	1

$\Gamma(\pi^+\mu^-\nu_\mu)/\Gamma_{\text{total}}$		$\Gamma_2/\Gamma$		
VALUE	EVTS	DOCUMENT ID	TECN	COMMENT
<b><math>0.2704 \pm 0.0007</math> OUR FIT</b>				Error includes scale factor of 1.1.
<b><math>0.2700 \pm 0.0008</math> OUR AVERAGE</b>				
$0.2698 \pm 0.0005 \pm 0.0015$	13M	<sup>1</sup> AMBROSINO 06	KLOE	
$0.2701 \pm 0.0009$		<sup>2</sup> ALEXOPOU... 04	KTEV	

<sup>1</sup> There are correlations between these five KLOE measurements:  $B(K_L \rightarrow \pi e \nu)$ ,  $B(K_L \rightarrow \pi \mu \nu)$ ,  $B(K_L \rightarrow 3\pi^0)$ ,  $B(K_L \rightarrow \pi^+\pi^-\pi^0)$ , and  $\tau_{K_L}$  measured in AMBROSINO 06. See the footnote for the  $\tau_{K_L}$  measurement for the correlation matrix.<sup>2</sup> For correlations with other ALEXOPOULOS 04 measurements, see the footnote with their  $B(K_L \rightarrow \pi e \nu)$  measurement.

$[\Gamma(\pi^+e^-\nu_e) + \Gamma(\pi^+\mu^-\nu_\mu)]/\Gamma_{\text{total}}$		$(\Gamma_1 + \Gamma_2)/\Gamma$		
VALUE	EVTS	DOCUMENT ID	TECN	COMMENT
<b><math>0.6760 \pm 0.0012</math> OUR FIT</b>				Error includes scale factor of 1.6.

$\Gamma(\pi^+\mu^-\nu_\mu)/\Gamma(\pi^+e^-\nu_e)$		$\Gamma_2/\Gamma_1$		
VALUE	EVTS	DOCUMENT ID	TECN	COMMENT
<b><math>0.6669 \pm 0.0027</math> OUR FIT</b>				Error includes scale factor of 1.2.
<b><math>0.666 \pm 0.004</math> OUR AVERAGE</b>				Error includes scale factor of 1.6.
••• We use the following data for averages but not for fits. •••				
$0.6740 \pm 0.0059$	13M	<sup>1</sup> AMBROSINO 06	KLOE	Not in fit
$0.6640 \pm 0.0014 \pm 0.0022$	394K	<sup>2</sup> ALEXOPOU... 04	KTEV	Not in fit
••• We do not use the following data for averages, fits, limits, etc. •••				
$0.702 \pm 0.011$	33k	CHO	80 HBC	
$0.662 \pm 0.037$	10k	WILLIAMS	74 ASPK	
$0.741 \pm 0.044$	6700	BRANDENB...	73 HBC	
$0.662 \pm 0.030$	1309	EVANS	73 HLBC	
$0.68 \pm 0.08$	3548	BASILE	70 OSPK	
$0.71 \pm 0.05$	770	BUDAGOV	68 HLBC	

<sup>1</sup> AMBROSINO 06 enters the fit via their separate measurements of these two modes.<sup>2</sup> ALEXOPOULOS 04 enters the fit via their separate measurements of these two modes.

$\Gamma((\pi\mu\text{atom})\nu)/\Gamma(\pi^+\mu^-\nu_\mu)$		$\Gamma_3/\Gamma_2$		
VALUE (units $10^{-7}$ )	EVTS	DOCUMENT ID	TECN	COMMENT
<b><math>3.90 \pm 0.39</math></b>	155	<sup>1</sup> ARONSON 86	SPEC	
••• We do not use the following data for averages, fits, limits, etc. •••				
seen	18	COOMBES	76 WIRE	
<sup>1</sup> ARONSON 86 quote theoretical value of $(4.31 \pm 0.08) \times 10^{-7}$ .				

$\Gamma(\pi^0\pi^\pm e^\mp \nu)/\Gamma_{\text{total}}$		$\Gamma_4/\Gamma$		
VALUE (units $10^{-5}$ )	CL% EVTS	DOCUMENT ID	TECN	COMMENT
<b><math>5.20 \pm 0.11</math> OUR AVERAGE</b>				
$5.21 \pm 0.07 \pm 0.09$	5402	BATLEY	04 NA48	
$5.16 \pm 0.20 \pm 0.22$	729	MAKOFF	93 E731	
••• We do not use the following data for averages, fits, limits, etc. •••				
$6.2 \pm 2.0$	16	CARROLL	80c SPEC	
$< 220$	90	<sup>1</sup> DONALDSON 74	SPEC	
<sup>1</sup> DONALDSON 74 uses $K_L^0 \rightarrow \pi^+\pi^-\pi^0$ (all $K_L^0$ ) decays = 0.126.				

$\Gamma(\pi^\pm e^\mp \nu e^\pm)/\Gamma(\pi^+\pi^-\pi^0)$		$\Gamma_5/\Gamma_7$		
VALUE (units $10^{-5}$ )	EVTS	DOCUMENT ID	TECN	COMMENT
<b><math>10.02 \pm 0.17 \pm 0.29</math></b>	19k	<sup>1</sup> ABOUZAID 07c	KTEV	$M_{ee} > 5 \text{ MeV}$ , $E_{ee}^* > 30 \text{ MeV}$
<sup>1</sup> $E_{ee}^*$ is the energy of the $e^+e^-$ pair in the kaon rest frame. ABOUZAID 07c reports $[\Gamma(K_L^0 \rightarrow \pi^\pm e^\mp \nu e^\pm)/\Gamma(K_L^0 \rightarrow \pi^+\pi^-\pi^0)] / [B(\pi^0 \rightarrow e^+e^-\gamma)] = (8.54 \pm 0.07 \pm 0.13) \times 10^{-3}$ which we multiply by our best value $B(\pi^0 \rightarrow e^+e^-\gamma) = (1.174 \pm 0.035) \times 10^{-2}$ . Our first error is their experiment's error and our second error is the systematic error from using our best value.				

## Hadronic modes,

including Charge conjugation×Parity Violating (CPV) modes

$\Gamma(3\pi^0)/\Gamma_{\text{total}}$		$\Gamma_6/\Gamma$		
VALUE	EVTS	DOCUMENT ID	TECN	COMMENT
<b><math>0.1952 \pm 0.0012</math> OUR FIT</b>				Error includes scale factor of 1.6.
<b><math>0.1969 \pm 0.0026</math> OUR AVERAGE</b>				Error includes scale factor of 2.0.
••• We use the following data for averages but not for fits. •••				
$0.1997 \pm 0.0003 \pm 0.0019$	13M	<sup>1</sup> AMBROSINO 06	KLOE	Not fitted
$0.1945 \pm 0.0018$		<sup>1</sup> ALEXOPOU... 04	KTEV	Not fitted

<sup>1</sup> We exclude these  $B(K_L \rightarrow 3\pi^0)$  measurements from our fit because the authors have constrained  $K_L$  branching fractions to sum to one. It enters our fit via the other measurements from the experiment and their correlations, along with our constraint that the fitted branching fractions sum to one.

$\Gamma(3\pi^0)/\Gamma(\pi^+e^-\nu_e)$		$\Gamma_6/\Gamma_1$		
VALUE	EVTS	DOCUMENT ID	TECN	COMMENT
<b><math>0.481 \pm 0.004</math> OUR FIT</b>				Error includes scale factor of 1.8.
••• We use the following data for averages but not for fits. •••				
<b><math>0.4782 \pm 0.0014 \pm 0.0053</math></b>	209K	<sup>1</sup> ALEXOPOU... 04	KTEV	Not in fit
••• We do not use the following data for averages, fits, limits, etc. •••				
$0.545 \pm 0.004 \pm 0.009$	38k	KREUTZ	95 NA31	

<sup>1</sup> This measurement enters the fit via their separate measurements of these two modes.

$\Gamma(3\pi^0)/[\Gamma(\pi^+e^-\nu_e) + \Gamma(\pi^+\mu^-\nu_\mu) + \Gamma(\pi^+\pi^-\pi^0)]$		$\Gamma_6/(\Gamma_1 + \Gamma_2 + \Gamma_7)$		
VALUE	EVTS	DOCUMENT ID	TECN	COMMENT
<b><math>0.2436 \pm 0.0018</math> OUR FIT</b>				Error includes scale factor of 1.6.
••• We do not use the following data for averages, fits, limits, etc. •••				
$0.251 \pm 0.014$	549	BUDAGOV	68 HLBC	ORSAY meas.
$0.277 \pm 0.021$	444	BUDAGOV	68 HLBC	Ecole polytec.meas
$0.31^{+0.07}_{-0.06}$	29	KULYUKINA	68 CC	
$0.24 \pm 0.08$	24	ANIKINA	64 CC	

See key on page 457

## Meson Particle Listings

 $K_L^0$  $\Gamma(3\pi^0)/\Gamma(\pi^+\pi^-\pi^0)$   $\Gamma_6/\Gamma_7$ 

VALUE	EVTS	DOCUMENT ID	TECN	COMMENT
<b>1.557±0.012 OUR FIT</b>				Error includes scale factor of 1.3.
•••				We use the following data for averages but not for fits. •••
<b>1.582±0.027</b>	13M	<sup>1</sup> AMBROSINO 06	KLOE	Not in fit
•••				We do not use the following data for averages, fits, limits, etc. •••
1.611±0.014±0.034	28k	KREUTZ 95	NA31	
1.65±0.07	883	BARMIN 72B	HLBC	Error statistical only
1.80±0.13	1010	BUDAGOV 68	HLBC	
2.0±0.6	188	ALEKSANYAN 64B	FBC	

<sup>1</sup>AMBROSINO 06 enters the fit via their separate measurements of these two modes. $\Gamma(\pi^+\pi^-\pi^0)/\Gamma_{total}$   $\Gamma_7/\Gamma$ 

VALUE	EVTS	DOCUMENT ID	TECN	COMMENT
<b>0.1254±0.0005 OUR FIT</b>				Error includes scale factor of 1.3.
<b>0.1255±0.0006 OUR AVERAGE</b>				
0.1263±0.0004±0.0011	13M	<sup>1</sup> AMBROSINO 06	KLOE	
0.1252±0.0007		<sup>2</sup> ALEXOPOU... 04	KTEV	

<sup>1</sup>There are correlations between these five KLOE measurements:  $B(K_L \rightarrow \pi e \nu)$ ,  $B(K_L \rightarrow \pi \mu \nu)$ ,  $B(K_L \rightarrow 3\pi^0)$ ,  $B(K_L \rightarrow \pi^+\pi^-\pi^0)$ , and  $\tau_{K_L}$  measured in AMBROSINO 06. See the footnote for the  $\tau_{K_L}$  measurement for the correlation matrix.<sup>2</sup>For correlations with other ALEXOPOULOS 04 measurements, see the footnote with their  $B(K_L \rightarrow \pi e \nu)$  measurement. $\Gamma(\pi^+\pi^-\pi^0)/\Gamma(\pi^\pm e^\mp \nu_e)$   $\Gamma_7/\Gamma_1$ 

VALUE	EVTS	DOCUMENT ID	TECN	COMMENT
<b>0.3092±0.0016 OUR FIT</b>				Error includes scale factor of 1.1.
•••				We use the following data for averages but not for fits. •••
<b>0.3078±0.0005±0.0017</b>	799K	<sup>1</sup> ALEXOPOU... 04	KTEV	Not in fit
•••				We do not use the following data for averages, fits, limits, etc. •••
0.336±0.003±0.007	28k	KREUTZ 95	NA31	

<sup>1</sup>This measurement enters the fit via their separate measurements for the two modes. $\Gamma(\pi^+\pi^-\pi^0)/[\Gamma(\pi^\pm e^\mp \nu_e) + \Gamma(\pi^\pm \mu^\mp \nu_\mu) + \Gamma(\pi^+\pi^-\pi^0)]$   $\Gamma_7/(\Gamma_1+\Gamma_2+\Gamma_7)$ 

VALUE	EVTS	DOCUMENT ID	TECN	COMMENT
<b>0.1565±0.0006 OUR FIT</b>				Error includes scale factor of 1.1.
•••				We do not use the following data for averages, fits, limits, etc. •••
0.163±0.003	6499	CHO 77	HBC	
0.1605±0.0038	1590	ALEXANDER 73B	HBC	
0.146±0.004	3200	BRANDENB... 73	HBC	
0.159±0.010	558	EVANS 73	HLBC	
0.167±0.016	1402	KULYUKINA 68	CC	
0.161±0.005		HOPKINS 67	HBC	
0.162±0.015	126	HAWKINS 66	HBC	
0.159±0.015	326	ASTBURY 65B	CC	
0.178±0.017	566	GUIDONI 65	HBC	
0.144±0.004	1729	HOPKINS 65	HBC	See HOPKINS 67

 $\Gamma(\pi^+\pi^-)/\Gamma_{total}$   $\Gamma_8/\Gamma$ 

VALUE (units $10^{-3}$ )	DOCUMENT ID	TECN	COMMENT
<b>1.967±0.010 OUR FIT</b>			Error includes scale factor of 1.5.
<b>1.975±0.012</b>	<sup>1</sup> ALEXOPOU... 04	KTEV	

<sup>1</sup>For correlations with other ALEXOPOULOS 04 measurements, see the footnote with their  $B(K_L \rightarrow \pi e \nu)$  measurement. $\Gamma(\pi^+\pi^-)/\Gamma(\pi^\pm e^\mp \nu_e)$   $\Gamma_8/\Gamma_1$ 

VALUE (units $10^{-3}$ )	EVTS	DOCUMENT ID	TECN	COMMENT
<b>4.849±0.020 OUR FIT</b>				Error includes scale factor of 1.1.
<b>4.840±0.020 OUR AVERAGE</b>				
4.826±0.022±0.016	47k	<sup>1</sup> LAI 07	NA48	
•••				We use the following data for averages but not for fits. •••
4.856±0.017±0.023	84k	<sup>2</sup> ALEXOPOU... 04	KTEV	Not in fit

<sup>1</sup>The LAI 07 central value of  $4.835 \times 10^{-3}$  has been reduced by 0.19% to  $4.826 \times 10^{-3}$  to subtract the contribution from the direct emission mode  $K_L^0 \rightarrow \pi^+\pi^-\gamma(\text{DE})$ .<sup>2</sup>This measurement enters the fit via their separate measurements for the two modes. $[\Gamma(\pi^+\pi^-) + \Gamma(\pi^+\pi^-\gamma(\text{DE}))]/\Gamma(\pi^\pm \mu^\mp \nu_\mu)$   $(\Gamma_8+\Gamma_{14})/\Gamma_2$ 

VALUE (units $10^{-3}$ )	EVTS	DOCUMENT ID	TECN	COMMENT
<b>7.38±0.04 OUR FIT</b>				Error includes scale factor of 1.4.
<b>7.275±0.042±0.054</b>	45k	<sup>1</sup> AMBROSINO 06F	KLOE	

<sup>1</sup>Fully inclusive. Taking  $B(K_L^0 \rightarrow \pi \mu \nu)$  from KLOE, AMBROSINO 06,  $B(K_L^0 \rightarrow \pi^+\pi^- + \pi^+\pi^-\gamma(\text{DE})) = (1.963 \pm 0.012 \pm 0.017) \times 10^{-3}$  is obtained. $\Gamma(\pi^+\pi^-)/[\Gamma(\pi^\pm e^\mp \nu_e) + \Gamma(\pi^\pm \mu^\mp \nu_\mu)]$   $\Gamma_8/(\Gamma_1+\Gamma_2)$ 

VALUE (units $10^{-3}$ )	EVTS	DOCUMENT ID	TECN	COMMENT
<b>2.909±0.013 OUR FIT</b>				Error includes scale factor of 1.3.
•••				We do not use the following data for averages, fits, limits, etc. •••
3.13±0.14	1687	COUPAL 85	SPEC	$\eta_{+-} = 2.28 \pm 0.06$
3.04±0.14	2703	DEVOE 77	SPEC	$\eta_{+-} = 2.25 \pm 0.05$
2.51±0.23	309	<sup>1</sup> DEBOUARD 67	OSPK	$\eta_{+-} = 2.00 \pm 0.09$
2.35±0.19	525	<sup>1</sup> FITCH 67	OSPK	$\eta_{+-} = 1.94 \pm 0.08$

<sup>1</sup>Old experiments excluded from fit. See subsection on  $\eta_{+-}$  in section on "PARAMETERS FOR  $K_L^0 \rightarrow 2\pi$  DECAY" below for average  $\eta_{+-}$  of these experiments and for note on discrepancy. $\Gamma(\pi^\pm e^\mp \nu_e)/\Gamma(2 \text{ tracks})$   $\Gamma_1/(\Gamma_1+\Gamma_2+0.03508\Gamma_6+\Gamma_7+\Gamma_8)$  $\Gamma(2 \text{ tracks}) = \Gamma(\pi^\pm e^\mp \nu_e) + \Gamma(\pi^\pm \mu^\mp \nu_\mu) + 0.03508 \Gamma(3\pi^0) + \Gamma(\pi^+\pi^-\pi^0) + \Gamma(\pi^+\pi^-)$  where 0.03508 is the fraction of  $3\pi^0$  events with one Dalitz decay ( $\pi^0 \rightarrow \gamma e^+ e^-$ ).

VALUE	EVTS	DOCUMENT ID	TECN	COMMENT
<b>0.5006±0.0009 OUR FIT</b>				Error includes scale factor of 1.3.
<b>0.4978±0.0035</b>	6.8M	LAI 04B	NA48	

 $\Gamma(\pi^+\pi^-)/[\Gamma(\pi^\pm e^\mp \nu_e) + \Gamma(\pi^\pm \mu^\mp \nu_\mu) + \Gamma(\pi^+\pi^-\pi^0)]$   $\Gamma_8/(\Gamma_1+\Gamma_2+\Gamma_7)$ 

VALUE (units $10^{-3}$ )	EVTS	DOCUMENT ID	TECN	COMMENT
<b>2.454±0.011 OUR FIT</b>				Error includes scale factor of 1.3.
•••				We do not use the following data for averages, fits, limits, etc. •••
2.60±0.07	4200	<sup>1</sup> MESSNER 73	ASPK	$\eta_{+-} = 2.23 \pm 0.05$

<sup>1</sup>From same data as  $\Gamma(\pi^+\pi^-)/\Gamma(\pi^+\pi^-\pi^0)$  MESSNER 73, but with different normalization. $\Gamma(\pi^+\pi^-)/\Gamma(\pi^+\pi^-\pi^0)$   $\Gamma_8/\Gamma_7$ 

VALUE (units $10^{-2}$ )	EVTS	DOCUMENT ID	TECN	COMMENT
<b>1.568±0.010 OUR FIT</b>				Error includes scale factor of 1.3.
•••				We do not use the following data for averages, fits, limits, etc. •••
1.64±0.04	4200	MESSNER 73	ASPK	$\eta_{+-} = 2.23$

<sup>1</sup>For correlations with other ALEXOPOULOS 04 measurements, see the footnote with their  $B(K_L \rightarrow \pi e \nu)$  measurement. $\Gamma(\pi^+\pi^-)/\Gamma_{total}$   $\Gamma_9/\Gamma$ 

VALUE (units $10^{-3}$ )	DOCUMENT ID	TECN	COMMENT
<b>0.864±0.006 OUR FIT</b>			Error includes scale factor of 1.8.
<b>0.865±0.012</b>	<sup>1</sup> ALEXOPOU... 04	KTEV	

<sup>1</sup>For correlations with other ALEXOPOULOS 04 measurements, see the footnote with their  $B(K_L \rightarrow \pi e \nu)$  measurement. $\Gamma(\pi^0\pi^0)/\Gamma(\pi^+\pi^-)$   $\Gamma_9/\Gamma_8$ 

VALUE	DOCUMENT ID	TECN	COMMENT
<b>0.4395±0.0023 OUR FIT</b>			Error includes scale factor of 2.0.
<b>0.4390±0.0012</b>	ETAFIT 12		

 $\Gamma(\pi^0\pi^0)/\Gamma(3\pi^0)$   $\Gamma_9/\Gamma_6$ 

VALUE (units $10^{-2}$ )	EVTS	DOCUMENT ID	TECN	COMMENT
<b>0.443±0.004 OUR FIT</b>				Error includes scale factor of 2.1.
•••				We use the following data for averages but not for fits. •••
<b>0.4446±0.0016±0.0019</b>	100K	<sup>1</sup> ALEXOPOU... 04	KTEV	Not in fit
•••				We do not use the following data for averages, fits, limits, etc. •••
0.37±0.08	29	BARMIN 70	HLBC	$\eta_{00} = 2.02 \pm 0.23$
0.32±0.15	30	BUDAGOV 70	HLBC	$\eta_{00} = 1.9 \pm 0.5$
0.46±0.11	57	BANNER 69	OSPK	$\eta_{00} = 2.2 \pm 0.3$

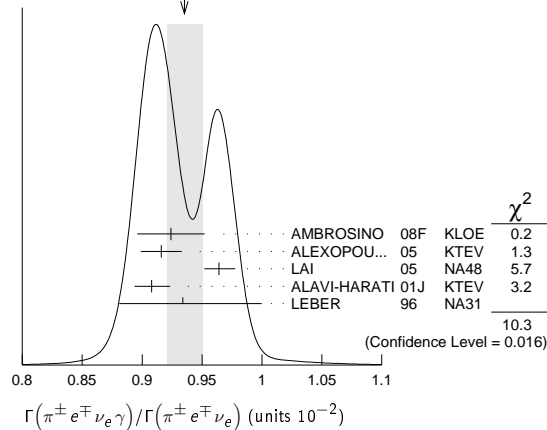
<sup>1</sup>This measurement enters the fit via their separate measurements for the two modes. $\Gamma(\pi^\pm e^\mp \nu_e \gamma)/\Gamma(\pi^\pm e^\mp \nu_e)$   $\Gamma_{10}/\Gamma_1$ 

VALUE (units $10^{-2}$ )	EVTS	DOCUMENT ID	TECN	COMMENT
<b>0.935±0.015 OUR AVERAGE</b>				Error includes scale factor of 1.9. See the ideogram below.
0.924±0.023±0.016	9k	<sup>1</sup> AMBROSINO 08F	KLOE	$E_\gamma^* > 30 \text{ MeV}$ , $\theta_{e\gamma}^* > 20^\circ$
0.916±0.017	4309	<sup>2</sup> ALEXOPOU... 05	KTEV	$E_\gamma^* > 30 \text{ MeV}$ , $\theta_{e\gamma}^* > 20^\circ$
0.964±0.008 $^{+0.011}_{-0.009}$	19K	LAI 05	NA48	$E_\gamma^* > 30 \text{ MeV}$ , $\theta_{e\gamma}^* > 20^\circ$
0.908±0.008 $^{+0.013}_{-0.012}$	15k	ALAVI-HARATI01J	KTEV	$E_\gamma^* \geq 30 \text{ MeV}$ , $\theta_{e\gamma}^* \geq 20^\circ$
0.934±0.036 $^{+0.055}_{-0.039}$	1384	LEBER 96	NA31	$E_\gamma^* \geq 30 \text{ MeV}$ , $\theta_{e\gamma}^* \geq 20^\circ$

<sup>1</sup>Direct emission contribution measured  $\langle X \rangle = -2.3 \pm 1.3 \pm 1.4$ .<sup>2</sup>Also measured cut  $E_\gamma^* > 10 \text{ MeV}$ ,  $\theta_{e\gamma}^* > 0^\circ$  14221 evts:  $\Gamma(\pi^\pm e^\mp \nu_e \gamma) / \Gamma(\pi^\pm e^\mp \nu_e) = (4.942 \pm 0.062)\%$ .

## Semileptonic modes with photons

## Meson Particle Listings

 $K_L^0$ WEIGHTED AVERAGE  
0.935±0.015 (Error scaled by 1.9) $\Gamma(\pi^\pm \mu^\mp \nu_\mu \gamma) / \Gamma(\pi^\pm \mu^\mp \nu_\mu)$   $\Gamma_{11}/\Gamma_2$ 

VALUE (units $10^{-3}$ )	EVTS	DOCUMENT ID	TECN	COMMENT
<b>2.09±0.08 OUR AVERAGE</b>				
2.09±0.09		<sup>1</sup> ALEXOPOU... 05	KTEV	$E_\gamma^* > 30$ MeV
2.08±0.17 <sup>+0.16</sup> <sub>-0.21</sub>	252	BENDER 98	NA48	$E_\gamma^* \geq 30$ MeV

<sup>1</sup> Also measured cut  $E_\gamma^* > 10$  MeV, 1385 evts:  $\Gamma(\pi^\pm \mu^\mp \nu_\mu \gamma) / \Gamma(\pi^\pm \mu^\mp \nu_\mu) = (0.530 \pm 0.014 \pm 0.012)\%$ .

Hadronic modes with photons or  $\ell\bar{\ell}$  pairs $\Gamma(\pi^0 \pi^0 \gamma) / \Gamma_{\text{total}}$   $\Gamma_{12}/\Gamma$ 

VALUE (units $10^{-6}$ )	CL%	DOCUMENT ID	TECN	COMMENT
<b>&lt; 0.243</b>	90	ABOUZAID 08B	KTEV	$K_L^0 \rightarrow \pi^0 \pi_D^0 \gamma, \pi_D^0 \rightarrow ee\gamma$
< 5.6	90	BARR 94	NA31	
<230	90	ROBERTS 94	E799	

••• We do not use the following data for averages, fits, limits, etc. •••

 $\Gamma(\pi^+ \pi^- \gamma) / \Gamma(\pi^+ \pi^- \pi^0)$   $\Gamma_{13}/\Gamma_7$ 

For earlier limits see our 1992 edition Physical Review D45 S1 (1992).

VALUE (units $10^{-4}$ )	EVTS	DOCUMENT ID	TECN	COMMENT
<b>&lt; 5.6</b>	90	BARR 94	NA31	
<230	90	ROBERTS 94	E799	

••• We do not use the following data for averages, fits, limits, etc. •••

1.23±0.13	516	<sup>1,2</sup> CARROLL 80B	SPEC	$E_\gamma^* > 20$ MeV
2.33±0.23	546	<sup>1,3</sup> CARROLL 80B	SPEC	
3.56±0.26	1062	<sup>1,4</sup> CARROLL 80B	SPEC	$E_\gamma^* > 20$ MeV

<sup>1</sup> CARROLL 80B quotes  $B(\pi^+ \pi^- \gamma)$  using normalization  $B(\pi^+ \pi^- \pi^0) = 0.1239$ . We divide by this value to obtain their measured  $\Gamma(\pi^+ \pi^- \gamma) / \Gamma(\pi^+ \pi^- \pi^0)$ .

<sup>2</sup> Internal Bremsstrahlung component only.

<sup>3</sup> Direct  $\gamma$  emission component only.

<sup>4</sup> Both IB and DE components.

 $\Gamma(\pi^+ \pi^- \gamma) / \Gamma(\pi^+ \pi^-)$   $\Gamma_{13}/\Gamma_8$ 

VALUE (units $10^{-2}$ )	EVTS	DOCUMENT ID	TECN	COMMENT
<b>2.11±0.08 OUR FIT</b>				Error includes scale factor of 2.9.
<b>2.11±0.08 OUR AVERAGE</b>				Error includes scale factor of 2.9.
2.08±0.02±0.02	8669	<sup>1</sup> ALAVI-HARATI 01B	KTEV	$E_\gamma^* > 20$ MeV
2.30±0.07	3136	RAMBERG 93	E731	$E_\gamma^* > 20$ MeV

<sup>1</sup> ALAVI-HARATI 01B includes both Direct Emission (DE) and Inner Bremsstrahlung (IB) processes.

 $\Gamma(\pi^+ \pi^- \gamma(\text{DE})) / \Gamma(\pi^+ \pi^-)$   $\Gamma_{14}/\Gamma_{13}$ 

These values assume that  $\Gamma(K_L^0 \rightarrow \pi^+ \pi^- \gamma) = \Gamma(K_L^0 \rightarrow \pi^+ \pi^- \gamma(\text{DE})) + \Gamma(K_L^0 \rightarrow \pi^+ \pi^- \gamma(\text{IB}))$ , the sum of widths for the direct emission (DE) and inner bremsstrahlung (IB) processes, with no IB-DE interference. DE assumes a form factor as described in RAMBERG 93.

VALUE	EVTS	DOCUMENT ID	TECN	COMMENT
<b>0.684±0.009 OUR FIT</b>				
<b>0.684±0.009 OUR AVERAGE</b>				
0.689±0.021	111k	ABOUZAID 06A	KTEV	$E_\gamma^* > 20$ MeV
0.683±0.011	8669	ALAVI-HARATI 01B	KTEV	$E_\gamma^* > 20$ MeV
0.685±0.041	3136	RAMBERG 93	E731	$E_\gamma^* > 20$ MeV

 $\Gamma(\pi^0 2\gamma) / \Gamma_{\text{total}}$   $\Gamma_{15}/\Gamma$ 

VALUE (units $10^{-6}$ )	CL%	EVTS	DOCUMENT ID	TECN	COMMENT
<b>1.273±0.033 OUR AVERAGE</b>					
1.28 ± 0.06 ± 0.01		1.4k	<sup>1</sup> ABOUZAID 08	KTEV	
1.27 ± 0.04 ± 0.01		2.5k	<sup>2</sup> LAI	02B	NA48

••• We do not use the following data for averages, fits, limits, etc. •••

1.68 ± 0.07 ± 0.08		884	<sup>3</sup> ALAVI-HARATI 99B	KTEV	
1.7 ± 0.2 ± 0.2		63	<sup>4</sup> BARR 92	NA31	
1.86 ± 0.60 ± 0.60		60	PAPADIMITR...91	E731	$m_{\gamma\gamma} > 280$ MeV
<5.1		90	PAPADIMITR...91	E731	$m_{\gamma\gamma} < 264$ MeV
2.1 ± 0.6		14	<sup>5</sup> BARR 90c	NA31	$m_{\gamma\gamma} > 280$ MeV

<sup>1</sup> ABOUZAID 08 reports  $(1.29 \pm 0.03 \pm 0.05) \times 10^{-6}$  from a measurement of  $[\Gamma(K_L^0 \rightarrow \pi^0 2\gamma) / \Gamma_{\text{total}}] / [B(K_L^0 \rightarrow \pi^0 \pi^0)]$  assuming  $B(K_L^0 \rightarrow \pi^0 \pi^0) = (8.69 \pm 0.04) \times 10^{-4}$ , which we rescale to our best value  $B(K_L^0 \rightarrow \pi^0 \pi^0) = (8.64 \pm 0.06) \times 10^{-4}$ . Our first error is their experiment's error and our second error is the systematic error from using our best value.

<sup>2</sup> LAI 02B reports  $[\Gamma(K_L^0 \rightarrow \pi^0 2\gamma) / \Gamma_{\text{total}}] / [B(K_L^0 \rightarrow \pi^0 \pi^0)] = (1.467 \pm 0.032 \pm 0.032) \times 10^{-3}$  which we multiply by our best value  $B(K_L^0 \rightarrow \pi^0 \pi^0) = (8.64 \pm 0.06) \times 10^{-4}$ . Our first error is their experiment's error and our second error is the systematic error from using our best value. They also find that  $B(\pi^0 2\gamma, m_{\gamma\gamma} < 110 \text{ MeV}) < 0.6 \times 10^{-8}$  (90% CL).

<sup>3</sup> ALAVI-HARATI 99B finds that  $\Gamma(\pi^0 2\gamma, m_{\gamma\gamma} < 240 \text{ MeV}) / \Gamma(\pi^0 2\gamma) = (17.3 \pm 1.3 \pm 1.5)\%$ . Superseded by ABOUZAID 08.

<sup>4</sup> BARR 92 find that  $\Gamma(\pi^0 2\gamma, m_{\gamma\gamma} < 240 \text{ MeV}) / \Gamma(\pi^0 2\gamma) < 0.09$  (90% CL).

<sup>5</sup> BARR 90c superseded by BARR 92.

 $\Gamma(\pi^0 \gamma e^+ e^-) / \Gamma_{\text{total}}$   $\Gamma_{16}/\Gamma$ 

VALUE (units $10^{-8}$ )	CL%	EVTS	DOCUMENT ID	TECN
<b>1.62±0.14±0.09</b>		125	<sup>1</sup> ABOUZAID 07D	KTEV

••• We do not use the following data for averages, fits, limits, etc. •••

2.34±0.35±0.13		44	ALAVI-HARATI 01E	KTEV
<71		90	MURAKAMI 99	SPEC

<sup>1</sup> ABOUZAID 07D includes 1997 (ALAVI-HARATI 01E) and 1999 data. It measures the ratio of  $B(K_L^0 \rightarrow \pi^0 \gamma e^+ e^-) / B(K_L^0 \rightarrow \pi^0 \pi_D^0)$ , where  $\pi_D^0$  is the Dalitz decaying  $\pi^0$ , and uses PDG 06 values  $B(K_L^0 \rightarrow \pi^0 \pi^0) = (8.69 \pm 0.04) \times 10^{-4}$ , and  $B(\pi_D^0 \rightarrow e^+ e^- \gamma) = (1.198 \pm 0.032) \times 10^{-2}$ . Supersedes ALAVI-HARATI 01E result.

Other modes with photons or  $\ell\bar{\ell}$  pairs $\Gamma(2\gamma) / \Gamma_{\text{total}}$   $\Gamma_{17}/\Gamma$ 

VALUE (units $10^{-4}$ )	EVTS	DOCUMENT ID	TECN	COMMENT
<b>5.47±0.04 OUR FIT</b>				Error includes scale factor of 1.1.

••• We do not use the following data for averages, fits, limits, etc. •••

4.54±0.84			<sup>1</sup> BANNER 72B	OSPK
4.5 ± 1.0		23	ENSTROM 71	OSPK $K_L^0$ 1.5-9 GeV/c
5.0 ± 1.0			<sup>2</sup> REPELLIN 71	OSPK
5.5 ± 1.1		90	KUNZ 68	OSPK Norm. to 3 $\pi(C+N)$

<sup>1</sup> This value uses  $(\eta_{00}/\eta_{+-})^2 = 1.05 \pm 0.14$ . In general,  $\Gamma(2\gamma) / \Gamma_{\text{total}} = [(4.32 \pm 0.55) \times 10^{-4}] [(\eta_{00}/\eta_{+-})^2]$ .

<sup>2</sup> Assumes regeneration amplitude in copper at 2 GeV is 22 mb. To evaluate for a given regeneration amplitude and error, multiply by (regeneration amplitude/22mb)<sup>2</sup>.

 $\Gamma(2\gamma) / \Gamma(3\pi^0)$   $\Gamma_{17}/\Gamma_6$ 

VALUE (units $10^{-3}$ )	EVTS	DOCUMENT ID	TECN	COMMENT
<b>2.802±0.017 OUR FIT</b>				
<b>2.802±0.018 OUR AVERAGE</b>				

2.79 ± 0.02 ± 0.02	27k	ADINOLFI 03	KLOE	
2.81 ± 0.01 ± 0.02		LAI 03	NA48	

••• We do not use the following data for averages, fits, limits, etc. •••

2.13 ± 0.43	28	BARMIN 71	HLBC	
2.24 ± 0.28	115	BANNER 69	OSPK	
2.5 ± 0.7	16	ARNOLD 68B	HLBC	Vacuum decay

 $\Gamma(2\gamma) / \Gamma(\pi^0 \pi^0)$   $\Gamma_{17}/\Gamma_9$ 

VALUE	EVTS	DOCUMENT ID	TECN
<b>0.633±0.006 OUR FIT</b>			Error includes scale factor of 1.4.
<b>0.632±0.004±0.008</b>	110k	BURKHARDT 87	NA31

 $\Gamma(3\gamma) / \Gamma_{\text{total}}$   $\Gamma_{18}/\Gamma$ 

VALUE	CL%	DOCUMENT ID	TECN
<b>&lt;7.4 × 10<sup>-8</sup></b>	90	<sup>1</sup> TUNG 11	K391

••• We do not use the following data for averages, fits, limits, etc. •••

<2.4 × 10 <sup>-7</sup>	90	<sup>2</sup> BARR 95c	NA31
-------------------------	----	-----------------------	------

<sup>1</sup> TUNG 11 reports the result assuming parity violating interaction and using 2005 data (Run-II and III). Assuming parity conserving or phase space interaction, the 90% upper limits obtained are  $7.5 \times 10^{-8}$  and  $8.6 \times 10^{-8}$ , respectively.

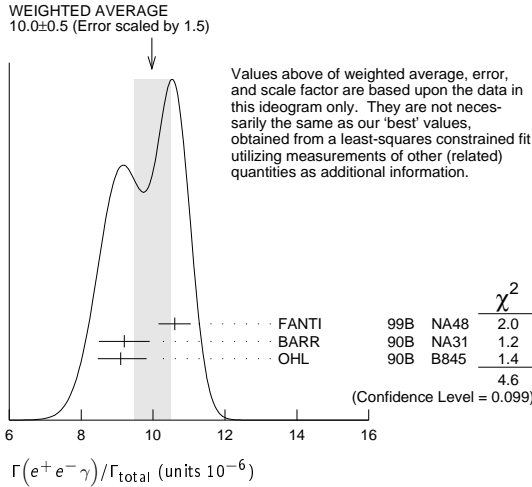
<sup>2</sup> Assumes a phase-space decay distribution.



$\Gamma(e^+e^-\gamma)/\Gamma_{total}$   $\Gamma_{19}/\Gamma$

VALUE (units $10^{-6}$ )	EVTS	DOCUMENT ID	TECN
<b>9.4 ± 0.4 OUR FIT</b>			
Error includes scale factor of 2.0.			
<b>10.0 ± 0.5 OUR AVERAGE</b>			
Error includes scale factor of 1.5. See the ideogram below.			
10.6 ± 0.2 ± 0.4	6864	<sup>1</sup> FANTI	99B NA48
9.2 ± 0.5 ± 0.5	1053	BARR	90B NA31
9.1 ± 0.4 ± 0.6 -0.5	919	OHL	90B B845

<sup>1</sup> For FANTI 99B, the ±0.4 systematic error includes for uncertainties in the calculation, primarily uncertainties in the  $\pi^0 \rightarrow e^+e^-\gamma$  and  $K_L^0 \rightarrow \pi^0\pi^0$  branching ratios, evaluated using our 1999 Web edition values.



$\Gamma(e^+e^-\gamma)/\Gamma(3\pi^0)$   $\Gamma_{19}/\Gamma_6$

VALUE (units $10^{-3}$ )	EVTS	DOCUMENT ID	TECN
<b>4.82 ± 0.21 OUR FIT</b>			
Error includes scale factor of 2.0.			
<b>4.63 ± 0.04 ± 0.13</b>	83k	<sup>1</sup> ABOUZAID	07B KTEV

<sup>1</sup> ABOUZAID 07B reports  $[\Gamma(K_L^0 \rightarrow e^+e^-\gamma)/\Gamma(K_L^0 \rightarrow 3\pi^0)] / [3\Gamma(\pi^0 \rightarrow 2\gamma)/\Gamma_{total} \times \Gamma(\pi^0 \rightarrow e^+e^-\gamma)/\Gamma_{total}] = (1.3302 \pm 0.0046 \pm 0.0103) \times 10^{-3}$  which we multiply by our best value  $3\Gamma(\pi^0 \rightarrow 2\gamma)/\Gamma_{total} \times \Gamma(\pi^0 \rightarrow e^+e^-\gamma)/\Gamma_{total} = 0.0348 \pm 0.0010$ . Our first error is their experiment's error and our second error is the systematic error from using our best value.

$\Gamma(\mu^+\mu^-)/\Gamma_{total}$   $\Gamma_{20}/\Gamma$

VALUE (units $10^{-7}$ )	EVTS	DOCUMENT ID	TECN
<b>3.59 ± 0.11 OUR AVERAGE</b>			
Error includes scale factor of 1.3.			
3.62 ± 0.04 ± 0.08	9100	ALAVI-HARATI01G	KTEV
3.4 ± 0.6 ± 0.4	45	FANTI	97 NA48
3.23 ± 0.23 ± 0.19	197	SPENCER	95 E799

$\Gamma(e^+e^-\gamma\gamma)/\Gamma_{total}$   $\Gamma_{21}/\Gamma$

VALUE (units $10^{-7}$ )	EVTS	DOCUMENT ID	TECN	COMMENT
<b>5.95 ± 0.33 OUR AVERAGE</b>				
5.84 ± 0.15 ± 0.32	1543	ALAVI-HARATI01F	KTEV	$E_\gamma^* > 5$ MeV
8.0 ± 1.5 ± 1.4 -1.2	40	SETZU	98 NA31	$E_\gamma^* > 5$ MeV
6.5 ± 1.2 ± 0.6	58	NAKAYA	94 E799	$E_\gamma^* > 5$ MeV
6.6 ± 3.2		MORSE	92 B845	$E_\gamma^* > 5$ MeV

$\Gamma(\mu^+\mu^-\gamma\gamma)/\Gamma_{total}$   $\Gamma_{22}/\Gamma$

VALUE (units $10^{-9}$ )	EVTS	DOCUMENT ID	TECN	COMMENT
<b>10.4 ± 7.5 ± 0.7</b>	4	ALAVI-HARATI00E	KTEV	$m_{\gamma\gamma} \geq 1$ MeV/c <sup>2</sup>

Charge conjugation × Parity (CP) or Lepton Family number (LF) violating modes, or  $\Delta S = 1$  weak neutral current (S1) modes

$\Gamma(\mu^+\mu^-)/\Gamma(\pi^+\pi^-)$   $\Gamma_{23}/\Gamma_8$

Test for  $\Delta S = 1$  weak neutral current. Allowed by higher-order electroweak interaction.

VALUE (units $10^{-6}$ )	EVTS	DOCUMENT ID	TECN	COMMENT
<b>3.48 ± 0.05 OUR AVERAGE</b>				
3.474 ± 0.057	6210	AMBROSE	00 B871	
3.87 ± 0.30	179	<sup>1</sup> AKAGI	95 SPEC	
3.38 ± 0.17	707	HEINSON	95 B791	

• • • We do not use the following data for averages, fits, limits, etc. • • •

3.9 ± 0.3 ± 0.1	178	<sup>2</sup> AKAGI	91B SPEC	ln AKAGI 95
3.45 ± 0.18 ± 0.13	368	<sup>3</sup> HEINSON	91 SPEC	ln HEINSON 95
4.1 ± 0.5	54	INAGAKI	89 SPEC	ln AKAGI 91B
2.8 ± 0.3 ± 0.2	87	MATHIAZHA...	89B SPEC	ln HEINSON 91

<sup>1</sup> AKAGI 95 gives this number multiplied by the PDG 1992 average for  $\Gamma(K_L^0 \rightarrow \pi^+\pi^-)/\Gamma_{total}$ .  
<sup>2</sup> AKAGI 91B give this number multiplied by the 1990 PDG average for  $\Gamma(K_L^0 \rightarrow \pi^+\pi^-)/\Gamma_{total}$ .  
<sup>3</sup> HEINSON 91 give  $\Gamma(K_L^0 \rightarrow \mu\mu)/\Gamma_{total}$ . We divide out the  $\Gamma(K_L^0 \rightarrow \pi^+\pi^-)/\Gamma_{total}$  PDG average which they used.

$\Gamma(e^+e^-)/\Gamma_{total}$   $\Gamma_{24}/\Gamma$

Test for  $\Delta S = 1$  weak neutral current. Allowed by higher-order electroweak interaction.

VALUE (units $10^{-10}$ )	CL%	EVTS	DOCUMENT ID	TECN
<b>0.087 ± 0.057 -0.041</b>		4	AMBROSE	98 B871

• • • We do not use the following data for averages, fits, limits, etc. • • •

<1.6	90	1	AKAGI	95 SPEC
<0.41	90	0	<sup>1</sup> ARISAKA	93B B791

<sup>1</sup> ARISAKA 93B includes all events with <6 MeV radiated energy.

$\Gamma(\pi^+\pi^-e^+e^-)/\Gamma_{total}$   $\Gamma_{25}/\Gamma$

Test for  $\Delta S = 1$  weak neutral current. Allowed by higher-order electroweak interaction.

VALUE (units $10^{-7}$ )	CL%	EVTS	DOCUMENT ID	TECN	COMMENT
<b>3.11 ± 0.19 OUR AVERAGE</b>					
3.08 ± 0.09 ± 0.18	1125		<sup>1</sup> LAI	03c NA48	
3.2 ± 0.6 ± 0.4	37		ADAMS	98 KTEV	
4.4 ± 1.3 ± 0.5	13		TAKEUCHI	98 SPEC	

• • • We do not use the following data for averages, fits, limits, etc. • • •

<4.6	90		NOMURA	97 SPEC	$m_{ee} > 4$ MeV
------	----	--	--------	---------	------------------

<sup>1</sup> LAI 03c second error is 0.15(syst) ± 0.10(norm) combined in quadrature. The normalization uses  $BR(K_L^0 \rightarrow \pi^+\pi^-\pi^0) * BR(\pi^0 \rightarrow e^+e^-) = (1.505 \pm 0.047) \times 10^{-3}$  from our 2000 Edition.

$\Gamma(\pi^0\pi^0e^+e^-)/\Gamma_{total}$   $\Gamma_{26}/\Gamma$

Test for  $\Delta S = 1$  weak neutral current. Allowed by higher-order electroweak interaction.

VALUE (units $10^{-9}$ )	CL%	EVTS	DOCUMENT ID	TECN
<b>&lt;6.6</b>	90	1	ALAVI-HARATI02C	E799

$\Gamma(\pi^0\pi^0\mu^+\mu^-)/\Gamma_{total}$   $\Gamma_{27}/\Gamma$

Test for  $\Delta S = 1$  weak neutral current. Allowed by higher-order electroweak interaction.

VALUE	CL%	DOCUMENT ID	TECN
<b>&lt;9.2 × 10<sup>-11</sup></b>	90	<sup>1</sup> ABOUZAID 11A	E799

<sup>1</sup> ABOUZAID 11A also reports  $B(K_L^0 \rightarrow \pi^0\pi^0X^0 \rightarrow \pi^0\pi^0\mu^+\mu^-) < 1.0 \times 10^{-10}$  at 90% C.L., where the  $X^0$  is a possible new neutral boson that was reported by PARK 05 with a mass of 214.3 ± 0.5 MeV/c<sup>2</sup>.

$\Gamma(\mu^+\mu^-e^+e^-)/\Gamma_{total}$   $\Gamma_{28}/\Gamma$

Test for  $\Delta S = 1$  weak neutral current. Allowed by higher-order electroweak interaction.

VALUE (units $10^{-9}$ )	CL%	EVTS	DOCUMENT ID	TECN	COMMENT
<b>2.69 ± 0.27 OUR AVERAGE</b>					
2.69 ± 0.24 ± 0.12	131		<sup>1</sup> ALAVI-HARATI03B	KTEV	
2.9 ± 6.7 -2.4	1		GU	96 E799	

• • • We do not use the following data for averages, fits, limits, etc. • • •

2.62 ± 0.40 ± 0.17	43		ALAVI-HARATI01H	KTEV	Sup. by ALAVI-HARATI 03B
--------------------	----	--	-----------------	------	--------------------------

<4900 90 BALATS 83 SPEC

<sup>1</sup> ALAVI-HARATI 03B also measures the linear slope  $\alpha = -1.59 \pm 0.37$ .

$\Gamma(e^+e^-e^+e^-)/\Gamma_{total}$   $\Gamma_{29}/\Gamma$

Test for  $\Delta S = 1$  weak neutral current. Allowed by higher-order electroweak interaction.

VALUE (units $10^{-8}$ )	EVTS	DOCUMENT ID	TECN	COMMENT
<b>3.56 ± 0.21 OUR AVERAGE</b>				
3.30 ± 0.24 ± 0.25	200		<sup>1</sup> LAI	05B NA48
3.72 ± 0.18 ± 0.23	441		ALAVI-HARATI01D	KTEV
3.96 ± 0.78 ± 0.32	27		GU	E799
3.07 ± 1.25 ± 0.26	6		VAGINS	93 B845

• • • We do not use the following data for averages, fits, limits, etc. • • •

6 ± 2 ± 1	18	<sup>2</sup> AKAGI	95 SPEC	$m_{ee} > 470$ MeV
7 ± 3 ± 2	6	<sup>2</sup> AKAGI	95 SPEC	$m_{ee} > 470$ MeV
10.4 ± 3.7 ± 1.1	8	<sup>3</sup> BARR	95 NA31	
6 ± 2 ± 1	18	AKAGI	93 CNTR	Sup. by AKAGI 95
4 ± 3	2	BARR	91 NA31	Sup. by BARR 95

<sup>1</sup> LAI 05B uses 1998 and 1999 data. Data are normalized to the observed events of  $K_L^0 \rightarrow \pi^+\pi^-\pi^0$  ( $\pi^0$  into Dalitz pair) and PDG 04 values are used for  $B(K_L^0 \rightarrow \pi^+\pi^-\pi^0)$  and  $B(\pi^0 \rightarrow e^+e^-)$ . The systematic error includes a normalization error of ±0.10.  
<sup>2</sup> Values are for the total branching fraction, acceptance-corrected for the  $m_{ee}$  cuts shown.  
<sup>3</sup> Distribution of angles between two  $e^+e^-$  pair planes favors  $CP=-1$  for  $K_L^0$ .

$\Gamma(\pi^0\mu^+\mu^-)/\Gamma_{total}$   $\Gamma_{30}/\Gamma$

Violates CP in leading order. Test for  $\Delta S = 1$  weak neutral current. Allowed by higher-order electroweak interaction.

VALUE (units $10^{-9}$ )	CL%	EVTS	DOCUMENT ID	TECN
<b>&lt;0.38</b>	90		ALAVI-HARATI00D	KTEV

• • • We do not use the following data for averages, fits, limits, etc. • • •

<5.1	90	0	HARRIS	93 E799
------	----	---	--------	---------

## Meson Particle Listings

 $K_L^0$  $\Gamma(\pi^0 e^+ e^-)/\Gamma_{\text{total}}$   $\Gamma_{31}/\Gamma$ 

Violates  $CP$  in leading order. Direct and indirect  $CP$ -violating contributions are expected to be comparable and to dominate the  $CP$ -conserving part. LAI 02B result suggests that  $CP$ -violation effects dominate. Test for  $\Delta S = 1$  weak neutral current. Allowed by higher-order electroweak interaction.

VALUE (units $10^{-10}$ )	CL%	EVTS	DOCUMENT ID	TECN	COMMENT
< 2.8	90		<sup>1</sup> ALAVI-HARATI 04A	KTEV	combined result
••• We do not use the following data for averages, fits, limits, etc. •••					
< 3.5	90		ALAVI-HARATI 04A	KTEV	
0.0047 <sup>+0.0022</sup> <sub>-0.0018</sub>			<sup>2</sup> LAI	02B NA48	$CP$ -conserving part
< 5.1	90	2	ALAVI-HARATI 01	KTEV	
0.01 to 0.02			ALAVI-HARATI 99B	KTEV	$CP$ -conserving part
< 43	90	0	HARRIS	93B E799	
< 75	90	0	BARKER	90 E731	
< 55	90	0	OHL	90 B845	
< 400	90		BARR	88 NA31	
< 3200	90		JASTRZEM...	88 SPEC	

<sup>1</sup> Combined result of ALAVI-HARATI 04A 1999-2000 data set and ALAVI-HARATI 01 1997 data set.

<sup>2</sup> LAI 02B uses the absence of a signal in  $K_L^0 \rightarrow \pi^0 \gamma \gamma$  with  $m(\gamma\gamma) < m(\pi^0)$  and their  $a_V$  value to predict this value.

 $\Gamma(\pi^0 \nu \bar{\nu})/\Gamma_{\text{total}}$   $\Gamma_{32}/\Gamma$ 

Violates  $CP$  in leading order. Test of direct  $CP$  violation since the indirect  $CP$ -violating and  $CP$ -conserving contributions are expected to be suppressed. Test of  $\Delta S = 1$  weak neutral current.

VALUE (units $10^{-7}$ )	CL%	DOCUMENT ID	TECN
< 0.26	90	<sup>1</sup> AHN 10	K391
••• We do not use the following data for averages, fits, limits, etc. •••			
< 0.67	90	<sup>2</sup> AHN 08	K391
< 2.1	90	<sup>3</sup> AHN 06	K391
< 5.9	90	ALAVI-HARATI 100	KTEV
< 16	90	ADAMS 99	KTEV
< 580	90	WEAVER 94	E799
< 2200	90	GRAHAM 92	CNTR

<sup>1</sup> Obtained combining Run-2 (AHN 08) and Run-3 data.

<sup>2</sup> Value obtained using data from February to April 2005.

<sup>3</sup> Value obtained analyzing 10% of data of RUN 1 (performed in 2004).

 $\Gamma(\pi^0 \pi^0 \nu \bar{\nu})/\Gamma_{\text{total}}$   $\Gamma_{33}/\Gamma$ 

VALUE	CL%	DOCUMENT ID	TECN
< $8.1 \times 10^{-7}$	90	<sup>1</sup> OGATA 11	K391
••• We do not use the following data for averages, fits, limits, etc. •••			
< $4.7 \times 10^{-5}$	90	<sup>2</sup> NIX 07	K391

<sup>1</sup> Using 2005 Run-1 data. OGATA 11 also sets a limit on the  $K_L^0 \rightarrow \pi^0 \pi^0 X \rightarrow$  invisible particles process: the limit on the branching fraction varied from  $7.0 \times 10^{-7}$  to  $4.0 \times 10^{-5}$  for the mass of  $X$  ranging from 50 to 200 MeV/ $c^2$ .

<sup>2</sup> Observed 1 event with expected background of  $0.43 \pm 0.35$  events. NIX 07 also measured  $B(K_L^0 \rightarrow \pi^0 \pi^0 P) < 1.2 \times 10^{-6}$  at 90% CL, where  $P$  is the pseudoscalar particle and  $m_P < 100$  MeV.

 $\Gamma(e^\pm \mu^\mp)/\Gamma_{\text{total}}$   $\Gamma_{34}/\Gamma$ 

Test of lepton family number conservation.

VALUE (units $10^{-11}$ )	CL%	EVTS	DOCUMENT ID	TECN
< 0.47	90		AMBROSE 98B	B871
••• We do not use the following data for averages, fits, limits, etc. •••				
< 9.4	90	0	AKAGI 95	SPEC
< 3.9	90	0	ARISAKA 93	B791
< 3.3	90	0	<sup>1</sup> ARISAKA 93	B791

<sup>1</sup> This is the combined result of ARISAKA 93 and MATHIAZHAGAN 89.

 $\Gamma(e^\pm e^\pm \mu^\mp \mu^\mp)/\Gamma_{\text{total}}$   $\Gamma_{35}/\Gamma$ 

Test of lepton family number conservation.

VALUE (units $10^{-11}$ )	CL%	EVTS	DOCUMENT ID	TECN	COMMENT
< 4.12	90	0	ALAVI-HARATI 03B	KTEV	
••• We do not use the following data for averages, fits, limits, etc. •••					
< 12.3	90	0	<sup>1</sup> ALAVI-HARATI 01H	KTEV	Sup. by ALAVI-HARATI 03B
< 610	90	0	<sup>1</sup> GU	96 E799	

<sup>1</sup> Assuming uniform phase space distribution.

 $\Gamma(\pi^0 \mu^\pm e^\mp)/\Gamma_{\text{total}}$   $\Gamma_{36}/\Gamma$ 

Test of lepton family number conservation.

VALUE (units $10^{-10}$ )	CL%	DOCUMENT ID	TECN
< 0.76	90	ABOUZAID 08c	KTEV
••• We do not use the following data for averages, fits, limits, etc. •••			
< 62	90	ARISAKA 98	E799

 $\Gamma(\pi^0 \pi^0 \mu^\pm e^\mp)/\Gamma_{\text{total}}$   $\Gamma_{37}/\Gamma$ 

Test of lepton family number conservation.

VALUE (units $10^{-10}$ )	CL%	DOCUMENT ID	TECN
< 1.7	90	ABOUZAID 08c	KTEV

### $V_{ud}$ , $V_{us}$ , THE CABIBBO ANGLE, AND CKM UNITARITY

Updated March 2012 by E. Blucher (Univ. of Chicago) and W.J. Marciano (BNL)

The Cabibbo-Kobayashi-Maskawa (CKM) [1,2] three-generation quark mixing matrix written in terms of the Wolfenstein parameters  $(\lambda, A, \rho, \eta)$  [3] nicely illustrates the orthonormality constraint of unitarity and central role played by  $\lambda$ .

$$V_{\text{CKM}} = \begin{pmatrix} V_{ud} & V_{us} & V_{ub} \\ V_{cd} & V_{cs} & V_{cb} \\ V_{td} & V_{ts} & V_{tb} \end{pmatrix} = \begin{pmatrix} 1 - \lambda^2/2 & \lambda & A\lambda^3(\rho - i\eta) \\ -\lambda & 1 - \lambda^2/2 & A\lambda^2 \\ A\lambda^3(1 - \rho - i\eta) & -A\lambda^2 & 1 \end{pmatrix} + \mathcal{O}(\lambda^4). \quad (1)$$

That cornerstone is a carryover from the two-generation Cabibbo angle,  $\lambda = \sin(\theta_{\text{Cabibbo}}) = V_{us}$ . Its value is a critical ingredient in determinations of the other parameters and in tests of CKM unitarity.

Unfortunately, the precise value of  $\lambda$  has been somewhat controversial in the past, with kaon decays suggesting [4]  $\lambda \simeq 0.220$ , while hyperon decays [5] and indirect determinations via nuclear  $\beta$ -decays imply a somewhat larger  $\lambda \simeq 0.225 - 0.230$ . That discrepancy is often discussed in terms of a deviation from the unitarity requirement

$$|V_{ud}|^2 + |V_{us}|^2 + |V_{ub}|^2 = 1. \quad (2)$$

For many years, using a value of  $V_{us}$  derived from  $K \rightarrow \pi e \nu$  ( $K_{e3}$ ) decays, that sum was consistently 2–2.5 sigma below unity, a potential signal [6] for new physics effects. Below, we discuss the current status of  $V_{ud}$ ,  $V_{us}$ , and their associated unitarity test in Eq. (2). (Since  $|V_{ub}|^2 \simeq 1 \times 10^{-5}$  is negligibly small, it is ignored in this discussion.)

$V_{ud}$

The value of  $V_{ud}$  has been obtained from superallowed nuclear, neutron, and pion decays. Currently, the most precise determination of  $V_{ud}$  comes from superallowed nuclear beta-decays [6] ( $0^+ \rightarrow 0^+$  transitions). Measuring their half-lives,  $t$ , and  $Q$  values which give the decay rate factor,  $f$ , leads to a precise determination of  $V_{ud}$  via the master formula [7–9]

$$|V_{ud}|^2 = \frac{2984.48(5) \text{ sec}}{ft(1 + \text{RC})} \quad (3)$$

where RC denotes the entire effect of electroweak radiative corrections, nuclear structure, and isospin violating nuclear effects. RC is nucleus-dependent, ranging from about +3.0% to +3.6% for the best measured superallowed decays. The most recent analysis of Hardy and Towner [10, 11] gives a weighted average (with errors combined in quadrature) of

$$V_{ud} = 0.97425(22) \text{ (superallowed)}, \quad (4)$$

which, assuming unitarity, corresponds to  $\lambda = 0.2255(10)$ . The new average value of  $V_{ud}$  is shifted upward compared to our 2007 value of 0.97418(27) primarily because of improvements in the experimental  $ft$  values and nuclear isospin breaking corrections employed. We note, however, that the possibility of additional nuclear coulombic corrections has been raised recently [12].

Combined measurements of the neutron lifetime,  $\tau_n$ , and the ratio of axial-vector/vector couplings,  $g_A \equiv G_A/G_V$ , via neutron decay asymmetries can also be used to determine  $V_{ud}$ :

$$|V_{ud}|^2 = \frac{4908.7(1.9) \text{ sec}}{\tau_n(1 + 3g_A^2)}, \quad (5)$$

where the error stems from uncertainties in the electroweak radiative corrections [8] due to hadronic loop effects. Those effects have been recently updated and their error was reduced by about a factor of 2 [9], leading to a  $\pm 0.0002$  theoretical uncertainty in  $V_{ud}$  (common to all  $V_{ud}$  extractions). Using the world averages from this *Review*

$$\begin{aligned} \tau_n^{\text{ave}} &= 880.1(1.1) \text{ sec} \\ g_A^{\text{ave}} &= 1.2701(25) \end{aligned} \quad (6)$$

leads to

$$V_{ud} = 0.9773(6)_{\tau_n} (16)_{g_A} (2)_{\text{RC}} \quad (7)$$

with the error dominated by  $g_A$  uncertainties (which have been expanded due to experimental inconsistencies). The new shorter neutron lifetime average (since the last review) now leads to a value of  $V_{ud}$  that is inconsistent with the superallowed nuclear beta decay result in Eq. (4). That disagreement suggests that a shift of  $g_A$  to about 1.275 (consistent with more modern day measurements [14]) is likely. Future neutron studies are expected to resolve these inconsistencies and significantly reduce the uncertainties in  $g_A$  and  $\tau_n$ , potentially making them the best way to determine  $V_{ud}$ .

The recently completed PIBETA experiment at PSI measured the very small ( $\mathcal{O}(10^{-8})$ ) branching ratio for  $\pi^+ \rightarrow \pi^0 e^+ \nu_e$  with about  $\pm 1/2\%$  precision. Their result gives [15]

$$V_{ud} = 0.9749(26) \left[ \frac{BR(\pi^+ \rightarrow e^+ \nu_e(\gamma))}{1.2352 \times 10^{-4}} \right]^{\frac{1}{2}} \quad (8)$$

which is normalized using the very precisely determined theoretical prediction for  $BR(\pi^+ \rightarrow e^+ \nu_e(\gamma)) = 1.2352(5) \times 10^{-4}$  [7], rather than the experimental branching ratio from this *Review* of  $1.230(4) \times 10^{-4}$  which would lower the value to  $V_{ud} = 0.9728(30)$ . Theoretical uncertainties in that determination are very small; however, much higher statistics would be required to make this approach competitive with others.

### $V_{us}$

$|V_{us}|$  may be determined from kaon decays, hyperon decays, and tau decays. Previous determinations have most often used  $K\ell 3$  decays:

$$\Gamma_{K\ell 3} = \frac{G_F^2 M_K^5}{192\pi^3} S_{EW} (1 + \delta_K^\ell + \delta_{SU2}) C^2 |V_{us}|^2 f_+^2(0) I_K^\ell. \quad (9)$$

Here,  $\ell$  refers to either  $e$  or  $\mu$ ,  $G_F$  is the Fermi constant,  $M_K$  is the kaon mass,  $S_{EW}$  is the short-distance radiative correction,  $\delta_K^\ell$  is the mode-dependent long-distance radiative correction,  $f_+(0)$  is the calculated form factor at zero momentum transfer for the  $\ell\nu$  system, and  $I_K^\ell$  is the phase-space integral, which depends on measured semileptonic form factors. For charged kaon decays,  $\delta_{SU2}$  is the deviation from one of the ratio of  $f_+(0)$  for the charged to neutral kaon decay; it is zero for the neutral kaon.  $C^2$  is 1 (1/2) for neutral (charged) kaon decays. Most determinations of  $|V_{us}|$  have been based only on  $K \rightarrow \pi e \nu$  decays;  $K \rightarrow \pi \mu \nu$  decays have not been used because of large uncertainties in  $I_K^\mu$ . The experimental measurements are the semileptonic decay widths (based on the semileptonic branching fractions and lifetime) and form factors (allowing calculation of the phase space integrals). Theory is needed for  $S_{EW}$ ,  $\delta_K^\ell$ ,  $\delta_{SU2}$ , and  $f_+(0)$ .

Many new measurements during the last few years have resulted in a significant shift in  $V_{us}$ . Most importantly, recent measurements of the  $K \rightarrow \pi e \nu$  branching fractions are significantly different than earlier PDG averages, probably as a result of inadequate treatment of radiation in older experiments. This effect was first observed by BNL E865 [16] in the charged kaon system and then by KTeV [17,18] in the neutral kaon system; subsequent measurements were made by KLOE [19–22], NA48 [23–25], and ISTRA+ [26]. Current averages (*e.g.*, by the PDG [27] or Flavianet [28]) of the semileptonic branching fractions are based only on recent, high-statistics experiments where the treatment of radiation is clear. In addition to measurements of branching fractions, new measurements of lifetimes [29] and form factors [30–34], have resulted in improved precision for all of the experimental inputs to  $V_{us}$ . Precise measurements of form factors for  $K_{\mu 3}$  decay now make it possible to use both semileptonic decay modes to extract  $V_{us}$ .

Following the analysis of the Flavianet group [28], one finds the values of  $|V_{us}| f_+(0)$  in Table 1. The average of these measurements gives

$$f_+(0) |V_{us}| = 0.21664(48). \quad (10)$$

Figure 1 shows a comparison of these results with the PDG evaluation from 2002 [35], as well as  $f_+(0)(1 - |V_{ud}|^2 - |V_{ub}|^2)^{1/2}$ , the expectation for  $f_+(0) |V_{us}|$  assuming unitarity, based on  $|V_{ud}| = 0.9742 \pm 0.0003$ ,  $|V_{ub}| = (3.6 \pm 0.7) \times 10^{-3}$ , and the lattice calculation of  $f_+(0) = 0.9644 \pm 0.0049$  [36] (Lattice calculations of  $f_+(0)$  have improved significantly in recent years, and therefore replace the classic calculation of Leutwyler and Roos [37].) Combining the result in Eq. (10) with the above value of  $f_+(0)$  gives

$$|V_{us}| = \lambda = 0.2246 \pm 0.0012. \quad (11)$$

# Meson Particle Listings

$K_L^0$

**Table 1:**  $|V_{us}|f_+(0)$  from  $K\ell 3$ .

Decay Mode	$ V_{us} f_+(0)$
$K^\pm e 3$	$0.2173 \pm 0.0008$
$K^\pm \mu 3$	$0.2176 \pm 0.0011$
$K_L e 3$	$0.2163 \pm 0.0006$
$K_L \mu 3$	$0.2168 \pm 0.0007$
$K_S e 3$	$0.2154 \pm 0.0013$
Average	$0.2166 \pm 0.0005$

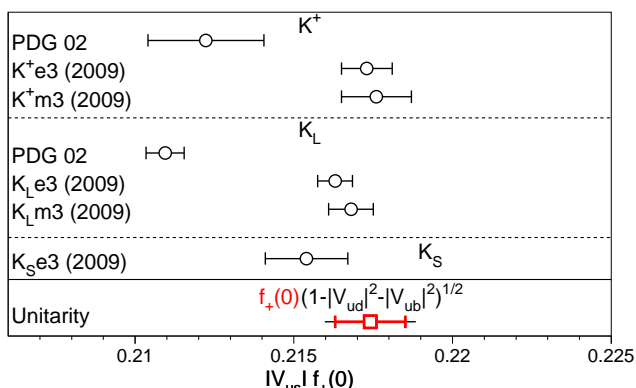


**Figure 1:** Comparison of determinations of  $|V_{us}|f_+(0)$  from this review (labeled 2009), from the PDG 2002, and with the prediction from unitarity using  $|V_{ud}|$  and the lattice calculation of  $f_+(0)$  [36]. For  $f_+(0)(1 - |V_{ud}|^2 - |V_{ub}|^2)^{1/2}$ , the inner error bars are from the quoted uncertainty in  $f_+(0)$ ; the total uncertainties include the  $|V_{ud}|$  and  $|V_{ub}|$  errors.

A value of  $V_{us}$  can also be obtained from a comparison of the radiative inclusive decay rates for  $K \rightarrow \mu\nu(\gamma)$  and  $\pi \rightarrow \mu\nu(\gamma)$  combined with a lattice gauge theory calculation of  $f_K/f_\pi$  via [42]

$$\frac{|V_{us}|f_K}{|V_{ud}|f_\pi} = 0.2387(4) \left[ \frac{\Gamma(K \rightarrow \mu\nu(\gamma))}{\Gamma(\pi \rightarrow \mu\nu(\gamma))} \right]^{\frac{1}{2}} \quad (12)$$

with the small error coming from electroweak radiative corrections. Employing

$$\frac{\Gamma(K \rightarrow \mu\nu(\gamma))}{\Gamma(\pi \rightarrow \mu\nu(\gamma))} = 1.3337(46), \quad (13)$$

which averages in the KLOE result [43],  $B(K \rightarrow \mu\nu(\gamma)) = 63.66(9)(15)\%$  and [44]

$$f_K/f_\pi = 1.189(7) \quad (14)$$

along with the value of  $V_{ud}$  in Eq. (4) leads to

$$|V_{us}| = 0.2259(5)(13). \quad (15)$$

It should be mentioned that hyperon decay fits suggest [5]

$$|V_{us}| = 0.2250(27) \text{ Hyperon Decays} \quad (16)$$

modulo SU(3) breaking effects that could shift that value up or down. We note that a recent representative effort [45] that incorporates SU(3) breaking found  $V_{us} = 0.226(5)$ . Similarly, inclusive strangeness changing tau decays give [46]

$$|V_{us}| = 0.2208(34) \text{ Tau Decays} \quad (17)$$

where the central value depends on the strange quark mass. However, a recent BaBar study [47] of  $\tau \rightarrow K\nu/\tau \rightarrow \pi\nu$  using the lattice value of  $f_K/f_\pi$  from Eq. (14) finds  $V_{us} = 0.2255(24)$ , in good agreement with other determinations.

Employing the value of  $V_{ud}$  in Eq. (4) and  $V_{us} = 0.2252(9)$ , the average of the  $K\ell 3$  (Eq. (11)) and  $K\mu 2$  (Eq. (15)) determinations of  $V_{us}$ , leads to the unitarity consistency check

$$|V_{ud}|^2 + |V_{us}|^2 + |V_{ub}|^2 = 0.9999(4)(4). \quad (18)$$

where the first error is the uncertainty from  $|V_{ud}|^2$  and the second error is the uncertainty from  $|V_{us}|^2$ .

### CKM Unitarity Constraints

The current good experimental agreement with unitarity,  $|V_{ud}|^2 + |V_{us}|^2 + |V_{ub}|^2 = 0.9999(6)$ , provides strong confirmation of Standard Model radiative corrections (which range between 3-4% depending on the nucleus used) at better than the 50 sigma level [48]. In addition, it implies constraints on “New Physics” effects at both the tree and quantum loop levels. Those effects could be in the form of contributions to nuclear beta decays,  $K$  decays and/or muon decays, with the last of these providing normalization via the muon lifetime [49], which is used to obtain the Fermi constant,  $G_\mu = 1.166371(6) \times 10^{-5} \text{GeV}^{-2}$ .

In the following sections, we illustrate the implications of CKM unitarity for (1) exotic muon decays [50] (beyond ordinary muon decay  $\mu^+ \rightarrow e^+\nu_e\bar{\nu}_\mu$ ) and (2) new heavy quark mixing  $V_{uD}$  [51]. Other examples in the literature [52,53] include  $Z_\chi$  boson quantum loop effects, supersymmetry, leptoquarks, compositeness etc.

### Exotic Muon Decays

If additional lepton flavor violating decays such as  $\mu^+ \rightarrow e^+\bar{\nu}_e\nu_\mu$  (wrong neutrinos) occur, they would cause confusion in searches for neutrino oscillations at, for example, muon storage rings/neutrino factories or other neutrino sources from muon decays. Calling the rate for all such decays  $\Gamma(\text{exotic } \mu \text{ decays})$ , they should be subtracted before the extraction of  $G_\mu$  and normalization of the CKM matrix. Since that is not done and unitarity works, one has (at one-sided 95% CL)

$$|V_{ud}|^2 + |V_{us}|^2 + |V_{ub}|^2 = 1 - BR(\text{exotic } \mu \text{ decays}) \geq 0.9989 \quad (19)$$

or

$$BR(\text{exotic } \mu \text{ decays}) < 0.001. \quad (20)$$

This bound is a factor of 10 better than the direct experimental bound on  $\mu^+ \rightarrow e^+\bar{\nu}_e\nu_\mu$ .

### New Heavy Quark Mixing

See key on page 457

Heavy  $D$  quarks naturally occur in fourth quark generation models and some heavy quark “new physics” scenarios such as  $E_6$  grand unification. Their mixing with ordinary quarks gives rise to  $V_{ud}$  which is constrained by unitarity (one sided 95% CL)

$$\begin{aligned} |V_{ud}|^2 + |V_{us}|^2 + |V_{ub}|^2 &= 1 - |V_{ud}|^2 > 0.9989 \\ |V_{ud}| &< 0.03. \end{aligned} \quad (21)$$

A similar constraint applies to heavy neutrino mixing and the couplings  $V_{\mu N}$  and  $V_{eN}$ .

### References

1. N. Cabibbo, Phys. Rev. Lett. **10**, 531 (1963).
2. M. Kobayashi and T. Maskawa, Prog. Theor. Phys. **49**, 652 (1973).
3. L. Wolfenstein, Phys. Rev. Lett. **51**, 1945 (1983).
4. S. Eidelman *et al.*, [Particle Data Group], Phys. Lett. **B592**, 1 (2004).
5. N. Cabibbo, E.C. Swallow, and R. Winston, Phys. Rev. Lett. **92**, 251803 (2004) [hep-ph/0307214].
6. J.C. Hardy and I.S. Towner, Phys. Rev. Lett. **94**, 092502 (2005) [nucl-th/0412050].
7. W.J. Marciano and A. Sirlin, Phys. Rev. Lett. **71**, 3629 (1993).
8. A. Czarnecki, W.J. Marciano, and A. Sirlin, Phys. Rev. **D70**, 093006 (2004) [hep-ph/0406324].
9. W.J. Marciano and A. Sirlin, Phys. Rev. Lett. **96**, 032002 (2006) [hep-ph/0510099].
10. J.C. Hardy and I.S. Towner, Phys. Rev. **C77**, 025501 (2008).
11. J.C. Hardy and I.S. Towner, Phys. Rev. **C79**, 055502 (2009).
12. G.A. Miller and A. Schwenk, Phys. Rev. **C78**, 035501 (2008); N. Auerbach, Phys. Rev. **C79**, 035502 (2009); H. Liang, N. Van Giai and J. Meng, Phys. Rev. **C79**, 064316 (2009).
13. A. Serebrov *et al.*, Phys. Lett. **B605**, 72 (2005) [nucl-ex/0408009].
14. H. Abele, Prog. in Part. Nucl. Phys. **60**, 1 (2008).
15. D. Pocanic *et al.*, Phys. Rev. Lett. **93**, 181803 (2004) [hep-ex/0312030].
16. A. Sher *et al.*, Phys. Rev. Lett. **91**, 261802 (2003).
17. T. Alexopoulos *et al.*, [KTeV Collab.], Phys. Rev. Lett. **93**, 181802 (2004) [hep-ex/0406001].
18. T. Alexopoulos *et al.*, [KTeV Collab.], Phys. Rev. **D70**, 092006 (2004) [hep-ex/0406002].
19. F. Ambrosino *et al.*, [KLOE Collab.], Phys. Lett. **B632**, 43 (2006) [hep-ex/0508027].
20. F. Ambrosino *et al.*, [KLOE Collab.], Phys. Lett. **B638**, 140 (2006) [hep-ex/0603041].
21. F. Ambrosino *et al.*, [KLOE Collab.], Phys. Lett. **B636**, 173 (2006) [hep-ex/0601026].
22. F. Ambrosino *et al.*, [KLOE Collab.], PoS **HEP2005**, 287 (2006) [Frascati Phys. Ser. **41**, 69 (2006)] [hep-ex/0510028].
23. A. Lai *et al.*, [NA48 Collab.], Phys. Lett. **B602**, 41 (2004) [hep-ex/0410059].
24. A. Lai *et al.*, [NA48 Collab.], Phys. Lett. **B645**, 26 (2007) [hep-ex/0611052].
25. J.R. Batley *et al.*, [NA48/2 Collab.], Eur. Phys. J. C **50**, 329 (2007) [hep-ex/0702015].
26. V.I. Romanovsky *et al.*, [hep-ex/0704.2052].
27. C. Amsler *et al.*, [Particle Data Group], Phys. Lett. **B667**, 1 (2008).
28. Flavianet Working Group on Precise SM Tests in K Decays, <http://www.lnf.infn.it/wg/vus>. For a recent detailed review, see M. Antonelli *et al.*, [hep-ph/0907.5386].
29. F. Ambrosino *et al.*, [KLOE Collab.], Phys. Lett. **B626**, 15 (2005) [hep-ex/0507088].
30. T. Alexopoulos *et al.*, [KTeV Collab.], Phys. Rev. **D70**, 092007 (2004) [hep-ex/0406003].
31. E. Abouzaid *et al.*, [KTeV Collab.], Phys. Rev. **D74**, 097101 (2006) [hep-ex/0608058].
32. F. Ambrosino *et al.*, [KLOE Collab.], Phys. Lett. **B636**, 166 (2006) [hep-ex/0601038].
33. A. Lai *et al.*, [NA48 Collab.], Phys. Lett. **B604**, 1 (2004) [hep-ex/0410065].
34. O.P. Yushchenko *et al.*, Phys. Lett. **B589**, 111 (2004) [hep-ex/0404030].
35. K. Hagiwara *et al.*, [Particle Data Group], Phys. Rev. **D66**, 1 (2002).
36. P.A. Boyle *et al.*, Phys. Rev. Lett. **100**, 141601 (2008).
37. H. Leutwyler and M. Roos, Z. Phys. **C25**, 91 (1984).
38. D. Becirevic *et al.*, Nucl. Phys. **B705**, 339 (2005) [hep-ph/0403217].
39. J. Bijnens and P. Talavera, Nucl. Phys. **B669**, 341 (2003).
40. V. Cirigliano *et al.*, JHEP **0504**, 006 (2005) [hep-ph/0503108].
41. M. Jamin, J.A. Oller, and A. Pich, JHEP **02**, 047 (2004).
42. W.J. Marciano, Phys. Rev. Lett. **93**, 231803 (2004) [hep-ph/0402299].
43. F. Ambrosino *et al.*, [KLOE Collab.], Phys. Lett. **B632**, 76 (2006) [hep-ex/0509045].
44. E. Follana *et al.*, Phys. Rev. Lett. **100**, 062002 (2008).
45. V. Mateu and A. Pich, JHEP **0510**, 041 (2005) [hep-ph/0509045].
46. E. Gamiz *et al.*, Phys. Rev. Lett. **94**, 011803 (2005) [hep-ph/0408044]; E. Gamiz *et al.*, arXiv:0709.0282 [hep-ph].
47. B. Aubert *et al.*, [BaBar Collab.], [hep-ex/0912.0242].
48. A. Sirlin, Rev. Mod. Phys. **50**, 573 (1978).
49. D.B. Chitwood *et al.*, Phys. Rev. Lett. **99**, 032001 (2007).
50. K.S. Babu and S. Pakvasa, hep-ph/0204236.
51. W. Marciano and A. Sirlin, Phys. Rev. Lett. **56**, 22 (1986); P. Langacker and D. London, Phys. Rev. **D38**, 886 (1988).
52. W. Marciano and A. Sirlin, Phys. Rev. **D35**, 1672 (1987).
53. R. Barbieri *et al.*, Phys. Lett. **156B**, 348 (1985); K. Hagiwara *et al.*, Phys. Rev. Lett. **75**, 3605 (1995); A. Kurylov and M. Ramsey-Musolf, Phys. Rev. Lett. **88**, 071804 (2000).

## Meson Particle Listings

 $K_L^0$ ENERGY DEPENDENCE OF  $K_L^0$  DALITZ PLOT

For discussion, see note on Dalitz plot parameters in the  $K^\pm$  section of the Particle Listings above. For definitions of  $a_V$ ,  $a_T$ ,  $a_U$ , and  $a_Y$ , see the earlier version of the same note in the 1982 edition of this Review published in Physics Letters **111B** 70 (1982).

$$|\text{matrix element}|^2 = 1 + gu + hu^2 + jv + kv^2 + fuv$$

$$\text{where } u = (s_3 - s_0) / m_\pi^2 \text{ and } v = (s_2 - s_1) / m_\pi^2$$

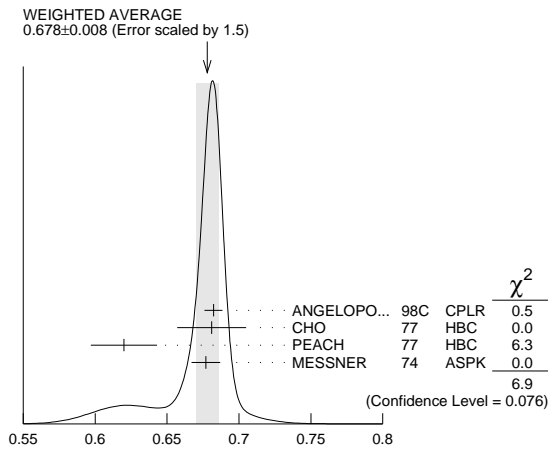
LINEAR COEFFICIENT  $g$  FOR  $K_L^0 \rightarrow \pi^+ \pi^- \pi^0$ 

VALUE	EVTS	DOCUMENT ID	TECN	COMMENT
<b>0.678 ± 0.008 OUR AVERAGE</b>				Error includes scale factor of 1.5. See the ideogram below.
0.6823 ± 0.0044 ± 0.0044	500k	ANGELOPO...	98c CPLR	
0.681 ± 0.024	6499	CHO	77 HBC	
0.620 ± 0.023	4709	PEACH	77 HBC	
0.677 ± 0.010	509k	MESSNER	74 ASPK	$a_Y = -0.917 \pm 0.013$
• • • We do not use the following data for averages, fits, limits, etc. • • •				
0.69 ± 0.07	192	<sup>1</sup> BALDO...	75 HLBC	
0.590 ± 0.022	56k	<sup>1</sup> BUCHANAN	75 SPEC	$a_U = -0.277 \pm 0.010$
0.619 ± 0.027	20k	<sup>1,2</sup> BISI	74 ASPK	$a_T = -0.282 \pm 0.011$
0.612 ± 0.032		<sup>1</sup> ALEXANDER	73B HBC	
0.73 ± 0.04	3200	<sup>1</sup> BRANDENB...	73 HBC	
0.608 ± 0.043	1486	<sup>1</sup> KRENZ	72 HLBC	$a_T = -0.277 \pm 0.018$
0.650 ± 0.012	29k	<sup>1</sup> ALBROW	70 ASPK	$a_Y = -0.858 \pm 0.015$
0.593 ± 0.022	36k	<sup>1,3</sup> BUCHANAN	70 SPEC	$a_U = -0.278 \pm 0.010$
0.664 ± 0.056	4400	<sup>1</sup> SMITH	70 OSPK	$a_T = -0.306 \pm 0.024$
0.400 ± 0.045	2446	<sup>1</sup> BASILE	68B OSPK	$a_T = -0.188 \pm 0.020$
0.649 ± 0.044	1350	<sup>1</sup> HOPKINS	67 HBC	$a_T = -0.294 \pm 0.018$
0.428 ± 0.055	1198	<sup>1</sup> NEFKENS	67 OSPK	$a_U = -0.204 \pm 0.025$

<sup>1</sup> Quadratic dependence required by some experiments. (See sections on "QUADRATIC COEFFICIENT  $h$ " and "QUADRATIC COEFFICIENT  $k$ " below.) Correlations prevent us from averaging results of fits not including  $g$ ,  $h$ , and  $k$  terms.

<sup>2</sup> BISI 74 value comes from quadratic fit with quad. term consistent with zero.  $g$  error is thus larger than if linear fit were used.

<sup>3</sup> BUCHANAN 70 result revised by BUCHANAN 75 to include radiative correlations and to use more reliable  $K_L^0$  momentum spectrum of second experiment (had same beam).



Linear coeff.  $g$  for  $K_L^0 \rightarrow \pi^+ \pi^- \pi^0$  matrix element squared

QUADRATIC COEFFICIENT  $h$  FOR  $K_L^0 \rightarrow \pi^+ \pi^- \pi^0$ 

VALUE	EVTS	DOCUMENT ID	TECN
<b>0.076 ± 0.006 OUR AVERAGE</b>			
0.061 ± 0.004 ± 0.015	500k	ANGELOPO...	98c CPLR
0.095 ± 0.032	6499	CHO	77 HBC
0.048 ± 0.036	4709	PEACH	77 HBC
0.079 ± 0.007	509k	MESSNER	74 ASPK

• • • We do not use the following data for averages, fits, limits, etc. • • •

-0.011 ± 0.018	29k	<sup>1</sup> ALBROW	70 ASPK
0.043 ± 0.052	4400	<sup>1</sup> SMITH	70 OSPK

See notes in section "LINEAR COEFFICIENT  $g$  FOR  $K_L^0 \rightarrow \pi^+ \pi^- \pi^0$  | MATRIX ELEMENT<sup>2</sup>" above.

<sup>1</sup> Quadratic coefficients  $h$  and  $k$  required by some experiments. (See section on "QUADRATIC COEFFICIENT  $k$ " below.) Correlations prevent us from averaging results of fits not including  $g$ ,  $h$ , and  $k$  terms.

QUADRATIC COEFFICIENT  $k$  FOR  $K_L^0 \rightarrow \pi^+ \pi^- \pi^0$ 

VALUE	EVTS	DOCUMENT ID	TECN
<b>0.0099 ± 0.0015 OUR AVERAGE</b>			
0.0104 ± 0.0017 ± 0.0024	500k	ANGELOPO...	98c CPLR
0.024 ± 0.010	6499	CHO	77 HBC
-0.008 ± 0.012	4709	PEACH	77 HBC
0.0097 ± 0.0018	509k	MESSNER	74 ASPK

LINEAR COEFFICIENT  $j$  FOR  $K_L^0 \rightarrow \pi^+ \pi^- \pi^0$  (CP-VIOLATING TERM)

Listed in CP-violation section below.

QUADRATIC COEFFICIENT  $f$  FOR  $K_L^0 \rightarrow \pi^+ \pi^- \pi^0$  (CP-VIOLATING TERM)

Listed in CP-violation section below.

QUADRATIC COEFFICIENT  $h$  FOR  $K_L^0 \rightarrow \pi^0 \pi^0 \pi^0$ 

No average is computed because not all measurements included the effect of final state rescattering.

VALUE (units $10^{-3}$ )	EVTS	DOCUMENT ID	TECN
+0.59 ± 0.20 ± 1.16	6.8M	<sup>1</sup> ABOUZAID	08A KTEV
-6.1 ± 0.9 ± 0.5	14.7M	<sup>2</sup> LAI	01B NA48
-3.3 ± 1.1 ± 0.7	5M	<sup>2,3</sup> SOMALWAR	92 E731

<sup>1</sup> Result obtained using CI3pl model of CABIBBO 05 to include  $\pi\pi$  rescattering effects. The systematic error includes an external error of  $1.06 \times 10^{-3}$  from the parametrization input of  $(a_0 - a_2) m_{\pi^+} = 0.268 \pm 0.017$  from BATLEY 06B.

<sup>2</sup> LAI 01B and SOMALWAR 92 results do not include  $\pi\pi$  final state rescattering effects.

<sup>3</sup> SOMALWAR 92 chose  $m_{\pi^+}$  as normalization to make it compatible with the Particle Data Group  $K_L^0 \rightarrow \pi^+ \pi^- \pi^0$  definitions.

 $K_L^0$  FORM FACTORS

For discussion, see note on form factors in the  $K^\pm$  section of the Particle Listings above.

In the form factor comments, the following symbols are used.

$f_+$  and  $f_-$  are form factors for the vector matrix element.

$f_S$  and  $f_T$  refer to the scalar and tensor term.

$$f_0(t) = f_+(t) + f_-(t) t / (m_K^2 - m_{\pi^+}^2)$$

$t$  = momentum transfer to the  $\pi$ .

$\lambda_+$  and  $\lambda_0$  are the linear expansion coefficients of  $f_+$  and  $f_0$ :

$$f_+(t) = f_+(0) (1 + \lambda_+ t / m_{\pi^+}^2)$$

For quadratic expansion

$$f_+(t) = f_+(0) (1 + \lambda'_+ t / m_{\pi^+}^2 + \lambda''_+ t^2 / m_{\pi^+}^4)$$

as used by KTeV. If there is a non-vanishing quadratic term, then  $\lambda_+$

represents an average slope, which is then different from  $\lambda'_+$ .

NA48 ( $K_{e3}$ ) and ISTRA quadratic expansion coefficients are converted with

$$\lambda'_+{}^{PDG} = \lambda_+{}^{NA48} \text{ and } \lambda''_+{}^{PDG} = 2 \lambda'_+{}^{NA48}$$

$$\lambda'_+{}^{PDG} = (\frac{m_{\pi^+}}{m_{\pi^0}})^2 \lambda_+{}^{ISTRA} \text{ and}$$

$$\lambda''_+{}^{PDG} = 2 (\frac{m_{\pi^+}}{m_{\pi^0}})^4 \lambda'_+{}^{ISTRA}$$

ISTRA linear expansion coefficients are converted with

$$\lambda_+{}^{PDG} = (\frac{m_{\pi^+}}{m_{\pi^0}})^2 \lambda_+{}^{ISTRA} \text{ and } \lambda_0{}^{PDG} = (\frac{m_{\pi^+}}{m_{\pi^0}})^2 \lambda_0{}^{ISTRA}$$

The pole parametrization is

$$f_+(t) = f_+(0) (\frac{M_V^2}{M_V^2 - t})$$

$$f_0(t) = f_0(0) (\frac{M_S^2}{M_S^2 - t})$$

where  $M_V$  and  $M_S$  are the vector and scalar pole masses.

The dispersive parametrization is

$$f_+(t) = f_+(0) \exp[\frac{t}{m_{\pi^+}^2} (\Lambda_+ + H(t))];$$

$$f_0(t) = f_0(0) \exp[\frac{t}{m_K^2 - m_{\pi^+}^2} (\ln[C] - G(t))];$$

where  $\Lambda_+$  is the slope parameter and  $\ln[C] = \ln[f_0(m_K^2 - m_{\pi^+}^2)]$

is the logarithm of the scalar form factor at the Callan-Treiman point.

$H(t)$  and  $G(t)$  are dispersive integrals.

The following abbreviations are used:

DP = Dalitz plot analysis.

PI =  $\pi$  spectrum analysis.

MU =  $\mu$  spectrum analysis.

POL =  $\mu$  polarization analysis.

BR =  $K_{\mu 3}^0 / K_{e 3}^0$  branching ratio analysis.

E = positron or electron spectrum analysis.

RC = radiative corrections.

 $\lambda_+$  (LINEAR ENERGY DEPENDENCE OF  $f_+$  IN  $K_{e 3}^0$  DECAY)

For radiative correction of  $K_{e 3}^0$  DP, see GINSBERG 67, BECHERRAWY 70, CIRIGLIANO 02, CIRIGLIANO 04, and ANDRE 07. Results labeled OUR FIT are discussed in the review "K<sub>23</sub><sup>±</sup> and K<sub>33</sub><sup>0</sup> Form Factors" in the  $K^\pm$  Listings. For earlier, lower statistics results, see the 2004 edition of this review, Physics Letters **B592** 1 (2004).

VALUE (units $10^{-2}$ )	EVTS	DOCUMENT ID	TECN	COMMENT
<b>2.82 ± 0.04 OUR FIT</b>				Error includes scale factor of 1.1. Assuming $\mu$ -e universality
<b>2.85 ± 0.04 OUR AVERAGE</b>				
2.86 ± 0.05 ± 0.04	2M	AMBROSINO	06D KLOE	
2.832 ± 0.037 ± 0.043	1.9M	ALEXOPOU...	04A KTEV	PI, no $\mu = e$
2.88 ± 0.04 ± 0.11	5.6M	<sup>1</sup> LAI	04c NA48	DP

See key on page 457

# Meson Particle Listings

$K_L^0$

• • • We do not use the following data for averages, fits, limits, etc. • • •

2.84 ± 0.07 ± 0.13	5.6M	<sup>2</sup> LAI	04c	NA48	DP
2.45 ± 0.12 ± 0.22	366k	APOSTOLA...	00	CPLR	DP
3.06 ± 0.34	74k	BIRULEV	81	SPEC	DP
3.12 ± 0.25	500k	GJESDAL	76	SPEC	DP
2.70 ± 0.28	25k	BLUMENTHAL75	SPEC	DP	

<sup>1</sup> Results from linear fit and assuming only vector and axial couplings.  
<sup>2</sup> Results from linear fit with  $|f_S/f_+|$  and  $|f_T/f_+|$  free.

## $\lambda_+$ (LINEAR ENERGY DEPENDENCE OF $f_+$ IN $K_{\mu 3}^0$ DECAY)

Results labeled OUR FIT are discussed in the review " $K_{\mu 3}^+$  and  $K_{\mu 3}^0$  Form Factors" in the  $K^\pm$  Listings. For earlier, lower statistics results, see the 2004 edition of this review, Physics Letters **B592** 1 (2004).

VALUE (units $10^{-2}$ )	EVTS	DOCUMENT ID	TECN	COMMENT
<b>2.82 ± 0.04 OUR FIT</b>	Error includes scale factor of 1.1. Assuming $\mu$ -e universality			
<b>2.71 ± 0.10 OUR FIT</b>	Error includes scale factor of 1.4. Not assuming $\mu$ -e universality			
2.67 ± 0.06 ± 0.08	2.3M	<sup>1</sup> LAI	07A	NA48 DP
2.745 ± 0.088 ± 0.063	1.5M	ALEXOPOU...	04A	KTEV DP, no $\mu = e$
2.813 ± 0.051	3.4M	ALEXOPOU...	04A	KTEV PI, DP, $\mu = e$
3.0 ± 0.3	1.6M	DONALDSON	74B	SPEC DP
• • • We do not use the following data for averages, fits, limits, etc. • • •				
4.27 ± 0.44	150k	BIRULEV	81	SPEC DP

<sup>1</sup> LAI 07A gives a correlation  $-0.40$  between their  $\lambda_0$  and  $\lambda_+$  measurements.

## $\lambda_0$ (LINEAR ENERGY DEPENDENCE OF $f_0$ IN $K_{\mu 3}^0$ DECAY)

Wherever possible, we have converted the above values of  $\xi(0)$  into values of  $\lambda_0$  using the associated  $\lambda_+^u$  and  $d\xi(0)/d\lambda_+$ . Results labeled OUR FIT are discussed in the review " $K_{\mu 3}^+$  and  $K_{\mu 3}^0$  Form Factors" in the  $K^\pm$  Listings. For earlier, lower statistics results, see the 2004 edition of this review, Physics Letters **B592** 1 (2004).

VALUE (units $10^{-2}$ )	$d\lambda_0/d\lambda_+$	EVTS	DOCUMENT ID	TECN	COMMENT
<b>1.38 ± 0.18 OUR FIT</b>	Error includes scale factor of 2.2. Assuming $\mu$ -e universality				
<b>1.42 ± 0.23 OUR FIT</b>	Error includes scale factor of 2.8. Not assuming $\mu$ -e universality				
1.17 ± 0.07 ± 0.10	2.3M	<sup>1</sup> LAI	07A	NA48 DP	
1.657 ± 0.125	-0.44	1.5M	<sup>2</sup> ALEXOPOU...	04A	KTEV DP, no $\mu = e$
1.635 ± 0.121	-0.85	3.4M	<sup>3</sup> ALEXOPOU...	04A	KTEV PI, DP, $\mu = e$
+ 1.9 ± 0.4	-0.47	1.6M	<sup>4</sup> DONALDSON	74B	SPEC DP

• • • We do not use the following data for averages, fits, limits, etc. • • •

3.41 ± 0.67 unknown 150k <sup>5</sup> BIRULEV 81 SPEC DP

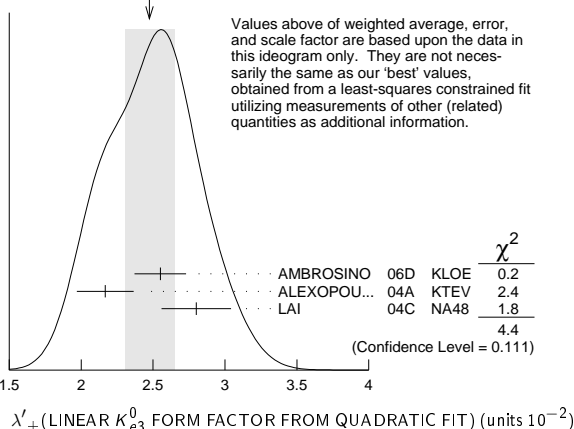
<sup>1</sup> LAI 07A gives a correlation  $-0.40$  between their  $\lambda_0$  and  $\lambda_+$  measurements.  
<sup>2</sup> ALEXOPOULOS 04A gives a correlation  $-0.38$  between their  $\lambda_0$  and  $\lambda_+$  measurements.  
<sup>3</sup> ALEXOPOULOS 04A gives a correlation  $-0.36$  between their  $\lambda_0$  and  $\lambda_+$  measurements.  
<sup>4</sup> DONALDSON 74B  $d\lambda_0/d\lambda_+$  obtained from figure 18.  
<sup>5</sup> BIRULEV 81 gives  $d\lambda_0/d\lambda_+ = -1.5$ , giving an unreasonably narrow error ellipse which dominates all other results. We use  $d\lambda_0/d\lambda_+ = 0$ .

## $\lambda'_+$ (LINEAR $K_{e3}^0$ FORM FACTOR FROM QUADRATIC FIT)

VALUE (units $10^{-2}$ )	EVTS	DOCUMENT ID	TECN	COMMENT
<b>2.40 ± 0.12 OUR FIT</b>	Error includes scale factor of 1.2. Assuming $\mu$ -e universality			
<b>2.49 ± 0.13 OUR FIT</b>	Error includes scale factor of 1.1. Not assuming $\mu$ -e universality			
<b>2.48 ± 0.17 OUR AVERAGE</b>	Error includes scale factor of 1.5. See the ideogram below.			
2.55 ± 0.15 ± 0.10	2M	<sup>1</sup> AMBROSINO	06D	KLOE
2.167 ± 0.137 ± 0.143	1.9M	<sup>2</sup> ALEXOPOU...	04A	KTEV PI, no $\mu = e$
2.80 ± 0.19 ± 0.15	5.6M	<sup>3</sup> LAI	04c	NA48 DP

<sup>1</sup> We use AMBROSINO 06D result in the fit not assuming  $\mu$ -e universality. This result enters the fit assuming  $\mu$ -e universality via AMBROSINO 07c measurement of  $\lambda'_+$  in  $K_{\mu 3}$  decays. AMBROSINO 06D gives a correlation  $-0.95$  between their  $\lambda'_+$  and  $\lambda''_+$ .  
<sup>2</sup> ALEXOPOULOS 04A gives a correlation  $-0.97$  between their  $\lambda'_+$  and  $\lambda''_+$ .  
<sup>3</sup> For LAI 04c we calculate a correlation  $-0.88$  between their  $\lambda'_+$  and  $\lambda''_+$ .

WEIGHTED AVERAGE  
 2.48 ± 0.17 (Error scaled by 1.5)

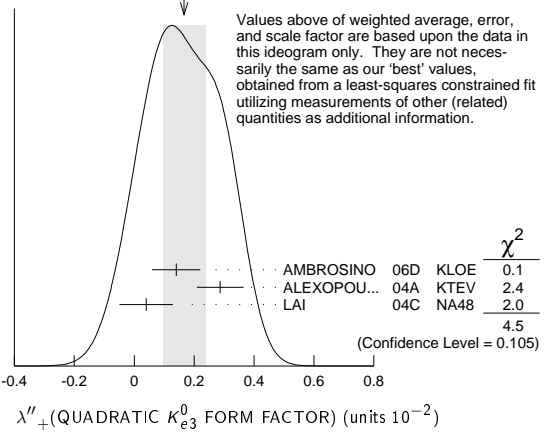


## $\lambda''_+$ (QUADRATIC $K_{e3}^0$ FORM FACTOR)

VALUE (units $10^{-2}$ )	EVTS	DOCUMENT ID	TECN	COMMENT
<b>0.20 ± 0.05 OUR FIT</b>	Error includes scale factor of 1.2. Assuming $\mu$ -e universality			
<b>0.16 ± 0.05 OUR FIT</b>	Error includes scale factor of 1.1. Not assuming $\mu$ -e universality			
<b>0.17 ± 0.07 OUR AVERAGE</b>	Error includes scale factor of 1.5. See the ideogram below.			
0.14 ± 0.07 ± 0.04	2M	<sup>1</sup> AMBROSINO	06D	KLOE
0.287 ± 0.057 ± 0.053	1.9M	<sup>2</sup> ALEXOPOU...	04A	KTEV PI, no $\mu = e$
0.04 ± 0.08 ± 0.04	5.6M	<sup>3,4</sup> LAI	04c	NA48 DP

<sup>1</sup> We use AMBROSINO 06D result in the fit not assuming  $\mu$ -e universality. This result enters the fit assuming  $\mu$ -e universality via AMBROSINO 07c measurement of  $\lambda''_+$  in  $K_{\mu 3}$  decays. AMBROSINO 06D gives a correlation  $-0.95$  between their  $\lambda'_+$  and  $\lambda''_+$ .  
<sup>2</sup> ALEXOPOULOS 04A gives a correlation  $-0.97$  between their  $\lambda'_+$  and  $\lambda''_+$ .  
<sup>3</sup> Values doubled to agree with PDG conventions described above.  
<sup>4</sup> LAI 04c gives a correlation  $-0.88$  between their  $\lambda'_+$  and  $\lambda''_+$ .

WEIGHTED AVERAGE  
 0.17 ± 0.07 (Error scaled by 1.5)



## $\lambda'_+$ (LINEAR $K_{\mu 3}^0$ FORM FACTOR FROM QUADRATIC FIT)

VALUE (units $10^{-2}$ )	EVTS	DOCUMENT ID	TECN	COMMENT
<b>2.40 ± 0.12 OUR FIT</b>	Error includes scale factor of 1.2. Assuming $\mu$ -e universality			
<b>1.89 ± 0.24 OUR FIT</b>	Not assuming $\mu$ -e universality			
2.23 ± 0.98 ± 0.37	1.8M	<sup>1</sup> AMBROSINO	07c	KLOE no $\mu = e$
2.56 ± 0.15 ± 0.09	3.8M	<sup>1</sup> AMBROSINO	07c	KLOE $\mu = e$
2.05 ± 0.22 ± 0.24	2.3M	<sup>1</sup> LAI	07A	NA48 DP
1.703 ± 0.319 ± 0.177	1.5M	<sup>1</sup> ALEXOPOU...	04A	KTEV DP, no $\mu = e$
2.064 ± 0.175	3.4M	<sup>1</sup> ALEXOPOU...	04A	KTEV PI, DP, $\mu = e$

<sup>1</sup> See section  $\lambda_0$  below for correlations.

## $\lambda''_+$ (QUADRATIC $K_{\mu 3}^0$ FORM FACTOR)

VALUE (units $10^{-2}$ )	EVTS	DOCUMENT ID	TECN	COMMENT
<b>0.20 ± 0.05 OUR FIT</b>	Error includes scale factor of 1.2. Assuming $\mu$ -e universality			
<b>0.37 ± 0.12 OUR FIT</b>	Error includes scale factor of 1.3. Not assuming $\mu$ -e universality			
0.48 ± 0.49 ± 0.16	1.8M	<sup>1</sup> AMBROSINO	07c	KLOE no $\mu = e$
0.15 ± 0.07 ± 0.04	3.8M	<sup>1</sup> AMBROSINO	07c	KLOE $\mu = e$
0.26 ± 0.09 ± 0.10	2.3M	<sup>1</sup> LAI	07A	NA48 DP
0.443 ± 0.131 ± 0.072	1.5M	<sup>1</sup> ALEXOPOU...	04A	KTEV DP, no $\mu = e$
0.320 ± 0.069	3.4M	<sup>1</sup> ALEXOPOU...	04A	KTEV PI, DP, $\mu = e$

<sup>1</sup> See section  $\lambda_0$  below for correlations.

## $\lambda_0$ (LINEAR $f_0$ $K_{\mu 3}^0$ FORM FACTOR FROM QUADRATIC FIT)

VALUE (units $10^{-2}$ )	EVTS	DOCUMENT ID	TECN	COMMENT
<b>1.16 ± 0.09 OUR FIT</b>	Error includes scale factor of 1.2. Assuming $\mu$ -e universality			
<b>1.07 ± 0.14 OUR FIT</b>	Error includes scale factor of 1.3. Not assuming $\mu$ -e universality			
0.91 ± 0.59 ± 0.26	1.8M	<sup>1</sup> AMBROSINO	07c	KLOE no $\mu = e$
1.54 ± 0.18 ± 0.13	3.8M	<sup>2</sup> AMBROSINO	07c	KLOE $\mu = e$
0.95 ± 0.11 ± 0.08	2.3M	<sup>3</sup> LAI	07A	NA48 DP
1.281 ± 0.136 ± 0.122	1.5M	<sup>4</sup> ALEXOPOU...	04A	KTEV DP, no $\mu = e$
1.372 ± 0.131	3.4M	<sup>5</sup> ALEXOPOU...	04A	KTEV PI, DP, $\mu = e$

<sup>1</sup> AMBROSINO 07c, not assuming  $\mu$ -e universality, gives a correlation matrix

$$\begin{matrix} \lambda'_+ & \lambda''_+ \\ \lambda''_+ & -0.97 & 1 \\ \lambda_0 & 0.81 & -0.91 \end{matrix}$$

<sup>2</sup> AMBROSINO 07c, assuming  $\mu$ -e universality, gives a correlation matrix

$$\begin{matrix} \lambda'_+ & \lambda''_+ \\ \lambda''_+ & -0.95 & 1 \\ \lambda_0 & 0.29 & -0.38 \end{matrix}$$

<sup>3</sup> LAI 07A gives a correlation matrix

$$\begin{matrix} \lambda'_+ & \lambda''_+ \\ \lambda''_+ & -0.96 & 1 \\ \lambda_0 & 0.63 & -0.73 \end{matrix}$$

# Meson Particle Listings

$K_L^0$

<sup>4</sup> ALEXOPOULOS 04A, not assuming  $\mu$ - $e$  universality, gives a correlation matrix

$$\begin{matrix} & \lambda'_+ & \lambda''_+ & \lambda_0 \\ \lambda'_+ & 1 & & \\ \lambda''_+ & -0.96 & 1 & \\ \lambda_0 & 0.65 & -0.75 & 1 \end{matrix}$$

<sup>5</sup> ALEXOPOULOS 04A, assuming  $\mu$ - $e$  universality, gives a correlation matrix

$$\begin{matrix} & \lambda'_+ & \lambda''_+ & \lambda_0 \\ \lambda'_+ & 1 & & \\ \lambda''_+ & -0.97 & 1 & \\ \lambda_0 & 0.34 & -0.44 & 1 \end{matrix}$$

## $M_V^e$ (POLE MASS FOR $K_{e3}^0$ DECAY)

VALUE (MeV)	EVTS	DOCUMENT ID	TECN	COMMENT
<b>878 ± 6</b>	<b>OUR FIT</b>	Error includes scale factor of 1.1. Assuming $\mu$ - $e$ universality		
<b>875 ± 5</b>	<b>OUR AVERAGE</b>			
870 ± 6 ± 7	2M	AMBROSINO 06D	KLOE	
881.03 ± 5.12 ± 4.94	1.9M	ALEXOPOU... 04A	KTEV	PI, no $\mu = e$
859 ± 18	5.6M	LAI 04C	NA48	

## $M_V^\mu$ (POLE MASS FOR $K_{\mu 3}^0$ DECAY)

VALUE (MeV)	EVTS	DOCUMENT ID	TECN	COMMENT
<b>878 ± 6</b>	<b>OUR FIT</b>	Error includes scale factor of 1.1. Assuming $\mu$ - $e$ universality		
<b>900 ± 21</b>	<b>OUR FIT</b>	Error includes scale factor of 1.7. Not assuming $\mu$ - $e$ universality		
905 ± 9 ± 17	2.3M	<sup>1</sup> LAI 07A	NA48	DP
889.19 ± 12.81 ± 9.92	1.5M	<sup>1</sup> ALEXOPOU... 04A	KTEV	DP, no $\mu = e$
882.32 ± 6.54	3.4M	<sup>1</sup> ALEXOPOU... 04A	KTEV	PI, DP, $\mu = e$

<sup>1</sup> See section  $M_S^\mu$  below for correlations.

## $M_S^\mu$ (POLE MASS FOR $K_{\mu 3}^0$ DECAY)

VALUE (MeV)	EVTS	DOCUMENT ID	TECN	COMMENT
<b>1252 ± 90</b>	<b>OUR FIT</b>	Error includes scale factor of 2.6. Assuming $\mu$ - $e$ universality		
<b>1222 ± 80</b>	<b>OUR FIT</b>	Error includes scale factor of 2.3. Not assuming $\mu$ - $e$ universality		
1400 ± 46 ± 53	2.3M	<sup>1</sup> LAI 07A	NA48	DP
1167.14 ± 28.30 ± 31.04	1.5M	<sup>2</sup> ALEXOPOU... 04A	KTEV	PI, no $\mu = e$
1173.80 ± 39.47	3.4M	<sup>3</sup> ALEXOPOU... 04A	KTEV	PI, DP, $\mu = e$

- <sup>1</sup> LAI 07A gives a correlation  $-0.47$  between their  $M_S^\mu$  and  $M_V^\mu$  measurements, not assuming  $\mu$ - $e$  universality.
- <sup>2</sup> ALEXOPOULOS 04A gives a correlation  $-0.46$  between their  $M_S^\mu$  and  $M_V^\mu$  and measurements, not assuming  $\mu$ - $e$  universality.
- <sup>3</sup> ALEXOPOULOS 04A gives a correlation  $-0.40$  between their  $M_S^\mu$  and  $M_V^\mu$  and measurements, assuming  $\mu$ - $e$  universality.

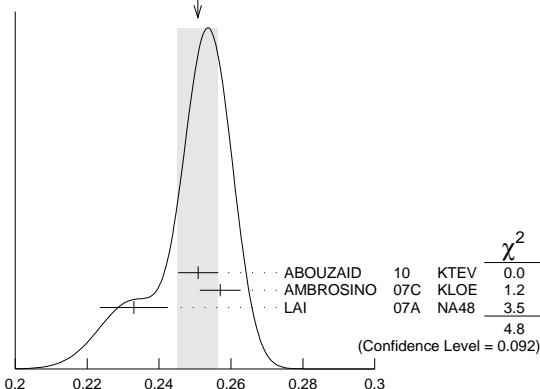
## $\Lambda_+$ (DISPERSIVE VECTOR FORM FACTOR FOR $K_{\mu 3}^0$ DECAY)

See the review on " $K_{e3}^0$  and  $K_{\mu 3}^0$  Form Factors" for details of the dispersive parametrization.

VALUE (units $10^{-1}$ )	EVTS	DOCUMENT ID	TECN	COMMENT
<b>0.251 ± 0.006</b>	<b>OUR AVERAGE</b>	Error includes scale factor of 1.5. See the ideogram below.		
0.2509 ± 0.0035 ± 0.0043	3.4M	<sup>1</sup> ABOUZAID 10	KTEV	$\mu = e$
0.257 ± 0.004 ± 0.004	3.8M	<sup>2</sup> AMBROSINO 07C	KLOE	$\mu = e$
0.233 ± 0.005 ± 0.008	2.3M	<sup>3</sup> LAI 07A	NA48	DP

- <sup>1</sup> Obtained from a sample of 1.9 M  $K_{e3}$  and 1.5 M  $K_{\mu 3}$ . The correlation between  $\Lambda_+$  and  $\ln(C)$  is  $-0.269$ .
- <sup>2</sup> AMBROSINO 07C results include 2M  $K_{e3}$  events from AMBROSINO 06D. The correlation between  $\Lambda_+$  and  $\ln(C)$  is  $-0.26$ .
- <sup>3</sup> LAI 07A gives a correlation  $-0.44$  between their  $\Lambda_+$  and  $\ln(C)$  measurements.

WEIGHTED AVERAGE  
0.251 ± 0.006 (Error scaled by 1.5)



$\Lambda_+$  (DISPERSIVE VECTOR FORM FACTOR FOR  $K_{\mu 3}^0$  DECAY) (units  $10^{-1}$ )

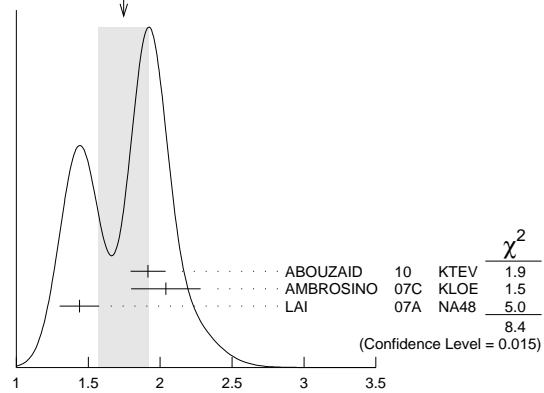
## $\ln(C)$ (DISPERSIVE SCALAR FORM FACTOR FOR $K_{\mu 3}^0$ DECAY)

See the review on " $K_{e3}^0$  and  $K_{\mu 3}^0$  Form Factors" for details of the dispersive parametrization.

VALUE (units $10^{-1}$ )	EVTS	DOCUMENT ID	TECN	COMMENT
<b>1.75 ± 0.18</b>	<b>OUR AVERAGE</b>	Error includes scale factor of 2.0. See the ideogram below.		
1.915 ± 0.078 ± 0.094	3.4M	<sup>1</sup> ABOUZAID 10	KTEV	$\mu = e$
2.04 ± 0.19 ± 0.15	3.8M	<sup>2</sup> AMBROSINO 07C	KLOE	$\mu = e$
1.438 ± 0.080 ± 0.112	2.3M	<sup>3</sup> LAI 07A	NA48	DP

- <sup>1</sup> Obtained from a sample of 1.9 M  $K_{e3}$  and 1.5 M  $K_{\mu 3}$ . The correlation between  $\Lambda_+$  and  $\ln(C)$  is  $-0.269$ .
- <sup>2</sup> AMBROSINO 07C results include 2M  $K_{e3}$  events from AMBROSINO 06D. We convert  $(\Lambda_+, A_0)$  to  $(\Lambda_+, \ln(C))$  parametrization using  $\ln(C) = (\Lambda_0 \cdot 11.713 + 0.0398) \pm 0.0041$ , where the error is due to theory parametrization of the form factor. The correlation between  $\Lambda_+$  and  $\ln(C)$  is  $-0.26$ .
- <sup>3</sup> LAI 07A gives a correlation  $-0.44$  between their  $\Lambda_+$  and  $\ln(C)$  measurements.

WEIGHTED AVERAGE  
1.75 ± 0.18 (Error scaled by 2.0)



$\ln(C)$  (DISPERSIVE SCALAR FORM FACTOR FOR  $K_{\mu 3}^0$  DECAY) (units  $10^{-1}$ )

## $a_1(t_0, Q^2)$ FORM FACTOR PARAMETER

See HILL 06 for a definition of this parameter.

VALUE	EVTS	DOCUMENT ID	TECN
<b>1.023 ± 0.028 ± 0.029</b>	2M	<sup>1</sup> ABOUZAID 06C	KTEV

<sup>1</sup>  $Q^2 = 2 \text{ GeV}^2$ ,  $t_0 = 0.49 (m_K - m_\pi)^2$ . Correlation between  $a_1$  and  $a_2$ :  $\rho_{12} = -0.064$ .

## $a_2(t_0, Q^2)$ FORM FACTOR PARAMETER

See HILL 06 for a definition of this parameter.

VALUE	EVTS	DOCUMENT ID	TECN
<b>0.75 ± 1.58 ± 1.47</b>	2M	<sup>1</sup> ABOUZAID 06C	KTEV

<sup>1</sup>  $Q^2 = 2 \text{ GeV}^2$ ,  $t_0 = 0.49 (m_K - m_\pi)^2$ . Correlation between  $a_1$  and  $a_2$ :  $\rho_{12} = -0.064$ .

## $|f_S/f_+|$ FOR $K_{e3}^0$ DECAY

Ratio of scalar to  $f_+$  couplings.

VALUE (units $10^{-2}$ )	CL%	EVTS	DOCUMENT ID	TECN	COMMENT
<b>1.5<sup>+0.7</sup><sub>-1.0</sub> ± 1.2</b>		5.6M	<sup>1</sup> LAI 04C	NA48	

• • • We do not use the following data for averages, fits, limits, etc. • • •

<9.5	95	18k	HILL 78	STRC	
<7.	68	48k	BIRULEV 76	SPEC	See also BIRULEV 81
<4.	68	25k	BLUMENTHAL75	SPEC	

<sup>1</sup> Results from linear fit with  $|f_S/f_+|$  and  $|f_T/f_+|$  free.

## $|f_T/f_+|$ FOR $K_{e3}^0$ DECAY

Ratio of tensor to  $f_+$  couplings.

VALUE (units $10^{-2}$ )	CL%	EVTS	DOCUMENT ID	TECN	COMMENT
<b>5<sup>+3</sup><sub>-4</sub> ± 3</b>		5.6M	<sup>1</sup> LAI 04C	NA48	

• • • We do not use the following data for averages, fits, limits, etc. • • •

<40.	95	18k	HILL 78	STRC	
<34.	68	48k	BIRULEV 76	SPEC	See also BIRULEV 81
<23.	68	25k	BLUMENTHAL75	SPEC	

<sup>1</sup> Results from linear fit with  $|f_S/f_+|$  and  $|f_T/f_+|$  free.

## $|f_T/f_+|$ FOR $K_{\mu 3}^0$ DECAY

Ratio of tensor to  $f_+$  couplings.

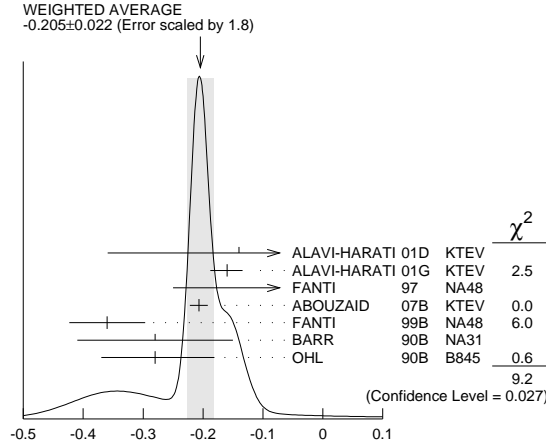
VALUE (units $10^{-2}$ )	DOCUMENT ID	TECN
<b>12. ± 12.</b>	BIRULEV 81	SPEC



**$\alpha_{K^*}$  DECAY FORM FACTOR FOR  $K_L \rightarrow \ell^+ \ell^- \gamma$ ,  $K_L^0 \rightarrow \ell^+ \ell^- \ell'^+ \ell'^-$** 

Average of all  $\alpha_{K^*}$  measurements (from each of three datablocks following this one) assuming lepton universality.

**VALUE** DOCUMENT ID  
**-0.205 ± 0.022 OUR AVERAGE** Includes data from the 3 datablocks that follow this one. Error includes scale factor of 1.8. See the ideogram below.



$\alpha_{K^*}$  DECAY FORM FACTOR FOR  $K_L \rightarrow \ell^+ \ell^- \gamma$ ,  $K_L^0 \rightarrow \ell^+ \ell^- \ell'^+ \ell'^-$

 **$\alpha_{K^*}$  DECAY FORM FACTOR FOR  $K_L \rightarrow e^+ e^- \gamma$** 

$\alpha_{K^*}$  is the constant in the model of BERGSTROM 83 which measures the relative strength of the vector-vector transition  $K_L \rightarrow K^* \gamma$  with  $K^* \rightarrow \rho, \omega, \phi \rightarrow \gamma^*$  and the pseudoscalar-pseudoscalar transition  $K_L \rightarrow \pi, \eta, \eta' \rightarrow \gamma \gamma^*$ .

**VALUE** EVTS DOCUMENT ID TECN  
 The data in this block is included in the average printed for a previous datablock.

**-0.217 ± 0.034 OUR AVERAGE** Error includes scale factor of 2.4.  
 -0.207 ± 0.012 ± 0.009 83k <sup>1</sup>ABOUZAID 07B KTEV  
 -0.36 ± 0.06 ± 0.02 6864 FANTI 99B NA48  
 -0.28 ± 0.13 BARR 90B NA31  
 -0.280 <sup>+0.099</sup>/<sub>-0.090</sub> OHL 90B B845

<sup>1</sup>ABOUZAID 07b measures  $C \alpha_{K^*} = -0.517 \pm 0.030 \pm 0.022$ . We assume  $C = 2.5$ , as in all other measurements.

 **$\alpha_{K^*}$  DECAY FORM FACTOR FOR  $K_L \rightarrow \mu^+ \mu^- \gamma$** 

$\alpha_{K^*}$  is the constant in the model of BERGSTROM 83 described in the previous section.

**VALUE** EVTS DOCUMENT ID TECN  
 The data in this block is included in the average printed for a previous datablock.

**-0.158 ± 0.027 OUR AVERAGE**  
 -0.160 <sup>+0.026</sup>/<sub>-0.028</sub> 9100 ALAVI-HARATI01G KTEV  
 -0.04 <sup>+0.24</sup>/<sub>-0.21</sub> FANTI 97 NA48

 **$\alpha_{K^*}^{\text{eff}}$  DECAY FORM FACTOR FOR  $K_L \rightarrow e^+ e^- e^+ e^-$** 

$\alpha_{K^*}^{\text{eff}}$  is the parameter describing the relative strength of an intermediate pseudoscalar decay amplitude and a vector meson decay amplitude in the model of BERGSTROM 83. It takes into account both the radiative effects and the form factor. Since there are two  $e^+ e^-$  pairs here compared with one in  $e^+ e^- \gamma$  decays, a factorized expression is used for the  $e^+ e^- e^+ e^-$  decay form factor.

**VALUE** EVTS DOCUMENT ID TECN  
 The data in this block is included in the average printed for a previous datablock.

**-0.14 ± 0.16 ± 0.15** 441 ALAVI-HARATI01D KTEV

 **$\alpha_{DIP}$  DECAY FORM FACTOR FOR  $K_L^0 \rightarrow \ell^+ \ell^- \gamma$ ,  $K_L^0 \rightarrow \ell^+ \ell^- \ell'^+ \ell'^-$** 

Average of all  $\alpha_{DIP}$  measurements (from each of three datablocks following this one) assuming lepton universality.

**VALUE** DOCUMENT ID  
**-1.69 ± 0.08 OUR AVERAGE** Includes data from the 3 datablocks that follow this one. Error includes scale factor of 1.7.

 **$\alpha_{DIP}$  DECAY FORM FACTOR FOR  $K_L^0 \rightarrow e^+ e^- \gamma$** 

$\alpha_{DIP}$  parameter in  $K_L^0 \rightarrow \gamma^* \gamma^*$  form factor by DAMBROSIO 98, motivated by vector meson dominance and a proper short distance behavior.

**VALUE** EVTS DOCUMENT ID TECN  
 The data in this block is included in the average printed for a previous datablock.

**-1.729 ± 0.043 ± 0.028** 83k ABOUZAID 07B KTEV

 **$\alpha_{DIP}$  DECAY FORM FACTOR FOR  $K_L^0 \rightarrow \mu^+ \mu^- \gamma$** 

$\alpha_{DIP}$  is a constant in the model of DAMBROSIO 98 described in the previous section.

**VALUE** EVTS DOCUMENT ID TECN  
 The data in this block is included in the average printed for a previous datablock.

**-1.54 ± 0.10** 9100 ALAVI-HARATI01G KTEV

 **$\alpha_{DIP}$  DECAY FORM FACTOR FOR  $K_L^0 \rightarrow e^+ e^- \mu^+ \mu^-$** 

$\alpha_{DIP}$  is a constant in the model of DAMBROSIO 98 described in the previous section.

**VALUE** EVTS DOCUMENT ID TECN  
 The data in this block is included in the average printed for a previous datablock.

**-1.59 ± 0.37** 131 ALAVI-HARATI03B KTEV

 **$a_1/a_2$  FORM FACTOR FOR M1 DIRECT EMISSION AMPLITUDE**

Form factor =  $\tilde{g}_{M1} \left[ 1 + \frac{a_1/a_2}{(M_\rho^2 - M_K^2) + 2M_K E_\gamma} \right]$  as described in ALAVI-HARATI 00b.

**VALUE** (GeV<sup>2</sup>) EVTS DOCUMENT ID TECN COMMENT  
**-0.737 ± 0.014 OUR AVERAGE**  
 -0.744 ± 0.027 ± 0.032 5241 <sup>1</sup>ABOUZAID 06 KTEV  $\pi^+ \pi^- e^+ e^-$   
 -0.738 ± 0.007 ± 0.018 111k <sup>2</sup>ABOUZAID 06A KTEV  $\pi^+ \pi^+ \gamma$   
 -0.81 <sup>+0.07</sup>/<sub>-0.13</sub> ± 0.02 <sup>3</sup>LAI 03c NA48  $\pi^+ \pi^- e^+ e^-$   
 -0.737 ± 0.026 ± 0.022 <sup>4</sup>ALAVI-HARATI01B  $\pi^+ \pi^- \gamma$   
 -0.720 ± 0.028 ± 0.009 1766 <sup>5</sup>ALAVI-HARATI00B KTEV  $\pi^+ \pi^- e^+ e^-$   
<sup>1</sup>ABOUZAID 06 also measured  $|\tilde{g}_{M1}| = 1.11 \pm 0.14$ .  
<sup>2</sup>ABOUZAID 06A also measured  $|\tilde{g}_{M1}| = 1.198 \pm 0.035 \pm 0.086$ .  
<sup>3</sup>LAI 03c also measured  $\tilde{g}_{M1} = 0.99 \pm 0.28$   
<sup>4</sup>ALAVI-HARATI 01B fit gives  $\chi^2/\text{DOF} = 38.8/27$ . Linear and quadratic fits give  $\chi^2/\text{DOF} = 43.2/27$  and  $37.6/26$  respectively.  
<sup>5</sup>ALAVI-HARATI 00b also measured  $|\tilde{g}_{M1}| = 1.35 \pm 0.20$   
<sub>-0.17</sub> ± 0.04.

 **$\bar{T}_S$  DECAY FORM FACTOR FOR  $K_L^0 \rightarrow \pi^\pm \pi^0 e^\mp \nu_e$** 

**VALUE** DOCUMENT ID TECN  
**0.049 ± 0.011 OUR AVERAGE** Error includes scale factor of 1.7.  
 0.052 ± 0.006 ± 0.002 BATLEY 04 NA48  
 0.010 ± 0.016 ± 0.017 MAKOFF 93 E731

 **$\bar{T}_P$  DECAY FORM FACTOR FOR  $K_L^0 \rightarrow \pi^\pm \pi^0 e^\mp \nu_e$** 

**VALUE** DOCUMENT ID TECN  
**-0.052 ± 0.012 OUR AVERAGE**  
 -0.051 ± 0.011 ± 0.005 BATLEY 04 NA48  
 -0.079 ± 0.049 ± 0.022 MAKOFF 93 E731

 **$\lambda_g$  DECAY FORM FACTOR FOR  $K_L^0 \rightarrow \pi^\pm \pi^0 e^\mp \nu_e$** 

**VALUE** DOCUMENT ID TECN  
**0.085 ± 0.020 OUR AVERAGE**  
 0.087 ± 0.019 ± 0.006 BATLEY 04 NA48  
 0.014 ± 0.087 ± 0.070 MAKOFF 93 E731

 **$\bar{T}$  DECAY FORM FACTOR FOR  $K_L^0 \rightarrow \pi^\pm \pi^0 e^\mp \nu_e$** 

**VALUE** DOCUMENT ID TECN  
**-0.30 ± 0.13 OUR AVERAGE**  
 -0.32 ± 0.12 ± 0.07 BATLEY 04 NA48  
 -0.07 ± 0.31 ± 0.31 MAKOFF 93 E731

 **$L_3$  CHIRAL PERT. THEO. PARAM. FOR  $K_L^0 \rightarrow \pi^\pm \pi^0 e^\mp \nu_e$** 

**VALUE** (units 10<sup>-3</sup>) DOCUMENT ID TECN  
**-3.96 ± 0.28 OUR AVERAGE** Error includes scale factor of 1.6.  
 -4.1 ± 0.2 BATLEY 04 NA48  
 -3.4 ± 0.4 <sup>1</sup>MAKOFF 93 E731

<sup>1</sup>MAKOFF 93 sign has been changed to negative to agree with the sign convention used in BATLEY 04.

 **$a_V$ , VECTOR MESON EXCHANGE CONTRIBUTION**

**VALUE** EVTS DOCUMENT ID TECN COMMENT  
**-0.43 ± 0.06 OUR AVERAGE** Error includes scale factor of 1.5.  
 -0.31 ± 0.05 ± 0.07 1.4k <sup>1</sup>ABOUZAID 08 KTEV  
 -0.46 ± 0.03 ± 0.04 LAI 02B NA48  $K_L^0 \rightarrow \pi^0 2\gamma$   
 -0.67 ± 0.21 ± 0.12 ALAVI-HARATI01E KTEV  $K_L^0 \rightarrow \pi^0 e^+ e^- \gamma$

••• We do not use the following data for averages, fits, limits, etc. •••

-0.72 ± 0.05 ± 0.06 <sup>2</sup>ALAVI-HARATI99B KTEV  $K_L^0 \rightarrow \pi^0 2\gamma$

<sup>1</sup>Using KTeV dataset collected in 1996, 1997, and 1999.

<sup>2</sup>Superseded by ABOUZAID 08.

**CP VIOLATION IN  $K_L$  DECAYS**

Updated April 2012 by L. Wolfenstein (Carnegie-Mellon University), C.-J. Lin (LBNL), and T.G. Trippe (LBNL).

The symmetries  $C$  (particle-antiparticle interchange) and  $P$  (space inversion) hold for strong and electromagnetic interactions. After the discovery of large  $C$  and  $P$  violation in the weak interactions, it appeared that the product  $CP$  was a good symmetry. In 1964  $CP$  violation was observed in  $K^0$  decays at a level given by the parameter  $\epsilon \approx 2.3 \times 10^{-3}$ .

A unified treatment of  $CP$  violation in  $K$ ,  $D$ ,  $B$ , and  $B_s$  mesons is given in "CP Violation in Meson Decays" by

# Meson Particle Listings

## $K_L^0$

D. Kirkby and Y. Nir in this *Review*. A more detailed review including a thorough discussion of the experimental techniques used to determine  $CP$  violation parameters is given in a book by K. Kleinknecht [1]. Here we give a concise summary of the formalism needed to define the parameters of  $CP$  violation in  $K_L$  decays, and a description of our fits for the best values of these parameters.

### 1. Formalism for $CP$ violation in Kaon decay:

$CP$  violation has been observed in the semi-leptonic decays  $K_L^0 \rightarrow \pi^\mp \ell^\pm \nu$ , and in the nonleptonic decay  $K_L^0 \rightarrow 2\pi$ . The experimental numbers that have been measured are

$$A_L = \frac{\Gamma(K_L^0 \rightarrow \pi^- \ell^+ \nu) - \Gamma(K_L^0 \rightarrow \pi^+ \ell^- \nu)}{\Gamma(K_L^0 \rightarrow \pi^- \ell^+ \nu) + \Gamma(K_L^0 \rightarrow \pi^+ \ell^- \nu)} \quad (1a)$$

$$\eta_{+-} = A(K_L^0 \rightarrow \pi^+ \pi^-) / A(K_S^0 \rightarrow \pi^+ \pi^-) \\ = |\eta_{+-}| e^{i\phi_{+-}} \quad (1b)$$

$$\eta_{00} = A(K_L^0 \rightarrow \pi^0 \pi^0) / A(K_S^0 \rightarrow \pi^0 \pi^0) \\ = |\eta_{00}| e^{i\phi_{00}} \quad (1c)$$

$CP$  violation can occur either in the  $K^0 - \bar{K}^0$  mixing or in the decay amplitudes. Assuming  $CPT$  invariance, the mass eigenstates of the  $K^0 - \bar{K}^0$  system can be written

$$|K_S\rangle = p|K^0\rangle + q|\bar{K}^0\rangle, \quad |K_L\rangle = p|K^0\rangle - q|\bar{K}^0\rangle. \quad (2)$$

If  $CP$  invariance held, we would have  $q = p$  so that  $K_S$  would be  $CP$ -even and  $K_L$   $CP$ -odd. (We define  $|\bar{K}^0\rangle$  as  $CP |K^0\rangle$ ).  $CP$  violation in  $K^0 - \bar{K}^0$  mixing is then given by the parameter  $\tilde{\epsilon}$  where

$$\frac{p}{q} = \frac{(1 + \tilde{\epsilon})}{(1 - \tilde{\epsilon})}. \quad (3)$$

$CP$  violation can also occur in the decay amplitudes

$$A(K^0 \rightarrow \pi\pi(I)) = A_I e^{i\delta_I}, \quad A(\bar{K}^0 \rightarrow \pi\pi(I)) = A_I^* e^{i\delta_I}, \quad (4)$$

where  $I$  is the isospin of  $\pi\pi$ ,  $\delta_I$  is the final-state phase shift, and  $A_I$  would be real if  $CP$  invariance held. The  $CP$ -violating observables are usually expressed in terms of  $\epsilon$  and  $\epsilon'$  defined by

$$\eta_{+-} = \epsilon + \epsilon', \quad \eta_{00} = \epsilon - 2\epsilon'. \quad (5a)$$

One can then show [2]

$$\epsilon = \tilde{\epsilon} + i (\text{Im } A_0 / \text{Re } A_0), \quad (5b)$$

$$\sqrt{2}\epsilon' = ie^{i(\delta_2 - \delta_0)} (\text{Re } A_2 / \text{Re } A_0) (\text{Im } A_2 / \text{Re } A_2 - \text{Im } A_0 / \text{Re } A_0), \quad (5c)$$

$$A_L = 2\text{Re } \epsilon / (1 + |\epsilon|^2) \approx 2\text{Re } \epsilon. \quad (5d)$$

In Eqs. (5a), small corrections [3] of order  $\epsilon' \times \text{Re } (A_2/A_0)$  are neglected, and Eq. (5d) assumes the  $\Delta S = \Delta Q$  rule.

The quantities  $\text{Im } A_0$ ,  $\text{Im } A_2$ , and  $\text{Im } \tilde{\epsilon}$  depend on the choice of phase convention, since one can change the phases of  $K^0$  and  $\bar{K}^0$  by a transformation of the strange quark state  $|s\rangle \rightarrow |s\rangle e^{i\alpha}$ ; of course, observables are unchanged. It is possible by a choice of phase convention to set  $\text{Im } A_0$  or  $\text{Im } A_2$  or  $\text{Im } \tilde{\epsilon}$  to zero, but none of these is zero with the usual phase conventions in the Standard Model. The choice  $\text{Im } A_0 = 0$  is called the

Wu-Yang phase convention [4], in which case  $\epsilon = \tilde{\epsilon}$ . The value of  $\epsilon'$  is independent of phase convention, and a nonzero value demonstrates  $CP$  violation in the decay amplitudes, referred to as direct  $CP$  violation. The possibility that direct  $CP$  violation is essentially zero, and that  $CP$  violation occurs only in the mixing matrix, was referred to as the superweak theory [5].

By applying  $CPT$  invariance and unitarity the phase of  $\epsilon$  is given approximately by

$$\phi_\epsilon \approx \tan^{-1} \frac{2(m_{K_L} - m_{K_S})}{\Gamma_{K_S} - \Gamma_{K_L}} \approx 43.52 \pm 0.05^\circ, \quad (6a)$$

while Eq. (5c) gives the phase of  $\epsilon'$  to be

$$\phi_{\epsilon'} = \delta_2 - \delta_0 + \frac{\pi}{2} \approx 42.3 \pm 1.5^\circ, \quad (6b)$$

where the numerical value is based on an analysis of  $\pi - \pi$  scattering using chiral perturbation theory [6]. The approximation in Eq. (6a) depends on the assumption that direct  $CP$  violation is very small in all  $K^0$  decays. This is expected to be good to a few tenths of a degree, as indicated by the small value of  $\epsilon'$  and of  $\eta_{+-}$  and  $\eta_{00}$ , the  $CP$ -violation parameters in the decays  $K_S \rightarrow \pi^+ \pi^- \pi^0$  [7], and  $K_S \rightarrow \pi^0 \pi^0 \pi^0$  [8]. The relation in Eq. (6a) is exact in the superweak theory, so this is sometimes called the superweak-phase  $\phi_{SW}$ . An important point for the analysis is that  $\cos(\phi_{\epsilon'} - \phi_\epsilon) \simeq 1$ . The consequence is that only two real quantities need be measured, the magnitude of  $\epsilon$  and the value of  $(\epsilon'/\epsilon)$ , including its sign. The measured quantity  $|\eta_{00}/\eta_{+-}|^2$  is very close to unity so that we can write

$$|\eta_{00}/\eta_{+-}|^2 \approx 1 - 6\text{Re } (\epsilon'/\epsilon) \approx 1 - 6\epsilon'/\epsilon, \quad (7a)$$

$$\text{Re } (\epsilon'/\epsilon) \approx \frac{1}{3}(1 - |\eta_{00}/\eta_{+-}|). \quad (7b)$$

From the experimental measurements in this edition of the *Review*, and the fits discussed in the next section, one finds

$$|\epsilon| = (2.228 \pm 0.011) \times 10^{-3}, \quad (8a)$$

$$\phi_\epsilon = (43.5 \pm 0.5)^\circ, \quad (8b)$$

$$\text{Re } (\epsilon'/\epsilon) \approx \epsilon'/\epsilon = (1.66 \pm 0.23) \times 10^{-3}, \quad (8c)$$

$$\phi_{+-} = (43.4 \pm 0.5)^\circ, \quad (8d)$$

$$\phi_{00} - \phi_{+-} = (0.34 \pm 0.32)^\circ, \quad (8e)$$

$$A_L = (3.32 \pm 0.06) \times 10^{-3}. \quad (8f)$$

Direct  $CP$  violation, as indicated by  $\epsilon'/\epsilon$ , is expected in the Standard Model. However, the numerical value cannot be reliably predicted because of theoretical uncertainties [9]. The value of  $A_L$  agrees with Eq. (5d). The values of  $\phi_{+-}$  and  $\phi_{00} - \phi_{+-}$  are used to set limits on  $CPT$  violation [see "Tests of Conservation Laws"].

## 2. Fits for $K_L^0$ $CP$ -violation parameters:

In recent years,  $K_L^0$   $CP$ -violation experiments have improved our knowledge of  $CP$ -violation parameters, and their consistency with the expectations of  $CPT$  invariance and unitarity. To determine the best values of the  $CP$ -violation parameters in  $K_L^0 \rightarrow \pi^+\pi^-$  and  $\pi^0\pi^0$  decay, we make two types of fits, one for the phases  $\phi_{+-}$  and  $\phi_{00}$  jointly with  $\Delta m$  and  $\tau_S$ , and the other for the amplitudes  $|\eta_{+-}|$  and  $|\eta_{00}|$  jointly with the  $K_L^0 \rightarrow \pi\pi$  branching fractions.

**Fits to  $\phi_{+-}$ ,  $\phi_{00}$ ,  $\Delta\phi$ ,  $\Delta m$ , and  $\tau_S$  data:** These are joint fits to the data on  $\phi_{+-}$ ,  $\phi_{00}$ , the phase difference  $\Delta\phi = \phi_{00} - \phi_{+-}$ , the  $K_L^0 - K_S^0$  mass difference  $\Delta m$ , and the  $K_S^0$  mean life  $\tau_S$ , including the effects of correlations.

Measurements of  $\phi_{+-}$  and  $\phi_{00}$  are highly correlated with  $\Delta m$  and  $\tau_S$ . Some measurements of  $\tau_S$  are correlated with  $\Delta m$ . The correlations are given in the footnotes of the  $\phi_{+-}$  and  $\phi_{00}$  sections of the  $K_L^0$  Listings, and the  $\tau_S$  section of the  $K_S^0$  Listings.

In most cases, the correlations are quoted as 100%, *i.e.*, with the value and error of  $\phi_{+-}$  or  $\phi_{00}$  given at a fixed value of  $\Delta m$  and  $\tau_S$ , with additional terms specifying the dependence of the value on  $\Delta m$  and  $\tau_S$ . These cases lead to diagonal bands in Figs. 1 and 2. The KTeV experiment [10] quotes its results as values of  $\Delta m$ ,  $\tau_S$ ,  $\phi_\epsilon$ ,  $\text{Re}(\epsilon'/\epsilon)$ , and  $\text{Im}(\epsilon'/\epsilon)$  with correlations, leading to the ellipses labeled “b.” The correlations for the KTeV measurements are given in the  $\text{Im}(\epsilon'/\epsilon)$  section of the  $K_L^0$  Listings. For small  $|\epsilon'/\epsilon|$ ,  $\phi_{+-} \approx \phi_\epsilon + \text{Im}(\epsilon'/\epsilon)$ .

**Table 1:** References, Document ID’s, and sources corresponding to the letter labels in the figures. The data are given in the  $\phi_{+-}$  and  $\Delta m$  sections of the  $K_L$  Listings, and the  $\tau_S$  section of the  $K_S$  Listings.

Label	Source	PDG Document ID	Ref.
a	this Review	OUR FIT	
b	FNAL KTeV	ABOUZAID 11	[10]
c	CERN CPLEAR	APOSTOLAKIS 99C	[11]
d	FNAL E773	SCHWINGENHEUER 95	[12]
e	FNAL E731	GIBBONS 93,93C	[13,14]
f	CERN	GEWENIGER 74B,74C	[15,16]
g	CERN NA31	CAROSI 90	[17]
h	CERN NA48	LAI 02C	[18]
i	CERN NA31	BERTANZA 97	[19]
j	this Review	SUPERWEAK 12	

The data on  $\tau_S$ ,  $\Delta m$ , and  $\phi_{+-}$  shown in Figs. 1 and 2 are combined with data on  $\phi_{00}$  and  $\phi_{00} - \phi_{+-}$  in two fits, one without assuming  $CPT$ , and the other with this assumption. The results without assuming  $CPT$  are shown as ellipses labeled “a.” These ellipses are seen to be in good agreement with the superweak phase

$$\phi_{\text{SW}} = \tan^{-1} \left( \frac{2\Delta m}{\Delta\Gamma} \right) = \tan^{-1} \left( \frac{2\Delta m \tau_S \tau_L}{\hbar(\tau_L - \tau_S)} \right). \quad (9)$$

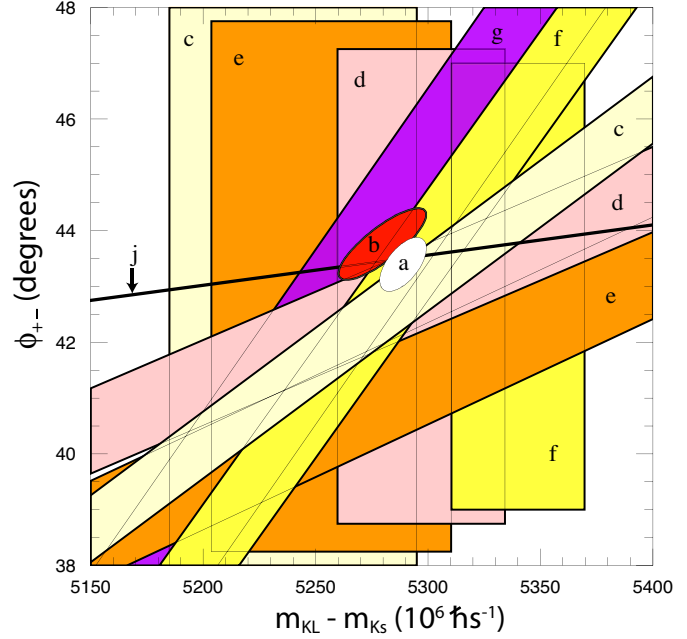


**Figure 1:**  $\phi_{+-}$  vs  $\Delta m$  for experiments which do not assume  $CPT$  invariance.  $\Delta m$  measurements appear as vertical bands spanning  $\Delta m \pm 1\sigma$ , cut near the top and bottom to aid the eye. Most  $\phi_{+-}$  measurements appear as diagonal bands spanning  $\phi_{+-} \pm \sigma_\phi$ . Data are labeled by letters: “b”–FNAL KTeV, “c”–CERN CPLEAR, “d”–FNAL E773, “e”–FNAL E731, “f”–CERN, “g”–CERN NA31, and are cited in Table 1. The narrow band “j” shows  $\phi_{\text{SW}}$ . The ellipse “a” shows the  $\chi^2 = 1$  contour of the fit result.

In Figs. 1 and 2,  $\phi_{\text{SW}}$  is shown as narrow bands labeled “j.”

Table 2 column 2, “Fit w/o  $CPT$ ,” gives the resulting fitted parameters, while Table 3 gives the correlation matrix for this fit. The white ellipses labeled “a” in Fig. 1 and Fig. 2 are the  $\chi^2 = 1$  contours for this fit.

For experiments which have dependencies on unseen fit parameters, that is, parameters other than those shown on the x or y axis of the figure, their band positions are evaluated using the fit results and their band widths include the fitted uncertainty in the unseen parameters. This is also true for the  $\phi_{\text{SW}}$  bands.

If  $CPT$  invariance and unitarity are assumed, then by Eq. (6a), the phase of  $\epsilon$  is constrained to be approximately equal to

$$\phi_{\text{SW}} = (43.5165 \pm 0.0002)^\circ + 54.1(\Delta m - 0.5290)^\circ + 32.0(\tau_S - 0.8958) \quad (10)$$

where we have linearized the  $\Delta m$  and  $\tau_S$  dependence of Eq. (9). The error  $\pm 0.0002$  is due to the uncertainty in  $\tau_L$ . Here  $\Delta m$  has units  $10^{10} \hbar s^{-1}$  and  $\tau_S$  has units  $10^{-10} s$ .

If in addition we use the observation that  $\text{Re}(\epsilon'/\epsilon) \ll 1$  and  $\cos(\phi_{\epsilon'} - \phi_\epsilon) \simeq 1$ , as well as the numerical value of  $\phi_{\epsilon'}$  given in

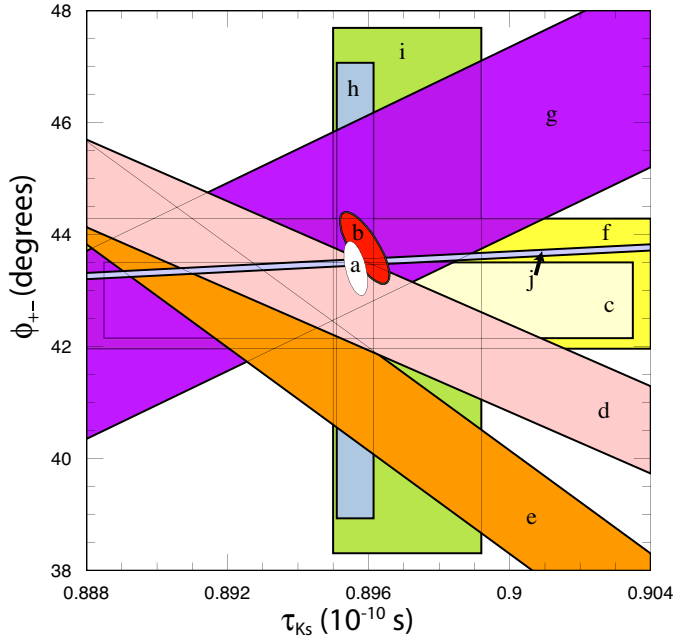


**Figure 2:**  $\phi_{+-}$  vs  $\tau_S$ .  $\tau_S$  measurements appear as vertical bands spanning  $\tau_S \pm 1\sigma$ , some of which are cut near the top and bottom to aid the eye. Most  $\phi_{+-}$  measurements appear as diagonal or horizontal bands spanning  $\phi_{+-} \pm \sigma_\phi$ . Data are labeled by letters: “b”–FNAL KTeV, “c”–CERN CPLEAR, “d”–FNAL E773, “e”–FNAL E731, “f”–CERN, “g”–CERN NA31, “h”–CERN NA48, “i”–CERN NA31, and are cited in Table 1. The narrow band “j” shows  $\phi_{SW}$ . The ellipse “a” shows the fit result’s  $\chi^2 = 1$  contour.

**Table 2:** Fit results for  $\phi_{+-}$ ,  $\Delta m$ ,  $\tau_S$ ,  $\phi_{00}$ ,  $\Delta\phi = \phi_{00} - \phi_{+-}$ , and  $\phi_\epsilon$  without and with the *CPT* assumption.

Quantity(units)	Fit w/o <i>CPT</i>	Fit w/ <i>CPT</i>
$\phi_{+-}(\circ)$	$43.4 \pm 0.5$ (S=1.2)	$43.51 \pm 0.05$ (S=1.2)
$\Delta m(10^{10}\hbar s^{-1})$	$0.5289 \pm 0.0010$	$0.5293 \pm 0.0009$ (S=1.3)
$\tau_S(10^{-10}s)$	$0.89564 \pm 0.00033$	$0.8954 \pm 0.0004$ (S=1.1)
$\phi_{00}(\circ)$	$43.7 \pm 0.6$ (S=1.2)	$43.52 \pm 0.05$ (S=1.3)
$\Delta\phi(\circ)$	$0.34 \pm 0.32$	$0.006 \pm 0.014$ (S=1.7)
$\phi_\epsilon(\circ)$	$43.5 \pm 0.5$ (S=1.3)	$43.52 \pm 0.05$ (S=1.2)
$\chi^2$	16.4	20.0
# Deg. Free.	14	16

Eq. (6b), then Eqs. (5a), which are sketched in Fig. 3, lead to the constraint

$$\begin{aligned}
 \phi_{00} - \phi_{+-} &\approx -3 \operatorname{Im} \left( \frac{\epsilon'}{\epsilon} \right) \\
 &\approx -3 \operatorname{Re} \left( \frac{\epsilon'}{\epsilon} \right) \tan(\phi_{\epsilon'} - \phi_\epsilon) \\
 &\approx 0.006^\circ \pm 0.008^\circ, \quad (11)
 \end{aligned}$$

so that  $\phi_{+-} \approx \phi_{00} \approx \phi_\epsilon \approx \phi_{SW}$ .

In the fit assuming *CPT*, we constrain  $\phi_\epsilon = \phi_{SW}$  using the linear expression in Eq. (10), and constrain  $\phi_{00} - \phi_{+-}$  using Eq. (11). These constraints are inserted into the Listings with the Document ID of SUPERWEAK 12. Some additional data for which the authors assumed *CPT* are added to this fit or substitute for other less precise data for which the authors did not make this assumption. See the Listings for details.

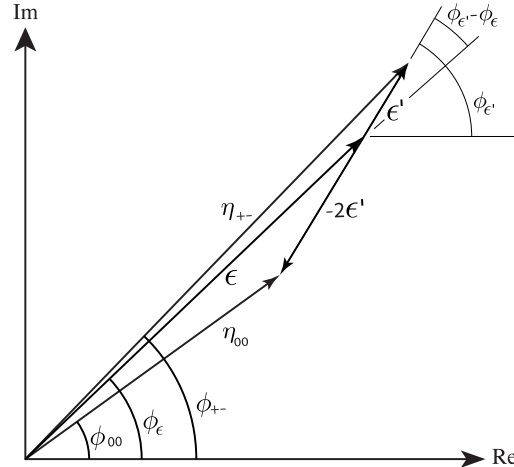


**Figure 3:** Sketch of Eqs. (5a). Not to scale.

The results of this fit are shown in Table 2, column 3, “Fit w/*CPT*,” and the correlation matrix is shown in Table 4. The  $\Delta m$  precision is improved by the *CPT* assumption.

**Table 3:** Correlation matrix for the results of the fit without the *CPT* assumption

	$\phi_{+-}$	$\Delta m$	$\tau_S$	$\phi_{00}$	$\Delta\phi$	$\phi_\epsilon$
$\phi_{+-}$	1.000	0.596	-0.488	0.827	-0.040	0.976
$\Delta m$	0.596	1.000	-0.572	0.487	-0.035	0.580
$\tau_S$	-0.488	-0.572	1.000	-0.423	-0.014	-0.484
$\phi_{00}$	0.827	0.487	-0.423	1.000	0.529	0.929
$\Delta\phi$	-0.040	-0.035	-0.014	0.529	1.000	0.178
$\phi_\epsilon$	0.976	0.580	-0.484	0.929	0.178	1.000

**Table 4:** Correlation matrix for the results of the fit with the *CPT* assumption

	$\phi_{+-}$	$\Delta m$	$\tau_S$	$\phi_{00}$	$\Delta\phi$	$\phi_\epsilon$
$\phi_{+-}$	1.000	0.972	-0.311	0.957	-0.105	0.995
$\Delta m$	0.972	1.000	-0.509	0.958	-0.007	0.977
$\tau_S$	-0.311	-0.509	1.000	-0.306	0.004	-0.312
$\phi_{00}$	0.957	0.958	-0.306	1.000	0.189	0.981
$\Delta\phi$	-0.105	-0.007	0.004	0.189	1.000	-0.006
$\phi_\epsilon$	0.995	0.977	-0.312	0.981	-0.006	1.000

**Fits for  $\epsilon'/\epsilon$ ,  $|\eta_{+-}|$ ,  $|\eta_{00}|$ , and  $B(K_L \rightarrow \pi\pi)$** 

We list measurements of  $|\eta_{+-}|$ ,  $|\eta_{00}|$ ,  $|\eta_{00}/\eta_{+-}|$ , and  $\epsilon'/\epsilon$ . Independent information on  $|\eta_{+-}|$  and  $|\eta_{00}|$  can be obtained from measurements of the  $K_L^0$  and  $K_S^0$  lifetimes ( $\tau_L$ ,  $\tau_S$ ), and branching ratios (B) to  $\pi\pi$ , using the relations

$$|\eta_{+-}| = \left[ \frac{B(K_L^0 \rightarrow \pi^+\pi^-)}{\tau_L} \frac{\tau_S}{B(K_S^0 \rightarrow \pi^+\pi^-)} \right]^{1/2}, \quad (12a)$$

$$|\eta_{00}| = \left[ \frac{B(K_L^0 \rightarrow \pi^0\pi^0)}{\tau_L} \frac{\tau_S}{B(K_S^0 \rightarrow \pi^0\pi^0)} \right]^{1/2}. \quad (12b)$$

For historical reasons, the branching ratio fits and the  $CP$ -violation fits are done separately, but we want to include the influence of  $|\eta_{+-}|$ ,  $|\eta_{00}|$ ,  $|\eta_{00}/\eta_{+-}|$ , and  $\epsilon'/\epsilon$  measurements on  $B(K_L^0 \rightarrow \pi^+\pi^-)$  and  $B(K_L^0 \rightarrow \pi^0\pi^0)$  and vice versa. We approximate a global fit to all of these measurements by first performing two independent fits: 1) BRFIT, a fit to the  $K_L^0$  branching ratios, rates, and mean life, and 2) ETAFIT, a fit to the  $|\eta_{+-}|$ ,  $|\eta_{00}|$ ,  $|\eta_{+-}/\eta_{00}|$ , and  $\epsilon'/\epsilon$  measurements. The results from fit 1, along with the  $K_S^0$  values from this edition, are used to compute values of  $|\eta_{+-}|$  and  $|\eta_{00}|$ , which are included as measurements in the  $|\eta_{00}|$  and  $|\eta_{+-}|$  sections with a document ID of BRFIT 12. Thus, the fit values of  $|\eta_{+-}|$  and  $|\eta_{00}|$  given in this edition include both the direct measurements and the results from the branching ratio fit.

The process is reversed in order to include the direct  $|\eta|$  measurements in the branching ratio fit. The results from fit 2 above (before including BRFIT 12 values) are used along with the  $K_L^0$  and  $K_S^0$  mean lives and the  $K_S^0 \rightarrow \pi\pi$  branching fractions to compute the  $K_L^0$  branching ratio  $\Gamma(K_L^0 \rightarrow \pi^0\pi^0)/\Gamma(K_L^0 \rightarrow \pi^+\pi^-)$ . This branching ratio value is included as a measurement in the branching ratio section with a document ID of ETAFIT 12. Thus, the  $K_L^0$  branching ratio fit values in this edition include the results of the direct measurement of  $|\eta_{00}/\eta_{+-}|$  and  $\epsilon'/\epsilon$ . Most individual measurements of  $|\eta_{+-}|$  and  $|\eta_{00}|$  enter our fits directly via the corresponding measurements of  $\Gamma(K_L^0 \rightarrow \pi^+\pi^-)/\Gamma(\text{total})$  and  $\Gamma(K_L^0 \rightarrow \pi^0\pi^0)/\Gamma(\text{total})$ , and those that do not have too large errors to have any influence on the fitted values of these branching ratios. A more detailed discussion of these fits is given in the 1990 edition of this *Review* [20].

**References**

- K. Kleinknecht, "Uncovering  $CP$  violation: experimental clarification in the neutral  $K$  meson and  $B$  meson systems," *Springer Tracts in Modern Physics*, vol. 195 (Springer Verlag 2003).
- B. Winstein and L. Wolfenstein, *Rev. Mod. Phys.* **65**, 1113 (1993).
- M.S. Sozzi, *Eur. Phys. J.* **C36**, 37 (2004).
- T.T. Wu and C.N. Yang, *Phys. Rev. Lett.* **13**, 380 (1964).
- L. Wolfenstein, *Phys. Rev. Lett.* **13**, 562 (1964);  
L. Wolfenstein, *Comm. Nucl. Part. Phys.* **21**, 275 (1994).
- G. Colangelo, J. Gasser, and H. Leutwyler, *Nucl. Phys.* **B603**, 125 (2001).
- R. Adler *et al.*, (CLEAR Collaboration), *Phys. Lett.* **B407**, 193 (1997);  
P. Bloch, *Proceedings of Workshop on K Physics* (Orsay 1996), ed. L. Iconomidou-Fayard, Edition Frontieres, Gif-sur-Yvette, France (1997) p. 307.
- A. Lai *et al.*, *Phys. Lett.* **B610**, 165 (2005).
- G. Buchalla, A.J. Buras, and M.E. Lautenbacher, *Rev. Mod. Phys.* **68**, 1125 (1996);  
S. Bosch *et al.*, *Nucl. Phys.* **B565**, 3 (2000);  
S. Bertolini, M. Fabrichesi, and J.O. Egg, *Rev. Mod. Phys.* **72**, 65 (2000).
- E. Abouzaid *et al.*, *Phys. Rev.* **D83**, 092001 (2011).
- A. Apostolakis *et al.*, *Phys. Lett.* **B458**, 545 (1999).
- B. Schwingerheuer *et al.*, *Phys. Rev. Lett.* **74**, 4376 (1995).
- L.K. Gibbons *et al.*, *Phys. Rev. Lett.* **70**, 1199 (1993) and footnote in Ref. 12.
- L.K. Gibbons, Thesis, RX-1487, Univ. of Chicago, 1993.
- C. Geweniger *et al.*, *Phys. Lett.* **48B**, 487 (1974).
- C. Geweniger *et al.*, *Phys. Lett.* **52B**, 108 (1974).
- R. Carosi *et al.*, *Phys. Lett.* **B237**, 303 (1990).
- A. Lai *et al.*, *Phys. Lett.* **B537**, 28 (2002).
- L. Bertanza *et al.*, *Z. Phys.* **C73**, 629 (1997).
- J.J. Hernandez *et al.*, Particle Data Group, *Phys. Lett.* **B239**, 1 (1990).

 **$CP$ -VIOLATION PARAMETERS IN  $K_L^0$  DECAYS****CHARGE ASYMMETRY IN  $K_{S3}^0$  DECAYS**

Such asymmetry violates  $CP$ . It is related to  $Re(\epsilon)$ .

 **$A_L$  = weighted average of  $A_L(\mu)$  and  $A_L(e)$** 

In previous editions and in the literature the symbol used for this asymmetry was  $\delta_L$  or  $\delta$ . We use  $A_L$  for consistency with  $B^0$  asymmetry notation and with recent  $K_S^0$  notation.

VALUE (%)	EVTS	DOCUMENT ID	TECN	COMMENT
<b>0.332 ± 0.006 OUR AVERAGE</b>		Includes data from the 2 datablocks that follow this one.		
0.333 ± 0.050	33M	WILLIAMS	73	ASPK $K_{\mu 3} + K_{e 3}$

 **$A_L(\mu) = [\Gamma(\pi^- \mu^+ \nu_\mu) - \Gamma(\pi^+ \mu^- \bar{\nu}_\mu)]/\text{SUM}$** 

Only the combined value below is put into the Meson Summary Table.

VALUE (%)	EVTS	DOCUMENT ID	TECN
The data in this block is included in the average printed for a previous datablock.			

**0.304 ± 0.025 OUR AVERAGE**

0.313 ± 0.029	15M	GEWENIGER	74	ASPK
0.278 ± 0.051	7.7M	PICCIONI	72	ASPK
• • • We do not use the following data for averages, fits, limits, etc. • • •				
0.60 ± 0.14	4.1M	MCCARTHY	73	CNTR
0.57 ± 0.17	1M	<sup>1</sup> PACIOTTI	69	OSPK
0.403 ± 0.134	1M	<sup>1</sup> DORFAN	67	OSPK

<sup>1</sup>PACIOTTI 69 is a reanalysis of DORFAN 67 and is corrected for  $\mu^+ \mu^-$  range difference in MCCARTHY 72.

 **$A_L(e) = [\Gamma(\pi^- e^+ \nu_e) - \Gamma(\pi^+ e^- \bar{\nu}_e)]/\text{SUM}$** 

Only the combined value below is put into the Meson Summary Table.

VALUE (%)	EVTS	DOCUMENT ID	TECN
The data in this block is included in the average printed for a previous datablock.			

**0.334 ± 0.007 OUR AVERAGE**

0.3322 ± 0.0058 ± 0.0047	298M	ALAVI-HARATI	102	
0.341 ± 0.018	34M	GEWENIGER	74	ASPK
0.318 ± 0.038	40M	FITCH	73	ASPK
0.346 ± 0.033	10M	MARX	70	CNTR
• • • We do not use the following data for averages, fits, limits, etc. • • •				
0.36 ± 0.18	600k	ASHFORD	72	ASPK
0.246 ± 0.059	10M	<sup>1</sup> SAAL	69	CNTR
0.224 ± 0.036	10M	<sup>1</sup> BENNETT	67	CNTR

<sup>1</sup>SAAL 69 is a reanalysis of BENNETT 67.

## Meson Particle Listings

 $K_L^0$ PARAMETERS FOR  $K_L^0 \rightarrow 2\pi$  DECAY

$$\eta_{+-} = A(K_L^0 \rightarrow \pi^+\pi^-) / A(K_S^0 \rightarrow \pi^+\pi^-)$$

$$\eta_{00} = A(K_L^0 \rightarrow \pi^0\pi^0) / A(K_S^0 \rightarrow \pi^0\pi^0)$$

The fitted values of  $|\eta_{+-}|$  and  $|\eta_{00}|$  given below are the results of a fit to  $|\eta_{+-}|$ ,  $|\eta_{00}|$ ,  $|\eta_{00}/\eta_{+-}|$ , and  $\text{Re}(e'/\epsilon)$ . Independent information on  $|\eta_{+-}|$  and  $|\eta_{00}|$  can be obtained from the fitted values of the  $K_L^0 \rightarrow \pi\pi$  and  $K_S^0 \rightarrow \pi\pi$  branching ratios and the  $K_L^0$  and  $K_S^0$  lifetimes. This information is included as data in the  $|\eta_{+-}|$  and  $|\eta_{00}|$  sections with a Document ID "BRFIT." See the note "CP violation in  $K_L$  decays" above for details.

$$|\eta_{00}| = |A(K_L^0 \rightarrow 2\pi^0) / A(K_S^0 \rightarrow 2\pi^0)|$$

VALUE (units $10^{-3}$ )	DOCUMENT ID	TECN	COMMENT
<b>2.220 ± 0.011 OUR FIT</b>	Error includes scale factor of 1.8.		
<b>2.243 ± 0.014</b>	BRFIT	12	
• • • We do not use the following data for averages, fits, limits, etc. • • •			
2.47 ± 0.31 ± 0.24	ANGELOPO...	98	CPLR
2.49 ± 0.40	1 ADLER	96B	CPLR Sup. by ANGELOPOULOS 98
2.33 ± 0.18	CHRISTENS...	79	ASPK
2.71 ± 0.37	2 WOLFF	71	OSPK Cu reg., $4\gamma$ 's
2.95 ± 0.63	2 CHOLLET	70	OSPK Cu reg., $4\gamma$ 's

<sup>1</sup> Error is statistical only.

<sup>2</sup> CHOLLET 70 gives  $|\eta_{00}| = (1.23 \pm 0.24) \times (\text{regeneration amplitude}, 2 \text{ GeV}/c \text{ Cu})/10000\text{mb}$ . WOLFF 71 gives  $|\eta_{00}| = (1.13 \pm 0.12) \times (\text{regeneration amplitude}, 2 \text{ GeV}/c \text{ Cu})/10000\text{mb}$ . We compute both  $|\eta_{00}|$  values for (regeneration amplitude, 2 GeV/c Cu) =  $24 \pm 2\text{mb}$ . This regeneration amplitude results from averaging over FAISSNER 69, extrapolated using optical-model calculations of Bohm et al., Physics Letters **27B** 594 (1968) and the data of BALATS 71. (From H. Faissner, private communication).

$$|\eta_{+-}| = |A(K_L^0 \rightarrow \pi^+\pi^-) / A(K_S^0 \rightarrow \pi^+\pi^-)|$$

VALUE (units $10^{-3}$ )	EVTS	DOCUMENT ID	TECN	COMMENT
<b>2.232 ± 0.011 OUR FIT</b>	Error includes scale factor of 1.8.			
<b>2.226 ± 0.007</b>	BRFIT	12		
• • • We do not use the following data for averages, fits, limits, etc. • • •				
2.223 ± 0.012	1	LAI	07	NA48
2.219 ± 0.013	2	AMBROSINO	06F	KLOE
2.228 ± 0.010	3	ALEXOPOU...	04	KTEV
2.286 ± 0.023 ± 0.026	70M	4	APOSTOLA...	99C CPLR $K^0\bar{K}^0$ asymmetry
2.310 ± 0.043 ± 0.031	5	ADLER	95B	CPLR $K^0\bar{K}^0$ asymmetry
2.32 ± 0.14 ± 0.03	10 <sup>5</sup>	ADLER	92B	CPLR $K^0\bar{K}^0$ asymmetry
2.30 ± 0.035		GEWENIGER	74B	ASPK

<sup>1</sup> Value obtained from the NA48 measurements of  $\Gamma(K_L^0 \rightarrow \pi^+\pi^-)/\Gamma(K_L^0 \rightarrow \pi e \nu_e)$  and  $\tau_{K_S^0}$  and KLOE measurements of  $B(K_S^0 \rightarrow \pi^+\pi^-)$  and  $\tau_{K_L^0}$ .  $\Gamma(K_L^0 \rightarrow \pi^+\pi^-)$

is defined to include the inner bremsstrahlung component  $\Gamma(K_L^0 \rightarrow \pi^+\pi^-\gamma(\text{IB}))$  but exclude the direct emission component  $B(K_S^0 \rightarrow \pi^+\pi^-(\text{DE}))$ . Their  $|\eta_{+-}|$  value is not directly used in our fit, but enters the fit via their branching ratio and lifetime measurements.

<sup>2</sup> AMBROSINO 06F uses KLOE branching ratios and  $\tau_L$  together with  $\tau_S$  from PDG 04. Their  $|\eta_{+-}|$  value is not directly used in our fit, but enters the fit via their branching ratio and lifetime measurements.

<sup>3</sup> ALEXOPOULOS 04  $|\eta_{+-}|$  uses their  $K_L^0 \rightarrow \pi\pi$  branching fractions,  $\tau_S = (0.8963 \pm 0.0005) \times 10^{-10}$  s from the average of KTeV and NA48  $\tau_S$  measurements, and assumes that  $\Gamma(K_S^0 \rightarrow \pi e \nu_e) = \Gamma(K_L^0 \rightarrow \pi e \nu_e)$  giving  $B(K_S^0 \rightarrow \pi e \nu_e) = 0.118\%$ . Their  $|\eta_{+-}|$  is not directly used in our fit, but enters our fit via their branching ratio measurements.

<sup>4</sup> APOSTOLAKIS 99C report  $(2.264 \pm 0.023 \pm 0.026 + 9.1[\tau_S - 0.8934]) \times 10^{-3}$ . We evaluate for our 2006 best value  $\tau_S = (0.8958 \pm 0.0005) \times 10^{-10}$  s.

<sup>5</sup> ADLER 95B report  $(2.312 \pm 0.043 \pm 0.030 - 1[\Delta m - 0.5274] + 9.1[\tau_S - 0.8926]) \times 10^{-3}$ . We evaluate for our 1996 best values  $\Delta m = (0.5304 \pm 0.0014) \times 10^{-10} \text{hs}^{-1}$  and  $\tau_S = (0.8927 \pm 0.0009) \times 10^{-10}$  s. Superseded by APOSTOLAKIS 99C.

$$|\epsilon| = (2|\eta_{+-}| + |\eta_{00}|)/3$$

This expression is a very good approximation, good to about one part in  $10^{-4}$  because of the small measured value of  $\phi_{00} - \phi_{+-}$  and small theoretical ambiguities.

VALUE (units $10^{-3}$ )	DOCUMENT ID	TECN	COMMENT
<b>2.228 ± 0.011 OUR FIT</b>	Error includes scale factor of 1.8.		

$$|\eta_{00}/\eta_{+-}|$$

VALUE	EVTS	DOCUMENT ID	TECN	COMMENT
<b>0.9950 ± 0.0007 OUR FIT</b>	Error includes scale factor of 1.6.			
<b>0.9930 ± 0.0020 OUR AVERAGE</b>				
0.9931 ± 0.0020	1,2	BARR	93D	NA31
0.9904 ± 0.0084 ± 0.0036	3	WOODS	88	E731
• • • We do not use the following data for averages, fits, limits, etc. • • •				
0.9939 ± 0.0013 ± 0.0015	1M	1 BARR	93D	NA31
0.9899 ± 0.0020 ± 0.0025	1	BURKHARDT	88	NA31

<sup>1</sup> This is the square root of the ratio  $R$  given by BURKHARDT 88 and BARR 93D.

<sup>2</sup> This is the combined results from BARR 93D and BURKHARDT 88, taking into account a common systematic uncertainty of 0.0014.

<sup>3</sup> We calculate  $|\eta_{00}/\eta_{+-}| = 1 - 3(\epsilon'/\epsilon)$  from WOODS 88 ( $\epsilon'/\epsilon$ ) value.

$$\text{Re}(\epsilon'/\epsilon) = (1 - |\eta_{00}/\eta_{+-}|)/3$$

We have neglected terms of order  $\omega \cdot \text{Re}(\epsilon'/\epsilon)$ , where  $\omega = \text{Re}(A_2)/\text{Re}(A_0) \approx 1/22$ . If included, this correction would lower  $\text{Re}(\epsilon'/\epsilon)$  by about  $0.04 \times 10^{-3}$ . See SOZZI 04.

VALUE (units $10^{-3}$ )	DOCUMENT ID	TECN	COMMENT
<b>1.66 ± 0.23 OUR FIT</b>	Error includes scale factor of 1.6.		
<b>1.68 ± 0.20 OUR AVERAGE</b>	Error includes scale factor of 1.4. See the ideogram below.		
1.92 ± 0.21	1	ABOUZAID	11 KTEV Assuming CPT
1.47 ± 0.22		BATLEY	02 NA48
0.74 ± 0.52 ± 0.29		GIBBONS	93B E731
• • • We use the following data for averages but not for fits. • • •			
2.3 ± 0.65	2,3	BARR	93D NA31
• • • We do not use the following data for averages, fits, limits, etc. • • •			
2.110 ± 0.343	1,4	ABOUZAID	11 KTEV Not assuming CPT
2.07 ± 0.28		ALAVI-HARATI	03 KTEV In ABOUZAID 11
1.53 ± 0.26		LAI	01C NA48 Incl. in BATLEY 02
2.80 ± 0.30 ± 0.28		ALAVI-HARATI	99D KTEV In ALAVI-HARATI 03
1.85 ± 0.45 ± 0.58		FANTI	99C NA48 In LAI 01C
2.0 ± 0.7	5	BARR	93D NA31
-0.4 ± 1.4 ± 0.6		PATTERSON	90 E731 in GIBBONS 93B
3.3 ± 1.1	5	BURKHARDT	88 NA31
3.2 ± 2.8 ± 1.2	2	WOODS	88 E731

<sup>1</sup> The two ABOUZAID 11 values use the same data. The fits are performed with and without CPT invariance requirement.

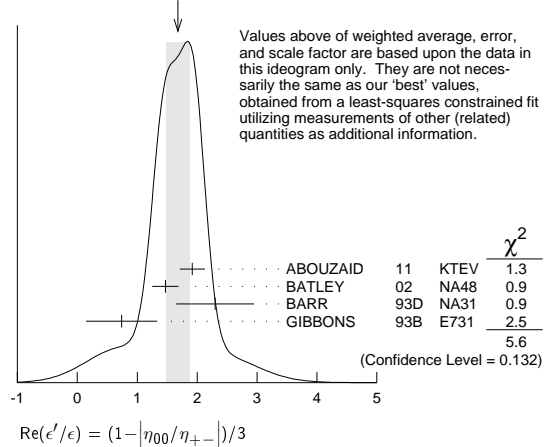
<sup>2</sup> These values are derived from  $|\eta_{00}/\eta_{+-}|$  measurements. They enter the average in this section but enter the fit via the  $|\eta_{00}/\eta_{+-}|$  only.

<sup>3</sup> This is the combined results from BARR 93D and BURKHARDT 88, taking into account their common systematic uncertainty.

<sup>4</sup> We use ABOUZAID 11  $\text{Re}(\epsilon'/\epsilon)$  value with CPT assumption in our fits for  $|\eta_{+-}|$ ,  $|\eta_{00}|$ , and  $\text{Re}(\epsilon'/\epsilon)$ .

<sup>5</sup> These values are derived from  $|\eta_{00}/\eta_{+-}|$  measurements.

WEIGHTED AVERAGE  
1.68±0.20 (Error scaled by 1.4)

 $\phi_{+-}$ , PHASE OF  $\eta_{+-}$ 

The dependence of the phase on  $\Delta m$  and  $\tau_S$  is given for each experiment in the comments below, where  $\Delta m$  is the  $K_L^0 - K_S^0$  mass difference in units  $10^{10} \text{hs}^{-1}$  and  $\tau_S$  is the  $K_S$  mean life in units  $10^{-10}$  s. We also give the regeneration phase  $\phi_r$  in the comments below.

OUR FIT is described in the note on "CP violation in  $K_L$  decays" in the  $K_L^0$  Particle Listings. Most experiments in this section are included in both the "Not Assuming CPT" and "Assuming CPT" fits. In the latter fit, they have little direct influence on  $\phi_{+-}$  because their errors are large compared to that assuming CPT, but they influence  $\Delta m$  and  $\tau_S$  through their dependencies on these parameters, which are given in the footnotes.

VALUE (°)	EVTS	DOCUMENT ID	TECN	COMMENT
<b>43.51 ± 0.05 OUR FIT</b>	Error includes scale factor of 1.2. Assuming CPT			
<b>43.4 ± 0.5 OUR FIT</b>	Error includes scale factor of 1.2. Not assuming CPT			
42.9 ± 0.6 ± 0.3	70M	1	APOSTOLA...	99C CPLR $K^0\bar{K}^0$ asymmetry
42.9 ± 0.8 ± 0.2		2,3	SCHWINGEN...	95 E773 CH <sub>1,1</sub> regenerator
41.4 ± 0.9 ± 0.2		3,4	GIBBONS	93 E731 B <sub>4</sub> C regenerator
44.5 ± 1.6 ± 0.6		5	CAROSI	90 NA31 Vacuum regen.
43.3 ± 1.0 ± 0.5		6	GEWENIGER	74B ASPK Vacuum regen.
• • • We do not use the following data for averages, fits, limits, etc. • • •				
43.76 ± 0.64		7	ABOUZAID	11 KTEV Not assuming CPT
44.12 ± 0.72 ± 1.20		8	ALAVI-HARATI	03 KTEV Not assuming CPT
42.5 ± 0.4 ± 0.3		9,10	ADLER	96C RVUE
43.4 ± 1.1 ± 0.3		11	ADLER	95B CPLR $K^0\bar{K}^0$ asymmetry
42.3 ± 4.4 ± 1.4		12	ADLER	92B CPLR $K^0\bar{K}^0$ asymmetry
47.7 ± 2.0 ± 0.9		3,13	KARLSSON	90 E731
44.3 ± 2.8 ± 0.2		14	CARITHERS	75 SPEC C regenerator

- <sup>1</sup> APOSTOLAKIS 99c measures  $\phi_{+-} = (43.19 \pm 0.53 \pm 0.28) + 300 [\Delta m - 0.5301]^\circ$ . We have adjusted the measurement to use our best values of  $(\Delta m = 0.5293 \pm 0.0009) (10^{10} \text{ h s}^{-1})$ . Our first error is their experiment's error and our second error is the systematic error from using our best values.
- <sup>2</sup> SCHWINGENHEUER 95 measures  $\phi_{+-} = (43.53 \pm 0.76) + 173 [\Delta m - 0.5282] - 275 [\tau_S - 0.8926]^\circ$ . We have adjusted the measurement to use our best values of  $(\Delta m = 0.5293 \pm 0.0009) (10^{10} \text{ h s}^{-1})$ ,  $(\tau_S = 0.8954 \pm 0.0004) (10^{-10} \text{ s})$ . Our first error is their experiment's error and our second error is the systematic error from using our best values.
- <sup>3</sup> These experiments measure  $\phi_{+-} - \phi_f$  and calculate the regeneration phase from the power law momentum dependence of the regeneration amplitude using analyticity and dispersion relations. SCHWINGENHEUER 95 [GIBBONS 93] includes a systematic error of  $0.35^\circ [0.5^\circ]$  for uncertainties in their modeling of the regeneration amplitude.
- <sup>4</sup> GIBBONS 93 measures  $\phi_{+-} = (42.21 \pm 0.9) + 189 [\Delta m - 0.5257] - 460 [\tau_S - 0.8922]^\circ$ . We have adjusted the measurement to use our best values of  $(\Delta m = 0.5293 \pm 0.0009) (10^{10} \text{ h s}^{-1})$ ,  $(\tau_S = 0.8954 \pm 0.0004) (10^{-10} \text{ s})$ . Our first error is their experiment's error and our second error is the systematic error from using our best values. This is actually reported in SCHWINGENHEUER 95, footnote 8. GIBBONS 93 reports  $\phi_{+-} (42.2 \pm 1.4)^\circ$ . They measure  $\phi_{+-} - \phi_f$  and calculate the regeneration phase  $\phi_f$  from the power law momentum dependence of the regeneration amplitude using analyticity. An error of  $0.6^\circ$  is included for possible uncertainties in the regeneration phase.
- <sup>5</sup> CAROSI 90 measures  $\phi_{+-} = (46.9 \pm 1.4 \pm 0.7) + 579 [\Delta m - 0.5351] + 303 [\tau_S - 0.8922]^\circ$ . We have adjusted the measurement to use our best values of  $(\Delta m = 0.5293 \pm 0.0009) (10^{10} \text{ h s}^{-1})$ ,  $(\tau_S = 0.8954 \pm 0.0004) (10^{-10} \text{ s})$ . Our first error is their experiment's error and our second error is the systematic error from using our best values.
- <sup>6</sup> GEWENIGER 74B measures  $\phi_{+-} = (49.4 \pm 1.0) + 565 [\Delta m - 0.540]^\circ$ . We have adjusted the measurement to use our best values of  $(\Delta m = 0.5293 \pm 0.0009) (10^{10} \text{ h s}^{-1})$ . Our first error is their experiment's error and our second error is the systematic error from using our best values.
- <sup>7</sup> Not independent of other phase parameters reported in ABOUZAID 11.
- <sup>8</sup> ALAVI-HARATI 03  $\phi_{+-}$  is correlated with their  $\Delta m = m_{K_L^0} - m_{K_S^0}$  and  $\tau_{K_S}$  measurements in the  $K_L^0$  and  $K_S^0$  sections respectively. The correlation coefficients are  $\rho(\phi_{+-}, \Delta m) = +0.955$ ,  $\rho(\phi_{+-}, \tau_S) = -0.871$ , and  $\rho(\tau_S, \Delta m) = -0.840$ . *CPT* is not assumed. Uses scintillator Pb regenerator. Superseded by ABOUZAID 11.
- <sup>9</sup> ADLER 96c measures  $\phi_{+-} = (43.82 \pm 0.41) + 339 [\Delta m - 0.5307] - 252 [\tau_S - 0.8922]^\circ$ . We have adjusted the measurement to use our best values of  $(\Delta m = 0.5293 \pm 0.0009) (10^{10} \text{ h s}^{-1})$ ,  $(\tau_S = 0.8954 \pm 0.0004) (10^{-10} \text{ s})$ . Our first error is their experiment's error and our second error is the systematic error from using our best values.
- <sup>10</sup> ADLER 96c is the result of a fit which includes nearly the same data as entered into the "OUR FIT" value in the 1996 edition of this Review (Physical Review **D54** 1 (1996)).
- <sup>11</sup> ADLER 95B measures  $\phi_{+-} = (42.7 \pm 0.9 \pm 0.6) + 316 [\Delta m - 0.5274] + 30 [\tau_S - 0.8926]^\circ$ . We have adjusted the measurement to use our best values of  $(\Delta m = 0.5293 \pm 0.0009) (10^{10} \text{ h s}^{-1})$ ,  $(\tau_S = 0.8954 \pm 0.0004) (10^{-10} \text{ s})$ . Our first error is their experiment's error and our second error is the systematic error from using our best values.
- <sup>12</sup> ADLER 92B quote separately two systematic errors:  $\pm 0.4$  from their experiment and  $\pm 1.0$  degrees due to the uncertainty in the value of  $\Delta m$ .
- <sup>13</sup> KARLSSON 90 systematic error does not include regeneration phase uncertainty.
- <sup>14</sup> CARITHERS 75 measures  $\phi_{+-} = (45.5 \pm 2.8) + 224 [\Delta m - 0.5348]^\circ$ . We have adjusted the measurement to use our best values of  $(\Delta m = 0.5293 \pm 0.0009) (10^{10} \text{ h s}^{-1})$ . Our first error is their experiment's error and our second error is the systematic error from using our best values.  $\phi_f = -40.9 \pm 2.6^\circ$ .

 **$\phi_{00}$ , PHASE OF  $\eta_{00}$** 

See comment in  $\phi_{+-}$  header above for treatment of  $\Delta m$  and  $\tau_S$  dependence, as well as for the inclusion of data in both the "Assuming *CPT*" and "Not Assuming *CPT*" fits.

OUR FIT is described in the note on "CP violation in  $K_L$  decays" in the  $K_L^0$  Particle Listings.

VALUE ( $^\circ$ )	DOCUMENT ID	TECN	COMMENT
<b>43.52 ± 0.05 OUR FIT</b>			Error includes scale factor of 1.3. Assuming <i>CPT</i>
<b>43.7 ± 0.6 OUR FIT</b>			Error includes scale factor of 1.2. Not assuming <i>CPT</i>
44.5 ± 2.3 ± 0.5	<sup>1</sup> CAROSI 90	NA31	
• • •			We do not use the following data for averages, fits, limits, etc. • • •
44.06 ± 0.68	<sup>2</sup> ABOUZAID 11	KTEV	Not assuming <i>CPT</i>
41.7 ± 5.9 ± 0.2	<sup>3</sup> ANGELOPOULOS 98	CPLR	
50.8 ± 7.1 ± 1.7	<sup>4</sup> ADLER 96B	CPLR	Sup. by ANGELOPOULOS 98
47.4 ± 1.4 ± 0.9	<sup>5</sup> KARLSSON 90	E731	

- <sup>1</sup> CAROSI 90 measures  $\phi_{00} = (47.1 \pm 2.1 \pm 1.0) + 579 [\Delta m - 0.5351] + 252 [\tau_S - 0.8922]^\circ$ . We have adjusted the measurement to use our best values of  $(\Delta m = 0.5293 \pm 0.0009) (10^{10} \text{ h s}^{-1})$ ,  $(\tau_S = 0.8954 \pm 0.0004) (10^{-10} \text{ s})$ . Our first error is their experiment's error and our second error is the systematic error from using our best values.
- <sup>2</sup> Not independent of other phase parameters reported in ABOUZAID 11.
- <sup>3</sup> ANGELOPOULOS 98 measures  $\phi_{00} = (42.0 \pm 5.6 \pm 1.9) + 240 [\Delta m - 0.5307]^\circ$ . We have adjusted the measurement to use our best values of  $(\Delta m = 0.5293 \pm 0.0009) (10^{10} \text{ h s}^{-1})$ . Our first error is their experiment's error and our second error is the systematic error from using our best values. The  $\tau_S$  dependence is negligible.
- <sup>4</sup> ADLER 96B identified initial neutral kaon individually as being a  $K^0$  or a  $\bar{K}^0$ . The systematic uncertainty is  $\pm 1.5^\circ$  combined in quadrature with  $\pm 0.8^\circ$  due to  $\Delta m$ .
- <sup>5</sup> KARLSSON 90 systematic error does not include regeneration phase uncertainty.

$$\phi_\epsilon = (2\phi_{+-} + \phi_{00})/3$$

This expression is a very good approximation, good to about  $10^{-3}$  degrees because of the small measured values of  $\phi_{00} - \phi_{+-}$  and  $\text{Re } \epsilon'/\epsilon$ , and small theoretical ambiguities.

VALUE ( $^\circ$ )	DOCUMENT ID	TECN	COMMENT
<b>43.52 ± 0.05 OUR FIT</b>			Error includes scale factor of 1.2. Assuming <i>CPT</i>
<b>43.5 ± 0.5 OUR FIT</b>			Error includes scale factor of 1.3. Not assuming <i>CPT</i>
43.5164 ± 0.0002 ± 0.0518	<sup>1</sup> SUPERWEAK 12		Assuming <i>CPT</i>
43.86 ± 0.63	<sup>2</sup> ABOUZAID 11	KTEV	Not assuming <i>CPT</i>

- <sup>1</sup> SUPERWEAK 12 is a fake measurement used to impose the *CPT* or Superweak constraint  $\phi_{+-} = \phi_{SW} = \tan^{-1} [2 \frac{\Delta m}{\hbar} (\frac{\tau_S \tau_L}{\tau_L - \tau_S})]$ . This "measurement" is linearized using values near the RPP 2004 edition values of  $\Delta m$ ,  $\tau_S$  and  $\tau_L$ , and then adjusted to our current values as described in the following "measurement". SUPERWEAK 12 measures  $\phi_\epsilon = (43.50258 \pm 0.00021) + 54.1 [\Delta m - 0.5289] + 32.0 [\tau_S - 0.89564]^\circ$ . We have adjusted the measurement to use our best values of  $(\Delta m = 0.5293 \pm 0.0009) (10^{10} \text{ h s}^{-1})$ ,  $(\tau_S = 0.8954 \pm 0.0004) (10^{-10} \text{ s})$ . Our first error is their experiment's error and our second error is the systematic error from using our best values.
- <sup>2</sup> ABOUZAID 11 uses the full KTeV dataset collected in 1996, 1997, and 1999. See  $\text{Im}(\epsilon'/\epsilon)$  section for correlation information.

$$\text{Im}(\epsilon'/\epsilon) = -(\phi_{00} - \phi_{+-})/3$$

For small  $|\epsilon'/\epsilon|$ ,  $\text{Im}(\epsilon'/\epsilon)$  is related to the phases of  $\eta_{00}$  and  $\eta_{+-}$  by the above expression.

VALUE ( $^\circ$ )	DOCUMENT ID	TECN	COMMENT
<b>-0.002 ± 0.005 OUR FIT</b>			Error includes scale factor of 1.7. Assuming <i>CPT</i>
<b>-0.11 ± 0.11 OUR FIT</b>			Not assuming <i>CPT</i>
<b>-0.0985 ± 0.1157</b>	<sup>1</sup> ABOUZAID 11	KTEV	Not assuming <i>CPT</i>

- <sup>1</sup> ABOUZAID 11 uses the full KTeV dataset collected in 1996, 1997, and 1999. The fit has  $\Delta m$ ,  $\tau_S$ ,  $\phi_\epsilon$ ,  $\text{Re}(\epsilon'/\epsilon)$ , and  $\text{Im}(\epsilon'/\epsilon)$  as free parameters. The reported value of  $\text{Im}(\epsilon'/\epsilon) = (-17.20 \pm 20.20) \times 10^{-4}$  rad. The correlation coefficients are  $\rho(\phi_\epsilon, \Delta m) = 0.828$ ,  $\rho(\phi_\epsilon, \tau_S) = -0.765$ ,  $\rho(\Delta m, \tau_S) = -0.858$ ,  $\rho(\text{Im}(\epsilon'/\epsilon), \phi_\epsilon) = -0.041$ ,  $\rho(\text{Im}(\epsilon'/\epsilon), \Delta m) = 0.026$ ,  $\rho(\text{Im}(\epsilon'/\epsilon), \tau_S) = -0.010$ .

**DECAY-PLANE ASYMMETRY IN  $\pi^+ \pi^- e^+ e^-$  DECAYS**

This is the *CP*-violating asymmetry

$$A = \frac{N_{\sin\phi\cos\phi>0.0} - N_{\sin\phi\cos\phi<0.0}}{N_{\sin\phi\cos\phi>0.0} + N_{\sin\phi\cos\phi<0.0}}$$

where  $\phi$  is the angle between the  $e^+ e^-$  and  $\pi^+ \pi^-$  planes in the  $K_L^0$  rest frame.

**CP ASYMMETRY  $A$  in  $K_L^0 \rightarrow \pi^+ \pi^- e^+ e^-$** 

VALUE (%)	DOCUMENT ID	TECN
<b>13.7 ± 1.5 OUR AVERAGE</b>		
13.6 ± 1.4 ± 1.5	ABOUZAID 06	KTEV
14.2 ± 3.0 ± 1.9	LAI 03C	NA48
13.6 ± 2.5 ± 1.2	ALAVI-HARATI 00B	KTEV

**PARAMETERS FOR  $e^+ e^- e^+ e^-$  DECAYS**

These are the *CP*-violating parameters in the  $\phi$  distribution, where  $\phi$  is the angle between the planes of the two  $e^+ e^-$  pairs in the kaon rest frame:

$$d\Gamma/d\phi \propto 1 + \beta_{CP} \cos(2\phi) + \gamma_{CP} \sin(2\phi)$$

 **$\beta_{CP}$  from  $K_L^0 \rightarrow e^+ e^- e^+ e^-$** 

VALUE	EVTS	DOCUMENT ID	TECN	COMMENT
<b>-0.19 ± 0.07 OUR AVERAGE</b>				
-0.13 ± 0.10 ± 0.03	200	<sup>1</sup> LAI	05B	NA48
-0.23 ± 0.09 ± 0.02	441	ALAVI-HARATI 01D	KTEV	$M_{e^+ e^-} > 8 \text{ MeV}/c^2$

- <sup>1</sup> LAI 05B obtains  $\beta_{CP} = -0.13 \pm 0.10$  (stat) if  $\gamma_{CP} = 0$  is assumed.

 **$\gamma_{CP}$  from  $K_L^0 \rightarrow e^+ e^- e^+ e^-$** 

VALUE	EVTS	DOCUMENT ID	TECN	COMMENT
<b>0.01 ± 0.11 OUR AVERAGE</b>				Error includes scale factor of 1.6.
+0.13 ± 0.10 ± 0.03	200	LAI	05B	NA48
-0.09 ± 0.09 ± 0.02	441	ALAVI-HARATI 01D	KTEV	$M_{e^+ e^-} > 8 \text{ MeV}/c^2$

**CHARGE ASYMMETRY IN  $\pi^+ \pi^- \pi^0$  DECAYS**

These are *CP*-violating charge-asymmetry parameters, defined at beginning of section "LINEAR COEFFICIENT  $g$  FOR  $K_L^0 \rightarrow \pi^+ \pi^- \pi^0$  above.

See also note on Dalitz plot parameters in  $K^\pm$  section and note on "CP violation in  $K_L$  decays" above.

**LINEAR COEFFICIENT  $j$  FOR  $K_L^0 \rightarrow \pi^+ \pi^- \pi^0$** 

VALUE	EVTS	DOCUMENT ID	TECN
<b>0.0012 ± 0.0008 OUR AVERAGE</b>			
0.0010 ± 0.0024 ± 0.0030	500k	ANGELOPOULOS 98C	CPLR
-0.001 ± 0.011	6499	CHO	77
0.001 ± 0.003	4709	PEACH	77
0.0013 ± 0.0009	3M	SCRIBANO	70
0.0 ± 0.017	4400	SMITH	70
0.001 ± 0.004	238k	BLANPIED	68

# Meson Particle Listings

$K_L^0$

## QUADRATIC COEFFICIENT $f$ FOR $K_L^0 \rightarrow \pi^+ \pi^- \pi^0$

VALUE	EVTs	DOCUMENT ID	TECN
<b>0.0045 ± 0.0024 ± 0.0059</b>	500k	ANGELOPO...	98c CPLR

### PARAMETERS for $K_L^0 \rightarrow \pi^+ \pi^- \gamma$ DECAY

$$|\eta_{+-\gamma}| = |A(K_L^0 \rightarrow \pi^+ \pi^- \gamma, CP \text{ violating})/A(K_S^0 \rightarrow \pi^+ \pi^- \gamma)|$$

VALUE (units $10^{-3}$ )	EVTs	DOCUMENT ID	TECN
<b>2.35 ± 0.07 OUR AVERAGE</b>			
2.359 ± 0.062 ± 0.040	9045	MATTHEWS	95 E773
2.15 ± 0.26 ± 0.20	3671	RAMBERG	93B E731

### $\phi_{+-\gamma}$ = phase of $\eta_{+-\gamma}$

VALUE (°)	EVTs	DOCUMENT ID	TECN
<b>44 ± 4 OUR AVERAGE</b>			
43.8 ± 3.5 ± 1.9	9045	MATTHEWS	95 E773
72 ± 23 ± 17	3671	RAMBERG	93B E731

$$|\epsilon'_{+-\gamma}|/\epsilon \text{ for } K_L^0 \rightarrow \pi^+ \pi^- \gamma$$

VALUE	CL%	EVTs	DOCUMENT ID	TECN
<b>&lt;0.3</b>	90	3671	1 RAMBERG	93B E731

<sup>1</sup> RAMBERG 93B limit on  $|\epsilon'_{+-\gamma}|/\epsilon$  assumes than any difference between  $\eta_{+-}$  and  $\eta_{+-\gamma}$  is due to direct CP violation.

$$|\mathcal{E}| \text{ for } K_L^0 \rightarrow \pi^+ \pi^- \gamma$$

This parameter is the amplitude of the direct emission of a CP violating E1 electric dipole photon.

VALUE	CL%	EVTs	DOCUMENT ID	TECN	COMMENT
<b>&lt;0.21</b>	90	111k	ABOUZAID	06A KTEV	$E_{\gamma}^* > 20$ MeV

## T VIOLATION TESTS IN $K_L^0$ DECAYS

### $\text{Im}(\xi)$ in $K_{\mu 3}^0$ DECAY (from transverse $\mu$ pol.)

Test of T reversal invariance.

VALUE	CL%	EVTs	DOCUMENT ID	TECN	COMMENT
<b>-0.007 ± 0.026 OUR AVERAGE</b>					
0.009 ± 0.030	12M		MORSE	80 CNTR	Polarization
0.35 ± 0.30	207k		1 CLARK	77 SPEC	POL, $t=0$
-0.085 ± 0.064	2.2M		2 SANDWEISS	73 CNTR	POL, $t=0$
-0.02 ± 0.08			LONGO	69 CNTR	POL, $t=3.3$
-0.2 ± 0.6			ABRAMS	68B OSPK	Polarization
0.012 ± 0.026			SCHMIDT	79 CNTR	Repl. by MORSE 80

<sup>1</sup> CLARK 77 value has additional  $\xi(0)$  dependence  $+0.21\text{Re}[\xi(0)]$ .  
<sup>2</sup> SANDWEISS 73 value corrected from value quoted in their paper due to new value of  $\text{Re}(\xi)$ . See footnote 4 of SCHMIDT 79.

## CPT-INVARIANCE TESTS IN $K_L^0$ DECAYS

### PHASE DIFFERENCE $\phi_{00} - \phi_{+-}$

Test of CPT.

OUR FIT is described in the note on "CP violation in  $K_L$  decays" in the  $K_L^0$  Particle Listings.

VALUE (°)	DOCUMENT ID	TECN	COMMENT
<b>0.006 ± 0.014 OUR FIT</b>	Error includes scale factor of 1.7. Assuming CPT		
<b>0.34 ± 0.32 OUR FIT</b>	Not assuming CPT		
0.006 ± 0.008	<sup>1</sup> SUPERWEAK 12		Assuming CPT
-0.30 ± 0.88	<sup>2</sup> SCHWINGEN...95		Combined E731, E773
0.30 ± 0.35	<sup>3</sup> ABOUZAID 11	KTEV	Not assuming CPT
0.39 ± 0.22 ± 0.45	<sup>4</sup> ALAVI-HARATI03	KTEV	
0.62 ± 0.71 ± 0.75	SCHWINGEN...95	E773	
-1.6 ± 1.2	<sup>5</sup> GIBBONS 93	E731	
0.2 ± 2.6 ± 1.2	<sup>6</sup> CAROSI 90	NA31	
-0.3 ± 2.4 ± 1.2	KARLSSON 90	E731	

<sup>1</sup> SUPERWEAK 12 is a fake experiment to constrain  $\phi_{00} - \phi_{+-}$  to a small value as described in the note "CP violation in  $K_L$  decays."  
<sup>2</sup> This SCHWINGENHEUER 95 values is the combined result of SCHWINGENHEUER 95 and GIBBONS 93, accounting for correlated systematic errors.  
<sup>3</sup> Not independent of other phase parameters reported in ABOUZAID 11.  
<sup>4</sup> ALAVI-HARATI 03 fit  $\text{Re}(\epsilon'/\epsilon)$ ,  $\text{Im}(\epsilon'/\epsilon)$ ,  $\Delta m$ ,  $\tau_S$ , and  $\phi_{+-}$  simultaneously, not assuming CPT. Phase difference is obtained from  $\phi_{00} - \phi_{+-} \approx -3\text{Im}(\epsilon'/\epsilon)$  for small  $|\epsilon'/\epsilon|$ . Superseded by ABOUZAID 11.  
<sup>5</sup> GIBBONS 93 give detailed dependence of systematic error on lifetime (see the section on the  $K_S^0$  mean life) and mass difference (see the section on  $m_{K_L^0} - m_{K_S^0}$ ).  
<sup>6</sup> CAROSI 90 is excluded from the fit because it is not independent of  $\phi_{+-}$  and  $\phi_{00}$  values.

### PHASE DIFFERENCE $\phi_{+-} - \phi_{SW}$

Test of CPT. The Superweak phase  $\phi_{SW} \equiv \tan^{-1}(2\Delta m/\Delta\Gamma)$  where  $\Delta m = m_{K_L^0} - m_{K_S^0}$  and  $\Delta\Gamma = \hbar(\tau_L - \tau_S)/(\tau_L\tau_S)$ .

VALUE (°)	DOCUMENT ID	TECN
<b>0.61 ± 0.62 ± 1.01</b>	<sup>1</sup> ALAVI-HARATI03	KTEV

<sup>1</sup> ALAVI-HARATI 03 fit is the same as their  $\phi_{+-}$ ,  $\tau_{K_S}$ ,  $\Delta m$  fit, except that the parameter  $\phi_{+-} - \phi_{SW}$  is used in place of  $\phi$ .

$$\text{Re}\left(\frac{2}{3}\eta_{+-} + \frac{1}{3}\eta_{00}\right) - \frac{A_f}{2}$$

VALUE (units $10^{-6}$ )	DOCUMENT ID	TECN	COMMENT
<b>-3 ± 35</b>	<sup>1</sup> ALAVI-HARATI02	E799	Uses $A_L$ from $K_{e3}$ decays

<sup>1</sup> ALAVI-HARATI 02 uses PDG 00 values of  $\eta_{+-}$  and  $\eta_{00}$ .

## $\Delta S = \Delta Q$ IN $K^0$ DECAYS

The relative amount of  $\Delta S \neq \Delta Q$  component present is measured by the parameter  $x$ , defined as

$$x = A(\bar{K}^0 \rightarrow \pi^- \ell^+ \nu)/A(K^0 \rightarrow \pi^- \ell^+ \nu)$$

We list  $\text{Re}\{x\}$  and  $\text{Im}\{x\}$  for  $K_{e3}$  and  $K_{\mu 3}$  combined.

$$x = A(\bar{K}^0 \rightarrow \pi^- \ell^+ \nu)/A(K^0 \rightarrow \pi^- \ell^+ \nu) = A(\Delta S = -\Delta Q)/A(\Delta S = \Delta Q)$$

### REAL PART OF $x$

VALUE	EVTs	DOCUMENT ID	TECN	COMMENT
<b>-0.0018 ± 0.0041 ± 0.0045</b>		ANGELOPO...	98D CPLR	$K_{e3}$ from $K^0$
0.10 <sup>+0.18</sup> / <sub>-0.19</sub>	79	SMITH	75B WIRE	$\pi^- p \rightarrow K^0 \Lambda$
0.04 ± 0.03	4724	NIEBERGALL	74 ASPK	$K^+ p \rightarrow K^0 p \pi^+$
-0.008 ± 0.044	1757	FACKLER	73 OSPK	$K_{e3}$ from $K^0$
-0.03 ± 0.07	1367	HART	73 OSPK	$K_{e3}$ from $K^0 \Lambda$
-0.070 ± 0.036	1079	MALLARY	73 OSPK	$K_{e3}$ from $K^0 \Lambda X$
0.03 ± 0.06	410	<sup>1</sup> BURGUN	72 HBC	$K^+ p \rightarrow K^0 p \pi^+$
0.04 <sup>+0.10</sup> / <sub>-0.13</sub>	100	<sup>2</sup> GRAHAM	72 OSPK	$K_{\mu 3}$ from $K^0 \Lambda$
-0.05 ± 0.09	442	<sup>2</sup> GRAHAM	72 OSPK	$\pi^- p \rightarrow K^0 \Lambda$
0.26 <sup>+0.10</sup> / <sub>-0.14</sub>	126	MANN	72 HBC	$K^- p \rightarrow n \bar{K}^0$
-0.13 ± 0.11	342	<sup>2</sup> MANTSCH	72 OSPK	$K_{e3}$ from $K^0 \Lambda$
0.04 <sup>+0.07</sup> / <sub>-0.08</sub>	222	<sup>1</sup> BURGUN	71 HBC	$K^+ p \rightarrow K^0 p \pi^+$
0.25 <sup>+0.07</sup> / <sub>-0.09</sub>	252	WEBBER	71 HBC	$K^- p \rightarrow n \bar{K}^0$
0.12 ± 0.09	215	<sup>3</sup> CHO	70 DBC	$K^+ d \rightarrow K^0 p p$
-0.020 ± 0.025		<sup>4</sup> BENNETT	69 CNTR	Charge asym+ Cu regen.
0.09 <sup>+0.14</sup> / <sub>-0.16</sub>	686	LITTENBERG	69 OSPK	$K^+ n \rightarrow K^0 p$
0.03 ± 0.03		<sup>4</sup> BENNETT	68 CNTR	
0.09 <sup>+0.07</sup> / <sub>-0.09</sub>	121	JAMES	68 HBC	$\bar{p} p$
0.17 <sup>+0.16</sup> / <sub>-0.35</sub>	116	FELDMAN	67B OSPK	$\pi^- p \rightarrow K^0 \Lambda$
0.17 ± 0.10	335	<sup>3</sup> HILL	67 DBC	$K^+ d \rightarrow K^0 p p$
0.035 <sup>+0.11</sup> / <sub>-0.13</sub>	196	AUBERT	65 HLBC	$K^+$ charge exch.
0.06 <sup>+0.18</sup> / <sub>-0.44</sub>	152	<sup>5</sup> BALDO...	65 HLBC	$K^+$ charge exch.
-0.08 <sup>+0.16</sup> / <sub>-0.28</sub>	109	<sup>6</sup> FRANZINI	65 HBC	$\bar{p} p$

<sup>1</sup> BURGUN 72 is a final result which includes BURGUN 71.  
<sup>2</sup> First GRAHAM 72 value is second GRAHAM 72 value combined with MANTSCH 72.  
<sup>3</sup> CHO 70 is analysis of unambiguous events in new data and HILL 67.  
<sup>4</sup> BENNETT 69 is a reanalysis of BENNETT 68.  
<sup>5</sup> BALDO-CEOLIN 65 gives  $x$  and  $\theta$  converted by us to  $\text{Re}(x)$  and  $\text{Im}(x)$ .  
<sup>6</sup> FRANZINI 65 gives  $x$  and  $\theta$  for  $\text{Re}(x)$  and  $\text{Im}(x)$ . See SCHMIDT 67.

### IMAGINARY PART OF $x$

Assumes  $m_{K_L^0} - m_{K_S^0}$  positive. See Listings above.

VALUE	EVTs	DOCUMENT ID	TECN	COMMENT
<b>0.0012 ± 0.0019 ± 0.0009</b>	640k	ANGELOPO...	01B CPLR	$K_{e3}$ from $K^0$
0.0012 ± 0.0019	640k	<sup>1</sup> ANGELOPO...	98E CPLR	$K_{e3}$ from $K^0$
-0.10 <sup>+0.16</sup> / <sub>-0.19</sub>	79	SMITH	75B WIRE	$\pi^- p \rightarrow K^0 \Lambda$
-0.06 ± 0.05	4724	NIEBERGALL	74 ASPK	$K^+ p \rightarrow K^0 p \pi^+$
-0.017 ± 0.060	1757	FACKLER	73 OSPK	$K_{e3}$ from $K^0$
0.09 ± 0.07	1367	HART	73 OSPK	$K_{e3}$ from $K^0 \Lambda$
0.107 <sup>+0.092</sup> / <sub>-0.074</sub>	1079	MALLARY	73 OSPK	$K_{e3}$ from $K^0 \Lambda X$
0.07 <sup>+0.06</sup> / <sub>-0.07</sub>	410	<sup>2</sup> BURGUN	72 HBC	$K^+ p \rightarrow K^0 p \pi^+$

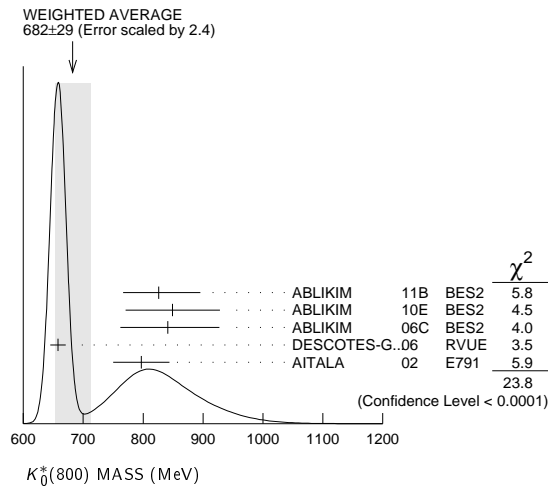
• • • We do not use the following data for averages, fits, limits, etc. • • •







- 7 Not seen by KOPP 01 using 7070 events of  $D^0 \rightarrow K^- \pi^+ \pi^0$ . LINK 02E and LINK 05I show clear evidence for a constant non-resonant scalar amplitude rather than  $K_0^*(800)$  in their high statistics analysis of  $D^+ \rightarrow K^- \pi^+ \mu^+ \nu_\mu$ .
- 8 AUBERT 07T does not find evidence for the charged  $K_0^*(800)$  using 11k events of  $D^0 \rightarrow K^- K^+ \pi^0$ .
- 9 S-Matrix pole. Supersedes BUGG 06. Combined analysis of ASTON 88, ABLIKIM 06c, AITALA 06, and LINK 09 using an s-dependent width with couplings to  $K\pi$  and  $K\eta'$ , and the Adler zero near thresholds.
- 10 T-matrix pole.
- 11 A Breit-Wigner mass and width.
- 12 S-matrix pole. Reanalysis of ASTON 88, AITALA 02, and ABLIKIM 06c using for the  $\kappa$  an s-dependent width with an Adler zero near threshold.
- 13 Breit-Wigner parameters. A significant S-wave can be also modeled as a non-resonant contribution.
- 14 Using ASTON 88.
- 15 T-matrix pole. Reanalysis of data from LINGLIN 73, ESTABROOKS 78, and ASTON 88 in the unitarized ChPT model.
- 16 T-matrix pole. Reanalysis of ASTON 88 data.
- 17 Reanalysis of ASTON 88 using interfering Breit-Wigner amplitudes.



- 26 T-matrix pole.
- 27 A Breit-Wigner mass and width.
- 28 S-matrix pole. Reanalysis of ASTON 88, AITALA 02, and ABLIKIM 06c using for the  $\kappa$  an s-dependent width with an Adler zero near threshold.
- 29 Statistical error only. A fit to the Dalitz plot including the  $K_0^*(800)^\pm$ ,  $K^*(892)^\pm$ , and  $\phi$  resonances modeled as Breit-Wigners. A significant S-wave can be also modeled as a non-resonant contribution.
- 30 Using ASTON 88.
- 31 T-matrix pole. Reanalysis of data from LINGLIN 73, ESTABROOKS 78, and ASTON 88 in the unitarized ChPT model.
- 32 T-matrix pole. Reanalysis of ASTON 88 data.
- 33 Reanalysis of ASTON 88 using interfering Breit-Wigner amplitudes.

**$K_0^*(800)$  REFERENCES**

ABLIKIM 11B	PL B698 183	M. Ablikim et al.	(BES II Collab.)
ABLIKIM 10E	PL B693 88	M. Ablikim et al.	(BES II Collab.)
BUGG 10	PR D81 014002	D.V. Bugg	(LOQM)
LINK 09	PL B681 14	J.M. Link et al.	(FNAL FOCUS Collab.)
BONVICINI 08A	PR D78 052001	G. Bonvicini et al.	(CLEO Collab.)
AUBERT 07T	PR D76 011102R	B. Aubert et al.	(BABAR Collab.)
EPIFANOV 07	PL B654 65	D. Epifanov et al.	(BELLE Collab.)
LINK 07B	PL B653 1	J.M. Link et al.	(FNAL FOCUS Collab.)
ABLIKIM 06C	PL B633 681	M. Ablikim et al.	(BES Collab.)
AITALA 06	PR D73 032004	E.M. Aitala et al.	(FNAL E791 Collab.)
Also	PR D74 059901 (errata.)	E.M. Aitala et al.	(FNAL E791 Collab.)
BUGG 06	PL B632 471	D.V. Bugg	(LOQM)
CRAWFIELD 06A	PR D74 031108R	C. Crawford et al.	(CLEO Collab.)
DESCOTES-G..06	EPJ C48 553	S. Descotes-Genon, B. Mousallam	
GUO 06	NP A773 78	F.K. Guo et al.	
ZHOU 06	NP A775 212	Z.Y. Zhou, H.Q. Zheng	
LINK 05I	PL B621 72	J.M. Link et al.	(FNAL FOCUS Collab.)
PELAEZ 04A	MPL A19 2879	J.R. Pelaez	
ZHENG 04	NP A733 235	H.Q. Zheng et al.	
BUGG 03	PL B572 1	D.V. Bugg	
AITALA 02	PRL 89 121801	E.M. Aitala et al.	(FNAL E791 Collab.)
LINK 02E	PL B535 43	J.M. Link et al.	(FNAL FOCUS Collab.)
KOPP 01	PR D63 092001	S. Kopp et al.	(CLEO Collab.)
ISHIDA 97B	PTP 98 621	S. Ishida et al.	
ASTON 88	NP B296 493	D. Aston et al.	(SLAC, NAGO, CINC, INUS)
ESTABROOKS 78	NP B133 490	P.G. Estabrooks et al.	(MCGI, CARL, DURH+)
LINGLIN 73	NP B55 408	D. Linglin	(CERN)
ROY 71	PL 36B 353	S.M. Roy	

**$K^*(892)$**

$I(J^P) = \frac{1}{2}(1^-)$

**$K^*(892)$  MASS**

**CHARGED ONLY, HADROPRODUCED**

VALUE (MeV)	EVTS	DOCUMENT ID	TECN	CHG	COMMENT
<b>891.66 ± 0.26 OUR AVERAGE</b>					
892.6 ± 0.5	5840	BAUBILLIER 84B	HBC	-	8.25 $K^- p \rightarrow \bar{K}^0 \pi^- p$
888 ± 3		NAPIER 84	SPEC	+	200 $\pi^- p \rightarrow 2K^0 X$
891 ± 1		NAPIER 84	SPEC	-	200 $\pi^- p \rightarrow 2K_S^0 X$
891.7 ± 2.1	3700	BARTH 83	HBC	+	70 $K^+ p \rightarrow K^0 \pi^+ X$
891 ± 1	4100	TOAFF 81	HBC	-	6.5 $K^+ p \rightarrow \bar{K}^0 \pi^- p$
892.8 ± 1.6		AJINENKO 80	HBC	+	32 $K^+ p \rightarrow K^0 \pi^+ X$
890.7 ± 0.9	1800	AGUILAR... 78B	HBC	±	0.76 $\bar{p} p \rightarrow K^\mp K_S^0 \pi^\pm$
886.6 ± 2.4	1225	BALAND 78	HBC	±	12 $\bar{p} p \rightarrow (K\pi)^\pm X$
891.7 ± 0.6	6706	COOPER 78	HBC	±	0.76 $\bar{p} p \rightarrow (K\pi)^\pm X$
891.9 ± 0.7	9000	1 PALER 75	HBC	-	14.3 $K^- p \rightarrow (K\pi)^- X$
892.2 ± 1.5	4404	AGUILAR... 71B	HBC	-	3.9, 4.6 $K^- p \rightarrow (K\pi)^- p$
891 ± 2	1000	CRENNELL 69D	DBC	-	3.9 $K^- N \rightarrow K^0 \pi^- X$
890 ± 3.0	720	BARLOW 67	HBC	±	1.2 $\bar{p} p \rightarrow (K^0 \pi)^\pm K^\mp$
889 ± 3.0	600	BARLOW 67	HBC	±	1.2 $\bar{p} p \rightarrow (K^0 \pi)^\pm K\pi$
891 ± 2.3	620	2 DEBAERE 67B	HBC	+	3.5 $K^+ p \rightarrow K^0 \pi^+ p$
891.0 ± 1.2	1700	3 WOJCICKI 64	HBC	-	1.7 $K^- p \rightarrow \bar{K}^0 \pi^- p$
• • • We do not use the following data for averages, fits, limits, etc. • • •					
893.5 ± 1.1	27k	4 ABELE 99D	CBAR	±	0.0 $\bar{p} p \rightarrow K^+ K^- \pi^0$
890.4 ± 0.2 ± 0.5	80 ± 0.8k	5 BIRD 89	LASS	-	11 $K^- p \rightarrow \bar{K}^0 \pi^- p$
890.0 ± 2.3	800	2,3 CLELAND 82	SPEC	+	30 $K^+ p \rightarrow K_S^0 \pi^+ p$
896.0 ± 1.1	3200	2,3 CLELAND 82	SPEC	+	50 $K^+ p \rightarrow K_S^0 \pi^+ p$
893 ± 1	3600	2,3 CLELAND 82	SPEC	-	50 $K^+ p \rightarrow K_S^0 \pi^- p$
896.0 ± 1.9	380	DELFOSSIE 81	SPEC	+	50 $K^\pm p \rightarrow K^\pm \pi^0 p$
886.0 ± 2.3	187	DELFOSSIE 81	SPEC	-	50 $K^\pm p \rightarrow K^\pm \pi^0 p$
894.2 ± 2.0	765	2 CLARK 73	HBC	-	3.13 $K^- p \rightarrow \bar{K}^0 \pi^- p$
894.3 ± 1.5	1150	2,3 CLARK 73	HBC	-	3.3 $K^- p \rightarrow \bar{K}^0 \pi^- p$
892.0 ± 2.6	341	2 SCHWEING...68	HBC	-	5.5 $K^- p \rightarrow \bar{K}^0 \pi^- p$

**CHARGED ONLY, PRODUCED IN  $\tau$  LEPTON DECAYS**

VALUE (MeV)	EVTS	DOCUMENT ID	TECN	COMMENT
<b>895.47 ± 0.20 ± 0.74</b>				
892.0 ± 0.5	53k	6 EPIFANOV 07	BELL	$\tau^- \rightarrow K_S^0 \pi^- \nu_\tau$
• • • We do not use the following data for averages, fits, limits, etc. • • •				
892.0 ± 0.5		7 BOITO 10	RVUE	$\tau^- \rightarrow K_S^0 \pi^- \nu_\tau$
892.0 ± 0.9		8,9 BOITO 09	RVUE	$\tau^- \rightarrow K_S^0 \pi^- \nu_\tau$
895.3 ± 0.2		8,10 JAMIN 08	RVUE	$\tau^- \rightarrow K_S^0 \pi^- \nu_\tau$
896.4 ± 0.9	11970	11 BONVICINI 02	CLEO	$\tau^- \rightarrow K^- \pi^0 \nu_\tau$
895 ± 2		12 BARATE 99R	ALEP	$\tau^- \rightarrow K^- \pi^0 \nu_\tau$

**$K_0^*(800)$  WIDTH**

VALUE (MeV)	EVTS	DOCUMENT ID	TECN	COMMENT
<b>547 ± 24 OUR AVERAGE</b>				
Error includes scale factor of 1.1.				
449 ± 156	+144 - 81	1338	18 ABLIKIM	11B BES2 $J/\psi \rightarrow K_S^0 K_S^0 \pi^+ \pi^-$
512 ± 80	+ 92 - 44	1421	19,20 ABLIKIM	10E BES2 $J/\psi \rightarrow K^\pm K_S^0 \pi^\mp \pi^0$
618 ± 90	+ 96 - 144	25k	19,21 ABLIKIM	06C BES2 $J/\psi \rightarrow \bar{K}^*(892)^0 K^+ \pi^-$
557 ± 24		22	DESCOTES-G..06	RVUE $\pi K \rightarrow \pi K$
410 ± 43 ± 87	15k	23,24	AITALA 02	E791 $D^+ \rightarrow K^- \pi^+ \pi^+$
• • • We do not use the following data for averages, fits, limits, etc. • • •				
658 ± 10 ± 44		25	BUGG 10	RVUE S-matrix pole
638.8 ± 4.4 ± 40.4	141k	26	BONVICINI 08A	CLEO $D^+ \rightarrow K^- \pi^+ \pi^+$
464 ± 28 ± 22	54k	27	LINK 07B	FOCS $D^+ \rightarrow K^- \pi^+ \pi^+$
684 ± 120		28	BUGG 06	RVUE
251 ± 48	0.6k	29	CRAWFIELD 06A	CLEO $D^0 \rightarrow K^+ K^- \pi^0$
606 ± 59		19,30	ZHOU 06	RVUE $K p \rightarrow K^- \pi^+ n$
470 ± 66		31	PELAEZ 04A	RVUE $K\pi \rightarrow K\pi$
724 ± 332		30	ZHENG 04	RVUE $K^- p \rightarrow K^- \pi^+ n$
772 ± 100		32	BUGG 03	RVUE $11 K^- p \rightarrow K^- \pi^+ n$
545 ± 235 - 110		33	ISHIDA 97B	RVUE $11 K^- p \rightarrow K^- \pi^+ n$

- 18 The Breit-Wigner parameters from a fit with seven intermediate resonances. The S-matrix pole position is  $(764 \pm 63^{+71}_{-54}) - i(306 \pm 149^{+143}_{-85})$  MeV.
- 19 S-matrix pole.
- 20 From a fit including ten additional resonances and energy-independent Breit-Wigner width.
- 21 A fit in the  $K_0^*(800) + K^*(892) + K^*(1410)$  model with mass and width of the  $K_0^*(800)$  from ABLIKIM 06c well describes the left slope of the  $K_S^0 \pi^-$  invariant mass spectrum in  $\tau^- \rightarrow K_S^0 \pi^- \nu_\tau$  decay studied by EPIFANOV 07.
- 22 S-matrix pole. Using Roy-Steiner equations (ROY 71) as well as unitarity, analyticity and crossing symmetry constraints.
- 23 Not seen by KOPP 01 using 7070 events of  $D^0 \rightarrow K^- \pi^+ \pi^0$ . LINK 02E and LINK 05I show clear evidence for a constant non-resonant scalar amplitude rather than  $K_0^*(800)$  in their high statistics analysis of  $D^+ \rightarrow K^- \pi^+ \mu^+ \nu_\mu$ .
- 24 AUBERT 07T does not find evidence for the charged  $K_0^*(800)$  using 11k events of  $D^0 \rightarrow K^- K^+ \pi^0$ .
- 25 S-Matrix pole. Supersedes BUGG 06. Combined analysis of ASTON 88, ABLIKIM 06c, AITALA 06, and LINK 09 using an s-dependent width with couplings to  $K\pi$  and  $K\eta'$ , and the Adler zero near thresholds.

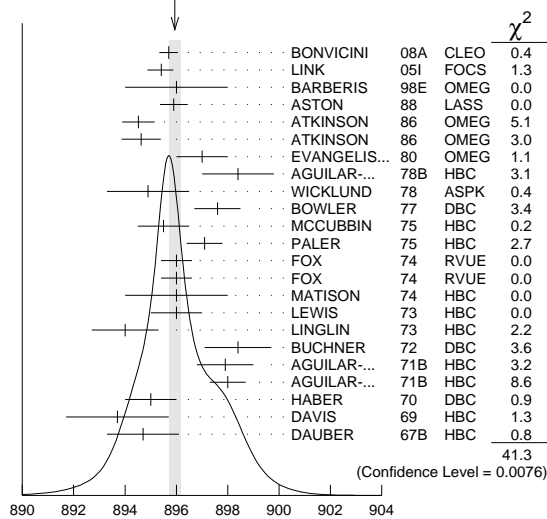
## Meson Particle Listings

 $K^*(892)$ 

## NEUTRAL ONLY

VALUE (MeV)	EVTS	DOCUMENT ID	TECN	COMMENT
<b>895.94 ± 0.22 OUR AVERAGE</b>		Error includes scale factor of 1.4. See the ideogram below.		
895.7 ± 0.2 ± 0.3	141k	<sup>13</sup> BONVICINI 08A	CLEO	$D^+ \rightarrow K^- \pi^+ \pi^+$
895.41 ± 0.32 <sup>+0.35</sup> <sub>-0.43</sub>	18k	<sup>14</sup> LINK 05I	FOCS	$D^+ \rightarrow K^- \pi^+ \mu^+ \nu_\mu$
896 ± 2		BARBERIS 98E	OMEG	$450 p p \rightarrow p_f p_s K^* \bar{K}^*$
895.9 ± 0.5 ± 0.2		ASTON 88	LASS	$11 K^- p \rightarrow K^- \pi^+ n$
894.52 ± 0.63	25k	<sup>1</sup> ATKINSON 86	OMEG	20-70 $\gamma p$
894.63 ± 0.76	20k	<sup>1</sup> ATKINSON 86	OMEG	20-70 $\gamma p$
897 ± 1	28k	EVANGELIS... 80	OMEG	$10 \pi^- p \rightarrow K^+ \pi^- (\Lambda, \Sigma)$
898.4 ± 1.4	1180	AGUILAR... 78B	HBC	$0.76 \bar{p} p \rightarrow K^\mp K_S^0 \pi^\pm$
894.9 ± 1.6		WICKLUND 78	ASPK	$3,4,6 K^\pm N \rightarrow (K\pi)^0 N$
897.6 ± 0.9		BOWLER 77	DBC	$5.4 K^+ d \rightarrow K^+ \pi^- p p$
895.5 ± 1.0	3600	MCCUBBIN 75	HBC	$3.6 K^- p \rightarrow K^- \pi^+ n$
897.1 ± 0.7	22k	<sup>1</sup> PALER 75	HBC	$14.3 K^- p \rightarrow (K\pi)^0 X$
896.0 ± 0.6	10k	FOX 74	RVUE	$2 K^- p \rightarrow K^- \pi^+ n$
896.0 ± 0.6		FOX 74	RVUE	$2 K^+ n \rightarrow K^+ \pi^- p$
896 ± 2		<sup>15</sup> MATISON 74	HBC	$12 K^+ p \rightarrow K^+ \pi^- \Delta$
896 ± 1	3186	LEWIS 73	HBC	$2.1-2.7 K^+ p \rightarrow K \pi \pi p$
894.0 ± 1.3		<sup>15</sup> LINGLIN 73	HBC	$2-13 K^+ p \rightarrow K^+ \pi^- \pi^+ p$
898.4 ± 1.3	1700	<sup>2</sup> BUCHNER 72	DBC	$4.6 K^+ n \rightarrow K^+ \pi^- p$
897.9 ± 1.1	2934	<sup>2</sup> AGUILAR... 71B	HBC	$3.9,4.6 K^- p \rightarrow K^- \pi^+ n$
898.0 ± 0.7	5362	<sup>2</sup> AGUILAR... 71B	HBC	$3.9,4.6 K^- p \rightarrow K^- \pi^+ \pi^- p$
895 ± 1	4300	<sup>3</sup> HABER 70	DBC	$3 K^- N \rightarrow K^- \pi^+ X$
893.7 ± 2.0	10k	DAVIS 69	HBC	$12 K^+ p \rightarrow K^+ \pi^- \pi^+ p$
894.7 ± 1.4	1040	<sup>2</sup> DAUBER 67B	HBC	$2.0 K^- p \rightarrow K^- \pi^+ \pi^- p$
• • • We do not use the following data for averages, fits, limits, etc. • • •				
894.9 ± 0.5 ± 0.7	14.4k	<sup>16</sup> MITCHELL 09A	CLEO	$D^+ \rightarrow K^+ K^- \pi^+$
896.2 ± 0.3	20k	<sup>8</sup> AUBERT 07AK	BABR	$10.6 e^+ e^- \rightarrow K^{*0} K^\pm \pi^\mp \gamma$
900.7 ± 1.1	5900	BARTH 83	HBC	$70 K^+ p \rightarrow K^+ \pi^- X$

WEIGHTED AVERAGE  
895.94 ± 0.22 (Error scaled by 1.4)



$K^*(892)^0$  mass (MeV)

- Inclusive reaction. Complicated background and phase-space effects.
- Mass errors enlarged by us to  $\Gamma/\sqrt{N}$ . See note.
- Number of events in peak reevaluated by us.
- K-matrix pole.
- From a partial wave amplitude analysis.
- From a fit in the  $K_S^0(800) + K^*(892) + K^*(1410)$  model.
- From the pole position of the  $K\pi$  vector form factor using EPIFANOV 07 and constraints from  $K_J$  decays in ANTONELLI 10.
- Systematic uncertainties not estimated.
- From the pole position of the  $K\pi$  vector form factor in the complex  $s$ -plane and using EPIFANOV 07 data.
- Reanalysis of EPIFANOV 07 using resonance chiral theory.
- Calculated by us from the shift by  $4.7 \pm 0.9$  MeV (statistical uncertainty only) reported in BONVICINI 02 with respect to the world average value from PDG 00.
- With mass and width of the  $K^*(1410)$  fixed at 1412 MeV and 227 MeV, respectively.
- From the isobar model with a complex pole for the  $\kappa$ .
- Fit to  $K\pi$  mass spectrum includes a non-resonant scalar component.
- From pole extrapolation.
- This value comes from a fit with  $\chi^2$  of 178/117.

 $K^*(892)$  MASSES AND MASS DIFFERENCES

Unrealistically small errors have been reported by some experiments. We use simple “realistic” tests for the minimum errors on the determination of a mass and width from a sample of  $N$  events:

$$\delta_{\min}(m) = \frac{\Gamma}{\sqrt{N}}, \quad \delta_{\min}(\Gamma) = 4 \frac{\Gamma}{\sqrt{N}}. \quad (1)$$

We consistently increase unrealistic errors before averaging. For a detailed discussion, see the 1971 edition of this Note.

 $m_{K^*(892)^0} - m_{K^*(892)^\pm}$ 

VALUE (MeV)	EVTS	DOCUMENT ID	TECN	CHG	COMMENT
<b>6.7 ± 1.2 OUR AVERAGE</b>					
7.7 ± 1.7	2980	AGUILAR... 78B	HBC	± 0	$0.76 \bar{p} p \rightarrow K^\mp K_S^0 \pi^\pm$
5.7 ± 1.7	7338	AGUILAR... 71B	HBC	- 0	$3.9,4.6 K^- p$
6.3 ± 4.1	283	<sup>17</sup> BARASH 67B	HBC		$0.0 \bar{p} p$

<sup>17</sup> Number of events in peak reevaluated by us.

 $K^*(892)$  RANGE PARAMETER

All from partial wave amplitude analyses.

VALUE (GeV <sup>-1</sup> )	EVTS	DOCUMENT ID	TECN	CHG	COMMENT
$3.96 \pm 0.54^{+1.31}_{-0.90}$	18k	<sup>18</sup> LINK 05I	FOCS	0	$D^+ \rightarrow K^- \pi^+ \mu^+ \nu_\mu$
3.4 ± 0.7		ASTON 88	LASS	0	$11 K^- p \rightarrow K^- \pi^+ n$
• • • We do not use the following data for averages, fits, limits, etc. • • •					
12.1 ± 3.2 ± 3.0		BIRD 89	LASS	-	$11 K^- p \rightarrow \bar{K}^0 \pi^- p$

<sup>18</sup> Fit to  $K\pi$  mass spectrum includes a non-resonant scalar component.

 $K^*(892)$  WIDTH

## CHARGED ONLY, HADROPRODUCED

VALUE (MeV)	EVTS	DOCUMENT ID	TECN	CHG	COMMENT
<b>50.8 ± 0.9 OUR FIT</b>					
<b>50.8 ± 0.9 OUR AVERAGE</b>					
49 ± 2	5840	BAUBILLIER 84B	HBC	-	$8.25 K^- p \rightarrow \bar{K}^0 \pi^- p$
56 ± 4		NAPIER 84	SPEC	-	$200 \pi^- p \rightarrow 2K_S^0 X$
51 ± 2	4100	TOAFF 81	HBC	-	$6.5 K^- p \rightarrow \bar{K}^0 \pi^- p$
50.5 ± 5.6		AJINENKO 80	HBC	±	$32 K^+ p \rightarrow K^0 \pi^+ X$
45.8 ± 3.6	1800	AGUILAR... 78B	HBC	±	$0.76 \bar{p} p \rightarrow K^\mp K_S^0 \pi^\pm$
52.0 ± 2.5	6706	<sup>19</sup> COOPER 78	HBC	±	$0.76 \bar{p} p \rightarrow (K\pi)^\pm X$
52.1 ± 2.2	9000	<sup>20</sup> PALER 75	HBC	-	$14.3 K^- p \rightarrow (K\pi)^-$
46.3 ± 6.7	765	<sup>19</sup> CLARK 73	HBC	-	$3.13 K^- p \rightarrow \bar{K}^0 \pi^- p$
48.2 ± 5.7	1150	<sup>19,21</sup> CLARK 73	HBC	-	$3.3 K^- p \rightarrow \bar{K}^0 \pi^- p$
54.3 ± 3.3	4404	<sup>19</sup> AGUILAR... 71B	HBC	-	$3.9,4.6 K^- p \rightarrow (K\pi)^-$
46 ± 5	1700	<sup>19,21</sup> WOJCIICKI 64	HBC	-	$1.7 K^- p \rightarrow \bar{K}^0 \pi^- p$
• • • We do not use the following data for averages, fits, limits, etc. • • •					
54.8 ± 1.7	27k	<sup>22</sup> ABELE 99D	CBAR	±	$0.0 \bar{p} p \rightarrow K^+ K^- \pi^0$
45.2 ± 1 ± 2	79.7 ± 0.8k	<sup>23</sup> BIRD 89	LASS	-	$11 K^- p \rightarrow \bar{K}^0 \pi^- p$
42.8 ± 7.1	3700	BARTH 83	HBC	+	$70 K^+ p \rightarrow K^0 \pi^+ X$
64.0 ± 9.2	800	<sup>19,21</sup> CLELAND 82	SPEC	+	$30 K^+ p \rightarrow K_S^0 \pi^+ p$
62.0 ± 4.4	3200	<sup>19,21</sup> CLELAND 82	SPEC	+	$50 K^+ p \rightarrow K_S^0 \pi^+ p$
55 ± 4	3600	<sup>19,21</sup> CLELAND 82	SPEC	-	$50 K^+ p \rightarrow K_S^0 \pi^- p$
62.6 ± 3.8	380	DELFOSE 81	SPEC	+	$50 K^\pm p \rightarrow K^\pm \pi^0 p$
50.5 ± 3.9	187	DELFOSE 81	SPEC	-	$50 K^\pm p \rightarrow K^\pm \pi^0 p$

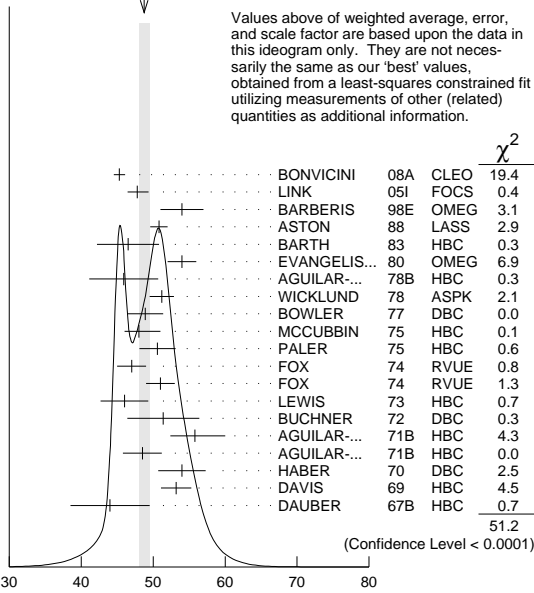
CHARGED ONLY, PRODUCED IN  $\tau$  LEPTON DECAYS

VALUE (MeV)	EVTS	DOCUMENT ID	TECN	COMMENT
<b>46.2 ± 0.6 ± 1.2</b>	53k	<sup>24</sup> EPIFANOV 07	BELL	$\tau^- \rightarrow K_S^0 \pi^- \nu_\tau$
• • • We do not use the following data for averages, fits, limits, etc. • • •				
46.5 ± 1.1		<sup>25</sup> BOITO 10	RVUE	$\tau^- \rightarrow K_S^0 \pi^- \nu_\tau$
46.2 ± 0.4		<sup>26,27</sup> BOITO 09	RVUE	$\tau^- \rightarrow K_S^0 \pi^- \nu_\tau$
47.5 ± 0.4		<sup>26,28</sup> JAMIN 08	RVUE	$\tau^- \rightarrow K_S^0 \pi^- \nu_\tau$
55 ± 8		<sup>29</sup> BARATE 99R	ALEP	$\tau^- \rightarrow K^- \pi^0 \nu_\tau$

**NEUTRAL ONLY**

VALUE (MeV)	EVTS	DOCUMENT ID	TECN	CHG	COMMENT
<b>48.7 ± 0.8 OUR FIT</b>					Error includes scale factor of 1.7.
<b>48.7 ± 0.7 OUR AVERAGE</b>					Error includes scale factor of 1.6. See the ideogram below.
45.3 ± 0.5 ± 0.6	141k	<sup>30</sup> BONVICINI 08A	CLEO		$D^+ \rightarrow K^- \pi^+ \pi^+$
47.79 ± 0.86 ± 1.32	18k	<sup>31</sup> LINK 05I	FOCS	0	$D^+ \rightarrow K^- \pi^+ \mu^+ \nu_\mu$
54 ± 3		BARBERIS 98E	OMEG		$450 p p \rightarrow p_f p_S K^* \bar{K}^*$
50.8 ± 0.8 ± 0.9		ASTON 88	LASS	0	$11 K^- p \rightarrow K^- \pi^+ n$
46.5 ± 4.3	5900	BARTH 83	HBC	0	$70 K^+ p \rightarrow K^+ \pi^- X$
54 ± 2	28k	EVANGELIS...80	OMEG	0	$10 \pi^- p \rightarrow K^+ \pi^- (\Lambda, \Sigma)$
45.9 ± 4.8	1180	AGUILAR-... 78B	HBC	0	$0.76 \bar{p} p \rightarrow K^\mp K_S^0 \pi^\pm$
51.2 ± 1.7		WICKLUND 78	ASPK	0	$3,4,6 K^\pm N \rightarrow (K\pi)^0 N$
48.9 ± 2.5		BOWLER 77	DBC	0	$5.4 K^+ d \rightarrow K^+ \pi^- p p$
48 ± 3	3600	MCCUBBIN 75	HBC	0	$3.6 K^- p \rightarrow K^- \pi^+ n$
50.6 ± 2.5	22k	<sup>20</sup> PALER 75	HBC	0	$14.3 K^- p \rightarrow (K\pi)^0 X$
47 ± 2	10k	FOX 74	RVUE	0	$2 K^- p \rightarrow K^- \pi^+ n$
51 ± 2		FOX 74	RVUE	0	$2 K^+ n \rightarrow K^+ \pi^- p$
46.0 ± 3.3	3186	<sup>19</sup> LEWIS 73	HBC	0	$2.1-2.7 K^+ p \rightarrow K\pi p$
51.4 ± 5.0	1700	<sup>19</sup> BUCHNER 72	DBC	0	$4.6 K^+ n \rightarrow K^+ \pi^- p$
55.8 ± 4.2	2934	<sup>19</sup> AGUILAR-... 71B	HBC	0	$3.9,4,6 K^- p \rightarrow K^- \pi^+ n$
48.5 ± 2.7	5362	AGUILAR-... 71B	HBC	0	$3.9,4,6 K^- p \rightarrow K^- \pi^+ \pi^- p$
54.0 ± 3.3	4300	<sup>19,21</sup> HABER 70	DBC	0	$3 K^- N \rightarrow K^- \pi^+ X$
53.2 ± 2.1	10k	<sup>19</sup> DAVIS 69	HBC	0	$12 K^+ p \rightarrow K^+ \pi^- \pi^+ p$
44 ± 5.5	1040	<sup>19</sup> DAUBER 67B	HBC	0	$2.0 K^- p \rightarrow K^- \pi^+ \pi^- p$
• • • We do not use the following data for averages, fits, limits, etc. • • •					
45.7 ± 1.1 ± 0.5	14.4k	<sup>32</sup> MITCHELL 09A	CLEO		$D_S^+ \rightarrow K^+ K^- \pi^+$
50.6 ± 0.9	20k	<sup>26</sup> AUBERT 07AK	BABR		$10.6 e^+ e^- \rightarrow K^* K^\pm \pi^\mp \gamma$

WEIGHTED AVERAGE  
48.7±0.7 (Error scaled by 1.6)



NEUTRAL ONLY (MeV)

- <sup>19</sup>Width errors enlarged by us to  $4 \times \Gamma/\sqrt{N}$ ; see note.
- <sup>20</sup>Inclusive reaction. Complicated background and phase-space effects.
- <sup>21</sup>Number of events in peak reevaluated by us.
- <sup>22</sup>K-matrix pole.
- <sup>23</sup>From a partial wave amplitude analysis.
- <sup>24</sup>From a fit in the  $K_S^0(800) + K^*(892) + K^*(1410)$  model.
- <sup>25</sup>From the pole position of the  $K\pi$  vector form factor using EPIFANOV 07 and constraints from  $K_{f3}$  decays in ANTONELLI 10.
- <sup>26</sup>Systematic uncertainties not estimated.
- <sup>27</sup>From the pole position of the  $K\pi$  vector form factor in the complex s-plane and using EPIFANOV 07 data.
- <sup>28</sup>Reanalysis of EPIFANOV 07 using resonance chiral theory.
- <sup>29</sup>With mass and width of the  $K^*(1410)$  fixed at 1412 MeV and 227 MeV, respectively.
- <sup>30</sup>From the isobar model with a complex pole for the  $\kappa$ .
- <sup>31</sup>Fit to  $K\pi$  mass spectrum includes a non-resonant scalar component.
- <sup>32</sup>This value comes from a fit with  $\chi^2$  of 178/117.

**$K^*(892)$  DECAY MODES**

Mode	Fraction ( $\Gamma_i/\Gamma$ )	Confidence level
$\Gamma_1$ $K\pi$	~ 100	%
$\Gamma_2$ $(K\pi)^\pm$	( 99.901 ± 0.009 ) %	
$\Gamma_3$ $(K\pi)^0$	( 99.761 ± 0.021 ) %	
$\Gamma_4$ $K^0 \gamma$	( 2.39 ± 0.21 ) × 10 <sup>-3</sup>	
$\Gamma_5$ $K^\pm \gamma$	( 9.9 ± 0.9 ) × 10 <sup>-4</sup>	
$\Gamma_6$ $K\pi\pi$	< 7	× 10 <sup>-4</sup> 95%

**CONSTRAINED FIT INFORMATION**

An overall fit to the total width and a partial width uses 13 measurements and one constraint to determine 3 parameters. The overall fit has a  $\chi^2 = 7.8$  for 11 degrees of freedom.

The following *off-diagonal* array elements are the correlation coefficients  $\langle \delta p_i \delta p_j \rangle / (\delta p_i \delta p_j)$ , in percent, from the fit to parameters  $p_i$ , including the branching fractions,  $x_i \equiv \Gamma_i/\Gamma_{\text{total}}$ . The fit constrains the  $x_i$  whose labels appear in this array to sum to one.

$x_5$	-100	
$\Gamma$	19	-19
	$x_2$	$x_5$

Mode	Rate (MeV)
$\Gamma_2$ $(K\pi)^\pm$	50.7 ± 0.9
$\Gamma_5$ $K^\pm \gamma$	0.050 ± 0.005

**CONSTRAINED FIT INFORMATION**

An overall fit to the total width and a partial width uses 21 measurements and one constraint to determine 3 parameters. The overall fit has a  $\chi^2 = 51.2$  for 19 degrees of freedom.

The following *off-diagonal* array elements are the correlation coefficients  $\langle \delta p_i \delta p_j \rangle / (\delta p_i \delta p_j)$ , in percent, from the fit to parameters  $p_i$ , including the branching fractions,  $x_i \equiv \Gamma_i/\Gamma_{\text{total}}$ . The fit constrains the  $x_i$  whose labels appear in this array to sum to one.

$x_4$	-100	
$\Gamma$	18	-18
	$x_3$	$x_4$

Mode	Rate (MeV)	Scale factor
$\Gamma_3$ $(K\pi)^0$	48.6 ± 0.8	1.7
$\Gamma_4$ $K^0 \gamma$	0.117 ± 0.010	

**$K^*(892)$  PARTIAL WIDTHS**

$\Gamma(K^0 \gamma)$	EVTS	DOCUMENT ID	TECN	CHG	COMMENT	$\Gamma_4$
<b>117 ± 10 OUR FIT</b>						
<b>116.5 ± 9.9</b>	584	CARLSMITH 86	SPEC	0	$K_L^0 A \rightarrow K_S^0 \pi^0 A$	

$\Gamma(K^\pm \gamma)$	DOCUMENT ID	TECN	CHG	COMMENT	$\Gamma_5$
<b>50 ± 5 OUR FIT</b>					
<b>50 ± 5 OUR AVERAGE</b>					
48 ± 11	BERG 83	SPEC	-	156 $K^- A \rightarrow \bar{K} \pi A$	
51 ± 5	CHANDLEE 83	SPEC	+	200 $K^+ A \rightarrow K \pi A$	

**$K^*(892)$  BRANCHING RATIOS**

$\Gamma(K^0 \gamma)/\Gamma_{\text{total}}$	DOCUMENT ID	TECN	CHG	COMMENT	$\Gamma_4/\Gamma$
<b>2.39 ± 0.21 OUR FIT</b>					
• • • We do not use the following data for averages, fits, limits, etc. • • •					
1.5 ± 0.7	CARITHERS 75B	CNTR	0	8-16 $\bar{K}^0 A$	

$\Gamma(K^\pm \gamma)/\Gamma_{\text{total}}$	DOCUMENT ID	TECN	CHG	COMMENT	$\Gamma_5/\Gamma$
<b>0.99 ± 0.09 OUR FIT</b>					
• • • We do not use the following data for averages, fits, limits, etc. • • •					
< 1.6	95	BEMPORAD 73	CNTR	+	10-16 $K^+ A$

# Meson Particle Listings

## K\*(892), K<sub>1</sub>(1270)

Γ(Kππ)/Γ((Kπ)±)						Γ <sub>6</sub> /Γ <sub>2</sub>
VALUE	CL%	DOCUMENT ID	TECN	CHG	COMMENT	
< 7 × 10 <sup>-4</sup>	95	JONGEJANS	78	HBC	4 K <sup>-</sup> p → pK <sup>0</sup> 2π	
••• We do not use the following data for averages, fits, limits, etc. •••						
< 20 × 10 <sup>-4</sup>		WOJCICKI	64	HBC	1.7 K <sup>-</sup> p → K <sup>0</sup> π <sup>-</sup> p	

### K\*(892) REFERENCES

ANTONELLI	10	EPJ C69 399	M. Antonelli et al.	(FlaviaNet Working Group)
BOITO	10	JHEP 1009 031	D.R. Boito, R. Escrivano, M. Jamin	(BARC)
BOITO	09	EPJ C59 821	D.R. Boito, R. Escrivano, M. Jamin	
MITCHELL	09A	PR D79 072008	R.E. Mitchell et al.	(CLEO Collab.)
BONVICINI	08A	PR D78 052001	G. Bonvicini et al.	(CLEO Collab.)
JAMIN	08	PL B664 78	M. Jamin, A. Pich, J. Portoles	
AUBERT	07AK	PR D76 012008	B. Aubert et al.	(BABAR Collab.)
EPIFANOV	07	PL B654 65	D. Epifanov et al.	(BELLE Collab.)
LINK	05I	PL B621 72	J.M. Link et al.	(FNAL FOCUS Collab.)
BONVICINI	02	PRL 88 11803	G. Bonvicini et al.	(CLEO Collab.)
PDG	00	EPJ C15 1	D.E. Groom et al.	
ABELE	99D	PL B468 178	A. Abele et al.	(Crystal Barrel Collab.)
BARATE	99R	EPJ C11 599	R. Barate et al.	(ALEPH Collab.)
BARBERIS	96E	PL B436 204	D. Barberis et al.	(Omega Expt.)
BIRD	89	SLAC-332	P.F. Bird	(SLAC)
ASTON	88	NP B296 493	D. Aston et al.	(SLAC, NAGO, CINC, INUS)
ATKINSON	86	ZPHY C30 521	M. Atkinson et al.	(BONN, CERN, GLAS+)
CARLSMITH	86	PRL 56 18	D. Carlsmith et al.	(EFT, SAFL)
BAUBILLIER	84B	ZPHY C26 37	M. Baubillier et al.	(BIRM, CERN, GLAS+)
NAPIER	84	PL 149B 514	A. Napier et al.	(TUFTS, ARIZ, FNAL, FLOR+)
BARTH	83	NP B223 296	M. Barth et al.	(BRUX, CERN, GENO, MONS+)
BERG	83	Thesis UMI 83-21652	D.M. Berg	(ROCH)
CHANDLEE	83	PRL 51 168	C. Handlee et al.	(ROCH, FNAL, MINN)
CLELAND	82	NP B208 189	W.E. Cleland et al.	(DURH, GEVA, LAUS+)
DELFOSE	81	NP B183 349	A. Delfosse et al.	(GEVA, LAUS)
TOAFF	81	PR D23 1500	S. Toaff et al.	(ANL, KANS)
AJINENKO	80	ZPHY C5 177	I.V. Ajinenko et al.	(SERP, BRUX, MONS+)
EVANGELIS...	80	NP B165 383	C. Evangelista et al.	(BARI, BONN, CERN+)
AGUILAR...	78B	NP B141 101	M. Aguilar-Benitez et al.	(MADR, TATA+)
BALAND	78	NP B140 220	J.F. Baland et al.	(MONS, BELG, CERN+)
COOPER	78	NP B136 365	A.M. Cooper et al.	(TATA, CERN, CDEF+)
JONGEJANS	78	NP B139 383	B. Jongejans et al.	(ZEEM, CERN, NIJM+)
WICKLUND	78	PR D17 1197	A.B. Wicklund et al.	(ANL)
BOWLER	77	NP B126 31	M.G. Bowler et al.	(OXF)
CARITHERS	75B	PRL 35 349	W.C.J. Carithers et al.	(ROCH, MCGI)
MCCUBBIN	75	NP B86 13	N.A. McCubbin, L. Lyons	(OXF)
PALER	75	NP B96 1	K. Paler et al.	(RHEL, SAFL, EPOL)
FOX	74	NP B80 403	G.C. Fox, M.L. Griss	(CIT)
MATISON	74	PR D9 1872	M.J. Matison et al.	(LBL)
BEMPORAD	73	NP B51 1	C. Bemporad et al.	(CERN, ETH, LOIC)
CLARK	73	NP B54 432	A.G. Clark, L. Lyons, D. Radojicic	(OXF)
LEWIS	73	NP B60 283	P.H. Lewis et al.	(LOWC, LOIC, CDEF)
LINGLIN	73	NP B55 408	D. Linglin	(CERN)
BUCHNER	72	NP B45 333	K. Buchner et al.	(MPIM, CERN, BRUX)
AGUILAR...	71B	PR D4 2583	M. Aguilar-Benitez, R.L. Eisner, J.B. Kinson	(BNL)
HABER	70	NP B17 289	R. Haber et al.	(REHO, SAFL, BGNA, EPOL)
CRENNELL	69D	PRL 22 487	D.J. Crennell et al.	(BNL)
DAVIS	69	PRL 23 1071	P.J. Davis et al.	(LRL)
SCHWEING...	68	PR 166 1317	F. Schweingruber et al.	(ANL, NWES)
BARASH	67B	PR 156 1399	N. Barash et al.	(COLU)
BARLOW	67	NC 50A 701	J. Barlow et al.	(CERN, CDEF, IRAD, LIVP)
DAUBER	67B	PR 153 1403	P.M. Dauber et al.	(UCLA)
DEBAERE	67B	NC 51A 401	W. de Baere et al.	(BRUX, CERN)
WOJCICKI	64	PR 135 B484	S.G. Wojcicki	(LRL)

### K<sub>1</sub>(1270)

$$I(J^P) = \frac{1}{2}(1^+)$$

### K<sub>1</sub>(1270) MASS

VALUE (MeV)	DOCUMENT ID
1272 ± 7 OUR AVERAGE	Includes data from the 2 datablocks that follow this one.

**PRODUCED BY K<sup>-</sup>, BACKWARD SCATTERING, HYPERON EXCHANGE**  
 VALUE (MeV) EVTS DOCUMENT ID TECN CHG COMMENT  
 The data in this block is included in the average printed for a previous datablock.

1275 ± 10	700	GAVILLET	78	HBC	+	4.2 K <sup>-</sup> p → Ξ <sup>-</sup> (Kππ) <sup>+</sup>
-----------	-----	----------	----	-----	---	--

**PRODUCED BY K BEAMS**  
 VALUE (MeV) DOCUMENT ID TECN CHG COMMENT  
 The data in this block is included in the average printed for a previous datablock.

1270 ± 10	1	DAUM	81c	CNTR	-	63 K <sup>-</sup> p → K <sup>-</sup> 2π
••• We do not use the following data for averages, fits, limits, etc. •••						
~1276	2	TORNQVIST	82B	RVUE		
~1300		VERGEEST	79	HBC	-	4.2 K <sup>-</sup> p → (K̄ππ) <sup>-</sup> p
1289 ± 25	3	CARNEGIE	77	ASPK	±	13 K <sup>±</sup> p → (Kππ) <sup>±</sup> p
~1300		BRANDENB...	76	ASPK	±	13 K <sup>±</sup> p → (Kππ) <sup>±</sup> p
~1270		OTTER	76	HBC	-	10,14,16 K <sup>-</sup> p → (K̄ππ) <sup>-</sup> p
1260		DAVIS	72	HBC	+	12 K <sup>+</sup> p
1234 ± 12		FIRESTONE	72B	DBC	+	12 K <sup>+</sup> d

<sup>1</sup> Well described in the chiral unitary approach of GENG 07 with two poles at 1195 and 1284 MeV and widths of 246 and 146 MeV, respectively.  
<sup>2</sup> From a unitarized quark-model calculation.  
<sup>3</sup> From a model-dependent fit with Gaussian background to BRANDENBURG 76 data.

### PRODUCED BY BEAMS OTHER THAN K MESONS

VALUE (MeV)	EVTS	DOCUMENT ID	TECN	CHG	COMMENT
1248.1 ± 3.3 ± 1.4		GULER	11	BELL	B <sup>+</sup> → J/ψ K <sup>+</sup> π <sup>+</sup> π <sup>-</sup>
••• We do not use the following data for averages, fits, limits, etc. •••					
1279 ± 10	25k	4 ABLIKIM	06c	BES2	J/ψ → K*(892) <sup>0</sup> K <sup>+</sup> π <sup>-</sup>
1294 ± 10	310	RODEBACK	81	HBC	4 π <sup>-</sup> p → Λ K 2π
1300	40	CRENNELL	72	HBC	0 4.5 π <sup>-</sup> p → Λ K 2π
1242 + 9 - 10		5 ASTIER	69	HBC	0 p̄p
1300	45	CRENNELL	67	HBC	0 6 π <sup>-</sup> p → Λ K 2π
Systematic errors not estimated.					
This was called the C meson.					

### PRODUCED IN τ LEPTON DECAYS

VALUE (MeV)	EVTS	DOCUMENT ID	TECN	CHG	COMMENT
1254 ± 33 ± 34	7k	ASNER	00B	CLEO	± τ <sup>-</sup> → K <sup>-</sup> π <sup>+</sup> π <sup>-</sup> ν <sub>τ</sub>

### K<sub>1</sub>(1270) WIDTH

VALUE (MeV)	DOCUMENT ID
90 ± 20 OUR ESTIMATE	This is only an educated guess; the error given is larger than the error on the average of the published values.
87 ± 7 OUR AVERAGE	Includes data from the 2 datablocks that follow this one.

### PRODUCED BY K<sup>-</sup>, BACKWARD SCATTERING, HYPERON EXCHANGE

VALUE (MeV)	EVTS	DOCUMENT ID	TECN	CHG	COMMENT	
75 ± 15	700	GAVILLET	78	HBC	+	4.2 K <sup>-</sup> p → Ξ <sup>-</sup> Kππ

### PRODUCED BY K BEAMS

VALUE (MeV)	DOCUMENT ID	TECN	CHG	COMMENT	
90 ± 8	6 DAUM	81c	CNTR	-	63 K <sup>-</sup> p → K <sup>-</sup> 2π
••• We do not use the following data for averages, fits, limits, etc. •••					
~150	VERGEEST	79	HBC	-	4.2 K <sup>-</sup> p → (K̄ππ) <sup>-</sup> p
150 ± 71	7 CARNEGIE	77	ASPK	±	13 K <sup>±</sup> p → (Kππ) <sup>±</sup> p
~200	BRANDENB...	76	ASPK	±	13 K <sup>±</sup> p → (Kππ) <sup>±</sup> p
120	DAVIS	72	HBC	+	12 K <sup>+</sup> p
188 ± 21	FIRESTONE	72B	DBC	+	12 K <sup>+</sup> d

<sup>6</sup> Well described in the chiral unitary approach of GENG 07 with two poles at 1195 and 1284 MeV and widths of 246 and 146 MeV, respectively.  
<sup>7</sup> From a model-dependent fit with Gaussian background to BRANDENBURG 76 data.

### PRODUCED BY BEAMS OTHER THAN K MESONS

VALUE (MeV)	EVTS	DOCUMENT ID	TECN	CHG	COMMENT
1195 ± 5.2 ± 6.7		GULER	11	BELL	B <sup>+</sup> → J/ψ K <sup>+</sup> π <sup>+</sup> π <sup>-</sup>
••• We do not use the following data for averages, fits, limits, etc. •••					
131 ± 21	25k	8 ABLIKIM	06c	BES2	J/ψ → K*(892) <sup>0</sup> K <sup>+</sup> π <sup>-</sup>
66 ± 15	310	RODEBACK	81	HBC	4 π <sup>-</sup> p → Λ K 2π
60	40	CRENNELL	72	HBC	0 4.5 π <sup>-</sup> p → Λ K 2π
127 + 7 - 25		ASTIER	69	HBC	0 p̄p
60	45	CRENNELL	67	HBC	0 6 π <sup>-</sup> p → Λ K 2π
Systematic errors not estimated.					

### PRODUCED IN τ LEPTON DECAYS

VALUE (MeV)	EVTS	DOCUMENT ID	TECN	CHG	COMMENT
260 + 90 - 70 ± 80	7k	ASNER	00B	CLEO	± τ <sup>-</sup> → K <sup>-</sup> π <sup>+</sup> π <sup>-</sup> ν <sub>τ</sub>

### K<sub>1</sub>(1270) DECAY MODES

Mode	Fraction (Γ <sub>i</sub> /Γ)
Γ <sub>1</sub> K ρ	(42 ± 6) %
Γ <sub>2</sub> K <sub>0</sub> <sup>0</sup> (1430) π	(28 ± 4) %
Γ <sub>3</sub> K*(892) π	(16 ± 5) %
Γ <sub>4</sub> K ω	(11.0 ± 2.0) %
Γ <sub>5</sub> K f <sub>0</sub> <sup>0</sup> (1370)	( 3.0 ± 2.0) %
Γ <sub>6</sub> γ K <sup>0</sup>	seen

### K<sub>1</sub>(1270) PARTIAL WIDTHS

VALUE (MeV)	DOCUMENT ID	TECN	CHG	COMMENT	
57 ± 5	MAZZUCATO	79	HBC	+	4.2 K <sup>-</sup> p → Ξ <sup>-</sup> (Kππ) <sup>+</sup>
75 ± 6	CARNEGIE	77B	ASPK	±	13 K <sup>±</sup> p → (Kππ) <sup>±</sup> p

### Γ(K<sub>0</sub><sup>0</sup>(1430) π)

VALUE (MeV)	DOCUMENT ID	TECN	CHG	COMMENT	
26 ± 6	CARNEGIE	77B	ASPK	±	13 K <sup>±</sup> p → (Kππ) <sup>±</sup> p

See key on page 457

# Meson Particle Listings

## $K_1(1270)$ , $K_1(1400)$

### $\Gamma(K^*(892)\pi)$ $\Gamma_3$

VALUE (MeV)	DOCUMENT ID	TECN	CHG	COMMENT
$14 \pm 11$	MAZZUCATO 79	HBC	+	$4.2 K^- p \rightarrow \Xi^-(K\pi\pi)^+$
$2 \pm 2$	CARNEGIE 77B	ASPK	$\pm$	$13 K^\pm p \rightarrow (K\pi\pi)^\pm p$

### $\Gamma(K\omega)$ $\Gamma_4$

VALUE (MeV)	DOCUMENT ID	TECN	CHG	COMMENT
$4 \pm 4$	MAZZUCATO 79	HBC	+	$4.2 K^- p \rightarrow \Xi^-(K\pi\pi)^+$
$24 \pm 3$	CARNEGIE 77B	ASPK	$\pm$	$13 K^\pm p \rightarrow (K\pi\pi)^\pm p$

### $\Gamma(K f_0(1370))$ $\Gamma_5$

VALUE (MeV)	DOCUMENT ID	TECN	CHG	COMMENT
$22 \pm 5$	CARNEGIE 77B	ASPK	$\pm$	$13 K^\pm p \rightarrow (K\pi\pi)^\pm p$

### $\Gamma(\gamma K^0)$ $\Gamma_6$

VALUE (keV)	DOCUMENT ID	TECN	COMMENT
$73.2 \pm 6.1 \pm 28.3$	ALAVI-HARATI 02B	KTEV	$K + A \rightarrow K^* + A$

### $K_1(1270)$ BRANCHING RATIOS

#### $\Gamma(K\rho)/\Gamma_{total}$ $\Gamma_1/\Gamma$

VALUE	DOCUMENT ID	TECN	COMMENT
$0.42 \pm 0.06$	<sup>9</sup> DAUM 81c	CNTR	$63 K^- p \rightarrow K^- 2\pi p$
$0.584 \pm 0.043$	<sup>10</sup> GULER 11	BELL	$B^+ \rightarrow J/\psi K^+ \pi^+ \pi^-$
dominant	RODEBACK 81	HBC	$4 \pi^- p \rightarrow \Lambda K 2\pi$

#### $\Gamma(K_0^*(1430)\pi)/\Gamma_{total}$ $\Gamma_2/\Gamma$

VALUE	DOCUMENT ID	TECN	COMMENT
$0.28 \pm 0.04$	<sup>9</sup> DAUM 81c	CNTR	$63 K^- p \rightarrow K^- 2\pi p$
$0.0201 \pm 0.0064$	<sup>10</sup> GULER 11	BELL	$B^+ \rightarrow J/\psi K^+ \pi^+ \pi^-$

#### $\Gamma(K^*(892)\pi)/\Gamma_{total}$ $\Gamma_3/\Gamma$

VALUE	DOCUMENT ID	TECN	COMMENT
$0.16 \pm 0.05$	<sup>9</sup> DAUM 81c	CNTR	$63 K^- p \rightarrow K^- 2\pi p$
$0.171 \pm 0.023$	<sup>10</sup> GULER 11	BELL	$B^+ \rightarrow J/\psi K^+ \pi^+ \pi^-$

#### $\Gamma(K\omega)/\Gamma_{total}$ $\Gamma_4/\Gamma$

VALUE	DOCUMENT ID	TECN	COMMENT
$0.11 \pm 0.02$	<sup>9</sup> DAUM 81c	CNTR	$63 K^- p \rightarrow K^- 2\pi p$
$0.225 \pm 0.052$	<sup>10</sup> GULER 11	BELL	$B^+ \rightarrow J/\psi K^+ \pi^+ \pi^-$

#### $\Gamma(K\omega)/\Gamma(K\rho)$ $\Gamma_4/\Gamma_1$

VALUE	CL%	DOCUMENT ID	TECN	COMMENT
$< 0.30$	95	RODEBACK 81	HBC	$4 \pi^- p \rightarrow \Lambda K 2\pi$

#### $\Gamma(K f_0(1370))/\Gamma_{total}$ $\Gamma_5/\Gamma$

VALUE	DOCUMENT ID	TECN	COMMENT
$0.03 \pm 0.02$	<sup>9</sup> DAUM 81c	CNTR	$63 K^- p \rightarrow K^- 2\pi p$

#### D-wave/S-wave RATIO FOR $K_1(1270) \rightarrow K^*(892)\pi$

VALUE	DOCUMENT ID	TECN	COMMENT
$1.0 \pm 0.7$	<sup>9</sup> DAUM 81c	CNTR	$63 K^- p \rightarrow K^- 2\pi p$

<sup>9</sup> Average from low and high  $t$  data.  
<sup>10</sup> Assuming that decays are saturated by the  $K\rho$ ,  $K_0^*(1430)\pi$ ,  $K^*(892)\pi$ ,  $K\omega$  decay modes and neglecting interference between them. The values  $B(\omega \rightarrow \pi^+\pi^-) = (1.53^{+0.11}_{-0.13})\%$  and  $B(K_0^*(1430) \rightarrow K\pi) = (93 \pm 10)\%$  are used. Systematic uncertainties not estimated.

### $K_1(1270)$ REFERENCES

GULER 11	PR D83 032005	H. Guler et al.	(BELLE Collab.)
GENG 07	PR D75 014017	L.S. Geng et al.	
ABLIKIM 06C	PL B633 681	M. Ablikim et al.	(BES Collab.)
ALAVI-HARATI 02B	PRL 89 072001	A. Alavi-Harati et al.	(FNAL KTeV Collab.)
ASNER 00B	PR D62 072006	D.M. Asner et al.	(CLEO Collab.)
TORNQVIST 82B	NP B303 268	N.A. Tornqvist	(HELS)
DAUM 81C	NP B187 1	C. Daum et al.	(AMST, CERN, CRAC, MPIM+)
RODEBACK 81	ZPHY C9 9	S. Rodeback et al.	(CERN, CDEF, MADR+)
MAZZUCATO 79	NP B156 532	M. Mazzucato et al.	(CERN, ZEEM, NIJM+)
VERGEEST 79	NP B158 265	J.S.M. Vergeest et al.	(NIJM, AMST, CERN+)
GAVILLET 78	PL 76B 517	P. Gavillet et al.	(AMST, CERN, NIJM+)
CARNEGIE 77	NP B127 509	R.K. Carnegie et al.	(SLAC)
CARNEGIE 77B	PL 68B 287	R.K. Carnegie et al.	(SLAC)
BRANDENB... 76	PRL 36 703	G.W. Brandenburg et al.	(SLAC) JP
OTTER 76	NP B106 77	G. Otter et al.	(AACH3, BERL, CERN, LOIC+)
CRENNELL 72	PR D6 1220	D.J. Crennell et al.	(BNL)
DAVIS 72	PR D5 2688	P.J. Davis et al.	(LBL)
FIRESTONE 72B	PR D5 505	A. Firestone et al.	(LBL)
ASTIER 69	NP B10 65	A. Astier et al.	(CDEF, CERN, IJNP, LJV) JP
CRENNELL 67	PRL 19 44	D.J. Crennell et al.	(BNL)

## $K_1(1400)$

$$I(J^P) = \frac{1}{2}(1^+)$$

### $K_1(1400)$ MASS

VALUE (MeV)	EVTS	DOCUMENT ID	TECN	CHG	COMMENT
<b>1403 ± 7 OUR AVERAGE</b>					
$1463 \pm 64 \pm 68$	7k	ASNER 00B	CLEO	$\pm$	$\tau^- \rightarrow K^- \pi^+ \pi^- \nu_\tau$
$1373 \pm 14 \pm 18$		<sup>1</sup> ASTON 87	LASS	0	$11 K^- p \rightarrow \bar{K}^0 \pi^+ \pi^- n$
$1392 \pm 18$		BAUBILLIER 82B	HBC	0	$8.25 K^- p \rightarrow K_S^0 \pi^+ \pi^- n$
$1410 \pm 25$		DAUM 81c	CNTR	-	$63 K^- p \rightarrow K^- 2\pi p$
$1415 \pm 15$		ETKIN 80	MPS	0	$6 K^- p \rightarrow \bar{K}^0 \pi^+ \pi^- n$
$1404 \pm 10$		<sup>2</sup> CARNEGIE 77	ASPK	$\pm$	$13 K^\pm p \rightarrow (K\pi\pi)^\pm p$
$1418 \pm 8$	25k	<sup>3</sup> ABLIKIM 06c	BES2		$J/\psi \rightarrow \bar{K}^*(892)^0 K^+ \pi^-$
$\sim 1350$		<sup>4</sup> TORNQVIST 82B	RVUE		
$\sim 1400$		VERGEEST 79	HBC	-	$4.2 K^- p \rightarrow (\bar{K}\pi\pi)^- p$
$\sim 1400$		BRANDENB... 76	ASPK	$\pm$	$13 K^\pm p \rightarrow (K\pi\pi)^\pm p$
1420		DAVIS 72	HBC	+	$12 K^+ p$
$1368 \pm 18$		FIRESTONE 72B	DBC	+	$12 K^+ d$

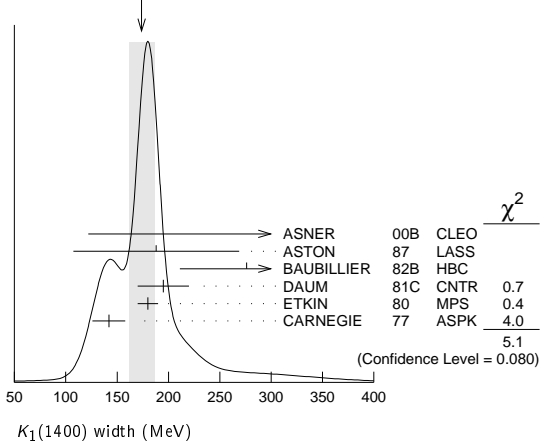
- <sup>1</sup> From partial-wave analysis of  $K^0 \pi^+ \pi^-$  system.
- <sup>2</sup> From a model-dependent fit with Gaussian background to BRANDENBURG 76 data.
- <sup>3</sup> Systematic errors not estimated.
- <sup>4</sup> From a unitarized quark-model calculation.

### $K_1(1400)$ WIDTH

VALUE (MeV)	EVTS	DOCUMENT ID	TECN	CHG	COMMENT
<b>174 ± 13 OUR AVERAGE</b>					Error includes scale factor of 1.6. See the ideogram below.
$300^{+370}_{-110} \pm 140$	7k	ASNER 00B	CLEO	$\pm$	$\tau^- \rightarrow K^- \pi^+ \pi^- \nu_\tau$
$188 \pm 54 \pm 60$		<sup>5</sup> ASTON 87	LASS	0	$11 K^- p \rightarrow \bar{K}^0 \pi^+ \pi^- n$
$276 \pm 65$		BAUBILLIER 82B	HBC	0	$8.25 K^- p \rightarrow K_S^0 \pi^+ \pi^- n$
$195 \pm 25$		DAUM 81c	CNTR	-	$63 K^- p \rightarrow K^- 2\pi p$
$180 \pm 10$		ETKIN 80	MPS	0	$6 K^- p \rightarrow \bar{K}^0 \pi^+ \pi^- n$
$142 \pm 16$		<sup>6</sup> CARNEGIE 77	ASPK	$\pm$	$13 K^\pm p \rightarrow (K\pi\pi)^\pm p$
$152 \pm 16$	25k	<sup>7</sup> ABLIKIM 06c	BES2		$J/\psi \rightarrow \bar{K}^*(892)^0 K^+ \pi^-$

- <sup>5</sup> From partial-wave analysis of  $K^0 \pi^+ \pi^-$  system.
- <sup>6</sup> From a model-dependent fit with Gaussian background to BRANDENBURG 76 data.
- <sup>7</sup> Systematic errors not estimated.

WEIGHTED AVERAGE  
174±13 (Error scaled by 1.6)



### $K_1(1400)$ DECAY MODES

Mode	Fraction ( $\Gamma_i/\Gamma$ )
$\Gamma_1$ $K^*(892)\pi$	$(94 \pm 6) \%$
$\Gamma_2$ $K\rho$	$(3.0 \pm 3.0) \%$
$\Gamma_3$ $K f_0(1370)$	$(2.0 \pm 2.0) \%$
$\Gamma_4$ $K\omega$	$(1.0 \pm 1.0) \%$
$\Gamma_5$ $K_0^*(1430)\pi$	not seen
$\Gamma_6$ $\gamma K^0$	seen

# Meson Particle Listings

## $K_1(1400)$ , $K^*(1410)$ , $K_0^*(1430)$

### $K_1(1400)$ PARTIAL WIDTHS

$\Gamma(K^*(892)\pi)$	$\Gamma_1$			
VALUE (MeV)	DOCUMENT ID	TECN	CHG	COMMENT
<b>117±10</b>	CARNEGIE	77	ASPK	± 13 $K^\pm p \rightarrow (K\pi\pi)^\pm p$
$\Gamma(K\rho)$	$\Gamma_2$			
VALUE (MeV)	DOCUMENT ID	TECN	CHG	COMMENT
<b>2±1</b>	CARNEGIE	77	ASPK	± 13 $K^\pm p \rightarrow (K\pi\pi)^\pm p$
$\Gamma(K\omega)$	$\Gamma_4$			
VALUE (MeV)	DOCUMENT ID	TECN	CHG	COMMENT
<b>23±12</b>	CARNEGIE	77	ASPK	± 13 $K^\pm p \rightarrow (K\pi\pi)^\pm p$
$\Gamma(\gamma K^0)$	$\Gamma_6$			
VALUE (keV)	DOCUMENT ID	TECN	COMMENT	
<b>280.8±23.2±40.4</b>	ALAVI-HARATI02B	KTEV	$K + A \rightarrow K^* + A$	

### $K_1(1400)$ BRANCHING RATIOS

$\Gamma(K^*(892)\pi)/\Gamma_{total}$	$\Gamma_1/\Gamma$		
VALUE	DOCUMENT ID	TECN	COMMENT
<b>0.94±0.06</b>	<sup>8</sup> DAUM	81c	CNTR 63 $K^- p \rightarrow K^- 2\pi p$
$\Gamma(K\rho)/\Gamma_{total}$	$\Gamma_2/\Gamma$		
VALUE	DOCUMENT ID	TECN	COMMENT
<b>0.03±0.03</b>	<sup>8</sup> DAUM	81c	CNTR 63 $K^- p \rightarrow K^- 2\pi p$
$\Gamma(K f_0(1370))/\Gamma_{total}$	$\Gamma_3/\Gamma$		
VALUE	DOCUMENT ID	TECN	COMMENT
<b>0.02±0.02</b>	<sup>8</sup> DAUM	81c	CNTR 63 $K^- p \rightarrow K^- 2\pi p$
$\Gamma(K\omega)/\Gamma_{total}$	$\Gamma_4/\Gamma$		
VALUE	DOCUMENT ID	TECN	COMMENT
<b>0.01±0.01</b>	<sup>8</sup> DAUM	81c	CNTR 63 $K^- p \rightarrow K^- 2\pi p$
$\Gamma(K_0^*(1430)\pi)/\Gamma_{total}$	$\Gamma_5/\Gamma$		
VALUE	DOCUMENT ID	TECN	COMMENT
not seen	<sup>8</sup> DAUM	81c	CNTR 63 $K^- p \rightarrow K^- 2\pi p$

### D-wave/S-wave RATIO FOR $K_1(1400) \rightarrow K^*(892)\pi$

VALUE	DOCUMENT ID	TECN	COMMENT
<b>0.04±0.01</b>	<sup>8</sup> DAUM	81c	CNTR 63 $K^- p \rightarrow K^- 2\pi p$

<sup>8</sup> Average from low and high  $t$  data.

### $K_1(1400)$ REFERENCES

ABLIKIM	06C	PL B633 681	M. Ablikim et al.	(BES Collab.)
ALAVI-HARATI	02B	PRL 89 072001	A. Alavi-Harati et al.	(FNAL KTeV Collab.)
ASNER	00B	PR D62 072006	D.M. Asner et al.	(CLEO Collab.)
ASTON	87	NP B292 693	D. Aston et al.	(SLAC, NAGO, CINC, INUS)
BAUBILLIER	82B	NP B202 21	M. Baubillier et al.	(BIRM, CERN, GLAS+)
TORNQVIST	82B	NP B203 268	N.A. Tornqvist	(HEL5)
DAUM	81C	PR B187 1	C. Daum et al.	(AMST, CERN, CRAC, MPIM+)
ETKIN	80	PR D22 42	A. Etkin et al.	(BNL, CUNY) JP
VERGEEST	79	NP B150 265	J.S.M. Vergeest et al.	(NUM, AMST, CERN+)
CARNEGIE	77	NP B127 509	R.K. Carnegie et al.	(SLAC)
BRANDENB...	76	PRL 36 703	G.W. Brandenburg et al.	(SLAC) JP
DAVIS	72	PR D5 2688	P.J. Davis et al.	(LBL)
FIRESTONE	72B	PR D5 505	A. Firestone et al.	(LBL)

## $K^*(1410)$

$$I(J^P) = \frac{1}{2}(1^-)$$

### $K^*(1410)$ MASS

VALUE (MeV)	DOCUMENT ID	TECN	CHG	COMMENT
<b>1414±15 OUR AVERAGE</b>	Error includes scale factor of 1.3.			
1380±21±19	ASTON	88	LASS	0 11 $K^- p \rightarrow K^- \pi^+ n$
1420±7±10	ASTON	87	LASS	0 11 $K^- p \rightarrow \bar{K}^0 \pi^+ \pi^- n$
••• We do not use the following data for averages, fits, limits, etc. •••				
1276 <sup>+72</sup> / <sub>-77</sub>	<sup>1,2</sup> BOITO	09	RVUE	$\tau^- \rightarrow K_S^0 \pi^- \nu_\tau$
1367±54	BIRD	89	LASS	- 11 $K^- p \rightarrow \bar{K}^0 \pi^- p$
1474±25	BAUBILLIER	82B	HBC	0 8.25 $K^- p \rightarrow \bar{K}^0 2\pi n$
1500±30	ETKIN	80	MPS	0 6 $K^- p \rightarrow \bar{K}^0 \pi^+ \pi^- n$
<sup>1</sup> From the pole position of the $K\pi$ vector form factor in the complex $s$ -plane and using EPIFANOV 07 data.				
<sup>2</sup> Systematic uncertainties not estimated.				
$K^*(1410)$ WIDTH				
VALUE (MeV)	DOCUMENT ID	TECN	CHG	COMMENT
<b>232±21 OUR AVERAGE</b>	Error includes scale factor of 1.1.			
176±52±22	ASTON	88	LASS	0 11 $K^- p \rightarrow K^- \pi^+ n$
240±18±12	ASTON	87	LASS	0 11 $K^- p \rightarrow \bar{K}^0 \pi^+ \pi^- n$

••• We do not use the following data for averages, fits, limits, etc. •••

198 <sup>+61</sup> / <sub>-87</sub>	<sup>3,4</sup> BOITO	09	RVUE	$\tau^- \rightarrow K_S^0 \pi^- \nu_\tau$
114±101	BIRD	89	LASS	- 11 $K^- p \rightarrow \bar{K}^0 \pi^- p$
275±65	BAUBILLIER	82B	HBC	0 8.25 $K^- p \rightarrow \bar{K}^0 2\pi n$
500±100	ETKIN	80	MPS	0 6 $K^- p \rightarrow \bar{K}^0 \pi^+ \pi^- n$
<sup>3</sup> From the pole position of the $K\pi$ vector form factor in the complex $s$ -plane and using EPIFANOV 07 data.				
<sup>4</sup> Systematic uncertainties not estimated.				

### $K^*(1410)$ DECAY MODES

Mode	Fraction ( $\Gamma_i/\Gamma$ )	Confidence level
$\Gamma_1$ $K^*(892)\pi$	> 40 %	95%
$\Gamma_2$ $K\pi$	(6.6±1.3) %	
$\Gamma_3$ $K\rho$	< 7 %	95%
$\Gamma_4$ $\gamma K^0$	seen	

### $K^*(1410)$ PARTIAL WIDTHS

$\Gamma(\gamma K^0)$	$\Gamma_4$			
VALUE (keV)	CL%	DOCUMENT ID	TECN	COMMENT
<b>&lt;52.9</b>	90	ALAVI-HARATI02B	KTEV	$K + A \rightarrow K^* + A$

### $K^*(1410)$ BRANCHING RATIOS

$\Gamma(K\rho)/\Gamma(K^*(892)\pi)$	$\Gamma_3/\Gamma_1$				
VALUE	CL%	DOCUMENT ID	TECN	CHG	COMMENT
<0.17	95	ASTON	84	LASS	0 11 $K^- p \rightarrow \bar{K}^0 2\pi n$
$\Gamma(K\pi)/\Gamma(K^*(892)\pi)$	$\Gamma_2/\Gamma_1$				
VALUE	CL%	DOCUMENT ID	TECN	CHG	COMMENT
<0.16	95	ASTON	84	LASS	0 11 $K^- p \rightarrow \bar{K}^0 2\pi n$
$\Gamma(K\pi)/\Gamma_{total}$	$\Gamma_2/\Gamma$				
VALUE	DOCUMENT ID	TECN	CHG	COMMENT	
<b>0.066±0.010±0.008</b>	ASTON	88	LASS	0 11 $K^- p \rightarrow K^- \pi^+ n$	

### $K^*(1410)$ REFERENCES

BOITO	09	EPL C59 021	D.R. Boito, R. Escribano, M. Jamin	(BELLE Collab.)
EPIFANOV	07	PL B654 05	D. Epifanov et al.	(BELLE Collab.)
ALAVI-HARATI	02B	PRL 89 072001	A. Alavi-Harati et al.	(FNAL KTeV Collab.)
BIRD	89	SLAC-332	P.F. Bird	(SLAC)
ASTON	88	NP B296 493	D. Aston et al.	(SLAC, NAGO, CINC, INUS)
ASTON	87	NP B292 693	D. Aston et al.	(SLAC, NAGO, CINC, INUS)
ASTON	84	PL 149B 258	D. Aston et al.	(SLAC, CARL, OTTA) JP
BAUBILLIER	82B	NP B202 21	M. Baubillier et al.	(BIRM, CERN, GLAS+)
ETKIN	80	PR D22 42	A. Etkin et al.	(BNL, CUNY) JP

## $K_0^*(1430)$

$$I(J^P) = \frac{1}{2}(0^+)$$

See our minireview in the 1994 edition and in this edition under the  $f_0(500)$ .

### $K_0^*(1430)$ MASS

VALUE (MeV)	EVTS	DOCUMENT ID	TECN	CHG	COMMENT
<b>1425 ±50 OUR ESTIMATE</b>					
••• We do not use the following data for averages, fits, limits, etc. •••					
1427 ± 4 ±13	1	BUGG	10	RVUE	S-matrix pole
1466.6±0.7±3.4 141k	2	BONVICINI	08A	CLEO	$D^+ \rightarrow K^- \pi^+ \pi^+$
~1412	3	LINK	07	FOCS	0 $D^+ \rightarrow K^- K^+ \pi^+$
1461.0±4.0±2.1 54k	4	LINK	07B	FOCS	$D^+ \rightarrow K^- \pi^+ \pi^+$
1406 ±29	5	BUGG	06	RVUE	
1435 ±6	6	ZHOU	06	RVUE	$K\rho \rightarrow K^- \pi^+ n$
1455 ±20 ±15		ABLIKIM	05Q	BES2	$\psi(2S) \rightarrow \gamma \pi^+ \pi^- K^+ K^-$
1456 ±8	7	ZHENG	04	RVUE	$K^- p \rightarrow K^- \pi^+ n$
~1419	8	BUGG	03	RVUE	11 $K^- p \rightarrow K^- \pi^+ n$
~1440	9	LI	03	RVUE	11 $K^- p \rightarrow K^- \pi^+ n$
1459 ±9	10	AITALA	02	E791	$D^+ \rightarrow K^- \pi^+ \pi^+$
~1440	11	JAMIN	00	RVUE	$K\rho \rightarrow K\rho$
1436 ±8	12	BARBERIS	98E	OMEG	$450 pp \rightarrow p_f p_S K^+ K^- \pi^+ \pi^-$
1415 ±25	8	ANISOVICH	97C	RVUE	11 $K^- p \rightarrow K^- \pi^+ n$
~1450	13	TORNQVIST	96	RVUE	$\pi\pi \rightarrow \pi\pi, K\bar{K}, K\pi$
1412 ±6	14	ASTON	88	LASS	0 11 $K^- p \rightarrow K^- \pi^+ n$
~1430		BAUBILLIER	84B	HBC	- 8.25 $K^- p \rightarrow \bar{K}^0 \pi^- p$
~1425	15,16	ESTABROOKS	78	ASPK	13 $K^\pm p \rightarrow K^\pm \pi^\pm (n, \Delta)$
~1450.0		MARTIN	78	SPEC	10 $K^\pm p \rightarrow K_S^0 \pi p$



See key on page 457

## Meson Particle Listings

 $K_0^*(1430), K_2^*(1430)$  $K_0^*(1430)$  REFERENCES

- 1 S-matrix pole. Supersedes BUGG 06. Combined analysis of ASTON 88, ABLIKIM 06c, AITALA 06, and LINK 09 using an s-dependent width with couplings to  $K\pi$  and  $K\eta'$ , and the Adler zero near thresholds.
- 2 From the isobar model with a complex pole for the  $\kappa$ .
- 3 From a non-parametric analysis.
- 4 A Breit-Wigner mass and width.
- 5 S-matrix pole. Reanalysis of ASTON 88, AITALA 02, and ABLIKIM 06c including the  $\kappa$  with an s-dependent width and an Adler zero near threshold.
- 6 S-matrix pole. Using ASTON 88 and assuming  $K_0^*(800), K_0^*(1950)$ .
- 7 Using ASTON 88 and assuming  $K_0^*(800)$ .
- 8 T-matrix pole. Reanalysis of ASTON 88 data.
- 9 Breit-Wigner fit. Using ASTON 88.
- 10 Assuming a low-mass scalar  $K\pi$  resonance,  $\kappa(800)$ .
- 11 T-matrix pole. Using data from ESTABROOKS 78 and ASTON 88.
- 12  $J^P$  not determined, could be  $K_2^*(1430)$ .
- 13 T-matrix pole.
- 14 Uses a model for the background, without this background they get a mass 1340 MeV, where the phase shift passes  $90^\circ$ .
- 15 Mass defined by pole position.
- 16 From elastic  $K\pi$  partial-wave analysis.

Author	Year	Document ID	TECN	CHG	COMMENT
BUGG	10	PR D81 014002			D.V. Bugg <i>et al.</i> (LOQM)
LINK	09	PL B681 14			J.M. Link <i>et al.</i> (FNAL FOCUS Collab.)
BONVICINI	08A	PR D78 052001			G. Bonvicini <i>et al.</i> (CLEO Collab.)
LINK	07	PL B648 156			J.M. Link <i>et al.</i> (FNAL FOCUS Collab.)
LINK	07B	PL B653 1			J.M. Link <i>et al.</i> (FNAL FOCUS Collab.)
ABLIKIM	06C	PL B633 681			M. Ablikim <i>et al.</i> (BES Collab.)
AITALA	06	PR D73 032004			E.M. Aitala <i>et al.</i> (FNAL E791 Collab.)
Also		PR D74 059901 (err.)			E.M. Aitala <i>et al.</i> (FNAL E791 Collab.)
BUGG	06	PL B632 471			D.V. Bugg (LOQM)
ZHOU	06	NP A775 212			Z.Y. Zhou, H.Q. Zheng
ABLIKIM	05Q	PR D72 092002			M. Ablikim <i>et al.</i> (BES Collab.)
ZHENG	04	NP A733 235			H.Q. Zheng <i>et al.</i>
BUGG	03	PL B572 1			D.V. Bugg
LI	03	PR D67 034025			L. Li, B. Zou, G. Li
AITALA	02	PRL 89 121801			E.M. Aitala <i>et al.</i> (FNAL E791 Collab.)
JAMIN	00	NP B587 331			M. Jamin <i>et al.</i>
BARBERIS	98E	PL B436 204			D. Barberis <i>et al.</i> (Omega Expt.)
ANISOVICH	97C	PL B413 137			A.V. Anisovich, A.V. Sarantsev
TORNQVIST	96	PRL 76 1575			N.A. Tornqvist, M. Roos (HELS)
ASTON	88	NP B296 493			D. Aston <i>et al.</i> (SLAC, NAGO, CIN, INUS)
BAUBILLIER	84B	ZPHY C26 37			M. Baubillier <i>et al.</i> (BIRM, CERN, GLAS+)
ESTABROOKS	78	NP B133 490			P.G. Estabrooks <i>et al.</i> (MCGI, CARL, DURH+)
MARTIN	78	NP B134 392			A.D. Martin <i>et al.</i> (DURH, GEVA)

 $K_2^*(1430)$ 

$$I(J^P) = \frac{1}{2}(2^+)$$

We consider that phase-shift analyses provide more reliable determinations of the mass and width.

 $K_0^*(1430)$  WIDTH

VALUE (MeV)	EVTS	DOCUMENT ID	TECN	CHG	COMMENT
-------------	------	-------------	------	-----	---------

**270 ± 80 OUR ESTIMATE**

• • • We do not use the following data for averages, fits, limits, etc. • • •						
270 ± 10 ± 40	17	BUGG	10	RVUE	S-matrix pole	
174.2 ± 1.9 ± 3.2 141k	18	BONVICINI	08A	CLEO	$D^+ \rightarrow K^- \pi^+ \pi^+$	
~ 500	19	LINK	07	FOCS 0	$D^+ \rightarrow K^- K^+ \pi^+$	
177.0 ± 8.0 ± 3.4 54k	20	LINK	07B	FOCS	$D^+ \rightarrow K^- \pi^+ \pi^+$	
350 ± 40	21	BUGG	06	RVUE		
288 ± 22	22	ZHOU	06	RVUE	$K\rho \rightarrow K^- \pi^+ n$	
270 ± 45 ± 30 -35		ABLIKIM	05Q	BES2	$\psi(2S) \rightarrow$ $\gamma \pi^+ \pi^- K^+ K^-$ $K^- \rho \rightarrow K^- \pi^+ n$	
217 ± 31	23	ZHENG	04	RVUE	$11 K^- \rho \rightarrow K^- \pi^+ n$	
~ 316	24	BUGG	03	RVUE	$11 K^- \rho \rightarrow K^- \pi^+ n$	
~ 350	25	LI	03	RVUE	$11 K^- \rho \rightarrow K^- \pi^+ n$	
175 ± 17	15k	26	AITALA	02	E791	$D^+ \rightarrow K^- \pi^+ \pi^+$
~ 300	27	JAMIN	00	RVUE	$K\rho \rightarrow K\rho$	
196 ± 45	28	BARBERIS	98E	OMEG	$450 \rho\rho \rightarrow$ $p_f p_s K^+ K^- \pi^+ \pi^-$	
330 ± 50	24	ANISOVICH	97C	RVUE	$11 K^- \rho \rightarrow K^- \pi^+ n$	
~ 320	29	TORNQVIST	96	RVUE	$\pi\pi \rightarrow \pi\pi, K\bar{K}, K\pi$	
294 ± 23		ASTON	88	LASS 0	$11 K^- \rho \rightarrow K^- \pi^+ n$	
~ 200		BAUBILLIER	84B	HBC -	$8.25 K^- \rho \rightarrow \bar{K}^0 \pi^- p$	
200 to 300	30	ESTABROOKS	78	ASPK	$13 K^\pm \rho \rightarrow$ $K^\pm \pi^\pm(n, \Delta)$	

- 17 S-matrix pole. Supersedes BUGG 06. Combined analysis of ASTON 88, ABLIKIM 06c, AITALA 06, and LINK 09 using an s-dependent width with couplings to  $K\pi$  and  $K\eta'$ , and the Adler zero near thresholds.
- 18 From the isobar model with a complex pole for the  $\kappa$ .
- 19 From a non-parametric analysis.
- 20 A Breit-Wigner mass and width.
- 21 S-matrix pole. Reanalysis of ASTON 88, AITALA 02, and ABLIKIM 06c including the  $\kappa$  with an s-dependent width and an Adler zero near threshold.
- 22 S-matrix pole. Using ASTON 88 and assuming  $K_0^*(800), K_0^*(1950)$ .
- 23 Using ASTON 88 and assuming  $K_0^*(800)$ .
- 24 T-matrix pole. Reanalysis of ASTON 88 data.
- 25 Breit-Wigner fit. Using ASTON 88.
- 26 Assuming a low-mass scalar  $K\pi$  resonance,  $\kappa(800)$ .
- 27 T-matrix pole. Using data from ESTABROOKS 78 and ASTON 88.
- 28  $J^P$  not determined, could be  $K_2^*(1430)$ .
- 29 T-matrix pole.
- 30 From elastic  $K\pi$  partial-wave analysis.

 $K_0^*(1430)$  DECAY MODES

Mode	Fraction ( $\Gamma_i/\Gamma$ )
$\Gamma_1 K\pi$	(93 ± 10) %

 $K_0^*(1430)$  BRANCHING RATIOS

$\Gamma(K\pi)/\Gamma_{\text{total}}$	DOCUMENT ID	TECN	CHG	COMMENT	$\Gamma_1/\Gamma$
0.93 ± 0.04 ± 0.09	ASTON	88	LASS 0	11 $K^- \rho \rightarrow K^- \pi^+ n$	

 $K_2^*(1430)$  MASSCHARGED ONLY, WITH FINAL STATE  $K\pi$ 

VALUE (MeV)	EVTS	DOCUMENT ID	TECN	CHG	COMMENT
<b>1425.6 ± 1.5 OUR AVERAGE</b>					Error includes scale factor of 1.1.
1420 ± 4	1587	BAUBILLIER	84B	HBC -	$8.25 K^- \rho \rightarrow$ $\bar{K}^0 \pi^- p$
1436 ± 5.5	400	1,2 CLELAND	82	SPEC +	$30 K^+ \rho \rightarrow K_S^0 \pi^+ p$
1430 ± 3.2	1500	1,2 CLELAND	82	SPEC +	$50 K^+ \rho \rightarrow K_S^0 \pi^+ p$
1430 ± 3.2	1200	1,2 CLELAND	82	SPEC -	$50 K^+ \rho \rightarrow K_S^0 \pi^- p$
1423 ± 5	935	TOAFF	81	HBC -	$6.5 K^- \rho \rightarrow$ $\bar{K}^0 \pi^- p$
1428.0 ± 4.6		3 MARTIN	78	SPEC +	$10 K^\pm \rho \rightarrow K_S^0 \pi p$
1423.8 ± 4.6		3 MARTIN	78	SPEC -	$10 K^\pm \rho \rightarrow K_S^0 \pi p$
1420.0 ± 3.1	1400	AGUILAR...	71B	HBC -	$3.9, 4.6 K^- \rho \rightarrow$ $K^+ \rho \rightarrow K^0 \pi^+ p$
1425 ± 8.0	225	1,2 BARNHAM	71C	HBC +	$3.9 K^- N \rightarrow$ $\bar{K}^0 \pi^- N$
1416 ± 10	220	CRENNELL	69D	DBC -	$9 K^+ \rho \rightarrow K^0 \pi^+ p$
1414 ± 13.0	60	1 LIND	69	HBC +	$5.5 K^- \rho \rightarrow \bar{K} \pi N$
1427 ± 12	63	1 SCHWEING...	68	HBC -	$4.6-5.0 K^- \rho \rightarrow$ $\bar{K}^0 \pi^- p$
1423 ± 11.0	39	1 BASSANO	67	HBC -	
• • • We do not use the following data for averages, fits, limits, etc. • • •					
1423.4 ± 2 ± 3	24809 ± 820	4 BIRD	89	LASS -	$11 K^- \rho \rightarrow \bar{K}^0 \pi^- p$

## NEUTRAL ONLY

VALUE (MeV)	EVTS	DOCUMENT ID	TECN	COMMENT
<b>1432.4 ± 1.3 OUR AVERAGE</b>				
1431.2 ± 1.8 ± 0.7		5 ASTON	88	LASS 11 $K^- \rho \rightarrow K^- \pi^+ n$
1434 ± 4 ± 6		5 ASTON	87	LASS 11 $K^- \rho \rightarrow \bar{K}^0 \pi^+ \pi^- n$
1433 ± 6 ± 10		5 ASTON	84B	LASS 11 $K^- \rho \rightarrow \bar{K}^0 2\pi n$
1471 ± 12		5 BAUBILLIER	82B	HBC 8.25 $K^- \rho \rightarrow NK_S^0 \pi\pi$
1428 ± 3		5 ASTON	81C	LASS 11 $K^- \rho \rightarrow K^- \pi^+ n$
1434 ± 2		5 ESTABROOKS	78	ASPK 13 $K^\pm \rho \rightarrow pK\pi$
1440 ± 10		5 BOWLER	77	DBC 5.5 $K^+ d \rightarrow K\pi pp$
• • • We do not use the following data for averages, fits, limits, etc. • • •				
1428.5 ± 3.9	1786 ± 127	6 AUBERT	07AK	BABR 10.6 $e^+ e^- \rightarrow$ $K_S^0 K^\pm \pi^\mp \gamma$
1420 ± 7	300	HENDRICK	76	DBC 8.25 $K^+ N \rightarrow K^+ \pi N$
1421.6 ± 4.2	800	MCCUBBIN	75	HBC 3.6 $K^- \rho \rightarrow K^- \pi^+ n$
1420.1 ± 4.3		7 LINGLIN	73	HBC 2-13 $K^+ \rho \rightarrow K^+ \pi^- X$
1419.1 ± 3.7	1800	AGUILAR...	71B	HBC 3.9, 4.6 $K^- \rho$
1416 ± 6	600	CORDS	71	DBC 9 $K^+ n \rightarrow K^+ \pi^- p$
1421.1 ± 2.6	2200	DAVIS	69	HBC 12 $K^+ \rho \rightarrow K^+ \pi^- X$

1 Errors enlarged by us to  $\Gamma/\sqrt{N}$ ; see the note with the  $K^*(892)$  mass.

2 Number of events in peak re-evaluated by us.

3 Systematic error added by us.

4 From a partial wave amplitude analysis.

5 From phase shift or partial-wave analysis.

6 Systematic errors not estimated.

7 From pole extrapolation, using world  $K^+ p$  data summary tape.

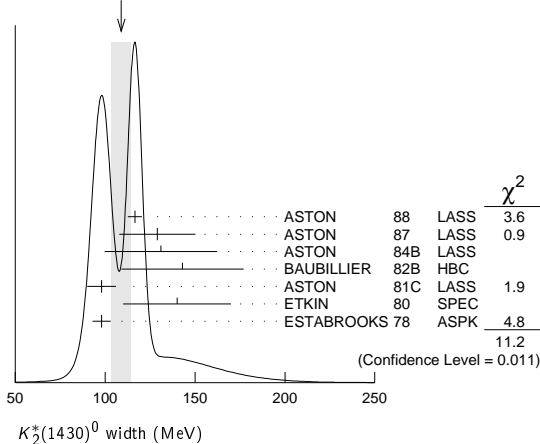
## Meson Particle Listings

 $K_2^*(1430)$  $K_2^*(1430)$  WIDTHCHARGED ONLY, WITH FINAL STATE  $K\pi$ 

VALUE (MeV)	EVTs	DOCUMENT ID	TECN	CHG	COMMENT
<b>98.5 ± 2.7 OUR FIT</b>					Error includes scale factor of 1.1.
<b>98.5 ± 2.9 OUR AVERAGE</b>					Error includes scale factor of 1.1.
109 ± 22	400	<sup>8,9</sup> CLELAND	82	SPEC +	30 $K^+p \rightarrow K_S^0 \pi^+ p$
124 ± 12.8	1500	<sup>8,9</sup> CLELAND	82	SPEC +	50 $K^+p \rightarrow K_S^0 \pi^+ p$
113 ± 12.8	1200	<sup>8,9</sup> CLELAND	82	SPEC -	50 $K^+p \rightarrow K_S^0 \pi^- p$
85 ± 16	935	TOAFF	81	HBC -	6.5 $K^-p \rightarrow \bar{K}^0 \pi^- p$
96.5 ± 3.8		MARTIN	78	SPEC +	10 $K^\pm p \rightarrow K_S^0 \pi p$
97.7 ± 4.0		MARTIN	78	SPEC -	10 $K^\pm p \rightarrow K_S^0 \pi p$
94.7 <sup>+15.1</sup> <sub>-12.5</sub>	1400	AGUILAR-...	71B	HBC -	3.9,4.6 $K^-p$
• • • We do not use the following data for averages, fits, limits, etc. • • •					
98 ± 4 ± 4	25k	<sup>10</sup> BIRD	89	LASS -	11 $K^-p \rightarrow \bar{K}^0 \pi^- p$

## NEUTRAL ONLY

VALUE (MeV)	EVTs	DOCUMENT ID	TECN	COMMENT
<b>109 ± 5 OUR AVERAGE</b>				Error includes scale factor of 1.9. See the ideogram below.
116.5 ± 3.6 ± 1.7	11	ASTON	88	LASS 11 $K^-p \rightarrow K^- \pi^+ n$
129 ± 15 ± 15	11	ASTON	87	LASS 11 $K^-p \rightarrow \bar{K}^0 \pi^+ \pi^- n$
131 ± 24 ± 20	11	ASTON	84B	LASS 11 $K^-p \rightarrow \bar{K}^0 2\pi n$
143 ± 34	11	BAUBILLIER	82B	HBC 8.25 $K^-p \rightarrow N K_S^0 \pi \pi$
98 ± 8	11	ASTON	81c	LASS 11 $K^-p \rightarrow K^- \pi^+ n$
140 ± 30	11	ETKIN	80	SPEC 6 $K^-p \rightarrow \bar{K}^0 \pi^+ \pi^- n$
98 ± 5	11	ESTABROOKS	78	ASPK 13 $K^\pm p \rightarrow \rho K \pi$
• • • We do not use the following data for averages, fits, limits, etc. • • •				
113.7 ± 9.2	1786 ± 127	<sup>12</sup> AUBERT	07AK	BABR 10.6 $e^+ e^- \rightarrow K_S^0 K^\pm \pi^\mp \gamma$
125 ± 29	300	<sup>8</sup> HENDRICK	76	DBC 8.25 $K^+ N \rightarrow K^+ \pi N$
116 ± 18	800	MCCUBBIN	75	HBC 3.6 $K^-p \rightarrow K^- \pi^+ n$
61 ± 14		<sup>13</sup> LINGLIN	73	HBC 2-13 $K^+ p \rightarrow K^+ \pi^+ X$
116.6 <sup>+10.3</sup> <sub>-15.5</sub>	1800	AGUILAR-...	71B	HBC 3.9,4.6 $K^-p$
144 ± 24.0	600	<sup>8</sup> CORDS	71	DBC 9 $K^+ n \rightarrow K^+ \pi^- p$
101 ± 10	2200	DAVIS	69	HBC 12 $K^+ p \rightarrow K^+ \pi^- \pi^+ p$

WEIGHTED AVERAGE  
109±5 (Error scaled by 1.9)<sup>8</sup> Errors enlarged by us to  $4\Gamma/\sqrt{N}$ ; see the note with the  $K^*(892)$  mass.<sup>9</sup> Number of events in peak re-evaluated by us.<sup>10</sup> From a partial wave amplitude analysis.<sup>11</sup> From phase shift or partial-wave analysis.<sup>12</sup> Systematic errors not estimated.<sup>13</sup> From pole extrapolation, using world  $K^+ p$  data summary tape. $K_2^*(1430)$  DECAY MODES

Mode	Fraction ( $\Gamma_i/\Gamma$ )	Scale factor/ Confidence level
$\Gamma_1$ $K\pi$	(49.9 ± 1.2) %	
$\Gamma_2$ $K^*(892)\pi$	(24.7 ± 1.5) %	
$\Gamma_3$ $K^*(892)\pi\pi$	(13.4 ± 2.2) %	
$\Gamma_4$ $K\rho$	( 8.7 ± 0.8) %	S=1.2
$\Gamma_5$ $K\omega$	( 2.9 ± 0.8) %	
$\Gamma_6$ $K^+\gamma$	( 2.4 ± 0.5) × 10 <sup>-3</sup>	S=1.1
$\Gamma_7$ $K\eta$	( 1.5 <sup>+3.4</sup> <sub>-1.0</sub> ) × 10 <sup>-3</sup>	S=1.3
$\Gamma_8$ $K\omega\pi$	< 7.2 × 10 <sup>-4</sup>	CL=95%
$\Gamma_9$ $K^0\gamma$	< 9 × 10 <sup>-4</sup>	CL=90%

## CONSTRAINED FIT INFORMATION

An overall fit to the total width, a partial width, and 10 branching ratios uses 31 measurements and one constraint to determine 8 parameters. The overall fit has a  $\chi^2 = 20.2$  for 24 degrees of freedom.

The following off-diagonal array elements are the correlation coefficients  $\langle \delta p_i \delta p_j \rangle / (\delta p_i \delta p_j)$ , in percent, from the fit to parameters  $p_i$ , including the branching fractions,  $x_i \equiv \Gamma_i/\Gamma_{\text{total}}$ . The fit constrains the  $x_i$  whose labels appear in this array to sum to one.

$x_2$	-9						
$x_3$	-40	-73					
$x_4$	-8	36	-52				
$x_5$	-11	-3	-26	-7			
$x_6$	-1	-1	-1	-1	0		
$x_7$	-4	-7	-5	-5	-2	0	
$\Gamma$	0	0	0	0	0	-13	0
	$x_1$	$x_2$	$x_3$	$x_4$	$x_5$	$x_6$	$x_7$

Mode	Rate (MeV)	Scale factor
$\Gamma_1$ $K\pi$	49.1 ± 1.8	
$\Gamma_2$ $K^*(892)\pi$	24.3 ± 1.6	
$\Gamma_3$ $K^*(892)\pi\pi$	13.2 ± 2.2	
$\Gamma_4$ $K\rho$	8.5 ± 0.8	1.2
$\Gamma_5$ $K\omega$	2.9 ± 0.8	
$\Gamma_6$ $K^+\gamma$	0.24 ± 0.05	1.1
$\Gamma_7$ $K\eta$	0.15 <sup>+0.33</sup> <sub>-0.10</sub>	1.3

 $K_2^*(1430)$  PARTIAL WIDTHS $\Gamma(K^+\gamma)$ 

VALUE (keV)	DOCUMENT ID	TECN	CHG	COMMENT	$\Gamma_6$
<b>241 ± 50 OUR FIT</b>				Error includes scale factor of 1.1.	
<b>240 ± 45</b>	CIHANGIR	82	SPEC +	200 $K^+ Z \rightarrow Z K^+ \pi^0, Z K_S^0 \pi^+$	

 $\Gamma(K^0\gamma)$ 

VALUE (keV)	CL%	DOCUMENT ID	TECN	CHG	COMMENT	$\Gamma_9$
< 5.4	90	ALAVI-HARATI02B	KTEV		$K^+ A \rightarrow K^+ + A$	
• • • We do not use the following data for averages, fits, limits, etc. • • •						
< 84	90	CARLSMITH	87	SPEC 0	60-200 $K_L^0 A \rightarrow K_S^0 \pi^0 A$	

 $K_2^*(1430)$  BRANCHING RATIOS $\Gamma(K\pi)/\Gamma_{\text{total}}$ 

VALUE	DOCUMENT ID	TECN	CHG	COMMENT	$\Gamma_1/\Gamma$
<b>0.499 ± 0.012 OUR FIT</b>					
<b>0.488 ± 0.014 OUR AVERAGE</b>					
0.485 ± 0.006 ± 0.020	<sup>14</sup> ASTON	88	LASS 0	11 $K^-p \rightarrow K^- \pi^+ n$	
0.49 ± 0.02	<sup>14</sup> ESTABROOKS	78	ASPK ±	13 $K^\pm p \rightarrow \rho K \pi$	

 $\Gamma(K^*(892)\pi)/\Gamma(K\pi)$ 

VALUE	DOCUMENT ID	TECN	CHG	COMMENT	$\Gamma_2/\Gamma_1$
<b>0.496 ± 0.034 OUR FIT</b>					
<b>0.47 ± 0.04 OUR AVERAGE</b>					
0.44 ± 0.09	ASTON	84B	LASS 0	11 $K^-p \rightarrow \bar{K}^0 2\pi n$	
0.62 ± 0.19	LAUSCHER	75	HBC 0	10,16 $K^-p \rightarrow K^- \pi^+ n$	
0.54 ± 0.16	DEHM	74	DBC 0	4.6 $K^+ N$	
0.47 ± 0.08	AGUILAR-...	71B	HBC	3.9,4.6 $K^-p$	
0.47 ± 0.10	BASSANO	67	HBC -0	4.6,5.0 $K^-p$	
0.45 ± 0.13	BADIER	65c	HBC -	3 $K^-p$	

 $\Gamma(K\omega)/\Gamma(K\pi)$ 

VALUE	DOCUMENT ID	TECN	CHG	COMMENT	$\Gamma_5/\Gamma_1$
<b>0.059 ± 0.017 OUR FIT</b>					
<b>0.070 ± 0.035 OUR AVERAGE</b>					
0.05 ± 0.04	AGUILAR-...	71B	HBC	3.9,4.6 $K^-p$	
0.13 ± 0.07	BASSOMPIE...	69	HBC 0	5 $K^+ p$	

 $\Gamma(K\rho)/\Gamma(K\pi)$ 

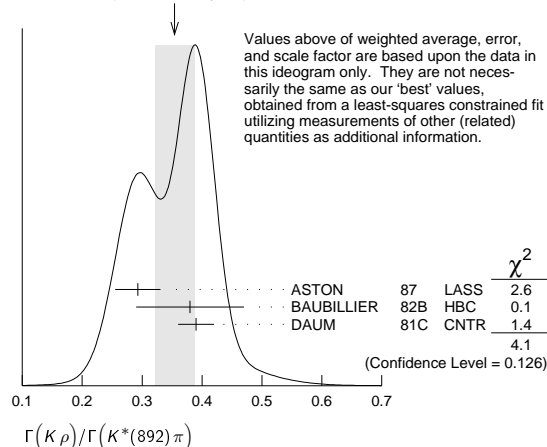
VALUE	DOCUMENT ID	TECN	CHG	COMMENT	$\Gamma_4/\Gamma_1$
<b>0.174 ± 0.017 OUR FIT</b>				Error includes scale factor of 1.2.	
<b>0.150 ± 0.029 OUR AVERAGE</b>					
0.18 ± 0.05	ASTON	84B	LASS 0	11 $K^-p \rightarrow \bar{K}^0 2\pi n$	
0.02 <sup>+0.10</sup> <sub>-0.02</sub>	DEHM	74	DBC 0	4.6 $K^+ N$	
0.16 ± 0.05	AGUILAR-...	71B	HBC	3.9,4.6 $K^-p$	
0.14 ± 0.10	BASSANO	67	HBC -0	4.6,5.0 $K^-p$	
0.14 ± 0.07	BADIER	65c	HBC -	3 $K^-p$	

See key on page 457

## Meson Particle Listings

 $K_2^*(1430)$ ,  $K(1460)$  $\Gamma(K\rho)/\Gamma(K^*(892)\pi)$  $\Gamma_4/\Gamma_2$ 

VALUE	DOCUMENT ID	TECN	CHG	COMMENT
<b>0.350 ± 0.031 OUR FIT</b>	Error includes scale factor of 1.4.			
<b>0.354 ± 0.033 OUR AVERAGE</b>	Error includes scale factor of 1.4. See the ideogram below.			
0.293 ± 0.032 ± 0.020	ASTON	87	LASS	0 11 $K^- p \rightarrow \bar{K}^0 \pi^+ \pi^- n$
0.38 ± 0.09	BAUBILLIER	82B	HBC	0 8.25 $K^- p \rightarrow N K_S^0 \pi \pi$
0.39 ± 0.03	DAUM	81c	CNTR	63 $K^- p \rightarrow K^- 2\pi$

WEIGHTED AVERAGE  
0.354 ± 0.033 (Error scaled by 1.4) $\Gamma(K\omega)/\Gamma(K^*(892)\pi)$  $\Gamma_5/\Gamma_2$ 

VALUE	DOCUMENT ID	TECN	CHG	COMMENT
<b>0.118 ± 0.034 OUR FIT</b>				
<b>0.10 ± 0.04</b>	FIELD	67	HBC	— 3.8 $K^- p$

 $\Gamma(K\eta)/\Gamma(K^*(892)\pi)$  $\Gamma_7/\Gamma_2$ 

VALUE	DOCUMENT ID	TECN	CHG	COMMENT
<b>0.006 ± 0.014 OUR FIT</b>	Error includes scale factor of 1.2.			
<b>0.07 ± 0.04</b>	FIELD	67	HBC	— 3.8 $K^- p$

 $\Gamma(K\eta)/\Gamma(K\pi)$  $\Gamma_7/\Gamma_1$ 

VALUE	CL%	DOCUMENT ID	TECN	CHG	COMMENT
<b>0.0030 ± 0.0070 OUR FIT</b>		Error includes scale factor of 1.3.			
<b>0 ± 0.0056</b>	15	ASTON	88B	LASS	— 11 $K^- p \rightarrow K^- \eta p$
...	We do not use the following data for averages, fits, limits, etc. ...				
<0.04	95	AGUILAR...	71B	HBC	3, 9, 4, 6 $K^- p$
<0.065	16	BASSOMPIE...	69	HBC	5, 0 $K^+ p$
<0.02		BISHOP	69	HBC	3.5 $K^+ p$

 $\Gamma(K^*(892)\pi\pi)/\Gamma_{\text{total}}$  $\Gamma_3/\Gamma$ 

VALUE	DOCUMENT ID	TECN	CHG	COMMENT	
<b>0.134 ± 0.022 OUR FIT</b>					
<b>0.12 ± 0.04</b>	17	GOLDBERG	76	HBC	— 3 $K^- p \rightarrow \rho \bar{K}^0 \pi \pi$

 $\Gamma(K^*(892)\pi\pi)/\Gamma(K\pi)$  $\Gamma_3/\Gamma_1$ 

VALUE	DOCUMENT ID	TECN	CHG	COMMENT	
<b>0.27 ± 0.05 OUR FIT</b>					
<b>0.21 ± 0.08</b>	16, 17	JONGEJANS	78	HBC	— 4 $K^- p \rightarrow \rho \bar{K}^0 \pi \pi$

 $\Gamma(K\omega\pi)/\Gamma_{\text{total}}$  $\Gamma_8/\Gamma$ 

VALUE (units $10^{-3}$ )	CL%	EVTS	DOCUMENT ID	TECN	COMMENT
<b>&lt;0.72</b>	95	0	JONGEJANS	78	HBC 4 $K^- p \rightarrow \rho \bar{K}^0 4\pi$

14 From phase shift analysis.

15 ASTON 88B quote &lt; 0.0092 at CL=95%. We convert this to a central value and 1 sigma error in order to be able to use it in our constrained fit.

16 Restated by us.

17 Assuming  $\pi\pi$  system has isospin 1, which is supported by the data. $K_2^*(1430)$  REFERENCES

AUBERT	07AK	PR D76 012008	B. Aubert et al.	(BABAR Collab.)
ALAVI-HARATI	02B	PRL 89 072001	A. Alavi-Harati et al.	(FNAL KTeV Collab.)
BIRD	89	SLAC-332	P.F. Bird	(SLAC)
ASTON	88	NP B296 493	D. Aston et al.	(SLAC, NAGO, CINC, INUS)
ASTON	88B	PL B201 169	D. Aston et al.	(SLAC, NAGO, CINC, INUS)
ASTON	87	NP B292 693	D. Aston et al.	(SLAC, NAGO, CINC, INUS)
CARLSMITH	87	PR D36 3502	D. Carlsmith et al.	(EFT, SACL)
ASTON	84B	NP B247 261	D. Aston et al.	(SLAC, CARL, OTTA)
BAUBILLIER	84B	ZPHY C26 37	M. Baubillier et al.	(BIRM, CERN, GLAS+)
BAUBILLIER	82B	NP B202 21	M. Baubillier et al.	(BIRM, CERN, GLAS+)
CHANGIR	82	PL 117B 123	S. Cihangir et al.	(FNAL, MINN, ROCH)
CLELAND	82	NP B208 189	W.E. Cleland et al.	(DURH, GEVA, LAUS+)
ASTON	81C	PL 106B 235	D. Aston et al.	(SLAC, CARL, OTTA) JP
DAUM	81C	NP B187 1	C. Daum et al.	(AMST, CERN, CRAC, MPIM+)
TOAFF	81	PR D23 1500	S. Toaff et al.	(ANL, KANS)

ETKIN	80	PR D22 42	A. Etkin et al.	(BNL, CUNY) JP
ESTABROOKS	78	NP B133 490	P.G. Estabrooks et al.	(MCGI, CARL, DURH+)
Also		PR D17 658	P.G. Estabrooks et al.	(MCGI, CARL, DURH+)
JONGEJANS	78	NP B139 383	B. Jongejans et al.	(ZEEM, CERN, NIJM+)
MARTIN	78	NP B134 392	A.D. Martin et al.	(DURH, GEVA)
BOWLER	77	NP B126 31	M.G. Bowler et al.	(OXF)
GOLDBERG	76	LNC 17 253	J. Goldberg	(HAIF)
HENDRICK	76	NP B112 189	K. Hendrickx et al.	(MONS, SACL, PARIS+)
LAUSCHER	75	NP B86 189	P. Lauscher et al.	(ABCLV Collab.) JP
MCCUBBIN	75	NP B86 13	N.A. McCubbin, L. Lyons	(OXF)
DEHM	74	NP B75 47	G. Dehm et al.	(MPIM, BRUX, MONS, CERN)
LINGLIN	73	NP B55 408	D. Linglin	(CERN)
AGUILAR...	71B	PR D4 2583	M. Aguilar-Benitez, R.L. Eisner, J.B. Kinson	(BNL)
BARNHAM	71C	NP B28 171	K.W.J. Barnham et al.	(BIRM, GLAS)
CORDS	71	PR D4 1974	D. Cords et al.	(PURD, UCD, IUPUI)
BASSOMPIE...	69	NP B13 189	G. Bassompierre et al.	(CERN, BRUX) JP
BISHOP	69	NP B9 403	J.M. Bishop et al.	(WISC)
CRENNELL	69D	PRL 22 487	D.J. Crennell et al.	(BNL)
DAVIS	69	PRL 23 1071	P.J. Davis et al.	(LRL)
LIND	69	NP B14 1	V.G. Lind et al.	(LRL) JP
SCHWEING...	68	PR 166 1317	F. Schweingruber et al.	(ANL, NWES)
Also		Thesis	F.L. Schweingruber	(NWES, NWES)
BASSANO	67	PRL 19 968	D. Bassano et al.	(BNL, SYRA)
FIELD	67	PL 24B 638	J.H. Field et al.	(UCSD)
BADIER	65C	PL 19 612	J. Badier et al.	(EPOL, SACL, AMST)

 $K(1460)$ 

$$I(J^P) = \frac{1}{2}(0^-)$$

OMITTED FROM SUMMARY TABLE

Observed in  $K\pi\pi$  partial-wave analysis. $K(1460)$  MASS

VALUE (MeV)	DOCUMENT ID	TECN	CHG	COMMENT
...	We do not use the following data for averages, fits, limits, etc. ...			
~ 1460	DAUM	81c	CNTR	— 63 $K^- p \rightarrow K^- 2\pi$
~ 1400	1	BRANDENB...	76B	ASPK ± 13 $K^\pm p \rightarrow K^\pm 2\pi$
1 Coupled mainly to $K f_0(1370)$ . Decay into $K^*(892)\pi$ seen.				

 $K(1460)$  WIDTH

VALUE (MeV)	DOCUMENT ID	TECN	CHG	COMMENT
...	We do not use the following data for averages, fits, limits, etc. ...			
~ 260	DAUM	81c	CNTR	— 63 $K^- p \rightarrow K^- 2\pi$
~ 250	2	BRANDENB...	76B	ASPK ± 13 $K^\pm p \rightarrow K^\pm 2\pi$
2 Coupled mainly to $K f_0(1370)$ . Decay into $K^*(892)\pi$ seen.				

 $K(1460)$  DECAY MODES

Mode	Fraction ( $\Gamma_i/\Gamma$ )
$\Gamma_1$ $K^*(892)\pi$	seen
$\Gamma_2$ $K\rho$	seen
$\Gamma_3$ $K_0^*(1430)\pi$	seen

 $K(1460)$  PARTIAL WIDTHS

$\Gamma(K^*(892)\pi)$	$\Gamma_1$		
VALUE (MeV)	DOCUMENT ID	TECN	COMMENT
...	We do not use the following data for averages, fits, limits, etc. ...		
~ 109	DAUM	81c	CNTR 63 $K^- p \rightarrow K^- 2\pi$
$\Gamma(K\rho)$	$\Gamma_2$		
VALUE (MeV)	DOCUMENT ID	TECN	COMMENT
...	We do not use the following data for averages, fits, limits, etc. ...		
~ 34	DAUM	81c	CNTR 63 $K^- p \rightarrow K^- 2\pi$
$\Gamma(K_0^*(1430)\pi)$	$\Gamma_3$		
VALUE (MeV)	DOCUMENT ID	TECN	COMMENT
...	We do not use the following data for averages, fits, limits, etc. ...		
~ 117	DAUM	81c	CNTR 63 $K^- p \rightarrow K^- 2\pi$

 $K(1460)$  REFERENCES

DAUM	81C	NP B187 1	C. Daum et al.	(AMST, CERN, CRAC, MPIM+)
BRANDENB...	76B	PRL 36 1239	G.W. Brandenburg et al.	(SLAC) JP

## Meson Particle Listings

 $K_2(1580)$ ,  $K(1630)$ ,  $K_1(1650)$ ,  $K^*(1680)$  $K_2(1580)$ 

$$I(J^P) = \frac{1}{2}(2^-)$$

OMITTED FROM SUMMARY TABLE

Seen in partial-wave analysis of the  $K^- \pi^+ \pi^-$  system. Needs confirmation. $K_2(1580)$  MASS

VALUE (MeV)	DOCUMENT ID	TECN	CHG	COMMENT
• • • We do not use the following data for averages, fits, limits, etc. • • •				
~ 1580	OTTER	79	-	10,14,16 $K^- p$

 $K_2(1580)$  WIDTH

VALUE (MeV)	DOCUMENT ID	TECN	CHG	COMMENT
• • • We do not use the following data for averages, fits, limits, etc. • • •				
~ 110	OTTER	79	-	10,14,16 $K^- p$

 $K_2(1580)$  DECAY MODES

Mode	Fraction ( $\Gamma_i/\Gamma$ )
$\Gamma_1$ $K^*(892)\pi$	seen
$\Gamma_2$ $K_2^*(1430)\pi$	possibly seen

 $K_2(1580)$  BRANCHING RATIOS

$\Gamma(K^*(892)\pi)/\Gamma_{\text{total}}$	DOCUMENT ID	TECN	CHG	COMMENT	$\Gamma_1/\Gamma$	
seen	OTTER	79	HBC	-	10,14,16 $K^- p$	
• • • We do not use the following data for averages, fits, limits, etc. • • •						
possibly seen	GULER	11	BELL	$B^+ \rightarrow J/\psi K^+ \pi^+ \pi^-$		

$\Gamma(K_2^*(1430)\pi)/\Gamma_{\text{total}}$	DOCUMENT ID	TECN	CHG	COMMENT	$\Gamma_2/\Gamma$
possibly seen	OTTER	79	HBC	-	10,14,16 $K^- p$

 $K_2(1580)$  REFERENCES

GULER	11	PR D83 032005	H. Guler et al.	(BELLE Collab.)
OTTER	79	NP B147 1	G. Otter et al.	(AACH3, BERL, CERN, LOIC+)JP

 $K(1630)$ 

$$I(J^P) = \frac{1}{2}(?^?)$$

OMITTED FROM SUMMARY TABLE

Seen as a narrow peak, compatible with the experimental resolution, in the invariant mass of the  $K_S^0 \pi^+ \pi^-$  system produced in  $\pi^- p$  interactions at high momentum transfers. $K(1630)$  MASS

VALUE (MeV)	EVTS	DOCUMENT ID	TECN	COMMENT
<b>1629 ± 7</b>	~ 75	KARNAUKHOV98	BC	16.0 $\pi^- p \rightarrow (K_S^0 \pi^+ \pi^-) X^+ \pi^- X^0$

 $K(1630)$  WIDTH

VALUE (MeV)	EVTS	DOCUMENT ID	TECN	COMMENT
<b>16 ± 19</b> <b>-16</b>	~ 75	<sup>1</sup> KARNAUKHOV98	BC	16.0 $\pi^- p \rightarrow (K_S^0 \pi^+ \pi^-) X^+ \pi^- X^0$

<sup>1</sup> Compatible with an experimental resolution of  $14 \pm 1$  MeV. $K(1630)$  DECAY MODES

Mode	Fraction ( $\Gamma_i/\Gamma$ )
$\Gamma_1$ $K_S^0 \pi^+ \pi^-$	

 $K(1630)$  REFERENCES

KARNAUKHOV 98	PAN 61 203	V.M. Karnaukhov, C. Coca, V.J. Moroz
	Translated from YAF 61 252.	

 $K_1(1650)$ 

$$I(J^P) = \frac{1}{2}(1^+)$$

OMITTED FROM SUMMARY TABLE

This entry contains various peaks in strange meson systems ( $K^+ \phi$ ,  $K \pi \pi$ ) reported in partial-wave analysis in the 1600–1900 mass region. $K_1(1650)$  MASS

VALUE (MeV)	DOCUMENT ID	TECN	CHG	COMMENT
<b>1650 ± 50</b>	FRAME	86	OMEG +	13 $K^+ p \rightarrow \phi K^+ p$
• • • We do not use the following data for averages, fits, limits, etc. • • •				
~ 1840	ARMSTRONG	83	OMEG -	18.5 $K^- p \rightarrow 3K p$
~ 1800	DAUM	81c	CNTR -	63 $K^- p \rightarrow K^- 2\pi p$

 $K_1(1650)$  WIDTH

VALUE (MeV)	DOCUMENT ID	TECN	CHG	COMMENT
<b>150 ± 50</b>	FRAME	86	OMEG +	13 $K^+ p \rightarrow \phi K^+ p$
• • • We do not use the following data for averages, fits, limits, etc. • • •				
~ 250	DAUM	81c	CNTR -	63 $K^- p \rightarrow K^- 2\pi p$

 $K_1(1650)$  DECAY MODES

Mode	Fraction ( $\Gamma_i/\Gamma$ )
$\Gamma_1$ $K \pi \pi$	
$\Gamma_2$ $K \phi$	

 $K_1(1650)$  REFERENCES

FRAME	86	NP B276 667	D. Frame et al.	(GLAS)
ARMSTRONG	83	NP B221 1	T.A. Armstrong et al.	(BARL BIRM, CERN+)
DAUM	81c	NP B187 1	C. Daum et al.	(AMST, CERN, CRAC, MPIM+)

 $K^*(1680)$ 

$$I(J^P) = \frac{1}{2}(1^-)$$

 $K^*(1680)$  MASS

VALUE (MeV)	DOCUMENT ID	TECN	CHG	COMMENT
<b>1717 ± 27 OUR AVERAGE</b>	Error includes scale factor of 1.4.			
1677 ± 10 ± 32	ASTON	88	LASS 0	11 $K^- p \rightarrow K^- \pi^+ n$
1735 ± 10 ± 20	ASTON	87	LASS 0	11 $K^- p \rightarrow \bar{K}^0 \pi^+ \pi^- n$
• • • We do not use the following data for averages, fits, limits, etc. • • •				
1678 ± 64	BIRD	89	LASS -	11 $K^- p \rightarrow \bar{K}^0 \pi^- p$
1800 ± 70	ETKIN	80	MPS 0	6 $K^- p \rightarrow \bar{K}^0 \pi^+ \pi^- n$
~ 1650	ESTABROOKS	78	ASPK 0	13 $K^\pm p \rightarrow K^\pm \pi^\pm n$

 $K^*(1680)$  WIDTH

VALUE (MeV)	DOCUMENT ID	TECN	CHG	COMMENT
<b>322 ± 110 OUR AVERAGE</b>	Error includes scale factor of 4.2.			
205 ± 16 ± 34	ASTON	88	LASS 0	11 $K^- p \rightarrow K^- \pi^+ n$
423 ± 18 ± 30	ASTON	87	LASS 0	11 $K^- p \rightarrow \bar{K}^0 \pi^+ \pi^- n$
• • • We do not use the following data for averages, fits, limits, etc. • • •				
454 ± 270	BIRD	89	LASS -	11 $K^- p \rightarrow \bar{K}^0 \pi^- p$
170 ± 30	ETKIN	80	MPS 0	6 $K^- p \rightarrow \bar{K}^0 \pi^+ \pi^- n$
250 to 300	ESTABROOKS	78	ASPK 0	13 $K^\pm p \rightarrow K^\pm \pi^\pm n$

 $K^*(1680)$  DECAY MODES

Mode	Fraction ( $\Gamma_i/\Gamma$ )
$\Gamma_1$ $K \pi$	(38.7 ± 2.5) %
$\Gamma_2$ $K \rho$	(31.4 ± 5.0 / -2.1) %
$\Gamma_3$ $K^*(892)\pi$	(29.9 ± 2.2 / -5.0) %

See key on page 457

Meson Particle Listings

$K^*(1680), K_2(1770)$

CONSTRAINED FIT INFORMATION

An overall fit to 4 branching ratios uses 4 measurements and one constraint to determine 3 parameters. The overall fit has a  $\chi^2 = 2.9$  for 2 degrees of freedom.

The following *off-diagonal* array elements are the correlation coefficients  $\langle \delta x_i \delta x_j \rangle / (\delta x_i \delta x_j)$ , in percent, from the fit to the branching fractions,  $x_i \equiv \Gamma_i / \Gamma_{\text{total}}$ . The fit constrains the  $x_i$  whose labels appear in this array to sum to one.

$x_2$	-36	
$x_3$	-39	-72
	$x_1$	$x_2$

$K^*(1680)$  BRANCHING RATIOS

$\Gamma(K\pi) / \Gamma_{\text{total}}$	DOCUMENT ID	TECN	CHG	COMMENT	$\Gamma_1 / \Gamma$
<b>0.387 ± 0.026 OUR FIT</b>					
<b>0.388 ± 0.014 ± 0.022</b>	ASTON	88	LASS	0	11 $K^- p \rightarrow K^- \pi^+ n$
$\Gamma(K\pi) / \Gamma(K^*(892)\pi)$	DOCUMENT ID	TECN	CHG	COMMENT	$\Gamma_1 / \Gamma_3$
<b>1.30 ± 0.23 OUR FIT</b>					
<b>2.8 ± 1.1</b>	ASTON	84	LASS	0	11 $K^- p \rightarrow \bar{K}^0 2\pi n$
$\Gamma(K\rho) / \Gamma(K\pi)$	DOCUMENT ID	TECN	CHG	COMMENT	$\Gamma_2 / \Gamma_1$
<b>0.81 ± 0.14 OUR FIT</b>					
<b>1.2 ± 0.4</b>	ASTON	84	LASS	0	11 $K^- p \rightarrow \bar{K}^0 2\pi n$
$\Gamma(K\rho) / \Gamma(K^*(892)\pi)$	DOCUMENT ID	TECN	CHG	COMMENT	$\Gamma_2 / \Gamma_3$
<b>1.05 ± 0.27 OUR FIT</b>					
<b>0.97 ± 0.09 ± 0.30 OUR FIT</b>	ASTON	87	LASS	0	11 $K^- p \rightarrow \bar{K}^0 \pi^+ \pi^- n$

$K^*(1680)$  REFERENCES

BIRD	89	SLAC-332	P.F. Bird	(SLAC)
ASTON	88	NP B296 493	D. Aston et al.	(SLAC, NAGO, CINC, INUS)
ASTON	87	NP B292 693	D. Aston et al.	(SLAC, NAGO, CINC, INUS)
ASTON	84	PL 149B 258	D. Aston et al.	(SLAC, CARL, OTTA) JP
ETKIN	80	PR D22 42	A. Etkin et al.	(BNL, CUNY) JP
ESTABROOKS	78	NP B133 490	P.G. Estabrooks et al.	(MCGI, CARL, DURH+) JP

$K_2(1770)$

$$I(J^P) = \frac{1}{2}(2^-)$$

See our mini-review in the 2004 edition of this Review, PDG 04.

$K_2(1770)$  MASS

VALUE (MeV)	EVTS	DOCUMENT ID	TECN	CHG	COMMENT
<b>1773 ± 8</b>		1 ASTON	93	LASS	11 $K^- p \rightarrow K^- \omega p$
••• We do not use the following data for averages, fits, limits, etc. •••					
1743 ± 15		TIKHOMIROV 03	SPEC		40.0 $\pi^- C \rightarrow K_S^0 K_S^0 K_L^0 X$
1810 ± 20		FRAME	86	OMEG +	13 $K^+ p \rightarrow \phi K^+ p$
~ 1730		ARMSTRONG	83	OMEG -	18.5 $K^- p \rightarrow 3Kp$
~ 1780		2 DAUM	81c	CNTR -	63 $K^- p \rightarrow K^- 2\pi p$
1710 ± 15	60	CHUNG	74	HBC -	7.3 $K^- p \rightarrow K^- \omega p$
1767 ± 6		BLIEDEN	72	MMS -	11-16 $K^- p$
1730 ± 20	306	3 FIRESTONE	72B	DBC +	12 $K^+ d$
1765 ± 40		4 COLLEY	71	HBC +	10 $K^+ p \rightarrow K 2\pi N$
1740		DENEGRI	71	DBC -	12.6 $K^- d \rightarrow \bar{K} 2\pi d$
1745 ± 20		AGUILAR-...	70c	HBC -	4.6 $K^- p$
1780 ± 15		BARTSCH	70c	HBC -	10.1 $K^- p$
1760 ± 15		LUDLAM	70	HBC -	12.6 $K^- p$

1 From a partial wave analysis of the  $K^- \omega$  system.  
 2 From a partial wave analysis of the  $K^- 2\pi$  system.  
 3 Produced in conjunction with excited deuteron.  
 4 Systematic errors added correspond to spread of different fits.

$K_2(1770)$  WIDTH

VALUE (MeV)	EVTS	DOCUMENT ID	TECN	CHG	COMMENT
<b>186 ± 14</b>		5 ASTON	93	LASS	11 $K^- p \rightarrow K^- \omega p$

••• We do not use the following data for averages, fits, limits, etc. •••

147 ± 70		TIKHOMIROV 03	SPEC		40.0 $\pi^- C \rightarrow K_S^0 K_S^0 K_L^0 X$
140 ± 40		FRAME	86	OMEG +	13 $K^+ p \rightarrow \phi K^+ p$
~ 220		ARMSTRONG	83	OMEG -	18.5 $K^- p \rightarrow 3Kp$
~ 210		6 DAUM	81c	CNTR -	63 $K^- p \rightarrow K^- 2\pi p$
110 ± 50		CHUNG	74	HBC -	7.3 $K^- p \rightarrow K^- \omega p$
100 ± 26		BLIEDEN	72	MMS -	11-16 $K^- p$
210 ± 30	60	7 FIRESTONE	72B	DBC +	12 $K^+ d$
90 ± 70		8 COLLEY	71	HBC +	10 $K^+ p \rightarrow K 2\pi N$
130		DENEGRI	71	DBC -	12.6 $K^- d \rightarrow \bar{K} 2\pi d$
100 ± 50		AGUILAR-...	70c	HBC -	4.6 $K^- p$
138 ± 40		BARTSCH	70c	HBC -	10.1 $K^- p$
50 ± 40		LUDLAM	70	HBC -	12.6 $K^- p$
-20					

5 From a partial wave analysis of the  $K^- \omega$  system.  
 6 From a partial wave analysis of the  $K^- 2\pi$  system.  
 7 Produced in conjunction with excited deuteron.  
 8 Systematic errors added correspond to spread of different fits.

$K_2(1770)$  DECAY MODES

Mode	Fraction ( $\Gamma_i / \Gamma$ )
$\Gamma_1$ $K \pi \pi$	
$\Gamma_2$ $K_2^*(1430) \pi$	dominant
$\Gamma_3$ $K^*(892) \pi$	seen
$\Gamma_4$ $K f_2(1270)$	seen
$\Gamma_5$ $K f_0(980)$	
$\Gamma_6$ $K \phi$	seen
$\Gamma_7$ $K \omega$	seen

$K_2(1770)$  BRANCHING RATIOS

$\Gamma(K_2^*(1430)\pi) / \Gamma(K\pi\pi)$   $\Gamma_2 / \Gamma_1$

VALUE	DOCUMENT ID	TECN	CHG	COMMENT
••• We do not use the following data for averages, fits, limits, etc. •••				
~ 0.03	DAUM	81c	CNTR	63 $K^- p \rightarrow K^- 2\pi p$
~ 1.0	9 FIRESTONE	72B	DBC +	12 $K^+ d$
< 1.0	COLLEY	71	HBC	10 $K^+ p$
0.2 ± 0.2	AGUILAR-...	70c	HBC -	4.6 $K^- p$
< 1.0	BARTSCH	70c	HBC -	10.1 $K^- p$
1.0	BARBARO-...	69	HBC +	12.0 $K^+ p$
9 Produced in conjunction with excited deuteron.				

$\Gamma(K^*(892)\pi) / \Gamma(K\pi\pi)$   $\Gamma_3 / \Gamma_1$

VALUE	DOCUMENT ID	TECN	COMMENT
••• We do not use the following data for averages, fits, limits, etc. •••			
~ 0.23	DAUM	81c	CNTR 63 $K^- p \rightarrow K^- 2\pi p$

$\Gamma(K f_2(1270)) / \Gamma(K\pi\pi)$   $\Gamma_4 / \Gamma_1$

VALUE	DOCUMENT ID	TECN	COMMENT
••• We do not use the following data for averages, fits, limits, etc. •••			
~ 0.74	DAUM	81c	CNTR 63 $K^- p \rightarrow K^- 2\pi p$

$\Gamma(K f_0(980)) / \Gamma_{\text{total}}$   $\Gamma_5 / \Gamma$

VALUE	DOCUMENT ID	TECN	COMMENT
••• We do not use the following data for averages, fits, limits, etc. •••			
possibly seen	TIKHOMIROV 03	SPEC	40.0 $\pi^- C \rightarrow K_S^0 K_S^0 K_L^0 X$

$\Gamma(K\phi) / \Gamma_{\text{total}}$   $\Gamma_6 / \Gamma$

VALUE	DOCUMENT ID	TECN	CHG	COMMENT
seen	ARMSTRONG 83	OMEG -		18.5 $K^- p \rightarrow K^- \phi N$

$\Gamma(K\omega) / \Gamma_{\text{total}}$   $\Gamma_7 / \Gamma$

VALUE	DOCUMENT ID	TECN	CHG	COMMENT
seen	OTTER 81	HBC ±		8.25, 10, 16 $K^\pm p$
seen	CHUNG 74	HBC -		7.3 $K^- p \rightarrow K^- \omega p$

# Meson Particle Listings

## $K_2(1770), K_3^*(1780)$

### $K_2(1770)$ REFERENCES

PDG	04	PL B592 1	S. Eidelman <i>et al.</i>	(PDG Collab.)
TIKHOMIROV	03	PAN 66 828	G.D. Tikhomirov <i>et al.</i>	
		Translated from YAF 66 860		
ASTON	93	PL B308 186	D. Aston <i>et al.</i>	(SLAC, NAGO, CINC, INUS)
FRAME	86	NP B276 667	D. Frame <i>et al.</i>	(GLAS)
ARMSTRONG	83	NP B221 1	T.A. Armstrong <i>et al.</i>	(BARI, BIRM, CERN+)
DAUM	81C	NP B187 1	C. Daum <i>et al.</i>	(AMST, CERN, CRAC, MPIM+)
OTTER	81	NP B181 1	G. Otter	(AACH3, BERL, LOIC, VIEN, BIRM+)
CHUNG	74	PL 51B 413	S.U. Chung <i>et al.</i>	(BNL)
BLIEDEN	72	PL 39B 668	H.R. Blieden <i>et al.</i>	(STON, NEAS)
FIRESTONE	72B	PR D5 505	A. Firestone <i>et al.</i>	(LBL)
COLLEY	71	NP B26 71	D.C. Colley <i>et al.</i>	(BIRM, GLAS)
DENEGRI	71	NP B28 13	D. Denegri <i>et al.</i>	(JHU)JP
AGUILAR...	70C	PRL 25 54	M. Aguilar-Benitez <i>et al.</i>	(BNL)
BARTSCH	70C	PL 33B 186	J. Bartsch <i>et al.</i>	(AACH, BERL, CERN+)
LUDLAM	70	PR D2 1234	T. Ludlam, J. Sandweiss, A.J. Slaughter	(YALE)
BARBARO...	69	PRL 22 1207	A. Barbaro-Galieri <i>et al.</i>	(LRL)

### $K_3^*(1780)$

$$I(J^P) = \frac{1}{2}(3^-)$$

### $K_3^*(1780)$ MASS

VALUE (MeV)	EVTS	DOCUMENT ID	TECN	CHG	COMMENT
<b>1776 ± 7 OUR AVERAGE</b>		Error includes scale factor of 1.1.			
1781 ± 8 ± 4		<sup>1</sup> ASTON	88	LASS	0 11 $K^- p \rightarrow K^- \pi^+ n$
1740 ± 14 ± 15		<sup>1</sup> ASTON	87	LASS	0 11 $K^- p \rightarrow \bar{K}^0 \pi^+ \pi^- n$
1779 ± 11		<sup>2</sup> BALDI	76	SPEC	+ 10 $K^+ p \rightarrow K^0 \pi^+ p$
1776 ± 26		<sup>3</sup> BRANDENB...	76D	ASPK	0 13 $K^\pm p \rightarrow K^\pm \pi^\mp N$
• • • We do not use the following data for averages, fits, limits, etc. • • •					
1720 ± 10 ± 15	6111	<sup>4</sup> BIRD	89	LASS	- 11 $K^- p \rightarrow \bar{K}^0 \pi^- p$
1749 ± 10		ASTON	88B	LASS	- 11 $K^- p \rightarrow K^- \eta p$
1780 ± 9	300	BAUBILLIER	84B	HBC	- 8.25 $K^- p \rightarrow \bar{K}^0 \pi^- p$
1790 ± 15		BAUBILLIER	82B	HBC	0 8.25 $K^- p \rightarrow K_S^0 2\pi N$
1784 ± 9	2060	CLELAND	82	SPEC	± 50 $K^+ p \rightarrow K_S^0 \pi^\pm p$
1786 ± 15		<sup>5</sup> ASTON	81D	LASS	0 11 $K^- p \rightarrow K^- \pi^+ n$
1762 ± 9	190	TOAFF	81	HBC	- 6.5 $K^- p \rightarrow \bar{K}^0 \pi^- p$
1850 ± 50		ETKIN	80	MPS	0 6 $K^- p \rightarrow \bar{K}^0 \pi^+ \pi^-$
1812 ± 28		BEUSCH	78	OMEG	10 $K^- p \rightarrow \bar{K}^0 \pi^+ \pi^- n$
1786 ± 8		CHUNG	78	MPS	0 6 $K^- p \rightarrow K^- \pi^+ n$

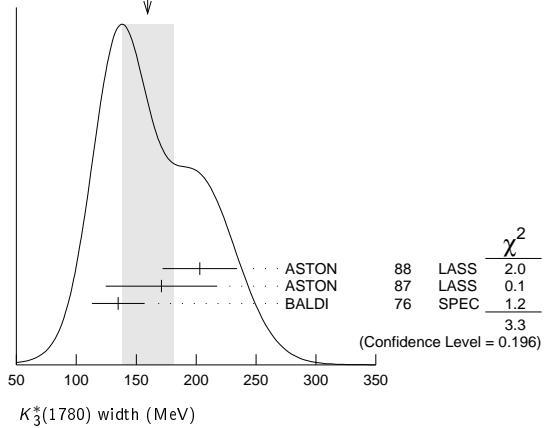
- <sup>1</sup> From energy-independent partial-wave analysis.
- <sup>2</sup> From a fit to  $Y_6^2$  moment.  $J^P = 3^-$  found.
- <sup>3</sup> Confirmed by phase shift analysis of ESTABROOKS 78, yields  $J^P = 3^-$ .
- <sup>4</sup> From a partial wave amplitude analysis.
- <sup>5</sup> From a fit to the  $Y_6^0$  moment.

### $K_3^*(1780)$ WIDTH

VALUE (MeV)	EVTS	DOCUMENT ID	TECN	CHG	COMMENT
<b>159 ± 21 OUR AVERAGE</b>		Error includes scale factor of 1.3. See the ideogram below.			
203 ± 30 ± 8		<sup>6</sup> ASTON	88	LASS	0 11 $K^- p \rightarrow K^- \pi^+ n$
171 ± 42 ± 20		<sup>6</sup> ASTON	87	LASS	0 11 $K^- p \rightarrow \bar{K}^0 \pi^+ \pi^- n$
135 ± 22		<sup>7</sup> BALDI	76	SPEC	+ 10 $K^+ p \rightarrow K^0 \pi^+ p$
• • • We do not use the following data for averages, fits, limits, etc. • • •					
187 ± 31 ± 20	6111	<sup>8</sup> BIRD	89	LASS	- 11 $K^- p \rightarrow \bar{K}^0 \pi^- p$
193 $\pm$ $\frac{51}{37}$		ASTON	88B	LASS	- 11 $K^- p \rightarrow K^- \eta p$
99 ± 30	300	BAUBILLIER	84B	HBC	- 8.25 $K^- p \rightarrow \bar{K}^0 \pi^- p$
~ 130		BAUBILLIER	82B	HBC	0 8.25 $K^- p \rightarrow K_S^0 2\pi N$
191 ± 24	2060	CLELAND	82	SPEC	± 50 $K^+ p \rightarrow K_S^0 \pi^\pm p$
225 ± 60		<sup>9</sup> ASTON	81D	LASS	0 11 $K^- p \rightarrow K^- \pi^+ n$
~ 80	190	TOAFF	81	HBC	- 6.5 $K^- p \rightarrow \bar{K}^0 \pi^- p$
240 ± 50		ETKIN	80	MPS	0 6 $K^- p \rightarrow \bar{K}^0 \pi^+ \pi^-$
181 ± 44		<sup>10</sup> BEUSCH	78	OMEG	10 $K^- p \rightarrow \bar{K}^0 \pi^+ \pi^- n$
96 ± 31		CHUNG	78	MPS	0 6 $K^- p \rightarrow K^- \pi^+ n$
270 ± 70		<sup>11</sup> BRANDENB...	76D	ASPK	0 13 $K^\pm p \rightarrow K^\pm \pi^\mp N$

- <sup>6</sup> From energy-independent partial-wave analysis.
- <sup>7</sup> From a fit to  $Y_6^2$  moment.  $J^P = 3^-$  found.
- <sup>8</sup> From a partial wave amplitude analysis.
- <sup>9</sup> From a fit to  $Y_6^0$  moment.
- <sup>10</sup> Errors enlarged by us to  $4\Gamma/\sqrt{N}$ ; see the note with the  $K^*(892)$  mass.
- <sup>11</sup> ESTABROOKS 78 find that BRANDENBURG 76D data are consistent with 175 MeV width. Not averaged.

WEIGHTED AVERAGE  
159 ± 21 (Error scaled by 1.3)



### $K_3^*(1780)$ DECAY MODES

Mode	Fraction ( $\Gamma_i/\Gamma$ )	Confidence level
$\Gamma_1$ $K \rho$	(31 ± 9) %	
$\Gamma_2$ $K^*(892)\pi$	(20 ± 5) %	
$\Gamma_3$ $K \pi$	(18.8 ± 1.0) %	
$\Gamma_4$ $K \eta$	(30 ± 13) %	
$\Gamma_5$ $K_2^*(1430)\pi$	< 16 %	95%

### CONSTRAINED FIT INFORMATION

An overall fit to 3 branching ratios uses 4 measurements and one constraint to determine 4 parameters. The overall fit has a  $\chi^2 = 0.0$  for 1 degrees of freedom.

The following *off-diagonal* array elements are the correlation coefficients  $\langle \delta x_i \delta x_j \rangle / (\delta x_i \delta x_j)$ , in percent, from the fit to the branching fractions,  $x_i \equiv \Gamma_i/\Gamma_{\text{total}}$ . The fit constrains the  $x_i$  whose labels appear in this array to sum to one.

$x_2$	85		
$x_3$	18	21	
$x_4$	-98	-94	-27
	$x_1$	$x_2$	$x_3$

### $K_3^*(1780)$ BRANCHING RATIOS

$\Gamma(K \rho)/\Gamma(K^*(892)\pi)$	DOCUMENT ID	TECN	CHG	COMMENT	$\Gamma_1/\Gamma_2$
<b>1.52 ± 0.23 OUR FIT</b>					
<b>1.52 ± 0.21 ± 0.10</b>	ASTON	87	LASS	0 11 $K^- p \rightarrow \bar{K}^0 \pi^+ \pi^- n$	
$\Gamma(K^*(892)\pi)/\Gamma(K \pi)$	DOCUMENT ID	TECN	CHG	COMMENT	$\Gamma_2/\Gamma_3$
<b>1.09 ± 0.26 OUR FIT</b>					
<b>1.09 ± 0.26</b>	ASTON	84B	LASS	0 11 $K^- p \rightarrow \bar{K}^0 2\pi n$	
$\Gamma(K \pi)/\Gamma_{\text{total}}$	DOCUMENT ID	TECN	CHG	COMMENT	$\Gamma_3/\Gamma$
<b>0.188 ± 0.010 OUR FIT</b>					
<b>0.188 ± 0.010 OUR AVERAGE</b>					
0.187 ± 0.008 ± 0.008	ASTON	88	LASS	0 11 $K^- p \rightarrow K^- \pi^+ n$	
0.19 ± 0.02	ESTABROOKS 78	ASPK	0	13 $K^\pm p \rightarrow K \pi N$	
$\Gamma(K \eta)/\Gamma(K \pi)$	DOCUMENT ID	TECN	CHG	COMMENT	$\Gamma_4/\Gamma_3$
<b>1.6 ± 0.7 OUR FIT</b>					
• • • We do not use the following data for averages, fits, limits, etc. • • •					
0.41 ± 0.050	<sup>12</sup> BIRD	89	LASS	- 11 $K^- p \rightarrow \bar{K}^0 \pi^- p$	
0.50 ± 0.18	ASTON	88B	LASS	- 11 $K^- p \rightarrow K^- \eta p$	

<sup>12</sup> This result supersedes ASTON 88B.

See key on page 457

## Meson Particle Listings

 $K_3^*(1780)$ ,  $K_2(1820)$ ,  $K(1830)$ ,  $K_0^*(1950)$  $\Gamma(K_2^*(1430)\pi)/\Gamma(K^*(892)\pi)$  $\Gamma_5/\Gamma_2$ 

VALUE	CL%	DOCUMENT ID	TECN	CHG	COMMENT
<0.78	95	ASTON	87	LASS	0 11 $K^-p \rightarrow \bar{K}^0\pi^+\pi^-n$

 $K_3^*(1780)$  REFERENCES

BIRD	89	SLAC-332	P.F. Bird	(SLAC)
ASTON	88	NP B296 493	D. Aston et al.	(SLAC, NAGO, CINC, INUS) JP
ASTON	88B	PL B201 169	D. Aston et al.	(SLAC, NAGO, CINC, INUS) JP
ASTON	87	NP B292 693	D. Aston et al.	(SLAC, NAGO, CINC, INUS) JP
ASTON	84B	NP B247 261	D. Aston et al.	(SLAC, CARL, OTTA) JP
BAUBILLIER	84B	ZPHY C26 37	M. Baubillier et al.	(BIRM, CERN, GLAS+) JP
BAUBILLIER	82B	NP B202 21	M. Baubillier et al.	(BIRM, CERN, GLAS+) JP
CLELAND	82	NP B208 189	W.E. Cleland et al.	(DURH, GEVA, LAUS+) JP
ASTON	81D	PL 99B 502	D. Aston et al.	(SLAC, CARL, OTTA) JP
TOAFF	81	PR D23 1500	S. Toaff et al.	(ANL, KANS) JP
ETKIN	80	PR D22 42	A. Etkin et al.	(BNL, CUNY) JP
BEUSCH	78	PL 74B 282	W. Beusch et al.	(CERN, AACH3, ETH) JP
CHUNG	78	PRL 40 355	S.U. Chung et al.	(BNL, BRAN, CUNY+) JP
ESTABROOKS	78	NP B133 490	P.G. Estabrooks et al.	(MCGI, CARL, DURH+) JP
Also		PR D17 658	P.G. Estabrooks et al.	(MCGI, CARL, DURH+) JP
BALDI	76	PL 63B 344	R. Baldi et al.	(GEVA) JP
BRANDENB...	76D	PL 60B 478	G.W. Brandenburg et al.	(SLAC) JP

 $K_2(1820)$ 

$I(J^P) = \frac{1}{2}(2^-)$

See our mini-review in the 2004 edition of this Review (PDG 04) under  $K_2(1770)$ . $K_2(1820)$  MASS

VALUE (MeV)	DOCUMENT ID	TECN	COMMENT
$1816 \pm 13$	<sup>1</sup> ASTON 93 LASS	11	$K^-p \rightarrow K^- \omega p$
~ 1840	<sup>2</sup> DAUM 81c CNTR	63	$K^-p \rightarrow K^- 2\pi p$

<sup>1</sup> From a partial wave analysis of the  $K^- \omega$  system.  
<sup>2</sup> From a partial wave analysis of the  $K^- 2\pi$  system.

 $K_2(1820)$  WIDTH

VALUE (MeV)	DOCUMENT ID	TECN	COMMENT
$276 \pm 35$	<sup>3</sup> ASTON 93 LASS	11	$K^-p \rightarrow K^- \omega p$
~ 230	<sup>4</sup> DAUM 81c CNTR	63	$K^-p \rightarrow K^- 2\pi p$

<sup>3</sup> From a partial wave analysis of the  $K^- \omega$  system.  
<sup>4</sup> From a partial wave analysis of the  $K^- 2\pi$  system.

 $K_2(1820)$  DECAY MODES

Mode	Fraction ( $\Gamma_i/\Gamma$ )
$\Gamma_1$ $K\pi\pi$	
$\Gamma_2$ $K_2^*(1430)\pi$	seen
$\Gamma_3$ $K^*(892)\pi$	seen
$\Gamma_4$ $Kf_2(1270)$	seen
$\Gamma_5$ $K\omega$	seen

 $K_2(1820)$  BRANCHING RATIOS

$\Gamma(K_2^*(1430)\pi)/\Gamma(K\pi\pi)$	$\Gamma_2/\Gamma_1$
~ 0.77	DAUM 81c CNTR 63 $K^-p \rightarrow \bar{K}2\pi p$

$\Gamma(K^*(892)\pi)/\Gamma(K\pi\pi)$	$\Gamma_3/\Gamma_1$
~ 0.05	DAUM 81c CNTR 63 $K^-p \rightarrow \bar{K}2\pi p$

$\Gamma(Kf_2(1270))/\Gamma(K\pi\pi)$	$\Gamma_4/\Gamma_1$
~ 0.18	DAUM 81c CNTR 63 $K^-p \rightarrow \bar{K}2\pi p$

 $K_2(1820)$  REFERENCES

PDG	04	PL B592 1	S. Eidelman et al.	(PDG Collab.)
ASTON	93	PL B308 186	D. Aston et al.	(SLAC, NAGO, CINC, INUS)
DAUM	81c	NP B187 1	C. Daum et al.	(AMST, CERN, CRAC, MPIM+)

 $K(1830)$ 

$I(J^P) = \frac{1}{2}(0^-)$

OMITTED FROM SUMMARY TABLE

Seen in partial-wave analysis of  $K^- \phi$  system. Needs confirmation. $K(1830)$  MASS

VALUE (MeV)	DOCUMENT ID	TECN	CHG	COMMENT
~ 1830	ARMSTRONG 83 OMEG	—	—	18.5 $K^-p \rightarrow 3Kp$

• • • We do not use the following data for averages, fits, limits, etc. • • •

 $K(1830)$  WIDTH

VALUE (MeV)	DOCUMENT ID	TECN	CHG	COMMENT
~ 250	ARMSTRONG 83 OMEG	—	—	18.5 $K^-p \rightarrow 3Kp$

• • • We do not use the following data for averages, fits, limits, etc. • • •

 $K(1830)$  DECAY MODES

Mode	Fraction ( $\Gamma_i/\Gamma$ )
$\Gamma_1$ $K\phi$	

 $K(1830)$  REFERENCES

ARMSTRONG 83	NP B221 1	T.A. Armstrong et al.	(BARI, BIRM, CERN+) JP
--------------	-----------	-----------------------	------------------------

 $K_0^*(1950)$ 

$I(J^P) = \frac{1}{2}(0^+)$

OMITTED FROM SUMMARY TABLE

Seen in partial-wave analysis of the  $K^- \pi^+$  system. Needs confirmation. $K_0^*(1950)$  MASS

VALUE (MeV)	DOCUMENT ID	TECN	CHG	COMMENT
$1945 \pm 10 \pm 20$	<sup>1</sup> ASTON 88 LASS	0	11	$K^-p \rightarrow K^- \pi^+ n$
1917 ± 12	<sup>2</sup> ZHOU 06 RVUE	—	—	$Kp \rightarrow K^- \pi^+ n$
1820 ± 40	<sup>3</sup> ANISOVICH 97C RVUE	11	11	$K^-p \rightarrow K^- \pi^+ n$

<sup>1</sup> We take the central value of the two solutions and the larger error given.  
<sup>2</sup> S-matrix pole. Using ASTON 88 and assuming  $K_0^*(800)$ ,  $K_0^*(1430)$ .  
<sup>3</sup> T-matrix pole. Reanalysis of ASTON 88 data.

 $K_0^*(1950)$  WIDTH

VALUE (MeV)	DOCUMENT ID	TECN	CHG	COMMENT
$201 \pm 34 \pm 79$	<sup>4</sup> ASTON 88 LASS	0	11	$K^-p \rightarrow K^- \pi^+ n$
145 ± 38	<sup>5</sup> ZHOU 06 RVUE	—	—	$Kp \rightarrow K^- \pi^+ n$
250 ± 100	<sup>6</sup> ANISOVICH 97C RVUE	11	11	$K^-p \rightarrow K^- \pi^+ n$

<sup>4</sup> We take the central value of the two solutions and the larger error given.  
<sup>5</sup> S-matrix pole. Using ASTON 88 and assuming  $K_0^*(800)$ ,  $K_0^*(1430)$ .  
<sup>6</sup> T-matrix pole. Reanalysis of ASTON 88 data.

 $K_0^*(1950)$  DECAY MODES

Mode	Fraction ( $\Gamma_i/\Gamma$ )
$\Gamma_1$ $K\pi$	(52 ± 14) %

 $K_0^*(1950)$  BRANCHING RATIOS

$\Gamma(K\pi)/\Gamma_{total}$	$\Gamma_1/\Gamma$
$0.52 \pm 0.08 \pm 0.12$	<sup>7</sup> ASTON 88 LASS 0 11 $K^-p \rightarrow K^- \pi^+ n$
~ 0.60	<sup>8</sup> ZHOU 06 RVUE $Kp \rightarrow K^- \pi^+ n$

<sup>7</sup> We take the central value of the two solutions and the larger error given.  
<sup>8</sup> S-matrix pole. Using ASTON 88 and assuming  $K_0^*(800)$ ,  $K_0^*(1430)$ .

 $K_0^*(1950)$  REFERENCES

ZHOU	06	NP A775 212	Z.Y. Zhou, H.Q. Zheng	
ANISOVICH	97C	PL B413 137	A.V. Anisovich, A.V. Sarantsev	
ASTON	88	NP B296 493	D. Aston et al.	(SLAC, NAGO, CINC, INUS)

## Meson Particle Listings

 $K_2^*(1980)$ ,  $K_4^*(2045)$  $K_2^*(1980)$ 

$$I(J^P) = \frac{1}{2}(2^+)$$

OMITTED FROM SUMMARY TABLE  
Needs confirmation. $K_2^*(1980)$  MASS

VALUE (MeV)	EVTS	DOCUMENT ID	TECN	CHG	COMMENT
<b>1973 ± 8 ± 25</b>		ASTON	87	LASS	0 11 $K^- p \rightarrow \bar{K}^0 \pi^+ \pi^- n$
• • • We do not use the following data for averages, fits, limits, etc. • • •					
2020 ± 20		TIKHOMIROV	03	SPEC	40.0 $\pi^- C \rightarrow K_S^0 K_S^0 K_L^0 X$
1978 ± 40	241 ± 47	BIRD	89	LASS	- 11 $K^- p \rightarrow \bar{K}^0 \pi^- p$

 $K_2^*(1980)$  WIDTH

VALUE (MeV)	EVTS	DOCUMENT ID	TECN	CHG	COMMENT
<b>373 ± 33 ± 60</b>		ASTON	87	LASS	0 11 $K^- p \rightarrow \bar{K}^0 \pi^+ \pi^- n$
• • • We do not use the following data for averages, fits, limits, etc. • • •					
180 ± 70		TIKHOMIROV	03	SPEC	40.0 $\pi^- C \rightarrow K_S^0 K_S^0 K_L^0 X$
398 ± 47	241 ± 47	BIRD	89	LASS	- 11 $K^- p \rightarrow \bar{K}^0 \pi^- p$

 $K_2^*(1980)$  DECAY MODES

Mode	Fraction ( $\Gamma_i/\Gamma$ )
$\Gamma_1$ $K^*(892)\pi$	possibly seen
$\Gamma_2$ $K\rho$	possibly seen
$\Gamma_3$ $K f_2(1270)$	possibly seen

 $K_2^*(1980)$  BRANCHING RATIOS

$\Gamma(K^*(892)\pi)/\Gamma_{\text{total}}$	$\Gamma_1/\Gamma$		
VALUE	DOCUMENT ID	TECN	COMMENT
possibly seen	GULER	11	BELL $B^+ \rightarrow J/\psi K^+ \pi^+ \pi^-$

$\Gamma(K\rho)/\Gamma_{\text{total}}$	$\Gamma_2/\Gamma$		
VALUE	DOCUMENT ID	TECN	COMMENT
possibly seen	GULER	11	BELL $B^+ \rightarrow J/\psi K^+ \pi^+ \pi^-$

$\Gamma(K\rho)/\Gamma(K^*(892)\pi)$	$\Gamma_2/\Gamma_1$			
VALUE	DOCUMENT ID	TECN	CHG	COMMENT
<b>1.49 ± 0.24 ± 0.09</b>	ASTON	87	LASS	0 11 $K^- p \rightarrow \bar{K}^0 \pi^+ \pi^- n$

$\Gamma(K f_2(1270))/\Gamma_{\text{total}}$	$\Gamma_3/\Gamma$		
VALUE	DOCUMENT ID	TECN	COMMENT
possibly seen	TIKHOMIROV	03	SPEC 40.0 $\pi^- C \rightarrow K_S^0 K_S^0 K_L^0 X$

 $K_2^*(1980)$  REFERENCES

GULER	11	PR D83 032005	H. Guler et al.	(BELLE Collab.)
TIKHOMIROV	03	PAN 66 828	G.D. Tikhomirov et al.	
		Translated from YAF 66 800.		
BIRD	89	SLAC-332	P.F. Bird	(SLAC)
ASTON	87	NP B292 693	D. Aston et al.	(SLAC, NAGO, CINC, INUS)

 $K_4^*(2045)$ 

$$I(J^P) = \frac{1}{2}(4^+)$$

 $K_4^*(2045)$  MASS

VALUE (MeV)	EVTS	DOCUMENT ID	TECN	CHG	COMMENT
<b>2045 ± 9 OUR AVERAGE</b>		Error includes scale factor of 1.1.			
2062 ± 14 ± 13		<sup>1</sup> ASTON	86	LASS	0 11 $K^- p \rightarrow K^- \pi^+ n$
2039 ± 10	400	<sup>2,3</sup> CLELAND	82	SPEC	± 50 $K^+ p \rightarrow K_S^0 \pi^\pm p$
2070 $^{+100}_{-40}$		<sup>4</sup> ASTON	81c	LASS	0 11 $K^- p \rightarrow K^- \pi^+ n$

• • • We do not use the following data for averages, fits, limits, etc. • • •

2079 ± 7	431	TORRES	86	MPSF	400 $pA \rightarrow 4KX$
2088 ± 20	650	BAUBILLIER	82	HBC	- 8.25 $K^- p \rightarrow K_S^0 \pi^- p$
2115 ± 46	488	CARMONY	77	HBC	0 9 $K^+ d \rightarrow K^+ \pi^+ s X$

- From a fit to all moments.
- From a fit to 8 moments.
- Number of events evaluated by us.
- From energy-independent partial-wave analysis.

 $K_4^*(2045)$  WIDTH

VALUE (MeV)	EVTS	DOCUMENT ID	TECN	CHG	COMMENT
<b>198 ± 30 OUR AVERAGE</b>		<sup>5</sup> ASTON	86	LASS	0 11 $K^- p \rightarrow K^- \pi^+ n$
221 ± 48 ± 27					
189 ± 35	400	<sup>6,7</sup> CLELAND	82	SPEC	± 50 $K^+ p \rightarrow K_S^0 \pi^\pm p$
• • • We do not use the following data for averages, fits, limits, etc. • • •					
61 ± 58	431	TORRES	86	MPSF	400 $pA \rightarrow 4KX$
170 $^{+100}_{-50}$	650	BAUBILLIER	82	HBC	- 8.25 $K^- p \rightarrow K_S^0 \pi^- p$
240 $^{+500}_{-100}$		<sup>8</sup> ASTON	81c	LASS	0 11 $K^- p \rightarrow K^- \pi^+ n$
300 ± 200		CARMONY	77	HBC	0 9 $K^+ d \rightarrow K^+ \pi^+ s X$

<sup>5</sup> From a fit to all moments.  
<sup>6</sup> From a fit to 8 moments.  
<sup>7</sup> Number of events evaluated by us.  
<sup>8</sup> From energy-independent partial-wave analysis.

 $K_4^*(2045)$  DECAY MODES

Mode	Fraction ( $\Gamma_i/\Gamma$ )
$\Gamma_1$ $K\pi$	(9.9 ± 1.2) %
$\Gamma_2$ $K^*(892)\pi\pi$	(9 ± 5) %
$\Gamma_3$ $K^*(892)\pi\pi\pi$	(7 ± 5) %
$\Gamma_4$ $\rho K\pi$	(5.7 ± 3.2) %
$\Gamma_5$ $\omega K\pi$	(5.0 ± 3.0) %
$\Gamma_6$ $\phi K\pi$	(2.8 ± 1.4) %
$\Gamma_7$ $\phi K^*(892)$	(1.4 ± 0.7) %

 $K_4^*(2045)$  BRANCHING RATIOS

$\Gamma(K\pi)/\Gamma_{\text{total}}$	$\Gamma_1/\Gamma$			
VALUE	DOCUMENT ID	TECN	CHG	COMMENT
<b>0.099 ± 0.012</b>	ASTON	88	LASS	0 11 $K^- p \rightarrow K^- \pi^+ n$

$\Gamma(K^*(892)\pi\pi)/\Gamma(K\pi)$	$\Gamma_2/\Gamma_1$			
VALUE	DOCUMENT ID	TECN	CHG	COMMENT
<b>0.89 ± 0.53</b>	BAUBILLIER	82	HBC	- 8.25 $K^- p \rightarrow p K_S^0 3\pi$

$\Gamma(K^*(892)\pi\pi\pi)/\Gamma(K\pi)$	$\Gamma_3/\Gamma_1$			
VALUE	DOCUMENT ID	TECN	CHG	COMMENT
<b>0.75 ± 0.49</b>	BAUBILLIER	82	HBC	- 8.25 $K^- p \rightarrow p K_S^0 3\pi$

$\Gamma(\rho K\pi)/\Gamma(K\pi)$	$\Gamma_4/\Gamma_1$			
VALUE	DOCUMENT ID	TECN	CHG	COMMENT
<b>0.58 ± 0.32</b>	BAUBILLIER	82	HBC	- 8.25 $K^- p \rightarrow p K_S^0 3\pi$

$\Gamma(\omega K\pi)/\Gamma(K\pi)$	$\Gamma_5/\Gamma_1$			
VALUE	DOCUMENT ID	TECN	CHG	COMMENT
<b>0.50 ± 0.30</b>	BAUBILLIER	82	HBC	- 8.25 $K^- p \rightarrow p K_S^0 3\pi$

$\Gamma(\phi K\pi)/\Gamma_{\text{total}}$	$\Gamma_6/\Gamma$		
VALUE	DOCUMENT ID	TECN	COMMENT
<b>0.028 ± 0.014</b>	<sup>9</sup> TORRES	86	MPSF 400 $pA \rightarrow 4KX$

$\Gamma(\phi K^*(892))/\Gamma_{\text{total}}$	$\Gamma_7/\Gamma$		
VALUE	DOCUMENT ID	TECN	COMMENT
<b>0.014 ± 0.007</b>	<sup>9</sup> TORRES	86	MPSF 400 $pA \rightarrow 4KX$

<sup>9</sup> Error determination is model dependent.

 $K_4^*(2045)$  REFERENCES

ASTON	88	NP B296 493	D. Aston et al.	(SLAC, NAGO, CINC, INUS)
ASTON	86	PL B180 308	D. Aston et al.	(SLAC, NAGO, CINC, INUS)
TORRES	86	PR D34 707	S. Torres et al.	(VPI, ARIZ, FNAL, FSU+)
BAUBILLIER	82	PL 118B 447	M. Baubillier et al.	(BIRM, CERN, GLAS+)
CLELAND	82	NP B208 189	W.E. Cleland et al.	(DURH, GEVA, LAUS+)
ASTON	81c	PL 106B 235	D. Aston et al.	(SLAC, CARL, OTTA) JP
CARMONY	77	PR D16 1251	D.D. Carmony et al.	(PURD, UCD, IUPUI)



See key on page 457

## Meson Particle Listings

 $K_2(2250)$ ,  $K_3(2320)$ ,  $K_5^*(2380)$ ,  $K_4(2500)$  $K_2(2250)$ 

$$I(J^P) = \frac{1}{2}(2^-)$$

OMITTED FROM SUMMARY TABLE

This entry contains various peaks in strange meson systems reported in the 2150–2260 MeV region, as well as enhancements seen in the antihyperon-nucleon system, either in the mass spectra or in the  $J^P = 2^-$  wave.

 $K_2(2250)$  MASS

VALUE (MeV)	EVTS	DOCUMENT ID	TECN	CHG	COMMENT
<b>2247±17 OUR AVERAGE</b>					
2200±40		<sup>1</sup> ARMSTRONG 83c	OMEG	–	18 $K^- p \rightarrow \Lambda \bar{p} X$
2235±50		<sup>1</sup> BAUBILLIER 81	HBC	–	8 $K^- p \rightarrow \Lambda \bar{p} X$
2260±20		<sup>1</sup> CLELAND 81	SPEC	±	50 $K^+ p \rightarrow \Lambda \bar{p} X$
• • • We do not use the following data for averages, fits, limits, etc. • • •					
2280±20		TIKHOMIROV 03	SPEC		40.0 $\pi^- C \rightarrow K_S^0 K_S^0 K_L^0 X$
2147±4	37	CHLIAPNIK... 79	HBC	+	32 $K^+ p \rightarrow \bar{\Lambda} p X$
2240±20	20	LISSAUER 70	HBC		9 $K^+ p$

<sup>1</sup>  $J^P = 2^-$  from moments analysis. $K_2(2250)$  WIDTH

VALUE (MeV)	EVTS	DOCUMENT ID	TECN	CHG	COMMENT
<b>180±30 OUR AVERAGE</b>					
Error includes scale factor of 1.4.					
150±30		<sup>2</sup> ARMSTRONG 83c	OMEG	–	18 $K^- p \rightarrow \Lambda \bar{p} X$
210±30		<sup>2</sup> CLELAND 81	SPEC	±	50 $K^+ p \rightarrow \Lambda \bar{p} X$
• • • We do not use the following data for averages, fits, limits, etc. • • •					
180±60		TIKHOMIROV 03	SPEC		40.0 $\pi^- C \rightarrow K_S^0 K_S^0 K_L^0 X$
~ 200		<sup>2</sup> BAUBILLIER 81	HBC	–	8 $K^- p \rightarrow \Lambda \bar{p} X$
~ 40	37	CHLIAPNIK... 79	HBC	+	32 $K^+ p \rightarrow \bar{\Lambda} p X$
80±20	20	LISSAUER 70	HBC		9 $K^+ p$

<sup>2</sup>  $J^P = 2^-$  from moments analysis. $K_2(2250)$  DECAY MODES

Mode	$\Gamma_i$
$K \pi \pi$	$\Gamma_1$
$K f_2(1270)$	$\Gamma_2$
$K^*(892) f_0(980)$	$\Gamma_3$
$\rho \bar{\Lambda}$	$\Gamma_4$

 $K_2(2250)$  REFERENCES

TIKHOMIROV 03	PAN 66 828	G.D. Tikhomirov et al.
ARMSTRONG 83c	Translated from YAF 66 850.	
ARMSTRONG 83c	NP B227 365	T.A. Armstrong et al.
BAUBILLIER 81	NP B183 1	M. Baubillier et al.
CLELAND 81	NP B184 1	W.E. Cleland et al.
CHLIAPNIK... 79	NP B158 253	P.V. Chliapnikov et al.
LISSAUER 70	NP B18 491	D. Lissauer et al.

 $K_3(2320)$ 

$$I(J^P) = \frac{1}{2}(3^+)$$

OMITTED FROM SUMMARY TABLE

Seen in the  $J^P = 3^+$  wave of the antihyperon-nucleon system. Needs confirmation.

 $K_3(2320)$  MASS

VALUE (MeV)	DOCUMENT ID	TECN	CHG	COMMENT
<b>2324±24 OUR AVERAGE</b>				
2330±40	<sup>1</sup> ARMSTRONG 83c	OMEG	–	18 $K^- p \rightarrow \Lambda \bar{p} X$
2320±30	<sup>1</sup> CLELAND 81	SPEC	±	50 $K^+ p \rightarrow \Lambda \bar{p} X$

<sup>1</sup>  $J^P = 3^+$  from moments analysis. $K_3(2320)$  WIDTH

VALUE (MeV)	DOCUMENT ID	TECN	CHG	COMMENT
<b>150±30</b>				
• • • We do not use the following data for averages, fits, limits, etc. • • •				
~ 250	<sup>2</sup> CLELAND 81	SPEC	±	50 $K^+ p \rightarrow \Lambda \bar{p} X$

<sup>2</sup>  $J^P = 3^+$  from moments analysis. $K_3(2320)$  DECAY MODES

Mode	$\Gamma_i$
$\rho \bar{\Lambda}$	$\Gamma_1$

 $K_3(2320)$  REFERENCES

ARMSTRONG 83c	NP B227 365	T.A. Armstrong et al.	(BARI, BIRM, CERN+)
CLELAND 81	NP B184 1	W.E. Cleland et al.	(PITT, GEVA, LAUS+)

 $K_5^*(2380)$ 

$$I(J^P) = \frac{1}{2}(5^-)$$

OMITTED FROM SUMMARY TABLE

Needs confirmation.

 $K_5^*(2380)$  MASS

VALUE (MeV)	DOCUMENT ID	TECN	CHG	COMMENT
<b>2382±14±19</b>				
	<sup>1</sup> ASTON	86	LASS	0

<sup>1</sup> From a fit to all the moments. $K_5^*(2380)$  WIDTH

VALUE (MeV)	DOCUMENT ID	TECN	CHG	COMMENT
<b>178±37±32</b>				
	<sup>2</sup> ASTON	86	LASS	0

<sup>2</sup> From a fit to all the moments. $K_5^*(2380)$  DECAY MODES

Mode	Fraction ( $\Gamma_i/\Gamma$ )
$K \pi$	$\Gamma_1$
	(6.1±1.2) %

 $K_5^*(2380)$  BRANCHING RATIOS

$\Gamma(K \pi)/\Gamma_{total}$	$\Gamma_1/\Gamma$
<b>0.061±0.012</b>	
	ASTON 88 LASS 0
	11 $K^- p \rightarrow K^- \pi^+ n$

 $K_5^*(2380)$  REFERENCES

ASTON 88	NP B296 493	D. Aston et al.	(SLAC, NAGO, CIN, INUS)
ASTON 86	PL B180 308	D. Aston et al.	(SLAC, NAGO, CIN, INUS)

 $K_4(2500)$ 

$$I(J^P) = \frac{1}{2}(4^-)$$

OMITTED FROM SUMMARY TABLE

Needs confirmation.

 $K_4(2500)$  MASS

VALUE (MeV)	DOCUMENT ID	TECN	CHG	COMMENT
<b>2490±20</b>				
	<sup>1</sup> CLELAND 81	SPEC	±	50 $K^+ p \rightarrow \Lambda \bar{p}$

<sup>1</sup>  $J^P = 4^-$  from moments analysis. $K_4(2500)$  WIDTH

VALUE (MeV)	DOCUMENT ID	TECN	CHG	COMMENT
• • • We do not use the following data for averages, fits, limits, etc. • • •				
~ 250	<sup>2</sup> CLELAND 81	SPEC	±	50 $K^+ p \rightarrow \Lambda \bar{p}$

<sup>2</sup>  $J^P = 4^-$  from moments analysis. $K_4(2500)$  DECAY MODES

Mode	$\Gamma_i$
$\rho \bar{\Lambda}$	$\Gamma_1$

 $K_4(2500)$  REFERENCES

CLELAND 81	NP B184 1	W.E. Cleland et al.	(PITT, GEVA, LAUS+)
------------	-----------	---------------------	---------------------

## Meson Particle Listings

## K(3100)

**K(3100)**

$$J^{PC} = ?^{?}(???)$$

OMITTED FROM SUMMARY TABLE

Narrow peak observed in several ( $\Lambda\bar{p}$  + pions) and ( $\bar{\Lambda}p$  + pions) states in  $\Sigma^-$  Be reactions by BOURQUIN 86 and in  $np$  and  $nA$  reactions by ALEEV 93. Not seen by BOEHNLEIN 91. If due to strong decays, this state has exotic quantum numbers ( $B=0, Q=+1, S=-1$  for  $\Lambda\bar{p}\pi^+\pi^+$  and  $I \geq 3/2$  for  $\Lambda\bar{p}\pi^-$ ). Needs confirmation.

**K(3100) MASS**

VALUE (MeV)

DOCUMENT ID

 $\approx 3100$  OUR ESTIMATE**3-BODY DECAYS**

VALUE (MeV)

DOCUMENT ID

TECN

COMMENT

**3054 ± 11 OUR AVERAGE**

3060 ± 7 ± 20

<sup>1</sup> ALEEV 93 BIS2 K(3100) →  $\Lambda\bar{p}\pi^+$ 

3056 ± 7 ± 20

<sup>1</sup> ALEEV 93 BIS2 K(3100) →  $\bar{\Lambda}p\pi^-$ 

3055 ± 8 ± 20

<sup>1</sup> ALEEV 93 BIS2 K(3100) →  $\Lambda\bar{p}\pi^-$ 

3045 ± 8 ± 20

<sup>1</sup> ALEEV 93 BIS2 K(3100) →  $\bar{\Lambda}p\pi^+$ **4-BODY DECAYS**

VALUE (MeV)

DOCUMENT ID

TECN

COMMENT

**3059 ± 11 OUR AVERAGE**

3067 ± 6 ± 20

<sup>1</sup> ALEEV 93 BIS2 K(3100) →  $\Lambda\bar{p}\pi^+\pi^+$ 

3060 ± 8 ± 20

<sup>1</sup> ALEEV 93 BIS2 K(3100) →  $\Lambda\bar{p}\pi^+\pi^-$ 

3055 ± 7 ± 20

<sup>1</sup> ALEEV 93 BIS2 K(3100) →  $\bar{\Lambda}p\pi^-\pi^-$ 

3052 ± 8 ± 20

<sup>1</sup> ALEEV 93 BIS2 K(3100) →  $\bar{\Lambda}p\pi^-\pi^+$ 

• • • We do not use the following data for averages, fits, limits, etc. • • •

3105 ± 30

BOURQUIN 86 SPEC K(3100) →  $\Lambda\bar{p}\pi^+\pi^+$ 

3115 ± 30

BOURQUIN 86 SPEC K(3100) →  $\Lambda\bar{p}\pi^+\pi^-$ **5-BODY DECAYS**

VALUE (MeV)

DOCUMENT ID

TECN

COMMENT

• • • We do not use the following data for averages, fits, limits, etc. • • •

3095 ± 30

BOURQUIN 86 SPEC K(3100) →  $\Lambda\bar{p}\pi^+\pi^+\pi^-$ <sup>1</sup> Supersedes ALEEV 90.**K(3100) WIDTH****3-BODY DECAYS**

VALUE (MeV)

DOCUMENT ID

TECN

COMMENT

• • • We do not use the following data for averages, fits, limits, etc. • • •

42 ± 16

<sup>2</sup> ALEEV 93 BIS2 K(3100) →  $\Lambda\bar{p}\pi^+$ 

36 ± 15

<sup>2</sup> ALEEV 93 BIS2 K(3100) →  $\bar{\Lambda}p\pi^-$ 

50 ± 18

<sup>2</sup> ALEEV 93 BIS2 K(3100) →  $\Lambda\bar{p}\pi^-$ 

30 ± 15

<sup>2</sup> ALEEV 93 BIS2 K(3100) →  $\bar{\Lambda}p\pi^+$ **4-BODY DECAYS**

VALUE (MeV)

CL%

DOCUMENT ID

TECN

COMMENT

• • • We do not use the following data for averages, fits, limits, etc. • • •

22 ± 8

<sup>2</sup> ALEEV 93 BIS2 K(3100) →  $\Lambda\bar{p}\pi^+\pi^+$ 

28 ± 12

<sup>2</sup> ALEEV 93 BIS2 K(3100) →  $\Lambda\bar{p}\pi^+\pi^-$ 

32 ± 15

<sup>2</sup> ALEEV 93 BIS2 K(3100) →  $\bar{\Lambda}p\pi^-\pi^-$ 

30 ± 15

<sup>2</sup> ALEEV 93 BIS2 K(3100) →  $\bar{\Lambda}p\pi^-\pi^+$ 

&lt; 30

90 BOURQUIN 86 SPEC K(3100) →  $\Lambda\bar{p}\pi^+\pi^+$ 

&lt; 80

90 BOURQUIN 86 SPEC K(3100) →  $\Lambda\bar{p}\pi^+\pi^-$ **5-BODY DECAYS**

VALUE (MeV)

CL%

DOCUMENT ID

TECN

COMMENT

• • • We do not use the following data for averages, fits, limits, etc. • • •

&lt; 30

90 BOURQUIN 86 SPEC K(3100) →  $\Lambda\bar{p}\pi^+\pi^+\pi^-$ <sup>2</sup> Supersedes ALEEV 90.**K(3100) DECAY MODES**

Mode

 $\Gamma_1$  K(3100)<sup>0</sup> →  $\Lambda\bar{p}\pi^+$  $\Gamma_2$  K(3100)<sup>--</sup> →  $\Lambda\bar{p}\pi^-$  $\Gamma_3$  K(3100)<sup>-</sup> →  $\Lambda\bar{p}\pi^+\pi^-$  $\Gamma_4$  K(3100)<sup>+</sup> →  $\Lambda\bar{p}\pi^+\pi^+$  $\Gamma_5$  K(3100)<sup>0</sup> →  $\Lambda\bar{p}\pi^+\pi^+\pi^-$  $\Gamma_6$  K(3100)<sup>0</sup> →  $\Sigma(1385)^+\bar{p}$  **$\Gamma(\Sigma(1385)^+\bar{p})/\Gamma(\Lambda\bar{p}\pi^+)$**  **$\Gamma_6/\Gamma_1$** 

VALUE

CL%

DOCUMENT ID

TECN

COMMENT

&lt; 0.04

90

ALEEV 93 BIS2 K(3100)<sup>0</sup> →  $\Sigma(1385)^+\bar{p}$ **K(3100) REFERENCES**

ALEEV	93	PAN 56 1358	A.N. Aleev <i>et al.</i>	(BIS-2 Collab.)
		Translated from YAF 56 100.		
BOEHNLEIN	91	NPBPS B21 174	A. Boehnlein <i>et al.</i>	(FLOR, BNL, IND+)
ALEEV	90	ZPHY C47 533	A.N. Aleev <i>et al.</i>	(BIS-2 Collab.)
BOURQUIN	86	PL B172 113	M.H. Bourquin <i>et al.</i>	(GEVA, RAL, HEIDP+)

# CHARMED MESONS

## ( $C = \pm 1$ )

$D^+ = c\bar{d}, D^0 = c\bar{u}, \bar{D}^0 = \bar{c}u, D^- = \bar{c}d,$  similarly for  $D^{*s}$

$D^\pm$

$$I(J^P) = \frac{1}{2}(0^-)$$

### $D^\pm$ MASS

The fit includes  $D^\pm, D^0, D_s^\pm, D^{*s}, D^{*0}, D_1(2420)^0, D_2^*(2460)^0,$  and  $D_{s1}(2536)^\pm$  mass and mass difference measurements.

VALUE (MeV)	EVTS	DOCUMENT ID	TECN	COMMENT
<b>1869.62 ± 0.15 OUR FIT</b>	Error includes scale factor of 1.1.			
<b>1869.5 ± 0.4 OUR AVERAGE</b>				
1869.53 ± 0.49 ± 0.20	110 ± 15	ANASHIN	10A	KEDR $e^+e^-$ at $\psi(3770)$
1870.0 ± 0.5 ± 1.0	317	BARLAG	90c	ACCM $\pi^-$ Cu 230 GeV
1869.4 ± 0.6		<sup>1</sup> TRILLING	81	RVUE $e^+e^-$ 3.77 GeV
••• We do not use the following data for averages, fits, limits, etc. •••				
1875 ± 10	9	ADAMOVIICH	87	EMUL Photoproduction
1860 ± 16	6	ADAMOVIICH	84	EMUL Photoproduction
1863 ± 4		DERRICK	84	HRS $e^+e^-$ 29 GeV
1868.4 ± 0.5		<sup>1</sup> SCHINDLER	81	MRK2 $e^+e^-$ 3.77 GeV
1874 ± 5		GOLDHABER	77	MRK1 $D^0, D^+$ recoil spectra
1868.3 ± 0.9		<sup>1</sup> PERUZZI	77	LGW $e^+e^-$ 3.77 GeV
1874 ± 11		PICCOLO	77	MRK1 $e^+e^-$ 4.03, 4.41 GeV
1876 ± 15	50	PERUZZI	76	MRK1 $K^\mp \pi^\pm \pi^\pm$

<sup>1</sup>PERUZZI 77 and SCHINDLER 81 errors do not include the 0.13% uncertainty in the absolute SPEAR energy calibration. TRILLING 81 uses the high precision  $J/\psi(1S)$  and  $\psi(2S)$  measurements of ZHOLENTZ 80 to determine this uncertainty and combines the PERUZZI 77 and SCHINDLER 81 results to obtain the value quoted.

### $D^\pm$ MEAN LIFE

Measurements with an error  $> 100 \times 10^{-15}$  s have been omitted from the Listings.

VALUE ( $10^{-15}$ s)	EVTS	DOCUMENT ID	TECN	COMMENT
<b>1040 ± 7 OUR AVERAGE</b>				
1039.4 ± 4.3 ± 7.0	110k	LINK	02F	FOCS $\gamma$ nucleus, $\approx 180$ GeV
1033.6 ± 22.1 ± 9.9 ± 12.7	3777	BONVICINI	99	CLEO $e^+e^- \approx \Upsilon(4S)$
1048 ± 15 ± 11	9k	FRABETTI	94d	E687 $D^+ \rightarrow K^- \pi^+ \pi^+$
••• We do not use the following data for averages, fits, limits, etc. •••				
1075 ± 40 ± 18	2455	FRABETTI	91	E687 $\gamma$ Be, $D^+ \rightarrow K^- \pi^+ \pi^+$
1030 ± 80 ± 60	200	ALVAREZ	90	NA14 $\gamma, D^+ \rightarrow K^- \pi^+ \pi^+$
1050 ± 77 ± 72	317	<sup>2</sup> BARLAG	90c	ACCM $\pi^-$ Cu 230 GeV
1050 ± 80 ± 70	363	ALBRECHT	88i	ARG $e^+e^-$ 10 GeV
1090 ± 30 ± 25	2992	RAAB	88	E691 Photoproduction

<sup>2</sup>BARLAG 90c estimates the systematic error to be negligible.

### $D^+$ DECAY MODES

Most decay modes (other than the semileptonic modes) that involve a neutral  $K$  meson are now given as  $K_S^0$  modes, not as  $\bar{K}^0$  modes. Nearly always it is a  $K_S^0$  that is measured, and interference between Cabibbo-allowed and doubly Cabibbo-suppressed modes can invalidate the assumption that  $2\Gamma(K_S^0) = \Gamma(\bar{K}^0)$ .

Mode	Fraction ( $\Gamma_i/\Gamma$ )	Scale factor/ Confidence level
<b>Inclusive modes</b>		
$\Gamma_1$ $D^+ \rightarrow e^+$ semileptonic	(16.07 ± 0.30) %	
$\Gamma_2$ $D^+ \rightarrow \mu^+$ anything	(17.6 ± 3.2) %	
$\Gamma_3$ $D^+ \rightarrow K^-$ anything	(25.7 ± 1.4) %	
$\Gamma_4$ $D^+ \rightarrow \bar{K}^0$ anything + $K^0$ anything	(61 ± 5) %	
$\Gamma_5$ $D^+ \rightarrow K^+$ anything	( 5.9 ± 0.8) %	
$\Gamma_6$ $D^+ \rightarrow K^*(892)^-$ anything	( 6 ± 5) %	
$\Gamma_7$ $D^+ \rightarrow \bar{K}^*(892)^0$ anything	(23 ± 5) %	
$\Gamma_8$ $D^+ \rightarrow K^*(892)^0$ anything	< 6.6 %	CL=90%
$\Gamma_9$ $D^+ \rightarrow \eta$ anything	( 6.3 ± 0.7) %	
$\Gamma_{10}$ $D^+ \rightarrow \eta'$ anything	( 1.04 ± 0.18) %	
$\Gamma_{11}$ $D^+ \rightarrow \phi$ anything	( 1.03 ± 0.12) %	

### Leptonic and semileptonic modes

$\Gamma_{12}$ $D^+ \rightarrow e^+ \nu_e$	< 8.8	$\times 10^{-6}$	CL=90%
$\Gamma_{13}$ $D^+ \rightarrow \mu^+ \nu_\mu$	( 3.82 ± 0.33)	$\times 10^{-4}$	
$\Gamma_{14}$ $D^+ \rightarrow \tau^+ \nu_\tau$	< 1.2	$\times 10^{-3}$	CL=90%
$\Gamma_{15}$ $D^+ \rightarrow \bar{K}^0 e^+ \nu_e$	( 8.83 ± 0.22) %		
$\Gamma_{16}$ $D^+ \rightarrow \bar{K}^0 \mu^+ \nu_\mu$	( 9.2 ± 0.6) %		
$\Gamma_{17}$ $D^+ \rightarrow K^- \pi^+ e^+ \nu_e$	( 4.00 ± 0.10) %		
$\Gamma_{18}$ $D^+ \rightarrow \bar{K}^*(892)^0 e^+ \nu_e,$ $\bar{K}^*(892)^0 \rightarrow K^- \pi^+$	( 3.68 ± 0.10) %		
$\Gamma_{19}$ $D^+ \rightarrow (K^- \pi^+)_{S\text{-wave}} e^+ \nu_e$	( 2.32 ± 0.10)	$\times 10^{-3}$	
$\Gamma_{20}$ $D^+ \rightarrow \bar{K}^*(1410)^0 e^+ \nu_e,$ $\bar{K}^*(1410)^0 \rightarrow K^- \pi^+$	< 6	$\times 10^{-3}$	CL=90%
$\Gamma_{21}$ $D^+ \rightarrow K_2^*(1430)^0 e^+ \nu_e,$ $K_2^*(1430)^0 \rightarrow K^- \pi^+$	< 5	$\times 10^{-4}$	CL=90%
$\Gamma_{22}$ $D^+ \rightarrow K^- \pi^+ e^+ \nu_e$ nonresonant	< 7	$\times 10^{-3}$	CL=90%
$\Gamma_{23}$ $D^+ \rightarrow K^- \pi^+ \mu^+ \nu_\mu$	( 3.8 ± 0.4) %		
$\Gamma_{24}$ $D^+ \rightarrow \bar{K}^*(892)^0 \mu^+ \nu_\mu,$ $\bar{K}^*(892)^0 \rightarrow K^- \pi^+$	( 3.52 ± 0.10) %		
$\Gamma_{25}$ $D^+ \rightarrow K^- \pi^+ \mu^+ \nu_\mu$ nonresonant	( 2.0 ± 0.5)	$\times 10^{-3}$	
$\Gamma_{26}$ $D^+ \rightarrow K^- \pi^+ \pi^0 \mu^+ \nu_\mu$	< 1.6	$\times 10^{-3}$	CL=90%
$\Gamma_{27}$ $D^+ \rightarrow \pi^0 e^+ \nu_e$	( 4.05 ± 0.18)	$\times 10^{-3}$	
$\Gamma_{28}$ $D^+ \rightarrow \eta e^+ \nu_e$	( 1.14 ± 0.10)	$\times 10^{-3}$	
$\Gamma_{29}$ $D^+ \rightarrow \rho^0 e^+ \nu_e$	( 2.2 ± 0.4)	$\times 10^{-3}$	
$\Gamma_{30}$ $D^+ \rightarrow \rho^0 \mu^+ \nu_\mu$	( 2.4 ± 0.4)	$\times 10^{-3}$	
$\Gamma_{31}$ $D^+ \rightarrow \omega e^+ \nu_e$	( 1.6 $^{+0.7}_{-0.6}$ )	$\times 10^{-3}$	
$\Gamma_{32}$ $D^+ \rightarrow \eta'(958) e^+ \nu_e$	( 2.2 ± 0.5)	$\times 10^{-4}$	
$\Gamma_{33}$ $D^+ \rightarrow \phi e^+ \nu_e$	< 9	$\times 10^{-5}$	CL=90%

Fractions of some of the following modes with resonances have already appeared above as submodes of particular charged-particle modes.

$\Gamma_{34}$ $D^+ \rightarrow \bar{K}^*(892)^0 e^+ \nu_e$	( 5.52 ± 0.15) %	
$\Gamma_{35}$ $D^+ \rightarrow \bar{K}^*(892)^0 \mu^+ \nu_\mu$	( 5.28 ± 0.15) %	
$\Gamma_{36}$ $D^+ \rightarrow \bar{K}_0^*(1430)^0 \mu^+ \nu_\mu$	< 2.4	$\times 10^{-4}$
$\Gamma_{37}$ $D^+ \rightarrow \bar{K}^*(1680)^0 \mu^+ \nu_\mu$	< 1.5	$\times 10^{-3}$

### Hadronic modes with a $\bar{K}$ or $\bar{K}K\bar{K}$

$\Gamma_{38}$ $D^+ \rightarrow K_S^0 \pi^+$	( 1.47 ± 0.07) %	S=2.0
$\Gamma_{39}$ $D^+ \rightarrow K_L^0 \pi^+$	( 1.46 ± 0.05) %	
$\Gamma_{40}$ $D^+ \rightarrow K^- 2\pi^+$	[a] ( 9.13 ± 0.19) %	
$\Gamma_{41}$ $D^+ \rightarrow (K^- \pi^+)_{S\text{-wave}} \pi^+$	( 7.32 ± 0.19) %	
$\Gamma_{42}$ $D^+ \rightarrow \bar{K}_0^*(800)^0 \pi^+,$ $\bar{K}_0^*(800)^0 \rightarrow K^- \pi^+$	[b] ( 1.21 ± 0.06) %	
$\Gamma_{43}$ $D^+ \rightarrow \bar{K}_0^*(1430)^0 \pi^+,$ $\bar{K}_0^*(1430)^0 \rightarrow K^- \pi^+$	( 1.01 ± 0.11) %	
$\Gamma_{44}$ $D^+ \rightarrow \bar{K}^*(892)^0 \pi^+,$ $\bar{K}^*(892)^0 \rightarrow K^- \pi^+$	not seen	
$\Gamma_{45}$ $D^+ \rightarrow \bar{K}^*(1410)^0 \pi^+,$ $\bar{K}^*(1410)^0 \rightarrow K^- \pi^+$	[b] ( 2.2 ± 0.7)	$\times 10^{-4}$
$\Gamma_{46}$ $D^+ \rightarrow \bar{K}_2^*(1430)^0 \pi^+,$ $\bar{K}_2^*(1430)^0 \rightarrow K^- \pi^+$	[b] ( 2.1 ± 1.1)	$\times 10^{-4}$
$\Gamma_{47}$ $D^+ \rightarrow \bar{K}^*(1680)^0 \pi^+,$ $\bar{K}^*(1680)^0 \rightarrow K^- \pi^+$	( 1.41 ± 0.26) %	
$\Gamma_{48}$ $D^+ \rightarrow K^- (2\pi^+)_{I=2}$	( 6.99 ± 0.27) %	
$\Gamma_{49}$ $D^+ \rightarrow K^- 2\pi^+$ nonresonant	( 4.8 ± 1.0) %	
$\Gamma_{50}$ $D^+ \rightarrow K_S^0 \pi^+ \pi^0$	( 1.3 ± 0.6) %	
$\Gamma_{51}$ $D^+ \rightarrow K_S^0 \rho^+$	( 9 ± 7)	$\times 10^{-3}$
$\Gamma_{52}$ $D^+ \rightarrow \bar{K}^*(892)^0 \pi^+,$ $\bar{K}^*(892)^0 \rightarrow K_S^0 \pi^0$	[c] ( 5.99 ± 0.18) %	
$\Gamma_{53}$ $D^+ \rightarrow K_S^0 \pi^+ \pi^0$ nonresonant	[c] ( 3.12 ± 0.11) %	
$\Gamma_{54}$ $D^+ \rightarrow K^- 2\pi^+ \pi^0$	[a] ( 5.6 ± 0.5)	$\times 10^{-3}$
$\Gamma_{55}$ $D^+ \rightarrow K_S^0 2\pi^+ \pi^-$	[a] ( 1.2 ± 0.4)	$\times 10^{-3}$
$\Gamma_{56}$ $D^+ \rightarrow K^- 3\pi^+ \pi^-$	( 2.2 ± 0.4)	$\times 10^{-3}$
$\Gamma_{57}$ $D^+ \rightarrow \bar{K}^*(892)^0 2\pi^+ \pi^-,$ $\bar{K}^*(892)^0 \rightarrow K^- \pi^+$	( 2.2 ± 0.4)	$\times 10^{-3}$
$\Gamma_{58}$ $D^+ \rightarrow \bar{K}^*(892)^0 \rho^0 \pi^+,$ $\bar{K}^*(892)^0 \rightarrow K^- \pi^+$	[d] ( 9.0 ± 1.8)	$\times 10^{-3}$
$\Gamma_{59}$ $D^+ \rightarrow \bar{K}^*(892)^0 a_1(1260)^+$		
$\Gamma_{60}$ $D^+ \rightarrow \bar{K}^*(892)^0 2\pi^+ \pi^- \text{ no-}\rho,$ $\bar{K}^*(892)^0 \rightarrow K^- \pi^+$		

## Meson Particle Listings

 $D^\pm$ 

$\Gamma_{61}$	$D^+ \rightarrow K^- \rho^0 2\pi^+$	$(1.68 \pm 0.27) \times 10^{-3}$	
$\Gamma_{62}$	$D^+ \rightarrow K^- 3\pi^+ \pi^-$ nonresonant	$(3.9 \pm 2.9) \times 10^{-4}$	
$\Gamma_{63}$	$D^+ \rightarrow K^+ 2K_S^0$	$(4.5 \pm 2.0) \times 10^{-3}$	
$\Gamma_{64}$	$D^+ \rightarrow K^+ K^- K_S^0 \pi^+$	$(2.4 \pm 0.6) \times 10^{-4}$	
<b>Pionic modes</b>			
$\Gamma_{65}$	$D^+ \rightarrow \pi^+ \pi^0$	$(1.19 \pm 0.06) \times 10^{-3}$	
$\Gamma_{66}$	$D^+ \rightarrow 2\pi^+ \pi^-$	$(3.18 \pm 0.18) \times 10^{-3}$	
$\Gamma_{67}$	$D^+ \rightarrow \rho^0 \pi^+$	$(8.1 \pm 1.5) \times 10^{-4}$	
$\Gamma_{68}$	$D^+ \rightarrow \pi^+ (\pi^+ \pi^-)_{S\text{-wave}}$	$(1.78 \pm 0.16) \times 10^{-3}$	
$\Gamma_{69}$	$D^+ \rightarrow \sigma \pi^+, \sigma \rightarrow \pi^+ \pi^-$	$(1.34 \pm 0.12) \times 10^{-3}$	
$\Gamma_{70}$	$D^+ \rightarrow f_0(980) \pi^+, f_0(980) \rightarrow \pi^+ \pi^-$	$(1.52 \pm 0.33) \times 10^{-4}$	
$\Gamma_{71}$	$D^+ \rightarrow f_0(1370) \pi^+, f_0(1370) \rightarrow \pi^+ \pi^-$	$(8 \pm 4) \times 10^{-5}$	
$\Gamma_{72}$	$D^+ \rightarrow f_2(1270) \pi^+, f_2(1270) \rightarrow \pi^+ \pi^-$	$(4.9 \pm 0.9) \times 10^{-4}$	
$\Gamma_{73}$	$D^+ \rightarrow \rho(1450)^0 \pi^+, \rho(1450)^0 \rightarrow \pi^+ \pi^-$	$< 8 \times 10^{-5}$	CL=95%
$\Gamma_{74}$	$D^+ \rightarrow f_0(1500) \pi^+, f_0(1500) \rightarrow \pi^+ \pi^-$	$(1.1 \pm 0.4) \times 10^{-4}$	
$\Gamma_{75}$	$D^+ \rightarrow f_0(1710) \pi^+, f_0(1710) \rightarrow \pi^+ \pi^-$	$< 5 \times 10^{-5}$	CL=95%
$\Gamma_{76}$	$D^+ \rightarrow f_0(1790) \pi^+, f_0(1790) \rightarrow \pi^+ \pi^-$	$< 6 \times 10^{-5}$	CL=95%
$\Gamma_{77}$	$D^+ \rightarrow (\pi^+ \pi^+)_{S\text{-wave}} \pi^-$	$< 1.2 \times 10^{-4}$	CL=95%
$\Gamma_{78}$	$D^+ \rightarrow 2\pi^+ \pi^-$ nonresonant	$< 1.1 \times 10^{-4}$	CL=95%
$\Gamma_{79}$	$D^+ \rightarrow \pi^+ 2\pi^0$	$(4.6 \pm 0.4) \times 10^{-3}$	
$\Gamma_{80}$	$D^+ \rightarrow 2\pi^+ \pi^- \pi^0$	$(1.13 \pm 0.08) \%$	
$\Gamma_{81}$	$D^+ \rightarrow \eta \pi^+, \eta \rightarrow \pi^+ \pi^- \pi^0$	$(8.0 \pm 0.5) \times 10^{-4}$	
$\Gamma_{82}$	$D^+ \rightarrow \omega \pi^+, \omega \rightarrow \pi^+ \pi^- \pi^0$	$< 3 \times 10^{-4}$	CL=90%
$\Gamma_{83}$	$D^+ \rightarrow 3\pi^+ 2\pi^-$	$(1.61 \pm 0.16) \times 10^{-3}$	

Fractions of some of the following modes with resonances have already appeared above as submodes of particular charged-particle modes.

$\Gamma_{84}$	$D^+ \rightarrow \eta \pi^+$	$(3.53 \pm 0.21) \times 10^{-3}$	
$\Gamma_{85}$	$D^+ \rightarrow \eta \pi^+ \pi^0$	$(1.38 \pm 0.35) \times 10^{-3}$	
$\Gamma_{86}$	$D^+ \rightarrow \omega \pi^+$	$< 3.4 \times 10^{-4}$	CL=90%
$\Gamma_{87}$	$D^+ \rightarrow \eta'(958) \pi^+$	$(4.67 \pm 0.29) \times 10^{-3}$	
$\Gamma_{88}$	$D^+ \rightarrow \eta'(958) \pi^+ \pi^0$	$(1.6 \pm 0.5) \times 10^{-3}$	

**Hadronic modes with a  $K\bar{K}$  pair**

$\Gamma_{89}$	$D^+ \rightarrow K^+ K_S^0$	$(2.83 \pm 0.16) \times 10^{-3}$	S=2.2
$\Gamma_{90}$	$D^+ \rightarrow K^+ K^- \pi^+$	[a] $(9.54 \pm 0.26) \times 10^{-3}$	S=1.1
$\Gamma_{91}$	$D^+ \rightarrow \phi \pi^+, \phi \rightarrow K^+ K^-$	$(2.65^{+0.08}_{-0.09}) \times 10^{-3}$	
$\Gamma_{92}$	$D^+ \rightarrow K^+ \bar{K}^*(892)^0, \bar{K}^*(892)^0 \rightarrow K^- \pi^+$	$(2.45^{+0.09}_{-0.14}) \times 10^{-3}$	
$\Gamma_{93}$	$D^+ \rightarrow K^+ \bar{K}_0^*(1430)^0, \bar{K}_0^*(1430)^0 \rightarrow K^- \pi^+$	$(1.79 \pm 0.34) \times 10^{-3}$	
$\Gamma_{94}$	$D^+ \rightarrow K^+ \bar{K}_2^*(1430)^0, \bar{K}_2^* \rightarrow K^- \pi^+$	$(1.6^{+1.2}_{-0.8}) \times 10^{-4}$	
$\Gamma_{95}$	$D^+ \rightarrow K^+ \bar{K}_0^*(800), \bar{K}_0^* \rightarrow K^- \pi^+$	$(6.7^{+3.4}_{-2.1}) \times 10^{-4}$	
$\Gamma_{96}$	$D^+ \rightarrow a_0(1450)^0 \pi^+, a_0^0 \rightarrow K^+ K^-$	$(4.4^{+7.0}_{-1.8}) \times 10^{-4}$	
$\Gamma_{97}$	$D^+ \rightarrow \phi(1680) \pi^+, \phi \rightarrow K^+ K^-$	$(4.9^{+4.0}_{-1.9}) \times 10^{-5}$	
$\Gamma_{98}$	$D^+ \rightarrow K^+ K^- \pi^+$ nonresonant	not seen	
$\Gamma_{99}$	$D^+ \rightarrow K^+ K_S^0 \pi^+ \pi^-$	$(1.75 \pm 0.18) \times 10^{-3}$	
$\Gamma_{100}$	$D^+ \rightarrow K_S^0 K^- 2\pi^+$	$(2.40 \pm 0.18) \times 10^{-3}$	
$\Gamma_{101}$	$D^+ \rightarrow K^+ K^- 2\pi^+ \pi^-$	$(2.2 \pm 1.2) \times 10^{-4}$	

A few poorly measured branching fractions:

$\Gamma_{102}$	$D^+ \rightarrow \phi \pi^+ \pi^0$	$(2.3 \pm 1.0) \%$	
$\Gamma_{103}$	$D^+ \rightarrow \phi \rho^+$	$< 1.5 \%$	CL=90%
$\Gamma_{104}$	$D^+ \rightarrow K^+ K^- \pi^+ \pi^0$ non- $\phi$	$(1.5^{+0.7}_{-0.6}) \%$	
$\Gamma_{105}$	$D^+ \rightarrow K^*(892)^+ K_S^0$	$(1.6 \pm 0.7) \%$	

**Doubly Cabibbo-suppressed modes**

$\Gamma_{106}$	$D^+ \rightarrow K^+ \pi^0$	$(1.83 \pm 0.26) \times 10^{-4}$	S=1.4
$\Gamma_{107}$	$D^+ \rightarrow K^+ \eta$	$(1.08 \pm 0.17) \times 10^{-4}$	
$\Gamma_{108}$	$D^+ \rightarrow K^+ \eta'(958)$	$(1.76 \pm 0.22) \times 10^{-4}$	
$\Gamma_{109}$	$D^+ \rightarrow K^+ \pi^+ \pi^-$	$(5.27 \pm 0.23) \times 10^{-4}$	
$\Gamma_{110}$	$D^+ \rightarrow K^+ \rho^0$	$(2.0 \pm 0.5) \times 10^{-4}$	
$\Gamma_{111}$	$D^+ \rightarrow K^*(892)^0 \pi^+, K^*(892)^0 \rightarrow K^+ \pi^-$	$(2.5 \pm 0.4) \times 10^{-4}$	
$\Gamma_{112}$	$D^+ \rightarrow K^+ f_0(980), f_0(980) \rightarrow \pi^+ \pi^-$	$(4.7 \pm 2.8) \times 10^{-5}$	
$\Gamma_{113}$	$D^+ \rightarrow K_2^*(1430)^0 \pi^+, K_2^*(1430)^0 \rightarrow K^+ \pi^-$	$(4.2 \pm 2.9) \times 10^{-5}$	
$\Gamma_{114}$	$D^+ \rightarrow K^+ \pi^+ \pi^-$ nonresonant	not seen	
$\Gamma_{115}$	$D^+ \rightarrow 2K^+ K^-$	$(8.7 \pm 2.0) \times 10^{-5}$	

 **$\Delta C = 1$  weak neutral current (CI) modes, or Lepton Family number (LF) or Lepton number (L) violating modes**

$\Gamma_{116}$	$D^+ \rightarrow \pi^+ e^+ e^-$	CI	$< 1.1 \times 10^{-6}$	CL=90%
$\Gamma_{117}$	$D^+ \rightarrow \pi^+ \phi, \phi \rightarrow e^+ e^-$	[e]	$(1.7^{+1.4}_{-0.9}) \times 10^{-6}$	
$\Gamma_{118}$	$D^+ \rightarrow \pi^+ \mu^+ \mu^-$	CI	$< 3.9 \times 10^{-6}$	CL=90%
$\Gamma_{119}$	$D^+ \rightarrow \pi^+ \phi, \phi \rightarrow \mu^+ \mu^-$	[e]	$(1.8 \pm 0.8) \times 10^{-6}$	
$\Gamma_{120}$	$D^+ \rightarrow \rho^+ \mu^+ \mu^-$	CI	$< 5.6 \times 10^{-4}$	CL=90%
$\Gamma_{121}$	$D^+ \rightarrow K^+ e^+ e^-$	[f]	$< 1.0 \times 10^{-6}$	CL=90%
$\Gamma_{122}$	$D^+ \rightarrow K^+ \mu^+ \mu^-$	[f]	$< 4.3 \times 10^{-6}$	CL=90%
$\Gamma_{123}$	$D^+ \rightarrow \pi^+ e^+ \mu^-$	LF	$< 2.9 \times 10^{-6}$	CL=90%
$\Gamma_{124}$	$D^+ \rightarrow \pi^+ e^- \mu^+$	LF	$< 3.6 \times 10^{-6}$	CL=90%
$\Gamma_{125}$	$D^+ \rightarrow K^+ e^+ \mu^-$	LF	$< 1.2 \times 10^{-6}$	CL=90%
$\Gamma_{126}$	$D^+ \rightarrow K^+ e^- \mu^+$	LF	$< 2.8 \times 10^{-6}$	CL=90%
$\Gamma_{127}$	$D^+ \rightarrow \pi^- 2e^+$	L	$< 1.1 \times 10^{-6}$	CL=90%
$\Gamma_{128}$	$D^+ \rightarrow \pi^- 2\mu^+$	L	$< 2.0 \times 10^{-6}$	CL=90%
$\Gamma_{129}$	$D^+ \rightarrow \pi^- e^+ \mu^+$	L	$< 2.0 \times 10^{-6}$	CL=90%
$\Gamma_{130}$	$D^+ \rightarrow \rho^- 2\mu^+$	L	$< 5.6 \times 10^{-4}$	CL=90%
$\Gamma_{131}$	$D^+ \rightarrow K^- 2e^+$	L	$< 9 \times 10^{-7}$	CL=90%
$\Gamma_{132}$	$D^+ \rightarrow K^- 2\mu^+$	L	$< 1.0 \times 10^{-5}$	CL=90%
$\Gamma_{133}$	$D^+ \rightarrow K^- e^+ \mu^+$	L	$< 1.9 \times 10^{-6}$	CL=90%
$\Gamma_{134}$	$D^+ \rightarrow K^*(892)^- 2\mu^+$	L	$< 8.5 \times 10^{-4}$	CL=90%

$\Gamma_{135}$  Unaccounted decay modes  $(51.2 \pm 1.0) \%$

[a] The branching fraction for this mode may differ from the sum of the submodes that contribute to it, due to interference effects. See the relevant papers.

[b] These subfractions of the  $K^- 2\pi^+$  mode are uncertain: see the Particle Listings.

[c] Submodes of the  $D^+ \rightarrow K^- 2\pi^+ \pi^0$  and  $K_S^0 2\pi^+ \pi^-$  modes were studied by ANJOS 92C and COFFMAN 92B, but with at most 142 events for the first mode and 229 for the second – not enough for precise results. With nothing new for 18 years, we refer to our 2008 edition, Physics Letters **B667** 1 (2008), for those results.

[d] The unseen decay modes of the resonances are included.

[e] This is *not* a test for the  $\Delta C=1$  weak neutral current, but leads to the  $\pi^+ \ell^+ \ell^-$  final state.

[f] This mode is not a useful test for a  $\Delta C=1$  weak neutral current because both quarks must change flavor in this decay.

See key on page 457

## CONSTRAINED FIT INFORMATION

An overall fit to 22 branching ratios uses 31 measurements and one constraint to determine 15 parameters. The overall fit has a  $\chi^2 = 32.1$  for 17 degrees of freedom.

The following *off-diagonal* array elements are the correlation coefficients  $\langle \delta x_i \delta x_j \rangle / (\delta x_i \delta x_j)$ , in percent, from the fit to the branching fractions,  $x_i \equiv \Gamma_i / \Gamma_{\text{total}}$ . The fit constrains the  $x_i$  whose labels appear in this array to sum to one.

x <sub>29</sub>	0													
x <sub>34</sub>	0	3												
x <sub>35</sub>	22	0	0											
x <sub>38</sub>	6	0	0	1										
x <sub>40</sub>	15	0	0	3	44									
x <sub>50</sub>	5	0	0	1	14	31								
x <sub>54</sub>	6	0	0	1	18	40	56							
x <sub>55</sub>	7	0	0	2	22	50	50	0						
x <sub>56</sub>	3	0	0	1	10	24	7	10	12					
x <sub>83</sub>	3	0	0	1	10	22	7	9	11	76				
x <sub>89</sub>	6	0	0	1	75	38	12	15	19	9				
x <sub>90</sub>	10	0	0	2	29	66	24	38	36	16				
x <sub>106</sub>	2	0	0	0	6	13	4	5	6	3				
x <sub>135</sub>	-75	-4	-15	-32	-32	-58	-54	-48	-42	-20				
	x <sub>16</sub>	x <sub>29</sub>	x <sub>34</sub>	x <sub>35</sub>	x <sub>38</sub>	x <sub>40</sub>	x <sub>50</sub>	x <sub>54</sub>	x <sub>55</sub>	x <sub>56</sub>				
x <sub>89</sub>	8													
x <sub>90</sub>	14	25												
x <sub>106</sub>	3	5	9											
x <sub>135</sub>	-18	-27	-43	-8										
	x <sub>83</sub>	x <sub>89</sub>	x <sub>90</sub>	x <sub>106</sub>										

D<sup>+</sup> BRANCHING RATIOS

Some now-obsolete measurements have been omitted from these Listings.

## c-quark decays

 $\Gamma(c \rightarrow e^+ \text{ anything}) / \Gamma(c \rightarrow \text{ anything})$ 

For the Summary Table, we only use the average of  $e^+$  and  $\mu^+$  measurements from  $Z^0 \rightarrow c\bar{c}$  decays; see the second data block below.

VALUE	EVTs	DOCUMENT ID	TECN	COMMENT
<b>0.103 ± 0.009 ± 0.008</b>	378	<sup>3</sup> ABBIENDI	99K	OPAL $Z^0 \rightarrow c\bar{c}$

<sup>3</sup> ABBIENDI 99K uses the excess of right-sign over wrong-sign leptons opposite reconstructed  $D^*(2010)^+ \rightarrow D^0 \pi^+$  decays in  $Z^0 \rightarrow c\bar{c}$ .

 $\Gamma(c \rightarrow \mu^+ \text{ anything}) / \Gamma(c \rightarrow \text{ anything})$ 

For the Summary Table, we only use the average of  $e^+$  and  $\mu^+$  measurements from  $Z^0 \rightarrow c\bar{c}$  decays; see the next data block.

VALUE	EVTs	DOCUMENT ID	TECN	COMMENT
<b>0.082 ± 0.005 OUR AVERAGE</b>				
0.073 ± 0.008 ± 0.002	73	KAYIS-TOPAK.05	CHRS	$\nu_\mu$ emulsion
0.095 ± 0.007 +0.014 -0.013	2829	ASTIER	00D	NOMD $\nu_\mu \text{Fe} \rightarrow \mu^- \mu^+$ X
0.090 ± 0.007 +0.007 -0.006	476	<sup>4</sup> ABBIENDI	99K	OPAL $Z^0 \rightarrow c\bar{c}$
0.086 ± 0.017 +0.008 -0.007	69	<sup>5</sup> ALBRECHT	92F	ARG $e^+ e^- \approx 10$ GeV
0.078 ± 0.009 ± 0.012		ONG	88	MRK2 $e^+ e^- 29$ GeV
0.078 ± 0.015 ± 0.02		BARTEL	87	JADE $e^+ e^- 34.6$ GeV
0.082 ± 0.012 +0.02 -0.01		ALTHOFF	84G	TASS $e^+ e^- 34.5$ GeV
• • • We do not use the following data for averages, fits, limits, etc. • • •				
0.093 ± 0.009 ± 0.009	88	KAYIS-TOPAK.02	CHRS	See KAYIS-TOPAKSU 05
0.089 ± 0.018 ± 0.025		BARTEL	85J	JADE See BARTEL 87

<sup>4</sup> ABBIENDI 99K uses the excess of right-sign over wrong-sign leptons opposite reconstructed  $D^*(2010)^+ \rightarrow D^0 \pi^+$  decays in  $Z^0 \rightarrow c\bar{c}$ .

<sup>5</sup> ALBRECHT 92F uses the excess of right-sign over wrong-sign leptons in a sample of events tagged by fully reconstructed  $D^*(2010)^+ \rightarrow D^0 \pi^+$  decays.

 $\Gamma(c \rightarrow \ell^+ \text{ anything}) / \Gamma(c \rightarrow \text{ anything})$ 

This is an average (not a sum) of  $e^+$  and  $\mu^+$  measurements.

VALUE	EVTs	DOCUMENT ID	TECN	COMMENT
<b>0.096 ± 0.004 OUR AVERAGE</b>				
0.0958 ± 0.0042 ± 0.0028	1828	<sup>6</sup> ABREU	00o	DLPH $Z^0 \rightarrow c\bar{c}$
0.095 ± 0.006 +0.007 -0.006	854	<sup>7</sup> ABBIENDI	99K	OPAL $Z^0 \rightarrow c\bar{c}$

<sup>6</sup> ABREU 00o uses leptons opposite fully reconstructed  $D^*(2010)^+, D^+$ , or  $D^0$  mesons.

<sup>7</sup> ABBIENDI 99K uses the excess of right-sign over wrong-sign leptons opposite reconstructed  $D^*(2010)^+ \rightarrow D^0 \pi^+$  decays in  $Z^0 \rightarrow c\bar{c}$ .

 $\Gamma(c \rightarrow D^*(2010)^+ \text{ anything}) / \Gamma(c \rightarrow \text{ anything})$ 

VALUE	EVTs	DOCUMENT ID	TECN	COMMENT
<b>0.255 ± 0.015 ± 0.008</b>	2371	<sup>8</sup> ABREU	00o	DLPH $Z^0 \rightarrow c\bar{c}$

<sup>8</sup> ABREU 00o uses slow pions opposite fully reconstructed  $D^*(2010)^+, D^+$ , or  $D^0$  mesons as a signal of  $D^*(2010)^-$  production.

## Inclusive modes

 $\Gamma(e^+ \text{ semileptonic}) / \Gamma_{\text{total}}$ 

The sum of our  $\bar{K}^0 e^+ \nu_e, \bar{K}^*(892)^0 e^+ \nu_e, \pi^0 e^+ \nu_e, \eta e^+ \nu_e, \rho^0 e^+ \nu_e,$  and  $\omega e^+ \nu_e$  branching fractions is  $15.3 \pm 0.4\%$ .

VALUE (%)	EVTs	DOCUMENT ID	TECN	COMMENT
<b>16.07 ± 0.30 OUR AVERAGE</b>				
16.13 ± 0.10 ± 0.29	26.2 ± 0.2k	<sup>9</sup> ASNER	10	CLEO $e^+ e^-$ at 3774 MeV
15.2 ± 0.9 ± 0.8	521 ± 32	ABLIKIM	07G	BES2 $e^+ e^- \approx \psi(3770)$
• • • We do not use the following data for averages, fits, limits, etc. • • •				
16.13 ± 0.20 ± 0.33	8798 ± 105	<sup>10</sup> ADAM	06A	CLEO See ASNER 10
17.0 ± 1.9 ± 0.7	158	BALTRUSAIT...	85B	MRK3 $e^+ e^- 3.77$ GeV
<sup>9</sup> Using the $D^+$ and $D^0$ lifetimes, ASNER 10 finds that the ratio of the $D^+$ and $D^0$ semileptonic widths is $0.985 \pm 0.015 \pm 0.024$ .				
<sup>10</sup> Using the $D^+$ and $D^0$ lifetimes, ADAM 06A finds that the ratio of the $D^+$ and $D^0$ inclusive $e^+$ widths is $0.985 \pm 0.028 \pm 0.015$ , consistent with the isospin-invariance prediction of 1.				

 $\Gamma(\mu^+ \text{ anything}) / \Gamma_{\text{total}}$ 

VALUE (%)	EVTs	DOCUMENT ID	TECN	COMMENT
<b>17.6 ± 2.7 ± 1.8</b>	100 ± 12	<sup>11</sup> ABLIKIM	08L	BES2 $e^+ e^- \approx \psi(3772)$
<sup>11</sup> ABLIKIM 08L finds the ratio of $D^+ \rightarrow \mu^+ X$ and $D^0 \rightarrow \mu^+ X$ branching fractions to be $2.59 \pm 0.70 \pm 0.25$ , in accord with the ratio of $D^+$ and $D^0$ lifetimes, $2.54 \pm 0.02$ .				

 $\Gamma(K^- \text{ anything}) / \Gamma_{\text{total}}$ 

VALUE (%)	EVTs	DOCUMENT ID	TECN	COMMENT
<b>25.7 ± 1.4 OUR AVERAGE</b>				
24.7 ± 1.3 ± 1.2	631 ± 33	ABLIKIM	07G	BES2 $e^+ e^- \approx \psi(3770)$
27.8 +3.6 -3.1		BARLAG	92C	ACCM $\pi^- \text{Cu} 230$ GeV
27.1 ± 2.3 ± 2.4		COFFMAN	91	MRK3 $e^+ e^- 3.77$ GeV

 $[\Gamma(K^0 \text{ anything}) + \Gamma(K^0 \text{ anything})] / \Gamma_{\text{total}}$ 

VALUE (%)	EVTs	DOCUMENT ID	TECN	COMMENT
<b>61 ± 5 OUR AVERAGE</b>				
60.5 ± 5.5 ± 3.3	244 ± 22	ABLIKIM	06U	BES2 $e^+ e^-$ at 3773 MeV
61.2 ± 6.5 ± 4.3		COFFMAN	91	MRK3 $e^+ e^- 3.77$ GeV

 $\Gamma(K^+ \text{ anything}) / \Gamma_{\text{total}}$ 

VALUE (%)	EVTs	DOCUMENT ID	TECN	COMMENT
<b>5.9 ± 0.8 OUR AVERAGE</b>				
6.1 ± 0.9 ± 0.4	189 ± 27	ABLIKIM	07G	BES2 $e^+ e^- \approx \psi(3770)$
5.5 ± 1.3 ± 0.9		COFFMAN	91	MRK3 $e^+ e^- 3.77$ GeV

 $\Gamma(K^*(892)^- \text{ anything}) / \Gamma_{\text{total}}$ 

VALUE (%)	EVTs	DOCUMENT ID	TECN	COMMENT
<b>5.7 ± 5.2 ± 0.7</b>	7.2 ± 6.5	ABLIKIM	06U	BES2 $e^+ e^-$ at 3773 MeV

 $\Gamma(\bar{K}^*(892)^0 \text{ anything}) / \Gamma_{\text{total}}$ 

VALUE (%)	EVTs	DOCUMENT ID	TECN	COMMENT
<b>23.2 ± 4.5 ± 3.0</b>	189 ± 36	ABLIKIM	05P	BES $e^+ e^- \approx 3773$ MeV

 $\Gamma(K^*(892)^0 \text{ anything}) / \Gamma_{\text{total}}$ 

VALUE (%)	CL%	DOCUMENT ID	TECN	COMMENT
<b>&lt;6.6</b>	90	ABLIKIM	05P	BES $e^+ e^- \approx 3773$ MeV

 $\Gamma(\eta \text{ anything}) / \Gamma_{\text{total}}$ 

This ratio includes  $\eta$  particles from  $\eta'$  decays.

VALUE (%)	EVTs	DOCUMENT ID	TECN	COMMENT
<b>6.3 ± 0.5 ± 0.5</b>	1972 ± 142	HUANG	06B	CLEO $e^+ e^-$ at $\psi(3770)$

 $\Gamma(\eta' \text{ anything}) / \Gamma_{\text{total}}$ 

VALUE (%)	EVTs	DOCUMENT ID	TECN	COMMENT
<b>1.04 ± 0.16 ± 0.09</b>	82 ± 13	HUANG	06B	CLEO $e^+ e^-$ at $\psi(3770)$

 $\Gamma(\phi \text{ anything}) / \Gamma_{\text{total}}$ 

VALUE (%)	EVTs	DOCUMENT ID	TECN	COMMENT
<b>1.03 ± 0.10 ± 0.07</b>	248 ± 21	HUANG	06B	CLEO $e^+ e^-$ at $\psi(3770)$

## Leptonic and semileptonic modes

 $\Gamma(e^+ \nu_e) / \Gamma_{\text{total}}$ 

VALUE	CL%	DOCUMENT ID	TECN	COMMENT
<b>&lt;8.8 × 10<sup>-6</sup></b>	90	EISENSTEIN	08	CLEO $e^+ e^-$ at $\psi(3770)$
• • • We do not use the following data for averages, fits, limits, etc. • • •				
<2.4 × 10 <sup>-5</sup>	90	ARTUSO	05A	CLEO See EISENSTEIN 08

## Meson Particle Listings

 $D^\pm$ 

$\Gamma(\mu^+ \nu_\mu)/\Gamma_{\text{total}}$   $\Gamma_{13}/\Gamma$   
 See the note on "Decay Constants of Charged Pseudoscalar Mesons" in the  $D_S^\pm$  Listings.

VALUE (units $10^{-4}$ )	EVTS	DOCUMENT ID	TECN	COMMENT
$3.82 \pm 0.32 \pm 0.09$	150 ± 12	12 EISENSTEIN 08	CLEO	$e^+e^-$ at $\psi(3770)$
• • • We do not use the following data for averages, fits, limits, etc. • • •				
$12.2 \pm 11.1 \pm 1.0$	3	13 ABLIKIM	05D BES	$e^+e^- \approx 3.773$ GeV
$4.40 \pm 0.66 \pm 0.09$	47 ± 7	14 ARTUSO	05A CLEO	See EISENSTEIN 08
$3.5 \pm 1.4 \pm 0.6$	7	15 BONVICINI	04A CLEO	Incl. in ARTUSO 05A
$8 \pm 16 \pm 5 \pm 2$	1	16 BAI	98B BES	$e^+e^- \rightarrow D^{*+} D^-$
12 EISENSTEIN 08, using the $D^+$ lifetime and assuming $ V_{cd}  =  V_{us} $ , gets $f_{D^+} = (205.8 \pm 8.5 \pm 2.5)$ MeV from this measurement.				
13 ABLIKIM 05D finds a background-subtracted $2.67 \pm 1.74$ $D^+ \rightarrow \mu^+ \nu_\mu$ events, and from this obtains $f_{D^+} = 371 \pm 129 \pm 25$ MeV.				
14 ARTUSO 05A obtains $f_{D^+} = 222.6 \pm 16.7 \pm 3.4$ MeV from this measurement.				
15 BONVICINI 04A finds eight events with an estimated background of one, and from the branching fraction obtains $f_{D^+} = 202 \pm 41 \pm 17$ MeV.				
16 BAI 98B obtains $f_{D^+} = (300 \pm 180 \pm 80) \pm (150 \pm 40)$ MeV from this measurement.				

$\Gamma(\tau^+ \nu_\tau)/\Gamma_{\text{total}}$   $\Gamma_{14}/\Gamma$   
 VALUE CL% DOCUMENT ID TECN COMMENT  
 $<1.2 \times 10^{-3}$  90 EISENSTEIN 08 CLEO  $e^+e^-$  at  $\psi(3770)$   
 • • • We do not use the following data for averages, fits, limits, etc. • • •  
 $<2.1 \times 10^{-3}$  90 RUBIN 06A CLEO See EISENSTEIN 08

$\Gamma(K^0 e^+ \nu_e)/\Gamma_{\text{total}}$   $\Gamma_{15}/\Gamma$   
 VALUE (%) EVTS DOCUMENT ID TECN COMMENT  
 **$8.83 \pm 0.22$  OUR AVERAGE**  
 $8.83 \pm 0.10 \pm 0.20$  8467 17 BESSON 09 CLEO  $e^+e^-$  at  $\psi(3770)$   
 $8.95 \pm 1.59 \pm 0.67$  34 ± 6 18 ABLIKIM 05A BES  $e^+e^-$  at  $\psi(3770)$   
 • • • We do not use the following data for averages, fits, limits, etc. • • •  
 $8.53 \pm 0.13 \pm 0.23$  19 DOBBS 08 CLEO See BESSON 09  
 $8.71 \pm 0.38 \pm 0.37$  545 ± 24 HUANG 05B CLEO See DOBBS 08  
 17 See the form-factor parameters near the end of this  $D^+$  Listing.  
 18 The ABLIKIM 05A result together with the  $D^0 \rightarrow K^- e^+ \nu_e$  branching fraction of ABLIKIM 04C and Particle Data Group lifetimes gives  $\Gamma(D^0 \rightarrow K^- e^+ \nu_e) / \Gamma(D^+ \rightarrow \bar{K}^0 e^+ \nu_e) = 1.08 \pm 0.22 \pm 0.07$ ; isospin invariance predicts the ratio is 1.0.  
 19 DOBBS 08 establishes  $|\frac{V_{cd}}{V_{cs}} \cdot \frac{f_{K^+}(0)}{f_{K^0}(0)}| = 0.188 \pm 0.008 \pm 0.002$  from the  $D^+$  and  $D^0$  decays to  $\bar{K}^+ e^+ \nu_e$  and  $\pi^+ e^+ \nu_e$ . It also finds  $\Gamma(D^0 \rightarrow K^- e^+ \nu_e) / \Gamma(D^+ \rightarrow \bar{K}^0 e^+ \nu_e) = 1.06 \pm 0.02 \pm 0.03$ ; isospin invariance predicts the ratio is 1.0.

$\Gamma(K^0 \mu^+ \nu_\mu)/\Gamma_{\text{total}}$   $\Gamma_{16}/\Gamma$   
 VALUE EVTS DOCUMENT ID TECN COMMENT  
 **$0.092 \pm 0.006$  OUR FIT**  
 **$0.103 \pm 0.023 \pm 0.008$**  29 ± 6 ABLIKIM 07 BES2  $e^+e^-$  at 3773 MeV

$\Gamma(K^0 \mu^+ \nu_\mu)/\Gamma(K^- 2\pi^+)$   $\Gamma_{16}/\Gamma_{40}$   
 VALUE EVTS DOCUMENT ID TECN COMMENT  
 **$1.00 \pm 0.07$  OUR FIT**  
 **$1.019 \pm 0.076 \pm 0.065$**  555 ± 39 LINK 04E FOCS  $\gamma$  nucleus,  $\bar{E}_\gamma \approx 180$  GeV

$\Gamma(K^- \pi^+ e^+ \nu_e)/\Gamma_{\text{total}}$   $\Gamma_{17}/\Gamma$   
 VALUE (units  $10^{-2}$ ) EVTS DOCUMENT ID TECN COMMENT  
 • • • We do not use the following data for averages, fits, limits, etc. • • •  
 $3.50 \pm 0.75 \pm 0.27$  29 ± 6 ABLIKIM 06O BES2  $e^+e^-$  at 3773 MeV  
 $3.5 \pm 1.2 \pm 0.4$  14 BAI 91 MRK3  $e^+e^- \approx 3.77$  GeV

$\Gamma(K^- \pi^+ e^+ \nu_e)/\Gamma(K^- 2\pi^+)$   $\Gamma_{17}/\Gamma_{40}$   
 VALUE EVTS DOCUMENT ID TECN COMMENT  
 **$0.4380 \pm 0.0036 \pm 0.0042$**  70k ± 363 DEL-AMO-SA..11I BABR  $e^+e^- \approx 10.6$  GeV

$\Gamma(\bar{K}^*(892)^0 e^+ \nu_e)/\Gamma_{\text{total}}$   $\Gamma_{34}/\Gamma$   
 Unseen decay modes of the  $\bar{K}^*(892)^0$  are included. See the end of the  $D^+$  Listings for measurements of  $D^+ \rightarrow \bar{K}^*(892)^0 e^+ \nu_e$  form-factor ratios.

VALUE (units $10^{-2}$ )	EVTS	DOCUMENT ID	TECN	COMMENT
<b><math>5.52 \pm 0.15</math> OUR FIT</b>				
<b><math>5.52 \pm 0.07 \pm 0.13</math></b>	$\approx 5k$	BRIERE 10	CLEO	$e^+e^-$ at $\psi(3770)$
• • • We do not use the following data for averages, fits, limits, etc. • • •				
$5.06 \pm 1.21 \pm 0.40$	28 ± 7	ABLIKIM 06O	BES2	$e^+e^-$ at 3773 MeV
$5.56 \pm 0.27 \pm 0.23$	422 ± 21	20 HUANG 05B	CLEO	$e^+e^-$ at $\psi(3770)$
20 HUANG 05B finds $\Gamma(D^0 \rightarrow K^{*0} e^+ \nu_e) / \Gamma(D^+ \rightarrow \bar{K}^{*0} e^+ \nu_e) = 0.98 \pm 0.08 \pm 0.04$ ; isospin invariance predicts the ratio is 1.0.				

$\Gamma(\bar{K}^*(892)^0 e^+ \nu_e)/\Gamma(K^- 2\pi^+)$   $\Gamma_{34}/\Gamma_{40}$   
 Unseen decay modes of the  $\bar{K}^*(892)^0$  are included. See the end of the  $D^+$  Listings for measurements of  $D^+ \rightarrow \bar{K}^*(892)^0 e^+ \nu_e$  form-factor ratios.

VALUE	EVTS	DOCUMENT ID	TECN	COMMENT
• • • We do not use the following data for averages, fits, limits, etc. • • •				
$0.74 \pm 0.04 \pm 0.05$		BRANDENB.. 02	CLEO	$e^+e^- \approx \gamma(4S)$
$0.62 \pm 0.15 \pm 0.09$	35	ADAMOVICH 91	OMEG	$\pi^- 340$ GeV
$0.55 \pm 0.08 \pm 0.10$	880	ALBRECHT 91	ARG	$e^+e^- \approx 10.4$ GeV
$0.49 \pm 0.04 \pm 0.05$		ANJOS 89B	E691	Photoproduction

$\Gamma(\bar{K}^*(892)^0 e^+ \nu_e, \bar{K}^*(892)^0 \rightarrow K^- \pi^+)/\Gamma(K^- \pi^+ e^+ \nu_e)$   $\Gamma_{18}/\Gamma_{17}$   
 VALUE (%) DOCUMENT ID TECN COMMENT  
 **$94.11 \pm 0.74 \pm 0.75$**  DEL-AMO-SA..11I BABR  $e^+e^- \approx 10.6$  GeV

$\Gamma(((K^- \pi^+) S\text{-wave } e^+ \nu_e)/\Gamma(K^- \pi^+ e^+ \nu_e))$   $\Gamma_{19}/\Gamma_{17}$   
 VALUE (%) DOCUMENT ID TECN COMMENT  
 **$5.79 \pm 0.16 \pm 0.15$**  DEL-AMO-SA..11I BABR  $e^+e^- \approx 10.6$  GeV

$\Gamma(\bar{K}^*(1410)^0 e^+ \nu_e, \bar{K}^*(1410)^0 \rightarrow K^- \pi^+)/\Gamma_{\text{total}}$   $\Gamma_{20}/\Gamma$   
 VALUE CL% DOCUMENT ID TECN COMMENT  
 $<6 \times 10^{-3}$  90 DEL-AMO-SA..11I BABR  $e^+e^- \approx 10.6$  GeV

$\Gamma(\bar{K}_2^*(1430)^0 e^+ \nu_e, \bar{K}_2^*(1430)^0 \rightarrow K^- \pi^+)/\Gamma_{\text{total}}$   $\Gamma_{21}/\Gamma$   
 VALUE CL% DOCUMENT ID TECN COMMENT  
 $<5 \times 10^{-4}$  90 DEL-AMO-SA..11I BABR  $e^+e^- \approx 10.6$  GeV

$\Gamma(K^- \pi^+ e^+ \nu_e \text{ nonresonant})/\Gamma_{\text{total}}$   $\Gamma_{22}/\Gamma$   
 VALUE CL% DOCUMENT ID TECN COMMENT  
 $<0.007$  90 ANJOS 89B E691 Photoproduction

$\Gamma(K^- \pi^+ \mu^+ \nu_\mu)/\Gamma(K^0 \mu^+ \nu_\mu)$   $\Gamma_{23}/\Gamma_{16}$   
 VALUE EVTS DOCUMENT ID TECN COMMENT  
 **$0.417 \pm 0.030 \pm 0.023$**  555 ± 39 LINK 04E FOCS  $\gamma$  nucleus,  $\bar{E}_\gamma \approx 180$  GeV

$\Gamma(\bar{K}^*(892)^0 \mu^+ \nu_\mu)/\Gamma_{\text{total}}$   $\Gamma_{35}/\Gamma$   
 VALUE (units  $10^{-2}$ ) EVTS DOCUMENT ID TECN COMMENT  
 **$5.28 \pm 0.15$  OUR FIT**  
 **$5.27 \pm 0.07 \pm 0.14$**   $\approx 5k$  BRIERE 10 CLEO  $e^+e^-$  at  $\psi(3770)$

$\Gamma(\bar{K}^*(892)^0 \mu^+ \nu_\mu)/\Gamma(K^0 \mu^+ \nu_\mu)$   $\Gamma_{35}/\Gamma_{16}$   
 Unseen decay modes of the  $\bar{K}^*(892)^0$  are included. See the end of the  $D^+$  Listings for measurements of  $D^+ \rightarrow \bar{K}^*(892)^0 e^+ \nu_e$  form-factor ratios.

VALUE EVTS DOCUMENT ID TECN COMMENT  
 **$0.58 \pm 0.04$  OUR FIT**  
 **$0.594 \pm 0.043 \pm 0.033$**  555 ± 39 LINK 04E FOCS  $\gamma$  nucleus,  $\bar{E}_\gamma \approx 180$  GeV

$\Gamma(\bar{K}^*(892)^0 \mu^+ \nu_\mu)/\Gamma(K^- 2\pi^+)$   $\Gamma_{35}/\Gamma_{40}$   
 Unseen decay modes of the  $\bar{K}^*(892)^0$  are included. See the end of the  $D^+$  Listings for measurements of  $D^+ \rightarrow \bar{K}^*(892)^0 e^+ \nu_e$  form-factor ratios.

VALUE	EVTS	DOCUMENT ID	TECN	COMMENT
<b><math>0.578 \pm 0.021</math> OUR FIT</b> Error includes scale factor of 1.1.				
<b><math>0.57 \pm 0.06</math> OUR AVERAGE</b> Error includes scale factor of 1.2.				
$0.72 \pm 0.10 \pm 0.05$		BRANDENB.. 02	CLEO	$e^+e^- \approx \gamma(4S)$
$0.56 \pm 0.04 \pm 0.06$	875	FRABETTI 93E	E687	$\gamma$ Be $\bar{E}_\gamma \approx 200$ GeV
$0.46 \pm 0.07 \pm 0.08$	224	KODA MA 92C	E653	$\pi^-$ emulsion 600 GeV
• • • We do not use the following data for averages, fits, limits, etc. • • •				
$0.602 \pm 0.010 \pm 0.021$	12k	21 LINK 02J	FOCS	$\gamma$ nucleus, $\approx 180$ GeV

21 This LINK 02J result includes the effects of an interference of a small S-wave  $K^- \pi^+$  amplitude with the dominant  $\bar{K}^{*0}$  amplitude. (The interference effect is reported in LINK 02E.) This result is redundant with results of LINK 04E elsewhere in these Listings.

$\Gamma(K^- \pi^+ \mu^+ \nu_\mu \text{ nonresonant})/\Gamma(K^- \pi^+ \mu^+ \nu_\mu)$   $\Gamma_{25}/\Gamma_{23}$   
 VALUE EVTS DOCUMENT ID TECN COMMENT  
 **$0.0530 \pm 0.0074 \pm 0.0099$**  14k LINK 05I FOCS  $\gamma$  nucleus,  $\bar{E}_\gamma \approx 180$  GeV

$\Gamma(K^- \pi^+ \pi^0 \mu^+ \nu_\mu)/\Gamma(K^- \pi^+ \mu^+ \nu_\mu)$   $\Gamma_{26}/\Gamma_{23}$   
 VALUE CL% DOCUMENT ID TECN COMMENT  
 $<0.042$  90 FRABETTI 93E E687  $\gamma$ Be  $\bar{E}_\gamma \approx 200$  GeV

$\Gamma(\bar{K}_0^*(1430)^0 \mu^+ \nu_\mu)/\Gamma(K^- \pi^+ \mu^+ \nu_\mu)$   $\Gamma_{36}/\Gamma_{23}$   
 Unseen decay modes of the  $\bar{K}_0^*(1430)^0$  are included.  
 VALUE EVTS DOCUMENT ID TECN COMMENT  
 $<0.0064$  90 LINK 05I FOCS  $\gamma$  nucleus,  $\bar{E}_\gamma \approx 180$  GeV

$\Gamma(\bar{K}^*(1680)^0 \mu^+ \nu_\mu)/\Gamma(K^- \pi^+ \mu^+ \nu_\mu)$   $\Gamma_{37}/\Gamma_{23}$   
 Unseen decay modes of the  $\bar{K}^*(1680)^0$  are included.  
 VALUE EVTS DOCUMENT ID TECN COMMENT  
 $<0.04$  90 LINK 05I FOCS  $\gamma$  nucleus,  $\bar{E}_\gamma \approx 180$  GeV

$\Gamma(\pi^0 e^+ \nu_e)/\Gamma_{\text{total}}$   $\Gamma_{27}/\Gamma$ 

VALUE (%)	EVTS	DOCUMENT ID	TECN	COMMENT
<b>0.405 ± 0.016 ± 0.009</b>	838	22 BESSON 09	CLEO	$e^+ e^-$ at $\psi(3770)$
• • • We do not use the following data for averages, fits, limits, etc. • • •				
0.373 ± 0.022 ± 0.013		23 DOBBS 08	CLEO	See BESSON 09
0.44 ± 0.06 ± 0.03	63 ± 9	HUANG 05B	CLEO	See DOBBS 08

<sup>22</sup> See the form-factor parameters near the end of this  $D^+$  Listing.

<sup>23</sup> DOBBS 08 establishes  $|\frac{V_{cd}}{V_{cs}} \cdot \frac{f_{\pi^+}(0)}{f_{K^+}(0)}| = 0.188 \pm 0.008 \pm 0.002$  from the  $D^+$  and  $D^0$  decays to  $\bar{K} e^+ \nu_e$  and  $\pi e^+ \nu_e$ . It finds  $\Gamma(D^0 \rightarrow \pi^- e^+ \nu_e) / \Gamma(D^+ \rightarrow \pi^0 e^+ \nu_e) = 2.03 \pm 0.14 \pm 0.08$ ; isospin invariance predicts the ratio is 2.0.

 $\Gamma(\eta e^+ \nu_e)/\Gamma_{\text{total}}$   $\Gamma_{28}/\Gamma$ 

VALUE (units $10^{-4}$ )	EVTS	DOCUMENT ID	TECN	COMMENT
<b>11.4 ± 0.9 ± 0.4</b>		YELTON 11	CLEO	$e^+ e^-$ at $\psi(3770)$
• • • We do not use the following data for averages, fits, limits, etc. • • •				
13.3 ± 2.0 ± 0.6	46 ± 8	MITCHELL 09B	CLEO	See YELTON 11

 $\Gamma(\rho^0 e^+ \nu_e)/\Gamma_{\text{total}}$   $\Gamma_{29}/\Gamma$ 

VALUE	EVTS	DOCUMENT ID	TECN	COMMENT
<b>0.0022 ± 0.0004 OUR FIT</b>				
<b>0.0021 ± 0.0004 ± 0.0001</b>	27 ± 6	24 HUANG 05B	CLEO	$e^+ e^-$ at $\psi(3770)$
<sup>24</sup> HUANG 05B finds $\Gamma(D^0 \rightarrow \rho^- e^+ \nu_e) / 2 \Gamma(D^+ \rightarrow \rho^0 e^+ \nu_e) = 1.2^{+0.4}_{-0.3} \pm 0.1$ ; isospin invariance predicts the ratio is 1.0.				

 $\Gamma(\rho^0 e^+ \nu_e)/\Gamma(\bar{K}^*(892)^0 e^+ \nu_e)$   $\Gamma_{29}/\Gamma_{34}$ 

VALUE	EVTS	DOCUMENT ID	TECN	COMMENT
<b>0.039 ± 0.007 OUR FIT</b>				
<b>0.045 ± 0.014 ± 0.009</b>	49	25 AITALA 97	E791	$\pi^-$ nucleus, 500 GeV
<sup>25</sup> AITALA 97 explicitly subtracts $D^+ \rightarrow \eta' e^+ \nu_e$ and other backgrounds to get this result.				

 $\Gamma(\rho^0 \mu^+ \nu_\mu)/\Gamma(\bar{K}^*(892)^0 \mu^+ \nu_\mu)$   $\Gamma_{30}/\Gamma_{35}$ 

VALUE	EVTS	DOCUMENT ID	TECN	COMMENT
<b>0.045 ± 0.007 OUR AVERAGE</b>				Error includes scale factor of 1.1.
0.041 ± 0.006 ± 0.004	320 ± 44	LINK 06B	FOCS	$\gamma A, \bar{E}_\gamma \approx 180$ GeV
0.051 ± 0.015 ± 0.009	54	26 AITALA 97	E791	$\pi^-$ nucleus, 500 GeV
0.079 ± 0.019 ± 0.013	39	27 FRABETTI 97	E687	$\gamma Be, \bar{E}_\gamma \approx 220$ GeV
<sup>26</sup> AITALA 97 explicitly subtracts $D^+ \rightarrow \eta' \mu^+ \nu_\mu$ and other backgrounds to get this result.				
<sup>27</sup> Because the reconstruction efficiency for photons is low, this FRABETTI 97 result also includes any $D^+ \rightarrow \eta' \mu^+ \nu_\mu \rightarrow \gamma \rho^0 \mu^+ \nu_\mu$ events in the numerator.				

 $\Gamma(\omega e^+ \nu_e)/\Gamma_{\text{total}}$   $\Gamma_{31}/\Gamma$ 

VALUE	EVTS	DOCUMENT ID	TECN	COMMENT
<b>0.0016 ± 0.0007 ± 0.0001</b>	$7.6^{+3.3}_{-2.7}$	HUANG 05B	CLEO	$e^+ e^-$ at $\psi(3770)$

 $\Gamma(\eta'(958) e^+ \nu_e)/\Gamma_{\text{total}}$   $\Gamma_{32}/\Gamma$ 

VALUE (units $10^{-4}$ )	CL%	DOCUMENT ID	TECN	COMMENT
<b>2.16 ± 0.53 ± 0.07</b>		YELTON 11	CLEO	$e^+ e^-$ at $\psi(3770)$
• • • We do not use the following data for averages, fits, limits, etc. • • •				
<3.5	90	MITCHELL 09B	CLEO	See YELTON 11

 $\Gamma(\phi e^+ \nu_e)/\Gamma_{\text{total}}$   $\Gamma_{33}/\Gamma$ 

VALUE	CL%	DOCUMENT ID	TECN	COMMENT
Unseen decay modes of the $\phi$ are included.				
<b>&lt;0.9 × 10<sup>-4</sup></b>	90	YELTON 11	CLEO	$e^+ e^-$ at $\psi(3770)$
• • • We do not use the following data for averages, fits, limits, etc. • • •				
<1.6 × 10 <sup>-4</sup>	90	MITCHELL 09B	CLEO	See YELTON 11
<0.0201	90	ABLIKIM 06P	BES2	$e^+ e^-$ at 3773 MeV
<0.0209	90	BAI 91	MRK3	$e^+ e^- \approx 3.77$ GeV

Hadronic modes with a  $\bar{K}$  or  $\bar{K} K \bar{K}$  $\Gamma(K_S^0 \pi^+)/\Gamma_{\text{total}}$   $\Gamma_{38}/\Gamma$ 

VALUE (units $10^{-2}$ )	EVTS	DOCUMENT ID	TECN	COMMENT
• • • We do not use the following data for averages, fits, limits, etc. • • •				
1.526 ± 0.022 ± 0.038		28 DOBBS 07	CLEO	See MENDEZ 10
1.55 ± 0.05 ± 0.06	2230 ± 60	28 HE 05	CLEO	See DOBBS 07
1.6 ± 0.3 ± 0.1	161	ADLER 88c	MRK3	$e^+ e^- 3.77$ GeV
<sup>28</sup> DOBBS 07 and HE 05 use single- and double-tagged events in an overall fit. DOBBS 07 supersedes HE 05.				

 $\Gamma(K_S^0 \pi^+)/\Gamma(K^- 2\pi^+)$   $\Gamma_{38}/\Gamma_{40}$ 

VALUE	EVTS	DOCUMENT ID	TECN	COMMENT
<b>0.161 ± 0.007 OUR FIT</b>				Error includes scale factor of 3.4.
<b>0.158 ± 0.007 OUR AVERAGE</b>				Error includes scale factor of 3.2.
0.1682 ± 0.0012 ± 0.0037	30k	MENDEZ 10	CLEO	$e^+ e^-$ at 3774 MeV
0.1530 ± 0.0023 ± 0.0016	10.6k	LINK 02B	FOCS	$\gamma$ nucleus, $\bar{E}_\gamma \approx 180$ GeV
• • • We do not use the following data for averages, fits, limits, etc. • • •				
0.174 ± 0.012 ± 0.011	473	29 BISHAI 97	CLEO	$e^+ e^- \approx \gamma(4S)$
0.137 ± 0.015 ± 0.016	264	ANJOS 90c	E691	Photoproduction
<sup>29</sup> See BISHAI 97 for an isospin analysis of $D^+ \rightarrow \bar{K} \pi$ amplitudes.				

 $\Gamma(K_L^0 \pi^+)/\Gamma_{\text{total}}$   $\Gamma_{39}/\Gamma$ 

VALUE (units $10^{-2}$ )	EVTS	DOCUMENT ID	TECN	COMMENT
<b>1.460 ± 0.040 ± 0.035</b>	2023 ± 54	30 HE 08	CLEO	$e^+ e^-$ at $\psi(3770)$
<sup>30</sup> The difference of CLEO $D^+ \rightarrow K_S^0 \pi^+$ and $K_L^0 \pi^+$ branching fractions over the sum (DOBBS 07 and HE 08) is $+0.022 \pm 0.016 \pm 0.018$ .				

 $\Gamma(K^- 2\pi^+)/\Gamma_{\text{total}}$   $\Gamma_{40}/\Gamma$ 

VALUE (units $10^{-2}$ )	EVTS	DOCUMENT ID	TECN	COMMENT
<b>9.13 ± 0.19 OUR FIT</b>				
<b>9.14 ± 0.10 ± 0.17</b>		31 DOBBS 07	CLEO	$e^+ e^-$ at $\psi(3770)$
• • • We do not use the following data for averages, fits, limits, etc. • • •				
9.5 ± 0.2 ± 0.3	15.1k ± 130	31 HE 05	CLEO	See DOBBS 07
9.3 ± 0.6 ± 0.8	1502	32 BALEST 94	CLEO	$e^+ e^- \approx \gamma(4S)$
6.4 $^{+1.5}_{-1.4}$		33 BARLAG 92c	ACCM	$\pi^-$ Cu 230 GeV
9.1 ± 1.3 ± 0.4	1164	ADLER 88c	MRK3	$e^+ e^- 3.77$ GeV
9.1 ± 1.9	239	34 SCHINDLER 81	MRK2	$e^+ e^- 3.771$ GeV

<sup>31</sup> DOBBS 07 and HE 05 use single- and double-tagged events in an overall fit. DOBBS 07 supersedes HE 05.

<sup>32</sup> BALEST 94 measures the ratio of  $D^+ \rightarrow K^- \pi^+ \pi^+$  and  $D^0 \rightarrow K^- \pi^+$  branching fractions to be  $2.35 \pm 0.16 \pm 0.16$  and uses their absolute measurement of the  $D^0 \rightarrow K^- \pi^+$  fraction (AKERIB 93).

<sup>33</sup> BARLAG 92c computes the branching fraction by topological normalization.

<sup>34</sup> SCHINDLER 81 (MARK-2) measures  $\sigma(e^+ e^- \rightarrow \psi(3770)) \times$  branching fraction to be  $0.38 \pm 0.05$  nb. We use the MARK-3 (ADLER 88c) value of  $\sigma = 4.2 \pm 0.6 \pm 0.3$  nb.

## DALITZ PLOT ANALYSIS FORMALISM

Revised March 2012 by D. Asner (Pacific Northwest National Laboratory) and C. Hanhart (Forschungszentrum Jülich).

**Introduction:** Weak nonleptonic decays of  $D$  and  $B$  mesons are expected to proceed dominantly through resonant two-body decays [1]; see Ref. 2 for a review of resonance phenomenology. The amplitudes are typically calculated with the Dalitz-plot analysis technique [3], which uses the minimum number of independent observable quantities. For three-body decays of a spin-0 particle to all pseudo-scalar final states, such as  $D$  or  $B \rightarrow abc$ , the decay rate [4] is

$$\Gamma = \frac{1}{(2\pi)^3 32\sqrt{s^3}} |\mathcal{M}|^2 dm_{ab}^2 dm_{bc}^2, \quad (1)$$

where  $m_{ij}$  is the invariant mass of particles  $i$  and  $j$ . Here the prefactor contains all kinematic factors, while  $|\mathcal{M}|^2$  contains the dynamics. The scatter plot in  $m_{ab}^2$  versus  $m_{bc}^2$  is the Dalitz plot. If  $|\mathcal{M}|^2$  is constant, the kinematically allowed region of the plot will be populated uniformly with events. Any variation in the population over the Dalitz plot is due to dynamic rather than kinematic effects. It is straightforward to extend the formalism beyond three-body final states.

**Formalism:** The amplitude for the process  $R \rightarrow rc, r \rightarrow ab$  where  $R$  is a  $D$  or  $B$  meson,  $r$  is an intermediate resonance, and  $a, b, c$  are pseudo-scalars, is given by

$$\begin{aligned} \mathcal{M}_r(J, L, l, m_{ab}, m_{bc}) &= \sum_{\lambda} \langle ab|r_{\lambda} \rangle T_r(m_{ab}) \langle cr_{\lambda}|R_J \rangle \quad (2) \\ &= Z(J, L, l, \vec{p}, \vec{q}) B_L^R(|\vec{p}|) B_L^r(|\vec{q}|) T_r(m_{ab}). \end{aligned}$$

The sum is over the helicity states  $\lambda$  of  $r$ ;  $J$  is the total angular momentum of  $R$  (for  $D$  and  $B$  decays,  $J = 0$ );  $L$  is the orbital angular momentum between  $r$  and  $c$ ;  $l$  is the orbital angular momentum between  $a$  and  $b$ ; (the spin of  $r$ );  $\vec{p}$  and  $\vec{q}$  are the momenta of  $c$  and of  $a$  in the  $r$  rest frame;  $Z$  describes the angular distribution of the final-state particles;  $B_L^R$  and  $B_L^r$  are

# Meson Particle Listings

$D^\pm$

the barrier factors for the production of  $rc$  and of  $ab$ ; and  $T_r$  is the dynamical function describing the resonance  $r$ .  $T_r$  is a phenomenological object, with the resonances modeled often by a Breit-Wigner form, although some more recent analyses use a  $K$ -matrix formalism [5–7] with the  $P$ -vector approximation [8] to describe the  $\pi\pi$  S-wave.

The nonresonant (NR) contribution to  $D \rightarrow abc$  is parametrized as constant (S-wave), with no variation in magnitude or phase across the Dalitz plot. The available phase space is much greater for  $B$  decays than for  $D$  decays, and the nonresonant contribution to  $B \rightarrow abc$  requires a more sophisticated parametrization. Experimentally, several parametrizations have been used [9,10]. Differences in the parametrizations of the NR contributions, and in  $Z$ ,  $B_L$ , and  $T_r$ , as well as in the set of resonances  $r$ , complicate the comparison of results from different experiments.

**Angular distribution  $Z$ :** The tensor or Zemach formalism [11,12] and the helicity formalism [13,12] yield identical descriptions of the angular distributions for the decay process  $R \rightarrow rc, r \rightarrow ab$  when  $a$ ,  $b$  and  $c$  all have spin 0. The angular distributions for  $L = 0, 1$ , and  $2$  are given in Table 1. For a derivation of the expressions, see, *e.g.*, Ref. 12. For final-state particles with non-zero spin (*e.g.*, radiative decays), the helicity formalism is required.

**Table 1:** Angular distributions for  $L = 0, 1, 2$  for the decay process  $R \rightarrow rc, r \rightarrow ab$  when  $a$ ,  $b$  and  $c$  all have spin 0. Here  $\theta$  is the angle between particles  $a$  and  $c$  in the rest frame of resonance  $r$ ,  $\sqrt{1+\zeta^2} = E_r/m_{ab}$  is a relativistic correction, where  $E_r = (m_R^2 + m_{ab}^2 - m_c^2)/2m_R$  is the energy of resonance  $r$  in the rest frame of  $R$ .

$J \rightarrow L+l$	Angular distribution
$0 \rightarrow 0+0$	uniform
$0 \rightarrow 1+1$	$(1+\zeta^2) \cos^2 \theta$
$0 \rightarrow 2+2$	$\left(\zeta^2 + \frac{3}{2}\right)^2 (\cos^2 \theta - 1/3)^2$

**Barrier Factor  $B_L$ :** The maximum angular momentum  $L$  in a strong decay is limited by the linear momentum  $q$ —the relative momentum of the decay particles in the center of mass frame of the decaying resonance. Decay particles moving slowly with an impact parameter (meson radius)  $d$  of order 1 fm have difficulty generating sufficient angular momentum to conserve the spin of the resonance. The Blatt-Weisskopf [14,15] functions  $B_L$ , given in Table 2, weight the reaction amplitudes to account for this spin-dependent effect. These functions are normalized to give  $B_L = 1$  for  $z = (|q|d)^2 = 1$ . Another common formulation,  $B'_L$ , also in Table 2, is normalized to give  $B'_L = 1$  for  $z = z_0 = (|q_0|d)^2$  where  $q_0$  is the value of  $q$  when  $m_{ab} = m_r$ . An important difference between the  $B_L$  and the  $B'_L$  is that the former include explicitly the centrifugal barrier,

while it is to be moved to the dynamical functions in the case of  $B'_L$ .

**Table 2:** Blatt-Weisskopf barrier factors weight the reaction amplitudes to account for spin-dependent effects (c.f. Sec. VIII.5 of Ref. 14). Two formulations with different normalization conditions (described in text) are shown.  $B_L$  is commonly used in Dalitz plot analyses;  $B'_L$  is commonly used with the helicity formalism.

$L$	$B_L(q)$	$B'_L(q, q_0)$
0	1	1
1	$\sqrt{\frac{2z}{1+z}}$	$\sqrt{\frac{1+z_0}{1+z}}$
2	$\sqrt{\frac{13z^2}{(z-3)^2+9z}}$	$\sqrt{\frac{(z_0-3)^2+9z_0}{(z-3)^2+9z}}$

where  $z = (|q|d)^2$  and  $z_0 = (|q_0|d)^2$

**Dynamical Function  $T_r$ :** The dynamical function  $T_r$  is derived from the  $S$ -matrix formalism [5]. In general, the amplitude that a final state  $f$  couples to an initial state  $i$  is  $S_{fi} = \langle f|S|i\rangle$ , where the scattering operator  $S$  is unitary:  $SS^\dagger = S^\dagger S = I$ . The Lorentz-invariant transition operator  $\hat{T}$  is defined by separating the probability that  $f = i$ , yielding

$$S = I + 2iT = I + 2i \{\rho\}^{1/2} \hat{T} \{\rho\}^{1/2}, \quad (3)$$

where  $I$  is the identity operator and  $\rho$  is the diagonal phase-space matrix. If channel  $i$  denotes the two-body state  $ab$ , then

$$\rho_{ii} = \rho_i = \frac{2q_i}{m_{ab}} \theta [m_{ab} - (m_a + m_b)], \quad (4)$$

where  $m_{ab}$  is the invariant mass of the system;

$$q_i = \frac{1}{2m_{ab}} \sqrt{(m_{ab}^2 - (m_a + m_b)^2)(m_{ab}^2 - (m_a - m_b)^2)} \quad (5)$$

is the momentum of  $a$  in the  $r$  rest frame, and  $\theta[\dots]$  is the step function. In the single-channel case, unitarity allows one to express  $S$  through a single parameter,  $S = e^{2i\delta}$ , and

$$\hat{T} = \frac{1}{\rho} e^{i\delta} \sin \delta. \quad (6)$$

There are three common formulations of the dynamical function. The Breit-Wigner form—the first term in a Taylor expansion about a  $T$ -matrix pole—is the simplest. The  $K$ -matrix formalism [5] is more general (allowing more than one  $T$ -matrix pole and coupled channels while preserving unitarity). The Flatté distribution [16] is used to parametrize resonances near threshold, located at  $s = (m_a + m_b)^2$ , and is equivalent to a one-pole, two-channel  $K$ -matrix.



**Breit-Wigner Formulation:**

The common formulation of a Breit-Wigner resonance decaying to spin-0 particles  $a$  and  $b$  is

$$T_r(m_{ab}) \propto \frac{1}{m_r^2 - m_{ab}^2 - im_r \Gamma_{ab}(m_{ab})}. \quad (7)$$

A standard formulation for the “mass-dependent” width  $\Gamma_{ab}$  reads

$$\Gamma_{ab}(m_{ab}) = \sum_i \Gamma_i^r \left( \frac{q_i}{q_r} \right)^{2L_i+1} \left( \frac{m_r}{m_{ab}} \right) B'_{L_i}(q_i, q_0)^2, \quad (8)$$

where  $q_i$ ,  $L_i$ ,  $\Gamma_i^r$  and  $B'_{L_i}(q_i, q_0)$  are the momentum and angular momentum of the decay products, the partial width and Blatt-Weisskopf barrier factor (see Table 2) for the decay of resonance  $r$  into channel  $i$ , respectively. A Breit-Wigner parametrization best describes isolated, non-overlapping resonances far from the threshold of additional decay channels. For the  $\rho(770)$  and  $\rho(1450)$  a more complex parametrization suggested by Gounaris-Sakurai [17] is often used [18-22]. Unitarity is violated when the dynamical function is parametrized as the sum of two or more overlapping Breit-Wigners — see the discussion below Eq. (13). The proximity of a threshold to a resonance distorts the line shape from a simple Breit-Wigner. Here the Flatté formula provides a better description and is discussed below.

***K-matrix Formulation***

The  $T$  matrix can be written as

$$\hat{T} = (I - i\hat{K}\rho)^{-1}\hat{K}, \quad (9)$$

where  $\hat{K}$  is the Lorentz-invariant  $K$ -matrix describing the scattering process and  $\rho$  is the phase-space factor defined below Eq. (3). Resonances appear as poles in the  $K$ -matrix:

$$\hat{K}_{ij} = \sum_\alpha \frac{\sqrt{m_\alpha \Gamma_{\alpha i}(m) m_\alpha \Gamma_{\alpha j}(m)}}{(m_\alpha^2 - m^2) \sqrt{\rho_i \rho_j}}. \quad (10)$$

The  $K$ -matrix is real by construction, and so the associated  $T$ -matrix respects unitarity. However, in the given form it has the wrong analytic structure. To improve it, some authors use the analytic continuation for the momentum  $q_i$ , defined in Eq. (5), to below-threshold values, where for  $m_a \neq m_b$  the phase space factor needs to be modified to avoid false singularities (see, *e.g.*, Ref. 7, Sec. 2.1). For further improvements see below.

For a single pole in a single channel,  $K = \rho\hat{K}$  is

$$K = \frac{m_0 \Gamma(m)}{m_0^2 - m^2} \quad (11)$$

and

$$T = K(1 - iK)^{-1} = \frac{m_0 \Gamma(m)}{m_0^2 - m^2 - im_0 \Gamma(m)}, \quad (12)$$

which is the relativistic Breit-Wigner formula. For two poles in a single channel,  $K$  is

$$K = \frac{m_\alpha \Gamma_\alpha(m)}{m_\alpha^2 - m^2} + \frac{m_\beta \Gamma_\beta(m)}{m_\beta^2 - m^2}. \quad (13)$$

If  $m_\alpha$  and  $m_\beta$  are far apart relative to the widths, the  $T$  matrix is approximately the sum of two Breit-Wigners,  $T(K_\alpha + K_\beta) \approx T(K_\alpha) + T(K_\beta)$ , each of the form of Eq. (12). This approximation is not valid for two nearby resonances, for it violates unitarity. For example, for  $m = m_\alpha$  the full, unitary  $K$ -matrix expression gives  $\text{Im}(T)=1$ , while the imaginary part of  $T(K_\alpha) + T(K_\beta)$  is  $1 + (m_\beta \Gamma_\beta)^2 / [(m_\beta^2 - m_\alpha^2)^2 + (m_\beta \Gamma_\beta)^2]$ .

This formulation, which applies to  $S$ -channel production in two-body scattering,  $ab \rightarrow cd$ , can be generalized to describe the production of resonances in processes such as the decay of charm mesons. The key assumption here is that the two-body system described by the  $K$ -matrix does *not* interact with the rest of the final state [8]. The validity of this assumption varies with the production process and is appropriate for reactions such as  $\pi^- p \rightarrow \pi^0 \pi^0 n$  in the several-GeV regime, and for semileptonic decays such as  $D \rightarrow K\pi\ell\nu$ . The assumption may be of limited validity for production processes such as  $p\bar{p} \rightarrow \pi\pi\pi$ ,  $D \rightarrow \pi\pi\pi$ ,  $D \rightarrow K\pi\pi$  and  $J/\psi \rightarrow \omega\pi\pi$ . In the last two cases, additional three-body rescatterings were found to be relevant. In the  $J/\psi$  decays, they appeared where the two-body amplitudes were very small [23]; in the  $D$  decays, they were shown to lead to a significant difference between the  $K\pi$  scattering phase and the phase extracted from the production process [24]. If three-body interactions are neglected, the two-body Lorentz-invariant amplitude,  $\hat{F}$ , is given by

$$\hat{F}_i = (I - i\hat{K}\rho)^{-1}\hat{P}_j = (\hat{T}\hat{K}^{-1})_{ij}\hat{P}_j, \quad (14)$$

where  $P$  is the production vector that parametrizes the resonance production in the open channels.

For the  $\pi\pi$  S-wave, a common formulation of the  $K$ -matrix [7,20,21,25] is

$$K_{ij}(s) = \left[ \sum_\alpha \left( \frac{g_i^{(\alpha)} g_j^{(\alpha)}}{m_\alpha^2 - s} \right) + f_{ij}^{sc} \frac{1 + s_0^{sc}}{s + s_0^{sc}} \right] \left[ \frac{(s - s_A)}{(s + s_{A0})} \right]. \quad (15)$$

The factor  $g_i^{(\alpha)}$  is the real coupling constant of the  $K$ -matrix pole  $m_\alpha$  to meson channel  $i$ ; the parameters  $f_{ij}^{sc}$  and  $s_0^{sc}$  describe a smooth part of the  $K$ -matrix elements; the second factor in square brackets, with  $s_A \sim (0.1-0.5)m_\pi^2$  contains the Adler zero and at the same time suppresses a false kinematical singularity; *e.g.*, in Ref. 25,  $s_{A0} = 0.15 \text{ GeV}^2$  and  $s_A = 0.5m_\pi^2$  were used. The number 1 has units  $\text{GeV}^2$ .

The production vector, with  $i = 1$  denoting  $\pi\pi$ , is

$$P_j(s) = \left[ \sum_\alpha \left( \frac{\beta_\alpha g_j^{(\alpha)}}{m_\alpha^2 - s} \right) + f_{1j}^{pr} \frac{1 + s_0^{pr}}{s + s_0^{pr}} \right], \quad (16)$$

where the free parameters of the Dalitz-plot fit are the complex production couplings  $\beta_\alpha$  and the production-vector background parameters  $f_{1j}^{pr}$  and  $s_0^{pr}$ . All other parameters are fixed by scattering experiments. Ref. 6 describes the  $\pi\pi$  scattering data with a 4-pole, 2-channel ( $\pi\pi$ ,  $K\bar{K}$ ) model, while Ref. 7 describes the scattering data with a 5-pole, 5-channel ( $\pi\pi$ ,  $K\bar{K}$ ,  $\eta\eta$ ,  $\eta'\eta'$  and  $4\pi$ ) model. The former has been implemented by

# Meson Particle Listings

## $D^\pm$

CLEO [26] and the latter by FOCUS [21] and BABAR [20]. In both cases, only the  $\pi\pi$  channel was analyzed. A more complete coupled-channel analysis would simultaneously fit all final states accessible by rescattering.

### Flatté Formalism

The Flatté formulation is used when a second channel opens close to a resonance. This situation occurs in the  $\pi\pi$  S-wave where the  $f_0(980)$  is near the  $K\bar{K}$  threshold, and in the  $\pi\eta$  channel where the  $a_0(980)$  also lies near the  $K\bar{K}$  threshold. The  $T$ -matrix is parameterized as

$$\hat{T}(m_{ab})_{ij} = \frac{g_i g_j}{m_i^2 - m_{ab}^2 - i(\rho_1 g_1^2 + \rho_2 g_2^2)}, \quad (17)$$

where  $\rho_1 g_1^2 + \rho_2 g_2^2 = m_0 \Gamma_r$ , when the phase spaces are evaluated at the resonance mass. For the  $a_0(980)$  resonance, the relevant coupling constants are  $g_1 = g_{\pi\eta}$  and  $g_2 = g_{KK}$ , and the phase space terms are  $\rho_1 = \rho_{\pi\eta}$  and  $\rho_2 = \rho_{KK}$ , with  $\rho_i$  defined in Eq. (4). For the  $f_0(980)$  the relevant coupling constants are  $g_1 = g_{\pi\pi}$  and  $g_2 = g_{KK}$ , and the phase space terms are  $\rho_1 = \rho_{\pi\pi}$  and  $\rho_2 = \rho_{KK}$ . The charged and neutral  $K$  channels are usually assumed to have the same coupling constant but different phase space factors, due to  $m_{K^+} \neq m_{K^0}$ ; the result is

$$\rho_{KK} = \frac{1}{2} \left( \sqrt{1 - \left(\frac{2m_{K^\pm}}{m_{KK}}\right)^2} + \sqrt{1 - \left(\frac{2m_{K^0}}{m_{KK}}\right)^2} \right). \quad (18)$$

The effect of using this expression compared to using the averaged kaon masses is confined in the region very near threshold and is significant only in between the two kaon thresholds. If the coupling of a resonance to the channel opening nearby is strong, the Flatté parametrization shows a scaling invariance and does not allow for an extraction of the parameters individually, but only of ratios [27].

### Further improvements:

The  $K$ -matrix described above usually allows one to get a proper fit of physical amplitudes and it is easy to deal with. However, it also has an important deficit: it violates constraints from analyticity — *e.g.*,  $\rho_{ii}$  has a pole at  $s = 0$ , and for unequal masses develops an unphysical cut. An analytic continuation of the amplitudes into the complex plane is not controlled, and typically the parameters of broad resonances come out wrong (see, *e.g.*, the minireview on scalar mesons). A method to improve the analytic properties was suggested in Refs. [25,28–30]. It basically amounts to replacing the phase-space factor  $i\rho_i$  in Eqs. 9 and 14 with an analytic function that produces the identical imaginary part. In the simplest case of a channel with equal masses the expressions are

$$-\frac{\rho_i}{\pi} \log \left| \frac{1 + \rho_i}{1 - \rho_i} \right|, \quad -\frac{2\rho_i}{\pi} \arctan \left( \frac{1}{\rho_i} \right), \quad -\frac{\rho_i}{\pi} \log \left| \frac{1 + \rho_i}{1 - \rho_i} \right| + i\rho_i$$

for  $m^2 < 0$ ,  $0 < m^2 < (m_a + m_b)^2$ , and  $(m_a + m_b)^2 < m^2$ , respectively. Here  $\rho_i = \sqrt{|1 - (m_a + m_b)^2/m^2|}$  for all values of  $m^2$ , extending the expression of Eq. (4) into the regime

below threshold. The more complicated expression for the case of different masses can be found, *e.g.*, in Ref. 29.

**Branching Ratios from Dalitz Plot Fits:** A fit to the Dalitz plot distribution using either a Breit-Wigner or a  $K$ -matrix formalism factorizes into a resonant contribution to the amplitude  $\mathcal{M}_j$  and a complex coefficient,  $a_j e^{i\delta_j}$ , where  $a_j$  and  $\delta_j$  are real. The definition of a rate of a single process, given a set of amplitudes  $a_j$  and phases  $\delta_j$ , is the square of the relevant matrix element (see Eq. (1)). The “fit fraction” is usually defined as the integral over the Dalitz plot ( $m_{ab}$  vs.  $m_{bc}$ ) of a single amplitude squared divided by the integral over the Dalitz plot of the square of the coherent sum of all amplitudes, or

$$\text{fit fraction}_j = \frac{\int |a_j e^{i\delta_j} \mathcal{M}_j|^2 dm_{ab}^2 dm_{bc}^2}{\int |\sum_k a_k e^{i\delta_k} \mathcal{M}_k|^2 dm_{ab}^2 dm_{bc}^2}, \quad (19)$$

where  $\mathcal{M}_j$  is defined in Eq. (2) and described in Ref. 31. In general, the sum of the fit fractions for all components will not be unity due to interference.

When the  $K$ -matrix of Eq. (9) is used to describe a wave (*e.g.*, the  $\pi\pi$  S-wave), then  $\mathcal{M}_j$  refers to the entire wave. In this case, it may not be straightforward to separate  $\mathcal{M}_j$  into a sum of individual resonances unless these are narrow and well separated.

**Reconstruction Efficiency and Resolution:** The efficiency for reconstructing an event as a function of position on the Dalitz plot is in general non-uniform. Typically, a Monte Carlo sample generated with a uniform distribution in phase space is used to determine the efficiency. The variation in efficiency across the Dalitz plot varies with experiment and decay mode. Most recent analyses utilize a full GEANT [32] detector simulation.

Finite detector resolution can usually be safely neglected, as most resonances are comparatively broad. Notable exceptions where detector resolution effects must be modeled are  $\phi \rightarrow K^+ K^-$ ,  $\omega \rightarrow \pi^+ \pi^-$ , and  $a_0 \rightarrow \eta \pi^0$ . One approach is to convolve the resolution function in the Dalitz-plot variables  $m_{ab}^2$  and  $m_{bc}^2$  with the function that parametrizes the resonant amplitudes. In high-statistics data samples, resolution effects near the phase-space boundary typically contribute to a poor goodness of fit. The momenta of the final-state particles can be recalculated with a  $D$  or  $B$  mass constraint, which forces the kinematic boundaries of the Dalitz plot to be strictly respected. If the three-body mass is not constrained, then the efficiency (and the parametrization of background) may also depend on the reconstructed mass.

**Backgrounds:** The contribution of background to  $D$  and  $B$  samples varies by experiment and final state. The background naturally falls into six categories: (1) Purely combinatoric background containing no resonances. (2) Combinatoric background containing intermediate resonances, such as a real  $K^*$  or  $\rho$ , plus additional random particles. (3) Final states containing identical particles as in  $D^0 \rightarrow K_S^0 \pi^0$  background to  $D^0 \rightarrow \pi^+ \pi^- \pi^0$

See key on page 457

and  $B \rightarrow D\pi$  background to  $B \rightarrow K\pi\pi$ . (4) Mistagged decays such as a real  $\overline{D}^0$  or  $\overline{B}^0$  incorrectly identified as a  $D^0$  or  $B^0$ . (5) Particle misidentification of the decay products, such as  $D^+ \rightarrow \pi^-\pi^+\pi^+$  or  $D_s^+ \rightarrow K^-K^+\pi^+$  reconstructed as  $D^+ \rightarrow K^-\pi^+\pi^+$ . (6) Background from decays of charged pions or kaons in flight.

The contribution from combinatoric background with intermediate resonances is distinct from the resonances in the signal because the former do *not* interfere with the latter since they are not from true resonances. The usual identification tag of the initial particle as a  $D^0$  or a  $\overline{D}^0$  is the charge of the distinctive slow pion in the decay sequence  $D^{*+} \rightarrow D^0\pi_s^+$  or  $D^{*-} \rightarrow \overline{D}^0\pi_s^-$ . Another possibility is the identification or “tagging” of one of the  $D$  mesons from  $\psi(3770) \rightarrow D^0\overline{D}^0$ , as is done for  $B$  mesons from  $\Upsilon(4S)$ . The mistagged background is subtle and may be mistakenly enumerated in the *signal* fraction determined by a  $D^0$  mass fit. Mistagged decays contain true  $\overline{D}^0$ 's or  $\overline{B}^0$ 's and so the resonances in the mistagged sample exhibit interference on the Dalitz plot.

## References

- M. Bauer, B. Stech, and M. Wirbel, *Z. Phys. C* **34**, 103 (1987); P. Bedaque, A. Das, and V.S. Mathur, *Phys. Rev. D* **49**, 269 (1994); L.-L. Chau and H.-Y. Cheng, *Phys. Rev. D* **36**, 137 (1987); K. Terasaki, *Int. J. Mod. Phys. A* **10**, 3207 (1995); F. Buccella, M. Lusignoli, and A. Pugliese, *Phys. Lett. B* **379**, 249 (1996).
- J.D. Jackson, *Nuovo Cim.* **34**, 1644 (1964).
- R.H. Dalitz, *Phil. Mag.* **44**, 1068 (1953).
- See the note on Kinematics in this *Review*.
- S.U. Chung *et al.*, *Ann. Physik.* **4**, 404 (1995).
- K.L. Au, D. Morgan, and M.R. Pennington, *Phys. Rev. D* **35**, 1633 (1987).
- V.V. Anisovich and A.V. Sarantsev, *Eur. Phys. J. A* **16**, 229 (2003).
- I.J.R. Aitchison, *Nucl. Phys.* **A189**, 417 (1972).
- A. Garmash *et al.* (Belle Collab.), *Phys. Rev. D* **71**, 092003 (2005).
- B. Aubert *et al.* (BABAR Collab.), [arXiv:hep-ex/0507094](https://arxiv.org/abs/hep-ex/0507094).
- C. Zemach, *Phys. Rev. B* **133**, 1201 (1964); C. Zemach, *Phys. Rev. B* **140**, 97 (1965).
- V. Filippini, A. Fontana, and A. Rotondi, *Phys. Rev. D* **51**, 2247 (1995).
- M. Jacob and G.C. Wick, *Annals Phys.* **7**, 404 (1959) [*Annals Phys.* **281**, 774 (2000)]; S.U. Chung, *Phys. Rev. D* **48**, 1225 (1993); J.D. Richman, CALT-68-1148.
- J. Blatt and V. Weisskopf, *Theoretical Nuclear Physics*, New York: John Wiley & Sons (1952).
- F. von Hippel and C. Quigg, *Phys. Rev. D* **5**, 624 (1972).
- S.M. Flatté, *Phys. Lett. B* **63**, 224 (1976).
- G.J. Gounaris and J.J. Sakarai, *Phys. Rev. Lett.* **21**, 244 (1968).
- B. Aubert *et al.* (BABAR Collab.), [arXiv:hep-ex/0408073](https://arxiv.org/abs/hep-ex/0408073).
- K. Abe *et al.* (Belle Collab.), [arXiv:hep-ex/0504013](https://arxiv.org/abs/hep-ex/0504013).
- B. Aubert *et al.* (BABAR Collab.), [arXiv:hep-ex/0507101](https://arxiv.org/abs/hep-ex/0507101).
- J.M. Link *et al.* (FOCUS Collab.), *Phys. Lett. B* **585**, 200 (2004).
- B. Aubert *et al.* (BABAR Collab.), [arXiv:hep-ex/0408099](https://arxiv.org/abs/hep-ex/0408099).
- B. Liu *et al.*, *Eur. Phys. J. C* **63**, 93 (2009).
- P. C. Magalhaes *et al.*, *Phys. Rev. D* **84** (2011) 094001.
- A. V. Anisovich *et al.*, *Phys. Rev. D* **84**, 076001 (2011).
- D. Cronin-Hennessy *et al.* (CLEO Collab.), *Phys. Rev. D* **72**, 031102 (2005).
- V. Baru *et al.*, *Eur. Phys. J. A* **23**, 523 (2005).
- M.R. Pennington *et al.*, *Eur. Phys. J.* **C56**, 1 (2008).
- J. A. Oller and E. Oset, *Phys. Rev. D* **60**, 074023 (1999).
- N. N. Achasov and A. V. Kiselev, *Phys. Rev. D* **83**, 054008 (2011).
- S. Kopp *et al.* (CLEO Collab.), *Phys. Rev. D* **63**, 092001 (2001).
- R. Brun *et al.*, GEANT 3.15, CERN Report No. DD/EE/84-1 (1987); R. Brun *et al.*, GEANT 3.21, CERN Program Library Long Writeup W5013 (1993), unpublished; S. Agostinelli *et al.* (GEANT4 Collab.), *Nucl. Instrum. Meth. A* **506**, 250 (2003).

## REVIEW OF D-MESON DALITZ PLOT ANALYSES

Revised April 2010 by D. Asner (Pacific Northwest National Laboratory)

The formalism of Dalitz-plot analysis is reviewed in the preceding note. Recent studies of multi-body decays of charm mesons probe a variety of physics, including  $\gamma/\phi_3$ ,  $D^0$ - $\overline{D}^0$  mixing, searches for  $CP$  violation, doubly Cabibbo-suppressed decays, and properties of S-wave  $\pi\pi$ ,  $K\pi$ , and  $K\overline{K}$  resonances. In the following, we discuss: (1)  $D^0 \rightarrow K_S^0\pi^+\pi^-$ ; (2) doubly Cabibbo-suppressed decays; and (3)  $CP$  violation. The properties of the light meson resonances determined in D-meson Dalitz-plot analyses are reported in the light unflavored meson section of this *Review*.

$D^0 \rightarrow K_S^0\pi^+\pi^-$ : Several experiments have analyzed  $D^0 \rightarrow K_S^0\pi^+\pi^-$  decay. A CLEO analysis [1] included ten resonances:  $K_S^0\rho^0$ ,  $K_S^0\omega$ ,  $K_S^0f_0(980)$ ,  $K_S^0f_2(1270)$ ,  $K_S^0f_0(1370)$ ,  $K^*(892)^-\pi^+$ ,  $K_0^*(1430)^-\pi^+$ ,  $K_2^*(1430)^-\pi^+$ ,  $K^*(1680)^-\pi^+$ , and the doubly Cabibbo-suppressed (DCS) mode  $K^*(892)^+\pi^-$ . The CLEO model does not provide a good description of higher-statistics BABAR and Belle data samples. An improved description is obtained in three ways: First, by adding more Breit-Wigner resonances. Second, following the methodology of FOCUS [2], by applying a  $K$ -matrix model [3–5] to the  $\pi\pi$  S-wave [6,7]. Third, by adding a parameterization to the  $K\pi$  S-wave motivated by the LASS experiment [8].

A BABAR analysis [7,9,10] added to the CLEO model the  $K^*(1410)^-\pi^+$ ,  $K_S^0\rho^0(1450)$ , the DCS modes  $K_0^*(1430)^+\pi^-$  and  $K_2^*(1430)^+\pi^-$ , and two Breit-Wigner  $\pi\pi$  S-wave contributions. A Belle analysis [11–13] included all the components of BABAR and added two more DCS modes,  $K^*(1410)^+\pi^-$  and

# Meson Particle Listings

## $D^\pm$

$K^*(1680)^+\pi^-$ . Recently, BABAR has modeled the  $\pi\pi$  S-wave using a  $K$ -matrix model for the  $\pi\pi$  and  $K\pi$  S-waves [14].

The primary motivation for the analysis of the decay  $D^0 \rightarrow K_S^0\pi^+\pi^-$  is to study  $D^0 - \bar{D}^0$  oscillations and the CKM angles. The quasi-two-body intermediate states include both  $CP$ -even and  $CP$ -odd eigenstates as well as doubly Cabibbo-suppressed channels. Time-dependent analyses of the Dalitz plot from CLEO [15] and Belle [6] simultaneously determined the strong transition amplitudes and phases, the mixing parameters  $x$  and  $y$  without phase or sign ambiguity, and the  $CP$ -violating parameter  $|q/p|$  and  $\text{Arg}(q/p)$ . See the note on “ $D^0 - \bar{D}^0$  Mixing” for a discussion.

The CKM angle  $\gamma/\phi_3$  [16] and the quark-mixing parameter  $\cos 2\beta/\phi_1$  [17] can be determined using the decays  $B^- \rightarrow D^{(*)}K^{(*)-}$  and  $\bar{B}^0 \rightarrow Dh^0$ , respectively, followed by the decay  $D \rightarrow K_S^0\pi^+\pi^-$ . The Belle and BABAR experiments measured  $\gamma/\phi_3$  (Belle [11–13] and BABAR [7,9,10,14,18]) and  $\cos 2\beta/\phi_1$  (Belle [19], BABAR [20]). In these analyses, a large systematic uncertainty in the relative phase between the  $D^0$  and  $\bar{D}^0$  amplitudes point by point across the Dalitz plot remains to be fully understood.

The quantum entangled production of  $D^0\bar{D}^0$  pairs from  $\psi(3770)$  enables a model-independent determination of the  $D^0/\bar{D}^0$  relative phase. Studying  $CP$ -tagged Dalitz plots [21,22] provides sensitivity to the cosine of the relative phase, while studying double-tagged Dalitz plots [22] probes both the cosine and sine of the  $D^0/\bar{D}^0$  phase difference. CLEO analyzed [23] the  $D^0 \rightarrow K_S^0\pi^+\pi^-$  and  $D^0 \rightarrow K_L^0\pi^+\pi^-$  samples using the  $CP$ -even tag modes  $K^+K^-$ ,  $\pi^+\pi^-$ ,  $K_L^0\pi^0$  (vs.  $K_S^0\pi^+\pi^-$  only), the  $CP$ -odd tag modes  $K_S^0\pi^0$ ,  $K_S^0\eta$ , and the double-tag modes  $(K_S^0\pi^+\pi^-)^2$  and  $(K_S^0\pi^+\pi^-)(K_L^0\pi^+\pi^-)$ . These measurements can reduce the model uncertainty on  $\gamma/\phi_3$  to about  $3^\circ$ .

**Doubly Cabibbo-Suppressed Decays:** There are two classes of multibody doubly Cabibbo-suppressed (DCS) decays of  $D$  mesons. The first consists of those in which the DCS and corresponding Cabibbo-favored (CF) decays populate distinct Dalitz plots; the pairs  $D^0 \rightarrow K^+\pi^-\pi^0$  and  $D^0 \rightarrow K^-\pi^+\pi^0$ , or  $D^+ \rightarrow K^+\pi^+\pi^-$  and  $D^+ \rightarrow K^-\pi^+\pi^+$ , are examples. Our average of three measurements of  $\Gamma(D^0 \rightarrow K^+\pi^-\pi^0)/\Gamma(D^0 \rightarrow K^-\pi^+\pi^0)$  is  $(2.20 \pm 0.10) \times 10^{-3}$ . Our average of four measurements of  $\Gamma(D^+ \rightarrow K^+\pi^-\pi^+)/\Gamma(D^+ \rightarrow K^-\pi^+\pi^+)$  is  $(5.77 \pm 0.22) \times 10^{-3}$ ; see the Particle Listings.

The second class consists of decays in which the DCS and CF modes populate the same Dalitz plot; for example,  $D^0 \rightarrow K^*\pi^+$  and  $D^0 \rightarrow K^*\pi^-$  both contribute to  $D^0 \rightarrow K_S^0\pi^+\pi^-$ . In this class, the potential for interference of DCS and CF amplitudes increases the sensitivity to the DCS amplitude and allows direct measurement of the relative strong phases between amplitudes. CLEO [1] and Belle [6] have measured the relative phase between  $D^0 \rightarrow K^*(892)^+\pi^-$  and  $D^0 \rightarrow K^*(892)^-\pi^+$  to be  $(189 \pm 10 \pm 3_{-5}^{+15})^\circ$  and  $(171.9 \pm 1.3)^\circ$  (statistical error only). These results are close to the  $180^\circ$  expected from Cabibbo factors and a small strong phase.

In addition, Belle [6] has results for both the relative phase (statistical errors only) and ratio  $R$  (central values only) of the DCS fit fraction relative to the CF fit fractions for  $K^*(892)^+\pi^-$ ,  $K_0^*(1430)^+\pi^-$ ,  $K_2^*(1430)^+\pi^-$ ,  $K^*(1410)^+\pi^-$ , and  $K^*(1680)^+\pi^-$ . The systematic uncertainties on  $R$  must be evaluated. The values for  $R$  in units of  $\tan^4\theta_c$  are  $2.94 \pm 0.12$ ,  $22.0 \pm 1.6$ ,  $34 \pm 4$ ,  $87 \pm 13$ , and  $500 \pm 500$ . For  $K^+\pi^-$ , the corresponding value for  $R_D$  is  $(1.28 \pm 0.02) \times \tan^4\theta_c$ . Similarly, BABAR [7] has reported central values for  $R$  for  $K^*(892)^+\pi^-$ ,  $K_0^*(1430)^+\pi^-$ , and  $K_2^*(1430)^+\pi^-$ . The values for  $R$  in units of  $\tan^4\theta_c$  are  $3.45 \pm 0.31$ ,  $7.7 \pm 3.0$ , and  $1.7 \pm 1.7$ , respectively. Recently, BABAR [14] has used a  $K$ -matrix formalism to describe the  $\pi\pi$  S-wave in  $K_S^0\pi^+\pi^-$ . The reported values for  $R$  in units of  $\tan^4\theta_c$  are  $2.78 \pm 0.11$ ,  $0.5 \pm 0.2$ , and  $1.4 \pm 0.5$ , respectively. The large differences in  $R$  among these final states could point to an interesting role for hadronic effects.

There are other ways, not involving DCS decays, in which  $D^0$  and  $\bar{D}^0$  singly Cabibbo-suppressed decays can populate the same Dalitz plot. Examples are  $D^0$  and  $\bar{D}^0$  decays to  $K_S^0K^+\pi^-$ , or to  $K_S^0K^-\pi^+$ . These final states can be used to study  $D^0 - \bar{D}^0$  mixing and the CKM angle  $\gamma/\phi_3$ .

**$CP$  Violation:** In the limit of  $CP$  conservation, charge conjugate decays will have the same Dalitz-plot distribution. The  $D^{*\pm}$  tag enables the discrimination between  $D^0$  and  $\bar{D}^0$ . The integrated  $CP$  violation across the Dalitz plot is determined in two ways. The first uses

$$A_{CP} = \int \left( \frac{|\mathcal{M}|^2 - |\bar{\mathcal{M}}|^2}{|\mathcal{M}|^2 + |\bar{\mathcal{M}}|^2} \right) dm_{ab}^2 dm_{bc}^2 / \int dm_{ab}^2 dm_{bc}^2, \quad (1)$$

where  $\mathcal{M}$  and  $\bar{\mathcal{M}}$  have the same normalization and represent the  $D^0$  and  $\bar{D}^0$  Dalitz-plot amplitudes for the three-body decay  $D \rightarrow abc$ , and  $m_{ab}$  ( $m_{bc}$ ) is the invariant mass of  $ab$  ( $bc$ ). The second uses the asymmetry in the efficiency-corrected  $D^0$  and  $\bar{D}^0$  yields,

$$A_{CP} = \frac{N_{D^0} - N_{\bar{D}^0}}{N_{D^0} + N_{\bar{D}^0}}. \quad (2)$$

These expressions are less sensitive to  $CP$  violation than are the individual resonant submodes [24–26]. Our Particle Listings give limits on  $CP$  violation for 12  $D^+$ , 52  $D^0$ , and 13  $D_S^+$  decay modes. No evidence of  $CP$  violation has been observed in  $D$ -meson decays.

The possibility of interference between  $CP$ -conserving and  $CP$ -violating amplitudes provides a more sensitive probe of  $CP$  violation. The constraints on the square of the  $CP$ -violating amplitudes obtained in the resonant submodes of  $D^0 \rightarrow K_S^0\pi^+\pi^-$  range from  $3.5 \times 10^{-4}$  to  $28.4 \times 10^{-4}$  at 95% confidence level [24]. A similar analysis has been performed by CLEO [25] searching for  $CP$  violation in  $D^+ \rightarrow K^+K^-\pi^+$ . The constraints on the square of the  $CP$ -violating amplitudes in the resonant submodes range from  $4 \times 10^{-4}$  to  $51 \times 10^{-4}$  at 95%. BABAR finds no evidence for  $CP$ -violating amplitudes in the resonant submodes of  $D^0 \rightarrow K^+K^-\pi^0$  and  $D^0 \rightarrow \pi^+\pi^-\pi^0$  [26].

## References

- H. Muramatsu *et al.* (CLEO Collab.), Phys. Rev. Lett. **89**, 251802 (2002).
- J.M. Link *et al.* (FOCUS Collab.), Phys. Lett. **B585**, 200 (2004).
- E. P. Wigner, Phys. Rev. **70**, 15 (1946).
- S. U. Chung *et al.*, Annalen Phys. **4**, 404 (1995).
- I. J. R. Aitchison, Nucl. Phys. **A189**, 417 (1972).
- L.M. Zhang *et al.* (Belle Collab.), Phys. Rev. Lett. **99**, 131803 (2007).
- B. Aubert *et al.* (BABAR Collab.), Phys. Rev. Lett. **95**, 121802 (2005).
- D. Aston *et al.* (LASS Collab.), Nucl. Phys. **B296**, 493 (1988).
- B. Aubert *et al.* (BABAR Collab.), hep-ex/0507101.
- B. Aubert *et al.* (BABAR Collab.), arXiv:hep-ex/0607104.
- A. Poluektov *et al.* (Belle Collab.), Phys. Rev. **D70**, 072003 (2004).
- K. Abe *et al.* (Belle Collab.), hep-ex/0411049.
- A. Poluektov *et al.* (Belle Collab.), Phys. Rev. **D73**, 112009 (2006).
- B. Aubert *et al.* (BABAR Collab.), Phys. Rev. **D78**, 034023 (2008).
- D.M. Asner *et al.* (CLEO Collab.), Phys. Rev. **D72**, 012001 (2005).
- A. Giri *et al.*, Phys. Rev. **D68**, 054018 (2003).
- A. Bondar, T. Gershon, and P. Krokovny, Phys. Lett. **B624**, 1 (2005).
- B. Aubert *et al.* (BABAR Collab.), Phys. Rev. **D79**, 072003 (2009).
- P. Krokovny *et al.* (Belle Collab.), Phys. Rev. Lett. **97**, 081801 (2006).
- B. Aubert *et al.* (BABAR Collab.), arXiv:hep-ex/0607105.
- A. Bondar and A. Poluektov, Eur. Phys. J. **C47**, 347 (2006).
- A. Bondar and A. Poluektov, arXiv:hep-ph/0703267.
- R. A. Briere *et al.* (CLEO Collab.), Phys. Rev. **D80**, 032002 (2009).
- D.M. Asner *et al.* (CLEO Collab.), Phys. Rev. **D70**, 091101R (2004).
- P. Rubin *et al.* (CLEO Collab.), Phys. Rev. **D78**, 072003 (2008).
- B. Aubert *et al.* (BABAR Collab.), Phys. Rev. **D78**, 051102 (2008).

 $\Gamma((K^-\pi^+)_{S\text{-wave}})/\Gamma(K^-2\pi^+)$   $\Gamma_{41}/\Gamma_{40}$ 

This is the "fit fraction" from the Dalitz-plot analysis. The  $K^-\pi^+$  S-wave includes a broad scalar  $\kappa$  ( $\bar{K}_0^*(800)$ ), the  $\bar{K}_0^*(1430)^0$ , and non-resonant background.

VALUE	DOCUMENT ID	TECN	COMMENT
<b>0.801 ± 0.012 OUR AVERAGE</b>			
0.8024 ± 0.0138 ± 0.0043	<sup>35</sup> LINK	09	FOCS MIPWA fit, 53k evts
0.838 ± 0.038	<sup>36</sup> BONVICINI	08A	CLEO QMIPWA fit, 141k evts
0.786 ± 0.014 ± 0.018	AITALA	06	E791 Dalitz fit, 15.1k events
••• We do not use the following data for averages, fits, limits, etc. •••			
0.8323 ± 0.0150 ± 0.0008	<sup>37</sup> LINK	07B	FOCS See LINK 09

<sup>35</sup> This LINK 09 model-independent partial-wave analysis of the  $K^-\pi^+$  S-wave slices the  $K^-\pi^+$  mass range into 39 bins.

<sup>36</sup> The BONVICINI 08A QMIPWA (quasi-model-independent partial-wave analysis) of the  $K^-\pi^+$  S-wave amplitude slices the  $K^-\pi^+$  mass range into 26 bins but keeps the Breit-Wigner  $\bar{K}_0^*(1430)^0$ .

<sup>37</sup> This LINK 07B fit uses a K matrix. The  $K^-\pi^+$  S-wave fit fraction given above breaks down into (207.3 ± 25.5 ± 12.4)% isospin-1/2 and (40.5 ± 9.6 ± 3.2)% isospin-3/2 — with large interference between the two. The isospin-1/2 component includes the  $\kappa$  (or  $\bar{K}_0^*(800)^0$ ) and  $\bar{K}_0^*(1430)^0$ .

 $\Gamma(\bar{K}_0^*(800)^0\pi^+, \bar{K}_0^*(800) \rightarrow K^-\pi^+)/\Gamma(K^-2\pi^+)$   $\Gamma_{42}/\Gamma_{40}$ 

This is the "fit fraction" from the Dalitz-plot analysis.

VALUE	DOCUMENT ID	TECN	COMMENT
••• We do not use the following data for averages, fits, limits, etc. •••			
0.478 ± 0.121 ± 0.053	AITALA	02	E791 See AITALA 06

 $\Gamma(\bar{K}^*(892)^0\pi^+, \bar{K}^*(892)^0 \rightarrow K^-\pi^+)/\Gamma(K^-2\pi^+)$   $\Gamma_{44}/\Gamma_{40}$ 

This is the "fit fraction" from the Dalitz-plot analysis.

VALUE	DOCUMENT ID	TECN	COMMENT
<b>0.111 ± 0.012 OUR AVERAGE</b>			Error includes scale factor of 3.7.
0.1236 ± 0.0034 ± 0.0034	LINK	09	FOCS MIPWA fit, 53k evts
0.0988 ± 0.0046	BONVICINI	08A	CLEO QMIPWA fit, 141k evts
0.119 ± 0.002 ± 0.020	AITALA	06	E791 Dalitz fit, 15.1k events
••• We do not use the following data for averages, fits, limits, etc. •••			
0.1361 ± 0.0041 ± 0.0030	<sup>38</sup> LINK	07B	FOCS See LINK 09
0.123 ± 0.010 ± 0.009	AITALA	02	E791 See AITALA 06
0.137 ± 0.006 ± 0.009	FRABETTI	94G	E687 Dalitz fit, 8800 evts
0.170 ± 0.009 ± 0.034	ANJOS	93	E691 $\gamma$ Be 90–260 GeV
0.14 ± 0.04 ± 0.04	ALVAREZ	91B	NA14 Photoproduction
0.13 ± 0.01 ± 0.07	ADLER	87	MRK3 $e^+e^-$ 3.77 GeV

<sup>38</sup> The statistical error on this LINK 07B value is corrected in LINK 09.

 $\Gamma(\bar{K}^*(1410)^0\pi^+, \bar{K}^{*0} \rightarrow K^-\pi^+)/\Gamma(K^-2\pi^+)$   $\Gamma_{45}/\Gamma_{40}$ 

VALUE (units $10^{-3}$ )	DOCUMENT ID	TECN	COMMENT
not seen	LINK	09	FOCS MIPWA fit, 53k evts
not seen	BONVICINI	08A	CLEO QMIPWA fit, 141k evts
••• We do not use the following data for averages, fits, limits, etc. •••			
4.8 ± 2.1 ± 1.7	LINK	07B	FOCS See LINK 09

 $\Gamma(\bar{K}_0^*(1430)^0\pi^+, \bar{K}_0^*(1430)^0 \rightarrow K^-\pi^+)/\Gamma(K^-2\pi^+)$   $\Gamma_{43}/\Gamma_{40}$ 

This is the "fit fraction" from the Dalitz-plot analysis.

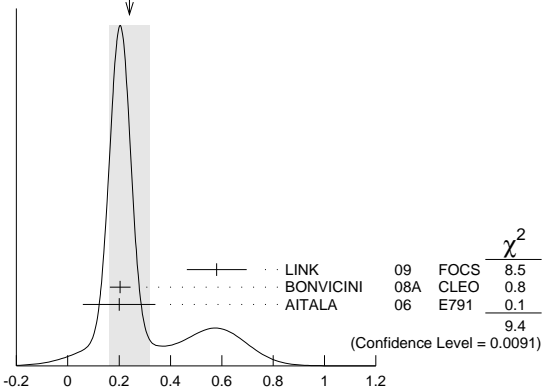
VALUE	DOCUMENT ID	TECN	COMMENT
<b>0.1330 ± 0.0062</b>	BONVICINI	08A	CLEO QMIPWA fit, 141k evts
••• We do not use the following data for averages, fits, limits, etc. •••			
0.125 ± 0.014 ± 0.005	AITALA	02	E791 See AITALA 06
0.284 ± 0.022 ± 0.059	FRABETTI	94G	E687 Dalitz fit, 8800 evts
0.248 ± 0.019 ± 0.017	ANJOS	93	E691 $\gamma$ Be 90–260 GeV

 $\Gamma(\bar{K}_2^*(1430)^0\pi^+, \bar{K}_2^*(1430)^0 \rightarrow K^-\pi^+)/\Gamma(K^-2\pi^+)$   $\Gamma_{46}/\Gamma_{40}$ 

This is the "fit fraction" from the Dalitz-plot analysis.

VALUE (units $10^{-2}$ )	DOCUMENT ID	TECN	COMMENT
<b>0.24 ± 0.08 OUR AVERAGE</b>			Error includes scale factor of 2.2. See the ideogram below.
0.58 ± 0.10 ± 0.06	LINK	09	FOCS MIPWA fit, 53k evts
0.204 ± 0.040	BONVICINI	08A	CLEO QMIPWA fit, 141k evts
0.2 ± 0.1 ± 0.1	AITALA	06	E791 Dalitz fit, 15.1k events
••• We do not use the following data for averages, fits, limits, etc. •••			
0.39 ± 0.09 ± 0.05	LINK	07B	FOCS See LINK 09
0.5 ± 0.1 ± 0.2	AITALA	02	E791 See AITALA 06

WEIGHTED AVERAGE  
0.24 ± 0.08 (Error scaled by 2.2)

 $\Gamma(\bar{K}_2^*(1430)^0\pi^+, \bar{K}_2^*(1430)^0 \rightarrow K^-\pi^+)/\Gamma(K^-2\pi^+)$   $\Gamma_{46}/\Gamma_{40}$  $\Gamma(\bar{K}^*(1680)^0\pi^+, \bar{K}^*(1680)^0 \rightarrow K^-\pi^+)/\Gamma(K^-2\pi^+)$   $\Gamma_{47}/\Gamma_{40}$ 

This is the "fit fraction" from the Dalitz-plot analysis.

VALUE (units $10^{-2}$ )	DOCUMENT ID	TECN	COMMENT
<b>0.23 ± 0.12 OUR AVERAGE</b>			
1.75 ± 0.62 ± 0.54	LINK	09	FOCS MIPWA fit, 53k evts
0.196 ± 0.118	BONVICINI	08A	CLEO QMIPWA fit, 141k evts
1.2 ± 0.6 ± 1.2	AITALA	06	E791 Dalitz fit, 15.1k events
••• We do not use the following data for averages, fits, limits, etc. •••			
1.90 ± 0.63 ± 0.43	LINK	07B	FOCS See LINK 09
2.5 ± 0.7 ± 0.3	AITALA	02	E791 See AITALA 06
4.7 ± 0.6 ± 0.7	FRABETTI	94G	E687 Dalitz fit, 8800 evts
3.0 ± 0.4 ± 1.3	ANJOS	93	E691 $\gamma$ Be 90–260 GeV

## Meson Particle Listings

 $D^\pm$  $\Gamma(K^-(2\pi^+)_{I=2})/\Gamma(K^-2\pi^+)$   $\Gamma_{48}/\Gamma_{40}$ 

VALUE	DOCUMENT ID	TECN	COMMENT
<b>0.155±0.028</b>	BONVICINI	08A	CLEO QMIPWA fit, 141k evts

 $\Gamma(K^-2\pi^+ \text{ nonresonant})/\Gamma(K^-2\pi^+)$   $\Gamma_{49}/\Gamma_{40}$ 

This is the "fit fraction" from the Dalitz-plot analysis. Later analyses find little need for this decay mode.

VALUE	DOCUMENT ID	TECN	COMMENT
••• We do not use the following data for averages, fits, limits, etc. •••			
0.130±0.058±0.044	AITALA	02	E791 See AITALA 06
0.998±0.037±0.072	FRABETTI	94G	E687 Dalitz fit, 8800 evts
0.838±0.088±0.275	ANJOS	93	E691 $\gamma$ Be 90-260 GeV
0.79 ±0.07 ±0.15	ADLER	87	MRK3 $e^+e^-$ 3.77 GeV

 $\Gamma(K_S^0\pi^+\pi^0)/\Gamma_{\text{total}}$   $\Gamma_{50}/\Gamma$ 

VALUE (units $10^{-2}$ )	EVTS	DOCUMENT ID	TECN	COMMENT
<b>6.99±0.27 OUR FIT</b>				
<b>6.99±0.09±0.25</b>		<sup>39</sup> DOBBS	07	CLEO $e^+e^-$ at $\psi(3770)$
••• We do not use the following data for averages, fits, limits, etc. •••				
7.2 ±0.2 ±0.4	5090±100	<sup>39</sup> HE	05	CLEO See DOBBS 07
5.1 ±1.3 ±0.8	159	ADLER	88c	MRK3 $e^+e^-$ 3.77 GeV
<sup>39</sup> DOBBS 07 and HE 05 use single- and double-tagged events in an overall fit. DOBBS 07 supersedes HE 05.				

 $\Gamma(K_S^0\rho^+)/\Gamma(K_S^0\pi^+\pi^0)$   $\Gamma_{51}/\Gamma_{50}$ 

VALUE	DOCUMENT ID	TECN	COMMENT
<b>0.68±0.08±0.12</b>	ADLER	87	MRK3 $e^+e^-$ 3.77 GeV

 $\Gamma(\bar{K}^*(892)^0\pi^+, \bar{K}^*(892)^0 \rightarrow K_S^0\pi^0)/\Gamma(K_S^0\pi^+\pi^0)$   $\Gamma_{52}/\Gamma_{50}$ 

VALUE	DOCUMENT ID	TECN	COMMENT
<b>0.19±0.06±0.06</b>	ADLER	87	MRK3 $e^+e^-$ 3.77 GeV

 $\Gamma(K_S^0\pi^+\pi^0 \text{ nonresonant})/\Gamma(K_S^0\pi^+\pi^0)$   $\Gamma_{53}/\Gamma_{50}$ 

VALUE	DOCUMENT ID	TECN	COMMENT
<b>0.13±0.07±0.08</b>	ADLER	87	MRK3 $e^+e^-$ 3.77 GeV

 $\Gamma(K^-2\pi^+\pi^0)/\Gamma_{\text{total}}$   $\Gamma_{54}/\Gamma$ 

See our 2008 Review (Physics Letters **B667** 1 (2008)) for measurements of submodes of this mode. There is nothing new since 1992, and the two papers, ANJOS 92c, with 91 ± 12 events above background, and COFFMAN 92b, with 142 ± 20 such events, could not determine submode fractions with much accuracy.

VALUE (units $10^{-2}$ )	EVTS	DOCUMENT ID	TECN	COMMENT
<b>5.99±0.18 OUR FIT</b>				
<b>5.98±0.08±0.16</b>		<sup>40</sup> DOBBS	07	CLEO $e^+e^-$ at $\psi(3770)$
••• We do not use the following data for averages, fits, limits, etc. •••				
6.0 ±0.2 ±0.2	4840±100	<sup>40</sup> HE	05	CLEO See DOBBS 07
5.8 ±1.2 ±1.2	142	COFFMAN	92b	MRK3 $e^+e^-$ 3.77 GeV
6.3 $^{+1.4}_{-1.3}$ ±1.2	175	BALTRUSAIT..86E	MRK3	See COFFMAN 92b

<sup>40</sup> DOBBS 07 and HE 05 use single- and double-tagged events in an overall fit. DOBBS 07 supersedes HE 05.

 $\Gamma(K_S^02\pi^+\pi^-)/\Gamma_{\text{total}}$   $\Gamma_{55}/\Gamma$ 

See our 2008 Review (Physics Letters **B667** 1 (2008)) for measurements of submodes of this mode. There is nothing new since 1992, and the two papers, ANJOS 92c, with 229 ± 17 events above background, and COFFMAN 92b, with 209 ± 20 such events, could not determine submode fractions with much accuracy.

VALUE (units $10^{-2}$ )	EVTS	DOCUMENT ID	TECN	COMMENT
<b>3.12 ±0.11 OUR FIT</b>				
<b>3.122±0.046±0.096</b>		<sup>41</sup> DOBBS	07	CLEO $e^+e^-$ at $\psi(3770)$
••• We do not use the following data for averages, fits, limits, etc. •••				
3.2 ±0.1 ±0.2	3210 ± 85	<sup>41</sup> HE	05	CLEO See DOBBS 07
2.1 $^{+1.0}_{-0.9}$		<sup>42</sup> BARLAG	92c	ACCM $\pi^-$ Cu 230 GeV
3.3 ±0.8 ±0.2	168	ADLER	88c	MRK3 $e^+e^-$ 3.77 GeV

<sup>41</sup> DOBBS 07 and HE 05 use single- and double-tagged events in an overall fit. DOBBS 07 supersedes HE 05.

<sup>42</sup> BARLAG 92c computes the branching fraction by topological normalization.

 $\Gamma(K^-3\pi^+\pi^-)/\Gamma(K^-2\pi^+)$   $\Gamma_{56}/\Gamma_{40}$ 

VALUE	EVTS	DOCUMENT ID	TECN	COMMENT
<b>0.061±0.005 OUR FIT</b>				Error includes scale factor of 1.1.
<b>0.062±0.008 OUR AVERAGE</b>				Error includes scale factor of 1.3.
0.058±0.002±0.006	2923	LINK	03D	FOCS $\gamma$ A, $\bar{E}_\gamma \approx 180$ GeV
0.077±0.008±0.010	239	FRABETTI	97c	E687 $\gamma$ Be, $\bar{E}_\gamma \approx 200$ GeV
••• We do not use the following data for averages, fits, limits, etc. •••				
0.09 ±0.01 ±0.01	113	ANJOS	90D	E691 Photoproduction

 $\Gamma(\bar{K}^*(892)^02\pi^+\pi^-, \bar{K}^*(892)^0 \rightarrow K^- \pi^+)/\Gamma(K^-3\pi^+\pi^-)$   $\Gamma_{57}/\Gamma_{56}$ 

VALUE	DOCUMENT ID	TECN	COMMENT
<b>0.21±0.04±0.06</b>	LINK	03D	FOCS $\gamma$ A, $\bar{E}_\gamma \approx 180$ GeV

 $\Gamma(\bar{K}^*(892)^0\rho^0\pi^+, \bar{K}^*(892)^0 \rightarrow K^- \pi^+)/\Gamma(K^-3\pi^+\pi^-)$   $\Gamma_{58}/\Gamma_{56}$ 

VALUE	DOCUMENT ID	TECN	COMMENT
<b>0.40±0.03±0.06</b>	LINK	03D	FOCS $\gamma$ A, $\bar{E}_\gamma \approx 180$ GeV

 $\Gamma(\bar{K}^*(892)^0\rho^0\pi^+, \bar{K}^*(892)^0 \rightarrow K^- \pi^+)/\Gamma(K^-2\pi^+)$   $\Gamma_{58}/\Gamma_{40}$ 

VALUE	DOCUMENT ID	TECN	COMMENT
••• We do not use the following data for averages, fits, limits, etc. •••			
0.016±0.007±0.004	FRABETTI	97c	E687 $\gamma$ Be, $\bar{E}_\gamma \approx 200$ GeV

 $\Gamma(\bar{K}^*(892)^02\pi^+\pi^-\text{non-}\rho, \bar{K}^*(892)^0 \rightarrow K^- \pi^+)/\Gamma(K^-2\pi^+)$   $\Gamma_{60}/\Gamma_{40}$ 

VALUE	DOCUMENT ID	TECN	COMMENT
••• We do not use the following data for averages, fits, limits, etc. •••			
0.032±0.010±0.008	FRABETTI	97c	E687 $\gamma$ Be, $\bar{E}_\gamma \approx 200$ GeV

 $\Gamma(K^- \rho^0 2\pi^+)/\Gamma(K^-3\pi^+\pi^-)$   $\Gamma_{61}/\Gamma_{56}$ 

VALUE	DOCUMENT ID	TECN	COMMENT
<b>0.30±0.04±0.01</b>	LINK	03D	FOCS $\gamma$ A, $\bar{E}_\gamma \approx 180$ GeV

 $\Gamma(K^- \rho^0 2\pi^+)/\Gamma(K^-2\pi^+)$   $\Gamma_{61}/\Gamma_{40}$ 

VALUE	DOCUMENT ID	TECN	COMMENT
••• We do not use the following data for averages, fits, limits, etc. •••			
0.034±0.009±0.005	FRABETTI	97c	E687 $\gamma$ Be, $\bar{E}_\gamma \approx 200$ GeV

 $\Gamma(\bar{K}^*(892)^0 a_1(1260)^+)/\Gamma(K^-2\pi^+)$   $\Gamma_{59}/\Gamma_{40}$ 

VALUE	DOCUMENT ID	TECN	COMMENT
<b>0.099±0.008±0.018</b>	LINK	03D	FOCS $\gamma$ A, $\bar{E}_\gamma \approx 180$ GeV

 $\Gamma(K^-3\pi^+\pi^- \text{ nonresonant})/\Gamma(K^-3\pi^+\pi^-)$   $\Gamma_{62}/\Gamma_{56}$ 

VALUE	CL%	DOCUMENT ID	TECN	COMMENT
<b>0.07 ±0.05±0.01</b>		LINK	03D	FOCS $\gamma$ A, $\bar{E}_\gamma \approx 180$ GeV
••• We do not use the following data for averages, fits, limits, etc. •••				
<0.026	90	FRABETTI	97c	E687 $\gamma$ Be, $\bar{E}_\gamma \approx 200$ GeV

 $\Gamma(K^+2K_S^0)/\Gamma(K^-2\pi^+)$   $\Gamma_{63}/\Gamma_{40}$ 

VALUE	EVTS	DOCUMENT ID	TECN	COMMENT
<b>0.049±0.022 OUR AVERAGE</b>				Error includes scale factor of 2.4.
0.035±0.010±0.005	39 ± 9	ALBRECHT	94I	ARG $e^+e^- \approx 10$ GeV
0.085±0.018	70 ± 12	AMMAR	91	CLEO $e^+e^- \approx 10.5$ GeV

 $\Gamma(K^+K^-K_S^0\pi^+)/\Gamma(K_S^02\pi^+\pi^-)$   $\Gamma_{64}/\Gamma_{55}$ 

VALUE (units $10^{-3}$ )	EVTS	DOCUMENT ID	TECN	COMMENT
<b>7.7±1.5±0.9</b>	35 ± 7	LINK	01c	FOCS $\gamma$ nucleus, $\bar{E}_\gamma \approx 180$ GeV

## Pionic modes

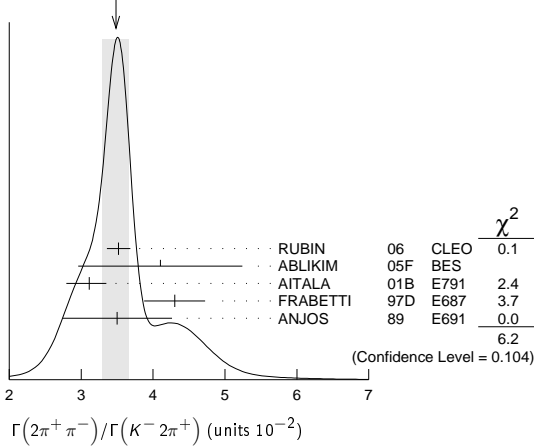
 $\Gamma(\pi^+\pi^0)/\Gamma(K^-2\pi^+)$   $\Gamma_{65}/\Gamma_{40}$ 

VALUE (units $10^{-2}$ )	EVTS	DOCUMENT ID	TECN	COMMENT
<b>1.31±0.06 OUR AVERAGE</b>				
1.29±0.04±0.05	2649 ± 76	MENDEZ	10	CLEO $e^+e^-$ at 3774 MeV
1.33±0.11±0.09	1229 ± 99	AUBERT,B	06F	BABR $e^+e^- \approx \gamma(4S)$
1.44±0.19±0.10	171 ± 22	ARMS	04	CLEO $e^+e^- \approx 10$ GeV
••• We do not use the following data for averages, fits, limits, etc. •••				
1.33±0.07±0.06	914 ± 46	RUBIN	06	CLEO See MENDEZ 10

 $\Gamma(2\pi^+\pi^-)/\Gamma(K^-2\pi^+)$   $\Gamma_{66}/\Gamma_{40}$ 

VALUE (units $10^{-2}$ )	EVTS	DOCUMENT ID	TECN	COMMENT
<b>3.48±0.19 OUR AVERAGE</b>				Error includes scale factor of 1.4. See the ideogram below.
3.52±0.11±0.12	3303 ± 95	RUBIN	06	CLEO $e^+e^-$ at $\psi(3770)$
4.1 ±1.1 ±0.3	85 ± 22	ABLIKIM	05F	BES $e^+e^- \approx \psi(3770)$
3.11±0.18 $^{+0.16}_{-0.26}$	1172	AITALA	01B	E791 $\pi^-$ nucleus, 500 GeV
4.3 ±0.3 ±0.3	236	FRABETTI	97D	E687 $\gamma$ Be $\approx 200$ GeV
3.5 ±0.7 ±0.3	83	ANJOS	89	E691 Photoproduction

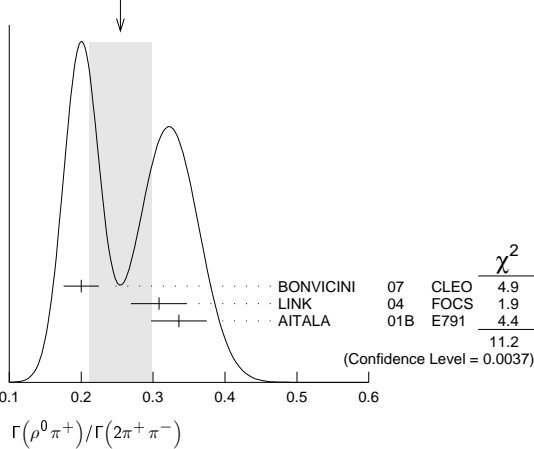
WEIGHTED AVERAGE  
3.48±0.19 (Error scaled by 1.4)



$\Gamma(\rho^0\pi^+)/\Gamma(2\pi^+\pi^-)$   $\Gamma_{67}/\Gamma_{66}$   
This is the "fit fraction" from the Dalitz-plot analysis.

VALUE	DOCUMENT ID	TECN	COMMENT
<b>0.25 ± 0.04 OUR AVERAGE</b>			Error includes scale factor of 2.4. See the ideogram below.
0.200 ± 0.023 ± 0.009	BONVICINI 07	CLEO	Dalitz fit, ≈ 2240 evts
0.3082 ± 0.0314 ± 0.0230	LINK 04	FOCS	Dalitz fit, 1527 ± 51 evts
0.336 ± 0.032 ± 0.022	AITALA 01B	E791	Dalitz fit, 1172 evts

WEIGHTED AVERAGE  
0.25±0.04 (Error scaled by 2.4)



$\Gamma(\pi^+(\pi^+\pi^-)_{S\text{-wave}})/\Gamma(2\pi^+\pi^-)$   $\Gamma_{68}/\Gamma_{66}$   
This is the "fit fraction" from the Dalitz-plot analysis. See also the next three data blocks.

VALUE	DOCUMENT ID	TECN	COMMENT
<b>0.5600 ± 0.0324 ± 0.0214</b>	43 LINK	04	FOCS Dalitz fit, 1527 ± 51 evts

<sup>43</sup>LINK 04 borrows a K-matrix parametrization from ANISOVICH 03 of the full  $\pi\pi$  S-wave isoscalar scattering amplitude to describe the  $\pi^+\pi^-$  S-wave component of the  $\pi^+\pi^+\pi^-$  state. The fit fraction given above is a sum over five  $f_0$  mesons, the  $f_0(980)$ ,  $f_0(1300)$ ,  $f_0(1200-1600)$ ,  $f_0(1500)$ , and  $f_0(1750)$ . See LINK 04 for details and discussion.

$\Gamma(\sigma\pi^+, \sigma \rightarrow \pi^+\pi^-)/\Gamma(2\pi^+\pi^-)$   $\Gamma_{69}/\Gamma_{66}$   
This is the "fit fraction" from the Dalitz-plot analysis.

VALUE	DOCUMENT ID	TECN	COMMENT
<b>0.422 ± 0.027 OUR AVERAGE</b>			
0.418 ± 0.014 ± 0.025	BONVICINI 07	CLEO	Dalitz fit, ≈ 2240 evts
0.463 ± 0.090 ± 0.021	AITALA 01B	E791	Dalitz fit, 1172 evts

$\Gamma(f_0(980)\pi^+, f_0(980) \rightarrow \pi^+\pi^-)/\Gamma(2\pi^+\pi^-)$   $\Gamma_{70}/\Gamma_{66}$   
This is the "fit fraction" from the Dalitz-plot analysis.

VALUE	DOCUMENT ID	TECN	COMMENT
<b>0.048 ± 0.010 OUR AVERAGE</b>			Error includes scale factor of 1.3.
0.041 ± 0.009 ± 0.003	BONVICINI 07	CLEO	Dalitz fit, ≈ 2240 evts
0.062 ± 0.013 ± 0.004	AITALA 01B	E791	Dalitz fit, 1172 evts

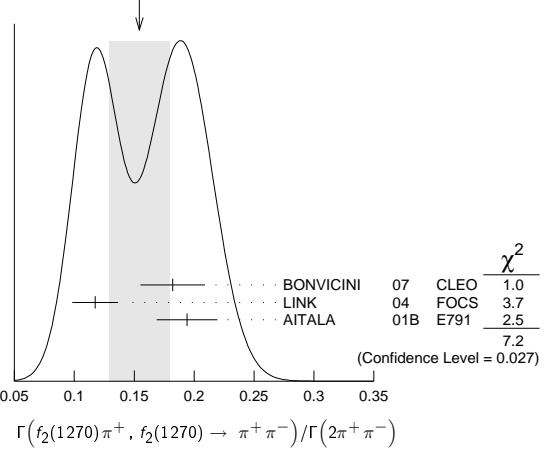
$\Gamma(f_0(1370)\pi^+, f_0(1370) \rightarrow \pi^+\pi^-)/\Gamma(2\pi^+\pi^-)$   $\Gamma_{71}/\Gamma_{66}$   
This is the "fit fraction" from the Dalitz-plot analysis.

VALUE	DOCUMENT ID	TECN	COMMENT
<b>0.024 ± 0.013 OUR AVERAGE</b>			
0.026 ± 0.018 ± 0.006	BONVICINI 07	CLEO	Dalitz fit, ≈ 2240 evts
0.023 ± 0.015 ± 0.008	AITALA 01B	E791	Dalitz fit, 1172 evts

$\Gamma(f_2(1270)\pi^+, f_2(1270) \rightarrow \pi^+\pi^-)/\Gamma(2\pi^+\pi^-)$   $\Gamma_{72}/\Gamma_{66}$   
This is the "fit fraction" from the Dalitz-plot analysis.

VALUE	DOCUMENT ID	TECN	COMMENT
<b>0.154 ± 0.025 OUR AVERAGE</b>			Error includes scale factor of 1.9. See the ideogram below.
0.182 ± 0.026 ± 0.007	BONVICINI 07	CLEO	Dalitz fit, ≈ 2240 evts
0.1174 ± 0.0190 ± 0.0029	LINK 04	FOCS	Dalitz fit, 1527 ± 51 evts
0.194 ± 0.025 ± 0.004	AITALA 01B	E791	Dalitz fit, 1172 evts

WEIGHTED AVERAGE  
0.154±0.025 (Error scaled by 1.9)



$\Gamma(\rho(1450)^0\pi^+, \rho(1450)^0 \rightarrow \pi^+\pi^-)/\Gamma(2\pi^+\pi^-)$   $\Gamma_{73}/\Gamma_{66}$   
This is the "fit fraction" from the Dalitz-plot analysis.

VALUE	CL%	DOCUMENT ID	TECN	COMMENT
<b>&lt;0.024</b>	95	BONVICINI 07	CLEO	Dalitz fit, ≈ 2240 evts
• • • We do not use the following data for averages, fits, limits, etc. • • •				
0.007 ± 0.007 ± 0.003		AITALA 01B	E791	Dalitz fit, 1172 evts

$\Gamma(f_0(1500)\pi^+, f_0(1500) \rightarrow \pi^+\pi^-)/\Gamma(2\pi^+\pi^-)$   $\Gamma_{74}/\Gamma_{66}$   
This is the "fit fraction" from the Dalitz-plot analysis.

VALUE	DOCUMENT ID	TECN	COMMENT
<b>0.034 ± 0.010 ± 0.008</b>	BONVICINI 07	CLEO	Dalitz fit, ≈ 2240 evts

$\Gamma(f_0(1710)\pi^+, f_0(1710) \rightarrow \pi^+\pi^-)/\Gamma(2\pi^+\pi^-)$   $\Gamma_{75}/\Gamma_{66}$   
This is the "fit fraction" from the Dalitz-plot analysis.

VALUE	CL%	DOCUMENT ID	TECN	COMMENT
<b>&lt;0.016</b>	95	BONVICINI 07	CLEO	Dalitz fit, ≈ 2240 evts

$\Gamma(f_0(1790)\pi^+, f_0(1790) \rightarrow \pi^+\pi^-)/\Gamma(2\pi^+\pi^-)$   $\Gamma_{76}/\Gamma_{66}$   
This is the "fit fraction" from the Dalitz-plot analysis.

VALUE	CL%	DOCUMENT ID	TECN	COMMENT
<b>&lt;0.02</b>	95	BONVICINI 07	CLEO	Dalitz fit, ≈ 2240 evts

$\Gamma((\pi^+\pi^+)_{S\text{-wave}}\pi^-)/\Gamma(2\pi^+\pi^-)$   $\Gamma_{77}/\Gamma_{66}$   
This is the "fit fraction" from the Dalitz-plot analysis.

VALUE	CL%	DOCUMENT ID	TECN	COMMENT
<b>&lt;0.037</b>	95	BONVICINI 07	CLEO	Dalitz fit, ≈ 2240 evts

$\Gamma(2\pi^+\pi^- \text{ nonresonant})/\Gamma(2\pi^+\pi^-)$   $\Gamma_{78}/\Gamma_{66}$   
This is the "fit fraction" from the Dalitz-plot analysis.

VALUE	CL%	DOCUMENT ID	TECN	COMMENT
<b>&lt;0.035</b>	95	BONVICINI 07	CLEO	Dalitz fit, ≈ 2240 evts
• • • We do not use the following data for averages, fits, limits, etc. • • •				
0.078 ± 0.060 ± 0.027		AITALA 01B	E791	Dalitz fit, 1172 evts

$\Gamma(\pi^+2\pi^0)/\Gamma(K^-2\pi^+)$   $\Gamma_{79}/\Gamma_{40}$

VALUE (units 10 <sup>-2</sup> )	EVTs	DOCUMENT ID	TECN	COMMENT
<b>5.0 ± 0.3 ± 0.3</b>	1535 ± 89	RUBIN 06	CLEO	$e^+e^-$ at $\psi(3770)$

$\Gamma(2\pi^+\pi^-\pi^0)/\Gamma(K^-2\pi^+)$   $\Gamma_{80}/\Gamma_{40}$

VALUE (units 10 <sup>-2</sup> )	EVTs	DOCUMENT ID	TECN	COMMENT
<b>12.4 ± 0.5 ± 0.6</b>	5701 ± 205	RUBIN 06	CLEO	$e^+e^-$ at $\psi(3770)$

$\Gamma(\eta\pi^+)/\Gamma_{\text{total}}$   $\Gamma_{84}/\Gamma$   
Unseen decay modes of the  $\eta$  are included.

VALUE (units 10 <sup>-4</sup> )	EVTs	DOCUMENT ID	TECN	COMMENT
<b>34.3 ± 1.4 ± 1.7</b>	1033 ± 42	ARTUSO 08	CLEO	See MENDEZ 10

• • • We do not use the following data for averages, fits, limits, etc. • • •

# Meson Particle Listings

## $D^{\pm}$

$\Gamma(\eta\pi^+)/\Gamma(K^-2\pi^+)$   $\Gamma_{84}/\Gamma_{40}$

Unseen decay modes of the  $\eta$  are included.

VALUE (units $10^{-2}$ )	EVTs	DOCUMENT ID	TECN	COMMENT
<b>3.87±0.09±0.19</b>	2940 ± 68	MENDEZ	10	CLEO $e^+e^-$ at 3774 MeV
● ● ● We do not use the following data for averages, fits, limits, etc. ● ● ●				
3.81±0.26±0.21	377 ± 26	RUBIN	06	CLEO See ARTUSO 08

$\Gamma(\omega\pi^+)/\Gamma_{total}$   $\Gamma_{86}/\Gamma$

Unseen decay modes of the  $\omega$  are included.

VALUE	CL%	DOCUMENT ID	TECN	COMMENT
<b>&lt;3.4 × 10<sup>-4</sup></b>	90	RUBIN	06	CLEO $e^+e^-$ at $\psi(3770)$

$\Gamma(3\pi^+2\pi^-)/\Gamma(K^-2\pi^+)$   $\Gamma_{83}/\Gamma_{40}$

VALUE (units $10^{-2}$ )	EVTs	DOCUMENT ID	TECN	COMMENT
<b>1.77±0.17 OUR FIT</b>				
<b>1.73±0.20±0.17</b>	732 ± 77	RUBIN	06	CLEO $e^+e^-$ at $\psi(3770)$
● ● ● We do not use the following data for averages, fits, limits, etc. ● ● ●				
2.3 ± 0.4 ± 0.2	58	FRABETTI	97c	E687 $\gamma$ Be, $\overline{E}_\gamma \approx 200$ GeV

$\Gamma(3\pi^+2\pi^-)/\Gamma(K^-3\pi^+\pi^-)$   $\Gamma_{83}/\Gamma_{56}$

VALUE	EVTs	DOCUMENT ID	TECN	COMMENT
<b>0.289±0.019 OUR FIT</b>				
<b>0.290±0.017±0.011</b>	835	LINK	03b	FOCS $\gamma$ A, $\overline{E}_\gamma \approx 180$ GeV

$\Gamma(\eta\pi^+\pi^0)/\Gamma_{total}$   $\Gamma_{85}/\Gamma$

VALUE (units $10^{-4}$ )	EVTs	DOCUMENT ID	TECN	COMMENT
<b>13.8±3.1±1.6</b>	149 ± 34	ARTUSO	08	CLEO $e^+e^-$ at $\psi(3770)$

$\Gamma(\eta'(958)\pi^+)/\Gamma_{total}$   $\Gamma_{87}/\Gamma$

Unseen decay modes of the  $\eta'(958)$  are included.

VALUE (units $10^{-4}$ )	EVTs	DOCUMENT ID	TECN	COMMENT
● ● ● We do not use the following data for averages, fits, limits, etc. ● ● ●				
44.2±2.5±2.9	352 ± 20	ARTUSO	08	CLEO See MENDEZ 10

$\Gamma(\eta'(958)\pi^+)/\Gamma(K^-2\pi^+)$   $\Gamma_{87}/\Gamma_{40}$

Unseen decay modes of the  $\eta'(958)$  are included.

VALUE (units $10^{-2}$ )	EVTs	DOCUMENT ID	TECN	COMMENT
<b>5.12±0.17±0.25</b>	1037 ± 35	MENDEZ	10	CLEO $e^+e^-$ at 3774 MeV

$\Gamma(\eta'(958)\pi^+\pi^0)/\Gamma_{total}$   $\Gamma_{88}/\Gamma$

Unseen decay modes of the  $\eta'(958)$  are included.

VALUE (units $10^{-4}$ )	EVTs	DOCUMENT ID	TECN	COMMENT
<b>15.7±4.3±2.5</b>	33 ± 9	ARTUSO	08	CLEO $e^+e^-$ at $\psi(3770)$

### Hadronic modes with a $K\overline{K}$ pair

$\Gamma(K^+K_S^0)/\Gamma_{total}$   $\Gamma_{89}/\Gamma$

VALUE (units $10^{-3}$ )	EVTs	DOCUMENT ID	TECN	COMMENT
● ● ● We do not use the following data for averages, fits, limits, etc. ● ● ●				
3.14±0.09±0.08	1971 ± 51	BONVICINI	08	CLEO See MENDEZ 10

$\Gamma(K^+K_S^0)/\Gamma(K_S^0\pi^+)$   $\Gamma_{89}/\Gamma_{38}$

VALUE	EVTs	DOCUMENT ID	TECN	COMMENT
<b>0.193 ± 0.007 OUR FIT</b>				Error includes scale factor of 3.2.
<b>0.1901 ± 0.0024 OUR AVERAGE</b>				
0.1899 ± 0.0011 ± 0.0022	101k ± 5.61	WON	09	BELL $e^+e^-$ at $\Upsilon(4S)$
0.1892 ± 0.0155 ± 0.0073	278 ± 21	ARMS	04	CLEO $e^+e^- \approx 10$ GeV
0.1996 ± 0.0119 ± 0.0096	949	LINK	02b	FOCS $\gamma$ A, $\overline{E}_\gamma \approx 180$ GeV
● ● ● We do not use the following data for averages, fits, limits, etc. ● ● ●				
0.222 ± 0.037 ± 0.013	63 ± 10	ABLIKIM	05F	BES $e^+e^- \approx \psi(3770)$
0.222 ± 0.041 ± 0.019	70	BISHAI	97	CLEO See ARMS 04
0.25 ± 0.04 ± 0.02	129	FRABETTI	95	E687 $\gamma$ Be $\overline{E}_\gamma \approx 200$ GeV
0.271 ± 0.065 ± 0.039	69	ANJOS	90c	E691 $\gamma$ Be
0.317 ± 0.086 ± 0.048	31	BALTRUSAIT..85E	MRK3	$e^+e^-$ 3.77 GeV
0.25 ± 0.15	6	SCHINDLER	81	MRK2 $e^+e^-$ 3.771 GeV

$\Gamma(K^+K_S^0)/\Gamma(K^-2\pi^+)$   $\Gamma_{89}/\Gamma_{40}$

VALUE (units $10^{-2}$ )	EVTs	DOCUMENT ID	TECN	COMMENT
<b>3.11±0.16 OUR FIT</b>				Error includes scale factor of 3.3.
<b>3.35±0.06±0.07</b>	5161 ± 86	MENDEZ	10	CLEO $e^+e^-$ at 3774 MeV
● ● ● We do not use the following data for averages, fits, limits, etc. ● ● ●				
3.02±0.18±0.15	949	LINK	02b	FOCS $\gamma$ nucleus, $\overline{E}_\gamma \approx 180$ GeV
44 This LINK 02b result is redundant with a result in the previous datablock.				

$\Gamma(K^+K^-\pi^+)/\Gamma_{total}$   $\Gamma_{90}/\Gamma$

VALUE (units $10^{-2}$ )	EVTs	DOCUMENT ID	TECN	COMMENT
<b>0.954±0.026 OUR FIT</b>				Error includes scale factor of 1.1.
<b>0.935±0.017±0.024</b>				
● ● ● We do not use the following data for averages, fits, limits, etc. ● ● ●				
0.97 ± 0.04 ± 0.04	1250 ± 40	<sup>45</sup> HE	05	CLEO See DOBBS 07
<sup>45</sup> DOBBS 07 and HE 05 use single- and double-tagged events in an overall fit. DOBBS 07 supersedes HE 05.				

$\Gamma(K^+K^-\pi^+)/\Gamma(K^-2\pi^+)$   $\Gamma_{90}/\Gamma_{40}$

VALUE	EVTs	DOCUMENT ID	TECN	COMMENT
<b>0.1045±0.0022 OUR FIT</b>				Error includes scale factor of 1.3.
<b>0.1058±0.0029 OUR AVERAGE</b>				Error includes scale factor of 1.4.
0.117 ± 0.013 ± 0.007	181 ± 20	ABLIKIM	05F	BES $e^+e^- \approx \psi(3770)$
0.107 ± 0.001 ± 0.002	43k	AUBERT	05s	BABR $e^+e^- \approx \Upsilon(4S)$
0.093 ± 0.010 <sup>+0.008</sup> / <sub>-0.006</sub>		JUN	00	SELX $\Sigma^-$ nucleus, 600 GeV
0.0976 ± 0.0042 ± 0.0046		FRABETTI	95b	E687 $\gamma$ Be, $\overline{E}_\gamma \approx 200$ GeV

$\Gamma(\phi\pi^+, \phi \rightarrow K^+K^-)/\Gamma(K^+K^-\pi^+)$   $\Gamma_{91}/\Gamma_{90}$

This is the "fit fraction" from the Dalitz-plot analysis.

VALUE (%)	DOCUMENT ID	TECN	COMMENT
<b>27.8±0.4<sup>+0.2</sup>/<sub>-0.5</sub></b>	RUBIN	08	CLEO Dalitz fit, 19,458±163 evts
● ● ● We do not use the following data for averages, fits, limits, etc. ● ● ●			
29.2 ± 3.1 ± 3.0	FRABETTI	95B	E687 Dalitz fit, 915 evts

$\Gamma(K^+K^*(892)^0, \overline{K}^*(892)^0 \rightarrow K^-\pi^+)/\Gamma(K^+K^-\pi^+)$   $\Gamma_{92}/\Gamma_{90}$

This is the "fit fraction" from the Dalitz-plot analysis.

VALUE (%)	DOCUMENT ID	TECN	COMMENT
<b>25.7±0.5<sup>+0.4</sup>/<sub>-1.2</sub></b>	RUBIN	08	CLEO Dalitz fit, 19,458±163 evts
● ● ● We do not use the following data for averages, fits, limits, etc. ● ● ●			
30.1 ± 2.0 ± 2.5	FRABETTI	95B	E687 Dalitz fit, 915 evts

$\Gamma(K^+K_S^0(1430)^0, \overline{K}_S^0(1430)^0 \rightarrow K^-\pi^+)/\Gamma(K^+K^-\pi^+)$   $\Gamma_{93}/\Gamma_{90}$

This is the "fit fraction" from the Dalitz-plot analysis.

VALUE (%)	DOCUMENT ID	TECN	COMMENT
<b>18.8±1.2<sup>+3.3</sup>/<sub>-3.4</sub></b>	RUBIN	08	CLEO Dalitz fit, 19,458±163 evts
● ● ● We do not use the following data for averages, fits, limits, etc. ● ● ●			
37.0 ± 3.5 ± 1.8	FRABETTI	95B	E687 Dalitz fit, 915 evts

$\Gamma(K^+K_S^0(1430)^0, \overline{K}_S^0 \rightarrow K^-\pi^+)/\Gamma(K^+K^-\pi^+)$   $\Gamma_{94}/\Gamma_{90}$

This is the "fit fraction" from the Dalitz-plot analysis.

VALUE (%)	DOCUMENT ID	TECN	COMMENT
<b>1.7±0.4<sup>+1.2</sup>/<sub>-0.7</sub></b>	RUBIN	08	CLEO Dalitz fit, 19,458±163 evts

$\Gamma(K^+K_S^0(800), \overline{K}_S^0 \rightarrow K^-\pi^+)/\Gamma(K^+K^-\pi^+)$   $\Gamma_{95}/\Gamma_{90}$

This is the "fit fraction" from the Dalitz-plot analysis.

VALUE (%)	DOCUMENT ID	TECN	COMMENT
<b>7.0±0.8<sup>+3.5</sup>/<sub>-2.0</sub></b>	RUBIN	08	CLEO Dalitz fit, 19,458±163 evts

$\Gamma(a_0(1450)^0\pi^+, a_0^0 \rightarrow K^+K^-)/\Gamma(K^+K^-\pi^+)$   $\Gamma_{96}/\Gamma_{90}$

This is the "fit fraction" from the Dalitz-plot analysis.

VALUE (%)	DOCUMENT ID	TECN	COMMENT
<b>4.6±0.6<sup>+7.2</sup>/<sub>-1.8</sub></b>	RUBIN	08	CLEO Dalitz fit, 19,458±163 evts

$\Gamma(\phi(1680)\pi^+, \phi \rightarrow K^+K^-)/\Gamma(K^+K^-\pi^+)$   $\Gamma_{97}/\Gamma_{90}$

This is the "fit fraction" from the Dalitz-plot analysis.

VALUE (%)	DOCUMENT ID	TECN	COMMENT
<b>0.51±0.11<sup>+0.37</sup>/<sub>-0.16</sub></b>	RUBIN	08	CLEO Dalitz fit, 19,458±163 evts

$\Gamma(K^*(892)^+K_S^0)/\Gamma(K_S^0\pi^+)$   $\Gamma_{105}/\Gamma_{38}$

Unseen decay modes of the  $K^*(892)^+$  are included.

VALUE	EVTs	DOCUMENT ID	TECN	COMMENT
<b>1.1 ± 0.3 ± 0.4</b>	67	FRABETTI	95	E687 $\gamma$ Be $\overline{E}_\gamma \approx 200$ GeV

$\Gamma(\phi\pi^+\pi^0)/\Gamma_{total}$   $\Gamma_{102}/\Gamma$

Unseen decay modes of the  $\phi$  are included.

VALUE	DOCUMENT ID	TECN	COMMENT
<b>0.023±0.010</b>	<sup>46</sup> BARLAG	92c	ACCM $\pi^-$ Cu 230 GeV
<sup>46</sup> BARLAG 92c computes the branching fraction using topological normalization.			

$\Gamma(\phi\rho^+)/\Gamma(K^-2\pi^+)$   $\Gamma_{103}/\Gamma_{40}$

Unseen decay modes of the  $\phi$  are included.

VALUE	CL%	DOCUMENT ID	TECN	COMMENT
<b>&lt;0.16</b>	90	DAOUDI	92	CLEO $e^+e^- \approx 10.5$ GeV

$\Gamma(K^+K^-\pi^+\pi^0 \text{ non-}\phi)/\Gamma_{total}$   $\Gamma_{104}/\Gamma$

VALUE	DOCUMENT ID	TECN	COMMENT
<b>0.015<sup>+0.007</sup>/<sub>-0.006</sub></b>	<sup>47</sup> BARLAG	92c	ACCM $\pi^-$ Cu 230 GeV
<sup>47</sup> BARLAG 92c computes the branching fraction using topological normalization.			

$\Gamma(K^+K^-\pi^+\pi^0 \text{ non-}\phi)/\Gamma(K^-2\pi^+)$   $\Gamma_{104}/\Gamma_{40}$

VALUE	CL%	DOCUMENT ID	TECN	COMMENT
<0.25	90	ANJOS	89E	E691 Photoproduction

$\Gamma(K^+K_S^0\pi^+\pi^-)/\Gamma(K_S^02\pi^+\pi^-)$   $\Gamma_{99}/\Gamma_{55}$

VALUE (units $10^{-2}$ )	EVTs	DOCUMENT ID	TECN	COMMENT
<b>5.62±0.39±0.40</b>	469 ± 32	LINK	01c	FOCS $\gamma$ nucleus, $\overline{E}_\gamma \approx 180$ GeV



$\Gamma(K_S^0 K^- 2\pi^+)/\Gamma(K_S^0 2\pi^+ \pi^-)$		$\Gamma_{100}/\Gamma_{55}$	
VALUE (units $10^{-2}$ )	EVTS	DOCUMENT ID	TECN COMMENT
<b>7.68 ± 0.41 ± 0.32</b>	670 ± 35	LINK	01c FOCS $\gamma$ nucleus, $\bar{E}_\gamma \approx 180$ GeV

$\Gamma(K^+ K^- 2\pi^+ \pi^-)/\Gamma(K^- 3\pi^+ \pi^-)$		$\Gamma_{101}/\Gamma_{56}$	
VALUE	EVTS	DOCUMENT ID	TECN COMMENT
<b>0.040 ± 0.009 ± 0.019</b>	38	LINK	03D FOCS $\gamma$ A, $\bar{E}_\gamma \approx 180$ GeV

## Doubly Cabibbo-suppressed modes

$\Gamma(K^+ \pi^0)/\Gamma_{total}$		$\Gamma_{106}/\Gamma$	
VALUE (units $10^{-4}$ )	EVTS	DOCUMENT ID	TECN COMMENT
<b>1.83 ± 0.26 OUR FIT</b>			Error includes scale factor of 1.4.
<b>2.52 ± 0.47 ± 0.26</b>	189 ± 37	AUBERT,B	06F BABR $e^+ e^- \approx \Upsilon(4S)$
• • • We do not use the following data for averages, fits, limits, etc. • • •			
2.28 ± 0.36 ± 0.17	148 ± 23	DYTMAN	06 CLEO See MENDEZ 10

$\Gamma(K^+ \pi^0)/\Gamma(K^- 2\pi^+)$		$\Gamma_{106}/\Gamma_{40}$	
VALUE (units $10^{-3}$ )	EVTS	DOCUMENT ID	TECN COMMENT
<b>2.01 ± 0.29 OUR FIT</b>			Error includes scale factor of 1.4.
<b>1.9 ± 0.2 ± 0.1</b>	343 ± 37	MENDEZ	10 CLEO $e^+ e^-$ at 3774 MeV

$\Gamma(K^+ \eta)/\Gamma(\eta \pi^+)$		$\Gamma_{107}/\Gamma_{84}$	
VALUE (%)	EVTS	DOCUMENT ID	TECN COMMENT
<b>3.06 ± 0.43 ± 0.14</b>	166 ± 23	WON	11 BELL $e^+ e^- \approx \Upsilon(4S)$

$\Gamma(K^+ \eta)/\Gamma(K^- 2\pi^+)$		$\Gamma_{107}/\Gamma_{40}$	
Unseen decay modes of the $\eta$ are included.			
VALUE (units $10^{-2}$ )	CL%	DOCUMENT ID	TECN COMMENT
<0.15	90	MENDEZ	10 CLEO $e^+ e^-$ at 3774 MeV
• • • We do not use the following data for averages, fits, limits, etc. • • •			

$\Gamma(K^+ \eta(958))/\Gamma(\eta(958) \pi^+)$		$\Gamma_{108}/\Gamma_{87}$	
VALUE (%)	EVTS	DOCUMENT ID	TECN COMMENT
<b>3.77 ± 0.39 ± 0.10</b>	180 ± 19	WON	11 BELL $e^+ e^- \approx \Upsilon(4S)$

$\Gamma(K^+ \eta(958))/\Gamma(K^- 2\pi^+)$		$\Gamma_{108}/\Gamma_{40}$	
Unseen decay modes of the $\eta(958)$ are included.			
VALUE (units $10^{-2}$ )	CL%	DOCUMENT ID	TECN COMMENT
<0.20	90	MENDEZ	10 CLEO $e^+ e^-$ at 3774 MeV
• • • We do not use the following data for averages, fits, limits, etc. • • •			

$\Gamma(K^+ \pi^+ \pi^-)/\Gamma(K^- 2\pi^+)$		$\Gamma_{109}/\Gamma_{40}$	
VALUE (units $10^{-3}$ )	EVTS	DOCUMENT ID	TECN COMMENT
<b>5.77 ± 0.22 OUR AVERAGE</b>			
5.69 ± 0.18 ± 0.14	2638 ± 84	KO	09 BELL $e^+ e^-$ at $\Upsilon(4S)$
6.5 ± 0.8 ± 0.4	189 ± 24	LINK	04F FOCS $\gamma$ A, $\bar{E}_\gamma \approx 180$ GeV
7.7 ± 1.7 ± 0.8	59 ± 13	AITALA	97C E791 $\pi^-$ A, 500 GeV
7.2 ± 2.3 ± 1.7	21	FRABETTI	95E E687 $\gamma$ Be, $\bar{E}_\gamma = 220$ GeV

$\Gamma(K^+ \rho^0)/\Gamma(K^+ \pi^+ \pi^-)$		$\Gamma_{110}/\Gamma_{109}$	
This is the "fit fraction" from the Dalitz-plot analysis.			
VALUE	DOCUMENT ID	TECN	COMMENT
<b>0.39 ± 0.09 OUR AVERAGE</b>			
0.3943 ± 0.0787 ± 0.0815	LINK	04F FOCS	Dalitz fit, 189 evts
0.37 ± 0.14 ± 0.07	AITALA	97C E791	Dalitz fit, 59 evts

$\Gamma(K^+ f_0(980), f_0(980) \rightarrow \pi^+ \pi^-)/\Gamma(K^+ \pi^+ \pi^-)$		$\Gamma_{112}/\Gamma_{109}$	
This is the "fit fraction" from the Dalitz-plot analysis.			
VALUE	DOCUMENT ID	TECN	COMMENT
<b>0.0892 ± 0.0333 ± 0.0412</b>	LINK	04F FOCS	Dalitz fit, 189 evts

$\Gamma(K^*(892)^0 \pi^+, K^*(892)^0 \rightarrow K^+ \pi^-)/\Gamma(K^+ \pi^+ \pi^-)$		$\Gamma_{111}/\Gamma_{109}$	
This is the "fit fraction" from the Dalitz-plot analysis.			
VALUE	DOCUMENT ID	TECN	COMMENT
<b>0.47 ± 0.08 OUR AVERAGE</b>			
0.5220 ± 0.0684 ± 0.0638	LINK	04F FOCS	Dalitz fit, 189 evts
0.35 ± 0.14 ± 0.01	AITALA	97C E791	Dalitz fit, 59 evts

$\Gamma(K_S^*(1430)^0 \pi^+, K_S^*(1430)^0 \rightarrow K^+ \pi^-)/\Gamma(K^+ \pi^+ \pi^-)$		$\Gamma_{113}/\Gamma_{109}$	
This is the "fit fraction" from the Dalitz-plot analysis.			
VALUE	DOCUMENT ID	TECN	COMMENT
<b>0.0803 ± 0.0372 ± 0.0391</b>	LINK	04F FOCS	Dalitz fit, 189 evts

$\Gamma(K^+ \pi^+ \pi^- \text{ nonresonant})/\Gamma(K^+ \pi^+ \pi^-)$		$\Gamma_{114}/\Gamma_{109}$	
This is the "fit fraction" from the Dalitz-plot analysis.			
VALUE	DOCUMENT ID	TECN	COMMENT
<0.36 ± 0.14 ± 0.07	48 AITALA	97C E791	Dalitz fit, 59 evts
• • • We do not use the following data for averages, fits, limits, etc. • • •			

<sup>48</sup>LINK 04F, with three times as many events, finds no need for a nonresonant amplitude.

$\Gamma(2K^+ K^-)/\Gamma(K^- 2\pi^+)$		$\Gamma_{115}/\Gamma_{40}$	
VALUE (units $10^{-4}$ )	EVTS	DOCUMENT ID	TECN COMMENT
<b>9.49 ± 2.17 ± 0.22</b>	65	<sup>49</sup> LINK	02i FOCS $\gamma$ nucleus, $\approx 180$ GeV

<sup>49</sup>LINK 02i finds little evidence for  $\phi K^+$  or  $f_0(980) K^+$  submodes.

## Rare or forbidden modes

$\Gamma(\pi^+ e^+ e^-)/\Gamma_{total}$		$\Gamma_{116}/\Gamma$	
A test for the $\Delta C = 1$ weak neutral current. Allowed by higher-order electroweak interactions.			
VALUE	CL%	EVTS	DOCUMENT ID TECN COMMENT
<1.1 × 10 <sup>-6</sup>	90	-3.9 ± 2.3	LEES 11G BABR $e^+ e^- \approx \Upsilon(4S)$

• • • We do not use the following data for averages, fits, limits, etc. • • •			
<5.9 × 10 <sup>-6</sup>	90		<sup>50</sup> RUBIN 10 CLEO $e^+ e^-$ at $\psi(3770)$
<7.4 × 10 <sup>-6</sup>	90		HE 05A CLEO See RUBIN 10
<5.2 × 10 <sup>-5</sup>	90		AITALA 99G E791 $\pi^-$ N 500 GeV
<1.1 × 10 <sup>-4</sup>	90		FRABETTI 97B E687 $\gamma$ Be, $\bar{E}_\gamma \approx 220$ GeV
<6.6 × 10 <sup>-5</sup>	90		AITALA 96 E791 $\pi^-$ N 500 GeV
<2.5 × 10 <sup>-3</sup>	90		WEIR 90B MRK2 $e^+ e^-$ 29 GeV
<2.6 × 10 <sup>-3</sup>	90	39	HAAS 88 CLEO $e^+ e^-$ 10 GeV

<sup>50</sup>This RUBIN 10 limit is for the  $e^+ e^-$  mass in the continuum away from the  $\phi(1020)$ . See the next data block.

$\Gamma(\pi^+ \phi, \phi \rightarrow e^+ e^-)/\Gamma_{total}$		$\Gamma_{117}/\Gamma$	
This is <i>not</i> a test for the $\Delta C = 1$ weak neutral current, but leads to the $\pi^+ e^+ e^-$ final state.			
VALUE	EVTS	DOCUMENT ID	TECN COMMENT
<b>(1.7 ± 1.4 ± 0.1) × 10<sup>-6</sup></b>	4	<sup>51</sup> RUBIN 10	CLEO $e^+ e^-$ at $\psi(3770)$

• • • We do not use the following data for averages, fits, limits, etc. • • •			
(2.7 ± 3.6 ± 0.2) × 10 <sup>-6</sup>	2	HE	05A CLEO See RUBIN 10

<sup>51</sup>This RUBIN 10 result is consistent with the known  $D^+ \rightarrow \phi \pi^+$  and  $\phi \rightarrow e^+ e^-$  fractions.

$\Gamma(\pi^+ \mu^+ \mu^-)/\Gamma_{total}$		$\Gamma_{118}/\Gamma$	
A test for the $\Delta C = 1$ weak neutral current. Allowed by higher-order electroweak interactions.			
VALUE	CL%	EVTS	DOCUMENT ID TECN COMMENT
<3.9 × 10 <sup>-6</sup>	90		<sup>52</sup> ABAZOV 08D D0 $p\bar{p}$ , $E_{cm} = 1.96$ TeV

• • • We do not use the following data for averages, fits, limits, etc. • • •			
<6.5 × 10 <sup>-6</sup>	90	-0.2 ± 2.9	LEES 11G BABR $e^+ e^- \approx \Upsilon(4S)$
<8.8 × 10 <sup>-6</sup>	90		LINK 03F FOCS $\gamma$ nucleus, $\bar{E}_\gamma \approx 180$ GeV
<1.5 × 10 <sup>-5</sup>	90		AITALA 99G E791 $\pi^-$ N 500 GeV
<8.9 × 10 <sup>-5</sup>	90		FRABETTI 97B E687 $\gamma$ Be, $\bar{E}_\gamma \approx 220$ GeV
<1.8 × 10 <sup>-5</sup>	90		AITALA 96 E791 $\pi^-$ N 500 GeV
<2.2 × 10 <sup>-4</sup>	90	0	KODAMA 95 E653 $\pi^-$ emulsion 600 GeV
<5.9 × 10 <sup>-3</sup>	90		WEIR 90B MRK2 $e^+ e^-$ 29 GeV
<2.9 × 10 <sup>-3</sup>	90	36	HAAS 88 CLEO $e^+ e^-$ 10 GeV

<sup>52</sup>This ABAZOV 08D limit is for the  $\mu^+ \mu^-$  mass in the continuum away from the  $\phi(1020)$ . See the next data block.

$\Gamma(\pi^+ \phi, \phi \rightarrow \mu^+ \mu^-)/\Gamma_{total}$		$\Gamma_{119}/\Gamma$	
This is <i>not</i> a test for the $\Delta C = 1$ weak neutral current, but leads to the $\pi^+ \mu^+ \mu^-$ final state.			
VALUE	DOCUMENT ID	TECN	COMMENT
<b>(1.8 ± 0.5 ± 0.6) × 10<sup>-6</sup></b>	<sup>53</sup> ABAZOV	08D D0	$p\bar{p}$ , $E_{cm} = 1.96$ TeV

<sup>53</sup>This ABAZOV 08D value is consistent with the known  $D^+ \rightarrow \phi \pi^+$  and  $\phi \rightarrow \mu^+ \mu^-$  fractions.

$\Gamma(\rho^+ \mu^+ \mu^-)/\Gamma_{total}$		$\Gamma_{120}/\Gamma$	
A test for the $\Delta C = 1$ weak neutral current. Allowed by higher-order electroweak interactions.			
VALUE	CL%	EVTS	DOCUMENT ID TECN COMMENT
<5.6 × 10 <sup>-4</sup>	90	0	KODAMA 95 E653 $\pi^-$ emulsion 600 GeV

$\Gamma(K^+ e^+ e^-)/\Gamma_{total}$		$\Gamma_{121}/\Gamma$	
Both quarks would have to change flavor for this decay to occur.			
VALUE	CL%	EVTS	DOCUMENT ID TECN COMMENT
<1.0 × 10 <sup>-6</sup>	90	-3.7 ± 4.4	LEES 11G BABR $e^+ e^- \approx \Upsilon(4S)$

• • • We do not use the following data for averages, fits, limits, etc. • • •			
<3.0 × 10 <sup>-6</sup>	90		RUBIN 10 CLEO $e^+ e^-$ at $\psi(3770)$
<6.2 × 10 <sup>-6</sup>	90		HE 05A CLEO See RUBIN 10
<2.0 × 10 <sup>-4</sup>	90		AITALA 99G E791 $\pi^-$ N 500 GeV
<2.0 × 10 <sup>-4</sup>	90		FRABETTI 97B E687 $\gamma$ Be, $\bar{E}_\gamma \approx 220$ GeV
<4.8 × 10 <sup>-3</sup>	90		WEIR 90B MRK2 $e^+ e^-$ 29 GeV







FRABETTI	95	PL B346 199	P.L. Frabetti et al.	(FNAL E687 Collab.)
FRABETTI	95B	PL B351 591	P.L. Frabetti et al.	(FNAL E687 Collab.)
FRABETTI	95E	PL B359 403	P.L. Frabetti et al.	(FNAL E687 Collab.)
KODAMA	95	PL B345 85	K. Kodama et al.	(FNAL E653 Collab.)
ALBRECHT	94I	ZPHY C64 375	H. Albrecht et al.	(ARGUS Collab.)
BALEST	94	PRL 72 2328	R. Balest et al.	(CLEO Collab.)
FRABETTI	94D	PL B323 459	P.L. Frabetti et al.	(FNAL E687 Collab.)
FRABETTI	94G	PL B331 217	P.L. Frabetti et al.	(FNAL E687 Collab.)
FRABETTI	94I	PR D50 R2953	P.L. Frabetti et al.	(FNAL E687 Collab.)
AKERIB	93	PRL 71 3070	D.S. Akerib et al.	(CLEO Collab.)
ANJOS	93	PR D48 56	J.C. Anjos et al.	(FNAL E691 Collab.)
FRABETTI	93E	PL B307 262	P.L. Frabetti et al.	(FNAL E687 Collab.)
ALBRECHT	92F	PL B278 202	H. Albrecht et al.	(ARGUS Collab.)
ANJOS	92C	PR D46 1941	J.C. Anjos et al.	(FNAL E691 Collab.)
BARLAG	92C	ZPHY C55 383	S. Barlag et al.	(ACCMOR Collab.)
Also		ZPHY C48 29	S. Barlag et al.	(ACCMOR Collab.)
COFFMAN	92B	PR D45 2196	D.M. Coffman et al.	(Mark III Collab.)
DAOUDI	92	PR D45 3965	M. Daoudi et al.	(CLEO Collab.)
KODAMA	92	PL B274 246	K. Kodama et al.	(FNAL E653 Collab.)
KODAMA	92C	PL B286 187	K. Kodama et al.	(FNAL E653 Collab.)
ADAMOVIICH	91	PL B268 142	M.I. Adamovich et al.	(WA82 Collab.)
ALBRECHT	91	PL B255 634	H. Albrecht et al.	(ARGUS Collab.)
ALVAREZ	91B	ZPHY C50 11	M.P. Alvarez et al.	(CERN NA14/2 Collab.)
AMMAR	91	PR D44 3383	R. Ammar et al.	(CLEO Collab.)
BAI	91	PRL 66 1011	Z. Bai et al.	(Mark III Collab.)
COFFMAN	91	PL B263 135	D.M. Coffman et al.	(Mark III Collab.)
FRABETTI	91	PL B263 584	P.L. Frabetti et al.	(FNAL E687 Collab.)
ALVAREZ	90	ZPHY C47 539	M.P. Alvarez et al.	(CERN NA14/2 Collab.)
ANJOS	90C	PR D41 2705	J.C. Anjos et al.	(FNAL E691 Collab.)
ANJOS	90D	PR D42 2414	J.C. Anjos et al.	(FNAL E691 Collab.)
ANJOS	90E	PRL 65 2630	J.C. Anjos et al.	(FNAL E691 Collab.)
BARLAG	90C	ZPHY C46 563	S. Barlag et al.	(ACCMOR Collab.)
WEIR	90B	PR D41 1384	A.J. Weir et al.	(Mark II Collab.)
ANJOS	89	PRL 62 125	J.C. Anjos et al.	(FNAL E691 Collab.)
ANJOS	89B	PRL 62 722	J.C. Anjos et al.	(FNAL E691 Collab.)
ANJOS	89E	PL B223 267	J.C. Anjos et al.	(FNAL E691 Collab.)
ADLER	88C	PRL 60 89	J. Adler et al.	(Mark III Collab.)
ALBRECHT	88I	PL B210 267	H. Albrecht et al.	(ARGUS Collab.)
HAAS	88	PRL 60 1614	P. Haas et al.	(CLEO Collab.)
ONG	88	PRL 60 2587	R.A. Ong et al.	(Mark II Collab.)
RAAB	88	PR D37 2391	J.R. Raab et al.	(FNAL E691 Collab.)
ADAMOVIICH	87	EPL 4 897	M.I. Adamovich et al.	(Photon Emission Collab.)
ADLER	87	PL B196 107	J. Adler et al.	(Mark III Collab.)
BARTEL	87	ZPHY C33 339	W. Bartel et al.	(JADE Collab.)
BALTRUSAITIS...86E		PRL 56 2140	R.M. Baltrusaitis et al.	(Mark III Collab.)
BALTRUSAITIS...85B		PRL 54 1976	R.M. Baltrusaitis et al.	(Mark III Collab.)
BALTRUSAITIS...85E		PRL 55 150	R.M. Baltrusaitis et al.	(Mark III Collab.)
BARTEL	85J	PL 163B 277	W. Bartel et al.	(JADE Collab.)
ADAMOVIICH	84	PL 140B 119	M.I. Adamovich et al.	(CERN WA58 Collab.)
ALTHOFF	84G	ZPHY C22 219	M. Althoff et al.	(TASSO Collab.)
DERRICK	84	PRL 53 1971	M. Derrick et al.	(HRS Collab.)
SCHINDLER	81	PR D24 78	R.H. Schindler et al.	(Mark II Collab.)
TRILLING	81	PRPL 75 57	G.H. Trilling	(LBL UCB J)
ZHOLENTZ	80	PL 96B 214	A.A. Zholents et al.	(NOVO)
Also		SJNP 34 814	A.A. Zholents et al.	(NOVO)
		Translated from YAF 34 1471.		
GOLDHABER	77	PL 69B 503	G. Goldhaber et al.	(Mark I Collab.)
PERUZZI	77	PRL 39 1301	I. Peruzzi et al.	(LGVW Collab.)
PICCOLO	77	PL 70B 260	M. Piccolo et al.	(Mark I Collab.)
PERUZZI	76	PRL 37 569	I. Peruzzi et al.	(Mark I Collab.)

## OTHER RELATED PAPERS

RICHMAN	95	RMP 67 893	J.D. Richman, P.R. Burchat	(UCSB, STAN)
ROSNER	95	CNPP 21 369	J. Rosner	(CHIC)

 $D^0$ 

$$I(J^P) = \frac{1}{2}(0^-)$$

 $D^0$  MASS

The fit includes  $D^\pm, D^0, D_s^\pm, D^{*\pm}, D^{*0}, D_s^{*\pm}, D_1(2420)^0, D_2^*(2460)^0$ , and  $D_{s1}(2536)^\pm$  mass and mass difference measurements.

VALUE (MeV)	EVTs	DOCUMENT ID	TECN	COMMENT
<b>1864.86 ± 0.13</b>	<b>OUR FIT</b>			
<b>1864.91 ± 0.17</b>	<b>OUR AVERAGE</b>			
1865.30 ± 0.33	±0.23 98 ± 13	ANASHIN	10A	KEDR $e^+e^-$ at $\psi(3770)$
1864.847 ± 0.150	±0.095 319 ± 18	CAWLFIELD	07	CLEO $D^0 \rightarrow K_S^0 \phi$
1864.6 ± 0.3	±1.0 641	BARLAG	90c	ACCM $\pi^- \text{Cu}$ 230 GeV
•••	We do not use the following data for averages, fits, limits, etc. •••			
1852 ± 7	16	ADAMOVIICH	87	EMUL Photoproduction
1856 ± 36	22	ADAMOVIICH	84b	EMUL Photoproduction
1861 ± 4		DERRICK	84	HRS $e^+e^-$ 29 GeV
1847 ± 7	1	FIORINO	81	EMUL $\gamma N \rightarrow \bar{D}^0 +$
1863.8 ± 0.5		1 SCHINDLER	81	MRK2 $e^+e^-$ 3.77 GeV
1864.7 ± 0.6		1 TRILLING	81	RVUE $e^+e^-$ 3.77 GeV
1863.0 ± 2.5	238	ASTON	80E	OMEG $\gamma p \rightarrow \bar{D}^0$
1860 ± 2	143	2 AVERY	80	SPEC $\gamma N \rightarrow D^{*+}$
1869 ± 4	35	2 AVERY	80	SPEC $\gamma N \rightarrow D^{*+}$
1854 ± 6	94	2 ATIYA	79	SPEC $\gamma N \rightarrow D^0 \bar{D}^0$
1850 ± 15	64	BALTAY	78c	HBC $\nu N \rightarrow K^0 \pi \pi$
1863 ± 3		GOLDHABER	77	MRK1 $D^0, D^+$ recoil spectra
1863.3 ± 0.9		1 PERUZZI	77	LGW $e^+e^-$ 3.77 GeV
1868 ± 11		PICCOLO	77	MRK1 $e^+e^-$ 4.03, 4.41 GeV
1865 ± 15	234	GOLDHABER	76	MRK1 $K\pi$ and $K3\pi$

<sup>1</sup> PERUZZI 77 and SCHINDLER 81 errors do not include the 0.13% uncertainty in the absolute SPEAR energy calibration. TRILLING 81 uses the high precision  $J/\psi(1S)$  and  $\psi(2S)$  measurements of ZHOLENTZ 80 to determine this uncertainty and combines the PERUZZI 77 and SCHINDLER 81 results to obtain the value quoted. TRILLING 81 enters the fit in the  $D^\pm$  mass, and PERUZZI 77 and SCHINDLER 81 enter in the  $m_{D^\pm} - m_{D^0}$ , below.

<sup>2</sup> Error does not include possible systematic mass scale shift, estimated to be less than 5 MeV.

 $m_{D^\pm} - m_{D^0}$ 

The fit includes  $D^\pm, D^0, D_s^\pm, D^{*\pm}, D^{*0}, D_s^{*\pm}, D_1(2420)^0, D_2^*(2460)^0$ , and  $D_{s1}(2536)^\pm$  mass and mass difference measurements.

VALUE (MeV)	DOCUMENT ID	TECN	COMMENT
<b>4.76 ± 0.10</b>	<b>OUR FIT</b>		Error includes scale factor of 1.1.
<b>4.74 ± 0.28</b>	<b>OUR AVERAGE</b>		
4.7 ± 0.3	1 SCHINDLER	81	MRK2 $e^+e^-$ 3.77 GeV
5.0 ± 0.8	1 PERUZZI	77	LGW $e^+e^-$ 3.77 GeV

<sup>1</sup> See the footnote on TRILLING 81 in the  $D^0$  and  $D^\pm$  sections on the mass.

 $D^0$  MEAN LIFE

Measurements with an error  $> 10 \times 10^{-15}$  s have been omitted from the average.

VALUE ( $10^{-15}$ s)	EVTs	DOCUMENT ID	TECN	COMMENT
<b>410.1 ± 1.5</b>	<b>OUR AVERAGE</b>			
409.6 ± 1.1 ± 1.5	210k	LINK	02F	FOCS $\gamma$ nucleus, $\approx 180$ GeV
407.9 ± 6.0 ± 4.3	10k	KUSHNIR..	01	SELX $K^- \pi^+, K^- \pi^+ \pi^+ \pi^-$
413 ± 3 ± 4	35k	AITALA	99E	E791 $K^- \pi^+$
408.5 ± 4.1 ± 3.5	± 3.4 25k	BONVICINI	99	CLE2 $e^+e^- \approx \Gamma(4S)$
413 ± 4 ± 3	16k	FRABETTI	94D	E687 $K^- \pi^+, K^- \pi^+ \pi^+ \pi^-$
•••	We do not use the following data for averages, fits, limits, etc. •••			
424 ± 11 ± 7	5118	FRABETTI	91	E687 $K^- \pi^+, K^- \pi^+ \pi^+ \pi^-$
417 ± 18 ± 15	890	ALVAREZ	90	NA14 $K^- \pi^+, K^- \pi^+ \pi^+ \pi^-$
388 +23 -21	641	1 BARLAG	90c	ACCM $\pi^- \text{Cu}$ 230 GeV
480 ± 40 ± 30	776	ALBRECHT	88I	ARG $e^+e^-$ 10 GeV
422 ± 8 ± 10	4212	RAAB	88	E691 Photoproduction
420 ± 50	90	BARLAG	87b	ACCM $K^-$ and $\pi^-$ 200 GeV

<sup>1</sup> BARLAG 90c estimate systematic error to be negligible.

 $D^0 - \bar{D}^0$  MIXING

Revised March 2012 by D. Asner (Pacific Northwest National Laboratory)

The detailed formalism for  $D^0 - \bar{D}^0$  mixing is presented in the note on “ $CP$  Violation in Meson Decays” in this *Review*. For completeness, we present an overview here. The time evolution of the  $D^0 - \bar{D}^0$  system is described by the Schrödinger equation

$$i \frac{\partial}{\partial t} \begin{pmatrix} D^0(t) \\ \bar{D}^0(t) \end{pmatrix} = \left( \mathbf{M} - \frac{i}{2} \mathbf{\Gamma} \right) \begin{pmatrix} D^0(t) \\ \bar{D}^0(t) \end{pmatrix}, \quad (1)$$

where the  $\mathbf{M}$  and  $\mathbf{\Gamma}$  matrices are Hermitian, and  $CPT$  invariance requires that  $M_{11} = M_{22} \equiv M$  and  $\Gamma_{11} = \Gamma_{22} \equiv \Gamma$ . The off-diagonal elements of these matrices describe the dispersive and absorptive parts of the mixing.

Because  $CP$  violation is expected to be quite small here, it is convenient to label the mass eigenstates by the  $CP$  quantum number in the limit of  $CP$  conservation. Thus, we write

$$|D_{1,2}\rangle = p|D^0\rangle \pm q|\bar{D}^0\rangle, \quad (2)$$

where

$$\left( \frac{q}{p} \right)^2 = \frac{M_{12}^* - \frac{i}{2}\Gamma_{12}^*}{M_{12} - \frac{i}{2}\Gamma_{12}}. \quad (3)$$

The normalization condition is  $|p|^2 + |q|^2 = 1$ . Our phase convention is  $CP|D^0\rangle = +|\bar{D}^0\rangle$ , and the sign is chosen so that  $D_1$  has  $CP$  even, or nearly so.

# Meson Particle Listings

## $D^0$

The corresponding eigenvalues are

$$\omega_{1,2} \equiv m_{1,2} - \frac{i}{2}\Gamma_{1,2} = \left(M - \frac{i}{2}\Gamma\right) \pm \frac{q}{p} \left(M_{12} - \frac{i}{2}\Gamma_{12}\right), \quad (4)$$

where  $m_{1,2}$  and  $\Gamma_{1,2}$  are the masses and widths of the  $D_{1,2}$ .

We define dimensionless mixing parameters  $x$  and  $y$  by

$$x \equiv (m_1 - m_2)/\Gamma = \Delta m/\Gamma \quad (5)$$

and

$$y \equiv (\Gamma_1 - \Gamma_2)/2\Gamma = \Delta\Gamma/2\Gamma, \quad (6)$$

where  $\Gamma \equiv (\Gamma_1 + \Gamma_2)/2$ . If  $CP$  is conserved, then  $M_{12}$  and  $\Gamma_{12}$  are real,  $\Delta m = 2M_{12}$ ,  $\Delta\Gamma = 2\Gamma_{12}$ , and  $p = q = 1/\sqrt{2}$ . The signs of  $\Delta m$  and  $\Delta\Gamma$  are to be determined experimentally.

The parameters  $x$  and  $y$  are measured in several ways. The most precise values are obtained using the time dependence of  $D$  decays. Since  $D^0\text{--}\bar{D}^0$  mixing is a small effect, the identifying tag of the initial particle as a  $D^0$  or a  $\bar{D}^0$  must be extremely accurate. The usual tag is the charge of the distinctive slow pion in the decay sequence  $D^{*+} \rightarrow D^0\pi^+$  or  $D^{*-} \rightarrow \bar{D}^0\pi^-$ . In current experiments, the probability of mistagging is about 0.1%. The large data samples produced at the  $B$ -factories allow the production flavor to also be determined by fully reconstructing charm on the ‘‘other side’’ of the event—significantly reducing the mistag rate [1]. Another tag of comparable accuracy is identification of one of the  $D$ 's produced from  $\psi(3770) \rightarrow D^0\bar{D}^0$  decays. Although time-dependent analyses are not possible at symmetric charm-threshold facilities (the  $D^0$  and  $\bar{D}^0$  do not travel far enough), the quantum-coherent  $C = -1$   $\psi(3770) \rightarrow D^0\bar{D}^0$  state provides time-integrated sensitivity [2,3].

**Time-Dependent Analyses:** We extend the formalism of this *Review's* note on ‘‘ $CP$  Violation in Meson Decays.’’ In addition to the ‘‘right-sign’’ instantaneous decay amplitudes  $\bar{A}_f \equiv \langle f|H|\bar{D}^0\rangle$  and  $A_{\bar{f}} \equiv \langle \bar{f}|H|D^0\rangle$  for  $CP$  conjugate final states  $f = K^+\pi^-, \dots$  and  $\bar{f} = K^-\pi^+, \dots$ , we include ‘‘wrong-sign’’ amplitudes  $\bar{A}_{\bar{f}} \equiv \langle \bar{f}|H|\bar{D}^0\rangle$  and  $A_f \equiv \langle f|H|D^0\rangle$ .

It is conventional to normalize the wrong-sign decay distributions to the integrated rate of right-sign decays and to express time in units of the precisely measured neutral  $D$ -meson mean lifetime,  $\tau_{D^0} = 1/\Gamma = 2/(\Gamma_1 + \Gamma_2)$ . Starting from a pure  $|D^0\rangle$  or  $|\bar{D}^0\rangle$  state at  $t = 0$ , the time-dependent rates of decay to wrong-sign final states relative to the integrated right-sign decay rates are, to leading order:

$$r(t) \equiv \frac{|\langle f|H|D^0(t)\rangle|^2}{|\bar{A}_f|^2} = \left|\frac{q}{p}\right|^2 \left|g_+(t)\lambda_f^{-1} + g_-(t)\right|^2, \quad (7)$$

and

$$\bar{r}(t) \equiv \frac{|\langle \bar{f}|H|\bar{D}^0(t)\rangle|^2}{|A_{\bar{f}}|^2} = \left|\frac{p}{q}\right|^2 \left|g_+(t)\lambda_{\bar{f}} + g_-(t)\right|^2. \quad (8)$$

where

$$\lambda_f \equiv q\bar{A}_f/pA_f, \quad \lambda_{\bar{f}} \equiv q\bar{A}_{\bar{f}}/pA_{\bar{f}}, \quad (9)$$

and

$$g_{\pm}(t) = \frac{1}{2} \left( e^{-iz_1 t} \pm e^{-iz_2 t} \right), \quad z_{1,2} = \frac{\omega_{1,2}}{\Gamma}. \quad (10)$$

Note that a change in the convention for the relative phase of  $D^0$  and  $\bar{D}^0$  would cancel between  $q/p$  and  $\bar{A}_f/A_f$  and leave  $\lambda_f$  unchanged. We expand  $r(t)$  and  $\bar{r}(t)$  to second order in  $x$  and  $y$  for modes in which the ratio of decay amplitudes,  $R_D = |A_f/\bar{A}_f|^2$ , is very small.

**Semileptonic decays:** Consider the final state  $f = K^+\ell^-\bar{\nu}_\ell$ , where  $A_f = \bar{A}_{\bar{f}} = 0$  in the Standard Model. The final state  $f$  is only accessible through mixing and  $r(t)$  is

$$r(t) = |g_-(t)|^2 \left|\frac{q}{p}\right|^2 \approx \frac{e^{-t}}{4} (x^2 + y^2) t^2 \left|\frac{q}{p}\right|^2. \quad (11)$$

For  $\bar{r}(t)$   $q/p$  is replaced by  $p/q$ . In the Standard Model,  $CP$  violation in charm mixing is small and  $|q/p| \approx 1$ . In the limit of  $CP$  conservation,  $r(t) = \bar{r}(t)$ , and the time-integrated mixing rate relative to the time-integrated right-sign decay rate for semileptonic decays is

$$R_M = \int_0^\infty r(t) dt = \left|\frac{q}{p}\right|^2 \frac{x^2 + y^2}{2 + x^2 - y^2} = \frac{1}{2}(x^2 + y^2). \quad (12)$$

**Table 1:** Results for  $R_M$  in  $D^0$  semileptonic decays.

Year	Exper.	Final state(s)	$R_M (\times 10^{-3})$	90% C.L.
2008	Belle [4]	$K^{(*)+}e^-\bar{\nu}_e$	$0.13 \pm 0.22 \pm 0.20$	$< 0.61 \times 10^{-3}$
2007	BaBar [1]	$K^{(*)+}e^-\bar{\nu}_e$	$0.04_{-0.60}^{+0.70}$	$(-1.3, 1.2) \times 10^{-3}$
2005*	Belle [5]	$K^{(*)+}e^-\bar{\nu}_e$	$0.02 \pm 0.47 \pm 0.14$	$< 1.0 \times 10^{-3}$
2005	CLEO [6]	$K^{(*)+}e^-\bar{\nu}_e$	$1.6 \pm 2.9 \pm 2.9$	$< 7.8 \times 10^{-3}$
2004*	BaBar [7]	$K^{(*)+}e^-\bar{\nu}_e$	$2.3 \pm 1.2 \pm 0.4$	$< 4.2 \times 10^{-3}$
2002*	FOCUS [8]	$K^+\mu^-\bar{\nu}_\mu$	$-0.76_{-0.93}^{+0.99}$	$< 1.01 \times 10^{-3}$
1996	E791 [9]	$K^+\ell^-\bar{\nu}_\ell$	$(1.1 \pm 3.0) \times 10^{-3}$	$< 5.0 \times 10^{-3}$
HFAG [10]			$0.13 \pm 0.27$	

\*These measurements are excluded from the HFAG average. The FOCUS result is unpublished, the BaBar result has been superseded by Ref. 1, and the Belle result has been superseded by Ref. 4.

Table 1 summarizes results for  $R_M$  from semileptonic decays; the world average from the Heavy Flavor Averaging Group (HFAG) [10] is  $R_M = (1.30 \pm 2.69) \times 10^{-4}$ .

**Wrong-sign decays to hadronic non- $CP$  eigenstates:**

Consider the final state  $f = K^+\pi^-$ , where  $A_f$  is doubly Cabibbo-suppressed. The ratio of decay amplitudes is

$$\frac{A_f}{\bar{A}_f} = -\sqrt{R_D} e^{-i\delta_f}, \quad \left|\frac{A_f}{\bar{A}_f}\right| \sim O(\tan^2 \theta_c), \quad (13)$$

where  $R_D$  is the doubly Cabibbo-suppressed (DCS) decay rate relative to the Cabibbo-favored (CF) rate,  $\delta_f$  is the strong phase difference between DCS and CF processes, and  $\theta_c$  is the Cabibbo angle. The minus sign originates from the sign of  $V_{us}$  relative to  $V_{cd}$ .

We characterize the violation of  $CP$  with the real-valued parameters  $A_M$ ,  $A_D$ , and  $\phi$ . We adopt the parametrization (see Refs. 11 and 12)

$$\left|\frac{q}{p}\right|^2 = \sqrt{\frac{1+A_M}{1-A_M}}, \quad (14)$$

$$\lambda_f^{-1} \equiv \frac{pA_f}{q\bar{A}_f} = -\sqrt{R_D} \left( \frac{(1+A_D)(1-A_M)}{(1-A_D)(1+A_M)} \right)^{1/4} e^{-i(\delta_f+\phi)}, \quad (15)$$

$$\lambda_{\bar{f}} \equiv \frac{q\bar{A}_{\bar{f}}}{pA_{\bar{f}}} = -\sqrt{R_D} \left( \frac{(1-A_D)(1+A_M)}{(1+A_D)(1-A_M)} \right)^{1/4} e^{-i(\delta_f-\phi)}, \quad (16)$$

and  $A_D$  is a measure of direct  $CP$  violation, while  $A_M$  is a measure of  $CP$  violation in mixing. From these relations, we obtain

$$\sqrt{\frac{1+A_D}{1-A_D}} = \frac{|A_f/\bar{A}_f|}{|\bar{A}_{\bar{f}}/A_{\bar{f}}|}, \quad (17)$$

The angle  $\phi$  measures  $CP$  violation in interference between mixing and decay. While  $A_M$  is independent of the decay process,  $A_D$  and  $\phi$ , in general, depend on  $f$ .

In general,  $\lambda_{\bar{f}}$  and  $\lambda_f^{-1}$  are independent complex numbers. More detail on  $CP$  violation in meson decays can be found in Ref. 13. To leading order, for  $A_D$  and  $A_M \ll 1$ ,

$$r(t) = e^{-t} \left[ R_D(1+A_D) + \sqrt{R_D(1+A_M)(1+A_D)} y'_- t + \frac{1}{2}(1+A_M)R_M t^2 \right] \quad (18)$$

and

$$\bar{r}(t) = e^{-t} \left[ R_D(1-A_D) + \sqrt{R_D(1-A_M)(1-A_D)} y'_+ t + \frac{1}{2}(1-A_M)R_M t^2 \right] \quad (19)$$

Here

$$y'_\pm \equiv y' \cos \phi \pm x' \sin \phi \\ = y \cos(\delta_{K\pi} \mp \phi) - x \sin(\delta_{K\pi} \mp \phi), \quad (20)$$

where

$$x' \equiv x \cos \delta_{K\pi} + y \sin \delta_{K\pi}, \\ y' \equiv y \cos \delta_{K\pi} - x \sin \delta_{K\pi}, \quad (21)$$

and  $R_M = (x^2 + y^2)/2 = (x'^2 + y'^2)/2$  is the mixing rate relative to the time-integrated Cabibbo-favored rate.

The three terms in Eq. (18) and Eq. (19) probe the three fundamental types of  $CP$  violation. In the limit of  $CP$  conservation,  $A_M$ ,  $A_D$ , and  $\phi$  are all zero. Then

$$r(t) = \bar{r}(t) = e^{-t} \left( R_D + \sqrt{R_D} y' t + \frac{1}{2} R_M t^2 \right), \quad (22)$$

and the time-integrated wrong-sign rate relative to the integrated right-sign rate is

$$R = \int_0^\infty r(t) dt = R_D + \sqrt{R_D} y' + R_M. \quad (23)$$

The ratio  $R$  is the most readily accessible experimental quantity. In Table 2 are reported the measurements of  $R$ ,  $R_D$  and  $A_D$  in  $D^0 \rightarrow K^+\pi^-$ , and their HFAG average [20] from a general fit; all allow for both mixing and  $CP$  violation. Typically, the fit parameters are  $R_D$ ,  $x'^2$ , and  $y'$ . Table 3 summarizes the results for  $x'^2$  and  $y'$ . Allowing for  $CP$  violation, the separate contributions to  $R$  can be extracted by fitting the  $D^0 \rightarrow K^+\pi^-$  and  $\bar{D}^0 \rightarrow K^-\pi^+$  decay rates.

**Table 2:** Results for  $R$ ,  $R_D$ , and  $A_D$  in  $D^0 \rightarrow K^+\pi^-$ .

Year	Exper.	$R(\times 10^{-3})$	$R_D(\times 10^{-3})$	$A_D(\%)$
2007	CDF [14]	$4.15 \pm 0.10$	$3.04 \pm 0.55$	—
2007	BaBar [15]	$3.53 \pm 0.08 \pm 0.04$	$3.03 \pm 0.16 \pm 0.10$	$-2.1 \pm 5.2 \pm 1.5$
2006	Belle [16]	$3.77 \pm 0.08 \pm 0.05$	$3.64 \pm 0.17$	$2.3 \pm 4.7$
2005*	FOCUS [17]	$4.29^{+0.63}_{-0.61} \pm 0.28$	$5.17^{+1.47}_{-1.58} \pm 0.76$	$13^{+33}_{-25} \pm 10$
2000*	CLEO [18]	$3.32^{+0.63}_{-0.65} \pm 0.40$	$4.8 \pm 1.2 \pm 0.4$	$-1^{+16}_{-17} \pm 1$
1998	E791 [19]	$6.8^{+3.4}_{-3.3} \pm 0.7$	—	—
Average		$3.80 \pm 0.05$	$3.31 \pm 0.08$ [20]	$-1.7 \pm 2.4$ [20]

\*These measurements are excluded from the HFAG average due to poor precision.

**Table 3:** Results on the time-dependence of  $r(t)$  in  $D^0 \rightarrow K^+\pi^-$  and  $\bar{D}^0 \rightarrow K^-\pi^+$  decays. The CDF result assumes no  $CP$  violation. The FOCUS, CLEO, and Belle results restrict  $x'^2$  to the physical region. The confidence intervals from FOCUS, CLEO, and BaBar are obtained from the fit, whereas Belle uses a Feldman-Cousins method, and CDF uses a Bayesian method.

Year	Exper.	$y'$ (%)	$x'^2 (\times 10^{-3})$
2007	CDF [14]	$0.85 \pm 0.76$	$-0.12 \pm 0.35$
2007	BaBar [15]	$0.97 \pm 0.44 \pm 0.31$	$-0.22 \pm 0.30 \pm 0.21$
2006	Belle [16]	$-2.8 < y' < 2.1$	$< 0.72$ (95% C.L.)
2005	FOCUS [17]	$-11.2 < y' < 6.7$	$< 8.0$ (95% C.L.)
2000	CLEO [18]	$-5.8 < y' < 1.0$	$< 0.81$ (95% C.L.)

Extraction of the mixing parameters  $x$  and  $y$  from the results in Table 3 requires knowledge of the relative strong phase  $\delta_{K\pi}$ . An interference effect that provides useful sensitivity to  $\delta_{K\pi}$  arises in the decay chain  $\psi(3770) \rightarrow D^0 \bar{D}^0 \rightarrow (f_{CP})(K^+\pi^-)$ , where  $f_{CP}$  denotes a  $CP$ -even or -odd eigenstate from  $D^0$  decay, such as  $K^+K^-$  or  $K_S^0\pi^0$ , respectively [23]. Here, the amplitude relation

$$\sqrt{2} A(D_\pm \rightarrow K^-\pi^+) = A(D^0 \rightarrow K^-\pi^+) \pm A(\bar{D}^0 \rightarrow K^-\pi^+). \quad (24)$$

where  $D_\pm$  denotes a  $CP$ -even or -odd eigenstate, implies that

$$\cos \delta_{K\pi} = \frac{|A(D_+ \rightarrow K^-\pi^+)|^2 - |A(D_- \rightarrow K^-\pi^+)|^2}{2\sqrt{R_D} |A(D^0 \rightarrow K^-\pi^+)|^2}. \quad (25)$$

This neglects  $CP$  violation and uses  $\sqrt{R_D} \ll 1$ .

For multibody final states, Eqs. (13)–(23) apply separately to each point in phase-space. Although  $x$  and  $y$  do not vary across the space, knowledge of the resonant substructure is

# Meson Particle Listings

## $D^0$

needed to extrapolate the strong phase difference  $\delta$  from point to point to determine  $x$  and  $y$ .

A time-dependent analysis of the process  $D^0 \rightarrow K^+\pi^-\pi^0$  from BaBar [21,22] determines the *relative* strong phase variation across the Dalitz plot and reports  $x'' = (2.61_{-0.68}^{+0.57} \pm 0.39)\%$ , and  $y'' = (-0.06_{-0.64}^{+0.55} \pm 0.34)\%$ , where  $x''$  and  $y''$  are defined as

$$\begin{aligned} x'' &\equiv x \cos \delta_{K\pi\pi^0} + y \sin \delta_{K\pi\pi^0}, \\ y'' &\equiv y \cos \delta_{K\pi\pi^0} - x \sin \delta_{K\pi\pi^0}, \end{aligned} \quad (26)$$

in parallel to  $x'$ ,  $y'$ , and  $\delta_{K\pi}$  of Eq. (21). Here  $\delta_{K\pi\pi^0}$  is the remaining strong phase difference between the DCS  $D^0 \rightarrow K^+\rho^-$  and the CF  $\overline{D}^0 \rightarrow K^+\rho^-$  amplitudes and does not vary across the Dalitz plot. Both strong phases,  $\delta_{K\pi}$  and  $\delta_{K\pi\pi^0}$ , can be determined from time-integrated  $CP$  asymmetries in correlated  $D^0\overline{D}^0$  produced at the  $\psi(3770)$  [23,24].

Both the sign and magnitude of  $x$  and  $y$  without phase or sign ambiguity may be measured using the time-dependent resonant substructure of multibody  $D^0$  decays [25,26]. In  $D^0 \rightarrow K_S^0\pi^+\pi^-$ , the DCS and CF decay amplitudes populate the same Dalitz plot, which allows direct measurement of the relative strong phases. CLEO [27], Belle [26], and BaBar [28] have measured the relative phase between  $D^0 \rightarrow K^*(892)^-\pi^+$  and  $D^0 \rightarrow K^*(892)^+\pi^-$  to be  $(189 \pm 10 \pm 3_{-5}^{+15})^\circ$ ,  $(171.9 \pm 1.3$  (stat. only) $)^\circ$ , and  $(177.6 \pm 1.1$  (stat. only) $)^\circ$ , respectively. These results are close to the  $180^\circ$  expected from Cabibbo factors and a small strong phase. Table 4 summarizes the results of a time-dependent Dalitz-plot analyses.

**Table 4:** Results from time-dependent Dalitz-plot analysis of  $D^0 \rightarrow K_S^0\pi^+\pi^-$  (CLEO and Belle) and  $D^0 \rightarrow K_S^0\pi^+\pi^-, K_S^0K^+K^-$  (BaBar). The errors are statistical, experimental systematic, and decay-model systematic, respectively.

No $CP$ Violation			
Year	Exper.	$x \times 10^{-3}$	$y \times 10^{-3}$
2010	BaBar [28]	$1.6 \pm 2.3 \pm 1.2 \pm 0.8$	$5.7 \pm 2.0 \pm 1.3 \pm 0.7$
2007	Belle [26]	$8.0 \pm 2.9_{-0.7}^{+0.9} \pm 1.4$	$3.3 \pm 2.4_{-1.2}^{+0.8} \pm 0.8$
2005	CLEO [25]	$19_{-33}^{+32} \pm 4 \pm 4$	$-14 \pm 24 \pm 8 \pm 4$
	HFAG [20]	$4.2 \pm 2.1$	$4.6 \pm 1.9$
With $CP$ Violation			
Year	Exper.	$ q/p $	$\phi$
2007	Belle [26]	$0.86_{-0.29}^{+0.30} \pm 0.06_{-0.03} \pm 0.08$	$(-14_{-18}^{+16} \pm 5 \pm 2)^\circ$

In addition, Belle [26] has results for both the relative phase (statistical errors only) and ratio  $R$  (central values only) of the DCS fit fraction relative to the CF fit fractions for  $K^*(892)^+\pi^-$ ,  $K_0^*(1430)^+\pi^-$ ,  $K_2^*(1430)^+\pi^-$ ,  $K^*(1410)^+\pi^-$ , and  $K^*(1680)^+\pi^-$ . The systematic uncertainties on  $R$  must be evaluated. The values for  $R$  in units of  $\tan^4\theta_c$  are  $2.94 \pm 0.12$ ,  $22.0 \pm 1.6$ ,  $34 \pm 4$ ,  $87 \pm 13$ , and  $500 \pm 500$ , respectively. For  $K^+\pi^-$ , the corresponding value for  $R_D$  is  $(1.28 \pm 0.02) \times \tan^4\theta_c$ .

Similarly, BaBar [28–30] has reported central values for  $R$  for  $K^*(892)^+\pi^-$ ,  $K_0^*(1430)^+\pi^-$ , and  $K_2^*(1430)^+\pi^-$ . The large differences in  $R$  among these final states could point to an interesting role for hadronic effects.

**Decays to  $CP$  Eigenstates:** When the final state  $f$  is a  $CP$  eigenstate, there is no distinction between  $f$  and  $\bar{f}$ , and  $A_f = A_{\bar{f}}$  and  $\overline{A}_{\bar{f}} = \overline{A}_f$ . We denote final states with  $CP$  eigenvalues  $\pm 1$  by  $f_\pm$  and write  $\lambda_\pm$  for  $\lambda_{f_\pm}$ .

The quantity  $y$  may be measured by comparing the rate for  $D^0$  decays to non- $CP$  eigenstates such as  $K^-\pi^+$  with decays to  $CP$  eigenstates such as  $K^+K^-$  [12]. If decays to  $K^+K^-$  have a shorter effective lifetime than those to  $K^-\pi^+$ ,  $y$  is positive.

In the limit of slow mixing ( $x, y \ll 1$ ) and the absence of direct  $CP$  violation ( $A_D = 0$ ), but allowing for small indirect  $CP$  violation ( $|A_M|, |\phi| \ll 1$ ), we can write

$$\lambda_\pm = \left| \frac{q}{p} \right| e^{\pm i\phi}. \quad (27)$$

In this scenario, to a good approximation, the decay rates for states that are initially  $D^0$  and  $\overline{D}^0$  to a  $CP$  eigenstate have exponential time dependence:

$$r_\pm(t) \propto \exp(-t/\tau_\pm), \quad (28)$$

$$\bar{r}_\pm(t) \propto \exp(-t/\bar{\tau}_\pm), \quad (29)$$

where  $\tau$  is measured in units of  $1/\Gamma$ .

The effective lifetimes are given by

$$1/\tau_\pm = 1 \pm \left| \frac{q}{p} \right| (y \cos \phi - x \sin \phi), \quad (30)$$

$$1/\bar{\tau}_\pm = 1 \pm \left| \frac{p}{q} \right| (y \cos \phi + x \sin \phi). \quad (31)$$

The effective decay rate to a  $CP$  eigenstate combining both  $D^0$  and  $\overline{D}^0$  decays is

$$r_\pm(t) + \bar{r}_\pm(t) \propto e^{-(1 \pm y_{CP})t}. \quad (32)$$

Here

$$y_{CP} = \frac{1}{2} \left( \left| \frac{q}{p} \right| + \left| \frac{p}{q} \right| \right) y \cos \phi - \frac{1}{2} \left( \left| \frac{q}{p} \right| - \left| \frac{p}{q} \right| \right) x \sin \phi \quad (33)$$

$$\approx y \cos \phi - A_M x \sin \phi. \quad (34)$$

If  $CP$  is conserved,  $y_{CP} = y$ .

All measurements of  $y_{CP}$  and  $A_\Gamma$  are relative to the  $D^0 \rightarrow K^-\pi^+$  decay rate. Table 5 summarizes the current status of measurements. Belle [35], BaBar [32,34], and LHCb [31] have reported  $y_{CP}$  and the decay-rate asymmetry for  $CP$  even final states

$$A_\Gamma = \frac{\bar{\tau}_+ - \tau_+}{\bar{\tau}_+ + \tau_+} = \frac{(1/\tau_+) - (1/\bar{\tau}_+)}{(1/\tau_+) + (1/\bar{\tau}_+)} \quad (35)$$

$$= \frac{1}{2} \left( \left| \frac{q}{p} \right| - \left| \frac{p}{q} \right| \right) y \cos \phi - \frac{1}{2} \left( \left| \frac{q}{p} \right| + \left| \frac{p}{q} \right| \right) x \sin \phi \quad (36)$$

$$\approx A_M y \cos \phi - x \sin \phi. \quad (37)$$



**Table 5:** Results for  $y_{CP}$  from  $D^0 \rightarrow K^+K^-$  and  $\pi^+\pi^-$ .

Year	Exper.	final state(s)	$y_{CP}(\%)$	$A_\Gamma(\times 10^{-3})$
2011	LHCb [31]	$K^+K^-\pi^+\pi^-$	$0.55 \pm 0.63 \pm 0.41$	$-0.59 \pm 0.59 \pm 0.21$
2009	BaBar [32]	$K^+K^-$	$1.16 \pm 0.22 \pm 0.18$	—
2009	Belle [33]	$K_S^0 K^+ K^-$	$0.11 \pm 0.61 \pm 0.52$	—
2008	BaBar* [34]	$K^+K^-\pi^+\pi^-$	$1.03 \pm 0.33 \pm 0.19$	$2.6 \pm 3.6 \pm 0.8$
2007	Belle [35]	$K^+K^-\pi^+\pi^-$	$1.31 \pm 0.32 \pm 0.25$	$0.1 \pm 3.0 \pm 1.5$
2001	CLEO [36]	$K^+K^-\pi^+\pi^-$	$-1.2 \pm 2.5 \pm 1.4$	—
2001	Belle [37]	$K^+K^-$	$-0.5 \pm 1.0^{+0.7}_{-0.8}$	—
2000	FOCUS [38]	$K^+K^-$	$3.42 \pm 1.39 \pm 0.74$	—
1999	E791 [39]	$K^+K^-$	$0.8 \pm 2.9 \pm 1.0$	—
HFAG [20]			$1.06 \pm 0.21$	$0.03 \pm 0.23$

\*This measurement is included in the result reported by Ref. 32.

Belle [33] has also reported  $y_{CP}$  for the final state  $K_S^0 K^+ K^-$  which is dominated by the  $CP$  odd final state  $K_S^0 \phi$ . If  $CP$  is conserved,  $A_\Gamma = 0$ .

Substantial work on the time-integrated  $CP$  asymmetries in decays to  $CP$  eigenstates are consistent [40]. Recently, LHCb has reported  $3.5\sigma$  evidence for the difference in time-integrated  $CP$  asymmetry,  $\Delta A_{CP} = A_K - A_\pi$ , between  $D^0 \rightarrow K^-K^+$  and  $D^0 \rightarrow \pi^-\pi^+$ , yielding  $\Delta A_{CP} = [-0.82 \pm 0.21(stat.) \pm 0.11(sys.)]\%$  [41]. Subsequently, CDF has reported  $\Delta A_{CP} = [-0.62 \pm 0.21(stat.) \pm 0.10(sys.)]\%$  [42].

**Coherent  $D^0\bar{D}^0$  Analyses:** Measurements of  $R_D$ ,  $\cos\delta_{K\pi}$ ,  $\sin\delta_{K\pi}$ ,  $x$ , and  $y$  can be determined simultaneously from a combined fit to the time-integrated single-tag (ST) and double-tag (DT) yields in correlated  $D^0\bar{D}^0$  produced at the  $\psi(3770)$  [23,24].

Due to quantum correlations in the  $C = -1$  and  $C = +1$   $D^0\bar{D}^0$  pairs produced in the reactions  $e^+e^- \rightarrow D^0\bar{D}^0(\pi^0)$  and  $e^+e^- \rightarrow D^0\bar{D}^0\gamma(\pi^0)$ , respectively, the time-integrated  $D^0\bar{D}^0$  decay rates are sensitive to interference between amplitudes for indistinguishable final states. The size of this interference is governed by the relevant amplitude ratios and can include contributions from  $D^0-\bar{D}^0$  mixing.

The following categories of final states are considered:

**$f$  or  $\bar{f}$ :** Hadronic states accessed from either  $D^0$  or  $\bar{D}^0$  decay but that are not  $CP$  eigenstates. An example is  $K^-\pi^+$ , which results from Cabibbo-favored  $D^0$  transitions or DCS  $\bar{D}^0$  transitions.

**$\ell^+$  or  $\ell^-$ :** Semileptonic or purely leptonic final states, which, in the absence of mixing, tag unambiguously the flavor of the parent  $D^0$ .

**$f_+$  or  $f_-$ :**  $CP$ -even and  $CP$ -odd eigenstates, respectively.

The decay rates for  $D^0\bar{D}^0$  pairs to all possible combinations of the above categories of final states are calculated in Ref. 2, for both  $C = -1$  and  $C = +1$ , reproducing the work of Ref. 3. Such  $D^0\bar{D}^0$  combinations, where both  $D$  final states are specified, are double tags. In addition, the rates for single tags, where either the  $D^0$  or  $\bar{D}^0$  is identified and the other neutral  $D$  decays generically are given in Ref. 2.

CLEO-c has reported results using 818 pb $^{-1}$  of  $e^+e^- \rightarrow \psi(3770)$  data [43–45], where the quantum-coherent  $D^0\bar{D}^0$  pairs are in the  $C = -1$  state. The values of  $y$ ,  $R_M$ ,  $\cos\delta_{K\pi}$ , and  $\sin\delta_{K\pi}$  are determined from a combined fit to the ST (hadronic only) and DT yields. The hadronic final states included are  $K^-\pi^+$  ( $f$ ),  $K^+\pi^-$  ( $\bar{f}$ ),  $K^-K^+$  ( $f_+$ ),  $\pi^+\pi^-$  ( $f_+$ ),  $K_S^0\pi^0\pi^0$  ( $f_+$ ),  $K_L^0\pi^0$  ( $f_+$ ),  $K_L^0\eta$  ( $f_+$ ),  $K_L^0\omega$  ( $f_+$ ),  $K_S^0\pi^0$  ( $f_-$ ),  $K_S^0\eta$  ( $f_-$ ),  $K_S^0\omega$  ( $f_-$ ), and  $K_L^0\pi^0\pi^0$  ( $f_-$ ), and  $K_S^0\pi^+\pi^-$  (mixture of  $f, \bar{f}, f_+$ , and  $f_-$ ). The two flavored final states,  $K^-\pi^+$  and  $K^+\pi^-$ , can be reached via CF or DCS transitions.

Semileptonic DT yields are also included, where one  $D$  is fully reconstructed in one of the hadronic modes listed above, and the other  $D$  is partially reconstructed in either  $D \rightarrow K\ell\nu$  or  $D \rightarrow K\mu\nu$ . When the lepton is accompanied by a flavor tag ( $D \rightarrow K^-\pi^+$  or  $K^+\pi^-$ ), both the “right-sign” and “wrong-sign” DT samples are used, where the electron and kaon charges are the same and opposite, respectively.

The main results of the CLEO-c analysis are the determination of  $\cos\delta_{K\pi} = 0.98^{+0.27}_{-0.20} \pm 0.08$ ,  $\sin\delta_{K\pi} = -0.04 \pm 0.49 \pm 0.08$ , and World Averages for the mixing parameters from an “extended” fit that combines the CLEO-c data with previous mixing and branching-ratio measurements [45]. These fits allow  $\cos\delta_{K\pi}$ ,  $\sin\delta_{K\pi}$  and  $x^2$  to be unphysical. Constraining  $\cos\delta_{K\pi}$  and  $\sin\delta_{K\pi}$  to  $[-1, +1]$ —that is interpreting  $\delta_{K\pi}$  as an angle—yields  $\delta_{K\pi} = (15^{+11}_{-17} \pm 7)^\circ$ . Note that measurements of  $y$  (Table 4 and Table 5) and  $y'$  (Table 3) contribute to the determination of  $\delta_{K\pi}$ .

**Summary of Experimental Results:** Several recent results indicate that charm mixing is at the upper end of the range of Standard Model estimates.

For  $D^0 \rightarrow K^+\pi^-$ , BaBar [15] and CDF [14] find evidence for oscillations with  $3.9\sigma$  ( $\Delta\text{Log}\mathcal{L}$ ) and  $3.8\sigma$  (Bayesian), respectively. The most precise measurement for mixing parameters is from Belle [16], which excludes  $x^2 = y' = 0$  at  $2.1\sigma$ .

For  $y_{CP}$  in  $D^0 \rightarrow K^+K^-$  and  $\pi^+\pi^-$ , Belle [35] and BaBar [32] find  $3.2\sigma$  and  $4.1\sigma$  effects. The most sensitive measurement of  $x$  and  $y$  is in  $D^0 \rightarrow K_S^0\pi^+\pi^-$ ,  $K_S^0K^+K^-$  from BaBar [28] and the no mixing solution is only excluded at  $1.9\sigma$ . The current situation would benefit from better knowledge of the strong phase difference  $\delta_{K\pi}$  than provided by the current CLEO-c result [45]. This would allow one to unfold  $x$  and  $y$  from the  $D^0 \rightarrow K^+\pi^-$  measurements of  $x'^2$  and  $y'$ , and directly compare them to the  $D^0 \rightarrow K_S^0\pi^+\pi^-$  results.

The experimental data consistently indicate that the  $D^0$  and  $\bar{D}^0$  do mix. The mixing is presumably dominated by long-range processes. Under the assumption that the observed mixing is due entirely to short-range processes, significant constraints on a variety of new physics models are obtained [46]. A serious limitation to the interpretation of charm oscillations in terms of New Physics is the theoretical uncertainty of the Standard Model prediction. However, recent evidence opens the window to searches for  $CP$  violation in mixing, which would provide unequivocal evidence of New Physics. The evidence for time

# Meson Particle Listings

## $D^0$

integrated  $CP$ -violation,  $\Delta A_{CP} \neq 0$ , observed by LHCb is intriguing. This result is marginally consistent with Standard Model expectation [47–49].

### HFAG Averaging of Charm Mixing Results:

The Heavy Flavor Averaging Group (HFAG) has made a global fit to all mixing measurements to obtain values of  $x$ ,  $y$ ,  $\delta_{K\pi}$ ,  $\delta_{K\pi\pi^0}$ ,  $R_D$ ,  $A_D \equiv (R_D^+ - R_D^-)/(R_D^+ + R_D^-)$ ,  $|q/p|$ ,  $\text{Arg}(q/p) \equiv \phi$ , and the time-integrated  $CP$  asymmetries  $A_K$  and  $A_\pi$ . Correlations among observables are taken into account by using the error matrices from the experiments. The measurements of  $D^0 \rightarrow K^{(*)}\ell^-\bar{\nu}$ ,  $K^+K^-$ ,  $\pi^+\pi^-$ ,  $K^+\pi^-$ ,  $K^+\pi^-\pi^0$ ,  $K^+\pi^-\pi^+\pi^-$ ,  $K_S^0\pi^+\pi^-$ , and  $K_S^0K^+K^-$  decays, as well as CLEO- $c$  results for double-tagged branching fractions measured at the  $\psi(3770)$  are used.

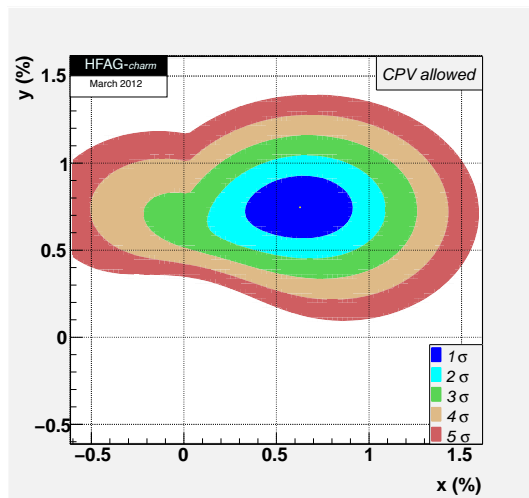


**Figure 1:** Two-dimensional  $1\sigma$ - $5\sigma$  contours for  $(x, y)$  from measurements of  $D^0 \rightarrow K^{(*)}\ell\nu$ ,  $h^+h^-$ ,  $K^+\pi^-$ ,  $K^+\pi^-\pi^0$ ,  $K^+\pi^-\pi^+\pi^-$ ,  $K_S^0\pi^+\pi^-$ , and  $K_S^0K^+K^-$  decays, and double-tagged branching fractions measured at the  $\psi(3770)$  resonance (from HFAG [20]).

**Table 6:** HFAG Charm Mixing Average allowing for  $CP$  violation [20].

Parameter	HFAG average	95% C.L. interval
$x(\%)$	$0.63^{+0.19}_{-0.20}$	[0.24, 0.99]
$y(\%)$	$0.75 \pm 0.12$	[0.51, 0.98]
$R_D(\%)$	$0.331 \pm 0.008$	[0.315, 0.347]
$\delta_{K\pi}(\circ)$	$22.1^{+9.7}_{-11.1}$	[-2.6, 40.6]
$\delta_{K\pi\pi^0}(\circ)$	$19 \pm 22$	[-26, 62]
$A_D(\%)$	$-1.7 \pm 2.4$	[-6.4, 3.0]
$ q/p $	$0.88^{+0.18}_{-0.16}$	[0.59, 1.26]
$\phi(\circ)$	$-10.1^{+9.5}_{-8.9}$	[-27.4, 8.7]
$A_K$	$-0.31 \pm 0.24$	[-0.78, 0.15]
$A_\pi$	$0.36 \pm 0.25$	[-0.13, 0.86]

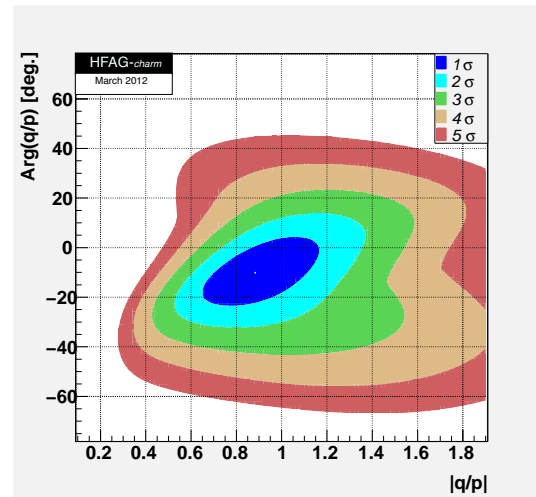


**Figure 2:** Two-dimensional  $1\sigma$ - $5\sigma$  contours for  $(|q/p|, \text{Arg}(q/p))$  from measurements of  $D^0 \rightarrow K^{(*)}\ell\nu$ ,  $h^+h^-$ ,  $K^+\pi^-$ ,  $K^+\pi^-\pi^0$ ,  $K^+\pi^-\pi^+\pi^-$ ,  $K_S^0\pi^+\pi^-$ , and  $K_S^0K^+K^-$  decays, and double-tagged branching fractions measured at the  $\psi(3770)$  resonance (from HFAG [20]).

For the global fit, confidence contours in the two dimensions  $(x, y)$  and  $(|q/p|, \phi)$  are obtained by letting, for any point in the two-dimensional plane, all other fit parameters take their preferred values. Figures 1 and 2 show the resulting 1-to-5  $\sigma$  contours. The fits exclude the no-mixing point  $(x = y = 0)$  at  $10.2\sigma$ , whether or not  $CP$  violation is allowed. The parameters  $x$  and  $y$  differ from zero by  $2.7\sigma$  and  $6.0\sigma$ , respectively. One-dimensional likelihood functions for parameters are obtained by allowing, for any value of the parameter, all other fit parameters to take their preferred values. The resulting likelihood functions give central values, 68.3% C.L. intervals, and 95% C.L. intervals as listed in Table 6.

From the results of the HFAG averaging, the following can be concluded: (1) Since  $CP$  violation is small and  $y_{CP}$  is positive, the  $CP$ -even state is shorter-lived, as in the  $K^0\bar{K}^0$  system; (2) However, since  $x$  appears to be positive, the  $CP$ -even state is heavier, unlike in the  $K^0\bar{K}^0$  system; (3) The strong phase difference  $\delta_{K\pi}$  is consistent with the SU(3) expectation of zero but large values are not excluded; (4) There is no evidence yet for  $CP$ -violation in  $D^0\bar{D}^0$  mixing. Observing  $CP$ -violation in mixing at the current level of sensitivity would indicate new physics.

### References

1. B. Aubert *et al.*, Phys. Rev. **D76**, 014018 (2007).
2. D.M. Asner and W.M. Sun, Phys. Rev. **D73**, 034024 (2006); Erratum-*ibid.*, **77**, 019901 (2008).
3. D. Atwood and A.A. Petrov, Phys. Rev. **D71**, 054032 (2005) Z.Z. Xing, Phys. Rev. **D55**, 196 (1997) M. Goldhaber and J.L. Rosner, Phys. Rev. **D15**, 1254 (1977).
4. U. Bitenc *et al.*, Phys. Rev. **D77**, 112003 (2008).
5. U. Bitenc *et al.*, Phys. Rev. **D72**, 071101R (2005).

See key on page 457

6. C. Cawfield *et al.*, Phys. Rev. **D71**, 077101 (2005).
7. B. Aubert *et al.*, Phys. Rev. **D70**, 091102R (2004).
8. K. Stenson, presented at the April Meeting of the American Physical Society (APS 03), Philadelphia, Pennsylvania, April 5-8, 2003; M. Hosack, (FOCUS Collab.), Fermilab-Thesis-2002-25.
9. E.M. Aitala *et al.*, Phys. Rev. Lett. **77**, 2384 (1996).
10. A.J. Schwartz, for the Heavy Flavor Averaging Group, arXiv:0911.1464 [hep-ex].
11. Y. Nir, Lectures given at 27th SLAC Summer Institute on Particle Physics: "CP Violation in and Beyond the Standard Model (SSI 99)," Stanford, California, 7-16 Jul 1999. Published in Trieste 1999, *Particle Physics*, pp. 165-243.
12. S. Bergmann *et al.*, Phys. Lett. **B486**, 418 (2000).
13. See the Note on "CP Violation in Meson Decays" in this Review.
14. T. Aaltonen, Phys. Rev. Lett. **100**, 121802 (2008).
15. B. Aubert *et al.*, Phys. Rev. Lett. **98**, 211802 (2007).
16. L.M. Zhang *et al.*, Phys. Rev. Lett. **96**, 151801 (2006).
17. J.M. Link *et al.*, Phys. Lett. **B607**, 51 (2005).
18. R. Godang *et al.*, Phys. Rev. Lett. **84**, 5038 (2000).
19. E.M. Aitala *et al.*, Phys. Rev. **D57**, 13 (1998).
20. Heavy Flavor Averaging Group, [www.slac.stanford.edu/xorg/hfag/charm/March12/results\\_mix+cpv.html](http://www.slac.stanford.edu/xorg/hfag/charm/March12/results_mix+cpv.html).
21. B. Aubert *et al.*, Phys. Rev. Lett. **97**, 221803 (2006).
22. B. Aubert *et al.*, Phys. Rev. Lett. **103**, 211801 (2009).
23. R.A. Briere *et al.*, (CLEO Collab.), CLNS 01-1742, (2001).
24. G. Cavoto *et al.*, Prepared for *3rd Workshop on the Unitarity Triangle: CKM 2005*, San Diego, California, 15-18 Mar 2005, hep-ph/0603019.
25. D.M. Asner *et al.*, Phys. Rev. **D72**, 012001 (2005).
26. L.M. Zhang *et al.*, Phys. Rev. Lett. **99**, 131803 (2007).
27. H. Muramatsu *et al.*, Phys. Rev. Lett. **89**, 251802 (2002).
28. P. del Amo Sanchez *et al.*, Phys. Rev. Lett. **105**, 081803 (2010).
29. B. Aubert *et al.*, Phys. Rev. Lett. **95**, 121802 (2005).
30. B. Aubert *et al.*, Phys. Rev. **D78**, 034023 (2008).
31. R. Aaij *et al.*, arXiv:1112.4698 [hep-ex].
32. B. Aubert *et al.*, Phys. Rev. **D80**, 071103R (2009).
33. A. Zupanc *et al.*, Phys. Rev. **D80**, 052006 (2009).
34. B. Aubert *et al.*, Phys. Rev. **D78**, 011105 (2008).
35. M. Staric *et al.*, Phys. Rev. Lett. **98**, 211803 (2007).
36. S.E. Csorna *et al.*, Phys. Rev. **D65**, 092001 (2002).
37. K. Abe *et al.*, Phys. Rev. Lett. **88**, 162001 (2002).
38. J.M. Link *et al.*, Phys. Lett. **B485**, 62 (2000).
39. E.M. Aitala *et al.*, Phys. Rev. Lett. **83**, 32 (1999).
40. See the tabulation of  $A_{CP}$  results in the  $D^0$  and  $D^+$  Listings in this Review.
41. R. Aaij *et al.*, arXiv:1112.0938 [hep-ex].
42. CDF public note 10784 (2012).
43. J.L. Rosner *et al.*, Phys. Rev. Lett. **100**, 221801 (2008).
44. D.M. Asner *et al.*, Phys. Rev. **D78**, 012001 (2008).
45. W.M. Sun *et al.*, presented at *Physics in Collision 2010 Conference*, Karlsruhe, Germany, September 2010. [www-ekp.physik.uni-karlsruhe.de/~jyothsna/](http://www-ekp.physik.uni-karlsruhe.de/~jyothsna/)

PIC2010\_Proceedings/013\_Werner\_Sun.pdf.

46. E. Golowich *et al.*, Phys. Rev. **D76**, 095009 (2007).
47. G. Isidori *et al.*, arXiv:1111.4987 [hep-ph].
48. E. Franco *et al.*, arXiv:1203.3131 [hep-ph].
49. M. Gersaback *et al.*, J. Phys. **G39**, 045005 (2012).

$$|m_{D_1^0} - m_{D_2^0}| = x \Gamma$$

The  $D_1^0$  and  $D_2^0$  are the mass eigenstates of the  $D^0$  meson, as described in the note on " $D^0$ - $\bar{D}^0$  Mixing," above. The experiments usually present  $x \equiv \Delta m/\Gamma$ . Then  $\Delta m = x \Gamma = x \hbar/\tau$ .

"OUR EVALUATION" comes from averages provided by the Heavy Flavor Averaging Group, see the note on " $D^0$ - $\bar{D}^0$  Mixing."

VALUE ( $10^{10} \text{ h s}^{-1}$ )	CL %	DOCUMENT ID	TECN	COMMENT
<b>1.44<sup>+0.48</sup><sub>-0.50</sub></b>		<b>OUR EVALUATION</b>		
<b>1.0 ± 0.8</b>		<b>OUR AVERAGE</b> Error includes scale factor of 1.5.		
0.39 ± 0.56 ± 0.35		<sup>1</sup> DEL-AMO-SA..10b	BABR	$e^+e^-$ , 10.6 GeV
1.98 ± 0.73 <sup>+0.32</sup> <sub>-0.41</sub>		<sup>2</sup> ZHANG	07B	BELL $\Delta m < 3.9$ , 95% CL
••• We do not use the following data for averages, fits, limits, etc. •••				
6.4 <sup>+1.4</sup> <sub>-1.7</sub> ± 1.0		<sup>3</sup> AUBERT	09AN	BABR $e^+e^-$ at 10.58 GeV
- 2 <sup>+7</sup> <sub>-6</sub>		<sup>4</sup> LOWREY	09	CLEO $e^+e^-$ at $\psi(3770)$
< 7	95	<sup>5</sup> ZHANG	06	BELL $e^+e^-$
-11 to +22		<sup>2</sup> ASNER	05	CLEO $e^+e^- \approx 10$ GeV
< 11	90	BITENC	05	BELL
< 30	90	CRAWFIELD	05	CLEO
< 7	95	<sup>5</sup> LI	05A	BELL See ZHANG 06
< 22	95	<sup>6</sup> LINK	05H	FOCS $\gamma$ nucleus
< 23	95	AUBERT	04Q	BABR
< 11	95	<sup>5</sup> AUBERT	03Z	BABR $e^+e^-$ , 10.6 GeV
< 7	95	<sup>7</sup> GODANG	00	CLE2 $e^+e^-$
< 32	90	<sup>8,9</sup> AITALA	98	E791 $\pi^-$ nucleus, 500 GeV
< 24	90	<sup>10</sup> AITALA	96C	E791 $\pi^-$ nucleus, 500 GeV
< 21	90	<sup>9,11</sup> ANJOS	88C	E691 Photoproduction

<sup>1</sup> DEL-AMO-SANCHEZ 10b uses 540,800 ± 800  $K_S^0 \pi^+ \pi^-$  and 79,900 ± 300  $K_S^0 K^+ K^-$  events in a time-dependent amplitude analysis of the  $D^0$  and  $\bar{D}^0$  Dalitz plots. No evidence was found for CP violation, and the values here assume no such violation.

<sup>2</sup> The ASNER 05 and ZHANG 07B values are from the time-dependent Dalitz-plot analysis of  $D^0 \rightarrow K_S^0 \pi^+ \pi^-$ . Decay-time information and interference on the Dalitz plot are used to distinguish doubly Cabibbo-suppressed decays from mixing and to measure the relative phase between  $D^0 \rightarrow K^{*+} \pi^-$  and  $\bar{D}^0 \rightarrow K^{*+} \pi^-$ . This value allows CP violation and is sensitive to the sign of  $\Delta m$ .

<sup>3</sup> The AUBERT 09AN values are inferred from the branching ratio  $\Gamma(D^0 \rightarrow K^+ \pi^- \pi^0 \text{ via } \bar{D}^0)/\Gamma(D^0 \rightarrow K^- \pi^+ \pi^0)$  given near the end of this Listings. Mixing is distinguished from DCS decays using decay-time information. Interference between mixing and DCS is allowed. The phase between  $D^0 \rightarrow K^+ \pi^- \pi^0$  and  $\bar{D}^0 \rightarrow K^+ \pi^- \pi^0$  is assumed to be small. The width difference here is  $y''$ , which is not the same as  $y_{CP}$  in the note on  $D^0$ - $\bar{D}^0$  mixing.

<sup>4</sup> LOWREY 09 uses quantum correlations in  $e^+e^- \rightarrow D^0 \bar{D}^0$  at the  $\psi(3770)$ . See below for coherence factors and average relative strong phases for both  $D^0 \rightarrow K^- \pi^+ \pi^0$  and  $D^0 \rightarrow K^- \pi^- 2\pi^+$ . A fit that includes external measurements of charm mixing parameters gets  $\Delta m = (2.34 \pm 0.61) \times 10^{10} \text{ h s}^{-1}$ .

<sup>5</sup> The AUBERT 03Z, LI 05A, and ZHANG 06 limits are inferred from the  $D^0$ - $\bar{D}^0$  mixing ratio  $\Gamma(K^+ \pi^- \text{ (via } \bar{D}^0))/\Gamma(K^- \pi^+)$  given near the end of this  $D^0$  Listings. Decay-time information is used to distinguish DCS decays from  $D^0$ - $\bar{D}^0$  mixing. The limit allows interference between the DCS and mixing ratios, and also allows CP violation. AUBERT 03Z assumes the strong phase between  $D^0 \rightarrow K^+ \pi^-$  and  $\bar{D}^0 \rightarrow K^+ \pi^-$  amplitudes is small; if an arbitrary phase is allowed, the limit degrades by 20%. The LI 05A and ZHANG 06 limits are valid for an arbitrary strong phase.

<sup>6</sup> This LINK 05H limit is inferred from the  $D^0$ - $\bar{D}^0$  mixing ratio  $\Gamma(K^+ \pi^- \text{ (via } \bar{D}^0))/\Gamma(K^- \pi^+)$  given near the end of this  $D^0$  Listings. Decay-time information is used to distinguish DCS decays from  $D^0$ - $\bar{D}^0$  mixing. The limit allows interference between the DCS and mixing ratios, and also allows CP violation. The strong phase between  $D^0 \rightarrow K^+ \pi^-$  and  $\bar{D}^0 \rightarrow K^+ \pi^-$  is assumed to be small. If an arbitrary relative strong phase is allowed, the limit degrades by 25%.

<sup>7</sup> This GODANG 00 limit is inferred from the  $D^0$ - $\bar{D}^0$  mixing ratio  $\Gamma(K^+ \pi^- \text{ (via } \bar{D}^0))/\Gamma(K^- \pi^+)$  given near the end of this  $D^0$  Listings. Decay-time information is used to distinguish DCS decays from  $D^0$ - $\bar{D}^0$  mixing. The limit allows interference between the DCS and mixing ratios, and also allows CP violation. The strong phase between  $D^0 \rightarrow K^+ \pi^-$  and  $\bar{D}^0 \rightarrow K^+ \pi^-$  is assumed to be small. If an arbitrary relative strong phase is allowed, the limit degrades by a factor of two.

<sup>8</sup> AITALA 98 allows interference between the doubly Cabibbo-suppressed and mixing amplitudes, and also allows CP violation in this term, but assumes that  $A_D = A_R = 0$ . See the note on " $D^0$ - $\bar{D}^0$  Mixing," above.

<sup>9</sup> This limit is inferred from  $R_M$  for  $f = K^+ \pi^-$  and  $f = K^+ \pi^- \pi^+ \pi^-$ . See the note on " $D^0$ - $\bar{D}^0$  Mixing," above. Decay-time information is used to distinguish doubly Cabibbo-suppressed decays from  $D^0$ - $\bar{D}^0$  mixing.

<sup>10</sup> This limit is inferred from  $R_M$  for  $f = K^+ \ell^- \bar{\nu}_\ell$ . See the note on " $D^0$ - $\bar{D}^0$  Mixing," above.

## Meson Particle Listings

 $D^0$ 

<sup>11</sup> ANJOS 88c assumes that  $y = 0$ . See the note on " $D^0$ - $\bar{D}^0$  Mixing," above. Without this assumption, the limit degrades by about a factor of two.

$$(\Gamma_{D_1^0} - \Gamma_{D_2^0})/\Gamma = 2y$$

The  $D_1^0$  and  $D_2^0$  are the mass eigenstates of the  $D^0$  meson, as described in the note on " $D^0$ - $\bar{D}^0$  Mixing," above.

Due to the strong phase difference between  $D^0 \rightarrow K^+\pi^-$  and  $\bar{D}^0 \rightarrow K^+\pi^-$ , we exclude from the average those measurements of  $y'$  that are inferred from the  $D^0$ - $\bar{D}^0$  mixing ratio  $\Gamma(K^+\pi^- \text{ via } \bar{D}^0) / \Gamma(K^+\pi^-)$  given near the end of this  $D^0$  Listings.

Some early results have been omitted. See our 2006 Review (Journal of Physics, G **33** 1 (2006)).

"OUR EVALUATION" comes from averages provided by the Heavy Flavor Averaging Group, see the note on " $D^0$ - $\bar{D}^0$  Mixing."

VALUE (units $10^{-2}$ )	EVTS	DOCUMENT ID	TECN	COMMENT
<b><math>1.60 \pm 0.25</math></b>				<b>OUR EVALUATION</b>
<b><math>1.36 \pm 0.33</math></b>				<b>OUR AVERAGE</b> Error includes scale factor of 1.3. See the ideogram below.
$0.55 \pm 0.63 \pm 0.41$		<sup>1</sup> AAIJ	12K LHCb	$pp$ at 7 TeV
$1.14 \pm 0.40 \pm 0.30$		<sup>2</sup> DEL-AMO-SA...	10D BABR	$e^+e^-$ , 10.6 GeV
$2.32 \pm 0.44 \pm 0.36$		<sup>3</sup> AUBERT	09A1 BABR	$e^+e^- \approx \Upsilon(4S)$
$0.22 \pm 1.22 \pm 1.04$		<sup>4</sup> ZUPANC	09 BELL	$e^+e^- \approx \Upsilon(4S)$
$2.62 \pm 0.64 \pm 0.50$	160k	<sup>5</sup> STARIC	07 BELL	$e^+e^- \approx \Upsilon(4S)$
$0.74 \pm 0.50 \pm 0.20$	534k	<sup>6</sup> ZHANG	07B BELL	$e^+e^- \approx \Upsilon(4S)$
$-1.0 \pm 2.0 \pm 1.4$	18k	<sup>7</sup> ABE	02I BELL	$e^+e^- \approx \Upsilon(4S)$
$-2.4 \pm 5.0 \pm 2.8$	3393	<sup>8</sup> CSORNA	02 CLE2	$e^+e^- \approx \Upsilon(4S)$
$6.84 \pm 2.78 \pm 1.48$	10k	<sup>7</sup> LINK	00 FOCUS	$\gamma$ nucleus
$+1.6 \pm 5.8 \pm 2.1$		<sup>7</sup> AITALA	99E E791	$K^-\pi^+$ , $K^+K^-$
• • • We do not use the following data for averages, fits, limits, etc. • • •				
$-0.12 \pm 1.10 \pm 1.28 \pm 0.68$		<sup>9</sup> AUBERT	09AN BABR	$e^+e^-$ at 10.58 GeV
$1.4 \pm 4.8 \pm 5.4$		<sup>10</sup> LOWREY	09 CLEO	$e^+e^-$ at $\psi(3770)$
$1.70 \pm 1.52$	$12.7 \pm 0.3k$	<sup>11</sup> AALTONEN	08E CDF	$p\bar{p}$ , $\sqrt{s} = 1.96$ TeV
$2.06 \pm 0.66 \pm 0.38$		<sup>12</sup> AUBERT	08U BABR	See AUBERT 09A1
$1.94 \pm 0.88 \pm 0.62$	$4030 \pm 90$	<sup>11</sup> AUBERT	07W BABR	$e^+e^- \approx 10.6$ GeV
$-0.7 \pm 4.9$	$4k \pm 88$	<sup>11,13</sup> ZHANG	06 BELL	$e^+e^-$
$-3.0 \pm 5.0 \pm 1.6$		<sup>6</sup> ASNER	05 CLEO	$e^+e^- \approx 10$ GeV
$-3.3 \pm 4.8 \pm 0.8$		<sup>11,13</sup> LI	05A BELL	See ZHANG 06
$-3.0 \pm 5.7$		<sup>11,13</sup> LINK	05H FOCUS	$\gamma$ nucleus
$-5.2 \pm 18.4 \pm 16.8$		<sup>14</sup> AUBERT	03P BABR	See AUBERT 08U
$1.6 \pm 0.8 \pm 1.0 \pm 0.8$	450k	<sup>11,13</sup> AUBERT	03Z BABR	$e^+e^-$ , 10.6 GeV
$1.6 \pm 6.2 \pm 12.8$		<sup>11</sup> GODANG	00 CLE2	$e^+e^-$
$-5.0 \pm 2.8 \pm 3.2 \pm 0.6$				

- <sup>1</sup> Compared the lifetimes of  $D^0$  decay to the  $CP$  eigenstate  $K^+K^-$  with  $D^0$  decay to  $\pi^+K^-$ . The values here assume no  $CP$  violation.
- <sup>2</sup> DEL-AMO-SANCHEZ 10D uses 540,800  $\pm 800$   $K_S^0\pi^+\pi^-$  and 79,900  $\pm 300$   $K_S^0K^+K^-$  events in a time-dependent amplitude analyses of the  $D^0$  and  $\bar{D}^0$  Dalitz plots. No evidence was found for  $CP$  violation, and the values here assume no such violation.
- <sup>3</sup> This combines the  $y_{CP} = (\tau_{K^+\pi^-}/\tau_{K^+K^-}) - 1$  using untagged  $K^-\pi^+$  and  $K^+K^+$  events of AUBERT 09A1 with the disjoint  $y_{CP}$  using tagged  $K^-\pi^+$ ,  $K^-K^+$ , and  $\pi^-\pi^+$  events of AUBERT 08U.
- <sup>4</sup> ZUPANC 09 uses a method based on measuring the mean decay time of  $D^0 \rightarrow K_S^0K^+K^-$  events for different  $K^+K^-$  mass intervals.
- <sup>5</sup> STARIC 07 compares the lifetimes of  $D^0$  decay to the  $CP$  eigenstates  $K^+K^-$  and  $\pi^+\pi^-$  with  $D^0$  decay to  $K^-\pi^+$ .
- <sup>6</sup> The ASNER 05 and ZHANG 07B values are from the time-dependent Dalitz-plot analysis of  $D^0 \rightarrow K_S^0\pi^+\pi^-$ . Decay-time information and interference on the Dalitz plot are used to distinguish doubly Cabibbo-suppressed decays from mixing and to measure the relative phase between  $D^0 \rightarrow K^{*+}\pi^-$  and  $\bar{D}^0 \rightarrow K^{*+}\pi^-$ . This limit allows  $CP$  violation.
- <sup>7</sup> LINK 00, AITALA 99E, and ABE 02I measure the lifetime difference between  $D^0 \rightarrow K^-K^+$  ( $CP$ even) decays and  $D^0 \rightarrow K^-\pi^+$  ( $CP$ mixed) decays, or  $y_{CP} = [\Gamma(CP^+) - \Gamma(CP^-)] / [\Gamma(CP^+) + \Gamma(CP^-)]$ . We list  $2y_{CP} = \Delta\Gamma/\Gamma$ .
- <sup>8</sup> CSORNA 02 measures the lifetime difference between  $D^0 \rightarrow K^-K^+$  and  $\pi^-\pi^+$  ( $CP$ even) decays and  $D^0 \rightarrow K^-\pi^+$  ( $CP$ mixed) decays, or  $y_{CP} = [\Gamma(CP^+) - \Gamma(CP^-)] / [\Gamma(CP^+) + \Gamma(CP^-)]$ . We list  $2y_{CP} = \Delta\Gamma/\Gamma$ .
- <sup>9</sup> The AUBERT 09AN values are inferred from the branching ratio  $\Gamma(D^0 \rightarrow K^+\pi^-\pi^0 \text{ via } \bar{D}^0) / \Gamma(D^0 \rightarrow K^-\pi^+\pi^0)$  given near the end of this Listings. Mixing is distinguished from DCS decays using decay-time information. Interference between mixing and DCS is allowed. The phase between  $D^0 \rightarrow K^+\pi^-\pi^0$  and  $\bar{D}^0 \rightarrow K^+\pi^-\pi^0$  is assumed to be small. The width difference here is  $y''$ , which is not the same as  $y_{CP}$  in the note on  $D^0$ - $\bar{D}^0$  mixing.
- <sup>10</sup> LOWREY 09 uses quantum correlations in  $e^+e^- \rightarrow D^0\bar{D}^0$  at the  $\psi(3770)$ . See below for coherence factors and average relative strong phases for both  $D^0 \rightarrow K^-\pi^+\pi^0$  and  $D^0 \rightarrow K^-\pi^-2\pi^+$ . A fit that includes external measurements of charm mixing parameters gets  $2y = (1.62 \pm 0.32) \times 10^{-2}$ .

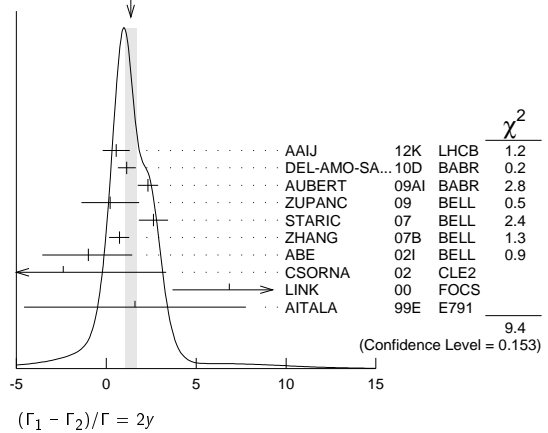
<sup>11</sup> The GODANG 00, AUBERT 03Z, LINK 05H, LI 05A, ZHANG 06, AUBERT 07W, and AALTONEN 08E limits are inferred from the  $D^0$ - $\bar{D}^0$  mixing ratio  $\Gamma(K^+\pi^- \text{ (via } \bar{D}^0)) / \Gamma(K^-\pi^+)$  given near the end of this  $D^0$  Listings. Decay-time information is used to distinguish DCS decays from  $D^0$ - $\bar{D}^0$  mixing. The limits allow interference between the DCS and mixing ratios, and all except AUBERT 07W and AALTONEN 08E also allow  $CP$  violation. The phase between  $D^0 \rightarrow K^+\pi^-$  and  $\bar{D}^0 \rightarrow K^+\pi^-$  is assumed to be small. This is a measurement of  $y'$  and is not the same as the  $y_{CP}$  of our note above on " $D^0$ - $\bar{D}^0$  Mixing."

<sup>12</sup> This value combines the results of AUBERT 08U and AUBERT 03P.

<sup>13</sup> The ranges of AUBERT 03Z, LINK 05H, LI 05A, and ZHANG 06 measurements are for 95% confidence level.

<sup>14</sup> AUBERT 03P measures  $Y \equiv 2\tau^0 / (\tau^+ + \tau^-) - 1$ , where  $\tau^0$  is the  $D^0 \rightarrow K^-\pi^+$  (and  $\bar{D}^0 \rightarrow K^+\pi^-$ ) lifetime, and  $\tau^+$  and  $\tau^-$  are the  $D^0$  and  $\bar{D}^0$  lifetimes to  $CP$ -even states (here  $K^-K^+$  and  $\pi^-\pi^+$ ). In the limit of  $CP$  conservation,  $Y = y \equiv \Delta\Gamma / 2\Gamma$  (we list  $2y = \Delta\Gamma/\Gamma$ ). AUBERT 03P also uses  $\tau^+ - \tau^-$  to get  $\Delta Y = -0.008 \pm 0.006 \pm 0.002$ .

WEIGHTED AVERAGE  
1.36 $\pm$ 0.33 (Error scaled by 1.3)

 $|q/p|$ 

The mass eigenstates  $D_1^0$  and  $D_2^0$  are related to the  $C = \pm 1$  states by  $|D_{1,2}^0\rangle = p|D^0\rangle + q|\bar{D}^0\rangle$ . See the note on " $D^0$ - $\bar{D}^0$  Mixing" above.

"OUR EVALUATION" comes from averages provided by the Heavy Flavor Averaging Group. This would include as-yet-unpublished results, see the note on " $D^0$ - $\bar{D}^0$  Mixing."

VALUE	DOCUMENT ID	TECN	COMMENT
<b><math>0.88 \pm 0.16</math></b>			<b>OUR EVALUATION</b> HFAG fit; see the note on " $D^0$ - $\bar{D}^0$ Mixing."
<b><math>0.86 \pm 0.30 \pm 0.10</math></b>	<sup>1</sup> ZHANG	07B BELL	$e^+e^- \approx \Upsilon(4S)$
<b><math>-0.29 \pm 0.08</math></b>			

<sup>1</sup> The phase of  $p/q$  is  $(-14 \pm 16 \pm 5)^\circ$ . The ZHANG 07B value is from the time-dependent Dalitz-plot analysis of  $D^0 \rightarrow K_S^0\pi^+\pi^-$ . Decay-time information and interference on the Dalitz plot are used to distinguish doubly Cabibbo-suppressed decays from mixing and to measure the relative phase between  $D^0 \rightarrow K^{*+}\pi^-$  and  $\bar{D}^0 \rightarrow K^{*+}\pi^-$ . This value allows  $CP$  violation.

 $A_\Gamma$ 

$A_\Gamma$  is the decay-rate asymmetry for  $CP$ -even final states  $A_\Gamma = (\bar{\tau}_+ - \tau_+) / (\bar{\tau}_+ + \tau_+)$ . See the note on " $D^0$ - $\bar{D}^0$  Mixing" above.

VALUE (units $10^{-3}$ )	DOCUMENT ID	TECN	COMMENT
<b><math>0.26 \pm 2.31</math></b>			<b>OUR EVALUATION</b>
<b><math>0.3 \pm 2.5</math></b>			<b>OUR AVERAGE</b>
$-5.9 \pm 5.9 \pm 2.1$	AAIJ	12K LHCb	$pp$ at 7 TeV
$+2.6 \pm 3.6 \pm 0.8$	AUBERT	08U BABR	$e^+e^- \approx \Upsilon(4S)$
$+0.1 \pm 3.0 \pm 2.5$	STARIC	07 BELL	$e^+e^- \approx \Upsilon(4S)$
• • • We do not use the following data for averages, fits, limits, etc. • • •			
$+8 \pm 6 \pm 2$	AUBERT	03P BABR	$e^+e^- \approx \Upsilon(4S)$

 $\cos \delta$ 

$\delta$  is the  $D^0 \rightarrow K^+\pi^-$  relative strong phase.

VALUE	DOCUMENT ID	TECN	COMMENT
<b><math>1.03 \pm 0.31</math></b>			<b>OUR EVALUATION</b>
<b><math>-0.17 \pm 0.06</math></b>	<sup>1</sup> ASNER	08 CLEO	$e^+e^- \rightarrow D^0\bar{D}^0$ , 3.77 GeV

<sup>1</sup> ASNER 08 uses quantum correlations in  $e^+e^- \rightarrow D^0\bar{D}^0$  at the  $\psi(3770)$ , where decay rates of  $CP$ -tagged  $K\pi$  final states depend on  $\cos \delta$  because of interfering amplitudes. The above measurement implies  $|\delta| < 75^\circ$  with a confidence level of 95%. A fit that includes external measurements of charm mixing parameters finds  $\cos \delta = 1.10 \pm 0.35 \pm 0.07$ . See also the note on " $D^0$ - $\bar{D}^0$  Mixing" p. 783 in our 2008 Review (PDG 08).

$D^0 \rightarrow K^- \pi^+ \pi^0$  COHERENCE FACTOR  $R_{K\pi\pi^0}$ 

See the note on ' $D^0$ - $\bar{D}^0$  Mixing' for the definition.  $R_{K\pi\pi^0}$  can have any value between 0 and 1. A value near 1 indicates the decay is dominated by a few intermediate states with limited interference.

VALUE	DOCUMENT ID	TECN	COMMENT
$0.78^{+0.11}_{-0.25}$	<sup>1</sup> LOWREY 09	CLEO	$e^+e^- \rightarrow D^0\bar{D}^0$ at $\psi(3770)$

<sup>1</sup> LOWREY 09 uses quantum correlations in  $e^+e^- \rightarrow D^0\bar{D}^0$  at the  $\psi(3770)$ , where the decay rates of CP-tagged  $K^- \pi^+ \pi^0$  final states depend on  $R_{K\pi\pi^0}$  and  $\delta^{K\pi\pi^0}$ . A fit that includes external measurements of charm mixing parameters gets  $R_{K\pi\pi^0} = 0.84 \pm 0.07$ .

 $D^0 \rightarrow K^- \pi^+ \pi^0$  AVERAGE RELATIVE STRONG PHASE  $\delta^{K\pi\pi^0}$ 

VALUE (°)	DOCUMENT ID	TECN	COMMENT
$239^{+32}_{-28}$	<sup>1</sup> LOWREY 09	CLEO	$e^+e^- \rightarrow D^0\bar{D}^0$ at $\psi(3770)$

<sup>1</sup> LOWREY 09 uses quantum correlations in  $e^+e^- \rightarrow D^0\bar{D}^0$  at the  $\psi(3770)$ , where the decay rates of CP-tagged  $K^- \pi^+ \pi^0$  final states depend on  $R_{K\pi\pi^0}$  and  $\delta^{K\pi\pi^0}$ . A fit that includes external measurements of charm mixing parameters gets  $\delta^{K\pi\pi^0} = (227^{+14}_{-17})^\circ$ .

 $D^0 \rightarrow K^- \pi^- 2\pi^+$  COHERENCE FACTOR  $R_{K3\pi}$ 

See the note on ' $D^0$ - $\bar{D}^0$  Mixing' for the definition.  $R_{K3\pi}$  can have any value between 0 and 1. A value near 1 indicates the decay is dominated by a few intermediate states with limited interference.

VALUE	DOCUMENT ID	TECN	COMMENT
$0.36^{+0.24}_{-0.30}$	<sup>1</sup> LOWREY 09	CLEO	$e^+e^- \rightarrow D^0\bar{D}^0$ at $\psi(3770)$

<sup>1</sup> LOWREY 09 uses quantum correlations in  $e^+e^- \rightarrow D^0\bar{D}^0$  at the  $\psi(3770)$ , where the decay rates of CP-tagged  $K^- \pi^- 2\pi^+$  final states depend on  $R_{K3\pi}$  and  $\delta^{K3\pi}$ . A fit that includes external measurements of charm mixing parameters gets  $R_{K3\pi} = 0.33^{+0.26}_{-0.23}$ .

 $D^0 \rightarrow K^- \pi^- 2\pi^+$  AVERAGE RELATIVE STRONG PHASE  $\delta^{K3\pi}$ 

VALUE (°)	DOCUMENT ID	TECN	COMMENT
$118^{+62}_{-53}$	<sup>1</sup> LOWREY 09	CLEO	$e^+e^- \rightarrow D^0\bar{D}^0$ at $\psi(3770)$

<sup>1</sup> LOWREY 09 uses quantum correlations in  $e^+e^- \rightarrow D^0\bar{D}^0$  at the  $\psi(3770)$ , where the decay rates of CP-tagged  $K^- \pi^- 2\pi^+$  final states depend on  $R_{K3\pi}$  and  $\delta^{K3\pi}$ . A fit that includes external measurements of charm mixing parameters gets  $\delta^{K3\pi} = (114^{+26}_{-23})^\circ$ .

D<sup>0</sup> DECAY MODES

Most decay modes (other than the semileptonic modes) that involve a neutral K meson are now given as  $K_S^0$  modes, not as  $\bar{K}^0$  modes. Nearly always it is a  $K_S^0$  that is measured, and interference between Cabibbo-allowed and doubly Cabibbo-suppressed modes can invalidate the assumption that  $2\Gamma(K_S^0) = \Gamma(\bar{K}^0)$ .

Mode	Fraction ( $\Gamma_i/\Gamma$ )	Scale factor/ Confidence level
<b>Topological modes</b>		
$\Gamma_1$ $D^0 \rightarrow 0$ -prongs	[a] (15 ± 6) %	
$\Gamma_2$ $D^0 \rightarrow 2$ -prongs	(70 ± 6) %	
$\Gamma_3$ $D^0 \rightarrow 4$ -prongs	[b] (14.5 ± 0.5) %	
$\Gamma_4$ $D^0 \rightarrow 6$ -prongs	[c] (6.4 ± 1.3) × 10 <sup>-4</sup>	
<b>Inclusive modes</b>		
$\Gamma_5$ $D^0 \rightarrow e^+$ anything	[d] (6.49 ± 0.11) %	
$\Gamma_6$ $D^0 \rightarrow \mu^+$ anything	(6.7 ± 0.6) %	
$\Gamma_7$ $D^0 \rightarrow K^-$ anything	(54.7 ± 2.8) %	S=1.3
$\Gamma_8$ $D^0 \rightarrow \bar{K}^0$ anything + $K^0$ anything	(47 ± 4) %	
$\Gamma_9$ $D^0 \rightarrow K^+$ anything	(3.4 ± 0.4) %	
$\Gamma_{10}$ $D^0 \rightarrow K^*(892)^-$ anything	(15 ± 9) %	
$\Gamma_{11}$ $D^0 \rightarrow \bar{K}^*(892)^0$ anything	(9 ± 4) %	
$\Gamma_{12}$ $D^0 \rightarrow K^*(892)^+ \pi^0$ anything	< 3.6 %	CL=90%
$\Gamma_{13}$ $D^0 \rightarrow K^*(892)^0$ anything	(2.8 ± 1.3) %	
$\Gamma_{14}$ $D^0 \rightarrow \eta$ anything	(9.5 ± 0.9) %	
$\Gamma_{15}$ $D^0 \rightarrow \eta'$ anything	(2.48 ± 0.27) %	
$\Gamma_{16}$ $D^0 \rightarrow \phi$ anything	(1.05 ± 0.11) %	
<b>Semileptonic modes</b>		
$\Gamma_{17}$ $D^0 \rightarrow K^- \ell^+ \nu_\ell$		
$\Gamma_{18}$ $D^0 \rightarrow K^- e^+ \nu_e$	(3.55 ± 0.04) %	S=1.2
$\Gamma_{19}$ $D^0 \rightarrow K^- \mu^+ \nu_\mu$	(3.30 ± 0.13) %	
$\Gamma_{20}$ $D^0 \rightarrow K^*(892)^- e^+ \nu_e$	(2.16 ± 0.16) %	
$\Gamma_{21}$ $D^0 \rightarrow K^*(892)^- \mu^+ \nu_\mu$	(1.90 ± 0.24) %	
$\Gamma_{22}$ $D^0 \rightarrow K^- \pi^0 e^+ \nu_e$	(1.6 ± 1.3 / 0.5) %	

$\Gamma_{23}$ $D^0 \rightarrow \bar{K}^0 \pi^- e^+ \nu_e$	(2.7 ± 0.9 / 0.7) %	
$\Gamma_{24}$ $D^0 \rightarrow K^- \pi^+ \pi^- e^+ \nu_e$	(2.8 ± 1.4 / 1.1) × 10 <sup>-4</sup>	
$\Gamma_{25}$ $D^0 \rightarrow K_1(1270)^- e^+ \nu_e$	(7.6 ± 4.0 / 3.1) × 10 <sup>-4</sup>	
$\Gamma_{26}$ $D^0 \rightarrow K^- \pi^+ \pi^- \mu^+ \nu_\mu$	< 1.2 × 10 <sup>-3</sup>	CL=90%
$\Gamma_{27}$ $D^0 \rightarrow (\bar{K}^*(892)\pi)^- \mu^+ \nu_\mu$	< 1.4 × 10 <sup>-3</sup>	CL=90%
$\Gamma_{28}$ $D^0 \rightarrow \pi^- e^+ \nu_e$	(2.89 ± 0.08) × 10 <sup>-3</sup>	S=1.1
$\Gamma_{29}$ $D^0 \rightarrow \pi^- \mu^+ \nu_\mu$	(2.37 ± 0.24) × 10 <sup>-3</sup>	
$\Gamma_{30}$ $D^0 \rightarrow \rho^- e^+ \nu_e$	(1.9 ± 0.4) × 10 <sup>-3</sup>	

Hadronic modes with one  $\bar{K}$ 

$\Gamma_{31}$ $D^0 \rightarrow K^- \pi^+$	(3.88 ± 0.05) %	S=1.2
$\Gamma_{32}$ $D^0 \rightarrow K_S^0 \pi^0$	(1.19 ± 0.04) %	
$\Gamma_{33}$ $D^0 \rightarrow K_S^0 \pi^0$	(10.0 ± 0.7) × 10 <sup>-3</sup>	
$\Gamma_{34}$ $D^0 \rightarrow K_S^0 \pi^+ \pi^-$	[e] (2.82 ± 0.19) %	S=1.1
$\Gamma_{35}$ $D^0 \rightarrow K_S^0 \rho^0$	(6.3 ± 0.7 / 0.8) × 10 <sup>-3</sup>	
$\Gamma_{36}$ $D^0 \rightarrow K_S^0 \omega, \omega \rightarrow \pi^+ \pi^-$	(2.0 ± 0.6) × 10 <sup>-4</sup>	
$\Gamma_{37}$ $D^0 \rightarrow K_S^0 (\pi^+ \pi^-)_{S\text{-wave}}$	(3.4 ± 0.8) × 10 <sup>-3</sup>	
$\Gamma_{38}$ $D^0 \rightarrow K_S^0 f_0(980), f_0(980) \rightarrow \pi^+ \pi^-$	(1.21 ± 0.40 / 0.24) × 10 <sup>-3</sup>	
$\Gamma_{39}$ $D^0 \rightarrow K_S^0 f_0(1370), f_0(1370) \rightarrow \pi^+ \pi^-$	(2.8 ± 0.9 / 1.3) × 10 <sup>-3</sup>	
$\Gamma_{40}$ $D^0 \rightarrow K_S^0 f_2(1270), f_2(1270) \rightarrow \pi^+ \pi^-$	(9 ± 10 / 6) × 10 <sup>-5</sup>	
$\Gamma_{41}$ $D^0 \rightarrow K^*(892)^- \pi^+, K^*(892)^- \rightarrow K_S^0 \pi^-$	(1.66 ± 0.15 / 0.17) %	
$\Gamma_{42}$ $D^0 \rightarrow K_0^*(1430)^- \pi^+, K_0^*(1430)^- \rightarrow K_S^0 \pi^-$	(2.69 ± 0.40 / 0.33) × 10 <sup>-3</sup>	
$\Gamma_{43}$ $D^0 \rightarrow K_2^*(1430)^- \pi^+, K_2^*(1430)^- \rightarrow K_S^0 \pi^-$	(3.4 ± 1.9 / 1.0) × 10 <sup>-4</sup>	
$\Gamma_{44}$ $D^0 \rightarrow K^*(1680)^- \pi^+, K^*(1680)^- \rightarrow K_S^0 \pi^-$	(4 ± 4) × 10 <sup>-4</sup>	
$\Gamma_{45}$ $D^0 \rightarrow K^*(892)^+ \pi^-, K^*(892)^+ \rightarrow K_S^0 \pi^+$	[f] (1.13 ± 0.60 / 0.34) × 10 <sup>-4</sup>	
$\Gamma_{46}$ $D^0 \rightarrow K_0^*(1430)^+ \pi^-, K_0^*(1430)^+ \rightarrow K_S^0 \pi^+$	[f] < 1.4 × 10 <sup>-5</sup>	CL=95%
$\Gamma_{47}$ $D^0 \rightarrow K_2^*(1430)^+ \pi^-, K_2^*(1430)^+ \rightarrow K_S^0 \pi^+$	[f] < 3.4 × 10 <sup>-5</sup>	CL=95%
$\Gamma_{48}$ $D^0 \rightarrow K_S^0 \pi^+ \pi^-$ nonresonant	(2.5 ± 6.0 / 1.6) × 10 <sup>-4</sup>	
$\Gamma_{49}$ $D^0 \rightarrow K^- \pi^+ \pi^0$	[e] (13.9 ± 0.5) %	S=1.7
$\Gamma_{50}$ $D^0 \rightarrow K^- \rho^+$	(10.8 ± 0.7) %	
$\Gamma_{51}$ $D^0 \rightarrow K^- \rho(1700)^+, \rho(1700)^+ \rightarrow \pi^+ \pi^0$	(7.9 ± 1.7) × 10 <sup>-3</sup>	
$\Gamma_{52}$ $D^0 \rightarrow K^*(892)^- \pi^+, K^*(892)^- \rightarrow K^- \pi^0$	(2.22 ± 0.40 / 0.19) %	
$\Gamma_{53}$ $D^0 \rightarrow \bar{K}^*(892)^0 \pi^0, \bar{K}^*(892)^0 \rightarrow K^- \pi^+$	(1.88 ± 0.23) %	
$\Gamma_{54}$ $D^0 \rightarrow K_0^*(1430)^- \pi^+, K_0^*(1430)^- \rightarrow K^- \pi^0$	(4.6 ± 2.1) × 10 <sup>-3</sup>	
$\Gamma_{55}$ $D^0 \rightarrow \bar{K}_0^*(1430)^0 \pi^0, \bar{K}_0^*(1430)^0 \rightarrow K^- \pi^+$	(5.7 ± 5.0 / 1.5) × 10 <sup>-3</sup>	
$\Gamma_{56}$ $D^0 \rightarrow K^*(1680)^- \pi^+, K^*(1680)^- \rightarrow K^- \pi^0$	(1.8 ± 0.7) × 10 <sup>-3</sup>	
$\Gamma_{57}$ $D^0 \rightarrow K^- \pi^+ \pi^0$ nonresonant	(1.11 ± 0.50 / 0.19) %	
$\Gamma_{58}$ $D^0 \rightarrow K_S^0 2\pi^0$	(9.1 ± 1.1) × 10 <sup>-3</sup>	S=2.2
$\Gamma_{59}$ $D^0 \rightarrow K_S^0 (2\pi^0)$ -S-wave	(2.6 ± 0.7) × 10 <sup>-3</sup>	
$\Gamma_{60}$ $D^0 \rightarrow \bar{K}^*(892)^0 \pi^0, \bar{K}^*(892)^0 \rightarrow K_S^0 \pi^0$	(7.8 ± 0.7) × 10 <sup>-3</sup>	
$\Gamma_{61}$ $D^0 \rightarrow \bar{K}^*(1430)^0 \pi^0, \bar{K}^{*0} \rightarrow K_S^0 \pi^0$	(4 ± 23) × 10 <sup>-5</sup>	
$\Gamma_{62}$ $D^0 \rightarrow \bar{K}^*(1680)^0 \pi^0, \bar{K}^{*0} \rightarrow K_S^0 \pi^0$	(1.0 ± 0.4) × 10 <sup>-3</sup>	
$\Gamma_{63}$ $D^0 \rightarrow K_S^0 f_2(1270), f_2 \rightarrow 2\pi^0$	(2.3 ± 1.1) × 10 <sup>-4</sup>	
$\Gamma_{64}$ $D^0 \rightarrow 2K_S^0, \text{one } K_S^0 \rightarrow 2\pi^0$	(3.2 ± 1.1) × 10 <sup>-4</sup>	
$\Gamma_{65}$ $D^0 \rightarrow K_S^0 2\pi^0$ nonresonant		
$\Gamma_{66}$ $D^0 \rightarrow K^- 2\pi^+ \pi^-$	[e] (8.07 ± 0.21 / 0.19) %	S=1.3









See key on page 457

$x_{172}$	1										
$x_{174}$	1	1									
$x_{175}$	1	0	0								
$x_{176}$	7	5	6	3							
$x_{177}$	1	0	1	0	3						
$x_{178}$	1	0	1	0	4	3					
$x_{180}$	1	0	1	0	3	2	9				
$x_{208}$	1	1	1	0	8	0	1	0			
$x_{212}$	3	2	3	1	15	1	2	1	2		
$x_{271}$	-3	-3	-4	-3	-14	-4	-18	-14	-2	-5	
	$x_{166}$	$x_{172}$	$x_{174}$	$x_{175}$	$x_{176}$	$x_{177}$	$x_{178}$	$x_{180}$	$x_{208}$	$x_{212}$	

**CONSTRAINED FIT INFORMATION**

An overall fit to 3 branching ratios uses 3 measurements and one constraint to determine 4 parameters. The overall fit has a  $\chi^2 = 0.0$  for 0 degrees of freedom.

The following *off-diagonal* array elements are the correlation coefficients  $\langle \delta x_i \delta x_j \rangle / (\delta x_i \delta x_j)$ , in percent, from the fit to the branching fractions,  $x_i \equiv \Gamma_i / \Gamma_{\text{total}}$ . The fit constrains the  $x_i$  whose labels appear in this array to sum to one.

$x_2$	-100		
$x_3$	-46	40	
$x_4$	0	0	0
	$x_1$	$x_2$	$x_3$

 **$D^0$  BRANCHING RATIOS**

Some older now obsolete results have been omitted from these Listings.

**Topological modes**

**$\Gamma(0\text{-prongs})/\Gamma_{\text{total}}$**   $\Gamma_1/\Gamma$   
This value is obtained by subtracting the branching fractions for 2-, 4-, and 6-prongs from unity.

VALUE	DOCUMENT ID
<b>0.15 ± 0.06 OUR FIT</b>	

**$\Gamma(4\text{-prongs})/\Gamma_{\text{total}}$**   $\Gamma_3/\Gamma$   
This is the sum of our  $K^- 2\pi^+ \pi^-$ ,  $K^- 2\pi^+ \pi^- \pi^0$ ,  $\bar{K}^0 2\pi^+ 2\pi^-$ ,  $K^+ 2K^- \pi^+$ ,  $2\pi^+ 2\pi^-$ ,  $2\pi^+ 2\pi^- \pi^0$ ,  $K^+ K^- \pi^+ \pi^-$ , and  $K^+ K^- \pi^+ \pi^- \pi^0$  branching fractions.

VALUE	DOCUMENT ID
<b>0.145 ± 0.005 OUR FIT</b>	
<b>0.145 ± 0.005</b>	PDG 12

**$\Gamma(4\text{-prongs})/\Gamma(2\text{-prongs})$**   $\Gamma_3/\Gamma_2$   
**0.207 ± 0.016 OUR FIT**  
**0.207 ± 0.016 ± 0.004** 226 ONENGUT 05 CHRS  $\nu_\mu$  emulsion,  $\bar{E}_\nu \approx 27$  GeV

**$\Gamma(6\text{-prongs})/\Gamma_{\text{total}}$**   $\Gamma_4/\Gamma$   
This is the sum of our  $K^- 3\pi^+ 2\pi^-$  and  $3\pi^+ 3\pi^-$  branching fractions.

VALUE (units $10^{-4}$ )	EVTs	DOCUMENT ID	TECN	COMMENT
<b>6.4 ± 1.3 OUR FIT</b>				
<b>6.4 ± 1.3</b>		PDG 12		
• • • We do not use the following data for averages, fits, limits, etc. • • •				
12 $\pm_{-9}^{+13} \pm 2$	3	ONENGUT 05	CHRS	$\nu_\mu$ emulsion, $\bar{E}_\nu \approx 27$ GeV

**Inclusive modes**

**$\Gamma(e^+ \text{ anything})/\Gamma_{\text{total}}$**   $\Gamma_5/\Gamma$   
The branching fractions for the  $K^- e^+ \nu_e$ ,  $K^*(892)^- e^+ \nu_e$ ,  $\pi^- e^+ \nu_e$ , and  $\rho^- e^+ \nu_e$  modes add up to  $6.20 \pm 0.17$  %.

VALUE (%)	EVTs	DOCUMENT ID	TECN	COMMENT
<b>6.49 ± 0.11 OUR AVERAGE</b>				
6.46 ± 0.09 ± 0.11	6584 ± 96	<sup>1</sup> ASNER 10	CLEO	$e^+ e^-$ at 3774 MeV
6.3 ± 0.7 ± 0.4	290 ± 32	ABLIKIM 07G	BES2	$e^+ e^- \approx \psi(3770)$
6.46 ± 0.17 ± 0.13	2246 ± 57	ADAM 06A	CLEO	See ASNER 10
6.9 ± 0.3 ± 0.5	1670	ALBRECHT 96C	ARG	$e^+ e^- \approx 10$ GeV
6.64 ± 0.18 ± 0.29	4609	KUBOTA 96B	CLE2	$e^+ e^- \approx \Upsilon(4S)$

<sup>1</sup> Using the  $D^+$  and  $D^0$  lifetimes, ASNER 10 finds that the ratio of the  $D^+$  and  $D^0$  semileptonic widths is  $0.985 \pm 0.015 \pm 0.024$ .

**$\Gamma(\mu^+ \text{ anything})/\Gamma_{\text{total}}$**   $\Gamma_6/\Gamma$   
**6.7 ± 0.6 OUR FIT**  
**6.4 ± 0.8 OUR AVERAGE**

VALUE (%)	EVTs	DOCUMENT ID	TECN	COMMENT
6.8 ± 1.5 ± 0.8	79 ± 10	<sup>1</sup> ABLIKIM 08L	BES2	$e^+ e^- \approx \psi(3772)$
6.5 ± 1.2 ± 0.3	36	KAYIS-TOPAK.05	CHRS	$\nu_\mu$ emulsion
6.0 ± 0.7 ± 1.2	310	ALBRECHT 96C	ARG	$e^+ e^- \approx 10$ GeV

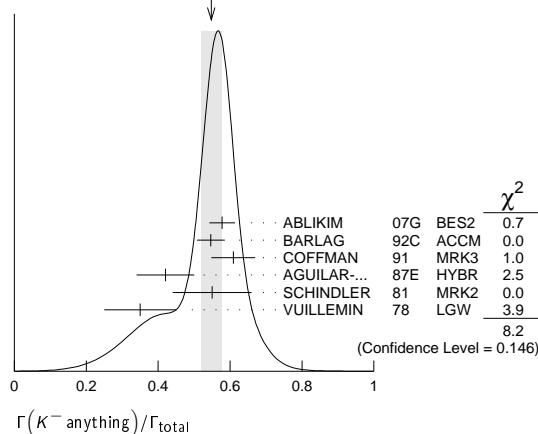
<sup>1</sup> ABLIKIM 08L finds the ratio of  $D^+ \rightarrow \mu^+ X$  and  $D^0 \rightarrow \mu^+ X$  branching fractions to be  $2.59 \pm 0.70 \pm 0.25$ , in accord with the ratio of  $D^+$  and  $D^0$  lifetimes,  $2.54 \pm 0.02$ .

**$\Gamma(K^- \text{ anything})/\Gamma_{\text{total}}$**   $\Gamma_7/\Gamma$

VALUE	EVTs	DOCUMENT ID	TECN	COMMENT
<b>0.547 ± 0.028 OUR AVERAGE</b>	Error	includes scale factor of 1.3. See the ideogram below.		
0.578 ± 0.016 ± 0.032	2098 ± 59	ABLIKIM 07G	BES2	$e^+ e^- \approx \psi(3770)$
0.546 $\pm_{-0.038}^{+0.039}$		<sup>1</sup> BARLAG 92c	ACCM	$\pi^-$ Cu 230 GeV
0.609 ± 0.032 ± 0.052		COFFMAN 91	MRK3	$e^+ e^-$ 3.77 GeV
0.42 ± 0.08		AGUILAR-... 87E	HYBR	$\pi p, pp$ 360, 400 GeV
0.55 ± 0.11	121	SCHINDLER 81	MRK2	$e^+ e^-$ 3.771 GeV
0.35 ± 0.10	19	VUILLEMIN 78	LGW	$e^+ e^-$ 3.772 GeV

<sup>1</sup> BARLAG 92c computes the branching fraction using topological normalization.

WEIGHTED AVERAGE  
0.547 ± 0.028 (Error scaled by 1.3)



**$[\Gamma(K^0 \text{ anything}) + \Gamma(K^- \text{ anything})]/\Gamma_{\text{total}}$**   $\Gamma_8/\Gamma$

VALUE	EVTs	DOCUMENT ID	TECN	COMMENT
<b>0.47 ± 0.04 OUR AVERAGE</b>				
0.476 ± 0.048 ± 0.030	250 ± 25	ABLIKIM 06u	BES2	$e^+ e^-$ at 3773 MeV
0.455 ± 0.050 ± 0.032		COFFMAN 91	MRK3	$e^+ e^-$ 3.77 GeV

**$\Gamma(K^+ \text{ anything})/\Gamma_{\text{total}}$**   $\Gamma_9/\Gamma$   
**0.034 ± 0.004 OUR AVERAGE**

VALUE	EVTs	DOCUMENT ID	TECN	COMMENT
0.035 ± 0.007 ± 0.003	119 ± 23	ABLIKIM 07G	BES2	$e^+ e^- \approx \psi(3770)$
0.034 $\pm_{-0.005}^{+0.007}$		<sup>1</sup> BARLAG 92c	ACCM	$\pi^-$ Cu 230 GeV
0.028 ± 0.009 ± 0.004		COFFMAN 91	MRK3	$e^+ e^-$ 3.77 GeV
0.03 $\pm_{-0.02}^{+0.05}$		AGUILAR-... 87E	HYBR	$\pi p, pp$ 360, 400 GeV
0.08 ± 0.03	25	SCHINDLER 81	MRK2	$e^+ e^-$ 3.771 GeV

<sup>1</sup> BARLAG 92c computes the branching fraction using topological normalization.

**$\Gamma(K^*(892)^- \text{ anything})/\Gamma_{\text{total}}$**   $\Gamma_{10}/\Gamma$

VALUE	EVTs	DOCUMENT ID	TECN	COMMENT
<b>0.153 ± 0.083 ± 0.019</b>	28 ± 15	ABLIKIM 06u	BES2	$e^+ e^-$ at 3773 MeV

**$\Gamma(\bar{K}^*(892)^0 \text{ anything})/\Gamma_{\text{total}}$**   $\Gamma_{11}/\Gamma$

VALUE	EVTs	DOCUMENT ID	TECN	COMMENT
<b>0.087 ± 0.040 ± 0.012</b>	96 ± 44	ABLIKIM 05P	BES	$e^+ e^- \approx 3773$ MeV

**$\Gamma(K^*(892)^+ \text{ anything})/\Gamma_{\text{total}}$**   $\Gamma_{12}/\Gamma$

VALUE	CL%	DOCUMENT ID	TECN	COMMENT
<b>&lt; 0.036</b>	90	ABLIKIM 06u	BES2	$e^+ e^-$ at 3773 MeV

**$\Gamma(K^*(892)^0 \text{ anything})/\Gamma_{\text{total}}$**   $\Gamma_{13}/\Gamma$

VALUE	EVTs	DOCUMENT ID	TECN	COMMENT
<b>0.028 ± 0.012 ± 0.004</b>	31 ± 12	ABLIKIM 05P	BES	$e^+ e^- \approx 3773$ MeV

**$\Gamma(\eta \text{ anything})/\Gamma_{\text{total}}$**   $\Gamma_{14}/\Gamma$

VALUE (units $10^{-2}$ )	EVTs	DOCUMENT ID	TECN	COMMENT
<b>9.5 ± 0.4 ± 0.8</b>	4463 ± 197	HUANG 06B	CLEO	$e^+ e^-$ at $\psi(3770)$

**$\Gamma(\eta' \text{ anything})/\Gamma_{\text{total}}$**   $\Gamma_{15}/\Gamma$

VALUE (units $10^{-2}$ )	EVTs	DOCUMENT ID	TECN	COMMENT
<b>2.48 ± 0.17 ± 0.21</b>	299 ± 21	HUANG 06B	CLEO	$e^+ e^-$ at $\psi(3770)$

**$\Gamma(\phi \text{ anything})/\Gamma_{\text{total}}$**   $\Gamma_{16}/\Gamma$

VALUE (units $10^{-2}$ )	EVTs	DOCUMENT ID	TECN	COMMENT
<b>1.05 ± 0.08 ± 0.07</b>	368 ± 24	HUANG 06B	CLEO	$e^+ e^-$ at $\psi(3770)$
• • • We do not use the following data for averages, fits, limits, etc. • • •				
1.71 $\pm_{-0.71}^{+0.76} \pm 0.17$	9	BAI 00c	BES	$e^+ e^- \rightarrow D\bar{D}^*, D^*\bar{D}^*$



$\Gamma(\pi^- \mu^+ \nu_\mu)/\Gamma(K^- \mu^+ \nu_\mu)$		$\Gamma_{29}/\Gamma_{19}$	
VALUE	EVTS	DOCUMENT ID	TECN COMMENT
<b>0.072±0.007 OUR FIT</b>			
<b>0.074±0.008±0.007</b>	288 ± 29	<sup>1</sup> LINK	05 FOCS $\gamma A, \bar{E}_\gamma \approx 180$ GeV
<sup>1</sup> LINK 05 finds the form-factor ratio $ f_0^{\pi^-}(0)/f_0^{K^-}(0) $ to be $0.85 \pm 0.04 \pm 0.04 \pm 0.01$ .			

$\Gamma(\rho^- e^+ \nu_e)/\Gamma_{total}$		$\Gamma_{30}/\Gamma$	
VALUE (units $10^{-2}$ )	EVTS	DOCUMENT ID	TECN COMMENT
<b>0.194±0.039±0.013</b>	31 ± 6	COAN	05 CLEO $e^+ e^-$ at $\psi(3770)$

Hadronic modes with a single  $\bar{K}$ 

$\Gamma(K^- \pi^+)/\Gamma_{total}$		$\Gamma_{31}/\Gamma$	
VALUE (units $10^{-2}$ )	EVTS	DOCUMENT ID	TECN COMMENT
<b>3.88 ± 0.05 OUR FIT</b>			Error includes scale factor of 1.2.
<b>3.91 ± 0.05 OUR AVERAGE</b>			Error includes scale factor of 1.1.
4.007±0.037±0.072	33.8 ± 0.3k	AUBERT	08L BABR $e^+ e^-$ at $\Upsilon(4S)$
3.891±0.035±0.069		<sup>1</sup> DOBBS	07 CLEO $e^+ e^-$ at $\psi(3770)$
3.82 ± 0.07 ± 0.12		<sup>2</sup> ARTUSO	98 CLE2 CLEO average
3.90 ± 0.09 ± 0.12	5392	<sup>3</sup> BARATE	97c ALEP From Z decays
3.41 ± 0.12 ± 0.28	1173 ± 37	<sup>3</sup> ALBRECHT	94F ARG $e^+ e^- \approx \Upsilon(4S)$
3.62 ± 0.34 ± 0.44		<sup>3</sup> DECAMP	91J ALEP From Z decays
• • • We do not use the following data for averages, fits, limits, etc. • • •			
3.91 ± 0.08 ± 0.09	10.3k ± 100	<sup>1</sup> HE	05 CLEO See DOBBS 07
3.81 ± 0.15 ± 0.16	1165	<sup>4</sup> ARTUSO	98 CLE2 $e^+ e^-$ at $\Upsilon(4S)$
3.69 ± 0.11 ± 0.16		<sup>5</sup> COAN	98 CLE2 See ARTUSO 98
4.5 ± 0.6 ± 0.4		<sup>6</sup> ALBRECHT	94 ARG $e^+ e^- \approx \Upsilon(4S)$
3.95 ± 0.08 ± 0.17	4208	<sup>3,7</sup> AKERIB	93 CLE2 See ARTUSO 98
4.5 ± 0.8 ± 0.5	56	<sup>3</sup> ABACHI	88 HRS $e^+ e^-$ 29 GeV
4.2 ± 0.4 ± 0.4	930	ADLER	88c MRK3 $e^+ e^-$ 3.77 GeV
4.1 ± 0.6	263 ± 17	<sup>8</sup> SCHINDLER	81 MRK2 $e^+ e^-$ 3.771 GeV
4.3 ± 1.0	130	<sup>9</sup> PERUZZI	77 LGW $e^+ e^-$ 3.77 GeV

<sup>1</sup> DOBBS 07 and HE 05 use single- and double-tagged events in an overall fit. DOBBS 07 supersedes HE 05.

<sup>2</sup> This combines the CLEO results of ARTUSO 98, COAN 98, and AKERIB 93.

<sup>3</sup> ABACHI 88, DECAMP 91J, AKERIB 93, ALBRECHT 94F, and BARATE 97c use  $D^*(2010)^+ \rightarrow D^0 \pi^+$  decays. The  $\pi^+$  is both slow and of low  $p_T$  with respect to the event thrust axis or nearest jet ( $\approx D^{*+}$  direction). The excess number of such  $\pi^+$ 's over background gives the number of  $D^*(2010)^+ \rightarrow D^0 \pi^+$  events, and the fraction with  $D^0 \rightarrow K^- \pi^+$  gives the  $D^0 \rightarrow K^- \pi^+$  branching fraction.

<sup>4</sup> ARTUSO 98, following ALBRECHT 94, uses  $D^0$  mesons from  $\bar{B}^0 \rightarrow D^*(2010)^+ X \ell^- \bar{\nu}_\ell$  decays. Our average uses the CLEO average of this value with the values of COAN 98 and AKERIB 93.

<sup>5</sup> COAN 98 assumes that  $\Gamma(B \rightarrow D X \ell^+ \nu)/\Gamma(B \rightarrow X \ell^+ \nu) = 1.0 - 3|V_{ub}/V_{cb}|^2 - 0.010 \pm 0.005$ , the last term accounting for  $\bar{B} \rightarrow D_s^+ K X \ell^- \bar{\nu}$ . COAN 98 is included in the CLEO average in ARTUSO 98.

<sup>6</sup> ALBRECHT 94 uses  $D^0$  mesons from  $\bar{B}^0 \rightarrow D^{*+} \ell^- \bar{\nu}_\ell$  decays. This is a different set of events than used by ALBRECHT 94F.

<sup>7</sup> This AKERIB 93 value includes radiative corrections; without them, the value is  $0.0391 \pm 0.0008 \pm 0.0017$ . AKERIB 93 is included in the CLEO average in ARTUSO 98.

<sup>8</sup> SCHINDLER 81 (MARK-2) measures  $\sigma(e^+ e^- \rightarrow \psi(3770)) \times$  branching fraction to be  $0.24 \pm 0.02$  nb. We use the MARK-3 (ADLER 88c) value of  $\sigma = 5.8 \pm 0.5 \pm 0.6$  nb.

<sup>9</sup> PERUZZI 77 (MARK-1) measures  $\sigma(e^+ e^- \rightarrow \psi(3770)) \times$  branching fraction to be  $0.25 \pm 0.05$  nb. We use the MARK-3 (ADLER 88c) value of  $\sigma = 5.8 \pm 0.5 \pm 0.6$  nb.

$\Gamma(K_S^0 \pi^0)/\Gamma_{total}$		$\Gamma_{32}/\Gamma$	
VALUE (units $10^{-2}$ )	EVTS	DOCUMENT ID	TECN COMMENT
• • • We do not use the following data for averages, fits, limits, etc. • • •			
1.240±0.017±0.056	614	HE	08 CLEO See MENDEZ 10

$\Gamma(K_S^0 \pi^0)/\Gamma(K^- \pi^+)$		$\Gamma_{32}/\Gamma_{31}$	
VALUE	EVTS	DOCUMENT ID	TECN COMMENT
• • • We do not use the following data for averages, fits, limits, etc. • • •			
0.68±0.12±0.11	119	ANJOS	92B E691 $\gamma$ Be 80–240 GeV

$\Gamma(K_S^0 \pi^0)/[\Gamma(K^- \pi^+) + \Gamma(K^+ \pi^-)]$		$\Gamma_{32}/(\Gamma_{31} + \Gamma_{212})$	
VALUE (units $10^{-2}$ )	EVTS	DOCUMENT ID	TECN COMMENT
<b>30.5 ± 0.9 OUR FIT</b>			
<b>30.4 ± 0.3 ± 0.9</b>	20k	MENDEZ	10 CLEO $e^+ e^-$ at 3774 MeV

$\Gamma(K_S^0 \pi^0)/\Gamma(K_S^0 \pi^+ \pi^-)$		$\Gamma_{32}/\Gamma_{34}$	
VALUE	EVTS	DOCUMENT ID	TECN COMMENT
<b>0.421 ± 0.029 OUR FIT</b>			
<b>0.44 ± 0.02 ± 0.05</b>	1942 ± 64	PROCARIO	93B CLE2 $e^+ e^-$ 10.36–10.7 GeV
• • • We do not use the following data for averages, fits, limits, etc. • • •			
0.34 ± 0.04 ± 0.02	92	<sup>1</sup> ALBRECHT	92P ARG $e^+ e^- \approx 10$ GeV
0.36 ± 0.04 ± 0.08	104	KINOSHITA	91 CLEO $e^+ e^- \sim 10.7$ GeV
<sup>1</sup> This value is calculated from numbers in Table 1 of ALBRECHT 92P.			

$\Gamma(K_L^0 \pi^0)/\Gamma_{total}$		$\Gamma_{33}/\Gamma$	
VALUE (units $10^{-2}$ )	EVTS	DOCUMENT ID	TECN COMMENT
<b>0.998 ± 0.049 ± 0.048</b>	1116	<sup>1</sup> HE	08 CLEO $e^+ e^-$ at $\psi(3770)$
<sup>1</sup> The difference of HE 08 $D^0 \rightarrow K_S^0 \pi^0$ and $K_L^0 \pi^0$ branching fractions over the sum is $0.108 \pm 0.025 \pm 0.024$ . This is consistent with U-spin symmetry and the Cabibbo angle.			

$\Gamma(K_S^0 \pi^+ \pi^-)/\Gamma_{total}$		$\Gamma_{34}/\Gamma$	
VALUE (units $10^{-2}$ )	EVTS	DOCUMENT ID	TECN COMMENT
• • • We do not use the following data for averages, fits, limits, etc. • • •			
2.52±0.20±0.25	284 ± 22	<sup>1</sup> ALBRECHT	94F ARG $e^+ e^- \approx \Upsilon(4S)$
3.2 ± 0.3 ± 0.5		ADLER	87 MRK3 $e^+ e^-$ 3.77 GeV
2.6 ± 0.8	32 ± 8	<sup>2</sup> SCHINDLER	81 MRK2 $e^+ e^-$ 3.771 GeV
4.0 ± 1.2	28	<sup>3</sup> PERUZZI	77 LGW $e^+ e^-$ 3.77 GeV

<sup>1</sup> See the footnote on the ALBRECHT 94F measurement of  $\Gamma(K^- \pi^+)/\Gamma_{total}$  for the method used.

<sup>2</sup> SCHINDLER 81 (MARK-2) measures  $\sigma(e^+ e^- \rightarrow \psi(3770)) \times$  branching fraction to be  $0.30 \pm 0.08$  nb. We use the MARK-3 (ADLER 88c) value of  $\sigma = 5.8 \pm 0.5 \pm 0.6$  nb.

<sup>3</sup> PERUZZI 77 (MARK-1) measures  $\sigma(e^+ e^- \rightarrow \psi(3770)) \times$  branching fraction to be  $0.46 \pm 0.12$  nb. We use the MARK-3 (ADLER 88c) value of  $\sigma = 5.8 \pm 0.5 \pm 0.6$  nb.

$\Gamma(K_S^0 \rho^+ \pi^-)/\Gamma(K^- \pi^+)$		$\Gamma_{34}/\Gamma_{31}$	
VALUE	EVTS	DOCUMENT ID	TECN COMMENT
<b>0.73 ± 0.05 OUR FIT</b>			Error includes scale factor of 1.1.
<b>0.81 ± 0.05 ± 0.08</b>	856 ± 35	FRABETTI	94J E687 $\gamma$ Be $\bar{E}_\gamma = 220$ GeV
• • • We do not use the following data for averages, fits, limits, etc. • • •			
0.85 ± 0.40	35	AVERY	80 SPEC $\gamma N \rightarrow D^{*+}$
1.4 ± 0.5	116	PICCOLO	77 MRK1 $e^+ e^-$ 4.03, 4.41 GeV

$\Gamma(K_S^0 \rho^0)/\Gamma(K_S^0 \pi^+ \pi^-)$		$\Gamma_{35}/\Gamma_{34}$	
VALUE	EVTS	DOCUMENT ID	TECN COMMENT
This is the "fit fraction" from the Dalitz-plot analysis.			
<b>0.224 ± 0.017 - 0.023 OUR AVERAGE</b>			Error includes scale factor of 1.7.
0.210 ± 0.016		<sup>1</sup> AUBERT	08AL BABR Dalitz fit, $\approx 487$ k evts
0.264 ± 0.009 ± 0.010 - 0.026		MURAMATSU	02 CLE2 Dalitz fit, 5299 evts

• • • We do not use the following data for averages, fits, limits, etc. • • •

0.267 ± 0.011 ± 0.009 - 0.028		ASNER	04A CLEO See MURAMATSU 02
0.350 ± 0.028 ± 0.067		FRABETTI	94G E687 Dalitz fit, 597 evts
0.227 ± 0.032 ± 0.009		ALBRECHT	93D ARG Dalitz fit, 440 evts
0.215 ± 0.051 ± 0.037		ANJOS	93 E691 $\gamma$ Be 90–260 GeV
0.20 ± 0.06 ± 0.03		FRABETTI	92B E687 $\gamma$ Be, $\bar{E}_\gamma = 221$ GeV
0.12 ± 0.01 ± 0.07		ADLER	87 MRK3 $e^+ e^-$ 3.77 GeV

<sup>1</sup> The error on this AUBERT 08AL value includes both statistical and systematic uncertainties; the latter dominates.

$\Gamma(K_S^0 \omega, \omega \rightarrow \pi^+ \pi^-)/\Gamma(K_S^0 \pi^+ \pi^-)$		$\Gamma_{36}/\Gamma_{34}$	
VALUE	EVTS	DOCUMENT ID	TECN COMMENT
<b>0.0073 ± 0.0020 OUR AVERAGE</b>			Error includes scale factor of 1.7.
0.009 ± 0.010		<sup>1</sup> AUBERT	08AL BABR Dalitz fit, $\approx 487$ k evts
0.0072 ± 0.0018 ± 0.0010 - 0.0009		MURAMATSU	02 CLE2 Dalitz fit, 5299 evts
• • • We do not use the following data for averages, fits, limits, etc. • • •			
0.0081 ± 0.0019 ± 0.0018 - 0.0010		ASNER	04A CLEO See MURAMATSU 02

<sup>1</sup> The error on this AUBERT 08AL value includes both statistical and systematic uncertainties; the latter dominates.

$\Gamma(K_S^0 (\pi^+ \pi^-)_{s\text{-wave}})/\Gamma(K_S^0 \pi^+ \pi^-)$		$\Gamma_{37}/\Gamma_{34}$	
VALUE	EVTS	DOCUMENT ID	TECN COMMENT
This is the "fit fraction" from the Dalitz-plot analysis. The $(\pi^+ \pi^-)_{s\text{-wave}}$ includes what in isobar models are the $f_0(980)$ and $f_0(1370)$ ; see the following two data blocks.			
<b>0.119 ± 0.026</b>		<sup>1</sup> AUBERT	08AL BABR Dalitz fit, $\approx 487$ k evts
<sup>1</sup> The error on this AUBERT 08AL value includes both statistical and systematic uncertainties; the latter dominates.			

$\Gamma(K_S^0 f_0(980), f_0(980) \rightarrow \pi^+ \pi^-)/\Gamma(K_S^0 \pi^+ \pi^-)$		$\Gamma_{38}/\Gamma_{34}$	
VALUE	EVTS	DOCUMENT ID	TECN COMMENT
This is the "fit fraction" from the Dalitz-plot analysis.			
<b>0.043 ± 0.005 ± 0.012 - 0.006</b>			Error includes scale factor of 1.7.
0.042 ± 0.005 ± 0.011 - 0.005		ASNER	04A CLEO See MURAMATSU 02
0.068 ± 0.016 ± 0.018		FRABETTI	94G E687 Dalitz fit, 597 evts
0.046 ± 0.018 ± 0.006		ALBRECHT	93D ARG Dalitz fit, 440 evts

$\Gamma(K_S^0 f_0(1370), f_0(1370) \rightarrow \pi^+ \pi^-)/\Gamma(K_S^0 \pi^+ \pi^-)$		$\Gamma_{39}/\Gamma_{34}$	
VALUE	EVTS	DOCUMENT ID	TECN COMMENT
This is the "fit fraction" from the Dalitz-plot analysis.			
<b>0.099 ± 0.011 ± 0.028 - 0.044</b>			Error includes scale factor of 1.7.
0.098 ± 0.014 ± 0.026 - 0.036		ASNER	04A CLEO See MURAMATSU 02
0.077 ± 0.022 ± 0.031		FRABETTI	94G E687 Dalitz fit, 597 evts
0.082 ± 0.028 ± 0.013		ALBRECHT	93D ARG Dalitz fit, 440 evts

• • • We do not use the following data for averages, fits, limits, etc. • • •

## Meson Particle Listings

 $D^0$ 

$\Gamma(K_S^0 f_2(1270), f_2(1270) \rightarrow \pi^+ \pi^-) / \Gamma(K_S^0 \pi^+ \pi^-)$   $\Gamma_{40}/\Gamma_{34}$   
This is the "fit fraction" from the Dalitz-plot analysis.

VALUE	DOCUMENT ID	TECN	COMMENT
<b>0.0032 ± 0.0035</b> <b>-0.0022</b> OUR AVERAGE			
0.006 ± 0.007	<sup>1</sup> AUBERT	08AL BABR	Dalitz fit, ≈ 487 k evts
0.0027 ± 0.0015 ± 0.0037 -0.0017	MURAMATSU 02	CLE2	Dalitz fit, 5 299 evts
• • • We do not use the following data for averages, fits, limits, etc. • • •			
0.0036 ± 0.0022 ± 0.0032 -0.0019	ASNER	04A CLEO	See MURAMATSU 02
0.037 ± 0.014 ± 0.017	FRABETTI	94G E687	Dalitz fit, 5 97 evts
0.050 ± 0.021 ± 0.008	ALBRECHT	93D ARG	Dalitz fit, 440 evts

<sup>1</sup> The error on this AUBERT 08AL value includes both statistical and systematic uncertainties; the latter dominates.

$\Gamma(K^*(892)^- \pi^+, K^*(892)^- \rightarrow K_S^0 \pi^-) / \Gamma(K_S^0 \pi^+ \pi^-)$   $\Gamma_{41}/\Gamma_{34}$   
This is the "fit fraction" from the Dalitz-plot analysis.

VALUE	DOCUMENT ID	TECN	COMMENT
<b>0.588 ± 0.034</b> <b>-0.050</b> OUR AVERAGE			Error includes scale factor of 2.0.
0.557 ± 0.028	<sup>1</sup> AUBERT	08AL BABR	Dalitz fit, ≈ 487 k evts
0.657 ± 0.013 ± 0.018 -0.040	MURAMATSU 02	CLE2	Dalitz fit, 5 299 evts
• • • We do not use the following data for averages, fits, limits, etc. • • •			
0.663 ± 0.013 ± 0.024 -0.043	ASNER	04A CLEO	See MURAMATSU 02
0.625 ± 0.036 ± 0.026	FRABETTI	94G E687	Dalitz fit, 5 97 evts
0.718 ± 0.042 ± 0.030	ALBRECHT	93D ARG	Dalitz fit, 440 evts
0.480 ± 0.097	ANJOS	93 E691	$\gamma$ Be 90–260 GeV
0.56 ± 0.04 ± 0.05	ADLER	87 MRK3	$e^+ e^-$ 3.77 GeV

<sup>1</sup> The error on this AUBERT 08AL value includes both statistical and systematic uncertainties; the latter dominates.

$\Gamma(K_S^0(1430)^- \pi^+, K_S^0(1430)^- \rightarrow K_S^0 \pi^-) / \Gamma(K_S^0 \pi^+ \pi^-)$   $\Gamma_{42}/\Gamma_{34}$   
This is the "fit fraction" from the Dalitz-plot analysis.

VALUE	DOCUMENT ID	TECN	COMMENT
<b>0.095 ± 0.014</b> <b>-0.010</b> OUR AVERAGE			
0.102 ± 0.015	<sup>1</sup> AUBERT	08AL BABR	Dalitz fit, ≈ 487 k evts
0.073 ± 0.007 ± 0.031 -0.011	MURAMATSU 02	CLE2	Dalitz fit, 5 299 evts
• • • We do not use the following data for averages, fits, limits, etc. • • •			
0.072 ± 0.007 ± 0.014 -0.013	ASNER	04A CLEO	See MURAMATSU 02
0.109 ± 0.027 ± 0.029	FRABETTI	94G E687	Dalitz fit, 5 97 evts
0.129 ± 0.034 ± 0.021	ALBRECHT	93D ARG	Dalitz fit, 440 evts

<sup>1</sup> The error on this AUBERT 08AL value includes both statistical and systematic uncertainties; the latter dominates.

$\Gamma(K_S^0(1430)^- \pi^+, K_S^0(1430)^- \rightarrow K_S^0 \pi^-) / \Gamma(K_S^0 \pi^+ \pi^-)$   $\Gamma_{43}/\Gamma_{34}$   
This is the "fit fraction" from the Dalitz-plot analysis.

VALUE	DOCUMENT ID	TECN	COMMENT
<b>0.0120 ± 0.0070</b> <b>-0.0035</b> OUR AVERAGE			
0.022 ± 0.016	<sup>1</sup> AUBERT	08AL BABR	Dalitz fit, ≈ 487 k evts
0.011 ± 0.002 ± 0.007 -0.003	MURAMATSU 02	CLE2	Dalitz fit, 5 299 evts
• • • We do not use the following data for averages, fits, limits, etc. • • •			
0.011 ± 0.002 ± 0.005 -0.003	ASNER	04A CLEO	See MURAMATSU 02

<sup>1</sup> The error on this AUBERT 08AL value includes both statistical and systematic uncertainties; the latter dominates.

$\Gamma(K^*(1680)^- \pi^+, K^*(1680)^- \rightarrow K_S^0 \pi^-) / \Gamma(K_S^0 \pi^+ \pi^-)$   $\Gamma_{44}/\Gamma_{34}$   
This is the "fit fraction" from the Dalitz-plot analysis.

VALUE	DOCUMENT ID	TECN	COMMENT
<b>0.016 ± 0.013</b> OUR AVERAGE			
0.007 ± 0.019	<sup>1</sup> AUBERT	08AL BABR	Dalitz fit, ≈ 487 k evts
0.022 ± 0.004 ± 0.018 -0.015	MURAMATSU 02	CLE2	Dalitz fit, 5 299 evts
• • • We do not use the following data for averages, fits, limits, etc. • • •			
0.023 ± 0.005 ± 0.007 -0.014	ASNER	04A CLEO	See MURAMATSU 02

<sup>1</sup> The error on this AUBERT 08AL value includes both statistical and systematic uncertainties; the latter dominates.

$\Gamma(K^*(892)^+ \pi^-, K^*(892)^+ \rightarrow K_S^0 \pi^+) / \Gamma(K_S^0 \pi^+ \pi^-)$   $\Gamma_{45}/\Gamma_{34}$   
This is the "fit fraction" from the Dalitz-plot analysis. This is a doubly Cabibbo-suppressed mode.

VALUE (units $10^{-3}$ )	DOCUMENT ID	TECN	COMMENT
<b>4.0 ± 2.0</b> <b>-1.2</b> OUR AVERAGE			
4.6 ± 2.3	<sup>1</sup> AUBERT	08AL BABR	Dalitz fit, ≈ 487 k evts
3.4 ± 1.3 ± 4.1 -0.4	MURAMATSU 02	CLE2	Dalitz fit, 5 299 evts
• • • We do not use the following data for averages, fits, limits, etc. • • •			
3.4 ± 1.3 ± 3.6 -0.5	ASNER	04A CLEO	See MURAMATSU 02

<sup>1</sup> The error on this AUBERT 08AL value includes both statistical and systematic uncertainties; the latter dominates.

$\Gamma(K_S^0(1430)^+ \pi^-, K_S^0(1430)^+ \rightarrow K_S^0 \pi^+) / \Gamma(K_S^0 \pi^+ \pi^-)$   $\Gamma_{46}/\Gamma_{34}$   
This is the "fit fraction" from the Dalitz-plot analysis. This is a doubly Cabibbo-suppressed mode.

VALUE	CL%	DOCUMENT ID	TECN	COMMENT
<b>&lt;5 × 10<sup>-4</sup></b>	95	AUBERT	08AL BABR	Dalitz fit, ≈ 487 k evts
$\Gamma(K_S^0(1430)^+ \pi^-, K_S^0(1430)^+ \rightarrow K_S^0 \pi^+) / \Gamma(K_S^0 \pi^+ \pi^-)$ $\Gamma_{47}/\Gamma_{34}$				
This is the "fit fraction" from the Dalitz-plot analysis. This is a doubly Cabibbo-suppressed mode.				
VALUE	CL%	DOCUMENT ID	TECN	COMMENT
<b>&lt;1.2 × 10<sup>-3</sup></b>	95	AUBERT	08AL BABR	Dalitz fit, ≈ 487 k evts

$\Gamma(K_S^0 \pi^+ \pi^- \text{ nonresonant}) / \Gamma(K_S^0 \pi^+ \pi^-)$   $\Gamma_{48}/\Gamma_{34}$   
This is the "fit fraction" from the Dalitz-plot analysis. Neither FRABETTI 94G nor ALBRECHT 93D (quoted in many of the earlier submodes of  $K_S^0 \pi^+ \pi^-$ ) sees evidence for a nonresonant component.

VALUE	DOCUMENT ID	TECN	COMMENT
<b>0.009 ± 0.004 ± 0.020</b> <b>-0.004</b>	MURAMATSU 02	CLE2	Dalitz fit, 5 299 evts
• • • We do not use the following data for averages, fits, limits, etc. • • •			
0.007 ± 0.007 ± 0.021 0.006	ASNER	04A CLEO	See MURAMATSU 02
0.263 ± 0.024 ± 0.041	ANJOS	93 E691	$\gamma$ Be 90–260 GeV
0.26 ± 0.08 ± 0.05	FRABETTI	92B E687	$\gamma$ Be, $E_\gamma = 221$ GeV
0.33 ± 0.05 ± 0.10	ADLER	87 MRK3	$e^+ e^-$ 3.77 GeV

$\Gamma(K^- \pi^+ \pi^0) / \Gamma_{\text{total}}$   $\Gamma_{49}/\Gamma$

VALUE (units $10^{-2}$ )	EVTS	DOCUMENT ID	TECN	COMMENT
<b>13.9 ± 0.5</b> OUR FIT				Error includes scale factor of 1.7.
<b>14.57 ± 0.12 ± 0.38</b>		<sup>1</sup> DOBBS	07 CLEO	$e^+ e^-$ at $\psi(3770)$
• • • We do not use the following data for averages, fits, limits, etc. • • •				
14.9 ± 0.3 ± 0.5	19k ± 150	<sup>1</sup> HE	05 CLEO	See DOBBS 07
13.3 ± 1.2 ± 1.3	931	ADLER	88c MRK3	$e^+ e^-$ 3.77 GeV
11.7 ± 4.3	37	<sup>2</sup> SCHINDLER	81 MRK2	$e^+ e^-$ 3.771 GeV

<sup>1</sup> DOBBS 07 and HE 05 use single- and double-tagged events in an overall fit. DOBBS 07 supersedes HE 05.

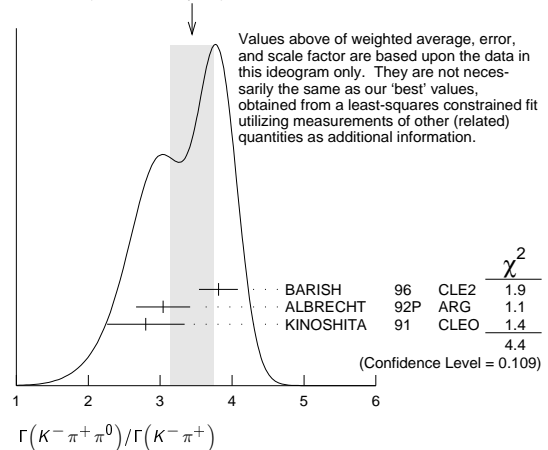
<sup>2</sup> SCHINDLER 81 (MARK-2) measures  $\sigma(e^+ e^- \rightarrow \psi(3770)) \times$  branching fraction to be  $0.68 \pm 0.23$  nb. We use the MARK-3 (ADLER 88c) value of  $\sigma = 5.8 \pm 0.5 \pm 0.6$  nb.

$\Gamma(K^- \pi^+ \pi^0) / \Gamma(K^- \pi^+)$   $\Gamma_{49}/\Gamma_{31}$

VALUE	EVTS	DOCUMENT ID	TECN	COMMENT
<b>3.58 ± 0.14</b> OUR FIT				Error includes scale factor of 1.9.
<b>3.44 ± 0.30</b> OUR AVERAGE				Error includes scale factor of 1.5. See the ideogram below.
3.81 ± 0.07 ± 0.26	10k	BARISH	96 CLE2	$e^+ e^- \approx \Upsilon(4S)$
3.04 ± 0.16 ± 0.34	931	<sup>1</sup> ALBRECHT	92P ARG	$e^+ e^- \approx 10$ GeV
2.8 ± 0.14 ± 0.52	1050	KINOSHITA	91 CLEO	$e^+ e^- \sim 10.7$ GeV

<sup>1</sup> This value is calculated from numbers in Table 1 of ALBRECHT 92P.

WEIGHTED AVERAGE  
3.44 ± 0.30 (Error scaled by 1.5)



$\Gamma(K^- \rho^+) / \Gamma(K^- \pi^+ \pi^0)$   $\Gamma_{50}/\Gamma_{49}$   
This is the "fit fraction" from the Dalitz-plot analysis.

VALUE	DOCUMENT ID	TECN	COMMENT
<b>0.78 ± 0.04</b> OUR AVERAGE			
0.788 ± 0.019 ± 0.048	KOPP	01 CLE2	Dalitz fit, ≈ 7,000 evts
0.765 ± 0.041 ± 0.054	FRABETTI	94G E687	Dalitz fit, 5 30 evts
• • • We do not use the following data for averages, fits, limits, etc. • • •			
0.647 ± 0.039 ± 0.150	ANJOS	93 E691	$\gamma$ Be 90–260 GeV
0.81 ± 0.03 ± 0.06	ADLER	87 MRK3	$e^+ e^-$ 3.77 GeV

$\Gamma(K^- \rho(1700)^+, \rho(1700)^+ \rightarrow \pi^+ \pi^0) / \Gamma(K^- \pi^+ \pi^0)$   $\Gamma_{51}/\Gamma_{49}$   
This is the "fit fraction" from the Dalitz-plot analysis.

VALUE	DOCUMENT ID	TECN	COMMENT
<b>0.057 ± 0.008 ± 0.009</b>	KOPP	01 CLE2	Dalitz fit, ≈ 7,000 evts

$\Gamma(K^*(892)^-\pi^+, K^*(892)^-\pi^0)/\Gamma(K^-\pi^+\pi^0)$   $\Gamma_{52}/\Gamma_{49}$ 

This is the "fit fraction" from the Dalitz-plot analysis.

VALUE	DOCUMENT ID	TECN	COMMENT
<b>0.160<sup>+0.025</sup><sub>-0.013</sub> OUR AVERAGE</b>			
0.161 $\pm$ 0.007 $\pm$ 0.027 <sub>-0.011</sub>	KOPP	01 CLE2	Dalitz fit, $\approx$ 7,000 evts
0.148 $\pm$ 0.028 $\pm$ 0.049	FRABETTI	94G E687	Dalitz fit, 530 evts
• • • We do not use the following data for averages, fits, limits, etc. • • •			
0.084 $\pm$ 0.011 $\pm$ 0.012	ANJOS	93 E691	$\gamma$ Be 90–260 GeV
0.12 $\pm$ 0.02 $\pm$ 0.03	ADLER	87 MRK3	$e^+e^-$ 3.77 GeV

 $\Gamma(\bar{K}^*(892)^0\pi^0, \bar{K}^*(892)^0\pi^0 \rightarrow K^-\pi^+)/\Gamma(K^-\pi^+\pi^0)$   $\Gamma_{53}/\Gamma_{49}$ 

This is the "fit fraction" from the Dalitz-plot analysis.

VALUE	DOCUMENT ID	TECN	COMMENT
<b>0.135<math>\pm</math>0.016 OUR AVERAGE</b>			
0.127 $\pm$ 0.009 $\pm$ 0.016	KOPP	01 CLE2	Dalitz fit, $\approx$ 7,000 evts
0.165 $\pm$ 0.031 $\pm$ 0.015	FRABETTI	94G E687	Dalitz fit, 530 evts
• • • We do not use the following data for averages, fits, limits, etc. • • •			
0.142 $\pm$ 0.018 $\pm$ 0.024	ANJOS	93 E691	$\gamma$ Be 90–260 GeV
0.13 $\pm$ 0.02 $\pm$ 0.03	ADLER	87 MRK3	$e^+e^-$ 3.77 GeV

 $\Gamma(K_S^0(1430)^-\pi^+, K_S^0(1430)^-\pi^0)/\Gamma(K^-\pi^+\pi^0)$   $\Gamma_{54}/\Gamma_{49}$ 

This is the "fit fraction" from the Dalitz-plot analysis.

VALUE	DOCUMENT ID	TECN	COMMENT
<b>0.033<math>\pm</math>0.006<math>\pm</math>0.014</b>	KOPP	01 CLE2	Dalitz fit, $\approx$ 7,000 evts

 $\Gamma(\bar{K}_0^*(1430)^0\pi^0, \bar{K}_0^*(1430)^0\pi^0 \rightarrow K^-\pi^+)/\Gamma(K^-\pi^+\pi^0)$   $\Gamma_{55}/\Gamma_{49}$ 

This is the "fit fraction" from the Dalitz-plot analysis.

VALUE	DOCUMENT ID	TECN	COMMENT
<b>0.041<math>\pm</math>0.006<math>\pm</math>0.032<sub>-0.009</sub></b>	KOPP	01 CLE2	Dalitz fit, $\approx$ 7,000 evts

 $\Gamma(K^*(1680)^-\pi^+, K^*(1680)^-\pi^0)/\Gamma(K^-\pi^+\pi^0)$   $\Gamma_{56}/\Gamma_{49}$ 

This is the "fit fraction" from the Dalitz-plot analysis.

VALUE	DOCUMENT ID	TECN	COMMENT
<b>0.013<math>\pm</math>0.003<math>\pm</math>0.004</b>	KOPP	01 CLE2	Dalitz fit, $\approx$ 7,000 evts

 $\Gamma(K^-\pi^+\pi^0 \text{ nonresonant})/\Gamma(K^-\pi^+\pi^0)$   $\Gamma_{57}/\Gamma_{49}$ 

This is the "fit fraction" from the Dalitz-plot analysis.

VALUE	EVTS	DOCUMENT ID	TECN	COMMENT
<b>0.080<math>\pm</math>0.040<sub>-0.014</sub> OUR AVERAGE</b>				
0.075 $\pm$ 0.009 $\pm$ 0.056 <sub>-0.011</sub>		KOPP	01 CLE2	Dalitz fit, $\approx$ 7,000 evts
0.101 $\pm$ 0.033 $\pm$ 0.040		FRABETTI	94G E687	Dalitz fit, 530 evts
• • • We do not use the following data for averages, fits, limits, etc. • • •				
0.036 $\pm$ 0.004 $\pm$ 0.018		ANJOS	93 E691	$\gamma$ Be 90–260 GeV
0.09 $\pm$ 0.02 $\pm$ 0.04		ADLER	87 MRK3	$e^+e^-$ 3.77 GeV
0.51 $\pm$ 0.22	21	SUMMERS	84 E691	Photoproduction

 $\Gamma(K_S^0(2\pi^0))/\Gamma_{\text{total}}$   $\Gamma_{58}/\Gamma$ 

VALUE (units  $10^{-3}$ )

VALUE	EVTS	DOCUMENT ID	TECN	COMMENT
<b>9.1<math>\pm</math>1.1 OUR AVERAGE</b>				Error includes scale factor of 2.2.
10.58 $\pm$ 0.38 $\pm$ 0.73	1259	LOWREY	11 CLEO	$e^+e^- \approx$ 3.77 GeV
8.34 $\pm$ 0.45 $\pm$ 0.42		ASNER	08 CLEO	$e^+e^- \rightarrow D^0\bar{D}^0$ , 3.77 GeV

 $\Gamma(K_S^0(2\pi^0)\text{-S-wave})/\Gamma(K_S^0(2\pi^0))$   $\Gamma_{59}/\Gamma_{58}$ 

VALUE (%)	DOCUMENT ID	TECN	COMMENT
<b>28.9<math>\pm</math>6.3<math>\pm</math>3.1</b>	LOWREY	11 CLEO	Dalitz analysis, 1259 evts

 $\Gamma(\bar{K}^*(892)^0\pi^0, \bar{K}^*(892)^0\pi^0 \rightarrow K_S^0\pi^0)/\Gamma(K_S^0(2\pi^0))$   $\Gamma_{60}/\Gamma_{32}$ 

VALUE (%)

VALUE (%)	DOCUMENT ID	TECN	COMMENT
<b>65.6<math>\pm</math>5.3<math>\pm</math>2.5</b>	LOWREY	11 CLEO	Dalitz analysis, 1259 evts
• • • We do not use the following data for averages, fits, limits, etc. • • •			
55 $\pm$ 13 <sub>-10</sub> $\pm$ 7	PROCARIO	93B CLE2	Dalitz plot fit, 122 evts

 $\Gamma(\bar{K}^*(1430)^0\pi^0, \bar{K}^*(1430)^0\pi^0 \rightarrow K_S^0\pi^0)/\Gamma(K_S^0(2\pi^0))$   $\Gamma_{61}/\Gamma_{58}$ 

VALUE (%)

VALUE (%)	DOCUMENT ID	TECN	COMMENT
<b>0.49<math>\pm</math>0.45<math>\pm</math>2.51</b>	LOWREY	11 CLEO	Dalitz analysis, 1259 evts

 $\Gamma(\bar{K}^*(1680)^0\pi^0, \bar{K}^*(1680)^0\pi^0 \rightarrow K_S^0\pi^0)/\Gamma(K_S^0(2\pi^0))$   $\Gamma_{62}/\Gamma_{58}$ 

VALUE (%)

VALUE (%)	DOCUMENT ID	TECN	COMMENT
<b>11.2<math>\pm</math>2.7<math>\pm</math>2.5</b>	LOWREY	11 CLEO	Dalitz analysis, 1259 evts

 $\Gamma(K_S^0 f_2(1270), f_2 \rightarrow 2\pi^0)/\Gamma(K_S^0(2\pi^0))$   $\Gamma_{63}/\Gamma_{58}$ 

VALUE (%)

VALUE (%)	DOCUMENT ID	TECN	COMMENT
<b>2.48<math>\pm</math>0.91<math>\pm</math>0.78</b>	LOWREY	11 CLEO	Dalitz analysis, 1259 evts

 $\Gamma(2K_S^0, \text{one } K_S^0 \rightarrow 2\pi^0)/\Gamma(K_S^0(2\pi^0))$   $\Gamma_{64}/\Gamma_{58}$ 

VALUE (%)

VALUE (%)	DOCUMENT ID	TECN	COMMENT
<b>3.46<math>\pm</math>0.92<math>\pm</math>0.66</b>	LOWREY	11 CLEO	Dalitz analysis, 1259 evts

 $\Gamma(K_S^0(2\pi^0 \text{ nonresonant})/\Gamma(K_S^0\pi^0)$   $\Gamma_{65}/\Gamma_{32}$ 

VALUE

VALUE	DOCUMENT ID	TECN	COMMENT
<b>0.37<math>\pm</math>0.08<math>\pm</math>0.04</b>	PROCARIO	93B CLE2	Dalitz plot fit, 122 evts

 $\Gamma(K^-\rho^+\pi^-)/\Gamma_{\text{total}}$   $\Gamma_{66}/\Gamma$ 

VALUE (units  $10^{-2}$ )

VALUE (units $10^{-2}$ )	EVTS	DOCUMENT ID	TECN	COMMENT
<b>8.07<math>\pm</math>0.21<sub>-0.19</sub> OUR FIT</b>				Error includes scale factor of 1.3.

8.17 $\pm$ 0.33 OUR AVERAGE Error includes scale factor of 1.7. See the ideogram below.

8.30 $\pm$ 0.07 $\pm$ 0.20	1 DOBBS	07 CLEO	$e^+e^-$ at $\psi(3770)$
7.9 $\pm$ 1.5 $\pm$ 0.9	2 ALBRECHT	94 ARG	$e^+e^- \approx \Upsilon(4S)$
6.80 $\pm$ 0.27 $\pm$ 0.57	1430 $\pm$ 52	3 ALBRECHT	94F ARG $e^+e^- \approx \Upsilon(4S)$
9.1 $\pm$ 0.8 $\pm$ 0.8	992	ADLER	88c MRK3 $e^+e^-$ 3.77 GeV
• • • We do not use the following data for averages, fits, limits, etc. • • •			
8.3 $\pm$ 0.2 $\pm$ 0.3	15k $\pm$ 130	1 HE	05 CLEO See DOBBS 07
11.7 $\pm$ 2.5	185	4 SCHINDLER	81 MRK2 $e^+e^-$ 3.77 GeV
6.2 $\pm$ 1.9	44	5 PERUZZI	77 LGW $e^+e^-$ 3.77 GeV

1 DOBBS 07 and HE 05 use single- and double-tagged events in an overall fit. DOBBS 07 supersedes HE 05.

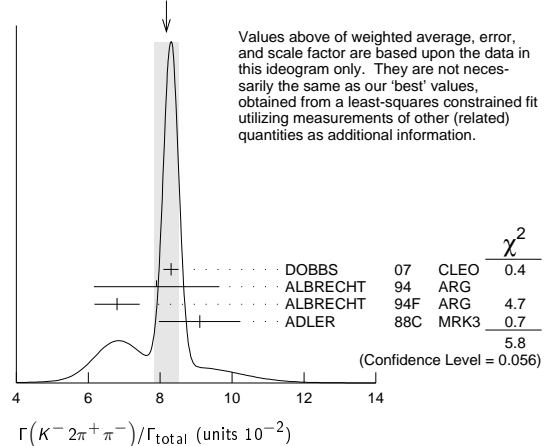
2 ALBRECHT 94 uses  $D^0$  mesons from  $\bar{B}^0 \rightarrow D^{*+} \ell^- \bar{\nu}_\ell$  decays. This is a different set of events than used by ALBRECHT 94F.

3 See the footnote on the ALBRECHT 94F measurement of  $\Gamma(K^-\pi^+)/\Gamma_{\text{total}}$  for the method used.

4 SCHINDLER 81 (MARK-2) measures  $\sigma(e^+e^- \rightarrow \psi(3770)) \times$  branching fraction to be  $0.68 \pm 0.11$  nb. We use the MARK-3 (ADLER 88c) value of  $\sigma = 5.8 \pm 0.5 \pm 0.6$  nb.

5 PERUZZI 77 (MARK-1) measures  $\sigma(e^+e^- \rightarrow \psi(3770)) \times$  branching fraction to be  $0.36 \pm 0.10$  nb. We use the MARK-3 (ADLER 88c) value of  $\sigma = 5.8 \pm 0.5 \pm 0.6$  nb.

WEIGHTED AVERAGE  
8.17 $\pm$ 0.33 (Error scaled by 1.7)


 $\Gamma(K^-\rho^+\pi^-)/\Gamma(K^-\pi^+)$   $\Gamma_{66}/\Gamma_{31}$ 

VALUE

VALUE	EVTS	DOCUMENT ID	TECN	COMMENT
<b>2.08<math>\pm</math>0.05 OUR FIT</b>				Error includes scale factor of 1.6.
<b>1.97<math>\pm</math>0.09 OUR AVERAGE</b>				

1.94 $\pm$ 0.07 $\pm$ 0.09 <sub>-0.11</sub>		JUN	00 SELX	$\Sigma^-$ nucleus, 600 GeV
1.7 $\pm$ 0.2 $\pm$ 0.2	1745	ANJOS	92c E691	$\gamma$ Be 90–260 GeV
1.90 $\pm$ 0.25 $\pm$ 0.20	337	ALVAREZ	91B NA14	Photoproduction
2.12 $\pm$ 0.16 $\pm$ 0.09		BORTOLETTO88	CLEO	$e^+e^-$ 10.55 GeV
2.17 $\pm$ 0.28 $\pm$ 0.23		ALBRECHT	85F ARG	$e^+e^-$ 10 GeV
• • • We do not use the following data for averages, fits, limits, etc. • • •				
2.0 $\pm$ 0.9	48	BAILEY	86 ACCM	$\pi^-$ Be fixed target
2.0 $\pm$ 1.0	10	BAILEY	83B SPEC	$\pi^-$ Be $\rightarrow D^0$
2.2 $\pm$ 0.8	214	PICCOLO	77 MRK1	$e^+e^-$ 4.03, 4.41 GeV

 $\Gamma(K^-\pi^+\rho^0 \text{ total})/\Gamma(K^-\rho^+\pi^-)$   $\Gamma_{67}/\Gamma_{66}$ 

This includes  $K^- a_1(1260)^+$ ,  $\bar{K}^*(892)^0 \rho^0$ , etc. The next entry gives the specifically 3-body fraction. We rely on the MARKIII and E691 full amplitude analyses of the  $K^-\pi^+\pi^+\pi^-$  channel for values of the resonant substructure.

VALUE

VALUE	DOCUMENT ID	TECN	COMMENT
<b>0.835<math>\pm</math>0.035 OUR AVERAGE</b>			

0.80 $\pm$ 0.03 $\pm$ 0.05	ANJOS	92c E691	1745 $K^-\pi^+\pi^+$ evts
0.855 $\pm$ 0.032 $\pm$ 0.030	COFFMAN	92B MRK3	1281 $\pm$ 45 $K^-\pi^+\pi^-$ evts
• • • We do not use the following data for averages, fits, limits, etc. • • •			
0.98 $\pm$ 0.12 $\pm$ 0.10	ALVAREZ	91B NA14	Photoproduction

## Meson Particle Listings

 $D^0$  $\Gamma(K^- \pi^+ \rho^0 \text{ 3-body})/\Gamma(K^- 2\pi^+ \pi^-)$   $\Gamma_{68}/\Gamma_{66}$ 

We rely on the MARKIII and E691 full amplitude analyses of the  $K^- \pi^+ \pi^+ \pi^-$  channel for values of the resonant substructure.

VALUE	EVTs	DOCUMENT ID	TECN	COMMENT
<b>0.063 ± 0.028 OUR AVERAGE</b>				
0.05 ± 0.03 ± 0.02		ANJOS	92c E691	1745 $K^- 2\pi^+ \pi^-$ evts
0.084 ± 0.022 ± 0.04		COFFMAN	92B MRK3	1281 ± 45 $K^- 2\pi^+ \pi^-$ evts
• • • We do not use the following data for averages, fits, limits, etc. • • •				
0.77 ± 0.06 ± 0.06		<sup>1</sup> ALVAREZ	91B NA14	Photoproduction
0.85 <sup>+0.11</sup> <sub>-0.22</sub>	180	PICCOLO	77 MRK1	$e^+ e^-$ 4.03, 4.41 GeV

<sup>1</sup> This value is for  $\rho^0(K^- \pi^+)$ -nonresonant. ALVAREZ 91B cannot determine what fraction of this is  $K^- a_1(1260)^+$ .

 $\Gamma(\bar{K}^*(892)^0 \rho^0)/\Gamma(K^- 2\pi^+ \pi^-)$   $\Gamma_{100}/\Gamma_{66}$ 

Unseen decay modes of the  $\bar{K}^*(892)^0$  are included. We rely on the MARKIII and E691 full amplitude analyses of the  $K^- \pi^+ \pi^+ \pi^-$  channel for values of the resonant substructure.

VALUE	EVTs	DOCUMENT ID	TECN	COMMENT
<b>0.195 ± 0.03 ± 0.03</b>		ANJOS	92c E691	1745 $K^- 2\pi^+ \pi^-$ evts
• • • We do not use the following data for averages, fits, limits, etc. • • •				
0.34 ± 0.09 ± 0.09		ALVAREZ	91B NA14	Photoproduction
0.75 ± 0.3	5	BAILEY	83B SPEC	$\pi Be \rightarrow D^0$
0.15 <sup>+0.16</sup> <sub>-0.15</sub>	20	PICCOLO	77 MRK1	$e^+ e^-$ 4.03, 4.41 GeV

 $\Gamma(\bar{K}^*(892)^0 \rho^0 \text{ transverse})/\Gamma(K^- 2\pi^+ \pi^-)$   $\Gamma_{101}/\Gamma_{66}$ 

Unseen decay modes of the  $\bar{K}^*(892)^0$  are included.

VALUE	DOCUMENT ID	TECN	COMMENT
<b>0.213 ± 0.024 ± 0.075</b>	COFFMAN 92B MRK3	1281 ± 45	$K^- 2\pi^+ \pi^-$ evts

 $\Gamma(\bar{K}^*(892)^0 \rho^0 \text{ S-wave})/\Gamma(K^- 2\pi^+ \pi^-)$   $\Gamma_{102}/\Gamma_{66}$ 

Unseen decay modes of the  $\bar{K}^*(892)^0$  are included.

VALUE	DOCUMENT ID	TECN	COMMENT
<b>0.375 ± 0.045 ± 0.06</b>	ANJOS 92c E691	1745	$K^- 2\pi^+ \pi^-$ evts

 $\Gamma(\bar{K}^*(892)^0 \rho^0 \text{ S-wave long.})/\Gamma_{\text{total}}$   $\Gamma_{103}/\Gamma$ 

Unseen decay modes of the  $\bar{K}^*(892)^0$  are included.

VALUE	CL%	DOCUMENT ID	TECN	COMMENT
<b>&lt;0.003</b>	90	COFFMAN	92B MRK3	1281 ± 45 $K^- 2\pi^+ \pi^-$ evts

 $\Gamma(\bar{K}^*(892)^0 \rho^0 \text{ P-wave})/\Gamma_{\text{total}}$   $\Gamma_{104}/\Gamma$ 

Unseen decay modes of the  $\bar{K}^*(892)^0$  are included.

VALUE	CL%	DOCUMENT ID	TECN	COMMENT
<b>&lt;0.003</b>	90	COFFMAN	92B MRK3	1281 ± 45 $K^- 2\pi^+ \pi^-$ evts

• • • We do not use the following data for averages, fits, limits, etc. • • •

 $\Gamma(\bar{K}^*(892)^0 \rho^0 \text{ D-wave})/\Gamma(K^- 2\pi^+ \pi^-)$   $\Gamma_{105}/\Gamma_{66}$ 

Unseen decay modes of the  $\bar{K}^*(892)^0$  are included.

VALUE	DOCUMENT ID	TECN	COMMENT
<b>0.255 ± 0.045 ± 0.06</b>	ANJOS 92c E691	1745	$K^- 2\pi^+ \pi^-$ evts

 $\Gamma(K^- \pi^+ f_0(980))/\Gamma_{\text{total}}$   $\Gamma_{106}/\Gamma$ 

VALUE	CL%	DOCUMENT ID	TECN	COMMENT
<b>&lt;0.011</b>	90	ANJOS	92c E691	1745 $K^- 2\pi^+ \pi^-$ evts

 $\Gamma(\bar{K}^*(892)^0 f_0(980))/\Gamma_{\text{total}}$   $\Gamma_{107}/\Gamma$ 

VALUE	CL%	DOCUMENT ID	TECN	COMMENT
<b>&lt;0.007</b>	90	ANJOS	92c E691	1745 $K^- 2\pi^+ \pi^-$ evts

 $\Gamma(K^- a_1(1260)^+)/\Gamma(K^- 2\pi^+ \pi^-)$   $\Gamma_{96}/\Gamma_{66}$ 

Unseen decay modes of the  $a_1(1260)^+$  are included, assuming that the  $a_1(1260)^+$  decays entirely to  $\rho\pi$  [or at least to  $(\pi\pi)_{J=1}\pi$ ].

VALUE	DOCUMENT ID	TECN	COMMENT
<b>0.97 ± 0.14 OUR AVERAGE</b>			
0.94 ± 0.13 ± 0.20	ANJOS 92c E691	1745	$K^- 2\pi^+ \pi^-$ evts
0.984 ± 0.048 ± 0.16	COFFMAN 92B MRK3	1281 ± 45	$K^- 2\pi^+ \pi^-$ evts

 $\Gamma(K^- a_2(1320)^+)/\Gamma_{\text{total}}$   $\Gamma_{97}/\Gamma$ 

Unseen decay modes of the  $a_2(1320)^+$  are included.

VALUE	CL%	DOCUMENT ID	TECN	COMMENT
<b>&lt;0.002</b>	90	ANJOS	92c E691	1745 $K^- 2\pi^+ \pi^-$ evts

• • • We do not use the following data for averages, fits, limits, etc. • • •

VALUE	CL%	DOCUMENT ID	TECN	COMMENT
<0.006	90	COFFMAN	92B MRK3	1281 ± 45 $K^- 2\pi^+ \pi^-$ evts

 $\Gamma(K_1(1270)^- \pi^+)/\Gamma(K^- 2\pi^+ \pi^-)$   $\Gamma_{108}/\Gamma_{66}$ 

Unseen decay modes of the  $K_1(1270)^-$  are included. The MARK3 and E691 experiments disagree considerably here.

VALUE	CL%	DOCUMENT ID	TECN	COMMENT
<b>0.194 ± 0.056 ± 0.088</b>		COFFMAN	92B MRK3	1281 ± 45 $K^- 2\pi^+ \pi^-$ evts
• • • We do not use the following data for averages, fits, limits, etc. • • •				
<0.013	90	ANJOS	92c E691	1745 $K^- 2\pi^+ \pi^-$ evts

 $\Gamma(K_1(1400)^- \pi^+)/\Gamma_{\text{total}}$   $\Gamma_{109}/\Gamma$ 

VALUE	CL%	DOCUMENT ID	TECN	COMMENT
<b>&lt;0.012</b>	90	COFFMAN	92B MRK3	1281 ± 45 $K^- 2\pi^+ \pi^-$ evts

 $\Gamma(K^*(1410)^- \pi^+)/\Gamma_{\text{total}}$   $\Gamma_{110}/\Gamma$ 

VALUE	CL%	DOCUMENT ID	TECN	COMMENT
• • • We do not use the following data for averages, fits, limits, etc. • • •				
<0.012	90	COFFMAN	92B MRK3	1281 ± 45 $K^- 2\pi^+ \pi^-$ evts

 $\Gamma(\bar{K}^*(892)^0 \pi^+ \pi^- \text{ total})/\Gamma(K^- 2\pi^+ \pi^-)$   $\Gamma_{98}/\Gamma_{66}$ 

This includes  $\bar{K}^*(892)^0 \rho^0$ , etc. The next entry gives the specifically 3-body fraction. Unseen decay modes of the  $\bar{K}^*(892)^0$  are included.

VALUE	DOCUMENT ID	TECN	COMMENT
<b>0.30 ± 0.06 ± 0.03</b>	ANJOS 92c E691	1745	$K^- 2\pi^+ \pi^-$ evts

 $\Gamma(\bar{K}^*(892)^0 \pi^+ \pi^- \text{ 3-body})/\Gamma(K^- 2\pi^+ \pi^-)$   $\Gamma_{99}/\Gamma_{66}$ 

Unseen decay modes of the  $\bar{K}^*(892)^0$  are included.

VALUE	DOCUMENT ID	TECN	COMMENT
<b>0.18 ± 0.04 OUR AVERAGE</b>			
0.165 ± 0.03 ± 0.045	ANJOS 92c E691	1745	$K^- 2\pi^+ \pi^-$ evts
0.210 ± 0.027 ± 0.06	COFFMAN 92B MRK3	1281 ± 45	$K^- 2\pi^+ \pi^-$ evts

 $\Gamma(K^- 2\pi^+ \pi^- \text{ nonresonant})/\Gamma(K^- 2\pi^+ \pi^-)$   $\Gamma_{74}/\Gamma_{66}$ 

VALUE	DOCUMENT ID	TECN	COMMENT
<b>0.233 ± 0.032 OUR AVERAGE</b>			
0.23 ± 0.02 ± 0.03	ANJOS 92c E691	1745	$K^- 2\pi^+ \pi^-$ evts
0.242 ± 0.025 ± 0.06	COFFMAN 92B MRK3	1281 ± 45	$K^- 2\pi^+ \pi^-$ evts

 $\Gamma(K_S^0 \pi^+ \pi^- \pi^0)/\Gamma_{\text{total}}$   $\Gamma_{75}/\Gamma$ 

VALUE (units $10^{-2}$ )	EVTs	DOCUMENT ID	TECN	COMMENT
<b>5.2 ± 0.6 OUR FIT</b>				
<b>5.2 ± 1.1 ± 1.2</b>	140	COFFMAN	92B MRK3	$e^+ e^-$ 3.77 GeV
• • • We do not use the following data for averages, fits, limits, etc. • • •				

6.7 <sup>+1.6</sup><sub>-1.7</sub> <sup>1</sup>BARLAG 92c ACCM  $\pi^- Cu$  230 GeV

<sup>1</sup> BARLAG 92c computes the branching fraction using topological normalization.

 $\Gamma(K_S^0 \pi^+ \pi^- \pi^0)/\Gamma(K_S^0 \pi^+ \pi^-)$   $\Gamma_{75}/\Gamma_{34}$ 

Branching fractions for submodes of this mode with narrow resonances (the  $\eta$ ,  $\omega$ ,  $\eta'$ ) are fairly well determined (see below). COFFMAN 92B gives fractions of  $K^*$  and  $\rho$  submodes, but with only 140 ± 28 events above background could not determine them with much accuracy. We omit those measurements here; they are in our 2008 Review (Physics Letters **B667** 1 (2008)).

VALUE	EVTs	DOCUMENT ID	TECN	COMMENT
<b>1.84 ± 0.20 OUR FIT</b>				
<b>1.86 ± 0.23 OUR AVERAGE</b>				
1.80 ± 0.20 ± 0.21	190	<sup>1</sup> ALBRECHT	92P ARG	$e^+ e^- \approx 10$ GeV
2.8 ± 0.8 ± 0.8	46	ANJOS	92c E691	$\gamma Be$ 90–260 GeV
1.85 ± 0.26 ± 0.30	158	KINOSHITA	91 CLEO	$e^+ e^- \sim 10.7$ GeV

<sup>1</sup> This value is calculated from numbers in Table 1 of ALBRECHT 92P.

 $\Gamma(K_S^0 \eta)/\Gamma_{\text{total}}$   $\Gamma_{93}/\Gamma$ 

Unseen decay modes of the  $\eta$  are included.

VALUE (units $10^{-3}$ )	DOCUMENT ID	TECN	COMMENT
• • • We do not use the following data for averages, fits, limits, etc. • • •			
4.42 ± 0.15 ± 0.28	ASNER 08 CLEO	See MENDEZ 10	

 $\Gamma(K_S^0 \eta)/[\Gamma(K^- \pi^+) + \Gamma(K^+ \pi^-)]$   $\Gamma_{93}/(\Gamma_{31} + \Gamma_{212})$ 

Unseen decay modes of the  $\eta$  are included.

VALUE (units $10^{-2}$ )	EVTs	DOCUMENT ID	TECN	COMMENT
<b>12.3 ± 0.8 OUR FIT</b>				
<b>12.3 ± 0.3 ± 0.7</b>	2864 ± 65	MENDEZ	10 CLEO	$e^+ e^-$ at 3774 MeV

 $\Gamma(K_S^0 \eta)/\Gamma(K_S^0 \pi^0)$   $\Gamma_{93}/\Gamma_{32}$ 

Unseen decay modes of the  $\eta$  are included.

VALUE	EVTs	DOCUMENT ID	TECN	COMMENT
• • • We do not use the following data for averages, fits, limits, etc. • • •				
0.32 ± 0.04 ± 0.03	225 ± 30	PROCARIO	93B CLE2	$\eta \rightarrow \gamma\gamma$

 $\Gamma(K_S^0 \eta)/\Gamma(K_S^0 \pi^+ \pi^-)$   $\Gamma_{93}/\Gamma_{34}$ 

Unseen decay modes of the  $\eta$  are included.

VALUE	EVTs	DOCUMENT ID	TECN	COMMENT
• • • We do not use the following data for averages, fits, limits, etc. • • •				
0.14 ± 0.02 ± 0.02	80 ± 12	PROCARIO	93B CLE2	$\eta \rightarrow \pi^+ \pi^- \pi^0$



# Meson Particle Listings

## $D^0$

$\Gamma(K_S^0 a_0(980)^0, a_0^0 \rightarrow K^+ K^-) / \Gamma(K_S^0 K^+ K^-)$   $\Gamma_{118} / \Gamma_{117}$   
 This is the “fit fraction” from the Dalitz-plot analysis, with interference.

VALUE	DOCUMENT ID	TECN	COMMENT
<b>0.664 ± 0.016 ± 0.070</b>	AUBERT,B	05J	BABR Dalitz fit, 12540 ± 112 evts

$\Gamma(K^- a_0(980)^+, a_0^+ \rightarrow K^+ K_S^0) / \Gamma(K_S^0 K^+ K^-)$   $\Gamma_{119} / \Gamma_{117}$   
 This is the “fit fraction” from the Dalitz-plot analysis, with interference.

VALUE	DOCUMENT ID	TECN	COMMENT
<b>0.134 ± 0.011 ± 0.037</b>	AUBERT,B	05J	BABR Dalitz fit, 12540 ± 112 evts

$\Gamma(K^+ a_0(980)^-, a_0^- \rightarrow K^- K_S^0) / \Gamma(K_S^0 K^+ K^-)$   $\Gamma_{120} / \Gamma_{117}$   
 This is a doubly Cabibbo-suppressed mode.

VALUE	CL%	DOCUMENT ID	TECN	COMMENT
<0.025	95	AUBERT,B	05J	BABR Dalitz fit, 12540 ± 112 evts

$\Gamma(K_S^0 f_0(980), f_0 \rightarrow K^+ K^-) / \Gamma(K_S^0 K^+ K^-)$   $\Gamma_{121} / \Gamma_{117}$

VALUE	CL%	DOCUMENT ID	TECN	COMMENT
<0.021	95	AUBERT,B	05J	BABR Dalitz fit, 12540 ± 112 evts

$\Gamma(K_S^0 \phi, \phi \rightarrow K^+ K^-) / \Gamma(K_S^0 K^+ K^-)$   $\Gamma_{122} / \Gamma_{117}$   
 This is the “fit fraction” from the Dalitz-plot analysis, with interference.

VALUE	DOCUMENT ID	TECN	COMMENT
<b>0.459 ± 0.007 ± 0.007</b>	AUBERT,B	05J	BABR Dalitz fit, 12540 ± 112 evts

$\Gamma(K_S^0 f_0(1370), f_0 \rightarrow K^+ K^-) / \Gamma(K_S^0 K^+ K^-)$   $\Gamma_{123} / \Gamma_{117}$   
 This is the “fit fraction” from the Dalitz-plot analysis, with interference.

VALUE	DOCUMENT ID	TECN	COMMENT
<b>0.038 ± 0.007 ± 0.023</b>	AUBERT,B	05J	BABR Dalitz fit, 12540 ± 112 evts

<sup>1</sup>AUBERT,B 05J calls the mode  $K_S^0 f_0(1400)$ , but insofar as it is seen here at all, it is certainly the same as  $f_0(1370)$ .

$\Gamma(3K_S^0) / \Gamma(K_S^0 \pi^+ \pi^-)$   $\Gamma_{124} / \Gamma_{34}$

VALUE (units 10 <sup>-2</sup> )	EVTs	DOCUMENT ID	TECN	COMMENT
<b>3.2 ± 0.4 OUR AVERAGE</b>				
3.58 ± 0.54 ± 0.52	170 ± 26	LINK	05A	FOCS $\gamma$ Be, $\bar{E}_\gamma \approx 180$ GeV
2.78 ± 0.38 ± 0.48	61	ASNER	96B	CLE2 $e^+ e^- \approx \Upsilon(4S)$
7.0 ± 2.4 ± 1.2	10 ± 3	FRABETTI	94J	E687 $\gamma$ Be, $\bar{E}_\gamma = 220$ GeV
3.2 ± 1.0	22	AMMAR	91	CLEO $e^+ e^- \approx 10.5$ GeV
3.4 ± 1.4 ± 1.0	5	ALBRECHT	90c	ARG $e^+ e^- \approx 10$ GeV

$\Gamma(K^+ 2K^- \pi^+) / \Gamma(K^- 2\pi^+ \pi^-)$   $\Gamma_{125} / \Gamma_{66}$

VALUE	EVTs	DOCUMENT ID	TECN	COMMENT
<b>0.0027 ± 0.0004 OUR AVERAGE</b>				Error includes scale factor of 1.1.
0.00257 ± 0.00034 ± 0.00024	143	LINK	03G	FOCS $\gamma$ A, $\bar{E}_\gamma \approx 180$ GeV
0.0054 ± 0.0016 ± 0.0008	18	AITALA	01D	E791 $\pi^-$ A, 500 GeV
0.0028 ± 0.0007 ± 0.0001	20	FRABETTI	95c	E687 $\gamma$ Be, $\bar{E}_\gamma \approx 200$ GeV

$\Gamma(\phi \bar{K}^*(892)^0, \phi \rightarrow K^+ K^-, \bar{K}^*(892)^0 \rightarrow K^- \pi^+) / \Gamma(K^+ 2K^- \pi^+)$   $\Gamma_{128} / \Gamma_{125}$

VALUE	DOCUMENT ID	TECN	COMMENT
<b>0.48 ± 0.06 ± 0.01</b>	LINK	03G	FOCS $\gamma$ A, $\bar{E}_\gamma \approx 180$ GeV

$\Gamma(K^- \pi^+ \phi, \phi \rightarrow K^+ K^-) / \Gamma(K^+ 2K^- \pi^+)$   $\Gamma_{127} / \Gamma_{125}$

VALUE	DOCUMENT ID	TECN	COMMENT
<b>0.18 ± 0.06 ± 0.04</b>	LINK	03G	FOCS $\gamma$ A, $\bar{E}_\gamma \approx 180$ GeV

$\Gamma(K^+ K^- \bar{K}^*(892)^0, \bar{K}^*(892)^0 \rightarrow K^- \pi^+) / \Gamma(K^+ 2K^- \pi^+)$   $\Gamma_{126} / \Gamma_{125}$

VALUE	DOCUMENT ID	TECN	COMMENT
<b>0.20 ± 0.07 ± 0.02</b>	LINK	03G	FOCS $\gamma$ A, $\bar{E}_\gamma \approx 180$ GeV

$\Gamma(K^+ 2K^- \pi^+ \text{nonresonant}) / \Gamma(K^+ 2K^- \pi^+)$   $\Gamma_{129} / \Gamma_{125}$

VALUE	DOCUMENT ID	TECN	COMMENT
<b>0.15 ± 0.06 ± 0.02</b>	LINK	03G	FOCS $\gamma$ A, $\bar{E}_\gamma \approx 180$ GeV

$\Gamma(2K_S^0 K^\pm \pi^\mp) / \Gamma(K_S^0 \pi^+ \pi^-)$   $\Gamma_{130} / \Gamma_{34}$

VALUE (units 10 <sup>-2</sup> )	EVTs	DOCUMENT ID	TECN	COMMENT
<b>2.12 ± 0.38 ± 0.20</b>	57 ± 10	LINK	05A	FOCS $\gamma$ Be, $\bar{E}_\gamma \approx 180$ GeV

Pionic modes

$\Gamma(\pi^+ \pi^-) / \Gamma(K^- \pi^+)$   $\Gamma_{131} / \Gamma_{31}$

VALUE (units 10 <sup>-2</sup> )	EVTs	DOCUMENT ID	TECN	COMMENT
<b>3.62 ± 0.05 OUR FIT</b>				
<b>3.59 ± 0.06 OUR AVERAGE</b>				
3.594 ± 0.054 ± 0.040	7334 ± 97	ACOSTA	05c	CDF $p\bar{p}, \sqrt{s} = 1.96$ TeV
3.53 ± 0.12 ± 0.06	3453	LINK	03	FOCS $\gamma$ A, $\bar{E}_\gamma \approx 180$ GeV
3.51 ± 0.16 ± 0.17	710	CSORNA	02	CLE2 $e^+ e^- \approx \Upsilon(4S)$
4.0 ± 0.2 ± 0.3	2043	AITALA	98c	E791 $\pi^-$ A, 500 GeV
• • • We do not use the following data for averages, fits, limits, etc. • • •				
3.62 ± 0.10 ± 0.08	2085 ± 54	RUBIN	06	CLEO See MENDEZ 10
3.4 ± 0.7 ± 0.1	76 ± 15	ABLIKIM	05F	BES $e^+ e^- \approx \psi(3770)$
4.3 ± 0.7 ± 0.3	177	FRABETTI	94c	E687 $\gamma$ Be $\bar{E}_\gamma = 220$ GeV
3.48 ± 0.30 ± 0.23	227	SELEN	93	CLE2 $e^+ e^- \approx \Upsilon(4S)$
5.5 ± 0.8 ± 0.5	120	ANJOS	91D	E691 Photoproduction
5.0 ± 0.7 ± 0.5	110	ALEXANDER	90	CLEO $e^+ e^- 10.5\text{--}11$ GeV

$\Gamma(\pi^+ \pi^-) / [\Gamma(K^- \pi^+) + \Gamma(K^+ \pi^-)]$   $\Gamma_{131} / (\Gamma_{31} + \Gamma_{212})$

VALUE (units 10 <sup>-2</sup> )	EVTs	DOCUMENT ID	TECN	COMMENT
<b>3.60 ± 0.05 OUR FIT</b>				
<b>3.70 ± 0.06 ± 0.09</b>	6210 ± 93	MENDEZ	10	CLEO $e^+ e^-$ at 3774 MeV

$\Gamma(2\pi^0) / \Gamma(K^- \pi^+)$   $\Gamma_{132} / \Gamma_{31}$

VALUE (units 10 <sup>-2</sup> )	EVTs	DOCUMENT ID	TECN	COMMENT
• • • We do not use the following data for averages, fits, limits, etc. • • •				
2.05 ± 0.13 ± 0.16	499 ± 32	RUBIN	06	CLEO See MENDEZ 10
2.2 ± 0.4 ± 0.4	40	SELEN	93	CLE2 $e^+ e^- \rightarrow \Upsilon(4S)$

$\Gamma(2\pi^0) / [\Gamma(K^- \pi^+) + \Gamma(K^+ \pi^-)]$   $\Gamma_{132} / (\Gamma_{31} + \Gamma_{212})$

VALUE (units 10 <sup>-2</sup> )	EVTs	DOCUMENT ID	TECN	COMMENT
<b>2.06 ± 0.12 OUR FIT</b>				
<b>2.06 ± 0.07 ± 0.10</b>	1567 ± 54	MENDEZ	10	CLEO $e^+ e^-$ at 3774 MeV

$\Gamma(\pi^+ \pi^- \pi^0) / \Gamma(K^- \pi^+)$   $\Gamma_{133} / \Gamma_{31}$

VALUE (units 10 <sup>-2</sup> )	EVTs	DOCUMENT ID	TECN	COMMENT
<b>37.0 ± 1.6 OUR FIT</b>				Error includes scale factor of 2.1.
<b>34.4 ± 0.5 ± 1.2</b>	11k ± 164	RUBIN	06	CLEO $e^+ e^-$ at $\psi(3770)$

$\Gamma(\pi^+ \pi^- \pi^0) / \Gamma(K^- \pi^+ \pi^0)$   $\Gamma_{133} / \Gamma_{49}$

VALUE (units 10 <sup>-2</sup> )	EVTs	DOCUMENT ID	TECN	COMMENT
<b>10.34 ± 0.24 OUR FIT</b>				Error includes scale factor of 2.2.
<b>10.41 ± 0.23 OUR AVERAGE</b>				Error includes scale factor of 2.0.
10.12 ± 0.04 ± 0.18	123k ± 490	ARINSTEIN	08	BELL $e^+ e^- \approx \Upsilon(4S)$
10.59 ± 0.06 ± 0.13	60k ± 343	AUBERT,B	06x	BABR $e^+ e^- \approx \Upsilon(4S)$

$\Gamma(\rho^+ \pi^-) / \Gamma(\pi^+ \pi^- \pi^0)$   $\Gamma_{134} / \Gamma_{133}$   
 This is the “fit fraction” from the Dalitz-plot analysis, with interference. See GASPERO 08 and BHATTACHARYA 10A for isospin decompositions of the  $D^0 \rightarrow \pi^+ \pi^0 \pi^-$  Dalitz plot, both based on the amplitudes of AUBERT 07BJ. They quantify the conclusion that the final state is dominantly isospin 0.

VALUE (units 10 <sup>-2</sup> )	DOCUMENT ID	TECN	COMMENT
<b>68.1 ± 0.6 OUR AVERAGE</b>			
67.8 ± 0.0 ± 0.6	AUBERT	07BJ	BABR Dalitz fit, 45k events
76.3 ± 1.9 ± 2.5	CRONIN-HEN..05	CLEO	$e^+ e^- \approx 10$ GeV

$\Gamma(\rho^0 \pi^0) / \Gamma(\pi^+ \pi^- \pi^0)$   $\Gamma_{135} / \Gamma_{133}$   
 This is the “fit fraction” from the Dalitz-plot analysis, with interference.

VALUE (units 10 <sup>-2</sup> )	DOCUMENT ID	TECN	COMMENT
<b>25.9 ± 1.1 OUR AVERAGE</b>			
26.2 ± 0.5 ± 1.1	AUBERT	07BJ	BABR Dalitz fit, 45k events
24.4 ± 2.0 ± 2.1	CRONIN-HEN..05	CLEO	$e^+ e^- \approx 10$ GeV

$\Gamma(\rho^- \pi^+) / \Gamma(\pi^+ \pi^- \pi^0)$   $\Gamma_{136} / \Gamma_{133}$   
 This is the “fit fraction” from the Dalitz-plot analysis, with interference.

VALUE (units 10 <sup>-2</sup> )	DOCUMENT ID	TECN	COMMENT
<b>34.6 ± 0.8 OUR AVERAGE</b>			
34.6 ± 0.8 ± 0.3	AUBERT	07BJ	BABR Dalitz fit, 45k events
34.5 ± 2.4 ± 1.3	CRONIN-HEN..05	CLEO	$e^+ e^- \approx 10$ GeV

$\Gamma(\rho(1450)^+ \pi^-, \rho(1450)^+ \rightarrow \pi^+ \pi^0) / \Gamma(\pi^+ \pi^- \pi^0)$   $\Gamma_{137} / \Gamma_{133}$

VALUE (units 10 <sup>-2</sup> )	DOCUMENT ID	TECN	COMMENT
<b>0.11 ± 0.07 ± 0.12</b>	AUBERT	07BJ	BABR Dalitz fit, 45k events

$\Gamma(\rho(1450)^0 \pi^0, \rho(1450)^0 \rightarrow \pi^+ \pi^-) / \Gamma(\pi^+ \pi^- \pi^0)$   $\Gamma_{138} / \Gamma_{133}$

VALUE (units 10 <sup>-2</sup> )	DOCUMENT ID	TECN	COMMENT
<b>0.30 ± 0.11 ± 0.07</b>	AUBERT	07BJ	BABR Dalitz fit, 45k events

$\Gamma(\rho(1450)^- \pi^+, \rho(1450)^- \rightarrow \pi^- \pi^0) / \Gamma(\pi^+ \pi^- \pi^0)$   $\Gamma_{139} / \Gamma_{133}$

VALUE (units 10 <sup>-2</sup> )	DOCUMENT ID	TECN	COMMENT
<b>1.79 ± 0.22 ± 0.12</b>	AUBERT	07BJ	BABR Dalitz fit, 45k events

$\Gamma(\rho(1700)^+ \pi^-, \rho(1700)^+ \rightarrow \pi^+ \pi^0) / \Gamma(\pi^+ \pi^- \pi^0)$   $\Gamma_{140} / \Gamma_{133}$

VALUE (units 10 <sup>-2</sup> )	DOCUMENT ID	TECN	COMMENT
<b>4.1 ± 0.7 ± 0.7</b>	AUBERT	07BJ	BABR Dalitz fit, 45k events

$\Gamma(\rho(1700)^0 \pi^0, \rho(1700)^0 \rightarrow \pi^+ \pi^-) / \Gamma(\pi^+ \pi^- \pi^0)$   $\Gamma_{141} / \Gamma_{133}$

VALUE (units 10 <sup>-2</sup> )	DOCUMENT ID	TECN	COMMENT
<b>5.0 ± 0.6 ± 1.0</b>	AUBERT	07BJ	BABR Dalitz fit, 45k events

$\Gamma(\rho(1700)^- \pi^+, \rho(1700)^- \rightarrow \pi^- \pi^0) / \Gamma(\pi^+ \pi^- \pi^0)$   $\Gamma_{142} / \Gamma_{133}$

VALUE (units 10 <sup>-2</sup> )	DOCUMENT ID	TECN	COMMENT
<b>3.2 ± 0.4 ± 0.6</b>	AUBERT	07BJ	BABR Dalitz fit, 45k events

$\Gamma(f_0(980) \pi^0, f_0(980) \rightarrow \pi^+ \pi^-) / \Gamma(\pi^+ \pi^- \pi^0)$   $\Gamma_{143} / \Gamma_{133}$

VALUE (units 10 <sup>-2</sup> )	CL%	DOCUMENT ID	TECN	COMMENT
<b>0.25 ± 0.04 ± 0.04</b>		AUBERT	07BJ	BABR Dalitz fit, 45k events
<0.026	95	<sup>1</sup> CRONIN-HEN..05	CLEO	$e^+ e^- \approx 10$ GeV

<sup>1</sup>THE CRONIN-HENNESSY 05 fit here includes, in addition to the three  $\rho$  charged states, only the  $f_0(980) \pi^0$  mode. See also the next entries for limits obtained in the same way for the  $f_0(500) \pi^0$  mode and for an S-wave  $\pi^+ \pi^-$  parametrized using a K-matrix. Our  $\rho$  branching ratios, given above, use the fit with the K-matrix S wave.





# Meson Particle Listings

## $D^0$

### $\Gamma(3\pi^+3\pi^-)/\Gamma(K^-3\pi^+2\pi^-)$ $\Gamma_{171}/\Gamma_{92}$

VALUE	DOCUMENT ID	TECN	COMMENT
1.93±0.47±0.48	<sup>1</sup> LINK	04B	FOCS $\gamma A, \bar{E}_\gamma \approx 180$ GeV

<sup>1</sup>This LINK 04B result is not independent of other results in these Listings.

### $\Gamma(\eta'(958)\pi^0)/\Gamma_{total}$ $\Gamma_{172}/\Gamma$

Unseen decay modes of the  $\eta'(958)$  are included.

VALUE (units $10^{-4}$ )	EVTS	DOCUMENT ID	TECN	COMMENT
8.1±1.5±0.6	50 ± 9	ARTUSO	08	CLEO See MENDEZ 10

### $\Gamma(\eta'(958)\pi^0)/[\Gamma(K^-\pi^+) + \Gamma(K^+\pi^-)]$ $\Gamma_{172}/(\Gamma_{31}+\Gamma_{212})$

Unseen decay modes of the  $\eta'(958)$  are included.

VALUE (units $10^{-2}$ )	EVTS	DOCUMENT ID	TECN	COMMENT
<b>2.3±0.4 OUR FIT</b>				
<b>2.3±0.3±0.2</b>	159 ± 19	MENDEZ	10	CLEO $e^+e^-$ at 3774 MeV

### $\Gamma(\eta'(958)\pi^+\pi^-)/\Gamma_{total}$ $\Gamma_{173}/\Gamma$

Unseen decay modes of the  $\eta'(958)$  are included.

VALUE (units $10^{-4}$ )	EVTS	DOCUMENT ID	TECN	COMMENT
<b>4.5±1.6±0.5</b>	21 ± 8	ARTUSO	08	CLEO $e^+e^-$ at $\psi(3770)$

### $\Gamma(2\eta)/\Gamma_{total}$ $\Gamma_{174}/\Gamma$

Unseen decay modes of the  $\eta$  are included.

VALUE (units $10^{-4}$ )	EVTS	DOCUMENT ID	TECN	COMMENT
16.7±1.4±1.3	255 ± 22	ARTUSO	08	CLEO See MENDEZ 10

### $\Gamma(2\eta)/[\Gamma(K^-\pi^+) + \Gamma(K^+\pi^-)]$ $\Gamma_{174}/(\Gamma_{31}+\Gamma_{212})$

Unseen decay modes of the  $\eta$  are included.

VALUE (units $10^{-2}$ )	EVTS	DOCUMENT ID	TECN	COMMENT
<b>4.3±0.5 OUR FIT</b>				
<b>4.3±0.3±0.4</b>	430 ± 29	MENDEZ	10	CLEO $e^+e^-$ at 3774 MeV

### $\Gamma(\eta\eta'(958))/\Gamma_{total}$ $\Gamma_{175}/\Gamma$

Unseen decay modes of the  $\eta$  and  $\eta'(958)$  are included.

VALUE (units $10^{-4}$ )	EVTS	DOCUMENT ID	TECN	COMMENT
12.6±2.5±1.1	46 ± 9	ARTUSO	08	CLEO See MENDEZ 10

### $\Gamma(\eta\eta'(958))/[\Gamma(K^-\pi^+) + \Gamma(K^+\pi^-)]$ $\Gamma_{175}/(\Gamma_{31}+\Gamma_{212})$

Unseen decay modes of the  $\eta$  and  $\eta'(958)$  are included.

VALUE (units $10^{-2}$ )	EVTS	DOCUMENT ID	TECN	COMMENT
<b>2.7±0.7 OUR FIT</b>				
<b>2.7±0.6±0.3</b>	66 ± 15	MENDEZ	10	CLEO $e^+e^-$ at 3774 MeV

### Hadronic modes with a $K\bar{K}$ pair

### $\Gamma(K^+K^-)/\Gamma_{total}$ $\Gamma_{176}/\Gamma$

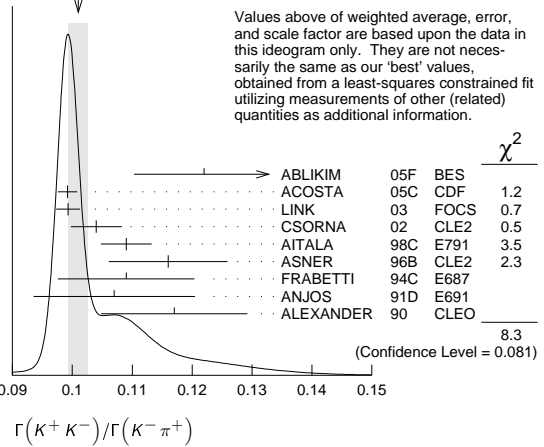
VALUE (units $10^{-3}$ )	EVTS	DOCUMENT ID	TECN	COMMENT
<b>3.96±0.08 OUR FIT</b>				Error includes scale factor of 1.4.
4.08±0.08±0.09	4746 ± 74	BONVICINI	08	CLEO See MENDEZ 10

### $\Gamma(K^+K^-)/\Gamma(K^-\pi^+)$ $\Gamma_{176}/\Gamma_{31}$

VALUE	EVTS	DOCUMENT ID	TECN	COMMENT
<b>0.1021±0.0015 OUR FIT</b>				Error includes scale factor of 1.7.
<b>0.1010±0.0016 OUR AVERAGE</b>				Error includes scale factor of 1.4. See the ideogram below.
0.122 ± 0.011 ± 0.004	242 ± 20	ABLIKIM	05F	BES $e^+e^- \approx \psi(3770)$
0.0992±0.0011±0.0012	16k±200	ACOSTA	05c	CDF $p\bar{p}, \sqrt{s}=1.96$ TeV
0.0993±0.0014±0.0014	11k	LINK	03	FOCS $\gamma$ nucleus, $\bar{E}_\gamma \approx 180$ GeV
0.1040±0.0033±0.0027	1900	CSORNA	02	CLE2 $e^+e^- \approx \Upsilon(4S)$
0.109 ± 0.003 ± 0.003	3317	AITALA	98c	E791 $\pi^-$ nucleus, 500 GeV
0.116 ± 0.007 ± 0.007	1102	ASNER	96B	CLE2 $e^+e^- \approx \Upsilon(4S)$
0.109 ± 0.007 ± 0.009	581	FRABETTI	94c	E687 $\gamma$ Be $\bar{E}_\gamma = 220$ GeV
0.107 ± 0.010 ± 0.009	193	ANJOS	91D	E691 Photoproduction
0.117 ± 0.010 ± 0.007	249	ALEXANDER	90	CLEO $e^+e^-$ 10.5–11 GeV
0.107 ± 0.029 ± 0.015	103	ADAMOVIICH	92	OMEG $\pi^-$ 340 GeV
0.138 ± 0.027 ± 0.010	155	FRABETTI	92	E687 $\gamma$ Be
0.16 ± 0.05	34	ALVAREZ	91B	NA14 Photoproduction
0.10 ± 0.02 ± 0.01	131	ALBRECHT	90c	ARG $e^+e^- \approx 10$ GeV
0.122 ± 0.018 ± 0.012	118	BALTRUSAIT..85E	MRK3	$e^+e^-$ 3.77 GeV
0.113 ± 0.030		ABRAMS	79D	MRK2 $e^+e^-$ 3.77 GeV

### WEIGHTED AVERAGE

0.1010±0.0016 (Error scaled by 1.4)



### $\Gamma(K^+K^-)/[\Gamma(K^-\pi^+) + \Gamma(K^+\pi^-)]$ $\Gamma_{176}/(\Gamma_{31}+\Gamma_{212})$

VALUE (units $10^{-2}$ )	EVTS	DOCUMENT ID	TECN	COMMENT
<b>10.18±0.15 OUR FIT</b>				Error includes scale factor of 1.7.
<b>10.41±0.11±0.12</b>	13.8k	MENDEZ	10	CLEO $e^+e^-$ at 3774 MeV

### $\Gamma(K^+K^-)/\Gamma(\pi^+\pi^-)$ $\Gamma_{176}/\Gamma_{131}$

The unused results here are redundant with  $\Gamma(K^+K^-)/\Gamma(K^-\pi^+)$  and  $\Gamma(\pi^+\pi^-)/\Gamma(K^-\pi^+)$  measurements by the same experiments.

VALUE	EVTS	DOCUMENT ID	TECN	COMMENT
2.760±0.040±0.034	7334	ACOSTA	05c	CDF $p\bar{p}, \sqrt{s}=1.96$ TeV
2.81 ± 0.10 ± 0.06		LINK	03	FOCS $\gamma$ nucleus, $\bar{E}_\gamma \approx 180$ GeV
2.96 ± 0.16 ± 0.15	710	CSORNA	02	CLE2 $e^+e^- \approx \Upsilon(4S)$
2.75 ± 0.15 ± 0.16		AITALA	98c	E791 $\pi^-$ nucleus, 500 GeV
2.53 ± 0.46 ± 0.19		FRABETTI	94c	E687 $\gamma$ Be $\bar{E}_\gamma = 220$ GeV
2.23 ± 0.81 ± 0.46		ADAMOVIICH	92	OMEG $\pi^-$ 340 GeV
1.95 ± 0.34 ± 0.22		ANJOS	91D	E691 Photoproduction
2.5 ± 0.7		ALBRECHT	90c	ARG $e^+e^- \approx 10$ GeV
2.35 ± 0.37 ± 0.28		ALEXANDER	90	CLEO $e^+e^-$ 10.5–11 GeV

### $\Gamma(2K_S^0)/\Gamma_{total}$ $\Gamma_{177}/\Gamma$

VALUE (units $10^{-4}$ )	EVTS	DOCUMENT ID	TECN	COMMENT
1.46±0.32±0.09	68 ± 15	BONVICINI	08	CLEO See MENDEZ 10

### $\Gamma(2K_S^0)/[\Gamma(K^-\pi^+) + \Gamma(K^+\pi^-)]$ $\Gamma_{177}/(\Gamma_{31}+\Gamma_{212})$

VALUE (units $10^{-2}$ )	EVTS	DOCUMENT ID	TECN	COMMENT
<b>0.45±0.11 OUR FIT</b>				Error includes scale factor of 2.5.
<b>0.41±0.04±0.02</b>	215 ± 23	MENDEZ	10	CLEO $e^+e^-$ at 3774 MeV

### $\Gamma(2K_S^0)/\Gamma(K_S^0\pi^+\pi^-)$ $\Gamma_{177}/\Gamma_{34}$

This is the same as  $\Gamma(K^0\bar{K}^0)/\Gamma(\bar{K}^0\pi^+\pi^-)$  because  $D^0 \rightarrow K_S^0 K_L^0$  is forbidden by CP conservation.

VALUE	EVTS	DOCUMENT ID	TECN	COMMENT
<b>0.0061±0.0015 OUR FIT</b>				Error includes scale factor of 2.2.
<b>0.0120±0.0022 OUR AVERAGE</b>				
0.0144±0.0032±0.0016	79 ± 17	LINK	05A	FOCS $\gamma$ Be, $\bar{E}_\gamma \approx 180$ GeV
0.0101±0.0022±0.0016	26	ASNER	96B	CLE2 $e^+e^- \approx \Upsilon(4S)$
0.039 ± 0.013 ± 0.013	20 ± 7	FRABETTI	94J	E687 $\gamma$ Be $\bar{E}_\gamma = 220$ GeV
0.021 +0.011 -0.008 ± 0.002	5	ALEXANDER	90	CLEO $e^+e^-$ 10.5–11 GeV

### $\Gamma(K_S^0 K^-\pi^+)/\Gamma(K^-\pi^+)$ $\Gamma_{178}/\Gamma_{31}$

VALUE	DOCUMENT ID	TECN	COMMENT
<b>0.086±0.013 OUR FIT</b>			Error includes scale factor of 1.1.
<b>0.08 ± 0.03</b>	<sup>1</sup> ANJOS	91	E691 $\gamma$ Be 80–240 GeV

<sup>1</sup>The factor 100 at the top of column 2 of Table I of ANJOS 91 should be omitted.

### $\Gamma(K_S^0 K^-\pi^+)/\Gamma(K_S^0\pi^+\pi^-)$ $\Gamma_{178}/\Gamma_{34}$

VALUE	EVTS	DOCUMENT ID	TECN	COMMENT
<b>0.118±0.017 OUR FIT</b>				Error includes scale factor of 1.1.
<b>0.119±0.021 OUR AVERAGE</b>				Error includes scale factor of 1.3.
0.108±0.019	61	AMMAR	91	CLEO $e^+e^- \approx 10.5$ GeV
0.16 ± 0.03 ± 0.02	39	ALBRECHT	90c	ARG $e^+e^- \approx 10$ GeV



# Meson Particle Listings

## $D^0$

$\Gamma(K_S^0 K^- 2\pi^+ \pi^-)/\Gamma(K_S^0 2\pi^+ 2\pi^-)$		$\Gamma_{201}/\Gamma_{86}$		
VALUE	CL%	DOCUMENT ID	TECN	COMMENT
<b>&lt;0.054</b>	90	LINK	04D	FOCS $\gamma A, \bar{E}_\gamma \approx 180$ GeV

$\Gamma(K^+ K^- \pi^+ \pi^- \pi^0)/\Gamma_{total}$		$\Gamma_{202}/\Gamma$		
VALUE	CL%	DOCUMENT ID	TECN	COMMENT
<b>0.0031 ± 0.0020</b>		<sup>1</sup> BARLAG	92c	ACCM $\pi^-$ Cu 230 GeV

<sup>1</sup> BARLAG 92c computes the branching fraction using topological normalization.

### Radiative modes

$\Gamma(\rho^0 \gamma)/\Gamma_{total}$		$\Gamma_{206}/\Gamma$		
VALUE	CL%	DOCUMENT ID	TECN	COMMENT
<b>&lt;2.4 × 10<sup>-4</sup></b>	90	ASNER	98	CLE2

$\Gamma(\omega \gamma)/\Gamma_{total}$		$\Gamma_{207}/\Gamma$		
VALUE	CL%	DOCUMENT ID	TECN	COMMENT
<b>&lt;2.4 × 10<sup>-4</sup></b>	90	ASNER	98	CLE2

$\Gamma(\phi \gamma)/\Gamma(K^+ K^-)$		$\Gamma_{208}/\Gamma_{76}$		
VALUE (units 10 <sup>-3</sup> )	EVTS	DOCUMENT ID	TECN	COMMENT
<b>6.8 ± 0.9 OUR FIT</b>				
<b>6.31<sup>+1.70+0.30</sup><sub>-1.48-0.36</sub></b>	28	TAJIMA	04	BELL $e^+ e^-$ at $\gamma(4S)$

$\Gamma(\phi \gamma)/\Gamma(K^- \pi^+)$		$\Gamma_{208}/\Gamma_{31}$		
VALUE (units 10 <sup>-4</sup> )	EVTS	DOCUMENT ID	TECN	COMMENT
<b>7.0 ± 0.9 OUR FIT</b>				
<b>7.15 ± 0.78 ± 0.69</b>	243 ± 25	AUBERT	08AZ	BABR $e^+ e^- \approx 10.6$ GeV

$\Gamma(K^*(892)^0 \gamma)/\Gamma(K^- \pi^+)$		$\Gamma_{209}/\Gamma_{31}$		
VALUE (units 10 <sup>-3</sup> )	EVTS	DOCUMENT ID	TECN	COMMENT
<b>8.43 ± 0.51 ± 0.70</b>	2286 ± 113	AUBERT	08AZ	BABR $e^+ e^- \approx 10.6$ GeV

### Doubly Cabibbo-suppressed / Mixing modes

$\Gamma(K^+ \ell^- \bar{\nu}_\ell \text{ via } \bar{D}^0)/\Gamma(K^- \ell^+ \nu_\ell)$		$\Gamma_{210}/\Gamma_{17}$		
VALUE	CL%	DOCUMENT ID	TECN	COMMENT
<b>&lt; 6.1 × 10<sup>-4</sup></b>	90	<sup>1</sup> BITENC	08	BELL $e^+ e^-$ , 10.58 GeV
<b>&lt;50 × 10<sup>-4</sup></b>	90	<sup>2</sup> AITALA	96c	E791 $\pi^-$ nucleus, 500 GeV

<sup>1</sup> The BITENC 08 right-sign sample includes about 15% of  $D^0 \rightarrow K^- \pi^0 \ell^+ \nu_\ell$  and other decays.

<sup>2</sup> AITALA 96c uses  $D^{*+} \rightarrow D^0 \pi^+$  (and charge conjugate) decays to identify the charm at production and  $D^0 \rightarrow K^- \ell^+ \nu_\ell$  (and charge conjugate) decays to identify the charm at decay.

$\Gamma(K^+ \text{ or } K^*(892)^+ e^- \bar{\nu}_e \text{ via } \bar{D}^0)/[\Gamma(K^- e^+ \nu_e) + \Gamma(K^*(892)^- e^+ \nu_e)]$		$\Gamma_{211}/(\Gamma_{18} + \Gamma_{20})$		
VALUE	CL%	DOCUMENT ID	TECN	COMMENT
<b>&lt;0.001</b>	90	BITENC	05	BELL $e^+ e^- \approx 10.6$ GeV
<b>-0.0013 &lt; R &lt; +0.0012</b>	90	AUBERT	07AB	BABR $e^+ e^- \approx 10.58$ GeV
<b>&lt;0.0078</b>	90	CRAWFIELD	05	CLEO $e^+ e^- \approx 10.6$ GeV
<b>&lt;0.0042</b>	90	AUBERT,B	04Q	BABR See AUBERT 07AB

This is a limit on  $R_M$  without the complications of possible doubly Cabibbo-suppressed decays that occur when using hadronic modes. For the limits on  $|m_1 - m_2|$  and  $(\Gamma_1 - \Gamma_2)/\Gamma$  that come from the best mixing limit, see near the beginning of these  $D^0$  Listings.

<sup>1</sup> The BITENC 08 right-sign sample includes about 15% of  $D^0 \rightarrow K^- \pi^0 \ell^+ \nu_\ell$  and other decays.

<sup>2</sup> AITALA 96c uses  $D^{*+} \rightarrow D^0 \pi^+$  (and charge conjugate) decays to identify the charm at production and  $D^0 \rightarrow K^- \ell^+ \nu_\ell$  (and charge conjugate) decays to identify the charm at decay.

$\Gamma(K^+ \pi^-)/\Gamma(K^- \pi^+)$		$\Gamma_{212}/\Gamma_{31}$		
VALUE	CL%	DOCUMENT ID	TECN	COMMENT
<b>&lt;0.001</b>	90	BITENC	05	BELL $e^+ e^- \approx 10.6$ GeV
<b>-0.0013 &lt; R &lt; +0.0012</b>	90	AUBERT	07AB	BABR $e^+ e^- \approx 10.58$ GeV
<b>&lt;0.0078</b>	90	CRAWFIELD	05	CLEO $e^+ e^- \approx 10.6$ GeV
<b>&lt;0.0042</b>	90	AUBERT,B	04Q	BABR See AUBERT 07AB

This is  $R$ , the time-integrated wrong-sign rate compared to the right-sign rate. See the note on " $D^0$ - $\bar{D}^0$  Mixing," near the start of the  $D^0$  Listings.

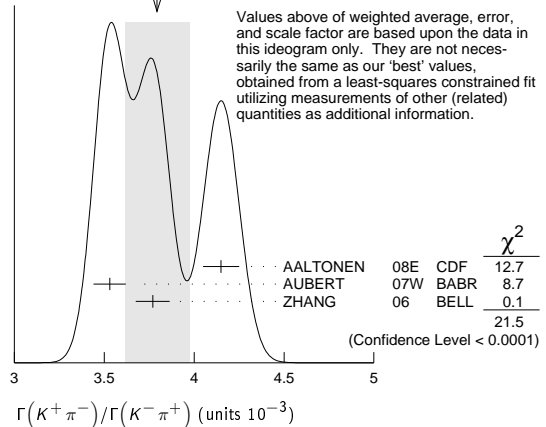
The experiments here use the charge of the pion in  $D^*(2010)^\pm \rightarrow (D^0 \text{ or } \bar{D}^0) \pi^\pm$  decay to tell whether a  $D^0$  or a  $\bar{D}^0$  was born. The  $D^0 \rightarrow K^+ \pi^-$  decay can occur directly by doubly Cabibbo-suppressed (DCS) decay, or indirectly by  $D^0 \rightarrow \bar{D}^0$  mixing followed by  $\bar{D}^0 \rightarrow K^+ \pi^-$  decay. Some of the experiments can use the decay-time information to disentangle the two mechanisms. Here, we list the experimental branching ratio, which if there is no mixing is the DCS ratio. See the next data block for values of the DCS ratio  $R_D$ , and the following data block for limits on the mixing ratio  $R_M$ . See the section on  $CP$ -violating asymmetries near the end of this  $D^0$  Listing for values of  $A_D$ , and the note on " $D^0$ - $\bar{D}^0$  Mixing" for limits on  $x'$  and  $y'$ .

Some early limits have been omitted from this Listing; see our 1998 edition (The European Physical Journal **C3** 1 (1998)) and our 2006 edition (Journal of Physics, G **33** 1 (2006)).

VALUE (units 10 <sup>-3</sup> )	EVTS	DOCUMENT ID	TECN	COMMENT
<b>3.79 ± 0.18 OUR AVERAGE</b>				Error includes scale factor of 3.3. See the ideogram below.
4.15 ± 0.10	12.7 ± 0.3k	<sup>1</sup> AALTONEN	08E	CDF $p\bar{p}, \sqrt{s} = 1.96$ TeV
3.53 ± 0.08 ± 0.04	4030 ± 90	<sup>2</sup> AUBERT	07w	BABR $e^+ e^- \approx 10.6$ GeV
3.77 ± 0.08 ± 0.05	4024 ± 88	<sup>1</sup> ZHANG	06	BELL $e^+ e^-$
• • • We do not use the following data for averages, fits, limits, etc. • • •				
4.05 ± 0.21 ± 0.11	2.0 ± 0.1k	<sup>3</sup> ABULENCIA	06x	CDF See AALTONEN 08E
3.81 ± 0.17 <sup>+0.08</sup> <sub>-0.16</sub>	845 ± 40	<sup>2</sup> LI	05A	BELL See ZHANG 06
4.29 <sup>+0.63</sup> <sub>-0.61</sub> ± 0.27	234	<sup>4</sup> LINK	05H	FOCS $\gamma$ nucleus
3.57 ± 0.22 ± 0.27		<sup>5</sup> AUBERT	03Z	BABR See AUBERT 07w
4.04 ± 0.85 ± 0.25	149	<sup>6</sup> LINK	01	FOCS $\gamma$ nucleus
3.32 <sup>+0.63</sup> <sub>-0.65</sub> ± 0.40	45	<sup>1</sup> GODANG	00	CLE2 $e^+ e^-$
6.8 <sup>+3.4</sup> <sub>-3.3</sub> ± 0.7	34	<sup>2</sup> AITALA	98	E791 $\pi^-$ nucl., 500 GeV

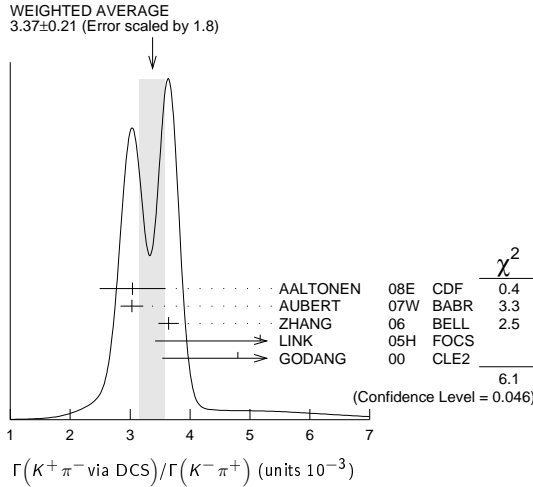
- <sup>1</sup> GODANG 00, ZHANG 06, and AALTONEN 08E allow  $CP$  violation.
- <sup>2</sup> AITALA 98, LI 05A, and AUBERT 07w assume no  $CP$  violation.
- <sup>3</sup> This ABULENCIA 06x result assumes no mixing.
- <sup>4</sup> This LINK 05H result assumes no mixing but allows  $CP$  violation. If neither mixing nor  $CP$  violation is allowed,  $R = (4.29 \pm 0.63 \pm 0.28) \times 10^{-3}$ .
- <sup>5</sup> This AUBERT 03z result allows  $CP$  violation. If  $CP$  violation is not allowed,  $R = 0.00359 \pm 0.00020 \pm 0.00027$ .
- <sup>6</sup> This LINK 01 result assumes no mixing or  $CP$  violation.

WEIGHTED AVERAGE  
3.79±0.18 (Error scaled by 3.3)



$\Gamma(K^+ \pi^- \text{ via DCS})/\Gamma(K^- \pi^+)$		$\Gamma_{213}/\Gamma_{31}$			
VALUE (units 10 <sup>-3</sup> )	CL%	EVTS	DOCUMENT ID	TECN	COMMENT
<b>3.37 ± 0.21 OUR AVERAGE</b>					Error includes scale factor of 1.8. See the ideogram below.
3.04 ± 0.55		12.7 ± 0.3k	AALTONEN	08E	CDF $p\bar{p}, \sqrt{s} = 1.96$ TeV
3.03 ± 0.16 ± 0.10		4030 ± 90	<sup>1</sup> AUBERT	07w	BABR $e^+ e^- \approx 10.6$ GeV
3.64 ± 0.17		4024 ± 88	<sup>2</sup> ZHANG	06	BELL $e^+ e^-$
5.17 <sup>+1.47</sup> <sub>-1.58</sub> ± 0.76		234	<sup>3</sup> LINK	05H	FOCS $\gamma$ nucleus
4.8 ± 1.2 ± 0.4		45	<sup>4</sup> GODANG	00	CLE2 $e^+ e^-$
• • • We do not use the following data for averages, fits, limits, etc. • • •					
2.87 ± 0.37		845 ± 40	LI	05A	BELL See ZHANG 06
2.3 < $R_D$ < 5.2	95		<sup>5</sup> AUBERT	03Z	BABR See AUBERT 07w
9.0 <sup>+12.0</sup> <sub>-10.9</sub> ± 4.4		34	<sup>6</sup> AITALA	98	E791 $\pi^-$ nucl., 500 GeV

- <sup>1</sup> This AUBERT 07w result is the same whether or not  $CP$  violation is allowed.
- <sup>2</sup> This ZHANG 06 assumes no  $CP$  violation.
- <sup>3</sup> This LINK 05H result allows  $CP$  violation. Allowing mixing but not  $CP$  violation,  $R_D = (3.81 \pm 1.67 \pm 0.92) \times 10^{-3}$ .
- <sup>4</sup> This GODANG 00 result allows  $CP$  violation.
- <sup>5</sup> This AUBERT 03z result allows  $CP$  violation. If only mixing is allowed, the 95% confidence level interval is  $(2.4 < R_D < 4.9) \times 10^{-3}$ .
- <sup>6</sup> This AITALA 98 result assumes no  $CP$  violation.



**$\Gamma(K^+\pi^- \text{ via } \bar{D}^0)/\Gamma(K^-\pi^+)$   $\Gamma_{214}/\Gamma_{31}$**   
 This is  $R_M$  in the note on " $D^0\text{-}\bar{D}^0$  Mixing" near the start of the  $D^0$  Listings. The experiments here (1) use the charge of the pion in  $D^*(2010)^\pm \rightarrow (D^0 \text{ or } \bar{D}^0)\pi^\pm$  decay to tell whether a  $D^0$  or a  $\bar{D}^0$  was born; and (2) use the decay-time distribution to disentangle doubly Cabibbo-suppressed decay and mixing. For the limits on  $|m_1 - m_2|$  and  $(\Gamma_1 - \Gamma_2)/\Gamma$  that come from the best mixing limit, see near the beginning of these  $D^0$  Listings.

VALUE	CL%	EVTS	DOCUMENT ID	TECN	COMMENT
<0.00040	95	1	ZHANG 06	BELL	$e^+e^-$
••• We do not use the following data for averages, fits, limits, etc. •••					
<0.00046	95	2	LI 05A	BELL	See ZHANG 06
<0.0063	95	3	LINK 05H	FOCS	$\gamma$ nucleus
<0.0013	95	4	AUBERT 03Z	BABR	$e^+e^-$ , 10.6 GeV
<0.00041	95	5	GODANG 00	CLE2	$e^+e^-$
<0.0092	95	6	BARATE 98W	ALEP	$e^+e^-$ at $Z^0$
<0.005	90	1 ± 4	ANJOS 88c	E691	Photoproduction

- This ZHANG 06 result allows  $CP$  violation, but the result does not change if  $CP$  violation is not allowed.
- This LI 05A result allows  $CP$  violation. The limit becomes  $< 0.00042$  (95% CL) if  $CP$  violation is not allowed.
- LINK 05H obtains the same result whether or not  $CP$  violation is allowed.
- This AUBERT 03Z result allows  $CP$  violation and assumes that the strong phase between  $D^0 \rightarrow K^+\pi^-$  and  $\bar{D}^0 \rightarrow K^+\pi^-$  is small, and limits only  $D^0 \rightarrow \bar{D}^0$  transitions via off-shell intermediate states. The limit on transitions via on-shell intermediate states is 0.0016.
- This GODANG 00 result allows  $CP$  violation and assumes that the strong phase between  $D^0 \rightarrow K^+\pi^-$  and  $\bar{D}^0 \rightarrow K^+\pi^-$  is small, and limits only  $D^0 \rightarrow \bar{D}^0$  transitions via off-shell intermediate states. The limit on transitions via on-shell intermediate states is 0.0017.
- This BARATE 98W result assumes no interference between the DCS and mixing amplitudes ( $\gamma = 0$  in the note on " $D^0\text{-}\bar{D}^0$  Mixing" near the start of the  $D^0$  Listings). When interference is allowed, the limit degrades to 0.036 (95% CL).
- This ANJOS 88c result assumes no interference between the DCS and mixing amplitudes ( $\gamma = 0$  in the note on " $D^0\text{-}\bar{D}^0$  Mixing" near the start of the  $D^0$  Listings). When interference is allowed, the limit degrades to 0.019.

**$\Gamma(K_S^0\pi^+\pi^- \text{ in } D^0 \rightarrow \bar{D}^0)/\Gamma(K_S^0\pi^+\pi^-)$   $\Gamma_{215}/\Gamma_{34}$**   
 This is  $R_M$  in the note on " $D^0\text{-}\bar{D}^0$  Mixing" near the start of the  $D^0$  Listings. The experiments here (1) use the charge of the pion in  $D^*(2010)^\pm \rightarrow (D^0 \text{ or } \bar{D}^0)\pi^\pm$  decay to tell whether a  $D^0$  or a  $\bar{D}^0$  was born; and (2) use the decay-time distribution to disentangle doubly Cabibbo-suppressed decay and mixing. For the limits on  $|m_1 - m_2|$  and  $(\Gamma_1 - \Gamma_2)/\Gamma$  that come from the best mixing limit, see near the beginning of these  $D^0$  Listings.

VALUE	CL%	DOCUMENT ID	TECN	COMMENT
<0.0063	95	1 ASNER 05	CLEO	$e^+e^- \approx 10$ GeV

- This ASNER 05 limit allows  $CP$  violation. If  $CP$  violation is not allowed, the limit is 0.0042 at 95% CL.

**$\Gamma(K^+\pi^-\pi^0)/\Gamma(K^-\pi^+\pi^0)$   $\Gamma_{219}/\Gamma_{49}$**   
 The experiments here use the charge of the pion in  $D^*(2010)^\pm \rightarrow (D^0 \text{ or } \bar{D}^0)\pi^\pm$  decay to tell whether a  $D^0$  or a  $\bar{D}^0$  was born. The  $D^0 \rightarrow K^+\pi^-\pi^0$  decay can occur directly by doubly Cabibbo-suppressed (DCS) decay, or indirectly by  $D^0 \rightarrow \bar{D}^0$  mixing followed by  $\bar{D}^0 \rightarrow K^+\pi^-\pi^0$  decay.

VALUE (units $10^{-3}$ )	CL%	EVTS	DOCUMENT ID	TECN	COMMENT
<b>2.20 ± 0.10 OUR AVERAGE</b>					
2.14 ± 0.08 ± 0.08	763 ± 51	1	AUBERT,B 06N	BABR	$e^+e^- \approx \gamma(4S)$
2.29 ± 0.15 ± 0.13	1978 ± 104		TIAN 05	BELL	$e^+e^- \approx \gamma(4S)$
4.3 ± 1.1 ± 1.0	38		BRANDENB... 01	CLE2	$e^+e^- \approx \gamma(4S)$

- This AUBERT,B 06N result assumes no mixing.

**$\Gamma(K^+\pi^-\pi^0 \text{ via } \bar{D}^0)/\Gamma(K^-\pi^+\pi^0)$   $\Gamma_{220}/\Gamma_{49}$**   
 This is  $R_M$  in the note on " $D^0\text{-}\bar{D}^0$  Mixing" near the start of the  $D^0$  Listings. The experiments here (1) use the charge of the pion in  $D^*(2010)^\pm \rightarrow (D^0 \text{ or } \bar{D}^0)\pi^\pm$  decay to tell whether a  $D^0$  or a  $\bar{D}^0$  was born; and (2) use the decay-time distribution to disentangle doubly Cabibbo-suppressed decay and mixing. For the limits on  $|m_1 - m_2|$  and  $(\Gamma_1 - \Gamma_2)/\Gamma$  that come from the best mixing limit, see near the beginning of these  $D^0$  Listings.

VALUE (units $10^{-3}$ )	CL%	DOCUMENT ID	TECN	COMMENT
<b>5.25 ± 0.25 ± 0.12</b>		AUBERT 09AN	BABR	$e^+e^-$ at 10.58 GeV

- We do not use the following data for averages, fits, limits, etc. •••
- | VALUE | CL% | DOCUMENT ID    | TECN | COMMENT                     |
|-------|-----|----------------|------|-----------------------------|
| <0.54 | 95  | 1 AUBERT,B 06N | BABR | $e^+e^- \approx \gamma(4S)$ |
- This AUBERT,B 06N limit assumes no  $CP$  violation. The measured value corresponding to the limit is  $(2.3 \pm 1.8 \pm 0.4) \times 10^{-4}$ . If  $CP$  violation is allowed, this becomes  $(1.0 \pm 2.2 \pm 0.7) \times 10^{-4}$ .

**$\Gamma(K^+\pi^+2\pi^-)/\Gamma(K^-2\pi^+\pi^-)$   $\Gamma_{221}/\Gamma_{66}$**   
 The experiments here use the charge of the pion in  $D^*(2010)^\pm \rightarrow (D^0 \text{ or } \bar{D}^0)\pi^\pm$  decay to tell whether a  $D^0$  or a  $\bar{D}^0$  was born. The  $D^0 \rightarrow K^+\pi^+\pi^-\pi^-$  decay can occur directly by doubly Cabibbo-suppressed (DCS) decay, or indirectly by  $D^0 \rightarrow \bar{D}^0$  mixing followed by  $\bar{D}^0 \rightarrow K^+\pi^+\pi^-\pi^-$  decay. Some of the experiments can use the decay-time information to disentangle the two mechanisms. Here, we list the experimental branching ratio, which if there is no mixing is the DCS ratio; in the next data block we give the limits on the mixing ratio.

Some early limits have been omitted from this Listing; see our 1998 edition (EPJ C3 1).

VALUE (units $10^{-3}$ )	CL%	EVTS	DOCUMENT ID	TECN	COMMENT
<b>3.24 ± 0.25 ± 0.22 OUR AVERAGE</b>					

3.20 ± 0.18 ± 0.18	1721 ± 75	1	TIAN 05	BELL	$e^+e^- \approx \gamma(4S)$
4.4 ± 1.3 ± 1.2 ± 0.4	54	1	DYTMAN 01	CLE2	$e^+e^- \approx \gamma(4S)$
2.5 ± 3.6 ± 0.3		2	AITALA 98	E791	$\pi^-$ nucl., 500 GeV

- We do not use the following data for averages, fits, limits, etc. •••
- | VALUE | CL% | EVTS   | DOCUMENT ID | TECN | COMMENT                   |
|-------|-----|--------|-------------|------|---------------------------|
| <18   | 90  | 1      | AMMAR 91    | CLEO | $e^+e^- \approx 10.5$ GeV |
| <18   | 90  | 5 ± 12 | 3 ANJOS 88c | E691 | Photoproduction           |
- AMMAR 91 cannot and DYTMAN 01 and TIAN 05 do not distinguish between doubly Cabibbo-suppressed decay and  $D^0\text{-}\bar{D}^0$  mixing.
  - This AITALA 98 result assumes no  $D^0\text{-}\bar{D}^0$  mixing ( $R_M$  in the note on " $D^0\text{-}\bar{D}^0$  Mixing"). It becomes  $-0.0020 \pm 0.0117 \pm 0.0035$  when mixing is allowed and decay-time information is used to distinguish doubly Cabibbo-suppressed decays from mixing.
  - ANJOS 88c uses decay-time information to distinguish doubly Cabibbo-suppressed (DCS) decays from  $D^0\text{-}\bar{D}^0$  mixing. However, the result assumes no interference between the DCS and mixing amplitudes ( $\gamma = 0$  in the note on " $D^0\text{-}\bar{D}^0$  Mixing" near the start of the  $D^0$  Listings). When interference is allowed, the limit degrades to 0.033.

**$\Gamma(K^+\pi^+2\pi^- \text{ via } \bar{D}^0)/\Gamma(K^-2\pi^+\pi^-)$   $\Gamma_{222}/\Gamma_{66}$**   
 This is a  $D^0\text{-}\bar{D}^0$  mixing limit. The experiments here (1) use the charge of the pion in  $D^*(2010)^\pm \rightarrow (D^0 \text{ or } \bar{D}^0)\pi^\pm$  decay to tell whether a  $D^0$  or a  $\bar{D}^0$  was born; and (2) use the decay-time distribution to disentangle doubly Cabibbo-suppressed decay and mixing. For the limits on  $|m_{D_1^0} - m_{D_2^0}|$  and  $(\Gamma_{D_1^0} - \Gamma_{D_2^0})/\Gamma_{D^0}$  that come from the best mixing limit, see near the beginning of these  $D^0$  Listings.

VALUE	CL%	EVTS	DOCUMENT ID	TECN	COMMENT
<0.005	90	0 ± 4	1 ANJOS 88c	E691	Photoproduction

- ANJOS 88c uses decay-time information to distinguish doubly Cabibbo-suppressed (DCS) decays from  $D^0\text{-}\bar{D}^0$  mixing. However, the result assumes no interference between the DCS and mixing amplitudes ( $\gamma = 0$  in the note on " $D^0\text{-}\bar{D}^0$  Mixing" near the start of the  $D^0$  Listings). When interference is allowed, the limit degrades to 0.007.

**$\Gamma(K^+\pi^- \text{ or } K^+\pi^+2\pi^- \text{ via } \bar{D}^0)/\Gamma(K^-\pi^+ \text{ or } K^-2\pi^+\pi^-)$   $\Gamma_{223}/\Gamma_0$**   
 This is a  $D^0\text{-}\bar{D}^0$  mixing limit. For the limits on  $|m_{D_1^0} - m_{D_2^0}|$  and  $(\Gamma_{D_1^0} - \Gamma_{D_2^0})/\Gamma_{D^0}$  that come from the best mixing limit, see near the beginning of these  $D^0$  Listings.

VALUE	CL%	DOCUMENT ID	TECN	COMMENT
<0.0085	90	1 AITALA 98	E791	$\pi^-$ nucleus, 500 GeV
<0.0037	90	2 ANJOS 88c	E691	Photoproduction

- We do not use the following data for averages, fits, limits, etc. •••
- AITALA 98 uses decay-time information to distinguish doubly Cabibbo-suppressed decays from  $D^0\text{-}\bar{D}^0$  mixing. The fit allows interference between the two amplitudes, and also allows  $CP$  violation in this term. The central value obtained is  $0.0039 \pm 0.0036 \pm 0.0032 \pm 0.0016$ . When interference is disallowed, the result becomes  $0.0021 \pm 0.0009 \pm 0.0002$ .
  - This combines results of ANJOS 88c on  $K^+\pi^-$  and  $K^+\pi^+\pi^-\pi^-$  (via  $\bar{D}^0$ ) reported in the data block above (see footnotes there). It assumes no interference.



See key on page 457

## Meson Particle Listings

 $D^0$ 

$\Gamma(\bar{K}^0 \mu^+ \mu^-)/\Gamma_{\text{total}}$   $\Gamma_{243}/\Gamma$   
Not a useful test for  $\Delta C=1$  weak neutral current because both quarks must change flavor.

VALUE	CL%	EVTS	DOCUMENT ID	TECN	COMMENT
$<2.6 \times 10^{-4}$	90	2	KODAMA	95 E653	$\pi^-$ emulsion 600 GeV
••• We do not use the following data for averages, fits, limits, etc. •••					
$<6.7 \times 10^{-4}$	90	1	FREYBERGER	96 CLE2	$e^+ e^- \approx \Upsilon(4S)$

$\Gamma(K^- \pi^+ e^+ e^-)/\Gamma_{\text{total}}$   $\Gamma_{244}/\Gamma$   
A test for the  $\Delta C = 1$  weak neutral current. Allowed by higher-order electroweak interactions.

VALUE	CL%	EVTS	DOCUMENT ID	TECN	COMMENT
$<3.85 \times 10^{-4}$	90	6	AITALA	01c E791	$\pi^-$ nucleus, 500 GeV

$\Gamma(\bar{K}^*(892)^0 e^+ e^-)/\Gamma_{\text{total}}$   $\Gamma_{245}/\Gamma$   
Not a useful test for  $\Delta C=1$  weak neutral current because both quarks must change flavor.

VALUE	CL%	EVTS	DOCUMENT ID	TECN	COMMENT
$<4.7 \times 10^{-5}$	90	2	AITALA	01c E791	$\pi^-$ nucleus, 500 GeV
••• We do not use the following data for averages, fits, limits, etc. •••					
$<1.4 \times 10^{-4}$	90	1	<sup>1</sup> FREYBERGER	96 CLE2	$e^+ e^- \approx \Upsilon(4S)$

<sup>1</sup>This FREYBERGER 96 limit is obtained using a phase-space model. The limit changes to  $<2.0 \times 10^{-4}$  using a photon pole amplitude model.

$\Gamma(K^- \pi^+ \mu^+ \mu^-)/\Gamma_{\text{total}}$   $\Gamma_{246}/\Gamma$   
A test for the  $\Delta C = 1$  weak neutral current. Allowed by higher-order electroweak interactions.

VALUE	CL%	EVTS	DOCUMENT ID	TECN	COMMENT
$<3.59 \times 10^{-4}$	90	12	AITALA	01c E791	$\pi^-$ nucleus, 500 GeV

$\Gamma(\bar{K}^*(892)^0 \mu^+ \mu^-)/\Gamma_{\text{total}}$   $\Gamma_{247}/\Gamma$   
Not a useful test for  $\Delta C=1$  weak neutral current because both quarks must change flavor.

VALUE	CL%	EVTS	DOCUMENT ID	TECN	COMMENT
$<2.4 \times 10^{-5}$	90	3	AITALA	01c E791	$\pi^-$ nucleus, 500 GeV
••• We do not use the following data for averages, fits, limits, etc. •••					
$<1.18 \times 10^{-3}$	90	1	<sup>1</sup> FREYBERGER	96 CLE2	$e^+ e^- \approx \Upsilon(4S)$

<sup>1</sup>This FREYBERGER 96 limit is obtained using a phase-space model. The limit changes to  $<1.0 \times 10^{-3}$  using a photon pole amplitude model.

$\Gamma(\pi^+ \pi^- \pi^0 \mu^+ \mu^-)/\Gamma_{\text{total}}$   $\Gamma_{248}/\Gamma$   
A test for the  $\Delta C=1$  weak neutral current. Allowed by higher-order electroweak interactions.

VALUE	CL%	EVTS	DOCUMENT ID	TECN	COMMENT
$<8.1 \times 10^{-4}$	90	1	KODAMA	95 E653	$\pi^-$ emulsion 600 GeV

$\Gamma(\mu^\pm e^\mp)/\Gamma_{\text{total}}$   $\Gamma_{249}/\Gamma$   
A test of lepton family number conservation.

VALUE	CL%	EVTS	DOCUMENT ID	TECN	COMMENT
$<2.6 \times 10^{-7}$	90		PETRIC	10 BELL	$e^+ e^- \approx \Upsilon(4S)$
••• We do not use the following data for averages, fits, limits, etc. •••					
$<8.1 \times 10^{-7}$	90	0	AUBERT,B	04Y BABR	$e^+ e^- \approx \Upsilon(4S)$
$<1.72 \times 10^{-5}$	90		PRIPSTEIN	00 E789	$p$ nucleus, 800 GeV
$<8.1 \times 10^{-6}$	90		AITALA	99G E791	$\pi^- N$ 500 GeV
$<1.9 \times 10^{-5}$	90	2	<sup>1</sup> FREYBERGER	96 CLE2	$e^+ e^- \approx \Upsilon(4S)$
$<1.0 \times 10^{-4}$	90	4	ALBRECHT	88G ARG	$e^+ e^-$ 10 GeV
$<2.7 \times 10^{-4}$	90	9	HAAS	88 CLEO	$e^+ e^-$ 10 GeV
$<1.2 \times 10^{-4}$	90		BECKER	87c MRK3	$e^+ e^-$ 3.77 GeV
$<9 \times 10^{-4}$	90		PALKA	87 SILI	200 GeV $\pi p$
$<21 \times 10^{-4}$	90	0	<sup>2</sup> RILES	87 MRK2	$e^+ e^-$ 29 GeV

<sup>1</sup>This is the corrected result given in the erratum to FREYBERGER 96.

<sup>2</sup>RILES 87 assumes  $B(D \rightarrow K\pi) = 3.0\%$  and has production model dependency.

$\Gamma(\pi^0 e^\pm \mu^\mp)/\Gamma_{\text{total}}$   $\Gamma_{250}/\Gamma$   
A test of lepton family number conservation. The value is for the sum of the two charge states.

VALUE	CL%	EVTS	DOCUMENT ID	TECN	COMMENT
$<8.6 \times 10^{-5}$	90	2	FREYBERGER	96 CLE2	$e^+ e^- \approx \Upsilon(4S)$

$\Gamma(\eta e^\pm \mu^\mp)/\Gamma_{\text{total}}$   $\Gamma_{251}/\Gamma$   
A test of lepton family number conservation. The value is for the sum of the two charge states.

VALUE	CL%	EVTS	DOCUMENT ID	TECN	COMMENT
$<1.0 \times 10^{-4}$	90	0	FREYBERGER	96 CLE2	$e^+ e^- \approx \Upsilon(4S)$

$\Gamma(\pi^+ \pi^- e^\pm \mu^\mp)/\Gamma_{\text{total}}$   $\Gamma_{252}/\Gamma$   
A test of lepton family-number conservation. The value is for the sum of the two charge states.

VALUE	CL%	EVTS	DOCUMENT ID	TECN	COMMENT
$<1.5 \times 10^{-5}$	90	1	AITALA	01c E791	$\pi^-$ nucleus, 500 GeV

$\Gamma(\rho^0 e^\pm \mu^\mp)/\Gamma_{\text{total}}$   $\Gamma_{253}/\Gamma$   
A test of lepton family number conservation. The value is for the sum of the two charge states.

VALUE	CL%	EVTS	DOCUMENT ID	TECN	COMMENT
$<4.9 \times 10^{-5}$	90	0	<sup>1</sup> FREYBERGER	96 CLE2	$e^+ e^- \approx \Upsilon(4S)$
••• We do not use the following data for averages, fits, limits, etc. •••					
$<6.6 \times 10^{-5}$	90	1	AITALA	01c E791	$\pi^-$ nucleus, 500 GeV

<sup>1</sup>This FREYBERGER 96 limit is obtained using a phase-space model. The limit changes to  $<5.0 \times 10^{-5}$  using a photon pole amplitude model.

$\Gamma(\omega e^\pm \mu^\mp)/\Gamma_{\text{total}}$   $\Gamma_{254}/\Gamma$   
A test of lepton family number conservation. The value is for the sum of the two charge states.

VALUE	CL%	EVTS	DOCUMENT ID	TECN	COMMENT
$<1.2 \times 10^{-4}$	90	0	<sup>1</sup> FREYBERGER	96 CLE2	$e^+ e^- \approx \Upsilon(4S)$

<sup>1</sup>This FREYBERGER 96 limit is obtained using a phase-space model. The same limit is obtained using a photon pole amplitude model.

$\Gamma(K^- K^+ e^\pm \mu^\mp)/\Gamma_{\text{total}}$   $\Gamma_{255}/\Gamma$   
A test of lepton family-number conservation. The value is for the sum of the two charge states.

VALUE	CL%	EVTS	DOCUMENT ID	TECN	COMMENT
$<1.8 \times 10^{-4}$	90	5	AITALA	01c E791	$\pi^-$ nucleus, 500 GeV

$\Gamma(\phi e^\pm \mu^\mp)/\Gamma_{\text{total}}$   $\Gamma_{256}/\Gamma$   
A test of lepton family number conservation. The value is for the sum of the two charge states.

VALUE	CL%	EVTS	DOCUMENT ID	TECN	COMMENT
$<3.4 \times 10^{-5}$	90	0	<sup>1</sup> FREYBERGER	96 CLE2	$e^+ e^- \approx \Upsilon(4S)$

••• We do not use the following data for averages, fits, limits, etc. •••

VALUE	CL%	EVTS	DOCUMENT ID	TECN	COMMENT
$<4.7 \times 10^{-5}$	90	0	AITALA	01c E791	$\pi^-$ nucleus, 500 GeV

<sup>1</sup>This FREYBERGER 96 limit is obtained using a phase-space model. The limit changes to  $<3.3 \times 10^{-5}$  using a photon pole amplitude model.

$\Gamma(\bar{K}^0 e^\pm \mu^\mp)/\Gamma_{\text{total}}$   $\Gamma_{257}/\Gamma$   
A test of lepton family number conservation. The value is for the sum of the two charge states.

VALUE	CL%	EVTS	DOCUMENT ID	TECN	COMMENT
$<1.0 \times 10^{-4}$	90	0	FREYBERGER	96 CLE2	$e^+ e^- \approx \Upsilon(4S)$

$\Gamma(K^- \pi^+ e^\pm \mu^\mp)/\Gamma_{\text{total}}$   $\Gamma_{258}/\Gamma$   
A test of lepton family-number conservation. The value is for the sum of the two charge states.

VALUE	CL%	EVTS	DOCUMENT ID	TECN	COMMENT
$<5.53 \times 10^{-4}$	90	15	AITALA	01c E791	$\pi^-$ nucleus, 500 GeV

$\Gamma(\bar{K}^*(892)^0 e^\pm \mu^\mp)/\Gamma_{\text{total}}$   $\Gamma_{259}/\Gamma$   
A test of lepton family number conservation. The value is for the sum of the two charge states.

VALUE	CL%	EVTS	DOCUMENT ID	TECN	COMMENT
$<8.3 \times 10^{-5}$	90	9	AITALA	01c E791	$\pi^-$ nucleus, 500 GeV
••• We do not use the following data for averages, fits, limits, etc. •••					
$<1.0 \times 10^{-4}$	90	0	<sup>1</sup> FREYBERGER	96 CLE2	$e^+ e^- \approx \Upsilon(4S)$

<sup>1</sup>This FREYBERGER 96 limit is obtained using a phase-space model. The same limit is obtained using a photon pole amplitude model.

$\Gamma(2\pi^- 2e^+ + c.c.)/\Gamma_{\text{total}}$   $\Gamma_{260}/\Gamma$   
A test of lepton-number conservation. The value is for the sum of the two charge states.

VALUE	CL%	EVTS	DOCUMENT ID	TECN	COMMENT
$<1.12 \times 10^{-4}$	90	1	AITALA	01c E791	$\pi^-$ nucleus, 500 GeV

$\Gamma(2\pi^- 2\mu^+ + c.c.)/\Gamma_{\text{total}}$   $\Gamma_{261}/\Gamma$   
A test of lepton-number conservation. The value is for the sum of the two charge states.

VALUE	CL%	EVTS	DOCUMENT ID	TECN	COMMENT
$<2.9 \times 10^{-5}$	90	1	AITALA	01c E791	$\pi^-$ nucleus, 500 GeV

$\Gamma(K^- \pi^- 2e^+ + c.c.)/\Gamma_{\text{total}}$   $\Gamma_{262}/\Gamma$   
A test of lepton-number conservation. The value is for the sum of the two charge states.

VALUE	CL%	EVTS	DOCUMENT ID	TECN	COMMENT
$<2.06 \times 10^{-4}$	90	2	AITALA	01c E791	$\pi^-$ nucleus, 500 GeV

$\Gamma(K^- \pi^- 2\mu^+ + c.c.)/\Gamma_{\text{total}}$   $\Gamma_{263}/\Gamma$   
A test of lepton-number conservation. The value is for the sum of the two charge states.

VALUE	CL%	EVTS	DOCUMENT ID	TECN	COMMENT
$<3.9 \times 10^{-4}$	90	14	AITALA	01c E791	$\pi^-$ nucleus, 500 GeV

$\Gamma(2K^- 2e^+ + c.c.)/\Gamma_{\text{total}}$   $\Gamma_{264}/\Gamma$   
A test of lepton-number conservation. The value is for the sum of the two charge states.

VALUE	CL%	EVTS	DOCUMENT ID	TECN	COMMENT
$<1.52 \times 10^{-4}$	90	2	AITALA	01c E791	$\pi^-$ nucleus, 500 GeV





$A_{CP}(K^*(892)^+ K^- \rightarrow K^+ K^- \pi^0)$  in  $D^0 \rightarrow K^*(892)^+ K^-, \bar{D}^0 \rightarrow K^*(892)^- K^+$

VALUE (%)	DOCUMENT ID	TECN	COMMENT
$-0.9 \pm 1.2 \pm 0.4$	AUBERT	08AO BABR	Table 1, -Col.5/2×Col.2

$A_{CP}(K^*(1410)^+ K^- \rightarrow K^+ K^- \pi^0)$  in  $D^0 \rightarrow K^*(1410)^+ K^-, \bar{D}^0 \rightarrow K^*(1410)^- K^+$

VALUE (%)	DOCUMENT ID	TECN	COMMENT
$-21 \pm 23 \pm 8$	AUBERT	08AO BABR	Table 1, -Col.5/2×Col.2

$A_{CP}((K^+ \pi^0)_{S\text{-wave}} K^- \rightarrow K^+ K^- \pi^0)$  in  $D^0 \rightarrow (K^+ \pi^0)_S K^-, \bar{D}^0 \rightarrow (K^- \pi^0)_S K^+$

VALUE (%)	DOCUMENT ID	TECN	COMMENT
$+7 \pm 15 \pm 3$	AUBERT	08AO BABR	Table 1, -Col.5/2×Col.2

$A_{CP}(\phi(1020) \pi^0 \rightarrow K^+ K^- \pi^0)$  in  $D^0, \bar{D}^0 \rightarrow \phi(1020) \pi^0$

VALUE (%)	DOCUMENT ID	TECN	COMMENT
$+1.1 \pm 2.1 \pm 0.5$	AUBERT	08AO BABR	Table 1, -Col.5/2×Col.2

$A_{CP}(f_0(980) \pi^0 \rightarrow K^+ K^- \pi^0)$  in  $D^0, \bar{D}^0 \rightarrow f_0(980) \pi^0$

VALUE (%)	DOCUMENT ID	TECN	COMMENT
$-3 \pm 19 \pm 1$	AUBERT	08AO BABR	Table 1, -Col.5/2×Col.2

$A_{CP}(a_0(980)^0 \pi^0 \rightarrow K^+ K^- \pi^0)$  in  $D^0, \bar{D}^0 \rightarrow a_0(980)^0 \pi^0$

VALUE (%)	DOCUMENT ID	TECN	COMMENT
$-5 \pm 16 \pm 2$	<sup>1</sup> AUBERT	08AO BABR	Table 1, -Col.5/2×Col.2

<sup>1</sup> This AUBERT 08AO value is obtained when the  $a_0(980)^0$  replaces the  $f_0(980)$  in the fit.

$A_{CP}(f_2'(1525) \pi^0 \rightarrow K^+ K^- \pi^0)$  in  $D^0, \bar{D}^0 \rightarrow f_2'(1525) \pi^0$

VALUE (%)	DOCUMENT ID	TECN	COMMENT
$0 \pm 50 \pm 150$	AUBERT	08AO BABR	Table 1, -Col.5/2×Col.2

$A_{CP}(K^*(892)^- K^+ \rightarrow K^+ K^- \pi^0)$  in  $D^0 \rightarrow K^*(892)^- K^+, \bar{D}^0 \rightarrow K^*(892)^+ K^-$

VALUE (%)	DOCUMENT ID	TECN	COMMENT
$-5 \pm 4 \pm 1$	AUBERT	08AO BABR	Table 1, -Col.5/2×Col.2

$A_{CP}(K^*(1410)^- K^+ \rightarrow K^+ K^- \pi^0)$  in  $D^0 \rightarrow K^*(1410)^- K^+, \bar{D}^0 \rightarrow K^*(1410)^+ K^-$

VALUE (%)	DOCUMENT ID	TECN	COMMENT
$-17 \pm 28 \pm 7$	AUBERT	08AO BABR	Table 1, -Col.5/2×Col.2

$A_{CP}((K^- \pi^0)_{S\text{-wave}} K^+ \rightarrow K^+ K^- \pi^0)$  in  $D^0 \rightarrow (K^- \pi^0)_S K^+, \bar{D}^0 \rightarrow (K^+ \pi^0)_S K^-$

VALUE (%)	DOCUMENT ID	TECN	COMMENT
$-7 \pm 40 \pm 8$	AUBERT	08AO BABR	Table 1, -Col.5/2×Col.2

$A_{CP}(K_S^0 \pi^0)$  in  $D^0, \bar{D}^0 \rightarrow K_S^0 \pi^0$

VALUE (%)	EVTS	DOCUMENT ID	TECN	COMMENT
$-0.27 \pm 0.21$ OUR AVERAGE				
$-0.28 \pm 0.19 \pm 0.10$	326k	KO	11	BELL $e^+ e^- \approx \Upsilon(4S)$
$+0.1 \pm 1.3$	9099	BONVICINI	01	CLE2 $e^+ e^- \approx 10.6$ GeV
••• We do not use the following data for averages, fits, limits, etc. •••				
$-1.8 \pm 3.0$		BARTELT	95	CLE2 See BONVICINI 01

$A_{CP}(K_S^0 \eta)$  in  $D^0, \bar{D}^0 \rightarrow K_S^0 \eta$

VALUE (%)	EVTS	DOCUMENT ID	TECN	COMMENT
$+0.54 \pm 0.51 \pm 0.16$	46k	KO	11	BELL $e^+ e^- \approx \Upsilon(4S)$

$A_{CP}(K_S^0 \eta')$  in  $D^0, \bar{D}^0 \rightarrow K_S^0 \eta'$

VALUE (%)	EVTS	DOCUMENT ID	TECN	COMMENT
$+0.98 \pm 0.67 \pm 0.14$	27k	KO	11	BELL $e^+ e^- \approx \Upsilon(4S)$

$A_{CP}(K_S^0 \phi)$  in  $D^0, \bar{D}^0 \rightarrow K_S^0 \phi$

VALUE (%)	DOCUMENT ID	TECN	COMMENT
$-2.8 \pm 9.4$	BARTELT	95	CLE2 $-18.2 < A_{CP} < +12.6\%$ (90%CL)

$A_{CP}(K^\mp \pi^\pm)$  in  $D^0 \rightarrow K^- \pi^+, \bar{D}^0 \rightarrow K^+ \pi^-$

VALUE (%)	EVTS	DOCUMENT ID	TECN	COMMENT
$0.1 \pm 0.7$ OUR AVERAGE				
$+0.5 \pm 0.4 \pm 0.9$	150k	MENDEZ	10	CLEO $e^+ e^-$ at 3774 MeV
$-0.4 \pm 0.5 \pm 0.9$		DOBBS	07	CLEO $e^+ e^-$ at $\psi(3770)$

$A_{CP}(K^\pm \pi^\mp)$  in  $D^0 \rightarrow K^+ \pi^-, \bar{D}^0 \rightarrow K^- \pi^+$

VALUE (%)	EVTS	DOCUMENT ID	TECN	COMMENT
$2.2 \pm 3.2$ OUR AVERAGE				
$-2.1 \pm 5.2 \pm 1.5$	4030 ± 90	AUBERT	07w BABR	$e^+ e^- \approx 10.6$ GeV
$+2.3 \pm 4.7$	4024 ± 88	<sup>1</sup> ZHANG	06	BELL $e^+ e^-$
$+18 \pm 14 \pm 4$		<sup>2</sup> LINK	05H FOCUS	$\gamma$ nucleus
$+9.5 \pm 6.1 \pm 8.3$		<sup>3</sup> AUBERT	03z BABR	$e^+ e^-$ , 10.6 GeV
$+2 \pm 19 \pm 1$	45	<sup>4</sup> GODANG	00	CLE2 $-0.43 < A_{CP} < +0.34$ (95%CL)

••• We do not use the following data for averages, fits, limits, etc. •••

$-8.0 \pm 7.7$	845 ± 40	<sup>5</sup> LI	05A BELL	See ZHANG 06
----------------	----------	-----------------	----------	--------------

<sup>1</sup> This ZHANG 06 result allows mixing.

<sup>2</sup> This LINK 05H result assumes no mixing. If mixing is allowed, it becomes  $0.13_{-0.25}^{+0.33} \pm 0.10$ .

<sup>3</sup> This AUBERT 03z limit assumes no mixing. If mixing is allowed, the 95% confidence-level interval is  $(-2.8 < A_D < 4.9) \times 10^{-3}$ .

<sup>4</sup> This GODANG 00 result assumes no  $D^0$ - $\bar{D}^0$  mixing; it becomes  $-0.01_{-0.17}^{+0.16} \pm 0.01$  when mixing is allowed.

<sup>5</sup> This LI 05A result allows mixing.

$A_{CP}(K^\mp \pi^\pm \pi^0)$  in  $D^0 \rightarrow K^- \pi^+ \pi^0, \bar{D}^0 \rightarrow K^+ \pi^- \pi^0$

VALUE (%)	DOCUMENT ID	TECN	COMMENT
$0.2 \pm 0.9$ OUR AVERAGE			
$+0.2 \pm 0.4 \pm 0.8$	DOBBS	07	CLEO $e^+ e^-$ at $\psi(3770)$
$-3.1 \pm 8.6$	<sup>1</sup> KOPP	01	CLE2 $e^+ e^- \approx 10.6$ GeV
<sup>1</sup> KOPP 01 fits separately the $D^0$ and $\bar{D}^0$ Dalitz plots and then calculates the integrated difference of normalized densities divided by the integrated sum.			

$A_{CP}(K^\pm \pi^\mp \pi^0)$  in  $D^0 \rightarrow K^+ \pi^- \pi^0, \bar{D}^0 \rightarrow K^- \pi^+ \pi^0$

VALUE (%)	EVTS	DOCUMENT ID	TECN	COMMENT
$0 \pm 5$ OUR AVERAGE				
$-0.6 \pm 5.3$	1978 ± 104	TIAN	05	BELL $e^+ e^- \approx \Upsilon(4S)$
$+9 \pm 25$	38	BRANDENB...	01	CLE2 $e^+ e^- \approx \Upsilon(4S)$

$A_{CP}(K_S^0 \pi^+ \pi^-)$  in  $D^0, \bar{D}^0 \rightarrow K_S^0 \pi^+ \pi^-$

VALUE (%)	EVTS	DOCUMENT ID	TECN	COMMENT
$-0.9 \pm 2.1 \pm 1.6$	4854	<sup>1</sup> ASNER	04A	CLEO $e^+ e^- \approx 10$ GeV

<sup>1</sup> This is the overall result of ASNER 04A; CP-violating limits are also given below for each of the 10 resonant submodes found in an amplitude analysis of the  $D^0$  and  $\bar{D}^0 \rightarrow K_S^0 \pi^+ \pi^-$  Dalitz plots. These limits range from  $< 3.5 \times 10^{-4}$  to  $28.4 \times 10^{-4}$  at 95% CL.

$A_{CP}(K^*(892)^\mp \pi^\pm \rightarrow K_S^0 \pi^+ \pi^-)$  in  $D^0 \rightarrow K^* \pi^+, \bar{D}^0 \rightarrow K^* \pi^-$

VALUE (units $10^{-4}$ )	CL%	DOCUMENT ID	TECN	COMMENT
$< 3.5$	95	<sup>1</sup> ASNER	04A	CLEO Dalitz fit, 4854 $D^0 + \bar{D}^0$ evts
<sup>1</sup> This ASNER 04A limit comes from an amplitude analysis of the $D^0$ and $\bar{D}^0 \rightarrow K_S^0 \pi^+ \pi^-$ Dalitz plots.				

$A_{CP}(K^*(892)^\pm \pi^\mp \rightarrow K_S^0 \pi^+ \pi^-)$  in  $D^0 \rightarrow K^* \pi^-, \bar{D}^0 \rightarrow K^* \pi^+$

VALUE (units $10^{-4}$ )	CL%	DOCUMENT ID	TECN	COMMENT
$< 7.8$	95	<sup>1</sup> ASNER	04A	CLEO Dalitz fit, 4854 $D^0 + \bar{D}^0$ evts
<sup>1</sup> This ASNER 04A limit comes from an amplitude analysis of the $D^0$ and $\bar{D}^0 \rightarrow K_S^0 \pi^+ \pi^-$ Dalitz plots.				

$A_{CP}(K_S^0 \rho^0 \rightarrow K_S^0 \pi^+ \pi^-)$  in  $D^0 \rightarrow \bar{K}^0 \rho^0, \bar{D}^0 \rightarrow K^0 \rho^0$

VALUE (units $10^{-4}$ )	CL%	DOCUMENT ID	TECN	COMMENT
$< 4.8$	95	<sup>1</sup> ASNER	04A	CLEO Dalitz fit, 4854 $D^0 + \bar{D}^0$ evts
<sup>1</sup> This ASNER 04A limit comes from an amplitude analysis of the $D^0$ and $\bar{D}^0 \rightarrow K_S^0 \pi^+ \pi^-$ Dalitz plots.				

$A_{CP}(K_S^0 \omega \rightarrow K_S^0 \pi^+ \pi^-)$  in  $D^0 \rightarrow \bar{K}^0 \omega, \bar{D}^0 \rightarrow K^0 \omega$

VALUE (units $10^{-4}$ )	CL%	DOCUMENT ID	TECN	COMMENT
$< 9.2$	95	<sup>1</sup> ASNER	04A	CLEO Dalitz fit, 4854 $D^0 + \bar{D}^0$ evts
<sup>1</sup> This ASNER 04A limit comes from an amplitude analysis of the $D^0$ and $\bar{D}^0 \rightarrow K_S^0 \pi^+ \pi^-$ Dalitz plots.				

$A_{CP}(K_S^0 f_0(980) \rightarrow K_S^0 \pi^+ \pi^-)$  in  $D^0 \rightarrow \bar{K}^0 f_0(980), \bar{D}^0 \rightarrow K^0 f_0(980)$

VALUE (units $10^{-4}$ )	CL%	DOCUMENT ID	TECN	COMMENT
$< 6.8$	95	<sup>1</sup> ASNER	04A	CLEO Dalitz fit, 4854 $D^0 + \bar{D}^0$ evts
<sup>1</sup> This ASNER 04A limit comes from an amplitude analysis of the $D^0$ and $\bar{D}^0 \rightarrow K_S^0 \pi^+ \pi^-$ Dalitz plots.				

$A_{CP}(K_S^0 f_2(1270) \rightarrow K_S^0 \pi^+ \pi^-)$  in  $D^0 \rightarrow \bar{K}^0 f_2(1270), \bar{D}^0 \rightarrow K^0 f_2(1270)$

VALUE (units $10^{-4}$ )	CL%	DOCUMENT ID	TECN	COMMENT
$< 13.5$	95	<sup>1</sup> ASNER	04A	CLEO Dalitz fit, 4854 $D^0 + \bar{D}^0$ evts
<sup>1</sup> This ASNER 04A limit comes from an amplitude analysis of the $D^0$ and $\bar{D}^0 \rightarrow K_S^0 \pi^+ \pi^-$ Dalitz plots.				

$A_{CP}(K_S^0 f_0(1370) \rightarrow K_S^0 \pi^+ \pi^-)$  in  $D^0 \rightarrow \bar{K}^0 f_0(1370), \bar{D}^0 \rightarrow K^0 f_0(1370)$

VALUE (units $10^{-4}$ )	CL%	DOCUMENT ID	TECN	COMMENT
$< 25.5$	95	<sup>1</sup> ASNER	04A	CLEO Dalitz fit, 4854 $D^0 + \bar{D}^0$ evts
<sup>1</sup> This ASNER 04A limit comes from an amplitude analysis of the $D^0$ and $\bar{D}^0 \rightarrow K_S^0 \pi^+ \pi^-$ Dalitz plots.				

$A_{CP}(K_0^*(1430)^\mp \pi^\pm \rightarrow K_S^0 \pi^+ \pi^-)$  in  $D^0 \rightarrow K_0^*(1430)^- \pi^+, \bar{D}^0 \rightarrow K_0^*(1430)^+ \pi^-$

VALUE (units $10^{-4}$ )	CL%	DOCUMENT ID	TECN	COMMENT
$< 9.0$	95	<sup>1</sup> ASNER	04A	CLEO Dalitz fit, 4854 $D^0 + \bar{D}^0$ evts
<sup>1</sup> This ASNER 04A limit comes from an amplitude analysis of the $D^0$ and $\bar{D}^0 \rightarrow K_S^0 \pi^+ \pi^-$ Dalitz plots.				

Meson Particle Listings

D<sup>0</sup>

A<sub>CP</sub>(K<sub>S</sub><sup>0</sup>(1430)<sup>±</sup>π<sup>±</sup> → K<sub>S</sub><sup>0</sup>π<sup>±</sup>π<sup>-</sup>) in D<sup>0</sup> → K<sub>S</sub><sup>0</sup>(1430)<sup>-</sup>π<sup>+</sup>, D<sup>0</sup> → K<sub>S</sub><sup>0</sup>(1430)<sup>+</sup>π<sup>-</sup>

Table with columns: VALUE (units 10<sup>-4</sup>), CL%, DOCUMENT ID, TECN, COMMENT. Value <6.5, CL% 95, ASNER 04A CLEO Dalitz fit, 4854 D<sup>0</sup>+D<sup>0</sup> epts. Comment: This ASNER 04A limit comes from an amplitude analysis of the D<sup>0</sup> and D<sup>0</sup> → K<sub>S</sub><sup>0</sup>π<sup>+</sup>π<sup>-</sup> Dalitz plots.

A<sub>CP</sub>(K\*(1680)<sup>±</sup>π<sup>±</sup> → K<sub>S</sub><sup>0</sup>π<sup>±</sup>π<sup>-</sup>) in D<sup>0</sup> → K\*(1680)<sup>-</sup>π<sup>+</sup>, D<sup>0</sup> → K\*(1680)<sup>+</sup>π<sup>-</sup>

Table with columns: VALUE (units 10<sup>-4</sup>), CL%, DOCUMENT ID, TECN, COMMENT. Value <28.4, CL% 95, ASNER 04A CLEO Dalitz fit, 4854 D<sup>0</sup>+D<sup>0</sup> epts. Comment: This ASNER 04A limit comes from an amplitude analysis of the D<sup>0</sup> and D<sup>0</sup> → K<sub>S</sub><sup>0</sup>π<sup>+</sup>π<sup>-</sup> Dalitz plots.

A<sub>CP</sub>(K<sup>-</sup>π<sup>+</sup>π<sup>+</sup>π<sup>-</sup>) in D<sup>0</sup> → K<sup>-</sup>π<sup>+</sup>π<sup>+</sup>π<sup>-</sup>, D<sup>0</sup> → K<sup>+</sup>π<sup>-</sup>π<sup>-</sup>π<sup>+</sup>

Table with columns: VALUE (%), DOCUMENT ID, TECN, COMMENT. Value +0.7±0.5±0.9, DOBBS 07 CLEO e<sup>+</sup>e<sup>-</sup> at ψ(3770)

A<sub>CP</sub>(K<sup>±</sup>π<sup>∓</sup>π<sup>±</sup>π<sup>-</sup>) in D<sup>0</sup> → K<sup>±</sup>π<sup>-</sup>π<sup>±</sup>π<sup>-</sup>, D<sup>0</sup> → K<sup>-</sup>π<sup>+</sup>π<sup>±</sup>π<sup>-</sup>

Table with columns: VALUE (%), EVTS, DOCUMENT ID, TECN, COMMENT. Value -1.8±4.4, EVTS 1721 ± 75, TIAN 05 BELL e<sup>+</sup>e<sup>-</sup> ≈ T(45)

A<sub>CP</sub>(K<sup>+</sup>K<sup>-</sup>π<sup>+</sup>π<sup>-</sup>) in D<sup>0</sup>, D<sup>0</sup> → K<sup>+</sup>K<sup>-</sup>π<sup>+</sup>π<sup>-</sup>

Table with columns: VALUE (%), EVTS, DOCUMENT ID, TECN, COMMENT. Value -8.2±5.6±4.7, EVTS 828 ± 46, LINK 05E FOCS γ A, E<sub>γ</sub> ≈ 180 GeV

D<sup>0</sup> CP-VIOLATING ASYMMETRY DIFFERENCES

ΔA<sub>CP</sub> = A<sub>CP</sub>(K<sup>+</sup>K<sup>-</sup>) - A<sub>CP</sub>(π<sup>+</sup>π<sup>-</sup>)

CP violation in these modes can come from the decay amplitudes (direct) and/or from mixing or interference of mixing and decay (indirect). The difference ΔA<sub>CP</sub> is primarily sensitive to the direct component, and only retains a second-order dependence on the indirect component for measurements where the mean decay time of the K<sup>+</sup>K<sup>-</sup> and π<sup>+</sup>π<sup>-</sup> samples are not identical. The results below are averaged assuming the indirect component can be neglected.

Table with columns: VALUE (%), EVTS, DOCUMENT ID, TECN, COMMENT. Value -0.65 ± 0.18 OUR AVERAGE. Data points from AAIJ, AALTONEN, AUBERT, STARIC.

Calculated from the AUBERT 08M values of A<sub>CP</sub>(K<sup>+</sup>K<sup>-</sup>) and A<sub>CP</sub>(π<sup>+</sup>π<sup>-</sup>). The systematic error here combines the systematic errors in quadrature, and therefore somewhat over-estimates it.

D<sup>0</sup>-D<sup>0</sup> T-VIOLATING DECAY-RATE ASYMMETRIES

D<sup>0</sup> and D<sup>0</sup> are distinguished by the charge of the parent D\*: D<sup>+</sup> → D<sup>0</sup>π<sup>+</sup> and D<sup>+</sup> → D<sup>0</sup>π<sup>-</sup>. Assuming CPT is good, T violation implies CP violation.

A<sub>Tviol</sub>(K<sup>+</sup>K<sup>-</sup>π<sup>+</sup>π<sup>-</sup>) in D<sup>0</sup>, D<sup>0</sup> → K<sup>+</sup>K<sup>-</sup>π<sup>+</sup>π<sup>-</sup>

C<sub>T</sub> ≡  $\vec{p}_{K^+} \cdot (\vec{p}_{\pi^+} \times \vec{p}_{\pi^-})$  is a T-odd correlation of the K<sup>+</sup>, π<sup>+</sup>, and π<sup>-</sup> momenta (evaluated in the D<sup>0</sup> rest frame) for the D<sup>0</sup>. C<sub>T</sub> ≡  $\vec{p}_{K^-} \cdot (\vec{p}_{\pi^-} \times \vec{p}_{\pi^+})$  is the corresponding quantity for the D<sup>0</sup>. A<sub>T</sub> ≡ [Γ(C<sub>T</sub> > 0) - Γ(C<sub>T</sub> < 0)] / [Γ(C<sub>T</sub> > 0) + Γ(C<sub>T</sub> < 0)] would, in the absence of strong phases, test for T violation in D<sup>0</sup> decays (the Γ's are partial widths). With A<sub>T</sub> ≡ [Γ(-C<sub>T</sub> > 0) - Γ(-C<sub>T</sub> < 0)] / [Γ(-C<sub>T</sub> > 0) + Γ(-C<sub>T</sub> < 0)], the asymmetry A<sub>Tviol</sub> ≡ 1/2(A<sub>T</sub> - A<sub>T</sub>) tests for T violation even with nonzero strong phases.

Table with columns: VALUE (units 10<sup>-3</sup>), EVTS, DOCUMENT ID, TECN, COMMENT. Value +1.0 ± 5.1 ± 4.4, EVTS 47k, DEL-AMO-SA...10 BABR e<sup>+</sup>e<sup>-</sup> ≈ 10.6 GeV. Comment: We do not use the following data for averages, fits, limits, etc.

D<sup>0</sup> CPT-VIOLATING DECAY-RATE ASYMMETRIES

A<sub>CP T</sub>(K<sup>±</sup>π<sup>±</sup>) in D<sup>0</sup> → K<sup>-</sup>π<sup>±</sup>, D<sup>0</sup> → K<sup>+</sup>π<sup>-</sup>

A<sub>CP T</sub>(t) is defined in terms of the time-dependent decay probabilities P(D<sup>0</sup> → K<sup>-</sup>π<sup>±</sup>) and P(D<sup>0</sup> → K<sup>+</sup>π<sup>-</sup>) by A<sub>CP T</sub>(t) = (P - P)/(P + P). For small mixing parameters x ≡ Δm/Γ and y ≡ ΔΓ/2Γ (as is the case), and times t, A<sub>CP T</sub>(t) reduces to [y Re ξ - x Im ξ] / Γ, where ξ is the CPT-violating parameter.

The following is actually y Re ξ - x Im ξ.

Table with columns: VALUE, DOCUMENT ID, TECN, COMMENT. Value 0.0083 ± 0.0065 ± 0.0041, LINK 03B FOCS γ nucleus, E<sub>γ</sub> ≈ 180 GeV

D<sup>0</sup> → K\*(892)<sup>-</sup>ℓ<sup>+</sup>ν<sub>ℓ</sub> FORM FACTORS

r<sub>V</sub> ≡ V(0)/A<sub>1</sub>(0) in D<sup>0</sup> → K\*(892)<sup>-</sup>ℓ<sup>+</sup>ν<sub>ℓ</sub>

Table with columns: VALUE, DOCUMENT ID, TECN, COMMENT. Value 1.71 ± 0.68 ± 0.34, LINK 05B FOCS K\*(892)<sup>-</sup>μ<sup>+</sup>ν<sub>μ</sub>

r<sub>2</sub> ≡ A<sub>2</sub>(0)/A<sub>1</sub>(0) in D<sup>0</sup> → K\*(892)<sup>-</sup>ℓ<sup>+</sup>ν<sub>ℓ</sub>

Table with columns: VALUE, DOCUMENT ID, TECN, COMMENT. Value 0.91 ± 0.37 ± 0.10, LINK 05B FOCS K\*(892)<sup>-</sup>μ<sup>+</sup>ν<sub>μ</sub>

D<sup>0</sup> → K<sup>-</sup>/π<sup>-</sup>ℓ<sup>+</sup>ν<sub>ℓ</sub> FORM FACTORS

f<sub>+</sub>(0) in D<sup>0</sup> → K<sup>-</sup>ℓ<sup>+</sup>ν<sub>ℓ</sub>

Table with columns: VALUE, DOCUMENT ID, TECN, COMMENT. Value 0.727 ± 0.007 ± 0.009, AUBERT 07BG BABR K<sup>-</sup>e<sup>+</sup>ν<sub>e</sub> 2-parameter fit

f<sub>+</sub>(0)|V<sub>cb</sub> in D<sup>0</sup> → K<sup>-</sup>ℓ<sup>+</sup>ν<sub>ℓ</sub>

Table with columns: VALUE, DOCUMENT ID, TECN, COMMENT. Value 0.726 ± 0.008 ± 0.004, BESSON 09 CLEO K<sup>-</sup>e<sup>+</sup>ν<sub>e</sub> 3-parameter fit

r<sub>1</sub> ≡ a<sub>1</sub>/a<sub>0</sub> in D<sup>0</sup> → K<sup>-</sup>ℓ<sup>+</sup>ν<sub>ℓ</sub>

Table with columns: VALUE, DOCUMENT ID, TECN, COMMENT. Value -2.65 ± 0.34 ± 0.08, BESSON 09 CLEO K<sup>-</sup>e<sup>+</sup>ν<sub>e</sub> 3-parameter fit

r<sub>2</sub> ≡ a<sub>1</sub>/a<sub>0</sub> in D<sup>0</sup> → K<sup>-</sup>ℓ<sup>+</sup>ν<sub>ℓ</sub>

Table with columns: VALUE, DOCUMENT ID, TECN, COMMENT. Value 13 ± 9 ± 1, BESSON 09 CLEO K<sup>-</sup>e<sup>+</sup>ν<sub>e</sub> 3-parameter fit

f<sub>+</sub>(0)|V<sub>cd</sub> in D<sup>0</sup> → π<sup>-</sup>ℓ<sup>+</sup>ν<sub>ℓ</sub>

Table with columns: VALUE, DOCUMENT ID, TECN, COMMENT. Value 0.152 ± 0.005 ± 0.001, BESSON 09 CLEO π<sup>-</sup>e<sup>+</sup>ν<sub>e</sub> 3-parameter fit

r<sub>1</sub> ≡ a<sub>1</sub>/a<sub>0</sub> in D<sup>0</sup> → π<sup>-</sup>ℓ<sup>+</sup>ν<sub>ℓ</sub>

Table with columns: VALUE, DOCUMENT ID, TECN, COMMENT. Value -2.80 ± 0.49 ± 0.04, BESSON 09 CLEO π<sup>-</sup>e<sup>+</sup>ν<sub>e</sub> 3-parameter fit

r<sub>2</sub> ≡ a<sub>1</sub>/a<sub>0</sub> in D<sup>0</sup> → π<sup>-</sup>ℓ<sup>+</sup>ν<sub>ℓ</sub>

Table with columns: VALUE, DOCUMENT ID, TECN, COMMENT. Value 6 ± 3 ± 0, BESSON 09 CLEO π<sup>-</sup>e<sup>+</sup>ν<sub>e</sub> 3-parameter fit

D<sup>0</sup> REFERENCES

List of references for D<sup>0</sup> decays, including AAIJ, AALTONEN, AUBERT, BESSON, STARIC, and others. Includes collaboration names like LHCb, Belle, and BABAR.



## Meson Particle Listings

 $D^*(2007)^0$ ,  $D^*(2010)^\pm$ 

<sup>2</sup>From simultaneous fit to  $D^*(2010)^+$ ,  $D^*(2007)^0$ ,  $D^+$ , and  $D^0$ .

 $D^*(2007)^0$  WIDTH

VALUE (MeV)	CL%	DOCUMENT ID	TECN	COMMENT
<2.1	90	<sup>3</sup> ABACHI	88B HRS	$D^{*0} \rightarrow D^+ \pi^-$

<sup>3</sup>Assuming  $m_{D^{*0}} = 2007.2 \pm 2.1$  MeV/ $c^2$ .

 $D^*(2007)^0$  DECAY MODES

$\bar{D}^*(2007)^0$  modes are charge conjugates of modes below.

Mode	Fraction ( $\Gamma_i/\Gamma$ )
$\Gamma_1$ $D^0 \pi^0$	(61.9±2.9) %
$\Gamma_2$ $D^0 \gamma$	(38.1±2.9) %

## CONSTRAINED FIT INFORMATION

An overall fit to a branching ratio uses 3 measurements and one constraint to determine 2 parameters. The overall fit has a  $\chi^2 = 0.5$  for 2 degrees of freedom.

The following *off-diagonal* array elements are the correlation coefficients  $\langle \delta x_i \delta x_j \rangle / (\delta x_i \delta x_j)$ , in percent, from the fit to the branching fractions,  $x_i \equiv \Gamma_i/\Gamma_{\text{total}}$ . The fit constrains the  $x_i$  whose labels appear in this array to sum to one.

$$x_2 \begin{vmatrix} -100 \\ x_1 \end{vmatrix}$$

 $D^*(2007)^0$  BRANCHING RATIOS

$\Gamma(D^0 \pi^0)/\Gamma(D^0 \gamma)$	$\Gamma_1/\Gamma_2$		
VALUE	DOCUMENT ID	TECN	COMMENT
<b>1.74±0.02±0.13</b>	AUBERT,BE	05G BABR	10.6 $e^+ e^- \rightarrow$ hadrons

$\Gamma(D^0 \pi^0)/\Gamma_{\text{total}}$	$\Gamma_1/\Gamma$			
VALUE	EVTS	DOCUMENT ID	TECN	COMMENT
<b>0.619±0.029 OUR FIT</b>				

• • • We do not use the following data for averages, fits, limits, etc. • • •

0.635±0.003±0.017	69k	<sup>4</sup> AUBERT,BE	05G BABR	10.6 $e^+ e^- \rightarrow$ hadrons
0.596±0.035±0.028	858	<sup>5</sup> ALBRECHT	95F ARG	$e^+ e^- \rightarrow$ hadrons
0.636±0.023±0.033	1097	<sup>5</sup> BUTLER	92 CLE2	$e^+ e^- \rightarrow$ hadrons

$\Gamma(D^0 \gamma)/\Gamma_{\text{total}}$	$\Gamma_2/\Gamma$			
VALUE	EVTS	DOCUMENT ID	TECN	COMMENT
<b>0.381±0.029 OUR FIT</b>				
<b>0.381±0.029 OUR AVERAGE</b>				

0.404±0.035±0.028	456	<sup>5</sup> ALBRECHT	95F ARG	$e^+ e^- \rightarrow$ hadrons
0.364±0.023±0.033	621	<sup>5</sup> BUTLER	92 CLE2	$e^+ e^- \rightarrow$ hadrons
0.37 ± 0.08 ± 0.08		ADLER	88D MRK3	$e^+ e^-$

• • • We do not use the following data for averages, fits, limits, etc. • • •

0.365±0.003±0.017	68k	<sup>4</sup> AUBERT,BE	05G BABR	10.6 $e^+ e^- \rightarrow$ hadrons
0.47 ± 0.23		LOW	87 HRS	29 GeV $e^+ e^-$
0.53 ± 0.13		BARTEL	85G JADE	$e^+ e^-$ , hadrons
0.47 ± 0.12		COLES	82 MRK2	$e^+ e^-$
0.45 ± 0.15		GOLDHABER	77 MRK1	$e^+ e^-$

<sup>4</sup>Derived from the ratio  $\Gamma(D^0 \pi^0) / \Gamma(D^0 \gamma)$  assuming that the branching fractions of  $D^{*0} \rightarrow D^0 \pi^0$  and  $D^{*0} \rightarrow D^0 \gamma$  decays sum to 100%

<sup>5</sup>The BUTLER 92 and ALBRECHT 95F branching ratios are not independent, they have been constrained by the authors to sum to 100%.

 $D^*(2007)^0$  REFERENCES

AUBERT,BE	05G	PR D72 091101	B. Aubert <i>et al.</i>	(BABAR Collab.)
ALBRECHT	95F	ZPHY C66 63	H. Albrecht <i>et al.</i>	(ARGUS Collab.)
BORTOLETTO	92B	PRL 69 2046	D. Bortoletto <i>et al.</i>	(CLEO Collab.)
BUTLER	92	PRL 69 2041	F. Butler <i>et al.</i>	(CLEO Collab.)
ABACHI	88B	PL B212 533	S. Abachi <i>et al.</i>	(ANL, IND, MICH, PURD+)
ADLER	88D	PL B208 152	J. Adler <i>et al.</i>	(Mark III Collab.)
LOW	87	PL B183 232	E.H. Low <i>et al.</i>	(HRS Collab.)
BARTEL	85G	PL 161B 197	W. Bartel <i>et al.</i>	(JADE Collab.)
COLES	82	PR D26 2190	M.W. Coles <i>et al.</i>	(LBL, SLAC)
SADROZINSKI	80	Madison Conf. 681	H.F.W. Sadrozinski <i>et al.</i>	(PRIN, CIT+)
GOLDHABER	77	PL 69B 503	G. Goldhaber <i>et al.</i>	(Mark I Collab.)
NGUYEN	77	PRL 39 262	H.K. Nguyen <i>et al.</i>	(LBL, SLAC)J

 $D^*(2010)^\pm$ 

$I(J^P) = \frac{1}{2}(1^-)$   
I, J, P need confirmation.

 $D^*(2010)^\pm$  MASS

The fit includes  $D^\pm$ ,  $D^0$ ,  $D_s^\pm$ ,  $D^{*±}$ ,  $D^{*0}$ ,  $D_s^{*±}$ ,  $D_1(2420)^0$ ,  $D_2^*(2460)^0$ , and  $D_{s1}(2536)^\pm$  mass and mass difference measurements.

VALUE (MeV)	DOCUMENT ID	TECN	CHG	COMMENT
<b>2010.28±0.13 OUR FIT</b>				

• • • We do not use the following data for averages, fits, limits, etc. • • •

2008 ± 3	<sup>1</sup> GOLDHABER	77 MRK1	±	$e^+ e^-$
2008.6 ± 1.0	<sup>2</sup> PERUZZI	77 LGW	±	$e^+ e^-$

<sup>1</sup>From simultaneous fit to  $D^*(2010)^+$ ,  $D^*(2007)^0$ ,  $D^+$ , and  $D^0$ ; not independent of FELDMAN 77B mass difference below.

<sup>2</sup>PERUZZI 77 mass not independent of FELDMAN 77B mass difference below and PERUZZI 77  $D^0$  mass value.

 $m_{D^*(2010)^+} - m_{D^+}$ 

The fit includes  $D^\pm$ ,  $D^0$ ,  $D_s^\pm$ ,  $D^{*±}$ ,  $D^{*0}$ ,  $D_s^{*±}$ ,  $D_1(2420)^0$ ,  $D_2^*(2460)^0$ , and  $D_{s1}(2536)^\pm$  mass and mass difference measurements.

VALUE (MeV)	EVTS	DOCUMENT ID	TECN	COMMENT
<b>140.66±0.10 OUR FIT</b>				Error includes scale factor of 1.1.
<b>140.64±0.08±0.06</b>	620	BORTOLETTO92B	CLE2	$e^+ e^- \rightarrow$ hadrons

 $m_{D^*(2010)^+} - m_{D^0}$ 

The fit includes  $D^\pm$ ,  $D^0$ ,  $D_s^\pm$ ,  $D^{*±}$ ,  $D^{*0}$ ,  $D_s^{*±}$ ,  $D_1(2420)^0$ ,  $D_2^*(2460)^0$ , and  $D_{s1}(2536)^\pm$  mass and mass difference measurements.

VALUE (MeV)	EVTS	DOCUMENT ID	TECN	COMMENT
<b>145.421±0.010 OUR FIT</b>				Error includes scale factor of 1.1.
<b>145.421±0.010 OUR AVERAGE</b>				

145.412±0.002±0.012		ANASTASSOV	02 CLE2	$D^{*±} \rightarrow D^0 \pi^\pm \rightarrow (K\pi)\pi^\pm$
145.54 ± 0.08	611	<sup>3</sup> ADINOLFI	99 BEAT	$D^{*±} \rightarrow D^0 \pi^\pm$
145.45 ± 0.02		<sup>3</sup> BREITWEG	99 ZEUS	$D^{*±} \rightarrow D^0 \pi^\pm \rightarrow (K\pi)\pi^\pm$
145.42 ± 0.05		<sup>3</sup> BREITWEG	99 ZEUS	$D^{*±} \rightarrow D^0 \pi^\pm \rightarrow (K^* 3\pi)\pi^\pm$
145.5 ± 0.15	103	<sup>4</sup> ADLOFF	97B H1	$D^{*±} \rightarrow D^0 \pi^\pm$
145.44 ± 0.08	152	<sup>4</sup> BREITWEG	97 ZEUS	$D^{*±} \rightarrow D^0 \pi^\pm$
145.42 ± 0.11	199	<sup>4</sup> BREITWEG	97 ZEUS	$D^{*±} \rightarrow D^0 \pi^\pm$
145.4 ± 0.2	48	<sup>4</sup> DERRICK	95 ZEUS	$D^{*±} \rightarrow D^0 \pi^\pm$
145.39 ± 0.06 ± 0.03		BARLAG	92B ACCM	$\pi^- 230$ GeV
145.5 ± 0.2	115	<sup>4</sup> ALEXANDER	91B OPAL	$D^{*±} \rightarrow D^0 \pi^\pm$
145.30 ± 0.06		<sup>4</sup> DECAAMP	91J ALEP	$D^{*±} \rightarrow D^0 \pi^\pm$
145.40 ± 0.05 ± 0.10		ABACHI	88B HRS	$D^{*±} \rightarrow D^0 \pi^\pm$
145.46 ± 0.07 ± 0.03		ALBRECHT	85F ARG	$D^{*±} \rightarrow D^0 \pi^\pm$
145.5 ± 0.3	28	BAILEY	83 SPEC	$D^{*±} \rightarrow D^0 \pi^\pm$
145.5 ± 0.3	60	FITCH	81 SPEC	$\pi^- A$
145.3 ± 0.5	30	FELDMAN	77B MRK1	$D^{*+} \rightarrow D^0 \pi^+$
• • • We do not use the following data for averages, fits, limits, etc. • • •				
145.44 ± 0.09	122	<sup>4</sup> BREITWEG	97B ZEUS	$D^{*±} \rightarrow D^0 \pi^\pm$
145.8 ± 1.5	16	AHLEN	83 HRS	$D^{*+} \rightarrow D^0 \pi^+$
145.1 ± 1.8	12	BAILEY	83 SPEC	$D^{*±} \rightarrow D^0 \pi^\pm$
145.1 ± 0.5	14	BAILEY	83 SPEC	$D^{*±} \rightarrow D^0 \pi^\pm$
145.5 ± 0.5	14	YELTON	82 MRK2	29 $e^+ e^- \rightarrow K^- \pi^+$
~ 145.5		• • •		
145.2 ± 0.6	2	BLIETSCHAU	79 BEBC	$\nu p$

<sup>3</sup>Statistical errors only.  
<sup>4</sup>Systematic error not evaluated.

 $m_{D^*(2010)^+} - m_{D^*(2007)^0}$ 

VALUE (MeV)	DOCUMENT ID	TECN	COMMENT
• • • We do not use the following data for averages, fits, limits, etc. • • •			

2.6±1.8	<sup>5</sup> PERUZZI	77 LGW	$e^+ e^-$
---------	----------------------	--------	-----------

<sup>5</sup>Not independent of FELDMAN 77B mass difference above, PERUZZI 77  $D^0$  mass, and GOLDHABER 77  $D^*(2007)^0$  mass.

 $D^*(2010)^\pm$  WIDTH

VALUE (keV)	CL%	EVTS	DOCUMENT ID	TECN	COMMENT
<b>96±4±22</b>			ANASTASSOV	02 CLE2	$D^{*±} \rightarrow D^0 \pi^\pm \rightarrow (K\pi)\pi^\pm$

• • • We do not use the following data for averages, fits, limits, etc. • • •

<131	90	110	BARLAG	92B ACCM	$\pi^- 230$ GeV
------	----	-----	--------	----------	-----------------

See key on page 457

Meson Particle Listings

$D^*(2010)^\pm, D_0^*(2400)^0, D_0^*(2400)^\pm$

$D^*(2010)^\pm$  DECAY MODES

$D^*(2010)^\pm$  modes are charge conjugates of the modes below.

Mode	Fraction ( $\Gamma_i/\Gamma$ )
$\Gamma_1 D^0 \pi^+$	(67.7±0.5) %
$\Gamma_2 D^+ \pi^0$	(30.7±0.5) %
$\Gamma_3 D^+ \gamma$	(1.6±0.4) %

CONSTRAINED FIT INFORMATION

An overall fit to 3 branching ratios uses 6 measurements and one constraint to determine 3 parameters. The overall fit has a  $\chi^2 = 0.3$  for 4 degrees of freedom.

The following *off-diagonal* array elements are the correlation coefficients  $\langle \delta x_i \delta x_j \rangle / (\delta x_i \delta x_j)$ , in percent, from the fit to the branching fractions,  $x_i \equiv \Gamma_i/\Gamma_{\text{total}}$ . The fit constrains the  $x_i$  whose labels appear in this array to sum to one.

$x_2$	-62	
$x_3$	-43	-44
	$x_1$	$x_2$

$D^*(2010)^+$  BRANCHING RATIOS

$\Gamma(D^0 \pi^+)/\Gamma_{\text{total}}$	$\Gamma_1/\Gamma$
<b>0.677 ± 0.005 OUR FIT</b>	
<b>0.677 ± 0.006 OUR AVERAGE</b>	
0.6759 ± 0.0029 ± 0.0064	6,7,8 BARTELT 98 CLE2 $e^+ e^-$
0.688 ± 0.024 ± 0.013	ALBRECHT 95F ARG $e^+ e^- \rightarrow$ hadrons
0.681 ± 0.010 ± 0.013	6 BUTLER 92 CLE2 $e^+ e^- \rightarrow$ hadrons
• • • We do not use the following data for averages, fits, limits, etc. • • •	
0.57 ± 0.04 ± 0.04	ADLER 88D MRK3 $e^+ e^-$
0.44 ± 0.10	COLES 82 MRK2 $e^+ e^-$
0.6 ± 0.15	8 GOLDHABER 77 MRK1 $e^+ e^-$

$\Gamma(D^+ \pi^0)/\Gamma_{\text{total}}$	$\Gamma_2/\Gamma$
<b>0.307 ± 0.005 OUR FIT</b>	
<b>0.3073 ± 0.0013 ± 0.0062</b>	
• • • We do not use the following data for averages, fits, limits, etc. • • •	
0.312 ± 0.011 ± 0.008	1404 ALBRECHT 95F ARG $e^+ e^- \rightarrow$ hadrons
0.308 ± 0.004 ± 0.008	6 BUTLER 92 CLE2 $e^+ e^- \rightarrow$ hadrons
0.26 ± 0.02 ± 0.02	ADLER 88D MRK3 $e^+ e^-$
0.34 ± 0.07	COLES 82 MRK2 $e^+ e^-$

$\Gamma(D^+ \gamma)/\Gamma_{\text{total}}$	$\Gamma_3/\Gamma$
<b>0.016 ± 0.004 OUR FIT</b>	
<b>0.016 ± 0.005 OUR AVERAGE</b>	
0.0168 ± 0.0042 ± 0.0029	6,7 BARTELT 98 CLE2 $e^+ e^-$
0.011 ± 0.014 ± 0.016	12 6 BUTLER 92 CLE2 $e^+ e^- \rightarrow$ hadrons
• • • We do not use the following data for averages, fits, limits, etc. • • •	
<0.052	90 ALBRECHT 95F ARG $e^+ e^- \rightarrow$ hadrons
0.17 ± 0.05 ± 0.05	ADLER 88D MRK3 $e^+ e^-$
0.22 ± 0.12	9 COLES 82 MRK2 $e^+ e^-$

6 The branching ratios are not independent, they have been constrained by the authors to sum to 100%.  
 7 Systematic error includes theoretical error on the prediction of the ratio of hadronic modes.  
 8 Assuming that isospin is conserved in the decay.  
 9 Not independent of  $\Gamma(D^0 \pi^+)/\Gamma_{\text{total}}$  and  $\Gamma(D^+ \pi^0)/\Gamma_{\text{total}}$  measurement.

$D^*(2010)^\pm$  REFERENCES

ANASTASSOV 02 PR D65 032003	A. Anastassov <i>et al.</i>	(CLEO Collab.)
ADINOLFI 99 NP B547 3	M. Adinolfi <i>et al.</i>	(Batrice Collab.)
BREITWEG 99 EPJ C6 67	J. Breitweg <i>et al.</i>	(ZEUS Collab.)
BARTELT 98 PRL 80 3919	J. Bartelt <i>et al.</i>	(CLEO Collab.)
ADLOFF 97B ZPHY C72 593	C. Adloff <i>et al.</i>	(HI Collab.)
BREITWEG 97 PL B401 192	J. Breitweg <i>et al.</i>	(ZEUS Collab.)
BREITWEG 97B PL B407 402	J. Breitweg <i>et al.</i>	(ZEUS Collab.)
ALBRECHT 95F ZPHY C66 63	H. Albrecht <i>et al.</i>	(ARGUS Collab.)
DERRICK 95 PL B349 225	M. Derrick <i>et al.</i>	(ZEUS Collab.)
BARLAG 92B PL B278 480	S. Barlag <i>et al.</i>	(ACCMOR Collab.)
BORTOLETTO 92B PRL 69 2046	D. Bortoletto <i>et al.</i>	(CLEO Collab.)
BUTLER 92 PRL 69 2041	F. Butler <i>et al.</i>	(CLEO Collab.)
ALEXANDER 91B PL B262 341	G. Alexander <i>et al.</i>	(OPAL Collab.)
DECAMP 91J PL B266 218	D. Decamp <i>et al.</i>	(ALEPH Collab.)
ABACHI 85B PL B212 533	S. Abachi <i>et al.</i>	(ANL, IND, MICH, PURD+)
ADLER 88D PL B208 152	J. Adler <i>et al.</i>	(Mark III Collab.)

ALBRECHT 85F PL 150B 235	H. Albrecht <i>et al.</i>	(ARGUS Collab.)
AHLEN 83 PRL 51 1147	S.P. Ahlen <i>et al.</i>	(ANL, IND, LBL+)
BAILEY 83 PL 132B 230	R. Bailey <i>et al.</i>	(AMST, BRIS, CERN, CRAC+)
COLES 82 PR D26 2190	M.W. Coles <i>et al.</i>	(LBL, SLAC)
YELTON 82 PRL 49 430	J.M. Yelton <i>et al.</i>	(SLAC, LBL, UCB+)
FITCH 81 PRL 46 761	V.L. Fitch <i>et al.</i>	(PRIN, SACL, TORI+)
AVERY 80 PRL 44 1309	P. Avery <i>et al.</i>	(ILL, FNAL, COLU)
BLIETSCHAU 79 PL 86B 108	J. Blietschau <i>et al.</i>	(AACH3, BONN, CERN+)
FELDMAN 77B PRL 38 1313	G.J. Feldman <i>et al.</i>	(Mark I Collab.)
GOLDHABER 77 PL 69B 503	G. Goldhaber <i>et al.</i>	(Mark I Collab.)
PERUZZI 77 PRL 39 1301	I. Peruzzi <i>et al.</i>	(LGW Collab.)

$D_0^*(2400)^0$

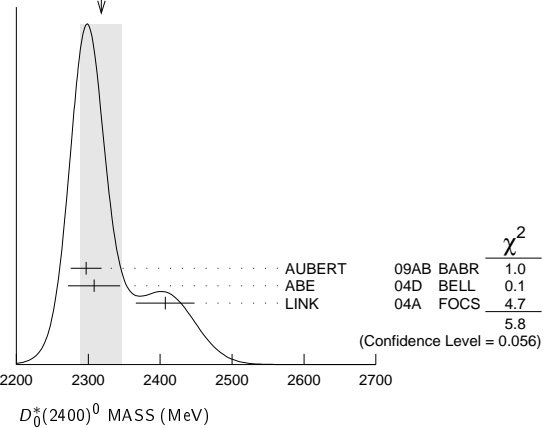
$I(J^P) = \frac{1}{2}(0^+)$

$J^P = 0^+$  assignment favored (ABE 04D).

$D_0^*(2400)^0$  MASS

VALUE (MeV)	EVTS	DOCUMENT ID	TECN	COMMENT
<b>2318 ± 29 OUR AVERAGE</b>		Error includes scale factor of 1.7. See the ideogram below.		
2297 ± 8 ± 20	3.4k	AUBERT	09AB BABR	$B^- \rightarrow D^+ \pi^- \pi^-$
2308 ± 17 ± 32		ABE	04D BELL	$B^- \rightarrow D^+ \pi^- \pi^-$
2407 ± 21 ± 35	9.8k	LINK	04A FOCS	$\gamma A$

WEIGHTED AVERAGE  
2318±29 (Error scaled by 1.7)



$D_0^*(2400)^0$  WIDTH

VALUE (MeV)	EVTS	DOCUMENT ID	TECN	COMMENT
<b>267 ± 40 OUR AVERAGE</b>				
273 ± 12 ± 48	3.4k	AUBERT	09AB BABR	$B^- \rightarrow D^+ \pi^- \pi^-$
276 ± 21 ± 63		ABE	04D BELL	$B^- \rightarrow D^+ \pi^- \pi^-$
240 ± 55 ± 59	9.8k	LINK	04A FOCS	$\gamma A$

$D_0^*(2400)^0$  DECAY MODES

Mode	Fraction ( $\Gamma_i/\Gamma$ )
$\Gamma_1 D^+ \pi^-$	seen

$D_0^*(2400)^0$  REFERENCES

AUBERT 09AB PR D79 112004	B. Aubert <i>et al.</i>	(BABAR Collab.)
ABE 04D PR D69 112002	K. Abe <i>et al.</i>	(BELLE Collab.)
LINK 04A PL B586 11	J.M. Link <i>et al.</i>	(FOCUS Collab.)

$D_0^*(2400)^\pm$

$I(J^P) = \frac{1}{2}(0^+)$

OMITTED FROM SUMMARY TABLE  
 $J, P$  need confirmation.

$D_0^*(2400)^\pm$  MASS

VALUE (MeV)	EVTS	DOCUMENT ID	TECN	COMMENT
<b>2403 ± 14 ± 35</b>	18.8k	LINK	04A FOCS	$\gamma A$

$D_0^*(2400)^\pm$  WIDTH

VALUE (MeV)	EVTS	DOCUMENT ID	TECN	COMMENT
<b>283 ± 24 ± 34</b>	18.8k	LINK	04A FOCS	$\gamma A$

# Meson Particle Listings

## $D_0^*(2400)^\pm, D_1(2420)^0$

### $D_0^*(2400)^\pm$ DECAY MODES

Mode	Fraction ( $\Gamma_i/\Gamma$ )
$\Gamma_1 D^0 \pi^+$	seen

### $D_0^*(2400)^\pm$ REFERENCES

LINK 04A PL B586 11 J.M. Link *et al.* (FOCUS Collab.)

## $D_1(2420)^0$

$I(J^P) = \frac{1}{2}(1^+)$   
I needs confirmation.

### $D_1(2420)^0$ MASS

The fit includes  $D^\pm, D^0, D_s^\pm, D^{*\pm}, D^{*0}, D_s^{*\pm}, D_1(2420)^0, D_2^*(2460)^0$ , and  $D_{s1}(2536)^\pm$  mass and mass difference measurements.

VALUE (MeV)	EVTS	DOCUMENT ID	TECN	COMMENT
<b>2421.3 ± 0.6 OUR FIT</b>				Error includes scale factor of 1.2.
<b>2420.9 ± 0.8 OUR AVERAGE</b>				Error includes scale factor of 1.2.
2420.1 ± 0.1 ± 0.8	103k	DEL-AMO-SA...10P	BABR	$e^+e^- \rightarrow D^{*+}\pi^-X$
2426 ± 3 ± 1	151	ABE	05A BELL	$B^- \rightarrow D^0\pi^+\pi^-\pi^-$
2421.4 ± 1.5 ± 0.9		<sup>1</sup> ABE	04D BELL	$B^- \rightarrow D^{*+}\pi^-\pi^-$
2421 $\pm \frac{1}{2} \pm 2$	286	AVERY	94C CLE2	$e^+e^- \rightarrow D^{*+}\pi^-X$
2422 ± 2 ± 2	51	FRABETTI	94B E687	$\gamma Be \rightarrow D^{*+}\pi^-X$
2428 ± 3 ± 2	279	AVERY	90 CLEO	$e^+e^- \rightarrow D^{*+}\pi^-X$
2414 ± 2 ± 5	171	ALBRECHT	89H ARG	$e^+e^- \rightarrow D^{*+}\pi^-X$
2428 ± 8 ± 5	171	ANJOS	89C TPS	$\gamma N \rightarrow D^{*+}\pi^-X$
• • • We do not use the following data for averages, fits, limits, etc. • • •				
2420.5 ± 2.1 ± 0.9	3110 ± 340	<sup>2</sup> CHEKANOV	09 ZEUS	$e^\pm p \rightarrow D^{*+}\pi^-X$
2421.7 ± 0.7 ± 0.6	7.5k	ABULENCIA	06A CDF	1900 $p\bar{p} \rightarrow D^{*+}\pi^-X$
2425 ± 3	235	<sup>3</sup> ABREU	98M DLPH	$e^+e^-$

<sup>1</sup> Fit includes the contribution from  $D_1^*(2430)^0$ .

<sup>2</sup> Calculated using the mass difference  $m(D_1^0) - m(D^{*+})_{PDG}$  reported below and  $m(D^{*+})_{PDG} = 2010.27 \pm 0.17$  MeV. The 0.17 MeV uncertainty of the PDG mass value should be added to the experimental uncertainty of 0.9 MeV.

<sup>3</sup> No systematic error given.

### $m_{D_1^0} - m_{D^{*+}}$

The fit includes  $D^\pm, D^0, D_s^\pm, D^{*\pm}, D^{*0}, D_s^{*\pm}, D_1(2420)^0, D_2^*(2460)^0$ , and  $D_{s1}(2536)^\pm$  mass and mass difference measurements.

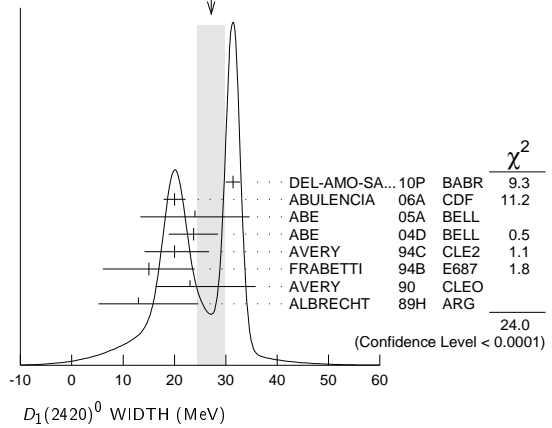
VALUE	EVTS	DOCUMENT ID	TECN	COMMENT
<b>411.0 ± 0.6 OUR FIT</b>				Error includes scale factor of 1.2.
<b>411.5 ± 0.8 OUR AVERAGE</b>				
410.2 ± 2.1 ± 0.9	3110 ± 340	CHEKANOV	09 ZEUS	$e^\pm p \rightarrow D^{*+}\pi^-X$
411.7 ± 0.7 ± 0.4	7.5k	ABULENCIA	06A CDF	1900 $p\bar{p} \rightarrow D^{*+}\pi^-X$

### $D_1(2420)^0$ WIDTH

VALUE (MeV)	EVTS	DOCUMENT ID	TECN	COMMENT
<b>27.1 ± 2.7 OUR AVERAGE</b>				Error includes scale factor of 2.4. See the ideogram below.
31.4 ± 0.5 ± 1.3	103k	DEL-AMO-SA...10P	BABR	$e^+e^- \rightarrow D^{*+}\pi^-X$
20.0 ± 1.7 ± 1.3	7.5k	ABULENCIA	06A CDF	1900 $p\bar{p} \rightarrow D^{*+}\pi^-X$
24 ± 7 ± 8	151	ABE	05A BELL	$B^- \rightarrow D^0\pi^+\pi^-\pi^-$
23.7 ± 2.7 ± 4.0		<sup>4</sup> ABE	04D BELL	$B^- \rightarrow D^{*+}\pi^-\pi^-$
20 $\pm \frac{6}{5} \pm 3$	286	AVERY	94C CLE2	$e^+e^- \rightarrow D^{*+}\pi^-X$
15 ± 8 ± 4	51	FRABETTI	94B E687	$\gamma Be \rightarrow D^{*+}\pi^-X$
23 $\pm \frac{8}{6} \pm \frac{10}{3}$	279	AVERY	90 CLEO	$e^+e^- \rightarrow D^{*+}\pi^-X$
13 ± 6 $\pm \frac{10}{5}$	171	ALBRECHT	89H ARG	$e^+e^- \rightarrow D^{*+}\pi^-X$
• • • We do not use the following data for averages, fits, limits, etc. • • •				
53.2 ± 7.2 $\pm \frac{3.3}{4.9}$	3110 ± 340	CHEKANOV	09 ZEUS	$e^\pm p \rightarrow D^{*+}\pi^-X$
58 ± 14 ± 10	171	ANJOS	89C TPS	$\gamma N \rightarrow D^{*+}\pi^-X$

<sup>4</sup> Fit includes the contribution from  $D_1^*(2430)^0$ .

WEIGHTED AVERAGE  
27.1 ± 2.7 (Error scaled by 2.4)



### $D_1(2420)^0$ DECAY MODES

$\bar{D}_1(2420)^0$  modes are charge conjugates of modes below.

Mode	Fraction ( $\Gamma_i/\Gamma$ )
$\Gamma_1 D^*(2010)^+\pi^-$	seen
$\Gamma_2 D^0\pi^+\pi^-$	seen
$\Gamma_3 D^0\rho^0$	
$\Gamma_4 D^0 f_0(500)$	
$\Gamma_5 D_0^*(2400)^+\pi^-$	
$\Gamma_6 D^+\pi^-$	not seen
$\Gamma_7 D^{*0}\pi^+\pi^-$	not seen

### $D_1(2420)^0$ BRANCHING RATIOS

$\Gamma(D^*(2010)^+\pi^-)/\Gamma_{total}$	VALUE	DOCUMENT ID	TECN	COMMENT	$\Gamma_1/\Gamma$
seen		ACKERSTAFF 97W	OPAL	$e^+e^- \rightarrow D^{*+}\pi^-X$	
seen		AVERY 90	CLEO	$e^+e^- \rightarrow D^{*+}\pi^-X$	
seen		ALBRECHT 89H	ARG	$e^+e^- \rightarrow D^{*+}\pi^-X$	
seen		ANJOS 89C	TPS	$\gamma N \rightarrow D^{*+}\pi^-X$	

$\Gamma(D^+\pi^-)/\Gamma(D^*(2010)^+\pi^-)$	VALUE	CL%	DOCUMENT ID	TECN	COMMENT	$\Gamma_6/\Gamma_1$
<0.24		90	AVERY 90	CLEO	$e^+e^- \rightarrow D^+\pi^-X$	

### $D_1(2420)^0$ POLARIZATION AMPLITUDE $A_{D_1}$

A polarization amplitude  $A_{D_1}$  is a parameter that depends on the initial polarization of the  $D_1$  and is sensitive to a possible S-wave contribution to its decay. For  $D_1$  decays the helicity angle,  $\theta_h$ , distribution varies like  $1 + A_{D_1} \cos^2\theta_h$ , where  $\theta_h$  is the angle in the  $D^*$  rest frame between the two pions emitted by the  $D_1 \rightarrow D^*\pi$  and the  $D^* \rightarrow D\pi$ .

Unpolarized  $D_1$  decaying purely via D-wave is predicted to give  $A_{D_1} = 3$ .

VALUE	EVTS	DOCUMENT ID	TECN	COMMENT
<b>5.72 ± 0.25 OUR AVERAGE</b>				
5.72 ± 0.25	103k	DEL-AMO-SA...10P	BABR	$e^+e^- \rightarrow D^{*+}\pi^-X$
5.9 $\pm \frac{3.0}{1.7} \pm \frac{2.4}{1.0}$		CHEKANOV 09	ZEUS	$e^\pm p \rightarrow D^{*+}\pi^-X$
• • • We do not use the following data for averages, fits, limits, etc. • • •				
3.8 ± 0.6 ± 0.8		<sup>5</sup> AUBERT	09Y	BABR $B^+ \rightarrow D_1^0 \ell^+ \nu_\ell$
2.74 $\pm \frac{1.40}{0.93}$		<sup>6</sup> AVERY	94C	CLE2 $e^+e^- \rightarrow D^{*+}\pi^-X$

<sup>5</sup> Assuming  $\Gamma(\Upsilon(4S) \rightarrow B^+B^-) / \Gamma(\Upsilon(4S) \rightarrow B^0\bar{B}^0) = 1.065 \pm 0.026$  and equal partial widths and helicity angle distributions for charged and neutral  $D_1$  mesons.

<sup>6</sup> Systematic uncertainties not estimated.

### $D_1(2420)^0$ REFERENCES

DEL-AMO-SA...10P	PR D82 111101	P. del Amo Sanchez <i>et al.</i>	(BABAR Collab.)
AUBERT 09Y	PRL 103 051803	B. Aubert <i>et al.</i>	(BABAR Collab.)
CHEKANOV 09	EPJ C60 25	S. Chekanov <i>et al.</i>	(ZEUS Collab.)
ABULENCIA 06A	PR D73 051104	A. Abulencia <i>et al.</i>	(CDF Collab.)
ABE 05A	PRL 94 221805	K. Abe <i>et al.</i>	(BELLE Collab.)
ABE 04D	PR D69 112002	K. Abe <i>et al.</i>	(BELLE Collab.)
ABREU 98M	PL B426 231	P. Abreu <i>et al.</i>	(DELPHI Collab.)
ACKERSTAFF 97W	ZPHY C76 425	K. Ackerstaff <i>et al.</i>	(OPAL Collab.)
AVERY 94C	PL B331 236	P. Avery <i>et al.</i>	(CLEO Collab.)
FRABETTI 94B	PRL 72 324	P.L. Frabetti <i>et al.</i>	(FNAL E687 Collab.)
AVERY 90	PR D41 774	P. Avery, D. Besson	(CLEO Collab.)
ALBRECHT 89H	PL B232 398	H. Albrecht <i>et al.</i>	(ARGUS Collab.)
ANJOS 89C	PRL 62 1717	J.C. Anjos <i>et al.</i>	(FNAL E691 Collab.)

See key on page 457

# Meson Particle Listings

## $D_1(2420)^\pm, D_1(2430)^0, D_2^*(2460)^0$

### $D_1(2420)^\pm$

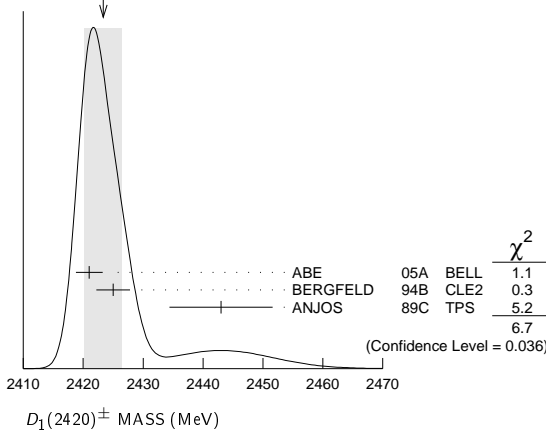
$I(J^P) = \frac{1}{2}(??)$   
 $I$  needs confirmation.

OMITTED FROM SUMMARY TABLE  
 Seen in  $D^*(2007)^0 \pi^\pm$ .  $J^P = 0^+$  ruled out.

#### $D_1(2420)^\pm$ MASS

VALUE (MeV)	EVTS	DOCUMENT ID	TECN	COMMENT
<b>2423.4 ± 3.1 OUR AVERAGE</b>		Error includes scale factor of 1.8.		See the ideogram below.
2421 ± 2 ± 1	124	ABE	05A	BELL $\bar{B}^0 \rightarrow D^+ \pi^+ \pi^- \pi^-$
2425 ± 2 ± 2	146	BERGFELD	94B	CLE2 $e^+ e^- \rightarrow D^{*0} \pi^+ X$
2443 ± 7 ± 5	190	ANJOS	89C	TPS $\gamma N \rightarrow D^0 \pi^+ X^0$

WEIGHTED AVERAGE  
 2423.4 ± 3.1 (Error scaled by 1.8)



#### $m_{D_1^+(2420)}^\pm - m_{D_1^0(2420)}$

VALUE (MeV)	DOCUMENT ID	TECN	COMMENT
<b>4 ± 2 ± 3</b>	BERGFELD	94B	CLE2 $e^+ e^- \rightarrow$ hadrons

#### $D_1(2420)^\pm$ WIDTH

VALUE (MeV)	EVTS	DOCUMENT ID	TECN	COMMENT
<b>25 ± 6 OUR AVERAGE</b>				
21 ± 5 ± 8	124	ABE	05A	BELL $\bar{B}^0 \rightarrow D^+ \pi^+ \pi^- \pi^-$
26 ± 8 ± 4	146	BERGFELD	94B	CLE2 $e^+ e^- \rightarrow D^{*0} \pi^+ X$
41 ± 19 ± 8	190	ANJOS	89C	TPS $\gamma N \rightarrow D^0 \pi^+ X^0$

#### $D_1(2420)^\pm$ DECAY MODES

$D_1^*(2420)^-$  modes are charge conjugates of modes below.

Mode	Fraction ( $\Gamma_i/\Gamma$ )
$\Gamma_1$ $D^*(2007)^0 \pi^+$	seen
$\Gamma_2$ $D^+ \pi^+ \pi^-$	seen
$\Gamma_3$ $D^+ \rho^0$	
$\Gamma_4$ $D^+ f_0(500)$	
$\Gamma_5$ $D_0^*(2400)^0 \pi^+$	
$\Gamma_6$ $D^0 \pi^+$	not seen
$\Gamma_7$ $D^{*+} \pi^+ \pi^-$	not seen

#### $D_1(2420)^\pm$ BRANCHING RATIOS

$\Gamma(D^*(2007)^0 \pi^+)/\Gamma_{\text{total}}$	$\Gamma_1/\Gamma$		
VALUE	DOCUMENT ID	TECN	COMMENT
seen	ANJOS	89C	TPS $\gamma N \rightarrow D^0 \pi^+ X^0$

$\Gamma(D^0 \pi^+)/\Gamma(D^*(2007)^0 \pi^+)$	$\Gamma_6/\Gamma_1$			
VALUE	CL%	DOCUMENT ID	TECN	COMMENT
<0.18	90	BERGFELD	94B	CLE2 $e^+ e^- \rightarrow$ hadrons

#### $D_1(2420)^\pm$ POLARIZATION AMPLITUDE $A_{D_1}$

A polarization amplitude  $A_{D_1}$  is a parameter that depends on the initial polarization of the  $D_1$  and is sensitive to a possible S-wave contribution to its decay. For  $D_1$  decays the helicity angle,  $\theta_h$ , distribution varies like

$1 + A_{D_1} \cos^2 \theta_h$ , where  $\theta_h$  is the angle in the  $D^*$  rest frame between the two pions emitted by the  $D_1 \rightarrow D^* \pi$  and the  $D^* \rightarrow D \pi$ .

Unpolarized  $D_1$  decaying purely via D-wave is predicted to give  $A_{D_1} = 3$ .

VALUE	DOCUMENT ID	TECN	COMMENT
• • • We do not use the following data for averages, fits, limits, etc. • • •			
3.8 ± 0.6 ± 0.8	<sup>1</sup> AUBERT	09Y	BABR $B^0 \rightarrow D_1^- \ell^+ \nu_\ell$
<sup>1</sup> Assuming $\Gamma(\Upsilon(4S) \rightarrow B^+ B^-) / \Gamma(\Upsilon(4S) \rightarrow B^0 \bar{B}^0) = 1.065 \pm 0.026$ and equal partial widths and helicity angle distributions for charged and neutral $D_1$ mesons.			

#### $D_1(2420)^\pm$ REFERENCES

AUBERT	09Y	PRL 103 051803	B. Aubert et al.	(BABAR Collab.)
ABE	05A	PRL 94 221805	K. Abe et al.	(BELLE Collab.)
BERGFELD	94B	PL B340 194	T. Bergfeld et al.	(CLEO Collab.)
ANJOS	89C	PRL 62 1717	J.C. Anjos et al.	(FNAL E691 Collab.)

### $D_1(2430)^0$

$I(J^P) = \frac{1}{2}(1^+)$

OMITTED FROM SUMMARY TABLE  
 $J = 1^+$  assignment favored (ABE 04D).

#### $D_1(2430)^0$ MASS

VALUE (MeV)	DOCUMENT ID	TECN	COMMENT
<b>2427 ± 26 ± 25</b>	ABE	04D	BELL $B^- \rightarrow D^{*+} \pi^- \pi^-$
• • • We do not use the following data for averages, fits, limits, etc. • • •			
2477 ± 28	<sup>1</sup> AUBERT	06L	BABR $\bar{B}^0 \rightarrow D^{*+} \omega \pi^-$
<sup>1</sup> Systematic errors not estimated.			

#### $D_1(2430)^0$ WIDTH

VALUE (MeV)	DOCUMENT ID	TECN	COMMENT
<b>384 ± 107 ± 74</b>	ABE	04D	BELL $B^- \rightarrow D^{*+} \pi^- \pi^-$
• • • We do not use the following data for averages, fits, limits, etc. • • •			
266 ± 97	<sup>2</sup> AUBERT	06L	BABR $\bar{B}^0 \rightarrow D^{*+} \omega \pi^-$
<sup>2</sup> Systematic errors not estimated.			

#### $D_1(2430)^0$ DECAY MODES

Mode	Fraction ( $\Gamma_i/\Gamma$ )
$\Gamma_1$ $D^*(2010)^+ \pi^-$	seen

#### $D_1(2430)^0$ REFERENCES

AUBERT	06L	PR D74 012001	B. Aubert et al.	(BABAR Collab.)
ABE	04D	PR D69 112002	K. Abe et al.	(BELLE Collab.)

### $D_2^*(2460)^0$

$I(J^P) = \frac{1}{2}(2^+)$

$J^P = 2^+$  assignment strongly favored (ALBRECHT 89B, ALBRECHT 89H), natural parity confirmed by the helicity analysis (DEL-AMO-SANCHEZ 10P),

#### $D_2^*(2460)^0$ MASS

The fit includes  $D^\pm, D^0, D_2^\pm, D^{*+}, D^{*0}, D_2^{*\pm}, D_1(2420)^0, D_2^*(2460)^0$ , and  $D_{s1}(2536)^\pm$  mass and mass difference measurements.

VALUE (MeV)	EVTS	DOCUMENT ID	TECN	COMMENT
<b>2462.6 ± 0.7 OUR FIT</b>		Error includes scale factor of 1.3.		
<b>2461.8 ± 0.8 OUR AVERAGE</b>		Error includes scale factor of 1.2.		
2462.2 ± 0.1 ± 0.8	243k	DEL-AMO-SA...10P	BABR	$e^+ e^- \rightarrow D^+ \pi^- X$
2460.4 ± 1.2 ± 2.2	3.4k	AUBERT	09AB	BABR $B^- \rightarrow D^+ \pi^- \pi^-$
2461.6 ± 2.1 ± 3.3		<sup>1</sup> ABE	04D	BELL $B^- \rightarrow D^+ \pi^- \pi^-$
2464.5 ± 1.1 ± 1.9	5.8k	<sup>1</sup> LINK	04A	FOCS $\gamma A$
2465 ± 3 ± 3	486	AVERY	94C	CLE2 $e^+ e^- \rightarrow D^+ \pi^- X$
2453 ± 3 ± 2	128	FRABETTI	94B	E687 $\gamma Be \rightarrow D^+ \pi^- X$
2461 ± 3 ± 1	440	AVERY	90	CLEO $e^+ e^- \rightarrow D^{*+} \pi^- X$
2455 ± 3 ± 5	337	ALBRECHT	89B	ARG $e^+ e^- \rightarrow D^+ \pi^- X$
2459 ± 3 ± 2	153	ANJOS	89C	TPS $\gamma N \rightarrow D^+ \pi^- X$
• • • We do not use the following data for averages, fits, limits, etc. • • •				
2469.1 ± 3.7 ± 1.3	1560 ± 230	<sup>2</sup> CHEKANOV	09	ZEUS $e^\pm p \rightarrow D^{(*)+} \pi^- X$
2463.3 ± 0.6 ± 0.8	20k	ABULENCIA	06A	CDF 1900 $p\bar{p} \rightarrow D^+ \pi^- X$
2461 ± 6	126	<sup>3</sup> ABREU	98M	DLPH $e^+ e^-$
2466 ± 7	1	ASRATYAN	95	BEBC 53,40 $\nu(\bar{\nu}) \rightarrow pX, dX$

## Meson Particle Listings

 $D_2^*(2460)^0$ 

<sup>1</sup> Fit includes the contribution from  $D_0^*(2400)^0$ .

<sup>2</sup> Calculated using the mass difference  $m(D_2^{*0}) - m(D^{*+})_{PDG}$  reported below and  $m(D^{*+})_{PDG} = 2010.27 \pm 0.17$  MeV. The 0.17 MeV uncertainty of the PDG mass value should be added to the experimental uncertainty of  $^{+1.2}_{-1.3}$  MeV.

<sup>3</sup> No systematic error given.

 $m_{D_2^0} - m_{D^+}$ 

The fit includes  $D^\pm, D^0, D_s^\pm, D^{*0}, D_s^{*0}, D_1(2420)^0, D_2^*(2460)^0$ , and  $D_{s1}(2536)^\pm$  mass and mass difference measurements.

VALUE (MeV)	EVTS	DOCUMENT ID	TECN	COMMENT
<b>593.0 ± 0.7 OUR FIT</b>				Error includes scale factor of 1.3.
<b>593.9 ± 0.6 ± 0.5</b>	20k	ABULENCIA 06A	CDF	1900 $p\bar{p} \rightarrow D^+ \pi^- X$

 $m_{D_2^0} - m_{D^{*+}}$ 

The fit includes  $D^\pm, D^0, D_s^\pm, D^{*0}, D_s^{*0}, D_1(2420)^0, D_2^*(2460)^0$ , and  $D_{s1}(2536)^\pm$  mass and mass difference measurements.

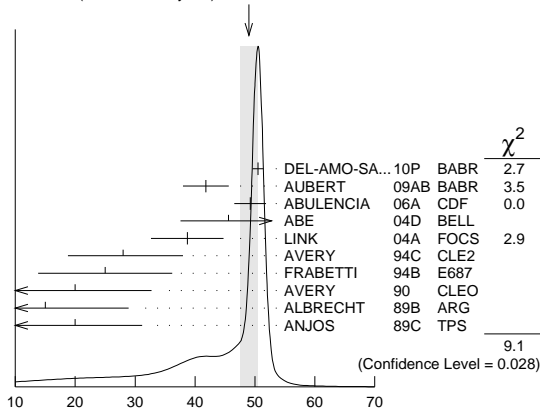
VALUE (MeV)	EVTS	DOCUMENT ID	TECN	COMMENT
<b>452.3 ± 0.7 OUR FIT</b>				Error includes scale factor of 1.3.
<b>458.8 ± 3.7 +1.2 -1.3</b>	1560 ± 230	CHEKANOV 09	ZEUS	$e^\pm p \rightarrow D^{(*)+} \pi^- X$

 $D_2^*(2460)^0$  WIDTH

VALUE (MeV)	EVTS	DOCUMENT ID	TECN	COMMENT
<b>49.0 ± 1.4 OUR AVERAGE</b>				Error includes scale factor of 1.7. See the ideogram below.
50.5 ± 0.6 ± 0.7	243k	DEL-AMO-SA...10P	BABR	$e^+ e^- \rightarrow D^+ \pi^- X$
41.8 ± 2.5 ± 2.9	3.4k	AUBERT 09AB	BABR	$B^- \rightarrow D^+ \pi^- \pi^-$
49.2 ± 2.3 ± 1.3	20k	ABULENCIA 06A	CDF	1900 $p\bar{p} \rightarrow D^+ \pi^- X$
45.6 ± 4.4 ± 6.7		<sup>4</sup> ABE 04D	BELL	$B^- \rightarrow D^+ \pi^- \pi^-$
38.7 ± 5.3 ± 2.9	5.8k	<sup>4</sup> LINK 04A	FOCS	$\gamma A$
28 + <sup>8</sup> / <sub>-7</sub> ± 6	486	AVERY 94C	CLE2	$e^+ e^- \rightarrow D^+ \pi^- X$
25 ± 10 ± 5	128	FRABETTI 94B	E687	$\gamma Be \rightarrow D^+ \pi^- X$
20 + <sup>9</sup> / <sub>-12</sub> + <sup>9</sup> / <sub>-10</sub>	440	AVERY 90	CLEO	$e^+ e^- \rightarrow D^{*+} \pi^- X$
15 + <sup>13</sup> / <sub>-10</sub> + <sup>5</sup> / <sub>-10</sub>	337	ALBRECHT 89B	ARG	$e^+ e^- \rightarrow D^+ \pi^- X$
20 ± 10 ± 5	153	ANJOS 89C	TPS	$\gamma N \rightarrow D^+ \pi^- X$

<sup>4</sup> Fit includes the contribution from  $D_0^*(2400)^0$ .

WEIGHTED AVERAGE  
49.0 ± 1.4 (Error scaled by 1.7)



$D_2^*(2460)^0$  WIDTH (MeV)

 $D_2^*(2460)^0$  DECAY MODES

$\bar{D}_2^*(2460)^0$  modes are charge conjugates of modes below.

Mode	Fraction ( $\Gamma_i/\Gamma$ )
$\Gamma_1$ $D^+ \pi^-$	seen
$\Gamma_2$ $D^*(2010)^+ \pi^-$	seen
$\Gamma_3$ $D^0 \pi^+ \pi^-$	not seen
$\Gamma_4$ $D^{*0} \pi^+ \pi^-$	not seen

 $D_2^*(2460)^0$  BRANCHING RATIOS

$\Gamma(D^+ \pi^-)/\Gamma_{\text{total}}$	VALUE	EVTS	DOCUMENT ID	TECN	COMMENT	$\Gamma_1/\Gamma$
seen	3.4k		AUBERT 09AB	BABR	$B^- \rightarrow D^+ \pi^- \pi^-$	
seen	337		ALBRECHT 89B	ARG	$e^+ e^- \rightarrow D^+ \pi^- X$	
seen			ANJOS 89C	TPS	$\gamma N \rightarrow D^+ \pi^- X$	

$\Gamma(D^*(2010)^+ \pi^-)/\Gamma_{\text{total}}$	VALUE	EVTS	DOCUMENT ID	TECN	COMMENT	$\Gamma_2/\Gamma$
seen			ACKERSTAFF 97W	OPAL	$e^+ e^- \rightarrow D^{*+} \pi^- X$	
seen			AVERY 90	CLEO	$e^+ e^- \rightarrow D^{*+} \pi^- X$	
seen			ALBRECHT 89H	ARG	$e^+ e^- \rightarrow D^* \pi^- X$	

$\Gamma(D^+ \pi^-)/\Gamma(D^*(2010)^+ \pi^-)$	VALUE	EVTS	DOCUMENT ID	TECN	COMMENT	$\Gamma_1/\Gamma_2$
<b>1.56 ± 0.16 OUR AVERAGE</b>						
1.47 ± 0.03 ± 0.16	379k		DEL-AMO-SA...10P	BABR	$e^+ e^- \rightarrow D^{(*)+} \pi^- X$	
2.8 ± 0.8 + <sup>0.5</sup> / <sub>-0.6</sub>	1560 ± 230		CHEKANOV 09	ZEUS	$e^\pm p \rightarrow D^{(*)+} \pi^- X$	
2.2 ± 0.7 ± 0.6			AVERY 94C	CLE2	$e^+ e^- \rightarrow D^{*+} \pi^- X$	
2.3 ± 0.8			AVERY 90	CLEO	$e^+ e^- \rightarrow D^{*+} \pi^- X$	
3.0 ± 1.1 ± 1.5			ALBRECHT 89H	ARG	$e^+ e^- \rightarrow D^* \pi^- X$	
• • • We do not use the following data for averages, fits, limits, etc. • • •						
1.9 ± 0.5			ABE 04D	BELL	$B^- \rightarrow D^{(*)+} \pi^- \pi^-$	

 $\Gamma(D^+ \pi^-)/[\Gamma(D^+ \pi^-) + \Gamma(D^*(2010)^+ \pi^-)]$ 

VALUE	EVTS	DOCUMENT ID	TECN	COMMENT
• • • We do not use the following data for averages, fits, limits, etc. • • •				
0.62 ± 0.03 ± 0.02	8414	<sup>5</sup> AUBERT 09Y	BABR	$B^+ \rightarrow D_2^0 \ell^+ \nu_\ell$

<sup>5</sup> Assuming  $\Gamma(\Upsilon(4S) \rightarrow B^+ B^-) / \Gamma(\Upsilon(4S) \rightarrow B^0 \bar{B}^0) = 1.065 \pm 0.026$  and equal partial widths for charged and neutral  $D_2^*$  mesons.

 $D_2^*(2460)^0$  POLARIZATION AMPLITUDE  $A_{D_2}$ 

A polarization amplitude  $A_{D_2}$  is a parameter that depends on the initial polarization of the  $D_2$ . For  $D_2$  decays the helicity angle,  $\theta_H$ , distribution varies like  $1 + A_{D_2} \cos(\theta_H)$ , where  $\theta_H$  is the angle in the  $D^*$  rest frame between the two pions emitted by the  $D_2 \rightarrow D^* \pi$  and  $D^* \rightarrow D \pi$ .

VALUE	EVTS	DOCUMENT ID	TECN	COMMENT
• • • We do not use the following data for averages, fits, limits, etc. • • •				
consistent with -1	243k	DEL-AMO-SA...10P	BABR	$e^+ e^- \rightarrow D^+ \pi^- X$
-0.74 + <sup>0.49</sup> / <sub>-0.38</sub>		<sup>6</sup> AVERY 94C	CLE2	$e^+ e^- \rightarrow D^{*+} \pi^- X$

<sup>6</sup> Systematic uncertainties not estimated.

 $D_2^*(2460)^0$  REFERENCES

DEL-AMO-SA...10P	PR D82 111101	P. del Amo Sanchez et al.	(BABAR Collab.)
AUBERT 09AB	PR D79 112004	B. Aubert et al.	(BABAR Collab.)
AUBERT 09Y	PRL 103 051803	B. Aubert et al.	(BABAR Collab.)
CHEKANOV 09	EPJ C60 25	S. Chekanov et al.	(ZEUS Collab.)
ABULENCIA 06A	PR D73 051104	A. Abulencia et al.	(CDF Collab.)
ABE 04D	PR D69 112002	K. Abe et al.	(BELLE Collab.)
LINK 04A	PL B586 11	J.M. Link et al.	(FOCUS Collab.)
ABREU 98M	PL B426 231	P. Abreu et al.	(DELPHI Collab.)
ACKERSTAFF 97W	ZPHY C76 425	K. Ackerstaff et al.	(OPAL Collab.)
ASRATYAN 95	ZPHY C68 43	A.E. Asratyan et al.	(BIRM, BELG, CERN+)
AVERY 94C	PL B331 236	P. Avery et al.	(CLEO Collab.)
FRABETTI 94B	PRL 72 324	P.L. Frabetti et al.	(FNAL E687 Collab.)
AVERY 90	PR D41 774	P. Avery, D. Besson	(CLEO Collab.)
ALBRECHT 89B	PL B221 422	H. Albrecht et al.	(ARGUS Collab.)
ALBRECHT 89H	PL B232 398	H. Albrecht et al.	(ARGUS Collab.)
ANJOS 89C	PRL 62 1717	J.C. Anjos et al.	(FNAL E691 Collab.)



See key on page 457

Meson Particle Listings

$D_2^*(2460)^\pm, D(2550)^0$

$D_2^*(2460)^\pm$

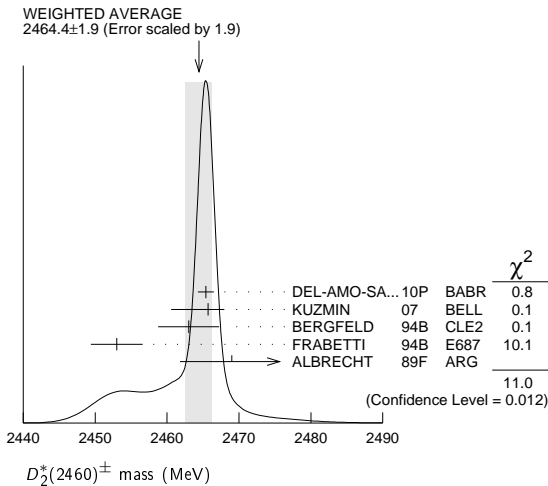
$I(J^P) = \frac{1}{2}(2^+)$

$J^P = 2^+$  assignment strongly favored(ALBRECHT 89B).

$D_2^*(2460)^\pm$  MASS

VALUE (MeV)	EVTS	DOCUMENT ID	TECN	COMMENT
<b>2464.4 ± 1.9 OUR AVERAGE</b>		Error includes scale factor of 1.9. See the ideogram below.		
2465.4 ± 0.2 ± 1.1	111k	<sup>1</sup> DEL-AMO-SA...10P	BABR	$e^+e^- \rightarrow D^0\pi^+X$
2465.7 ± 1.8 <sup>+1.4</sup> <sub>-4.8</sub>	2909	KUZMIN	07 BELL	$e^+e^- \rightarrow$ hadrons
2463 ± 3 ± 3	310	BERGFELD	94B CLE2	$e^+e^- \rightarrow D^0\pi^+X$
2453 ± 3 ± 2	185	FRABETTI	94B E687	$\gamma\text{Be} \rightarrow D^0\pi^+X$
2469 ± 4 ± 6		ALBRECHT	89F ARG	$e^+e^- \rightarrow D^0\pi^+X$
2467.6 ± 1.5 ± 0.8	3.5k	<sup>2</sup> LINK	04A FOCS	$\gamma A$

• • • We do not use the following data for averages, fits, limits, etc. • • •  
<sup>1</sup> At a fixed width of 50.5 MeV.  
<sup>2</sup> Fit includes the contribution from  $D_0^*(2400)^\pm$ . Not independent of the corresponding mass difference measurement,  $(m_{D_2^*(2460)^\pm} - (m_{D_2^*(2460)^0})$ .



$m_{D_2^*(2460)^\pm} - m_{D_2^*(2460)^0}$

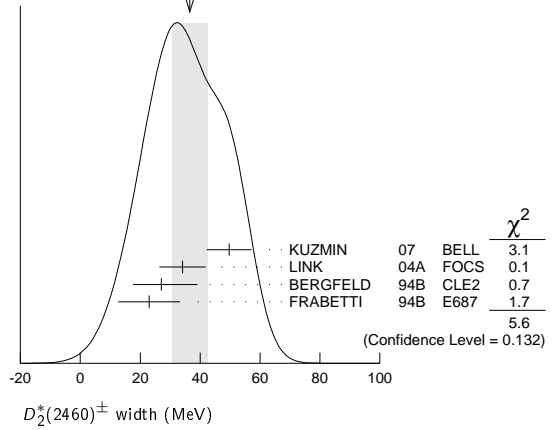
VALUE (MeV)	DOCUMENT ID	TECN	COMMENT
<b>2.4 ± 1.7 OUR AVERAGE</b>			
3.1 ± 1.9 ± 0.9	LINK 04A FOCS	$\gamma A$	
- 2 ± 4 ± 4	BERGFELD 94B CLE2	$e^+e^- \rightarrow$ hadrons	
0 ± 4	FRABETTI 94B E687	$\gamma\text{Be} \rightarrow D\pi X$	
14 ± 5 ± 8	ALBRECHT 89F ARG	$e^+e^- \rightarrow D^0\pi^+X$	

$D_2^*(2460)^\pm$  WIDTH

VALUE (MeV)	EVTS	DOCUMENT ID	TECN	COMMENT
<b>37 ± 6 OUR AVERAGE</b>		Error includes scale factor of 1.4. See the ideogram below.		
49.7 ± 3.8 ± 6.4	2909	KUZMIN	07 BELL	$e^+e^- \rightarrow$ hadrons
34.1 ± 6.5 ± 4.2	3.5k	<sup>3</sup> LINK	04A FOCS	$\gamma A$
27 <sup>+11</sup> <sub>-8</sub> ± 5	310	BERGFELD	94B CLE2	$e^+e^- \rightarrow D^0\pi^+X$
23 ± 9 ± 5	185	FRABETTI	94B E687	$\gamma\text{Be} \rightarrow D^0\pi^+X$

<sup>3</sup> Fit includes the contribution from  $D_0^*(2400)^\pm$ .

WEIGHTED AVERAGE  
37 ± 6 (Error scaled by 1.4)



$D_2^*(2460)^\pm$  DECAY MODES

$D_2^*(2460)^-$  modes are charge conjugates of modes below.

Mode	Fraction ( $\Gamma_i/\Gamma$ )
$\Gamma_1 D^0\pi^+$	seen
$\Gamma_2 D^{*0}\pi^+$	seen
$\Gamma_3 D^+\pi^+\pi^-$	not seen
$\Gamma_4 D^{*+}\pi^+\pi^-$	not seen

$D_2^*(2460)^\pm$  BRANCHING RATIOS

$\Gamma(D^0\pi^+)/\Gamma_{\text{total}}$	$\Gamma_1/\Gamma$
VALUE	DOCUMENT ID TECN COMMENT
seen	ALBRECHT 89F ARG $e^+e^- \rightarrow D^0\pi^+X$

$\Gamma(D^0\pi^+)/\Gamma(D^{*0}\pi^+)$	$\Gamma_1/\Gamma_2$
VALUE	DOCUMENT ID TECN COMMENT
<b>1.9 ± 1.1 ± 0.3</b>	BERGFELD 94B CLE2 $e^+e^- \rightarrow$ hadrons

$\Gamma(D^0\pi^+)/[\Gamma(D^0\pi^+) + \Gamma(D^{*0}\pi^+)]$	$\Gamma_1/(\Gamma_1 + \Gamma_2)$
VALUE	EVTS DOCUMENT ID TECN COMMENT

• • • We do not use the following data for averages, fits, limits, etc. • • •

0.62 ± 0.03 ± 0.02 3361 <sup>4</sup> AUBERT 09Y BABR  $\bar{B}^0 \rightarrow D_2^{*+} \ell^- \nu_\ell$

<sup>4</sup> Assuming  $\Gamma(\Upsilon(4S) \rightarrow B^+B^-) / \Gamma(\Upsilon(4S) \rightarrow B^0\bar{B}^0) = 1.065 \pm 0.026$  and equal partial widths for charged and neutral  $D_2^*$  mesons.

$D_2^*(2460)^\pm$  REFERENCES

DEL-AMO-SA...10P	PR D82 111101	P. del Amo Sanchez et al.	(BABAR Collab.)
AUBERT 09Y	PRL 103 051803	B. Aubert et al.	(BABAR Collab.)
KUZMIN 07	PR D76 012006	A. Kuzmin et al.	(BELLE Collab.)
LINK 04A	PL B586 11	J.M. Link et al.	(FOCUS Collab.)
BERGFELD 94B	PL B340 194	T. Bergfeld et al.	(CLEO Collab.)
FRABETTI 94B	PRL 72 324	P.L. Frabetti et al.	(FNAL E687 Collab.)
ALBRECHT 89B	PL B221 422	H. Albrecht et al.	(ARGUS Collab.)
ALBRECHT 89F	PL B231 208	H. Albrecht et al.	(ARGUS Collab.)

$D(2550)^0$

$I(J^P) = \frac{1}{2}(0^-)$

OMITTED FROM SUMMARY TABLE

$J^P = 0^-$  assignment based on the helicity analysis (DEL-AMO-SANCHEZ 10P).

$D(2550)^0$  MASS

VALUE (MeV)	EVTS	DOCUMENT ID	TECN	COMMENT
<b>2539.4 ± 4.5 ± 6.8</b>	34k	DEL-AMO-SA...10P	BABR	$e^+e^- \rightarrow D^{*+}\pi^-X$

$D(2550)^0$  WIDTH

VALUE (MeV)	EVTS	DOCUMENT ID	TECN	COMMENT
<b>130 ± 12 ± 13</b>	34k	DEL-AMO-SA...10P	BABR	$e^+e^- \rightarrow D^{*+}\pi^-X$

## Meson Particle Listings

 $D(2550)^0$ ,  $D(2600)$ ,  $D^*(2640)^\pm$ ,  $D(2750)$  $D(2550)^0$  DECAY MODES

Mode	Fraction ( $\Gamma_i/\Gamma$ )
$\Gamma_1$ $D^{*+}\pi^-$	seen

 $D(2550)^0$  REFERENCES

DEL-AMO-SA...10P PR D82 111101 P. del Amo Sanchez et al. (BABAR Collab.)

 **$D(2600)$** 

$$I(J^P) = \frac{1}{2}(??)$$

OMITTED FROM SUMMARY TABLE

 $J^P$  consistent with natural parity (DEL-AMO-SANCHEZ 10P). $D(2600)$  MASS

VALUE (MeV)	EVTS	DOCUMENT ID	TECN	CHG	COMMENT
<b>2612 ± 6</b> OUR AVERAGE					Error includes scale factor of 1.9.
2608.7 ± 2.4 ± 2.5	26k	DEL-AMO-SA...10P	BABR	0	$e^+e^- \rightarrow D^+\pi^- X$
2621.3 ± 3.7 ± 4.2	13k	<sup>1</sup> DEL-AMO-SA...10P	BABR	+	$e^+e^- \rightarrow D^0\pi^+ X$

<sup>1</sup>At a fixed width of 93 MeV. $D(2600)$  WIDTH

VALUE (MeV)	EVTS	DOCUMENT ID	TECN	COMMENT
<b>93 ± 6 ± 13</b>	26k	DEL-AMO-SA...10P	BABR	$e^+e^- \rightarrow D^+\pi^- X$

 $D(2600)$  DECAY MODES

Mode	Fraction ( $\Gamma_i/\Gamma$ )
$\Gamma_1$ $D\pi$	seen
$\Gamma_2$ $D^+\pi^-$	seen
$\Gamma_3$ $D^0\pi^\pm$	seen
$\Gamma_4$ $D^*\pi$	seen
$\Gamma_5$ $D^{*+}\pi^-$	seen

 $D(2600)$  BRANCHING RATIOS

$\Gamma(D^+\pi^-)/\Gamma(D^{*+}\pi^-)$	$\Gamma_2/\Gamma_5$			
<b>0.32 ± 0.02 ± 0.09</b>				
VALUE	EVTS	DOCUMENT ID	TECN	COMMENT
	76k	DEL-AMO-SA...10P	BABR	$e^+e^- \rightarrow D^{*+}\pi^- X$

 $D(2600)$  REFERENCES

DEL-AMO-SA...10P PR D82 111101 P. del Amo Sanchez et al. (BABAR Collab.)

 **$D^*(2640)^\pm$** 

$$I(J^P) = \frac{1}{2}(??)$$

OMITTED FROM SUMMARY TABLE

Seen in Z decays by ABREU 98M. Not seen by ABBIENDI 01N and CHEKANOV 09. Needs confirmation.

 $D^*(2640)^\pm$  MASS

VALUE (MeV)	EVTS	DOCUMENT ID	TECN	COMMENT
<b>2637 ± 2 ± 6</b>	66 ± 14	ABREU	98M	DLPH $e^+e^- \rightarrow D^{*+}\pi^+\pi^- X$

 $D^*(2640)^\pm$  WIDTH

VALUE (MeV)	CL%	DOCUMENT ID	TECN	COMMENT
<b>&lt;15</b>	95	ABREU	98M	DLPH $e^+e^- \rightarrow D^{*+}\pi^+\pi^- X$

 $D^*(2640)^+$  DECAY MODES $D^*(2640)^-$  modes are charge conjugates of modes below.

Mode	Fraction ( $\Gamma_i/\Gamma$ )
$\Gamma_1$ $D^*(2010)^+\pi^+\pi^-$	seen

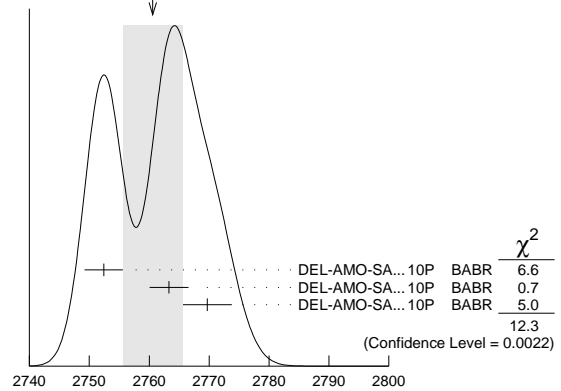
 $D^*(2640)^\pm$  REFERENCESCHEKANOV 09 EPJ C60 25 S. Chekanov et al. (ZEUS Collab.)  
ABBIENDI 01N EPJ C20 445 G. Abbiendi et al. (OPAL Collab.)  
ABREU 98M PL B426 231 P. Abreu et al. (DELPHI Collab.) **$D(2750)$** 

$$I(J^P) = \frac{1}{2}(??)$$

OMITTED FROM SUMMARY TABLE

 $D(2750)$  MASS

VALUE (MeV)	EVTS	DOCUMENT ID	TECN	CHG	COMMENT
<b>2761 ± 5</b> OUR AVERAGE					Error includes scale factor of 2.5. See the ideogram below.
2752.4 ± 1.7 ± 2.7	23.5k	<sup>1</sup> DEL-AMO-SA...10P	BABR	0	$e^+e^- \rightarrow D^{*+}\pi^- X$
2763.3 ± 2.3 ± 2.3	11.3k	<sup>1</sup> DEL-AMO-SA...10P	BABR	0	$e^+e^- \rightarrow D^+\pi^- X$
2769.7 ± 3.8 ± 1.5	5.7k	<sup>1,2</sup> DEL-AMO-SA...10P	BABR	+	$e^+e^- \rightarrow D^0\pi^+ X$

<sup>1</sup>The states observed in the  $D^*\pi$  and  $D\pi$  final states are not necessarily the same.<sup>2</sup>At a fixed width of 60.9 MeV.WEIGHTED AVERAGE  
2761 ± 5 (Error scaled by 2.5)

D(2750) MASS (MeV)

 $D(2750)$  WIDTH

VALUE (MeV)	EVTS	DOCUMENT ID	TECN	COMMENT
<b>63 ± 6</b> OUR AVERAGE				
71 ± 6 ± 11	23.5k	<sup>3</sup> DEL-AMO-SA...10P	BABR	$e^+e^- \rightarrow D^{*+}\pi^- X$
60.9 ± 5.1 ± 3.6	11.3k	<sup>3</sup> DEL-AMO-SA...10P	BABR	$e^+e^- \rightarrow D^+\pi^- X$

<sup>3</sup>The states observed in the  $D^*\pi$  and  $D\pi$  final states are not necessarily the same. $D(2750)$  DECAY MODES

Mode	Fraction ( $\Gamma_i/\Gamma$ )
$\Gamma_1$ $D\pi$	seen
$\Gamma_2$ $D^+\pi^-$	seen
$\Gamma_3$ $D^0\pi^\pm$	seen
$\Gamma_4$ $D^*\pi$	seen
$\Gamma_5$ $D^{*+}\pi^-$	seen

 $D(2750)$  BRANCHING RATIOS

$\Gamma(D^+\pi^-)/\Gamma(D^{*+}\pi^-)$	$\Gamma_2/\Gamma_5$			
<b>0.42 ± 0.05 ± 0.11</b>				
VALUE	EVTS	DOCUMENT ID	TECN	COMMENT
	34.8k	<sup>4</sup> DEL-AMO-SA...10P	BABR	$e^+e^- \rightarrow D^{*+}\pi^- X$

<sup>4</sup>The states observed in the  $D^*\pi$  and  $D\pi$  final states are not necessarily the same. $D(2750)$  POLARIZATION AMPLITUDE  $A_D$ 

A polarization amplitude  $A_D$  is a parameter that depends on the initial polarization of the  $D(2750)$ . For  $D(2750)$  decays the helicity angle,  $\theta_H$ , distribution varies like  $1 + A_D \cos(\theta_H)$ , where  $\theta_H$  is the angle in the  $D^*$  rest frame between the two pions emitted by the  $D(2750) \rightarrow D^*\pi$  and  $D^* \rightarrow D\pi$ .

VALUE	EVTS	DOCUMENT ID	TECN	COMMENT
<b>-0.33 ± 0.28</b>	23.5k	<sup>5</sup> DEL-AMO-SA...10P	BABR	$e^+e^- \rightarrow D^{*+}\pi^- X$

<sup>5</sup>Systematic uncertainties not estimated. The states observed in the  $D^*\pi$  and  $D\pi$  final states are not necessarily the same. $D(2750)$  REFERENCES

DEL-AMO-SA...10P PR D82 111101 P. del Amo Sanchez et al. (BABAR Collab.)

# CHARMED, STRANGE MESONS ( $C = S = \pm 1$ )

$$D_s^+ = c\bar{s}, D_s^- = \bar{c}s, \text{ similarly for } D_s^{*\prime}s$$

## $D_s^\pm$

$$I(J^P) = 0(0^-)$$

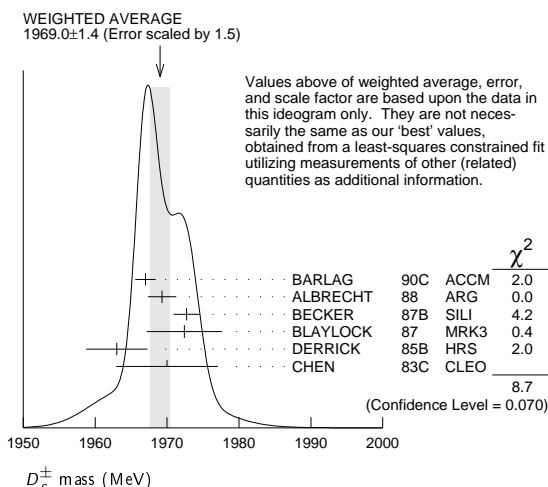
The angular distributions of the decays of the  $\phi$  and  $\bar{K}^*(892)^0$  in the  $\phi\pi^+$  and  $K^+\bar{K}^*(892)^0$  modes strongly indicate that the spin is zero. The parity given is that expected of a  $c\bar{s}$  ground state.

### $D_s^\pm$ MASS

The fit includes  $D_s^\pm, D^0, D_s^{*\pm}, D^{*0}, D_s^{*\prime\pm}, D_1(2420)^0, D_2^*(2460)^0$ , and  $D_{s1}(2536)^\pm$  mass and mass difference measurements. Measurements of the  $D_s^\pm$  mass with an error greater than 10 MeV are omitted from the fit and average. A number of early measurements have been omitted altogether.

VALUE (MeV)	EVTS	DOCUMENT ID	TECN	COMMENT
<b>1968.49 ± 0.32 OUR FIT</b>		Error includes scale factor of 1.3.		
<b>1969.0 ± 1.4 OUR AVERAGE</b>		Error includes scale factor of 1.5. See the ideogram below.		
1967.0 ± 1.0 ± 1.0	54	BARLAG	90c	ACCM $\pi^-$ Cu 230 GeV
1969.3 ± 1.4 ± 1.4		ALBRECHT	88	ARG $e^+e^-$ 9.4–10.6 GeV
1972.7 ± 1.5 ± 1.0	21	BECKER	87b	SILI 200 GeV $\pi, K, p$
1972.4 ± 3.7 ± 3.7	27	BLAYLOCK	87	MRK3 $e^+e^-$ 4.14 GeV
1963 ± 3 ± 3	30	DERRICK	85b	HRS $e^+e^-$ 29 GeV
1970 ± 5 ± 5	104	CHEN	83c	CLEO $e^+e^-$ 10.5 GeV
••• We do not use the following data for averages, fits, limits, etc. •••				
1968.3 ± 0.7 ± 0.7	290	<sup>1</sup> ANJOS	88	E691 Photoproduction
1980 ± 15	6	USHIDA	86	EMUL $\nu$ wideband
1973.6 ± 2.6 ± 3.0	163	ALBRECHT	85d	ARG $e^+e^-$ 10 GeV
1948 ± 28 ± 10	65	AIHARA	84d	TPC $e^+e^-$ 29 GeV
1975 ± 9 ± 10	49	ALTHOFF	84	TASS $e^+e^-$ 14–25 GeV
1975 ± 4	3	BAILEY	84	ACCM hadron <sup>+</sup> Be → $\phi\pi^+X$

<sup>1</sup> ANJOS 88 enters the fit via  $m_{D_s^\pm} - m_{D^\pm}$  (see below).



### $m_{D_s^\pm} - m_{D^\pm}$

The fit includes  $D_s^\pm, D^0, D_s^{*\pm}, D^{*0}, D_s^{*\prime\pm}, D_1(2420)^0, D_2^*(2460)^0$ , and  $D_{s1}(2536)^\pm$  mass and mass difference measurements.

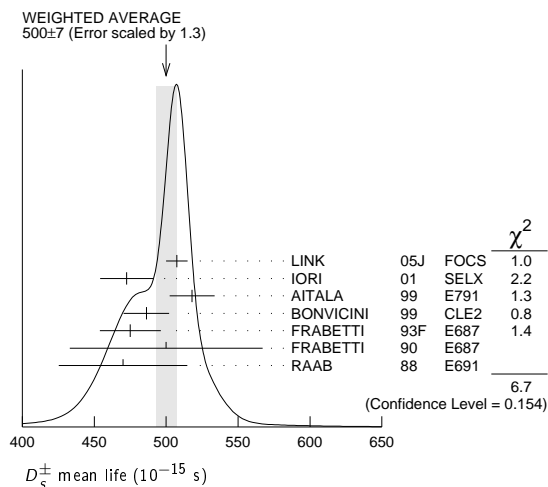
VALUE (MeV)	EVTS	DOCUMENT ID	TECN	COMMENT
<b>98.87 ± 0.29 OUR FIT</b>		Error includes scale factor of 1.4.		
<b>98.85 ± 0.25 OUR AVERAGE</b>		Error includes scale factor of 1.1.		
99.41 ± 0.38 ± 0.21		ACOSTA	03d	CDF2 $\bar{p}p, \sqrt{s} = 1.96$ TeV
98.4 ± 0.1 ± 0.3	48k	AUBERT	02g	BABR $e^+e^- \approx \Upsilon(4S)$
99.5 ± 0.6 ± 0.3		BROWN	94	CLE2 $e^+e^- \approx \Upsilon(4S)$
98.5 ± 1.5	555	CHEN	89	CLEO $e^+e^-$ 10.5 GeV
99.0 ± 0.8	290	ANJOS	88	E691 Photoproduction

### $D_s^\pm$ MEAN LIFE

Measurements with an error greater than  $100 \times 10^{-15}$  s or with fewer than 100 events have been omitted from the Listings.

VALUE ( $10^{-15}$ s)	EVTS	DOCUMENT ID	TECN	COMMENT
<b>500 ± 7 OUR AVERAGE</b>		Error includes scale factor of 1.3. See the ideogram below.		
507.4 ± 5.5 ± 5.1	13.6k	LINK	05j	FOCS $\phi\pi^+$ and $\bar{K}^{*0}K^+$
472.5 ± 17.2 ± 6.6	760	IORI	01	SELX 600 GeV $\Sigma^-, \pi^-, p$
518 ± 14 ± 7	1662	AITALA	99	E791 $\pi^-$ nucleus, 500 GeV
486.3 ± 15.0 <sup>+</sup> ± 4.9 <sup>-</sup>	2167	<sup>2</sup> BONVICINI	99	CLE2 $e^+e^- \approx \Upsilon(4S)$
475 ± 20 ± 7	900	FRABETTI	93f	E687 $\gamma$ Be, $\phi\pi^+$
500 ± 60 ± 30	104	FRABETTI	90	E687 $\gamma$ Be, $\phi\pi^+$
470 ± 40 ± 20	228	RAAB	88	E691 Photoproduction

<sup>2</sup> BONVICINI 99 obtains  $1.19 \pm 0.04$  for the ratio of  $D_s^\pm$  to  $D^0$  lifetimes.



### $D_s^\pm$ DECAY MODES

Unless otherwise noted, the branching fractions for modes with a resonance in the final state include all the decay modes of the resonance.  $D_s^\pm$  modes are charge conjugates of the modes below.

Mode	Fraction ( $\Gamma_i/\Gamma$ )	Scale factor / Confidence level
<b>Inclusive modes</b>		
$\Gamma_1$ $e^+$ semileptonic	[a] ( 6.5 ± 0.4 ) %	
$\Gamma_2$ $\pi^+$ anything	(119.3 ± 1.4) %	
$\Gamma_3$ $\pi^-$ anything	( 43.2 ± 0.9 ) %	
$\Gamma_4$ $\pi^0$ anything	(123 ± 7) %	
$\Gamma_5$ $K^-$ anything	( 18.7 ± 0.5 ) %	
$\Gamma_6$ $K^+$ anything	( 28.9 ± 0.7 ) %	
$\Gamma_7$ $K_S^0$ anything	( 19.0 ± 1.1 ) %	
$\Gamma_8$ $\eta$ anything	[b] ( 29.9 ± 2.8 ) %	
$\Gamma_9$ $\omega$ anything	( 6.1 ± 1.4 ) %	
$\Gamma_{10}$ $\eta'$ anything	[c] ( 11.7 ± 1.8 ) %	
$\Gamma_{11}$ $f_0(980)$ anything, $f_0 \rightarrow \pi^+\pi^-$	< 1.3 %	CL=90%
$\Gamma_{12}$ $\phi$ anything	( 15.7 ± 1.0 ) %	
$\Gamma_{13}$ $K^+K^-$ anything	( 15.8 ± 0.7 ) %	
$\Gamma_{14}$ $K_S^0 K^+$ anything	( 5.8 ± 0.5 ) %	
$\Gamma_{15}$ $K_S^0 K^-$ anything	( 1.9 ± 0.4 ) %	
$\Gamma_{16}$ $2K_S^0$ anything	( 1.70 ± 0.32 ) %	
$\Gamma_{17}$ $2K^+$ anything	< 2.6 × 10 <sup>-3</sup>	CL=90%
$\Gamma_{18}$ $2K^-$ anything	< 6 × 10 <sup>-4</sup>	CL=90%
<b>Leptonic and semileptonic modes</b>		
$\Gamma_{19}$ $e^+\nu_e$	< 1.2 × 10 <sup>-4</sup>	CL=90%
$\Gamma_{20}$ $\mu^+\nu_\mu$	( 5.90 ± 0.33 ) × 10 <sup>-3</sup>	
$\Gamma_{21}$ $\tau^+\nu_\tau$	( 5.43 ± 0.31 ) %	
$\Gamma_{22}$ $K^+K^-e^+\nu_e$	—	
$\Gamma_{23}$ $\phi e^+\nu_e$	[d] ( 2.49 ± 0.14 ) %	
$\Gamma_{24}$ $\eta e^+\nu_e + \eta'(958) e^+\nu_e$	[d] ( 3.66 ± 0.37 ) %	
$\Gamma_{25}$ $\eta e^+\nu_e$	[d] ( 2.67 ± 0.29 ) %	S=1.1
$\Gamma_{26}$ $\eta'(958) e^+\nu_e$	[d] ( 9.9 ± 2.3 ) × 10 <sup>-3</sup>	
$\Gamma_{27}$ $\omega e^+\nu_e$	[e] < 2.0 × 10 <sup>-3</sup>	CL=90%
$\Gamma_{28}$ $K^0 e^+\nu_e$	( 3.7 ± 1.0 ) × 10 <sup>-3</sup>	
$\Gamma_{29}$ $K^*(892)^0 e^+\nu_e$	[d] ( 1.8 ± 0.7 ) × 10 <sup>-3</sup>	
$\Gamma_{30}$ $f_0(980) e^+\nu_e, f_0 \rightarrow \pi^+\pi^-$	( 2.00 ± 0.32 ) × 10 <sup>-3</sup>	

## Meson Particle Listings

 $D_s^\pm$ 

Hadronic modes with a $K\bar{K}$ pair			
$\Gamma_{31}$	$K^+ K_S^0$	( 1.48±0.08 ) %	
$\Gamma_{32}$	$K^+ K^- \pi^+$	[f] ( 5.49±0.27 ) %	
$\Gamma_{33}$	$\phi \pi^+$	[d,g] ( 4.5 ±0.4 ) %	
$\Gamma_{34}$	$\phi \pi^+, \phi \rightarrow K^+ K^-$	[g] ( 2.28±0.12 ) %	
$\Gamma_{35}$	$K^+ \bar{K}^*(892)^0, \bar{K}^{*0} \rightarrow K^- \pi^+$	( 2.63±0.13 ) %	
$\Gamma_{36}$	$f_0(980) \pi^+, f_0 \rightarrow K^+ K^-$	( 1.16±0.32 ) %	
$\Gamma_{37}$	$f_0(1370) \pi^+, f_0 \rightarrow K^+ K^-$	( 7 ±5 ) ×10 <sup>-4</sup>	
$\Gamma_{38}$	$f_0(1710) \pi^+, f_0 \rightarrow K^+ K^-$	( 6.7 ±2.9 ) ×10 <sup>-4</sup>	
$\Gamma_{39}$	$K^+ \bar{K}_0^*(1430)^0, \bar{K}_0^{*0} \rightarrow K^- \pi^+$	( 1.9 ±0.4 ) ×10 <sup>-3</sup>	
$\Gamma_{40}$	$K^0 \bar{K}^0 \pi^+$	—	
$\Gamma_{41}$	$K^*(892) \bar{K}^0$	[d] ( 5.4 ±1.2 ) %	
$\Gamma_{42}$	$K^+ K^- \pi^+ \pi^0$	( 5.6 ±0.5 ) %	
$\Gamma_{43}$	$\phi \rho^+$	[d] ( 8.4 $\begin{smallmatrix} +1.9 \\ -2.3 \end{smallmatrix}$ ) %	
$\Gamma_{44}$	$K_S^0 K^- 2\pi^+$	( 1.64±0.12 ) %	
$\Gamma_{45}$	$K^*(892) \bar{K}^*(892)^0$	[d] ( 7.2 ±2.6 ) %	
$\Gamma_{46}$	$K^+ K_S^0 \pi^+ \pi^-$	( 9.6 ±1.3 ) ×10 <sup>-3</sup>	
$\Gamma_{47}$	$K^+ K^- 2\pi^+ \pi^-$	( 8.8 ±1.6 ) ×10 <sup>-3</sup>	
$\Gamma_{48}$	$\phi 2\pi^+ \pi^-$	[d] ( 1.21±0.16 ) %	
$\Gamma_{49}$	$K^+ K^- \rho^0 \pi^+$ non- $\phi$	< 2.6 ×10 <sup>-4</sup>	CL=90%
$\Gamma_{50}$	$\phi \rho^0 \pi^+, \phi \rightarrow K^+ K^-$	( 6.6 ±1.3 ) ×10 <sup>-3</sup>	
$\Gamma_{51}$	$\phi a_1(1260)^+, \phi \rightarrow K^+ K^-, a_1^+ \rightarrow \rho^0 \pi^+$	( 7.5 ±1.3 ) ×10 <sup>-3</sup>	
$\Gamma_{52}$	$K^+ K^- 2\pi^+ \pi^-$ nonresonant	( 9 ±7 ) ×10 <sup>-4</sup>	
$\Gamma_{53}$	$2K_S^0 2\pi^+ \pi^-$	( 8.3 ±3.5 ) ×10 <sup>-4</sup>	
Hadronic modes without $K$ 's			
$\Gamma_{54}$	$\pi^+ \pi^0$	< 3.4 ×10 <sup>-4</sup>	CL=90%
$\Gamma_{55}$	$2\pi^+ \pi^-$	( 1.10±0.06 ) %	
$\Gamma_{56}$	$\rho^0 \pi^+$	( 2.0 ±1.2 ) ×10 <sup>-4</sup>	
$\Gamma_{57}$	$\pi^+ (\pi^+ \pi^-)_{S\text{-wave}}$	[h] ( 9.2 ±0.6 ) ×10 <sup>-3</sup>	
$\Gamma_{58}$	$f_0(980) \pi^+, f_0 \rightarrow \pi^+ \pi^-$		
$\Gamma_{59}$	$f_0(1370) \pi^+, f_0 \rightarrow \pi^+ \pi^-$		
$\Gamma_{60}$	$f_0(1500) \pi^+, f_0 \rightarrow \pi^+ \pi^-$		
$\Gamma_{61}$	$f_2(1270) \pi^+, f_2 \rightarrow \pi^+ \pi^-$	( 1.11±0.20 ) ×10 <sup>-3</sup>	
$\Gamma_{62}$	$\rho(1450)^0 \pi^+, \rho^0 \rightarrow \pi^+ \pi^-$	( 3.0 ±2.0 ) ×10 <sup>-4</sup>	
$\Gamma_{63}$	$\pi^+ 2\pi^0$	( 6.5 ±1.3 ) ×10 <sup>-3</sup>	
$\Gamma_{64}$	$2\pi^+ \pi^- \pi^0$	—	
$\Gamma_{65}$	$\eta \pi^+$	[d] ( 1.83±0.15 ) %	
$\Gamma_{66}$	$\omega \pi^+$	[d] ( 2.5 ±0.7 ) ×10 <sup>-3</sup>	
$\Gamma_{67}$	$3\pi^+ 2\pi^-$	( 8.0 ±0.9 ) ×10 <sup>-3</sup>	
$\Gamma_{68}$	$2\pi^+ \pi^- 2\pi^0$	—	
$\Gamma_{69}$	$\eta \rho^+$	[d] ( 8.9 ±0.8 ) %	
$\Gamma_{70}$	$\eta \pi^+ \pi^0$ 3-body	[d] < 5 %	CL=90%
$\Gamma_{71}$	$\omega \pi^+ \pi^0$	[d] ( 2.8 ±0.7 ) %	
$\Gamma_{72}$	$3\pi^+ 2\pi^- \pi^0$	( 4.9 ±3.2 ) %	
$\Gamma_{73}$	$\omega 2\pi^+ \pi^-$	[d] ( 1.6 ±0.5 ) %	
$\Gamma_{74}$	$\eta'(958) \pi^+$	[c,d] ( 3.94±0.33 ) %	
$\Gamma_{75}$	$3\pi^+ 2\pi^- 2\pi^0$	—	
$\Gamma_{76}$	$\omega \eta \pi^+$	[d] < 2.13 %	CL=90%
$\Gamma_{77}$	$\eta'(958) \rho^+$	[c,d] ( 12.5 ±2.2 ) %	
$\Gamma_{78}$	$\eta'(958) \pi^+ \pi^0$ 3-body	[d] < 1.8 %	CL=90%
Modes with one or three $K$ 's			
$\Gamma_{79}$	$K^+ \pi^0$	( 6.2 ±2.1 ) ×10 <sup>-4</sup>	
$\Gamma_{80}$	$K_S^0 \pi^+$	( 1.21±0.08 ) ×10 <sup>-3</sup>	
$\Gamma_{81}$	$K^+ \eta$	[d] ( 1.75±0.35 ) ×10 <sup>-3</sup>	
$\Gamma_{82}$	$K^+ \omega$	[d] < 2.4 ×10 <sup>-3</sup>	CL=90%
$\Gamma_{83}$	$K^+ \eta'(958)$	[d] ( 1.8 ±0.6 ) ×10 <sup>-3</sup>	
$\Gamma_{84}$	$K^+ \pi^+ \pi^-$	( 6.9 ±0.5 ) ×10 <sup>-3</sup>	
$\Gamma_{85}$	$K^+ \rho^0$	( 2.7 ±0.5 ) ×10 <sup>-3</sup>	
$\Gamma_{86}$	$K^+ \rho(1450)^0, \rho^0 \rightarrow \pi^+ \pi^-$	( 7.3 ±2.6 ) ×10 <sup>-4</sup>	
$\Gamma_{87}$	$K^*(892)^0 \pi^+, K^{*0} \rightarrow K^+ \pi^-$	( 1.50±0.26 ) ×10 <sup>-3</sup>	
$\Gamma_{88}$	$K^*(1410)^0 \pi^+, K^{*0} \rightarrow K^+ \pi^-$	( 1.30±0.31 ) ×10 <sup>-3</sup>	
$\Gamma_{89}$	$K^*(1430)^0 \pi^+, K^{*0} \rightarrow K^+ \pi^-$	( 5 ±4 ) ×10 <sup>-4</sup>	
$\Gamma_{90}$	$K^+ \pi^+ \pi^-$ nonresonant	( 1.1 ±0.4 ) ×10 <sup>-3</sup>	
$\Gamma_{91}$	$K^0 \pi^+ \pi^0$	( 1.00±0.18 ) %	
$\Gamma_{92}$	$K_S^0 2\pi^+ \pi^-$	( 2.9 ±1.1 ) ×10 <sup>-3</sup>	
$\Gamma_{93}$	$K^+ \omega \pi^0$	[d] < 8.2 ×10 <sup>-3</sup>	CL=90%
$\Gamma_{94}$	$K^+ \omega \pi^+ \pi^-$	[d] < 5.4 ×10 <sup>-3</sup>	CL=90%
$\Gamma_{95}$	$K^+ \omega \eta$	[d] < 7.9 ×10 <sup>-3</sup>	CL=90%
$\Gamma_{96}$	$2K^+ K^-$	( 2.20±0.23 ) ×10 <sup>-4</sup>	
$\Gamma_{97}$	$\phi K^+, \phi \rightarrow K^+ K^-$	( 9.0 ±2.1 ) ×10 <sup>-5</sup>	
Doubly Cabibbo-suppressed modes			
$\Gamma_{98}$	$2K^+ \pi^-$	( 1.28±0.14 ) ×10 <sup>-4</sup>	
$\Gamma_{99}$	$K^+ K^*(892)^0, K^{*0} \rightarrow K^+ \pi^-$	( 6.0 ±3.5 ) ×10 <sup>-5</sup>	
Baryon-antibaryon mode			
$\Gamma_{100}$	$\rho \bar{\rho}$	( 1.3 ±0.4 ) ×10 <sup>-3</sup>	
$\Delta C = 1$ weak neutral current (C1) modes, Lepton family number (LF), or Lepton number (L) violating modes			
$\Gamma_{101}$	$\pi^+ e^+ e^-$	[i] < 1.3 ×10 <sup>-5</sup>	CL=90%
$\Gamma_{102}$	$\pi^+ \phi, \phi \rightarrow e^+ e^-$	[j] ( 6 $\begin{smallmatrix} +8 \\ -4 \end{smallmatrix}$ ) ×10 <sup>-6</sup>	
$\Gamma_{103}$	$\pi^+ \mu^+ \mu^-$	[i] < 2.6 ×10 <sup>-5</sup>	CL=90%
$\Gamma_{104}$	$K^+ e^+ e^-$	CI < 3.7 ×10 <sup>-6</sup>	CL=90%
$\Gamma_{105}$	$K^+ \mu^+ \mu^-$	CI < 2.1 ×10 <sup>-5</sup>	CL=90%
$\Gamma_{106}$	$K^*(892)^+ \mu^+ \mu^-$	CI < 1.4 ×10 <sup>-3</sup>	CL=90%
$\Gamma_{107}$	$\pi^+ e^+ \mu^-$	LF < 1.2 ×10 <sup>-5</sup>	CL=90%
$\Gamma_{108}$	$\pi^+ e^- \mu^+$	LF < 2.0 ×10 <sup>-5</sup>	CL=90%
$\Gamma_{109}$	$K^+ e^+ \mu^-$	LF < 1.4 ×10 <sup>-5</sup>	CL=90%
$\Gamma_{110}$	$K^+ e^- \mu^+$	LF < 9.7 ×10 <sup>-6</sup>	CL=90%
$\Gamma_{111}$	$\pi^- 2e^+$	L < 4.1 ×10 <sup>-6</sup>	CL=90%
$\Gamma_{112}$	$\pi^- 2\mu^+$	L < 1.4 ×10 <sup>-5</sup>	CL=90%
$\Gamma_{113}$	$\pi^- e^+ \mu^+$	L < 8.4 ×10 <sup>-6</sup>	CL=90%
$\Gamma_{114}$	$K^- 2e^+$	L < 5.2 ×10 <sup>-6</sup>	CL=90%
$\Gamma_{115}$	$K^- 2\mu^+$	L < 1.3 ×10 <sup>-5</sup>	CL=90%
$\Gamma_{116}$	$K^- e^+ \mu^+$	L < 6.1 ×10 <sup>-6</sup>	CL=90%
$\Gamma_{117}$	$K^*(892)^- 2\mu^+$	L < 1.4 ×10 <sup>-3</sup>	CL=90%

[a] This is the purely  $e^+$  semileptonic branching fraction: the  $e^+$  fraction from  $\tau^+$  decays has been subtracted off. The sum of our (non- $\tau$ )  $e^+$  exclusive fractions — an  $e^+ \nu_e$  with an  $\eta, \eta', \phi, K^0, K^{*0}$ , or  $f_0(980)$  — is  $7.0 \pm 0.4$  %

[b] This fraction includes  $\eta$  from  $\eta'$  decays.

[c] Two times (to include  $\mu$  decays) the  $\eta' e^+ \nu_e$  branching fraction, plus the  $\eta' \pi^+, \eta' \rho^+$ , and  $\eta' K^+$  fractions, is  $(18.6 \pm 2.3)$ %, which considerably exceeds the inclusive  $\eta'$  fraction of  $(11.7 \pm 1.8)$ %. Our best guess is that the  $\eta' \rho^+$  fraction,  $(12.5 \pm 2.2)$ %, is too large.

[d] This branching fraction includes all the decay modes of the final-state resonance.

[e] A test for  $u\bar{u}$  or  $d\bar{d}$  content in the  $D_s^\pm$ . Neither Cabibbo-favored nor Cabibbo-suppressed decays can contribute, and  $\omega-\phi$  mixing is an unlikely explanation for any fraction above about  $2 \times 10^{-4}$ .

[f] The branching fraction for this mode may differ from the sum of the submodes that contribute to it, due to interference effects. See the relevant papers.

[g] We decouple the  $D_s^\pm \rightarrow \phi \pi^\pm$  branching fraction obtained from mass projections (and used to get some of the other branching fractions) from the  $D_s^\pm \rightarrow \phi \pi^\pm, \phi \rightarrow K^+ K^-$  branching fraction obtained from the Dalitz-plot analysis of  $D_s^\pm \rightarrow K^+ K^- \pi^\pm$ . That is, the ratio of these two branching fractions is not exactly the  $\phi \rightarrow K^+ K^-$  branching fraction 0.491.

[h] This is the average of a model-independent and a  $K$ -matrix parametrization of the  $\pi^+ \pi^-$   $S$ -wave and is a sum over several  $f_0$  mesons.

[i] This mode is not a useful test for a  $\Delta C=1$  weak neutral current because both quarks must change flavor in this decay.

[j] This is *not* a test for the  $\Delta C=1$  weak neutral current, but leads to the  $\pi^+ \ell^+ \ell^-$  final state.

See key on page 457

**CONSTRAINED FIT INFORMATION**

An overall fit to 16 branching ratios uses 17 measurements and one constraint to determine 12 parameters. The overall fit has a  $\chi^2 = 2.4$  for 6 degrees of freedom.

The following *off-diagonal* array elements are the correlation coefficients  $\langle \delta x_i \delta x_j \rangle / (\delta x_i \delta x_j)$ , in percent, from the fit to the branching fractions,  $x_i \equiv \Gamma_i / \Gamma_{\text{total}}$ . The fit constrains the  $x_i$  whose labels appear in this array to sum to one.

$x_{25}$	16																			
$x_{26}$	12	2																		
$x_{31}$	0	0	0																	
$x_{32}$	0	0	0	76																
$x_{42}$	0	0	0	42	48															
$x_{44}$	0	0	0	51	59	32														
$x_{55}$	0	0	0	59	74	37	45													
$x_{65}$	0	0	0	67	51	29	35	40												
$x_{66}$	0	0	0	11	8	5	6	6	16											
$x_{84}$	0	0	0	37	45	22	28	33	25	4										
	$x_{23}$	$x_{25}$	$x_{26}$	$x_{31}$	$x_{32}$	$x_{42}$	$x_{44}$	$x_{55}$	$x_{65}$	$x_{66}$										

 **$D_s^+$  BRANCHING FRACTIONS**

Written April 2010 by J.L. Rosner (University of Chicago) and C.G. Wohl (LBNL).

More than a dozen papers on the  $D_s^+$ , most of them from the CLEO experiment, have been published since the 2008 Review. We now know enough to attempt an overview of the branching fractions. Figure 1 shows a partial breakdown of the fractions. The rest of this note is about how the figure was constructed. The values shown make heavy use of CLEO measurements of inclusive branching fractions [1]. For other data and references cited in the following, see the Listings.

**Modes with leptons:** The bottom  $(20.0 \pm 0.9)\%$  of Fig. 1 shows the fractions for the exclusive modes that include leptons. Measured  $e^+\nu_e$  fractions have been doubled to get the semileptonic  $\ell^+\nu$  fractions. The sum of the exclusive  $e^+\nu_e$  fractions is  $(6.9 \pm 0.4)\%$ , consistent with an inclusive semileptonic  $e^+\nu_e$  measurement of  $(6.5 \pm 0.4)\%$ . There seems to be little missing here.

**Inclusive hadronic  $K\bar{K}$  fractions:** The Cabibbo-favored  $c \rightarrow s$  decay in  $D_s^+$  decay produces a final state with both an  $s$  and an  $\bar{s}$ ; and thus decay modes with a  $K\bar{K}$  pair or with an  $\eta$ ,  $\omega$ ,  $\eta'$ , or  $\phi$  predominate (see, for example, in Fig. 1 the fractions with leptons). We consider the  $K\bar{K}$  modes first. A complete picture of the exclusive  $K\bar{K}$  charge modes is not yet possible, because branching fractions for more than half of those modes have yet to be measured. However, CLEO has measured the inclusive  $K^+$ ,  $K^-$ ,  $K_S^0$ ,  $K^+K^-$ ,  $K^+K_S^0$ ,  $K^-K_S^0$ , and  $2K_S^0$  fractions (which include modes with leptons) [1]. And each of these inclusive fractions  $f$  with a  $K_S^0$  is equal to the corresponding fraction with a  $K_L^0$ :  $f(K^+K_L^0) = f(K^+K_S^0)$ ,  $f(2K_L^0) = f(2K_S^0)$ , etc. Therefore, of all inclusive fractions pairing a  $K^+$ ,  $K_S^0$ , or  $K_L^0$  with a  $K^-$ ,  $K_S^0$ , or  $K_L^0$ , we know all but  $f(K_S^0K_L^0)$ .

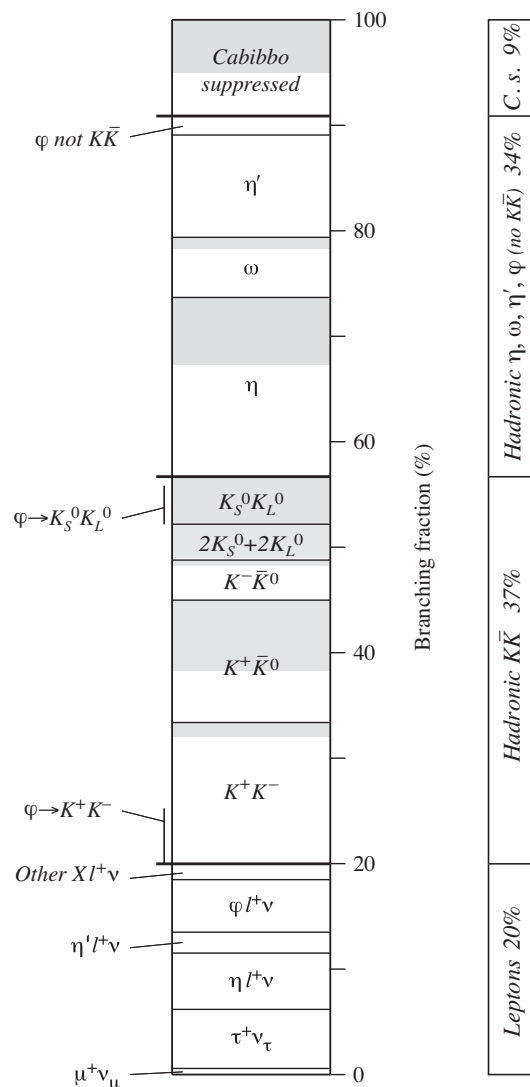


**Figure :** A partial breakdown of  $D_s^+$  branching fractions. Shading indicates parts of bins allotted to as-yet unmeasured exclusive modes. The inclusive hadronic  $\phi$  fraction is spread over three bins. See the text for further explanations.

We can get that fraction. The total  $K_S^0$  fraction is

$$f(K_S^0) = f(K^+K_S^0) + f(K^-K_S^0) + 2f(2K_S^0) + f(K_S^0K_L^0) + f(\text{single } K_S^0),$$

where  $f(\text{single } K_S^0)$  is the sum of the branching fractions for modes such as  $K_S^0\pi^+2\pi^0$  with a  $K_S^0$  and no second  $K$ . The  $K_S^0\pi^+2\pi^0$  mode is in fact the only unmeasured single- $K_S^0$  mode (throughout, we shall assume that fractions for modes with a  $K$  or  $K\bar{K}$  and more than three pions are negligible), and we shall take its fraction to be the same as for the  $K_S^02\pi^+\pi^-$  mode,  $(0.29 \pm 0.11)\%$ . Any reasonable deviation from this value would be too small to matter much in the following. Adding the several small single- $K_S^0$  branching fractions, including those from semileptonic modes, we get  $f(\text{single } K_S^0) = (1.67 \pm 0.26)\%$ .

# Meson Particle Listings

$D_s^\pm$

Using this, we have:

$$\begin{aligned} f(K_S^0 K_L^0) &= f(K_S^0) - f(K^+ K_S^0) - f(K^- K_S^0) - 2f(2K_S^0) \\ &\quad - f(\text{single } K_S^0) \\ &= (19.0 \pm 1.1) - (5.8 \pm 0.5) - (1.9 \pm 0.4) \\ &\quad - 2 \times (1.70 \pm 0.32) - (1.67 \pm 0.26) \\ &= (6.2 \pm 1.4)\% . \end{aligned}$$

Here and below we treat the errors as uncorrelated, although often they are not. However, our main aim is to get numbers for Fig. 1; errors will be secondary.

There is a check on our result: The  $\phi$  inclusive branching fraction is  $(15.7 \pm 1.0)\%$ , of which 34%, or  $(5.34 \pm 0.34)\%$  of  $D_s^\pm$  decays, produces a  $K_S^0 K_L^0$ . Our  $f(K_S^0 K_L^0) = (6.2 \pm 1.4)\%$  has to be at least this large—and it is.

We now make a table. The first column gives the various particle pairings; here we use  $f(K^+ \bar{K}^0) = 2f(K^+ K_S^0)$ , and likewise for  $f(K^- K^0)$ . The second column gives the inclusive branching fractions; the third column gives the fractions for  $K^+ K^-$  and  $K_S^0 K_L^0$  from  $\phi \ell^+ \nu$  decay; the last column subtracts these off to get the purely hadronic  $K\bar{K}$  inclusive fractions.

$K^+ K^-$	15.8 (0.7)%	2.44 (0.14)%	13.4 (0.7)%
$K^+ \bar{K}^0$	11.6 (1.0)		11.6 (1.0)
$K^- K^0$	3.8 (0.8)		3.8 (0.8)
$K_S^0 K_S^0 + K_L^0 K_L^0$	3.4 (0.64)		3.4 (0.64)
$K_S^0 K_L^0$	6.2 (1.4)	1.69 (0.10)	4.5 (1.4) .

The values in the last column are shown in Fig. 1. Their sum is  $(36.7 \pm 2.1)\%$ .

We can add more information to the figure by summing up measured branching fractions for exclusive modes within each bin:

$K^+ K^-$  modes—The sum of measured  $K^+ K^- \pi^+$ ,  $K^+ K^- \pi^+ \pi^0$ , and  $K^+ K^- 2\pi^+ \pi^-$  branching fractions is  $(12.0 \pm 0.6)\%$ . That leaves  $(1.4 \pm 0.9)\%$  for the  $K^+ K^- \pi^+ 2\pi^0$  mode, which is the only other  $K^+ K^-$  mode with three or fewer pions. In Fig. 1, this unmeasured part of the  $K^+ K^-$  bin is shaded.

$K^+ \bar{K}^0$  modes—Twice the sum of measured  $K^+ K_S^0$  and  $K^+ K_S^0 \pi^+ \pi^-$  branching fractions is  $(4.9 \pm 0.3)\%$ . This leaves  $(6.7 \pm 1.0)\%$  for the unmeasured  $K^+ \bar{K}^0$  modes (there are four such modes with three or fewer pions). This is shaded in the figure.

$K^- K^0$  modes—Twice the  $K^- K_S^0 2\pi^+$  fraction is  $(3.28 \pm 0.24)\%$ , which leaves about  $(0.5 \pm 0.8)\%$  for  $K^- K^0 2\pi^+ \pi^0$ , the only other  $K^- K^0$  mode with three or fewer pions.

$K^0 \bar{K}^0$  modes—The only measurement of  $K^0 \bar{K}^0$  decays is of the  $2K_S^0 2\pi^+ \pi^-$  fraction,  $(0.084 \pm 0.035)\%$ ; so nearly everything is shaded here. However, most of the  $K_S^0 K_L^0$  fraction is accounted for by  $\phi$  decays (see below).

**Inclusive hadronic  $\eta$ ,  $\omega$ ,  $\eta'$ , and  $\phi$  fractions:** These are easier. We start with the inclusive branching fractions, and then, to avoid double counting, subtract: (1) fractions for modes

with leptons; (2)  $\eta$  mesons that are included in the inclusive  $\eta'$  fraction; and (3)  $K^+ K^-$  and  $K_S^0 K_L^0$  from  $\phi$  decays:

$$\begin{aligned} f(\eta \text{ hadronic}) &= f(\eta \text{ inclusive}) - 0.65 f(\eta' \text{ inclusive}) \\ &\quad - f(\eta \ell^+ \nu) = (17.0 \pm 3.1)\% \end{aligned}$$

$$\begin{aligned} f(\omega \text{ hadronic}) &= f(\omega \text{ inclusive}) - 0.03 f(\eta' \text{ inclusive}) \\ &= (5.7 \pm 1.4)\% \end{aligned}$$

$$\begin{aligned} f(\eta' \text{ hadronic}) &= f(\eta' \text{ inclusive}) - f(\eta' \ell^+ \nu) \\ &= (9.7 \pm 1.9)\% \end{aligned}$$

$$\begin{aligned} f(\phi \text{ hadronic, } \not\rightarrow K\bar{K}) &= 0.17 [f(\phi \text{ inclusive}) \\ &\quad - f(\phi \ell^+ \nu)] = (1.8 \pm 0.2)\% . \end{aligned}$$

The factors 0.65, 0.03, and 0.17 are the  $\eta' \rightarrow \eta$ ,  $\eta' \rightarrow \omega$ , and  $\phi \not\rightarrow K\bar{K}$  branching fractions. Figure 1 shows the results; the sum is  $(34.2 \pm 3.9)\%$ , which is about equal to the hadronic  $K\bar{K}$  total.

Note that the bin marked  $\phi$  near the top of Fig. 1 includes neither the  $\phi \ell^+ \nu$  decays nor the 83% of other  $\phi$  decays that produce a  $K\bar{K}$  pair. Compared to the size of that  $\phi$  bin, there is twice as much  $\phi$  in the  $K_S^0 K_L^0$  bin, and nearly three times as much in the  $K^+ K^-$  bin. These contributions are indicated in those bins.

Again, we can show how much of each bin is accounted for by measured exclusive branching fractions:

$\eta$  modes—The sum of  $\eta \pi^+$ ,  $\eta \rho^+$ , and  $\eta K^+$  branching fractions is  $(10.6 \pm 0.8)\%$ , which leaves a good part of the inclusive hadronic  $\eta$  fraction,  $(17.0 \pm 3.1)\%$ , to be accounted for. This is shaded in the figure.

$\omega$  modes—The sum of  $\omega \pi^+$ ,  $\omega \pi^+ \pi^0$ , and  $\omega 2\pi^+ \pi^-$  fractions is  $(4.6 \pm 0.9)\%$ , which is nearly as large as the inclusive hadronic  $\omega$  fraction,  $(5.7 \pm 1.4)\%$ .

$\eta'$  modes—The sum of  $\eta' \pi^+$ ,  $\eta' \rho^+$ , and  $\eta' K^+$  fractions is  $(16.5 \pm 2.2)\%$ , which is much larger than the inclusive hadronic  $\eta'$  fraction,  $(9.7 \pm 1.9)\%$ . If an exclusive measurement is at fault, it almost has to be the  $\eta' \rho^+$  fraction, which is  $(12.5 \pm 2.2)\%$ . It has been suggested that some of this signal might instead be misidentified kinematic reflections of other modes [2].

**Cabibbo-suppressed modes:** Remaining is  $(9.1 \pm 4.5)\%$  for hadronic Cabibbo-suppressed modes having no  $\eta$ ,  $\omega$ ,  $\eta'$ , or  $\phi$ . The contributions are:

$K^0 + pions$ —Above, we found that  $f(\text{single } K_S^0) = (1.67 \pm 0.26)\%$ ; subtracting leptonic contributions leaves  $(1.20 \pm 0.24)\%$ . The hadronic single- $K^0$  fraction is twice this,  $(2.40 \pm 0.48)\%$ .

$K^+ + pions$ —The  $K^+ \pi^0$  and  $K^+ \pi^+ \pi^-$  fractions sum to  $(0.77 \pm 0.05)\%$ . Much of the  $K^+ n\pi$  modes, where  $n \geq 3$ , is already in the  $\eta$ ,  $\omega$ , and  $\eta'$  bins, and the rest is not measured. The total  $K^+$  fraction wanted here is probably in the 1-to-2% range.

$Multi-pions$ —The  $2\pi^+ \pi^-$ ,  $\pi^+ 2\pi^0$ , and  $3\pi^+ 2\pi^-$  fractions total  $(2.6 \pm 0.2)\%$ . Modes not measured might double this.

The sum of the three contributions is certainly not inconsistent with the Cabibbo-suppressed total of  $(9.1 \pm 4.5)\%$ . The sum of actually measured fractions is  $(4.2 \pm 0.2)\%$ .

**A model:** With CLEO about to publish inclusive branching fractions [1], Gronau and Rosner predicted those fractions using a “statistical isospin” model [2]. Consider, say, the  $D_s^+ \rightarrow K\bar{K}\pi$  charge modes: the  $K^+K^-\pi^+$  branching fraction is measured, the  $K^+\bar{K}^0\pi^0$  and  $K^0\bar{K}^0\pi^+$  fractions are not. The statistical isospin model assumes that all the independent isospin amplitudes for  $D_s^+ \rightarrow K\bar{K}\pi$  decay are equal in magnitude and incoherent in phase—in which case, the ratio of the three fractions here is 3:3:2. (Actually, use was also made of the fact that  $D_s^+ \rightarrow K\bar{K}\pi$  decay is dominated by  $\phi\pi^+$ ,  $K^+\bar{K}^{*0}$ , and  $K^{*+}\bar{K}^0$  submodes; but the estimated charge-mode ratios were not far from 3:3:2.) A different, quark-antiquark pair-production model was used to estimate systematic uncertainties.

In this way, unmeasured exclusive fractions were calculated from measured exclusive fractions (the latter were taken from the 2008 Review, and so did not benefit from recent results). In the hadronic sector, the measured total of 59.4% of  $D_s^+$  decays led to an estimated total of 24.2% for unmeasured modes. Weighted counts of  $\pi^+$ ,  $K_S^0$ , etc., were then made to get the inclusive fractions.

Of interest here is that the sum of all the exclusive fractions—a way-stop in getting the inclusive values—was a nearly correct 103%. In the absence of complete measurements, the model is a way to, in effect, average over ignorance. It probably works better summed over a number of charge-mode sets than in detail. It is known to sometimes give incorrect results when there are sufficient measurements to test it.

## References

1. S. Dobbs *et al.*, Phys. Rev. **D79**, 112008 (2009).
2. M. Gronau and J.L. Rosner, Phys. Rev. **D79**, 074022 (2009).

### $D_s^\pm$ BRANCHING RATIOS

A number of older, now obsolete results have been omitted. They may be found in earlier editions.

#### Inclusive modes

$\Gamma(e^+ \text{ semileptonic})/\Gamma_{\text{total}}$		$\Gamma_1/\Gamma$	
This is the purely $e^+$ semileptonic branching fraction: the $e^+$ fraction from $\tau^+$ decays has been subtracted off. The sum of our (non- $\tau$ ) $e^+$ exclusive fractions — an $e^+\nu_e$ with an $\eta$ , $\eta'$ , $\phi$ , $K^0$ , $K^{*0}$ , or $f_0(980)$ — is $6.90 \pm 0.4\%$			
VALUE (units $10^{-2}$ )	EVTS	DOCUMENT ID	TECN COMMENT
<b><math>6.52 \pm 0.39 \pm 0.15</math></b>	536 ± 29	<sup>3</sup> ASNER	10 CLEO $e^+e^-$ at 3774 MeV
<sup>3</sup> Using the $D_s^+$ and $D^0$ lifetimes, ASNER 10 finds that the ratio of the $D_s^+$ and $D^0$ semileptonic widths is $0.828 \pm 0.051 \pm 0.025$ .			

$\Gamma(\pi^+ \text{ anything})/\Gamma_{\text{total}}$		$\Gamma_2/\Gamma$	
Events with two $\pi^+$ 's count twice, etc. But $\pi^+$ 's from $K_S^0 \rightarrow \pi^+\pi^-$ are not included.			
VALUE (units $10^{-2}$ )	DOCUMENT ID	TECN	COMMENT
<b><math>119.3 \pm 1.2 \pm 0.7</math></b>	DOBBS	09	CLEO $e^+e^-$ at 4170 MeV

$\Gamma(\pi^- \text{ anything})/\Gamma_{\text{total}}$		$\Gamma_3/\Gamma$	
Events with two $\pi^-$ 's count twice, etc. But $\pi^-$ 's from $K_S^0 \rightarrow \pi^+\pi^-$ are not included.			
VALUE (units $10^{-2}$ )	DOCUMENT ID	TECN	COMMENT
<b><math>43.2 \pm 0.9 \pm 0.3</math></b>	DOBBS	09	CLEO $e^+e^-$ at 4170 MeV

$\Gamma(\pi^0 \text{ anything})/\Gamma_{\text{total}}$		$\Gamma_4/\Gamma$	
Events with two $\pi^0$ 's count twice, etc. But $\pi^0$ 's from $K_S^0 \rightarrow 2\pi^0$ are not included.			
VALUE (units $10^{-2}$ )	DOCUMENT ID	TECN	COMMENT
<b><math>123.4 \pm 3.8 \pm 5.3</math></b>	DOBBS	09	CLEO $e^+e^-$ at 4170 MeV

$\Gamma(K^- \text{ anything})/\Gamma_{\text{total}}$		$\Gamma_5/\Gamma$	
VALUE (units $10^{-2}$ )	DOCUMENT ID	TECN	COMMENT
<b><math>18.7 \pm 0.5 \pm 0.2</math></b>	DOBBS	09	CLEO $e^+e^-$ at 4170 MeV

$\Gamma(K^+ \text{ anything})/\Gamma_{\text{total}}$		$\Gamma_6/\Gamma$	
VALUE (units $10^{-2}$ )	DOCUMENT ID	TECN	COMMENT
<b><math>28.9 \pm 0.6 \pm 0.3</math></b>	DOBBS	09	CLEO $e^+e^-$ at 4170 MeV

$\Gamma(K_S^0 \text{ anything})/\Gamma_{\text{total}}$		$\Gamma_7/\Gamma$	
VALUE (units $10^{-2}$ )	DOCUMENT ID	TECN	COMMENT
<b><math>19.0 \pm 1.0 \pm 0.4</math></b>	DOBBS	09	CLEO $e^+e^-$ at 4170 MeV

$\Gamma(\eta \text{ anything})/\Gamma_{\text{total}}$		$\Gamma_8/\Gamma$	
This ratio includes $\eta$ particles from $\eta'$ decays.			
VALUE (units $10^{-2}$ )	EVTS	DOCUMENT ID	TECN COMMENT
<b><math>29.9 \pm 2.2 \pm 1.7</math></b>		DOBBS	09 CLEO $e^+e^-$ at 4170 MeV
••• We do not use the following data for averages, fits, limits, etc. •••			
$23.5 \pm 3.1 \pm 2.0$	674 ± 91	HUANG	06B CLEO See DOBBS 09

$\Gamma(\omega \text{ anything})/\Gamma_{\text{total}}$		$\Gamma_9/\Gamma$	
VALUE (units $10^{-2}$ )	DOCUMENT ID	TECN	COMMENT
<b><math>6.1 \pm 1.4 \pm 0.3</math></b>	DOBBS	09	CLEO $e^+e^-$ at 4170 MeV

$\Gamma(\eta' \text{ anything})/\Gamma_{\text{total}}$		$\Gamma_{10}/\Gamma$	
VALUE (units $10^{-2}$ )	EVTS	DOCUMENT ID	TECN COMMENT
<b><math>11.7 \pm 1.7 \pm 0.7</math></b>		DOBBS	09 CLEO $e^+e^-$ at 4170 MeV
••• We do not use the following data for averages, fits, limits, etc. •••			
$8.7 \pm 1.9 \pm 0.8$	68 ± 15	HUANG	06B CLEO See DOBBS 09

$\Gamma(f_0(980) \text{ anything, } f_0 \rightarrow \pi^+\pi^-)/\Gamma_{\text{total}}$		$\Gamma_{11}/\Gamma$	
VALUE (units $10^{-2}$ )	CL%	DOCUMENT ID	TECN COMMENT
<b>&lt;1.3</b>	90	DOBBS	09 CLEO $e^+e^-$ at 4170 MeV

$\Gamma(\phi \text{ anything})/\Gamma_{\text{total}}$		$\Gamma_{12}/\Gamma$	
VALUE (units $10^{-2}$ )	EVTS	DOCUMENT ID	TECN COMMENT
<b><math>15.7 \pm 0.8 \pm 0.6</math></b>		DOBBS	09 CLEO $e^+e^-$ at 4170 MeV
••• We do not use the following data for averages, fits, limits, etc. •••			
$16.1 \pm 1.2 \pm 1.1$	398 ± 27	HUANG	06B CLEO See DOBBS 09

$\Gamma(K^+K^- \text{ anything})/\Gamma_{\text{total}}$		$\Gamma_{13}/\Gamma$	
VALUE (units $10^{-2}$ )	DOCUMENT ID	TECN	COMMENT
<b><math>15.8 \pm 0.6 \pm 0.3</math></b>	DOBBS	09	CLEO $e^+e^-$ at 4170 MeV

$\Gamma(K_S^0 K^+ \text{ anything})/\Gamma_{\text{total}}$		$\Gamma_{14}/\Gamma$	
VALUE (units $10^{-2}$ )	DOCUMENT ID	TECN	COMMENT
<b><math>5.8 \pm 0.5 \pm 0.1</math></b>	DOBBS	09	CLEO $e^+e^-$ at 4170 MeV

$\Gamma(K_S^0 K^- \text{ anything})/\Gamma_{\text{total}}$		$\Gamma_{15}/\Gamma$	
VALUE (units $10^{-2}$ )	DOCUMENT ID	TECN	COMMENT
<b><math>1.9 \pm 0.4 \pm 0.1</math></b>	DOBBS	09	CLEO $e^+e^-$ at 4170 MeV

$\Gamma(2K_S^0 \text{ anything})/\Gamma_{\text{total}}$		$\Gamma_{16}/\Gamma$	
VALUE (units $10^{-2}$ )	DOCUMENT ID	TECN	COMMENT
<b><math>1.7 \pm 0.3 \pm 0.1</math></b>	DOBBS	09	CLEO $e^+e^-$ at 4170 MeV

$\Gamma(2K^+ \text{ anything})/\Gamma_{\text{total}}$		$\Gamma_{17}/\Gamma$	
VALUE (units $10^{-2}$ )	CL%	DOCUMENT ID	TECN COMMENT
<b>&lt;0.26</b>	90	DOBBS	09 CLEO $e^+e^-$ at 4170 MeV

$\Gamma(2K^- \text{ anything})/\Gamma_{\text{total}}$		$\Gamma_{18}/\Gamma$	
VALUE (units $10^{-2}$ )	CL%	DOCUMENT ID	TECN COMMENT
<b>&lt;0.06</b>	90	DOBBS	09 CLEO $e^+e^-$ at 4170 MeV

#### Leptonic and semileptonic modes

# Meson Particle Listings

$D_s^\pm$

## DECAY CONSTANTS OF CHARGED PSEUDO-SCALAR MESONS

Revised February 2012 by J. Rosner (Univ. Chicago) and S. Stone (Syracuse Univ.)

**Introduction:** Charged mesons formed from a quark and an antiquark can decay to a charged lepton pair when these objects annihilate via a virtual  $W$  boson [1]. Fig. 1 illustrates this process for the purely leptonic decay of a  $D^+$  meson.

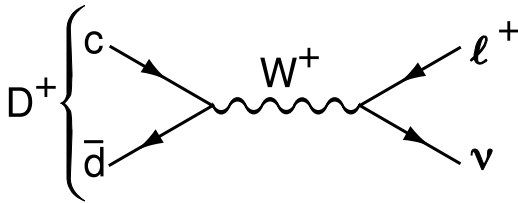


**Figure 1:** The annihilation process for pure  $D^+$  leptonic decays in the Standard Model.

Similar quark-antiquark annihilations via a virtual  $W^+$  to the  $\ell^+\nu$  final states occur for the  $\pi^+$ ,  $K^+$ ,  $D_s^+$ , and  $B^+$  mesons. (Charge-conjugate particles and decays are implied.) Let  $P$  be any of these pseudoscalar mesons. To lowest order, the decay width is

$$\Gamma(P \rightarrow \ell\nu) = \frac{G_F^2}{8\pi} f_P^2 m_\ell^2 M_P \left(1 - \frac{m_\ell^2}{M_P^2}\right)^2 |V_{q_1 q_2}|^2. \quad (1)$$

Here  $M_P$  is the  $P$  mass,  $m_\ell$  is the  $\ell$  mass,  $V_{q_1 q_2}$  is the Cabibbo-Kobayashi-Maskawa (CKM) matrix element between the constituent quarks  $q_1 \bar{q}_2$  in  $P$ , and  $G_F$  is the Fermi coupling constant. The parameter  $f_P$  is the decay constant, and is related to the wave-function overlap of the quark and antiquark.

The decay  $P^\pm$  starts with a spin-0 meson, and ends up with a left-handed neutrino or right-handed antineutrino. By angular momentum conservation, the  $\ell^\pm$  must then also be left-handed or right-handed, respectively. In the  $m_\ell = 0$  limit, the decay is forbidden, and can only occur as a result of the finite  $\ell$  mass. This helicity suppression is the origin of the  $m_\ell^2$  dependence of the decay width.

There is a complication in measuring purely leptonic decay rates. The process  $P \rightarrow \ell\nu\gamma$  is not simply a radiative correction, although radiative corrections contribute. The  $P$  can make a transition to a virtual  $P^*$ , emitting a real photon, and the  $P^*$  decays into  $\ell\nu$ , avoiding helicity suppression. The importance of this amplitude depends on the decaying particle and the detection technique. The  $\ell\nu\gamma$  rate for a heavy particle such as  $B$  decaying into a light particle such as a muon can be larger than the width without photon emission [2]. On the other hand, for decays into a  $\tau^\pm$ , the helicity suppression is mostly broken and these effects appear to be small.

Measurements of purely leptonic decay branching fractions and lifetimes allow an experimental determination of the product  $|V_{q_1 q_2}| f_P$ . If the CKM element is well known from other

measurements, then  $f_P$  can be well measured. If, on the other hand, the CKM element is not well measured, having theoretical input on  $f_P$  can allow a determination of the CKM element. The importance of measuring  $\Gamma(P \rightarrow \ell\nu)$  depends on the particle being considered. For example, the measurement of  $\Gamma(B^- \rightarrow \tau^- \bar{\nu})$  provides an indirect determination of  $|V_{ub}|$  provided that  $f_B$  is provided by theory. In addition,  $f_B$  is crucial for using measurements of  $B^0$ - $\bar{B}^0$  mixing to extract information on the fundamental CKM parameters. Knowledge of  $f_{B_s}$  is also needed, but it cannot be directly measured as the  $B_s$  is neutral, so the violation of the SU(3) relation  $f_{B_s} = f_B$  must be estimated theoretically. This difficulty does not occur for  $D$  mesons as both the  $D^+$  and  $D_s^+$  are charged, allowing the direct measurement of SU(3) breaking and a direct comparison with theory.

For  $B^-$  and  $D_s^+$  decays, the existence of a charged Higgs boson (or any other charged object beyond the Standard Model) would modify the decay rates; however, this would not necessarily be true for the  $D^+$  [3,4]. More generally, the ratio of  $\tau\nu$  to  $\mu\nu$  decays can serve as one probe of lepton universality [3,5].

As  $|V_{ud}|$  has been quite accurately measured in super-allowed  $\beta$  decays [6], with a value of 0.97425(22) [7], measurements of  $\Gamma(\pi^+ \rightarrow \mu^+\nu)$  yield a value for  $f_\pi$ . Similarly,  $|V_{us}|$  has been well measured in semileptonic kaon decays, so a value for  $f_K$  from  $\Gamma(K^- \rightarrow \mu^-\bar{\nu})$  can be compared to theoretical calculations. Lattice gauge theory calculations, however, have been claimed to be very accurate in determining  $f_K$ , and these have been used to predict  $|V_{us}|$  [8].

**$D^+$  and  $D_s^+$  decay constants:** We review current measurements, starting with the charm system. The CLEO collaboration has performed the only measurement of the branching fraction for  $D^+ \rightarrow \mu^+\nu$  [9]. CLEO uses  $e^+e^-$  collisions at the  $\psi(3770)$  resonant energy where  $D^-D^+$  pairs are copiously produced. They fully reconstruct one of the  $D$ 's, find a candidate muon track of opposite sign to the tag, and then use kinematical constraints to infer the existence of a missing neutrino and hence the  $\mu\nu$  decay of the other  $D$ . They find  $\mathcal{B}(D^+ \rightarrow \mu^+\nu) = (3.82 \pm 0.32 \pm 0.09) \times 10^{-4}$ . We use the well-measured  $D^+$  lifetime of 1.040(7) ps, and assuming  $|V_{cd}|$  equals  $|V_{us}| = 0.2246(12)$  [7] minus higher order correction terms [10], we find  $|V_{cd}| = 0.2245(12)$ . The CLEO branching fraction result then translates into a value of

$$f_{D^+} = (206.7 \pm 8.5 \pm 2.5) \text{ MeV}.$$

This result includes a 1% correction (lowering) of the rate due to the presence of the radiative  $\mu^+\nu\gamma$  final state based on the estimate by Dobrescu and Kronfeld [11].

Before we compare this result with theoretical predictions, we discuss the  $D_s^+$ . Measurements of  $f_{D_s^+}$  have been made by several groups and are listed in Table 1 [12–16]. We exclude older values obtained by normalizing to  $D_s^+$  decay modes that are not well defined. Many measurements, for example, used



the  $\phi\pi^+$  mode. This decay is a subset of the  $D_s^+ \rightarrow K^+K^-\pi^+$  channel which has interferences from other modes populating the  $K^+K^-$  mass region near the  $\phi$ , the most prominent of which is the  $f_0(980)$ . Thus the extraction of effective  $\phi\pi^+$  rate is sensitive to the mass resolution of the experiment and the cuts used to define the  $\phi$  mass region [17,18]. The CLEO, BaBar, and Belle  $\mu^+\nu$  results rely on fully reconstructing all the final-state particles except for the neutrino and using a missing-mass technique to infer the existence of the neutrino. CLEO uses  $e^+e^- \rightarrow D_s D_s^*$  collisions at 4170 MeV, while Babar and Belle use  $e^+e^- \rightarrow DK n \pi D_s^*$  collisions at energies near the  $\Upsilon(4S)$ .

**Table 1:** Experimental results for  $\mathcal{B}(D_s^+ \rightarrow \mu^+\nu)$ ,  $\mathcal{B}(D_s^+ \rightarrow \tau^+\nu)$ , and  $f_{D_s^+}$ . Numbers for  $f_{D_s^+}$  have been extracted using updated values for masses and  $|V_{cs}|$  (see text). Radiative corrections and systematic uncertainties for errors on the  $D_s^+$  lifetime and mass have been included. Common systematic errors in the CLEO results have been taken into account.

Experiment	Mode	$\mathcal{B}(\%)$	$f_{D_s^+}$ (MeV)
CLEO-c [12]	$\mu^+\nu$	$0.565 \pm 0.045 \pm 0.017$	$257.6 \pm 10.3 \pm 4.3$
BaBar [16]	$\mu^+\nu$	$0.602 \pm 0.038 \pm 0.034$	$265.9 \pm 8.4 \pm 7.7$
Belle [13]	$\mu^+\nu$	$0.638 \pm 0.076 \pm 0.057$	$274 \pm 16 \pm 12$
Average	$\mu^+\nu$	$0.589 \pm 0.033$	$263.0 \pm 7.3$
CLEO-c [12]	$\tau^+\nu$ ( $\pi^+\bar{\nu}$ )	$6.42 \pm 0.81 \pm 0.18$	$278.0 \pm 17.5 \pm 4.4$
CLEO-c [14]	$\tau^+\nu$ ( $\rho^+\bar{\nu}$ )	$5.52 \pm 0.57 \pm 0.21$	$257.8 \pm 13.3 \pm 5.2$
CLEO-c [15]	$\tau^+\nu$ ( $e^+\nu\bar{\nu}$ )	$5.30 \pm 0.47 \pm 0.22$	$252.6 \pm 11.1 \pm 5.2$
BaBar [16]	$\tau^+\nu$ ( $e^+/\mu^+\nu\bar{\nu}$ )	$5.00 \pm 0.35 \pm 0.49$	$245.4 \pm 8.6 \pm 12.2$
Average	$\tau^+\nu$	$5.43 \pm 0.31$	$255.7 \pm 7.2$

When selecting the  $\tau^+ \rightarrow \pi^+\bar{\nu}$  and  $\tau^+ \rightarrow \rho^+\bar{\nu}$  decay modes, CLEO uses both calculation of the missing-mass and the fact that there should be no extra energy in the event beyond that deposited by the measured tagged  $D_s^-$  and the  $\tau^+$  decay products. The  $\tau^+ \rightarrow e^+\nu\bar{\nu}$  mode, however, uses only no extra energy. BaBar measures  $\Gamma(D_s^+ \rightarrow \tau^+\nu)/\Gamma(D_s^+ \rightarrow \bar{K}^0 K^+)$  using the  $\tau^+ \rightarrow e^+\nu\bar{\nu}$  mode.

We extract the decay constant from the measured branching ratios using the  $D_s^+$  mass of 1.96847(33) GeV, the  $\tau^+$  mass of 1.77682(16) GeV, and a lifetime of 0.500(7) ps. We use the first-order correction  $|V_{cs}| = |V_{ud}| - |V_{cb}|^2/2$  [10]; taking  $|V_{ud}| = 0.97425(22)$  [6], and  $|V_{cb}| = 0.04$  from an average of exclusive and inclusive semileptonic  $B$  decay results as discussed in Ref. [19], we find  $|V_{cs}| = 0.97345(22)$ . CLEO has included the radiative correction of 1% in the  $\mu^+\nu$  rate listed in the Table [11] (the  $\tau^+\nu$  rates need not be corrected). Other theoretical calculations show that the  $\mu^+\nu\gamma$  rate is a factor of 40–100 below the  $\mu^+\nu$  rate for charm [20]. As this is a small effect we do not attempt to correct the other measurements.

The average decay constant cannot simply be obtained by averaging the values in Table 1 since there are correlated errors between the  $\mu^+\nu$  and  $\tau^+\nu$  values. Table 2 gives the average values of  $f_{D_s}$  where the experiments have included the correlations.

**Table 2:** Experimental results for  $f_{D_s^+}$  taking into account the common systematic errors in the  $\mu^+\nu$  and  $\tau^+\nu$  measurements.

Experiment	$f_{D_s^+}$ (MeV)
CLEO-c	$259.0 \pm 6.2 \pm 3.0$
BaBar	$258.8 \pm 6.4 \pm 7.5$
Belle	$273.8 \pm 16.3 \pm 12.2$
Average of $\mu^+\nu + \tau^+\nu$	$260.0 \pm 5.4$

Our experimental average is

$$f_{D_s^+} = (260.0 \pm 5.4) \text{ MeV.}$$

Furthermore, the ratio of branching fractions is found to be

$$R \equiv \frac{\mathcal{B}(D_s^+ \rightarrow \tau^+\nu)}{\mathcal{B}(D_s^+ \rightarrow \mu^+\nu)} = 9.2 \pm 0.7,$$

where a value of 9.76 is predicted in the Standard Model. Assuming lepton universality then we can derive improved values for the leptonic decay branching fractions of

$$\mathcal{B}(D_s^+ \rightarrow \mu^+\nu) = (5.75 \pm 0.24) \times 10^{-3}, \quad \text{and}$$

$$\mathcal{B}(D_s^+ \rightarrow \tau^+\nu) = (5.61 \pm 0.24) \times 10^{-2}.$$

The experimentally determined ratio of decay constants is  $f_{D_s^+}/f_{D^+} = 1.26 \pm 0.06$ .

Table 3 compares the experimental  $f_{D_s^+}$  with theoretical calculations [21–27]. While most theories give values lower than the  $f_{D_s^+}$  measurement, the errors are sufficiently large, in most cases, to declare success.

Upper limits on  $f_{D^+}$  and  $f_{D_s}$  of 230 and 270 MeV, respectively, have been determined using two-point correlation functions by Khodjamirian [28]. Both the  $D^+$  and  $D_s^+$  values are safely below this limit.

Akeroyd and Chen [29] pointed out that leptonic decay widths are modified in two-Higgs-doublet models (2HDM). Specifically, for the  $D^+$  and  $D_s^+$ , Eq. (1) is modified by a factor  $r_q$  multiplying the right-hand side [30]:

$$r_q = \left[ 1 + \left( \frac{1}{m_c + m_q} \right) \left( \frac{M_{D_q}}{M_{H^+}} \right)^2 \left( m_c - \frac{m_q \tan^2 \beta}{1 + \epsilon_0 \tan \beta} \right) \right]^2,$$

## Meson Particle Listings

 $D_s^\pm$ 

**Table 3:** Theoretical predictions of  $f_{D_s^+}$ ,  $f_{D^+}$ , and  $f_{D_s^+}/f_{D^+}$ . Quenched lattice calculations are omitted, while PQL indicates a partially-quenched lattice calculation. (Only selected results having errors are included.)

Model	$f_{D_s^+}$ (MeV)	$f_{D^+}$ (MeV)	$f_{D_s^+}/f_{D^+}$
Experiment (our averages)	$260.0 \pm 5.4$	$206.7 \pm 8.9$	$1.26 \pm 0.06$
Lattice (HPQCD) [21]	$248.0 \pm 2.5$	$213 \pm 4$	$1.164 \pm 0.018$
Lattice (FNAL+MILC) [22]	$260.1 \pm 10.8$	$218.9 \pm 11.3$	$1.188 \pm 0.025$
PQL [23]	$244 \pm 8$	$197 \pm 9$	$1.24 \pm 0.03$
QCD sum rules [24]	$205 \pm 22$	$177 \pm 21$	$1.16 \pm 0.01 \pm 0.03$
QCD sum rules [25]	$245.3 \pm 15.7 \pm 4.5$	$206.2 \pm 7.3 \pm 5.1$	$1.193 \pm 0.025 \pm 0.007$
Field correlators [26]	$260 \pm 10$	$210 \pm 10$	$1.24 \pm 0.03$
Light front [27]	$268.3 \pm 19.1$	206 (fixed)	$1.30 \pm 0.04$

where  $m_{H^+}$  is the charged Higgs mass,  $M_{D_q}$  is the mass of the  $D$  meson (containing the light quark  $q$ ),  $m_c$  is the charm quark mass,  $m_q$  is the light-quark mass, and  $\tan\beta$  is the ratio of the vacuum expectation values of the two Higgs doublets. In models where the fermion mass arises from coupling to more than one vacuum expectation value  $\epsilon_0$  can be non-zero, perhaps as large as 0.01. For the  $D^+$ ,  $m_d \ll m_c$ , and the change due to the  $H^+$  is very small. For the  $D_s^+$ , however, the effect can be substantial.

A major concern is the need for the Standard Model (SM) value of  $f_{D_s^+}$ . We can take that from a theoretical model. Our most aggressive choice is that of the unquenched lattice calculation [21], because it claims the smallest error. Since the charged Higgs would lower the rate compared to the SM, in principle, experiment gives a lower limit on the charged Higgs mass. However, the value for the predicted decay constant using this model is 2.0 standard deviations *below* the measurement. If this small discrepancy is to be taken seriously, either (a) the model of Ref. [21] is not representative; (b) no value of  $m_{H^+}$  in the two-Higgs doublet model will satisfy the constraint at 99% confidence level; or (c) there is new physics, different from the 2HDM, that interferes constructively with the SM amplitude such as in the R-parity-violating model of Akeroyd and Recksiegel [31].

To sum up, the situation is not clear. To set limits on new physics we need an independent calculation of  $f_{D_s}$  with comparable accuracy, and more precise measurements would also be useful.

**The  $B^+$  decay constant:** The Belle and BaBar collaborations have found evidence for  $B^- \rightarrow \tau^- \bar{\nu}$  decay in  $e^+e^- \rightarrow B^- B^+$  collisions at the  $\Upsilon(4S)$  energy. The analysis relies on reconstructing a hadronic or semi-leptonic  $B$  decay tag, finding a  $\tau$  candidate in the remaining track and or photon candidates, and examining the extra energy in the event which should be close to zero for a real  $\tau^-$  decay to  $e^- \bar{\nu}$  or  $\mu^- \bar{\nu}$  opposite a  $B^+$  tag. The results are listed in Table 4.

**Table 4:** Experimental results for  $\mathcal{B}(B^- \rightarrow \tau^- \bar{\nu})$ . We have computed an average for the two Belle measurements assuming that the systematic errors are fully correlated.

Experiment	Tag	$\mathcal{B}$ (units of $10^{-4}$ )
Belle [32]	Hadronic	$1.79_{-0.49-0.51}^{+0.56+0.46}$
Belle [33]	Semileptonic	$1.54_{-0.37-0.31}^{+0.38+0.29}$
Belle	Our average	$1.62 \pm 0.40$
BaBar [34]	Hadronic	$1.80_{-0.54}^{+0.57} \pm 0.26$
BaBar [35]	Semileptonic	$1.7 \pm 0.8 \pm 0.2$
BaBar	Average [34]	$1.76 \pm 0.49$
	Our average	$1.68 \pm 0.31$

There are large backgrounds under the signals in all cases. The systematic errors are also quite large, on the order of 20%. Thus, the significance of the signals is not that large. Belle quotes  $3.5\sigma$  and  $3.6\sigma$  for their hadronic and semileptonic tags, while BaBar quotes  $3.3\sigma$  and  $2.3\sigma$  for these tags. We note that the four central values are remarkably close to the average considering the large errors on all the measurements. More accuracy would be useful to investigate the effects of new physics.

We extract a SM value using Eq. (1). Here theory provides a value of  $f_B = (194 \pm 9)$  MeV [36]. We also need a value for  $|V_{ub}|$ . Here significant differences arise between using inclusive charmless semileptonic decays and the exclusive decay  $B \rightarrow \pi \ell^+ \nu$  [37]. The inclusive decays give rise to a value of  $|V_{ub}| = (4.27 \pm 0.38) \times 10^{-3}$  while the exclusive measurements yield  $|V_{ub}| = (3.38 \pm 0.36) \times 10^{-3}$ , where the errors are dominantly theoretical [38]. Their average, enlarging the error in the standard manner because the results differ, is  $|V_{ub}| = (3.80 \pm 0.44) \times 10^{-3}$ . Using these values and the PDG values for the  $B^+$  mass and lifetime, we arrive at the SM prediction for the  $\tau^- \bar{\nu}$  branching fraction of  $(0.96 \pm 0.24) \times 10^{-4}$ . This value is about

See key on page 457

a factor of two smaller than the measurements. There is a 6.6% probability that the data and the SM prediction are consistent. This difference is more clearly seen by examining the correlation between the CKM angle  $\beta$  and  $\mathcal{B}(B^- \rightarrow \tau^- \bar{\nu})$ . The CKM fitter group provides a fit to a large number of measurements involving heavy quark transitions [39]. The point in Fig. 2 shows the directly measured values, while the predictions from their fit without the direct measurements are also shown. There is about a factor of two discrepancy between the measured value of  $\mathcal{B}(B^- \rightarrow \tau^- \bar{\nu})$  and the fit prediction.

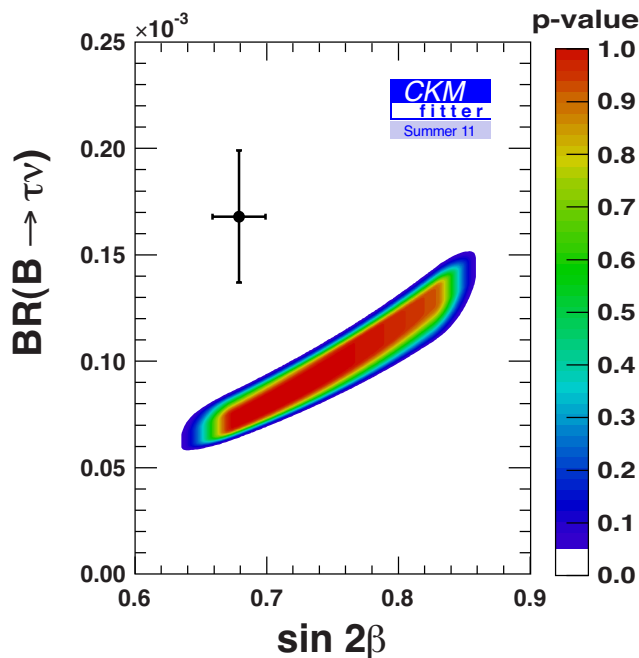


**Figure 2:** Measured and predicted values of  $\mathcal{B}(B^- \rightarrow \tau^- \bar{\nu})$  versus  $\sin 2\beta$  from the CKM fitter group [39]. The point with error bars shows the measured values, while the predictions are in shaded contours, with the shading related to the confidence level.

**$\pi^+$  and  $K^+$  decay constants:** The sum of branching fractions for  $\pi^- \rightarrow \mu^- \bar{\nu}$  and  $\pi^- \rightarrow \mu^- \bar{\nu} \gamma$  is 99.98770(4)%. The two modes are difficult to separate experimentally, so we use this sum, with Eq. (1) modified to include photon emission and radiative corrections [40]. The branching fraction together with the lifetime 26.033(5) ns gives

$$f_{\pi^-} = (130.41 \pm 0.03 \pm 0.20) \text{ MeV} .$$

The first error is due to the error on  $|V_{ud}|$ , 0.97425(22) [6]; the second is due to the higher-order corrections, and is much larger.

Similarly, the sum of branching fractions for  $K^- \rightarrow \mu^- \bar{\nu}$  and  $K^- \rightarrow \mu^- \bar{\nu} \gamma$  is 63.55(11)%, and the lifetime is 12.3840(193) ns [41]. Measurements of semileptonic kaon decays provide a

value for the product  $f_+(0)|V_{us}|$ , where  $f_+(0)$  is the form-factor at zero four-momentum transfer between the initial state kaon and the final state pion. We use a value for  $f_+(0)|V_{us}|$  of 0.21664(48) [41]. The  $f_+(0)$  must be determined theoretically. We follow Blucher and Marciano [7] in using the lattice calculation  $f_+(0) = 0.9644 \pm 0.0049$  [42], since it appears to be more precise than the classic Leutwyler-Roos calculation  $f_+(0) = 0.961 \pm 0.008$  [43]. [Other recent averages are  $0.956 \pm 0.008$  [49] and  $0.9588 \pm 0.0044$  [44].] Using the value from Ref. [42], the result is  $|V_{us}| = 0.2246 \pm 0.0012$ , consistent with the hyperon decay value of  $0.2250 \pm 0.0027$  [45]. We derive

$$f_{K^-} = (156.1 \pm 0.2 \pm 0.8 \pm 0.2) \text{ MeV} .$$

The first error is due to the error on  $\Gamma$ ; the second is due to the CKM factor  $|V_{us}|$ , and the third is due to the higher-order corrections. The largest source of error in these corrections depends on the QCD part, which is based on one calculation in the large  $N_c$  framework. We have doubled the quoted error here; this would probably be unnecessary if other calculations were to come to similar conclusions. A large part of the additional uncertainty vanishes in the ratio of the  $K^-$  and  $\pi^-$  decay constants, which is

$$f_{K^-}/f_{\pi^-} = 1.197 \pm 0.002 \pm 0.006 \pm 0.001 .$$

The first error is due to the measured decay rates; the second is due to the uncertainties on the CKM factors; the third is due to the uncertainties in the radiative correction ratio.

These measurements have been used in conjunction with calculations of  $f_K/f_\pi$  in order to find a value for  $|V_{us}|/|V_{ud}|$ . Three recent lattice predictions of  $f_K/f_\pi$  are  $1.189 \pm 0.007$  [46],  $1.192 \pm 0.007 \pm 0.006$  [47], and  $1.197 \pm 0.002^{+0.003}_{-0.007}$  [48], yielding an average by the FLAG group of  $1.195 \pm 0.005$  [49]. (A new average  $1.1872 \pm 0.0041$  is quoted with statistical errors only [50]). Together with the precisely measured  $|V_{ud}|$ , this gives an independent measure of  $|V_{us}|$  [8,41].

## References

1. For the version of this review on the arXiv (including an Abstract) see J. L. Rosner and S. Stone, "Leptonic Decays of Charged Pseudoscalar Mesons – 2012," arXiv:1201.2401.
2. Most predictions for the rate for  $B^- \rightarrow \mu^- \bar{\nu}$  are in the range of 1 to 20 times the rate for  $B^- \rightarrow \mu^- \bar{\nu}$ . See G. Burdman, T. Goldman, and D. Wyler, Phys. Rev. **D51**, 111 (1995); P. Colangelo, F. De Fazio, and G. Nardulli, Phys. Lett. **B372**, 331 (1996); *ibid.*, **386**, 328 (1996); A. Khodjamirian, G. Stoll, and D. Wyler, Phys. Lett. **B358**, 129 (1995); G. Eilam, I. Halperin, and R. Mendel, Phys. Lett. **B361**, 137 (1995); D. Atwood, G. Eilam, and A. Soni, Mod. Phys. Lett. **A11**, 1061 (1996); C.Q. Geng and C.C. Lih, Phys. Rev. **D57**, 5697 (1998) and Mod. Phys. Lett. **A15**, 2087 (2000); G.P. Korchemsky, D. Pirjol, and T. M. Yan, Phys. Rev. **D61**, 114510 (2000); C.W. Hwang, Eur. Phys. J. **C46**, 379 (2006).
3. W.-S. Hou, Phys. Rev. **D48**, 2342 (1993).

## Meson Particle Listings

 $D_s^\pm$ 

4. See, for example, A.G. Akeroyd and S. Recksiegel, Phys. Lett. **B554**, 38 (2003); A.G. Akeroyd, Prog. Theor. Phys. **111**, 295 (2004).
5. J.L. Hewett, hep-ph/9505246, presented at *Lafex International School on High Energy Physics (LISHEP95)*, Rio de Janeiro, Brazil, Feb. 6-22, 1995.
6. I.S. Towner and J.C. Hardy, Phys. Rev. **C79**, 055502 (2009); *ibid.* **77**, 025501 (2008).
7. E. Blucher and W. J. Marciano, “ $V_{ud}$ ,  $V_{us}$ , The Cabibbo Angle and CKM Unitarity” in K. Nakamura *et al.*, (Particle Data Group), J. Phys. **G37**, 075021 (2010).
8. W. J. Marciano, Phys. Rev. Lett. **93**, 231803 (2004); A. Jüttner, PoS LAT2007, 014 (2007) [arXiv:0711.1239].
9. B. I. Eisenstein *et al.* (CLEO Collab.), Phys. Rev. **D78**, 052003 (2008). See also M. Artuso *et al.* (CLEO Collab.), Phys. Rev. Lett. **95**, 251801 (2005).
10. J. Charles *et al.*, Eur. Phys. J. **C41**, 1 (2005).
11. B. A. Dobrescu and A. S. Kronfeld, Phys. Rev. Lett. **100**, 241802 (2008).
12. J.P. Alexander *et al.* (CLEO Collab.), Phys. Rev. **D79**, 052001 (2009); M. Artuso *et al.* (CLEO Collab.), Phys. Rev. Lett. **99**, 071802 (2007).
13. L. Widhalm *et al.* (Belle Collab.), Phys. Rev. Lett. **100**, 241801 (2008).
14. P. Naik *et al.* (CLEO Collab.), Phys. Rev. **D80**, 112004 (2009).
15. P.U.E. Onyisi *et al.* (CLEO Collab.), Phys. Rev. **D79**, 052002 (2009); K. M. Ecklund *et al.* (CLEO Collab.), Phys. Rev. Lett. **100**, 161801 (2008).
16. P. del Amo Sanchez *et al.* (BaBar Collab.), Phys. Rev. **D82**, 091103 (2010) [arXiv:1008.4080] We do not use the previous BaBar result from a subsample of data as reported in J.P. Lee *et al.* (BaBar Collab.), [arXiv:1003.3063].
17. See J. Alexander *et al.* (CLEO Collab.), Phys. Rev. Lett. **100**, 161804 (2008).
18. We have not included a BaBar result:  $\mathcal{B}(D_s^+ \rightarrow \mu^+ \nu) = (6.67 \pm 0.83 \pm 0.26 \pm 0.66) \times 10^{-3}$  and  $f_{D_s^+} = (281 \pm 17 \pm 7 \pm 14)$  MeV based on  $\mathcal{B}(D_s^+ \rightarrow \phi \pi^+) = (4.71 \pm 0.46)\%$ . These measurements determined the ratio of the leptonic decay to a hadronic decay, usually  $\Gamma(D_s^+ \rightarrow \ell^+ \nu) / \Gamma(D_s^+ \rightarrow \phi \pi^+)$ . See B. Aubert *et al.* (BABAR Collab.), Phys. Rev. Lett. **98**, 141801 (2007).
19. M. Artuso, E. Barberio, and S. Stone, PMC Physics A, 3:3 (2009) [arXiv:0902.3743].
20. See most papers in Ref. 2 and C.D. Lü and G.L. Song, Phys. Lett. **B562**, 75 (2003).
21. C.T.H. Davies *et al.* (HPQCD Collab.), Phys. Rev. **D82**, 114504 (2010) [arXiv:1008.4018].
22. A. Bazavov *et al.* (Fermilab/MILC Collab.), [arXiv:1112.3051], submitted to Phys. Rev. D.
23. B. Blossier *et al.*, JHEP **0907**, 043 (2009) [arXiv:0904.0954].
24. J. Bordes, J. Peñarrocha, and K. Schilcher, JHEP **0511**, 014 (2005).
25. W. Lucha, D. Melikhov, and S. Simula, Phys. Lett. **B701**, 82 (2011).
26. A.M. Badalian *et al.*, Phys. Rev. **D75**, 116001 (2007); see also A.M. Badalian and B.L.G. Bakker, [hep-ph/0702229].
27. C.-W. Hwang, Phys. Rev. **D81**, 054022 (2010) [arXiv:0910.0145].
28. A. Khodjamirian, Phys. Rev. **D79**, 031503 (2009).
29. A.G. Akeroyd and C.H. Chen, Phys. Rev. **D75**, 075004 (2007).
30. A.G. Akeroyd and F. Mahmoudi, JHEP **0904**, 121 (2009).
31. A.G. Akeroyd and S. Recksiegel, Phys. Lett. **B554**, 38 (2003).
32. K. Ikado *et al.* (Belle Collab.), Phys. Rev. Lett. **97**, 251802 (2006).
33. K. Hara *et al.* (Belle Collab.), Phys. Rev. **D82**, 071101R (2010).
34. P. del Amo Sanchez *et al.* (BaBar Collab.), contribution to *35th Int. Conf. on High Energy Physics (ICHEP)*, Paris (2010) [arXiv:1008.0104].
35. B. Aubert *et al.* (BaBar Collab.), Phys. Rev. **D81**, 051101R (2010).
36. A. Bazavov *et al.* (Fermilab/MILC Collab.) [22] calculate  $f_B = 196.9 \pm 8.9$  MeV, while E. Gamiz *et al.* (HPQCD Collab.) Phys. Rev. **D80**, 014503 (2009) find  $f_B = 190 \pm 13$  MeV. We average the two results assuming the errors are fully correlated.
37. See the discussion in M. Artuso, E. Barberio and S. Stone, Ref. 19.
38. R. Kowalewski and T. Mannel, in K. Nakamura *et al.* (Particle Data Group), J. Phys. **G37**, 075021 (2010), p. 1014 See also P. Urquijo, “Exclusive (Semi) Leptonic Decays at Belle,” presented at EPS, Grenoble, France, July, 2011.
39. J. Charles *et al.* (CKMfitter Group), Phys. Rev. **D85**, 1 (2011) [arXiv:1106.4041 [hep-ph]], updated results and plots available at: <http://ckmfitter.in2p3.fr>.
40. W.J. Marciano and A. Sirlin, Phys. Rev. Lett. **71**, 3629 (1993); V. Cirigliano and I. Rosell, JHEP **0710**, 005 (2007).
41. Flavianet Working Group on Precise SM Tests in K Decays, M. Antonelli *et al.*, Nucl. Phys. Proc. Suppl. **83**, 181 (2008), updated periodically at: <http://www.lnf.infn.it/wg/vus>. For a recent detailed review, see M. Antonelli *et al.*, [arXiv:0907.5386] (2009).
42. P.A. Boyle *et al.*, Phys. Rev. Lett. **100**, 141601 (2008).
43. H. Leutwyler and M. Roos, Z. Phys. **C25**, 91 (1984).
44. J. Laiho, E. Lunghi, and R. Van de Water, Phys. Rev. **D81**, 034503 (2010), and periodic updates on <http://www.latticeaverages.org>.
45. N. Cabibbo, E.C. Swallow, and R. Winston, Phys. Rev. Lett. **92**, 251803 (2004).
46. E. Follana *et al.*, (HPQCD and UKQCD Collab.), Phys. Rev. Lett. **100**, 062002 (2008).
47. S. Durr *et al.*, Phys. Rev. **D81**, 054507 (2010) [arXiv:1001.4692].
48. A. Bazavov *et al.* (MILC Collab.), PoS LAT 2010 074 [arXiv:1012.0868].
49. G. Colangelo *et al.* (FLAG working group of FLAVIANET), Eur. Phys. J. **C71**, 1695 (2011) [arXiv:1011.4408].
50. A. Bazavov *et al.* (MILC Collab.), presented at *XXIX International Symposium on Lattice Field Theory*, 2011, Lake Tahoe, California, to be published by *Proceedings of Science* [arXiv:1111.4314].

$\Gamma(e^+ \nu_e)/\Gamma_{\text{total}}$		$\Gamma_{19}/\Gamma$	
VALUE	CL%	DOCUMENT ID	TECN COMMENT
$<1.2 \times 10^{-4}$	90	ALEXANDER 09	CLEO $e^+e^-$ at 4170 MeV
••• We do not use the following data for averages, fits, limits, etc. •••			
$<2.3 \times 10^{-4}$	90	DEL-AMO-SA...10j	BABR $e^+e^-$ , 10.58 GeV
$<1.3 \times 10^{-4}$	90	PEDLAR 07A	CLEO See ALEXANDER 09

$\Gamma(\mu^+ \nu_\mu)/\Gamma_{\text{total}}$		$\Gamma_{20}/\Gamma$	
VALUE (units $10^{-3}$ )	EVTS	DOCUMENT ID	TECN COMMENT
<b>5.90±0.33 OUR AVERAGE</b>			
$6.02 \pm 0.38 \pm 0.34$	275 ± 17	<sup>4</sup> DEL-AMO-SA...10j	BABR $e^+e^-$ , 10.58 GeV
$5.65 \pm 0.45 \pm 0.17$	235 ± 14	ALEXANDER 09	CLEO $e^+e^-$ at 4170 MeV
$6.44 \pm 0.76 \pm 0.57$	169 ± 18	<sup>5</sup> WIDHALM 08	BELL $e^+e^- \approx \Upsilon(4S)$
••• We do not use the following data for averages, fits, limits, etc. •••			
$5.94 \pm 0.66 \pm 0.31$	88	<sup>6</sup> PEDLAR 07A	CLEO See ALEXANDER 09
$6.8 \pm 1.1 \pm 1.8$	553	<sup>7</sup> HEISTER 02i	ALEP Z decays

<sup>4</sup> DEL-AMO-SANCHEZ 10j uses  $\mu^+ \nu_\mu$  and  $\tau^+ \nu_\tau$  events together to get  $f_{D_s} = (258.6 \pm 6.4 \pm 7.5)$  MeV.

<sup>5</sup> WIDHALM 08 gets  $f_{D_s} = (275 \pm 16 \pm 12)$  MeV from the branching fraction.

<sup>6</sup> PEDLAR 07A also fits  $\mu^+$  and  $\tau^+$  events together and gets an effective  $\mu^+ \nu_\mu$  branching fraction of  $(6.38 \pm 0.59 \pm 0.33) \times 10^{-3}$

<sup>7</sup> This HEISTER 02i result is not actually an independent measurement of the absolute  $\mu^+ \nu_\mu$  branching fraction, but is in fact based on our  $\phi\pi^+$  branching fraction of 3.6 ± 0.9%, so it cannot be included in our overall fit. HEISTER 02i combines its  $D_s^+ \rightarrow \tau^+ \nu_\tau$  and  $\mu^+ \nu_\mu$  branching fractions to get  $f_{D_s} = (285 \pm 19 \pm 40)$  MeV.

$\Gamma(\mu^+ \nu_\mu)/\Gamma(\phi\pi^+)$		$\Gamma_{20}/\Gamma_{33}$	
VALUE	EVTS	DOCUMENT ID	TECN COMMENT
••• We do not use the following data for averages, fits, limits, etc. •••			
$0.143 \pm 0.018 \pm 0.006$	489 ± 55	<sup>8</sup> AUBERT 07v	BABR $e^+e^- \approx \Upsilon(4S)$
$0.23 \pm 0.06 \pm 0.04$	18	<sup>9</sup> ALEXANDROV 00	BEAT $\pi^-$ nucleus, 350 GeV
$0.173 \pm 0.023 \pm 0.035$	182	<sup>10</sup> CHADHA 98	CLE2 $e^+e^- \approx \Upsilon(4S)$
$0.245 \pm 0.052 \pm 0.074$	39	<sup>11</sup> ACOSTA 94	CLE2 See CHADHA 98

<sup>8</sup> AUBERT 07v gets  $f_{D_s^+} = (283 \pm 17 \pm 16)$  MeV, using  $\Gamma(D_s^+ \rightarrow \phi\pi^+)/\Gamma(\text{total}) = (4.71 \pm 0.46)\%$ .

<sup>9</sup> ALEXANDROV 00 uses  $r_D^2/r_{D_s}^2 = 0.82 \pm 0.09$  from a lattice-gauge-theory calculation to get the relative numbers of  $D^+ \rightarrow \mu^+ \nu_\mu$  and  $D_s^+ \rightarrow \mu^+ \nu_\mu$  events. The present result leads to  $f_{D_s} = (323 \pm 44 \pm 36)$  MeV.

<sup>10</sup> CHADHA 98 obtains  $f_{D_s} = (280 \pm 19 \pm 28 \pm 34)$  MeV from this measurement, using  $\Gamma(D_s^+ \rightarrow \phi\pi^+)/\Gamma(\text{total}) = 0.036 \pm 0.009$ .

<sup>11</sup> ACOSTA 94 obtains  $f_{D_s} = (344 \pm 37 \pm 52 \pm 42)$  MeV from this measurement, using  $\Gamma(D_s^+ \rightarrow \phi\pi^+)/\Gamma(\text{total}) = 0.037 \pm 0.009$ .

$\Gamma(\tau^+ \nu_\tau)/\Gamma_{\text{total}}$		$\Gamma_{21}/\Gamma$	
VALUE (units $10^{-2}$ )	EVTS	DOCUMENT ID	TECN COMMENT
<b>5.43±0.31 OUR AVERAGE</b>			
$5.00 \pm 0.35 \pm 0.49$	748 ± 53	<sup>12</sup> DEL-AMO-SA...10j	BABR $e^- \bar{\nu}_e \nu_\tau, \mu^- \bar{\nu}_\mu \nu_\tau$
$6.42 \pm 0.81 \pm 0.18$	126 ± 16	<sup>13</sup> ALEXANDER 09	CLEO $\tau^+ \rightarrow \pi^+ \bar{\nu}_\tau$
$5.52 \pm 0.57 \pm 0.21$	155 ± 17	<sup>13</sup> NAIK 09A	CLEO $\tau^+ \rightarrow \rho^+ \bar{\nu}_\tau$
$5.30 \pm 0.47 \pm 0.22$	181 ± 16	<sup>13</sup> ONYISI 09	CLEO $\tau^+ \rightarrow e^+ \nu_e \bar{\nu}_\tau$
••• We do not use the following data for averages, fits, limits, etc. •••			
$6.17 \pm 0.71 \pm 0.34$	102	<sup>14</sup> ECKLUND 08	CLEO See ONYISI 09
$8.0 \pm 1.3 \pm 0.4$	47	<sup>14</sup> PEDLAR 07A	CLEO See ALEXANDER 09
$5.79 \pm 0.77 \pm 1.84$	881	<sup>15</sup> HEISTER 02i	ALEP Z decays
$7.0 \pm 2.1 \pm 2.0$	22	<sup>16</sup> ABBIENDI 01L	OPAL $D_s^{*+} \rightarrow \gamma D_s^+$ from Z's
$7.4 \pm 2.8 \pm 2.4$	16	<sup>17</sup> ACCIARRI 97f	L3 $D_s^{*+} \rightarrow \gamma D_s^+$ from Z's

<sup>12</sup> DEL-AMO-SANCHEZ 10j uses  $\mu^+ \nu_\mu$  and  $\tau^+ \nu_\tau$  events together to get  $f_{D_s} = (258.6 \pm 6.4 \pm 7.5)$  MeV.

<sup>13</sup> ALEXANDER 09, NAIK 09A, and ONYISI 09 use different  $\tau$  decay modes and are independent. The three papers combined give  $f_{D_s} = (259.7 \pm 7.8 \pm 3.4)$  MeV.

<sup>14</sup> ECKLUND 08 and PEDLAR 07A are independent: ECKLUND 08 uses  $\tau^+ \rightarrow e^+ \nu_e \bar{\nu}_\tau$  events, PEDLAR 07A uses  $\tau^+ \rightarrow \pi^+ \bar{\nu}_\tau$  events.

<sup>15</sup> HEISTER 02i combines its  $D_s^+ \rightarrow \tau^+ \nu_\tau$  and  $\mu^+ \nu_\mu$  branching fractions to get  $f_{D_s} = (285 \pm 19 \pm 40)$  MeV.

<sup>16</sup> This ABBIENDI 01L value gives a decay constant  $f_{D_s}$  of  $(286 \pm 44 \pm 41)$  MeV.

<sup>17</sup> The second ACCIARRI 97f error here combines in quadrature systematic (0.016) and normalization (0.018) errors. The branching fraction gives  $f_{D_s} = (309 \pm 58 \pm 33 \pm 38)$  MeV.

$\Gamma(\tau^+ \nu_\tau)/\Gamma(\mu^+ \nu_\mu)$		$\Gamma_{21}/\Gamma_{20}$	
VALUE	EVTS	DOCUMENT ID	TECN COMMENT
••• We do not use the following data for averages, fits, limits, etc. •••			
$11.0 \pm 1.4 \pm 0.6$	102	<sup>18</sup> ECKLUND 08	CLEO See ONYISI 09
<sup>18</sup> This ECKLUND 08 value also uses results from PEDLAR 07A, and it is not independent of other results in these Listings. Combined with earlier CLEO results, the decay constant $f_{D_s}$ is $274 \pm 10 \pm 5$ MeV.			

$\Gamma(K^+ K^- e^+ \nu_e)/\Gamma(K^+ K^- \pi^+)$		$\Gamma_{22}/\Gamma_{32}$	
VALUE	DOCUMENT ID	TECN	COMMENT
••• We do not use the following data for averages, fits, limits, etc. •••			
$0.558 \pm 0.007 \pm 0.016$	<sup>19</sup> AUBERT 08AN	BABR	$e^+e^-$ at $\Upsilon(4S)$
<sup>19</sup> This AUBERT 08AN ratio is only for the $K^+ K^-$ mass in the range 1.01-to-1.03 GeV in the numerator and 1.0095-to-1.0295 GeV in the denominator.			

$\Gamma(\phi e^+ \nu_e)/\Gamma_{\text{total}}$		$\Gamma_{23}/\Gamma$	
VALUE (units $10^{-2}$ )	EVTS	DOCUMENT ID	TECN COMMENT
See the end of the $D_s^\pm$ Listings for measurements of $D_s^+ \rightarrow \phi e^+ \nu_e$ form factors. Unseen decay modes of the $\phi$ are included.			
<b>2.49±0.14 OUR FIT</b>			
<b>2.54±0.14 OUR AVERAGE</b>			
$2.36 \pm 0.23 \pm 0.13$	106 ± 10	ECKLUND 09	CLEO $e^+e^-$ at 4170 MeV
$2.61 \pm 0.03 \pm 0.17$	(25 ± 0.5)k	AUBERT 08AN	BABR $e^+e^-$ at $\Upsilon(4S)$
••• We do not use the following data for averages, fits, limits, etc. •••			
$2.29 \pm 0.37 \pm 0.11$	45	YELTON 09	CLEO See ECKLUND 09

$\Gamma(\phi e^+ \nu_e)/\Gamma(\phi\pi^+)$		$\Gamma_{23}/\Gamma_{33}$		
VALUE	EVTS	DOCUMENT ID	TECN COMMENT	
As noted in the comment column, most of these measurements use $\phi\mu^+ \nu_\mu$ events in addition to or instead of $\phi e^+ \nu_e$ events.				
••• We do not use the following data for averages, fits, limits, etc. •••				
$0.540 \pm 0.033 \pm 0.048$	793	LINK 02j	FOCS Uses $\phi\mu^+ \nu_\mu$	
$0.54 \pm 0.05 \pm 0.04$	367	BUTLER 94	CLE2 Uses $\phi e^+ \nu_e$ and $\phi\mu^+ \nu_\mu$	
$0.58 \pm 0.17 \pm 0.07$	97	FRABETTI 93g	E687 Uses $\phi\mu^+ \nu_\mu$	
$0.57 \pm 0.15 \pm 0.15$	104	ALBRECHT 91	ARG Uses $\phi e^+ \nu_e$	
$0.49 \pm 0.10$	$\frac{+0.10}{-0.14}$	54	ALEXANDER 90b	CLEO Uses $\phi e^+ \nu_e$ and $\phi\mu^+ \nu_\mu$

$\Gamma(\eta e^+ \nu_e)/\Gamma_{\text{total}}$		$\Gamma_{25}/\Gamma$	
VALUE (units $10^{-2}$ )	EVTS	DOCUMENT ID	TECN COMMENT
Unseen decay modes of the $\eta$ are included.			
<b>2.67±0.29 OUR FIT</b> Error includes scale factor of 1.1.			
<b>2.48±0.29±0.13</b>	82	YELTON 09	CLEO $e^+e^-$ at 4170 MeV

$\Gamma(\eta e^+ \nu_e)/\Gamma(\phi e^+ \nu_e)$		$\Gamma_{25}/\Gamma_{23}$	
VALUE	EVTS	DOCUMENT ID	TECN COMMENT
Unseen decay modes of the $\eta$ and the $\phi$ are included.			
<b>1.07±0.12 OUR FIT</b> Error includes scale factor of 1.1.			
<b>1.24±0.12±0.15</b>	440	<sup>20</sup> BRANDENB... 95	CLE2 $e^+e^- \approx \Upsilon(4S)$
<sup>20</sup> BRANDENBURG 95 uses both $e^+$ and $\mu^+$ events and makes a phase-space adjustment to use the $\mu^+$ events as $e^+$ events.			

$\Gamma(\eta'(958) e^+ \nu_e)/\Gamma_{\text{total}}$		$\Gamma_{26}/\Gamma$	
VALUE (units $10^{-2}$ )	EVTS	DOCUMENT ID	TECN COMMENT
Unseen decay modes of the $\eta'(958)$ are included.			
<b>0.99±0.23 OUR FIT</b>			
<b>0.91±0.33±0.05</b>	7.5	YELTON 09	CLEO $e^+e^-$ at 4170 MeV

$\Gamma(\eta'(958) e^+ \nu_e)/\Gamma(\phi e^+ \nu_e)$		$\Gamma_{26}/\Gamma_{23}$	
VALUE	EVTS	DOCUMENT ID	TECN COMMENT
Unseen decay modes of the resonances are included.			
<b>0.40±0.09 OUR FIT</b>			
<b>0.43±0.11±0.07</b>	29	<sup>21</sup> BRANDENB... 95	CLE2 $e^+e^- \approx \Upsilon(4S)$
<sup>21</sup> BRANDENBURG 95 uses both $e^+$ and $\mu^+$ events and makes a phase-space adjustment to use the $\mu^+$ events as $e^+$ events.			

$[\Gamma(\eta e^+ \nu_e) + \Gamma(\eta'(958) e^+ \nu_e)]/\Gamma(\phi e^+ \nu_e)$		$\Gamma_{24}/\Gamma_{23} = (\Gamma_{25} + \Gamma_{26})/\Gamma_{23}$	
VALUE	DOCUMENT ID	TECN	COMMENT
Unseen decay modes of the resonances are included.			
••• We do not use the following data for averages, fits, limits, etc. •••			
$1.67 \pm 0.17 \pm 0.17$	<sup>22</sup> BRANDENB... 95	CLE2	$e^+e^- \approx \Upsilon(4S)$
<sup>22</sup> This BRANDENBURG 95 data is redundant with data in previous blocks.			

$\Gamma(\omega e^+ \nu_e)/\Gamma_{\text{total}}$		$\Gamma_{27}/\Gamma$	
VALUE (%)	CL%	DOCUMENT ID	TECN COMMENT
A test for $u\bar{u}$ or $d\bar{d}$ content in the $D_s^+$ . Neither Cabibbo-favored nor Cabibbo-suppressed decays can contribute, and $\omega - \phi$ mixing is an unlikely explanation for any fraction above about $2 \times 10^{-4}$ .			
<b>&lt;0.20</b>	90	MARTIN 11	CLEO $e^+e^-$ at 4170 MeV

$\Gamma(K^0 e^+ \nu_e)/\Gamma_{\text{total}}$		$\Gamma_{28}/\Gamma$	
VALUE (units $10^{-2}$ )	EVTS	DOCUMENT ID	TECN COMMENT
<b>0.37±0.10±0.02</b>	14	YELTON 09	CLEO $e^+e^-$ at 4170 MeV

$\Gamma(K^*(892)^0 e^+ \nu_e)/\Gamma_{\text{total}}$		$\Gamma_{29}/\Gamma$	
VALUE (units $10^{-2}$ )	EVTS	DOCUMENT ID	TECN COMMENT
Unseen decay modes of the $K^*(892)^0$ are included.			
<b>0.18±0.07±0.01</b>	7.5	YELTON 09	CLEO $e^+e^-$ at 4170 MeV

## Meson Particle Listings

 $D_s^\pm$ 

$\Gamma(f_0(980)e^+\nu_e, f_0 \rightarrow \pi^+\pi^-)/\Gamma_{\text{total}}$					$\Gamma_{30}/\Gamma$
VALUE (units $10^{-2}$ )	EVTS	DOCUMENT ID	TECN	COMMENT	
<b>0.20±0.03±0.01</b>	44 ± 7	ECKLUND 09	CLEO	$e^+e^-$ at 4170 MeV	
• • • We do not use the following data for averages, fits, limits, etc. • • •					
0.13±0.04±0.01	13	YELTON 09	CLEO	See ECKLUND 09	

Hadronic modes with a  $K\bar{K}$  pair.

$\Gamma(K^+K_S^0)/\Gamma_{\text{total}}$					$\Gamma_{31}/\Gamma$
VALUE (units $10^{-2}$ )	DOCUMENT ID	TECN	COMMENT		
<b>1.48±0.08 OUR FIT</b>					
<b>1.49±0.07±0.05</b>	23	ALEXANDER 08	CLEO	$e^+e^-$ at 4.17 GeV	
23 ALEXANDER 08 uses single- and double-tagged events in an overall fit. The correlation matrix for the branching fractions is used in the fit.					

$\Gamma(K^+K^-\pi^+)/\Gamma_{\text{total}}$					$\Gamma_{32}/\Gamma$
VALUE (units $10^{-2}$ )	DOCUMENT ID	TECN	COMMENT		
<b>5.49±0.27 OUR FIT</b>					
<b>5.50±0.23±0.16</b>	24	ALEXANDER 08	CLEO	$e^+e^-$ at 4.17 GeV	
24 ALEXANDER 08 uses single- and double-tagged events in an overall fit. The correlation matrix for the branching fractions is used in the fit.					

$\Gamma(\phi\pi^+)/\Gamma_{\text{total}}$					$\Gamma_{33}/\Gamma$
The results here are model-independent. For earlier, model-dependent results, see our PDG 06 edition. We decouple the $D_s^+ \rightarrow \phi\pi^+$ branching fraction obtained from mass projections (and used to get some of the other branching fractions) from the $D_s^+ \rightarrow \phi\pi^+, \phi \rightarrow K^+K^-$ branching fraction obtained from the Dalitz-plot analysis of $D_s^+ \rightarrow K^+K^-\pi^+$ . That is, the ratio of these two branching fractions is not exactly the $\phi \rightarrow K^+K^-$ branching fraction 0.491.					

VALUE (units $10^{-2}$ )	EVTS	DOCUMENT ID	TECN	COMMENT
<b>4.5 ± 0.4 OUR AVERAGE</b>				
4.62±0.36±0.51		25 AUBERT 06N	BABR	$e^+e^-$ at $\gamma(4S)$
4.81±0.52±0.38	212 ± 19	26 AUBERT 05v	BABR	$e^+e^- \approx \gamma(4S)$
3.59±0.77±0.48		27 ARTUSO 96	CLE2	$e^+e^-$ at $\gamma(4S)$
• • • We do not use the following data for averages, fits, limits, etc. • • •				
3.9	+5.1 +1.8 -1.9 -1.1	28 BAI	95c BES	$e^+e^-$ 4.03 GeV

25 This AUBERT 06N measurement uses  $\bar{B}^0 \rightarrow D_s^{(*)-}D^{(*)+}$  and  $B^- \rightarrow D_s^{(*)-}D^{(*)0}$  decays, including some from other papers. However, the result is independent of AUBERT 05v.

26 AUBERT 05v uses the ratio of  $B^0 \rightarrow D^{*-}D_s^{*+}$  events seen in two different ways, in both of which the  $D^{*-} \rightarrow \bar{D}^0\pi^-$  decay is fully reconstructed: (1) The  $D_s^{*+} \rightarrow D_s^+\gamma$ ,  $D_s^+ \rightarrow \phi\pi^+$  decay is fully reconstructed. (2) The number of events in the  $D_s^+$  peak in the missing mass spectrum against the  $D^{*-}\gamma$  is measured.

27 ARTUSO 96 uses partially reconstructed  $\bar{B}^0 \rightarrow D^{*+}D_s^{*-}$  decays to get a model-independent value for  $\Gamma(D_s^- \rightarrow \phi\pi^-)/\Gamma(D^0 \rightarrow K^-\pi^+)$  of  $0.92 \pm 0.20 \pm 0.11$ .

28 BAI 95c uses  $e^+e^- \rightarrow D_s^+D_s^-$  events in which one or both of the  $D_s^\pm$  are observed to obtain the first model-independent measurement of the  $D_s^+ \rightarrow \phi\pi^+$  branching fraction, without assumptions about  $\sigma(D_s^\pm)$ . However, with only two "doubly-tagged" events, the statistical error is very large.

$\Gamma(\phi\pi^+, \phi \rightarrow K^+K^-)/\Gamma(K^+K^-\pi^+)$					$\Gamma_{34}/\Gamma_{32}$
This is the "fit fraction" from the Dalitz-plot analysis. We decouple the $D_s^+ \rightarrow \phi\pi^+$ branching fraction obtained from mass projections (and used to get some of the other branching fractions) from the $D_s^+ \rightarrow \phi\pi^+, \phi \rightarrow K^+K^-$ branching fraction obtained from the Dalitz-plot analysis of $D_s^+ \rightarrow K^+K^-\pi^+$ . That is, the ratio of these two branching fractions is not exactly the $\phi \rightarrow K^+K^-$ branching fraction 0.491.					

VALUE (%)	DOCUMENT ID	TECN	COMMENT
<b>41.6±0.8 OUR AVERAGE</b>			
41.4±0.8±0.5	DEL-AMO-SA...11G	BABR	Dalitz fit, 96k±369 evts
42.2±1.6±0.3	MITCHELL 09A	CLEO	Dalitz fit, 12k evts
• • • We do not use the following data for averages, fits, limits, etc. • • •			
39.6±3.3±4.7	FRABETTI 95B	E687	Dalitz fit, 701 evts

$\Gamma(K^+\bar{K}^*(892)^0, \bar{K}^{*0} \rightarrow K^-\pi^+)/\Gamma(K^+K^-\pi^+)$					$\Gamma_{35}/\Gamma_{32}$
This is the "fit fraction" from the Dalitz-plot analysis.					
VALUE (%)	DOCUMENT ID	TECN	COMMENT		
<b>47.8±0.6 OUR AVERAGE</b>					
47.9±0.5±0.5	DEL-AMO-SA...11G	BABR	Dalitz fit, 96k±369 evts		
47.4±1.5±0.4	MITCHELL 09A	CLEO	Dalitz fit, 12k evts		
• • • We do not use the following data for averages, fits, limits, etc. • • •					
47.8±4.6±4.0	FRABETTI 95B	E687	Dalitz fit, 701 evts		

$\Gamma(f_0(980)\pi^+, f_0 \rightarrow K^+K^-)/\Gamma(K^+K^-\pi^+)$					$\Gamma_{36}/\Gamma_{32}$
This is the "fit fraction" from the Dalitz-plot analysis.					
VALUE (%)	DOCUMENT ID	TECN	COMMENT		
<b>21 ± 6 OUR AVERAGE</b>					
16.4±0.7±2.0	DEL-AMO-SA...11G	BABR	Dalitz fit, 96k±369 evts		
28.2±1.9±1.8	MITCHELL 09A	CLEO	Dalitz fit, 12k evts		
• • • We do not use the following data for averages, fits, limits, etc. • • •					
11.0±3.5±2.6	FRABETTI 95B	E687	Dalitz fit, 701 evts		

$\Gamma(f_0(1370)\pi^+, f_0 \rightarrow K^+K^-)/\Gamma(K^+K^-\pi^+)$					$\Gamma_{37}/\Gamma_{32}$
This is the "fit fraction" from the Dalitz-plot analysis.					
VALUE (%)	DOCUMENT ID	TECN	COMMENT		
<b>1.3±0.8 OUR AVERAGE</b>					
1.1±0.1±0.2	DEL-AMO-SA...11G	BABR	Dalitz fit, 96k±369 evts		
4.3±0.6±0.5	MITCHELL 09A	CLEO	Dalitz fit, 12k evts		

$\Gamma(f_0(1710)\pi^+, f_0 \rightarrow K^+K^-)/\Gamma(K^+K^-\pi^+)$					$\Gamma_{38}/\Gamma_{32}$
This is the "fit fraction" from the Dalitz-plot analysis.					
VALUE (%)	DOCUMENT ID	TECN	COMMENT		
<b>1.2±0.5 OUR AVERAGE</b>					
1.1±0.1±0.1	DEL-AMO-SA...11G	BABR	Dalitz fit, 96k±369 evts		
3.4±0.5±0.3	MITCHELL 09A	CLEO	Dalitz fit, 12k evts		
• • • We do not use the following data for averages, fits, limits, etc. • • •					
3.4±2.3±3.5	FRABETTI 95B	E687	Dalitz fit, 701 evts		

$\Gamma(K^+\bar{K}_S^*(1430)^0, \bar{K}_S^{*0} \rightarrow K^-\pi^+)/\Gamma(K^+K^-\pi^+)$					$\Gamma_{39}/\Gamma_{32}$
This is the "fit fraction" from the Dalitz-plot analysis.					
VALUE (%)	DOCUMENT ID	TECN	COMMENT		
<b>3.4±0.7 OUR AVERAGE</b>					
2.4±0.3±1.0	DEL-AMO-SA...11G	BABR	Dalitz fit, 96k±369 evts		
3.9±0.5±0.5	MITCHELL 09A	CLEO	Dalitz fit, 12k evts		
• • • We do not use the following data for averages, fits, limits, etc. • • •					
9.3±3.2±3.2	FRABETTI 95B	E687	Dalitz fit, 701 evts		

$\Gamma(K^*(892)^+\bar{K}^0)/\Gamma(\phi\pi^+)$					$\Gamma_{41}/\Gamma_{33}$
Unseen decay modes of the resonances are included.					
VALUE	DOCUMENT ID	TECN	COMMENT		
<b>1.20±0.21±0.13</b>					
	CHEN 89	CLEO	$e^+e^-$ 10 GeV		

$\Gamma(K^+K^-\pi^+\pi^0)/\Gamma_{\text{total}}$					$\Gamma_{42}/\Gamma$
VALUE (units $10^{-2}$ )	DOCUMENT ID	TECN	COMMENT		
<b>5.6 ± 0.5 OUR FIT</b>					
<b>5.65±0.29±0.40</b>	29	ALEXANDER 08	CLEO	$e^+e^-$ at 4.17 GeV	
29 ALEXANDER 08 uses single- and double-tagged events in an overall fit. The correlation matrix for the branching fractions is used in the fit.					

$\Gamma(\phi\rho^+)/\Gamma(\phi\pi^+)$					$\Gamma_{43}/\Gamma_{33}$
VALUE	EVTS	DOCUMENT ID	TECN	COMMENT	
<b>1.86±0.26±0.29</b>	253	AVERY 92	CLE2	$e^+e^- \approx 10.5$ GeV	

$\Gamma(K_S^0K^-2\pi^+)/\Gamma_{\text{total}}$					$\Gamma_{44}/\Gamma$
VALUE (units $10^{-2}$ )	DOCUMENT ID	TECN	COMMENT		
<b>1.64±0.12 OUR FIT</b>					
<b>1.64±0.10±0.07</b>	30	ALEXANDER 08	CLEO	$e^+e^-$ at 4.17 GeV	
30 ALEXANDER 08 uses single- and double-tagged events in an overall fit. The correlation matrix for the branching fractions is used in the fit.					

$\Gamma(K^*(892)^+\bar{K}^*(892)^0)/\Gamma(\phi\pi^+)$					$\Gamma_{45}/\Gamma_{33}$
Unseen decay modes of the resonances are included.					
VALUE	DOCUMENT ID	TECN	COMMENT		
<b>1.6±0.4±0.4</b>					
	ALBRECHT 92B	ARG	$e^+e^- \approx 10.4$ GeV		

$\Gamma(K^+K_S^0\pi^+\pi^-)/\Gamma(K_S^0K^-2\pi^+)$					$\Gamma_{46}/\Gamma_{44}$
VALUE	EVTS	DOCUMENT ID	TECN	COMMENT	
<b>0.586±0.052±0.043</b>	476	LINK	01c	FOCS $\gamma$ nucleus, $\bar{E}_\gamma \approx 180$ GeV	

$\Gamma(K^+K^-2\pi^+\pi^-)/\Gamma(K^+K^-\pi^+)$					$\Gamma_{47}/\Gamma_{32}$
VALUE	EVTS	DOCUMENT ID	TECN	COMMENT	
<b>0.160±0.027 OUR AVERAGE</b>					
0.150±0.019±0.025	240	LINK	03D	FOCS $\gamma$ A, $\bar{E}_\gamma \approx 180$ GeV	
0.188±0.036±0.040	75	FRABETTI 97C	E687	$\gamma$ Be, $\bar{E}_\gamma \approx 200$ GeV	

$\Gamma(\phi 2\pi^+\pi^-)/\Gamma(\phi\pi^+)$					$\Gamma_{48}/\Gamma_{33}$
VALUE	EVTS	DOCUMENT ID	TECN	COMMENT	
<b>0.269±0.027 OUR AVERAGE</b>					
0.249±0.024±0.021	136	LINK	03D	FOCS $\gamma$ A, $\bar{E}_\gamma \approx 180$ GeV	
0.28 ± 0.06 ± 0.01	40	FRABETTI 97C	E687	$\gamma$ Be, $\bar{E}_\gamma \approx 200$ GeV	
0.58 ± 0.21 ± 0.10	21	FRABETTI 92	E687	$\gamma$ Be	
0.42 ± 0.13 ± 0.07	19	ANJOS 88	E691	Photoproduction	
1.11 ± 0.37 ± 0.28	62	ALBRECHT 85D	ARG	$e^+e^-$ 10 GeV	

$\Gamma(K^+K^-\rho^+\pi^-)/\Gamma(K^+K^-2\pi^+\pi^-)$					$\Gamma_{49}/\Gamma_{47}$
VALUE	CL%	DOCUMENT ID	TECN	COMMENT	
<b>&lt;0.03</b>	90	LINK	03D	FOCS $\gamma$ A, $\bar{E}_\gamma \approx 180$ GeV	

$\Gamma(\phi\rho^0\pi^+, \phi \rightarrow K^+K^-)/\Gamma(K^+K^-2\pi^+\pi^-)$					$\Gamma_{50}/\Gamma_{47}$
VALUE	DOCUMENT ID	TECN	COMMENT		
<b>0.75±0.06±0.04</b>					
	LINK	03D	FOCS $\gamma$ A, $\bar{E}_\gamma \approx 180$ GeV		

$\Gamma(\phi a_1(1260)^+, \phi \rightarrow K^+K^-, a_1^+ \rightarrow \rho^0\pi^+)/\Gamma(K^+K^-\pi^+)$					$\Gamma_{51}/\Gamma_{32}$
VALUE	DOCUMENT ID	TECN	COMMENT		
<b>0.137±0.019±0.011</b>					
	LINK	03D	FOCS $\gamma$ A, $\bar{E}_\gamma \approx 180$ GeV		

$\Gamma(K^+ K^- 2\pi^+ \pi^- \text{ nonresonant})/\Gamma(K^+ K^- 2\pi^+ \pi^-)$				$\Gamma_{52}/\Gamma_{47}$
VALUE	DOCUMENT ID	TECN	COMMENT	
$0.10 \pm 0.06 \pm 0.05$	LINK	03D	FOCS $\gamma A, \bar{E}_\gamma \approx 180$ GeV	

$\Gamma(2K_S^0 2\pi^+ \pi^-)/\Gamma(K_S^0 K^- 2\pi^+)$				$\Gamma_{53}/\Gamma_{44}$
VALUE	EVTS	DOCUMENT ID	TECN	COMMENT
$0.051 \pm 0.015 \pm 0.015$	37 ± 10	LINK	04D	FOCS $\gamma A, \bar{E}_\gamma \approx 180$ GeV

## Pionic modes

$\Gamma(\pi^+ \pi^0)/\Gamma(K^+ K_S^0)$				$\Gamma_{54}/\Gamma_{31}$
VALUE (units $10^{-2}$ )	CL%	DOCUMENT ID	TECN	COMMENT
<2.3	90	MENDEZ	10	CLEO $e^+ e^-$ at 4170 MeV
••• We do not use the following data for averages, fits, limits, etc. •••				
<4.1	90	ADAMS	07A	CLEO See MENDEZ 10

$\Gamma(2\pi^+ \pi^-)/\Gamma_{\text{total}}$				$\Gamma_{55}/\Gamma$
VALUE (units $10^{-2}$ )	DOCUMENT ID	TECN	COMMENT	
$1.10 \pm 0.06$ OUR FIT				
$1.11 \pm 0.07 \pm 0.04$	31	ALEXANDER	08	CLEO $e^+ e^-$ at 4.17 GeV

<sup>31</sup> ALEXANDER 08 uses single- and double-tagged events in an overall fit. The correlation matrix for the branching fractions is used in the fit.

$\Gamma(2\pi^+ \pi^-)/\Gamma(K^+ K^- \pi^+)$				$\Gamma_{55}/\Gamma_{32}$
VALUE	EVTS	DOCUMENT ID	TECN	COMMENT
$0.200 \pm 0.008$ OUR FIT				
$0.199 \pm 0.004 \pm 0.009$	$\approx 10.5k$	AUBERT	09o	BABR $e^+ e^- \approx 10.6$ GeV
••• We do not use the following data for averages, fits, limits, etc. •••				
$0.265 \pm 0.041 \pm 0.031$	98	FRABETTI	97D	E687 $\gamma Be \approx 200$ GeV

$\Gamma(\rho^0 \pi^+)/\Gamma(2\pi^+ \pi^-)$				$\Gamma_{56}/\Gamma_{55}$
VALUE	CL%	DOCUMENT ID	TECN	COMMENT
$0.018 \pm 0.005 \pm 0.010$		AUBERT	09o	BABR Dalitz fit, $\approx 10.5k$ evts
••• We do not use the following data for averages, fits, limits, etc. •••				
not seen		LINK	04	FOCS Dalitz fit, 1475 ± 50 evts
$0.058 \pm 0.023 \pm 0.037$		AITALA	01A	E791 Dalitz fit, 848 evts
<0.073	90	FRABETTI	97D	E687 $\gamma Be \approx 200$ GeV

$\Gamma(\pi^+ (\pi^+ \pi^-)_{S\text{-wave}})/\Gamma(2\pi^+ \pi^-)$				$\Gamma_{57}/\Gamma_{55}$
This is the "fit fraction" from the Dalitz-plot analysis. See also KLEMP 08, which uses 568 $D^+ \rightarrow 3\pi$ decays (over 280 background events) from FNAL E791 to study various parametrizations of the decay amplitudes. The emphasis there is more on S-wave $\pi\pi$ decay products — 20 different solutions are given — than on $D_S^+$ fit fractions.				
VALUE	DOCUMENT ID	TECN	COMMENT	
$0.833 \pm 0.020$ OUR AVERAGE				
$0.830 \pm 0.009 \pm 0.019$	32	AUBERT	09o	BABR Dalitz fit, $\approx 10.5k$ evts
$0.8704 \pm 0.0560 \pm 0.0438$	33	LINK	04	FOCS Dalitz fit, 1475 ± 50 evts

<sup>32</sup> AUBERT 09o gives the amplitude and phase of the  $\pi^+ \pi^-$  S-wave in 29  $\pi^+ \pi^-$  invariant-mass bins.  
<sup>33</sup> LINK 04 borrows a K-matrix parametrization from ANISOVICH 03 of the full  $\pi\pi$  S-wave isoscalar scattering amplitude to describe the  $\pi^+ \pi^-$  S-wave component of the  $\pi^+ \pi^+ \pi^-$  state. The fit fraction given above is a sum over five  $f_0$  mesons, the  $f_0(980)$ ,  $f_0(1300)$ ,  $f_0(1200-1600)$ ,  $f_0(1500)$ , and  $f_0(1750)$ . See LINK 04 for details and discussion.

$\Gamma(f_0(980) \pi^+, f_0 \rightarrow \pi^+ \pi^-)/\Gamma(2\pi^+ \pi^-)$				$\Gamma_{58}/\Gamma_{55}$
This is the "fit fraction" from the Dalitz-plot analysis. See above for the full $\pi^+ (\pi^+ \pi^-)_{S\text{-wave}}$ fit fraction.				
VALUE	DOCUMENT ID	TECN	COMMENT	
••• We do not use the following data for averages, fits, limits, etc. •••				
$0.565 \pm 0.043 \pm 0.047$		AITALA	01A	E791 Dalitz fit, 848 evts
$1.074 \pm 0.140 \pm 0.043$		FRABETTI	97D	E687 $\gamma Be \approx 200$ GeV

$\Gamma(f_0(1300) \pi^+, f_0 \rightarrow \pi^+ \pi^-)/\Gamma(2\pi^+ \pi^-)$				$\Gamma_{59}/\Gamma_{55}$
This is the "fit fraction" from the Dalitz-plot analysis. See above for the full $\pi^+ (\pi^+ \pi^-)_{S\text{-wave}}$ fit fraction.				
VALUE	DOCUMENT ID	TECN	COMMENT	
••• We do not use the following data for averages, fits, limits, etc. •••				
$0.324 \pm 0.077 \pm 0.017$		AITALA	01A	E791 Dalitz fit, 848 evts

$\Gamma(f_0(1500) \pi^+, f_0 \rightarrow \pi^+ \pi^-)/\Gamma(2\pi^+ \pi^-)$				$\Gamma_{60}/\Gamma_{55}$
This is the "fit fraction" from the Dalitz-plot analysis. See above for the full $\pi^+ (\pi^+ \pi^-)_{S\text{-wave}}$ fit fraction.				
VALUE	DOCUMENT ID	TECN	COMMENT	
••• We do not use the following data for averages, fits, limits, etc. •••				
$0.274 \pm 0.114 \pm 0.019$		FRABETTI	97D	E687 $\gamma Be \approx 200$ GeV

<sup>34</sup> FRABETTI 97D calls this mode  $S(1475) \pi^+$ , but finds the mass and width of this  $S(1475)$  to be in excellent agreement with those of the  $f_0(1500)$ .

$\Gamma(f_2(1270) \pi^+, f_2 \rightarrow \pi^+ \pi^-)/\Gamma(2\pi^+ \pi^-)$				$\Gamma_{61}/\Gamma_{55}$
This is the "fit fraction" from the Dalitz-plot analysis.				
VALUE	DOCUMENT ID	TECN	COMMENT	
<b>0.101 ± 0.018 OUR AVERAGE</b>				
$0.101 \pm 0.015 \pm 0.011$		AUBERT	09o	BABR Dalitz fit, $\approx 10.5k$ evts
$0.0974 \pm 0.0449 \pm 0.0294$		LINK	04	FOCS Dalitz fit, 1475 ± 50 evts

••• We do not use the following data for averages, fits, limits, etc. •••

$0.197 \pm 0.033 \pm 0.006$		AITALA	01A	E791 Dalitz fit, 848 evts
$0.123 \pm 0.056 \pm 0.018$		FRABETTI	97D	E687 $\gamma Be \approx 200$ GeV

$\Gamma(\rho(1450)^0 \pi^+, \rho^0 \rightarrow \pi^+ \pi^-)/\Gamma(2\pi^+ \pi^-)$				$\Gamma_{62}/\Gamma_{55}$
This is the "fit fraction" from the Dalitz-plot analysis.				
VALUE	DOCUMENT ID	TECN	COMMENT	
<b>0.027 ± 0.018 OUR AVERAGE</b>				
$0.023 \pm 0.008 \pm 0.017$		AUBERT	09o	BABR Dalitz fit, $\approx 10.5k$ evts
$0.0656 \pm 0.0343 \pm 0.0440$		LINK	04	FOCS Dalitz fit, 1475 ± 50 evts

••• We do not use the following data for averages, fits, limits, etc. •••

$0.044 \pm 0.021 \pm 0.002$		AITALA	01A	E791 Dalitz fit, 848 evts
-----------------------------	--	--------	-----	---------------------------

$\Gamma(\pi^+ 2\pi^0)/\Gamma_{\text{total}}$				$\Gamma_{63}/\Gamma$
VALUE (units $10^{-2}$ )	EVTS	DOCUMENT ID	TECN	COMMENT
$0.65 \pm 0.13 \pm 0.03$	72 ± 16	NAIK	09A	CLEO $e^+ e^-$ at 4170 MeV

$\Gamma(2\pi^+ \pi^- \pi^0)/\Gamma(\phi \pi^+)$				$\Gamma_{64}/\Gamma_{33}$
VALUE	CL%	DOCUMENT ID	TECN	COMMENT
••• We do not use the following data for averages, fits, limits, etc. •••				
<3.3	90	ANJOS	89E	E691 Photoproduction

$\Gamma(\eta \pi^+)/\Gamma_{\text{total}}$				$\Gamma_{65}/\Gamma$
Unseen decay modes of the $\eta$ are included.				
VALUE (units $10^{-2}$ )	DOCUMENT ID	TECN	COMMENT	
••• We do not use the following data for averages, fits, limits, etc. •••				
$1.58 \pm 0.11 \pm 0.18$	35	ALEXANDER	08	CLEO See MENDEZ 10
<sup>35</sup> ALEXANDER 08 uses single- and double-tagged events in an overall fit.				

$\Gamma(\eta \pi^+)/\Gamma(K^+ K_S^0)$				$\Gamma_{65}/\Gamma_{31}$
Unseen decay modes of the $\eta$ are included.				
VALUE	EVTS	DOCUMENT ID	TECN	COMMENT
$1.23 \pm 0.08$ OUR FIT				
$1.236 \pm 0.043 \pm 0.063$	2587 ± 89	MENDEZ	10	CLEO $e^+ e^-$ at 4170 MeV

$\Gamma(\eta \pi^+)/\Gamma(\phi \pi^+)$				$\Gamma_{65}/\Gamma_{33}$
Unseen decay modes of the resonances are included.				
VALUE	EVTS	DOCUMENT ID	TECN	COMMENT
••• We do not use the following data for averages, fits, limits, etc. •••				
$0.48 \pm 0.03 \pm 0.04$	920	JESSOP	98	CLE2 $e^+ e^- \approx \Upsilon(4S)$
$0.54 \pm 0.09 \pm 0.06$	165	ALEXANDER	92	CLE2 See JESSOP 98

$\Gamma(\omega \pi^+)/\Gamma_{\text{total}}$				$\Gamma_{66}/\Gamma$
Unseen decay modes of the $\omega$ are included.				
VALUE (units $10^{-2}$ )	EVTS	DOCUMENT ID	TECN	COMMENT
$0.25 \pm 0.07$ OUR FIT				
$0.21 \pm 0.09 \pm 0.01$	6 ± 2.4	GE	09A	CLEO $e^+ e^-$ at 4170 MeV

$\Gamma(\omega \pi^+)/\Gamma(\eta \pi^+)$				$\Gamma_{66}/\Gamma_{65}$
Unseen decay modes of the resonances are included.				
VALUE	DOCUMENT ID	TECN	COMMENT	
<b>0.14 ± 0.04 OUR FIT</b>				
$0.16 \pm 0.04 \pm 0.03$		BALEST	97	CLE2 $e^+ e^- \approx \Upsilon(4S)$

$\Gamma(2\pi^+ 2\pi^-)/\Gamma(K^+ K^- \pi^+)$				$\Gamma_{67}/\Gamma_{32}$
VALUE	EVTS	DOCUMENT ID	TECN	COMMENT
<b>0.146 ± 0.014 OUR AVERAGE</b>				
$0.145 \pm 0.011 \pm 0.010$	671	LINK	03D	FOCS $\gamma A, \bar{E}_\gamma \approx 180$ GeV
$0.158 \pm 0.042 \pm 0.031$	37	FRABETTI	97C	E687 $\gamma Be, \bar{E}_\gamma \approx 200$ GeV

$\Gamma(\eta \rho^+)/\Gamma_{\text{total}}$				$\Gamma_{69}/\Gamma$
Unseen decay modes of the $\eta$ are included.				
VALUE (units $10^{-2}$ )	EVTS	DOCUMENT ID	TECN	COMMENT
$8.9 \pm 0.6 \pm 0.5$	328 ± 22	NAIK	09A	CLEO $\eta \rightarrow 2\gamma$

$\Gamma(\eta \rho^+)/\Gamma(\phi \pi^+)$				$\Gamma_{69}/\Gamma_{33}$
Unseen decay modes of the resonances are included.				
VALUE	EVTS	DOCUMENT ID	TECN	COMMENT
••• We do not use the following data for averages, fits, limits, etc. •••				
$2.98 \pm 0.20 \pm 0.39$	447	JESSOP	98	CLE2 $e^+ e^- \approx \Upsilon(4S)$
$2.86 \pm 0.38_{-0.38}$	217	AVERY	92	CLE2 See JESSOP 98

$\Gamma(\eta \pi^+ \pi^0 \text{ 3-body})/\Gamma(\phi \pi^+)$				$\Gamma_{70}/\Gamma_{33}$	
Unseen decay modes of the resonances are included.					
VALUE	CL%	DOCUMENT ID	TECN	COMMENT	
<1.1	90	JESSOP	98	CLE2 $e^+ e^- \approx \Upsilon(4S)$	
••• We do not use the following data for averages, fits, limits, etc. •••					
<0.82	90	36	DAOUDI	92	CLE2 See JESSOP 98

<sup>36</sup> We use the JESSOP 98 limit, even though the DAOUDI 92 limit, from the same experiment but with a much smaller data sample, is more restrictive.

## Meson Particle Listings

 $D_s^\pm$ 

$\Gamma(\omega\pi^+\pi^0)/\Gamma_{\text{total}}$   $\Gamma_{71}/\Gamma$   
 Unseen decay modes of the  $\omega$  are included.

VALUE (units $10^{-2}$ )	EVTS	DOCUMENT ID	TECN	COMMENT
$2.78 \pm 0.65 \pm 0.25$	$34 \pm 7.9$	GE	09A	CLEO $e^+e^-$ at 4170 MeV

$\Gamma(3\pi^+2\pi^-\pi^0)/\Gamma_{\text{total}}$   $\Gamma_{72}/\Gamma$

VALUE	DOCUMENT ID	TECN	COMMENT
$0.049 \pm 0.033$ $-0.030$	BARLAG	92c	ACCM $\pi^-$ 230 GeV

$\Gamma(\omega 2\pi^+\pi^-)/\Gamma_{\text{total}}$   $\Gamma_{73}/\Gamma$   
 Unseen decay modes of the  $\omega$  are included.

VALUE (units $10^{-2}$ )	EVTS	DOCUMENT ID	TECN	COMMENT
$1.58 \pm 0.45 \pm 0.09$	$29 \pm 8.2$	GE	09A	CLEO $e^+e^-$ at 4170 MeV

$\Gamma(\eta'(958)\pi^+)/\Gamma_{\text{total}}$   $\Gamma_{74}/\Gamma$   
 Unseen decay modes of the  $\eta'(958)$  are included.

VALUE (units $10^{-2}$ )	DOCUMENT ID	TECN	COMMENT
$3.77 \pm 0.25 \pm 0.30$	37 ALEXANDER	08	CLEO See MENDEZ 10
$37$	ALEXANDER	08	uses single- and double-tagged events in an overall fit.

$\Gamma(\eta'(958)\pi^+)/\Gamma(K^+K_S^0)$   $\Gamma_{74}/\Gamma_{31}$   
 Unseen decay modes of the  $\eta'(958)$  are included.

VALUE	EVTS	DOCUMENT ID	TECN	COMMENT
$2.654 \pm 0.088 \pm 0.139$	$1436 \pm 47$	MENDEZ	10	CLEO $e^+e^-$ at 4170 MeV

$\Gamma(\eta'(958)\pi^+)/\Gamma(\phi\pi^+)$   $\Gamma_{74}/\Gamma_{33}$   
 Unseen decay modes of the resonances are included.

VALUE	EVTS	DOCUMENT ID	TECN	COMMENT
$1.03 \pm 0.06 \pm 0.07$	537	JESSOP	98	CLE2 $e^+e^- \approx \Upsilon(4S)$
$1.20 \pm 0.15 \pm 0.11$	281	ALEXANDER	92	CLE2 See JESSOP 98
$2.5 \pm 1.0 \pm 1.5$ $-0.4$	22	ALVAREZ	91	NA14 Photoproduction
$2.5 \pm 0.5 \pm 0.3$	215	ALBRECHT	90d	ARG $e^+e^- \approx 10.4$ GeV

$\Gamma(\omega\eta\pi^+)/\Gamma_{\text{total}}$   $\Gamma_{76}/\Gamma$   
 Unseen decay modes of the  $\omega$  and  $\eta$  are included.

VALUE	CL%	DOCUMENT ID	TECN	COMMENT
$<2.13 \times 10^{-2}$	90	GE	09A	CLEO $e^+e^-$ at 4170 MeV

$\Gamma(\eta'(958)\pi^+)/\Gamma(\phi\pi^+)$   $\Gamma_{77}/\Gamma_{33}$   
 Unseen decay modes of the resonances are included.

VALUE	EVTS	DOCUMENT ID	TECN	COMMENT
$2.78 \pm 0.28 \pm 0.30$	137	JESSOP	98	CLE2 $e^+e^- \approx \Upsilon(4S)$
$3.44 \pm 0.62 \pm 0.44$ $-0.46$	68	AVERY	92	CLE2 See JESSOP 98

$\Gamma(\eta'(958)\pi^+\pi^0\text{-body})/\Gamma(\phi\pi^+)$   $\Gamma_{78}/\Gamma_{33}$   
 Unseen decay modes of the resonances are included.

VALUE	CL%	DOCUMENT ID	TECN	COMMENT
$<0.4$	90	JESSOP	98	CLE2 $e^+e^- \approx \Upsilon(4S)$
$<0.85$	90	DAOUDI	92	CLE2 See JESSOP 98

Modes with one or three  $K$ 's

$\Gamma(K^+\pi^0)/\Gamma(K^+K_S^0)$   $\Gamma_{79}/\Gamma_{31}$

VALUE (units $10^{-2}$ )	EVTS	DOCUMENT ID	TECN	COMMENT
$4.2 \pm 1.4 \pm 0.2$	$202 \pm 70$	MENDEZ	10	CLEO $e^+e^-$ at 4170 MeV
$5.5 \pm 1.3 \pm 0.7$	$141 \pm 34$	ADAMS	07A	CLEO See MENDEZ 10

$\Gamma(K_S^0\pi^+)/\Gamma(K^+K_S^0)$   $\Gamma_{80}/\Gamma_{31}$

VALUE (units $10^{-2}$ )	EVTS	DOCUMENT ID	TECN	COMMENT
$8.12 \pm 0.28$ OUR AVERAGE				
$8.5 \pm 0.7 \pm 0.2$	$393 \pm 33$	MENDEZ	10	CLEO $e^+e^-$ at 4170 MeV
$8.03 \pm 0.24 \pm 0.19$	$17.6k \pm 481$	WON	09	BELL $e^+e^-$ at $\Upsilon(4S)$
$10.4 \pm 2.4 \pm 1.4$	$113 \pm 26$	LINK	08	FOCS $\gamma A, \bar{E}_\gamma \approx 180$ GeV
$8.2 \pm 0.9 \pm 0.2$	$206 \pm 22$	ADAMS	07A	CLEO See MENDEZ 10

$\Gamma(K^+\eta)/\Gamma(K^+K_S^0)$   $\Gamma_{81}/\Gamma_{31}$   
 Unseen decay modes of the  $\eta$  are included.

VALUE (units $10^{-2}$ )	EVTS	DOCUMENT ID	TECN	COMMENT
$11.8 \pm 2.2 \pm 0.6$	$222 \pm 41$	MENDEZ	10	CLEO $e^+e^-$ at 4170 MeV

$\Gamma(K^+\eta)/\Gamma(\eta\pi^+)$   $\Gamma_{81}/\Gamma_{65}$

VALUE (units $10^{-2}$ )	EVTS	DOCUMENT ID	TECN	COMMENT
$8.9 \pm 1.5 \pm 0.4$	$113 \pm 18$	ADAMS	07A	CLEO See MENDEZ 10

$\Gamma(K^+\omega)/\Gamma_{\text{total}}$   $\Gamma_{82}/\Gamma$   
 Unseen decay modes of the  $\omega$  are included.

VALUE (units $10^{-2}$ )	CL%	DOCUMENT ID	TECN	COMMENT
$<0.24$	90	GE	09A	CLEO $e^+e^-$ at 4170 MeV

$\Gamma(K^+\eta'(958))/\Gamma(K^+K_S^0)$   $\Gamma_{83}/\Gamma_{31}$   
 Unseen decay modes of the  $\eta'(958)$  are included.

VALUE (units $10^{-2}$ )	EVTS	DOCUMENT ID	TECN	COMMENT
$11.8 \pm 3.6 \pm 0.7$	$56 \pm 17$	MENDEZ	10	CLEO $e^+e^-$ at 4170 MeV

$\Gamma(K^+\eta'(958))/\Gamma(\eta'(958)\pi^+)$   $\Gamma_{83}/\Gamma_{74}$

VALUE (units $10^{-2}$ )	EVTS	DOCUMENT ID	TECN	COMMENT
$4.2 \pm 1.3 \pm 0.3$	$28 \pm 9$	ADAMS	07A	CLEO See MENDEZ 10

$\Gamma(K^+\pi^+\pi^-)/\Gamma_{\text{total}}$   $\Gamma_{84}/\Gamma$

VALUE (units $10^{-2}$ )	DOCUMENT ID	TECN	COMMENT
$0.69 \pm 0.05$ OUR FIT			
$0.69 \pm 0.05 \pm 0.03$	38 ALEXANDER	08	CLEO $e^+e^-$ at 4.17 GeV
$38$	ALEXANDER	08	uses single- and double-tagged events in an overall fit. The correlation matrix for the branching fractions is used in the fit.

$\Gamma(K^+\pi^+\pi^-)/\Gamma(K^+K^-\pi^+)$   $\Gamma_{84}/\Gamma_{32}$

VALUE	EVTS	DOCUMENT ID	TECN	COMMENT
$0.126 \pm 0.009$ OUR FIT				
$0.127 \pm 0.007 \pm 0.014$	$567 \pm 31$	LINK	04F	FOCS $\gamma A, \bar{E}_\gamma \approx 180$ GeV

$\Gamma(K^+\rho^0)/\Gamma(K^+\pi^+\pi^-)$   $\Gamma_{85}/\Gamma_{84}$   
 This is the "fit fraction" from the Dalitz-plot analysis.

VALUE	DOCUMENT ID	TECN	COMMENT
$0.3883 \pm 0.0531 \pm 0.0261$	LINK	04F	FOCS Dalitz fit, 567 evts

$\Gamma(K^+\rho(1450)^0, \rho^0 \rightarrow \pi^+\pi^-)/\Gamma(K^+\pi^+\pi^-)$   $\Gamma_{86}/\Gamma_{84}$   
 This is the "fit fraction" from the Dalitz-plot analysis.

VALUE	DOCUMENT ID	TECN	COMMENT
$0.1062 \pm 0.0351 \pm 0.0104$	LINK	04F	FOCS Dalitz fit, 567 evts

$\Gamma(K^*(892)^0\pi^+, K^{*0} \rightarrow K^+\pi^-)/\Gamma(K^+\pi^+\pi^-)$   $\Gamma_{87}/\Gamma_{84}$   
 This is the "fit fraction" from the Dalitz-plot analysis.

VALUE	DOCUMENT ID	TECN	COMMENT
$0.2164 \pm 0.0321 \pm 0.0114$	LINK	04F	FOCS Dalitz fit, 567 evts

$\Gamma(K^*(1410)^0\pi^+, K^{*0} \rightarrow K^+\pi^-)/\Gamma(K^+\pi^+\pi^-)$   $\Gamma_{88}/\Gamma_{84}$   
 This is the "fit fraction" from the Dalitz-plot analysis.

VALUE	DOCUMENT ID	TECN	COMMENT
$0.1882 \pm 0.0403 \pm 0.0122$	LINK	04F	FOCS Dalitz fit, 567 evts

$\Gamma(K^*(1430)^0\pi^+, K^{*0} \rightarrow K^+\pi^-)/\Gamma(K^+\pi^+\pi^-)$   $\Gamma_{89}/\Gamma_{84}$   
 This is the "fit fraction" from the Dalitz-plot analysis.

VALUE	DOCUMENT ID	TECN	COMMENT
$0.0765 \pm 0.0500 \pm 0.0170$	LINK	04F	FOCS Dalitz fit, 567 evts

$\Gamma(K^+\pi^+\pi^- \text{ nonresonant})/\Gamma(K^+\pi^+\pi^-)$   $\Gamma_{90}/\Gamma_{84}$   
 This is the "fit fraction" from the Dalitz-plot analysis.

VALUE	DOCUMENT ID	TECN	COMMENT
$0.1588 \pm 0.0492 \pm 0.0153$	LINK	04F	FOCS Dalitz fit, 567 evts

$\Gamma(K^0\pi^+\pi^0)/\Gamma_{\text{total}}$   $\Gamma_{91}/\Gamma$

VALUE (units $10^{-2}$ )	EVTS	DOCUMENT ID	TECN	COMMENT
$1.00 \pm 0.18 \pm 0.04$	$44 \pm 8$	NAIK	09A	CLEO $e^+e^-$ at 4170 MeV

$\Gamma(K_S^0 2\pi^+\pi^-)/\Gamma(K_S^0 K^-\pi^+)$   $\Gamma_{92}/\Gamma_{44}$

VALUE	EVTS	DOCUMENT ID	TECN	COMMENT
$0.18 \pm 0.04 \pm 0.05$	$179 \pm 36$	LINK	08	FOCS $\gamma A, \bar{E}_\gamma \approx 180$ GeV

$\Gamma(K^+\omega\pi^0)/\Gamma_{\text{total}}$   $\Gamma_{93}/\Gamma$   
 Unseen decay modes of the  $\omega$  are included.

VALUE (units $10^{-2}$ )	CL%	DOCUMENT ID	TECN	COMMENT
$<0.82$	90	GE	09A	CLEO $e^+e^-$ at 4170 MeV

$\Gamma(K^+\omega\pi^+\pi^-)/\Gamma_{\text{total}}$   $\Gamma_{94}/\Gamma$   
 Unseen decay modes of the  $\omega$  are included.

VALUE (units $10^{-2}$ )	CL%	DOCUMENT ID	TECN	COMMENT
$<0.54$	90	GE	09A	CLEO $e^+e^-$ at 4170 MeV

$\Gamma(K^+\omega\eta)/\Gamma_{\text{total}}$   $\Gamma_{95}/\Gamma$   
 Unseen decay modes of the  $\omega$  and  $\eta$  are included.

VALUE (units $10^{-2}$ )	CL%	DOCUMENT ID	TECN	COMMENT
$<0.79$	90	GE	09A	CLEO $e^+e^-$ at 4170 MeV

$\Gamma(2K^+K^-)/\Gamma(K^+K^-\pi^+)$   $\Gamma_{96}/\Gamma_{32}$

VALUE (units $10^{-3}$ )	EVTS	DOCUMENT ID	TECN	COMMENT
$4.0 \pm 0.3 \pm 0.2$	$748 \pm 60$	DEL-AMO-SA..11g	BABR	$e^+e^- \approx \Upsilon(4S)$
$8.95 \pm 2.12 \pm 2.24$ $-2.31$	31	LINK	02i	FOCS $\gamma$ nucleus, $\approx 180$ GeV



$\Gamma(\phi K^+, \phi \rightarrow K^+ K^-)/\Gamma(2K^+ K^-)$				$\Gamma_{97}/\Gamma_{96}$
VALUE	DOCUMENT ID	TECN	COMMENT	
$0.41 \pm 0.08 \pm 0.03$	DEL-AMO-SA..11G	BABR	$e^+ e^- \approx \mathcal{T}(4S)$	

## Doubly Cabibbo-suppressed modes

$\Gamma(2K^+ \pi^-)/\Gamma(K^+ K^- \pi^+)$				$\Gamma_{98}/\Gamma_{32}$
VALUE (units $10^{-3}$ )	EVTS	DOCUMENT ID	TECN	COMMENT
<b><math>2.33 \pm 0.23</math> OUR AVERAGE</b>				
$2.3 \pm 0.3 \pm 0.2$	356 ± 52	DEL-AMO-SA..11G	BABR	$e^+ e^- \approx \mathcal{T}(4S)$
$2.29 \pm 0.28 \pm 0.12$	281 ± 34	KO 09	BELL	$e^+ e^-$ at $\mathcal{T}(4S)$
$5.2 \pm 1.7 \pm 1.1$	27 ± 9	LINK	05K	FOCS <0.78%, CL = 90%

$\Gamma(K^+ K^*(892)^0, K^{*0} \rightarrow K^+ \pi^-)/\Gamma(2K^+ \pi^-)$				$\Gamma_{99}/\Gamma_{98}$
VALUE	DOCUMENT ID	TECN	COMMENT	
$0.47 \pm 0.22 \pm 0.15$	DEL-AMO-SA..11G	BABR	$e^+ e^- \approx \mathcal{T}(4S)$	

## Baryon-antibaryon mode

$\Gamma(p\bar{p})/\Gamma_{\text{total}}$				$\Gamma_{100}/\Gamma$
This is the only baryonic mode allowed kinematically.				
VALUE (units $10^{-3}$ )	EVTS	DOCUMENT ID	TECN	COMMENT
$1.30 \pm 0.36 \pm 0.12$ $-0.16$	13.0 ± 3.6	ATHAR 08	CLEO	$e^+ e^-$ , $E_{\text{cm}} \approx 4170$ MeV

## Rare or forbidden modes

$\Gamma(\pi^+ e^+ e^-)/\Gamma_{\text{total}}$				$\Gamma_{101}/\Gamma$	
This mode is not a useful test for a $\Delta C=1$ weak neutral current because both quarks must change flavor in this decay.					
VALUE	CL%	EVTS	DOCUMENT ID	TECN	COMMENT
$< 13 \times 10^{-6}$	90	8 ± 35	LEES	11G	BABR $e^+ e^- \approx \mathcal{T}(4S)$
••• We do not use the following data for averages, fits, limits, etc. •••					
$< 2.2 \times 10^{-5}$	90		<sup>39</sup> RUBIN	10	CLEO $e^+ e^-$ at 4170 MeV
$< 27 \times 10^{-5}$	90		AITALA	99G	E791 $\pi^- N$ 500 GeV
<sup>39</sup> This RUBIN 10 limit is for the $e^+ e^-$ mass in the continuum away from the $\phi(1020)$ . See the next data block.					

$\Gamma(\pi^+ \phi, \phi \rightarrow e^+ e^-)/\Gamma_{\text{total}}$				$\Gamma_{102}/\Gamma$
This is not a test for the $\Delta C=1$ weak neutral current, but leads to the $\pi^+ e^+ e^-$ final state.				
VALUE	EVTS	DOCUMENT ID	TECN	COMMENT
$(6 \pm 8 \pm 1) \times 10^{-6}$	3	RUBIN 10	CLEO	$e^+ e^-$ at 4170 MeV

$\Gamma(\pi^+ \mu^+ \mu^-)/\Gamma_{\text{total}}$				$\Gamma_{103}/\Gamma$	
This mode is not a useful test for a $\Delta C=1$ weak neutral current because both quarks must change flavor in this decay.					
VALUE	CL%	EVTS	DOCUMENT ID	TECN	COMMENT
$< 2.6 \times 10^{-5}$	90		LINK	03F	FOCS $\gamma$ nucleus, $\bar{E}_\gamma \approx 180$ GeV
••• We do not use the following data for averages, fits, limits, etc. •••					
$< 43 \times 10^{-6}$	90	20 ± 16	LEES	11G	BABR $e^+ e^- \approx \mathcal{T}(4S)$
$< 1.4 \times 10^{-4}$	90		AITALA	99G	E791 $\pi^- N$ 500 GeV
$< 4.3 \times 10^{-4}$	90	0	KODAMA	95	E653 $\pi^-$ emulsion 600 GeV

$\Gamma(K^+ e^+ e^-)/\Gamma_{\text{total}}$				$\Gamma_{104}/\Gamma$	
A test for the $\Delta C=1$ weak neutral current. Allowed by higher-order electroweak interactions.					
VALUE	CL%	EVTS	DOCUMENT ID	TECN	COMMENT
$< 3.7 \times 10^{-6}$	90	-5.7 ± 6.1	LEES	11G	BABR $e^+ e^- \approx \mathcal{T}(4S)$
••• We do not use the following data for averages, fits, limits, etc. •••					
$< 5.2 \times 10^{-5}$	90		RUBIN	10	CLEO $e^+ e^-$ at 4170 MeV
$< 1.6 \times 10^{-3}$	90		AITALA	99G	E791 $\pi^- N$ 500 GeV

$\Gamma(K^+ \mu^+ \mu^-)/\Gamma_{\text{total}}$				$\Gamma_{105}/\Gamma$	
A test for the $\Delta C=1$ weak neutral current. Allowed by higher-order electroweak interactions.					
VALUE	CL%	EVTS	DOCUMENT ID	TECN	COMMENT
$< 21 \times 10^{-6}$	90	4.8 ± 6.0	LEES	11G	BABR $e^+ e^- \approx \mathcal{T}(4S)$
••• We do not use the following data for averages, fits, limits, etc. •••					
$< 3.6 \times 10^{-5}$	90		LINK	03F	FOCS $\gamma$ nucleus, $\bar{E}_\gamma \approx 180$ GeV
$< 1.4 \times 10^{-4}$	90		AITALA	99G	E791 $\pi^- N$ 500 GeV
$< 5.9 \times 10^{-4}$	90	0	KODAMA	95	E653 $\pi^-$ emulsion 600 GeV

$\Gamma(K^*(892)^+ \mu^+ \mu^-)/\Gamma_{\text{total}}$				$\Gamma_{106}/\Gamma$	
A test for the $\Delta C=1$ weak neutral current. Allowed by higher-order electroweak interactions.					
VALUE	CL%	EVTS	DOCUMENT ID	TECN	COMMENT
$< 1.4 \times 10^{-3}$	90	0	KODAMA	95	E653 $\pi^-$ emulsion 600 GeV

$\Gamma(\pi^+ e^+ \mu^-)/\Gamma_{\text{total}}$				$\Gamma_{107}/\Gamma$	
A test of lepton-family-number conservation.					
VALUE	CL%	EVTS	DOCUMENT ID	TECN	COMMENT
$< 12 \times 10^{-6}$	90	-3 ± 11	LEES	11G	BABR $e^+ e^- \approx \mathcal{T}(4S)$

$\Gamma(\pi^+ e^- \mu^+)/\Gamma_{\text{total}}$				$\Gamma_{108}/\Gamma$	
A test of lepton-family-number conservation.					
VALUE	CL%	EVTS	DOCUMENT ID	TECN	COMMENT
$< 20 \times 10^{-6}$	90	9.3 ± 7.8	LEES	11G	BABR $e^+ e^- \approx \mathcal{T}(4S)$

$\Gamma(K^+ e^+ \mu^-)/\Gamma_{\text{total}}$				$\Gamma_{109}/\Gamma$	
A test of lepton-family-number conservation.					
VALUE	CL%	EVTS	DOCUMENT ID	TECN	COMMENT
$< 14 \times 10^{-6}$	90	9.1 ± 6.6	LEES	11G	BABR $e^+ e^- \approx \mathcal{T}(4S)$

$\Gamma(K^+ e^- \mu^+)/\Gamma_{\text{total}}$				$\Gamma_{110}/\Gamma$	
A test of lepton-family-number conservation.					
VALUE	CL%	EVTS	DOCUMENT ID	TECN	COMMENT
$< 9.7 \times 10^{-6}$	90	3.4 ± 7.3	LEES	11G	BABR $e^+ e^- \approx \mathcal{T}(4S)$

$\Gamma(\pi^- 2e^+)/\Gamma_{\text{total}}$				$\Gamma_{111}/\Gamma$	
A test of lepton-number conservation.					
VALUE	CL%	EVTS	DOCUMENT ID	TECN	COMMENT
$< 4.1 \times 10^{-6}$	90	-5.7 ± 14	LEES	11G	BABR $e^+ e^- \approx \mathcal{T}(4S)$
••• We do not use the following data for averages, fits, limits, etc. •••					
$< 1.8 \times 10^{-5}$	90		RUBIN	10	CLEO $e^+ e^-$ at 4170 MeV
$< 69 \times 10^{-5}$	90		AITALA	99G	E791 $\pi^- N$ 500 GeV

$\Gamma(\pi^- 2\mu^+)/\Gamma_{\text{total}}$				$\Gamma_{112}/\Gamma$	
A test of lepton-number conservation.					
VALUE	CL%	EVTS	DOCUMENT ID	TECN	COMMENT
$< 14 \times 10^{-6}$	90	0.6 ± 5.8	LEES	11G	BABR $e^+ e^- \approx \mathcal{T}(4S)$
••• We do not use the following data for averages, fits, limits, etc. •••					
$< 2.9 \times 10^{-5}$	90		LINK	03F	FOCS $\gamma$ nucleus, $\bar{E}_\gamma \approx 180$ GeV
$< 8.2 \times 10^{-5}$	90		AITALA	99G	E791 $\pi^- N$ 500 GeV
$< 4.3 \times 10^{-4}$	90	0	KODAMA	95	E653 $\pi^-$ emulsion 600 GeV

$\Gamma(\pi^- e^+ \mu^+)/\Gamma_{\text{total}}$				$\Gamma_{113}/\Gamma$	
A test of lepton-number conservation.					
VALUE	CL%	EVTS	DOCUMENT ID	TECN	COMMENT
$< 8.4 \times 10^{-6}$	90	-0.2 ± 7.9	LEES	11G	BABR $e^+ e^- \approx \mathcal{T}(4S)$
••• We do not use the following data for averages, fits, limits, etc. •••					
$< 7.3 \times 10^{-4}$	90		AITALA	99G	E791 $\pi^- N$ 500 GeV

$\Gamma(K^- 2e^+)/\Gamma_{\text{total}}$				$\Gamma_{114}/\Gamma$	
A test of lepton-number conservation.					
VALUE	CL%	EVTS	DOCUMENT ID	TECN	COMMENT
$< 5.2 \times 10^{-6}$	90	2.3 ± 8.6	LEES	11G	BABR $e^+ e^- \approx \mathcal{T}(4S)$
••• We do not use the following data for averages, fits, limits, etc. •••					
$< 1.7 \times 10^{-5}$	90		RUBIN	10	CLEO $e^+ e^-$ at 4170 MeV
$< 63 \times 10^{-5}$	90		AITALA	99G	E791 $\pi^- N$ 500 GeV

$\Gamma(K^- 2\mu^+)/\Gamma_{\text{total}}$				$\Gamma_{115}/\Gamma$	
A test of lepton-number conservation.					
VALUE	CL%	EVTS	DOCUMENT ID	TECN	COMMENT
$< 1.3 \times 10^{-5}$	90	-2.3 ± 5.7	LEES	11G	BABR $e^+ e^- \approx \mathcal{T}(4S)$
••• We do not use the following data for averages, fits, limits, etc. •••					
$< 1.8 \times 10^{-4}$	90		AITALA	99G	E791 $\pi^- N$ 500 GeV
$< 5.9 \times 10^{-4}$	90	0	KODAMA	95	E653 $\pi^-$ emulsion 600 GeV

$\Gamma(K^- e^+ \mu^+)/\Gamma_{\text{total}}$				$\Gamma_{116}/\Gamma$	
A test of lepton-number conservation.					
VALUE	CL%	EVTS	DOCUMENT ID	TECN	COMMENT
$< 6.1 \times 10^{-6}$	90	-14 ± 9	LEES	11G	BABR $e^+ e^- \approx \mathcal{T}(4S)$
••• We do not use the following data for averages, fits, limits, etc. •••					
$< 6.8 \times 10^{-4}$	90		AITALA	99G	E791 $\pi^- N$ 500 GeV

$\Gamma(K^*(892)^- 2\mu^+)/\Gamma_{\text{total}}$				$\Gamma_{117}/\Gamma$	
A test of lepton-number conservation.					
VALUE	CL%	EVTS	DOCUMENT ID	TECN	COMMENT
$< 1.4 \times 10^{-3}$	90	0	KODAMA	95	E653 $\pi^-$ emulsion 600 GeV

 $D_s^+ - D_s^-$  CP-VIOLATING DECAY-RATE ASYMMETRIES

This is the difference of the  $D_s^+$  and  $D_s^-$  partial widths divided by the sum of the widths.

$A_{CP}(\mu^\pm \nu)$ in $D_s^+ \rightarrow \mu^+ \nu$ , $D_s^- \rightarrow \mu^- \bar{\nu}_\mu$			
VALUE (%)	DOCUMENT ID	TECN	COMMENT
$+4.8 \pm 6.1$	ALEXANDER 09	CLEO	$e^+ e^-$ at 4170 MeV



ACCIARRI	97F	PL B396 327	M. Acciarri <i>et al.</i>	(L3 Collab.)
BALEST	97	PRL 79 1436	R. Balest <i>et al.</i>	(CLEO Collab.)
FRABETTI	97C	PL B401 131	P.L. Frabetti <i>et al.</i>	(FNAL E687 Collab.)
FRABETTI	97D	PL B407 79	P.L. Frabetti <i>et al.</i>	(FNAL E687 Collab.)
ARTUSO	96	PL B378 364	M. Artuso <i>et al.</i>	(CLEO Collab.)
BAI	95C	PR D52 3781	J.Z. Bai <i>et al.</i>	(BES Collab.)
BRANDENB...	95	PRL 75 3804	G.W. Brandenburg <i>et al.</i>	(CLEO Collab.)
FRABETTI	95B	PL B351 591	P.L. Frabetti <i>et al.</i>	(FNAL E687 Collab.)
KODAMA	95	PL B345 85	K. Kodama <i>et al.</i>	(FNAL E653 Collab.)
ACOSTA	94	PR D49 5690	D. Acosta <i>et al.</i>	(CLEO Collab.)
AVERY	94B	PL B337 405	P. Avery <i>et al.</i>	(CLEO Collab.)
BROWN	94	PR D50 1884	D. Brown <i>et al.</i>	(CLEO Collab.)
BUTLER	94	PL B324 255	F. Butler <i>et al.</i>	(CLEO Collab.)
FRABETTI	94F	PL B328 187	P.L. Frabetti <i>et al.</i>	(FNAL E687 Collab.)
FRABETTI	93F	PRL 71 827	P.L. Frabetti <i>et al.</i>	(FNAL E687 Collab.)
FRABETTI	93G	PL B313 253	P.L. Frabetti <i>et al.</i>	(FNAL E687 Collab.)
KODAMA	93	PL B309 483	K. Kodama <i>et al.</i>	(FNAL E653 Collab.)
ALBRECHT	92B	ZPHY C53 361	H. Albrecht <i>et al.</i>	(ARGUS Collab.)
ALEXANDER	92	PRL 68 1275	J. Alexander <i>et al.</i>	(CLEO Collab.)
AVERY	92	PRL 68 1279	P. Avery <i>et al.</i>	(CLEO Collab.)
BARLAG	92C	ZPHY C55 383	S. Barlag <i>et al.</i>	(ACCMOR Collab.)
Also		ZPHY C48 29	S. Barlag <i>et al.</i>	(ACCMOR Collab.)
DAOUDI	92	PR D45 3965	M. Daoudi <i>et al.</i>	(CLEO Collab.)
FRABETTI	92	PL B281 167	P.L. Frabetti <i>et al.</i>	(FNAL E687 Collab.)
ALBRECHT	91	PL B255 634	H. Albrecht <i>et al.</i>	(ARGUS Collab.)
ALVAREZ	91	PL B255 639	M.P. Alvarez <i>et al.</i>	(CERN NA14/2 Collab.)
ALBRECHT	90D	PL B245 315	H. Albrecht <i>et al.</i>	(ARGUS Collab.)
ALEXANDER	90B	PRL 65 1531	J. Alexander <i>et al.</i>	(CLEO Collab.)
BARLAG	90C	ZPHY C46 563	S. Barlag <i>et al.</i>	(ACCMOR Collab.)
FRABETTI	90	PL B251 639	P.L. Frabetti <i>et al.</i>	(FNAL E687 Collab.)
ANJOS	89E	PL B223 267	J.C. Anjos <i>et al.</i>	(FNAL E691 Collab.)
CHEN	89	PL B226 192	W.Y. Chen <i>et al.</i>	(CLEO Collab.)
ALBRECHT	88	PL B207 349	H. Albrecht <i>et al.</i>	(ARGUS Collab.)
ANJOS	88	PRL 60 897	J.C. Anjos <i>et al.</i>	(FNAL E691 Collab.)
RAAB	88	PR D37 2391	J.R. Raab <i>et al.</i>	(FNAL E691 Collab.)
BECKER	87B	PL B184 277	H. Becker <i>et al.</i>	(NA11 and NA32 Collab.)
BLAYLOCK	87	PRL 58 2171	G.T. Blaylock <i>et al.</i>	(Mark III Collab.)
USHIDA	86	PRL 56 1767	N. Ushida <i>et al.</i>	(FNAL E531 Collab.)
ALBRECHT	85D	PL 153B 343	H. Albrecht <i>et al.</i>	(ARGUS Collab.)
DERRICK	85B	PRL 54 2568	M. Derrick <i>et al.</i>	(HRS Collab.)
AIHARA	84D	PRL 53 2465	H. Aihara <i>et al.</i>	(TPC Collab.)
ALTHOFF	84	PL 136B 130	M. Althoff <i>et al.</i>	(TASSO Collab.)
BAILEY	84	PL 139B 320	R. Bailey <i>et al.</i>	(ACCMOR Collab.)
CHEN	83C	PRL 51 634	A. Chen <i>et al.</i>	(CLEO Collab.)

OTHER RELATED PAPERS

RICHMAN	95	RMP 67 893	J.D. Richman, P.R. Burchat	(UCSB, STAN)
---------	----	------------	----------------------------	--------------

$D_s^{*\pm}$

 $I(J^P) = 0(?^?)$   
 $J^P$  is natural, width and decay modes consistent with  $1^-$ .

$D_s^{*\pm}$  MASS

The fit includes  $D^\pm, D^0, D_s^\pm, D^{*\pm}, D^{*0}, D_s^{*\pm}, D_1(2420)^0, D_2^*(2460)^0$ , and  $D_{s1}(2536)^\pm$  mass and mass difference measurements.

VALUE (MeV)	EVTS	DOCUMENT ID	TECN	COMMENT
<b>2112.3 ± 0.5 OUR FIT</b>				Error includes scale factor of 1.1.
<b>2106.6 ± 2.1 ± 2.7</b>	1	BLAYLOCK	87	MRK3 $e^+e^- \rightarrow D_s^{*\pm}\gamma X$

<sup>1</sup> Assuming  $D_s^{*\pm}$  mass = 1968.7 ± 0.9 MeV.

$m_{D_s^{*\pm}} - m_{D_s^\pm}$

The fit includes  $D^\pm, D^0, D_s^\pm, D^{*\pm}, D^{*0}, D_s^{*\pm}, D_1(2420)^0, D_2^*(2460)^0$ , and  $D_{s1}(2536)^\pm$  mass and mass difference measurements.

VALUE (MeV)	EVTS	DOCUMENT ID	TECN	COMMENT
<b>143.8 ± 0.4 OUR FIT</b>				
<b>143.9 ± 0.4 OUR AVERAGE</b>				
143.76 ± 0.39 ± 0.40		GRONBERG	95	CLE2 $e^+e^-$
144.22 ± 0.47 ± 0.37		BROWN	94	CLE2 $e^+e^-$
142.5 ± 0.8 ± 1.5		<sup>2</sup> ALBRECHT	88	ARG $e^+e^- \rightarrow D_s^{*\pm}\gamma X$
139.5 ± 8.3 ± 9.7	60	AIHARA	84D	TPC $e^+e^- \rightarrow$ hadrons
• • • We do not use the following data for averages, fits, limits, etc. • • •				
143.0 ± 18.0	8	ASRATYAN	85	HLBC FNAL 15-ft, $\mu^2$ H
110 ± 46		BRANDELIK	79	DASP $e^+e^- \rightarrow D_s^{*\pm}\gamma X$

<sup>2</sup> Result includes data of ALBRECHT 84B.

$D_s^{*\pm}$  WIDTH

VALUE (MeV)	CL%	DOCUMENT ID	TECN	COMMENT
<b>&lt; 1.9</b>	90	GRONBERG	95	CLE2 $e^+e^-$
<b>&lt; 4.5</b>	90	ALBRECHT	88	ARG $E_{cm}^e = 10.2$ GeV
• • • We do not use the following data for averages, fits, limits, etc. • • •				
< 4.9	90	BROWN	94	CLE2 $e^+e^-$
< 22	90	BLAYLOCK	87	MRK3 $e^+e^- \rightarrow D_s^{*\pm}\gamma X$

$D_s^{*+}$  DECAY MODES

$D_s^{*-}$  modes are charge conjugates of the modes below.

Mode	Fraction ( $\Gamma_i/\Gamma$ )
$\Gamma_1 D_s^{*+} \gamma$	(94.2 ± 0.7) %
$\Gamma_2 D_s^{*+} \pi^0$	(5.8 ± 0.7) %

CONSTRAINED FIT INFORMATION

An overall fit to a branching ratio uses 2 measurements and one constraint to determine 2 parameters. The overall fit has a  $\chi^2 = 0.0$  for 1 degrees of freedom.

The following *off-diagonal* array elements are the correlation coefficients  $\langle \delta x_i \delta x_j \rangle / (\delta x_i \cdot \delta x_j)$ , in percent, from the fit to the branching fractions,  $x_i \equiv \Gamma_i/\Gamma_{total}$ . The fit constrains the  $x_i$  whose labels appear in this array to sum to one.

$x_2$	-100
$x_1$	

$D_s^{*+}$  BRANCHING RATIOS

$\Gamma(D_s^{*+} \gamma)/\Gamma_{total}$	VALUE	EVTS	DOCUMENT ID	TECN	COMMENT	$\Gamma_1/\Gamma$
<b>0.942 ± 0.007 OUR FIT</b>						
0.942 ± 0.004 ± 0.006	16k	<sup>3</sup> AUBERT, BE	05G	BABR	10.6 $e^+e^- \rightarrow$ hadrons	
seen		ASRATYAN	91	HLBC	$\tau_\mu$ Ne	
seen		ALBRECHT	88	ARG	$e^+e^- \rightarrow D_s^{*+} \gamma X$	
seen		AIHARA	84D			
seen		ALBRECHT	84B			
seen		BRANDELIK	79			

$\Gamma(D_s^{*+} \pi^0)/\Gamma_{total}$	VALUE	EVTS	DOCUMENT ID	TECN	COMMENT	$\Gamma_2/\Gamma$
• • • We do not use the following data for averages, fits, limits, etc. • • •						
0.059 ± 0.004 ± 0.006	560	<sup>3</sup> AUBERT, BE	05G	BABR	10.6 $e^+e^- \rightarrow$ hadrons	

$\Gamma(D_s^{*+} \pi^0)/\Gamma(D_s^{*+} \gamma)$	VALUE	DOCUMENT ID	TECN	COMMENT	$\Gamma_2/\Gamma_1$
<b>0.062 ± 0.008 OUR FIT</b>					
<b>0.062 ± 0.008 OUR AVERAGE</b>					
0.062 ± 0.005 ± 0.006		AUBERT, BE	05G	BABR	10.6 $e^+e^- \rightarrow$ hadrons
0.062 ± 0.020 ± 0.018		GRONBERG	95	CLE2	$e^+e^-$

<sup>3</sup> Derived from the ratio  $\Gamma(D_s^{*+} \pi^0) / \Gamma(D_s^{*+} \gamma)$  assuming that the branching fractions of  $D_s^{*+} \rightarrow D_s^{*+} \pi^0$  and  $D_s^{*+} \rightarrow D_s^{*+} \gamma$  decays sum to 100%.

$D_{s0}^{*+}$  REFERENCES

AUBERT, BE	05G	PR D72 091101	B. Aubert <i>et al.</i>	(BABAR Collab.)
GRONBERG	95	PRL 75 3232	J. Gronberg <i>et al.</i>	(CLEO Collab.)
BROWN	94	PR D50 1884	D. Brown <i>et al.</i>	(CLEO Collab.)
ASRATYAN	91	PL B257 525	A.E. Asratyan <i>et al.</i>	(ITEP, BELG, SACL+)
ALBRECHT	88	PL B207 349	H. Albrecht <i>et al.</i>	(ARGUS Collab.)
BLAYLOCK	87	PRL 58 2171	G.T. Blaylock <i>et al.</i>	(Mark III Collab.)
ASRATYAN	85	PL 156B 441	A.E. Asratyan <i>et al.</i>	(ITEP, SERP)
AIHARA	84D	PRL 53 2465	H. Aihara <i>et al.</i>	(TPC Collab.)
ALBRECHT	84B	PL 146B 111	H. Albrecht <i>et al.</i>	(ARGUS Collab.)
BRANDELIK	79	PL 80B 412	R. Brandelik <i>et al.</i>	(DASP Collab.)

$D_{s0}^*(2317)^\pm$

$I(J^P) = 0(0^+)$   
 $J, P$  need confirmation.

AUBERT 06P does not observe neutral and doubly charged partners of the  $D_{s0}^*(2317)^\pm$ .

$D_{s0}^*(2317)^\pm$  MASS

The fit includes  $D^\pm, D^0, D_s^\pm, D^{*\pm}, D^{*0}, D_s^{*\pm}, D_1(2420)^0, D_2^*(2460)^0$ , and  $D_{s1}(2536)^\pm$  mass and mass difference measurements.

VALUE (MeV)	EVTS	DOCUMENT ID	TECN	COMMENT
<b>2317.8 ± 0.6 OUR FIT</b>				Error includes scale factor of 1.1.
<b>2318.0 ± 1.0 OUR AVERAGE</b>				Error includes scale factor of 1.4.
2319.6 ± 0.2 ± 1.4	3180	AUBERT	06P	BABR 10.6 $e^+e^- \rightarrow D_s^{*+} \pi^0 X$
2317.3 ± 0.4 ± 0.8	1022	<sup>1</sup> AUBERT	04E	BABR 10.6 $e^+e^-$

# Meson Particle Listings

## $D_{s0}^*(2317)^\pm, D_{s1}(2460)^\pm$

• • • We do not use the following data for averages, fits, limits, etc. • • •

VALUE	EVTS	DOCUMENT ID	TECN	COMMENT
2317.2±1.3	88	<sup>2</sup> AUBERT,B	04s BABR	$B \rightarrow D_{s0}^{(*)}(2317)^+ \bar{D}^{(*)}$
2317.2±0.5±0.9	761	<sup>3</sup> MIKAMI	04 BELL	10.6 e <sup>+</sup> e <sup>-</sup>
2316.8±0.4±3.0	1267±53	<sup>3,4</sup> AUBERT	03G BABR	10.6 e <sup>+</sup> e <sup>-</sup>
2317.6±1.3	273±33	<sup>3,5</sup> AUBERT	03G BABR	10.6 e <sup>+</sup> e <sup>-</sup>
2319.8±2.1±2.0	24	<sup>3</sup> KROKOVNY	03B BELL	10.6 e <sup>+</sup> e <sup>-</sup>

<sup>1</sup> Supersedes AUBERT 03G.  
<sup>2</sup> Systematic errors not evaluated.  
<sup>3</sup> Not independent of the corresponding  $m_{D_{s0}^*(2317)} - m_{D_s}$ .  
<sup>4</sup> From  $D_s^+ \rightarrow K^+ K^- \pi^+$  decay.  
<sup>5</sup> From  $D_s^+ \rightarrow K^+ K^- \pi^+ \pi^0$  decay.

### $m_{D_{s0}^*(2317)^\pm} - m_{D_s^\pm}$

The fit includes  $D^\pm, D^0, D_s^\pm, D^{*\pm}, D^{*0}, D_1(2420)^0, D_2^*(2460)^0$ , and  $D_{s1}(2536)^\pm$  mass and mass difference measurements.

VALUE (MeV)	EVTS	DOCUMENT ID	TECN	COMMENT
<b>349.3±0.6 OUR FIT</b>	Error includes scale factor of 1.1.			
<b>349.2±0.7 OUR AVERAGE</b>				
348.7±0.5±0.7	761	MIKAMI	04 BELL	10.6 e <sup>+</sup> e <sup>-</sup>
350.0±1.2±1.0	135	BESSON	03 CLE2	10.6 e <sup>+</sup> e <sup>-</sup>
351.3±2.1±1.9	24	<sup>6</sup> KROKOVNY	03B BELL	10.6 e <sup>+</sup> e <sup>-</sup>

• • • We do not use the following data for averages, fits, limits, etc. • • •

349.6±0.4±3.0	1267	<sup>7,8</sup> AUBERT	03G BABR	10.6 e <sup>+</sup> e <sup>-</sup>
350.2±1.3	273	<sup>9,10</sup> AUBERT	03G BABR	10.6 e <sup>+</sup> e <sup>-</sup>

<sup>6</sup> Recalculated by us using  $m_{D_s^+} = 1968.5 \pm 0.6$  MeV.  
<sup>7</sup> From  $D_s^+ \rightarrow K^+ K^- \pi^+$  decay.  
<sup>8</sup> Recalculated by us using  $m_{D_s^+} = 1967.20 \pm 0.03$  MeV.  
<sup>9</sup> From  $D_s^+ \rightarrow K^+ K^- \pi^+ \pi^0$  decay.  
<sup>10</sup> Recalculated by us using  $m_{D_s^+} = 1967.4 \pm 0.2$  MeV. Systematic errors not estimated.

### $D_{s0}^*(2317)^\pm$ WIDTH

VALUE (MeV)	CL%	EVTS	DOCUMENT ID	TECN	COMMENT
<b>&lt; 3.8</b>	95	3180	AUBERT	06P BABR	10.6 e <sup>+</sup> e <sup>-</sup> → $D_s^+ \pi^0 X$

• • • We do not use the following data for averages, fits, limits, etc. • • •

< 4.6	90	761	MIKAMI	04 BELL	10.6 e <sup>+</sup> e <sup>-</sup>
<10			AUBERT	03G BABR	10.6 e <sup>+</sup> e <sup>-</sup>
< 7	90	135	BESSON	03 CLE2	10.6 e <sup>+</sup> e <sup>-</sup>

### $D_{s0}^*(2317)^\pm$ DECAY MODES

$D_{s0}^*(2317)^-$  modes are charge conjugates of modes below.

Mode	Fraction ( $\Gamma_i/\Gamma$ )
$\Gamma_1$ $D_s^+ \pi^0$	seen
$\Gamma_2$ $D_s^+ \gamma$	
$\Gamma_3$ $D_s^{*+}(2112) \gamma$	
$\Gamma_4$ $D_s^+ \gamma \gamma$	
$\Gamma_5$ $D_s^{*+}(2112) \pi^0$	
$\Gamma_6$ $D_s^{*+} \pi^+ \pi^-$	
$\Gamma_7$ $D_s^+ \pi^0 \pi^0$	not seen

### $D_{s0}^*(2317)^\pm$ BRANCHING RATIOS

$\Gamma(D_s^+ \pi^0)/\Gamma_{total}$	$\Gamma_1/\Gamma$
seen	1540 ± 62

$\Gamma(D_s^+ \gamma)/\Gamma(D_s^+ \pi^0)$	$\Gamma_2/\Gamma_1$
<b>&lt;0.05</b>	90
<0.14	95
<0.052	90

• • • We do not use the following data for averages, fits, limits, etc. • • •

95	AUBERT	06P BABR	10.6 e <sup>+</sup> e <sup>-</sup>
90	BESSON	03 CLE2	10.6 e <sup>+</sup> e <sup>-</sup>

$\Gamma(D_s^{*+}(2112) \gamma)/\Gamma(D_s^+ \pi^0)$	$\Gamma_3/\Gamma_1$
<b>&lt;0.059</b>	90
<0.16	95
<0.18	90

• • • We do not use the following data for averages, fits, limits, etc. • • •

95	AUBERT	06P BABR	10.6 e <sup>+</sup> e <sup>-</sup>
90	MIKAMI	04 BELL	10.6 e <sup>+</sup> e <sup>-</sup>

$\Gamma(D_s^{*+} \gamma \gamma)/\Gamma(D_s^+ \pi^0)$	$\Gamma_4/\Gamma_1$
<b>&lt;0.18</b>	95

• • • We do not use the following data for averages, fits, limits, etc. • • •

95	AUBERT	06P BABR	10.6 e <sup>+</sup> e <sup>-</sup>
90	AUBERT	03G BABR	10.6 e <sup>+</sup> e <sup>-</sup>

$\Gamma(D_s^{*+}(2112) \pi^0)/\Gamma(D_s^+ \pi^0)$	$\Gamma_5/\Gamma_1$
<b>&lt;0.11</b>	90

• • • We do not use the following data for averages, fits, limits, etc. • • •

90	BESSON	03 CLE2	10.6 e <sup>+</sup> e <sup>-</sup>
----	--------	---------	------------------------------------

$\Gamma(D_s^{*+} \pi^+ \pi^-)/\Gamma(D_s^+ \pi^0)$	$\Gamma_6/\Gamma_1$
<b>&lt;0.004</b>	90
<0.005	95
<0.019	90

• • • We do not use the following data for averages, fits, limits, etc. • • •

90	MIKAMI	04 BELL	10.6 e <sup>+</sup> e <sup>-</sup>
95	AUBERT	06P BABR	10.6 e <sup>+</sup> e <sup>-</sup>
90	BESSON	03 CLE2	10.6 e <sup>+</sup> e <sup>-</sup>

$\Gamma(D_s^+ \pi^0 \pi^0)/\Gamma(D_s^+ \pi^0)$	$\Gamma_7/\Gamma_1$
<b>&lt;0.25</b>	95

• • • We do not use the following data for averages, fits, limits, etc. • • •

95	AUBERT	06P BABR	10.6 e <sup>+</sup> e <sup>-</sup>
----	--------	----------	------------------------------------

### $D_{s0}^*(2317)^\pm$ REFERENCES

AUBERT	06P	PR D74 032007	B. Aubert et al.	(BABAR Collab.)
AUBERT	04E	PR D69 031101R	B. Aubert et al.	(BABAR Collab.)
AUBERT,B	04S	PRL 93 181801	B. Aubert et al.	(BABAR Collab.)
MIKAMI	04	PRL 92 012002	Y. Mikami et al.	(BELLE Collab.)
AUBERT	03G	PRL 90 242001	B. Aubert et al.	(BABAR Collab.)
BESSON	03	PR D68 032002	D. Besson et al.	(CLEO Collab.)
KROKOVNY	03B	PRL 91 262002	P. Krokovny et al.	(BELLE Collab.)

## $D_{s1}(2460)^\pm$

$$I(J^P) = 0(1^+)$$

### $D_{s1}(2460)^\pm$ MASS

The fit includes  $D^\pm, D^0, D_s^\pm, D^{*\pm}, D^{*0}, D_1(2420)^0, D_2^*(2460)^0$ , and  $D_{s1}(2536)^\pm$  mass and mass difference measurements.

VALUE (MeV)	EVTS	DOCUMENT ID	TECN	COMMENT
<b>2459.6±0.6 OUR FIT</b>	Error includes scale factor of 1.1.			
<b>2459.6±0.9 OUR AVERAGE</b>	Error includes scale factor of 1.3.			
2460.1±0.2±0.8		<sup>1</sup> AUBERT	06P BABR	10.6 e <sup>+</sup> e <sup>-</sup>
2458.0±1.0±1.0	195	AUBERT	04E BABR	10.6 e <sup>+</sup> e <sup>-</sup>

• • • We do not use the following data for averages, fits, limits, etc. • • •

2459.5±1.2±3.7	920	AUBERT	06P BABR	10.6 e <sup>+</sup> e <sup>-</sup> → $D_s^+ \gamma X$
2458.6±1.0±2.5	560	AUBERT	06P BABR	10.6 e <sup>+</sup> e <sup>-</sup> → $D_s^+ \pi^0 \gamma X$
2460.2±0.2±0.8	123	AUBERT	06P BABR	10.6 e <sup>+</sup> e <sup>-</sup> → $D_s^+ \pi^+ \pi^- X$
2458.9±1.5	112	<sup>2</sup> AUBERT,B	04s BABR	$B \rightarrow D_{s1}(2460)^+ \bar{D}^{(*)}$
2461.1±1.6	139	<sup>3</sup> AUBERT,B	04s BABR	$B \rightarrow D_{s1}(2460)^+ \bar{D}^{(*)}$
2456.5±1.3±1.3	126	<sup>4,5</sup> MIKAMI	04 BELL	10.6 e <sup>+</sup> e <sup>-</sup>
2459.5±1.3±2.0	152	<sup>6,7</sup> MIKAMI	04 BELL	10.6 e <sup>+</sup> e <sup>-</sup>
2459.9±0.9±1.6	60	<sup>6,7</sup> MIKAMI	04 BELL	10.6 e <sup>+</sup> e <sup>-</sup>
2459.2±1.6±2.0	57	KROKOVNY	03B BELL	10.6 e <sup>+</sup> e <sup>-</sup>

<sup>1</sup> The average of the values obtained from the  $D_s^+ \gamma, D_s^+ \pi^0 \gamma, D_s^+ \pi^+ \pi^-$  final state.  
<sup>2</sup> Systematic errors not evaluated. From the decay to  $D_s^{*+} \pi^0$ .  
<sup>3</sup> Systematic errors not evaluated. From the decay to  $D_s^+ \gamma$ .  
<sup>4</sup> Not independent of the corresponding  $m_{D_{s1}(2460)^\pm} - m_{D_s^{*\pm}}$ .  
<sup>5</sup> Using  $m_{D_s^{*+}} = 2112.4 \pm 0.7$  MeV.  
<sup>6</sup> Not independent of the corresponding  $m_{D_{s1}(2460)^\pm} - m_{D_s^\pm}$ .  
<sup>7</sup> Using  $m_{D_s^+} = 1968.5 \pm 0.6$  MeV.

### $m_{D_{s1}(2460)^\pm} - m_{D_s^{*\pm}}$

The fit includes  $D^\pm, D^0, D_s^\pm, D^{*\pm}, D^{*0}, D_1(2420)^0, D_2^*(2460)^0$ , and  $D_{s1}(2536)^\pm$  mass and mass difference measurements.

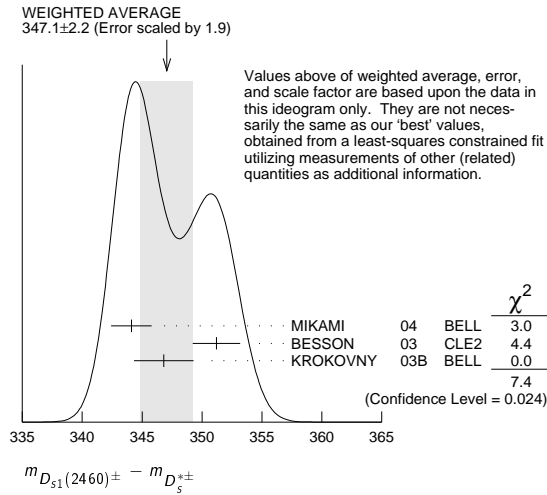
VALUE (MeV)	EVTS	DOCUMENT ID	TECN	COMMENT
<b>347.2±0.7 OUR FIT</b>	Error includes scale factor of 1.2.			
<b>347.1±2.2 OUR AVERAGE</b>	Error includes scale factor of 1.9. See the ideogram below.			
344.1±1.3±1.1	126	MIKAMI	04 BELL	10.6 e <sup>+</sup> e <sup>-</sup>
351.2±1.7±1.0	41	BESSON	03 CLE2	10.6 e <sup>+</sup> e <sup>-</sup>
346.8±1.6±1.9	57	<sup>8</sup> KROKOVNY	03B BELL	10.6 e <sup>+</sup> e <sup>-</sup>

See key on page 457

Meson Particle Listings

$D_{s1}(2460)^\pm$

<sup>8</sup> Recalculated by us using  $m_{D_s^{*+}} = 2112.4 \pm 0.7$  MeV.



$m_{D_{s1}(2460)^\pm} - m_{D_s^\pm}$

The fit includes  $D^\pm, D^0, D_s^\pm, D_s^{*0}, D_s^{*\pm}, D_1(2420)^0, D_2^*(2460)^0$ , and  $D_{s1}(2536)^\pm$  mass and mass difference measurements.

VALUE (MeV)	EVTs	DOCUMENT ID	TECN	COMMENT
<b>491.1 ± 0.7 OUR FIT</b>	Error includes scale factor of 1.1.			
<b>491.3 ± 1.4 OUR AVERAGE</b>				
491.0 ± 1.3 ± 1.9	152	<sup>9</sup> MIKAMI	04 BELL	10.6 e <sup>+</sup> e <sup>-</sup>
491.4 ± 0.9 ± 1.5	60	<sup>10</sup> MIKAMI	04 BELL	10.6 e <sup>+</sup> e <sup>-</sup>

<sup>9</sup> From the decay to  $D_s^\pm \gamma$ .  
<sup>10</sup> From the decay to  $D_s^\pm \pi^+ \pi^-$ .

$D_{s1}(2460)^\pm$  WIDTH

VALUE (MeV)	CL%	EVTs	DOCUMENT ID	TECN	COMMENT
<b>&lt; 3.5</b>	95	123	AUBERT	06P BABR	10.6 e <sup>+</sup> e <sup>-</sup> → $D_s^\pm \pi^+ \pi^- X$
<b>&lt; 6.3</b>	95	560	AUBERT	06P BABR	10.6 e <sup>+</sup> e <sup>-</sup> → $D_s^\pm \pi^0 \gamma X$
< 10		195	AUBERT	04E BABR	10.6 e <sup>+</sup> e <sup>-</sup>
< 5.5		126	MIKAMI	04 BELL	10.6 e <sup>+</sup> e <sup>-</sup>
< 7		41	BESSON	03 CLE2	10.6 e <sup>+</sup> e <sup>-</sup>

• • • We do not use the following data for averages, fits, limits, etc. • • •

$D_{s1}(2460)^+$  DECAY MODES

$D_{s1}(2460)^-$  modes are charge conjugates of the modes below.

Mode	Fraction ( $\Gamma_i/\Gamma$ )	Scale factor/ Confidence level
$\Gamma_1$ $D_s^{*+} \pi^0$	(48 ± 11) %	
$\Gamma_2$ $D_s^+ \gamma$	(18 ± 4) %	
$\Gamma_3$ $D_s^+ \pi^+ \pi^-$	(4.3 ± 1.3) %	S=1.1
$\Gamma_4$ $D_s^{*+} \gamma$	< 8 %	CL=90%
$\Gamma_5$ $D_{s0}^*(2317)^+ \gamma$	(3.7 <sup>+5.0</sup> <sub>-2.4</sub> ) %	
$\Gamma_6$ $D_s^+ \pi^0$		
$\Gamma_7$ $D_s^+ \pi^0 \pi^0$		
$\Gamma_8$ $D_s^+ \gamma \gamma$		

CONSTRAINED FIT INFORMATION

An overall fit to 7 branching ratios uses 8 measurements and one constraint to determine 5 parameters. The overall fit has a  $\chi^2 = 3.4$  for 4 degrees of freedom.

The following off-diagonal array elements are the correlation coefficients  $\langle \delta x_i \delta x_j \rangle / (\delta x_i \delta x_j)$ , in percent, from the fit to the branching fractions,  $x_i \equiv \Gamma_i/\Gamma_{\text{total}}$ . The fit constrains the  $x_i$  whose labels appear in this array to sum to one.

$x_2$	80		
$x_3$	68	62	
$x_5$	-3	25	26
	$x_1$	$x_2$	$x_3$

$D_{s1}(2460)^\pm$  BRANCHING RATIOS

$\Gamma(D_s^{*+} \pi^0)/\Gamma_{\text{total}}$	VALUE	CL%	EVTs	DOCUMENT ID	TECN	COMMENT	$\Gamma_1/\Gamma$
<b>0.48 ± 0.11 OUR FIT</b>							
<b>0.56 ± 0.13 ± 0.09</b>				<sup>11</sup> AUBERT	06N BABR	$B \rightarrow D_{s1}(2460)^- \bar{D}^{(*)}$	
• • • We do not use the following data for averages, fits, limits, etc. • • •							
seen			41	BESSON	03 CLE2	10.6 e <sup>+</sup> e <sup>-</sup>	
<sup>11</sup> Evaluated in AUBERT 06N including measurements from AUBERT,B 04s.							
$\Gamma(D_s^+ \gamma)/\Gamma_{\text{total}}$	VALUE	CL%	EVTs	DOCUMENT ID	TECN	COMMENT	$\Gamma_2/\Gamma$
<b>0.18 ± 0.04 OUR FIT</b>							
<b>0.16 ± 0.04 ± 0.03</b>				<sup>12</sup> AUBERT	06N BABR	$B \rightarrow D_{s1}(2460)^- \bar{D}^{(*)}$	
<sup>12</sup> Evaluated in AUBERT 06N including measurements from AUBERT,B 04s.							
$\Gamma(D_s^+ \gamma)/\Gamma(D_s^{*+} \pi^0)$	VALUE	CL%	EVTs	DOCUMENT ID	TECN	COMMENT	$\Gamma_2/\Gamma_1$
<b>0.38 ± 0.05 OUR FIT</b>							
<b>0.44 ± 0.09 OUR AVERAGE</b>							
0.55 ± 0.13 ± 0.08			152	MIKAMI	04 BELL	10.6 e <sup>+</sup> e <sup>-</sup>	
0.38 ± 0.11 ± 0.04			38	KROKOVNY	03B BELL	10.6 e <sup>+</sup> e <sup>-</sup>	
• • • We do not use the following data for averages, fits, limits, etc. • • •							
0.274 ± 0.045 ± 0.020			251	<sup>13</sup> AUBERT,B	04s BABR	$B \rightarrow D_{s1}(2460)^+ \bar{D}^{(*)}$	
< 0.49			90	BESSON	03 CLE2	10.6 e <sup>+</sup> e <sup>-</sup>	
<sup>13</sup> Used by AUBERT 06N in their measurement of $B(D_s^{*-} \pi^0)$ and $B(D_s^- \gamma)$ .							
$\Gamma(D_s^+ \pi^+ \pi^-)/\Gamma(D_s^{*+} \pi^0)$	VALUE	CL%	EVTs	DOCUMENT ID	TECN	COMMENT	$\Gamma_3/\Gamma_1$
<b>0.090 ± 0.020 OUR FIT</b>						Error includes scale factor of 1.2.	
<b>0.14 ± 0.04 ± 0.02</b>				60	MIKAMI	04 BELL	10.6 e <sup>+</sup> e <sup>-</sup>
• • • We do not use the following data for averages, fits, limits, etc. • • •							
< 0.08			90	BESSON	03 CLE2	10.6 e <sup>+</sup> e <sup>-</sup>	
$\Gamma(D_s^{*+} \gamma)/\Gamma(D_s^{*+} \pi^0)$	VALUE	CL%	EVTs	DOCUMENT ID	TECN	COMMENT	$\Gamma_4/\Gamma_1$
<b>&lt; 0.16</b>				90	BESSON	03 CLE2	10.6 e <sup>+</sup> e <sup>-</sup>
• • • We do not use the following data for averages, fits, limits, etc. • • •							
< 0.31			90	MIKAMI	04 BELL	10.6 e <sup>+</sup> e <sup>-</sup>	
$\Gamma(D_{s0}^*(2317)^+ \gamma)/\Gamma(D_s^{*+} \pi^0)$	VALUE	CL%	EVTs	DOCUMENT ID	TECN	COMMENT	$\Gamma_5/\Gamma_1$
<b>&lt; 0.22</b>				95	AUBERT	04E BABR	10.6 e <sup>+</sup> e <sup>-</sup>
• • • We do not use the following data for averages, fits, limits, etc. • • •							
< 0.58			90	BESSON	03 CLE2	10.6 e <sup>+</sup> e <sup>-</sup>	
$\Gamma(D_s^{*+} \pi^0)/[\Gamma(D_s^{*+} \pi^0) + \Gamma(D_{s0}^*(2317)^+ \gamma)]$	VALUE	CL%	EVTs	DOCUMENT ID	TECN	COMMENT	$\Gamma_1/(\Gamma_1 + \Gamma_5)$
<b>0.93 ± 0.09 OUR FIT</b>							
<b>0.97 ± 0.09 ± 0.05</b>				AUBERT	06P BABR	10.6 e <sup>+</sup> e <sup>-</sup>	
$\Gamma(D_s^+ \gamma)/[\Gamma(D_s^{*+} \pi^0) + \Gamma(D_{s0}^*(2317)^+ \gamma)]$	VALUE	CL%	EVTs	DOCUMENT ID	TECN	COMMENT	$\Gamma_2/(\Gamma_1 + \Gamma_5)$
<b>0.35 ± 0.04 OUR FIT</b>							
<b>0.337 ± 0.036 ± 0.038</b>				AUBERT	06P BABR	10.6 e <sup>+</sup> e <sup>-</sup>	
$\Gamma(D_s^+ \pi^+ \pi^-)/[\Gamma(D_s^{*+} \pi^0) + \Gamma(D_{s0}^*(2317)^+ \gamma)]$	VALUE	CL%	EVTs	DOCUMENT ID	TECN	COMMENT	$\Gamma_3/(\Gamma_1 + \Gamma_5)$
<b>0.083 ± 0.017 OUR FIT</b>						Error includes scale factor of 1.2.	
<b>0.077 ± 0.013 ± 0.008</b>				AUBERT	06P BABR	10.6 e <sup>+</sup> e <sup>-</sup>	
$\Gamma(D_s^{*+} \gamma)/[\Gamma(D_s^{*+} \pi^0) + \Gamma(D_{s0}^*(2317)^+ \gamma)]$	VALUE	CL%	EVTs	DOCUMENT ID	TECN	COMMENT	$\Gamma_4/(\Gamma_1 + \Gamma_5)$
<b>&lt; 0.24</b>				95	AUBERT	06P BABR	10.6 e <sup>+</sup> e <sup>-</sup>
$\Gamma(D_{s0}^*(2317)^+ \gamma)/[\Gamma(D_s^{*+} \pi^0) + \Gamma(D_{s0}^*(2317)^+ \gamma)]$	VALUE	CL%	EVTs	DOCUMENT ID	TECN	COMMENT	$\Gamma_5/(\Gamma_1 + \Gamma_5)$
<b>&lt; 0.25</b>				95	AUBERT	06P BABR	10.6 e <sup>+</sup> e <sup>-</sup>
$\Gamma(D_s^+ \pi^0)/[\Gamma(D_s^{*+} \pi^0) + \Gamma(D_{s0}^*(2317)^+ \gamma)]$	VALUE	CL%	EVTs	DOCUMENT ID	TECN	COMMENT	$\Gamma_6/(\Gamma_1 + \Gamma_5)$
<b>&lt; 0.042</b>				95	AUBERT	06P BABR	10.6 e <sup>+</sup> e <sup>-</sup>
$\Gamma(D_s^+ \pi^0 \pi^0)/[\Gamma(D_s^{*+} \pi^0) + \Gamma(D_{s0}^*(2317)^+ \gamma)]$	VALUE	CL%	EVTs	DOCUMENT ID	TECN	COMMENT	$\Gamma_7/(\Gamma_1 + \Gamma_5)$
<b>&lt; 0.68</b>				95	AUBERT	06P BABR	10.6 e <sup>+</sup> e <sup>-</sup>
$\Gamma(D_s^+ \gamma \gamma)/[\Gamma(D_s^{*+} \pi^0) + \Gamma(D_{s0}^*(2317)^+ \gamma)]$	VALUE	CL%	EVTs	DOCUMENT ID	TECN	COMMENT	$\Gamma_8/(\Gamma_1 + \Gamma_5)$
<b>&lt; 0.33</b>				95	AUBERT	06P BABR	10.6 e <sup>+</sup> e <sup>-</sup>

# Meson Particle Listings

## $D_{s1}(2460)^\pm, D_{s1}(2536)^\pm$

### $D_{s1}(2460)^\pm$ REFERENCES

AUBERT	06N	PR D74 031103R	B. Aubert et al.	(BABAR Collab.)
AUBERT	06P	PR D74 032007	B. Aubert et al.	(BABAR Collab.)
AUBERT	04E	PR D69 031101R	B. Aubert et al.	(BABAR Collab.)
AUBERT,B	04S	PRL 93 181801	B. Aubert et al.	(BABAR Collab.)
MIKAMI	04	PRL 92 012002	Y. Mikami et al.	(BELLE Collab.)
BESS ON	03	PR D68 032002	D. Besson et al.	(CLEO Collab.)
KROKOVNY	03B	PRL 91 262002	P. Krokovny et al.	(BELLE Collab.)

### $D_{s1}(2536)^\pm$

$I(J^P) = 0(1^+)$   
 $J, P$  need confirmation.

Seen in  $D^*(2010)^+ K^0, D^*(2007)^0 K^+,$  and  $D_s^+ \pi^+ \pi^-$ . Not seen in  $D^+ K^0$  or  $D^0 K^+$ .  $J^P = 1^+$  assignment strongly favored.

### $D_{s1}(2536)^\pm$ MASS

The fit includes  $D^\pm, D^0, D_s^\pm, D^{*\pm}, D^{*0}, D_s^{*\pm}, D_1(2420)^0, D_2^*(2460)^0,$  and  $D_{s1}(2536)^\pm$  mass and mass difference measurements.

VALUE (MeV)	EVTS	DOCUMENT ID	TECN	COMMENT
<b>2535.12 ± 0.13 OUR FIT</b>				
<b>2535.18 ± 0.24 OUR AVERAGE</b>				
2535.7 ± 0.6 ± 0.5	46 ± 9	<sup>1</sup> ABAZOV	09G D0	$B_s^0 \rightarrow D_{s1}^- \mu^+ \nu_\mu X$
2534.78 ± 0.31 ± 0.40	182	AUBERT	08B BABR	$B \rightarrow \overline{D}^{(*)} D^* K$
2534.6 ± 0.3 ± 0.7	193	AUBERT	06P BABR	$10.6 e^+ e^- \rightarrow D_s^+ \pi^+ \pi^- X$
2535.3 ± 0.7	92	<sup>2</sup> HEISTER	02B ALEP	$e^+ e^- \rightarrow D^{*+} K^0 X,$ $D^{*0} K^+ X$
2534.2 ± 1.2	9	ASRATYAN	94 BEBC	$\nu N \rightarrow D^{*0} K^0 X, D^{*0} K^\pm X$
2535 ± 0.6 ± 1	75	FRABETTI	94B E687	$\gamma Be \rightarrow D^{*+} K^0 X,$ $D^{*0} K^+ X$
2535.3 ± 0.2 ± 0.5	134	ALEXANDER	93 CLE2	$e^+ e^- \rightarrow D^{*0} K^+ X$
2534.8 ± 0.6 ± 0.6	44	ALEXANDER	93 CLE2	$e^+ e^- \rightarrow D^{*+} K^0 X$
2535.2 ± 0.5 ± 1.5	28	ALBRECHT	92R ARG	$10.4 e^+ e^- \rightarrow D^{*+} K^0 X,$ $D^{*0} K^+ X$
2536.6 ± 0.7 ± 0.4		AVERY	90 CLEO	$e^+ e^- \rightarrow D^{*+} K^0 X$
2535.9 ± 0.6 ± 2.0		ALBRECHT	89E ARG	$D_{s1}^* \rightarrow D^*(2010) K^0$

• • • We do not use the following data for averages, fits, limits, etc. • • •

2534.1 ± 0.6	116	<sup>3</sup> AUSHEV	11 BELL	$B \rightarrow D_{s1}(2536)^+ D^{(*)}$
2535.08 ± 0.01 ± 0.15	8038	<sup>4</sup> LEES	11B BABR	$10.6 e^+ e^- \rightarrow D^{*+} K_S^0 X$

2535.57<sup>+0.44</sup><sub>-0.41</sub> ± 0.10 236 ± 30 <sup>5</sup> CHEKANOV 09 ZEUS  $e^\pm p \rightarrow D^{*+} K_S^0 X,$   
 $D^{*0} K^+ X$

2535 ± 28 <sup>6</sup> ASRATYAN 88 HLBC  $\nu N \rightarrow D_s \gamma X$

<sup>1</sup> Using the  $D^*(2010)^\pm$  mass of 2010.0 ± 0.4 MeV from PDG 06.  
<sup>2</sup> Calculated using  $m(D^*(2010)^\pm) = 2010.0 \pm 0.5$  MeV,  $m(D^*(2007)^0) = 2006.7 \pm 0.5$  MeV, and the mass difference below.  
<sup>3</sup> Systematic uncertainties not evaluated.  
<sup>4</sup> Calculated using the mass difference  $m(D_{s1}^+) - m(D^{*+})_{PDG}$  below and  $m(D^{*+})_{PDG} = 2010.25 \pm 0.14$  MeV. Assuming S-wave decay of the  $D_{s1}(2536)$  to  $D^{*+} K_S^0$ , using a Breit-Wigner line shape corresponding to L=0.  
<sup>5</sup> Calculated using the mass difference  $m(D_{s1}^+) - m(D^{*+})_{PDG}$  reported below and  $m(D^{*+})_{PDG} = 2010.27 \pm 0.17$  MeV.  
<sup>6</sup> Not seen in  $D^* K$ .

### $m_{D_{s1}(2536)^\pm} - m_{D_s^*(2111)}$

The fit includes  $D^\pm, D^0, D_s^\pm, D^{*\pm}, D^{*0}, D_s^{*\pm}, D_1(2420)^0, D_2^*(2460)^0,$  and  $D_{s1}(2536)^\pm$  mass and mass difference measurements.

VALUE (MeV)	DOCUMENT ID	TECN	COMMENT
<b>422.8 ± 0.5 OUR FIT</b>	Error includes scale factor of 1.1.		
<b>424 ± 2.8</b>	ASRATYAN 88 HLBC	HLBC	$D_s^{*\pm} \gamma$

### $m_{D_{s1}(2536)^\pm} - m_{D^*(2010)^\pm}$

The fit includes  $D^\pm, D^0, D_s^\pm, D^{*\pm}, D^{*0}, D_s^{*\pm}, D_1(2420)^0, D_2^*(2460)^0,$  and  $D_{s1}(2536)^\pm$  mass and mass difference measurements.

VALUE (MeV)	EVTS	DOCUMENT ID	TECN	COMMENT
<b>524.84 ± 0.04 OUR FIT</b>				
<b>524.84 ± 0.04 OUR AVERAGE</b>				
524.83 ± 0.01 ± 0.04	8038	<sup>7</sup> LEES	11B BABR	$10.6 e^+ e^- \rightarrow D^{*+} K_S^0 X$
525.30 <sup>+0.44</sup> <sub>-0.41</sub> ± 0.10	236 ± 30	CHEKANOV 09 ZEUS	ZEUS	$e^\pm p \rightarrow D^{*+} K_S^0 X,$ $D^{*0} K^+ X$
525.3 ± 0.6 ± 0.1	41	HEISTER	02B ALEP	$e^+ e^- \rightarrow D^{*+} K^0 X$

<sup>7</sup> Assuming S-wave decay of the  $D_{s1}(2536)$  to  $D^{*+} K_S^0$ , using a Breit-Wigner line shape corresponding to L=0.

### $m_{D_{s1}(2536)^\pm} - m_{D^*(2007)^0}$

The fit includes  $D^\pm, D^0, D_s^\pm, D^{*\pm}, D^{*0}, D_s^{*\pm}, D_1(2420)^0, D_2^*(2460)^0,$  and  $D_{s1}(2536)^\pm$  mass and mass difference measurements.

VALUE (MeV)	EVTS	DOCUMENT ID	TECN	COMMENT
<b>528.14 ± 0.08 OUR FIT</b>				
<b>528.1 ± 1.5 OUR AVERAGE</b>				
528.7 ± 1.9 ± 0.5	51	HEISTER	02B ALEP	$e^+ e^- \rightarrow D^{*0} K^+ X$
527.3 ± 2.2	29	ACKERSTAFF	97W OPAL	$e^+ e^- \rightarrow D^{*0} K^+ X$

### $D_{s1}(2536)^\pm$ WIDTH

VALUE (MeV)	CL% EVTS	DOCUMENT ID	TECN	COMMENT
<b>0.92 ± 0.03 ± 0.04</b>	8038	<sup>8</sup> LEES	11B BABR	$10.6 e^+ e^- \rightarrow D^{*+} K_S^0 X$
0.75 ± 0.23	116	<sup>9</sup> AUSHEV	11 BELL	$B \rightarrow D_{s1}(2536)^+ D^{(*)}$
< 2.5	95 193	AUBERT	06P BABR	$10.6 e^+ e^- \rightarrow D_s^+ \pi^+ \pi^- X$
< 3.2	90 75	FRABETTI	94B E687	$\gamma Be \rightarrow D^{*+} K^0 X,$ $D^{*0} K^+ X$
< 2.3	90	ALEXANDER	93 CLEO	$e^+ e^- \rightarrow D^{*0} K^+ X$
< 3.9	90	ALBRECHT	92R ARG	$10.4 e^+ e^- \rightarrow D^{*0} K^+ X$
< 5.44	90	AVERY	90 CLEO	$e^+ e^- \rightarrow D^{*+} K^0 X$
< 4.6	90	ALBRECHT	89E ARG	$D_{s1}^* \rightarrow D^*(2010) K^0$

<sup>8</sup> Assuming S-wave decay of the  $D_{s1}(2536)$  to  $D^{*+} K_S^0$ , using a Breit-Wigner line shape corresponding to L=0.  
<sup>9</sup> Systematic uncertainties not evaluated.

### $D_{s1}(2536)^+$ DECAY MODES

$D_{s1}(2536)^-$  modes are charge conjugates of the modes below.

Mode	Fraction ( $\Gamma_i/\Gamma$ )
$\Gamma_1$ $D^*(2010)^+ K^0$	seen
$\Gamma_2$ $(D^*(2010)^+ K^0)_{S-wave}$	
$\Gamma_3$ $(D^*(2010)^+ K^0)_{D-wave}$	
$\Gamma_4$ $D^+ \pi^- K^+$	
$\Gamma_5$ $D^*(2007)^0 K^+$	seen
$\Gamma_6$ $D^+ K^0$	not seen
$\Gamma_7$ $D^0 K^+$	not seen
$\Gamma_8$ $D_s^{*+} \gamma$	possibly seen
$\Gamma_9$ $D_s^+ \pi^+ \pi^-$	seen

### $D_{s1}(2536)^+$ BRANCHING RATIOS

$\Gamma(D^*(2007)^0 K^+)/\Gamma(D^*(2010)^+ K^0)$	$\Gamma_5/\Gamma_1$			
VALUE	EVTS	DOCUMENT ID	TECN	COMMENT
<b>1.18 ± 0.16 OUR AVERAGE</b>				
0.88 ± 0.24 ± 0.08	116	AUSHEV	11 BELL	$B \rightarrow D_{s1}(2536)^+ D^{(*)}$
2.3 ± 0.6 ± 0.3	236 ± 30	CHEKANOV 09 ZEUS	ZEUS	$e^\pm p \rightarrow D^{*+} K_S^0 X,$ $D^{*0} K^+ X$
1.32 ± 0.47 ± 0.23	92	<sup>10</sup> HEISTER	02B ALEP	$e^+ e^- \rightarrow D^{*+} K^0 X,$ $D^{*0} K^+ X$
1.9 <sup>+1.1</sup> <sub>-0.9</sub> ± 0.4	35	<sup>10</sup> ACKERSTAFF	97W OPAL	$e^+ e^- \rightarrow D^{*0} K^+ X,$ $D^{*+} K^0 X$
1.1 ± 0.3		ALEXANDER 93 CLEO	CLEO	$e^+ e^- \rightarrow D^{*0} K^+ X, D^{*+} K^0 X$
1.4 ± 0.3 ± 0.2		<sup>11</sup> ALBRECHT 92R ARG	ARG	$10.4 e^+ e^- \rightarrow D^{*0} K^+ X, D^{*+} K^0 X$

<sup>10</sup> Ratio of the production rates measured in  $Z^0$  decays.  
<sup>11</sup> Evaluated by us from published inclusive cross-sections.

$\Gamma((D^*(2010)^+ K^0)_{S-wave})/\Gamma(D^*(2010)^+ K^0)$	$\Gamma_2/\Gamma_1$			
VALUE	EVTS	DOCUMENT ID	TECN	COMMENT
<b>0.72 ± 0.05 ± 0.01</b>	5485	BALAGURA 08 BELL	BELL	$10.6 e^+ e^- \rightarrow D^{*+} K^0 X$

$\Gamma(D^+ \pi^- K^+)/\Gamma(D^*(2010)^+ K^0)$	$\Gamma_4/\Gamma_1$			
VALUE (units 10 <sup>-2</sup> )	EVTS	DOCUMENT ID	TECN	COMMENT
<b>3.27 ± 0.18 ± 0.37</b>	1264	BALAGURA 08 BELL	BELL	$10.6 e^+ e^- \rightarrow D^+ \pi^- K^+ X$

$\Gamma(D^+ K^0)/\Gamma(D^*(2010)^+ K^0)$	$\Gamma_6/\Gamma_1$			
VALUE	CL%	DOCUMENT ID	TECN	COMMENT
< 0.40	90	ALEXANDER 93 CLEO	CLEO	$e^+ e^- \rightarrow D^{*+} K^0 X$
< 0.43	90	ALBRECHT 89E ARG	ARG	$D_{s1}^* \rightarrow D^*(2010) K^0$

See key on page 457

Meson Particle Listings

$D_{s1}(2536)^\pm, D_{s2}(2573), D_{s1}^*(2700)^\pm$

$\Gamma(D^0 K^+)/\Gamma(D^*(2007)^0 K^+)$   $\Gamma_7/\Gamma_5$

VALUE	CL%	DOCUMENT ID	TECN	COMMENT
<0.12	90	ALEXANDER 93	CLEO	$e^+ e^- \rightarrow D^{*0} K^+ X$

$\Gamma(D_s^{*+} \gamma)/\Gamma_{total}$   $\Gamma_8/\Gamma$

possibly seen

DOCUMENT ID	TECN	COMMENT
ASRATYAN 88	HLBC	$\nu N \rightarrow D_s \gamma \gamma X$

$\Gamma(D_s^{*+} \gamma)/\Gamma(D^*(2007)^0 K^+)$   $\Gamma_8/\Gamma_5$

VALUE	CL%	DOCUMENT ID	TECN	COMMENT
<0.42	90	ALEXANDER 93	CLEO	$e^+ e^- \rightarrow D^{*0} K^+ X$

$\Gamma(D_s^+ \pi^+ \pi^-)/\Gamma_{total}$   $\Gamma_9/\Gamma$

seen

DOCUMENT ID	TECN	COMMENT
AUBERT 06P BABR	10.6	$e^+ e^- \rightarrow D_s^+ \pi^+ \pi^- X$

$D_{s1}(2536)^\pm$  REFERENCES

AUSHEV 11 PR D83 051102	T. Aushev et al.	(BELLE Collab.)
LEES 11B PR D83 072003	J.P. Lees et al.	(BABAR Collab.)
ABAZOV 09G PRL 102 051801	V.M. Abazov et al.	(DO Collab.)
CHEKANOV 09 EPJ C60 25	S. Chekanov et al.	(ZEUS Collab.)
AUBERT 08B PR D77 011102R	B. Aubert et al.	(BABAR Collab.)
BALAGURA 08 PR D77 032001	V. Balagura et al.	(BELLE Collab.)
AUBERT 06P PR D74 032007	B. Aubert et al.	(BABAR Collab.)
PDG 06 JPG 33 1	W.-M. Yao et al.	(PDG Collab.)
HEISTER 02B PL B526 34	A. Heister et al.	(ALEPH Collab.)
ACKERSTAFF 97W ZPHY C76 425	K. Ackerstaff et al.	(OPAL Collab.)
ASRATYAN 94 ZPHY C61 563	A.E. Asratyan et al.	(BIRM, BELG, CERNA)
FRABETTI 94B PRL 72 324	P.L. Frabetti et al.	(FNAL E687 Collab.)
ALEXANDER 93 PL B303 377	J. Alexander et al.	(CLEO Collab.)
ALBRECHT 92R PL B297 425	H. Albrecht et al.	(ARGUS Collab.)
AVERY 90 PR D41 774	P. Avery, D. Besson	(CLEO Collab.)
ALBRECHT 89E PL B230 162	H. Albrecht et al.	(ARGUS Collab.)
ASRATYAN 88 ZPHY C40 483	A.E. Asratyan et al.	(ITEP, SERP)

$D_{s2}^*(2573)$   $J(P) = 0(??)$

$J^P$  is natural, width and decay modes consistent with  $2^+$ .

$D_{s2}^*(2573)$  MASS

VALUE (MeV)	EVTS	DOCUMENT ID	TECN	COMMENT
<b>2571.9 ± 0.8 OUR AVERAGE</b>				
2569.4 ± 1.6 ± 0.5	82 ± 17	AAIJ 11A	LHCB	$B_s \rightarrow D_{s2}^*(2573) \mu \bar{\nu} X$
2572.2 ± 0.3 ± 1.0		AUBERT, BE 06E	BABR	$e^+ e^- \rightarrow D K X$
2574.5 ± 3.3 ± 1.6		ALBRECHT 96	ARG	$e^+ e^- \rightarrow D^0 K^+ X$
2573.2 ± 1.7 ± 0.9	217	KUBOTA 94	CLE2	$e^+ e^- \sim 10.5$ GeV

• • • We do not use the following data for averages, fits, limits, etc. • • •

2570.0 ± 4.3	25	<sup>1</sup> EVDOKIMOV 04	SELX	600 $\Sigma^- A \rightarrow D^0 K^+ X$
2568.6 ± 3.2	64	<sup>2</sup> HEISTER 02B	ALEP	$e^+ e^- \rightarrow D^0 K^+ X$

<sup>1</sup> Not independent of the mass difference below.  
<sup>2</sup> Calculated using  $m_{D^0} = 1864.5 \pm 0.5$  MeV and the mass difference below.

$m_{D_{s2}^*(2573)} - m_{D^0}$

VALUE (MeV)	EVTS	DOCUMENT ID	TECN	COMMENT
<b>704 ± 3 ± 1</b>	64	HEISTER 02B	ALEP	$e^+ e^- \rightarrow D^0 K^+ X$

• • • We do not use the following data for averages, fits, limits, etc. • • •

705.4 ± 4.3	25	<sup>3</sup> EVDOKIMOV 04	SELX	600 $\Sigma^- A \rightarrow D^0 K^+ X$
-------------	----	---------------------------	------	--

<sup>3</sup> Systematic errors not estimated.

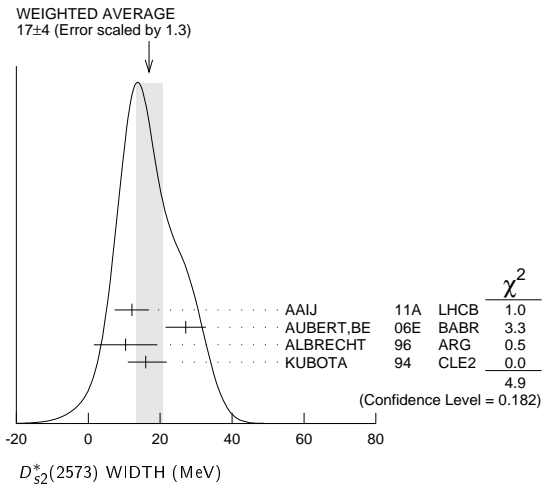
$D_{s2}^*(2573)$  WIDTH

VALUE (MeV)	EVTS	DOCUMENT ID	TECN	COMMENT
<b>17 ± 4 OUR AVERAGE</b>				Error includes scale factor of 1.3. See the ideogram below.
12.1 ± 4.5 ± 1.6	82 ± 17	AAIJ 11A	LHCB	$B_s \rightarrow D_{s2}^*(2573) \mu \bar{\nu} X$
27.1 ± 0.6 ± 5.6		AUBERT, BE 06E	BABR	$e^+ e^- \rightarrow D K X$
10.4 ± 8.3 ± 3.0		ALBRECHT 96	ARG	$e^+ e^- \rightarrow D^0 K^+ X$
16 ± 5 ± 3	217	KUBOTA 94	CLE2	$e^+ e^- \sim 10.5$ GeV

• • • We do not use the following data for averages, fits, limits, etc. • • •

14 ± 9 ± 6	25	<sup>4</sup> EVDOKIMOV 04	SELX	600 $\Sigma^- A \rightarrow D^0 K^+ X$
------------	----	---------------------------	------	--

<sup>4</sup> Systematic errors not estimated.



$D_{s2}^*(2573)^+$  DECAY MODES

$D_{s2}^*(2573)^-$  modes are charge conjugates of the modes below.

Mode	Fraction ( $\Gamma_i/\Gamma$ )
$\Gamma_1 D^0 K^+$	seen
$\Gamma_2 D^*(2007)^0 K^+$	not seen

$D_{s2}^*(2573)^+$  BRANCHING RATIOS

$\Gamma(D^0 K^+)/\Gamma_{total}$   $\Gamma_1/\Gamma$

VALUE	EVTS	DOCUMENT ID	TECN	CHG	COMMENT
seen	217	KUBOTA 94	CLE2	±	$e^+ e^- \sim 10.5$ GeV

$\Gamma(D^*(2007)^0 K^+)/\Gamma(D^0 K^+)$   $\Gamma_2/\Gamma_1$

VALUE	CL%	DOCUMENT ID	TECN	CHG	COMMENT
<0.33	90	KUBOTA 94	CLE2	+	$e^+ e^- \sim 10.5$ GeV

$D_{s2}^*(2573)$  REFERENCES

AAIJ 11A PL B698 14	R. Aaij et al.	(LHCB Collab.)
AUBERT, BE 06E PRL 97 222001	B. Aubert et al.	(BABAR Collab.)
EVDOKIMOV 04 PRL 93 242001	A.V. Evdokimov et al.	(SELEX Collab.)
HEISTER 02B PL B526 34	A. Heister et al.	(ALEPH Collab.)
ALBRECHT 96 ZPHY C69 405	H. Albrecht et al.	(ARGUS Collab.)
KUBOTA 94 PRL 72 1972	Y. Kubota et al.	(CLEO Collab.)

$D_{s1}^*(2700)^\pm$   $J(P) = 0(1^-)$

OMITTED FROM SUMMARY TABLE

$D_{s1}^*(2700)^+$  MASS

VALUE (MeV)	EVTS	DOCUMENT ID	TECN	COMMENT
<b>2709 ± 9 OUR AVERAGE</b>				
2710 ± 2 ± 12 ± 7	10.4k	<sup>1</sup> AUBERT 09AR	BABR	$e^+ e^- \rightarrow D^{(*)} K X$
2708 ± 9 ± 11 ± 10	182	BRODZICKA 08	BELL	$B^+ \rightarrow D^0 \bar{D}^0 K^+$

• • • We do not use the following data for averages, fits, limits, etc. • • •

2688 ± 4 ± 3		<sup>2</sup> AUBERT, BE 06E	BABR	10.6 $e^+ e^- \rightarrow D K X$
--------------	--	-----------------------------	------	----------------------------------

<sup>1</sup> From simultaneous fits to the two  $DK$  mass spectra and to the total  $D^* K$  mass spectrum.  
<sup>2</sup> Superseded by AUBERT 09AR.

$D_{s1}^*(2700)^+$  WIDTH

VALUE (MeV)	EVTS	DOCUMENT ID	TECN	COMMENT
<b>125 ± 30 OUR AVERAGE</b>				
149 ± 7 ± 39 ± 52	10.4k	<sup>3</sup> AUBERT 09AR	BABR	$e^+ e^- \rightarrow D^{(*)} K X$
108 ± 23 ± 36 ± 31	182	BRODZICKA 08	BELL	$B^+ \rightarrow D^0 \bar{D}^0 K^+$

• • • We do not use the following data for averages, fits, limits, etc. • • •

112 ± 7 ± 36		<sup>4</sup> AUBERT, BE 06E	BABR	10.6 $e^+ e^- \rightarrow D K X$
--------------	--	-----------------------------	------	----------------------------------

<sup>3</sup> From simultaneous fits to the two  $DK$  mass spectra and to the total  $D^* K$  mass spectrum.  
<sup>4</sup> Superseded by AUBERT 09AR.

# Meson Particle Listings

$D_{s1}^*(2700)^\pm, D_{sJ}^*(2860)^\pm, D_{sJ}(3040)^\pm$

## $D_{s1}^*(2700)^\pm$ DECAY MODES

Mode
$\Gamma_1$ $DK$
$\Gamma_2$ $D^0 K^+$
$\Gamma_3$ $D^+ K_S^0$
$\Gamma_4$ $D^* K$
$\Gamma_5$ $D^{*0} K^+$
$\Gamma_6$ $D^{*+} K_S^0$

## $D_{s1}^*(2700)^\pm$ BRANCHING RATIOS

$\Gamma(D^* K)/\Gamma(DK)$	$\Gamma_4/\Gamma_1$			
VALUE	EVTS	DOCUMENT ID	TECN	COMMENT
$0.91 \pm 0.13 \pm 0.12$	10.4k	<sup>5</sup> AUBERT	09AR BABR	$e^+ e^- \rightarrow D^{(*)} KX$

<sup>5</sup> From the average of the corresponding ratios with  $D^{(*)0} K^+$  and  $D^{(*)+} K_S^0$ .

$\Gamma(D^{*0} K^+)/\Gamma(D^0 K^+)$	$\Gamma_5/\Gamma_2$			
VALUE	EVTS	DOCUMENT ID	TECN	COMMENT
$0.88 \pm 0.14 \pm 0.14$	7716	<sup>6</sup> AUBERT	09AR BABR	$e^+ e^- \rightarrow D^{(*)} KX$

<sup>6</sup> From the  $D^{*0} K^+$  and  $D^0 K^+$ , where  $D^{*0} \rightarrow D^0 \pi^0$ .

$\Gamma(D^{*+} K_S^0)/\Gamma(D^+ K_S^0)$	$\Gamma_6/\Gamma_3$			
VALUE	EVTS	DOCUMENT ID	TECN	COMMENT
$1.14 \pm 0.39 \pm 0.23$	2700	<sup>7</sup> AUBERT	09AR BABR	$e^+ e^- \rightarrow D^{(*)} KX$

<sup>7</sup> From the  $D^{*+} K_S^0$  and  $D^+ K_S^0$ , where  $D^{*+} \rightarrow D^+ \pi^0$ .

## $D_{s1}^*(2700)^\pm$ REFERENCES

AUBERT	09AR	PR D80 092003	B. Aubert <i>et al.</i>	(BABAR Collab.)
BRODZICKA	08	PRL 100 092001	J. Brodzicka <i>et al.</i>	(BELLE Collab.)
AUBERT, BE	06E	PRL 97 222001	B. Aubert <i>et al.</i>	(BABAR Collab.)

**$D_{sJ}^*(2860)^\pm$**   $I(J^P) = 0(?)^?$

OMITTED FROM SUMMARY TABLE  
Observed by AUBERT, BE 06E and AUBERT 09AR in inclusive production of  $DK$  and  $D^* K$  in  $e^+ e^-$  annihilation.  $J^P$  is natural.

## $D_{sJ}^*(2860)^+$ MASS

VALUE (MeV)	EVTS	DOCUMENT ID	TECN	COMMENT
$2862 \pm 2 \pm 5$	3122	<sup>1</sup> AUBERT	09AR BABR	$e^+ e^- \rightarrow D^{(*)} KX$

• • • We do not use the following data for averages, fits, limits, etc. • • •

$2856.6 \pm 1.5 \pm 5.0$		<sup>2</sup> AUBERT, BE	06E BABR	$e^+ e^- \rightarrow DKX$
--------------------------	--	-------------------------	----------	---------------------------

<sup>1</sup> From simultaneous fits to the two  $DK$  mass spectra and to the total  $D^* K$  mass spectrum.  
<sup>2</sup> Superseded by AUBERT 09AR.

## $D_{sJ}^*(2860)^+$ WIDTH

VALUE (MeV)	EVTS	DOCUMENT ID	TECN	COMMENT
$48 \pm 3 \pm 6$	3122	<sup>3</sup> AUBERT	09AR BABR	$e^+ e^- \rightarrow D^{(*)} KX$

• • • We do not use the following data for averages, fits, limits, etc. • • •

$47 \pm 7 \pm 10$		<sup>4</sup> AUBERT, BE	06E BABR	$e^+ e^- \rightarrow DKX$
-------------------	--	-------------------------	----------	---------------------------

<sup>3</sup> From simultaneous fits to the two  $DK$  mass spectra and to the total  $D^* K$  mass spectrum.  
<sup>4</sup> Superseded by AUBERT 09AR.

## $D_{sJ}^*(2860)^\pm$ DECAY MODES

Mode
$\Gamma_1$ $DK$
$\Gamma_2$ $D^0 K^+$
$\Gamma_3$ $D^+ K_S^0$
$\Gamma_4$ $D^* K$
$\Gamma_5$ $D^{*0} K^+$
$\Gamma_6$ $D^{*+} K_S^0$

## $D_{sJ}^*(2860)^\pm$ BRANCHING RATIOS

$\Gamma(D^* K)/\Gamma(DK)$	$\Gamma_4/\Gamma_1$			
VALUE	EVTS	DOCUMENT ID	TECN	COMMENT
$1.10 \pm 0.15 \pm 0.19$	3122	<sup>5</sup> AUBERT	09AR BABR	$e^+ e^- \rightarrow D^{(*)} KX$

<sup>5</sup> From the average of the corresponding ratios with  $D^{(*)0} K^+$  and  $D^{(*)+} K_S^0$ .

$\Gamma(D^{*0} K^+)/\Gamma(D^0 K^+)$	$\Gamma_5/\Gamma_2$			
VALUE	EVTS	DOCUMENT ID	TECN	COMMENT
$1.04 \pm 0.17 \pm 0.20$	2241	<sup>6</sup> AUBERT	09AR BABR	$e^+ e^- \rightarrow D^{(*)} KX$

<sup>6</sup> From the  $D^{*0} K^+$  and  $D^0 K^+$ , where  $D^{*0} \rightarrow D^0 \pi^0$ .

$\Gamma(D^{*+} K_S^0)/\Gamma(D^+ K_S^0)$	$\Gamma_6/\Gamma_3$			
VALUE	EVTS	DOCUMENT ID	TECN	COMMENT
$1.38 \pm 0.35 \pm 0.49$	881	<sup>7</sup> AUBERT	09AR BABR	$e^+ e^- \rightarrow D^{(*)} KX$

<sup>7</sup> From the  $D^{*+} K_S^0$  and  $D^+ K_S^0$ , where  $D^{*+} \rightarrow D^+ \pi^0$ .

## $D_{sJ}^*(2860)^\pm$ REFERENCES

AUBERT	09AR	PR D80 092003	B. Aubert <i>et al.</i>	(BABAR Collab.)
AUBERT, BE	06E	PRL 97 222001	B. Aubert <i>et al.</i>	(BABAR Collab.)

**$D_{sJ}(3040)^\pm$**   $I(J^P) = 0(?)^?$

OMITTED FROM SUMMARY TABLE  
Observed by AUBERT 09AR in inclusive production of  $D^* K$  in  $e^+ e^-$  annihilation.

## $D_{sJ}(3040)^+$ MASS

VALUE (MeV)	DOCUMENT ID	TECN	COMMENT
$3044 \pm 8 \pm 30$	AUBERT	09AR BABR	$e^+ e^- \rightarrow D^* KX$

## $D_{sJ}(3040)^+$ WIDTH

VALUE (MeV)	DOCUMENT ID	TECN	COMMENT
$239 \pm 35 \pm 46$	AUBERT	09AR BABR	$e^+ e^- \rightarrow D^* KX$

## $D_{sJ}(3040)^\pm$ DECAY MODES

Mode
$\Gamma_1$ $D^* K$
$\Gamma_2$ $D^{*0} K^+$
$\Gamma_3$ $D^{*+} K_S^0$

## $D_{sJ}(3040)^\pm$ REFERENCES

AUBERT	09AR	PR D80 092003	B. Aubert <i>et al.</i>	(BABAR Collab.)
--------	------	---------------	-------------------------	-----------------

## OTHER RELATED PAPERS

SUN	09	PR D80 074037	Z.-F. Sun, X. Lin
-----	----	---------------	-------------------



See key on page 457

## Meson Particle Listings

*B* Meson Production and Decay, *b*-flavored hadrons**BOTTOM MESONS**

$$(B = \pm 1)$$

$$B^+ = u\bar{d}, B^0 = d\bar{b}, \bar{B}^0 = \bar{d}b, B^- = \bar{u}b, \text{ similarly for } B^{*s}$$

***B*-particle organization**

Many measurements of *B* decays involve admixtures of *B* hadrons. Previously we arbitrarily included such admixtures in the  $B^\pm$  section, but because of their importance we have created two new sections: “ $B^\pm/B^0$  Admixture” for  $\Upsilon(4S)$  results and “ $B^\pm/B^0/B_s^0/b$ -baryon Admixture” for results at higher energies. Most inclusive decay branching fractions and  $\chi_b$  at high energy are found in the Admixture sections.  $B^0$ - $\bar{B}^0$  mixing data are found in the  $B^0$  section, while  $B_s^0$ - $\bar{B}_s^0$  mixing data and  $B$ - $\bar{B}$  mixing data for a  $B^0/B_s^0$  admixture are found in the  $B_s^0$  section. *CP*-violation data are found in the  $B^\pm$ ,  $B^0$ , and  $B^\pm/B^0$  Admixture sections. *b*-baryons are found near the end of the Baryon section. Recently, we also created a new section: “ $V_{cb}$  and  $V_{ub}$  CKM Matrix Elements.”

The organization of the *B* sections is now as follows, where bullets indicate particle sections and brackets indicate reviews.

[Production and Decay of *b*-flavored Hadrons]

[A Short Note on HFAG Activities]

- $B^\pm$ 
  - mass, mean life
  - branching fractions
  - polarization in  $B^\pm$  decay
  - CP* violation
- $B^0$ 
  - mass, mean life
  - branching fractions
  - [Polarization in *B* decay]
  - polarization in  $B^0$  decay
  - [ $B$ - $\bar{B}$  Mixing]
  - $B^0$ - $\bar{B}^0$  mixing
  - CP* violation
- $B^\pm/B^0$  Admixture
  - branching fractions, *CP* violation
  - CP* violation
- $B^\pm/B^0/B_s^0/b$ -baryon Admixture
  - mean life
  - production fractions
  - branching fractions
  - $\chi_b$  at high energy
  - production fractions in hadronic *Z* decay
- $V_{cb}$  and  $V_{ub}$  CKM Matrix Elements
  - [Determination of  $V_{cb}$  and  $V_{ub}$ ]

- $B^*$ 
  - mass
- $B_1(5721)^0$ 
  - mass
- $B_J^*(5732)$ 
  - mass, width
- $B_2(5747)^0$ 
  - mass
- $B_s^0$ 
  - mass, mean life
  - branching fractions
  - polarization in  $B_s^0$  decay
  - $B_s^0$ - $\bar{B}_s^0$  mixing
- $B_s^*$ 
  - mass
- $B_{s,J}^*(5850)$ 
  - mass, width
- $B_c^\pm$ 
  - mass, mean life
  - branching fractions

At the end of Baryon Listings:

- $\Lambda_b$ 
  - mass, mean life
  - branching fractions
- $\Sigma_b, \Sigma_b^*$ 
  - mass
- $\Xi_b^0, \Xi_b^-$ 
  - mean life
- $\Omega_b^-$ 
  - mass, mean life
  - branching fractions
- *b*-baryon Admixture
  - mean life
  - branching fractions

**PRODUCTION AND DECAY OF *b*-FLAVORED HADRONS**

Updated March 2012 by M. Kreps (U. of Warwick, Coventry, UK), J.G. Smith (U. of Colorado, Boulder, USA), and Y. Kwon (Yonsei U., Seoul, Korea).

The *b* quark belongs to the third generation of quarks and is the weak-doublet partner of the *t* quark. The existence of the third-generation quark doublet was proposed in 1973 by Kobayashi and Maskawa [1] in their model of the quark mixing matrix (“CKM” matrix), and confirmed four years later by the first observation of a  $b\bar{b}$  meson [2]. In the KM model, *CP* violation is explained within the Standard Model (SM) by an irreducible phase of the  $3 \times 3$  unitary matrix. The regular pattern of the three lepton and quark families is one of the most intriguing puzzles in particle physics. The existence of families gives rise to many of the free parameters in the SM, including the fermion masses, and the elements of the CKM matrix.

Since the *b* quark is the lighter element of the third-generation quark doublet, the decays of *b*-flavored hadrons occur via generation-changing processes through this matrix. Because of this, and the fact that the CKM matrix is close to a  $3 \times 3$  unit matrix, many interesting features such as loop and box diagrams, flavor oscillations, as well as large *CP* asymmetries, can be observed in the weak decays of *b*-flavored hadrons.

The CKM matrix is parameterized by three real parameters and one complex phase. This complex phase can become a source of *CP* violation in *B* meson decays. A crucial milestone was the first observation of *CP* violation in the *B* meson system in 2001, by the BaBar [3] and Belle [4] collaborations. They measured a large value for the parameter  $\sin 2\beta$  ( $= \sin 2\phi_1$ ) [5], almost four decades after the discovery of a small *CP* asymmetry in neutral kaons. A more detailed discussion of the CKM matrix and *CP* violation can be found elsewhere in this Review [6,7].

Recent developments in the physics of *b*-hadrons include the observation of direct *CP* violation, results for rare higher-order weak decays, investigations of heavier *b*-hadrons ( $B_s$ ,  $B_c$ , baryons, excited states), measurement of the  $B_s$ -mixing frequency, increasingly accurate determinations of the CKM matrix parameters.

The structure of this mini-review is organized as follows. After a brief description of theory and terminology, we discuss *b*-quark production and current results on spectroscopy

# Meson Particle Listings

## *b*-flavored hadrons

and lifetimes of *b*-flavored hadrons. We then discuss some basic properties of *B*-meson decays, followed by summaries of hadronic, rare, and electroweak penguin decays of *B*-mesons. There are separate mini-reviews for  $B\bar{B}$  mixing [8] and the extraction of the CKM matrix elements  $V_{cb}$  and  $V_{ub}$  from *B*-meson decays [9] in this *Review*.

**Theory and terminology:** The ground states of *b*-flavored hadrons decay via weak interactions. In most hadrons, the *b*-quark is accompanied by light-partner quarks (*d*, *u*, or *s*), and the decay modes are well described by the decay of the *b* quark (spectator model) [10]. The dominant decay mode of a *b* quark is  $b \rightarrow cW^{*-}$  (referred to as a “tree” or “spectator” decay), where the virtual *W* materializes either into a pair of leptons  $\ell\bar{\nu}$  (“semileptonic decay”), or into a pair of quarks which then hadronizes. The decays in which the spectator quark combines with one of the quarks from  $W^*$  to form one of the final state hadrons are suppressed by a factor  $\sim (1/3)^2$ , because the colors of the two quarks from different sources must match (“color-suppression”).

Many aspects of *B* decays can be understood through the Heavy Quark Effective Theory (HQET) [11]. This has been particularly successful for semileptonic decays. For further discussion of HQET, see for instance Ref. 12. For hadronic decays, one typically uses effective Hamiltonian calculations that rely on a perturbative expansion with Wilson coefficients. In addition, some form of the factorization hypothesis is commonly used, where, in analogy with semileptonic decays, two-body hadronic decays of *B* mesons are expressed as the product of two independent hadronic currents, one describing the formation of a charm meson (in case of the dominant  $b \rightarrow cW^{*-}$  decays), and the other the hadronization of the remaining  $\bar{u}d$  (or  $\bar{c}s$ ) system from the virtual  $W^-$ . Qualitatively, for a *B* decay with a large energy release, the  $\bar{u}d$  pair (produced as a color singlet) travels fast enough to leave the interaction region without influencing the charm meson. This is known to work well for the dominant spectator decays [13]. There are several common implementations of these ideas for hadronic *B* decays, the most common of which are QCD factorization (QCDF) [14], perturbative QCD (pQCD) [15], and soft collinear effective theory (SCET) [16].

The transition  $b \rightarrow u$  is suppressed by  $|V_{ub}/V_{cb}|^2 \sim (0.1)^2$  relative to  $b \rightarrow c$  transitions. The transition  $b \rightarrow s$  is a flavor-changing neutral-current (FCNC) process, and although not allowed in the SM as a tree-process, can occur via more complex loop diagrams (denoted “penguin” decays). The rates for such processes are comparable or larger than CKM-suppressed  $b \rightarrow u$  processes. Penguin processes involving  $b \rightarrow d$  transitions are also possible, and have been observed [17,18]. Other decay processes discussed in this *Review* include *W*-exchange (a *W* is exchanged between initial-state quarks), penguin annihilation (the gluon from a penguin loop attaches to the spectator quark, similar to an exchange diagram), and pure-annihilation (the initial quarks annihilate to a virtual *W*, which then decays).

**Production and spectroscopy:** The bound states of a  $\bar{b}$  antiquark and a *u*, *d*, *s*, or *c* quark are referred to as the  $B_u$  ( $B^+$ ),  $B_d$  ( $B^0$ ),  $B_s$ , and  $B_c$  mesons, respectively. The  $B_c$  is the heaviest of the ground-state *b*-flavored mesons, and the most difficult to produce: it was observed for the first time in the semileptonic mode by CDF in 1998 [19], but its mass was accurately determined only in 2006, from the fully reconstructed mode  $B_c^+ \rightarrow J/\psi\pi^+$  [20].

The first excited meson is called the  $B^*$  meson, while  $B^{**}$  is the generic name for the four orbitally excited ( $L = 1$ ) *B*-meson states that correspond to the *P*-wave mesons in the charm system,  $D^{**}$ . Excited states of the  $B_s$  meson are similarly named  $B_s^*$  and  $B_s^{**}$ . Of the possible bound  $\bar{b}b$  states, the  $\Upsilon$  series (S-wave) and the  $\chi_b$  (P-wave) are well studied. The pseudoscalar ground state  $\eta_b$  also has been observed by BaBar [21] (and confirmed by CLEO [22]), indirectly through the decay  $\Upsilon(3S) \rightarrow \gamma\eta_b$ . See Ref. 23 for classification and naming of these and other states.

Experimental studies of *b* decays have been performed in  $e^+e^-$  collisions at the  $\Upsilon(4S)$  (ARGUS, CLEO, Belle, BaBar) and  $\Upsilon(5S)$  (CLEO, Belle) resonances, as well as at higher energies, at the *Z* resonance (SLC, LEP) and in  $p\bar{p}$  collisions (Tevatron). The  $e^+e^- \rightarrow b\bar{b}$  production cross-section at the *Z*,  $\Upsilon(4S)$ , and  $\Upsilon(5S)$  resonances are about 6.6 *nb*, 1.1 *nb*, and 0.3 *nb* respectively. High-energy hadron collisions produce *b*-flavored hadrons of all species with much larger cross-sections:  $\sigma(p\bar{p} \rightarrow bX, |\eta| < 1) \sim 30 \mu\text{b}$  at the Tevatron ( $\sqrt{s} = 1.96 \text{ TeV}$ ), and even higher at the energies of the LHC  $pp$  collider (up to a factor of ten at  $\sqrt{s} = 14 \text{ TeV}$ ).

BaBar and Belle have accumulated respectively 560  $\text{fb}^{-1}$  and 1020  $\text{fb}^{-1}$  of data, of which 433  $\text{fb}^{-1}$  and 710  $\text{fb}^{-1}$  respectively are at the  $\Upsilon(4S)$  resonance; CDF and D0 have currently accumulated about 10  $\text{fb}^{-1}$  each. At the LHC, CMS and ATLAS have collected 5  $\text{fb}^{-1}$  of data and LHCb has collected about 1  $\text{fb}^{-1}$ . These numbers indicate that the majority of *b*-quarks have been produced in hadron collisions, but the large backgrounds cause the hadron collider experiments to have lower selection efficiency. Only the few decay modes for which triggering and reconstruction are easiest have been studied so far in hadron collisions. These have included final states with leptons, and exclusive modes with all charged particles in the final state. In contrast, detectors operating at  $e^+e^-$  colliders (“B-Factories”) have a high efficiency for most decays, and have provided large samples of a rich variety of decays of  $B^0$  and  $B^+$  mesons.

In hadron collisions, most production happens as  $b\bar{b}$  pairs, either via *s*-channel production or gluon-splitting, with a smaller fraction of single *b*-quarks produced by flavor excitation. The total *b*-production cross section is an interesting test of our understanding of QCD processes. For many years, experimental measurements have been several times higher than predictions. With improved measurements [24], more accurate input parameters, and more advanced calculations [25], the discrepancy between theory and data is now much reduced, although the

presence of inconsistencies among existing measurements makes further studies desirable.

Each quark of a  $b\bar{b}$  pair produced in hadron collisions hadronizes separately and incoherently from the other, but it is still possible, although difficult, to obtain a statistical indication of the charge of a produced  $b/\bar{b}$  quark (“flavor tag” or “charge tag”) from the accompanying particles produced in the hadronization process, or from the decay products of the other quark. The momentum spectrum of produced  $b$ -quarks typically peaks near the  $b$ -quark mass, and extends to much higher momenta, dropping by about a decade for every ten GeV. This implies typical decay lengths of the order of a millimeter; the resolution for the decay vertex must be more precise than this to resolve the fast oscillations of  $B_s$  mesons.

In  $e^+e^-$  colliders, since the  $B$  mesons are very slow in the  $\Upsilon(4S)$  rest frame, asymmetric beam energies are used to boost the decay products to improve the precision of time-dependent measurements that are crucial for the study of  $CP$  violation. At KEKB, the boost is  $\beta\gamma = 0.43$ , and the typical  $B$ -meson decay length is dilated from  $\approx 20 \mu\text{m}$  to  $\approx 200 \mu\text{m}$ . PEP-II uses a slightly larger boost,  $\beta\gamma = 0.55$ . The two  $B$  mesons produced in  $\Upsilon(4S)$  decay are in a coherent quantum state, which makes it easier than in hadron collisions to infer the charge state of one  $B$  meson from observation of the other; however, the coherence also requires determination of the decay time of both mesons, rather than just one, in order to perform time-dependent  $CP$ -violation measurements.

For the measurement of branching fractions, the initial composition of the data sample must be known. The  $\Upsilon(4S)$  resonance decays predominantly to  $B^0\bar{B}^0$  and  $B^+B^-$ ; the current experimental upper limit for non- $B\bar{B}$  decays of the  $\Upsilon(4S)$  is less than 4% at the 95% confidence level (CL) [26]. The only known modes of this category are decays to lower  $\Upsilon$  states and a pion pair, observed with branching fractions of order  $10^{-4}$  [27]. The ratio  $f_+/f_0$  of the fractions of charged to neutral  $B$  productions from  $\Upsilon(4S)$  decays has been measured by CLEO, BaBar, and Belle in various ways. They typically use pairs of isospin-related decays of  $B^+$  and  $B^0$ , such that it can be assumed that  $\Gamma(B^+ \rightarrow x^+) = \Gamma(B^0 \rightarrow x^0)$ . In this way, the ratio of the number of events observed in these modes is proportional to  $(f_+\tau_+)/ (f_0\tau_0)$  [28–31]. BaBar has also performed an independent measurement of  $f_0$  with a different method that does not require isospin symmetry or the value of the lifetime ratio, based on the number of events with one or two reconstructed  $B^0 \rightarrow D^{*-}\ell^+\nu$  decays [32]. The combined result, from the current average of  $\tau_+/\tau_0$ , is  $f_+/f_0 = 1.055 \pm 0.025$  [33]. Though the current  $2.2\sigma$  discrepancy with equal production of  $B^+B^-$  and  $B^0\bar{B}^0$  pairs is somewhat larger than previous averages, we still assume  $f_+/f_0 = 1$  in this mini-review except where explicitly stated otherwise. This assumption is also supported by the near equality of the  $B^+$  and  $B^0$  masses: our fit of CLEO, ARGUS, and CDF measurements yields  $m(B^0) = 5279.50 \pm 0.33 \text{ MeV}/c^2$ ,  $m(B^+) = 5279.13 \pm 0.31 \text{ MeV}/c^2$ , and  $m(B^0) - m(B^+) = 0.37 \pm 0.24 \text{ MeV}/c^2$ . The latest measurement

from the LHCb agrees well with those and further improves precision [34].

CLEO and Belle have also collected some data at the  $\Upsilon(5S)$  resonance [35,36]. Belle has accumulated more than  $100 \text{ fb}^{-1}$  at this resonance. This resonance does not provide the simple final states of the  $\Upsilon(4S)$ : there are seven possible final states with a pair of non-strange  $B$  mesons and three with a pair of strange  $B$  mesons ( $B_s^*\bar{B}_s^*$ ,  $B_s^*\bar{B}_s$ , and  $B_s\bar{B}_s^*$ ). The fraction of events with a pair of  $B_s$  mesons over the total number of events with a pair of  $b$ -flavored hadrons has been measured to be  $f_s[\Upsilon(5S)] = 0.199 \pm 0.030$ , of which 90% is  $B_s^*\bar{B}_s^*$  events. A few branching fractions of the  $B_s$  have been measured in this way; if the precision of  $f_s$  were improved, they would become the most accurate. Belle has observed a few new  $B_s$  modes that are difficult to reconstruct in hadron colliders and the most precise mass measurement of the  $B_s^*$  meson has been obtained [36,37]. However, the small boost of  $B_s$  mesons produced in this way prevents resolution of their fast oscillations for time-dependent measurements; these are only accessible in hadron collisions or at the  $Z$  peak.

In high-energy collisions, the produced  $b$  or  $\bar{b}$  quarks can hadronize with different probabilities into the full spectrum of  $b$ -hadrons, either in their ground or excited states. Table 1 shows the measured fractions  $f_d$ ,  $f_u$ ,  $f_s$ , and  $f_{\text{baryon}}$  of  $B^0$ ,  $B^+$ ,  $B_s^0$ , and  $b$  baryons, respectively, in an unbiased sample of weakly decaying  $b$  hadrons produced at the  $Z$  resonance or in  $p\bar{p}$  collisions [33]. The results were obtained from a fit where the sum of the fractions were constrained to equal 1.0, neglecting production of  $B_c$  mesons. The observed yields of  $B_c$  mesons at the Tevatron [19] yields  $f_c = 0.2\%$ , in agreement with expectations [38], and well below the current experimental uncertainties in the other fractions.

**Table 1:** Fractions of weakly-decaying  $b$ -hadron species in  $Z \rightarrow b\bar{b}$  decay, in  $p\bar{p}$  collisions at  $\sqrt{s} = 1.8 \text{ TeV}$  and combination of fractions in  $Z \rightarrow b\bar{b}$  decay at Tevatron,  $p\bar{p}$  and  $pp$  collisions at LHC.

$b$ hadron	Fraction at Z [%]	Fraction at $p\bar{p}$ [%]	Combined [%]
$B^+, B^0$	$40.3 \pm 0.9$	$33.9 \pm 3.9$	$40.1 \pm 0.8$
$B_s$	$10.3 \pm 0.9$	$11.1 \pm 1.4$	$10.5 \pm 0.6$
$b$ baryons	$9.0 \pm 1.5$	$21.2 \pm 6.9$	$9.3 \pm 1.6$

The combined values assume identical hadronization in  $p\bar{p}$  collisions and in  $Z$  decay. These could in principle differ, because of the different momentum distributions of the  $b$ -quark in these processes; the sample used in the  $p\bar{p}$  measurements has momenta close to the  $b$  mass, rather than  $m_Z/2$ . A test of the agreement between production fractions may be given by comparison of values of the average time-integrated mixing probability parameter  $\bar{\chi} = f_d\chi_d + f_s\chi_s$  [8]. This is an important input in the determination of the world-averages of production fractions. The current measurements of  $\bar{\chi}$  from LEP and the

# Meson Particle Listings

## *b*-flavored hadrons

Tevatron differ by  $1.8\sigma$  [33]. This slight discrepancy increases the uncertainty in the combined fractions in Table 1. It should be noted that the combination is not well defined as both the CDF and LHCb experiments observe a significant dependence of the  $\Lambda_b$  production fraction on transverse momentum. With the availability of large samples of *b*-flavored mesons and baryons at  $p\bar{p}$  colliders, the limited knowledge of these fractions has become an important limiting factor in the determination of their branching fractions.

Excited *B*-meson states have been observed by CLEO, LEP, CUSB, D0, and CDF. The current world average of the  $B^*-B$  mass difference is  $45.78 \pm 0.35 \text{ MeV}/c^2$ . Evidence for  $B^{**}$  ( $L=1$ ) production has been initially obtained at LEP [39], as a broad resonance in the mass of an inclusively reconstructed bottom hadron candidate combined with a charged pion from the primary vertex. Detailed results from exclusive modes have been obtained at the Tevatron, allowing separation of the narrow states  $B_1$  and  $B_2^*$  and also a measurement of the  $B_2^*$  width [40].

Also the narrow  $B_s^{**}$  states, first sighted by OPAL as a single broad enhancement in the  $B^+K$  mass spectrum [41], have now been clearly observed and separately measured at the Tevatron [42]:  $M(B_{s1}) = 5829.4 \pm 0.7 \text{ MeV}/c^2$  (CDF) and  $M(B_{s2}^*) = 5839.7 \pm 0.7 \text{ MeV}/c^2$  (CDF),  $M(B_{s2}^*) = 5839.6 \pm 1.1 \pm 0.7 \text{ MeV}/c^2$  (D0).

Baryon states containing a *b* quark are labeled according to the same scheme used for non-*b* baryons, with the addition of a *b* subscript [23]. For many years, the only well-established *b* baryon was the  $\Lambda_b^0$  (quark composition  $udb$ ), with only indirect evidence for  $\Xi_b$  ( $dsb$ ) production from LEP [43]. This situation has changed dramatically in the past few years due to the large samples being accumulated at the Tevatron and LHCb. Clear signals of four strongly-decaying baryon states,  $\Sigma_b^+$ ,  $\Sigma_b^{*+}$  ( $uub$ ),  $\Sigma_b^-$ ,  $\Sigma_b^{*-}$  ( $ddb$ ) have been obtained by CDF in  $\Lambda_b^0\pi^\pm$  final states [44]. The strange bottom baryon  $\Xi_b^\pm$  was observed in the exclusive mode  $\Xi_b^\pm \rightarrow J/\psi\Xi^\pm$  by D0 [45], and CDF [46]. More recently CDF has also observed the  $\Xi_b$  in the  $\Xi_c\pi$  final state [47]. The relative production of  $\Xi_b$  and  $\Lambda_b$  baryons has been found to be consistent with the  $B_s$  to  $B_d$  production ratio [45]. Observation of the doubly-strange bottom baryon  $\Omega_b^-$  has been published by both D0 [48] and CDF [49]. However the masses measured by the two experiments show a large discrepancy. The resolution appears to be provided by LHCb; they recently presented a preliminary measurement of the  $\Omega_b^-$  mass consistent with the CDF measurement [50]. Apart from the discrepancy on  $\Omega_b^-$  mass, the masses of all these new baryons have been measured to a precision of a few  $\text{MeV}/c^2$ , and found to be in agreement with predictions from HQET.

**Lifetimes:** Precise lifetimes are key in extracting the weak parameters that are important for understanding the role of the CKM matrix in *CP* violation, such as the determination of  $V_{cb}$  and  $B_s\bar{B}_s$  mixing parameters. In the naive spectator model, the heavy quark can decay only via the external spectator

mechanism, and thus, the lifetimes of all mesons and baryons containing *b* quarks would be equal. Non-spectator effects, such as the interference between contributing amplitudes, modify this simple picture and give rise to a lifetime hierarchy for *b*-flavored hadrons similar to the one in the charm sector. However, since the lifetime differences are expected to scale as  $1/m_Q^2$ , where  $m_Q$  is the mass of the heavy quark, the variations in the *b* system are expected to be only 10% or less [51]. We expect:

$$\tau(B^+) \geq \tau(B^0) \approx \tau(B_s) > \tau(\Lambda_b^0) \gg \tau(B_c^+) . \quad (1)$$

For the  $B_c^+$ , both quarks decay weakly, so the lifetime is much shorter.

Measurements of the lifetimes of the different *b*-flavored hadrons thus provide a means to determine the importance of non-spectator mechanisms in the *b* sector. Over the past decade, the precision of silicon vertex detectors and the increasing availability of fully-reconstructed samples has resulted in much-reduced statistical and systematic uncertainties ( $\sim 1\%$ ). The averaging of precision results from different experiments is a complex task that requires careful treatment of correlated systematic uncertainties; the world averages given in Table 2 have been determined by the Heavy Flavor Averaging Group (HFAG) [33].

**Table 2:** Summary of inclusive and exclusive world-average *b*-hadron lifetime measurements. For the two  $B_s$  averages, see text below.

Particle	Lifetime [ps]
$B^+$	$1.641 \pm 0.008$
$B^0$	$1.519 \pm 0.007$
$B_s$ (flavor-specific)	$1.463 \pm 0.032$
$B_s$ ( $1/\Gamma_s$ )	$1.495 \pm 0.015$
$B_c^+$	$0.453 \pm 0.041$
$\Lambda_b^0$	$1.425 \pm 0.032$
$\Xi_b^-$	$1.56^{+0.27}_{-0.25}$
$\Omega_b^-$	$1.13^{+0.53}_{-0.40}$
$\Xi_b$ mixture	$1.49^{+0.19}_{-0.18}$
<i>b</i> -baryon mixture	$1.382 \pm 0.029$
<i>b</i> -hadron mixture	$1.568 \pm 0.009$

The short  $B_c^+$  lifetime is in good agreement with predictions [52]. For precision comparisons with theory, lifetime ratios are more sensitive. Experimentally we find:

$$\frac{\tau_{B^+}}{\tau_{B^0}} = 1.079 \pm 0.007, \quad \frac{\tau_{B_s}}{\tau_{B^0}} = 0.984 \pm 0.011,$$

$$\frac{\tau_{\Lambda_b}}{\tau_{B^0}} = 0.938 \pm 0.022,$$

while theory makes the following predictions [51,53]

$$\frac{\tau_{B^+}}{\tau_{B^0}} = 1.06 \pm 0.02, \quad \frac{\tau_{B_s}}{\tau_{B^0}} = 1.00 \pm 0.01, \quad \frac{\tau_{\Lambda_b}}{\tau_{B^0}} = 0.88 \pm 0.05.$$

The ratio of  $B^+$  to  $B^0$  lifetimes has a precision of better than 1%, and is significantly different from 1.0, in agreement

with predictions [51]. The ratio of  $B_s$  to  $B^0$  lifetimes is expected to be very close to 1.0; while there used to be mild tension between experiment and theory, the discrepancy is disappearing with newer measurements with large samples of fully reconstructed  $B_s$  decays [54]. The  $\Lambda_b$  lifetime has a history of discrepancies. Predictions were higher than data before the introduction of higher-order effects lowered them. The precision of the measurements has recently been improved by more than a factor of two by two CDF measurements [57,58]. The measurements are in marginal agreement with each other and previous measurements; the new world average is somewhat larger than the theoretical predictions. The most significant discrepancy comes from the CDF measurement in  $\Lambda_b \rightarrow J/\psi \Lambda$  channel which differs by  $3.3\sigma$  from the average of all other measurements. With more data available at both D0 and CDF and large samples available at LHCb, new results will hopefully resolve this discrepancy in the near future.

Neutral  $B$  mesons are two-component systems similar to neutral kaons, with a light (L) and a heavy (H) mass eigenstate, and independent decay widths  $\Gamma_L$  and  $\Gamma_H$ . The SM predicts a non-zero width difference  $\Delta\Gamma = \Gamma_L - \Gamma_H > 0$  for both  $B_s$  and  $B_d$ . For  $B_d$ ,  $\Delta\Gamma_d/\Gamma_d$  is expected to be  $\sim 0.2\%$ . Analysis of BaBar and DELPHI data on  $CP$ -specific modes of the  $B^0$  yield a combined result:  $\Delta\Gamma_d/\Gamma_d = 0.015 \pm 0.018$  [33]. The issue is much more interesting for the  $B_s$ , since the SM expectation for  $\Delta\Gamma_s/\Gamma_s$  is of order 10%. This potentially non-negligible difference requires care when defining the  $B_s$  lifetime. As indicated in Table 2, two different lifetimes are defined for the  $B_s$  meson: one is defined as  $1/\Gamma_s$ , where  $\Gamma_s$  is the average width of the two mass eigenstates  $(\Gamma_L + \Gamma_H)/2$ ; the other is obtained from “flavor-specific” (*e.g.*, semileptonic) decays and depends both on  $\Gamma_s$  and  $\Delta\Gamma_s$ . Experimentally, the quantity  $\Delta\Gamma_s$  can be accessed by measuring lifetimes in decays into  $CP$  eigenstates, which in the standard model are expected to be close approximations to the mass eigenstates. This has been done with the  $J/\psi\phi$  mode, where the two  $CP$  eigenstates are distinguished by angular distributions, and in  $B_s \rightarrow K^+K^-$  or  $B_s \rightarrow J/\psi f_0(980)$  which are  $CP$ -eigenstates. The current experimental information is dominated by measurements on the  $J/\psi\phi$  mode performed by CDF, D0 and LHCb experiments. By appropriately combining all published measurements of  $J/\psi\phi$  lifetimes and flavor-specific lifetimes, the HFAG group obtains a world-average  $\Delta\Gamma_s/\Gamma_s = 0.092^{+0.051}_{-0.054}$  [33], which is compatible with zero; the latest theoretical predictions yield  $\Delta\Gamma_s/\Gamma_s = 0.133 \pm 0.032$  [59], in agreement with measurements within the large uncertainties on both. From the theoretical point of view, the best quantity to use is  $\Delta\Gamma_s/\Delta M_s$ , which is much less affected by hadronic uncertainties [59]. Exploiting the very accurate measurement of  $\Delta M_s$  now available [60], this can be turned into a SM prediction with an uncertainty of only 20%:  $\Delta\Gamma_s/\Gamma_s = 0.137 \pm 0.027$ . This is likely to be of importance in future comparisons, as the experimental precision improves with the growth of Tevatron samples. Further improvements are coming from lifetime measurements in the  $CP$ -eigenstates

such as  $B_s \rightarrow K^+K^-$  [61] and  $B_s \rightarrow J/\psi f_0(980)$  [62], and alternative (model-dependent) determinations via the  $B_s \rightarrow D_s^{(*)+} D_s^{(*)-}$  branching fraction [63].

The width difference  $\Delta\Gamma_s$  is connected to the  $B_s$  mixing phase  $\phi_s$  by  $\Delta\Gamma_s = \Gamma_{12} \cos \phi_s$ , where  $\Gamma_{12}$  is the off-diagonal term of the decay matrix [6,8,59]. The early measurements by CDF [64] and D0 [65] have produced CL contours in the  $(\phi_s, \Delta\Gamma)$  plane, and both observe a mild deviation, in the same direction, from the expectation of the Standard model of the phase  $\phi_s$  near  $\Delta\Gamma = 0$ . The possibility of a large value of  $\phi_s$  has attracted significant interest, as it would be very clean evidence for the existence of new sources of  $CP$  violation beyond the standard model. However the latest measurements from CDF [66], D0 [67] and LHCb [68], which provide significant improvements over initial measurements, show good agreement with the standard model. The LHCb experiment also used the decay  $B_s \rightarrow J/\psi f_0(980)$  to measure  $\phi_s$  [69]. While this measurement is not as precise as the one from  $B_s \rightarrow J/\psi\phi$ , it does not require analysis of angular distributions, which simplifies the analysis. It should be noted that all above measurements have a two-fold ambiguity in their results. We can resolve this ambiguity using the interference between the decays to  $J/\psi\phi$  and  $J/\psi K^+K^-$ , where  $K^+K^-$  is in relative S-wave state. This has been used by LHCb experiment to determine the sign of the  $\Delta\Gamma_s$  to be positive [70].

***B meson decay properties:*** Semileptonic  $B$  decays  $B \rightarrow X_c \ell \nu$  and  $B \rightarrow X_u \ell \nu$  provide an excellent way to measure the magnitude of the CKM elements  $|V_{cb}|$  and  $|V_{ub}|$  respectively, because the strong interaction effects are much simplified due to the two leptons in the final state. Both exclusive and inclusive decays can be used, and the nature of uncertainties are quite complementary. For exclusive decay analysis, knowledge of the form factors for the exclusive hadronic system  $X_{c(u)}$  is required. For inclusive analysis, it is usually necessary to restrict the available phase-space of the decay products to suppress backgrounds; subsequently uncertainties are introduced in the extrapolation to the full phase-space. Moreover, restriction to a small corner of the phase-space may result in breakdown of the operator-product expansion scheme, thus making theoretical calculations unreliable. A more detailed discussion of  $B$  semileptonic decays and the extraction of  $|V_{cb}|$  and  $|V_{ub}|$  is given elsewhere in this *Review* [9].

On the other hand, hadronic decays of  $B$  are complicated because of strong interaction effects caused by the surrounding cloud of light quarks and gluons. While this complicates the extraction of CKM matrix elements, it also provides a great opportunity to study perturbative and non-perturbative QCD, hadronization, and Final State Interaction (FSI) effects. Pure-penguin decays were first established by the observation of  $B \rightarrow K^* \gamma$  [71]. Some observed decay modes such as  $B^0 \rightarrow D_s^- K^+$ , may be interpreted as evidence of a  $W$ -exchange process [72]. The evidence for the decay  $B^+ \rightarrow \tau^+ \nu$  from Belle [73] and BaBar [74] is the first sign of a pure annihilation decay. There

# Meson Particle Listings

## *b*-flavored hadrons

is growing evidence that penguin annihilation processes may be important in decays with two vector mesons in the final state [75].

**Hadronic decays:** Most of the hadronic  $B$  decays involve  $b \rightarrow c$  transition at the quark level, resulting in a charmed hadron or charmonium in the final state. Other types of hadronic decays are very rare and will be discussed separately in the next section. The experimental results on hadronic  $B$  decays have steadily improved over the past few years, and the measurements have reached sufficient precision to challenge our understanding of the dynamics of these decays. With the good neutral particle detection and hadron identification capabilities of  $B$ -factory detectors, a substantial fraction of hadronic  $B$  decay events can be fully reconstructed. Because of the kinematic constraint of  $\Upsilon(4S)$ , the energy sum of the final-state particles of a  $B$  meson decay is always equal to one half of the total energy in the center of mass frame. As a result, the two variables,  $\Delta E$  (energy difference) and  $M_B$  ( $B$  candidate mass with a beam-energy constraint) are very effective for suppressing combinatorial background both from  $\Upsilon(4S)$  and  $e^+e^- \rightarrow q\bar{q}$  continuum events. In particular, the energy-constraint in  $M_B$  improves the signal resolution by almost an order of magnitude.

The kinematically clean environment of  $B$  meson decays provides an excellent opportunity to search for new states. For instance, quark-level  $b \rightarrow c\bar{c}s$  decays have been used to search for new charmonium and charm-strange mesons and study their properties in detail. In 2003, BaBar discovered a new narrow charm-strange state  $D_{sJ}^*(2317)$  [76], and CLEO observed a similar state  $D_{sJ}(2460)$  [77]. The properties of these new states were studied in the  $B$  meson decays,  $B \rightarrow DD_{sJ}^*(2317)$  and  $B \rightarrow DD_{sJ}(2460)$  by Belle [78]. Further studies of  $D_{sJ}^{(*)}$  meson production in  $B$  decays have been made by Belle [79] and BaBar [80]. Now these charm-strange meson states are identified as  $D_{s0}^*(2317)$  and  $D_{s1}(2460)$ , respectively.

More recently, Belle observed a new  $D_{sJ}$  meson produced in  $B^+ \rightarrow \bar{D}^0 D_{sJ} \rightarrow \bar{D}^0 D^0 K^+$  [81]. Combined with a subsequent measurement by BaBar [82], the mass and width of this state are determined to be  $2709_{-6}^{+9}$  MeV/ $c^2$  and  $125 \pm 30$  MeV, respectively. An analysis of the helicity angle distribution determines its spin-parity to be  $1^-$ .

A variety of exotic particles have been discovered in  $B$  decays. Belle found the  $X(3872)$  state [83], which is confirmed by CDF [84] and BaBar [85]. Analyzing their full  $\Upsilon(4S)$  data sample, Belle finds a new upper limit on the width of  $X(3872)$  to be  $\Gamma_{X(3872)} < 1.2$  MeV [86], improving on the existing limit by nearly a factor of 2. Radiative decays of  $X(3872)$  can play a crucial role in understanding the nature of the particle. For example, in the molecular model the decay of  $X(3872)$  to  $\psi'\gamma$  is expected to be highly suppressed in comparison to the decay to  $J/\psi\gamma$  [87]. BaBar has seen the evidence for the decay to  $J/\psi\gamma$  [88]. The ratio  $R \equiv \mathcal{B}(X(3872) \rightarrow \psi'\gamma)/\mathcal{B}(X(3872) \rightarrow J/\psi\gamma)$  is measured to be  $3.4 \pm 1.4$  by BaBar [89], while Belle obtains  $R < 2.1$  at 90% CL [90].

Belle has observed a near-threshold enhancement in the  $J/\psi\omega$  invariant mass for  $B \rightarrow J/\psi\omega K$  decays [91]. BaBar has studied  $B \rightarrow J/\psi\pi^+\pi^-K$ , finding an excess of  $J/\psi\pi^+\pi^-$  events with a mass just above 4.2 GeV/ $c^2$ ; this is consistent with the  $Y(4260)$  that was observed by BaBar in ISR (Initial State Radiation) events [93]. A Belle study of  $B \rightarrow \psi'K\pi^\pm$  [94] finds a state called  $X(4430)^\pm$  that decays to  $\psi'\pi^\pm$ . Since it is charged, it could not be a charmonium state. This state was searched for by BaBar with similar sensitivity but was not found [95]. In a Dalitz plot analysis of  $\bar{B}^0 \rightarrow \chi_{c1}K^-\pi^+$ , Belle has observed two resonance-like structures in the  $\chi_{c1}\pi^+$  mass distribution [96], labelled as  $X(4050)^\pm$  and  $X(4250)^\pm$  in this *Review*, while no evidence is found by BaBar in a search with similar sensitivity [97].

The hadronic decays  $\bar{B}^0 \rightarrow D^{(*)0}h^0$ , where  $h^0$  stands for light neutral mesons such as  $\pi^0, \eta^{(\prime)}, \rho^0, \omega$ , proceed through color-suppressed diagrams, hence they provide useful tests on the factorization models. Both Belle and BaBar have made comprehensive measurements of such color-suppressed hadronic decays of  $\bar{B}^0$  [98].

Information on  $B_s$  and  $\Lambda_b$  decays is limited, though improving with recent studies of large samples at the Tevatron and LHC experiments. Recent additions are decays of  $B_s \rightarrow J/\psi f_0(980)$  [62,99],  $B_s \rightarrow J/\psi f_2'(1525)$  [100], and  $\Lambda_b \rightarrow \Lambda_c\pi^+\pi^-\pi^-$  [101]. For the later, not only the total rate is measured, but also structure involving decays through excited  $\Lambda_c$  and  $\Sigma_c$  baryons.

There have been hundreds of publications on hadronic  $B$  decays to open-charm and charmonium final states mostly from the  $B$ -factory experiments. These results are nicely summarized in a recent report by HFAG [33].

**Rare  $B$  decays:** All  $B$ -meson decays that do not occur through the  $b \rightarrow c$  transition are usually called rare  $B$  decays. These include both semileptonic and hadronic  $b \rightarrow u$  decays that are suppressed at leading order by the small CKM matrix element  $V_{ub}$ , as well as higher-order  $b \rightarrow s(d)$  processes such as electroweak and gluonic penguin decays.

Charmless  $B$  meson decays into two-body hadronic final states such as  $B \rightarrow \pi\pi$  and  $K\pi$  are experimentally clean, and provide good opportunities to probe new physics and search for indirect and direct  $CP$  violations. Since the final state particles in these decays tend to have larger momenta than average  $B$  decay products, the event environment is cleaner than for  $b \rightarrow c$  decays. Branching fractions are typically around  $10^{-5}$ . Over the past decade, many such modes have been observed by BaBar, Belle, and CLEO. More recently, comparable samples of the modes with all charged final particles have been reconstructed in  $p\bar{p}$  collisions by CDF by triggering on the impact parameter of the charged tracks. This has also allowed observation of charmless decays of the  $B_s$ , in final states such as  $\phi\phi$  [102],  $K^+K^-$  [103], and  $K^-\pi^+$  [104], and of charmless decays of the  $\Lambda_b^0$  baryon [104]. Charmless  $B_s$  modes are related to corresponding  $B^0$  modes by U-spin symmetry, and are determined

by similar amplitudes. Combining the observables from  $B_s$  and  $B^0$  modes is a further way of eliminating hadronic uncertainties and extracting relevant CKM information [105].

Because of relatively high-momenta for final state particles, the dominant source of background in  $e^+e^-$  collisions is  $q\bar{q}$  continuum events; sophisticated background suppression techniques exploiting event shape variables are essential for these analyses. In hadron collisions, the dominant background comes from QCD or partially reconstructed heavy flavors, and is similarly suppressed by a combination of kinematic and isolation requirements. The results are in general consistent among the experiments.

BaBar [106] and Belle [107] have observed the decays  $B^+ \rightarrow \bar{K}^0 K^+$  and  $B^0 \rightarrow K^0 \bar{K}^0$ . The world-average branching fractions are  $\mathcal{B}(B^0 \rightarrow K^0 \bar{K}^0) = (0.96^{+0.20}_{-0.18}) \times 10^{-6}$  and  $\mathcal{B}(B^+ \rightarrow \bar{K}^0 K^+) = (1.36 \pm 0.27) \times 10^{-6}$ . These are the first observations of hadronic  $b \rightarrow d$  transitions, with significance  $> 5\sigma$  for all four measurements.  $CP$  asymmetries have even been measured for these modes, though with large errors.

Most rare decay modes including  $B^0 \rightarrow K^+ \pi^-$  have contributions from both  $b \rightarrow u$  tree and  $b \rightarrow sg$  penguin processes. If the size of the two contributions are comparable, the interference between them may result in direct  $CP$  violation, seen experimentally as a charge asymmetry in the decay rate measurement. BaBar [108], Belle [109], and CDF [103] have measured the direct  $CP$  violating asymmetry in  $B^0 \rightarrow K^+ \pi^-$  decays. The BaBar and Belle measurements constitute observation of direct  $CP$  violation with a significance of more than  $5\sigma$ . The world average for this quantity is now rather precise,  $-0.098 \pm 0.013$ . There are sum rules [110] that relate the decay rates and decay-rate asymmetries between the four  $K\pi$  charge states. The experimental measurements of the other three modes are not yet precise enough to test these sum rules.

There is now evidence for direct  $CP$  violation in three other decays:  $B^+ \rightarrow \rho^0 K^+$  [111],  $B^+ \rightarrow \eta K^+$  [112], and  $B^0 \rightarrow \eta K^{*0}$  [113]. The significance is typically 3–4 $\sigma$ , though the significance for the  $B^+ \rightarrow \eta K^+$  decay is now nearly  $5\sigma$  with the recent Belle measurement [112]. In at least the first two cases, a large direct  $CP$  violation might be expected since the penguin amplitude is suppressed so the tree and penguin amplitudes may have comparable magnitudes.

The decay  $B^0 \rightarrow \pi^+ \pi^-$  can be used to extract the CKM angle  $\alpha$ . This is complicated by the presence of significant contributions from penguin diagrams. An isospin analysis [114] can be used to untangle the penguin complications. The decay  $B^0 \rightarrow \pi^0 \pi^0$ , which is now measured by both BaBar and Belle, is crucial in this analysis. Unfortunately the amount of penguin pollution in the  $B \rightarrow \pi\pi$  system is rather large. In the past few years, measurements in the  $B^0 \rightarrow \rho\rho$  system have produced more precise values of  $\alpha$ , since penguin amplitudes are generally smaller for decays with vector mesons. An important ingredient in the analysis is the  $B^0 \rightarrow \rho^0 \rho^0$  branching fraction. The average of measurements from BaBar and Belle BaBar [115] yields a branching fraction of  $(0.73 \pm 0.28) \times 10^{-6}$ . This is only 3% of the

$\rho^+ \rho^-$  branching fraction, much smaller than the corresponding ratio in the  $\pi\pi$  system.

The decay  $B \rightarrow a_1 \pi$  has been seen by BaBar. An analysis of the time evolution of this decay [116] together with measurements of other related decays has been used to measure the CKM angle  $\alpha$  [117] in agreement with the more precise measurements from the  $\rho\rho$  system.

Since  $B \rightarrow \rho\rho$  has two vector mesons in the final state, the  $CP$  eigenvalue of the final state depends on the longitudinal polarization fraction  $f_L$  for the decay. Therefore, a measurement of  $f_L$  is needed to extract the CKM angle  $\alpha$ . Both BaBar and Belle have measured  $f_L$  for the decays  $\rho^+ \rho^-$  and  $\rho^+ \rho^0$  and in both cases the measurements show  $f_L > 0.9$ , making a complete angular analysis unnecessary.

By analyzing the angular distributions of the  $B$  decays to two vector mesons, we can learn a lot about both weak- and strong-interaction dynamics in  $B$  decays. Decays that are penguin-dominated surprisingly have values of  $f_L$  near 0.5. The list of such decays has now grown to include  $B \rightarrow \phi K^*$ ,  $B \rightarrow \rho K^*$ , and  $B \rightarrow \omega K^*$ . The reasons for this "polarization puzzle" are not fully understood. A detailed description of the angular analysis of  $B$  decays to two vector mesons can be found in a separate mini-review [118] in this *Review*.

There has been substantial progress in measurements of many other rare- $B$  decays. The decay  $B \rightarrow \eta' K$  stood out as the largest rare- $B$  decay for many years. The reasons for the large rate are now largely understood [14,119]. However, there are now measurements of several 3-body or quasi-3-body modes with similarly large branching fractions. States seen so far include  $K\pi\pi$  (three charge states) [120],  $KKK$  (four charge states) [121], and  $K^* \pi\pi$  (two charged states) [122]. Many of these analyses now include Dalitz plot treatments with many intermediate resonances. There has also been an observation of the decay  $B^+ \rightarrow K^+ K^- \pi^+$  by BaBar [123], noteworthy because an even number of kaons is typically indicative of suppressed  $b \rightarrow d$  transitions as discussed above.

Belle [73] and BaBar [74] have found evidence for  $B^+ \rightarrow \tau^+ \nu$ ; the average branching fraction, with a significance of nearly  $5\sigma$  is  $(165 \pm 34) \times 10^{-6}$ . This is somewhat larger than, though consistent with, the value expected in the SM. This is the first observation of a pure annihilation decay. A substantial region of parameter space of charged Higgs mass vs.  $\tan\beta$  is excluded by the measurements of this mode.

**Electroweak penguin decays:** More than a decade has passed since the CLEO experiment first observed an exclusive radiative  $b \rightarrow s\gamma$  transition,  $B \rightarrow K^*(892)\gamma$  [71], thus providing the first evidence for the one-loop FCNC electromagnetic penguin decay. Using much larger data samples, both Belle and BaBar have updated this analysis [124] with an average branching fraction  $\mathcal{B}(B^0 \rightarrow K^{*0}\gamma) = (43.3 \pm 1.5) \times 10^{-6}$ , and have added several new decay modes such as  $B \rightarrow K_{1\gamma}$ ,  $K_2^*(1430)\gamma$ , *etc.* [125]. With a sample of 24 fb $^{-1}$  at  $\Upsilon(5S)$ , Belle observed the radiative penguin decay of  $B_s \rightarrow \phi\gamma$  with a branching fraction  $(57^{+22}_{-19}) \times 10^{-6}$  [126].

# Meson Particle Listings

## *b*-flavored hadrons

Compared to  $b \rightarrow s\gamma$ , the  $b \rightarrow d\gamma$  transitions such as  $B \rightarrow \rho\gamma$ , are suppressed by the small CKM element  $V_{td}$ . Both Belle and BaBar have observed these decays [17,18]. The world average  $\mathcal{B}(B \rightarrow (\rho, \omega)\gamma) = (1.28 \pm 0.21) \times 10^{-6}$ . This can be used to calculate  $|V_{td}/V_{ts}|$  [127]; the measured values are  $0.233_{-0.032}^{+0.033}$  from BaBar [18] and  $0.195_{-0.024}^{+0.025}$  from Belle [17].

The observed radiative penguin branching fractions can constrain a large class of SM extensions [128]. However, due to the uncertainties in the hadronization, only the inclusive  $b \rightarrow s\gamma$  rate can be reliably compared with theoretical calculations. This rate can be measured from the endpoint of the inclusive photon spectrum in  $B$  decay. By combining the measurements of  $B \rightarrow X_s\gamma$  from CLEO, BaBar, and Belle experiments [129,130], HFAG obtains the new average:  $\mathcal{B}(B \rightarrow X_s\gamma) = (3.55 \pm 0.24 \pm 0.09) \times 10^{-4}$  [33] for  $E_\gamma \geq 1.6$  GeV. Consistent results have been reported by ALEPH for inclusive  $b$ -hadrons produced at the  $Z$ . The measured branching fraction can be compared to theoretical calculations. Recent calculations of  $\mathcal{B}(b \rightarrow s\gamma)$  at NNLO level predict the values of  $(3.15 \pm 0.23) \times 10^{-4}$  [131] and  $(2.98 \pm 0.26) \times 10^{-4}$  [132], where the latter is calculated requiring  $E_\gamma \geq 1.6$  GeV.

The  $CP$  asymmetry in  $b \rightarrow s\gamma$  is extensively studied theoretically both in the SM and beyond [133]. According to the SM, the  $CP$  asymmetry in  $b \rightarrow s\gamma$  is smaller than 1%, but some non-SM models allow significantly larger  $CP$  asymmetry ( $\sim 10\%$ ) without altering the inclusive branching fraction. The current world average is  $A_{CP} = -0.012 \pm 0.028$ , again dominated by BaBar and Belle [134]. In addition to the  $CP$  asymmetry, BaBar also measured the isospin asymmetry  $\Delta_{0-} = 0.06 \pm 0.17$  in  $b \rightarrow s\gamma$  by measuring the companion  $B$  with full reconstruction in the hadronic decay modes [135].

In addition, all three experiments have measured the inclusive photon energy spectrum for  $b \rightarrow s\gamma$ , and by analyzing the shape of the spectrum they obtain the first and second moments for photon energies. Belle has measured these moments covering the widest range in the photon energy ( $1.7 < E_\gamma < 2.8$  GeV) [130]. These results can be used to extract non-perturbative HQET parameters that are needed for precise determination of the CKM matrix element  $V_{ub}$ .

Additional information on FCNC processes can be obtained from  $B \rightarrow X_s\ell^+\ell^-$  decays, which are mediated by electroweak penguin and  $W$ -box diagrams. Their branching fractions have been measured by Belle [136], BaBar [137], and CDF [138]. Average branching fractions over all charged and neutral modes have been determined from BaBar and Belle data for  $B \rightarrow K\ell^+\ell^-$ :  $(0.45 \pm 0.04) \times 10^{-6}$  and for  $B \rightarrow K^*(892)\ell^+\ell^-$ :  $(1.08 \pm 0.11) \times 10^{-6}$ , consistent with the SM expectation.  $B$ -factory experiments also measured the branching fractions for inclusive  $B \rightarrow X_s\ell^+\ell^-$  decays [139], with an average of  $(3.66_{-0.77}^{+0.76}) \times 10^{-6}$  [140]. Recently corresponding decays of  $B_s$  and  $\Lambda_b$  were observed [138,141]. Branching fraction for the decay  $B_s \rightarrow \phi\mu^+\mu^-$  is measured to be  $(1.47 \pm 0.24 \pm 0.46) \times 10^{-6}$  and for the decay  $\Lambda_b \rightarrow \Lambda\mu^+\mu^-$  to be  $(1.73 \pm 0.42 \pm 0.55) \times 10^{-6}$ . Excitement was generated by measurements of forward-backward

asymmetry in  $B \rightarrow K^*(892)\ell^+\ell^-$  decays, which exhibited mild tension with the standard model in earlier measurements. The most recent measurements by CDF [142] and LHCb [143] agree with standard model, suggesting that the earlier discrepancy was mainly due to statistical fluctuations.

Finally the decays  $B_{(s)}^0 \rightarrow e^+e^-$  and  $\mu^+\mu^-$  are interesting since they only proceed at second order in weak interactions in the SM, but may have large contributions from supersymmetric loops, proportional to  $(\tan\beta)^6$ . Experiments at Tevatron,  $B$ -factories and now also LHC have obtained results that exclude a portion of the region allowed by SUSY models. The most stringent limits in these modes are obtained by LHCb. The limits in the  $\mu^+\mu^-$  mode are:  $< 1.4 \times 10^{-8}$  and  $< 3.2 \times 10^{-9}$  at 95% confidence level, respectively, for  $B_s$  and  $B^0$  [144]. For the  $B_s$  mode, the result is about factor of five above SM predictions [145]. It should be noted, that the most recent search by CDF observes an excess above expected background [146]. While the branching fraction for decay  $B_s \rightarrow \mu^+\mu^-$  of  $(1.8_{-0.9}^{+1.1}) \times 10^{-8}$  is extracted, CDF concludes that most plausible explanation for the excess is a statistical fluctuation. The limits for the  $e^+e^-$  modes are:  $< 2.8 \times 10^{-7}$  and  $< 8.3 \times 10^{-8}$ , respectively, for  $B_s$  and  $B^0$  [147]. There are also limits for lepton flavor-violating channels  $B_{(s)}^0 \rightarrow e^+\mu^-$ , which are around  $10^{-7}$  [147].

**Summary and Outlook:** The study of  $B$  mesons continues to be one of the most productive fields in particle physics. With the two asymmetric  $B$ -factory experiments Belle and BaBar, we now have a combined data sample of well over  $1 \text{ ab}^{-1}$ .  $CP$  violation has been firmly established in many decays of  $B$  mesons. Evidence for direct  $CP$  violation has been observed. Many rare decays resulting from hadronic  $b \rightarrow u$  transitions and  $b \rightarrow s(d)$  penguin decays have been observed, and the emerging pattern is still full of surprises. Despite the remarkable successes of the  $B$ -factory experiments, many fundamental questions in the flavor sector remain unanswered.

At Fermilab, CDF and D0 each has accumulated about  $10 \text{ fb}^{-1}$ , which is the equivalent of about  $10^{12}$   $b$ -hadrons produced. In spite of the low trigger efficiency of hadronic experiments, a selection of modes have been reconstructed in large quantities, giving a start to a program of studies on  $B_s$  and  $b$ -flavored baryons, in which a first major step has been the determination of the  $B_s$  oscillation frequency.

As Tevatron and  $B$ -factories stop their taking data, the new experiments at the LHC have become very active. The LHC accelerator performed very well in 2011. The general purpose experiments ATLAS and CMS collected about  $5 \text{ fb}^{-1}$  while LHCb collected about  $1 \text{ fb}^{-1}$ . LHCb, which is almost fully dedicated to studies of  $b$ - and  $c$ -hadrons, has a very large data sample. Of particular note is the sensitivity of the LHC experiments for the decay  $B_s \rightarrow \mu^+\mu^-$  which is expected to approach the standard model level in 2012.

In addition, two projects for next generation high-luminosity  $B$ -factories at KEK and Frascati are approved. Their aim to increase samples to  $\sim 50 \text{ ab}^{-1}$  will make it possible to explore the



See key on page 457

indirect evidence of new physics beyond the SM in the heavy-flavor particles (*b*, *c*, and  $\tau$ ), in a way that is complementary to the LHC.

These experiments promise a rich spectrum of rare and precise measurements that have the potential to fundamentally affect our understanding of the SM and *CP*-violating phenomena.

## References

1. M. Kobayashi and T. Maskawa, *Prog. Theor. Phys.* **49**, 652 (1973).
2. S. W. Herb *et al.*, *Phys. Rev. Lett.* **39**, 252 (1977).
3. B. Aubert *et al.* (BaBar Collab.), *Phys. Rev. Lett.* **87**, 091801 (2001).
4. K. Abe *et al.* (Belle Collab.), *Phys. Rev. Lett.* **87**, 091802 (2001).
5. Currently two different notations ( $\phi_1, \phi_2, \phi_3$ ) and ( $\alpha, \beta, \gamma$ ) are used in the literature for CKM unitarity angles. In this mini-review, we use the latter notation following the other mini-reviews in this *Review*. The two notations are related by  $\phi_1 = \beta$ ,  $\phi_2 = \alpha$  and  $\phi_3 = \gamma$ .
6. See the “*CP* Violation in Meson Decays” by D. Kirkby and Y. Nir in this *Review*.
7. See the “CKM Quark Mixing Matrix,” by A. Cecucci, Z. Ligeti, and Y. Sakai, in this *Review*.
8. See the “Review on *B*- $\bar{B}$  Mixing,” by O. Schneider in this *Review*.
9. See the “Determination of  $|V_{cb}|$  and  $|V_{ub}|$ ,” by R. Kowalewski and T. Mannel in this *Review*.
10. The  $B_c$  is a special case, where a weak decay of the *c* quark is also possible, but the spectator model still applies.
11. B. Grinstein, *Nucl. Phys.* **B339**, 253 (1990); H. Georgi, *Phys. Lett.* **B240**, 447 (1990); A.F. Falk *et al.*, *Nucl. Phys.* **B343**, 1 (1990); E. Eichten and B. Hill, *Phys. Lett.* **B234**, 511 (1990).
12. “Heavy-Quark and Soft-Collinear Effective Theory” by C.W. Bauer and M. Neubert in this *Review*.
13. M. Neubert, “Aspects of QCD Factorization,” [hep-ph/0110093](#), *Proceedings of HF9*, Pasadena (2001) and references therein; Z. Ligeti *et al.*, *Phys. Lett.* **B507**, 142 (2001).
14. M. Beneke *et al.*, *Phys. Rev. Lett.* **83**, 1914 (1999); *Nucl. Phys.* **B591**, 313 (2000); *Nucl. Phys.* **B606**, 245 (2001); M. Beneke and M. Neubert, *Nucl. Phys.* **B675**, 333 (2003).
15. Y.Y. Keum, H-n. Li, and A.I. Sanda, *Phys. Lett.* **B504**, 6 (2001); *Phys. Rev.* **D63**, 054008 (2001); Y.Y. Keum and H-n. Li, *Phys. Rev.* **D63**, 074006 (2001); C.D. Lü, K. Ukai, and M.Z. Yang, *Phys. Rev.* **D63**, 074009 (2001); C.D. Lü and M.Z. Yang, *Eur. Phys. J.* **C23**, 275 (2002).
16. C.W. Bauer, S. Fleming, and M.E. Luke, *Phys. Rev.* **D63**, 014006 (2001); C.W. Bauer *et al.*, *Phys. Rev.* **D63**, 114020 (2001); C.W. Bauer and I.W. Stewart, *Phys. Lett.* **B516**, 134 (2001).
17. N. Taniguchi *et al.* (Belle Collab.), *Phys. Rev. Lett.* **101**, 111801 (2008).
18. B. Aubert *et al.* (BaBar Collab.), *Phys. Rev.* **D78**, 112001 (2008).
19. F. Abe *et al.* (CDF Collab.), *Phys. Rev. Lett.* **81**, 2432 (1998); F. Abe *et al.* (CDF Collab.), *Phys. Rev.* **D58**, 112004 (1998).
20. D. Acosta *et al.* (CDF Collab.), *Phys. Rev. Lett.* **96**, 082002 (2006).
21. B. Aubert *et al.* (BABAR Collaboration), *Phys. Rev. Lett.* **101**, 071801 (2008) [Erratum-ibid. **102**, 029901 (2009)].
22. G. Bonvicini, *et al.* (CLEO Collaboration), *Phys. Rev.* **D81**, 031104 (2010).
23. See the note on “Naming scheme for hadrons,” by M. Roos and C.G. Wohl in this *Review*.
24. A. Abulencia *et al.* (CDF Collab.), *Phys. Rev.* **D75**, 012010 (2007), and references therein.
25. M. Cacciari *et al.*, *JHEP* **9805**, 007 (1998); S. Frixione and B. R. Webber, *JHEP* **0206**, 029 (2002); M. Cacciari *et al.*, *JHEP* **0407**, 033 (2004); M. Cacciari *et al.*, *JHEP* **0604**, 006 (2006), and references therein.
26. B. Barish *et al.* (CLEO Collab.), *Phys. Rev. Lett.* **76**, 1570 (1996).
27. B. Aubert *et al.* (BaBar Collab.), *Phys. Rev. Lett.* **96**, 232001 (2006); A. Sokolov *et al.* (Belle Collab.), *Phys. Rev.* **D75**, 071103 (R) (2007).
28. J.P. Alexander *et al.* (CLEO Collab.), *Phys. Rev. Lett.* **86**, 2737 (2001).
29. B. Aubert *et al.* (BaBar Collab.), *Phys. Rev.* **D65**, 032001 (2001); B. Aubert *et al.* (BaBar Collab.), *Phys. Rev.* **D69**, 071101 (2004).
30. S.B. Athar *et al.* (CLEO Collab.), *Phys. Rev.* **D66**, 052003 (2002).
31. N.C. Hastings *et al.* (Belle Collab.), *Phys. Rev.* **D67**, 052004 (2003).
32. B. Aubert *et al.* (BaBar Collab.), *Phys. Rev. Lett.* **95**, 042001 (2005).
33. E. Barberio *et al.* (Heavy Flavor Averaging Group), “Averages of *b*-hadron, *c*-hadron, and tau-lepton Properties,” [arXiv:1010.1589 \[hep-ex\]](#), and online update at <http://www.slac.stanford.edu/xorg/hfag/>.
34. R. Aaij *et al.* (LHCb Collab.), *Phys. Lett.* **B708**, 241 (2012).
35. G.S. Huang *et al.* (CLEO Collab.), *Phys. Rev.* **D75**, 012002 (2007).
36. R. Louvot *et al.* (Belle Collab.), *Phys. Rev. Lett.* **102**, 021801 (2009).
37. R. Louvot [Belle Collaboration], *Proceedings of EPS09*, Krakov, Poland (2009), [arXiv:0909.2160 \[hep-ex\]](#).
38. M. Lusignoli, M. Masetti, and S. Petrarca, *Phys. Lett.* **B266**, 142 (1991); K. Cheung, *Phys. Lett.* **B472**, 408 (2000).
39. P. Abreu *et al.* (DELPHI Collab.), *Phys. Lett.* **B345**, 598 (1995).
40. T. Aaltonen *et al.* (CDF Collaboration), *Phys. Rev. Lett.* **102**, 102003 (2009); V.M..
41. R. Akers *et al.* (OPAL Collab.), *Z. Phys.* **C66**, 19 (1995).
42. T. Aaltonen *et al.* (CDF Collab.), *Phys. Rev. Lett.* **100**, 082001 (2008); V.M. Abazov *et al.* (D0 Collab.), *Phys. Rev. Lett.* **100**, 082002 (2008).
43. D. Buskulic *et al.* (ALEPH Collab.), *Phys. Lett.* **B384**, 449 (1996); P. Abreu *et al.* (DELPHI Collab.), *Z. Phys.* **C68**, 541 (1995).

## Meson Particle Listings

*b*-flavored hadrons

- 
44. T. Aaltonen *et al.* (CDF Collab.), Phys. Rev. Lett. **99**, 202001 (2007).
45. V.M. Abazov *et al.* (D0 Collab.), Phys. Rev. Lett. **99**, 052001 (2007).
46. T. Aaltonen *et al.* (CDF Collab.), Phys. Rev. Lett. **99**, 052002 (2007).
47. T. Aaltonen *et al.* (CDF Collab.), Phys. Rev. Lett. **107**, 102001 (2011).
48. V. M. Abazov *et al.* (D0 Collab.), Phys. Rev. Lett. **101**, 232002 (2008).
49. T. Aaltonen *et al.* (CDF Collab.), Phys. Rev. D **80**, 072003 (2009).
50. LHCb Collab., LHCb-CONF-2011-060 (2011), unpublished.
51. C. Tarantino, Eur. Phys. J. **C33**, S895 (2004); F. Gabbiani *et al.*, Phys. Rev. **D68**, 114006 (2003); F. Gabbiani *et al.*, Phys. Rev. **D70**, 094031 (2004).
52. C.H. Chang *et al.*, Phys. Rev. **D64**, 014003 (2001); V.V. Kiselev, A.E. Kovalsky, and A.K. Likhoded, Nucl. Phys. **B585**, 353 (2000); V.V. Kiselev, [arXiv:hep-ph/0308214](https://arxiv.org/abs/hep-ph/0308214), and references therein.
53. I.I. Bigi *et al.*, in *B Decays*, 2nd ed., S. Stone (ed.), World Scientific, Singapore, 1994.
54. T. Aaltonen *et al.* (CDF Collab.), Phys. Rev. Lett. **107**, 272001 (2007).
55. A. Abulencia *et al.* (CDF Collab.), Phys. Rev. Lett. **98**, 122001 (2007).
56. V.M. Abazov *et al.* (D0 Collab.), Phys. Rev. Lett. **99**, 182001 (2007); V.M. Abazov *et al.* (D0 Collab.), Phys. Rev. Lett. **99**, 142001 (2007).
57. T. Aaltonen *et al.* (CDF Collab.), Phys. Rev. Lett. **104**, 102002 (2010).
58. T. Aaltonen *et al.* (CDF Collab.), Phys. Rev. Lett. **106**, 121804 (2011).
59. A. Lenz and U. Nierste, JHEP **0706**, 072 (2007) and numerical update in [arXiv:1102.4274 \[hep-ph\]](https://arxiv.org/abs/1102.4274).
60. A. Abulencia *et al.* (CDF Collab.), Phys. Rev. Lett. **97**, 242003 (2006).
61. R. Aaij *et al.* (LHCb Collab.), Phys. Lett. **B707**, 349 (2012).
62. A. Abulencia *et al.* (CDF Collab.), Phys. Rev. **D84**, 052012 (2012).
63. R. Barate *et al.* (ALEPH Collab.), Phys. Lett. **B486**, 286 (2000); V.M. Abazov *et al.* (D0 Collab.), Phys. Rev. Lett. **99**, 241801 (2007).
64. T. Aaltonen *et al.* (CDF Collab.), Phys. Rev. Lett. **100**, 121803 (2008).
65. V.M. Abazov *et al.* (D0 Collab.), Phys. Rev. **D76**, 057101 (2007).
66. T. Aaltonen *et al.* (CDF Collab.), Phys. Rev. Lett. **100**, 121803 (2012).
67. V. M. Abazov *et al.* (D0 Collab.), Phys. Rev. **D85**, 032006 (2012).
68. R. Aaij *et al.* (LHCb Collab.), Phys. Rev. Lett. **108**, 101803 (2012).
69. R. Aaij *et al.* (LHCb Collab.), Phys. Lett. **B707**, 497 (2012).
70. R. Aaij *et al.* [LHCb Collaboration], [arXiv:1202.4717 \[hep-ex\]](https://arxiv.org/abs/1202.4717), Submitted to Phys. Rev. Lett.
71. R. Ammar *et al.* (CLEO Collab.), Phys. Rev. Lett. **71**, 674 (1993).
72. P. Krokovny *et al.* (Belle Collab.), Phys. Rev. Lett. **89**, 231804 (2002); B. Aubert *et al.* (BaBar Collab.), Phys. Rev. Lett. **98**, 081801 (2007).
73. K. Ikado *et al.* (Belle Collab.), Phys. Rev. Lett. **97**, 251802 (2006); K. Hara *et al.* (Belle Collab.), Phys. Rev. **D82**, 071101 (2010).
74. B. Aubert *et al.* (BaBar Collab.), Phys. Rev. **D77**, 011107 (2008); B. Aubert *et al.* (BaBar Collab.), Phys. Rev. **D81**, 051101 (2010).
75. M. Beneke, J. Rohrer, and D. Yang, Nucl. Phys. **B774**, 64 (2007).
76. B. Aubert *et al.* (BaBar Collab.), Phys. Rev. Lett. **90**, 242001 (2003).
77. D. Besson *et al.* (CLEO Collab.), Phys. Rev. **D68**, 032002 (2003).
78. P. Krokovny *et al.* (Belle Collab.), Phys. Rev. Lett. **91**, 262002 (2003).
79. Y. Mikami *et al.* (Belle Collab.), Phys. Rev. Lett. **92**, 012002 (2004).
80. B. Aubert *et al.* (BaBar Collab.), Phys. Rev. Lett. **93**, 181801 (2004).
81. J. Brodzicka *et al.* (Belle Collab.), Phys. Rev. Lett. **100**, 092001 (2008).
82. B. Aubert *et al.* (BaBar Collab.), Phys. Rev. **D80**, 092003 (2009).
83. S.-K. Choi *et al.* (Belle Collab.), Phys. Rev. Lett. **91**, 262001 (2003).
84. D. Acosta *et al.* (CDF II Collab.), Phys. Rev. Lett. **93**, 072001 (2004).
85. B. Aubert *et al.* (BaBar Collab.), Phys. Rev. **D71**, 071103 (2005).
86. S.-K. Choi *et al.* (Belle Collab.), Phys. Rev. **D84**, 052004 (2011).
87. E.S. Swanson, Phys. Rep. **429**, 243 (2006).
88. B. Aubert *et al.* (BaBar Collab.), Phys. Rev. **D74**, 071101 (2006).
89. B. Aubert *et al.* (BaBar Collab.), Phys. Rev. Lett. **102**, 132001 (2009).
90. V. Bhardwaj *et al.* (Belle Collab.), Phys. Rev. Lett. **107**, 091803 (2011).
91. S.-K. Choi *et al.* (Belle Collab.), Phys. Rev. Lett. **94**, 182002 (2005).
92. B. Aubert *et al.* (BaBar Collab.), Phys. Rev. **D73**, 011101 (2006).
93. B. Aubert *et al.* (BaBar Collab.), Phys. Rev. Lett. **95**, 142001 (2005).
94. S.-K. Choi *et al.* (Belle Collab.), Phys. Rev. Lett. **100**, 142001 (2008); R. Mizuk *et al.* (Belle Collab.), Phys. Rev. **D80**, 031104 (2009).
95. B. Aubert *et al.* (BaBar Collab.), Phys. Rev. **D79**, 112001 (2009).
96. R. Mizuk *et al.* (Belle Collab.), Phys. Rev. **D78**, 072004 (2008).
97. J. P. Lees *et al.* (BaBar Collab.), Phys. Rev. **D85**, 052003 (2012).
98. J. P. Lees *et al.* (BaBar Collab.), Phys. Rev. **D84**, 112007 (2011); S. Blyth *et al.* (Belle Collab.), Phys. Rev. **D74**, 092002 (2006).

- 
99. R. Aaij *et al.* (LHCb Collab.), Phys. Lett. **B698**, 115 (2011); J. Li *et al.* (Belle Collab.), Phys. Rev. Lett. **106**, 121802 (2011); V. M. Abazov *et al.* (D0 Collab.), Phys. Rev. **D85**, 011103 (2012).
100. R. Aaij *et al.* (LHCb Collab.), Phys. Rev. Lett. **707**, 497 (2012).
101. R. Aaij *et al.* (LHCb Collab.), Phys. Rev. **D84**, 092001 (2011); *ibid.* Phys. Rev. **D85**, 039904 (2012); T. Aaltonen *et al.* (CDF Collab.), Phys. Rev. **D85**, 032003 (2012).
102. T. Aaltonen *et al.* (CDF Collab.), Phys. Rev. Lett. **107**, 261802 (2011).
103. T. Aaltonen *et al.* (CDF Collab.), Phys. Rev. Lett. **106**, 181802 (2011).
104. T. Aaltonen *et al.* (CDF Collab.), Phys. Rev. Lett. **103**, 031801 (2009).
105. R. Fleischer, Phys. Lett. **B459**, 306 (1999); D. London and J. Matias, Phys. Rev. **D70**, 031502 (2004).
106. B. Aubert *et al.* (BaBar Collab.), Phys. Rev. Lett. **97**, 171805 (2006).
107. S.-W. Lin *et al.* (Belle Collab.), Phys. Rev. Lett. **98**, 181804 (2007).
108. B. Aubert *et al.* (BaBar Collab.), Phys. Rev. Lett. **99**, 021603 (2007).
109. S.-W. Lin *et al.* (Belle Collab.), Nature **452** 332(2008).
110. See for example M. Gronau and J.L. Rosner, Phys. Rev. **D71**, 074019 (2005); M. Gronau, Phys. Lett. **B627**, 82 (2005).
111. B. Aubert *et al.* (BaBar Collab.), Phys. Rev. **D78**, 012004 (2008); A. Garmash *et al.* (Belle Collab.), Phys. Rev. Lett. **96**, 251803 (2006).
112. C.-T. Hoi *et al.* (Belle Collab.), Phys. Rev. Lett. **108**, 031801 (2012); B. Aubert *et al.* (BaBar Collab.), Phys. Rev. **D80**, 112002 (2009).
113. B. Aubert *et al.* (BaBar Collab.), Phys. Rev. Lett. **97**, 201802 (2006); C.H. Wang *et al.* (Belle Collab.), Phys. Rev. **D75**, 092005 (2007).
114. M. Gronau and D. London, Phys. Rev. Lett. **65**, 3381 (1990).
115. B. Aubert *et al.* (BaBar Collab.), Phys. Rev. **D78**, 071104 (2008); C.C. Chiang *et al.* (Belle Collab.), Phys. Rev. **D78**, 111102 (2008).
116. B. Aubert *et al.* (BaBar Collab.), Phys. Rev. Lett. **98**, 181803 (2007).
117. B. Aubert *et al.* (BaBar Collab.), Phys. Rev. **D81**, 052009 (2010).
118. See the “Polarization in *B* Decays,” by A. Gritsan and J.G. Smith in this *Review*.
119. A. Williamson and J. Zupan, Phys. Rev. **D74**, 014003 (2006).
120. B. Aubert *et al.* (BaBar Collab.), Phys. Rev. **D78**, 012004 (2008); A. Garmash *et al.* (Belle Collab.), Phys. Rev. Lett. **96**, 251803 (2006); P. Chang *et al.* (Belle Collab.), Phys. Lett. **B599**, 148 (2004); J.P. Lees *et al.* (BaBar Collab.), Phys. Rev. **D83**, 112010 (2011); A. Garmash *et al.* (Belle Collab.), Phys. Rev. **D75**, 012006 (2007); B. Aubert *et al.* (BaBar Collab.), Phys. Rev. **D80**, 112001 (2009).
121. A. Garmash *et al.* (Belle Collab.), Phys. Rev. **D71**, 092003 (2005); B. Aubert *et al.* (BaBar Collab.), Phys. Rev. **D74**, 032003 (2006); A. Garmash *et al.* (Belle Collab.), Phys. Rev. **D69**, 012001 (2004); B. Aubert *et al.* (BaBar Collab.), Phys. Rev. Lett. **93**, 181805 (2004); B. Aubert *et al.* (BaBar Collab.), Phys. Rev. Lett. **95**, 011801 (2005).
122. B. Aubert *et al.* (BaBar Collab.), Phys. Rev. **D74**, 051104R (2006); B. Aubert *et al.* (BaBar Collab.), Phys. Rev. **D76**, 071104R (2007).
123. B. Aubert *et al.* (BaBar Collab.), Phys. Rev. Lett. **99**, 221801 (2007).
124. M. Nakao *et al.* (Belle Collab.), Phys. Rev. **D69**, 112001 (2004); B. Aubert *et al.* (BaBar Collab.), Phys. Rev. Lett. **103**, 211802 (2009).
125. B. Aubert *et al.* (BaBar Collab.), Phys. Rev. **D70**, 091105R (2004); H. Yang *et al.* (Belle Collab.), Phys. Rev. Lett. **94**, 111802 (2005); S. Nishida *et al.* (Belle Collab.), Phys. Lett. **B610**, 23 (2005); B. Aubert *et al.* (BaBar Collab.), Phys. Rev. **D74**, 031102R (2004).
126. J. Wicht *et al.* (Belle Collab.), Phys. Rev. Lett. **100**, 121801 (2008).
127. A. Ali *et al.*, Phys. Lett. **B595**, 323 (2004); P. Ball, G. Jones, and R. Zwicky, Phys. Rev. **D75**, 054004 (2007).
128. J.L. Hewett, Phys. Rev. Lett. **70**, 1045 (1993).
129. S. Chen *et al.* (CLEO Collab.), Phys. Rev. Lett. **87**, 251807 (2001); B. Aubert *et al.* (BaBar Collab.), Phys. Rev. Lett. **97**, 171803 (2006).
130. A. Limosani *et al.* (Belle Collab.), Phys. Rev. Lett. **103**, 241801 (2009).
131. M. Misiak *et al.*, Phys. Rev. Lett. **98**, 022002 (2007).
132. T. Becher and M. Neubert, Phys. Rev. Lett. **98**, 022003 (2007).
133. L. Wolfenstein and Y.L. Wu, Phys. Rev. Lett. **73**, 2809 (1994); H.M. Asatrian and A. Ioannian, Phys. Rev. **D54**, 5642 (1996); M. Ciuchini *et al.*, Phys. Lett. **B388**, 353 (1996); S. Baek and P. Ko, Phys. Rev. Lett. **83**, 488 (1998); A.L. Kagan and M. Neubert, Phys. Rev. **D58**, 094012 (1998); K. Kiers *et al.*, Phys. Rev. **D62**, 116004 (2000).
134. S. Nishida *et al.* (Belle Collab.), Phys. Rev. Lett. **93**, 031803 (2004); B. Aubert *et al.* (BaBar Collab.), Phys. Rev. Lett. **101**, 171804 (2008).
135. B. Aubert *et al.* (BaBar Collab.), Phys. Rev. **D77**, 051103 (2008).
136. J.-T. Wei *et al.* (Belle Collab.), Phys. Rev. Lett. **103**, 171801 (2009).
137. B. Aubert *et al.* (BaBar Collab.), Phys. Rev. Lett. **102**, 091803 (2009).
138. T. Aaltonen *et al.* (CDF Collab.), Phys. Rev. Lett. **107**, 201802 (2011).
139. M. Iwasaki *et al.* (Belle Collab.), Phys. Rev. **D72**, 092005 (2005); B. Aubert *et al.* (BaBar Collab.), Phys. Rev. Lett. **93**, 081802 (2004).
140. The average is calculated by HFAG [33] including the recent unpublished value by Belle.
141. T. Aaltonen *et al.* (CDF Collab.), Phys. Rev. Lett. **106**, 161801 (2011).
142. T. Aaltonen *et al.* (CDF Collab.), Phys. Rev. Lett. **108**, 081807 (2012).
143. R. Aaij *et al.*, arXiv:1112.3515 [hep-ex].
144. R. Aaij *et al.* (LHCb Collab.), Phys. Lett. **B708**, 55 (2012).

# Meson Particle Listings

## $b$ -flavored hadrons, $b$ -flavored hadrons, $B^\pm$

145. G. Buchalla and A.J. Buras, Nucl. Phys. **B400**, 225 (1993); A.J. Buras, Phys. Lett. **B566**, 115 (2003).  
 146. T. Aaltonen *et al.* (CDF Collab.), Phys. Rev. Lett. **107**, 239903 (2011).  
 147. T. Aaltonen *et al.* (CDF Collab.), Phys. Rev. Lett. **102**, 201801 (2009).

### A NOTE ON HFAG ACTIVITIES

The Heavy Flavor Averaging Group (HFAG) has been formed, continuing the activities of the LEP Heavy Flavor Steering group, to provide the averages for measurements dedicated to the  $b$ -flavor related quantities. The HFAG consists of representatives and contacts from the experimental groups: BaBar, Belle, CDF, CLEO, DØ, LEP, SLD, and LHCb.

In the averaging the input parameters used in the various analyses are adjusted (rescaled) to common values, and all known correlations are taken into account. The HFAG has seven sub-groups providing averages for  $b$ -hadron lifetimes and  $B$ -oscillation parameters,  $CP$ -violation measurements, semileptonic parameters, rare branching fractions,  $b$ -hadron decays to charm, charm mixing and decays, and  $\tau$  decays. The averages provided by the HFAG are listed as "OUR EVALUATION" with a corresponding note.

The most up-to-date and complete listing of averages and more detailed information on the averaging procedures are available at:

<http://www.slac.stanford.edu/xorg/hfag>.

**$B^\pm$**

$$I(J^P) = \frac{1}{2}(0^-)$$

Quantum numbers not measured. Values shown are quark-model predictions.

See also the  $B^\pm/B^0$  ADMIXTURE and  $B^\pm/B^0/B_s^0/b$ -baryon ADMIXTURE sections.

### $B^\pm$ MASS

The fit uses  $m_{B^{*+}}$  ( $m_{B^0} - m_{B^+}$ ), and  $m_{B^0}$  to determine  $m_{B^+}$ ,  $m_{B^0}$ , and the mass difference.

VALUE (MeV)	EVTS	DOCUMENT ID	TECN	COMMENT
<b>5279.25 ± 0.17 OUR FIT</b>				
<b>5279.25 ± 0.26 OUR AVERAGE</b>				
5279.38 ± 0.11 ± 0.33		<sup>1</sup> AAIJ	12E LHCb	$p\bar{p}$ at 7 TeV
5279.10 ± 0.41 ± 0.36		<sup>2</sup> ACOSTA	06 CDF	$p\bar{p}$ at 1.96 TeV
5279.1 ± 0.4 ± 0.4	526	<sup>3</sup> CSORNA	00 CLE2	$e^+e^- \rightarrow \Upsilon(4S)$
5279.1 ± 1.7 ± 1.4	147	ABE	96B CDF	$p\bar{p}$ at 1.8 TeV
• • • We do not use the following data for averages, fits, limits, etc. • • •				
5278.8 ± 0.54 ± 2.0	362	ALAM	94 CLE2	$e^+e^- \rightarrow \Upsilon(4S)$
5278.3 ± 0.4 ± 2.0		BORTOLETTO	092 CLEO	$e^+e^- \rightarrow \Upsilon(4S)$
5280.5 ± 1.0 ± 2.0		<sup>4</sup> ALBRECHT	90J ARG	$e^+e^- \rightarrow \Upsilon(4S)$
5275.8 ± 1.3 ± 3.0	32	ALBRECHT	87c ARG	$e^+e^- \rightarrow \Upsilon(4S)$
5278.2 ± 1.8 ± 3.0	12	<sup>5</sup> ALBRECHT	87D ARG	$e^+e^- \rightarrow \Upsilon(4S)$
5278.6 ± 0.8 ± 2.0		BEBEK	87 CLEO	$e^+e^- \rightarrow \Upsilon(4S)$

<sup>1</sup> Uses  $B^+ \rightarrow J/\psi K^+$  fully reconstructed decays.

<sup>2</sup> Uses exclusively reconstructed final states containing a  $J/\psi \rightarrow \mu^+ \mu^-$  decays.

<sup>3</sup> CSORNA 00 uses fully reconstructed 526  $B^+ \rightarrow J/\psi(\ell^+) K^+$  events and invariant masses without beam constraint.

<sup>4</sup> ALBRECHT 90J assumes 10580 for  $\Upsilon(4S)$  mass. Supersedes ALBRECHT 87c and ALBRECHT 87D.

<sup>5</sup> Found using fully reconstructed decays with  $J/\psi(1S)$ . ALBRECHT 87D assume  $m_{\Upsilon(4S)} = 10577$  MeV.

### $B^\pm$ MEAN LIFE

See  $B^\pm/B^0/B_s^0/b$ -baryon ADMIXTURE section for data on  $B$ -hadron mean life averaged over species of bottom particles.

"OUR EVALUATION" is an average using rescaled values of the data listed below. The average and rescaling were performed by the Heavy Flavor Averaging Group (HFAG) and are described at <http://www.slac.stanford.edu/xorg/hfag/>. The averaging/rescaling procedure takes into account correlations between the measurements and asymmetric lifetime errors.

VALUE ( $10^{-12}$ s)	EVTS	DOCUMENT ID	TECN	COMMENT
<b>1.641 ± 0.008 OUR EVALUATION</b>				
1.639 ± 0.009 ± 0.009		<sup>1</sup> AALTONEN	11 CDF	$p\bar{p}$ at 1.96 TeV
1.663 ± 0.023 ± 0.015		<sup>2</sup> AALTONEN	11B CDF	$p\bar{p}$ at 1.96 TeV
1.635 ± 0.011 ± 0.011		<sup>3</sup> ABE	05B BELL	$e^+e^- \rightarrow \Upsilon(4S)$
1.624 ± 0.014 ± 0.018		<sup>4</sup> ABDALLAH	04E DLPH	$e^+e^- \rightarrow Z$
1.636 ± 0.058 ± 0.025		<sup>5</sup> ACOSTA	02C CDF	$p\bar{p}$ at 1.8 TeV
1.673 ± 0.032 ± 0.023		<sup>6</sup> AUBERT	01F BABR	$e^+e^- \rightarrow \Upsilon(4S)$
1.648 ± 0.049 ± 0.035		<sup>7</sup> BARATE	00R ALEP	$e^+e^- \rightarrow Z$
1.643 ± 0.037 ± 0.025		<sup>8</sup> ABBIENDI	99J OPAL	$e^+e^- \rightarrow Z$
1.637 ± 0.058 ± 0.045 ± 0.043		<sup>7</sup> ABE	98Q CDF	$p\bar{p}$ at 1.8 TeV
1.66 ± 0.06 ± 0.03		<sup>8</sup> ACCIARRI	98s L3	$e^+e^- \rightarrow Z$
1.66 ± 0.06 ± 0.05		<sup>8</sup> ABE	97J SLD	$e^+e^- \rightarrow Z$
1.58 +0.21 -0.18 +0.04 -0.03	94	<sup>5</sup> BUSKULIC	96J ALEP	$e^+e^- \rightarrow Z$
1.61 ± 0.16 ± 0.12		<sup>7,9</sup> ABREU	95Q DLPH	$e^+e^- \rightarrow Z$
1.72 ± 0.08 ± 0.06		<sup>10</sup> ADAM	95 DLPH	$e^+e^- \rightarrow Z$
1.52 ± 0.14 ± 0.09		<sup>7</sup> AKERS	95T OPAL	$e^+e^- \rightarrow Z$
• • • We do not use the following data for averages, fits, limits, etc. • • •				
1.695 ± 0.026 ± 0.015		<sup>6</sup> ABE	02H BELL	Repl. by ABE 05B
1.68 ± 0.07 ± 0.02		<sup>5</sup> ABE	98B CDF	Repl. by ACOSTA 02C
1.56 ± 0.13 ± 0.06		<sup>7</sup> ABE	96C CDF	Repl. by ABE 98Q
1.58 ± 0.09 ± 0.03		<sup>11</sup> BUSKULIC	96J ALEP	$e^+e^- \rightarrow Z$
1.58 ± 0.09 ± 0.04		<sup>7</sup> BUSKULIC	96J ALEP	Repl. by BARATE 00R
1.70 ± 0.09		<sup>12</sup> ADAM	95 DLPH	$e^+e^- \rightarrow Z$
1.61 ± 0.16 ± 0.05	148	<sup>5</sup> ABE	94D CDF	Repl. by ABE 98B
1.30 +0.33 -0.29 ± 0.16	92	<sup>7</sup> ABREU	93D DLPH	Sup. by ABREU 95Q
1.56 ± 0.19 ± 0.13	134	<sup>10</sup> ABREU	93G DLPH	Sup. by ADAM 95
1.51 +0.30 -0.28 ± 0.12 ± 0.14	59	<sup>7</sup> ACTON	93C OPAL	Sup. by AKERS 95T
1.47 +0.22 -0.19 ± 0.15 ± 0.14	77	<sup>7</sup> BUSKULIC	93D ALEP	Sup. by BUSKULIC 96J

<sup>1</sup> Measured mean life using fully reconstructed decays ( $J/\psi K^{(*)}$ ).

<sup>2</sup> Measured using  $B^- \rightarrow D^0 \pi^-$  with  $D^0 \rightarrow K^- \pi^+$  events that were selected using a silicon vertex trigger.

<sup>3</sup> Measurement performed using a combined fit of  $CP$ -violation, mixing and lifetimes.

<sup>4</sup> Measurement performed using an inclusive reconstruction and  $B$  flavor identification technique.

<sup>5</sup> Measured mean life using fully reconstructed decays.

<sup>6</sup> Events are selected in which one  $B$  meson is fully reconstructed while the second  $B$  meson is reconstructed inclusively.

<sup>7</sup> Data analyzed using  $D/D^* \ell X$  event vertices.

<sup>8</sup> Data analyzed using charge of secondary vertex.

<sup>9</sup> ABREU 95Q assumes  $B(B^0 \rightarrow D^{*-} \ell^+ \nu_\ell) = 3.2 \pm 1.7\%$ .

<sup>10</sup> Data analyzed using vertex-charge technique to tag  $B$  charge.

<sup>11</sup> Combined result of  $D/D^* \ell X$  analysis and fully reconstructed  $B$  analysis.

<sup>12</sup> Combined ABREU 95Q and ADAM 95 result.

### $B^+$ DECAY MODES

$B^-$  modes are charge conjugates of the modes below. Modes which do not identify the charge state of the  $B$  are listed in the  $B^\pm/B^0$  ADMIXTURE section.

The branching fractions listed below assume 50%  $B^0 \bar{B}^0$  and 50%  $B^+ B^-$  production at the  $\Upsilon(4S)$ . We have attempted to bring older measurements up to date by rescaling their assumed  $\Upsilon(4S)$  production ratio to 50:50 and their assumed  $D, D_s, D^*$ , and  $\psi$  branching ratios to current values whenever this would affect our averages and best limits significantly.

Indentation is used to indicate a subchannel of a previous reaction. All resonant subchannels have been corrected for resonance branching fractions to the final state so the sum of the subchannel branching fractions can exceed that of the final state.

For inclusive branching fractions, e.g.,  $B \rightarrow D^\pm$  anything, the values usually are multiplicities, not branching fractions. They can be greater than one.

Mode	Fraction ( $\Gamma_i/\Gamma$ )	Scale factor/ Confidence level
<b>Semileptonic and leptonic modes</b>		
$\Gamma_1$ $\ell^+ \nu_\ell$ anything	[a] ( 10.99 $\pm$ 0.28 ) %	
$\Gamma_2$ $e^+ \nu_e X_c$	( 10.8 $\pm$ 0.4 ) %	
$\Gamma_3$ $D \ell^+ \nu_\ell$ anything	( 9.8 $\pm$ 0.7 ) %	
$\Gamma_4$ $\overline{D}^0 \ell^+ \nu_\ell$	[a] ( 2.26 $\pm$ 0.11 ) %	
$\Gamma_5$ $\overline{D}^0 \tau^+ \nu_\tau$	( 7.7 $\pm$ 2.5 ) $\times 10^{-3}$	
$\Gamma_6$ $\overline{D}^*(2007)^0 \ell^+ \nu_\ell$	[a] ( 5.70 $\pm$ 0.19 ) %	
$\Gamma_7$ $\overline{D}^*(2007)^0 \tau^+ \nu_\tau$	( 2.04 $\pm$ 0.30 ) %	
$\Gamma_8$ $D^- \pi^+ \ell^+ \nu_\ell$	( 4.2 $\pm$ 0.5 ) $\times 10^{-3}$	
$\Gamma_9$ $\overline{D}_0^*(2420)^0 \ell^+ \nu_\ell \times$ $B(\overline{D}_0^{*0} \rightarrow D^- \pi^+)$	( 2.5 $\pm$ 0.5 ) $\times 10^{-3}$	
$\Gamma_{10}$ $\overline{D}_2^*(2460)^0 \ell^+ \nu_\ell \times$ $B(\overline{D}_2^{*0} \rightarrow D^- \pi^+)$	( 1.53 $\pm$ 0.16 ) $\times 10^{-3}$	
$\Gamma_{11}$ $D^*(n \pi \ell^+ \nu_\ell (n \geq 1))$	( 1.87 $\pm$ 0.26 ) %	
$\Gamma_{12}$ $D^{*-} \pi^+ \ell^+ \nu_\ell$	( 6.1 $\pm$ 0.6 ) $\times 10^{-3}$	
$\Gamma_{13}$ $D_s^- K^+ \ell^+ \nu_\ell$	( 6.1 $\pm$ 1.2 ) $\times 10^{-4}$	
$\Gamma_{14}$ $\overline{D}_1(2420)^0 \ell^+ \nu_\ell \times B(\overline{D}_1^0 \rightarrow$ $D^{*-} \pi^+)$	( 3.03 $\pm$ 0.20 ) $\times 10^{-3}$	
$\Gamma_{15}$ $\overline{D}_1^*(2430)^0 \ell^+ \nu_\ell \times B(\overline{D}_1^{*0} \rightarrow$ $D^{*-} \pi^+)$	( 2.7 $\pm$ 0.6 ) $\times 10^{-3}$	
$\Gamma_{16}$ $\overline{D}_2^*(2460)^0 \ell^+ \nu_\ell \times$ $B(\overline{D}_2^{*0} \rightarrow D^{*-} \pi^+)$	( 1.01 $\pm$ 0.24 ) $\times 10^{-3}$	S=2.0
$\Gamma_{17}$ $\pi^0 \ell^+ \nu_\ell$	( 7.78 $\pm$ 0.28 ) $\times 10^{-5}$	
$\Gamma_{18}$ $\pi^0 e^+ \nu_e$		
$\Gamma_{19}$ $\eta \ell^+ \nu_\ell$	( 3.9 $\pm$ 0.8 ) $\times 10^{-5}$	S=1.3
$\Gamma_{20}$ $\eta' \ell^+ \nu_\ell$	( 2.3 $\pm$ 0.8 ) $\times 10^{-5}$	
$\Gamma_{21}$ $\omega \ell^+ \nu_\ell$	[a] ( 1.15 $\pm$ 0.17 ) $\times 10^{-4}$	
$\Gamma_{22}$ $\omega \mu^+ \nu_\mu$		
$\Gamma_{23}$ $\rho^0 \ell^+ \nu_\ell$	[a] ( 1.07 $\pm$ 0.13 ) $\times 10^{-4}$	
$\Gamma_{24}$ $p \bar{p} e^+ \nu_e$	< 5.2 $\times 10^{-3}$	CL=90%
$\Gamma_{25}$ $e^+ \nu_e$	< 9.8 $\times 10^{-7}$	CL=90%
$\Gamma_{26}$ $\mu^+ \nu_\mu$	< 1.0 $\times 10^{-6}$	CL=90%
$\Gamma_{27}$ $\tau^+ \nu_\tau$	( 1.65 $\pm$ 0.34 ) $\times 10^{-4}$	
$\Gamma_{28}$ $\ell^+ \nu_\ell \gamma$	< 1.56 $\times 10^{-5}$	CL=90%
$\Gamma_{29}$ $e^+ \nu_e \gamma$	< 1.7 $\times 10^{-5}$	CL=90%
$\Gamma_{30}$ $\mu^+ \nu_\mu \gamma$	< 2.4 $\times 10^{-5}$	CL=90%
<b>Inclusive modes</b>		
$\Gamma_{31}$ $D^0 X$	( 8.6 $\pm$ 0.7 ) %	
$\Gamma_{32}$ $\overline{D}^0 X$	( 79 $\pm$ 4 ) %	
$\Gamma_{33}$ $D^+ X$	( 2.5 $\pm$ 0.5 ) %	
$\Gamma_{34}$ $D^- X$	( 9.9 $\pm$ 1.2 ) %	
$\Gamma_{35}$ $D_s^+ X$	( 7.9 $\pm$ 1.4 -1.3 ) %	
$\Gamma_{36}$ $D_s^- X$	( 1.10 $\pm$ 0.40 -0.32 ) %	
$\Gamma_{37}$ $\Lambda_c^+ X$	( 2.1 $\pm$ 0.9 -0.6 ) %	
$\Gamma_{38}$ $\overline{\Lambda}_c^- X$	( 2.8 $\pm$ 1.1 -0.9 ) %	
$\Gamma_{39}$ $\bar{c} X$	( 97 $\pm$ 4 ) %	
$\Gamma_{40}$ $c X$	( 23.4 $\pm$ 2.2 -1.8 ) %	
$\Gamma_{41}$ $\bar{c} c X$	( 120 $\pm$ 6 ) %	
<b>D, D*, or D<sub>s</sub> modes</b>		
$\Gamma_{42}$ $\overline{D}^0 \pi^+$	( 4.81 $\pm$ 0.15 ) $\times 10^{-3}$	
$\Gamma_{43}$ $D_{CP(+)} \pi^+$	[b] ( 2.5 $\pm$ 0.4 ) $\times 10^{-3}$	
$\Gamma_{44}$ $D_{CP(-)} \pi^+$	[b] ( 2.0 $\pm$ 0.4 ) $\times 10^{-3}$	
$\Gamma_{45}$ $\overline{D}^0 \rho^+$	( 1.34 $\pm$ 0.18 ) %	
$\Gamma_{46}$ $\overline{D}^0 K^+$	( 3.65 $\pm$ 0.33 ) $\times 10^{-4}$	
$\Gamma_{47}$ $D_{CP(+)} K^+$	[b] ( 2.18 $\pm$ 0.26 ) $\times 10^{-4}$	
$\Gamma_{48}$ $D_{CP(-)} K^+$	[b] ( 1.97 $\pm$ 0.24 ) $\times 10^{-4}$	
$\Gamma_{49}$ $[K^+ \pi^-]_D K^+$	[c] < 2.8 $\times 10^{-7}$	CL=90%
$\Gamma_{50}$ $[K^+ \pi^-]_D K^+$	[c] < 1.8 $\times 10^{-5}$	CL=90%
$\Gamma_{51}$ $[K^+ \pi^+ \pi^0]_D K^+$		
$\Gamma_{52}$ $[K^+ \pi^- \pi^0]_D K^+$		
$\Gamma_{53}$ $[K^+ \pi^+ \pi^0]_D K^*(892)^+$	[c]	
$\Gamma_{54}$ $[K^+ \pi^- \pi^0]_D K^*(892)^+$	[c]	
$\Gamma_{55}$ $[K^+ \pi^+ \pi^0]_D \pi^+$	[c] ( 6.3 $\pm$ 1.1 ) $\times 10^{-7}$	
$\Gamma_{56}$ $[K^+ \pi^- \pi^0]_D \pi^+$	( 2.0 $\pm$ 0.4 ) $\times 10^{-4}$	
$\Gamma_{57}$ $[K^+ \pi^+ \pi^0]_{(D \pi)} \pi^+$		
$\Gamma_{58}$ $[K^+ \pi^-]_{(D \pi)} \pi^+$		
$\Gamma_{59}$ $[K^- \pi^+]_{(D \gamma)} \pi^+$		
$\Gamma_{60}$ $[K^+ \pi^-]_{(D \gamma)} \pi^+$		
$\Gamma_{61}$ $[K^- \pi^+]_{(D \pi)} K^+$		
$\Gamma_{62}$ $[K^+ \pi^-]_{(D \pi)} K^+$		
$\Gamma_{63}$ $[K^- \pi^+]_{(D \gamma)} K^+$		
$\Gamma_{64}$ $[K^+ \pi^-]_{(D \gamma)} K^+$		
$\Gamma_{65}$ $[\pi^+ \pi^- \pi^0]_D K^-$	( 4.6 $\pm$ 0.9 ) $\times 10^{-6}$	
$\Gamma_{66}$ $\overline{D}^0 K^*(892)^+$	( 5.3 $\pm$ 0.4 ) $\times 10^{-4}$	
$\Gamma_{67}$ $D_{CP(-)} K^*(892)^+$	[b] ( 2.7 $\pm$ 0.8 ) $\times 10^{-4}$	
$\Gamma_{68}$ $D_{CP(+)} K^*(892)^+$	[b] ( 5.8 $\pm$ 1.1 ) $\times 10^{-4}$	
$\Gamma_{69}$ $\overline{D}^0 K^+ \overline{K}^0$	( 5.5 $\pm$ 1.6 ) $\times 10^{-4}$	
$\Gamma_{70}$ $\overline{D}^0 K^+ \overline{K}^*(892)^0$	( 7.5 $\pm$ 1.7 ) $\times 10^{-4}$	
$\Gamma_{71}$ $\overline{D}^0 \pi^+ \pi^+ \pi^-$	( 5.7 $\pm$ 2.2 ) $\times 10^{-3}$	S=3.6
$\Gamma_{72}$ $\overline{D}^0 \pi^+ \pi^+ \pi^-$ nonresonant	( 5 $\pm$ 4 ) $\times 10^{-3}$	
$\Gamma_{73}$ $\overline{D}^0 \pi^+ \rho^0$	( 4.2 $\pm$ 3.0 ) $\times 10^{-3}$	
$\Gamma_{74}$ $\overline{D}^0 a_1(1260)^+$	( 4 $\pm$ 4 ) $\times 10^{-3}$	
$\Gamma_{75}$ $\overline{D}^0 \omega \pi^+$	( 4.1 $\pm$ 0.9 ) $\times 10^{-3}$	
$\Gamma_{76}$ $D^*(2010)^- \pi^+ \pi^+$	( 1.35 $\pm$ 0.22 ) $\times 10^{-3}$	
$\Gamma_{77}$ $\overline{D}_1(2420)^0 \pi^+ \times B(\overline{D}_1^0 \rightarrow$ $D^*(2010)^- \pi^+)$	( 5.3 $\pm$ 2.3 ) $\times 10^{-4}$	
$\Gamma_{78}$ $D^- \pi^+ \pi^+$	( 1.07 $\pm$ 0.05 ) $\times 10^{-3}$	
$\Gamma_{79}$ $D^+ K^0$	< 2.9 $\times 10^{-6}$	CL=90%
$\Gamma_{80}$ $D^+ K^{*0}$	< 3.0 $\times 10^{-6}$	CL=90%
$\Gamma_{81}$ $\overline{D}^*(2007)^0 \pi^+$	( 5.18 $\pm$ 0.26 ) $\times 10^{-3}$	
$\Gamma_{82}$ $\overline{D}_{CP(+)}^0 \pi^+$	[d] ( 2.9 $\pm$ 0.7 ) $\times 10^{-3}$	
$\Gamma_{83}$ $\overline{D}_{CP(-)}^0 \pi^+$	[d] ( 2.6 $\pm$ 1.0 ) $\times 10^{-3}$	
$\Gamma_{84}$ $\overline{D}^*(2007)^0 \omega \pi^+$	( 4.5 $\pm$ 1.2 ) $\times 10^{-3}$	
$\Gamma_{85}$ $\overline{D}^*(2007)^0 \rho^+$	( 9.8 $\pm$ 1.7 ) $\times 10^{-3}$	
$\Gamma_{86}$ $\overline{D}^*(2007)^0 K^+$	( 4.20 $\pm$ 0.34 ) $\times 10^{-4}$	
$\Gamma_{87}$ $\overline{D}_{CP(+)}^0 K^+$	[d] ( 2.8 $\pm$ 0.4 ) $\times 10^{-4}$	
$\Gamma_{88}$ $\overline{D}_{CP(-)}^0 K^+$	[d] ( 2.31 $\pm$ 0.33 ) $\times 10^{-4}$	
$\Gamma_{89}$ $\overline{D}^*(2007)^0 K^*(892)^+$	( 8.1 $\pm$ 1.4 ) $\times 10^{-4}$	
$\Gamma_{90}$ $\overline{D}^*(2007)^0 K^+ \overline{K}^0$	< 1.06 $\times 10^{-3}$	CL=90%
$\Gamma_{91}$ $\overline{D}^*(2007)^0 K^+ K^*(892)^0$	( 1.5 $\pm$ 0.4 ) $\times 10^{-3}$	
$\Gamma_{92}$ $\overline{D}^*(2007)^0 \pi^+ \pi^+ \pi^-$	( 1.03 $\pm$ 0.12 ) %	
$\Gamma_{93}$ $\overline{D}^*(2007)^0 a_1(1260)^+$	( 1.9 $\pm$ 0.5 ) %	
$\Gamma_{94}$ $\overline{D}^*(2007)^0 \pi^- \pi^+ \pi^+ \pi^0$	( 1.8 $\pm$ 0.4 ) %	
$\Gamma_{95}$ $\overline{D}^{*0} 3\pi^+ 2\pi^-$	( 5.7 $\pm$ 1.2 ) $\times 10^{-3}$	
$\Gamma_{96}$ $D^*(2010)^+ \pi^0$	< 3.6 $\times 10^{-6}$	
$\Gamma_{97}$ $D^*(2010)^+ K^0$	< 9.0 $\times 10^{-6}$	CL=90%
$\Gamma_{98}$ $D^*(2010)^- \pi^+ \pi^+ \pi^0$	( 1.5 $\pm$ 0.7 ) %	
$\Gamma_{99}$ $D^*(2010)^- \pi^+ \pi^+ \pi^+ \pi^-$	( 2.6 $\pm$ 0.4 ) $\times 10^{-3}$	
$\Gamma_{100}$ $\overline{D}^{*0} \pi^+$	[e] ( 5.9 $\pm$ 1.3 ) $\times 10^{-3}$	
$\Gamma_{101}$ $\overline{D}_1^+(2420)^0 \pi^+$	( 1.5 $\pm$ 0.6 ) $\times 10^{-3}$	S=1.3
$\Gamma_{102}$ $\overline{D}_1(2420)^0 \pi^+ \times B(\overline{D}_1^0 \rightarrow$ $\overline{D}^0 \pi^+ \pi^-)$	( 2.5 $\pm$ 1.7 -1.4 ) $\times 10^{-4}$	S=4.0
$\Gamma_{103}$ $\overline{D}_1(2420)^0 \pi^+ \times B(\overline{D}_1^0 \rightarrow$ $\overline{D}^0 \pi^+ \pi^- (nonresonant))$	( 2.3 $\pm$ 1.0 ) $\times 10^{-4}$	
$\Gamma_{104}$ $\overline{D}_2^*(2462)^0 \pi^+$ $\times B(\overline{D}_2^{*0}(2462)^0 \rightarrow D^- \pi^+)$	( 3.5 $\pm$ 0.4 ) $\times 10^{-4}$	
$\Gamma_{105}$ $\overline{D}_2^*(2462)^0 \pi^+ \times B(\overline{D}_2^{*0} \rightarrow$ $\overline{D}^0 \pi^- \pi^+)$	( 2.3 $\pm$ 1.1 ) $\times 10^{-4}$	
$\Gamma_{106}$ $\overline{D}_2^*(2462)^0 \pi^+ \times B(\overline{D}_2^{*0} \rightarrow$ $\overline{D}^0 \pi^- \pi^+ (nonresonant))$	< 1.7 $\times 10^{-4}$	CL=90%
$\Gamma_{107}$ $\overline{D}_2^*(2462)^0 \pi^+ \times B(\overline{D}_2^{*0} \rightarrow$ $D^*(2010)^- \pi^+)$	( 2.2 $\pm$ 1.1 ) $\times 10^{-4}$	
$\Gamma_{108}$ $\overline{D}_0^*(2400)^0 \pi^+$ $\times B(\overline{D}_0^{*0}(2400)^0 \rightarrow D^- \pi^+)$	( 6.4 $\pm$ 1.4 ) $\times 10^{-4}$	
$\Gamma_{109}$ $\overline{D}_1(2421)^0 \pi^+$ $\times B(\overline{D}_1^0(2421)^0 \rightarrow D^{*-} \pi^+)$	( 6.8 $\pm$ 1.5 ) $\times 10^{-4}$	
$\Gamma_{110}$ $\overline{D}_2^*(2462)^0 \pi^+$ $\times B(\overline{D}_2^{*0}(2462)^0 \rightarrow D^{*-} \pi^+)$	( 1.8 $\pm$ 0.5 ) $\times 10^{-4}$	
$\Gamma_{111}$ $\overline{D}_1^+(2427)^0 \pi^+$ $\times B(\overline{D}_1^0(2427)^0 \rightarrow D^{*-} \pi^+)$	( 5.0 $\pm$ 1.2 ) $\times 10^{-4}$	
$\Gamma_{112}$ $\overline{D}_1(2420)^0 \pi^+ \times B(\overline{D}_1^0 \rightarrow$ $\overline{D}^{*0} \pi^+ \pi^-)$	< 6 $\times 10^{-6}$	CL=90%
$\Gamma_{113}$ $\overline{D}_1^+(2420)^0 \rho^+$	< 1.4 $\times 10^{-3}$	CL=90%
$\Gamma_{114}$ $\overline{D}_2^*(2460)^0 \pi^+$	< 1.3 $\times 10^{-3}$	CL=90%

## Meson Particle Listings

 $B^\pm$ 

$\Gamma_{115}$	$\bar{D}_s^0(2460)^0 \pi^+ \times B(\bar{D}_s^0 \pi^+ \pi^-)$	$< 2.2$	$\times 10^{-5}$	CL=90%	$\Gamma_{163}$	$D_s^{*+} \rho^0$	$< 4$	$\times 10^{-4}$	CL=90%
$\Gamma_{116}$	$\bar{D}_s^0(2460)^0 \rho^+$	$< 4.7$	$\times 10^{-3}$	CL=90%	$\Gamma_{164}$	$D_s^+ \omega$	$< 4$	$\times 10^{-4}$	CL=90%
$\Gamma_{117}$	$\bar{D}_s^0 D_s^+$	$(10.0 \pm 1.7)$	$\times 10^{-3}$		$\Gamma_{165}$	$D_s^{*+} \omega$	$< 6$	$\times 10^{-4}$	CL=90%
$\Gamma_{118}$	$D_{s0}(2317)^+ \bar{D}^0 \times$ $B(D_{s0}(2317)^+ \rightarrow D_s^+ \pi^0)$	$(7.3 \pm 2.2)$	$\times 10^{-4}$		$\Gamma_{166}$	$D_s^+ a_1(1260)^0$	$< 1.8$	$\times 10^{-3}$	CL=90%
$\Gamma_{119}$	$D_{s0}(2317)^+ \bar{D}^0 \times$ $B(D_{s0}(2317)^+ \rightarrow D_s^{*+} \gamma)$	$< 7.6$	$\times 10^{-4}$	CL=90%	$\Gamma_{167}$	$D_s^+ a_1(1260)^0$	$< 1.3$	$\times 10^{-3}$	CL=90%
$\Gamma_{120}$	$D_{s0}(2317)^+ \bar{D}^*(2007)^0 \times$ $B(D_{s0}(2317)^+ \rightarrow D_s^+ \pi^0)$	$(9 \pm 7)$	$\times 10^{-4}$		$\Gamma_{168}$	$D_s^+ \phi$	$< 1.9$	$\times 10^{-6}$	CL=90%
$\Gamma_{121}$	$D_{sJ}(2457)^+ \bar{D}^0$	$(3.1 \pm 1.0)$	$\times 10^{-3}$		$\Gamma_{169}$	$D_s^+ \phi$	$< 1.2$	$\times 10^{-5}$	CL=90%
$\Gamma_{122}$	$D_{sJ}(2457)^+ \bar{D}^0 \times$ $B(D_{sJ}(2457)^+ \rightarrow D_s^+ \gamma)$	$(4.6 \pm 1.3)$	$\times 10^{-4}$		$\Gamma_{170}$	$D_s^+ \bar{K}^0$	$< 8$	$\times 10^{-4}$	CL=90%
$\Gamma_{123}$	$D_{sJ}(2457)^+ \bar{D}^0 \times$ $B(D_{sJ}(2457)^+ \rightarrow D_s^+ \pi^+ \pi^-)$	$< 2.2$	$\times 10^{-4}$	CL=90%	$\Gamma_{171}$	$D_s^+ \bar{K}^0$	$< 9$	$\times 10^{-4}$	CL=90%
$\Gamma_{124}$	$D_{sJ}(2457)^+ \bar{D}^0 \times$ $B(D_{sJ}(2457)^+ \rightarrow D_s^+ \pi^0)$	$< 2.7$	$\times 10^{-4}$	CL=90%	$\Gamma_{172}$	$D_s^+ \bar{K}^*(892)^0$	$< 4$	$\times 10^{-4}$	CL=90%
$\Gamma_{125}$	$D_{sJ}(2457)^+ \bar{D}^0 \times$ $B(D_{sJ}(2457)^+ \rightarrow D_s^{*+} \gamma)$	$< 9.8$	$\times 10^{-4}$	CL=90%	$\Gamma_{173}$	$D_s^+ \bar{K}^*(892)^0$	$< 3.5$	$\times 10^{-4}$	CL=90%
$\Gamma_{126}$	$D_{sJ}(2457)^+ \bar{D}^*(2007)^0$	$(1.20 \pm 0.30)$	%		$\Gamma_{174}$	$D_s^- \pi^+ K^+$	$(1.80 \pm 0.22)$	$\times 10^{-4}$	
$\Gamma_{127}$	$D_{sJ}(2457)^+ \bar{D}^*(2007)^0 \times$ $B(D_{sJ}(2457)^+ \rightarrow D_s^+ \gamma)$	$(1.4 \pm 0.7)$	$\times 10^{-3}$		$\Gamma_{175}$	$D_s^- \pi^+ K^+$	$(1.45 \pm 0.24)$	$\times 10^{-4}$	
$\Gamma_{128}$	$\bar{D}^0 D_{s1}(2536)^+ \times$ $B(D_{s1}(2536)^+ \rightarrow D^*(2007)^0 K^+ + D^*(2010)^+ K^0)$	$(4.0 \pm 1.0)$	$\times 10^{-4}$		$\Gamma_{176}$	$D_s^- \pi^+ K^*(892)^+$	$< 5$	$\times 10^{-3}$	CL=90%
$\Gamma_{129}$	$\bar{D}^0 D_{s1}(2536)^+ \times$ $B(D_{s1}(2536)^+ \rightarrow D^*(2007)^0 K^+)$	$(2.2 \pm 0.7)$	$\times 10^{-4}$		$\Gamma_{177}$	$D_s^- \pi^+ K^*(892)^+$	$< 7$	$\times 10^{-3}$	CL=90%
$\Gamma_{130}$	$\bar{D}^*(2007)^0 D_{s1}(2536)^+ \times$ $B(D_{s1}(2536)^+ \rightarrow D^*(2007)^0 K^+)$	$(5.5 \pm 1.6)$	$\times 10^{-4}$		$\Gamma_{178}$	$D_s^- K^+ K^+$	$(1.1 \pm 0.4)$	$\times 10^{-5}$	
$\Gamma_{131}$	$\bar{D}^0 D_{s1}(2536)^+ \times$ $B(D_{s1}(2536)^+ \rightarrow D^{*+} K^0)$	$(2.3 \pm 1.1)$	$\times 10^{-4}$		$\Gamma_{179}$	$D_s^- K^+ K^+$	$< 1.5$	$\times 10^{-5}$	CL=90%
$\Gamma_{132}$	$\bar{D}^0 D_{sJ}(2700)^+ \times$ $B(D_{sJ}(2700)^+ \rightarrow D^0 K^+)$	$(1.13 \pm 0.26)$	$\times 10^{-3}$		<b>Charmonium modes</b>				
$\Gamma_{133}$	$\bar{D}^{*0} D_{s1}(2536)^+ \times$ $B(D_{s1}(2536)^+ \rightarrow D^{*+} K^0)$	$(3.9 \pm 2.6)$	$\times 10^{-4}$		$\Gamma_{180}$	$\eta_c K^+$	$(9.6 \pm 1.2)$	$\times 10^{-4}$	
$\Gamma_{134}$	$\bar{D}^{*0} D_{sJ}(2573)^+ \times$ $B(D_{sJ}(2573)^+ \rightarrow D^0 K^+)$	$< 2$	$\times 10^{-4}$	CL=90%	$\Gamma_{181}$	$\eta_c K^+, \eta_c \rightarrow K_S^0 K^\mp \pi^\pm$	$(2.7 \pm 0.6)$	$\times 10^{-5}$	
$\Gamma_{135}$	$\bar{D}^*(2007)^0 D_{sJ}(2573)^+ \times$ $B(D_{sJ}(2573)^+ \rightarrow D^0 K^+)$	$< 5$	$\times 10^{-4}$	CL=90%	$\Gamma_{182}$	$\eta_c K^*(892)^+$	$(1.1 \pm 0.5)$	$\times 10^{-3}$	
$\Gamma_{136}$	$\bar{D}^0 D_s^{*+}$	$(7.6 \pm 1.6)$	$\times 10^{-3}$		$\Gamma_{183}$	$\eta_c(2S) K^+$	$(3.4 \pm 1.8)$	$\times 10^{-4}$	
$\Gamma_{137}$	$\bar{D}^*(2007)^0 D_s^+$	$(8.2 \pm 1.7)$	$\times 10^{-3}$		$\Gamma_{184}$	$\eta_c(2S) K^+, \eta_c(2S) \rightarrow K_S^0 K^\mp \pi^\pm$	$(3.4 \pm 1.6)$	$\times 10^{-6}$	
$\Gamma_{138}$	$\bar{D}^*(2007)^0 D_s^{*+}$	$(1.71 \pm 0.24)$	%		$\Gamma_{185}$	$J/\psi(1S) K^+$	$(1.016 \pm 0.033)$	$\times 10^{-3}$	
$\Gamma_{139}$	$D_s^{(*)+} \bar{D}^{*0}$	$(2.7 \pm 1.2)$	%		$\Gamma_{186}$	$J/\psi(1S) K^+ \pi^+ \pi^-$	$(8.1 \pm 1.3)$	$\times 10^{-4}$	S=2.5
$\Gamma_{140}$	$\bar{D}_s^*(2007)^0 D^*(2010)^+$	$(8.1 \pm 1.7)$	$\times 10^{-4}$		$\Gamma_{187}$	$h_c(1P) K^+ \times B(h_c(1P) \rightarrow J/\psi \pi^+ \pi^-)$	$< 3.4$	$\times 10^{-6}$	CL=90%
$\Gamma_{141}$	$\bar{D}^0 D^*(2010)^+ + \bar{D}^*(2007)^0 D^+$	$< 1.30$	%	CL=90%	$\Gamma_{188}$	$X(3872) K^+$	$< 3.2$	$\times 10^{-4}$	CL=90%
$\Gamma_{142}$	$\bar{D}^0 D^*(2010)^+$	$(3.9 \pm 0.5)$	$\times 10^{-4}$		$\Gamma_{189}$	$X(3872) K^+ \times B(X \rightarrow J/\psi \pi^+ \pi^-)$	$(8.6 \pm 0.8)$	$\times 10^{-6}$	
$\Gamma_{143}$	$\bar{D}^0 D^+$	$(3.8 \pm 0.4)$	$\times 10^{-4}$		$\Gamma_{190}$	$X(3872) K^+ \times B(X \rightarrow J/\psi \gamma)$	$(2.1 \pm 0.4)$	$\times 10^{-6}$	S=1.1
$\Gamma_{144}$	$\bar{D}^0 D^+ K^0$	$(1.55 \pm 0.21)$	$\times 10^{-3}$		$\Gamma_{191}$	$X(3872) K^*(892)^+ \times B(X \rightarrow J/\psi \gamma)$	$< 4.8$	$\times 10^{-6}$	CL=90%
$\Gamma_{145}$	$D^+ \bar{D}^*(2007)^0$	$(6.3 \pm 1.7)$	$\times 10^{-4}$		$\Gamma_{192}$	$X(3872) K^+ \times B(X \rightarrow \psi(2S) \gamma)$	$(4 \pm 4)$	$\times 10^{-6}$	S=2.5
$\Gamma_{146}$	$\bar{D}^*(2007)^0 D^+ K^0$	$(2.1 \pm 0.5)$	$\times 10^{-3}$		$\Gamma_{193}$	$X(3872) K^*(892)^+ \times B(X \rightarrow \psi(2S) \gamma)$	$< 2.8$	$\times 10^{-5}$	CL=90%
$\Gamma_{147}$	$\bar{D}^0 \bar{D}^*(2010)^+ K^0$	$(3.8 \pm 0.4)$	$\times 10^{-3}$		$\Gamma_{194}$	$X(3872) K^+ \times B(X \rightarrow D^0 \bar{D}^0)$	$< 6.0$	$\times 10^{-5}$	CL=90%
$\Gamma_{148}$	$\bar{D}^*(2007)^0 D^*(2010)^+ K^0$	$(9.2 \pm 1.2)$	$\times 10^{-3}$		$\Gamma_{195}$	$X(3872) K^+ \times B(X \rightarrow D^+ D^-)$	$< 4.0$	$\times 10^{-5}$	CL=90%
$\Gamma_{149}$	$\bar{D}^0 D^0 K^+$	$(1.45 \pm 0.33)$	$\times 10^{-3}$	S=2.6	$\Gamma_{196}$	$X(3872) K^+ \times B(X \rightarrow D^0 \bar{D}^0 \pi^0)$	$(1.0 \pm 0.4)$	$\times 10^{-4}$	
$\Gamma_{150}$	$\bar{D}^*(2007)^0 D^0 K^+$	$(2.26 \pm 0.23)$	$\times 10^{-3}$		$\Gamma_{197}$	$X(3872) K^+ \times B(X \rightarrow \bar{D}^{*0} D^0)$	$(8.5 \pm 2.6)$	$\times 10^{-5}$	S=1.4
$\Gamma_{151}$	$\bar{D}^0 D^*(2007)^0 K^+$	$(6.3 \pm 0.5)$	$\times 10^{-3}$		$\Gamma_{198}$	$X(3872) K^+ \times B(X(3872) \rightarrow J/\psi(1S) \eta)$	$< 7.7$	$\times 10^{-6}$	CL=90%
$\Gamma_{152}$	$\bar{D}^*(2007)^0 D^*(2007)^0 K^+$	$(1.12 \pm 0.13)$	%		$\Gamma_{199}$	$X(3872)^+ K^0 \times B(X(3872)^+ \rightarrow [f] J/\psi(1S) \pi^+ \pi^0)$	$< 6.1$	$\times 10^{-6}$	CL=90%
$\Gamma_{153}$	$D^- D^+ K^+$	$(2.2 \pm 0.7)$	$\times 10^{-4}$		$\Gamma_{200}$	$X(4430)^+ K^0 \times B(X^+ \rightarrow J/\psi \pi^+)$	$< 1.5$	$\times 10^{-5}$	CL=95%
$\Gamma_{154}$	$D^- D^*(2010)^+ K^+$	$(6.3 \pm 1.1)$	$\times 10^{-4}$		$\Gamma_{201}$	$X(4430)^+ K^0 \times B(X^+ \rightarrow \psi(2S) \pi^+)$	$< 4.7$	$\times 10^{-5}$	CL=95%
$\Gamma_{155}$	$D^*(2010)^- D^+ K^+$	$(6.0 \pm 1.3)$	$\times 10^{-4}$		$\Gamma_{202}$	$X(4260)^0 K^+ \times B(X^0 \rightarrow J/\psi \pi^+ \pi^-)$	$< 2.9$	$\times 10^{-5}$	CL=95%
$\Gamma_{156}$	$D^*(2010)^- D^*(2010)^+ K^+$	$(1.32 \pm 0.18)$	$\times 10^{-3}$		$\Gamma_{203}$	$X(3915)^0 K^+ \times B(X^0 \rightarrow J/\psi \gamma)$	$< 1.4$	$\times 10^{-5}$	CL=90%
$\Gamma_{157}$	$(\bar{D}^+ \bar{D}^*)(D^+ D^*) K$	$(4.05 \pm 0.30)$	%		$\Gamma_{204}$	$Z(3930)^0 K^+ \times B(Z^0 \rightarrow J/\psi \gamma)$	$< 2.5$	$\times 10^{-6}$	CL=90%
$\Gamma_{158}$	$D_s^+ \pi^0$	$(1.6 \pm 0.5)$	$\times 10^{-5}$		$\Gamma_{205}$	$J/\psi(1S) K^*(892)^+$	$(1.43 \pm 0.08)$	$\times 10^{-3}$	
$\Gamma_{159}$	$D_s^{*+} \pi^0$	$< 2.6$	$\times 10^{-4}$	CL=90%	$\Gamma_{206}$	$J/\psi(1S) K(1270)^+$	$(1.8 \pm 0.5)$	$\times 10^{-3}$	
$\Gamma_{160}$	$D_s^+ \eta$	$< 4$	$\times 10^{-4}$	CL=90%	$\Gamma_{207}$	$J/\psi(1S) K(1400)^+$	$< 5$	$\times 10^{-4}$	CL=90%
$\Gamma_{161}$	$D_s^{*+} \eta$	$< 6$	$\times 10^{-4}$	CL=90%	$\Gamma_{208}$	$J/\psi(1S) \eta K^+$	$(1.08 \pm 0.33)$	$\times 10^{-4}$	
$\Gamma_{162}$	$D_s^+ \rho^0$	$< 3.0$	$\times 10^{-4}$	CL=90%	$\Gamma_{209}$	$J/\psi(1S) \eta' K^+$	$< 8.8$	$\times 10^{-5}$	CL=90%
					$\Gamma_{210}$	$J/\psi(1S) \phi K^+$	$(5.2 \pm 1.7)$	$\times 10^{-5}$	S=1.2
					$\Gamma_{211}$	$J/\psi(1S) \omega K^+$	$(3.20 \pm 0.60)$	$\times 10^{-4}$	
					$\Gamma_{212}$	$X(3872) K^+ \times B(X \rightarrow J/\psi \omega)$	$(6.0 \pm 2.2)$	$\times 10^{-6}$	
					$\Gamma_{213}$	$X(3915) K^+ \times B(X \rightarrow J/\psi \omega)$	$(3.0 \pm 0.9)$	$\times 10^{-5}$	
					$\Gamma_{214}$	$J/\psi(1S) \pi^+$	$(4.9 \pm 0.4)$	$\times 10^{-5}$	S=1.2
					$\Gamma_{215}$	$J/\psi(1S) \rho^+$	$(5.0 \pm 0.8)$	$\times 10^{-5}$	
					$\Gamma_{216}$	$J/\psi(1S) \pi^+ \pi^0$ nonresonant	$< 7.3$	$\times 10^{-6}$	CL=90%
					$\Gamma_{217}$	$J/\psi(1S) a_1(1260)^+$	$< 1.2$	$\times 10^{-3}$	CL=90%
					$\Gamma_{218}$	$J/\psi(1S) \rho \bar{\lambda}$	$(1.18 \pm 0.31)$	$\times 10^{-5}$	







$\Gamma_{465}$	$\rho^- e^+ \mu^+$	L	< 3.3	$\times 10^{-6}$	CL=90%
$\Gamma_{466}$	$K^- e^+ e^+$	L	< 1.0	$\times 10^{-6}$	CL=90%
$\Gamma_{467}$	$K^- \mu^+ \mu^+$	L	< 4.1	$\times 10^{-8}$	CL=90%
$\Gamma_{468}$	$K^- e^+ \mu^+$	L	< 2.0	$\times 10^{-6}$	CL=90%
$\Gamma_{469}$	$K^*(892)^- e^+ e^+$	L	< 2.8	$\times 10^{-6}$	CL=90%
$\Gamma_{470}$	$K^*(892)^- \mu^+ \mu^+$	L	< 8.3	$\times 10^{-6}$	CL=90%
$\Gamma_{471}$	$K^*(892)^- e^+ \mu^+$	L	< 4.4	$\times 10^{-6}$	CL=90%
$\Gamma_{472}$	$D^- e^+ e^+$	L	< 2.6	$\times 10^{-6}$	CL=90%
$\Gamma_{473}$	$D^- e^+ \mu^+$	L	< 1.8	$\times 10^{-6}$	CL=90%
$\Gamma_{474}$	$D^- \mu^+ \mu^+$	L	< 1.1	$\times 10^{-6}$	CL=90%
$\Gamma_{475}$	$\Lambda^0 \mu^+$	L,B	< 6	$\times 10^{-8}$	CL=90%
$\Gamma_{476}$	$\Lambda^0 e^+$	L,B	< 3.2	$\times 10^{-8}$	CL=90%
$\Gamma_{477}$	$\bar{\Lambda}^0 \mu^+$	L,B	< 6	$\times 10^{-8}$	CL=90%
$\Gamma_{478}$	$\bar{\Lambda}^0 e^+$	L,B	< 8	$\times 10^{-8}$	CL=90%

- [a] An  $\ell$  indicates an  $e$  or a  $\mu$  mode, not a sum over these modes.  
 [b] An  $CP(\pm 1)$  indicates the  $CP=+1$  and  $CP=-1$  eigenstates of the  $D^0$ - $\bar{D}^0$  system.  
 [c]  $D$  denotes  $D^0$  or  $\bar{D}^0$ .  
 [d]  $D_{CP^\pm}^0$  decays into  $D^0 \pi^0$  with the  $D^0$  reconstructed in  $CP$ -even eigenstates  $K^+ K^-$  and  $\pi^+ \pi^-$ .  
 [e]  $\bar{D}^{**}$  represents an excited state with mass  $2.2 < M < 2.8$  GeV/ $c^2$ .  
 [f]  $X(3872)^+$  is a hypothetical charged partner of the  $X(3872)$ .  
 [g]  $\Theta(1710)^{++}$  is a possible narrow pentaquark state and  $G(2220)$  is a possible glueball resonance.  
 [h]  $(\bar{\Lambda}_c^- p)_s$  denotes a low-mass enhancement near 3.35 GeV/ $c^2$ .

### CONSTRAINED FIT INFORMATION

An overall fit to 18 branching ratios uses 48 measurements and one constraint to determine 12 parameters. The overall fit has a  $\chi^2 = 38.8$  for 37 degrees of freedom.

The following *off-diagonal* array elements are the correlation coefficients  $\langle \delta x_i \delta x_j \rangle / (\delta x_i \delta x_j)$ , in percent, from the fit to the branching fractions,  $x_i \equiv \Gamma_i / \Gamma_{\text{total}}$ . The fit constrains the  $x_i$  whose labels appear in this array to sum to one.

$x_7$	14										
$x_{42}$	0	0									
$x_{71}$	0	0	8								
$x_{102}$	0	0	1	13							
$x_{185}$	0	0	0	0	0						
$x_{205}$	0	0	0	0	0	0					
$x_{214}$	0	0	0	0	0	36	0				
$x_{223}$	0	0	0	0	0	13	0	5			
$x_{443}$	0	0	0	0	0	27	0	10	4		
$x_{448}$	0	0	0	0	0	0	12	0	0		
	$x_6$	$x_7$	$x_{42}$	$x_{71}$	$x_{102}$	$x_{185}$	$x_{205}$	$x_{214}$	$x_{223}$	$x_{443}$	$x_{448}$

### $B^+$ BRANCHING RATIOS

$\Gamma(\ell^+ \nu_\ell \text{ anything}) / \Gamma_{\text{total}}$	$\Gamma_1 / \Gamma$		
"OUR EVALUATION" is an average using rescaled values of the data listed below. The average and rescaling were performed by the Heavy Flavor Averaging Group (HFAG) and are described at <a href="http://www.slac.stanford.edu/xorg/hfag/">http://www.slac.stanford.edu/xorg/hfag/</a> . The averaging/rescaling procedure takes into account correlations between the measurements.			
VALUE (units $10^{-2}$ )	DOCUMENT ID	TECN	COMMENT
<b>10.99 ± 0.28 OUR EVALUATION</b>			
<b>10.76 ± 0.32 OUR AVERAGE</b>	Error includes scale factor of 1.1.		
11.17 ± 0.25 ± 0.28	1 URQUIJO	07 BELL	$e^+ e^- \rightarrow \Upsilon(4S)$
10.28 ± 0.26 ± 0.39	2 AUBERT,B	06Y BABR	$e^+ e^- \rightarrow \Upsilon(4S)$
10.25 ± 0.57 ± 0.65	3 ARTUSO	97 CLE2	$e^+ e^- \rightarrow \Upsilon(4S)$
• • • We do not use the following data for averages, fits, limits, etc. • • •			
11.15 ± 0.26 ± 0.41	4 OKABE	05 BELL	Repl. by URQUIJO 07
10.1 ± 1.8 ± 1.5	ATHANAS	94 CLE2	Sup. by ARTUSO 97

- <sup>1</sup> URQUIJO 07 report a measurement of  $(10.34 \pm 0.23 \pm 0.25)\%$  for the partial branching fraction of  $B^+ \rightarrow e^+ \nu_e X_c$  decay with electron energy above 0.6 GeV. We converted the result to  $B^+ \rightarrow e^+ \nu_e X$  branching fraction.  
<sup>2</sup> The measurements are obtained for charged and neutral  $B$  mesons partial rates of semileptonic decay to electrons with momentum above 0.6 GeV/ $c$  in the  $B$  rest frame. The best precision on the ratio is achieved for a momentum threshold of 1.0 GeV:  $B(B^+ \rightarrow e^+ \nu_e X) / B(B^0 \rightarrow e^+ \nu_e X) = 1.074 \pm 0.041 \pm 0.026$ .  
<sup>3</sup> ARTUSO 97 uses partial reconstruction of  $B \rightarrow D^* \ell \nu_\ell$  and inclusive semileptonic branching ratio from BARISH 96b  $(0.1049 \pm 0.0017 \pm 0.0043)$ .  
<sup>4</sup> The measurements are obtained for charged and neutral  $B$  mesons partial rates of semileptonic decay to electrons with momentum above 0.6 GeV/ $c$  in the  $B$  rest frame, and their ratio of  $B(B^+ \rightarrow e^+ \nu_e X) / B(B^0 \rightarrow e^+ \nu_e X) = 1.08 \pm 0.05 \pm 0.02$ .

$\Gamma(e^+ \nu_e X_c) / \Gamma_{\text{total}}$	$\Gamma_2 / \Gamma$		
VALUE (units $10^{-2}$ )	DOCUMENT ID	TECN	COMMENT
<b>10.79 ± 0.25 ± 0.27</b>	1 URQUIJO	07 BELL	$e^+ e^- \rightarrow \Upsilon(4S)$

- <sup>1</sup> Measure the independent  $B^+$  and  $B^0$  partial branching fractions with electron threshold energies of 0.4 GeV.

$\Gamma(D^0 \ell^+ \nu_\ell) / \Gamma_{\text{total}}$	$\Gamma_4 / \Gamma$		
"OUR EVALUATION" is an average using rescaled values of the data listed below. The average and rescaling were performed by the Heavy Flavor Averaging Group (HFAG) and are described at <a href="http://www.slac.stanford.edu/xorg/hfag/">http://www.slac.stanford.edu/xorg/hfag/</a> . The averaging/rescaling procedure takes into account correlations between the measurements. $\ell = e$ or $\mu$ , not sum over $e$ and $\mu$ modes.			
VALUE	DOCUMENT ID	TECN	COMMENT
<b>0.0226 ± 0.0011 OUR EVALUATION</b>			
<b>0.0229 ± 0.0008 OUR AVERAGE</b>			
0.0229 ± 0.0008 ± 0.0009	1 AUBERT	10 BABR	$e^+ e^- \rightarrow \Upsilon(4S)$
0.0234 ± 0.0003 ± 0.0013	AUBERT	09A BABR	$e^+ e^- \rightarrow \Upsilon(4S)$
0.0221 ± 0.0013 ± 0.0019	2 BARTELT	99 CLE2	$e^+ e^- \rightarrow \Upsilon(4S)$
0.016 ± 0.006 ± 0.003	3 FULTON	91 CLEO	$e^+ e^- \rightarrow \Upsilon(4S)$
• • • We do not use the following data for averages, fits, limits, etc. • • •			
0.0233 ± 0.0009 ± 0.0009	1 AUBERT	08Q BABR	Repl. by AUBERT 09A
0.0194 ± 0.0015 ± 0.0034	4 ATHANAS	97 CLE2	Repl. by BARTELT 99

- <sup>1</sup> Uses a fully reconstructed  $B$  meson as a tag on the recoil side.  
<sup>2</sup> Assumes equal production of  $B^+$  and  $B^0$  at the  $\Upsilon(4S)$ .  
<sup>3</sup> FULTON 91 assumes equal production of  $B^0 \bar{B}^0$  and  $B^+ B^-$  at the  $\Upsilon(4S)$ .  
<sup>4</sup> ATHANAS 97 uses missing energy and missing momentum to reconstruct neutrino.

$\Gamma(D^0 \ell^+ \nu_\ell) / \Gamma(\ell^+ \nu_\ell \text{ anything})$	$\Gamma_4 / \Gamma_1$		
VALUE	DOCUMENT ID	TECN	COMMENT
<b>0.255 ± 0.009 ± 0.009</b>	1 AUBERT	10 BABR	$e^+ e^- \rightarrow \Upsilon(4S)$

- <sup>1</sup> Uses a fully reconstructed  $B$  meson on the recoil side.

$\Gamma(D^0 \tau^+ \nu_\tau) / \Gamma_{\text{total}}$	$\Gamma_5 / \Gamma$		
VALUE (units $10^{-2}$ )	DOCUMENT ID	TECN	COMMENT
<b>0.77 ± 0.22 ± 0.12</b>	1 BOZEK	10 BELL	$e^+ e^- \rightarrow \Upsilon(4S)$
• • • We do not use the following data for averages, fits, limits, etc. • • •			
0.67 ± 0.37 ± 0.13	2 AUBERT	08N BABR	Repl. by AUBERT 09s

- <sup>1</sup> Assumes equal production of  $B^+$  and  $B^0$  at the  $\Upsilon(4S)$ .  
<sup>2</sup> Uses a fully reconstructed  $B$  meson as a tag on the recoil side.

$\Gamma(D^0 \tau^+ \nu_\tau) / \Gamma(D^0 \ell^+ \nu_\ell)$	$\Gamma_5 / \Gamma_4$		
VALUE	DOCUMENT ID	TECN	COMMENT
<b>0.314 ± 0.170 ± 0.049</b>	1 AUBERT	09s BABR	$e^+ e^- \rightarrow \Upsilon(4S)$

- <sup>1</sup> Uses a fully reconstructed  $B$  meson as a tag on the recoil side.

$\Gamma(D^0 \ell^+ \nu_\ell) / \Gamma(D \ell^+ \nu_\ell \text{ anything})$	$\Gamma_4 / \Gamma_3$		
VALUE	DOCUMENT ID	TECN	COMMENT
<b>0.227 ± 0.014 ± 0.016</b>	1 AUBERT	07AN BABR	$e^+ e^- \rightarrow \Upsilon(4S)$

- <sup>1</sup> Uses a fully reconstructed  $B$  meson on the recoil side.

$\Gamma(\bar{D}^*(2007)^0 \ell^+ \nu_\ell) / \Gamma_{\text{total}}$	$\Gamma_6 / \Gamma$			
"OUR EVALUATION" is an average using rescaled values of the data listed below. The average and rescaling were performed by the Heavy Flavor Averaging Group (HFAG) and are described at <a href="http://www.slac.stanford.edu/xorg/hfag/">http://www.slac.stanford.edu/xorg/hfag/</a> . The averaging/rescaling procedure takes into account correlations between the measurements. $\ell = e$ or $\mu$ , not sum over $e$ and $\mu$ modes.				
VALUE	EVTS	DOCUMENT ID	TECN	COMMENT
<b>0.0570 ± 0.0019 OUR EVALUATION</b>				
<b>0.0559 ± 0.0026 OUR FIT</b>	Error includes scale factor of 1.5.			
<b>0.0558 ± 0.0026 OUR AVERAGE</b>	Error includes scale factor of 1.5. See the ideogram below.			
0.0540 ± 0.0002 ± 0.0021	AUBERT	09A BABR	$e^+ e^- \rightarrow \Upsilon(4S)$	
0.0556 ± 0.0008 ± 0.0041	1 AUBERT	08AT BABR	$e^+ e^- \rightarrow \Upsilon(4S)$	
0.0650 ± 0.0020 ± 0.0043	2 ADAM	03 CLE2	$e^+ e^- \rightarrow \Upsilon(4S)$	
0.066 ± 0.016 ± 0.015	3 ALBRECHT	92C ARG	$e^+ e^- \rightarrow \Upsilon(4S)$	
• • • We do not use the following data for averages, fits, limits, etc. • • •				
0.0583 ± 0.0015 ± 0.0030	4 AUBERT	08Q BABR	Repl. by AUBERT 09A	
0.0650 ± 0.0020 ± 0.0043	5 BRIERE	02 CLE2	$e^+ e^- \rightarrow \Upsilon(4S)$	
0.0513 ± 0.0054 ± 0.0064	6 BARISH	95 CLE2	Repl. by ADAM 03	
seen	7 SANGHERA	93 CLE2	$e^+ e^- \rightarrow \Upsilon(4S)$	
0.041 ± 0.008 ± 0.008	8 FULTON	91 CLEO	$e^+ e^- \rightarrow \Upsilon(4S)$	
0.070 ± 0.018 ± 0.014	9 ANTREASYAN	90B CBAL	$e^+ e^- \rightarrow \Upsilon(4S)$	

- <sup>1</sup> Measured using the dependence of  $B^- \rightarrow D^{*0} e^- \bar{\nu}_e$  decay differential rate and the form factor description by CAPRINI 98.  
<sup>2</sup> Simultaneous measurements of both  $B^0 \rightarrow D^*(2010) \ell \nu$  and  $B^+ \rightarrow \bar{D}(2007)^0 \ell \nu$ .  
<sup>3</sup> ALBRECHT 92c reports  $0.058 \pm 0.014 \pm 0.013$ . We rescale using the method described in STONE 94 but with the updated PDG 94  $B(D^0 \rightarrow K^- \pi^+)$ . Assumes equal production of  $B^0 \bar{B}^0$  and  $B^+ B^-$  at the  $\Upsilon(4S)$ .  
<sup>4</sup> Uses a fully reconstructed  $B$  meson as a tag on the recoil side.  
<sup>5</sup> The results are based on the same analysis and data sample reported in ADAM 03.  
<sup>6</sup> BARISH 95 use  $B(D^0 \rightarrow K^- \pi^+) = (3.91 \pm 0.08 \pm 0.17)\%$  and  $B(D^{*0} \rightarrow D^0 \pi^0) = (63.6 \pm 2.3 \pm 3.3)\%$ .  
<sup>7</sup> Combining  $\bar{D}^{*0} \ell^+ \nu_\ell$  and  $\bar{D}^{*0} \ell^+ \nu_\ell$  SANGHERA 93 test  $V-A$  structure and fit the decay angular distributions to obtain  $A_{FB} = 3/4 * (\Gamma^- - \Gamma^+) / \Gamma = 0.14 \pm 0.06 \pm 0.03$ .

# Meson Particle Listings

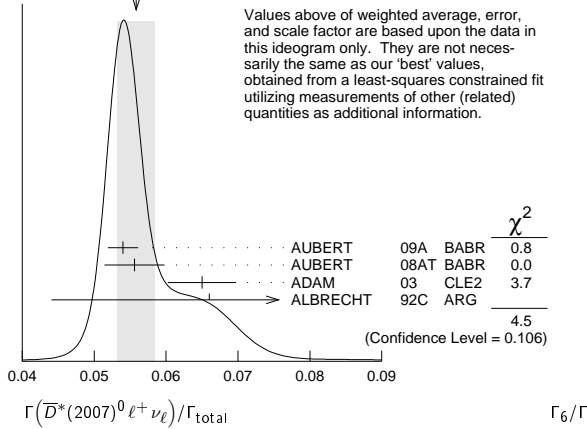
$B^\pm$

Assuming a value of  $V_{cb}$ , they measure  $V, A_1,$  and  $A_2,$  the three form factors for the  $D^* \ell \nu_\ell$  decay, where results are slightly dependent on model assumptions.

<sup>8</sup> Assumes equal production of  $B^0 \bar{B}^0$  and  $B^+ B^-$  at the  $\Upsilon(4S)$ . Uncorrected for  $D$  and  $D^*$  branching ratio assumptions.

<sup>9</sup> ANTREASYAN 90B is average over  $B$  and  $\bar{D}^*(2010)$  charge states.

WEIGHTED AVERAGE  
0.0558±0.0026 (Error scaled by 1.5)



$\Gamma(\bar{D}^*(2007)^0 \tau^+ \nu_\tau) / \Gamma_{total}$   $\Gamma_7 / \Gamma$

VALUE (units $10^{-2}$ )	DOCUMENT ID	TECN	COMMENT
<b>2.04 ± 0.30 OUR FIT</b>			
2.12 ± 0.28 ± 0.29	<sup>1</sup> BOZEK 10	BELL	$e^+ e^- \rightarrow \Upsilon(4S)$
2.25 ± 0.48 ± 0.28	<sup>2</sup> AUBERT 08N	BABR	Repl. by AUBERT 09s

• • • We do not use the following data for averages, fits, limits, etc. • • •

<sup>1</sup> Assumes equal production of  $B^+$  and  $B^0$  at the  $\Upsilon(4S)$ .  
<sup>2</sup> Uses a fully reconstructed  $B$  meson as a tag on the recoil side.

$\Gamma(\bar{D}^*(2007)^0 \tau^+ \nu_\tau) / \Gamma(\bar{D}^*(2007)^0 \ell^+ \nu_\ell)$   $\Gamma_7 / \Gamma_6$

VALUE	DOCUMENT ID	TECN	COMMENT
<b>0.36 ± 0.05 OUR FIT</b>			
0.346 ± 0.073 ± 0.034	<sup>1</sup> AUBERT 09s	BABR	$e^+ e^- \rightarrow \Upsilon(4S)$

<sup>1</sup> Uses a fully reconstructed  $B$  meson as a tag on the recoil side.

$\Gamma(\bar{D}^*(2007)^0 \ell^+ \nu_\ell) / \Gamma(D \ell^+ \nu_\ell \text{ anything})$   $\Gamma_6 / \Gamma_3$

VALUE	DOCUMENT ID	TECN	COMMENT
<b>0.582 ± 0.018 ± 0.030</b>	<sup>1</sup> AUBERT 07AN	BABR	$e^+ e^- \rightarrow \Upsilon(4S)$

<sup>1</sup> Uses a fully reconstructed  $B$  meson on the recoil side.

$\Gamma(D^{(*)} n \pi \ell^+ \nu_\ell (n \geq 1)) / \Gamma(D \ell^+ \nu_\ell \text{ anything})$   $\Gamma_{11} / \Gamma_3$

VALUE	DOCUMENT ID	TECN	COMMENT
<b>0.191 ± 0.013 ± 0.019</b>	<sup>1</sup> AUBERT 07AN	BABR	$e^+ e^- \rightarrow \Upsilon(4S)$

<sup>1</sup> Uses a fully reconstructed  $B$  meson on the recoil side.

$\Gamma(D^- \pi^+ \ell^+ \nu_\ell) / \Gamma_{total}$   $\Gamma_8 / \Gamma$

VALUE (units $10^{-3}$ )	DOCUMENT ID	TECN	COMMENT
<b>4.2 ± 0.5 OUR AVERAGE</b>			
4.2 ± 0.6 ± 0.3	<sup>1</sup> AUBERT 08Q	BABR	$e^+ e^- \rightarrow \Upsilon(4S)$
4.2 ± 0.6 ± 0.2	<sup>1,2</sup> LIVENTSEV 08	BELL	$e^+ e^- \rightarrow \Upsilon(4S)$
5.5 ± 0.9 ± 0.3	<sup>3</sup> LIVENTSEV 05	BELL	Repl. by LIVENTSEV 08

• • • We do not use the following data for averages, fits, limits, etc. • • •

<sup>1</sup> Uses a fully reconstructed  $B$  meson as a tag on the recoil side.  
<sup>2</sup> LIVENTSEV 08 reports  $(4.0 \pm 0.4 \pm 0.6) \times 10^{-3}$  from a measurement of  $[\Gamma(B^+ \rightarrow D^- \pi^+ \ell^+ \nu_\ell) / \Gamma_{total}] / [B(B^+ \rightarrow \bar{D}^0 \ell^+ \nu_\ell)]$  assuming  $B(B^+ \rightarrow \bar{D}^0 \ell^+ \nu_\ell) = (2.15 \pm 0.22) \times 10^{-2}$ , which we rescale to our best value  $B(B^+ \rightarrow \bar{D}^0 \ell^+ \nu_\ell) = (2.26 \pm 0.11) \times 10^{-2}$ . Our first error is their experiment's error and our second error is the systematic error from using our best value.  
<sup>3</sup> LIVENTSEV 05 reports  $[\Gamma(B^+ \rightarrow D^- \pi^+ \ell^+ \nu_\ell) / \Gamma_{total}] / [B(B^0 \rightarrow D^- \ell^+ \nu_\ell)] = 0.25 \pm 0.03 \pm 0.03$  which we multiply by our best value  $B(B^0 \rightarrow D^- \ell^+ \nu_\ell) = (2.18 \pm 0.12) \times 10^{-2}$ . Our first error is their experiment's error and our second error is the systematic error from using our best value.

$\Gamma(\bar{D}_s^*(2420)^0 \ell^+ \nu_\ell \times B(\bar{D}_s^0 \rightarrow D^- \pi^+)) / \Gamma_{total}$   $\Gamma_9 / \Gamma$

VALUE (units $10^{-3}$ )	DOCUMENT ID	TECN	COMMENT
<b>2.5 ± 0.5 OUR AVERAGE</b>			
2.6 ± 0.5 ± 0.4	<sup>1</sup> AUBERT 08BL	BABR	$e^+ e^- \rightarrow \Upsilon(4S)$
2.4 ± 0.4 ± 0.6	<sup>1</sup> LIVENTSEV 08	BELL	$e^+ e^- \rightarrow \Upsilon(4S)$

<sup>1</sup> Uses a fully reconstructed  $B$  meson as a tag on the recoil side.

$\Gamma(\bar{D}_s^*(2460)^0 \ell^+ \nu_\ell \times B(\bar{D}_s^0 \rightarrow D^- \pi^+)) / \Gamma_{total}$   $\Gamma_{10} / \Gamma$

VALUE (units $10^{-3}$ )	DOCUMENT ID	TECN	COMMENT
<b>1.53 ± 0.16 OUR AVERAGE</b>			
1.42 ± 0.15 ± 0.15	<sup>1</sup> AUBERT 09Y	BABR	$e^+ e^- \rightarrow \Upsilon(4S)$
1.5 ± 0.2 ± 0.2	<sup>2</sup> AUBERT 08BL	BABR	$e^+ e^- \rightarrow \Upsilon(4S)$
2.2 ± 0.3 ± 0.4	<sup>2</sup> LIVENTSEV 08	BELL	$e^+ e^- \rightarrow \Upsilon(4S)$

<sup>1</sup> Uses a simultaneous fit of all  $B$  semileptonic decays without full reconstruction of events. AUBERT 09Y reports  $B(B^+ \rightarrow \bar{D}_s^*(2460)^0 \ell^+ \nu_\ell) \cdot B(\bar{D}_s^*(2460)^0 \rightarrow D^{(*)-} \pi^+) = (2.29 \pm 0.23 \pm 0.21) \times 10^{-3}$  and the authors have provided us the individual measurement.  
<sup>2</sup> Uses a fully reconstructed  $B$  meson as a tag on the recoil side.

$\Gamma(D^{*-} \pi^+ \ell^+ \nu_\ell) / \Gamma_{total}$   $\Gamma_{12} / \Gamma$

VALUE (units $10^{-3}$ )	DOCUMENT ID	TECN	COMMENT
<b>6.1 ± 0.6 OUR AVERAGE</b>			
5.9 ± 0.5 ± 0.4	<sup>1</sup> AUBERT 08Q	BABR	$e^+ e^- \rightarrow \Upsilon(4S)$
6.7 ± 1.1 ± 0.3	<sup>1,2</sup> LIVENTSEV 08	BELL	$e^+ e^- \rightarrow \Upsilon(4S)$
5.9 ± 1.4 ± 0.1	<sup>3,4</sup> LIVENTSEV 05	BELL	Repl. by LIVENTSEV 08

<sup>1</sup> Uses a fully reconstructed  $B$  meson as a tag on the recoil side.  
<sup>2</sup> LIVENTSEV 08 reports  $(6.4 \pm 0.8 \pm 0.9) \times 10^{-3}$  from a measurement of  $[\Gamma(B^+ \rightarrow D^{*-} \pi^+ \ell^+ \nu_\ell) / \Gamma_{total}] / [B(B^+ \rightarrow \bar{D}^0 \ell^+ \nu_\ell)]$  assuming  $B(B^+ \rightarrow \bar{D}^0 \ell^+ \nu_\ell) = (2.15 \pm 0.22) \times 10^{-2}$ , which we rescale to our best value  $B(B^+ \rightarrow \bar{D}^0 \ell^+ \nu_\ell) = (2.26 \pm 0.11) \times 10^{-2}$ . Our first error is their experiment's error and our second error is the systematic error from using our best value.  
<sup>3</sup> Excludes  $D^{*+}$  contribution to  $D \pi$  modes.  
<sup>4</sup> LIVENTSEV 05 reports  $[\Gamma(B^+ \rightarrow D^{*-} \pi^+ \ell^+ \nu_\ell) / \Gamma_{total}] / [B(B^0 \rightarrow D^{*+} \pi^0 \ell^+ \nu_\ell)] = 0.12 \pm 0.02 \pm 0.02$  which we multiply by our best value  $B(B^0 \rightarrow D^{*+} \pi^0 \ell^+ \nu_\ell) = (4.95 \pm 0.11) \times 10^{-2}$ . Our first error is their experiment's error and our second error is the systematic error from using our best value.

$\Gamma(D_s^{*-} K^+ \ell^+ \nu_\ell) / \Gamma_{total}$   $\Gamma_{13} / \Gamma$

VALUE (units $10^{-4}$ )	DOCUMENT ID	TECN	COMMENT
<b>6.13 ± 1.03 ± 0.67</b>	<sup>1</sup> DEL-AMO-SA...11L	BABR	$e^+ e^- \rightarrow \Upsilon(4S)$

<sup>1</sup> Assumes equal production of  $B^+$  and  $B^0$  at the  $\Upsilon(4S)$ .

$\Gamma(\bar{D}_1(2420)^0 \ell^+ \nu_\ell \times B(\bar{D}_1^0 \rightarrow D^{*-} \pi^+)) / \Gamma_{total}$   $\Gamma_{14} / \Gamma$

VALUE (units $10^{-3}$ )	DOCUMENT ID	TECN	COMMENT
<b>3.03 ± 0.20 OUR AVERAGE</b>			
2.97 ± 0.17 ± 0.17	<sup>1</sup> AUBERT 09Y	BABR	$e^+ e^- \rightarrow \Upsilon(4S)$
2.9 ± 0.3 ± 0.3	<sup>2</sup> AUBERT 08BL	BABR	$e^+ e^- \rightarrow \Upsilon(4S)$
4.2 ± 0.7 ± 0.7	<sup>2</sup> LIVENTSEV 08	BELL	$e^+ e^- \rightarrow \Upsilon(4S)$
3.73 ± 0.85 ± 0.57	<sup>3</sup> ANASTASSOV 98	CLE2	$e^+ e^- \rightarrow \Upsilon(4S)$

<sup>1</sup> Uses a simultaneous measurement of all  $B$  semileptonic decays without full reconstruction of events.  
<sup>2</sup> Uses a fully reconstructed  $B$  meson as a tag on the recoil side.  
<sup>3</sup> Assumes equal production of  $B^+$  and  $B^0$  at the  $\Upsilon(4S)$ .

$\Gamma(\bar{D}_1^*(2430)^0 \ell^+ \nu_\ell \times B(\bar{D}_1^0 \rightarrow D^{*-} \pi^+)) / \Gamma_{total}$   $\Gamma_{15} / \Gamma$

VALUE (units $10^{-3}$ )	CL%	DOCUMENT ID	TECN	COMMENT
<b>2.7 ± 0.4 ± 0.5</b>		<sup>1</sup> AUBERT 08BL	BABR	$e^+ e^- \rightarrow \Upsilon(4S)$
<0.7	90	<sup>1</sup> LIVENTSEV 08	BELL	$e^+ e^- \rightarrow \Upsilon(4S)$

• • • We do not use the following data for averages, fits, limits, etc. • • •

<sup>1</sup> Uses a fully reconstructed  $B$  meson as a tag on the recoil side.

$\Gamma(\bar{D}_s^*(2460)^0 \ell^+ \nu_\ell \times B(\bar{D}_s^0 \rightarrow D^{*-} \pi^+)) / \Gamma_{total}$   $\Gamma_{16} / \Gamma$

VALUE (units $10^{-3}$ )	CL%	DOCUMENT ID	TECN	COMMENT
<b>1.01 ± 0.24 OUR AVERAGE</b>				Error includes scale factor of 2.0.
0.87 ± 0.11 ± 0.07		<sup>1</sup> AUBERT 09Y	BABR	$e^+ e^- \rightarrow \Upsilon(4S)$
1.5 ± 0.2 ± 0.2		<sup>2</sup> AUBERT 08BL	BABR	$e^+ e^- \rightarrow \Upsilon(4S)$
1.8 ± 0.6 ± 0.3		<sup>2</sup> LIVENTSEV 08	BELL	$e^+ e^- \rightarrow \Upsilon(4S)$
<1.6	90	<sup>3</sup> ANASTASSOV 98	CLE2	$e^+ e^- \rightarrow \Upsilon(4S)$

• • • We do not use the following data for averages, fits, limits, etc. • • •

<sup>1</sup> Uses a simultaneous fit of all  $B$  semileptonic decays without full reconstruction of events. AUBERT 09Y reports  $B(B^+ \rightarrow \bar{D}_s^*(2460)^0 \ell^+ \nu_\ell) \cdot B(\bar{D}_s^*(2460)^0 \rightarrow D^{(*)-} \pi^+) = (2.29 \pm 0.23 \pm 0.21) \times 10^{-3}$  and the authors have provided us the individual measurement.  
<sup>2</sup> Uses a fully reconstructed  $B$  meson as a tag on the recoil side.  
<sup>3</sup> Assumes equal production of  $B^+$  and  $B^0$  at the  $\Upsilon(4S)$ .

$\Gamma(\pi^0 \ell^+ \nu_\ell) / \Gamma_{total}$   $\Gamma_{17} / \Gamma$

"OUR EVALUATION" is an average using rescaled values of the data listed below. The average and rescaling were performed by the Heavy Flavor Averaging Group (HFAG) and are described at <http://www.slac.stanford.edu/xorg/hfag/>. The averaging/rescaling procedure takes into account correlations between the measurements.

VALUE (units $10^{-4}$ )	DOCUMENT ID	TECN	COMMENT
<b>0.778 ± 0.028 OUR EVALUATION</b>			
<b>0.72 ± 0.04 OUR AVERAGE</b>			
0.705 ± 0.025 ± 0.035	<sup>1</sup> DEL-AMO-SA...11C	BABR	$e^+ e^- \rightarrow \Upsilon(4S)$
0.82 ± 0.09 ± 0.05	<sup>1</sup> AUBERT 08AV	BABR	$e^+ e^- \rightarrow \Upsilon(4S)$
0.77 ± 0.14 ± 0.08	<sup>2</sup> HOKUUE 07	BELL	$e^+ e^- \rightarrow \Upsilon(4S)$
0.74 ± 0.05 ± 0.10	<sup>3</sup> AUBERT,B 05o	BABR	Repl. by DEL-AMO-SANCHEZ 11c

• • • We do not use the following data for averages, fits, limits, etc. • • •

- 1 Using isospin relation,  $B^+$  and  $B^0$  branching fractions are combined.  
 2 The signal events are tagged by a second  $B$  meson reconstructed in the semileptonic mode  $B \rightarrow D^{(*)} \ell \nu_{\ell}$ .  
 3  $B^+$  and  $B^0$  decays combined assuming isospin symmetry. Systematic errors include both experimental and form-factor uncertainties.

 $\Gamma(\pi^0 e^+ \nu_e)/\Gamma_{\text{total}}$   $\Gamma_{18}/\Gamma$ 

VALUE (units $10^{-4}$ )	CL%	DOCUMENT ID	TECN	COMMENT
<b>0.9 ± 0.2 ± 0.2</b>				
0.9 ± 0.2 ± 0.2		<sup>1</sup> ALEXANDER 96T	CLE2	$e^+ e^- \rightarrow \mathcal{T}(4S)$
<22	90	ANTREASIAN 90B	CBAL	$e^+ e^- \rightarrow \mathcal{T}(4S)$

<sup>1</sup> Derived based in the reported  $B^0$  result by assuming isospin symmetry:  $\Gamma(B^0 \rightarrow \pi^- \ell^+ \nu) = 2\Gamma(B^+ \rightarrow \pi^0 \ell^+ \nu)$ .

 $\Gamma(\eta \ell^+ \nu_e)/\Gamma_{\text{total}}$   $\Gamma_{19}/\Gamma$ 

VALUE (units $10^{-4}$ )	CL%	DOCUMENT ID	TECN	COMMENT
<b>0.39 ± 0.08 OUR AVERAGE</b>				
Error includes scale factor of 1.3.				
0.36 ± 0.05 ± 0.04		<sup>1</sup> DEL-AMO-SA...11F	BABR	$e^+ e^- \rightarrow \mathcal{T}(4S)$
0.64 ± 0.20 ± 0.03		<sup>2</sup> AUBERT 08AV	BABR	$e^+ e^- \rightarrow \mathcal{T}(4S)$

• • • We do not use the following data for averages, fits, limits, etc. • • •

0.31 ± 0.06 ± 0.08		<sup>3</sup> AUBERT 09Q	BABR	Repl. by DEL-AMO-SANCHEZ 11F
<1.01	90	<sup>4</sup> ADAM 07	CLE2	$e^+ e^- \rightarrow \mathcal{T}(4S)$
0.84 ± 0.31 ± 0.18		<sup>5</sup> ATHAR 03	CLE2	Repl. by ADAM 07

- 1 Uses the neutrino reconstruction technique. Assumes  $B(Y(4S) \rightarrow B^+ B^-) = (51.6 \pm 0.6)\%$  and  $B(Y(4S) \rightarrow B^0 \bar{B}^0) = (48.4 \pm 0.6)\%$ .  
 2 Assumes equal production of  $B^+$  and  $B^0$  at the  $\mathcal{T}(4S)$ .  
 3 Uses the neutrino reconstruction technique. Assumes  $B(\mathcal{T}(4S) \rightarrow B^+ B^-) = (51.6 \pm 0.6)\%$  and  $B(\mathcal{T}(4S) \rightarrow B^0 \bar{B}^0) = (48.4 \pm 0.6)\%$ .  
 4 The  $B^0$  and  $B^+$  results are combined assuming the isospin,  $B$  lifetimes, and relative charged/neutral  $B$  production at the  $\mathcal{T}(4S)$ .  
 5 ATHAR 03 reports systematic errors  $0.16 \pm 0.09$ , which are experimental systematic and systematic due to model dependence. We combine these in quadrature.

 $\Gamma(\eta' \ell^+ \nu_e)/\Gamma_{\text{total}}$   $\Gamma_{20}/\Gamma$ 

VALUE (units $10^{-4}$ )	CL%	DOCUMENT ID	TECN	COMMENT
<b>0.23 ± 0.08 OUR AVERAGE</b>				
0.24 ± 0.08 ± 0.03		<sup>1</sup> DEL-AMO-SA...11F	BABR	$e^+ e^- \rightarrow \mathcal{T}(4S)$
0.04 ± 0.22 ± 0.05 -0.02		<sup>2</sup> AUBERT 08AV	BABR	$e^+ e^- \rightarrow \mathcal{T}(4S)$
2.66 ± 0.80 ± 0.56		<sup>3</sup> ADAM 07	CLE2	$e^+ e^- \rightarrow \mathcal{T}(4S)$

- 1 Uses the neutrino reconstruction technique. Assumes  $B(Y(4S) \rightarrow B^+ B^-) = (51.6 \pm 0.6)\%$  and  $B(Y(4S) \rightarrow B^0 \bar{B}^0) = (48.4 \pm 0.6)\%$ .  
 2 Assumes equal production of  $B^+$  and  $B^0$  at the  $\mathcal{T}(4S)$ .  
 3 The  $B^0$  and  $B^+$  results are combined assuming the isospin,  $B$  lifetimes, and relative charged/neutral  $B$  production at the  $\mathcal{T}(4S)$ . Corresponds to 90% CL interval  $(1.20-4.46) \times 10^{-4}$ .

 $\Gamma(\omega \ell^+ \nu_e)/\Gamma_{\text{total}}$   $\Gamma_{21}/\Gamma$ 

VALUE (units $10^{-4}$ )	CL%	DOCUMENT ID	TECN	COMMENT
<b>1.15 ± 0.17 OUR AVERAGE</b>				
1.14 ± 0.16 ± 0.08		<sup>1</sup> AUBERT 09Q	BABR	$e^+ e^- \rightarrow \mathcal{T}(4S)$
1.3 ± 0.4 ± 0.4		<sup>2</sup> SCHWA NDA 04	BELL	$e^+ e^- \rightarrow \mathcal{T}(4S)$

• • • We do not use the following data for averages, fits, limits, etc. • • •

<2.1	90	<sup>3</sup> BEAN 93B	CLE2	$e^+ e^- \rightarrow \mathcal{T}(4S)$
------	----	-----------------------	------	---------------------------------------

- 1 Uses  $B(\mathcal{T}(4S) \rightarrow B^+ B^-) = (51.6 \pm 0.6)\%$  and  $B(\mathcal{T}(4S) \rightarrow B^0 \bar{B}^0) = (48.4 \pm 0.6)\%$ .  
 2 Assumes equal production of  $B^+$  and  $B^0$  at the  $\mathcal{T}(4S)$ .  
 3 BEAN 93B limit set using ISGW Model. Using isospin and the quark model to combine  $\Gamma(\rho^0 \ell^+ \nu_e)$  and  $\Gamma(\rho^- \ell^+ \nu_e)$  with this result, they obtain a limit  $<(1.6-2.7) \times 10^{-4}$  at 90% CL for  $B^+ \rightarrow \omega \ell^+ \nu_e$ . The range corresponds to the ISGW, WSB, and KS models. An upper limit on  $|V_{ub}/V_{cb}| < 0.8-0.13$  at 90% CL is derived as well.

 $\Gamma(\omega \mu^+ \nu_{\mu})/\Gamma_{\text{total}}$   $\Gamma_{22}/\Gamma$ 

VALUE	CL%	DOCUMENT ID	TECN	COMMENT
<b>• • • We do not use the following data for averages, fits, limits, etc. • • •</b>				
seen		<sup>1</sup> ALBRECHT 91c	ARG	

- 1 In ALBRECHT 91c, one event is fully reconstructed providing evidence for the  $b \rightarrow u$  transition.

 $\Gamma(\rho^0 \ell^+ \nu_e)/\Gamma_{\text{total}}$   $\Gamma_{23}/\Gamma$ 

VALUE (units $10^{-4}$ )	CL%	DOCUMENT ID	TECN	COMMENT
<b>1.07 ± 0.13 OUR AVERAGE</b>				
0.94 ± 0.08 ± 0.14		<sup>1</sup> DEL-AMO-SA...11c	BABR	$e^+ e^- \rightarrow \mathcal{T}(4S)$
1.33 ± 0.23 ± 0.18		<sup>2</sup> HOKUUE 07	BELL	$e^+ e^- \rightarrow \mathcal{T}(4S)$
1.34 ± 0.15 ± 0.28 -0.32		<sup>3</sup> BEHRENS 00	CLE2	$e^+ e^- \rightarrow \mathcal{T}(4S)$

• • • We do not use the following data for averages, fits, limits, etc. • • •

1.16 ± 0.11 ± 0.30		<sup>1</sup> AUBERT,B 05o	BABR	Repl. by DEL-AMO-SANCHEZ 11c
1.40 ± 0.21 ± 0.32 -0.33		<sup>3</sup> BEHRENS 00	CLE2	$e^+ e^- \rightarrow \mathcal{T}(4S)$
1.2 ± 0.2 ± 0.3 -0.4		<sup>3</sup> ALEXANDER 96T	CLE2	$e^+ e^- \rightarrow \mathcal{T}(4S)$
<2.1	90	<sup>4</sup> BEAN 93B	CLE2	$e^+ e^- \rightarrow \mathcal{T}(4S)$

- 1  $B^+$  and  $B^0$  decays combined assuming isospin symmetry. Systematic errors include both experimental and form-factor uncertainties.  
 2 The signal events are tagged by a second  $B$  meson reconstructed in the semileptonic mode  $B \rightarrow D^{(*)} \ell \nu_{\ell}$ .  
 3 Derived based in the reported  $B^0$  result by assuming isospin symmetry:  $\Gamma(B^0 \rightarrow \rho^- \ell^+ \nu) = 2\Gamma(B^+ \rightarrow \rho^0 \ell^+ \nu) \approx 2\Gamma(B^+ \rightarrow \omega \ell^+ \nu)$ .  
 4 BEAN 93B limit set using ISGW Model. Using isospin and the quark model to combine  $\Gamma(\omega^0 \ell^+ \nu_e)$  and  $\Gamma(\rho^- \ell^+ \nu_e)$  with this result, they obtain a limit  $<(1.6-2.7) \times 10^{-4}$  at 90% CL for  $B^+ \rightarrow \rho^0 \ell^+ \nu_e$ . The range corresponds to the ISGW, WSB, and KS models. An upper limit on  $|V_{ub}/V_{cb}| < 0.8-0.13$  at 90% CL is derived as well.

 $\Gamma(\rho^0 e^+ \nu_e)/\Gamma_{\text{total}}$   $\Gamma_{24}/\Gamma$ 

VALUE	CL%	DOCUMENT ID	TECN	COMMENT
<b>&lt;5.2 × 10<sup>-3</sup></b>				
<5.2 × 10 <sup>-3</sup>	90	<sup>1</sup> ADAM 03B	CLE2	$e^+ e^- \rightarrow \mathcal{T}(4S)$

<sup>1</sup> Based on phase-space model; if  $V-A$  model is used, the 90% CL upper limit becomes  $<1.2 \times 10^{-3}$ .

 $\Gamma(e^+ \nu_e)/\Gamma_{\text{total}}$   $\Gamma_{25}/\Gamma$ 

VALUE (units $10^{-6}$ )	CL%	DOCUMENT ID	TECN	COMMENT
<b>&lt; 0.98</b>				
< 0.98	90	<sup>1</sup> SATOYAMA 07	BELL	$e^+ e^- \rightarrow \mathcal{T}(4S)$

• • • We do not use the following data for averages, fits, limits, etc. • • •

< 8	90	<sup>1</sup> AUBERT 10E	BABR	$e^+ e^- \rightarrow \mathcal{T}(4S)$
< 1.9	90	<sup>1</sup> AUBERT 09V	BABR	$e^+ e^- \rightarrow \mathcal{T}(4S)$
< 5.2	90	<sup>1</sup> AUBERT 08AD	BABR	$e^+ e^- \rightarrow \mathcal{T}(4S)$
< 15	90	ARTUSO 95	CLE2	$e^+ e^- \rightarrow \mathcal{T}(4S)$

<sup>1</sup> Assumes equal production of  $B^+$  and  $B^0$  at the  $\mathcal{T}(4S)$ .

 $\Gamma(\mu^+ \nu_{\mu})/\Gamma_{\text{total}}$   $\Gamma_{26}/\Gamma$ 

VALUE (units $10^{-6}$ )	CL%	DOCUMENT ID	TECN	COMMENT
<b>&lt; 1.0</b>				
< 1.0	90	<sup>1</sup> AUBERT 09V	BABR	$e^+ e^- \rightarrow \mathcal{T}(4S)$

• • • We do not use the following data for averages, fits, limits, etc. • • •

< 11	90	<sup>1</sup> AUBERT 10E	BABR	$e^+ e^- \rightarrow \mathcal{T}(4S)$
< 5.6	90	<sup>1</sup> AUBERT 08AD	BABR	$e^+ e^- \rightarrow \mathcal{T}(4S)$
< 1.7	90	<sup>1</sup> SATOYAMA 07	BELL	$e^+ e^- \rightarrow \mathcal{T}(4S)$
< 6.6	90	AUBERT 04o	BABR	Repl. by AUBERT 09V
< 21	90	ARTUSO 95	CLE2	$e^+ e^- \rightarrow \mathcal{T}(4S)$

<sup>1</sup> Assumes equal production of  $B^+$  and  $B^0$  at the  $\mathcal{T}(4S)$ .

 $\Gamma(\tau^+ \nu_{\tau})/\Gamma_{\text{total}}$   $\Gamma_{27}/\Gamma$ 

See the note on "Decay Constants of Charged Pseudoscalar Mesons" in the  $D_s^+$  Listings.

VALUE (units $10^{-4}$ )	CL%	DOCUMENT ID	TECN	COMMENT
<b>1.65 ± 0.34 OUR AVERAGE</b>				
1.7 ± 0.8 ± 0.2		<sup>1,2</sup> AUBERT 10E	BABR	$e^+ e^- \rightarrow \mathcal{T}(4S)$
1.54 <sup>+0.38+0.29</sup> -0.37-0.31		<sup>1,3</sup> HARA 10	BELL	$e^+ e^- \rightarrow \mathcal{T}(4S)$
1.8 <sup>+0.9+0.45</sup> -0.8		<sup>1,4</sup> AUBERT 08D	BABR	$e^+ e^- \rightarrow \mathcal{T}(4S)$
1.79 <sup>+0.56+0.46</sup> -0.49-0.51		<sup>1,4</sup> IKADO 06	BELL	$e^+ e^- \rightarrow \mathcal{T}(4S)$

- • • We do not use the following data for averages, fits, limits, etc. • • •
- |                 |    |                            |      |                                       |
|-----------------|----|----------------------------|------|---------------------------------------|
| 0.9 ± 0.6 ± 0.1 |    | <sup>1,2</sup> AUBERT 07AL | BABR | Repl. by AUBERT 10E                   |
| < 2.6           | 90 | <sup>1</sup> AUBERT 06K    | BABR | $e^+ e^- \rightarrow \mathcal{T}(4S)$ |
| < 4.2           | 90 | <sup>1</sup> AUBERT,B 05B  | BABR | Repl. by AUBERT 06K                   |
| < 8.3           | 90 | <sup>5</sup> BARATE 01E    | ALEP | $e^+ e^- \rightarrow Z$               |
| < 8.4           | 90 | <sup>1</sup> BROWDER 01    | CLE2 | $e^+ e^- \rightarrow \mathcal{T}(4S)$ |
| < 5.7           | 90 | <sup>6</sup> ACCIARRI 97F  | L3   | $e^+ e^- \rightarrow Z$               |
| < 104           | 90 | <sup>7</sup> ALBRECHT 95D  | ARG  | $e^+ e^- \rightarrow \mathcal{T}(4S)$ |
| < 22            | 90 | ARTUSO 95                  | CLE2 | $e^+ e^- \rightarrow \mathcal{T}(4S)$ |
| < 18            | 90 | <sup>8</sup> BUSKULIC 95   | ALEP | $e^+ e^- \rightarrow Z$               |

- 1 Assumes equal production of  $B^+$  and  $B^0$  at the  $\mathcal{T}(4S)$ .  
 2 Requires one reconstructed semileptonic  $B$  decay  $B^- \rightarrow D^0 \ell^- \bar{\nu}_{\ell} X$  in the recoil.  
 3 Requires one reconstructed semileptonic  $B$  decay  $B^- \rightarrow D^{(*)0} \ell^- \bar{\nu}_{\ell} X$  in the recoil.  
 4 The analysis is based on a sample of events with one fully reconstructed tag  $B$  in a hadronic decay mode  $B^- \rightarrow D^{(*)0} X^-$ .  
 5 The energy-flow and  $b$ -tagging algorithms were used.  
 6 ACCIARRI 97F uses missing-energy technique and  $f(b \rightarrow B^-) = (38.2 \pm 2.5)\%$ .  
 7 ALBRECHT 95D uses full reconstruction of one  $B$  decay as tag.  
 8 BUSKULIC 95 uses same missing-energy technique as in  $\bar{b} \rightarrow \tau^+ \nu_{\tau} X$ , but analysis is restricted to endpoint region of missing-energy distribution.

 $\Gamma(\ell^+ \nu_{\ell} \gamma)/\Gamma_{\text{total}}$   $\Gamma_{28}/\Gamma$ 

VALUE	CL%	DOCUMENT ID	TECN	COMMENT
<b>&lt;15.6 × 10<sup>-6</sup></b>				
<15.6 × 10 <sup>-6</sup>	90	<sup>1</sup> AUBERT 09AT	BABR	$e^+ e^- \rightarrow \mathcal{T}(4S)$

<sup>1</sup> Assumes equal production of  $B^+$  and  $B^0$  at the  $\mathcal{T}(4S)$ .

 $\Gamma(e^+ \nu_e \gamma)/\Gamma_{\text{total}}$   $\Gamma_{29}/\Gamma$ 

VALUE	CL%	DOCUMENT ID	TECN	COMMENT
<b>&lt; 17 × 10<sup>-6</sup></b>				
< 17 × 10 <sup>-6</sup>	90	<sup>1</sup> AUBERT 09AT	BABR	$e^+ e^- \rightarrow \mathcal{T}(4S)$

• • • We do not use the following data for averages, fits, limits, etc. • • •

< 200 × 10 <sup>-6</sup>	90	<sup>2</sup> BROWDER 97	CLE2	$e^+ e^- \rightarrow \mathcal{T}(4S)$
--------------------------	----	-------------------------	------	---------------------------------------

<sup>1</sup> Assumes equal production of  $B^+$  and  $B^0$  at the  $\mathcal{T}(4S)$ .  
<sup>2</sup> BROWDER 97 uses the hermiticity of the CLEO II detector to reconstruct the neutrino energy and momentum.

## Meson Particle Listings

 $B^\pm$  $\Gamma(\mu^+ \nu_\mu \gamma)/\Gamma_{\text{total}}$   $\Gamma_{30}/\Gamma$ 

VALUE	CL%	DOCUMENT ID	TECN	COMMENT
$<24 \times 10^{-6}$	90	<sup>1</sup> AUBERT	09AT	BABR $e^+ e^- \rightarrow \Upsilon(4S)$
$<52 \times 10^{-6}$	90	<sup>2</sup> BROWDER	97	CLE2 $e^+ e^- \rightarrow \Upsilon(4S)$

<sup>1</sup> Assumes equal production of  $B^+$  and  $B^0$  at the  $\Upsilon(4S)$ .  
<sup>2</sup> BROWDER 97 uses the hermiticity of the CLEOII detector to reconstruct the neutrino energy and momentum.

 $\Gamma(D^0 X)/\Gamma_{\text{total}}$   $\Gamma_{31}/\Gamma$ 

VALUE	DOCUMENT ID	TECN	COMMENT
$0.086 \pm 0.006 \pm 0.004$	<sup>1</sup> AUBERT	07N	BABR $e^+ e^- \rightarrow \Upsilon(4S)$
$0.098 \pm 0.009 \pm 0.006$	<sup>1</sup> AUBERT, BE	04B	BABR Repl. by AUBERT 07N

<sup>1</sup> Events are selected by completely reconstructing one  $B$  and searching for a reconstructed charmed particle in the rest of the event. The last error includes systematic and charm branching ratio uncertainties.

 $\Gamma(\overline{D}^0 X)/\Gamma_{\text{total}}$   $\Gamma_{32}/\Gamma$ 

VALUE	DOCUMENT ID	TECN	COMMENT
$0.786 \pm 0.016 \pm 0.034$ $-0.033$	<sup>1</sup> AUBERT	07N	BABR $e^+ e^- \rightarrow \Upsilon(4S)$
$0.793 \pm 0.025 \pm 0.045$ $-0.044$	<sup>1</sup> AUBERT, BE	04B	BABR Repl. by AUBERT 07N

<sup>1</sup> Events are selected by completely reconstructing one  $B$  and searching for a reconstructed charmed particle in the rest of the event. The last error includes systematic and charm branching ratio uncertainties.

 $\Gamma(D^0 X)/[\Gamma(D^0 X) + \Gamma(\overline{D}^0 X)]$   $\Gamma_{31}/(\Gamma_{31} + \Gamma_{32})$ 

VALUE	DOCUMENT ID	TECN	COMMENT
$0.098 \pm 0.007 \pm 0.001$	AUBERT	07N	BABR $e^+ e^- \rightarrow \Upsilon(4S)$
$0.110 \pm 0.010 \pm 0.003$	AUBERT, BE	04B	BABR Repl. by AUBERT 07N

 $\Gamma(D^+ X)/\Gamma_{\text{total}}$   $\Gamma_{33}/\Gamma$ 

VALUE	DOCUMENT ID	TECN	COMMENT
$0.025 \pm 0.005 \pm 0.002$	<sup>1</sup> AUBERT	07N	BABR $e^+ e^- \rightarrow \Upsilon(4S)$
$0.038 \pm 0.009 \pm 0.005$	<sup>1</sup> AUBERT, BE	04B	BABR Repl. by AUBERT 07N

<sup>1</sup> Events are selected by completely reconstructing one  $B$  and searching for a reconstructed charmed particle in the rest of the event. The last error includes systematic and charm branching ratio uncertainties.

 $\Gamma(D^- X)/\Gamma_{\text{total}}$   $\Gamma_{34}/\Gamma$ 

VALUE	DOCUMENT ID	TECN	COMMENT
$0.099 \pm 0.008 \pm 0.009$	<sup>1</sup> AUBERT	07N	BABR $e^+ e^- \rightarrow \Upsilon(4S)$
$0.098 \pm 0.012 \pm 0.014$	<sup>1</sup> AUBERT, BE	04B	BABR Repl. by AUBERT 07N

<sup>1</sup> Events are selected by completely reconstructing one  $B$  and searching for a reconstructed charmed particle in the rest of the event. The last error includes systematic and charm branching ratio uncertainties.

 $\Gamma(D^+ X)/[\Gamma(D^+ X) + \Gamma(D^- X)]$   $\Gamma_{33}/(\Gamma_{33} + \Gamma_{34})$ 

VALUE	DOCUMENT ID	TECN	COMMENT
$0.204 \pm 0.035 \pm 0.001$	AUBERT	07N	BABR $e^+ e^- \rightarrow \Upsilon(4S)$
$0.278 \pm 0.052 \pm 0.009$	AUBERT, BE	04B	BABR Repl. by AUBERT 07N

 $\Gamma(D_s^+ X)/\Gamma_{\text{total}}$   $\Gamma_{35}/\Gamma$ 

VALUE	DOCUMENT ID	TECN	COMMENT
$0.079 \pm 0.006 \pm 0.013$ $-0.011$	<sup>1</sup> AUBERT	07N	BABR $e^+ e^- \rightarrow \Upsilon(4S)$
$0.143 \pm 0.016 \pm 0.051$ $-0.034$	<sup>1</sup> AUBERT, BE	04B	BABR Repl. by AUBERT 07N

<sup>1</sup> Events are selected by completely reconstructing one  $B$  and searching for a reconstructed charmed particle in the rest of the event. The last error includes systematic and charm branching ratio uncertainties.

 $\Gamma(D_s^- X)/\Gamma_{\text{total}}$   $\Gamma_{36}/\Gamma$ 

VALUE	CL%	DOCUMENT ID	TECN	COMMENT
$0.011 \pm 0.004 \pm 0.002$ $-0.003 - 0.001$		<sup>1</sup> AUBERT	07N	BABR $e^+ e^- \rightarrow \Upsilon(4S)$
$<0.022$	90	<sup>1</sup> AUBERT, BE	04B	BABR Repl. by AUBERT 07N

<sup>1</sup> Events are selected by completely reconstructing one  $B$  and searching for a reconstructed charmed particle in the rest of the event. The last error includes systematic and charm branching ratio uncertainties.

 $\Gamma(D_s^+ X)/[\Gamma(D_s^+ X) + \Gamma(D_s^- X)]$   $\Gamma_{35}/(\Gamma_{35} + \Gamma_{36})$ 

VALUE	DOCUMENT ID	TECN	COMMENT
$0.884 \pm 0.038 \pm 0.002$	AUBERT	07N	BABR $e^+ e^- \rightarrow \Upsilon(4S)$
$0.966 \pm 0.039 \pm 0.012$	AUBERT, BE	04B	BABR Repl. by AUBERT 07N

 $\Gamma(D_s^- X)/[\Gamma(D_s^+ X) + \Gamma(D_s^- X)]$   $\Gamma_{36}/(\Gamma_{35} + \Gamma_{36})$ 

VALUE	CL%	DOCUMENT ID	TECN	COMMENT
$<0.126$	90	AUBERT, BE	04B	BABR $e^+ e^- \rightarrow \Upsilon(4S)$

 $\Gamma(\Lambda_c^+ X)/\Gamma_{\text{total}}$   $\Gamma_{37}/\Gamma$ 

VALUE	DOCUMENT ID	TECN	COMMENT
$0.021 \pm 0.005 \pm 0.008$ $-0.004$	<sup>1</sup> AUBERT	07N	BABR $e^+ e^- \rightarrow \Upsilon(4S)$
$0.029 \pm 0.008 \pm 0.011$ $-0.007$	<sup>1</sup> AUBERT, BE	04B	BABR Repl. by AUBERT 07N

<sup>1</sup> Events are selected by completely reconstructing one  $B$  and searching for a reconstructed charmed particle in the rest of the event. The last error includes systematic and charm branching ratio uncertainties.

 $\Gamma(\overline{\Lambda}_c^- X)/\Gamma_{\text{total}}$   $\Gamma_{38}/\Gamma$ 

VALUE	DOCUMENT ID	TECN	COMMENT
$0.028 \pm 0.005 \pm 0.010$ $-0.007$	<sup>1</sup> AUBERT	07N	BABR $e^+ e^- \rightarrow \Upsilon(4S)$
$0.035 \pm 0.008 \pm 0.013$ $-0.009$	<sup>1</sup> AUBERT, BE	04B	BABR Repl. by AUBERT 07N

<sup>1</sup> Events are selected by completely reconstructing one  $B$  and searching for a reconstructed charmed particle in the rest of the event. The last error includes systematic and charm branching ratio uncertainties.

 $\Gamma(\Lambda_c^+ X)/[\Gamma(\Lambda_c^+ X) + \Gamma(\overline{\Lambda}_c^- X)]$   $\Gamma_{37}/(\Gamma_{37} + \Gamma_{38})$ 

VALUE	DOCUMENT ID	TECN	COMMENT
$0.427 \pm 0.071 \pm 0.001$	AUBERT	07N	BABR $e^+ e^- \rightarrow \Upsilon(4S)$
$0.452 \pm 0.090 \pm 0.003$	AUBERT, BE	04B	BABR Repl. by AUBERT 07N

 $\Gamma(\overline{\Sigma}^+ X)/\Gamma_{\text{total}}$   $\Gamma_{39}/\Gamma$ 

VALUE	DOCUMENT ID	TECN	COMMENT
$0.968 \pm 0.019 \pm 0.041$ $-0.039$	<sup>1</sup> AUBERT	07N	BABR $e^+ e^- \rightarrow \Upsilon(4S)$
$0.983 \pm 0.030 \pm 0.054$ $-0.051$	<sup>1</sup> AUBERT, BE	04B	BABR Repl. by AUBERT 07N

<sup>1</sup> Events are selected by completely reconstructing one  $B$  and searching for a reconstructed charmed particle in the rest of the event. The last error includes systematic and charm branching ratio uncertainties.

 $\Gamma(c X)/\Gamma_{\text{total}}$   $\Gamma_{40}/\Gamma$ 

VALUE	DOCUMENT ID	TECN	COMMENT
$0.234 \pm 0.012 \pm 0.018$ $-0.014$	<sup>1</sup> AUBERT	07N	BABR $e^+ e^- \rightarrow \Upsilon(4S)$
$0.330 \pm 0.022 \pm 0.055$ $-0.037$	<sup>1</sup> AUBERT, BE	04B	BABR Repl. by AUBERT 07N

<sup>1</sup> Events are selected by completely reconstructing one  $B$  and searching for a reconstructed charmed particle in the rest of the event. The last error includes systematic and charm branching ratio uncertainties.

 $\Gamma(\overline{\Sigma}^+ X)/\Gamma_{\text{total}}$   $\Gamma_{41}/\Gamma$ 

VALUE	DOCUMENT ID	TECN	COMMENT
$1.202 \pm 0.023 \pm 0.053$ $-0.049$	<sup>1</sup> AUBERT	07N	BABR $e^+ e^- \rightarrow \Upsilon(4S)$
$1.313 \pm 0.037 \pm 0.088$ $-0.075$	<sup>1</sup> AUBERT, BE	04B	BABR Repl. by AUBERT 07N

<sup>1</sup> Events are selected by completely reconstructing one  $B$  and searching for a reconstructed charmed particle in the rest of the event. The last error includes systematic and charm branching ratio uncertainties.

 $\Gamma(\overline{D}^0 \pi^+)/\Gamma_{\text{total}}$   $\Gamma_{42}/\Gamma$ 

VALUE (units $10^{-3}$ )	EVTS	DOCUMENT ID	TECN	COMMENT
<b><math>4.81 \pm 0.15</math> OUR FIT</b>				
<b><math>4.84 \pm 0.15</math> OUR AVERAGE</b>				
$4.90 \pm 0.07 \pm 0.22$		<sup>1</sup> AUBERT	07N	BABR $e^+ e^- \rightarrow \Upsilon(4S)$
$5.3 \pm 0.6 \pm 0.3$		<sup>2</sup> ABULENCIA	06J	CDF $p\overline{p}$ at 1.96 TeV
$4.49 \pm 0.21 \pm 0.23$		<sup>3</sup> AUBERT, BE	06J	BABR $e^+ e^- \rightarrow \Upsilon(4S)$
$4.97 \pm 0.12 \pm 0.29$		<sup>1,4</sup> AHMED	02B	CLE2 $e^+ e^- \rightarrow \Upsilon(4S)$
$5.0 \pm 0.7 \pm 0.6$	54	<sup>5</sup> BORTOLETTO	92	CLEO $e^+ e^- \rightarrow \Upsilon(4S)$
$5.4 \pm 1.8 \pm 1.2$ $-1.5 - 0.9$	14	<sup>6</sup> BEBEK	87	CLEO $e^+ e^- \rightarrow \Upsilon(4S)$
$4.76 \pm 0.26 \pm 0.05$ $-0.06$		<sup>7</sup> AUBERT, B	04P	BABR Repl. by AUBERT 07N
$5.5 \pm 0.4 \pm 0.5$	304	<sup>8</sup> ALAM	94	CLE2 Repl. by AHMED 02B
$2.0 \pm 0.8 \pm 0.6$	12	<sup>5</sup> ALBRECHT	90J	ARG $e^+ e^- \rightarrow \Upsilon(4S)$
$1.9 \pm 1.0 \pm 0.6$	7	<sup>9</sup> ALBRECHT	88K	ARG $e^+ e^- \rightarrow \Upsilon(4S)$

<sup>1</sup> Events are selected by completely reconstructing one  $B$  and searching for a reconstructed charmed particle in the rest of the event. The last error includes systematic and charm branching ratio uncertainties.

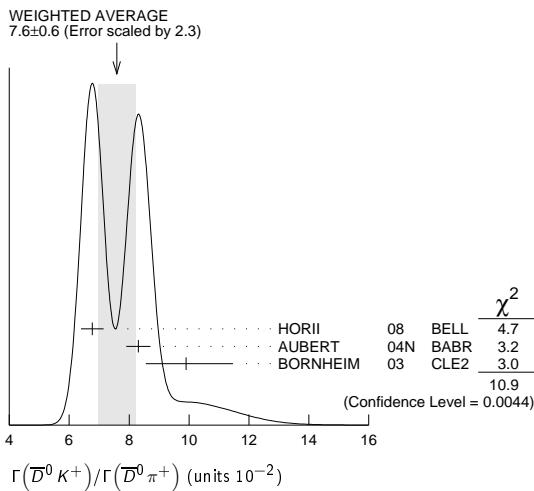
- Assumes equal production of  $B^+$  and  $B^0$  at the  $\Upsilon(4S)$ .
- ABULENCIA 06J reports  $[\Gamma(B^+ \rightarrow \bar{D}^0 \pi^+)/\Gamma_{\text{total}}] / [B(B^0 \rightarrow D^- \pi^+)] = 1.97 \pm 0.10 \pm 0.21$  which we multiply by our best value  $B(B^0 \rightarrow D^- \pi^+) = (2.68 \pm 0.13) \times 10^{-3}$ . Our first error is their experiment's error and our second error is the systematic error from using our best value.
- Uses a missing-mass method. Does not depend on  $D$  branching fractions or  $B^+/B^0$  production rates.
- AHMED 02B reports an additional uncertainty on the branching ratios to account for 4.5% uncertainty on relative production of  $B^0$  and  $B^+$ , which is not included here.
- Assumes equal production of  $B^+$  and  $B^0$  at the  $\Upsilon(4S)$  and uses the MarkIII branching fractions for the  $D$ .
- BEBEK 87 value has been updated in BERKELMAN 91 to use same assumptions as noted for BORTOLETTO 92.
- AUBERT,B 04P reports  $[\Gamma(B^+ \rightarrow \bar{D}^0 \pi^+)/\Gamma_{\text{total}}] \times [B(D^0 \rightarrow K^- \pi^+)] = (1.846 \pm 0.032 \pm 0.097) \times 10^{-4}$  which we divide by our best value  $B(D^0 \rightarrow K^- \pi^+) = (3.88 \pm 0.05) \times 10^{-2}$ . Our first error is their experiment's error and our second error is the systematic error from using our best value.
- ALAM 94 assume equal production of  $B^+$  and  $B^0$  at the  $\Upsilon(4S)$  and use the CLEOII absolute  $B(D^0 \rightarrow K^- \pi^+)$  and the PDG 1992  $B(D^0 \rightarrow K^- \pi^+ \pi^0)/B(D^0 \rightarrow K^- \pi^+)$  and  $B(D^0 \rightarrow K^- 2\pi^+ \pi^-)/B(D^0 \rightarrow K^- \pi^+)$ .
- ALBRECHT 88k assumes  $B^0 \bar{B}^0 : B^+ B^-$  ratio is 45:55. Superseded by ALBRECHT 90J.

$\Gamma(\bar{D}^0 \rho^+)/\Gamma_{\text{total}}$   $\Gamma_{45}/\Gamma$

VALUE	EVTs	DOCUMENT ID	TECN	COMMENT
<b>0.0134 ± 0.0018 OUR AVERAGE</b>				
0.0135 ± 0.0012 ± 0.0015	212	<sup>1</sup> ALAM 94	CLE2	$e^+ e^- \rightarrow \Upsilon(4S)$
0.013 ± 0.004 ± 0.004	19	<sup>2</sup> ALBRECHT 90J	ARG	$e^+ e^- \rightarrow \Upsilon(4S)$
• • • We do not use the following data for averages, fits, limits, etc. • • •				
0.021 ± 0.008 ± 0.009	10	<sup>3</sup> ALBRECHT 88k	ARG	$e^+ e^- \rightarrow \Upsilon(4S)$
<sup>1</sup> ALAM 94 assume equal production of $B^+$ and $B^0$ at the $\Upsilon(4S)$ and use the CLEOII absolute $B(D^0 \rightarrow K^- \pi^+)$ and the PDG 1992 $B(D^0 \rightarrow K^- \pi^+ \pi^0)/B(D^0 \rightarrow K^- \pi^+)$ and $B(D^0 \rightarrow K^- 2\pi^+ \pi^-)/B(D^0 \rightarrow K^- \pi^+)$ .				
<sup>2</sup> Assumes equal production of $B^+$ and $B^0$ at the $\Upsilon(4S)$ and uses the MarkIII branching fractions for the $D$ .				
<sup>3</sup> ALBRECHT 88k assumes $B^0 \bar{B}^0 : B^+ B^-$ ratio is 45:55.				

$\Gamma(\bar{D}^0 K^+)/\Gamma(\bar{D}^0 \pi^+)$   $\Gamma_{46}/\Gamma_{42}$

VALUE (units $10^{-2}$ )	DOCUMENT ID	TECN	COMMENT
<b>7.6 ± 0.6 OUR AVERAGE</b>	Error includes scale factor of 2.3. See the ideogram below.		
6.77 ± 0.23 ± 0.30	HORII 08	BELL	$e^+ e^- \rightarrow \Upsilon(4S)$
8.31 ± 0.35 ± 0.20	AUBERT 04N	BABR	$e^+ e^- \rightarrow \Upsilon(4S)$
9.9 <sup>+1.4</sup> <sub>-1.2</sub> ± 0.7 ± 0.6	BORNHEIM 03	CLE2	$e^+ e^- \rightarrow \Upsilon(4S)$
• • • We do not use the following data for averages, fits, limits, etc. • • •			
9.4 ± 0.9 ± 0.7	ABE 03D	BELL	Repl. by SWAIN 03
7.7 ± 0.5 ± 0.6	SWAIN 03	BELL	Repl. by HORII 08
7.9 ± 0.9 ± 0.6	ABE 01I	BELL	Repl. by ABE 03D
5.5 ± 1.4 ± 0.5	ATHANAS 98	CLE2	Repl. by BORNHEIM 03



$\Gamma(D_{CP(+1)} K^+)/\Gamma(D_{CP(+1)} \pi^+)$   $\Gamma_{47}/\Gamma_{43}$

VALUE	DOCUMENT ID	TECN	COMMENT
<b>0.086 ± 0.009 OUR AVERAGE</b>			
0.086 ± 0.008 ± 0.007	<sup>1,2</sup> ABE 06	BELL	$e^+ e^- \rightarrow \Upsilon(4S)$
0.088 ± 0.016 ± 0.005	<sup>3</sup> AUBERT 04N	BABR	$e^+ e^- \rightarrow \Upsilon(4S)$
• • • We do not use the following data for averages, fits, limits, etc. • • •			
0.125 ± 0.036 ± 0.010	<sup>3</sup> ABE 03D	BELL	Repl. by SWAIN 03
0.093 ± 0.018 ± 0.008	<sup>3</sup> SWAIN 03	BELL	Repl. by ABE 06

- Reports a double ratio of  $B(B^+ \rightarrow D_{CP(+1)} K^+)/B(B^+ \rightarrow D_{CP(+1)} \pi^+)$  and  $B(B^+ \rightarrow \bar{D}^0 K^+)/B(B^+ \rightarrow \bar{D}^0 \pi^+)$ ,  $1.13 \pm 0.16 \pm 0.08$ . We multiply by our best value of  $B(B^+ \rightarrow \bar{D}^0 K^+)/B(B^+ \rightarrow \bar{D}^0 \pi^+) = 0.083 \pm 0.006$ . Our first error is their experiment's error and the second error is systematic error from using our best value.
- ABE 06 reports  $[\Gamma(B^+ \rightarrow D_{CP(+1)} K^+)/\Gamma(B^+ \rightarrow D_{CP(+1)} \pi^+)] / [\Gamma(B^+ \rightarrow \bar{D}^0 K^+)/\Gamma(B^+ \rightarrow \bar{D}^0 \pi^+)] = 1.13 \pm 0.06 \pm 0.08$  which we multiply by our best value  $\Gamma(B^+ \rightarrow \bar{D}^0 K^+)/\Gamma(B^+ \rightarrow \bar{D}^0 \pi^+) = 0.076 \pm 0.006$ . Our first error is their experiment's error and our second error is the systematic error from using our best value.
- $CP=+1$  eigenstate of  $D^0 \bar{D}^0$  system is reconstructed via  $K^+ K^-$  and  $\pi^+ \pi^-$ .

$\Gamma(D_{CP(+1)} K^+)/\Gamma(\bar{D}^0 K^+)$   $\Gamma_{47}/\Gamma_{46}$

VALUE	DOCUMENT ID	TECN	COMMENT
<b>0.60 ± 0.05 OUR AVERAGE</b>			
0.65 ± 0.12 ± 0.06	<sup>1</sup> AALTONEN 10A	CDF	$p\bar{p}$ at 1.96 TeV
0.590 ± 0.045 ± 0.025	<sup>2</sup> DEL-AMO-SA...10G	BABR	$e^+ e^- \rightarrow \Upsilon(4S)$
• • • We do not use the following data for averages, fits, limits, etc. • • •			
0.53 ± 0.05 ± 0.025	AUBERT 08AA	BABR	Repl. by DEL-AMO-SANCHEZ 10G
0.45 ± 0.06 ± 0.02	AUBERT 06J	BABR	Repl. by AUBERT 08AA
<sup>1</sup> Reports $R_{CP+} = 2 (B(B^- \rightarrow D_{CP(+1)} K^-) + B(B^+ \rightarrow D_{CP(+1)} K^+)) / (B(B^- \rightarrow D^0 K^-) + B(B^+ \rightarrow \bar{D}^0 K^+)) = 1.30 \pm 0.24 \pm 0.12$ that we have divided by 2.			
<sup>2</sup> Reports $R_{CP+} = 1.18 \pm 0.09 \pm 0.05$ that we have divided by 2.			

$\Gamma(D_{CP(-1)} K^+)/\Gamma(D_{CP(-1)} \pi^+)$   $\Gamma_{48}/\Gamma_{44}$

VALUE	DOCUMENT ID	TECN	COMMENT
<b>0.097 ± 0.016 ± 0.007</b>	<sup>1</sup> ABE 06	BELL	$e^+ e^- \rightarrow \Upsilon(4S)$
• • • We do not use the following data for averages, fits, limits, etc. • • •			
0.119 ± 0.028 ± 0.006	<sup>2</sup> ABE 03D	BELL	Repl. by SWAIN 03
0.108 ± 0.019 ± 0.007	<sup>2</sup> SWAIN 03	BELL	Repl. by ABE 06
<sup>1</sup> Reports a double ratio of $B(B^+ \rightarrow D_{CP(-1)} K^+)/B(B^+ \rightarrow D_{CP(-1)} \pi^+)$ and $B(B^+ \rightarrow \bar{D}^0 K^+)/B(B^+ \rightarrow \bar{D}^0 \pi^+)$ , $1.17 \pm 0.14 \pm 0.14$ . We multiply by our best value of $B(B^+ \rightarrow \bar{D}^0 K^+)/B(B^+ \rightarrow \bar{D}^0 \pi^+) = 0.083 \pm 0.006$ . Our first error is their experiment's error and the second error is systematic error from using our best value.			
<sup>2</sup> $CP=-1$ eigenstate of $D^0 \bar{D}^0$ system is reconstructed via $K_S^0 \pi^0$ , $K_S^0 \omega$ , $K_S^0 \phi$ , $K_S^0 \eta$ , and $K_S^0 \eta'$ .			

$\Gamma(D_{CP(-1)} K^+)/\Gamma(\bar{D}^0 K^+)$   $\Gamma_{48}/\Gamma_{46}$

VALUE	DOCUMENT ID	TECN	COMMENT
<b>0.54 ± 0.04 ± 0.02</b>	<sup>1</sup> DEL-AMO-SA...10G	BABR	$e^+ e^- \rightarrow \Upsilon(4S)$
• • • We do not use the following data for averages, fits, limits, etc. • • •			
0.515 ± 0.05 ± 0.025	AUBERT 08AA	BABR	Repl. by DEL-AMO-SANCHEZ 10G
0.43 ± 0.05 ± 0.02	AUBERT 06J	BABR	Repl. by AUBERT 08AA
<sup>1</sup> Reports $R_{CP+} = 1.07 \pm 0.08 \pm 0.04$ that we have divided by 2.			

$\Gamma([K^- \pi^+]_D K^+)/\Gamma_{\text{total}}$   $\Gamma_{49}/\Gamma$

VALUE	CL%	DOCUMENT ID	TECN	COMMENT
<b>&lt; 2.8 × 10<sup>-7</sup></b>	90	HORII 08	BELL	$e^+ e^- \rightarrow \Upsilon(4S)$
• • • We do not use the following data for averages, fits, limits, etc. • • •				
< 6.3 × 10 <sup>-7</sup>	90	SAIGO 05	BELL	$e^+ e^- \rightarrow \Upsilon(4S)$

$\Gamma([K^- \pi^+]_D K^+)/\Gamma([K^+ \pi^-]_D K^+)$   $\Gamma_{49}/\Gamma_{50}$

VALUE (units $10^{-3}$ )	CL%	DOCUMENT ID	TECN	COMMENT
<b>15.6 ± 3.3 OUR AVERAGE</b>				
22.0 ± 8.6 ± 2.6		<sup>1</sup> AALTONEN 11AJ	CDF	$p\bar{p}$ at 1.96 TeV
16.3 <sup>+4.4</sup> <sub>-4.1</sub> ± 0.7 ± 1.3		HORII 11	BELL	$e^+ e^- \rightarrow \Upsilon(4S)$
11 ± 6 ± 2		DEL-AMO-SA...10H	BABR	$e^+ e^- \rightarrow \Upsilon(4S)$
• • • We do not use the following data for averages, fits, limits, etc. • • •				
7.8 <sup>+6.2</sup> <sub>-5.7</sub> ± 2.0 ± 2.8		HORII 08	BELL	Repl. by HORII 11
< 29	90	<sup>2</sup> AUBERT 05G	BABR	Repl. by DEL-AMO-SANCHEZ 10H
< 44	90	<sup>3</sup> SAIGO 05	BELL	$e^+ e^- \rightarrow \Upsilon(4S)$
< 26	90	<sup>4</sup> AUBERT,B 04L	BABR	Repl. by AUBERT 05G

- AALTONEN 11AJ also measures the ratio separately for  $B^+$  ( $R^+(K)$ ) and  $B^-$  ( $R^-(K)$ ) and obtains:  $R^+(K) = (42.6 \pm 13.7 \pm 2.8) \times 10^{-3}$ ,  $R^-(K) = (3.8 \pm 10.3 \pm 2.7) \times 10^{-3}$ .
- AUBERT 05G extract a constraint on the magnitude of the ratio of amplitudes  $|A(B^+ \rightarrow D^0 K^+) / A(B^+ \rightarrow \bar{D}^0 K^+)| < 0.23$  at 90% CL (Bayesian). Similar measurements from  $B^+ \rightarrow D^{*0} K^+$  are also reported.
- SAIGO 05 extract a constraint on the magnitude of the ratio of amplitudes  $|A(B^+ \rightarrow D^0 K^+) / A(B^+ \rightarrow \bar{D}^0 K^+)| < 0.27$  at 90% CL.
- AUBERT,B 04L extract a constraint on the magnitude of the ratio of amplitudes  $|A(B^+ \rightarrow D^0 K^+) / A(B^+ \rightarrow \bar{D}^0 K^+)| < 0.22$  at 90% CL.



$\Gamma(\bar{D}_1(2420)^0 \pi^+ \times B(\bar{D}_1^0 \rightarrow D^*(2010)^- \pi^+))/\Gamma(D^0 \pi^+ \pi^+ \pi^-)$   $\Gamma_{77}/\Gamma_{71}$ 

VALUE (units $10^{-2}$ )	DOCUMENT ID	TECN	COMMENT
<b>9.3 ± 1.6 ± 0.9</b>	1 AAIJ	11E	LHCB $p\bar{p}$ at 7 TeV

<sup>1</sup> Uses  $B(D^*(2010)^+ \rightarrow D^0 \pi^+) = (67.7 \pm 0.5)\%$ .

 $\Gamma(D^- \pi^+ \pi^+)/\Gamma_{total}$   $\Gamma_{78}/\Gamma$ 

VALUE (units $10^{-3}$ )	CL%	EVTS	DOCUMENT ID	TECN	COMMENT
<b>1.07 ± 0.05 OUR AVERAGE</b>					
1.08 ± 0.03 ± 0.05			1 AUBERT	09AB	BABR $e^+e^- \rightarrow \Upsilon(4S)$
1.02 ± 0.04 ± 0.15			1 ABE	04D	BELL $e^+e^- \rightarrow \Upsilon(4S)$
• • • We do not use the following data for averages, fits, limits, etc. • • •					
<1.4	90		2 ALAM	94	CLE2 $e^+e^- \rightarrow \Upsilon(4S)$
<7	90		3 BORTOLETTO92	CLEO	$e^+e^- \rightarrow \Upsilon(4S)$
2.5 $^{+4.1}_{-2.3}$ $^{+2.4}_{-0.8}$		1	4 BEBEK	87	CLEO $e^+e^- \rightarrow \Upsilon(4S)$

- <sup>1</sup> Assumes equal production of  $B^+$  and  $B^0$  at the  $\Upsilon(4S)$ .  
<sup>2</sup> ALAM 94 assume equal production of  $B^+$  and  $B^0$  at the  $\Upsilon(4S)$  and use the MarkIII  $B(D^+ \rightarrow K^- 2\pi^+)$ .  
<sup>3</sup> BORTOLETTO 92 assumes equal production of  $B^+$  and  $B^0$  at the  $\Upsilon(4S)$  and uses Mark III branching fractions for the  $D$ . The product branching fraction into  $D_0^*(2340)\pi$  followed by  $D_0^*(2340) \rightarrow D\pi$  is  $< 0.005$  at 90%CL and into  $D_2^*(2460)$  followed by  $D_2^*(2460) \rightarrow D\pi$  is  $< 0.004$  at 90%CL.  
<sup>4</sup> BEBEK 87 assume the  $\Upsilon(4S)$  decays 43% to  $B^0\bar{B}^0$ .  $B(D^- \rightarrow K^+\pi^-\pi^-) = (9.1 \pm 1.3 \pm 0.4)\%$  is assumed.

 $\Gamma(D^+ K^0)/\Gamma_{total}$   $\Gamma_{79}/\Gamma$ 

VALUE (units $10^{-6}$ )	CL%	DOCUMENT ID	TECN	COMMENT
<b>&lt;2.9</b>	90	1 DEL-AMO-SA...10k	BABR	$e^+e^- \rightarrow \Upsilon(4S)$
• • • We do not use the following data for averages, fits, limits, etc. • • •				
<5.0	90	1 AUBERT,B	05E	BABR Repl. by DEL-AMO-SANCHEZ 10k

<sup>1</sup> Assumes equal production of  $B^+$  and  $B^0$  at the  $\Upsilon(4S)$ .

 $\Gamma(D^+ K^{*0})/\Gamma_{total}$   $\Gamma_{80}/\Gamma$ 

VALUE (units $10^{-6}$ )	CL%	DOCUMENT ID	TECN	COMMENT
<b>&lt;3.0</b>	90	1 DEL-AMO-SA...10k	BABR	$e^+e^- \rightarrow \Upsilon(4S)$

<sup>1</sup> Assumes equal production of  $B^+$  and  $B^0$  at the  $\Upsilon(4S)$ .

 $\Gamma(\bar{D}^*(2007)^0 \pi^+)/\Gamma_{total}$   $\Gamma_{81}/\Gamma$ 

VALUE (units $10^{-3}$ )	EVTS	DOCUMENT ID	TECN	COMMENT
<b>5.18 ± 0.26 OUR AVERAGE</b>				
5.52 ± 0.17 ± 0.42		1 AUBERT	07H	BABR $e^+e^- \rightarrow \Upsilon(4S)$
5.5 ± 0.4 ± 0.2		2,3 AUBERT,BE	06J	BABR $e^+e^- \rightarrow \Upsilon(4S)$
4.34 ± 0.47 ± 0.18		4 BRANDENB...	98	CLE2 $e^+e^- \rightarrow \Upsilon(4S)$
5.2 ± 0.7 ± 0.7	71	5 ALAM	94	CLE2 $e^+e^- \rightarrow \Upsilon(4S)$
7.2 ± 1.8 ± 1.6		6 BORTOLETTO92	CLEO	$e^+e^- \rightarrow \Upsilon(4S)$
4.0 ± 1.4 ± 1.2	9	7 ALBRECHT	90J	ARG $e^+e^- \rightarrow \Upsilon(4S)$
2.7 ± 4.4		7 BEBEK	87	CLEO $e^+e^- \rightarrow \Upsilon(4S)$

- <sup>1</sup> Assumes equal production of  $B^+$  and  $B^0$  at the  $\Upsilon(4S)$ .  
<sup>2</sup> AUBERT,BE 06J reports  $[\Gamma(B^+ \rightarrow \bar{D}^*(2007)^0 \pi^+)/\Gamma_{total}] / [B(B^+ \rightarrow \bar{D}^0 \pi^+)] = 1.14 \pm 0.07 \pm 0.04$  which we multiply by our best value  $B(B^+ \rightarrow \bar{D}^0 \pi^+) = (4.81 \pm 0.15) \times 10^{-3}$ . Our first error is their experiment's error and our second error is the systematic error from using our best value.  
<sup>3</sup> Uses a missing-mass method. Does not depend on  $D$  branching fractions or  $B^+/\bar{B}^0$  production rates.  
<sup>4</sup> BRANDENBURG 98 assume equal production of  $B^+$  and  $B^0$  at  $\Upsilon(4S)$  and use the  $D^*$  reconstruction technique. The first error is their experiment's error and the second error is the systematic error from the PDG 96 value of  $B(D^* \rightarrow D\pi)$ .  
<sup>5</sup> ALAM 94 assume equal production of  $B^+$  and  $B^0$  at the  $\Upsilon(4S)$  and use the CLEOII  $B(D^*(2007)^0 \rightarrow D^0 \pi^0)$  and absolute  $B(D^0 \rightarrow K^- \pi^+)$  and the PDG 1992  $B(D^0 \rightarrow K^- \pi^+ \pi^0)/B(D^0 \rightarrow K^- \pi^+)$  and  $B(D^0 \rightarrow K^- 2\pi^+ \pi^-)/B(D^0 \rightarrow K^- \pi^+)$ .  
<sup>6</sup> Assumes equal production of  $B^+$  and  $B^0$  at the  $\Upsilon(4S)$  and uses MarkIII branching fractions for the  $D$  and  $D^*(2010)$ .  
<sup>7</sup> This is a derived branching ratio, using the inclusive pion spectrum and other two-body  $B$  decays. BEBEK 87 assume the  $\Upsilon(4S)$  decays 43% to  $B^0\bar{B}^0$ .

 $\Gamma(\bar{D}^*(2007)^0 \omega \pi^+)/\Gamma_{total}$   $\Gamma_{84}/\Gamma$ 

VALUE	DOCUMENT ID	TECN	COMMENT
<b>0.0045 ± 0.0010 ± 0.0007</b>	1 ALEXANDER	01B	CLE2 $e^+e^- \rightarrow \Upsilon(4S)$

<sup>1</sup> Assumes equal production of  $B^+$  and  $B^0$  at the  $\Upsilon(4S)$ . The signal is consistent with all observed  $\omega \pi^+$  having proceeded through the  $\rho^+$  resonance at mass  $1349 \pm 25 \pm 10$  MeV and width  $547 \pm 86 \pm 46 \pm 45$  MeV.

 $\Gamma(\bar{D}^*(2007)^0 \rho^+)/\Gamma_{total}$   $\Gamma_{85}/\Gamma$ 

VALUE	EVTS	DOCUMENT ID	TECN	COMMENT
<b>0.0098 ± 0.0017 OUR AVERAGE</b>				
0.0098 ± 0.0006 ± 0.0017		1 CSORNA	03	CLE2 $e^+e^- \rightarrow \Upsilon(4S)$
0.010 ± 0.006 ± 0.004	7	2 ALBRECHT	90J	ARG $e^+e^- \rightarrow \Upsilon(4S)$
• • • We do not use the following data for averages, fits, limits, etc. • • •				
0.0168 ± 0.0021 ± 0.0028	86	3 ALAM	94	CLE2 $e^+e^- \rightarrow \Upsilon(4S)$

<sup>1</sup> Assumes equal production of  $B^0$  and  $B^+$  at the  $\Upsilon(4S)$  resonance. The second error combines the systematic and theoretical uncertainties in quadrature. CSORNA 03 includes data used in ALAM 94. A full angular fit to three complex helicity amplitudes is performed.

<sup>2</sup> Assumes equal production of  $B^+$  and  $B^0$  at the  $\Upsilon(4S)$  and uses MarkIII branching fractions for the  $D$  and  $D^*(2010)$ .

<sup>3</sup> ALAM 94 assume equal production of  $B^+$  and  $B^0$  at the  $\Upsilon(4S)$  and use the CLEOII  $B(D^*(2007)^0 \rightarrow D^0 \pi^0)$  and absolute  $B(D^0 \rightarrow K^- \pi^+)$  and the PDG 1992  $B(D^0 \rightarrow K^- \pi^+ \pi^0)/B(D^0 \rightarrow K^- \pi^+)$  and  $B(D^0 \rightarrow K^- 2\pi^+ \pi^-)/B(D^0 \rightarrow K^- \pi^+)$ . The nonresonant  $\pi^+ \pi^0$  contribution under the  $\rho^+$  is negligible.

 $\Gamma(\bar{D}^*(2007)^0 K^+)/\Gamma_{total}$   $\Gamma_{86}/\Gamma$ 

VALUE (units $10^{-4}$ )	DOCUMENT ID	TECN	COMMENT
<b>4.20 ± 0.34 OUR AVERAGE</b>			
4.21 $^{+0.30}_{-0.26}$ ± 0.21	1 AUBERT	05N	BABR $e^+e^- \rightarrow \Upsilon(4S)$
4.0 ± 1.1 ± 0.2	2 ABE	01I	BELL $e^+e^- \rightarrow \Upsilon(4S)$

<sup>1</sup> AUBERT 05N reports  $[\Gamma(B^+ \rightarrow \bar{D}^*(2007)^0 K^+)/\Gamma_{total}] / [B(B^+ \rightarrow \bar{D}^*(2007)^0 \pi^+)] = 0.0813 \pm 0.0040 \pm 0.0042 \pm 0.0031$  which we multiply by our best value  $B(B^+ \rightarrow \bar{D}^*(2007)^0 \pi^+) = (5.18 \pm 0.26) \times 10^{-3}$ . Our first error is their experiment's error and our second error is the systematic error from using our best value.

<sup>2</sup> ABE 01I reports  $[\Gamma(B^+ \rightarrow \bar{D}^*(2007)^0 K^+)/\Gamma_{total}] / [B(B^+ \rightarrow \bar{D}^*(2007)^0 \pi^+)] = 0.078 \pm 0.019 \pm 0.009$  which we multiply by our best value  $B(B^+ \rightarrow \bar{D}^*(2007)^0 \pi^+) = (5.18 \pm 0.26) \times 10^{-3}$ . Our first error is their experiment's error and our second error is the systematic error from using our best value.

 $\Gamma(\bar{D}_{CP(1)}^{*0} K^+)/\Gamma_{total}$   $\Gamma_{87}/\Gamma$ 

VALUE (units $10^{-4}$ )	DOCUMENT ID	TECN	COMMENT
<b>2.75 ± 0.29 ± 0.23</b>	1 AUBERT	08BF	BABR $e^+e^- \rightarrow \Upsilon(4S)$

<sup>1</sup> AUBERT 08BF reports  $[\Gamma(B^+ \rightarrow \bar{D}_{CP(1)}^{*0} K^+)/\Gamma_{total}] / [B(B^+ \rightarrow \bar{D}^*(2007)^0 K^+)] = 0.655 \pm 0.065 \pm 0.020$  which we multiply by our best value  $B(B^+ \rightarrow \bar{D}^*(2007)^0 K^+) = (4.20 \pm 0.34) \times 10^{-4}$ . Our first error is their experiment's error and our second error is the systematic error from using our best value.

 $\Gamma(\bar{D}_{CP(1)}^{*0} K^+)/\Gamma(\bar{D}_{CP(1)}^{*0} \pi^+)$   $\Gamma_{87}/\Gamma_{82}$ 

VALUE	DOCUMENT ID	TECN	COMMENT
<b>0.095 ± 0.017 OUR AVERAGE</b>			
0.11 ± 0.02 ± 0.02	1 ABE	06	BELL $e^+e^- \rightarrow \Upsilon(4S)$
0.086 ± 0.021 ± 0.007	2 AUBERT	05N	BABR $e^+e^- \rightarrow \Upsilon(4S)$

<sup>1</sup> Reports a double ratio of  $B(B^+ \rightarrow \bar{D}_{CP(1)}^{*0} K^+)/B(B^+ \rightarrow \bar{D}_{CP(1)}^{*0} \pi^+)$  and  $B(B^+ \rightarrow \bar{D}^{*0} K^+)/B(B^+ \rightarrow \bar{D}^{*0} \pi^+) = 1.41 \pm 0.25 \pm 0.06$ . We multiply by our best value of  $B(B^+ \rightarrow \bar{D}^{*0} K^+)/B(B^+ \rightarrow \bar{D}^{*0} \pi^+) = 0.080 \pm 0.011$ . Our first error is their experiment's error and the second error is systematic error from using our best value.

<sup>2</sup> Uses  $D^{*0} \rightarrow D^0 \pi^0$  with  $D^0$  reconstructed in the  $CP$ -even eigenstates  $K^+ K^-$  and  $\pi^+ \pi^-$ .

 $\Gamma(\bar{D}_{CP(1)}^{*0} K^+)/\Gamma_{total}$   $\Gamma_{88}/\Gamma$ 

VALUE (units $10^{-4}$ )	DOCUMENT ID	TECN	COMMENT
<b>2.31 ± 0.27 ± 0.20</b>	1 AUBERT	08BF	BABR $e^+e^- \rightarrow \Upsilon(4S)$

<sup>1</sup> AUBERT 08BF reports  $[\Gamma(B^+ \rightarrow \bar{D}_{CP(1)}^{*0} K^+)/\Gamma_{total}] / [B(B^+ \rightarrow \bar{D}^*(2007)^0 K^+)] = 0.55 \pm 0.06 \pm 0.02$  which we multiply by our best value  $B(B^+ \rightarrow \bar{D}^*(2007)^0 K^+) = (4.20 \pm 0.34) \times 10^{-4}$ . Our first error is their experiment's error and our second error is the systematic error from using our best value.

 $\Gamma(\bar{D}_{CP(1)}^{*0} K^+)/\Gamma(D_{CP(1)}^{*0} \pi^+)$   $\Gamma_{88}/\Gamma_{83}$ 

VALUE	DOCUMENT ID	TECN	COMMENT
<b>0.09 ± 0.03 ± 0.01</b>	1 ABE	06	BELL $e^+e^- \rightarrow \Upsilon(4S)$

<sup>1</sup> Reports a double ratio of  $B(B^+ \rightarrow (D_{CP(1)}^{*0})^0 K^+)/B(B^+ \rightarrow (D_{CP(1)}^{*0})^0 \pi^+)$  and  $B(B^+ \rightarrow \bar{D}^{*0} K^+)/B(B^+ \rightarrow \bar{D}^{*0} \pi^+) = 1.15 \pm 0.31 \pm 0.12$ . We multiply by our best value of  $B(B^+ \rightarrow \bar{D}^{*0} K^+)/B(B^+ \rightarrow \bar{D}^{*0} \pi^+) = 0.080 \pm 0.011$ . Our first error is their experiment's error and the second error is systematic error from using our best value.

 $\Gamma(\bar{D}^*(2007)^0 K^*(892)^+)/\Gamma_{total}$   $\Gamma_{89}/\Gamma$ 

VALUE (units $10^{-4}$ )	DOCUMENT ID	TECN	COMMENT
<b>8.1 ± 1.4 OUR AVERAGE</b>			
8.3 ± 1.1 ± 1.0	1 AUBERT	04K	BABR $e^+e^- \rightarrow \Upsilon(4S)$
7.2 ± 2.2 ± 2.6	2 MAHAPATRA	02	CLE2 $e^+e^- \rightarrow \Upsilon(4S)$

<sup>1</sup> Assumes equal production of  $B^+$  and  $B^0$  at the  $\Upsilon(4S)$ .  
<sup>2</sup> Assumes equal production of  $B^+$  and  $B^0$  at the  $\Upsilon(4S)$  and an unpolarized final state.

 $\Gamma(\bar{D}^*(2007)^0 K^+ \bar{K}^0)/\Gamma_{total}$   $\Gamma_{90}/\Gamma$ 

VALUE (units $10^{-4}$ )	CL%	DOCUMENT ID	TECN	COMMENT
<b>&lt;10.6</b>	90	1 DRUTSKOY	02	BELL $e^+e^- \rightarrow \Upsilon(4S)$

<sup>1</sup> Assumes equal production of  $B^+$  and  $B^0$  at the  $\Upsilon(4S)$ .





$\Gamma(\overline{D}_1^*(2427)^0 \pi^+ \times B(\overline{D}_1^*(2427)^0 \rightarrow D^{*-} \pi^+))/\Gamma_{\text{total}}$		$\Gamma_{111}/\Gamma$	
VALUE (units $10^{-4}$ )	CL%	DOCUMENT ID	TECN COMMENT
<b><math>5.0 \pm 0.4 \pm 1.1</math></b>		<sup>1</sup> ABE 04D BELL	$e^+ e^- \rightarrow \Upsilon(4S)$

<sup>1</sup> Assumes equal production of  $B^+$  and  $B^0$  at the  $\Upsilon(4S)$ .

$\Gamma(\overline{D}_1^*(2420)^0 \pi^+ \times B(\overline{D}_1^*(2420)^0 \rightarrow \overline{D}^{*0} \pi^+ \pi^-))/\Gamma_{\text{total}}$		$\Gamma_{112}/\Gamma$	
VALUE (units $10^{-4}$ )	CL%	DOCUMENT ID	TECN COMMENT
<b><math>&lt;0.06</math></b>	90	<sup>1</sup> ABE 05A BELL	$e^+ e^- \rightarrow \Upsilon(4S)$

<sup>1</sup> Assumes equal production of  $B^+$  and  $B^0$  at the  $\Upsilon(4S)$ .

$\Gamma(\overline{D}_1^*(2420)^0 \rho^+)/\Gamma_{\text{total}}$		$\Gamma_{113}/\Gamma$	
VALUE	CL%	DOCUMENT ID	TECN COMMENT
<b><math>&lt;0.0014</math></b>	90	<sup>1</sup> ALAM 94	CLE2 $e^+ e^- \rightarrow \Upsilon(4S)$

<sup>1</sup> ALAM 94 assume equal production of  $B^+$  and  $B^0$  at the  $\Upsilon(4S)$  and use the CLEO II  $B(D^*(2010)^+ \rightarrow D^0 \pi^+)$  assuming  $B(D_1^*(2420)^0 \rightarrow D^*(2010)^+ \pi^-) = 67\%$ .

$\Gamma(\overline{D}_2^*(2460)^0 \pi^+)/\Gamma_{\text{total}}$		$\Gamma_{114}/\Gamma$	
VALUE	CL%	DOCUMENT ID	TECN COMMENT
<b><math>&lt;0.0013</math></b>	90	<sup>1</sup> ALAM 94	CLE2 $e^+ e^- \rightarrow \Upsilon(4S)$

• • • We do not use the following data for averages, fits, limits, etc. • • •

$<0.0028$	90	<sup>2</sup> ALAM 94	CLE2 $e^+ e^- \rightarrow \Upsilon(4S)$
$<0.0023$	90	<sup>3</sup> ALBRECHT 94D ARG	$e^+ e^- \rightarrow \Upsilon(4S)$

<sup>1</sup> ALAM 94 assume equal production of  $B^+$  and  $B^0$  at the  $\Upsilon(4S)$  and use the Mark III  $B(D^+ \rightarrow K^- 2\pi^+)$  and  $B(D_2^*(2460)^0 \rightarrow D^+ \pi^-) = 30\%$ .

<sup>2</sup> ALAM 94 assume equal production of  $B^+$  and  $B^0$  at the  $\Upsilon(4S)$  and use the Mark III  $B(D^+ \rightarrow K^- 2\pi^+)$ , the CLEO II  $B(D^*(2010)^+ \rightarrow D^0 \pi^+)$  and  $B(D_2^*(2460)^0 \rightarrow D^*(2010)^+ \pi^-) = 20\%$ .

<sup>3</sup> ALBRECHT 94D assume equal production of  $B^+$  and  $B^0$  at the  $\Upsilon(4S)$  and use the CLEO II  $B(D^*(2010)^+ \rightarrow D^0 \pi^+)$  and  $B(D_2^*(2460)^0 \rightarrow D^*(2010)^+ \pi^-) = 30\%$ .

$\Gamma(\overline{D}_2^*(2460)^0 \pi^+ \times B(\overline{D}_2^*(2460)^0 \rightarrow \overline{D}^{*0} \pi^+ \pi^-))/\Gamma_{\text{total}}$		$\Gamma_{115}/\Gamma$	
VALUE (units $10^{-4}$ )	CL%	DOCUMENT ID	TECN COMMENT
<b><math>&lt;0.22</math></b>	90	<sup>1</sup> ABE 05A BELL	$e^+ e^- \rightarrow \Upsilon(4S)$

<sup>1</sup> Assumes equal production of  $B^+$  and  $B^0$  at the  $\Upsilon(4S)$ .

$\Gamma(\overline{D}_2^*(2460)^0 \rho^+)/\Gamma_{\text{total}}$		$\Gamma_{116}/\Gamma$	
VALUE	CL%	DOCUMENT ID	TECN COMMENT
<b><math>&lt;0.0047</math></b>	90	<sup>1</sup> ALAM 94	CLE2 $e^+ e^- \rightarrow \Upsilon(4S)$
$<0.005$	90	<sup>2</sup> ALAM 94	CLE2 $e^+ e^- \rightarrow \Upsilon(4S)$

<sup>1</sup> ALAM 94 assume equal production of  $B^+$  and  $B^0$  at the  $\Upsilon(4S)$  and use the Mark III  $B(D^+ \rightarrow K^- 2\pi^+)$  and  $B(D_2^*(2460)^0 \rightarrow D^+ \pi^-) = 30\%$ .

<sup>2</sup> ALAM 94 assume equal production of  $B^+$  and  $B^0$  at the  $\Upsilon(4S)$  and use the Mark III  $B(D^+ \rightarrow K^- 2\pi^+)$ , the CLEO II  $B(D^*(2010)^+ \rightarrow D^0 \pi^+)$  and  $B(D_2^*(2460)^0 \rightarrow D^*(2010)^+ \pi^-) = 20\%$ .

$\Gamma(\overline{D}^0 D_s^+)/\Gamma_{\text{total}}$		$\Gamma_{117}/\Gamma$	
VALUE	EVTS	DOCUMENT ID	TECN COMMENT
<b><math>0.0100 \pm 0.0017</math> OUR AVERAGE</b>			
$0.0095 \pm 0.0020 \pm 0.0008$		<sup>1</sup> AUBERT 06N BABR	$e^+ e^- \rightarrow \Upsilon(4S)$
$0.0098 \pm 0.0026 \pm 0.0009$		<sup>2</sup> GIBAUT 96 CLE2	$e^+ e^- \rightarrow \Upsilon(4S)$
$0.014 \pm 0.008 \pm 0.001$		<sup>3</sup> ALBRECHT 92G ARG	$e^+ e^- \rightarrow \Upsilon(4S)$
$0.013 \pm 0.006 \pm 0.001$	5	<sup>4</sup> BORTOLETTO90 CLEO	$e^+ e^- \rightarrow \Upsilon(4S)$

<sup>1</sup> AUBERT 06N reports  $(0.92 \pm 0.14 \pm 0.18) \times 10^{-2}$  from a measurement of  $[\Gamma(B^+ \rightarrow \overline{D}^0 D_s^+)/\Gamma_{\text{total}}] \times [B(D_s^+ \rightarrow \phi \pi^+)]$  assuming  $B(D_s^+ \rightarrow \phi \pi^+) = 0.0462 \pm 0.0062$ , which we rescale to our best value  $B(D_s^+ \rightarrow \phi \pi^+) = (4.5 \pm 0.4) \times 10^{-2}$ . Our first error is their experiment's error and our second error is the systematic error from using our best value.

<sup>2</sup> GIBAUT 96 reports  $0.0126 \pm 0.0022 \pm 0.0025$  from a measurement of  $[\Gamma(B^+ \rightarrow \overline{D}^0 D_s^+)/\Gamma_{\text{total}}] \times [B(D_s^+ \rightarrow \phi \pi^+)]$  assuming  $B(D_s^+ \rightarrow \phi \pi^+) = 0.035$ , which we rescale to our best value  $B(D_s^+ \rightarrow \phi \pi^+) = (4.5 \pm 0.4) \times 10^{-2}$ . Our first error is their experiment's error and our second error is the systematic error from using our best value.

<sup>3</sup> ALBRECHT 92G reports  $0.024 \pm 0.012 \pm 0.004$  from a measurement of  $[\Gamma(B^+ \rightarrow \overline{D}^0 D_s^+)/\Gamma_{\text{total}}] \times [B(D_s^+ \rightarrow \phi \pi^+)]$  assuming  $B(D_s^+ \rightarrow \phi \pi^+) = 0.027$ , which we rescale to our best value  $B(D_s^+ \rightarrow \phi \pi^+) = (4.5 \pm 0.4) \times 10^{-2}$ . Our first error is their experiment's error and our second error is the systematic error from using our best value. Assumes PDG 1990  $D^0$  branching ratios, e.g.,  $B(D^0 \rightarrow K^- \pi^+) = 3.71 \pm 0.25\%$ .

<sup>4</sup> BORTOLETTO 90 reports  $0.029 \pm 0.013$  from a measurement of  $[\Gamma(B^+ \rightarrow \overline{D}^0 D_s^+)/\Gamma_{\text{total}}] \times [B(D_s^+ \rightarrow \phi \pi^+)]$  assuming  $B(D_s^+ \rightarrow \phi \pi^+) = 0.02$ , which we rescale to our best value  $B(D_s^+ \rightarrow \phi \pi^+) = (4.5 \pm 0.4) \times 10^{-2}$ . Our first error is their experiment's error and our second error is the systematic error from using our best value.

$\Gamma(D_{s0}(2317)^+ \overline{D}^0 \times B(D_{s0}(2317)^+ \rightarrow D_s^+ \pi^0))/\Gamma_{\text{total}}$		$\Gamma_{118}/\Gamma$	
VALUE (units $10^{-3}$ )	CL%	DOCUMENT ID	TECN COMMENT
<b><math>0.73 \pm 0.22</math> OUR AVERAGE</b>			
$0.80 \pm 0.35$		<sup>1,2</sup> AUBERT,B 04S BABR	$e^+ e^- \rightarrow \Upsilon(4S)$
$0.65 \pm 0.26$		<sup>1,3</sup> KROKOVNY 03B BELL	$e^+ e^- \rightarrow \Upsilon(4S)$

$0.21 \pm 0.07$

$0.65 \pm 0.26$   
 $0.24 \pm 0.06$

<sup>1</sup> Assumes equal production of  $B^+$  and  $B^0$  at the  $\Upsilon(4S)$ .

<sup>2</sup> AUBERT,B 04S reports  $(1.0 \pm 0.3 \pm 0.4) \times 10^{-3}$  from a measurement of  $[\Gamma(B^+ \rightarrow D_{s0}(2317)^+ \overline{D}^0 \times B(D_{s0}(2317)^+ \rightarrow D_s^+ \pi^0))/\Gamma_{\text{total}}] \times [B(D_s^+ \rightarrow \phi \pi^+)]$  assuming  $B(D_s^+ \rightarrow \phi \pi^+) = 0.036 \pm 0.009$ , which we rescale to our best value  $B(D_s^+ \rightarrow \phi \pi^+) = (4.5 \pm 0.4) \times 10^{-2}$ . Our first error is their experiment's error and our second error is the systematic error from using our best value.

<sup>3</sup> KROKOVNY 03B reports  $(0.81 \pm 0.30 \pm 0.24) \times 10^{-3}$  from a measurement of  $[\Gamma(B^+ \rightarrow D_{s0}(2317)^+ \overline{D}^0 \times B(D_{s0}(2317)^+ \rightarrow D_s^+ \pi^0))/\Gamma_{\text{total}}] \times [B(D_s^+ \rightarrow \phi \pi^+)]$  assuming  $B(D_s^+ \rightarrow \phi \pi^+) = 0.036 \pm 0.009$ , which we rescale to our best value  $B(D_s^+ \rightarrow \phi \pi^+) = (4.5 \pm 0.4) \times 10^{-2}$ . Our first error is their experiment's error and our second error is the systematic error from using our best value.

$\Gamma(D_{s0}(2317)^+ \overline{D}^0 \times B(D_{s0}(2317)^+ \rightarrow D_s^+ \gamma))/\Gamma_{\text{total}}$		$\Gamma_{119}/\Gamma$	
VALUE (units $10^{-3}$ )	CL%	DOCUMENT ID	TECN COMMENT
<b><math>&lt;0.76</math></b>	90	<sup>1</sup> KROKOVNY 03B BELL	$e^+ e^- \rightarrow \Upsilon(4S)$

<sup>1</sup> Assumes equal production of  $B^+$  and  $B^0$  at the  $\Upsilon(4S)$ .

$\Gamma(D_{s0}(2317)^+ \overline{D}^* (2007)^0 \times B(D_{s0}(2317)^+ \rightarrow D_s^+ \pi^0))/\Gamma_{\text{total}}$		$\Gamma_{120}/\Gamma$	
VALUE (units $10^{-3}$ )	CL%	DOCUMENT ID	TECN COMMENT
<b><math>0.9 \pm 0.6 \pm 0.4</math></b>		<sup>1</sup> AUBERT,B 04S BABR	$e^+ e^- \rightarrow \Upsilon(4S)$

<sup>1</sup> Assumes equal production of  $B^+$  and  $B^0$  at the  $\Upsilon(4S)$ .

$\Gamma(D_{sJ}(2457)^+ \overline{D}^0)/\Gamma_{\text{total}}$		$\Gamma_{121}/\Gamma$	
VALUE (units $10^{-3}$ )	CL%	DOCUMENT ID	TECN COMMENT
<b><math>3.1 \pm 1.0</math> OUR AVERAGE</b>			
$4.3 \pm 1.6 \pm 1.3$		<sup>1</sup> AUBERT 06N BABR	$e^+ e^- \rightarrow \Upsilon(4S)$
$4.6 \pm 1.8$		<sup>2,3</sup> AUBERT,B 04S BABR	$e^+ e^- \rightarrow \Upsilon(4S)$
$2.1 \pm 1.1$		<sup>2,4</sup> KROKOVNY 03B BELL	$e^+ e^- \rightarrow \Upsilon(4S)$

$0.5 \pm 0.5$

$1.1 \pm 0.5$

$0.9 \pm 0.5$

<sup>1</sup> Uses a missing-mass method in the events that one of the  $B$  mesons is fully reconstructed.

<sup>2</sup> Assumes equal production of  $B^+$  and  $B^0$  at the  $\Upsilon(4S)$ .

<sup>3</sup> AUBERT,B 04S reports  $[\Gamma(B^+ \rightarrow D_{sJ}(2457)^+ \overline{D}^0)/\Gamma_{\text{total}}] \times [B(D_{s1}(2460)^+ \rightarrow D_s^+ \pi^0)] = (2.2 \pm 0.8 \pm 0.3) \times 10^{-3}$  which we divide by our best value  $B(D_{s1}(2460)^+ \rightarrow D_s^+ \pi^0) = (48 \pm 11) \times 10^{-2}$ . Our first error is their experiment's error and our second error is the systematic error from using our best value.

<sup>4</sup> KROKOVNY 03B reports  $[\Gamma(B^+ \rightarrow D_{sJ}(2457)^+ \overline{D}^0)/\Gamma_{\text{total}}] \times [B(D_{s1}(2460)^+ \rightarrow D_s^+ \pi^0)] = (1.0 \pm 0.5 \pm 0.1) \times 10^{-3}$  which we divide by our best value  $B(D_{s1}(2460)^+ \rightarrow D_s^+ \pi^0) = (48 \pm 11) \times 10^{-2}$ . Our first error is their experiment's error and our second error is the systematic error from using our best value.

$\Gamma(D_{sJ}(2457)^+ \overline{D}^0 \times B(D_{sJ}(2457)^+ \rightarrow D_s^+ \gamma))/\Gamma_{\text{total}}$		$\Gamma_{122}/\Gamma$	
VALUE (units $10^{-3}$ )	CL%	DOCUMENT ID	TECN COMMENT
<b><math>0.46 \pm 0.13</math> OUR AVERAGE</b>			
$0.48 \pm 0.19 \pm 0.04$		<sup>1,2</sup> AUBERT,B 04S BABR	$e^+ e^- \rightarrow \Upsilon(4S)$
$0.45 \pm 0.15$		<sup>1,3</sup> KROKOVNY 03B BELL	$e^+ e^- \rightarrow \Upsilon(4S)$

$0.11 \pm 0.04$

$0.13 \pm 0.04$

$0.14 \pm 0.04$

<sup>1</sup> Assumes equal production of  $B^+$  and  $B^0$  at the  $\Upsilon(4S)$ .

<sup>2</sup> AUBERT,B 04S reports  $(0.6 \pm 0.2 \pm 0.2) \times 10^{-3}$  from a measurement of  $[\Gamma(B^+ \rightarrow D_{sJ}(2457)^+ \overline{D}^0 \times B(D_{sJ}(2457)^+ \rightarrow D_s^+ \gamma))/\Gamma_{\text{total}}] \times [B(D_s^+ \rightarrow \phi \pi^+)]$  assuming  $B(D_s^+ \rightarrow \phi \pi^+) = 0.036 \pm 0.009$ , which we rescale to our best value  $B(D_s^+ \rightarrow \phi \pi^+) = (4.5 \pm 0.4) \times 10^{-2}$ . Our first error is their experiment's error and our second error is the systematic error from using our best value.

<sup>3</sup> KROKOVNY 03B reports  $(0.56 \pm 0.16 \pm 0.17) \times 10^{-3}$  from a measurement of  $[\Gamma(B^+ \rightarrow D_{sJ}(2457)^+ \overline{D}^0 \times B(D_{sJ}(2457)^+ \rightarrow D_s^+ \gamma))/\Gamma_{\text{total}}] \times [B(D_s^+ \rightarrow \phi \pi^+)]$  assuming  $B(D_s^+ \rightarrow \phi \pi^+) = 0.036 \pm 0.009$ , which we rescale to our best value  $B(D_s^+ \rightarrow \phi \pi^+) = (4.5 \pm 0.4) \times 10^{-2}$ . Our first error is their experiment's error and our second error is the systematic error from using our best value.

$\Gamma(D_{sJ}(2457)^+ \overline{D}^0 \times B(D_{sJ}(2457)^+ \rightarrow D_s^+ \pi^+ \pi^-))/\Gamma_{\text{total}}$		$\Gamma_{123}/\Gamma$	
VALUE (units $10^{-3}$ )	CL%	DOCUMENT ID	TECN COMMENT
<b><math>&lt;0.22</math></b>	90	<sup>1</sup> KROKOVNY 03B BELL	$e^+ e^- \rightarrow \Upsilon(4S)$

<sup>1</sup> Assumes equal production of  $B^+$  and  $B^0$  at the  $\Upsilon(4S)$ .

$\Gamma(D_{sJ}(2457)^+ \overline{D}^0 \times B(D_{sJ}(2457)^+ \rightarrow D_s^+ \pi^0))/\Gamma_{\text{total}}$		$\Gamma_{124}/\Gamma$	
VALUE (units $10^{-3}$ )	CL%	DOCUMENT ID	TECN COMMENT
<b><math>&lt;0.27</math></b>	90	<sup>1</sup> KROKOVNY 03B BELL	$e^+ e^- \rightarrow \Upsilon(4S)$

<sup>1</sup> Assumes equal production of  $B^+$  and  $B^0$  at the  $\Upsilon(4S)$ .

$\Gamma(D_{sJ}(2457)^+ \overline{D}^0 \times B(D_{sJ}(2457)^+ \rightarrow D_s^+ \gamma))/\Gamma_{\text{total}}$		$\Gamma_{125}/\Gamma$	
VALUE (units $10^{-3}$ )	CL%	DOCUMENT ID	TECN COMMENT
<b><math>&lt;0.98</math></b>	90	<sup>1</sup> KROKOVNY 03B BELL	$e^+ e^- \rightarrow \Upsilon(4S)$

<sup>1</sup> Assumes equal production of  $B^+$  and  $B^0$  at the  $\Upsilon(4S)$ .

## Meson Particle Listings

 $B^\pm$  $\Gamma(D_{sJ}(2457)^+ \bar{D}^*(2007)^0)/\Gamma_{\text{total}}$   $\Gamma_{126}/\Gamma$ 

VALUE (units $10^{-3}$ )	DOCUMENT ID	TECN	COMMENT
<b>12.0 ± 3.0 OUR AVERAGE</b>			
11.2 ± 2.6 ± 2.0	<sup>1</sup> AUBERT	06N	BABR $e^+e^- \rightarrow \Upsilon(4S)$
16 $^{+8}_{-6} \pm 4$	<sup>2,3</sup> AUBERT,B	04s	BABR $e^+e^- \rightarrow \Upsilon(4S)$

- <sup>1</sup> Uses a missing-mass method in the events that one of the  $B$  mesons is fully reconstructed.  
<sup>2</sup> AUBERT,B 04s reports  $[\Gamma(B^+ \rightarrow D_{sJ}(2457)^+ \bar{D}^*(2007)^0)/\Gamma_{\text{total}}] \times [B(D_{s1}(2460)^+ \rightarrow D_s^{*+} \pi^0)] = (7.6 \pm 1.7 \pm_{2.4}^{3.2}) \times 10^{-3}$  which we divide by our best value  $B(D_{s1}(2460)^+ \rightarrow D_s^{*+} \pi^0) = (48 \pm 11) \times 10^{-2}$ . Our first error is their experiment's error and our second error is the systematic error from using our best value.  
<sup>3</sup> Assumes equal production of  $B^+$  and  $B^0$  at the  $\Upsilon(4S)$ .

 $\Gamma(D_{sJ}(2457)^+ \bar{D}^*(2007)^0 \times B(D_{sJ}(2457)^+ \rightarrow D_s^{*+} \gamma))/\Gamma_{\text{total}}$   $\Gamma_{127}/\Gamma$ 

VALUE (units $10^{-3}$ )	DOCUMENT ID	TECN	COMMENT
<b>1.4 ± 0.4 <math>^{+0.6}_{-0.4}</math></b>	<sup>1</sup> AUBERT,B	04s	BABR $e^+e^- \rightarrow \Upsilon(4S)$

- <sup>1</sup> Assumes equal production of  $B^+$  and  $B^0$  at the  $\Upsilon(4S)$ .

 $\Gamma(\bar{D}^0 D_{s1}(2536)^+ \times B(D_{s1}(2536)^+ \rightarrow D^*(2007)^0 K^+))/\Gamma_{\text{total}}$   $\Gamma_{129}/\Gamma$ 

VALUE (units $10^{-4}$ )	CL%	DOCUMENT ID	TECN	COMMENT
<b>2.16 ± 0.52 ± 0.45</b>		<sup>1</sup> AUBERT	08B	BABR $e^+e^- \rightarrow \Upsilon(4S)$

- • • We do not use the following data for averages, fits, limits, etc. • • •  
 < 90 AUBERT 03x BABR Repl. by AUBERT 08B  
<sup>1</sup> Assumes equal production of  $B^+$  and  $B^0$  at the  $\Upsilon(4S)$ .

 $\Gamma(\bar{D}^0 D_{s1}(2536)^+ \times B(D_{s1}(2536)^+ \rightarrow D^*(2007)^0 K^+ + D^*(2010)^+ K^0))/\Gamma_{\text{total}}$   $\Gamma_{128}/\Gamma$ 

VALUE (units $10^{-4}$ )	DOCUMENT ID	TECN	COMMENT
<b>3.97 ± 0.85 ± 0.56</b>	<sup>1,2</sup> AUSHEV	11	BELL $e^+e^- \rightarrow \Upsilon(4S)$

- <sup>1</sup> Uses  $\Gamma(D^*(2007)^0 \rightarrow D^0 \pi^0) / \Gamma(D^*(2007)^0 \rightarrow D^0 \gamma) = 1.74 \pm 0.13$  and  $\Gamma(D_{s1}(2536)^+ \rightarrow D^*(2007)^0 K^+) / \Gamma(D_{s1}(2536)^+ \rightarrow D^*(2010)^+ K^0) = 1.36 \pm 0.2$ .  
<sup>2</sup> Assumes equal production of  $B^+$  and  $B^0$  at the  $\Upsilon(4S)$ .

 $\Gamma(\bar{D}^*(2007)^0 D_{s1}(2536)^+ \times B(D_{s1}(2536)^+ \rightarrow D^*(2007)^0 K^+))/\Gamma_{\text{total}}$   $\Gamma_{130}/\Gamma$ 

VALUE (units $10^{-4}$ )	CL%	DOCUMENT ID	TECN	COMMENT
<b>5.46 ± 1.17 ± 1.04</b>		<sup>1</sup> AUBERT	08B	BABR $e^+e^- \rightarrow \Upsilon(4S)$

- • • We do not use the following data for averages, fits, limits, etc. • • •  
 < 7 90 AUBERT 03x BABR Repl. by AUBERT 08B  
<sup>1</sup> Assumes equal production of  $B^+$  and  $B^0$  at the  $\Upsilon(4S)$ .

 $\Gamma(\bar{D}^0 D_{s1}(2536)^+ \times B(D_{s1}(2536)^+ \rightarrow D^{*+} K^0))/\Gamma_{\text{total}}$   $\Gamma_{131}/\Gamma$ 

VALUE (units $10^{-4}$ )	DOCUMENT ID	TECN	COMMENT
<b>2.30 ± 0.98 ± 0.43</b>	<sup>1</sup> AUBERT	08B	BABR $e^+e^- \rightarrow \Upsilon(4S)$

- <sup>1</sup> Assumes equal production of  $B^+$  and  $B^0$  at the  $\Upsilon(4S)$ .

 $\Gamma(\bar{D}^0 D_{sJ}(2700)^+ \times B(D_{sJ}(2700)^+ \rightarrow D^0 K^+))/\Gamma_{\text{total}}$   $\Gamma_{132}/\Gamma$ 

VALUE (units $10^{-4}$ )	DOCUMENT ID	TECN	COMMENT
<b>11.3 ± 2.2 <math>^{+1.4}_{-2.8}</math></b>	<sup>1</sup> BRODZICKA	08	BELL $e^+e^- \rightarrow \Upsilon(4S)$

- <sup>1</sup> Assumes equal production of  $B^+$  and  $B^0$  at the  $\Upsilon(4S)$ .

 $\Gamma(\bar{D}^*(2007)^0 D_{s1}(2536)^+ \times B(D_{s1}(2536)^+ \rightarrow D^{*+} K^0))/\Gamma_{\text{total}}$   $\Gamma_{133}/\Gamma$ 

VALUE (units $10^{-4}$ )	DOCUMENT ID	TECN	COMMENT
<b>3.92 ± 2.46 ± 0.83</b>	<sup>1</sup> AUBERT	08B	BABR $e^+e^- \rightarrow \Upsilon(4S)$

- <sup>1</sup> Assumes equal production of  $B^+$  and  $B^0$  at the  $\Upsilon(4S)$ .

 $\Gamma(\bar{D}^*(2007)^0 D_{sJ}(2573)^+ \times B(D_{sJ}(2573)^+ \rightarrow D^0 K^+))/\Gamma_{\text{total}}$   $\Gamma_{134}/\Gamma$ 

VALUE (units $10^{-4}$ )	CL%	DOCUMENT ID	TECN	COMMENT
<b>&lt; 2</b>	90	AUBERT	03x	BABR $e^+e^- \rightarrow \Upsilon(4S)$

 $\Gamma(\bar{D}^*(2007)^0 D_{sJ}(2573)^+ \times B(D_{sJ}(2573)^+ \rightarrow D^0 K^+))/\Gamma_{\text{total}}$   $\Gamma_{135}/\Gamma$ 

VALUE (units $10^{-4}$ )	CL%	DOCUMENT ID	TECN	COMMENT
<b>&lt; 5</b>	90	AUBERT	03x	BABR $e^+e^- \rightarrow \Upsilon(4S)$

 $\Gamma(\bar{D}^0 D_s^{*+})/\Gamma_{\text{total}}$   $\Gamma_{136}/\Gamma$ 

VALUE	DOCUMENT ID	TECN	COMMENT
<b>0.0076 ± 0.0016 OUR AVERAGE</b>			
0.0079 ± 0.0017 ± 0.0007	<sup>1</sup> AUBERT	06N	BABR $e^+e^- \rightarrow \Upsilon(4S)$
0.0068 ± 0.0025 ± 0.0006	<sup>2</sup> GIBAUT	96	CLE2 $e^+e^- \rightarrow \Upsilon(4S)$
0.010 ± 0.007 ± 0.001	<sup>3</sup> ALBRECHT	92G	ARG $e^+e^- \rightarrow \Upsilon(4S)$

- <sup>1</sup> AUBERT 06N reports  $(0.77 \pm 0.15 \pm 0.13) \times 10^{-2}$  from a measurement of  $[\Gamma(B^+ \rightarrow \bar{D}^0 D_s^{*+})/\Gamma_{\text{total}}] \times [B(D_s^+ \rightarrow \phi \pi^+)]$  assuming  $B(D_s^+ \rightarrow \phi \pi^+) = 0.0462 \pm 0.0062$ , which we rescale to our best value  $B(D_s^+ \rightarrow \phi \pi^+) = (4.5 \pm 0.4) \times 10^{-2}$ . Our first error is their experiment's error and our second error is the systematic error from using our best value.  
<sup>2</sup> GIBAUT 96 reports  $0.0087 \pm 0.0027 \pm 0.0017$  from a measurement of  $[\Gamma(B^+ \rightarrow \bar{D}^0 D_s^{*+})/\Gamma_{\text{total}}] \times [B(D_s^+ \rightarrow \phi \pi^+)]$  assuming  $B(D_s^+ \rightarrow \phi \pi^+) = 0.035$ , which we rescale to our best value  $B(D_s^+ \rightarrow \phi \pi^+) = (4.5 \pm 0.4) \times 10^{-2}$ . Our first error is their experiment's error and our second error is the systematic error from using our best value.  
<sup>3</sup> ALBRECHT 92G reports  $0.016 \pm 0.012 \pm 0.003$  from a measurement of  $[\Gamma(B^+ \rightarrow \bar{D}^0 D_s^{*+})/\Gamma_{\text{total}}] \times [B(D_s^+ \rightarrow \phi \pi^+)]$  assuming  $B(D_s^+ \rightarrow \phi \pi^+) = 0.027$ , which we rescale to our best value  $B(D_s^+ \rightarrow \phi \pi^+) = (4.5 \pm 0.4) \times 10^{-2}$ . Our first error is their experiment's error and our second error is the systematic error from using our best value. Assumes PDG 1990  $D^0$  branching ratios, e.g.,  $B(D^0 \rightarrow K^- \pi^+) = 3.71 \pm 0.25\%$ .

 $\Gamma(\bar{D}^*(2007)^0 D_s^+)/\Gamma_{\text{total}}$   $\Gamma_{137}/\Gamma$ 

VALUE	DOCUMENT ID	TECN	COMMENT
<b>0.0082 ± 0.0017 OUR AVERAGE</b>			
0.0078 ± 0.0018 ± 0.0007	<sup>1</sup> AUBERT	06N	BABR $e^+e^- \rightarrow \Upsilon(4S)$
0.011 ± 0.004 ± 0.001	<sup>2</sup> GIBAUT	96	CLE2 $e^+e^- \rightarrow \Upsilon(4S)$
0.008 ± 0.006 ± 0.001	<sup>3</sup> ALBRECHT	92G	ARG $e^+e^- \rightarrow \Upsilon(4S)$

- <sup>1</sup> AUBERT 06N reports  $(0.76 \pm 0.15 \pm 0.13) \times 10^{-2}$  from a measurement of  $[\Gamma(B^+ \rightarrow \bar{D}^*(2007)^0 D_s^+)/\Gamma_{\text{total}}] \times [B(D_s^+ \rightarrow \phi \pi^+)]$  assuming  $B(D_s^+ \rightarrow \phi \pi^+) = 0.0462 \pm 0.0062$ , which we rescale to our best value  $B(D_s^+ \rightarrow \phi \pi^+) = (4.5 \pm 0.4) \times 10^{-2}$ . Our first error is their experiment's error and our second error is the systematic error from using our best value.  
<sup>2</sup> GIBAUT 96 reports  $0.0140 \pm 0.0043 \pm 0.0035$  from a measurement of  $[\Gamma(B^+ \rightarrow \bar{D}^*(2007)^0 D_s^+)/\Gamma_{\text{total}}] \times [B(D_s^+ \rightarrow \phi \pi^+)]$  assuming  $B(D_s^+ \rightarrow \phi \pi^+) = 0.035$ , which we rescale to our best value  $B(D_s^+ \rightarrow \phi \pi^+) = (4.5 \pm 0.4) \times 10^{-2}$ . Our first error is their experiment's error and our second error is the systematic error from using our best value.  
<sup>3</sup> ALBRECHT 92G reports  $0.013 \pm 0.009 \pm 0.002$  from a measurement of  $[\Gamma(B^+ \rightarrow \bar{D}^*(2007)^0 D_s^+)/\Gamma_{\text{total}}] \times [B(D_s^+ \rightarrow \phi \pi^+)]$  assuming  $B(D_s^+ \rightarrow \phi \pi^+) = 0.027$ , which we rescale to our best value  $B(D_s^+ \rightarrow \phi \pi^+) = (4.5 \pm 0.4) \times 10^{-2}$ . Our first error is their experiment's error and our second error is the systematic error from using our best value. Assumes PDG 1990  $D^0$  and  $D^*(2007)^0$  branching ratios, e.g.,  $B(D^0 \rightarrow K^- \pi^+) = 3.71 \pm 0.25\%$  and  $B(D^*(2007)^0 \rightarrow D^0 \pi^0) = 55 \pm 6\%$ .

 $\Gamma(\bar{D}^*(2007)^0 D_s^{*+})/\Gamma_{\text{total}}$   $\Gamma_{138}/\Gamma$ 

VALUE	DOCUMENT ID	TECN	COMMENT
<b>0.0171 ± 0.0024 OUR AVERAGE</b>			
0.0167 ± 0.0019 ± 0.0015	<sup>1</sup> AUBERT	06N	BABR $e^+e^- \rightarrow \Upsilon(4S)$
0.024 ± 0.009 ± 0.002	<sup>2</sup> GIBAUT	96	CLE2 $e^+e^- \rightarrow \Upsilon(4S)$
0.019 ± 0.010 ± 0.002	<sup>3</sup> ALBRECHT	92G	ARG $e^+e^- \rightarrow \Upsilon(4S)$

- <sup>1</sup> AUBERT 06N reports  $(1.62 \pm 0.22 \pm 0.18) \times 10^{-2}$  from a measurement of  $[\Gamma(B^+ \rightarrow \bar{D}^*(2007)^0 D_s^{*+})/\Gamma_{\text{total}}] \times [B(D_s^+ \rightarrow \phi \pi^+)]$  assuming  $B(D_s^+ \rightarrow \phi \pi^+) = 0.0462 \pm 0.0062$ , which we rescale to our best value  $B(D_s^+ \rightarrow \phi \pi^+) = (4.5 \pm 0.4) \times 10^{-2}$ . Our first error is their experiment's error and our second error is the systematic error from using our best value.  
<sup>2</sup> GIBAUT 96 reports  $0.0310 \pm 0.0088 \pm 0.0065$  from a measurement of  $[\Gamma(B^+ \rightarrow \bar{D}^*(2007)^0 D_s^{*+})/\Gamma_{\text{total}}] \times [B(D_s^+ \rightarrow \phi \pi^+)]$  assuming  $B(D_s^+ \rightarrow \phi \pi^+) = 0.035$ , which we rescale to our best value  $B(D_s^+ \rightarrow \phi \pi^+) = (4.5 \pm 0.4) \times 10^{-2}$ . Our first error is their experiment's error and our second error is the systematic error from using our best value.  
<sup>3</sup> ALBRECHT 92G reports  $0.031 \pm 0.016 \pm 0.005$  from a measurement of  $[\Gamma(B^+ \rightarrow \bar{D}^*(2007)^0 D_s^{*+})/\Gamma_{\text{total}}] \times [B(D_s^+ \rightarrow \phi \pi^+)]$  assuming  $B(D_s^+ \rightarrow \phi \pi^+) = 0.027$ , which we rescale to our best value  $B(D_s^+ \rightarrow \phi \pi^+) = (4.5 \pm 0.4) \times 10^{-2}$ . Our first error is their experiment's error and our second error is the systematic error from using our best value. Assumes PDG 1990  $D^0$  and  $D^*(2007)^0$  branching ratios, e.g.,  $B(D^0 \rightarrow K^- \pi^+) = 3.71 \pm 0.25\%$  and  $B(D^*(2007)^0 \rightarrow D^0 \pi^0) = 55 \pm 6\%$ .

 $\Gamma(D_s^{*+} \bar{D}^{*0})/\Gamma_{\text{total}}$   $\Gamma_{139}/\Gamma$ 

VALUE	DOCUMENT ID	TECN	COMMENT
<b>(2.73 ± 0.93 ± 0.68) × 10<sup>-2</sup></b>	<sup>1</sup> AHMED	00B	CLE2 $e^+e^- \rightarrow \Upsilon(4S)$

- <sup>1</sup> AHMED 00B reports their experiment's uncertainties  $(\pm 0.78 \pm 0.48 \pm 0.68)\%$ , where the first error is statistical, the second is systematic, and the third is the uncertainty in the  $D_s \rightarrow \phi \pi$  branching fraction. We combine the first two in quadrature.

 $\Gamma(\bar{D}^*(2007)^0 D^*(2010)^+)/\Gamma_{\text{total}}$   $\Gamma_{140}/\Gamma$ 

VALUE (units $10^{-4}$ )	CL%	DOCUMENT ID	TECN	COMMENT
<b>8.1 ± 1.2 ± 1.2</b>		<sup>1</sup> AUBERT,B	06A	BABR $e^+e^- \rightarrow \Upsilon(4S)$

- • • We do not use the following data for averages, fits, limits, etc. • • •  
 < 110 90 BARATE 98Q ALEP  $e^+e^- \rightarrow Z$   
<sup>1</sup> Assumes equal production of  $B^+$  and  $B^0$  at the  $\Upsilon(4S)$ .

 $[\Gamma(\bar{D}^0 D^*(2010)^+) + \Gamma(\bar{D}^*(2007)^0 D^+)]/\Gamma_{\text{total}}$   $\Gamma_{141}/\Gamma$ 

VALUE (units $10^{-4}$ )	CL%	DOCUMENT ID	TECN	COMMENT
<b>&lt; 130</b>	90	BARATE	98Q	ALEP $e^+e^- \rightarrow Z$

See key on page 457

## Meson Particle Listings

 $B^\pm$  $\Gamma(\bar{D}^0 D^*(2010)^+)/\Gamma_{\text{total}}$   $\Gamma_{142}/\Gamma$ 

VALUE (units $10^{-4}$ )	DOCUMENT ID	TECN	COMMENT
<b>3.9 ± 0.5 OUR AVERAGE</b>			
3.6 ± 0.5 ± 0.4	<sup>1</sup> AUBERT,B	06A	BABR $e^+e^- \rightarrow \Upsilon(4S)$
4.57 ± 0.71 ± 0.56	<sup>1</sup> MAJUMDER	05	BELL $e^+e^- \rightarrow \Upsilon(4S)$

<sup>1</sup> Assumes equal production of  $B^+$  and  $B^0$  at the  $\Upsilon(4S)$ .

 $\Gamma(\bar{D}^0 D^+)/\Gamma_{\text{total}}$   $\Gamma_{143}/\Gamma$ 

VALUE (units $10^{-4}$ )	CL%	DOCUMENT ID	TECN	COMMENT
<b>3.8 ± 0.4 OUR AVERAGE</b>				
3.85 ± 0.31 ± 0.38		<sup>1</sup> ADACHI	08	BELL $e^+e^- \rightarrow \Upsilon(4S)$
3.8 ± 0.6 ± 0.5		<sup>1</sup> AUBERT,B	06A	BABR $e^+e^- \rightarrow \Upsilon(4S)$
••• We do not use the following data for averages, fits, limits, etc. •••				
4.83 ± 0.78 ± 0.58		<sup>1</sup> MAJUMDER	05	BELL Repl. by ADACHI 08
<67	90	BARATE	98Q	ALEP $e^+e^- \rightarrow Z$

<sup>1</sup> Assumes equal production of  $B^+$  and  $B^0$  at the  $\Upsilon(4S)$ .

 $\Gamma(\bar{D}^0 D^+ K^0)/\Gamma_{\text{total}}$   $\Gamma_{144}/\Gamma$ 

VALUE (units $10^{-3}$ )	CL%	DOCUMENT ID	TECN	COMMENT
<b>1.55 ± 0.17 ± 0.13</b>		<sup>1</sup> DEL-AMO-SA...11B	BABR	$e^+e^- \rightarrow \Upsilon(4S)$
••• We do not use the following data for averages, fits, limits, etc. •••				
<2.8	90	<sup>1</sup> AUBERT	03x	BABR Repl. by DEL-AMO-SANCHEZ 11B

<sup>1</sup> Assumes equal production of  $B^+$  and  $B^0$  at the  $\Upsilon(4S)$ .

 $\Gamma(D^+ \bar{D}^*(2007)^0)/\Gamma_{\text{total}}$   $\Gamma_{145}/\Gamma$ 

VALUE (units $10^{-4}$ )	DOCUMENT ID	TECN	COMMENT
<b>6.3 ± 1.4 ± 1.0</b>	<sup>1</sup> AUBERT,B	06A	BABR $e^+e^- \rightarrow \Upsilon(4S)$

<sup>1</sup> Assumes equal production of  $B^+$  and  $B^0$  at the  $\Upsilon(4S)$ .

 $\Gamma(\bar{D}^*(2007)^0 D^+ K^0)/\Gamma_{\text{total}}$   $\Gamma_{146}/\Gamma$ 

VALUE (units $10^{-3}$ )	CL%	DOCUMENT ID	TECN	COMMENT
<b>2.06 ± 0.38 ± 0.30</b>		<sup>1</sup> DEL-AMO-SA...11B	BABR	$e^+e^- \rightarrow \Upsilon(4S)$
••• We do not use the following data for averages, fits, limits, etc. •••				
<6.1	90	<sup>1</sup> AUBERT	03x	BABR Repl. by DEL-AMO-SANCHEZ 11B

<sup>1</sup> Assumes equal production of  $B^+$  and  $B^0$  at the  $\Upsilon(4S)$ .

 $\Gamma(\bar{D}^0 \bar{D}^*(2010)^+ K^0)/\Gamma_{\text{total}}$   $\Gamma_{147}/\Gamma$ 

VALUE (units $10^{-3}$ )	DOCUMENT ID	TECN	COMMENT
<b>3.81 ± 0.31 ± 0.23</b>	<sup>1</sup> DEL-AMO-SA...11B	BABR	$e^+e^- \rightarrow \Upsilon(4S)$
••• We do not use the following data for averages, fits, limits, etc. •••			
5.2 $^{+1.0}_{-0.9}$ ± 0.7	<sup>1</sup> AUBERT	03x	BABR Repl. by DEL-AMO-SANCHEZ 11B

<sup>1</sup> Assumes equal production of  $B^+$  and  $B^0$  at the  $\Upsilon(4S)$ .

 $\Gamma(\bar{D}^*(2007)^0 D^*(2010)^+ K^0)/\Gamma_{\text{total}}$   $\Gamma_{148}/\Gamma$ 

VALUE (units $10^{-3}$ )	DOCUMENT ID	TECN	COMMENT
<b>9.17 ± 0.83 ± 0.90</b>	<sup>1</sup> DEL-AMO-SA...11B	BABR	$e^+e^- \rightarrow \Upsilon(4S)$
••• We do not use the following data for averages, fits, limits, etc. •••			
7.8 $^{+2.3}_{-2.1}$ ± 1.4	<sup>1</sup> AUBERT	03x	BABR Repl. by DEL-AMO-SANCHEZ 11B

<sup>1</sup> Assumes equal production of  $B^+$  and  $B^0$  at the  $\Upsilon(4S)$ .

 $\Gamma(\bar{D}^0 D^0 K^+)/\Gamma_{\text{total}}$   $\Gamma_{149}/\Gamma$ 

VALUE (units $10^{-3}$ )	DOCUMENT ID	TECN	COMMENT
<b>1.45 ± 0.33 OUR AVERAGE</b>			Error includes scale factor of 2.6.
1.31 ± 0.07 ± 0.12	<sup>1</sup> DEL-AMO-SA...11B	BABR	$e^+e^- \rightarrow \Upsilon(4S)$
2.22 ± 0.22 $^{+0.26}_{-0.24}$	<sup>1</sup> BRODZICKA	08	BELL $e^+e^- \rightarrow \Upsilon(4S)$
••• We do not use the following data for averages, fits, limits, etc. •••			
1.17 ± 0.21 ± 0.15	<sup>1</sup> CHISTOV	04	BELL Repl. by BRODZICKA 08
1.9 ± 0.3 ± 0.3	<sup>1</sup> AUBERT	03x	BABR Repl. by DEL-AMO-SANCHEZ 11B

<sup>1</sup> Assumes equal production of  $B^+$  and  $B^0$  at the  $\Upsilon(4S)$ .

 $\Gamma(\bar{D}^*(2007)^0 D^0 K^+)/\Gamma_{\text{total}}$   $\Gamma_{150}/\Gamma$ 

VALUE (units $10^{-3}$ )	CL%	DOCUMENT ID	TECN	COMMENT
<b>2.26 ± 0.16 ± 0.17</b>		<sup>1</sup> DEL-AMO-SA...11B	BABR	$e^+e^- \rightarrow \Upsilon(4S)$
••• We do not use the following data for averages, fits, limits, etc. •••				
<3.8	90	<sup>1</sup> AUBERT	03x	BABR Repl. by DEL-AMO-SANCHEZ 11B

<sup>1</sup> Assumes equal production of  $B^+$  and  $B^0$  at the  $\Upsilon(4S)$ .

 $\Gamma(\bar{D}^0 D^*(2007)^0 K^+)/\Gamma_{\text{total}}$   $\Gamma_{151}/\Gamma$ 

VALUE (units $10^{-3}$ )	DOCUMENT ID	TECN	COMMENT
<b>6.32 ± 0.19 ± 0.45</b>	<sup>1</sup> DEL-AMO-SA...11B	BABR	$e^+e^- \rightarrow \Upsilon(4S)$
••• We do not use the following data for averages, fits, limits, etc. •••			
4.7 ± 0.7 ± 0.7	<sup>1</sup> AUBERT	03x	BABR Repl. by DEL-AMO-SANCHEZ 11B

<sup>1</sup> Assumes equal production of  $B^+$  and  $B^0$  at the  $\Upsilon(4S)$ .

 $\Gamma(\bar{D}^*(2007)^0 D^*(2007)^0 K^+)/\Gamma_{\text{total}}$   $\Gamma_{152}/\Gamma$ 

VALUE (units $10^{-3}$ )	DOCUMENT ID	TECN	COMMENT
<b>11.23 ± 0.36 ± 1.26</b>	<sup>1</sup> DEL-AMO-SA...11B	BABR	$e^+e^- \rightarrow \Upsilon(4S)$
••• We do not use the following data for averages, fits, limits, etc. •••			
5.3 $^{+1.1}_{-1.0}$ ± 1.2	<sup>1</sup> AUBERT	03x	BABR Repl. by DEL-AMO-SANCHEZ 11B

<sup>1</sup> Assumes equal production of  $B^+$  and  $B^0$  at the  $\Upsilon(4S)$ .

 $\Gamma(D^- D^+ K^+)/\Gamma_{\text{total}}$   $\Gamma_{153}/\Gamma$ 

VALUE (units $10^{-3}$ )	CL%	DOCUMENT ID	TECN	COMMENT
<b>0.22 ± 0.05 ± 0.05</b>		<sup>1</sup> DEL-AMO-SA...11B	BABR	$e^+e^- \rightarrow \Upsilon(4S)$
••• We do not use the following data for averages, fits, limits, etc. •••				
<0.90	90	<sup>1</sup> CHISTOV	04	BELL $e^+e^- \rightarrow \Upsilon(4S)$
<0.4	90	<sup>1</sup> AUBERT	03x	BABR Repl. by DEL-AMO-SANCHEZ 11B

<sup>1</sup> Assumes equal production of  $B^+$  and  $B^0$  at the  $\Upsilon(4S)$ .

 $\Gamma(D^- D^*(2010)^+ K^+)/\Gamma_{\text{total}}$   $\Gamma_{154}/\Gamma$ 

VALUE (units $10^{-3}$ )	CL%	DOCUMENT ID	TECN	COMMENT
<b>0.63 ± 0.09 ± 0.06</b>		<sup>1</sup> DEL-AMO-SA...11B	BABR	$e^+e^- \rightarrow \Upsilon(4S)$
••• We do not use the following data for averages, fits, limits, etc. •••				
<0.7	90	<sup>1</sup> AUBERT	03x	BABR Repl. by DEL-AMO-SANCHEZ 11B

<sup>1</sup> Assumes equal production of  $B^+$  and  $B^0$  at the  $\Upsilon(4S)$ .

 $\Gamma(D^*(2010)^- D^+ K^+)/\Gamma_{\text{total}}$   $\Gamma_{155}/\Gamma$ 

VALUE (units $10^{-3}$ )	DOCUMENT ID	TECN	COMMENT
<b>0.60 ± 0.10 ± 0.08</b>	<sup>1</sup> DEL-AMO-SA...11B	BABR	$e^+e^- \rightarrow \Upsilon(4S)$
••• We do not use the following data for averages, fits, limits, etc. •••			
1.5 ± 0.3 ± 0.2	<sup>1</sup> AUBERT	03x	BABR Repl. by DEL-AMO-SANCHEZ 11B

<sup>1</sup> Assumes equal production of  $B^+$  and  $B^0$  at the  $\Upsilon(4S)$ .

 $\Gamma(D^*(2010)^- D^*(2010)^+ K^+)/\Gamma_{\text{total}}$   $\Gamma_{156}/\Gamma$ 

VALUE (units $10^{-3}$ )	CL%	DOCUMENT ID	TECN	COMMENT
<b>1.32 ± 0.13 ± 0.12</b>		<sup>1</sup> DEL-AMO-SA...11B	BABR	$e^+e^- \rightarrow \Upsilon(4S)$
••• We do not use the following data for averages, fits, limits, etc. •••				
<1.8	90	<sup>1</sup> AUBERT	03x	BABR Repl. by DEL-AMO-SANCHEZ 11B

<sup>1</sup> Assumes equal production of  $B^+$  and  $B^0$  at the  $\Upsilon(4S)$ .

 $\Gamma((\bar{D}^+ \bar{D}^*(2010)^+)(D^+ D^*) K)/\Gamma_{\text{total}}$   $\Gamma_{157}/\Gamma$ 

VALUE (units $10^{-2}$ )	DOCUMENT ID	TECN	COMMENT
<b>4.05 ± 0.11 ± 0.28</b>	<sup>1</sup> DEL-AMO-SA...11B	BABR	$e^+e^- \rightarrow \Upsilon(4S)$
••• We do not use the following data for averages, fits, limits, etc. •••			
3.5 ± 0.3 ± 0.5	<sup>1</sup> AUBERT	03x	BABR Repl. by DEL-AMO-SANCHEZ 11B

<sup>1</sup> Assumes equal production of  $B^+$  and  $B^0$  at the  $\Upsilon(4S)$ .

 $\Gamma(D_s^+ \pi^0)/\Gamma_{\text{total}}$   $\Gamma_{158}/\Gamma$ 

VALUE (units $10^{-5}$ )	CL%	DOCUMENT ID	TECN	COMMENT
<b>1.6 <math>^{+0.6}_{-0.5}</math> ± 0.1</b>		<sup>1</sup> AUBERT	07M	BABR $e^+e^- \rightarrow \Upsilon(4S)$
••• We do not use the following data for averages, fits, limits, etc. •••				
<16	90	<sup>2</sup> ALEXANDER	93B	CLE2 $e^+e^- \rightarrow \Upsilon(4S)$

<sup>1</sup> AUBERT 07M reports  $[\Gamma(B^+ \rightarrow D_s^+ \pi^0)/\Gamma_{\text{total}}] \times [B(D_s^+ \rightarrow \phi\pi^+)] = (7.0 \pm 2.4 + 0.6) \times 10^{-7}$  which we divide by our best value  $B(D_s^+ \rightarrow \phi\pi^+) = (4.5 \pm 0.4) \times 10^{-2}$ . Our first error is their experiment's error and our second error is the systematic error from using our best value.

<sup>2</sup> ALEXANDER 93B reports  $< 2.0 \times 10^{-4}$  from a measurement of  $[\Gamma(B^+ \rightarrow D_s^+ \pi^0)/\Gamma_{\text{total}}] \times [B(D_s^+ \rightarrow \phi\pi^+)]$  assuming  $B(D_s^+ \rightarrow \phi\pi^+) = 0.037$ , which we rescale to our best value  $B(D_s^+ \rightarrow \phi\pi^+) = 4.5 \times 10^{-2}$ .

 $[\Gamma(D_s^+ \pi^0) + \Gamma(D_s^{*+} \pi^0)]/\Gamma_{\text{total}}$   $(\Gamma_{158} + \Gamma_{159})/\Gamma$ 

VALUE	CL%	DOCUMENT ID	TECN	COMMENT
<b>&lt;5 × 10<sup>-4</sup></b>	90	<sup>1</sup> ALBRECHT	93E	ARG $e^+e^- \rightarrow \Upsilon(4S)$

<sup>1</sup> ALBRECHT 93E reports  $< 0.9 \times 10^{-3}$  from a measurement of  $[\Gamma(B^+ \rightarrow D_s^+ \pi^0) + \Gamma(B^+ \rightarrow D_s^{*+} \pi^0)]/\Gamma_{\text{total}} \times [B(D_s^+ \rightarrow \phi\pi^+)]$  assuming  $B(D_s^+ \rightarrow \phi\pi^+) = 0.027$ , which we rescale to our best value  $B(D_s^+ \rightarrow \phi\pi^+) = 4.5 \times 10^{-2}$ .

 $\Gamma(D_s^{*+} \pi^0)/\Gamma_{\text{total}}$   $\Gamma_{159}/\Gamma$ 

VALUE	CL%	DOCUMENT ID	TECN	COMMENT
<b>&lt;2.6 × 10<sup>-4</sup></b>	90	<sup>1</sup> ALEXANDER	93B	CLE2 $e^+e^- \rightarrow \Upsilon(4S)$

<sup>1</sup> ALEXANDER 93B reports  $< 3.2 \times 10^{-4}$  from a measurement of  $[\Gamma(B^+ \rightarrow D_s^{*+} \pi^0)/\Gamma_{\text{total}}] \times [B(D_s^+ \rightarrow \phi\pi^+)]$  assuming  $B(D_s^+ \rightarrow \phi\pi^+) = 0.037$ , which we rescale to our best value  $B(D_s^+ \rightarrow \phi\pi^+) = 4.5 \times 10^{-2}$ .



See key on page 457

## Meson Particle Listings

 $B^\pm$  $\Gamma(D_s^- \pi^+ K^+)/\Gamma_{\text{total}}$   $\Gamma_{174}/\Gamma$ 

VALUE (units $10^{-4}$ )	CL%	DOCUMENT ID	TECN	COMMENT
<b>1.80 ± 0.22 OUR AVERAGE</b>				
1.71 $^{+0.08}_{-0.07} \pm 0.25$		1 WIECHCZYN...09	BELL	$e^+ e^- \rightarrow \Upsilon(4S)$
2.02 ± 0.13 ± 0.38		1 AUBERT 08G	BABR	$e^+ e^- \rightarrow \Upsilon(4S)$
• • • We do not use the following data for averages, fits, limits, etc. • • •				
<7	90	2 ALBRECHT 93E	ARG	$e^+ e^- \rightarrow \Upsilon(4S)$
1 Assumes equal production of $B^+$ and $B^0$ at the $\Upsilon(4S)$ .				
2 ALBRECHT 93E reports $< 1.1 \times 10^{-3}$ from a measurement of $[\Gamma(B^+ \rightarrow D_s^- \pi^+ K^+)/\Gamma_{\text{total}}] \times [B(D_s^+ \rightarrow \phi\pi^+)]$ assuming $B(D_s^+ \rightarrow \phi\pi^+) = 0.027$ , which we rescale to our best value $B(D_s^+ \rightarrow \phi\pi^+) = 4.5 \times 10^{-2}$ .				

 $\Gamma(D_s^{*-} \pi^+ K^+)/\Gamma_{\text{total}}$   $\Gamma_{175}/\Gamma$ 

VALUE (units $10^{-4}$ )	CL%	DOCUMENT ID	TECN	COMMENT
<b>1.45 ± 0.24 OUR AVERAGE</b>				
1.31 $^{+0.13}_{-0.12} \pm 0.28$		1 WIECHCZYN...09	BELL	$e^+ e^- \rightarrow \Upsilon(4S)$
1.67 ± 0.16 ± 0.35		1 AUBERT 08G	BABR	$e^+ e^- \rightarrow \Upsilon(4S)$
• • • We do not use the following data for averages, fits, limits, etc. • • •				
<10	90	2 ALBRECHT 93E	ARG	$e^+ e^- \rightarrow \Upsilon(4S)$
1 Assumes equal production of $B^+$ and $B^0$ at the $\Upsilon(4S)$ .				
2 ALBRECHT 93E reports $< 1.6 \times 10^{-3}$ from a measurement of $[\Gamma(B^+ \rightarrow D_s^{*-} \pi^+ K^+)/\Gamma_{\text{total}}] \times [B(D_s^+ \rightarrow \phi\pi^+)]$ assuming $B(D_s^+ \rightarrow \phi\pi^+) = 0.027$ , which we rescale to our best value $B(D_s^+ \rightarrow \phi\pi^+) = 4.5 \times 10^{-2}$ .				

 $\Gamma(D_s^- \pi^+ K^*(892)^+)/\Gamma_{\text{total}}$   $\Gamma_{176}/\Gamma$ 

VALUE	CL%	DOCUMENT ID	TECN	COMMENT
<b>&lt;5 × 10<sup>-3</sup></b>	90	1 ALBRECHT 93E	ARG	$e^+ e^- \rightarrow \Upsilon(4S)$
1 ALBRECHT 93E reports $< 8.6 \times 10^{-3}$ from a measurement of $[\Gamma(B^+ \rightarrow D_s^- \pi^+ K^*(892)^+)/\Gamma_{\text{total}}] \times [B(D_s^+ \rightarrow \phi\pi^+)]$ assuming $B(D_s^+ \rightarrow \phi\pi^+) = 0.027$ , which we rescale to our best value $B(D_s^+ \rightarrow \phi\pi^+) = 4.5 \times 10^{-2}$ .				

 $\Gamma(D_s^{*-} \pi^+ K^*(892)^+)/\Gamma_{\text{total}}$   $\Gamma_{177}/\Gamma$ 

VALUE	CL%	DOCUMENT ID	TECN	COMMENT
<b>&lt;7 × 10<sup>-3</sup></b>	90	1 ALBRECHT 93E	ARG	$e^+ e^- \rightarrow \Upsilon(4S)$
1 ALBRECHT 93E reports $< 1.1 \times 10^{-2}$ from a measurement of $[\Gamma(B^+ \rightarrow D_s^{*-} \pi^+ K^*(892)^+)/\Gamma_{\text{total}}] \times [B(D_s^+ \rightarrow \phi\pi^+)]$ assuming $B(D_s^+ \rightarrow \phi\pi^+) = 0.027$ , which we rescale to our best value $B(D_s^+ \rightarrow \phi\pi^+) = 4.5 \times 10^{-2}$ .				

 $\Gamma(D_s^- K^+ K^+)/\Gamma_{\text{total}}$   $\Gamma_{178}/\Gamma$ 

VALUE (units $10^{-4}$ )	CL%	DOCUMENT ID	TECN	COMMENT
<b>0.11 ± 0.04 ± 0.02</b>		1 AUBERT 08G	BABR	$e^+ e^- \rightarrow \Upsilon(4S)$
1 Assumes equal production of $B^+$ and $B^0$ at the $\Upsilon(4S)$ .				

 $\Gamma(D_s^{*-} K^+ K^+)/\Gamma_{\text{total}}$   $\Gamma_{179}/\Gamma$ 

VALUE (units $10^{-4}$ )	CL%	DOCUMENT ID	TECN	COMMENT
<b>&lt;0.15</b>	90	1 AUBERT 08G	BABR	$e^+ e^- \rightarrow \Upsilon(4S)$
1 Assumes equal production of $B^+$ and $B^0$ at the $\Upsilon(4S)$ .				

 $\Gamma(\eta_c K^+)/\Gamma_{\text{total}}$   $\Gamma_{180}/\Gamma$ 

VALUE (units $10^{-3}$ )	CL%	DOCUMENT ID	TECN	COMMENT
<b>0.96 ± 0.12 OUR AVERAGE</b>				
0.87 ± 0.15		1,2 AUBERT 06E	BABR	$e^+ e^- \rightarrow \Upsilon(4S)$
1.28 $^{+0.26}_{-0.20} \pm 0.16$		3 AUBERT,B 05L	BABR	$e^+ e^- \rightarrow \Upsilon(4S)$
1.25 ± 0.14 $^{+0.39}_{-0.40}$		4 FANG 03	BELL	$e^+ e^- \rightarrow \Upsilon(4S)$
0.69 $^{+0.26}_{-0.21} \pm 0.22$		5 EDWARDS 01	CLE2	$e^+ e^- \rightarrow \Upsilon(4S)$
• • • We do not use the following data for averages, fits, limits, etc. • • •				
1.03 ± 0.12 $^{+0.09}_{-0.08}$		2,6 AUBERT,B 04B	BABR	$e^+ e^- \rightarrow \Upsilon(4S)$

- 1 Perform measurements of absolute branching fractions using a missing mass technique.
- 2 The ratio of  $B(B^\pm \rightarrow K^\pm \eta_c) B(\eta_c \rightarrow K\bar{K}\pi) = (7.4 \pm 0.5 \pm 0.7) \times 10^{-5}$  reported in AUBERT,B 04B and  $B(B^\pm \rightarrow K^\pm \eta_c) = (8.7 \pm 1.5) \times 10^{-3}$  reported in AUBERT 06E contribute to the determination of  $B(\eta_c \rightarrow K\bar{K}\pi)$ , which is used by others for normalization.
- 3 AUBERT,B 05L reports  $[\Gamma(B^+ \rightarrow \eta_c K^+)/\Gamma_{\text{total}}] \times [B(\eta_c(1S) \rightarrow p\bar{p})] = (1.8^{+0.3}_{-0.2} \pm 0.2) \times 10^{-6}$  which we divide by our best value  $B(\eta_c(1S) \rightarrow p\bar{p}) = (1.41 \pm 0.17) \times 10^{-3}$ . Our first error is their experiment's error and our second error is the systematic error from using our best value.
- 4 Assumes equal production of  $B^+$  and  $B^0$  at the  $\Upsilon(4S)$ .
- 5 EDWARDS 01 assumes equal production of  $B^0$  and  $B^+$  at the  $\Upsilon(4S)$ . The correlated uncertainties (28.3%) from  $B(J/\psi(1S) \rightarrow \gamma\eta_c)$  in those modes have been accounted for.
- 6 AUBERT,B 04B reports  $[\Gamma(B^+ \rightarrow \eta_c K^+)/\Gamma_{\text{total}}] \times [B(\eta_c(1S) \rightarrow K\bar{K}\pi)] = (0.074 \pm 0.005 \pm 0.007) \times 10^{-3}$  which we divide by our best value  $B(\eta_c(1S) \rightarrow K\bar{K}\pi) = (7.2 \pm 0.6) \times 10^{-2}$ . Our first error is their experiment's error and our second error is the systematic error from using our best value.

 $\Gamma(B^+ \rightarrow \eta_c K^+)/\Gamma_{\text{total}} \times \Gamma(\eta_c(1S) \rightarrow \gamma\gamma)/\Gamma_{\text{total}}$   $\Gamma_{180}/\Gamma \times \Gamma_{29}^{\eta_c(1S)}/\Gamma_{\eta_c(1S)}$ 

VALUE (units $10^{-6}$ )	CL%	DOCUMENT ID	TECN	COMMENT
<b>0.22<math>^{+0.09}_{-0.07} \pm 0.04</math></b>		1 WICHT 08	BELL	$e^+ e^- \rightarrow \Upsilon(4S)$
1 Assumes equal production of $B^+$ and $B^0$ at the $\Upsilon(4S)$ .				

 $\Gamma(\eta_c K^+, \eta_c \rightarrow K_S^0 K^\mp \pi^\pm)/\Gamma_{\text{total}}$   $\Gamma_{181}/\Gamma$ 

VALUE (units $10^{-6}$ )	CL%	DOCUMENT ID	TECN	COMMENT
<b>26.7 ± 1.4<math>^{+5.7}_{-5.5}</math></b>		1,2 VINOKUROVA 11	BELL	$e^+ e^- \rightarrow \Upsilon(4S)$
1 Assumes equal production of $B^0$ and $B^+$ from Upsilon(4S) decays.				
2 VINOKUROVA 11 reports $(26.7 \pm 1.4^{+2.9}_{-2.6} \pm 4.9) \times 10^{-6}$ , where the first uncertainty is statistical, the second is due to systematics, and the third comes from interference of $\eta_c(1S) \rightarrow K_S^0 K^\pm \pi^\mp$ with nonresonant $K_S^0 K^\pm \pi^\mp$ . We combined both systematic uncertainties to single values.				

 $\Gamma(\eta_c K^*(892)^+)/\Gamma_{\text{total}}$   $\Gamma_{182}/\Gamma$ 

VALUE (units $10^{-3}$ )	CL%	DOCUMENT ID	TECN	COMMENT
<b>1.1<math>^{+0.5}_{-0.4} \pm 0.1</math></b>		1,2 AUBERT 07AV	BABR	$e^+ e^- \rightarrow \Upsilon(4S)$
1 AUBERT 07AV reports $[\Gamma(B^+ \rightarrow \eta_c K^*(892)^+)/\Gamma_{\text{total}}] \times [B(\eta_c(1S) \rightarrow p\bar{p})] = (1.57^{+0.56}_{-0.46} \pm 0.45) \times 10^{-6}$ which we divide by our best value $B(\eta_c(1S) \rightarrow p\bar{p}) = (1.41 \pm 0.17) \times 10^{-3}$ . Our first error is their experiment's error and our second error is the systematic error from using our best value.				
2 Assumes equal production of $B^+$ and $B^0$ at the $\Upsilon(4S)$ .				

 $\Gamma(\eta_c(2S) K^+)/\Gamma_{\text{total}}$   $\Gamma_{183}/\Gamma$ 

VALUE (units $10^{-4}$ )	CL%	DOCUMENT ID	TECN	COMMENT
<b>3.4 ± 1.8 ± 0.3</b>		1 AUBERT 06E	BABR	$e^+ e^- \rightarrow \Upsilon(4S)$
1 Perform measurements of absolute branching fractions using a missing mass technique.				

 $\Gamma(B^+ \rightarrow h_c(1P) K^+)/\Gamma_{\text{total}} \times \Gamma(h_c(1P) \rightarrow \eta_c(1S)\gamma)/\Gamma_{\text{total}}$   $\Gamma_{238}/\Gamma \times \Gamma_{4}^{h_c(1P)}/\Gamma_{h_c(1P)}$ 

VALUE (units $10^{-4}$ )	CL%	DOCUMENT ID	TECN	COMMENT
<b>&lt;0.48</b>	90	1 AUBERT 08AB	BABR	$e^+ e^- \rightarrow \Upsilon(4S)$
1 Uses the production ratio of $(B^+ B^-)/(B^0 \bar{B}^0) = 1.026 \pm 0.032$ at $\Upsilon(4S)$ .				

 $\Gamma(B^+ \rightarrow \eta_c(2S) K^+)/\Gamma_{\text{total}} \times \Gamma(\eta_c(2S) \rightarrow \gamma\gamma)/\Gamma_{\text{total}}$   $\Gamma_{183}/\Gamma \times \Gamma_{14}^{\eta_c(2S)}/\Gamma_{\eta_c(2S)}$ 

VALUE (units $10^{-6}$ )	CL%	DOCUMENT ID	TECN	COMMENT
<b>&lt;0.18</b>	90	1 WICHT 08	BELL	$e^+ e^- \rightarrow \Upsilon(4S)$
1 Assumes equal production of $B^+$ and $B^0$ at the $\Upsilon(4S)$ .				

 $\Gamma(\eta_c(2S) K^+, \eta_c(2S) \rightarrow K_S^0 K^\mp \pi^\pm)/\Gamma_{\text{total}}$   $\Gamma_{184}/\Gamma$ 

VALUE (units $10^{-6}$ )	CL%	DOCUMENT ID	TECN	COMMENT
<b>3.4<math>^{+2.2}_{-1.5} \pm 0.5</math></b>		1,2 VINOKUROVA 11	BELL	$e^+ e^- \rightarrow \Upsilon(4S)$
1 Assumes equal production of $B^0$ and $B^+$ from Upsilon(4S) decays.				
2 The first uncertainty includes both statistical and interference effects while the second is due to systematics.				

 $\Gamma(J/\psi(1S) K^+)/\Gamma_{\text{total}}$   $\Gamma_{185}/\Gamma$ 

VALUE (units $10^{-4}$ )	CL%	DOCUMENT ID	TECN	COMMENT
<b>10.16 ± 0.33 OUR FIT</b>				
<b>10.22 ± 0.35 OUR AVERAGE</b>				
8.1 ± 1.3 ± 0.7		1 AUBERT 06E	BABR	$e^+ e^- \rightarrow \Upsilon(4S)$
10.61 ± 0.15 ± 0.48		2 AUBERT 05J	BABR	$e^+ e^- \rightarrow \Upsilon(4S)$
10.1 ± 1.0 ± 0.3		3 AUBERT,B 05L	BABR	$e^+ e^- \rightarrow \Upsilon(4S)$
10.1 ± 0.2 ± 0.7		2 ABE 03B	BELL	$e^+ e^- \rightarrow \Upsilon(4S)$
10.2 ± 0.8 ± 0.7		2 JESSOP 97	CLE2	$e^+ e^- \rightarrow \Upsilon(4S)$
9.3 ± 3.1 ± 0.1		4 BORTOLETTO92	CLEO	$e^+ e^- \rightarrow \Upsilon(4S)$
8.1 ± 3.5 ± 0.1	6	5 ALBRECHT 90J	ARG	$e^+ e^- \rightarrow \Upsilon(4S)$
• • • We do not use the following data for averages, fits, limits, etc. • • •				
10.1 ± 0.3 ± 0.5		2 AUBERT 02	BABR	Repl. by AUBERT 05J
11.0 ± 1.5 ± 0.9	59	2 ALAM 94	CLE2	Repl. by JESSOP 97
22 ± 10 ± 2		BUSKULIC 92G	ALEP	$e^+ e^- \rightarrow Z$
7 ± 4	3	6 ALBRECHT 87D	ARG	$e^+ e^- \rightarrow \Upsilon(4S)$
10 ± 7 ± 2	3	7 BEBEK 87	CLEO	$e^+ e^- \rightarrow \Upsilon(4S)$
9 ± 5	3	8 ALAM 86	CLEO	$e^+ e^- \rightarrow \Upsilon(4S)$

- 1 Perform measurements of absolute branching fractions using a missing mass technique.
- 2 Assumes equal production of  $B^+$  and  $B^0$  at the  $\Upsilon(4S)$ .
- 3 AUBERT,B 05L reports  $[\Gamma(B^+ \rightarrow J/\psi(1S) K^+)/\Gamma_{\text{total}}] \times [B(J/\psi(1S) \rightarrow p\bar{p})] = (2.2 \pm 0.2 \pm 0.1) \times 10^{-6}$  which we divide by our best value  $B(J/\psi(1S) \rightarrow p\bar{p}) = (2.17 \pm 0.07) \times 10^{-3}$ . Our first error is their experiment's error and our second error is the systematic error from using our best value.
- 4 BORTOLETTO 92 reports  $(8 \pm 2 \pm 2) \times 10^{-4}$  from a measurement of  $[\Gamma(B^+ \rightarrow J/\psi(1S) K^+)/\Gamma_{\text{total}}] \times [B(J/\psi(1S) \rightarrow e^+ e^-)]$  assuming  $B(J/\psi(1S) \rightarrow e^+ e^-) = 0.069 \pm 0.009$ , which we rescale to our best value  $B(J/\psi(1S) \rightarrow e^+ e^-) = (5.94 \pm 0.06) \times 10^{-2}$ . Our first error is their experiment's error and our second error is the

# Meson Particle Listings

$B^\pm$

systematic error from using our best value. Assumes equal production of  $B^+$  and  $B^0$  at the  $\Upsilon(4S)$ .

<sup>5</sup> ALBRECHT 90j reports  $(7 \pm 3 \pm 1) \times 10^{-4}$  from a measurement of  $[\Gamma(B^+ \rightarrow J/\psi(1S) K^+) / \Gamma_{\text{total}}] \times [B(J/\psi(1S) \rightarrow e^+ e^-)]$  assuming  $B(J/\psi(1S) \rightarrow e^+ e^-) = 0.069 \pm 0.009$ , which we rescale to our best value  $B(J/\psi(1S) \rightarrow e^+ e^-) = (5.94 \pm 0.06) \times 10^{-2}$ . Our first error is their experiment's error and our second error is the systematic error from using our best value. Assumes equal production of  $B^+$  and  $B^0$  at the  $\Upsilon(4S)$ .

<sup>6</sup> ALBRECHT 87d assume  $B^+ B^- / B^0 \bar{B}^0$  ratio is 55/45. Superseded by ALBRECHT 90j.

<sup>7</sup> BEBEK 87 value has been updated in BERKELMAN 91 to use same assumptions as noted for BORTOLETTO 92.

<sup>8</sup> ALAM 86 assumes  $B^\pm / B^0$  ratio is 60/40.

$\Gamma(\eta_c K^+) / \Gamma(J/\psi(1S) K^+)$		$\Gamma_{180} / \Gamma_{185}$	
VALUE	DOCUMENT ID	TECN	COMMENT
<b>1.33 ± 0.10 ± 0.43</b>	<sup>1</sup> AUBERT,B	04B	BABR $e^+ e^- \rightarrow \Upsilon(4S)$

<sup>1</sup> Uses BABAR measurement of  $B(B^+ \rightarrow J/\psi K^+) = (10.1 \pm 0.3 \pm 0.5) \times 10^{-4}$ .

$\Gamma(B^+ \rightarrow J/\psi(1S) K^+) / \Gamma_{\text{total}} \times \Gamma(J/\psi(1S) \rightarrow \gamma\gamma) / \Gamma_{\text{total}}$		$\Gamma_{185} / \Gamma \times \Gamma_{191}^{J/\psi(1S)} / \Gamma_{J/\psi(1S)}$	
VALUE (units $10^{-6}$ )	DOCUMENT ID	TECN	COMMENT
<b>&lt;0.16</b>	<sup>1</sup> WICHT	08	BELL $e^+ e^- \rightarrow \Upsilon(4S)$

<sup>1</sup> Assumes equal production of  $B^+$  and  $B^0$  at the  $\Upsilon(4S)$ .

$\Gamma(J/\psi(1S) K^+ \pi^+ \pi^-) / \Gamma_{\text{total}}$		$\Gamma_{186} / \Gamma$	
VALUE (units $10^{-3}$ )	DOCUMENT ID	TECN	COMMENT

VALUE (units $10^{-3}$ )	DOCUMENT ID	TECN	COMMENT
<b>0.81 ± 0.13 OUR AVERAGE</b>	Error includes scale factor of 2.5. See the ideogram below.		
0.716 ± 0.010 ± 0.060	<sup>1</sup> GULER	11	BELL $e^+ e^- \rightarrow \Upsilon(4S)$
1.16 ± 0.07 ± 0.09	<sup>1</sup> AUBERT	05R	BABR $e^+ e^- \rightarrow \Upsilon(4S)$
0.69 ± 0.18 ± 0.12	<sup>2</sup> ACOSTA	02F	CDF $p\bar{p}$ 1.8 TeV
1.39 ± 0.82 ± 0.01	<sup>3</sup> BORTOLETTO92	CLEO	$e^+ e^- \rightarrow \Upsilon(4S)$
1.39 ± 0.91 ± 0.01	<sup>6</sup> <sup>4</sup> ALBRECHT	87D	ARG $e^+ e^- \rightarrow \Upsilon(4S)$

• • • We do not use the following data for averages, fits, limits, etc. • • •  
 <1.9      90      <sup>5</sup> ALBRECHT 90j ARG  $e^+ e^- \rightarrow \Upsilon(4S)$

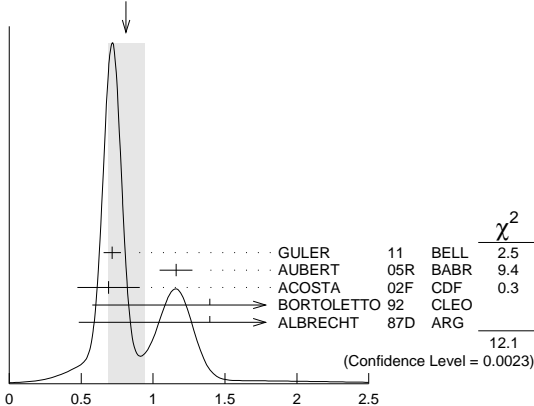
<sup>1</sup> Assumes equal production of  $B^+$  and  $B^0$  at the  $\Upsilon(4S)$ .  
<sup>2</sup> ACOSTA 02F uses as reference of  $B(B \rightarrow J/\psi(1S) K^+) = (10.1 \pm 0.6) \times 10^{-4}$ . The second error includes the systematic error and the uncertainties of the branching ratio.

<sup>3</sup> BORTOLETTO 92 reports  $(1.2 \pm 0.6 \pm 0.4) \times 10^{-3}$  from a measurement of  $[\Gamma(B^+ \rightarrow J/\psi(1S) K^+ \pi^+ \pi^-) / \Gamma_{\text{total}}] \times [B(J/\psi(1S) \rightarrow e^+ e^-)]$  assuming  $B(J/\psi(1S) \rightarrow e^+ e^-) = 0.069 \pm 0.009$ , which we rescale to our best value  $B(J/\psi(1S) \rightarrow e^+ e^-) = (5.94 \pm 0.06) \times 10^{-2}$ . Our first error is their experiment's error and our second error is the systematic error from using our best value. Assumes equal production of  $B^+$  and  $B^0$  at the  $\Upsilon(4S)$ .

<sup>4</sup> ALBRECHT 87d reports  $(1.2 \pm 0.8) \times 10^{-3}$  from a measurement of  $[\Gamma(B^+ \rightarrow J/\psi(1S) K^+ \pi^+ \pi^-) / \Gamma_{\text{total}}] \times [B(J/\psi(1S) \rightarrow e^+ e^-)]$  assuming  $B(J/\psi(1S) \rightarrow e^+ e^-) = 0.069 \pm 0.009$ , which we rescale to our best value  $B(J/\psi(1S) \rightarrow e^+ e^-) = (5.94 \pm 0.06) \times 10^{-2}$ . Our first error is their experiment's error and our second error is the systematic error from using our best value. They actually report  $0.0011 \pm 0.0007$  assuming  $B^+ B^- / B^0 \bar{B}^0$  ratio is 55/45. We rescale to 50/50. Analysis explicitly removes  $B^+ \rightarrow \psi(2S) K^+$ .

<sup>5</sup> ALBRECHT 90j reports  $< 1.6 \times 10^{-3}$  from a measurement of  $[\Gamma(B^+ \rightarrow J/\psi(1S) K^+ \pi^+ \pi^-) / \Gamma_{\text{total}}] \times [B(J/\psi(1S) \rightarrow e^+ e^-)]$  assuming  $B(J/\psi(1S) \rightarrow e^+ e^-) = 0.069$ , which we rescale to our best value  $B(J/\psi(1S) \rightarrow e^+ e^-) = 5.94 \times 10^{-2}$ . Assumes equal production of  $B^+$  and  $B^0$  at the  $\Upsilon(4S)$ .

WEIGHTED AVERAGE  
 0.81 ± 0.13 (Error scaled by 2.5)



$\Gamma(h_c(1P) K^+ \times B(h_c(1P) \rightarrow J/\psi \pi^+ \pi^-)) / \Gamma_{\text{total}}$		$\Gamma_{187} / \Gamma$	
VALUE	CL%	DOCUMENT ID	TECN

**<3.4 × 10<sup>-6</sup>**      90      <sup>1</sup> AUBERT      05R      BABR  $e^+ e^- \rightarrow \Upsilon(4S)$

<sup>1</sup> Assumes equal production of  $B^+$  and  $B^0$  at the  $\Upsilon(4S)$ .

$\Gamma(X(3872) K^+) / \Gamma_{\text{total}}$		$\Gamma_{188} / \Gamma$	
VALUE	CL%	DOCUMENT ID	TECN

**<3.2 × 10<sup>-4</sup>**      90      <sup>1</sup> AUBERT      06E      BABR  $e^+ e^- \rightarrow \Upsilon(4S)$

<sup>1</sup> Perform measurements of absolute branching fractions using a missing mass technique.

$\Gamma(B^+ \rightarrow X(3872) K^+) / \Gamma_{\text{total}} \times \Gamma(X(3872) \rightarrow \gamma\gamma) / \Gamma_{\text{total}}$		$\Gamma_{188} / \Gamma \times \Gamma_{191}^{X(3872)} / \Gamma_{X(3872)}$	
VALUE (units $10^{-6}$ )	CL%	DOCUMENT ID	TECN

**<0.24**      90      <sup>1</sup> WICHT      08      BELL  $e^+ e^- \rightarrow \Upsilon(4S)$

<sup>1</sup> Assumes equal production of  $B^+$  and  $B^0$  at the  $\Upsilon(4S)$ .

$\Gamma(X(3872) K^+ \times B(X \rightarrow J/\psi \pi^+ \pi^-)) / \Gamma_{\text{total}}$		$\Gamma_{189} / \Gamma$	
VALUE (units $10^{-6}$ )	CL%	DOCUMENT ID	TECN

**8.6 ± 0.8 OUR AVERAGE**

8.63 ± 0.82 ± 0.52      <sup>1</sup> CHOI      11      BELL  $e^+ e^- \rightarrow \Upsilon(4S)$

8.4 ± 1.5 ± 0.7      <sup>1</sup> AUBERT      08Y      BABR  $e^+ e^- \rightarrow \Upsilon(4S)$

• • • We do not use the following data for averages, fits, limits, etc. • • •

10.1 ± 2.5 ± 1.0      <sup>1</sup> AUBERT      06      BABR Repl. by AUBERT 08Y

12.8 ± 4.1      <sup>1</sup> AUBERT      05R      BABR Repl. by AUBERT 06

12.8 ± 2.8 ± 0.7      <sup>2</sup> CHOI      03      BELL Repl. by CHOI 11

<sup>1</sup> Assumes equal production of  $B^+$  and  $B^0$  at the  $\Upsilon(4S)$ .

<sup>2</sup> CHOI 03 reports  $[\Gamma(B^+ \rightarrow X(3872) K^+ \times B(X \rightarrow J/\psi \pi^+ \pi^-)) / \Gamma_{\text{total}}] / [B(B^+ \rightarrow \psi(2S) K^+)] = 0.0200 \pm 0.0038 \pm 0.0023$  which we multiply by our best value  $B(B^+ \rightarrow \psi(2S) K^+) = (6.39 \pm 0.33) \times 10^{-4}$ . Our first error is their experiment's error and our second error is the systematic error from using our best value.

$\Gamma(X(3872) K^+ \times B(X \rightarrow J/\psi \gamma)) / \Gamma_{\text{total}}$		$\Gamma_{190} / \Gamma$	
VALUE (units $10^{-6}$ )	CL%	DOCUMENT ID	TECN

**2.1 ± 0.4 OUR AVERAGE**      Error includes scale factor of 1.1.

1.78 ± 0.48 ± 0.12      <sup>1</sup> BHARDWAJ      11      BELL  $e^+ e^- \rightarrow \Upsilon(4S)$

2.8 ± 0.8 ± 0.1      <sup>2</sup> AUBERT      09B      BABR  $e^+ e^- \rightarrow \Upsilon(4S)$

• • • We do not use the following data for averages, fits, limits, etc. • • •

3.3 ± 1.0 ± 0.3      <sup>1</sup> AUBERT,BE      06M      BABR Repl. by AUBERT 09B

<sup>1</sup> Assumes equal production of  $B^+$  and  $B^0$  at the  $\Upsilon(4S)$ .

<sup>2</sup> Uses  $B(\Upsilon(4S) \rightarrow B^+ B^-) = (51.6 \pm 0.6)\%$  and  $B(\Upsilon(4S) \rightarrow B^0 \bar{B}^0) = (48.4 \pm 0.6)\%$ .

$\Gamma(X(3872) K^*(892)^+ \times B(X \rightarrow J/\psi \gamma)) / \Gamma_{\text{total}}$		$\Gamma_{191} / \Gamma$	
VALUE (units $10^{-6}$ )	CL%	DOCUMENT ID	TECN

**<4.8**      90      <sup>1</sup> AUBERT      09B      BABR  $e^+ e^- \rightarrow \Upsilon(4S)$

<sup>1</sup> Uses  $B(\Upsilon(4S) \rightarrow B^+ B^-) = (51.6 \pm 0.6)\%$  and  $B(\Upsilon(4S) \rightarrow B^0 \bar{B}^0) = (48.4 \pm 0.6)\%$ .

$\Gamma(X(3872) K^+ \times B(X \rightarrow \psi(2S) \gamma)) / \Gamma_{\text{total}}$		$\Gamma_{192} / \Gamma$	
VALUE (units $10^{-6}$ )	CL%	DOCUMENT ID	TECN

**4 ± 4 OUR AVERAGE**      Error includes scale factor of 2.5.

0.83 ± 1.98 ± 0.44      <sup>1,2</sup> BHARDWAJ      11      BELL  $e^+ e^- \rightarrow \Upsilon(4S)$

9.5 ± 2.7 ± 0.6      <sup>3</sup> AUBERT      09B      BABR  $e^+ e^- \rightarrow \Upsilon(4S)$

<sup>1</sup> BHARDWAJ 11 measurement is equivalent to a limit of  $< 3.45 \times 10^{-6}$  at 90% CL.

<sup>2</sup> Assumes equal production of  $B^+$  and  $B^0$  at the  $\Upsilon(4S)$ .

<sup>3</sup> Uses  $B(\Upsilon(4S) \rightarrow B^+ B^-) = (51.6 \pm 0.6)\%$  and  $B(\Upsilon(4S) \rightarrow B^0 \bar{B}^0) = (48.4 \pm 0.6)\%$ .

$\Gamma(X(3872) K^*(892)^+ \times B(X \rightarrow \psi(2S) \gamma)) / \Gamma_{\text{total}}$		$\Gamma_{193} / \Gamma$	
VALUE (units $10^{-6}$ )	CL%	DOCUMENT ID	TECN

**<28**      90      <sup>1</sup> AUBERT      09B      BABR  $e^+ e^- \rightarrow \Upsilon(4S)$

<sup>1</sup> Uses  $B(\Upsilon(4S) \rightarrow B^+ B^-) = (51.6 \pm 0.6)\%$  and  $B(\Upsilon(4S) \rightarrow B^0 \bar{B}^0) = (48.4 \pm 0.6)\%$ .

$\Gamma(X(3872) K^+ \times B(X \rightarrow D^0 \bar{D}^0)) / \Gamma_{\text{total}}$		$\Gamma_{194} / \Gamma$	
VALUE	CL%	DOCUMENT ID	TECN

**<6.0 × 10<sup>-5</sup>**      90      <sup>1</sup> CHISTOV      04      BELL  $e^+ e^- \rightarrow \Upsilon(4S)$

<sup>1</sup> Assumes equal production of  $B^+$  and  $B^0$  at the  $\Upsilon(4S)$ .

$\Gamma(X(3872) K^+ \times B(X \rightarrow D^+ D^-)) / \Gamma_{\text{total}}$		$\Gamma_{195} / \Gamma$	
VALUE	CL%	DOCUMENT ID	TECN

**<4.0 × 10<sup>-5</sup>**      90      <sup>1</sup> CHISTOV      04      BELL  $e^+ e^- \rightarrow \Upsilon(4S)$

<sup>1</sup> Assumes equal production of  $B^+$  and  $B^0$  at the  $\Upsilon(4S)$ .

$\Gamma(X(3872) K^+ \times B(X \rightarrow D^0 \bar{D}^0 \pi^0)) / \Gamma_{\text{total}}$		$\Gamma_{196} / \Gamma$	
VALUE (units $10^{-4}$ )	CL%	DOCUMENT ID	TECN

**1.02 ± 0.31 ± 0.21**      <sup>1</sup> GOKHROO      06      BELL  $e^+ e^- \rightarrow \Upsilon(4S)$

• • • We do not use the following data for averages, fits, limits, etc. • • •

<0.6      90      <sup>2</sup> CHISTOV      04      BELL Repl. by GOKHROO 06

<sup>1</sup> Measure the near-threshold enhancements in the  $(D^0 \bar{D}^0 \pi^0)$  system at a mass  $3875.2 \pm 0.7 \pm 0.3 \pm 0.8$  MeV/c<sup>2</sup>.

<sup>2</sup> Assumes equal production of  $B^+$  and  $B^0$  at the  $\Upsilon(4S)$ .

$\Gamma(X(3872)K^+ \times B(X \rightarrow \bar{D}^{*0}D^0))/\Gamma_{\text{total}}$   $\Gamma_{197}/\Gamma$ 

VALUE (units $10^{-4}$ )	DOCUMENT ID	TECN	COMMENT
<b>0.85 ± 0.26 OUR AVERAGE</b>	Error includes scale factor of 1.4.		
0.77 ± 0.16 ± 0.10	<sup>1</sup> AUSHEV 10	BELL	$e^+e^- \rightarrow \Upsilon(4S)$
1.67 ± 0.36 ± 0.47	<sup>1</sup> AUBERT 08B	BABR	$e^+e^- \rightarrow \Upsilon(4S)$

<sup>1</sup> Assumes equal production of  $B^+$  and  $B^0$  at the  $\Upsilon(4S)$ .

 $\Gamma(X(3872)K^+ \times B(X(3872) \rightarrow J/\psi(1S)\eta))/\Gamma_{\text{total}}$   $\Gamma_{198}/\Gamma$ 

VALUE	CL%	DOCUMENT ID	TECN	COMMENT
<b>&lt; 7.7 × 10<sup>-6</sup></b>	90	<sup>1</sup> AUBERT 04Y	BABR	$e^+e^- \rightarrow \Upsilon(4S)$

<sup>1</sup> Assumes equal production of  $B^+$  and  $B^0$  at the  $\Upsilon(4S)$ .

 $\Gamma(X(3872)^+K^0 \times B(X(3872)^+ \rightarrow J/\psi(1S)\pi^+\pi^0))/\Gamma_{\text{total}}$   $\Gamma_{199}/\Gamma$ 

VALUE (units $10^{-6}$ )	CL%	DOCUMENT ID	TECN	COMMENT
<b>&lt; 6.1</b>	90	<sup>1,2</sup> CHOI 11	BELL	$e^+e^- \rightarrow \Upsilon(4S)$
<b>&lt; 22</b>	90	<sup>3</sup> AUBERT 05B	BABR	$e^+e^- \rightarrow \Upsilon(4S)$

• • • We do not use the following data for averages, fits, limits, etc. • • •

<sup>1</sup> Assumes  $\pi^+\pi^0$  originates from  $\rho^+$ .  
<sup>2</sup> Assumes equal production of  $B^+$  and  $B^0$  at the  $\Upsilon(4S)$ .  
<sup>3</sup> Assumes equal production of  $B^+$  and  $B^0$  at the  $\Upsilon(4S)$ . The isovector-X hypothesis is excluded with a likelihood test at  $1 \times 10^{-4}$  level.

 $\Gamma(X(4430)^+K^0 \times B(X^+ \rightarrow J/\psi\pi^+))/\Gamma_{\text{total}}$   $\Gamma_{200}/\Gamma$ 

VALUE (units $10^{-5}$ )	CL%	DOCUMENT ID	TECN	COMMENT
<b>&lt; 1.5</b>	95	<sup>1</sup> AUBERT 09AA	BABR	$e^+e^- \rightarrow \Upsilon(4S)$

<sup>1</sup> Assumes equal production of  $B^+$  and  $B^0$  at the  $\Upsilon(4S)$ .

 $\Gamma(X(4430)^+K^0 \times B(X^+ \rightarrow \psi(2S)\pi^+))/\Gamma_{\text{total}}$   $\Gamma_{201}/\Gamma$ 

VALUE (units $10^{-5}$ )	CL%	DOCUMENT ID	TECN	COMMENT
<b>&lt; 4.7</b>	95	<sup>1</sup> AUBERT 09AA	BABR	$e^+e^- \rightarrow \Upsilon(4S)$

<sup>1</sup> Assumes equal production of  $B^+$  and  $B^0$  at the  $\Upsilon(4S)$ .

 $\Gamma(X(4260)^0K^+ \times B(X^0 \rightarrow J/\psi\pi^+\pi^-))/\Gamma_{\text{total}}$   $\Gamma_{202}/\Gamma$ 

VALUE (units $10^{-6}$ )	CL%	DOCUMENT ID	TECN	COMMENT
<b>&lt; 29</b>	95	<sup>1</sup> AUBERT 06	BABR	$e^+e^- \rightarrow \Upsilon(4S)$

<sup>1</sup> Assumes equal production of  $B^+$  and  $B^0$  at the  $\Upsilon(4S)$ .

 $\Gamma(X(3915)^0K^+ \times B(X^0 \rightarrow J/\psi\gamma))/\Gamma_{\text{total}}$   $\Gamma_{203}/\Gamma$ 

VALUE (units $10^{-6}$ )	CL%	DOCUMENT ID	TECN	COMMENT
<b>&lt; 14</b>	90	<sup>1</sup> AUBERT, BE 06M	BABR	$e^+e^- \rightarrow \Upsilon(4S)$

<sup>1</sup> Assumes equal production of  $B^+$  and  $B^0$  at the  $\Upsilon(4S)$ .

 $\Gamma(Z(3930)^0K^+ \times B(Z^0 \rightarrow J/\psi\gamma))/\Gamma_{\text{total}}$   $\Gamma_{204}/\Gamma$ 

VALUE (units $10^{-6}$ )	CL%	DOCUMENT ID	TECN	COMMENT
<b>&lt; 2.5</b>	90	<sup>1</sup> AUBERT, BE 06M	BABR	$e^+e^- \rightarrow \Upsilon(4S)$

<sup>1</sup> Assumes equal production of  $B^+$  and  $B^0$  at the  $\Upsilon(4S)$ .

 $\Gamma(J/\psi(1S)K^*(892)^+)/\Gamma_{\text{total}}$   $\Gamma_{205}/\Gamma$ 

For polarization information see the Listings at the end of the " $B^0$  Branching Ratios" section.

VALUE (units $10^{-3}$ )	EVTS	DOCUMENT ID	TECN	COMMENT
<b>1.43 ± 0.08 OUR FIT</b>				
<b>1.43 ± 0.08 OUR AVERAGE</b>				
1.74 <sup>+0.36</sup> <sub>-0.31</sub> ± 0.06		<sup>1,2</sup> AUBERT 07AV	BABR	$e^+e^- \rightarrow \Upsilon(4S)$
1.454 ± 0.047 ± 0.097		<sup>2</sup> AUBERT 05J	BABR	$e^+e^- \rightarrow \Upsilon(4S)$
1.28 ± 0.07 ± 0.14		<sup>2</sup> ABE 02N	BELL	$e^+e^- \rightarrow \Upsilon(4S)$
1.41 ± 0.23 ± 0.24		<sup>2</sup> JESSOP 97	CLE2	$e^+e^- \rightarrow \Upsilon(4S)$
1.58 ± 0.47 ± 0.27		<sup>3</sup> ABE 96H	CDF	$p\bar{p}$ at 1.8 TeV
1.51 ± 1.08 ± 0.02		<sup>4</sup> BORTOLETTO 92	CLEO	$e^+e^- \rightarrow \Upsilon(4S)$
1.86 ± 1.30 ± 0.02	2	<sup>5</sup> ALBRECHT 90J	ARG	$e^+e^- \rightarrow \Upsilon(4S)$
1.37 ± 0.09 ± 0.11		<sup>2</sup> AUBERT 02	BABR	Repl. by AUBERT 05J
1.78 ± 0.51 ± 0.23	13	<sup>2</sup> ALAM 94	CLE2	Sup. by JESSOP 97

<sup>1</sup> AUBERT 07AV reports  $[\Gamma(B^+ \rightarrow J/\psi(1S)K^*(892)^+)/\Gamma_{\text{total}}] \times [B(J/\psi(1S) \rightarrow p\bar{p})] = (3.78 \pm 0.72 \pm 0.28 \pm 0.64 \pm 0.23) \times 10^{-6}$  which we divide by our best value  $B(J/\psi(1S) \rightarrow p\bar{p}) = (2.17 \pm 0.07) \times 10^{-3}$ . Our first error is their experiment's error and our second error is the systematic error from using our best value.

<sup>2</sup> Assumes equal production of  $B^+$  and  $B^0$  at the  $\Upsilon(4S)$ .

<sup>3</sup> ABE 96H assumes that  $B(B^+ \rightarrow J/\psi K^+) = (1.02 \pm 0.14) \times 10^{-3}$ .

<sup>4</sup> BORTOLETTO 92 reports  $(1.3 \pm 0.9 \pm 0.3) \times 10^{-3}$  from a measurement of  $[\Gamma(B^+ \rightarrow J/\psi(1S)K^*(892)^+)/\Gamma_{\text{total}}] \times [B(J/\psi(1S) \rightarrow e^+e^-)]$  assuming  $B(J/\psi(1S) \rightarrow e^+e^-) = 0.069 \pm 0.009$ , which we rescale to our best value  $B(J/\psi(1S) \rightarrow e^+e^-) = (5.94 \pm 0.06) \times 10^{-2}$ . Our first error is their experiment's error and our second error is the systematic error from using our best value. Assumes equal production of  $B^+$  and  $B^0$  at the  $\Upsilon(4S)$ .

<sup>5</sup> ALBRECHT 90J reports  $(1.6 \pm 1.1 \pm 0.3) \times 10^{-3}$  from a measurement of  $[\Gamma(B^+ \rightarrow J/\psi(1S)K^*(892)^+)/\Gamma_{\text{total}}] \times [B(J/\psi(1S) \rightarrow e^+e^-)]$  assuming  $B(J/\psi(1S) \rightarrow e^+e^-) = 0.069 \pm 0.009$ , which we rescale to our best value  $B(J/\psi(1S) \rightarrow e^+e^-) = (5.94 \pm 0.06) \times 10^{-2}$ . Our first error is their experiment's error and our second error is the systematic error from using our best value. Assumes equal production of  $B^+$  and  $B^0$  at the  $\Upsilon(4S)$ .

 $\Gamma(J/\psi(1S)K^*(892)^+)/\Gamma(J/\psi(1S)K^+)$   $\Gamma_{205}/\Gamma_{185}$ 

VALUE	DOCUMENT ID	TECN	COMMENT
<b>1.39 ± 0.09 OUR AVERAGE</b>			
1.37 ± 0.05 ± 0.08	AUBERT 05J	BABR	$e^+e^- \rightarrow \Upsilon(4S)$
1.45 ± 0.20 ± 0.17	<sup>1</sup> JESSOP 97	CLE2	$e^+e^- \rightarrow \Upsilon(4S)$
1.92 ± 0.60 ± 0.17	ABE 96Q	CDF	$p\bar{p}$
• • • We do not use the following data for averages, fits, limits, etc. • • •			
1.37 ± 0.10 ± 0.08	<sup>2</sup> AUBERT 02	BABR	Repl. by AUBERT 05J

<sup>1</sup> JESSOP 97 assumes equal production of  $B^+$  and  $B^0$  at the  $\Upsilon(4S)$ . The measurement is actually measured as an average over kaon charged and neutral states.  
<sup>2</sup> Assumes equal production of  $B^+$  and  $B^0$  at the  $\Upsilon(4S)$ .

 $\Gamma(J/\psi(1S)K(1270)^+)/\Gamma_{\text{total}}$   $\Gamma_{206}/\Gamma$ 

VALUE (units $10^{-3}$ )	DOCUMENT ID	TECN	COMMENT
<b>1.80 ± 0.34 ± 0.39</b>	<sup>1</sup> ABE 01L	BELL	$e^+e^- \rightarrow \Upsilon(4S)$

<sup>1</sup> Uses the PDG value of  $B(B^+ \rightarrow J/\psi(1S)K^+) = (1.00 \pm 0.10) \times 10^{-3}$ .

 $\Gamma(J/\psi(1S)K(1400)^+)/\Gamma(J/\psi(1S)K(1270)^+)$   $\Gamma_{207}/\Gamma_{206}$ 

VALUE	CL%	DOCUMENT ID	TECN	COMMENT
<b>&lt; 0.30</b>	90	ABE 01L	BELL	$e^+e^- \rightarrow \Upsilon(4S)$

 $\Gamma(J/\psi(1S)\eta K^+)/\Gamma_{\text{total}}$   $\Gamma_{208}/\Gamma$ 

VALUE (units $10^{-5}$ )	DOCUMENT ID	TECN	COMMENT
<b>10.8 ± 2.3 ± 2.4</b>	<sup>1</sup> AUBERT 04Y	BABR	$e^+e^- \rightarrow \Upsilon(4S)$

<sup>1</sup> Assumes equal production of  $B^+$  and  $B^0$  at the  $\Upsilon(4S)$ .

 $\Gamma(J/\psi(1S)\eta' K^+)/\Gamma_{\text{total}}$   $\Gamma_{209}/\Gamma$ 

VALUE (units $10^{-5}$ )	CL%	DOCUMENT ID	TECN	COMMENT
<b>&lt; 8.8</b>	90	<sup>1</sup> XIE 07	BELL	$e^+e^- \rightarrow \Upsilon(4S)$

<sup>1</sup> Assumes equal production of  $B^+$  and  $B^0$  at the  $\Upsilon(4S)$ .

 $\Gamma(J/\psi(1S)\phi K^+)/\Gamma_{\text{total}}$   $\Gamma_{210}/\Gamma$ 

VALUE	DOCUMENT ID	TECN	COMMENT
<b>(5.2 ± 1.7) × 10<sup>-5</sup> OUR AVERAGE</b>			Error includes scale factor of 1.2.
(4.4 ± 1.4 ± 0.5) × 10 <sup>-5</sup>	<sup>1</sup> AUBERT 03o	BABR	$e^+e^- \rightarrow \Upsilon(4S)$
(8.8 <sup>+3.5</sup> <sub>-3.0</sub> ± 1.3) × 10 <sup>-5</sup>	<sup>2</sup> ANASTASSOV 00	CLE2	$e^+e^- \rightarrow \Upsilon(4S)$

<sup>1</sup> Assumes equal production of  $B^+$  and  $B^0$  at the  $\Upsilon(4S)$ .

<sup>2</sup> ANASTASSOV 00 finds 10 events on a background of  $0.5 \pm 0.2$ . Assumes equal production of  $B^0$  and  $B^+$  at the  $\Upsilon(4S)$ , a uniform Dalitz plot distribution, isotropic  $J/\psi(1S)$  and  $\phi$  decays, and  $B(B^+ \rightarrow J/\psi(1S)\phi K^+) = B(B^0 \rightarrow J/\psi(1S)\phi K^0)$ .

 $\Gamma(J/\psi(1S)\omega K^+)/\Gamma_{\text{total}}$   $\Gamma_{211}/\Gamma$ 

VALUE (units $10^{-4}$ )	DOCUMENT ID	TECN	COMMENT
<b>3.2 ± 0.1 <sup>+0.6</sup><sub>-0.3</sub></b>	<sup>1</sup> DEL-AMO-SA...10B	BABR	$e^+e^- \rightarrow \Upsilon(4S)$
• • • We do not use the following data for averages, fits, limits, etc. • • •			
3.5 ± 0.2 ± 0.4	<sup>1</sup> AUBERT 08W	BABR	Repl. by DEL-AMO-SANCHEZ 10B

<sup>1</sup> Assumes equal production of  $B^+$  and  $B^0$  at the  $\Upsilon(4S)$ .

 $\Gamma(X(3872)K^+ \times B(X \rightarrow J/\psi\omega))/\Gamma_{\text{total}}$   $\Gamma_{212}/\Gamma$ 

VALUE (units $10^{-6}$ )	DOCUMENT ID	TECN	COMMENT
<b>6 ± 2 ± 1</b>	<sup>1</sup> DEL-AMO-SA...10B	BABR	$e^+e^- \rightarrow \Upsilon(4S)$

<sup>1</sup> Assumes equal production of  $B^+$  and  $B^0$  at the  $\Upsilon(4S)$ .

 $\Gamma(X(3915)K^+ \times B(X \rightarrow J/\psi\omega))/\Gamma_{\text{total}}$   $\Gamma_{213}/\Gamma$ 

VALUE (units $10^{-5}$ )	DOCUMENT ID	TECN	COMMENT
<b>3.0 ± 0.7 ± 0.5 <sup>-0.6</sup><sub>-0.3</sub></b>	<sup>1</sup> DEL-AMO-SA...10B	BABR	$e^+e^- \rightarrow \Upsilon(4S)$
• • • We do not use the following data for averages, fits, limits, etc. • • •			
4.9 <sup>+1.0</sup> <sub>-0.9</sub> ± 0.5	<sup>1</sup> AUBERT 08W	BABR	Repl. by DEL-AMO-SANCHEZ 10B

<sup>1</sup> Assumes equal production of  $B^+$  and  $B^0$  at the  $\Upsilon(4S)$ .

 $\Gamma(J/\psi(1S)\pi^+)/\Gamma_{\text{total}}$   $\Gamma_{214}/\Gamma$ 

VALUE	DOCUMENT ID	TECN	COMMENT
<b>(4.9 ± 0.4) × 10<sup>-5</sup> OUR FIT</b>			Error includes scale factor of 1.2.
<b>(3.8 ± 0.6 ± 0.3) × 10<sup>-5</sup></b>	<sup>1</sup> ABE 03B	BELL	$e^+e^- \rightarrow \Upsilon(4S)$

<sup>1</sup> Assumes equal production of  $B^+$  and  $B^0$  at the  $\Upsilon(4S)$ .

 $\Gamma(J/\psi(1S)\pi^+)/\Gamma(J/\psi(1S)K^+)$   $\Gamma_{214}/\Gamma_{185}$ 

VALUE	EVTS	DOCUMENT ID	TECN	COMMENT
<b>0.049 ± 0.004 OUR FIT</b>				Error includes scale factor of 1.1.
<b>0.052 ± 0.004 OUR AVERAGE</b>				
0.0486 ± 0.0082 ± 0.0015		ABULENCIA 09	CDF	$p\bar{p}$ at 1.96 TeV
0.0537 ± 0.0045 ± 0.0011		AUBERT 04P	BABR	$e^+e^- \rightarrow \Upsilon(4S)$
0.050 <sup>+0.019</sup> <sub>-0.017</sub> ± 0.001		ABE 96R	CDF	$p\bar{p}$ 1.8 TeV
0.052 ± 0.024		BISHAI 96	CLE2	$e^+e^- \rightarrow \Upsilon(4S)$
• • • We do not use the following data for averages, fits, limits, etc. • • •				
0.0391 ± 0.0078 ± 0.0019		AUBERT 02F	BABR	Repl. by AUBERT 04P
0.043 ± 0.023	5	<sup>1</sup> ALEXANDER 95	CLE2	Sup. by BISHAI 96

<sup>1</sup> Assumes equal production of  $B^+B^-$  and  $B^0\bar{B}^0$  on  $\Upsilon(4S)$ .

## Meson Particle Listings

 $B^\pm$  $\Gamma(J/\psi(1S)\rho^+)/\Gamma_{\text{total}}$   $\Gamma_{215}/\Gamma$ 

VALUE (units $10^{-5}$ )	CL%	DOCUMENT ID	TECN	COMMENT
<b><math>5.0 \pm 0.7 \pm 0.3</math></b>		<sup>1</sup> AUBERT	07AC	BABR $e^+e^- \rightarrow \Upsilon(4S)$
• • • We do not use the following data for averages, fits, limits, etc. • • •				
<77	90	BISHAI	96	CLE2 $e^+e^- \rightarrow \Upsilon(4S)$

<sup>1</sup> Assumes equal production of  $B^+$  and  $B^0$  at the  $\Upsilon(4S)$ .

 $\Gamma(J/\psi(1S)\pi^+\pi^0\text{nonresonant})/\Gamma_{\text{total}}$   $\Gamma_{216}/\Gamma$ 

VALUE (units $10^{-5}$ )	CL%	DOCUMENT ID	TECN	COMMENT
<b>&lt;0.73</b>	90	<sup>1</sup> AUBERT	07AC	BABR $e^+e^- \rightarrow \Upsilon(4S)$

<sup>1</sup> Assumes equal production of  $B^+$  and  $B^0$  at the  $\Upsilon(4S)$ .

 $\Gamma(J/\psi(1S)a_1(1260)^+)/\Gamma_{\text{total}}$   $\Gamma_{217}/\Gamma$ 

VALUE	CL%	DOCUMENT ID	TECN	COMMENT
<b>&lt;1.2 <math>\times 10^{-3}</math></b>	90	BISHAI	96	CLE2 $e^+e^- \rightarrow \Upsilon(4S)$

 $\Gamma(J/\psi(1S)\rho^0)/\Gamma_{\text{total}}$   $\Gamma_{218}/\Gamma$ 

VALUE (units $10^{-6}$ )	CL%	DOCUMENT ID	TECN	COMMENT
<b><math>11.8 \pm 3.1</math> OUR AVERAGE</b>				
$11.7 \pm 2.8^{+1.8}_{-2.3}$		<sup>1</sup> XIE	05	BELL $e^+e^- \rightarrow \Upsilon(4S)$
$12^{+9}_{-6}$		<sup>1</sup> AUBERT	03K	BABR $e^+e^- \rightarrow \Upsilon(4S)$

• • • We do not use the following data for averages, fits, limits, etc. • • •

VALUE	CL%	DOCUMENT ID	TECN	COMMENT
<41	90	ZANG	04	BELL $e^+e^- \rightarrow \Upsilon(4S)$

<sup>1</sup> Assumes equal production of  $B^+$  and  $B^0$  at the  $\Upsilon(4S)$ .

 $\Gamma(J/\psi(1S)\Sigma^0\rho)/\Gamma_{\text{total}}$   $\Gamma_{219}/\Gamma$ 

VALUE	CL%	DOCUMENT ID	TECN	COMMENT
<b>&lt;1.1 <math>\times 10^{-5}</math></b>	90	<sup>1</sup> XIE	05	BELL $e^+e^- \rightarrow \Upsilon(4S)$

<sup>1</sup> Assumes equal production of  $B^+$  and  $B^0$  at the  $\Upsilon(4S)$ .

 $\Gamma(J/\psi(1S)D^+)/\Gamma_{\text{total}}$   $\Gamma_{220}/\Gamma$ 

VALUE (units $10^{-5}$ )	CL%	DOCUMENT ID	TECN	COMMENT
<b>&lt;12</b>	90	<sup>1</sup> AUBERT	05U	BABR $e^+e^- \rightarrow \Upsilon(4S)$

<sup>1</sup> Assumes equal production of  $B^+$  and  $B^0$  at the  $\Upsilon(4S)$ .

 $\Gamma(J/\psi(1S)\bar{D}^0\pi^+)/\Gamma_{\text{total}}$   $\Gamma_{221}/\Gamma$ 

VALUE (units $10^{-5}$ )	CL%	DOCUMENT ID	TECN	COMMENT
<b>&lt;2.5</b>	90	<sup>1</sup> ZHANG	05B	BELL $e^+e^- \rightarrow \Upsilon(4S)$
• • • We do not use the following data for averages, fits, limits, etc. • • •				
<5.2	90	<sup>1</sup> AUBERT	05R	BABR $e^+e^- \rightarrow \Upsilon(4S)$

<sup>1</sup> Assumes equal production of  $B^+$  and  $B^0$  at the  $\Upsilon(4S)$ .

 $\Gamma(\psi(2S)\pi^+)/\Gamma_{\text{total}}$   $\Gamma_{222}/\Gamma$ 

VALUE (units $10^{-5}$ )	CL%	DOCUMENT ID	TECN	COMMENT
<b><math>2.44 \pm 0.22 \pm 0.20</math></b>		<sup>1</sup> BHARDWAJ	08	BELL $e^+e^- \rightarrow \Upsilon(4S)$

<sup>1</sup> Assumes equal production of  $B^+$  and  $B^0$  at the  $\Upsilon(4S)$ .

 $\Gamma(\psi(2S)\pi^+)/\Gamma(\psi(2S)K^+)$   $\Gamma_{222}/\Gamma_{223}$ 

VALUE (units $10^{-2}$ )	CL%	DOCUMENT ID	TECN	COMMENT
<b><math>3.99 \pm 0.36 \pm 0.17</math></b>		BHARDWAJ	08	BELL $e^+e^- \rightarrow \Upsilon(4S)$

 $\Gamma(\psi(2S)K^+)/\Gamma_{\text{total}}$   $\Gamma_{223}/\Gamma$ 

VALUE (units $10^{-4}$ )	EVTs	DOCUMENT ID	TECN	COMMENT
<b><math>6.39 \pm 0.33</math> OUR FIT</b>				
<b><math>6.5 \pm 0.4</math> OUR AVERAGE</b>				
$6.65 \pm 0.17 \pm 0.55$		<sup>1</sup> GULER	11	BELL $e^+e^- \rightarrow \Upsilon(4S)$
$4.9 \pm 1.6 \pm 0.4$		<sup>2</sup> AUBERT	06E	BABR $e^+e^- \rightarrow \Upsilon(4S)$
$6.17 \pm 0.32 \pm 0.44$		<sup>1</sup> AUBERT	05J	BABR $e^+e^- \rightarrow \Upsilon(4S)$
$7.8 \pm 0.7 \pm 0.9$		<sup>1</sup> RICHICHI	01	CLE2 $e^+e^- \rightarrow \Upsilon(4S)$
$18 \pm 8 \pm 4$	5	<sup>1</sup> ALBRECHT	90J	ARG $e^+e^- \rightarrow \Upsilon(4S)$

• • • We do not use the following data for averages, fits, limits, etc. • • •

$6.9 \pm 0.6$		<sup>1</sup> ABE	03B	BELL Repl. by GULER 11
$6.4 \pm 0.5 \pm 0.8$		<sup>1</sup> AUBERT	02	BABR Repl. by AUBERT 05J
$6.1 \pm 2.3 \pm 0.9$	7	<sup>1</sup> ALAM	94	CLE2 Repl. by RICHICHI 01
<5 at 90% CL		<sup>1</sup> BORTOLETTO	92	CLEO $e^+e^- \rightarrow \Upsilon(4S)$
$22 \pm 17$	3	<sup>3</sup> ALBRECHT	87D	ARG $e^+e^- \rightarrow \Upsilon(4S)$

<sup>1</sup> Assumes equal production of  $B^+$  and  $B^0$  at the  $\Upsilon(4S)$ .  
<sup>2</sup> Perform measurements of absolute branching fractions using a missing mass technique.  
<sup>3</sup> ALBRECHT 87D assume  $B^+B^-/B^0\bar{B}^0$  ratio is 55/45. Superseded by ALBRECHT 90J.

 $\Gamma(\psi(2S)K^+)/\Gamma(J/\psi(1S)K^+)$   $\Gamma_{223}/\Gamma_{185}$ 

VALUE	DOCUMENT ID	TECN	COMMENT
<b><math>0.629 \pm 0.035</math> OUR FIT</b>			
<b><math>0.60 \pm 0.07</math> OUR AVERAGE</b>			
$0.63 \pm 0.05 \pm 0.08$	ABAZOV	09Y	D0 $p\bar{p}$ at 1.96 TeV
$0.558 \pm 0.082 \pm 0.056$	ABE	98O	CDF $p\bar{p}$ 1.8 TeV

• • • We do not use the following data for averages, fits, limits, etc. • • •

$0.64 \pm 0.06 \pm 0.07$	<sup>1</sup> AUBERT	02	BABR $e^+e^- \rightarrow \Upsilon(4S)$
--------------------------	---------------------	----	--

<sup>1</sup> Assumes equal production of  $B^+$  and  $B^0$  at the  $\Upsilon(4S)$ .

 $\Gamma(\psi(2S)K^*(892)^+)/\Gamma_{\text{total}}$   $\Gamma_{224}/\Gamma$ 

VALUE (units $10^{-4}$ )	CL%	DOCUMENT ID	TECN	COMMENT
<b><math>6.7 \pm 1.4</math> OUR AVERAGE</b>				Error includes scale factor of 1.3.
$5.92 \pm 0.85 \pm 0.89$		<sup>1</sup> AUBERT	05J	BABR $e^+e^- \rightarrow \Upsilon(4S)$
$9.2 \pm 1.9 \pm 1.2$		<sup>1</sup> RICHICHI	01	CLE2 $e^+e^- \rightarrow \Upsilon(4S)$

• • • We do not use the following data for averages, fits, limits, etc. • • •

<30	90	<sup>1</sup> ALAM	94	CLE2 Repl. by RICHICHI 01
<35	90	<sup>1</sup> BORTOLETTO	92	CLEO $e^+e^- \rightarrow \Upsilon(4S)$
<49	90	<sup>1</sup> ALBRECHT	90J	ARG $e^+e^- \rightarrow \Upsilon(4S)$

<sup>1</sup> Assumes equal production of  $B^+$  and  $B^0$  at the  $\Upsilon(4S)$ .

 $\Gamma(\psi(2S)K^*(892)^+)/\Gamma(\psi(2S)K^+)$   $\Gamma_{224}/\Gamma_{223}$ 

VALUE	DOCUMENT ID	TECN	COMMENT
<b><math>0.96 \pm 0.15 \pm 0.09</math></b>	AUBERT	05J	BABR $e^+e^- \rightarrow \Upsilon(4S)$

 $\Gamma(\psi(2S)K^+\pi^+\pi^-)/\Gamma_{\text{total}}$   $\Gamma_{225}/\Gamma$ 

VALUE (units $10^{-4}$ )	EVTs	DOCUMENT ID	TECN	COMMENT
<b><math>4.3 \pm 0.5</math> OUR AVERAGE</b>				
$4.31 \pm 0.20 \pm 0.50$		<sup>1</sup> GULER	11	BELL $e^+e^- \rightarrow \Upsilon(4S)$
$19 \pm 11 \pm 4$	3	<sup>1</sup> ALBRECHT	90J	ARG $e^+e^- \rightarrow \Upsilon(4S)$

<sup>1</sup> Assumes equal production of  $B^+$  and  $B^0$  at the  $\Upsilon(4S)$ .

 $\Gamma(\psi(3770)K^+)/\Gamma_{\text{total}}$   $\Gamma_{226}/\Gamma$ 

VALUE (units $10^{-3}$ )	DOCUMENT ID	TECN	COMMENT
<b><math>0.49 \pm 0.13</math> OUR AVERAGE</b>			
$3.5 \pm 2.5 \pm 0.3$	<sup>1</sup> AUBERT	06E	BABR $e^+e^- \rightarrow \Upsilon(4S)$
$0.48 \pm 0.11 \pm 0.07$	<sup>2</sup> CHISTOV	04	BELL $e^+e^- \rightarrow \Upsilon(4S)$

<sup>1</sup> Perform measurements of absolute branching fractions using a missing mass technique.  
<sup>2</sup> Assumes equal production of  $B^+$  and  $B^0$  at the  $\Upsilon(4S)$ .

 $\Gamma(\psi(3770)K^+ \times B(\psi \rightarrow D^0\bar{D}^0))/\Gamma_{\text{total}}$   $\Gamma_{227}/\Gamma$ 

VALUE (units $10^{-4}$ )	DOCUMENT ID	TECN	COMMENT
<b><math>1.6 \pm 0.4</math> OUR AVERAGE</b>			Error includes scale factor of 1.1.
$1.41 \pm 0.30 \pm 0.22$	<sup>1</sup> AUBERT	08B	BABR $e^+e^- \rightarrow \Upsilon(4S)$
$2.2 \pm 0.5 \pm 0.3$	<sup>1</sup> BRODZICKA	08	BELL $e^+e^- \rightarrow \Upsilon(4S)$

• • • We do not use the following data for averages, fits, limits, etc. • • •

$3.4 \pm 0.8 \pm 0.5$	<sup>1</sup> CHISTOV	04	BELL Repl. by BRODZICKA 08
-----------------------	----------------------	----	----------------------------

<sup>1</sup> Assumes equal production of  $B^+$  and  $B^0$  at the  $\Upsilon(4S)$ .

 $\Gamma(\psi(3770)K^+ \times B(\psi \rightarrow D^+D^-))/\Gamma_{\text{total}}$   $\Gamma_{228}/\Gamma$ 

VALUE (units $10^{-4}$ )	DOCUMENT ID	TECN	COMMENT
<b><math>0.94 \pm 0.35</math> OUR AVERAGE</b>			
$0.84 \pm 0.32 \pm 0.21$	<sup>1</sup> AUBERT	08B	BABR $e^+e^- \rightarrow \Upsilon(4S)$
$1.4 \pm 0.8 \pm 0.2$	<sup>1</sup> CHISTOV	04	BELL $e^+e^- \rightarrow \Upsilon(4S)$

<sup>1</sup> Assumes equal production of  $B^+$  and  $B^0$  at the  $\Upsilon(4S)$ .

 $\Gamma(\chi_{c0}\pi^+ \times B(\chi_{c0} \rightarrow \pi^+\pi^-))/\Gamma_{\text{total}}$   $\Gamma_{229}/\Gamma$ 

VALUE (units $10^{-6}$ )	CL%	DOCUMENT ID	TECN	COMMENT
<b>&lt;0.1</b>	90	<sup>1</sup> AUBERT	09L	BABR $e^+e^- \rightarrow \Upsilon(4S)$

• • • We do not use the following data for averages, fits, limits, etc. • • •

<0.3	90	<sup>1</sup> AUBERT,B	05G	BABR Repl. by AUBERT 09L
------	----	-----------------------	-----	--------------------------

<sup>1</sup> Assumes equal production of  $B^+$  and  $B^0$  at the  $\Upsilon(4S)$ .

 $\Gamma(\chi_{c0}(1P)K^+)/\Gamma_{\text{total}}$   $\Gamma_{230}/\Gamma$ 

VALUE (units $10^{-4}$ )	CL%	DOCUMENT ID	TECN	COMMENT
<b><math>1.34^{+0.19}_{-0.16}</math> OUR AVERAGE</b>				
$1.8 \pm 0.8 \pm 0.1$		<sup>1</sup> LEES	11I	BABR $e^+e^- \rightarrow \Upsilon(4S)$
$1.23^{+0.27}_{-0.25} \pm 0.06$		<sup>2,3</sup> AUBERT	08AI	BABR $e^+e^- \rightarrow \Upsilon(4S)$
$1.84 \pm 0.32 \pm 0.31$		<sup>2,4</sup> AUBERT	06O	BABR $e^+e^- \rightarrow \Upsilon(4S)$
$5.2 \pm 2.4 \pm 0.4$		<sup>5</sup> AUBERT,BE	06M	BABR $e^+e^- \rightarrow \Upsilon(4S)$
$1.12 \pm 0.12^{+0.30}_{-0.20}$		<sup>2</sup> GARMASH	06	BELL $e^+e^- \rightarrow \Upsilon(4S)$

• • • We do not use the following data for averages, fits, limits, etc. • • •

<5	90	<sup>2,6</sup> WICHT	08	BELL $e^+e^- \rightarrow \Upsilon(4S)$
<1.8	90	<sup>7</sup> AUBERT	06E	BABR $e^+e^- \rightarrow \Upsilon(4S)$
<8.9	90	<sup>2</sup> AUBERT	05K	BABR $e^+e^- \rightarrow \Upsilon(4S)$
$1.39 \pm 0.49 \pm 0.11$		<sup>8</sup> AUBERT,B	05N	BABR Repl. by AUBERT 08AI
$1.96 \pm 0.35^{+2.00}_{-0.42}$		<sup>2</sup> GARMASH	05	BELL Repl. by GARMASH 06
$2.7 \pm 0.7$		<sup>9</sup> AUBERT	04T	BABR Repl. by AUBERT,B 04P
$3.0 \pm 0.8 \pm 0.3$		<sup>10</sup> AUBERT,B	04P	BABR Repl. by AUBERT,B 05N
$6.0^{+2.1}_{-1.8} \pm 1.1$		<sup>11</sup> ABE	02B	BELL Repl. by GARMASH 05
<4.8	90	<sup>12</sup> EDWARDS	01	CLE2 $e^+e^- \rightarrow \Upsilon(4S)$



- <sup>1</sup> LEES 11i reports  $[\Gamma(B^+ \rightarrow \chi_{c0}(1P) K^+)/\Gamma_{\text{total}}] \times [B(\chi_{c0}(1P) \rightarrow \pi\pi)] = (1.53 \pm 0.66 \pm 0.27) \times 10^{-6}$  which we divide by our best value  $B(\chi_{c0}(1P) \rightarrow \pi\pi) = (8.5 \pm 0.4) \times 10^{-3}$ . Our first error is their experiment's error and our second error is the systematic error from using our best value.
- <sup>2</sup> Assumes equal production of  $B^+$  and  $B^0$  at the  $\Upsilon(4S)$ .
- <sup>3</sup> AUBERT 08A1 reports  $(0.70 \pm 0.10^{+0.12}_{-0.10}) \times 10^{-6}$  for  $B(B^+ \rightarrow \chi_{c0} K^+) \times B(\chi_{c0} \rightarrow \pi^+ \pi^-)$ . We compute  $B(B^+ \rightarrow \chi_{c0} K^+)$  using the PDG value  $B(\chi_{c0} \rightarrow \pi\pi) = (8.5 \pm 0.4) \times 10^{-3}$  and 2/3 for the  $\pi^+ \pi^-$  fraction. Our first error is their experiment's error and the second error is systematic error from using our best value.
- <sup>4</sup> Measured in the  $B^+ \rightarrow K^+ K^- K^+$  decay.
- <sup>5</sup> AUBERT, BE 06M reports  $[\Gamma(B^+ \rightarrow \chi_{c0}(1P) K^+)/\Gamma_{\text{total}}] \times [B(\chi_{c0}(1P) \rightarrow \gamma J/\psi(1S))] = (6.1 \pm 2.6 \pm 1.1) \times 10^{-6}$  which we divide by our best value  $B(\chi_{c0}(1P) \rightarrow \gamma J/\psi(1S)) = (1.17 \pm 0.08) \times 10^{-2}$ . Our first error is their experiment's error and our second error is the systematic error from using our best value. The significance of the observed signal is  $2.4 \sigma$ .
- <sup>6</sup> WICHT 08 reports  $[\Gamma(B^+ \rightarrow \chi_{c0}(1P) K^+)/\Gamma_{\text{total}}] \times [B(\chi_{c0}(1P) \rightarrow \gamma\gamma)] < 0.11 \times 10^{-6}$  which we divide by our best value  $B(\chi_{c0}(1P) \rightarrow \gamma\gamma) = 2.23 \times 10^{-4}$ .
- <sup>7</sup> Perform measurements of absolute branching fractions using a missing mass technique.
- <sup>8</sup> AUBERT, B 05N reports  $(0.66 \pm 0.22 \pm 0.08) \times 10^{-6}$  for  $B(B^+ \rightarrow \chi_c^0 K^+) \times B(\chi_c^0 \rightarrow \pi^+ \pi^-)$ . We compute  $B(B^+ \rightarrow \chi_c^0 K^+)$  using the PDG value  $B(\chi_c^0 \rightarrow \pi^+ \pi^-) = (7.1 \pm 0.6) \times 10^{-3}$  and 2/3 for the  $\pi^+ \pi^-$  fraction.
- <sup>9</sup> The measurement performed using decay channels  $\chi_c^0 \rightarrow \pi^+ \pi^-$  and  $\chi_c^0 \rightarrow K^+ K^-$ . The ratio of the branching ratios for these channels is found to be consistent with world average.
- <sup>10</sup> AUBERT 04P reports  $B(B^+ \rightarrow \chi_c^0 K^+) \times B(\chi_c^0 \rightarrow \pi^+ \pi^-) = (1.5 \pm 0.4 \pm 0.1) \times 10^{-6}$  and used PDG value of  $B(\chi_c^0 \rightarrow \pi\pi) = (7.4 \pm 0.8) \times 10^{-3}$  and Clebsch-Gordan coefficient to compute  $B(B^+ \rightarrow \chi_c^0 K^+)$ .
- <sup>11</sup> ABE 02B measures the ratio of  $B(B^+ \rightarrow \chi_c^0 K^+)/B(B^+ \rightarrow J/\psi(1S) K^+) = 0.60 \pm 0.21 - 0.18 \pm 0.05 \pm 0.08$ , where the third error is due to the uncertainty in the  $B(\chi_c^0 \rightarrow \pi^+ \pi^-)$ , and uses  $B(B^+ \rightarrow J/\psi(1S) K^+) = (10.0 \pm 1.0) \times 10^{-4}$  to obtain the result.
- <sup>12</sup> EDWARDS 01 assumes equal production of  $B^0$  and  $B^+$  at the  $\Upsilon(4S)$ . The correlated uncertainties (28.3)% from  $B(J/\psi(1S) \rightarrow \eta \eta_c)$  in those modes have been accounted for.

$\Gamma(\chi_{c0} K^*(892)^+)/\Gamma_{\text{total}}$		$\Gamma_{231}/\Gamma$		
VALUE (units $10^{-4}$ )	CL%	DOCUMENT ID	TECN	COMMENT
<b>&lt; 2.1</b>	90	<sup>1</sup> AUBERT	08BD BABR	$e^+ e^- \rightarrow \Upsilon(4S)$
••• We do not use the following data for averages, fits, limits, etc. •••				
<28.6	90	<sup>1</sup> AUBERT	05K BABR	Repl. by AUBERT 08BD
<sup>1</sup> Assumes equal production of $B^+$ and $B^0$ at the $\Upsilon(4S)$ .				

$\Gamma(\chi_{c2} \pi^+ \times B(\chi_{c2} \rightarrow \pi^+ \pi^-))/\Gamma_{\text{total}}$		$\Gamma_{232}/\Gamma$		
VALUE (units $10^{-6}$ )	CL%	DOCUMENT ID	TECN	COMMENT
<b>&lt; 0.1</b>	90	<sup>1</sup> AUBERT	09L BABR	$e^+ e^- \rightarrow \Upsilon(4S)$
<sup>1</sup> Assumes equal production of $B^+$ and $B^0$ at the $\Upsilon(4S)$ .				

$\Gamma(\chi_{c2} K^+)/\Gamma_{\text{total}}$		$\Gamma_{233}/\Gamma$		
VALUE (units $10^{-5}$ )	CL%	DOCUMENT ID	TECN	COMMENT
<b><math>1.11 \pm 0.36</math> <math>-0.34 \pm 0.09</math></b>		<sup>1</sup> BHARDWAJ	11 BELL	$e^+ e^- \rightarrow \Upsilon(4S)$
••• We do not use the following data for averages, fits, limits, etc. •••				
< 1.8	90	<sup>2</sup> AUBERT	09B BABR	$e^+ e^- \rightarrow \Upsilon(4S)$
< 20	90	<sup>3</sup> AUBERT	06E BABR	$e^+ e^- \rightarrow \Upsilon(4S)$
< 2.9	90	<sup>1</sup> SONI	06 BELL	Repl. by BHARDWAJ 11
< 3.0	90	<sup>1</sup> AUBERT	05K BABR	Repl. by AUBERT 06E
<sup>1</sup> Assumes equal production of $B^+$ and $B^0$ at the $\Upsilon(4S)$ .				
<sup>2</sup> Uses $\chi_{c1,2} \rightarrow J/\psi \gamma$ . Assumes $B(\Upsilon(4S) \rightarrow B^+ B^-) = (51.6 \pm 0.6)\%$ and $B(\Upsilon(4S) \rightarrow B^0 \bar{B}^0) = (48.4 \pm 0.6)\%$ .				
<sup>3</sup> Perform measurements of absolute branching fractions using a missing mass technique.				

$\Gamma(B^+ \rightarrow \chi_{c2} K^+)/\Gamma_{\text{total}} \times \Gamma(\chi_{c2}(1P) \rightarrow \gamma\gamma)/\Gamma_{\text{total}}$		$\Gamma_{233}/\Gamma \times \Gamma_{\chi_{c2}(1P)}/\Gamma_{\chi_{c2}(1P)}$		
VALUE (units $10^{-6}$ )	CL%	DOCUMENT ID	TECN	COMMENT
<b>&lt; 0.09</b>	90	<sup>1</sup> WICHT	08 BELL	$e^+ e^- \rightarrow \Upsilon(4S)$
<sup>1</sup> Assumes equal production of $B^+$ and $B^0$ at the $\Upsilon(4S)$ .				

$\Gamma(\chi_{c2} K^*(892)^+)/\Gamma_{\text{total}}$		$\Gamma_{234}/\Gamma$		
VALUE	CL%	DOCUMENT ID	TECN	COMMENT
<b>&lt; <math>12 \times 10^{-5}</math></b>	90	<sup>1</sup> AUBERT	09B BABR	$e^+ e^- \rightarrow \Upsilon(4S)$
••• We do not use the following data for averages, fits, limits, etc. •••				
< $12.7 \times 10^{-5}$	90	<sup>2</sup> SONI	06 BELL	$e^+ e^- \rightarrow \Upsilon(4S)$
< $1.2 \times 10^{-5}$	90	<sup>2</sup> AUBERT	05K BABR	Repl. by AUBERT 09B
<sup>1</sup> Uses $\chi_{c1,2} \rightarrow J/\psi \gamma$ . Assumes $B(\Upsilon(4S) \rightarrow B^+ B^-) = (51.6 \pm 0.6)\%$ and $B(\Upsilon(4S) \rightarrow B^0 \bar{B}^0) = (48.4 \pm 0.6)\%$ .				
<sup>2</sup> Assumes equal production of $B^+$ and $B^0$ at the $\Upsilon(4S)$ .				

$\Gamma(\chi_{c1}(1P) \pi^+)/\Gamma_{\text{total}}$		$\Gamma_{235}/\Gamma$		
VALUE (units $10^{-5}$ )		DOCUMENT ID	TECN	COMMENT
<b><math>2.2 \pm 0.4 \pm 0.3</math></b>		<sup>1</sup> KUMAR	06 BELL	$e^+ e^- \rightarrow \Upsilon(4S)$
<sup>1</sup> Assumes equal production of $B^+$ and $B^0$ at the $\Upsilon(4S)$ .				

$\Gamma(\chi_{c1}(1P) K^+)/\Gamma_{\text{total}}$		$\Gamma_{236}/\Gamma$		
VALUE (units $10^{-4}$ )	EVTS	DOCUMENT ID	TECN	COMMENT
<b><math>4.79 \pm 0.23</math> OUR AVERAGE</b>				
4.94 ± 0.11 ± 0.33		<sup>1</sup> BHARDWAJ	11 BELL	$e^+ e^- \rightarrow \Upsilon(4S)$
4.5 ± 0.1 ± 0.3		<sup>2</sup> AUBERT	09B BABR	$e^+ e^- \rightarrow \Upsilon(4S)$
8.1 ± 1.4 ± 0.7		<sup>3</sup> AUBERT	06E BABR	$e^+ e^- \rightarrow \Upsilon(4S)$
15.5 ± 5.4 ± 2.0		<sup>4</sup> ACOSTA	02F CDF	$p\bar{p}$ 1.8 TeV
••• We do not use the following data for averages, fits, limits, etc. •••				
5.1 ± 0.4 ± 0.2		<sup>5</sup> AUBERT, BE	06M BABR	Repl. by AUBERT 09B
4.49 ± 0.19 ± 0.53		<sup>1</sup> SONI	06 BELL	Repl. by BHARDWAJ 11
5.79 ± 0.26 ± 0.65		<sup>1</sup> AUBERT	05J BABR	Repl. by AUBERT, BE 06M
6.0 ± 0.9 ± 0.3		<sup>6</sup> AUBERT	02 BABR	Repl. by AUBERT 05J
9.7 ± 4.0 ± 0.9	6	<sup>1</sup> ALAM	94 CLE2	$e^+ e^- \rightarrow \Upsilon(4S)$
19 ± 13 ± 6		<sup>7</sup> ALBRECHT	92E ARG	$e^+ e^- \rightarrow \Upsilon(4S)$
<sup>1</sup> Assumes equal production of $B^+$ and $B^0$ at the $\Upsilon(4S)$ .				
<sup>2</sup> Uses $\chi_{c1,2} \rightarrow J/\psi \gamma$ . Assumes $B(\Upsilon(4S) \rightarrow B^+ B^-) = (51.6 \pm 0.6)\%$ and $B(\Upsilon(4S) \rightarrow B^0 \bar{B}^0) = (48.4 \pm 0.6)\%$ .				
<sup>3</sup> Perform measurements of absolute branching fractions using a missing mass technique.				
<sup>4</sup> ACOSTA 02F uses as reference of $B(B \rightarrow J/\psi(1S) K^+) = (10.1 \pm 0.6) \times 10^{-4}$ . The second error includes the systematic error and the uncertainties of the branching ratio.				
<sup>5</sup> AUBERT, BE 06M reports $[\Gamma(B^+ \rightarrow \chi_{c1}(1P) K^+)/\Gamma_{\text{total}}] \times [B(\chi_{c1}(1P) \rightarrow \gamma J/\psi(1S))] = (1.76 \pm 0.07 \pm 0.12) \times 10^{-4}$ which we divide by our best value $B(\chi_{c1}(1P) \rightarrow \gamma J/\psi(1S)) = (34.4 \pm 1.5) \times 10^{-2}$ . Our first error is their experiment's error and our second error is the systematic error from using our best value.				
<sup>6</sup> AUBERT 02 reports $(7.5 \pm 0.9 \pm 0.8) \times 10^{-4}$ from a measurement of $[\Gamma(B^+ \rightarrow \chi_{c1}(1P) K^+)/\Gamma_{\text{total}}] \times [B(\chi_{c1}(1P) \rightarrow \gamma J/\psi(1S))]$ assuming $B(\chi_{c1}(1P) \rightarrow \gamma J/\psi(1S)) = 0.273 \pm 0.016$ , which we rescale to our best value $B(\chi_{c1}(1P) \rightarrow \gamma J/\psi(1S)) = (34.4 \pm 1.5) \times 10^{-2}$ . Our first error is their experiment's error and our second error is the systematic error from using our best value. Assumes equal production of $B^+$ and $B^0$ at the $\Upsilon(4S)$ .				
<sup>7</sup> ALBRECHT 92E assumes no $\chi_{c2}(1P)$ production and $B(\Upsilon(4S) \rightarrow B^+ B^-) = 50\%$ .				

$\Gamma(\chi_{c1}(1P) K^+)/\Gamma(J/\psi(1S) K^+)$		$\Gamma_{236}/\Gamma_{185}$		
VALUE		DOCUMENT ID	TECN	COMMENT
<b><math>0.60 \pm 0.07 \pm 0.03</math></b>		<sup>1</sup> AUBERT	02 BABR	$e^+ e^- \rightarrow \Upsilon(4S)$
<sup>1</sup> AUBERT 02 reports $0.75 \pm 0.08 \pm 0.05$ from a measurement of $[\Gamma(B^+ \rightarrow \chi_{c1}(1P) K^+)/\Gamma(B^+ \rightarrow J/\psi(1S) K^+)] \times [B(\chi_{c1}(1P) \rightarrow \gamma J/\psi(1S))]$ assuming $B(\chi_{c1}(1P) \rightarrow \gamma J/\psi(1S)) = 0.273 \pm 0.016$ , which we rescale to our best value $B(\chi_{c1}(1P) \rightarrow \gamma J/\psi(1S)) = (34.4 \pm 1.5) \times 10^{-2}$ . Our first error is their experiment's error and our second error is the systematic error from using our best value. Assumes equal production of $B^+$ and $B^0$ at the $\Upsilon(4S)$ .				

$\Gamma(\chi_{c1}(1P) \pi^+)/\Gamma(\chi_{c1}(1P) K^+)$		$\Gamma_{235}/\Gamma_{236}$		
VALUE		DOCUMENT ID	TECN	COMMENT
<b><math>0.043 \pm 0.008 \pm 0.003</math></b>		<sup>1</sup> KUMAR	06 BELL	$e^+ e^- \rightarrow \Upsilon(4S)$
<sup>1</sup> Assumes equal production of $B^+$ and $B^0$ at the $\Upsilon(4S)$ .				

$\Gamma(\chi_{c1}(1P) K^*(892)^+)/\Gamma_{\text{total}}$		$\Gamma_{237}/\Gamma$		
VALUE (units $10^{-4}$ )	CL%	DOCUMENT ID	TECN	COMMENT
<b><math>3.0 \pm 0.6</math> OUR AVERAGE</b>		Error includes scale factor of 1.1.		
2.6 ± 0.5 ± 0.4		<sup>1</sup> AUBERT	09B BABR	$e^+ e^- \rightarrow \Upsilon(4S)$
4.05 ± 0.59 ± 0.95		<sup>2</sup> SONI	06 BELL	$e^+ e^- \rightarrow \Upsilon(4S)$
••• We do not use the following data for averages, fits, limits, etc. •••				
2.94 ± 0.95 ± 0.98		<sup>2</sup> AUBERT	05J BABR	Repl. by AUBERT 09B
< 21	90	<sup>2</sup> ALAM	94 CLE2	$e^+ e^- \rightarrow \Upsilon(4S)$
<sup>1</sup> Uses $\chi_{c1,2} \rightarrow J/\psi \gamma$ . Assumes $B(\Upsilon(4S) \rightarrow B^+ B^-) = (51.6 \pm 0.6)\%$ and $B(\Upsilon(4S) \rightarrow B^0 \bar{B}^0) = (48.4 \pm 0.6)\%$ .				
<sup>2</sup> Assumes equal production of $B^+$ and $B^0$ at the $\Upsilon(4S)$ .				

$\Gamma(\chi_{c1}(1P) K^*(892)^+)/\Gamma(\chi_{c1}(1P) K^+)$		$\Gamma_{237}/\Gamma_{236}$		
VALUE		DOCUMENT ID	TECN	COMMENT
<b><math>0.51 \pm 0.17 \pm 0.16</math></b>		AUBERT	05J BABR	$e^+ e^- \rightarrow \Upsilon(4S)$

$\Gamma(h_c(1P) K^+)/\Gamma_{\text{total}}$		$\Gamma_{238}/\Gamma$		
VALUE (units $10^{-5}$ )	EVTS	DOCUMENT ID	TECN	COMMENT
<b>&lt; 3.8</b>	90	<sup>1</sup> FANG	06 BELL	$e^+ e^- \rightarrow \Upsilon(4S)$
<sup>1</sup> Assumes equal production of $B^+$ and $B^0$ at the $\Upsilon(4S)$ and $B(h_c \rightarrow \eta_c \gamma) = 50\%$ .				

$\Gamma(K^0 \pi^+)/\Gamma_{\text{total}}$		$\Gamma_{239}/\Gamma$		
VALUE (units $10^{-6}$ )	CL%	DOCUMENT ID	TECN	COMMENT
<b><math>23.1 \pm 1.0</math> OUR AVERAGE</b>				
22.8 ± 0.8 ± 1.3		<sup>1</sup> LIN	07 BELL	$e^+ e^- \rightarrow \Upsilon(4S)$
23.9 ± 1.1 ± 1.0		<sup>1</sup> AUBERT, BE	06C BABR	$e^+ e^- \rightarrow \Upsilon(4S)$
18.8 ± 3.7 ± 2.1 - 3.3 - 1.8		<sup>1</sup> BORNHEIM	03 CLE2	$e^+ e^- \rightarrow \Upsilon(4S)$

## Meson Particle Listings

 $B^\pm$ 

• • • We do not use the following data for averages, fits, limits, etc. • • •

$26.0 \pm 1.3 \pm 1.0$	1	AUBERT, BE	05E	BABR	Repl. by AUBERT, BE 06C
$22.3 \pm 1.7 \pm 1.1$	1	AUBERT	04M	BABR	Repl. by AUBERT, BE 05E
$22.0 \pm 1.9 \pm 1.1$	1	CHAO	04	BELL	Repl. by LIN 07
$19.4 \pm 3.1 \pm 1.6$	1	CASEY	02	BELL	Repl. by CHAO 04
$13.7 \pm 5.7 \pm 1.9$ $-4.8 - 1.8$	1	ABE	01H	BELL	Repl. by CASEY 02
$18.2 \pm 3.3 \pm 2.0$ $-3.0 - 2.0$	1	AUBERT	01E	BABR	Repl. by AUBERT 04M
$18.2 \pm 4.6 \pm 1.6$ $-4.0 - 1.6$	1	CRONIN-HEN..00	CLE2		Repl. by BORNHEIM 03
$23 \pm 11 \pm 3.6$ $-10$		GODANG	98	CLE2	Repl. by CRONIN-HENNESSY 00
< 48	90	ASNER	96	CLE2	Repl. by GODANG 98
< 190	90	ALBRECHT	91B	ARG	$e^+e^- \rightarrow \Upsilon(4S)$
< 100	90	2 AVERY	89B	CLEO	$e^+e^- \rightarrow \Upsilon(4S)$
< 680	90	AVERY	87	CLEO	$e^+e^- \rightarrow \Upsilon(4S)$

<sup>1</sup> Assumes equal production of  $B^+$  and  $B^0$  at the  $\Upsilon(4S)$ .

<sup>2</sup> AVERY 89B reports  $< 9 \times 10^{-5}$  assuming the  $\Upsilon(4S)$  decays 43% to  $B^0\bar{B}^0$ . We rescale to 50%.

$\Gamma(K^+\pi^0)/\Gamma_{\text{total}}$   $\Gamma_{240}/\Gamma$

VALUE (units $10^{-6}$ )	CL%	DOCUMENT ID	TECN	COMMENT
<b><math>12.9 \pm 0.6</math> OUR AVERAGE</b>				
$13.6 \pm 0.6 \pm 0.7$		1 AUBERT	07BC	BABR $e^+e^- \rightarrow \Upsilon(4S)$
$12.4 \pm 0.5 \pm 0.6$		1 LIN	07A	BELL $e^+e^- \rightarrow \Upsilon(4S)$
$12.9 \pm 2.4 \pm 1.2$ $-2.2 - 1.1$		1 BORNHEIM	03	CLE2 $e^+e^- \rightarrow \Upsilon(4S)$
• • • We do not use the following data for averages, fits, limits, etc. • • •				
$12.0 \pm 0.7 \pm 0.6$		1 AUBERT	05L	BABR Repl. by AUBERT 07bc
$12.0 \pm 1.3 \pm 1.3$ $-0.9$		1 CHAO	04	BELL Repl. by LIN 07A
$12.8 \pm 1.2 \pm 1.0$ $-1.1$		1 AUBERT	03L	BABR Repl. by AUBERT 05L
$13.0 \pm 2.5 \pm 1.3$ $-2.4$		1 CASEY	02	BELL Repl. by CHAO 04
$16.3 \pm 3.5 \pm 1.6$ $-3.3 - 1.8$		1 ABE	01H	BELL Repl. by CASEY 02
$10.8 \pm 2.1 \pm 1.0$ $-1.9$		1 AUBERT	01E	BABR Repl. by AUBERT 03L
$11.6 \pm 3.0 \pm 1.4$ $-2.7 - 1.3$		1 CRONIN-HEN..00	CLE2	Repl. by BORNHEIM 03
< 16	90	GODANG	98	CLE2 Repl. by CRONIN-HENNESSY 00
< 14	90	ASNER	96	CLE2 Repl. by GODANG 98

<sup>1</sup> Assumes equal production of  $B^+$  and  $B^0$  at the  $\Upsilon(4S)$ .

$\Gamma(K^+\pi^0)/\Gamma(K^0\pi^+)$   $\Gamma_{240}/\Gamma_{239}$

VALUE	DOCUMENT ID	TECN	COMMENT
<b><math>0.54 \pm 0.03 \pm 0.04</math></b>	LIN	07A	BELL $e^+e^- \rightarrow \Upsilon(4S)$
• • • We do not use the following data for averages, fits, limits, etc. • • •			
$2.38 \pm 0.98 \pm 0.39$ $-1.10 - 0.26$	ABE	01H	BELL Repl. by LIN 07A

$\Gamma(\eta'K^+)/\Gamma_{\text{total}}$   $\Gamma_{241}/\Gamma$

VALUE (units $10^{-6}$ )	DOCUMENT ID	TECN	COMMENT
<b><math>70.6 \pm 2.5</math> OUR AVERAGE</b>			
$71.5 \pm 1.3 \pm 3.2$	1 AUBERT	09AV	BABR $e^+e^- \rightarrow \Upsilon(4S)$
$64 \pm 10 \pm 2$	1,2 WICHT	08	BELL $e^+e^- \rightarrow \Upsilon(4S)$
$69.2 \pm 2.2 \pm 3.7$	1 SCHUEMANN	06	BELL $e^+e^- \rightarrow \Upsilon(4S)$
$80 \pm 10 \pm 7$	1 RICHICHI	00	CLE2 $e^+e^- \rightarrow \Upsilon(4S)$
• • • We do not use the following data for averages, fits, limits, etc. • • •			
$70.0 \pm 1.5 \pm 2.8$	1 AUBERT	07AE	BABR Repl. by AUBERT 09AV
$68.9 \pm 2.0 \pm 3.2$	1 AUBERT	05M	BABR Repl. by AUBERT 07AE
$76.9 \pm 3.5 \pm 4.4$	1 AUBERT	03W	BABR Repl. by AUBERT 05M
$79 \pm 12 \pm 9$ $-11$	1 ABE	01M	BELL Repl. by SCHUEMANN 06
$70 \pm 8 \pm 5$	1 AUBERT	01G	BABR Repl. by AUBERT 03W
$65 \pm 15 \pm 9$ $-14$	BEHRENS	98	CLE2 Repl. by RICHICHI 00

<sup>1</sup> Assumes equal production of  $B^+$  and  $B^0$  at the  $\Upsilon(4S)$ .

<sup>2</sup> WICHT 08 reports  $[\Gamma(B^+ \rightarrow \eta'K^+)/\Gamma_{\text{total}}] \times [B(\eta'(958) \rightarrow \gamma\gamma)] = (1.40 \pm 0.16 \pm 0.15 - 0.12) \times 10^{-6}$  which we divide by our best value  $B(\eta'(958) \rightarrow \gamma\gamma) = (2.18 \pm 0.08) \times 10^{-2}$ . Our first error is their experiment's error and our second error is the systematic error from using our best value.

$\Gamma(\eta'K^*(892)^+)/\Gamma_{\text{total}}$   $\Gamma_{242}/\Gamma$

VALUE (units $10^{-6}$ )	CL%	DOCUMENT ID	TECN	COMMENT
<b><math>4.8 \pm 1.6 \pm 0.8</math></b> $-1.4$		1 DEL-AMO-SA..10A	BABR	$e^+e^- \rightarrow \Upsilon(4S)$
• • • We do not use the following data for averages, fits, limits, etc. • • •				
$4.9 \pm 1.9 \pm 0.8$ $-1.7$		1 AUBERT	07E	BABR Repl. by DEL-AMO-SANCHEZ 10A
< 2.9	90	1 SCHUEMANN	07	BELL $e^+e^- \rightarrow \Upsilon(4S)$
< 14	90	1 AUBERT, B	04D	BABR Repl. by AUBERT 07E
< 35	90	1 RICHICHI	00	CLE2 $e^+e^- \rightarrow \Upsilon(4S)$
< 13	90	BEHRENS	98	CLE2 Repl. by RICHICHI 00

<sup>1</sup> Assumes equal production of  $B^+$  and  $B^0$  at the  $\Upsilon(4S)$ .

$\Gamma(\eta'K_2^*(1430)^+)/\Gamma_{\text{total}}$   $\Gamma_{243}/\Gamma$

VALUE (units $10^{-6}$ )	DOCUMENT ID	TECN	COMMENT
<b><math>5.2 \pm 1.9 \pm 1.0</math></b>	1 DEL-AMO-SA..10A	BABR	$e^+e^- \rightarrow \Upsilon(4S)$
<sup>1</sup> Assumes equal production of $B^+$ and $B^0$ at the $\Upsilon(4S)$ .			

$\Gamma(\eta'K_2^*(1430)^+)/\Gamma_{\text{total}}$   $\Gamma_{244}/\Gamma$

VALUE (units $10^{-6}$ )	DOCUMENT ID	TECN	COMMENT
<b><math>28.0 \pm 4.6 \pm 2.6</math></b> $-4.3$	1 DEL-AMO-SA..10A	BABR	$e^+e^- \rightarrow \Upsilon(4S)$
<sup>1</sup> Assumes equal production of $B^+$ and $B^0$ at the $\Upsilon(4S)$ .			

$\Gamma(\eta K^+)/\Gamma_{\text{total}}$   $\Gamma_{245}/\Gamma$

VALUE (units $10^{-6}$ )	CL%	DOCUMENT ID	TECN	COMMENT
<b><math>2.4 \pm 0.4</math> OUR AVERAGE</b>				Error includes scale factor of 1.7.
$2.12 \pm 0.23 \pm 0.11$		1 HOI	12	BELL $e^+e^- \rightarrow \Upsilon(4S)$
$2.94 \pm 0.39 \pm 0.21$ $-0.34$		1 AUBERT	09AV	BABR $e^+e^- \rightarrow \Upsilon(4S)$
$2.2 \pm 2.8 \pm 2.2$		1 RICHICHI	00	CLE2 $e^+e^- \rightarrow \Upsilon(4S)$
• • • We do not use the following data for averages, fits, limits, etc. • • •				
$2.21 \pm 0.48 \pm 0.01$ $-0.42$		1,2 WICHT	08	BELL Repl. by HOI 12
$3.7 \pm 0.4 \pm 0.1$		1 AUBERT	07AE	BABR Repl. by AUBERT 09AV
$1.9 \pm 0.3 \pm 0.2$ $-0.1$		1 CHANG	07B	BELL Repl. by HOI 12
$3.3 \pm 0.6 \pm 0.3$		1 AUBERT, B	05K	BABR Repl. by AUBERT 07AE
$2.1 \pm 0.6 \pm 0.2$		1 CHANG	05A	BELL Repl. by CHANG 07B
$3.4 \pm 0.8 \pm 0.2$		1 AUBERT	04H	BABR Repl. by AUBERT, B 05K
< 14	90	BEHRENS	98	CLE2 Repl. by RICHICHI 00

<sup>1</sup> Assumes equal production of  $B^+$  and  $B^0$  at the  $\Upsilon(4S)$ .

<sup>2</sup> WICHT 08 reports  $[\Gamma(B^+ \rightarrow \eta K^+)/\Gamma_{\text{total}}] \times [B(\eta \rightarrow 2\gamma)] = (0.87 \pm 0.16 \pm 0.10 - 0.15 - 0.07) \times 10^{-6}$  which we divide by our best value  $B(\eta \rightarrow 2\gamma) = (39.31 \pm 0.20) \times 10^{-2}$ . Our first error is their experiment's error and our second error is the systematic error from using our best value.

$\Gamma(\eta K^*(892)^+)/\Gamma_{\text{total}}$   $\Gamma_{246}/\Gamma$

VALUE (units $10^{-6}$ )	CL%	DOCUMENT ID	TECN	COMMENT
<b><math>19.3 \pm 1.6</math> OUR AVERAGE</b>				
$19.3 \pm 2.0 \pm 1.5$ $-1.9$		1 WANG	07B	BELL $e^+e^- \rightarrow \Upsilon(4S)$
$18.9 \pm 1.8 \pm 1.3$		1 AUBERT, B	06H	BABR $e^+e^- \rightarrow \Upsilon(4S)$
$26.4 \pm 9.6 \pm 3.3$ $-8.2$		1 RICHICHI	00	CLE2 $e^+e^- \rightarrow \Upsilon(4S)$

• • • We do not use the following data for averages, fits, limits, etc. • • •

$25.6 \pm 4.0 \pm 2.4$		1 AUBERT, B	04D	BABR Repl. by AUBERT, B 06H
< 30	90	BEHRENS	98	CLE2 Repl. by RICHICHI 00

<sup>1</sup> Assumes equal production of  $B^+$  and  $B^0$  at the  $\Upsilon(4S)$ .

$\Gamma(\eta K_0^*(1430)^+)/\Gamma_{\text{total}}$   $\Gamma_{247}/\Gamma$

VALUE (units $10^{-6}$ )	DOCUMENT ID	TECN	COMMENT
<b><math>18.2 \pm 2.6 \pm 2.6</math></b>	1 AUBERT, B	06H	BABR $e^+e^- \rightarrow \Upsilon(4S)$
<sup>1</sup> Assumes equal production of $B^+$ and $B^0$ at the $\Upsilon(4S)$ .			

$\Gamma(\eta K_2^*(1430)^+)/\Gamma_{\text{total}}$   $\Gamma_{248}/\Gamma$

VALUE (units $10^{-6}$ )	DOCUMENT ID	TECN	COMMENT
<b><math>9.1 \pm 2.7 \pm 1.4</math></b>	1 AUBERT, B	06H	BABR $e^+e^- \rightarrow \Upsilon(4S)$
<sup>1</sup> Assumes equal production of $B^+$ and $B^0$ at the $\Upsilon(4S)$ .			

$\Gamma(\eta(1295)K^+ \times B(\eta(1295) \rightarrow \eta\pi\pi))/\Gamma_{\text{total}}$   $\Gamma_{249}/\Gamma$

VALUE (units $10^{-6}$ )	DOCUMENT ID	TECN	COMMENT
<b><math>2.9 \pm 0.9 \pm 0.2</math></b> $-0.7$	1 AUBERT	08X	BABR $e^+e^- \rightarrow \Upsilon(4S)$
<sup>1</sup> Assumes equal production of $B^+$ and $B^0$ at the $\Upsilon(4S)$ .			

$\Gamma(\eta(1405)K^+ \times B(\eta(1405) \rightarrow \eta\pi\pi))/\Gamma_{\text{total}}$   $\Gamma_{250}/\Gamma$

VALUE (units $10^{-6}$ )	CL%	DOCUMENT ID	TECN	COMMENT
<b>&lt; 1.3</b>	90	1 AUBERT	08X	BABR $e^+e^- \rightarrow \Upsilon(4S)$
<sup>1</sup> Assumes equal production of $B^+$ and $B^0$ at the $\Upsilon(4S)$ .				

$\Gamma(\eta(1405)K^+ \times B(\eta(1405) \rightarrow K^*K))/\Gamma_{\text{total}}$   $\Gamma_{251}/\Gamma$

VALUE (units $10^{-6}$ )	CL%	DOCUMENT ID	TECN	COMMENT
<b>&lt; 1.2</b>	90	1 AUBERT	08X	BABR $e^+e^- \rightarrow \Upsilon(4S)$
<sup>1</sup> Assumes equal production of $B^+$ and $B^0$ at the $\Upsilon(4S)$ .				

$\Gamma(\eta(1475)K^+ \times B(\eta(1475) \rightarrow K^*K))/\Gamma_{\text{total}}$   $\Gamma_{252}/\Gamma$

VALUE (units $10^{-6}$ )	DOCUMENT ID	TECN	COMMENT
<b><math>13.8 \pm 1.8 \pm 1.0</math></b> $-1.7 - 0.6$	1 AUBERT	08X	BABR $e^+e^- \rightarrow \Upsilon(4S)$
<sup>1</sup> Assumes equal production of $B^+$ and $B^0$ at the $\Upsilon(4S)$ .			

$\Gamma(f_1(1285)K^+)/\Gamma_{\text{total}}$   $\Gamma_{253}/\Gamma$ 

VALUE (units $10^{-6}$ )	CL%	DOCUMENT ID	TECN	COMMENT
<2.0	90	<sup>1</sup> AUBERT 08x	BABR	$e^+e^- \rightarrow \Upsilon(4S)$

<sup>1</sup> Assumes equal production of  $B^+$  and  $B^0$  at the  $\Upsilon(4S)$ .

 $\Gamma(f_1(1420)K^+ \times B(f_1(1420) \rightarrow \eta\pi\pi))/\Gamma_{\text{total}}$   $\Gamma_{254}/\Gamma$ 

VALUE (units $10^{-6}$ )	CL%	DOCUMENT ID	TECN	COMMENT
<2.9	90	<sup>1</sup> AUBERT 08x	BABR	$e^+e^- \rightarrow \Upsilon(4S)$

<sup>1</sup> Assumes equal production of  $B^+$  and  $B^0$  at the  $\Upsilon(4S)$ .

 $\Gamma(f_1(1420)K^+ \times B(f_1(1420) \rightarrow K^*K))/\Gamma_{\text{total}}$   $\Gamma_{255}/\Gamma$ 

VALUE (units $10^{-6}$ )	CL%	DOCUMENT ID	TECN	COMMENT
<4.1	90	<sup>1</sup> AUBERT 08x	BABR	$e^+e^- \rightarrow \Upsilon(4S)$

<sup>1</sup> Assumes equal production of  $B^+$  and  $B^0$  at the  $\Upsilon(4S)$ .

 $\Gamma(\phi(1680)K^+ \times B(\phi(1680) \rightarrow K^*K))/\Gamma_{\text{total}}$   $\Gamma_{256}/\Gamma$ 

VALUE (units $10^{-6}$ )	CL%	DOCUMENT ID	TECN	COMMENT
<3.4	90	<sup>1</sup> AUBERT 08x	BABR	$e^+e^- \rightarrow \Upsilon(4S)$

<sup>1</sup> Assumes equal production of  $B^+$  and  $B^0$  at the  $\Upsilon(4S)$ .

 $\Gamma(\omega K^+)/\Gamma_{\text{total}}$   $\Gamma_{257}/\Gamma$ 

VALUE (units $10^{-6}$ )	CL%	DOCUMENT ID	TECN	COMMENT
<b>6.7 ± 0.8 OUR AVERAGE</b>				Error includes scale factor of 1.8.
6.3 ± 0.5 ± 0.3		<sup>1</sup> AUBERT 07AE	BABR	$e^+e^- \rightarrow \Upsilon(4S)$
8.1 ± 0.6 ± 0.6		<sup>1</sup> JEN 06	BELL	$e^+e^- \rightarrow \Upsilon(4S)$
3.2 ± $\frac{2.4}{-1.9}$ ± 0.8		<sup>1</sup> JESSOP 00	CLE2	$e^+e^- \rightarrow \Upsilon(4S)$

• • • We do not use the following data for averages, fits, limits, etc. • • •

6.1 ± 0.6 ± 0.4		<sup>1</sup> AUBERT,B 06E	BABR	AUBERT 07AE
4.8 ± 0.8 ± 0.4		<sup>1</sup> AUBERT 04H	BABR	Repl. by AUBERT,B 06E
6.5 ± $\frac{1.3}{-1.2}$ ± 0.6		<sup>1</sup> WANG 04A	BELL	Repl. by JEN 06
9.2 ± $\frac{2.6}{-2.3}$ ± 1.0		<sup>1</sup> LU 02	BELL	Repl. by WANG 04A
<4	90	<sup>1</sup> AUBERT 01G	BABR	$e^+e^- \rightarrow \Upsilon(4S)$
1.5 ± $\frac{7}{-6}$ ± 2		<sup>1</sup> BERGFELD 98	CLE2	Repl. by JESSOP 00

<sup>1</sup> Assumes equal production of  $B^+$  and  $B^0$  at the  $\Upsilon(4S)$ .

 $\Gamma(\omega K^*(892^+)/\Gamma_{\text{total}}$   $\Gamma_{258}/\Gamma$ 

VALUE (units $10^{-6}$ )	CL%	DOCUMENT ID	TECN	COMMENT
< 7.4	90	<sup>1</sup> AUBERT 09H	BABR	$e^+e^- \rightarrow \Upsilon(4S)$

• • • We do not use the following data for averages, fits, limits, etc. • • •

< 3.4	90	<sup>1</sup> AUBERT,B 06T	BABR	Repl. by AUBERT 09H
< 7.4	90	<sup>1</sup> AUBERT 05O	BABR	Repl. by AUBERT,B 06T
< 87	90	<sup>1</sup> BERGFELD 98	CLE2	

<sup>1</sup> Assumes equal production of  $B^+$  and  $B^0$  at the  $\Upsilon(4S)$ .

 $\Gamma(\omega(K\pi)_0^{*+})/\Gamma_{\text{total}}$   $\Gamma_{259}/\Gamma$ 

( $K\pi)_0^{*+}$  is the total S-wave composed of  $K_0^*(1430)$  and nonresonant that are described using LASS shape.

VALUE (units $10^{-6}$ )	DOCUMENT ID	TECN	COMMENT
<b>27.5 ± 3.0 ± 2.6</b>	<sup>1</sup> AUBERT 09H	BABR	$e^+e^- \rightarrow \Upsilon(4S)$

<sup>1</sup> Assumes equal production of  $B^+$  and  $B^0$  at the  $\Upsilon(4S)$ .

 $\Gamma(\omega K_0^*(1430)^+)/\Gamma_{\text{total}}$   $\Gamma_{260}/\Gamma$ 

VALUE (units $10^{-6}$ )	DOCUMENT ID	TECN	COMMENT
<b>24.0 ± 2.6 ± 4.4</b>	<sup>1</sup> AUBERT 09H	BABR	$e^+e^- \rightarrow \Upsilon(4S)$

<sup>1</sup> Assumes equal production of  $B^+$  and  $B^0$  at the  $\Upsilon(4S)$ .

 $\Gamma(\omega K_2^*(1430)^+)/\Gamma_{\text{total}}$   $\Gamma_{261}/\Gamma$ 

VALUE (units $10^{-6}$ )	DOCUMENT ID	TECN	COMMENT
<b>21.5 ± 3.6 ± 2.4</b>	<sup>1</sup> AUBERT 09H	BABR	$e^+e^- \rightarrow \Upsilon(4S)$

<sup>1</sup> Assumes equal production of  $B^+$  and  $B^0$  at the  $\Upsilon(4S)$ .

 $\Gamma(a_0(980)^0 K^+ \times B(a_0(980)^0 \rightarrow \eta\pi^0))/\Gamma_{\text{total}}$   $\Gamma_{263}/\Gamma$ 

VALUE (units $10^{-6}$ )	CL%	DOCUMENT ID	TECN	COMMENT
<2.5	90	<sup>1</sup> AUBERT,BE 04	BABR	$e^+e^- \rightarrow \Upsilon(4S)$

<sup>1</sup> Assumes equal production of charged and neutral B mesons from  $\Upsilon(4S)$  decays.

 $\Gamma(a_0(980)^+ K^0 \times B(a_0(980)^+ \rightarrow \eta\pi^+))/\Gamma_{\text{total}}$   $\Gamma_{262}/\Gamma$ 

VALUE (units $10^{-6}$ )	CL%	DOCUMENT ID	TECN	COMMENT
<3.9	90	<sup>1</sup> AUBERT,BE 04	BABR	$e^+e^- \rightarrow \Upsilon(4S)$

<sup>1</sup> Assumes equal production of charged and neutral B mesons from  $\Upsilon(4S)$  decays.

 $\Gamma(K^*(892)^0\pi^+)/\Gamma_{\text{total}}$   $\Gamma_{264}/\Gamma$ 

VALUE (units $10^{-6}$ )	CL%	DOCUMENT ID	TECN	COMMENT
<b>10.1 ± 0.9 OUR AVERAGE</b>				
10.8 ± 0.6 ± $\frac{+1.2}{-1.4}$		<sup>1</sup> AUBERT 08AI	BABR	$e^+e^- \rightarrow \Upsilon(4S)$
9.67 ± 0.64 ± $\frac{+0.81}{-0.89}$		<sup>1</sup> GARMASH 06	BELL	$e^+e^- \rightarrow \Upsilon(4S)$

• • • We do not use the following data for averages, fits, limits, etc. • • •

13.5 ± 1.2 ± $\frac{+0.8}{-0.9}$		<sup>1</sup> AUBERT,B 05N	BABR	Repl. by AUBERT 08AI
9.8 ± 0.9 ± $\frac{+1.1}{-1.2}$		<sup>1</sup> GARMASH 05	BELL	Repl. by GARMASH 06
15.5 ± 1.8 ± $\frac{+1.5}{-4.0}$		<sup>1,2</sup> AUBERT,B 04P	BABR	Repl. by AUBERT,B 05N
19.4 ± $\frac{+4.2}{-3.9}$ ± 4.1		<sup>3</sup> GARMASH 02	BELL	Repl. by GARMASH 05
<119	90	<sup>4</sup> ABE 00c	SLD	$e^+e^- \rightarrow Z$
< 16	90	<sup>1</sup> JESSOP 00	CLE2	$e^+e^- \rightarrow \Upsilon(4S)$
<390	90	<sup>5</sup> ADAM 96D	DLPH	$e^+e^- \rightarrow Z$
< 41	90	<sup>5</sup> ASNER 96	CLE2	Repl. by JESSOP 00
<480	90	<sup>5</sup> ABREU 95N	DLPH	Sup. by ADAM 96D
<170	90	ALBRECHT 91B	ARG	$e^+e^- \rightarrow \Upsilon(4S)$
<150	90	<sup>6</sup> AVERY 89B	CLEO	$e^+e^- \rightarrow \Upsilon(4S)$
<260	90	AVERY 87	CLEO	$e^+e^- \rightarrow \Upsilon(4S)$

- <sup>1</sup> Assumes equal production of  $B^+$  and  $B^0$  at the  $\Upsilon(4S)$ .  
<sup>2</sup> AUBERT 04P also report a branching ratio for  $B^+ \rightarrow$  "higher  $K^*$  resonances"  $\pi^+$ ,  $K^* \rightarrow K^+\pi^-$ ,  $(25.1 \pm 2.0 \pm \frac{+11.0}{-5.7}) \times 10^{-6}$ .  
<sup>3</sup> Uses a reference decay mode  $B^+ \rightarrow \bar{D}^0\pi^+$  and  $\bar{D}^0 \rightarrow K^+\pi^-$  with  $B(B^+ \rightarrow \bar{D}^0\pi^+) \cdot B(\bar{D}^0 \rightarrow K^+\pi^-) = (20.3 \pm 2.0) \times 10^{-5}$ .  
<sup>4</sup> ABE 00c assumes  $B(Z \rightarrow b\bar{b}) = (21.7 \pm 0.1)\%$  and the B fractions  $f_{B^0} = f_{B^+} = (39.7 \pm \frac{1.8}{-2.2})\%$  and  $f_{B_s} = (10.5 \pm \frac{1.8}{-2.2})\%$ .  
<sup>5</sup> Assumes a  $B^0$ ,  $B^-$  production fraction of 0.39 and a  $B_s$  production fraction of 0.12.  
<sup>6</sup> AVERY 89B reports  $< 1.3 \times 10^{-4}$  assuming the  $\Upsilon(4S)$  decays 43% to  $B^0\bar{B}^0$ . We rescale to 50%.

 $\Gamma(K^*(892^+)\pi^0)/\Gamma_{\text{total}}$   $\Gamma_{265}/\Gamma$ 

VALUE (units $10^{-6}$ )	CL%	DOCUMENT ID	TECN	COMMENT
<b>8.2 ± 1.5 ± 1.1</b>		<sup>1</sup> LEES 11i	BABR	$e^+e^- \rightarrow \Upsilon(4S)$

• • • We do not use the following data for averages, fits, limits, etc. • • •

6.9 ± 2.0 ± 1.3		<sup>1</sup> AUBERT 05x	BABR	Repl. by LEES 11i
<31	90	<sup>1</sup> JESSOP 00	CLE2	$e^+e^- \rightarrow \Upsilon(4S)$
<99	90	ASNER 96	CLE2	Repl. by JESSOP 00

<sup>1</sup> Assumes equal production of  $B^+$  and  $B^0$  at the  $\Upsilon(4S)$ .

 $\Gamma(K^+\pi^-\pi^+)/\Gamma_{\text{total}}$   $\Gamma_{266}/\Gamma$ 

VALUE (units $10^{-6}$ )	DOCUMENT ID	TECN	COMMENT
<b>51.0 ± 2.9 OUR AVERAGE</b>			
54.4 ± 1.1 ± 4.6	<sup>1</sup> AUBERT 08AI	BABR	$e^+e^- \rightarrow \Upsilon(4S)$
48.8 ± 1.1 ± 3.6	<sup>1</sup> GARMASH 06	BELL	$e^+e^- \rightarrow \Upsilon(4S)$

• • • We do not use the following data for averages, fits, limits, etc. • • •

64.1 ± 2.4 ± 4.0	<sup>1</sup> AUBERT,B 05N	BABR	Repl. by AUBERT 08AI
46.6 ± 2.1 ± 4.3	<sup>1</sup> GARMASH 05	BELL	Repl. by GARMASH 06
53.6 ± 3.1 ± 5.1	<sup>1</sup> GARMASH 04	BELL	Repl. by GARMASH 05
59.1 ± 3.8 ± 3.2	<sup>2</sup> AUBERT 03M	BABR	Repl. by AUBERT,B 05N
55.6 ± 5.8 ± 7.7	<sup>3</sup> GARMASH 02	BELL	Repl. by GARMASH 04

- <sup>1</sup> Assumes equal production of  $B^+$  and  $B^0$  at the  $\Upsilon(4S)$ .  
<sup>2</sup> Assumes equal production of  $B^0$  and  $B^+$  at the  $\Upsilon(4S)$ ; charm and charmonium contributions are subtracted, otherwise no assumptions about intermediate resonances.  
<sup>3</sup> Uses a reference decay mode  $B^+ \rightarrow \bar{D}^0\pi^+$  and  $\bar{D}^0 \rightarrow K^+\pi^-$  with  $B(B^+ \rightarrow \bar{D}^0\pi^+) \cdot B(\bar{D}^0 \rightarrow K^+\pi^-) = (20.3 \pm 2.0) \times 10^{-5}$ .

 $\Gamma(K^+\pi^-\pi^+ \text{ nonresonant})/\Gamma_{\text{total}}$   $\Gamma_{267}/\Gamma$ 

VALUE (units $10^{-6}$ )	CL%	DOCUMENT ID	TECN	COMMENT
<b>16.3 ± 2.1 OUR AVERAGE</b>				
9.3 ± 1.0 ± $\frac{+6.9}{-1.7}$		<sup>1,2</sup> AUBERT 08AI	BABR	$e^+e^- \rightarrow \Upsilon(4S)$
16.9 ± 1.3 ± $\frac{+1.7}{-1.6}$		<sup>1</sup> GARMASH 06	BELL	$e^+e^- \rightarrow \Upsilon(4S)$

• • • We do not use the following data for averages, fits, limits, etc. • • •

2.9 ± 0.6 ± $\frac{+0.8}{-0.5}$		<sup>1</sup> AUBERT,B 05N	BABR	Repl. by AUBERT 08AI
17.3 ± 1.7 ± $\frac{+17.2}{-8.0}$		<sup>1</sup> GARMASH 05	BELL	Repl. by GARMASH 06
< 17	90	<sup>1</sup> AUBERT,B 04P	BABR	Repl. by AUBERT,B 05N
<330	90	<sup>3</sup> ADAM 96D	DLPH	$e^+e^- \rightarrow Z$
< 28	90	BERGFELD 96B	CLE2	$e^+e^- \rightarrow \Upsilon(4S)$
<400	90	<sup>3</sup> ABREU 95N	DLPH	Sup. by ADAM 96D
<330	90	ALBRECHT 91E	ARG	$e^+e^- \rightarrow \Upsilon(4S)$
<190	90	<sup>4</sup> AVERY 89B	CLEO	$e^+e^- \rightarrow \Upsilon(4S)$

- <sup>1</sup> Assumes equal production of  $B^+$  and  $B^0$  at the  $\Upsilon(4S)$ .  
<sup>2</sup> Calculate the total nonresonant contribution by combining the S-wave composed of  $K_0^*(1430)$  and nonresonant that are described using LASS shape.  
<sup>3</sup> Assumes a  $B^0$ ,  $B^-$  production fraction of 0.39 and a  $B_s$  production fraction of 0.12.  
<sup>4</sup> AVERY 89B reports  $< 1.7 \times 10^{-4}$  assuming the  $\Upsilon(4S)$  decays 43% to  $B^0\bar{B}^0$ . We rescale to 50%.

## Meson Particle Listings

 $B^\pm$ 

$\Gamma(\omega(782)K^+)/\Gamma_{\text{total}}$   $\Gamma_{268}/\Gamma$

VALUE (units $10^{-6}$ )	DOCUMENT ID	TECN	COMMENT
$5.9^{+8.8+0.5}_{-9.0-0.4}$	1,2 AUBERT	08AI	BABR $e^+e^- \rightarrow \Upsilon(4S)$

<sup>1</sup> Assumes equal production of  $B^+$  and  $B^0$  at the  $\Upsilon(4S)$ .

<sup>2</sup> AUBERT 08AI reports  $[\Gamma(B^+ \rightarrow \omega(782)K^+)/\Gamma_{\text{total}}] \times [B(\omega(782) \rightarrow \pi^+\pi^-)] = (0.09 \pm 0.13^{+0.036}_{-0.045}) \times 10^{-6}$  which we divide by our best value  $B(\omega(782) \rightarrow \pi^+\pi^-) = (1.53^{+0.11}_{-0.13}) \times 10^{-2}$ . Our first error is their experiment's error and our second error is the systematic error from using our best value.

$\Gamma(K^+ f_0(980) \times B(f_0(980) \rightarrow \pi^+\pi^-))/\Gamma_{\text{total}}$   $\Gamma_{269}/\Gamma$

VALUE (units $10^{-6}$ )	CL%	DOCUMENT ID	TECN	COMMENT
<b>9.4 <math>\pm</math> 1.0 OUR AVERAGE</b>				

10.3  $\pm$  0.5  $\pm$  2.0  $\pm$  1.4 <sup>1</sup> AUBERT 08AI BABR  $e^+e^- \rightarrow \Upsilon(4S)$

8.78  $\pm$  0.82  $\pm$  0.85  $\pm$  1.76 <sup>1</sup> GARMASH 06 BELL  $e^+e^- \rightarrow \Upsilon(4S)$

• • • We do not use the following data for averages, fits, limits, etc. • • •

9.47  $\pm$  0.97  $\pm$  0.62  $\pm$  0.88 <sup>1</sup> AUBERT,B 05N BABR Repl. by AUBERT 08AI

7.55  $\pm$  1.24  $\pm$  1.63  $\pm$  1.18 <sup>1</sup> GARMASH 05 BELL Repl. by GARMASH 06

9.2  $\pm$  1.2  $\pm$  2.1  $\pm$  2.6 <sup>2</sup> AUBERT,B 04P BABR Repl. by AUBERT,B 05N

9.6  $\pm$  2.5  $\pm$  3.7  $\pm$  1.7 <sup>3</sup> GARMASH 02 BELL Repl. by GARMASH 05

<80 90 <sup>4</sup> AVERY 89B CLEO  $e^+e^- \rightarrow \Upsilon(4S)$

<sup>1</sup> Assumes equal production of  $B^+$  and  $B^0$  at the  $\Upsilon(4S)$ .

<sup>2</sup> AUBERT,B 04P also reports  $B(B^+ \rightarrow \text{"higher } f^0 \text{ resonances"} \pi^+, f(980)^0 \rightarrow \pi^+\pi^-) = (3.2 \pm 1.2^{+6.0}_{-2.9}) \times 10^{-6}$ .

<sup>3</sup> Uses a reference decay mode  $B^+ \rightarrow \bar{D}^0 \pi^+$  and  $\bar{D}^0 \rightarrow K^+\pi^-$  with  $B(B^+ \rightarrow \bar{D}^0 \pi^+) \times B(\bar{D}^0 \rightarrow K^+\pi^-) = (20.3 \pm 2.0) \times 10^{-5}$ . Only charged pions from the  $f_0(980)$  are used.

<sup>4</sup> AVERY 89B reports  $< 7 \times 10^{-5}$  assuming the  $\Upsilon(4S)$  decays 43% to  $B^0 \bar{B}^0$ . We rescale to 50%.

$\Gamma(f_2(1270)^0 K^+)/\Gamma_{\text{total}}$   $\Gamma_{270}/\Gamma$

VALUE (units $10^{-6}$ )	CL%	DOCUMENT ID	TECN	COMMENT
<b>1.07 <math>\pm</math> 0.27 OUR AVERAGE</b>				

0.88  $\pm$  0.38  $\pm$  0.01  $\pm$  0.33  $\pm$  0.03 <sup>1,2</sup> AUBERT 08AI BABR  $e^+e^- \rightarrow \Upsilon(4S)$

1.33  $\pm$  0.30  $\pm$  0.23  $\pm$  0.34 <sup>1</sup> GARMASH 06 BELL  $e^+e^- \rightarrow \Upsilon(4S)$

• • • We do not use the following data for averages, fits, limits, etc. • • •

<16 90 <sup>3</sup> AUBERT,B 05N BABR Repl. by AUBERT 08AI

<2.3 90 <sup>4</sup> GARMASH 05 BELL Repl. by GARMASH 06

<sup>1</sup> Assumes equal production of  $B^+$  and  $B^0$  at the  $\Upsilon(4S)$ .

<sup>2</sup> AUBERT 08AI reports  $(0.50 \pm 0.15^{+0.15}_{-0.11}) \times 10^{-6}$  for  $B(B^+ \rightarrow f_2(1270)K^+) \times B(f_2 \rightarrow \pi^+\pi^-)$ . We compute  $B(B^+ \rightarrow f_2(1270)K^+)$  using the PDG value  $B(f_2(1270) \rightarrow \pi\pi) = (84.8 \pm 2.4^{+1.2}_{-1.2}) \times 10^{-2}$  and 2/3 for the  $\pi^+\pi^-$  fraction. Our first error is their experiment's error and the second error is systematic error from using our best value.

<sup>3</sup> AUBERT,B 05N reports  $8.9 \times 10^{-6}$  at 90% CL for  $B(B^+ \rightarrow f_2(1270)K^+) \times B(f_2(1270) \rightarrow \pi^+\pi^-)$ . We rescaled it using the PDG value  $B(f_2(1270) \rightarrow \pi\pi) = 84.7\%$  and 2/3 for the  $\pi^+\pi^-$  fraction.

<sup>4</sup> GARMASH 05 reports  $1.3 \times 10^{-6}$  at 90% CL for  $B(B^+ \rightarrow f_2(1270)K^+) \times B(f_2(1270) \rightarrow \pi^+\pi^-)$ . We rescaled it using the PDG value  $B(f_2(1270) \rightarrow \pi\pi) = 84.7\%$  and 2/3 for the  $\pi^+\pi^-$  fraction.

$\Gamma(f_0(1370)^0 K^+ \times B(f_0(1370)^0 \rightarrow \pi^+\pi^-))/\Gamma_{\text{total}}$   $\Gamma_{271}/\Gamma$

VALUE	CL%	DOCUMENT ID	TECN	COMMENT
<b>&lt;10.7 <math>\times</math> 10<sup>-6</sup></b>	90	<sup>1</sup> AUBERT,B	05N	BABR $e^+e^- \rightarrow \Upsilon(4S)$

<sup>1</sup> Assumes equal production of  $B^+$  and  $B^0$  at the  $\Upsilon(4S)$ .

$\Gamma(\rho^0(1450)K^+ \times B(\rho^0(1450) \rightarrow \pi^+\pi^-))/\Gamma_{\text{total}}$   $\Gamma_{272}/\Gamma$

VALUE	CL%	DOCUMENT ID	TECN	COMMENT
<b>&lt;11.7 <math>\times</math> 10<sup>-6</sup></b>	90	<sup>1</sup> AUBERT,B	05N	BABR $e^+e^- \rightarrow \Upsilon(4S)$

<sup>1</sup> Assumes equal production of  $B^+$  and  $B^0$  at the  $\Upsilon(4S)$ .

$\Gamma(f_0(1500)K^+ \times B(f_0(1500) \rightarrow \pi^+\pi^-))/\Gamma_{\text{total}}$   $\Gamma_{273}/\Gamma$

VALUE (units $10^{-6}$ )	CL%	DOCUMENT ID	TECN	COMMENT
<b>0.73 <math>\pm</math> 0.21 <math>\pm</math> 0.47 <math>\pm</math> 0.48</b>		<sup>1</sup> AUBERT	08AI	BABR $e^+e^- \rightarrow \Upsilon(4S)$

• • • We do not use the following data for averages, fits, limits, etc. • • •

<4.4 90 <sup>1</sup> AUBERT,B 05N BABR Repl. by AUBERT 08AI

<sup>1</sup> Assumes equal production of  $B^+$  and  $B^0$  at the  $\Upsilon(4S)$ .

$\Gamma(f_2'(1525)K^+ \times B(f_2'(1525) \rightarrow \pi^+\pi^-))/\Gamma_{\text{total}}$   $\Gamma_{274}/\Gamma$

VALUE	CL%	DOCUMENT ID	TECN	COMMENT
<b>&lt;3.4 <math>\times</math> 10<sup>-6</sup></b>	90	<sup>1</sup> AUBERT,B	05N	BABR $e^+e^- \rightarrow \Upsilon(4S)$

<sup>1</sup> Assumes equal production of  $B^+$  and  $B^0$  at the  $\Upsilon(4S)$ .

$\Gamma(K^+ \rho^0)/\Gamma_{\text{total}}$   $\Gamma_{275}/\Gamma$

VALUE (units $10^{-6}$ )	CL%	DOCUMENT ID	TECN	COMMENT
<b>3.7 <math>\pm</math> 0.5 OUR AVERAGE</b>				

3.56  $\pm$  0.45  $\pm$  0.57  $\pm$  0.46 <sup>1</sup> AUBERT 08AI BABR  $e^+e^- \rightarrow \Upsilon(4S)$

3.89  $\pm$  0.47  $\pm$  0.43  $\pm$  0.41 <sup>1</sup> GARMASH 06 BELL  $e^+e^- \rightarrow \Upsilon(4S)$

• • • We do not use the following data for averages, fits, limits, etc. • • •

5.07  $\pm$  0.75  $\pm$  0.55  $\pm$  0.88 <sup>1</sup> AUBERT,B 05N BABR Repl. by AUBERT 08AI

4.78  $\pm$  0.75  $\pm$  1.01  $\pm$  0.97 <sup>1</sup> GARMASH 05 BELL Repl. by GARMASH 06

<6.2 90 <sup>2</sup> AUBERT,B 04P BABR Repl. by AUBERT,B 05N

<12 90 <sup>3</sup> GARMASH 02 BELL  $e^+e^- \rightarrow \Upsilon(4S)$

<86 90 <sup>4</sup> ABE 00C SLD  $e^+e^- \rightarrow Z$

<17 90 <sup>1</sup> JESSOP 00 CLE2  $e^+e^- \rightarrow \Upsilon(4S)$

<120 90 <sup>5</sup> ADAM 96D DLPH  $e^+e^- \rightarrow Z$

<19 90 <sup>5</sup> ASNER 96 CLE2 Repl. by JESSOP 00

<190 90 <sup>5</sup> ABREU 95N DLPH Sup. by ADAM 96D

<180 90 <sup>6</sup> ALBRECHT 91B ARG  $e^+e^- \rightarrow \Upsilon(4S)$

<80 90 <sup>6</sup> AVERY 89B CLEO  $e^+e^- \rightarrow \Upsilon(4S)$

<260 90 <sup>6</sup> AVERY 87 CLEO  $e^+e^- \rightarrow \Upsilon(4S)$

<sup>1</sup> Assumes equal production of  $B^+$  and  $B^0$  at the  $\Upsilon(4S)$ .

<sup>2</sup> AUBERT 04P reports a central value of  $(3.9 \pm 1.2^{+1.3}_{-3.5}) \times 10^{-6}$  for this branching ratio.

<sup>3</sup> Uses a reference decay mode  $B^+ \rightarrow \bar{D}^0 \pi^+$  and  $\bar{D}^0 \rightarrow K^+\pi^-$  with  $B(B^+ \rightarrow \bar{D}^0 \pi^+) \times B(\bar{D}^0 \rightarrow K^+\pi^-) = (20.3 \pm 2.0) \times 10^{-5}$ .

<sup>4</sup> ABE 00C assumes  $B(Z \rightarrow b\bar{b}) = (21.7 \pm 0.1)\%$  and the  $B$  fractions  $f_{B^0} = f_{B^+} = (39.7 \pm 1.8^{+2.2}_{-2.2})\%$  and  $f_{B_s} = (10.5 \pm 1.8^{+2.2}_{-2.2})\%$ .

<sup>5</sup> Assumes production fractions  $f_{B^0} = f_{B^+} = 0.39$  and  $f_{B_s} = 0.12$ .

<sup>6</sup> AVERY 89B reports  $< 7 \times 10^{-5}$  assuming the  $\Upsilon(4S)$  decays 43% to  $B^0 \bar{B}^0$ . We rescale to 50%.

$\Gamma(K_S^0(1430)^0 \pi^+)/\Gamma_{\text{total}}$   $\Gamma_{276}/\Gamma$

VALUE (units $10^{-6}$ )	DOCUMENT ID	TECN	COMMENT
<b>45 <math>\pm</math> 9 OUR AVERAGE</b>			Error includes scale factor of 1.5.

32.0  $\pm$  1.2  $\pm$  10.8  $\pm$  6.0 <sup>1</sup> AUBERT 08AI BABR  $e^+e^- \rightarrow \Upsilon(4S)$

51.6  $\pm$  1.7  $\pm$  7.0  $\pm$  7.5 <sup>1</sup> GARMASH 06 BELL  $e^+e^- \rightarrow \Upsilon(4S)$

• • • We do not use the following data for averages, fits, limits, etc. • • •

44.4  $\pm$  2.2  $\pm$  5.3 <sup>1,2</sup> AUBERT,B 05N BABR Repl. by AUBERT 08AI

45.0  $\pm$  2.9  $\pm$  15.0  $\pm$  10.7 <sup>1</sup> GARMASH 05 BELL Repl. by GARMASH 06

<sup>1</sup> Assumes equal production of  $B^+$  and  $B^0$  at the  $\Upsilon(4S)$ .

<sup>2</sup> See erratum: AUBERT, BE 06A.

$\Gamma(K_S^0(1430)^0 \pi^+)/\Gamma_{\text{total}}$   $\Gamma_{277}/\Gamma$

VALUE (units $10^{-6}$ )	CL%	DOCUMENT ID	TECN	COMMENT
<b>5.6 <math>\pm</math> 2.5 <math>\pm</math> 0.1</b>		<sup>1,2</sup> AUBERT	08AI	BABR $e^+e^- \rightarrow \Upsilon(4S)$

• • • We do not use the following data for averages, fits, limits, etc. • • •

<23 90 <sup>3</sup> AUBERT,B 05N BABR Repl. by AUBERT 08AI

<6.9 90 <sup>4</sup> GARMASH 05 BELL  $e^+e^- \rightarrow \Upsilon(4S)$

<680 90 <sup>4</sup> ALBRECHT 91B ARG  $e^+e^- \rightarrow \Upsilon(4S)$

<sup>1</sup> Assumes equal production of  $B^+$  and  $B^0$  at the  $\Upsilon(4S)$ .

<sup>2</sup> AUBERT 08AI reports  $(1.85 \pm 0.41^{+0.61}_{-0.29}) \times 10^{-6}$  for  $B(B^+ \rightarrow K_S^0(1430)^0 \pi^+) \times B(K_S^0(1430)^0 \rightarrow K^+\pi^-)$ . We compute  $B(B^+ \rightarrow K_S^0(1430)^0 \pi^+)$  using the PDG value  $B(K_S^0(1430)^0 \rightarrow K\pi) = (49.9 \pm 1.2) \times 10^{-2}$  and 2/3 for the  $K^+\pi^-$  fraction. Our first error is their experiment's error and the second error is systematic error from using our best value.

<sup>3</sup> AUBERT,B 05N reports  $7.7 \times 10^{-6}$  at 90% CL for  $B(B^+ \rightarrow K_S^0(1430)^0 \pi^+) \times B(K_S^0(1430)^0 \rightarrow K^+\pi^-)$ . We rescaled it using the PDG value  $B(K_S^0(1430)^0 \rightarrow K\pi) = 49.9\%$  and 2/3 for the  $K^+\pi^-$  fraction.

<sup>4</sup> GARMASH 05 reports  $2.3 \times 10^{-6}$  at 90% CL for  $B(B^+ \rightarrow K_S^0(1430)^0 \pi^+) \times B(K_S^0(1430)^0 \rightarrow K^+\pi^-)$ . We rescaled it using the PDG value  $B(K_S^0(1430)^0 \rightarrow K\pi) = 49.9\%$  and 2/3 for the  $K^+\pi^-$  mode.

$\Gamma(K^*(1410)^0 \pi^+)/\Gamma_{\text{total}}$   $\Gamma_{278}/\Gamma$

VALUE (units $10^{-6}$ )	CL%	DOCUMENT ID	TECN	COMMENT
<b>&lt;45</b>	90	<sup>1</sup> GARMASH	05	BELL $e^+e^- \rightarrow \Upsilon(4S)$

<sup>1</sup> GARMASH 05 reports  $2.0 \times 10^{-6}$  at 90% CL for  $B(B^+ \rightarrow K^*(1410)^0 \pi^+) \times B(K^*(1410)^0 \rightarrow K^+\pi^-)$ . We rescaled it using the PDG value  $B(K^*(1410)^0 \rightarrow K\pi) = 6.6\%$  and 2/3 for the  $K^+\pi^-$  mode.

$\Gamma(K^*(1680)^0 \pi^+)/\Gamma_{\text{total}}$   $\Gamma_{279}/\Gamma$

VALUE (units $10^{-6}$ )	CL%	DOCUMENT ID	TECN	COMMENT
<b>&lt;12</b>	90	<sup>1</sup> GARMASH	05	BELL $e^+e^- \rightarrow \Upsilon(4S)$

• • • We do not use the following data for averages, fits, limits, etc. • • •

<15 90 <sup>2</sup> AUBERT,B 05N BABR  $e^+e^- \rightarrow \Upsilon(4S)$

<sup>1</sup> GARMASH 05 reports  $3.1 \times 10^{-6}$  at 90% CL for  $B(B^+ \rightarrow K^*(1680)^0 \pi^+) \times B(K^*(1680)^0 \rightarrow K^+ \pi^-)$ . We rescaled it using the PDG value  $B(K^*(1680)^0 \rightarrow K\pi) = 38.7\%$  and  $2/3$  for the  $K^+ \pi^-$  mode.  
<sup>2</sup> AUBERT,B 05N reports  $3.8 \times 10^{-6}$  at 90% CL for  $B(B^+ \rightarrow K^*(1680)^0 \pi^+) \times B(K^*(1680)^0 \rightarrow K^+ \pi^-)$ . We rescaled it using the PDG value  $B(K^*(1680)^0 \rightarrow K\pi) = 38.7\%$  and  $2/3$  for the  $K^+ \pi^-$  fraction.

$\Gamma(K^+ \pi^0 \pi^0)/\Gamma_{total}$		$\Gamma_{280}/\Gamma$	
VALUE (units $10^{-6}$ )	CL%	DOCUMENT ID	TECN COMMENT
$16.2 \pm 1.2 \pm 1.5$	90	<sup>1</sup> LEES 11i	BABR $e^+ e^- \rightarrow \Upsilon(4S)$
<sup>1</sup> Assumes equal production of $B^+$ and $B^0$ at the $\Upsilon(4S)$ .			

$\Gamma(f_0(980) K^+ \times B(f_0 \rightarrow \pi^0 \pi^0))/\Gamma_{total}$		$\Gamma_{281}/\Gamma$	
VALUE (units $10^{-6}$ )	CL%	DOCUMENT ID	TECN COMMENT
$2.8 \pm 0.6 \pm 0.5$	90	<sup>1</sup> LEES 11i	BABR $e^+ e^- \rightarrow \Upsilon(4S)$
<sup>1</sup> Assumes equal production of $B^+$ and $B^0$ at the $\Upsilon(4S)$ .			

$\Gamma(K^- \pi^+ \pi^+)/\Gamma_{total}$		$\Gamma_{282}/\Gamma$	
VALUE (units $10^{-6}$ )	CL%	DOCUMENT ID	TECN COMMENT
$<0.95$	90	<sup>1</sup> AUBERT 08BE	BABR $e^+ e^- \rightarrow \Upsilon(4S)$
• • • We do not use the following data for averages, fits, limits, etc. • • •			
$<4.5$	90	<sup>1</sup> GARMASH 04	BELL $e^+ e^- \rightarrow \Upsilon(4S)$
$<1.8$	90	<sup>2</sup> AUBERT 03M	BABR Repl. by AUBERT 08BE
$<7.0$	90	<sup>3</sup> GARMASH 02	BELL $e^+ e^- \rightarrow \Upsilon(4S)$

<sup>1</sup> Assumes equal production of  $B^+$  and  $B^0$  at the  $\Upsilon(4S)$ .  
<sup>2</sup> Assumes equal production of  $B^0$  and  $B^+$  at the  $\Upsilon(4S)$ ; charm and charmonium contributions are subtracted, otherwise no assumptions about intermediate resonances.  
<sup>3</sup> Uses a reference decay mode  $B^+ \rightarrow \bar{D}^0 \pi^+$  and  $\bar{D}^0 \rightarrow K^+ \pi^-$  with  $B(B^+ \rightarrow \bar{D}^0 \pi^+) \cdot B(\bar{D}^0 \rightarrow K^+ \pi^-) = (20.3 \pm 2.0) \times 10^{-5}$ .

$\Gamma(K^- \pi^+ \pi^+ \text{ nonresonant})/\Gamma_{total}$		$\Gamma_{283}/\Gamma$	
VALUE (units $10^{-6}$ )	CL%	DOCUMENT ID	TECN COMMENT
$<56$	90	BERGFELD 96B	CLE2 $e^+ e^- \rightarrow \Upsilon(4S)$

$\Gamma(K_1^+(1270)^0 \pi^+)/\Gamma_{total}$		$\Gamma_{284}/\Gamma$	
VALUE	CL%	DOCUMENT ID	TECN COMMENT
$<4.0 \times 10^{-5}$	90	<sup>1</sup> AUBERT 10D	BABR $e^+ e^- \rightarrow \Upsilon(4S)$
<sup>1</sup> Assumes equal production of $B^+$ and $B^0$ at the $\Upsilon(4S)$ .			

$\Gamma(K_1^+(1400)^0 \pi^+)/\Gamma_{total}$		$\Gamma_{285}/\Gamma$	
VALUE	CL%	DOCUMENT ID	TECN COMMENT
$<3.9 \times 10^{-5}$	90	<sup>1</sup> AUBERT 10D	BABR $e^+ e^- \rightarrow \Upsilon(4S)$
• • • We do not use the following data for averages, fits, limits, etc. • • •			
$<2.6 \times 10^{-3}$	90	ALBRECHT 91B	ARG $e^+ e^- \rightarrow \Upsilon(4S)$
<sup>1</sup> Assumes equal production of $B^+$ and $B^0$ at the $\Upsilon(4S)$ .			

$\Gamma(K^0 \pi^+ \pi^0)/\Gamma_{total}$		$\Gamma_{286}/\Gamma$	
VALUE	CL%	DOCUMENT ID	TECN COMMENT
$<66 \times 10^{-6}$	90	<sup>1</sup> ECKHART 02	CLE2 $e^+ e^- \rightarrow \Upsilon(4S)$
<sup>1</sup> Assumes equal production of $B^+$ and $B^0$ at the $\Upsilon(4S)$ .			

$\Gamma(K^0 \rho^+)/\Gamma_{total}$		$\Gamma_{287}/\Gamma$	
VALUE (units $10^{-6}$ )	CL%	DOCUMENT ID	TECN COMMENT
$8.0^{+1.4}_{-1.3} \pm 0.6$	90	AUBERT 07Z	BABR $e^+ e^- \rightarrow \Upsilon(4S)$
• • • We do not use the following data for averages, fits, limits, etc. • • •			
$<48$	90	ASNER 96	CLE2 $e^+ e^- \rightarrow \Upsilon(4S)$

$\Gamma(K^*(892)^+ \pi^+ \pi^-)/\Gamma_{total}$		$\Gamma_{288}/\Gamma$	
VALUE (units $10^{-6}$ )	CL%	DOCUMENT ID	TECN COMMENT
$75.3 \pm 6.0 \pm 8.1$	90	<sup>1</sup> AUBERT,B 06U	BABR $e^+ e^- \rightarrow \Upsilon(4S)$
• • • We do not use the following data for averages, fits, limits, etc. • • •			
$<1100$	90	ALBRECHT 91E	ARG $e^+ e^- \rightarrow \Upsilon(4S)$
<sup>1</sup> Assumes equal production of $B^+$ and $B^0$ at the $\Upsilon(4S)$ .			

$\Gamma(K^*(892)^+ \rho^0)/\Gamma_{total}$		$\Gamma_{289}/\Gamma$	
VALUE (units $10^{-6}$ )	CL%	DOCUMENT ID	TECN COMMENT
$4.6 \pm 1.0 \pm 0.4$	90	<sup>1</sup> DEL-AMO-SA..11D	BABR $e^+ e^- \rightarrow \Upsilon(4S)$
• • • We do not use the following data for averages, fits, limits, etc. • • •			
$< 6.1$	90	<sup>1</sup> AUBERT,B 06G	BABR Repl. by DEL-AMO-SANCHEZ 11D
$10.6^{+3.0}_{-2.6} \pm 2.4$	90	<sup>1</sup> AUBERT 03V	BABR Repl. by AUBERT,B 06G
$< 74$	90	<sup>2</sup> GODANG 02	CLE2 $e^+ e^- \rightarrow \Upsilon(4S)$
$<900$	90	ALBRECHT 91B	ARG $e^+ e^- \rightarrow \Upsilon(4S)$

<sup>1</sup> Assumes equal production of  $B^+$  and  $B^0$  at the  $\Upsilon(4S)$ .  
<sup>2</sup> Assumes a helicity 00 configuration. For a helicity 11 configuration, the limit decreases to  $4.9 \times 10^{-5}$ .

$\Gamma(K^*(892)^+ f_0(980))/\Gamma_{total}$		$\Gamma_{290}/\Gamma$	
VALUE (units $10^{-6}$ )	CL%	DOCUMENT ID	TECN COMMENT
$4.2 \pm 0.6 \pm 0.3$	90	<sup>1</sup> DEL-AMO-SA..11D	BABR $e^+ e^- \rightarrow \Upsilon(4S)$
• • • We do not use the following data for averages, fits, limits, etc. • • •			
$5.2 \pm 1.2 \pm 0.5$	90	<sup>1</sup> AUBERT,B 06G	BABR Repl. by DEL-AMO-SANCHEZ 11D
<sup>1</sup> Assumes equal production of $B^+$ and $B^0$ at the $\Upsilon(4S)$ .			

$\Gamma(a_1^+ K^0)/\Gamma_{total}$		$\Gamma_{291}/\Gamma$	
VALUE (units $10^{-6}$ )	CL%	DOCUMENT ID	TECN COMMENT
$34.9 \pm 5.0 \pm 4.4$	90	<sup>1,2</sup> AUBERT 08F	BABR $e^+ e^- \rightarrow \Upsilon(4S)$
<sup>1</sup> Assumes equal production of $B^+$ and $B^0$ at the $\Upsilon(4S)$ . <sup>2</sup> Assumes $a_1^\pm$ decays only to $3\pi$ and $B(a_1^\pm \rightarrow \pi^\pm \pi^\mp \pi^\pm) = 0.5$ .			

$\Gamma(b_1^+ K^0 \times B(b_1^+ \rightarrow \omega \pi^+))/\Gamma_{total}$		$\Gamma_{292}/\Gamma$	
VALUE (units $10^{-6}$ )	CL%	DOCUMENT ID	TECN COMMENT
$9.6 \pm 1.7 \pm 0.9$	90	<sup>1</sup> AUBERT 08AG	BABR $e^+ e^- \rightarrow \Upsilon(4S)$
<sup>1</sup> Assumes equal production of $B^+$ and $B^0$ at the $\Upsilon(4S)$ .			

$\Gamma(K^*(892)^0 \rho^+)/\Gamma_{total}$		$\Gamma_{293}/\Gamma$	
VALUE (units $10^{-6}$ )	CL%	DOCUMENT ID	TECN COMMENT
$9.2 \pm 1.5$	90	<b>OUR AVERAGE</b>	
$9.6 \pm 1.7 \pm 1.5$	90	<sup>1</sup> AUBERT,B 06G	BABR $e^+ e^- \rightarrow \Upsilon(4S)$
$8.9 \pm 1.7 \pm 1.2$	90	<sup>1</sup> ZHANG 05D	BELL $e^+ e^- \rightarrow \Upsilon(4S)$
<sup>1</sup> Assumes equal production of $B^+$ and $B^0$ at the $\Upsilon(4S)$ .			

$\Gamma(K_1^+(1400)^+ \rho^0)/\Gamma_{total}$		$\Gamma_{294}/\Gamma$	
VALUE	CL%	DOCUMENT ID	TECN COMMENT
$<7.8 \times 10^{-4}$	90	ALBRECHT 91B	ARG $e^+ e^- \rightarrow \Upsilon(4S)$

$\Gamma(K_2^+(1430)^+ \rho^0)/\Gamma_{total}$		$\Gamma_{295}/\Gamma$	
VALUE	CL%	DOCUMENT ID	TECN COMMENT
$<1.5 \times 10^{-3}$	90	ALBRECHT 91B	ARG $e^+ e^- \rightarrow \Upsilon(4S)$

$\Gamma(b_1^0 K^+ \times B(b_1^0 \rightarrow \omega \pi^0))/\Gamma_{total}$		$\Gamma_{296}/\Gamma$	
VALUE (units $10^{-6}$ )	CL%	DOCUMENT ID	TECN COMMENT
$9.1 \pm 1.7 \pm 1.0$	90	<sup>1</sup> AUBERT 07Bi	BABR $e^+ e^- \rightarrow \Upsilon(4S)$
<sup>1</sup> Assumes equal production of $B^+$ and $B^0$ at the $\Upsilon(4S)$ .			

$\Gamma(b_1^+ K^*0 \times B(b_1^+ \rightarrow \omega \pi^+))/\Gamma_{total}$		$\Gamma_{297}/\Gamma$	
VALUE	CL%	DOCUMENT ID	TECN COMMENT
$<5.9 \times 10^{-6}$	90	<sup>1</sup> AUBERT 09AF	BABR $e^+ e^- \rightarrow \Upsilon(4S)$
<sup>1</sup> Assumes equal production of $B^+$ and $B^0$ at the $\Upsilon(4S)$ .			

$\Gamma(b_1^0 K^{*+} \times B(b_1^0 \rightarrow \omega \pi^0))/\Gamma_{total}$		$\Gamma_{298}/\Gamma$	
VALUE	CL%	DOCUMENT ID	TECN COMMENT
$<6.7 \times 10^{-6}$	90	<sup>1</sup> AUBERT 09AF	BABR $e^+ e^- \rightarrow \Upsilon(4S)$
<sup>1</sup> Assumes equal production of $B^+$ and $B^0$ at the $\Upsilon(4S)$ .			

$\Gamma(K^+ \bar{K}^0)/\Gamma_{total}$		$\Gamma_{299}/\Gamma$	
VALUE (units $10^{-6}$ )	CL%	DOCUMENT ID	TECN COMMENT
$1.36 \pm 0.27$	90	<b>OUR AVERAGE</b>	
$1.22^{+0.32+0.13}_{-0.28-0.16}$	90	<sup>1</sup> LIN 07	BELL $e^+ e^- \rightarrow \Upsilon(4S)$
$1.61 \pm 0.44 \pm 0.09$	90	<sup>1</sup> AUBERT,BE 06C	BABR $e^+ e^- \rightarrow \Upsilon(4S)$
• • • We do not use the following data for averages, fits, limits, etc. • • •			
$1.0 \pm 0.4 \pm 0.1$	90	<sup>1</sup> ABE 05G	BELL Repl. by LIN 07
$1.5 \pm 0.5 \pm 0.1$	90	<sup>1</sup> AUBERT,BE 05E	BABR Repl. by AUBERT,BE 06C
$< 2.5$	90	<sup>1</sup> AUBERT 04M	BABR Repl. by AUBERT,BE 05E
$< 3.3$	90	<sup>1</sup> CHAO 04	BELL $e^+ e^- \rightarrow \Upsilon(4S)$
$< 3.3$	90	<sup>1</sup> BORNHEIM 03	CLE2 $e^+ e^- \rightarrow \Upsilon(4S)$
$< 2.0$	90	<sup>1</sup> CASEY 02	BELL Repl. by CHAO 04
$< 5.0$	90	<sup>1</sup> ABE 01H	BELL $e^+ e^- \rightarrow \Upsilon(4S)$
$< 2.4$	90	<sup>1</sup> AUBERT 01E	BABR $e^+ e^- \rightarrow \Upsilon(4S)$
$< 5.1$	90	<sup>1</sup> CRONIN-HEN..00	CLE2 $e^+ e^- \rightarrow \Upsilon(4S)$
$<21$	90	GODANG 98	CLE2 Repl. by CRONIN-HENNESSY 00
<sup>1</sup> Assumes equal production of $B^+$ and $B^0$ at the $\Upsilon(4S)$ .			

$\Gamma(\bar{K}^0 K^+ \pi^0)/\Gamma_{total}$		$\Gamma_{300}/\Gamma$	
VALUE	CL%	DOCUMENT ID	TECN COMMENT
$<24 \times 10^{-6}$	90	<sup>1</sup> ECKHART 02	CLE2 $e^+ e^- \rightarrow \Upsilon(4S)$
<sup>1</sup> Assumes equal production of $B^+$ and $B^0$ at the $\Upsilon(4S)$ .			

$\Gamma(K^+ K_S^0 K_S^0)/\Gamma_{total}$		$\Gamma_{301}/\Gamma$	
VALUE (units $10^{-6}$ )	CL%	DOCUMENT ID	TECN COMMENT
$11.5 \pm 1.3$	90	<b>OUR AVERAGE</b>	
$10.7 \pm 1.2 \pm 1.0$	90	<sup>1</sup> AUBERT,B 04V	BABR $e^+ e^- \rightarrow \Upsilon(4S)$
$13.4 \pm 1.9 \pm 1.5$	90	<sup>1</sup> GARMASH 04	BELL $e^+ e^- \rightarrow \Upsilon(4S)$
<sup>1</sup> Assumes equal production of $B^+$ and $B^0$ at the $\Upsilon(4S)$ .			





## Meson Particle Listings

 $B^\pm$  $\Gamma(\eta K^+ \gamma)/\Gamma_{\text{total}}$   $\Gamma_{339}/\Gamma$ 

VALUE (units $10^{-6}$ )	DOCUMENT ID	TECN	COMMENT
<b>7.9 ± 0.9 OUR AVERAGE</b>			
7.7 ± 1.0 ± 0.4	1,2 AUBERT	09	BABR $e^+e^- \rightarrow \Upsilon(4S)$
8.4 ± 1.5 ± 1.2 -0.9	2,3 NISHIDA	05	BELL $e^+e^- \rightarrow \Upsilon(4S)$
• • • We do not use the following data for averages, fits, limits, etc. • • •			
10.0 ± 1.3 ± 0.5	1,2 AUBERT,B	06M	BABR Repl. by AUBERT 09
<sup>1</sup> $m_{\eta K} < 3.25 \text{ GeV}/c^2$ .			
<sup>2</sup> Assumes equal production of $B^+$ and $B^0$ at the $\Upsilon(4S)$ .			
<sup>3</sup> $m_{\eta K} < 2.4 \text{ GeV}/c^2$			

 $\Gamma(\eta' K^+ \gamma)/\Gamma_{\text{total}}$   $\Gamma_{340}/\Gamma$ 

VALUE (units $10^{-6}$ )	DOCUMENT ID	TECN	COMMENT
<b>2.9 ± 1.0 -0.9 OUR AVERAGE</b>			
3.6 ± 1.2 ± 0.4	1,2 WEDD	10	BELL $e^+e^- \rightarrow \Upsilon(4S)$
1.9 ± 1.5 ± 0.1 -1.2	1,3 AUBERT,B	06M	BABR $e^+e^- \rightarrow \Upsilon(4S)$
<sup>1</sup> Assumes equal production of $B^+$ and $B^0$ at the $\Upsilon(4S)$ .			
<sup>2</sup> $m_{\eta' K} < 3.4 \text{ GeV}/c^2$ .			
<sup>3</sup> Set the upper limit of $4.2 \times 10^{-6}$ at 90% CL with $m_{\eta' K} < 3.25 \text{ GeV}/c^2$ .			

 $\Gamma(\phi K^+ \gamma)/\Gamma_{\text{total}}$   $\Gamma_{341}/\Gamma$ 

VALUE (units $10^{-6}$ )	DOCUMENT ID	TECN	COMMENT
<b>2.7 ± 0.4 OUR AVERAGE</b>			Error includes scale factor of 1.2.
2.48 ± 0.30 ± 0.24	1 SAHOO	11A	BELL $e^+e^- \rightarrow \Upsilon(4S)$
3.5 ± 0.6 ± 0.4	1 AUBERT	07Q	BABR $e^+e^- \rightarrow \Upsilon(4S)$
• • • We do not use the following data for averages, fits, limits, etc. • • •			
3.4 ± 0.9 ± 0.4	1 DRUTSKOY	04	BELL Repl. by SAHOO 11A
<sup>1</sup> Assumes equal production of $B^+$ and $B^0$ at $\Upsilon(4S)$ .			

 $\Gamma(K^+ \pi^- \pi^+ \gamma)/\Gamma_{\text{total}}$   $\Gamma_{342}/\Gamma$ 

VALUE (units $10^{-5}$ )	DOCUMENT ID	TECN	COMMENT
<b>2.76 ± 0.22 OUR AVERAGE</b>			Error includes scale factor of 1.2.
2.95 ± 0.13 ± 0.20	1,2 AUBERT	07R	BABR $e^+e^- \rightarrow \Upsilon(4S)$
2.50 ± 0.18 ± 0.22	2,3 YANG	05	BELL $e^+e^- \rightarrow \Upsilon(4S)$
• • • We do not use the following data for averages, fits, limits, etc. • • •			
2.4 ± 0.5 ± 0.4 -0.2	2,4 NISHIDA	02	BELL Repl. by YANG 05
<sup>1</sup> $M_{K\pi\pi} < 1.8 \text{ GeV}/c^2$ .			
<sup>2</sup> Assumes equal production of $B^+$ and $B^0$ at the $\Upsilon(4S)$ .			
<sup>3</sup> $M_{K\pi\pi} < 2.0 \text{ GeV}/c^2$ .			
<sup>4</sup> $M_{K\pi\pi} < 2.4 \text{ GeV}/c^2$ .			

 $\Gamma(K^*(892)^0 \pi^+ \gamma)/\Gamma_{\text{total}}$   $\Gamma_{343}/\Gamma$ 

VALUE	DOCUMENT ID	TECN	COMMENT
<b>(2.0 ± 0.7 ± 0.2) × 10<sup>-5</sup></b>			
2.0 ± 0.7 ± 0.2	1,2 NISHIDA	02	BELL $e^+e^- \rightarrow \Upsilon(4S)$
<sup>1</sup> Assumes equal production of $B^+$ and $B^0$ at the $\Upsilon(4S)$ .			
<sup>2</sup> $M_{K\pi\pi} < 2.4 \text{ GeV}/c^2$ .			

 $\Gamma(K^+ \rho^0 \gamma)/\Gamma_{\text{total}}$   $\Gamma_{344}/\Gamma$ 

VALUE	CL%	DOCUMENT ID	TECN	COMMENT
<b>&lt; 2.0 × 10<sup>-5</sup></b>	90	1,2 NISHIDA	02	BELL $e^+e^- \rightarrow \Upsilon(4S)$
<sup>1</sup> Assumes equal production of $B^+$ and $B^0$ at the $\Upsilon(4S)$ .				
<sup>2</sup> $M_{K\pi\pi} < 2.4 \text{ GeV}/c^2$ .				

 $\Gamma(K^+ \pi^- \pi^+ \gamma \text{ nonresonant})/\Gamma_{\text{total}}$   $\Gamma_{345}/\Gamma$ 

VALUE	CL%	DOCUMENT ID	TECN	COMMENT
<b>&lt; 9.2 × 10<sup>-6</sup></b>	90	1,2 NISHIDA	02	BELL $e^+e^- \rightarrow \Upsilon(4S)$
<sup>1</sup> Assumes equal production of $B^+$ and $B^0$ at the $\Upsilon(4S)$ .				
<sup>2</sup> $M_{K\pi\pi} < 2.4 \text{ GeV}/c^2$ .				

 $\Gamma(K^0 \pi^+ \pi^0 \gamma)/\Gamma_{\text{total}}$   $\Gamma_{346}/\Gamma$ 

VALUE (units $10^{-5}$ )	DOCUMENT ID	TECN	COMMENT
<b>4.56 ± 0.42 ± 0.31</b>			
4.56 ± 0.42 ± 0.31	1,2 AUBERT	07R	BABR $e^+e^- \rightarrow \Upsilon(4S)$
<sup>1</sup> $M_{K\pi\pi} < 1.8 \text{ GeV}/c^2$ .			
<sup>2</sup> Assumes equal production of $B^+$ and $B^0$ at the $\Upsilon(4S)$ .			

 $\Gamma(K_1(1400)^+ \gamma)/\Gamma_{\text{total}}$   $\Gamma_{347}/\Gamma$ 

VALUE (units $10^{-9}$ )	CL%	DOCUMENT ID	TECN	COMMENT
<b>&lt; 1.5</b>	90	1 YANG	05	BELL $e^+e^- \rightarrow \Upsilon(4S)$
• • • We do not use the following data for averages, fits, limits, etc. • • •				
< 5.0	90	1 NISHIDA	02	BELL Repl. by YANG 05
< 220	90	2 ALBRECHT	89G	ARG $e^+e^- \rightarrow \Upsilon(4S)$
<sup>1</sup> Assumes equal production of $B^+$ and $B^0$ at the $\Upsilon(4S)$ .				
<sup>2</sup> ALBRECHT 89G reports < 0.0020 assuming the $\Upsilon(4S)$ decays 45% to $B^0 \bar{B}^0$ . We rescale to 50%.				

 $\Gamma(K_2^*(1430)^+ \gamma)/\Gamma_{\text{total}}$   $\Gamma_{348}/\Gamma$ 

VALUE (units $10^{-5}$ )	CL%	DOCUMENT ID	TECN	COMMENT
<b>1.45 ± 0.40 ± 0.15</b>				
1.45 ± 0.40 ± 0.15	90	1 AUBERT,B	04U	BABR $e^+e^- \rightarrow \Upsilon(4S)$
• • • We do not use the following data for averages, fits, limits, etc. • • •				
< 140	90	2 ALBRECHT	89G	ARG $e^+e^- \rightarrow \Upsilon(4S)$
<sup>1</sup> Assumes equal production of $B^+$ and $B^0$ at the $\Upsilon(4S)$ .				
<sup>2</sup> ALBRECHT 89G reports < 0.0013 assuming the $\Upsilon(4S)$ decays 45% to $B^0 \bar{B}^0$ . We rescale to 50%.				

 $\Gamma(K^*(1680)^+ \gamma)/\Gamma_{\text{total}}$   $\Gamma_{349}/\Gamma$ 

VALUE	CL%	DOCUMENT ID	TECN	COMMENT
<b>&lt; 0.0019</b>	90	1 ALBRECHT	89G	ARG $e^+e^- \rightarrow \Upsilon(4S)$
<sup>1</sup> ALBRECHT 89G reports < 0.0017 assuming the $\Upsilon(4S)$ decays 45% to $B^0 \bar{B}^0$ . We rescale to 50%.				

 $\Gamma(K_3^*(1780)^+ \gamma)/\Gamma_{\text{total}}$   $\Gamma_{350}/\Gamma$ 

VALUE (units $10^{-6}$ )	CL%	DOCUMENT ID	TECN	COMMENT
<b>&lt; 39</b>	90	1,2 NISHIDA	05	BELL $e^+e^- \rightarrow \Upsilon(4S)$
• • • We do not use the following data for averages, fits, limits, etc. • • •				
< 5500	90	3 ALBRECHT	89G	ARG $e^+e^- \rightarrow \Upsilon(4S)$
<sup>1</sup> Assumes equal production of $B^+$ and $B^0$ at the $\Upsilon(4S)$ .				
<sup>2</sup> Uses $B(K_3^*(1780) \rightarrow \eta K) = 0.11 \pm 0.05$ .				
<sup>3</sup> ALBRECHT 89G reports < 0.005 assuming the $\Upsilon(4S)$ decays 45% to $B^0 \bar{B}^0$ . We rescale to 50%.				

 $\Gamma(K_4^*(2045)^+ \gamma)/\Gamma_{\text{total}}$   $\Gamma_{351}/\Gamma$ 

VALUE	CL%	DOCUMENT ID	TECN	COMMENT
<b>&lt; 0.0099</b>	90	1 ALBRECHT	89G	ARG $e^+e^- \rightarrow \Upsilon(4S)$
<sup>1</sup> ALBRECHT 89G reports < 0.0090 assuming the $\Upsilon(4S)$ decays 45% to $B^0 \bar{B}^0$ . We rescale to 50%.				

 $\Gamma(\rho^+ \gamma)/\Gamma_{\text{total}}$   $\Gamma_{352}/\Gamma$ 

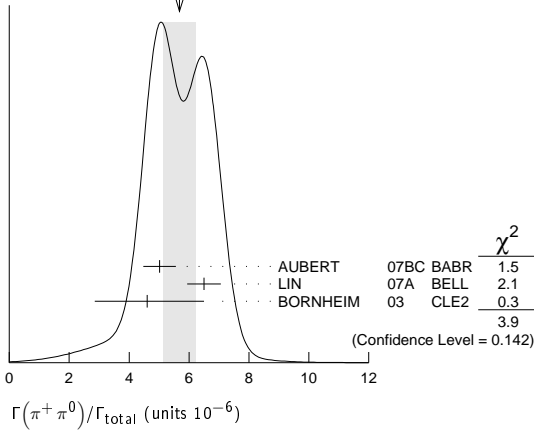
VALUE (units $10^{-6}$ )	CL%	DOCUMENT ID	TECN	COMMENT
<b>0.98 ± 0.25 OUR AVERAGE</b>				
1.20 ± 0.42 ± 0.20 -0.37	90	1 AUBERT	08BH	BABR $e^+e^- \rightarrow \Upsilon(4S)$
0.87 ± 0.29 ± 0.09 -0.27 - 0.11	90	1 TANIGUCHI	08	BELL $e^+e^- \rightarrow \Upsilon(4S)$
• • • We do not use the following data for averages, fits, limits, etc. • • •				
1.10 ± 0.37 ± 0.09 -0.33	90	1 AUBERT	07L	BABR Repl. by AUBERT 08BH
0.55 ± 0.42 ± 0.09 -0.36 - 0.08	90	1 MOHAPATRA	06	BELL Repl. by TANIGUCHI 08
0.9 ± 0.6 ± 0.1 -0.5	90	1 AUBERT	05	BABR Repl. by AUBERT 07L
< 2.2	90	1 MOHAPATRA	05	BELL $e^+e^- \rightarrow \Upsilon(4S)$
< 2.1	90	1 AUBERT	04c	BABR $e^+e^- \rightarrow \Upsilon(4S)$
< 13	90	1,2 COAN	00	CLE2 $e^+e^- \rightarrow \Upsilon(4S)$
<sup>1</sup> Assumes equal production of $B^+$ and $B^0$ at $\Upsilon(4S)$ .				
<sup>2</sup> No evidence for a nonresonant $K\pi\gamma$ contamination was seen; the central value assumes no contamination.				

 $\Gamma(\pi^+ \pi^0)/\Gamma_{\text{total}}$   $\Gamma_{353}/\Gamma$ 

VALUE (units $10^{-6}$ )	CL%	DOCUMENT ID	TECN	COMMENT
<b>5.7 ± 0.5 OUR AVERAGE</b>				Error includes scale factor of 1.4. See the ideogram below.
5.02 ± 0.46 ± 0.29	90	1 AUBERT	07Bc	BABR $e^+e^- \rightarrow \Upsilon(4S)$
6.5 ± 0.4 ± 0.4	90	1 LIN	07A	BELL $e^+e^- \rightarrow \Upsilon(4S)$
4.6 ± 1.8 ± 0.6 -1.6 - 0.7	90	1 BORNHEIM	03	CLE2 $e^+e^- \rightarrow \Upsilon(4S)$
• • • We do not use the following data for averages, fits, limits, etc. • • •				
5.8 ± 0.6 ± 0.4	90	1 AUBERT	05L	BABR Repl. by AUBERT 07Bc
5.0 ± 1.2 ± 0.5	90	1 CHAO	04	BELL Repl. by LIN 07A
5.5 ± 1.0 ± 0.6 -1.9	90	1 AUBERT	03L	BABR Repl. by AUBERT 05L
7.4 ± 2.3 ± 0.9 -2.2	90	1 CASEY	02	BELL Repl. by CHAO 04
< 13.4	90	1 ABE	01H	BELL $e^+e^- \rightarrow \Upsilon(4S)$
< 9.6	90	1 AUBERT	01E	BABR $e^+e^- \rightarrow \Upsilon(4S)$
< 12.7	90	1 CRONIN-HEN.	00	CLE2 $e^+e^- \rightarrow \Upsilon(4S)$
< 20	90	1 GODANG	98	CLE2 Repl. by CRONIN-HENNESSY 00
< 17	90	1 ASNER	96	CLE2 Repl. by GODANG 98
< 240	90	1 ALBRECHT	90B	ARG $e^+e^- \rightarrow \Upsilon(4S)$
< 2300	90	2 BEBEK	87	CLEO $e^+e^- \rightarrow \Upsilon(4S)$
<sup>1</sup> Assumes equal production of $B^+$ and $B^0$ at the $\Upsilon(4S)$ .				
<sup>2</sup> BEBEK 87 assume the $\Upsilon(4S)$ decays 43% to $B^0 \bar{B}^0$ .				



WEIGHTED AVERAGE  
5.7±0.5 (Error scaled by 1.4)



**Γ(π<sup>+</sup>π<sup>0</sup>)/Γ(K<sup>0</sup>π<sup>+</sup>)** Γ<sub>353</sub>/Γ<sub>239</sub>

VALUE	DOCUMENT ID	TECN	COMMENT
<b>0.285 ± 0.02 ± 0.02</b>	LIN	07A	BELL e <sup>+</sup> e <sup>-</sup> → Υ(4S)

**Γ(π<sup>+</sup>π<sup>+</sup>π<sup>-</sup>)/Γ<sub>total</sub>** Γ<sub>354</sub>/Γ

VALUE (units 10 <sup>-6</sup> )	CL%	DOCUMENT ID	TECN	COMMENT
<b>15.2 ± 0.6<sup>+1.3</sup><sub>-1.2</sub></b>		<sup>1</sup> AUBERT	09L	BABR e <sup>+</sup> e <sup>-</sup> → Υ(4S)

- • • We do not use the following data for averages, fits, limits, etc. • • •
- |                  |    |                         |     |  |
|------------------|----|-------------------------|-----|--|
| 16.2 ± 1.2 ± 0.9 |    | <sup>1</sup> AUBERT,B   | 05G | BABR Repl. by AUBERT 09L                   |
| 10.9 ± 3.3 ± 1.6 |    | <sup>1</sup> AUBERT     | 03M | BABR Repl. by AUBERT 05G                   |
| <130             | 90 | <sup>2</sup> ADAM       | 96D | DLPH e <sup>+</sup> e <sup>-</sup> → Z     |
| <220             | 90 | <sup>3</sup> ABREU      | 95W | DLPH Sup. by ADAM 96D                      |
| <450             | 90 | <sup>4</sup> ALBRECHT   | 90B | ARG e <sup>+</sup> e <sup>-</sup> → Υ(4S)  |
| <190             | 90 | <sup>5</sup> BORTOLETTO | 089 | CLEO e <sup>+</sup> e <sup>-</sup> → Υ(4S) |
- Assumes equal production of B<sup>0</sup> and B<sup>+</sup> at the Υ(4S); charm and charmonium contributions are subtracted, otherwise no assumptions about intermediate resonances.
  - ADAM 96D assumes f<sub>B<sup>0</sup></sub> = f<sub>B<sup>-</sup></sub> = 0.39 and f<sub>B<sub>s</sub></sub> = 0.12.
  - Assumes a B<sup>0</sup>, B<sup>-</sup> production fraction of 0.39 and a B<sub>s</sub> production fraction of 0.12.
  - ALBRECHT 90B limit assumes equal production of B<sup>0</sup>B<sup>0</sup> and B<sup>+</sup>B<sup>-</sup> at Υ(4S).
  - BORTOLETTO 89 reports < 1.7 × 10<sup>-4</sup> assuming the Υ(4S) decays 43% to B<sup>0</sup>B<sup>0</sup>. We rescale to 50%.

**Γ(ρ<sup>0</sup>π<sup>+</sup>)/Γ<sub>total</sub>** Γ<sub>355</sub>/Γ

VALUE (units 10 <sup>-6</sup> )	CL%	DOCUMENT ID	TECN	COMMENT
<b>8.3 ± 1.2 OUR AVERAGE</b>				

- |  |  |                     |     |  |
|--|--|---------------------|-----|--|
| 8.1 ± 0.7 <sup>+1.3</sup> <sub>-1.6</sub>  |  | <sup>1</sup> AUBERT | 09L | BABR e <sup>+</sup> e <sup>-</sup> → Υ(4S) |
| 8.0 <sup>+2.3</sup> <sub>-2.0</sub> ± 0.7  |  | <sup>1</sup> GORDON | 02  | BELL e <sup>+</sup> e <sup>-</sup> → Υ(4S) |
| 10.4 <sup>+3.3</sup> <sub>-3.4</sub> ± 2.1 |  | <sup>1</sup> JESSOP | 00  | CLE2 e <sup>+</sup> e <sup>-</sup> → Υ(4S) |
- • • We do not use the following data for averages, fits, limits, etc. • • •
- |   |    |                         |     |  |
|---|----|-------------------------|-----|--|
| 8.8 ± 1.0 <sup>+0.6</sup> <sub>-0.9</sub> |    | <sup>1</sup> AUBERT,B   | 05G | BABR Repl. by AUBERT 09L                   |
| 9.5 ± 1.1 ± 0.9                           |    | <sup>1</sup> AUBERT     | 04Z | BABR Repl. by AUBERT 05G                   |
| < 83                                      | 90 | <sup>2</sup> ABE        | 00C | SLD e <sup>+</sup> e <sup>-</sup> → Z      |
| <160                                      | 90 | <sup>3</sup> ADAM       | 96D | DLPH e <sup>+</sup> e <sup>-</sup> → Z     |
| < 43                                      | 90 | <sup>4</sup> ASNER      | 96  | CLE2 Repl. by JESSOP 00                    |
| <260                                      | 90 | <sup>4</sup> ABREU      | 95N | DLPH Sup. by ADAM 96D                      |
| <150                                      | 90 | <sup>1</sup> ALBRECHT   | 90B | ARG e <sup>+</sup> e <sup>-</sup> → Υ(4S)  |
| <170                                      | 90 | <sup>5</sup> BORTOLETTO | 089 | CLEO e <sup>+</sup> e <sup>-</sup> → Υ(4S) |
| <230                                      | 90 | <sup>5</sup> BEBEK      | 87  | CLEO e <sup>+</sup> e <sup>-</sup> → Υ(4S) |
| <600                                      | 90 | GILES                   | 84  | CLEO Repl. by BEBEK 87                     |
- Assumes equal production of B<sup>+</sup> and B<sup>0</sup> at the Υ(4S).
  - ABE 00C assumes B(Z → bD) = (21.7 ± 0.1)% and the B fractions f<sub>B<sup>0</sup></sub> = f<sub>B<sup>+</sup></sub> = (39.7 ± 1.8<sup>+2.2</sup><sub>-2.2</sub>)% and f<sub>B<sub>s</sub></sub> = (10.5 ± 1.8<sup>+2.2</sup><sub>-2.2</sub>)%.
  - ADAM 96D assumes f<sub>B<sup>0</sup></sub> = f<sub>B<sup>-</sup></sub> = 0.39 and f<sub>B<sub>s</sub></sub> = 0.12.
  - Assumes a B<sup>0</sup>, B<sup>-</sup> production fraction of 0.39 and a B<sub>s</sub> production fraction of 0.12.
  - Papers assume the Υ(4S) decays 43% to B<sup>0</sup>B<sup>0</sup>. We rescale to 50%.

**[Γ(K\*(892)<sup>0</sup>π<sup>+</sup>) + Γ(ρ<sup>0</sup>π<sup>+</sup>)]/Γ<sub>total</sub>** (Γ<sub>264</sub> + Γ<sub>355</sub>)/Γ

VALUE (units 10 <sup>-6</sup> )	DOCUMENT ID	TECN	COMMENT
<b>170 ± 120<sup>+20</sup><sub>-20</sub></b>	<sup>1</sup> ADAM	96D	DLPH e <sup>+</sup> e <sup>-</sup> → Z

<sup>1</sup> ADAM 96D assumes f<sub>B<sup>0</sup></sub> = f<sub>B<sup>-</sup></sub> = 0.39 and f<sub>B<sub>s</sub></sub> = 0.12.

**Γ(π<sup>+</sup>f<sub>0</sub>(980) × B(f<sub>0</sub>(980) → π<sup>+</sup>π<sup>-</sup>)/Γ<sub>total</sub>** Γ<sub>356</sub>/Γ

VALUE (units 10 <sup>-6</sup> )	CL%	DOCUMENT ID	TECN	COMMENT
< 1.5	90	<sup>1</sup> AUBERT	09L	BABR e <sup>+</sup> e <sup>-</sup> → Υ(4S)

- • • We do not use the following data for averages, fits, limits, etc. • • •
- |       |    |                         |     |  |
|-------|----|-------------------------|-----|--|
| < 3.0 | 90 | <sup>1</sup> AUBERT,B   | 05G | BABR Repl. by AUBERT 09L                   |
| <140  | 90 | <sup>2</sup> BORTOLETTO | 089 | CLEO e <sup>+</sup> e <sup>-</sup> → Υ(4S) |
- Assumes equal production of B<sup>+</sup> and B<sup>0</sup> at the Υ(4S).
  - BORTOLETTO 89 reports < 1.2 × 10<sup>-4</sup> assuming the Υ(4S) decays 43% to B<sup>0</sup>B<sup>0</sup>. We rescale to 50%.

**Γ(π<sup>+</sup>f<sub>2</sub>(1270)/Γ<sub>total</sub>** Γ<sub>357</sub>/Γ

VALUE (units 10 <sup>-6</sup> )	CL%	DOCUMENT ID	TECN	COMMENT
<b>1.59 ± 0.66 ± 0.02<sup>+0.43</sup><sub>-0.05</sub></b>		<sup>1,2</sup> AUBERT	09L	BABR e <sup>+</sup> e <sup>-</sup> → Υ(4S)

- • • We do not use the following data for averages, fits, limits, etc. • • •
- |                 |    |                         |     |  |
|-----------------|----|-------------------------|-----|--|
| 4.1 ± 1.3 ± 0.1 |    | <sup>2,3</sup> AUBERT,B | 05G | BABR Repl. by AUBERT 09L                   |
| <240            | 90 | <sup>4</sup> BORTOLETTO | 089 | CLEO e <sup>+</sup> e <sup>-</sup> → Υ(4S) |
- AUBERT 09L reports [Γ(B<sup>+</sup> → π<sup>+</sup>f<sub>2</sub>(1270))/Γ<sub>total</sub>] × [B(f<sub>2</sub>(1270) → π<sup>+</sup>π<sup>-</sup>)] = (0.9 ± 0.2 ± 0.1<sup>+0.3</sup><sub>-0.1</sub>) × 10<sup>-6</sup> which we divide by our best value B(f<sub>2</sub>(1270) → π<sup>+</sup>π<sup>-</sup>) = (5.65 ± 1.6<sup>+1.6</sup><sub>-0.8</sub>) × 10<sup>-2</sup>. Our first error is their experiment's error and our second error is the systematic error from using our best value.
  - Assumes equal production of B<sup>+</sup> and B<sup>0</sup> at the Υ(4S).
  - AUBERT,B 05G reports [Γ(B<sup>+</sup> → π<sup>+</sup>f<sub>2</sub>(1270))/Γ<sub>total</sub>] × [B(f<sub>2</sub>(1270) → π<sup>+</sup>π<sup>-</sup>)] = (2.3 ± 0.6 ± 0.4) × 10<sup>-6</sup> which we divide by our best value B(f<sub>2</sub>(1270) → π<sup>+</sup>π<sup>-</sup>) = (5.65 ± 1.6<sup>+1.6</sup><sub>-0.8</sub>) × 10<sup>-2</sup>. Our first error is their experiment's error and our second error is the systematic error from using our best value.
  - BORTOLETTO 89 reports < 2.1 × 10<sup>-4</sup> assuming the Υ(4S) decays 43% to B<sup>0</sup>B<sup>0</sup>. We rescale to 50%.

**Γ(ρ(1450)<sup>0</sup>π<sup>+</sup> × B(ρ<sup>0</sup> → π<sup>+</sup>π<sup>-</sup>)/Γ<sub>total</sub>** Γ<sub>358</sub>/Γ

VALUE (units 10 <sup>-6</sup> )	CL%	DOCUMENT ID	TECN	COMMENT
<b>1.4 ± 0.4 ± 0.5<sup>+0.8</sup><sub>-0.8</sub></b>		<sup>1</sup> AUBERT	09L	BABR e <sup>+</sup> e <sup>-</sup> → Υ(4S)

- • • We do not use the following data for averages, fits, limits, etc. • • •
- |      |    |                       |     |                          |
|------|----|-----------------------|-----|--------------------------|
| <2.3 | 90 | <sup>1</sup> AUBERT,B | 05G | BABR Repl. by AUBERT 09L |
|------|----|-----------------------|-----|--------------------------|
- Assumes equal production of B<sup>+</sup> and B<sup>0</sup> at the Υ(4S).

**Γ(f<sub>0</sub>(1370)π<sup>+</sup> × B(f<sub>0</sub>(1370) → π<sup>+</sup>π<sup>-</sup>)/Γ<sub>total</sub>** Γ<sub>359</sub>/Γ

VALUE (units 10 <sup>-6</sup> )	CL%	DOCUMENT ID	TECN	COMMENT
<4.0	90	<sup>1</sup> AUBERT	09L	BABR e <sup>+</sup> e <sup>-</sup> → Υ(4S)

- • • We do not use the following data for averages, fits, limits, etc. • • •
- |      |    |                       |     |                          |
|------|----|-----------------------|-----|--------------------------|
| <3.0 | 90 | <sup>1</sup> AUBERT,B | 05G | BABR Repl. by AUBERT 09L |
|------|----|-----------------------|-----|--------------------------|
- Assumes equal production of B<sup>+</sup> and B<sup>0</sup> at the Υ(4S).

**Γ(f<sub>0</sub>(500)π<sup>+</sup> × B(f<sub>0</sub>(500) → π<sup>+</sup>π<sup>-</sup>)/Γ<sub>total</sub>** Γ<sub>360</sub>/Γ

VALUE (units 10 <sup>-6</sup> )	CL%	DOCUMENT ID	TECN	COMMENT
<4.1	90	<sup>1</sup> AUBERT,B	05G	BABR e <sup>+</sup> e <sup>-</sup> → Υ(4S)

**Γ(π<sup>+</sup>π<sup>-</sup>π<sup>+</sup> nonresonant)/Γ<sub>total</sub>** Γ<sub>361</sub>/Γ

VALUE (units 10 <sup>-6</sup> )	CL%	DOCUMENT ID	TECN	COMMENT
<b>5.3 ± 0.7<sup>+1.3</sup><sub>-0.8</sub></b>		<sup>1</sup> AUBERT	09L	BABR e <sup>+</sup> e <sup>-</sup> → Υ(4S)

- • • We do not use the following data for averages, fits, limits, etc. • • •
- |       |    |                       |     |  |
|-------|----|-----------------------|-----|--|
| < 4.6 | 90 | <sup>1</sup> AUBERT,B | 05G | BABR Repl. by AUBERT 09L                   |
| <41   | 90 | BERGFELD              | 96B | CLE2 e <sup>+</sup> e <sup>-</sup> → Υ(4S) |
- Assumes equal production of B<sup>+</sup> and B<sup>0</sup> at the Υ(4S).

**Γ(π<sup>+</sup>π<sup>0</sup>π<sup>0</sup>)/Γ<sub>total</sub>** Γ<sub>362</sub>/Γ

VALUE	CL%	DOCUMENT ID	TECN	COMMENT
<8.9 × 10 <sup>-4</sup>	90	<sup>1</sup> ALBRECHT	90B	ARG e <sup>+</sup> e <sup>-</sup> → Υ(4S)

**Γ(ρ<sup>+</sup>π<sup>0</sup>)/Γ<sub>total</sub>** Γ<sub>363</sub>/Γ

VALUE (units 10 <sup>-6</sup> )	CL%	DOCUMENT ID	TECN	COMMENT
<b>10.9 ± 1.4 OUR AVERAGE</b>				

- |  |  |                     |     |  |
|--|--|---------------------|-----|--|
| 10.2 ± 1.4 ± 0.9                           |  | <sup>1</sup> AUBERT | 07X | BABR e <sup>+</sup> e <sup>-</sup> → Υ(4S) |
| 13.2 ± 2.3 <sup>+1.4</sup> <sub>-1.9</sub> |  | <sup>1</sup> ZHANG  | 05A | BELL e <sup>+</sup> e <sup>-</sup> → Υ(4S) |
- • • We do not use the following data for averages, fits, limits, etc. • • •
- |                  |    |                       |     |  |
|------------------|----|-----------------------|-----|--|
| 10.9 ± 1.9 ± 1.9 |    | <sup>1</sup> AUBERT   | 04Z | BABR Repl. by AUBERT 07X                   |
| < 43             | 90 | <sup>1,2</sup> JESSOP | 00  | CLE2 e <sup>+</sup> e <sup>-</sup> → Υ(4S) |
| < 77             | 90 | ASNER                 | 96  | CLE2 Repl. by JESSOP 00                    |
| <550             | 90 | <sup>1</sup> ALBRECHT | 90B | ARG e <sup>+</sup> e <sup>-</sup> → Υ(4S)  |
- Assumes equal production of B<sup>+</sup> and B<sup>0</sup> at the Υ(4S).
  - Assumes no nonresonant contributions of B<sup>+</sup> → π<sup>+</sup>π<sup>0</sup>π<sup>0</sup>.

**Γ(π<sup>+</sup>π<sup>-</sup>π<sup>+</sup>π<sup>0</sup>)/Γ<sub>total</sub>** Γ<sub>364</sub>/Γ

VALUE	CL%	DOCUMENT ID	TECN	COMMENT
<4.0 × 10 <sup>-3</sup>	90	<sup>1</sup> ALBRECHT	90B	ARG e <sup>+</sup> e <sup>-</sup> → Υ(4S)

<sup>1</sup> ALBRECHT 90B limit assumes equal production of B<sup>0</sup>B<sup>0</sup> and B<sup>+</sup>B<sup>-</sup> at Υ(4S).

## Meson Particle Listings

 $B^\pm$  $\Gamma(\rho^+\rho^0)/\Gamma_{\text{total}}$   $\Gamma_{365}/\Gamma$ 

VALUE (units $10^{-6}$ )	CL%	DOCUMENT ID	TECN	COMMENT
<b>24.0±1.9 OUR AVERAGE</b>				
23.7±1.4±1.4		<sup>1</sup> AUBERT	09G BABR	$e^+e^- \rightarrow \Upsilon(4S)$
31.7±7.1+ $\frac{3.8}{-6.7}$		<sup>1,2</sup> ZHANG	03B BELL	$e^+e^- \rightarrow \Upsilon(4S)$

• • • We do not use the following data for averages, fits, limits, etc. • • •

16.8±2.2±2.3		<sup>1</sup> AUBERT,BE	06G BABR	Repl. by AUBERT 09G
22.5+ $\frac{5.7}{-5.4}$ ±5.8		<sup>1</sup> AUBERT	03V BABR	Repl. by AUBERT,BE 06G
< 1000	90	<sup>1</sup> ALBRECHT	90B ARG	$e^+e^- \rightarrow \Upsilon(4S)$

<sup>1</sup> Assumes equal production of  $B^+$  and  $B^0$  at the  $\Upsilon(4S)$ .  
<sup>2</sup> The systematic error includes the error associated with the helicity-mix uncertainty.

 $\Gamma(\rho^+\rho_0(980) \times B(\rho_0(980) \rightarrow \pi^+\pi^-))/\Gamma_{\text{total}}$   $\Gamma_{366}/\Gamma$ 

VALUE (units $10^{-6}$ )	CL%	DOCUMENT ID	TECN	COMMENT
<b>&lt;2.0</b>	90	<sup>1</sup> AUBERT	09G BABR	$e^+e^- \rightarrow \Upsilon(4S)$

• • • We do not use the following data for averages, fits, limits, etc. • • •

<1.9	90	<sup>1</sup> AUBERT,BE	06G BABR	Repl. by AUBERT 09G
------	----	------------------------	----------	---------------------

<sup>1</sup> Assumes equal production of  $B^+$  and  $B^0$  at the  $\Upsilon(4S)$ .

 $\Gamma(a_1(1260)^+\pi^0)/\Gamma_{\text{total}}$   $\Gamma_{367}/\Gamma$ 

VALUE (units $10^{-6}$ )	CL%	DOCUMENT ID	TECN	COMMENT
<b>26.4±5.4±4.1</b>		<sup>1,2</sup> AUBERT	07BL BABR	$e^+e^- \rightarrow \Upsilon(4S)$

• • • We do not use the following data for averages, fits, limits, etc. • • •

<1700	90	<sup>1</sup> ALBRECHT	90B ARG	$e^+e^- \rightarrow \Upsilon(4S)$
-------	----	-----------------------	---------	-----------------------------------

<sup>1</sup> Assumes equal production of  $B^+$  and  $B^0$  at the  $\Upsilon(4S)$ .  
<sup>2</sup> Assumes  $a_1^+$  decays only to  $3\pi$  and  $B(a_1^+ \rightarrow \pi^\pm\pi^\mp\pi^+) = 0.5$ .

 $\Gamma(a_1(1260)^0\pi^+)/\Gamma_{\text{total}}$   $\Gamma_{368}/\Gamma$ 

VALUE (units $10^{-6}$ )	CL%	DOCUMENT ID	TECN	COMMENT
<b>20.4±4.7±3.4</b>		<sup>1,2</sup> AUBERT	07BL BABR	$e^+e^- \rightarrow \Upsilon(4S)$

• • • We do not use the following data for averages, fits, limits, etc. • • •

<900	90	<sup>1</sup> ALBRECHT	90B ARG	$e^+e^- \rightarrow \Upsilon(4S)$
------	----	-----------------------	---------	-----------------------------------

<sup>1</sup> Assumes equal production of  $B^+$  and  $B^0$  at the  $\Upsilon(4S)$ .  
<sup>2</sup> Assumes  $a_1^0$  decays only to  $3\pi$  and  $B(a_1^0 \rightarrow \pi^\pm\pi^\mp\pi^0) = 1.0$ .

 $\Gamma(\omega\pi^+)/\Gamma_{\text{total}}$   $\Gamma_{369}/\Gamma$ 

VALUE (units $10^{-6}$ )	CL%	DOCUMENT ID	TECN	COMMENT
<b>6.9±0.5 OUR AVERAGE</b>				
6.7±0.5±0.4		<sup>1</sup> AUBERT	07AE BABR	$e^+e^- \rightarrow \Upsilon(4S)$
6.9±0.6±0.5		<sup>1</sup> JEN	06 BELL	$e^+e^- \rightarrow \Upsilon(4S)$
11.3+ $\frac{3.3}{-2.9}$ ±1.4		<sup>1</sup> JESSOP	00 CLE2	$e^+e^- \rightarrow \Upsilon(4S)$

• • • We do not use the following data for averages, fits, limits, etc. • • •

6.1±0.7±0.4		<sup>1</sup> AUBERT,B	06E BABR	Repl. by AUBERT 07AE
5.5±0.9±0.5		<sup>1</sup> AUBERT	04H BABR	Repl. by AUBERT,B 06E
5.7+ $\frac{1.4}{-1.3}$ ±0.6		<sup>1</sup> WANG	04A BELL	Repl. by JEN 06
4.2+ $\frac{2.0}{-1.8}$ ±0.5		<sup>1</sup> LU	02 BELL	Repl. by WANG 04A
6.6+ $\frac{2.1}{-1.8}$ ±0.7		<sup>1</sup> AUBERT	01G BABR	Repl. by AUBERT 04H
< 23	90	<sup>1</sup> BERGFELD	98 CLE2	Repl. by JESSOP 00
<400	90	<sup>1</sup> ALBRECHT	90B ARG	$e^+e^- \rightarrow \Upsilon(4S)$

<sup>1</sup> Assumes equal production of  $B^+$  and  $B^0$  at the  $\Upsilon(4S)$ .

 $\Gamma(\omega\rho^+)/\Gamma_{\text{total}}$   $\Gamma_{370}/\Gamma$ 

VALUE (units $10^{-6}$ )	CL%	DOCUMENT ID	TECN	COMMENT
<b>15.9±1.6±1.4</b>		<sup>1</sup> AUBERT	09H BABR	$e^+e^- \rightarrow \Upsilon(4S)$

• • • We do not use the following data for averages, fits, limits, etc. • • •

10.6±2.1+ $\frac{1.6}{-1.0}$		<sup>1</sup> AUBERT,B	06T BABR	Repl. by AUBERT 09H
12.6+ $\frac{3.7}{-3.3}$ ±1.6		<sup>1</sup> AUBERT	05O BABR	Repl. by AUBERT,B 06T
<61	90	<sup>1</sup> BERGFELD	98 CLE2	

<sup>1</sup> Assumes equal production of  $B^+$  and  $B^0$  at the  $\Upsilon(4S)$ .

 $\Gamma(\eta\pi^+)/\Gamma_{\text{total}}$   $\Gamma_{371}/\Gamma$ 

VALUE (units $10^{-6}$ )	CL%	DOCUMENT ID	TECN	COMMENT
<b>4.02±0.27 OUR AVERAGE</b>				
4.07±0.26±0.21		<sup>1</sup> HOI	12 BELL	$e^+e^- \rightarrow \Upsilon(4S)$
4.00±0.40±0.24		<sup>1</sup> AUBERT	09AV BABR	$e^+e^- \rightarrow \Upsilon(4S)$
1.2+ $\frac{2.8}{-1.2}$		<sup>1</sup> RICHICHI	00 CLE2	$e^+e^- \rightarrow \Upsilon(4S)$

• • • We do not use the following data for averages, fits, limits, etc. • • •

5.0 ± 0.5 ± 0.3		<sup>1</sup> AUBERT	07AE BABR	Repl. by AUBERT 09AV
4.2 ± 0.4 ± 0.2		<sup>1</sup> CHANG	07B BELL	Repl. by HOI 12
5.1 ± 0.6 ± 0.3		<sup>1</sup> AUBERT,B	05K BABR	Repl. by AUBERT 07AE
4.8 ± 0.7 ± 0.3		<sup>1</sup> CHANG	05A BELL	Repl. by CHANG 07B
5.3 ± 1.0 ± 0.3		<sup>1</sup> AUBERT	04H BABR	Repl. by AUBERT,B 05K
< 15	90	BEHRENS	98 CLE2	Repl. by RICHICHI 00
<700	90	ALBRECHT	90B ARG	$e^+e^- \rightarrow \Upsilon(4S)$

<sup>1</sup> Assumes equal production of  $B^+$  and  $B^0$  at the  $\Upsilon(4S)$ .

 $\Gamma(\eta\rho^+)/\Gamma_{\text{total}}$   $\Gamma_{372}/\Gamma$ 

VALUE (units $10^{-6}$ )	CL%	DOCUMENT ID	TECN	COMMENT
<b>7.0±2.9 OUR AVERAGE</b>				Error includes scale factor of 2.8.
9.9±1.2±0.8		<sup>1</sup> AUBERT	08AH BABR	$e^+e^- \rightarrow \Upsilon(4S)$
4.1+ $\frac{1.4}{-1.3}$ ±0.4		<sup>1</sup> WANG	07B BELL	$e^+e^- \rightarrow \Upsilon(4S)$

• • • We do not use the following data for averages, fits, limits, etc. • • •

8.4±1.9±1.1		<sup>1</sup> AUBERT,B	05K BABR	Repl. by AUBERT 08AH
<14	90	<sup>1</sup> AUBERT,B	04D BABR	Repl. by AUBERT,B 05K
<15	90	<sup>1</sup> RICHICHI	00 CLE2	$e^+e^- \rightarrow \Upsilon(4S)$
<32	90	BEHRENS	98 CLE2	Repl. by RICHICHI 00

<sup>1</sup> Assumes equal production of  $B^+$  and  $B^0$  at the  $\Upsilon(4S)$ .

 $\Gamma(\eta'\pi^+)/\Gamma_{\text{total}}$   $\Gamma_{373}/\Gamma$ 

VALUE (units $10^{-6}$ )	CL%	DOCUMENT ID	TECN	COMMENT
<b>2.7 ± 0.9 OUR AVERAGE</b>				Error includes scale factor of 1.9.
3.5 ± 0.6 ± 0.2		<sup>1</sup> AUBERT	09AV BABR	$e^+e^- \rightarrow \Upsilon(4S)$
1.76+ $\frac{0.67+0.15}{-0.62-0.14}$		<sup>1</sup> SCHUEMANN	06 BELL	$e^+e^- \rightarrow \Upsilon(4S)$

• • • We do not use the following data for averages, fits, limits, etc. • • •

3.9 ± 0.7 ± 0.3		<sup>1</sup> AUBERT	07AE BABR	Repl. by AUBERT 09AV
4.0 ± 0.8 ± 0.4		<sup>1</sup> AUBERT,B	05K BABR	Repl. by AUBERT 07AE
< 4.5	90	<sup>1</sup> AUBERT	04H BABR	Repl. by AUBERT,B 05K
< 7.0	90	<sup>1</sup> ABE	01M BELL	$e^+e^- \rightarrow \Upsilon(4S)$
<12	90	<sup>1</sup> AUBERT	01G BABR	$e^+e^- \rightarrow \Upsilon(4S)$
<12	90	<sup>1</sup> RICHICHI	00 CLE2	$e^+e^- \rightarrow \Upsilon(4S)$
<31	90	BEHRENS	98 CLE2	Repl. by RICHICHI 00

<sup>1</sup> Assumes equal production of  $B^+$  and  $B^0$  at the  $\Upsilon(4S)$ .

 $\Gamma(\eta'\rho^+)/\Gamma_{\text{total}}$   $\Gamma_{374}/\Gamma$ 

VALUE (units $10^{-6}$ )	CL%	DOCUMENT ID	TECN	COMMENT
<b>9.7+<math>\frac{1.9}{-1.8}</math>±1.1</b>		<sup>1</sup> DEL-AMO-SA...	10A BABR	$e^+e^- \rightarrow \Upsilon(4S)$

• • • We do not use the following data for averages, fits, limits, etc. • • •

8.7+ $\frac{3.1+2.3}{-2.8-1.3}$		<sup>1</sup> AUBERT	07E BABR	Repl. by DEL-AMO-SANCHEZ 10A
< 5.8	90	<sup>1</sup> SCHUEMANN	07 BELL	$e^+e^- \rightarrow \Upsilon(4S)$
<22	90	<sup>1</sup> AUBERT,B	04D BABR	Repl. by AUBERT 07E
<33	90	<sup>1</sup> RICHICHI	00 CLE2	$e^+e^- \rightarrow \Upsilon(4S)$
<47	90	BEHRENS	98 CLE2	Repl. by RICHICHI 00

<sup>1</sup> Assumes equal production of  $B^+$  and  $B^0$  at the  $\Upsilon(4S)$ .

 $\Gamma(\phi\pi^+)/\Gamma_{\text{total}}$   $\Gamma_{375}/\Gamma$ 

VALUE (units $10^{-6}$ )	CL%	DOCUMENT ID	TECN	COMMENT
<b>&lt; 0.24</b>	90	<sup>1</sup> AUBERT,B	06C BABR	$e^+e^- \rightarrow \Upsilon(4S)$

• • • We do not use the following data for averages, fits, limits, etc. • • •

< 0.41	90	<sup>1</sup> AUBERT	04A BABR	Repl. by AUBERT,B 06C
< 1.4	90	<sup>1</sup> AUBERT	01D BABR	Repl. by AUBERT 07E
<153	90	<sup>2</sup> ABE	00C SLD	$e^+e^- \rightarrow Z$
< 5	90	<sup>1</sup> BERGFELD	98 CLE2	

<sup>1</sup> Assumes equal production of  $B^+$  and  $B^0$  at the  $\Upsilon(4S)$ .  
<sup>2</sup> ABE 00C assumes  $B(Z \rightarrow b\bar{b}) = (21.7 \pm 0.1)\%$  and the  $B$  fractions  $f_{B^0} = f_{B^+} = (39.7 \pm 1.8)\%$  and  $f_{B_s} = (10.5 \pm 2.2)\%$ .

 $\Gamma(\phi\rho^+)/\Gamma_{\text{total}}$   $\Gamma_{376}/\Gamma$ 

VALUE (units $10^{-6}$ )	CL%	DOCUMENT ID	TECN	COMMENT
<b>&lt; 3.0</b>	90	<sup>1</sup> AUBERT	08BK BABR	$e^+e^- \rightarrow \Upsilon(4S)$

• • • We do not use the following data for averages, fits, limits, etc. • • •

<16		<sup>1</sup> BERGFELD	98 CLE2	
-----	--	-----------------------	---------	--

<sup>1</sup> Assumes equal production of  $B^+$  and  $B^0$  at the  $\Upsilon(4S)$ .

 $\Gamma(a_0(980)^0\pi^+ \times B(a_0(980)^0 \rightarrow \eta\pi^0))/\Gamma_{\text{total}}$   $\Gamma_{377}/\Gamma$ 

VALUE (units $10^{-6}$ )	CL%	DOCUMENT ID	TECN	COMMENT
<b>&lt;5.8</b>	90	<sup>1</sup> AUBERT,BE	04 BABR	$e^+e^- \rightarrow \Upsilon(4S)$

<sup>1</sup> Assumes equal production of charged and neutral  $B$  mesons from  $\Upsilon(4S)$  decays.

 $\Gamma(a_0(980)^+\pi^0 \times B(a_0^+ \rightarrow \eta\pi^+))/\Gamma_{\text{total}}$   $\Gamma_{378}/\Gamma$ 

VALUE (units $10^{-6}$ )	CL%	DOCUMENT ID	TECN	COMMENT
<b>&lt;1.4</b>	90	<sup>1</sup> AUBERT	08A BABR	$e^+e^- \rightarrow \Upsilon(4S)$

<sup>1</sup> Assumes equal production of  $B^+$  and  $B^0$  at the  $\Upsilon(4S)$ .

 $\Gamma(\pi^+\pi^+\pi^-\pi^-)/\Gamma_{\text{total}}$   $\Gamma_{379}/\Gamma$ 

VALUE	CL%	DOCUMENT ID	TECN	COMMENT
<b>&lt;8.6 × 10<sup>-4</sup></b>		<sup>1</sup> ALBRECHT	90B ARG	$e^+e^- \rightarrow \Upsilon(4S)$

<sup>1</sup> ALBRECHT 90B limit assumes equal production of  $B^0\bar{B}^0$  and  $B^+B^-$  at  $\Upsilon(4S)$ .

$\Gamma(\rho^0 a_1(1260)^+)/\Gamma_{\text{total}}$   $\Gamma_{380}/\Gamma$ 

VALUE	CL%	DOCUMENT ID	TECN	COMMENT
$<6.2 \times 10^{-4}$	90	<sup>1</sup> BORTOLETTO89	CLEO	$e^+e^- \rightarrow \Upsilon(4S)$
••• We do not use the following data for averages, fits, limits, etc. •••				
$<6.0 \times 10^{-4}$	90	<sup>2</sup> ALBRECHT 90B	ARG	$e^+e^- \rightarrow \Upsilon(4S)$
$<3.2 \times 10^{-3}$	90	<sup>1</sup> BEBEK 87	CLEO	$e^+e^- \rightarrow \Upsilon(4S)$
<sup>1</sup> BORTOLETTO 89 reports $< 5.4 \times 10^{-4}$ assuming the $\Upsilon(4S)$ decays 43% to $B^0\bar{B}^0$ . We rescale to 50%.				
<sup>2</sup> ALBRECHT 90B limit assumes equal production of $B^0\bar{B}^0$ and $B^+B^-$ at $\Upsilon(4S)$ .				

 $\Gamma(\rho^0 a_2(1320)^+)/\Gamma_{\text{total}}$   $\Gamma_{381}/\Gamma$ 

VALUE	CL%	DOCUMENT ID	TECN	COMMENT
$<7.2 \times 10^{-4}$	90	<sup>1</sup> BORTOLETTO89	CLEO	$e^+e^- \rightarrow \Upsilon(4S)$
••• We do not use the following data for averages, fits, limits, etc. •••				
$<2.6 \times 10^{-3}$	90	<sup>2</sup> BEBEK 87	CLEO	$e^+e^- \rightarrow \Upsilon(4S)$
<sup>1</sup> BORTOLETTO 89 reports $< 6.3 \times 10^{-4}$ assuming the $\Upsilon(4S)$ decays 43% to $B^0\bar{B}^0$ . We rescale to 50%.				
<sup>2</sup> BEBEK 87 reports $< 2.3 \times 10^{-3}$ assuming the $\Upsilon(4S)$ decays 43% to $B^0\bar{B}^0$ . We rescale to 50%.				

 $\Gamma(b_1^0 \pi^+ \times B(b_1^0 \rightarrow \omega \pi^0))/\Gamma_{\text{total}}$   $\Gamma_{382}/\Gamma$ 

VALUE (units $10^{-6}$ )	CL%	DOCUMENT ID	TECN	COMMENT
$6.7 \pm 1.7 \pm 1.0$		<sup>1</sup> AUBERT 07B1	BABR	$e^+e^- \rightarrow \Upsilon(4S)$
<sup>1</sup> Assumes equal production of $B^+$ and $B^0$ at the $\Upsilon(4S)$ .				

 $\Gamma(b_1^+ \pi^0 \times B(b_1^+ \rightarrow \omega \pi^+))/\Gamma_{\text{total}}$   $\Gamma_{383}/\Gamma$ 

VALUE (units $10^{-6}$ )	CL%	DOCUMENT ID	TECN	COMMENT
$<3.3$	90	<sup>1</sup> AUBERT 08AG	BABR	$e^+e^- \rightarrow \Upsilon(4S)$
<sup>1</sup> Assumes equal production of $B^+$ and $B^0$ at the $\Upsilon(4S)$ .				

 $\Gamma(\pi^+ \pi^+ \pi^+ \pi^- \pi^- \pi^0)/\Gamma_{\text{total}}$   $\Gamma_{384}/\Gamma$ 

VALUE	CL%	DOCUMENT ID	TECN	COMMENT
$<6.3 \times 10^{-3}$	90	<sup>1</sup> ALBRECHT 90B	ARG	$e^+e^- \rightarrow \Upsilon(4S)$
<sup>1</sup> ALBRECHT 90B limit assumes equal production of $B^0\bar{B}^0$ and $B^+B^-$ at $\Upsilon(4S)$ .				

 $\Gamma(b_1^+ \rho^0 \times B(b_1^+ \rightarrow \omega \pi^+))/\Gamma_{\text{total}}$   $\Gamma_{385}/\Gamma$ 

VALUE	CL%	DOCUMENT ID	TECN	COMMENT
$<5.2 \times 10^{-6}$	90	<sup>1</sup> AUBERT 09AF	BABR	$e^+e^- \rightarrow \Upsilon(4S)$
<sup>1</sup> Assumes equal production of $B^+$ and $B^0$ at the $\Upsilon(4S)$ .				

 $\Gamma(b_1^0 \rho^+ \times B(b_1^0 \rightarrow \omega \pi^0))/\Gamma_{\text{total}}$   $\Gamma_{387}/\Gamma$ 

VALUE	CL%	DOCUMENT ID	TECN	COMMENT
$<3.3 \times 10^{-6}$	90	<sup>1</sup> AUBERT 09AF	BABR	$e^+e^- \rightarrow \Upsilon(4S)$
<sup>1</sup> Assumes equal production of $B^+$ and $B^0$ at the $\Upsilon(4S)$ .				

 $\Gamma(a_1(1260)^+ a_1(1260)^0)/\Gamma_{\text{total}}$   $\Gamma_{386}/\Gamma$ 

VALUE	CL%	DOCUMENT ID	TECN	COMMENT
$<1.3 \times 10^{-2}$	90	<sup>1</sup> ALBRECHT 90B	ARG	$e^+e^- \rightarrow \Upsilon(4S)$
<sup>1</sup> ALBRECHT 90B limit assumes equal production of $B^0\bar{B}^0$ and $B^+B^-$ at $\Upsilon(4S)$ .				

 $\Gamma(h^+ \pi^0)/\Gamma_{\text{total}}$   $\Gamma_{388}/\Gamma$ 

VALUE (units $10^{-6}$ )	CL%	DOCUMENT ID	TECN	COMMENT
$16 \pm 5 \pm 3.6$		GODANG 98	CLE2	$e^+e^- \rightarrow \Upsilon(4S)$

 $\Gamma(\omega h^+)/\Gamma_{\text{total}}$   $\Gamma_{389}/\Gamma$ 

VALUE (units $10^{-6}$ )	CL%	DOCUMENT ID	TECN	COMMENT
$13.8 \pm 2.7 \pm 2.4$				<b>OUR AVERAGE</b>

$13.4 \pm 3.3 \pm 1.1$		<sup>1</sup> LU 02	BELL	$e^+e^- \rightarrow \Upsilon(4S)$
$14.3 \pm 3.6 \pm 2.0$		<sup>1</sup> JESSOP 00	CLE2	$e^+e^- \rightarrow \Upsilon(4S)$
••• We do not use the following data for averages, fits, limits, etc. •••				
$25 \pm 8 \pm 3$		<sup>1</sup> BERGFELD 98	CLE2	Repl. by JESSOP 00
<sup>1</sup> Assumes equal production of $B^+$ and $B^0$ at the $\Upsilon(4S)$ .				

 $\Gamma(h^+ X^0(\text{Familon}))/\Gamma_{\text{total}}$   $\Gamma_{390}/\Gamma$ 

VALUE (units $10^{-6}$ )	CL%	DOCUMENT ID	TECN	COMMENT
$<49$		<sup>1</sup> AMMAR 01B	CLE2	$e^+e^- \rightarrow \Upsilon(4S)$
<sup>1</sup> AMMAR 01B searched for the two-body decay of the $B$ meson to a massless neutral feebly-interacting particle $X^0$ such as the familon, the Nambu-Goldstone boson associated with a spontaneously broken global family symmetry.				

 $\Gamma(\rho \bar{p} \pi^+)/\Gamma_{\text{total}}$   $\Gamma_{391}/\Gamma$ 

VALUE (units $10^{-6}$ )	CL%	DOCUMENT ID	TECN	COMMENT
$1.62 \pm 0.20$				<b>OUR AVERAGE</b>
$1.60 \pm 0.22 \pm 0.12$		<sup>1,2,3</sup> WEI 08	BELL	$e^+e^- \rightarrow \Upsilon(4S)$
$1.69 \pm 0.29 \pm 0.26$		<sup>1</sup> AUBERT 07AV	BABR	$e^+e^- \rightarrow \Upsilon(4S)$
••• We do not use the following data for averages, fits, limits, etc. •••				
$3.06 \pm 0.73 \pm 0.37$		<sup>1,3</sup> WANG 04	BELL	Repl. by WEI 08
$< 3.7$	90	<sup>1,2</sup> ABE 02K	BELL	Repl. by WANG 04
$<500$	90	<sup>4</sup> ABREU 95N	DLPH	Repl. by ADAM 96D
$<160$	90	<sup>5</sup> BEBEK 89	CLEO	$e^+e^- \rightarrow \Upsilon(4S)$
$570 \pm 150 \pm 210$		<sup>6</sup> ALBRECHT 88F	ARG	$e^+e^- \rightarrow \Upsilon(4S)$
<sup>1</sup> Assumes equal production of $B^+$ and $B^0$ at the $\Upsilon(4S)$ .				
<sup>2</sup> Explicitly vetoes resonant production of $p\bar{p}$ from Charmonium states.				
<sup>3</sup> Also provides results with $m_{p\bar{p}} < 2.85 \text{ GeV}/c^2$ and angular asymmetry of $p\bar{p}$ system.				
<sup>4</sup> Assumes a $B^0, B^-$ production fraction of 0.39 and a $B_s$ production fraction of 0.12.				
<sup>5</sup> BEBEK 89 reports $< 1.4 \times 10^{-4}$ assuming the $\Upsilon(4S)$ decays 43% to $B^0\bar{B}^0$ . We rescale to 50%.				
<sup>6</sup> ALBRECHT 88F reports $(5.2 \pm 1.4 \pm 1.9) \times 10^{-4}$ assuming the $\Upsilon(4S)$ decays 45% to $B^0\bar{B}^0$ . We rescale to 50%.				

 $\Gamma(\rho \bar{p} \pi^+ \text{nonresonant})/\Gamma_{\text{total}}$   $\Gamma_{392}/\Gamma$ 

VALUE (units $10^{-6}$ )	CL%	DOCUMENT ID	TECN	COMMENT
$<53$	90	BERGFELD 96B	CLE2	$e^+e^- \rightarrow \Upsilon(4S)$

 $\Gamma(\rho \bar{p} \pi^+ \pi^+ \pi^-)/\Gamma_{\text{total}}$   $\Gamma_{393}/\Gamma$ 

VALUE	CL%	DOCUMENT ID	TECN	COMMENT
$<5.2 \times 10^{-4}$	90	<sup>1</sup> ALBRECHT 88F	ARG	$e^+e^- \rightarrow \Upsilon(4S)$
<sup>1</sup> ALBRECHT 88F reports $< 4.7 \times 10^{-4}$ assuming the $\Upsilon(4S)$ decays 45% to $B^0\bar{B}^0$ . We rescale to 50%.				

 $\Gamma(\rho \bar{p} K^+)/\Gamma_{\text{total}}$   $\Gamma_{394}/\Gamma$ 

VALUE (units $10^{-6}$ )	CL%	DOCUMENT ID	TECN	COMMENT
$5.9 \pm 0.5$				<b>OUR AVERAGE</b> Error includes scale factor of 1.5.
$5.54 \pm 0.27 \pm 0.36$		<sup>1,2,3</sup> WEI 08	BELL	$e^+e^- \rightarrow \Upsilon(4S)$
$6.7 \pm 0.5 \pm 0.4$		<sup>1,3</sup> AUBERT,B 05L	BABR	$e^+e^- \rightarrow \Upsilon(4S)$
••• We do not use the following data for averages, fits, limits, etc. •••				
$4.59 \pm 0.38 \pm 0.50$		<sup>1,2,3</sup> WANG 05A	BELL	Repl. by WEI 08
$5.66 \pm 0.67 \pm 0.62$		<sup>1,2,3</sup> WANG 04	BELL	Repl. by WANG 05A
$4.3 \pm 1.1 \pm 0.9$		<sup>1,2</sup> ABE 02K	BELL	Repl. by WANG 04
<sup>1</sup> Assumes equal production of $B^+$ and $B^0$ at the $\Upsilon(4S)$ .				
<sup>2</sup> Explicitly vetoes resonant production of $p\bar{p}$ from Charmonium states.				
<sup>3</sup> Provides also results with $m_{p\bar{p}} < 2.85 \text{ GeV}/c^2$ and angular asymmetry of $p\bar{p}$ system.				

 $\Gamma(\theta(1710)^{++} \bar{p} \times B(\theta(1710)^{++} \rightarrow p K^+))/\Gamma_{\text{total}}$   $\Gamma_{395}/\Gamma$ 

VALUE (units $10^{-6}$ )	CL%	DOCUMENT ID	TECN	COMMENT
$<0.091$	90	<sup>1</sup> WANG 05A	BELL	$e^+e^- \rightarrow \Upsilon(4S)$
••• We do not use the following data for averages, fits, limits, etc. •••				
$<0.1$	90	<sup>1,2</sup> AUBERT,B 05L	BABR	$e^+e^- \rightarrow \Upsilon(4S)$
<sup>1</sup> Assumes equal production of $B^+$ and $B^0$ at the $\Upsilon(4S)$ .				
<sup>2</sup> Provides upper limits depending on the pentaquark masses between 1.43 to 2.0 $\text{GeV}/c^2$ .				

 $\Gamma(f_J(2220) K^+ \times B(f_J(2220) \rightarrow p \bar{p}))/\Gamma_{\text{total}}$   $\Gamma_{396}/\Gamma$ 

VALUE (units $10^{-6}$ )	CL%	DOCUMENT ID	TECN	COMMENT
$<0.41$	90	<sup>1</sup> WANG 05A	BELL	$e^+e^- \rightarrow \Upsilon(4S)$
<sup>1</sup> Assumes equal production of $B^+$ and $B^0$ at the $\Upsilon(4S)$ .				

 $\Gamma(\rho \bar{\Lambda}(1520))/\Gamma_{\text{total}}$   $\Gamma_{397}/\Gamma$ 

VALUE (units $10^{-6}$ )	CL%	DOCUMENT ID	TECN	COMMENT
$<1.5$	90	<sup>1</sup> AUBERT,B 05L	BABR	$e^+e^- \rightarrow \Upsilon(4S)$
<sup>1</sup> Assumes equal production of $B^+$ and $B^0$ at the $\Upsilon(4S)$ .				

 $\Gamma(\rho \bar{p} K^+ \text{nonresonant})/\Gamma_{\text{total}}$   $\Gamma_{398}/\Gamma$ 

VALUE (units $10^{-6}$ )	CL%	DOCUMENT ID	TECN	COMMENT
$<89$	90	BERGFELD 96B	CLE2	$e^+e^- \rightarrow \Upsilon(4S)$

 $\Gamma(\rho \bar{p} K^*(892)^+)/\Gamma_{\text{total}}$   $\Gamma_{399}/\Gamma$ 

VALUE (units $10^{-6}$ )	CL%	DOCUMENT ID	TECN	COMMENT
$3.6 \pm 0.8 \pm 0.7$				<b>OUR AVERAGE</b>
$3.38 \pm 0.73 \pm 0.39$		<sup>1,2</sup> CHEN 08c	BELL	$e^+e^- \rightarrow \Upsilon(4S)$
$5.3 \pm 1.5 \pm 1.3$		<sup>2</sup> AUBERT 07AV	BABR	$e^+e^- \rightarrow \Upsilon(4S)$
••• We do not use the following data for averages, fits, limits, etc. •••				
$10.3 \pm 3.6 \pm 1.3 \pm 2.8 \pm 1.7$		<sup>2,3</sup> WANG 04	BELL	Repl. by CHEN 08c
<sup>1</sup> Explicitly vetoes resonant production of $p\bar{p}$ from charmonium states.				
<sup>2</sup> Assumes equal production of $B^+$ and $B^0$ at the $\Upsilon(4S)$ .				
<sup>3</sup> Explicitly vetoes resonant production of $p\bar{p}$ from charmonium states. The branching fraction for $M_{p\bar{p}} < 2.85 \text{ GeV}/c^2$ is also reported.				

## Meson Particle Listings

 $B^\pm$  $\Gamma(f_j(2220)K^{*+} \times B(f_j(2220) \rightarrow p\bar{p}))/\Gamma_{\text{total}}$   $\Gamma_{400}/\Gamma$ 

VALUE (units $10^{-6}$ )	CL%	DOCUMENT ID	TECN	COMMENT
<b>&lt;0.77</b>	90	<sup>1</sup> AUBERT	07AV	BABR $e^+e^- \rightarrow \Upsilon(4S)$

<sup>1</sup> Assumes equal production of  $B^+$  and  $B^0$  at the  $\Upsilon(4S)$ .

 $\Gamma(\rho\bar{\Lambda})/\Gamma_{\text{total}}$   $\Gamma_{401}/\Gamma$ 

VALUE (units $10^{-6}$ )	CL%	DOCUMENT ID	TECN	COMMENT
<b>&lt; 0.32</b>	90	<sup>1</sup> TSAI	07	BELL $e^+e^- \rightarrow \Upsilon(4S)$
••• We do not use the following data for averages, fits, limits, etc. •••				
< 0.49	90	<sup>1</sup> CHANG	05	BELL Repl. by TSAI 07
< 1.5	90	<sup>1</sup> BORNHEIM	03	CLE2 $e^+e^- \rightarrow \Upsilon(4S)$
< 2.2	90	<sup>1</sup> ABE	02O	BELL $e^+e^- \rightarrow \Upsilon(4S)$
< 2.6	90	<sup>1</sup> COAN	99	CLE2 $e^+e^- \rightarrow \Upsilon(4S)$
<60	90	<sup>2</sup> AVERY	89B	CLEO $e^+e^- \rightarrow \Upsilon(4S)$
<93	90	<sup>3</sup> ALBRECHT	88F	ARG $e^+e^- \rightarrow \Upsilon(4S)$

<sup>1</sup> Assumes equal production of  $B^+$  and  $B^0$  at the  $\Upsilon(4S)$ .

<sup>2</sup> AVERY 89B reports  $< 5 \times 10^{-5}$  assuming the  $\Upsilon(4S)$  decays 43% to  $B^0\bar{B}^0$ . We rescale to 50%.

<sup>3</sup> ALBRECHT 88F reports  $< 8.5 \times 10^{-5}$  assuming the  $\Upsilon(4S)$  decays 45% to  $B^0\bar{B}^0$ . We rescale to 50%.

 $\Gamma(\rho\bar{\Lambda}\gamma)/\Gamma_{\text{total}}$   $\Gamma_{402}/\Gamma$ 

VALUE (units $10^{-6}$ )	CL%	DOCUMENT ID	TECN	COMMENT
<b><math>2.45^{+0.44}_{-0.38} \pm 0.22</math></b>		<sup>1</sup> WANG	07c	BELL $e^+e^- \rightarrow \Upsilon(4S)$
••• We do not use the following data for averages, fits, limits, etc. •••				
$2.16^{+0.58}_{-0.53} \pm 0.20$		<sup>1</sup> LEE	05	BELL Repl. by WANG 07c
<3.9	90	<sup>2</sup> EDWARDS	03	CLE2 $e^+e^- \rightarrow \Upsilon(4S)$

<sup>1</sup> Assumes equal production of  $B^+$  and  $B^0$  at the  $\Upsilon(4S)$ .

<sup>2</sup> Corresponds to  $E_\gamma > 1.5$  GeV. The limit changes to  $3.3 \times 10^{-6}$  for  $E_\gamma > 2.0$  GeV.

 $\Gamma(\rho\bar{\Lambda}\pi^0)/\Gamma_{\text{total}}$   $\Gamma_{403}/\Gamma$ 

VALUE (units $10^{-6}$ )	CL%	DOCUMENT ID	TECN	COMMENT
<b><math>3.00^{+0.61}_{-0.53} \pm 0.33</math></b>		<sup>1</sup> WANG	07c	BELL $e^+e^- \rightarrow \Upsilon(4S)$

<sup>1</sup> Assumes equal production of  $B^+$  and  $B^0$  at the  $\Upsilon(4S)$ .

 $\Gamma(\rho\Sigma(1385)^0)/\Gamma_{\text{total}}$   $\Gamma_{404}/\Gamma$ 

VALUE (units $10^{-6}$ )	CL%	DOCUMENT ID	TECN	COMMENT
<b>&lt;0.47</b>	90	<sup>1</sup> WANG	07c	BELL $e^+e^- \rightarrow \Upsilon(4S)$

<sup>1</sup> Assumes equal production of  $B^+$  and  $B^0$  at the  $\Upsilon(4S)$ .

 $\Gamma(\Delta^+\bar{\Lambda})/\Gamma_{\text{total}}$   $\Gamma_{405}/\Gamma$ 

VALUE (units $10^{-6}$ )	CL%	DOCUMENT ID	TECN	COMMENT
<b>&lt;0.82</b>	90	<sup>1</sup> WANG	07c	BELL $e^+e^- \rightarrow \Upsilon(4S)$

<sup>1</sup> Assumes equal production of  $B^+$  and  $B^0$  at the  $\Upsilon(4S)$ .

 $\Gamma(\rho\Sigma\gamma)/\Gamma_{\text{total}}$   $\Gamma_{406}/\Gamma$ 

VALUE (units $10^{-6}$ )	CL%	DOCUMENT ID	TECN	COMMENT
<b>&lt;4.6</b>	90	<sup>1</sup> LEE	05	BELL $e^+e^- \rightarrow \Upsilon(4S)$
••• We do not use the following data for averages, fits, limits, etc. •••				
<7.9	90	<sup>2</sup> EDWARDS	03	CLE2 $e^+e^- \rightarrow \Upsilon(4S)$

<sup>1</sup> Assumes equal production of  $B^+$  and  $B^0$  at the  $\Upsilon(4S)$ .

<sup>2</sup> Corresponds to  $E_\gamma > 1.5$  GeV. The limit changes to  $6.4 \times 10^{-6}$  for  $E_\gamma > 2.0$  GeV.

 $\Gamma(\rho\bar{\Lambda}\pi^+\pi^-)/\Gamma_{\text{total}}$   $\Gamma_{407}/\Gamma$ 

VALUE (units $10^{-6}$ )	CL%	DOCUMENT ID	TECN	COMMENT
<b><math>5.92^{+0.88}_{-0.84} \pm 0.69</math></b>		<sup>1</sup> CHEN	09c	BELL $e^+e^- \rightarrow \Upsilon(4S)$

••• We do not use the following data for averages, fits, limits, etc. •••

<200	90	<sup>2</sup> ALBRECHT	88F	ARG $e^+e^- \rightarrow \Upsilon(4S)$
------	----	-----------------------	-----	---------------------------------------

<sup>1</sup> Assumes equal production of  $B^+$  and  $B^0$  at the  $\Upsilon(4S)$ .

<sup>2</sup> ALBRECHT 88F reports  $< 1.8 \times 10^{-4}$  assuming the  $\Upsilon(4S)$  decays 45% to  $B^0\bar{B}^0$ . We rescale to 50%.

 $\Gamma(\rho\bar{\Lambda}\rho^0)/\Gamma_{\text{total}}$   $\Gamma_{408}/\Gamma$ 

VALUE (units $10^{-6}$ )	CL%	DOCUMENT ID	TECN	COMMENT
<b><math>4.78^{+0.67}_{-0.64} \pm 0.60</math></b>		<sup>1</sup> CHEN	09c	BELL $e^+e^- \rightarrow \Upsilon(4S)$

<sup>1</sup> Assumes equal production of  $B^+$  and  $B^0$  at the  $\Upsilon(4S)$ .

 $\Gamma(\rho\bar{\Lambda}\eta(1270))/\Gamma_{\text{total}}$   $\Gamma_{409}/\Gamma$ 

VALUE (units $10^{-6}$ )	CL%	DOCUMENT ID	TECN	COMMENT
<b><math>2.03^{+0.77}_{-0.72} \pm 0.27</math></b>		<sup>1</sup> CHEN	09c	BELL $e^+e^- \rightarrow \Upsilon(4S)$

<sup>1</sup> Assumes equal production of  $B^+$  and  $B^0$  at the  $\Upsilon(4S)$ .

 $\Gamma(\Lambda\bar{\Lambda}\pi^+)/\Gamma_{\text{total}}$   $\Gamma_{410}/\Gamma$ 

VALUE (units $10^{-6}$ )	CL%	DOCUMENT ID	TECN	COMMENT
<b>&lt;0.94</b>	90	<sup>1,2</sup> CHANG	09	BELL Repl. by CHANG 09
••• We do not use the following data for averages, fits, limits, etc. •••				
<2.8	90	<sup>2</sup> LEE	04	BELL $e^+e^- \rightarrow \Upsilon(4S)$

<sup>1</sup> For  $m_{\Lambda\bar{\Lambda}} < 2.85$  GeV/ $c^2$ .

<sup>2</sup> Assumes equal production of  $B^+$  and  $B^0$  at the  $\Upsilon(4S)$ .

 $\Gamma(\Lambda\bar{\Lambda}K^+)/\Gamma_{\text{total}}$   $\Gamma_{411}/\Gamma$ 

VALUE (units $10^{-6}$ )	CL%	DOCUMENT ID	TECN	COMMENT
<b><math>3.38^{+0.41}_{-0.36} \pm 0.41</math></b>		<sup>1,2</sup> CHANG	09	BELL $e^+e^- \rightarrow \Upsilon(4S)$
••• We do not use the following data for averages, fits, limits, etc. •••				
$2.91^{+0.9}_{-0.70} \pm 0.38$		<sup>2</sup> LEE	04	BELL Repl. by CHANG 09

<sup>1</sup> Excluding charmonium events in  $2.85 < m_{\Lambda\bar{\Lambda}} < 3.128$  GeV/ $c^2$  and  $3.315 < m_{\Lambda\bar{\Lambda}} < 3.735$  GeV/ $c^2$ . Measurements in various  $m_{\Lambda\bar{\Lambda}}$  bins are also reported.

<sup>2</sup> Assumes equal production of  $B^+$  and  $B^0$  at the  $\Upsilon(4S)$ .

 $\Gamma(\Lambda\bar{\Lambda}K^{*+})/\Gamma_{\text{total}}$   $\Gamma_{412}/\Gamma$ 

VALUE (units $10^{-6}$ )	CL%	DOCUMENT ID	TECN	COMMENT
<b><math>2.19^{+1.13}_{-0.88} \pm 0.33</math></b>		<sup>1,2</sup> CHANG	09	BELL $e^+e^- \rightarrow \Upsilon(4S)$

<sup>1</sup> For  $m_{\Lambda\bar{\Lambda}} < 2.85$  GeV/ $c^2$ .

<sup>2</sup> Assumes equal production of  $B^+$  and  $B^0$  at the  $\Upsilon(4S)$ .

 $\Gamma(\Delta^0\bar{p})/\Gamma_{\text{total}}$   $\Gamma_{413}/\Gamma$ 

VALUE (units $10^{-6}$ )	CL%	DOCUMENT ID	TECN	COMMENT
<b>&lt; 1.38</b>	90	<sup>1</sup> WEI	08	BELL $e^+e^- \rightarrow \Upsilon(4S)$
••• We do not use the following data for averages, fits, limits, etc. •••				
<380	90	<sup>2</sup> BORTOLETTO	089	CLEO $e^+e^- \rightarrow \Upsilon(4S)$

<sup>1</sup> Assumes equal production of  $B^+$  and  $B^0$  at the  $\Upsilon(4S)$ .

<sup>2</sup> BORTOLETTO 89 reports  $< 3.3 \times 10^{-4}$  assuming the  $\Upsilon(4S)$  decays 43% to  $B^0\bar{B}^0$ . We rescale to 50%.

 $\Gamma(\Delta^{++}\bar{p})/\Gamma_{\text{total}}$   $\Gamma_{414}/\Gamma$ 

VALUE (units $10^{-6}$ )	CL%	DOCUMENT ID	TECN	COMMENT
<b>&lt; 0.14</b>	90	<sup>1</sup> WEI	08	BELL $e^+e^- \rightarrow \Upsilon(4S)$
••• We do not use the following data for averages, fits, limits, etc. •••				
<150	90	<sup>2</sup> BORTOLETTO	089	CLEO $e^+e^- \rightarrow \Upsilon(4S)$

<sup>1</sup> Assumes equal production of  $B^+$  and  $B^0$  at the  $\Upsilon(4S)$ .

<sup>2</sup> BORTOLETTO 89 reports  $< 1.3 \times 10^{-4}$  assuming the  $\Upsilon(4S)$  decays 43% to  $B^0\bar{B}^0$ . We rescale to 50%.

 $\Gamma(D^+\rho\bar{p})/\Gamma_{\text{total}}$   $\Gamma_{415}/\Gamma$ 

VALUE	CL%	DOCUMENT ID	TECN	COMMENT
<b>&lt; <math>1.5 \times 10^{-5}</math></b>	90	<sup>1</sup> ABE	02W	BELL $e^+e^- \rightarrow \Upsilon(4S)$

<sup>1</sup> Assumes equal production of  $B^+$  and  $B^0$  at the  $\Upsilon(4S)$ .

 $\Gamma(D^*(2010)^+\rho\bar{p})/\Gamma_{\text{total}}$   $\Gamma_{416}/\Gamma$ 

VALUE	CL%	DOCUMENT ID	TECN	COMMENT
<b>&lt; <math>1.5 \times 10^{-5}</math></b>	90	<sup>1</sup> ABE	02W	BELL $e^+e^- \rightarrow \Upsilon(4S)$

<sup>1</sup> Assumes equal production of  $B^+$  and  $B^0$  at the  $\Upsilon(4S)$ .

 $\Gamma(\rho\bar{\Lambda}^0\bar{D}^0)/\Gamma_{\text{total}}$   $\Gamma_{417}/\Gamma$ 

VALUE (units $10^{-5}$ )	CL%	DOCUMENT ID	TECN	COMMENT
<b><math>1.43^{+0.28}_{-0.25} \pm 0.18</math></b>		<sup>1,2</sup> CHEN	11F	BELL $e^+e^- \rightarrow \Upsilon(4S)$

<sup>1</sup> Uses  $B(\Lambda \rightarrow p\pi^-) = 63.9 \pm 0.5\%$ ,  $B(D^0 \rightarrow K^-\pi^+) = 3.89 \pm 0.05\%$ , and  $B(D^0 \rightarrow K^-\pi^+\pi^0) = 13.9 \pm 0.5\%$ .

<sup>2</sup> Assumes equal production of  $B^0$  and  $B^+$  from Upsilon(4S) decays.

 $\Gamma(\rho\bar{\Lambda}^0\bar{D}^*(2007)^0)/\Gamma_{\text{total}}$   $\Gamma_{418}/\Gamma$ 

VALUE (units $10^{-5}$ )	CL%	DOCUMENT ID	TECN	COMMENT
<b>&lt;5</b>	90	<sup>1,2,3</sup> CHEN	11F	BELL $e^+e^- \rightarrow \Upsilon(4S)$

<sup>1</sup> CHEN 11F reports  $< 4.8 \times 10^{-5}$  from a measurement of  $[\Gamma(B^+ \rightarrow \rho\bar{\Lambda}^0\bar{D}^*(2007)^0)/\Gamma_{\text{total}}] / [B(D^*(2007)^0 \rightarrow D^0\pi^0)]$  assuming  $B(D^*(2007)^0 \rightarrow D^0\pi^0) = (61.9 \pm 2.9) \times 10^{-2}$ .

<sup>2</sup> Uses  $B(\Lambda \rightarrow p\pi^-) = 63.9 \pm 0.5\%$  and  $B(D^0 \rightarrow K^-\pi^+) = 3.89 \pm 0.05\%$ .

<sup>3</sup> Assumes equal production of  $B^0$  and  $B^+$  from Upsilon(4S) decays.

 $\Gamma(\bar{\Lambda}_c^- p\pi^+)/\Gamma_{\text{total}}$   $\Gamma_{419}/\Gamma$ 

VALUE (units $10^{-4}$ )	DOCUMENT ID	TECN	COMMENT
<b><math>2.8 \pm 0.8</math> OUR AVERAGE</b>			
$3.4 \pm 0.1 \pm 0.9$	<sup>1,2</sup> AUBERT	08BN	BABR $e^+e^- \rightarrow \Upsilon(4S)$
$2.0 \pm 0.3 \pm 0.5$	<sup>1,3</sup> GABYSHEV	06A	BELL $e^+e^- \rightarrow \Upsilon(4S)$
$2.4 \pm 0.6 \pm 0.6$	<sup>1,4</sup> DYTMAN	02	CLE2 $e^+e^- \rightarrow \Upsilon(4S)$
••• We do not use the following data for averages, fits, limits, etc. •••			
$1.9 \pm 0.5 \pm 0.5$	<sup>1,5</sup> GABYSHEV	02	BELL Repl. by GABYSHEV 06A
$6.2^{+2.3}_{-2.0} \pm 1.6$	<sup>1,6</sup> FU	97	CLE2 Repl. by DYTMAN 02

<sup>1</sup> Assumes equal production of  $B^+$  and  $B^0$  at the  $\Upsilon(4S)$ .

<sup>2</sup> AUBERT 08BN reports  $(3.4 \pm 0.1 \pm 0.9) \times 10^{-4}$  from a measurement of  $[\Gamma(B^+ \rightarrow \bar{A}_C^- \rho \pi^+)/\Gamma_{\text{total}}] \times [B(\Lambda_C^+ \rightarrow p K^- \pi^+)]$  assuming  $B(\Lambda_C^+ \rightarrow p K^- \pi^+) = (5.0 \pm 1.3) \times 10^{-2}$ .

<sup>3</sup> GABYSHEV 06A reports  $(2.01 \pm 0.15 \pm 0.20) \times 10^{-4}$  from a measurement of  $[\Gamma(B^+ \rightarrow \bar{A}_C^- \rho \pi^+)/\Gamma_{\text{total}}] \times [B(\Lambda_C^+ \rightarrow p K^- \pi^+)]$  assuming  $B(\Lambda_C^+ \rightarrow p K^- \pi^+) = 0.05$ , which we rescale to our best value  $B(\Lambda_C^+ \rightarrow p K^- \pi^+) = (5.0 \pm 1.3) \times 10^{-2}$ . Our first error is their experiment's error and our second error is the systematic error from using our best value.

<sup>4</sup> DYTMAN 02 reports  $(2.4 \pm 0.63 \pm 0.62) \times 10^{-4}$  from a measurement of  $[\Gamma(B^+ \rightarrow \bar{A}_C^- \rho \pi^+)/\Gamma_{\text{total}}] \times [B(\Lambda_C^+ \rightarrow p K^- \pi^+)]$  assuming  $B(\Lambda_C^+ \rightarrow p K^- \pi^+) = 0.05$ , which we rescale to our best value  $B(\Lambda_C^+ \rightarrow p K^- \pi^+) = (5.0 \pm 1.3) \times 10^{-2}$ . Our first error is their experiment's error and our second error is the systematic error from using our best value.

<sup>5</sup> GABYSHEV 02 reports  $(1.87 \pm 0.51 \pm 0.49) \times 10^{-4}$  from a measurement of  $[\Gamma(B^+ \rightarrow \bar{A}_C^- \rho \pi^+)/\Gamma_{\text{total}}] \times [B(\Lambda_C^+ \rightarrow p K^- \pi^+)]$  assuming  $B(\Lambda_C^+ \rightarrow p K^- \pi^+) = 0.05$ , which we rescale to our best value  $B(\Lambda_C^+ \rightarrow p K^- \pi^+) = (5.0 \pm 1.3) \times 10^{-2}$ . Our first error is their experiment's error and our second error is the systematic error from using our best value.

<sup>6</sup> FU 97 uses PDG 96 values of  $\Lambda_C$  branching fraction.

$\Gamma(\bar{A}_C^- \Delta(1232)^+)/\Gamma_{\text{total}}$		$\Gamma_{420}/\Gamma$		
VALUE (units $10^{-5}$ )	CL%	DOCUMENT ID	TECN	COMMENT
<1.9	90	GABYSHEV	06A	BELL $e^+ e^- \rightarrow \Upsilon(4S)$

$\Gamma(\bar{A}_C^- \Delta_X(1600)^+)/\Gamma_{\text{total}}$		$\Gamma_{421}/\Gamma$		
VALUE (units $10^{-5}$ )	CL%	DOCUMENT ID	TECN	COMMENT
<b>5.9 ± 1.2 ± 1.5</b>		1 GABYSHEV	06A	BELL $e^+ e^- \rightarrow \Upsilon(4S)$

<sup>1</sup> GABYSHEV 06A reports  $(5.9 \pm 1.0 \pm 0.6) \times 10^{-5}$  from a measurement of  $[\Gamma(B^+ \rightarrow \bar{A}_C^- \Delta_X(1600)^+)/\Gamma_{\text{total}}] \times [B(\Lambda_C^+ \rightarrow p K^- \pi^+)]$  assuming  $B(\Lambda_C^+ \rightarrow p K^- \pi^+) = 0.05$ , which we rescale to our best value  $B(\Lambda_C^+ \rightarrow p K^- \pi^+) = (5.0 \pm 1.3) \times 10^{-2}$ . Our first error is their experiment's error and our second error is the systematic error from using our best value.

$\Gamma(\bar{A}_C^- \Delta_X(2420)^+)/\Gamma_{\text{total}}$		$\Gamma_{422}/\Gamma$		
VALUE (units $10^{-5}$ )	CL%	DOCUMENT ID	TECN	COMMENT
<b>4.7 ± 1.1 ± 1.0 ± 1.2</b>		1 GABYSHEV	06A	BELL $e^+ e^- \rightarrow \Upsilon(4S)$

<sup>1</sup> GABYSHEV 06A reports  $(4.7 \pm 1.0 \pm 0.9 \pm 0.4) \times 10^{-5}$  from a measurement of  $[\Gamma(B^+ \rightarrow \bar{A}_C^- \Delta_X(2420)^+)/\Gamma_{\text{total}}] \times [B(\Lambda_C^+ \rightarrow p K^- \pi^+)]$  assuming  $B(\Lambda_C^+ \rightarrow p K^- \pi^+) = 0.05$ , which we rescale to our best value  $B(\Lambda_C^+ \rightarrow p K^- \pi^+) = (5.0 \pm 1.3) \times 10^{-2}$ . Our first error is their experiment's error and our second error is the systematic error from using our best value.

$\Gamma(\bar{A}_C^- \rho_s \pi^+)/\Gamma_{\text{total}}$		$\Gamma_{423}/\Gamma$		
VALUE (units $10^{-5}$ )	CL%	DOCUMENT ID	TECN	COMMENT
<b>3.9 ± 0.9 ± 0.8 ± 1.0</b>		1 GABYSHEV	06A	BELL $e^+ e^- \rightarrow \Upsilon(4S)$

<sup>1</sup> GABYSHEV 06A reports  $(3.9 \pm 0.8 \pm 0.7 \pm 0.4) \times 10^{-5}$  from a measurement of  $[\Gamma(B^+ \rightarrow \bar{A}_C^- \rho_s \pi^+)/\Gamma_{\text{total}}] \times [B(\Lambda_C^+ \rightarrow p K^- \pi^+)]$  assuming  $B(\Lambda_C^+ \rightarrow p K^- \pi^+) = 0.05$ , which we rescale to our best value  $B(\Lambda_C^+ \rightarrow p K^- \pi^+) = (5.0 \pm 1.3) \times 10^{-2}$ . Our first error is their experiment's error and our second error is the systematic error from using our best value.

$\Gamma(\bar{\Sigma}_C(2520)^0 \rho)/\Gamma_{\text{total}}$		$\Gamma_{424}/\Gamma$		
VALUE (units $10^{-5}$ )	CL%	DOCUMENT ID	TECN	COMMENT
<0.3	90	1,2 AUBERT	08BN	BABR $e^+ e^- \rightarrow \Upsilon(4S)$
••• We do not use the following data for averages, fits, limits, etc. •••				
<2.7	90	1,2 GABYSHEV	06A	BELL $e^+ e^- \rightarrow \Upsilon(4S)$
<4.6	90	1,2 GABYSHEV	02	BELL Repl. by GABYSHEV 06A

<sup>1</sup> Assumes equal production of  $B^+$  and  $B^0$  at the  $\Upsilon(4S)$ .

<sup>2</sup> Uses the value for  $\Lambda_C \rightarrow p K^- \pi^+$  branching ratio  $(5.0 \pm 1.3)\%$ .

$\Gamma(\bar{\Sigma}_C(2520)^0 \rho)/\Gamma(\bar{A}_C^- \rho \pi^+)$		$\Gamma_{424}/\Gamma_{419}$		
VALUE (units $10^{-3}$ )	CL%	DOCUMENT ID	TECN	COMMENT
<9	90	AUBERT	08BN	BABR $e^+ e^- \rightarrow \Upsilon(4S)$

$\Gamma(\bar{\Sigma}_C(2800)^0 \rho)/\Gamma_{\text{total}}$		$\Gamma_{425}/\Gamma$		
VALUE (units $10^{-5}$ )	CL%	DOCUMENT ID	TECN	COMMENT
<b>3.3 ± 0.9 ± 0.9</b>		1 AUBERT	08BN	BABR $e^+ e^- \rightarrow \Upsilon(4S)$

<sup>1</sup> AUBERT 08BN reports  $[\Gamma(B^+ \rightarrow \bar{\Sigma}_C(2800)^0 \rho)/\Gamma_{\text{total}}] / [B(B^+ \rightarrow \bar{A}_C^- \rho \pi^+)] = 0.117 \pm 0.023 \pm 0.024$  which we multiply by our best value  $B(B^+ \rightarrow \bar{A}_C^- \rho \pi^+) = (2.8 \pm 0.8) \times 10^{-4}$ . Our first error is their experiment's error and our second error is the systematic error from using our best value.

$\Gamma(\bar{A}_C^- \rho \pi^+ \pi^0)/\Gamma_{\text{total}}$		$\Gamma_{426}/\Gamma$		
VALUE (units $10^{-3}$ )	CL%	DOCUMENT ID	TECN	COMMENT
<b>1.81 ± 0.29 ± 0.52 ± 0.50</b>		1,2 DYTMAN	02	CLE2 $e^+ e^- \rightarrow \Upsilon(4S)$

••• We do not use the following data for averages, fits, limits, etc. •••

<3.12 90 <sup>3</sup>FU 97 CLE2  $e^+ e^- \rightarrow \Upsilon(4S)$

<sup>1</sup> Assumes equal production of  $B^+$  and  $B^0$  at the  $\Upsilon(4S)$ .

<sup>2</sup> DYTMAN 02 measurement uses  $B(\Lambda_C^+ \rightarrow \bar{p} K^+ \pi^-) = 5.0 \pm 1.3\%$ . The second error includes the systematic and the uncertainty of the branching ratio.

<sup>3</sup> FU 97 uses PDG 96 values of  $\Lambda_C$  branching ratio.

$\Gamma(\bar{A}_C^- \rho \pi^+ \pi^+ \pi^-)/\Gamma_{\text{total}}$		$\Gamma_{427}/\Gamma$		
VALUE (units $10^{-3}$ )	CL%	DOCUMENT ID	TECN	COMMENT
<b>2.25 ± 0.25 ± 0.63 ± 0.61</b>		1,2 DYTMAN	02	CLE2 $e^+ e^- \rightarrow \Upsilon(4S)$

••• We do not use the following data for averages, fits, limits, etc. •••

<1.46 90 <sup>3</sup>FU 97 CLE2  $e^+ e^- \rightarrow \Upsilon(4S)$

<sup>1</sup> Assumes equal production of  $B^+$  and  $B^0$  at the  $\Upsilon(4S)$ .

<sup>2</sup> DYTMAN 02 measurement uses  $B(\Lambda_C^+ \rightarrow \bar{p} K^+ \pi^-) = 5.0 \pm 1.3\%$ . The second error includes the systematic and the uncertainty of the branching ratio.

<sup>3</sup> FU 97 uses PDG 96 values of  $\Lambda_C$  branching ratio.

$\Gamma(\bar{A}_C^- \rho \pi^+ \pi^+ \pi^- \pi^0)/\Gamma_{\text{total}}$		$\Gamma_{428}/\Gamma$		
VALUE	CL%	DOCUMENT ID	TECN	COMMENT
<1.34 × 10 <sup>-2</sup>	90	1 FU	97	CLE2 $e^+ e^- \rightarrow \Upsilon(4S)$

<sup>1</sup> FU 97 uses PDG 96 values of  $\Lambda_C$  branching ratio.

$\Gamma(\Lambda_C^+ \Lambda_C^- K^+)/\Gamma_{\text{total}}$		$\Gamma_{429}/\Gamma$		
VALUE (units $10^{-4}$ )	CL%	DOCUMENT ID	TECN	COMMENT
<b>8.7 ± 3.5 OUR AVERAGE</b>				
11 ± 1 ± 6		1,2 AUBERT	08H	BABR $e^+ e^- \rightarrow \Upsilon(4S)$
8 ± 1 ± 4		2,3 GABYSHEV	06	BELL $e^+ e^- \rightarrow \Upsilon(4S)$

<sup>1</sup> AUBERT 08H reports  $(1.14 \pm 0.15 \pm 0.62) \times 10^{-3}$  from a measurement of  $[\Gamma(B^+ \rightarrow \Lambda_C^+ \Lambda_C^- K^+)/\Gamma_{\text{total}}] \times [B(\Lambda_C^+ \rightarrow p K^- \pi^+)]$  assuming  $B(\Lambda_C^+ \rightarrow p K^- \pi^+) = (5.0 \pm 1.3) \times 10^{-2}$ .

<sup>2</sup> Assumes equal production of  $B^+$  and  $B^0$  at the  $\Upsilon(4S)$ .

<sup>3</sup> GABYSHEV 06 reports  $(7.9 \pm 1.0 \pm 0.9 \pm 3.6) \times 10^{-4}$  from a measurement of  $[\Gamma(B^+ \rightarrow \Lambda_C^+ \Lambda_C^- K^+)/\Gamma_{\text{total}}] \times [B(\Lambda_C^+ \rightarrow p K^- \pi^+)]$  assuming  $B(\Lambda_C^+ \rightarrow p K^- \pi^+) = (5.0 \pm 1.3) \times 10^{-2}$ .

$\Gamma(\bar{\Sigma}_C(2455)^0 \rho)/\Gamma_{\text{total}}$		$\Gamma_{430}/\Gamma$		
VALUE (units $10^{-5}$ )	CL%	DOCUMENT ID	TECN	COMMENT
<b>3.7 ± 0.8 ± 1.0</b>		1,2 GABYSHEV	06A	BELL $e^+ e^- \rightarrow \Upsilon(4S)$

••• We do not use the following data for averages, fits, limits, etc. •••

<8 90 <sup>1,3</sup>DYTMAN 02 CLE2  $e^+ e^- \rightarrow \Upsilon(4S)$

<9.3 90 <sup>1,4</sup>GABYSHEV 02 BELL Repl. by GABYSHEV 06A

<sup>1</sup> Assumes equal production of  $B^+$  and  $B^0$  at the  $\Upsilon(4S)$ .

<sup>2</sup> GABYSHEV 06A reports  $(3.7 \pm 0.7 \pm 0.4) \times 10^{-5}$  from a measurement of  $[\Gamma(B^+ \rightarrow \bar{\Sigma}_C(2455)^0 \rho)/\Gamma_{\text{total}}] \times [B(\Lambda_C^+ \rightarrow p K^- \pi^+)]$  assuming  $B(\Lambda_C^+ \rightarrow p K^- \pi^+) = 0.05$ , which we rescale to our best value  $B(\Lambda_C^+ \rightarrow p K^- \pi^+) = (5.0 \pm 1.3) \times 10^{-2}$ . Our first error is their experiment's error and our second error is the systematic error from using our best value.

<sup>3</sup> DYTMAN 02 measurement uses  $B(\Lambda_C^+ \rightarrow \bar{p} K^+ \pi^-) = 5.0 \pm 1.3\%$ . The second error includes the systematic and the uncertainty of the branching ratio.

<sup>4</sup> Uses the value for  $\Lambda_C \rightarrow p K^- \pi^+$  branching ratio  $(5.0 \pm 1.3)\%$ .

$\Gamma(\bar{\Sigma}_C(2455)^0 \rho)/\Gamma(\bar{A}_C^- \rho \pi^+)$		$\Gamma_{430}/\Gamma_{419}$		
VALUE	CL%	DOCUMENT ID	TECN	COMMENT
<b>0.123 ± 0.012 ± 0.008</b>		1 AUBERT	08BN	BABR $e^+ e^- \rightarrow \Upsilon(4S)$

<sup>1</sup> Assumes equal production of  $B^+$  and  $B^0$  at the  $\Upsilon(4S)$ .

$\Gamma(\bar{\Sigma}_C(2455)^0 \rho \pi^0)/\Gamma_{\text{total}}$		$\Gamma_{431}/\Gamma$		
VALUE (units $10^{-4}$ )	CL%	DOCUMENT ID	TECN	COMMENT
<b>4.4 ± 1.4 ± 1.1</b>		1,2 DYTMAN	02	CLE2 $e^+ e^- \rightarrow \Upsilon(4S)$

<sup>1</sup> DYTMAN 02 reports  $(4.4 \pm 1.4) \times 10^{-4}$  from a measurement of  $[\Gamma(B^+ \rightarrow \bar{\Sigma}_C(2455)^0 \rho \pi^0)/\Gamma_{\text{total}}] \times [B(\Lambda_C^+ \rightarrow p K^- \pi^+)]$  assuming  $B(\Lambda_C^+ \rightarrow p K^- \pi^+) = 0.05$ , which we rescale to our best value  $B(\Lambda_C^+ \rightarrow p K^- \pi^+) = (5.0 \pm 1.3) \times 10^{-2}$ . Our first error is their experiment's error and our second error is the systematic error from using our best value.

<sup>2</sup> Assumes equal production of  $B^+$  and  $B^0$  at the  $\Upsilon(4S)$ .

$\Gamma(\bar{\Sigma}_C(2455)^0 \rho \pi^- \pi^+)/\Gamma_{\text{total}}$		$\Gamma_{432}/\Gamma$		
VALUE (units $10^{-4}$ )	CL%	DOCUMENT ID	TECN	COMMENT
<b>4.4 ± 1.3 ± 1.1</b>		1,2 DYTMAN	02	CLE2 $e^+ e^- \rightarrow \Upsilon(4S)$

<sup>1</sup> DYTMAN 02 reports  $(4.4 \pm 1.3) \times 10^{-4}$  from a measurement of  $[\Gamma(B^+ \rightarrow \bar{\Sigma}_C(2455)^0 \rho \pi^- \pi^+)/\Gamma_{\text{total}}] \times [B(\Lambda_C^+ \rightarrow p K^- \pi^+)]$  assuming  $B(\Lambda_C^+ \rightarrow p K^- \pi^+) = 0.05$ , which we rescale to our best value  $B(\Lambda_C^+ \rightarrow p K^- \pi^+) = (5.0 \pm 1.3) \times 10^{-2}$ . Our first error is their experiment's error and our second error is the systematic error from using our best value.

<sup>2</sup> Assumes equal production of  $B^+$  and  $B^0$  at the  $\Upsilon(4S)$ .

## Meson Particle Listings

 $B^\pm$  $\Gamma(\Sigma_c(2455)^{--} p \pi^+ \pi^+)/\Gamma_{\text{total}}$   $\Gamma_{433}/\Gamma$ 

VALUE (units $10^{-4}$ )	DOCUMENT ID	TECN	COMMENT
$2.8 \pm 1.0 \pm 0.7$	1,2 DYTMAN	02	CLE2 $e^+e^- \rightarrow \Upsilon(4S)$

- <sup>1</sup>DYTMAN 02 reports  $(2.8 \pm 1.0) \times 10^{-4}$  from a measurement of  $[\Gamma(B^+ \rightarrow \Sigma_c(2455)^{--} p \pi^+ \pi^+)/\Gamma_{\text{total}}] \times [B(\Lambda_c^+ \rightarrow p K^- \pi^+)]$  assuming  $B(\Lambda_c^+ \rightarrow p K^- \pi^+) = 0.05$ , which we rescale to our best value  $B(\Lambda_c^+ \rightarrow p K^- \pi^+) = (5.0 \pm 1.3) \times 10^{-2}$ . Our first error is their experiment's error and our second error is the systematic error from using our best value.
- <sup>2</sup>Assumes equal production of  $B^+$  and  $B^0$  at the  $\Upsilon(4S)$ .

 $\Gamma(\Lambda_c(2593)^- \bar{\Lambda}_c(2625)^- p \pi^+)/\Gamma_{\text{total}}$   $\Gamma_{434}/\Gamma$ 

VALUE	CL%	DOCUMENT ID	TECN	COMMENT
$< 1.9 \times 10^{-4}$	90	1,2 DYTMAN	02	CLE2 $e^+e^- \rightarrow \Upsilon(4S)$

- <sup>1</sup>Assumes equal production of  $B^+$  and  $B^0$  at the  $\Upsilon(4S)$ .
- <sup>2</sup>DYTMAN 02 measurement uses  $B(\Lambda_c^- \rightarrow \bar{p} K^+ \pi^-) = 5.0 \pm 1.3\%$ . The second error includes the systematic and the uncertainty of the branching ratio.

 $\Gamma(\Xi_c^0 \Lambda_c^+ \times B(\Xi_c^0 \rightarrow \Xi^+ \pi^-))/\Gamma_{\text{total}}$   $\Gamma_{435}/\Gamma$ 

VALUE (units $10^{-5}$ )	DOCUMENT ID	TECN	COMMENT
<b><math>3.0 \pm 1.1</math> OUR AVERAGE</b>			

$2.5 \pm 0.9 \pm 0.6$	1,2 AUBERT	08H	BABR $e^+e^- \rightarrow \Upsilon(4S)$
$5.6^{+1.9}_{-1.5} \pm 1.9$	2,3 CHISTOV	06A	BELL $e^+e^- \rightarrow \Upsilon(4S)$

- <sup>1</sup>AUBERT 08H reports  $(2.51 \pm 0.89 \pm 0.61) \times 10^{-5}$  from a measurement of  $[\Gamma(B^+ \rightarrow \Xi_c^0 \Lambda_c^+ \times B(\Xi_c^0 \rightarrow \Xi^+ \pi^-))/\Gamma_{\text{total}}] \times [B(\Lambda_c^+ \rightarrow p K^- \pi^+)]$  assuming  $B(\Lambda_c^+ \rightarrow p K^- \pi^+) = (5.0 \pm 1.3) \times 10^{-2}$ .
- <sup>2</sup>Assumes equal production of  $B^+$  and  $B^0$  at the  $\Upsilon(4S)$ .
- <sup>3</sup>CHISTOV 06A reports  $(5.6^{+1.9}_{-1.5} \pm 1.9) \times 10^{-5}$  from a measurement of  $[\Gamma(B^+ \rightarrow \Xi_c^0 \Lambda_c^+ \times B(\Xi_c^0 \rightarrow \Xi^+ \pi^-))/\Gamma_{\text{total}}] \times [B(\Lambda_c^+ \rightarrow p K^- \pi^+)]$  assuming  $B(\Lambda_c^+ \rightarrow p K^- \pi^+) = (5.0 \pm 1.3) \times 10^{-2}$ .

 $\Gamma(\Xi_c^0 \Lambda_c^+ \times B(\Xi_c^0 \rightarrow \Lambda K^+ \pi^-))/\Gamma_{\text{total}}$   $\Gamma_{436}/\Gamma$ 

VALUE (units $10^{-5}$ )	DOCUMENT ID	TECN	COMMENT
<b><math>2.6 \pm 1.1</math> OUR AVERAGE</b>	Error includes scale factor of 1.1.		

$1.7 \pm 0.9 \pm 0.5$	1,2 AUBERT	08H	BABR $e^+e^- \rightarrow \Upsilon(4S)$
$4.0^{+1.1}_{-0.9} \pm 1.3$	2,3 CHISTOV	06A	BELL $e^+e^- \rightarrow \Upsilon(4S)$

- <sup>1</sup>AUBERT 08H reports  $(1.70 \pm 0.93 \pm 0.53) \times 10^{-5}$  from a measurement of  $[\Gamma(B^+ \rightarrow \Xi_c^0 \Lambda_c^+ \times B(\Xi_c^0 \rightarrow \Lambda K^+ \pi^-))/\Gamma_{\text{total}}] \times [B(\Lambda_c^+ \rightarrow p K^- \pi^+)]$  assuming  $B(\Lambda_c^+ \rightarrow p K^- \pi^+) = (5.0 \pm 1.3) \times 10^{-2}$ .
- <sup>2</sup>Assumes equal production of  $B^+$  and  $B^0$  at the  $\Upsilon(4S)$ .
- <sup>3</sup>CHISTOV 06A reports  $(4.0^{+1.1}_{-0.9} \pm 1.3) \times 10^{-5}$  from a measurement of  $[\Gamma(B^+ \rightarrow \Xi_c^0 \Lambda_c^+ \times B(\Xi_c^0 \rightarrow \Lambda K^+ \pi^-))/\Gamma_{\text{total}}] \times [B(\Lambda_c^+ \rightarrow p K^- \pi^+)]$  assuming  $B(\Lambda_c^+ \rightarrow p K^- \pi^+) = (5.0 \pm 1.3) \times 10^{-2}$ .

 $\Gamma(\pi^+ \ell^+ \ell^-)/\Gamma_{\text{total}}$   $\Gamma_{437}/\Gamma$ 

VALUE	CL%	DOCUMENT ID	TECN	COMMENT
$< 4.9 \times 10^{-8}$	90	1 WEI	08A	BELL $e^+e^- \rightarrow \Upsilon(4S)$

- • • We do not use the following data for averages, fits, limits, etc. • • •
- |                        |    |          |      |  |
|------------------------|----|----------|------|--|
| $< 1.2 \times 10^{-7}$ | 90 | 1 AUBERT | 07AG | BABR $e^+e^- \rightarrow \Upsilon(4S)$ |
|------------------------|----|----------|------|--|

<sup>1</sup>Assumes equal production of  $B^+$  and  $B^0$  at the  $\Upsilon(4S)$ .

 $\Gamma(\pi^+ e^+ e^-)/\Gamma_{\text{total}}$   $\Gamma_{438}/\Gamma$ 

VALUE	CL%	DOCUMENT ID	TECN	COMMENT
$< 8.0 \times 10^{-8}$	90	1 WEI	08A	BELL $e^+e^- \rightarrow \Upsilon(4S)$

- • • We do not use the following data for averages, fits, limits, etc. • • •
- |                        |    |          |      |  |
|------------------------|----|----------|------|--|
| $< 1.8 \times 10^{-7}$ | 90 | 1 AUBERT | 07AG | BABR $e^+e^- \rightarrow \Upsilon(4S)$ |
| $< 3.9 \times 10^{-3}$ | 90 | 2 WEIR   | 90B  | MRK2 $e^+e^-$ 29 GeV                   |

- <sup>1</sup>Assumes equal production of  $B^+$  and  $B^0$  at the  $\Upsilon(4S)$ .
- <sup>2</sup>WEIR 90B assumes  $B^+$  production cross section from LUND.

 $\Gamma(\pi^+ \mu^+ \mu^-)/\Gamma_{\text{total}}$   $\Gamma_{439}/\Gamma$ 

VALUE	CL%	DOCUMENT ID	TECN	COMMENT
$< 6.9 \times 10^{-8}$	90	1 WEI	08A	BELL $e^+e^- \rightarrow \Upsilon(4S)$

- • • We do not use the following data for averages, fits, limits, etc. • • •
- |                        |    |          |      |  |
|------------------------|----|----------|------|--|
| $< 2.8 \times 10^{-7}$ | 90 | 1 AUBERT | 07AG | BABR $e^+e^- \rightarrow \Upsilon(4S)$ |
| $< 9.1 \times 10^{-3}$ | 90 | 2 WEIR   | 90B  | MRK2 $e^+e^-$ 29 GeV                   |

- <sup>1</sup>Assumes equal production of  $B^+$  and  $B^0$  at the  $\Upsilon(4S)$ .
- <sup>2</sup>WEIR 90B assumes  $B^+$  production cross section from LUND.

 $\Gamma(\pi^+ \nu \bar{\nu})/\Gamma_{\text{total}}$   $\Gamma_{440}/\Gamma$ 

VALUE	CL%	DOCUMENT ID	TECN	COMMENT
$< 1.0 \times 10^{-4}$	90	1 AUBERT	05H	BABR $e^+e^- \rightarrow \Upsilon(4S)$

- • • We do not use the following data for averages, fits, limits, etc. • • •
- |                        |    |        |     |  |
|------------------------|----|--------|-----|--|
| $< 1.7 \times 10^{-4}$ | 90 | 1 CHEN | 07D | BELL $e^+e^- \rightarrow \Upsilon(4S)$ |
|------------------------|----|--------|-----|--|

<sup>1</sup>Assumes equal production of  $B^+$  and  $B^0$  at the  $\Upsilon(4S)$ .

 $\Gamma(K^+ \ell^+ \ell^-)/\Gamma_{\text{total}}$   $\Gamma_{441}/\Gamma$ 

VALUE (units $10^{-7}$ )	DOCUMENT ID	TECN	COMMENT
<b><math>5.1 \pm 0.5</math> OUR AVERAGE</b>			

$4.8 \pm 0.9 \pm 0.2$	1 AUBERT	09T	BABR $e^+e^- \rightarrow \Upsilon(4S)$
$5.3^{+0.6}_{-0.5} \pm 0.3$	1 WEI	09A	BELL $e^+e^- \rightarrow \Upsilon(4S)$

- • • We do not use the following data for averages, fits, limits, etc. • • •

$3.8^{+0.9}_{-0.8} \pm 0.2$	1 AUBERT,B	06J	BABR Repl. by AUBERT 09T
$5.3^{+1.1}_{-1.0} \pm 0.3$	1 ISHIKAWA	03	BELL Repl. by WEI 09A

- <sup>1</sup>Assumes equal production of  $B^+$  and  $B^0$  at the  $\Upsilon(4S)$ .

 $\Gamma(K^+ e^+ e^-)/\Gamma_{\text{total}}$   $\Gamma_{442}/\Gamma$ 

VALUE (units $10^{-7}$ )	CL%	DOCUMENT ID	TECN	COMMENT
<b><math>5.5 \pm 0.7</math> OUR AVERAGE</b>				

$5.1^{+1.2}_{-1.1} \pm 0.2$	1 AUBERT	09T	BABR $e^+e^- \rightarrow \Upsilon(4S)$
$5.7^{+0.9}_{-0.8} \pm 0.3$	1 WEI	09A	BELL $e^+e^- \rightarrow \Upsilon(4S)$

- • • We do not use the following data for averages, fits, limits, etc. • • •

$4.2^{+1.2}_{-1.1} \pm 0.2$	1 AUBERT,B	06J	BABR Repl. by AUBERT 09T
$10.5^{+2.5}_{-2.2} \pm 0.7$	1 AUBERT	03U	BABR Repl. by AUBERT,B 06J

$6.3^{+1.9}_{-1.7} \pm 0.3$	2 ISHIKAWA	03	BELL Repl. by WEI 09A
-----------------------------	------------	----	-----------------------

$< 14$	90	1 ABE	02	BELL $e^+e^- \rightarrow \Upsilon(4S)$
$< 9$	90	1 AUBERT	02L	BABR $e^+e^- \rightarrow \Upsilon(4S)$

$< 24$	90	3 ANDERSON	01B	CLE2 $e^+e^- \rightarrow \Upsilon(4S)$
$< 990$	90	4 ALBRECHT	91E	ARG $e^+e^- \rightarrow \Upsilon(4S)$

$< 68000$	90	5 WEIR	90B	MRK2 $e^+e^-$ 29 GeV
$< 600$	90	6 AVERY	89B	CLEO $e^+e^- \rightarrow \Upsilon(4S)$
$< 2500$	90	7 AVERY	87	CLEO $e^+e^- \rightarrow \Upsilon(4S)$

- <sup>1</sup>Assumes equal production of  $B^+$  and  $B^0$  at the  $\Upsilon(4S)$ .
- <sup>2</sup>Assumes equal production of  $B^0$  and  $B^+$  at  $\Upsilon(4S)$ . The second error is a total of systematic uncertainties including model dependence.
- <sup>3</sup>The result is for di-lepton masses above 0.5 GeV.

<sup>4</sup>ALBRECHT 91E reports  $< 9.0 \times 10^{-5}$  assuming the  $\Upsilon(4S)$  decays 45% to  $B^0 \bar{B}^0$ . We rescale to 50%.

<sup>5</sup>WEIR 90B assumes  $B^+$  production cross section from LUND.

<sup>6</sup>AVERY 89B reports  $< 5 \times 10^{-5}$  assuming the  $\Upsilon(4S)$  decays 43% to  $B^0 \bar{B}^0$ . We rescale to 50%.

<sup>7</sup>AVERY 87 reports  $< 2.1 \times 10^{-4}$  assuming the  $\Upsilon(4S)$  decays 40% to  $B^0 \bar{B}^0$ . We rescale to 50%.

 $\Gamma(K^+ \mu^+ \mu^-)/\Gamma_{\text{total}}$   $\Gamma_{443}/\Gamma$ 

VALUE (units $10^{-7}$ )	CL%	DOCUMENT ID	TECN	COMMENT
<b><math>4.8 \pm 0.4</math> OUR FIT</b>				
<b><math>5.1^{+0.8}_{-0.7}</math> OUR AVERAGE</b>				

$4.1^{+1.6}_{-1.5} \pm 0.2$	1 AUBERT	09T	BABR $e^+e^- \rightarrow \Upsilon(4S)$
$5.3^{+0.8}_{-0.7} \pm 0.3$	1 WEI	09A	BELL $e^+e^- \rightarrow \Upsilon(4S)$

- • • We do not use the following data for averages, fits, limits, etc. • • •

$3.1^{+1.5}_{-1.2} \pm 0.3$	1 AUBERT,B	06J	BABR Repl. by AUBERT 09T
$0.7^{+1.9}_{-1.1} \pm 0.2$	1 AUBERT	03U	BABR Repl. by AUBERT,B 06J

$4.5^{+1.4}_{-1.2} \pm 0.3$	2 ISHIKAWA	03	BELL Repl. by WEI 09A
-----------------------------	------------	----	-----------------------

$9.8^{+4.6}_{-3.6} \pm 1.6$	1 ABE	02	BELL Repl. by ISHIKAWA 03
-----------------------------	-------	----	---------------------------

$< 12$	90	1 AUBERT	02L	BABR $e^+e^- \rightarrow \Upsilon(4S)$
$< 36.8$	90	3 ANDERSON	01B	CLE2 $e^+e^- \rightarrow \Upsilon(4S)$

$< 52$	90	4 AFFOLDER	99B	CDF $p\bar{p}$ at 1.8 TeV
$< 100$	90	5 ABE	96L	CDF Repl. by AFFOLDER 99B

$< 2400$	90	6 ALBRECHT	91E	ARG $e^+e^- \rightarrow \Upsilon(4S)$
$< 64000$	90	7 WEIR	90B	MRK2 $e^+e^-$ 29 GeV
$< 1700$	90	8 AVERY	89B	CLEO $e^+e^- \rightarrow \Upsilon(4S)$
$< 3800$	90	9 AVERY	87	CLEO $e^+e^- \rightarrow \Upsilon(4S)$

- <sup>1</sup>Assumes equal production of  $B^+$  and  $B^0$  at the  $\Upsilon(4S)$ .
- <sup>2</sup>Assumes equal production of  $B^0$  and  $B^+$  at  $\Upsilon(4S)$ . The second error is a total of systematic uncertainties including model dependence.

<sup>3</sup>The result is for di-lepton masses above 0.5 GeV.

<sup>4</sup>AFFOLDER 99B measured relative to  $B^+ \rightarrow J/\psi(1S) K^+$ .

<sup>5</sup>ABE 96L measured relative to  $B^+ \rightarrow J/\psi(1S) K^+$  using PDG 94 branching ratios.

<sup>6</sup>ALBRECHT 91E reports  $< 2.2 \times 10^{-4}$  assuming the  $\Upsilon(4S)$  decays 45% to  $B^0 \bar{B}^0$ . We rescale to 50%.

<sup>7</sup>WEIR 90B assumes  $B^+$  production cross section from LUND.

<sup>8</sup>AVERY 89B reports  $< 1.5 \times 10^{-4}$  assuming the  $\Upsilon(4S)$  decays 43% to  $B^0 \bar{B}^0$ . We rescale to 50%.

<sup>9</sup>AVERY 87 reports  $< 3.2 \times 10^{-4}$  assuming the  $\Upsilon(4S)$  decays 40% to  $B^0 \bar{B}^0$ . We rescale to 50%.

$\Gamma(K^+\mu^+\mu^-)/\Gamma(J/\psi(1S)K^+)$  $\Gamma_{443}/\Gamma_{185}$ 

VALUE (units $10^{-3}$ )	CL%	DOCUMENT ID	TECN	COMMENT
<b>0.47±0.04 OUR FIT</b>				
<b>0.46±0.04±0.02</b>		AALTONEN	11A1 CDF	$p\bar{p}$ at 1.96 TeV
••• We do not use the following data for averages, fits, limits, etc. •••				
0.38±0.05±0.02		AALTONEN	11L CDF	Repl. by AALTONEN 11A1
0.59±0.15±0.03		AALTONEN	09B CDF	Repl. by AALTONEN 11L

 $\Gamma(K^+\nu)/\Gamma_{total}$  $\Gamma_{444}/\Gamma$ 

Test for  $\Delta B=1$  weak neutral current. Allowed by higher-order electroweak interactions.

VALUE	CL%	DOCUMENT ID	TECN	COMMENT
<b>&lt;1.3 × 10<sup>-5</sup></b>	90	<sup>1</sup> DEL-AMO-SAL0q	BABR	$e^+e^- \rightarrow \Upsilon(4S)$
••• We do not use the following data for averages, fits, limits, etc. •••				
<1.4 × 10 <sup>-5</sup>	90	<sup>1</sup> CHEN	07D BELL	$e^+e^- \rightarrow \Upsilon(4S)$
<5.2 × 10 <sup>-5</sup>	90	<sup>1</sup> AUBERT	05H BABR	$e^+e^- \rightarrow \Upsilon(4S)$
<2.4 × 10 <sup>-4</sup>	90	<sup>1</sup> BROWDER	01 CLE2	$e^+e^- \rightarrow \Upsilon(4S)$

<sup>1</sup> Assumes equal production of  $B^+$  and  $B^0$  at the  $\Upsilon(4S)$ .

 $\Gamma(\rho^+\nu)/\Gamma_{total}$  $\Gamma_{445}/\Gamma$ 

Test for  $\Delta B=1$  weak neutral current. Allowed by higher-order electroweak interaction.

VALUE	CL%	DOCUMENT ID	TECN	COMMENT
<b>&lt;1.5 × 10<sup>-4</sup></b>	90	<sup>1</sup> CHEN	07D BELL	$e^+e^- \rightarrow \Upsilon(4S)$

<sup>1</sup> Assumes equal production of  $B^+$  and  $B^0$  at the  $\Upsilon(4S)$ .

 $\Gamma(K^*(892)^+\ell^+\ell^-)/\Gamma_{total}$  $\Gamma_{446}/\Gamma$ 

Test for  $\Delta B=1$  weak neutral current. Allowed by higher-order electroweak interactions.

VALUE (units $10^{-7}$ )	CL%	DOCUMENT ID	TECN	COMMENT
<b>12.9±2.1 OUR AVERAGE</b>				
14.0 <sup>+4.0</sup> <sub>-3.7</sub> ±0.9		<sup>1</sup> AUBERT	09T BABR	$e^+e^- \rightarrow \Upsilon(4S)$
12.4 <sup>+2.3</sup> <sub>-2.1</sub> ±1.3		<sup>1</sup> WEI	09A BELL	$e^+e^- \rightarrow \Upsilon(4S)$
••• We do not use the following data for averages, fits, limits, etc. •••				
7.3 <sup>+5.0</sup> <sub>-4.2</sub> ±2.1		<sup>1</sup> AUBERT,B	06J BABR	Repl. by AUBERT 09T
<22	90	<sup>1</sup> ISHIKAWA	03 BELL	$e^+e^- \rightarrow \Upsilon(4S)$

<sup>1</sup> Assumes equal production of  $B^+$  and  $B^0$  at the  $\Upsilon(4S)$ .

 $\Gamma(K^*(892)^+\nu)/\Gamma_{total}$  $\Gamma_{449}/\Gamma$ 

Test for  $\Delta B=1$  weak neutral current. Allowed by higher-order electroweak interaction.

VALUE	CL%	DOCUMENT ID	TECN	COMMENT
<b>&lt;8 × 10<sup>-5</sup></b>	90	AUBERT	08Bc BABR	$e^+e^- \rightarrow \Upsilon(4S)$
••• We do not use the following data for averages, fits, limits, etc. •••				
<1.4 × 10 <sup>-4</sup>	90	<sup>1</sup> CHEN	07D BELL	$e^+e^- \rightarrow \Upsilon(4S)$

<sup>1</sup> Assumes equal production of  $B^+$  and  $B^0$  at the  $\Upsilon(4S)$ .

 $\Gamma(K^*(892)^+e^+e^-)/\Gamma_{total}$  $\Gamma_{447}/\Gamma$ 

Test for  $\Delta B=1$  weak neutral current. Allowed by higher-order electroweak interactions.

VALUE (units $10^{-7}$ )	CL%	DOCUMENT ID	TECN	COMMENT
<b>15.5<sup>+4.0</sup><sub>-3.1</sub> OUR AVERAGE</b>				
13.8 <sup>+4.7</sup> <sub>-4.2</sub> ±0.8		<sup>1</sup> AUBERT	09T BABR	$e^+e^- \rightarrow \Upsilon(4S)$
17.3 <sup>+5.0</sup> <sub>-4.2</sub> ±2.0		<sup>1</sup> WEI	09A BELL	$e^+e^- \rightarrow \Upsilon(4S)$
••• We do not use the following data for averages, fits, limits, etc. •••				
7.5 <sup>+7.6</sup> <sub>-6.5</sub> ±3.8		<sup>1</sup> AUBERT,B	06J BABR	Repl. by AUBERT 09T
2.0 <sup>+13.4</sup> <sub>-8.7</sub> ±2.8		<sup>1</sup> AUBERT	03U BABR	$e^+e^- \rightarrow \Upsilon(4S)$
< 46	90	<sup>2</sup> ISHIKAWA	03 BELL	$e^+e^- \rightarrow \Upsilon(4S)$
< 89	90	<sup>1</sup> ABE	02L BELL	Repl. by ISHIKAWA 03
< 95	90	<sup>1</sup> AUBERT	02L BABR	$e^+e^- \rightarrow \Upsilon(4S)$
<6900	90	<sup>3</sup> ALBRECHT	91E ARG	$e^+e^- \rightarrow \Upsilon(4S)$

<sup>1</sup> Assumes equal production of  $B^+$  and  $B^0$  at the  $\Upsilon(4S)$ .<sup>2</sup> Assumes equal production of  $B^0$  and  $B^+$  at  $\Upsilon(4S)$ . The second error is a total of systematic uncertainties including model dependence.<sup>3</sup> ALBRECHT 91E reports  $< 6.3 \times 10^{-4}$  assuming the  $\Upsilon(4S)$  decays 45% to  $B^0\bar{B}^0$ . We rescale to 50%. $\Gamma(K^*(892)^+\mu^+\mu^-)/\Gamma_{total}$  $\Gamma_{448}/\Gamma$ 

Test for  $\Delta B=1$  weak neutral current. Allowed by higher-order electroweak interactions.

VALUE (units $10^{-7}$ )	CL%	DOCUMENT ID	TECN	COMMENT
<b>10.7± 2.2 OUR FIT</b>				
<b>11.6<sup>+3.1</sup><sub>-2.7</sub> OUR AVERAGE</b>				
14.6 <sup>+7.9</sup> <sub>-7.5</sub> ±1.2		<sup>1</sup> AUBERT	09T BABR	$e^+e^- \rightarrow \Upsilon(4S)$
11.1 <sup>+3.2</sup> <sub>-2.7</sub> ±1.0		<sup>1</sup> WEI	09A BELL	$e^+e^- \rightarrow \Upsilon(4S)$
••• We do not use the following data for averages, fits, limits, etc. •••				
9.7 <sup>+9.4</sup> <sub>-6.9</sub> ±1.4		<sup>1</sup> AUBERT,B	06J BABR	Repl. by AUBERT 09T
30.7 <sup>+25.8</sup> <sub>-17.8</sub> ±4.2		<sup>1</sup> AUBERT	03U BABR	$e^+e^- \rightarrow \Upsilon(4S)$
6.5 <sup>+6.9+1.5</sup> <sub>-5.3-1.6</sub>		<sup>2</sup> ISHIKAWA	03 BELL	Repl. by WEI 09A
< 39	90	<sup>1</sup> ABE	02L BELL	Repl. by ISHIKAWA 03
< 170	90	<sup>1</sup> AUBERT	02L BABR	$e^+e^- \rightarrow \Upsilon(4S)$
<12000	90	<sup>3</sup> ALBRECHT	91E ARG	$e^+e^- \rightarrow \Upsilon(4S)$

<sup>1</sup> Assumes equal production of  $B^+$  and  $B^0$  at the  $\Upsilon(4S)$ .<sup>2</sup> Assumes equal production of  $B^0$  and  $B^+$  at  $\Upsilon(4S)$ . The second error is a total of systematic uncertainties including model dependence. The 90% C.L. upper limit is  $2.2 \times 10^{-6}$ .<sup>3</sup> ALBRECHT 91E reports  $< 1.1 \times 10^{-3}$  assuming the  $\Upsilon(4S)$  decays 45% to  $B^0\bar{B}^0$ . We rescale to 50%. $\Gamma(K^*(892)^+\mu^+\mu^-)/\Gamma(J/\psi(1S)K^*(892)^+)$  $\Gamma_{448}/\Gamma_{205}$ 

VALUE (units $10^{-3}$ )	CL%	DOCUMENT ID	TECN	COMMENT
<b>0.75±0.15 OUR FIT</b>				
<b>0.67±0.22±0.04</b>		AALTONEN	11A1 CDF	$p\bar{p}$ at 1.96 TeV

 $\Gamma(\pi^+e^+\mu^-)/\Gamma_{total}$  $\Gamma_{450}/\Gamma$ 

Test of lepton family number conservation.

VALUE	CL%	DOCUMENT ID	TECN	COMMENT
<b>&lt;0.0064</b>	90	<sup>1</sup> WEIR	90B MRK2	$e^+e^-$ 29 GeV

<sup>1</sup> WEIR 90B assumes  $B^+$  production cross section from LUND.

 $\Gamma(\pi^+e^-\mu^-)/\Gamma_{total}$  $\Gamma_{451}/\Gamma$ 

Test of lepton family number conservation.

VALUE	CL%	DOCUMENT ID	TECN	COMMENT
<b>&lt;0.0064</b>	90	<sup>1</sup> WEIR	90B MRK2	$e^+e^-$ 29 GeV

<sup>1</sup> WEIR 90B assumes  $B^+$  production cross section from LUND.

 $\Gamma(\pi^+e^\pm\mu^\mp)/\Gamma_{total}$  $\Gamma_{452}/\Gamma$ 

VALUE	CL%	DOCUMENT ID	TECN	COMMENT
<b>&lt;1.7 × 10<sup>-7</sup></b>	90	<sup>1</sup> AUBERT	07Ag BABR	$e^+e^- \rightarrow \Upsilon(4S)$

<sup>1</sup> Assumes equal production of  $B^+$  and  $B^0$  at the  $\Upsilon(4S)$ .

 $\Gamma(K^+e^+\mu^-)/\Gamma_{total}$  $\Gamma_{453}/\Gamma$ 

Test of lepton family number conservation.

VALUE (units $10^{-7}$ )	CL%	DOCUMENT ID	TECN	COMMENT
<b>&lt;0.91</b>	90	<sup>1</sup> AUBERT,B	06J BABR	$e^+e^- \rightarrow \Upsilon(4S)$
••• We do not use the following data for averages, fits, limits, etc. •••				
<8	90	<sup>1</sup> AUBERT	02L BABR	Repl. by AUBERT,B 06J
<6.4 × 10 <sup>4</sup>	90	<sup>2</sup> WEIR	90B MRK2	$e^+e^-$ 29 GeV

<sup>1</sup> Assumes equal production of  $B^+$  and  $B^0$  at the  $\Upsilon(4S)$ .

<sup>2</sup> WEIR 90B assumes  $B^+$  production cross section from LUND.

 $\Gamma(K^+e^-\mu^+)/\Gamma_{total}$  $\Gamma_{454}/\Gamma$ 

Test of lepton family number conservation.

VALUE (units $10^{-7}$ )	CL%	DOCUMENT ID	TECN	COMMENT
<b>&lt;1.3</b>	90	<sup>1</sup> AUBERT,B	06J BABR	$e^+e^- \rightarrow \Upsilon(4S)$
••• We do not use the following data for averages, fits, limits, etc. •••				
<6.4 × 10 <sup>4</sup>	90	<sup>2</sup> WEIR	90B MRK2	$e^+e^-$ 29 GeV

<sup>1</sup> Assumes equal production of  $B^+$  and  $B^0$  at the  $\Upsilon(4S)$ .

<sup>2</sup> WEIR 90B assumes  $B^+$  production cross section from LUND.

 $\Gamma(K^+e^\pm\mu^\mp)/\Gamma_{total}$  $\Gamma_{455}/\Gamma$ 

VALUE (units $10^{-7}$ )	CL%	DOCUMENT ID	TECN	COMMENT
<b>&lt;0.91</b>	90	<sup>1</sup> AUBERT,B	06J BABR	$e^+e^- \rightarrow \Upsilon(4S)$

<sup>1</sup> Assumes equal production of  $B^+$  and  $B^0$  at the  $\Upsilon(4S)$ .

 $\Gamma(K^+\mu^\pm\tau^\mp)/\Gamma_{total}$  $\Gamma_{456}/\Gamma$ 

Test of lepton family number conservation.

VALUE (units $10^{-6}$ )	CL%	DOCUMENT ID	TECN	COMMENT
<b>&lt;77</b>	90	<sup>1</sup> AUBERT	07AZ BABR	$e^+e^- \rightarrow \Upsilon(4S)$

<sup>1</sup> Uses a fully reconstructed hadronic  $B$  decay as a tag on the recoil side.

 $\Gamma(K^*(892)^+e^+\mu^-)/\Gamma_{total}$  $\Gamma_{457}/\Gamma$ 

VALUE (units $10^{-7}$ )	CL%	DOCUMENT ID	TECN	COMMENT
<b>&lt;13</b>	90	<sup>1</sup> AUBERT,B	06J BABR	$e^+e^- \rightarrow \Upsilon(4S)$

<sup>1</sup> Assumes equal production of  $B^+$  and  $B^0$  at the  $\Upsilon(4S)$ .

 $\Gamma(K^*(892)^+e^-\mu^+)/\Gamma_{total}$  $\Gamma_{458}/\Gamma$ 

VALUE (units $10^{-7}$ )	CL%	DOCUMENT ID	TECN	COMMENT
<b>&lt;9.9</b>	90	<sup>1</sup> AUBERT,B	06J BABR	$e^+e^- \rightarrow \Upsilon(4S)$

<sup>1</sup> Assumes equal production of  $B^+$  and  $B^0$  at the  $\Upsilon(4S)$ .

 $\Gamma(K^*(892)^+e^\pm\mu^\mp)/\Gamma_{total}$  $\Gamma_{459}/\Gamma$ 

Test of lepton family number conservation.

VALUE	CL%	DOCUMENT ID	TECN	COMMENT
<b>&lt;1.4 × 10<sup>-6</sup></b>	90	<sup>1</sup> AUBERT,B	06J BABR	$e^+e^- \rightarrow \Upsilon(4S)$
••• We do not use the following data for averages, fits, limits, etc. •••				
<7.9 × 10 <sup>-6</sup>	90	<sup>1</sup> AUBERT	02L BABR	Repl. by AUBERT,B 06J

<sup>1</sup> Assumes equal production of  $B^+$  and  $B^0$  at the  $\Upsilon(4S)$ .

## Meson Particle Listings

 $B^\pm$  $\Gamma(\pi^- e^+ e^+)/\Gamma_{\text{total}}$   $\Gamma_{460}/\Gamma$ 

Test of total lepton number conservation.

VALUE	CL%	DOCUMENT ID	TECN	COMMENT
$<4.4 \times 10^{-6}$	90	<sup>1</sup> EDWARDS 02B	CLE2	$e^+ e^- \rightarrow \Upsilon(4S)$

••• We do not use the following data for averages, fits, limits, etc. •••

$<0.0039$	90	<sup>2</sup> WEIR 90B	MRK2	$e^+ e^-$ 29 GeV
-----------	----	-----------------------	------	------------------

<sup>1</sup> Assumes equal production of  $B^+$  and  $B^0$  at the  $\Upsilon(4S)$ .  
<sup>2</sup> WEIR 90B assumes  $B^+$  production cross section from LUND.

 $\Gamma(\pi^- \mu^+ \mu^+)/\Gamma_{\text{total}}$   $\Gamma_{461}/\Gamma$ 

Test of total lepton number conservation.

VALUE	CL%	DOCUMENT ID	TECN	COMMENT
$<4.4 \times 10^{-8}$	90	AAIJ	12C	LHCB $p\bar{p}$ at 7 TeV

••• We do not use the following data for averages, fits, limits, etc. •••

$<1.4 \times 10^{-6}$	90	<sup>1</sup> EDWARDS 02B	CLE2	$e^+ e^- \rightarrow \Upsilon(4S)$
$<9.1 \times 10^{-3}$	90	<sup>2</sup> WEIR 90B	MRK2	$e^+ e^-$ 29 GeV

<sup>1</sup> Assumes equal production of  $B^+$  and  $B^0$  at the  $\Upsilon(4S)$ .  
<sup>2</sup> WEIR 90B assumes  $B^+$  production cross section from LUND.

 $\Gamma(\pi^- e^+ \mu^+)/\Gamma_{\text{total}}$   $\Gamma_{462}/\Gamma$ 

Test of total lepton number conservation.

VALUE	CL%	DOCUMENT ID	TECN	COMMENT
$<1.3 \times 10^{-6}$	90	<sup>1</sup> EDWARDS 02B	CLE2	$e^+ e^- \rightarrow \Upsilon(4S)$

••• We do not use the following data for averages, fits, limits, etc. •••

$<0.0064$	90	<sup>2</sup> WEIR 90B	MRK2	$e^+ e^-$ 29 GeV
-----------	----	-----------------------	------	------------------

<sup>1</sup> Assumes equal production of  $B^+$  and  $B^0$  at the  $\Upsilon(4S)$ .  
<sup>2</sup> WEIR 90B assumes  $B^+$  production cross section from LUND.

 $\Gamma(\rho^- e^+ e^+)/\Gamma_{\text{total}}$   $\Gamma_{463}/\Gamma$ 

Test of total lepton number conservation.

VALUE (units $10^{-6}$ )	CL%	DOCUMENT ID	TECN	COMMENT
$<2.6$	90	<sup>1</sup> EDWARDS 02B	CLE2	$e^+ e^- \rightarrow \Upsilon(4S)$

<sup>1</sup> Assumes equal production of  $B^+$  and  $B^0$  at the  $\Upsilon(4S)$ .

 $\Gamma(\rho^- \mu^+ \mu^+)/\Gamma_{\text{total}}$   $\Gamma_{464}/\Gamma$ 

Test of total lepton number conservation.

VALUE (units $10^{-6}$ )	CL%	DOCUMENT ID	TECN	COMMENT
$<5.0$	90	<sup>1</sup> EDWARDS 02B	CLE2	$e^+ e^- \rightarrow \Upsilon(4S)$

<sup>1</sup> Assumes equal production of  $B^+$  and  $B^0$  at the  $\Upsilon(4S)$ .

 $\Gamma(\rho^- e^+ \mu^+)/\Gamma_{\text{total}}$   $\Gamma_{465}/\Gamma$ 

Test of total lepton number conservation.

VALUE (units $10^{-6}$ )	CL%	DOCUMENT ID	TECN	COMMENT
$<3.3$	90	<sup>1</sup> EDWARDS 02B	CLE2	$e^+ e^- \rightarrow \Upsilon(4S)$

<sup>1</sup> Assumes equal production of  $B^+$  and  $B^0$  at the  $\Upsilon(4S)$ .

 $\Gamma(K^- e^+ e^+)/\Gamma_{\text{total}}$   $\Gamma_{466}/\Gamma$ 

Test of total lepton number conservation.

VALUE	CL%	DOCUMENT ID	TECN	COMMENT
$<1.0 \times 10^{-6}$	90	<sup>1</sup> EDWARDS 02B	CLE2	$e^+ e^- \rightarrow \Upsilon(4S)$

••• We do not use the following data for averages, fits, limits, etc. •••

$<0.0039$	90	<sup>2</sup> WEIR 90B	MRK2	$e^+ e^-$ 29 GeV
-----------	----	-----------------------	------	------------------

<sup>1</sup> Assumes equal production of  $B^+$  and  $B^0$  at the  $\Upsilon(4S)$ .  
<sup>2</sup> WEIR 90B assumes  $B^+$  production cross section from LUND.

 $\Gamma(K^- \mu^+ \mu^+)/\Gamma_{\text{total}}$   $\Gamma_{467}/\Gamma$ 

Test of total lepton number conservation.

VALUE	CL%	DOCUMENT ID	TECN	COMMENT
$<1.0 \times 10^{-6}$	90	<sup>1</sup> EDWARDS 02B	CLE2	$e^+ e^- \rightarrow \Upsilon(4S)$

••• We do not use the following data for averages, fits, limits, etc. •••

$<0.0039$	90	<sup>2</sup> WEIR 90B	MRK2	$e^+ e^-$ 29 GeV
-----------	----	-----------------------	------	------------------

<sup>1</sup> Assumes equal production of  $B^+$  and  $B^0$  at the  $\Upsilon(4S)$ .  
<sup>2</sup> WEIR 90B assumes  $B^+$  production cross section from LUND.

 $\Gamma(K^- e^+ \mu^+)/\Gamma_{\text{total}}$   $\Gamma_{468}/\Gamma$ 

Test of total lepton number conservation.

VALUE	CL%	DOCUMENT ID	TECN	COMMENT
$<2.0 \times 10^{-6}$	90	<sup>1</sup> EDWARDS 02B	CLE2	$e^+ e^- \rightarrow \Upsilon(4S)$

••• We do not use the following data for averages, fits, limits, etc. •••

$<0.0064$	90	<sup>2</sup> WEIR 90B	MRK2	$e^+ e^-$ 29 GeV
-----------	----	-----------------------	------	------------------

<sup>1</sup> Assumes equal production of  $B^+$  and  $B^0$  at the  $\Upsilon(4S)$ .  
<sup>2</sup> WEIR 90B assumes  $B^+$  production cross section from LUND.

 $\Gamma(K^*(892)^- e^+ e^+)/\Gamma_{\text{total}}$   $\Gamma_{469}/\Gamma$ 

Test of total lepton number conservation.

VALUE (units $10^{-6}$ )	CL%	DOCUMENT ID	TECN	COMMENT
$<2.8$	90	<sup>1</sup> EDWARDS 02B	CLE2	$e^+ e^- \rightarrow \Upsilon(4S)$

<sup>1</sup> Assumes equal production of  $B^+$  and  $B^0$  at the  $\Upsilon(4S)$ .

 $\Gamma(K^*(892)^- \mu^+ \mu^+)/\Gamma_{\text{total}}$   $\Gamma_{470}/\Gamma$ 

Test of total lepton number conservation.

VALUE (units $10^{-6}$ )	CL%	DOCUMENT ID	TECN	COMMENT
$<8.3$	90	<sup>1</sup> EDWARDS 02B	CLE2	$e^+ e^- \rightarrow \Upsilon(4S)$

<sup>1</sup> Assumes equal production of  $B^+$  and  $B^0$  at the  $\Upsilon(4S)$ .

 $\Gamma(K^*(892)^- e^+ \mu^+)/\Gamma_{\text{total}}$   $\Gamma_{471}/\Gamma$ 

Test of total lepton number conservation.

VALUE (units $10^{-6}$ )	CL%	DOCUMENT ID	TECN	COMMENT
$<4.4$	90	<sup>1</sup> EDWARDS 02B	CLE2	$e^+ e^- \rightarrow \Upsilon(4S)$

<sup>1</sup> Assumes equal production of  $B^+$  and  $B^0$  at the  $\Upsilon(4S)$ .

 $\Gamma(D^- e^+ e^+)/\Gamma_{\text{total}}$   $\Gamma_{472}/\Gamma$ 

Test of total lepton number conservation.

VALUE	CL%	DOCUMENT ID	TECN	COMMENT
$<2.6 \times 10^{-6}$	90	<sup>1</sup> SEON 11	BELL	$e^+ e^- \rightarrow \Upsilon(4S)$

<sup>1</sup> Assumes equal production of  $B^0$  and  $B^+$  from Upsilon(4S) decays. Uses  $D^- \rightarrow K^+ \pi^- \pi^-$  mode and 3-body phase-space hypothesis for the signal decays.

 $\Gamma(D^- e^+ \mu^+)/\Gamma_{\text{total}}$   $\Gamma_{473}/\Gamma$ 

Test of total lepton number conservation.

VALUE	CL%	DOCUMENT ID	TECN	COMMENT
$<1.8 \times 10^{-6}$	90	<sup>1</sup> SEON 11	BELL	$e^+ e^- \rightarrow \Upsilon(4S)$

<sup>1</sup> Assumes equal production of  $B^0$  and  $B^+$  from Upsilon(4S) decays. Uses  $D^- \rightarrow K^+ \pi^- \pi^-$  mode and 3-body phase-space hypothesis for the signal decays.

 $\Gamma(D^- \mu^+ \mu^+)/\Gamma_{\text{total}}$   $\Gamma_{474}/\Gamma$ 

Test of total lepton number conservation.

VALUE	CL%	DOCUMENT ID	TECN	COMMENT
$<1.1 \times 10^{-6}$	90	<sup>1</sup> SEON 11	BELL	$e^+ e^- \rightarrow \Upsilon(4S)$

<sup>1</sup> Assumes equal production of  $B^0$  and  $B^+$  from Upsilon(4S) decays. Uses  $D^- \rightarrow K^+ \pi^- \pi^-$  mode and 3-body phase-space hypothesis for the signal decays.

 $\Gamma(\Lambda^0 \mu^+)/\Gamma_{\text{total}}$   $\Gamma_{475}/\Gamma$ 

Test of total lepton number conservation.

VALUE	CL%	DOCUMENT ID	TECN	COMMENT
$<6 \times 10^{-8}$	90	<sup>1,2</sup> DEL-AMO-SA...11k	BABR	$e^+ e^- \rightarrow \Upsilon(4S)$

<sup>1</sup> DEL-AMO-SANCHEZ 11k reports  $< 6.1 \times 10^{-8}$  from a measurement of  $[\Gamma(B^+ \rightarrow \Lambda^0 e^+)/\Gamma_{\text{total}}] \times [B(\Lambda \rightarrow p\pi^-)]$  assuming  $B(\Lambda \rightarrow p\pi^-) = (63.9 \pm 0.5) \times 10^{-2}$ .  
<sup>2</sup> Uses  $B(\Upsilon(4S) \rightarrow B^0 \bar{B}^0) = (51.6 \pm 0.6)\%$  and  $B(\Upsilon(4S) \rightarrow B^+ B^-) = (48.4 \pm 0.6)\%$ .

 $\Gamma(\Lambda^0 e^+)/\Gamma_{\text{total}}$   $\Gamma_{476}/\Gamma$ 

Test of total lepton number conservation.

VALUE	CL%	DOCUMENT ID	TECN	COMMENT
$<3.2 \times 10^{-8}$	90	<sup>1,2</sup> DEL-AMO-SA...11k	BABR	$e^+ e^- \rightarrow \Upsilon(4S)$

<sup>1</sup> DEL-AMO-SANCHEZ 11k reports  $< 3.2 \times 10^{-8}$  from a measurement of  $[\Gamma(B^+ \rightarrow \Lambda^0 e^+)/\Gamma_{\text{total}}] \times [B(\Lambda \rightarrow p\pi^-)]$  assuming  $B(\Lambda \rightarrow p\pi^-) = (63.9 \pm 0.5) \times 10^{-2}$ .  
<sup>2</sup> Uses  $B(\Upsilon(4S) \rightarrow B^0 \bar{B}^0) = (51.6 \pm 0.6)\%$  and  $B(\Upsilon(4S) \rightarrow B^+ B^-) = (48.4 \pm 0.6)\%$ .

 $\Gamma(\bar{\Lambda}^0 \mu^+)/\Gamma_{\text{total}}$   $\Gamma_{477}/\Gamma$ 

Test of total lepton number conservation.

VALUE	CL%	DOCUMENT ID	TECN	COMMENT
$<6 \times 10^{-8}$	90	<sup>1,2</sup> DEL-AMO-SA...11k	BABR	$e^+ e^- \rightarrow \Upsilon(4S)$

<sup>1</sup> DEL-AMO-SANCHEZ 11k reports  $< 6.2 \times 10^{-8}$  from a measurement of  $[\Gamma(B^+ \rightarrow \bar{\Lambda}^0 \mu^+)/\Gamma_{\text{total}}] \times [B(\Lambda \rightarrow p\pi^-)]$  assuming  $B(\Lambda \rightarrow p\pi^-) = (63.9 \pm 0.5) \times 10^{-2}$ .  
<sup>2</sup> Uses  $B(\Upsilon(4S) \rightarrow B^0 \bar{B}^0) = (51.6 \pm 0.6)\%$  and  $B(\Upsilon(4S) \rightarrow B^+ B^-) = (48.4 \pm 0.6)\%$ .

 $\Gamma(\bar{\Lambda}^0 e^+)/\Gamma_{\text{total}}$   $\Gamma_{478}/\Gamma$ 

Test of total lepton number conservation.

VALUE	CL%	DOCUMENT ID	TECN	COMMENT
$<8 \times 10^{-8}$	90	<sup>1,2</sup> DEL-AMO-SA...11k	BABR	$e^+ e^- \rightarrow \Upsilon(4S)$

<sup>1</sup> DEL-AMO-SANCHEZ 11k reports  $< 8.1 \times 10^{-8}$  from a measurement of  $[\Gamma(B^+ \rightarrow \bar{\Lambda}^0 e^+)/\Gamma_{\text{total}}] \times [B(\Lambda \rightarrow p\pi^-)]$  assuming  $B(\Lambda \rightarrow p\pi^-) = (63.9 \pm 0.5) \times 10^{-2}$ .  
<sup>2</sup> Uses  $B(\Upsilon(4S) \rightarrow B^0 \bar{B}^0) = (51.6 \pm 0.6)\%$  and  $B(\Upsilon(4S) \rightarrow B^+ B^-) = (48.4 \pm 0.6)\%$ .

POLARIZATION IN  $B^+$  DECAY

In decays involving two vector mesons, one can distinguish among the states in which meson polarizations are both longitudinal (L) or both are transverse and parallel (||) or perpendicular ( $\perp$ ) to each other with the parameters  $\Gamma_L/\Gamma$ ,  $\Gamma_{\perp}/\Gamma$ , and the relative phases  $\phi_{||}$  and  $\phi_{\perp}$ . See the definitions in the note on "Polarization in B Decays" review in the  $B^0$  Particle Listings.

 $\Gamma_L/\Gamma$  in  $B^+ \rightarrow \bar{D}^{*0} \rho^+$ 

VALUE	DOCUMENT ID	TECN	COMMENT
$0.892 \pm 0.018 \pm 0.016$	CSORNA 03	CLE2	$e^+ e^- \rightarrow \Upsilon(4S)$

 $\Gamma_L/\Gamma$  in  $B^+ \rightarrow \bar{D}^{*0} K^{*+}$ 

VALUE	DOCUMENT ID	TECN	COMMENT
$0.86 \pm 0.06 \pm 0.03$	AUBERT 04k	BABR	$e^+ e^- \rightarrow \Upsilon(4S)$

 $\Gamma_L/\Gamma$  in  $B^+ \rightarrow J/\psi K^{*+}$ 

VALUE	DOCUMENT ID	TECN	COMMENT
$0.604 \pm 0.015 \pm 0.018$	ITOH 05	BELL	$e^+ e^- \rightarrow \Upsilon(4S)$



$\Gamma_\perp/\Gamma$ in $B^+ \rightarrow J/\psi K^{*+}$	DOCUMENT ID	TECN	COMMENT
0.180±0.014±0.010	ITOH	05	BELL $e^+e^- \rightarrow \Upsilon(4S)$

$\Gamma_L/\Gamma$ in $B^+ \rightarrow \omega K^{*+}$	DOCUMENT ID	TECN	COMMENT
0.41±0.18±0.05	AUBERT	09H	BABR $e^+e^- \rightarrow \Upsilon(4S)$

$\Gamma_L/\Gamma$ in $B^+ \rightarrow \omega K_2^*(1430)^+$	DOCUMENT ID	TECN	COMMENT
0.56±0.10±0.04	AUBERT	09H	BABR $e^+e^- \rightarrow \Upsilon(4S)$

$\Gamma_L/\Gamma$ in $B^+ \rightarrow K^{*+} \bar{K}^{*0}$	DOCUMENT ID	TECN	COMMENT
0.75 <sup>+0.16</sup> <sub>-0.26</sub> ±0.03	<sup>1</sup> AUBERT	09F	BABR $e^+e^- \rightarrow \Upsilon(4S)$

<sup>1</sup> Assumes equal production of  $B^+$  and  $B^0$  at the  $\Upsilon(4S)$ .

$\Gamma_L/\Gamma$ in $B^+ \rightarrow \phi K^*(892)^+$	DOCUMENT ID	TECN	COMMENT
0.50±0.05 OUR AVERAGE			
0.49±0.05±0.03	AUBERT	07BA	BABR $e^+e^- \rightarrow \Upsilon(4S)$
0.52±0.08±0.03	CHEN	05A	BELL $e^+e^- \rightarrow \Upsilon(4S)$
••• We do not use the following data for averages, fits, limits, etc. •••			
0.46±0.12±0.03	AUBERT	03v	BABR Repl. by AUBERT 07Ba

$\Gamma_\perp/\Gamma$ in $B^+ \rightarrow \phi K^{*+}$	DOCUMENT ID	TECN	COMMENT
0.20±0.05 OUR AVERAGE			
0.21±0.05±0.02	AUBERT	07BA	BABR $e^+e^- \rightarrow \Upsilon(4S)$
0.19±0.08±0.02	CHEN	05A	BELL $e^+e^- \rightarrow \Upsilon(4S)$

$\phi_\parallel$ in $B^+ \rightarrow \phi K^{*+}$	DOCUMENT ID	TECN	COMMENT
2.34±0.18 OUR AVERAGE			
2.47±0.20±0.07	AUBERT	07BA	BABR $e^+e^- \rightarrow \Upsilon(4S)$
2.10±0.28±0.04	CHEN	05A	BELL $e^+e^- \rightarrow \Upsilon(4S)$

$\phi_\perp$ in $B^+ \rightarrow \phi K^{*+}$	DOCUMENT ID	TECN	COMMENT
2.58±0.17 OUR AVERAGE			
2.69±0.20±0.03	AUBERT	07BA	BABR $e^+e^- \rightarrow \Upsilon(4S)$
2.31±0.30±0.07	CHEN	05A	BELL $e^+e^- \rightarrow \Upsilon(4S)$

$\delta_0(B^+ \rightarrow \phi K^{*+})$	DOCUMENT ID	TECN	COMMENT
3.07±0.18±0.06	AUBERT	07BA	BABR $e^+e^- \rightarrow \Upsilon(4S)$

$A_{CP}^0(B^+ \rightarrow \phi K^{*+})$	DOCUMENT ID	TECN	COMMENT
0.17±0.11±0.02	AUBERT	07BA	BABR $e^+e^- \rightarrow \Upsilon(4S)$

$A_{CP}^1(B^+ \rightarrow \phi K^{*+})$	DOCUMENT ID	TECN	COMMENT
0.22±0.24±0.08	AUBERT	07BA	BABR $e^+e^- \rightarrow \Upsilon(4S)$

$\Delta\phi_\parallel(B^+ \rightarrow \phi K^{*+})$	DOCUMENT ID	TECN	COMMENT
0.07±0.20±0.05	AUBERT	07BA	BABR $e^+e^- \rightarrow \Upsilon(4S)$

$\Delta\phi_\perp(B^+ \rightarrow \phi K^{*+})$	DOCUMENT ID	TECN	COMMENT
0.19±0.20±0.07	AUBERT	07BA	BABR $e^+e^- \rightarrow \Upsilon(4S)$

$\Delta\delta_0(B^+ \rightarrow \phi K^{*+})$	DOCUMENT ID	TECN	COMMENT
0.20±0.18±0.03	AUBERT	07BA	BABR $e^+e^- \rightarrow \Upsilon(4S)$

$\Gamma_L/\Gamma$ in $B^+ \rightarrow \phi K_1(1270)^+$	DOCUMENT ID	TECN	COMMENT
0.46 <sup>+0.12+0.06</sup> <sub>-0.13-0.07</sub>	AUBERT	08Bi	BABR $e^+e^- \rightarrow \Upsilon(4S)$

$\Gamma_L/\Gamma$ in $B^+ \rightarrow \phi K_2^*(1430)^+$	DOCUMENT ID	TECN	COMMENT
0.80 <sup>+0.09</sup> <sub>-0.10</sub> ±0.03	AUBERT	08Bi	BABR $e^+e^- \rightarrow \Upsilon(4S)$

$\delta_0(B^+ \rightarrow \phi K_2^*(1430)^+)$	DOCUMENT ID	TECN	COMMENT
3.59±0.19±0.12	AUBERT	08Bi	BABR $e^+e^- \rightarrow \Upsilon(4S)$

$\Delta\delta_0(B^+ \rightarrow \phi K_2^*(1430)^+)$	DOCUMENT ID	TECN	COMMENT
-0.05±0.19±0.06	AUBERT	08Bi	BABR $e^+e^- \rightarrow \Upsilon(4S)$

$\Gamma_L/\Gamma$ in $B^+ \rightarrow \rho^0 K^*(892)^+$	DOCUMENT ID	TECN	COMMENT
0.78±0.12±0.03	DEL-AMO-SA...11D	BABR	$e^+e^- \rightarrow \Upsilon(4S)$
••• We do not use the following data for averages, fits, limits, etc. •••			
0.96 <sup>+0.04</sup> <sub>-0.15</sub> ±0.04	AUBERT	03v	BABR Repl. by DEL-AMO-SANCHEZ 11D

$\Gamma_L/\Gamma(B^+ \rightarrow K^*(892)^0 \rho^+)$	DOCUMENT ID	TECN	COMMENT
0.48±0.08 OUR AVERAGE			
0.52±0.10±0.04	AUBERT,B	06G	BABR $e^+e^- \rightarrow \Upsilon(4S)$
0.43±0.11 <sup>+0.05</sup> <sub>-0.02</sub>	ZHANG	05D	BELL $e^+e^- \rightarrow \Upsilon(4S)$

$\Gamma_L/\Gamma$ in $B^+ \rightarrow \rho^+ \rho^0$	DOCUMENT ID	TECN	COMMENT
0.950±0.016 OUR AVERAGE			
0.950±0.015±0.006	AUBERT	09G	BABR $e^+e^- \rightarrow \Upsilon(4S)$
0.948±0.106±0.021	ZHANG	03B	BELL $e^+e^- \rightarrow \Upsilon(4S)$
••• We do not use the following data for averages, fits, limits, etc. •••			
0.905±0.042 <sup>+0.023</sup> <sub>-0.027</sub>	AUBERT,BE	06G	BABR Repl. by AUBERT 09G
0.97 <sup>+0.03</sup> <sub>-0.07</sub> ±0.04	AUBERT	03v	BABR Repl. by AUBERT,BE 06G

$\Gamma_L/\Gamma$ in $B^+ \rightarrow \omega \rho^+$	DOCUMENT ID	TECN	COMMENT
0.90±0.05±0.03	AUBERT	09H	BABR $e^+e^- \rightarrow \Upsilon(4S)$
••• We do not use the following data for averages, fits, limits, etc. •••			
0.82±0.11±0.02	AUBERT,B	06T	BABR Repl. by AUBERT 09H
0.88 <sup>+0.12</sup> <sub>-0.15</sub> ±0.03	AUBERT	05o	BABR Repl. by AUBERT,B 06T

$\Gamma_L/\Gamma$ in $B^+ \rightarrow p\bar{p} K^*(892)^+$	DOCUMENT ID	TECN	COMMENT
0.32±0.17±0.09	CHEN	08c	BELL $e^+e^- \rightarrow \Upsilon(4S)$

CP VIOLATION

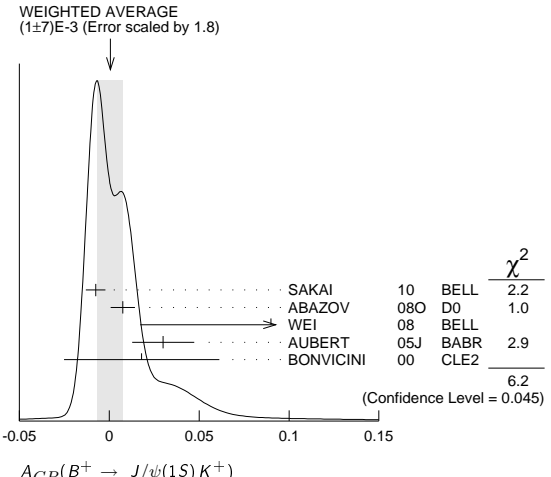
$A_{CP}$  is defined as

$$\frac{B(B^- \rightarrow \bar{f}) - B(B^+ \rightarrow f)}{B(B^- \rightarrow \bar{f}) + B(B^+ \rightarrow f)}$$

the CP-violation charge asymmetry of exclusive  $B^-$  and  $B^+$  decay.

$A_{CP}(B^+ \rightarrow J/\psi(1S) K^+)$	DOCUMENT ID	TECN	COMMENT
( 1 ± 7 ) × 10 <sup>-3</sup> OUR AVERAGE			Error includes scale factor of 1.8.
See the ideogram below.			
-0.0076±0.0050±0.0022	SAKAI	10	BELL $e^+e^- \rightarrow \Upsilon(4S)$
0.0075±0.0061±0.0030	<sup>1</sup> ABAZOV	08o	D0 $p\bar{p}$ at 1.96 TeV
0.09 ± 0.07 ± 0.02	<sup>2</sup> WEI	08	BELL $e^+e^- \rightarrow \Upsilon(4S)$
0.030 ± 0.014 ± 0.010	<sup>3</sup> AUBERT	05J	BABR $e^+e^- \rightarrow \Upsilon(4S)$
0.018 ± 0.043 ± 0.004	<sup>4</sup> BONVICINI	00	CLE2 $e^+e^- \rightarrow \Upsilon(4S)$
••• We do not use the following data for averages, fits, limits, etc. •••			
0.03 ± 0.015 ± 0.006	AUBERT	04P	BABR Repl. by AUBERT 05J
-0.026 ± 0.022 ± 0.017	ABE	03B	BELL Repl. by SAKAI 10
0.003 ± 0.030 ± 0.004	AUBERT	02F	BABR Repl. by AUBERT 04P

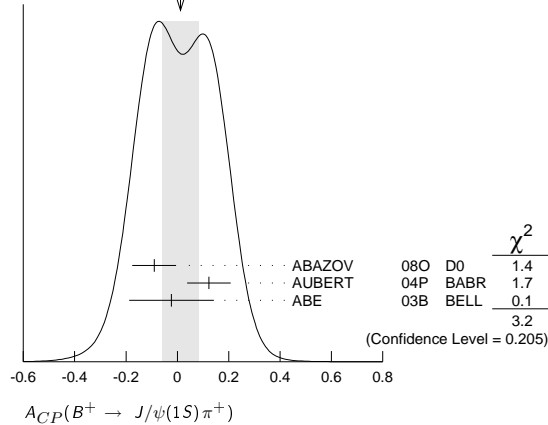
- <sup>1</sup> Uses  $J/\psi \rightarrow \mu^+ \mu^-$  decay.
- <sup>2</sup> Uses  $B^+ \rightarrow J/\psi K^+$ , where  $J/\psi \rightarrow p\bar{p}$ .
- <sup>3</sup> The result reported corresponds to  $-A_{CP}$ .
- <sup>4</sup> A +0.3% correction is applied due to a slightly higher reconstruction efficiency for the positive kaons.



## Meson Particle Listings

 $B^\pm$  $A_{CP}(B^+ \rightarrow J/\psi(1S)\pi^+)$ 

VALUE	DOCUMENT ID	TECN	COMMENT
<b><math>0.01 \pm 0.07</math> OUR AVERAGE</b>	Error includes scale factor of 1.3. See the ideogram below.		
$-0.09 \pm 0.08 \pm 0.03$	<sup>1</sup> ABAZOV	08o D0	$p\bar{p}$ at 1.96 TeV
$+0.123 \pm 0.085 \pm 0.004$	AUBERT	04P BABR	$e^+e^- \rightarrow \Upsilon(4S)$
$-0.023 \pm 0.164 \pm 0.015$	ABE	03B BELL	$e^+e^- \rightarrow \Upsilon(4S)$
••• We do not use the following data for averages, fits, limits, etc. •••			
$+0.01 \pm 0.22 \pm 0.01$	AUBERT	02F BABR	Repl. by AUBERT 04P

<sup>1</sup> Uses  $J/\psi \rightarrow \mu^+\mu^-$  decay.WEIGHTED AVERAGE  
 $0.01 \pm 0.07$  (Error scaled by 1.3) $A_{CP}(B^+ \rightarrow J/\psi\rho^+)$ 

VALUE	DOCUMENT ID	TECN	COMMENT
<b><math>-0.11 \pm 0.12 \pm 0.08</math></b>	AUBERT	07Ac BABR	$e^+e^- \rightarrow \Upsilon(4S)$

 $A_{CP}(B^+ \rightarrow J/\psi K^*(892)^+)$ 

VALUE	DOCUMENT ID	TECN	COMMENT
<b><math>-0.048 \pm 0.029 \pm 0.016</math></b>	<sup>1</sup> AUBERT	05j BABR	$e^+e^- \rightarrow \Upsilon(4S)$

<sup>1</sup> The result reported corresponds to  $-A_{CP}$ . $A_{CP}(B^+ \rightarrow \eta_c K^+)$ 

VALUE	DOCUMENT ID	TECN	COMMENT
<b><math>-0.16 \pm 0.08 \pm 0.02</math></b>	<sup>1</sup> WEI	08 BELL	$e^+e^- \rightarrow \Upsilon(4S)$

<sup>1</sup> Uses  $B^+ \rightarrow \eta_c K^+$ , where  $\eta_c \rightarrow p\bar{p}$ . $A_{CP}(B^+ \rightarrow \psi(2S)\pi^+)$ 

VALUE	DOCUMENT ID	TECN	COMMENT
<b><math>0.022 \pm 0.085 \pm 0.016</math></b>	BHARDWAJ	08 BELL	$e^+e^- \rightarrow \Upsilon(4S)$

 $A_{CP}(B^+ \rightarrow \psi(2S)K^+)$ 

VALUE	DOCUMENT ID	TECN	COMMENT
<b><math>-0.025 \pm 0.024</math> OUR AVERAGE</b>			
$0.052 \pm 0.059 \pm 0.020$	AUBERT	05j BABR	$e^+e^- \rightarrow \Upsilon(4S)$
$-0.042 \pm 0.020 \pm 0.017$	ABE	03B BELL	$e^+e^- \rightarrow \Upsilon(4S)$
$0.02 \pm 0.091 \pm 0.01$	<sup>1</sup> BONVICINI	00 CLE2	$e^+e^- \rightarrow \Upsilon(4S)$

<sup>1</sup> A +0.3% correction is applied due to a slightly higher reconstruction efficiency for the positive kaons. $A_{CP}(B^+ \rightarrow \psi(2S)K^*(892)^+)$ 

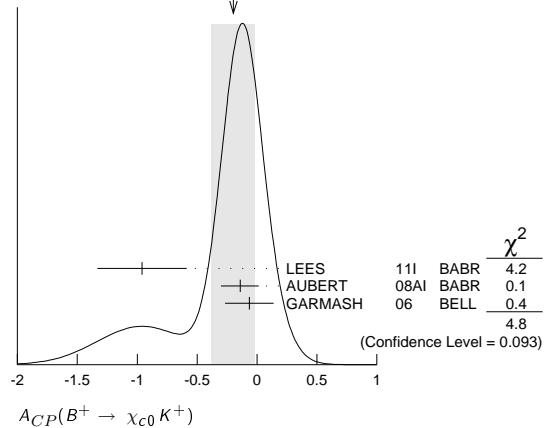
VALUE	DOCUMENT ID	TECN	COMMENT
<b><math>0.077 \pm 0.207 \pm 0.051</math></b>	<sup>1</sup> AUBERT	05j BABR	$e^+e^- \rightarrow \Upsilon(4S)$

<sup>1</sup> The result reported corresponds to  $-A_{CP}$ . $A_{CP}(B^+ \rightarrow \chi_{c1}(1P)\pi^+)$ 

VALUE	DOCUMENT ID	TECN	COMMENT
<b><math>0.07 \pm 0.18 \pm 0.02</math></b>	KUMAR	06 BELL	$e^+e^- \rightarrow \Upsilon(4S)$

 $A_{CP}(B^+ \rightarrow \chi_{c0} K^+)$ 

VALUE	DOCUMENT ID	TECN	COMMENT
<b><math>-0.20 \pm 0.18</math> OUR AVERAGE</b>	Error includes scale factor of 1.5. See the ideogram below.		
$-0.96 \pm 0.37 \pm 0.04$	LEES	11i BABR	$e^+e^- \rightarrow \Upsilon(4S)$
$-0.14 \pm 0.15 \pm 0.03$	AUBERT	08AI BABR	$e^+e^- \rightarrow \Upsilon(4S)$
$-0.065 \pm 0.20 \pm 0.035$	GARMASH	06 BELL	$e^+e^- \rightarrow \Upsilon(4S)$

WEIGHTED AVERAGE  
 $-0.20 \pm 0.18$  (Error scaled by 1.5) $A_{CP}(B^+ \rightarrow \chi_{c1} K^+)$ 

VALUE	DOCUMENT ID	TECN	COMMENT
<b><math>-0.009 \pm 0.033</math> OUR AVERAGE</b>			
$-0.01 \pm 0.03 \pm 0.02$	KUMAR	06 BELL	$e^+e^- \rightarrow \Upsilon(4S)$
$-0.003 \pm 0.076 \pm 0.017$	<sup>1</sup> AUBERT	05j BABR	$e^+e^- \rightarrow \Upsilon(4S)$

<sup>1</sup> The result reported corresponds to  $-A_{CP}$ . $A_{CP}(B^+ \rightarrow \chi_{c1} K^*(892)^+)$ 

VALUE	DOCUMENT ID	TECN	COMMENT
<b><math>0.471 \pm 0.378 \pm 0.268</math></b>	<sup>1</sup> AUBERT	05j BABR	$e^+e^- \rightarrow \Upsilon(4S)$

<sup>1</sup> The result reported corresponds to  $-A_{CP}$ . $A_{CP}(B^+ \rightarrow \bar{D}^0 \pi^+)$ 

VALUE	DOCUMENT ID	TECN	COMMENT
<b><math>-0.008 \pm 0.008</math></b>	ABE	06 BELL	$e^+e^- \rightarrow \Upsilon(4S)$

 $A_{CP}(B^+ \rightarrow D_{CP(+)} \pi^+)$ 

VALUE	DOCUMENT ID	TECN	COMMENT
<b><math>0.035 \pm 0.024</math></b>	ABE	06 BELL	$e^+e^- \rightarrow \Upsilon(4S)$

 $A_{CP}(B^+ \rightarrow D_{CP(-)} \pi^+)$ 

VALUE	DOCUMENT ID	TECN	COMMENT
<b><math>0.017 \pm 0.026</math></b>	ABE	06 BELL	$e^+e^- \rightarrow \Upsilon(4S)$

 $A_{CP}(B^+ \rightarrow \bar{D}^0 K^+)$ 

VALUE	DOCUMENT ID	TECN	COMMENT
<b><math>0.066 \pm 0.036</math></b>	ABE	06 BELL	$e^+e^- \rightarrow \Upsilon(4S)$

••• We do not use the following data for averages, fits, limits, etc. •••

$0.003 \pm 0.080 \pm 0.037$	<sup>1</sup> ABE	03b BELL	Repl. by SWAIN 03
$0.04 \pm 0.06 \pm 0.03$	<sup>2</sup> SWAIN	03 BELL	Repl. by ABE 06

<sup>1</sup> Corresponds to 90% confidence range  $-0.15 < A_{CP} < 0.16$ .<sup>2</sup> Corresponds to 90% confidence range  $-0.07 < A_{CP} < 0.15$ . $r_B(B^+ \rightarrow D^0 K^+)$  $r_B^{(*)}$  and  $\delta_B^{(*)}$  are the amplitude ratios and relative strong phases between the amplitudes of  $A(B^+ \rightarrow D^{(*)0} K^+)$  and  $A(B^+ \rightarrow \bar{D}^{(*)0} K^+)$ ,

VALUE	CL%	DOCUMENT ID	TECN	COMMENT
<b><math>0.113 \pm 0.024</math> <math>-0.021</math> OUR AVERAGE</b>				
$0.096 \pm 0.029 \pm 0.006$	<sup>1</sup> 90	DEL-AMO-SA..10F	BABR	$e^+e^- \rightarrow \Upsilon(4S)$
$0.095 \pm 0.051$ $-0.041$	<sup>2</sup> 90	DEL-AMO-SA..10H	BABR	$e^+e^- \rightarrow \Upsilon(4S)$
$0.160 \pm 0.040 \pm 0.051$ $-0.038 \pm 0.015$	<sup>3</sup> 90	POLUEKTOV 10	BELL	$e^+e^- \rightarrow \Upsilon(4S)$

••• We do not use the following data for averages, fits, limits, etc. •••

$< 0.13$	90	LEES	11D BABR	$e^+e^- \rightarrow \Upsilon(4S)$
$0.086 \pm 0.032 \pm 0.015$	<sup>5</sup> 90	AUBERT	08AL BABR	Repl. by DEL-AMO-SANCHEZ 10F
$< 0.19$	90	HORII	08 BELL	$e^+e^- \rightarrow \Upsilon(4S)$
$0.159 \pm 0.054$ $-0.056 \pm 0.050$	<sup>6</sup> 90	POLUEKTOV 06	BELL	Repl. by POLUEKTOV 10
$0.12 \pm 0.08 \pm 0.05$	<sup>7</sup> 90	AUBERT,B	05Y BABR	Repl. by AUBERT 08AL

<sup>1</sup> Uses Dalitz plot analysis of  $\bar{D}^0 \rightarrow K_S^0 \pi^+ \pi^-$ ,  $K_S^0 K^+ K^-$  decays from  $B^+ \rightarrow D^{(*)} K^{(*)+}$  modes. The corresponding two standard deviation interval is  $0.037 < r_B < 0.155$ .<sup>2</sup> Uses the Cabibbo suppressed decay of  $B^+ \rightarrow \bar{D}^0 K^+$  followed by  $\bar{D}^0 \rightarrow K^- \pi^+$ .<sup>3</sup> Uses Dalitz plot analysis of  $\bar{D}^0 \rightarrow K_S^0 \pi^+ \pi^-$  decays from  $B^+ \rightarrow D^0 K^+$  modes. The corresponding two standard deviation interval is  $0.084 < r_B < 0.239$ .<sup>4</sup> Uses decays of neutral  $D$  to  $K^- \pi^+ \pi^0$ .

See key on page 457

# Meson Particle Listings

## $B^\pm$

- <sup>5</sup> Uses Dalitz plot analysis of  $\overline{D}^0 \rightarrow K_S^0 \pi^+ \pi^-$  and  $\overline{D}^0 \rightarrow K_S^0 K^+ K^-$  decays coming from  $B^\pm \rightarrow D^{(*)} K^{(*)\pm}$  modes.  
<sup>6</sup> Uses a Dalitz plot analysis of the  $\overline{D}^0 \rightarrow K_S^0 \pi^+ \pi^-$  decays; Combines the  $D K^+$ ,  $D^* K^+$  and  $D K^{*+}$  modes.  
<sup>7</sup> Uses a Dalitz analysis of neutral  $D$  decays to  $K_S^0 \pi^+ \pi^-$  in the processes  $B^\pm \rightarrow D^{(*)} K^\pm, D^* \rightarrow D \pi^0, D \gamma$ .

### $\delta_B(B^+ \rightarrow D^0 K^+)$

VALUE (°)	DOCUMENT ID	TECN	COMMENT
<b>125 ± 16 OUR AVERAGE</b>			
119 $\frac{+19}{-20} \pm 4$	<sup>1</sup> DEL-AMO-SA...10F	BABR	$e^+ e^- \rightarrow \Upsilon(4S)$
136.7 $\frac{+13.0}{-15.8} \pm 23.2$	<sup>2</sup> POLUEKTOV 10	BELL	$e^+ e^- \rightarrow \Upsilon(4S)$
109 $\frac{+27}{-30} \pm 8$	<sup>3</sup> AUBERT	08AL BABR	Repl. by DEL-AMO-SANCHEZ 10F
145.7 $\frac{+19.0}{-19.7} \pm 23.1$	<sup>4</sup> POLUEKTOV 06	BELL	Repl. by POLUEKTOV 10
104 $\pm 45 \frac{+23}{-32}$	<sup>5</sup> AUBERT,B	05V BABR	Repl. by AUBERT 08AL

- • • We do not use the following data for averages, fits, limits, etc. • • •
- <sup>1</sup> Uses Dalitz plot analysis of  $\overline{D}^0 \rightarrow K_S^0 \pi^+ \pi^-$ ,  $K_S^0 K^+ K^-$  decays from  $B^+ \rightarrow D^{(*)} K^{(*)+}$  modes. The corresponding two standard deviation interval is  $75^\circ < \delta_B < 157^\circ$ .  
<sup>2</sup> Uses Dalitz plot analysis of  $\overline{D}^0 \rightarrow K_S^0 \pi^+ \pi^-$  decays from  $B^+ \rightarrow D^0 K^+$  modes. The corresponding two standard deviation interval is  $102.2^\circ < \delta_B < 162.3^\circ$ .  
<sup>3</sup> Uses Dalitz plot analysis of  $\overline{D}^0 \rightarrow K_S^0 \pi^+ \pi^-$  and  $\overline{D}^0 \rightarrow K_S^0 K^+ K^-$  decays coming from  $B^\pm \rightarrow D^{(*)} K^{(*)\pm}$  modes.  
<sup>4</sup> Uses a Dalitz plot analysis of the  $\overline{D}^0 \rightarrow K_S^0 \pi^+ \pi^-$  decays; Combines the  $D K^+$ ,  $D^* K^+$  and  $D K^{*+}$  modes.  
<sup>5</sup> Uses a Dalitz analysis of neutral  $D$  decays to  $K_S^0 \pi^+ \pi^-$  in the processes  $B^\pm \rightarrow D^{(*)} K^\pm, D^* \rightarrow D \pi^0, D \gamma$ .

### $r_B(B^+ \rightarrow DK^{*+})$

$r_B$  and  $\delta_B$  are the amplitude ratios and relative strong phases between the amplitudes of  $A_{CP}(B^+ \rightarrow DK^{*+})$  and  $A_{CP}(B^+ \rightarrow \overline{D} K^{*+})$ ,

VALUE	DOCUMENT ID	TECN	COMMENT
<b>0.34 ± 0.09 OUR AVERAGE</b>			Error includes scale factor of 1.3.
0.31 ± 0.07	<sup>1</sup> AUBERT	09AJ BABR	$e^+ e^- \rightarrow \Upsilon(4S)$
0.564 $\frac{+0.216}{-0.155} \pm 0.093$	<sup>2</sup> POLUEKTOV 06	BELL	$e^+ e^- \rightarrow \Upsilon(4S)$
0.181 $\frac{+0.088}{-0.108} \pm 0.042$	<sup>3</sup> AUBERT	08AL BABR	Repl. by AUBERT 09AJ

- • • We do not use the following data for averages, fits, limits, etc. • • •
- <sup>1</sup> Obtained by combining the GLW and ADS methods. The 2-sigma range corresponds to [0.17, 0.43].  
<sup>2</sup> Uses a Dalitz plot analysis of the  $\overline{D}^0 \rightarrow K_S^0 \pi^+ \pi^-$  decays; Combines the  $D K^+$ ,  $D^* K^+$  and  $D K^{*+}$  modes.  
<sup>3</sup> Uses Dalitz plot analysis of  $\overline{D}^0 \rightarrow K_S^0 \pi^+ \pi^-$  and  $\overline{D}^0 \rightarrow K_S^0 K^+ K^-$  decays coming from  $B^\pm \rightarrow D^{(*)} K^{(*)\pm}$  modes.

### $\delta_B(B^+ \rightarrow DK^{*+})$

VALUE (°)	DOCUMENT ID	TECN	COMMENT
<b>157 ± 70 OUR AVERAGE</b>			Error includes scale factor of 2.0.
104 $\frac{+39}{-37} \pm 18$	<sup>1</sup> AUBERT	08AL BABR	$e^+ e^- \rightarrow \Upsilon(4S)$
242.6 $\frac{+20.2}{-23.2} \pm 49.4$	<sup>2</sup> POLUEKTOV 06	BELL	$e^+ e^- \rightarrow \Upsilon(4S)$

- <sup>1</sup> Uses Dalitz plot analysis of  $\overline{D}^0 \rightarrow K_S^0 \pi^+ \pi^-$  and  $\overline{D}^0 \rightarrow K_S^0 K^+ K^-$  decays coming from  $B^\pm \rightarrow D^{(*)} K^{(*)\pm}$  modes.  
<sup>2</sup> Uses a Dalitz plot analysis of the  $\overline{D}^0 \rightarrow K_S^0 \pi^+ \pi^-$  decays; Combines the  $D K^+$ ,  $D^* K^+$  and  $D K^{*+}$  modes.

### $A_{CP}(B^+ \rightarrow [K^-\pi^+]_D K^+)$

VALUE	DOCUMENT ID	TECN	COMMENT
<b>-0.50 ± 0.21 OUR AVERAGE</b>			
-0.82 ± 0.44 ± 0.09	AALTONEN 11AJ	CDF	$p\overline{p}$ at 1.96 TeV
-0.39 $\frac{+0.26}{-0.28} \pm 0.04$	HORII 11	BELL	$e^+ e^- \rightarrow \Upsilon(4S)$
-0.86 ± 0.47 $\frac{+0.12}{-0.16}$	DEL-AMO-SA...10H	BABR	$e^+ e^- \rightarrow \Upsilon(4S)$
-0.1 $\frac{+0.8}{-1.0} \pm 0.4$	HORII 08	BELL	Repl. by HORII 11
+0.88 $\frac{+0.77}{-0.62} \pm 0.06$	SAIGO 05	BELL	Repl. by HORII 08

### $A_{CP}(B^+ \rightarrow [K^-\pi^+]_{\overline{D}} K^*(892)^+)$

VALUE	DOCUMENT ID	TECN	COMMENT
<b>-0.34 ± 0.43 ± 0.16</b>			
	AUBERT	09AJ BABR	$e^+ e^- \rightarrow \Upsilon(4S)$
-0.22 ± 0.61 ± 0.17	AUBERT,B	05V BABR	Repl. by AUBERT 09AJ

• • • We do not use the following data for averages, fits, limits, etc. • • •

### $A_{CP}(B^+ \rightarrow [K^-\pi^+]_D \pi^+)$

VALUE	DOCUMENT ID	TECN	COMMENT
<b>0.00 ± 0.09 OUR AVERAGE</b>			
0.13 ± 0.25 ± 0.02	AALTONEN 11AJ	CDF	$p\overline{p}$ at 1.96 TeV
-0.04 ± 0.11 $\frac{+0.02}{-0.01}$	HORII 11	BELL	$e^+ e^- \rightarrow \Upsilon(4S)$
0.03 ± 0.17 ± 0.04	DEL-AMO-SA...10H	BABR	$e^+ e^- \rightarrow \Upsilon(4S)$
-0.02 $\frac{+0.15}{-0.16} \pm 0.04$	HORII 08	BELL	Repl. by HORII 11
+0.30 $\frac{+0.29}{-0.25} \pm 0.06$	SAIGO 05	BELL	Repl. by HORII 08

### $A_{CP}(B^+ \rightarrow [K^-\pi^+]_{(D\pi)} \pi^+)$

VALUE	DOCUMENT ID	TECN	COMMENT
<b>-0.09 ± 0.27 ± 0.05</b>			
	DEL-AMO-SA...10H	BABR	$e^+ e^- \rightarrow \Upsilon(4S)$

### $A_{CP}(B^+ \rightarrow [K^-\pi^+]_{(D\gamma)} \pi^+)$

VALUE	DOCUMENT ID	TECN	COMMENT
<b>-0.65 ± 0.55 ± 0.22</b>			
	DEL-AMO-SA...10H	BABR	$e^+ e^- \rightarrow \Upsilon(4S)$

### $A_{CP}(B^+ \rightarrow [K^-\pi^+]_{(D\pi)} K^+)$

VALUE	DOCUMENT ID	TECN	COMMENT
<b>0.77 ± 0.35 ± 0.12</b>			
	DEL-AMO-SA...10H	BABR	$e^+ e^- \rightarrow \Upsilon(4S)$

### $A_{CP}(B^+ \rightarrow [K^-\pi^+]_{(D\gamma)} K^+)$

VALUE	DOCUMENT ID	TECN	COMMENT
<b>0.36 ± 0.94 ± 0.25</b>			
	DEL-AMO-SA...10H	BABR	$e^+ e^- \rightarrow \Upsilon(4S)$

### $A_{CP}(B^+ \rightarrow [\pi^+\pi^-\pi^0]_D K^+)$

VALUE	DOCUMENT ID	TECN	COMMENT
<b>-0.02 ± 0.15 ± 0.03</b>			
	<sup>1</sup> AUBERT	07BJ BABR	$e^+ e^- \rightarrow \Upsilon(4S)$
-0.02 ± 0.16 ± 0.03	AUBERT,B	05T BABR	Repl. by AUBERT 07BJ

- • • We do not use the following data for averages, fits, limits, etc. • • •
- <sup>1</sup> Uses a Dalitz plot analysis of  $D^0 \rightarrow \pi^+ \pi^- \pi^0$ . Also reports the one-sigma regions:  $0.06 < r_B < 0.78$ ,  $-30^\circ < \gamma < 76^\circ$ , and  $-27^\circ < \delta < 78^\circ$ .

### $A_{CP}(B^+ \rightarrow D_{CP(+1)} K^+)$

VALUE	DOCUMENT ID	TECN	COMMENT
<b>0.24 ± 0.06 OUR AVERAGE</b>			Error includes scale factor of 1.1.
0.39 ± 0.17 ± 0.04	AALTONEN 10A	CDF	$p\overline{p}$ at 1.96 TeV
0.25 ± 0.06 ± 0.02	<sup>1</sup> DEL-AMO-SA...10G	BABR	$e^+ e^- \rightarrow \Upsilon(4S)$
0.06 ± 0.14 ± 0.05	ABE 06	BELL	$e^+ e^- \rightarrow \Upsilon(4S)$
0.27 ± 0.09 ± 0.04	AUBERT	08AA BABR	Repl. by DEL-AMO-SANCHEZ 10G
0.35 ± 0.13 ± 0.04	AUBERT	06J BABR	Repl. by AUBERT 08AA
0.07 ± 0.17 ± 0.06	AUBERT	04N BABR	Repl. by AUBERT 06J
0.29 ± 0.26 ± 0.05	<sup>2</sup> ABE	03D BELL	Repl. by SWAIN 03
0.06 ± 0.19 ± 0.04	<sup>3</sup> SWAIN	03 BELL	Repl. by ABE 06

- <sup>1</sup> Reports the first evidence for direct  $CP$  violation in  $B \rightarrow DK$  decays with 3.6 standard deviations.  
<sup>2</sup> Corresponds to 90% confidence range  $-0.14 < A_{CP} < 0.73$ .  
<sup>3</sup> Corresponds to 90% confidence range  $-0.26 < A_{CP} < 0.38$ .

### $A_{CP}(B^+ \rightarrow D_{CP(-1)} K^+)$

VALUE	DOCUMENT ID	TECN	COMMENT
<b>-0.10 ± 0.07 OUR AVERAGE</b>			
-0.09 ± 0.07 ± 0.02	DEL-AMO-SA...10G	BABR	$e^+ e^- \rightarrow \Upsilon(4S)$
-0.12 ± 0.14 ± 0.05	ABE 06	BELL	$e^+ e^- \rightarrow \Upsilon(4S)$
-0.09 ± 0.09 ± 0.02	AUBERT	08AA BABR	Repl. by DEL-AMO-SANCHEZ 10G
-0.06 ± 0.13 ± 0.04	AUBERT	06J BABR	Repl. by AUBERT 08AA
-0.22 ± 0.24 ± 0.04	<sup>1</sup> ABE	03D BELL	Repl. by SWAIN 03
-0.19 ± 0.17 ± 0.05	<sup>2</sup> SWAIN	03 BELL	Repl. by ABE 06

- <sup>1</sup> Corresponds to 90% confidence range  $-0.62 < A_{CP} < 0.18$ .  
<sup>2</sup> Corresponds to 90% confidence range  $-0.47 < A_{CP} < 0.11$ .

### $A_{CP}(B^+ \rightarrow \overline{D}^{*0} \pi^+)$

VALUE	DOCUMENT ID	TECN	COMMENT
<b>-0.014 ± 0.015</b>			
	ABE 06	BELL	$e^+ e^- \rightarrow \Upsilon(4S)$

### $A_{CP}(B^+ \rightarrow (D_{CP(+1)}^*)^0 \pi^+)$

VALUE	DOCUMENT ID	TECN	COMMENT
<b>-0.021 ± 0.045</b>			
	ABE 06	BELL	$e^+ e^- \rightarrow \Upsilon(4S)$

### $A_{CP}(B^+ \rightarrow (D_{CP(-1)}^*)^0 \pi^+)$

VALUE	DOCUMENT ID	TECN	COMMENT
<b>-0.090 ± 0.051</b>			
	ABE 06	BELL	$e^+ e^- \rightarrow \Upsilon(4S)$

## Meson Particle Listings

 $B^\pm$  $A_{CP}(B^+ \rightarrow D^{*0} K^+)$ 

VALUE	DOCUMENT ID	TECN	COMMENT
<b><math>-0.07 \pm 0.04</math> OUR AVERAGE</b>			
$-0.06 \pm 0.04 \pm 0.01$	AUBERT	08BF BABR	$e^+ e^- \rightarrow \Upsilon(4S)$
$-0.089 \pm 0.086$	ABE	06 BELL	$e^+ e^- \rightarrow \Upsilon(4S)$

 $r_B^*(B^+ \rightarrow D^{*0} K^+)$ 

$r_B^{(*)}$  and  $\delta_B^{(*)}$  are the amplitude ratios and relative strong phases between the amplitudes of  $A(B^+ \rightarrow D^{(*)0} K^+)$  and  $A(B^+ \rightarrow \bar{D}^{(*)0} K^+)$ ,

VALUE	DOCUMENT ID	TECN	COMMENT
<b><math>0.123^{+0.025}_{-0.029}</math> OUR AVERAGE</b>			
$0.133^{+0.042}_{-0.039} \pm 0.013$	1 DEL-AMO-SA...10F	BABR	$e^+ e^- \rightarrow \Upsilon(4S)$
$0.096^{+0.035}_{-0.051}$	2 DEL-AMO-SA...10H	BABR	$e^+ e^- \rightarrow \Upsilon(4S)$
$0.196^{+0.072+0.064}_{-0.069-0.017}$	3 POLUEKTOV 10	BELL	$e^+ e^- \rightarrow \Upsilon(4S)$
$0.135 \pm 0.050 \pm 0.012$	4 AUBERT	08AL BABR	Repl. by DEL-AMO-SANCHEZ 10F
$0.175^{+0.108}_{-0.099} \pm 0.050$	5 POLUEKTOV 06	BELL	Repl. by POLUEKTOV 10
$0.17 \pm 0.10 \pm 0.04$	6 AUBERT,B	05Y BABR	Repl. by AUBERT 08AL

- • • We do not use the following data for averages, fits, limits, etc. • • •
- 1 Uses Dalitz plot analysis of  $\bar{D}^0 \rightarrow K_S^0 \pi^+ \pi^-$ ,  $K_S^0 K^+ K^-$  decays from  $B^+ \rightarrow D^{(*)} K^{(*)+}$  modes. The corresponding two standard deviation interval is  $0.049 < r_B^* < 0.215$ .
- 2 Uses the Cabibbo suppressed decay of  $B^+ \rightarrow \bar{D}^* K^+$  followed by  $\bar{D}^* \rightarrow \bar{D} \pi^0$  or  $\bar{D} \gamma$ , and  $\bar{D} \rightarrow K^- \pi^+$ .
- 3 Uses Dalitz plot analysis of  $\bar{D}^0 \rightarrow K_S^0 \pi^+ \pi^-$  decays from  $B^+ \rightarrow D^{*0} K^+$  modes. The corresponding two standard deviation interval is  $0.061 < r_B^* < 0.271$ .
- 4 Uses Dalitz plot analysis of  $\bar{D}^0 \rightarrow K_S^0 \pi^+ \pi^-$  and  $\bar{D}^0 \rightarrow K_S^0 K^+ K^-$  decays coming from  $B^\pm \rightarrow D^{(*)} K^{(*)\pm}$  modes.
- 5 Uses a Dalitz plot analysis of the  $\bar{D}^0 \rightarrow K_S^0 \pi^+ \pi^-$  decays; Combines the  $D K^+$ ,  $D^* K^+$  and  $D K^{*+}$  modes.
- 6 Uses a Dalitz analysis of neutral  $D$  decays to  $K_S^0 \pi^+ \pi^-$  in the processes  $B^\pm \rightarrow D^{(*)} K^\pm$ ,  $D^* \rightarrow D \pi^0$ ,  $D \gamma$ .

 $\delta_B^*(B^+ \rightarrow D^{*0} K^+)$ 

VALUE (°)	DOCUMENT ID	TECN	COMMENT
<b><math>300 \pm 30</math> OUR AVERAGE</b>			Error includes scale factor of 1.7.
$278 \pm 21 \pm 6$	1 DEL-AMO-SA...10F	BABR	$e^+ e^- \rightarrow \Upsilon(4S)$
$341.9^{+18.0}_{-19.6} \pm 23.1$	2 POLUEKTOV 10	BELL	$e^+ e^- \rightarrow \Upsilon(4S)$
$297^{+27}_{-29} \pm 6.4$	3 AUBERT	08AL BABR	Repl. by DEL-AMO-SANCHEZ 10F
$302.0^{+33.8}_{-35.1} \pm 23.7$	4 POLUEKTOV 06	BELL	Repl. by POLUEKTOV 10
$296 \pm 41 \pm \frac{20}{19}$	5 AUBERT,B	05Y BABR	Repl. by AUBERT 08AL

- • • We do not use the following data for averages, fits, limits, etc. • • •
- 1 Uses Dalitz plot analysis of  $\bar{D}^0 \rightarrow K_S^0 \pi^+ \pi^-$ ,  $K_S^0 K^+ K^-$  decays from  $B^+ \rightarrow D^{(*)} K^{(*)+}$  modes. The corresponding two standard deviation interval is  $236^\circ < \delta_B^* < 322^\circ$ .
- 2 Uses Dalitz plot analysis of  $\bar{D}^0 \rightarrow K_S^0 \pi^+ \pi^-$  decays from  $B^+ \rightarrow D^* K^+$  modes. The corresponding two standard deviation interval is  $296.5^\circ < \delta_B^* < 382.7^\circ$ .
- 3 Uses Dalitz plot analysis of  $\bar{D}^0 \rightarrow K_S^0 \pi^+ \pi^-$  and  $\bar{D}^0 \rightarrow K_S^0 K^+ K^-$  decays coming from  $B^\pm \rightarrow D^{(*)} K^{(*)\pm}$  modes.
- 4 Uses a Dalitz plot analysis of the  $\bar{D}^0 \rightarrow K_S^0 \pi^+ \pi^-$  decays; Combines the  $D K^+$ ,  $D^* K^+$  and  $D K^{*+}$  modes.
- 5 Uses a Dalitz analysis of neutral  $D$  decays to  $K_S^0 \pi^+ \pi^-$  in the processes  $B^\pm \rightarrow D^{(*)} K^\pm$ ,  $D^* \rightarrow D \pi^0$ ,  $D \gamma$ .

 $A_{CP}(B^+ \rightarrow D_{CP(+)}^{*0} K^+)$ 

VALUE	DOCUMENT ID	TECN	COMMENT
<b><math>-0.12 \pm 0.08</math> OUR AVERAGE</b>			
$-0.11 \pm 0.09 \pm 0.01$	AUBERT	08BF BABR	$e^+ e^- \rightarrow \Upsilon(4S)$
$-0.20 \pm 0.22 \pm 0.04$	ABE	06 BELL	$e^+ e^- \rightarrow \Upsilon(4S)$
$-0.10 \pm 0.23^{+0.03}_{-0.04}$	AUBERT	05N BABR	Repl. by AUBERT 08BF

 $A_{CP}(B^+ \rightarrow D_{CP(-)}^{*0} K^+)$ 

VALUE	DOCUMENT ID	TECN	COMMENT
<b><math>0.07 \pm 0.10</math> OUR AVERAGE</b>			
$+0.06 \pm 0.10 \pm 0.02$	AUBERT	08BF BABR	$e^+ e^- \rightarrow \Upsilon(4S)$
$+0.13 \pm 0.30 \pm 0.08$	ABE	06 BELL	$e^+ e^- \rightarrow \Upsilon(4S)$

 $A_{CP}(B^+ \rightarrow D_{CP(+)} K^*(892)^+)$ 

VALUE	DOCUMENT ID	TECN	COMMENT
<b><math>+0.09 \pm 0.13 \pm 0.06</math></b>	AUBERT	09AJ BABR	$e^+ e^- \rightarrow \Upsilon(4S)$
$-0.08 \pm 0.19 \pm 0.08$	AUBERT,B	05U BABR	Repl. by AUBERT 09AJ

 $A_{CP}(B^+ \rightarrow D_{CP(-)} K^*(892)^+)$ 

VALUE	DOCUMENT ID	TECN	COMMENT
<b><math>-0.23 \pm 0.21 \pm 0.07</math></b>	AUBERT	09AJ BABR	$e^+ e^- \rightarrow \Upsilon(4S)$
$-0.26 \pm 0.40 \pm 0.12$	AUBERT,B	05U BABR	Repl. by AUBERT 09AJ

 $A_{CP}(B^+ \rightarrow D^{*+} \bar{D}^{*0})$ 

VALUE	DOCUMENT ID	TECN	COMMENT
<b><math>-0.15 \pm 0.11 \pm 0.02</math></b>	AUBERT,B	06A BABR	$e^+ e^- \rightarrow \Upsilon(4S)$

 $A_{CP}(B^+ \rightarrow D^{*+} \bar{D}^0)$ 

VALUE	DOCUMENT ID	TECN	COMMENT
<b><math>-0.06 \pm 0.13 \pm 0.02</math></b>	AUBERT,B	06A BABR	$e^+ e^- \rightarrow \Upsilon(4S)$

 $A_{CP}(B^+ \rightarrow D^+ \bar{D}^{*0})$ 

VALUE	DOCUMENT ID	TECN	COMMENT
<b><math>0.13 \pm 0.18 \pm 0.04</math></b>	AUBERT,B	06A BABR	$e^+ e^- \rightarrow \Upsilon(4S)$

 $A_{CP}(B^+ \rightarrow D^+ \bar{D}^0)$ 

VALUE	DOCUMENT ID	TECN	COMMENT
<b><math>-0.03 \pm 0.07</math> OUR AVERAGE</b>			
$0.00 \pm 0.08 \pm 0.02$	ADACHI	08 BELL	$e^+ e^- \rightarrow \Upsilon(4S)$
$-0.13 \pm 0.14 \pm 0.02$	AUBERT,B	06A BABR	$e^+ e^- \rightarrow \Upsilon(4S)$

 $A_{CP}(B^+ \rightarrow K_S^0 \pi^+)$ 

VALUE	DOCUMENT ID	TECN	COMMENT
<b><math>0.009 \pm 0.029</math> OUR AVERAGE</b>			Error includes scale factor of 1.2.
$0.03 \pm 0.03 \pm 0.01$	LIN	07 BELL	$e^+ e^- \rightarrow \Upsilon(4S)$
$-0.029 \pm 0.039 \pm 0.010$	1 AUBERT,BE	06c BABR	$e^+ e^- \rightarrow \Upsilon(4S)$
$0.18 \pm 0.24$	2 CHEN	00 CLE2	$e^+ e^- \rightarrow \Upsilon(4S)$
$-0.09 \pm 0.05 \pm 0.01$	3 AUBERT,BE	05E BABR	Repl. by AUBERT,BE 06c
$-0.05 \pm 0.05 \pm 0.01$	4 CHAO	05A BELL	Repl. by LIN 07
$-0.05 \pm 0.08 \pm 0.01$	5 AUBERT	04M BABR	Repl. by AUBERT,BE 05E
$0.07^{+0.09+0.01}_{-0.08-0.03}$	6 UNNO	03 BELL	Repl. by CHAO 05A
$0.46 \pm 0.15 \pm 0.02$	7 CASEY	02 BELL	Repl. by UNNO 03
$0.098^{+0.430+0.020}_{-0.343-0.063}$	8 ABE	01k BELL	Repl. by CASEY 02
$-0.21 \pm 0.18 \pm 0.03$	9 AUBERT	01E BABR	Repl. by AUBERT 04M

- 1 Corresponds to 90% confidence range  $-0.092 < A_{CP} < 0.036$ .
- 2 Corresponds to 90% confidence range  $-0.22 < A_{CP} < 0.56$ .
- 3 Corresponds to 90% confidence range  $-0.16 < A_{CP} < -0.02$ .
- 4 Corresponds to a 90% CL interval of  $-0.04 < A_{CP} < 0.13$ .
- 5 90% CL interval  $-0.18 < A_{CP} < 0.08$ .
- 6 Corresponds to 90% confidence range  $-0.10 < A_{CP} < +0.22$ .
- 7 Corresponds to 90% confidence range  $+0.19 < A_{CP} < +0.72$ .
- 8 Corresponds to 90% confidence range  $-0.53 < A_{CP} < 0.82$ .
- 9 Corresponds to 90% confidence range  $-0.51 < A_{CP} < 0.09$ .

 $A_{CP}(B^+ \rightarrow K^+ \pi^0)$ 

VALUE	DOCUMENT ID	TECN	COMMENT
<b><math>0.051 \pm 0.025</math> OUR AVERAGE</b>			
$0.07 \pm 0.03 \pm 0.01$	LIN	08 BELL	$e^+ e^- \rightarrow \Upsilon(4S)$
$0.030 \pm 0.039 \pm 0.010$	AUBERT	07bc BABR	$e^+ e^- \rightarrow \Upsilon(4S)$
$-0.29 \pm 0.23$	1 CHEN	00 CLE2	$e^+ e^- \rightarrow \Upsilon(4S)$
$0.06 \pm 0.06 \pm 0.01$	2 AUBERT	05L BABR	Repl. by AUBERT 07bc
$0.06 \pm 0.06 \pm 0.02$	2 CHAO	05A BELL	Repl. by CHAO 04B
$0.04 \pm 0.05 \pm 0.02$	3 CHAO	04B BELL	Repl. by LIN 08
$-0.09 \pm 0.09 \pm 0.01$	4 AUBERT	03L BABR	Repl. by AUBERT 05L
$-0.02 \pm 0.19 \pm 0.02$	5 CASEY	02 BELL	Repl. by CHAO 04B
$-0.059^{+0.222+0.055}_{-0.196-0.017}$	6 ABE	01k BELL	Repl. by CASEY 02
$0.00 \pm 0.18 \pm 0.04$	7 AUBERT	01E BABR	Repl. by AUBERT 03L

- • • We do not use the following data for averages, fits, limits, etc. • • •
- 1 Corresponds to 90% confidence range  $-0.67 < A_{CP} < 0.09$ .
- 2 Corresponds to a 90% CL interval of  $-0.06 < A_{CP} < 0.18$ .
- 3 Corresponds to 90% CL interval of  $-0.05 < A_{CP} < 0.13$ .
- 4 Corresponds to 90% confidence range  $-0.24 < A_{CP} < 0.06$ .
- 5 Corresponds to 90% confidence range  $-0.35 < A_{CP} < +0.30$ .
- 6 Corresponds to 90% confidence range  $-0.40 < A_{CP} < 0.36$ .
- 7 Corresponds to 90% confidence range  $-0.30 < A_{CP} < +0.30$ .

 $A_{CP}(B^+ \rightarrow \eta' K^+)$ 

VALUE	DOCUMENT ID	TECN	COMMENT
<b><math>0.013 \pm 0.017</math> OUR AVERAGE</b>			
$0.008^{+0.017}_{-0.018} \pm 0.009$	AUBERT	09av BABR	$e^+ e^- \rightarrow \Upsilon(4S)$
$0.028 \pm 0.028 \pm 0.021$	SCHUEMANN	06 BELL	$e^+ e^- \rightarrow \Upsilon(4S)$
$0.03 \pm 0.12$	1 CHEN	00 CLE2	$e^+ e^- \rightarrow \Upsilon(4S)$



## Meson Particle Listings

 $B^\pm$  $A_{CP}(B^+ \rightarrow K^{*+} \pi^+ \pi^-)$ 

VALUE	DOCUMENT ID	TECN	COMMENT
$0.07 \pm 0.07 \pm 0.04$	AUBERT,B	06U	BABR $e^+ e^- \rightarrow \Upsilon(4S)$

 $A_{CP}(B^+ \rightarrow \rho^0 K^*(892)^+)$ 

VALUE	DOCUMENT ID	TECN	COMMENT
$0.31 \pm 0.13 \pm 0.03$	DEL-AMO-SA...11D	BABR	$e^+ e^- \rightarrow \Upsilon(4S)$
••• We do not use the following data for averages, fits, limits, etc. •••			
$0.20^{+0.32}_{-0.29} \pm 0.04$	AUBERT	03V	BABR Repl. by DEL-A MO-SANCHEZ 11D

 $A_{CP}(B^+ \rightarrow K^*(892)^+ f_0(980))$ 

VALUE	DOCUMENT ID	TECN	COMMENT
$-0.15 \pm 0.12 \pm 0.03$	DEL-AMO-SA...11D	BABR	$e^+ e^- \rightarrow \Upsilon(4S)$
••• We do not use the following data for averages, fits, limits, etc. •••			
$-0.34 \pm 0.21 \pm 0.03$	AUBERT,B	06G	BABR Repl. by DEL-AMO-SANCHEZ 11D

 $A_{CP}(B^+ \rightarrow a_1^+ K^0)$ 

VALUE	DOCUMENT ID	TECN	COMMENT
$+0.12 \pm 0.11 \pm 0.02$	AUBERT	08F	BABR $e^+ e^- \rightarrow \Upsilon(4S)$

 $A_{CP}(B^+ \rightarrow b_1^+ K^0)$ 

VALUE	DOCUMENT ID	TECN	COMMENT
$-0.03 \pm 0.15 \pm 0.02$	AUBERT	08AG	BABR $e^+ e^- \rightarrow \Upsilon(4S)$

 $A_{CP}(B^+ \rightarrow K^*(892)^0 \rho^+)$ 

VALUE	DOCUMENT ID	TECN	COMMENT
$-0.01 \pm 0.16 \pm 0.02$	AUBERT,B	06G	BABR $e^+ e^- \rightarrow \Upsilon(4S)$

 $A_{CP}(B^+ \rightarrow b_1^0 K^+)$ 

VALUE	DOCUMENT ID	TECN	COMMENT
$-0.46 \pm 0.20 \pm 0.02$	AUBERT	07B1	BABR $e^+ e^- \rightarrow \Upsilon(4S)$

 $A_{CP}(B^+ \rightarrow K^0 K^+)$ 

VALUE	DOCUMENT ID	TECN	COMMENT
<b><math>0.12 \pm 0.18</math> OUR AVERAGE</b>			
$0.13^{+0.23}_{-0.24} \pm 0.02$	LIN	07	BELL $e^+ e^- \rightarrow \Upsilon(4S)$
$0.10 \pm 0.26 \pm 0.03$	<sup>1</sup> AUBERT,BE	06C	BABR $e^+ e^- \rightarrow \Upsilon(4S)$
••• We do not use the following data for averages, fits, limits, etc. •••			
$0.15 \pm 0.33 \pm 0.03$	<sup>2</sup> AUBERT,BE	05E	BABR Repl. by AUBERT,BE 06C

<sup>1</sup> Corresponds to 90% confidence range  $-0.31 < A_{CP} < 0.54$ .

<sup>2</sup> Corresponds to 90% confidence range  $-0.43 < A_{CP} < 0.68$ .

 $A_{CP}(B^+ \rightarrow K^+ K_S^0 K_S^0)$ 

VALUE	DOCUMENT ID	TECN	COMMENT
<b><math>-0.04 \pm 0.11 \pm 0.02</math></b>	<sup>1</sup> AUBERT,B	04V	BABR $e^+ e^- \rightarrow \Upsilon(4S)$
<sup>1</sup> Corresponds to 90% confidence range $-0.23 < A_{CP} < 0.15$ .			

 $A_{CP}(B^+ \rightarrow K^+ K^- \pi^+)$ 

VALUE	DOCUMENT ID	TECN	COMMENT
<b><math>0.00 \pm 0.10 \pm 0.03</math></b>	AUBERT	07BB	BABR $e^+ e^- \rightarrow \Upsilon(4S)$

 $A_{CP}(B^+ \rightarrow K^+ K^- K^+)$ 

VALUE	DOCUMENT ID	TECN	COMMENT
<b><math>-0.017 \pm 0.026 \pm 0.015</math></b>	AUBERT	06O	BABR $e^+ e^- \rightarrow \Upsilon(4S)$
••• We do not use the following data for averages, fits, limits, etc. •••			
$0.02 \pm 0.07 \pm 0.03$	AUBERT	03M	BABR Repl. by AUBERT 06o

 $A_{CP}(B^+ \rightarrow \phi K^+)$ 

VALUE	DOCUMENT ID	TECN	COMMENT
<b><math>-0.01 \pm 0.06</math> OUR AVERAGE</b>			
$0.00 \pm 0.08 \pm 0.02$	AUBERT	06O	BABR $e^+ e^- \rightarrow \Upsilon(4S)$
$-0.07 \pm 0.17^{+0.03}_{-0.02}$	ACOSTA	05J	CDF $p\bar{p}$ at 1.96 TeV
$0.01 \pm 0.12 \pm 0.05$	<sup>1</sup> CHEN	03B	BELL $e^+ e^- \rightarrow \Upsilon(4S)$
••• We do not use the following data for averages, fits, limits, etc. •••			
$0.04 \pm 0.09 \pm 0.01$	<sup>2</sup> AUBERT	04A	BABR Repl. by AUBERT 06o
$-0.05 \pm 0.20 \pm 0.03$	<sup>3</sup> AUBERT	02E	BABR $e^+ e^- \rightarrow \Upsilon(4S)$
<sup>1</sup> Corresponds to 90% confidence range $-0.20 < A_{CP} < 0.22$ .			
<sup>2</sup> Corresponds to 90% confidence range $-0.10 < A_{CP} < 0.18$ .			
<sup>3</sup> Corresponds to 90% confidence range $-0.37 < A_{CP} < 0.28$ .			

 $A_{CP}(B^+ \rightarrow X_0(1550) K^+)$ 

VALUE	DOCUMENT ID	TECN	COMMENT
<b><math>-0.04 \pm 0.07 \pm 0.02</math></b>	<sup>1</sup> AUBERT	06O	BABR $e^+ e^- \rightarrow \Upsilon(4S)$
<sup>1</sup> Measured in the $B^+ \rightarrow K^+ K^- K^+$ decay.			

 $A_{CP}(B^+ \rightarrow K^{*+} K^+ K^-)$ 

VALUE	DOCUMENT ID	TECN	COMMENT
<b><math>0.11 \pm 0.08 \pm 0.03</math></b>	AUBERT,B	06U	BABR $e^+ e^- \rightarrow \Upsilon(4S)$

 $A_{CP}(B^+ \rightarrow \phi K^*(892)^+)$ 

VALUE	DOCUMENT ID	TECN	COMMENT
<b><math>-0.01 \pm 0.08</math> OUR AVERAGE</b>			
$0.00 \pm 0.09 \pm 0.04$	AUBERT	07BA	BABR $e^+ e^- \rightarrow \Upsilon(4S)$
$-0.02 \pm 0.14 \pm 0.03$	<sup>1</sup> CHEN	05A	BELL $e^+ e^- \rightarrow \Upsilon(4S)$
••• We do not use the following data for averages, fits, limits, etc. •••			
$0.16 \pm 0.17 \pm 0.03$	AUBERT	03V	BABR Repl. by AUBERT 07Ba
$-0.13 \pm 0.29^{+0.08}_{-0.11}$	<sup>2</sup> CHEN	03B	BELL Repl. by CHEN 05A
$-0.43^{+0.36}_{-0.30} \pm 0.06$	<sup>3</sup> AUBERT	02E	BABR Repl. by AUBERT 03V
<sup>1</sup> Corresponds to 90% confidence range $-0.25 < A_{CP} < 0.22$ .			
<sup>2</sup> Corresponds to 90% confidence range $-0.64 < A_{CP} < 0.36$ .			
<sup>3</sup> Corresponds to 90% confidence range $-0.88 < A_{CP} < 0.18$ .			

 $A_{CP}(B^+ \rightarrow \phi(K\pi)_0^{*+})$ 

VALUE	DOCUMENT ID	TECN	COMMENT
<b><math>0.04 \pm 0.15 \pm 0.04</math></b>	AUBERT	08B1	BABR $e^+ e^- \rightarrow \Upsilon(4S)$

 $A_{CP}(B^+ \rightarrow \phi K_1(1270)^+)$ 

VALUE	DOCUMENT ID	TECN	COMMENT
<b><math>0.15 \pm 0.19 \pm 0.05</math></b>	AUBERT	08B1	BABR $e^+ e^- \rightarrow \Upsilon(4S)$

 $A_{CP}(B^+ \rightarrow \phi K_2^*(1430)^+)$ 

VALUE	DOCUMENT ID	TECN	COMMENT
<b><math>-0.23 \pm 0.19 \pm 0.06</math></b>	AUBERT	08B1	BABR $e^+ e^- \rightarrow \Upsilon(4S)$

 $A_{CP}(B^+ \rightarrow K^+ \phi\phi)$ 

VALUE	DOCUMENT ID	TECN	COMMENT
<b><math>-0.10 \pm 0.08 \pm 0.02</math></b>	<sup>1</sup> LEES	11A	BABR $e^+ e^- \rightarrow \Upsilon(4S)$
<sup>1</sup> $m_{\phi\phi} < 2.85$ GeV/c <sup>2</sup> .			

 $A_{CP}(B^+ \rightarrow K^+ [\phi\phi]_{\eta_c})$ 

VALUE	DOCUMENT ID	TECN	COMMENT
<b><math>0.09 \pm 0.10 \pm 0.02</math></b>	<sup>1</sup> LEES	11A	BABR $e^+ e^- \rightarrow \Upsilon(4S)$
<sup>1</sup> $m_{\phi\phi}$ is consistent with $\eta_c$ mass [2.94, 3.02] GeV/c <sup>2</sup> .			

 $A_{CP}(B^+ \rightarrow K^*(892)^+ \gamma)$ 

VALUE	DOCUMENT ID	TECN	COMMENT
<b><math>+0.018 \pm 0.028 \pm 0.007</math></b>	AUBERT	09A0	BABR $e^+ e^- \rightarrow \Upsilon(4S)$

 $A_{CP}(B^+ \rightarrow \eta K^+ \gamma)$ 

VALUE	DOCUMENT ID	TECN	COMMENT
<b><math>-0.12 \pm 0.07</math> OUR AVERAGE</b>			
$-0.09 \pm 0.10 \pm 0.01$	<sup>1</sup> AUBERT	09	BABR $e^+ e^- \rightarrow \Upsilon(4S)$
$-0.16 \pm 0.09 \pm 0.06$	<sup>2</sup> NISHIDA	05	BELL $e^+ e^- \rightarrow \Upsilon(4S)$
••• We do not use the following data for averages, fits, limits, etc. •••			
$-0.09 \pm 0.12 \pm 0.01$	<sup>1</sup> AUBERT,B	06M	BABR Repl. by AUBERT 09
<sup>1</sup> $m_{\eta K} < 3.25$ GeV/c <sup>2</sup> .			
<sup>2</sup> $m_{\eta K} < 2.4$ GeV/c <sup>2</sup> .			

 $A_{CP}(B^+ \rightarrow \phi K^+ \gamma)$ 

VALUE	DOCUMENT ID	TECN	COMMENT
<b><math>-0.13 \pm 0.11</math> OUR AVERAGE</b>			Error includes scale factor of 1.1.
$-0.03 \pm 0.11 \pm 0.08$	SAHOO	11A	BELL $e^+ e^- \rightarrow \Upsilon(4S)$
$-0.26 \pm 0.14 \pm 0.05$	AUBERT	07Q	BABR $e^+ e^- \rightarrow \Upsilon(4S)$

 $A_{CP}(B^+ \rightarrow \rho^+ \gamma)$ 

VALUE	DOCUMENT ID	TECN	COMMENT
<b><math>-0.11 \pm 0.32 \pm 0.09</math></b>	TANIGUCHI	08	BELL $e^+ e^- \rightarrow \Upsilon(4S)$

 $A_{CP}(B^+ \rightarrow \pi^+ \pi^0)$ 

VALUE	DOCUMENT ID	TECN	COMMENT
<b><math>0.06 \pm 0.05</math> OUR AVERAGE</b>			
$0.07 \pm 0.06 \pm 0.01$	LIN	08	BELL $e^+ e^- \rightarrow \Upsilon(4S)$
$0.03 \pm 0.08 \pm 0.01$	AUBERT	07Bc	BABR $e^+ e^- \rightarrow \Upsilon(4S)$
••• We do not use the following data for averages, fits, limits, etc. •••			
$-0.01 \pm 0.10 \pm 0.02$	<sup>1</sup> AUBERT	05L	BABR Repl. by AUBERT 07Bc
$0.00 \pm 0.10 \pm 0.02$	<sup>2</sup> CHAO	05A	BELL Repl. by CHAO 04B
$-0.02 \pm 0.10 \pm 0.01$	<sup>3</sup> CHAO	04B	BELL Repl. by LIN 08
$-0.03^{+0.18}_{-0.17} \pm 0.02$	<sup>4</sup> AUBERT	03L	BABR Repl. by AUBERT 05L
$0.30 \pm 0.30^{+0.06}_{-0.04}$	<sup>5</sup> CASEY	02	BELL Repl. by CHAO 04B
<sup>1</sup> Corresponds to a 90% CL interval of $-0.19 < A_{CP} < 0.21$ .			
<sup>2</sup> Corresponds to a 90% CL interval of $-0.17 < A_{CP} < 0.16$ .			
<sup>3</sup> This corresponds to 90% CL interval of $-0.18 < A_{CP} < 0.14$ .			
<sup>4</sup> Corresponds to 90% confidence range $-0.32 < A_{CP} < 0.27$ .			
<sup>5</sup> Corresponds to 90% confidence range $-0.23 < A_{CP} < +0.86$ .			

$A_{CP}(B^+ \rightarrow \pi^+ \pi^- \pi^+)$ 

VALUE	DOCUMENT ID	TECN	COMMENT
$0.032 \pm 0.044 \pm 0.040$ $-0.037$	AUBERT	09L BABR	$e^+ e^- \rightarrow \Upsilon(4S)$
• • • We do not use the following data for averages, fits, limits, etc. • • •			
$-0.007 \pm 0.077 \pm 0.025$	AUBERT,B	05G BABR	Repl. by AUBERT 09L
$-0.39 \pm 0.33 \pm 0.12$	AUBERT	03M BABR	Repl. by AUBERT 05G

 $A_{CP}(B^+ \rightarrow \rho^0 \pi^+)$ 

VALUE	DOCUMENT ID	TECN	COMMENT
$0.18 \pm 0.07 \pm 0.05$ $-0.15$	AUBERT	09L BABR	$e^+ e^- \rightarrow \Upsilon(4S)$
• • • We do not use the following data for averages, fits, limits, etc. • • •			
$-0.074 \pm 0.120 \pm 0.035$ $-0.055$	AUBERT,B	05G BABR	Repl. by AUBERT 09L
$-0.19 \pm 0.11 \pm 0.02$	AUBERT	04Z BABR	Repl. by AUBERT,B 05G

 $A_{CP}(B^+ \rightarrow f_2(1270) \pi^+)$ 

VALUE	DOCUMENT ID	TECN	COMMENT
$0.41 \pm 0.25 \pm 0.18$ $-0.15$	AUBERT	09L BABR	$e^+ e^- \rightarrow \Upsilon(4S)$
• • • We do not use the following data for averages, fits, limits, etc. • • •			
$-0.004 \pm 0.247 \pm 0.028$ $-0.032$	AUBERT,B	05G BABR	Repl. by AUBERT 09L

 $A_{CP}(B^+ \rightarrow \rho^0(1450) \pi^+)$ 

VALUE	DOCUMENT ID	TECN	COMMENT
$-0.06 \pm 0.28 \pm 0.23$ $-0.40$	AUBERT	09L BABR	$e^+ e^- \rightarrow \Upsilon(4S)$

 $A_{CP}(B^+ \rightarrow f_0(1370) \pi^+)$ 

VALUE	DOCUMENT ID	TECN	COMMENT
$0.72 \pm 0.15 \pm 0.16$	AUBERT	09L BABR	$e^+ e^- \rightarrow \Upsilon(4S)$

 $A_{CP}(B^+ \rightarrow \pi^+ \pi^- \pi^+ \text{ nonresonant})$ 

VALUE	DOCUMENT ID	TECN	COMMENT
$-0.14 \pm 0.14 \pm 0.18$ $-0.08$	AUBERT	09L BABR	$e^+ e^- \rightarrow \Upsilon(4S)$

 $A_{CP}(B^+ \rightarrow \rho^+ \pi^0)$ 

VALUE	DOCUMENT ID	TECN	COMMENT
$0.02 \pm 0.11$ OUR AVERAGE			
$-0.01 \pm 0.13 \pm 0.02$	AUBERT	07X BABR	$e^+ e^- \rightarrow \Upsilon(4S)$
$0.06 \pm 0.17 \pm 0.04$ $-0.05$	ZHANG	05A BELL	$e^+ e^- \rightarrow \Upsilon(4S)$
• • • We do not use the following data for averages, fits, limits, etc. • • •			
$0.24 \pm 0.16 \pm 0.06$	AUBERT	04Z BABR	Repl. by AUBERT 07X

 $A_{CP}(B^+ \rightarrow \rho^+ \rho^0)$ 

VALUE	DOCUMENT ID	TECN	COMMENT
$-0.05 \pm 0.05$ OUR AVERAGE			
$-0.054 \pm 0.055 \pm 0.010$	AUBERT	09G BABR	$e^+ e^- \rightarrow \Upsilon(4S)$
$0.00 \pm 0.22 \pm 0.03$	ZHANG	03B BELL	$e^+ e^- \rightarrow \Upsilon(4S)$
• • • We do not use the following data for averages, fits, limits, etc. • • •			
$-0.12 \pm 0.13 \pm 0.10$	AUBERT,BE	06G BABR	Repl. by AUBERT 09G
$-0.19 \pm 0.23 \pm 0.03$	AUBERT	03V BABR	Repl. by AUBERT,BE 06G

 $A_{CP}(B^+ \rightarrow \omega \pi^+)$ 

VALUE	DOCUMENT ID	TECN	COMMENT
$-0.04 \pm 0.06$ OUR AVERAGE			
$-0.02 \pm 0.08 \pm 0.01$	AUBERT	07AE BABR	$e^+ e^- \rightarrow \Upsilon(4S)$
$-0.02 \pm 0.09 \pm 0.01$	JEN	06 BELL	$e^+ e^- \rightarrow \Upsilon(4S)$
$-0.34 \pm 0.25$	<sup>1</sup> CHEN	00 CLE2	$e^+ e^- \rightarrow \Upsilon(4S)$
• • • We do not use the following data for averages, fits, limits, etc. • • •			
$-0.01 \pm 0.10 \pm 0.01$	AUBERT,B	06E BABR	Repl. by AUBERT 07AE
$0.03 \pm 0.16 \pm 0.01$	AUBERT	04H BABR	Repl. by AUBERT,B 06E
$0.50 \pm 0.23 \pm 0.20$ $-0.02$	<sup>2</sup> WANG	04A BELL	Repl. by JEN 06
$-0.01 \pm 0.29 \pm 0.03$ $-0.31$	<sup>3</sup> AUBERT	02E BABR	Repl. by AUBERT 04H

<sup>1</sup> Corresponds to 90% confidence range  $-0.75 < A_{CP} < 0.07$ .

<sup>2</sup> Corresponds to 90% CL interval  $-0.25 < A_{CP} < 0.41$

<sup>3</sup> Corresponds to 90% confidence range  $-0.50 < A_{CP} < 0.46$ .

 $A_{CP}(B^+ \rightarrow \omega \rho^+)$ 

VALUE	DOCUMENT ID	TECN	COMMENT
$-0.20 \pm 0.09 \pm 0.02$	AUBERT	09H BABR	$e^+ e^- \rightarrow \Upsilon(4S)$
• • • We do not use the following data for averages, fits, limits, etc. • • •			
$0.04 \pm 0.18 \pm 0.02$	AUBERT,B	06T BABR	Repl. by AUBERT 09H
$0.05 \pm 0.26 \pm 0.02$	AUBERT	05O BABR	Repl. by AUBERT,B 06T

 $A_{CP}(B^+ \rightarrow \eta \pi^+)$ 

VALUE	DOCUMENT ID	TECN	COMMENT
$-0.14 \pm 0.07$ OUR AVERAGE			Error includes scale factor of 1.4.
$-0.19 \pm 0.06 \pm 0.01$	HOI	12 BELL	$e^+ e^- \rightarrow \Upsilon(4S)$
$-0.03 \pm 0.09 \pm 0.03$	AUBERT	09AV BABR	$e^+ e^- \rightarrow \Upsilon(4S)$
• • • We do not use the following data for averages, fits, limits, etc. • • •			
$-0.08 \pm 0.10 \pm 0.01$	AUBERT	07AE BABR	Repl. by AUBERT 09AV
$-0.23 \pm 0.09 \pm 0.02$	CHANG	07B BELL	Repl. by HOI 12
$-0.13 \pm 0.12 \pm 0.01$	AUBERT,B	05K BABR	Repl. by AUBERT 07AE
$0.07 \pm 0.15 \pm 0.03$	CHANG	05A BELL	Repl. by CHANG 07B
$-0.44 \pm 0.18 \pm 0.01$	AUBERT	04H BABR	Repl. by AUBERT,B 05K

 $A_{CP}(B^+ \rightarrow \eta \rho^+)$ 

VALUE	DOCUMENT ID	TECN	COMMENT
$0.11 \pm 0.11$ OUR AVERAGE			
$0.13 \pm 0.11 \pm 0.02$	AUBERT	08AH BABR	$e^+ e^- \rightarrow \Upsilon(4S)$
$-0.04 \pm 0.34 \pm 0.01$ $-0.32$	WANG	07B BELL	$e^+ e^- \rightarrow \Upsilon(4S)$
• • • We do not use the following data for averages, fits, limits, etc. • • •			
$0.02 \pm 0.18 \pm 0.02$	AUBERT,B	05K BABR	Repl. by AUBERT 08AH

 $A_{CP}(B^+ \rightarrow \eta' \pi^+)$ 

VALUE	DOCUMENT ID	TECN	COMMENT
$0.06 \pm 0.16$ OUR AVERAGE			
$0.03 \pm 0.17 \pm 0.02$	AUBERT	09AV BABR	$e^+ e^- \rightarrow \Upsilon(4S)$
$0.20 \pm 0.37 \pm 0.04$ $-0.36$	SCHUEMANN	06 BELL	$e^+ e^- \rightarrow \Upsilon(4S)$
• • • We do not use the following data for averages, fits, limits, etc. • • •			
$0.21 \pm 0.17 \pm 0.01$	AUBERT	07AE BABR	Repl. by AUBERT 09AV
$0.14 \pm 0.16 \pm 0.01$	AUBERT,B	05K BABR	Repl. by AUBERT 07AE

 $A_{CP}(B^+ \rightarrow \eta' \rho^+)$ 

VALUE	DOCUMENT ID	TECN	COMMENT
$0.26 \pm 0.17 \pm 0.02$	DEL-AMO-SA...10A	BABR	$e^+ e^- \rightarrow \Upsilon(4S)$
• • • We do not use the following data for averages, fits, limits, etc. • • •			
$0.04 \pm 0.28 \pm 0.02$	<sup>1</sup> AUBERT	07E BABR	Repl. by DEL-AMO-SANCHEZ 10A

<sup>1</sup> Reports  $A_{CP}$  with the opposite sign convention.

 $A_{CP}(B^+ \rightarrow b_1^0 \pi^+)$ 

VALUE	DOCUMENT ID	TECN	COMMENT
$+0.05 \pm 0.16 \pm 0.02$	AUBERT	07BI BABR	$e^+ e^- \rightarrow \Upsilon(4S)$

 $A_{CP}(B^+ \rightarrow \rho \bar{\rho} \pi^+)$ 

VALUE	DOCUMENT ID	TECN	COMMENT
$0.00 \pm 0.04$ OUR AVERAGE			
$-0.02 \pm 0.05 \pm 0.02$	<sup>1</sup> WEI	08 BELL	$e^+ e^- \rightarrow \Upsilon(4S)$
$+0.04 \pm 0.07 \pm 0.04$	AUBERT	07AV BABR	$e^+ e^- \rightarrow \Upsilon(4S)$
• • • We do not use the following data for averages, fits, limits, etc. • • •			
$-0.16 \pm 0.22 \pm 0.01$	WANG	04 BELL	Repl. by WEI 08

<sup>1</sup> Requires  $m_{\rho \bar{\rho}} < 2.85 \text{ GeV}/c^2$ .

 $A_{CP}(B^+ \rightarrow \rho \bar{\rho} K^+)$ 

VALUE	DOCUMENT ID	TECN	COMMENT
$-0.16 \pm 0.07$ OUR AVERAGE			
$-0.17 \pm 0.10 \pm 0.02$	<sup>1</sup> WEI	08 BELL	$e^+ e^- \rightarrow \Upsilon(4S)$
$-0.16 \pm 0.07 \pm 0.04$ $-0.08$	<sup>1</sup> AUBERT,B	05L BABR	$e^+ e^- \rightarrow \Upsilon(4S)$
• • • We do not use the following data for averages, fits, limits, etc. • • •			
$-0.05 \pm 0.11 \pm 0.01$	WANG	04 BELL	Repl. by WEI 08

<sup>1</sup> Requires  $m_{\rho \bar{\rho}} < 2.85 \text{ GeV}/c^2$ .

 $A_{CP}(B^+ \rightarrow \rho \bar{\rho} K^*(892)^+)$ 

VALUE	DOCUMENT ID	TECN	COMMENT
$0.21 \pm 0.16$ OUR AVERAGE			Error includes scale factor of 1.4.
$-0.01 \pm 0.19 \pm 0.02$	CHEN	08c BELL	$e^+ e^- \rightarrow \Upsilon(4S)$
$+0.32 \pm 0.13 \pm 0.05$	AUBERT	07AV BABR	$e^+ e^- \rightarrow \Upsilon(4S)$

 $A_{CP}(B^+ \rightarrow \rho \bar{\rho} \eta)$ 

VALUE	DOCUMENT ID	TECN	COMMENT
$+0.17 \pm 0.16 \pm 0.05$	WANG	07c BELL	$e^+ e^- \rightarrow \Upsilon(4S)$

 $A_{CP}(B^+ \rightarrow \rho \bar{\rho} \pi^0)$ 

VALUE	DOCUMENT ID	TECN	COMMENT
$+0.01 \pm 0.17 \pm 0.04$	WANG	07c BELL	$e^+ e^- \rightarrow \Upsilon(4S)$

 $A_{CP}(B^+ \rightarrow K^+ \ell^+ \ell^-)$ 

VALUE	DOCUMENT ID	TECN	COMMENT
$-0.01 \pm 0.09$ OUR AVERAGE			Error includes scale factor of 1.1.
$-0.18 \pm 0.18 \pm 0.01$	AUBERT	09T BABR	$e^+ e^- \rightarrow \Upsilon(4S)$
$+0.04 \pm 0.10 \pm 0.02$	WEI	09A BELL	$e^+ e^- \rightarrow \Upsilon(4S)$
• • • We do not use the following data for averages, fits, limits, etc. • • •			
$-0.07 \pm 0.22 \pm 0.02$	AUBERT,B	06J BABR	Repl. by AUBERT 09T









See key on page 457

# Meson Particle Listings

## $B^0$

VALUE (MeV)	$m_{B^0} - m_{B^+}$		
	DOCUMENT ID	TECN	COMMENT
<b>0.32 ± 0.06 OUR FIT</b>			
<b>0.32 ± 0.05 OUR AVERAGE</b>			
0.20 ± 0.17 ± 0.11	1 AAIJ	12E LHCb	$p\bar{p}$ at 7 TeV
0.33 ± 0.05 ± 0.03	2 AUBERT	08AF BABR	$e^+e^- \rightarrow \Upsilon(4S)$
0.53 ± 0.67 ± 0.14	3 ACOSTA	06 CDF	$p\bar{p}$ at 1.96 TeV
0.41 ± 0.25 ± 0.19	ALAM	94 CLE2	$e^+e^- \rightarrow \Upsilon(4S)$
-0.4 ± 0.6 ± 0.5	BORTOLETTO	092 CLEO	$e^+e^- \rightarrow \Upsilon(4S)$
-0.9 ± 1.2 ± 0.5	ALBRECHT	90J ARG	$e^+e^- \rightarrow \Upsilon(4S)$
2.0 ± 1.1 ± 0.3	4 BEBEK	87 CLEO	$e^+e^- \rightarrow \Upsilon(4S)$

1 Uses exclusively reconstructed final states containing a  $J/\psi \rightarrow \mu^+\mu^-$  decay.  
 2 Uses the  $B$ -momentum distributions in the  $e^+e^-$  rest frame.  
 3 Uses exclusively reconstructed final states containing a  $J/\psi \rightarrow \mu^+\mu^-$  decays.  
 4 BEBEK 87 actually measure the difference between half of  $E_{cm}$  and the  $B^\pm$  or  $B^0$  mass, so the  $m_{B^0} - m_{B^\pm}$  is more accurate. Assume  $m_{\Upsilon(4S)} = 10580$  MeV.

**$B^0$  MEAN LIFE**

See  $B^\pm/B^0/B_s^0/b$ -baryon ADMIXTURE section for data on  $B$ -hadron mean life averaged over species of bottom particles.

"OUR EVALUATION" is an average using rescaled values of the data listed below. The average and rescaling were performed by the Heavy Flavor Averaging Group (HFAG) and are described at <http://www.slac.stanford.edu/xorg/hfag/>. The averaging/rescaling procedure takes into account correlations between the measurements and asymmetric lifetime errors.

VALUE ( $10^{-12}$ s)	EVTS	DOCUMENT ID	TECN	COMMENT
<b>1.519 ± 0.007 OUR EVALUATION</b>				
1.507 ± 0.010 ± 0.008	1	AALTONEN	11 CDF	$p\bar{p}$ at 1.96 TeV
1.414 ± 0.018 ± 0.034	2	ABAZOV	09E D0	$p\bar{p}$ at 1.96 TeV
1.501 ± 0.078 ± 0.050	3	ABAZOV	07s D0	$p\bar{p}$ at 1.96 TeV
1.504 ± 0.013 ± 0.018	4	AUBERT	06G BABR	$e^+e^- \rightarrow \Upsilon(4S)$
1.534 ± 0.008 ± 0.010	5	ABE	05B BELL	$e^+e^- \rightarrow \Upsilon(4S)$
1.531 ± 0.021 ± 0.031	6	ABDALLAH	04E DLPH	$e^+e^- \rightarrow Z$
1.523 ± 0.024 ± 0.022	7	AUBERT	03C BABR	$e^+e^- \rightarrow \Upsilon(4S)$
1.533 ± 0.034 ± 0.038	8	AUBERT	03H BABR	$e^+e^- \rightarrow \Upsilon(4S)$
1.497 ± 0.073 ± 0.032	9	ACOSTA	02C CDF	$p\bar{p}$ at 1.8 TeV
1.529 ± 0.012 ± 0.029	10	AUBERT	02H BABR	$e^+e^- \rightarrow \Upsilon(4S)$
1.546 ± 0.032 ± 0.022	11	AUBERT	01F BABR	$e^+e^- \rightarrow \Upsilon(4S)$
1.541 ± 0.028 ± 0.023	10	ABBIENDI,G	00B OPAL	$e^+e^- \rightarrow Z$
1.518 ± 0.053 ± 0.034	12	BARATE	00R ALEP	$e^+e^- \rightarrow Z$
1.523 ± 0.057 ± 0.053	13	ABBIENDI	99J OPAL	$e^+e^- \rightarrow Z$
1.474 ± 0.039 ± 0.052	12	ABE	98Q CDF	$p\bar{p}$ at 1.8 TeV
1.52 ± 0.06 ± 0.04	13	ACCIARRI	98s L3	$e^+e^- \rightarrow Z$
1.64 ± 0.08 ± 0.08	13	ABE	97J SLD	$e^+e^- \rightarrow Z$
1.532 ± 0.041 ± 0.040	14	ABREU	97F DLPH	$e^+e^- \rightarrow Z$
1.25 ± 0.15 ± 0.05	121	9	BUSKULIC	96J ALEP $e^+e^- \rightarrow Z$
1.49 ± 0.17 ± 0.08		15	BUSKULIC	96J ALEP $e^+e^- \rightarrow Z$
1.61 ± 0.14 ± 0.08		12,16	ABREU	95Q DLPH $e^+e^- \rightarrow Z$
1.63 ± 0.14 ± 0.13		17	ADAM	95 DLPH $e^+e^- \rightarrow Z$
1.53 ± 0.12 ± 0.08		12,18	AKERS	95T OPAL $e^+e^- \rightarrow Z$

• • • We do not use the following data for averages, fits, limits, etc. • • •

1.524 ± 0.030 ± 0.016	3	ABULENCIA	07A CDF	Repl. by AALTONEN 11
1.473 ± 0.052 ± 0.023	2	ABAZOV	05B D0	Repl. by ABAZOV 05w
1.40 ± 0.11 ± 0.03	3	ABAZOV	05c D0	Repl. by ABAZOV 07s
1.530 ± 0.043 ± 0.023	2	ABAZOV	05w D0	Repl. by ABAZOV 09E
1.54 ± 0.05 ± 0.02	19	ACOSTA	05 CDF	Repl. by AALTONEN 11
1.554 ± 0.030 ± 0.019	11	ABE	02H BELL	Repl. by ABE 05b
1.58 ± 0.09 ± 0.02	9	ABE	98B CDF	Repl. by ACOSTA 02c
1.54 ± 0.08 ± 0.06	12	ABE	96C CDF	Repl. by ABE 98Q
1.55 ± 0.06 ± 0.03	20	BUSKULIC	96J ALEP	$e^+e^- \rightarrow Z$
1.61 ± 0.07 ± 0.04	12	BUSKULIC	96J ALEP	Repl. by BARATE 00R
1.62 ± 0.12	21	ADAM	95 DLPH	$e^+e^- \rightarrow Z$
1.57 ± 0.18 ± 0.08	121	9	ABE	94D CDF Repl. by ABE 98b
1.17 ± 0.29 ± 0.16	96	12	ABREU	93D DLPH Sup. by ABREU 95Q
1.55 ± 0.25 ± 0.18	76	17	ABREU	93G DLPH Sup. by ADAM 95
1.51 ± 0.24 ± 0.12	78	12	ACTON	93C OPAL Sup. by AKERS 95T

1.52 +0.20 +0.07 -0.18 -0.13	77	12	BUSKULIC	93D ALEP	Sup. by BUSKULIC 96J
1.20 +0.52 +0.16 -0.36 -0.14	15	22	WAGNER	90 MRK2	$E_{cm}^{ee} = 29$ GeV
0.82 +0.57 -0.37 ± 0.27	23	AVERILL	89 HRS	$E_{cm}^{ee} = 29$ GeV	

1 Measured mean life using fully reconstructed decays ( $J/\psi K^{(*)}$ ).  
 2 Measured mean life using  $B^0 \rightarrow J/\psi K^{*0}$  decays.  
 3 Measured mean life using  $B^0 \rightarrow J/\psi K_S$  decays.  
 4 Measured using a simultaneous fit of the  $B^0$  lifetime and  $\bar{B}^0 B^0$  oscillation frequency  $\Delta m_d$  in the partially reconstructed  $B^0 \rightarrow D^{*-} \ell \nu$  decays.  
 5 Measurement performed using a combined fit of  $CP$ -violation, mixing and lifetimes.  
 6 Measurement performed using an inclusive reconstruction and  $B$  flavor identification technique.  
 7 AUBERT 03c uses a sample of approximately 14,000 exclusively reconstructed  $B^0 \rightarrow D^{*}(2010)^- \ell \nu$  and simultaneously measures the lifetime and oscillation frequency.  
 8 Measurement performed with decays  $B^0 \rightarrow D^{*-} \pi^+$  and  $B^0 \rightarrow D^{*-} \rho^+$  using a partial reconstruction technique.  
 9 Measured mean life using fully reconstructed decays.  
 10 Data analyzed using partially reconstructed  $\bar{B}^0 \rightarrow D^{*+} \ell^- \bar{\nu}$  decays.  
 11 Events are selected in which one  $B$  meson is fully reconstructed while the second  $B$  meson is reconstructed inclusively.  
 12 Data analyzed using  $D/D^* \ell X$  event vertices.  
 13 Data analyzed using charge of secondary vertex.  
 14 Data analyzed using inclusive  $D/D^* \ell X$ .  
 15 Measured mean life using partially reconstructed  $D^{*-} \pi^+ X$  vertices.  
 16 ABREU 95Q assumes  $B(B^0 \rightarrow D^{*-} \ell^+ \nu_\ell) = 3.2 \pm 1.7\%$ .  
 17 Data analyzed using vertex-charge technique to tag  $B$  charge.  
 18 AKERS 95T assumes  $B(B^0 \rightarrow D_s^{(*)} D^{0(*)}) = 5.0 \pm 0.9\%$  to find  $B^+/B^0$  yield.  
 19 Measured using the time-dependent angular analysis of  $B_d^0 \rightarrow J/\psi K^{*0}$  decays.  
 20 Combined result of  $D/D^* \ell X$  analysis, fully reconstructed  $B$  analysis, and partially reconstructed  $D^{*-} \pi^+ X$  analysis.  
 21 Combined ABREU 95Q and ADAM 95 result.  
 22 WAGNER 90 tagged  $B^0$  mesons by their decays into  $D^{*-} e^+ \nu$  and  $D^{*-} \mu^+ \nu$  where the  $D^{*-}$  is tagged by its decay into  $\pi^- \bar{D}^0$ .  
 23 AVERILL 89 is an estimate of the  $B^0$  mean lifetime assuming that  $B^0 \rightarrow D^{*+} X$  always.

**MEAN LIFE RATIO  $\tau_{B^+}/\tau_{B^0}$**

**$\tau_{B^+}/\tau_{B^0}$  (direct measurements)**

"OUR EVALUATION" is an average using rescaled values of the data listed below. The average and rescaling were performed by the Heavy Flavor Averaging Group (HFAG) and are described at <http://www.slac.stanford.edu/xorg/hfag/>. The averaging/rescaling procedure takes into account correlations between the measurements and asymmetric lifetime errors.

VALUE	EVTS	DOCUMENT ID	TECN	COMMENT
<b>1.079 ± 0.007 OUR EVALUATION</b>				
1.088 ± 0.009 ± 0.004	1	AALTONEN	11 CDF	$p\bar{p}$ at 1.96 TeV
1.080 ± 0.016 ± 0.014	2	ABAZOV	05D D0	$p\bar{p}$ at 1.96 TeV
1.066 ± 0.008 ± 0.008	3	ABE	05B BELL	$e^+e^- \rightarrow \Upsilon(4S)$
1.060 ± 0.021 ± 0.024	4	ABDALLAH	04E DLPH	$e^+e^- \rightarrow Z$
1.093 ± 0.066 ± 0.028	5	ACOSTA	02C CDF	$p\bar{p}$ at 1.8 TeV
1.082 ± 0.026 ± 0.012	6	AUBERT	01F BABR	$e^+e^- \rightarrow \Upsilon(4S)$
1.085 ± 0.059 ± 0.018	2	BARATE	00R ALEP	$e^+e^- \rightarrow Z$
1.079 ± 0.064 ± 0.041	7	ABBIENDI	99J OPAL	$e^+e^- \rightarrow Z$
1.110 ± 0.056 ± 0.033	2	ABE	98Q CDF	$p\bar{p}$ at 1.8 TeV
1.09 ± 0.07 ± 0.03	7	ACCIARRI	98s L3	$e^+e^- \rightarrow Z$
1.01 ± 0.07 ± 0.06	7	ABE	97J SLD	$e^+e^- \rightarrow Z$
1.27 ± 0.23 ± 0.03	5	BUSKULIC	96J ALEP	$e^+e^- \rightarrow Z$
1.00 ± 0.17 ± 0.10	2,8	ABREU	95Q DLPH	$e^+e^- \rightarrow Z$
1.06 ± 0.13 ± 0.10	9	ADAM	95 DLPH	$e^+e^- \rightarrow Z$
0.99 ± 0.14 ± 0.05	2,10	AKERS	95T OPAL	$e^+e^- \rightarrow Z$

• • • We do not use the following data for averages, fits, limits, etc. • • •

1.091 ± 0.023 ± 0.014	6	ABE	02H BELL	Repl. by ABE 05B
1.06 ± 0.07 ± 0.02	5	ABE	98B CDF	Repl. by ACOSTA 02c
1.01 ± 0.11 ± 0.02	2	ABE	96C CDF	Repl. by ABE 98Q
1.03 ± 0.08 ± 0.02	11	BUSKULIC	96J ALEP	$e^+e^- \rightarrow Z$
0.98 ± 0.08 ± 0.03	2	BUSKULIC	96J ALEP	Repl. by BARATE 00R
1.02 ± 0.16 ± 0.05	269	5	ABE	94D CDF Repl. by ABE 98b
1.11 ± 0.51 ± 0.11	188	2	ABREU	93D DLPH Sup. by ABREU 95Q
1.01 ± 0.29 ± 0.12	253	9	ABREU	93G DLPH Sup. by ADAM 95
1.0 ± 0.33 ± 0.25 ± 0.08	130	ACTON	93C OPAL	Sup. by AKERS 95T
0.96 ± 0.19 ± 0.12	154	2	BUSKULIC	93D ALEP Sup. by BUSKULIC 96J

## Meson Particle Listings

 $B^0$ 

- <sup>1</sup> Measured mean life using fully reconstructed decays ( $J/\psi K^{(*)}$ ).
- <sup>2</sup> Data analyzed using  $D/D^* \mu X$  vertices.
- <sup>3</sup> Measurement performed using a combined fit of  $CP$ -violation, mixing and lifetimes.
- <sup>4</sup> Measurement performed using an inclusive reconstruction and  $B$  flavor identification technique.
- <sup>5</sup> Measured using fully reconstructed decays.
- <sup>6</sup> Events are selected in which one  $B$  meson is fully reconstructed while the second  $B$  meson is reconstructed inclusively.
- <sup>7</sup> Data analyzed using charge of secondary vertex.
- <sup>8</sup> ABREU 95Q assumes  $B(B^0 \rightarrow D^{*-} \ell^+ \nu_\ell) = 3.2 \pm 1.7\%$ .
- <sup>9</sup> Data analyzed using vertex-charge technique to tag  $B$  charge.
- <sup>10</sup> AKERS 95T assumes  $B(B^0 \rightarrow D_s^{(*)} D^0)^{(*)} = 5.0 \pm 0.9\%$  to find  $B^+/B^0$  yield.
- <sup>11</sup> Combined result of  $D/D^* \ell X$  analysis and fully reconstructed  $B$  analysis.

 $\tau_{B^+}/\tau_{B^0}$  (inferred from branching fractions)

These measurements are inferred from the branching fractions for semileptonic decay or other spectator-dominated decays by assuming that the rates for such decays are equal for  $B^0$  and  $B^+$ . We do not use measurements which assume equal production of  $B^0$  and  $B^+$  because of the large uncertainty in the production ratio.

“OUR EVALUATION” has been obtained by the Heavy Flavor Averaging Group (HFAG) by taking into account correlations between measurements.

VALUE	CL% <sub>EVTS</sub>	DOCUMENT ID	TECN	COMMENT
<b>1.076 ± 0.034 OUR EVALUATION</b>				
<b>1.07 ± 0.04 OUR AVERAGE</b>				
1.07 ± 0.04 ± 0.03		URQUIJO	07	BELL $e^+ e^- \rightarrow \Upsilon(4S)$
1.067 ± 0.041 ± 0.033		AUBERT,B	06Y	BABR $e^+ e^- \rightarrow \Upsilon(4S)$
• • • We do not use the following data for averages, fits, limits, etc. • • •				
0.95 <sup>+0.117</sup> / <sub>-0.080</sub> ± 0.091		1 ARTUSO	97	CLE2 $e^+ e^- \rightarrow \Upsilon(4S)$
1.15 ± 0.17 ± 0.06		2 JESSOP	97	CLE2 $e^+ e^- \rightarrow \Upsilon(4S)$
0.93 ± 0.18 ± 0.12		3 ATHANAS	94	CLE2 Sup. by ARTUSO 97
0.91 ± 0.27 ± 0.21		4 ALBRECHT	92C	ARG $e^+ e^- \rightarrow \Upsilon(4S)$
1.0 ± 0.4	29	4,5 ALBRECHT	92G	ARG $e^+ e^- \rightarrow \Upsilon(4S)$
0.89 ± 0.19 ± 0.13		4 FULTON	91	CLEO $e^+ e^- \rightarrow \Upsilon(4S)$
1.00 ± 0.23 ± 0.14		4 ALBRECHT	89L	ARG $e^+ e^- \rightarrow \Upsilon(4S)$
0.49 to 2.3	90	6 BEAN	87B	CLEO $e^+ e^- \rightarrow \Upsilon(4S)$

- <sup>1</sup> ARTUSO 97 uses partial reconstruction of  $B \rightarrow D^* \ell \nu_\ell$  and independent of  $B^0$  and  $B^+$  production fraction.
- <sup>2</sup> Assumes equal production of  $B^+$  and  $B^0$  at the  $\Upsilon(4S)$ .
- <sup>3</sup> ATHANAS 94 uses events tagged by fully reconstructed  $B^-$  decays and partially or fully reconstructed  $B^0$  decays.
- <sup>4</sup> Assumes equal production of  $B^0$  and  $B^+$ .
- <sup>5</sup> ALBRECHT 92G data analyzed using  $B \rightarrow D_s \bar{D}, D_s \bar{D}^*, D_s^* \bar{D}, D_s^* \bar{D}^*$  events.
- <sup>6</sup> BEAN 87B assume the fraction of  $B^0 \bar{B}^0$  events at the  $\Upsilon(4S)$  is 0.41.

 $\text{sgn}(\text{Re}(\lambda_{CP})) \Delta\Gamma_{B_d^0} / \Gamma_{B_d^0}$ 

$\Gamma_{B_d^0}$  and  $\Delta\Gamma_{B_d^0}$  are the decay rate average and difference between two  $B_d^0$   $CP$  eigenstates (light – heavy). The  $\lambda_{CP}$  characterizes  $B^0$  and  $\bar{B}^0$  decays to states of charmonium plus  $K_L^0$ , see the review on “ $CP$  Violation” in the reviews section.

“OUR EVALUATION” has been obtained by the Heavy Flavor Averaging Group (HFAG) by taking into account correlations between measurements.

VALUE (units $10^{-2}$ )	DOCUMENT ID	TECN	COMMENT
<b>1.5 ± 1.8 OUR EVALUATION</b>			
<b>1.5 ± 1.9 OUR AVERAGE</b> Includes data from the datablock that follows this one.			
1.7 ± 1.8 ± 1.1	1 HIGUCHI	12	BELL $e^+ e^- \rightarrow \Upsilon(4S)$
0.8 ± 3.7 ± 1.8	2 AUBERT,B	04c	BABR $e^+ e^- \rightarrow \Upsilon(4S)$
<sup>1</sup> Reports $-\Delta\Gamma_d/\Gamma_d$ using $B^0 \rightarrow J/\psi K_S^0, J/\psi K_L^0, D^- \pi^+, D^{*-} \pi^+, D^{*-} \rho^+$ , and $D^{*-} \ell^+ \nu$ decays.			
<sup>2</sup> Corresponds to 90% confidence range $[-0.084, 0.068]$ .			

 $|\Delta\Gamma_{B_d^0}|/\Gamma_{B_d^0}$ 

VALUE	CL%	DOCUMENT ID	TECN	COMMENT
The data in this block is included in the average printed for a previous datablock.				
<b>&lt;0.18</b>				
0.80	95	1 ABDALLAH	03B	DLPH $e^+ e^- \rightarrow Z$
• • • We do not use the following data for averages, fits, limits, etc. • • •				
<0.80	95	2,3 BEHRENS	00B	CLE2 $e^+ e^- \rightarrow \Upsilon(4S)$
<sup>1</sup> Using the measured $\tau_{B^0} = 1.55 \pm 0.03$ ps.				
<sup>2</sup> BEHRENS 00B uses high-momentum lepton tags and partially reconstructed $\bar{B}^0 \rightarrow D^{*+} \pi^-, \rho^-$ decays to determine the flavor of the $B$ meson.				
<sup>3</sup> Assumes $\Delta m_d = 0.478 \pm 0.018$ ps <sup>-1</sup> and $\tau_{B^0} = 1.548 \pm 0.032$ ps.				

 $B^0$  DECAY MODES

$\bar{B}^0$  modes are charge conjugates of the modes below. Reactions indicate the weak decay vertex and do not include mixing. Modes which do not identify the charge state of the  $B$  are listed in the  $B^\pm/B^0$  ADMIXTURE section.

The branching fractions listed below assume 50%  $B^0 \bar{B}^0$  and 50%  $B^+ B^-$  production at the  $\Upsilon(4S)$ . We have attempted to bring older measurements up to date by rescaling their assumed  $\Upsilon(4S)$  production ratio to 50:50 and their assumed  $D, D_s, D^*$ , and  $\psi$  branching ratios to current values whenever this would affect our averages and best limits significantly.

Indentation is used to indicate a subchannel of a previous reaction. All resonant subchannels have been corrected for resonance branching fractions to the final state so the sum of the subchannel branching fractions can exceed that of the final state.

For inclusive branching fractions, e.g.,  $B \rightarrow D^\pm$  anything, the values usually are multiplicities, not branching fractions. They can be greater than one.

Mode	Fraction ( $\Gamma_i/\Gamma$ )	Scale factor/ Confidence level
$\Gamma_1$ $\ell^+ \nu_\ell$ anything	[a] ( 10.33 ± 0.28 ) %	
$\Gamma_2$ $e^+ \nu_e X_c$	( 10.1 ± 0.4 ) %	
$\Gamma_3$ $D \ell^+ \nu_\ell$ anything	( 9.2 ± 0.8 ) %	
$\Gamma_4$ $D^- \ell^+ \nu_\ell$	[a] ( 2.18 ± 0.12 ) %	
$\Gamma_5$ $D^- \tau^+ \nu_\tau$	( 1.1 ± 0.4 ) %	
$\Gamma_6$ $D^*(2010)^- \ell^+ \nu_\ell$	[a] ( 4.95 ± 0.11 ) %	
$\Gamma_7$ $D^*(2010)^- \tau^+ \nu_\tau$	( 1.5 ± 0.5 ) %	S=1.4
$\Gamma_8$ $\bar{D}^0 \pi^- \ell^+ \nu_\ell$	( 4.3 ± 0.6 ) × 10 <sup>-3</sup>	
$\Gamma_9$ $D_0^*(2400)^- \ell^+ \nu_\ell \times$ $B(D_0^{*-} \rightarrow \bar{D}^0 \pi^-)$	( 3.0 ± 1.2 ) × 10 <sup>-3</sup>	S=1.8
$\Gamma_{10}$ $D_2^*(2460)^- \ell^+ \nu_\ell \times$ $B(D_2^{*-} \rightarrow \bar{D}^0 \pi^-)$	( 1.21 ± 0.33 ) × 10 <sup>-3</sup>	S=1.8
$\Gamma_{11}$ $\bar{D}^*(n) \pi^- \ell^+ \nu_\ell$ (n ≥ 1)	( 2.3 ± 0.5 ) %	
$\Gamma_{12}$ $\bar{D}^{*0} \pi^- \ell^+ \nu_\ell$	( 4.9 ± 0.8 ) × 10 <sup>-3</sup>	
$\Gamma_{13}$ $D_1(2420)^- \ell^+ \nu_\ell \times$ $B(D_1^- \rightarrow \bar{D}^{*0} \pi^-)$	( 2.80 ± 0.28 ) × 10 <sup>-3</sup>	
$\Gamma_{14}$ $D_1'(2430)^- \ell^+ \nu_\ell \times$ $B(D_1'^- \rightarrow \bar{D}^{*0} \pi^-)$	( 3.1 ± 0.9 ) × 10 <sup>-3</sup>	
$\Gamma_{15}$ $D_2^*(2460)^- \ell^+ \nu_\ell \times$ $B(D_2^{*-} \rightarrow \bar{D}^{*0} \pi^-)$	( 6.8 ± 1.2 ) × 10 <sup>-4</sup>	
$\Gamma_{16}$ $\rho^- \ell^+ \nu_\ell$	[a] ( 2.34 ± 0.28 ) × 10 <sup>-4</sup>	
$\Gamma_{17}$ $\pi^- \ell^+ \nu_\ell$	[a] ( 1.44 ± 0.05 ) × 10 <sup>-4</sup>	
$\Gamma_{18}$ $\pi^- \mu^+ \nu_\mu$		

## Inclusive modes

$\Gamma_{19}$ $K^\pm$ anything	( 78 ± 8 ) %	
$\Gamma_{20}$ $D^0 X$	( 8.1 ± 1.5 ) %	
$\Gamma_{21}$ $\bar{D}^0 X$	( 47.4 ± 2.8 ) %	
$\Gamma_{22}$ $D^+ X$	< 3.9 %	CL=90%
$\Gamma_{23}$ $D^- X$	( 36.9 ± 3.3 ) %	
$\Gamma_{24}$ $D_s^+ X$	( 10.3 ± <sup>2.1</sup> / <sub>1.8</sub> ) %	
$\Gamma_{25}$ $D_s^- X$	< 2.6 %	CL=90%
$\Gamma_{26}$ $\Lambda_c^+ X$	< 3.1 %	CL=90%
$\Gamma_{27}$ $\bar{\Lambda}_c^- X$	( 5.0 ± <sup>2.1</sup> / <sub>1.5</sub> ) %	
$\Gamma_{28}$ $\bar{c} X$	( 95 ± 5 ) %	
$\Gamma_{29}$ $c X$	( 24.6 ± 3.1 ) %	
$\Gamma_{30}$ $\bar{c} c X$	( 119 ± 6 ) %	

 $D, D^*, \text{ or } D_s$  modes

$\Gamma_{31}$ $D^- \pi^+$	( 2.68 ± 0.13 ) × 10 <sup>-3</sup>	
$\Gamma_{32}$ $D^- \rho^+$	( 7.8 ± 1.3 ) × 10 <sup>-3</sup>	
$\Gamma_{33}$ $D^- K^0 \pi^+$	( 4.9 ± 0.9 ) × 10 <sup>-4</sup>	
$\Gamma_{34}$ $D^- K^*(892)^+$	( 4.5 ± 0.7 ) × 10 <sup>-4</sup>	
$\Gamma_{35}$ $D^- \omega \pi^+$	( 2.8 ± 0.6 ) × 10 <sup>-3</sup>	
$\Gamma_{36}$ $D^- K^+$	( 1.97 ± 0.21 ) × 10 <sup>-4</sup>	
$\Gamma_{37}$ $D^- K^+ \bar{K}^0$	< 3.1 × 10 <sup>-4</sup>	CL=90%
$\Gamma_{38}$ $D^- K^+ \bar{K}^*(892)^0$	( 8.8 ± 1.9 ) × 10 <sup>-4</sup>	
$\Gamma_{39}$ $\bar{D}^0 \pi^+ \pi^-$	( 8.4 ± 0.9 ) × 10 <sup>-4</sup>	
$\Gamma_{40}$ $D^*(2010)^- \pi^+$	( 2.76 ± 0.13 ) × 10 <sup>-3</sup>	
$\Gamma_{41}$ $D^- \pi^+ \pi^+ \pi^-$	( 6.4 ± 0.7 ) × 10 <sup>-3</sup>	
$\Gamma_{42}$ $(D^- \pi^+ \pi^+ \pi^-)$ nonresonant	( 3.9 ± 1.9 ) × 10 <sup>-3</sup>	
$\Gamma_{43}$ $D^- \pi^+ \rho^0$	( 1.1 ± 1.0 ) × 10 <sup>-3</sup>	
$\Gamma_{44}$ $D^- a_1(1260)^+$	( 6.0 ± 3.3 ) × 10 <sup>-3</sup>	
$\Gamma_{45}$ $D^*(2010)^- \pi^+ \pi^0$	( 1.5 ± 0.5 ) %	

Γ <sub>46</sub>	$D^*(2010)^- \rho^+$	( 6.8 ± 0.9 ) × 10 <sup>-3</sup>		Γ <sub>92</sub>	$D^- D_{s1}(2536)^+ \times$ $B(D_{s1}(2536)^+ \rightarrow$ $D^{*0} K^+)$	( 1.7 ± 0.6 ) × 10 <sup>-4</sup>	
Γ <sub>47</sub>	$D^*(2010)^- K^+$	( 2.14 ± 0.16 ) × 10 <sup>-4</sup>		Γ <sub>93</sub>	$D^- D_{s1}(2536)^+ \times$ $B(D_{s1}(2536)^+ \rightarrow$ $D^{*+} K^0)$	( 2.6 ± 1.1 ) × 10 <sup>-4</sup>	
Γ <sub>48</sub>	$D^*(2010)^- K^0 \pi^+$	( 3.0 ± 0.8 ) × 10 <sup>-4</sup>		Γ <sub>94</sub>	$D^*(2010)^- D_{s1}(2536)^+ \times$ $B(D_{s1}(2536)^+ \rightarrow D^{*0} K^+$ $+ D^{*+} K^0)$	( 5.0 ± 1.4 ) × 10 <sup>-4</sup>	
Γ <sub>49</sub>	$D^*(2010)^- K^*(892)^+$	( 3.3 ± 0.6 ) × 10 <sup>-4</sup>		Γ <sub>95</sub>	$D^*(2010)^- D_{s1}(2536)^+ \times$ $B(D_{s1}(2536)^+ \rightarrow$ $D^{*0} K^+)$	( 3.3 ± 1.1 ) × 10 <sup>-4</sup>	
Γ <sub>50</sub>	$D^*(2010)^- K^+ \bar{K}^0$	< 4.7 × 10 <sup>-4</sup>	CL=90%	Γ <sub>96</sub>	$D^{*-} D_{s1}(2536)^+ \times$ $B(D_{s1}(2536)^+ \rightarrow$ $D^{*+} K^0)$	( 5.0 ± 1.7 ) × 10 <sup>-4</sup>	
Γ <sub>51</sub>	$D^*(2010)^- K^+ \bar{K}^*(892)^0$	( 1.29 ± 0.33 ) × 10 <sup>-3</sup>		Γ <sub>97</sub>	$D^- D_{sJ}(2573)^+ \times$ $B(D_{sJ}(2573)^+ \rightarrow D^0 K^+)$	< 1 × 10 <sup>-4</sup>	CL=90%
Γ <sub>52</sub>	$D^*(2010)^- \pi^+ \pi^+ \pi^-$	( 7.0 ± 0.8 ) × 10 <sup>-3</sup>	S=1.3	Γ <sub>98</sub>	$D^*(2010)^- D_{sJ}(2573)^+ \times$ $B(D_{sJ}(2573)^+ \rightarrow D^0 K^+)$	< 2 × 10 <sup>-4</sup>	CL=90%
Γ <sub>53</sub>	$(D^*(2010)^- \pi^+ \pi^+ \pi^-)$ non-resonant	( 0.0 ± 2.5 ) × 10 <sup>-3</sup>		Γ <sub>99</sub>	$D^+ \pi^-$	( 7.8 ± 1.4 ) × 10 <sup>-7</sup>	
Γ <sub>54</sub>	$D^*(2010)^- \pi^+ \rho^0$	( 5.7 ± 3.2 ) × 10 <sup>-3</sup>		Γ <sub>100</sub>	$D_s^+ \pi^-$	( 2.16 ± 0.26 ) × 10 <sup>-5</sup>	
Γ <sub>55</sub>	$D^*(2010)^- a_1(1260)^+$	( 1.30 ± 0.27 ) %		Γ <sub>101</sub>	$D_s^+ \pi^-$	( 2.1 ± 0.4 ) × 10 <sup>-5</sup>	S=1.4
Γ <sub>56</sub>	$D^*(2010)^- \pi^+ \pi^+ \pi^- \pi^0$	( 1.76 ± 0.27 ) %		Γ <sub>102</sub>	$D_s^+ \rho^-$	< 2.4 × 10 <sup>-5</sup>	CL=90%
Γ <sub>57</sub>	$D^{*-} 3\pi^+ 2\pi^-$	( 4.7 ± 0.9 ) × 10 <sup>-3</sup>		Γ <sub>103</sub>	$D_s^+ \rho^-$	( 4.1 ± 1.3 ) × 10 <sup>-5</sup>	
Γ <sub>58</sub>	$\bar{D}^*(2010)^- \omega \pi^+$	( 2.89 ± 0.30 ) × 10 <sup>-3</sup>		Γ <sub>104</sub>	$D_s^+ a_0^-$	< 1.9 × 10 <sup>-5</sup>	CL=90%
Γ <sub>59</sub>	$D_1(2430)^0 \omega \times$ $B(D_1(2430)^0 \rightarrow D^{*-} \pi^+)$	( 4.1 ± 1.6 ) × 10 <sup>-4</sup>		Γ <sub>105</sub>	$D_s^+ a_0^-$	< 3.6 × 10 <sup>-5</sup>	CL=90%
Γ <sub>60</sub>	$\bar{D}^{*-} \pi^+$	[b] ( 2.1 ± 1.0 ) × 10 <sup>-3</sup>		Γ <sub>106</sub>	$D_s^+ a_1(1260)^-$	< 2.1 × 10 <sup>-3</sup>	CL=90%
Γ <sub>61</sub>	$D_1(2420)^- \pi^+ \times B(D_1^- \rightarrow$ $D^- \pi^+ \pi^-)$	( 1.00 ± 0.21 / 0.25 ) × 10 <sup>-4</sup>		Γ <sub>107</sub>	$D_s^+ a_1(1260)^-$	< 1.7 × 10 <sup>-3</sup>	CL=90%
Γ <sub>62</sub>	$D_1(2420)^- \pi^+ \times B(D_1^- \rightarrow$ $D^{*-} \pi^+ \pi^-)$	< 3.3 × 10 <sup>-5</sup>	CL=90%	Γ <sub>108</sub>	$D_s^+ a_2^-$	< 1.9 × 10 <sup>-4</sup>	CL=90%
Γ <sub>63</sub>	$\bar{D}_2^*(2460)^- \pi^+ \times$ $B(D_2^*(2460)^- \rightarrow D^0 \pi^-)$	( 2.15 ± 0.35 ) × 10 <sup>-4</sup>		Γ <sub>109</sub>	$D_s^+ a_2^-$	< 2.0 × 10 <sup>-4</sup>	CL=90%
Γ <sub>64</sub>	$\bar{D}_0^*(2400)^- \pi^+ \times$ $B(D_0^*(2400)^- \rightarrow D^0 \pi^-)$	( 6.0 ± 3.0 ) × 10 <sup>-5</sup>		Γ <sub>110</sub>	$D_s^- K^+$	( 2.2 ± 0.5 ) × 10 <sup>-5</sup>	S=1.8
Γ <sub>65</sub>	$D_2^*(2460)^- \pi^+ \times B(D_2^* \rightarrow$ $D^{*-} \pi^+ \pi^-)$	< 2.4 × 10 <sup>-5</sup>	CL=90%	Γ <sub>111</sub>	$D_s^{*-} K^+$	( 2.19 ± 0.30 ) × 10 <sup>-5</sup>	
Γ <sub>66</sub>	$\bar{D}_s^*(2460)^- \rho^+$	< 4.9 × 10 <sup>-3</sup>	CL=90%	Γ <sub>112</sub>	$D_s^- K^*(892)^+$	( 3.5 ± 1.0 ) × 10 <sup>-5</sup>	
Γ <sub>67</sub>	$D^0 \bar{D}^0$	< 4.3 × 10 <sup>-5</sup>	CL=90%	Γ <sub>113</sub>	$D_s^{*-} K^*(892)^+$	( 3.2 ± 1.5 / 1.3 ) × 10 <sup>-5</sup>	
Γ <sub>68</sub>	$D^{*0} \bar{D}^0$	< 2.9 × 10 <sup>-4</sup>	CL=90%	Γ <sub>114</sub>	$D_s^- \pi^+ K^0$	( 1.10 ± 0.33 ) × 10 <sup>-4</sup>	
Γ <sub>69</sub>	$D^- D^+$	( 2.11 ± 0.31 ) × 10 <sup>-4</sup>	S=1.2	Γ <sub>115</sub>	$D_s^- \pi^+ K^0$	< 1.10 × 10 <sup>-4</sup>	CL=90%
Γ <sub>70</sub>	$D^- D_s^+$	( 7.2 ± 0.8 ) × 10 <sup>-3</sup>		Γ <sub>116</sub>	$D_s^- \pi^+ K^*(892)^0$	< 3.0 × 10 <sup>-3</sup>	CL=90%
Γ <sub>71</sub>	$D^*(2010)^- D_s^+$	( 8.0 ± 1.1 ) × 10 <sup>-3</sup>		Γ <sub>117</sub>	$D_s^{*-} \pi^+ K^*(892)^0$	< 1.6 × 10 <sup>-3</sup>	CL=90%
Γ <sub>72</sub>	$D^- D_s^{*+}$	( 7.4 ± 1.6 ) × 10 <sup>-3</sup>		Γ <sub>118</sub>	$\bar{D}^0 K^0$	( 5.2 ± 0.7 ) × 10 <sup>-5</sup>	
Γ <sub>73</sub>	$D^*(2010)^- D_s^{*+}$	( 1.77 ± 0.14 ) %		Γ <sub>119</sub>	$\bar{D}^0 K^+ \pi^-$	( 8.8 ± 1.7 ) × 10 <sup>-5</sup>	
Γ <sub>74</sub>	$D_{s0}(2317)^- K^+ \times$ $B(D_{s0}(2317)^- \rightarrow D_s^- \pi^0)$	( 4.2 ± 1.4 ) × 10 <sup>-5</sup>		Γ <sub>120</sub>	$\bar{D}^0 K^*(892)^0$	( 4.2 ± 0.6 ) × 10 <sup>-5</sup>	
Γ <sub>75</sub>	$D_{s0}(2317)^- \pi^+ \times$ $B(D_{s0}(2317)^- \rightarrow D_s^- \pi^0)$	< 2.5 × 10 <sup>-5</sup>	CL=90%	Γ <sub>121</sub>	$D_2^*(2460)^- K^+ \times$ $B(D_2^*(2460)^- \rightarrow \bar{D}^0 \pi^-)$	( 1.8 ± 0.5 ) × 10 <sup>-5</sup>	
Γ <sub>76</sub>	$D_{sJ}(2457)^- K^+ \times$ $B(D_{sJ}(2457)^- \rightarrow D_s^- \pi^0)$	< 9.4 × 10 <sup>-6</sup>	CL=90%	Γ <sub>122</sub>	$\bar{D}^0 K^+ \pi^-$ non-resonant	< 3.7 × 10 <sup>-5</sup>	CL=90%
Γ <sub>77</sub>	$D_{sJ}(2457)^- \pi^+ \times$ $B(D_{sJ}(2457)^- \rightarrow D_s^- \pi^0)$	< 4.0 × 10 <sup>-6</sup>	CL=90%	Γ <sub>123</sub>	$\bar{D}^0 \pi^0$	( 2.63 ± 0.14 ) × 10 <sup>-4</sup>	
Γ <sub>78</sub>	$D_s^- D_s^+$	< 3.6 × 10 <sup>-5</sup>	CL=90%	Γ <sub>124</sub>	$\bar{D}^0 \rho^0$	( 3.2 ± 0.5 ) × 10 <sup>-4</sup>	
Γ <sub>79</sub>	$D_s^{*-} D_s^+$	< 1.3 × 10 <sup>-4</sup>	CL=90%	Γ <sub>125</sub>	$\bar{D}^0 f_2$	( 1.2 ± 0.4 ) × 10 <sup>-4</sup>	
Γ <sub>80</sub>	$D_s^{*+} D_s^+$	< 2.4 × 10 <sup>-4</sup>	CL=90%	Γ <sub>126</sub>	$\bar{D}^0 \eta$	( 2.36 ± 0.32 ) × 10 <sup>-4</sup>	S=2.5
Γ <sub>81</sub>	$D_{s0}(2317)^+ D^- \times$ $B(D_{s0}(2317)^+ \rightarrow D_s^+ \pi^0)$	( 9.7 ± 4.0 / 3.3 ) × 10 <sup>-4</sup>	S=1.5	Γ <sub>127</sub>	$\bar{D}^0 \eta'$	( 1.38 ± 0.16 ) × 10 <sup>-4</sup>	S=1.3
Γ <sub>82</sub>	$D_{s0}(2317)^+ D^- \times$ $B(D_{s0}(2317)^+ \rightarrow D_s^{*+} \gamma)$	< 9.5 × 10 <sup>-4</sup>	CL=90%	Γ <sub>128</sub>	$\bar{D}^0 \omega$	( 2.53 ± 0.16 ) × 10 <sup>-4</sup>	
Γ <sub>83</sub>	$D_{s0}(2317)^+ D^*(2010)^- \times$ $B(D_{s0}(2317)^+ \rightarrow D_s^+ \pi^0)$	( 1.5 ± 0.6 ) × 10 <sup>-3</sup>		Γ <sub>129</sub>	$D^0 \phi$	< 1.16 × 10 <sup>-5</sup>	CL=90%
Γ <sub>84</sub>	$D_{sJ}(2457)^+ D^-$	( 3.5 ± 1.1 ) × 10 <sup>-3</sup>		Γ <sub>130</sub>	$D^0 K^+ \pi^-$	( 6 ± 4 ) × 10 <sup>-6</sup>	
Γ <sub>85</sub>	$D_{sJ}(2457)^+ D^- \times$ $B(D_{sJ}(2457)^+ \rightarrow D_s^+ \gamma)$	( 6.5 ± 1.7 / 1.4 ) × 10 <sup>-4</sup>		Γ <sub>131</sub>	$D^0 K^*(892)^0$	< 1.1 × 10 <sup>-5</sup>	CL=90%
Γ <sub>86</sub>	$D_{sJ}(2457)^+ D^- \times$ $B(D_{sJ}(2457)^+ \rightarrow D_s^{*+} \gamma)$	< 6.0 × 10 <sup>-4</sup>	CL=90%	Γ <sub>132</sub>	$\bar{D}^{*0} \gamma$	< 2.5 × 10 <sup>-5</sup>	CL=90%
Γ <sub>87</sub>	$D_{sJ}(2457)^+ D^- \times$ $B(D_{sJ}(2457)^+ \rightarrow$ $D_s^+ \pi^+ \pi^-)$	< 2.0 × 10 <sup>-4</sup>	CL=90%	Γ <sub>133</sub>	$\bar{D}^*(2007)^0 \pi^0$	( 2.2 ± 0.6 ) × 10 <sup>-4</sup>	S=2.6
Γ <sub>88</sub>	$D_{sJ}(2457)^+ D^- \times$ $B(D_{sJ}(2457)^+ \rightarrow D_s^+ \pi^0)$	< 3.6 × 10 <sup>-4</sup>	CL=90%	Γ <sub>134</sub>	$\bar{D}^*(2007)^0 \rho^0$	< 5.1 × 10 <sup>-4</sup>	CL=90%
Γ <sub>89</sub>	$D^*(2010)^- D_{sJ}(2457)^+$	( 9.3 ± 2.2 ) × 10 <sup>-3</sup>		Γ <sub>135</sub>	$\bar{D}^*(2007)^0 \eta$	( 2.3 ± 0.6 ) × 10 <sup>-4</sup>	S=2.8
Γ <sub>90</sub>	$D_{sJ}(2457)^+ D^*(2010) \times$ $B(D_{sJ}(2457)^+ \rightarrow D_s^+ \gamma)$	( 2.3 ± 0.9 / 0.7 ) × 10 <sup>-3</sup>		Γ <sub>136</sub>	$\bar{D}^*(2007)^0 \eta'$	( 1.40 ± 0.22 ) × 10 <sup>-4</sup>	
Γ <sub>91</sub>	$D^- D_{s1}(2536)^+ \times$ $B(D_{s1}(2536)^+ \rightarrow D^{*0} K^+$ $+ D^{*+} K^0)$	( 2.8 ± 0.7 ) × 10 <sup>-4</sup>		Γ <sub>137</sub>	$\bar{D}^*(2007)^0 \pi^+ \pi^-$	( 6.2 ± 2.2 ) × 10 <sup>-4</sup>	
				Γ <sub>138</sub>	$\bar{D}^*(2007)^0 K^0$	( 3.6 ± 1.2 ) × 10 <sup>-5</sup>	
				Γ <sub>139</sub>	$\bar{D}^*(2007)^0 K^*(892)^0$	< 6.9 × 10 <sup>-5</sup>	CL=90%
				Γ <sub>140</sub>	$D^*(2007)^0 K^*(892)^0$	< 4.0 × 10 <sup>-5</sup>	CL=90%
				Γ <sub>141</sub>	$D^*(2007)^0 \pi^+ \pi^+ \pi^- \pi^-$	( 2.7 ± 0.5 ) × 10 <sup>-3</sup>	
				Γ <sub>142</sub>	$D^*(2010)^+ D^*(2010)^-$	( 8.2 ± 0.9 ) × 10 <sup>-4</sup>	
				Γ <sub>143</sub>	$\bar{D}^*(2007)^0 \omega$	( 3.6 ± 1.1 ) × 10 <sup>-4</sup>	S=3.1
				Γ <sub>144</sub>	$D^*(2010)^+ D^-$	( 6.1 ± 1.5 ) × 10 <sup>-4</sup>	S=1.6
				Γ <sub>145</sub>	$D^*(2007)^0 \bar{D}^*(2007)^0$	< 9 × 10 <sup>-5</sup>	CL=90%
				Γ <sub>146</sub>	$D^- D^0 K^+$	( 1.07 ± 0.11 ) × 10 <sup>-3</sup>	
				Γ <sub>147</sub>	$D^- D^*(2007)^0 K^+$	( 3.5 ± 0.4 ) × 10 <sup>-3</sup>	
				Γ <sub>148</sub>	$D^*(2010)^- D^0 K^+$	( 2.47 ± 0.21 ) × 10 <sup>-3</sup>	
				Γ <sub>149</sub>	$D^*(2010)^- D^*(2007)^0 K^+$	( 1.06 ± 0.09 ) %	
				Γ <sub>150</sub>	$D^- D^+ K^0$	( 7.5 ± 1.7 ) × 10 <sup>-4</sup>	

## Meson Particle Listings

 $B^0$ 

$\Gamma_{151}$	$D^*(2010)^- D^+ K^0 + D^- D^*(2010)^+ K^0$	$(6.4 \pm 0.5) \times 10^{-3}$		$\Gamma_{211}$	$\chi_{c1}(1P) K^*(892)^0$	$(2.22^{+0.40}_{-0.31}) \times 10^{-4}$	S=1.6
$\Gamma_{152}$	$D^*(2010)^- D^*(2010)^+ K^0$	$(8.1 \pm 0.7) \times 10^{-3}$		$\Gamma_{212}$	$X(4051)^+ K^- \times B(X^+ \rightarrow \chi_{c1} \pi^+)$	$(3.0^{+4.0}_{-1.8}) \times 10^{-5}$	
$\Gamma_{153}$	$D^* - D_{s1}(2536)^+ \times B(D_{s1}(2536)^+ \rightarrow D^{*+} K^0)$	$(8.0 \pm 2.4) \times 10^{-4}$		$\Gamma_{213}$	$X(4248)^+ K^- \times B(X^+ \rightarrow \chi_{c1} \pi^+)$	$(4.0^{+20.0}_{-1.0}) \times 10^{-5}$	
$\Gamma_{154}$	$\bar{D}^0 D^0 K^0$	$(2.7 \pm 1.1) \times 10^{-4}$		<b>K or K* modes</b>			
$\Gamma_{155}$	$\bar{D}^0 D^*(2007)^0 K^0 + \bar{D}^*(2007)^0 D^0 K^0$	$(1.1 \pm 0.5) \times 10^{-3}$		$\Gamma_{214}$	$K^+ \pi^-$	$(1.94 \pm 0.06) \times 10^{-5}$	
$\Gamma_{156}$	$\bar{D}^*(2007)^0 D^*(2007)^0 K^0$	$(2.4 \pm 0.9) \times 10^{-3}$		$\Gamma_{215}$	$K^0 \pi^0$	$(9.5 \pm 0.8) \times 10^{-6}$	S=1.3
$\Gamma_{157}$	$(\bar{D} + \bar{D}^*)(D + D^*) K$	$(3.68 \pm 0.26) \%$		$\Gamma_{216}$	$\eta' K^0$	$(6.6 \pm 0.4) \times 10^{-5}$	S=1.4
<b>Charmonium modes</b>				$\Gamma_{217}$	$\eta' K^*(892)^0$	$(3.1 \pm 0.9) \times 10^{-6}$	
$\Gamma_{158}$	$\eta_c K^0$	$(8.3 \pm 1.2) \times 10^{-4}$		$\Gamma_{218}$	$\eta' K_0^*(1430)^0$	$(6.3 \pm 1.6) \times 10^{-6}$	
$\Gamma_{159}$	$\eta_c K^*(892)^0$	$(6.4 \pm 0.9) \times 10^{-4}$		$\Gamma_{219}$	$\eta' K_2^*(1430)^0$	$(1.37 \pm 0.32) \times 10^{-5}$	
$\Gamma_{160}$	$\eta_c(2S) K^{*0}$	$< 3.9 \times 10^{-4}$	CL=90%	$\Gamma_{220}$	$\eta K^0$	$(1.23^{+0.27}_{-0.24}) \times 10^{-6}$	
$\Gamma_{161}$	$h_c(1P) K^{*0}$	$< 4 \times 10^{-4}$	CL=90%	$\Gamma_{221}$	$\eta K^*(892)^0$	$(1.59 \pm 0.10) \times 10^{-5}$	
$\Gamma_{162}$	$J/\psi(1S) K^0$	$(8.74 \pm 0.32) \times 10^{-4}$		$\Gamma_{222}$	$\eta K_0^*(1430)^0$	$(1.10 \pm 0.22) \times 10^{-5}$	
$\Gamma_{163}$	$J/\psi(1S) K^+ \pi^-$	$(1.2 \pm 0.6) \times 10^{-3}$		$\Gamma_{223}$	$\eta K_2^*(1430)^0$	$(9.6 \pm 2.1) \times 10^{-6}$	
$\Gamma_{164}$	$J/\psi(1S) K^*(892)^0$	$(1.34 \pm 0.06) \times 10^{-3}$		$\Gamma_{224}$	$\omega K^0$	$(5.0 \pm 0.6) \times 10^{-6}$	
$\Gamma_{165}$	$J/\psi(1S) \eta K_S^0$	$(8 \pm 4) \times 10^{-5}$		$\Gamma_{225}$	$a_0(980)^0 K^0 \times B(a_0(980)^0 \rightarrow \eta \pi^0)$	$< 7.8 \times 10^{-6}$	CL=90%
$\Gamma_{166}$	$J/\psi(1S) \eta' K_S^0$	$< 2.5 \times 10^{-5}$	CL=90%	$\Gamma_{226}$	$b_1^0 K^0 \times B(b_1^0 \rightarrow \omega \pi^0)$	$< 7.8 \times 10^{-6}$	CL=90%
$\Gamma_{167}$	$J/\psi(1S) \phi K^0$	$(9.4 \pm 2.6) \times 10^{-5}$		$\Gamma_{227}$	$a_0(980)^\pm K^\mp \times B(a_0(980)^\pm \rightarrow \eta \pi^\pm)$	$< 1.9 \times 10^{-6}$	CL=90%
$\Gamma_{168}$	$J/\psi(1S) \omega K^0$	$(2.3 \pm 0.4) \times 10^{-4}$		$\Gamma_{228}$	$b_1^- K^+ \times B(b_1^- \rightarrow \omega \pi^-)$	$(7.4 \pm 1.4) \times 10^{-6}$	
$\Gamma_{169}$	$X(3872) K^0 \times B(X \rightarrow J/\psi \omega)$	$(6.0 \pm 3.2) \times 10^{-6}$		$\Gamma_{229}$	$b_1^0 K^{*0} \times B(b_1^0 \rightarrow \omega \pi^0)$	$< 8.0 \times 10^{-6}$	CL=90%
$\Gamma_{170}$	$X(3915) K^0 \times B(X \rightarrow J/\psi \omega)$	$(2.1 \pm 0.9) \times 10^{-5}$		$\Gamma_{230}$	$b_1^- K^{*+} \times B(b_1^- \rightarrow \omega \pi^-)$	$< 5.0 \times 10^{-6}$	CL=90%
$\Gamma_{171}$	$J/\psi(1S) K(1270)^0$	$(1.3 \pm 0.5) \times 10^{-3}$		$\Gamma_{231}$	$a_0(1450)^\pm K^\mp \times B(a_0(1450)^\pm \rightarrow \eta \pi^\pm)$	$< 3.1 \times 10^{-6}$	CL=90%
$\Gamma_{172}$	$J/\psi(1S) \pi^0$	$(1.76 \pm 0.16) \times 10^{-5}$	S=1.1	$\Gamma_{232}$	$K_S^0 X^0$ (Familon)	$< 5.3 \times 10^{-5}$	CL=90%
$\Gamma_{173}$	$J/\psi(1S) \eta$	$(9.5 \pm 1.9) \times 10^{-6}$		$\Gamma_{233}$	$\omega K^*(892)^0$	$(2.0 \pm 0.5) \times 10^{-6}$	
$\Gamma_{174}$	$J/\psi(1S) \pi^+ \pi^-$	$(4.6 \pm 0.9) \times 10^{-5}$		$\Gamma_{234}$	$\omega(K\pi)_0^{*0}$	$(1.84 \pm 0.25) \times 10^{-5}$	
$\Gamma_{175}$	$J/\psi(1S) \pi^+ \pi^-$ nonresonant	$< 1.2 \times 10^{-5}$	CL=90%	$\Gamma_{235}$	$\omega K_0^*(1430)^0$	$(1.60 \pm 0.34) \times 10^{-5}$	
$\Gamma_{176}$	$J/\psi(1S) f_2$	$< 4.6 \times 10^{-6}$	CL=90%	$\Gamma_{236}$	$\omega K_2^*(1430)^0$	$(1.01 \pm 0.23) \times 10^{-5}$	
$\Gamma_{177}$	$J/\psi(1S) \rho^0$	$(2.7 \pm 0.4) \times 10^{-5}$		$\Gamma_{237}$	$\omega K^+ \pi^-$ nonresonant	$(5.1 \pm 1.0) \times 10^{-6}$	
$\Gamma_{178}$	$J/\psi(1S) \omega$	$< 2.7 \times 10^{-4}$	CL=90%	$\Gamma_{238}$	$K^+ \pi^- \pi^0$	$(3.78 \pm 0.32) \times 10^{-5}$	
$\Gamma_{179}$	$J/\psi(1S) \phi$	$< 9.4 \times 10^{-7}$	CL=90%	$\Gamma_{239}$	$K^+ \rho^-$	$(7.0 \pm 0.9) \times 10^{-6}$	
$\Gamma_{180}$	$J/\psi(1S) \eta'(958)$	$< 6.3 \times 10^{-5}$	CL=90%	$\Gamma_{240}$	$K^+ \rho(1450)^-$	$(2.4 \pm 1.2) \times 10^{-6}$	
$\Gamma_{181}$	$J/\psi(1S) K^0 \pi^+ \pi^-$	$(1.0 \pm 0.4) \times 10^{-3}$		$\Gamma_{241}$	$K^+ \rho(1700)^-$	$(6 \pm 7) \times 10^{-7}$	
$\Gamma_{182}$	$J/\psi(1S) K^0 \rho^0$	$(5.4 \pm 3.0) \times 10^{-4}$		$\Gamma_{242}$	$(K^+ \pi^- \pi^0)$ non-resonant	$(2.8 \pm 0.6) \times 10^{-6}$	
$\Gamma_{183}$	$J/\psi(1S) K^*(892)^+ \pi^-$	$(8 \pm 4) \times 10^{-4}$		$\Gamma_{243}$	$(K\pi)_0^{*+} \pi^- \times B((K\pi)_0^{*+} \rightarrow K^+ \pi^0)$	$(3.4 \pm 0.5) \times 10^{-5}$	
$\Gamma_{184}$	$J/\psi(1S) K^*(892)^0 \pi^+ \pi^-$	$(6.6 \pm 2.2) \times 10^{-4}$		$\Gamma_{244}$	$(K\pi)_0^{*0} \pi^0 \times B((K\pi)_0^{*0} \rightarrow K^+ \pi^-)$	$(8.6 \pm 1.7) \times 10^{-6}$	
$\Gamma_{185}$	$X(3872)^- K^+$	$< 5 \times 10^{-4}$	CL=90%	$\Gamma_{245}$	$K_2^*(1430)^0 \pi^0$	$< 4.0 \times 10^{-6}$	CL=90%
$\Gamma_{186}$	$X(3872)^- K^+ \times B(X(3872)^- \rightarrow J/\psi \pi^+ \pi^-)$	$< 4.2 \times 10^{-6}$	CL=90%	$\Gamma_{246}$	$K^*(1680)^0 \pi^0$	$< 7.5 \times 10^{-6}$	CL=90%
$\Gamma_{187}$	$X(3872) K^0 \times B(X \rightarrow J/\psi \pi^+ \pi^-)$	$(4.3 \pm 1.3) \times 10^{-6}$		$\Gamma_{247}$	$K_x^{*0} \pi^0$	[d] $(6.1 \pm 1.6) \times 10^{-6}$	
$\Gamma_{188}$	$X(3872) K^0 \times B(X \rightarrow J/\psi \gamma)$	$< 2.4 \times 10^{-6}$	CL=90%	$\Gamma_{248}$	$K^0 \pi^+ \pi^-$ charmless	$(4.96 \pm 0.20) \times 10^{-5}$	
$\Gamma_{189}$	$X(3872) K^*(892)^0 \times B(X \rightarrow J/\psi \gamma)$	$< 2.8 \times 10^{-6}$	CL=90%	$\Gamma_{249}$	$K^0 \pi^+ \pi^-$ non-resonant	$(1.47^{+0.40}_{-0.26}) \times 10^{-5}$	S=2.1
$\Gamma_{190}$	$X(3872) K^0 \times B(X \rightarrow \psi(2S) \gamma)$	$< 6.62 \times 10^{-6}$	CL=90%	$\Gamma_{250}$	$K^0 \rho^0$	$(4.7 \pm 0.6) \times 10^{-6}$	
$\Gamma_{191}$	$X(3872) K^*(892)^0 \times B(X \rightarrow \psi(2S) \gamma)$	$< 4.4 \times 10^{-6}$	CL=90%	$\Gamma_{251}$	$K^*(892)^+ \pi^-$	$(8.4 \pm 0.8) \times 10^{-6}$	
$\Gamma_{192}$	$X(3872) K^0 \times B(X \rightarrow D^0 \bar{D}^0 \pi^0)$	$(1.7 \pm 0.8) \times 10^{-4}$		$\Gamma_{252}$	$K_0^*(1430)^+ \pi^-$	$(3.3 \pm 0.7) \times 10^{-5}$	S=2.0
$\Gamma_{193}$	$X(3872) K^0 \times B(X \rightarrow \bar{D}^{*0} D^0)$	$(1.2 \pm 0.4) \times 10^{-4}$		$\Gamma_{253}$	$K_x^{*+} \pi^-$	[d] $(5.1 \pm 1.6) \times 10^{-6}$	
$\Gamma_{194}$	$X(4430)^\pm K^\mp \times B(X^\pm \rightarrow \psi(2S) \pi^\pm)$	$(3.2^{+6.0}_{-1.8}) \times 10^{-5}$		$\Gamma_{254}$	$K^*(1410)^+ \pi^- \times B(K^*(1410)^+ \rightarrow K^0 \pi^+)$	$< 3.8 \times 10^{-6}$	CL=90%
$\Gamma_{195}$	$X(4430)^\pm K^\mp \times B(X^\pm \rightarrow J/\psi \pi^\pm)$	$< 4 \times 10^{-6}$	CL=95%	$\Gamma_{255}$	$f_0(980) K^0 \times B(f_0(980) \rightarrow \pi^+ \pi^-)$	$(7.0 \pm 0.9) \times 10^{-6}$	
$\Gamma_{196}$	$J/\psi(1S) \rho \bar{\rho}$	$< 8.3 \times 10^{-7}$	CL=90%	$\Gamma_{256}$	$f_2(1270) K^0$	$(2.7^{+1.3}_{-1.2}) \times 10^{-6}$	
$\Gamma_{197}$	$J/\psi(1S) \gamma$	$< 1.6 \times 10^{-6}$	CL=90%	$\Gamma_{257}$	$f_x(1300) K^0 \times B(f_x \rightarrow \pi^+ \pi^-)$	$(1.8 \pm 0.7) \times 10^{-6}$	
$\Gamma_{198}$	$J/\psi(1S) \bar{D}^0$	$< 1.3 \times 10^{-5}$	CL=90%	$\Gamma_{258}$	$K^*(892)^0 \pi^0$	$(3.3 \pm 0.6) \times 10^{-6}$	
$\Gamma_{199}$	$\psi(2S) K^0$	$(6.2 \pm 0.5) \times 10^{-4}$		$\Gamma_{259}$	$K_2^*(1430)^+ \pi^-$	$< 6 \times 10^{-6}$	CL=90%
$\Gamma_{200}$	$\psi(3770) K^0 \times B(\psi \rightarrow \bar{D}^0 D^0)$	$< 1.23 \times 10^{-4}$	CL=90%	$\Gamma_{260}$	$K^*(1680)^+ \pi^-$	$< 1.0 \times 10^{-5}$	CL=90%
$\Gamma_{201}$	$\psi(3770) K^0 \times B(\psi \rightarrow D^- D^+)$	$< 1.88 \times 10^{-4}$	CL=90%	$\Gamma_{261}$	$K^+ \pi^- \pi^+ \pi^-$	[e] $< 2.3 \times 10^{-4}$	CL=90%
$\Gamma_{202}$	$\psi(2S) K^+ \pi^-$	$(5.7 \pm 0.4) \times 10^{-4}$		$\Gamma_{262}$	$\rho^0 K^+ \pi^-$	$(2.8 \pm 0.7) \times 10^{-6}$	
$\Gamma_{203}$	$\psi(2S) K^*(892)^0$	$(6.1 \pm 0.5) \times 10^{-4}$	S=1.1	$\Gamma_{263}$	$f_0(980) K^+ \pi^-$	$(1.4^{+0.5}_{-0.6}) \times 10^{-6}$	
$\Gamma_{204}$	$\chi_{c0}(1P) K^0$	$(1.4^{+0.6}_{-0.5}) \times 10^{-4}$		$\Gamma_{264}$	$K^+ \pi^- \pi^+ \pi^-$ nonresonant	$< 2.1 \times 10^{-6}$	CL=90%
$\Gamma_{205}$	$\chi_{c0} K^*(892)^0$	$(1.7 \pm 0.4) \times 10^{-4}$		$\Gamma_{265}$	$K^*(892)^0 \pi^+ \pi^-$	$(5.5 \pm 0.5) \times 10^{-5}$	
$\Gamma_{206}$	$\chi_{c2} K^0$	$< 1.5 \times 10^{-5}$	CL=90%	$\Gamma_{266}$	$K^*(892)^0 \rho^0$	$(3.4^{+1.7}_{-1.3}) \times 10^{-6}$	S=1.8
$\Gamma_{207}$	$\chi_{c2} K^*(892)^0$	$(6.6 \pm 1.9) \times 10^{-5}$		$\Gamma_{267}$	$K^*(892)^0 f_0(980)$	$< 2.2 \times 10^{-6}$	CL=90%
$\Gamma_{208}$	$\chi_{c1}(1P) \pi^0$	$(1.12 \pm 0.28) \times 10^{-5}$		$\Gamma_{268}$	$K_1(1270)^+ \pi^-$	$< 3.0 \times 10^{-5}$	CL=90%
$\Gamma_{209}$	$\chi_{c1}(1P) K^0$	$(3.93 \pm 0.27) \times 10^{-4}$					
$\Gamma_{210}$	$\chi_{c1}(1P) K^- \pi^+$	$(3.8 \pm 0.4) \times 10^{-4}$					







$\Gamma(e^+ \nu_e X_c)/\Gamma_{total}$	$\Gamma_2/\Gamma$
VALUE (units $10^{-2}$ )	DOCUMENT ID TECN COMMENT
<b>10.08 ± 0.30 ± 0.22</b>	1 URQUIJO 07 BELL $e^+e^- \rightarrow \Upsilon(4S)$

1 Measure the independent B<sup>+</sup> and B<sup>0</sup> partial branching fractions with electron threshold energies of 0.4 GeV.

$\Gamma(D^- \ell^+ \nu_\ell)/\Gamma_{total}$	$\Gamma_4/\Gamma$
ℓ denotes e or μ, not the sum.	

“OUR EVALUATION” is an average using rescaled values of the data listed below. The average and rescaling were performed by the Heavy Flavor Averaging Group (HFAG) and are described at <http://www.slac.stanford.edu/xorg/hfag/>. The averaging/rescaling procedure takes into account correlations between the measurements.

VALUE	DOCUMENT ID	TECN	COMMENT
<b>0.0218 ± 0.0012 OUR EVALUATION</b>			
<b>0.0218 ± 0.0012 OUR AVERAGE</b>			
0.0221 ± 0.0011 ± 0.0011	1 AUBERT 10 BABR $e^+e^- \rightarrow \Upsilon(4S)$		
0.0213 ± 0.0012 ± 0.0039	ABE 02E BELL $e^+e^- \rightarrow \Upsilon(4S)$		
0.0209 ± 0.0013 ± 0.0018	2 BARTELT 99 CLE2 $e^+e^- \rightarrow \Upsilon(4S)$		
0.0235 ± 0.0020 ± 0.0044	3 BUSKULIC 97 ALEP $e^+e^- \rightarrow Z$		
• • • We do not use the following data for averages, fits, limits, etc. • • •			
0.0221 ± 0.0011 ± 0.0012	1 AUBERT 08Q BABR Repl. by AUBERT 10		
0.0187 ± 0.0015 ± 0.0032	4 ATHANAS 97 CLE2 Repl. by BARTELT 99		
0.018 ± 0.006 ± 0.003	5 FULTON 91 CLEO $e^+e^- \rightarrow \Upsilon(4S)$		
0.020 ± 0.007 ± 0.006	6 ALBRECHT 89J ARG $e^+e^- \rightarrow \Upsilon(4S)$		

- 1 Uses a fully reconstructed B meson as a tag on the recoil side.
- 2 Assumes equal production of B<sup>+</sup> and B<sup>0</sup> at the  $\Upsilon(4S)$ .
- 3 BUSKULIC 97 assumes fraction (B<sup>+</sup>) = fraction (B<sup>0</sup>) = (37.8 ± 2.2)% and PDG 96 values for B lifetime and branching ratio of D\* and D decays.
- 4 ATHANAS 97 uses missing energy and missing momentum to reconstruct neutrino.
- 5 FULTON 91 assumes assuming equal production of B<sup>0</sup> and B<sup>+</sup> at the  $\Upsilon(4S)$  and uses Mark III D and D\* branching ratios.
- 6 ALBRECHT 89J reports 0.018 ± 0.006 ± 0.005. We rescale using the method described in STONE 94 but with the updated PDG 94 B(D<sup>0</sup> → K<sup>-</sup>π<sup>+</sup>).

$\Gamma(D^- \ell^+ \nu_\ell)/\Gamma(\ell^+ \nu_\ell \text{ anything})$	$\Gamma_4/\Gamma_1$
VALUE	DOCUMENT ID TECN COMMENT
<b>0.230 ± 0.011 ± 0.011</b>	1 AUBERT 10 BABR $e^+e^- \rightarrow \Upsilon(4S)$

1 Uses a fully reconstructed B meson on the recoil side.

$\Gamma(D^- \ell^+ \nu_\ell)/\Gamma(D \ell^+ \nu_\ell \text{ anything})$	$\Gamma_4/\Gamma_3$
VALUE	DOCUMENT ID TECN COMMENT
<b>0.215 ± 0.016 ± 0.013</b>	1 AUBERT 07AN BABR $e^+e^- \rightarrow \Upsilon(4S)$

1 Uses a fully reconstructed B meson on the recoil side.

$\Gamma(D^- \tau^+ \nu_\tau)/\Gamma_{total}$	$\Gamma_5/\Gamma$
VALUE (units $10^{-2}$ )	DOCUMENT ID TECN COMMENT
• • • We do not use the following data for averages, fits, limits, etc. • • •	
1.04 ± 0.35 ± 0.18	1 AUBERT 08N BABR Repl. by AUBERT 09s

1 Uses a fully reconstructed B meson as a tag on the recoil side.

$\Gamma(D^- \tau^+ \nu_\tau)/\Gamma(D^- \ell^+ \nu_\ell)$	$\Gamma_5/\Gamma_4$
VALUE	DOCUMENT ID TECN COMMENT
<b>0.489 ± 0.165 ± 0.069</b>	1 AUBERT 09s BABR $e^+e^- \rightarrow \Upsilon(4S)$

1 Uses a fully reconstructed B meson as a tag on the recoil side.

$\Gamma(D^*(2010)^- \ell^+ \nu_\ell)/\Gamma_{total}$	$\Gamma_6/\Gamma$
--	-------------------

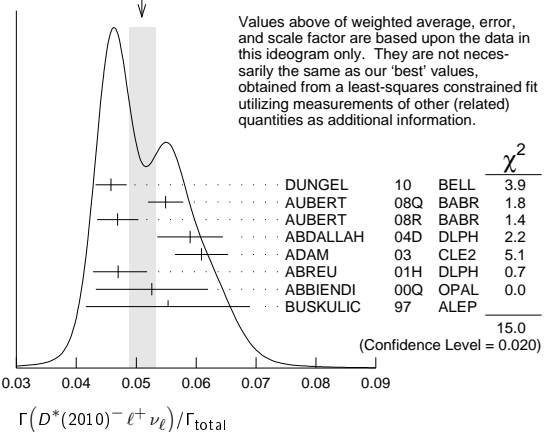
“OUR EVALUATION” is an average using rescaled values of the data listed below. The average and rescaling were performed by the Heavy Flavor Averaging Group (HFAG) and are described at <http://www.slac.stanford.edu/xorg/hfag/>. The averaging/rescaling procedure takes into account correlations between the measurements.

VALUE	EVTs	DOCUMENT ID	TECN	COMMENT
<b>0.0495 ± 0.0011 OUR EVALUATION</b>				
<b>0.0511 ± 0.0023 OUR FIT</b>				Error includes scale factor of 1.6.
<b>0.0509 ± 0.0022 OUR AVERAGE</b>				Error includes scale factor of 1.6. See the ideogram below.
0.0458 ± 0.0003 ± 0.0026	1 DUNGEL 10 BELL $e^+e^- \rightarrow \Upsilon(4S)$			
0.0549 ± 0.0016 ± 0.0025	2 AUBERT 08Q BABR $e^+e^- \rightarrow \Upsilon(4S)$			
0.0469 ± 0.0004 ± 0.0034	3 AUBERT 08R BABR $e^+e^- \rightarrow \Upsilon(4S)$			
0.0590 ± 0.0022 ± 0.0050	4 ABDALLAH 04D DLPH $e^+e^- \rightarrow Z^0$			
0.0609 ± 0.0019 ± 0.0040	5 ADAM 03 CLE2 $e^+e^- \rightarrow \Upsilon(4S)$			
0.0470 ± 0.0013 <sup>+</sup> ± 0.0036 <sup>-</sup>	6 ABREU 01H DLPH $e^+e^- \rightarrow Z$			
0.0526 ± 0.0020 ± 0.0046	7 ABBIENDI 00Q OPAL $e^+e^- \rightarrow Z$			
0.0553 ± 0.0026 ± 0.0052	8 BUSKULIC 97 ALEP $e^+e^- \rightarrow Z$			
• • • We do not use the following data for averages, fits, limits, etc. • • •				
0.0490 ± 0.0007 <sup>+</sup> ± 0.0036 <sup>-</sup>	4 AUBERT 05E BABR Repl. by AUBERT 08R			
0.0539 ± 0.0011 ± 0.0034	9 ABDALLAH 04D DLPH $e^+e^- \rightarrow Z^0$			
0.0459 ± 0.0023 ± 0.0040	10 ABE 02F BELL Repl. by DUNGEL 10			
0.0609 ± 0.0019 ± 0.0040	11 BRIERE 02 CLE2 $e^+e^- \rightarrow \Upsilon(4S)$			
0.0508 ± 0.0021 ± 0.0066	12 ACKERSTAFF 97G OPAL Repl. by ABBIENDI 00Q			
0.0552 ± 0.0017 ± 0.0068	13 ABREU 96P DLPH Repl. by ABREU 01H			
0.0449 ± 0.0032 ± 0.0039	376 14 BARISH 95 CLE2 Repl. by ADAM 03			
0.0518 ± 0.0030 ± 0.0062	410 15 BUSKULIC 95N ALEP Sup. by BUSKULIC 97			

0.045 ± 0.003 ± 0.004	16 ALBRECHT 94 ARG $e^+e^- \rightarrow \Upsilon(4S)$
0.047 ± 0.005 ± 0.005	235 17 ALBRECHT 93 ARG $e^+e^- \rightarrow \Upsilon(4S)$
seen	398 18 SANGHERA 93 CLE2 $e^+e^- \rightarrow \Upsilon(4S)$
0.070 ± 0.018 ± 0.014	19 ANTREASIAN 90B CBAL $e^+e^- \rightarrow \Upsilon(4S)$
	20 ALBRECHT 89c ARG $e^+e^- \rightarrow \Upsilon(4S)$
0.060 ± 0.010 ± 0.014	21 ALBRECHT 89J ARG $e^+e^- \rightarrow \Upsilon(4S)$
0.040 ± 0.004 ± 0.006	22 BORTOLETTO 89B CLEO $e^+e^- \rightarrow \Upsilon(4S)$
0.070 ± 0.012 ± 0.019	47 23 ALBRECHT 87J ARG $e^+e^- \rightarrow \Upsilon(4S)$

- 1 Uses fully reconstructed D\*<sup>-</sup>ℓ<sup>+</sup>ν events (ℓ = e or μ).
- 2 Uses a fully reconstructed B meson as a tag on the recoil side.
- 3 Measured using fully reconstructed D\* sample and a simultaneous fit to the Caprini-Lellouch-Neubert form factor parameters: ρ<sup>2</sup> = 1.191 ± 0.048 ± 0.028, R<sub>1</sub>(1) = 1.429 ± 0.061 ± 0.044, and R<sub>2</sub>(1) = 0.827 ± 0.038 ± 0.022.
- 4 Measured using fully reconstructed D\* sample.
- 5 Uses the combined fit of both B<sup>0</sup> → D\*(2010)<sup>-</sup>ℓν and B<sup>+</sup> →  $\bar{D}(2007)^0$ ℓν samples.
- 6 ABREU 01H measured using about 5000 partial reconstructed D\* sample.
- 7 ABBIENDI 00Q assumes the fraction B(b → B<sup>0</sup>) = (39.7<sup>+1.8</sup><sub>-2.2</sub>)%. This result is an average of two methods using exclusive and partial D\* reconstruction.
- 8 BUSKULIC 97 assumes fraction (B<sup>+</sup>) = fraction (B<sup>0</sup>) = (37.8 ± 2.2)% and PDG 96 values for B lifetime and D\* and D branching fractions.
- 9 Combines with previous partial reconstructed D\* measurement.
- 10 Assumes equal production of B<sup>+</sup> and B<sup>0</sup> at the  $\Upsilon(4S)$ .
- 11 The results are based on the same analysis and data sample reported in ADAM 03.
- 12 ACKERSTAFF 97G assumes fraction (B<sup>+</sup>) = fraction (B<sup>0</sup>) = (37.8 ± 2.2)% and PDG 96 values for B lifetime and branching ratio of D\* and D decays.
- 13 ABREU 96P result is the average of two methods using exclusive and partial D\* reconstruction.
- 14 BARISH 95 use B(D<sup>0</sup> → K<sup>-</sup>π<sup>+</sup>) = (3.91 ± 0.08 ± 0.17)% and B(D\*<sup>+</sup> → D<sup>0</sup>π<sup>+</sup>) = (68.1 ± 1.0 ± 1.3)%.
- 15 BUSKULIC 95N assumes fraction (B<sup>+</sup>) = fraction (B<sup>0</sup>) = 38.2 ± 1.3 ± 2.2% and τ<sub>B<sup>0</sup></sub> = 1.58 ± 0.06 ps. Γ(D\*<sup>-</sup>ℓ<sup>+</sup>ν<sub>ℓ</sub>)/total = [5.18 - 0.13(fraction(B<sup>0</sup>)-38.2)-1.5(τ<sub>B<sup>0</sup></sub>-1.58)]%.
- 16 ALBRECHT 94 assumes B(D\*<sup>+</sup> → D<sup>0</sup>π<sup>+</sup>) = 68.1 ± 1.0 ± 1.3%. Uses partial reconstruction of D\*<sup>+</sup> and is independent of D<sup>0</sup> branching ratios.
- 17 ALBRECHT 93 reports 0.052 ± 0.005 ± 0.006. We rescale using the method described in STONE 94 but with the updated PDG 94 B(D<sup>0</sup> → K<sup>-</sup>π<sup>+</sup>). We have taken their average e and μ value. They also obtain α = 2αΓ<sup>0</sup>/(Γ<sup>-</sup> + Γ<sup>+</sup>) - 1 = 1.1 ± 0.4 ± 0.2, A<sub>FB</sub> = 3/4\*(Γ<sup>-</sup> - Γ<sup>+</sup>)/Γ = 0.2 ± 0.08 ± 0.06 and a value of |V<sub>cb</sub>| = 0.036-0.045 depending on model assumptions.
- 18 Combining  $\bar{D}^{*0} \ell^+ \nu_\ell$  and  $\bar{D}^{*-} \ell^+ \nu_\ell$  SANGHERA 93 test V-A structure and fit the decay angular distributions to obtain A<sub>FB</sub> = 3/4\*(Γ<sup>-</sup> - Γ<sup>+</sup>)/Γ = 0.14 ± 0.06 ± 0.03. Assuming a value of V<sub>cb</sub>, they measure V, A<sub>1</sub>, and A<sub>2</sub>, the three form factors for the D\*ℓν<sub>ℓ</sub> decay, where results are slightly dependent on model assumptions.
- 19 ANTREASIAN 90B is average over B and  $\bar{D}^*(2010)$  charge states.
- 20 The measurement of ALBRECHT 89c suggests a D\* polarization γ<sub>L</sub>/γ<sub>T</sub> of 0.85 ± 0.45, or α = 0.7 ± 0.9.
- 21 ALBRECHT 89J is ALBRECHT 87J value rescaled using B(D\*(2010)<sup>-</sup> → D<sup>0</sup>π<sup>-</sup>) = 0.57 ± 0.04 ± 0.04. Superseded by ALBRECHT 93.
- 22 We have taken average of the BORTOLETTO 89B values for electrons and muons, 0.046 ± 0.005 ± 0.007. We rescale using the method described in STONE 94 but with the updated PDG 94 B(D<sup>0</sup> → K<sup>-</sup>π<sup>+</sup>). The measurement suggests a D\* polarization parameter value α = 0.65 ± 0.66 ± 0.25.
- 23 ALBRECHT 87J assume μ-e universality, the B(Υ(4S) → B<sup>0</sup> $\bar{B}^0$ ) = 0.45, the B(D<sup>0</sup> → K<sup>-</sup>π<sup>+</sup>) = (0.042 ± 0.004 ± 0.004), and the B(D\*(2010)<sup>-</sup> → D<sup>0</sup>π<sup>-</sup>) = 0.49 ± 0.08. Superseded by ALBRECHT 89J.

WEIGHTED AVERAGE  
0.0509 ± 0.0022 (Error scaled by 1.6)



Values above of weighted average, error, and scale factor are based upon the data in this ideogram only. They are not necessarily the same as our ‘best’ values, obtained from a least-squares constrained fit utilizing measurements of other (related) quantities as additional information.

	$\chi^2$
DUNGEL 10 BELL	3.9
AUBERT 08Q BABR	1.8
AUBERT 08R BABR	1.4
ABDALLAH 04D DLPH	2.2
ADAM 03 CLE2	5.1
ABREU 01H DLPH	0.7
ABBIENDI 00Q OPAL	0.0
BUSKULIC 97 ALEP	15.0

(Confidence Level = 0.020)

$\Gamma(D^*(2010)^- \ell^+ \nu_\ell)/\Gamma(D \ell^+ \nu_\ell \text{ anything})$	$\Gamma_6/\Gamma_3$
VALUE	DOCUMENT ID TECN COMMENT
<b>0.537 ± 0.031 ± 0.036</b>	1 AUBERT 07AN BABR $e^+e^- \rightarrow \Upsilon(4S)$

1 Uses a fully reconstructed B meson on the recoil side.

# Meson Particle Listings

## B<sup>0</sup>

$\Gamma(D^{*0}(2010)^- \tau^+ \nu_\tau) / \Gamma_{total}$   $\Gamma_7 / \Gamma$

VALUE (units 10 <sup>-2</sup> )	DOCUMENT ID	TECN	COMMENT
<b>1.5 ± 0.5 OUR FIT</b>			Error includes scale factor of 1.4.
<b>2.02 ± 0.40 ± 0.37</b>	<sup>1</sup> MATYJA 07	BELL	e <sup>+</sup> e <sup>-</sup> → T(4S)
<b>• • •</b> We do not use the following data for averages, fits, limits, etc. <b>• • • •</b>			
1.11 ± 0.51 ± 0.06	<sup>2</sup> AUBERT 08N	BABR	Repl. by AUBERT 09s
<sup>1</sup> Observed in the recoil of the accompanying B meson.			
<sup>2</sup> Uses a fully reconstructed B meson as a tag on the recoil side.			

$\Gamma(D^{*0}(2010)^- \tau^+ \nu_\tau) / \Gamma(D^{*0}(2010)^- \ell^+ \nu_\ell)$   $\Gamma_7 / \Gamma_6$

VALUE	DOCUMENT ID	TECN	COMMENT
<b>0.29 ± 0.10 OUR FIT</b>			Error includes scale factor of 1.4.
<b>0.207 ± 0.095 ± 0.008</b>	<sup>1</sup> AUBERT 09s	BABR	e <sup>+</sup> e <sup>-</sup> → T(4S)
<sup>1</sup> Uses a fully reconstructed B meson as a tag on the recoil side.			

$\Gamma(\overline{D}^0 \pi^- \ell^+ \nu_\ell) / \Gamma_{total}$   $\Gamma_8 / \Gamma$

VALUE (units 10 <sup>-3</sup> )	DOCUMENT ID	TECN	COMMENT
<b>4.3 ± 0.6 OUR AVERAGE</b>			
4.3 ± 0.8 ± 0.3	<sup>1</sup> AUBERT 08q	BABR	e <sup>+</sup> e <sup>-</sup> → T(4S)
4.3 ± 0.9 ± 0.2	<sup>1,2</sup> LIVENTSEV 08	BELL	e <sup>+</sup> e <sup>-</sup> → T(4S)
<b>• • •</b> We do not use the following data for averages, fits, limits, etc. <b>• • • •</b>			
3.4 ± 1.0 ± 0.2	<sup>3</sup> LIVENTSEV 05	BELL	Repl. by LIVENTSEV 08
<sup>1</sup> Uses a fully reconstructed B meson as a tag on the recoil side.			
<sup>2</sup> LIVENTSEV 08 reports (4.2 ± 0.7 ± 0.6) × 10 <sup>-3</sup> from a measurement of $[\Gamma(B^0 \rightarrow \overline{D}^0 \pi^- \ell^+ \nu_\ell) / \Gamma_{total}] / [B(B^0 \rightarrow D^- \ell^+ \nu_\ell)]$ assuming $B(B^0 \rightarrow D^- \ell^+ \nu_\ell) = (2.12 \pm 0.20) \times 10^{-2}$ , which we rescale to our best value $B(B^0 \rightarrow D^- \ell^+ \nu_\ell) = (2.18 \pm 0.12) \times 10^{-2}$ . Our first error is their experiment's error and our second error is the systematic error from using our best value.			
<sup>3</sup> LIVENTSEV 05 reports $[\Gamma(B^0 \rightarrow \overline{D}^0 \pi^- \ell^+ \nu_\ell) / \Gamma_{total}] / [B(B^+ \rightarrow \overline{D}^0 \ell^+ \nu_\ell)] = 0.15 \pm 0.03 \pm 0.03$ which we multiply by our best value $B(B^+ \rightarrow \overline{D}^0 \ell^+ \nu_\ell) = (2.26 \pm 0.11) \times 10^{-2}$ . Our first error is their experiment's error and our second error is the systematic error from using our best value.			

$\Gamma(D_1^0(2400)^- \ell^+ \nu_\ell \times B(D_1^{*0} \rightarrow \overline{D}^0 \pi^-)) / \Gamma_{total}$   $\Gamma_9 / \Gamma$

VALUE (units 10 <sup>-3</sup> )	DOCUMENT ID	TECN	COMMENT
<b>3.0 ± 1.2 OUR AVERAGE</b>			Error includes scale factor of 1.8.
4.4 ± 0.8 ± 0.6	<sup>1</sup> AUBERT 08BL	BABR	e <sup>+</sup> e <sup>-</sup> → T(4S)
2.0 ± 0.7 ± 0.5	<sup>1</sup> LIVENTSEV 08	BELL	e <sup>+</sup> e <sup>-</sup> → T(4S)
<sup>1</sup> Uses a fully reconstructed B meson as a tag on the recoil side.			

$\Gamma(D_2^*(2460)^- \ell^+ \nu_\ell \times B(D_2^{*-} \rightarrow \overline{D}^0 \pi^-)) / \Gamma_{total}$   $\Gamma_{10} / \Gamma$

VALUE (units 10 <sup>-3</sup> )	DOCUMENT ID	TECN	COMMENT
<b>1.21 ± 0.33 OUR AVERAGE</b>			Error includes scale factor of 1.8.
1.10 ± 0.17 ± 0.08	<sup>1</sup> AUBERT 09Y	BABR	e <sup>+</sup> e <sup>-</sup> → T(4S)
2.2 ± 0.4 ± 0.4	<sup>2</sup> LIVENTSEV 08	BELL	e <sup>+</sup> e <sup>-</sup> → T(4S)
<sup>1</sup> Uses a simultaneous fit of all B semileptonic decays without full reconstruction of events. AUBERT 09Y reports $B(B^0 \rightarrow \overline{D}_2^*(2460)^- \ell^+ \nu_\ell) \cdot B(\overline{D}_2^*(2460)^- \rightarrow \overline{D}^{(*)0} \pi^-) = (1.77 \pm 0.26 \pm 0.11) \times 10^{-3}$ and the authors have provided us the individual measurement.			
<sup>2</sup> Uses a fully reconstructed B meson as a tag on the recoil side.			

$\Gamma(\overline{D}^{(*)n} \pi \ell^+ \nu_\ell (n \geq 1)) / \Gamma(D \ell^+ \nu_\ell \text{ anything})$   $\Gamma_{11} / \Gamma_3$

VALUE	DOCUMENT ID	TECN	COMMENT
<b>0.248 ± 0.032 ± 0.030</b>	<sup>1</sup> AUBERT 07AN	BABR	e <sup>+</sup> e <sup>-</sup> → T(4S)
<sup>1</sup> Uses a fully reconstructed B meson on the recoil side.			

$\Gamma(\overline{D}^{*0} \pi^- \ell^+ \nu_\ell) / \Gamma_{total}$   $\Gamma_{12} / \Gamma$

VALUE (units 10 <sup>-3</sup> )	DOCUMENT ID	TECN	COMMENT
<b>4.9 ± 0.8 OUR AVERAGE</b>			
4.8 ± 0.8 ± 0.4	<sup>1</sup> AUBERT 08q	BABR	e <sup>+</sup> e <sup>-</sup> → T(4S)
5.8 ± 2.2 ± 0.3	<sup>1,2</sup> LIVENTSEV 08	BELL	e <sup>+</sup> e <sup>-</sup> → T(4S)
<b>• • •</b> We do not use the following data for averages, fits, limits, etc. <b>• • • •</b>			
5.7 ± 1.3 ± 0.2	<sup>3,4</sup> LIVENTSEV 05	BELL	Repl. by LIVENTSEV 08
<sup>1</sup> Uses a fully reconstructed B meson as a tag on the recoil side.			
<sup>2</sup> LIVENTSEV 08 reports (5.6 ± 2.1 ± 0.8) × 10 <sup>-3</sup> from a measurement of $[\Gamma(B^0 \rightarrow \overline{D}^{*0} \pi^- \ell^+ \nu_\ell) / \Gamma_{total}] / [B(B^0 \rightarrow D^- \ell^+ \nu_\ell)]$ assuming $B(B^0 \rightarrow D^- \ell^+ \nu_\ell) = (2.12 \pm 0.20) \times 10^{-2}$ , which we rescale to our best value $B(B^0 \rightarrow D^- \ell^+ \nu_\ell) = (2.18 \pm 0.12) \times 10^{-2}$ . Our first error is their experiment's error and our second error is the systematic error from using our best value.			
<sup>3</sup> Excludes D <sup>*+</sup> contribution to D <sub>π</sub> modes.			
<sup>4</sup> LIVENTSEV 05 reports $[\Gamma(B^0 \rightarrow \overline{D}^{*0} \pi^- \ell^+ \nu_\ell) / \Gamma_{total}] / [B(B^+ \rightarrow \overline{D}^{*0} \ell^+ \nu_\ell)] = 0.10 \pm 0.02 \pm 0.01$ which we multiply by our best value $B(B^+ \rightarrow \overline{D}^{*0} \ell^+ \nu_\ell) = (5.70 \pm 0.19) \times 10^{-2}$ . Our first error is their experiment's error and our second error is the systematic error from using our best value.			

$\Gamma(D_1(2420)^- \ell^+ \nu_\ell \times B(D_1^- \rightarrow \overline{D}^{*0} \pi^-)) / \Gamma_{total}$   $\Gamma_{13} / \Gamma$

VALUE (units 10 <sup>-3</sup> )	DOCUMENT ID	TECN	COMMENT
<b>2.80 ± 0.28 OUR AVERAGE</b>			
2.78 ± 0.24 ± 0.25	<sup>1</sup> AUBERT 09Y	BABR	e <sup>+</sup> e <sup>-</sup> → T(4S)
2.7 ± 0.4 ± 0.3	<sup>2</sup> AUBERT 08BL	BABR	e <sup>+</sup> e <sup>-</sup> → T(4S)
5.4 ± 1.9 ± 0.9	<sup>2</sup> LIVENTSEV 08	BELL	e <sup>+</sup> e <sup>-</sup> → T(4S)
<sup>1</sup> Uses a simultaneous measurement of all B semileptonic decays without full reconstruction of events.			
<sup>2</sup> Uses a fully reconstructed B meson as a tag on the recoil side.			

$\Gamma(D_1^+(2430)^- \ell^+ \nu_\ell \times B(D_1^- \rightarrow \overline{D}^{*0} \pi^-)) / \Gamma_{total}$   $\Gamma_{14} / \Gamma$

VALUE (units 10 <sup>-3</sup> )	CL%	DOCUMENT ID	TECN	COMMENT
<b>3.1 ± 0.7 ± 0.5</b>		<sup>1</sup> AUBERT 08BL	BABR	e <sup>+</sup> e <sup>-</sup> → T(4S)
<b>• • •</b> We do not use the following data for averages, fits, limits, etc. <b>• • • •</b>				
<5.0		<sup>1</sup> LIVENTSEV 08	BELL	e <sup>+</sup> e <sup>-</sup> → T(4S)
<sup>1</sup> Uses a fully reconstructed B meson as a tag on the recoil side.				

$\Gamma(D_2^*(2460)^- \ell^+ \nu_\ell \times B(D_2^{*-} \rightarrow \overline{D}^{*0} \pi^-)) / \Gamma_{total}$   $\Gamma_{15} / \Gamma$

VALUE (units 10 <sup>-3</sup> )	CL%	DOCUMENT ID	TECN	COMMENT
<b>0.68 ± 0.12 OUR AVERAGE</b>				
0.67 ± 0.12 ± 0.05		<sup>1</sup> AUBERT 09Y	BABR	e <sup>+</sup> e <sup>-</sup> → T(4S)
0.7 ± 0.2 ± 0.2		<sup>2</sup> AUBERT 08BL	BABR	e <sup>+</sup> e <sup>-</sup> → T(4S)
<b>• • •</b> We do not use the following data for averages, fits, limits, etc. <b>• • • •</b>				
<3.0		<sup>2</sup> LIVENTSEV 08	BELL	e <sup>+</sup> e <sup>-</sup> → T(4S)
<sup>1</sup> Uses a simultaneous fit of all B semileptonic decays without full reconstruction of events. AUBERT 09Y reports $B(B^0 \rightarrow \overline{D}_2^*(2460)^- \ell^+ \nu_\ell) \cdot B(\overline{D}_2^*(2460)^- \rightarrow \overline{D}^{(*)0} \pi^-) = (1.77 \pm 0.26 \pm 0.11) \times 10^{-3}$ and the authors have provided us the individual measurement.				
<sup>2</sup> Uses a fully reconstructed B meson as a tag on the recoil side.				

$\Gamma(\rho^-(\ell^+ \nu_\ell) / \Gamma_{total}$   $\Gamma_{16} / \Gamma$

$\ell = e \text{ or } \mu, \text{ not sum over } e \text{ and } \mu \text{ modes.}$

"OUR EVALUATION" has been obtained by the Heavy Flavor Averaging Group (HFAG) by including both B<sup>0</sup> and B<sup>+</sup> decays. The average assumes equality of the semileptonic decay width for these isospin conjugate states.

VALUE (units 10 <sup>-4</sup> )	CL%	DOCUMENT ID	TECN	COMMENT
<b>2.34 ± 0.15 ± 0.24 OUR EVALUATION</b>				Error includes scale factor of 1.4. See the ideogram below.
<b>2.07 ± 0.34 OUR AVERAGE</b>				
1.75 ± 0.15 ± 0.27		<sup>1</sup> DEL-AMO-SA.11c	BABR	e <sup>+</sup> e <sup>-</sup> → T(4S)
2.93 ± 0.37 ± 0.37		<sup>2</sup> ADAM 07	CLE2	e <sup>+</sup> e <sup>-</sup> → T(4S)
2.17 ± 0.54 ± 0.32		<sup>3</sup> HOKUUE 07	BELL	e <sup>+</sup> e <sup>-</sup> → T(4S)
<b>• • •</b> We do not use the following data for averages, fits, limits, etc. <b>• • • •</b>				
2.14 ± 0.21 ± 0.56		<sup>1</sup> AUBERT,B 05o	BABR	Repl. by DEL-AMO-SANCHEZ 11c
2.17 ± 0.34 ± 0.62 ± 0.68		<sup>4</sup> ATHAR 03	CLE2	Repl. by ADAM 07
3.29 ± 0.42 ± 0.72		<sup>5</sup> AUBERT 03E	BABR	Repl. by AUBERT,B 05o
2.57 ± 0.29 ± 0.53 ± 0.62		<sup>6</sup> BEHRENS 00	CLE2	Repl. by ADAM 07
2.69 ± 0.41 ± 0.61 ± 0.64		<sup>7</sup> BEHRENS 00	CLE2	e <sup>+</sup> e <sup>-</sup> → T(4S)
2.5 ± 0.4 ± 0.7 ± 0.9		<sup>8</sup> ALEXANDER 96T	CLE2	Repl. by BEHRENS 00
<4.1		<sup>9</sup> BEAN 93B	CLE2	e <sup>+</sup> e <sup>-</sup> → T(4S)

<sup>1</sup> B<sup>+</sup> and B<sup>0</sup> decays combined assuming isospin symmetry. Systematic errors include both experimental and form-factor uncertainties.

<sup>2</sup> The B<sup>0</sup> and B<sup>+</sup> results are combined assuming the isospin, B lifetimes, and relative charged/neutral B production at the T(4S).

<sup>3</sup> The signal events are tagged by a second B meson reconstructed in the semileptonic mode B → D<sup>(\*)</sup>ℓνℓ.

<sup>4</sup> ATHAR 03 reports systematic errors <sup>+0.47</sup>-0.50 ± 0.41 ± 0.01, which are experimental systematic, systematic due to residual form-factor uncertainties in the signal, and systematic due to residual form-factor uncertainties in the cross-feed modes, respectively. We combine these in quadrature.

<sup>5</sup> Uses isospin constraints and extrapolation to all electron energies according to five different form-factor calculations. The second error combines the systematic and theoretical uncertainties in quadrature.

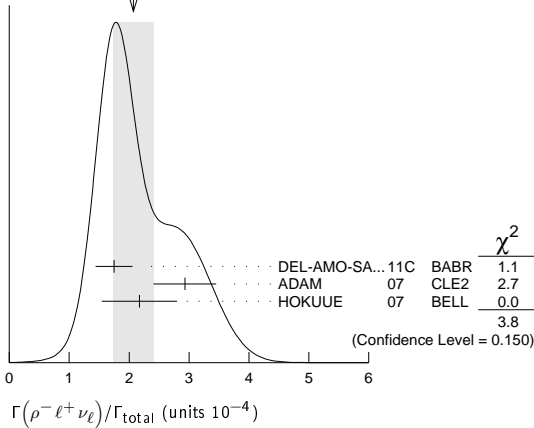
<sup>6</sup> Averaging with ALEXANDER 96T results including experimental and theoretical correlations considered, BEHRENS 00 reports systematic errors <sup>+0.33</sup>-0.46 ± 0.41, where the second error is theoretical model dependence. We combine these in quadrature.

<sup>7</sup> BEHRENS 00 reports <sup>+0.35</sup>-0.40 ± 0.50, where the second error is the theoretical model dependence. We combine these in quadrature. B<sup>+</sup> and B<sup>0</sup> decays combined using isospin symmetry:  $\Gamma(B^0 \rightarrow \rho^-(\ell^+ \nu) - 2\Gamma(B^+ \rightarrow \rho^0(\ell^+ \nu) \approx 2\Gamma(B^+ \rightarrow \omega(\ell^+ \nu))$ . No evidence for ωℓν is reported.

<sup>8</sup> ALEXANDER 96T reports <sup>+0.5</sup>-0.7 ± 0.5 where the second error is the theoretical model dependence. We combine these in quadrature. B<sup>+</sup> and B<sup>0</sup> decays combined using isospin symmetry:  $\Gamma(B^0 \rightarrow \rho^-(\ell^+ \nu) \approx 2\Gamma(B^+ \rightarrow \rho^0(\ell^+ \nu) \approx 2\Gamma(B^+ \rightarrow \omega(\ell^+ \nu))$ . No evidence for ωℓν is reported.

<sup>9</sup> BEAN 93B limit set using ISGW Model. Using isospin and the quark model to combine  $\Gamma(\rho^0(\ell^+ \nu))$  and  $\Gamma(\omega(\ell^+ \nu))$  with this result, they obtain a limit <(1.6-2.7) × 10<sup>-4</sup> at 90% CL for B<sup>+</sup> → (ω or ρ<sup>0</sup>)ℓ<sup>+</sup>νℓ. The range corresponds to the ISGW, WSB, and KS models. An upper limit on  $|V_{ub}/V_{cb}| < 0.08-0.13$  at 90% CL is derived as well.

WEIGHTED AVERAGE  
2.07±0.34 (Error scaled by 1.4)



$\Gamma(\pi^- \ell^+ \nu_\ell)/\Gamma_{total}$   $\Gamma_{17}/\Gamma$   
"OUR EVALUATION" is provided by the Heavy Flavor Averaging Group (HFAG) and the procedure is described at <http://www.slac.stanford.edu/xorg/hfag/>.

VALUE (units 10 <sup>-4</sup> )	DOCUMENT ID	TECN	COMMENT
<b>1.441 ± 0.052 OUR EVALUATION</b>			
<b>1.44 ± 0.05 OUR AVERAGE</b>			
1.41 ± 0.05 ± 0.07	<sup>1</sup> DEL-AMO-SA...11c	BABR	$e^+ e^- \rightarrow \Upsilon(4S)$
1.42 ± 0.05 ± 0.08	<sup>2</sup> DEL-AMO-SA...11f	BABR	$e^+ e^- \rightarrow \Upsilon(4S)$
1.49 ± 0.04 ± 0.07	<sup>2</sup> HA	BELL	$e^+ e^- \rightarrow \Upsilon(4S)$
1.54 ± 0.17 ± 0.09	<sup>1</sup> AUBERT	08AV	BABR $e^+ e^- \rightarrow \Upsilon(4S)$
1.37 ± 0.15 ± 0.11	<sup>3,4</sup> ADAM	07	CLE2 $e^+ e^- \rightarrow \Upsilon(4S)$
1.38 ± 0.19 ± 0.14	<sup>5</sup> HOKUUE	07	BELL $e^+ e^- \rightarrow \Upsilon(4S)$
• • • We do not use the following data for averages, fits, limits, etc. • • •			
1.46 ± 0.07 ± 0.08	<sup>6</sup> AUBERT	07J	BABR Repl. by DEL-AMO-SANCHEZ 11F
1.33 ± 0.17 ± 0.11	<sup>7</sup> AUBERT,B	06K	BABR Repl. by AUBERT 08AV
1.38 ± 0.10 ± 0.18	<sup>8</sup> AUBERT,B	05o	BABR Repl. by DEL-AMO-SANCHEZ 11c
1.33 ± 0.18 ± 0.13	<sup>9</sup> ATHAR	03	CLE2 Repl. by ATHAR 03
1.8 ± 0.4 ± 0.4	<sup>10</sup> ALEXANDER	96T	CLE2 Repl. by ATHAR 03

- Using isospin relation,  $B^+$  and  $B^0$  branching fractions are combined.
- Uses the neutrino reconstruction technique. Assumes  $B(\Upsilon(4S) \rightarrow B^+ B^-) = (51.6 \pm 0.6)\%$  and  $B(\Upsilon(4S) \rightarrow B^0 \bar{B}^0) = (48.4 \pm 0.6)\%$ .
- The  $B^0$  and  $B^+$  results are combined assuming the isospin,  $B$  lifetimes, and relative charged/neutral  $B$  production at the  $\Upsilon(4S)$ .
- Also report the rate for  $q^2 > 16 \text{ GeV}^2$  of  $(0.41 \pm 0.08 \pm 0.04) \times 10^{-4}$  from which they obtain  $|V_{ub}| = 3.6 \pm 0.4 \pm 0.2_{-0.4}^{+0.6}$  (last error is from theory).
- The signal events are tagged by a second  $B$  meson reconstructed in the semileptonic mode  $B \rightarrow D^{(*)} \ell \nu_\ell$ .
- The analysis uses events in which the signal  $B$  decays are reconstructed with an innovative loose neutrino reconstruction technique.
- The signals are tagged by a second  $B$  meson reconstructed in a semileptonic or hadronic decay. The  $B^0$  and  $B^+$  results are combined assuming the isospin symmetry.
- $B^+$  and  $B^0$  decays combined assuming isospin symmetry. Systematic errors include both experimental and form-factor uncertainties.
- ATHAR 03 reports systematic errors  $0.11 \pm 0.01 \pm 0.07$ , which are experimental systematic, systematic due to residual form-factor uncertainties in the signal, and systematic due to residual form-factor uncertainties in the cross-feed modes, respectively. We combine these in quadrature.
- ALEXANDER 96T gives systematic errors  $\pm 0.3 \pm 0.2$  where the second error reflects the estimated model dependence. We combine these in quadrature. Assumes isospin symmetry:  $\Gamma(B^0 \rightarrow \pi^- \ell^+ \nu) = 2 \times \Gamma(B^+ \rightarrow \pi^0 \ell^+ \nu)$ .

$\Gamma(\pi^- \mu^+ \nu_\mu)/\Gamma_{total}$   $\Gamma_{18}/\Gamma$

VALUE	DOCUMENT ID	TECN	COMMENT
• • • We do not use the following data for averages, fits, limits, etc. • • •			
seen	<sup>1</sup> ALBRECHT	91c	ARG
<sup>1</sup> In ALBRECHT 91c, one event is fully reconstructed providing evidence for the $b \rightarrow u$ transition.			

$\Gamma(K^\pm \text{ anything})/\Gamma_{total}$   $\Gamma_{19}/\Gamma$

VALUE	DOCUMENT ID	TECN	COMMENT
<b>0.78 ± 0.08</b>	<sup>1</sup> ALBRECHT	96D	ARG $e^+ e^- \rightarrow \Upsilon(4S)$
<sup>1</sup> Average multiplicity.			

$\Gamma(D^0 X)/\Gamma_{total}$   $\Gamma_{20}/\Gamma$

VALUE	DOCUMENT ID	TECN	COMMENT
<b>0.081 ± 0.014 ± 0.005</b>	<sup>1</sup> AUBERT	07N	BABR $e^+ e^- \rightarrow \Upsilon(4S)$
• • • We do not use the following data for averages, fits, limits, etc. • • •			
0.063 ± 0.019 ± 0.005	<sup>1</sup> AUBERT,BE	04B	BABR Repl. by AUBERT 07N

<sup>1</sup> Events are selected by completely reconstructing one  $B$  and searching for a reconstructed charmed particle in the rest of the event. The last error includes systematic and charm branching ratio uncertainties.

$\Gamma(D^0 X)/\Gamma_{total}$   $\Gamma_{21}/\Gamma$

VALUE	DOCUMENT ID	TECN	COMMENT
<b>0.474 ± 0.020 ± 0.020</b> <sub>-0.019</sub>	<sup>1</sup> AUBERT	07N	BABR $e^+ e^- \rightarrow \Upsilon(4S)$
• • • We do not use the following data for averages, fits, limits, etc. • • •			
0.511 ± 0.031 ± 0.028	<sup>1</sup> AUBERT,BE	04B	BABR Repl. by AUBERT 07N

<sup>1</sup> Events are selected by completely reconstructing one  $B$  and searching for a reconstructed charmed particle in the rest of the event. The last error includes systematic and charm branching ratio uncertainties.

$\Gamma(D^0 X)/[\Gamma(D^0 X) + \Gamma(D^0 \bar{X})]$   $\Gamma_{20}/(\Gamma_{20} + \Gamma_{21})$

VALUE	DOCUMENT ID	TECN	COMMENT
<b>0.146 ± 0.022 ± 0.006</b>	AUBERT	07N	BABR $e^+ e^- \rightarrow \Upsilon(4S)$
• • • We do not use the following data for averages, fits, limits, etc. • • •			
0.110 ± 0.031 ± 0.008	AUBERT,BE	04B	BABR Repl. by AUBERT 07N

$\Gamma(D^+ X)/\Gamma_{total}$   $\Gamma_{22}/\Gamma$

VALUE	CL%	DOCUMENT ID	TECN	COMMENT
<b>&lt;0.039</b>	90	<sup>1</sup> AUBERT	07N	BABR $e^+ e^- \rightarrow \Upsilon(4S)$
• • • We do not use the following data for averages, fits, limits, etc. • • •				
<0.051	90	<sup>1</sup> AUBERT,BE	04B	BABR Repl. by AUBERT 07N

<sup>1</sup> Events are selected by completely reconstructing one  $B$  and searching for a reconstructed charmed particle in the rest of the event. The last error includes systematic and charm branching ratio uncertainties.

$\Gamma(D^- X)/\Gamma_{total}$   $\Gamma_{23}/\Gamma$

VALUE	DOCUMENT ID	TECN	COMMENT
<b>0.369 ± 0.016 ± 0.030</b> <sub>-0.027</sub>	<sup>1</sup> AUBERT	07N	BABR $e^+ e^- \rightarrow \Upsilon(4S)$
• • • We do not use the following data for averages, fits, limits, etc. • • •			
0.397 ± 0.030 ± 0.040 <sub>-0.038</sub>	<sup>1</sup> AUBERT,BE	04B	BABR Repl. by AUBERT 07N

<sup>1</sup> Events are selected by completely reconstructing one  $B$  and searching for a reconstructed charmed particle in the rest of the event. The last error includes systematic and charm branching ratio uncertainties.

$\Gamma(D^+ X)/[\Gamma(D^+ X) + \Gamma(D^- X)]$   $\Gamma_{22}/(\Gamma_{22} + \Gamma_{23})$

VALUE	DOCUMENT ID	TECN	COMMENT
<b>0.058 ± 0.028 ± 0.006</b>	AUBERT	07N	BABR $e^+ e^- \rightarrow \Upsilon(4S)$
• • • We do not use the following data for averages, fits, limits, etc. • • •			
0.055 ± 0.040 ± 0.006	AUBERT,BE	04B	BABR Repl. by AUBERT 07N

$\Gamma(D_s^+ X)/\Gamma_{total}$   $\Gamma_{24}/\Gamma$

VALUE	DOCUMENT ID	TECN	COMMENT
<b>0.103 ± 0.012 ± 0.017</b> <sub>-0.014</sub>	<sup>1</sup> AUBERT	07N	BABR $e^+ e^- \rightarrow \Upsilon(4S)$
• • • We do not use the following data for averages, fits, limits, etc. • • •			
0.109 ± 0.021 ± 0.039 <sub>-0.024</sub>	<sup>1</sup> AUBERT,BE	04B	BABR Repl. by AUBERT 07N

<sup>1</sup> Events are selected by completely reconstructing one  $B$  and searching for a reconstructed charmed particle in the rest of the event. The last error includes systematic and charm branching ratio uncertainties.

$\Gamma(D_s^- X)/\Gamma_{total}$   $\Gamma_{25}/\Gamma$

VALUE	CL%	DOCUMENT ID	TECN	COMMENT
<b>&lt;0.026</b>	90	<sup>1</sup> AUBERT	07N	BABR $e^+ e^- \rightarrow \Upsilon(4S)$
• • • We do not use the following data for averages, fits, limits, etc. • • •				
<0.087	90	<sup>1</sup> AUBERT,BE	04B	BABR Repl. by AUBERT 07N

<sup>1</sup> Events are selected by completely reconstructing one  $B$  and searching for a reconstructed charmed particle in the rest of the event. The last error includes systematic and charm branching ratio uncertainties.

$\Gamma(D_s^+ X)/[\Gamma(D_s^+ X) + \Gamma(D_s^- X)]$   $\Gamma_{24}/(\Gamma_{24} + \Gamma_{25})$

VALUE	DOCUMENT ID	TECN	COMMENT
<b>0.879 ± 0.066 ± 0.005</b>	AUBERT	07N	BABR $e^+ e^- \rightarrow \Upsilon(4S)$
• • • We do not use the following data for averages, fits, limits, etc. • • •			
0.733 ± 0.092 ± 0.010	AUBERT,BE	04B	BABR Repl. by AUBERT 07N

$\Gamma(A_c^+ X)/\Gamma_{total}$   $\Gamma_{26}/\Gamma$

VALUE	CL%	DOCUMENT ID	TECN	COMMENT
<b>&lt;0.031</b>	90	<sup>1</sup> AUBERT	07N	BABR $e^+ e^- \rightarrow \Upsilon(4S)$
• • • We do not use the following data for averages, fits, limits, etc. • • •				
<0.038	90	<sup>1</sup> AUBERT,BE	04B	BABR Repl. by AUBERT 07N

<sup>1</sup> Events are selected by completely reconstructing one  $B$  and searching for a reconstructed charmed particle in the rest of the event. The last error includes systematic and charm branching ratio uncertainties.

$\Gamma(\bar{A}_c^- X)/\Gamma_{total}$   $\Gamma_{27}/\Gamma$

VALUE	DOCUMENT ID	TECN	COMMENT
<b>0.05 ± 0.010 ± 0.019</b> <sub>-0.011</sub>	<sup>1</sup> AUBERT	07N	BABR $e^+ e^- \rightarrow \Upsilon(4S)$
• • • We do not use the following data for averages, fits, limits, etc. • • •			
0.049 ± 0.017 ± 0.018 <sub>-0.011</sub>	<sup>1</sup> AUBERT,BE	04B	BABR Repl. by AUBERT 07N

<sup>1</sup> Events are selected by completely reconstructing one  $B$  and searching for a reconstructed charmed particle in the rest of the event. The last error includes systematic and charm branching ratio uncertainties.

## Meson Particle Listings

 $B^0$ 

$$\frac{\Gamma(\Lambda_c^+ X)}{\Gamma(\Lambda_c^+ X) + \Gamma(\bar{\Lambda}_c^+ X)} \quad \Gamma_{26}/(\Gamma_{26} + \Gamma_{27})$$

VALUE	DOCUMENT ID	TECN	COMMENT
$0.243^{+0.119}_{-0.121} \pm 0.003$	AUBERT	07N	BABR $e^+e^- \rightarrow \Upsilon(4S)$
• • • We do not use the following data for averages, fits, limits, etc. • • •			
$0.286 \pm 0.142 \pm 0.007$	AUBERT, BE	04B	BABR Repl. by AUBERT 07N

$$\frac{\Gamma(\bar{c} X)}{\Gamma_{\text{total}}} \quad \Gamma_{28}/\Gamma$$

VALUE	DOCUMENT ID	TECN	COMMENT
$0.947 \pm 0.030^{+0.045}_{-0.040}$	<sup>1</sup> AUBERT	07N	BABR $e^+e^- \rightarrow \Upsilon(4S)$
• • • We do not use the following data for averages, fits, limits, etc. • • •			
$1.039 \pm 0.051^{+0.063}_{-0.058}$	<sup>1</sup> AUBERT, BE	04B	BABR Repl. by AUBERT 07N

<sup>1</sup> Events are selected by completely reconstructing one  $B$  and searching for a reconstructed charmed particle in the rest of the event. The last error includes systematic and charm branching ratio uncertainties.

$$\frac{\Gamma(c X)}{\Gamma_{\text{total}}} \quad \Gamma_{29}/\Gamma$$

VALUE	DOCUMENT ID	TECN	COMMENT
$0.246 \pm 0.024^{+0.021}_{-0.017}$	<sup>1</sup> AUBERT	07N	BABR $e^+e^- \rightarrow \Upsilon(4S)$
• • • We do not use the following data for averages, fits, limits, etc. • • •			
$0.237 \pm 0.036^{+0.041}_{-0.027}$	<sup>1</sup> AUBERT, BE	04B	BABR Repl. by AUBERT 07N

<sup>1</sup> Events are selected by completely reconstructing one  $B$  and searching for a reconstructed charmed particle in the rest of the event. The last error includes systematic and charm branching ratio uncertainties.

$$\frac{\Gamma(\bar{c} c X)}{\Gamma_{\text{total}}} \quad \Gamma_{30}/\Gamma$$

VALUE	DOCUMENT ID	TECN	COMMENT
$1.193 \pm 0.030^{+0.053}_{-0.049}$	<sup>1</sup> AUBERT	07N	BABR $e^+e^- \rightarrow \Upsilon(4S)$
• • • We do not use the following data for averages, fits, limits, etc. • • •			
$1.276 \pm 0.062^{+0.088}_{-0.074}$	<sup>1</sup> AUBERT, BE	04B	BABR Repl. by AUBERT 07N

<sup>1</sup> Events are selected by completely reconstructing one  $B$  and searching for a reconstructed charmed particle in the rest of the event. The last error includes systematic and charm branching ratio uncertainties.

$$\frac{\Gamma(D^- \pi^+)}{\Gamma_{\text{total}}} \quad \Gamma_{31}/\Gamma$$

VALUE (units $10^{-3}$ )	EVTS	DOCUMENT ID	TECN	COMMENT
<b>2.68 ± 0.13 OUR FIT</b>				
<b>2.68 ± 0.13 OUR AVERAGE</b>				
$2.55 \pm 0.05 \pm 0.16$		<sup>1</sup> AUBERT	07H	BABR $e^+e^- \rightarrow \Upsilon(4S)$
$3.03 \pm 0.23 \pm 0.23$		<sup>2</sup> AUBERT, BE	06J	BABR $e^+e^- \rightarrow \Upsilon(4S)$
$2.68 \pm 0.12 \pm 0.24$		<sup>1,3</sup> AHMED	02B	CLE2 $e^+e^- \rightarrow \Upsilon(4S)$
$2.7 \pm 0.6 \pm 0.5$		<sup>4</sup> BORTOLETTO	92	CLEO $e^+e^- \rightarrow \Upsilon(4S)$
$4.8 \pm 1.1 \pm 1.1$	22	<sup>5</sup> ALBRECHT	90J	ARG $e^+e^- \rightarrow \Upsilon(4S)$
$5.1^{+2.8}_{-2.5} \pm 1.3$	4	<sup>6</sup> BEBEK	87	CLEO $e^+e^- \rightarrow \Upsilon(4S)$
• • • We do not use the following data for averages, fits, limits, etc. • • •				
$2.90 \pm 0.21 \pm 0.14$		<sup>1,7</sup> AUBERT, B	04O	BABR Repl. by AUBERT 07H
$2.9 \pm 0.4 \pm 0.1$	81	<sup>8</sup> ALAM	94	CLE2 Repl. by AHMED 02B
$3.1 \pm 1.3 \pm 1.0$	7	<sup>5</sup> ALBRECHT	88K	ARG $e^+e^- \rightarrow \Upsilon(4S)$

<sup>1</sup> Assumes equal production of  $B^+$  and  $B^0$  at the  $\Upsilon(4S)$ .  
<sup>2</sup> Uses a missing-mass method. Does not depend on  $D$  branching fractions or  $B^+/B^0$  production rates.

<sup>3</sup> AHMED 02B reports an additional uncertainty on the branching ratios to account for 4.5% uncertainty on relative production of  $B^0$  and  $B^+$ , which is not included here.

<sup>4</sup> BORTOLETTO 92 assumes equal production of  $B^+$  and  $B^0$  at the  $\Upsilon(4S)$  and uses Mark III branching fractions for the  $D$ .

<sup>5</sup> ALBRECHT 88K assumes  $B^0\bar{B}^0:B^+B^-$  production ratio is 45:55. Superseded by ALBRECHT 90J which assumes 50:50.

<sup>6</sup> BEBEK 87 value has been updated in BERKELMAN 91 to use same assumptions as noted for BORTOLETTO 92.

<sup>7</sup> AUBERT, B 04O reports  $[\Gamma(B^0 \rightarrow D^- \pi^+)/\Gamma_{\text{total}}] \times [B(D^+ \rightarrow K_S^0 \pi^+)] = (42.7 \pm 2.1 \pm 2.2) \times 10^{-6}$  which we divide by our best value  $B(D^+ \rightarrow K_S^0 \pi^+) = (1.47 \pm 0.07) \times 10^{-2}$ . Our first error is their experiment's error and our second error is the systematic error from using our best value.

<sup>8</sup> ALAM 94 reports  $[\Gamma(B^0 \rightarrow D^- \pi^+)/\Gamma_{\text{total}}] \times [B(D^+ \rightarrow K^- 2\pi^+)] = (0.265 \pm 0.032 \pm 0.023) \times 10^{-3}$  which we divide by our best value  $B(D^+ \rightarrow K^- 2\pi^+) = (9.13 \pm 0.19) \times 10^{-2}$ . Our first error is their experiment's error and our second error is the systematic error from using our best value. Assumes equal production of  $B^+$  and  $B^0$  at the  $\Upsilon(4S)$ .

$$\frac{\Gamma(D^- \ell^+ \nu_\ell)}{\Gamma(D^- \pi^+)} \quad \Gamma_4/\Gamma_{31}$$

VALUE	DOCUMENT ID	TECN	COMMENT
<b>9.9 ± 1.0 ± 0.9</b>	AALTONEN	09E	CDF $p\bar{p}$ at 1.96 TeV

$$\frac{\Gamma(D^- \rho^+)}{\Gamma_{\text{total}}} \quad \Gamma_{32}/\Gamma$$

VALUE	EVTS	DOCUMENT ID	TECN	COMMENT
<b>0.0078 ± 0.0013 OUR AVERAGE</b>				
$0.0077 \pm 0.0013 \pm 0.0002$	79	<sup>1</sup> ALAM	94	CLE2 $e^+e^- \rightarrow \Upsilon(4S)$
$0.009 \pm 0.005 \pm 0.003$	9	<sup>2</sup> ALBRECHT	90J	ARG $e^+e^- \rightarrow \Upsilon(4S)$
• • • We do not use the following data for averages, fits, limits, etc. • • •				
$0.022 \pm 0.012 \pm 0.009$	6	<sup>2</sup> ALBRECHT	88K	ARG $e^+e^- \rightarrow \Upsilon(4S)$

<sup>1</sup> ALAM 94 reports  $[\Gamma(B^0 \rightarrow D^- \rho^+)/\Gamma_{\text{total}}] \times [B(D^+ \rightarrow K^- 2\pi^+)] = 0.000704 \pm 0.000096 \pm 0.000070$  which we divide by our best value  $B(D^+ \rightarrow K^- 2\pi^+) = (9.13 \pm 0.19) \times 10^{-2}$ . Our first error is their experiment's error and our second error is the systematic error from using our best value. Assumes equal production of  $B^+$  and  $B^0$  at the  $\Upsilon(4S)$ .

<sup>2</sup> ALBRECHT 88K assumes  $B^0\bar{B}^0:B^+B^-$  production ratio is 45:55. Superseded by ALBRECHT 90J which assumes 50:50.

$$\frac{\Gamma(D^- K^0 \pi^+)}{\Gamma_{\text{total}}} \quad \Gamma_{33}/\Gamma$$

VALUE (units $10^{-4}$ )	DOCUMENT ID	TECN	COMMENT
<b>4.9 ± 0.7 ± 0.5</b>	<sup>1</sup> AUBERT, BE	05B	BABR $e^+e^- \rightarrow \Upsilon(4S)$

<sup>1</sup> Assumes equal production of  $B^+$  and  $B^0$  at the  $\Upsilon(4S)$ .

$$\frac{\Gamma(D^- K^*(892)^+)}{\Gamma_{\text{total}}} \quad \Gamma_{34}/\Gamma$$

VALUE (units $10^{-4}$ )	DOCUMENT ID	TECN	COMMENT
<b>4.5 ± 0.7 OUR AVERAGE</b>			
$4.6 \pm 0.6 \pm 0.5$	<sup>1</sup> AUBERT, BE	05B	BABR $e^+e^- \rightarrow \Upsilon(4S)$
$3.7 \pm 1.5 \pm 1.0$	<sup>1</sup> MAHAPATRA	02	CLE2 $e^+e^- \rightarrow \Upsilon(4S)$

<sup>1</sup> Assumes equal production of  $B^+$  and  $B^0$  at the  $\Upsilon(4S)$ .

$$\frac{\Gamma(D^- \omega \pi^+)}{\Gamma_{\text{total}}} \quad \Gamma_{35}/\Gamma$$

VALUE (units $10^{-4}$ )	DOCUMENT ID	TECN	COMMENT
<b>0.0028 ± 0.0005 ± 0.0004</b>	<sup>1</sup> ALEXANDER	01B	CLE2 $e^+e^- \rightarrow \Upsilon(4S)$

<sup>1</sup> Assumes equal production of  $B^+$  and  $B^0$  at the  $\Upsilon(4S)$ . The signal is consistent with all observed  $\omega \pi^+$  having proceeded through the  $\rho^{+}$  resonance at mass  $1349 \pm 25^{+10}_{-5}$  MeV and width  $547 \pm 86^{+46}_{-45}$  MeV.

$$\frac{\Gamma(D^- K^+)}{\Gamma_{\text{total}}} \quad \Gamma_{36}/\Gamma$$

VALUE (units $10^{-4}$ )	DOCUMENT ID	TECN	COMMENT
<b>1.97 ± 0.21 OUR AVERAGE</b>			
$2.01 \pm 0.18 \pm 0.14$	<sup>1</sup> AAIJ	11F	LHCb $pp$ at 7 TeV
$1.8 \pm 0.4 \pm 0.1$	<sup>2</sup> ABE	01I	BELL $e^+e^- \rightarrow \Upsilon(4S)$

<sup>1</sup> AAIJ 11F reports  $(2.01 \pm 0.18 \pm 0.14) \times 10^{-4}$  from a measurement of  $[\Gamma(B^0 \rightarrow D^- K^+)/\Gamma_{\text{total}}] / [B(B^0 \rightarrow D^- \pi^+)]$  assuming  $B(B^0 \rightarrow D^- \pi^+) = (2.68 \pm 0.13) \times 10^{-3}$ .

<sup>2</sup> ABE 01I reports  $[\Gamma(B^0 \rightarrow D^- K^+)/\Gamma_{\text{total}}] / [B(B^0 \rightarrow D^- \pi^+)] = (6.8 \pm 1.5 \pm 0.7) \times 10^{-2}$  which we multiply by our best value  $B(B^0 \rightarrow D^- \pi^+) = (2.68 \pm 0.13) \times 10^{-3}$ . Our first error is their experiment's error and our second error is the systematic error from using our best value.

$$\frac{\Gamma(D^- K^+ \bar{K}^0)}{\Gamma_{\text{total}}} \quad \Gamma_{37}/\Gamma$$

VALUE (units $10^{-4}$ )	CL%	DOCUMENT ID	TECN	COMMENT
<b>&lt; 3.1</b>	90	<sup>1</sup> DRUTSKOY	02	BELL $e^+e^- \rightarrow \Upsilon(4S)$

<sup>1</sup> Assumes equal production of  $B^+$  and  $B^0$  at the  $\Upsilon(4S)$ .

$$\frac{\Gamma(D^- K^+ \bar{K}^*(892)^0)}{\Gamma_{\text{total}}} \quad \Gamma_{38}/\Gamma$$

VALUE (units $10^{-4}$ )	DOCUMENT ID	TECN	COMMENT
<b>8.8 ± 1.1 ± 1.5</b>	<sup>1</sup> DRUTSKOY	02	BELL $e^+e^- \rightarrow \Upsilon(4S)$

<sup>1</sup> Assumes equal production of  $B^+$  and  $B^0$  at the  $\Upsilon(4S)$ .

$$\frac{\Gamma(D^0 \pi^+ \pi^-)}{\Gamma_{\text{total}}} \quad \Gamma_{39}/\Gamma$$

VALUE (units $10^{-4}$ )	CL%	EVTS	DOCUMENT ID	TECN	COMMENT
<b>8.4 ± 0.4 ± 0.8</b>			<sup>1</sup> KUZMIN	07	BELL $e^+e^- \rightarrow \Upsilon(4S)$
• • • We do not use the following data for averages, fits, limits, etc. • • •					
$8.0 \pm 0.6 \pm 1.5$			<sup>1,2</sup> SATPATHY	03	BELL Repl. by KUZMIN 07
$< 16$	90		<sup>1</sup> ALAM	94	CLE2 $e^+e^- \rightarrow \Upsilon(4S)$
$< 70$	90		<sup>3</sup> BORTOLETTO	92	CLEO $e^+e^- \rightarrow \Upsilon(4S)$
$< 340$	90		<sup>4</sup> BEBEK	87	CLEO $e^+e^- \rightarrow \Upsilon(4S)$
$700 \pm 500$		5	<sup>5</sup> BEHREND	83	CLEO $e^+e^- \rightarrow \Upsilon(4S)$

<sup>1</sup> Assumes equal production of  $B^+$  and  $B^0$  at the  $\Upsilon(4S)$ .

<sup>2</sup> No assumption about the intermediate mechanism is made in the analysis.

<sup>3</sup> BORTOLETTO 92 assumes equal production of  $B^+$  and  $B^0$  at the  $\Upsilon(4S)$  and uses Mark III branching fractions for the  $D$ . The product branching fraction into  $D_1^*(2340)\pi$  followed by  $D_1^*(2340) \rightarrow D^0 \pi$  is  $< 0.0001$  at 90% CL and into  $D_2^*(2460)$  followed by  $D_2^*(2460) \rightarrow D^0 \pi$  is  $< 0.0004$  at 90% CL.

<sup>4</sup> BEBEK 87 assume the  $\Upsilon(4S)$  decays 43% to  $B^0\bar{B}^0$ . We rescale to 50%.  $B(D^0 \rightarrow K^- \pi^+) = (4.2 \pm 0.4 \pm 0.4)\%$  and  $B(D^0 \rightarrow K^- \pi^+ \pi^-) = (9.1 \pm 0.8 \pm 0.8)\%$  were used.

<sup>5</sup> Corrected by us using assumptions:  $B(D^0 \rightarrow K^- \pi^+) = (0.042 \pm 0.006)$  and  $B(\Upsilon(4S) \rightarrow B^0\bar{B}^0) = 50\%$ . The product branching ratio is  $B(B^0 \rightarrow \bar{D}^0 \pi^+ \pi^-)B(\bar{D}^0 \rightarrow K^+ \pi^-) = (0.39 \pm 0.26) \times 10^{-2}$ .

See key on page 457

Meson Particle Listings

$B^0$

$\Gamma(D^*(2010)^-\pi^+)/\Gamma_{total}$   $\Gamma_{40}/\Gamma$

Table with columns: VALUE (units 10^-3), EVTS, DOCUMENT ID, TECN, COMMENT. Contains rows for OUR AVERAGE (2.76 ± 0.13) and individual experiments like AUBERT, BRANDENBURG, ALAM, BORTOLETTO92, ALBRECHT, BEBEK, AKERS, ALBRECHT 87c, ARG, GILES.

Assumes equal production of B+ and B0 at the T(4S).
AUBERT, BE 06j reports [Γ(B0 → D\*(2010)-π+)/Γtotal] / [B(B0 → D-π+)] = 0.99 ± 0.11 ± 0.08...
ALBRECHT 90j reports (2.8 ± 0.9 ± 0.6) × 10^-3 from a measurement of [Γ(B0 → D\*(2010)-π+)/Γtotal] × [B(D\*(2010)+ → D0π+)]...
ALBRECHT 87c use PDG 86 branching ratios for D and D\*(2010) and assume B(T(4S) → B+B-) = 55% and B(T(4S) → B0B0) = 45%.

$\Gamma(D^*(2010)^-\ell^+\nu_\ell)/\Gamma(D^*(2010)^-\pi^+)$   $\Gamma_6/\Gamma_{40}$

Table with columns: VALUE, DOCUMENT ID, TECN, COMMENT. Contains row: 16.5 ± 2.3 ± 1.1 AALTONEN 09E CDF p p-bar at 1.96 TeV

$\Gamma(D^-\pi^+\pi^+\pi^-)/\Gamma_{total}$   $\Gamma_{41}/\Gamma$

Table with columns: VALUE, DOCUMENT ID, TECN, COMMENT. Contains row: 0.0080 ± 0.0021 ± 0.0014 BORTOLETTO92 CLEO e+e- → T(4S)

BORTOLETTO 92 assumes equal production of B+ and B0 at the T(4S) and uses Mark III branching fractions for the D.

$\Gamma(D^-\pi^+\pi^+\pi^-)/(D^-\pi^+)$   $\Gamma_{41}/\Gamma_{31}$

Table with columns: VALUE, DOCUMENT ID, TECN, COMMENT. Contains row: 2.38 ± 0.23 OUR FIT, 2.38 ± 0.11 ± 0.21 AAIJ 11E LHCB pp at 7 TeV

$\Gamma(D^-\pi^+\pi^+\pi^- \text{ nonresonant})/\Gamma_{total}$   $\Gamma_{42}/\Gamma$

Table with columns: VALUE, DOCUMENT ID, TECN, COMMENT. Contains row: 0.0039 ± 0.0014 ± 0.0013 BORTOLETTO92 CLEO e+e- → T(4S)

BORTOLETTO 92 assumes equal production of B+ and B0 at the T(4S) and uses Mark III branching fractions for the D.

$\Gamma(D^-\pi^+\rho^0)/\Gamma_{total}$   $\Gamma_{43}/\Gamma$

Table with columns: VALUE, DOCUMENT ID, TECN, COMMENT. Contains row: 0.0011 ± 0.0009 ± 0.0004 BORTOLETTO92 CLEO e+e- → T(4S)

BORTOLETTO 92 assumes equal production of B+ and B0 at the T(4S) and uses Mark III branching fractions for the D.

$\Gamma(D^-\pi_1(1260)^+)/\Gamma_{total}$   $\Gamma_{44}/\Gamma$

Table with columns: VALUE, DOCUMENT ID, TECN, COMMENT. Contains row: 0.0060 ± 0.0022 ± 0.0024 BORTOLETTO92 CLEO e+e- → T(4S)

BORTOLETTO 92 assumes equal production of B+ and B0 at the T(4S) and uses Mark III branching fractions for the D.

$\Gamma(D^*(2010)^-\pi^+\pi^0)/\Gamma_{total}$   $\Gamma_{45}/\Gamma$

Table with columns: VALUE, EVTS, DOCUMENT ID, TECN, COMMENT. Contains row: 0.0152 ± 0.0052 ± 0.0001 51 ALBRECHT 90j ARG e+e- → T(4S)

We do not use the following data for averages, fits, limits, etc.
0.015 ± 0.008 ± 0.008 8 2 ALBRECHT 87c ARG e+e- → T(4S)

ALBRECHT 90j reports 0.018 ± 0.004 ± 0.005 from a measurement of [Γ(B0 → D\*(2010)-π+π0)/Γtotal] × [B(D\*(2010)+ → D0π+)]...
ALBRECHT 87c use PDG 86 branching ratios for D and D\*(2010) and assume B(T(4S) → B+B-) = 55% and B(T(4S) → B0B0) = 45%.

$\Gamma(D^*(2010)^-\rho^+)/\Gamma_{total}$   $\Gamma_{46}/\Gamma$

Table with columns: VALUE, EVTS, DOCUMENT ID, TECN, COMMENT. Contains row: 0.0068 ± 0.0009 OUR AVERAGE, 1 CSORNA 03 CLE2 e+e- → T(4S)

We do not use the following data for averages, fits, limits, etc.
0.0074 ± 0.0010 ± 0.0014 76 4,5 ALAM 94 CLE2 e+e- → T(4S)
0.081 ± 0.029 +0.059/-0.024 19 6 CHEN 85 CLEO e+e- → T(4S)
Assumes equal production of B0 and B+ at the T(4S) resonance. The second error combines the systematic and theoretical uncertainties in quadrature.

$\Gamma(D^*(2010)^-K^+)/\Gamma_{total}$   $\Gamma_{47}/\Gamma$

Table with columns: VALUE (units 10^-4), DOCUMENT ID, TECN, COMMENT. Contains row: 2.14 ± 0.16 OUR AVERAGE, 1 AUBERT 06A BABR e+e- → T(4S)

AUBERT 06A reports [Γ(B0 → D\*(2010)-K+)/Γtotal] / [B(B0 → D\*(2010)-π+)] = 0.0776 ± 0.0034 ± 0.0029...
ABE 01i reports [Γ(B0 → D\*(2010)-K+)/Γtotal] / [B(B0 → D\*(2010)-π+)] = 0.074 ± 0.015 ± 0.006...

$\Gamma(D^*(2010)^-K^0\pi^+)/\Gamma_{total}$   $\Gamma_{48}/\Gamma$

Table with columns: VALUE (units 10^-4), DOCUMENT ID, TECN, COMMENT. Contains row: 3.0 ± 0.7 ± 0.3 AUBERT, BE 05B BABR e+e- → T(4S)

Assumes equal production of B+ and B0 at the T(4S).

$\Gamma(D^*(2010)^-K^*(892)^+)/\Gamma_{total}$   $\Gamma_{49}/\Gamma$

Table with columns: VALUE (units 10^-4), DOCUMENT ID, TECN, COMMENT. Contains row: 3.3 ± 0.6 OUR AVERAGE, 1 AUBERT, BE 05B BABR e+e- → T(4S)

Assumes equal production of B+ and B0 at the T(4S).
Assumes equal production of B+ and B0 at the T(4S) and an unpolarized final state.

# Meson Particle Listings

$B^0$

## $\Gamma(D^*(2010)^- K^+ \bar{K}^0)/\Gamma_{total}$ $\Gamma_{50}/\Gamma$

VALUE (units $10^{-4}$ )	CL%	DOCUMENT ID	TECN	COMMENT
<b>&lt;4.7</b>	90	<sup>1</sup> DRUTSKOY 02	BELL	$e^+e^- \rightarrow \Upsilon(4S)$

<sup>1</sup> Assumes equal production of  $B^+$  and  $B^0$  at the  $\Upsilon(4S)$ .

## $\Gamma(D^*(2010)^- K^+ \bar{K}^*(892)^0)/\Gamma_{total}$ $\Gamma_{51}/\Gamma$

VALUE (units $10^{-4}$ )	DOCUMENT ID	TECN	COMMENT
<b>12.9 ± 2.2 ± 2.5</b>	<sup>1</sup> DRUTSKOY 02	BELL	$e^+e^- \rightarrow \Upsilon(4S)$

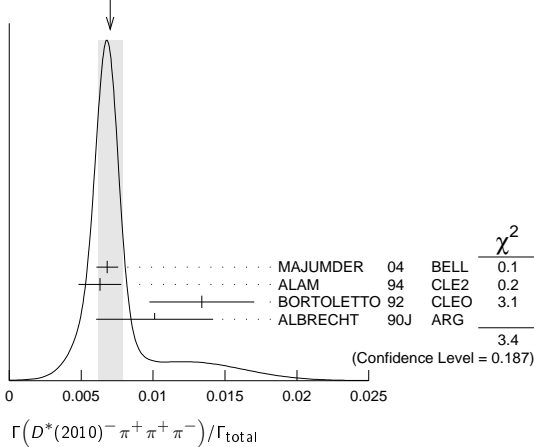
<sup>1</sup> Assumes equal production of  $B^+$  and  $B^0$  at the  $\Upsilon(4S)$ .

## $\Gamma(D^*(2010)^- \pi^+ \pi^+ \pi^-)/\Gamma_{total}$ $\Gamma_{52}/\Gamma$

VALUE	CL%	DOCUMENT ID	TECN	COMMENT
<b>0.0070 ± 0.0008 OUR AVERAGE</b>		Error includes scale factor of 1.3. See the ideogram below.		
0.00681 ± 0.00023 ± 0.00072		<sup>1</sup> MAJUMDER 04	BELL	$e^+e^- \rightarrow \Upsilon(4S)$
0.0063 ± 0.0010 ± 0.0011		<sup>2,3</sup> ALAM 94	CLE2	$e^+e^- \rightarrow \Upsilon(4S)$
0.0134 ± 0.0036 ± 0.0001		<sup>4</sup> BORTOLETTO 92	CLEO	$e^+e^- \rightarrow \Upsilon(4S)$
0.0101 ± 0.0041 ± 0.0001		<sup>5</sup> ALBRECHT 90J	ARG	$e^+e^- \rightarrow \Upsilon(4S)$
0.033 ± 0.009 ± 0.016		<sup>6</sup> ALBRECHT 87c	ARG	$e^+e^- \rightarrow \Upsilon(4S)$
<0.042	90	<sup>7</sup> BEBEK 87	CLEO	$e^+e^- \rightarrow \Upsilon(4S)$

<sup>1</sup> Assumes equal production of  $B^+$  and  $B^0$  at the  $\Upsilon(4S)$ .  
<sup>2</sup> ALAM 94 assume equal production of  $B^+$  and  $B^0$  at the  $\Upsilon(4S)$  and use the CLEO II  $B(D^*(2010)^+ \rightarrow D^0 \pi^+)$  and absolute  $B(D^0 \rightarrow K^- \pi^+)$  and the PDG 1992  $B(D^0 \rightarrow K^- \pi^+ \pi^0)/B(D^0 \rightarrow K^- \pi^+)$  and  $B(D^0 \rightarrow K^- 2\pi^+ \pi^-)/B(D^0 \rightarrow K^- \pi^+)$ .  
<sup>3</sup> The three pion mass is required to be between 1.0 and 1.6 GeV consistent with an  $a_1$  meson. (If this channel is dominated by  $a_1^+$ , the branching ratio for  $\bar{D}^* a_1^+$  is twice that for  $\bar{D}^* \pi^+ \pi^+ \pi^-$ .)  
<sup>4</sup> BORTOLETTO 92 reports  $0.0159 \pm 0.0028 \pm 0.0037$  from a measurement of  $[\Gamma(B^0 \rightarrow D^*(2010)^- \pi^+ \pi^+ \pi^-)/\Gamma_{total}] \times [B(D^*(2010)^+ \rightarrow D^0 \pi^+)]$  assuming  $B(D^*(2010)^+ \rightarrow D^0 \pi^+) = 0.57 \pm 0.06$ , which we rescale to our best value  $B(D^*(2010)^+ \rightarrow D^0 \pi^+) = (67.7 \pm 0.5) \times 10^{-2}$ . Our first error is their experiment's error and our second error is the systematic error from using our best value. Assumes equal production of  $B^+$  and  $B^0$  at the  $\Upsilon(4S)$  and uses Mark III branching fractions for the  $D$ .  
<sup>5</sup> ALBRECHT 90J reports  $0.012 \pm 0.003 \pm 0.004$  from a measurement of  $[\Gamma(B^0 \rightarrow D^*(2010)^- \pi^+ \pi^+ \pi^-)/\Gamma_{total}] \times [B(D^*(2010)^+ \rightarrow D^0 \pi^+)]$  assuming  $B(D^*(2010)^+ \rightarrow D^0 \pi^+) = 0.57 \pm 0.06$ , which we rescale to our best value  $B(D^*(2010)^+ \rightarrow D^0 \pi^+) = (67.7 \pm 0.5) \times 10^{-2}$ . Our first error is their experiment's error and our second error is the systematic error from using our best value. Assumes equal production of  $B^+$  and  $B^0$  at the  $\Upsilon(4S)$  and uses Mark III branching fractions for the  $D$ .  
<sup>6</sup> ALBRECHT 87c use PDG 86 branching ratios for  $D$  and  $D^*(2010)$  and assume  $B(\Upsilon(4S) \rightarrow B^+ B^-) = 55\%$  and  $B(\Upsilon(4S) \rightarrow B^0 \bar{B}^0) = 45\%$ . Superseded by ALBRECHT 90J.  
<sup>7</sup> BEBEK 87 value has been updated in BERKELMAN 91 to use same assumptions as noted for BORTOLETTO 92.

WEIGHTED AVERAGE  
0.0070 ± 0.0008 (Error scaled by 1.3)



## $\Gamma((D^*(2010)^- \pi^+ \pi^+ \pi^-)_{nonresonant})/\Gamma_{total}$ $\Gamma_{53}/\Gamma$

VALUE	DOCUMENT ID	TECN	COMMENT
<b>0.0000 ± 0.0019 ± 0.0016</b>	<sup>1</sup> BORTOLETTO 92	CLEO	$e^+e^- \rightarrow \Upsilon(4S)$

<sup>1</sup> BORTOLETTO 92 assumes equal production of  $B^+$  and  $B^0$  at the  $\Upsilon(4S)$  and uses Mark III branching fractions for the  $D$  and  $D^*(2010)$ .

## $\Gamma(D^*(2010)^- \pi^+ \rho^0)/\Gamma_{total}$ $\Gamma_{54}/\Gamma$

VALUE	DOCUMENT ID	TECN	COMMENT
<b>0.00573 ± 0.00317 ± 0.00004</b>	<sup>1</sup> BORTOLETTO 92	CLEO	$e^+e^- \rightarrow \Upsilon(4S)$

<sup>1</sup> BORTOLETTO 92 reports  $0.0068 \pm 0.0032 \pm 0.0021$  from a measurement of  $[\Gamma(B^0 \rightarrow D^*(2010)^- \pi^+ \rho^0)/\Gamma_{total}] \times [B(D^*(2010)^+ \rightarrow D^0 \pi^+)]$  assuming  $B(D^*(2010)^+ \rightarrow D^0 \pi^+) = 0.57 \pm 0.06$ , which we rescale to our best value  $B(D^*(2010)^+ \rightarrow D^0 \pi^+) = (67.7 \pm 0.5) \times 10^{-2}$ . Our first error is their experiment's error and our second error is the systematic error from using our best value. Assumes equal production of  $B^+$  and  $B^0$  at the  $\Upsilon(4S)$  and uses Mark III branching fractions for the  $D$ .

## $\Gamma(D^*(2010)^- a_1(1260)^+)/\Gamma_{total}$ $\Gamma_{55}/\Gamma$

VALUE	DOCUMENT ID	TECN	COMMENT
<b>0.0130 ± 0.0027 OUR AVERAGE</b>			
0.0126 ± 0.0020 ± 0.0022	<sup>1,2</sup> ALAM 94	CLE2	$e^+e^- \rightarrow \Upsilon(4S)$
0.0152 ± 0.0070 ± 0.0001	<sup>3</sup> BORTOLETTO 92	CLEO	$e^+e^- \rightarrow \Upsilon(4S)$

<sup>1</sup> ALAM 94 value is twice their  $\Gamma(D^*(2010)^- \pi^+ \pi^+ \pi^-)/\Gamma_{total}$  value based on their observation that the three pions are dominantly in the  $a_1(1260)$  mass range 1.0 to 1.6 GeV.  
<sup>2</sup> ALAM 94 assume equal production of  $B^+$  and  $B^0$  at the  $\Upsilon(4S)$  and use the CLEO II  $B(D^*(2010)^+ \rightarrow D^0 \pi^+)$  and absolute  $B(D^0 \rightarrow K^- \pi^+)$  and the PDG 1992  $B(D^0 \rightarrow K^- \pi^+ \pi^0)/B(D^0 \rightarrow K^- \pi^+)$  and  $B(D^0 \rightarrow K^- 2\pi^+ \pi^-)/B(D^0 \rightarrow K^- \pi^+)$ .  
<sup>3</sup> BORTOLETTO 92 reports  $0.018 \pm 0.006 \pm 0.006$  from a measurement of  $[\Gamma(B^0 \rightarrow D^*(2010)^- a_1(1260)^+)/\Gamma_{total}] \times [B(D^*(2010)^+ \rightarrow D^0 \pi^+)]$  assuming  $B(D^*(2010)^+ \rightarrow D^0 \pi^+) = 0.57 \pm 0.06$ , which we rescale to our best value  $B(D^*(2010)^+ \rightarrow D^0 \pi^+) = (67.7 \pm 0.5) \times 10^{-2}$ . Our first error is their experiment's error and our second error is the systematic error from using our best value. Assumes equal production of  $B^+$  and  $B^0$  at the  $\Upsilon(4S)$  and uses Mark III branching fractions for the  $D$ .

## $\Gamma(D^*(2010)^- \pi^+ \pi^+ \pi^- \pi^0)/\Gamma_{total}$ $\Gamma_{56}/\Gamma$

VALUE	EVTs	DOCUMENT ID	TECN	COMMENT
<b>0.0176 ± 0.0027 OUR AVERAGE</b>				
0.0172 ± 0.0014 ± 0.0024		<sup>1</sup> ALEXANDER 01B	CLE2	$e^+e^- \rightarrow \Upsilon(4S)$
0.0345 ± 0.0181 ± 0.0003	28	<sup>2</sup> ALBRECHT 90J	ARG	$e^+e^- \rightarrow \Upsilon(4S)$

<sup>1</sup> Assumes equal production of  $B^+$  and  $B^0$  at the  $\Upsilon(4S)$ . The signal is consistent with all observed  $\omega\pi^+$  having proceeded through the  $\rho^+$  resonance at mass  $1349 \pm 25 \pm 10$  MeV and width  $547 \pm 86 \pm 46$  MeV.  
<sup>2</sup> ALBRECHT 90J reports  $0.041 \pm 0.015 \pm 0.016$  from a measurement of  $[\Gamma(B^0 \rightarrow D^*(2010)^- \pi^+ \pi^+ \pi^- \pi^0)/\Gamma_{total}] \times [B(D^*(2010)^+ \rightarrow D^0 \pi^+)]$  assuming  $B(D^*(2010)^+ \rightarrow D^0 \pi^+) = 0.57 \pm 0.06$ , which we rescale to our best value  $B(D^*(2010)^+ \rightarrow D^0 \pi^+) = (67.7 \pm 0.5) \times 10^{-2}$ . Our first error is their experiment's error and our second error is the systematic error from using our best value. Assumes equal production of  $B^+$  and  $B^0$  at the  $\Upsilon(4S)$  and uses Mark III branching fractions for the  $D$ .

## $\Gamma(D^{*-} 3\pi^+ 2\pi^-)/\Gamma_{total}$ $\Gamma_{57}/\Gamma$

VALUE (units $10^{-3}$ )	DOCUMENT ID	TECN	COMMENT
<b>4.72 ± 0.59 ± 0.71</b>	<sup>1</sup> MAJUMDER 04	BELL	$e^+e^- \rightarrow \Upsilon(4S)$

<sup>1</sup> Assumes equal production of  $B^+$  and  $B^0$  at the  $\Upsilon(4S)$ .

## $\Gamma(\bar{D}^*(2010)^- \omega \pi^+)/\Gamma_{total}$ $\Gamma_{58}/\Gamma$

VALUE (units $10^{-3}$ )	DOCUMENT ID	TECN	COMMENT
<b>2.89 ± 0.30 OUR AVERAGE</b>			
2.88 ± 0.21 ± 0.31	<sup>1</sup> AUBERT 06L	BABR	$e^+e^- \rightarrow \Upsilon(4S)$
2.9 ± 0.3 ± 0.4	<sup>1,2</sup> ALEXANDER 01B	CLE2	$e^+e^- \rightarrow \Upsilon(4S)$

<sup>1</sup> Assumes equal production of  $B^+$  and  $B^0$  at the  $\Upsilon(4S)$ .  
<sup>2</sup> The signal is consistent with all observed  $\omega\pi^+$  having proceeded through the  $\rho^+$  resonance at mass  $1349 \pm 25 \pm 10$  MeV and width  $547 \pm 86 \pm 46$  MeV.

## $\Gamma(D_1(2430)^0 \omega \times B(D_1(2430)^0 \rightarrow D^{*-} \pi^+))/\Gamma_{total}$ $\Gamma_{59}/\Gamma$

VALUE (units $10^{-4}$ )	DOCUMENT ID	TECN	COMMENT
<b>4.1 ± 1.2 ± 1.1</b>	<sup>1</sup> AUBERT 06L	BABR	$e^+e^- \rightarrow \Upsilon(4S)$

<sup>1</sup> Obtained by fitting the events with  $\cos \theta_{D^*} < 0.5$  and scaling up the result by a factor of 4/3. No interference effects between  $B^0 \rightarrow D_1^0 \omega$  and  $D^* \omega \pi$  are assumed.

## $\Gamma(\bar{D}^{*-} \pi^+)/\Gamma_{total}$ $\Gamma_{60}/\Gamma$

$D^{*-}$  represents an excited state with mass  $2.2 < M < 2.8$  GeV/ $c^2$ .

VALUE (units $10^{-3}$ )	DOCUMENT ID	TECN	COMMENT
<b>2.1 ± 1.0 ± 0.1</b>	<sup>1,2</sup> AUBERT, BE 06J	BABR	$e^+e^- \rightarrow \Upsilon(4S)$

<sup>1</sup> AUBERT, BE 06J reports  $[\Gamma(B^0 \rightarrow \bar{D}^{*-} \pi^+)/\Gamma_{total}] / [B(B^0 \rightarrow D^- \pi^+)] = 0.77 \pm 0.22 \pm 0.29$  which we multiply by our best value  $B(B^0 \rightarrow D^- \pi^+) = (2.68 \pm 0.13) \times 10^{-3}$ . Our first error is their experiment's error and our second error is the systematic error from using our best value.  
<sup>2</sup> Uses a missing-mass method. Does not depend on  $D$  branching fractions or  $B^+/B^0$  production rates.

## $\Gamma(D_1(2420)^- \pi^+ \times B(D_1^- \rightarrow D^- \pi^+ \pi^-))/\Gamma_{total}$ $\Gamma_{61}/\Gamma$

VALUE (units $10^{-4}$ )	DOCUMENT ID	TECN	COMMENT
<b>1.00 ± 0.21 ± 0.25 OUR FIT</b>			
0.89 ± 0.15 ± 0.17	<sup>1</sup> ABE 05A	BELL	$e^+e^- \rightarrow \Upsilon(4S)$

<sup>1</sup> Assumes equal production of  $B^+$  and  $B^0$  at the  $\Upsilon(4S)$ .

See key on page 457

Meson Particle Listings

$B^0$

$\Gamma(D_1(2420)^- \pi^+ \times B(D_1^- \rightarrow D^- \pi^+ \pi^-))/\Gamma(D^- \pi^+ \pi^+ \pi^-)$   $\Gamma_{61}/\Gamma_{41}$   
 VALUE (units  $10^{-4}$ ) DOCUMENT ID TECN COMMENT

**1.57 ± 0.35 OUR FIT**  
**2.1 ± 0.5 ± 0.3**

AAIJ 11E LHCB  $p\bar{p}$  at 7 TeV

$\Gamma(D_1(2420)^- \pi^+ \times B(D_1^- \rightarrow D^{*-} \pi^+ \pi^-))/\Gamma_{total}$   $\Gamma_{62}/\Gamma$   
 VALUE (units  $10^{-4}$ ) CL% DOCUMENT ID TECN COMMENT

**<0.33** 90 <sup>1</sup>ABE 05A BELL  $e^+ e^- \rightarrow \Upsilon(4S)$

<sup>1</sup> Assumes equal production of  $B^+$  and  $B^0$  at the  $\Upsilon(4S)$ .

$\Gamma(D_2^*(2460)^- \pi^+ \times B(D_2^{*-}(2460)^- \rightarrow D^0 \pi^-))/\Gamma_{total}$   $\Gamma_{63}/\Gamma$   
 VALUE (units  $10^{-4}$ ) CL% DOCUMENT ID TECN COMMENT

**2.15 ± 0.17 ± 0.31** 1,2 KUZMIN 07 BELL  $e^+ e^- \rightarrow \Upsilon(4S)$   
 • • • We do not use the following data for averages, fits, limits, etc. • • •  
 <14.7 90 <sup>1</sup>ALAM 94 CLE2  $e^+ e^- \rightarrow \Upsilon(4S)$

<sup>1</sup> Assumes equal production of  $B^+$  and  $B^0$  at the  $\Upsilon(4S)$ .  
<sup>2</sup> Our second uncertainty combines systematics and model errors quoted in the paper.

$\Gamma(D_2^*(2400)^- \pi^+ \times B(D_2^{*0}(2400)^- \rightarrow D^0 \pi^-))/\Gamma_{total}$   $\Gamma_{64}/\Gamma$   
 VALUE (units  $10^{-4}$ ) DOCUMENT ID TECN COMMENT

**0.60 ± 0.13 ± 0.27** 1,2 KUZMIN 07 BELL  $e^+ e^- \rightarrow \Upsilon(4S)$

<sup>1</sup> Assumes equal production of  $B^+$  and  $B^0$  at the  $\Upsilon(4S)$ .  
<sup>2</sup> Our second uncertainty combines systematics and model errors quoted in the paper.

$\Gamma(D_2^*(2460)^- \pi^+ \times B((D_2^*)^- \rightarrow D^{*-} \pi^+ \pi^-))/\Gamma_{total}$   $\Gamma_{65}/\Gamma$   
 VALUE (units  $10^{-4}$ ) CL% DOCUMENT ID TECN COMMENT

**<0.24** 90 <sup>1</sup>ABE 05A BELL  $e^+ e^- \rightarrow \Upsilon(4S)$

<sup>1</sup> Assumes equal production of  $B^+$  and  $B^0$  at the  $\Upsilon(4S)$ .

$\Gamma(D_2^*(2460)^- \rho^+)/\Gamma_{total}$   $\Gamma_{66}/\Gamma$   
 VALUE CL% DOCUMENT ID TECN COMMENT

**<0.0049** 90 <sup>1</sup>ALAM 94 CLE2  $e^+ e^- \rightarrow \Upsilon(4S)$

<sup>1</sup> ALAM 94 assumes equal production of  $B^+$  and  $B^0$  at the  $\Upsilon(4S)$  and use the CLEO II absolute  $B(D^0 \rightarrow K^- \pi^+)$  and  $B(D_2^*(2460)^+ \rightarrow D^0 \pi^+) = 30\%$ .

$\Gamma(D^0 \bar{D}^0)/\Gamma_{total}$   $\Gamma_{67}/\Gamma$   
 VALUE (units  $10^{-4}$ ) CL% DOCUMENT ID TECN COMMENT

**<0.43** 90 <sup>1</sup>ADACHI 08 BELL  $e^+ e^- \rightarrow \Upsilon(4S)$

• • • We do not use the following data for averages, fits, limits, etc. • • •  
 <0.6 90 <sup>1</sup>AUBERT,B 06A BABR  $e^+ e^- \rightarrow \Upsilon(4S)$

<sup>1</sup> Assumes equal production of  $B^+$  and  $B^0$  at the  $\Upsilon(4S)$ .

$\Gamma(D^{*0} \bar{D}^0)/\Gamma_{total}$   $\Gamma_{68}/\Gamma$   
 VALUE (units  $10^{-4}$ ) CL% DOCUMENT ID TECN COMMENT

**<2.9** 90 <sup>1</sup>AUBERT,B 06A BABR  $e^+ e^- \rightarrow \Upsilon(4S)$

<sup>1</sup> Assumes equal production of  $B^+$  and  $B^0$  at the  $\Upsilon(4S)$ .

$\Gamma(D^- D^+)/\Gamma_{total}$   $\Gamma_{69}/\Gamma$   
 VALUE (units  $10^{-4}$ ) CL% DOCUMENT ID TECN COMMENT

**2.11 ± 0.31 OUR AVERAGE** Error includes scale factor of 1.2.  
 1.97 ± 0.20 ± 0.20 <sup>1</sup>FRATINA 07 BELL  $e^+ e^- \rightarrow \Upsilon(4S)$   
 2.8 ± 0.4 ± 0.5 <sup>1</sup>AUBERT,B 06A BABR  $e^+ e^- \rightarrow \Upsilon(4S)$

• • • We do not use the following data for averages, fits, limits, etc. • • •  
 1.91 ± 0.51 ± 0.30 <sup>1</sup>MAJUMDER 05 BELL Repl. by FRATINA 07  
 < 9.4 90 <sup>1</sup>LIPELES 00 CLE2  $e^+ e^- \rightarrow \Upsilon(4S)$   
 <59 90 BARATE 98Q ALEP  $e^+ e^- \rightarrow Z$   
 <12 90 ASNER 97 CLE2  $e^+ e^- \rightarrow \Upsilon(4S)$

<sup>1</sup> Assumes equal production of  $B^+$  and  $B^0$  at the  $\Upsilon(4S)$ .

$\Gamma(D^- D_S^+)/\Gamma_{total}$   $\Gamma_{70}/\Gamma$   
 VALUE EVTS DOCUMENT ID TECN COMMENT

**0.0072 ± 0.0008 OUR AVERAGE**

0.0073 ± 0.0004 ± 0.0007 <sup>1</sup>ZUPANC 07 BELL  $e^+ e^- \rightarrow \Upsilon(4S)$   
 0.0066 ± 0.0014 ± 0.0006 <sup>2</sup>AUBERT 06N BABR  $e^+ e^- \rightarrow \Upsilon(4S)$   
 0.0068 ± 0.0024 ± 0.0006 <sup>3</sup>GIBAUT 96 CLE2  $e^+ e^- \rightarrow \Upsilon(4S)$   
 0.010 ± 0.009 ± 0.001 <sup>4</sup>ALBRECHT 92G ARG  $e^+ e^- \rightarrow \Upsilon(4S)$   
 0.0053 ± 0.0030 ± 0.0005 <sup>5</sup>BORTOLETTO92 CLEO  $e^+ e^- \rightarrow \Upsilon(4S)$

• • • We do not use the following data for averages, fits, limits, etc. • • •  
 0.012 ± 0.007 3 <sup>6</sup>BORTOLETTO90 CLEO  $e^+ e^- \rightarrow \Upsilon(4S)$

<sup>1</sup> ZUPANC 07 reports  $(7.5 \pm 0.2 \pm 1.1) \times 10^{-3}$  from a measurement of  $[\Gamma(B^0 \rightarrow D^- D_S^+)/\Gamma_{total}] \times [B(D_S^+ \rightarrow \phi \pi^+)]$  assuming  $B(D_S^+ \rightarrow \phi \pi^+) = (4.4 \pm 0.6) \times 10^{-2}$ , which we rescale to our best value  $B(D_S^+ \rightarrow \phi \pi^+) = (4.5 \pm 0.4) \times 10^{-2}$ . Our first error is their experiment's error and our second error is the systematic error from using our best value.

<sup>2</sup> AUBERT 06N reports  $(0.64 \pm 0.13 \pm 0.10) \times 10^{-2}$  from a measurement of  $[\Gamma(B^0 \rightarrow D^- D_S^+)/\Gamma_{total}] \times [B(D_S^+ \rightarrow \phi \pi^+)]$  assuming  $B(D_S^+ \rightarrow \phi \pi^+) = 0.0462 \pm 0.0062$ , which we rescale to our best value  $B(D_S^+ \rightarrow \phi \pi^+) = (4.5 \pm 0.4) \times 10^{-2}$ . Our first error is their experiment's error and our second error is the systematic error from using our best value.

<sup>3</sup> GIBAUT 96 reports  $0.0087 \pm 0.0024 \pm 0.0020$  from a measurement of  $[\Gamma(B^0 \rightarrow D^- D_S^+)/\Gamma_{total}] \times [B(D_S^+ \rightarrow \phi \pi^+)]$  assuming  $B(D_S^+ \rightarrow \phi \pi^+) = 0.035$ , which we rescale to our best value  $B(D_S^+ \rightarrow \phi \pi^+) = (4.5 \pm 0.4) \times 10^{-2}$ . Our first error is their experiment's error and our second error is the systematic error from using our best value.

<sup>4</sup> ALBRECHT 92G reports  $0.017 \pm 0.013 \pm 0.006$  from a measurement of  $[\Gamma(B^0 \rightarrow D^- D_S^+)/\Gamma_{total}] \times [B(D_S^+ \rightarrow \phi \pi^+)]$  assuming  $B(D_S^+ \rightarrow \phi \pi^+) = 0.027$ , which we rescale to our best value  $B(D_S^+ \rightarrow \phi \pi^+) = (4.5 \pm 0.4) \times 10^{-2}$ . Our first error is their experiment's error and our second error is the systematic error from using our best value. Assumes PDG 1990  $D^+$  branching ratios, e.g.,  $B(D^+ \rightarrow K^- 2\pi^+) = 7.7 \pm 1.0\%$ .

<sup>5</sup> BORTOLETTO 92 reports  $0.0080 \pm 0.0045 \pm 0.0030$  from a measurement of  $[\Gamma(B^0 \rightarrow D^- D_S^+)/\Gamma_{total}] \times [B(D_S^+ \rightarrow \phi \pi^+)]$  assuming  $B(D_S^+ \rightarrow \phi \pi^+) = 0.030 \pm 0.011$ , which we rescale to our best value  $B(D_S^+ \rightarrow \phi \pi^+) = (4.5 \pm 0.4) \times 10^{-2}$ . Our first error is their experiment's error and our second error is the systematic error from using our best value. Assumes equal production of  $B^+$  and  $B^0$  at the  $\Upsilon(4S)$  and uses Mark III branching fractions for the  $D$ .

<sup>6</sup> BORTOLETTO 90 assume  $B(D_S \rightarrow \phi \pi^+) = 2\%$ . Superseded by BORTOLETTO 92.

$\Gamma(D^*(2010)^- D_S^+)/\Gamma_{total}$   $\Gamma_{71}/\Gamma$   
 VALUE EVTS DOCUMENT ID TECN COMMENT

**0.0080 ± 0.0011 OUR AVERAGE**

0.0073 ± 0.0013 ± 0.0007 <sup>1</sup>AUBERT 06N BABR  $e^+ e^- \rightarrow \Upsilon(4S)$   
 0.0083 ± 0.0015 ± 0.0007 <sup>2</sup>AUBERT 03i BABR  $e^+ e^- \rightarrow \Upsilon(4S)$   
 0.0088 ± 0.0017 ± 0.0008 <sup>3</sup>AHMED 00B CLE2  $e^+ e^- \rightarrow \Upsilon(4S)$   
 0.008 ± 0.006 ± 0.001 <sup>4</sup>ALBRECHT 92G ARG  $e^+ e^- \rightarrow \Upsilon(4S)$   
 0.011 ± 0.006 ± 0.001 <sup>5</sup>BORTOLETTO92 CLEO  $e^+ e^- \rightarrow \Upsilon(4S)$

• • • We do not use the following data for averages, fits, limits, etc. • • •  
 0.0072 ± 0.0022 ± 0.0006 <sup>6</sup>GIBAUT 96 CLE2 Repl. by AHMED 00B  
 0.024 ± 0.014 3 <sup>7</sup>BORTOLETTO90 CLEO  $e^+ e^- \rightarrow \Upsilon(4S)$

<sup>1</sup> AUBERT 06N reports  $(0.71 \pm 0.13 \pm 0.09) \times 10^{-2}$  from a measurement of  $[\Gamma(B^0 \rightarrow D^*(2010)^- D_S^+)/\Gamma_{total}] \times [B(D_S^+ \rightarrow \phi \pi^+)]$  assuming  $B(D_S^+ \rightarrow \phi \pi^+) = 0.0462 \pm 0.0062$ , which we rescale to our best value  $B(D_S^+ \rightarrow \phi \pi^+) = (4.5 \pm 0.4) \times 10^{-2}$ . Our first error is their experiment's error and our second error is the systematic error from using our best value.

<sup>2</sup> AUBERT 03i reports  $0.0103 \pm 0.0014 \pm 0.0013$  from a measurement of  $[\Gamma(B^0 \rightarrow D^*(2010)^- D_S^+)/\Gamma_{total}] \times [B(D_S^+ \rightarrow \phi \pi^+)]$  assuming  $B(D_S^+ \rightarrow \phi \pi^+) = 0.036$ , which we rescale to our best value  $B(D_S^+ \rightarrow \phi \pi^+) = (4.5 \pm 0.4) \times 10^{-2}$ . Our first error is their experiment's error and our second error is the systematic error from using our best value.

<sup>3</sup> AHMED 00B reports  $0.0110 \pm 0.0018 \pm 0.0011$  from a measurement of  $[\Gamma(B^0 \rightarrow D^*(2010)^- D_S^+)/\Gamma_{total}] \times [B(D_S^+ \rightarrow \phi \pi^+)]$  assuming  $B(D_S^+ \rightarrow \phi \pi^+) = 0.036$ , which we rescale to our best value  $B(D_S^+ \rightarrow \phi \pi^+) = (4.5 \pm 0.4) \times 10^{-2}$ . Our first error is their experiment's error and our second error is the systematic error from using our best value.

<sup>4</sup> ALBRECHT 92G reports  $0.014 \pm 0.010 \pm 0.003$  from a measurement of  $[\Gamma(B^0 \rightarrow D^*(2010)^- D_S^+)/\Gamma_{total}] \times [B(D_S^+ \rightarrow \phi \pi^+)]$  assuming  $B(D_S^+ \rightarrow \phi \pi^+) = 0.027$ , which we rescale to our best value  $B(D_S^+ \rightarrow \phi \pi^+) = (4.5 \pm 0.4) \times 10^{-2}$ . Our first error is their experiment's error and our second error is the systematic error from using our best value. Assumes PDG 1990  $D^+$  and  $D^*(2010)^+$  branching ratios, e.g.,  $B(D^0 \rightarrow K^- \pi^+) = 3.71 \pm 0.25\%$ ,  $B(D^+ \rightarrow K^- 2\pi^+) = 7.1 \pm 1.0\%$ , and  $B(D^*(2010)^+ \rightarrow D^0 \pi^+) = 55 \pm 4\%$ .

<sup>5</sup> BORTOLETTO 92 reports  $0.016 \pm 0.009 \pm 0.006$  from a measurement of  $[\Gamma(B^0 \rightarrow D^*(2010)^- D_S^+)/\Gamma_{total}] \times [B(D_S^+ \rightarrow \phi \pi^+)]$  assuming  $B(D_S^+ \rightarrow \phi \pi^+) = 0.030 \pm 0.011$ , which we rescale to our best value  $B(D_S^+ \rightarrow \phi \pi^+) = (4.5 \pm 0.4) \times 10^{-2}$ . Our first error is their experiment's error and our second error is the systematic error from using our best value. Assumes equal production of  $B^+$  and  $B^0$  at the  $\Upsilon(4S)$  and uses Mark III branching fractions for the  $D$  and  $D^*(2010)$ .

<sup>6</sup> GIBAUT 96 reports  $0.0093 \pm 0.0023 \pm 0.0016$  from a measurement of  $[\Gamma(B^0 \rightarrow D^*(2010)^- D_S^+)/\Gamma_{total}] \times [B(D_S^+ \rightarrow \phi \pi^+)]$  assuming  $B(D_S^+ \rightarrow \phi \pi^+) = 0.035$ , which we rescale to our best value  $B(D_S^+ \rightarrow \phi \pi^+) = (4.5 \pm 0.4) \times 10^{-2}$ . Our first error is their experiment's error and our second error is the systematic error from using our best value.

<sup>7</sup> BORTOLETTO 90 assume  $B(D_S \rightarrow \phi \pi^+) = 2\%$ . Superseded by BORTOLETTO 92.

$\Gamma(D^- D_S^{*+})/\Gamma_{total}$   $\Gamma_{72}/\Gamma$   
 VALUE DOCUMENT ID TECN COMMENT

**0.0074 ± 0.0016 OUR AVERAGE**

0.0071 ± 0.0016 ± 0.0006 <sup>1</sup>AUBERT 06N BABR  $e^+ e^- \rightarrow \Upsilon(4S)$   
 0.0078 ± 0.0032 ± 0.0007 <sup>2</sup>GIBAUT 96 CLE2  $e^+ e^- \rightarrow \Upsilon(4S)$   
 0.016 ± 0.012 ± 0.001 <sup>3</sup>ALBRECHT 92G ARG  $e^+ e^- \rightarrow \Upsilon(4S)$

## Meson Particle Listings

 $B^0$ 

<sup>1</sup>AUBERT 06N reports  $(0.69 \pm 0.16 \pm 0.09) \times 10^{-2}$  from a measurement of  $[\Gamma(B^0 \rightarrow D^- D_s^{*+})/\Gamma_{\text{total}}] \times [B(D_s^+ \rightarrow \phi\pi^+)]$  assuming  $B(D_s^+ \rightarrow \phi\pi^+) = 0.0462 \pm 0.0062$ , which we rescale to our best value  $B(D_s^+ \rightarrow \phi\pi^+) = (4.5 \pm 0.4) \times 10^{-2}$ . Our first error is their experiment's error and our second error is the systematic error from using our best value.

<sup>2</sup>GIBAUT 96 reports  $0.0100 \pm 0.0035 \pm 0.0022$  from a measurement of  $[\Gamma(B^0 \rightarrow D^- D_s^{*+})/\Gamma_{\text{total}}] \times [B(D_s^+ \rightarrow \phi\pi^+)]$  assuming  $B(D_s^+ \rightarrow \phi\pi^+) = 0.035$ , which we rescale to our best value  $B(D_s^+ \rightarrow \phi\pi^+) = (4.5 \pm 0.4) \times 10^{-2}$ . Our first error is their experiment's error and our second error is the systematic error from using our best value.

<sup>3</sup>ALBRECHT 92G reports  $0.027 \pm 0.017 \pm 0.009$  from a measurement of  $[\Gamma(B^0 \rightarrow D^- D_s^{*+})/\Gamma_{\text{total}}] \times [B(D_s^+ \rightarrow \phi\pi^+)]$  assuming  $B(D_s^+ \rightarrow \phi\pi^+) = 0.027$ , which we rescale to our best value  $B(D_s^+ \rightarrow \phi\pi^+) = (4.5 \pm 0.4) \times 10^{-2}$ . Our first error is their experiment's error and our second error is the systematic error from using our best value. Assumes PDG 1990  $D^+$  branching ratios, e.g.,  $B(D^+ \rightarrow K^- 2\pi^+) = 7.7 \pm 1.0\%$ .

$\Gamma(D^*(2010)^- D_s^{*+})/\Gamma_{\text{total}}$	DOCUMENT ID	TECN	COMMENT	$\Gamma_{73}/\Gamma$
<b>0.0177 ± 0.0014 OUR AVERAGE</b>				
0.0173 ± 0.0018 ± 0.0015	<sup>1</sup> AUBERT 06N	BABR	$e^+ e^- \rightarrow \Upsilon(4S)$	
0.0188 ± 0.0009 ± 0.0017	<sup>2</sup> AUBERT 05V	BABR	$e^+ e^- \rightarrow \Upsilon(4S)$	
0.0158 ± 0.0027 ± 0.0014	<sup>3</sup> AUBERT 03I	BABR	$e^+ e^- \rightarrow \Upsilon(4S)$	
0.015 ± 0.004 ± 0.001	<sup>4</sup> AHMED 00B	CLE2	$e^+ e^- \rightarrow \Upsilon(4S)$	
0.016 ± 0.009 ± 0.001	<sup>5</sup> ALBRECHT 92G	ARG	$e^+ e^- \rightarrow \Upsilon(4S)$	
• • • We do not use the following data for averages, fits, limits, etc. • • •				
0.016 ± 0.005 ± 0.001	<sup>6</sup> GIBAUT 96	CLE2	Repl. by AHMED 00B	

<sup>1</sup>AUBERT 06N reports  $(1.68 \pm 0.21 \pm 0.19) \times 10^{-2}$  from a measurement of  $[\Gamma(B^0 \rightarrow D^*(2010)^- D_s^{*+})/\Gamma_{\text{total}}] \times [B(D_s^+ \rightarrow \phi\pi^+)]$  assuming  $B(D_s^+ \rightarrow \phi\pi^+) = 0.0462 \pm 0.0062$ , which we rescale to our best value  $B(D_s^+ \rightarrow \phi\pi^+) = (4.5 \pm 0.4) \times 10^{-2}$ . Our first error is their experiment's error and our second error is the systematic error from using our best value.

<sup>2</sup>A partial reconstruction technique is used and the result is independent of the particle decay rate of  $D_s^+$  meson. It also provides a model-independent determination of  $B(D_s^+ \rightarrow \phi\pi^+) = (4.81 \pm 0.52 \pm 0.38)\%$ .

<sup>3</sup>AUBERT 03I reports  $0.0197 \pm 0.0015 \pm 0.0030$  from a measurement of  $[\Gamma(B^0 \rightarrow D^*(2010)^- D_s^{*+})/\Gamma_{\text{total}}] \times [B(D_s^+ \rightarrow \phi\pi^+)]$  assuming  $B(D_s^+ \rightarrow \phi\pi^+) = 0.036$ , which we rescale to our best value  $B(D_s^+ \rightarrow \phi\pi^+) = (4.5 \pm 0.4) \times 10^{-2}$ . Our first error is their experiment's error and our second error is the systematic error from using our best value.

<sup>4</sup>AHMED 00B reports  $0.0182 \pm 0.0037 \pm 0.0025$  from a measurement of  $[\Gamma(B^0 \rightarrow D^*(2010)^- D_s^{*+})/\Gamma_{\text{total}}] \times [B(D_s^+ \rightarrow \phi\pi^+)]$  assuming  $B(D_s^+ \rightarrow \phi\pi^+) = 0.036$ , which we rescale to our best value  $B(D_s^+ \rightarrow \phi\pi^+) = (4.5 \pm 0.4) \times 10^{-2}$ . Our first error is their experiment's error and our second error is the systematic error from using our best value.

<sup>5</sup>ALBRECHT 92G reports  $0.026 \pm 0.014 \pm 0.006$  from a measurement of  $[\Gamma(B^0 \rightarrow D^*(2010)^- D_s^{*+})/\Gamma_{\text{total}}] \times [B(D_s^+ \rightarrow \phi\pi^+)]$  assuming  $B(D_s^+ \rightarrow \phi\pi^+) = 0.027$ , which we rescale to our best value  $B(D_s^+ \rightarrow \phi\pi^+) = (4.5 \pm 0.4) \times 10^{-2}$ . Our first error is their experiment's error and our second error is the systematic error from using our best value. Assumes PDG 1990  $D^+$  and  $D^*(2010)^+$  branching ratios, e.g.,  $B(D^0 \rightarrow K^- \pi^+) = 3.71 \pm 0.25\%$ ,  $B(D^+ \rightarrow K^- 2\pi^+) = 7.1 \pm 1.0\%$ , and  $B(D^*(2010)^+ \rightarrow D^0 \pi^+) = 55 \pm 4\%$ .

<sup>6</sup>GIBAUT 96 reports  $0.0203 \pm 0.0050 \pm 0.0036$  from a measurement of  $[\Gamma(B^0 \rightarrow D^*(2010)^- D_s^{*+})/\Gamma_{\text{total}}] \times [B(D_s^+ \rightarrow \phi\pi^+)]$  assuming  $B(D_s^+ \rightarrow \phi\pi^+) = 0.035$ , which we rescale to our best value  $B(D_s^+ \rightarrow \phi\pi^+) = (4.5 \pm 0.4) \times 10^{-2}$ . Our first error is their experiment's error and our second error is the systematic error from using our best value.

$[\Gamma(D^*(2010)^- D_s^{*+}) + \Gamma(D^*(2010)^- D_s^{*+})]/\Gamma_{\text{total}}$	EVTS	DOCUMENT ID	TECN	COMMENT	$(\Gamma_{71} + \Gamma_{73})/\Gamma$
<b>2.5 ± 0.4 OUR AVERAGE</b>					
2.40 ± 0.35 ± 0.22		<sup>1</sup> AUBERT 03I	BABR	$e^+ e^- \rightarrow \Upsilon(4S)$	
3.3 ± 0.9 ± 0.3	22	<sup>2</sup> BORTOLETTO90	CLEO	$e^+ e^- \rightarrow \Upsilon(4S)$	

<sup>1</sup>AUBERT 03I reports  $(3.00 \pm 0.19 \pm 0.39) \times 10^{-2}$  from a measurement of  $[\Gamma(B^0 \rightarrow D^*(2010)^- D_s^{*+}) + \Gamma(B^0 \rightarrow D^*(2010)^- D_s^{*+})]/\Gamma_{\text{total}}] \times [B(D_s^+ \rightarrow \phi\pi^+)]$  assuming  $B(D_s^+ \rightarrow \phi\pi^+) = 0.036$ , which we rescale to our best value  $B(D_s^+ \rightarrow \phi\pi^+) = (4.5 \pm 0.4) \times 10^{-2}$ . Our first error is their experiment's error and our second error is the systematic error from using our best value.

<sup>2</sup>BORTOLETTO 90 reports  $(7.5 \pm 2.0) \times 10^{-2}$  from a measurement of  $[\Gamma(B^0 \rightarrow D^*(2010)^- D_s^{*+}) + \Gamma(B^0 \rightarrow D^*(2010)^- D_s^{*+})]/\Gamma_{\text{total}}] \times [B(D_s^+ \rightarrow \phi\pi^+)]$  assuming  $B(D_s^+ \rightarrow \phi\pi^+) = 0.02$ , which we rescale to our best value  $B(D_s^+ \rightarrow \phi\pi^+) = (4.5 \pm 0.4) \times 10^{-2}$ . Our first error is their experiment's error and our second error is the systematic error from using our best value.

$\Gamma(D_{s0}(2317)^- K^+ \times B(D_{s0}(2317)^- \rightarrow D_s^- \pi^0))/\Gamma_{\text{total}}$	DOCUMENT ID	TECN	COMMENT	$\Gamma_{74}/\Gamma$
<b>4.2 ± 1.4 ± 0.4</b>				
	<sup>1</sup> DRUTSKOY 05	BELL	$e^+ e^- \rightarrow \Upsilon(4S)$	

<sup>1</sup>DRUTSKOY 05 reports  $(5.3^{+1.5}_{-1.3} \pm 1.6) \times 10^{-5}$  from a measurement of  $[\Gamma(B^0 \rightarrow D_{s0}(2317)^- K^+ \times B(D_{s0}(2317)^- \rightarrow D_s^- \pi^0))/\Gamma_{\text{total}}] \times [B(D_s^+ \rightarrow \phi\pi^+)]$  assuming  $B(D_s^+ \rightarrow \phi\pi^+) = 0.036 \pm 0.009$ , which we rescale to our best value  $B(D_s^+ \rightarrow \phi\pi^+) = (4.5 \pm 0.4) \times 10^{-2}$ . Our first error is their experiment's error and our second error is the systematic error from using our best value.

$\Gamma(D_{s0}(2317)^- \pi^+ \times B(D_{s0}(2317)^- \rightarrow D_s^- \pi^0))/\Gamma_{\text{total}}$	DOCUMENT ID	TECN	COMMENT	$\Gamma_{75}/\Gamma$
<b>&lt; 2.5</b>	90	<sup>1</sup> DRUTSKOY 05	BELL	$e^+ e^- \rightarrow \Upsilon(4S)$

<sup>1</sup>Assumes equal production of  $B^+$  and  $B^0$  at the  $\Upsilon(4S)$ .

$\Gamma(D_{sJ}(2457)^- K^+ \times B(D_{sJ}(2457)^- \rightarrow D_s^- \pi^0))/\Gamma_{\text{total}}$	DOCUMENT ID	TECN	COMMENT	$\Gamma_{76}/\Gamma$
<b>&lt; 0.94</b>	90	<sup>1</sup> DRUTSKOY 05	BELL	$e^+ e^- \rightarrow \Upsilon(4S)$

<sup>1</sup>Assumes equal production of  $B^+$  and  $B^0$  at the  $\Upsilon(4S)$ .

$\Gamma(D_{sJ}(2457)^- \pi^+ \times B(D_{sJ}(2457)^- \rightarrow D_s^- \pi^0))/\Gamma_{\text{total}}$	DOCUMENT ID	TECN	COMMENT	$\Gamma_{77}/\Gamma$
<b>&lt; 0.40</b>	90	<sup>1</sup> DRUTSKOY 05	BELL	$e^+ e^- \rightarrow \Upsilon(4S)$

<sup>1</sup>Assumes equal production of  $B^+$  and  $B^0$  at the  $\Upsilon(4S)$ .

$\Gamma(D_s^- D_s^+)/\Gamma_{\text{total}}$	DOCUMENT ID	TECN	COMMENT	$\Gamma_{78}/\Gamma$
<b>&lt; 3.6 × 10<sup>-5</sup></b>	90	<sup>1</sup> ZUPANC 07	BELL	$e^+ e^- \rightarrow \Upsilon(4S)$

• • • We do not use the following data for averages, fits, limits, etc. • • •

< 10 × 10 <sup>-5</sup>	90	<sup>1</sup> AUBERT, BE 05F	BABR	$e^+ e^- \rightarrow \Upsilon(4S)$
-------------------------	----	-----------------------------	------	------------------------------------

<sup>1</sup>Assumes equal production of  $B^+$  and  $B^0$  at the  $\Upsilon(4S)$ .

$\Gamma(D_s^- D_s^+)/\Gamma_{\text{total}}$	DOCUMENT ID	TECN	COMMENT	$\Gamma_{79}/\Gamma$
<b>&lt; 1.3 × 10<sup>-4</sup></b>	90	<sup>1</sup> AUBERT, BE 05F	BABR	$e^+ e^- \rightarrow \Upsilon(4S)$

<sup>1</sup>Assumes equal production of  $B^+$  and  $B^0$  at the  $\Upsilon(4S)$ .

$\Gamma(D_s^- D_s^+)/\Gamma_{\text{total}}$	DOCUMENT ID	TECN	COMMENT	$\Gamma_{80}/\Gamma$
<b>&lt; 2.4 × 10<sup>-4</sup></b>	90	<sup>1</sup> AUBERT, BE 05F	BABR	$e^+ e^- \rightarrow \Upsilon(4S)$

<sup>1</sup>Assumes equal production of  $B^+$  and  $B^0$  at the  $\Upsilon(4S)$ .

$\Gamma(D_{s0}(2317)^+ D^- \times B(D_{s0}(2317)^+ \rightarrow D_s^+ \pi^0))/\Gamma_{\text{total}}$	DOCUMENT ID	TECN	COMMENT	$\Gamma_{81}/\Gamma$
<b>0.97 ± 0.40 ± 0.33 OUR AVERAGE</b>				Error includes scale factor of 1.5.

1.4 ± 0.5 ± 0.1

<sup>1,2</sup>AUBERT, B 04s

0.69 ± 0.29 ± 0.06

<sup>1,3</sup>KROKOVNY 03B

<sup>1</sup>Assumes equal production of  $B^+$  and  $B^0$  at the  $\Upsilon(4S)$ .

<sup>2</sup>AUBERT, B 04s reports  $(1.8 \pm 0.4^{+0.7}_{-0.5}) \times 10^{-3}$  from a measurement of  $[\Gamma(B^0 \rightarrow D_{s0}(2317)^+ D^- \times B(D_{s0}(2317)^+ \rightarrow D_s^+ \pi^0))/\Gamma_{\text{total}}] \times [B(D_s^+ \rightarrow \phi\pi^+)]$  assuming  $B(D_s^+ \rightarrow \phi\pi^+) = 0.036 \pm 0.009$ , which we rescale to our best value  $B(D_s^+ \rightarrow \phi\pi^+) = (4.5 \pm 0.4) \times 10^{-2}$ . Our first error is their experiment's error and our second error is the systematic error from using our best value.

<sup>3</sup>KROKOVNY 03B reports  $(0.86^{+0.33}_{-0.26} \pm 0.26) \times 10^{-3}$  from a measurement of  $[\Gamma(B^0 \rightarrow D_{s0}(2317)^+ D^- \times B(D_{s0}(2317)^+ \rightarrow D_s^+ \pi^0))/\Gamma_{\text{total}}] \times [B(D_s^+ \rightarrow \phi\pi^+)]$  assuming  $B(D_s^+ \rightarrow \phi\pi^+) = 0.036 \pm 0.009$ , which we rescale to our best value  $B(D_s^+ \rightarrow \phi\pi^+) = (4.5 \pm 0.4) \times 10^{-2}$ . Our first error is their experiment's error and our second error is the systematic error from using our best value.

$\Gamma(D_{s0}(2317)^+ D^- \times B(D_{s0}(2317)^+ \rightarrow D_s^+ \gamma))/\Gamma_{\text{total}}$	DOCUMENT ID	TECN	COMMENT	$\Gamma_{82}/\Gamma$
<b>&lt; 0.95</b>	90	<sup>1</sup> KROKOVNY 03B	BELL	$e^+ e^- \rightarrow \Upsilon(4S)$

<sup>1</sup>Assumes equal production of  $B^+$  and  $B^0$  at the  $\Upsilon(4S)$ .

$\Gamma(D_{s0}(2317)^+ D^*(2010)^- \times B(D_{s0}(2317)^+ \rightarrow D_s^+ \pi^0))/\Gamma_{\text{total}}$	DOCUMENT ID	TECN	COMMENT	$\Gamma_{83}/\Gamma$
<b>1.5 ± 0.4 ± 0.5 ± 0.4</b>				
	<sup>1</sup> AUBERT, B 04s	BABR	$e^+ e^- \rightarrow \Upsilon(4S)$	

<sup>1</sup>Assumes equal production of  $B^+$  and  $B^0$  at the  $\Upsilon(4S)$ .

$\Gamma(D_{sJ}(2457)^+ D^-)/\Gamma_{\text{total}}$	DOCUMENT ID	TECN	COMMENT	$\Gamma_{84}/\Gamma$
<b>3.5 ± 1.1 OUR AVERAGE</b>				
2.6 ± 1.5 ± 0.7	<sup>1</sup> AUBERT 06N	BABR	$e^+ e^- \rightarrow \Upsilon(4S)$	
4.8 ± 2.2 ± 1.1	<sup>2,3</sup> AUBERT, B 04s	BABR	$e^+ e^- \rightarrow \Upsilon(4S)$	

3.9 ± 1.5 ± 0.9

<sup>2,4</sup>KROKOVNY 03B

$e^+ e^- \rightarrow \Upsilon(4S)$



- <sup>1</sup> Uses a missing-mass method in the events that one of the B mesons is fully reconstructed.  
<sup>2</sup> Assumes equal production of B<sup>+</sup> and B<sup>0</sup> at the T(4S).  
<sup>3</sup> AUBERT,B 04s reports  $[\Gamma(B^0 \rightarrow D_{sJ}(2457)^+ D^-) / \Gamma_{\text{total}}] \times [B(D_{s1}(2460)^+ \rightarrow D_s^{*+} \pi^0)] = (2.3 \pm_{-0.7}^{+1.0} \pm 0.3) \times 10^{-3}$  which we divide by our best value B(D<sub>s1</sub>(2460)<sup>+</sup> → D<sub>s</sub><sup>\*+</sup> π<sup>0</sup>) = (48 ± 11) × 10<sup>-2</sup>. Our first error is their experiment's error and our second error is the systematic error from using our best value.  
<sup>4</sup> KROKOVNY 03B reports  $[\Gamma(B^0 \rightarrow D_{sJ}(2457)^+ D^-) / \Gamma_{\text{total}}] \times [B(D_{s1}(2460)^+ \rightarrow D_s^{*+} \pi^0)] = (1.9 \pm_{-0.6}^{+0.7} \pm 0.2) \times 10^{-3}$  which we divide by our best value B(D<sub>s1</sub>(2460)<sup>+</sup> → D<sub>s</sub><sup>\*+</sup> π<sup>0</sup>) = (48 ± 11) × 10<sup>-2</sup>. Our first error is their experiment's error and our second error is the systematic error from using our best value.

VALUE (units 10 <sup>-3</sup> )	DOCUMENT ID	TECN	COMMENT	Γ <sub>85</sub> /Γ
---------------------------------	-------------	------	---------	--------------------

**0.65 ±<sub>-0.14</sub><sup>+0.17</sup> OUR AVERAGE**

0.64 ± <sub>-0.16</sub> <sup>+0.24</sup> ± 0.06	1,2	AUBERT,B	04s BABR e <sup>+</sup> e <sup>-</sup> → T(4S)
0.66 ± <sub>-0.19</sub> <sup>+0.21</sup> ± 0.06	1,3	KROKOVNY	03B BELL e <sup>+</sup> e <sup>-</sup> → T(4S)

- <sup>1</sup> Assumes equal production of B<sup>+</sup> and B<sup>0</sup> at the T(4S).  
<sup>2</sup> AUBERT,B 04s reports  $(0.8 \pm_{-0.2}^{+0.3} \pm 0.3) \times 10^{-3}$  from a measurement of  $[\Gamma(B^0 \rightarrow D_{sJ}(2457)^+ D^- \times B(D_{sJ}(2457)^+ \rightarrow D_s^{*+} \gamma)) / \Gamma_{\text{total}}] \times [B(D_s^+ \rightarrow \phi \pi^+)]$  assuming B(D<sub>s</sub><sup>+</sup> → φπ<sup>+</sup>) = 0.036 ± 0.009, which we rescale to our best value B(D<sub>s</sub><sup>+</sup> → φπ<sup>+</sup>) = (4.5 ± 0.4) × 10<sup>-2</sup>. Our first error is their experiment's error and our second error is the systematic error from using our best value.  
<sup>3</sup> KROKOVNY 03B reports  $(0.82 \pm_{-0.19}^{+0.22} \pm 0.25) \times 10^{-3}$  from a measurement of  $[\Gamma(B^0 \rightarrow D_{sJ}(2457)^+ D^- \times B(D_{sJ}(2457)^+ \rightarrow D_s^{*+} \gamma)) / \Gamma_{\text{total}}] \times [B(D_s^+ \rightarrow \phi \pi^+)]$  assuming B(D<sub>s</sub><sup>+</sup> → φπ<sup>+</sup>) = 0.036 ± 0.009, which we rescale to our best value B(D<sub>s</sub><sup>+</sup> → φπ<sup>+</sup>) = (4.5 ± 0.4) × 10<sup>-2</sup>. Our first error is their experiment's error and our second error is the systematic error from using our best value.

VALUE (units 10 <sup>-3</sup> )	CL%	DOCUMENT ID	TECN	COMMENT	Γ <sub>86</sub> /Γ
---------------------------------	-----	-------------	------	---------	--------------------

<0.60	90	1	KROKOVNY 03B BELL e <sup>+</sup> e <sup>-</sup> → T(4S)
-------	----	---	---

- <sup>1</sup> Assumes equal production of B<sup>+</sup> and B<sup>0</sup> at the T(4S).  
<sup>2</sup> AUBERT,B 04s reports  $[\Gamma(B^0 \rightarrow D^*(2010)^- D_{sJ}(2457)^+ \rightarrow D_s^{*+} \pi^+ \pi^-) / \Gamma_{\text{total}}] \times [B(D_s^+ \rightarrow \phi \pi^+)] = (5.5 \pm_{-1.6}^{+1.2} \pm 2.2) \times 10^{-3}$  which we divide by our best value B(D<sub>s1</sub>(2460)<sup>+</sup> → D<sub>s</sub><sup>\*+</sup> π<sup>0</sup>) = (48 ± 11) × 10<sup>-2</sup>. Our first error is their experiment's error and our second error is the systematic error from using our best value.  
<sup>3</sup> Assumes equal production of B<sup>+</sup> and B<sup>0</sup> at the T(4S).

VALUE (units 10 <sup>-3</sup> )	CL%	DOCUMENT ID	TECN	COMMENT	Γ <sub>88</sub> /Γ
---------------------------------	-----	-------------	------	---------	--------------------

<0.36	90	1	KROKOVNY 03B BELL e <sup>+</sup> e <sup>-</sup> → T(4S)
-------	----	---	---

- <sup>1</sup> Assumes equal production of B<sup>+</sup> and B<sup>0</sup> at the T(4S).  
<sup>2</sup> AUBERT,B 04s reports  $[\Gamma(B^0 \rightarrow D^*(2010)^- D_{sJ}(2457)^+ \rightarrow D_s^{*+} \pi^0) / \Gamma_{\text{total}}] \times [B(D_s^+ \rightarrow \phi \pi^+)] = (5.5 \pm_{-1.6}^{+1.2} \pm 2.2) \times 10^{-3}$  which we divide by our best value B(D<sub>s1</sub>(2460)<sup>+</sup> → D<sub>s</sub><sup>\*+</sup> π<sup>0</sup>) = (48 ± 11) × 10<sup>-2</sup>. Our first error is their experiment's error and our second error is the systematic error from using our best value.  
<sup>3</sup> Assumes equal production of B<sup>+</sup> and B<sup>0</sup> at the T(4S).

VALUE (units 10 <sup>-3</sup> )	CL%	DOCUMENT ID	TECN	COMMENT	Γ <sub>87</sub> /Γ
---------------------------------	-----	-------------	------	---------	--------------------

<0.20	90	1	KROKOVNY 03B BELL e <sup>+</sup> e <sup>-</sup> → T(4S)
-------	----	---	---

- <sup>1</sup> Assumes equal production of B<sup>+</sup> and B<sup>0</sup> at the T(4S).  
<sup>2</sup> AUBERT,B 04s reports  $[\Gamma(B^0 \rightarrow D^*(2010)^- D_{sJ}(2457)^+ \rightarrow D_s^{*+} \pi^+ \pi^-) / \Gamma_{\text{total}}] \times [B(D_s^+ \rightarrow \phi \pi^+)] = (5.5 \pm_{-1.6}^{+1.2} \pm 2.2) \times 10^{-3}$  which we divide by our best value B(D<sub>s1</sub>(2460)<sup>+</sup> → D<sub>s</sub><sup>\*+</sup> π<sup>0</sup>) = (48 ± 11) × 10<sup>-2</sup>. Our first error is their experiment's error and our second error is the systematic error from using our best value.  
<sup>3</sup> Assumes equal production of B<sup>+</sup> and B<sup>0</sup> at the T(4S).

VALUE (units 10 <sup>-3</sup> )	CL%	DOCUMENT ID	TECN	COMMENT	Γ <sub>89</sub> /Γ
---------------------------------	-----	-------------	------	---------	--------------------

9.3 ± 2.2 OUR AVERAGE				
-----------------------	--	--	--	--

8.8 ± 2.0 ± 1.4		1	AUBERT 06N BABR e <sup>+</sup> e <sup>-</sup> → T(4S)
-----------------	--	---	---

11 ± <sub>-4</sub> <sup>+5</sup> ± 3		2,3	AUBERT,B 04s BABR e <sup>+</sup> e <sup>-</sup> → T(4S)
--------------------------------------	--	-----	---

- <sup>1</sup> Uses a missing-mass method in the events that one of the B mesons is fully reconstructed.  
<sup>2</sup> AUBERT,B 04s reports  $[\Gamma(B^0 \rightarrow D^*(2010)^- D_{sJ}(2457)^+ \rightarrow D_s^{*+} \pi^0) / \Gamma_{\text{total}}] \times [B(D_{s1}(2460)^+ \rightarrow D_s^{*+} \pi^0)] = (5.5 \pm_{-1.6}^{+1.2} \pm 2.2) \times 10^{-3}$  which we divide by our best value B(D<sub>s1</sub>(2460)<sup>+</sup> → D<sub>s</sub><sup>\*+</sup> π<sup>0</sup>) = (48 ± 11) × 10<sup>-2</sup>. Our first error is their experiment's error and our second error is the systematic error from using our best value.  
<sup>3</sup> Assumes equal production of B<sup>+</sup> and B<sup>0</sup> at the T(4S).

VALUE (units 10 <sup>-3</sup> )	CL%	DOCUMENT ID	TECN	COMMENT	Γ <sub>88</sub> /Γ
---------------------------------	-----	-------------	------	---------	--------------------

<0.36	90	1	KROKOVNY 03B BELL e <sup>+</sup> e <sup>-</sup> → T(4S)
-------	----	---	---

- <sup>1</sup> Assumes equal production of B<sup>+</sup> and B<sup>0</sup> at the T(4S).

VALUE (units 10 <sup>-4</sup> )	DOCUMENT ID	TECN	COMMENT	Γ <sub>93</sub> /Γ
---------------------------------	-------------	------	---------	--------------------

2.61 ± 1.03 ± 0.31	1	AUBERT	08B BABR e <sup>+</sup> e <sup>-</sup> → T(4S)
--------------------	---	--------	--

<sup>1</sup> Assumes equal production of B<sup>+</sup> and B<sup>0</sup> at the T(4S).

VALUE (units 10 <sup>-4</sup> )	DOCUMENT ID	TECN	COMMENT	Γ <sub>94</sub> /Γ = (Γ <sub>95</sub> + Γ <sub>96</sub> )/Γ
---------------------------------	-------------	------	---------	---

5.01 ± 1.21 ± 0.70	1,2	AUSHEV	11 BELL e <sup>+</sup> e <sup>-</sup> → T(4S)
--------------------	-----	--------	---

- <sup>1</sup> Uses  $\Gamma(D^*(2007)^0 \rightarrow D^0 \pi^0) / \Gamma(D^*(2007)^0 \rightarrow D^0 \gamma) = 1.74 \pm 0.13$  and  $\Gamma(D_{s1}(2536)^+ \rightarrow D^*(2007)^0 K^+) / \Gamma(D_{s1}(2536)^+ \rightarrow D^*(2010)^+ K^0) = 1.36 \pm 0.2$ .  
<sup>2</sup> Assumes equal production of B<sup>+</sup> and B<sup>0</sup> at the T(4S).

VALUE (units 10 <sup>-4</sup> )	CL%	DOCUMENT ID	TECN	COMMENT	Γ <sub>95</sub> /Γ
---------------------------------	-----	-------------	------	---------	--------------------

3.32 ± 0.88 ± 0.66		1	AUBERT 08B BABR e <sup>+</sup> e <sup>-</sup> → T(4S)
--------------------	--	---	---

- • • We do not use the following data for averages, fits, limits, etc. • • •  
 <7 90 AUBERT 03x BABR Repl. by AUBERT 08B  
<sup>1</sup> Assumes equal production of B<sup>+</sup> and B<sup>0</sup> at the T(4S).

VALUE (units 10 <sup>-4</sup> )	CL%	DOCUMENT ID	TECN	COMMENT	Γ <sub>96</sub> /Γ
---------------------------------	-----	-------------	------	---------	--------------------

5.00 ± 1.51 ± 0.67		1	AUBERT 08B BABR e <sup>+</sup> e <sup>-</sup> → T(4S)
--------------------	--	---	---

<sup>1</sup> Assumes equal production of B<sup>+</sup> and B<sup>0</sup> at the T(4S).

VALUE (units 10 <sup>-4</sup> )	CL%	DOCUMENT ID	TECN	COMMENT	Γ <sub>97</sub> /Γ
---------------------------------	-----	-------------	------	---------	--------------------

<1	90	AUBERT	03x BABR e <sup>+</sup> e <sup>-</sup> → T(4S)
----	----	--------	--

VALUE (units 10 <sup>-4</sup> )	CL%	DOCUMENT ID	TECN	COMMENT	Γ <sub>98</sub> /Γ
---------------------------------	-----	-------------	------	---------	--------------------

<2	90	AUBERT	03x BABR e <sup>+</sup> e <sup>-</sup> → T(4S)
----	----	--------	--

VALUE (units 10 <sup>-7</sup> )	DOCUMENT ID	TECN	COMMENT	Γ <sub>99</sub> /Γ
---------------------------------	-------------	------	---------	--------------------

7.8 ± 1.3 ± 0.4	1,2	DAS	10 BELL e <sup>+</sup> e <sup>-</sup> → T(4S)
-----------------	-----	-----	---

- <sup>1</sup> DAS 10 reports  $[\Gamma(B^0 \rightarrow D^+ \pi^-) / \Gamma_{\text{total}}] / [B(B^0 \rightarrow D^- \pi^+)] = (2.92 \pm 0.38 \pm 0.31) \times 10^{-4}$  which we multiply by our best value B(B<sup>0</sup> → D<sup>-</sup> π<sup>+</sup>) = (2.68 ± 0.13) × 10<sup>-3</sup>. Our first error is their experiment's error and our second error is the systematic error from using our best value.  
<sup>2</sup> Derived using  $\tan(\theta_C) f_D / f_{D_s} \sqrt{B(B^0 \rightarrow D_s^+ \pi^-) / B(B^0 \rightarrow D^- \pi^+)}$  by assuming the flavor SU(3) symmetry, where θ<sub>C</sub> is the Cabibbo angle, f<sub>D</sub> (f<sub>D<sub>s</sub></sub>) is the D (D<sub>s</sub>) meson decay constant.

VALUE (units 10 <sup>-6</sup> )	CL%	DOCUMENT ID	TECN	COMMENT	Γ <sub>100</sub> /Γ
---------------------------------	-----	-------------	------	---------	---------------------

21.6 ± 2.6 OUR AVERAGE				
------------------------	--	--	--	--

19.9 ± 2.6 ± 1.8		1	DAS 10 BELL e <sup>+</sup> e <sup>-</sup> → T(4S)
------------------	--	---	---

25 ± 4 ± 2		1	AUBERT 08AJ BABR e <sup>+</sup> e <sup>-</sup> → T(4S)
------------	--	---	--

- • • We do not use the following data for averages, fits, limits, etc. • • •  
 14.0 ± 3.5 ± 1.3 2 AUBERT 07K BABR Repl. by AUBERT 08AJ  
 25 ± 9 ± 2 3 AUBERT 03D BABR Repl. by AUBERT 07K  
 19 ±<sub>-7</sub><sup>+9</sup> ± 2 4 KROKOVNY 02 BELL Repl. by DAS 10  
 < 220 90 5 ALEXANDER 93B CLE2 e<sup>+</sup>e<sup>-</sup> → T(4S)  
 < 1300 90 6 BORTOLETTO90 CLEO e<sup>+</sup>e<sup>-</sup> → T(4S)

<sup>1</sup> Assumes equal production of B<sup>+</sup> and B<sup>0</sup> at the T(4S).

<sup>2</sup> AUBERT 07K reports  $[\Gamma(B^0 \rightarrow D_s^+ \pi^-) / \Gamma_{\text{total}}] \times [B(D_s^+ \rightarrow \phi \pi^+)] = (0.63 \pm 0.15 \pm 0.05) \times 10^{-6}$  which we divide by our best value B(D<sub>s</sub><sup>+</sup> → φπ<sup>+</sup>) = (4.5 ± 0.4) × 10<sup>-2</sup>. Our first error is their experiment's error and our second error is the systematic error from using our best value.  
<sup>3</sup> AUBERT 03D reports  $[\Gamma(B^0 \rightarrow D_s^+ \pi^-) / \Gamma_{\text{total}}] \times [B(D_s^+ \rightarrow \phi \pi^+)] = (1.13 \pm 0.33 \pm 0.21) \times 10^{-6}$  which we divide by our best value B(D<sub>s</sub><sup>+</sup> → φπ<sup>+</sup>) = (4.5 ± 0.4) × 10<sup>-2</sup>. Our first error is their experiment's error and our second error is the systematic error from using our best value.

<sup>4</sup> KROKOVNY 02 reports  $[\Gamma(B^0 \rightarrow D_s^+ \pi^-) / \Gamma_{\text{total}}] \times [B(D_s^+ \rightarrow \phi \pi^+)] = (0.86 \pm_{-0.30}^{+0.37} \pm 0.11) \times 10^{-6}$  which we divide by our best value B(D<sub>s</sub><sup>+</sup> → φπ<sup>+</sup>) = (4.5 ± 0.4) × 10<sup>-2</sup>. Our first error is their experiment's error and our second error is the systematic error from using our best value.  
<sup>5</sup> ALEXANDER 93B reports < 270 × 10<sup>-6</sup> from a measurement of  $[\Gamma(B^0 \rightarrow D_s^+ \pi^-) / \Gamma_{\text{total}}] \times [B(D_s^+ \rightarrow \phi \pi^+)]$  assuming B(D<sub>s</sub><sup>+</sup> → φπ<sup>+</sup>) = 0.037, which we rescale to our best value B(D<sub>s</sub><sup>+</sup> → φπ<sup>+</sup>) = 4.5 × 10<sup>-2</sup>.

<sup>6</sup> BORTOLETTO 90 assume B(D<sub>s</sub> → φπ<sup>+</sup>) = 2%.

## Meson Particle Listings

 $B^0$ 

$$\frac{\Gamma(D_s^+ \pi^-) + \Gamma(D_s^- K^+)}{\Gamma_{\text{total}}} \quad (\Gamma_{100} + \Gamma_{110})/\Gamma$$

VALUE (units $10^{-5}$ )	CL%	DOCUMENT ID	TECN	COMMENT
$<1.0 \times 10^{-3}$	90	<sup>1</sup> ALBRECHT 93E	ARG	$e^+e^- \rightarrow \mathcal{T}(4S)$
<sup>1</sup> ALBRECHT 93E reports $<1.7 \times 10^{-3}$ from a measurement of $[\Gamma(B^0 \rightarrow D_s^+ \pi^-) + \Gamma(B^0 \rightarrow D_s^- K^+)]/\Gamma_{\text{total}} \times [B(D_s^+ \rightarrow \phi\pi^+)]$ assuming $B(D_s^+ \rightarrow \phi\pi^+) = 0.027$ , which we rescale to our best value $B(D_s^+ \rightarrow \phi\pi^+) = 4.5 \times 10^{-2}$ .				

$$\frac{\Gamma(D_s^{*+} \pi^-)}{\Gamma_{\text{total}}} \quad \Gamma_{101}/\Gamma$$

VALUE (units $10^{-5}$ )	CL%	DOCUMENT ID	TECN	COMMENT
<b><math>2.1 \pm 0.4</math> OUR AVERAGE</b>		Error includes scale factor of 1.4.		
$1.75 \pm 0.34 \pm 0.20$		<sup>1</sup> JOSHI 10	BELL	$e^+e^- \rightarrow \mathcal{T}(4S)$
$2.6^{+0.5}_{-0.4} \pm 0.2$		<sup>1</sup> AUBERT 08AJ	BABR	$e^+e^- \rightarrow \mathcal{T}(4S)$
• • • We do not use the following data for averages, fits, limits, etc. • • •				
$2.9 \pm 0.7 \pm 0.3$		<sup>2</sup> AUBERT 07K	BABR	Repl. by AUBERT 08AJ
$<4.1$	90	AUBERT 03D	BABR	Repl. by AUBERT 07K
$<40$	90	<sup>3</sup> ALEXANDER 93B	CLE2	$e^+e^- \rightarrow \mathcal{T}(4S)$

- <sup>1</sup> Assumes equal production of  $B^+$  and  $B^0$  at the  $\mathcal{T}(4S)$ .  
<sup>2</sup> AUBERT 07K reports  $[\Gamma(B^0 \rightarrow D_s^{*+} \pi^-)/\Gamma_{\text{total}}] \times [B(D_s^+ \rightarrow \phi\pi^+)] = (1.32 \pm 0.27 \pm 0.15) \times 10^{-6}$  which we divide by our best value  $B(D_s^+ \rightarrow \phi\pi^+) = (4.5 \pm 0.4) \times 10^{-2}$ . Our first error is their experiment's error and our second error is the systematic error from using our best value.  
<sup>3</sup> ALEXANDER 93B reports  $<44 \times 10^{-5}$  from a measurement of  $[\Gamma(B^0 \rightarrow D_s^{*+} \pi^-)/\Gamma_{\text{total}}] \times [B(D_s^+ \rightarrow \phi\pi^+)]$  assuming  $B(D_s^+ \rightarrow \phi\pi^+) = 0.037$ , which we rescale to our best value  $B(D_s^+ \rightarrow \phi\pi^+) = 4.5 \times 10^{-2}$ .

$$\frac{\Gamma(D_s^{*+} \pi^-) + \Gamma(D_s^{*+} K^+)}{\Gamma_{\text{total}}} \quad (\Gamma_{101} + \Gamma_{111})/\Gamma$$

VALUE (units $10^{-5}$ )	CL%	DOCUMENT ID	TECN	COMMENT
$<7 \times 10^{-4}$	90	<sup>1</sup> ALBRECHT 93E	ARG	$e^+e^- \rightarrow \mathcal{T}(4S)$
<sup>1</sup> ALBRECHT 93E reports $<1.2 \times 10^{-3}$ from a measurement of $[\Gamma(B^0 \rightarrow D_s^{*+} \pi^-) + \Gamma(B^0 \rightarrow D_s^{*+} K^+)]/\Gamma_{\text{total}} \times [B(D_s^+ \rightarrow \phi\pi^+)]$ assuming $B(D_s^+ \rightarrow \phi\pi^+) = 0.027$ , which we rescale to our best value $B(D_s^+ \rightarrow \phi\pi^+) = 4.5 \times 10^{-2}$ .				

$$\frac{\Gamma(D_s^+ \rho^-)}{\Gamma_{\text{total}}} \quad \Gamma_{102}/\Gamma$$

VALUE (units $10^{-5}$ )	CL%	DOCUMENT ID	TECN	COMMENT
<b><math>&lt;2.4</math></b>	90	<sup>1</sup> AUBERT 08AJ	BABR	$e^+e^- \rightarrow \mathcal{T}(4S)$
• • • We do not use the following data for averages, fits, limits, etc. • • •				
$<130$	90	<sup>2</sup> ALBRECHT 93E	ARG	$e^+e^- \rightarrow \mathcal{T}(4S)$
$<50$	90	<sup>3</sup> ALEXANDER 93B	CLE2	$e^+e^- \rightarrow \mathcal{T}(4S)$

- <sup>1</sup> Assumes equal production of  $B^+$  and  $B^0$  at the  $\mathcal{T}(4S)$ .  
<sup>2</sup> ALBRECHT 93E reports  $<2.2 \times 10^{-3}$  from a measurement of  $[\Gamma(B^0 \rightarrow D_s^+ \rho^-)/\Gamma_{\text{total}}] \times [B(D_s^+ \rightarrow \phi\pi^+)]$  assuming  $B(D_s^+ \rightarrow \phi\pi^+) = 0.027$ , which we rescale to our best value  $B(D_s^+ \rightarrow \phi\pi^+) = 4.5 \times 10^{-2}$ .  
<sup>3</sup> ALEXANDER 93B reports  $<6.6 \times 10^{-4}$  from a measurement of  $[\Gamma(B^0 \rightarrow D_s^+ \rho^-)/\Gamma_{\text{total}}] \times [B(D_s^+ \rightarrow \phi\pi^+)]$  assuming  $B(D_s^+ \rightarrow \phi\pi^+) = 0.037$ , which we rescale to our best value  $B(D_s^+ \rightarrow \phi\pi^+) = 4.5 \times 10^{-2}$ .

$$\frac{\Gamma(D_s^{*+} \rho^-)}{\Gamma_{\text{total}}} \quad \Gamma_{103}/\Gamma$$

VALUE (units $10^{-5}$ )	CL%	DOCUMENT ID	TECN	COMMENT
<b><math>4.1^{+1.3}_{-1.2} \pm 0.4</math></b>		<sup>1</sup> AUBERT 08AJ	BABR	$e^+e^- \rightarrow \mathcal{T}(4S)$
• • • We do not use the following data for averages, fits, limits, etc. • • •				
$<150$	90	<sup>2</sup> ALBRECHT 93E	ARG	$e^+e^- \rightarrow \mathcal{T}(4S)$
$<60$	90	<sup>3</sup> ALEXANDER 93B	CLE2	$e^+e^- \rightarrow \mathcal{T}(4S)$

- <sup>1</sup> Assumes equal production of  $B^+$  and  $B^0$  at the  $\mathcal{T}(4S)$ .  
<sup>2</sup> ALBRECHT 93E reports  $<2.5 \times 10^{-3}$  from a measurement of  $[\Gamma(B^0 \rightarrow D_s^{*+} \rho^-)/\Gamma_{\text{total}}] \times [B(D_s^+ \rightarrow \phi\pi^+)]$  assuming  $B(D_s^+ \rightarrow \phi\pi^+) = 0.027$ , which we rescale to our best value  $B(D_s^+ \rightarrow \phi\pi^+) = 4.5 \times 10^{-2}$ .  
<sup>3</sup> ALEXANDER 93B reports  $<7.4 \times 10^{-4}$  from a measurement of  $[\Gamma(B^0 \rightarrow D_s^{*+} \rho^-)/\Gamma_{\text{total}}] \times [B(D_s^+ \rightarrow \phi\pi^+)]$  assuming  $B(D_s^+ \rightarrow \phi\pi^+) = 0.037$ , which we rescale to our best value  $B(D_s^+ \rightarrow \phi\pi^+) = 4.5 \times 10^{-2}$ .

$$\frac{\Gamma(D_s^+ a_0^-)}{\Gamma_{\text{total}}} \quad \Gamma_{104}/\Gamma$$

VALUE (units $10^{-5}$ )	CL%	DOCUMENT ID	TECN	COMMENT
<b><math>&lt;1.9</math></b>	90	<sup>1</sup> AUBERT 06X	BABR	$e^+e^- \rightarrow \mathcal{T}(4S)$
<sup>1</sup> Assumes equal production of $B^+$ and $B^0$ at the $\mathcal{T}(4S)$ .				

$$\frac{\Gamma(D_s^{*+} a_0^-)}{\Gamma_{\text{total}}} \quad \Gamma_{105}/\Gamma$$

VALUE (units $10^{-5}$ )	CL%	DOCUMENT ID	TECN	COMMENT
<b><math>&lt;3.6</math></b>	90	<sup>1</sup> AUBERT 06X	BABR	$e^+e^- \rightarrow \mathcal{T}(4S)$
<sup>1</sup> Assumes equal production of $B^+$ and $B^0$ at the $\mathcal{T}(4S)$ .				

$$\frac{\Gamma(D_s^+ a_1(1260)^-)}{\Gamma_{\text{total}}} \quad \Gamma_{106}/\Gamma$$

VALUE (units $10^{-5}$ )	CL%	DOCUMENT ID	TECN	COMMENT
<b><math>&lt;2.1 \times 10^{-3}</math></b>	90	<sup>1</sup> ALBRECHT 93E	ARG	$e^+e^- \rightarrow \mathcal{T}(4S)$
<sup>1</sup> ALBRECHT 93E reports $<3.5 \times 10^{-3}$ from a measurement of $[\Gamma(B^0 \rightarrow D_s^+ a_1(1260)^-)/\Gamma_{\text{total}}] \times [B(D_s^+ \rightarrow \phi\pi^+)]$ assuming $B(D_s^+ \rightarrow \phi\pi^+) = 0.027$ , which we rescale to our best value $B(D_s^+ \rightarrow \phi\pi^+) = 4.5 \times 10^{-2}$ .				

$$\frac{\Gamma(D_s^{*+} a_1(1260)^-)}{\Gamma_{\text{total}}} \quad \Gamma_{107}/\Gamma$$

VALUE (units $10^{-5}$ )	CL%	DOCUMENT ID	TECN	COMMENT
<b><math>&lt;1.7 \times 10^{-3}</math></b>	90	<sup>1</sup> ALBRECHT 93E	ARG	$e^+e^- \rightarrow \mathcal{T}(4S)$
<sup>1</sup> ALBRECHT 93E reports $<2.9 \times 10^{-3}$ from a measurement of $[\Gamma(B^0 \rightarrow D_s^{*+} a_1(1260)^-)/\Gamma_{\text{total}}] \times [B(D_s^+ \rightarrow \phi\pi^+)]$ assuming $B(D_s^+ \rightarrow \phi\pi^+) = 0.027$ , which we rescale to our best value $B(D_s^+ \rightarrow \phi\pi^+) = 4.5 \times 10^{-2}$ .				

$$\frac{\Gamma(D_s^+ a_2^-)}{\Gamma_{\text{total}}} \quad \Gamma_{108}/\Gamma$$

VALUE (units $10^{-5}$ )	CL%	DOCUMENT ID	TECN	COMMENT
<b><math>&lt;19</math></b>	90	<sup>1</sup> AUBERT 06X	BABR	$e^+e^- \rightarrow \mathcal{T}(4S)$
<sup>1</sup> Assumes equal production of $B^+$ and $B^0$ at the $\mathcal{T}(4S)$ .				

$$\frac{\Gamma(D_s^{*+} a_2^-)}{\Gamma_{\text{total}}} \quad \Gamma_{109}/\Gamma$$

VALUE (units $10^{-5}$ )	CL%	DOCUMENT ID	TECN	COMMENT
<b><math>&lt;20</math></b>	90	<sup>1</sup> AUBERT 06X	BABR	$e^+e^- \rightarrow \mathcal{T}(4S)$
<sup>1</sup> Assumes equal production of $B^+$ and $B^0$ at the $\mathcal{T}(4S)$ .				

$$\frac{\Gamma(D_s^- K^+)}{\Gamma_{\text{total}}} \quad \Gamma_{110}/\Gamma$$

VALUE (units $10^{-5}$ )	CL%	DOCUMENT ID	TECN	COMMENT
<b><math>22 \pm 5</math> OUR AVERAGE</b>		Error includes scale factor of 1.8.		
$19.1 \pm 2.4 \pm 1.7$		<sup>1</sup> DAS 10	BELL	$e^+e^- \rightarrow \mathcal{T}(4S)$
$29 \pm 4 \pm 2$		<sup>1</sup> AUBERT 08AJ	BABR	$e^+e^- \rightarrow \mathcal{T}(4S)$
• • • We do not use the following data for averages, fits, limits, etc. • • •				
$27 \pm 5 \pm 2$		<sup>2</sup> AUBERT 07K	BABR	Repl. by AUBERT 08AJ
$26 \pm 10 \pm 2$		<sup>3</sup> AUBERT 03D	BABR	Repl. by AUBERT 07K
$36^{+11}_{-10} \pm 3$		<sup>4</sup> KROKOVNY 02	BELL	Repl. by DAS 10
$<190$	90	<sup>5</sup> ALEXANDER 93B	CLE2	$e^+e^- \rightarrow \mathcal{T}(4S)$
$<1300$	90	<sup>6</sup> BORTOLETTO 90	CLEO	$e^+e^- \rightarrow \mathcal{T}(4S)$

- <sup>1</sup> Assumes equal production of  $B^+$  and  $B^0$  at the  $\mathcal{T}(4S)$ .  
<sup>2</sup> AUBERT 07K reports  $[\Gamma(B^0 \rightarrow D_s^- K^+)/\Gamma_{\text{total}}] \times [B(D_s^+ \rightarrow \phi\pi^+)] = (1.21 \pm 0.17 \pm 0.11) \times 10^{-6}$  which we divide by our best value  $B(D_s^+ \rightarrow \phi\pi^+) = (4.5 \pm 0.4) \times 10^{-2}$ . Our first error is their experiment's error and our second error is the systematic error from using our best value.  
<sup>3</sup> AUBERT 03D reports  $[\Gamma(B^0 \rightarrow D_s^- K^+)/\Gamma_{\text{total}}] \times [B(D_s^+ \rightarrow \phi\pi^+)] = (1.16 \pm 0.36 \pm 0.24) \times 10^{-6}$  which we divide by our best value  $B(D_s^+ \rightarrow \phi\pi^+) = (4.5 \pm 0.4) \times 10^{-2}$ . Our first error is their experiment's error and our second error is the systematic error from using our best value.  
<sup>4</sup> KROKOVNY 02 reports  $[\Gamma(B^0 \rightarrow D_s^- K^+)/\Gamma_{\text{total}}] \times [B(D_s^+ \rightarrow \phi\pi^+)] = (1.61^{+0.45}_{-0.38} \pm 0.21) \times 10^{-6}$  which we divide by our best value  $B(D_s^+ \rightarrow \phi\pi^+) = (4.5 \pm 0.4) \times 10^{-2}$ . Our first error is their experiment's error and our second error is the systematic error from using our best value.  
<sup>5</sup> ALEXANDER 93B reports  $<230 \times 10^{-6}$  from a measurement of  $[\Gamma(B^0 \rightarrow D_s^- K^+)/\Gamma_{\text{total}}] \times [B(D_s^+ \rightarrow \phi\pi^+)]$  assuming  $B(D_s^+ \rightarrow \phi\pi^+) = 0.037$ , which we rescale to our best value  $B(D_s^+ \rightarrow \phi\pi^+) = 4.5 \times 10^{-2}$ .  
<sup>6</sup> BORTOLETTO 90 assume  $B(D_s \rightarrow \phi\pi^+) = 2\%$ .

$$\frac{\Gamma(D_s^{*-} K^+)}{\Gamma_{\text{total}}} \quad \Gamma_{111}/\Gamma$$

VALUE (units $10^{-5}$ )	CL%	DOCUMENT ID	TECN	COMMENT
<b><math>2.19 \pm 0.30</math> OUR AVERAGE</b>				
$2.02 \pm 0.33 \pm 0.22$		<sup>1</sup> JOSHI 10	BELL	$e^+e^- \rightarrow \mathcal{T}(4S)$
$2.4 \pm 0.4 \pm 0.2$		<sup>1</sup> AUBERT 08AJ	BABR	$e^+e^- \rightarrow \mathcal{T}(4S)$
• • • We do not use the following data for averages, fits, limits, etc. • • •				
$2.2 \pm 0.6 \pm 0.2$		<sup>2</sup> AUBERT 07K	BABR	Repl. by AUBERT 08AJ
$<2.5$	90	AUBERT 03D	BABR	Repl. by AUBERT 07K
$<14$	90	<sup>3</sup> ALEXANDER 93B	CLE2	$e^+e^- \rightarrow \mathcal{T}(4S)$

- <sup>1</sup> Assumes equal production of  $B^+$  and  $B^0$  at the  $\mathcal{T}(4S)$ .  
<sup>2</sup> AUBERT 07K reports  $[\Gamma(B^0 \rightarrow D_s^{*-} K^+)/\Gamma_{\text{total}}] \times [B(D_s^+ \rightarrow \phi\pi^+)] = (0.97 \pm 0.24 \pm 0.12) \times 10^{-6}$  which we divide by our best value  $B(D_s^+ \rightarrow \phi\pi^+) = (4.5 \pm 0.4) \times 10^{-2}$ . Our first error is their experiment's error and our second error is the systematic error from using our best value.  
<sup>3</sup> ALEXANDER 93B reports  $<17 \times 10^{-5}$  from a measurement of  $[\Gamma(B^0 \rightarrow D_s^{*-} K^+)/\Gamma_{\text{total}}] \times [B(D_s^+ \rightarrow \phi\pi^+)]$  assuming  $B(D_s^+ \rightarrow \phi\pi^+) = 0.037$ , which we rescale to our best value  $B(D_s^+ \rightarrow \phi\pi^+) = 4.5 \times 10^{-2}$ .

See key on page 457

# Meson Particle Listings

$B^0$

$\Gamma(D_s^- K^*(892)^+)/\Gamma_{total}$	$\Gamma_{112}/\Gamma$			
VALUE (units $10^{-5}$ )	CL%	DOCUMENT ID	TECN	COMMENT

$3.5^{+1.0}_{-0.9} \pm 0.4$		1 AUBERT	08AJ	BABR $e^+e^- \rightarrow \Upsilon(4S)$
<280	90	2 ALBRECHT	93E	ARG $e^+e^- \rightarrow \Upsilon(4S)$
< 80	90	3 ALEXANDER	93B	CLE2 $e^+e^- \rightarrow \Upsilon(4S)$

• • • We do not use the following data for averages, fits, limits, etc. • • •

<sup>1</sup> Assumes equal production of  $B^+$  and  $B^0$  at the  $\Upsilon(4S)$ .

<sup>2</sup> ALBRECHT 93E reports  $< 4.6 \times 10^{-3}$  from a measurement of  $[\Gamma(B^0 \rightarrow D_s^- K^*(892)^+)/\Gamma_{total}] \times [B(D_s^+ \rightarrow \phi\pi^+)]$  assuming  $B(D_s^+ \rightarrow \phi\pi^+) = 0.027$ , which we rescale to our best value  $B(D_s^+ \rightarrow \phi\pi^+) = 4.5 \times 10^{-2}$ .

<sup>3</sup> ALEXANDER 93B reports  $< 9.7 \times 10^{-4}$  from a measurement of  $[\Gamma(B^0 \rightarrow D_s^- K^*(892)^+)/\Gamma_{total}] \times [B(D_s^+ \rightarrow \phi\pi^+)]$  assuming  $B(D_s^+ \rightarrow \phi\pi^+) = 0.037$ , which we rescale to our best value  $B(D_s^+ \rightarrow \phi\pi^+) = 4.5 \times 10^{-2}$ .

$\Gamma(D_s^{*-} K^*(892)^+)/\Gamma_{total}$	$\Gamma_{113}/\Gamma$			
VALUE (units $10^{-5}$ )	CL%	DOCUMENT ID	TECN	COMMENT

$3.2^{+1.4}_{-1.2} \pm 0.4$		1 AUBERT	08AJ	BABR $e^+e^- \rightarrow \Upsilon(4S)$
<350	90	2 ALBRECHT	93E	ARG $e^+e^- \rightarrow \Upsilon(4S)$
< 90	90	3 ALEXANDER	93B	CLE2 $e^+e^- \rightarrow \Upsilon(4S)$

• • • We do not use the following data for averages, fits, limits, etc. • • •

<sup>1</sup> Assumes equal production of  $B^+$  and  $B^0$  at the  $\Upsilon(4S)$ .

<sup>2</sup> ALBRECHT 93E reports  $< 5.8 \times 10^{-3}$  from a measurement of  $[\Gamma(B^0 \rightarrow D_s^{*-} K^*(892)^+)/\Gamma_{total}] \times [B(D_s^+ \rightarrow \phi\pi^+)]$  assuming  $B(D_s^+ \rightarrow \phi\pi^+) = 0.027$ , which we rescale to our best value  $B(D_s^+ \rightarrow \phi\pi^+) = 4.5 \times 10^{-2}$ .

<sup>3</sup> ALEXANDER 93B reports  $< 11.0 \times 10^{-4}$  from a measurement of  $[\Gamma(B^0 \rightarrow D_s^{*-} K^*(892)^+)/\Gamma_{total}] \times [B(D_s^+ \rightarrow \phi\pi^+)]$  assuming  $B(D_s^+ \rightarrow \phi\pi^+) = 0.037$ , which we rescale to our best value  $B(D_s^+ \rightarrow \phi\pi^+) = 4.5 \times 10^{-2}$ .

$\Gamma(D_s^- \pi^+ K^0)/\Gamma_{total}$	$\Gamma_{114}/\Gamma$			
VALUE (units $10^{-4}$ )	CL%	DOCUMENT ID	TECN	COMMENT

$1.10 \pm 0.26 \pm 0.20$		1 AUBERT	08G	BABR $e^+e^- \rightarrow \Upsilon(4S)$
<40	90	2 ALBRECHT	93E	ARG $e^+e^- \rightarrow \Upsilon(4S)$

• • • We do not use the following data for averages, fits, limits, etc. • • •

<sup>1</sup> Assumes equal production of  $B^+$  and  $B^0$  at the  $\Upsilon(4S)$ .

<sup>2</sup> ALBRECHT 93E reports  $< 7.3 \times 10^{-3}$  from a measurement of  $[\Gamma(B^0 \rightarrow D_s^- \pi^+ K^0)/\Gamma_{total}] \times [B(D_s^+ \rightarrow \phi\pi^+)]$  assuming  $B(D_s^+ \rightarrow \phi\pi^+) = 0.027$ , which we rescale to our best value  $B(D_s^+ \rightarrow \phi\pi^+) = 4.5 \times 10^{-2}$ .

$\Gamma(D_s^{*-} \pi^+ K^0)/\Gamma_{total}$	$\Gamma_{115}/\Gamma$			
VALUE (units $10^{-4}$ )	CL%	DOCUMENT ID	TECN	COMMENT

< 1.10	90	1 AUBERT	08G	BABR $e^+e^- \rightarrow \Upsilon(4S)$
<25	90	2 ALBRECHT	93E	ARG $e^+e^- \rightarrow \Upsilon(4S)$

• • • We do not use the following data for averages, fits, limits, etc. • • •

<sup>1</sup> Assumes equal production of  $B^+$  and  $B^0$  at the  $\Upsilon(4S)$ .

<sup>2</sup> ALBRECHT 93E reports  $< 4.2 \times 10^{-3}$  from a measurement of  $[\Gamma(B^0 \rightarrow D_s^{*-} \pi^+ K^0)/\Gamma_{total}] \times [B(D_s^+ \rightarrow \phi\pi^+)]$  assuming  $B(D_s^+ \rightarrow \phi\pi^+) = 0.027$ , which we rescale to our best value  $B(D_s^+ \rightarrow \phi\pi^+) = 4.5 \times 10^{-2}$ .

$\Gamma(D_s^- \pi^+ K^*(892)^0)/\Gamma_{total}$	$\Gamma_{116}/\Gamma$			
VALUE	CL%	DOCUMENT ID	TECN	COMMENT

< $3.0 \times 10^{-3}$	90	1 ALBRECHT	93E	ARG $e^+e^- \rightarrow \Upsilon(4S)$
------------------------	----	------------	-----	---------------------------------------

<sup>1</sup> ALBRECHT 93E reports  $< 5.0 \times 10^{-3}$  from a measurement of  $[\Gamma(B^0 \rightarrow D_s^- \pi^+ K^*(892)^0)/\Gamma_{total}] \times [B(D_s^+ \rightarrow \phi\pi^+)]$  assuming  $B(D_s^+ \rightarrow \phi\pi^+) = 0.027$ , which we rescale to our best value  $B(D_s^+ \rightarrow \phi\pi^+) = 4.5 \times 10^{-2}$ .

$\Gamma(D_s^{*-} \pi^+ K^*(892)^0)/\Gamma_{total}$	$\Gamma_{117}/\Gamma$			
VALUE	CL%	DOCUMENT ID	TECN	COMMENT

< $1.6 \times 10^{-3}$	90	1 ALBRECHT	93E	ARG $e^+e^- \rightarrow \Upsilon(4S)$
------------------------	----	------------	-----	---------------------------------------

<sup>1</sup> ALBRECHT 93E reports  $< 2.7 \times 10^{-3}$  from a measurement of  $[\Gamma(B^0 \rightarrow D_s^{*-} \pi^+ K^*(892)^0)/\Gamma_{total}] \times [B(D_s^+ \rightarrow \phi\pi^+)]$  assuming  $B(D_s^+ \rightarrow \phi\pi^+) = 0.027$ , which we rescale to our best value  $B(D_s^+ \rightarrow \phi\pi^+) = 4.5 \times 10^{-2}$ .

$\Gamma(\bar{D}^0 K^0)/\Gamma_{total}$	$\Gamma_{118}/\Gamma$			
VALUE (units $10^{-5}$ )	CL%	DOCUMENT ID	TECN	COMMENT

<b>5.2 ± 0.7 OUR AVERAGE</b>		1 AUBERT,B	06L	BABR $e^+e^- \rightarrow \Upsilon(4S)$
$5.3 \pm 0.7 \pm 0.3$		1 KROKOVNY	03	BELL $e^+e^- \rightarrow \Upsilon(4S)$
$5.0^{+1.3}_{-1.2} \pm 0.6$				

<sup>1</sup> Assumes equal production of  $B^+$  and  $B^0$  at the  $\Upsilon(4S)$ .

$\Gamma(\bar{D}^0 K^+ \pi^-)/\Gamma_{total}$	$\Gamma_{119}/\Gamma$			
VALUE (units $10^{-5}$ )	CL%	DOCUMENT ID	TECN	COMMENT

<b>88 ± 15 ± 9</b>		1 AUBERT	06A	BABR $e^+e^- \rightarrow \Upsilon(4S)$
--------------------	--	----------	-----	--

<sup>1</sup> Assumes equal production of  $B^+$  and  $B^0$  at the  $\Upsilon(4S)$ .

$\Gamma(\bar{D}^0 K^*(892)^0)/\Gamma_{total}$	$\Gamma_{120}/\Gamma$			
VALUE (units $10^{-5}$ )	CL%	DOCUMENT ID	TECN	COMMENT

<b>4.2 ± 0.6 OUR AVERAGE</b>		1 AUBERT,B	06L	BABR $e^+e^- \rightarrow \Upsilon(4S)$
$4.0 \pm 0.7 \pm 0.3$		1 KROKOVNY	03	BELL $e^+e^- \rightarrow \Upsilon(4S)$
$4.8^{+1.1}_{-1.0} \pm 0.5$				

• • • We do not use the following data for averages, fits, limits, etc. • • •

<sup>1</sup> Assumes equal production of  $B^+$  and  $B^0$  at the  $\Upsilon(4S)$ .

$\Gamma(D_2^{*-}(2460)^- K^+ \times B(D_2^{*+}(2460)^- \rightarrow \bar{D}^0 \pi^-))/\Gamma_{total}$	$\Gamma_{121}/\Gamma$			
VALUE (units $10^{-6}$ )	CL%	DOCUMENT ID	TECN	COMMENT

<b>18.3 ± 4.0 ± 3.1</b>		1 AUBERT	06A	BABR $e^+e^- \rightarrow \Upsilon(4S)$
-------------------------	--	----------	-----	--

<sup>1</sup> Assumes equal production of  $B^+$  and  $B^0$  at the  $\Upsilon(4S)$ .

$\Gamma(\bar{D}^0 K^+ \pi^- \text{ non-resonant})/\Gamma_{total}$	$\Gamma_{122}/\Gamma$			
VALUE (units $10^{-6}$ )	CL%	DOCUMENT ID	TECN	COMMENT

<37	90	1 AUBERT	06A	BABR $e^+e^- \rightarrow \Upsilon(4S)$
-----	----	----------	-----	--

<sup>1</sup> Assumes equal production of  $B^+$  and  $B^0$  at the  $\Upsilon(4S)$ .

$\Gamma(\bar{D}^0 \rho^0)/\Gamma_{total}$	$\Gamma_{123}/\Gamma$			
VALUE (units $10^{-4}$ )	CL%	DOCUMENT ID	TECN	COMMENT

<b>2.63 ± 0.14 OUR AVERAGE</b>		1 LEES	11M	BABR $e^+e^- \rightarrow \Upsilon(4S)$
$2.69 \pm 0.09 \pm 0.13$		1 BLYTH	06	BELL $e^+e^- \rightarrow \Upsilon(4S)$
$2.25 \pm 0.14 \pm 0.35$		1 COAN	02	CLE2 $e^+e^- \rightarrow \Upsilon(4S)$
$2.74^{+0.36}_{-0.32} \pm 0.55$				

• • • We do not use the following data for averages, fits, limits, etc. • • •

<sup>1</sup> AUBERT 04B BABR Repl. by LEES 11M

<sup>1</sup> ABE 02J BELL Repl. by BLYTH 06

<sup>2</sup> NEMAT 98 CLE2 Repl. by COAN 02

<sup>3</sup> ALAM 94 CLE2 Repl. by NEMAT 98

<sup>1</sup> Assumes equal production of  $B^+$  and  $B^0$  at the  $\Upsilon(4S)$ .

<sup>2</sup> NEMAT 98 assumes equal production of  $B^+$  and  $B^0$  at the  $\Upsilon(4S)$  and use the PDG 96 values for  $D^0, D^{*0}, \eta, \eta',$  and  $\omega$  branching fractions.

<sup>3</sup> ALAM 94 assume equal production of  $B^+$  and  $B^0$  at the  $\Upsilon(4S)$  and use the CLEO II absolute  $B(D^0 \rightarrow K^-\pi^+)$  and the PDG 1992  $B(D^0 \rightarrow K^-\pi^+\pi^0)/B(D^0 \rightarrow K^-\pi^+)$  and  $B(D^0 \rightarrow K^-2\pi^+\pi^-)/B(D^0 \rightarrow K^-\pi^+)$ .

$\Gamma(\bar{D}^0 f_2)/\Gamma_{total}$	$\Gamma_{124}/\Gamma$			
VALUE (units $10^{-4}$ )	CL%	DOCUMENT ID	TECN	COMMENT

<b>3.19 ± 0.20 ± 0.45</b>		1,2 KUZMIN	07	BELL $e^+e^- \rightarrow \Upsilon(4S)$
$2.9 \pm 1.0 \pm 0.4$		1 SATPATHY	03	BELL Repl. by KUZMIN 07
< 3.1	90	3 NEMAT 98	CLE2	$e^+e^- \rightarrow \Upsilon(4S)$
< 5.5	90	4 ALAM 94	CLE2	Repl. by NEMAT 98
< 6.0	90	5 BORTOLETTO 92	CLEO	$e^+e^- \rightarrow \Upsilon(4S)$
<27.0	90	6 ALBRECHT	88K	ARG $e^+e^- \rightarrow \Upsilon(4S)$

• • • We do not use the following data for averages, fits, limits, etc. • • •

<sup>1</sup> Assumes equal production of  $B^+$  and  $B^0$  at the  $\Upsilon(4S)$ .

<sup>2</sup> Our second uncertainty combines systematics and model errors quoted in the paper.

<sup>3</sup> NEMAT 98 assumes equal production of  $B^+$  and  $B^0$  at the  $\Upsilon(4S)$  and use the PDG 96 values for  $D^0, D^{*0}, \eta, \eta',$  and  $\omega$  branching fractions.

<sup>4</sup> ALAM 94 assume equal production of  $B^+$  and  $B^0$  at the  $\Upsilon(4S)$  and use the CLEO II absolute  $B(D^0 \rightarrow K^-\pi^+)$  and the PDG 1992  $B(D^0 \rightarrow K^-\pi^+\pi^0)/B(D^0 \rightarrow K^-\pi^+)$  and  $B(D^0 \rightarrow K^-2\pi^+\pi^-)/B(D^0 \rightarrow K^-\pi^+)$ .

<sup>5</sup> BORTOLETTO 92 assumes equal production of  $B^+$  and  $B^0$  at the  $\Upsilon(4S)$  and uses Mark III branching fractions for the  $D$ .

<sup>6</sup> ALBRECHT 88K reports  $< 0.003$  assuming  $B^0 \bar{B}^0, B^+ B^-$  production ratio is 45:55. We rescale to 50%.

$\Gamma(\bar{D}^0 \eta)/\Gamma_{total}$	$\Gamma_{125}/\Gamma$			
VALUE (units $10^{-4}$ )	CL%	DOCUMENT ID	TECN	COMMENT

<b>1.20 ± 0.18 ± 0.38</b>		1,2 KUZMIN	07	BELL $e^+e^- \rightarrow \Upsilon(4S)$
---------------------------	--	------------	----	--

<sup>1</sup> Assumes equal production of  $B^+$  and  $B^0$  at the  $\Upsilon(4S)$ .

<sup>2</sup> Our second uncertainty combines systematics and model errors quoted in the paper.

$\Gamma(\bar{D}^0 \eta)/\Gamma_{total}$	$\Gamma_{126}/\Gamma$			
VALUE (units $10^{-4}$ )	CL%	DOCUMENT ID	TECN	COMMENT

<b>2.36 ± 0.32 OUR AVERAGE</b>		Error includes scale factor of 2.5.		
$2.53 \pm 0.09 \pm 0.11$		1 LEES	11M	BABR $e^+e^- \rightarrow \Upsilon(4S)$
$1.77 \pm 0.16 \pm 0.21$		1 BLYTH	06	BELL $e^+e^- \rightarrow \Upsilon(4S)$

• • • We do not use the following data for averages, fits, limits, etc. • • •

<sup>1</sup> AUBERT 04B BABR Repl. by LEES 11M

<sup>1</sup> ABE 02J BELL Repl. by BLYTH 06

<sup>2</sup> NEMAT 98 CLE2  $e^+e^- \rightarrow \Upsilon(4S)$

<sup>3</sup> ALAM 94 CLE2 Repl. by NEMAT 98

## Meson Particle Listings

 $B^0$ 

- <sup>1</sup> Assumes equal production of  $B^+$  and  $B^0$  at the  $\Upsilon(4S)$ .  
<sup>2</sup> NEMAT1 98 assumes equal production of  $B^+$  and  $B^0$  at the  $\Upsilon(4S)$  and use the PDG 96 values for  $D^0$ ,  $D^{*0}$ ,  $\eta$ ,  $\eta'$ , and  $\omega$  branching fractions.  
<sup>3</sup> ALAM 94 assume equal production of  $B^+$  and  $B^0$  at the  $\Upsilon(4S)$  and use the CLEOII absolute  $B(D^0 \rightarrow K^- \pi^+)$  and the PDG 1992  $B(D^0 \rightarrow K^- \pi^+ \pi^0)/B(D^0 \rightarrow K^- \pi^+)$  and  $B(D^0 \rightarrow K^- 2\pi^+ \pi^-)/B(D^0 \rightarrow K^- \pi^+)$ .

$\Gamma(D^0 \eta)/\Gamma_{total}$		$\Gamma_{127}/\Gamma$		
VALUE (units $10^{-4}$ )	CL%	DOCUMENT ID	TECN	COMMENT
<b><math>1.38 \pm 0.16</math></b>	<b>OUR AVERAGE</b>	Error includes scale factor of 1.3.		
$1.48 \pm 0.13 \pm 0.07$		<sup>1</sup> LEES	11M BABR	$e^+ e^- \rightarrow \Upsilon(4S)$
$1.14 \pm 0.20^{+0.10}_{-0.13}$		<sup>1</sup> SCHUMANN	05 BELL	$e^+ e^- \rightarrow \Upsilon(4S)$

- • • We do not use the following data for averages, fits, limits, etc. • • •
- |                       |    |                     |          |                                    |
|-----------------------|----|---------------------|----------|------------------------------------|
| $1.7 \pm 0.4 \pm 0.2$ |    | <sup>1</sup> AUBERT | 04B BABR | Repl. by LEES 11M                  |
| $<9.4$                | 90 | <sup>2</sup> NEMAT1 | 98 CLE2  | $e^+ e^- \rightarrow \Upsilon(4S)$ |
| $<8.6$                | 90 | <sup>3</sup> ALAM   | 94 CLE2  | Repl. by NEMAT1 98                 |

- <sup>1</sup> Assumes equal production of  $B^+$  and  $B^0$  at the  $\Upsilon(4S)$ .  
<sup>2</sup> NEMAT1 98 assumes equal production of  $B^+$  and  $B^0$  at the  $\Upsilon(4S)$  and use the PDG 96 values for  $D^0$ ,  $D^{*0}$ ,  $\eta$ ,  $\eta'$ , and  $\omega$  branching fractions.  
<sup>3</sup> ALAM 94 assume equal production of  $B^+$  and  $B^0$  at the  $\Upsilon(4S)$  and use the CLEOII absolute  $B(D^0 \rightarrow K^- \pi^+)$  and the PDG 1992  $B(D^0 \rightarrow K^- \pi^+ \pi^0)/B(D^0 \rightarrow K^- \pi^+)$  and  $B(D^0 \rightarrow K^- 2\pi^+ \pi^-)/B(D^0 \rightarrow K^- \pi^+)$ .

$\Gamma(D^0 \eta')/\Gamma(D^0 \eta)$		$\Gamma_{127}/\Gamma_{126}$		
VALUE		DOCUMENT ID	TECN	COMMENT
<b><math>0.54 \pm 0.07 \pm 0.01</math></b>		LEES	11M BABR	$e^+ e^- \rightarrow \Upsilon(4S)$
• • • We do not use the following data for averages, fits, limits, etc. • • •				
$0.7 \pm 0.2 \pm 0.1$		AUBERT	04B BABR	Repl. by LEES 11M

$\Gamma(D^0 \omega)/\Gamma_{total}$		$\Gamma_{128}/\Gamma$		
VALUE (units $10^{-4}$ )	CL%	DOCUMENT ID	TECN	COMMENT
<b><math>2.53 \pm 0.16</math></b>	<b>OUR AVERAGE</b>			
$2.57 \pm 0.11 \pm 0.14$		<sup>1</sup> LEES	11M BABR	$e^+ e^- \rightarrow \Upsilon(4S)$
$2.37 \pm 0.23 \pm 0.28$		<sup>1</sup> BLYTH	06 BELL	$e^+ e^- \rightarrow \Upsilon(4S)$
• • • We do not use the following data for averages, fits, limits, etc. • • •				
$3.0 \pm 0.3 \pm 0.4$		<sup>1</sup> AUBERT	04B BABR	Repl. by LEES 11M
$1.8 \pm 0.5^{+0.4}_{-0.3}$		<sup>1</sup> ABE	02J BELL	Repl. by BLYTH 06
$<5.1$	90	<sup>2</sup> NEMAT1	98 CLE2	$e^+ e^- \rightarrow \Upsilon(4S)$
$<6.3$	90	<sup>3</sup> ALAM	94 CLE2	Repl. by NEMAT1 98

- <sup>1</sup> Assumes equal production of  $B^+$  and  $B^0$  at the  $\Upsilon(4S)$ .  
<sup>2</sup> NEMAT1 98 assumes equal production of  $B^+$  and  $B^0$  at the  $\Upsilon(4S)$  and use the PDG 96 values for  $D^0$ ,  $D^{*0}$ ,  $\eta$ ,  $\eta'$ , and  $\omega$  branching fractions.  
<sup>3</sup> ALAM 94 assume equal production of  $B^+$  and  $B^0$  at the  $\Upsilon(4S)$  and use the CLEOII absolute  $B(D^0 \rightarrow K^- \pi^+)$  and the PDG 1992  $B(D^0 \rightarrow K^- \pi^+ \pi^0)/B(D^0 \rightarrow K^- \pi^+)$  and  $B(D^0 \rightarrow K^- 2\pi^+ \pi^-)/B(D^0 \rightarrow K^- \pi^+)$ .

$\Gamma(D^0 \phi)/\Gamma_{total}$		$\Gamma_{129}/\Gamma$		
VALUE (units $10^{-6}$ )	CL%	DOCUMENT ID	TECN	COMMENT
<b><math>&lt;11.6</math></b>	90	<sup>1</sup> AUBERT	07A0 BABR	$e^+ e^- \rightarrow \Upsilon(4S)$

- <sup>1</sup> Assumes equal production of  $B^+$  and  $B^0$  at the  $\Upsilon(4S)$ .

$\Gamma(D^0 K^+ \pi^-)/\Gamma_{total}$		$\Gamma_{130}/\Gamma$		
VALUE (units $10^{-6}$ )	CL%	DOCUMENT ID	TECN	COMMENT
• • • We do not use the following data for averages, fits, limits, etc. • • •				
$<19$	90	<sup>1</sup> AUBERT	06A BABR	Repl. by AUBERT 09AE

- <sup>1</sup> Assumes equal production of  $B^+$  and  $B^0$  at the  $\Upsilon(4S)$ .

$\Gamma(D^0 K^+ \pi^-)/\Gamma(D^0 K^+ \pi^-)$		$\Gamma_{130}/\Gamma_{119}$		
VALUE		DOCUMENT ID	TECN	COMMENT
<b><math>0.068 \pm 0.042</math></b>		<sup>1</sup> AUBERT	09AE BABR	$e^+ e^- \rightarrow \Upsilon(4S)$

- <sup>1</sup> Reports a signal at the level of 2.5 standard deviations after combining results from  $D^0 \rightarrow K^+ \pi^-$ ,  $K^+ \pi^- \pi^0$ , and  $K^+ \pi^- \pi^+ \pi^-$ .

$\Gamma(D^0 K^*(892)^0)/\Gamma_{total}$		$\Gamma_{131}/\Gamma$		
VALUE (units $10^{-5}$ )	CL%	DOCUMENT ID	TECN	COMMENT
<b><math>&lt;1.1</math></b>	90	<sup>1</sup> AUBERT,B	06L BABR	$e^+ e^- \rightarrow \Upsilon(4S)$
• • • We do not use the following data for averages, fits, limits, etc. • • •				
$<1.8$	90	<sup>1</sup> KROKOVNY	03 BELL	$e^+ e^- \rightarrow \Upsilon(4S)$

- <sup>1</sup> Assumes equal production of  $B^+$  and  $B^0$  at the  $\Upsilon(4S)$ .

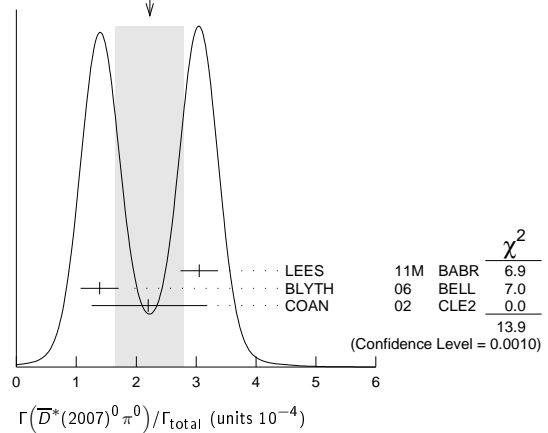
$\Gamma(D^{*0} \gamma)/\Gamma_{total}$		$\Gamma_{132}/\Gamma$		
VALUE	CL%	DOCUMENT ID	TECN	COMMENT
<b><math>&lt;2.5 \times 10^{-5}</math></b>	90	<sup>1</sup> AUBERT,B	05Q BABR	$e^+ e^- \rightarrow \Upsilon(4S)$
• • • We do not use the following data for averages, fits, limits, etc. • • •				
$<5.0 \times 10^{-5}$	90	<sup>1</sup> ARTUSO	00 CLE2	$e^+ e^- \rightarrow \Upsilon(4S)$

- <sup>1</sup> Assumes equal production of  $B^+$  and  $B^0$  at the  $\Upsilon(4S)$ .

 $\Gamma(D^{*0}(2007)^0 \pi^0)/\Gamma_{total}$   $\Gamma_{133}/\Gamma$ 

VALUE (units $10^{-4}$ )	CL%	DOCUMENT ID	TECN	COMMENT
<b><math>2.2 \pm 0.6</math></b>	<b>OUR AVERAGE</b>	Error includes scale factor of 2.6. See the ideogram below.		
$3.05 \pm 0.14 \pm 0.28$		<sup>1</sup> LEES	11M BABR	$e^+ e^- \rightarrow \Upsilon(4S)$
$1.39 \pm 0.18 \pm 0.26$		<sup>1</sup> BLYTH	06 BELL	$e^+ e^- \rightarrow \Upsilon(4S)$
$2.20^{+0.59}_{-0.52} \pm 0.79$		<sup>1</sup> COAN	02 CLE2	$e^+ e^- \rightarrow \Upsilon(4S)$
• • • We do not use the following data for averages, fits, limits, etc. • • •				
$2.9 \pm 0.4 \pm 0.5$		<sup>1</sup> AUBERT	04B BABR	Repl. by LEES 11M
$2.7 \pm 0.8^{+0.5}_{-0.6}$		<sup>1</sup> ABE	02J BELL	Repl. by BLYTH 06
$<4.4$	90	<sup>2</sup> NEMAT1	98 CLE2	Repl. by COAN 02
$<9.7$	90	<sup>3</sup> ALAM	94 CLE2	Repl. by NEMAT1 98

- <sup>1</sup> Assumes equal production of  $B^+$  and  $B^0$  at the  $\Upsilon(4S)$ .  
<sup>2</sup> NEMAT1 98 assumes equal production of  $B^+$  and  $B^0$  at the  $\Upsilon(4S)$  and use the PDG 96 values for  $D^0$ ,  $D^{*0}$ ,  $\eta$ ,  $\eta'$ , and  $\omega$  branching fractions.  
<sup>3</sup> ALAM 94 assume equal production of  $B^+$  and  $B^0$  at the  $\Upsilon(4S)$  and use the CLEOII  $B(D^{*0}(2007)^0 \rightarrow D^0 \pi^0)$  and absolute  $B(D^0 \rightarrow K^- \pi^+)$  and the PDG 1992  $B(D^0 \rightarrow K^- \pi^+ \pi^0)/B(D^0 \rightarrow K^- \pi^+)$  and  $B(D^0 \rightarrow K^- 2\pi^+ \pi^-)/B(D^0 \rightarrow K^- \pi^+)$ .

WEIGHTED AVERAGE  
2.2±0.6 (Error scaled by 2.6) $\Gamma(D^0 \pi^0)/\Gamma(D^{*0}(2007)^0 \pi^0)$   $\Gamma_{123}/\Gamma_{133}$ 

VALUE	CL%	DOCUMENT ID	TECN	COMMENT
<b><math>0.90 \pm 0.08</math></b>	<b>OUR AVERAGE</b>			
$0.88 \pm 0.05 \pm 0.06$		LEES	11M BABR	$e^+ e^- \rightarrow \Upsilon(4S)$
$1.62 \pm 0.23 \pm 0.35$		BLYTH	06 BELL	$e^+ e^- \rightarrow \Upsilon(4S)$
• • • We do not use the following data for averages, fits, limits, etc. • • •				
$1.0 \pm 0.1 \pm 0.2$		AUBERT	04B BABR	Repl. by LEES 11M

 $\Gamma(D^{*0}(2007)^0 \rho^0)/\Gamma_{total}$   $\Gamma_{134}/\Gamma$ 

VALUE	CL%	DOCUMENT ID	TECN	COMMENT
<b><math>&lt;5.1 \times 10^{-4}</math></b>	90	<sup>1</sup> SATPATHY	03 BELL	$e^+ e^- \rightarrow \Upsilon(4S)$
• • • We do not use the following data for averages, fits, limits, etc. • • •				
$<0.00056$	90	<sup>2</sup> NEMAT1	98 CLE2	$e^+ e^- \rightarrow \Upsilon(4S)$
$<0.00117$	90	<sup>3</sup> ALAM	94 CLE2	Repl. by NEMAT1 98

- <sup>1</sup> Assumes equal production of  $B^+$  and  $B^0$  at the  $\Upsilon(4S)$ .  
<sup>2</sup> NEMAT1 98 assumes equal production of  $B^+$  and  $B^0$  at the  $\Upsilon(4S)$  and use the PDG 96 values for  $D^0$ ,  $D^{*0}$ ,  $\eta$ ,  $\eta'$ , and  $\omega$  branching fractions.  
<sup>3</sup> ALAM 94 assume equal production of  $B^+$  and  $B^0$  at the  $\Upsilon(4S)$  and use the CLEOII  $B(D^{*0}(2007)^0 \rightarrow D^0 \pi^0)$  and absolute  $B(D^0 \rightarrow K^- \pi^+)$  and the PDG 1992  $B(D^0 \rightarrow K^- \pi^+ \pi^0)/B(D^0 \rightarrow K^- \pi^+)$  and  $B(D^0 \rightarrow K^- 2\pi^+ \pi^-)/B(D^0 \rightarrow K^- \pi^+)$ .

 $\Gamma(D^{*0}(2007)^0 \eta)/\Gamma_{total}$   $\Gamma_{135}/\Gamma$ 

VALUE (units $10^{-4}$ )	CL%	DOCUMENT ID	TECN	COMMENT
<b><math>2.3 \pm 0.6</math></b>	<b>OUR AVERAGE</b>	Error includes scale factor of 2.8.		
$2.69 \pm 0.14 \pm 0.23$		<sup>1</sup> LEES	11M BABR	$e^+ e^- \rightarrow \Upsilon(4S)$
$1.40 \pm 0.28 \pm 0.26$		<sup>1</sup> BLYTH	06 BELL	$e^+ e^- \rightarrow \Upsilon(4S)$
• • • We do not use the following data for averages, fits, limits, etc. • • •				
$2.6 \pm 0.4 \pm 0.4$		<sup>1</sup> AUBERT	04B BABR	Repl. by LEES 11M
$<4.6$	90	<sup>1</sup> ABE	02J BELL	$e^+ e^- \rightarrow \Upsilon(4S)$
$<2.6$	90	<sup>2</sup> NEMAT1	98 CLE2	$e^+ e^- \rightarrow \Upsilon(4S)$
$<6.9$	90	<sup>3</sup> ALAM	94 CLE2	Repl. by NEMAT1 98

- <sup>1</sup> Assumes equal production of  $B^+$  and  $B^0$  at the  $\Upsilon(4S)$ .  
<sup>2</sup> NEMAT1 98 assumes equal production of  $B^+$  and  $B^0$  at the  $\Upsilon(4S)$  and use the PDG 96 values for  $D^0$ ,  $D^{*0}$ ,  $\eta$ ,  $\eta'$ , and  $\omega$  branching fractions.  
<sup>3</sup> ALAM 94 assume equal production of  $B^+$  and  $B^0$  at the  $\Upsilon(4S)$  and use the CLEOII  $B(D^{*0}(2007)^0 \rightarrow D^0 \pi^0)$  and absolute  $B(D^0 \rightarrow K^- \pi^+)$  and the PDG 1992  $B(D^0 \rightarrow K^- \pi^+ \pi^0)/B(D^0 \rightarrow K^- \pi^+)$  and  $B(D^0 \rightarrow K^- 2\pi^+ \pi^-)/B(D^0 \rightarrow K^- \pi^+)$ .

$\Gamma(\bar{D}^0\eta)/\Gamma(\bar{D}^*(2007)^0\eta)$   $\Gamma_{126}/\Gamma_{135}$ 

VALUE	DOCUMENT ID	TECN	COMMENT
<b>0.99±0.10 OUR AVERAGE</b>			
0.97±0.07±0.07	LEES	11M	BABR $e^+e^- \rightarrow \Upsilon(4S)$
1.27±0.29±0.25	BLYTH	06	BELL $e^+e^- \rightarrow \Upsilon(4S)$
••• We do not use the following data for averages, fits, limits, etc. •••			
0.9 ± 0.2 ± 0.1	AUBERT	04B	BABR Repl. by LEES 11M

 $\Gamma(\bar{D}^*(2007)^0\eta')/\Gamma(\bar{D}^*(2007)^0\eta)$   $\Gamma_{136}/\Gamma_{135}$ 

VALUE	DOCUMENT ID	TECN	COMMENT
<b>0.61±0.14±0.02</b>			
1.21±0.34±0.22	LEES	11M	BABR $e^+e^- \rightarrow \Upsilon(4S)$
••• We do not use the following data for averages, fits, limits, etc. •••			
0.5 ± 0.3 ± 0.1	AUBERT	04B	BABR Repl. by LEES 11M

 $\Gamma(\bar{D}^*(2007)^0\eta')/\Gamma_{total}$   $\Gamma_{136}/\Gamma$ 

VALUE (units $10^{-4}$ )	CL%	DOCUMENT ID	TECN	COMMENT
<b>1.40±0.22 OUR AVERAGE</b>				
1.48±0.22±0.13		<sup>1</sup> LEES	11M	BABR $e^+e^- \rightarrow \Upsilon(4S)$
1.21±0.34±0.22		<sup>1</sup> SCHUMANN	05	BELL $e^+e^- \rightarrow \Upsilon(4S)$
••• We do not use the following data for averages, fits, limits, etc. •••				
1.3 ± 0.7 ± 0.2		<sup>1,2</sup> AUBERT	04B	BABR Repl. by LEES 11M
<14	90	BRANDENB...	98	CLE2 $e^+e^- \rightarrow \Upsilon(4S)$
<19	90	<sup>3</sup> NEMAT1	98	CLE2 $e^+e^- \rightarrow \Upsilon(4S)$
<27	90	<sup>4</sup> ALAM	94	CLE2 Repl. by NEMAT1 98

- Assumes equal production of  $B^+$  and  $B^0$  at the  $\Upsilon(4S)$ .
- Reports an upper limit  $< 2.6 \times 10^{-4}$  at 90% CL.
- NEMAT1 98 assumes equal production of  $B^+$  and  $B^0$  at the  $\Upsilon(4S)$  and use the PDG 96 values for  $D^0$ ,  $D^{*0}$ ,  $\eta$ ,  $\eta'$ , and  $\omega$  branching fractions.
- ALAM 94 assume equal production of  $B^+$  and  $B^0$  at the  $\Upsilon(4S)$  and use the CLEO11  $B(D^{*0}(2007)^0 \rightarrow D^0\pi^0)$  and absolute  $B(D^0 \rightarrow K^-\pi^+)$  and the PDG 1992  $B(D^0 \rightarrow K^-\pi^+\pi^0)/B(D^0 \rightarrow K^-\pi^+)$  and  $B(D^0 \rightarrow K^-\pi^+\pi^-)/B(D^0 \rightarrow K^-\pi^+)$ .

 $\Gamma(\bar{D}^0\eta')/\Gamma(\bar{D}^*(2007)^0\eta')$   $\Gamma_{127}/\Gamma_{136}$ 

VALUE	DOCUMENT ID	TECN	COMMENT
<b>0.96±0.18±0.06</b>			
0.97±0.07±0.07	LEES	11M	BABR $e^+e^- \rightarrow \Upsilon(4S)$
••• We do not use the following data for averages, fits, limits, etc. •••			
1.3 ± 0.8 ± 0.2	AUBERT	04B	BABR Repl. by LEES 11M

 $\Gamma(\bar{D}^*(2007)^0\pi^+\pi^-)/\Gamma_{total}$   $\Gamma_{137}/\Gamma$ 

VALUE	DOCUMENT ID	TECN	COMMENT
<b>(6.2±1.2±1.8) × 10<sup>-4</sup></b>			
1.2 SATPATHY	03	BELL	$e^+e^- \rightarrow \Upsilon(4S)$
<sup>1</sup> Assumes equal production of $B^+$ and $B^0$ at the $\Upsilon(4S)$ .			
<sup>2</sup> No assumption about the intermediate mechanism is made in the analysis.			

 $\Gamma(\bar{D}^*(2007)^0K^0)/\Gamma_{total}$   $\Gamma_{138}/\Gamma$ 

VALUE (units $10^{-5}$ )	CL%	DOCUMENT ID	TECN	COMMENT
<b>3.6±1.2±0.3</b>				
3.6 ± 1.2 ± 0.3		<sup>1</sup> AUBERT,B	06L	BABR $e^+e^- \rightarrow \Upsilon(4S)$
••• We do not use the following data for averages, fits, limits, etc. •••				
<6.6	90	<sup>1</sup> KROKOVNY	03	BELL $e^+e^- \rightarrow \Upsilon(4S)$
<sup>1</sup> Assumes equal production of $B^+$ and $B^0$ at the $\Upsilon(4S)$ .				

 $\Gamma(\bar{D}^*(2007)^0K^*(892)^0)/\Gamma_{total}$   $\Gamma_{139}/\Gamma$ 

VALUE	CL%	DOCUMENT ID	TECN	COMMENT
<b>&lt;6.9 × 10<sup>-5</sup></b>				
<6.9 × 10 <sup>-5</sup>	90	<sup>1</sup> KROKOVNY	03	BELL $e^+e^- \rightarrow \Upsilon(4S)$
<sup>1</sup> Assumes equal production of $B^+$ and $B^0$ at the $\Upsilon(4S)$ .				

 $\Gamma(D^*(2007)^0K^*(892)^0)/\Gamma_{total}$   $\Gamma_{140}/\Gamma$ 

VALUE	CL%	DOCUMENT ID	TECN	COMMENT
<b>&lt;4.0 × 10<sup>-5</sup></b>				
<4.0 × 10 <sup>-5</sup>	90	<sup>1</sup> KROKOVNY	03	BELL $e^+e^- \rightarrow \Upsilon(4S)$
<sup>1</sup> Assumes equal production of $B^+$ and $B^0$ at the $\Upsilon(4S)$ .				

 $\Gamma(D^*(2007)^0\pi^+\pi^-\pi^-)/\Gamma_{total}$   $\Gamma_{141}/\Gamma$ 

VALUE (units $10^{-3}$ )	DOCUMENT ID	TECN	COMMENT
<b>2.7 ± 0.5 OUR AVERAGE</b>			
2.60±0.47±0.37	<sup>1</sup> MAJUMDER	04	BELL $e^+e^- \rightarrow \Upsilon(4S)$
3.0 ± 0.7 ± 0.6	<sup>1</sup> EDWARDS	02	CLE2 $e^+e^- \rightarrow \Upsilon(4S)$
<sup>1</sup> Assumes equal production of $B^+$ and $B^0$ at the $\Upsilon(4S)$ .			

 $\Gamma(D^*(2007)^0\pi^+\pi^-\pi^-)/\Gamma(D^*(2010)^-\pi^+\pi^-\pi^0)$   $\Gamma_{141}/\Gamma_{56}$ 

VALUE	DOCUMENT ID	TECN	COMMENT
<b>0.17±0.04±0.02</b>			
0.17±0.04±0.02	<sup>1</sup> EDWARDS	02	CLE2 $e^+e^- \rightarrow \Upsilon(4S)$
<sup>1</sup> Assumes equal production of $B^+$ and $B^0$ at the $\Upsilon(4S)$ .			

 $\Gamma(D^*(2010)^+D^*(2010)^-)/\Gamma_{total}$   $\Gamma_{142}/\Gamma$ 

VALUE (units $10^{-4}$ )	CL%	DOCUMENT ID	TECN	COMMENT
<b>8.2±0.9 OUR AVERAGE</b>				
8.1±0.6±1.0		<sup>1</sup> AUBERT,B	06A	BABR $e^+e^- \rightarrow \Upsilon(4S)$
8.1±0.8±1.1		<sup>1</sup> MIYAKE	05	BELL $e^+e^- \rightarrow \Upsilon(4S)$
9.9 <sup>+4.2</sup> <sub>-3.3</sub> ±1.2		<sup>1</sup> LIPELES	00	CLE2 $e^+e^- \rightarrow \Upsilon(4S)$
••• We do not use the following data for averages, fits, limits, etc. •••				
8.3±1.6±1.2		<sup>1,2</sup> AUBERT	02M	BABR Repl. by AUBERT,B 06B
6.2 <sup>+4.0</sup> <sub>-2.9</sub> ±1.0		<sup>3</sup> ARTUSO	99	CLE2 Repl. by LIPELES 00
<61	90	<sup>4</sup> BARATE	98Q	ALEP $e^+e^- \rightarrow Z$
<22	90	<sup>5</sup> ASNER	97	CLE2 Repl. by ARTUSO 99

- Assumes equal production of  $B^+$  and  $B^0$  at the  $\Upsilon(4S)$ .
- AUBERT 02M also assumes the measured CP-odd fraction of the final states is  $0.22 \pm 0.18 \pm 0.03$ .
- ARTUSO 99 uses  $B(\Upsilon(4S) \rightarrow B^0\bar{B}^0) = (48 \pm 4)\%$ .
- BARATE 98Q (ALEPH) observes 2 events with an expected background of  $0.10 \pm 0.03$  which corresponds to a branching ratio of  $(2.3 \pm 1.9 \pm 0.4) \times 10^{-3}$ .
- ASNER 97 at CLEO observes 1 event with an expected background of  $0.022 \pm 0.011$ . This corresponds to a branching ratio of  $(5.3 \pm 7.1 \pm 1.0) \times 10^{-4}$ .

 $\Gamma(\bar{D}^*(2007)^0\omega)/\Gamma_{total}$   $\Gamma_{143}/\Gamma$ 

VALUE (units $10^{-4}$ )	CL%	DOCUMENT ID	TECN	COMMENT
<b>3.6 ± 1.1 OUR AVERAGE</b>				Error includes scale factor of 3.1.
4.55±0.24±0.39		<sup>1</sup> LEES	11M	BABR $e^+e^- \rightarrow \Upsilon(4S)$
2.29±0.39±0.40		<sup>1</sup> BLYTH	06	BELL $e^+e^- \rightarrow \Upsilon(4S)$
••• We do not use the following data for averages, fits, limits, etc. •••				
4.2 ± 0.7 ± 0.9	90	<sup>1</sup> AUBERT	04B	BABR Repl. by LEES 11M
< 7.9	90	<sup>1</sup> ABE	02J	BELL $e^+e^- \rightarrow \Upsilon(4S)$
< 7.4	90	<sup>2</sup> NEMAT1	98	CLE2 $e^+e^- \rightarrow \Upsilon(4S)$
<21	90	<sup>3</sup> ALAM	94	CLE2 Repl. by NEMAT1 98

- Assumes equal production of  $B^+$  and  $B^0$  at the  $\Upsilon(4S)$ .
- NEMAT1 98 assumes equal production of  $B^+$  and  $B^0$  at the  $\Upsilon(4S)$  and use the PDG 96 values for  $D^0$ ,  $D^{*0}$ ,  $\eta$ ,  $\eta'$ , and  $\omega$  branching fractions.
- ALAM 94 assume equal production of  $B^+$  and  $B^0$  at the  $\Upsilon(4S)$  and use the CLEO11  $B(D^*(2007)^0 \rightarrow D^0\pi^0)$  and absolute  $B(D^0 \rightarrow K^-\pi^+)$  and the PDG 1992  $B(D^0 \rightarrow K^-\pi^+\pi^0)/B(D^0 \rightarrow K^-\pi^+)$  and  $B(D^0 \rightarrow K^-\pi^+\pi^-)/B(D^0 \rightarrow K^-\pi^+)$ .

 $\Gamma(\bar{D}^0\omega)/\Gamma(\bar{D}^*(2007)^0\omega)$   $\Gamma_{128}/\Gamma_{143}$ 

VALUE	DOCUMENT ID	TECN	COMMENT
<b>0.58±0.06 OUR AVERAGE</b>			
0.56±0.04±0.04	LEES	11M	BABR $e^+e^- \rightarrow \Upsilon(4S)$
1.04±0.20±0.17	BLYTH	06	BELL $e^+e^- \rightarrow \Upsilon(4S)$
••• We do not use the following data for averages, fits, limits, etc. •••			
0.7 ± 0.1 ± 0.1	AUBERT	04B	BABR Repl. by LEES 11M

 $\Gamma(D^*(2010)^+D^-)/\Gamma_{total}$   $\Gamma_{144}/\Gamma$ 

VALUE (units $10^{-4}$ )	CL%	DOCUMENT ID	TECN	COMMENT
<b>6.1±1.5 OUR AVERAGE</b>				Error includes scale factor of 1.6.
5.7±0.7±0.7		<sup>1</sup> AUBERT,B	06A	BABR $e^+e^- \rightarrow \Upsilon(4S)$
11.7±2.6 <sup>+2.2</sup> <sub>-2.5</sub>		<sup>1,2</sup> ABE	02Q	BELL $e^+e^- \rightarrow \Upsilon(4S)$
••• We do not use the following data for averages, fits, limits, etc. •••				
8.8±1.0±1.3		<sup>1</sup> AUBERT	03J	BABR Repl. by AUBERT,B 06B
14.8±3.8 <sup>+2.8</sup> <sub>-3.1</sub>		<sup>1,3</sup> ABE	02Q	BELL $e^+e^- \rightarrow \Upsilon(4S)$
< 6.3	90	<sup>1</sup> LIPELES	00	CLE2 $e^+e^- \rightarrow \Upsilon(4S)$
<56	90	BARATE	98Q	ALEP $e^+e^- \rightarrow Z$
<18	90	ASNER	97	CLE2 $e^+e^- \rightarrow \Upsilon(4S)$

- Assumes equal production of  $B^+$  and  $B^0$  at the  $\Upsilon(4S)$ .
- The measurement is performed using fully reconstructed  $D^*$  and  $D^+$  decays.
- The measurement is performed using a partial reconstruction technique for the  $D^*$  and fully reconstructed  $D^+$  decays as a cross check.

 $\Gamma(D^*(2007)^0\bar{D}^*(2007)^0)/\Gamma_{total}$   $\Gamma_{145}/\Gamma$ 

VALUE (units $10^{-4}$ )	CL%	DOCUMENT ID	TECN	COMMENT
<b>&lt; 0.9</b>				
< 0.9	90	<sup>1</sup> AUBERT,B	06A	BABR $e^+e^- \rightarrow \Upsilon(4S)$
••• We do not use the following data for averages, fits, limits, etc. •••				
<270	90	BARATE	98Q	ALEP $e^+e^- \rightarrow Z$
<sup>1</sup> Assumes equal production of $B^+$ and $B^0$ at the $\Upsilon(4S)$ .				

 $\Gamma(D^-D^0K^+)/\Gamma_{total}$   $\Gamma_{146}/\Gamma$ 

VALUE (units $10^{-3}$ )	DOCUMENT ID	TECN	COMMENT
<b>1.07±0.07±0.09</b>			
1.07±0.07±0.09	<sup>1</sup> DEL-AMO-SA...	11B	BABR $e^+e^- \rightarrow \Upsilon(4S)$
••• We do not use the following data for averages, fits, limits, etc. •••			
1.7 ± 0.3 ± 0.3	<sup>1</sup> AUBERT	03X	BABR Repl. by DEL-AMO-SANCHEZ 11B

- Assumes equal production of  $B^+$  and  $B^0$  at the  $\Upsilon(4S)$ .

## Meson Particle Listings

 $B^0$  $\Gamma(D^- D^*(2007)^0 K^+)/\Gamma_{\text{total}}$   $\Gamma_{147}/\Gamma$ 

VALUE (units $10^{-3}$ )	DOCUMENT ID	TECN	COMMENT
<b>3.46 ± 0.18 ± 0.37</b>	<sup>1</sup> DEL-AMO-SA...11B	BABR	$e^+ e^- \rightarrow \Upsilon(4S)$
• • • We do not use the following data for averages, fits, limits, etc. • • •			
4.6 ± 0.7 ± 0.7	<sup>1</sup> AUBERT	03x BABR	Repl. by DEL-AMO-SANCHEZ 11B

<sup>1</sup> Assumes equal production of  $B^+$  and  $B^0$  at the  $\Upsilon(4S)$ . $\Gamma(D^*(2010)^- D^0 K^+)/\Gamma_{\text{total}}$   $\Gamma_{148}/\Gamma$ 

VALUE (units $10^{-3}$ )	DOCUMENT ID	TECN	COMMENT
<b>2.47 ± 0.10 ± 0.18</b>	<sup>1</sup> DEL-AMO-SA...11B	BABR	$e^+ e^- \rightarrow \Upsilon(4S)$
• • • We do not use the following data for averages, fits, limits, etc. • • •			
3.1 $^{+0.4}_{-0.3}$ ± 0.4	<sup>1</sup> AUBERT	03x BABR	Repl. by DEL-AMO-SANCHEZ 11B

<sup>1</sup> Assumes equal production of  $B^+$  and  $B^0$  at the  $\Upsilon(4S)$ . $\Gamma(D^*(2010)^- D^*(2007)^0 K^+)/\Gamma_{\text{total}}$   $\Gamma_{149}/\Gamma$ 

VALUE (units $10^{-3}$ )	DOCUMENT ID	TECN	COMMENT
<b>10.6 ± 0.33 ± 0.86</b>	<sup>1</sup> DEL-AMO-SA...11B	BABR	$e^+ e^- \rightarrow \Upsilon(4S)$
• • • We do not use the following data for averages, fits, limits, etc. • • •			
11.8 ± 1.0 ± 1.7	<sup>1</sup> AUBERT	03x BABR	Repl. by DEL-AMO-SANCHEZ 11B

<sup>1</sup> Assumes equal production of  $B^+$  and  $B^0$  at the  $\Upsilon(4S)$ . $\Gamma(D^- D^+ K^0)/\Gamma_{\text{total}}$   $\Gamma_{150}/\Gamma$ 

VALUE (units $10^{-3}$ )	CL%	DOCUMENT ID	TECN	COMMENT
<b>0.75 ± 0.12 ± 0.12</b>		<sup>1</sup> DEL-AMO-SA...11B	BABR	$e^+ e^- \rightarrow \Upsilon(4S)$
• • • We do not use the following data for averages, fits, limits, etc. • • •				
<1.7	90	<sup>1</sup> AUBERT	03x BABR	Repl. by DEL-AMO-SANCHEZ 11B

<sup>1</sup> Assumes equal production of  $B^+$  and  $B^0$  at the  $\Upsilon(4S)$ . $[\Gamma(D^*(2010)^- D^+ K^0) + \Gamma(D^- D^*(2010)^+ K^0)]/\Gamma_{\text{total}}$   $\Gamma_{151}/\Gamma$ 

VALUE (units $10^{-3}$ )	DOCUMENT ID	TECN	COMMENT
<b>6.41 ± 0.36 ± 0.39</b>	<sup>1</sup> DEL-AMO-SA...11B	BABR	$e^+ e^- \rightarrow \Upsilon(4S)$
• • • We do not use the following data for averages, fits, limits, etc. • • •			
6.5 ± 1.2 ± 1.0	<sup>1</sup> AUBERT	03x BABR	Repl. by DEL-AMO-SANCHEZ 11B

<sup>1</sup> Assumes equal production of  $B^+$  and  $B^0$  at the  $\Upsilon(4S)$ . $\Gamma(D^*(2010)^- D^*(2010)^+ K^0)/\Gamma_{\text{total}}$   $\Gamma_{152}/\Gamma$ 

VALUE (units $10^{-3}$ )	DOCUMENT ID	TECN	COMMENT
<b>8.1 ± 0.7 OUR AVERAGE</b>			
8.26 ± 0.43 ± 0.67	<sup>1</sup> DEL-AMO-SA...11B	BABR	$e^+ e^- \rightarrow \Upsilon(4S)$
6.8 ± 0.8 ± 1.4	<sup>1,2</sup> DALSENO	07 BELL	$e^+ e^- \rightarrow \Upsilon(4S)$
8.8 ± 0.8 ± 1.4	<sup>1,2</sup> AUBERT,B	06q BABR	$e^+ e^- \rightarrow \Upsilon(4S)$
• • • We do not use the following data for averages, fits, limits, etc. • • •			
8.8 $^{+1.5}_{-1.4}$ ± 1.3	<sup>1</sup> AUBERT	03x BABR	Repl. by AUBERT,B 06q

<sup>1</sup> Assumes equal production of  $B^+$  and  $B^0$  at the  $\Upsilon(4S)$ .<sup>2</sup> The result is rescaled by a factor of 2 to convert from  $K_S^0$  to  $K^0$ . $\Gamma(D^* D_{s1}(2536)^+ \times B(D_{s1}(2536)^+ \rightarrow D^* K^0))/\Gamma_{\text{total}}$   $\Gamma_{153}/\Gamma$ 

VALUE (units $10^{-4}$ )	DOCUMENT ID	TECN	COMMENT
<b>8.0 ± 2.4 OUR AVERAGE</b>			
7.6 $^{+4.8+1.6}_{-4.2-1.4}$	<sup>1,2</sup> DALSENO	07 BELL	$e^+ e^- \rightarrow \Upsilon(4S)$
8.2 ± 2.6 ± 1.2	<sup>1,2</sup> AUBERT,B	06q BABR	$e^+ e^- \rightarrow \Upsilon(4S)$

<sup>1</sup> Assumes equal production of  $B^+$  and  $B^0$  at the  $\Upsilon(4S)$ .<sup>2</sup> The result is rescaled by a factor of 2 to convert from  $K_S^0$  to  $K^0$ . $\Gamma(D^0 D^0 K^0)/\Gamma_{\text{total}}$   $\Gamma_{154}/\Gamma$ 

VALUE (units $10^{-3}$ )	CL%	DOCUMENT ID	TECN	COMMENT
<b>0.27 ± 0.10 ± 0.05</b>		<sup>1</sup> DEL-AMO-SA...11B	BABR	$e^+ e^- \rightarrow \Upsilon(4S)$
• • • We do not use the following data for averages, fits, limits, etc. • • •				
<1.4	90	<sup>1</sup> AUBERT	03x BABR	Repl. by DEL-AMO-SANCHEZ 11B

<sup>1</sup> Assumes equal production of  $B^+$  and  $B^0$  at the  $\Upsilon(4S)$ . $[\Gamma(D^0 D^*(2007)^0 K^0) + \Gamma(D^*(2007)^0 D^0 K^0)]/\Gamma_{\text{total}}$   $\Gamma_{155}/\Gamma$ 

VALUE (units $10^{-3}$ )	CL%	DOCUMENT ID	TECN	COMMENT
<b>1.08 ± 0.32 ± 0.36</b>		<sup>1</sup> DEL-AMO-SA...11B	BABR	$e^+ e^- \rightarrow \Upsilon(4S)$
• • • We do not use the following data for averages, fits, limits, etc. • • •				
<3.7	90	<sup>1</sup> AUBERT	03x BABR	Repl. by DEL-AMO-SANCHEZ 11B

<sup>1</sup> Assumes equal production of  $B^+$  and  $B^0$  at the  $\Upsilon(4S)$ . $\Gamma(\bar{D}^*(2007)^0 D^*(2007)^0 K^0)/\Gamma_{\text{total}}$   $\Gamma_{156}/\Gamma$ 

VALUE (units $10^{-3}$ )	CL%	DOCUMENT ID	TECN	COMMENT
<b>2.40 ± 0.55 ± 0.67</b>		<sup>1</sup> DEL-AMO-SA...11B	BABR	$e^+ e^- \rightarrow \Upsilon(4S)$
• • • We do not use the following data for averages, fits, limits, etc. • • •				
<6.6	90	<sup>1</sup> AUBERT	03x BABR	Repl. by DEL-AMO-SANCHEZ 11B

<sup>1</sup> Assumes equal production of  $B^+$  and  $B^0$  at the  $\Upsilon(4S)$ . $\Gamma((\bar{D} + \bar{D}^*)(D + D^*)K)/\Gamma_{\text{total}}$   $\Gamma_{157}/\Gamma$ 

VALUE (units $10^{-2}$ )	DOCUMENT ID	TECN	COMMENT
<b>3.68 ± 0.10 ± 0.24</b>	<sup>1</sup> DEL-AMO-SA...11B	BABR	$e^+ e^- \rightarrow \Upsilon(4S)$
• • • We do not use the following data for averages, fits, limits, etc. • • •			
4.3 ± 0.3 ± 0.6	<sup>1</sup> AUBERT	03x BABR	Repl. by DEL-AMO-SANCHEZ 11B

<sup>1</sup> Assumes equal production of  $B^+$  and  $B^0$  at the  $\Upsilon(4S)$ . $\Gamma(\eta_c K^0)/\Gamma_{\text{total}}$   $\Gamma_{158}/\Gamma$ 

VALUE (units $10^{-3}$ )	DOCUMENT ID	TECN	COMMENT
<b>0.83 ± 0.12 OUR AVERAGE</b>			
0.59 $^{+0.20}_{-0.19}$ ± 0.07	<sup>1,2</sup> AUBERT	07AV BABR	$e^+ e^- \rightarrow \Upsilon(4S)$
0.91 ± 0.15 $^{+0.08}_{-0.07}$	<sup>1,3</sup> AUBERT,B	04B BABR	$e^+ e^- \rightarrow \Upsilon(4S)$
1.23 ± 0.23 $^{+0.40}_{-0.41}$	<sup>1</sup> FANG	03 BELL	$e^+ e^- \rightarrow \Upsilon(4S)$
1.09 $^{+0.55}_{-0.42}$ ± 0.33	<sup>4</sup> EDWARDS	01 CLE2	$e^+ e^- \rightarrow \Upsilon(4S)$

<sup>1</sup> Assumes equal production of  $B^+$  and  $B^0$  at the  $\Upsilon(4S)$ .<sup>2</sup> AUBERT 07AV reports  $[\Gamma(B^0 \rightarrow \eta_c K^0)/\Gamma_{\text{total}}] \times [B(\eta_c(1S) \rightarrow p\bar{p})] = (0.83 \pm 0.28 \pm 0.05) \times 10^{-6}$  which we divide by our best value  $B(\eta_c(1S) \rightarrow p\bar{p}) = (1.41 \pm 0.17) \times 10^{-3}$ . Our first error is their experiment's error and our second error is the systematic error from using our best value.<sup>3</sup> AUBERT,B 04B reports  $[\Gamma(B^0 \rightarrow \eta_c K^0)/\Gamma_{\text{total}}] \times [B(\eta_c(1S) \rightarrow K\bar{K}\pi)] = (0.0648 \pm 0.0085 \pm 0.0071) \times 10^{-3}$  which we divide by our best value  $B(\eta_c(1S) \rightarrow K\bar{K}\pi) = (7.2 \pm 0.6) \times 10^{-2}$ . Our first error is their experiment's error and our second error is the systematic error from using our best value.<sup>4</sup> EDWARDS 01 assumes equal production of  $B^0$  and  $B^+$  at the  $\Upsilon(4S)$ . The correlated uncertainties (28.3)% from  $B(J/\psi(1S) \rightarrow \gamma\eta_c)$  in those modes have been accounted for. $\Gamma(\eta_c K^0)/\Gamma(J/\psi(1S) K^0)$   $\Gamma_{158}/\Gamma_{162}$ 

VALUE	DOCUMENT ID	TECN	COMMENT
<b>1.39 ± 0.20 ± 0.45</b>	<sup>1</sup> AUBERT,B	04B BABR	$e^+ e^- \rightarrow \Upsilon(4S)$

<sup>1</sup> Uses BABAR measurement of  $B(B^0 \rightarrow J/\psi K^0) = (8.5 \pm 0.5 \pm 0.6) \times 10^{-4}$ . $\Gamma(\eta_c K^*(892)^0)/\Gamma_{\text{total}}$   $\Gamma_{159}/\Gamma$ 

VALUE (units $10^{-3}$ )	DOCUMENT ID	TECN	COMMENT
<b>0.64 ± 0.09 OUR AVERAGE</b>			
0.60 ± 0.08 ± 0.07	<sup>1,2</sup> AUBERT	08AB BABR	$e^+ e^- \rightarrow \Upsilon(4S)$
0.73 $^{+0.23}_{-0.21}$ ± 0.09	<sup>3,4</sup> AUBERT	07AV BABR	$e^+ e^- \rightarrow \Upsilon(4S)$
1.62 ± 0.32 $^{+0.55}_{-0.60}$	<sup>4</sup> FANG	03 BELL	$e^+ e^- \rightarrow \Upsilon(4S)$

<sup>1</sup> AUBERT 08AB reports  $[\Gamma(B^0 \rightarrow \eta_c K^*(892)^0)/\Gamma_{\text{total}}] / [B(B^+ \rightarrow \eta_c K^+)] = 0.62 \pm 0.06 \pm 0.05$  which we multiply by our best value  $B(B^+ \rightarrow \eta_c K^+) = (9.6 \pm 1.2) \times 10^{-4}$ . Our first error is their experiment's error and our second error is the systematic error from using our best value.<sup>2</sup> Uses the production ratio of  $(B^+ B^-)/(B^0 \bar{B}^0) = 1.026 \pm 0.032$  at  $\Upsilon(4S)$ .<sup>3</sup> AUBERT 07AV reports  $[\Gamma(B^0 \rightarrow \eta_c K^*(892)^0)/\Gamma_{\text{total}}] \times [B(\eta_c(1S) \rightarrow p\bar{p})] = (1.03 \pm 0.27 \pm 0.24) \times 10^{-6}$  which we divide by our best value  $B(\eta_c(1S) \rightarrow p\bar{p}) = (1.41 \pm 0.17) \times 10^{-3}$ . Our first error is their experiment's error and our second error is the systematic error from using our best value.<sup>4</sup> Assumes equal production of  $B^+$  and  $B^0$  at the  $\Upsilon(4S)$ . $\Gamma(\eta_c(2S) K^0)/\Gamma_{\text{total}}$   $\Gamma_{160}/\Gamma$ 

VALUE (units $10^{-4}$ )	CL%	DOCUMENT ID	TECN	COMMENT
<b>&lt;3.9</b>	90	<sup>1</sup> AUBERT	08AB BABR	$e^+ e^- \rightarrow \Upsilon(4S)$

<sup>1</sup> Uses the production ratio of  $(B^+ B^-)/(B^0 \bar{B}^0) = 1.026 \pm 0.032$  at  $\Upsilon(4S)$ . $\Gamma(B^0 \rightarrow h_c(1P) K^0)/\Gamma_{\text{total}} \times \Gamma(h_c(1P) \rightarrow \eta_c(1S)\gamma)/\Gamma_{\text{total}}$  $\Gamma_{161}/\Gamma \times \Gamma_{164}^{h_c(1P)}/\Gamma_{h_c(1P)}$ 

VALUE (units $10^{-4}$ )	CL%	DOCUMENT ID	TECN	COMMENT
<b>&lt;2.2</b>	90	<sup>1</sup> AUBERT	08AB BABR	$e^+ e^- \rightarrow \Upsilon(4S)$

<sup>1</sup> Uses the production ratio of  $(B^+ B^-)/(B^0 \bar{B}^0) = 1.026 \pm 0.032$  at  $\Upsilon(4S)$ . $\Gamma(\eta_c K^*(892)^0)/\Gamma(\eta_c K^0)$   $\Gamma_{159}/\Gamma_{158}$ 

VALUE	DOCUMENT ID	TECN	COMMENT
<b>1.33 ± 0.36 <math>^{+0.24}_{-0.33}</math></b>	FANG	03 BELL	$e^+ e^- \rightarrow \Upsilon(4S)$

See key on page 457

# Meson Particle Listings

$B^0$

## $\Gamma(J/\psi(1S)K^0)/\Gamma_{total}$ $\Gamma_{162}/\Gamma$

VALUE (units $10^{-4}$ )	CL%	EVTS	DOCUMENT ID	TECN	COMMENT
<b>8.74 ± 0.32 OUR FIT</b>					
<b>8.71 ± 0.32 OUR AVERAGE</b>					
8.6	+1.3 -1.2	±0.3	1,2	AUBERT 07AV	BABR $e^+e^- \rightarrow \Upsilon(4S)$
8.69	±0.22	±0.30	2	AUBERT 05J	BABR $e^+e^- \rightarrow \Upsilon(4S)$
7.9	±0.4	±0.9	2	ABE 03B	BELL $e^+e^- \rightarrow \Upsilon(4S)$
9.5	±0.8	±0.6	2	AVERY 00	CLE2 $e^+e^- \rightarrow \Upsilon(4S)$
11.5	±2.3	±1.7	3	ABE 96H	CDF $p\bar{p}$ at 1.8 TeV
7.0	±4.1	±0.1	4	BORTOLETTO92	CLEO $e^+e^- \rightarrow \Upsilon(4S)$
9.3	±7.2	±0.1	2	ALBRECHT 90J	ARG $e^+e^- \rightarrow \Upsilon(4S)$

• • • We do not use the following data for averages, fits, limits, etc. • • •

8.3 ± 0.4 ± 0.5      2 AUBERT 02      BABR      Repl. by AUBERT 05J

8.5 <sup>+1.4</sup><sub>-1.2</sub> ± 0.6      2 JESSOP 97      CLE2      Repl. by AVERY 00

7.5 ± 2.4 ± 0.8      10      4 ALAM 94      CLE2      Sup. by JESSOP 97

<5.0      90      ALAM 86      CLEO  $e^+e^- \rightarrow \Upsilon(4S)$

1 AUBERT 07AV reports  $[\Gamma(B^0 \rightarrow J/\psi(1S)K^0)/\Gamma_{total}] \times [B(J/\psi(1S) \rightarrow p\bar{p})] = (1.87^{+0.28}_{-0.26} \pm 0.07) \times 10^{-6}$  which we divide by our best value  $B(J/\psi(1S) \rightarrow p\bar{p}) = (2.17 \pm 0.07) \times 10^{-3}$ . Our first error is their experiment's error and our second error is the systematic error from using our best value.

2 Assumes equal production of  $B^+$  and  $B^0$  at the  $\Upsilon(4S)$ .

3 ABE 96H assumes that  $B(B^+ \rightarrow J/\psi K^+) = (1.02 \pm 0.14) \times 10^{-3}$ .

4 BORTOLETTO 92 reports  $(6 \pm 3 \pm 2) \times 10^{-4}$  from a measurement of  $[\Gamma(B^0 \rightarrow J/\psi(1S)K^0)/\Gamma_{total}] \times [B(J/\psi(1S) \rightarrow e^+e^-)]$  assuming  $B(J/\psi(1S) \rightarrow e^+e^-) = 0.069 \pm 0.009$ , which we rescale to our best value  $B(J/\psi(1S) \rightarrow e^+e^-) = (5.94 \pm 0.06) \times 10^{-2}$ . Our first error is their experiment's error and our second error is the systematic error from using our best value. Assumes equal production of  $B^+$  and  $B^0$  at the  $\Upsilon(4S)$ .

5 ALBRECHT 90J reports  $(8 \pm 6 \pm 2) \times 10^{-4}$  from a measurement of  $[\Gamma(B^0 \rightarrow J/\psi(1S)K^0)/\Gamma_{total}] \times [B(J/\psi(1S) \rightarrow e^+e^-)]$  assuming  $B(J/\psi(1S) \rightarrow e^+e^-) = 0.069 \pm 0.009$ , which we rescale to our best value  $B(J/\psi(1S) \rightarrow e^+e^-) = (5.94 \pm 0.06) \times 10^{-2}$ . Our first error is their experiment's error and our second error is the systematic error from using our best value. Assumes equal production of  $B^+$  and  $B^0$  at the  $\Upsilon(4S)$ .

## $\Gamma(J/\psi(1S)K^+\pi^-)/\Gamma_{total}$ $\Gamma_{163}/\Gamma$

VALUE (units $10^{-3}$ )	CL%	EVTS	DOCUMENT ID	TECN	COMMENT
<b>1.16 ± 0.56 ± 0.01</b>					
• • • We do not use the following data for averages, fits, limits, etc. • • •					
<1.3		90	2	ALBRECHT 87D	ARG $e^+e^- \rightarrow \Upsilon(4S)$
<6.3		90	2	GILES 84	CLEO $e^+e^- \rightarrow \Upsilon(4S)$

1 BORTOLETTO 92 reports  $(1.0 \pm 0.4 \pm 0.3) \times 10^{-3}$  from a measurement of  $[\Gamma(B^0 \rightarrow J/\psi(1S)K^+\pi^-)/\Gamma_{total}] \times [B(J/\psi(1S) \rightarrow e^+e^-)]$  assuming  $B(J/\psi(1S) \rightarrow e^+e^-) = 0.069 \pm 0.009$ , which we rescale to our best value  $B(J/\psi(1S) \rightarrow e^+e^-) = (5.94 \pm 0.06) \times 10^{-2}$ . Our first error is their experiment's error and our second error is the systematic error from using our best value. Assumes equal production of  $B^+$  and  $B^0$  at the  $\Upsilon(4S)$ .

2 ALBRECHT 87D assume  $B^+B^-/B^0\bar{B}^0$  ratio is 55/45.  $K\pi$  system is specifically selected as nonresonant.

## $\Gamma(J/\psi(1S)K^*(892)^0)/\Gamma_{total}$ $\Gamma_{164}/\Gamma$

VALUE (units $10^{-3}$ )	EVTS	DOCUMENT ID	TECN	COMMENT	
<b>1.34 ± 0.06 OUR FIT</b>					
<b>1.33 ± 0.06 OUR AVERAGE</b>					
1.30	+0.22 -0.21	±0.04	1,2	AUBERT 07AV	BABR $e^+e^- \rightarrow \Upsilon(4S)$
1.309	±0.026	±0.077	2	AUBERT 05J	BABR $e^+e^- \rightarrow \Upsilon(4S)$
1.29	±0.05	±0.13	2	ABE 02N	BELL $e^+e^- \rightarrow \Upsilon(4S)$
1.74	±0.20	±0.18	3	ABE 98O	CDF $p\bar{p}$ 1.8 TeV
1.32	±0.17	±0.17	4	JESSOP 97	CLE2 $e^+e^- \rightarrow \Upsilon(4S)$
1.28	±0.66	±0.01	5	BORTOLETTO92	CLEO $e^+e^- \rightarrow \Upsilon(4S)$
1.28	±0.60	±0.01	6	ALBRECHT 90J	ARG $e^+e^- \rightarrow \Upsilon(4S)$
4.07	±1.82	±0.04	5	BEBEK 87	CLEO $e^+e^- \rightarrow \Upsilon(4S)$

• • • We do not use the following data for averages, fits, limits, etc. • • •

1.24 ± 0.05 ± 0.09      2 AUBERT 02      BABR      Repl. by AUBERT 05J

1.36 ± 0.27 ± 0.22      8 ABE 96H      CDF      Sup. by ABE 98O

1.69 ± 0.31 ± 0.18      29      9 ALAM 94      CLE2      Sup. by JESSOP 97

4.0 ± 0.30      10 ALBRECHT 94G      ARG  $e^+e^- \rightarrow \Upsilon(4S)$

3.3 ± 0.18      5      11 ALBAJAR 91E      UA1  $E_{cm}^{pp} = 630$  GeV

4.1 ± 0.18      5      12 ALBRECHT 87D      ARG  $e^+e^- \rightarrow \Upsilon(4S)$

1 AUBERT 07AV reports  $[\Gamma(B^0 \rightarrow J/\psi(1S)K^*(892)^0)/\Gamma_{total}] \times [B(J/\psi(1S) \rightarrow p\bar{p})] = (2.82^{+0.30+0.36}_{-0.28-0.35}) \times 10^{-6}$  which we divide by our best value  $B(J/\psi(1S) \rightarrow p\bar{p}) = (2.17 \pm 0.07) \times 10^{-3}$ . Our first error is their experiment's error and our second error is the systematic error from using our best value.

2 Assumes equal production of  $B^+$  and  $B^0$  at the  $\Upsilon(4S)$ .

3 ABE 98O reports  $[B(B^0 \rightarrow J/\psi(1S)K^*(892)^0)]/[B(B^+ \rightarrow J/\psi(1S)K^+)] = 1.76 \pm 0.14 \pm 0.15$ . We multiply by our best value  $B(B^+ \rightarrow J/\psi(1S)K^+) = (9.9 \pm 1.0) \times 10^{-4}$ . Our first error is their experiment's error and our second error is the systematic error from using our best value.

4 Assumes equal production of  $B^+$  and  $B^0$  at the  $\Upsilon(4S)$ .

5 BORTOLETTO 92 reports  $(1.1 \pm 0.5 \pm 0.3) \times 10^{-3}$  from a measurement of  $[\Gamma(B^0 \rightarrow J/\psi(1S)K^*(892)^0)/\Gamma_{total}] \times [B(J/\psi(1S) \rightarrow e^+e^-)]$  assuming  $B(J/\psi(1S) \rightarrow e^+e^-) = 0.069 \pm 0.009$ , which we rescale to our best value  $B(J/\psi(1S) \rightarrow e^+e^-) = (5.94 \pm 0.06) \times 10^{-2}$ . Our first error is their experiment's error and our second error is the systematic error from using our best value. Assumes equal production of  $B^+$  and  $B^0$  at the  $\Upsilon(4S)$ .

6 ALBRECHT 90J reports  $(1.1 \pm 0.5 \pm 0.2) \times 10^{-3}$  from a measurement of  $[\Gamma(B^0 \rightarrow J/\psi(1S)K^*(892)^0)/\Gamma_{total}] \times [B(J/\psi(1S) \rightarrow e^+e^-)]$  assuming  $B(J/\psi(1S) \rightarrow e^+e^-) = 0.069 \pm 0.009$ , which we rescale to our best value  $B(J/\psi(1S) \rightarrow e^+e^-) = (5.94 \pm 0.06) \times 10^{-2}$ . Our first error is their experiment's error and our second error is the systematic error from using our best value. Assumes equal production of  $B^+$  and  $B^0$  at the  $\Upsilon(4S)$ .

7 BEBEK 87 reports  $(3.5 \pm 1.6 \pm 0.3) \times 10^{-3}$  from a measurement of  $[\Gamma(B^0 \rightarrow J/\psi(1S)K^*(892)^0)/\Gamma_{total}] \times [B(J/\psi(1S) \rightarrow e^+e^-)]$  assuming  $B(J/\psi(1S) \rightarrow e^+e^-) = 0.069 \pm 0.009$ , which we rescale to our best value  $B(J/\psi(1S) \rightarrow e^+e^-) = (5.94 \pm 0.06) \times 10^{-2}$ . Our first error is their experiment's error and our second error is the systematic error from using our best value. Updated in BORTOLETTO 92 to use the same assumptions.

8 ABE 96H assumes that  $B(B^+ \rightarrow J/\psi K^+) = (1.02 \pm 0.14) \times 10^{-3}$ .

9 The neutral and charged  $B$  events together are predominantly longitudinally polarized,  $\Gamma_L/\Gamma = 0.080 \pm 0.08 \pm 0.05$ . This can be compared with a prediction using HQET, 0.73 (KRAMER 92). This polarization indicates that the  $B \rightarrow \psi K^*$  decay is dominated by the  $CP = -1$   $CP$  eigenstate. Assumes equal production of  $B^+$  and  $B^0$  at the  $\Upsilon(4S)$ .

10 ALBRECHT 94G measures the polarization in the vector-vector decay to be predominantly longitudinal,  $\Gamma_T/\Gamma = 0.03 \pm 0.16 \pm 0.15$  making the neutral decay a  $CP$  eigenstate when the  $K^*$  decays through  $K_S^0 \pi^0$ .

11 ALBAJAR 91E assumes  $B^0$  production fraction of 36%.

12 ALBRECHT 87D assume  $B^+B^-/B^0\bar{B}^0$  ratio is 55/45. Superseded by ALBRECHT 90J.

13 ALAM 86 assumes  $B^\pm/B^0$  ratio is 60/40. The observation of the decay  $B^+ \rightarrow J/\psi K^*(892)^+$  (HAAS 85) has been retracted in this paper.

## $\Gamma(J/\psi(1S)K^*(892)^0)/\Gamma(J/\psi(1S)K^0)$ $\Gamma_{164}/\Gamma_{162}$

VALUE	DOCUMENT ID	TECN	COMMENT
<b>1.50 ± 0.09 OUR AVERAGE</b>			
1.51 ± 0.05 ± 0.08	AUBERT 05J	BABR	$e^+e^- \rightarrow \Upsilon(4S)$
1.39 ± 0.36 ± 0.10	ABE 96Q	CDF	$p\bar{p}$
• • • We do not use the following data for averages, fits, limits, etc. • • •			
1.49 ± 0.10 ± 0.08	1 AUBERT 02	BABR	Repl. by AUBERT 05J
1 Assumes equal production of $B^+$ and $B^0$ at the $\Upsilon(4S)$ .			

## $\Gamma(J/\psi(1S)\eta K_S^0)/\Gamma_{total}$ $\Gamma_{165}/\Gamma$

VALUE (units $10^{-5}$ )	DOCUMENT ID	TECN	COMMENT
<b>8.4 ± 2.6 ± 2.7</b>			
1 AUBERT 04Y      BABR $e^+e^- \rightarrow \Upsilon(4S)$			
1 Assumes equal production of $B^+$ and $B^0$ at the $\Upsilon(4S)$ .			

## $\Gamma(J/\psi(1S)\eta' K_S^0)/\Gamma_{total}$ $\Gamma_{166}/\Gamma$

VALUE (units $10^{-5}$ )	CL%	DOCUMENT ID	TECN	COMMENT
<2.5		90	1	XIE 07      BELL $e^+e^- \rightarrow \Upsilon(4S)$
1 Assumes equal production of $B^+$ and $B^0$ at the $\Upsilon(4S)$ .				

## $\Gamma(J/\psi(1S)\omega K^0)/\Gamma_{total}$ $\Gamma_{168}/\Gamma$

VALUE (units $10^{-4}$ )	DOCUMENT ID	TECN	COMMENT
<b>2.3 ± 0.3 ± 0.3</b>			
1 DEL-AMO-SA...10B      BABR $e^+e^- \rightarrow \Upsilon(4S)$			
• • • We do not use the following data for averages, fits, limits, etc. • • •			
3.1 ± 0.6 ± 0.3	1 AUBERT 08W	BABR	Repl. by DEL-AMO-SANCHEZ 10B
1 Assumes equal production of $B^+$ and $B^0$ at the $\Upsilon(4S)$ .			

## $\Gamma(X(3872)K^0 \times B(X \rightarrow J/\psi\omega))/\Gamma_{total}$ $\Gamma_{169}/\Gamma$

VALUE (units $10^{-6}$ )	DOCUMENT ID	TECN	COMMENT
<b>6 ± 3 ± 1</b>			
1 DEL-AMO-SA...10B      BABR $e^+e^- \rightarrow \Upsilon(4S)$			
1 Assumes equal production of $B^+$ and $B^0$ at the $\Upsilon(4S)$ .			

## $\Gamma(X(3915)K^0 \times B(X \rightarrow J/\psi\omega))/\Gamma_{total}$ $\Gamma_{170}/\Gamma$

VALUE (units $10^{-5}$ )	DOCUMENT ID	TECN	COMMENT
<b>2.1 ± 0.9 ± 0.3</b>			
1 DEL-AMO-SA...10B      BABR $e^+e^- \rightarrow \Upsilon(4S)$			
• • • We do not use the following data for averages, fits, limits, etc. • • •			
1.3 ± 1.3 ± 0.2	1,2 AUBERT 08W	BABR	Repl. by DEL-AMO-SANCHEZ 10B
1 Assumes equal production of $B^+$ and $B^0$ at the $\Upsilon(4S)$ .			
2 Corresponds to upper limit of $3.9 \times 10^{-5}$ at 90% CL.			

## $\Gamma(J/\psi(1S)\phi K^0)/\Gamma_{total}$ $\Gamma_{167}/\Gamma$

VALUE	DOCUMENT ID	TECN	COMMENT
<b>( 9.4 ± 2.6 ) × 10<sup>-5</sup> OUR AVERAGE</b>			
(10.2 ± 3.8 ± 1.0) × 10 <sup>-5</sup>	1 AUBERT 03O	BABR	$e^+e^- \rightarrow \Upsilon(4S)$
( 8.8 ± 3.5 ± 1.3 ) × 10 <sup>-5</sup>	2 ANASTASSOV 00	CLE2	$e^+e^- \rightarrow \Upsilon(4S)$
1 Assumes equal production of $B^+$ and $B^0$ at the $\Upsilon(4S)$ .			
2 ANASTASSOV 00 finds 10 events on a background of 0.5 ± 0.2. Assumes equal production of $B^0$ and $B^+$ at the $\Upsilon(4S)$ , a uniform Dalitz plot distribution, isotropic $J/\psi(1S)$ and $\phi$ decays, and $B(B^+ \rightarrow J/\psi(1S)\phi K^+) = B(B^0 \rightarrow J/\psi(1S)\phi K^0)$ .			







## Meson Particle Listings

 $B^0$ 

- <sup>1</sup> Assumes equal production of  $B^+$  and  $B^0$  at the  $\Upsilon(4S)$ .  
<sup>2</sup> Uses  $\chi_{c1,2} \rightarrow J/\psi\gamma$ . Assumes  $B(\Upsilon(4S) \rightarrow B^+B^-) = (51.6 \pm 0.6)\%$  and  $B(\Upsilon(4S) \rightarrow B^0\bar{B}^0) = (48.4 \pm 0.6)\%$ .  
<sup>3</sup> AVERY 00 reports  $(3.9^{+1.9}_{-1.3} \pm 0.4) \times 10^{-4}$  from a measurement of  $[\Gamma(B^0 \rightarrow \chi_{c1}(1P)K^0)/\Gamma_{\text{total}}] \times [B(\chi_{c1}(1P) \rightarrow \gamma J/\psi(1S))]$  assuming  $B(\chi_{c1}(1P) \rightarrow \gamma J/\psi(1S)) = 0.273 \pm 0.016$ , which we rescale to our best value  $B(\chi_{c1}(1P) \rightarrow \gamma J/\psi(1S)) = (34.4 \pm 1.5) \times 10^{-2}$ . Our first error is their experiment's error and our second error is the systematic error from using our best value. Assumes equal production of  $B^+$  and  $B^0$  at the  $\Upsilon(4S)$ .  
<sup>4</sup> AUBERT 02 reports  $(5.4 \pm 1.4 \pm 1.1) \times 10^{-4}$  from a measurement of  $[\Gamma(B^0 \rightarrow \chi_{c1}(1P)K^0)/\Gamma_{\text{total}}] \times [B(\chi_{c1}(1P) \rightarrow \gamma J/\psi(1S))]$  assuming  $B(\chi_{c1}(1P) \rightarrow \gamma J/\psi(1S)) = 0.273 \pm 0.016$ , which we rescale to our best value  $B(\chi_{c1}(1P) \rightarrow \gamma J/\psi(1S)) = (34.4 \pm 1.5) \times 10^{-2}$ . Our first error is their experiment's error and our second error is the systematic error from using our best value. Assumes equal production of  $B^+$  and  $B^0$  at the  $\Upsilon(4S)$ .

$\Gamma(\chi_{c1}(1P)K^0)/\Gamma(J/\psi(1S)K^0)$		$\Gamma_{209}/\Gamma_{162}$	
VALUE	DOCUMENT ID	TECN	COMMENT
<b><math>0.52 \pm 0.16 \pm 0.02</math></b>	1 AUBERT	02	BABR $e^+e^- \rightarrow \Upsilon(4S)$

- <sup>1</sup> AUBERT 02 reports  $0.66 \pm 0.11 \pm 0.17$  from a measurement of  $[\Gamma(B^0 \rightarrow \chi_{c1}(1P)K^0)/\Gamma(B^0 \rightarrow J/\psi(1S)K^0)] \times [B(\chi_{c1}(1P) \rightarrow \gamma J/\psi(1S))]$  assuming  $B(\chi_{c1}(1P) \rightarrow \gamma J/\psi(1S)) = 0.273 \pm 0.016$ , which we rescale to our best value  $B(\chi_{c1}(1P) \rightarrow \gamma J/\psi(1S)) = (34.4 \pm 1.5) \times 10^{-2}$ . Our first error is their experiment's error and our second error is the systematic error from using our best value. Assumes equal production of  $B^+$  and  $B^0$  at the  $\Upsilon(4S)$ .

$\Gamma(\chi_{c1}(1P)K^-\pi^+)/\Gamma_{\text{total}}$		$\Gamma_{210}/\Gamma$	
VALUE (units $10^{-4}$ )	DOCUMENT ID	TECN	COMMENT
<b><math>3.83 \pm 0.10 \pm 0.39</math></b>	1 MIZUK	08	BELL $e^+e^- \rightarrow \Upsilon(4S)$

- <sup>1</sup> Assumes equal production of  $B^+$  and  $B^0$  at the  $\Upsilon(4S)$ .

$\Gamma(\chi_{c1}(1P)K^*(892)^0)/\Gamma_{\text{total}}$		$\Gamma_{211}/\Gamma$		
VALUE (units $10^{-4}$ )	CL%	DOCUMENT ID	TECN	COMMENT
<b><math>2.22^{+0.40}_{-0.31}</math> OUR AVERAGE</b>		Error includes scale factor of 1.6.		
2.5 $\pm 0.2 \pm 0.2$		1 AUBERT	09b	BABR $e^+e^- \rightarrow \Upsilon(4S)$
$1.73^{+0.15+0.34}_{-0.12-0.22}$		2 MIZUK	08	BELL $e^+e^- \rightarrow \Upsilon(4S)$

- • • We do not use the following data for averages, fits, limits, etc. • • •
- |                          |          |        |      |  |
|--------------------------|----------|--------|------|--|
| 3.14 $\pm 0.34 \pm 0.72$ | 2 SONI   | 06     | BELL | Repl. by MIZUK 08                      |
| 3.27 $\pm 0.42 \pm 0.64$ | 2 AUBERT | 05j    | BABR | Repl. by AUBERT 09b                    |
| 3.8 $\pm 1.3 \pm 0.2$    | 3 AUBERT | 02     | BABR | Repl. by AUBERT 05j                    |
| <21                      | 90       | 4 ALAM | 94   | CLE2 $e^+e^- \rightarrow \Upsilon(4S)$ |

- <sup>1</sup> Uses  $\chi_{c1,2} \rightarrow J/\psi\gamma$ . Assumes  $B(\Upsilon(4S) \rightarrow B^+B^-) = (51.6 \pm 0.6)\%$  and  $B(\Upsilon(4S) \rightarrow B^0\bar{B}^0) = (48.4 \pm 0.6)\%$ .  
<sup>2</sup> Assumes equal production of  $B^+$  and  $B^0$  at the  $\Upsilon(4S)$ .  
<sup>3</sup> AUBERT 02 reports  $(4.8 \pm 1.4 \pm 0.9) \times 10^{-4}$  from a measurement of  $[\Gamma(B^0 \rightarrow \chi_{c1}(1P)K^*(892)^0)/\Gamma_{\text{total}}] \times [B(\chi_{c1}(1P) \rightarrow \gamma J/\psi(1S))]$  assuming  $B(\chi_{c1}(1P) \rightarrow \gamma J/\psi(1S)) = 0.273 \pm 0.016$ , which we rescale to our best value  $B(\chi_{c1}(1P) \rightarrow \gamma J/\psi(1S)) = (34.4 \pm 1.5) \times 10^{-2}$ . Our first error is their experiment's error and our second error is the systematic error from using our best value. Assumes equal production of  $B^+$  and  $B^0$  at the  $\Upsilon(4S)$ .  
<sup>4</sup> BORTOLETTO 92 assumes equal production of  $B^+$  and  $B^0$  at the  $\Upsilon(4S)$ .

$\Gamma(X(4051)^+K^- \times B(X^+ \rightarrow \chi_{c1}\pi^+))/\Gamma_{\text{total}}$		$\Gamma_{212}/\Gamma$	
VALUE (units $10^{-5}$ )	DOCUMENT ID	TECN	COMMENT
<b><math>3.0^{+1.5+3.7}_{-0.8-1.6}</math></b>	1 MIZUK	08	BELL $e^+e^- \rightarrow \Upsilon(4S)$

- <sup>1</sup> Assumes equal production of  $B^+$  and  $B^0$  at the  $\Upsilon(4S)$ .

$\Gamma(X(4248)^+K^- \times B(X^+ \rightarrow \chi_{c1}\pi^+))/\Gamma_{\text{total}}$		$\Gamma_{213}/\Gamma$	
VALUE (units $10^{-5}$ )	DOCUMENT ID	TECN	COMMENT
<b><math>4.0^{+2.3+19.7}_{-0.9-0.5}</math></b>	1 MIZUK	08	BELL $e^+e^- \rightarrow \Upsilon(4S)$

- <sup>1</sup> Assumes equal production of  $B^+$  and  $B^0$  at the  $\Upsilon(4S)$ .

$\Gamma(\chi_{c1}(1P)K^*(892)^0)/\Gamma(\chi_{c1}(1P)K^0)$		$\Gamma_{211}/\Gamma_{209}$	
VALUE	DOCUMENT ID	TECN	COMMENT
<b><math>0.72 \pm 0.11 \pm 0.12</math></b>	AUBERT	05j	BABR $e^+e^- \rightarrow \Upsilon(4S)$

- • • We do not use the following data for averages, fits, limits, etc. • • •
- |                          |          |    |      |                     |
|--------------------------|----------|----|------|---------------------|
| 0.89 $\pm 0.34 \pm 0.17$ | 1 AUBERT | 02 | BABR | Repl. by AUBERT 05j |
|--------------------------|----------|----|------|---------------------|
- <sup>1</sup> Assumes equal production of  $B^+$  and  $B^0$  at the  $\Upsilon(4S)$ .

$\Gamma(K^+\pi^-)/\Gamma_{\text{total}}$		$\Gamma_{214}/\Gamma$		
VALUE (units $10^{-6}$ )	CL%	DOCUMENT ID	TECN	COMMENT
<b><math>19.4 \pm 0.6</math> OUR FIT</b>				
<b><math>19.4 \pm 0.6</math> OUR AVERAGE</b>				
19.1 $\pm 0.6 \pm 0.6$		1 AUBERT	07b	BABR $e^+e^- \rightarrow \Upsilon(4S)$
19.9 $\pm 0.4 \pm 0.8$		1 LIN	07a	BELL $e^+e^- \rightarrow \Upsilon(4S)$
18.0 $^{+2.3+1.2}_{-2.1-0.9}$		1 BORNHEIM	03	CLE2 $e^+e^- \rightarrow \Upsilon(4S)$

- • • We do not use the following data for averages, fits, limits, etc. • • •

18.5 $\pm 1.0 \pm 0.7$	1 CHAO	04	BELL	Repl. by LIN 07a	
17.9 $\pm 0.9 \pm 0.7$	1 AUBERT	02q	BABR	Repl. by AUBERT 07b	
22.5 $\pm 1.9 \pm 1.8$	1 CASEY	02	BELL	Repl. by CHAO 04	
19.3 $^{+3.4+1.5}_{-3.2-0.6}$	1 ABE	01H	BELL	Repl. by CASEY 02	
16.7 $\pm 1.6 \pm 1.3$	1 AUBERT	01E	BABR	Repl. by AUBERT 02q	
< 66	2 ABE	00c	SLD	$e^+e^- \rightarrow Z$	
17.2 $^{+2.5}_{-2.4} \pm 1.2$	1 CRONIN-HEN..00	CLE2		Repl. by BORNHEIM 03	
15 $^{+5}_{-4} \pm 1.4$	GODANG	98	CLE2	Repl. by CRONIN-HENNESSY 00	
24 $^{+17}_{-11} \pm 2$	3 ADAM	96d	DLPH	$e^+e^- \rightarrow Z$	
< 17	90	ASNER	96	CLE2	Sup. by ADAM 96d
< 30	90	4 BUSKULIC	96v	ALEP	$e^+e^- \rightarrow Z$
< 90	90	5 ABREU	95N	DLPH	Sup. by ADAM 96d
< 81	90	6 AKERS	94L	OPAL	$e^+e^- \rightarrow Z$
< 26	90	7 BATTLE	93	CLE2	$e^+e^- \rightarrow \Upsilon(4S)$
< 180	90	ALBRECHT	91B	ARG	$e^+e^- \rightarrow \Upsilon(4S)$
< 90	90	8 AVERY	89B	CLEO	$e^+e^- \rightarrow \Upsilon(4S)$
< 320	90	AVERY	87	CLEO	$e^+e^- \rightarrow \Upsilon(4S)$

- <sup>1</sup> Assumes equal production of  $B^+$  and  $B^0$  at the  $\Upsilon(4S)$ .  
<sup>2</sup> ABE 00c assumes  $B(Z \rightarrow b\bar{b}) = (21.7 \pm 0.1)\%$  and the  $B$  fractions  $f_{B^0} = f_{B^+} = (39.7^{+1.8}_{-2.2}\%)$  and  $f_{B_s} = (10.5^{+1.8}_{-2.2}\%)$ .  
<sup>3</sup> ADAM 96d assumes  $f_{B^0} = f_{B^-} = 0.39$  and  $f_{B_s} = 0.12$ . Contributions from  $B^0$  and  $B_s$  decays cannot be separated. Limits are given for the weighted average of the decay rates for the two neutral  $B$  mesons.  
<sup>4</sup> BUSKULIC 96v assumes PDG 96 production fractions for  $B^0, B^+, B_s, b$  baryons.  
<sup>5</sup> Assumes a  $B^0, B^-$  production fraction of 0.39 and a  $B_s$  production fraction of 0.12. Contributions from  $B^0$  and  $B_s$  decays cannot be separated. Limits are given for the weighted average of the decay rates for the two neutral  $B$  mesons.  
<sup>6</sup> Assumes  $B(Z \rightarrow b\bar{b}) = 0.217$  and  $B^0(B_s^0)$  fraction 39.5% (12%).  
<sup>7</sup> BATTLE 93 assumes equal production of  $B^0\bar{B}^0$  and  $B^+B^-$  at  $\Upsilon(4S)$ .  
<sup>8</sup> Assumes the  $\Upsilon(4S)$  decays 43% to  $B^0\bar{B}^0$ .

$\Gamma(K^+\pi^-)/\Gamma(K^0\pi^0)$		$\Gamma_{214}/\Gamma_{215}$		
VALUE	DOCUMENT ID	TECN	COMMENT	
<b><math>2.16 \pm 0.16 \pm 0.16</math></b>	LIN	07a	BELL $e^+e^- \rightarrow \Upsilon(4S)$	
1.20 $^{+0.50+0.22}_{-0.58-0.32}$	1 ABE	01H	BELL	Repl. by LIN 07a

- <sup>1</sup> Assumes equal production of  $B^+$  and  $B^0$  at the  $\Upsilon(4S)$ .

$[\Gamma(K^+\pi^-) + \Gamma(\pi^+\pi^-)]/\Gamma_{\text{total}}$		$(\Gamma_{214} + \Gamma_{330})/\Gamma$		
VALUE (units $10^{-6}$ )	EVTS	DOCUMENT ID	TECN	COMMENT
<b><math>19 \pm 6</math> OUR AVERAGE</b>				
28 $^{+15}_{-10} \pm 20$		1 ADAM	96d	DLPH $e^+e^- \rightarrow Z$
18 $^{+6+3}_{-5-4}$	17.2	ASNER	96	CLE2 $e^+e^- \rightarrow \Upsilon(4S)$

- • • We do not use the following data for averages, fits, limits, etc. • • •

24 $^{+8}_{-7} \pm 2$	2 BATTLE	93	CLE2	$e^+e^- \rightarrow \Upsilon(4S)$
-----------------------	----------	----	------	-----------------------------------

<sup>1</sup> ADAM 96d assumes  $f_{B^0} = f_{B^-} = 0.39$  and  $f_{B_s} = 0.12$ . Contributions from  $B^0$  and  $B_s$  decays cannot be separated. Limits are given for the weighted average of the decay rates for the two neutral  $B$  mesons.  
<sup>2</sup> BATTLE 93 assumes equal production of  $B^0\bar{B}^0$  and  $B^+B^-$  at  $\Upsilon(4S)$ .

$\Gamma(K^0\pi^0)/\Gamma_{\text{total}}$		$\Gamma_{215}/\Gamma$		
VALUE (units $10^{-6}$ )	CL%	DOCUMENT ID	TECN	COMMENT
<b><math>9.5 \pm 0.8</math> OUR AVERAGE</b>		Error includes scale factor of 1.3.		
8.7 $\pm 0.5 \pm 0.6$		1 FUJIKAWA	10a	BELL $e^+e^- \rightarrow \Upsilon(4S)$
10.3 $\pm 0.7 \pm 0.6$		1 AUBERT	08E	BABR $e^+e^- \rightarrow \Upsilon(4S)$
12.8 $^{+4.0+1.7}_{-3.3-1.4}$		1 BORNHEIM	03	CLE2 $e^+e^- \rightarrow \Upsilon(4S)$

- • • We do not use the following data for averages, fits, limits, etc. • • •
- |                               |                  |        |      |                       |                             |
|-------------------------------|------------------|--------|------|-----------------------|-----------------------------|
| 9.2 $\pm 0.7 \pm 0.6$         | 1 LIN            | 07a    | BELL | Repl. by FUJIKAWA 10a |                             |
| 11.4 $\pm 0.9 \pm 0.6$        | 1 AUBERT         | 05y    | BABR | Repl. by AUBERT 08E   |                             |
| 11.4 $\pm 1.7 \pm 0.8$        | 1 AUBERT         | 04M    | BABR | Repl. by AUBERT 05y   |                             |
| 11.7 $^{+2.3+1.2}_{-1.3}$     | 1 CHAO           | 04     | BELL | Repl. by LIN 07a      |                             |
| 8.0 $^{+3.3}_{-3.1} \pm 1.6$  | 1 CASEY          | 02     | BELL | Repl. by CHAO 04      |                             |
| 16.0 $^{+7.2+2.5}_{-5.9-2.7}$ | 1 ABE            | 01H    | BELL | Repl. by CASEY 02     |                             |
| 8.2 $^{+3.1+1.2}_{-2.7}$      | 1 AUBERT         | 01E    | BABR | Repl. by AUBERT 04M   |                             |
| 14.6 $^{+5.9+2.4}_{-5.1-3.3}$ | 1 CRONIN-HEN..00 | CLE2   |      | Repl. by BORNHEIM 03  |                             |
| < 41                          | 90               | GODANG | 98   | CLE2                  | Repl. by CRONIN-HENNESSY 00 |
| < 40                          | 90               | ASNER  | 96   | CLE2                  | Rep. by GODANG 98           |

- <sup>1</sup> Assumes equal production of  $B^+$  and  $B^0$  at the  $\Upsilon(4S)$ .

$\Gamma(\eta' K^0)/\Gamma_{\text{total}}$   $\Gamma_{216}/\Gamma$ 

VALUE (units $10^{-6}$ )	DOCUMENT ID	TECN	COMMENT
<b>66 ± 4 OUR AVERAGE</b>	Error includes scale factor of 1.4.		
68.5 ± 2.2 ± 3.1	<sup>1</sup> AUBERT	09AV	BABR $e^+e^- \rightarrow \Upsilon(4S)$
58.9 ± 3.5 ± 4.3	<sup>1</sup> SCHUEMANN 06	BELL	$e^+e^- \rightarrow \Upsilon(4S)$
89 ± 18 ± 9	<sup>1</sup> RICHICHI	00	CLE2 $e^+e^- \rightarrow \Upsilon(4S)$
• • • We do not use the following data for averages, fits, limits, etc. • • •			
66.6 ± 2.6 ± 2.8	<sup>1</sup> AUBERT	07AE	BABR Repl. by AUBERT 09AV
67.4 ± 3.3 ± 3.2	<sup>1</sup> AUBERT	05M	BABR AUBERT 07AE
60.6 ± 5.6 ± 4.6	<sup>1</sup> AUBERT	03W	BABR Repl. by AUBERT 05M
55 ± 19 ± 8	<sup>1</sup> ABE	01M	BELL Repl. by SCHUEMANN 06
42 ± 13 ± 4	<sup>1</sup> AUBERT	01G	BABR Repl. by AUBERT 03W
47 ± 27 ± 9	BEHRENS	98	CLE2 Repl. by RICHICHI 00

<sup>1</sup> Assumes equal production of  $B^+$  and  $B^0$  at the  $\Upsilon(4S)$ .

 $\Gamma(\eta' K^*(892)^0)/\Gamma_{\text{total}}$   $\Gamma_{217}/\Gamma$ 

VALUE (units $10^{-6}$ )	CL%	DOCUMENT ID	TECN	COMMENT
<b>3.1 ± 0.9 ± 0.3</b>		<sup>1</sup> DEL-AMO-SA...10A	BABR	$e^+e^- \rightarrow \Upsilon(4S)$
• • • We do not use the following data for averages, fits, limits, etc. • • •				
3.8 ± 1.1 ± 0.5		<sup>1</sup> AUBERT	07E	BABR Repl. by DEL-AMO-SANCHEZ 10A
< 2.6	90	<sup>1</sup> SCHUEMANN 07	BELL	$e^+e^- \rightarrow \Upsilon(4S)$
< 7.6	90	<sup>1</sup> AUBERT,B	04D	BABR Repl. by AUBERT 07E
< 24	90	<sup>1</sup> RICHICHI	00	CLE2 $e^+e^- \rightarrow \Upsilon(4S)$
< 39	90	BEHRENS	98	CLE2 Repl. by RICHICHI 00

<sup>1</sup> Assumes equal production of  $B^+$  and  $B^0$  at the  $\Upsilon(4S)$ .

 $\Gamma(\eta' K_0^*(1430)^0)/\Gamma_{\text{total}}$   $\Gamma_{218}/\Gamma$ 

VALUE (units $10^{-6}$ )	DOCUMENT ID	TECN	COMMENT
<b>6.3 ± 1.3 ± 0.9</b>	<sup>1</sup> DEL-AMO-SA...10A	BABR	$e^+e^- \rightarrow \Upsilon(4S)$

<sup>1</sup> Assumes equal production of  $B^+$  and  $B^0$  at the  $\Upsilon(4S)$ .

 $\Gamma(\eta' K_2^*(1430)^0)/\Gamma_{\text{total}}$   $\Gamma_{219}/\Gamma$ 

VALUE (units $10^{-6}$ )	DOCUMENT ID	TECN	COMMENT
<b>13.7 ± 3.0 ± 2.9 ± 1.2</b>	<sup>1</sup> DEL-AMO-SA...10A	BABR	$e^+e^- \rightarrow \Upsilon(4S)$

<sup>1</sup> Assumes equal production of  $B^+$  and  $B^0$  at the  $\Upsilon(4S)$ .

 $\Gamma(\eta K^0)/\Gamma_{\text{total}}$   $\Gamma_{220}/\Gamma$ 

VALUE (units $10^{-6}$ )	CL%	DOCUMENT ID	TECN	COMMENT
<b>1.23 ± 0.27 ± 0.24 OUR AVERAGE</b>				
1.27 ± 0.33 ± 0.08		<sup>1</sup> HOI	12	BELL $e^+e^- \rightarrow \Upsilon(4S)$
1.15 ± 0.43 ± 0.09		<sup>1</sup> AUBERT	09AV	BABR $e^+e^- \rightarrow \Upsilon(4S)$
• • • We do not use the following data for averages, fits, limits, etc. • • •				
< 1.9	90	<sup>1</sup> CHANG	07B	BELL Repl. by HOI 12
< 2.9	90	<sup>1</sup> AUBERT,B	06V	BABR $e^+e^- \rightarrow \Upsilon(4S)$
< 2.5	90	<sup>1</sup> AUBERT,B	05K	BABR $e^+e^- \rightarrow \Upsilon(4S)$
< 2.0	90	<sup>1</sup> CHANG	05A	BELL Repl. by CHANG 07B
< 5.2	90	<sup>1</sup> AUBERT	04H	BABR Repl. by AUBERT,B 05K
< 9.3	90	<sup>1</sup> RICHICHI	00	CLE2 $e^+e^- \rightarrow \Upsilon(4S)$
< 33	90	BEHRENS	98	CLE2 Repl. by RICHICHI 00

<sup>1</sup> Assumes equal production of  $B^+$  and  $B^0$  at the  $\Upsilon(4S)$ .

 $\Gamma(\eta K^*(892)^0)/\Gamma_{\text{total}}$   $\Gamma_{221}/\Gamma$ 

VALUE (units $10^{-6}$ )	CL%	DOCUMENT ID	TECN	COMMENT
<b>15.9 ± 1.0 OUR AVERAGE</b>				
15.2 ± 1.2 ± 1.0		<sup>1</sup> WANG	07B	BELL $e^+e^- \rightarrow \Upsilon(4S)$
16.5 ± 1.1 ± 0.8		<sup>1</sup> AUBERT,B	06H	BABR $e^+e^- \rightarrow \Upsilon(4S)$
13.8 ± 5.5 ± 1.6		<sup>1</sup> RICHICHI	00	CLE2 $e^+e^- \rightarrow \Upsilon(4S)$
• • • We do not use the following data for averages, fits, limits, etc. • • •				
18.6 ± 2.3 ± 1.2		<sup>1</sup> AUBERT,B	04D	BABR Repl. by AUBERT,B 06H
< 30	90	BEHRENS	98	CLE2 Repl. by RICHICHI 00

<sup>1</sup> Assumes equal production of  $B^+$  and  $B^0$  at the  $\Upsilon(4S)$ .

 $\Gamma(\eta K_0^*(1430)^0)/\Gamma_{\text{total}}$   $\Gamma_{222}/\Gamma$ 

VALUE (units $10^{-6}$ )	DOCUMENT ID	TECN	COMMENT
<b>11.0 ± 1.6 ± 1.5</b>	<sup>1</sup> AUBERT,B	06H	BABR $e^+e^- \rightarrow \Upsilon(4S)$

<sup>1</sup> Assumes equal production of  $B^+$  and  $B^0$  at the  $\Upsilon(4S)$ .

 $\Gamma(\eta K_2^*(1430)^0)/\Gamma_{\text{total}}$   $\Gamma_{223}/\Gamma$ 

VALUE (units $10^{-6}$ )	DOCUMENT ID	TECN	COMMENT
<b>9.6 ± 1.8 ± 1.1</b>	<sup>1</sup> AUBERT,B	06H	BABR $e^+e^- \rightarrow \Upsilon(4S)$

<sup>1</sup> Assumes equal production of  $B^+$  and  $B^0$  at the  $\Upsilon(4S)$ .

 $\Gamma(\omega K^0)/\Gamma_{\text{total}}$   $\Gamma_{224}/\Gamma$ 

VALUE (units $10^{-6}$ )	CL%	DOCUMENT ID	TECN	COMMENT
<b>5.0 ± 0.6 OUR AVERAGE</b>				
5.4 ± 0.8 ± 0.3		<sup>1</sup> AUBERT	07AE	BABR $e^+e^- \rightarrow \Upsilon(4S)$
4.4 ± 0.8 ± 0.4		<sup>1</sup> JEN	06	BELL $e^+e^- \rightarrow \Upsilon(4S)$
10.0 ± 5.4 ± 1.4		<sup>1</sup> JESSOP	00	CLE2 $e^+e^- \rightarrow \Upsilon(4S)$
• • • We do not use the following data for averages, fits, limits, etc. • • •				
6.2 ± 1.0 ± 0.4		<sup>1</sup> AUBERT,B	06E	BABR Repl. by AUBERT 07AE
5.9 ± 1.6 ± 0.5		<sup>1</sup> AUBERT	04H	BABR Repl. by AUBERT,B 06E
4.0 ± 1.9 ± 0.5		<sup>1</sup> WANG	04A	BELL Repl. by JEN 06
< 13	90	<sup>1</sup> AUBERT	01G	BABR Repl. by AUBERT 04H
< 57	90	<sup>1</sup> BERGFELD	98	CLE2 Repl. by JESSOP 00

<sup>1</sup> Assumes equal production of  $B^+$  and  $B^0$  at the  $\Upsilon(4S)$ .

 $\Gamma(a_0(980)^0 K^0 \times B(a_0(980)^0 \rightarrow \eta\pi^0))/\Gamma_{\text{total}}$   $\Gamma_{225}/\Gamma$ 

VALUE (units $10^{-6}$ )	CL%	DOCUMENT ID	TECN	COMMENT
<b>&lt; 7.8</b>	90	<sup>1</sup> AUBERT,BE	04	BABR $e^+e^- \rightarrow \Upsilon(4S)$

<sup>1</sup> Assumes equal production of charged and neutral  $B$  mesons from  $\Upsilon(4S)$  decays.

 $\Gamma(b_1^0 K^0 \times B(b_1^0 \rightarrow \omega\pi^0))/\Gamma_{\text{total}}$   $\Gamma_{226}/\Gamma$ 

VALUE (units $10^{-6}$ )	CL%	DOCUMENT ID	TECN	COMMENT
<b>&lt; 7.8</b>	90	<sup>1</sup> AUBERT	08AG	BABR $e^+e^- \rightarrow \Upsilon(4S)$

<sup>1</sup> Assumes equal production of  $B^+$  and  $B^0$  at the  $\Upsilon(4S)$ .

 $\Gamma(a_0(980)^\pm K^\mp \times B(a_0(980)^\pm \rightarrow \eta\pi^\pm))/\Gamma_{\text{total}}$   $\Gamma_{227}/\Gamma$ 

VALUE (units $10^{-6}$ )	CL%	DOCUMENT ID	TECN	COMMENT
<b>&lt; 1.9</b>	90	<sup>1</sup> AUBERT	07Y	BABR $e^+e^- \rightarrow \Upsilon(4S)$
< 2.1	90	<sup>1</sup> AUBERT,BE	04	BABR Repl. by AUBERT 07Y

<sup>1</sup> Assumes equal production of  $B^+$  and  $B^0$  at the  $\Upsilon(4S)$ .

 $\Gamma(b_1^- K^+ \times B(b_1^- \rightarrow \omega\pi^-))/\Gamma_{\text{total}}$   $\Gamma_{228}/\Gamma$ 

VALUE (units $10^{-6}$ )	DOCUMENT ID	TECN	COMMENT
<b>7.4 ± 1.0 ± 1.0</b>	<sup>1</sup> AUBERT	07Bi	BABR $e^+e^- \rightarrow \Upsilon(4S)$

<sup>1</sup> Assumes equal production of  $B^+$  and  $B^0$  at the  $\Upsilon(4S)$ .

 $\Gamma(b_1^0 K^{*0} \times B(b_1^0 \rightarrow \omega\pi^0))/\Gamma_{\text{total}}$   $\Gamma_{229}/\Gamma$ 

VALUE	CL%	DOCUMENT ID	TECN	COMMENT
<b>&lt; 8.0 × 10<sup>-6</sup></b>	90	<sup>1</sup> AUBERT	09AF	BABR $e^+e^- \rightarrow \Upsilon(4S)$

<sup>1</sup> Assumes equal production of  $B^+$  and  $B^0$  at the  $\Upsilon(4S)$ .

 $\Gamma(b_1^- K^{*+} \times B(b_1^- \rightarrow \omega\pi^-))/\Gamma_{\text{total}}$   $\Gamma_{230}/\Gamma$ 

VALUE	CL%	DOCUMENT ID	TECN	COMMENT
<b>&lt; 5.0 × 10<sup>-6</sup></b>	90	<sup>1</sup> AUBERT	09AF	BABR $e^+e^- \rightarrow \Upsilon(4S)$

<sup>1</sup> Assumes equal production of  $B^+$  and  $B^0$  at the  $\Upsilon(4S)$ .

 $\Gamma(a_0(1450)^\pm K^\mp \times B(a_0(1450)^\pm \rightarrow \eta\pi^\pm))/\Gamma_{\text{total}}$   $\Gamma_{231}/\Gamma$ 

VALUE (units $10^{-6}$ )	CL%	DOCUMENT ID	TECN	COMMENT
<b>&lt; 3.1</b>	90	<sup>1</sup> AUBERT	07Y	BABR $e^+e^- \rightarrow \Upsilon(4S)$

<sup>1</sup> Assumes equal production of  $B^+$  and  $B^0$  at the  $\Upsilon(4S)$ .

 $\Gamma(K_0^*(800) \times X^0(\text{Familon}))/\Gamma_{\text{total}}$   $\Gamma_{232}/\Gamma$ 

VALUE (units $10^{-6}$ )	CL%	DOCUMENT ID	TECN	COMMENT
<b>&lt; 53</b>	90	<sup>1</sup> AMMAR	01B	CLE2 $e^+e^- \rightarrow \Upsilon(4S)$

<sup>1</sup> AMMAR 01B searched for the two-body decay of the  $B$  meson to a massless neutral feebly-interacting particle  $X^0$  such as the familon, the Nambu-Goldstone boson associated with a spontaneously broken global family symmetry.

 $\Gamma(\omega K^*(892)^0)/\Gamma_{\text{total}}$   $\Gamma_{233}/\Gamma$ 

VALUE (units $10^{-6}$ )	CL%	DOCUMENT ID	TECN	COMMENT
<b>2.0 ± 0.5 OUR AVERAGE</b>				
2.2 ± 0.6 ± 0.2		<sup>1</sup> AUBERT	09H	BABR $e^+e^- \rightarrow \Upsilon(4S)$
1.8 ± 0.7 ± 0.3		<sup>1</sup> GOLDENZWE..08	BELL	$e^+e^- \rightarrow \Upsilon(4S)$
• • • We do not use the following data for averages, fits, limits, etc. • • •				
< 4.2	90	<sup>1</sup> AUBERT,B	06T	BABR Repl. by AUBERT 09H
< 6.0	90	<sup>1</sup> AUBERT	05o	BABR Repl. by AUBERT,B 06T
< 23	90	<sup>1</sup> BERGFELD	98	CLE2

<sup>1</sup> Assumes equal production of  $B^+$  and  $B^0$  at the  $\Upsilon(4S)$ .

 $\Gamma(\omega(K\pi)_0^{*0})/\Gamma_{\text{total}}$   $\Gamma_{234}/\Gamma$ 

VALUE (units $10^{-6}$ )	DOCUMENT ID	TECN	COMMENT
<b>18.4 ± 1.8 ± 1.7</b>	<sup>1</sup> AUBERT	09H	BABR $e^+e^- \rightarrow \Upsilon(4S)$

<sup>1</sup> Assumes equal production of  $B^+$  and  $B^0$  at the  $\Upsilon(4S)$ .

## Meson Particle Listings

 $B^0$  $\Gamma(\omega K_0^*(1430)^0)/\Gamma_{\text{total}}$   $\Gamma_{235}/\Gamma$ 

VALUE (units $10^{-6}$ )	DOCUMENT ID	TECN	COMMENT
<b>16.0 ± 1.6 ± 3.0</b>	<sup>1</sup> AUBERT	09H	BABR $e^+e^- \rightarrow \Upsilon(4S)$

<sup>1</sup> Assumes equal production of  $B^+$  and  $B^0$  at the  $\Upsilon(4S)$ .

 $\Gamma(\omega K_2^*(1430)^0)/\Gamma_{\text{total}}$   $\Gamma_{236}/\Gamma$ 

VALUE (units $10^{-6}$ )	DOCUMENT ID	TECN	COMMENT
<b>10.1 ± 2.0 ± 1.1</b>	<sup>1</sup> AUBERT	09H	BABR $e^+e^- \rightarrow \Upsilon(4S)$

<sup>1</sup> Assumes equal production of  $B^+$  and  $B^0$  at the  $\Upsilon(4S)$ .

 $\Gamma(\omega K^+\pi^- \text{ nonresonant})/\Gamma_{\text{total}}$   $\Gamma_{237}/\Gamma$ 

VALUE (units $10^{-6}$ )	DOCUMENT ID	TECN	COMMENT
<b>5.1 ± 0.7 ± 0.7</b>	<sup>1,2</sup> GOLDENZWE..08	BELL	$e^+e^- \rightarrow \Upsilon(4S)$

<sup>1</sup> Assumes equal production of  $B^+$  and  $B^0$  at the  $\Upsilon(4S)$ .  
<sup>2</sup> For the  $K\pi$  mass range 0.755–1.250 GeV/ $c^2$ , excluding  $K^*(892)$ .

 $\Gamma(K^+\pi^-\pi^0)/\Gamma_{\text{total}}$   $\Gamma_{238}/\Gamma$ 

VALUE (units $10^{-6}$ )	CL%	DOCUMENT ID	TECN	COMMENT
<b>37.8 ± 3.2 OUR AVERAGE</b>				
38.5 ± 1.0 ± 3.9		<sup>1,2</sup> LEES	11	BABR $e^+e^- \rightarrow \Upsilon(4S)$
36.6 <sup>+4.2</sup> <sub>-4.3</sub> ± 3.0		<sup>1</sup> CHANG	04	BELL $e^+e^- \rightarrow \Upsilon(4S)$
• • • We do not use the following data for averages, fits, limits, etc. • • •				
35.7 <sup>+2.6</sup> <sub>-1.5</sub> ± 2.2		<sup>1</sup> AUBERT	08AQ	BABR Repl. by LEES 11
<40	90	<sup>1</sup> ECKHART	02	CLE2 $e^+e^- \rightarrow \Upsilon(4S)$

<sup>1</sup> Assumes equal production of  $B^+$  and  $B^0$  at the  $\Upsilon(4S)$ .  
<sup>2</sup> Uses Dalitz plot analysis of  $B^0 \rightarrow K^+\pi^-\pi^0$  decays.

 $\Gamma(K^+\rho^-)/\Gamma_{\text{total}}$   $\Gamma_{239}/\Gamma$ 

VALUE (units $10^{-6}$ )	CL%	DOCUMENT ID	TECN	COMMENT
<b>7.0 ± 0.9 OUR AVERAGE</b>				
6.6 ± 0.5 ± 0.8		<sup>1,2</sup> LEES	11	BABR $e^+e^- \rightarrow \Upsilon(4S)$
15.1 <sup>+3.4</sup> <sub>-3.3</sub> ± 2.4		<sup>1</sup> CHANG	04	BELL $e^+e^- \rightarrow \Upsilon(4S)$
• • • We do not use the following data for averages, fits, limits, etc. • • •				
8.0 <sup>+0.8</sup> <sub>-1.3</sub> ± 0.6		<sup>1</sup> AUBERT	08AQ	BABR Repl. by LEES 11
7.3 <sup>+1.3</sup> <sub>-1.2</sub> ± 1.3		<sup>1</sup> AUBERT	03T	BABR Repl. by AUBERT 08AQ
<32	90	<sup>1</sup> JESSOP	00	CLE2 $e^+e^- \rightarrow \Upsilon(4S)$
<35	90	ASNER	96	CLE2 Repl. by JESSOP 00

<sup>1</sup> Assumes equal production of  $B^+$  and  $B^0$  at the  $\Upsilon(4S)$ .  
<sup>2</sup> Uses Dalitz plot analysis of  $B^0 \rightarrow K^+\pi^-\pi^0$  decays.

 $\Gamma(K^+\rho(1450)^-)/\Gamma_{\text{total}}$   $\Gamma_{240}/\Gamma$ 

VALUE (units $10^{-6}$ )	CL%	DOCUMENT ID	TECN	COMMENT
<b>2.4 ± 1.0 ± 0.6</b>		<sup>1,2</sup> LEES	11	BABR $e^+e^- \rightarrow \Upsilon(4S)$
• • • We do not use the following data for averages, fits, limits, etc. • • •				
<2.1	90	<sup>1</sup> AUBERT	08AQ	BABR Repl. by LEES 11

<sup>1</sup> Assumes equal production of  $B^+$  and  $B^0$  at the  $\Upsilon(4S)$ .  
<sup>2</sup> Uses Dalitz plot analysis of  $B^0 \rightarrow K^+\pi^-\pi^0$  decays.

 $\Gamma(K^+\rho(1700)^-)/\Gamma_{\text{total}}$   $\Gamma_{241}/\Gamma$ 

VALUE (units $10^{-6}$ )	CL%	DOCUMENT ID	TECN	COMMENT
<b>0.6 ± 0.6 ± 0.4</b>		<sup>1,2</sup> LEES	11	BABR $e^+e^- \rightarrow \Upsilon(4S)$
• • • We do not use the following data for averages, fits, limits, etc. • • •				
<1.1	90	<sup>1</sup> AUBERT	08AQ	BABR Repl. by LEES 11

<sup>1</sup> Assumes equal production of  $B^+$  and  $B^0$  at the  $\Upsilon(4S)$ .  
<sup>2</sup> Uses Dalitz plot analysis of  $B^0 \rightarrow K^+\pi^-\pi^0$  decays.

 $\Gamma((K^+\pi^-\pi^0) \text{ non-resonant})/\Gamma_{\text{total}}$   $\Gamma_{242}/\Gamma$ 

VALUE (units $10^{-6}$ )	CL%	DOCUMENT ID	TECN	COMMENT
<b>2.8 ± 0.5 ± 0.4</b>		<sup>1,2</sup> LEES	11	BABR $e^+e^- \rightarrow \Upsilon(4S)$
• • • We do not use the following data for averages, fits, limits, etc. • • •				
4.4 ± 0.9 ± 0.5		<sup>1</sup> AUBERT	08AQ	BABR Repl. by LEES 11
<9.4	90	<sup>1</sup> CHANG	04	BELL $e^+e^- \rightarrow \Upsilon(4S)$

<sup>1</sup> Assumes equal production of  $B^+$  and  $B^0$  at the  $\Upsilon(4S)$ .  
<sup>2</sup> Uses Dalitz plot analysis of  $B^0 \rightarrow K^+\pi^-\pi^0$  decays. The quoted value is only for the flat part of the non-resonant component.

 $\Gamma((K\pi)_0^{*+}\pi^- \times B((K\pi)_0^{*+} \rightarrow K^+\pi^0))/\Gamma_{\text{total}}$   $\Gamma_{243}/\Gamma$ 

VALUE (units $10^{-6}$ )	DOCUMENT ID	TECN	COMMENT
<b>34.2 ± 2.4 ± 4.1</b>	<sup>1,2</sup> LEES	11	BABR $e^+e^- \rightarrow \Upsilon(4S)$
• • • We do not use the following data for averages, fits, limits, etc. • • •			
9.4 <sup>+1.1</sup> <sub>-1.3</sub> ± 2.3	<sup>1</sup> AUBERT	08AQ	BABR Repl. by LEES 11

<sup>1</sup> Assumes equal production of  $B^+$  and  $B^0$  at the  $\Upsilon(4S)$ .  
<sup>2</sup> Uses Dalitz plot analysis of  $B^0 \rightarrow K^+\pi^-\pi^0$  decays.

 $\Gamma((K\pi)_0^{*0}\pi^0 \times B((K\pi)_0^{*0} \rightarrow K^+\pi^-))/\Gamma_{\text{total}}$   $\Gamma_{244}/\Gamma$ 

VALUE (units $10^{-6}$ )	DOCUMENT ID	TECN	COMMENT
<b>8.6 ± 1.1 ± 1.3</b>	<sup>1,2</sup> LEES	11	BABR $e^+e^- \rightarrow \Upsilon(4S)$
• • • We do not use the following data for averages, fits, limits, etc. • • •			
8.7 <sup>+1.1</sup> <sub>-0.9</sub> ± 2.8	<sup>1</sup> AUBERT	08AQ	BABR Repl. by LEES 11

<sup>1</sup> Assumes equal production of  $B^+$  and  $B^0$  at the  $\Upsilon(4S)$ .  
<sup>2</sup> Uses Dalitz plot analysis of  $B^0 \rightarrow K^+\pi^-\pi^0$  decays.

 $\Gamma(K_2^*(1430)^0\pi^0)/\Gamma_{\text{total}}$   $\Gamma_{245}/\Gamma$ 

VALUE (units $10^{-6}$ )	CL%	DOCUMENT ID	TECN	COMMENT
<b>&lt;4.0</b>	90	<sup>1</sup> AUBERT	08AQ	BABR $e^+e^- \rightarrow \Upsilon(4S)$

<sup>1</sup> Assumes equal production of  $B^+$  and  $B^0$  at the  $\Upsilon(4S)$ .

 $\Gamma(K^*(1680)^0\pi^0)/\Gamma_{\text{total}}$   $\Gamma_{246}/\Gamma$ 

VALUE (units $10^{-6}$ )	CL%	DOCUMENT ID	TECN	COMMENT
<b>&lt;7.5</b>	90	<sup>1</sup> AUBERT	08AQ	BABR $e^+e^- \rightarrow \Upsilon(4S)$

<sup>1</sup> Assumes equal production of  $B^+$  and  $B^0$  at the  $\Upsilon(4S)$ .

 $\Gamma(K_x^{*0}\pi^0)/\Gamma_{\text{total}}$   $\Gamma_{247}/\Gamma$ 

VALUE (units $10^{-6}$ )	DOCUMENT ID	TECN	COMMENT
<b>6.1 ± 1.6 ± 0.5</b> <b>-1.5 - 0.6</b>	<sup>1</sup> CHANG	04	BELL $e^+e^- \rightarrow \Upsilon(4S)$

$K_x^{*0}$  stands for the possible candidates of  $K^*(1410)$ ,  $K_0^*(1430)$  and  $K_2^*(1430)$ .  
<sup>1</sup> Assumes equal production of  $B^+$  and  $B^0$  at the  $\Upsilon(4S)$ .

 $\Gamma(K^0\pi^+\pi^- \text{ charmless})/\Gamma_{\text{total}}$   $\Gamma_{248}/\Gamma$ 

VALUE (units $10^{-6}$ )	CL%	DOCUMENT ID	TECN	COMMENT
<b>49.6 ± 2.0 OUR AVERAGE</b>				
50.2 ± 1.5 ± 1.8		<sup>1</sup> AUBERT	09AU	BABR $e^+e^- \rightarrow \Upsilon(4S)$
47.5 ± 2.4 ± 3.7		<sup>2</sup> GARMASH	07	BELL $e^+e^- \rightarrow \Upsilon(4S)$
50 <sup>+10</sup> <sub>-9</sub> ± 7		<sup>1</sup> ECKHART	02	CLE2 $e^+e^- \rightarrow \Upsilon(4S)$
• • • We do not use the following data for averages, fits, limits, etc. • • •				
43.0 ± 2.3 ± 2.3		<sup>1</sup> AUBERT	06I	BABR Repl. by AUBERT 09AU
43.7 ± 3.8 ± 3.4		<sup>1</sup> AUBERT,B	04O	BABR Repl. by AUBERT 06I
45.4 ± 5.2 ± 5.9		<sup>1</sup> GARMASH	04	BELL Repl. by GARMASH 07
<440	90	ALBRECHT	91E	ARG $e^+e^- \rightarrow \Upsilon(4S)$

<sup>1</sup> Assumes equal production of  $B^+$  and  $B^0$  at the  $\Upsilon(4S)$ .  
<sup>2</sup> Uses Dalitz plot analysis of the  $B^0 \rightarrow K^0\pi^+\pi^-$  final state decays.

 $\Gamma(K^0\pi^+\pi^- \text{ non-resonant})/\Gamma_{\text{total}}$   $\Gamma_{249}/\Gamma$ 

VALUE (units $10^{-6}$ )	DOCUMENT ID	TECN	COMMENT
<b>14.7<sup>+4.0</sup><sub>-2.6</sub> OUR AVERAGE</b>	Error includes scale factor of 2.1.		
11.1 <sup>+2.5</sup> <sub>-1.0</sub> ± 0.9	<sup>1</sup> AUBERT	09AU	BABR $e^+e^- \rightarrow \Upsilon(4S)$
19.9 ± 2.5 <sup>+1.7</sup> <sub>-2.0</sub>	<sup>2</sup> GARMASH	07	BELL $e^+e^- \rightarrow \Upsilon(4S)$

<sup>1</sup> Assumes equal production of  $B^+$  and  $B^0$  at the  $\Upsilon(4S)$ .  
<sup>2</sup> Uses Dalitz plot analysis of the  $B^0 \rightarrow K^0\pi^+\pi^-$  final state decays.

 $\Gamma(K^0\rho^0)/\Gamma_{\text{total}}$   $\Gamma_{250}/\Gamma$ 

VALUE (units $10^{-6}$ )	CL%	DOCUMENT ID	TECN	COMMENT
<b>4.7 ± 0.6 OUR AVERAGE</b>				
4.4 <sup>+0.7</sup> <sub>-0.6</sub> ± 0.3		<sup>1</sup> AUBERT	09AU	BABR $e^+e^- \rightarrow \Upsilon(4S)$
6.1 ± 1.0 <sup>+1.1</sup> <sub>-1.2</sub>		<sup>2</sup> GARMASH	07	BELL $e^+e^- \rightarrow \Upsilon(4S)$
• • • We do not use the following data for averages, fits, limits, etc. • • •				
4.9 ± 0.8 ± 0.9		<sup>1</sup> AUBERT	07F	BABR Repl. by AUBERT 09AU
< 39	90	ASNER	96	CLEO $e^+e^- \rightarrow \Upsilon(4S)$
< 320	90	ALBRECHT	91B	ARG $e^+e^- \rightarrow \Upsilon(4S)$
< 500	90	<sup>3</sup> AVERY	89B	CLEO $e^+e^- \rightarrow \Upsilon(4S)$
<64000	90	<sup>4</sup> AVERY	87	CLEO $e^+e^- \rightarrow \Upsilon(4S)$

<sup>1</sup> Assumes equal production of  $B^+$  and  $B^0$  at the  $\Upsilon(4S)$ .  
<sup>2</sup> Uses Dalitz plot analysis of the  $B^0 \rightarrow K^0\pi^+\pi^-$  final state decays.  
<sup>3</sup> AVERY 89B reports  $< 5.8 \times 10^{-4}$  assuming the  $\Upsilon(4S)$  decays 43% to  $B^0\bar{B}^0$ . We rescale to 50%.  
<sup>4</sup> AVERY 87 reports  $< 0.08$  assuming the  $\Upsilon(4S)$  decays 40% to  $B^0\bar{B}^0$ . We rescale to 50%.

 $\Gamma(K^*(892)^+\pi^-)/\Gamma_{\text{total}}$   $\Gamma_{251}/\Gamma$ 

VALUE (units $10^{-6}$ )	CL%	DOCUMENT ID	TECN	COMMENT
<b>8.4 ± 0.8 OUR AVERAGE</b>				
8.0 ± 1.1 ± 0.8		<sup>1,2</sup> LEES	11	BABR $e^+e^- \rightarrow \Upsilon(4S)$
8.3 <sup>+0.9</sup> <sub>-0.8</sub> ± 0.8		<sup>2,3</sup> AUBERT	09AU	BABR $e^+e^- \rightarrow \Upsilon(4S)$
8.4 ± 1.1 <sup>+1.0</sup> <sub>-0.9</sub>		<sup>3</sup> GARMASH	07	BELL $e^+e^- \rightarrow \Upsilon(4S)$
16 <sup>+6</sup> <sub>-5</sub> ± 2		<sup>2</sup> ECKHART	02	CLE2 $e^+e^- \rightarrow \Upsilon(4S)$

See key on page 457

# Meson Particle Listings

## $B^0$

• • • We do not use the following data for averages, fits, limits, etc. • • •

$12.6^{+2.7}_{-1.6} \pm 0.9$	1,2	AUBERT	08AQ	BABR	Repl. by LEES 11
$11.0 \pm 1.5 \pm 0.71$	2	AUBERT	06i	BABR	Repl. by AUBERT 09AU
$12.9 \pm 2.4 \pm 1.4$	2	AUBERT,B	04o	BABR	Repl. by AUBERT 06i
$14.8^{+4.6+2.8}_{-4.4-1.3}$	2	CHANG	04	BELL	Repl. by GARMASH 07
< 72	90	ASNER	96	CLE2	$e^+e^- \rightarrow \Upsilon(4S)$
< 620	90	ALBRECHT	91B	ARG	$e^+e^- \rightarrow \Upsilon(4S)$
< 380	90	AVERY	89B	CLEO	$e^+e^- \rightarrow \Upsilon(4S)$
< 560	90	AVERY	87	CLEO	$e^+e^- \rightarrow \Upsilon(4S)$

- <sup>1</sup> Uses Dalitz plot analysis of  $B^0 \rightarrow K^+ \pi^- \pi^0$  decays.
- <sup>2</sup> Assumes equal production of  $B^+$  and  $B^0$  at the  $\Upsilon(4S)$ .
- <sup>3</sup> Uses Dalitz plot analysis of the  $B^0 \rightarrow K^0 \pi^+ \pi^-$  final state decays.
- <sup>4</sup> AVERY 89B reports  $< 4.4 \times 10^{-4}$  assuming the  $\Upsilon(4S)$  decays 43% to  $B^0 \bar{B}^0$ . We rescale to 50%.
- <sup>5</sup> AVERY 87 reports  $< 7 \times 10^{-4}$  assuming the  $\Upsilon(4S)$  decays 40% to  $B^0 \bar{B}^0$ . We rescale to 50%.

$\Gamma(K_S^0(1430)^+ \pi^-) / \Gamma_{total}$   $\Gamma_{252} / \Gamma$

VALUE (units $10^{-6}$ )	DOCUMENT ID	TECN	COMMENT
<b>33 ± 7 OUR AVERAGE</b>	Error includes scale factor of 2.0.		
$29.9^{+2.3}_{-1.7} \pm 3.6$	1,2	AUBERT	09AU BABR $e^+e^- \rightarrow \Upsilon(4S)$
$49.7 \pm 3.8^{+6.8}_{-8.2}$	2	GARMASH	07 BELL $e^+e^- \rightarrow \Upsilon(4S)$

- <sup>1</sup> Assumes equal production of  $B^+$  and  $B^0$  at the  $\Upsilon(4S)$ .
- <sup>2</sup> Uses Dalitz plot analysis of the  $B^0 \rightarrow K^0 \pi^+ \pi^-$  final state decays.

$\Gamma(K_x^{*+} \pi^-) / \Gamma_{total}$   $\Gamma_{253} / \Gamma$

$K_x^{*+}$  stands for the possible candidates of  $K^*(1410)$ ,  $K_S^*(1430)$  and  $K_2^*(1430)$ .

VALUE (units $10^{-6}$ )	DOCUMENT ID	TECN	COMMENT
<b>5.1 ± 1.5 ± 0.6 - 0.7</b>	1	CHANG	04 BELL $e^+e^- \rightarrow \Upsilon(4S)$

- <sup>1</sup> Assumes equal production of  $B^+$  and  $B^0$  at the  $\Upsilon(4S)$ .

$\Gamma(K^*(1410)^+ \pi^- \times B(K^*(1410)^+ \rightarrow K^0 \pi^+)) / \Gamma_{total}$   $\Gamma_{254} / \Gamma$

VALUE (units $10^{-6}$ )	CL%	DOCUMENT ID	TECN	COMMENT
<b>&lt; 3.8</b>	90	1	GARMASH	07 BELL $e^+e^- \rightarrow \Upsilon(4S)$

- <sup>1</sup> Uses Dalitz plot analysis of the  $B^0 \rightarrow K^0 \pi^+ \pi^-$  final state decays.

$\Gamma(f_0(980) K^0 \times B(f_0(980) \rightarrow \pi^+ \pi^-)) / \Gamma_{total}$   $\Gamma_{255} / \Gamma$

VALUE (units $10^{-6}$ )	CL%	DOCUMENT ID	TECN	COMMENT
<b>7.0 ± 0.9 OUR AVERAGE</b>				
$6.9 \pm 0.8 \pm 0.6$	1	AUBERT	09AU BABR	$e^+e^- \rightarrow \Upsilon(4S)$
$7.6 \pm 1.7^{+0.9}_{-1.3}$	2	GARMASH	07 BELL	$e^+e^- \rightarrow \Upsilon(4S)$

- • • We do not use the following data for averages, fits, limits, etc. • • •
- |                       |    |        |       |      |  |
|-----------------------|----|--------|-------|------|--|
| $5.5 \pm 0.7 \pm 0.6$ | 1  | AUBERT | 06i   | BABR | Repl. by AUBERT 09AU                   |
| < 360                 | 90 | 3      | AVERY | 89B  | CLEO $e^+e^- \rightarrow \Upsilon(4S)$ |
- <sup>1</sup> Assumes equal production of  $B^+$  and  $B^0$  at the  $\Upsilon(4S)$ .
  - <sup>2</sup> Uses Dalitz plot analysis of the  $B^0 \rightarrow K^0 \pi^+ \pi^-$  final state decays.
  - <sup>3</sup> AVERY 89B reports  $< 4.2 \times 10^{-4}$  assuming the  $\Upsilon(4S)$  decays 43% to  $B^0 \bar{B}^0$ . We rescale to 50%.

$\Gamma(f_2(1270) K^0) / \Gamma_{total}$   $\Gamma_{256} / \Gamma$

VALUE (units $10^{-6}$ )	CL%	DOCUMENT ID	TECN	COMMENT
<b>2.7 ± 1.0 ± 0.8 ± 0.9</b>				
	1	AUBERT	09AU BABR	$e^+e^- \rightarrow \Upsilon(4S)$

- • • We do not use the following data for averages, fits, limits, etc. • • •
- |       |    |   |         |         |                                   |
|-------|----|---|---------|---------|-----------------------------------|
| < 2.5 | 90 | 2 | GARMASH | 07 BELL | $e^+e^- \rightarrow \Upsilon(4S)$ |
|-------|----|---|---------|---------|-----------------------------------|
- <sup>1</sup> Assumes equal production of  $B^+$  and  $B^0$  at the  $\Upsilon(4S)$ .
  - <sup>2</sup> GARMASH 07 reports  $B(B^0 \rightarrow f_2(1270) K^0) \times B(f_2(1270) \rightarrow \pi^+ \pi^-) < 1.4 \times 10^{-6}$  using Dalitz plot analysis. We compute  $B(B^0 \rightarrow f_2(1270) K^0)$  using the PDG value  $B(f_2(1270) \rightarrow \pi\pi) = 84.8 \times 10^{-2}$  and 2/3 for the  $\pi^+ \pi^-$  fraction.

$\Gamma(f_x(1300) K^0 \times B(f_x \rightarrow \pi^+ \pi^-)) / \Gamma_{total}$   $\Gamma_{257} / \Gamma$

VALUE (units $10^{-6}$ )	DOCUMENT ID	TECN	COMMENT
<b>1.81 ± 0.55 ± 0.48</b>	1	AUBERT	09AU BABR $e^+e^- \rightarrow \Upsilon(4S)$

- <sup>1</sup> Assumes equal production of  $B^+$  and  $B^0$  at the  $\Upsilon(4S)$ .

$\Gamma(K^*(892)^0 \rho^0) / \Gamma_{total}$   $\Gamma_{258} / \Gamma$

VALUE (units $10^{-6}$ )	CL%	DOCUMENT ID	TECN	COMMENT
<b>3.3 ± 0.5 ± 0.4</b>				
	1,2	LEES	11 BABR	$e^+e^- \rightarrow \Upsilon(4S)$

• • • We do not use the following data for averages, fits, limits, etc. • • •

$3.6 \pm 0.7 \pm 0.4$	1,2	AUBERT	08AQ	BABR	Repl. by LEES 11
< 3.5	90	2	CHANG	04 BELL	$e^+e^- \rightarrow \Upsilon(4S)$
< 3.6	90	JESSOP	00	CLE2	$e^+e^- \rightarrow \Upsilon(4S)$
< 28	90	ASNER	96	CLE2	Repl. by JESSOP 00

- <sup>1</sup> Uses Dalitz plot analysis of  $B^0 \rightarrow K^+ \pi^- \pi^0$  decays.
- <sup>2</sup> Assumes equal production of  $B^+$  and  $B^0$  at the  $\Upsilon(4S)$ .

$\Gamma(K_2^*(1430)^+ \pi^-) / \Gamma_{total}$   $\Gamma_{259} / \Gamma$

VALUE (units $10^{-6}$ )	CL%	DOCUMENT ID	TECN	COMMENT
<b>&lt; 6</b>	90	1	GARMASH	07 BELL $e^+e^- \rightarrow \Upsilon(4S)$

• • • We do not use the following data for averages, fits, limits, etc. • • •

< 16.2	90	2,3	AUBERT	08AQ BABR $e^+e^- \rightarrow \Upsilon(4S)$
< 18	90	3	GARMASH	04 BELL Repl. by GARMASH 07
< 2600	90	ALBRECHT	91B	ARG $e^+e^- \rightarrow \Upsilon(4S)$

- <sup>1</sup> GARMASH 07 reports  $B(B^0 \rightarrow K_2^*(1430)^+ \pi^-) \times B(K_2^*(1430)^+ \rightarrow K^0 \pi^+) < 2.1 \times 10^{-6}$  using Dalitz plot analysis. We compute  $B(B^0 \rightarrow K_2^*(1430)^+ \pi^-)$  using the PDG value  $B(K_2^*(1430) \rightarrow K\pi) = 49.9 \times 10^{-2}$  and 2/3 for the  $K^0 \pi^+$  fraction.
- <sup>2</sup> Uses Dalitz plot analysis of  $B^0 \rightarrow K^+ \pi^- \pi^0$  decays.
- <sup>3</sup> Assumes equal production of  $B^+$  and  $B^0$  at the  $\Upsilon(4S)$ .

$\Gamma(K^*(1680)^+ \pi^-) / \Gamma_{total}$   $\Gamma_{260} / \Gamma$

VALUE (units $10^{-6}$ )	CL%	DOCUMENT ID	TECN	COMMENT
<b>&lt; 10</b>	90	1	GARMASH	07 BELL $e^+e^- \rightarrow \Upsilon(4S)$

• • • We do not use the following data for averages, fits, limits, etc. • • •

< 25	90	2,3	AUBERT	08AQ BABR $e^+e^- \rightarrow \Upsilon(4S)$
------	----	-----	--------	---

- <sup>1</sup> GARMASH 07 reports  $B(B^0 \rightarrow K^*(1680)^+ \pi^-) \times B(K^*(1680)^+ \rightarrow K^0 \pi^+) < 2.6 \times 10^{-6}$  using Dalitz plot analysis. We compute  $B(B^0 \rightarrow K^*(1680)^+ \pi^-)$  using the PDG value  $B(K^*(1680) \rightarrow K\pi) = 38.7 \times 10^{-2}$  and 2/3 for the  $K^0 \pi^+$  fraction.
- <sup>2</sup> Uses Dalitz plot analysis of  $B^0 \rightarrow K^+ \pi^- \pi^0$  decays.
- <sup>3</sup> Assumes equal production of  $B^+$  and  $B^0$  at the  $\Upsilon(4S)$ .

$\Gamma(K^+ \pi^- \pi^+ \pi^-) / \Gamma_{total}$   $\Gamma_{261} / \Gamma$

VALUE	CL%	DOCUMENT ID	TECN	COMMENT
<b>&lt; 2.3 × 10<sup>-4</sup></b>	90	1	ADAM	96D DLPH $e^+e^- \rightarrow Z$

• • • We do not use the following data for averages, fits, limits, etc. • • •

< 2.1 × 10 <sup>-4</sup>	90	2	ABREU	95N DLPH Sup. by ADAM 96D
--------------------------	----	---	-------	---------------------------

- <sup>1</sup> ADAM 96D assumes  $f_{B^0} = f_{B^-} = 0.39$  and  $f_{B_S} = 0.12$ . Contributions from  $B^0$  and  $B_S$  decays cannot be separated. Limits are given for the weighted average of the decay rates for the two neutral  $B$  mesons.
- <sup>2</sup> Assumes a  $B^0$ ,  $B^-$  production fraction of 0.39 and a  $B_S$  production fraction of 0.12. Contributions from  $B^0$  and  $B_S$  decays cannot be separated. Limits are given for the weighted average of the decay rates for the two neutral  $B$  mesons.

$\Gamma(\rho^0 K^+ \pi^-) / \Gamma_{total}$   $\Gamma_{262} / \Gamma$

VALUE (units $10^{-6}$ )	DOCUMENT ID	TECN	COMMENT
<b>2.8 ± 0.5 ± 0.5</b>	1,2	KYEONG	09 BELL $e^+e^- \rightarrow \Upsilon(4S)$

- <sup>1</sup> Assumes equal production of  $B^+$  and  $B^0$  at the  $\Upsilon(4S)$ .
- <sup>2</sup> Required  $0.75 < m_{K^+ \pi^-} < 1.20$  GeV/c<sup>2</sup>.

$\Gamma(f_0(980) K^+ \pi^-) / \Gamma_{total}$   $\Gamma_{263} / \Gamma$

VALUE (units $10^{-6}$ )	DOCUMENT ID	TECN	COMMENT
<b>1.4 ± 0.4 ± 0.3 - 0.4</b>	1,2	KYEONG	09 BELL $e^+e^- \rightarrow \Upsilon(4S)$

- <sup>1</sup> Assumes equal production of  $B^+$  and  $B^0$  at the  $\Upsilon(4S)$ .
- <sup>2</sup> Required  $0.75 < m_{K^+ K^-} < 1.2$  GeV/c<sup>2</sup>.

$\Gamma(K^+ \pi^- \pi^+ \pi^- \text{ nonresonant}) / \Gamma_{total}$   $\Gamma_{264} / \Gamma$

VALUE	CL%	DOCUMENT ID	TECN	COMMENT
<b>&lt; 2.1 × 10<sup>-6</sup></b>	90	1,2	KYEONG	09 BELL $e^+e^- \rightarrow \Upsilon(4S)$

- <sup>1</sup> Assumes equal production of  $B^+$  and  $B^0$  at the  $\Upsilon(4S)$ .
- <sup>2</sup> Required  $0.55 < m_{\pi^+ \pi^-} < 1.42$  and  $0.75 < m_{K^+ \pi^-} < 1.20$  GeV/c<sup>2</sup>.

$\Gamma(K^*(892)^0 \rho^+ \pi^-) / \Gamma_{total}$   $\Gamma_{265} / \Gamma$

VALUE (units $10^{-6}$ )	CL%	DOCUMENT ID	TECN	COMMENT
<b>54.5 ± 2.9 ± 4.3</b>				
	1	AUBERT	07As	BABR $e^+e^- \rightarrow \Upsilon(4S)$

• • • We do not use the following data for averages, fits, limits, etc. • • •

$4.5^{+1.1+0.9}_{-1.0-1.6}$	1,2	KYEONG	09 BELL	$e^+e^- \rightarrow \Upsilon(4S)$
< 1400	90	ALBRECHT	91E	ARG $e^+e^- \rightarrow \Upsilon(4S)$

- <sup>1</sup> Assumes equal production of  $B^+$  and  $B^0$  at the  $\Upsilon(4S)$ .
- <sup>2</sup> Required  $0.55 < m_{\pi^+ \pi^-} < 1.42$  GeV/c<sup>2</sup>.

$\Gamma(K^*(892)^0 \rho^0) / \Gamma_{total}$   $\Gamma_{266} / \Gamma$

VALUE (units $10^{-6}$ )	CL%	DOCUMENT ID	TECN	COMMENT
<b>3.4 ± 1.7 - 1.3 OUR AVERAGE</b>				Error includes scale factor of 1.8.
$2.1^{+0.8+0.9}_{-0.7-0.5}$	1	KYEONG	09 BELL	$e^+e^- \rightarrow \Upsilon(4S)$
$5.6 \pm 0.9 \pm 1.3$	1	AUBERT,B	06G	BABR $e^+e^- \rightarrow \Upsilon(4S)$

- • • We do not use the following data for averages, fits, limits, etc. • • •
- |       |    |          |        |         |  |
|-------|----|----------|--------|---------|--|
| < 34  | 90 | 2        | GODANG | 02 CLE2 | $e^+e^- \rightarrow \Upsilon(4S)$      |
| < 286 | 90 | 3        | ABE    | 00C     | SLD $e^+e^- \rightarrow Z$             |
| < 460 | 90 | ALBRECHT | 91B    | ARG     | $e^+e^- \rightarrow \Upsilon(4S)$      |
| < 580 | 90 | 4        | AVERY  | 89B     | CLEO $e^+e^- \rightarrow \Upsilon(4S)$ |
| < 960 | 90 | 5        | AVERY  | 87      | CLEO $e^+e^- \rightarrow \Upsilon(4S)$ |

## Meson Particle Listings

 $B^0$ 

- <sup>1</sup> Assumes equal production of  $B^+$  and  $B^0$  at the  $\Upsilon(4S)$ .  
<sup>2</sup> Assumes a helicity 00 configuration. For a helicity 11 configuration, the limit decreases to  $2.4 \times 10^{-5}$ .  
<sup>3</sup> ABE 00c assumes  $B(Z \rightarrow b\bar{b}) = (21.7 \pm 0.1)\%$  and the  $B$  fractions  $f_{B^0} = f_{B^+} = (39.7^{+1.8}_{-2.2})\%$  and  $f_{B_s} = (10.5^{+1.8}_{-2.2})\%$ .  
<sup>4</sup> AVERY 89B reports  $< 6.7 \times 10^{-4}$  assuming the  $\Upsilon(4S)$  decays 43% to  $B^0\bar{B}^0$ . We rescale to 50%.  
<sup>5</sup> AVERY 87 reports  $< 1.2 \times 10^{-3}$  assuming the  $\Upsilon(4S)$  decays 40% to  $B^0\bar{B}^0$ . We rescale to 50%.

 $\Gamma(K^*(892)^0 f_0(980))/\Gamma_{\text{total}}$   $\Gamma_{267}/\Gamma$ 

VALUE (units $10^{-6}$ )	CL%	DOCUMENT ID	TECN	COMMENT
$< 2.2$	90	<sup>1</sup> KYEONG 09	BELL	$e^+e^- \rightarrow \Upsilon(4S)$
••• We do not use the following data for averages, fits, limits, etc. •••				
$< 4.3$	90	<sup>1</sup> AUBERT,B 06G	BABR	$e^+e^- \rightarrow \Upsilon(4S)$
$< 170$	90	<sup>2</sup> AVERY 89B	CLEO	$e^+e^- \rightarrow \Upsilon(4S)$

- <sup>1</sup> Assumes equal production of  $B^+$  and  $B^0$  at the  $\Upsilon(4S)$ .  
<sup>2</sup> AVERY 89B reports  $< 2.0 \times 10^{-4}$  assuming the  $\Upsilon(4S)$  decays 43% to  $B^0\bar{B}^0$ . We rescale to 50%.

 $\Gamma(K_1(1270)^+ \pi^-)/\Gamma_{\text{total}}$   $\Gamma_{268}/\Gamma$ 

VALUE	CL%	DOCUMENT ID	TECN	COMMENT
$< 3.0 \times 10^{-5}$	90	<sup>1</sup> AUBERT 10D	BABR	$e^+e^- \rightarrow \Upsilon(4S)$

- <sup>1</sup> Assumes equal production of  $B^+$  and  $B^0$  at the  $\Upsilon(4S)$ .

 $\Gamma(K_1(1400)^+ \pi^-)/\Gamma_{\text{total}}$   $\Gamma_{269}/\Gamma$ 

VALUE	CL%	DOCUMENT ID	TECN	COMMENT
$< 2.7 \times 10^{-5}$	90	<sup>1</sup> AUBERT 10D	BABR	$e^+e^- \rightarrow \Upsilon(4S)$
••• We do not use the following data for averages, fits, limits, etc. •••				
$< 1.1 \times 10^{-3}$	90	ALBRECHT 91B	ARG	$e^+e^- \rightarrow \Upsilon(4S)$

- <sup>1</sup> Assumes equal production of  $B^+$  and  $B^0$  at the  $\Upsilon(4S)$ .

 $\Gamma(a_1(1260)^- K^+)/\Gamma_{\text{total}}$   $\Gamma_{270}/\Gamma$ 

VALUE (units $10^{-6}$ )	CL%	DOCUMENT ID	TECN	COMMENT
$16.3 \pm 2.9 \pm 2.3$		<sup>1,2</sup> AUBERT 08F	BABR	$e^+e^- \rightarrow \Upsilon(4S)$
••• We do not use the following data for averages, fits, limits, etc. •••				
$< 230$	90	<sup>3</sup> ADAM 96D	DLPH	$e^+e^- \rightarrow Z$
$< 390$	90	<sup>4</sup> ABREU 95N	DLPH	Sup. by ADAM 96D

- <sup>1</sup> Assumes equal production of  $B^+$  and  $B^0$  at the  $\Upsilon(4S)$ .  
<sup>2</sup> Assumes  $a_1^\pm$  decays only to  $3\pi$  and  $B(a_1^\pm \rightarrow \pi^\pm \pi^\mp \pi^\pm) = 0.5$ .  
<sup>3</sup> ADAM 96D assumes  $f_{B^0} = f_{B^-} = 0.39$  and  $f_{B_s} = 0.12$ . Contributions from  $B^0$  and  $B_s$  decays cannot be separated. Limits are given for the weighted average of the decay rates for the two neutral  $B$  mesons.  
<sup>4</sup> Assumes a  $B^0, B^-$  production fraction of 0.39 and a  $B_s$  production fraction of 0.12. Contributions from  $B^0$  and  $B_s^0$  decays cannot be separated. Limits are given for the weighted average of the decay rates for the two neutral  $B$  mesons.

 $\Gamma(K^*(892)^+ \rho^-)/\Gamma_{\text{total}}$   $\Gamma_{271}/\Gamma$ 

VALUE (units $10^{-6}$ )	CL%	DOCUMENT ID	TECN	COMMENT
$< 12.0$	90	<sup>1</sup> AUBERT,B 06G	BABR	$e^+e^- \rightarrow \Upsilon(4S)$

- <sup>1</sup> Assumes equal production of  $B^+$  and  $B^0$  at the  $\Upsilon(4S)$ .

 $\Gamma(K_1(1400)^0 \rho^0)/\Gamma_{\text{total}}$   $\Gamma_{272}/\Gamma$ 

VALUE	CL%	DOCUMENT ID	TECN	COMMENT
$< 3.0 \times 10^{-3}$	90	ALBRECHT 91B	ARG	$e^+e^- \rightarrow \Upsilon(4S)$

 $\Gamma(K^+ K^-)/\Gamma_{\text{total}}$   $\Gamma_{273}/\Gamma$ 

VALUE (units $10^{-6}$ )	CL%	DOCUMENT ID	TECN	COMMENT
$< 0.41$	90	<sup>1</sup> LIN 07	BELL	$e^+e^- \rightarrow \Upsilon(4S)$
••• We do not use the following data for averages, fits, limits, etc. •••				
$< 0.7$	90	<sup>2</sup> AALTONEN 09c	CDF	$p\bar{p}$ at 1.96 TeV
$< 0.5$	90	<sup>1</sup> AUBERT 07B	BABR	$e^+e^- \rightarrow \Upsilon(4S)$
$< 1.8$	90	<sup>3</sup> ABULENCIA,A 06D	CDF	Repl. by AALTONEN 09c
$< 0.37$	90	ABE 05G	BELL	Repl. by LIN 07
$< 0.7$	90	CHAO 04	BELL	$e^+e^- \rightarrow \Upsilon(4S)$
$< 0.8$	90	<sup>1</sup> BORNHEIM 03	CLE2	$e^+e^- \rightarrow \Upsilon(4S)$
$< 0.6$	90	<sup>1</sup> AUBERT 02Q	BABR	$e^+e^- \rightarrow \Upsilon(4S)$
$< 0.9$	90	<sup>1</sup> CASEY 02	BELL	$e^+e^- \rightarrow \Upsilon(4S)$
$< 2.7$	90	<sup>1</sup> ABE 01H	BELL	$e^+e^- \rightarrow \Upsilon(4S)$
$< 2.5$	90	<sup>1</sup> AUBERT 01E	BABR	$e^+e^- \rightarrow \Upsilon(4S)$
$< 66$	90	<sup>4</sup> ABE 00c	SLD	$e^+e^- \rightarrow Z$
$< 1.9$	90	<sup>1</sup> CRONIN-HEN..00	CLE2	$e^+e^- \rightarrow \Upsilon(4S)$
$< 4.3$	90	GODANG 98	CLE2	Repl. by CRONIN-HENNESSY 00
$< 46$		<sup>5</sup> ADAM 96D	DLPH	$e^+e^- \rightarrow Z$
$< 4$	90	ASNER 96	CLE2	Repl. by GODANG 98
$< 18$	90	<sup>6</sup> BUSKULIC 96v	ALEP	$e^+e^- \rightarrow Z$
$< 120$	90	<sup>7</sup> ABREU 95N	DLPH	Sup. by ADAM 96D
$< 7$	90	<sup>1</sup> BATTLE 93	CLE2	$e^+e^- \rightarrow \Upsilon(4S)$

- <sup>1</sup> Assumes equal production of  $B^+$  and  $B^0$  at the  $\Upsilon(4S)$ .  
<sup>2</sup> Obtains this result from  $B(K^+ K^-)/B(K^+ \pi^-) = 0.020 \pm 0.008 \pm 0.006$ , assuming  $B(B^0 \rightarrow K^+ \pi^-) = (19.4 \pm 0.6) \times 10^{-6}$ .  
<sup>3</sup> ABULENCIA,A 06D obtains this from  $\Gamma(K^+ K^-)/\Gamma(K^+ \pi^-) < 0.10$  at 90% CL, assuming  $B(B^0 \rightarrow K^+ \pi^-) = (18.9 \pm 0.7) \times 10^{-6}$ .  
<sup>4</sup> ABE 00c assumes  $B(Z \rightarrow b\bar{b}) = (21.7 \pm 0.1)\%$  and the  $B$  fractions  $f_{B^0} = f_{B^+} = (39.7^{+1.8}_{-2.2})\%$  and  $f_{B_s} = (10.5^{+1.8}_{-2.2})\%$ .  
<sup>5</sup> ADAM 96D assumes  $f_{B^0} = f_{B^-} = 0.39$  and  $f_{B_s} = 0.12$ . Contributions from  $B^0$  and  $B_s$  decays cannot be separated. Limits are given for the weighted average of the decay rates for the two neutral  $B$  mesons.  
<sup>6</sup> BUSKULIC 96v assumes PDG 96 production fractions for  $B^0, B^+, B_s, b$  baryons.  
<sup>7</sup> Assumes a  $B^0, B^-$  production fraction of 0.39 and a  $B_s$  production fraction of 0.12. Contributions from  $B^0$  and  $B_s^0$  decays cannot be separated. Limits are given for the weighted average of the decay rates for the two neutral  $B$  mesons.

 $\Gamma(K^0 \bar{K}^0)/\Gamma_{\text{total}}$   $\Gamma_{274}/\Gamma$ 

VALUE (units $10^{-6}$ )	CL%	DOCUMENT ID	TECN	COMMENT
$0.96^{+0.20}_{-0.18}$		<b>OUR AVERAGE</b>		
$0.87^{+0.25}_{-0.20} \pm 0.09$		<sup>1</sup> LIN 07	BELL	$e^+e^- \rightarrow \Upsilon(4S)$
$1.08 \pm 0.28 \pm 0.11$		<sup>1</sup> AUBERT,BE 06c	BABR	$e^+e^- \rightarrow \Upsilon(4S)$
••• We do not use the following data for averages, fits, limits, etc. •••				
$0.8 \pm 0.3 \pm 0.9$		<sup>1</sup> ABE 05G	BELL	Repl. by LIN 07
$1.19^{+0.40}_{-0.35} \pm 0.13$		<sup>1</sup> AUBERT,BE 05E	BABR	Repl. by AUBERT,BE 06c
$< 1.8$	90	<sup>1</sup> AUBERT 04M	BABR	$e^+e^- \rightarrow \Upsilon(4S)$
$< 1.5$	90	<sup>1</sup> CHAO 04	BELL	Repl. by ABE 05G
$< 3.3$	90	<sup>1</sup> BORNHEIM 03	CLE2	$e^+e^- \rightarrow \Upsilon(4S)$
$< 4.1$	90	<sup>1</sup> CASEY 02	BELL	$e^+e^- \rightarrow \Upsilon(4S)$
$< 17$	90	GODANG 98	CLE2	$e^+e^- \rightarrow \Upsilon(4S)$

- <sup>1</sup> Assumes equal production of  $B^+$  and  $B^0$  at the  $\Upsilon(4S)$ .

 $\Gamma(K^0 K^- \pi^+)/\Gamma_{\text{total}}$   $\Gamma_{275}/\Gamma$ 

VALUE (units $10^{-6}$ )	CL%	DOCUMENT ID	TECN	COMMENT
$6.4 \pm 1.0 \pm 0.6$		<sup>1</sup> DEL-AMO-SA..10E	BABR	$e^+e^- \rightarrow \Upsilon(4S)$
••• We do not use the following data for averages, fits, limits, etc. •••				
$< 18$	90	<sup>1</sup> GARMASH 04	BELL	$e^+e^- \rightarrow \Upsilon(4S)$
$< 21$	90	<sup>1</sup> ECKHART 02	CLE2	$e^+e^- \rightarrow \Upsilon(4S)$

- <sup>1</sup> Assumes equal production of  $B^+$  and  $B^0$  at the  $\Upsilon(4S)$ .

 $[\Gamma(\bar{K}^{*0} K^0) + \Gamma(K^{*0} \bar{K}^0)]/\Gamma_{\text{total}}$   $\Gamma_{276}/\Gamma$ 

VALUE (units $10^{-6}$ )	CL%	DOCUMENT ID	TECN	COMMENT
$< 1.9$		<sup>1</sup> AUBERT,BE 06N	BABR	$e^+e^- \rightarrow \Upsilon(4S)$

- <sup>1</sup> Assumes equal production of  $B^+$  and  $B^0$  at the  $\Upsilon(4S)$ .

 $\Gamma(K^+ K^- \pi^0)/\Gamma_{\text{total}}$   $\Gamma_{277}/\Gamma$ 

VALUE	CL%	DOCUMENT ID	TECN	COMMENT
$< 19 \times 10^{-6}$	90	<sup>1</sup> ECKHART 02	CLE2	$e^+e^- \rightarrow \Upsilon(4S)$

- <sup>1</sup> Assumes equal production of  $B^+$  and  $B^0$  at the  $\Upsilon(4S)$ .

 $\Gamma(K_S^0 K_S^0 \pi^0)/\Gamma_{\text{total}}$   $\Gamma_{278}/\Gamma$ 

VALUE	CL%	DOCUMENT ID	TECN	COMMENT
$< 0.9 \times 10^{-6}$	90	<sup>1</sup> AUBERT 09AD	BABR	$e^+e^- \rightarrow \Upsilon(4S)$

- <sup>1</sup> Assumes equal production of  $B^+$  and  $B^0$  at the  $\Upsilon(4S)$ .

 $\Gamma(K_S^0 K_S^0 \eta)/\Gamma_{\text{total}}$   $\Gamma_{279}/\Gamma$ 

VALUE	CL%	DOCUMENT ID	TECN	COMMENT
$< 1.0 \times 10^{-6}$	90	<sup>1</sup> AUBERT 09AD	BABR	$e^+e^- \rightarrow \Upsilon(4S)$

- <sup>1</sup> Assumes equal production of  $B^+$  and  $B^0$  at the  $\Upsilon(4S)$ .

 $\Gamma(K_S^0 K_S^0 \eta')/\Gamma_{\text{total}}$   $\Gamma_{280}/\Gamma$ 

VALUE	CL%	DOCUMENT ID	TECN	COMMENT
$< 2.0 \times 10^{-6}$	90	<sup>1</sup> AUBERT 09AD	BABR	$e^+e^- \rightarrow \Upsilon(4S)$

- <sup>1</sup> Assumes equal production of  $B^+$  and  $B^0$  at the  $\Upsilon(4S)$ .

 $\Gamma(K^0 K^+ K^-)/\Gamma_{\text{total}}$   $\Gamma_{281}/\Gamma$ 

VALUE (units $10^{-6}$ )	CL%	DOCUMENT ID	TECN	COMMENT
$24.7 \pm 2.3$		<b>OUR AVERAGE</b>		
$23.8 \pm 2.0 \pm 1.6$		<sup>1</sup> AUBERT,B 04V	BABR	$e^+e^- \rightarrow \Upsilon(4S)$
$28.3 \pm 3.3 \pm 4.0$		<sup>1</sup> GARMASH 04	BELL	$e^+e^- \rightarrow \Upsilon(4S)$

- We do not use the following data for averages, fits, limits, etc. •••  
 $< 1300$  90 ALBRECHT 91E ARG  $e^+e^- \rightarrow \Upsilon(4S)$   
<sup>1</sup> Assumes equal production of  $B^+$  and  $B^0$  at the  $\Upsilon(4S)$ .

See key on page 457

# Meson Particle Listings

## $B^0$

### $\Gamma(K^0\phi)/\Gamma_{total}$ $\Gamma_{282}/\Gamma$

VALUE (units $10^{-6}$ )	CL%	DOCUMENT ID	TECN	COMMENT
<b>8.6<sup>+1.3</sup><sub>-1.1</sub> OUR AVERAGE</b>				
8.4 <sup>+1.5</sup> <sub>-1.3</sub> ± 0.5		<sup>1</sup> AUBERT	04A	BABR $e^+e^- \rightarrow \Upsilon(4S)$
9.0 <sup>+2.2</sup> <sub>-1.8</sub> ± 0.7		<sup>1</sup> CHEN	03B	BELL $e^+e^- \rightarrow \Upsilon(4S)$
• • • We do not use the following data for averages, fits, limits, etc. • • •				
8.1 <sup>+3.1</sup> <sub>-2.5</sub> ± 0.8		<sup>1</sup> AUBERT	01D	BABR $e^+e^- \rightarrow \Upsilon(4S)$
< 12.3	90	<sup>1</sup> BRIERE	01	CLE2 $e^+e^- \rightarrow \Upsilon(4S)$
< 31	90	<sup>1</sup> BERGFELD	98	CLE2
< 88	90	ASNER	96	CLE2 $e^+e^- \rightarrow \Upsilon(4S)$
< 720	90	ALBRECHT	91B	ARG $e^+e^- \rightarrow \Upsilon(4S)$
< 420	90	<sup>2</sup> AVERY	89B	CLEO $e^+e^- \rightarrow \Upsilon(4S)$
< 1000	90	<sup>3</sup> AVERY	87	CLEO $e^+e^- \rightarrow \Upsilon(4S)$

- <sup>1</sup> Assumes equal production of  $B^+$  and  $B^0$  at the  $\Upsilon(4S)$ .
- <sup>2</sup> AVERY 89B reports  $< 4.9 \times 10^{-4}$  assuming the  $\Upsilon(4S)$  decays 43% to  $B^0\bar{B}^0$ . We rescale to 50%.
- <sup>3</sup> AVERY 87 reports  $< 1.3 \times 10^{-3}$  assuming the  $\Upsilon(4S)$  decays 40% to  $B^0\bar{B}^0$ . We rescale to 50%.

### $\Gamma(K_S^0 K_S^0 K_S^0)/\Gamma_{total}$ $\Gamma_{283}/\Gamma$

VALUE (units $10^{-6}$ )	CL%	DOCUMENT ID	TECN	COMMENT
<b>6.2<sup>+1.2</sup><sub>-1.1</sub> OUR AVERAGE</b> Error includes scale factor of 1.3.				
6.9 <sup>+0.9</sup> <sub>-0.8</sub> ± 0.6		<sup>1</sup> AUBERT,B	05	BABR $e^+e^- \rightarrow \Upsilon(4S)$
4.2 <sup>+1.6</sup> <sub>-1.3</sub> ± 0.8		<sup>1</sup> GARMASH	04	BELL $e^+e^- \rightarrow \Upsilon(4S)$

- <sup>1</sup> Assumes equal production of  $B^+$  and  $B^0$  at the  $\Upsilon(4S)$ .

### $\Gamma(K_S^0 K_S^0 K_L^0)/\Gamma_{total}$ $\Gamma_{284}/\Gamma$

VALUE (units $10^{-6}$ )	CL%	DOCUMENT ID	TECN	COMMENT
<b>&lt; 16</b>	90	<sup>1</sup> AUBERT,B	06R	BABR $e^+e^- \rightarrow \Upsilon(4S)$

- <sup>1</sup> Assumes equal production of  $B^+$  and  $B^0$  at the  $\Upsilon(4S)$ .

### $\Gamma(K^*(892)^0 K^+ K^-)/\Gamma_{total}$ $\Gamma_{285}/\Gamma$

VALUE (units $10^{-6}$ )	CL%	DOCUMENT ID	TECN	COMMENT
<b>27.5 ± 1.3 ± 2.2</b>				
		<sup>1</sup> AUBERT	07As	BABR $e^+e^- \rightarrow \Upsilon(4S)$
• • • We do not use the following data for averages, fits, limits, etc. • • •				
< 610	90	ALBRECHT	91E	ARG $e^+e^- \rightarrow \Upsilon(4S)$

- <sup>1</sup> Assumes equal production of  $B^+$  and  $B^0$  at the  $\Upsilon(4S)$ .

### $\Gamma(K^*(892)^0 \phi)/\Gamma_{total}$ $\Gamma_{286}/\Gamma$

VALUE (units $10^{-6}$ )	CL%	DOCUMENT ID	TECN	COMMENT
<b>9.8 ± 0.6 OUR AVERAGE</b>				
9.7 ± 0.5 ± 0.5		<sup>1</sup> AUBERT	08Bg	BABR $e^+e^- \rightarrow \Upsilon(4S)$
10.0 <sup>+1.6</sup> <sub>-1.5</sub> ± 0.7		<sup>1</sup> CHEN	03B	BELL $e^+e^- \rightarrow \Upsilon(4S)$
11.5 <sup>+4.5</sup> <sub>-3.7</sub> ± 1.8		<sup>1</sup> BRIERE	01	CLE2 $e^+e^- \rightarrow \Upsilon(4S)$

• • • We do not use the following data for averages, fits, limits, etc. • • •				
9.2 ± 0.7 ± 0.6		<sup>1</sup> AUBERT	07D	BABR Repl. by AUBERT 08Bg
9.2 ± 0.9 ± 0.5		<sup>1</sup> AUBERT,B	04W	BABR Repl. by AUBERT 07D
11.2 ± 1.3 ± 0.8		<sup>1</sup> AUBERT	03V	BABR Repl. by AUBERT,B 04W
8.7 <sup>+2.5</sup> <sub>-2.1</sub> ± 1.1		<sup>1</sup> AUBERT	01D	BABR Repl. by AUBERT 03V
< 384	90	<sup>2</sup> ABE	00c	SLD $e^+e^- \rightarrow Z$
< 21	90	<sup>1</sup> BERGFELD	98	CLE2
< 43	90	ASNER	96	CLE2 $e^+e^- \rightarrow \Upsilon(4S)$
< 320	90	ALBRECHT	91B	ARG $e^+e^- \rightarrow \Upsilon(4S)$
< 380	90	<sup>3</sup> AVERY	89B	CLEO $e^+e^- \rightarrow \Upsilon(4S)$
< 380	90	<sup>4</sup> AVERY	87	CLEO $e^+e^- \rightarrow \Upsilon(4S)$

- <sup>1</sup> Assumes equal production of  $B^+$  and  $B^0$  at the  $\Upsilon(4S)$ .
- <sup>2</sup> ABE 00c assumes  $B(Z \rightarrow b\bar{b}) = (21.7 \pm 0.1)\%$  and the  $B$  fractions  $f_{B^0} = f_{B^+} = (39.7^{+1.8}_{-2.2})\%$  and  $f_{B_s} = (10.5^{+1.8}_{-2.2})\%$ .
- <sup>3</sup> AVERY 89B reports  $< 4.4 \times 10^{-4}$  assuming the  $\Upsilon(4S)$  decays 43% to  $B^0\bar{B}^0$ . We rescale to 50%.
- <sup>4</sup> AVERY 87 reports  $< 4.7 \times 10^{-4}$  assuming the  $\Upsilon(4S)$  decays 40% to  $B^0\bar{B}^0$ . We rescale to 50%.

### $\Gamma(K^+ K^- \pi^+ \pi^- \text{nonresonant})/\Gamma_{total}$ $\Gamma_{287}/\Gamma$

VALUE (units $10^{-6}$ )	CL%	DOCUMENT ID	TECN	COMMENT
<b>&lt; 71.7</b>	90	<sup>1,2</sup> CHIANG	10	BELL $e^+e^- \rightarrow \Upsilon(4S)$

- <sup>1</sup> Measured in the range  $0.7 < m_{K\pi} < 1.7$  and corrected using PS assumption for the full  $K\pi$  mass range.
- <sup>2</sup> Assumes equal production of  $B^+$  and  $B^0$  at the  $\Upsilon(4S)$ .

### $\Gamma(K^*(892)^0 K^- \pi^+)/\Gamma_{total}$ $\Gamma_{288}/\Gamma$

VALUE (units $10^{-6}$ )	CL%	DOCUMENT ID	TECN	COMMENT
<b>4.5 ± 1.3 OUR AVERAGE</b>				
2.11 <sup>+5.63</sup> <sub>-5.26</sub> ± 4.85		<sup>1,2</sup> CHIANG	10	BELL $e^+e^- \rightarrow \Upsilon(4S)$
4.6 ± 1.1 ± 0.8		<sup>2</sup> AUBERT	07As	BABR $e^+e^- \rightarrow \Upsilon(4S)$

- <sup>1</sup> Measured in the range  $0.7 < m_{K\pi} < 1.7$  and corrected using PS assumption for the full  $K\pi$  mass range. The quoted result is equivalent to the upper limit of  $< 13.9 \times 10^{-6}$  at 90% CL.
- <sup>2</sup> Assumes equal production of  $B^+$  and  $B^0$  at the  $\Upsilon(4S)$ .

### $\Gamma(K^*(892)^0 \bar{K}^*(892)^0)/\Gamma_{total}$ $\Gamma_{289}/\Gamma$

VALUE (units $10^{-6}$ )	CL%	DOCUMENT ID	TECN	COMMENT
<b>0.8 ± 0.5 OUR AVERAGE</b> Error includes scale factor of 2.2.				
0.26 <sup>+0.33</sup> <sub>-0.29</sub> ± 0.10		<sup>1,2</sup> CHIANG	10	BELL $e^+e^- \rightarrow \Upsilon(4S)$
1.28 <sup>+0.35</sup> <sub>-0.30</sub> ± 0.11		<sup>2</sup> AUBERT	08i	BABR $e^+e^- \rightarrow \Upsilon(4S)$

- • • We do not use the following data for averages, fits, limits, etc. • • •
- < 22
 90 | <sup>3</sup> GODANG | 02 | CLE2  $e^+e^- \rightarrow \Upsilon(4S)$ |
- < 469
 90 | <sup>4</sup> ABE | 00c | SLD  $e^+e^- \rightarrow Z$ |
- <sup>1</sup> Measured in the range  $0.7 < m_{K\pi} < 1.7$  and corrected using PS assumption for the full  $K\pi$  mass range. The quoted result is equivalent to the upper limit of  $< 0.8 \times 10^{-6}$  at 90% CL.
- <sup>2</sup> Assumes equal production of  $B^+$  and  $B^0$  at the  $\Upsilon(4S)$ .
- <sup>3</sup> Assumes a helicity 00 configuration. For a helicity 11 configuration, the limit decreases to  $1.9 \times 10^{-5}$ .
- <sup>4</sup> ABE 00c assumes  $B(Z \rightarrow b\bar{b}) = (21.7 \pm 0.1)\%$  and the  $B$  fractions  $f_{B^0} = f_{B^+} = (39.7^{+1.8}_{-2.2})\%$  and  $f_{B_s} = (10.5^{+1.8}_{-2.2})\%$ .

### $\Gamma(K^+ K^+ \pi^- \text{nonresonant})/\Gamma_{total}$ $\Gamma_{290}/\Gamma$

VALUE (units $10^{-6}$ )	CL%	DOCUMENT ID	TECN	COMMENT
<b>&lt; 6.0</b>	90	<sup>1</sup> CHIANG	10	BELL $e^+e^- \rightarrow \Upsilon(4S)$

- <sup>1</sup> Assumes equal production of  $B^+$  and  $B^0$  at the  $\Upsilon(4S)$ .

### $\Gamma(K^*(892)^0 K^+ \pi^-)/\Gamma_{total}$ $\Gamma_{291}/\Gamma$

VALUE (units $10^{-6}$ )	CL%	DOCUMENT ID	TECN	COMMENT
<b>&lt; 2.2</b>				
		<sup>1</sup> AUBERT	07As	BABR $e^+e^- \rightarrow \Upsilon(4S)$
< 7.6	90	<sup>1</sup> CHIANG	10	BELL $e^+e^- \rightarrow \Upsilon(4S)$

- <sup>1</sup> Assumes equal production of  $B^+$  and  $B^0$  at the  $\Upsilon(4S)$ .

### $\Gamma(K^*(892)^0 K^*(892)^0)/\Gamma_{total}$ $\Gamma_{292}/\Gamma$

VALUE (units $10^{-6}$ )	CL%	DOCUMENT ID	TECN	COMMENT
<b>&lt; 0.2</b>				
		<sup>1</sup> CHIANG	10	BELL $e^+e^- \rightarrow \Upsilon(4S)$
< 0.41	90	<sup>1</sup> AUBERT	08i	BABR $e^+e^- \rightarrow \Upsilon(4S)$
< 37	90	<sup>2</sup> GODANG	02	CLE2 $e^+e^- \rightarrow \Upsilon(4S)$

- <sup>1</sup> Assumes equal production of  $B^+$  and  $B^0$  at the  $\Upsilon(4S)$ .
- <sup>2</sup> Assumes a helicity 00 configuration. For a helicity 11 configuration, the limit decreases to  $2.9 \times 10^{-5}$ .

### $\Gamma(K^*(892)^+ K^*(892)^-)/\Gamma_{total}$ $\Gamma_{293}/\Gamma$

VALUE (units $10^{-6}$ )	CL%	DOCUMENT ID	TECN	COMMENT
<b>&lt; 2.0</b>				
		<sup>1</sup> AUBERT	08AP	BABR $e^+e^- \rightarrow \Upsilon(4S)$
• • • We do not use the following data for averages, fits, limits, etc. • • •				
< 141	90	<sup>2</sup> GODANG	02	CLE2 $e^+e^- \rightarrow \Upsilon(4S)$

- <sup>1</sup> Assumes equal production of  $B^+$  and  $B^0$  at the  $\Upsilon(4S)$ .
- <sup>2</sup> Assumes a helicity 00 configuration. For a helicity 11 configuration, the limit decreases to  $8.9 \times 10^{-5}$ .

### $\Gamma(K_1(1400)^0 \phi)/\Gamma_{total}$ $\Gamma_{294}/\Gamma$

VALUE	CL%	DOCUMENT ID	TECN	COMMENT
<b>&lt; 5.0 × 10<sup>-3</sup></b>	90	ALBRECHT	91B	ARG $e^+e^- \rightarrow \Upsilon(4S)$

### $\Gamma(\phi(K\pi)_0^0(1.60 < m_{K\pi} < 2.15))/\Gamma_{total}$ $\Gamma_{295}/\Gamma$

VALUE (units $10^{-6}$ )	CL%	DOCUMENT ID	TECN	COMMENT
<b>4.3 ± 0.6 ± 0.4</b>				
		<sup>1</sup> AUBERT	08Bg	BABR $e^+e^- \rightarrow \Upsilon(4S)$
• • • We do not use the following data for averages, fits, limits, etc. • • •				
5.0 ± 0.8 ± 0.3		<sup>1</sup> AUBERT	07D	BABR Repl. by AUBERT 08Bg

- <sup>1</sup> Assumes equal production of  $B^+$  and  $B^0$  at the  $\Upsilon(4S)$ .

### $\Gamma(\phi(K\pi)_0^0(1.60 < m_{K\pi} < 2.15))/\Gamma_{total}$ $\Gamma_{296}/\Gamma$

VALUE (units $10^{-6}$ )	CL%	DOCUMENT ID	TECN	COMMENT
<b>&lt; 1.7</b>				
		<sup>1</sup> AUBERT	07A0	BABR $e^+e^- \rightarrow \Upsilon(4S)$

- <sup>1</sup> Assumes equal production of  $B^+$  and  $B^0$  at the  $\Upsilon(4S)$ .





See key on page 457

## Meson Particle Listings

 $B^0$ 

$\Gamma(K^*(892)^0 X(214) \times B(X \rightarrow \mu^+ \mu^-))/\Gamma_{\text{total}}$   $\Gamma_{317}/\Gamma$   
 $X(214)$  is a hypothetical particle of mass 214 MeV/ $c^2$  reported by the HyperCP experiment (PARK 05)

VALUE (units $10^{-8}$ )	CL%	DOCUMENT ID	TECN	COMMENT
<2.26	90	1,2 HYUN	10	BELL $e^+ e^- \rightarrow \Upsilon(4S)$

- <sup>1</sup> Assumes equal production of  $B^+$  and  $B^0$  at the  $\Upsilon(4S)$ .  
<sup>2</sup> Based on scalar nature of  $X$  particle. With a vector  $X$  assumption, the upper limit is  $2.27 \times 10^{-8}$ .

$\Gamma(K^0 \pi^+ \pi^- \gamma)/\Gamma_{\text{total}}$   $\Gamma_{318}/\Gamma$   
 VALUE (units  $10^{-5}$ )

VALUE (units $10^{-5}$ )	CL%	DOCUMENT ID	TECN	COMMENT
<b>1.95 ± 0.22 OUR AVERAGE</b>				
1.85 ± 0.21 ± 0.12		1,2 AUBERT	07R	BABR $e^+ e^- \rightarrow \Upsilon(4S)$
2.40 ± 0.4 ± 0.3		2,3 YANG	05	BELL $e^+ e^- \rightarrow \Upsilon(4S)$

- <sup>1</sup>  $M_{K\pi\pi} < 1.8$  GeV/ $c^2$ .  
<sup>2</sup> Assumes equal production of  $B^+$  and  $B^0$  at the  $\Upsilon(4S)$ .  
<sup>3</sup>  $M_{K\pi\pi} < 2.0$  GeV/ $c^2$ .

$\Gamma(K^+ \pi^- \pi^0 \gamma)/\Gamma_{\text{total}}$   $\Gamma_{319}/\Gamma$   
 VALUE (units  $10^{-5}$ )

VALUE (units $10^{-5}$ )	CL%	DOCUMENT ID	TECN	COMMENT
<b>4.07 ± 0.22 ± 0.31</b>		1,2 AUBERT	07R	BABR $e^+ e^- \rightarrow \Upsilon(4S)$

- <sup>1</sup>  $M_{K\pi\pi} < 1.8$  GeV/ $c^2$ .  
<sup>2</sup> Assumes equal production of  $B^+$  and  $B^0$  at the  $\Upsilon(4S)$ .

$\Gamma(K_1(1270)^0 \gamma)/\Gamma_{\text{total}}$   $\Gamma_{320}/\Gamma$   
 VALUE (units  $10^{-5}$ )

VALUE (units $10^{-5}$ )	CL%	DOCUMENT ID	TECN	COMMENT
< 5.8	90	1 YANG	05	BELL $e^+ e^- \rightarrow \Upsilon(4S)$

- • • We do not use the following data for averages, fits, limits, etc. • • •  
 <700 90 <sup>2</sup> ALBRECHT 89G ARG  $e^+ e^- \rightarrow \Upsilon(4S)$

- <sup>1</sup> Assumes equal production of  $B^+$  and  $B^0$  at the  $\Upsilon(4S)$ .  
<sup>2</sup> ALBRECHT 89G reports < 0.0078 assuming the  $\Upsilon(4S)$  decays 45% to  $B^0 \bar{B}^0$ . We rescale to 50%.

$\Gamma(K_1(1400)^0 \gamma)/\Gamma_{\text{total}}$   $\Gamma_{321}/\Gamma$   
 VALUE (units  $10^{-5}$ )

VALUE (units $10^{-5}$ )	CL%	DOCUMENT ID	TECN	COMMENT
< 1.2	90	1 YANG	05	BELL $e^+ e^- \rightarrow \Upsilon(4S)$

- • • We do not use the following data for averages, fits, limits, etc. • • •  
 <430 90 <sup>2</sup> ALBRECHT 89G ARG  $e^+ e^- \rightarrow \Upsilon(4S)$

- <sup>1</sup> Assumes equal production of  $B^+$  and  $B^0$  at the  $\Upsilon(4S)$ .  
<sup>2</sup> ALBRECHT 89G reports < 0.0048 assuming the  $\Upsilon(4S)$  decays 45% to  $B^0 \bar{B}^0$ . We rescale to 50%.

$\Gamma(K_2^*(1430)^0 \gamma)/\Gamma_{\text{total}}$   $\Gamma_{322}/\Gamma$   
 VALUE (units  $10^{-5}$ )

VALUE (units $10^{-5}$ )	CL%	DOCUMENT ID	TECN	COMMENT
<b>1.24 ± 0.24 OUR AVERAGE</b>				
1.22 ± 0.25 ± 0.10		1 AUBERT,B	04U	BABR $e^+ e^- \rightarrow \Upsilon(4S)$
1.3 ± 0.5 ± 0.1		1 NISHIDA	02	BELL $e^+ e^- \rightarrow \Upsilon(4S)$

- • • We do not use the following data for averages, fits, limits, etc. • • •  
 <40 90 <sup>2</sup> ALBRECHT 89G ARG  $e^+ e^- \rightarrow \Upsilon(4S)$

- <sup>1</sup> Assumes equal production of  $B^+$  and  $B^0$  at the  $\Upsilon(4S)$ .  
<sup>2</sup> ALBRECHT 89G reports <  $4.4 \times 10^{-4}$  assuming the  $\Upsilon(4S)$  decays 45% to  $B^0 \bar{B}^0$ . We rescale to 50%.

$\Gamma(K^*(1680)^0 \gamma)/\Gamma_{\text{total}}$   $\Gamma_{323}/\Gamma$   
 VALUE

VALUE	CL%	DOCUMENT ID	TECN	COMMENT
<0.0020	90	1 ALBRECHT	89G	ARG $e^+ e^- \rightarrow \Upsilon(4S)$

- <sup>1</sup> ALBRECHT 89G reports < 0.0022 assuming the  $\Upsilon(4S)$  decays 45% to  $B^0 \bar{B}^0$ . We rescale to 50%.

$\Gamma(K_3^*(1780)^0 \gamma)/\Gamma_{\text{total}}$   $\Gamma_{324}/\Gamma$   
 VALUE (units  $10^{-6}$ )

VALUE (units $10^{-6}$ )	CL%	DOCUMENT ID	TECN	COMMENT
< 83	90	1,2 NISHIDA	05	BELL $e^+ e^- \rightarrow \Upsilon(4S)$

- • • We do not use the following data for averages, fits, limits, etc. • • •  
 <10000 90 <sup>3</sup> ALBRECHT 89G ARG  $e^+ e^- \rightarrow \Upsilon(4S)$

- <sup>1</sup> Assumes equal production of  $B^+$  and  $B^0$  at the  $\Upsilon(4S)$ .  
<sup>2</sup> Uses  $B(K_3^*(1780) \rightarrow \eta K) = 0.11^{+0.05}_{-0.04}$ .  
<sup>3</sup> ALBRECHT 89G reports < 0.011 assuming the  $\Upsilon(4S)$  decays 45% to  $B^0 \bar{B}^0$ . We rescale to 50%.

$\Gamma(K_2^*(2045)^0 \gamma)/\Gamma_{\text{total}}$   $\Gamma_{325}/\Gamma$   
 VALUE

VALUE	CL%	DOCUMENT ID	TECN	COMMENT
<0.0043	90	1 ALBRECHT	89G	ARG $e^+ e^- \rightarrow \Upsilon(4S)$

- <sup>1</sup> ALBRECHT 89G reports < 0.0048 assuming the  $\Upsilon(4S)$  decays 45% to  $B^0 \bar{B}^0$ . We rescale to 50%.

$\Gamma(\rho^0 \gamma)/\Gamma_{\text{total}}$   $\Gamma_{326}/\Gamma$   
 VALUE (units  $10^{-6}$ )

VALUE (units $10^{-6}$ )	CL%	DOCUMENT ID	TECN	COMMENT
<b>0.86 ± 0.15 OUR AVERAGE</b>				
0.97 <sup>+0.24</sup> <sub>-0.22</sub> ± 0.06		1 AUBERT	08BH	BABR $e^+ e^- \rightarrow \Upsilon(4S)$
0.78 <sup>+0.17+0.09</sup> <sub>-0.16-0.10</sub>		1 TANIGUCHI	08	BELL $e^+ e^- \rightarrow \Upsilon(4S)$

- • • We do not use the following data for averages, fits, limits, etc. • • •  
 0.79 <sup>+0.22</sup> <sub>-0.20</sub> ± 0.06 1 AUBERT 07L BABR Repl. by AUBERT 08BH

- 1.25 <sup>+0.37+0.07</sup> <sub>-0.33-0.06</sub> 1 MOHAPATRA 06 BELL Repl. by TANIGUCHI 08

- 0.0 ± 0.2 ± 0.1 90 1 AUBERT 05 BABR Repl. by AUBERT 07L  
 < 0.8 90 1 MOHAPATRA 05 BELL  $e^+ e^- \rightarrow \Upsilon(4S)$   
 < 1.2 90 1 AUBERT 04c BABR  $e^+ e^- \rightarrow \Upsilon(4S)$   
 < 1.7 90 1 COAN 00 CLE2  $e^+ e^- \rightarrow \Upsilon(4S)$

$\Gamma(\rho^0 X(214) \times B(X \rightarrow \mu^+ \mu^-))/\Gamma_{\text{total}}$   $\Gamma_{327}/\Gamma$   
 $X(214)$  is a hypothetical particle of mass 214 MeV/ $c^2$  reported by the HyperCP experiment (PARK 05)

VALUE (units $10^{-8}$ )	CL%	DOCUMENT ID	TECN	COMMENT
<1.73	90	1,2 HYUN	10	BELL $e^+ e^- \rightarrow \Upsilon(4S)$

- <sup>1</sup> Assumes equal production of  $B^+$  and  $B^0$  at the  $\Upsilon(4S)$ .  
<sup>2</sup> The result is the same for a scalar or vector  $X$  particle.

$\Gamma(\rho^0 \gamma)/\Gamma(K^*(892)^0 \gamma)$   $\Gamma_{326}/\Gamma_{314}$   
 VALUE (units  $10^{-2}$ )

VALUE (units $10^{-2}$ )	CL%	DOCUMENT ID	TECN	COMMENT
<b>2.06 <sup>+0.45</sup> <sub>-0.43</sub> ± 0.14</b>		TANIGUCHI	08	BELL $e^+ e^- \rightarrow \Upsilon(4S)$

$\Gamma(\omega \gamma)/\Gamma_{\text{total}}$   $\Gamma_{328}/\Gamma$   
 VALUE (units  $10^{-6}$ )

VALUE (units $10^{-6}$ )	CL%	DOCUMENT ID	TECN	COMMENT
<b>0.44 <sup>+0.18</sup> <sub>-0.16</sub> OUR AVERAGE</b>				
0.50 <sup>+0.27</sup> <sub>-0.23</sub> ± 0.09		1 AUBERT	08BH	BABR $e^+ e^- \rightarrow \Upsilon(4S)$
0.40 <sup>+0.19</sup> <sub>-0.17</sub> ± 0.13		1 TANIGUCHI	08	BELL $e^+ e^- \rightarrow \Upsilon(4S)$

- • • We do not use the following data for averages, fits, limits, etc. • • •  
 0.40 <sup>+0.24</sup> <sub>-0.20</sub> ± 0.05 1 AUBERT 07L BABR Repl. by AUBERT 08BH

- 0.56 <sup>+0.34+0.05</sup> <sub>-0.27-0.10</sub> 1 MOHAPATRA 06 BELL Repl. by TANIGUCHI 08  
 <1.0 90 1 AUBERT 05 BABR Repl. by AUBERT 07L  
 <0.8 90 1 MOHAPATRA 05 BELL Repl. by MOHAPATRA 06  
 <1.0 90 1 AUBERT 04c BABR  $e^+ e^- \rightarrow \Upsilon(4S)$   
 <9.2 90 1 COAN 00 CLE2  $e^+ e^- \rightarrow \Upsilon(4S)$

- <sup>1</sup> Assumes equal production of  $B^+$  and  $B^0$  at the  $\Upsilon(4S)$ .

$\Gamma(\phi \gamma)/\Gamma_{\text{total}}$   $\Gamma_{329}/\Gamma$   
 VALUE

VALUE	CL%	DOCUMENT ID	TECN	COMMENT
<8.5 × 10 <sup>-7</sup>	90	1 AUBERT,BE	05c	BABR $e^+ e^- \rightarrow \Upsilon(4S)$

- • • We do not use the following data for averages, fits, limits, etc. • • •  
 <0.33 × 10<sup>-5</sup> 90 1 COAN 00 CLE2  $e^+ e^- \rightarrow \Upsilon(4S)$

$\Gamma(\pi^+ \pi^-)/\Gamma_{\text{total}}$   $\Gamma_{330}/\Gamma$   
 VALUE (units  $10^{-6}$ )

VALUE (units $10^{-6}$ )	CL%	DOCUMENT ID	TECN	COMMENT
<b>5.15 ± 0.22 OUR FIT</b>				
<b>5.18 ± 0.24 OUR AVERAGE</b>				
5.5 ± 0.4 ± 0.3		1 AUBERT	07B	BABR $e^+ e^- \rightarrow \Upsilon(4S)$
5.1 ± 0.2 ± 0.2		1 LIN	07A	BELL $e^+ e^- \rightarrow \Upsilon(4S)$
4.5 <sup>+1.4</sup> <sub>-1.2</sub> ± 0.5		1 BORNHEIM	03	CLE2 $e^+ e^- \rightarrow \Upsilon(4S)$

- • • We do not use the following data for averages, fits, limits, etc. • • •  
 4.4 ± 0.6 ± 0.3 1 CHAO 04 BELL Repl. by LIN 07A  
 4.7 ± 0.6 ± 0.2 1 AUBERT 02Q BABR Repl. by AUBERT 07B  
 5.4 ± 1.2 ± 0.5 1 CASEY 02 BELL Repl. by CHAO 04

- 5.6 <sup>+2.3</sup> <sub>-2.0</sub> ± 0.4 1 ABE 01H BELL Repl. by CASEY 02  
 4.1 ± 1.0 ± 0.7 1 AUBERT 01E BABR Repl. by AUBERT 02Q  
 < 67 2 ABE 00c SLD  $e^+ e^- \rightarrow Z$

- 4.3 <sup>+1.6</sup> <sub>-1.4</sub> ± 0.5 1 CRONIN-HEN..00 CLE2 Repl. by BORNHEIM 03  
 < 15 90 GODANG 98 CLE2 Repl. by CRONIN-HENNESSY 00

- < 45 90 3 ADAM 96D DLPH  $e^+ e^- \rightarrow Z$   
 < 20 90 ASNER 96 CLE2 Repl. by GODANG 98  
 < 41 90 4 BUSKULIC 96v ALEP  $e^+ e^- \rightarrow Z$

- < 55 90 5 ABREU 95N DLPH Sup. by ADAM 96D  
 < 47 90 6 AKERS 94L OPAL  $e^+ e^- \rightarrow Z$   
 < 29 90 1 BATTLE 93 CLE2  $e^+ e^- \rightarrow \Upsilon(4S)$

- < 130 90 1 ALBRECHT 90B ARG  $e^+ e^- \rightarrow \Upsilon(4S)$   
 < 77 90 7 BORTOLETTO89 CLEO  $e^+ e^- \rightarrow \Upsilon(4S)$   
 < 260 90 7 BEBEK 87 CLEO  $e^+ e^- \rightarrow \Upsilon(4S)$   
 < 500 90 GILES 84 CLEO  $e^+ e^- \rightarrow \Upsilon(4S)$

## Meson Particle Listings

 $B^0$ 

- <sup>1</sup> Assumes equal production of  $B^+$  and  $B^0$  at the  $\Upsilon(4S)$ .  
<sup>2</sup> ABE 00c assumes  $B(Z \rightarrow b\bar{b}) = (21.7 \pm 0.1)\%$  and the  $B$  fractions  $f_{B^0} = f_{B^+} = (39.7^{+1.8}_{-2.2})\%$  and  $f_{B_s^0} = (10.5^{+1.8}_{-2.2})\%$ .  
<sup>3</sup> ADAM 96d assumes  $f_{B^0} = f_{B^-} = 0.39$  and  $f_{B_s} = 0.12$ .  
<sup>4</sup> BUSKULIC 96v assumes PDG 96 production fractions for  $B^0$ ,  $B^+$ ,  $B_s$ ,  $b$  baryons.  
<sup>5</sup> Assumes a  $B^0$ ,  $B^-$  production fraction of 0.39 and a  $B_s$  production fraction of 0.12.  
<sup>6</sup> Assumes  $B(Z \rightarrow b\bar{b}) = 0.217$  and  $B_d^0$  ( $B_s^0$ ) fraction 39.5% (12%).  
<sup>7</sup> Paper assumes the  $\Upsilon(4S)$  decays 43% to  $B^0\bar{B}^0$ . We rescale to 50%.

 $\Gamma(\pi^+\pi^-)/\Gamma(K^+\pi^-)$   $\Gamma_{330}/\Gamma_{214}$ 

VALUE (units $10^{-6}$ )	CL%	DOCUMENT ID	TECN	COMMENT
<b>0.265 ± 0.013 OUR FIT</b>				
<b>0.259 ± 0.017 ± 0.016</b>		AALTONEN 11N	CDF	$p\bar{p}$ at 1.96 TeV
• • • We do not use the following data for averages, fits, limits, etc. • • •				
0.21 ± 0.05 ± 0.03		ABULENCIA,A 06d	CDF	Repl. by AALTONEN 11N

 $\Gamma(\pi^0\pi^0)/\Gamma_{total}$   $\Gamma_{331}/\Gamma$ 

VALUE (units $10^{-6}$ )	CL%	DOCUMENT ID	TECN	COMMENT
<b>1.62 ± 0.31 OUR AVERAGE</b>		Error includes scale factor of 1.3.		
1.47 ± 0.25 ± 0.12		<sup>1</sup> AUBERT	07bc	BABR $e^+e^- \rightarrow \Upsilon(4S)$
2.3 +0.4 +0.2 -0.5 -0.3		<sup>1</sup> CHAO	05	BELL $e^+e^- \rightarrow \Upsilon(4S)$
• • • We do not use the following data for averages, fits, limits, etc. • • •				
1.17 ± 0.32 ± 0.10		<sup>1</sup> AUBERT	05L	BABR Repl. by AUBERT 07bc
< 3.6	90	<sup>1</sup> AUBERT	03L	BABR $e^+e^- \rightarrow \Upsilon(4S)$
2.1 ± 0.6 ± 0.3		<sup>1</sup> AUBERT	03s	BABR Repl. by AUBERT 05L
< 4.4	90	<sup>1</sup> BORNHEIM	03	CLE2 $e^+e^- \rightarrow \Upsilon(4S)$
1.7 ± 0.6 ± 0.2		<sup>1</sup> LEE	03	BELL Repl. by CHAO 05
< 5.7	90	<sup>1</sup> ASNER	02	CLE2 $e^+e^- \rightarrow \Upsilon(4S)$
< 6.4	90	<sup>1</sup> CASEY	02	BELL $e^+e^- \rightarrow \Upsilon(4S)$
< 9.3	90	GODANG	98	CLE2 Repl. by ASNER 02
< 9.1	90	ASNER	96	CLE2 Repl. by GODANG 98
< 60	90	<sup>2</sup> ACCIARRI	95H L3	$e^+e^- \rightarrow Z$

- <sup>1</sup> Assumes equal production of  $B^+$  and  $B^0$  at the  $\Upsilon(4S)$ .  
<sup>2</sup> ACCIARRI 95H assumes  $f_{B^0} = 39.5 \pm 4.0$  and  $f_{B_s} = 12.0 \pm 3.0\%$ .

 $\Gamma(\eta\pi^0)/\Gamma_{total}$   $\Gamma_{332}/\Gamma$ 

VALUE (units $10^{-6}$ )	CL%	DOCUMENT ID	TECN	COMMENT
<b>&lt; 1.5</b>	90	<sup>1</sup> AUBERT	08AH	BABR $e^+e^- \rightarrow \Upsilon(4S)$
• • • We do not use the following data for averages, fits, limits, etc. • • •				
< 1.3	90	<sup>1</sup> AUBERT	06W	BABR Repl. by AUBERT 08AH
< 2.5	90	<sup>1</sup> CHANG	05A	BELL $e^+e^- \rightarrow \Upsilon(4S)$
< 2.5	90	<sup>1</sup> AUBERT,B	04D	BABR Repl. by AUBERT 06W
< 2.9	90	<sup>1</sup> RICHICHI	00	CLE2 $e^+e^- \rightarrow \Upsilon(4S)$
< 8	90	BEHRENS	98	CLE2 Repl. by RICHICHI 00
< 250	90	<sup>2</sup> ACCIARRI	95H L3	$e^+e^- \rightarrow Z$
< 1800	90	<sup>1</sup> ALBRECHT	90B	ARG $e^+e^- \rightarrow \Upsilon(4S)$

- <sup>1</sup> Assumes equal production of  $B^+$  and  $B^0$  at the  $\Upsilon(4S)$ .  
<sup>2</sup> ACCIARRI 95H assumes  $f_{B^0} = 39.5 \pm 4.0$  and  $f_{B_s} = 12.0 \pm 3.0\%$ .

 $\Gamma(\eta)/\Gamma_{total}$   $\Gamma_{333}/\Gamma$ 

VALUE (units $10^{-6}$ )	CL%	DOCUMENT ID	TECN	COMMENT
<b>&lt; 1.0</b>	90	<sup>1</sup> AUBERT	09AV	BABR $e^+e^- \rightarrow \Upsilon(4S)$
• • • We do not use the following data for averages, fits, limits, etc. • • •				
< 1.8	90	<sup>1</sup> AUBERT,B	06V	BABR Repl. by AUBERT 09AV
< 2.0	90	<sup>1</sup> CHANG	05A	BELL $e^+e^- \rightarrow \Upsilon(4S)$
< 2.8	90	<sup>1</sup> AUBERT,B	04X	BABR $e^+e^- \rightarrow \Upsilon(4S)$
< 18	90	BEHRENS	98	CLE2 $e^+e^- \rightarrow \Upsilon(4S)$
< 410	90	<sup>2</sup> ACCIARRI	95H L3	$e^+e^- \rightarrow Z$

- <sup>1</sup> Assumes equal production of  $B^+$  and  $B^0$  at the  $\Upsilon(4S)$ .  
<sup>2</sup> ACCIARRI 95H assumes  $f_{B^0} = 39.5 \pm 4.0$  and  $f_{B_s} = 12.0 \pm 3.0\%$ .

 $\Gamma(\eta'\pi^0)/\Gamma_{total}$   $\Gamma_{334}/\Gamma$ 

VALUE (units $10^{-6}$ )	CL%	DOCUMENT ID	TECN	COMMENT
<b>1.2 ± 0.6 OUR AVERAGE</b>		Error includes scale factor of 1.7.		
0.9 ± 0.4 ± 0.1		<sup>1</sup> AUBERT	08AH	BABR $e^+e^- \rightarrow \Upsilon(4S)$
2.8 ± 1.0 ± 0.3		<sup>1</sup> SCHUEMANN	06	BELL $e^+e^- \rightarrow \Upsilon(4S)$
• • • We do not use the following data for averages, fits, limits, etc. • • •				
0.8 +0.8 +0.1 -0.6		<sup>1</sup> AUBERT	06W	BABR Repl. by AUBERT 08AH
1.0 +1.4 +0.8 -1.0	90	<sup>1</sup> AUBERT,B	04D	BABR Repl. by AUBERT 06W
< 5.7	90	<sup>1</sup> RICHICHI	00	CLE2 $e^+e^- \rightarrow \Upsilon(4S)$
< 11	90	BEHRENS	98	CLE2 Repl. by RICHICHI 00

- <sup>1</sup> Assumes equal production of  $B^+$  and  $B^0$  at the  $\Upsilon(4S)$ .

 $\Gamma(\eta'\eta)/\Gamma_{total}$   $\Gamma_{335}/\Gamma$ 

VALUE (units $10^{-6}$ )	CL%	DOCUMENT ID	TECN	COMMENT
<b>&lt; 1.7</b>	90	<sup>1</sup> AUBERT	09AV	BABR $e^+e^- \rightarrow \Upsilon(4S)$
• • • We do not use the following data for averages, fits, limits, etc. • • •				
< 6.5	90	<sup>1</sup> SCHUEMANN	07	BELL $e^+e^- \rightarrow \Upsilon(4S)$
< 2.4	90	<sup>1</sup> AUBERT,B	06V	BABR Repl. by AUBERT 09AV
< 10	90	<sup>1</sup> AUBERT,B	04X	BABR Repl. by AUBERT,B 06V
< 47	90	BEHRENS	98	CLE2 $e^+e^- \rightarrow \Upsilon(4S)$

- <sup>1</sup> Assumes equal production of  $B^+$  and  $B^0$  at the  $\Upsilon(4S)$ .

 $\Gamma(\eta)/\Gamma_{total}$   $\Gamma_{336}/\Gamma$ 

VALUE (units $10^{-6}$ )	CL%	DOCUMENT ID	TECN	COMMENT
<b>&lt; 1.2</b>	90	<sup>1</sup> AUBERT	08AH	BABR $e^+e^- \rightarrow \Upsilon(4S)$
• • • We do not use the following data for averages, fits, limits, etc. • • •				
< 4.5	90	<sup>1</sup> SCHUEMANN	07	BELL $e^+e^- \rightarrow \Upsilon(4S)$
< 1.7	90	<sup>1</sup> AUBERT	06W	BABR Repl. by AUBERT 08AH
< 4.6	90	<sup>1</sup> AUBERT,B	04X	BABR $e^+e^- \rightarrow \Upsilon(4S)$
< 27	90	BEHRENS	98	CLE2 $e^+e^- \rightarrow \Upsilon(4S)$

- <sup>1</sup> Assumes equal production of  $B^+$  and  $B^0$  at the  $\Upsilon(4S)$ .

 $\Gamma(\eta'\rho^0)/\Gamma_{total}$   $\Gamma_{337}/\Gamma$ 

VALUE (units $10^{-6}$ )	CL%	DOCUMENT ID	TECN	COMMENT
<b>&lt; 1.3</b>	90	<sup>1</sup> SCHUEMANN	07	BELL $e^+e^- \rightarrow \Upsilon(4S)$
• • • We do not use the following data for averages, fits, limits, etc. • • •				
< 2.8	90	<sup>1</sup> DEL-AMO-SA...10A	BABR	$e^+e^- \rightarrow \Upsilon(4S)$
< 3.7	90	AUBERT	07E	BABR Repl. by DEL-AMO-SANCHEZ 10A
< 4.3	90	<sup>1</sup> AUBERT,B	04D	BABR Repl. by AUBERT 07E
< 12	90	<sup>1</sup> RICHICHI	00	CLE2 $e^+e^- \rightarrow \Upsilon(4S)$
< 23	90	BEHRENS	98	CLE2 Repl. by RICHICHI 00

- <sup>1</sup> Assumes equal production of  $B^+$  and  $B^0$  at the  $\Upsilon(4S)$ .

 $\Gamma(\eta'\rho(980) \times B(\rho(980) \rightarrow \pi^+\pi^-))/\Gamma_{total}$   $\Gamma_{338}/\Gamma$ 

VALUE (units $10^{-6}$ )	CL%	DOCUMENT ID	TECN	COMMENT
<b>&lt; 0.9</b>	90	<sup>1</sup> DEL-AMO-SA...10A	BABR	$e^+e^- \rightarrow \Upsilon(4S)$
• • • We do not use the following data for averages, fits, limits, etc. • • •				
< 1.5	90	AUBERT	07E	BABR Repl. by DEL-AMO-SANCHEZ 10A

- <sup>1</sup> Assumes equal production of  $B^+$  and  $B^0$  at the  $\Upsilon(4S)$ .

 $\Gamma(\eta\rho^0)/\Gamma_{total}$   $\Gamma_{339}/\Gamma$ 

VALUE (units $10^{-6}$ )	CL%	DOCUMENT ID	TECN	COMMENT
<b>&lt; 1.5</b>	90	<sup>1</sup> AUBERT	07Y	BABR $e^+e^- \rightarrow \Upsilon(4S)$
• • • We do not use the following data for averages, fits, limits, etc. • • •				
< 1.9	90	<sup>1</sup> WANG	07B	BELL $e^+e^- \rightarrow \Upsilon(4S)$
< 1.5	90	<sup>1</sup> AUBERT,B	04D	BABR Repl. by AUBERT 07Y
< 10	90	<sup>1</sup> RICHICHI	00	CLE2 $e^+e^- \rightarrow \Upsilon(4S)$
< 13	90	BEHRENS	98	CLE2 Repl. by RICHICHI 00

- <sup>1</sup> Assumes equal production of  $B^+$  and  $B^0$  at the  $\Upsilon(4S)$ .

 $\Gamma(\eta\rho(980) \times B(\rho(980) \rightarrow \pi^+\pi^-))/\Gamma_{total}$   $\Gamma_{340}/\Gamma$ 

VALUE (units $10^{-6}$ )	CL%	DOCUMENT ID	TECN	COMMENT
<b>&lt; 0.4</b>	90	<sup>1</sup> AUBERT	07Y	BABR $e^+e^- \rightarrow \Upsilon(4S)$

- <sup>1</sup> Assumes equal production of  $B^+$  and  $B^0$  at the  $\Upsilon(4S)$ .

 $\Gamma(\omega\eta)/\Gamma_{total}$   $\Gamma_{341}/\Gamma$ 

VALUE (units $10^{-6}$ )	CL%	DOCUMENT ID	TECN	COMMENT
<b>0.94 +0.35 ± 0.09 -0.30</b>		<sup>1</sup> AUBERT	09AV	BABR $e^+e^- \rightarrow \Upsilon(4S)$
• • • We do not use the following data for averages, fits, limits, etc. • • •				
< 1.9	90	<sup>1</sup> AUBERT,B	05K	BABR Repl. by AUBERT 09AV
4.0 +1.3 +0.4 -1.2		<sup>1</sup> AUBERT,B	04X	BABR Repl. by AUBERT,B 05K
< 12	90	<sup>1</sup> BERGFELD	98	CLE2

- <sup>1</sup> Assumes equal production of  $B^+$  and  $B^0$  at the  $\Upsilon(4S)$ .

 $\Gamma(\omega\eta')/\Gamma_{total}$   $\Gamma_{342}/\Gamma$ 

VALUE (units $10^{-6}$ )	CL%	DOCUMENT ID	TECN	COMMENT
<b>1.01 +0.46 ± 0.09 -0.38</b>		<sup>1</sup> AUBERT	09AV	BABR $e^+e^- \rightarrow \Upsilon(4S)$
• • • We do not use the following data for averages, fits, limits, etc. • • •				
< 2.2	90	<sup>1</sup> SCHUEMANN	07	BELL $e^+e^- \rightarrow \Upsilon(4S)$
< 2.8	90	<sup>1</sup> AUBERT,B	04X	BABR $e^+e^- \rightarrow \Upsilon(4S)$
< 60	90	<sup>1</sup> BERGFELD	98	CLE2

- <sup>1</sup> Assumes equal production of  $B^+$  and  $B^0$  at the  $\Upsilon(4S)$ .

$\Gamma(\omega\rho^0)/\Gamma_{\text{total}}$   $\Gamma_{343}/\Gamma$ 

VALUE (units $10^{-6}$ )	CL%	DOCUMENT ID	TECN	COMMENT
< 1.6	90	<sup>1</sup> AUBERT 09H	BABR	$e^+e^- \rightarrow \Upsilon(4S)$
••• We do not use the following data for averages, fits, limits, etc. •••				
< 1.5	90	<sup>1</sup> AUBERT,B 06T	BABR	Repl. by AUBERT 09H
< 3.3	90	<sup>1</sup> AUBERT 05o	BABR	Repl. by AUBERT,B 06T
<11	90	<sup>1</sup> BERGFELD 98	CLE2	

<sup>1</sup> Assumes equal production of  $B^+$  and  $B^0$  at the  $\Upsilon(4S)$ .

 $\Gamma(\omega f_0(980) \times B(f_0(980) \rightarrow \pi^+\pi^-))/\Gamma_{\text{total}}$   $\Gamma_{344}/\Gamma$ 

VALUE (units $10^{-6}$ )	CL%	DOCUMENT ID	TECN	COMMENT
<1.5	90	<sup>1</sup> AUBERT 09H	BABR	$e^+e^- \rightarrow \Upsilon(4S)$
••• We do not use the following data for averages, fits, limits, etc. •••				
<1.5	90	<sup>1</sup> AUBERT,B 06T	BABR	Repl. by AUBERT 09H

<sup>1</sup> Assumes equal production of  $B^+$  and  $B^0$  at the  $\Upsilon(4S)$ .

 $\Gamma(\omega\omega)/\Gamma_{\text{total}}$   $\Gamma_{345}/\Gamma$ 

VALUE (units $10^{-6}$ )	CL%	DOCUMENT ID	TECN	COMMENT
< 4.0	90	<sup>1</sup> AUBERT,B 06T	BABR	$e^+e^- \rightarrow \Upsilon(4S)$
••• We do not use the following data for averages, fits, limits, etc. •••				
<19	90	<sup>1</sup> BERGFELD 98	CLE2	

<sup>1</sup> Assumes equal production of  $B^+$  and  $B^0$  at the  $\Upsilon(4S)$ .

 $\Gamma(\phi\pi^0)/\Gamma_{\text{total}}$   $\Gamma_{346}/\Gamma$ 

VALUE (units $10^{-6}$ )	CL%	DOCUMENT ID	TECN	COMMENT
<0.28	90	<sup>1</sup> AUBERT,B 06c	BABR	$e^+e^- \rightarrow \Upsilon(4S)$
••• We do not use the following data for averages, fits, limits, etc. •••				
<1.0	90	<sup>1</sup> AUBERT,B 04D	BABR	Repl. by AUBERT,B 06c
<5	90	<sup>1</sup> BERGFELD 98	CLE2	

<sup>1</sup> Assumes equal production of  $B^+$  and  $B^0$  at the  $\Upsilon(4S)$ .

 $\Gamma(\phi\eta)/\Gamma_{\text{total}}$   $\Gamma_{347}/\Gamma$ 

VALUE (units $10^{-6}$ )	CL%	DOCUMENT ID	TECN	COMMENT
<0.5	90	<sup>1</sup> AUBERT 09Av	BABR	$e^+e^- \rightarrow \Upsilon(4S)$
••• We do not use the following data for averages, fits, limits, etc. •••				
<0.6	90	<sup>1</sup> AUBERT,B 06v	BABR	Repl. by AUBERT 09Av
<1.0	90	<sup>1</sup> AUBERT,B 04x	BABR	Repl. by AUBERT,B 06v
<9	90	<sup>1</sup> BERGFELD 98	CLE2	

<sup>1</sup> Assumes equal production of  $B^+$  and  $B^0$  at the  $\Upsilon(4S)$ .

 $\Gamma(\phi\eta')/\Gamma_{\text{total}}$   $\Gamma_{348}/\Gamma$ 

VALUE (units $10^{-6}$ )	CL%	DOCUMENT ID	TECN	COMMENT
< 0.5	90	<sup>1</sup> SCHUEMANN 07	BELL	$e^+e^- \rightarrow \Upsilon(4S)$
••• We do not use the following data for averages, fits, limits, etc. •••				
< 1.1	90	<sup>1</sup> AUBERT 09Av	BABR	$e^+e^- \rightarrow \Upsilon(4S)$
< 1.0	90	<sup>1</sup> AUBERT,B 06v	BABR	Repl. by AUBERT 09Av
< 4.5	90	<sup>1</sup> AUBERT,B 04x	BABR	Repl. by AUBERT,B 06v
<31	90	<sup>1</sup> BERGFELD 98	CLE2	

<sup>1</sup> Assumes equal production of  $B^+$  and  $B^0$  at the  $\Upsilon(4S)$ .

 $\Gamma(\phi\rho^0)/\Gamma_{\text{total}}$   $\Gamma_{349}/\Gamma$ 

VALUE (units $10^{-6}$ )	CL%	DOCUMENT ID	TECN	COMMENT
< 0.33	90	<sup>1</sup> AUBERT 08BK	BABR	$e^+e^- \rightarrow \Upsilon(4S)$
••• We do not use the following data for averages, fits, limits, etc. •••				
<156	90	<sup>2</sup> ABE 00c	SLD	$e^+e^- \rightarrow Z$
< 13	90	<sup>1</sup> BERGFELD 98	CLE2	

<sup>1</sup> Assumes equal production of  $B^+$  and  $B^0$  at the  $\Upsilon(4S)$ .  
<sup>2</sup> ABE 00c assumes  $B(Z \rightarrow b\bar{b}) = (21.7 \pm 0.1)\%$  and the  $B$  fractions  $f_{B^0} = f_{B^+} = (39.7^{+1.8}_{-2.2}\%)$  and  $f_{B_s} = (10.5^{+1.8}_{-2.2}\%)$ .

 $\Gamma(\phi f_0(980) \times B(f_0 \rightarrow \pi^+\pi^-))/\Gamma_{\text{total}}$   $\Gamma_{350}/\Gamma$ 

VALUE (units $10^{-6}$ )	CL%	DOCUMENT ID	TECN	COMMENT
<0.38	90	<sup>1</sup> AUBERT 08BK	BABR	$e^+e^- \rightarrow \Upsilon(4S)$

<sup>1</sup> Assumes equal production of  $B^+$  and  $B^0$  at the  $\Upsilon(4S)$ .

 $\Gamma(\phi\omega)/\Gamma_{\text{total}}$   $\Gamma_{351}/\Gamma$ 

VALUE (units $10^{-6}$ )	CL%	DOCUMENT ID	TECN	COMMENT
< 1.2	90	<sup>1</sup> AUBERT,B 06T	BABR	$e^+e^- \rightarrow \Upsilon(4S)$
••• We do not use the following data for averages, fits, limits, etc. •••				
<21	90	<sup>1</sup> BERGFELD 98	CLE2	

<sup>1</sup> Assumes equal production of  $B^+$  and  $B^0$  at the  $\Upsilon(4S)$ .

 $\Gamma(\phi\phi)/\Gamma_{\text{total}}$   $\Gamma_{352}/\Gamma$ 

VALUE	CL%	DOCUMENT ID	TECN	COMMENT
<2 $\times 10^{-7}$	90	<sup>1</sup> AUBERT 08BK	BABR	$e^+e^- \rightarrow \Upsilon(4S)$
••• We do not use the following data for averages, fits, limits, etc. •••				
<1.5 $\times 10^{-6}$	90	<sup>1</sup> AUBERT,B 04X	BABR	Repl. by AUBERT 08BK
<3.21 $\times 10^{-4}$	90	<sup>2</sup> ABE 00c	SLD	$e^+e^- \rightarrow Z$
<1.2 $\times 10^{-5}$	90	<sup>1</sup> BERGFELD 98	CLE2	
<3.9 $\times 10^{-5}$	90	ASNER 96	CLE2	$e^+e^- \rightarrow \Upsilon(4S)$

<sup>1</sup> Assumes equal production of  $B^+$  and  $B^0$  at the  $\Upsilon(4S)$ .  
<sup>2</sup> ABE 00c assumes  $B(Z \rightarrow b\bar{b}) = (21.7 \pm 0.1)\%$  and the  $B$  fractions  $f_{B^0} = f_{B^+} = (39.7^{+1.8}_{-2.2}\%)$  and  $f_{B_s} = (10.5^{+1.8}_{-2.2}\%)$ .

 $\Gamma(a_0(980)^\pm \pi^\mp \times B(a_0(980)^\pm \rightarrow \eta\pi^\pm))/\Gamma_{\text{total}}$   $\Gamma_{353}/\Gamma$ 

VALUE (units $10^{-6}$ )	CL%	DOCUMENT ID	TECN	COMMENT
<3.1	90	<sup>1</sup> AUBERT 07Y	BABR	$e^+e^- \rightarrow \Upsilon(4S)$
••• We do not use the following data for averages, fits, limits, etc. •••				
<5.1	90	<sup>1</sup> AUBERT,BE 04	BABR	Repl. by AUBERT 07Y

<sup>1</sup> Assumes equal production of  $B^+$  and  $B^0$  at the  $\Upsilon(4S)$ .

 $\Gamma(a_0(1450)^\pm \pi^\mp \times B(a_0(1450)^\pm \rightarrow \eta\pi^\pm))/\Gamma_{\text{total}}$   $\Gamma_{354}/\Gamma$ 

VALUE (units $10^{-6}$ )	CL%	DOCUMENT ID	TECN	COMMENT
<2.3	90	<sup>1</sup> AUBERT 07Y	BABR	$e^+e^- \rightarrow \Upsilon(4S)$

<sup>1</sup> Assumes equal production of  $B^+$  and  $B^0$  at the  $\Upsilon(4S)$ .

 $\Gamma(\pi^+\pi^-\pi^0)/\Gamma_{\text{total}}$   $\Gamma_{355}/\Gamma$ 

VALUE	CL%	DOCUMENT ID	TECN	COMMENT
<7.2 $\times 10^{-4}$	90	<sup>1</sup> ALBRECHT 90B	ARG	$e^+e^- \rightarrow \Upsilon(4S)$

<sup>1</sup> ALBRECHT 90B limit assumes equal production of  $B^0\bar{B}^0$  and  $B^+B^-$  at  $\Upsilon(4S)$ .

 $\Gamma(\rho^0\pi^0)/\Gamma_{\text{total}}$   $\Gamma_{356}/\Gamma$ 

VALUE (units $10^{-6}$ )	CL%	DOCUMENT ID	TECN	COMMENT
<b>2.0 <math>\pm 0.5</math> OUR AVERAGE</b>				
3.0 $\pm 0.5 \pm 0.7$		<sup>1,2</sup> KUSAKA 08	BELL	$e^+e^- \rightarrow \Upsilon(4S)$
1.4 $\pm 0.6 \pm 0.3$		<sup>1</sup> AUBERT 04z	BABR	$e^+e^- \rightarrow \Upsilon(4S)$
1.6 $^{+2.0}_{-1.4} \pm 0.8$		<sup>1</sup> JESSOP 00	CLEO	$e^+e^- \rightarrow \Upsilon(4S)$
••• We do not use the following data for averages, fits, limits, etc. •••				
3.12 $^{+0.88+0.60}_{-0.82-0.76}$		<sup>1</sup> DRAGIC 06	BELL	Repl. by KUSAKA 08
5.1 $\pm 1.6 \pm 0.9$		DRAGIC 04	BELL	Repl. by DRAGIC 06
< 5.3	90	<sup>1</sup> GORDON 02	BELL	Repl. by DRAGIC 04
< 24	90	ASNER 96	CLEO	Repl. by JESSOP 00
<400	90	<sup>1</sup> ALBRECHT 90B	ARG	$e^+e^- \rightarrow \Upsilon(4S)$

<sup>1</sup> Assumes equal production of  $B^+$  and  $B^0$  at the  $\Upsilon(4S)$ .  
<sup>2</sup> This is the first measurement that excludes contributions from  $\rho(1450)$  and  $\rho(1570)$  resonances.

 $\Gamma(\rho^\mp\pi^\pm)/\Gamma_{\text{total}}$   $\Gamma_{357}/\Gamma$ 

VALUE (units $10^{-6}$ )	CL%	DOCUMENT ID	TECN	COMMENT
<b>23.0 <math>\pm 2.3</math> OUR AVERAGE</b>				
22.6 $\pm 1.1 \pm 4.4$		<sup>1,2</sup> KUSAKA 08	BELL	$e^+e^- \rightarrow \Upsilon(4S)$
22.6 $\pm 1.8 \pm 2.2$		<sup>1</sup> AUBERT 03t	BABR	$e^+e^- \rightarrow \Upsilon(4S)$
27.6 $^{+8.4}_{-7.4} \pm 4.2$		<sup>1</sup> JESSOP 00	CLE2	$e^+e^- \rightarrow \Upsilon(4S)$
••• We do not use the following data for averages, fits, limits, etc. •••				
20.8 $^{+6.0+2.8}_{-6.3-3.1}$		<sup>1</sup> GORDON 02	BELL	Repl. by KUSAKA 08
< 88	90	ASNER 96	CLE2	Repl. by JESSOP 00
< 520	90	<sup>1</sup> ALBRECHT 90B	ARG	$e^+e^- \rightarrow \Upsilon(4S)$
<5200	90	<sup>3</sup> BEBEK 87	CLEO	$e^+e^- \rightarrow \Upsilon(4S)$

<sup>1</sup> Assumes equal production of  $B^+$  and  $B^0$  at the  $\Upsilon(4S)$ .  
<sup>2</sup> This is the first measurement that excludes contributions from  $\rho(1450)$  and  $\rho(1570)$  resonances.  
<sup>3</sup> BEBEK 87 reports  $< 6.1 \times 10^{-3}$  assuming the  $\Upsilon(4S)$  decays 43% to  $B^0\bar{B}^0$ . We rescale to 50%.

 $\Gamma(\pi^+\pi^-\pi^+\pi^-)/\Gamma_{\text{total}}$   $\Gamma_{358}/\Gamma$ 

VALUE	CL%	DOCUMENT ID	TECN	COMMENT
<19.3 $\times 10^{-6}$	90	<sup>1</sup> CHIANG 08	BELL	$e^+e^- \rightarrow \Upsilon(4S)$
••• We do not use the following data for averages, fits, limits, etc. •••				
<23.1 $\times 10^{-6}$	90	<sup>1</sup> AUBERT 08BB	BABR	$e^+e^- \rightarrow \Upsilon(4S)$
< 2.3 $\times 10^{-4}$	90	<sup>2</sup> ADAM 96D	DLPH	$e^+e^- \rightarrow Z$
< 2.8 $\times 10^{-4}$	90	<sup>3</sup> ABREU 95N	DLPH	Sup. by ADAM 96D
< 6.7 $\times 10^{-4}$	90	<sup>1</sup> ALBRECHT 90B	ARG	$e^+e^- \rightarrow \Upsilon(4S)$

<sup>1</sup> Assumes equal production of  $B^+$  and  $B^0$  at the  $\Upsilon(4S)$ .  
<sup>2</sup> ADAM 96D assumes  $f_{B^0} = f_{B^-} = 0.39$  and  $f_{B_s} = 0.12$ .  
<sup>3</sup> Assumes a  $B^0, B^-$  production fraction of 0.39 and a  $B_s$  production fraction of 0.12.



See key on page 457

Meson Particle Listings

B<sup>0</sup>

Γ(a<sub>1</sub>(1260)<sup>+</sup>a<sub>1</sub>(1260)<sup>-</sup> × B<sup>2</sup>(a<sub>1</sub><sup>+</sup> → 2π<sup>+</sup>π<sup>-</sup>)/Γ<sub>total</sub> Γ<sub>379</sub>/Γ

VALUE (units 10 <sup>-6</sup> )	CL%	DOCUMENT ID	TECN	COMMENT
11.8 ± 2.6 ± 1.6		1 AUBERT 09AL	BABR	e <sup>+</sup> e <sup>-</sup> → T(4S)

- • • We do not use the following data for averages, fits, limits, etc. • • •
  - <6000 90 1 ALBRECHT 90B ARG e<sup>+</sup>e<sup>-</sup> → T(4S)
  - <2800 90 2 BORTOLETTO 89 CLEO e<sup>+</sup>e<sup>-</sup> → T(4S)
- <sup>1</sup> Assumes equal production of B<sup>0</sup> $\bar{B}^0$  and B<sup>+</sup>B<sup>-</sup> at T(4S).  
<sup>2</sup> BORTOLETTO 89 reports < 3.2 × 10<sup>-3</sup> assuming the T(4S) decays 43% to B<sup>0</sup> $\bar{B}^0$ . We rescale to 50%.

Γ(π<sup>+</sup>π<sup>+</sup>π<sup>+</sup>π<sup>-</sup>π<sup>-</sup>π<sup>-</sup>π<sup>-</sup>)/Γ<sub>total</sub> Γ<sub>380</sub>/Γ

VALUE	CL%	DOCUMENT ID	TECN	COMMENT
< 1.1 × 10 <sup>-2</sup>	90	1 ALBRECHT 90B	ARG	e <sup>+</sup> e <sup>-</sup> → T(4S)

<sup>1</sup> ALBRECHT 90B limit assumes equal production of B<sup>0</sup> $\bar{B}^0$  and B<sup>+</sup>B<sup>-</sup> at T(4S).

Γ(ρ $\bar{\rho}$ )/Γ<sub>total</sub> Γ<sub>381</sub>/Γ

VALUE (units 10 <sup>-6</sup> )	CL%	DOCUMENT ID	TECN	COMMENT
< 0.11	90	1 TSAI 07	BELL	e <sup>+</sup> e <sup>-</sup> → T(4S)

- • • We do not use the following data for averages, fits, limits, etc. • • •
- < 0.41 90 1 CHANG 05 BELL e<sup>+</sup>e<sup>-</sup> → T(4S)
- < 0.27 90 1 AUBERT 04U BABR e<sup>+</sup>e<sup>-</sup> → T(4S)
- < 1.4 90 1 BORNHEIM 03 CLE2 e<sup>+</sup>e<sup>-</sup> → T(4S)
- < 1.2 90 1 ABE 02O BELL e<sup>+</sup>e<sup>-</sup> → T(4S)
- < 7.0 90 1 COAN 99 CLE2 e<sup>+</sup>e<sup>-</sup> → T(4S)
- < 18 90 2 BUSKULIC 96V ALEP e<sup>+</sup>e<sup>-</sup> → Z
- < 350 90 3 ABREU 95N DLPH Sup. by ADAM 96D
- < 34 90 4 BORTOLETTO 89 CLEO e<sup>+</sup>e<sup>-</sup> → T(4S)
- < 120 90 5 ALBRECHT 88F ARG e<sup>+</sup>e<sup>-</sup> → T(4S)
- < 170 90 4 BEBEK 87 CLEO e<sup>+</sup>e<sup>-</sup> → T(4S)

- <sup>1</sup> Assumes equal production of B<sup>+</sup> and B<sup>0</sup> at the T(4S).
- <sup>2</sup> BUSKULIC 96V assumes PDG 96 production fractions for B<sup>0</sup>, B<sup>+</sup>, B<sub>S</sub>, b baryons.
- <sup>3</sup> Assumes a B<sup>0</sup>, B<sup>-</sup> production fraction of 0.39 and a B<sub>S</sub> production fraction of 0.12.
- <sup>4</sup> Paper assumes the T(4S) decays 43% to B<sup>0</sup> $\bar{B}^0$ . We rescale to 50%.
- <sup>5</sup> ALBRECHT 88F reports < 1.3 × 10<sup>-4</sup> assuming the T(4S) decays 45% to B<sup>0</sup> $\bar{B}^0$ . We rescale to 50%.

Γ(ρ $\bar{\rho}$ π<sup>+</sup>π<sup>-</sup>)/Γ<sub>total</sub> Γ<sub>382</sub>/Γ

VALUE (units 10 <sup>-4</sup> )	CL%	DOCUMENT ID	TECN	COMMENT
< 2.5	90	1 BEBEK 89	CLEO	e <sup>+</sup> e <sup>-</sup> → T(4S)

- • • We do not use the following data for averages, fits, limits, etc. • • •
  - < 9.5 90 2 ABREU 95N DLPH Sup. by ADAM 96D
  - 5.4 ± 1.8 ± 2.0 3 ALBRECHT 88F ARG e<sup>+</sup>e<sup>-</sup> → T(4S)
- <sup>1</sup> BEBEK 89 reports < 2.9 × 10<sup>-4</sup> assuming the T(4S) decays 43% to B<sup>0</sup> $\bar{B}^0$ . We rescale to 50%.  
<sup>2</sup> Assumes a B<sup>0</sup>, B<sup>-</sup> production fraction of 0.39 and a B<sub>S</sub> production fraction of 0.12.  
<sup>3</sup> ALBRECHT 88F reports 6.0 ± 2.0 ± 2.2 assuming the T(4S) decays 45% to B<sup>0</sup> $\bar{B}^0$ . We rescale to 50%.

Γ(ρ $\bar{\rho}$ K<sup>0</sup>)/Γ<sub>total</sub> Γ<sub>383</sub>/Γ

VALUE (units 10 <sup>-6</sup> )	CL%	DOCUMENT ID	TECN	COMMENT
2.66 ± 0.32 OUR AVERAGE				

- 2.51<sup>+0.35</sup><sub>-0.29</sub> ± 0.21 1,2 CHEN 08c BELL e<sup>+</sup>e<sup>-</sup> → T(4S)
  - 3.0 ± 0.5 ± 0.3 2 AUBERT 07AV BABR e<sup>+</sup>e<sup>-</sup> → T(4S)
- • • We do not use the following data for averages, fits, limits, etc. • • •
  - 2.40<sup>+0.64</sup><sub>-0.44</sub> ± 0.28 2,3,4 WANG 05A BELL Repl. by CHEN 08c
  - 1.88<sup>+0.77</sup><sub>-0.60</sub> ± 0.23 2,3,5 WANG 04 BELL Repl. by WANG 05A
  - < 7.2 90 2,3 ABE 02K BELL Repl. by WANG 04
- <sup>1</sup> Explicitly vetoes resonant production of ρ $\bar{\rho}$  from charmonium states.  
<sup>2</sup> Assumes equal production of B<sup>+</sup> and B<sup>0</sup> at the T(4S).  
<sup>3</sup> Explicitly vetoes resonant production of ρ $\bar{\rho}$  from charmonium states and ρK<sup>0</sup> production from Λ<sub>C</sub>.  
<sup>4</sup> Provides also results with M<sub>ρ $\bar{\rho}$</sub>  < 2.85 GeV/c<sup>2</sup> and angular asymmetry of ρ $\bar{\rho}$  system.  
<sup>5</sup> The branching fraction for M<sub>ρ $\bar{\rho}$</sub>  < 2.85 is also reported.

Γ(Θ(1540)<sup>+</sup> $\bar{\rho}$  × B(Θ(1540)<sup>+</sup> → ρK<sub>S</sub><sup>0</sup>)/Γ<sub>total</sub> Γ<sub>384</sub>/Γ

VALUE (units 10 <sup>-6</sup> )	CL%	DOCUMENT ID	TECN	COMMENT
< 0.05	90	1 AUBERT 07AV	BABR	e <sup>+</sup> e <sup>-</sup> → T(4S)

- • • We do not use the following data for averages, fits, limits, etc. • • •
  - < 0.23 90 1 WANG 05A BELL e<sup>+</sup>e<sup>-</sup> → T(4S)
- <sup>1</sup> Assumes equal production of B<sup>+</sup> and B<sup>0</sup> at the T(4S).

Γ(f<sub>J</sub>(2220)K<sup>0</sup> × B(f<sub>J</sub>(2220) → ρ $\bar{\rho}$ )/Γ<sub>total</sub> Γ<sub>385</sub>/Γ

VALUE (units 10 <sup>-6</sup> )	CL%	DOCUMENT ID	TECN	COMMENT
< 0.45	90	1 AUBERT 07AV	BABR	e <sup>+</sup> e <sup>-</sup> → T(4S)

<sup>1</sup> Assumes equal production of B<sup>+</sup> and B<sup>0</sup> at the T(4S).

Γ(ρ $\bar{\rho}$ K<sup>\*</sup>(892)<sup>0</sup>)/Γ<sub>total</sub> Γ<sub>386</sub>/Γ

VALUE (units 10 <sup>-6</sup> )	CL%	DOCUMENT ID	TECN	COMMENT
1.24 <sup>+0.28</sup> <sub>-0.25</sub> OUR AVERAGE				

- 1.18<sup>+0.29</sup><sub>-0.25</sub> ± 0.11 1,2 CHEN 08c BELL e<sup>+</sup>e<sup>-</sup> → T(4S)
  - 1.47 ± 0.45 ± 0.40 2 AUBERT 07AV BABR e<sup>+</sup>e<sup>-</sup> → T(4S)
- • • We do not use the following data for averages, fits, limits, etc. • • •
  - < 7.6 90 2 WANG 04 BELL e<sup>+</sup>e<sup>-</sup> → T(4S)
- <sup>1</sup> Explicitly vetoes resonant production of ρ $\bar{\rho}$  from charmonium states.  
<sup>2</sup> Assumes equal production of B<sup>+</sup> and B<sup>0</sup> at the T(4S).

Γ(f<sub>J</sub>(2220)K<sub>0</sub><sup>\*</sup> × B(f<sub>J</sub>(2220) → ρ $\bar{\rho}$ )/Γ<sub>total</sub> Γ<sub>387</sub>/Γ

VALUE (units 10 <sup>-6</sup> )	CL%	DOCUMENT ID	TECN	COMMENT
< 0.15	90	1 AUBERT 07AV	BABR	e <sup>+</sup> e <sup>-</sup> → T(4S)

<sup>1</sup> Assumes equal production of B<sup>+</sup> and B<sup>0</sup> at the T(4S).

Γ(ρ $\bar{\rho}$ π<sup>-</sup>)/Γ<sub>total</sub> Γ<sub>388</sub>/Γ

VALUE (units 10 <sup>-6</sup> )	CL%	DOCUMENT ID	TECN	COMMENT
3.14 ± 0.29 OUR AVERAGE				

- 3.07 ± 0.31 ± 0.23 1 AUBERT 09AC BABR e<sup>+</sup>e<sup>-</sup> → T(4S)
  - 3.23<sup>+0.33</sup><sub>-0.29</sub> ± 0.29 1 WANG 07c BELL e<sup>+</sup>e<sup>-</sup> → T(4S)
- • • We do not use the following data for averages, fits, limits, etc. • • •
  - 2.62<sup>+0.44</sup><sub>-0.40</sub> ± 0.31 1,2 WANG 05A BELL Repl. by WANG 07c
  - 3.97<sup>+1.00</sup><sub>-0.80</sub> ± 0.56 1 WANG 03 BELL Repl. by WANG 05A
  - < 13 90 1 COAN 99 CLE2 e<sup>+</sup>e<sup>-</sup> → T(4S)
  - < 180 90 3 ALBRECHT 88F ARG e<sup>+</sup>e<sup>-</sup> → T(4S)

- <sup>1</sup> Assumes equal production of B<sup>+</sup> and B<sup>0</sup> at the T(4S).
- <sup>2</sup> Provides also results with M<sub>ρ $\bar{\rho}$</sub>  < 2.85 GeV/c<sup>2</sup> and angular asymmetry of ρ $\bar{\rho}$  system.
- <sup>3</sup> ALBRECHT 88F reports < 2.0 × 10<sup>-4</sup> assuming the T(4S) decays 45% to B<sup>0</sup> $\bar{B}^0$ . We rescale to 50%.

Γ(ρ $\Sigma$ (1385)<sup>-</sup>)/Γ<sub>total</sub> Γ<sub>389</sub>/Γ

VALUE (units 10 <sup>-6</sup> )	CL%	DOCUMENT ID	TECN	COMMENT
< 0.26	90	1 WANG 07c	BELL	e <sup>+</sup> e <sup>-</sup> → T(4S)

<sup>1</sup> Assumes equal production of B<sup>+</sup> and B<sup>0</sup> at the T(4S).

Γ(Δ<sup>0</sup>Λ)/Γ<sub>total</sub> Γ<sub>390</sub>/Γ

VALUE (units 10 <sup>-6</sup> )	CL%	DOCUMENT ID	TECN	COMMENT
< 0.93	90	1 WANG 07c	BELL	e <sup>+</sup> e <sup>-</sup> → T(4S)

<sup>1</sup> Assumes equal production of B<sup>+</sup> and B<sup>0</sup> at the T(4S).

Γ(ρ $\bar{\rho}$ K<sup>-</sup>)/Γ<sub>total</sub> Γ<sub>391</sub>/Γ

VALUE (units 10 <sup>-6</sup> )	CL%	DOCUMENT ID	TECN	COMMENT
< 0.82	90	1 WANG 03	BELL	e <sup>+</sup> e <sup>-</sup> → T(4S)

<sup>1</sup> Assumes equal production of B<sup>+</sup> and B<sup>0</sup> at the T(4S).

Γ(ρ $\Sigma$ <sup>0</sup>π<sup>-</sup>)/Γ<sub>total</sub> Γ<sub>392</sub>/Γ

VALUE	CL%	DOCUMENT ID	TECN	COMMENT
< 3.8 × 10 <sup>-6</sup>	90	1 WANG 03	BELL	e <sup>+</sup> e <sup>-</sup> → T(4S)

<sup>1</sup> Assumes equal production of B<sup>+</sup> and B<sup>0</sup> at the T(4S).

Γ(Λ)/Γ<sub>total</sub> Γ<sub>393</sub>/Γ

VALUE (units 10 <sup>-6</sup> )	CL%	DOCUMENT ID	TECN	COMMENT
< 0.32	90	1 TSAI 07	BELL	e <sup>+</sup> e <sup>-</sup> → T(4S)

- • • We do not use the following data for averages, fits, limits, etc. • • •
  - < 0.69 90 1 CHANG 05 BELL Repl. by TSAI 07
  - < 1.2 90 1 BORNHEIM 03 CLE2 e<sup>+</sup>e<sup>-</sup> → T(4S)
  - < 1.0 90 1 ABE 02O BELL Repl. by CHANG 05
  - < 3.9 90 1 COAN 99 CLE2 e<sup>+</sup>e<sup>-</sup> → T(4S)
- <sup>1</sup> Assumes equal production of B<sup>+</sup> and B<sup>0</sup> at the T(4S).

Γ(ΛΛK<sup>0</sup>)/Γ<sub>total</sub> Γ<sub>394</sub>/Γ

VALUE (units 10 <sup>-6</sup> )	CL%	DOCUMENT ID	TECN	COMMENT
4.76 <sup>+0.84</sup> <sub>-0.68</sub> ± 0.61		1,2 CHANG 09	BELL	e <sup>+</sup> e <sup>-</sup> → T(4S)

- <sup>1</sup> Excluding charmonium events in 2.85 < m<sub>ΛΛ</sub> < 3.128 GeV/c<sup>2</sup> and 3.315 < m<sub>ΛΛ</sub> < 3.735 GeV/c<sup>2</sup>. Measurements in various m<sub>ΛΛ</sub> bins are also reported.
- <sup>2</sup> Assumes equal production of B<sup>+</sup> and B<sup>0</sup> at the T(4S).

Γ(ΛΛK<sup>\*0</sup>)/Γ<sub>total</sub> Γ<sub>395</sub>/Γ

VALUE (units 10 <sup>-6</sup> )	CL%	DOCUMENT ID	TECN	COMMENT
2.46 <sup>+0.87</sup> <sub>-0.72</sub> ± 0.34		1,2 CHANG 09	BELL	e <sup>+</sup> e <sup>-</sup> → T(4S)

- <sup>1</sup> Excluding charmonium events in 2.85 < m<sub>ΛΛ</sub> < 3.128 GeV/c<sup>2</sup> and 3.315 < m<sub>ΛΛ</sub> < 3.735 GeV/c<sup>2</sup>. Measurements in various m<sub>ΛΛ</sub> bins are also reported.
- <sup>2</sup> Assumes equal production of B<sup>+</sup> and B<sup>0</sup> at the T(4S).

## Meson Particle Listings

 $B^0$ 

$\Gamma(\Lambda D^0)/\Gamma_{\text{total}}$   $\Gamma_{396}/\Gamma$   
 VALUE (units  $10^{-5}$ ) DOCUMENT ID TECN COMMENT

$1.05^{+0.57}_{-0.44} \pm 0.14$  <sup>1</sup> CHANG 09 BELL  $e^+e^- \rightarrow \Upsilon(4S)$   
<sup>1</sup> Assumes equal production of  $B^+$  and  $B^0$  at the  $\Upsilon(4S)$ .

$\Gamma(\Delta^0 \bar{D}^0)/\Gamma_{\text{total}}$   $\Gamma_{397}/\Gamma$   
 VALUE CL% DOCUMENT ID TECN COMMENT

$<0.0015$  90 <sup>1</sup> BORTOLETTO89 CLEO  $e^+e^- \rightarrow \Upsilon(4S)$   
<sup>1</sup> BORTOLETTO 89 reports  $< 0.0018$  assuming  $\Upsilon(4S)$  decays 43% to  $B^0 \bar{B}^0$ . We rescale to 50%.

$\Gamma(\Delta^{++} \bar{D}^{--})/\Gamma_{\text{total}}$   $\Gamma_{398}/\Gamma$   
 VALUE CL% DOCUMENT ID TECN COMMENT

$<1.1 \times 10^{-4}$  90 <sup>1</sup> BORTOLETTO89 CLEO  $e^+e^- \rightarrow \Upsilon(4S)$   
<sup>1</sup> BORTOLETTO 89 reports  $< 1.3 \times 10^{-4}$  assuming  $\Upsilon(4S)$  decays 43% to  $B^0 \bar{B}^0$ . We rescale to 50%.

$\Gamma(\bar{D}^0 \rho \bar{p})/\Gamma_{\text{total}}$   $\Gamma_{399}/\Gamma$   
 VALUE (units  $10^{-4}$ ) DOCUMENT ID TECN COMMENT

$1.14 \pm 0.09$  OUR AVERAGE  
 $1.13 \pm 0.06 \pm 0.08$  <sup>1</sup> AUBERT,B 06s BABR  $e^+e^- \rightarrow \Upsilon(4S)$   
 $1.18 \pm 0.15 \pm 0.16$  <sup>1</sup> ABE 02w BELL  $e^+e^- \rightarrow \Upsilon(4S)$   
<sup>1</sup> Assumes equal production of  $B^+$  and  $B^0$  at the  $\Upsilon(4S)$ .

$\Gamma(D_s^- \bar{\Lambda} p)/\Gamma_{\text{total}}$   $\Gamma_{400}/\Gamma$   
 VALUE (units  $10^{-5}$ ) DOCUMENT ID TECN COMMENT

$2.8 \pm 0.8 \pm 0.3$  <sup>1,2</sup> MEDVEDEVA 07 BELL  $e^+e^- \rightarrow \Upsilon(4S)$   
<sup>1</sup> Assumes equal production of  $B^+$  and  $B^0$  at the  $\Upsilon(4S)$ .  
<sup>2</sup> MEDVEDEVA 07 reports  $(2.9 \pm 0.7 \pm 0.5 \pm 0.4) \times 10^{-5}$  from a measurement of  $[\Gamma(B^0 \rightarrow D_s^- \bar{\Lambda} p)/\Gamma_{\text{total}}] \times [B(D_s^+ \rightarrow \phi \pi^+)]$  assuming  $B(D_s^+ \rightarrow \phi \pi^+) = (4.4 \pm 0.6) \times 10^{-2}$ , which we rescale to our best value  $B(D_s^+ \rightarrow \phi \pi^+) = (4.5 \pm 0.4) \times 10^{-2}$ . Our first error is their experiment's error and our second error is the systematic error from using our best value.

$\Gamma(\bar{D}^*(2007)^0 \rho \bar{p})/\Gamma_{\text{total}}$   $\Gamma_{401}/\Gamma$   
 VALUE (units  $10^{-4}$ ) DOCUMENT ID TECN COMMENT

$1.03 \pm 0.13$  OUR AVERAGE  
 $1.01 \pm 0.10 \pm 0.09$  <sup>1</sup> AUBERT,B 06s BABR  $e^+e^- \rightarrow \Upsilon(4S)$   
 $1.20^{+0.33}_{-0.29} \pm 0.21$  <sup>1</sup> ABE 02w BELL  $e^+e^- \rightarrow \Upsilon(4S)$   
<sup>1</sup> Assumes equal production of  $B^+$  and  $B^0$  at the  $\Upsilon(4S)$ .

$\Gamma(D^*(2010)^- \rho \pi)/\Gamma_{\text{total}}$   $\Gamma_{402}/\Gamma$   
 VALUE (units  $10^{-4}$ ) DOCUMENT ID TECN COMMENT

$14.5^{+3.4}_{-3.0} \pm 2.7$  <sup>1</sup> ANDERSON 01 CLE2  $e^+e^- \rightarrow \Upsilon(4S)$   
<sup>1</sup> Assumes equal production of  $B^+$  and  $B^0$  at the  $\Upsilon(4S)$ .

$\Gamma(D^- \rho \bar{p} \pi^+)/\Gamma_{\text{total}}$   $\Gamma_{403}/\Gamma$   
 VALUE (units  $10^{-4}$ ) DOCUMENT ID TECN COMMENT

$3.38 \pm 0.14 \pm 0.29$  <sup>1</sup> AUBERT,B 06s BABR  $e^+e^- \rightarrow \Upsilon(4S)$   
<sup>1</sup> Assumes equal production of  $B^+$  and  $B^0$  at the  $\Upsilon(4S)$ .

$\Gamma(D^*(2010)^- \rho \bar{p} \pi^+)/\Gamma_{\text{total}}$   $\Gamma_{404}/\Gamma$   
 VALUE (units  $10^{-4}$ ) DOCUMENT ID TECN COMMENT

$5.0 \pm 0.5$  OUR AVERAGE  
 $4.81 \pm 0.22 \pm 0.44$  <sup>1</sup> AUBERT,B 06s BABR  $e^+e^- \rightarrow \Upsilon(4S)$   
 $6.5^{+1.3}_{-1.2} \pm 1.0$  <sup>1</sup> ANDERSON 01 CLE2  $e^+e^- \rightarrow \Upsilon(4S)$   
<sup>1</sup> Assumes equal production of  $B^+$  and  $B^0$  at the  $\Upsilon(4S)$ .

$\Gamma(\Theta_c^- \bar{p} \pi^+ \times B(\Theta_c \rightarrow D^- \rho))/\Gamma_{\text{total}}$   $\Gamma_{405}/\Gamma$   
 VALUE (units  $10^{-6}$ ) CL% DOCUMENT ID TECN COMMENT

$<9$  90 <sup>1</sup> AUBERT,B 06s BABR  $e^+e^- \rightarrow \Upsilon(4S)$   
<sup>1</sup> Assumes equal production of  $B^+$  and  $B^0$  at the  $\Upsilon(4S)$ .

$\Gamma(\Theta_c^- \bar{p} \pi^+ \times B(\Theta_c \rightarrow D^{*-} \rho))/\Gamma_{\text{total}}$   $\Gamma_{406}/\Gamma$   
 VALUE (units  $10^{-6}$ ) CL% DOCUMENT ID TECN COMMENT

$<14$  90 <sup>1</sup> AUBERT,B 06s BABR  $e^+e^- \rightarrow \Upsilon(4S)$   
<sup>1</sup> Assumes equal production of  $B^+$  and  $B^0$  at the  $\Upsilon(4S)$ .

$\Gamma(\Sigma_c^- \Delta^{++})/\Gamma_{\text{total}}$   $\Gamma_{407}/\Gamma$   
 VALUE CL% DOCUMENT ID TECN COMMENT

$<1.0 \times 10^{-3}$  90 <sup>1</sup> PROCARIO 94 CLE2  $e^+e^- \rightarrow \Upsilon(4S)$   
<sup>1</sup> PROCARIO 94 reports  $< 0.0012$  from a measurement of  $[\Gamma(B^0 \rightarrow \Sigma_c^- \Delta^{++})/\Gamma_{\text{total}}] \times [B(\Lambda_c^+ \rightarrow p K^- \pi^+)]$  assuming  $B(\Lambda_c^+ \rightarrow p K^- \pi^+) = 0.043$ , which we rescale to our best value  $B(\Lambda_c^+ \rightarrow p K^- \pi^+) = 5.0 \times 10^{-2}$ .

$\Gamma(\Lambda_c^- \rho \pi^+ \pi^-)/\Gamma_{\text{total}}$   $\Gamma_{408}/\Gamma$   
 VALUE (units  $10^{-3}$ ) DOCUMENT ID TECN COMMENT

$1.3 \pm 0.4$  OUR AVERAGE  
 $1.7^{+0.3}_{-0.2} \pm 0.4$  <sup>1</sup> DYTMAN 02 CLE2  $e^+e^- \rightarrow \Upsilon(4S)$   
 $1.10 \pm 0.20 \pm 0.29$  <sup>2</sup> GABYSHEV 02 BELL  $e^+e^- \rightarrow \Upsilon(4S)$   
 • • • We do not use the following data for averages, fits, limits, etc. • • •  
 $1.33^{+0.46}_{-0.42} \pm 0.37$  <sup>3</sup> FU 97 CLE2 Repl. by DYTMAN 02

<sup>1</sup> DYTMAN 02 reports  $(1.67^{+0.27}_{-0.25}) \times 10^{-3}$  from a measurement of  $[\Gamma(B^0 \rightarrow \Lambda_c^- \rho \pi^+ \pi^-)/\Gamma_{\text{total}}] \times [B(\Lambda_c^+ \rightarrow p K^- \pi^+)]$  assuming  $B(\Lambda_c^+ \rightarrow p K^- \pi^+) = 0.05$ , which we rescale to our best value  $B(\Lambda_c^+ \rightarrow p K^- \pi^+) = (5.0 \pm 1.3) \times 10^{-2}$ . Our first error is their experiment's error and our second error is the systematic error from using our best value.  
<sup>2</sup> GABYSHEV 02 reports  $(1.1 \pm 0.2) \times 10^{-3}$  from a measurement of  $[\Gamma(B^0 \rightarrow \Lambda_c^- \rho \pi^+ \pi^-)/\Gamma_{\text{total}}] \times [B(\Lambda_c^+ \rightarrow p K^- \pi^+)]$  assuming  $B(\Lambda_c^+ \rightarrow p K^- \pi^+) = 0.05$ , which we rescale to our best value  $B(\Lambda_c^+ \rightarrow p K^- \pi^+) = (5.0 \pm 1.3) \times 10^{-2}$ . Our first error is their experiment's error and our second error is the systematic error from using our best value.  
<sup>3</sup> FU 97 uses PDG 96 values of  $\Lambda_c$  branching fraction.

$\Gamma(\Lambda_c^- \rho)/\Gamma_{\text{total}}$   $\Gamma_{409}/\Gamma$   
 VALUE (units  $10^{-5}$ ) CL% DOCUMENT ID TECN COMMENT

$2.0 \pm 0.4$  OUR AVERAGE  
 $1.9 \pm 0.2 \pm 0.5$  <sup>1,2</sup> AUBERT 08BN BABR  $e^+e^- \rightarrow \Upsilon(4S)$   
 $2.19^{+0.56}_{-0.49} \pm 0.65$  <sup>1,3</sup> GABYSHEV 03 BELL  $e^+e^- \rightarrow \Upsilon(4S)$   
 • • • We do not use the following data for averages, fits, limits, etc. • • •  
 $2.10^{+0.67+0.77}_{-0.55-0.46}$  <sup>1,4</sup> AUBERT 07AV BABR Repl. by AUBERT 08BN  
 $< 9$  90 <sup>1,5</sup> DYTMAN 02 CLE2  $e^+e^- \rightarrow \Upsilon(4S)$   
 $< 3.1$  90 <sup>1,4</sup> GABYSHEV 02 BELL  $e^+e^- \rightarrow \Upsilon(4S)$   
 $< 21$  90 <sup>6</sup> FU 97 CLE2  $e^+e^- \rightarrow \Upsilon(4S)$

<sup>1</sup> Assumes equal production of  $B^+$  and  $B^0$  at the  $\Upsilon(4S)$ .  
<sup>2</sup> AUBERT 08BN reports  $(1.89 \pm 0.21 \pm 0.49) \times 10^{-5}$  from a measurement of  $[\Gamma(B^0 \rightarrow \Lambda_c^- \rho)/\Gamma_{\text{total}}] \times [B(\Lambda_c^+ \rightarrow p K^- \pi^+)]$  assuming  $B(\Lambda_c^+ \rightarrow p K^- \pi^+) = (5.0 \pm 1.3) \times 10^{-2}$ .  
<sup>3</sup> The second error for GABYSHEV 03 includes the systematic and the error of  $\Lambda_c \rightarrow \bar{p} K^+ \pi^-$  decay branching fraction.  
<sup>4</sup> Uses the value for  $\Lambda_c \rightarrow p K^- \pi^+$  branching ratio  $(5.0 \pm 1.3)\%$ .  
<sup>5</sup> DYTMAN 02 measurement uses  $B(\Lambda_c^- \rightarrow \bar{p} K^+ \pi^-) = 5.0 \pm 1.3\%$ . The second error includes the systematic and the uncertainty of the branching ratio.  
<sup>6</sup> FU 97 uses PDG 96 values of  $\Lambda_c$  branching ratio.

$\Gamma(\Lambda_c^- \rho \pi^0)/\Gamma_{\text{total}}$   $\Gamma_{410}/\Gamma$   
 VALUE (units  $10^{-4}$ ) CL% DOCUMENT ID TECN COMMENT

$1.9 \pm 0.2 \pm 0.5$  <sup>1,2</sup> AUBERT 10H BABR  $e^+e^- \rightarrow \Upsilon(4S)$   
 • • • We do not use the following data for averages, fits, limits, etc. • • •  
 $<5.9$  90 <sup>3</sup> FU 97 CLE2  $e^+e^- \rightarrow \Upsilon(4S)$   
<sup>1</sup> AUBERT 10H reports  $(1.94 \pm 0.17 \pm 0.52) \times 10^{-4}$  from a measurement of  $[\Gamma(B^0 \rightarrow \Lambda_c^- \rho \pi^0)/\Gamma_{\text{total}}] \times [B(\Lambda_c^+ \rightarrow p K^- \pi^+)]$  assuming  $B(\Lambda_c^+ \rightarrow p K^- \pi^+) = (5.0 \pm 1.3) \times 10^{-2}$ .  
<sup>2</sup> Assumes equal production of  $B^+$  and  $B^0$  at the  $\Upsilon(4S)$ .  
<sup>3</sup> FU 97 uses PDG 96 values of  $\Lambda_c$  branching ratio.

$\Gamma(\Sigma_c(2455)^- \rho)/\Gamma_{\text{total}}$   $\Gamma_{411}/\Gamma$   
 VALUE (units  $10^{-6}$ ) DOCUMENT ID TECN COMMENT

$<30$  <sup>1,2</sup> AUBERT 10H BABR  $e^+e^- \rightarrow \Upsilon(4S)$   
<sup>1</sup> AUBERT 10H reports  $[\Gamma(B^0 \rightarrow \Sigma_c(2455)^- \rho)/\Gamma_{\text{total}}] \times [B(\Lambda_c^+ \rightarrow p K^- \pi^+)] < 1.5 \times 10^{-6}$  which we divide by our best value  $B(\Lambda_c^+ \rightarrow p K^- \pi^+) = 5.0 \times 10^{-2}$ .  
<sup>2</sup> Assumes equal production of  $B^+$  and  $B^0$  at the  $\Upsilon(4S)$ .

$\Gamma(\Lambda_c^- \rho \pi^+ \pi^- \pi^0)/\Gamma_{\text{total}}$   $\Gamma_{412}/\Gamma$   
 VALUE CL% DOCUMENT ID TECN COMMENT

$<5.07 \times 10^{-3}$  90 <sup>1</sup> FU 97 CLE2  $e^+e^- \rightarrow \Upsilon(4S)$   
<sup>1</sup> FU 97 uses PDG 96 values of  $\Lambda_c$  branching ratio.

$\Gamma(\Lambda_c^- \rho \pi^+ \pi^- \pi^+ \pi^-)/\Gamma_{\text{total}}$   $\Gamma_{413}/\Gamma$   
 VALUE CL% DOCUMENT ID TECN COMMENT

$<2.74 \times 10^{-3}$  90 <sup>1</sup> FU 97 CLE2  $e^+e^- \rightarrow \Upsilon(4S)$   
<sup>1</sup> FU 97 uses PDG 96 values of  $\Lambda_c$  branching ratio.

$\Gamma(\Lambda_c^- \rho \pi^+ \pi^-)/\Gamma_{\text{total}}$   $\Gamma_{414}/\Gamma$   
 VALUE (units  $10^{-4}$ ) DOCUMENT ID TECN COMMENT

$11.2 \pm 0.5 \pm 3.2$  <sup>1,2</sup> PARK 07 BELL  $e^+e^- \rightarrow \Upsilon(4S)$   
<sup>1</sup> Assumes equal production of  $B^+$  and  $B^0$  at the  $\Upsilon(4S)$ .  
<sup>2</sup> PARK 07 reports  $(11.2 \pm 0.5 \pm 3.2) \times 10^{-4}$  from a measurement of  $[\Gamma(B^0 \rightarrow \Lambda_c^- \rho \pi^+ \pi^-)/\Gamma_{\text{total}}] \times [B(\Lambda_c^+ \rightarrow p K^- \pi^+)]$  assuming  $B(\Lambda_c^+ \rightarrow p K^- \pi^+) = (5.0 \pm 1.3) \times 10^{-2}$ .

See key on page 457

## Meson Particle Listings

 $B^0$  $\Gamma(\bar{\Lambda}_c^- \rho \pi^+ \pi^- (\text{nonresonant}))/\Gamma_{\text{total}}$   $\Gamma_{415}/\Gamma$ 

VALUE (units $10^{-4}$ )	DOCUMENT ID	TECN	COMMENT
<b><math>6.4 \pm 0.4 \pm 1.9</math></b>	1,2 PARK 07	BELL	$e^+ e^- \rightarrow \Upsilon(4S)$

- <sup>1</sup> Assumes equal production of  $B^+$  and  $B^0$  at the  $\Upsilon(4S)$ .  
<sup>2</sup> PARK 07 reports  $(6.4 \pm 0.4 \pm 1.9) \times 10^{-4}$  from a measurement of  $[\Gamma(B^0 \rightarrow \bar{\Lambda}_c^- \rho \pi^+ \pi^- (\text{nonresonant}))/\Gamma_{\text{total}}] \times [B(\Lambda_c^+ \rightarrow \rho K^- \pi^+)]$  assuming  $B(\Lambda_c^+ \rightarrow \rho K^- \pi^+) = (5.0 \pm 1.3) \times 10^{-2}$ .

 $\Gamma(\bar{\Sigma}_c(2520)^- \rho \pi^+)/\Gamma_{\text{total}}$   $\Gamma_{416}/\Gamma$ 

VALUE (units $10^{-4}$ )	DOCUMENT ID	TECN	COMMENT
<b><math>1.2 \pm 0.1 \pm 0.4</math></b>	1,2 PARK 07	BELL	$e^+ e^- \rightarrow \Upsilon(4S)$

- • • We do not use the following data for averages, fits, limits, etc. • • •  
 $1.6 \pm 0.6 \pm 0.4$  <sup>3</sup> GABYSHEV 02 BELL Repl. by PARK 07

- <sup>1</sup> Assumes equal production of  $B^+$  and  $B^0$  at the  $\Upsilon(4S)$ .  
<sup>2</sup> PARK 07 reports  $(1.2 \pm 0.1 \pm 0.4) \times 10^{-4}$  from a measurement of  $[\Gamma(B^0 \rightarrow \bar{\Sigma}_c(2520)^- \rho \pi^+)/\Gamma_{\text{total}}] \times [B(\Lambda_c^+ \rightarrow \rho K^- \pi^+)]$  assuming  $B(\Lambda_c^+ \rightarrow \rho K^- \pi^+) = (5.0 \pm 1.3) \times 10^{-2}$ .  
<sup>3</sup> GABYSHEV 02 reports  $(1.63^{+0.64}_{-0.58}) \times 10^{-4}$  from a measurement of  $[\Gamma(B^0 \rightarrow \bar{\Sigma}_c(2520)^- \rho \pi^+)/\Gamma_{\text{total}}] \times [B(\Lambda_c^+ \rightarrow \rho K^- \pi^+)]$  assuming  $B(\Lambda_c^+ \rightarrow \rho K^- \pi^+) = 0.05$ , which we rescale to our best value  $B(\Lambda_c^+ \rightarrow \rho K^- \pi^+) = (5.0 \pm 1.3) \times 10^{-2}$ . Our first error is their experiment's error and our second error is the systematic error from using our best value.

 $\Gamma(\bar{\Sigma}_c(2520)^0 \rho \pi^-)/\Gamma_{\text{total}}$   $\Gamma_{417}/\Gamma$ 

VALUE	CL%	DOCUMENT ID	TECN	COMMENT
<b><math>&lt;0.38 \times 10^{-4}</math></b>	90	1 PARK 07	BELL	$e^+ e^- \rightarrow \Upsilon(4S)$

- • • We do not use the following data for averages, fits, limits, etc. • • •  
 $<1.21 \times 10^{-4}$  90 <sup>1,2</sup> GABYSHEV 02 BELL Repl. by PARK 07  
<sup>1</sup> Assumes equal production of  $B^+$  and  $B^0$  at the  $\Upsilon(4S)$ .  
<sup>2</sup> Uses the value for  $\Lambda_c \rightarrow \rho K^- \pi^+$  branching ratio  $(5.0 \pm 1.3)\%$ .

 $\Gamma(\bar{\Sigma}_c(2455)^0 N^0 \times B(N^0 \rightarrow \rho \pi^-))/\Gamma_{\text{total}}$   $\Gamma_{419}/\Gamma$ 

VALUE (units $10^{-4}$ )	DOCUMENT ID	TECN	COMMENT
<b><math>0.80 \pm 0.15 \pm 0.25</math></b>	1,2 KIM 08	BELL	$e^+ e^- \rightarrow \Upsilon(4S)$

- $N^0$  is the  $N(1440) P_{11}$  or  $N(1535) S_{11}$  or an admixture of the two baryonic states.  
<sup>1</sup> Assumes equal production of  $B^+$  and  $B^0$  at the  $\Upsilon(4S)$ .  
<sup>2</sup> KIM 08 reports  $(0.80 \pm 0.15 \pm 0.25) \times 10^{-4}$  from a measurement of  $[\Gamma(B^0 \rightarrow \bar{\Sigma}_c(2455)^0 N^0 \times B(N^0 \rightarrow \rho \pi^-))/\Gamma_{\text{total}}] \times [B(\Lambda_c^+ \rightarrow \rho K^- \pi^+)]$  assuming  $B(\Lambda_c^+ \rightarrow \rho K^- \pi^+) = (5.0 \pm 1.3) \times 10^{-2}$ .

 $\Gamma(\bar{\Sigma}_c(2455)^0 \rho \pi^-)/\Gamma_{\text{total}}$   $\Gamma_{418}/\Gamma$ 

VALUE (units $10^{-4}$ )	CL%	DOCUMENT ID	TECN	COMMENT
<b><math>1.5 \pm 0.5</math> OUR AVERAGE</b>				

- $1.4 \pm 0.2 \pm 0.4$  <sup>1,2</sup> PARK 07 BELL  $e^+ e^- \rightarrow \Upsilon(4S)$   
 $2.2 \pm 0.7 \pm 0.6$  <sup>3</sup> DYTMAN 02 CLE2  $e^+ e^- \rightarrow \Upsilon(4S)$   
 • • • We do not use the following data for averages, fits, limits, etc. • • •  
 $0.5^{+0.5}_{-0.4} \pm 0.1$  90 <sup>4</sup> GABYSHEV 02 BELL Repl. by PARK 07

- <sup>1</sup> Assumes equal production of  $B^+$  and  $B^0$  at the  $\Upsilon(4S)$ .  
<sup>2</sup> PARK 07 reports  $(1.4 \pm 0.2 \pm 0.4) \times 10^{-4}$  from a measurement of  $[\Gamma(B^0 \rightarrow \bar{\Sigma}_c(2455)^0 \rho \pi^-)/\Gamma_{\text{total}}] \times [B(\Lambda_c^+ \rightarrow \rho K^- \pi^+)]$  assuming  $B(\Lambda_c^+ \rightarrow \rho K^- \pi^+) = (5.0 \pm 1.3) \times 10^{-2}$ .  
<sup>3</sup> DYTMAN 02 reports  $(2.2 \pm 0.7) \times 10^{-4}$  from a measurement of  $[\Gamma(B^0 \rightarrow \bar{\Sigma}_c(2455)^0 \rho \pi^-)/\Gamma_{\text{total}}] \times [B(\Lambda_c^+ \rightarrow \rho K^- \pi^+)]$  assuming  $B(\Lambda_c^+ \rightarrow \rho K^- \pi^+) = 0.05$ , which we rescale to our best value  $B(\Lambda_c^+ \rightarrow \rho K^- \pi^+) = (5.0 \pm 1.3) \times 10^{-2}$ . Our first error is their experiment's error and our second error is the systematic error from using our best value.  
<sup>4</sup> GABYSHEV 02 reports  $(0.48^{+0.46}_{-0.41}) \times 10^{-4}$  from a measurement of  $[\Gamma(B^0 \rightarrow \bar{\Sigma}_c(2455)^0 \rho \pi^-)/\Gamma_{\text{total}}] \times [B(\Lambda_c^+ \rightarrow \rho K^- \pi^+)]$  assuming  $B(\Lambda_c^+ \rightarrow \rho K^- \pi^+) = 0.05$ , which we rescale to our best value  $B(\Lambda_c^+ \rightarrow \rho K^- \pi^+) = (5.0 \pm 1.3) \times 10^{-2}$ . Our first error is their experiment's error and our second error is the systematic error from using our best value.

 $\Gamma(\bar{\Sigma}_c(2455)^- \rho \pi^+)/\Gamma_{\text{total}}$   $\Gamma_{420}/\Gamma$ 

VALUE (units $10^{-4}$ )	DOCUMENT ID	TECN	COMMENT
<b><math>2.2 \pm 0.7</math> OUR AVERAGE</b>			

- $2.1 \pm 0.2 \pm 0.6$  <sup>1,2</sup> PARK 07 BELL  $e^+ e^- \rightarrow \Upsilon(4S)$   
 $3.7 \pm 1.1 \pm 1.0$  <sup>3</sup> DYTMAN 02 CLE2  $e^+ e^- \rightarrow \Upsilon(4S)$   
 • • • We do not use the following data for averages, fits, limits, etc. • • •  
 $2.4^{+0.8}_{-0.7} \pm 0.6$  <sup>4</sup> GABYSHEV 02 BELL Repl. by PARK 07

- <sup>1</sup> Assumes equal production of  $B^+$  and  $B^0$  at the  $\Upsilon(4S)$ .  
<sup>2</sup> PARK 07 reports  $(2.1 \pm 0.2 \pm 0.6) \times 10^{-4}$  from a measurement of  $[\Gamma(B^0 \rightarrow \bar{\Sigma}_c(2455)^- \rho \pi^+)/\Gamma_{\text{total}}] \times [B(\Lambda_c^+ \rightarrow \rho K^- \pi^+)]$  assuming  $B(\Lambda_c^+ \rightarrow \rho K^- \pi^+) = (5.0 \pm 1.3) \times 10^{-2}$ .  
<sup>3</sup> DYTMAN 02 reports  $(3.7 \pm 1.1) \times 10^{-4}$  from a measurement of  $[\Gamma(B^0 \rightarrow \bar{\Sigma}_c(2455)^- \rho \pi^+)/\Gamma_{\text{total}}] \times [B(\Lambda_c^+ \rightarrow \rho K^- \pi^+)]$  assuming  $B(\Lambda_c^+ \rightarrow \rho K^- \pi^+) = 0.05$ , which we rescale to our best value  $B(\Lambda_c^+ \rightarrow \rho K^- \pi^+) = (5.0 \pm 1.3) \times 10^{-2}$ . Our first error is their experiment's error and our second error is the systematic error from using our best value.  
<sup>4</sup> GABYSHEV 02 reports  $(2.38^{+0.75}_{-0.69}) \times 10^{-4}$  from a measurement of  $[\Gamma(B^0 \rightarrow \bar{\Sigma}_c(2455)^- \rho \pi^+)/\Gamma_{\text{total}}] \times [B(\Lambda_c^+ \rightarrow \rho K^- \pi^+)]$  assuming  $B(\Lambda_c^+ \rightarrow \rho K^- \pi^+) = 0.05$ , which we rescale to our best value  $B(\Lambda_c^+ \rightarrow \rho K^- \pi^+) = (5.0 \pm 1.3) \times 10^{-2}$ . Our first error is their experiment's error and our second error is the systematic error from using our best value.

 $\Gamma(\bar{\Lambda}_c^- \rho K^+ \pi^-)/\Gamma_{\text{total}}$   $\Gamma_{421}/\Gamma$ 

VALUE (units $10^{-5}$ )	DOCUMENT ID	TECN	COMMENT
<b><math>4.3 \pm 0.8 \pm 1.2</math></b>	1,2 AUBERT 09AG BABR	BELL	$e^+ e^- \rightarrow \Upsilon(4S)$

- <sup>1</sup> AUBERT 09AG reports  $(4.33 \pm 0.82 \pm 0.33 \pm 1.13) \times 10^{-5}$  from a measurement of  $[\Gamma(B^0 \rightarrow \bar{\Lambda}_c^- \rho K^+ \pi^-)/\Gamma_{\text{total}}] \times [B(\Lambda_c^+ \rightarrow \rho K^- \pi^+)]$  assuming  $B(\Lambda_c^+ \rightarrow \rho K^- \pi^+) = (5.0 \pm 1.3) \times 10^{-2}$ .  
<sup>2</sup> Assumes equal production of  $B^+$  and  $B^0$  at the  $\Upsilon(4S)$ .

 $\Gamma(\bar{\Sigma}_c(2455)^- \rho K^+ \times B(\bar{\Sigma}_c^- \rightarrow \bar{\Lambda}_c^- \pi^-))/\Gamma_{\text{total}}$   $\Gamma_{422}/\Gamma$ 

VALUE (units $10^{-5}$ )	DOCUMENT ID	TECN	COMMENT
<b><math>1.11 \pm 0.30 \pm 0.30</math></b>	1,2 AUBERT 09AG BABR	BELL	$e^+ e^- \rightarrow \Upsilon(4S)$

- <sup>1</sup> AUBERT 09AG reports  $(1.11 \pm 0.30 \pm 0.09 \pm 0.29) \times 10^{-5}$  from a measurement of  $[\Gamma(B^0 \rightarrow \bar{\Sigma}_c(2455)^- \rho K^+ \times B(\bar{\Sigma}_c^- \rightarrow \bar{\Lambda}_c^- \pi^-))/\Gamma_{\text{total}}] \times [B(\Lambda_c^+ \rightarrow \rho K^- \pi^+)]$  assuming  $B(\Lambda_c^+ \rightarrow \rho K^- \pi^+) = (5.0 \pm 1.3) \times 10^{-2}$ .  
<sup>2</sup> Assumes equal production of  $B^+$  and  $B^0$  at the  $\Upsilon(4S)$ .

 $\Gamma(\bar{\Lambda}_c^- \rho K^*(892)^0)/\Gamma_{\text{total}}$   $\Gamma_{423}/\Gamma$ 

VALUE (units $10^{-5}$ )	CL%	DOCUMENT ID	TECN	COMMENT
<b><math>&lt;2.42</math></b>	90	1 AUBERT 09AG BABR	BELL	$e^+ e^- \rightarrow \Upsilon(4S)$

- <sup>1</sup> Assumes equal production of  $B^+$  and  $B^0$  at the  $\Upsilon(4S)$ .

 $\Gamma(\bar{\Lambda}_c^- \Lambda K^+)/\Gamma_{\text{total}}$   $\Gamma_{424}/\Gamma$ 

VALUE (units $10^{-5}$ )	DOCUMENT ID	TECN	COMMENT
<b><math>3.8 \pm 0.8 \pm 1.0</math></b>	1,2 LEES 11F BABR	BELL	$e^+ e^- \rightarrow \Upsilon(4S)$

- <sup>1</sup> Assumes equal production of  $B^0$  and  $B^+$  from Upsilon(4S) decays.  
<sup>2</sup> LEES 11F reports  $(3.8 \pm 0.8 \pm 0.2 \pm 1.0) \times 10^{-5}$  from a measurement of  $[\Gamma(B^0 \rightarrow \bar{\Lambda}_c^- \Lambda K^+)/\Gamma_{\text{total}}] / [B(\Lambda_c^+ \rightarrow \rho K^- \pi^+)] / [B(\Lambda \rightarrow p \pi^-)]$  assuming  $B(\Lambda_c^+ \rightarrow \rho K^- \pi^+) = (5.0 \pm 1.3) \times 10^{-2}$ ,  $B(\Lambda \rightarrow p \pi^-) = (63.9 \pm 0.5) \times 10^{-2}$ . The reported uncertainties are statistical, systematic, and  $\bar{\Lambda}_c^-$  branching fraction uncertainty.

 $\Gamma(\bar{\Lambda}_c^- \Lambda_c^+)/\Gamma_{\text{total}}$   $\Gamma_{425}/\Gamma$ 

VALUE (units $10^{-5}$ )	CL%	DOCUMENT ID	TECN	COMMENT
<b><math>&lt;6.2</math></b>	90	1 UCHIDA 08 BELL	BELL	$e^+ e^- \rightarrow \Upsilon(4S)$

- <sup>1</sup> Assumes equal production of  $B^+$  and  $B^0$  at the  $\Upsilon(4S)$ .

 $\Gamma(\bar{\Lambda}_c(2593)^- / \bar{\Lambda}_c(2625)^- \rho)/\Gamma_{\text{total}}$   $\Gamma_{426}/\Gamma$ 

VALUE	CL%	DOCUMENT ID	TECN	COMMENT
<b><math>&lt;1.1 \times 10^{-4}</math></b>	90	1,2 DYTMAN 02 CLE2	BELL	$e^+ e^- \rightarrow \Upsilon(4S)$

- <sup>1</sup> Assumes equal production of  $B^+$  and  $B^0$  at the  $\Upsilon(4S)$ .  
<sup>2</sup> DYTMAN 02 measurement uses  $B(\Lambda_c^- \rightarrow \bar{p} K^+ \pi^-) = 5.0 \pm 1.3\%$ . The second error includes the systematic and the uncertainty of the branching ratio.

 $\Gamma(\bar{\Xi}_c^- \Lambda_c^+ \times B(\bar{\Xi}_c^- \rightarrow \Xi^+ \pi^- \pi^-))/\Gamma_{\text{total}}$   $\Gamma_{427}/\Gamma$ 

VALUE (units $10^{-5}$ )	DOCUMENT ID	TECN	COMMENT
<b><math>2.2 \pm 2.3</math> OUR AVERAGE</b>			Error includes scale factor of 1.9.

- $1.5 \pm 1.1 \pm 0.4$  <sup>1,2</sup> AUBERT 08H BABR  $e^+ e^- \rightarrow \Upsilon(4S)$   
 $9.3^{+3.7}_{-2.8} \pm 3.1$  <sup>2,3</sup> CHISTOV 06A BELL  $e^+ e^- \rightarrow \Upsilon(4S)$

- <sup>1</sup> AUBERT 08H reports  $(1.5 \pm 1.07 \pm 0.44) \times 10^{-5}$  from a measurement of  $[\Gamma(B^0 \rightarrow \bar{\Xi}_c^- \Lambda_c^+ \times B(\bar{\Xi}_c^- \rightarrow \Xi^+ \pi^- \pi^-))/\Gamma_{\text{total}}] \times [B(\Lambda_c^+ \rightarrow \rho K^- \pi^+)]$  assuming  $B(\Lambda_c^+ \rightarrow \rho K^- \pi^+) = (5.0 \pm 1.3) \times 10^{-2}$ .  
<sup>2</sup> Assumes equal production of  $B^+$  and  $B^0$  at the  $\Upsilon(4S)$ .  
<sup>3</sup> CHISTOV 06A reports  $(9.3^{+3.7}_{-2.8} \pm 3.1) \times 10^{-5}$  from a measurement of  $[\Gamma(B^0 \rightarrow \bar{\Xi}_c^- \Lambda_c^+ \times B(\bar{\Xi}_c^- \rightarrow \Xi^+ \pi^- \pi^-))/\Gamma_{\text{total}}] \times [B(\Lambda_c^+ \rightarrow \rho K^- \pi^+)]$  assuming  $B(\Lambda_c^+ \rightarrow \rho K^- \pi^+) = (5.0 \pm 1.3) \times 10^{-2}$ .

# Meson Particle Listings

## $B^0$

### $\Gamma(\Lambda_c^+ \Lambda_c^- K^0)/\Gamma_{total}$ $\Gamma_{428}/\Gamma$

VALUE (units  $10^{-4}$ )      DOCUMENT ID      TECN      COMMENT

#### $5.4 \pm 3.2$ OUR AVERAGE

$3.8 \pm 3.1 \pm 2.1$	1,2	AUBERT	08H	BABR	$e^+ e^- \rightarrow \Upsilon(4S)$
$8 \text{ }^{+3}_{-2} \pm 4$	2,3	GABYSHEV	06	BELL	$e^+ e^- \rightarrow \Upsilon(4S)$

- 1 AUBERT 08H reports  $(0.38 \pm 0.31 \pm 0.21) \times 10^{-3}$  from a measurement of  $[\Gamma(B^0 \rightarrow \Lambda_c^+ \Lambda_c^- K^0)/\Gamma_{total}] \times [B(\Lambda_c^+ \rightarrow pK^- \pi^+)]$  assuming  $B(\Lambda_c^+ \rightarrow pK^- \pi^+) = (5.0 \pm 1.3) \times 10^{-2}$ .
- 2 Assumes equal production of  $B^+$  and  $B^0$  at the  $\Upsilon(4S)$ .
- 3 GABYSHEV 06 reports  $(7.9^{+2.9}_{-2.3} \pm 4.3) \times 10^{-4}$  from a measurement of  $[\Gamma(B^0 \rightarrow \Lambda_c^+ \Lambda_c^- K^0)/\Gamma_{total}] \times [B(\Lambda_c^+ \rightarrow pK^- \pi^+)]$  assuming  $B(\Lambda_c^+ \rightarrow pK^- \pi^+) = (5.0 \pm 1.3) \times 10^{-2}$ .

### $\Gamma(\gamma)/\Gamma_{total}$ $\Gamma_{429}/\Gamma$

Test for  $\Delta B=1$  weak neutral current. Allowed by higher-order electroweak interactions.

VALUE      CL%      DOCUMENT ID      TECN      COMMENT

$<3.2 \times 10^{-7}$	90	1 DEL-AMO-SA...11A	BABR	$e^+ e^- \rightarrow \Upsilon(4S)$
$<6.2 \times 10^{-7}$	90	1 VILLA	06	BELL $e^+ e^- \rightarrow \Upsilon(4S)$
$<1.7 \times 10^{-6}$	90	1 AUBERT	01I	BABR $e^+ e^- \rightarrow \Upsilon(4S)$
$<3.9 \times 10^{-5}$	90	2 ACCIARRI	95I	L3 $e^+ e^- \rightarrow Z$

- • • We do not use the following data for averages, fits, limits, etc. • • •
- 1 Assumes equal production of  $B^+$  and  $B^0$  at the  $\Upsilon(4S)$ .
  - 2 ACCIARRI 95I assumes  $f_{B^0} = 39.5 \pm 4.0$  and  $f_{B_s} = 12.0 \pm 3.0\%$ .

### $\Gamma(e^+ e^-)/\Gamma_{total}$ $\Gamma_{430}/\Gamma$

Test for  $\Delta B=1$  weak neutral current. Allowed by higher-order electroweak interactions.

VALUE      CL%      DOCUMENT ID      TECN      COMMENT

$<8.3 \times 10^{-8}$	90	AALTONEN	09P	CDF	$p\bar{p}$ at 1.96 TeV
$<11.3 \times 10^{-8}$	90	1 AUBERT	08P	BABR	$e^+ e^- \rightarrow \Upsilon(4S)$
$<6.1 \times 10^{-8}$	90	1 AUBERT	05W	BABR	Repl. by AUBERT 08P
$<1.9 \times 10^{-7}$	90	1 CHANG	03	BELL	$e^+ e^- \rightarrow \Upsilon(4S)$
$<8.3 \times 10^{-7}$	90	1 BERGFELD	00B	CLE2	$e^+ e^- \rightarrow \Upsilon(4S)$
$<1.4 \times 10^{-5}$	90	2 ACCIARRI	97B	L3	$e^+ e^- \rightarrow Z$
$<5.9 \times 10^{-6}$	90	AMMAR	94	CLE2	Repl. by BERGFELD 00B
$<2.6 \times 10^{-5}$	90	3 AVERY	89B	CLEO	$e^+ e^- \rightarrow \Upsilon(4S)$
$<7.6 \times 10^{-5}$	90	4 ALBRECHT	87D	ARG	$e^+ e^- \rightarrow \Upsilon(4S)$
$<6.4 \times 10^{-5}$	90	5 AVERY	87	CLEO	$e^+ e^- \rightarrow \Upsilon(4S)$
$<3 \times 10^{-4}$	90	GILES	84	CLEO	Repl. by AVERY 87

- • • We do not use the following data for averages, fits, limits, etc. • • •
- 1 Assumes equal production of  $B^+$  and  $B^0$  at the  $\Upsilon(4S)$ .
  - 2 ACCIARRI 97B assume PDG 96 production fractions for  $B^+$ ,  $B^0$ ,  $B_s$ , and  $\Lambda_b$ .
  - 3 AVERY 89B reports  $<3 \times 10^{-5}$  assuming the  $\Upsilon(4S)$  decays 43% to  $B^0 \bar{B}^0$ . We rescale to 50%.
  - 4 ALBRECHT 87D reports  $<8.5 \times 10^{-5}$  assuming the  $\Upsilon(4S)$  decays 45% to  $B^0 \bar{B}^0$ . We rescale to 50%.
  - 5 AVERY 87 reports  $<8 \times 10^{-5}$  assuming the  $\Upsilon(4S)$  decays 40% to  $B^0 \bar{B}^0$ . We rescale to 50%.

### $\Gamma(e^+ e^- \gamma)/\Gamma_{total}$ $\Gamma_{431}/\Gamma$

Test for  $\Delta B=1$  weak neutral current. Allowed by higher-order electroweak interactions.

VALUE      CL%      DOCUMENT ID      TECN      COMMENT

$<1.2 \times 10^{-7}$	90	AUBERT	08C	BABR	$e^+ e^- \rightarrow \Upsilon(4S)$
-----------------------	----	--------	-----	------	------------------------------------

### $\Gamma(\mu^+ \mu^-)/\Gamma_{total}$ $\Gamma_{432}/\Gamma$

Test for  $\Delta B=1$  weak neutral current. Allowed by higher-order electroweak interactions.

VALUE      CL%      DOCUMENT ID      TECN      COMMENT

$<1.4 \times 10^{-9}$	90	1 CHATRCHYAN12A	CMS	$p\bar{p}$ at 7 TeV
$<2.6 \times 10^{-9}$	90	2 AAIJ	12A	LHCB $p\bar{p}$ at 7 TeV
$<1.2 \times 10^{-8}$	90	3 AAIJ	11B	LHCB Repl. by AAIJ 12A
$<5.0 \times 10^{-9}$	90	4 AALTONEN	11AG	CDF $p\bar{p}$ at 1.96 TeV
$<3.7 \times 10^{-9}$	90	1 CHATRCHYAN11T	CMS	Repl. by CHATRCHYAN 12A
$<1.5 \times 10^{-8}$	90	5 AALTONEN	08I	CDF Repl. by AALTONEN 11AG
$<5.2 \times 10^{-8}$	90	6 AUBERT	08P	BABR $e^+ e^- \rightarrow \Upsilon(4S)$
$<3.9 \times 10^{-8}$	90	7 ABULENCIA	05	CDF Repl. by AALTONEN 08I
$<8.3 \times 10^{-8}$	90	6 AUBERT	05W	BABR $e^+ e^- \rightarrow \Upsilon(4S)$
$<1.5 \times 10^{-7}$	90	8 ACOSTA	04D	CDF $p\bar{p}$ at 1.96 TeV
$<1.6 \times 10^{-7}$	90	6 CHANG	03	BELL $e^+ e^- \rightarrow \Upsilon(4S)$
$<6.1 \times 10^{-7}$	90	6 BERGFELD	00B	CLE2 $e^+ e^- \rightarrow \Upsilon(4S)$
$<4.0 \times 10^{-5}$	90	ABBOTT	98B	D0 $p\bar{p}$ 1.8 TeV
$<6.8 \times 10^{-7}$	90	9 ABE	98	CDF $p\bar{p}$ at 1.8 TeV
$<1.0 \times 10^{-5}$	90	10 ACCIARRI	97B	L3 $e^+ e^- \rightarrow Z$
$<1.6 \times 10^{-6}$	90	11 ABE	96L	CDF Repl. by ABE 98
$<5.9 \times 10^{-6}$	90	AMMAR	94	CLE2 $e^+ e^- \rightarrow \Upsilon(4S)$
$<8.3 \times 10^{-6}$	90	12 ALBAJAR	91C	UA1 $E_{cm}^{p\bar{p}} = 630$ GeV
$<1.2 \times 10^{-5}$	90	13 ALBAJAR	91C	UA1 $E_{cm}^{p\bar{p}} = 630$ GeV
$<4.3 \times 10^{-5}$	90	14 AVERY	89B	CLEO $e^+ e^- \rightarrow \Upsilon(4S)$
$<4.5 \times 10^{-5}$	90	15 ALBRECHT	87D	ARG $e^+ e^- \rightarrow \Upsilon(4S)$
$<7.7 \times 10^{-5}$	90	16 AVERY	87	CLEO $e^+ e^- \rightarrow \Upsilon(4S)$
$<2 \times 10^{-4}$	90	GILES	84	CLEO Repl. by AVERY 87

- 1 Uses  $B(B^+ \rightarrow J/\psi K^+ \rightarrow \mu^+ \mu^- K^+) = (6.0 \pm 0.2) \times 10^{-5}$ .
- 2 Uses  $B(B^+ \rightarrow J/\psi K^+ \rightarrow \mu^+ \mu^- K^+) = (6.01 \pm 0.21) \times 10^{-5}$  and  $B(B^0 \rightarrow K^+ \pi^-) = (1.94 \pm 0.06) \times 10^{-5}$  for normalization.

- 3 Uses  $B$  production ratio  $f(\bar{b} \rightarrow B^+) / f(\bar{b} \rightarrow B_s^0) = 3.71 \pm 0.47$  and three normalization modes.
- 4 Uses  $B(B^+ \rightarrow J/\psi K^+ \rightarrow \mu^+ \mu^- K^+) = (6.01 \pm 0.21) \times 10^{-5}$ .
- 5 Uses  $B(B^+ \rightarrow J/\psi K^+) B(J/\psi \rightarrow \mu^+ \mu^-) = (5.94 \pm 0.21) \times 10^{-5}$ .
- 6 Assumes equal production of  $B^+$  and  $B^0$  at the  $\Upsilon(4S)$ .
- 7 Uses  $B(B^+ \rightarrow J/\psi K^+) B(J/\psi \rightarrow \mu^+ \mu^-) = (5.88 \pm 0.26) \times 10^{-5}$ .
- 8 Assumes production cross-section  $\sigma(B_s^0)/\sigma(B^+) = 0.100/0.391$  and the CDF measured value of  $\sigma(B^+) = 3.6 \pm 0.6 \mu b$ .
- 9 ABE 98 assumes production of  $\sigma(B^0) = \sigma(B^+)$  and  $\sigma(B_s^0)/\sigma(B^0) = 1/3$ . They normalize to their measured  $\sigma(B^0, p_T(B) > 6, |y| < 1.0) = 2.39 \pm 0.32 \pm 0.44 \mu b$ .
- 10 ACCIARRI 97B assume PDG 96 production fractions for  $B^+$ ,  $B^0$ ,  $B_s$ , and  $\Lambda_b$ .
- 11 ABE 96L assumes equal  $B^0$  and  $B^+$  production. They normalize to their measured  $\sigma(B^+, p_T(B) > 6 \text{ GeV}/c, |y| < 1) = 2.39 \pm 0.54 \mu b$ .
- 12  $B^0$  and  $B_s^0$  are not separated.
- 13 Obtained from unseparated  $B^0$  and  $B_s^0$  measurement by assuming a  $B^0 : B_s^0$  ratio 2:1.
- 14 AVERY 89B reports  $<5 \times 10^{-3}$  assuming the  $\Upsilon(4S)$  decays 43% to  $B^0 \bar{B}^0$ . We rescale to 50%.
- 15 ALBRECHT 87D reports  $<5 \times 10^{-5}$  assuming the  $\Upsilon(4S)$  decays 45% to  $B^0 \bar{B}^0$ . We rescale to 50%.
- 16 AVERY 87 reports  $<9 \times 10^{-5}$  assuming the  $\Upsilon(4S)$  decays 40% to  $B^0 \bar{B}^0$ . We rescale to 50%.

### $\Gamma(\mu^+ \mu^- \gamma)/\Gamma_{total}$ $\Gamma_{433}/\Gamma$

Test for  $\Delta B=1$  weak neutral current. Allowed by higher-order electroweak interactions.

VALUE      CL%      DOCUMENT ID      TECN      COMMENT

$<1.6 \times 10^{-7}$	90	AUBERT	08C	BABR	$e^+ e^- \rightarrow \Upsilon(4S)$
-----------------------	----	--------	-----	------	------------------------------------

### $\Gamma(\tau^+ \tau^-)/\Gamma_{total}$ $\Gamma_{434}/\Gamma$

Test for  $\Delta B=1$  weak neutral current. Allowed by higher-order electroweak interactions.

VALUE      CL%      DOCUMENT ID      TECN      COMMENT

$<4.1 \times 10^{-3}$	90	1 AUBERT	06S	BABR	$e^+ e^- \rightarrow \Upsilon(4S)$
-----------------------	----	----------	-----	------	------------------------------------

- • • We do not use the following data for averages, fits, limits, etc. • • •
- 1 Assumes equal production of  $B^+$  and  $B^0$  at the  $\Upsilon(4S)$ .

### $\Gamma(\pi^0 \ell^+ \ell^-)/\Gamma_{total}$ $\Gamma_{435}/\Gamma$

VALUE      CL%      DOCUMENT ID      TECN      COMMENT

$<1.2 \times 10^{-7}$	90	1 AUBERT	07AG	BABR	$e^+ e^- \rightarrow \Upsilon(4S)$
-----------------------	----	----------	------	------	------------------------------------

- • • We do not use the following data for averages, fits, limits, etc. • • •

$<1.5 \times 10^{-7}$	90	1 WEI	08A	BELL	$e^+ e^- \rightarrow \Upsilon(4S)$
-----------------------	----	-------	-----	------	------------------------------------

- • • We do not use the following data for averages, fits, limits, etc. • • •
- 1 Assumes equal production of  $B^+$  and  $B^0$  at the  $\Upsilon(4S)$ .

### $\Gamma(\pi^0 \nu \bar{\nu})/\Gamma_{total}$ $\Gamma_{436}/\Gamma$

Test for  $\Delta B=1$  weak neutral current. Allowed by higher-order electroweak interaction.

VALUE      CL%      DOCUMENT ID      TECN      COMMENT

$<2.2 \times 10^{-4}$	90	1 CHEN	07D	BELL	$e^+ e^- \rightarrow \Upsilon(4S)$
-----------------------	----	--------	-----	------	------------------------------------

- • • We do not use the following data for averages, fits, limits, etc. • • •
- 1 Assumes equal production of  $B^+$  and  $B^0$  at the  $\Upsilon(4S)$ .

### $\Gamma(\pi^0 e^+ e^-)/\Gamma_{total}$ $\Gamma_{436}/\Gamma$

VALUE      CL%      DOCUMENT ID      TECN      COMMENT

$<1.4 \times 10^{-7}$	90	1 AUBERT	07AG	BABR	$e^+ e^- \rightarrow \Upsilon(4S)$
-----------------------	----	----------	------	------	------------------------------------

- • • We do not use the following data for averages, fits, limits, etc. • • •

$<2.3 \times 10^{-7}$	90	1 WEI	08A	BELL	$e^+ e^- \rightarrow \Upsilon(4S)$
-----------------------	----	-------	-----	------	------------------------------------

- • • We do not use the following data for averages, fits, limits, etc. • • •
- 1 Assumes equal production of  $B^+$  and  $B^0$  at the  $\Upsilon(4S)$ .

### $\Gamma(\pi^0 \mu^+ \mu^-)/\Gamma_{total}$ $\Gamma_{437}/\Gamma$

VALUE      CL%      DOCUMENT ID      TECN      COMMENT

$<1.8 \times 10^{-7}$	90	1 WEI	08A	BELL	$e^+ e^- \rightarrow \Upsilon(4S)$
-----------------------	----	-------	-----	------	------------------------------------

- • • We do not use the following data for averages, fits, limits, etc. • • •

$<5.1 \times 10^{-7}$	90	1 AUBERT	07AG	BABR	$e^+ e^- \rightarrow \Upsilon(4S)$
-----------------------	----	----------	------	------	------------------------------------

- • • We do not use the following data for averages, fits, limits, etc. • • •
- 1 Assumes equal production of  $B^+$  and  $B^0$  at the  $\Upsilon(4S)$ .

### $\Gamma(K^0 \ell^+ \ell^-)/\Gamma_{total}$ $\Gamma_{439}/\Gamma$

VALUE (units  $10^{-7}$ )      CL%      DOCUMENT ID      TECN      COMMENT

$3.1 \text{ }^{+0.8}_{-0.7}$ OUR AVERAGE				
$2.1 \text{ }^{+1.5}_{-1.3} \pm 0.2$	90	1 AUBERT	09T	BABR $e^+ e^- \rightarrow \Upsilon(4S)$
$3.4 \text{ }^{+0.9}_{-0.8} \pm 0.2$	90	1 WEI	09A	BELL $e^+ e^- \rightarrow \Upsilon(4S)$
$2.9 \text{ }^{+1.6}_{-1.3} \pm 0.3$	90	1 AUBERT,B	06J	BABR Repl. by AUBERT 09T
$<6.8$	90	1 ISHIKAWA	03	BELL $e^+ e^- \rightarrow \Upsilon(4S)$

- • • We do not use the following data for averages, fits, limits, etc. • • •
- 1 Assumes equal production of  $B^0$  and  $B^+$  at  $\Upsilon(4S)$ .



$\Gamma(K^0 e^+ e^-)/\Gamma_{total}$   
Test for  $\Delta B=1$  weak neutral current. Allowed by higher-order electroweak interactions.

Table with 5 columns: VALUE (units 10^-7), CL%, DOCUMENT ID, TECN, COMMENT. Includes 'OUR AVERAGE' and data points from AUBERT, WEI, etc.

1 Assumes equal production of B+ and B0 at the T(4S).  
2 Assumes equal production of B0 and B+ at T(4S).  
3 The result is for di-lepton masses above 0.5 GeV.  
4 AVERY 87 reports < 6.5 x 10^-4 assuming the T(4S) decays 40% to B0 B0-bar. We rescale to 50%.

$\Gamma(K^0 \nu \bar{\nu})/\Gamma_{total}$   
Test for  $\Delta B = 1$  weak neutral current. Allowed by higher-order electroweak interaction.

Table with 5 columns: VALUE, CL%, DOCUMENT ID, TECN, COMMENT. Includes 'OUR FIT' and data points from CHEN.

1 Assumes equal production of B+ and B0 at the T(4S).

$\Gamma(\rho^0 \nu \bar{\nu})/\Gamma_{total}$   
Test for  $\Delta B = 1$  weak neutral current. Allowed by higher-order electroweak interaction.

Table with 5 columns: VALUE, CL%, DOCUMENT ID, TECN, COMMENT. Includes data point from CHEN.

1 Assumes equal production of B+ and B0 at the T(4S).

$\Gamma(K^0 \mu^+ \mu^-)/\Gamma_{total}$   
Test for  $\Delta B=1$  weak neutral current. Allowed by higher-order electroweak interactions.

Table with 5 columns: VALUE (units 10^-7), CL%, DOCUMENT ID, TECN, COMMENT. Includes 'OUR FIT' and 'OUR AVERAGE' and data points from AUBERT, WEI, etc.

1 Assumes equal production of B+ and B0 at the T(4S).  
2 Assumes equal production of B0 and B+ at T(4S). The second error is a total of systematic uncertainties including model dependence.  
3 The result is for di-lepton masses above 0.5 GeV.  
4 AVERY 87 reports < 4.5 x 10^-4 assuming the T(4S) decays 40% to B0 B0-bar. We rescale to 50%.

$\Gamma(K^0 \mu^+ \mu^-)/\Gamma(J/\psi(1S) K^0)$

Table with 4 columns: VALUE (units 10^-3), DOCUMENT ID, TECN, COMMENT. Includes data point from AALTONEN.

$\Gamma(K^*(892)^0 e^+ e^-)/\Gamma_{total}$   
Test for  $\Delta B=1$  weak neutral current. Allowed by higher-order electroweak interactions.

Table with 5 columns: VALUE (units 10^-7), CL%, DOCUMENT ID, TECN, COMMENT. Includes 'OUR AVERAGE' and data points from AUBERT, WEI, etc.

••• We do not use the following data for averages, fits, limits, etc. •••

Table with 5 columns: VALUE, CL%, DOCUMENT ID, TECN, COMMENT. Includes data points from AUBERT, WEI, etc.

1 Assumes equal production of B0 and B+ at T(4S).

$\Gamma(K^*(892)^0 e^+ e^-)/\Gamma_{total}$   
Test for  $\Delta B=1$  weak neutral current. Allowed by higher-order electroweak interactions.

Table with 5 columns: VALUE (units 10^-7), CL%, DOCUMENT ID, TECN, COMMENT. Includes 'OUR AVERAGE' and data points from AUBERT, WEI, etc.

1 Assumes equal production of B+ and B0 at the T(4S).  
2 Assumes equal production of B0 and B+ at T(4S).

$\Gamma(K^*(892)^0 \mu^+ \mu^-)/\Gamma_{total}$   
Test for  $\Delta B=1$  weak neutral current. Allowed by higher-order electroweak interactions.

Table with 5 columns: VALUE (units 10^-7), CL%, DOCUMENT ID, TECN, COMMENT. Includes 'OUR FIT' and 'OUR AVERAGE' and data points from AUBERT, WEI, etc.

1 Assumes equal production of B+ and B0 at the T(4S).  
2 Assumes equal production of B0 and B+ at T(4S). The second error is a total of systematic uncertainties including model dependence.  
3 AFFOLDER 99B measured relative to B0 -> J/psi(1S) K\*(892)0.  
4 ABE 96L measured relative to B0 -> J/psi(1S) K\*(892)0 using PDG 94 branching ratios.  
5 ALBAJAR 91C assumes 36% of B-bar quarks give B0 mesons.

$\Gamma(K^*(892)^0 \mu^+ \mu^-)/\Gamma(J/\psi(1S) K^*(892)^0)$

Table with 5 columns: VALUE (units 10^-3), CL%, DOCUMENT ID, TECN, COMMENT. Includes 'OUR FIT' and data points from AALTONEN.

••• We do not use the following data for averages, fits, limits, etc. •••

Table with 5 columns: VALUE, CL%, DOCUMENT ID, TECN, COMMENT. Includes data points from AALTONEN.

1 Assumes equal production of B+ and B0 at the T(4S).  
2 ADAM 96D assumes fB0 = fB- = 0.39 and fBs = 0.12.

$\Gamma(K^*(892)^0 \nu \bar{\nu})/\Gamma_{total}$   
Test for  $\Delta B=1$  weak neutral current. Allowed by higher-order electroweak interactions.

Table with 5 columns: VALUE, CL%, DOCUMENT ID, TECN, COMMENT. Includes data points from AUBERT, CHEN, ADAM.

1 Assumes equal production of B+ and B0 at the T(4S).  
2 ADAM 96D assumes fB0 = fB- = 0.39 and fBs = 0.12.

$\Gamma(\phi \nu \bar{\nu})/\Gamma_{total}$   
Test for  $\Delta B = 1$  weak neutral current. Allowed by higher-order electroweak interaction.

Table with 5 columns: VALUE, CL%, DOCUMENT ID, TECN, COMMENT. Includes data point from CHEN.

1 Assumes equal production of B+ and B0 at the T(4S).

$\Gamma(e^{\pm} \mu^{\mp})/\Gamma_{total}$   
Test of lepton family number conservation. Allowed by higher-order electroweak interactions.

Table with 5 columns: VALUE, CL%, DOCUMENT ID, TECN, COMMENT. Includes data point from AALTONEN.

## Meson Particle Listings

 $B^0$ 

• • • We do not use the following data for averages, fits, limits, etc. • • •

$< 9.2 \times 10^{-8}$	90	1	AUBERT	08P	BABR	$e^+e^- \rightarrow \Upsilon(4S)$
$< 1.8 \times 10^{-7}$	90	1	AUBERT	05W	BABR	$e^+e^- \rightarrow \Upsilon(4S)$
$< 1.7 \times 10^{-7}$	90	1	CHANG	03	BELL	$e^+e^- \rightarrow \Upsilon(4S)$
$< 15 \times 10^{-7}$	90	1	BERGFELD	00B	CLE2	$e^+e^- \rightarrow \Upsilon(4S)$
$< 3.5 \times 10^{-6}$	90		ABE	98V	CDF	$p\bar{p}$ at 1.8 TeV
$< 1.6 \times 10^{-5}$	90	2	ACCIARRI	97B	L3	$e^+e^- \rightarrow Z$
$< 5.9 \times 10^{-6}$	90		AMMAR	94	CLE2	$e^+e^- \rightarrow \Upsilon(4S)$
$< 3.4 \times 10^{-5}$	90	3	AVERY	89B	CLEO	$e^+e^- \rightarrow \Upsilon(4S)$
$< 4.5 \times 10^{-5}$	90	4	ALBRECHT	87D	ARG	$e^+e^- \rightarrow \Upsilon(4S)$
$< 7.7 \times 10^{-5}$	90	5	AVERY	87	CLEO	$e^+e^- \rightarrow \Upsilon(4S)$
$< 3 \times 10^{-4}$	90		GILES	84	CLEO	Repl. by AVERY 87

- Assumes equal production of  $B^+$  and  $B^0$  at the  $\Upsilon(4S)$ .
- ACCIARRI 97B assume PDG 96 production fractions for  $B^+$ ,  $B^0$ ,  $B_s$ , and  $\Lambda_b$ .
- Paper assumes the  $\Upsilon(4S)$  decays 43% to  $B^0\bar{B}^0$ . We rescale to 50%.
- ALBRECHT 87D reports  $< 5 \times 10^{-5}$  assuming the  $\Upsilon(4S)$  decays 45% to  $B^0\bar{B}^0$ . We rescale to 50%.
- AVERY 87 reports  $< 9 \times 10^{-5}$  assuming the  $\Upsilon(4S)$  decays 40% to  $B^0\bar{B}^0$ . We rescale to 50%.

$\Gamma(\pi^0 e^\pm \mu^\mp)/\Gamma_{\text{total}}$					$\Gamma_{450}/\Gamma$	
VALUE	CL%	DOCUMENT ID	TECN	COMMENT		
$< 1.4 \times 10^{-7}$	90	1	AUBERT	07AG	BABR $e^+e^- \rightarrow \Upsilon(4S)$	

- Assumes equal production of  $B^+$  and  $B^0$  at the  $\Upsilon(4S)$ .

$\Gamma(K^0 e^\pm \mu^\mp)/\Gamma_{\text{total}}$					$\Gamma_{451}/\Gamma$	
Test of lepton family number conservation.						
VALUE (units $10^{-7}$ )	CL%	DOCUMENT ID	TECN	COMMENT		
$< 2.7$	90	1	AUBERT,B	06J	BABR $e^+e^- \rightarrow \Upsilon(4S)$	

• • • We do not use the following data for averages, fits, limits, etc. • • •

$< 40$	90	1	AUBERT	02L	BABR	Repl. by AUBERT,B 06J
--------	----	---	--------	-----	------	-----------------------

- Assumes equal production of  $B^+$  and  $B^0$  at the  $\Upsilon(4S)$ .

$\Gamma(K^*(892)^0 e^+ \mu^-)/\Gamma_{\text{total}}$					$\Gamma_{452}/\Gamma$	
VALUE (units $10^{-7}$ )	CL%	DOCUMENT ID	TECN	COMMENT		
$< 5.3$	90	1	AUBERT,B	06J	BABR $e^+e^- \rightarrow \Upsilon(4S)$	

- Assumes equal production of  $B^0$  and  $B^+$  at  $\Upsilon(4S)$ .

$\Gamma(K^*(892)^0 e^- \mu^+)/\Gamma_{\text{total}}$					$\Gamma_{453}/\Gamma$	
VALUE (units $10^{-7}$ )	CL%	DOCUMENT ID	TECN	COMMENT		
$< 3.4$	90	1	AUBERT,B	06J	BABR $e^+e^- \rightarrow \Upsilon(4S)$	

- Assumes equal production of  $B^0$  and  $B^+$  at  $\Upsilon(4S)$ .

$\Gamma(K^*(892)^0 e^\pm \mu^\mp)/\Gamma_{\text{total}}$					$\Gamma_{454}/\Gamma$	
Test of lepton family number conservation.						
VALUE (units $10^{-7}$ )	CL%	DOCUMENT ID	TECN	COMMENT		
$< 5.8$	90	1	AUBERT,B	06J	BABR $e^+e^- \rightarrow \Upsilon(4S)$	

• • • We do not use the following data for averages, fits, limits, etc. • • •

$< 34$	90	1	AUBERT	02L	BABR	Repl. by AUBERT,B 06J
--------	----	---	--------	-----	------	-----------------------

- Assumes equal production of  $B^+$  and  $B^0$  at the  $\Upsilon(4S)$ .

$\Gamma(e^\pm \tau^\mp)/\Gamma_{\text{total}}$					$\Gamma_{455}/\Gamma$	
Test of lepton family number conservation. Allowed by higher-order electroweak interactions.						
VALUE	CL%	DOCUMENT ID	TECN	COMMENT		
$< 2.8 \times 10^{-5}$	90	1	AUBERT	08AD	BABR $e^+e^- \rightarrow \Upsilon(4S)$	

• • • We do not use the following data for averages, fits, limits, etc. • • •

$< 1.1 \times 10^{-4}$	90		BORNHEIM	04	CLE2	$e^+e^- \rightarrow \Upsilon(4S)$
$< 5.3 \times 10^{-4}$	90		AMMAR	94	CLE2	Repl. by BORNHEIM 04

- Assumes equal production of  $B^+$  and  $B^0$  at the  $\Upsilon(4S)$ .

$\Gamma(\mu^\pm \tau^\mp)/\Gamma_{\text{total}}$					$\Gamma_{456}/\Gamma$	
Test of lepton family number conservation. Allowed by higher-order electroweak interactions.						
VALUE	CL%	DOCUMENT ID	TECN	COMMENT		
$< 2.2 \times 10^{-5}$	90	1	AUBERT	08AD	BABR $e^+e^- \rightarrow \Upsilon(4S)$	

• • • We do not use the following data for averages, fits, limits, etc. • • •

$< 3.8 \times 10^{-5}$	90		BORNHEIM	04	CLE2	$e^+e^- \rightarrow \Upsilon(4S)$
$< 8.3 \times 10^{-4}$	90		AMMAR	94	CLE2	Repl. by BORNHEIM 04

- Assumes equal production of  $B^+$  and  $B^0$  at the  $\Upsilon(4S)$ .

$\Gamma(\text{invisible})/\Gamma_{\text{total}}$					$\Gamma_{457}/\Gamma$	
VALUE (units $10^{-5}$ )	CL%	DOCUMENT ID	TECN	COMMENT		
$< 22$	90	1	AUBERT,B	04J	BABR $e^+e^- \rightarrow \Upsilon(4S)$	

- Uses the fully reconstructed  $B^0 \rightarrow D^*(*)-\ell^+\nu_\ell$  events as a tag.

$\Gamma(\nu\bar{\nu}\gamma)/\Gamma_{\text{total}}$					$\Gamma_{458}/\Gamma$	
VALUE (units $10^{-5}$ )	CL%	DOCUMENT ID	TECN	COMMENT		
$< 4.7$	90	1	AUBERT,B	04J	BABR $e^+e^- \rightarrow \Upsilon(4S)$	

- Uses the fully reconstructed  $B^0 \rightarrow D^*(*)-\ell^+\nu_\ell$  events as a tag.

$\Gamma(\Lambda_c^+ \mu^-)/\Gamma_{\text{total}}$					$\Gamma_{459}/\Gamma$
VALUE	CL%	DOCUMENT ID	TECN	COMMENT	
$< 1.8 \times 10^{-6}$	90	1,2	DEL-AMO-SA..11k	BABR $e^+e^- \rightarrow \Upsilon(4S)$	

- DEL-AMO-SANCHEZ 11k reports  $< 180 \times 10^{-8}$  from a measurement of  $[\Gamma(B^0 \rightarrow \Lambda_c^+ \mu^-)/\Gamma_{\text{total}}] \times [B(\Lambda_c^+ \rightarrow pK^- \pi^+)]$  assuming  $B(\Lambda_c^+ \rightarrow pK^- \pi^+) = (5.0 \pm 1.3) \times 10^{-2}$ .

- Uses  $B(\Upsilon(4S) \rightarrow B^0\bar{B}^0) = (51.6 \pm 0.6)\%$  and  $B(\Upsilon(4S) \rightarrow B^+B^-) = (48.4 \pm 0.6)\%$ .

$\Gamma(\Lambda_c^+ e^-)/\Gamma_{\text{total}}$					$\Gamma_{460}/\Gamma$
VALUE	CL%	DOCUMENT ID	TECN	COMMENT	
$< 5 \times 10^{-6}$	90	1,2	DEL-AMO-SA..11k	BABR $e^+e^- \rightarrow \Upsilon(4S)$	

- DEL-AMO-SANCHEZ 11k reports  $< 520 \times 10^{-8}$  from a measurement of  $[\Gamma(B^0 \rightarrow \Lambda_c^+ e^-)/\Gamma_{\text{total}}] \times [B(\Lambda_c^+ \rightarrow pK^- \pi^+)]$  assuming  $B(\Lambda_c^+ \rightarrow pK^- \pi^+) = (5.0 \pm 1.3) \times 10^{-2}$ .

- Uses  $B(\Upsilon(4S) \rightarrow B^0\bar{B}^0) = (51.6 \pm 0.6)\%$  and  $B(\Upsilon(4S) \rightarrow B^+B^-) = (48.4 \pm 0.6)\%$ .

POLARIZATION IN  $B$  DECAYS

Revised February 2012 by A. V. Gritsan (Johns Hopkins University) and J. G. Smith (University of Colorado at Boulder).

We review the notation used in polarization measurements in particle production and decay, with a particular emphasis on the  $B$  decays and the  $CP$ -violating observables in polarization measurements. We look at several examples of vector-vector and vector-tensor  $B$  meson decays, while more details about the theory and experimental results in  $B$  decays can be found in a separate mini-review [1] in this *Review*.

Figure 1 illustrates angular observables in an example of the sequential process  $ab \rightarrow X \rightarrow P_1 P_2 \rightarrow (p_{11} p_{12})(p_{21} p_{22})$  [2]. The angular distributions are of particular interest because they are sensitive to spin correlations and reveal properties of particles and their interactions, such as quantum numbers and couplings. In the case of a spin-zero particle  $X$ , such as  $B$  meson or a Higgs boson, there are no spin correlations in the production mechanism and the decay chain is to be analyzed. The angular distribution of decay products can be expressed as a function of three helicity angles which describe the alignment of the particles in the decay chain. The analyzer of the  $B$ -daughter polarization is normally chosen for two-body decays, as the direction of the daughters in the center-of-mass of the parent (*e.g.*,  $\rho \rightarrow 2\pi$ ) [3], and for three-body decays as the normal to the decay plane (*e.g.*,  $\omega \rightarrow 3\pi$ ) [4]. An equivalent set of transversity angles is sometimes used in polarization analyses [5]. The differential decay width depends on complex amplitudes  $A_{\lambda_1 \lambda_2}$ , corresponding to the  $X$ -daughter helicity states  $\lambda_i$ .

In the case of a spin-zero  $B$ -meson decay, its daughter helicities are constrained to  $\lambda_1 = \lambda_2 = \lambda$ . Therefore we simplify amplitude notation as  $A_\lambda$ . Moreover, most  $B$ -decay polarization analyses are limited to the case when the spin of one of the  $B$ -meson daughters is 1. In that case, there are only three independent amplitudes corresponding to  $\lambda = 0$  or  $\pm 1$  [6], where the last two can be expressed in terms of parity-even and parity-odd amplitudes  $A_{\parallel, \perp} = (A_{+1} \pm A_{-1})/\sqrt{2}$ . The overall decay amplitude involves three complex terms proportional to the above amplitudes and the Wigner  $d$  functions of helicity angles. The exact angular dependence would depend on the quantum numbers of the  $B$ -meson daughters and of their decay products, and can be found in the literature [6,7]. The

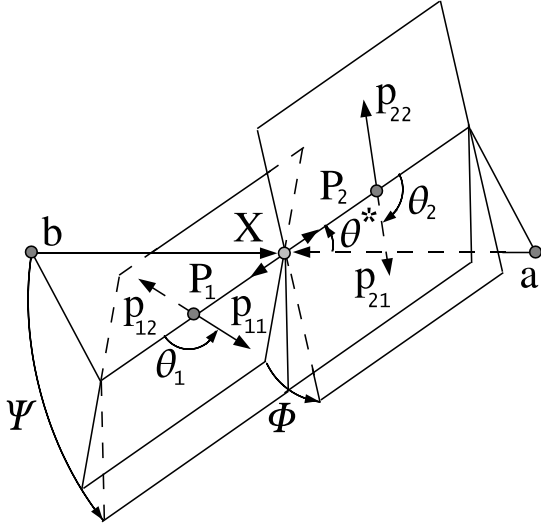


**Figure 1:** Definition of the production and helicity angles in the sequential process  $ab \rightarrow X \rightarrow P_1 P_2 \rightarrow (p_{11} p_{12})(p_{21} p_{22})$ . The three helicity angles include  $\theta_1$  and  $\theta_2$ , defined in the rest frame of the two daughters  $P_1$  and  $P_2$ , and  $\Phi$ , defined in the  $X$  frame as the angle between the two decay planes. The two production angles  $\theta^*$  and  $\Psi$  are defined in the  $X$  frame, where  $\Psi$  is the angle between the production plane and the average of the two decay planes.

differential decay rate would involve six real quantities  $\alpha_i$ , including interference terms,

$$\frac{d\Gamma}{\Gamma d\cos\theta_1 d\cos\theta_2 d\Phi} = \sum_i \alpha_i f_i(\cos\theta_1, \cos\theta_2, \Phi), \quad (1)$$

where each  $f_i(\cos\theta_1, \cos\theta_2, \Phi)$  has unique angular dependence specific to particle quantum numbers, and the  $\alpha_i$  parameters are defined as:

$$\alpha_1 = \frac{|A_0|^2}{\sum |A_\lambda|^2} = f_L, \quad (2)$$

$$\alpha_2 = \frac{|A_\parallel|^2 + |A_\perp|^2}{\sum |A_\lambda|^2} = (1 - f_L), \quad (3)$$

$$\alpha_3 = \frac{|A_\parallel|^2 - |A_\perp|^2}{\sum |A_\lambda|^2} = (1 - f_L - 2f_\perp), \quad (4)$$

$$\alpha_4 = \frac{\Im m(A_\perp A_\parallel^*)}{\sum |A_\lambda|^2} = \sqrt{f_\perp(1 - f_L - f_\perp)} \sin(\phi_\perp - \phi_\parallel), \quad (5)$$

$$\alpha_5 = \frac{\Re e(A_\parallel A_0^*)}{\sum |A_\lambda|^2} = \sqrt{f_L(1 - f_L - f_\perp)} \cos(\phi_\parallel), \quad (6)$$

$$\alpha_6 = \frac{\Im m(A_\perp A_0^*)}{\sum |A_\lambda|^2} = \sqrt{f_\perp f_L} \sin(\phi_\perp), \quad (7)$$

where the amplitudes have been expressed with the help of polarization parameters  $f_L$ ,  $f_\perp$ ,  $\phi_\parallel$ , and  $\phi_\perp$  defined in Table 1. Note that the terms proportional to  $\Re e(A_\perp A_\parallel^*)$ ,  $\Im m(A_\parallel A_0^*)$ , and  $\Re e(A_\perp A_0^*)$  are absent in Eqs. (2-7). However, these terms may appear for some three-body decays of a  $B$ -meson daughter, see Ref. 7.

**Table 1:** Rate, polarization, and  $CP$ -asymmetry parameters defined for the  $B$ -meson decays to mesons with non-zero spin. Numerical examples are shown for the  $B^0 \rightarrow \varphi K^*(892)^0$  decay. The first six parameters are defined under the assumption of no  $CP$  violation in decay, while they are averaged between the  $\bar{B}$  and  $B$  parameters in general. The last six parameters involve differences between the  $\bar{B}$  and  $B$  meson decay parameters. The phase convention  $\delta_0$  is chosen with respect to a single  $A_{00}$  amplitude from a reference  $B$  decay mode, which is  $B^0 \rightarrow \varphi K_0^*(1430)^0$  for numerical results.

parameter	definition	average
$\mathcal{B}$	$\Gamma/\Gamma_{\text{total}}$	$(9.8 \pm 0.6) \times 10^{-6}$
$f_L$	$ A_0 ^2/\sum  A_\lambda ^2$	$0.480 \pm 0.030$
$f_\perp$	$ A_\perp ^2/\sum  A_\lambda ^2$	$0.24 \pm 0.05$
$\phi_\parallel - \pi$	$\arg(A_\parallel/A_0) - \pi$	$-0.74 \pm 0.13$
$\phi_\perp - \pi$	$\arg(A_\perp/A_0) - \pi$	$-0.75 \pm 0.13$
$\delta_0 - \pi$	$\arg(A_{00}/A_0) - \pi$	$-0.32 \pm 0.17$
$A_{CP}$	$(\bar{\Gamma} - \Gamma)/(\bar{\Gamma} + \Gamma)$	$+0.01 \pm 0.05$
$A_{CP}^0$	$(\bar{f}_L - f_L)/(\bar{f}_L + f_L)$	$+0.04 \pm 0.06$
$A_{CP}^\perp$	$(\bar{f}_\perp - f_\perp)/(\bar{f}_\perp + f_\perp)$	$-0.11 \pm 0.12$
$\Delta\phi_\parallel$	$(\bar{\phi}_\parallel - \phi_\parallel)/2$	$+0.11 \pm 0.22$
$\Delta\phi_\perp$	$(\bar{\phi}_\perp - \phi_\perp - \pi)/2$	$+0.08 \pm 0.22$
$\Delta\delta_0$	$(\bar{\delta}_0 - \delta_0)/2$	$+0.27 \pm 0.16$

Overall, six real parameters describe three complex amplitudes  $A_0$ ,  $A_\parallel$ , and  $A_\perp$ . These could be chosen to be the four polarization parameters  $f_L$ ,  $f_\perp$ ,  $\phi_\parallel$ , and  $\phi_\perp$ , one overall size normalization, such as decay rate  $\Gamma$ , or branching fraction  $\mathcal{B}$ , and one overall phase  $\delta_0$ . The phase convention is arbitrary for an isolated  $B$  decay mode. However, for several  $B$  decays, the relative phase could produce meaningful and observable effects through interference with other  $B$  decays with the same final states, such as for  $B \rightarrow VK_J^*$  with  $J = 0, 1, 2, 3, 4, \dots$ . The phase could be referenced to the single  $B \rightarrow VK_0^*$  amplitude  $A_{00}$  in such a case, as shown in Table 1. Here  $V$  stands for any spin-one vector meson.

Moreover,  $CP$  violation can be tested in the angular distribution of the decay as the difference between the  $B$  and  $\bar{B}$ . Each of the six real parameters describing the three complex amplitudes would have a counterpart  $CP$ -asymmetry term, corresponding to three direct- $CP$  asymmetries in three amplitudes, and three  $CP$ -violating phase differences, equivalent to the phase measurements from the mixing-induced  $CP$  asymmetries in the time evolution of  $B$ -decays [1]. In Table 1 and Ref. 8, these are chosen to be the direct- $CP$  asymmetries in the overall decay rate  $\mathcal{A}_{CP}$ , in the  $f_L$  fraction  $\mathcal{A}_{CP}^0$ , and in the  $f_\perp$  fraction  $\mathcal{A}_{CP}^\perp$ , and three weak phase differences:

$$\Delta\phi_\parallel = \frac{1}{2} \arg(\bar{A}_\parallel A_0 / A_\parallel \bar{A}_0), \quad (8)$$

$$\Delta\phi_\perp = \frac{1}{2} \arg(\bar{A}_\perp A_0 / A_\perp \bar{A}_0) - \frac{\pi}{2}, \quad (9)$$

## Meson Particle Listings

 $B^0$ 

$$\Delta\delta_0 = \frac{1}{2}\arg(\bar{A}_{00}A_0/A_{00}\bar{A}_0). \quad (10)$$

The  $\frac{\pi}{2}$  term in Eq. (9) reflects the fact that  $A_\perp$  and  $\bar{A}_\perp$  differ in phase by  $\pi$  if  $CP$  is conserved. The two parameters  $\Delta\phi_\parallel$  and  $\Delta\phi_\perp$  are equivalent to triple-product asymmetries constructed from the vectors describing the decay angular distribution [9]. The  $CP$ -violating phase difference in the reference decay mode [8] is, in the Wolfenstein CKM quark-mixing phase convention,

$$\Delta\phi_{00} = \frac{1}{2}\arg(A_{00}/\bar{A}_{00}). \quad (11)$$

This can be measured only together with the mixing-induced phase difference for some of the neutral  $B$ -meson decays similar to other mixing-induced  $CP$  asymmetry measurements [1].

It may not always be possible to have a phase-reference decay mode which would define  $\delta_0$  and  $\Delta\delta_0$  parameters. In that case, it may be possible to define the phase difference directly similarly to Eq. (11):

$$\Delta\phi_0 = \frac{1}{2}\arg(A_0/\bar{A}_0). \quad (12)$$

One can measure the angles of the CKM unitarity triangle, assuming Standard Model contributions to the  $\Delta\phi_0$  and  $B$ -mixing phases. Examples include measurements of  $\beta = \phi_1$  with  $B \rightarrow J/\psi K^*$  and  $\alpha = \phi_2$  with  $B \rightarrow \rho\rho$ .

Most of the  $B$  decays that arise from tree-level  $b \rightarrow c$  transitions have the amplitude hierarchy  $|A_0| > |A_+| > |A_-|$  which is expected from analyses based on quark-helicity conservation [10]. The larger the mass of the vector-meson daughters, the weaker the inequality. The  $B$  meson decays to heavy vector particles with charm, such as  $B \rightarrow J/\psi K^*$ ,  $\psi(2S)K^*$ ,  $\chi_{c1}K^*$ ,  $D^*\rho$ ,  $D^*K^*$ ,  $D^*D^*$ , and  $D^*D_s^*$ , show a substantial fraction of the amplitudes corresponding to transverse polarization of the vector mesons ( $A_{\pm 1}$ ), in agreement with the factorization prediction. The detailed amplitude analysis of the  $B \rightarrow J/\psi K^*$  decays has been performed by the BABAR [11], Belle [12], CDF [13], CLEO [14], and D0 [15] collaborations. Most analyses are performed under the assumption of the absence of direct  $CP$  violation. The parameter values are given in the particle listing of this *Review*. The difference between the strong phases  $\phi_\parallel$  and  $\phi_\perp$  deviates significantly from zero. The recent measurements [11,12] of  $CP$ -violating terms similar to those in  $B \rightarrow \varphi K^*$  [8] shown in Table 1 are consistent with zero.

In addition, the mixing-induced  $CP$ -violating asymmetry is measured in the  $B^0 \rightarrow J/\psi K^{*0}$  decay [1,11,12] where angular analysis allows one to separate  $CP$ -eigenstate amplitudes. This allows one to resolve the sign ambiguity of the  $\cos 2\beta$  ( $\cos 2\phi_1$ ) term that appears in the time-dependent angular distribution due to interference of parity-even and parity-odd terms. This analysis relies on the knowledge of discrete ambiguities in the strong phases  $\phi_\parallel$  and  $\phi_\perp$ , as discussed below. The BABAR experiment used a method based on the dependence on the  $K\pi$  invariant mass of the interference between the  $S$ - and  $P$ -waves to resolve the discrete ambiguity in the determination of the

strong phases ( $\phi_\parallel, \phi_\perp$ ) in  $B \rightarrow J/\psi K^*$  decays [11]. The result is in agreement with the amplitude hierarchy expectation [10]. The CDF [16], D0 [17], and LHCb [18] experiments have studied the  $B_s^0 \rightarrow J/\psi\varphi$  decay and provided the lifetime, polarization, and phase measurements.

The amplitude hierarchy  $|A_0| \gg |A_+| \gg |A_-|$  was expected in  $B$  decays to light vector particles in both penguin transitions [19,20] and tree-level transitions [10]. There is confirmation by the BABAR and Belle experiments of predominantly longitudinal polarization in the tree-level  $b \rightarrow u$  transition, such as  $B^0 \rightarrow \rho^+\rho^-$  [21],  $B^+ \rightarrow \rho^0\rho^+$  [22], and  $B^+ \rightarrow \omega\rho^+$  [23]; this is consistent with the analysis of the quark helicity conservation [10]. Because the longitudinal amplitude dominates the decay, a detailed amplitude analysis is not possible with current  $B$  samples, and limits on the transverse amplitude fraction are obtained. The fraction of transverse polarization is large in decays to heavier mesons such as  $B^0 \rightarrow a_1(1260)^+a_1(1260)^-$  [24]. Only limits have been set for  $B^0 \rightarrow \omega\rho^0, \omega\omega$  [23]; there is some evidence for  $B^0 \rightarrow \rho^0\rho^0$  [25] decays. The small values for these branching fractions indicates that  $b \rightarrow d$  penguin pollution is small in the charmless, strangeless vector-vector  $B$  decays.

The interest in the polarization and  $CP$ -asymmetry measurements in penguin transition, such as  $b \rightarrow s$  decays  $B \rightarrow \varphi K^*$ ,  $\rho K^*$ ,  $\omega K^*$ , or  $B_s^0 \rightarrow \varphi\varphi$ , and  $b \rightarrow d$  decay  $B \rightarrow K^*\bar{K}^*$ , is motivated by their potential sensitivity to physics beyond the Standard Model. The decay amplitudes for  $B \rightarrow \varphi K^*$  have been measured by the BABAR and Belle experiments [8,26,27]. The fractions of longitudinal polarization are  $f_L = 0.50 \pm 0.05$  for the  $B^+ \rightarrow \varphi K^{*+}$  decay and  $f_L = 0.48 \pm 0.03$  for the  $B^0 \rightarrow \varphi K^{*0}$  decay. These indicate significant departure from the naive expectation of predominant longitudinal polarization, suggesting other contributions to the decay amplitude, previously neglected, either within the Standard Model, such as penguin annihilation [28] or QCD rescattering [29], or from physics beyond the Standard Model [30]. The complete set of twelve amplitude parameters measured in the  $B^0 \rightarrow \varphi K^{*0}$  decay is given in Table 1. Several other parameters could be constructed from the above twelve parameters, as suggested in Ref. 31.

The discrete ambiguity in the phase ( $\phi_\parallel, \phi_\perp, \Delta\phi_\parallel, \Delta\phi_\perp$ ) measurements has been resolved by BABAR in favor of  $|A_+| \gg |A_-|$  through interference between the  $S$ - and  $P$ -waves of  $K\pi$ . The search for vector-tensor and vector-axialvector  $B \rightarrow \varphi K_J^{(*)}$  decays with  $J = 1, 2, 3, 4$  revealed a large fraction of longitudinal polarization in the decay  $B \rightarrow \varphi K_2^*(1430)$  with  $f_L = 0.90_{-0.07}^{+0.06}$  [8,32], but large contribution of transverse amplitude in  $B \rightarrow \varphi K_1(1270)$  with  $f_L = 0.46_{-0.15}^{+0.13}$  [33].

Like  $B \rightarrow \varphi K^*$ , the decays  $B \rightarrow \rho K^*$  and  $B \rightarrow \omega K^*$  may be sensitive to New Physics. Measurements of the longitudinal polarization fraction in  $B^+ \rightarrow \rho^0 K^{*0}$ ,  $B^+ \rightarrow \rho^+ K^{*0}$  [34] and in both vector-vector and vector-tensor final states of  $B \rightarrow \omega K_J^*$  [23] reveal a large fraction of transverse polarization, indicating an anomaly similar to  $B \rightarrow \varphi K^*$  except for a different

pattern in vector-tensor final states. A large transverse polarization is also observed in the  $B_s^0 \rightarrow \varphi\varphi$  decays by CDF [37] and  $B_s^0 \rightarrow K^{*0}\bar{K}^{*0}$  decays by LHCb [36]. At the same time, first measurement of the polarization in the  $b \rightarrow d$  penguin decays  $B \rightarrow K^*\bar{K}^*$  indicates a large fraction of longitudinal polarization [35]. The polarization pattern in penguin-dominated  $B$ -meson decays is not fully understood [28,29,30].

The three-body semileptonic  $B$ -meson decays, such as  $B \rightarrow V\ell_1\ell_2$ , share many features with the two-body  $B \rightarrow VV$  decays. Their differential decay width can be parameterized with the two helicity angles defined in the  $V$  and  $(\ell_1\ell_2)$  frames and with the azimuthal angle, as defined in Fig. 1. However, since the  $(\ell_1\ell_2)$  pair does not come from an on-shell particle, the angular distribution is unique to each point in the dilepton mass  $m_{\ell\ell}$  spectrum. The polarization measurements as a function of  $m_{\ell\ell}$  provide complementary information on physics beyond the Standard Model, as discussed for  $B \rightarrow K^*\ell^+\ell^-$  decay in Ref. 38. The current data in this mode has been analyzed by the BABAR, Belle, and CDF experiments [39].

The examples of the angular distributions and observables in  $B \rightarrow K^*\ell^+\ell^-$  are discussed in Ref. 38. Typically two angular observables have been measured in this decay in certain ranges of the dilepton mass  $m_{\ell\ell}$  [39]. One parameter is the fraction of longitudinal polarization  $F_L$ , which is determined by the  $K^*$  angular distribution and is similar to  $f_L$  defined for exclusive two-body decays. The other parameter is the forward-backward asymmetry of the lepton pair  $A_{FB}$ , which is the asymmetry of the decay rate with positive and negative values of  $\cos\theta_1$ .

In summary, there has been considerable recent interest in the polarization measurements of  $B$ -meson decays because they reveal both weak- and strong-interaction dynamics [28–30,40]. New measurements will further elucidate the pattern of spin alignment measurements in rare  $B$  decays, and further test the Standard Model and strong interaction dynamics, including the non-factorizable contributions to the  $B$ -decay amplitudes.

## References

1. Y. Kwon, G. Punzi, and J. G. Smith, “Production and Decay of  $b$ -Flavored Hadrons,” mini-review in this *Review*.
2. For a recent example and further references see Y. Y. Gao *et al.*, Phys. Rev. **D81**, 075022 (2010).
3. M. Jacob and G. C. Wick, Ann. Phys. **7**, 404 (1959).
4. S. M. Berman and M. Jacob, Phys. Rev. **139**, 1023 (1965).
5. I. Dunietz *et al.*, Phys. Rev. **D43**, 2193 (1991).
6. G. Kramer and W. F. Palmer, Phys. Rev. **D45**, 193 (1992).
7. A. Datta *et al.*, Phys. Rev. **D77**, 114025 (2008).
8. BABAR Collab., B. Aubert *et al.*, Phys. Rev. Lett. **93**, 231804 (2004); Phys. Rev. Lett. **98**, 051801 (2007); Phys. Rev. **D78**, 092008 (2008).
9. G. Valencia, Phys. Rev. **D39**, 3339 (1998); A. Datta and D. London, Int. J. Mod. Phys. **A19**, 2505 (2004).
10. A. Ali *et al.*, Z. Physik **C1**, 269 (1979); M. Suzuki, Phys. Rev. **D64**, 117503 (2001).
11. BABAR Collab., B. Aubert *et al.*, Phys. Rev. **D71**, 032005 (2005); Phys. Rev. **D76**, 031102 (2007).
12. Belle Collab., R. Itoh *et al.*, Phys. Rev. Lett. **95**, 091601 (2005).
13. CDF Collab., T. Affolder *et al.*, Phys. Rev. Lett. **85**, 4668 (2000); CDF Collab., D. Acosta *et al.*, Phys. Rev. Lett. **94**, 101803 (2005).
14. CLEO Collab., C. P. Jessop, Phys. Rev. Lett. **79**, 4533 (1997).
15. D0 Collab., V. M. Abazov *et al.*, Phys. Rev. Lett. **102**, 032001 (2009).
16. CDF Collab., T. Aaltonen *et al.*, Phys. Rev. Lett. **100**, 121803 (2008).
17. D0 Collab., V. M. Abazov *et al.*, Phys. Rev. Lett. **98**, 121801 (2007); Phys. Rev. **D85**, 032006 (2012)..
18. LHCb Collab., R. Aaij *et al.*, Phys. Rev. Lett. **108**, 101803 (2012).
19. H. Y. Cheng and K. C. Yang, Phys. Lett. **B511**, 40 (2001); C. H. Chen, Y. Y. Keum, and H. n. Li, Phys. Rev. **D66**, 054013 (2002).
20. A. L. Kagan, Phys. Lett. **B601**, 151 (2004); Y. Grossman, Int. J. Mod. Phys. **A19**, 907 (2004).
21. Belle Collab., A. Somov *et al.*, Phys. Rev. Lett. **96**, 171801 (2006); BABAR Collab., B. Aubert *et al.*, Phys. Rev. **D76**, 052007 (2007).
22. Belle Collab., J. Zhang *et al.*, Phys. Rev. Lett. **91**, 221801 (2003); BABAR Collab., B. Aubert *et al.*, Phys. Rev. Lett. **102**, 141802 (2009).
23. BABAR Collab., B. Aubert *et al.*, Phys. Rev. **D74**, 051102 (2006); Phys. Rev. **D79**, 052005 (2009).
24. BABAR Collab., B. Aubert *et al.*, Phys. Rev. **D80**, 092007 (2009).
25. BABAR Collab., B. Aubert *et al.*, Phys. Rev. **D78**, 071104 (2008).
26. Belle Collab., K. F. Chen *et al.*, Phys. Rev. Lett. **94**, 221804 (2005).
27. BABAR Collab., B. Aubert *et al.*, Phys. Rev. Lett. **99**, 201802 (2007).
28. A. L. Kagan, Phys. Lett. **B601**, 151 (2004); H. n. Li and S. Mishima, Phys. Rev. **D71**, 054025 (2005); C.-H. Chen *et al.*, Phys. Rev. **D72**, 054011 (2005); M. Beneke *et al.*, Phys. Rev. Lett. **96**, 141801 (2006); C.-H. Chen and C.-Q. Geng, Phys. Rev. **D75**, 054010 (2007); A. Datta *et al.*, Phys. Rev. **D76**, 034015 (2007); M. Beneke, J. Rohrer, and D. Yang, Nucl. Phys. **B774**, 64 (2007); H.-Y. Cheng and K.-C. Yang, Phys. Rev. **D78**, 094001 (2008).
29. C. W. Bauer *et al.*, Phys. Rev. **D70**, 054015 (2004); P. Colangelo *et al.*, Phys. Lett. **B597**, 291 (2004); M. Ladisa *et al.*, Phys. Rev. **D70**, 114025 (2004); H. Y. Cheng *et al.*, Phys. Rev. **D71**, 014030 (2005); H. Y. Cheng and K. C. Yang, Phys. Rev. **D83**, 034001 (2011).
30. Y. Grossman, Int. J. Mod. Phys. **A19**, 907 (2004); E. Alvarez *et al.*, Phys. Rev. **D70**, 115014 (2004); P. K. Das and K. C. Yang, Phys. Rev. **D71**, 094002 (2005); C. H. Chen and C. Q. Geng, Phys. Rev. **D71**, 115004 (2005); Y. D. Yang *et al.*, Phys. Rev. **D72**, 015009 (2005); K. C. Yang, Phys. Rev. **72**, 034009 (2005); S. Baek, Phys. Rev. **D72**, 094008 (2005); C. S. Huang *et al.*, Phys. Rev. **D73**, 034026 (2006); C. H. Chen and H. Hatanaka, Phys.

## Meson Particle Listings

 $B^0$ 

Rev. **D73**, 075003 (2006); A. Faessler *et al.*, Phys. Rev. **D75**, 074029 (2007).

31. D. London, N. Sinha, and R. Sinha, Phys. Rev. **D69**, 114013 (2004).
32. BABAR Collab., B. Aubert *et al.*, Phys. Rev. **D76**, 051103 (2007).
33. BABAR Collab., B. Aubert *et al.*, Phys. Rev. Lett. **101**, 161801 (2008).
34. Belle Collab., J. Zhang *et al.*, Phys. Rev. Lett. **95**, 141801 (2005); BABAR Collab., B. Aubert *et al.*, Phys. Rev. Lett. **97**, 201801 (2006); Phys. Rev. **D83**, 051101 (2011).
35. BABAR Collab., B. Aubert *et al.*, Phys. Rev. Lett. **100**, 081801 (2008), Phys. Rev. **D79**, 051102 (2009).
36. LHCb Collab., R. Aaij *et al.*, Phys. Lett. B **709**, 50 (2012).
37. CDF Collab., T. Aaltonen *et al.*, Phys. Rev. Lett. **107**, 261802 (2011).
38. G. Burdman, Phys. Rev. **D52**, 6400 (1995); F. Kruger and J. Matias, Phys. Rev. **D71**, 094009 (2005); E. Lunghi and J. Matias, JHEP **0704**, 058 (2007); J. Matias *et al.*, arXiv:1202.4266 [hep-ph].
39. Belle Collab., J.-T. Wei *et al.*, Phys. Rev. Lett. **103**, 171801 (2009); BABAR Collab., B. Aubert *et al.*, Phys. Rev. **D79**, 031102 (2009); CDF Collab., T. Aaltonen *et al.*, Phys. Rev. Lett. **107**, 201802 (2011); CDF Collab., T. Aaltonen *et al.*, Phys. Rev. Lett. **108**, 081807 (2012).
40. C. H. Chen and H. n. Li, Phys. Rev. **D71**, 114008 (2005).

POLARIZATION IN  $B^0$  DECAY

In decays involving two vector mesons, one can distinguish among the states in which meson polarizations are both longitudinal (L) or both are transverse and parallel ( $\parallel$ ) or perpendicular ( $\perp$ ) to each other with the parameters  $\Gamma_L/\Gamma$ ,  $\Gamma_\perp/\Gamma$ , and the relative phases  $\phi_\parallel$  and  $\phi_\perp$ . See the definitions in the note on "Polarization in  $B$  Decays" review in the  $B^0$  Particle Listings.

 $\Gamma_L/\Gamma$  in  $B^0 \rightarrow J/\psi(1S)K^*(892)^0$ 

VALUE	EVTS	DOCUMENT ID	TECN	COMMENT
<b>0.570 ± 0.008 OUR AVERAGE</b>				
0.587 ± 0.011 ± 0.013		<sup>1</sup> ABAZOV	09E D0	$p\bar{p}$ at 1.96 TeV
0.556 ± 0.009 ± 0.010		<sup>2</sup> AUBERT	07AD BABR	$e^+e^- \rightarrow \Upsilon(4S)$
0.562 ± 0.026 ± 0.018		ACOSTA	05 CDF	$p\bar{p}$ at 1.96 TeV
0.574 ± 0.012 ± 0.009		ITOH	05 BELL	$e^+e^- \rightarrow \Upsilon(4S)$
0.59 ± 0.06 ± 0.01		<sup>3</sup> AFFOLDER	00N CDF	$p\bar{p}$ at 1.8 TeV
0.52 ± 0.07 ± 0.04		<sup>4</sup> JESSOP	97 CLE2	$e^+e^- \rightarrow \Upsilon(4S)$
0.65 ± 0.10 ± 0.04	65	ABE	95Z CDF	$p\bar{p}$ at 1.8 TeV
0.97 ± 0.16 ± 0.15	13	<sup>5</sup> ALBRECHT	94G ARG	$e^+e^- \rightarrow \Upsilon(4S)$
• • • We do not use the following data for averages, fits, limits, etc. • • •				
0.566 ± 0.012 ± 0.005		<sup>2</sup> AUBERT	05P BABR	Repl. by AUBERT 07AD
0.62 ± 0.02 ± 0.03		<sup>6</sup> ABE	02N BELL	Repl. by ITOH 05
0.597 ± 0.028 ± 0.024		<sup>7</sup> AUBERT	01H BABR	Repl. by AUBERT 07AD
0.80 ± 0.08 ± 0.05	42	<sup>5</sup> ALAM	94 CLE2	Sup. by JESSOP 97

<sup>1</sup> Measured the angular and lifetime parameters for the time-dependent angular untagged decays  $B_d^0 \rightarrow J/\psi K^{*0}$  and  $B_s^0 \rightarrow J/\psi \phi$ .

<sup>2</sup> Obtained by combining the  $B^0$  and  $B^+$  modes.

<sup>3</sup> AFFOLDER 00N measurements are based on 190  $B^0$  candidates obtained from a data sample of  $89 \text{ pb}^{-1}$ . The  $P$ -wave fraction is found to be  $0.13^{+0.12}_{-0.05} \pm 0.06$ .

<sup>4</sup> JESSOP 97 is the average over a mixture of  $B^0$  and  $B^+$  decays. The  $P$ -wave fraction is found to be  $0.16 \pm 0.08 \pm 0.04$ .

<sup>5</sup> Averaged over an admixture of  $B^0$  and  $B^+$  decays.

<sup>6</sup> Averaged over an admixture of  $B^0$  and  $B^+$  decays and the  $P$  wave fraction is  $(19 \pm 2 \pm 3)\%$ .

<sup>7</sup> Averaged over an admixture of  $B^0$  and  $B^-$  decays and the  $P$  wave fraction is  $(16.0 \pm 3.2 \pm 1.4) \times 10^{-2}$ .

 $\Gamma_\perp/\Gamma$  in  $B^0 \rightarrow J/\psi K^{*0}$ 

VALUE	DOCUMENT ID	TECN	COMMENT
<b>0.219 ± 0.010 OUR AVERAGE</b>			Error includes scale factor of 1.2.
0.230 ± 0.013 ± 0.025	<sup>1</sup> ABAZOV	09E D0	$p\bar{p}$ at 1.96 TeV
0.233 ± 0.010 ± 0.005	<sup>2</sup> AUBERT	07AD BABR	$e^+e^- \rightarrow \Upsilon(4S)$
0.215 ± 0.032 ± 0.006	ACOSTA	05 CDF	$p\bar{p}$ at 1.96 TeV
0.195 ± 0.012 ± 0.008	ITOH	05 BELL	$e^+e^- \rightarrow \Upsilon(4S)$

<sup>1</sup> Measured the angular and lifetime parameters for the time-dependent angular untagged decays  $B_d^0 \rightarrow J/\psi K^{*0}$  and  $B_s^0 \rightarrow J/\psi \phi$ .

<sup>2</sup> Obtained by combining the  $B^0$  and  $B^+$  modes.

 $\phi_\parallel$  in  $B^0 \rightarrow J/\psi K^{*0}$ 

VALUE (rad)	DOCUMENT ID	TECN	COMMENT
<b>−2.86 ± 0.11 OUR AVERAGE</b>			Error includes scale factor of 1.5.
−2.69 ± 0.08 ± 0.11	<sup>1</sup> ABAZOV	09E D0	$p\bar{p}$ at 1.96 TeV
−2.93 ± 0.08 ± 0.04	<sup>2</sup> AUBERT	07AD BABR	$e^+e^- \rightarrow \Upsilon(4S)$

<sup>1</sup> Obtained  $\phi_\parallel$  as  $\delta_2 - \delta_1$ , assuming they are uncorrelated.

<sup>2</sup> Obtained by combining the  $B^0$  and  $B^+$  modes.

 $\phi_\perp$  in  $B^0 \rightarrow J/\psi K^{*0}$ 

VALUE (rad)	DOCUMENT ID	TECN	COMMENT
<b>3.01 ± 0.14 OUR AVERAGE</b>			Error includes scale factor of 2.9.
3.21 ± 0.06 ± 0.06	ABAZOV	09E D0	$p\bar{p}$ at 1.96 TeV
2.91 ± 0.05 ± 0.03	<sup>1</sup> AUBERT	07AD BABR	$e^+e^- \rightarrow \Upsilon(4S)$

<sup>1</sup> Obtained by combining the  $B^0$  and  $B^+$  modes.

 $\Gamma_L/\Gamma$  in  $B^0 \rightarrow \psi(2S)K^*(892)^0$ 

VALUE	DOCUMENT ID	TECN	COMMENT
<b>0.46 ± 0.04 OUR AVERAGE</b>			
0.448 <sup>+0.040 +0.040</sup> <sub>−0.027 −0.053</sub>	MIZUK	09 BELL	$e^+e^- \rightarrow \Upsilon(4S)$
0.48 ± 0.05 ± 0.02	<sup>1</sup> AUBERT	07AD BABR	$e^+e^- \rightarrow \Upsilon(4S)$
0.45 ± 0.11 ± 0.04	<sup>2</sup> RICHICHI	01 CLE2	$e^+e^- \rightarrow \Upsilon(4S)$

<sup>1</sup> Obtained by combining the  $B^0$  and  $B^+$  modes.

<sup>2</sup> Averages between charged and neutral  $B$  mesons.

 $\Gamma_\perp/\Gamma$  in  $B^0 \rightarrow \psi(2S)K^{*0}$ 

VALUE	DOCUMENT ID	TECN	COMMENT
<b>0.30 ± 0.06 ± 0.02</b>			
	<sup>1</sup> AUBERT	07AD BABR	$e^+e^- \rightarrow \Upsilon(4S)$

<sup>1</sup> Obtained by combining the  $B^0$  and  $B^+$  modes.

 $\phi_\parallel$  in  $B^0 \rightarrow \psi(2S)K^{*0}$ 

VALUE (rad)	DOCUMENT ID	TECN	COMMENT
<b>−2.8 ± 0.4 ± 0.1</b>			
	<sup>1</sup> AUBERT	07AD BABR	$e^+e^- \rightarrow \Upsilon(4S)$

<sup>1</sup> Obtained by combining the  $B^0$  and  $B^+$  modes.

 $\phi_\perp$  in  $B^0 \rightarrow \psi(2S)K^{*0}$ 

VALUE (rad)	DOCUMENT ID	TECN	COMMENT
<b>2.8 ± 0.3 ± 0.1</b>			
	<sup>1</sup> AUBERT	07AD BABR	$e^+e^- \rightarrow \Upsilon(4S)$

<sup>1</sup> Obtained by combining the  $B^0$  and  $B^+$  modes.

 $\Gamma_L/\Gamma$  in  $B^0 \rightarrow \chi_{c1} K^*(892)^0$ 

VALUE	DOCUMENT ID	TECN	COMMENT
<b>0.83 <sup>+0.06</sup><sub>−0.08</sub> OUR AVERAGE</b>			Error includes scale factor of 1.3.
0.947 <sup>+0.038 +0.046</sup> <sub>−0.048 −0.099</sub>	MIZUK	08 BELL	$e^+e^- \rightarrow \Upsilon(4S)$
0.77 ± 0.07 ± 0.04	<sup>1</sup> AUBERT	07AD BABR	$e^+e^- \rightarrow \Upsilon(4S)$

<sup>1</sup> Obtained by combining the  $B^0$  and  $B^+$  modes.

 $\Gamma_\perp/\Gamma$  in  $B^0 \rightarrow \chi_{c1} K^*(892)^0$ 

VALUE	DOCUMENT ID	TECN	COMMENT
<b>0.03 ± 0.04 ± 0.02</b>			
	<sup>1</sup> AUBERT	07AD BABR	$e^+e^- \rightarrow \Upsilon(4S)$

<sup>1</sup> Obtained by combining the  $B^0$  and  $B^+$  modes.

 $\phi_\parallel$  in  $B^0 \rightarrow \chi_{c1} K^*(892)^0$ 

VALUE (rad)	DOCUMENT ID	TECN	COMMENT
<b>0.0 ± 0.3 ± 0.1</b>			
	<sup>1</sup> AUBERT	07AD BABR	$e^+e^- \rightarrow \Upsilon(4S)$

<sup>1</sup> Obtained by combining the  $B^0$  and  $B^+$  modes.

 $\Gamma_L/\Gamma$  in  $B^0 \rightarrow D_s^* D^{*-}$ 

VALUE	DOCUMENT ID	TECN	COMMENT
<b>0.52 ± 0.05 OUR AVERAGE</b>			
0.519 ± 0.050 ± 0.028	<sup>1</sup> AUBERT	03I BABR	$e^+e^- \rightarrow \Upsilon(4S)$
0.506 ± 0.139 ± 0.036	AHMED	00B CLE2	$e^+e^- \rightarrow \Upsilon(4S)$

<sup>1</sup> Measurement performed using partial reconstruction of  $D^{*-}$  decay.

 $\Gamma_\perp/\Gamma$  in  $B^0 \rightarrow D^{*-} \rho^+$ 

VALUE	EVTS	DOCUMENT ID	TECN	COMMENT
<b>0.885 ± 0.016 ± 0.012</b>				
		CSORNA	03 CLE2	$e^+e^- \rightarrow \Upsilon(4S)$

• • • We do not use the following data for averages, fits, limits, etc. • • •

0.93 ± 0.05 ± 0.05 76 ALAM 94 CLE2  $e^+e^- \rightarrow \Upsilon(4S)$

 $\Gamma_L/\Gamma$  in  $B^0 \rightarrow D_s^{*+} \rho^-$ 

VALUE	DOCUMENT ID	TECN	COMMENT
<b>0.84 <sup>+0.26</sup><sub>−0.28</sub> ± 0.13</b>			
	<sup>1</sup> AUBERT	08AJ BABR	$e^+e^- \rightarrow \Upsilon(4S)$

<sup>1</sup> Assumes equal production of  $B^+$  and  $B^0$  at the  $\Upsilon(4S)$ .

 $\Gamma_\perp/\Gamma$  in  $B^0 \rightarrow D_s^{*+} K^{*-}$ 

VALUE	DOCUMENT ID	TECN	COMMENT
<b>0.92 <sup>+0.37</sup><sub>−0.31</sub> ± 0.07</b>			
	<sup>1</sup> AUBERT	08AJ BABR	$e^+e^- \rightarrow \Upsilon(4S)$

<sup>1</sup> Assumes equal production of  $B^+$  and  $B^0$  at the  $\Upsilon(4S)$ .

$\Gamma_L/\Gamma$  in  $B^0 \rightarrow D^{*+} D^{*-}$ 

VALUE	DOCUMENT ID	TECN	COMMENT
$0.57 \pm 0.08 \pm 0.02$	MIYAKE	05	BELL $e^+ e^- \rightarrow \Upsilon(4S)$

 $\Gamma_L/\Gamma$  in  $B^0 \rightarrow D^{*+} D^{*-}$ 

VALUE	DOCUMENT ID	TECN	COMMENT
<b><math>0.150 \pm 0.025</math> OUR AVERAGE</b>			
$0.158 \pm 0.028 \pm 0.006$	AUBERT	09c	BABR $e^+ e^- \rightarrow \Upsilon(4S)$
$0.125 \pm 0.043 \pm 0.023$	VERVINK	09	BELL $e^+ e^- \rightarrow \Upsilon(4S)$
• • • We do not use the following data for averages, fits, limits, etc. • • •			
$0.143 \pm 0.034 \pm 0.008$	AUBERT	07B0	BABR Repl. by AUBERT 09c
$0.125 \pm 0.044 \pm 0.007$	AUBERT,BE	05A	BABR Repl. by AUBERT 07B0
$0.19 \pm 0.08 \pm 0.01$	MIYAKE	05	BELL Repl. by VERVINK 09
$0.063 \pm 0.055 \pm 0.009$	AUBERT	03Q	BABR Repl. by AUBERT,BE 05A

 $\Gamma_L/\Gamma$  in  $B^0 \rightarrow \bar{D}^{*0} \omega$ 

VALUE	DOCUMENT ID	TECN	COMMENT
<b><math>0.665 \pm 0.047 \pm 0.015</math></b>	LEES	11m	BABR $e^+ e^- \rightarrow \Upsilon(4S)$

 $\Gamma_L/\Gamma$  in  $B^0 \rightarrow D^{*-} \omega \pi^+$ 

VALUE	DOCUMENT ID	TECN	COMMENT
<b><math>0.654 \pm 0.042 \pm 0.016</math></b>	<sup>1</sup> AUBERT	06L	BABR $e^+ e^- \rightarrow \Upsilon(4S)$

<sup>1</sup>Invariant mass of the  $[\omega \pi]$  system is restricted in the region 1.1 and 1.9 GeV.

 $\Gamma_L/\Gamma$  in  $B^0 \rightarrow \omega K^{*0}$ 

VALUE	DOCUMENT ID	TECN	COMMENT
<b><math>0.69 \pm 0.13</math> OUR AVERAGE</b>			
$0.72 \pm 0.14 \pm 0.02$	AUBERT	09H	BABR $e^+ e^- \rightarrow \Upsilon(4S)$
$0.56 \pm 0.29 \pm 0.18$ $-0.08$	GOLDENZWE..08	BELL	$e^+ e^- \rightarrow \Upsilon(4S)$

 $\Gamma_L/\Gamma$  in  $B^0 \rightarrow \omega K_2^*(1430)^0$ 

VALUE	DOCUMENT ID	TECN	COMMENT
<b><math>0.45 \pm 0.12 \pm 0.02</math></b>	AUBERT	09H	BABR $e^+ e^- \rightarrow \Upsilon(4S)$

 $\Gamma_L/\Gamma$  in  $B^0 \rightarrow K^{*0} \bar{K}^{*0}$ 

VALUE	DOCUMENT ID	TECN	COMMENT
<b><math>0.80 \pm 0.10</math> <math>-0.12 \pm 0.06</math></b>	AUBERT	08i	BABR $e^+ e^- \rightarrow \Upsilon(4S)$

 $\Gamma_L/\Gamma$  in  $B^0 \rightarrow \phi K^*(892)^0$ 

VALUE	DOCUMENT ID	TECN	COMMENT
<b><math>0.480 \pm 0.030</math> OUR AVERAGE</b>			
$0.494 \pm 0.034 \pm 0.013$	AUBERT	08BG	BABR $e^+ e^- \rightarrow \Upsilon(4S)$
$0.45 \pm 0.05 \pm 0.02$	CHEN	05A	BELL $e^+ e^- \rightarrow \Upsilon(4S)$
• • • We do not use the following data for averages, fits, limits, etc. • • •			
$0.506 \pm 0.040 \pm 0.015$	AUBERT	07D	BABR Repl. by AUBERT 08BG
$0.52 \pm 0.05 \pm 0.02$	<sup>1</sup> AUBERT,B	04W	BABR Repl. by AUBERT 07D
$0.65 \pm 0.07 \pm 0.02$	AUBERT	03V	BABR Repl. by AUBERT,B 04W
$0.41 \pm 0.10 \pm 0.04$	CHEN	03B	BELL Repl. by CHEN 05A

<sup>1</sup>AUBERT,B 04W also measures the fraction of parity-odd transverse contribution  $f_{\perp} = 0.22 \pm 0.05 \pm 0.02$  and the phases of the parity-even and parity-odd transverse amplitudes relative to the longitudinal amplitude.

 $\Gamma_{\perp}/\Gamma$  in  $B^0 \rightarrow \phi K^{*0}$ 

VALUE	DOCUMENT ID	TECN	COMMENT
<b><math>0.24 \pm 0.05</math> OUR AVERAGE</b>			Error includes scale factor of 1.5.
$0.212 \pm 0.032 \pm 0.013$	AUBERT	08BG	BABR $e^+ e^- \rightarrow \Upsilon(4S)$
$0.31 \pm 0.06 \pm 0.02$ $-0.05$	<sup>1</sup> CHEN	05A	BELL $e^+ e^- \rightarrow \Upsilon(4S)$

• • • We do not use the following data for averages, fits, limits, etc. • • •

$0.227 \pm 0.038 \pm 0.013$	AUBERT	07D	BABR Repl. by AUBERT 08BG
$0.22 \pm 0.05 \pm 0.02$	AUBERT,B	04W	BABR Repl. by AUBERT 07D

<sup>1</sup>This quantity was recalculated by the BELLE authors from numbers in the original paper.

 $\phi_{\parallel}$  in  $B^0 \rightarrow \phi K^{*0}$ 

VALUE (rad)	DOCUMENT ID	TECN	COMMENT
<b><math>2.40 \pm 0.13</math> OUR AVERAGE</b>			
$2.40 \pm 0.13 \pm 0.08$	AUBERT	08BG	BABR $e^+ e^- \rightarrow \Upsilon(4S)$
$2.40 \pm 0.28 \pm 0.07$ $-0.24$	<sup>1</sup> CHEN	05A	BELL $e^+ e^- \rightarrow \Upsilon(4S)$
• • • We do not use the following data for averages, fits, limits, etc. • • •			
$2.31 \pm 0.14 \pm 0.08$	AUBERT	07D	BABR Repl. by AUBERT 08BG
$2.34 \pm 0.23 \pm 0.05$ $-0.20$	AUBERT,B	04W	BABR Repl. by AUBERT 07D

<sup>1</sup>This quantity was recalculated by the BELLE authors from numbers in the original paper.

 $\phi_{\perp}$  in  $B^0 \rightarrow \phi K^{*0}$ 

VALUE (rad)	DOCUMENT ID	TECN	COMMENT
<b><math>2.39 \pm 0.13</math> OUR AVERAGE</b>			
$2.35 \pm 0.13 \pm 0.09$	AUBERT	08BG	BABR $e^+ e^- \rightarrow \Upsilon(4S)$
$2.51 \pm 0.25 \pm 0.06$	<sup>1</sup> CHEN	05A	BELL $e^+ e^- \rightarrow \Upsilon(4S)$
• • • We do not use the following data for averages, fits, limits, etc. • • •			
$2.24 \pm 0.15 \pm 0.09$	AUBERT	07D	BABR Repl. by AUBERT 08BG
$2.47 \pm 0.25 \pm 0.05$	AUBERT,B	04W	BABR Repl. by AUBERT 07D

<sup>1</sup>This quantity was recalculated by the BELLE authors from numbers in the original paper.

 $\delta_0(B^0 \rightarrow \phi K^{*0})$ 

VALUE (rad)	DOCUMENT ID	TECN	COMMENT
<b><math>2.82 \pm 0.15 \pm 0.09</math></b>	AUBERT	08BG	BABR $e^+ e^- \rightarrow \Upsilon(4S)$
• • • We do not use the following data for averages, fits, limits, etc. • • •			
$2.78 \pm 0.17 \pm 0.09$	AUBERT	07D	BABR Repl. by AUBERT 08BG

 $A_{CP}^{0}$  in  $B^0 \rightarrow \phi K^{*0}$ 

VALUE	DOCUMENT ID	TECN	COMMENT
<b><math>0.04 \pm 0.06</math> OUR AVERAGE</b>			
$0.01 \pm 0.07 \pm 0.02$	AUBERT	08BG	BABR $e^+ e^- \rightarrow \Upsilon(4S)$
$0.13 \pm 0.12 \pm 0.04$	<sup>1</sup> CHEN	05A	BELL $e^+ e^- \rightarrow \Upsilon(4S)$
• • • We do not use the following data for averages, fits, limits, etc. • • •			
$-0.03 \pm 0.08 \pm 0.02$	AUBERT	07D	BABR Repl. by AUBERT 08BG
$-0.06 \pm 0.10 \pm 0.01$	AUBERT,B	04W	BABR Repl. by AUBERT 07D

<sup>1</sup>This quantity was recalculated by the BELLE authors from numbers in the original paper.

 $A_{CP}^{\perp}$  in  $B^0 \rightarrow \phi K^{*0}$ 

VALUE	DOCUMENT ID	TECN	COMMENT
<b><math>-0.11 \pm 0.12</math> OUR AVERAGE</b>			
$-0.04 \pm 0.15 \pm 0.06$	AUBERT	08BG	BABR $e^+ e^- \rightarrow \Upsilon(4S)$
$-0.20 \pm 0.18 \pm 0.04$	<sup>1</sup> CHEN	05A	BELL $e^+ e^- \rightarrow \Upsilon(4S)$
• • • We do not use the following data for averages, fits, limits, etc. • • •			
$-0.03 \pm 0.16 \pm 0.05$	AUBERT	07D	BABR Repl. by AUBERT 08BG
$-0.10 \pm 0.24 \pm 0.05$	AUBERT,B	04W	BABR Repl. by AUBERT 07D

<sup>1</sup>This quantity was recalculated by the BELLE authors from numbers in the original paper.

 $\Delta\phi_{\parallel}$  in  $B^0 \rightarrow \phi K^{*0}$ 

VALUE (rad)	DOCUMENT ID	TECN	COMMENT
<b><math>0.11 \pm 0.22</math> OUR AVERAGE</b>			Error includes scale factor of 1.7.
$0.22 \pm 0.12 \pm 0.08$	AUBERT	08BG	BABR $e^+ e^- \rightarrow \Upsilon(4S)$
$-0.32 \pm 0.27 \pm 0.07$	<sup>1</sup> CHEN	05A	BELL $e^+ e^- \rightarrow \Upsilon(4S)$
• • • We do not use the following data for averages, fits, limits, etc. • • •			
$0.24 \pm 0.14 \pm 0.08$	AUBERT	07D	BABR Repl. by AUBERT 08BG
$0.27 \pm 0.20 \pm 0.05$ $-0.23$	AUBERT,B	04W	BABR Repl. by AUBERT 07D

<sup>1</sup>This quantity was recalculated by the BELLE authors from numbers in the original paper.

 $\Delta\phi_{\perp}$  in  $B^0 \rightarrow \phi K^{*0}$ 

VALUE (rad)	DOCUMENT ID	TECN	COMMENT
<b><math>0.08 \pm 0.22</math> OUR AVERAGE</b>			Error includes scale factor of 1.7.
$0.21 \pm 0.13 \pm 0.08$	AUBERT	08BG	BABR $e^+ e^- \rightarrow \Upsilon(4S)$
$-0.30 \pm 0.25 \pm 0.06$	<sup>1</sup> CHEN	05A	BELL $e^+ e^- \rightarrow \Upsilon(4S)$
• • • We do not use the following data for averages, fits, limits, etc. • • •			
$0.19 \pm 0.15 \pm 0.08$	AUBERT	07D	BABR Repl. by AUBERT 08BG
$0.36 \pm 0.25 \pm 0.05$	AUBERT,B	04W	BABR Repl. by AUBERT 07D

<sup>1</sup>This quantity was recalculated by the BELLE authors from numbers in the original paper.

 $\Delta\delta_0(B^0 \rightarrow \phi K^{*0})$ 

VALUE (rad)	DOCUMENT ID	TECN	COMMENT
<b><math>0.27 \pm 0.14 \pm 0.08</math></b>	AUBERT	08BG	BABR $e^+ e^- \rightarrow \Upsilon(4S)$
• • • We do not use the following data for averages, fits, limits, etc. • • •			
$0.21 \pm 0.17 \pm 0.08$	AUBERT	07D	BABR Repl. by AUBERT 08BG

 $\Delta\phi_{00}(B^0 \rightarrow \phi K_2^*(1430)^0)$ 

VALUE (rad)	DOCUMENT ID	TECN	COMMENT
<b><math>0.28 \pm 0.42 \pm 0.04</math></b>	AUBERT	08BG	BABR $e^+ e^- \rightarrow \Upsilon(4S)$

 $\Gamma_L/\Gamma$  in  $B^0 \rightarrow \phi K_2^*(1430)^0$ 

VALUE	DOCUMENT ID	TECN	COMMENT
<b><math>0.901 \pm 0.046 \pm 0.037</math> <math>-0.058</math></b>	AUBERT	08BG	BABR $e^+ e^- \rightarrow \Upsilon(4S)$
• • • We do not use the following data for averages, fits, limits, etc. • • •			
$0.853 \pm 0.061 \pm 0.036$ $-0.069$	AUBERT	07D	BABR Repl. by AUBERT 08BG

 $\Gamma_{\perp}/\Gamma$  in  $B^0 \rightarrow \phi K_2^*(1430)^0$ 

VALUE	DOCUMENT ID	TECN	COMMENT
<b><math>0.002 \pm 0.018 \pm 0.031</math> <math>-0.002</math></b>	AUBERT	08BG	BABR $e^+ e^- \rightarrow \Upsilon(4S)$
• • • We do not use the following data for averages, fits, limits, etc. • • •			
$0.045 \pm 0.049 \pm 0.013$ $-0.040$	AUBERT	07D	BABR Repl. by AUBERT 08BG

 $\phi_{\parallel}$  in  $B^0 \rightarrow \phi K_2^*(1430)^0$ 

VALUE (rad)	DOCUMENT ID	TECN	COMMENT
<b><math>3.96 \pm 0.38 \pm 0.06</math></b>	AUBERT	08BG	BABR $e^+ e^- \rightarrow \Upsilon(4S)$
• • • We do not use the following data for averages, fits, limits, etc. • • •			
$2.90 \pm 0.39 \pm 0.06$	AUBERT	07D	BABR Repl. by AUBERT 08BG

 $\phi_{\perp}$  in  $B^0 \rightarrow \phi K_2^*(1430)^0$ 

VALUE (rad)	DOCUMENT ID	TECN	COMMENT
• • • We do not use the following data for averages, fits, limits, etc. • • •			
$5.72 \pm 0.55 \pm 0.11$ $-0.87$	AUBERT	07D	BABR Repl. by AUBERT 08BG

## Meson Particle Listings

 $B^0$  $\delta_0(B^0 \rightarrow \phi K_2^*(1430)^0)$ 

VALUE (rad)	DOCUMENT ID	TECN	COMMENT
$3.41 \pm 0.13 \pm 0.13$	AUBERT	08BG BABR	$e^+ e^- \rightarrow \Upsilon(4S)$
• • • We do not use the following data for averages, fits, limits, etc. • • •			
$3.54^{+0.12}_{-0.14} \pm 0.06$	AUBERT	07D BABR	Repl. by AUBERT 08BG

 $A_{CP}^0$  in  $B^0 \rightarrow \phi K_2^*(1430)^0$ 

VALUE	DOCUMENT ID	TECN	COMMENT
$-0.05 \pm 0.06 \pm 0.01$	AUBERT	08BG BABR	$e^+ e^- \rightarrow \Upsilon(4S)$

 $\Delta\phi_{||}(B^0 \rightarrow \phi K_2^*(1430)^0)$ 

VALUE (rad)	DOCUMENT ID	TECN	COMMENT
$-1.00 \pm 0.38 \pm 0.09$	AUBERT	08BG BABR	$e^+ e^- \rightarrow \Upsilon(4S)$

 $\Delta\delta_0$  in  $B^0 \rightarrow \phi K_2^*(1430)^0$ 

VALUE (rad)	DOCUMENT ID	TECN	COMMENT
$0.11 \pm 0.13 \pm 0.06$	AUBERT	08BG BABR	$e^+ e^- \rightarrow \Upsilon(4S)$

 $\Gamma_L/\Gamma$  in  $B^0 \rightarrow K^*(892)^0 \rho^0$ 

VALUE	DOCUMENT ID	TECN	COMMENT
$0.57 \pm 0.09 \pm 0.08$	AUBERT,B	06G BABR	$e^+ e^- \rightarrow \Upsilon(4S)$

 $\Gamma_L/\Gamma$  in  $B^0 \rightarrow \rho^+ \rho^-$ 

VALUE	DOCUMENT ID	TECN	COMMENT
$0.977^{+0.028}_{-0.024}$ OUR AVERAGE			
$0.992 \pm 0.024^{+0.026}_{-0.013}$	AUBERT	07BF BABR	$e^+ e^- \rightarrow \Upsilon(4S)$
$0.941^{+0.034}_{-0.040} \pm 0.030$	SOMOV	06 BELL	$e^+ e^- \rightarrow \Upsilon(4S)$
• • • We do not use the following data for averages, fits, limits, etc. • • •			
$0.978 \pm 0.014^{+0.021}_{-0.029}$	AUBERT,B	05C BABR	Repl. by AUBERT 07BF
$0.98^{+0.02}_{-0.08} \pm 0.03$	AUBERT	04G BABR	Repl. by AUBERT,B 04R
$0.99 \pm 0.03^{+0.04}_{-0.03}$	AUBERT,B	04R BABR	Repl. by AUBERT,B 05C

 $\Gamma_L/\Gamma$  in  $B^0 \rightarrow \rho^0 \rho^0$ 

VALUE	DOCUMENT ID	TECN	COMMENT
$0.75^{+0.11}_{-0.14} \pm 0.05$	AUBERT	08BB BABR	$e^+ e^- \rightarrow \Upsilon(4S)$
• • • We do not use the following data for averages, fits, limits, etc. • • •			
$0.87 \pm 0.13 \pm 0.04$	AUBERT	07G BABR	Repl. by AUBERT 08BB

 $\Gamma_L/\Gamma$  in  $B^0 \rightarrow a_1(1260)^+ a_1(1260)^-$ 

VALUE	DOCUMENT ID	TECN	COMMENT
$0.31 \pm 0.22 \pm 0.10$	AUBERT	09AL BABR	$e^+ e^- \rightarrow \Upsilon(4S)$

 $\Gamma_L/\Gamma$  in  $B^0 \rightarrow \rho \bar{\rho} K^*(892)^0$ 

VALUE	DOCUMENT ID	TECN	COMMENT
$1.01 \pm 0.13 \pm 0.03$	CHEN	08C BELL	$e^+ e^- \rightarrow \Upsilon(4S)$

 $\Gamma_L/\Gamma$  in  $B^0 \rightarrow \Lambda \bar{\Lambda} K^*(892)^0$ 

VALUE	DOCUMENT ID	TECN	COMMENT
$0.60 \pm 0.22 \pm 0.08$	CHANG	09 BELL	$e^+ e^- \rightarrow \Upsilon(4S)$

 $B^0-\bar{B}^0$  MIXING

Updated April 2012 by O. Schneider (Ecole Polytechnique Fédérale de Lausanne).

There are two neutral  $B^0-\bar{B}^0$  meson systems,  $B_d^0-\bar{B}_d^0$  and  $B_s^0-\bar{B}_s^0$  (generically denoted  $B_q^0-\bar{B}_q^0$ ,  $q = s, d$ ), which exhibit particle-antiparticle mixing [1]. This mixing phenomenon is described in Ref. 2. In the following, we adopt the notation introduced in Ref. 2, and assume  $CPT$  conservation throughout. In each system, the light (L) and heavy (H) mass eigenstates,

$$|B_{L,H}\rangle = p|B_q^0\rangle \pm q|\bar{B}_q^0\rangle, \quad (1)$$

have a mass difference  $\Delta m_q = m_H - m_L > 0$ , and a total decay width difference  $\Delta\Gamma_q = \Gamma_L - \Gamma_H$ . In the absence of  $CP$  violation in the mixing,  $|q/p| = 1$ , these differences are given by  $\Delta m_q = 2|M_{12}|$  and  $|\Delta\Gamma_q| = 2|\Gamma_{12}|$ , where  $M_{12}$  and  $\Gamma_{12}$  are the

off-diagonal elements of the mass and decay matrices [2]. The evolution of a pure  $|B_q^0\rangle$  or  $|\bar{B}_q^0\rangle$  state at  $t = 0$  is given by

$$|B_q^0(t)\rangle = g_+(t)|B_q^0\rangle + \frac{q}{p}g_-(t)|\bar{B}_q^0\rangle, \quad (2)$$

$$|\bar{B}_q^0(t)\rangle = g_+(t)|\bar{B}_q^0\rangle + \frac{p}{q}g_-(t)|B_q^0\rangle, \quad (3)$$

which means that the flavor states remain unchanged (+) or oscillate into each other (-) with time-dependent probabilities proportional to

$$|g_{\pm}(t)|^2 = \frac{e^{-\Gamma_q t}}{2} \left[ \cosh\left(\frac{\Delta\Gamma_q}{2}t\right) \pm \cos(\Delta m_q t) \right], \quad (4)$$

where  $\Gamma_q = (\Gamma_H + \Gamma_L)/2$ . In the absence of  $CP$  violation, the time-integrated mixing probability  $\int |g_-(t)|^2 dt / (\int |g_-(t)|^2 dt + \int |g_+(t)|^2 dt)$  is given by

$$\chi_q = \frac{x_q^2 + y_q^2}{2(x_q^2 + 1)}, \quad \text{where} \quad x_q = \frac{\Delta m_q}{\Gamma_q}, \quad y_q = \frac{\Delta\Gamma_q}{2\Gamma_q}. \quad (5)$$

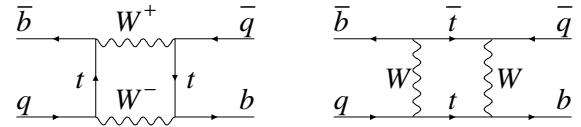


**Figure 1:** Dominant box diagrams for the  $B_q^0 \rightarrow \bar{B}_q^0$  transitions ( $q = d$  or  $s$ ). Similar diagrams exist where one or both  $t$  quarks are replaced with  $c$  or  $u$  quarks.

*Standard Model predictions and phenomenology*

In the Standard Model, the transitions  $B_q^0 \rightarrow \bar{B}_q^0$  and  $\bar{B}_q^0 \rightarrow B_q^0$  are due to the weak interaction. They are described, at the lowest order, by box diagrams involving two  $W$  bosons and two up-type quarks (see Fig. 1), as is the case for  $K^0-\bar{K}^0$  mixing. However, the long range interactions arising from intermediate virtual states are negligible for the neutral  $B$  meson systems, because the large  $B$  mass is off the region of hadronic resonances. The calculation of the dispersive and absorptive parts of the box diagrams yields the following predictions for the off-diagonal element of the mass and decay matrices [3],

$$M_{12} = -\frac{G_F^2 m_W^2 \eta_B m_{B_q} B_{B_q} f_{B_q}^2}{12\pi^2} S_0(m_i^2/m_W^2) (V_{tq}^* V_{tb})^2, \quad (6)$$

$$\Gamma_{12} = \frac{G_F^2 m_b^2 \eta_B' m_{B_q} B_{B_q} f_{B_q}^2}{8\pi} \times \left[ (V_{tq}^* V_{tb})^2 + V_{tq}^* V_{tb} V_{cq}^* V_{cb} \mathcal{O}\left(\frac{m_c^2}{m_b^2}\right) + (V_{cq}^* V_{cb})^2 \mathcal{O}\left(\frac{m_c^4}{m_b^4}\right) \right], \quad (7)$$

where  $G_F$  is the Fermi constant,  $m_W$  the  $W$  boson mass, and  $m_i$  the mass of quark  $i$ ;  $m_{B_q}$ ,  $f_{B_q}$  and  $B_{B_q}$  are the  $B_q^0$  mass, weak decay constant and bag parameter, respectively. The known function  $S_0(x_t)$  can be approximated very well by  $0.784 x_t^{0.76}$  [4], and  $V_{ij}$  are the elements of the CKM matrix [5].



The QCD corrections  $\eta_B$  and  $\eta'_B$  are of order unity. The only non-negligible contributions to  $M_{12}$  are from box diagrams involving two top quarks. The phases of  $M_{12}$  and  $\Gamma_{12}$  satisfy

$$\phi_M - \phi_\Gamma = \pi + \mathcal{O}\left(\frac{m_c^2}{m_b^2}\right), \quad (8)$$

implying that the mass eigenstates have mass and width differences of opposite signs. This means that, like in the  $K^0-\bar{K}^0$  system, the heavy state is expected to have a smaller decay width than that of the light state:  $\Gamma_H < \Gamma_L$ . Hence,  $\Delta\Gamma = \Gamma_L - \Gamma_H$  is expected to be positive in the Standard Model.

Furthermore, the quantity

$$\left|\frac{\Gamma_{12}}{M_{12}}\right| \simeq \frac{3\pi}{2} \frac{m_b^2}{m_W^2} \frac{1}{S_0(m_t^2/m_W^2)} \sim \mathcal{O}\left(\frac{m_b^2}{m_t^2}\right) \quad (9)$$

is small, and a power expansion of  $|q/p|^2$  yields

$$\left|\frac{q}{p}\right|^2 = 1 + \left|\frac{\Gamma_{12}}{M_{12}}\right| \sin(\phi_M - \phi_\Gamma) + \mathcal{O}\left(\left|\frac{\Gamma_{12}}{M_{12}}\right|^2\right). \quad (10)$$

Therefore, considering both Eqs. (8) and (9), the  $CP$ -violating parameter

$$1 - \left|\frac{q}{p}\right|^2 \simeq \text{Im}\left(\frac{\Gamma_{12}}{M_{12}}\right) \quad (11)$$

is expected to be very small:  $\sim \mathcal{O}(10^{-3})$  for the  $B_d^0-\bar{B}_d^0$  system and  $\lesssim \mathcal{O}(10^{-4})$  for the  $B_s^0-\bar{B}_s^0$  system [6].

In the approximation of negligible  $CP$  violation in mixing, the ratio  $\Delta\Gamma_q/\Delta m_q$  is equal to the small quantity  $|\Gamma_{12}/M_{12}|$  of Eq. (9); it is hence independent of CKM matrix elements, *i.e.*, the same for the  $B_d^0-\bar{B}_d^0$  and  $B_s^0-\bar{B}_s^0$  systems. Calculations [7] yield  $\sim 5 \times 10^{-3}$  with a  $\sim 20\%$  uncertainty. Given the published experimental knowledge [8] on the mixing parameter  $x_q$

$$\begin{cases} x_d = 0.770 \pm 0.008 & (B_d^0-\bar{B}_d^0 \text{ system}) \\ x_s = 26.49 \pm 0.29 & (B_s^0-\bar{B}_s^0 \text{ system}) \end{cases}, \quad (12)$$

the Standard Model thus predicts that  $\Delta\Gamma_d/\Gamma_d$  is very small (below 1%), but  $\Delta\Gamma_s/\Gamma_s$  considerably larger ( $\sim 10\%$ ). These width differences are caused by the existence of final states to which both the  $B_q^0$  and  $\bar{B}_q^0$  mesons can decay. Such decays involve  $b \rightarrow c\bar{q}$  quark-level transitions, which are Cabibbo-suppressed if  $q = d$  and Cabibbo-allowed if  $q = s$ .

A complete set of Standard Model predictions for all mixing parameters in both the  $B_d^0-\bar{B}_d^0$  and  $B_s^0-\bar{B}_s^0$  systems can be found in Ref. 7.

### Experimental issues and methods for oscillation analyses

Time-integrated measurements of  $B^0-\bar{B}^0$  mixing were published for the first time in 1987 by UA1 [9] and ARGUS [10], and since then by many other experiments. These measurements are typically based on counting same-sign and opposite-sign lepton pairs from the semileptonic decay of the produced  $b\bar{b}$  pairs. Such analyses cannot easily separate the contributions from the different  $b$ -hadron species, therefore, the clean environment of  $\Upsilon(4S)$  machines (where only  $B_d^0$  and charged  $B_u$  mesons are produced) is in principle best suited to measure  $\chi_d$ .

However, better sensitivity is obtained from time-dependent analyses aiming at the direct measurement of the oscillation frequencies  $\Delta m_d$  and  $\Delta m_s$ , from the proper time distributions of  $B_d^0$  or  $B_s^0$  candidates identified through their decay in (mostly) flavor-specific modes, and suitably tagged as mixed or unmixed. This is particularly true for the  $B_s^0-\bar{B}_s^0$  system, where the large value of  $x_s$  implies maximal mixing, *i.e.*,  $\chi_s \simeq 1/2$ . In such analyses, the  $B_d^0$  or  $B_s^0$  mesons are either fully reconstructed, partially reconstructed from a charm meson, selected from a lepton with the characteristics of a  $b \rightarrow \ell^-$  decay, or selected from a reconstructed displaced vertex. At high-energy colliders (LEP, SLC, Tevatron, LHC), the proper time  $t = \frac{m_B}{p}L$  is measured from the distance  $L$  between the production vertex and the  $B$  decay vertex, and from an estimate of the  $B$  momentum  $p$ . At asymmetric  $B$  factories (KEKB, PEP-II), producing  $e^+e^- \rightarrow \Upsilon(4S) \rightarrow B_d^0\bar{B}_d^0$  events with a boost  $\beta\gamma$  ( $= 0.425, 0.55$ ), the proper time difference between the two  $B$  candidates is estimated as  $\Delta t \simeq \frac{\Delta z}{\beta\gamma c}$ , where  $\Delta z$  is the spatial separation between the two  $B$  decay vertices along the boost direction. In all cases, the good resolution needed on the vertex positions is obtained with silicon detectors.

The average statistical significance  $\mathcal{S}$  of a  $B_d^0$  or  $B_s^0$  oscillation signal can be approximated as [11]

$$\mathcal{S} \approx \sqrt{N/2} f_{\text{sig}} (1 - 2\eta) e^{-(\Delta m \sigma_t)^2/2}, \quad (13)$$

where  $N$  is the number of selected and tagged candidates,  $f_{\text{sig}}$  is the fraction of signal in that sample,  $\eta$  is the total mistag probability, and  $\sigma_t$  is the resolution on proper time (or proper time difference). The quantity  $\mathcal{S}$  decreases very quickly as  $\Delta m$  increases; this dependence is controlled by  $\sigma_t$ , which is therefore a critical parameter for  $\Delta m_s$  analyses. At high-energy colliders, the proper time resolution  $\sigma_t \sim \frac{m_B}{\langle p \rangle} \sigma_L \oplus t \frac{\sigma_p}{p}$  includes a constant contribution due to the decay length resolution  $\sigma_L$  (typically 0.04–0.3 ps), and a term due to the relative momentum resolution  $\sigma_p/p$  (typically 10–20% for partially reconstructed decays), which increases with proper time. At  $B$  factories, the boost of the  $B$  mesons is estimated from the known beam energies, and the term due to the spatial resolution dominates (typically 1–1.5 ps because of the much smaller  $B$  boost).

In order to tag a  $B$  candidate as mixed or unmixed, it is necessary to determine its flavor both in the initial state and in the final state. The initial and final state mistag probabilities,  $\eta_i$  and  $\eta_f$ , degrade  $\mathcal{S}$  by a total factor  $(1 - 2\eta) = (1 - 2\eta_i)(1 - 2\eta_f)$ . In lepton-based analyses, the final state is tagged by the charge of the lepton from  $b \rightarrow \ell^-$  decays; the largest contribution to  $\eta_f$  is then due to  $\bar{b} \rightarrow \bar{c} \rightarrow \ell^-$  decays. Alternatively, the charge of a reconstructed charm meson ( $D^{*-}$  from  $B_d^0$  or  $D_s^-$  from  $B_s^0$ ), or that of a kaon hypothesized to come from a  $b \rightarrow c \rightarrow s$  decay [12], can be used. For fully-inclusive analyses based on topological vertexing, final-state tagging techniques include jet-charge [13] and charge-dipole [14,15] methods. At high-energy colliders, the methods to tag the initial state (*i.e.*, the state at production), can be divided into two groups: the ones that tag

# Meson Particle Listings

## $B^0$

the initial charge of the  $\bar{b}$  quark contained in the  $B$  candidate itself (same-side tag), and the ones that tag the initial charge of the other  $b$  quark produced in the event (opposite-side tag). On the same side, the sign of a charged pion or kaon from the primary vertex is correlated with the production state of the  $B_d^0$  or  $B_s^0$  if that particle is a decay product of a  $B^{**}$  state or the first in the fragmentation chain [16,17]. Jet- and vertex-charge techniques work on both sides and on the opposite side, respectively. Finally, the charge of a lepton from  $b \rightarrow \ell^-$  or of a kaon from  $b \rightarrow c \rightarrow s$  can be used as opposite side tags, keeping in mind that their performance is degraded due to integrated mixing. At SLC, the beam polarization produced a sizeable forward-backward asymmetry in the  $Z \rightarrow b\bar{b}$  decays, and provided another very interesting and effective initial state tag based on the polar angle of the  $B$  candidate [14]. Initial state tags have also been combined to reach  $\eta_i \sim 26\%$  at LEP [17,18], or even 22% at SLD [14] with full efficiency. In the case  $\eta_f = 0$ , this corresponds to an effective tagging efficiency  $Q = \epsilon D^2 = \epsilon(1 - 2\eta)^2$ , where  $\epsilon$  is the tagging efficiency, in the range 23 – 31%. The equivalent figure achieved by CDF during Tevatron Run I was  $\sim 3.5\%$  [19], reflecting the fact that tagging is more difficult at hadron colliders. The current CDF and DØ analyses of Tevatron Run II data reach  $\epsilon D^2 = (1.8 \pm 0.1)\%$  [20] and  $(2.5 \pm 0.2)\%$  [21] for opposite-side tagging, while same-side kaon tagging (for  $B_s^0$  analyses) is contributing an additional 3.7 – 4.8% at CDF [20], and pushes the combined performance to  $(4.7 \pm 0.5)\%$  at DØ [22]. LHCb, operating in the forward region at the LHC where the environment is different in terms of track multiplicity and  $b$ -hadron production kinematics, has reported  $\epsilon D^2 = (2.10 \pm 0.25)\%$  [23] for opposite-side tagging and  $(1.3 \pm 0.4)\%$  [24] for same-side kaon tagging.

At  $B$  factories, the flavor of a  $B_d^0$  meson at production cannot be determined, since the two neutral  $B$  mesons produced in a  $\Upsilon(4S)$  decay evolve in a coherent  $P$ -wave state where they keep opposite flavors at any time. However, as soon as one of them decays, the other follows a time-evolution given by Eqs. (2) or (3), where  $t$  is replaced with  $\Delta t$  (which will take negative values half of the time). Hence, the “initial state” tag of a  $B$  can be taken as the final-state tag of the other  $B$ . Effective tagging efficiencies  $Q$  of 30% are achieved by BaBar and Belle [25], using different techniques including  $b \rightarrow \ell^-$  and  $b \rightarrow c \rightarrow s$  tags. It is worth noting that, in this case, mixing of the other  $B$  (*i.e.*, the coherent mixing occurring before the first  $B$  decay) does not contribute to the mistag probability.

In the absence of experimental observation of a decay-width difference, oscillation analyses typically neglected  $\Delta\Gamma$  in Eq. (4), and described the data with the physics functions  $\Gamma e^{-\Gamma t}(1 \pm \cos(\Delta m t))/2$  (high-energy colliders) or  $\Gamma e^{-\Gamma|\Delta t|}(1 \pm \cos(\Delta m \Delta t))/4$  (asymmetric  $\Upsilon(4S)$  machines). As can be seen from Eq. (4), a non-zero value of  $\Delta\Gamma$  would effectively reduce the oscillation amplitude with a small time-dependent factor that would be very difficult to distinguish from time resolution effects. Measurements of  $\Delta m$  are usually extracted from the data using a maximum likelihood fit.

### $\Delta m_d$ and $\Delta\Gamma_d$ measurements

Many  $B_d^0$ - $\bar{B}_d^0$  oscillations analyses have been published [26] by the ALEPH [27], DELPHI [15,28], L3 [29], OPAL [30,31] BaBar [32], Belle [33], CDF [16], DØ [21], and LHCb [34] collaborations. Although a variety of different techniques have been used, the individual  $\Delta m_d$  results obtained at high-energy colliders have remarkably similar precision. Their average is compatible with the recent and more precise measurements from asymmetric  $B$  factories. The systematic uncertainties are not negligible; they are often dominated by sample composition, mistag probability, or  $b$ -hadron lifetime contributions. Before being combined, the measurements are adjusted on the basis of a common set of input values, including the  $b$ -hadron lifetimes and fractions published in this *Review*. Some measurements are statistically correlated. Systematic correlations arise both from common physics sources (fragmentation fractions, lifetimes, branching ratios of  $b$  hadrons), and from purely experimental or algorithmic effects (efficiency, resolution, tagging, background description). Combining all published measurements [15,16,21,27–34] and accounting for all identified correlations yields  $\Delta m_d = 0.507 \pm 0.003(\text{stat}) \pm 0.003(\text{syst}) \text{ ps}^{-1}$  [8], a result dominated by the  $B$  factories.

On the other hand, ARGUS and CLEO have published time-integrated measurements [35–37], which average to  $\chi_d = 0.182 \pm 0.015$ . Following Ref. 37, the width difference  $\Delta\Gamma_d$  could in principle be extracted from the measured value of  $\Gamma_d$  and the above averages for  $\Delta m_d$  and  $\chi_d$  (see Eq. (5)), provided that  $\Delta\Gamma_d$  has a negligible impact on the  $\Delta m_d$  measurements. However, direct time-dependent studies published by DELPHI [15], BaBar [38] and Belle [39] provide stronger constraints, which can be combined to yield [8]

$$\text{sign}(\text{Re}\lambda_{CP})\Delta\Gamma_d/\Gamma_d = 0.015 \pm 0.018,$$

where  $\text{sign}(\text{Re}\lambda_{CP}) = +1$  is expected in the Standard Model.

Assuming  $\Delta\Gamma_d = 0$  and no  $CP$  violation in mixing, and using the measured  $B_d^0$  lifetime of  $1.519 \pm 0.007 \text{ ps}$ , the  $\Delta m_d$  and  $\chi_d$  results are combined to yield the world average

$$\Delta m_d = 0.507 \pm 0.004 \text{ ps}^{-1} \quad (14)$$

or, equivalently,

$$\chi_d = 0.1862 \pm 0.0023. \quad (15)$$

This  $\Delta m_d$  value provides an estimate of  $2|M_{12}|$ , and can be used with Eq. (6) to extract  $|V_{td}|$  within the Standard Model [40]. The main experimental uncertainties on the result come from  $m_t$  and  $\Delta m_d$ , but are completely negligible with respect to the uncertainty due to the hadronic matrix element  $f_{B_d}\sqrt{B_{B_d}} = 211 \pm 12 \text{ MeV}$  obtained from lattice QCD calculations [41].

### $\Delta m_s$ and $\Delta\Gamma_s$ measurements

After many years of intense search at LEP and SLC,  $B_s^0$ - $\bar{B}_s^0$  oscillations were first observed in 2006 by CDF using  $1 \text{ fb}^{-1}$  of Tevatron Run II data [20]. A year later DØ reported an independent preliminary evidence using  $2.4 \text{ fb}^{-1}$  of data [46]. Recently LHCb obtained the most precise results

using  $0.036 \text{ fb}^{-1}$  [34] and  $0.34 \text{ fb}^{-1}$  [24] of data collected at the LHC in 2010 and 2011, respectively. While the average of the published measurements of  $\Delta m_s$  [20,34] is

$$\Delta m_s = 17.69 \pm 0.08 \text{ ps}^{-1}, \quad (16)$$

including also the preliminary LHCb measurement [24] and taking systematic correlations into account yields

$$\Delta m_s = 17.719 \pm 0.036(\text{stat}) \pm 0.023(\text{syst}) \text{ ps}^{-1}. \quad (17)$$

The information on  $|V_{ts}|$  obtained in the framework of the Standard Model is hampered by the hadronic uncertainty, as in the  $B_d^0$  case. However, several uncertainties cancel in the frequency ratio

$$\frac{\Delta m_s}{\Delta m_d} = \frac{m_{B_s}}{m_{B_d}} \xi^2 \left| \frac{V_{ts}}{V_{td}} \right|^2, \quad (18)$$

where  $\xi = (f_{B_s} \sqrt{B_{B_s}}) / (f_{B_d} \sqrt{B_{B_d}}) = 1.237 \pm 0.032$  is an SU(3) flavor-symmetry breaking factor obtained from lattice QCD calculations [41]. Using the measurements of Eqs. (14) and (16), one can extract

$$\left| \frac{V_{td}}{V_{ts}} \right| = 0.2111 \pm 0.0010(\text{exp}) \pm 0.0055(\text{lattice}), \quad (19)$$

in good agreement with (but much more precise than) the value obtained from the ratio of the  $b \rightarrow d\gamma$  and  $b \rightarrow s\gamma$  transition rates observed at the  $B$  factories [40].

The CKM matrix can be constrained using experimental results on observables such as  $\Delta m_d$ ,  $\Delta m_s$ ,  $|V_{ub}/V_{cb}|$ ,  $\epsilon_K$ , and  $\sin(2\beta)$  together with theoretical inputs and unitarity conditions [40,47,48]. The constraint from our knowledge on the ratio  $\Delta m_s/\Delta m_d$  is more effective in limiting the position of the apex of the CKM unitarity triangle than the one obtained from the  $\Delta m_d$  measurements alone, due to the reduced hadronic uncertainty in Eq. (18). We also note that the measured value of  $\Delta m_s$  is consistent with the Standard Model prediction obtained from CKM fits where no experimental information on  $\Delta m_s$  is used, *e.g.*,  $19.0 \pm 1.5 \text{ ps}^{-1}$  [47] or  $18.1^{+2.2}_{-2.1} \text{ ps}^{-1}$  [48].

Information on  $\Delta\Gamma_s$  can be obtained from the study of the proper time distribution of untagged  $B_s^0$  samples [49]. In the case of an inclusive  $B_s^0$  selection [50], or a semileptonic (or flavor-specific)  $B_s^0$  decay selection [18,51], both the short- and long-lived components are present, and the proper time distribution is a superposition of two exponentials with decay constants  $\Gamma_{L,H} = \Gamma_s \pm \Delta\Gamma_s/2$ . In principle, this provides sensitivity to both  $\Gamma_s$  and  $(\Delta\Gamma_s/\Gamma_s)^2$ . Ignoring  $\Delta\Gamma_s$  and fitting for a single exponential leads to an estimate of  $\Gamma_s$  with a relative bias proportional to  $(\Delta\Gamma_s/\Gamma_s)^2$ . An alternative approach, which is directly sensitive to first order in  $\Delta\Gamma_s/\Gamma_s$ , is to determine the effective lifetime of untagged  $B_s^0$  candidates decaying to (fairly pure)  $CP$  eigenstates; measurements exist for  $B_s^0 \rightarrow D_s^{(*)+} D_s^{(*)-}$  [52],  $B_s^0 \rightarrow K^+ K^-$  [53], and  $B_s^0 \rightarrow J/\psi f_0(980)$  [54]. The extraction of  $1/\Gamma_s$  and  $\Delta\Gamma_s$  from such measurements, discussed in detail in Ref. [55], requires additional information in the form of theoretical assumptions

or external inputs on weak phases and hadronic parameters. In what follows, only the effective lifetimes from the decays to the pure  $CP$  eigenstates  $K^+ K^-$  and  $J/\psi f_0(980)$  will be used, under the assumption that these decays are dominated by a single weak phase.

The best sensitivity to  $1/\Gamma_s$  and  $\Delta\Gamma_s$  is achieved by the recent time-dependent measurements of the  $B_s^0 \rightarrow J/\psi\phi$  decay rates performed at CDF [56,57], DØ [58] and LHCb [59,60], where the  $CP$ -even and  $CP$ -odd amplitudes are separated statistically through a full angular analysis. In particular LHCb obtained the first observation of a non-zero value of  $\Delta\Gamma_s$  [60]. These studies use both untagged and tagged  $B_s^0$  candidates and are optimized for the measurement of the  $CP$ -violating phase  $\phi_s$ , defined as the weak phase difference between the  $B_s^0\text{-}\bar{B}_s^0$  mixing amplitude and the  $b \rightarrow c\bar{c}s$  decay amplitude. The Standard Model prediction for  $\phi_s$ , if Penguin pollution is neglected, is equal to  $-2\beta_s = -2\arg(-(V_{ts}V_{tb}^*)/(V_{cs}V_{cb}^*)) = -0.0363^{+0.0016}_{-0.0015}$  [48]. With a Gaussian constraint on  $\phi_s$  to this Standard Model expectation, a combination [8] of the published  $B_s^0 \rightarrow J/\psi\phi$  analyses [56,58,59] and of the lifetime measurements with flavor-specific [18,51] and pure  $CP$  [53,54] final states yields

$$\Delta\Gamma_s = +0.100 \pm 0.013 \text{ ps}^{-1} \quad \text{and} \quad 1/\Gamma_s = 1.497 \pm 0.015 \text{ ps}, \quad (20)$$

or, equivalently,

$$1/\Gamma_L = 1.393 \pm 0.019 \text{ ps} \quad \text{and} \quad 1/\Gamma_H = 1.618 \pm 0.024 \text{ ps}, \quad (21)$$

in good agreement with the Standard Model prediction  $\Delta\Gamma_s = 0.087 \pm 0.021 \text{ ps}^{-1}$  [7].

The positive sign of  $\Delta\Gamma_s$  is due to the constraint applied on  $\phi_s$ . In absence of such constraint, there would be two mirror solutions related by the transformation  $(\Delta\Gamma_s, \phi_s) \rightarrow (-\Delta\Gamma_s, \pi - \phi_s)$ . Recently the LHCb collaboration analyzed the  $B_s^0 \rightarrow J/\psi K^+ K^-$  decay, considering that the  $K^+ K^-$  system can be in a P-wave or S-wave state, and measured the dependence of the strong phase difference between the P-wave and S-wave amplitudes as a function of the  $K^+ K^-$  invariant mass [61]. This allowed, for the first time, the unambiguous determination of the sign of  $\Delta\Gamma_s$ , which was found to be positive at the  $4.7\sigma$  level.

Independent estimates of  $\Delta\Gamma_s/\Gamma_s$  obtained from measurements of the  $B_s^0 \rightarrow D_s^{(*)+} D_s^{(*)-}$  branching fractions [52,62] are no longer included in the average, since they are based on the questionable [7] assumption that these decays account for all  $CP$ -even final states.

#### Average $b$ -hadron mixing probability and $b$ -hadron production fractions at high energy

Mixing measurements can significantly improve our knowledge on the fractions  $f_u$ ,  $f_d$ ,  $f_s$ , and  $f_{\text{baryon}}$ , defined as the fractions of  $B_u$ ,  $B_d^0$ ,  $B_s^0$ , and  $b$ -baryons in an unbiased sample of weakly decaying  $b$  hadrons produced in high-energy collisions.

# Meson Particle Listings

## $B^0$

Indeed, time-integrated mixing analyses using lepton pairs from  $b\bar{b}$  events at high energy measure the quantity

$$\bar{\chi} = f'_d \chi_d + f'_s \chi_s, \quad (22)$$

where  $f'_d$  and  $f'_s$  are the fractions of  $B_d^0$  and  $B_s^0$  hadrons in a sample of semileptonic  $b$ -hadron decays. Assuming that all  $b$  hadrons have the same semileptonic decay width implies  $f'_q = f_q/(\Gamma_q \tau_b)$  ( $q = s, d$ ), where  $\tau_b$  is the average  $b$ -hadron lifetime. Hence  $\bar{\chi}$  measurements performed at LEP [63] and Tevatron [64,65,66], together with the  $\chi_d$  average of Eq. (15) and the very good approximation  $\chi_s = 1/2$  (in fact  $\chi_s = 0.499292 \pm 0.000016$  from Eqs. (5), (16) and (20)), provide constraints on the fractions  $f_d$  and  $f_s$ . In what follows, we use the preliminary  $\bar{\chi}$  result from CDF [65] instead of the published one [64]. Averages based on published data only can be found in the full listings of this *Review*.

The LEP experiments have measured  $\mathcal{B}(\bar{b} \rightarrow B_s^0) \times \mathcal{B}(B_s^0 \rightarrow D_s^- \ell^+ \nu_\ell X)$  [67],  $\mathcal{B}(b \rightarrow \Lambda_b^0) \times \mathcal{B}(\Lambda_b^0 \rightarrow \Lambda_c^+ \ell^- \bar{\nu}_\ell X)$  [68], and  $\mathcal{B}(b \rightarrow \Xi_b^-) \times \mathcal{B}(\Xi_b^- \rightarrow \Xi^- \ell^- \bar{\nu}_\ell X)$  [69] from partially reconstructed final states including a lepton,  $f_{\text{baryon}}$  from protons identified in  $b$  events [70], and the production rate of charged  $b$  hadrons [71]. The  $b$ -hadron fraction ratios measured at CDF are based on double semileptonic  $K^* \mu \mu$  and  $\phi \mu \mu$  final states [72] and lepton-charm final states [73]; in addition CDF and DØ have both measured strange  $b$ -baryon production [74]. On the other hand, fraction ratios have been studied by LHCb using fully reconstructed hadronic  $B_s^0$  and  $B_d^0$  decays [75], as well as semileptonic decays [76]. Both CDF and LHCb observe that the ratio  $f_{\Lambda_b^0}/(f_u + f_d)$  decreases with the transverse momentum of the lepton+charm system, indicating that the  $b$ -hadron fractions are not the same in different environments. We therefore provide sets of fractions separately for LEP and Tevatron (and no complete set for LHCb, where strange  $b$ -baryon production has not been measured yet). A combination of all the available information under the constraints  $f_u = f_d$ ,  $f_u + f_d + f_s + f_{\text{baryon}} = 1$ , and Eq. (22), yields the averages shown in Table 1.

**Table 1:**  $\bar{\chi}$  and  $b$ -hadron fractions (see text).

	in $Z$ decays [8]	at Tevatron [8]	at LHCb [76]
$\bar{\chi}$	$0.1259 \pm 0.0042$	$0.127 \pm 0.008$	
$f_u = f_d$	$0.403 \pm 0.009$	$0.330 \pm 0.030$	
$f_s$	$0.103 \pm 0.009$	$0.103 \pm 0.012$	
$f_{\text{baryon}}$	$0.090 \pm 0.015$	$0.236 \pm 0.067$	
$f_s/f_d$	$0.256 \pm 0.025$	$0.311 \pm 0.037$	$0.267^{+0.021}_{-0.020}$

### $CP$ -violation studies

Evidence for  $CP$  violation in  $B_q^0 - \bar{B}_q^0$  mixing has been searched for, both with flavor-specific and inclusive  $B_q^0$  decays, in samples where the initial flavor state is tagged, usually with a lepton from the other  $b$ -hadron in the event. In the

case of semileptonic (or other flavor-specific) decays, where the final-state tag is also available, the following asymmetry [2]

$$\mathcal{A}_{\text{SL}}^q = \frac{N(\bar{B}_q^0(t) \rightarrow \ell^+ \nu_\ell X) - N(B_q^0(t) \rightarrow \ell^- \bar{\nu}_\ell X)}{N(\bar{B}_q^0(t) \rightarrow \ell^+ \nu_\ell X) + N(B_q^0(t) \rightarrow \ell^- \bar{\nu}_\ell X)} \simeq 1 - |q/p|_q^2 \quad (23)$$

has been measured either in time-integrated analyses at CLEO [37,77], CDF [78] and DØ [79], or in time-dependent analyses at LEP [31,80], BaBar [38,81], Belle [82] and DØ [83]. In the inclusive case, also investigated at LEP [80,84], no final-state tag is used, and the asymmetry [85]

$$\frac{N(B_q^0(t) \rightarrow \text{all}) - N(\bar{B}_q^0(t) \rightarrow \text{all})}{N(B_q^0(t) \rightarrow \text{all}) + N(\bar{B}_q^0(t) \rightarrow \text{all})} \simeq \mathcal{A}_{\text{SL}}^q \left[ \frac{x_q}{2} \sin(\Delta m_q t) - \sin^2 \left( \frac{\Delta m_q t}{2} \right) \right] \quad (24)$$

must be measured as a function of the proper time to extract information on  $CP$  violation.

The DØ collaboration measures a like-sign dimuon charge asymmetry in semileptonic  $b$  decays that deviates by  $3.9\sigma$  from the Standard Model prediction [79]. In all other cases, asymmetries compatible with zero (and the Standard Model) have been found, with a precision limited by the available statistics. Most of the analyses at high energy don't disentangle the  $B_d^0$  and  $B_s^0$  contributions, and either quote a mean asymmetry or a measurement of  $\mathcal{A}_{\text{SL}}^d$  assuming  $\mathcal{A}_{\text{SL}}^s = 0$ : we no longer include these in the average. An exception is the latest dimuon DØ analysis [79], which separates the two contributions by exploiting their dependence on the muon impact parameter cut. The resulting measurements of  $\mathcal{A}_{\text{SL}}^d$  and  $\mathcal{A}_{\text{SL}}^s$  are then both compatible with the Standard Model. They are also correlated. We therefore perform a two-dimensional average of all published measurements [37,38,77,79,81–83] and obtain [8]

$$\mathcal{A}_{\text{SL}}^d = -0.0033 \pm 0.0033, \quad \text{or } |q/p|_d = 1.0017 \pm 0.0017, \quad (25)$$

$$\mathcal{A}_{\text{SL}}^s = -0.0105 \pm 0.0064, \quad \text{or } |q/p|_s = 1.0052 \pm 0.0032, \quad (26)$$

with a correlation coefficient of  $-0.57$  between  $\mathcal{A}_{\text{SL}}^d$  and  $\mathcal{A}_{\text{SL}}^s$ . These results show no evidence of  $CP$  violation and don't constrain yet the Standard Model.

$CP$  violation induced by  $B_s^0 - \bar{B}_s^0$  mixing in  $b \rightarrow c\bar{c}s$  decays has been a field of very active study in the past couple of years. In addition to the previously mentioned  $B_s^0 \rightarrow J/\psi \phi$  studies, the recently observed  $CP$ -odd decay mode  $B_s^0 \rightarrow J/\psi \phi(980)$ ,  $f_0(980) \rightarrow \pi^+ \pi^-$  has also been analyzed by LHCb to measure  $\phi_s$ , without the need for an angular analysis [86]. A two-dimensional fit [8] of all published analyses [56,58,59,86] in the  $(\phi_s, \Delta\Gamma_s)$  plane, shown on Fig. 2, yields  $\phi_s = -0.14^{+0.16}_{-0.11}$ . This is consistent with the Standard Model expectation, although with a large uncertainty. The fit is then repeated, but using the external constraint provided by the measured semileptonic asymmetry of Eq. (26), which depends on  $\Delta\Gamma_s$  and on the mixing phase difference  $\phi_M - \phi_\Gamma - \pi = \arg(-M_{12}/\Gamma_{12})$  of Eq. (8). Since New Physics is expected to affect  $\arg(-M_{12}/\Gamma_{12})$

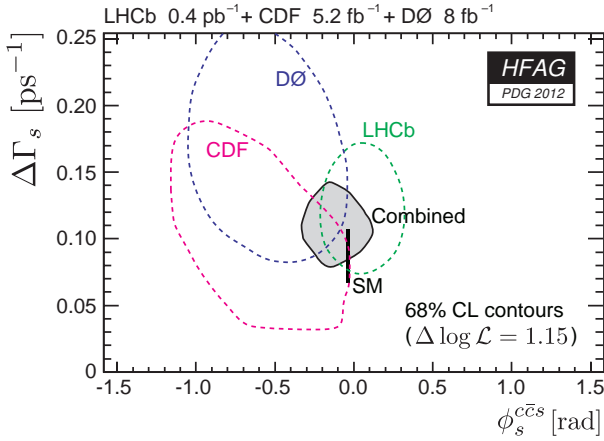


**Figure 2:** 68% CL contours in the  $(\phi_s, \Delta\Gamma_s)$  plane, showing the measurements from CDF [56], DØ [58] and LHCb [59,86], with their combination [8]. The unphysical mirror solution with  $\Delta\Gamma_s < 0$  [61] is not shown. The thin rectangle represents the Standard Model predictions of  $\phi_s$  [48] and  $\Delta\Gamma_s$  [7].

and  $\phi_s$  in the same way, the constraint is implemented under the assumption that a new phase in  $B_s^0$  mixing would not change the difference  $\arg(-M_{12}/\Gamma_{12}) - \phi_s$  from its Standard Model value [7]. The result is [8]

$$\phi_s = -0.17^{+0.14}_{-0.11}, \quad (27)$$

still not showing any sign of  $CP$  violation or New Physics. The precision on this average will soon improve significantly. Indeed it does not include yet the preliminary updates of CDF [57] and LHCb [60], nor a new preliminary LHCb measurement using  $B_s^0 \rightarrow J/\psi\pi^+\pi^-$  decays [87]. The LHCb preliminary combined value is  $\phi_s = -0.002 \pm 0.083(\text{stat}) \pm 0.027(\text{syst})$  [60].

### Summary

$B^0-\bar{B}^0$  mixing has been and still is a field of intense study. While relatively little experimental progress was achieved in the  $B_d^0$  sector during the past years, impressive new  $B_s^0$  results became available from CDF, DØ and LHCb. The mass difference in the  $B_s^0-\bar{B}_s^0$  system is now known to a relative precision which is significantly better than that in the  $B_d^0-\bar{B}_d^0$  system. The non-zero decay width difference in the  $B_s^0-\bar{B}_s^0$  system is now firmly established, with a relative difference of  $(15 \pm 2)\%$ . Its sign has been determined: the heavy state of the  $B_s^0-\bar{B}_s^0$  system lives longer than the light state. In contrast, the relative decay width difference in the  $B_d^0-\bar{B}_d^0$  system,  $(1.5 \pm 1.8)\%$ , is still consistent with zero.  $CP$  violation in mixing has not been observed yet, with precisions on the semileptonic asymmetries below 1%. A quantum step has been achieved in the measurement of the mixing-induced phase  $\phi_s$  in  $B_s^0$  decays proceeding through the  $b \rightarrow c\bar{c}s$  transition, with a Gaussian uncertainty reaching the 0.1 radian level. Despite these significant improvements, all observations remain consistent with the Standard Model expectations.

However, the measurements where New Physics might show up are still statistically limited. More results are expected in the future, especially from LHCb in the  $B_s^0$  sector, with promising prospects for the investigation of the  $CP$ -violating phase  $\arg(-M_{12}/\Gamma_{12})$  and an expected uncertainty on  $\phi_s$  of  $\sim 0.05$  radian by the time of the next edition of this *Review*.

Mixing studies have clearly reached the stage of precision measurements, where much effort is needed, both on the experimental and theoretical sides, in particular to further reduce the hadronic uncertainties of lattice QCD calculations. In the long term, a stringent check of the consistency of the  $B_d^0$  and  $B_s^0$  mixing amplitudes (magnitudes and phases) with all other measured flavor-physics observables will be possible within the Standard Model, leading to very tight limits on (or otherwise a long-awaited surprise about) New Physics.

### References

1. T.D. Lee and C.S. Wu, *Ann. Rev. Nucl. Sci.* **16**, 511 (1966); I.I. Bigi and A.I. Sanda, “ $CP$  violation,” Cambridge Univ. Press, 2000; G.C. Branco, L. Lavoura, and J.P. Silva, “ $CP$  violation,” Clarendon Press Oxford, 1999.
2. See the review on  $CP$  violation in meson decays by D. Kirkby and Y. Nir in this publication.
3. A.J. Buras, W. Slominski, and H. Steger, *Nucl. Phys.* **B245**, 369 (1984).
4. T. Inami and C.S. Lim, *Prog. Theor. Phys.* **65**, 297 (1981); for the power-like approximation, see A.J. Buras and R. Fleischer, page 91 in “Heavy Flavours II,” eds. A.J. Buras and M. Lindner, Singapore World Scientific, 1998.
5. M. Kobayashi and K. Maskawa, *Prog. Theor. Phys.* **49**, 652 (1973).
6. I.I. Bigi *et al.*, in “ $CP$  violation,” ed. C. Jarlskog, Singapore World Scientific, 1989.
7. A. Lenz and U. Nierste, [arXiv:1102.4274 \[hep-ph\]](https://arxiv.org/abs/1102.4274); A. Lenz and U. Nierste, *JHEP* **0607**, 072 (2007).
8. D. Asner *et al.* (HFAG), “Averages of  $b$ -hadron,  $c$ -hadron, and  $\tau$ -lepton properties,” [arXiv:1010.1589v3 \[hep-ex\]](https://arxiv.org/abs/1010.1589v3), September 2011; the combined results on  $b$ -hadron fractions, lifetimes and mixing parameters published in this *Review* have been obtained by the  $B$  oscillations working group of the Heavy Flavor Averaging Group (HFAG), using the methods and procedures described in Chapter 3 of the above paper, after updating the list of inputs; for more information, see <http://www.slac.stanford.edu/xorg/hfag/osc/>.
9. C. Albajar *et al.* (UA1 Collab.), *Phys. Lett.* **B186**, 247 (1987).
10. H. Albrecht *et al.* (ARGUS Collab.), *Phys. Lett.* **B192**, 245 (1987).
11. H.-G. Moser and A. Roussarie, *Nucl. Instrum. Methods* **384**, 491 (1997).
12. SLD Collab., SLAC-PUB-7228, SLAC-PUB-7229, and SLAC-PUB-7230, *28th Int. Conf. on High Energy Physics*, Warsaw, 1996; J. Wittlin, PhD thesis, SLAC-R-582, 2001.
13. ALEPH Collab., contrib. 596 to *Int. Europhysics Conf. on High Energy Physics*, Jerusalem, 1997.
14. K. Abe *et al.* (SLD Collab.), *Phys. Rev.* **D67**, 012006 (2003).

## Meson Particle Listings

 $B^0$ 

15. J. Abdallah *et al.* (DELPHI Collab.), *Eur. Phys. J.* **C28**, 155 (2003).
16. F. Abe *et al.* (CDF Collab.), *Phys. Rev. Lett.* **80**, 2057 (1998) and *Phys. Rev.* **D59**, 032001 (1999); *Phys. Rev.* **D60**, 051101 (1999); *Phys. Rev.* **D60**, 072003 (1999); T. Affolder *et al.* (CDF Collab.), *Phys. Rev.* **D60**, 112004 (1999).
17. R. Barate *et al.* (ALEPH Collab.), *Eur. Phys. J.* **C4**, 367 (1998); *Eur. Phys. J.* **C7**, 553 (1999).
18. P. Abreu *et al.* (DELPHI Collab.), *Eur. Phys. J.* **C16**, 555 (2000); *Eur. Phys. J.* **C18**, 229 (2000).
19. See tagging summary on page 160 of K. Anikeev *et al.*, “ $B$  physics at the Tevatron: Run II and beyond,” FERMILAB-PUB-01/97, hep-ph/0201071, and references therein.
20. A. Abulencia *et al.* (CDF Collab.), *Phys. Rev. Lett.* **97**, 242003 (2006).
21. V.M. Abazov *et al.* (DØ Collab.), *Phys. Rev.* **D74**, 112002 (2006).
22. V.M. Abazov *et al.* (DØ Collab.), *Phys. Rev. Lett.* **101**, 241801 (2008).
23. R. Aaij *et al.* (LHCb Collab.), arXiv:1202.4979 [hep-ex], submitted to *Eur. Phys. J.* **C**.
24. LHCb Collab., LHCb note CERN-LHCb-CONF-2011-050, November 2011.
25. B. Aubert *et al.* (BaBar Collab.), *Phys. Rev. Lett.* **94**, 161803 (2005); K.-F. Chen *et al.* (Belle Collab.), *Phys. Rev.* **D72**, 012004 (2005).
26. Throughout this paper, we omit references of results that have been superseded by new published measurements.
27. D. Buskulic *et al.* (ALEPH Collab.), *Z. Phys.* **C75**, 397 (1997).
28. P. Abreu *et al.* (DELPHI Collab.), *Z. Phys.* **C76**, 579 (1997).
29. M. Acciarri *et al.* (L3 Collab.), *Eur. Phys. J.* **C5**, 195 (1998).
30. G. Alexander *et al.* (OPAL Collab.), *Z. Phys.* **C72**, 377 (1996); K. Ackerstaff *et al.* (OPAL Collab.), *Z. Phys.* **C76**, 417 (1997); G. Abbiendi *et al.* (OPAL Collab.), *Phys. Lett.* **B493**, 266 (2000).
31. K. Ackerstaff *et al.* (OPAL Collab.), *Z. Phys.* **C76**, 401 (1997).
32. B. Aubert *et al.* (BaBar Collab.), *Phys. Rev. Lett.* **88**, 221802 (2002) and *Phys. Rev.* **D66**, 032003 (2002); *Phys. Rev. Lett.* **88**, 221803 (2002); *Phys. Rev.* **D67**, 072002 (2003); *Phys. Rev.* **D73**, 012004 (2006).
33. N.C. Hastings *et al.* (Belle Collab.), *Phys. Rev.* **D67**, 052004 (2003); Y. Zheng *et al.* (Belle Collab.), *Phys. Rev.* **D67**, 092004 (2003); K. Abe *et al.* (Belle Collab.), *Phys. Rev.* **D71**, 072003 (2005).
34. R. Aaij *et al.* (LHCb Collab.), *Phys. Lett.* **B709**, 177 (2012).
35. H. Albrecht *et al.* (ARGUS Collab.), *Z. Phys.* **C55**, 357 (1992); *Phys. Lett.* **B324**, 249 (1994).
36. J. Bartelt *et al.* (CLEO Collab.), *Phys. Rev. Lett.* **71**, 1680 (1993).
37. B.H. Behrens *et al.* (CLEO Collab.), *Phys. Lett.* **B490**, 36 (2000).
38. B. Aubert *et al.* (BaBar Collab.), *Phys. Rev. Lett.* **92**, 181801 (2004) and *Phys. Rev.* **D70**, 012007 (2004).
39. T. Higuchi *et al.* (Belle Collab.), arXiv:1203.0930 [hep-ex], to appear in *Phys. Rev. D*.
40. See the review on the CKM quark-mixing matrix by A. Ceccucci, Z. Ligeti, and Y. Sakai in this publication.
41. J. Laiho, E. Lunghi, and R.S. Van de Water, *Phys. Rev.* **D81**, 034503 (2010), with updated results available at <http://www.latticeaverages.org>; we use the end-2011 averages of  $f_{B_d}\sqrt{B_{B_d}}$  and  $\xi$  combining the unquenched calculations of Refs. [42,43] and [43–45], respectively.
42. C.M. Bouchard *et al.*, arXiv:1112.5642 [hep-lat].
43. E. Gamiz *et al.* (HPQCD Collab.), *Phys. Rev.* **D80**, 014503 (2009).
44. R.T. Evans, A.X. El-Khadra, and E. Gamiz, PoS LATTICE 2008, 052 (2008).
45. C. Albertus *et al.* (RBC and UKQCD Collab.), *Phys. Rev.* **D82**, 014505 (2010).
46. DØ Collab., DØ note 5474-CONF, August 2007.
47. M. Bona *et al.* (UTfit Collab.), arXiv:hep-ph/0606167v2; updated results at <http://www.utfit.org/>.
48. J. Charles *et al.* (CKMfitter Group), *Phys. Rev.* **D84**, 033005 (2011); updated results at <http://ckmfitter.in2p3.fr/>.
49. K. Hartkorn and H.-G. Moser, *Eur. Phys. J.* **C8**, 381 (1999).
50. M. Acciarri *et al.* (L3 Collab.), *Phys. Lett.* **B438**, 417 (1998).
51. D. Buskulic *et al.* (ALEPH Collab.), *Phys. Lett.* **B377**, 205 (1996); K. Ackerstaff *et al.* (OPAL Collab.), *Phys. Lett.* **B426**, 161 (1998); F. Abe *et al.* (CDF Collab.), *Phys. Rev.* **D59**, 032004 (1999); V.M. Abazov *et al.* (DØ Collab.), *Phys. Rev. Lett.* **97**, 241801 (2006); T. Aaltonen *et al.* (CDF Collab.), *Phys. Rev. Lett.* **107**, 272001 (2011).
52. R. Barate *et al.* (ALEPH Collab.), *Phys. Lett.* **B486**, 286 (2000).
53. R. Aaij *et al.* (LHCb Collab.), *Phys. Lett.* **B707**, 349 (2012).
54. T. Aaltonen *et al.* (CDF Collab.), *Phys. Rev.* **D84**, 052012 (2011).
55. R. Fleischer and R. Knegjens, *Eur. Phys. J.* **C71**, 1789 (2011).
56. T. Aaltonen *et al.* (CDF Collab.), arXiv:1112.1726 [hep-ex], to appear in *Phys. Rev. D*.
57. CDF Collab., CDF note 10778, March 2012.
58. V.M. Abazov *et al.* (DØ Collab.), *Phys. Rev.* **D85**, 032006 (2012).
59. R. Aaij *et al.* (LHCb Collab.), *Phys. Rev. Lett.* **108**, 101803 (2012).
60. LHCb Collab., LHCb note CERN-LHCb-CONF-2012-002, March 2012.
61. R. Aaij *et al.* (LHCb Collab.), arXiv:1202.4717 [hep-ex], to appear in *Phys. Rev. Lett.*
62. S. Esen *et al.* (Belle Collab.), *Phys. Rev. Lett.* **105**, 201802 (2010); V.M. Abazov *et al.* (DØ Collab.), *Phys. Rev. Lett.* **102**, 091801 (2009); A. Abulencia *et al.* (CDF Collab.), *Phys. Rev. Lett.* **100**, 021803 (2008).
63. ALEPH, DELPHI, L3, OPAL, and SLD Collabs.; *Physics Reports* **427**, 257 (2006); we use the  $\bar{\chi}$  average given in Eq. (5.39).
64. D. Acosta *et al.* (CDF Collab.), *Phys. Rev.* **D69**, 012002 (2004).

65. CDF Collab., CDF note 10335, January 2011.

66. V.M. Abazov *et al.* (DØ Collab.), Phys. Rev. **D74**, 092001 (2006).

67. P. Abreu *et al.* (DELPHI Collab.), Phys. Lett. **B289**, 199 (1992); P.D. Acton *et al.* (OPAL Collab.), Phys. Lett. **B295**, 357 (1992); D. Buskulic *et al.* (ALEPH Collab.), Phys. Lett. **B361**, 221 (1995).

68. P. Abreu *et al.* (DELPHI Collab.), Z. Phys. **C68**, 375 (1995); R. Barate *et al.* (ALEPH Collab.), Eur. Phys. J. **C2**, 197 (1998).

69. D. Buskulic *et al.* (ALEPH Collab.), Phys. Lett. **B384**, 449 (1996); J. Abdallah *et al.* (DELPHI Collab.), Eur. Phys. J. **C44**, 299 (2005).

70. R. Barate *et al.* (ALEPH Collab.), Eur. Phys. J. **C5**, 205 (1998).

71. J. Abdallah *et al.* (DELPHI Collab.), Phys. Lett. **B576**, 29 (2003).

72. F. Abe *et al.* (CDF Collab.), Phys. Rev. **D60**, 092005 (1999).

73. T. Aaltonen *et al.* (CDF Collab.), Phys. Rev. **D77**, 072003 (2008); T. Affolder *et al.* (CDF Collab.), Phys. Rev. Lett. **84**, 1663 (2000); the measurement of  $f_{\text{baryon}}/f_d$  in the latter paper has been updated based on T. Aaltonen *et al.* (CDF Collab.), Phys. Rev. **D79**, 032001 (2009).

74. V.M. Abazov *et al.* (DØ Collab.), Phys. Rev. Lett. **99**, 052001 (2007); V.M. Abazov *et al.* (DØ Collab.), Phys. Rev. Lett. **101**, 232002 (2008); T. Aaltonen *et al.* (CDF Collab.), Phys. Rev. **D80**, 072003 (2009).

75. R. Aaij *et al.* (LHCb Collab.), Phys. Rev. Lett. **107**, 211801 (2011).

76. R. Aaij *et al.* (LHCb Collab.), Phys. Rev. **D85**, 032008 (2012).

77. D.E. Jaffe *et al.* (CLEO Collab.), Phys. Rev. Lett. **86**, 5000 (2001).

78. F. Abe *et al.* (CDF Collab.), Phys. Rev. **D55**, 2546 (1997).

79. V.M. Abazov *et al.* (DØ Collab.), Phys. Rev. **D84**, 052007 (2011).

80. R. Barate *et al.* (ALEPH Collab.), Eur. Phys. J. **C20**, 431 (2001).

81. B. Aubert *et al.* (BaBar Collab.), Phys. Rev. Lett. **96**, 251802 (2006).

82. E. Nakano *et al.* (Belle Collab.), Phys. Rev. **D73**, 112002 (2006).

83. V.M. Abazov *et al.* (DØ Collab.), Phys. Rev. **D82**, 012003 (2010).

84. G. Abbiendi *et al.* (OPAL Collab.), Eur. Phys. J. **C12**, 609 (2000).

85. M. Beneke, G. Buchalla, and I. Dunietz, Phys. Lett. **B393**, 132 (1997); I. Dunietz, Eur. Phys. J. **C7**, 197 (1999).

86. R. Aaij *et al.* (LHCb Collab.), Phys. Lett. **B707**, 497 (2012).

87. P. Clarke (for the LHCb Collab.), LHCb-TALK-2012-029, talk at *47th Rencontres de Moriond on Electroweak and Unified Theories*, La Thuile, Italy, March 2012.

**$B^0-\bar{B}^0$  MIXING PARAMETERS**

For a discussion of  $B^0-\bar{B}^0$  mixing see the note on “ $B^0-\bar{B}^0$  Mixing” in the  $B^0$  Particle Listings above.

$\chi_d$  is a measure of the time-integrated  $B^0-\bar{B}^0$  mixing probability that a produced  $B^0(\bar{B}^0)$  decays as a  $\bar{B}^0(B^0)$ . Mixing violates  $\Delta B \neq 2$  rule.

$$\chi_d = \frac{x_d^2}{2(1+x_d^2)}$$

$$x_d = \frac{\Delta m_{B^0}}{\Gamma_{B^0}} = (m_{B_H^0} - m_{B_L^0}) \tau_{B^0}$$

where  $H, L$  stand for heavy and light states of two  $B^0$  CP eigenstates and  $\tau_{B^0} = \frac{1}{0.5(\Gamma_{B_H^0} + \Gamma_{B_L^0})}$ .

**$\chi_d$**

This  $B^0-\bar{B}^0$  mixing parameter is the probability (integrated over time) that a produced  $B^0$  (or  $\bar{B}^0$ ) decays as a  $\bar{B}^0$  (or  $B^0$ ), e.g. for inclusive lepton decays

$$\chi_d = \frac{\Gamma(B^0 \rightarrow \ell^- X \text{ (via } \bar{B}^0)) / \Gamma(B^0 \rightarrow \ell^\pm X)}{\Gamma(\bar{B}^0 \rightarrow \ell^+ X \text{ (via } B^0)) / \Gamma(\bar{B}^0 \rightarrow \ell^\pm X)}$$

Where experiments have measured the parameter  $r = \chi/(1-\chi)$ , we have converted to  $\chi$ . Mixing violates the  $\Delta B \neq 2$  rule.

Note that the measurement of  $\chi$  at energies higher than the  $\Upsilon(4S)$  have not separated  $\chi_d$  from  $\chi_s$  where the subscripts indicate  $B^0(Dd)$  or  $B_s^0(\bar{B}s)$ . They are listed in the  $B^\pm/B^0/B_s^\pm/b$ -baryon ADMIXTURE section.

The experiments at  $\Upsilon(4S)$  make an assumption about the  $B^0\bar{B}^0$  fraction and about the ratio of the  $B^\pm$  and  $B^0$  semileptonic branching ratios (usually that it equals one).

“OUR EVALUATION” is an average using rescaled values of the data listed below. The average and rescaling were performed by the Heavy Flavor Averaging Group (HFAG) and are described at <http://www.slac.stanford.edu/xorg/hfag/>. The averaging/rescaling procedure takes into account correlations between the measurements, includes  $\chi_d$  calculated from  $\Delta m_{B^0}$  and  $\tau_{B^0}$ .

VALUE	CL%	DOCUMENT ID	TECN	COMMENT
<b>0.1862±0.0023</b>				<b>OUR EVALUATION</b>
<b>0.182 ±0.015</b>				<b>OUR AVERAGE</b>
0.198 ±0.013 ±0.014		1 BEHRENS	00B CLE2	$e^+e^- \rightarrow \Upsilon(4S)$
0.16 ±0.04 ±0.04		2 ALBRECHT	94 ARG	$e^+e^- \rightarrow \Upsilon(4S)$
0.149 ±0.023 ±0.022		3 BARTELT	93 CLE2	$e^+e^- \rightarrow \Upsilon(4S)$
0.171 ±0.048		4 ALBRECHT	92L ARG	$e^+e^- \rightarrow \Upsilon(4S)$
• • • We do not use the following data for averages, fits, limits, etc. • • •				
0.20 ±0.13 ±0.12		5 ALBRECHT	96D ARG	$e^+e^- \rightarrow \Upsilon(4S)$
0.19 ±0.07 ±0.09		6 ALBRECHT	96B ARG	$e^+e^- \rightarrow \Upsilon(4S)$
0.24 ±0.12		7 ELSEN	90 JADE	$e^+e^- \rightarrow 35\text{-}44 \text{ GeV}$
0.158 $\pm_{-0.05}^{+0.052}$ $\pm_{-0.05}^{+0.059}$		ARTUSO	89 CLEO	$e^+e^- \rightarrow \Upsilon(4S)$
0.17 ±0.05		8 ALBRECHT	87I ARG	$e^+e^- \rightarrow \Upsilon(4S)$
<0.19	90	9 BEAN	87B CLEO	$e^+e^- \rightarrow \Upsilon(4S)$
<0.27	90	10 AVERY	84 CLEO	$e^+e^- \rightarrow \Upsilon(4S)$

- 1 BEHRENS 00B uses high-momentum lepton tags and partially reconstructed  $\bar{B}^0 \rightarrow D^{*+} \pi^-, \rho^-$  decays to determine the flavor of the B meson.
- 2 ALBRECHT 94 reports  $r=0.194 \pm 0.062 \pm 0.054$ . We convert to  $\chi$  for comparison. Uses tagged events (lepton + pion from  $D^*$ ).
- 3 BARTELT 93 analysis performed using tagged events (lepton+pion from  $D^*$ ). Using dilepton events they obtain  $0.157 \pm 0.016 \pm_{-0.028}^{+0.033}$ .
- 4 ALBRECHT 92L is a combined measurement employing several lepton-based techniques. It uses all previous ARGUS data in addition to new data and therefore supersedes ALBRECHT 87I. A value of  $r = 20.6 \pm 7.0\%$  is directly measured. The value can be used to measure  $x = \Delta M/\Gamma = 0.72 \pm 0.15$  for the  $B_d$  meson. Assumes  $f_{+,-}/f_0 = 1.0 \pm 0.05$  and uses  $\tau_{B^\pm}/\tau_{B^0} = (0.95 \pm 0.14) (f_{+,-}/f_0)$ .
- 5 Uses  $D^{*+} K^\pm$  correlations.
- 6 Uses  $(D^{*+} \ell^-) K^\pm$  correlations.
- 7 These experiments see a combination of  $B_s$  and  $B_d$  mesons.
- 8 ALBRECHT 87I is inclusive measurement with like-sign dileptons, with tagged B decays plus leptons, and one fully reconstructed event. Measures  $r=0.21 \pm 0.08$ . We convert to  $\chi$  for comparison. Superseded by ALBRECHT 92L.
- 9 BEAN 87B measured  $r < 0.24$ ; we converted to  $\chi$ .
- 10 Same-sign dilepton events. Limit assumes semileptonic BR for  $B^+$  and  $B^0$  equal. If  $B^0/B^\pm$  ratio  $< 0.58$ , no limit exists. The limit was corrected in BEAN 87B from  $r < 0.30$  to  $r < 0.37$ . We converted this limit to  $\chi$ .

**$\Delta m_{B^0} = m_{B_H^0} - m_{B_L^0}$**

$\Delta m_{B^0}$  is a measure of  $2\pi$  times the  $B^0-\bar{B}^0$  oscillation frequency in time-dependent mixing experiments.

The second “OUR EVALUATION” is an average using rescaled values of the data listed below. The average and rescaling were performed by the Heavy Flavor Averaging Group (HFAG) and are described at <http://www.slac.stanford.edu/xorg/hfag/>. The averaging/rescaling procedure takes into account correlations between the measurements.

The first “OUR EVALUATION”, also provided by the HFAG, includes  $\Delta m_d$  calculated from  $\chi_d$  measured at  $\Upsilon(4S)$ .

## Meson Particle Listings

 $B^0$ 

VALUE ( $10^{12} \text{ s}^{-1}$ )	DOCUMENT ID	TECN	COMMENT
<b>0.507±0.004 OUR EVALUATION</b>	First		
<b>0.507±0.004 OUR EVALUATION</b>	Second		
0.499±0.032±0.003	1 AAIJ	12i LHCB	$pp$ at 7 TeV
0.506±0.020±0.016	2 ABZOV	06w D0	$p\bar{p}$ at 1.96 TeV
0.511±0.007 <sup>+0.007</sup> <sub>-0.006</sub>	3 AUBERT	06g BABR	$e^+e^- \rightarrow \Upsilon(4S)$
0.511±0.005±0.006	4 ABE	05b BELL	$e^+e^- \rightarrow \Upsilon(4S)$
0.531±0.025±0.007	5 ABDALLAH	03b DLPH	$e^+e^- \rightarrow Z$
0.503±0.008±0.010	6 HASTINGS	03 BELL	$e^+e^- \rightarrow \Upsilon(4S)$
0.509±0.017±0.020	7 ZHENG	03 BELL	$e^+e^- \rightarrow \Upsilon(4S)$
0.516±0.016±0.010	8 AUBERT	02i BABR	$e^+e^- \rightarrow \Upsilon(4S)$
0.493±0.012±0.009	9 AUBERT	02j BABR	$e^+e^- \rightarrow \Upsilon(4S)$
0.497±0.024±0.025	10 ABBIENDI,G	00b OPAL	$e^+e^- \rightarrow Z$
0.503±0.064±0.071	11 ABE	99k CDF	$p\bar{p}$ at 1.8 TeV
0.500±0.052±0.043	12 ABE	99q CDF	$p\bar{p}$ at 1.8 TeV
0.516±0.009 <sup>+0.029</sup> <sub>-0.035</sub>	13 AFFOLDER	99c CDF	$p\bar{p}$ at 1.8 TeV
0.471 <sup>+0.078</sup> <sub>-0.068</sub> ±0.033 <sub>-0.034</sub>	14 ABE	98c CDF	$p\bar{p}$ at 1.8 TeV
0.458±0.046±0.032	15 ACCIARRI	98D L3	$e^+e^- \rightarrow Z$
0.437±0.043±0.044	16 ACCIARRI	98D L3	$e^+e^- \rightarrow Z$
0.472±0.049±0.053	17 ACCIARRI	98D L3	$e^+e^- \rightarrow Z$
0.523±0.072±0.043	18 ABREU	97N DLPH	$e^+e^- \rightarrow Z$
0.493±0.042±0.027	16 ABREU	97N DLPH	$e^+e^- \rightarrow Z$
0.499±0.053±0.015	19 ABREU	97N DLPH	$e^+e^- \rightarrow Z$
0.480±0.040±0.051	15 ABREU	97N DLPH	$e^+e^- \rightarrow Z$
0.444±0.029 <sup>+0.020</sup> <sub>-0.017</sub>	16 ACKERSTAFF	97u OPAL	$e^+e^- \rightarrow Z$
0.430±0.043 <sup>+0.028</sup> <sub>-0.030</sub>	15 ACKERSTAFF	97v OPAL	$e^+e^- \rightarrow Z$
0.482±0.044±0.024	20 BUSKULIC	97D ALEP	$e^+e^- \rightarrow Z$
0.404±0.045±0.027	16 BUSKULIC	97D ALEP	$e^+e^- \rightarrow Z$
0.452±0.039±0.044	15 BUSKULIC	97D ALEP	$e^+e^- \rightarrow Z$
0.539±0.060±0.024	21 ALEXANDER	96v OPAL	$e^+e^- \rightarrow Z$
0.567±0.089 <sup>+0.029</sup> <sub>-0.023</sub>	22 ALEXANDER	96v OPAL	$e^+e^- \rightarrow Z$
• • • We do not use the following data for averages, fits, limits, etc. • • •			
0.492±0.018±0.013	23 AUBERT	03c BABR	Repl. by AUBERT 06g
0.516±0.016±0.010	24 AUBERT	02n BABR	$e^+e^- \rightarrow \Upsilon(4S)$
0.494±0.012±0.015	25 HARA	02 BELL	Repl. by ABE 05b
0.528±0.017±0.011	26 TOMURA	02 BELL	Repl. by ABE 05b
0.463±0.008±0.016	9 ABE	01d BELL	Repl. by HASTINGS 03
0.444±0.028±0.028	27 ACCIARRI	98D L3	$e^+e^- \rightarrow Z$
0.497±0.035	28 ABREU	97N DLPH	$e^+e^- \rightarrow Z$
0.467±0.022 <sup>+0.017</sup> <sub>-0.015</sub>	29 ACKERSTAFF	97v OPAL	$e^+e^- \rightarrow Z$
0.446±0.032	30 BUSKULIC	97D ALEP	$e^+e^- \rightarrow Z$
0.531 <sup>+0.050</sup> <sub>-0.046</sub> ±0.078	31 ABREU	96q DLPH	Sup. by ABREU 97N
0.496 <sup>+0.055</sup> <sub>-0.051</sub> ±0.043	15 ACCIARRI	96E L3	Repl. by ACCIARRI 98D
0.548±0.050 <sup>+0.023</sup> <sub>-0.019</sub>	32 ALEXANDER	96v OPAL	$e^+e^- \rightarrow Z$
0.496±0.046	33 AKERS	95j OPAL	Repl. by ACKERSTAFF 97v
0.462 <sup>+0.040</sup> <sub>-0.053</sub> ±0.052 <sub>-0.035</sub>	15 AKERS	95j OPAL	Repl. by ACKERSTAFF 97v
0.50 ±0.12 ±0.06	18 ABREU	94M DLPH	Sup. by ABREU 97N
0.508±0.075±0.025	21 AKERS	94c OPAL	Repl. by ALEXANDER 96v
0.57 ±0.11 ±0.02	22 AKERS	94H OPAL	Repl. by ALEXANDER 96v
0.50 <sup>+0.07</sup> <sub>-0.06</sub> ±0.11 <sub>-0.10</sub>	15 BUSKULIC	94B ALEP	Sup. by BUSKULIC 97D
0.52 <sup>+0.10</sup> <sub>-0.11</sub> ±0.04 <sub>-0.03</sub>	22 BUSKULIC	93k ALEP	Sup. by BUSKULIC 97D

- 1 Measured using  $B^0 \rightarrow D^-\pi^+$ .
- 2 Uses opposite-side flavor-tagging with  $B \rightarrow D^{(*)}\mu\nu\mu X$  events.
- 3 Measured using a simultaneous fit of the  $B^0$  lifetime and  $\bar{B}^0 B^0$  oscillation frequency  $\Delta m_d$  in the partially reconstructed  $B^0 \rightarrow D^{*-}\ell\nu$  decays.
- 4 Measurement performed using a combined fit of  $CP$ -violation, mixing and lifetimes.
- 5 Events with a high transverse momentum lepton were removed and an inclusively reconstructed vertex was required.
- 6 HASTINGS 03 measurement based on the time evolution of dilepton events. It also reports  $f_+/f_0 = 1.01 \pm 0.03 \pm 0.09$  and  $CPT$  violation parameters in  $B^0\text{-}\bar{B}^0$  mixing.
- 7 ZHENG 03 data analyzed using partially reconstructed  $\bar{B}^0 \rightarrow D^{*-}\pi^+$  decay and a flavor tag based on the charge of the lepton from the accompanying  $B$  decay.
- 8 Uses a tagged sample of fully-reconstructed neutral  $B$  decays at  $\Upsilon(4S)$ .
- 9 Measured based on the time evolution of dilepton events in  $\Upsilon(4S)$  decays.
- 10 Data analyzed using partially reconstructed  $\bar{B}^0 \rightarrow D^{*+}\ell^-\bar{\nu}$  decay and a combination of flavor tags from the rest of the event.
- 11 Uses di-muon events.
- 12 Uses jet-charge and lepton-flavor tagging.
- 13 Uses  $\ell^- D^{*+} - \ell$  events.
- 14 Uses  $\pi-B$  in the same side.
- 15 Uses  $\ell\text{-}\ell$ .
- 16 Uses  $\ell\text{-}Q_{\text{hem}}$ .
- 17 Uses  $\ell\text{-}\ell$  with impact parameters.
- 18 Uses  $D^{*+}\text{-}Q_{\text{hem}}$ .
- 19 Uses  $\pi_s^{\pm}\ell\text{-}Q_{\text{hem}}$ .
- 20 Uses  $D^{*+}\text{-}\ell/Q_{\text{hem}}$ .

- 21 Uses  $D^{*+}\ell\text{-}Q_{\text{hem}}$ .
- 22 Uses  $D^{*+}\ell$ .
- 23 AUBERT 03c uses a sample of approximately 14,000 exclusively reconstructed  $B^0 \rightarrow D^{*}(2010)^-\ell\nu$  and simultaneously measures the lifetime and oscillation frequency.
- 24 AUBERT 02n result based on the same analysis and data sample reported in AUBERT 02i.
- 25 Uses a tagged sample of  $B^0$  decays reconstructed in the mode  $B^0 \rightarrow D^{*}\ell\nu$ .
- 26 Uses a tagged sample of fully-reconstructed hadronic  $B^0$  decays at  $\Upsilon(4S)$ .
- 27 ACCIARRI 98D combines results from  $\ell\text{-}\ell$ ,  $\ell\text{-}Q_{\text{hem}}$ , and  $\ell\text{-}\ell$  with impact parameters.
- 28 ABREU 97N combines results from  $D^{*+}\text{-}Q_{\text{hem}}$ ,  $\ell\text{-}Q_{\text{hem}}$ ,  $\pi_s^{\pm}\ell\text{-}Q_{\text{hem}}$ , and  $\ell\text{-}\ell$ .
- 29 ACKERSTAFF 97v combines results from  $\ell\text{-}\ell$ ,  $\ell\text{-}Q_{\text{hem}}$ ,  $D^{*}\text{-}\ell$ , and  $D^{*+}\text{-}Q_{\text{hem}}$ .
- 30 BUSKULIC 97D combines results from  $D^{*+}\text{-}\ell/Q_{\text{hem}}$ ,  $\ell\text{-}Q_{\text{hem}}$ , and  $\ell\text{-}\ell$ .
- 31 ABREU 96Q analysis performed using lepton, kaon, and jet-charge tags.
- 32 ALEXANDER 96v combines results from  $D^{*+}\text{-}\ell$  and  $D^{*+}\ell\text{-}Q_{\text{hem}}$ .
- 33 AKERS 95j combines results from charge measurement,  $D^{*+}\ell\text{-}Q_{\text{hem}}$  and  $\ell\text{-}\ell$ .

$\chi_d = \Delta m_{B^0}/\Gamma_{B^0}$

The second "OUR EVALUATION" is an average using rescaled values of the data listed below. The average and rescaling were performed by the Heavy Flavor Averaging Group (HFAG) and are described at <http://www.slac.stanford.edu/xorg/hfag/>. The averaging/rescaling procedure takes into account correlations between the measurements.

The first "OUR EVALUATION", also provided by the HFAG, includes  $\chi_d$  measured at  $\Upsilon(4S)$ .

VALUE	DOCUMENT ID
<b>0.770±0.008 OUR EVALUATION</b>	First
<b>0.770±0.008 OUR EVALUATION</b>	Second

$\text{Re}(\lambda_{CP} / |\lambda_{CP}|) \text{Re}(z)$

The  $\lambda_{CP}$  characterizes  $B^0$  and  $\bar{B}^0$  decays to states of charmonium plus  $K^0$ . Parameter  $z$  is used to describe  $CPT$  violation in mixing, see the review on "CP Violation" in the reviews section.

VALUE	DOCUMENT ID	TECN	COMMENT
<b>0.014±0.035±0.034</b>	1 AUBERT,B	04c BABR	$e^+e^- \rightarrow \Upsilon(4S)$

1 Corresponds to 90% confidence range  $[-0.072, 0.101]$ .

$\Delta\Gamma \text{Re}(z)$

VALUE	DOCUMENT ID	TECN	COMMENT
<b>-0.0071±0.0039±0.0020</b>	AUBERT	06t BABR	$e^+e^- \rightarrow \Upsilon(4S)$

$\text{Re}(z)$

VALUE (units $10^{-2}$ )	DOCUMENT ID	TECN	COMMENT
<b>1.9± 3.7±3.3</b>	1 HIGUCHI	12 BELL	$e^+e^- \rightarrow \Upsilon(4S)$

- • • We do not use the following data for averages, fits, limits, etc. • • •
- 0 ±12 ±1
- 2 HASTINGS 03 BELL Repl. by HIGUCHI 12
- 1 Measured using  $B^0 \rightarrow J/\psi K_S^0, J/\psi K_L^0, D^-\pi^+, D^{*-}\pi^+, D^{*-}\rho^+, \text{ and } D^{*-}\ell^+\nu$  decays.
- 2 Measured using inclusive dilepton events from  $B^0$  decay.

$\text{Im}(z)$

VALUE (units $10^{-2}$ )	DOCUMENT ID	TECN	COMMENT
<b>-0.8 ±0.4 OUR AVERAGE</b>			
-0.57±0.33±0.33	1 HIGUCHI	12 BELL	$e^+e^- \rightarrow \Upsilon(4S)$
-1.39±0.73±0.32	2 AUBERT	06t BABR	$e^+e^- \rightarrow \Upsilon(4S)$

- • • We do not use the following data for averages, fits, limits, etc. • • •
- 3.8 ±2.9 ±2.5
- 3 AUBERT,B 04c BABR Repl. by AUBERT 06T
- 3 ±1 ±3
- 4 HASTINGS 03 BELL Repl. by HIGUCHI 12
- 1 Measured using  $B^0 \rightarrow J/\psi K_S^0, J/\psi K_L^0, D^-\pi^+, D^{*-}\pi^+, D^{*-}\rho^+, \text{ and } D^{*-}\ell^+\nu$  decays.
- 2 Assuming  $\Delta\Gamma = 0$ , the result becomes  $\text{Im}(z) = -0.0037 \pm 0.0046$ .
- 3 Corresponds to 90% confidence range  $[-0.028, 0.104]$ .
- 4 Measured using inclusive dilepton events from  $B^0$  decay.

## CP VIOLATION PARAMETERS

$\text{Re}(\epsilon_{B^0})/(1+|\epsilon_{B^0}|^2)$

$CP$  impurity in  $B^0_d$  system. It is obtained from either  $a_{\ell\ell}$ , the charge asymmetry in like-sign dilepton events or  $a_{CP}$ , the time-dependent asymmetry of inclusive  $B^0$  and  $\bar{B}^0$  decays.

The second "OUR EVALUATION" is an average using rescaled values of the data listed below. The average and rescaling were performed by the Heavy Flavor Averaging Group (HFAG) and are described at <http://www.slac.stanford.edu/xorg/hfag/>. The averaging/rescaling procedure takes into account correlations between the measurements. It assumes there is no  $CP$  violation in  $B_s$  mixing.

The first "OUR EVALUATION", also provided by the HFAG, uses the measurements from  $B$ -factories only.



See key on page 457

## Meson Particle Listings

 $B^0$ 

VALUE (units $10^{-3}$ )	DOCUMENT ID	TECN	COMMENT
<b><math>-0.8 \pm 0.8</math> OUR EVALUATION</b>			
<b><math>0.0 \pm 0.9</math> OUR AVERAGE</b>			
$-0.3 \pm 1.3$	1 ABAZOV	11u D0	$p\bar{p}$ at 1.96 TeV
$0.4 \pm 1.3 \pm 0.9$	2 AUBERT	06T BABR	$e^+e^- \rightarrow \Upsilon(4S)$
$-0.3 \pm 2.0 \pm 2.1$	3 NAKANO	06 BELL	$e^+e^- \rightarrow \Upsilon(4S)$
$1.2 \pm 2.9 \pm 3.6$	4 AUBERT	02k BABR	$e^+e^- \rightarrow \Upsilon(4S)$
$-3.2 \pm 6.5$	5 BARATE	01D ALEP	$e^+e^- \rightarrow Z$
$3.5 \pm 10.3 \pm 1.5$	6 JAFFE	01 CLE2	$e^+e^- \rightarrow \Upsilon(4S)$
$1.2 \pm 13.8 \pm 3.2$	7 ABBIENDI	99j OPAL	$e^+e^- \rightarrow Z$
$2 \pm 7 \pm 3$	8 ACKERSTAFF	97u OPAL	$e^+e^- \rightarrow Z$
$-2.3 \pm 1.1 \pm 0.8$	9 ABAZOV	06s D0	Repl. by ABAZOV 11u
$-14.7 \pm 6.7 \pm 5.7$	10 AUBERT,B	04c BABR	Repl. by AUBERT 06T
$4 \pm 18 \pm 3$	11 BEHRENS	00b CLE2	Repl. by JAFFE 01
< 45	12 BARTELT	93 CLE2	$e^+e^- \rightarrow \Upsilon(4S)$

- 1 Uses the dimuon charge asymmetry with different impact parameters from which it reports  $A_{SL}^d = (-1.2 \pm 5.2) \times 10^{-3}$ .
- 2 AUBERT 06T reports  $|q/p| - 1 = (-0.8 \pm 2.7 \pm 1.9) \times 10^{-3}$ . We convert to  $(1 - |q/p|^2)/4$ .
- 3 Uses the charge asymmetry in like-sign dilepton events and reports  $|q/p| = 1.0005 \pm 0.0040 \pm 0.0043$ .
- 4 AUBERT 02k uses the charge asymmetry in like-sign dilepton events.
- 5 BARATE 01D measured by investigating time-dependent asymmetries in semileptonic and fully inclusive  $B^0$  decays.
- 6 JAFFE 01 finds  $a_{\ell\ell} = 0.013 \pm 0.050 \pm 0.005$  and combines with the previous BEHRENS 00b independent measurement.
- 7 Data analyzed using the time-dependent asymmetry of inclusive  $B^0$  decay. The production flavor of  $B^0$  mesons is determined using both the jet charge and the charge of secondary vertex in the opposite hemisphere.
- 8 ACKERSTAFF 97u assumes  $CP$  T and is based on measuring the charge asymmetry in a sample of  $B^0$  decays defined by lepton and  $Q_{\text{hem}}$  tags. If  $CP$  T is not invoked,  $\text{Re}(\epsilon_B) = -0.006 \pm 0.010 \pm 0.006$  is found. The indirect  $CP$  T violation parameter is determined to  $\text{Im}(\delta B) = -0.020 \pm 0.016 \pm 0.006$ .
- 9 Uses the dimuon charge asymmetry.
- 10 AUBERT 04c reports  $|q/p| = 1.029 \pm 0.013 \pm 0.011$  and we converted it to  $(1 - |q/p|^2)/4$ .
- 11 BEHRENS 00b uses high-momentum lepton tags and partially reconstructed  $\bar{B}^0 \rightarrow D^{*+} \pi^-, \rho^-$  decays to determine the flavor of the  $B$  meson.
- 12 BARTELT 93 finds  $a_{\ell\ell} = 0.031 \pm 0.096 \pm 0.032$  which corresponds to  $|a_{\ell\ell}| < 0.18$ , which yields the above  $|\text{Re}(\epsilon_{B^0})/(1 + |\epsilon_{B^0}|^2)|$ .

 $A_{T/CP}$  $A_{T/CP}$  is defined as

$$\frac{P(\bar{B}^0 \rightarrow B^0) - P(B^0 \rightarrow \bar{B}^0)}{P(\bar{B}^0 \rightarrow B^0) + P(B^0 \rightarrow \bar{B}^0)}$$

the  $CP$  T invariant asymmetry between the oscillation probabilities  $P(\bar{B}^0 \rightarrow B^0)$  and  $P(B^0 \rightarrow \bar{B}^0)$ .

VALUE	DOCUMENT ID	TECN	COMMENT
<b><math>0.005 \pm 0.012 \pm 0.014</math></b>	1 AUBERT	02k BABR	$e^+e^- \rightarrow \Upsilon(4S)$

1 AUBERT 02k uses the charge asymmetry in like-sign dilepton events.

 $A_{CP}(B^0 \rightarrow D^*(2010)^+ D^-)$  $A_{CP}$  is defined as

$$\frac{B(\bar{B}^0 \rightarrow \bar{f}) - B(B^0 \rightarrow f)}{B(\bar{B}^0 \rightarrow \bar{f}) + B(B^0 \rightarrow f)}$$

the  $CP$ -violation charge asymmetry of exclusive  $B^0$  and  $\bar{B}^0$  decay.

VALUE	DOCUMENT ID	TECN	COMMENT
<b><math>0.02 \pm 0.04</math> OUR AVERAGE</b>			
$+0.008 \pm 0.048 \pm 0.013$	AUBERT	09c BABR	$e^+e^- \rightarrow \Upsilon(4S)$
$+0.07 \pm 0.08 \pm 0.04$	1 AUSHEV	04 BELL	$e^+e^- \rightarrow \Upsilon(4S)$
$-0.12 \pm 0.06 \pm 0.02$	AUBERT	07Al BABR	Repl. by AUBERT 09c
$-0.03 \pm 0.10 \pm 0.02$	AUBERT,B	06A BABR	Repl. by AUBERT 07Al
$-0.03 \pm 0.11 \pm 0.05$	AUBERT	03J BABR	Repl. by AUBERT,B 06B

1 Combines results from fully and partially reconstructed  $B^0 \rightarrow D^{*+} D^-$  decays. $A_{CP}(B^0 \rightarrow K^+ \pi^-)$ 

VALUE	DOCUMENT ID	TECN	COMMENT
<b><math>-0.097 \pm 0.012</math> OUR AVERAGE</b>			
$-0.086 \pm 0.023 \pm 0.009$	AALTONEN	11n CDF	$p\bar{p}$ at 1.96 TeV
$-0.094 \pm 0.018 \pm 0.008$	LIN	08 BELL	$e^+e^- \rightarrow \Upsilon(4S)$
$-0.107 \pm 0.018 \pm 0.007$	AUBERT	07AF BABR	$e^+e^- \rightarrow \Upsilon(4S)$
$-0.04 \pm 0.16$	1 CHEN	00 CLE2	$e^+e^- \rightarrow \Upsilon(4S)$
$-0.013 \pm 0.078 \pm 0.012$	2 ABULENCIA,A	06D CDF	Repl. by AALTONEN 11n
$-0.088 \pm 0.035 \pm 0.013$	3 CHAO	05A BELL	Repl. by CHAO 04B
$-0.133 \pm 0.030 \pm 0.009$	4 AUBERT,B	04k BABR	Repl. by AUBERT 07AF
$-0.101 \pm 0.025 \pm 0.005$	5 CHAO	04B BELL	Repl. by LIN 08
$-0.07 \pm 0.08 \pm 0.02$	6 AUBERT	02D BABR	Repl. by AUBERT 02Q
$-0.102 \pm 0.050 \pm 0.016$	7 AUBERT	02Q BABR	Repl. by AUBERT,B 04k
$-0.06 \pm 0.09 \pm 0.01$	8 CASEY	02 BELL	Repl. by CHAO 04B
$0.044 \pm 0.186 \pm 0.018$	9 ABE	01k BELL	Repl. by CASEY 02
$-0.167 \pm 0.021$	10 AUBERT	01E BABR	Repl. by AUBERT 02Q

- 1 Corresponds to 90% confidence range  $-0.30 < A_{CP} < 0.22$ .
- 2 Corresponds to a 90% CL interval of  $-0.15 < A_{CP} < -0.03$ .
- 3 Based on a total signal yield of  $N(K^-\pi^+) + N(K^+\pi^-) = 1606 \pm 51$  events.
- 4 CHAO 04B reports significance of 3.9 standard deviation for deviation of  $A_{CP}$  from zero.
- 5 Corresponds to 90% confidence range  $-0.21 < A_{CP} < 0.07$ .
- 6 Corresponds to 90% confidence range  $-0.188 < A_{CP} < -0.016$ .
- 7 Corresponds to 90% confidence range  $-0.21 < A_{CP} < +0.09$ .
- 8 Corresponds to 90% confidence range  $-0.25 < A_{CP} < 0.37$ .
- 9 Corresponds to 90% confidence range  $-0.35 < A_{CP} < -0.03$ .

 $A_{CP}(B^0 \rightarrow \eta' K^*(892)^0)$ 

VALUE	DOCUMENT ID	TECN	COMMENT
<b><math>0.02 \pm 0.23 \pm 0.02</math></b>	DEL-AMO-SA...10A	BABR	$e^+e^- \rightarrow \Upsilon(4S)$
$0.08 \pm 0.25 \pm 0.02$	1 AUBERT	07E BABR	Repl. by DEL-AMO-SANCHEZ 10A

1 Reports  $A_{CP}$  with the opposite sign convention. $A_{CP}(B^0 \rightarrow \eta' K_0^*(1430)^0)$ 

VALUE	DOCUMENT ID	TECN	COMMENT
<b><math>-0.19 \pm 0.17 \pm 0.02</math></b>	DEL-AMO-SA...10A	BABR	$e^+e^- \rightarrow \Upsilon(4S)$

 $A_{CP}(B^0 \rightarrow \eta' K_2^*(1430)^0)$ 

VALUE	DOCUMENT ID	TECN	COMMENT
<b><math>0.14 \pm 0.18 \pm 0.02</math></b>	DEL-AMO-SA...10A	BABR	$e^+e^- \rightarrow \Upsilon(4S)$

 $A_{CP}(B^0 \rightarrow \eta K^*(892)^0)$ 

VALUE	DOCUMENT ID	TECN	COMMENT
<b><math>0.19 \pm 0.05</math> OUR AVERAGE</b>			
$0.17 \pm 0.08 \pm 0.01$	WANG	07B BELL	$e^+e^- \rightarrow \Upsilon(4S)$
$0.21 \pm 0.06 \pm 0.02$	AUBERT,B	06H BABR	$e^+e^- \rightarrow \Upsilon(4S)$
$0.02 \pm 0.11 \pm 0.02$	AUBERT,B	04D BABR	Repl. by AUBERT,B 06H

 $A_{CP}(B^0 \rightarrow \eta K_0^*(1430)^0)$ 

VALUE	DOCUMENT ID	TECN	COMMENT
<b><math>0.06 \pm 0.13 \pm 0.02</math></b>	AUBERT,B	06H BABR	$e^+e^- \rightarrow \Upsilon(4S)$

 $A_{CP}(B^0 \rightarrow \eta K_2^*(1430)^0)$ 

VALUE	DOCUMENT ID	TECN	COMMENT
<b><math>-0.07 \pm 0.19 \pm 0.02</math></b>	AUBERT,B	06H BABR	$e^+e^- \rightarrow \Upsilon(4S)$

 $A_{CP}(B^0 \rightarrow b_1 K^+)$ 

VALUE	DOCUMENT ID	TECN	COMMENT
<b><math>-0.07 \pm 0.12 \pm 0.02</math></b>	AUBERT	07Bl BABR	$e^+e^- \rightarrow \Upsilon(4S)$

 $A_{CP}(B^0 \rightarrow \omega K^*0)$ 

VALUE	DOCUMENT ID	TECN	COMMENT
<b><math>0.45 \pm 0.25 \pm 0.02</math></b>	AUBERT	09H BABR	$e^+e^- \rightarrow \Upsilon(4S)$

 $A_{CP}(B^0 \rightarrow \omega(K\pi)_0^+0)$ 

VALUE	DOCUMENT ID	TECN	COMMENT
<b><math>-0.07 \pm 0.09 \pm 0.02</math></b>	AUBERT	09H BABR	$e^+e^- \rightarrow \Upsilon(4S)$

 $A_{CP}(B^0 \rightarrow \omega K_2^*(1430)^0)$ 

VALUE	DOCUMENT ID	TECN	COMMENT
<b><math>-0.37 \pm 0.17 \pm 0.02</math></b>	AUBERT	09H BABR	$e^+e^- \rightarrow \Upsilon(4S)$

 $A_{CP}(B^0 \rightarrow K^+ \pi^- \pi^0)$ 

VALUE (units $10^{-2}$ )	DOCUMENT ID	TECN	COMMENT
<b><math>0 \pm 6</math> OUR AVERAGE</b>			
$-3.0 \pm 4.5 \pm 5.5$	1 AUBERT	08AQ BABR	$e^+e^- \rightarrow \Upsilon(4S)$
$7 \pm 11 \pm 1$	2 CHANG	04 BELL	$e^+e^- \rightarrow \Upsilon(4S)$

1 Uses Dalitz plot analysis of  $B^0 \rightarrow K^+ \pi^- \pi^0$  decays.2 Corresponds to 90% confidence range  $-0.12 < A_{CP} < 0.26$ . $A_{CP}(B^0 \rightarrow \rho^- K^+)$ 

VALUE	DOCUMENT ID	TECN	COMMENT
<b><math>0.20 \pm 0.11</math> OUR AVERAGE</b>			
$0.20 \pm 0.09 \pm 0.08$	1 LEES	11 BABR	$e^+e^- \rightarrow \Upsilon(4S)$
$0.22 \pm 0.22 \pm 0.06$	2 CHANG	04 BELL	$e^+e^- \rightarrow \Upsilon(4S)$
$-0.23 \pm 0.02$			
$0.11 \pm 0.14 \pm 0.07$	1 AUBERT	08AQ BABR	Repl. by LEES 11
$-0.28 \pm 0.17 \pm 0.08$	3 AUBERT	03T BABR	Repl. by AUBERT 08AQ

1 Uses Dalitz plot analysis of  $B^0 \rightarrow K^+ \pi^- \pi^0$  decays.2 Corresponds to 90% confidence range  $-0.18 < A_{CP} < 0.64$ .3 The result reported corresponds to  $-A_{CP}$ . $A_{CP}(B^0 \rightarrow \rho(1450)^- K^+)$ 

VALUE	DOCUMENT ID	TECN	COMMENT
<b><math>-0.10 \pm 0.32 \pm 0.09</math></b>	1 LEES	11 BABR	$e^+e^- \rightarrow \Upsilon(4S)$

1 Uses Dalitz plot analysis of  $B^0 \rightarrow K^+ \pi^- \pi^0$  decays.



$A_{CP}(B^0 \rightarrow \rho \bar{\lambda} \pi^-)$ 

VALUE	DOCUMENT ID	TECN	COMMENT
<b>0.04 ± 0.07 OUR AVERAGE</b>			
+0.10 ± 0.10 ± 0.02	AUBERT	09Ac	BABR $e^+ e^- \rightarrow \Upsilon(4S)$
-0.02 ± 0.10 ± 0.03	WANG	07c	BELL $e^+ e^- \rightarrow \Upsilon(4S)$

 $A_{CP}(B^0 \rightarrow K^{*0} \ell^+ \ell^-)$ 

VALUE	DOCUMENT ID	TECN	COMMENT
<b>-0.05 ± 0.10 OUR AVERAGE</b>			
0.02 ± 0.20 ± 0.02	AUBERT	09t	BABR $e^+ e^- \rightarrow \Upsilon(4S)$
-0.08 ± 0.12 ± 0.02	WEI	09A	BELL $e^+ e^- \rightarrow \Upsilon(4S)$

 $A_{CP}(B^0 \rightarrow K^{*0} e^+ e^-)$ 

VALUE	DOCUMENT ID	TECN	COMMENT
<b>-0.21 ± 0.19 ± 0.02</b>	WEI	09A	BELL $e^+ e^- \rightarrow \Upsilon(4S)$

 $A_{CP}(B^0 \rightarrow K^{*0} \mu^+ \mu^-)$ 

VALUE	DOCUMENT ID	TECN	COMMENT
<b>+0.00 ± 0.15 ± 0.03</b>	WEI	09A	BELL $e^+ e^- \rightarrow \Upsilon(4S)$

 $C_{D^*(2010)^- D^+}(B^0 \rightarrow D^*(2010)^- D^+)$ 

VALUE	DOCUMENT ID	TECN	COMMENT
<b>0.07 ± 0.14 OUR AVERAGE</b>			
0.00 ± 0.17 ± 0.03	AUBERT	09c	BABR $e^+ e^- \rightarrow \Upsilon(4S)$
0.23 ± 0.25 ± 0.06	<sup>1</sup> AUSHEV	04	BELL $e^+ e^- \rightarrow \Upsilon(4S)$
••• We do not use the following data for averages, fits, limits, etc. •••			
0.23 ± 0.15 ± 0.04	AUBERT	07A1	BABR Repl. by AUBERT 09c
0.17 ± 0.24 ± 0.04	AUBERT,B	05z	BABR Repl. by AUBERT 07A1
-0.22 ± 0.37 ± 0.10	AUBERT	03j	BABR Repl. by AUBERT,B 05z
<sup>1</sup> Combines results from fully and partially reconstructed $B^0 \rightarrow D^{*\pm} D^\mp$ decays.			

 $S_{D^*(2010)^- D^+}(B^0 \rightarrow D^*(2010)^- D^+)$ 

VALUE	DOCUMENT ID	TECN	COMMENT
<b>-0.78 ± 0.21 OUR AVERAGE</b>			
-0.73 ± 0.23 ± 0.050	AUBERT	09c	BABR $e^+ e^- \rightarrow \Upsilon(4S)$
-0.96 ± 0.43 ± 0.12	<sup>1</sup> AUSHEV	04	BELL $e^+ e^- \rightarrow \Upsilon(4S)$
••• We do not use the following data for averages, fits, limits, etc. •••			
-0.44 ± 0.22 ± 0.06	AUBERT	07A1	BABR Repl. by AUBERT 09c
-0.29 ± 0.33 ± 0.07	AUBERT,B	05z	BABR Repl. by AUBERT 07A1
-0.24 ± 0.69 ± 0.12	AUBERT	03j	BABR Repl. by AUBERT,B 05z
<sup>1</sup> Combines results from fully and partially reconstructed $B^0 \rightarrow D^{*\pm} D^\mp$ decays.			

 $C_{D^*(2010)^+ D^-}(B^0 \rightarrow D^*(2010)^+ D^-)$ 

VALUE	DOCUMENT ID	TECN	COMMENT
<b>-0.09 ± 0.22 OUR AVERAGE</b>	Error includes scale factor of 1.6.		
+0.08 ± 0.17 ± 0.04	AUBERT	09c	BABR $e^+ e^- \rightarrow \Upsilon(4S)$
-0.37 ± 0.22 ± 0.06	<sup>1</sup> AUSHEV	04	BELL $e^+ e^- \rightarrow \Upsilon(4S)$
••• We do not use the following data for averages, fits, limits, etc. •••			
+0.18 ± 0.15 ± 0.04	AUBERT	07A1	BABR Repl. by AUBERT 09c
+0.09 ± 0.25 ± 0.06	AUBERT,B	05z	BABR Repl. by AUBERT 07A1
-0.47 ± 0.40 ± 0.12	AUBERT	03j	BABR Repl. by AUBERT,B 05z
<sup>1</sup> Combines results from fully and partially reconstructed $B^0 \rightarrow D^{*\pm} D^\mp$ decays.			

 $S_{D^*(2010)^+ D^-}(B^0 \rightarrow D^*(2010)^+ D^-)$ 

VALUE	DOCUMENT ID	TECN	COMMENT
<b>-0.61 ± 0.19 OUR AVERAGE</b>			
-0.62 ± 0.21 ± 0.03	AUBERT	09c	BABR $e^+ e^- \rightarrow \Upsilon(4S)$
-0.55 ± 0.39 ± 0.12	<sup>1</sup> AUSHEV	04	BELL $e^+ e^- \rightarrow \Upsilon(4S)$
••• We do not use the following data for averages, fits, limits, etc. •••			
-0.79 ± 0.21 ± 0.06	AUBERT	07A1	BABR Repl. by AUBERT 09c
-0.54 ± 0.35 ± 0.07	AUBERT,B	05z	BABR Repl. by AUBERT 07A1
-0.82 ± 0.75 ± 0.14	AUBERT	03j	BABR Repl. by AUBERT,B 05z
<sup>1</sup> Combines results from fully and partially reconstructed $B^0 \rightarrow D^{*\pm} D^\mp$ decays.			

 $C_{D^{*+} D^{*-}}(B^0 \rightarrow D^{*+} D^{*-})$ 

VALUE	DOCUMENT ID	TECN	COMMENT
<b>-0.01 ± 0.09 OUR AVERAGE</b>	Error includes scale factor of 1.2.		
0.05 ± 0.09 ± 0.02	AUBERT	09c	BABR $e^+ e^- \rightarrow \Upsilon(4S)$
-0.15 ± 0.13 ± 0.04	<sup>1</sup> VERVINK	09	BELL $e^+ e^- \rightarrow \Upsilon(4S)$
••• We do not use the following data for averages, fits, limits, etc. •••			
-0.02 ± 0.11 ± 0.02	<sup>2</sup> AUBERT	07B0	BABR Repl. by AUBERT 09c
0.26 ± 0.26 ± 0.06	<sup>1</sup> MIYAKE	05	BELL Repl. by VERVINK 09
0.28 ± 0.23 ± 0.02	<sup>3</sup> AUBERT	03q	BABR Repl. by AUBERT 07B0

<sup>1</sup> Belle Collab. quotes  $A_{D^{*+} D^{*-}}$  which is equal to  $-C_{D^{*+} D^{*-}}$ .

<sup>2</sup> Assumes both  $CP$ -even and  $CP$ -odd states having the  $CP$  asymmetry.

<sup>3</sup> AUBERT 03q reports  $|\lambda|=0.75 \pm 0.19 \pm 0.02$  and  $\text{Im}(\lambda)=0.05 \pm 0.29 \pm 0.10$ . We convert them to  $S$  and  $C$  parameters taking into account correlations.

 $S_{D^{*+} D^{*-}}(B^0 \rightarrow D^{*+} D^{*-})$ 

VALUE	DOCUMENT ID	TECN	COMMENT
<b>-0.76 ± 0.14 OUR AVERAGE</b>			
-0.70 ± 0.16 ± 0.03	<sup>1</sup> AUBERT	09c	BABR $e^+ e^- \rightarrow \Upsilon(4S)$
-0.96 ± 0.25 $^{+0.13}_{-0.16}$	VERVINK	09	BELL $e^+ e^- \rightarrow \Upsilon(4S)$
••• We do not use the following data for averages, fits, limits, etc. •••			
-0.66 ± 0.19 ± 0.04	<sup>1</sup> AUBERT	07B0	BABR Repl. by AUBERT 09c
-0.75 ± 0.56 ± 0.12	MIYAKE	05	BELL Repl. by VERVINK 09
0.06 ± 0.37 ± 0.13	<sup>2</sup> AUBERT	03q	BABR Repl. by AUBERT 07B0
<sup>1</sup> Assumes both $CP$ -even and $CP$ -odd states having the $CP$ asymmetry.			
<sup>2</sup> AUBERT 03q reports $ \lambda =0.75 \pm 0.19 \pm 0.02$ and $\text{Im}(\lambda)=0.05 \pm 0.29 \pm 0.10$ . We convert them to $S$ and $C$ parameters taking into account correlations.			

 $C_+(B^0 \rightarrow D^{*+} D^{*-})$ 

See the note in the  $C_{\pi\pi}$  datablock, but for  $CP$  even final state.

VALUE	DOCUMENT ID	TECN	COMMENT
<b>0.00 ± 0.12 ± 0.02</b>	AUBERT	09c	BABR $e^+ e^- \rightarrow \Upsilon(4S)$
••• We do not use the following data for averages, fits, limits, etc. •••			
-0.05 ± 0.14 ± 0.02	AUBERT	07B0	BABR Repl. by AUBERT 09c
+0.06 ± 0.17 ± 0.03	<sup>1</sup> AUBERT,BE	05A	BABR Repl. by AUBERT 07B0
<sup>1</sup> AUBERT,BE 05A reports a $CP$ -odd fraction $R_{\perp} = 0.125 \pm 0.044 \pm 0.007$ .			

 $S_+(B^0 \rightarrow D^{*+} D^{*-})$ 

See the note in the  $S_{\pi\pi}$  datablock, but for  $CP$  even final state.

VALUE	DOCUMENT ID	TECN	COMMENT
<b>-0.76 ± 0.16 ± 0.04</b>	AUBERT	09c	BABR $e^+ e^- \rightarrow \Upsilon(4S)$
••• We do not use the following data for averages, fits, limits, etc. •••			
-0.72 ± 0.19 ± 0.05	AUBERT	07B0	BABR Repl. by AUBERT 09c
-0.75 ± 0.25 ± 0.03	<sup>1</sup> AUBERT,BE	05A	BABR Repl. by AUBERT 07B0
<sup>1</sup> AUBERT,BE 05A reports a $CP$ -odd fraction $R_{\perp} = 0.125 \pm 0.044 \pm 0.007$ .			

 $C_-(B^0 \rightarrow D^{*+} D^{*-})$ 

See the note in the  $C_{\pi\pi}$  datablock, but for  $CP$  odd final state.

VALUE	DOCUMENT ID	TECN	COMMENT
<b>+0.41 ± 0.49 ± 0.08</b>	AUBERT	09c	BABR $e^+ e^- \rightarrow \Upsilon(4S)$
••• We do not use the following data for averages, fits, limits, etc. •••			
+0.23 ± 0.67 ± 0.10	AUBERT	07B0	BABR Repl. by AUBERT 09c
-0.20 ± 0.96 ± 0.11	<sup>1</sup> AUBERT,BE	05A	BABR Repl. by AUBERT 07B0
<sup>1</sup> AUBERT,BE 05A reports a $CP$ -odd fraction $R_{\perp} = 0.125 \pm 0.044 \pm 0.007$ .			

 $S_-(B^0 \rightarrow D^{*+} D^{*-})$ 

See the note in the  $S_{\pi\pi}$  datablock, but for  $CP$  odd final state.

VALUE	DOCUMENT ID	TECN	COMMENT
<b>-1.80 ± 0.70 ± 0.16</b>	AUBERT	09c	BABR $e^+ e^- \rightarrow \Upsilon(4S)$
••• We do not use the following data for averages, fits, limits, etc. •••			
-1.83 ± 1.04 ± 0.23	AUBERT	07B0	BABR Repl. by AUBERT 09c
-1.75 ± 1.78 ± 0.22	<sup>1</sup> AUBERT,BE	05A	BABR Repl. by AUBERT 07B0
<sup>1</sup> AUBERT,BE 05A reports a $CP$ -odd fraction $R_{\perp} = 0.125 \pm 0.044 \pm 0.007$ .			

 $C(B^0 \rightarrow D^*(2010)^+ D^*(2010)^- K_S^0)$ 

VALUE	DOCUMENT ID	TECN	COMMENT
<b>0.01 ± 0.28 ± 0.09</b>	<sup>1</sup> DALSENO	07	BELL $e^+ e^- \rightarrow \Upsilon(4S)$
<sup>1</sup> Reports value of $A$ which is equal to $-C$ .			

 $S(B^0 \rightarrow D^*(2010)^+ D^*(2010)^- K_S^0)$ 

VALUE	DOCUMENT ID	TECN	COMMENT
<b>0.06 <math>^{+0.45}_{-0.44} \pm 0.06</math></b>	<sup>1</sup> DALSENO	07	BELL $e^+ e^- \rightarrow \Upsilon(4S)$
<sup>1</sup> This value includes an unknown $CP$ dilution factor $D$ due to possible contributions from intermediate resonances and different partial waves.			

 $C_{D^+ D^-}(B^0 \rightarrow D^+ D^-)$ 

VALUE	DOCUMENT ID	TECN	COMMENT
<b>-0.5 ± 0.4 OUR AVERAGE</b>	Error includes scale factor of 2.5.		
-0.07 ± 0.23 ± 0.03	AUBERT	09c	BABR $e^+ e^- \rightarrow \Upsilon(4S)$
-0.91 ± 0.23 ± 0.06	<sup>1</sup> FRATINA	07	BELL $e^+ e^- \rightarrow \Upsilon(4S)$
••• We do not use the following data for averages, fits, limits, etc. •••			
+0.11 ± 0.22 ± 0.07	AUBERT	07A1	BABR Repl. by AUBERT 09c
+0.11 ± 0.35 ± 0.06	AUBERT,B	05z	BABR Repl. by AUBERT 07A1
<sup>1</sup> The paper reports $A$ , which is equal to $-C$ .			

 $S_{D^+ D^-}(B^0 \rightarrow D^+ D^-)$ 

VALUE	DOCUMENT ID	TECN	COMMENT
<b>-0.87 ± 0.26 OUR AVERAGE</b>			
-0.63 ± 0.36 ± 0.05	AUBERT	09c	BABR $e^+ e^- \rightarrow \Upsilon(4S)$
-1.13 ± 0.37 ± 0.09	FRATINA	07	BELL $e^+ e^- \rightarrow \Upsilon(4S)$
••• We do not use the following data for averages, fits, limits, etc. •••			
-0.54 ± 0.34 ± 0.06	AUBERT	07A1	BABR Repl. by AUBERT 09c
-0.29 ± 0.63 ± 0.06	AUBERT,B	05z	BABR Repl. by AUBERT 07A1

## Meson Particle Listings

 $B^0$  $C_{J/\psi(1S)\pi^0}(B^0 \rightarrow J/\psi(1S)\pi^0)$ 

VALUE	DOCUMENT ID	TECN	COMMENT
<b><math>-0.13 \pm 0.13</math> OUR AVERAGE</b>			
$-0.20 \pm 0.19 \pm 0.03$	AUBERT	08AU	BABR $e^+e^- \rightarrow \Upsilon(4S)$
$-0.08 \pm 0.16 \pm 0.05$	<sup>1</sup> LEE	08A	BELL $e^+e^- \rightarrow \Upsilon(4S)$
• • • We do not use the following data for averages, fits, limits, etc. • • •			
$-0.21 \pm 0.26 \pm 0.06$	AUBERT,B	06B	BABR Repl. by AUBERT 08AU
$0.01 \pm 0.29 \pm 0.03$	<sup>1</sup> KATAOKA	04	BELL Repl. by LEE 08A
$0.38 \pm 0.41 \pm 0.09$	AUBERT	03N	BABR Repl. by AUBERT,B 06B

<sup>1</sup> Belle Collab. quotes  $A_{J/\psi\pi^0}$  which is equal to  $-C_{J/\psi\pi^0}$ . $S_{J/\psi(1S)\pi^0}(B^0 \rightarrow J/\psi(1S)\pi^0)$ 

VALUE	DOCUMENT ID	TECN	COMMENT
<b><math>-0.94 \pm 0.29</math> OUR AVERAGE</b>			Error includes scale factor of 1.9.
$-1.23 \pm 0.21 \pm 0.04$	AUBERT	08AU	BABR $e^+e^- \rightarrow \Upsilon(4S)$
$-0.65 \pm 0.21 \pm 0.05$	LEE	08A	BELL $e^+e^- \rightarrow \Upsilon(4S)$
• • • We do not use the following data for averages, fits, limits, etc. • • •			
$-0.68 \pm 0.30 \pm 0.04$	AUBERT,B	06B	BABR Repl. by AUBERT 08AU
$-0.72 \pm 0.42 \pm 0.09$	KATAOKA	04	BELL Repl. by LEE 08A
$0.05 \pm 0.49 \pm 0.16$	AUBERT	03N	BABR Repl. by AUBERT,B 06B

 $C_{D_{CP}^{(*)}\rho^0}(B^0 \rightarrow D_{CP}^{(*)}\rho^0)$ 

VALUE	DOCUMENT ID	TECN	COMMENT
<b><math>-0.23 \pm 0.16 \pm 0.04</math></b>	AUBERT	07AJ	BABR $e^+e^- \rightarrow \Upsilon(4S)$

 $S_{D_{CP}^{(*)}\rho^0}(B^0 \rightarrow D_{CP}^{(*)}\rho^0)$ 

VALUE	DOCUMENT ID	TECN	COMMENT
<b><math>-0.56 \pm 0.23 \pm 0.05</math></b>	AUBERT	07AJ	BABR $e^+e^- \rightarrow \Upsilon(4S)$

 $C_{K^0\pi^0}(B^0 \rightarrow K^0\pi^0)$ 

VALUE	DOCUMENT ID	TECN	COMMENT
<b><math>0.00 \pm 0.13</math> OUR AVERAGE</b>			Error includes scale factor of 1.4.
$-0.14 \pm 0.13 \pm 0.06$	<sup>1</sup> FUJIKAWA	10A	BELL $e^+e^- \rightarrow \Upsilon(4S)$
$+0.13 \pm 0.13 \pm 0.03$	AUBERT	09I	BABR $e^+e^- \rightarrow \Upsilon(4S)$
• • • We do not use the following data for averages, fits, limits, etc. • • •			
$+0.24 \pm 0.15 \pm 0.03$	AUBERT	08E	BABR Repl. by AUBERT 09I
$+0.05 \pm 0.14 \pm 0.05$	<sup>1</sup> CHAO	07	BELL Repl. by FUJIKAWA 10A
$+0.06 \pm 0.18 \pm 0.03$	AUBERT	05Y	BABR Repl. by AUBERT 08E
$-0.16 \pm 0.29 \pm 0.05$	<sup>1,2</sup> CHAO	05A	BELL Repl. by CHEN 05B
$+0.11 \pm 0.20 \pm 0.09$	<sup>1</sup> CHEN	05B	BELL Repl. by CHAO 07
$-0.03 \pm 0.36 \pm 0.11$	<sup>1</sup> AUBERT	04M	BABR Repl. by AUBERT,B 04M
$+0.40 \pm 0.27 \pm 0.09$	<sup>3</sup> AUBERT,B	04M	BABR Repl. by AUBERT 05Y

<sup>1</sup> Reports A which is equal to  $-C$ .<sup>2</sup> Corresponds to a 90% CL interval of  $-0.33 < A_{CP} < 0.64$ .<sup>3</sup> Based on a total signal yield of  $122 \pm 16$  events. $S_{K^0\pi^0}(B^0 \rightarrow K^0\pi^0)$ 

VALUE	DOCUMENT ID	TECN	COMMENT
<b><math>0.58 \pm 0.17</math> OUR AVERAGE</b>			
$0.67 \pm 0.31 \pm 0.08$	FUJIKAWA	10A	BELL $e^+e^- \rightarrow \Upsilon(4S)$
$+0.55 \pm 0.20 \pm 0.03$	AUBERT	09I	BABR $e^+e^- \rightarrow \Upsilon(4S)$
• • • We do not use the following data for averages, fits, limits, etc. • • •			
$+0.40 \pm 0.23 \pm 0.03$	AUBERT	08E	BABR Repl. by AUBERT 09I
$+0.33 \pm 0.35 \pm 0.08$	CHAO	07	BELL Repl. by FUJIKAWA 10A
$+0.35 \pm 0.30 \pm 0.04$	AUBERT	05Y	BABR Repl. by AUBERT 08E
$+0.32 \pm 0.61 \pm 0.13$	CHEN	05B	BELL Repl. by CHAO 07
$+0.48 \pm 0.38 \pm 0.06$	<sup>1</sup> AUBERT,B	04M	BABR Repl. by AUBERT 05Y

<sup>1</sup> Based on a total signal yield of  $122 \pm 16$  events. $C_{\eta(958)K_S^0}(B^0 \rightarrow \eta(958)K_S^0)$ See updated measurements in  $C_{\eta'K^0}$ 

VALUE	DOCUMENT ID	TECN	COMMENT
<b><math>-0.04 \pm 0.20</math> OUR AVERAGE</b>			Error includes scale factor of 2.5.
$-0.21 \pm 0.10 \pm 0.02$	AUBERT	05M	BABR $e^+e^- \rightarrow \Upsilon(4S)$
$0.19 \pm 0.11 \pm 0.05$	<sup>1</sup> CHEN	05B	BELL $e^+e^- \rightarrow \Upsilon(4S)$
• • • We do not use the following data for averages, fits, limits, etc. • • •			
$-0.26 \pm 0.22 \pm 0.03$	<sup>1</sup> ABE	03C	BELL Repl. by ABE 03H
$0.01 \pm 0.16 \pm 0.04$	<sup>1</sup> ABE	03H	BELL Repl. by CHEN 05B
$0.10 \pm 0.22 \pm 0.04$	AUBERT	03W	BABR Repl. by AUBERT 05M
$-0.13 \pm 0.32 \pm 0.06$	<sup>1</sup> CHEN	02B	BELL Repl. by ABE 03C

<sup>1</sup> Belle Collab. quotes  $A_{\eta(958)K_S^0}$  which is equal to  $-C_{\eta(958)K_S^0}$ . $S_{\eta(958)K_S^0}(B^0 \rightarrow \eta(958)K_S^0)$ See updated measurements in  $S_{\eta'K^0}$ 

VALUE	DOCUMENT ID	TECN	COMMENT
<b><math>0.43 \pm 0.17</math> OUR AVERAGE</b>			Error includes scale factor of 1.5.
$0.30 \pm 0.14 \pm 0.02$	AUBERT	05M	BABR $e^+e^- \rightarrow \Upsilon(4S)$
$+0.65 \pm 0.18 \pm 0.04$	CHEN	05B	BELL $e^+e^- \rightarrow \Upsilon(4S)$
• • • We do not use the following data for averages, fits, limits, etc. • • •			
$0.71 \pm 0.37 \pm 0.05$	ABE	03C	BELL Repl. by ABE 03H
$0.43 \pm 0.27 \pm 0.05$	ABE	03H	BELL Repl. by CHEN 05B
$0.02 \pm 0.34 \pm 0.03$	AUBERT	03W	BABR Repl. by AUBERT 05M
$0.28 \pm 0.55 \pm 0.07$	CHEN	02B	BELL Repl. by ABE 03C

 $C_{\eta'K^0}(B^0 \rightarrow \eta'K^0)$ 

VALUE	DOCUMENT ID	TECN	COMMENT
<b><math>-0.05 \pm 0.05</math> OUR AVERAGE</b>			
$-0.08 \pm 0.06 \pm 0.02$	AUBERT	09I	BABR $e^+e^- \rightarrow \Upsilon(4S)$
$0.01 \pm 0.07 \pm 0.05$	<sup>1,2</sup> CHEN	07	BELL $e^+e^- \rightarrow \Upsilon(4S)$
• • • We do not use the following data for averages, fits, limits, etc. • • •			
$-0.16 \pm 0.07 \pm 0.03$	<sup>1</sup> AUBERT	07A	BABR Repl. by AUBERT 09I

<sup>1</sup> The mixing-induced CP violation is reported with a significance of more than 5 standard deviations in this  $b \rightarrow s$  penguin dominated mode.<sup>2</sup> The paper reports A, which is equal to  $-C$ . $S_{\eta'K^0}(B^0 \rightarrow \eta'K^0)$ 

VALUE	DOCUMENT ID	TECN	COMMENT
<b><math>0.60 \pm 0.07</math> OUR AVERAGE</b>			
$+0.57 \pm 0.08 \pm 0.02$	AUBERT	09I	BABR $e^+e^- \rightarrow \Upsilon(4S)$
$0.64 \pm 0.10 \pm 0.04$	<sup>1</sup> CHEN	07	BELL $e^+e^- \rightarrow \Upsilon(4S)$
• • • We do not use the following data for averages, fits, limits, etc. • • •			
$0.58 \pm 0.10 \pm 0.03$	<sup>1</sup> AUBERT	07A	BABR Repl. by AUBERT 09I

<sup>1</sup> The mixing-induced CP violation is reported with a significance of more than 5 standard deviations in this  $b \rightarrow s$  penguin dominated mode. $C_{\omega K_S^0}(B^0 \rightarrow \omega K_S^0)$ 

VALUE	DOCUMENT ID	TECN	COMMENT
<b><math>-0.30 \pm 0.28</math> OUR AVERAGE</b>			Error includes scale factor of 1.6.
$-0.52 \pm 0.22 \pm 0.03$	AUBERT	09I	BABR $e^+e^- \rightarrow \Upsilon(4S)$
$+0.09 \pm 0.29 \pm 0.06$	<sup>1</sup> CHAO	07	BELL $e^+e^- \rightarrow \Upsilon(4S)$
• • • We do not use the following data for averages, fits, limits, etc. • • •			
$-0.55 \pm 0.28 \pm 0.03$	AUBERT,B	06E	BABR Repl. by AUBERT 09I
$-0.27 \pm 0.48 \pm 0.15$	<sup>1</sup> CHEN	05B	BELL Repl. by CHAO 07

<sup>1</sup> Belle Collab. quotes  $A_{\omega K_S^0}$  which is equal to  $-C_{\omega K_S^0}$ . $S_{\omega K_S^0}(B^0 \rightarrow \omega K_S^0)$ 

VALUE	DOCUMENT ID	TECN	COMMENT
<b><math>0.43 \pm 0.24</math> OUR AVERAGE</b>			
$+0.55 \pm 0.26 \pm 0.02$	AUBERT	09I	BABR $e^+e^- \rightarrow \Upsilon(4S)$
$+0.11 \pm 0.46 \pm 0.07$	CHAO	07	BELL $e^+e^- \rightarrow \Upsilon(4S)$
• • • We do not use the following data for averages, fits, limits, etc. • • •			
$+0.51 \pm 0.35 \pm 0.02$	AUBERT,B	06E	BABR Repl. by AUBERT 09I
$+0.76 \pm 0.65 \pm 0.13$	CHEN	05B	BELL Repl. by CHAO 07

 $C(B^0 \rightarrow K_S^0\pi^0\pi^0)$ 

VALUE	DOCUMENT ID	TECN	COMMENT
<b><math>0.23 \pm 0.52 \pm 0.13</math></b>	AUBERT	07AQ	BABR $e^+e^- \rightarrow \Upsilon(4S)$

 $S(B^0 \rightarrow K_S^0\pi^0\pi^0)$ 

VALUE	DOCUMENT ID	TECN	COMMENT
<b><math>0.72 \pm 0.71 \pm 0.08</math></b>	AUBERT	07AQ	BABR $e^+e^- \rightarrow \Upsilon(4S)$

 $C_{\rho^0 K_S^0}(B^0 \rightarrow \rho^0 K_S^0)$ 

VALUE	DOCUMENT ID	TECN	COMMENT
<b><math>-0.04 \pm 0.20</math> OUR AVERAGE</b>			
$-0.05 \pm 0.26 \pm 0.10$	<sup>1</sup> AUBERT	09AU	BABR $e^+e^- \rightarrow \Upsilon(4S)$
$-0.03 \pm 0.24 \pm 0.15$	<sup>2,3</sup> DALSENO	09	BELL $e^+e^- \rightarrow \Upsilon(4S)$
• • • We do not use the following data for averages, fits, limits, etc. • • •			
$0.64 \pm 0.41 \pm 0.20$	AUBERT	07F	BABR Repl. by AUBERT 09AU

<sup>1</sup> Uses Dalitz plot analysis of  $B^0 \rightarrow K^0\pi^+\pi^-$  decays and the first of two equivalent solutions is used.<sup>2</sup> Quotes  $A_{\rho^0(K_S^0)}$  which is equal to  $-C_{\rho^0 K_S^0}$ .<sup>3</sup> Uses Dalitz plot analysis of  $B^0 \rightarrow K^0\pi^+\pi^-$  decays and the first of two consistent solutions that may be preferred.

See key on page 457

Meson Particle Listings

$B^0$

$S_{\rho^0 K_S^0} (B^0 \rightarrow \rho^0 K_S^0)$

VALUE	DOCUMENT ID	TECN	COMMENT
<b><math>0.50 \pm 0.17</math></b> OUR AVERAGE			
$0.35 \pm 0.26$	<sup>1</sup> AUBERT	09AU BABR	$e^+ e^- \rightarrow \Upsilon(4S)$
$0.64 \pm 0.19$	<sup>2</sup> DALSENO	09 BELL	$e^+ e^- \rightarrow \Upsilon(4S)$
$0.20 \pm 0.52 \pm 0.24$	AUBERT	07F BABR	Repl. by AUBERT 09AU

• • • We do not use the following data for averages, fits, limits, etc. • • •

<sup>1</sup> Uses Dalitz plot analysis of  $B^0 \rightarrow K^0 \pi^+ \pi^-$  decays and the first of two equivalent solutions is used.

<sup>2</sup> Uses Dalitz plot analysis of  $B^0 \rightarrow K^0 \pi^+ \pi^-$  decays and the first of two consistent solutions that may be preferred.

$C_{f_0(980) K_S^0} (B^0 \rightarrow f_0(980) K_S^0)$

VALUE	DOCUMENT ID	TECN	COMMENT
<b><math>0.14 \pm 0.17</math></b> OUR AVERAGE			
$0.30 \pm 0.29 \pm 0.14$	<sup>1,2</sup> NAKAHAMA	10 BELL	$e^+ e^- \rightarrow \Upsilon(4S)$
$0.08 \pm 0.19 \pm 0.05$	<sup>3</sup> AUBERT	09AU BABR	$e^+ e^- \rightarrow \Upsilon(4S)$
$+0.06 \pm 0.17 \pm 0.11$	<sup>1,4</sup> DALSENO	09 BELL	Repl. by NAKAHAMA 10
$-0.41 \pm 0.23 \pm 0.07$	<sup>1</sup> AUBERT	07AX BABR	Repl. by AUBERT 09AU
$+0.15 \pm 0.15 \pm 0.07$	<sup>1</sup> CHAO	07 BELL	Repl. by DALSENO 09
$+0.39 \pm 0.27 \pm 0.09$	<sup>1</sup> CHEN	05B BELL	Repl. by CHAO 07

• • • We do not use the following data for averages, fits, limits, etc. • • •

<sup>1</sup> Quotes  $A_{f_0(980) K_S^0}$  which is equal to  $-C_{f_0(980) K_S^0}$ .

<sup>2</sup> Uses Dalitz plot analysis of  $B^0 \rightarrow K_S^0 K^+ K^-$  decays and the first of four consistent solutions that may be preferred.

<sup>3</sup> Uses Dalitz plot analysis of  $B^0 \rightarrow K^0 \pi^+ \pi^-$  decays and the first of two equivalent solutions is used.

<sup>4</sup> Uses Dalitz plot analysis of  $B^0 \rightarrow K^0 \pi^+ \pi^-$  decays and the first of two consistent solutions that may be preferred.

$S_{f_0(980) K_S^0} (B^0 \rightarrow f_0(980) K_S^0)$

VALUE	DOCUMENT ID	TECN	COMMENT
<b><math>-0.73 \pm 0.27</math></b> OUR AVERAGE			Error includes scale factor of 1.6.
$-0.96 \pm 0.21$	<sup>1</sup> AUBERT	09AU BABR	$e^+ e^- \rightarrow \Upsilon(4S)$
$-0.43 \pm 0.22$	<sup>2</sup> DALSENO	09 BELL	$e^+ e^- \rightarrow \Upsilon(4S)$
$-0.25 \pm 0.26 \pm 0.10$	<sup>3</sup> AUBERT	07AX BABR	Repl. by AUBERT 09AU
$+0.18 \pm 0.23 \pm 0.11$	CHAO	07 BELL	Repl. by DALSENO 09
$+0.47 \pm 0.41 \pm 0.08$	CHEN	05B BELL	Repl. by CHAO 07

• • • We do not use the following data for averages, fits, limits, etc. • • •

<sup>1</sup> Uses Dalitz plot analysis of  $B^0 \rightarrow K^0 \pi^+ \pi^-$  decays and the first of two equivalent solutions is used.

<sup>2</sup> Uses Dalitz plot analysis of  $B^0 \rightarrow K^0 \pi^+ \pi^-$  decays and the first of two consistent solutions that may be preferred.

<sup>3</sup> Reports  $\beta_{eff}$ . We quote  $S$  obtained from epaps: E-PRLTAO-99-076741.

$S_{f_2(1270) K_S^0} (B^0 \rightarrow f_2(1270) K_S^0)$

VALUE	DOCUMENT ID	TECN	COMMENT
<b><math>-0.48 \pm 0.52 \pm 0.12</math></b>	<sup>1</sup> AUBERT	09AU BABR	$e^+ e^- \rightarrow \Upsilon(4S)$

<sup>1</sup> Uses Dalitz plot analysis of  $B^0 \rightarrow K^0 \pi^+ \pi^-$  decays and the first of two equivalent solutions is used.

$C_{f_2(1270) K_S^0} (B^0 \rightarrow f_2(1270) K_S^0)$

VALUE	DOCUMENT ID	TECN	COMMENT
<b><math>0.28 \pm 0.35</math></b> OUR AVERAGE			
$0.28 \pm 0.35 \pm 0.11$	<sup>1</sup> AUBERT	09AU BABR	$e^+ e^- \rightarrow \Upsilon(4S)$

<sup>1</sup> Uses Dalitz plot analysis of  $B^0 \rightarrow K^0 \pi^+ \pi^-$  decays and the first of two equivalent solutions is used.

$S_{f_x(1300) K_S^0} (B^0 \rightarrow f_x(1300) K_S^0)$

VALUE	DOCUMENT ID	TECN	COMMENT
<b><math>-0.20 \pm 0.52 \pm 0.10</math></b>	<sup>1</sup> AUBERT	09AU BABR	$e^+ e^- \rightarrow \Upsilon(4S)$

<sup>1</sup> Uses Dalitz plot analysis of  $B^0 \rightarrow K^0 \pi^+ \pi^-$  decays and the first of two equivalent solutions is used.

$C_{f_x(1300) K_S^0} (B^0 \rightarrow f_x(1300) K_S^0)$

VALUE	DOCUMENT ID	TECN	COMMENT
<b><math>0.13 \pm 0.33</math></b> OUR AVERAGE			
$0.13 \pm 0.33 \pm 0.10$	<sup>1</sup> AUBERT	09AU BABR	$e^+ e^- \rightarrow \Upsilon(4S)$

<sup>1</sup> Uses Dalitz plot analysis of  $B^0 \rightarrow K^0 \pi^+ \pi^-$  decays and the first of two equivalent solutions is used.

$S_{K^0 \pi^+ \pi^-} (B^0 \rightarrow K^0 \pi^+ \pi^- \text{ nonresonant})$

VALUE	DOCUMENT ID	TECN	COMMENT
<b><math>-0.01 \pm 0.31 \pm 0.10</math></b>	<sup>1</sup> AUBERT	09AU BABR	$e^+ e^- \rightarrow \Upsilon(4S)$

<sup>1</sup> Uses Dalitz plot analysis of  $B^0 \rightarrow K^0 \pi^+ \pi^-$  decays and the first of two equivalent solutions is used.

$C_{K^0 \pi^+ \pi^-} (B^0 \rightarrow K^0 \pi^+ \pi^- \text{ nonresonant})$

VALUE	DOCUMENT ID	TECN	COMMENT
<b><math>0.01 \pm 0.25 \pm 0.08</math></b>	<sup>1</sup> AUBERT	09AU BABR	$e^+ e^- \rightarrow \Upsilon(4S)$

<sup>1</sup> Uses Dalitz plot analysis of  $B^0 \rightarrow K^0 \pi^+ \pi^-$  decays and the first of two equivalent solutions is used.

$C_{K_S^0 K_S^0} (B^0 \rightarrow K_S^0 K_S^0)$

VALUE	DOCUMENT ID	TECN	COMMENT
<b><math>0.0 \pm 0.4</math></b> OUR AVERAGE			Error includes scale factor of 1.4.
$+0.38 \pm 0.38 \pm 0.05$	<sup>1</sup> NAKAHAMA	08 BELL	$e^+ e^- \rightarrow \Upsilon(4S)$
$-0.40 \pm 0.41 \pm 0.06$	AUBERT, BE	06c BABR	$e^+ e^- \rightarrow \Upsilon(4S)$

<sup>1</sup> Reports  $A_{K_S^0 K_S^0}$  which equals to  $-C_{K_S^0 K_S^0}$ .

$S_{K_S^0 K_S^0} (B^0 \rightarrow K_S^0 K_S^0)$

VALUE	DOCUMENT ID	TECN	COMMENT
<b><math>-0.8 \pm 0.5</math></b> OUR AVERAGE			
$-0.38 \pm 0.69$	NAKAHAMA	08 BELL	$e^+ e^- \rightarrow \Upsilon(4S)$
$-1.28 \pm 0.80 \pm 0.11$	AUBERT, BE	06c BABR	$e^+ e^- \rightarrow \Upsilon(4S)$

$C_{K^+ K^- K_S^0} (B^0 \rightarrow K^+ K^- K_S^0 \text{ nonresonant})$

VALUE	DOCUMENT ID	TECN	COMMENT
<b><math>0.09 \pm 0.09</math></b> OUR AVERAGE			
$0.14 \pm 0.11 \pm 0.09$	<sup>1,2</sup> NAKAHAMA	10 BELL	$e^+ e^- \rightarrow \Upsilon(4S)$
$0.054 \pm 0.102 \pm 0.060$	<sup>1,3</sup> AUBERT	07AX BABR	$e^+ e^- \rightarrow \Upsilon(4S)$
$0.09 \pm 0.10 \pm 0.05$	<sup>1,3</sup> CHAO	07 BELL	Repl. by NAKAHAMA 10
$0.10 \pm 0.14 \pm 0.04$	<sup>3</sup> AUBERT	05T BABR	Repl. by AUBERT 07AX
$0.09 \pm 0.12 \pm 0.07$	<sup>1</sup> CHEN	05B BELL	Repl. by CHAO 07
$-0.10 \pm 0.19 \pm 0.10$	<sup>3</sup> AUBERT, B	04V BABR	Repl. by AUBERT 05T
$0.40 \pm 0.33 \pm 0.28$	<sup>1</sup> ABE	03c BELL	Repl. by ABE 03H
$0.17 \pm 0.16 \pm 0.04$	<sup>1,3</sup> ABE	03H BELL	Repl. by CHEN 05B

• • • We do not use the following data for averages, fits, limits, etc. • • •

<sup>1</sup> Quotes  $A_{K^+ K^- K_S^0}$  which is equal to  $-C_{K^+ K^- K_S^0}$ .

<sup>2</sup> Uses Dalitz plot analysis of  $B^0 \rightarrow K_S^0 K^+ K^-$  decays and the first of four consistent solutions that may be preferred.

<sup>3</sup> Excludes the events from  $B^0 \rightarrow \phi K_S^0$  decay. The results are derived from a combined sample of  $K^+ K^- K_S^0$  and  $K^+ K^- K_L^0$  decays.

$S_{K^+ K^- K_S^0} (B^0 \rightarrow K^+ K^- K_S^0 \text{ nonresonant})$

VALUE	DOCUMENT ID	TECN	COMMENT
<b><math>-0.74 \pm 0.12</math></b> OUR AVERAGE			
$-0.764 \pm 0.111 \pm 0.071$	<sup>1,2</sup> AUBERT	07AX BABR	$e^+ e^- \rightarrow \Upsilon(4S)$
$-0.68 \pm 0.15 \pm 0.21$	<sup>1</sup> CHAO	07 BELL	$e^+ e^- \rightarrow \Upsilon(4S)$
$-0.42 \pm 0.17 \pm 0.03$	<sup>1,3</sup> AUBERT	05T BABR	Repl. by AUBERT 07AX
$-0.49 \pm 0.18 \pm 0.04$	CHEN	05B BELL	Repl. by CHAO 07
$-0.56 \pm 0.25 \pm 0.04$	<sup>1,4</sup> AUBERT, B	04V BABR	Repl. by AUBERT 05T
$-0.49 \pm 0.43 \pm 0.11$	ABE	03c BELL	Repl. by ABE 03H
$-0.51 \pm 0.26 \pm 0.05$	<sup>1,5</sup> ABE	03H BELL	Repl. by CHEN 05B

• • • We do not use the following data for averages, fits, limits, etc. • • •

<sup>1</sup> Excludes events from  $B^0 \rightarrow \phi K_S^0$  decay. The results are derived from a combined sample of  $K^+ K^- K_S^0$  and  $K^+ K^- K_L^0$  decays.

<sup>2</sup> Reports  $\beta_{eff}$ . We quote  $S$  obtained from epaps: E-PRLTAO-99-076741.

<sup>3</sup> The measured  $CP$ -even final states fraction is  $0.89 \pm 0.08 \pm 0.06$ .

<sup>4</sup> The measured  $CP$ -even final states fraction is  $0.98 \pm 0.15 \pm 0.04$ .

<sup>5</sup> The measured  $CP$ -even final states fraction is  $1.03 \pm 0.15 \pm 0.05$ .

$C_{K^+ K^- K_S^0} (B^0 \rightarrow K^+ K^- K_S^0 \text{ inclusive})$

VALUE	DOCUMENT ID	TECN	COMMENT
<b><math>0.015 \pm 0.077 \pm 0.053</math></b>	<sup>1,2</sup> AUBERT	07AX BABR	$e^+ e^- \rightarrow \Upsilon(4S)$

<sup>1</sup> Measured using full Dalitz plot fit including  $\phi$  component.

<sup>2</sup> The results are derived from a combined sample of  $K^+ K^- K_S^0$  and  $K^+ K^- K_L^0$  decays.

$S_{K^+ K^- K_S^0} (B^0 \rightarrow K^+ K^- K_S^0 \text{ inclusive})$

VALUE	DOCUMENT ID	TECN	COMMENT
<b><math>-0.647 \pm 0.116 \pm 0.040</math></b>	<sup>1</sup> AUBERT	07AX BABR	$e^+ e^- \rightarrow \Upsilon(4S)$

<sup>1</sup> Measured using full Dalitz plot fit including  $\phi$  component.

$C_{\phi K_S^0} (B^0 \rightarrow \phi K_S^0)$

VALUE	DOCUMENT ID	TECN	COMMENT
<b><math>0.03 \pm 0.14</math></b> OUR AVERAGE			
$-0.04 \pm 0.20 \pm 0.10$	<sup>1,2</sup> NAKAHAMA	10 BELL	$e^+ e^- \rightarrow \Upsilon(4S)$
$0.08 \pm 0.18 \pm 0.04$	<sup>1,3</sup> AUBERT	07AX BABR	$e^+ e^- \rightarrow \Upsilon(4S)$

## Meson Particle Listings

 $B^0$ 

• • • We do not use the following data for averages, fits, limits, etc. • • •

$-0.07 \pm 0.15 \pm 0.05$	<sup>1,3</sup> CHEN	07	BELL	Repl. by NAKAHAMA 10
$0.00 \pm 0.23 \pm 0.05$	<sup>3</sup> AUBERT	05T	BABR	Repl. by AUBERT 07AX
$-0.08 \pm 0.22 \pm 0.09$	<sup>1,3</sup> CHEN	05B	BELL	Repl. by CHEN 07
$0.01 \pm 0.33 \pm 0.10$	<sup>3</sup> AUBERT,B	04G	BABR	Repl. by AUBERT 05T
$0.56 \pm 0.41 \pm 0.16$	<sup>1</sup> ABE	03C	BELL	Repl. by ABE 03H
$0.15 \pm 0.29 \pm 0.07$	<sup>1</sup> ABE	03H	BELL	Repl. by CHEN 05B

<sup>1</sup> Quotes  $A_{\phi K_S^0}$  which is equal to  $-C_{\phi K_S^0}$ .

<sup>2</sup> Uses Dalitz plot analysis of  $B^0 \rightarrow K_S^0 K^+ K^-$  decays and the first of four consistent solutions that may be preferred.

<sup>3</sup> Result combines  $B$ -meson final states  $\phi K_S^0$  and  $\phi K_L^0$  by assuming  $S_{\phi K_S^0} = -S_{\phi K_L^0}$

 $S_{\phi K_S^0}(B^0 \rightarrow \phi K_S^0)$ 

VALUE	DOCUMENT ID	TECN	COMMENT
<b><math>0.39 \pm 0.17</math> OUR AVERAGE</b>			
$0.21 \pm 0.26 \pm 0.11$	<sup>1,2</sup> AUBERT	07AX	BABR $e^+ e^- \rightarrow \Upsilon(4S)$
$0.50 \pm 0.21 \pm 0.06$	<sup>1</sup> CHEN	07	BELL $e^+ e^- \rightarrow \Upsilon(4S)$
• • • We do not use the following data for averages, fits, limits, etc. • • •			
$0.50 \pm 0.25 \pm 0.07$	<sup>1</sup> AUBERT	05T	BABR Repl. by AUBERT 07AX
$0.08 \pm 0.33 \pm 0.09$	<sup>1</sup> CHEN	05B	BELL Repl. by CHEN 07
$0.47 \pm 0.34 \pm 0.08$	<sup>1</sup> AUBERT,B	04G	BABR Repl. by AUBERT 05T
$-0.73 \pm 0.64 \pm 0.22$	ABE	03C	BELL Repl. by ABE 03H
$-0.96 \pm 0.50 \pm 0.09$	ABE	03H	BELL Repl. by CHEN 05B

<sup>1</sup> Result combines  $B$ -meson final states  $\phi K_S^0$  and  $\phi K_L^0$  by assuming  $S_{\phi K_S^0} = -S_{\phi K_L^0}$

<sup>2</sup> Reports  $\beta_{eff}$ . We quote  $S$  obtained from epaps: E-PRLTAO-99-076741.

 $C_{K_S K_S}(B^0 \rightarrow K_S K_S K_S)$ 

VALUE	DOCUMENT ID	TECN	COMMENT
<b><math>-0.15 \pm 0.16</math> OUR AVERAGE</b>			Error includes scale factor of 1.1.
$+0.02 \pm 0.21 \pm 0.05$	AUBERT	07AT	BABR $e^+ e^- \rightarrow \Upsilon(4S)$
$-0.31 \pm 0.20 \pm 0.07$	<sup>1</sup> CHEN	07	BELL $e^+ e^- \rightarrow \Upsilon(4S)$
• • • We do not use the following data for averages, fits, limits, etc. • • •			
$-0.34 \pm 0.28 \pm 0.05$	AUBERT,B	05	BABR Repl. by AUBERT 07AT
$-0.54 \pm 0.34 \pm 0.09$	<sup>1</sup> SUMISAWA	05	BELL Repl. by CHEN 07

<sup>1</sup> Belle Collab. quotes  $A_{K_S K_S K_S}$  which is equal to  $-C_{K_S K_S K_S}$ .

 $S_{K_S K_S}(B^0 \rightarrow K_S K_S K_S)$ 

VALUE	DOCUMENT ID	TECN	COMMENT
<b><math>-0.4 \pm 0.5</math> OUR AVERAGE</b>			Error includes scale factor of 2.5.
$-0.71 \pm 0.24 \pm 0.04$	AUBERT	07AT	BABR $e^+ e^- \rightarrow \Upsilon(4S)$
$0.30 \pm 0.32 \pm 0.08$	CHEN	07	BELL $e^+ e^- \rightarrow \Upsilon(4S)$
• • • We do not use the following data for averages, fits, limits, etc. • • •			
$-0.71 \pm 0.38 \pm 0.04$	AUBERT,B	05	BABR Repl. by AUBERT 07AT
$1.26 \pm 0.68 \pm 0.20$	SUMISAWA	05	BELL Repl. by CHEN 07.

 $C_{K_S^0 \pi^0 \gamma}(B^0 \rightarrow K_S^0 \pi^0 \gamma)$ 

VALUE	DOCUMENT ID	TECN	COMMENT
<b><math>+0.36 \pm 0.33 \pm 0.04</math></b>	<sup>1</sup> AUBERT	08BA	BABR $e^+ e^- \rightarrow \Upsilon(4S)$
• • • We do not use the following data for averages, fits, limits, etc. • • •			
$+0.20 \pm 0.20 \pm 0.06$	<sup>2,3</sup> USHIRODA	06	BELL $e^+ e^- \rightarrow \Upsilon(4S)$
$-1.0 \pm 0.5 \pm 0.2$	<sup>1</sup> AUBERT,B	05P	BABR Repl. by AUBERT 08BA
$-0.03 \pm 0.34 \pm 0.11$	<sup>3</sup> USHIRODA	05	BELL Repl. by USHIRODA 06

<sup>1</sup> Requires  $1.1 < M_{K_S^0 \pi^0} < 1.8$  GeV/c<sup>2</sup>.

<sup>2</sup> Requires  $M_{K_S^0 \pi^0} < 1.8$  GeV/c<sup>2</sup>.

<sup>3</sup> Reports  $A_{K_S^0 \pi^0 \gamma}$ , which is  $-C_{K_S^0 \pi^0 \gamma}$ .

 $S_{K_S^0 \pi^0 \gamma}(B^0 \rightarrow K_S^0 \pi^0 \gamma)$ 

VALUE	DOCUMENT ID	TECN	COMMENT
<b><math>-0.78 \pm 0.59 \pm 0.09</math></b>	<sup>1</sup> AUBERT	08BA	BABR $e^+ e^- \rightarrow \Upsilon(4S)$
• • • We do not use the following data for averages, fits, limits, etc. • • •			
$-0.10 \pm 0.31 \pm 0.07$	<sup>2</sup> USHIRODA	06	BELL $e^+ e^- \rightarrow \Upsilon(4S)$
$+0.9 \pm 1.0 \pm 0.2$	<sup>1</sup> AUBERT,B	05P	BABR Repl. by AUBERT 08BA
$-0.58 \pm 0.46 \pm 0.11$	USHIRODA	05	BELL Repl. by USHIRODA 06

<sup>1</sup> Requires  $1.1 < M_{K_S^0 \pi^0} < 1.8$  GeV/c<sup>2</sup>.

<sup>2</sup> Requires  $M_{K_S^0 \pi^0} < 1.8$  GeV/c<sup>2</sup>.

 $C_{K^*(892)^0 \gamma}(B^0 \rightarrow K^*(892)^0 \gamma)$ 

VALUE	DOCUMENT ID	TECN	COMMENT
<b><math>-0.04 \pm 0.16</math> OUR AVERAGE</b>			Error includes scale factor of 1.2.
$-0.14 \pm 0.16 \pm 0.03$	<sup>1</sup> AUBERT	08BA	BABR $e^+ e^- \rightarrow \Upsilon(4S)$
$+0.20 \pm 0.24 \pm 0.05$	<sup>1,2</sup> USHIRODA	06	BELL $e^+ e^- \rightarrow \Upsilon(4S)$
• • • We do not use the following data for averages, fits, limits, etc. • • •			
$-0.40 \pm 0.23 \pm 0.03$	AUBERT,B	05P	BABR Repl. by AUBERT 08BA
$-0.57 \pm 0.32 \pm 0.09$	<sup>3</sup> AUBERT,B	04Z	BABR Repl. by AUBERT,B 05P

<sup>1</sup> Requires  $0.8 < M_{K_S^0 \pi^0} < 1.0$  GeV/c<sup>2</sup>.

<sup>2</sup> Reports value of  $A$  which is equal to  $-C$ .

<sup>3</sup> Based on a total signal of  $105 \pm 14$  events with  $K^*(892)^0 \rightarrow K_S^0 \pi^0$  only.

 $S_{K^*(892)^0 \gamma}(B^0 \rightarrow K^*(892)^0 \gamma)$ 

VALUE	DOCUMENT ID	TECN	COMMENT
<b><math>-0.15 \pm 0.22</math> OUR AVERAGE</b>			
$-0.03 \pm 0.29 \pm 0.03$	<sup>1</sup> AUBERT	08BA	BABR $e^+ e^- \rightarrow \Upsilon(4S)$
$-0.32 \pm 0.36 \pm 0.05$	<sup>1</sup> USHIRODA	06	BELL $e^+ e^- \rightarrow \Upsilon(4S)$
• • • We do not use the following data for averages, fits, limits, etc. • • •			
$-0.21 \pm 0.40 \pm 0.05$	AUBERT,B	05P	BABR Repl. by AUBERT 08BA
$-0.79 \pm 0.63 \pm 0.10$	<sup>2</sup> USHIRODA	05	BELL Repl. by USHIRODA 06
$0.25 \pm 0.63 \pm 0.14$	<sup>3</sup> AUBERT,B	04Z	BABR Repl. by AUBERT,B 05P

<sup>1</sup> Requires  $0.8 < M_{K_S^0 \pi^0} < 1.0$  GeV/c<sup>2</sup>.

<sup>2</sup> Assumes  $C(B^0 \rightarrow K^*(892)^0 \gamma) = 0$ .

<sup>3</sup> Based on a total signal of  $105 \pm 14$  events with  $K^*(892)^0 \rightarrow K_S^0 \pi^0$  only.

 $C_{\eta K^0 \gamma}(B^0 \rightarrow \eta K^0 \gamma)$ 

VALUE	DOCUMENT ID	TECN	COMMENT
<b><math>-0.32 \pm 0.40 \pm 0.07</math></b>	<sup>1</sup> AUBERT	09	BABR $e^+ e^- \rightarrow \Upsilon(4S)$
$1 m_{\eta K} < 3.25$ GeV/c <sup>2</sup> .			

 $S_{\eta K^0 \gamma}(B^0 \rightarrow \eta K^0 \gamma)$ 

VALUE	DOCUMENT ID	TECN	COMMENT
<b><math>-0.18 \pm 0.49 \pm 0.12</math></b>	<sup>1</sup> AUBERT	09	BABR $e^+ e^- \rightarrow \Upsilon(4S)$
$1 m_{\eta K} < 3.25$ GeV/c <sup>2</sup> .			

 $C_{K^0 \phi \gamma}(B^0 \rightarrow K^0 \phi \gamma)$ 

VALUE	DOCUMENT ID	TECN	COMMENT
<b><math>-0.35 \pm 0.58 \pm 0.10</math></b>	<sup>1</sup> SAHOO	11A	BELL $e^+ e^- \rightarrow \Upsilon(4S)$
$-0.23$			
$1$ Reports value of $A$ , which is equal to $-C$ .			

 $S_{K^0 \phi \gamma}(B^0 \rightarrow K^0 \phi \gamma)$ 

VALUE	DOCUMENT ID	TECN	COMMENT
<b><math>0.74 \pm 0.72 \pm 0.10</math></b>	SAHOO	11A	BELL $e^+ e^- \rightarrow \Upsilon(4S)$
$-1.05$			

 $C(B^0 \rightarrow K_S^0 \rho^0 \gamma)$ 

VALUE	DOCUMENT ID	TECN	COMMENT
<b><math>-0.05 \pm 0.18 \pm 0.06</math></b>	<sup>1,2</sup> LI	08F	BELL $e^+ e^- \rightarrow \Upsilon(4S)$
$1$ Requires $M_{K_S^0 \pi^+ \pi^-} < 1.8$ GeV/c <sup>2</sup> and $0.6 < M_{\pi^+ \pi^-} < 0.9$ GeV/c <sup>2</sup> .			
$2$ Reports value of $A_{eff}$ which is equal to $-C$ , and includes the non-resonant $\pi^+ \pi^-$ contribution in the $\rho^0$ region.			

 $S(B^0 \rightarrow K_S^0 \rho^0 \gamma)$ 

VALUE	DOCUMENT ID	TECN	COMMENT
<b><math>+0.11 \pm 0.33 \pm 0.05</math></b>	<sup>1</sup> LI	08F	BELL $e^+ e^- \rightarrow \Upsilon(4S)$
$-0.09$			
$1$ Requires $M_{K_S^0 \pi^+ \pi^-} < 1.8$ GeV/c <sup>2</sup> .			

 $C(B^0 \rightarrow \rho^0 \gamma)$ 

VALUE	DOCUMENT ID	TECN	COMMENT
<b><math>+0.44 \pm 0.49 \pm 0.14</math></b>	<sup>1</sup> USHIRODA	08	BELL $e^+ e^- \rightarrow \Upsilon(4S)$
$1$ Reports value of $A$ which is equal to $-C$ .			

 $S(B^0 \rightarrow \rho^0 \gamma)$ 

VALUE	DOCUMENT ID	TECN	COMMENT
<b><math>-0.83 \pm 0.65 \pm 0.18</math></b>	USHIRODA	08	BELL $e^+ e^- \rightarrow \Upsilon(4S)$

 $C_{\pi \pi}(B^0 \rightarrow \pi^+ \pi^-)$ 

$C_{\pi \pi}$  is defined as  $(1-|\lambda|^2)/(1+|\lambda|^2)$ , where the quantity  $\lambda=q/p \bar{A}_f/A_f$  is a phase convention independent observable quantity for the final state  $f$ . For details, see the review on "CP Violation" in the Reviews section.

VALUE	DOCUMENT ID	TECN	COMMENT
<b><math>-0.38 \pm 0.17</math> OUR AVERAGE</b>			Error includes scale factor of 2.6.
$-0.21 \pm 0.09 \pm 0.02$	AUBERT	07AF	BABR $e^+ e^- \rightarrow \Upsilon(4S)$
$-0.55 \pm 0.08 \pm 0.05$	<sup>1</sup> ISHINO	07	BELL $e^+ e^- \rightarrow \Upsilon(4S)$

• • • We do not use the following data for averages, fits, limits, etc. • • •

Table with 5 columns: VALUE, DOCUMENT ID, TECN, COMMENT. Rows include data from ABE, AUBERT, BELL, and SHINO.

1 Paper reports A<sub>ππ</sub> which equals to -C<sub>ππ</sub>.
2 Corresponds to 90% confidence range -1.0 < C<sub>ππ</sub> < 0.47.
3 Corresponds to 90% confidence range -0.72 < C<sub>ππ</sub> < 0.12.

S<sub>ππ</sub>(B<sup>0</sup> → π<sup>+</sup>π<sup>-</sup>)
S<sub>ππ</sub> = 2Imλ/(1+|λ|<sup>2</sup>), see the note in the C<sub>ππ</sub> datablock above.

Table with 5 columns: VALUE, DOCUMENT ID, TECN, COMMENT. Rows include data from AUBERT and ISHINO.

1 Rule out the CP-conserving case, C<sub>ππ</sub> = S<sub>ππ</sub> = 0, at the 5.4 sigma level.
2 Rule out the CP-conserving case, C<sub>ππ</sub> = S<sub>ππ</sub> = 0, at the 5.2 sigma level.
3 Corresponds to 90% confidence range -0.89 < S<sub>ππ</sub> < 0.85.
4 Corresponds to 90% confidence range -0.54 < S<sub>ππ</sub> < 0.58.

C<sub>π<sup>0</sup>π<sup>0</sup></sub>(B<sup>0</sup> → π<sup>0</sup>π<sup>0</sup>)
-0.48 ± 0.30 OUR AVERAGE

Table with 5 columns: VALUE, DOCUMENT ID, TECN, COMMENT. Rows include data from AUBERT and CHAO.

• • • We do not use the following data for averages, fits, limits, etc. • • •
1 Belle Collab. quotes A<sub>π<sup>0</sup>π<sup>0</sup></sub> which is equal to -C<sub>π<sup>0</sup>π<sup>0</sup></sub>.
2 Corresponds to a 90% CL interval of -0.88 < A<sub>CP</sub> < 0.64.

C<sub>ρπ</sub>(B<sup>0</sup> → ρ<sup>+</sup>π<sup>-</sup>)
0.01 ± 0.14 OUR AVERAGE

Table with 5 columns: VALUE, DOCUMENT ID, TECN, COMMENT. Rows include data from AUBERT and KUSAKA.

• • • We do not use the following data for averages, fits, limits, etc. • • •
0.25 ± 0.17 ± 0.02 / -0.06
0.36 ± 0.18 ± 0.04

S<sub>ρπ</sub>(B<sup>0</sup> → ρ<sup>+</sup>π<sup>-</sup>)
0.01 ± 0.09 OUR AVERAGE

Table with 5 columns: VALUE, DOCUMENT ID, TECN, COMMENT. Rows include data from AUBERT and KUSAKA.

• • • We do not use the following data for averages, fits, limits, etc. • • •
-0.28 ± 0.23 ± 0.10 / -0.08
0.19 ± 0.24 ± 0.03

ΔC<sub>ρπ</sub>(B<sup>0</sup> → ρ<sup>+</sup>π<sup>-</sup>)
ΔC<sub>ρπ</sub> describes the asymmetry between the rates Γ(B<sup>0</sup> → ρ<sup>+</sup>π<sup>-</sup>) + Γ(B<sup>0</sup> → ρ<sup>-</sup>π<sup>+</sup>) and Γ(B<sup>0</sup> → ρ<sup>-</sup>π<sup>+</sup>) + Γ(B<sup>0</sup> → ρ<sup>+</sup>π<sup>-</sup>).

Table with 5 columns: VALUE, DOCUMENT ID, TECN, COMMENT. Rows include data from AUBERT and KUSAKA.

• • • We do not use the following data for averages, fits, limits, etc. • • •
0.38 ± 0.18 ± 0.02 / -0.04
0.28 ± 0.18 ± 0.04

ΔS<sub>ρπ</sub>(B<sup>0</sup> → ρ<sup>+</sup>π<sup>-</sup>)
ΔS<sub>ρπ</sub> is related to the strong phase difference between the amplitudes contributing to B<sup>0</sup> → ρ<sup>+</sup>π<sup>-</sup>.

Table with 5 columns: VALUE, DOCUMENT ID, TECN, COMMENT. Rows include data from AUBERT and KUSAKA.

• • • We do not use the following data for averages, fits, limits, etc. • • •
-0.30 ± 0.24 ± 0.09
0.15 ± 0.25 ± 0.03

C<sub>ρ<sup>0</sup>π<sup>0</sup></sub>(B<sup>0</sup> → ρ<sup>0</sup>π<sup>0</sup>)
0.3 ± 0.4 OUR AVERAGE

Table with 5 columns: VALUE, DOCUMENT ID, TECN, COMMENT. Rows include data from AUBERT and KUSAKA.

• • • We do not use the following data for averages, fits, limits, etc. • • •
0.53 ± 0.67 ± 0.10 / -0.84 - 0.15
1 Quotes A<sub>ρ<sup>0</sup>π<sup>0</sup></sub> which is equal to -C<sub>ρ<sup>0</sup>π<sup>0</sup></sub>.

S<sub>ρ<sup>0</sup>π<sup>0</sup></sub>(B<sup>0</sup> → ρ<sup>0</sup>π<sup>0</sup>)
0.1 ± 0.4 OUR AVERAGE

Table with 5 columns: VALUE, DOCUMENT ID, TECN, COMMENT. Rows include data from AUBERT and KUSAKA.

C<sub>a<sub>1</sub>π</sub>(B<sup>0</sup> → a<sub>1</sub>(1260)<sup>+</sup>π<sup>-</sup>)
-0.10 ± 0.15 ± 0.09

Table with 5 columns: VALUE, DOCUMENT ID, TECN, COMMENT. Rows include data from AUBERT.

S<sub>a<sub>1</sub>π</sub>(B<sup>0</sup> → a<sub>1</sub>(1260)<sup>+</sup>π<sup>-</sup>)
0.37 ± 0.21 ± 0.07

Table with 5 columns: VALUE, DOCUMENT ID, TECN, COMMENT. Rows include data from AUBERT.

ΔC<sub>a<sub>1</sub>π</sub>(B<sup>0</sup> → a<sub>1</sub>(1260)<sup>+</sup>π<sup>-</sup>)
ΔC<sub>a<sub>1</sub>π</sub> describes the asymmetry between the rates Γ(B<sup>0</sup> → a<sub>1</sub><sup>+</sup>π<sup>-</sup>) + Γ(B<sup>0</sup> → a<sub>1</sub><sup>-</sup>π<sup>+</sup>) and Γ(B<sup>0</sup> → a<sub>1</sub><sup>-</sup>π<sup>+</sup>) + Γ(B<sup>0</sup> → a<sub>1</sub><sup>+</sup>π<sup>-</sup>).

Table with 5 columns: VALUE, DOCUMENT ID, TECN, COMMENT. Rows include data from AUBERT.

ΔS<sub>a<sub>1</sub>π</sub>(B<sup>0</sup> → a<sub>1</sub>(1260)<sup>+</sup>π<sup>-</sup>)
ΔS<sub>a<sub>1</sub>π</sub> is related to the strong phase difference between the amplitudes contributing to B<sup>0</sup> → a<sub>1</sub>π decays.

Table with 5 columns: VALUE, DOCUMENT ID, TECN, COMMENT. Rows include data from AUBERT.

C(B<sup>0</sup> → b<sub>1</sub><sup>-</sup>K<sup>+</sup>)
-0.22 ± 0.23 ± 0.05

Table with 5 columns: VALUE, DOCUMENT ID, TECN, COMMENT. Rows include data from AUBERT.

ΔC(B<sup>0</sup> → b<sub>1</sub><sup>-</sup>π<sup>+</sup>)
-1.04 ± 0.23 ± 0.08

Table with 5 columns: VALUE, DOCUMENT ID, TECN, COMMENT. Rows include data from AUBERT.

C<sub>ρ<sup>0</sup>ρ<sup>0</sup></sub>(B<sup>0</sup> → ρ<sup>0</sup>ρ<sup>0</sup>)
0.2 ± 0.8 ± 0.3

Table with 5 columns: VALUE, DOCUMENT ID, TECN, COMMENT. Rows include data from AUBERT.

S<sub>ρ<sup>0</sup>ρ<sup>0</sup></sub>(B<sup>0</sup> → ρ<sup>0</sup>ρ<sup>0</sup>)
0.3 ± 0.7 ± 0.2

Table with 5 columns: VALUE, DOCUMENT ID, TECN, COMMENT. Rows include data from AUBERT.

C<sub>ρρ</sub>(B<sup>0</sup> → ρ<sup>+</sup>ρ<sup>-</sup>)
-0.05 ± 0.13 OUR AVERAGE

Table with 5 columns: VALUE, DOCUMENT ID, TECN, COMMENT. Rows include data from AUBERT and SOMOV.

• • • We do not use the following data for averages, fits, limits, etc. • • •
-0.00 ± 0.30 ± 0.09
-0.03 ± 0.18 ± 0.09
-0.17 ± 0.27 ± 0.14
1 BELLE Collab. quotes A<sub>CP</sub> which is equal to -C.

S<sub>ρρ</sub>(B<sup>0</sup> → ρ<sup>+</sup>ρ<sup>-</sup>)
-0.06 ± 0.17 OUR AVERAGE

Table with 5 columns: VALUE, DOCUMENT ID, TECN, COMMENT. Rows include data from AUBERT and SOMOV.





• • • We do not use the following data for averages, fits, limits, etc. • • •

$0.714 \pm 0.032 \pm 0.018$	<sup>2</sup> AUBERT	07AY	BABR	Repl. by AUBERT 09K
$0.728 \pm 0.056 \pm 0.023$	<sup>8</sup> ABE	05B	BELL	Repl. by CHEN 07
$0.722 \pm 0.040 \pm 0.023$	<sup>9</sup> AUBERT	05F	BABR	Repl. by AUBERT 07AY
$0.99 \pm 0.14 \pm 0.06$	<sup>10</sup> ABE	02U	BELL	$e^+e^- \rightarrow \Upsilon(4S)$
$0.719 \pm 0.074 \pm 0.035$	<sup>11</sup> ABE	02Z	BELL	Repl. by ABE 05B
$0.59 \pm 0.14 \pm 0.05$	<sup>12</sup> AUBERT	02N	BABR	$e^+e^- \rightarrow \Upsilon(4S)$
$0.741 \pm 0.067 \pm 0.034$	<sup>13</sup> AUBERT	02P	BABR	Repl. by AUBERT 05F
$0.58 \pm 0.32 \pm 0.09$ $-0.34 \pm 0.10$	ABASHIAN	01	BELL	Repl. by ABE 01G
$0.99 \pm 0.14 \pm 0.06$	<sup>14</sup> ABE	01G	BELL	Repl. by ABE 02Z
$0.34 \pm 0.20 \pm 0.05$	AUBERT	01	BABR	Repl. by AUBERT 01B
$0.59 \pm 0.14 \pm 0.05$	<sup>14</sup> AUBERT	01B	BABR	Repl. by AUBERT 02P
$1.8 \pm 1.1 \pm 0.3$	<sup>15</sup> ABE	98U	CDF	Repl. by AFFOLDER 00C

<sup>1</sup> Uses Dalitz plot analysis of  $B^0 \rightarrow K^0 \pi^+ \pi^-$  decays and the first of two equivalent solutions.

<sup>2</sup> Measurement based on  $B^0 \rightarrow c\bar{c}K^{(*)0}$  decays.

<sup>3</sup> Based on  $B^0 \rightarrow \psi(2S) K_S^0$  decays.

<sup>4</sup> Measurement in which the  $J/\psi$  decays to hadrons or to muons that do not satisfy the standard identification criteria.

<sup>5</sup> AFFOLDER 00C uses about 400  $B^0 \rightarrow J/\psi(1S) K_S^0$  events. The production flavor of  $B^0$  was determined using three tagging algorithms: a same-side tag, a jet-charge tag, and a soft-lepton tag.

<sup>6</sup> BARATE 00Q uses 23 candidates for  $B^0 \rightarrow J/\psi(1S) K_S^0$  decays. A combination of jet-charge, vertex-charge, and same-side tagging techniques were used to determine the  $B^0$  production flavor.

<sup>7</sup> ACKERSTAFF 98Z uses 24 candidates for  $B_d^0 \rightarrow J/\psi(1S) K_S^0$  decay. A combination of jet-charge and vertex-charge techniques were used to tag the  $B_d^0$  production flavor.

<sup>8</sup> Measurement based on  $152 \times 10^6 B\bar{B}$  pairs.

<sup>9</sup> Measurement based on  $227 \times 10^6 B\bar{B}$  pairs.

<sup>10</sup> ABE 02U result is based on the same analysis and data sample reported in ABE 01G.

<sup>11</sup> ABE 02Z result is based on  $85 \times 10^6 B\bar{B}$  pairs.

<sup>12</sup> AUBERT 02N result based on the same analysis and data sample reported in AUBERT 01B.

<sup>13</sup> AUBERT 02P result is based on  $88 \times 10^6 B\bar{B}$  pairs.

<sup>14</sup> First observation of CP violation in  $B^0$  meson system.

<sup>15</sup> ABE 98U uses  $198 \pm 17 B_d^0 \rightarrow J/\psi(1S) K_S^0$  events. The production flavor of  $B^0$  was determined using the same side tagging technique.

### $C_{J/\psi(nS)K^0}(B^0 \rightarrow J/\psi(nS)K^0)$

"OUR EVALUATION" is an average using rescaled values of the data listed below.

The average and rescaling were performed by the Heavy Flavor Averaging Group (HFAG) and are described at <http://www.slac.stanford.edu/xorg/hfag/>. The averaging/rescaling procedure takes into account correlations between the measurements.

VALUE (units  $10^{-2}$ )

**$0.5 \pm 2.0$  OUR EVALUATION**  
 **$0.0 \pm 1.8$  OUR AVERAGE**

$+8.9 \pm 7.6 \pm 2.0$	<sup>1</sup> AUBERT	09K	BABR	$e^+e^- \rightarrow \Upsilon(4S)$
$+1.6 \pm 2.3 \pm 1.8$	AUBERT	09K	BABR	$e^+e^- \rightarrow \Upsilon(4S)$
$-4 \pm 7 \pm 5$	<sup>1,2</sup> SAHOO	08	BELL	$e^+e^- \rightarrow \Upsilon(4S)$
$-1.8 \pm 2.1 \pm 1.4$	<sup>2</sup> CHEN	07	BELL	$e^+e^- \rightarrow \Upsilon(4S)$

<sup>1</sup> Based on  $B^0 \rightarrow \psi(2S) K_S^0$  decays.

<sup>2</sup> The paper reports A, which is equal to  $-C$ .

### $S_{J/\psi(nS)K^0}(B^0 \rightarrow J/\psi(nS)K^0)$

"OUR EVALUATION" is an average using rescaled values of the data listed below.

The average and rescaling were performed by the Heavy Flavor Averaging Group (HFAG) and are described at <http://www.slac.stanford.edu/xorg/hfag/>. The averaging/rescaling procedure takes into account correlations between the measurements.

VALUE

**$0.676 \pm 0.021$  OUR EVALUATION**  
 **$0.67 \pm 0.04$  OUR AVERAGE**

Error includes scale factor of 1.6. See the ideogram below.

$0.897 \pm 0.100 \pm 0.036$	<sup>1</sup> AUBERT	09K	BABR	$e^+e^- \rightarrow \Upsilon(4S)$
$0.666 \pm 0.031 \pm 0.013$	AUBERT	09K	BABR	$e^+e^- \rightarrow \Upsilon(4S)$
$0.650 \pm 0.029 \pm 0.018$	<sup>2</sup> SAHOO	08	BELL	$e^+e^- \rightarrow \Upsilon(4S)$
$0.79 \pm 0.41 \pm 0.44$	<sup>3</sup> AFFOLDER	00C	CDF	$p\bar{p}$ at 1.8 TeV
$0.84 \pm 0.82 \pm 0.16$ $-1.04$	<sup>4</sup> BARATE	00Q	ALEP	$e^+e^- \rightarrow Z$
$3.2 \pm 1.8 \pm 2.0$	<sup>5</sup> ACKERSTAFF	98Z	OPAL	$e^+e^- \rightarrow Z$

• • • We do not use the following data for averages, fits, limits, etc. • • •

$0.72 \pm 0.09 \pm 0.03$	<sup>1</sup> SAHOO	08	BELL	$e^+e^- \rightarrow \Upsilon(4S)$
$0.642 \pm 0.031 \pm 0.017$	CHEN	07	BELL	$e^+e^- \rightarrow \Upsilon(4S)$

<sup>1</sup> Based on  $B^0 \rightarrow \psi(2S) K_S^0$  decays.

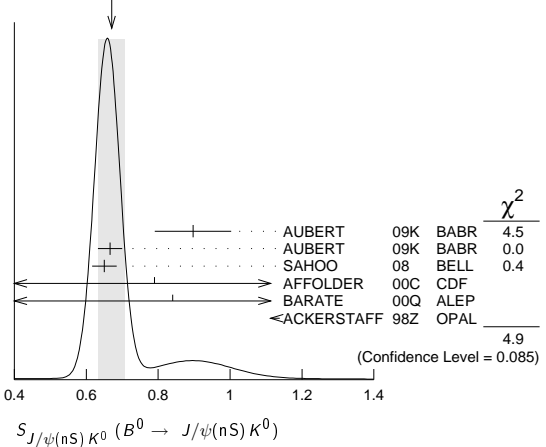
<sup>2</sup> Combined result of CHEN 07 and SAHOO 08.

<sup>3</sup> AFFOLDER 00C uses about 400  $B^0 \rightarrow J/\psi(1S) K_S^0$  events. The production flavor of  $B^0$  was determined using three tagging algorithms: a same-side tag, a jet-charge tag, and a soft-lepton tag.

<sup>4</sup> BARATE 00Q uses 23 candidates for  $B^0 \rightarrow J/\psi(1S) K_S^0$  decays. A combination of jet-charge, vertex-charge, and same-side tagging techniques were used to determine the  $B^0$  production flavor.

<sup>5</sup> ACKERSTAFF 98Z uses 24 candidates for  $B_d^0 \rightarrow J/\psi(1S) K_S^0$  decay. A combination of jet-charge and vertex-charge techniques were used to tag the  $B_d^0$  production flavor.

WEIGHTED AVERAGE  
 $0.67 \pm 0.04$  (Error scaled by 1.6)



### $C_{J/\psi K^*0}(B^0 \rightarrow J/\psi K^*0)$

VALUE	DOCUMENT ID	TECN	COMMENT
<b><math>0.025 \pm 0.083 \pm 0.054</math></b>	<sup>1</sup> AUBERT	09K	BABR $e^+e^- \rightarrow \Upsilon(4S)$

<sup>1</sup> Based on  $B^0 \rightarrow J/\psi K^*0, K^*0 \rightarrow K_S^0 \pi^0$ .

### $S_{J/\psi K^*0}(B^0 \rightarrow J/\psi K^*0)$

VALUE	DOCUMENT ID	TECN	COMMENT
<b><math>0.601 \pm 0.239 \pm 0.087</math></b>	<sup>1,2</sup> AUBERT	09K	BABR $e^+e^- \rightarrow \Upsilon(4S)$

<sup>1</sup> Based on  $B^0 \rightarrow J/\psi K^*0, K^*0 \rightarrow K_S^0 \pi^0$ .

<sup>2</sup> This  $S_{J/\psi K^*0}$  value has been corrected for the dilution of the  $\sin(\Delta M \Delta t)$  coefficient of the CP asymmetry by a factor of  $1 - R_{\perp}$ , which arises from the mixture of CP-even and CP-odd B decay amplitudes.

### $C_{\chi_{c0} K_S^0}(B^0 \rightarrow \chi_{c0} K_S^0)$

VALUE	DOCUMENT ID	TECN	COMMENT
<b><math>-0.29 \pm 0.53 \pm 0.06</math></b>	<sup>1</sup> AUBERT	09AU	BABR $e^+e^- \rightarrow \Upsilon(4S)$

<sup>1</sup> Uses Dalitz plot analysis of  $B^0 \rightarrow K^0 \pi^+ \pi^-$  decays and the first of two equivalent solutions is used.

### $S_{\chi_{c0} K_S^0}(B^0 \rightarrow \chi_{c0} K_S^0)$

VALUE	DOCUMENT ID	TECN	COMMENT
<b><math>-0.69 \pm 0.52 \pm 0.08</math></b>	<sup>1</sup> AUBERT	09AU	BABR $e^+e^- \rightarrow \Upsilon(4S)$

<sup>1</sup> Uses Dalitz plot analysis of  $B^0 \rightarrow K^0 \pi^+ \pi^-$  decays and the first of two equivalent solutions is used.

### $C_{\chi_{c1} K_S^0}(B^0 \rightarrow \chi_{c1} K_S^0)$

VALUE	DOCUMENT ID	TECN	COMMENT
<b><math>0.129 \pm 0.109 \pm 0.025</math></b>	AUBERT	09K	BABR $e^+e^- \rightarrow \Upsilon(4S)$

### $S_{\chi_{c1} K_S^0}(B^0 \rightarrow \chi_{c1} K_S^0)$

VALUE	DOCUMENT ID	TECN	COMMENT
<b><math>0.614 \pm 0.160 \pm 0.040</math></b>	AUBERT	09K	BABR $e^+e^- \rightarrow \Upsilon(4S)$

### $\sin(2\beta_{\text{eff}})(B^0 \rightarrow \phi K^0)$

VALUE	DOCUMENT ID	TECN	COMMENT
<b><math>0.22 \pm 0.27 \pm 0.12</math></b>	AUBERT	07AX	BABR $e^+e^- \rightarrow \Upsilon(4S)$

• • • We do not use the following data for averages, fits, limits, etc. • • •

$0.50 \pm 0.25 \pm 0.07$ $-0.04$	<sup>1</sup> AUBERT	05T	BABR Repl. by AUBERT 07AX
-------------------------------------	---------------------	-----	---------------------------

<sup>1</sup> Obtained by constraining  $C = 0$ .

### $\sin(2\beta_{\text{eff}})(B^0 \rightarrow \phi K_0^*(1430)^0)$

VALUE	DOCUMENT ID	TECN	COMMENT
<b><math>0.97 \pm 0.03</math></b> <b><math>-0.52</math></b>	<sup>1</sup> AUBERT	08BG	BABR $e^+e^- \rightarrow \Upsilon(4S)$

<sup>1</sup> Measured using the CP-violation phase difference  $\Delta\phi_{00}$  between the B and  $\bar{B}$  decay amplitude.

### $\sin(2\beta_{\text{eff}})(B^0 \rightarrow K^+ K^- K_S^0)$

VALUE	DOCUMENT ID	TECN	COMMENT
<b><math>0.77 \pm 0.11 \pm 0.07</math></b> <b><math>-0.04</math></b>	AUBERT	07AX	BABR $e^+e^- \rightarrow \Upsilon(4S)$

• • • We do not use the following data for averages, fits, limits, etc. • • •

$0.55 \pm 0.22 \pm 0.12$	<sup>1</sup> AUBERT	05T	BABR Repl. by AUBERT 07AX
--------------------------	---------------------	-----	---------------------------

<sup>1</sup> Obtained by constraining  $C = 0$ .

## Meson Particle Listings

 $B^0$  $\sin(2\beta_{\text{eff}})(B^0 \rightarrow [K_S^0 \pi^+ \pi^-]_{D^*(*)} h^0)$ 

VALUE	DOCUMENT ID	TECN	COMMENT
<b>0.45 ± 0.28 OUR AVERAGE</b>			
0.29 ± 0.34 ± 0.06	AUBERT	07BH BABR	$e^+ e^- \rightarrow \Upsilon(4S)$
0.78 ± 0.44 ± 0.22	KROKOVNY	06 BELL	$e^+ e^- \rightarrow \Upsilon(4S)$

 $|\lambda|(B^0 \rightarrow [K_S^0 \pi^+ \pi^-]_{D^*(*)} h^0)$ 

VALUE	DOCUMENT ID	TECN	COMMENT
<b>1.01 ± 0.08 ± 0.02</b>	AUBERT	07BH BABR	$e^+ e^- \rightarrow \Upsilon(4S)$

 $|\sin(2\beta + \gamma)|$ 

$\beta$  ( $\phi_1$ ) and  $\gamma$  ( $\phi_3$ ) are angles of CKM unitarity triangle, see the review on "CP Violation" in the Reviews section.

VALUE	CL%	DOCUMENT ID	TECN	COMMENT
<b>&gt;0.40</b>	90	1 AUBERT	06Y BABR	$e^+ e^- \rightarrow \Upsilon(4S)$
• • • We do not use the following data for averages, fits, limits, etc. • • •				
>0.13	95	2 RONGA	06 BELL	$e^+ e^- \rightarrow \Upsilon(4S)$
>0.07	95	2 RONGA	06 BELL	$e^+ e^- \rightarrow \Upsilon(4S)$
>0.35	90	3 AUBERT	05Z BABR	$e^+ e^- \rightarrow \Upsilon(4S)$
>0.69	68	4 AUBERT	04W BABR	$e^+ e^- \rightarrow \Upsilon(4S)$
>0.58	95	5 AUBERT	04W BABR	Repl. by AUBERT 05Z

- 1 Uses fully reconstructed  $B^0 \rightarrow D^{(*)\pm} \pi^\mp$  and  $D^\pm \rho^\mp$  decays and some theoretical assumptions.
- 2 Combines the results from fully reconstructed and partially reconstructed  $D^{(*)}\pi$  events by taking weighted averages. Assumes that systematic errors from physics parameters and fit biases in the two measurements are 100% correlated.
- 3 Uses partially reconstructed  $B^0 \rightarrow D^{*\pm} \pi^\mp$  decays and some theoretical assumptions.
- 4 Uses fully reconstructed  $B^0 \rightarrow D^{(*)\pm} \pi^\mp$  decays and some theoretical assumptions, such as the SU(3) symmetry relation.
- 5 Combining this measurement with the results from AUBERT 04W for fully reconstructed  $B^0 \rightarrow D^{(*)\pm} \pi^\mp$  and some theoretical assumptions, such as the SU(3) symmetry relation.

 $2\beta + \gamma$ 

VALUE (°)	DOCUMENT ID	TECN	COMMENT
<b>83 ± 53 ± 20</b>	1 AUBERT	08AC BABR	$e^+ e^- \rightarrow \Upsilon(4S)$

- 1 Used a time-dependent Dalitz-plot analysis of  $B^0 \rightarrow D^\mp K^0 \pi^\pm$  assuming the ratio of the  $b \rightarrow u$  and  $b \rightarrow c$  decay amplitudes to be 0.3.

 $\gamma(B^0 \rightarrow D^0 K^{*0})$ 

VALUE (°)	DOCUMENT ID	TECN	COMMENT
<b>162 ± 56</b>	1 AUBERT	09R BABR	$e^+ e^- \rightarrow \Upsilon(4S)$

- 1 Uses Dalitz plot analysis of  $D^0 \rightarrow K_S^0 \pi^+ \pi^-$  decays coming from  $B^0 \rightarrow D^0 K^{*0}$  modes. The corresponding 95% CL interval is  $77^\circ < \gamma < 247^\circ$ . A 180 degree ambiguity is implied.

 $\alpha$ 

For angle  $\alpha$  ( $\phi_2$ ) of the CKM unitarity triangle, see the review on "CP violation" in the reviews section.

VALUE (°)	DOCUMENT ID	TECN	COMMENT
<b>90 ± 5 OUR AVERAGE</b>			
79 ± 7 ± 11	1 AUBERT	10D BABR	$e^+ e^- \rightarrow \Upsilon(4S)$
92.4 + 6.0 - 6.5	2 AUBERT	09G BABR	$e^+ e^- \rightarrow \Upsilon(4S)$
88 ± 17	3 SOMOV	06 BELL	$e^+ e^- \rightarrow \Upsilon(4S)$
• • • We do not use the following data for averages, fits, limits, etc. • • •			
78.6 ± 7.3	4 AUBERT	07O BABR	$e^+ e^- \rightarrow \Upsilon(4S)$
100 ± 13	5 AUBERT,B	05C BABR	Repl. by AUBERT 09G
102 + 16 - 12 ± 14	6 AUBERT,B	04R BABR	Repl. by AUBERT,B 05C

- 1 Obtained using the time dependent analysis of  $B^0 \rightarrow a_1(1260)^\pm \pi^\mp$  and branching fraction measurements of  $B \rightarrow a_1(1260) K$  and  $B \rightarrow K_1 \pi$ .
- 2 Based on the favored  $B \rightarrow \rho\rho$  isospin method.
- 3 Obtained using isospin relation and selecting a solution closest to the CKM best fit average; the 90% CL allowed interval is  $59^\circ < \phi_2 (= \alpha) < 115^\circ$ .
- 4 The angle  $\alpha_{\text{eff}}$  is obtained using the measured CP parameters of  $B^0 \rightarrow a_1(1260)^\pm \pi^\mp$  and choosing one of the four solutions that is compatible with the result of SM-based fits.
- 5 Obtained using isospin relation and selecting a solution closest to the CKM best fit average; 90% CL allowed interval is  $79^\circ < \alpha < 123^\circ$ .
- 6 Obtained from the measured CP parameters of the longitudinal polarization by selecting the solution closest to the CKM best fit central value of  $\alpha = 95^\circ - 98^\circ$ .

 $B^0 \rightarrow D^{*-} \ell^+ \nu_\ell$  FORM FACTORS

VALUE	DOCUMENT ID	TECN	COMMENT
<b>1.41 ± 0.04 OUR AVERAGE</b>			
1.401 ± 0.034 ± 0.018	1 DUNGEL	10 BELL	$e^+ e^- \rightarrow \Upsilon(4S)$
1.56 ± 0.07 ± 0.15	AUBERT	09A BABR	$e^+ e^- \rightarrow \Upsilon(4S)$
1.18 ± 0.30 ± 0.12	DUBOSCQ	96 CLE2	$e^+ e^- \rightarrow \Upsilon(4S)$
• • • We do not use the following data for averages, fits, limits, etc. • • •			
1.429 ± 0.061 ± 0.044	AUBERT	08R BABR	Repl. by AUBERT 09A
1.396 ± 0.060 ± 0.044	AUBERT,B	06Z BABR	Repl. by AUBERT 08R

- 1 Uses fully reconstructed  $D^{*-} \ell^+ \nu$  events ( $\ell = e$  or  $\mu$ ).

 $R_2$  (form factor ratio  $\sim A_2/A_1$ )

VALUE	DOCUMENT ID	TECN	COMMENT
<b>0.85 ± 0.05 OUR AVERAGE</b>			Error includes scale factor of 1.9.
0.864 ± 0.024 ± 0.008	1 DUNGEL	10 BELL	$e^+ e^- \rightarrow \Upsilon(4S)$
0.66 ± 0.05 ± 0.09	AUBERT	09A BABR	$e^+ e^- \rightarrow \Upsilon(4S)$
0.71 ± 0.22 ± 0.07	DUBOSCQ	96 CLE2	$e^+ e^- \rightarrow \Upsilon(4S)$
• • • We do not use the following data for averages, fits, limits, etc. • • •			
0.827 ± 0.038 ± 0.022	AUBERT	08R BABR	Repl. by AUBERT 09A
0.885 ± 0.040 ± 0.026	AUBERT,B	06Z BABR	Repl. by AUBERT 08R

- 1 Uses fully reconstructed  $D^{*-} \ell^+ \nu$  events ( $\ell = e$  or  $\mu$ ).

 $\rho_{A_1}^2$  (form factor slope)

VALUE	DOCUMENT ID	TECN	COMMENT
<b>1.204 ± 0.031 OUR AVERAGE</b>			
1.214 ± 0.034 ± 0.009	1 DUNGEL	10 BELL	$e^+ e^- \rightarrow \Upsilon(4S)$
1.22 ± 0.02 ± 0.07	AUBERT	09A BABR	$e^+ e^- \rightarrow \Upsilon(4S)$
0.91 ± 0.15 ± 0.06	DUBOSCQ	96 CLE2	$e^+ e^- \rightarrow \Upsilon(4S)$
• • • We do not use the following data for averages, fits, limits, etc. • • •			
1.191 ± 0.048 ± 0.028	AUBERT	08R BABR	Repl. by AUBERT 09A
1.145 ± 0.059 ± 0.046	AUBERT,B	06Z BABR	Repl. by AUBERT 08R

- 1 Uses fully reconstructed  $D^{*-} \ell^+ \nu$  events ( $\ell = e$  or  $\mu$ ).

PARTIAL BRANCHING FRACTIONS IN  $B^0 \rightarrow K^{(*)0} \ell^+ \ell^-$ 

VALUE (units $10^{-7}$ )	DOCUMENT ID	TECN	COMMENT
<b>1.80 ± 0.36 ± 0.11</b>	AALTONEN	11AI CDF	$p\bar{p}$ at 1.96 TeV

VALUE (units $10^{-7}$ )	DOCUMENT ID	TECN	COMMENT
<b>0.84 ± 0.28 ± 0.06</b>	AALTONEN	11AI CDF	$p\bar{p}$ at 1.96 TeV

VALUE (units $10^{-7}$ )	DOCUMENT ID	TECN	COMMENT
<b>1.73 ± 0.43 ± 0.15</b>	AALTONEN	11AI CDF	$p\bar{p}$ at 1.96 TeV

VALUE (units $10^{-7}$ )	DOCUMENT ID	TECN	COMMENT
<b>1.77 ± 0.36 ± 0.12</b>	AALTONEN	11AI CDF	$p\bar{p}$ at 1.96 TeV

VALUE (units $10^{-7}$ )	DOCUMENT ID	TECN	COMMENT
<b>1.34 ± 0.26 ± 0.08</b>	AALTONEN	11AI CDF	$p\bar{p}$ at 1.96 TeV

VALUE (units $10^{-7}$ )	DOCUMENT ID	TECN	COMMENT
<b>0.97 ± 0.26 ± 0.07</b>	AALTONEN	11AI CDF	$p\bar{p}$ at 1.96 TeV

VALUE (units $10^{-7}$ )	DOCUMENT ID	TECN	COMMENT
<b>1.42 ± 0.41 ± 0.12</b>	AALTONEN	11AI CDF	$p\bar{p}$ at 1.96 TeV

VALUE (units $10^{-7}$ )	DOCUMENT ID	TECN	COMMENT
<b>2.60 ± 0.45 ± 0.17</b>	AALTONEN	11AI CDF	$p\bar{p}$ at 1.96 TeV

VALUE (units $10^{-7}$ )	DOCUMENT ID	TECN	COMMENT
<b>0.31 ± 0.37 ± 0.02</b>	AALTONEN	11AI CDF	$p\bar{p}$ at 1.96 TeV

VALUE (units $10^{-7}$ )	DOCUMENT ID	TECN	COMMENT
<b>0.93 ± 0.49 ± 0.07</b>	AALTONEN	11AI CDF	$p\bar{p}$ at 1.96 TeV

VALUE (units $10^{-7}$ )	DOCUMENT ID	TECN	COMMENT
<b>0.66 ± 0.51 ± 0.05</b>	AALTONEN	11AI CDF	$p\bar{p}$ at 1.96 TeV

VALUE (units $10^{-7}$ )	DOCUMENT ID	TECN	COMMENT
<b>-0.03 ± 0.22 ± 0.01</b>	AALTONEN	11AI CDF	$p\bar{p}$ at 1.96 TeV

VALUE (units $10^{-7}$ )	DOCUMENT ID	TECN	COMMENT
<b>0.73 ± 0.26 ± 0.06</b>	AALTONEN	11AI CDF	$p\bar{p}$ at 1.96 TeV

VALUE (units $10^{-7}$ )	DOCUMENT ID	TECN	COMMENT
<b>0.21 ± 0.18 ± 0.16</b>	AALTONEN	11AI CDF	$p\bar{p}$ at 1.96 TeV

See key on page 457

Meson Particle Listings

B<sup>0</sup>

B(B<sup>0</sup> → K<sup>0</sup>ℓ<sup>+</sup>ℓ<sup>-</sup>) (1.0 < q<sup>2</sup> < 6.0 GeV<sup>2</sup>/c<sup>2</sup>)

Table with columns: VALUE (units 10<sup>-7</sup>), DOCUMENT ID, TECN, COMMENT. Row: 0.98±0.61±0.08, AALTONEN 11A1 CDF, pP at 1.96 TeV

B(B<sup>0</sup> → K<sup>0</sup>ℓ<sup>+</sup>ℓ<sup>-</sup>) (0.0 < q<sup>2</sup> < 4.3 GeV<sup>2</sup>/c<sup>2</sup>)

Table with columns: VALUE (units 10<sup>-7</sup>), DOCUMENT ID, TECN, COMMENT. Row: 1.27±0.62±0.10, AALTONEN 11A1 CDF, pP at 1.96 TeV

B<sup>0</sup> REFERENCES

Main reference table for B<sup>0</sup>. Columns: Author, Year, Ref ID, Journal, Comment. Includes entries like AAJ, AAIJ, CHATRCHYAN, HIGUCHI, HOI, etc.

Continuation of B<sup>0</sup> references. Columns: Author, Year, Ref ID, Journal, Comment. Includes entries like AUBERT, CHIANG, CHOI, GOLDENZWEIG, etc.



See key on page 457

Meson Particle Listings
B0, B±/B0 ADMIXTURE

Table listing meson particles with columns for particle name, quantum numbers, production methods, and references. Includes a section for B±/B0 ADMIXTURE and B DECAY MODES.

# Meson Particle Listings

## $B^\pm/B^0$ ADMIXTURE

Mode	Fraction ( $\Gamma_i/\Gamma$ )	Scale factor/ Confidence level
<b>Semileptonic and leptonic modes</b>		
$\Gamma_1$ $e^+ \nu_e$ anything	[a] ( 10.72 ± 0.13 ) %	
$\Gamma_2$ $\bar{p} e^+ \nu_e$ anything	< 5.9	$\times 10^{-4}$ CL=90%
$\Gamma_3$ $\mu^+ \nu_\mu$ anything	[a] ( 10.72 ± 0.13 ) %	
$\Gamma_4$ $\ell^+ \nu_\ell$ anything	[a,b] ( 10.72 ± 0.13 ) %	
$\Gamma_5$ $D^- \ell^+ \nu_\ell$ anything	[b] ( 2.8 ± 0.9 ) %	
$\Gamma_6$ $\bar{D}^0 \ell^+ \nu_\ell$ anything	[b] ( 7.2 ± 1.4 ) %	
$\Gamma_7$ $\bar{D} \ell \nu_\ell$	( 2.39 ± 0.12 ) %	
$\Gamma_8$ $D \tau^+ \nu_\tau$	( 8.6 ± 2.7 ) $\times 10^{-3}$	
$\Gamma_9$ $D^{*-} \ell^+ \nu_\ell$ anything	[c] ( 6.7 ± 1.3 ) $\times 10^{-3}$	
$\Gamma_{10}$ $D^{*0} \ell^+ \nu_\ell$ anything	( 1.62 ± 0.33 ) %	
$\Gamma_{11}$ $D^{*+} \nu_\tau$	( 2.7 ± 0.7 ) %	
$\Gamma_{12}$ $\bar{D}^{*+} \ell^+ \nu_\ell$	[b,d] ( 2.7 ± 0.7 ) %	
$\Gamma_{13}$ $\bar{D}_1(2420) \ell^+ \nu_\ell$ anything	( 3.8 ± 1.3 ) $\times 10^{-3}$	S=2.4
$\Gamma_{14}$ $D \pi \ell^+ \nu_\ell$ anything + $D^* \pi \ell^+ \nu_\ell$ anything	( 2.6 ± 0.5 ) %	S=1.5
$\Gamma_{15}$ $D \pi \ell^+ \nu_\ell$ anything	( 1.5 ± 0.6 ) %	
$\Gamma_{16}$ $D^* \pi \ell^+ \nu_\ell$ anything	( 1.9 ± 0.4 ) %	
$\Gamma_{17}$ $\bar{D}_2^*(2460) \ell^+ \nu_\ell$ anything	( 4.4 ± 1.6 ) $\times 10^{-3}$	
$\Gamma_{18}$ $D^{*-} \pi^+ \ell^+ \nu_\ell$ anything	( 1.00 ± 0.34 ) %	
$\Gamma_{19}$ $D_s^- \ell^+ \nu_\ell$ anything	[b] < 7	$\times 10^{-3}$ CL=90%
$\Gamma_{20}$ $D_s^- \ell^+ \nu_\ell K^+$ anything	[b] < 5	$\times 10^{-3}$ CL=90%
$\Gamma_{21}$ $D_s^- \ell^+ \nu_\ell K^0$ anything	[b] < 7	$\times 10^{-3}$ CL=90%
$\Gamma_{22}$ $\ell^+ \nu_\ell$ charm	( 10.51 ± 0.13 ) %	
$\Gamma_{23}$ $X_u \ell^+ \nu_\ell$	( 2.08 ± 0.30 ) $\times 10^{-3}$	
$\Gamma_{24}$ $K^+ \ell^+ \nu_\ell$ anything	[b] ( 6.2 ± 0.5 ) %	
$\Gamma_{25}$ $K^- \ell^+ \nu_\ell$ anything	[b] ( 10 ± 4 ) $\times 10^{-3}$	
$\Gamma_{26}$ $K^0/\bar{K}^0 \ell^+ \nu_\ell$ anything	[b] ( 4.5 ± 0.5 ) %	
<b>D, D*, or D<sub>s</sub> modes</b>		
$\Gamma_{27}$ $D^\pm$ anything	( 23.7 ± 1.3 ) %	
$\Gamma_{28}$ $D^0/\bar{D}^0$ anything	( 62.7 ± 2.9 ) %	S=1.3
$\Gamma_{29}$ $D^{*0}(2010)^\pm$ anything	( 22.5 ± 1.5 ) %	
$\Gamma_{30}$ $D^*(2007)^0$ anything	( 26.0 ± 2.7 ) %	
$\Gamma_{31}$ $D_s^\pm$ anything	[e] ( 8.3 ± 0.8 ) %	
$\Gamma_{32}$ $D_s^{*\pm}$ anything	( 6.3 ± 1.0 ) %	
$\Gamma_{33}$ $D_s^{*\pm} \bar{D}^{(*)}$	( 3.4 ± 0.6 ) %	
$\Gamma_{34}$ $\bar{D} D_{s0}(2317)$		
$\Gamma_{35}$ $\bar{D} D_{sJ}(2457)$		
$\Gamma_{36}$ $D^{(*)} \bar{D}^{(*)} K^0 + D^{(*)} \bar{D}^{(*)} K^\pm$	[e,f] ( 7.1 + 2.7 / - 1.7 ) %	
$\Gamma_{37}$ $b \rightarrow c \bar{s}$	( 22 ± 4 ) %	
$\Gamma_{38}$ $D_s^{(*)} \bar{D}^{(*)}$	[e,f] ( 3.9 ± 0.4 ) %	
$\Gamma_{39}$ $D^* D^*(2010)^\pm$	[e] < 5.9	$\times 10^{-3}$ CL=90%
$\Gamma_{40}$ $D D^*(2010)^\pm + D^* D^\pm$	[e] < 5.5	$\times 10^{-3}$ CL=90%
$\Gamma_{41}$ $D D^\pm$	[e] < 3.1	$\times 10^{-3}$ CL=90%
$\Gamma_{42}$ $D_s^{(*)} \pm \bar{D}^{(*)} X(n\pi^\pm)$	[e,f] ( 9 + 5 / - 4 ) %	
$\Gamma_{43}$ $D^*(2010)\gamma$	< 1.1	$\times 10^{-3}$ CL=90%
$\Gamma_{44}$ $D_s^+ \pi^-, D_s^{*+} \pi^-, D_s^+ \rho^-, D_s^{*+} \rho^-, D_s^+ \pi^0, D_s^{*+} \pi^0, D_s^\pm \eta, D_s^{*+} \eta, D_s^+ \rho^0, D_s^{*+} \rho^0, D_s^+ \omega, D_s^{*+} \omega$	[e] < 4	$\times 10^{-4}$ CL=90%
$\Gamma_{45}$ $D_{s1}(2536)^+$ anything	< 9.5	$\times 10^{-3}$ CL=90%
<b>Charmonium modes</b>		
$\Gamma_{46}$ $J/\psi(1S)$ anything	( 1.094 ± 0.032 ) %	S=1.1
$\Gamma_{47}$ $J/\psi(1S)$ (direct) anything	( 7.8 ± 0.4 ) $\times 10^{-3}$	S=1.1
$\Gamma_{48}$ $\psi(2S)$ anything	( 3.07 ± 0.21 ) $\times 10^{-3}$	
$\Gamma_{49}$ $\chi_{c1}(1P)$ anything	( 3.86 ± 0.27 ) $\times 10^{-3}$	
$\Gamma_{50}$ $\chi_{c1}(1P)$ (direct) anything	( 3.22 ± 0.25 ) $\times 10^{-3}$	
$\Gamma_{51}$ $\chi_{c2}(1P)$ anything	( 1.3 ± 0.4 ) $\times 10^{-3}$	S=1.9
$\Gamma_{52}$ $\chi_{c2}(1P)$ (direct) anything	( 1.65 ± 0.31 ) $\times 10^{-3}$	
$\Gamma_{53}$ $\eta_c(1S)$ anything	< 9	$\times 10^{-3}$ CL=90%
$\Gamma_{54}$ $KX(3872) \times B(X \rightarrow D^0 \bar{D}^0 \pi^0)$	( 1.2 ± 0.4 ) $\times 10^{-4}$	
$\Gamma_{55}$ $KX(3872) \times B(X \rightarrow D^{*0} D^0)$	( 8.0 ± 2.2 ) $\times 10^{-5}$	
$\Gamma_{56}$ $KX(3940) \times B(X \rightarrow D^{*0} D^0)$	< 6.7	$\times 10^{-5}$ CL=90%
$\Gamma_{57}$ $KX(3915) \times B(X \rightarrow \omega J/\psi)$	[g] ( 7.1 ± 3.4 ) $\times 10^{-5}$	
<b>K or K* modes</b>		
$\Gamma_{58}$ $K^\pm$ anything	[e] ( 78.9 ± 2.5 ) %	
$\Gamma_{59}$ $K^+$ anything	( 66 ± 5 ) %	
$\Gamma_{60}$ $K^-$ anything	( 13 ± 4 ) %	
$\Gamma_{61}$ $K^0/\bar{K}^0$ anything	[e] ( 64 ± 4 ) %	
$\Gamma_{62}$ $K^*(892)^\pm$ anything	( 18 ± 6 ) %	
$\Gamma_{63}$ $K^*(892)^0/\bar{K}^*(892)^0$ anything	[e] ( 14.6 ± 2.6 ) %	
$\Gamma_{64}$ $K^*(892)\gamma$	( 4.2 ± 0.6 ) $\times 10^{-5}$	
$\Gamma_{65}$ $\eta K \gamma$	( 8.5 + 1.8 / - 1.6 ) $\times 10^{-6}$	
$\Gamma_{66}$ $K_1(1400)\gamma$	< 1.27	$\times 10^{-4}$ CL=90%
$\Gamma_{67}$ $K_2^*(1430)\gamma$	( 1.7 + 0.6 / - 0.5 ) $\times 10^{-5}$	
$\Gamma_{68}$ $K_2(1770)\gamma$	< 1.2	$\times 10^{-3}$ CL=90%
$\Gamma_{69}$ $K_3^*(1780)\gamma$	< 3.7	$\times 10^{-5}$ CL=90%
$\Gamma_{70}$ $K_4^*(2045)\gamma$	< 1.0	$\times 10^{-3}$ CL=90%
$\Gamma_{71}$ $K \eta'(958)$	( 8.3 ± 1.1 ) $\times 10^{-5}$	
$\Gamma_{72}$ $K^*(892) \eta'(958)$	( 4.1 ± 1.1 ) $\times 10^{-6}$	
$\Gamma_{73}$ $K \eta$	< 5.2	$\times 10^{-6}$ CL=90%
$\Gamma_{74}$ $K^*(892) \eta$	( 1.8 ± 0.5 ) $\times 10^{-5}$	
$\Gamma_{75}$ $K \phi \phi$	( 2.3 ± 0.9 ) $\times 10^{-6}$	
$\Gamma_{76}$ $\bar{b} \rightarrow \bar{s} \gamma$	( 3.53 ± 0.24 ) $\times 10^{-4}$	
$\Gamma_{77}$ $\bar{b} \rightarrow \bar{d} \gamma$	( 9.2 ± 3.0 ) $\times 10^{-6}$	
$\Gamma_{78}$ $\bar{b} \rightarrow \bar{s}$ gluon	< 6.8	% CL=90%
$\Gamma_{79}$ $\eta'$ anything	( 2.6 + 0.5 / - 0.8 ) $\times 10^{-4}$	
$\Gamma_{80}$ $\eta'$ anything	( 4.2 ± 0.9 ) $\times 10^{-4}$	
$\Gamma_{81}$ $K^+$ gluon (charmless)	< 1.87	$\times 10^{-4}$ CL=90%
$\Gamma_{82}$ $K^0$ gluon (charmless)	( 1.9 ± 0.7 ) $\times 10^{-4}$	
<b>Light unflavored meson modes</b>		
$\Gamma_{83}$ $\rho \gamma$	( 1.39 ± 0.25 ) $\times 10^{-6}$	S=1.2
$\Gamma_{84}$ $\rho/\omega \gamma$	( 1.30 ± 0.23 ) $\times 10^{-6}$	S=1.2
$\Gamma_{85}$ $\pi^\pm$ anything	[e,h] ( 358 ± 7 ) %	
$\Gamma_{86}$ $\pi^0$ anything	( 235 ± 11 ) %	
$\Gamma_{87}$ $\eta$ anything	( 17.6 ± 1.6 ) %	
$\Gamma_{88}$ $\rho^0$ anything	( 21 ± 5 ) %	
$\Gamma_{89}$ $\omega$ anything	< 81	% CL=90%
$\Gamma_{90}$ $\phi$ anything	( 3.43 ± 0.12 ) %	
$\Gamma_{91}$ $\phi K^*(892)$	< 2.2	$\times 10^{-5}$ CL=90%
$\Gamma_{92}$ $\bar{b} \rightarrow \bar{d}$ gluon		
$\Gamma_{93}$ $\pi^+$ gluon (charmless)	( 3.7 ± 0.8 ) $\times 10^{-4}$	
<b>Baryon modes</b>		
$\Gamma_{94}$ $\Lambda_c^+ / \bar{\Lambda}_c^-$ anything	( 4.5 ± 1.2 ) %	
$\Gamma_{95}$ $\Lambda_c^+$ anything		
$\Gamma_{96}$ $\bar{\Lambda}_c^-$ anything		
$\Gamma_{97}$ $\bar{\Lambda}_c^- e^+$ anything	< 1.1	$\times 10^{-3}$ CL=90%
$\Gamma_{98}$ $\bar{\Lambda}_c^- p$ anything	( 2.6 ± 0.8 ) %	
$\Gamma_{99}$ $\bar{\Lambda}_c^- p e^+ \nu_e$	< 1.0	$\times 10^{-3}$ CL=90%
$\Gamma_{100}$ $\Sigma_c^{*--}$ anything	( 4.2 ± 2.4 ) $\times 10^{-3}$	
$\Gamma_{101}$ $\bar{\Sigma}_c^{*0}$ anything	< 9.6	$\times 10^{-3}$ CL=90%
$\Gamma_{102}$ $\bar{\Sigma}_c^0$ anything	( 4.6 ± 2.4 ) $\times 10^{-3}$	
$\Gamma_{103}$ $\bar{\Sigma}_c^0 N(N = p \text{ or } n)$	< 1.5	$\times 10^{-3}$ CL=90%
$\Gamma_{104}$ $\Xi_c^0$ anything	( 1.93 ± 0.30 ) $\times 10^{-4}$	S=1.1
	$\times B(\Xi_c^0 \rightarrow \Xi^- \pi^+)$	
$\Gamma_{105}$ $\Xi_c^\pm$ anything	( 4.5 + 1.3 / - 1.2 ) $\times 10^{-4}$	
	$\times B(\Xi_c^\pm \rightarrow \Xi^- \pi^+ \pi^+)$	
$\Gamma_{106}$ $p/\bar{p}$ anything	[e] ( 8.0 ± 0.4 ) %	
$\Gamma_{107}$ $p/\bar{p}$ (direct) anything	[e] ( 5.5 ± 0.5 ) %	
$\Gamma_{108}$ $\Lambda/\bar{\Lambda}$ anything	[e] ( 4.0 ± 0.5 ) %	
$\Gamma_{109}$ $\Lambda$ anything		
$\Gamma_{110}$ $\bar{\Lambda}$ anything		
$\Gamma_{111}$ $\Xi^-/\bar{\Xi}^+$ anything	[e] ( 2.7 ± 0.6 ) $\times 10^{-3}$	
$\Gamma_{112}$ baryons anything	( 6.8 ± 0.6 ) %	
$\Gamma_{113}$ $p\bar{p}$ anything	( 2.47 ± 0.23 ) %	
$\Gamma_{114}$ $\Lambda\bar{\Lambda}$ anything	[e] ( 2.5 ± 0.4 ) %	
$\Gamma_{115}$ $\Lambda\bar{\Lambda}$ anything	< 5	$\times 10^{-3}$ CL=90%
<b>Lepton Family number (LF) violating modes or <math>\Delta B = 1</math> weak neutral current (<math>B_1</math>) modes</b>		
$\Gamma_{116}$ $s e^+ e^-$	$B_1$ ( 4.7 ± 1.3 ) $\times 10^{-6}$	
$\Gamma_{117}$ $s \mu^+ \mu^-$	$B_1$ ( 4.3 ± 1.2 ) $\times 10^{-6}$	
$\Gamma_{118}$ $s \ell^+ \ell^-$	$B_1$ [b] ( 4.5 ± 1.0 ) $\times 10^{-6}$	
$\Gamma_{119}$ $\pi \ell^+ \ell^-$	$B_1$ < 6.2	$\times 10^{-8}$ CL=90%
$\Gamma_{120}$ $K e^+ e^-$	$B_1$ ( 4.4 ± 0.6 ) $\times 10^{-7}$	

See key on page 457

Meson Particle Listings  
 $B^\pm/B^0$  ADMIXTURE

$\Gamma_{121}$	$K^*(892)e^+e^-$	B1	( 1.19 ± 0.20 ) × 10 <sup>-6</sup>	S=1.2
$\Gamma_{122}$	$K\mu^+\mu^-$	B1	( 4.4 ± 0.4 ) × 10 <sup>-7</sup>	
$\Gamma_{123}$	$K^*(892)\mu^+\mu^-$	B1	( 1.06 ± 0.09 ) × 10 <sup>-6</sup>	
$\Gamma_{124}$	$K\ell^+\ell^-$	B1	( 4.5 ± 0.4 ) × 10 <sup>-7</sup>	
$\Gamma_{125}$	$K^*(892)\ell^+\ell^-$	B1	( 1.08 ± 0.11 ) × 10 <sup>-6</sup>	
$\Gamma_{126}$	$K\nu\bar{\nu}$	B1	< 1.4	× 10 <sup>-5</sup> CL=90%
$\Gamma_{127}$	$K^*\nu\bar{\nu}$	B1	< 8	× 10 <sup>-5</sup> CL=90%
$\Gamma_{128}$	$s e^\pm \mu^\mp$	LF	[e] < 2.2	× 10 <sup>-5</sup> CL=90%
$\Gamma_{129}$	$\pi e^\pm \mu^\mp$	LF	< 9.2	× 10 <sup>-8</sup> CL=90%
$\Gamma_{130}$	$\rho e^\pm \mu^\mp$	LF	< 3.2	× 10 <sup>-6</sup> CL=90%
$\Gamma_{131}$	$K e^\pm \mu^\mp$	LF	< 3.8	× 10 <sup>-8</sup> CL=90%
$\Gamma_{132}$	$K^*(892)e^\pm \mu^\mp$	LF	< 5.1	× 10 <sup>-7</sup> CL=90%

[a] These values are model dependent.

[b] An  $\ell$  indicates an  $e$  or a  $\mu$  mode, not a sum over these modes.

[c] Here "anything" means at least one particle observed.

[d]  $D^{**}$  stands for the sum of the  $D(1^1P_1)$ ,  $D(1^3P_0)$ ,  $D(1^3P_1)$ ,  $D(1^3P_2)$ ,  $D(2^1S_0)$ , and  $D(2^1S_1)$  resonances.

[e] The value is for the sum of the charge states or particle/antiparticle states indicated.

[f]  $D^*(\bar{D}^*)$  stands for the sum of  $D^*\bar{D}^*$ ,  $D^*\bar{D}$ ,  $D\bar{D}^*$ , and  $D\bar{D}$ .[g]  $X(3915)$  denotes a near-threshold enhancement in the  $\omega J/\psi$  mass spectrum.

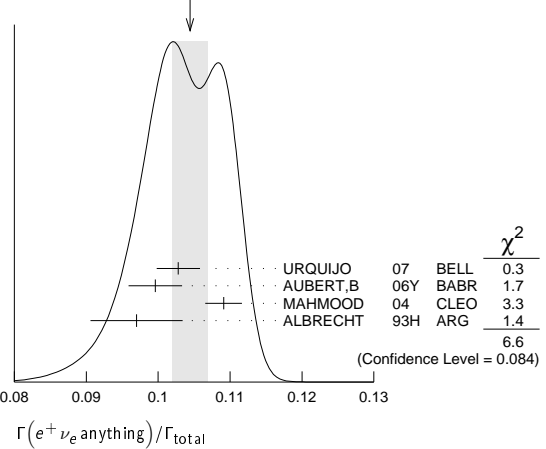
[h] Inclusive branching fractions have a multiplicity definition and can be greater than 100%.

<sup>11</sup> YANAGISAWA 91 also measures an average semileptonic branching ratio at the  $\Upsilon(5S)$  of 9.6–10.5% depending on assumptions about the relative production of different  $B$  meson species.

<sup>12</sup> ALBRECHT 90H uses the model of ALTARELLI 82 to correct over all lepton momenta. 0.099 ± 0.006 is obtained using ISGUR 89B.

<sup>13</sup> Using data above  $p(e) = 2.4$  GeV, WACHS 89 determine  $\sigma(B \rightarrow e\nu\mu)/\sigma(B \rightarrow e\nu\text{charm}) < 0.065$  at 90% CL.

<sup>14</sup> Ratio  $\sigma(b \rightarrow e\nu\mu)/\sigma(b \rightarrow e\nu\text{charm}) < 0.055$  at CL = 90%.

WEIGHTED AVERAGE  
0.1044±0.0025 (Error scaled by 1.5) $B^\pm/B^0$  ADMIXTURE BRANCHING RATIOS

$\Gamma(e^+ \nu_e \text{ anything})/\Gamma_{\text{total}}$   $\Gamma_1/\Gamma$   
These branching fraction values are model dependent.

"OUR EVALUATION" is an average using rescaled values of the data listed below. The average and rescaling were performed by the Heavy Flavor Averaging Group (HFAG) and are described at <http://www.slac.stanford.edu/xorg/hfag/>. The averaging/rescaling procedure takes into account correlations between the measurements.

VALUE	DOCUMENT ID	TECN	COMMENT
The data in this block is included in the average printed for a previous datablock.			

**0.1072 ± 0.0013 OUR EVALUATION**

**0.1044 ± 0.0025 OUR AVERAGE** Error includes scale factor of 1.5. See the ideogram below.

0.1028 ± 0.0018 ± 0.0024	<sup>1</sup> URQUIJO	07	BELL	$e^+e^- \rightarrow \Upsilon(4S)$
0.0996 ± 0.0019 ± 0.0032	<sup>2</sup> AUBERT,B	06Y	BABR	$e^+e^- \rightarrow \Upsilon(4S)$
0.1091 ± 0.0009 ± 0.0024	<sup>3</sup> MAHMOOD	04	CLEO	$e^+e^- \rightarrow \Upsilon(4S)$
0.097 ± 0.005 ± 0.004	<sup>4</sup> ALBRECHT	93H	ARG	$e^+e^- \rightarrow \Upsilon(4S)$
• • • We do not use the following data for averages, fits, limits, etc. • • •				
0.1085 ± 0.0021 ± 0.0036	<sup>5</sup> OKABE	05	BELL	Repl. by URQUIJO 07
0.1083 ± 0.0016 ± 0.0006	<sup>6</sup> AUBERT	04X	BABR	Repl. by AUBERT,B 06Y
0.1036 ± 0.0006 ± 0.0023	<sup>7</sup> AUBERT,B	04A	BABR	$e^+e^- \rightarrow \Upsilon(4S)$
0.1087 ± 0.0018 ± 0.0030	<sup>8</sup> AUBERT	03	BABR	Repl. by AUBERT 04x
0.109 ± 0.0012 ± 0.0049	<sup>9</sup> ABE	02Y	BELL	Repl. by OKABE 05
0.1049 ± 0.0017 ± 0.0043	<sup>10</sup> BARISH	96B	CLE2	Repl. by MAHMOOD 04
0.100 ± 0.004 ± 0.003	<sup>11</sup> YANAGISAWA	91	CSB2	$e^+e^- \rightarrow \Upsilon(4S)$
0.103 ± 0.006 ± 0.002	<sup>12</sup> ALBRECHT	90H	ARG	$e^+e^- \rightarrow \Upsilon(4S)$
0.117 ± 0.004 ± 0.010	<sup>13</sup> WACHS	89	CBAL	Direct $e$ at $\Upsilon(4S)$
0.120 ± 0.007 ± 0.005	CHEN	84	CLEO	Direct $e$ at $\Upsilon(4S)$
0.132 ± 0.008 ± 0.014	<sup>14</sup> KLOPFEN...	83B	CUSB	Direct $e$ at $\Upsilon(4S)$

<sup>1</sup> URQUIJO 07 report a measurement of  $(10.07 \pm 0.18 \pm 0.21)\%$  for the partial branching fraction of  $B \rightarrow e\nu_e X_c$  decay with electron energy above 0.6 GeV. We converted the result to  $B \rightarrow e\nu_e X$  branching fraction.

<sup>2</sup> The measurements are obtained for charged and neutral  $B$  mesons partial rates of semileptonic decay to electrons with momentum above 0.6 GeV/c in the  $B$  rest frame. The best precision on the ratio is achieved for a momentum threshold of 1.0 GeV:  $B(B^+ \rightarrow e^+ \nu_e X) / B(B^0 \rightarrow e^+ \nu_e X) = 1.074 \pm 0.041 \pm 0.026$ .

<sup>3</sup> Uses charge and angular correlations in  $\Upsilon(4S)$  events with a high-momentum lepton and an additional electron.

<sup>4</sup> ALBRECHT 93H analysis performed using tagged semileptonic decays of the  $B$ . This technique is almost model independent for the lepton branching ratio.

<sup>5</sup> The measurements are obtained for charged and neutral  $B$  mesons partial rates of semileptonic decay to electrons with momentum above 0.6 GeV/c in the  $B$  rest frame, and their ratio of  $B(B^+ \rightarrow e^+ \nu_e X)/B(B^0 \rightarrow e^+ \nu_e X) = 1.08 \pm 0.05 \pm 0.02$ .

<sup>6</sup> The semileptonic branching ratio,  $|V_{cb}|$  and other heavy-quark parameters are determined from a simultaneous fit to moments of the hadronic-mass and lepton-energy distribution.

<sup>7</sup> Uses the high-momentum lepton tag method and requires the electron energy above 0.6 GeV.

<sup>8</sup> Uses the high-momentum lepton tag method. They also report  $|V_{cb}| = 0.0423 \pm 0.0007(\text{exp}) \pm 0.0020(\text{theo.})$ .

<sup>9</sup> Uses the high-momentum lepton tag method. ABE 02y also reports  $|V_{cb}| = 0.0408 \pm 0.0010(\text{exp}) \pm 0.0025(\text{theo.})$ . The second error is due to uncertainties of theoretical inputs.

<sup>10</sup> BARISH 96B analysis performed using tagged semileptonic decays of the  $B$ . This technique is almost model independent for the lepton branching ratio.

$\Gamma(\bar{D}e^+ \nu_e \text{ anything})/\Gamma_{\text{total}}$   $\Gamma_2/\Gamma$

VALUE	CL%	DOCUMENT ID	TECN	COMMENT
<b>&lt; 5.9 × 10<sup>-4</sup></b>	90	<sup>1</sup> ADAM	03B	CLE2 $e^+e^- \rightarrow \Upsilon(4S)$
• • • We do not use the following data for averages, fits, limits, etc. • • •				
< 0.0016	90	ALBRECHT	90H	ARG $e^+e^- \rightarrow \Upsilon(4S)$
<sup>1</sup> Based on V–A model.				

$\Gamma(\mu^+ \nu_\mu \text{ anything})/\Gamma_{\text{total}}$   $\Gamma_3/\Gamma$

These branching fraction values are model dependent.

"OUR EVALUATION" is an average using rescaled values of the data listed below. The average and rescaling were performed by the Heavy Flavor Averaging Group (HFAG) and are described at <http://www.slac.stanford.edu/xorg/hfag/>. The averaging/rescaling procedure takes into account correlations between the measurements.

VALUE	DOCUMENT ID	TECN	COMMENT
The data in this block is included in the average printed for a previous datablock.			

**0.1072 ± 0.0013 OUR EVALUATION**

• • • We do not use the following data for averages, fits, limits, etc. • • •

0.100 ± 0.006 ± 0.002	<sup>1</sup> ALBRECHT	90H	ARG	$e^+e^- \rightarrow \Upsilon(4S)$
0.108 ± 0.006 ± 0.01	CHEN	84	CLEO	Direct $\mu$ at $\Upsilon(4S)$
0.112 ± 0.009 ± 0.01	LEVMAN	84	CUSB	Direct $\mu$ at $\Upsilon(4S)$

<sup>1</sup> ALBRECHT 90H uses the model of ALTARELLI 82 to correct over all lepton momenta. 0.097 ± 0.006 is obtained using ISGUR 89B.

$\Gamma(\ell^+ \nu_\ell \text{ anything})/\Gamma_{\text{total}}$   $\Gamma_4/\Gamma$

These branching fraction values are model dependent.

"OUR EVALUATION" is an average using rescaled values of the data listed below. The average and rescaling were performed by the Heavy Flavor Averaging Group (HFAG) and are described at <http://www.slac.stanford.edu/xorg/hfag/>. The averaging/rescaling procedure takes into account correlations between the measurements.

VALUE	DOCUMENT ID	TECN	COMMENT
<b>0.1072 ± 0.0013 OUR EVALUATION</b>			
<b>0.1044 ± 0.0025 OUR AVERAGE</b> Includes data from the 2 datablocks that follow this one. Error includes scale factor of 1.5. See the ideogram below.			

• • • We do not use the following data for averages, fits, limits, etc. • • •

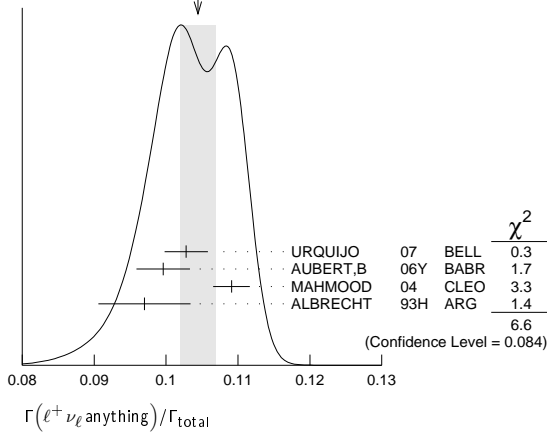
0.108 ± 0.002 ± 0.0056	<sup>1</sup> HENDERSON	92	CLEO	$e^+e^- \rightarrow \Upsilon(4S)$
------------------------	------------------------	----	------	-----------------------------------

<sup>1</sup> HENDERSON 92 measurement employs  $e$  and  $\mu$ . The systematic error contains 0.004 in quadrature from model dependence. The authors average a variation of the Isgur, Scora, Grinstein, and Wise model with that of the Altarelli-Cabibbo-Corbò-Maiani-Martinelli model for semileptonic decays to correct the acceptance.

Meson Particle Listings

$B^\pm/B^0$  ADMIXTURE

WEIGHTED AVERAGE  
0.1044±0.0025 (Error scaled by 1.5)



$\Gamma(D^- \ell^+ \nu_\ell \text{ anything})/\Gamma(\ell^+ \nu_\ell \text{ anything})$   $\Gamma_5/\Gamma_4$   
ℓ = e or μ.

VALUE	DOCUMENT ID	TECN	COMMENT
0.26±0.07±0.04	1 FULTON 91	CLEO	$e^+e^- \rightarrow \Upsilon(4S)$

1 FULTON 91 uses  $B(D^+ \rightarrow K^- \pi^+ \pi^+) = (9.1 \pm 1.3 \pm 0.4)\%$  as measured by MARK III.

$\Gamma(\bar{D}^0 \ell^+ \nu_\ell \text{ anything})/\Gamma(\ell^+ \nu_\ell \text{ anything})$   $\Gamma_6/\Gamma_4$   
ℓ = e or μ.

VALUE	DOCUMENT ID	TECN	COMMENT
0.67±0.09±0.10	1 FULTON 91	CLEO	$e^+e^- \rightarrow \Upsilon(4S)$

1 FULTON 91 uses  $B(D^0 \rightarrow K^- \pi^+) = (4.2 \pm 0.4 \pm 0.4)\%$  as measured by MARK III.

$\Gamma(\bar{D} \ell \nu_\ell)/\Gamma(\ell^+ \nu_\ell \text{ anything})$   $\Gamma_7/\Gamma_4$

VALUE	DOCUMENT ID	TECN	COMMENT
0.223±0.006±0.009	1 AUBERT 10	BABR	$e^+e^- \rightarrow \Upsilon(4S)$

1 Uses a fully reconstructed B meson as a tag on the recoil side.

$\Gamma(D \tau^+ \nu_\tau)/\Gamma_{\text{total}}$   $\Gamma_8/\Gamma$

VALUE (units $10^{-2}$ )	DOCUMENT ID	TECN	COMMENT
0.86±0.24±0.12	1 AUBERT 08N	BABR	$e^+e^- \rightarrow \Upsilon(4S)$

1 Uses a fully reconstructed B meson as a tag on the recoil side.

$\Gamma(D^{*+} \ell^+ \nu_\ell \text{ anything})/\Gamma_{\text{total}}$   $\Gamma_9/\Gamma$

VALUE (units $10^{-2}$ )	DOCUMENT ID	TECN	COMMENT
0.67±0.08±0.10	ABDALLAH 04D	DLPH	$e^+e^- \rightarrow Z^0$
0.6 ± 0.3 ± 0.1	1 BARISH 95	CLE2	$e^+e^- \rightarrow \Upsilon(4S)$

••• We do not use the following data for averages, fits, limits, etc. •••  
1 BARISH 95 use  $B(D^0 \rightarrow K^- \pi^+) = (3.91 \pm 0.08 \pm 0.17)\%$  and  $B(D^{*+} \rightarrow D^0 \pi^+) = (68.1 \pm 1.0 \pm 1.3)\%$ .

$\Gamma(D^{*0} \ell^+ \nu_\ell \text{ anything})/\Gamma_{\text{total}}$   $\Gamma_{10}/\Gamma$

VALUE (units $10^{-2}$ )	DOCUMENT ID	TECN	COMMENT
0.6±0.6±0.1	1 BARISH 95	CLE2	$e^+e^- \rightarrow \Upsilon(4S)$

••• We do not use the following data for averages, fits, limits, etc. •••  
1 BARISH 95 use  $B(D^0 \rightarrow K^- \pi^+) = (3.91 \pm 0.08 \pm 0.17)\%$ ,  $B(D^{*+} \rightarrow D^0 \pi^+) = (68.1 \pm 1.0 \pm 1.3)\%$ ,  $B(D^{*0} \rightarrow D^0 \pi^0) = (63.6 \pm 2.3 \pm 3.3)\%$ .

$\Gamma(D^{*+} \tau^+ \nu_\tau)/\Gamma_{\text{total}}$   $\Gamma_{11}/\Gamma$

VALUE (units $10^{-2}$ )	DOCUMENT ID	TECN	COMMENT
1.62±0.31±0.11	1 AUBERT 08N	BABR	$e^+e^- \rightarrow \Upsilon(4S)$

1 Uses a fully reconstructed B meson as a tag on the recoil side. The results are normalized to the  $B^+$  decay rate.

$\Gamma(\bar{D}^{**} \ell^+ \nu_\ell)/\Gamma_{\text{total}}$   $\Gamma_{12}/\Gamma$

$D^{**}$  stands for the sum of the  $D(1^1P_1)$ ,  $D(1^3P_0)$ ,  $D(1^3P_1)$ ,  $D(1^3P_2)$ ,  $D(2^1S_0)$ , and  $D(2^1S_1)$  resonances. ℓ = e or μ, not sum over e and μ modes.

VALUE	CL%	EVTs	DOCUMENT ID	TECN	COMMENT
0.027±0.005±0.005		63	1 ALBRECHT 93	ARG	$e^+e^- \rightarrow \Upsilon(4S)$

••• We do not use the following data for averages, fits, limits, etc. •••  
<0.028 95 2 BARISH 95 CLE2  $e^+e^- \rightarrow \Upsilon(4S)$   
1 ALBRECHT 93 assumes the GISW model to correct for unseen modes. Using the BHKT model, the result becomes  $0.023 \pm 0.006 \pm 0.004$ . Assumes  $B(D^{*+} \rightarrow D^0 \pi^+) = 68.1\%$ ,  $B(D^0 \rightarrow K^- \pi^+) = 3.65\%$ ,  $B(D^0 \rightarrow K^- \pi^+ \pi^- \pi^+) = 7.5\%$ . We have taken their average e and μ value.  
2 BARISH 95 use  $B(D^0 \rightarrow K^- \pi^+) = (3.91 \pm 0.08 \pm 0.17)\%$ , assume all nonresonant channels are zero, and use GISW model for relative abundances of  $D^{**}$  states.

$\Gamma(\bar{D}_1(2420) \ell^+ \nu_\ell \text{ anything})/\Gamma_{\text{total}}$   $\Gamma_{13}/\Gamma$

VALUE	DOCUMENT ID	TECN	COMMENT
0.0038±0.0013 OUR AVERAGE	Error includes scale factor of 2.4.		
0.0033±0.0006	1 ABAZOV 05o	D0	$p\bar{p}$ at 1.96 TeV
0.0074±0.0016	2 BUSKULIC 97B	ALEP	$e^+e^- \rightarrow Z$

••• We do not use the following data for averages, fits, limits, etc. •••  
seen 3 BUSKULIC 95B ALEP Repl. by BUSKULIC 97B  
1 Assumes  $B(D_1 \rightarrow D^* \pi) = 1$ ,  $B(D_1 \rightarrow D^* \pi^\pm) = 2/3$ , and  $B(b \rightarrow B) = 0.397$ .  
2 BUSKULIC 97B assumes  $B(D_1(2420) \rightarrow D^* \pi) = 1$ ,  $B(D_1(2420) \rightarrow D^* \pi^\pm) = 2/3$ , and  $B(b \rightarrow B) = 0.378 \pm 0.022$ .  
3 BUSKULIC 95B reports  $f_B \times B(B \rightarrow \bar{D}_1(2420)^0 \ell^+ \nu_\ell \text{ anything}) \times B(\bar{D}_1(2420)^0 \rightarrow \bar{D}^*(2010)^- \pi^+) = (2.04 \pm 0.58 \pm 0.34)10^{-3}$ , where  $f_B$  is the production fraction for a single B charge state.

$[\Gamma(D \pi \ell^+ \nu_\ell \text{ anything}) + \Gamma(D^* \pi \ell^+ \nu_\ell \text{ anything})]/\Gamma_{\text{total}}$   $\Gamma_{14}/\Gamma$

VALUE	DOCUMENT ID	TECN	COMMENT
0.026 ± 0.005 OUR AVERAGE	Error includes scale factor of 1.5.		
0.0340±0.0052±0.0032	1 ABREU 00R	DLPH	$e^+e^- \rightarrow Z$
0.0226±0.0029±0.0033	2 BUSKULIC 97B	ALEP	$e^+e^- \rightarrow Z$

1 Assumes no contribution from  $B_s$  and b baryons. Further assumes contributions from single pion ( $D \pi$  and  $D^* \pi$ ) states only, allowing isospin conservation to relate the relative  $\pi^0$  and  $\pi^\pm$  rates.  
2 BUSKULIC 97B assumes  $B(b \rightarrow B) = 0.378 \pm 0.022$  and uses isospin invariance by assuming that all observed  $D^0 \pi^+$ ,  $D^{*0} \pi^+$ ,  $D^+ \pi^-$ , and  $D^{*+} \pi^-$  are from  $D^{**}$  states. A correction has been applied to account for the production of  $B_s^0$  and  $\Lambda_b^0$ .

$\Gamma(D \pi \ell^+ \nu_\ell \text{ anything})/\Gamma_{\text{total}}$   $\Gamma_{15}/\Gamma$

VALUE	DOCUMENT ID	TECN	COMMENT
0.0154±0.0061	ABREU 00R	DLPH	$e^+e^- \rightarrow Z$

$\Gamma(D^* \pi \ell^+ \nu_\ell \text{ anything})/\Gamma_{\text{total}}$   $\Gamma_{16}/\Gamma$

VALUE	DOCUMENT ID	TECN	COMMENT
0.0186±0.0038	ABREU 00R	DLPH	$e^+e^- \rightarrow Z$

$\Gamma(\bar{D}_2^*(2460) \ell^+ \nu_\ell \text{ anything})/\Gamma_{\text{total}}$   $\Gamma_{17}/\Gamma$

VALUE	CL%	DOCUMENT ID	TECN	COMMENT
0.0044±0.0016		1 ABAZOV 05o	D0	$p\bar{p}$ at 1.96 TeV
<0.0065	95	2 BUSKULIC 97B	ALEP	$e^+e^- \rightarrow Z$
not seen		3 BUSKULIC 95B	ALEP	$e^+e^- \rightarrow Z$

••• We do not use the following data for averages, fits, limits, etc. •••  
1 Assumes  $B(D_2^{*+} \rightarrow D^* \pi^\pm) = 0.30 \pm 0.06$  and  $B(b \rightarrow B) = 0.397$ .  
2 A revised number based on BUSKULIC 97B which assumes  $B(D_2^*(2460) \rightarrow D^* \pi^\pm) = 0.20$  and  $B(b \rightarrow B) = 0.378 \pm 0.022$ .  
3 BUSKULIC 95B reports  $f_B \times B(B \rightarrow \bar{D}_2^*(2460)^0 \ell^+ \nu_\ell \text{ anything}) \times B(\bar{D}_2^*(2460)^0 \rightarrow \bar{D}^*(2010)^- \pi^+) \leq 0.81 \times 10^{-3}$  at CL=95%, where  $f_B$  is the production fraction for a single B charge state.

$\Gamma(B \rightarrow \bar{D}_2^*(2460) \ell^+ \nu_\ell \text{ anything}) \times B(D_2^*(2460) \rightarrow D^* \pi^+)$   
 $\Gamma(B \rightarrow \bar{D}_1(2420) \ell^+ \nu_\ell \text{ anything}) \times B(D_1(2420) \rightarrow D^* \pi^+)$

VALUE	DOCUMENT ID	TECN	COMMENT
0.39±0.09±0.12	ABAZOV 05o	D0	$p\bar{p}$ at 1.96 TeV

$\Gamma(D^{*-} \pi^+ \ell^+ \nu_\ell \text{ anything})/\Gamma_{\text{total}}$   $\Gamma_{18}/\Gamma$

VALUE (units $10^{-3}$ )	DOCUMENT ID	TECN	COMMENT
10.0±2.7±2.1	1 BUSKULIC 95B	ALEP	$e^+e^- \rightarrow Z$

1 BUSKULIC 95B reports  $f_B \times B(B \rightarrow \bar{D}^*(2010)^- \pi^+ \ell^+ \nu_\ell \text{ anything}) = (3.7 \pm 1.0 \pm 0.7)10^{-3}$ . Above value assumes  $f_B = 0.37 \pm 0.03$ .

$\Gamma(D_s^- \ell^+ \nu_\ell \text{ anything})/\Gamma_{\text{total}}$   $\Gamma_{19}/\Gamma$

VALUE	CL%	DOCUMENT ID	TECN	COMMENT
<7 × 10 <sup>-3</sup>	90	1 ALBRECHT 93E	ARG	$e^+e^- \rightarrow \Upsilon(4S)$

1 ALBRECHT 93E reports <0.012 from a measurement of  $[\Gamma(B \rightarrow D_s^- \ell^+ \nu_\ell \text{ anything})/\Gamma_{\text{total}}] \times [B(D_s^+ \rightarrow \phi \pi^+)]$  assuming  $B(D_s^+ \rightarrow \phi \pi^+) = 0.027$ , which we rescale to our best value  $B(D_s^+ \rightarrow \phi \pi^+) = 4.5 \times 10^{-2}$ .

$\Gamma(D_s^- \ell^+ \nu_\ell K^+ \text{ anything})/\Gamma_{\text{total}}$   $\Gamma_{20}/\Gamma$

VALUE	CL%	DOCUMENT ID	TECN	COMMENT
<5 × 10 <sup>-3</sup>	90	1 ALBRECHT 93E	ARG	$e^+e^- \rightarrow \Upsilon(4S)$

1 ALBRECHT reports <0.008 from a measurement of  $[\Gamma(B \rightarrow D_s^- \ell^+ \nu_\ell K^+ \text{ anything})/\Gamma_{\text{total}}] \times [B(D_s^+ \rightarrow \phi \pi^+)]$  assuming  $B(D_s^+ \rightarrow \phi \pi^+) = 0.027$ , which we rescale to our best value  $B(D_s^+ \rightarrow \phi \pi^+) = 4.5 \times 10^{-2}$ .

$\Gamma(D_s^- \ell^+ \nu_\ell K^0 \text{ anything})/\Gamma_{\text{total}}$   $\Gamma_{21}/\Gamma$

VALUE	CL%	DOCUMENT ID	TECN	COMMENT
<7 × 10 <sup>-3</sup>	90	1 ALBRECHT 93E	ARG	$e^+e^- \rightarrow \Upsilon(4S)$

1 ALBRECHT reports <0.012 from a measurement of  $[\Gamma(B \rightarrow D_s^- \ell^+ \nu_\ell K^0 \text{ anything})/\Gamma_{\text{total}}] \times [B(D_s^+ \rightarrow \phi \pi^+)]$  assuming  $B(D_s^+ \rightarrow \phi \pi^+) = 0.027$ , which we rescale to our best value  $B(D_s^+ \rightarrow \phi \pi^+) = 4.5 \times 10^{-2}$ .



See key on page 457

# Meson Particle Listings

## $B^\pm/B^0$ ADMIXTURE

### $\Gamma(\ell^+ \nu_\ell \text{ charm})/\Gamma_{\text{total}}$ $\Gamma_{22}/\Gamma$

"OUR EVALUATION" is an average using rescaled values of the data listed below. The average and rescaling were performed by the Heavy Flavor Averaging Group (HFAG) and are described at <http://www.slac.stanford.edu/xorg/hfag/>. The averaging/rescaling procedure takes into account correlations between the measurements.

VALUE	DOCUMENT ID	TECN	COMMENT
<b>0.1051 ± 0.0013 OUR EVALUATION</b>			
<b>0.1058 ± 0.0015 OUR AVERAGE</b>			
0.1064 ± 0.0017 ± 0.0006	<sup>1</sup> AUBERT	10A BABR	$e^+ e^- \rightarrow \Upsilon(4S)$
0.1044 ± 0.0019 ± 0.0022	<sup>2</sup> URQUIJO	07 BELL	$e^+ e^- \rightarrow \Upsilon(4S)$
• • • We do not use the following data for averages, fits, limits, etc. • • •			
0.1061 ± 0.0016 ± 0.0006	<sup>3</sup> AUBERT	04x BABR	Repl. by AUBERT 10A

- Obtained from a combined fit to the moments of observed spectra in inclusive  $B \rightarrow X_c \ell^+ \nu_\ell$  decay.
- Measured the independent  $B^+$  and  $B^0$  partial branching fractions with electron energy above 0.4 GeV.
- The semileptonic branching ratio,  $|V_{cb}|$  and other heavy-quark parameters are determined from a simultaneous fit to moments of the hadronic-mass and lepton-energy distribution.

### $\Gamma(X_{cb} \ell^+ \nu_\ell)/\Gamma_{\text{total}}$ $\Gamma_{23}/\Gamma$

"OUR EVALUATION" is an average using rescaled values of the data listed below. The average and rescaling were performed by the Heavy Flavor Averaging Group (HFAG) and are described at <http://www.slac.stanford.edu/xorg/hfag/>. The averaging/rescaling procedure takes into account correlations between the measurements.

VALUE (units $10^{-3}$ )	DOCUMENT ID	TECN	COMMENT
<b>2.08 ± 0.30 OUR EVALUATION</b>			
<b>2.33 ± 0.22 OUR AVERAGE</b>			
2.27 ± 0.26 $^{+0.37}_{-0.33}$	<sup>1</sup> AUBERT	06H BABR	$e^+ e^- \rightarrow \Upsilon(4S)$
2.53 ± 0.24 ± 0.24	<sup>2</sup> AUBERT,B	05x BABR	$e^+ e^- \rightarrow \Upsilon(4S)$
2.80 ± 0.52 ± 0.41	<sup>3</sup> LIMOSANI	05 BELL	$e^+ e^- \rightarrow \Upsilon(4S)$
1.77 ± 0.29 ± 0.38	<sup>4</sup> BORNHEIM	02 CLE2	$e^+ e^- \rightarrow \Upsilon(4S)$
• • • We do not use the following data for averages, fits, limits, etc. • • •			
1.963 ± 0.173 ± 0.159	<sup>5</sup> URQUIJO	10 BELL	$e^+ e^- \rightarrow \Upsilon(4S)$
	<sup>6</sup> AUBERT	08As BABR	$e^+ e^- \rightarrow \Upsilon(4S)$
2.24 ± 0.27 ± 0.47	<sup>7,8</sup> AUBERT	04i BABR	Repl. by AUBERT,B 05x

- Obtained from the partial rate  $\Delta B = (0.572 \pm 0.041 \pm 0.065) \times 10^{-3}$  for the electron momentum interval of 2.0–2.6 GeV/c based on BLNP method.
- Determined from the partial rate  $\Delta B = (4.41 \pm 0.42 \pm 0.42) \times 10^{-4}$  measured for electron energy > 2 GeV and hadronic mass squared < 3.5 GeV<sup>2</sup>, and calculated acceptance 0.174 in that region. The  $V_{ub}$  is measured as  $(4.41 \pm 0.30^{+0.65}_{-0.47} \pm 0.28) \times 10^{-3}$ .
- Uses electrons in the momentum interval 1.9–2.6 GeV/c in the center-of-mass frame. The  $V_{ub}$  is found to be  $(5.08 \pm 0.47^{+0.49}_{-0.48}) \times 10^{-3}$ .
- BORNHEIM 02 uses the observed yield of leptons from semileptonic  $B$  decays in the end-point momentum interval 2.2–2.6 GeV/c with recent CLEO-2 data on  $B \rightarrow X_S \gamma$ . The  $V_{ub}$  is found to be  $(4.08 \pm 0.34 \pm 0.53) \times 10^{-3}$ .
- Uses a multivariate analysis method and requires lepton momentum in the  $B$  rest frame,  $p_T^{*B} > 1.0$  GeV/c.
- Measures several partial branching fractions in different phase space regions. The most precise result is obtained in the region for hadronic mass  $M_X < 1.55$  GeV/c<sup>2</sup>, and is  $\Delta B = (1.18 \pm 0.09 \pm 0.07) \times 10^{-3}$ . The corresponding  $|V_{ub}|$  from the BLNP method is  $(4.27 \pm 0.16 \pm 0.13 \pm 0.30) \times 10^{-3}$ , where the last uncertainty comes from the theoretical prediction of the partial rate in the given phase-space region.
- Used BaBar measurement of Semileptonic branching fraction  $B(B \rightarrow X \ell \nu_\ell) = (10.87 \pm 0.18 \pm 0.30)\%$  to convert the ratio of rates to branching fraction.
- The third error includes the systematics and theoretical errors summed in quadrature.

### $\Gamma(X_{cb} \ell^+ \nu_\ell)/\Gamma(\ell^+ \nu_\ell \text{ anything})$ $\Gamma_{23}/\Gamma_4$

$\ell$  denotes  $e$  or  $\mu$ , not the sum. These experiments measure this ratio in very limited momentum intervals.

VALUE (units $10^{-2}$ )	CL%	EVTS	DOCUMENT ID	TECN	COMMENT
<b>2.06 ± 0.25 ± 0.42</b>			<sup>1</sup> AUBERT	04i BABR	$e^+ e^- \rightarrow \Upsilon(4S)$
• • • We do not use the following data for averages, fits, limits, etc. • • •					
			<sup>2</sup> ALBRECHT	94c ARG	$e^+ e^- \rightarrow \Upsilon(4S)$
	107		<sup>3</sup> BARTELT	93B CLE2	$e^+ e^- \rightarrow \Upsilon(4S)$
	77		<sup>4</sup> ALBRECHT	91c ARG	$e^+ e^- \rightarrow \Upsilon(4S)$
	41		<sup>5</sup> ALBRECHT	90 ARG	$e^+ e^- \rightarrow \Upsilon(4S)$
	76		<sup>6</sup> FULTON	90 CLEO	$e^+ e^- \rightarrow \Upsilon(4S)$
<4.0	90		<sup>7</sup> BEHRENDIS	87 CLEO	$e^+ e^- \rightarrow \Upsilon(4S)$
<4.0	90		CHEN	84 CLEO	Direct $e$ at $\Upsilon(4S)$
<5.5	90		KLOPFEN...	83B CUSB	Direct $e$ at $\Upsilon(4S)$

- The third error includes the systematics and theoretical errors summed in quadrature.
- ALBRECHT 94c find  $\Gamma(b \rightarrow c)/\Gamma(b \rightarrow \text{all}) = 0.99 \pm 0.02 \pm 0.04$ .
- BARTELT 93B (CLEO II) measures an excess of  $107 \pm 15 \pm 11$  leptons in the lepton momentum interval 2.3–2.6 GeV/c which is attributed to  $b \rightarrow u \ell \nu_\ell$ . This corresponds to a model-dependent partial branching ratio  $\Delta B_{ub}$  between  $(1.15 \pm 0.16 \pm 0.15) \times 10^{-4}$ , as evaluated using the KS model (KOERNER 88), and  $(1.54 \pm 0.22 \pm 0.20) \times 10^{-4}$  using the ACCMM model (ARTUSO 93). The corresponding values of  $|V_{ub}|/|V_{cb}|$  are  $0.056 \pm 0.006$  and  $0.076 \pm 0.008$ , respectively.
- ALBRECHT 91c result supersedes ALBRECHT 90. Two events are fully reconstructed providing evidence for the  $b \rightarrow u$  transition. Using the model of ALTARELLI 82, they obtain  $|V_{ub}|/|V_{cb}| = 0.11 \pm 0.012$  from 77 leptons in the 2.3–2.6 GeV momentum range.

<sup>5</sup> ALBRECHT 90 observes  $41 \pm 10$  excess  $e$  and  $\mu$  (lepton) events in the momentum interval  $p = 2.3\text{--}2.6$  GeV signaling the presence of the  $b \rightarrow u$  transition. The events correspond to a model-dependent measurement of  $|V_{ub}|/|V_{cb}| = 0.10 \pm 0.01$ .

<sup>6</sup> FULTON 90 observe  $76 \pm 20$  excess  $e$  and  $\mu$  (lepton) events in the momentum interval  $p = 2.4\text{--}2.6$  GeV signaling the presence of the  $b \rightarrow u$  transition. The average branching ratio,  $(1.8 \pm 0.4 \pm 0.3) \times 10^{-4}$ , corresponds to a model-dependent measurement of approximately  $|V_{ub}|/|V_{cb}| = 0.1$  using  $B(b \rightarrow c \ell \nu) = 10.2 \pm 0.2 \pm 0.7\%$ .

<sup>7</sup> The quoted possible limits range from 0.018 to 0.04 for the ratio, depending on which model or momentum range is chosen. We select the most conservative limit they have calculated. This corresponds to a limit on  $|V_{ub}|/|V_{cb}| < 0.20$ . While the endpoint technique employed is more robust than their previous results in CHEN 84, these results do not provide a numerical improvement in the limit.

### $\Gamma(K^+ \ell^+ \nu_\ell \text{ anything})/\Gamma(\ell^+ \nu_\ell \text{ anything})$ $\Gamma_{24}/\Gamma_4$

$\ell$  denotes  $e$  or  $\mu$ , not the sum.

VALUE	DOCUMENT ID	TECN	COMMENT
<b>0.58 ± 0.05 OUR AVERAGE</b>			
0.594 ± 0.021 ± 0.056	ALBRECHT	94c ARG	$e^+ e^- \rightarrow \Upsilon(4S)$
0.54 ± 0.07 ± 0.06	<sup>1</sup> ALAM	87B CLEO	$e^+ e^- \rightarrow \Upsilon(4S)$

<sup>1</sup> ALAM 87B measurement relies on lepton-kaon correlations.

### $\Gamma(K^- \ell^+ \nu_\ell \text{ anything})/\Gamma(\ell^+ \nu_\ell \text{ anything})$ $\Gamma_{25}/\Gamma_4$

$\ell$  denotes  $e$  or  $\mu$ , not the sum.

VALUE	DOCUMENT ID	TECN	COMMENT
<b>0.092 ± 0.035 OUR AVERAGE</b>			
0.086 ± 0.011 ± 0.044	ALBRECHT	94c ARG	$e^+ e^- \rightarrow \Upsilon(4S)$
0.10 ± 0.05 ± 0.02	<sup>1</sup> ALAM	87B CLEO	$e^+ e^- \rightarrow \Upsilon(4S)$

<sup>1</sup> ALAM 87B measurement relies on lepton-kaon correlations.

### $\Gamma(K^0/\bar{K}^0 \ell^+ \nu_\ell \text{ anything})/\Gamma(\ell^+ \nu_\ell \text{ anything})$ $\Gamma_{26}/\Gamma_4$

$\ell$  denotes  $e$  or  $\mu$ , not the sum. Sum over  $K^0$  and  $\bar{K}^0$  states.

VALUE	DOCUMENT ID	TECN	COMMENT
<b>0.42 ± 0.05 OUR AVERAGE</b>			
0.452 ± 0.038 ± 0.056	<sup>1</sup> ALBRECHT	94c ARG	$e^+ e^- \rightarrow \Upsilon(4S)$
0.39 ± 0.06 ± 0.04	<sup>2</sup> ALAM	87B CLEO	$e^+ e^- \rightarrow \Upsilon(4S)$

<sup>1</sup> ALBRECHT 94c assume a  $K^0/\bar{K}^0$  multiplicity twice that of  $K_S^0$ .

<sup>2</sup> ALAM 87B measurement relies on lepton-kaon correlations.

### $\langle n_c \rangle$

VALUE	DOCUMENT ID	TECN	COMMENT
<b>1.10 ± 0.05</b>	<sup>1</sup> GIBBONS	97B CLE2	$e^+ e^- \rightarrow \Upsilon(4S)$

• • • We do not use the following data for averages, fits, limits, etc. • • •

0.98 ± 0.16 ± 0.12	<sup>2</sup> ALAM	87B CLEO	$e^+ e^- \rightarrow \Upsilon(4S)$
--------------------	-------------------	----------	------------------------------------

<sup>1</sup> GIBBONS 97B from charm counting using  $B(D_S^+ \rightarrow \phi \pi) = 0.036 \pm 0.009$  and  $B(\Lambda_c^+ \rightarrow p K^- \pi^+) = 0.044 \pm 0.006$ .

<sup>2</sup> From the difference between  $K^-$  and  $K^+$  widths. ALAM 87B measurement relies on lepton-kaon correlations. It does not consider the possibility of  $B\bar{B}$  mixing. We have thus removed it from the average.

### $\Gamma(D^\pm \text{ anything})/\Gamma_{\text{total}}$ $\Gamma_{27}/\Gamma$

VALUE	EVTS	DOCUMENT ID	TECN	COMMENT
<b>0.237 ± 0.013 OUR AVERAGE</b>				

0.237 ± 0.013 ± 0.005	<sup>1</sup> GIBBONS	97B CLE2	$e^+ e^- \rightarrow \Upsilon(4S)$
0.25 ± 0.04 ± 0.01	<sup>2</sup> BORTOLETTO92	CLEO	$e^+ e^- \rightarrow \Upsilon(4S)$
0.229 ± 0.053 ± 0.005	<sup>3</sup> ALBRECHT	91H ARG	$e^+ e^- \rightarrow \Upsilon(4S)$

• • • We do not use the following data for averages, fits, limits, etc. • • •

0.208 ± 0.049 ± 0.004	20k	<sup>4</sup> BORTOLETTO87	CLEO	Sup. by BORTOLETTO 92
-----------------------	-----	---------------------------	------	-----------------------

<sup>1</sup> GIBBONS 97B reports  $[\Gamma(B \rightarrow D^\pm \text{ anything})/\Gamma_{\text{total}}] \times [B(D^+ \rightarrow K^- 2\pi^+)] = 0.0216 \pm 0.0008 \pm 0.00082$  which we divide by our best value  $B(D^+ \rightarrow K^- 2\pi^+) = (9.13 \pm 0.19) \times 10^{-2}$ . Our first error is their experiment's error and our second error is the systematic error from using our best value.

<sup>2</sup> BORTOLETTO 92 reports  $[\Gamma(B \rightarrow D^\pm \text{ anything})/\Gamma_{\text{total}}] \times [B(D^+ \rightarrow K^- 2\pi^+)] = 0.0226 \pm 0.0030 \pm 0.0018$  which we divide by our best value  $B(D^+ \rightarrow K^- 2\pi^+) = (9.13 \pm 0.19) \times 10^{-2}$ . Our first error is their experiment's error and our second error is the systematic error from using our best value.

<sup>3</sup> ALBRECHT 91H reports  $[\Gamma(B \rightarrow D^\pm \text{ anything})/\Gamma_{\text{total}}] \times [B(D^+ \rightarrow K^- 2\pi^+)] = 0.0209 \pm 0.0027 \pm 0.0040$  which we divide by our best value  $B(D^+ \rightarrow K^- 2\pi^+) = (9.13 \pm 0.19) \times 10^{-2}$ . Our first error is their experiment's error and our second error is the systematic error from using our best value.

<sup>4</sup> BORTOLETTO 87 reports  $[\Gamma(B \rightarrow D^\pm \text{ anything})/\Gamma_{\text{total}}] \times [B(D^+ \rightarrow K^- 2\pi^+)] = 0.019 \pm 0.004 \pm 0.002$  which we divide by our best value  $B(D^+ \rightarrow K^- 2\pi^+) = (9.13 \pm 0.19) \times 10^{-2}$ . Our first error is their experiment's error and our second error is the systematic error from using our best value.

### $\Gamma(D^0/\bar{D}^0 \text{ anything})/\Gamma_{\text{total}}$ $\Gamma_{28}/\Gamma$

VALUE	EVTS	DOCUMENT ID	TECN	COMMENT
<b>0.627 ± 0.029 OUR AVERAGE</b>				Error includes scale factor of 1.3. See the ideogram below.

0.648 ± 0.025 $^{+0.007}_{-0.008}$	<sup>1</sup> GIBBONS	97B CLE2	$e^+ e^- \rightarrow \Upsilon(4S)$
0.60 ± 0.05 ± 0.01	<sup>2</sup> BORTOLETTO92	CLEO	$e^+ e^- \rightarrow \Upsilon(4S)$
0.50 ± 0.08 ± 0.01	<sup>3</sup> ALBRECHT	91H ARG	$e^+ e^- \rightarrow \Upsilon(4S)$

• • • We do not use the following data for averages, fits, limits, etc. • • •

0.54 ± 0.07 ± 0.01	21k	<sup>4</sup> BORTOLETTO87	CLEO	$e^+ e^- \rightarrow \Upsilon(4S)$
0.62 ± 0.19 ± 0.01		<sup>5</sup> GREEN	83 CLEO	Repl. by BORTOLETTO 87

## Meson Particle Listings

 $B^\pm/B^0$  ADMIXTURE

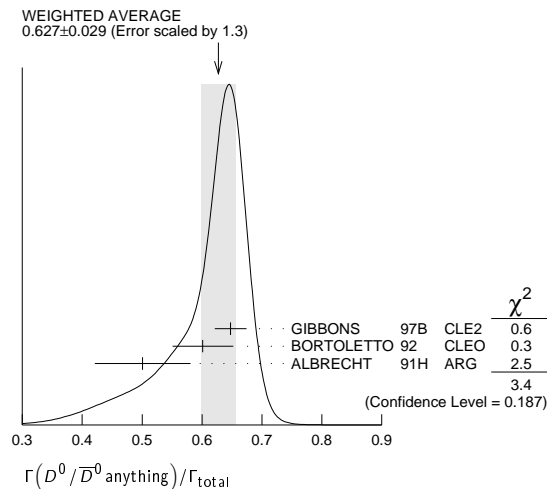
<sup>1</sup> GIBBONS 97B reports  $[\Gamma(B \rightarrow D^0/\bar{D}^0 \text{ anything})/\Gamma_{\text{total}}] \times [B(D^0 \rightarrow K^- \pi^+)] = 0.0251 \pm 0.0006 \pm 0.00075$  which we divide by our best value  $B(D^0 \rightarrow K^- \pi^+) = (3.88 \pm 0.05) \times 10^{-2}$ . Our first error is their experiment's error and our second error is the systematic error from using our best value.

<sup>2</sup> BORTOLETTO 92 reports  $[\Gamma(B \rightarrow D^0/\bar{D}^0 \text{ anything})/\Gamma_{\text{total}}] \times [B(D^0 \rightarrow K^- \pi^+)] = 0.0233 \pm 0.0012 \pm 0.0014$  which we divide by our best value  $B(D^0 \rightarrow K^- \pi^+) = (3.88 \pm 0.05) \times 10^{-2}$ . Our first error is their experiment's error and our second error is the systematic error from using our best value.

<sup>3</sup> ALBRECHT 91H reports  $[\Gamma(B \rightarrow D^0/\bar{D}^0 \text{ anything})/\Gamma_{\text{total}}] \times [B(D^0 \rightarrow K^- \pi^+)] = 0.0194 \pm 0.0015 \pm 0.0025$  which we divide by our best value  $B(D^0 \rightarrow K^- \pi^+) = (3.88 \pm 0.05) \times 10^{-2}$ . Our first error is their experiment's error and our second error is the systematic error from using our best value.

<sup>4</sup> BORTOLETTO 87 reports  $[\Gamma(B \rightarrow D^0/\bar{D}^0 \text{ anything})/\Gamma_{\text{total}}] \times [B(D^0 \rightarrow K^- \pi^+)] = 0.0210 \pm 0.0015 \pm 0.0021$  which we divide by our best value  $B(D^0 \rightarrow K^- \pi^+) = (3.88 \pm 0.05) \times 10^{-2}$ . Our first error is their experiment's error and our second error is the systematic error from using our best value.

<sup>5</sup> GREEN 83 reports  $[\Gamma(B \rightarrow D^0/\bar{D}^0 \text{ anything})/\Gamma_{\text{total}}] \times [B(D^0 \rightarrow K^- \pi^+)] = 0.024 \pm 0.006 \pm 0.004$  which we divide by our best value  $B(D^0 \rightarrow K^- \pi^+) = (3.88 \pm 0.05) \times 10^{-2}$ . Our first error is their experiment's error and our second error is the systematic error from using our best value.

 $\Gamma(D^*(2010)^\pm \text{ anything})/\Gamma_{\text{total}}$   $\Gamma_{29}/\Gamma$ 

VALUE	EVTS	DOCUMENT ID	TECN	COMMENT
<b>0.225 ± 0.015 OUR AVERAGE</b>				
0.247 ± 0.019 ± 0.01		<sup>1</sup> GIBBONS 97B	CLE2	$e^+e^- \rightarrow \Upsilon(4S)$
0.205 ± 0.019 ± 0.007		<sup>2</sup> ALBRECHT 96D	ARG	$e^+e^- \rightarrow \Upsilon(4S)$
0.230 ± 0.028 ± 0.009		<sup>3</sup> BORTOLETTO 92	CLEO	$e^+e^- \rightarrow \Upsilon(4S)$
• • • We do not use the following data for averages, fits, limits, etc. • • •				
0.283 ± 0.053 ± 0.002		<sup>4</sup> ALBRECHT 91H	ARG	Sup. by ALBRECHT 96D
0.22 ± 0.04 $^{+0.07}_{-0.04}$	5200	<sup>5</sup> BORTOLETTO 87	CLEO	$e^+e^- \rightarrow \Upsilon(4S)$
0.27 ± 0.06 $^{+0.08}_{-0.06}$	510	<sup>6</sup> CSORNA	85	CLEO Repl. by BORTOLETTO 87

<sup>1</sup> GIBBONS 97B reports  $B(B \rightarrow D^*(2010)^\pm \text{ anything}) = 0.239 \pm 0.015 \pm 0.014 \pm 0.009$  using CLEO measured  $D$  and  $D^*$  branching fractions. We rescale to our PDG 96 values of  $D$  and  $D^*$  branching ratios. Our first error is their experiment's error and our second error is the systematic error from using our best value.

<sup>2</sup> ALBRECHT 96D reports  $B(B \rightarrow D^*(2010)^\pm \text{ anything}) = 0.196 \pm 0.019$  using CLEO measured  $B(D^*(2010)^\pm \rightarrow D^0 \pi^\pm) = 0.681 \pm 0.01 \pm 0.013$ ,  $B(D^0 \rightarrow K^- \pi^+) = 0.0401 \pm 0.0014$ ,  $B(D^0 \rightarrow K^- \pi^+ \pi^+ \pi^-) = 0.081 \pm 0.005$ . We rescale to our PDG 96 values of  $D$  and  $D^*$  branching ratios. Our first error is their experiment's error and our second error is the systematic error from using our best value.

<sup>3</sup> BORTOLETTO 92 reports  $B(B \rightarrow D^*(2010)^\pm \text{ anything}) = 0.25 \pm 0.03 \pm 0.04$  using MARK II  $B(D^*(2010)^\pm \rightarrow D^0 \pi^\pm) = 0.57 \pm 0.06$  and  $B(D^0 \rightarrow K^- \pi^+) = 0.042 \pm 0.008$ . We rescale to our PDG 96 values of  $D$  and  $D^*$  branching ratios. Our first error is their experiment's error and our second error is the systematic error from using our best value.

<sup>4</sup> ALBRECHT 91H reports  $0.348 \pm 0.060 \pm 0.035$  from a measurement of  $[\Gamma(B \rightarrow D^*(2010)^\pm \text{ anything})/\Gamma_{\text{total}}] \times [B(D^*(2010)^\pm \rightarrow D^0 \pi^\pm)]$  assuming  $B(D^*(2010)^\pm \rightarrow D^0 \pi^\pm) = 0.55 \pm 0.04$ , which we rescale to our best value  $B(D^*(2010)^\pm \rightarrow D^0 \pi^\pm) = (67.7 \pm 0.5) \times 10^{-2}$ . Our first error is their experiment's error and our second error is the systematic error from using our best value. Uses the PDG 90  $B(D^0 \rightarrow K^- \pi^+) = 0.0371 \pm 0.0025$ .

<sup>5</sup> BORTOLETTO 87 uses old MARK III (BALTRUSAITIS 86E) branching ratios  $B(D^0 \rightarrow K^- \pi^+) = 0.056 \pm 0.004 \pm 0.003$  and also assumes  $B(D^*(2010)^\pm \rightarrow D^0 \pi^\pm) = 0.60 \pm 0.08$ . The product branching ratio for  $B(B \rightarrow D^*(2010)^\pm) B(D^*(2010)^\pm \rightarrow D^0 \pi^\pm)$  is  $0.13 \pm 0.02 \pm 0.012$ . Superseded by BORTOLETTO 92.

<sup>6</sup>  $V-A$  momentum spectrum used to extrapolate below  $p = 1$  GeV. We correct the value assuming  $B(D^0 \rightarrow K^- \pi^+) = 0.042 \pm 0.006$  and  $B(D^{*+} \rightarrow D^0 \pi^+) = 0.6 \pm 0.08$ . The product branching fraction is  $B(B \rightarrow D^{*+} X) \cdot B(D^{*+} \rightarrow \pi^+ D^0) \cdot B(D^0 \rightarrow K^- \pi^+) = (68 \pm 15 \pm 9) \times 10^{-4}$ .

 $\Gamma(D^*(2007)^0 \text{ anything})/\Gamma_{\text{total}}$   $\Gamma_{30}/\Gamma$ 

VALUE	DOCUMENT ID	TECN	COMMENT
<b>0.260 ± 0.023 ± 0.015</b>	<sup>1</sup> GIBBONS 97B	CLE2	$e^+e^- \rightarrow \Upsilon(4S)$

<sup>1</sup> GIBBONS 97B reports  $B(B \rightarrow D^*(2007)^0 \text{ anything}) = 0.247 \pm 0.012 \pm 0.018 \pm 0.018$  using CLEO measured  $D$  and  $D^*$  branching fractions. We rescale to our PDG 96 values of  $D$  and  $D^*$  branching ratios. Our first error is their experiment's error and our second error is the systematic error from using our best value.

 $\Gamma(D_s^\pm \text{ anything})/\Gamma_{\text{total}}$   $\Gamma_{31}/\Gamma$ 

VALUE	EVTS	DOCUMENT ID	TECN	COMMENT
<b>0.083 ± 0.008 OUR AVERAGE</b>				

0.089 ± 0.010 ± 0.008		<sup>1</sup> ARTUSO 05B	CLE2	$e^+e^- \rightarrow \Upsilon(5S)$
0.087 ± 0.005 ± 0.008		<sup>2</sup> AUBERT 02G	BABR	$e^+e^- \rightarrow \Upsilon(4S)$
0.065 ± 0.011 ± 0.006		<sup>3</sup> ALBRECHT 92G	ARG	$e^+e^- \rightarrow \Upsilon(4S)$
0.068 ± 0.010 ± 0.006	257	<sup>4</sup> BORTOLETTO 90	CLEO	$e^+e^- \rightarrow \Upsilon(4S)$
0.085 ± 0.022 ± 0.008		<sup>5</sup> HAAS 86	CLEO	$e^+e^- \rightarrow \Upsilon(4S)$

• • • We do not use the following data for averages, fits, limits, etc. • • •

0.094 ± 0.007 ± 0.008		<sup>6</sup> GIBAUT 96	CLE2	Repl. by ARTUSO 05B
0.094 ± 0.024 ± 0.008		<sup>7</sup> ALBRECHT 87H	ARG	$e^+e^- \rightarrow \Upsilon(4S)$

<sup>1</sup> ARTUSO 05B reports  $0.0905 \pm 0.0025 \pm 0.0140$  from a measurement of  $[\Gamma(B \rightarrow D_s^\pm \text{ anything})/\Gamma_{\text{total}}] \times [B(D_s^\pm \rightarrow \phi \pi^\pm)]$  assuming  $B(D_s^\pm \rightarrow \phi \pi^\pm) = (4.4 \pm 0.5) \times 10^{-2}$ , which we rescale to our best value  $B(D_s^\pm \rightarrow \phi \pi^\pm) = (4.5 \pm 0.4) \times 10^{-2}$ . Our first error is their experiment's error and our second error is the systematic error from using our best value.

<sup>2</sup> AUBERT 02G reports  $[\Gamma(B \rightarrow D_s^\pm \text{ anything})/\Gamma_{\text{total}}] \times [B(D_s^\pm \rightarrow \phi \pi^\pm)] = 0.00393 \pm 0.00007 \pm 0.00021$  which we divide by our best value  $B(D_s^\pm \rightarrow \phi \pi^\pm) = (4.5 \pm 0.4) \times 10^{-2}$ . Our first error is their experiment's error and our second error is the systematic error from using our best value.

<sup>3</sup> ALBRECHT 92G reports  $[\Gamma(B \rightarrow D_s^\pm \text{ anything})/\Gamma_{\text{total}}] \times [B(D_s^\pm \rightarrow \phi \pi^\pm)] = 0.00292 \pm 0.00039 \pm 0.00031$  which we divide by our best value  $B(D_s^\pm \rightarrow \phi \pi^\pm) = (4.5 \pm 0.4) \times 10^{-2}$ . Our first error is their experiment's error and our second error is the systematic error from using our best value.

<sup>4</sup> BORTOLETTO 90 reports  $[\Gamma(B \rightarrow D_s^\pm \text{ anything})/\Gamma_{\text{total}}] \times [B(D_s^\pm \rightarrow \phi \pi^\pm)] = 0.00306 \pm 0.00047$  which we divide by our best value  $B(D_s^\pm \rightarrow \phi \pi^\pm) = (4.5 \pm 0.4) \times 10^{-2}$ . Our first error is their experiment's error and our second error is the systematic error from using our best value.

<sup>5</sup> HAAS 86 reports  $[\Gamma(B \rightarrow D_s^\pm \text{ anything})/\Gamma_{\text{total}}] \times [B(D_s^\pm \rightarrow \phi \pi^\pm)] = 0.0038 \pm 0.0010$  which we divide by our best value  $B(D_s^\pm \rightarrow \phi \pi^\pm) = (4.5 \pm 0.4) \times 10^{-2}$ . Our first error is their experiment's error and our second error is the systematic error from using our best value. 64 ± 22% decays are 2-body.

<sup>6</sup> GIBAUT 96 reports  $0.1211 \pm 0.0039 \pm 0.0088$  from a measurement of  $[\Gamma(B \rightarrow D_s^\pm \text{ anything})/\Gamma_{\text{total}}] \times [B(D_s^\pm \rightarrow \phi \pi^\pm)]$  assuming  $B(D_s^\pm \rightarrow \phi \pi^\pm) = 0.035$ , which we rescale to our best value  $B(D_s^\pm \rightarrow \phi \pi^\pm) = (4.5 \pm 0.4) \times 10^{-2}$ . Our first error is their experiment's error and our second error is the systematic error from using our best value.

<sup>7</sup> ALBRECHT 87H reports  $[\Gamma(B \rightarrow D_s^\pm \text{ anything})/\Gamma_{\text{total}}] \times [B(D_s^\pm \rightarrow \phi \pi^\pm)] = 0.0042 \pm 0.0009 \pm 0.0006$  which we divide by our best value  $B(D_s^\pm \rightarrow \phi \pi^\pm) = (4.5 \pm 0.4) \times 10^{-2}$ . Our first error is their experiment's error and our second error is the systematic error from using our best value. 46 ± 16% of  $B \rightarrow D_s X$  decays are 2-body. Superseded by ALBRECHT 92G.

 $\Gamma(D_s^{*\pm} \text{ anything})/\Gamma_{\text{total}}$   $\Gamma_{32}/\Gamma$ 

VALUE	DOCUMENT ID	TECN	COMMENT
<b>0.063 ± 0.009 ± 0.006</b>	<sup>1</sup> AUBERT 02G	BABR	$e^+e^- \rightarrow \Upsilon(4S)$

<sup>1</sup> AUBERT 02G reports  $[\Gamma(B \rightarrow D_s^{*\pm} \text{ anything})/\Gamma_{\text{total}}] \times [B(D_s^{*\pm} \rightarrow \phi \pi^\pm)] = 0.00284 \pm 0.00029 \pm 0.00025$  which we divide by our best value  $B(D_s^{*\pm} \rightarrow \phi \pi^\pm) = (4.5 \pm 0.4) \times 10^{-2}$ . Our first error is their experiment's error and our second error is the systematic error from using our best value.

 $\Gamma(D_s^{*\pm} \bar{D}^{(*)})/\Gamma(D_s^{*\pm} \text{ anything})$   $\Gamma_{33}/\Gamma_{32}$ 

VALUE	DOCUMENT ID	TECN	COMMENT
<b>0.533 ± 0.037 ± 0.037</b>	AUBERT 02G	BABR	$e^+e^- \rightarrow \Upsilon(4S)$

 $\Gamma(\bar{D} D_{s0}(2317))/\Gamma_{\text{total}}$   $\Gamma_{34}/\Gamma$ 

VALUE	DOCUMENT ID	TECN	COMMENT
seen	<sup>1</sup> KROKOVNY 03B	BELL	$e^+e^- \rightarrow \Upsilon(4S)$

<sup>1</sup> The product branching ratio for  $B(B \rightarrow \bar{D} D_{s0}(2317)^+) \times B(D_{s0}(2317)^+ \rightarrow D_s \pi^0)$  is measured to be  $(8.5 \pm 2.1 \pm 1.9 \pm 2.6) \times 10^{-4}$ .

 $\Gamma(\bar{D} D_{sJ}(2457))/\Gamma_{\text{total}}$   $\Gamma_{35}/\Gamma$ 

VALUE	DOCUMENT ID	TECN	COMMENT
seen	<sup>1</sup> KROKOVNY 03B	BELL	$e^+e^- \rightarrow \Upsilon(4S)$

<sup>1</sup> The product branching ratio for  $B(B \rightarrow \bar{D} D_{sJ}(2457)^+) \times B(D_{sJ}(2457)^+ \rightarrow D_s^{*+} \pi^0, D_s^+ \gamma)$  are measured to be  $(17.8 \pm 4.5 \pm 5.3) \times 10^{-4}$  and  $(6.7 \pm 1.3 \pm 2.0) \times 10^{-4}$ , respectively.

 $[\Gamma(D^{(*)} \bar{D}^{(*)} K^0) + \Gamma(D^{(*)} \bar{D}^{(*)} K^\pm)]/\Gamma_{\text{total}}$   $\Gamma_{36}/\Gamma$ 

VALUE	DOCUMENT ID	TECN	COMMENT
<b>0.071 ± 0.025 ± 0.010</b> <b>-0.015 ± 0.009</b>	<sup>1</sup> BARATE 98Q	ALEP	$e^+e^- \rightarrow Z$

<sup>1</sup> The systematic error includes the uncertainties due to the charm branching ratios.

# Meson Particle Listings

## $B^\pm/B^0$ ADMIXTURE

$\Gamma(B \rightarrow c\bar{c}s)/\Gamma_{\text{total}}$		$\Gamma_{37}/\Gamma$	
VALUE	DOCUMENT ID	TECN	COMMENT
<b>0.219 ± 0.037</b>	1 COAN	98	CLE2 $e^+e^- \rightarrow \Upsilon(4S)$

<sup>1</sup> COAN 98 uses  $D$ - $\ell$  correlation.

$\Gamma(D_s^{(*)}\bar{D}^{(*)})/\Gamma(D_s^\pm \text{ anything})$		$\Gamma_{38}/\Gamma_{31}$	
VALUE	DOCUMENT ID	TECN	COMMENT
<b>0.469 ± 0.017 OUR AVERAGE</b>	Sum over modes. Error includes scale factor of 1.1.		
0.464 ± 0.013 ± 0.015	AUBERT	02G	BABR $e^+e^- \rightarrow \Upsilon(4S)$
0.56 $\begin{smallmatrix} +0.21 & +0.09 \\ -0.15 & -0.08 \end{smallmatrix}$	1 BARATE	98Q	ALEP $e^+e^- \rightarrow Z$
0.457 ± 0.019 ± 0.037	GIBAUT	96	CLE2 $e^+e^- \rightarrow \Upsilon(4S)$
0.58 ± 0.07 ± 0.09	ALBRECHT	92G	ARG $e^+e^- \rightarrow \Upsilon(4S)$
0.56 ± 0.10	BORTOLETTO	090	CLEO $e^+e^- \rightarrow \Upsilon(4S)$

<sup>1</sup> BARATE 98Q measures  $B(B \rightarrow D_s^{(*)}\bar{D}^{(*)}) = 0.056^{+0.021+0.009+0.019}_{-0.015-0.008-0.011}$ , where the third error results from the uncertainty on the different  $D$  branching ratios and is dominated by the uncertainty on  $B(D_s^+ \rightarrow \phi\pi^+)$ . We divide  $B(B \rightarrow D_s^{(*)}\bar{D}^{(*)})$  by our best value of  $B(B \rightarrow D_s \text{ anything}) = 0.1 \pm 0.025$ .

$\Gamma(D^* D^*(2010)^\pm)/\Gamma_{\text{total}}$		$\Gamma_{39}/\Gamma$	
VALUE	DOCUMENT ID	TECN	COMMENT
<b>&lt;5.9 × 10<sup>-3</sup></b>	90	BARATE	98Q ALEP $e^+e^- \rightarrow Z$

$[\Gamma(D D^*(2010)^\pm) + \Gamma(D^* D^\pm)]/\Gamma_{\text{total}}$		$\Gamma_{40}/\Gamma$	
VALUE	DOCUMENT ID	TECN	COMMENT
<b>&lt;5.5 × 10<sup>-3</sup></b>	90	BARATE	98Q ALEP $e^+e^- \rightarrow Z$

$\Gamma(D D^\pm)/\Gamma_{\text{total}}$		$\Gamma_{41}/\Gamma$	
VALUE	DOCUMENT ID	TECN	COMMENT
<b>&lt;3.1 × 10<sup>-3</sup></b>	90	BARATE	98Q ALEP $e^+e^- \rightarrow Z$

$\Gamma(D_s^{(*)}\bar{D}^{(*)}X(n\pi^\pm))/\Gamma_{\text{total}}$		$\Gamma_{42}/\Gamma$	
VALUE	DOCUMENT ID	TECN	COMMENT
<b>0.094 <math>\begin{smallmatrix} +0.040 &amp; +0.034 \\ -0.031 &amp; -0.024 \end{smallmatrix}</math></b>	1 BARATE	98Q	ALEP $e^+e^- \rightarrow Z$

<sup>1</sup> The systematic error includes the uncertainties due to the charm branching ratios.

$\Gamma(D^*(2010)\gamma)/\Gamma_{\text{total}}$		$\Gamma_{43}/\Gamma$	
VALUE	DOCUMENT ID	TECN	COMMENT
<b>&lt;1.1 × 10<sup>-3</sup></b>	90	1 LESIAK	92 CBAL $e^+e^- \rightarrow \Upsilon(4S)$

<sup>1</sup> LESIAK 92 set a limit on the inclusive process  $B(B \rightarrow s\gamma) < 2.8 \times 10^{-3}$  at 90% CL for the range of masses of 892–2045 MeV, independent of assumptions about s-quark hadronization.

$\Gamma(D_s^+ \pi^-, D_s^{*+} \pi^-, D_s^+ \rho^-, D_s^{*+} \rho^-, D_s^+ \pi^0, D_s^{*+} \pi^0, D_s^+ \eta, D_s^{*+} \eta, D_s^+ \rho^0, D_s^{*+} \rho^0, D_s^+ \omega, D_s^{*+} \omega)/\Gamma_{\text{total}}$		$\Gamma_{44}/\Gamma$	
VALUE	DOCUMENT ID	TECN	COMMENT
<b>&lt;4 × 10<sup>-4</sup></b>	90	1 ALEXANDER	93B CLE2 $e^+e^- \rightarrow \Upsilon(4S)$

<sup>1</sup> ALEXANDER 93B reports  $< 4.8 \times 10^{-4}$  from a measurement of  $[\Gamma(B \rightarrow D_s^+ \pi^-, D_s^{*+} \pi^-, D_s^+ \rho^-, D_s^{*+} \rho^-, D_s^+ \pi^0, D_s^{*+} \pi^0, D_s^+ \eta, D_s^{*+} \eta, D_s^+ \rho^0, D_s^{*+} \rho^0, D_s^+ \omega, D_s^{*+} \omega)/\Gamma_{\text{total}}] \times [B(D_s^+ \rightarrow \phi\pi^+)]$  assuming  $B(D_s^+ \rightarrow \phi\pi^+) = 0.037$ , which we rescale to our best value  $B(D_s^+ \rightarrow \phi\pi^+) = 4.5 \times 10^{-2}$ . This branching ratio limit provides a model-dependent upper limit  $|V_{ub}|/|V_{cb}| < 0.16$  at CL=90%.

$\Gamma(D_{s1}(2536)^+ \text{ anything})/\Gamma_{\text{total}}$		$\Gamma_{45}/\Gamma$	
VALUE	DOCUMENT ID	TECN	COMMENT
<b>&lt;0.0095</b>	90	1 BISHAI	98 CLE2 $e^+e^- \rightarrow \Upsilon(4S)$

<sup>1</sup> Assuming factorization, the decay constant  $f_{D_{s1}^+}$  is at least a factor of 2.5 times smaller than  $f_{D_s^+}$ .

$\Gamma(J/\psi(1S) \text{ anything})/\Gamma_{\text{total}}$		$\Gamma_{46}/\Gamma$	
VALUE (units 10 <sup>-2</sup> )	DOCUMENT ID	TECN	COMMENT
<b>1.094 ± 0.032 OUR AVERAGE</b>	Error includes scale factor of 1.1.		
1.057 ± 0.012 ± 0.040	1 AUBERT	03F	BABR $e^+e^- \rightarrow \Upsilon(4S)$
1.121 ± 0.013 ± 0.042	ANDERSON	02	CLE2 $e^+e^- \rightarrow \Upsilon(4S)$
1.30 ± 0.45 ± 0.01	2 MASCHMANN	90	CBAL $e^+e^- \rightarrow \Upsilon(4S)$
1.24 ± 0.27 ± 0.01	3 ALBRECHT	87D	ARG $e^+e^- \rightarrow \Upsilon(4S)$
1.36 ± 0.24 ± 0.01	4 ALAM	86	CLEO $e^+e^- \rightarrow \Upsilon(4S)$
••• We do not use the following data for averages, fits, limits, etc. •••			
1.13 ± 0.06 ± 0.01	1489	5 BALEST	95B CLE2 $e^+e^- \rightarrow \Upsilon(4S)$
1.4 $\begin{smallmatrix} +0.6 \\ -0.5 \end{smallmatrix}$	7	6 ALBRECHT	85H ARG $e^+e^- \rightarrow \Upsilon(4S)$
1.1 ± 0.21 ± 0.23	46	7 HAAS	85 CLEO Repl. by ALAM 86

<sup>1</sup> AUBERT 03F also reports the momentum distribution and helicity of  $J/\psi \rightarrow \ell^+ \ell^-$  in the  $\Upsilon(4S)$  center-of-mass frame.

<sup>2</sup> MASCHMANN 90 reports  $(1.12 \pm 0.33 \pm 0.25) \times 10^{-2}$  from a measurement of  $[\Gamma(B \rightarrow J/\psi(1S) \text{ anything})/\Gamma_{\text{total}}] \times [B(J/\psi(1S) \rightarrow e^+e^-)]$  assuming  $B(J/\psi(1S) \rightarrow e^+e^-) = 0.069 \pm 0.009$ , which we rescale to our best value  $B(J/\psi(1S) \rightarrow e^+e^-) = (5.94 \pm 0.06) \times 10^{-2}$ . Our first error is their experiment's error and our second error is the systematic error from using our best value.

<sup>3</sup> ALBRECHT 87D reports  $(1.07 \pm 0.16 \pm 0.22) \times 10^{-2}$  from a measurement of  $[\Gamma(B \rightarrow J/\psi(1S) \text{ anything})/\Gamma_{\text{total}}] \times [B(J/\psi(1S) \rightarrow e^+e^-)]$  assuming  $B(J/\psi(1S) \rightarrow e^+e^-) = 0.069 \pm 0.009$ , which we rescale to our best value  $B(J/\psi(1S) \rightarrow e^+e^-) = (5.94 \pm 0.06) \times 10^{-2}$ . Our first error is their experiment's error and our second error is the systematic error from using our best value. ALBRECHT 87D find the branching ratio for  $J/\psi$  not from  $\psi(2S)$  to be  $0.0081 \pm 0.0023$ .

<sup>4</sup> ALAM 86 reports  $(1.09 \pm 0.16 \pm 0.21) \times 10^{-2}$  from a measurement of  $[\Gamma(B \rightarrow J/\psi(1S) \text{ anything})/\Gamma_{\text{total}}] \times [B(J/\psi(1S) \rightarrow \mu^+ \mu^-)]$  assuming  $B(J/\psi(1S) \rightarrow \mu^+ \mu^-) = 0.074 \pm 0.012$ , which we rescale to our best value  $B(J/\psi(1S) \rightarrow \mu^+ \mu^-) = (5.93 \pm 0.06) \times 10^{-2}$ . Our first error is their experiment's error and our second error is the systematic error from using our best value.

<sup>5</sup> BALEST 95B reports  $(1.12 \pm 0.04 \pm 0.06) \times 10^{-2}$  from a measurement of  $[\Gamma(B \rightarrow J/\psi(1S) \text{ anything})/\Gamma_{\text{total}}] \times [B(J/\psi(1S) \rightarrow e^+e^-)]$  assuming  $B(J/\psi(1S) \rightarrow e^+e^-) = 0.0599 \pm 0.0025$ , which we rescale to our best value  $B(J/\psi(1S) \rightarrow e^+e^-) = (5.94 \pm 0.06) \times 10^{-2}$ . Our first error is their experiment's error and our second error is the systematic error from using our best value. They measure  $J/\psi(1S) \rightarrow e^+e^-$  and  $\mu^+ \mu^-$  and use PDG 1994 values for the branching fractions. The rescaling is the same for either mode so we use  $e^+e^-$ .

<sup>6</sup> Statistical and systematic errors were added in quadrature. ALBRECHT 85H also report a CL = 90% limit of 0.007 for  $B \rightarrow J/\psi(1S) + X$  where  $m_X < 1$  GeV.

<sup>7</sup> Dimuon and dielectron events used.

$\Gamma(J/\psi(1S) \text{ (direct) anything})/\Gamma_{\text{total}}$		$\Gamma_{47}/\Gamma$	
VALUE	DOCUMENT ID	TECN	COMMENT
<b>0.0078 ± 0.0004 OUR AVERAGE</b>	Error includes scale factor of 1.1.		
0.00740 ± 0.00023 ± 0.00043	1 AUBERT	03F	BABR $e^+e^- \rightarrow \Upsilon(4S)$
0.00813 ± 0.00017 ± 0.00037	2 ANDERSON	02	CLE2 $e^+e^- \rightarrow \Upsilon(4S)$
••• We do not use the following data for averages, fits, limits, etc. •••			
0.0080 ± 0.0008	3 BALEST	95B	CLE2 $e^+e^- \rightarrow \Upsilon(4S)$

<sup>1</sup> AUBERT 03F also reports the helicity of  $J/\psi \rightarrow \ell^+ \ell^-$  produced directly in  $B$  decay.

<sup>2</sup> Also reports the measurement of  $J/\psi \rightarrow \ell^+ \ell^-$  polarization produced directly from  $B$  decay.

<sup>3</sup> BALEST 95B assume PDG 1994 values for sub mode branching ratios.  $J/\psi(1S)$  mesons are reconstructed in  $J/\psi(1S) \rightarrow e^+e^-$  and  $J/\psi(1S) \rightarrow \mu^+ \mu^-$ . The  $B \rightarrow J/\psi(1S)X$  branching ratio contains  $J/\psi(1S)$  mesons directly from  $B$  decays and also from feeddown through  $\psi(2S) \rightarrow J/\psi(1S)$ ,  $\chi_{c1}(1P) \rightarrow J/\psi(1S)$ , or  $\chi_{c2}(1P) \rightarrow J/\psi(1S)$ . Using the measured inclusive rates, BALEST 95B corrects for the feeddown and finds the  $B \rightarrow J/\psi(1S) \text{ (direct) } X$  branching ratio.

$\Gamma(\psi(2S) \text{ anything})/\Gamma_{\text{total}}$		$\Gamma_{48}/\Gamma$	
VALUE	DOCUMENT ID	TECN	COMMENT
<b>0.00307 ± 0.00021 OUR AVERAGE</b>	EVTs Error includes scale factor of 1.1.		
0.00297 ± 0.00020 ± 0.00020	AUBERT	03F	BABR $e^+e^- \rightarrow \Upsilon(4S)$
0.00316 ± 0.00014 ± 0.00028	1 ANDERSON	02	CLE2 $e^+e^- \rightarrow \Upsilon(4S)$
0.0046 ± 0.0017 ± 0.0011	8	ALBRECHT	87D ARG $e^+e^- \rightarrow \Upsilon(4S)$
••• We do not use the following data for averages, fits, limits, etc. •••			
0.0034 ± 0.0004 ± 0.0003	240	2 BALEST	95B CLE2 $e^+e^- \rightarrow \Upsilon(4S)$

<sup>1</sup> Also reports the measurement of  $\psi(2S) \rightarrow \ell^+ \ell^-$  polarization produced directly from  $B$  decay.

<sup>2</sup> BALEST 95B assume PDG 1994 values for sub mode branching ratios. They find  $B(B \rightarrow \psi(2S)X, \psi(2S) \rightarrow \ell^+ \ell^-) = 0.30 \pm 0.05 \pm 0.04$  and  $B(B \rightarrow \psi(2S)X, \psi(2S) \rightarrow J/\psi(1S) \pi^+ \pi^-) = 0.37 \pm 0.05 \pm 0.05$ . Weighted average is quoted for  $B(B \rightarrow \psi(2S)X)$ .

$\Gamma(\chi_{c1}(1P) \text{ anything})/\Gamma_{\text{total}}$		$\Gamma_{49}/\Gamma$	
VALUE	DOCUMENT ID	TECN	COMMENT
<b>0.00386 ± 0.00027 OUR AVERAGE</b>	EVTs Error includes scale factor of 1.1.		
0.00367 ± 0.00035 ± 0.00044	AUBERT	03F	BABR $e^+e^- \rightarrow \Upsilon(4S)$
0.00363 ± 0.00022 ± 0.00034	1 ABE	02L	BELL $e^+e^- \rightarrow \Upsilon(4S)$
0.00435 ± 0.00029 ± 0.00040	ANDERSON	02	CLE2 $e^+e^- \rightarrow \Upsilon(4S)$
••• We do not use the following data for averages, fits, limits, etc. •••			
0.00329 ± 0.00035 ± 0.00014	2 CHEN	01	CLE2 $e^+e^- \rightarrow \Upsilon(4S)$
0.0040 ± 0.0006 ± 0.0004	112	3 BALEST	95B CLE2 Repl. by CHEN 01
0.0105 ± 0.0035 ± 0.0025	4	ALBRECHT	92E ARG $e^+e^- \rightarrow \Upsilon(4S)$

<sup>1</sup> ABE 02L uses PDG 01 values for  $B(J/\psi(1S) \rightarrow \ell^+ \ell^-)$  and  $B(\chi_{c1,c2} \rightarrow J/\psi(1S)\gamma)$ .

<sup>2</sup> CHEN 01 reports  $0.00414 \pm 0.00031 \pm 0.00040$  from a measurement of  $[\Gamma(B \rightarrow \chi_{c1}(1P) \text{ anything})/\Gamma_{\text{total}}] \times [B(\chi_{c1}(1P) \rightarrow \gamma J/\psi(1S))]$  assuming  $B(\chi_{c1}(1P) \rightarrow \gamma J/\psi(1S)) = 0.273 \pm 0.016$ , which we rescale to our best value  $B(\chi_{c1}(1P) \rightarrow \gamma J/\psi(1S)) = (34.4 \pm 1.5) \times 10^{-2}$ . Our first error is their experiment's error and our second error is the systematic error from using our best value. Assumes equal production of  $B^+$  and  $B^0$  at the  $\Upsilon(4S)$ .

<sup>3</sup> BALEST 95B assume  $B(\chi_{c1}(1P) \rightarrow J/\psi(1S)\gamma) = (27.3 \pm 1.6) \times 10^{-2}$ , the PDG 1994 value. Fit to  $\psi$ -photon invariant mass distribution allows for a  $\chi_{c1}(1P)$  and a  $\chi_{c2}(1P)$  component.

<sup>4</sup> ALBRECHT 92E assumes no  $\chi_{c2}(1P)$  production.

# Meson Particle Listings

## $B^\pm/B^0$ ADMIXTURE

### $\Gamma(\chi_{c1}(1P)(\text{direct anything})/\Gamma_{\text{total}})$ $\Gamma_{50}/\Gamma$

VALUE	DOCUMENT ID	TECN	COMMENT	$\Gamma_{50}/\Gamma$
<b>0.00322 ± 0.00025 OUR AVERAGE</b>				
0.00341 ± 0.00035 ± 0.00042	AUBERT	03F	BABR $e^+e^- \rightarrow \Upsilon(4S)$	
0.00332 ± 0.00022 ± 0.00034	<sup>1</sup> ABE	02L	BELL $e^+e^- \rightarrow \Upsilon(4S)$	
0.0030 ± 0.0004 ± 0.0001	<sup>2</sup> CHEN	01	CLE2 $e^+e^- \rightarrow \Upsilon(4S)$	
0.0037 ± 0.0007	<sup>3</sup> BALEST	95B	CLE2 Repl. by CHEN 01	

• • • We do not use the following data for averages, fits, limits, etc. • • •

<sup>1</sup> ABE 02L uses PDG 01 values for  $B(J/\psi(1S) \rightarrow \ell^+\ell^-)$  and  $B(\chi_{c1,c2} \rightarrow J/\psi(1S)\gamma)$ .

<sup>2</sup> CHEN 01 reports  $0.00383 \pm 0.00031 \pm 0.00040$  from a measurement of  $[\Gamma(B \rightarrow \chi_{c1}(1P)(\text{direct anything})/\Gamma_{\text{total}}) \times [B(\chi_{c1}(1P) \rightarrow \gamma J/\psi(1S))] \text{ assuming } B(\chi_{c1}(1P) \rightarrow \gamma J/\psi(1S)) = 0.273 \pm 0.016, \text{ which we rescale to our best value } B(\chi_{c1}(1P) \rightarrow \gamma J/\psi(1S)) = (34.4 \pm 1.5) \times 10^{-2}.$  Our first error is their experiment's error and our second error is the systematic error from using our best value. Assumes equal production of  $B^+$  and  $B^0$  at the  $\Upsilon(4S)$ .

<sup>3</sup> BALEST 95B assume PDG 1994 values.  $J/\psi(1S)$  mesons are reconstructed in the  $e^+e^-$  and  $\mu^+\mu^-$  modes. The  $B \rightarrow \chi_{c1}(1P)X$  branching ratio contains  $\chi_{c1}(1P)$  mesons directly from  $B$  decays and also from feeddown through  $\psi(2S) \rightarrow \chi_{c1}(1P)\gamma$ . Using the measured inclusive rates, BALEST 95B corrects for the feeddown and finds the  $B \rightarrow \chi_{c1}(1P)(\text{direct})X$  branching ratio.

### $\Gamma(\chi_{c2}(1P)\text{anything})/\Gamma_{\text{total}}$ $\Gamma_{51}/\Gamma$

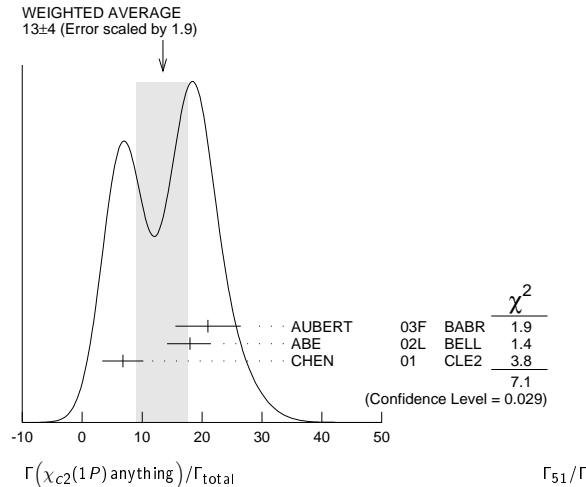
VALUE (units $10^{-4}$ )	CL%	EVTS	DOCUMENT ID	TECN	COMMENT	$\Gamma_{51}/\Gamma$
<b>13 ± 4 OUR AVERAGE</b>					Error includes scale factor of 1.9. See the ideogram below.	
21.0 ± 4.5 ± 3.1			AUBERT	03F	BABR $e^+e^- \rightarrow \Upsilon(4S)$	
18.0 <sup>+2.3</sup> <sub>-2.8</sub> ± 2.6			<sup>1</sup> ABE	02L	BELL $e^+e^- \rightarrow \Upsilon(4S)$	
6.8 ± 3.4 ± 0.3			<sup>2</sup> CHEN	01	CLE2 $e^+e^- \rightarrow \Upsilon(4S)$	
<0.38	90	35	<sup>3</sup> BALEST	95B	CLE2 Repl. by CHEN 01	

• • • We do not use the following data for averages, fits, limits, etc. • • •

<sup>1</sup> ABE 02L uses PDG 01 values for  $B(J/\psi(1S) \rightarrow \ell^+\ell^-)$  and  $B(\chi_{c1,c2} \rightarrow J/\psi(1S)\gamma)$ .

<sup>2</sup> CHEN 01 reports  $(9.8 \pm 4.8 \pm 1.5) \times 10^{-4}$  from a measurement of  $[\Gamma(B \rightarrow \chi_{c2}(1P)\text{anything})/\Gamma_{\text{total}}] \times [B(\chi_{c2}(1P) \rightarrow \gamma J/\psi(1S))] \text{ assuming } B(\chi_{c2}(1P) \rightarrow \gamma J/\psi(1S)) = 0.135 \pm 0.011, \text{ which we rescale to our best value } B(\chi_{c2}(1P) \rightarrow \gamma J/\psi(1S)) = (19.5 \pm 0.8) \times 10^{-2}.$  Our first error is their experiment's error and our second error is the systematic error from using our best value. Assumes equal production of  $B^+$  and  $B^0$  at the  $\Upsilon(4S)$ .

<sup>3</sup> BALEST 95B assume  $B(\chi_{c2}(1P) \rightarrow J/\psi(1S)\gamma) = (13.5 \pm 1.1) \times 10^{-2}$ , the PDG 1994 value.  $J/\psi(1S)$  mesons are reconstructed in the  $e^+e^-$  and  $\mu^+\mu^-$  modes, and PDG 1994 branching fractions are used. If interpreted as signal, the  $35 \pm 13$  events correspond to  $B(B \rightarrow \chi_{c2}(1P)X) = (0.25 \pm 0.10 \pm 0.03) \times 10^{-2}$ .



### $\Gamma(\chi_{c2}(1P)(\text{direct anything})/\Gamma_{\text{total}})$ $\Gamma_{52}/\Gamma$

VALUE	DOCUMENT ID	TECN	COMMENT	$\Gamma_{52}/\Gamma$
<b>0.00165 ± 0.00031 OUR AVERAGE</b>				
0.00190 ± 0.00045 ± 0.00029	AUBERT	03F	BABR $e^+e^- \rightarrow \Upsilon(4S)$	
0.00153 <sup>+0.00023</sup> <sub>-0.00028</sub> ± 0.00027	<sup>1</sup> ABE	02L	BELL $e^+e^- \rightarrow \Upsilon(4S)$	

<sup>1</sup> ABE 02L uses PDG 01 values for  $B(J/\psi(1S) \rightarrow \ell^+\ell^-)$  and  $B(\chi_{c1,c2} \rightarrow J/\psi(1S)\gamma)$ .

### $\Gamma(\eta_c(1S)\text{anything})/\Gamma_{\text{total}}$ $\Gamma_{53}/\Gamma$

VALUE	CL%	DOCUMENT ID	TECN	COMMENT	$\Gamma_{53}/\Gamma$
<b>&lt;0.009</b>	90	<sup>1</sup> BALEST	95B	CLE2 $e^+e^- \rightarrow \Upsilon(4S)$	

<sup>1</sup> BALEST 95B assume PDG 1994 values for sub mode branching ratios.  $J/\psi(1S)$  mesons are reconstructed in  $J/\psi(1S) \rightarrow e^+e^-$  and  $J/\psi(1S) \rightarrow \mu^+\mu^-$ . Search region  $2960 < m_{\eta_c(1S)} < 3010$  MeV/ $c^2$ .

### $\Gamma(KX(3872) \times B(X \rightarrow D^0\bar{D}^0\pi^0))/\Gamma_{\text{total}}$ $\Gamma_{54}/\Gamma$

VALUE (units $10^{-4}$ )	DOCUMENT ID	TECN	COMMENT	$\Gamma_{54}/\Gamma$
<b>1.22 ± 0.31<sup>+0.23</sup><sub>-0.30</sub></b>	<sup>1</sup> GOKHROO	06	BELL $e^+e^- \rightarrow \Upsilon(4S)$	

<sup>1</sup> Measure the near-threshold enhancements in the  $(D^0\bar{D}^0\pi^0)$  system at a mass  $3875.2 \pm 0.7<sup>+0.3</sup><sub>-1.6</sub> \pm 0.8$  MeV/ $c^2$ .

### $\Gamma(KX(3872) \times B(X \rightarrow D^{*0}D^0))/\Gamma_{\text{total}}$ $\Gamma_{55}/\Gamma$

VALUE (units $10^{-4}$ )	DOCUMENT ID	TECN	COMMENT	$\Gamma_{55}/\Gamma$
<b>0.80 ± 0.20 ± 0.10</b>	AUSHEV	10	BELL $e^+e^- \rightarrow \Upsilon(4S)$	

### $\Gamma(KX(3940) \times B(X \rightarrow D^{*0}D^0))/\Gamma_{\text{total}}$ $\Gamma_{56}/\Gamma$

VALUE (units $10^{-4}$ )	CL%	DOCUMENT ID	TECN	COMMENT	$\Gamma_{56}/\Gamma$
<b>&lt;0.67</b>	90	AUSHEV	10	BELL $e^+e^- \rightarrow \Upsilon(4S)$	

### $\Gamma(KX(3915) \times B(X \rightarrow \omega J/\psi))/\Gamma_{\text{total}}$ $\Gamma_{57}/\Gamma$

VALUE (units $10^{-5}$ )	DOCUMENT ID	TECN	COMMENT	$\Gamma_{57}/\Gamma$
<b>7.1 ± 1.3 ± 3.1</b>	<sup>1</sup> CHOI	05	BELL $e^+e^- \rightarrow \Upsilon(4S)$	

<sup>1</sup> CHOI 05 reports the observation of a near-threshold enhancement in the  $\omega J/\psi$  mass spectrum in exclusive  $B \rightarrow K\omega J/\psi$ . The new state, denoted as  $X(3915)$ , is measured to have a mass of  $3943 \pm 11 \pm 13$  GeV/ $c^2$  and a width  $\Gamma = 87 \pm 22 \pm 26$  MeV.

### $\Gamma(K^\pm\text{anything})/\Gamma_{\text{total}}$ $\Gamma_{58}/\Gamma$

VALUE	DOCUMENT ID	TECN	COMMENT	$\Gamma_{58}/\Gamma$
<b>0.789 ± 0.025 OUR AVERAGE</b>				
0.82 ± 0.01 ± 0.05	ALBRECHT	94C	ARG $e^+e^- \rightarrow \Upsilon(4S)$	
0.775 ± 0.015 ± 0.025	<sup>1</sup> ALBRECHT	93I	ARG $e^+e^- \rightarrow \Upsilon(4S)$	
0.85 ± 0.07 ± 0.09	ALAM	87B	CLEO $e^+e^- \rightarrow \Upsilon(4S)$	
<0.38	90	35	<sup>3</sup> BALEST	

• • • We do not use the following data for averages, fits, limits, etc. • • •

seen <sup>2</sup> BRODY 82 CLEO  $e^+e^- \rightarrow \Upsilon(4S)$

seen <sup>3</sup> GIANNINI 82 CUSB  $e^+e^- \rightarrow \Upsilon(4S)$

<sup>1</sup> ALBRECHT 93I value is not independent of the sum of  $B \rightarrow K^+$  anything and  $B \rightarrow K^-$  anything ALBRECHT 94C values.

<sup>2</sup> Assuming  $\Upsilon(4S) \rightarrow B\bar{B}$ , a total of  $3.38 \pm 0.34 \pm 0.68$  kaons per  $\Upsilon(4S)$  decay is found (the second error is systematic). In the context of the standard  $B$ -decay model, this leads to a value for  $(b\text{-quark} \rightarrow c\text{-quark})/(b\text{-quark} \rightarrow \text{all})$  of  $1.09 \pm 0.33 \pm 0.13$ .

<sup>3</sup> GIANNINI 82 at CESR-CUSB observed  $1.58 \pm 0.35$   $K^0$  per hadronic event much higher than  $0.82 \pm 0.10$  below threshold. Consistent with predominant  $b \rightarrow cX$  decay.

### $\Gamma(K^+\text{anything})/\Gamma_{\text{total}}$ $\Gamma_{59}/\Gamma$

VALUE	DOCUMENT ID	TECN	COMMENT	$\Gamma_{59}/\Gamma$
<b>0.66 ± 0.05</b>	<sup>1</sup> ALBRECHT	94C	ARG $e^+e^- \rightarrow \Upsilon(4S)$	
<0.38	90	35	<sup>3</sup> BALEST	
0.620 ± 0.013 ± 0.038	<sup>2</sup> ALBRECHT	94C	ARG $e^+e^- \rightarrow \Upsilon(4S)$	
0.66 ± 0.05 ± 0.07	<sup>2</sup> ALAM	87B	CLEO $e^+e^- \rightarrow \Upsilon(4S)$	

• • • We do not use the following data for averages, fits, limits, etc. • • •

<sup>1</sup> Measurement relies on lepton-kaon correlations. It is for the weak decay vertex and does not include mixing of the neutral  $B$  meson. Mixing effects were corrected for by assuming a mixing parameter  $r$  of  $(18.1 \pm 4.3)\%$ .

<sup>2</sup> Measurement relies on lepton-kaon correlations. It includes production through mixing of the neutral  $B$  meson.

### $\Gamma(K^-\text{anything})/\Gamma_{\text{total}}$ $\Gamma_{60}/\Gamma$

VALUE	DOCUMENT ID	TECN	COMMENT	$\Gamma_{60}/\Gamma$
<b>0.13 ± 0.04</b>	<sup>1</sup> ALBRECHT	94C	ARG $e^+e^- \rightarrow \Upsilon(4S)$	
<0.38	90	35	<sup>3</sup> BALEST	
0.165 ± 0.011 ± 0.036	<sup>2</sup> ALBRECHT	94C	ARG $e^+e^- \rightarrow \Upsilon(4S)$	
0.19 ± 0.05 ± 0.02	<sup>2</sup> ALAM	87B	CLEO $e^+e^- \rightarrow \Upsilon(4S)$	

• • • We do not use the following data for averages, fits, limits, etc. • • •

<sup>1</sup> Measurement relies on lepton-kaon correlations. It is for the weak decay vertex and does not include mixing of the neutral  $B$  meson. Mixing effects were corrected for by assuming a mixing parameter  $r$  of  $(18.1 \pm 4.3)\%$ .

<sup>2</sup> Measurement relies on lepton-kaon correlations. It includes production through mixing of the neutral  $B$  meson.

### $\Gamma(K^0/\bar{K}^0\text{anything})/\Gamma_{\text{total}}$ $\Gamma_{61}/\Gamma$

VALUE	DOCUMENT ID	TECN	COMMENT	$\Gamma_{61}/\Gamma$
<b>0.64 ± 0.04 OUR AVERAGE</b>				
0.642 ± 0.010 ± 0.042	<sup>1</sup> ALBRECHT	94C	ARG $e^+e^- \rightarrow \Upsilon(4S)$	
0.63 ± 0.06 ± 0.06	ALAM	87B	CLEO $e^+e^- \rightarrow \Upsilon(4S)$	

<sup>1</sup> ALBRECHT 94C assume a  $K^0/\bar{K}^0$  multiplicity twice that of  $K_S^0$ .

### $\Gamma(K^*(892)^\pm\text{anything})/\Gamma_{\text{total}}$ $\Gamma_{62}/\Gamma$

VALUE	DOCUMENT ID	TECN	COMMENT	$\Gamma_{62}/\Gamma$
<b>0.182 ± 0.054 ± 0.024</b>	ALBRECHT	94J	ARG $e^+e^- \rightarrow \Upsilon(4S)$	

### $\Gamma(K^*(892)^0/\bar{K}^*(892)^0\text{anything})/\Gamma_{\text{total}}$ $\Gamma_{63}/\Gamma$

VALUE	DOCUMENT ID	TECN	COMMENT	$\Gamma_{63}/\Gamma$
<b>0.146 ± 0.016 ± 0.020</b>	ALBRECHT	94J	ARG $e^+e^- \rightarrow \Upsilon(4S)$	







## Meson Particle Listings

 $B^\pm/B^0$  ADMIXTURE

$\Gamma(s\mu^+\mu^-)/\Gamma_{\text{total}}$   $\Gamma_{117}/\Gamma$   
Test for  $\Delta B = 1$  weak neutral current. Allowed by higher-order electroweak interactions.

VALUE (units $10^{-6}$ )	CL%	DOCUMENT ID	TECN	COMMENT
<b>4.3 ± 1.2 OUR AVERAGE</b>				
4.13 ± 1.05 <sup>+0.85</sup> <sub>-0.81</sub>		1 IWASAKI	05 BELL	$e^+e^- \rightarrow \Upsilon(4S)$
5.0 ± 2.8 ± 1.2		AUBERT,B	04I BABR	$e^+e^- \rightarrow \Upsilon(4S)$
• • • We do not use the following data for averages, fits, limits, etc. • • •				
7.9 ± 2.1 <sup>+2.1</sup> <sub>-1.5</sub>		KANEKO	03 BELL	Repl. by IWASAKI 05
< 58	90	GLENN	98 CLEO	$e^+e^- \rightarrow \Upsilon(4S)$
< 17000	90	CHADWICK	81 CLEO	$e^+e^- \rightarrow \Upsilon(4S)$
<sup>1</sup> Requires $M_{\ell^+\ell^-} > 0.2 \text{ GeV}/c^2$ .				

$[\Gamma(s e^+ e^-) + \Gamma(s\mu^+\mu^-)]/\Gamma_{\text{total}}$   $(\Gamma_{116} + \Gamma_{117})/\Gamma$   
Test for  $\Delta B = 1$  weak neutral current. Allowed by higher-order electroweak interactions.

VALUE	CL%	DOCUMENT ID	TECN	COMMENT
<b>&lt; 4.2 × 10<sup>-5</sup></b>	90	GLENN	98 CLEO	$e^+e^- \rightarrow \Upsilon(4S)$
• • • We do not use the following data for averages, fits, limits, etc. • • •				
< 0.0024	90	1 BEAN	87 CLEO	Repl. by GLENN 98
< 0.0062	90	2 AVERY	84 CLEO	Repl. by BEAN 87
<sup>1</sup> BEAN 87 reports $[(\mu^+\mu^-) + (e^+e^-)]/2$ and we converted it.				
<sup>2</sup> Determine ratio of $B^+$ to $B^0$ semileptonic decays to be in the range 0.25–2.9.				

$\Gamma(s\ell^+\ell^-)/\Gamma_{\text{total}}$   $\Gamma_{118}/\Gamma$   
Test for  $\Delta B = 1$  weak neutral current.

VALUE (units $10^{-6}$ )	CL%	DOCUMENT ID	TECN	COMMENT
<b>4.5 ± 1.0 OUR AVERAGE</b>				
4.11 ± 0.83 <sup>+0.85</sup> <sub>-0.81</sub>		1 IWASAKI	05 BELL	$e^+e^- \rightarrow \Upsilon(4S)$
5.6 ± 1.5 ± 1.3		2 AUBERT,B	04I BABR	$e^+e^- \rightarrow \Upsilon(4S)$
• • • We do not use the following data for averages, fits, limits, etc. • • •				
6.1 ± 1.4 <sup>+1.4</sup> <sub>-1.1</sub>		2 KANEKO	03 BELL	Repl. by IWASAKI 05
<sup>1</sup> Requires $M_{\ell^+\ell^-} > 0.2 \text{ GeV}/c^2$ .				
<sup>2</sup> Requires $M_{e^+e^-} > 0.2 \text{ GeV}/c^2$ .				

$\Gamma(\pi\ell^+\ell^-)/\Gamma_{\text{total}}$   $\Gamma_{119}/\Gamma$   
Test for  $\Delta B = 1$  weak neutral current.

VALUE	CL%	DOCUMENT ID	TECN	COMMENT
<b>&lt; 6.2 × 10<sup>-8</sup></b>	90	1 WEI	08A BELL	$e^+e^- \rightarrow \Upsilon(4S)$
• • • We do not use the following data for averages, fits, limits, etc. • • •				
< 9.1 × 10 <sup>-8</sup>	90	1 AUBERT	07AG BABR	$e^+e^- \rightarrow \Upsilon(4S)$
<sup>1</sup> Assumes equal production of $B^+$ and $B^0$ at the $\Upsilon(4S)$ .				

$\Gamma(K e^+ e^-)/\Gamma_{\text{total}}$   $\Gamma_{120}/\Gamma$   
Test for  $\Delta B = 1$  weak neutral current. Allowed by higher-order electroweak interactions.

VALUE (units $10^{-7}$ )	CL%	DOCUMENT ID	TECN	COMMENT
<b>4.4 ± 0.6 OUR AVERAGE</b>				
3.9 <sup>+0.9</sup> <sub>-0.8</sub> ± 0.2		1 AUBERT	09T BABR	$e^+e^- \rightarrow \Upsilon(4S)$
4.8 <sup>+0.8</sup> <sub>-0.7</sub> ± 0.3		1 WEI	09A BELL	$e^+e^- \rightarrow \Upsilon(4S)$
• • • We do not use the following data for averages, fits, limits, etc. • • •				
3.3 <sup>+0.9</sup> <sub>-0.8</sub> ± 0.2		1 AUBERT,B	06J BABR	Repl. by AUBERT 09T
7.4 <sup>+1.8</sup> <sub>-1.6</sub> ± 0.5		1 AUBERT	03U BABR	Repl. by AUBERT,B 06J
4.8 <sup>+1.5</sup> <sub>-1.3</sub> ± 0.3		1,2 ISHIKAWA	03 BELL	Repl. by WEI 09A
< 13	90	ABE	02 BELL	Repl. by ISHIKAWA 03
<sup>1</sup> Assumes equal production of $B^+$ and $B^0$ at the $\Upsilon(4S)$ .				
<sup>2</sup> The second error is a total of systematic uncertainties including model dependence.				

$\Gamma(K^*(892) e^+ e^-)/\Gamma_{\text{total}}$   $\Gamma_{121}/\Gamma$   
Test for  $\Delta B = 1$  weak neutral current. Allowed by higher-order electroweak interactions.

VALUE (units $10^{-7}$ )	CL%	DOCUMENT ID	TECN	COMMENT
<b>11.9 ± 2.0 OUR AVERAGE</b>				Error includes scale factor of 1.2.
9.9 <sup>+2.3</sup> <sub>-2.1</sub> ± 0.6		1 AUBERT	09T BABR	$e^+e^- \rightarrow \Upsilon(4S)$
13.9 <sup>+2.3</sup> <sub>-2.0</sub> ± 1.2		1 WEI	09A BELL	$e^+e^- \rightarrow \Upsilon(4S)$
• • • We do not use the following data for averages, fits, limits, etc. • • •				
9.7 <sup>+3.0</sup> <sub>-2.7</sub> ± 1.4		1 AUBERT,B	06J BABR	Repl. by AUBERT 09T
9.8 <sup>+5.0</sup> <sub>-4.2</sub> ± 1.1		1 AUBERT	03U BABR	Repl. by AUBERT,B 06J
14.0 <sup>+5.2</sup> <sub>-4.6</sub> ± 1.2		2 ISHIKAWA	03 BELL	Repl. by WEI 09A
< 56	90	ABE	02 BELL	Repl. by ISHIKAWA 03
<sup>1</sup> Assumes equal production of $B^+$ and $B^0$ at the $\Upsilon(4S)$ .				
<sup>2</sup> Assumes equal production of $B^0$ and $B^+$ at $\Upsilon(4S)$ . The second error is a total of systematic uncertainties including model dependence.				

$\Gamma(K\mu^+\mu^-)/\Gamma_{\text{total}}$   $\Gamma_{122}/\Gamma$   
Test for  $\Delta B = 1$  weak neutral current. Allowed by higher-order electroweak interactions.

VALUE (units $10^{-7}$ )	DOCUMENT ID	TECN	COMMENT
<b>4.4 ± 0.4 OUR AVERAGE</b>			
4.2 ± 0.4 ± 0.2	AALTONEN	11A CDF	$p\bar{p}$ at 1.96 TeV
4.1 <sup>+1.3</sup> <sub>-1.2</sub> ± 0.2	1 AUBERT	09T BABR	$e^+e^- \rightarrow \Upsilon(4S)$
5.0 ± 0.6 ± 0.3	1 WEI	09A BELL	$e^+e^- \rightarrow \Upsilon(4S)$
• • • We do not use the following data for averages, fits, limits, etc. • • •			
3.5 <sup>+1.3</sup> <sub>-1.1</sub> ± 0.3	1 AUBERT,B	06J BABR	Repl. by AUBERT 09T
4.5 <sup>+2.3</sup> <sub>-1.9</sub> ± 0.4	1 AUBERT	03U BABR	Repl. by AUBERT,B 06J
4.8 <sup>+1.2</sup> <sub>-1.1</sub> ± 0.4	1,2 ISHIKAWA	03 BELL	Repl. by WEI 09A
9.9 <sup>+4.0</sup> <sub>-3.2</sub> ± 1.0	ABE	02 BELL	Repl. by ISHIKAWA 03
<sup>1</sup> Assumes equal production of $B^+$ and $B^0$ at the $\Upsilon(4S)$ .			
<sup>2</sup> The second error is a total of systematic uncertainties including model dependence.			

$\Gamma(K\mu^+\mu^-)/\Gamma(K e^+ e^-)$   $\Gamma_{122}/\Gamma_{120}$

VALUE	DOCUMENT ID	TECN	COMMENT
<b>1.02 ± 0.18 OUR AVERAGE</b>			
0.96 <sup>+0.44</sup> <sub>-0.34</sub> ± 0.05	AUBERT	09T BABR	$e^+e^- \rightarrow \Upsilon(4S)$
1.03 ± 0.19 ± 0.06	WEI	09A BELL	$e^+e^- \rightarrow \Upsilon(4S)$
• • • We do not use the following data for averages, fits, limits, etc. • • •			
1.06 ± 0.48 ± 0.08	AUBERT,B	06J BABR	Repl. by AUBERT 09T

$\Gamma(K^*(892)\mu^+\mu^-)/\Gamma_{\text{total}}$   $\Gamma_{123}/\Gamma$   
Test for  $\Delta B = 1$  weak neutral current. Allowed by higher-order electroweak interactions.

VALUE (units $10^{-7}$ )	CL%	DOCUMENT ID	TECN	COMMENT
<b>10.6 ± 0.9 OUR AVERAGE</b>				
10.1 ± 1.0 ± 0.5		AALTONEN	11A CDF	$p\bar{p}$ at 1.96 TeV
13.5 <sup>+3.5</sup> <sub>-3.3</sub> ± 1.0		1 AUBERT	09T BABR	$e^+e^- \rightarrow \Upsilon(4S)$
11.0 <sup>+1.6</sup> <sub>-1.4</sub> ± 0.8		1 WEI	09A BELL	$e^+e^- \rightarrow \Upsilon(4S)$
• • • We do not use the following data for averages, fits, limits, etc. • • •				
8.8 <sup>+3.5</sup> <sub>-3.0</sub> ± 1.2		1 AUBERT,B	06J BABR	Repl. by AUBERT 09T
12.7 <sup>+7.6</sup> <sub>-6.1</sub> ± 1.6		1 AUBERT	03U BABR	Repl. by AUBERT,B 06J
11.7 <sup>+3.6</sup> <sub>-3.1</sub> ± 1.0		2 ISHIKAWA	03 BELL	Repl. by WEI 09A
< 31	90	ABE	02 BELL	Repl. by ISHIKAWA 03
<sup>1</sup> Assumes equal production of $B^+$ and $B^0$ at the $\Upsilon(4S)$ .				
<sup>2</sup> Assumes equal production of $B^0$ and $B^+$ at $\Upsilon(4S)$ . The second error is a total of systematic uncertainties including model dependence.				

$\Gamma(K^*(892)\mu^+\mu^-)/\Gamma(K^*(892) e^+ e^-)$   $\Gamma_{123}/\Gamma_{121}$

VALUE	DOCUMENT ID	TECN	COMMENT
<b>0.92 ± 0.21 OUR AVERAGE</b>			Error includes scale factor of 1.2.
1.37 <sup>+0.53</sup> <sub>-0.40</sub> ± 0.09	AUBERT	09T BABR	$e^+e^- \rightarrow \Upsilon(4S)$
0.83 ± 0.17 ± 0.08	WEI	09A BELL	$e^+e^- \rightarrow \Upsilon(4S)$
• • • We do not use the following data for averages, fits, limits, etc. • • •			
0.91 ± 0.45 ± 0.06	AUBERT,B	06J BABR	Repl. by AUBERT 09T

$\Gamma(K\ell^+\ell^-)/\Gamma_{\text{total}}$   $\Gamma_{124}/\Gamma$   
Test for  $\Delta B = 1$  weak neutral current. Allowed by higher-order electroweak interactions.

VALUE (units $10^{-7}$ )	CL%	DOCUMENT ID	TECN	COMMENT
<b>4.5 ± 0.4 OUR AVERAGE</b>				
3.9 ± 0.7 ± 0.2		1 AUBERT	09T BABR	$e^+e^- \rightarrow \Upsilon(4S)$
4.8 <sup>+0.5</sup> <sub>-0.4</sub> ± 0.3		WEI	09A BELL	$e^+e^- \rightarrow \Upsilon(4S)$
• • • We do not use the following data for averages, fits, limits, etc. • • •				
3.4 ± 0.7 ± 0.2		1 AUBERT,B	06J BABR	Repl. by AUBERT 09T
6.5 <sup>+1.4</sup> <sub>-1.3</sub> ± 0.4		2 AUBERT	03U BABR	Repl. by AUBERT,B 06J
4.8 <sup>+1.0</sup> <sub>-0.9</sub> ± 0.3		3 ISHIKAWA	03 BELL	Repl. by WEI 09A
7.5 <sup>+2.5</sup> <sub>-2.1</sub> ± 0.6		4 ABE	02 BELL	Repl. by ISHIKAWA 03
< 5.1	90	1 AUBERT	02L BABR	$e^+e^- \rightarrow \Upsilon(4S)$
< 17	90	5 ANDERSON	01B CLE2	$e^+e^- \rightarrow \Upsilon(4S)$
<sup>1</sup> Assumes equal production of $B^+$ and $B^0$ at the $\Upsilon(4S)$ .				
<sup>2</sup> Assumes all four $B \rightarrow K\ell^+\ell^-$ modes having equal partial widths in the fit.				
<sup>3</sup> Assumes equal production rate for charge and neutral $B$ meson pairs, isospin invariance, lepton universality for $B \rightarrow K\ell^+\ell^-$ , and $B(B \rightarrow K^*(892)\mu^+\mu^-) = 1.33$ . The second error is total systematic uncertainties including model dependence.				
<sup>4</sup> Assumes lepton universality.				
<sup>5</sup> The result is for di-lepton masses above 0.5 GeV.				



See key on page 457

# Meson Particle Listings

## $B^\pm/B^0$ ADMIXTURE

$\Gamma(K^*(892)\ell^+\ell^-)/\Gamma_{\text{total}}$   $\Gamma_{125}/\Gamma$   
 Test for  $\Delta B = 1$  weak neutral current. Allowed by higher-order electroweak interactions.

VALUE (units $10^{-7}$ )	CL%	DOCUMENT ID	TECN	COMMENT
<b><math>10.8 \pm 1.1</math> OUR AVERAGE</b>				
$11.1^{+1.9}_{-1.8} \pm 0.7$		<sup>1</sup> AUBERT	09T BABR	$e^+e^- \rightarrow \Upsilon(4S)$
$10.7^{+1.1}_{-1.0} \pm 0.9$		WEI	09A BELL	$e^+e^- \rightarrow \Upsilon(4S)$
• • • We do not use the following data for averages, fits, limits, etc. • • •				
$7.8^{+1.9}_{-1.7} \pm 1.1$		<sup>1</sup> AUBERT,B	06J BABR	Repl. by AUBERT 09T
$8.8^{+3.3}_{-2.9} \pm 1.0$		<sup>2</sup> AUBERT	03U BABR	Repl. by AUBERT,B 06J
$11.5^{+2.6}_{-2.4} \pm 0.8$		<sup>3</sup> ISHIKAWA	03 BELL	Repl. by WEI 09A
<31	90	<sup>1,4</sup> AUBERT	02L BABR	Repl. by AUBERT 03U
<33	90	<sup>5</sup> ANDERSON	01B CLE2	$e^+e^- \rightarrow \Upsilon(4S)$

- <sup>1</sup> Assumes equal production of  $B^+$  and  $B^0$  at the  $\Upsilon(4S)$ .  
<sup>2</sup> Assumes the partial width ratio of electron and muon modes to be  $\Gamma(B \rightarrow K^*(892)e^+e^-)/\Gamma(B \rightarrow K^*(892)\mu^+\mu^-) = 1.33$ .  
<sup>3</sup> Assumes equal production rate for charge and neutral  $B$  meson pairs, isospin invariance, lepton universality for  $B \rightarrow K\ell^+\ell^-$ , and  $B(B \rightarrow K^*(892)\mu^+\mu^-) = 1.33$ . The second error is total systematic uncertainties including model dependence.  
<sup>4</sup> For averaging  $K^*(892)\mu^+\mu^-$  and  $K^*(892)e^+e^-$  modes, AUBERT 02L assumed  $B(B \rightarrow K^*(892)e^+e^-)/B(B \rightarrow K^*(892)\mu^+\mu^-) = 1.2$ .  
<sup>5</sup> The result is for di-lepton masses above 0.5 GeV.

$\Gamma(K\nu\bar{\nu})/\Gamma_{\text{total}}$   $\Gamma_{126}/\Gamma$   
 Test for  $\Delta B = 1$  weak neutral current.

VALUE	CL%	DOCUMENT ID	TECN	COMMENT
<b><math>&lt;1.4 \times 10^{-5}</math></b>	90	<sup>1</sup> DEL-AMO-SA..10Q	BABR	$e^+e^- \rightarrow \Upsilon(4S)$

- <sup>1</sup> Assumes equal production of  $B^+$  and  $B^0$  at the  $\Upsilon(4S)$ .

$\Gamma(K^*\nu\bar{\nu})/\Gamma_{\text{total}}$   $\Gamma_{127}/\Gamma$   
 Test for  $\Delta B = 1$  weak neutral current.

VALUE (units $10^{-5}$ )	CL%	DOCUMENT ID	TECN	COMMENT
<b>&lt;8</b>	90	AUBERT	08Bc BABR	$e^+e^- \rightarrow \Upsilon(4S)$

$\Gamma(se^\pm\mu^\mp)/\Gamma_{\text{total}}$   $\Gamma_{128}/\Gamma$   
 Test for lepton family number conservation. Allowed by higher-order electroweak interactions.

VALUE	CL%	DOCUMENT ID	TECN	COMMENT
<b><math>&lt;2.2 \times 10^{-5}</math></b>	90	GLENN	98 CLEO	$e^+e^- \rightarrow \Upsilon(4S)$

$\Gamma(\pi e^\pm\mu^\mp)/\Gamma_{\text{total}}$   $\Gamma_{129}/\Gamma$   
 Test of lepton family number conservation.

VALUE	CL%	DOCUMENT ID	TECN	COMMENT
<b><math>&lt;9.2 \times 10^{-8}</math></b>	90	<sup>1</sup> AUBERT	07AG BABR	$e^+e^- \rightarrow \Upsilon(4S)$
• • • We do not use the following data for averages, fits, limits, etc. • • •				
$<1.6 \times 10^{-6}$	90	<sup>1</sup> EDWARDS	02B CLE2	$e^+e^- \rightarrow \Upsilon(4S)$

- <sup>1</sup> Assumes equal production of  $B^+$  and  $B^0$  at the  $\Upsilon(4S)$ .

$\Gamma(\rho e^\pm\mu^\mp)/\Gamma_{\text{total}}$   $\Gamma_{130}/\Gamma$   
 Test of lepton family number conservation.

VALUE	CL%	DOCUMENT ID	TECN	COMMENT
<b><math>&lt;3.2 \times 10^{-6}</math></b>	90	<sup>1</sup> EDWARDS	02B CLE2	$e^+e^- \rightarrow \Upsilon(4S)$

- <sup>1</sup> Assumes equal production of  $B^+$  and  $B^0$  at the  $\Upsilon(4S)$ .

$\Gamma(K e^\pm\mu^\mp)/\Gamma_{\text{total}}$   $\Gamma_{131}/\Gamma$   
 Test of lepton family number conservation.

VALUE (units $10^{-7}$ )	CL%	DOCUMENT ID	TECN	COMMENT
<b>&lt; 0.38</b>	90	<sup>1</sup> AUBERT,B	06J BABR	$e^+e^- \rightarrow \Upsilon(4S)$
• • • We do not use the following data for averages, fits, limits, etc. • • •				
<16	90	<sup>1</sup> EDWARDS	02B CLE2	$e^+e^- \rightarrow \Upsilon(4S)$

- <sup>1</sup> Assumes equal production of  $B^+$  and  $B^0$  at the  $\Upsilon(4S)$ .

$\Gamma(K^*(892)e^\pm\mu^\mp)/\Gamma_{\text{total}}$   $\Gamma_{132}/\Gamma$   
 Test of lepton family number conservation.

VALUE (units $10^{-7}$ )	CL%	DOCUMENT ID	TECN	COMMENT
<b>&lt; 5.1</b>	90	<sup>1</sup> AUBERT,B	06J BABR	$e^+e^- \rightarrow \Upsilon(4S)$
• • • We do not use the following data for averages, fits, limits, etc. • • •				
<62	90	<sup>1</sup> EDWARDS	02B CLE2	$e^+e^- \rightarrow \Upsilon(4S)$

- <sup>1</sup> Assumes equal production of  $B^+$  and  $B^0$  at the  $\Upsilon(4S)$ .

### CP VIOLATION

$A_{CP}$  is defined as

$$\frac{B(\bar{B} \rightarrow \bar{f}) - B(B \rightarrow f)}{B(\bar{B} \rightarrow \bar{f}) + B(B \rightarrow f)},$$

the CP-violation charge asymmetry of inclusive  $B^\pm$  and  $B^0$  decay.

### $A_{CP}(B \rightarrow K^*(892)\gamma)$

VALUE	DOCUMENT ID	TECN	COMMENT
<b><math>-0.003 \pm 0.017</math> OUR AVERAGE</b>			
$-0.003 \pm 0.017 \pm 0.007$	<sup>1</sup> AUBERT	09A0 BABR	$e^+e^- \rightarrow \Upsilon(4S)$
$-0.015 \pm 0.044 \pm 0.012$	<sup>2</sup> NAKAO	04 BELL	$e^+e^- \rightarrow \Upsilon(4S)$
$+0.08 \pm 0.13 \pm 0.03$	<sup>2</sup> COAN	00 CLE2	$e^+e^- \rightarrow \Upsilon(4S)$
• • • We do not use the following data for averages, fits, limits, etc. • • •			
$-0.013 \pm 0.036 \pm 0.010$	<sup>3</sup> AUBERT,BE	04A BABR	Repl. by AUBERT 09A0
$-0.044 \pm 0.076 \pm 0.012$	<sup>4</sup> AUBERT	02c BABR	Repl. by AUBERT,BE 04A

- <sup>1</sup> Corresponds to a 90% CL interval  $-0.033 < A_{CP} < 0.028$ .

- <sup>2</sup> Assumes equal production of  $B^+$  and  $B^0$  at the  $\Upsilon(4S)$ .

- <sup>3</sup> Corresponds to a 90% CL allowed region,  $-0.074 < A_{CP} < 0.049$ .

- <sup>4</sup> A 90% CL range is  $-0.170 < A_{CP} < 0.082$ .

### $A_{CP}(B \rightarrow s\gamma)$

VALUE	DOCUMENT ID	TECN	COMMENT
<b><math>-0.008 \pm 0.029</math> OUR AVERAGE</b>			
$-0.011 \pm 0.030 \pm 0.014$	<sup>1</sup> AUBERT	08Bj BABR	$e^+e^- \rightarrow \Upsilon(4S)$
$+0.002 \pm 0.050 \pm 0.030$	<sup>2</sup> NISHIDA	04 BELL	$e^+e^- \rightarrow \Upsilon(4S)$
• • • We do not use the following data for averages, fits, limits, etc. • • •			
$+0.025 \pm 0.050 \pm 0.015$	<sup>3</sup> AUBERT,B	04E BABR	Repl. by AUBERT 08Bj

- <sup>1</sup> Uses a sum of exclusively reconstructed  $B \rightarrow X_S$  decay modes, with  $X_S$  mass between 0.6 and 2.8 GeV/ $c^2$ .

- <sup>2</sup> This measurement is performed inclusively for recoil mass  $X_S$  less than 2.1 GeV, which corresponds to  $-0.093 < A_{CP} < 0.096$  at 90% CL.

- <sup>3</sup> Corresponds to  $-0.06 < A_{CP} < 0.11$  at 90% CL.

### $A_{CP}(B \rightarrow (s+d)\gamma)$

VALUE	DOCUMENT ID	TECN	COMMENT
<b><math>-0.09 \pm 0.07</math> OUR AVERAGE</b>			
$-0.10 \pm 0.18 \pm 0.05$	<sup>1</sup> AUBERT	080 BABR	$e^+e^- \rightarrow \Upsilon(4S)$
$-0.110 \pm 0.115 \pm 0.017$	AUBERT,BE	06B BABR	$e^+e^- \rightarrow \Upsilon(4S)$
$-0.079 \pm 0.108 \pm 0.022$	<sup>2</sup> COAN	01 CLE2	$e^+e^- \rightarrow \Upsilon(4S)$

- <sup>1</sup> Uses a fully reconstructed  $B$  meson as a tag on the recoil side. Requires  $E_\gamma > 2.2$  GeV.

- <sup>2</sup> Corresponds to  $-0.27 < A_{CP} < 0.10$  at 90% CL.

### $A_{CP}(B \rightarrow X_S\ell^+\ell^-)$

VALUE	DOCUMENT ID	TECN	COMMENT
<b><math>-0.22 \pm 0.26 \pm 0.02</math></b>	<sup>1</sup> AUBERT,B	04I BABR	$e^+e^- \rightarrow \Upsilon(4S)$

- <sup>1</sup> The final state flavor is determined by the kaon and pion charges where modes with  $X_S = K_S^0, K_S^0\pi^0$  or  $K_S^0\pi^+\pi^-$  are not used.

### $A_{CP}(B \rightarrow K^*e^+e^-)$

VALUE	DOCUMENT ID	TECN	COMMENT
<b><math>-0.18 \pm 0.15 \pm 0.01</math></b>	WEI	09A BELL	$e^+e^- \rightarrow \Upsilon(4S)$

### $A_{CP}(B \rightarrow K^*\mu^+\mu^-)$

VALUE	DOCUMENT ID	TECN	COMMENT
<b><math>-0.03 \pm 0.13 \pm 0.02</math></b>	WEI	09A BELL	$e^+e^- \rightarrow \Upsilon(4S)$

### $A_{CP}(B \rightarrow K^*\ell^+\ell^-)$

VALUE	DOCUMENT ID	TECN	COMMENT
<b><math>-0.07 \pm 0.08</math> OUR AVERAGE</b>			
$+0.01^{+0.16}_{-0.15} \pm 0.01$	AUBERT	09T BABR	$e^+e^- \rightarrow \Upsilon(4S)$
$-0.10 \pm 0.10 \pm 0.01$	WEI	09A BELL	$e^+e^- \rightarrow \Upsilon(4S)$

### $A_{CP}(B \rightarrow \eta\text{anything})$

VALUE	DOCUMENT ID	TECN	COMMENT
<b><math>-0.13 \pm 0.04^{+0.02}_{-0.03}</math></b>	<sup>1</sup> NISHIMURA	10 BELL	$e^+e^- \rightarrow \Upsilon(4S)$

- <sup>1</sup> Uses  $B \rightarrow \eta X_S$  with  $0.4 < m_{X_S} < 2.6$  GeV/ $c^2$ .

### POLARIZATION IN B DECAY

In decays involving two vector mesons, one can distinguish among the states in which meson polarizations are both longitudinal ( $L$ ) or both are transverse and parallel ( $\parallel$ ) or perpendicular ( $\perp$ ) to each other with the parameters  $\Gamma_L/\Gamma$ ,  $\Gamma_\perp/\Gamma$ , and the relative phases  $\phi_\parallel$  and  $\phi_\perp$ . See the definitions in the note on "Polarization in B Decays" review in the  $B^0$  Particle Listings.

### $F_L(B \rightarrow K^*\ell^+\ell^-) (q^2 > 0.1 \text{ GeV}^2/c^2)$

VALUE	DOCUMENT ID	TECN	COMMENT
<b><math>0.63^{+0.18}_{-0.19} \pm 0.05</math></b>	<sup>1</sup> AUBERT,B	06J BABR	$e^+e^- \rightarrow \Upsilon(4S)$

- <sup>1</sup> Results with different  $q^2$  cuts are also reported.

## Meson Particle Listings

 $B^\pm/B^0$  ADMIXTURE $F_L(B \rightarrow K^* \ell^+ \ell^-) (m_{\ell\ell} < 2.5 \text{ GeV}/c^2)$ 

VALUE	DOCUMENT ID	TECN	COMMENT
$0.35 \pm 0.16 \pm 0.04$	AUBERT	09N	BABR $e^+ e^- \rightarrow \Upsilon(4S)$

 $F_L(B \rightarrow K^* \ell^+ \ell^-) (m_{\ell\ell} > 3.2 \text{ GeV}/c^2)$ 

VALUE	DOCUMENT ID	TECN	COMMENT
$0.71 \pm 0.20 \pm 0.04$	AUBERT	09N	BABR $e^+ e^- \rightarrow \Upsilon(4S)$

 $F_L(B \rightarrow K^* \ell^+ \ell^-) (q^2 < 2.0 \text{ GeV}^2/c^2)$ 

VALUE	DOCUMENT ID	TECN	COMMENT
<b><math>0.35 \pm 0.17</math> OUR AVERAGE</b>			
$0.53 \pm 0.32 \pm 0.07$	AALTONEN	11L	CDF $p\bar{p}$ at 1.96 TeV
$0.29 \pm 0.21 \pm 0.02$	WEI	09A	BELL $e^+ e^- \rightarrow \Upsilon(4S)$

 $F_L(B \rightarrow K^* \ell^+ \ell^-) (2.0 < q^2 < 4.3 \text{ GeV}^2/c^2)$ 

VALUE	DOCUMENT ID	TECN	COMMENT
<b><math>0.60 \pm 0.20</math> OUR AVERAGE</b>			
$0.40 \pm 0.32 \pm 0.08$	AALTONEN	11L	CDF $p\bar{p}$ at 1.96 TeV
$0.71 \pm 0.24 \pm 0.05$	WEI	09A	BELL $e^+ e^- \rightarrow \Upsilon(4S)$

 $F_L(B \rightarrow K^* \ell^+ \ell^-) (4.3 < q^2 < 8.6 \text{ GeV}^2/c^2)$ 

VALUE	DOCUMENT ID	TECN	COMMENT
<b><math>0.74 \pm 0.15</math> OUR AVERAGE</b>			

$0.82 \pm 0.19 \pm 0.07$	AALTONEN	11L	CDF $p\bar{p}$ at 1.96 TeV
$0.64 \pm 0.23 \pm 0.07$	WEI	09A	BELL $e^+ e^- \rightarrow \Upsilon(4S)$

 $F_L(B \rightarrow K^* \ell^+ \ell^-) (10.09 < q^2 < 12.86 \text{ GeV}^2/c^2)$ 

VALUE	DOCUMENT ID	TECN	COMMENT
<b><math>0.23 \pm 0.12</math> OUR AVERAGE</b>			
$0.31 \pm 0.19 \pm 0.02$	AALTONEN	11L	CDF $p\bar{p}$ at 1.96 TeV
$0.17 \pm 0.17 \pm 0.03$	WEI	09A	BELL $e^+ e^- \rightarrow \Upsilon(4S)$

 $F_L(B \rightarrow K^* \ell^+ \ell^-) (14.18 < q^2 < 16.0 \text{ GeV}^2/c^2)$ 

VALUE	DOCUMENT ID	TECN	COMMENT
<b><math>0.34 \pm 0.31</math> OUR AVERAGE</b> Error includes scale factor of 2.1.			
$0.55 \pm 0.17 \pm 0.02$	AALTONEN	11L	CDF $p\bar{p}$ at 1.96 TeV
$-0.15 \pm 0.27 \pm 0.07$	WEI	09A	BELL $e^+ e^- \rightarrow \Upsilon(4S)$

 $F_L(B \rightarrow K^* \ell^+ \ell^-) (16.0 < q^2 \text{ GeV}^2/c^2)$ 

VALUE	DOCUMENT ID	TECN	COMMENT
<b><math>0.11 \pm 0.12</math> OUR AVERAGE</b>			
$0.09 \pm 0.18 \pm 0.03$	AALTONEN	11L	CDF $p\bar{p}$ at 1.96 TeV
$0.12 \pm 0.15 \pm 0.02$	WEI	09A	BELL $e^+ e^- \rightarrow \Upsilon(4S)$

 $F_L(B \rightarrow K^* \ell^+ \ell^-) (1.0 < q^2 < 6.0 \text{ GeV}^2/c^2)$ 

VALUE	DOCUMENT ID	TECN	COMMENT
<b><math>0.60 \pm 0.18</math> OUR AVERAGE</b>			
$0.50 \pm 0.27 \pm 0.03$	AALTONEN	11L	CDF $p\bar{p}$ at 1.96 TeV
$0.67 \pm 0.23 \pm 0.05$	WEI	09A	BELL $e^+ e^- \rightarrow \Upsilon(4S)$

 $F_L(B \rightarrow K^* \ell^+ \ell^-) (0.0 < q^2 < 4.3 \text{ GeV}^2/c^2)$ 

VALUE	DOCUMENT ID	TECN	COMMENT
<b><math>0.47 \pm 0.23</math> OUR AVERAGE</b>			
$0.47 \pm 0.23 \pm 0.03$	AALTONEN	11L	CDF $p\bar{p}$ at 1.96 TeV

PARTIAL BRANCHING FRACTIONS IN  $B \rightarrow K^{(*)} \ell^+ \ell^-$  $B(B \rightarrow K^* \ell^+ \ell^-) (q^2 < 2.0 \text{ GeV}^2/c^2)$ 

VALUE (units $10^{-7}$ )	DOCUMENT ID	TECN	COMMENT
<b><math>1.61 \pm 0.26</math> OUR AVERAGE</b>			
$1.73 \pm 0.33 \pm 0.10$	AALTONEN	11A1	CDF $p\bar{p}$ at 1.96 TeV
$1.46 \pm 0.40 \pm 0.35$	WEI	09A	BELL $e^+ e^- \rightarrow \Upsilon(4S)$
••• We do not use the following data for averages, fits, limits, etc. •••			
$0.98 \pm 0.40 \pm 0.09$	AALTONEN	11L	CDF Repl. by AALTONEN 11A1

 $B(B \rightarrow K^* \ell^+ \ell^-) (2.0 < q^2 < 4.3 \text{ GeV}^2/c^2)$ 

VALUE (units $10^{-7}$ )	DOCUMENT ID	TECN	COMMENT
<b><math>0.84 \pm 0.20</math> OUR AVERAGE</b>			
$0.82 \pm 0.26 \pm 0.06$	AALTONEN	11A1	CDF $p\bar{p}$ at 1.96 TeV
$0.86 \pm 0.31 \pm 0.07$	WEI	09A	BELL $e^+ e^- \rightarrow \Upsilon(4S)$
••• We do not use the following data for averages, fits, limits, etc. •••			
$1.00 \pm 0.38 \pm 0.09$	AALTONEN	11L	CDF Repl. by AALTONEN 11A1

 $B(B \rightarrow K^* \ell^+ \ell^-) (4.3 < q^2 < 8.68 \text{ GeV}^2/c^2)$ 

VALUE (units $10^{-7}$ )	DOCUMENT ID	TECN	COMMENT
<b><math>1.60 \pm 0.35</math> OUR AVERAGE</b>			
$1.72 \pm 0.41 \pm 0.14$	AALTONEN	11A1	CDF $p\bar{p}$ at 1.96 TeV
$1.37 \pm 0.47 \pm 0.39$	WEI	09A	BELL $e^+ e^- \rightarrow \Upsilon(4S)$
••• We do not use the following data for averages, fits, limits, etc. •••			
$1.69 \pm 0.57 \pm 0.15$	AALTONEN	11L	CDF Repl. by AALTONEN 11A1

 $B(B \rightarrow K^* \ell^+ \ell^-) (10.09 < q^2 < 12.86 \text{ GeV}^2/c^2)$ 

VALUE (units $10^{-7}$ )	DOCUMENT ID	TECN	COMMENT
<b><math>1.95 \pm 0.28</math> OUR AVERAGE</b>			
$1.77 \pm 0.34 \pm 0.11$	AALTONEN	11A1	CDF $p\bar{p}$ at 1.96 TeV
$2.24 \pm 0.44 \pm 0.19$	WEI	09A	BELL $e^+ e^- \rightarrow \Upsilon(4S)$
••• We do not use the following data for averages, fits, limits, etc. •••			
$1.97 \pm 0.47 \pm 0.17$	AALTONEN	11L	CDF Repl. by AALTONEN 11A1

 $B(B \rightarrow K^* \ell^+ \ell^-) (14.18 < q^2 < 16.0 \text{ GeV}^2/c^2)$ 

VALUE (units $10^{-7}$ )	DOCUMENT ID	TECN	COMMENT
<b><math>1.14 \pm 0.19</math> OUR AVERAGE</b>			
$1.21 \pm 0.24 \pm 0.07$	AALTONEN	11A1	CDF $p\bar{p}$ at 1.96 TeV
$1.05 \pm 0.29 \pm 0.08$	WEI	09A	BELL $e^+ e^- \rightarrow \Upsilon(4S)$
••• We do not use the following data for averages, fits, limits, etc. •••			
$1.51 \pm 0.36 \pm 0.13$	AALTONEN	11L	CDF Repl. by AALTONEN 11A1

 $B(B \rightarrow K^* \ell^+ \ell^-) (16.0 < q^2 \text{ GeV}^2/c^2)$ 

VALUE (units $10^{-7}$ )	DOCUMENT ID	TECN	COMMENT
<b><math>1.3 \pm 0.6</math> OUR AVERAGE</b> Error includes scale factor of 3.2.			
$0.88 \pm 0.22 \pm 0.05$	AALTONEN	11A1	CDF $p\bar{p}$ at 1.96 TeV
$2.04 \pm 0.27 \pm 0.24$	WEI	09A	BELL $e^+ e^- \rightarrow \Upsilon(4S)$
••• We do not use the following data for averages, fits, limits, etc. •••			
$1.35 \pm 0.37 \pm 0.12$	AALTONEN	11L	CDF Repl. by AALTONEN 11A1

 $B(B \rightarrow K^* \ell^+ \ell^-) (1.0 < q^2 < 6.0 \text{ GeV}^2/c^2)$ 

VALUE (units $10^{-7}$ )	DOCUMENT ID	TECN	COMMENT
<b><math>1.48 \pm 0.30</math> OUR AVERAGE</b>			
$1.48 \pm 0.39 \pm 0.12$	AALTONEN	11A1	CDF $p\bar{p}$ at 1.96 TeV
$1.49 \pm 0.45 \pm 0.12$	WEI	09A	BELL $e^+ e^- \rightarrow \Upsilon(4S)$
••• We do not use the following data for averages, fits, limits, etc. •••			
$1.60 \pm 0.54 \pm 0.14$	AALTONEN	11L	CDF Repl. by AALTONEN 11A1

 $B(B \rightarrow K^* \ell^+ \ell^-) (0.0 < q^2 < 4.3 \text{ GeV}^2/c^2)$ 

VALUE (units $10^{-7}$ )	DOCUMENT ID	TECN	COMMENT
<b><math>2.53 \pm 0.43 \pm 0.15</math></b>	AALTONEN	11A1	CDF $p\bar{p}$ at 1.96 TeV
••• We do not use the following data for averages, fits, limits, etc. •••			
$1.98 \pm 0.55 \pm 0.18$	AALTONEN	11L	CDF Repl. by AALTONEN 11A1

 $B(B \rightarrow K \ell^+ \ell^-) (q^2 < 2.0 \text{ GeV}^2/c^2)$ 

VALUE (units $10^{-7}$ )	DOCUMENT ID	TECN	COMMENT
<b><math>0.46 \pm 0.22</math> OUR AVERAGE</b> Error includes scale factor of 2.4.			
$0.33 \pm 0.10 \pm 0.02$	AALTONEN	11A1	CDF $p\bar{p}$ at 1.96 TeV
$0.81 \pm 0.18 \pm 0.05$	WEI	09A	BELL $e^+ e^- \rightarrow \Upsilon(4S)$
••• We do not use the following data for averages, fits, limits, etc. •••			
$0.38 \pm 0.16 \pm 0.03$	AALTONEN	11L	CDF Repl. by AALTONEN 11A1

 $B(B \rightarrow K \ell^+ \ell^-) (2.0 < q^2 < 4.3 \text{ GeV}^2/c^2)$ 

VALUE (units $10^{-7}$ )	DOCUMENT ID	TECN	COMMENT
<b><math>0.61 \pm 0.15</math> OUR AVERAGE</b> Error includes scale factor of 1.5.			
$0.77 \pm 0.14 \pm 0.05$	AALTONEN	11A1	CDF $p\bar{p}$ at 1.96 TeV
$0.46 \pm 0.14 \pm 0.12$	WEI	09A	BELL $e^+ e^- \rightarrow \Upsilon(4S)$
••• We do not use the following data for averages, fits, limits, etc. •••			
$0.58 \pm 0.19 \pm 0.04$	AALTONEN	11L	CDF Repl. by AALTONEN 11A1

 $B(B \rightarrow K \ell^+ \ell^-) (4.3 < q^2 < 8.68 \text{ GeV}^2/c^2)$ 

VALUE (units $10^{-7}$ )	DOCUMENT ID	TECN	COMMENT
<b><math>1.03 \pm 0.13</math> OUR AVERAGE</b>			
$1.05 \pm 0.17 \pm 0.07$	AALTONEN	11A1	CDF $p\bar{p}$ at 1.96 TeV
$1.00 \pm 0.19 \pm 0.06$	WEI	09A	BELL $e^+ e^- \rightarrow \Upsilon(4S)$
••• We do not use the following data for averages, fits, limits, etc. •••			
$0.93 \pm 0.25 \pm 0.06$	AALTONEN	11L	CDF Repl. by AALTONEN 11A1

 $B(B \rightarrow K \ell^+ \ell^-) (10.09 < q^2 < 12.86 \text{ GeV}^2/c^2)$ 

VALUE (units $10^{-7}$ )	DOCUMENT ID	TECN	COMMENT
<b><math>0.50 \pm 0.09</math> OUR AVERAGE</b>			
$0.48 \pm 0.10 \pm 0.03$	AALTONEN	11A1	CDF $p\bar{p}$ at 1.96 TeV
$0.55 \pm 0.16 \pm 0.03$	WEI	09A	BELL $e^+ e^- \rightarrow \Upsilon(4S)$
••• We do not use the following data for averages, fits, limits, etc. •••			
$0.72 \pm 0.17 \pm 0.05$	AALTONEN	11L	CDF Repl. by AALTONEN 11A1

# Meson Particle Listings

## $B^\pm/B^0$ ADMIXTURE

### $B(B \rightarrow K\ell^+\ell^-)$ ( $14.18 < q^2 < 16.0 \text{ GeV}^2/c^2$ )

VALUE (units $10^{-7}$ )	DOCUMENT ID	TECN	COMMENT
<b><math>0.49^{+0.08}_{-0.07}</math> OUR AVERAGE</b>			
$0.52 \pm 0.09 \pm 0.03$	AALTONEN	11A1	CDF $p\bar{p}$ at 1.96 TeV
$0.38^{+0.19}_{-0.12} \pm 0.02$	WEI	09A	BELL $e^+e^- \rightarrow \Upsilon(4S)$
••• We do not use the following data for averages, fits, limits, etc. •••			
$0.38 \pm 0.12 \pm 0.03$	AALTONEN	11L	CDF Repl. by AALTONEN 11A1

### $B(B \rightarrow K\ell^+\ell^-)$ ( $16.0 < q^2 < 6.0 \text{ GeV}^2/c^2$ )

VALUE (units $10^{-7}$ )	DOCUMENT ID	TECN	COMMENT
<b><math>0.49 \pm 0.24</math> OUR AVERAGE</b>	Error includes scale factor of 2.8.		
$0.38 \pm 0.09 \pm 0.02$	AALTONEN	11A1	CDF $p\bar{p}$ at 1.96 TeV
$0.98^{+0.20}_{-0.18} \pm 0.06$	WEI	09A	BELL $e^+e^- \rightarrow \Upsilon(4S)$
••• We do not use the following data for averages, fits, limits, etc. •••			
$0.35 \pm 0.13 \pm 0.02$	AALTONEN	11L	CDF Repl. by AALTONEN 11A1

### $B(B \rightarrow K\ell^+\ell^-)$ ( $1.0 < q^2 < 6.0 \text{ GeV}^2/c^2$ )

VALUE (units $10^{-7}$ )	DOCUMENT ID	TECN	COMMENT
<b><math>1.32 \pm 0.15</math> OUR AVERAGE</b>			
$1.29 \pm 0.18 \pm 0.08$	AALTONEN	11A1	CDF $p\bar{p}$ at 1.96 TeV
$1.36^{+0.23}_{-0.21} \pm 0.08$	WEI	09A	BELL $e^+e^- \rightarrow \Upsilon(4S)$
••• We do not use the following data for averages, fits, limits, etc. •••			
$1.01 \pm 0.26 \pm 0.07$	AALTONEN	11L	CDF Repl. by AALTONEN 11A1

### $B(B \rightarrow K\ell^+\ell^-)$ ( $0.0 < q^2 < 4.3 \text{ GeV}^2/c^2$ )

VALUE (units $10^{-7}$ )	DOCUMENT ID	TECN	COMMENT
<b><math>1.07 \pm 0.17 \pm 0.07</math></b>	AALTONEN	11A1	CDF $p\bar{p}$ at 1.96 TeV
••• We do not use the following data for averages, fits, limits, etc. •••			
$0.96 \pm 0.25 \pm 0.06$	AALTONEN	11L	CDF Repl. by AALTONEN 11A1

### LEPTON FORWARD-BACKWARD ASYMMETRY IN $B \rightarrow K^{(*)}\ell^+\ell^-$ DECAY

The forward-backward angular asymmetry of the lepton pair in  $B \rightarrow K^{(*)}\ell^+\ell^-$  decay is defined as

$$A_{FB}(s) = \frac{N(\cos\theta > 0) - N(\cos\theta < 0)}{N(\cos\theta > 0) + N(\cos\theta < 0)},$$

where  $s = q^2/m_B^2$ , and  $\theta$  is the angle of the lepton with respect to the flight direction of the  $B$  meson, measured in the dilepton rest frame. In addition, the fraction of longitudinal polarization  $F_L$  of the  $K^*$  and  $F_{S_1}$ , the relative contribution from scalar and pseudoscalar penguin amplitudes in  $B \rightarrow K\ell^+\ell^-$ , can be measured from the angular distribution of its decay products.

### $A_{FB}(B \rightarrow K^*\ell^+\ell^-)$ ( $q^2 > 0.1 \text{ GeV}^2/c^2$ )

VALUE	CL%	DOCUMENT ID	TECN	COMMENT
<b><math>0.50 \pm 0.15 \pm 0.02</math></b>		<sup>1</sup> ISHIKAWA	06	BELL $e^+e^- \rightarrow \Upsilon(4S)$
••• We do not use the following data for averages, fits, limits, etc. •••				
$> 0.55$	95	<sup>2</sup> AUBERT,B	06J	BABR $e^+e^- \rightarrow \Upsilon(4S)$
<sup>1</sup> Using an unbinned max. likelihood fits to the $M_{bc}$ distribution in five $q^2$ bins for $\cos\theta > 0$ and $\cos\theta < 0$ .				
<sup>2</sup> Results with different $q^2$ cuts are also reported.				

### $A_{FB}(B \rightarrow K^*\ell^+\ell^-)$ ( $q^2 < 2.0 \text{ GeV}^2/c^2$ )

VALUE	DOCUMENT ID	TECN	COMMENT
<b><math>0.45^{+0.25}_{-0.30}</math> OUR AVERAGE</b>			
$0.13^{+1.65}_{-0.75} \pm 0.25$	AALTONEN	11L	CDF $p\bar{p}$ at 1.96 TeV
$0.47^{+0.26}_{-0.32} \pm 0.03$	WEI	09A	BELL $e^+e^- \rightarrow \Upsilon(4S)$

### $A_{FB}(B \rightarrow K^*\ell^+\ell^-)$ ( $2.0 < q^2 < 4.3 \text{ GeV}^2/c^2$ )

VALUE	DOCUMENT ID	TECN	COMMENT
<b><math>0.14 \pm 0.27</math> OUR AVERAGE</b>			
$0.19^{+0.40}_{-0.41} \pm 0.14$	AALTONEN	11L	CDF $p\bar{p}$ at 1.96 TeV
$0.11^{+0.31}_{-0.36} \pm 0.07$	WEI	09A	BELL $e^+e^- \rightarrow \Upsilon(4S)$

### $A_{FB}(B \rightarrow K^*\ell^+\ell^-)$ ( $4.3 < q^2 < 8.6 \text{ GeV}^2/c^2$ )

VALUE	DOCUMENT ID	TECN	COMMENT
<b><math>0.24 \pm 0.24</math> OUR AVERAGE</b>	Error includes scale factor of 1.3.		
$-0.06^{+0.30}_{-0.28} \pm 0.05$	AALTONEN	11L	CDF $p\bar{p}$ at 1.96 TeV
$0.45^{+0.15}_{-0.21} \pm 0.15$	WEI	09A	BELL $e^+e^- \rightarrow \Upsilon(4S)$

### $A_{FB}(B \rightarrow K^*\ell^+\ell^-)$ ( $10.09 < q^2 < 12.86 \text{ GeV}^2/c^2$ )

VALUE	DOCUMENT ID	TECN	COMMENT
<b><math>0.53 \pm 0.15</math> OUR AVERAGE</b>			
$0.66^{+0.23}_{-0.20} \pm 0.07$	AALTONEN	11L	CDF $p\bar{p}$ at 1.96 TeV
$0.43^{+0.18}_{-0.20} \pm 0.03$	WEI	09A	BELL $e^+e^- \rightarrow \Upsilon(4S)$

### $A_{FB}(B \rightarrow K^*\ell^+\ell^-)$ ( $14.18 < q^2 < 16.0 \text{ GeV}^2/c^2$ )

VALUE	DOCUMENT ID	TECN	COMMENT
<b><math>0.53^{+0.13}_{-0.15}</math> OUR AVERAGE</b>			
$0.42 \pm 0.16 \pm 0.09$	AALTONEN	11L	CDF $p\bar{p}$ at 1.96 TeV
$0.70^{+0.16}_{-0.22} \pm 0.10$	WEI	09A	BELL $e^+e^- \rightarrow \Upsilon(4S)$

### $A_{FB}(B \rightarrow K^*\ell^+\ell^-)$ ( $16.0 < q^2 < 6.0 \text{ GeV}^2/c^2$ )

VALUE	DOCUMENT ID	TECN	COMMENT
<b><math>0.67^{+0.10}_{-0.14}</math> OUR AVERAGE</b>			
$0.70^{+0.16}_{-0.25} \pm 0.10$	AALTONEN	11L	CDF $p\bar{p}$ at 1.96 TeV
$0.66^{+0.11}_{-0.16} \pm 0.04$	WEI	09A	BELL $e^+e^- \rightarrow \Upsilon(4S)$

### $A_{FB}(B \rightarrow K^*\ell^+\ell^-)$ ( $1.0 < q^2 < 6.0 \text{ GeV}^2/c^2$ )

VALUE	DOCUMENT ID	TECN	COMMENT
<b><math>0.32 \pm 0.23</math> OUR AVERAGE</b>			
$0.43^{+0.36}_{-0.37} \pm 0.06$	AALTONEN	11L	CDF $p\bar{p}$ at 1.96 TeV
$0.26^{+0.27}_{-0.30} \pm 0.07$	WEI	09A	BELL $e^+e^- \rightarrow \Upsilon(4S)$

### $A_{FB}(B \rightarrow K^*\ell^+\ell^-)$ ( $0.0 < q^2 < 4.3 \text{ GeV}^2/c^2$ )

VALUE	DOCUMENT ID	TECN	COMMENT
<b><math>0.21^{+0.31}_{-0.33} \pm 0.05</math></b>	AALTONEN	11L	CDF $p\bar{p}$ at 1.96 TeV

### $A_{FB}(B \rightarrow K^*\ell^+\ell^-)$ ( $m_{\ell\ell} < 2.5 \text{ GeV}/c^2$ )

VALUE	DOCUMENT ID	TECN	COMMENT
<b><math>0.24^{+0.18}_{-0.23} \pm 0.05</math></b>	AUBERT	09N	BABR $e^+e^- \rightarrow \Upsilon(4S)$

### $A_{FB}(B \rightarrow K^*\ell^+\ell^-)$ ( $m_{\ell\ell} > 3.2 \text{ GeV}/c^2$ )

VALUE	DOCUMENT ID	TECN	COMMENT
<b><math>0.76^{+0.52}_{-0.32} \pm 0.07</math></b>	AUBERT	09N	BABR $e^+e^- \rightarrow \Upsilon(4S)$

### $A_{FB}(B \rightarrow K\ell^+\ell^-)$ ( $q^2 > 0.1 \text{ GeV}^2/c^2$ )

VALUE	DOCUMENT ID	TECN	COMMENT
<b><math>0.11 \pm 0.12</math> OUR AVERAGE</b>			
$0.15^{+0.21}_{-0.23} \pm 0.08$	<sup>1</sup> AUBERT,B	06J	BABR $e^+e^- \rightarrow \Upsilon(4S)$
$0.10 \pm 0.14 \pm 0.01$	<sup>2</sup> ISHIKAWA	06	BELL $e^+e^- \rightarrow \Upsilon(4S)$
<sup>1</sup> Results with different $q^2$ cuts are also reported.			
<sup>2</sup> Using an unbinned max. likelihood fits to the $M_{bc}$ distribution in five $q^2$ bins for $\cos\theta > 0$ and $\cos\theta < 0$ .			

### $A_{FB}(B \rightarrow K\ell^+\ell^-)$ ( $q^2 < 2.0 \text{ GeV}^2/c^2$ )

VALUE	DOCUMENT ID	TECN	COMMENT
<b><math>-0.02 \pm 0.26</math> OUR AVERAGE</b>			
$-0.15^{+0.46}_{-0.39} \pm 0.08$	AALTONEN	11L	CDF $p\bar{p}$ at 1.96 TeV
$0.06^{+0.32}_{-0.35} \pm 0.02$	WEI	09A	BELL $e^+e^- \rightarrow \Upsilon(4S)$

### $A_{FB}(B \rightarrow K\ell^+\ell^-)$ ( $2.0 < q^2 < 4.3 \text{ GeV}^2/c^2$ )

VALUE	DOCUMENT ID	TECN	COMMENT
<b><math>0.2 \pm 0.6</math> OUR AVERAGE</b>	Error includes scale factor of 2.2.		
$0.72^{+0.40}_{-0.35} \pm 0.07$	AALTONEN	11L	CDF $p\bar{p}$ at 1.96 TeV
$-0.43^{+0.38}_{-0.40} \pm 0.09$	WEI	09A	BELL $e^+e^- \rightarrow \Upsilon(4S)$

### $A_{FB}(B \rightarrow K\ell^+\ell^-)$ ( $4.3 < q^2 < 8.6 \text{ GeV}^2/c^2$ )

VALUE	DOCUMENT ID	TECN	COMMENT
<b><math>-0.20^{+0.10}_{-0.13}</math> OUR AVERAGE</b>			
$-0.20^{+0.17}_{-0.28} \pm 0.03$	AALTONEN	11L	CDF $p\bar{p}$ at 1.96 TeV
$-0.20^{+0.12}_{-0.14} \pm 0.03$	WEI	09A	BELL $e^+e^- \rightarrow \Upsilon(4S)$

### $A_{FB}(B \rightarrow K\ell^+\ell^-)$ ( $10.09 < q^2 < 12.86 \text{ GeV}^2/c^2$ )

VALUE	DOCUMENT ID	TECN	COMMENT
<b><math>-0.15^{+0.13}_{-0.12}</math> OUR AVERAGE</b>			
$-0.10^{+0.17}_{-0.15} \pm 0.07$	AALTONEN	11L	CDF $p\bar{p}$ at 1.96 TeV
$-0.21^{+0.17}_{-0.15} \pm 0.06$	WEI	09A	BELL $e^+e^- \rightarrow \Upsilon(4S)$

### $A_{FB}(B \rightarrow K\ell^+\ell^-)$ ( $14.18 < q^2 < 16.0 \text{ GeV}^2/c^2$ )

VALUE	DOCUMENT ID	TECN	COMMENT
<b><math>0.03^{+0.27}_{-0.14}</math> OUR AVERAGE</b>			
$0.03^{+0.49}_{-0.16} \pm 0.04$	AALTONEN	11L	CDF $p\bar{p}$ at 1.96 TeV
$0.04^{+0.32}_{-0.26} \pm 0.05$	WEI	09A	BELL $e^+e^- \rightarrow \Upsilon(4S)$

## Meson Particle Listings

 $B^\pm/B^0$  ADMIXTURE $A_{FB}(B \rightarrow K\ell^+\ell^-)$  ( $16.0 < q^2 \text{ GeV}^2/c^2$ )

VALUE	DOCUMENT ID	TECN	COMMENT
<b><math>0.03 \pm_{-0.08}^{+0.10}</math> OUR AVERAGE</b>			
$0.07 \pm_{-0.23}^{+0.30} \pm 0.02$	AALTONEN	11L	CDF $p\bar{p}$ at 1.96 TeV
$0.02 \pm_{-0.08}^{+0.11} \pm 0.02$	WEI	09A	BELL $e^+e^- \rightarrow \Upsilon(4S)$

 $A_{FB}(B \rightarrow K\ell^+\ell^-)$  ( $1.0 < q^2 < 6.0 \text{ GeV}^2/c^2$ )

VALUE	DOCUMENT ID	TECN	COMMENT
<b><math>-0.01 \pm_{-0.13}^{+0.13}</math> OUR AVERAGE</b>			
$0.08 \pm_{-0.22}^{+0.27} \pm 0.07$	AALTONEN	11L	CDF $p\bar{p}$ at 1.96 TeV
$-0.04 \pm_{-0.16}^{+0.13} \pm 0.05$	WEI	09A	BELL $e^+e^- \rightarrow \Upsilon(4S)$

 $A_{FB}(B \rightarrow K\ell^+\ell^-)$  ( $0.0 < q^2 < 4.3 \text{ GeV}^2/c^2$ )

VALUE	DOCUMENT ID	TECN	COMMENT
<b><math>0.36 \pm_{-0.26}^{+0.24} \pm 0.06</math></b>	AALTONEN	11L	CDF $p\bar{p}$ at 1.96 TeV

 $F_S(B \rightarrow K\ell^+\ell^-)$  ( $q^2 > 0.1 \text{ GeV}^2/c^2$ )

VALUE	DOCUMENT ID	TECN	COMMENT
<b><math>0.81 \pm_{-0.61}^{+0.58} \pm 0.46</math></b>	<sup>1</sup> AUBERT,B	06J	BABR $e^+e^- \rightarrow \Upsilon(4S)$

<sup>1</sup> Results with different  $q^2$  cuts are also reported.

## ISOSPIN ASYMMETRY

$\Delta_{0-}$  is defined as

$$\frac{\Gamma(B^0 \rightarrow f_\gamma) - \Gamma(B^+ \rightarrow f_\gamma)}{\Gamma(B^0 \rightarrow f) + \Gamma(B^+ \rightarrow f)}$$

the isospin asymmetry of inclusive neutral and charged B decay.

 $\Delta_{0-}(B(B \rightarrow X_S \gamma))$ 

VALUE	DOCUMENT ID	TECN	COMMENT
<b><math>-0.01 \pm_{-0.06}^{+0.06}</math> OUR AVERAGE</b>			
$-0.06 \pm_{-0.15}^{+0.15} \pm 0.07$	<sup>1,2</sup> AUBERT	08o	BABR $e^+e^- \rightarrow \Upsilon(4S)$
$-0.006 \pm_{-0.058}^{+0.058} \pm 0.026$	AUBERT,B	05R	BABR $e^+e^- \rightarrow \Upsilon(4S)$

<sup>1</sup> The result is for  $E_\gamma > 2.2 \text{ GeV}$ .

<sup>2</sup> Uses a fully reconstructed B meson as a tag on the recoil side.

 $\Delta_{0+}(B \rightarrow K^*(892) \gamma)$ 

$\Delta_{0+}$  describes the isospin asymmetry between  $\Gamma(B^0 \rightarrow K^*(892)^0 \gamma)$  and  $\Gamma(B^+ \rightarrow K^*(892)^+ \gamma)$ .

VALUE	DOCUMENT ID	TECN	COMMENT
<b><math>0.052 \pm_{-0.026}^{+0.026}</math> OUR AVERAGE</b>			
$0.066 \pm_{-0.021}^{+0.021} \pm 0.022$	<sup>1</sup> AUBERT	09A0	BABR $e^+e^- \rightarrow \Upsilon(4S)$
$0.012 \pm_{-0.044}^{+0.044} \pm 0.026$	NAKAO	04	BELL $e^+e^- \rightarrow \Upsilon(4S)$
$0.050 \pm_{-0.045}^{+0.045} \pm 0.037$	<sup>2</sup> AUBERT,BE	04A	BABR Repl. by AUBERT 09A0

<sup>1</sup> Uses the production ratio of charged and neutral B from  $\Upsilon(4S)$  decays and the lifetime ratio  $\tau_{B^+}/\tau_{B^0} = 1.071 \pm 0.009$ . The 90% CL interval is  $0.017 < \Delta_{0+} < 0.116$

<sup>2</sup> Uses the production ratio of charged and neutral B from  $\Upsilon(4S)$  decays  $R^{+0} = 1.006 \pm 0.048$  and the lifetime ratio of  $\tau_{B^+}/\tau_{B^0} = 1.083 \pm 0.017$ . The 90% CL interval is  $-0.046 < \Delta_{0+} < 0.146$ .

 $\Delta_{\rho\gamma} = \Gamma(B^+ \rightarrow \rho^+ \gamma) / (2 \cdot \Gamma(B^0 \rightarrow \rho^0 \gamma)) - 1$ 

VALUE	DOCUMENT ID	TECN	COMMENT
<b><math>-0.46 \pm_{-0.17}^{+0.17}</math> OUR AVERAGE</b>			
$-0.43 \pm_{-0.22}^{+0.25} \pm 0.10$	AUBERT	08BH	BABR $e^+e^- \rightarrow \Upsilon(4S)$
$-0.40 \pm_{-0.19}^{+0.21} \pm 0.08$	TANIGUCHI	08	BELL $e^+e^- \rightarrow \Upsilon(4S)$

 $\Delta_{0-}(B(B \rightarrow K\ell^+\ell^-))$ 

VALUE	DOCUMENT ID	TECN	COMMENT
<b><math>-0.40 \pm_{-0.30}^{+0.34}</math> OUR AVERAGE</b>			Error includes scale factor of 1.9.
$-1.43 \pm_{-0.85}^{+0.56} \pm 0.05$	<sup>1,2</sup> AUBERT	09T	BABR $e^+e^- \rightarrow \Upsilon(4S)$
$-0.31 \pm_{-0.14}^{+0.17} \pm 0.08$	<sup>3</sup> WEI	09A	BELL $e^+e^- \rightarrow \Upsilon(4S)$

<sup>1</sup> For  $0.1 < m_{\ell^+\ell^-}^2 < 7.02 \text{ GeV}^2/c^4$ .

<sup>2</sup> Assumes equal production of  $B^+$  and  $B^0$  at the  $\Upsilon(4S)$ .

<sup>3</sup> For  $q^2 < 8.68 \text{ GeV}^2/c^2$ .

 $\Delta_{0-}(B(B \rightarrow K^*\ell^+\ell^-))$ 

VALUE	DOCUMENT ID	TECN	COMMENT
<b><math>-0.44 \pm_{-0.13}^{+0.13}</math> OUR AVERAGE</b>			Error includes scale factor of 1.1.
$-0.56 \pm_{-0.15}^{+0.17} \pm 0.03$	<sup>1,2</sup> AUBERT	09T	BABR $e^+e^- \rightarrow \Upsilon(4S)$
$-0.29 \pm_{-0.16}^{+0.16} \pm 0.09$	<sup>3</sup> WEI	09A	BELL $e^+e^- \rightarrow \Upsilon(4S)$

<sup>1</sup> For  $0.1 < m_{\ell^+\ell^-}^2 < 7.02 \text{ GeV}^2/c^4$ .

<sup>2</sup> Assumes equal production of  $B^+$  and  $B^0$  at the  $\Upsilon(4S)$ .

<sup>3</sup> For  $q^2 < 8.68 \text{ GeV}^2/c^2$ .

 $\Delta_{0-}(B(B \rightarrow K^{(*)}\ell^+\ell^-))$ 

VALUE	DOCUMENT ID	TECN	COMMENT
<b><math>-0.45 \pm_{-0.17}^{+0.17}</math> OUR AVERAGE</b>			Error includes scale factor of 1.7.
$-0.64 \pm_{-0.14}^{+0.15} \pm 0.03$	<sup>1,2</sup> AUBERT	09T	BABR $e^+e^- \rightarrow \Upsilon(4S)$
$-0.30 \pm_{-0.11}^{+0.12} \pm 0.08$	<sup>3</sup> WEI	09A	BELL $e^+e^- \rightarrow \Upsilon(4S)$

<sup>1</sup> For  $0.1 < m_{\ell^+\ell^-}^2 < 7.02 \text{ GeV}^2/c^4$ .

<sup>2</sup> Assumes equal production of  $B^+$  and  $B^0$  at the  $\Upsilon(4S)$ .

<sup>3</sup> For  $q^2 < 8.68 \text{ GeV}^2/c^2$ .

 $B \rightarrow X_c \ell \nu$  HADRONIC MASS MOMENTS $\langle M_X^2 - \overline{M}_B^2 \rangle$  (First Moments)

VALUE ( $\text{GeV}^2$ )	DOCUMENT ID	TECN	COMMENT
<b><math>0.36 \pm_{-0.08}^{+0.08}</math> OUR AVERAGE</b>			Error includes scale factor of 1.8.
$0.467 \pm_{-0.012}^{+0.038} \pm 0.068$	<sup>1</sup> ACOSTA	05F	CDF $p\bar{p}$ at 1.96 TeV
$0.293 \pm_{-0.012}^{+0.012} \pm 0.058$	<sup>2</sup> CSORNA	04	CLE2 $e^+e^- \rightarrow \Upsilon(4S)$
$0.251 \pm_{-0.023}^{+0.023} \pm 0.062$	<sup>3</sup> CRONIN-HEN..01B	CLE2	$e^+e^- \rightarrow \Upsilon(4S)$

<sup>1</sup> Moments are measured with a minimum lepton momentum of  $0.7 \text{ GeV}/c$  in the B rest frame;

<sup>2</sup> Uses minimum lepton energy of  $1.5 \text{ GeV}$  and also reports moments with  $E_\ell > 1.0 \text{ GeV}$ .

<sup>3</sup> The leptons are required to have  $P_\ell > 1.5 \text{ GeV}/c$ .

 $\langle M_X^2 \rangle$  (First Moments)

VALUE ( $\text{GeV}^2$ )	DOCUMENT ID	TECN	COMMENT
<b><math>4.156 \pm_{-0.029}^{+0.029}</math> OUR AVERAGE</b>			
$4.144 \pm_{-0.028}^{+0.028} \pm 0.022$	<sup>1</sup> SCHWANDA	07	BELL $e^+e^- \rightarrow \Upsilon(4S)$
$4.18 \pm_{-0.04}^{+0.04} \pm 0.03$	<sup>1</sup> AUBERT,B	04	BABR $e^+e^- \rightarrow \Upsilon(4S)$

<sup>1</sup> The leptons are required to have  $E_\ell > 1.5 \text{ GeV}/c$ .

 $\langle (M_X^2 - \overline{M}_X^2)^2 \rangle$  (Second Moments)

VALUE ( $\text{GeV}^4$ )	DOCUMENT ID	TECN	COMMENT
<b><math>0.55 \pm_{-0.08}^{+0.08}</math> OUR AVERAGE</b>			
$0.515 \pm_{-0.061}^{+0.061} \pm 0.064$	<sup>1</sup> SCHWANDA	07	BELL $e^+e^- \rightarrow \Upsilon(4S)$
$0.629 \pm_{-0.031}^{+0.031} \pm 0.143$	<sup>2</sup> CSORNA	04	CLE2 $e^+e^- \rightarrow \Upsilon(4S)$
$1.05 \pm_{-0.26}^{+0.26} \pm 0.13$	<sup>3</sup> ACOSTA	05F	CDF $p\bar{p}$ at 1.96 TeV
$0.576 \pm_{-0.048}^{+0.048} \pm 0.168$	<sup>1</sup> CRONIN-HEN..01B	CLE2	$e^+e^- \rightarrow \Upsilon(4S)$

<sup>1</sup> The leptons are required to have  $E_\ell > 1.5 \text{ GeV}/c$ .

<sup>2</sup> Uses minimum lepton energy of  $1.5 \text{ GeV}$  and also reports moments with  $E_\ell > 1.0 \text{ GeV}$ .

<sup>3</sup> Moments are measured with a minimum lepton momentum of  $0.7 \text{ GeV}/c$  in the B rest frame;

 $\langle (M_X^2 - \overline{M}_B^2)^2 \rangle$  (Second Moments)

VALUE ( $\text{GeV}^4$ )	DOCUMENT ID	TECN	COMMENT
<b><math>0.639 \pm_{-0.056}^{+0.056} \pm 0.178</math></b>	<sup>1</sup> CRONIN-HEN..01B	CLE2	$e^+e^- \rightarrow \Upsilon(4S)$

<sup>1</sup> The leptons are required to have  $E_\ell > 1.5 \text{ GeV}/c$ .

 $B \rightarrow X_c \ell \nu$  LEPTON MOMENTUM MOMENTS $R_0 (\Gamma_{E_l > 1.7 \text{ GeV}} / \Gamma_{E_l > 1.5 \text{ GeV}})$ 

VALUE	DOCUMENT ID	TECN	COMMENT
<b><math>0.6187 \pm_{-0.0014}^{+0.0014} \pm 0.0016</math></b>	<sup>1</sup> MAHMOOD	03	CLE2 $e^+e^- \rightarrow \Upsilon(4S)$

<sup>1</sup> The leptons are required to have  $E_l > 1.5 \text{ GeV}$  in the B rest frame.

 $R_1 (\langle E_l \rangle_{E_l > 1.5 \text{ GeV}})$ 

VALUE	DOCUMENT ID	TECN	COMMENT
<b><math>1.7797 \pm_{-0.0018}^{+0.0018}</math> OUR AVERAGE</b>			Error includes scale factor of 1.8. See the ideogram below.
$1.7743 \pm_{-0.0019}^{+0.0019} \pm 0.0014$	<sup>1</sup> AUBERT,B	04A	BABR $e^+e^- \rightarrow \Upsilon(4S)$
$1.7792 \pm_{-0.0021}^{+0.0021} \pm 0.0027$	<sup>2</sup> MAHMOOD	04	CLE0 $e^+e^- \rightarrow \Upsilon(4S)$
$1.7810 \pm_{-0.0007}^{+0.0007} \pm 0.0009$	<sup>3</sup> MAHMOOD	03	CLE2 $e^+e^- \rightarrow \Upsilon(4S)$

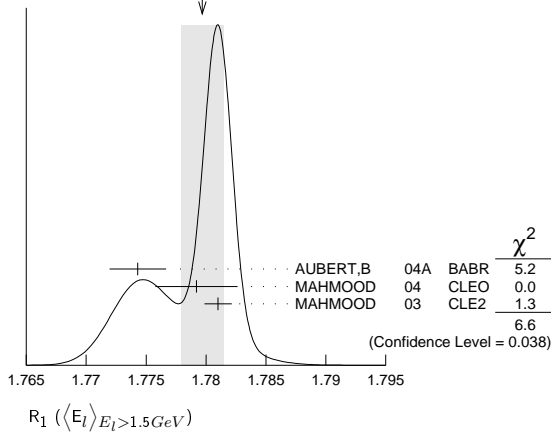
<sup>1</sup> The leptons are required to have  $E_l > 1.5 \text{ GeV}$  in the B rest frame. The result with  $E_l > 0.6 \text{ GeV}$  is also given.

<sup>2</sup> Uses  $E_e > 1.5 \text{ GeV}$  and also reports moments with other minimum minimum  $E_e$  conditions, as low as  $E_e > 0.6 \text{ GeV}$ .

<sup>3</sup> The leptons are required to have  $E_l > 1.5 \text{ GeV}$  in the B rest frame.

Meson Particle Listings
B±/B0 ADMIXTURE

WEIGHTED AVERAGE
1.7797±0.0018 (Error scaled by 1.8)



R2 <math>(\langle E\_l^2 \rangle - \bar{E}\_l^2)\_{E\_l > 1.5 \text{ GeV}}</math>

Table with columns: VALUE (10^-3 GeV^2), DOCUMENT ID, TECN, COMMENT. Includes our average 30.8 ± 0.8 and individual entries from AUBERT.B, MAHMOOD, etc.

1 The leptons are required to have E\_l > 1.5 GeV in the B rest frame. The result with E\_l > 0.6 GeV is also given.
2 Uses E\_e > 1.5 GeV and also reports moments with other minimum minimum E\_e conditions, as low as E\_e > 0.6 GeV.

R3 <math>(\langle E\_l^3 \rangle - \bar{E}\_l^3)\_{E\_l > 1.5 \text{ GeV}}</math>

Table with columns: VALUE (10^-3 GeV^3), DOCUMENT ID, TECN, COMMENT. Includes our average 2.12 ± 0.47 ± 0.20 and individual entries from AUBERT.B, etc.

1 The leptons are required to have E\_l > 1.5 GeV in the B rest frame. The result with E\_l > 0.6 GeV is also given.

B -> Xs gamma PHOTON ENERGY MOMENTS

<math>\langle E\_\gamma \rangle</math>

Table with columns: VALUE (GeV), DOCUMENT ID, TECN, COMMENT. Includes our average 2.306 ± 0.014 and individual entries from LIMOSANI, AUBERT, etc.

1 The result is for E\_gamma > 1.9 GeV.
2 Uses a fully reconstructed B meson as a tag on the recoil side.
3 Results for different E\_gamma threshold values are also measured.

<math>\langle E\_\gamma^2 \rangle - \langle E\_\gamma \rangle^2</math>

Table with columns: VALUE (10^-2 GeV^2), DOCUMENT ID, TECN, COMMENT. Includes our average 2.99 ± 0.28 and individual entries from LIMOSANI, AUBERT, etc.

1 The result is for E\_gamma > 1.9 GeV.
2 Uses a fully reconstructed B meson as a tag on the recoil side.
3 Results for different E\_gamma threshold values are also measured.

B±/B0 ADMIXTURE REFERENCES

List of references for B±/B0 admixture, including authors like Lees, Aaltonen, Urquijo, Schwanda, etc., and experiment names like BABAR, Belle, CLEO, etc.

Main list of references for meson particle listings, including authors like Aubert, Schwanda, Taniguchi, Wei, etc., and experiment names like BABAR, Belle, CLEO, etc.

## Meson Particle Listings

 $B^\pm/B^0$  ADMIXTURE,  $B^\pm/B^0/B_s^0/b$ -baryon ADMIXTURE

FULTON	91	PR D43 651	R. Fulton et al.	(CLEO Collab.)
YANAGISAWA	91	PRL 66 2436	C. Yanagisawa et al.	(CUSB II Collab.)
ALBRECHT	90	PL B234 409	H. Albrecht et al.	(ARGUS Collab.)
ALBRECHT	90H	PL B249 359	H. Albrecht et al.	(ARGUS Collab.)
BORTOLETTO	90	PRL 64 2117	D. Bortoletto et al.	(CLEO Collab.)
Also		PR D45 21	D. Bortoletto et al.	(CLEO Collab.)
FULTON	90	PRL 64 16	R. Fulton et al.	(CLEO Collab.)
MASCHMANN	90	ZPHY C46 555	W.S. Maschmann et al.	(Crystal Ball Collab.)
FDG	90	PL B239 1	J.J. Hernandez et al.	(IFIC, BOST, CIT+)
ALBRECHT	89K	ZPHY C42 519	H. Albrecht et al.	(ARGUS Collab.)
ISGUR	89B	PR D39 799	N. Isgur et al.	(TNT0, CIT)
WACHS	89	ZPHY C42 33	K. Wachs et al.	(Crystal Ball Collab.)
ALBRECHT	88E	PL B210 263	H. Albrecht et al.	(ARGUS Collab.)
ALBRECHT	88H	PL B210 258	H. Albrecht et al.	(ARGUS Collab.)
KOERNER	88	ZPHY C38 511	J.G. Korner, G.A. Schuler	(MANZ, DESY)
ALAM	87	PRL 59 22	M.S. Alam et al.	(CLEO Collab.)
ALAM	87B	PRL 58 1814	M.S. Alam et al.	(CLEO Collab.)
ALBRECHT	87D	PL B199 451	H. Albrecht et al.	(ARGUS Collab.)
ALBRECHT	87H	PL B187 425	H. Albrecht et al.	(ARGUS Collab.)
BEAN	87	PR D35 3533	A. Bean et al.	(CLEO Collab.)
BEHRENDIS	87	PRL 59 407	S. Behrendis et al.	(CLEO Collab.)
BORTOLETTO	87	PR D35 19	D. Bortoletto et al.	(CLEO Collab.)
ALAM	86	PR D34 3279	M.S. Alam et al.	(CLEO Collab.)
BALTUSAITIS...	86E	PRL 56 2140	R.M. Baltusaitis et al.	(Mark III Collab.)
BORTOLETTO	86	PRL 56 800	D. Bortoletto et al.	(CLEO Collab.)
HAAS	86	PRL 56 2781	J. Haas et al.	(CLEO Collab.)
ALBRECHT	85H	PL 162B 395	H. Albrecht et al.	(ARGUS Collab.)
CSORNA	85	PRL 54 1894	S.E. Csorna et al.	(CLEO Collab.)
HAAS	85	PRL 55 1248	J. Haas et al.	(CLEO Collab.)
AVERY	84	PRL 53 1309	P. Avery et al.	(CLEO Collab.)
CHEN	84	PR 52 1084	A. Chen et al.	(CLEO Collab.)
LEVMAN	84	PL 141B 271	G.M. Levman et al.	(CUSB Collab.)
ALAM	83B	PRL 51 1143	M.S. Alam et al.	(CLEO Collab.)
GREEN	83	PRL 51 347	J. Green et al.	(CLEO Collab.)
KLOPFEN...	83B	PL 130B 444	C. Klopfenstein et al.	(CUSB Collab.)
ALTARELLI	82	NP B208 365	G. Altarelli et al.	(ROMA, INFN, FRAS)
BRODY	82	PRL 48 1070	A.D. Brody et al.	(CLEO Collab.)
GIANNINI	82	NP B206 1	G. Giannini et al.	(CUSB Collab.)
BEBEK	81	PRL 46 84	C. Bebek et al.	(CLEO Collab.)
CHADWICK	81	PRL 46 88	K. Chadwick et al.	(CLEO Collab.)
ABRAMS	80	PRL 44 10	G.S. Abrams et al.	(SLAC, LBL)

0.98 ± 0.12 ± 0.13	ONG	89	MRK2	$E_{cm}^{90} = 29$ GeV
1.17 $^{+0.27}_{-0.22}$ $^{+0.17}_{-0.16}$	KLEM	88	DLCO	$E_{cm}^{90} = 29$ GeV
1.29 ± 0.20 ± 0.21	25 ASH	87	MAC	$E_{cm}^{90} = 29$ GeV
1.02 $^{+0.42}_{-0.39}$	301 26 BROM	87	HRS	$E_{cm}^{90} = 29$ GeV

- Measurement performed using an inclusive reconstruction and  $B$  flavor identification technique.
- Measured using inclusive  $J/\psi(1S) \rightarrow \mu^+ \mu^-$  vertex.
- ACCIARRI 98 uses inclusively reconstructed secondary vertex and lepton impact parameter.
- ACKERSTAFF 97F uses inclusively reconstructed secondary vertices.
- BUSKULIC 96F analyzed using 3D impact parameter.
- ABE,K 95b uses an inclusive topological technique.
- ABREU 94L uses charged particle impact parameters. Their result from inclusively reconstructed secondary vertices is superseded by ABREU 96E.
- ACTON 93L and ADRIANI 93K analyzed using lepton ( $e$  and  $\mu$ ) impact parameter at Z.
- BUSKULIC 93o analyzed using dipole method.
- Combines ABREU 96E secondary vertex result with ABREU 94L impact parameter result.
- From proper time distribution of  $b \rightarrow J/\psi(1S)$  anything.
- ABE 93i analyzed using  $J/\psi(1S) \rightarrow \mu\mu$  vertices.
- ABREU 93d data analyzed using  $D/D^* \ell$  anything event vertices.
- ABREU 93c data analyzed using charged and neutral vertices.
- ACTON 93c analyzed using  $D/D^* \ell$  anything event vertices.
- ABREU 92 is combined result of muon and hadron impact parameter analyses. Hadron tracks gave  $(12.7 \pm 0.4 \pm 1.2) \times 10^{-13}$  s for an admixture of  $B$  species weighted by production fraction and mean charge multiplicity, while muon tracks gave  $(13.0 \pm 1.0 \pm 0.8) \times 10^{-13}$  s for an admixture weighted by production fraction and semileptonic branching fraction.
- ACTON 92 is combined result of muon and electron impact parameter analyses.
- BUSKULIC 92f uses the lepton impact parameter distribution for data from the 1991 run.
- BUSKULIC 92g use  $J/\psi(1S)$  tags to measure the average  $b$  lifetime. This is comparable to other methods only if the  $J/\psi(1S)$  branching fractions of the different  $b$ -flavored hadrons are in the same ratio.
- Using  $Z \rightarrow e^+ X$  or  $\mu^+ X$ , ADEVA 91H determined the average lifetime for an admixture of  $B$  hadrons from the impact parameter distribution of the lepton.
- Using  $Z \rightarrow J/\psi(1S) X$ ,  $J/\psi(1S) \rightarrow \ell^+ \ell^-$ , ALEXANDER 91G determined the average lifetime for an admixture of  $B$  hadrons from the decay point of the  $J/\psi(1S)$ .
- Using  $Z \rightarrow e X$  or  $\mu X$ , DECAAMP 91C determines the average lifetime for an admixture of  $B$  hadrons from the signed impact parameter distribution of the lepton.
- HAGEMANN 90 uses electrons and muons in an impact parameter analysis.
- LYONS 90 combine the results of the  $B$  lifetime measurements of ONG 89, BRAUN-SCHWEIG 89B, KLEM 88, and ASH 87, and JADE data by private communication. They use statistical techniques which include variation of the error with the mean life, and possible correlations between the systematic errors. This result is not independent of the measured results used in our average.
- We have combined an overall scale error of 15% in quadrature with the systematic error of  $\pm 0.7$  to obtain  $\pm 2.1$  systematic error.
- Statistical and systematic errors were combined by BROM 87.

 $B^\pm/B^0/B_s^0/b$ -baryon ADMIXTURE $B^\pm/B^0/B_s^0/b$ -baryon ADMIXTURE MEAN LIFE

Each measurement of the  $B$  mean life is an average over an admixture of various bottom mesons and baryons which decay weakly. Different techniques emphasize different admixtures of produced particles, which could result in a different  $B$  mean life.

"OUR EVALUATION" is an average using rescaled values of the data listed below. The average and rescaling were performed by the Heavy Flavor Averaging Group (HFAG) and are described at <http://www.slac.stanford.edu/xorg/hfag/>. The averaging/rescaling procedure takes into account correlations between the measurements and asymmetric lifetime errors, but ignores the small differences due to different techniques.

VALUE ( $10^{-12}$ s)	EVTS	DOCUMENT ID	TECN	COMMENT
<b>1.568 ± 0.009 OUR EVALUATION</b>				
1.570 ± 0.005 ± 0.008		<sup>1</sup> ABDALLAH 04E	DLPH	$e^+ e^- \rightarrow Z$
1.533 ± 0.015 $^{+0.035}_{-0.031}$		<sup>2</sup> ABE 98b	CDF	$p\bar{p}$ at 1.8 TeV
1.549 ± 0.009 ± 0.015		<sup>3</sup> ACCIARRI 98	L3	$e^+ e^- \rightarrow Z$
1.611 ± 0.010 ± 0.027		<sup>4</sup> ACKERSTAFF 97F	OPAL	$e^+ e^- \rightarrow Z$
1.582 ± 0.011 ± 0.027		<sup>4</sup> ABREU 96E	DLPH	$e^+ e^- \rightarrow Z$
1.533 ± 0.013 ± 0.022	19.8k	<sup>5</sup> BUSKULIC 96F	ALEP	$e^+ e^- \rightarrow Z$
1.564 ± 0.030 ± 0.036		<sup>6</sup> ABE,K 95b	SLD	$e^+ e^- \rightarrow Z$
1.542 ± 0.021 ± 0.045		<sup>7</sup> ABREU 94L	DLPH	$e^+ e^- \rightarrow Z$
1.523 ± 0.034 ± 0.038	5372	<sup>8</sup> ACTON 93L	OPAL	$e^+ e^- \rightarrow Z$
1.511 ± 0.022 ± 0.078		<sup>9</sup> BUSKULIC 93o	ALEP	$e^+ e^- \rightarrow Z$
• • • We do not use the following data for averages, fits, limits, etc. • • •				
1.575 ± 0.010 ± 0.026		<sup>10</sup> ABREU 96E	DLPH	$e^+ e^- \rightarrow Z$
1.50 $^{+0.24}_{-0.21}$ ± 0.03		<sup>11</sup> ABREU 94P	DLPH	$e^+ e^- \rightarrow Z$
1.46 ± 0.06 ± 0.06	5344	<sup>12</sup> ABE 93j	CDF	Repl. by ABE 98b
1.23 $^{+0.14}_{-0.13}$ ± 0.15	188	<sup>13</sup> ABREU 93d	DLPH	Sup. by ABREU 94L
1.49 ± 0.11 ± 0.12	253	<sup>14</sup> ABREU 93g	DLPH	Sup. by ABREU 94L
1.51 $^{+0.16}_{-0.14}$ ± 0.11	130	<sup>15</sup> ACTON 93c	OPAL	$e^+ e^- \rightarrow Z$
1.535 ± 0.035 ± 0.028	7357	<sup>8</sup> ADRIANI 93K	L3	Repl. by ACCIARRI 98
1.28 ± 0.10		<sup>16</sup> ABREU 92	DLPH	Sup. by ABREU 94L
1.37 ± 0.07 ± 0.06	1354	<sup>17</sup> ACTON 92	OPAL	Sup. by ACTON 93L
1.49 ± 0.03 ± 0.06		<sup>18</sup> BUSKULIC 92F	ALEP	Sup. by BUSKULIC 96F
1.35 $^{+0.19}_{-0.17}$ ± 0.05		<sup>19</sup> BUSKULIC 92g	ALEP	$e^+ e^- \rightarrow Z$
1.32 ± 0.08 ± 0.09	1386	<sup>20</sup> ADEVA 91H	L3	Sup. by ADRIANI 93K
1.32 $^{+0.31}_{-0.25}$ ± 0.15	37	<sup>21</sup> ALEXANDER 91G	OPAL	$e^+ e^- \rightarrow Z$
1.29 ± 0.06 ± 0.10	2973	<sup>22</sup> DECAAMP 91C	ALEP	Sup. by BUSKULIC 92F
1.36 $^{+0.25}_{-0.23}$		<sup>23</sup> HAGEMANN 90	JADE	$E_{cm}^{90} = 35$ GeV
1.13 ± 0.15		<sup>24</sup> LYONS 90	RVUE	
1.35 ± 0.10 ± 0.24		BRAUNSCH... 89b	TASS	$E_{cm}^{90} = 35$ GeV

CHARGED  $b$ -HADRON ADMIXTURE MEAN LIFE

VALUE ( $10^{-12}$ s)	DOCUMENT ID	TECN	COMMENT
<b>1.72 ± 0.08 ± 0.06</b>	<sup>27</sup> ADAM 95	DLPH	$e^+ e^- \rightarrow Z$
<sup>27</sup> ADAM 95 data analyzed using vertex-charge technique to tag $b$ -hadron charge.			

NEUTRAL  $b$ -HADRON ADMIXTURE MEAN LIFE

VALUE ( $10^{-12}$ s)	DOCUMENT ID	TECN	COMMENT
<b>1.58 ± 0.11 ± 0.09</b>	<sup>28</sup> ADAM 95	DLPH	$e^+ e^- \rightarrow Z$
<sup>28</sup> ADAM 95 data analyzed using vertex-charge technique to tag $b$ -hadron charge.			

MEAN LIFE RATIO  $\tau^{\text{charged } b\text{-hadron}}/\tau^{\text{neutral } b\text{-hadron}}$ 

VALUE	DOCUMENT ID	TECN	COMMENT
<b>1.09 <math>^{+0.11}_{-0.10}</math> ± 0.08</b>	<sup>29</sup> ADAM 95	DLPH	$e^+ e^- \rightarrow Z$
<sup>29</sup> ADAM 95 data analyzed using vertex-charge technique to tag $b$ -hadron charge.			

$$|\Delta\tau_b|/\tau_{b,\bar{b}}$$

$\tau_{b,\bar{b}}$  and  $|\Delta\tau_b|$  are the mean life average and difference between  $b$  and  $\bar{b}$  hadrons.

VALUE	DOCUMENT ID	TECN	COMMENT
<b>-0.001 ± 0.012 ± 0.008</b>	<sup>30</sup> ABBIENDI 99j	OPAL	$e^+ e^- \rightarrow Z$

- Data analyzed using both the jet charge and the charge of secondary vertex in the opposite hemisphere.

See key on page 457

# Meson Particle Listings

## $B^\pm/B^0/B_s^0/b$ -baryon ADMIXTURE

### $\bar{b}$ PRODUCTION FRACTIONS AND DECAY MODES

The branching fraction measurements are for an admixture of  $B$  mesons and baryons at energies above the  $T(4S)$ . Only the highest energy results (LHC, LEP, Tevatron,  $Sp\bar{p}S$ ) are used in the branching fraction averages. In the following, we assume that the production fractions are the same at the LHC, LEP, and at the Tevatron.

For inclusive branching fractions, e.g.,  $B \rightarrow D^\pm$  anything, the values usually are multiplicities, not branching fractions. They can be greater than one.

The modes below are listed for a  $\bar{b}$  initial state.  $b$  modes are their charge conjugates. Reactions indicate the weak decay vertex and do not include mixing.

Mode	Fraction ( $\Gamma_i/\Gamma$ )	Scale factor/ Confidence level
------	--------------------------------	-----------------------------------

### PRODUCTION FRACTIONS

The production fractions for weakly decaying  $b$ -hadrons at high energy have been calculated from the best values of mean lives, mixing parameters, and branching fractions in this edition by the Heavy Flavor Averaging Group (HFAG) as described in the note " $B^0$ - $\bar{B}^0$  Mixing" in the  $B^0$  Particle Listings. The production fractions in  $b$ -hadronic  $Z$  decay or  $p\bar{p}$  collisions at the Tevatron are also listed at the end of the section. Values assume

$$B(\bar{b} \rightarrow B^+) = B(\bar{b} \rightarrow B^0)$$

$$B(\bar{b} \rightarrow B^+) + B(\bar{b} \rightarrow B^0) + B(\bar{b} \rightarrow B_s^0) + B(b \rightarrow b\text{-baryon}) = 100\%.$$

The correlation coefficients between production fractions are also reported:

$$\text{cor}(B_s^0, b\text{-baryon}) = -0.277$$

$$\text{cor}(B_s^0, B^\pm=B^0) = -0.119$$

$$\text{cor}(b\text{-baryon}, B^\pm=B^0) = -0.921.$$

The notation for production fractions varies in the literature ( $f_d, d_{B^0}, f(b \rightarrow \bar{B}^0), \text{Br}(b \rightarrow \bar{B}^0)$ ). We use our own branching fraction notation here,  $B(\bar{b} \rightarrow B^0)$ .

Note these production fractions are  $b$ -hadronization fractions, not the conventional branching fractions of  $b$ -quark to a  $B$ -hadron, which may have considerable dependence on the initial and final state kinematic and production environment.

$\Gamma_1$	$B^+$	( 40.1 $\pm$ 0.8 ) %
$\Gamma_2$	$B^0$	( 40.1 $\pm$ 0.8 ) %
$\Gamma_3$	$B_s^0$	( 10.5 $\pm$ 0.6 ) %
$\Gamma_4$	$b$ -baryon	( 9.3 $\pm$ 1.6 ) %

### DECAY MODES

#### Semileptonic and leptonic modes

$\Gamma_5$	$\nu$ anything	( 23.1 $\pm$ 1.5 ) %	
$\Gamma_6$	$\ell^+ \nu_\ell$ anything	[a] ( 10.69 $\pm$ 0.22 ) %	
$\Gamma_7$	$e^+ \nu_e$ anything	( 10.86 $\pm$ 0.35 ) %	
$\Gamma_8$	$\mu^+ \nu_\mu$ anything	( 10.95 $\pm$ $^{0.29}_{-0.25}$ ) %	
$\Gamma_9$	$D^- \ell^+ \nu_\ell$ anything	[a] ( 2.27 $\pm$ 0.35 ) %	S=1.7
$\Gamma_{10}$	$D^- \pi^+ \ell^+ \nu_\ell$ anything	( 4.9 $\pm$ 1.9 ) $\times 10^{-3}$	
$\Gamma_{11}$	$D^- \pi^- \ell^+ \nu_\ell$ anything	( 2.6 $\pm$ 1.6 ) $\times 10^{-3}$	
$\Gamma_{12}$	$\bar{D}^0 \ell^+ \nu_\ell$ anything	[a] ( 6.84 $\pm$ 0.35 ) %	
$\Gamma_{13}$	$\bar{D}^0 \pi^- \ell^+ \nu_\ell$ anything	( 1.07 $\pm$ 0.27 ) %	
$\Gamma_{14}$	$\bar{D}^0 \pi^+ \ell^+ \nu_\ell$ anything	( 2.3 $\pm$ 1.6 ) $\times 10^{-3}$	
$\Gamma_{15}$	$D^{*-} \ell^+ \nu_\ell$ anything	[a] ( 2.75 $\pm$ 0.19 ) %	
$\Gamma_{16}$	$D^{*-} \pi^- \ell^+ \nu_\ell$ anything	( 6 $\pm$ 7 ) $\times 10^{-4}$	
$\Gamma_{17}$	$D^{*-} \pi^+ \ell^+ \nu_\ell$ anything	( 4.8 $\pm$ 1.0 ) $\times 10^{-3}$	
$\Gamma_{18}$	$\bar{D}_j^0 \ell^+ \nu_\ell$ anything $\times$ $B(\bar{D}_j^0 \rightarrow D^{*+} \pi^-)$	[a,b] ( 2.6 $\pm$ 0.9 ) $\times 10^{-3}$	
$\Gamma_{19}$	$D_j^- \ell^+ \nu_\ell$ anything $\times$ $B(D_j^- \rightarrow D^0 \pi^-)$	[a,b] ( 7.0 $\pm$ 2.3 ) $\times 10^{-3}$	
$\Gamma_{20}$	$\bar{D}_2^*(2460)^0 \ell^+ \nu_\ell$ anything $\times B(\bar{D}_2^*(2460)^0 \rightarrow$ $D^{*-} \pi^+)$	< 1.4 $\times 10^{-3}$	CL=90%
$\Gamma_{21}$	$D_2^*(2460)^- \ell^+ \nu_\ell$ anything $\times B(D_2^*(2460)^- \rightarrow$ $D^0 \pi^-)$	( 4.2 $\pm$ $^{1.5}_{-1.8}$ ) $\times 10^{-3}$	
$\Gamma_{22}$	$\bar{D}_2^*(2460)^0 \ell^+ \nu_\ell$ anything $\times B(\bar{D}_2^*(2460)^0 \rightarrow$ $D^- \pi^+)$	( 1.6 $\pm$ 0.8 ) $\times 10^{-3}$	
$\Gamma_{23}$	charmless $\ell \bar{\nu}_\ell$	[a] ( 1.7 $\pm$ 0.5 ) $\times 10^{-3}$	

$\Gamma_{24}$	$\tau^+ \nu_\tau$ anything	( 2.41 $\pm$ 0.23 ) %
$\Gamma_{25}$	$D^{*-} \tau \nu_\tau$ anything	( 9 $\pm$ 4 ) $\times 10^{-3}$
$\Gamma_{26}$	$\bar{c} \rightarrow \ell^- \bar{\nu}_\ell$ anything	[a] ( 8.02 $\pm$ 0.19 ) %
$\Gamma_{27}$	$c \rightarrow \ell^+ \nu$ anything	( 1.6 $\pm$ $^{0.4}_{0.5}$ ) %

### Charmed meson and baryon modes

$\Gamma_{28}$	$\bar{D}^0$ anything	( 59.8 $\pm$ 2.9 ) %	
$\Gamma_{29}$	$D^0 D_s^\pm$ anything	[c] ( 9.1 $\pm$ $^{4.0}_{2.8}$ ) %	
$\Gamma_{30}$	$D^\mp D_s^\pm$ anything	[c] ( 4.0 $\pm$ $^{2.3}_{1.8}$ ) %	
$\Gamma_{31}$	$\bar{D}^0 D^0$ anything	[c] ( 5.1 $\pm$ $^{2.0}_{1.8}$ ) %	
$\Gamma_{32}$	$D^0 D^\pm$ anything	[c] ( 2.7 $\pm$ $^{1.8}_{1.6}$ ) %	
$\Gamma_{33}$	$D^\pm D^\mp$ anything	[c] < 9 $\times 10^{-3}$	CL=90%
$\Gamma_{34}$	$D^0$ anything		
$\Gamma_{35}$	$D^+$ anything		
$\Gamma_{36}$	$D^-$ anything	( 23.3 $\pm$ 1.7 ) %	
$\Gamma_{37}$	$D^*(2010)^+$ anything	( 17.3 $\pm$ 2.0 ) %	
$\Gamma_{38}$	$D_1(2420)^0$ anything	( 5.0 $\pm$ 1.5 ) %	
$\Gamma_{39}$	$D^*(2010)^\mp D_s^\pm$ anything	[c] ( 3.3 $\pm$ $^{1.6}_{-1.3}$ ) %	
$\Gamma_{40}$	$D^0 D^*(2010)^\pm$ anything	[c] ( 3.0 $\pm$ $^{1.1}_{0.9}$ ) %	
$\Gamma_{41}$	$D^*(2010)^\pm D^\mp$ anything	[c] ( 2.5 $\pm$ $^{1.2}_{1.0}$ ) %	
$\Gamma_{42}$	$D^*(2010)^\pm D^*(2010)^\mp$ anything	[c] ( 1.2 $\pm$ 0.4 ) %	
$\Gamma_{43}$	$\bar{D} D$ anything	( 10 $\pm$ $^{11}_{-10}$ ) %	
$\Gamma_{44}$	$D_2^*(2460)^0$ anything	( 4.7 $\pm$ 2.7 ) %	
$\Gamma_{45}$	$D_s^-$ anything	( 14.7 $\pm$ 2.1 ) %	
$\Gamma_{46}$	$D_s^+$ anything	( 10.1 $\pm$ 3.1 ) %	
$\Gamma_{47}$	$\Lambda_c^+$ anything	( 9.7 $\pm$ 2.9 ) %	
$\Gamma_{48}$	$\bar{c}/c$ anything	[d] ( 116.2 $\pm$ 3.2 ) %	

### Charmonium modes

$\Gamma_{49}$	$J/\psi(1S)$ anything	( 1.16 $\pm$ 0.10 ) %
$\Gamma_{50}$	$\psi(2S)$ anything	( 4.8 $\pm$ 2.4 ) $\times 10^{-3}$
$\Gamma_{51}$	$\chi_{c1}(1P)$ anything	( 1.4 $\pm$ 0.4 ) %

### K or K\* modes

$\Gamma_{52}$	$\bar{S}\gamma$	( 3.1 $\pm$ 1.1 ) $\times 10^{-4}$	
$\Gamma_{53}$	$\bar{S}\bar{\nu}\nu$	< 6.4 $\times 10^{-4}$	CL=90%
$\Gamma_{54}$	$K^\pm$ anything	( 74 $\pm$ 6 ) %	
$\Gamma_{55}$	$K_S^0$ anything	( 29.0 $\pm$ 2.9 ) %	

### Pion modes

$\Gamma_{56}$	$\pi^\pm$ anything	( 397 $\pm$ 21 ) %
$\Gamma_{57}$	$\pi^0$ anything	[d] ( 278 $\pm$ 60 ) %
$\Gamma_{58}$	$\phi$ anything	( 2.82 $\pm$ 0.23 ) %

### Baryon modes

$\Gamma_{59}$	$p/\bar{p}$ anything	( 13.1 $\pm$ 1.1 ) %
---------------	----------------------	----------------------

### Other modes

$\Gamma_{60}$	charged anything	[d] ( 497 $\pm$ 7 ) %
$\Gamma_{61}$	hadron <sup>+</sup> hadron <sup>-</sup>	( 1.7 $\pm$ $^{1.0}_{0.7}$ ) $\times 10^{-5}$
$\Gamma_{62}$	charmless	( 7 $\pm$ 21 ) $\times 10^{-3}$

### Baryon modes

$\Gamma_{63}$	$\Lambda/\bar{\Lambda}$ anything	( 5.9 $\pm$ 0.6 ) %
$\Gamma_{64}$	$b$ -baryon anything	( 10.2 $\pm$ 2.8 ) %

### $\Delta B = 1$ weak neutral current ( $B1$ ) modes

$\Gamma_{65}$	$e^+ e^-$ anything	$B1$	
$\Gamma_{66}$	$\mu^+ \mu^-$ anything	$B1$	< 3.2 $\times 10^{-4}$
$\Gamma_{67}$	$\nu\bar{\nu}$ anything	$B1$	

[a] An  $\ell$  indicates an  $e$  or a  $\mu$  mode, not a sum over these modes.

[b]  $D_j$  represents an unresolved mixture of pseudoscalar and tensor  $D^{**}$  ( $P$ -wave) states.

[c] The value is for the sum of the charge states or particle/antiparticle states indicated.

[d] Inclusive branching fractions have a multiplicity definition and can be greater than 100%.







## Meson Particle Listings

 $B^\pm/B^0/B_s^0/b$ -baryon ADMIXTURE

<sup>84</sup> Uses the combination of lepton transverse momentum spectrum and the correlation between the charge of the lepton and opposite jet charge. The first error is statistic and the second error is the total systematic error including the modeling.

<sup>85</sup> The experimental systematic and model uncertainties are combined in quadrature.

<sup>86</sup> ABBIENDI 00E result is determined by comparing the distribution of several kinematic variables of leptonic events in a lifetime tagged  $Z \rightarrow b\bar{b}$  sample using artificial neural network techniques. The first error is statistic; the second error is the total systematic error.

<sup>87</sup> ABREU 95D give systematic errors  $\pm 0.0033$  (model) and  $0.0032$  ( $R_c$ ). We combine these in quadrature. This result is from the same global fit as their  $\Gamma(\bar{b} \rightarrow \ell^+ \nu_\ell X)$  data.

<sup>88</sup> BUSKULIC 94G uses  $e$  and  $\mu$  events. This value is from the same global fit as their  $\Gamma(\bar{b} \rightarrow \ell^+ \nu_\ell \text{anything})/\Gamma_{\text{total}}$  data.

<sup>89</sup> AKERS 93B analysis performed using single and dilepton events.

$\Gamma(c \rightarrow \ell^+ \nu \text{ anything})/\Gamma_{\text{total}}$		$\Gamma_{27}/\Gamma$	
VALUE	DOCUMENT ID	TECN	COMMENT
$0.0161 \pm 0.0020 \pm 0.0034$ $-0.0047$	90 ABREU	01L	DLPH $e^+ e^- \rightarrow Z$

<sup>90</sup> The experimental systematic and model uncertainties are combined in quadrature.

$\Gamma(\bar{D}^0 \text{ anything})/\Gamma_{\text{total}}$		$\Gamma_{28}/\Gamma$	
VALUE	DOCUMENT ID	TECN	COMMENT
$0.598 \pm 0.029 \pm 0.007$ $-0.008$	91 BUSKULIC	96Y	ALEP $e^+ e^- \rightarrow Z$

<sup>91</sup> BUSKULIC 96Y reports  $0.605 \pm 0.024 \pm 0.016$  from a measurement of  $[\Gamma(\bar{b} \rightarrow \bar{D}^0 \text{ anything})/\Gamma_{\text{total}}] \times [B(D^0 \rightarrow K^- \pi^+)]$  assuming  $B(D^0 \rightarrow K^- \pi^+) = 0.0383$ , which we rescale to our best value  $B(D^0 \rightarrow K^- \pi^+) = (3.88 \pm 0.05) \times 10^{-2}$ . Our first error is their experiment's error and our second error is the systematic error from using our best value.

$\Gamma(D^0 D_s^\pm \text{ anything})/\Gamma_{\text{total}}$		$\Gamma_{29}/\Gamma$	
VALUE	DOCUMENT ID	TECN	COMMENT
$0.091 \pm 0.020 \pm 0.034$ $-0.018 - 0.022$	92 BARATE	98Q	ALEP $e^+ e^- \rightarrow Z$

<sup>92</sup> The systematic error includes the uncertainties due to the charm branching ratios.

$\Gamma(D^\mp D_s^\pm \text{ anything})/\Gamma_{\text{total}}$		$\Gamma_{30}/\Gamma$	
VALUE	DOCUMENT ID	TECN	COMMENT
$0.040 \pm 0.017 \pm 0.016$ $-0.014 - 0.011$	93 BARATE	98Q	ALEP $e^+ e^- \rightarrow Z$

<sup>93</sup> The systematic error includes the uncertainties due to the charm branching ratios.

$[\Gamma(D^0 D_s^\pm \text{ anything}) + \Gamma(D^\mp D_s^\pm \text{ anything})]/\Gamma_{\text{total}}$		$(\Gamma_{29} + \Gamma_{30})/\Gamma$	
VALUE	DOCUMENT ID	TECN	COMMENT
$0.131 \pm 0.026 \pm 0.048$ $-0.022 - 0.031$	94 BARATE	98Q	ALEP $e^+ e^- \rightarrow Z$

<sup>94</sup> The systematic error includes the uncertainties due to the charm branching ratios.

$\Gamma(\bar{D}^0 D^0 \text{ anything})/\Gamma_{\text{total}}$		$\Gamma_{31}/\Gamma$	
VALUE	DOCUMENT ID	TECN	COMMENT
$0.051 \pm 0.016 \pm 0.012$ $-0.014 - 0.011$	95 BARATE	98Q	ALEP $e^+ e^- \rightarrow Z$

<sup>95</sup> The systematic error includes the uncertainties due to the charm branching ratios.

$\Gamma(D^0 D^\pm \text{ anything})/\Gamma_{\text{total}}$		$\Gamma_{32}/\Gamma$	
VALUE	DOCUMENT ID	TECN	COMMENT
$0.027 \pm 0.015 \pm 0.010$ $-0.013 - 0.009$	96 BARATE	98Q	ALEP $e^+ e^- \rightarrow Z$

<sup>96</sup> The systematic error includes the uncertainties due to the charm branching ratios.

$[\Gamma(\bar{D}^0 D^0 \text{ anything}) + \Gamma(D^0 D^\pm \text{ anything})]/\Gamma_{\text{total}}$		$(\Gamma_{31} + \Gamma_{32})/\Gamma$	
VALUE	DOCUMENT ID	TECN	COMMENT
$0.078 \pm 0.020 \pm 0.018$ $-0.018 - 0.016$	97 BARATE	98Q	ALEP $e^+ e^- \rightarrow Z$

<sup>97</sup> The systematic error includes the uncertainties due to the charm branching ratios.

$\Gamma(D^\pm D^\mp \text{ anything})/\Gamma_{\text{total}}$		$\Gamma_{33}/\Gamma$		
VALUE	CL%	DOCUMENT ID	TECN	COMMENT
$<0.009$	90	BARATE	98Q	ALEP $e^+ e^- \rightarrow Z$

$[\Gamma(D^0 \text{ anything}) + \Gamma(D^+ \text{ anything})]/\Gamma_{\text{total}}$		$(\Gamma_{34} + \Gamma_{35})/\Gamma$	
VALUE	DOCUMENT ID	TECN	COMMENT
$0.093 \pm 0.017 \pm 0.014$	98 ABDALLAH	03E	DLPH $e^+ e^- \rightarrow Z$

<sup>98</sup> The second error is the total of systematic uncertainties including the branching fractions used in the measurement.

$\Gamma(D^- \text{ anything})/\Gamma_{\text{total}}$		$\Gamma_{36}/\Gamma$	
VALUE	DOCUMENT ID	TECN	COMMENT
$0.233 \pm 0.016 \pm 0.005$	99 BUSKULIC	96Y	ALEP $e^+ e^- \rightarrow Z$

<sup>99</sup> BUSKULIC 96Y reports  $0.234 \pm 0.013 \pm 0.010$  from a measurement of  $[\Gamma(\bar{b} \rightarrow D^- \text{ anything})/\Gamma_{\text{total}}] \times [B(D^+ \rightarrow K^- 2\pi^+)]$  assuming  $B(D^+ \rightarrow K^- 2\pi^+) = 0.091$ , which we rescale to our best value  $B(D^+ \rightarrow K^- 2\pi^+) = (9.13 \pm 0.19) \times 10^{-2}$ . Our first error is their experiment's error and our second error is the systematic error from using our best value.

$\Gamma(D^*(2010)^+ \text{ anything})/\Gamma_{\text{total}}$		$\Gamma_{37}/\Gamma$	
VALUE	DOCUMENT ID	TECN	COMMENT
$0.173 \pm 0.016 \pm 0.012$	100 ACKERSTAFF	98E	OPAL $e^+ e^- \rightarrow Z$

<sup>100</sup> Uses lepton tags to select  $Z \rightarrow b\bar{b}$  events.

$\Gamma(D_1(2420)^0 \text{ anything})/\Gamma_{\text{total}}$		$\Gamma_{38}/\Gamma$	
VALUE	DOCUMENT ID	TECN	COMMENT
$0.050 \pm 0.014 \pm 0.006$	101 ACKERSTAFF	97W	OPAL $e^+ e^- \rightarrow Z$

<sup>101</sup> ACKERSTAFF 97W assumes  $B(D_2^*(2460)^0 \rightarrow D^{*+} \pi^-) = 0.21 \pm 0.04$  and  $\Gamma_{b\bar{b}}/\Gamma_{\text{hadrons}} = 0.216$  at  $Z$  decay.

$\Gamma(D^*(2010)^\mp D_s^\pm \text{ anything})/\Gamma_{\text{total}}$		$\Gamma_{39}/\Gamma$	
VALUE	DOCUMENT ID	TECN	COMMENT
$0.033 \pm 0.010 \pm 0.012$ $-0.009 - 0.009$	102 BARATE	98Q	ALEP $e^+ e^- \rightarrow Z$

<sup>102</sup> The systematic error includes the uncertainties due to the charm branching ratios.

$\Gamma(D^0 D^*(2010)^\pm \text{ anything})/\Gamma_{\text{total}}$		$\Gamma_{40}/\Gamma$	
VALUE	DOCUMENT ID	TECN	COMMENT
$0.030 \pm 0.009 \pm 0.007$ $-0.008 - 0.005$	103 BARATE	98Q	ALEP $e^+ e^- \rightarrow Z$

<sup>103</sup> The systematic error includes the uncertainties due to the charm branching ratios.

$\Gamma(D^*(2010)^\pm D^\mp \text{ anything})/\Gamma_{\text{total}}$		$\Gamma_{41}/\Gamma$	
VALUE	DOCUMENT ID	TECN	COMMENT
$0.025 \pm 0.010 \pm 0.006$ $-0.009 - 0.005$	104 BARATE	98Q	ALEP $e^+ e^- \rightarrow Z$

<sup>104</sup> The systematic error includes the uncertainties due to the charm branching ratios.

$\Gamma(D^*(2010)^\pm D^*(2010)^\mp \text{ anything})/\Gamma_{\text{total}}$		$\Gamma_{42}/\Gamma$	
VALUE	DOCUMENT ID	TECN	COMMENT
$0.012 \pm 0.004 \pm 0.002$ $-0.003$	105 BARATE	98Q	ALEP $e^+ e^- \rightarrow Z$

<sup>105</sup> The systematic error includes the uncertainties due to the charm branching ratios.

$\Gamma(\bar{D} D \text{ anything})/\Gamma_{\text{total}}$		$\Gamma_{43}/\Gamma$	
VALUE	DOCUMENT ID	TECN	COMMENT
$0.10 \pm 0.032 \pm 0.107$ $-0.095$	106 ABBIENDI	04I	OPAL $e^+ e^- \rightarrow Z$

<sup>106</sup> Measurement performed using an inclusive identification of  $B$  mesons and the  $D$  candidates.

$\Gamma(D_2^*(2460)^0 \text{ anything})/\Gamma_{\text{total}}$		$\Gamma_{44}/\Gamma$	
VALUE	DOCUMENT ID	TECN	COMMENT
$0.047 \pm 0.024 \pm 0.013$	107 ACKERSTAFF	97W	OPAL $e^+ e^- \rightarrow Z$

<sup>107</sup> ACKERSTAFF 97W assumes  $B(D_2^*(2460)^0 \rightarrow D^{*+} \pi^-) = 0.21 \pm 0.04$  and  $\Gamma_{b\bar{b}}/\Gamma_{\text{hadrons}} = 0.216$  at  $Z$  decay.

$\Gamma(D_s^- \text{ anything})/\Gamma_{\text{total}}$		$\Gamma_{45}/\Gamma$	
VALUE	DOCUMENT ID	TECN	COMMENT
$0.147 \pm 0.017 \pm 0.013$	108 BUSKULIC	96Y	ALEP $e^+ e^- \rightarrow Z$

<sup>108</sup> BUSKULIC 96Y reports  $0.183 \pm 0.019 \pm 0.009$  from a measurement of  $[\Gamma(\bar{b} \rightarrow D_s^- \text{ anything})/\Gamma_{\text{total}}] \times [B(D_s^+ \rightarrow \phi \pi^+)]$  assuming  $B(D_s^+ \rightarrow \phi \pi^+) = 0.036$ , which we rescale to our best value  $B(D_s^+ \rightarrow \phi \pi^+) = (4.5 \pm 0.4) \times 10^{-2}$ . Our first error is their experiment's error and our second error is the systematic error from using our best value.

$\Gamma(D_s^+ \text{ anything})/\Gamma_{\text{total}}$		$\Gamma_{46}/\Gamma$	
VALUE	DOCUMENT ID	TECN	COMMENT
$0.101 \pm 0.010 \pm 0.029$	109 ABDALLAH	03E	DLPH $e^+ e^- \rightarrow Z$

<sup>109</sup> The second error is the total of systematic uncertainties including the branching fractions used in the measurement.

$\Gamma(b \rightarrow \Lambda_c^+ \text{ anything})/\Gamma_{\text{total}}$		$\Gamma_{47}/\Gamma$	
VALUE	DOCUMENT ID	TECN	COMMENT
$0.097 \pm 0.013 \pm 0.025$	110 BUSKULIC	96Y	ALEP $e^+ e^- \rightarrow Z$

<sup>110</sup> BUSKULIC 96Y reports  $0.110 \pm 0.014 \pm 0.006$  from a measurement of  $[\Gamma(b \rightarrow \Lambda_c^+ \text{ anything})/\Gamma_{\text{total}}] \times [B(\Lambda_c^+ \rightarrow p K^- \pi^+)]$  assuming  $B(\Lambda_c^+ \rightarrow p K^- \pi^+) = 0.044$ , which we rescale to our best value  $B(\Lambda_c^+ \rightarrow p K^- \pi^+) = (5.0 \pm 1.3) \times 10^{-2}$ . Our first error is their experiment's error and our second error is the systematic error from using our best value.

$\Gamma(\bar{c} / c \text{ anything})/\Gamma_{\text{total}}$		$\Gamma_{48}/\Gamma$	
VALUE	DOCUMENT ID	TECN	COMMENT
$1.162 \pm 0.032$ OUR AVERAGE			
$1.12 \pm 0.11$ $-0.10$	111 ABBIENDI	04I	OPAL $e^+ e^- \rightarrow Z$
$1.166 \pm 0.031 \pm 0.080$	112 ABREU	00	DLPH $e^+ e^- \rightarrow Z$
$1.147 \pm 0.041$	113 ABREU	98D	DLPH $e^+ e^- \rightarrow Z$
$1.230 \pm 0.036 \pm 0.065$	114 BUSKULIC	96Y	ALEP $e^+ e^- \rightarrow Z$



## Meson Particle Listings

 $B^\pm/B^0/B_s^0/b$ -baryon ADMIXTURE

"OUR EVALUATION" is an average using rescaled values of the data listed below. The average and rescaling were performed by the Heavy Flavor Averaging Group (HFAG) and are described at <http://www.slac.stanford.edu/xorg/hfag/>. The averaging/rescaling procedure takes into account correlations between the measurements.

VALUE	EVTS	DOCUMENT ID	TECN	COMMENT
<b>0.1284 ± 0.0069 OUR EVALUATION</b>				
<b>0.129 ± 0.004 OUR AVERAGE</b>				
0.132 ± 0.001 ± 0.024		134 ABAZOV	06s D0	$p\bar{p}$ at 1.96 TeV
0.152 ± 0.007 ± 0.011		135 ACOSTA	04A CDF	$p\bar{p}$ at 1.8 TeV
0.1312 ± 0.0049 ± 0.0042		136 ABBIENDI	03P OPAL	$e^+e^- \rightarrow Z$
0.127 ± 0.013 ± 0.006		137 ABREU	01L DLPH	$e^+e^- \rightarrow Z$
0.1192 ± 0.0068 ± 0.0051		138 ACCIARRI	99D L3	$e^+e^- \rightarrow Z$
0.121 ± 0.016 ± 0.006		139 ABREU	94J DLPH	$e^+e^- \rightarrow Z$
0.114 ± 0.014 ± 0.008		140 BUSKULIC	94G ALEP	$e^+e^- \rightarrow Z$
0.129 ± 0.022		141 BUSKULIC	92B ALEP	$e^+e^- \rightarrow Z$
0.176 ± 0.031 ± 0.032	1112	142 ABE	91G CDF	$p\bar{p}$ 1.8 TeV
0.148 ± 0.029 ± 0.017		143 ALBAJAR	91D UA1	$p\bar{p}$ 630 GeV
• • • We do not use the following data for averages, fits, limits, etc. • • •				
0.131 ± 0.020 ± 0.016		144 ABE	97I CDF	Repl. by ACOSTA 04A
0.1107 ± 0.0062 ± 0.0055		145 ALEXANDER	96 OPAL	Repl. by ABBIENDI 03P
0.136 ± 0.037 ± 0.040		146 UENO	96 AMY	$e^+e^-$ at 57.9 GeV
0.144 ± 0.014 ± 0.017 -0.011		147 ABREU	94F DLPH	Sup. by ABREU 94J
0.131 ± 0.014		148 ABREU	94J DLPH	$e^+e^- \rightarrow Z$
0.123 ± 0.012 ± 0.008		ACCARRI	94D L3	Repl. by ACCIARRI 99D
0.157 ± 0.020 ± 0.032		149 ALBAJAR	94 UA1	$\sqrt{s} = 630$ GeV
0.121 ± 0.044 ± 0.017 -0.040	1665	150 ABREU	93C DLPH	Sup. by ABREU 94J
0.143 ± 0.022 ± 0.007 -0.021		151 AKERS	93B OPAL	Sup. by ALEXANDER 96
0.145 ± 0.041 ± 0.018 -0.035		152 ACTON	92C OPAL	$e^+e^- \rightarrow Z$
0.121 ± 0.017 ± 0.006		153 ADEVA	92C L3	Sup. by ACCIARRI 94D
0.132 ± 0.22 ± 0.015 -0.012	823	154 DECAMP	91 ALEP	$e^+e^- \rightarrow Z$
0.178 ± 0.049 ± 0.020 -0.040		155 ADEVA	90P L3	$e^+e^- \rightarrow Z$
0.17 ± 0.15 ± 0.08 -0.08	156,157	WEIR	90 MRK2	$e^+e^-$ 29 GeV
0.21 ± 0.29 ± 0.15 -0.15	156	BAND	88 MAC	$E_{cm}^{ee} = 29$ GeV
>0.02 at 90% CL	156	BAND	88 MAC	$E_{cm}^{ee} = 29$ GeV
0.121 ± 0.047	156,158	ALBAJAR	87C UA1	Repl. by ALBAJAR 91D
<0.12 at 90% CL	156,159	SCHAAD	85 MRK2	$E_{cm}^{ee} = 29$ GeV

- 134 Uses the dimuon charge asymmetry. Averaged over the mix of  $b$ -flavored hadrons.
- 135 Measurement performed using events containing a dimuon or an  $e/\mu$  pair.
- 136 The average  $B$  mixing parameter is determined simultaneously with  $b$  and  $c$  forward-backward asymmetries in the fit.
- 137 The experimental systematic and model uncertainties are combined in quadrature.
- 138 ACCIARRI 99D uses maximum-likelihood fits to extract  $\chi_b$  as well as the  $A_{FB}^b$  in  $Z \rightarrow b\bar{b}$  events containing prompt leptons.
- 139 This ABREU 94J result is from 5182  $\ell\ell$  and 279  $\ell e$  events. The systematic error includes 0.004 for model dependence.
- 140 BUSKULIC 94G data analyzed using  $ee$ ,  $e\mu$ , and  $\mu\mu$  events.
- 141 BUSKULIC 92B uses a jet charge technique combined with electrons and muons.
- 142 ABE 91G measurement of  $\chi$  is done with  $e\mu$  and  $ee$  events.
- 143 ALBAJAR 91D measurement of  $\chi$  is done with dimuons.
- 144 Uses di-muon events.
- 145 ALEXANDER 96 uses a maximum likelihood fit to simultaneously extract  $\chi$  as well as the forward-backward asymmetries in  $e^+e^- \rightarrow Z \rightarrow b\bar{b}$  and  $cc$ .
- 146 UENO 96 extracted  $\chi$  from the energy dependence of the forward-backward asymmetry.
- 147 ABREU 94F uses the average electric charge sum of the jets recoiling against a  $b$ -quark jet tagged by a high  $p_T$  muon. The result is for  $\bar{\chi} = f_d\chi_d + 0.9f_s\chi_s$ .
- 148 This ABREU 94J result combines  $\ell\ell$ ,  $\ell e$ , and jet-charge  $\ell$  (ABREU 94F) analyses. It is for  $\bar{\chi} = f_d\chi_d + 0.96f_s\chi_s$ .
- 149 ALBAJAR 94 uses dimuon events. Not independent of ALBAJAR 91D.
- 150 ABREU 93C data analyzed using  $ee$ ,  $e\mu$ , and  $\mu\mu$  events.
- 151 AKERS 93B analysis performed using dilepton events.
- 152 ACTON 92C uses electrons and muons. Superseded by AKERS 93B.
- 153 ADEVA 92C uses electrons and muons.
- 154 DECAMP 91 done with opposite and like-sign dileptons. Superseded by BUSKULIC 92B.
- 155 ADEVA 90P measurement uses  $ee$ ,  $e\mu$ , and  $\mu\mu$  events from 118k events at the Z. Superseded by ADEVA 92C.
- 156 These experiments are not in the average because the combination of  $B_s$  and  $B_d$  mesons which they see could differ from those at higher energy.
- 157 The WEIR 90 measurement supersedes the limit obtained in SCHAAD 85. The 90% CL are 0.06 and 0.38.
- 158 ALBAJAR 87C measured  $\chi = (\bar{B}^0 \rightarrow B^0 \rightarrow \mu^+ X)$  divided by the average production weighted semileptonic branching fraction for  $B$  hadrons at 546 and 630 GeV.
- 159 Limit is average probability for hadron containing  $B$  quark to produce a positive lepton.

CP VIOLATION PARAMETERS IN SEMILEPTONIC  $b$ -HADRON DECAYS. $\text{Re}(\epsilon_b) / (1 + |\epsilon_b|^2)$ 

CP impurity in semileptonic  $b$ -hadron decays.

VALUE (units $10^{-3}$ )	DOCUMENT ID	TECN	COMMENT
<b>-1.97 ± 0.43 ± 0.23</b>	160 ABAZOV	11U D0	$p\bar{p}$ at 1.96 TeV
• • • We do not use the following data for averages, fits, limits, etc. • • •			
-2.39 ± 0.63 ± 0.37	161 ABAZOV	10H D0	Repl. by ABAZOV 11U
160 ABAZOV 11U reports a measurement of like-sign dimuon charge asymmetry of $A_{SL}^b = (-7.87 \pm 1.72 \pm 0.93) \times 10^{-3}$ in semileptonic $b$ -hadron decays.			
161 ABAZOV 10H reports a measurement of like-sign dimuon charge asymmetry of $A_{SL}^b = (-9.57 \pm 2.51 \pm 1.46) \times 10^{-3}$ in semileptonic $b$ -hadron decays. Using the measured production ratio of $B_d^0$ and $B_s^0$ , and the asymmetry of $B_d^0 A_{SL}^d = (-4.7 \pm 4.6) \times 10^{-3}$ measured from $B$ -factories, they obtain the asymmetry for $B_s^0$ as $A_{SL}^s = (-14.6 \pm 7.5) \times 10^{-3}$ .			

## B-HADRON PRODUCTION FRACTIONS IN HADRONIC Z DECAY

The production fractions of  $b$ -hadrons in hadronic Z decays have been calculated using the best values of mean lives, mixing parameters and branching fractions in this edition by the Heavy Flavor Averaging Group (HFAG) (see <http://www.slac.stanford.edu/xorg/hfag/>).

The values reported below assume:

$$f(\bar{b} \rightarrow B^+) = f(\bar{b} \rightarrow B^0)$$

$$f(\bar{b} \rightarrow B^+) + f(\bar{b} \rightarrow B^0) + f(\bar{b} \rightarrow B_s^0) + f(b \rightarrow b\text{-baryon}) = 1$$

The values are:

$$f(\bar{b} \rightarrow B^+) = f(\bar{b} \rightarrow B^0) = 0.403 \pm 0.009$$

$$f(\bar{b} \rightarrow B_s^0) = 0.103 \pm 0.009$$

$$f(b \rightarrow b\text{-baryon}) = 0.090 \pm 0.015$$

and their correlation coefficients are:

$$\text{cor}(B_s^0, b\text{-baryon}) = +0.036$$

$$\text{cor}(B_s^0, B^+ = B^0) = -0.522$$

$$\text{cor}(b\text{-baryon}, B^+ = B^0) = -0.871$$

as obtained using a time-integrated mixing parameter  $\bar{\chi} = 0.1259 \pm 0.0042$  given by a fit to heavy quark quantities with asymmetries removed (see the note "The Z boson").

B-HADRON PRODUCTION FRACTIONS IN  $p\bar{p}$  COLLISIONS AT Tevatron

The production fractions for  $b$ -hadrons in  $p\bar{p}$  collisions at the Tevatron have been calculated from the best values of mean lifetimes, mixing parameters, and branching fractions in this edition by the Heavy Flavor Averaging Group (HFAG) (see <http://www.slac.stanford.edu/xorg/hfag/>).

The values reported below assume:

$$f(\bar{b} \rightarrow B^+) = f(\bar{b} \rightarrow B^0)$$

$$f(\bar{b} \rightarrow B^+) + f(\bar{b} \rightarrow B^0) + f(\bar{b} \rightarrow B_s^0) + f(b \rightarrow b\text{-baryon}) = 1$$

The values are:

$$f(\bar{b} \rightarrow B^+) = f(\bar{b} \rightarrow B^0) = 0.339 \pm 0.031$$

$$f(\bar{b} \rightarrow B_s^0) = 0.111 \pm 0.014$$

$$f(b \rightarrow b\text{-baryon}) = 0.212 \pm 0.069$$

and their correlation coefficients are:

$$\text{cor}(B_s^0, b\text{-baryon}) = -0.581$$

$$\text{cor}(B_s^0, B^+ = B^0) = +0.425$$

$$\text{cor}(b\text{-baryon}, B^+ = B^0) = -0.984$$

as obtained with the Tevatron average of time-integrated mixing parameter  $\bar{\chi} = 0.147 \pm 0.011$ .

 $B^\pm/B^0/B_s^0/b$ -baryon ADMIXTURE REFERENCES

AALJ	12J	PR D85 032008	R. Aaji et al.	(LHCb Collab.)
AALJ	11F	PRL 107 211801	R. Aaji et al.	(LHCb Collab.)
ABAZOV	11U	PR D84 052007	V.M. Abazov et al.	(D0 Collab.)
ABAZOV	10H	PR D82 032001	V.M. Abazov et al.	(D0 Collab.)
Also		PRL 105 081801	V.M. Abazov et al.	(D0 Collab.)
AALTONEN	09E	PR D79 032001	T. Aaltonen et al.	(CDF Collab.)
AALTONEN	08N	PR D77 072003	T. Aaltonen et al.	(CDF Collab.)
ABAZOV	06S	PR D74 092001	V.M. Abazov et al.	(D0 Collab.)
ABBIENDI	04I	EPJ C35 149	G. Abbiendi et al.	(OPAL Collab.)
ABDALLAH	04E	EPJ C33 307	J. Abdallah et al.	(DELPHI Collab.)
ACOSTA	04A	PR D69 012002	D. Acosta et al.	(CDF Collab.)
ABBIENDI	03M	EPJ C30 467	G. Abbiendi et al.	(OPAL Collab.)
ABBIENDI	03P	PL B577 18	G. Abbiendi et al.	(OPAL Collab.)
ABDALLAH	03E	PL B561 26	J. Abdallah et al.	(DELPHI Collab.)
ABDALLAH	03K	PL B576 29	J. Abdallah et al.	(DELPHI Collab.)
HEISTER	02G	EPJ C22 613	A. Heister et al.	(ALEPH Collab.)
ABBIENDI	01Q	PL B520 1	G. Abbiendi et al.	(OPAL Collab.)
ABBIENDI	01R	EPJ C21 399	G. Abbiendi et al.	(OPAL Collab.)
ABREU	01L	EPJ C20 455	P. Abreu et al.	(DELPHI Collab.)
BARATE	01E	EPJ C19 213	R. Barate et al.	(ALEPH Collab.)
ABBIENDI	00E	EPJ C13 225	G. Abbiendi et al.	(OPAL Collab.)
ABBIENDI	00Z	PL B492 13	G. Abbiendi et al.	(OPAL Collab.)
ABREU	00I	EPJ C12 225	P. Abreu et al.	(DELPHI Collab.)
ABREU	00C	PL B496 43	P. Abreu et al.	(DELPHI Collab.)
ABREU	00D	PL B478 14	P. Abreu et al.	(DELPHI Collab.)
ABREU	00R	PL B475 407	P. Abreu et al.	(DELPHI Collab.)
ACCIARRI	00I	EPJ C13 47	M. Acciarri et al.	(L3 Collab.)
AFFOLDER	00E	PRL 84 1663	T. Affolder et al.	(CDF Collab.)
ABBIENDI	99J	EPJ C12 609	G. Abbiendi et al.	(OPAL Collab.)
ABE	99P	PR D60 092005	F. Abe et al.	(CDF Collab.)
ACCIARRI	99D	PL B448 152	M. Acciarri et al.	(L3 Collab.)
BARATE	99G	EPJ C6 555	R. Barate et al.	(ALEPH Collab.)

See key on page 457

## Meson Particle Listings

 $B^\pm/B^0/B_s^0/b$ -baryon ADMIXTURE,  $V_{cb}$  and  $V_{ub}$  CKM Matrix Elements

ABBOTT	98B	PL B423 419	B. Abbott <i>et al.</i>	(D0 Collab.)
ABE	98B	PR D57 5382	F. Abe <i>et al.</i>	(CDF Collab.)
ABREU	98D	PL B426 193	P. Abreu <i>et al.</i>	(DELPHI Collab.)
ABREU	98H	PL B425 399	P. Abreu <i>et al.</i>	(DELPHI Collab.)
ACCIARRI	98	PL B416 220	M. Acciari <i>et al.</i>	(L3 Collab.)
ACCIARRI	98K	PL B436 174	M. Acciari <i>et al.</i>	(L3 Collab.)
ACKERSTAFF	98E	EPJ C1 439	K. Ackerstaff <i>et al.</i>	(OPAL Collab.)
BARATE	98I	PL B429 169	R. Barate <i>et al.</i>	(ALEPH Collab.)
BARATE	98Q	EPJ C4 387	R. Barate <i>et al.</i>	(ALEPH Collab.)
BARATE	98V	EPJ C5 205	R. Barate <i>et al.</i>	(ALEPH Collab.)
GLENN	98	PRL 80 2289	S. Glenn <i>et al.</i>	(CLEO Collab.)
ABE	97I	PR D55 2546	F. Abe <i>et al.</i>	(CDF Collab.)
ACKERSTAFF	97F	ZPHY C73 397	K. Ackerstaff <i>et al.</i>	(OPAL Collab.)
ACKERSTAFF	97N	ZPHY C74 423	K. Ackerstaff <i>et al.</i>	(OPAL Collab.)
ACKERSTAFF	97W	ZPHY C76 425	K. Ackerstaff <i>et al.</i>	(OPAL Collab.)
ABREU	96E	PL B377 195	P. Abreu <i>et al.</i>	(DELPHI Collab.)
ACCIARRI	96C	ZPHY C71 379	M. Acciari <i>et al.</i>	(L3 Collab.)
ADAM	96	ZPHY C69 561	W. Adam <i>et al.</i>	(DELPHI Collab.)
ADAM	96D	ZPHY C72 207	W. Adam <i>et al.</i>	(DELPHI Collab.)
ALEXANDER	96	ZPHY C70 357	G. Alexander <i>et al.</i>	(OPAL Collab.)
BUSKULIC	96F	PL B369 151	D. Buskulic <i>et al.</i>	(ALEPH Collab.)
BUSKULIC	96V	PL B384 471	D. Buskulic <i>et al.</i>	(ALEPH Collab.)
BUSKULIC	96Y	PL B388 648	D. Buskulic <i>et al.</i>	(ALEPH Collab.)
GROSSMAN	96	NP B465 369	Y. Grossman, Z. Ligeti, E. Nardi	(REHO, CIT)
Also		NP B480 753 (erratum)	Y. Grossman, Z. Ligeti, E. Nardi	
PDG	96	PR D54 1	R. M. Barnett <i>et al.</i>	
UENO	96	PL B381 365	K. Ueno <i>et al.</i>	(AMY Collab.)
ABE,K	95B	PRL 75 3624	K. Abe <i>et al.</i>	(SLD Collab.)
ABREU	95C	PL B347 447	P. Abreu <i>et al.</i>	(DELPHI Collab.)
ABREU	95D	ZPHY C66 323	P. Abreu <i>et al.</i>	(DELPHI Collab.)
ADAM	95	ZPHY C68 363	W. Adam <i>et al.</i>	(DELPHI Collab.)
AKERS	95Q	ZPHY C67 57	R. Akers <i>et al.</i>	(OPAL Collab.)
BUSKULIC	95	PL B343 444	D. Buskulic <i>et al.</i>	(ALEPH Collab.)
ABREU	94F	PL B322 459	P. Abreu <i>et al.</i>	(DELPHI Collab.)
ABREU	94J	PL B332 488	P. Abreu <i>et al.</i>	(DELPHI Collab.)
ABREU	94L	ZPHY C63 3	P. Abreu <i>et al.</i>	(DELPHI Collab.)
ABREU	94P	PL B341 109	P. Abreu <i>et al.</i>	(DELPHI Collab.)
ACCIARRI	94C	PL B332 201	M. Acciari <i>et al.</i>	(L3 Collab.)
ACCIARRI	94D	PL B335 542	M. Acciari <i>et al.</i>	(L3 Collab.)
ALBAJAR	94	ZPHY C61 41	C. Albajar <i>et al.</i>	(UA1 Collab.)
BUSKULIC	94G	ZPHY C62 179	D. Buskulic <i>et al.</i>	(ALEPH Collab.)
ABE	93E	PL B313 288	K. Abe <i>et al.</i>	(VENUS Collab.)
ABE	93J	PRL 71 3421	F. Abe <i>et al.</i>	(CDF Collab.)
ABREU	93C	PL B301 145	P. Abreu <i>et al.</i>	(DELPHI Collab.)
ABREU	93D	ZPHY C57 181	P. Abreu <i>et al.</i>	(DELPHI Collab.)
ABREU	93G	PL B312 253	P. Abreu <i>et al.</i>	(DELPHI Collab.)
ACTON	93C	PL B307 247	P.D. Acton <i>et al.</i>	(OPAL Collab.)
ACTON	93L	ZPHY C60 217	P.D. Acton <i>et al.</i>	(OPAL Collab.)
ADRIANI	93J	PL B317 467	O. Adriani <i>et al.</i>	(L3 Collab.)
ADRIANI	93K	PL B317 474	O. Adriani <i>et al.</i>	(L3 Collab.)
ADRIANI	93L	PL B317 637	O. Adriani <i>et al.</i>	(L3 Collab.)
AKERS	93B	ZPHY C60 199	R. Akers <i>et al.</i>	(OPAL Collab.)
BUSKULIC	93B	PL B298 479	D. Buskulic <i>et al.</i>	(ALEPH Collab.)
BUSKULIC	93O	PL B314 459	D. Buskulic <i>et al.</i>	(ALEPH Collab.)
ABREU	92	ZPHY C53 567	P. Abreu <i>et al.</i>	(DELPHI Collab.)
ACTON	92	PL B274 513	D.P. Acton <i>et al.</i>	(OPAL Collab.)
ACTON	92C	PL B276 379	D.P. Acton <i>et al.</i>	(OPAL Collab.)
ADEVA	92C	PL B288 395	B. Adeva <i>et al.</i>	(L3 Collab.)
ADRIANI	92	PL B288 412	O. Adriani <i>et al.</i>	(L3 Collab.)
BUSKULIC	92B	PL B284 177	D. Buskulic <i>et al.</i>	(ALEPH Collab.)
BUSKULIC	92F	PL B295 174	D. Buskulic <i>et al.</i>	(ALEPH Collab.)
BUSKULIC	92G	PL B295 396	D. Buskulic <i>et al.</i>	(ALEPH Collab.)
ABE	91G	PRL 67 3351	F. Abe <i>et al.</i>	(CDF Collab.)
ADEVA	91C	PL B261 177	B. Adeva <i>et al.</i>	(L3 Collab.)
ADEVA	91H	PL B270 111	B. Adeva <i>et al.</i>	(L3 Collab.)
ALBAJAR	91C	PL B262 163	C. Albajar <i>et al.</i>	(UA1 Collab.)
ALBAJAR	91D	PL B262 171	C. Albajar <i>et al.</i>	(UA1 Collab.)
ALEXANDER	91G	PL B266 485	G. Alexander <i>et al.</i>	(OPAL Collab.)
DECAMP	91	PL B258 236	D. Decamp <i>et al.</i>	(ALEPH Collab.)
DECAMP	91C	PL B257 492	D. Decamp <i>et al.</i>	(ALEPH Collab.)
ADEVA	90P	PL B252 703	B. Adeva <i>et al.</i>	(L3 Collab.)
BEHREND	90D	ZPHY C47 333	H.J. Behrend <i>et al.</i>	(CELLO Collab.)
HAGEMANN	90	ZPHY C48 401	J. Hagemann <i>et al.</i>	(JADE Collab.)
LYONS	90	PR D41 982	L. Lyons, A.J. Martin, D.H. Saxon	(OXF, BRIS+)
WEIR	90	PL B240 289	A.J. Weir <i>et al.</i>	(Mark II Collab.)
BRAUNSCHWIG	89B	ZPHY C44 1	R. Braunschweig <i>et al.</i>	(TASSO Collab.)
ONG	89	PRL 62 1236	R.A. Ong <i>et al.</i>	(Mark II Collab.)
BAND	88	PL B200 221	H.R. Band <i>et al.</i>	(MAC Collab.)
KLEM	88	PR D37 41	D.E. Klem <i>et al.</i>	(DELCO Collab.)
ONG	88	PRL 60 2587	R.A. Ong <i>et al.</i>	(Mark II Collab.)
ALBAJAR	87C	PL B186 247	C. Albajar <i>et al.</i>	(UA1 Collab.)
ASH	87	PRL 58 640	W.W. Ash <i>et al.</i>	(MAC Collab.)
BARTEL	87	ZPHY C33 339	W. Bartel <i>et al.</i>	(JADE Collab.)
BROM	87	PL B195 301	J.M. Brom <i>et al.</i>	(HRS Collab.)
PAL	86	PR D33 2708	T. Pal <i>et al.</i>	(DELCO Collab.)
AIHARA	85	ZPHY C27 39	H. Aihara <i>et al.</i>	(TPC Collab.)
BARTEL	85J	PL 163B 277	W. Bartel <i>et al.</i>	(JADE Collab.)
SCHAAD	85	PL 160B 189	T. Schaad <i>et al.</i>	(Mark II Collab.)
ALTHOFF	84G	ZPHY C22 219	M. Althoff <i>et al.</i>	(TASSO Collab.)
ALTHOFF	84J	PL 146B 443	M. Althoff <i>et al.</i>	(TASSO Collab.)
KOOP	84	PRL 52 970	D.E. Koop <i>et al.</i>	(DELCO Collab.)
ADEVA	83	PRL 50 799	B. Adeva <i>et al.</i>	(Mark-J Collab.)
ADEVA	83B	PRL 51 443	B. Adeva <i>et al.</i>	(Mark-J Collab.)
BARTEL	83B	PL 132B 241	W. Bartel <i>et al.</i>	(JADE Collab.)
FERNANDEZ	83D	PRL 50 2054	E. Fernandez <i>et al.</i>	(MAC Collab.)
MATTEUZZI	83	PL 129B 141	C. Matteuzzi <i>et al.</i>	(Mark II Collab.)
NELSON	83	PRL 50 1542	M.E. Nelson <i>et al.</i>	(Mark II Collab.)

 $V_{cb}$  and  $V_{ub}$  CKM Matrix Elements

OMITTED FROM SUMMARY TABLE

DETERMINATION OF  $V_{cb}$  AND  $V_{ub}$ 

Updated February 2012 by R. Kowalewski (Univ. of Victoria, Canada) and T. Mannel (Univ. of Siegen, Germany)

## INTRODUCTION

Precision determinations of  $|V_{ub}|$  and  $|V_{cb}|$  are central to testing the CKM sector of the Standard Model, and complement the measurements of CP asymmetries in  $B$  decays. The length of the side of the unitarity triangle opposite the well-measured angle  $\beta$  is proportional to the ratio  $|V_{ub}|/|V_{cb}|$ , making its determination a high priority of the heavy-flavor physics program.

The semileptonic transitions  $b \rightarrow c\ell\bar{\nu}_\ell$  and  $b \rightarrow u\ell\bar{\nu}_\ell$  provide two avenues for determining these CKM matrix elements, namely through inclusive and exclusive final states. The experimental and theoretical techniques underlying these two avenues are independent, providing a crucial cross-check on our understanding. Recent measurements and calculations are reflected in the values quoted in this article, which is an update on the previous review [1]. The leptonic decay  $B^- \rightarrow \tau\bar{\nu}$  can also be used to extract  $|V_{ub}|$ , but we do not use this information at present since none of the current experimental measurements have a significance above 3.6 $\sigma$ .

The theory underlying the determination of  $|V_{qb}|$  is mature, in particular for  $|V_{cb}|$ . Most of the theoretical approaches use the fact that the mass  $m_b$  of the  $b$  quark is large compared to the scale  $\Lambda_{\text{QCD}}$  that determines low-energy hadronic physics. The basis for precise calculations is a systematic expansion in powers of  $\Lambda/m_b$ , where  $\Lambda \sim 500 - 700$  MeV is a hadronic scale of the order of  $\Lambda_{\text{QCD}}$ , using effective-field-theory methods to separate non-perturbative from perturbative contributions. The expansion in  $\Lambda/m_b$  and  $\alpha_s$  works well enough to enable a precision determination of  $|V_{cb}|$  and  $|V_{ub}|$  in semileptonic decays.

The large data samples available at the  $B$  factories enable analyses where one  $B$  meson from an  $\Upsilon(4S)$  decay is fully reconstructed, allowing a recoiling semileptonic  $B$  decay to be studied with high purity. Improved knowledge of  $\bar{B} \rightarrow X_c\ell\bar{\nu}_\ell$  decays allows partial rates for  $\bar{B} \rightarrow X_u\ell\bar{\nu}_\ell$  transitions to be measured in regions previously considered inaccessible, increasing the acceptance for  $\bar{B} \rightarrow X_u\ell\bar{\nu}_\ell$  transitions and reducing theoretical uncertainties.

Experimental measurements of the exclusive  $\bar{B} \rightarrow \pi\ell\bar{\nu}_\ell$  decay are quite precise, and recent improvements in the theoretical calculation of the form factor normalization have enabled a determination of  $|V_{ub}|$  from this decay with an uncertainty below 10%.

Throughout this review the numerical results quoted are based on the methods of the Heavy Flavor Averaging Group [2].

# Meson Particle Listings

## $V_{cb}$ and $V_{ub}$ CKM Matrix Elements

### DETERMINATION OF $|V_{cb}|$

*Summary:* The determination of  $|V_{cb}|$  from  $\bar{B} \rightarrow D^* \ell \bar{\nu}_\ell$  decays is currently at a relative precision of about 2%. The main limitation is the knowledge of the form factor near the maximum momentum transfer to the leptons. For the  $\bar{B} \rightarrow D \ell \bar{\nu}_\ell$  channel experimental measurements have recently been substantially improved, allowing this channel to provide a meaningful cross-check on  $\bar{B} \rightarrow D^* \ell \bar{\nu}_\ell$ .

Determinations of  $|V_{cb}|$  from inclusive decays are currently below 2% relative uncertainty. The limitations arise mainly from our ignorance of higher-order perturbative and non-perturbative corrections.

The values obtained from inclusive and exclusive determinations are marginally consistent with each other:

$$|V_{cb}| = (41.9 \pm 0.7) \times 10^{-3} \quad (\text{inclusive}) \quad (1)$$

$$|V_{cb}| = (39.6 \pm 0.9) \times 10^{-3} \quad (\text{exclusive}). \quad (2)$$

An average of the above gives  $|V_{cb}| = (40.9 \pm 0.6) \times 10^{-3}$ , with  $p(\chi^2) = 0.04$ . Scaling the error by  $\sqrt{\chi^2/1} = 2.0$  we quote

$$|V_{cb}| = (40.9 \pm 1.1) \times 10^{-3}. \quad (3)$$

### $|V_{cb}|$ from exclusive decays

Exclusive determinations of  $|V_{cb}|$  are based on a study of semileptonic  $B$  decays into the ground state charmed mesons  $D$  and  $D^*$ . The main uncertainties in this approach stem from our ignorance of the form factors describing the  $B \rightarrow D$  and  $B \rightarrow D^*$  transitions. However, in the limit of infinite bottom and charm quark masses only a single form factor appears, the Isgur-Wise function [3], which depends on the product of the four-velocities  $v$  and  $v'$  of the initial and final-state hadrons.

The extraction of  $|V_{cb}|$  is based on the distribution of the variable  $w \equiv v \cdot v'$ , which corresponds to the energy of the final state  $D^{(*)}$  meson in the rest frame of the decay. Heavy Quark Symmetry (HQS) [3,4] predicts the normalization of the rate at  $w = 1$ , the point of maximum momentum transfer to the leptons, and  $|V_{cb}|$  is obtained from an extrapolation of the measured spectrum to  $w = 1$ . This extrapolation relies on a parametrization of the form factor, as explained below.

A precise determination requires corrections to the HQS prediction for the normalization as well as some information on the slope of the form factors near the point  $w = 1$ , since the phase space vanishes there. The corrections to the HQS prediction due to finite quark masses are given in terms of the symmetry-breaking parameter

$$\frac{1}{\mu} = \frac{1}{m_c} - \frac{1}{m_b},$$

which is essentially  $1/m_c$  for realistic quark masses. HQS ensures that those matrix elements that correspond to the currents that generate the HQS are normalized at  $w = 1$ ; as a result, some of the form factors either vanish or are normalized to unity at  $w = 1$ . Due to Luke's Theorem [5] (which is an application of the Ademollo-Gatto theorem [6] to heavy

quarks), the leading correction to those form factors normalized due to HQS is quadratic in  $1/\mu$ , while for the form factors that vanish in the infinite mass limit the corrections are in general linear in  $1/m_c$  and  $1/m_b$ . Thus we have, using the definitions as in Eq. (2.84) of Ref. [7]

$$\begin{aligned} h_i(1) &= 1 + \mathcal{O}(1/\mu^2) & \text{for } i = +, V, A_1, A_3, \\ h_i(1) &= \mathcal{O}(1/m_c, 1/m_b) & \text{for } i = -, A_2. \end{aligned} \quad (4)$$

In addition to these corrections, there are perturbatively calculable radiative corrections from QCD and QED, which will be discussed in the relevant sections. Both - radiative corrections as well as  $1/m_{b,c}$  corrections - are considered in the framework of Heavy Quark Effective Theory (HQET) [8], which provides for a systematic expansion.

### $\bar{B} \rightarrow D^* \ell \bar{\nu}_\ell$

The decay rate for  $\bar{B} \rightarrow D^* \ell \bar{\nu}_\ell$  is given by

$$\frac{d\Gamma}{dw}(\bar{B} \rightarrow D^* \ell \bar{\nu}_\ell) = \frac{G_F^2}{48\pi^3} |V_{cb}|^2 m_{D^*}^3 (w^2 - 1)^{1/2} P(w) (\eta_{\text{em}} \mathcal{F}(w))^2, \quad (5)$$

where  $P(w)$  is a phase space factor with  $P(1) = 12(m_B - m_{D^*})^2$  and  $\mathcal{F}(w)$  is dominated by the axial vector form factor  $h_{A_1}$  as  $w \rightarrow 1$ . Furthermore,  $\eta_{\text{em}} = 1.007$  accounts for the electroweak corrections to the four-fermion operator mediating the semileptonic decay [11]. In the infinite-mass limit, the HQS normalization gives  $\mathcal{F}(1) = 1$ .

The form factor  $\mathcal{F}(w)$  must be parametrized to perform an extrapolation to the zero-recoil point. A frequently used one-parameter form motivated by analyticity and unitarity is [9,10]

$$\begin{aligned} \mathcal{F}(w) &= \eta_A \left[ 1 + \delta_{1/m^2} + \dots \right] \\ &= \left[ 1 - 8\rho_{A_1}^2 z + (53\rho_{A_1}^2 - 15)z^2 - (231\rho_{A_1}^2 - 91)z^3 \right] \end{aligned} \quad (6)$$

with  $z = (\sqrt{w+1} - \sqrt{2})/(\sqrt{w+1} + \sqrt{2})$  originating from a conformal transformation. The parameter  $\rho_{A_1}^2$  is the slope of the form factor at  $w = 1$ . The factor  $\eta_A$  is the QCD short-distance radiative correction [12] to the form factor

$$\eta_A = 0.960 \pm 0.007, \quad (7)$$

and  $\delta_{1/m^2}$  comes from non-perturbative  $1/m^2$  corrections.

Improved lattice simulations that include effects from finite quark masses are used to calculate the deviation of  $\mathcal{F}(1)$  from unity. A recent calculation gives

$$\mathcal{F}(1) = 0.902 \pm 0.017, \quad (8)$$

where the factor  $\eta_{\text{em}}$  has been divided out from the value quoted in Ref. [13] and the errors have been added in quadrature. The leading uncertainties are due to heavy-quark discretization and chiral extrapolation errors.

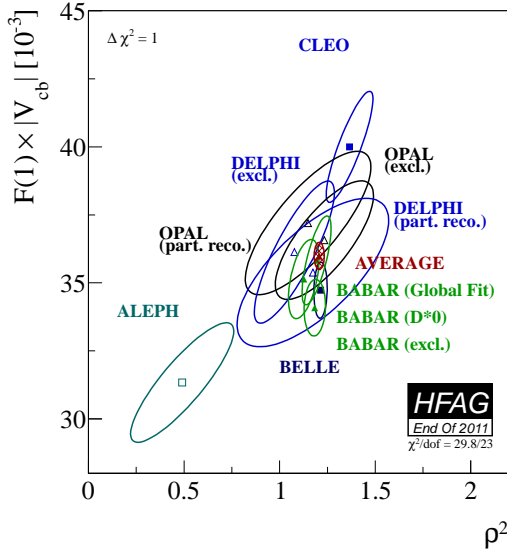


**Figure 1:** Measurements of  $|V_{cb}|\mathcal{F}(1)$  vs.  $\rho_{A_1}^2$  are shown as  $\Delta\chi^2 = 1$  ellipses.

Non-lattice estimates based on sum rules for the form factor tend to yield lower values for  $\mathcal{F}(1)$  [14,15,16]. Omitting the contributions from excited states, the sum rules indicate that  $\mathcal{F}(1) < 0.93$ . Including an estimate for the contribution of the excited states yields  $\mathcal{F}(1) = 0.86 \pm 0.01 \pm 0.02$  [16], where the second uncertainty originates from the estimate for the excited states.

Many experiments [17–25] have measured the differential rate as a function of  $w$ . Fig. 1 shows corresponding values of  $\mathcal{F}(1)|V_{cb}|$  and  $\rho_{A_1}^2$  (as defined in Ref. [10]). These measurements are input to a four-dimensional fit [26] for  $\mathcal{F}(1)|V_{cb}|$ ,  $\rho_{A_1}^2$  and the form factor ratios  $R_1 \propto A_2/A_1$  and  $R_2 \propto V/A_1$ . The leading sources of uncertainty on  $\mathcal{F}(1)|V_{cb}|$  are due to detection efficiencies and  $D^{(*)}$  decay branching fractions, while for  $\rho_{A_1}^2$  the uncertainties in  $R_1$  and  $R_2$  still dominate. Recent BABAR measurements, one using  $\overline{B}^0 \rightarrow D^{*0}\ell\overline{\nu}_\ell$  decays [23] and the other using a global fit to  $\overline{B} \rightarrow D\ell\overline{\nu}_\ell X$  decays [24] are completely insensitive to uncertainties related to the reconstruction of the charged pion from  $D^* \rightarrow D\pi$  decays; both measurements agree with the average given below.

The fit gives  $\mathcal{F}(1)|V_{cb}| = (36.0 \pm 0.5) \times 10^{-3}$  with a  $p$ -value of 0.15. Along with the lattice value given above for  $\mathcal{F}(1)$  this yields

$$|V_{cb}| = (39.6 \pm 0.6_{\text{exp}} \pm 0.8_{\text{theo}}) \times 10^{-3} \quad (\overline{B} \rightarrow D^*\ell\overline{\nu}_\ell, \text{ LQCD}), \quad (9)$$

The value of  $\mathcal{F}(1)$  obtained from QCD sum rules results in a larger value for  $|V_{cb}|$ :

$$|V_{cb}| = (41.6 \pm 0.6_{\text{exp}} \pm 1.9_{\text{theo}}) \times 10^{-3} \quad (\overline{B} \rightarrow D^*\ell\overline{\nu}_\ell, \text{ SR}). \quad (10)$$

### $\overline{B} \rightarrow D\ell\overline{\nu}_\ell$

The differential rate for  $\overline{B} \rightarrow D\ell\overline{\nu}_\ell$  is given by

$$\frac{d\Gamma}{dw}(\overline{B} \rightarrow D\ell\overline{\nu}_\ell) = \frac{G_F^2}{48\pi^3} |V_{cb}|^2 (m_B + m_D)^2 m_D^3 (w^2 - 1)^{3/2} (\eta_{\text{em}} \mathcal{G}(w))^2. \quad (11)$$

The form factor is

$$\mathcal{G}(w) = h_+(w) - \frac{m_B - m_D}{m_B + m_D} h_-(w), \quad (12)$$

where  $h_+$  is normalized to unity in the infinite-mass limit due to HQS and  $h_-$  vanishes in the heavy-mass limit. Thus

$$\mathcal{G}(1) = 1 + \mathcal{O}\left(\frac{m_B - m_D}{m_B + m_D} \frac{1}{m_c}\right) \quad (13)$$

and the corrections to the HQET predictions are parametrically larger than was the case for  $\overline{B} \rightarrow D^*\ell\overline{\nu}_\ell$ .

In order to get a more precise prediction for the form factor  $\mathcal{G}(1)$  the heavy-quark expansion can be supplemented by additional assumptions. It has been argued in Ref. [27] that in a limit in which the kinetic energy  $\mu_\pi^2$  is equal to the chromomagnetic moment  $\mu_G^2$  (these quantities are discussed below in more detail) one may obtain the value

$$\mathcal{G}(1) = 1.04 \pm 0.01_{\text{power}} \pm 0.01_{\text{pert}}. \quad (14)$$

Lattice calculations including effects beyond the heavy mass limit have become available, and hence the fact that deviations from the HQET predictions are parametrically larger than in the case  $\overline{B} \rightarrow D^*\ell\overline{\nu}_\ell$  is irrelevant. These unquenched calculations quote a value (preliminary, from 2005) [28]

$$\mathcal{G}(1) = 1.074 \pm 0.018 \pm 0.016. \quad (15)$$

The measurements of  $\overline{B} \rightarrow D\ell\overline{\nu}_\ell$  have improved substantially in the last few years. The new measurements [24,29] are consistent with previous measurements [17,30,31] but significantly more precise. The average of these inputs [26] gives  $\mathcal{G}(1)|V_{cb}| = (42.6 \pm 0.7 \pm 1.4) \times 10^{-3}$ . Using the value given in Eq. (15) for  $\mathcal{G}(1)$ , accounting for the electroweak correction and conservatively adding the theory uncertainties linearly results in

$$|V_{cb}| = (39.4 \pm 1.4 \pm 1.3) \times 10^{-3} \quad (\overline{B} \rightarrow D\ell\overline{\nu}_\ell, \text{ LQCD}), \quad (16)$$

where the first uncertainty is from experiment and the second from theory.

Using the non-lattice estimate from Eq. (14) one finds  $|V_{cb}| = (40.7 \pm 1.5 \pm 0.8) \times 10^{-3}$ .

Measuring the differential rate at  $w = 1$  is more difficult in  $\overline{B} \rightarrow D\ell\overline{\nu}_\ell$  decays than in  $\overline{B} \rightarrow D^*\ell\overline{\nu}_\ell$  decays, since the rate is smaller and the background from misreconstructed  $\overline{B} \rightarrow D^*\ell\overline{\nu}_\ell$  decays is significant; this is reflected in the larger experimental uncertainty. The  $B$  factories address these limitations by studying decays recoiling against fully reconstructed  $B$  mesons or doing a global fit to  $\overline{B} \rightarrow X_c\ell\overline{\nu}_\ell$  decays. Theoretical input

# Meson Particle Listings

## $V_{cb}$ and $V_{ub}$ CKM Matrix Elements

on the shape of the  $w$  spectrum in  $\bar{B} \rightarrow D\ell\bar{\nu}_\ell$  is valuable, as precise measurements of the total rate are easier; recent measurements [24,29] of  $\mathcal{B}(\bar{B} \rightarrow D\ell\bar{\nu}_\ell)$  have uncertainties of  $\sim 5\%$ .

The determinations from  $\bar{B} \rightarrow D^*\ell\bar{\nu}_\ell$  and  $\bar{B} \rightarrow D\ell\bar{\nu}_\ell$  decays are consistent, and their uncertainties are largely uncorrelated. Averaging these two lattice-based results gives

$$|V_{cb}| = (39.6 \pm 0.9) \times 10^{-3} \quad (\text{exclusive}). \quad (17)$$

### Prospects for Lattice determinations of the $B \rightarrow D^{(*)}$ form factors

Lattice determinations of the  $B \rightarrow D^{(*)}$  form factors naturally build in heavy-quark symmetries, so all uncertainties scale with the deviation of the form factor from unity [32,33]. In combination with unquenched calculations, i.e. calculations with realistic sea quarks, one obtains quite precise calculations of the form factors, now at the 2% level. The dominant uncertainties are due to the chiral extrapolation from the light quark masses used in the numerical lattice computation to realistic up and down quark masses, and to discretization errors. These sources of uncertainty will be reduced with larger lattice sizes and smaller lattice spacings.

A further ongoing development is the extension of these calculations to nonzero recoil. Such calculations are especially helpful for avoiding the  $w \rightarrow 1$  extrapolation in  $B \rightarrow D$ .

### Decays to Excited $D$ Meson States

Above the ground state  $D$  and  $D^*$  mesons lie four positive-parity states with one unit of orbital angular momentum, generically denoted as  $D^{**}$ . In the heavy mass limit they form two spin symmetry doublets with  $j_\ell = 1/2$  and  $j_\ell = 3/2$ , where  $j_\ell$  is the total angular momentum of the light degrees of freedom. The doublet with  $j_\ell = 3/2$  is expected to be narrow while the states with  $j_\ell = 1/2$  should be broad, consistent with experimental measurements. Furthermore, one expects that in the heavy mass limit  $\Gamma(B \rightarrow D^{**}(j_\ell = 3/2)\ell\bar{\nu}) \gg \Gamma(B \rightarrow D^{**}(j_\ell = 1/2)\ell\bar{\nu})$  [34,35,36]. Measurements indicate that this expectation may be violated, although the experimental situation is not clear. BELLE [37] and BABAR [38] report different results for the broad states and the experiments do not have the sensitivity to identify the spin-parity of these states. It has been suggested that decays to radially excited charm mesons may play a role in this puzzle [39]. If a violation is confirmed, it may indicate substantial mixing between the two spin symmetry doublets, which can occur due to terms of order  $1/m_c$ . However, the impact on the exclusive  $|V_{cb}|$  determination is expected to be small, since the zero-recoil point is protected against corrections of order  $1/m_c$  by Luke's theorem.

### $|V_{cb}|$ from inclusive decays

At present the most precise determinations of  $|V_{cb}|$  come from inclusive decays. The method is based on a measurement of the total semileptonic decay rate, together with the leptonic energy and the hadronic invariant mass spectra of inclusive

semileptonic decays. The total decay rate can be calculated quite reliably in terms of non-perturbative parameters that can be extracted from the information contained in the spectra.

### Inclusive semileptonic rate

The theoretical foundation for the calculation of the total semileptonic rate is the Operator Product Expansion (OPE) which yields the Heavy Quark Expansion (HQE), a systematic expansion in inverse powers of the  $b$ -quark mass [40,41]. The validity of the OPE is proven in the deep Euclidean region for the momenta (which is satisfied, *e.g.*, in deep inelastic scattering), but its application to heavy-quark decays requires a continuation to time-like momenta  $p_B^2 = M_B^2$ , where possible contributions which are exponentially damped in the Euclidean region could become oscillatory. The validity of the OPE for inclusive decays is equivalent to the assumption of parton-hadron duality, hereafter referred to simply as duality, and possible oscillatory contributions would be an indication of duality violation.

Duality-violating effects are hard to quantify. In practice, they would appear as unnaturally large coefficients of higher order terms in the  $1/m$  expansion [42]. The description of  $\sim 60$  measurements in terms of  $\sim 6$  free parameters in global fits to  $\bar{B} \rightarrow X_c\ell\bar{\nu}_\ell$  decays provides a non-trivial testing ground for the HQE predictions. Present fits include terms up to order  $1/m_b^3$ , the coefficients of which have sizes as expected a priori by theory and are in quantitative agreement with extractions from other observables. The consistency of the data with these OPE fits will be discussed later; no indication is found that terms of order  $1/m_b^4$  or higher are large, and there is no evidence for duality violations in the data. Thus duality or, likewise, the validity of the OPE, is assumed in the analysis, and no further uncertainty is assigned to potential duality violations.

The OPE result for the total rate can be written schematically (the details of the expression can be found, *e.g.*, in Ref. [43]) as

$$\begin{aligned} \Gamma = & |V_{cb}|^2 \hat{\Gamma}_0 m_b^5(\mu) (1 + A_{\text{ew}}) \times \\ & \left[ z_0^{(0)}(r) + \frac{\alpha_s(\mu)}{\pi} z_0^{(1)}(r) + \left( \frac{\alpha_s(\mu)}{\pi} \right)^2 z_0^{(2)}(r) + \dots \right. \\ & + \frac{\mu_\pi^2}{m_b^2} \left( z_2^{(0)}(r) + \frac{\alpha_s(\mu)}{\pi} z_2^{(1)}(r) + \dots \right) \\ & + \frac{\mu_G^2}{m_b^2} \left( y_2^{(0)}(r) + \frac{\alpha_s(\mu)}{\pi} y_2^{(1)}(r) + \dots \right) \\ & + \frac{\rho_D^3}{m_b^3} \left( z_3^{(0)}(r) + \frac{\alpha_s(\mu)}{\pi} z_3^{(1)}(r) + \dots \right) \\ & + \frac{\rho_{\text{LS}}^3}{m_b^3} \left( y_3^{(0)}(r) + \frac{\alpha_s(\mu)}{\pi} y_3^{(1)}(r) + \dots \right) \\ & \left. + z_4 \left( r, \frac{s_i}{m_b^4}, \frac{\alpha_s(\mu)}{\pi} \right) + \dots \right] \quad (18) \end{aligned}$$

where  $A_{\text{ew}}$  denotes the electroweak corrections,  $r$  is the ratio  $m_c/m_b$  and the  $y_i$  and  $z_i$  are known functions which appear in the perturbative expansion of the different orders of the heavy mass expansion. A similar expansion can be set up for



moments of the distributions of charged-lepton energy, hadronic invariant mass and hadronic energy.

This expression is known up to order  $1/m_b^5$ , where the terms of order  $1/m_b^n$  with  $n > 2$  have been computed only at tree level [44,45,46,47]. The leading term is the parton model, which is known completely to order  $\alpha_s$  and  $\alpha_s^2$  [48–50], and the terms of order  $\alpha_s^{n+1}\beta_0^n$  (where  $\beta_0$  is the first coefficient of the QCD  $\beta$  function,  $\beta_0 = (33 - 2n_f)/3$ ) have been included by the usual BLM procedure [43,51,52]. Furthermore, the corrections of order  $\alpha_s\mu_\pi^2/m_b^2$  have been computed [53].

Starting at order  $1/m_b^3$  contributions with an infrared sensitivity to the charm mass  $m_c$  appear [46,54,112]. At order  $1/m_b^3$  this “intrinsic charm” contribution is a  $\log(m_c)$  in the coefficient of the Darwin term  $\rho_D^3$ . At higher orders, terms such as  $1/m_b^3 \times 1/m_c^2$  and  $\alpha_s(m_c)1/m_b^3 \times 1/m_c$  appear, which are comparable in size to the contributions of order  $1/m_b^4$ .

The HQE parameters are given in terms of forward matrix elements; the parameters entering the expansion for orders up to  $1/m_b^3$  are

$$\begin{aligned}\bar{\Lambda} &= M_B - m_b, \\ \mu_\pi^2 &= -\langle B|\bar{b}(iD_\perp)^2b|B\rangle, \\ \mu_G^2 &= \langle B|\bar{b}(iD_\perp^\mu)(iD_\perp^\nu)\sigma_{\mu\nu}b|B\rangle, \\ \rho_D^3 &= \langle B|\bar{b}(iD_{\perp\mu})(ivD)(iD_\perp^\nu)b|B\rangle, \\ \rho_{LS}^3 &= \langle B|\bar{b}(iD_\perp^\mu)(ivD)(iD_\perp^\nu)\sigma_{\mu\nu}b|B\rangle.\end{aligned}\quad (19)$$

The hadronic parameters of the orders  $1/m_b^4$  and  $1/m_b^5$  can be found in Ref. [47] while the five hadronic parameters  $s_i$  of the order  $1/m_b^4$  can be found in Ref. [45]; these have not yet been included in the fits. The non-perturbative matrix elements depend on the renormalization scale  $\mu$ , on the chosen renormalization scheme and on the quark mass  $m_b$ , and may eventually be calculated in Lattice QCD. The rates and the spectra depend strongly on  $m_b$  (or equivalently on  $\bar{\Lambda}$ ), which makes the discussion of renormalization issues mandatory.

Using the pole mass definition for the heavy quark masses, it is well known that the corresponding perturbative series of decay rates does not converge very well, making a precision determination of  $|V_{cb}|$  in such a scheme impossible. The solution to this problem is to choose an appropriate “short-distance” mass definition. Frequently used mass definitions are the kinetic scheme [14], or the 1S scheme [56]. Both of these schemes have been applied to semileptonic  $b \rightarrow c$  transitions, yielding comparable results and uncertainties.

The 1S scheme eliminates the  $b$  quark pole mass by relating it to the perturbative expression for the mass of the 1S state of the  $\Upsilon$  system. The physical mass of the  $\Upsilon(1S)$  contains non-perturbative contributions, which have been estimated in Ref. [57]. These non-perturbative contributions are small; nevertheless, the best determination of the  $b$  quark mass in the 1S scheme is obtained from sum rules for  $e^+e^- \rightarrow b\bar{b}$  [58].

Alternatively one may use a short-distance mass definition such as the  $\overline{\text{MS}}$  mass  $m_b^{\overline{\text{MS}}}(m_b)$ . However, it has been argued that the scale  $m_b$  is unnaturally high for  $B$  decays, while

for smaller scales  $\mu \sim 1\text{ GeV}$   $m_b^{\overline{\text{MS}}}(\mu)$  is under poor control. For this reason the so-called “kinetic mass”  $m_b^{\text{kin}}(\mu)$ , has been proposed. It is the mass entering the non-relativistic expression for the kinetic energy of a heavy quark, and is defined using heavy-quark sum rules [14].

The HQE parameters also depend on the renormalization scale and scheme. The matrix elements given in Eq. (19) are defined with the full QCD fields and states, which is the definition frequently used in the kinetic scheme. Sometimes slightly different parameters  $\lambda_1$  and  $\lambda_2$  are used, which are defined in the infinite mass limit. The relation between these parameters is

$$\begin{aligned}\bar{\Lambda}_{\text{HQET}} &= \lim_{m_b \rightarrow \infty} \bar{\Lambda}, \quad -\lambda_1 = \lim_{m_b \rightarrow \infty} \mu_\pi^2, \\ \lambda_2 &= \lim_{m_b \rightarrow \infty} \mu_G^2, \quad \rho_1 = \lim_{m_b \rightarrow \infty} \rho_D^3, \\ \rho_2 &= \lim_{m_b \rightarrow \infty} \rho_{LS}^3.\end{aligned}\quad (20)$$

Defining the kinetic energy and the chromomagnetic moment in the infinite-mass limit (as, *e.g.*, in the 1S scheme) requires that  $1/m_b$  corrections to the matrix elements defined in Eq. (19) be taken into account once one goes beyond order  $1/m_b^2$ . As a result, additional quantities  $\mathcal{T}_1 \cdots \mathcal{T}_4$  appear at order  $1/m_b^3$ . However, these quantities are correlated such that the total number of non-perturbative parameters to order  $1/m_b^3$  is the same as in the scheme where  $m_b$  is kept finite in the matrix elements which define the non-perturbative parameters. A detailed discussion of these issues can be found in Ref. [59].

In order to define the HQE parameters properly one must adopt a renormalization scheme, as was done for the heavy quark mass. Since all these parameters can again be determined by heavy-quark sum rules, one may adopt a scheme similar to the kinetic scheme for the quark mass. The HQE parameters in the kinetic scheme depend on powers of the renormalization scale  $\mu$ , and the above relations are valid in the limit  $\mu \rightarrow 0$ , leaving only logarithms of  $\mu$ .

Some of these parameters also appear in the relation for the heavy hadron masses. The quantity  $\bar{\Lambda}$  is determined once a definition is specified for the quark mass. The parameter  $\mu_G^2$  can be extracted from the mass splitting in the lowest spin-symmetry doublet of heavy mesons [60]

$$\mu_G^2(\mu) = \frac{3}{4}C_G(\mu, m_b)(M_{B^*}^2 - M_B^2), \quad (21)$$

where  $C_G(\mu, m_b)$  is a perturbatively-computable coefficient which depends on the scheme. In the kinetic scheme we have

$$\mu_G^2(1\text{ GeV}) = 0.35_{-0.02}^{+0.03} \text{ GeV}^2. \quad (22)$$

#### Determination of HQE Parameters and $|V_{cb}|$

Several experiments have measured moments in  $\bar{B} \rightarrow X_c \ell \bar{\nu}_\ell$  decays [61–69] as a function of the minimum lepton momentum. The measurements of the moments of the electron energy spectrum (0<sup>th</sup>–3<sup>rd</sup>) and of the squared hadronic mass spectrum (0<sup>th</sup>–2<sup>nd</sup>) have statistical uncertainties that are roughly equal

# Meson Particle Listings

## $V_{cb}$ and $V_{ub}$ CKM Matrix Elements

to their systematic uncertainties. They can be improved with more data and significant effort. The sets of moments measured by each experiment have strong correlations; the full statistical and systematic correlation matrices are required to allow these to be used in a global fit. Measurements of photon energy moments (0<sup>th</sup>-2<sup>nd</sup>) in  $B \rightarrow X_s \gamma$  decays [70–74] as a function of the minimum accepted photon energy are still primarily statistics limited.

Global fits to the full set of moments [69,71,75–78] have been performed in the 1S and kinetic schemes. The semileptonic moments alone determine a linear combination of  $m_b$  and  $m_c$  very accurately but leave the orthogonal combination poorly determined [79]; additional input is required to allow a precise determination of  $m_b$ . This additional information can come from the radiative  $B \rightarrow X_s \gamma$  moments, which provide complementary information on  $m_b$  and  $\mu_\pi^2$ , or from precise determinations of the charm quark mass [80,81]. The values obtained in the kinetic scheme fits [77] with these two constraints are consistent. Based on the charm quark mass constraint [80],  $m_c^{\overline{\text{MS}}}(3 \text{ GeV}) = 0.998 \pm 0.029 \text{ GeV}$ ,

$$|V_{cb}| = (41.88 \pm 0.44 \pm 0.59) \times 10^{-3} \quad (23)$$

$$m_b^{\text{kin}} = 4.560 \pm 0.023 \text{ GeV} \quad (24)$$

$$\mu_\pi^2(\text{kin}) = 0.453 \pm 0.036 \text{ GeV}^2, \quad (25)$$

where the first error on  $|V_{cb}|$  includes experimental and theoretical uncertainties and the second error is from the estimated accuracy of the HQE for the total semileptonic rate.

Theoretical uncertainties are estimated and included in performing the fits. The  $\chi^2/\text{dof}$  is substantially below unity in all fits, suggesting that the theoretical uncertainties may be overestimated. In any case, the low  $\chi^2$  shows no evidence for duality violations at a significant level. Similar values for the parameters are obtained when only experimental uncertainties are used in the fits. If the photon energy spectrum moments from  $\overline{B} \rightarrow X_s \gamma$  are used in place of the constraint on the charm quark mass, the results change by only small amounts, e.g.,  $m_b^{\text{kin}}$  increases to  $4.574 \pm 0.032 \text{ GeV}$ . The mass in the  $\overline{\text{MS}}$  scheme corresponding to Eq. (24) is  $m_b^{\overline{\text{MS}}} = 4.19 \pm 0.04 \text{ GeV}$ , which can be compared with a recent value obtained using relativistic sum rules [82],  $m_b^{\overline{\text{MS}}} = 4.163 \pm 0.016 \text{ GeV}$ , and provides a non-trivial cross-check.

A fit to the same moments in the 1S scheme gives [78]

$$|V_{cb}| = (41.96 \pm 0.45 \pm 0.07) \times 10^{-3} \quad (26)$$

$$m_b^{1\text{S}} = 4.691 \pm 0.037 \text{ GeV} \quad (27)$$

$$\lambda_1(1\text{S}) = -0.362 \pm 0.067 \text{ GeV}^2, \quad (28)$$

where the last error on  $|V_{cb}|$  is due to the uncertainties in the B meson lifetimes. This fit uses semileptonic and radiative moments and constrains the chromomagnetic operator using the mass difference between the  $D$  and  $D^*$  mesons. This independent fit gives consistent results for  $|V_{cb}|$  and, after translation to a common renormalization scheme, for  $m_b$  and  $\mu_\pi^2$ .

The precision of the global fit results can be further improved. Some of the measurements, in particular of the  $\overline{B} \rightarrow X_s \gamma$  photon energy spectrum, can be improved by using the full B-factory data sets. Improvements can be made in the theory by calculating higher order perturbative corrections to the coefficients of the HQE parameters, in particular the still missing  $\alpha_s \mu_G^2$  corrections, which are presently only known for  $B \rightarrow X_s \gamma$  [84]. The inclusion of still higher order moments may improve the sensitivity of the fits to higher order terms in the HQE.

### Determination of $|V_{ub}|$

*Summary:* The determination of  $|V_{ub}|$  is the focus of significant experimental and theoretical work. The determinations based on inclusive semileptonic decays using different calculational ansätze are consistent. The largest parametric uncertainty comes from the error on  $m_b$ . Significant progress has been made in determinations of  $|V_{ub}|$  from  $\overline{B} \rightarrow \pi \ell \overline{\nu}_\ell$  decays by using combined fits to theory and experimental data as a function of  $q^2$ . Further improvements in the form factor normalization are needed to improve the precision.

The values obtained from inclusive and exclusive determinations are

$$|V_{ub}| = (4.41 \pm 0.15 \pm_{0.17}^{0.15}) \times 10^{-3} \quad (\text{inclusive}), \quad (29)$$

$$|V_{ub}| = (3.23 \pm 0.31) \times 10^{-3} \quad (\text{exclusive}). \quad (30)$$

The two determinations are independent, and the dominant uncertainties are on multiplicative factors. The inclusive and exclusive values are weighted by their relative errors and the uncertainties are treated as normally distributed. The resulting average has  $p(\chi^2) = 0.01$ , so we scale the error by  $\sqrt{\chi^2/1} = 2.6$  to find

$$|V_{ub}| = (4.15 \pm 0.49) \times 10^{-3}. \quad (31)$$

Given the poor consistency between the two determinations, this average should be treated with caution.

### $|V_{ub}|$ from inclusive decays

The theoretical description of inclusive  $\overline{B} \rightarrow X_u \ell \overline{\nu}_\ell$  decays is based on the Heavy Quark Expansion, as for  $\overline{B} \rightarrow X_c \ell \overline{\nu}_\ell$  decays, and leads to a predicted total decay rate with uncertainties below 5% [85,86]. Unfortunately, the total decay rate is hard to measure due to the large background from CKM-favored  $\overline{B} \rightarrow X_c \ell \overline{\nu}_\ell$  transitions. Technically, the calculation of the partial decay rate in regions of phase space where  $\overline{B} \rightarrow X_c \ell \overline{\nu}_\ell$  decays are suppressed is different from what has been described above, since it requires the introduction of a non-perturbative distribution function, the “shape function” (SF) [87,88]. Due to this, the theoretical input for the extraction on  $V_{ub}$  from inclusive decays is more challenging. The shape function becomes important when the light-cone momentum component  $P_+ \equiv E_X - |P_X|$  is not large compared to  $\Lambda_{QCD}$ . This additional difficulty can be addressed in two complementary ways. The leading shape function can either be measured in the radiative decay  $\overline{B} \rightarrow X_s \gamma$ , or be modeled with

constraints on the 0<sup>th</sup>-2<sup>nd</sup> moments, and the results applied to the calculation of the  $\overline{B} \rightarrow X_u \ell \overline{\nu}_\ell$  partial decay rate [89–91]; in such an approach the largest challenges are for the theory. Alternatively, measurements of  $\overline{B} \rightarrow X_u \ell \overline{\nu}_\ell$  partial decay rates can be extended further into the  $\overline{B} \rightarrow X_c \ell \overline{\nu}_\ell$ -allowed region, enabling a simplified theoretical (pure HQE) treatment [92] but requiring precise experimental knowledge of the  $\overline{B} \rightarrow X_c \ell \overline{\nu}_\ell$  background.

The shape function is a universal property of  $B$  mesons at leading order. It has been recognized for many years [87,88] that the leading SF can be measured in  $\overline{B} \rightarrow X_s \gamma$  decays. However, sub-leading shape functions [93–98] arise at each order in  $1/m_b$ , and differ in semileptonic and radiative  $B$  decays. The form of the SFs cannot be calculated from first principles. Prescriptions that relate directly the partial rates for  $\overline{B} \rightarrow X_s \gamma$  and  $\overline{B} \rightarrow X_u \ell \overline{\nu}_\ell$  decays and thereby avoid any parameterization of the leading SF are available [99–102]; uncertainties due to sub-leading SFs remain in these approaches. Existing measurements have tended to use parameterizations of the leading SF that respect constraints on the zeroth, first and second moments. At leading order the first and second moments are equal to  $\overline{\Lambda} = M_B - m_b$  and  $\mu_\pi^2$ , respectively. The relations between SF moments and the non-perturbative parameters of the HQE are known to second order in  $\alpha_s$  [103]. As a result, measurements of HQE parameters from global fits to  $\overline{B} \rightarrow X_c \ell \overline{\nu}_\ell$  and  $\overline{B} \rightarrow X_s \gamma$  moments can be used to constrain the SF moments, as well as provide accurate values of  $m_b$  and other parameters for use in determining  $|V_{ub}|$ . The possibility of measuring these HQE parameters directly from moments in  $\overline{B} \rightarrow X_u \ell \overline{\nu}_\ell$  decays has been explored [104], but the experimental precision achievable there is not competitive with other approaches.

A recent development is to use appropriate basis functions to approximate the shape function, thereby also including the known short-distance contributions as well as the renormalization properties of the SF [105], in order to allow a global fit of all inclusive  $B$  meson decay data.

The calculations that are used for the fits performed by HFAG are documented in Refs. [89] (BLNP), [106] (GGOU), [107] (DGE) and [92] (BLL).

The calculations start from the triple differential rate using the variables

$$P_l = M_B - 2E_l, \quad P_- = E_X + |\vec{P}_X|, \quad P_+ = E_X - |\vec{P}_X| \quad (32)$$

for which the differential rate becomes

$$\frac{d^3\Gamma}{dP_+ dP_- dP_l} = \frac{G_F^2 |V_{ub}|^2}{16\pi^2} (M_B - P_+) \quad (33)$$

$$\left\{ (P_- - P_l)(M_B - P_- + P_l - P_+) \mathcal{F}_1 \right. \\ \left. + (M_B - P_-)(P_- - P_+) \mathcal{F}_2 + (P_- - P_l)(P_l - P_+) \mathcal{F}_3 \right\}.$$

The “structure functions”  $\mathcal{F}_i$  can be calculated using factorization theorems that have been proven to subleading order in the  $1/m_b$  expansion.

The BLNP [89] calculation uses these factorization theorems to write the  $\mathcal{F}_i$  in terms of perturbatively calculable hard coefficients  $H$  and jet functions  $J$ , which are convolved with the (soft) light-cone distribution functions  $S$ , the shape functions of the  $B$  meson. The BLNP calculation has been updated to include the full  $\mathcal{O}(\alpha_s^2)$  contributions [108].

The leading order term in the  $1/m_b$  expansion of the  $\mathcal{F}_i$  contains a single non-perturbative function and is calculated to subleading order in  $\alpha_s$ , while at subleading order in the  $1/m_b$  expansion there are several independent non-perturbative functions which have been calculated only at tree level in the  $\alpha_s$  expansion.

To extract the non-perturbative input one can study the photon energy spectrum in  $B \rightarrow X_s \gamma$  [91]. This spectrum is known at a similar accuracy as the  $P_+$  spectrum in  $B \rightarrow X_u \ell \overline{\nu}_\ell$ . Going to subleading order in the  $1/m_b$  expansion requires the modeling of subleading SFs, a large variety of which were studied in Ref. [89].

A distinct approach (GGOU) [106] uses a hard, Wilsonian cut-off that matches the definition of the kinetic mass. The non-perturbative input is similar to what is used in BLNP, but the shape functions are defined differently. In particular, they are defined at finite  $m_b$  and depend on the light-cone component  $k_+$  of the  $b$  quark momentum and on the momentum transfer  $q^2$  to the leptons. These functions include sub-leading effects to all orders; as a result they are non-universal, with one shape function corresponding to each structure function in Eq. (33). Their  $k_+$  moments can be computed in the OPE and related to observables and to the shape functions defined in Ref. [89].

Going to subleading order in  $\alpha_s$  requires the definition of a renormalization scheme for the HQE parameters and for the SF. It has been noted that the relation between the moments of the SF and the forward matrix elements of local operators is plagued by ultraviolet problems which require additional renormalization. A possible scheme for improving this behavior has been suggested in Refs. [89,91], which introduce a particular definition of the quark mass (the so-called shape function scheme) based on the first moment of the measured spectrum. Likewise, the HQE parameters can be defined from measured moments of spectra, corresponding to moments of the SF.

One can also attempt to calculate the SF by using additional assumptions. One possible approach (DGE) is the so-called “dressed gluon exponentiation” [107], where the perturbative result is continued into the infrared regime using the renormalon structure obtained in the large  $\beta_0$  limit, where  $\beta_0$  has been defined following Eq. (18).

While attempts to quantify the SF are important, the impact of uncertainties in the SF is significantly reduced in some recent measurements that cover a larger portion of the  $\overline{B} \rightarrow X_u \ell \overline{\nu}_\ell$  phase space. Several measurements using a combination of cuts on the leptonic momentum transfer  $q^2$  and the hadronic invariant mass  $m_X$  as suggested in Ref. [109] have been made. Measurements of the electron spectrum in

# Meson Particle Listings

## $V_{cb}$ and $V_{ub}$ CKM Matrix Elements

$\bar{B} \rightarrow X_u \ell \bar{\nu}_\ell$  decays have been made down to momenta of 1.9 GeV or even lower, where SF uncertainties are not dominant. Of course, determining  $\bar{B} \rightarrow X_u \ell \bar{\nu}_\ell$  partial rates in charm-dominated regions can bring in a strong dependence on the modeling of the  $\bar{B} \rightarrow X_u \ell \bar{\nu}_\ell$  spectrum, which is problematic. The measurements quoted below have used a variety of functional forms to parameterize the leading SF; in no case does this lead to more than a 2% uncertainty on  $|V_{ub}|$ .

Weak Annihilation [110,111,106] (WA) can in principle contribute significantly in the restricted region (at high  $q^2$ ) accepted by measurements of  $\bar{B} \rightarrow X_u \ell \bar{\nu}_\ell$  decays. An estimate [92] based on leptonic  $D_s$  decays [111,112] leads to a  $\sim 2\%$  uncertainty on the total  $\bar{B} \rightarrow X_u \ell \bar{\nu}_\ell$  rate from the  $\Upsilon(4S)$ . The differential spectrum from WA decays is not well known, but they are expected to contribute predominantly at high  $q^2$ . More recent investigations of WA [112,113,114] confirm that WA is a small effect, but may become a significant source of uncertainty for  $|V_{ub}|$  measurements that only accept a small fraction,  $f_u$ , of the full  $\bar{B} \rightarrow X_u \ell \bar{\nu}_\ell$  phase space. Model-dependent limits on WA were determined in Ref. [115], where the CLEO data were fitted to combinations of WA models and a spectator  $\bar{B} \rightarrow X_u \ell \bar{\nu}_\ell$  component and background. More direct experimental constraints [116] on WA have recently been made by comparing the  $\bar{B} \rightarrow X_u \ell \bar{\nu}_\ell$  decay rates of charged and neutral  $B$  mesons. However, these constraints are not sensitive to the isoscalar contribution to WA. The sensitivity of  $|V_{ub}|$  determinations to WA can also be reduced by removing the region at high  $q^2$  in those measurements where  $q^2$  is determined.

### Measurements

We summarize the measurements used in the determination of  $|V_{ub}|$  below. Given the improved precision and more rigorous theoretical interpretation of the recent measurements, earlier determinations [117–120] will not be further considered in this review.

Inclusive electron momentum measurements [121–123] reconstruct a single charged electron to determine a partial decay rate for  $\bar{B} \rightarrow X_u \ell \bar{\nu}_\ell$  near the kinematic endpoint. This results in a high  $\mathcal{O}(50\%)$  selection efficiency and only modest sensitivity to the modeling of detector response. The decay rate can be cleanly extracted for  $E_e > 2.3$  GeV, but this is deep in the SF region, where theoretical uncertainties are large. Measurements down to 2.0 or 1.9 GeV exist, but have low ( $< 1/10$ ) signal-to-background (S/B) ratio, making the control of the  $\bar{B} \rightarrow X_c \ell \bar{\nu}_\ell$  background a crucial point. In these analyses the inclusive electron momentum spectrum from  $B\bar{B}$  events is determined by subtracting the  $e^+e^- \rightarrow q\bar{q}$  continuum background using data samples collected just below  $B\bar{B}$  threshold. The continuum-subtracted spectrum is fitted to a combination of a model  $\bar{B} \rightarrow X_u \ell \bar{\nu}_\ell$  spectrum and several components ( $D\ell\bar{\nu}_\ell$ ,  $D^*\ell\bar{\nu}_\ell$ , ...) of the  $\bar{B} \rightarrow X_c \ell \bar{\nu}_\ell$  background. The resulting  $|V_{ub}|$  values for various  $E_e$  cuts are given in Table 1. The leading uncertainty at the lower lepton momentum cuts comes from the  $\bar{B} \rightarrow X_c \ell \bar{\nu}_\ell$  background. Prospects for

reducing further the lepton momentum cut are improving in light of better knowledge of the semileptonic decays to higher mass  $X_c \ell \bar{\nu}$  states [124,37]. The determination of  $|V_{ub}|$  from these measurements is discussed below.

An untagged “neutrino reconstruction” measurement [125] from BABAR uses a combination [126] of a high-energy electron with a measurement of the missing momentum vector. This allows a much higher S/B  $\sim 0.7$  at the same  $E_e$  cut and a  $\mathcal{O}(5\%)$  selection efficiency, but at the cost of a smaller accepted phase space for  $\bar{B} \rightarrow X_u \ell \bar{\nu}_\ell$  decays and uncertainties associated with the determination of the missing momentum. A control sample of  $\Upsilon(4S) \rightarrow B\bar{B}$  decays where one  $B$  is reconstructed as  $\bar{B} \rightarrow D^0(X)e\bar{\nu}$  with  $D^0 \rightarrow K^-\pi^+$  is used to reduce uncertainties from detector and background modeling. The corresponding values for  $|V_{ub}|$  are given in Table 1.

The large samples accumulated at the  $B$  factories allow studies in which one  $B$  meson is fully reconstructed and the recoiling  $B$  decays semileptonically [127–130]. The experiments can fully reconstruct a “tag”  $B$  candidate in about 0.5% (0.3%) of  $B^+B^-$  ( $B^0\bar{B}^0$ ) events. An electron or muon with center-of-mass momentum above 1.0 GeV is required amongst the charged tracks not assigned to the tag  $B$  and the remaining particles are assigned to the  $X_u$  system. The full set of kinematic properties ( $E_\ell$ ,  $m_X$ ,  $q^2$ , etc.) are available for studying the semileptonically decaying  $B$ , making possible selections that accept up to 70% of the full  $\bar{B} \rightarrow X_u \ell \bar{\nu}_\ell$  rate. Despite requirements (e.g. on the square of the missing mass) aimed at rejecting events with additional missing particles, undetected or mis-measured particles from  $\bar{B} \rightarrow X_c \ell \bar{\nu}_\ell$  decay (e.g.,  $K_L^0$  and additional neutrinos) remain an important source of uncertainty. Measurements with the largest kinematic acceptance (i.e.  $E_\ell > 1$  GeV) lead to the smallest theoretical and overall uncertainties on  $|V_{ub}|$ .

BABAR [127] and BELLE [128,129] have measured partial rates with cuts on  $m_X$ ,  $m_X$  and  $q^2$ , and  $P_+$  based on large samples of  $B\bar{B}$  events. Correlations amongst these related partial rates are taken into account in the average given in Table 1. In each case the experimental systematics have significant contributions from the modeling of  $\bar{B} \rightarrow X_u \ell \bar{\nu}_\ell$  and  $\bar{B} \rightarrow X_c \ell \bar{\nu}_\ell$  decays and from the detector response to charged particles, photons and neutral hadrons.

### Determination of $|V_{ub}|$

The determination of  $|V_{ub}|$  from the measured partial rates requires input from theory. The BLNP, GGOU and DGE calculations described previously are used to determine  $|V_{ub}|$  from all measured partial  $\bar{B} \rightarrow X_u \ell \bar{\nu}_\ell$  rates; the values [26] are given in Table 1. The  $m_b$  input values used are derived from the fitted value in equation Eq. (24):  $m_b^{SF} = 4.588 \pm 0.025$  GeV for BLNP,  $m_b^{\text{kin}} = 4.560 \pm 0.023$  GeV for GGOU, and  $m_b^{\overline{MS}} = 4.194 \pm 0.043$  GeV for DGE. The larger uncertainties on  $m_b^{SF}$  and  $m_b^{\overline{MS}}$  reflect the effect of scheme translations, which are done at fixed-order in  $\alpha_s$ .

As an illustration of the relative sizes of the uncertainties entering  $|V_{ub}|$  we give the error breakdown for the GGOU average: statistical—2.0%; experimental—1.7%;  $\overline{B} \rightarrow X_c \ell \overline{\nu}_\ell$  modeling—1.3%;  $\overline{B} \rightarrow X_u \ell \overline{\nu}_\ell$  modeling—1.9%; HQE parameters—1.9%; higher-order corrections—1.4%;  $q^2$  modeling—1.3%; Weak Annihilation— $^{+0}_{-1.9}\%$ ; SF form—0.2%. The uncertainty on  $m_b$  dominates the uncertainty on  $|V_{ub}|$  from HQE parameters, but no longer dominates the overall uncertainty.

The correlations amongst the multiple BABAR recoil-based measurements [127] are fully accounted for in the average. The statistical correlations amongst the other measurements used in the average are tiny (due to small overlaps among signal events and large differences in S/B ratios) and have been ignored. Correlated systematic and theoretical errors are taken into account, both within an experiment and between experiments.

**Table 1:**  $|V_{ub}|$  (in units of  $10^{-5}$ ) from inclusive  $\overline{B} \rightarrow X_u \ell \overline{\nu}_\ell$  measurements. The first uncertainty on  $|V_{ub}|$  is experimental, while the second includes both theoretical and HQE parameter uncertainties. The values are listed in order of increasing  $f_u$  (0.19 to 0.90); those below the horizontal bar are based on recoil methods.

Ref.	cut	BLNP	GGOU	DGE
[121]	$E_e > 2.1$	$419 \pm 49 \begin{smallmatrix} +26 \\ -34 \end{smallmatrix}$	$393 \pm 46 \begin{smallmatrix} +22 \\ -29 \end{smallmatrix}$	$382 \pm 45 \begin{smallmatrix} +23 \\ -26 \end{smallmatrix}$
[125]	$E_e - q^2$	$466 \pm 31 \begin{smallmatrix} +31 \\ -36 \end{smallmatrix}$	not avail.	$432 \pm 29 \begin{smallmatrix} +24 \\ -29 \end{smallmatrix}$
[123]	$E_e > 2.0$	$448 \pm 25 \begin{smallmatrix} +27 \\ -28 \end{smallmatrix}$	$429 \pm 24 \begin{smallmatrix} +18 \\ -24 \end{smallmatrix}$	$428 \pm 24 \begin{smallmatrix} +22 \\ -24 \end{smallmatrix}$
[122]	$E_e > 1.9$	$488 \pm 45 \begin{smallmatrix} +24 \\ -27 \end{smallmatrix}$	$475 \pm 44 \begin{smallmatrix} +17 \\ -22 \end{smallmatrix}$	$479 \pm 44 \begin{smallmatrix} +21 \\ -24 \end{smallmatrix}$
[127]	$m_X - q^2$	$425 \pm 23 \begin{smallmatrix} +23 \\ -25 \end{smallmatrix}$	$417 \pm 22 \begin{smallmatrix} +22 \\ -25 \end{smallmatrix}$	$419 \pm 22 \begin{smallmatrix} +18 \\ -19 \end{smallmatrix}$
[127]	$P_+$	$402 \pm 25 \begin{smallmatrix} +24 \\ -23 \end{smallmatrix}$	$375 \pm 23 \begin{smallmatrix} +30 \\ -32 \end{smallmatrix}$	$410 \pm 25 \begin{smallmatrix} +37 \\ -26 \end{smallmatrix}$
[127]	$m_X$	$397 \pm 22 \pm 20$	$394 \pm 22 \begin{smallmatrix} +16 \\ -17 \end{smallmatrix}$	$416 \pm 23 \begin{smallmatrix} +22 \\ -12 \end{smallmatrix}$
[127]	$E_e > 1$	$428 \pm 24 \begin{smallmatrix} +18 \\ -20 \end{smallmatrix}$	$435 \pm 24 \begin{smallmatrix} +9 \\ -10 \end{smallmatrix}$	$440 \pm 24 \begin{smallmatrix} +13 \\ -13 \end{smallmatrix}$
[129]	$E_e > 1$	$447 \pm 27 \begin{smallmatrix} +19 \\ -21 \end{smallmatrix}$	$454 \pm 27 \begin{smallmatrix} +10 \\ -11 \end{smallmatrix}$	$460 \pm 27 \begin{smallmatrix} +11 \\ -13 \end{smallmatrix}$
		$440 \pm 15 \begin{smallmatrix} +19 \\ -21 \end{smallmatrix}$	$439 \pm 15 \begin{smallmatrix} +12 \\ -14 \end{smallmatrix}$	$445 \pm 15 \begin{smallmatrix} +15 \\ -16 \end{smallmatrix}$

The theoretical calculations produce very similar results for  $|V_{ub}|$ ; the standard deviation of the theory predictions for the endpoint rate is 4.6%, for the  $m_X - q^2$  rate is 2.2%, and for the  $E_e > 1$  GeV rate is 0.8%. The  $|V_{ub}|$  values do not show a marked trend versus the kinematic acceptance,  $f_u$ , for  $\overline{B} \rightarrow X_u \ell \overline{\nu}_\ell$  decays. The  $p$ -values of the averages are in the range 30-50%, indicating that the ratios of calculated partial widths in the different phase space regions are in good agreement with ratios of measured partial branching fractions.

A recent calculation [108] at NNLO accuracy of the leading term in the partial rate for kinematically restrictive cuts (e.g. near the electron endpoint energy) shows a surprisingly large change from the NLO calculation used in the BLNP method, increasing  $|V_{ub}|$  by up to  $\sim 8\%$  for some measurements. These updated calculations are not reflected in the BLNP values shown in Table 1. In the GGOU and the DGE approaches the inclusion of the dominant  $\alpha_s^2 \beta_0$  contributions do not suggest large  $\alpha_s^2$  corrections in these methods.

All calculations yield compatible  $|V_{ub}|$  values and similar error estimates. We take the arithmetic mean of the values and errors to find

$$|V_{ub}| = (4.41 \pm 0.15_{\text{exp}} \begin{smallmatrix} +0.15 \\ -0.17 \end{smallmatrix} \text{ th}) \times 10^{-3} \quad (\text{inclusive}). \quad (34)$$

As was the case with  $|V_{cb}|$ , it is hard to assign an uncertainty to  $|V_{ub}|$  for possible duality violations. However, theoretical arguments suggest that duality should hold even better in  $b \rightarrow u \ell \overline{\nu}_\ell$  than in  $b \rightarrow c \ell \overline{\nu}_\ell$  [42]. In any case, unless duality violations are much larger in  $\overline{B} \rightarrow X_u \ell \overline{\nu}_\ell$  decays than in  $\overline{B} \rightarrow X_c \ell \overline{\nu}_\ell$  decays, the precision of the  $|V_{ub}|$  determination is not yet at the level where duality violations are likely to be significant.

Hadronization uncertainties also impact the  $|V_{ub}|$  determination. The theoretical expressions are valid at the parton level and do not incorporate any resonant structure (e.g.  $\overline{B} \rightarrow \pi \ell \overline{\nu}_\ell$ ); this must be added “by hand” to the simulated  $\overline{B} \rightarrow X_u \ell \overline{\nu}_\ell$  event samples, since the detailed final state multiplicity and structure impacts the estimates of experimental acceptance and efficiency. The experiments have adopted procedures to input resonant structure while preserving the appropriate behavior in the kinematic variables averaged over the sample. The resulting uncertainties have been estimated to be  $\sim 1$ -2% on  $|V_{ub}|$ .

A separate class of analyses follows the strategy discussed in Refs. [99–102], where integrals of differential distributions in  $\overline{B} \rightarrow X_u \ell \overline{\nu}_\ell$  decays are compared with corresponding integrals in  $\overline{B} \rightarrow X_s \gamma$  decays to extract  $|V_{ub}|$ , thereby eliminating the need to model the leading shape function. A study [132] using the measured BABAR electron spectrum in  $\overline{B} \rightarrow X_u \ell \overline{\nu}_\ell$  decays provides  $|V_{ub}|$  determinations using all available “SF-free” calculations; the resulting  $|V_{ub}|$  values have total uncertainties of  $\sim 12\%$  and are compatible with the average quoted above.

The BLL [109] calculation can be used for measurements [128,130,131] with cuts on  $m_X$  and  $q^2$ . Using the same HQE parameter input as above yields a  $|V_{ub}|$  value of  $(4.62 \pm 0.20 \pm 0.29) \times 10^{-3}$ , which is about 7% higher than the values obtained from the calculations used in Table 1 for these measurements.

### Status and outlook

At present, as indicated by the average given above, the uncertainty on  $|V_{ub}|$  from inclusive decays is at the 5% level. Are these uncertainties justified? The uncertainty on  $m_b$  was discussed in detail above. The uncertainties quoted in the calculations due to matching scales, higher order corrections, etc., are at the few percent level on  $|V_{ub}|$ . While these uncertainties are inherently difficult to quantify, the calculations take different approaches yet produce similar estimates. Experimental uncertainties have been assessed independently by BaBar and Belle. An important common source of uncertainty comes from modelling the  $\overline{B} \rightarrow X_u \ell \overline{\nu}_\ell$  decays. Better measurements of these exclusive decays would be helpful in this regard, as would improved knowledge of the main  $\overline{B} \rightarrow X_c \ell \overline{\nu}_\ell$  decays.

# Meson Particle Listings

## $V_{cb}$ and $V_{ub}$ CKM Matrix Elements

### $|V_{ub}|$ from exclusive decays

Exclusive charmless semileptonic decays offer a complementary means of determining  $|V_{ub}|$ . For the experiments, the specification of the final state provides better background rejection, but the lower branching fraction reflects itself in lower yields compared with inclusive decays. For theory, the calculation of the form factors for  $\overline{B} \rightarrow X_u \ell \overline{\nu}_\ell$  decays is challenging, but brings in a different set of uncertainties from those encountered in inclusive decays. In this review we focus on  $\overline{B} \rightarrow \pi \ell \overline{\nu}_\ell$ , as it is the most promising mode for both experiment and theory, and recent improvements have been made in both areas. Measurements of other exclusive states can be found in Refs. [135–140,154].

**$\overline{B} \rightarrow \pi \ell \overline{\nu}_\ell$  form factor calculations** The relevant form factors for the decay  $\overline{B} \rightarrow \pi \ell \overline{\nu}_\ell$  are usually defined as

$$\begin{aligned} \langle \pi(p_\pi) | V^\mu | B(p_B) \rangle = & \quad (35) \\ f_+(q^2) \left[ p_B^\mu + p_\pi^\mu - \frac{m_B^2 - m_\pi^2}{q^2} q^\mu \right] + f_0(q^2) \frac{m_B^2 - m_\pi^2}{q^2} q^\mu \end{aligned}$$

in terms of which the rate becomes (in the limit  $m_\ell \rightarrow 0$ )

$$\frac{d\Gamma}{dq^2} = \frac{G_F^2 |V_{ub}|^2}{24\pi^3} |p_\pi|^3 |f_+(q^2)|^2, \quad (36)$$

where  $p_\pi$  is the momentum of pion in the  $B$  meson rest frame.

Currently available non-perturbative methods for the calculation of the form factors include lattice QCD (LQCD) and light-cone sum rules (LCSR). The two methods are complementary in phase space, since the lattice calculation is restricted to the kinematical range of high momentum transfer  $q^2$  to the leptons, to avoid large discretization errors, while light-cone sum rules provide information near  $q^2 = 0$ . Interpolations between these two regions can be constrained by unitarity and analyticity.

Unquenched simulations, for which quark loop effects in the QCD vacuum are fully incorporated, have become quite common, and the first results based on these simulations for the  $\overline{B} \rightarrow \pi \ell \overline{\nu}_\ell$  form factors have been obtained by the Fermilab/MILC collaboration [141] and the HPQCD collaboration [142]. The two calculations differ in the way the  $b$  quark is simulated, with HPQCD using nonrelativistic QCD and Fermilab/MILC the so-called Fermilab heavy-quark method; they agree within the quoted errors.

In order to obtain the partially-integrated differential rate, the BK parameterization [143]

$$f_+(q^2) = \frac{c_B(1 - \alpha_B)}{(1 - \tilde{q}^2)(1 - \alpha_B \tilde{q}^2)}, \quad (37)$$

$$f_0(q^2) = \frac{c_B(1 - \alpha_B)}{(1 - \tilde{q}^2/\beta_B)}, \quad (38)$$

with  $\tilde{q}^2 \equiv q^2/m_{B^*}^2$  has been used frequently to extrapolate to small values of  $q^2$ . It includes the leading pole contribution from  $B^*$ , and higher poles are modeled by a single pole. The heavy-quark scaling is satisfied if the parameters  $c_B$ ,  $\alpha_B$  and  $\beta_B$  scale appropriately. However, the BK parameterization should

be used with some caution, since it is not consistent with SCET [144]. More recently, analyticity and unitarity bounds have been employed to constrain the form factors. Making use of the heavy-quark limit, stringent constraints on the shape of the form factor can be derived [144], and the conformal mapping of the kinematical variables onto the complex unit disc yields a rapidly converging series in this variable. The use of lattice data in combination with a data point at small  $q^2$  from SCET or sum rules provides a stringent constraint on the shape of the form factor [145]. The form factor parametrization given in Ref. [145] has been applied to the extraction of  $|V_{ub}|$  from  $B \rightarrow \pi \ell \overline{\nu}_\ell$  using lattice data in Ref. [141].

Much work remains to be done, since the current combined statistical plus systematic errors in the lattice results are still at the  $\sim 10\%$  level on  $|V_{ub}|$  and need to be reduced. Reduction of errors to the  $\sim 5\text{--}6\%$  level for  $|V_{ub}|$  will be feasible within the next few years, with the inclusion of numerical data at lighter pion masses and finer lattice spacings, as well as possibly two-loop or nonperturbative matching between lattice and continuum heavy-to-light current operators.

Another established non-perturbative approach to obtain the form factors is through Light-Cone QCD Sum Rules (LCSR), where the heavy mass limit has been discussed from the point of view of SCET in Ref. [147]. The sum-rule approach provides an approximation for the product  $f_B f_+(q^2)$ , valid in the region  $0 < q^2 < \sim 12 \text{ GeV}^2$ . The determination of  $f_+(q^2)$  itself requires knowledge of the decay constant  $f_B$ , which usually is obtained by replacing  $f_B$  by its two-point QCD (SVZ) sum rule [148] in terms of perturbative and condensate contributions. The advantage of this procedure is the approximate cancellation of various theoretical uncertainties in the ratio  $(f_B f_+)/f_B$ . The LCSR for  $f_B f_+$  is based on the light-cone OPE of the relevant vacuum-to-pion correlation function, calculated in full QCD at finite  $b$ -quark mass. The resulting expressions actually comprise a triple expansion: in the twist  $t$  of the operators near the light-cone, in  $\alpha_s$ , and in the deviation of the pion distribution amplitudes from their asymptotic form, which is fixed from conformal symmetry.

There are multiple sources of uncertainties in the LCSR calculation, which are discussed in Refs. [149,150]. Currently, a total uncertainty slightly larger than  $10\%$  on  $|V_{ub}|$  is extracted from a LCSR calculation of

$$\begin{aligned} \Delta\zeta(0, q_{max}^2) &= \frac{G_F^2}{24\pi^3} \int_0^{q_{max}^2} dq^2 p_\pi^3 |f_+(q^2)|^2 \\ &= \frac{1}{|V_{ub}|^2 \tau_{B_0}} \int_0^{q_{max}^2} dq^2 \frac{d\mathcal{B}(B \rightarrow \pi \ell \nu)}{dq^2} \end{aligned} \quad (39)$$

which turn out to be [151]

$$\Delta\zeta(0, 12 \text{ GeV}^2) = 4.59_{-0.85}^{+1.00} \text{ ps}^{-1}. \quad (40)$$

It is interesting to note that the results from the LQCD and LCSR are consistent with each other when either the

See key on page 457

## Meson Particle Listings

### $V_{cb}$ and $V_{ub}$ CKM Matrix Elements

BK parameterization or parametrizations based on conformal mappings [145,146] are used to relate them. This increases confidence in the theoretical predictions for the rate of  $\bar{B} \rightarrow \pi \ell \bar{\nu}_\ell$ . This is complementary to the lattice results at large values of  $q^2$ , and the results from LCSR smoothly extrapolate the lattice data to small values of  $q^2$ .

An alternative determination of  $|V_{ub}|$  has been proposed by several authors [152,153] based on a model-independent relation between rare decays such as  $\bar{B} \rightarrow K^* \ell^+ \ell^-$  and  $\bar{B} \rightarrow \rho \ell \bar{\nu}_\ell$ . However, it requires a precise measurement of the  $\bar{B} \rightarrow K^* \ell^+ \ell^-$  decay, which is a task for ultra-high-rate experiments.

#### $\bar{B} \rightarrow \pi \ell \bar{\nu}_\ell$ measurements

The  $\bar{B} \rightarrow \pi \ell \bar{\nu}_\ell$  measurements fall into two broad classes: untagged, in which case the reconstruction of the missing momentum of the event serves as an estimator for the unseen neutrino, and tagged, in which the second  $B$  meson in the event is fully reconstructed in either a hadronic or semileptonic decay mode. The tagged measurements have high and uniform acceptance, S/B as high as 10, but low statistics. The untagged measurements have somewhat higher background levels (S/B < 1) and make slightly more restrictive kinematic cuts, but have adequate statistics to measure the  $q^2$  dependence of the form factor.

**Table 2:** Total and partial branching fractions for  $\bar{B}^0 \rightarrow \pi^+ \ell^- \bar{\nu}_\ell$ , scaled to a common set of external inputs. The uncertainties are from statistics and systematics. Measurements of  $\mathcal{B}(B^- \rightarrow \pi^0 \ell^- \bar{\nu}_\ell)$  have been multiplied by a factor  $2\tau_{B^0}/\tau_{B^+}$  to obtain the values below.

	$\mathcal{B} \times 10^4$	$\mathcal{B}(q^2 > 16) \times 10^4$
CLEO $\pi^+, \pi^0$ [139]	$1.38 \pm 0.15 \pm 0.11$	$0.41 \pm 0.08 \pm 0.04$
BABAR $\pi^+, \pi^0$ [140]	$1.41 \pm 0.05 \pm 0.08$	$0.32 \pm 0.02 \pm 0.03$
BABAR $\pi^+$ [154]	$1.42 \pm 0.05 \pm 0.07$	$0.33 \pm 0.03 \pm 0.03$
BELLE $\pi^+, \pi^0$ [155]	$1.49 \pm 0.04 \pm 0.07$	$0.40 \pm 0.02 \pm 0.02$
BELLE SL $\pi^+$ [156]	$1.42 \pm 0.19 \pm 0.15$	$0.37 \pm 0.10 \pm 0.04$
BELLE SL $\pi^0$ [156]	$1.41 \pm 0.26 \pm 0.15$	$0.36 \pm 0.15 \pm 0.04$
BELLE had $\pi^+$ [157]	$1.12 \pm 0.18 \pm 0.05$	$0.26 \pm 0.08 \pm 0.01$
BELLE had $\pi^0$ [157]	$1.22 \pm 0.22 \pm 0.05$	$0.41 \pm 0.11 \pm 0.02$
BABAR SL $\pi^+$ [158]	$1.39 \pm 0.21 \pm 0.08$	$0.46 \pm 0.13 \pm 0.03$
BABAR SL $\pi^0$ [158]	$1.78 \pm 0.28 \pm 0.15$	$0.44 \pm 0.17 \pm 0.06$
BABAR had $\pi^+$ [159]	$1.07 \pm 0.27 \pm 0.19$	$0.65 \pm 0.20 \pm 0.13$
BABAR had $\pi^0$ [159]	$1.52 \pm 0.41 \pm 0.30$	$0.48 \pm 0.22 \pm 0.12$
Average	$1.42 \pm 0.03 \pm 0.04$	$0.37 \pm 0.01 \pm 0.02$

CLEO has analyzed  $\bar{B} \rightarrow \pi \ell \bar{\nu}_\ell$  and  $\bar{B} \rightarrow \rho \ell \bar{\nu}_\ell$  using an untagged analysis [139]. Similar analyses have been done at BABAR [140,154] and BELLE [155]. The leading systematic uncertainties in the untagged  $\bar{B} \rightarrow \pi \ell \bar{\nu}_\ell$  analyses are associated with modeling the missing momentum reconstruction, with backgrounds from  $\bar{B} \rightarrow X_u \ell \bar{\nu}_\ell$  decays and  $e^+ e^- \rightarrow q \bar{q}$  continuum events, and with varying the form factor for the  $\bar{B} \rightarrow \rho \ell \bar{\nu}_\ell$  decay. The values obtained for the full and partial

branching fractions [26] are listed in Table 2 above the horizontal line. These BABAR and BELLE measurements provide the differential  $\bar{B} \rightarrow \pi \ell \bar{\nu}_\ell$  rate versus  $q^2$ , shown in Fig. 2, which is used in the determination of  $|V_{ub}|$  discussed below.

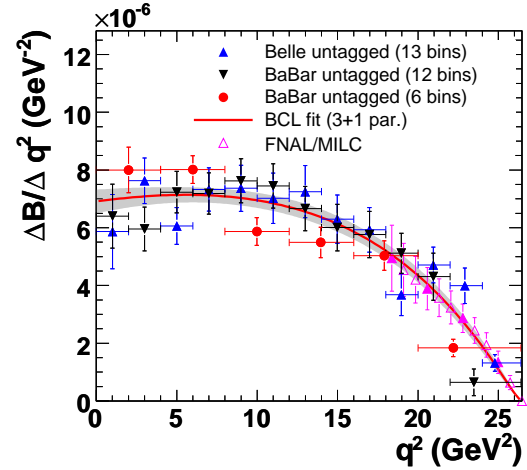


**Figure 2:** The untagged measurements of the differential  $\bar{B} \rightarrow \pi \ell \bar{\nu}_\ell$  branching fraction versus  $q^2$  that are used together with lattice calculations in the determination of  $|V_{ub}|$ .

Analyses [156,158] based on reconstructing a  $B$  in the  $\bar{D}^{(*)} \ell^+ \nu_\ell$  decay mode and looking for a  $\bar{B} \rightarrow \pi \ell \bar{\nu}_\ell$  or  $\bar{B} \rightarrow \rho \ell \bar{\nu}_\ell$  decay amongst the remaining particles in the event make use of the fact that the  $B$  and  $\bar{B}$  are back-to-back in the  $\Upsilon(4S)$  frame to construct a discriminant variable that provides a signal-to-noise ratio above unity for all  $q^2$  bins. A related technique was discussed in Ref. [161]. BABAR [158] and BELLE [157] have also used their samples of  $B$  mesons reconstructed in hadronic decay modes to measure exclusive charmless semileptonic decays giving very clean but low-yield samples. The resulting full and partial branching fractions are given in Table 2. The averages take account of correlations and common systematic uncertainties, and have  $p(\chi^2) > 0.5$  in each case.

$|V_{ub}|$  can be obtained from the average  $\bar{B} \rightarrow \pi \ell \bar{\nu}_\ell$  branching fraction and the measured  $q^2$  spectrum. Using the average [26] of partial branching fractions in the  $q^2 < 12 \text{ GeV}^2$  region,  $(0.81 \pm 0.02 \pm 0.03) \times 10^{-4}$ , along with an LCSR calculation of the theoretical rate [151] gives

$$|V_{ub}| = (3.40 \pm 0.07_{\text{exp}}^{+0.37}_{-0.32} \text{theo}) \times 10^{-3} \quad (\text{LCSR}, q^2 < 12 \text{ GeV}^2). \quad (41)$$

Fits to the measured  $q^2$  spectrum using a theoretically motivated parameterization (e.g. "BCL" from Ref. [146]) remove most of the model dependence from theoretical uncertainties in the shape of the spectrum. Recent determinations [26,141] of  $|V_{ub}|$  from  $\bar{B} \rightarrow \pi \ell \bar{\nu}_\ell$  decays have used simultaneous fits (see

# Meson Particle Listings

## $V_{cb}$ and $V_{ub}$ CKM Matrix Elements

also Refs. [162]) to the experimental partial rate and lattice points versus  $q^2$ . A fit [26] to the untagged measurements incorporates the full statistical and systematic uncertainties in the measured spectrum and uses four lattice points in the region  $q^2 > 16 \text{ GeV}^2$ , taking into account their correlations. The fit, shown in Fig. 2, has  $p(\chi^2) = 2.2\%$ . If the tagged measurements, which are less consistent in the  $q^2 < 8 \text{ GeV}^2$  region, are included, the fit gives  $p(\chi^2) < 0.01\%$ . We quote the result from the untagged measurements and add the difference ( $0.09 \times 10^{-3}$ ) between the  $|V_{ub}|$  values from the two fits as an additional uncertainty to find

$$|V_{ub}| = (3.23 \pm 0.31) \times 10^{-3} \quad (\text{exclusive}). \quad (42)$$

The largest contributions to the uncertainty come from lattice systematic and statistical errors, which will be further improved in the future.

### Conclusion

The study of semileptonic  $B$  meson decays continues to be an active area for both theory and experiment. Substantial progress has been made in the application of HQE calculations to inclusive decays, where fits to moments of  $\overline{B} \rightarrow X_c \ell \overline{\nu}_\ell$  decays provide precise values for  $|V_{cb}|$  and, in conjunction with  $B \rightarrow X_s \gamma$  decays or input on  $m_c$ , provide precise and consistent values for  $m_b$ . The values from the inclusive and exclusive  $|V_{cb}|$  determinations are in reasonable agreement.

Continued improvements in measurements of inclusive  $\overline{B} \rightarrow X_u \ell \overline{\nu}_\ell$  decays, along with additional theoretical studies of higher order contributions and improved knowledge of  $m_b$ , have strengthened our determination of  $|V_{ub}|$ . Further progress in this area is possible, but will require better theoretical control over higher order terms, and improved experimental knowledge of the  $\overline{B} \rightarrow X_c \ell \overline{\nu}_\ell$  background.

Progress in both  $b \rightarrow u$  and  $b \rightarrow c$  exclusive channels depends crucially on progress in lattice calculations. Here the prospects are good, since unquenched calculations are now available for the semileptonic form factors discussed here, as well as for other hadronic weak matrix elements needed to obtain the elements and phase of the CKM matrix [163,164]. Projections for future uncertainties from lattice calculations can be found in Ref. [165].

The measurements of the  $\overline{B} \rightarrow \pi \ell \overline{\nu}_\ell$  branching fraction have uncertainties below 4%, and the measured  $q^2$  dependence is reasonably precise. Reducing the theoretical uncertainties to a comparable level will require significant effort, but is clearly vital.

The difference between the values for  $|V_{ub}|$  obtained from inclusive and exclusive decays has persisted for many years, despite significant improvements in both theory and experiment for both methods. How to reconcile these results remains an intriguing puzzle.

Both  $|V_{cb}|$  and  $|V_{ub}|$  are indispensable inputs into unitarity triangle fits. In particular, knowing  $|V_{ub}|$  with good precision allows a test of CKM unitarity in the most direct way, by

comparing the length of the  $|V_{ub}|$  side of the unitarity triangle with the measurement of  $\sin(2\beta)$ . This comparison of a “tree” process ( $b \rightarrow u$ ) with a “loop-induced” process ( $B^0 - \overline{B}^0$  mixing) provides sensitivity to possible contributions from new physics. While the effort required to further improve our knowledge of these CKM matrix elements is large, it is well motivated.

The authors would like to acknowledge helpful input from C. Bozzi, J. Dingfelder, P. Gambino, A. Kronfeld, V. Luth, F. Muheim, C. Schwanda, P. Urquijo and R. Van de Water.

### References

1. See R. Kowalewski and T. Mannel, J. Phys. **G37**, 075021 (2010).
2. E. Barberio *et al.*, [arXiv:0704.3575](https://arxiv.org/abs/0704.3575).
3. N. Isgur and M.B. Wise, Phys. Lett. **B232**, 113 (1989); *ibid.* **B237**, 527 (1990).
4. M.A. Shifman and M.B. Voloshin, Sov. J. Nucl. Phys. **47**, 511 (1988) [*Yad. Fiz.* **47**, 801 (1988)].
5. M.E. Luke, Phys. Lett. **B252**, 447 (1990).
6. M. Ademollo and R. Gatto, Phys. Rev. Lett. **13**, 264 (1964).
7. A.V. Manohar and M.B. Wise, Camb. Monogr. Part. Phys. Nucl. Phys. Cosmol. **10**,1(2000).
8. B. Grinstein, Nucl. Phys. **B339**, 253 (1990); H. Georgi, Phys. Lett. **B240**, 447 (1990); A.F. Falk *et al.*, Nucl. Phys. **B343**, 1 (1990); E. Eichten and B. Hill, Phys. Lett. **B234**, 511 (1990).
9. C.G. Boyd, B. Grinstein, and R.F. Lebed, Phys. Rev. **D56**, 6895 (1997); *ibid.*, Phys. Rev. Lett. **74**, 4603 (1995); C.G. Boyd and M.J. Savage, Phys. Rev. **D56**, 303 (1997).
10. I. Caprini *et al.*, Nucl. Phys. **B530**, 153 (1998).
11. A. Sirlin, Nucl. Phys. **B196**, 83 (1982).
12. A. Czarnecki and K. Melnikov, Nucl. Phys. **B505**, 65 (1997).
13. Jon A. Bailey *et al.*, Fermilab Lattice and MILC collaborations, *Proceedings of Science LATTICE2010* (2010) 311. This is an update of C. Bernard *et al.*, Phys. Rev. **D79**, 014506 (2009).
14. I.I.Y. Bigi *et al.*, Phys. Rev. **D52**, 196 (1995).
15. A. Kapustin *et al.*, Phys. Lett. B **375**, 327 (1996).
16. P. Gambino, T. Mannel and N. Uraltsev, Phys. Rev. **D81**, 113002 (2010).
17. D. Buskulic *et al.*, (ALEPH Collab.), Phys. Lett. **B395**, 373 (1997).
18. G. Abbiendi *et al.*, (OPAL Collab.), Phys. Lett. **B482**, 15 (2000).
19. P. Abreu *et al.*, (DELPHI Collab.), Phys. Lett. **B510**, 55 (2001).
20. J. Abdallah *et al.*, (DELPHI Collab.), Eur. Phys. J. **C33**, 213 (2004).
21. N.E. Adam *et al.*, (CLEO Collab.), Phys. Rev. **D67**, 032001 (2003).
22. B. Aubert *et al.*, (BABAR Collab.), Phys. Rev. **D77**, 032002 (2008).
23. B. Aubert *et al.*, (BABAR Collab.), Phys. Rev. Lett. **100**, 231803 (2008).
24. B. Aubert *et al.*, (BABAR Collab.), Phys. Rev. **D79**, 012002 (2009).



See key on page 457

## Meson Particle Listings

 $V_{cb}$  and  $V_{ub}$  CKM Matrix Elements

- 
25. W. Dungen *et al.*, (BELLE Collab.), Phys. Rev. **D82**, 112007 (2010).
26. [slac.stanford.edu/xorg/hfag2/semi/EndOfYear11/](http://slac.stanford.edu/xorg/hfag2/semi/EndOfYear11/).
27. N. Uraltsev, Phys. Lett. **B585**, 253 (2004).
28. M. Okamoto *et al.*, Nucl. Phys. (Proc. Supp.) **B140**, 461 (2005). A. Kronfeld, talk presented at the workshop CKM05, San Diego, CA - Workshop on the Unitarity Triangle, 15-18 March 2005.
29. B. Aubert *et al.*, (BABAR Collab.), Phys. Rev. Lett. **104**, 011802 (2010).
30. J. E. Bartelt *et al.*, (CLEO Collab.), Phys. Rev. Lett. **82**, 3746 (1999).
31. K. Abe *et al.*, (BELLE Collab.), Phys. Lett. **B526**, 247 (2002).
32. S. Hashimoto *et al.*, Phys. Rev. **D66**, 014503 (2002).
33. S. Hashimoto *et al.*, Phys. Rev. **D61**, 014502 (2000).
34. A.K. Leibovich *et al.*, Phys. Rev. D **57**, 308 (1998).
35. N. Uraltsev, [arXiv:hep-ph/0409125](https://arxiv.org/abs/hep-ph/0409125).
36. I.I. Bigi *et al.*, Eur. Phys. J. C **52**, 975 (2007).
37. D. Liventsev *et al.*, (BELLE Collab.), Phys. Rev. **D77**, 091503 (2008).
38. B. Aubert *et al.*, (BABAR Collab.), Phys. Rev. Lett. **101**, 261802 (2008).
39. F. Bernlochner, Z. Ligeti, and S. Turczyk, [arXiv:1202.1834](https://arxiv.org/abs/1202.1834).
40. A.V. Manohar and M.B. Wise, Phys. Rev. **D49**, 1310 (1994).
41. I.I.Y. Bigi *et al.*, Phys. Rev. Lett. **71**, 496 (1993), Phys. Lett. **B323**, 408 (1994).
42. M.A. Shifman, [hep-ph/0009131](https://arxiv.org/abs/hep-ph/0009131), I.I.Y. Bigi and N. Uraltsev, Int. J. Mod. Phys. **A16**, 5201 (2001).
43. D. Benson *et al.*, Nucl. Phys. **B665**, 367 (2003).
44. M. Gremm and A. Kapustin, Phys. Rev. **D55**, 6924 (1997).
45. B. M. Dassinger, T. Mannel, and S. Turczyk, JHEP **0703**, 087 (2007).
46. I. I. Bigi, N. Uraltsev, and R. Zwicky, Eur. Phys. J. **C50**, 539 (2007).
47. T. Mannel, S. Turczyk, and N. Uraltsev, JHEP **1011**, 109 (2010).
48. A. Pak and A. Czarnecki, Phys. Rev. D **78**, 114015 (2008).
49. S. Biswas and K. Melnikov, JHEP **1002**, 089 (2010).
50. P. Gambino, JHEP **1109**, 055 (2011).
51. P. Gambino and N. Uraltsev, Eur. Phys. J. **C34**, 181 (2004).
52. V. Aquila *et al.*, Nucl. Phys. B **719**, 77 (2005).
53. T. Becher, H. Boos, and E. Lunghi, JHEP **0712**, 062 (2007).
54. C. Breidenbach *et al.*, Phys. Rev. D **78**, 014022 (2008).
55. I. Bigi *et al.*, [arXiv:0911.3322](https://arxiv.org/abs/0911.3322).
56. A.H. Hoang *et al.*, Phys. Rev. **D59**, 074017 (1999).
57. H. Leutwyler, Phys. Lett. **B98**, 447 (1981); M.B. Voloshin, Sov. J. Nucl. Phys. **36**, 143 (1982).
58. A.H. Hoang, Phys. Rev. D **61**, 034005 (2000).
59. C.W. Bauer *et al.*, Phys. Rev. **D70**, 094017 (2004).
60. N. Uraltsev, Phys. Lett. B **545**, 337 (2002).
61. S.E. Csorna *et al.*, (CLEO Collab.), Phys. Rev. **D70**, 032002 (2004).
62. A.H. Mahmood *et al.*, (CLEO Collab.), Phys. Rev. **D70**, 032003 (2004).
63. B. Aubert *et al.*, (BABAR Collab.), Phys. Rev. **D69**, 111103 (2004).
64. B. Aubert *et al.*, (BABAR Collab.), Phys. Rev. **D69**, 111104 (2004).
65. C. Schwanda *et al.*, (BELLE Collab.), Phys. Rev. **D75**, 032005 (2007).
66. P. Urquijo *et al.*, (BELLE Collab.), Phys. Rev. **D75**, 032001 (2007).
67. J. Abdallah *et al.*, (DELPHI Collab.), Eur. Phys. J. **C45**, 35 (2006).
68. D. Acosta *et al.*, (CDF Collab.), Phys. Rev. **D71**, 051103 (2005).
69. B. Aubert *et al.*, (BABAR Collab.), Phys. Rev. **D81**, 032003 (2010).
70. A. Limosani *et al.* [BELLE Collab.], Phys. Rev. Lett. **103**, 241801 (2009).
71. C. Schwanda *et al.*, (BELLE Collab.), Phys. Rev. **D78**, 032016 (2008).
72. B. Aubert *et al.*, (BABAR Collab.), Phys. Rev. **D72**, 052004 (2005).
73. B. Aubert *et al.*, (BABAR Collab.), Phys. Rev. Lett. **97**, 171803 (2006).
74. S. Chen *et al.*, (CLEO Collab.), Phys. Rev. Lett. **87**, 251807 (2001).
75. M. Battaglia *et al.*, Phys. Lett. **B556**, 41 (2003).
76. B. Aubert *et al.*, (BABAR Collab.), Phys. Rev. Lett. **93**, 011803 (2004).
77. O. Buchmüller and H. Flächer, [hep-ph/0507253](https://arxiv.org/abs/hep-ph/0507253); updated in Ref. [26].
78. C. W. Bauer *et al.*, Phys. Rev. **D70**, 094017 (2004); updated in Ref. [26].
79. See section 5.4.2 of M. Antonelli *et al.*, Phys. Reports **494**, 197 (2010).
80. B. Dehnadi, *et al.*, [arXiv:1102.2264](https://arxiv.org/abs/1102.2264).
81. I. Allison *et al.*, (HPQCD Collab.), Phys. Rev. **D78**, 054513 (2008).
82. Chetyrkin *et al.*, Phys. Rev. **D80**, 074010 (2009).
83. M. Neubert, Phys. Rev. D **72**, 074025 (2005).
84. T. Ewerth, P. Gambino, and S. Nandi, Nucl. Phys. B **830**, 278 (2010).
85. A. H. Hoang *et al.*, Phys. Rev. **D59**, 074017 (1999).
86. N. Uraltsev, Int. J. Mod. Phys. **A14**, 4641 (1999).
87. M. Neubert, Phys. Rev. **D49**, 4623 (1994); *ibid.* **D49**, 3392 (1994).
88. I. Bigi *et al.*, Int. J. Mod. Phys. **A9**, 2467 (1994).
89. B.O. Lange, M. Neubert, and G. Paz, Phys. Rev. **D72**, 073006 (2005).
90. C. W. Bauer *et al.*, Phys. Lett. **B543**, 261 (2002).
91. T. Mannel and S. Recksiegel, Phys. Rev. **D60**, 114040 (1999).
92. C. W. Bauer, Z. Ligeti, and M. E. Luke, Phys. Rev. **D64**, 113004 (2001).
93. C. W. Bauer *et al.*, Phys. Rev. **D68**, 094001 (2003).
94. S. W. Bosch *et al.*, JHEP **0411**, 073 (2004).

## Meson Particle Listings

 $V_{cb}$  and  $V_{ub}$  CKM Matrix Elements

95. A. W. Leibovich *et al.*, Phys. Lett. **B539**, 242 (2002).
96. M. Neubert, Phys. Lett. **B543**, 269 (2002).
97. K.S.M.Lee and I.W. Stewart, Nucl. Phys. **B721**, 325 (2005).
98. M. Beneke *et al.*, JHEP **0506**, 071 (2005).
99. M. Neubert, Phys. Lett. **B513**, 88 (2001); Phys. Lett. **B543**, 269 (2002).
100. A.K. Leibovich *et al.*, Phys. Rev. **D61**, 053006 (2000); **62**, 014010 (2000); Phys. Lett. **B486**, 86 (2000); **513**, 83 (2001).
101. A.H. Hoang *et al.*, Phys. Rev. **D71**, 093007 (2005).
102. B. Lange *et al.*, JHEP **0510**, 084 (2005); B. Lange, JHEP **0601**, 104 (2006).
103. M. Neubert, Phys. Lett. **B612**, 13 (2005).
104. P. Gambino, G. Ossola, and N. Uraltsev, JHEP **0509**, 010 (2005).
105. Z. Ligeti, I. W. Stewart, and F. J. Tackmann, Phys. Rev. D **78**, 114014 (2008).
106. P. Gambino *et al.*, JHEP **0710**, 058 (2007).
107. J.R. Andersen and E. Gardi, JHEP **0601**, 097 (2006).
108. C. Greub, M. Neubert, and B.D. Pecjak, Eur. Phys. J. **C65**, 501(2010).
109. C. W. Bauer *et al.*, Phys. Rev. **D64**, 113004 (2001); Phys. Lett. **B479**, 395 (2000).
110. I. I. Y. Bigi and N. G. Uraltsev, Nucl. Phys. **B423**, 33 (1994).
111. M.B. Voloshin, Phys. Lett. **B515**, 74 (2001).
112. I. Bigi, T. Mannel, S. Turczyk and N. Uraltsev, JHEP **1004**, 073 (2010).
113. Z. Ligeti, M. Luke, and A. V. Manohar, Phys. Rev. **D82**, 033003 (2010).
114. P. Gambino and J. F. Kamenik, Nucl. Phys. **B840**,424 (2010).
115. J.L. Rosner *et al.*, (CLEO Collab.), Phys. Rev. Lett. **96**, 121801 (2006).
116. B. Aubert *et al.*, (BABAR Collab.), arXiv:0708.1753.
117. R. Barate *et al.*, (ALEPH Collab.), Eur. Phys. J. **C6**, 555 (1999).
118. M. Acciarri *et al.*, (L3 Collab.), Phys. Lett. **B436**, 174 (1998).
119. G. Abbiendi *et al.*, (OPAL Collab.), Eur. Phys. J. **C21**, 399 (2001).
120. P. Abreu *et al.*, (DELPHI Collab.), Phys. Lett. **B478**, 14 (2000).
121. A. Bornheim *et al.*, (CLEO Collab.), Phys. Rev. Lett. **88**, 231803 (2002).
122. A. Limosani *et al.*, (BELLE Collab.), Phys. Lett. **B621**, 28 (2005).
123. B. Aubert *et al.*, (BABAR Collab.), Phys. Rev. **D73**, 012006 (2006).
124. B. Aubert *et al.*, (BABAR Collab.), Phys. Rev. **D76**, 051101 (2007); updated in arXiv:0708.1738.
125. B. Aubert *et al.*, (BABAR Collab.), Phys. Rev. Lett. **95**, 111801 (2005), Erratum-*ibid.* **97**, 019903(E) (2006).
126. R. Kowalewski and S. Menke, Phys. Lett. **B541**, 29 (2002).
127. J. P. Lees *et al.*, (BABAR Collab.), arXiv:1112.0702.
128. I. Bizjak *et al.*, (BELLE Collab.), Phys. Rev. Lett. **95**, 241801 (2005).
129. P. Urquijo *et al.*, (BELLE Collab.), Phys. Rev. Lett. **104**, 021801 (2010).
130. B. Aubert *et al.*, (BABAR Collab.), Phys. Rev. Lett. **96**, 221801 (2006).
131. H. Kakuno *et al.*, (BELLE Collab.), Phys. Rev. Lett. **92**, 101801 (2004).
132. V. Golubev, Y. Skovpen, and V. Luth, Phys. Rev. **D76**, 114003 (2007).
133. J.H. Kuhn, M. Steinhauser, and C. Sturm, Nucl. Phys. B **778**, 192 (2007).
134. I. Allison *et al.* [HPQCD Collab.], Phys. Rev. **D78**, 054513 (2008).
135. B. Aubert *et al.*, (BABAR Collab.), Phys. Rev. Lett. **90**, 181801 (2003).
136. T. Hokuue *et al.*, (BELLE Collab.), Phys. Lett. **B648**, 139 (2007).
137. B. Aubert *et al.*, (BABAR Collab.), Phys. Rev. **D79**, 052011 (2008).
138. C. Schwanda *et al.*, (BELLE Collab.), Phys. Rev. Lett. **93**, 131803 (2004).
139. N. E. Adam *et al.*, (CLEO Collab.), Phys. Rev. Lett. **99**, 041802 (2007); Phys. Rev. **D76**, 012007 (2007); supercedes Phys. Rev. **D68**, 072003 (2003).
140. P. del Amo Sanchez *et al.*, (BABAR Collab.), Phys. Rev. **D83**, 032007 (2011); supercedes B. Aubert *et al.*, (BABAR Collab.), Phys. Rev. **D72**, 051102 (2005).
141. J. Bailey *et al.*, (Fermilab/MILC), Phys. Rev. **D79**, 054507 (2009).
142. E. Dalgic *et al.*, (HPQCD), Phys. Rev. **D73**, 074502 (2006), Erratum-*ibid.* **D75** 119906 (2007).
143. D. Becirevic and A. B. Kaidalov, Phys. Lett. **B478**, 417 (2000).
144. T. Becher and R. J. Hill, Phys. Lett. **B633**, 61 (2006).
145. M. C. Arnesen *et al.*, Phys. Rev. Lett. **95**, 071802 (2005).
146. C. Bourrely, I. Caprini, and L. Lellouch, Phys. Rev. **D79**, 013008 (2009).
147. T. Hurth *et al.*, hep-ph/0509167.
148. M.A. Shifman, A.I. Vainshtein, and V.I. Zakharov, Nucl. Phys. **B147**, 385 (1979); *ibid.* **B147**, 448 (1979).
149. P. Ball and R. Zwicky, Phys. Rev. **D71**, 014015 (2005).
150. G. Duplancic *et al.*, JHEP **0804**, 014 (2008).
151. A. Khodjamirian *et al.*, Phys. Rev. **D83**, 094031 (2011).
152. N. Isgur and M.B. Wise, Phys. Rev. **D42**, 2388 (1990).
153. B. Grinstein and D. Pirjol, Phys. Rev. **D70**, 114005 (2004).
154. P. del Amo Sanchez *et al.*, (BABAR Collab.), Phys. Rev. **D83**, 052011 (2011).
155. H. Ha *et al.*, (BELLE Collab.), Phys. Rev. **D83**, 071101 (2011).
156. K. Abe *et al.*, (BELLE Collab.), Phys. Lett. **B648**, 139 (2007).
157. I. Adachi *et al.*, (BELLE Collab.), arXiv:0812.1414.
158. B. Aubert *et al.*, (BABAR Collab.), Phys. Rev. Lett. **101**, 081801 (2008).
159. B. Aubert *et al.*, (BABAR Collab.), Phys. Rev. Lett. **97**, 211801 (2006).
160. D. Scora and N. Isgur, Phys. Rev. **D52**, 2783 (1995).
161. W. Brower and H. Paar, Nucl. Instrum. Methods **A421**, 411 (1999).

See key on page 457

# Meson Particle Listings

## $V_{cb}$ and $V_{ub}$ CKM Matrix Elements

162. P. Ball, arXiv:0705.2290,; J.M. Flynn and J. Nieves, Phys. Lett. **B649**, 269 (2007); T. Becher and R.J. Hill, Phys. Lett. **B633**, 61 (2006); M. Arnesen *et al.*, Phys. Rev. Lett. **95**, 071802 (2005).
163. J. Laiho, E. Lunghi, and R. S. Van de Water, Phys. Rev. D **81**, 034503 (2010) [arXiv:0910.2928 [hep-ph]].
164. G. Colangelo, *et al.*, Eur. Phys. J. C **71**, 1695 (2011) [arXiv:1011.4408 [hep-lat]].
165. USQCD Collab. (2011), [www.usqcd.org/documents/HiIntensityFlavor.pdf](http://www.usqcd.org/documents/HiIntensityFlavor.pdf).

### $V_{cb}$ MEASUREMENTS

For the discussion of  $V_{cb}$  measurements, which is not repeated here, see the review on "Determination of  $|V_{cb}|$  and  $|V_{ub}|$ ."

The CKM matrix element  $|V_{cb}|$  can be determined by studying the rate of the semileptonic decay  $B \rightarrow D^{(*)} \ell \nu$  as a function of the recoil kinematics of  $D^{(*)}$  mesons. Taking advantage of theoretical constraints on the normalization and a linear  $\omega$  dependence of the form factors ( $F(\omega)$ ,  $G(\omega)$ ) provided by Heavy Quark Effective Theory (HQET), the  $|V_{cb}| \times F(\omega)$  and  $\rho^2$  ( $a^2$ ) can be simultaneously extracted from data, where  $\omega$  is the scalar product of the two-meson four velocities,  $F(1)$  is the form factor at zero recoil ( $\omega=1$ ) and  $\rho^2$  is the slope, sometimes denoted as  $a^2$ . Using the theoretical input of  $F(1)$ , a value of  $|V_{cb}|$  can be obtained.

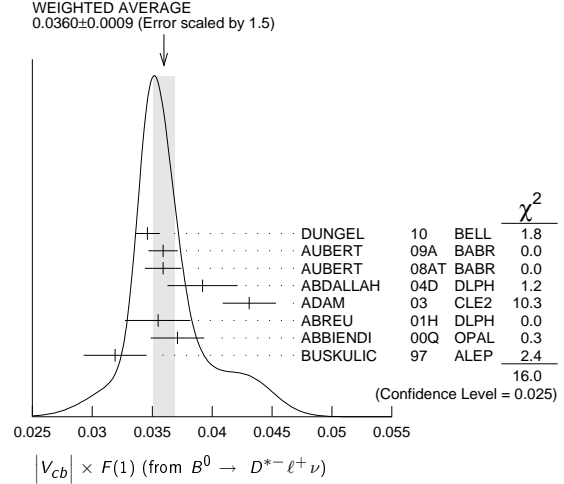
"OUR EVALUATION" is an average using rescaled values of the data listed below. The average and rescaling were performed by the Heavy Flavor Averaging Group (HFAG) and are described at <http://www.slac.stanford.edu/xorg/hfag/>. The averaging/rescaling procedure takes into account correlations between the measurements.

### $|V_{cb}| \times F(1)$ (from $B^0 \rightarrow D^{*-} \ell^+ \nu$ )

VALUE	DOCUMENT ID	TECN	COMMENT
<b>0.03590 ± 0.00045 OUR EVALUATION</b>	with $\rho^2=1.207 \pm 0.026$ and a correlation 0.32. The fitted $\chi^2$ is 29.7 for 23 degrees of freedom.		
<b>0.0360 ± 0.0009 OUR AVERAGE</b>	Error includes scale factor of 1.5. See the ideogram below.		
0.0346 ± 0.0002 ± 0.0010	1 DUNGEL	10 BELL	$e^+ e^- \rightarrow \Upsilon(4S)$
0.0359 ± 0.0002 ± 0.0012	2 AUBERT	09A BABR	$e^+ e^- \rightarrow \Upsilon(4S)$
0.0359 ± 0.0006 ± 0.0014	3 AUBERT	08AT BABR	$e^+ e^- \rightarrow \Upsilon(4S)$
0.0392 ± 0.0018 ± 0.0023	4 ABDALLAH	04D DLPH	$e^+ e^- \rightarrow Z^0$
0.0431 ± 0.0013 ± 0.0018	5 ADAM	03 CLE2	$e^+ e^- \rightarrow \Upsilon(4S)$
0.0355 ± 0.0014 ± 0.0023	6 ABREU	01H DLPH	$e^+ e^- \rightarrow Z$
0.0371 ± 0.0010 ± 0.0020	7 ABBIENDI	00Q OPAL	$e^+ e^- \rightarrow Z$
0.0319 ± 0.0018 ± 0.0019	8 BUSKULIC	97 ALEP	$e^+ e^- \rightarrow Z$
• • • We do not use the following data for averages, fits, limits, etc. • • •			
0.0344 ± 0.0003 ± 0.0011	9 AUBERT	08R BABR	Repl. by AUBERT 09A
0.0355 ± 0.0003 ± 0.0016	10 AUBERT	05E BABR	Repl. by AUBERT 08R
0.0377 ± 0.0011 ± 0.0019	11 ABDALLAH	04D DLPH	$e^+ e^- \rightarrow Z^0$
0.0354 ± 0.0019 ± 0.0018	12 ABE	02F BELL	Repl. by DUNGEL 10
0.0431 ± 0.0013 ± 0.0018	13 BRIERE	02 CLE2	$e^+ e^- \rightarrow \Upsilon(4S)$
0.0328 ± 0.0019 ± 0.0022	ACKERSTAFF	97G OPAL	Repl. by ABBIENDI 00Q
0.0350 ± 0.0019 ± 0.0023	14 ABREU	96P DLPH	Repl. by ABREU 01H
0.0351 ± 0.0019 ± 0.0020	15 BARISH	95 CLE2	Repl. by ADAM 03
0.0314 ± 0.0023 ± 0.0025	BUSKULIC	95N ALEP	Repl. by BUSKULIC 97

- 1 Uses fully reconstructed  $D^{*-} \ell^+ \nu$  events ( $\ell = e$  or  $\mu$ ).
- 2 Obtained from a global fit to  $B \rightarrow D^{(*)} \ell \nu$  events, with reconstructed  $D^0 \ell$  and  $D^+ \ell$  final states and  $\rho^2 = 1.22 \pm 0.02 \pm 0.07$ .
- 3 Measured using the dependence of  $B^- \rightarrow D^{*0} e^- \bar{\nu}_e$  decay differential rate and the form factor description by CAPRINI 98 with  $\rho^2 = 1.16 \pm 0.06 \pm 0.08$ .
- 4 Measurement using fully reconstructed  $D^*$  sample with a  $\rho^2 = 1.32 \pm 0.15 \pm 0.33$ .
- 5 Average of the  $B^0 \rightarrow D^*(2010)^- \ell^+ \nu$  and  $B^+ \rightarrow \bar{D}^*(2007)^+ \ell^+ \nu$  modes with  $\rho^2 = 1.61 \pm 0.09 \pm 0.21$  and  $f_{\pm} = 0.521 \pm 0.012$ .
- 6 ABREU 01H measured using about 5000 partial reconstructed  $D^*$  sample with a  $\rho^2 = 1.34 \pm 0.14 \pm 0.24$ .
- 7 ABBIENDI 00Q: measured using both inclusively and exclusively reconstructed  $D^{*\pm}$  samples with a  $\rho^2 = 1.21 \pm 0.12 \pm 0.20$ . The statistical and systematic correlations between  $|V_{cb}| \times F(1)$  and  $\rho^2$  are 0.90 and 0.54 respectively.
- 8 BUSKULIC 97: measured using exclusively reconstructed  $D^{*\pm}$  with a  $a^2 = 0.31 \pm 0.17 \pm 0.08$ . The statistical correlation is 0.92.
- 9 Measured using fully reconstructed  $D^*$  sample and a simultaneous fit to the Caprini-Lellouch-Neubert form factor parameters:  $\rho^2 = 1.191 \pm 0.048 \pm 0.028$ ,  $R_1(1) = 1.429 \pm 0.061 \pm 0.044$ , and  $R_2(1) = 0.827 \pm 0.038 \pm 0.022$ .
- 10 Measurement using fully reconstructed  $D^*$  sample with a  $\rho^2 = 1.29 \pm 0.03 \pm 0.27$ .
- 11 Combines with previous partial reconstructed  $D^*$  measurement with a  $\rho^2 = 1.39 \pm 0.10 \pm 0.33$ .
- 12 Measured using exclusive  $B^0 \rightarrow D^*(892)^- e^+ \nu$  decays with  $\rho^2 = 1.35 \pm 0.17 \pm 0.19$  and a correlation of 0.91.
- 13 BRIERE 02 result is based on the same analysis and data sample reported in ADAM 03.
- 14 ABREU 96P: measured using both inclusively and exclusively reconstructed  $D^{*\pm}$  samples.

- 15 BARISH 95: measured using both exclusive reconstructed  $B^0 \rightarrow D^{*-} \ell^+ \nu$  and  $B^+ \rightarrow D^{*0} \ell^+ \nu$  samples. They report their experiment's uncertainties  $\pm 0.0019 \pm 0.0018 \pm 0.0008$ , where the first error is statistical, the second is systematic, and the third is the uncertainty in the lifetimes. We combine the last two in quadrature.



### $|V_{cb}| \times G(1)$ (from $B \rightarrow D^- \ell^+ \nu$ )

VALUE	DOCUMENT ID	TECN	COMMENT
<b>0.04264 ± 0.00153 OUR EVALUATION</b>	with $\rho^2=1.186 \pm 0.054$ and a correlation 0.83. The fitted $\chi^2$ is 0.5 for 8 degrees of freedom.		
<b>0.0421 ± 0.0016 OUR AVERAGE</b>			
0.0423 ± 0.0019 ± 0.0014	16 AUBERT	10 BABR	$e^+ e^- \rightarrow \Upsilon(4S)$
0.0431 ± 0.0008 ± 0.0023	17 AUBERT	09A BABR	$e^+ e^- \rightarrow \Upsilon(4S)$
0.0411 ± 0.0044 ± 0.0052	18 ABE	02E BELL	$e^+ e^- \rightarrow \Upsilon(4S)$
0.0416 ± 0.0047 ± 0.0037	19 BARTELT	99 CLE2	$e^+ e^- \rightarrow \Upsilon(4S)$
0.0278 ± 0.0068 ± 0.0065	20 BUSKULIC	97 ALEP	$e^+ e^- \rightarrow Z$
• • • We do not use the following data for averages, fits, limits, etc. • • •			
0.0337 ± 0.0044 ± 0.0072	21 ATHANAS	97 CLE2	Repl. by BARTELT 99

- 16 Obtained from a fit to the combined  $B \rightarrow \bar{D} \ell^+ \nu \ell$  sample in which a hadronic decay of the second  $B$  meson is fully reconstructed and  $\rho^2 = 1.20 \pm 0.09 \pm 0.04$ .
- 17 Obtained from a global fit to  $B \rightarrow D^{(*)} \ell \nu$  events, with reconstructed  $D^0 \ell$  and  $D^+ \ell$  final states and  $\rho^2 = 1.20 \pm 0.04 \pm 0.07$ .
- 18 Using the missing energy and momentum to extract kinematic information about the undetected neutrino in the  $B^0 \rightarrow D^- \ell^+ \nu$  decay.
- 19 BARTELT 99: measured using both exclusive reconstructed  $B^0 \rightarrow D^- \ell^+ \nu$  and  $B^+ \rightarrow D^0 \ell^+ \nu$  samples.
- 20 BUSKULIC 97: measured using exclusively reconstructed  $D^{*\pm}$  with a  $a^2 = -0.05 \pm 0.53 \pm 0.38$ . The statistical correlation is 0.99.
- 21 ATHANAS 97: measured using both exclusive reconstructed  $B^0 \rightarrow D^- \ell^+ \nu$  and  $B^+ \rightarrow D^0 \ell^+ \nu$  samples with a  $\rho^2 = 0.59 \pm 0.22 \pm 0.12 \pm 0.59$ . They report their experiment's uncertainties  $\pm 0.0044 \pm 0.0048 \pm 0.0053$ , where the first error is statistical, the second is systematic, and the third is the uncertainty due to the form factor model variations. We combine the last two in quadrature.

### $V_{ub}$ MEASUREMENTS

For the discussion of  $V_{ub}$  measurements, which is not repeated here, see the review on "Determination of  $|V_{cb}|$  and  $|V_{ub}|$ ."

The CKM matrix element  $|V_{ub}|$  can be determined by studying the rate of the charmless semileptonic decay  $b \rightarrow u \ell \nu$ . The relevant branching ratio measurements based on exclusive and inclusive decays can be found in the  $B$  Listings, and are not repeated here.

### $V_{cb}$ and $V_{ub}$ CKM Matrix Elements REFERENCES

AUBERT	10	PRL 104 011802	B. Aubert <i>et al.</i>	(BABAR Collab.)
DUNGEL	10	PR D82 112007	W. Dungenl <i>et al.</i>	(BELLE Collab.)
AUBERT	09A	PR D79 012002	B. Aubert <i>et al.</i>	(BABAR Collab.)
AUBERT	08AT	PRL 100 231803	B. Aubert <i>et al.</i>	(BABAR Collab.)
AUBERT	08R	PR D77 032002	B. Aubert <i>et al.</i>	(BABAR Collab.)
AUBERT	05E	PR D71 051502R	B. Aubert <i>et al.</i>	(BABAR Collab.)
ABDALLAH	04D	EPJ C33 213	J. Abdallah <i>et al.</i>	(DELPHI Collab.)
ADAM	03	PR D67 032001	N.E. Adam <i>et al.</i>	(CLEO Collab.)
ABE	02E	PL B526 258	K. Abe <i>et al.</i>	(BELLE Collab.)
ABE	02F	PL B526 247	K. Abe <i>et al.</i>	(BELLE Collab.)
BRIERE	02	PRL 89 081803	R. Briere <i>et al.</i>	(CLEO Collab.)
ABREU	01H	PL B510 55	P. Abreu <i>et al.</i>	(DELPHI Collab.)
ABBIENDI	00Q	PL B482 15	G. Abbiendi <i>et al.</i>	(OPAL Collab.)
BARTELT	99	PRL 82 3746	J. Bartelt <i>et al.</i>	(CLEO Collab.)
CAPRINI	98	NP B530 153	I. Caprini, L. Lellouch, M. Neubert	(BCIP, CERN)
ACKERSTAFF	97G	PL B395 128	K. Akerstaff <i>et al.</i>	(OPAL Collab.)
ATHANAS	97	PRL 79 2208	M. Athanas <i>et al.</i>	(CLEO Collab.)
BUSKULIC	97	PL B395 373	D. Buskulic <i>et al.</i>	(ALEPH Collab.)
ABREU	96P	ZPHY C71 539	P. Abreu <i>et al.</i>	(DELPHI Collab.)
BARISH	95	PR D51 1014	B.C. Barish <i>et al.</i>	(CLEO Collab.)
BUSKULIC	95N	PL B359 236	D. Buskulic <i>et al.</i>	(ALEPH Collab.)

## Meson Particle Listings

 $B^*$ ,  $B_s^*(5732)$ ,  $B_1(5721)^0$  **$B^*$** 

$$I(J^P) = \frac{1}{2}(1^-)$$

$I, J, P$  need confirmation. Quantum numbers shown are quark-model predictions.

 **$B^*$  MASS**

From mass difference below and the average of our  $B$  masses ( $m_{B^\pm} + m_{B^0}$ )/2.

VALUE (MeV)	DOCUMENT ID
<b>5325.2 ± 0.4 OUR FIT</b>	

 **$m_{B^*} - m_B$** 

VALUE (MeV)	EVTS	DOCUMENT ID	TECN	COMMENT
<b>45.78 ± 0.35 OUR FIT</b>				
<b>45.78 ± 0.35 OUR AVERAGE</b>				
46.2 ± 0.3 ± 0.8		<sup>1</sup> ACKERSTAFF 97M	OPAL	$e^+e^- \rightarrow Z$
45.3 ± 0.35 ± 0.87	4227	<sup>1</sup> BUSKULIC 96D	ALEP	$E_{cm}^{ee} = 88-94$ GeV
45.5 ± 0.3 ± 0.8		<sup>1</sup> ABREU 95R	DLPH	$E_{cm}^{ee} = 88-94$ GeV
46.3 ± 1.9	1378	<sup>1</sup> ACCIARRI 95B	L3	$E_{cm}^{ee} = 88-94$ GeV
46.4 ± 0.3 ± 0.8		<sup>2</sup> AKERIB 91	CLE2	$e^+e^- \rightarrow \gamma X$
45.6 ± 0.8		<sup>2</sup> WU 91	CSB2	$e^+e^- \rightarrow \gamma X, \gamma \ell X$
45.4 ± 1.0		<sup>3</sup> LEE-FRANZINI 90	CSB2	$e^+e^- \rightarrow \Upsilon(5S)$

• • • We do not use the following data for averages, fits, limits, etc. • • •

52 ± 2 ± 4 1400 <sup>4</sup> HAN 85 CUSB  $e^+e^- \rightarrow \gamma eX$

<sup>1</sup>  $u, d, s$  flavor averaged.

<sup>2</sup> These papers report  $E_\gamma$  in the  $B^*$  center of mass. The  $m_{B^*} - m_B$  is 0.2 MeV higher.  $E_{cm} = 10.61-10.7$  GeV. Admixture of  $B^0$  and  $B^+$  mesons, but not  $B_s$ .

<sup>3</sup> LEE-FRANZINI 90 value is for an admixture of  $B^0$  and  $B^+$ . They measure  $46.7 \pm 0.4 \pm 0.2$  MeV for an admixture of  $B^0, B^+,$  and  $B_s$ , and use the shape of the photon line to separate the above value.

<sup>4</sup> HAN 85 is for  $E_{cm} = 10.6-11.2$  GeV, giving an admixture of  $B^0, B^+,$  and  $B_s$ .

$$|(m_{B^{*+}} - m_{B^+}) - (m_{B^{*0}} - m_{B^0})|$$

VALUE (MeV)	CL%	DOCUMENT ID	TECN	COMMENT
<b>&lt; 6</b>	95	ABREU 95R	DLPH	$E_{cm}^{ee} = 88-94$ GeV

 **$B^*$  DECAY MODES**

Mode	Fraction ( $\Gamma_i/\Gamma$ )
$\Gamma_1$ $B\gamma$	dominant

 **$B^*$  REFERENCES**

ACKERSTAFF 97M	ZPHY C74 413	K. Ackerstaff et al.	(OPAL Collab.)
BUSKULIC 96D	ZPHY C69 393	D. Buskulic et al.	(ALEPH Collab.)
ABREU 95R	ZPHY C68 353	P. Abreu et al.	(DELPHI Collab.)
ACCIARRI 95B	PL B345 589	M. Acciarri et al.	(L3 Collab.)
AKERIB 91	PRL 67 1692	D.S. Akerib et al.	(CLEO Collab.)
WU 91	PL B273 177	Q.W. Wu et al.	(CUSB II Collab.)
LEE-FRANZINI 90	PRL 65 2947	J. Lee-Franzini et al.	(CUSB II Collab.)
HAN 85	PRL 55 36	K. Han et al.	(COLU, LSU, MPIM, STON)

 **$B_s^*(5732)$**   
or  $B^{**}$ 

$$I(J^P) = ?(??)$$

$I, J, P$  need confirmation.

OMITTED FROM SUMMARY TABLE

Signal can be interpreted as stemming from several narrow and broad resonances. Needs confirmation.

 **$B_s^*(5732)$  MASS**

VALUE (MeV)	EVTS	DOCUMENT ID	TECN	COMMENT
<b>5698 ± 8 OUR AVERAGE</b>				Error includes scale factor of 1.2.
5710 ± 20		<sup>1</sup> AFFOLDER 01F	CDF	$p\bar{p}$ at 1.8 TeV
5695 <sup>+17</sup> <sub>-19</sub>		<sup>2</sup> BARATE 98L	ALEP	$e^+e^- \rightarrow Z$
5704 ± 4 ± 10	1944	<sup>3</sup> BUSKULIC 96D	ALEP	$E_{cm}^{ee} = 88-94$ GeV
5732 ± 5 ± 20	2157	ABREU 95B	DLPH	$E_{cm}^{ee} = 88-94$ GeV
5681 ± 11	1738	AKERS 95E	OPAL	$E_{cm}^{ee} = 88-94$ GeV
• • • We do not use the following data for averages, fits, limits, etc. • • •				
5713 ± 2		<sup>4</sup> ACCIARRI 99N	L3	$e^+e^- \rightarrow Z$

<sup>1</sup> AFFOLDER 01F uses the reconstructed  $B$  meson through semileptonic decay channels. The fraction of light  $B$  mesons that are produced at  $L=1$   $B^{**}$  states is measured to be  $0.28 \pm 0.06 \pm 0.03$ .

<sup>2</sup> BARATE 98L uses fully reconstructed  $B$  mesons to search for  $B^{**}$  production in the  $B\pi^\pm$  system. In the framework of heavy quark symmetry (HQSS), they also measured the mass of  $B_2^*$  to be  $5739^{+8+6}_{-11-4}$  MeV/ $c^2$  and the relative production rate of  $B(b \rightarrow B_2^* \rightarrow B^{(*)}\pi)/B(b \rightarrow B_{u,d}) = (31 \pm 9^{+6}_{-5})\%$ .

<sup>3</sup> Using  $m_{B\pi} - m_B = 424 \pm 4 \pm 10$  MeV.

<sup>4</sup> ACCIARRI 99N uses inclusive reconstructed  $B$  mesons to search for  $B^{**}$  production in the  $B^{(*)}\pi^\pm$  system. In the framework of HQET, they measured the mass of  $B_1^*$  and  $B_2^*$  to be  $5670 \pm 10 \pm 13$  MeV and  $5768 \pm 5 \pm 6$  with the  $B(b \rightarrow B^{**}) = (32 \pm 3 \pm 6) \times 10^{-2}$ . They also reported the evidence for the existence of an excited  $B$ -meson state or mixture of states in the region 5.9–6.0 GeV.

 **$B_s^*(5732)$  WIDTH**

VALUE (MeV)	EVTS	DOCUMENT ID	TECN	COMMENT
<b>128 ± 18 OUR AVERAGE</b>				
145 ± 28	2157	ABREU 95B	DLPH	$E_{cm}^{ee} = 88-94$ GeV
116 ± 24	1738	AKERS 95E	OPAL	$E_{cm}^{ee} = 88-94$ GeV

 **$B_s^*(5732)$  DECAY MODES**

Mode	Fraction ( $\Gamma_i/\Gamma$ )
$\Gamma_1$ $B^*\pi + B\pi$	dominant
$\Gamma_2$ $B^*\pi(X)$	[a] (85 ± 29) %

[a] X refers to decay modes with or without additional accompanying decay particles.

 **$B_s^*(5732)$  BRANCHING RATIOS**

X refers to decay modes with or without additional accompanying decay particles.

$\Gamma(B^*\pi(X))/\Gamma_{total}$	$\Gamma_2/\Gamma$
<b>0.85<sup>+0.26</sup><sub>-0.27</sub> ± 0.12</b>	
	ABBIENDI 02E
	OPAL
	$e^+e^- \rightarrow Z$

 **$B_s^*(5732)$  REFERENCES**

ABBIENDI 02E	EPJ C23 437	G. Abbiendi et al.	(OPAL Collab.)
AFFOLDER 01F	PR D64 072002	T. Affolder et al.	(CDF Collab.)
ACCIARRI 99N	PL B465 323	M. Acciarri et al.	(L3 Collab.)
BARATE 98L	PL B425 215	R. Barate et al.	(ALEPH Collab.)
BUSKULIC 96D	ZPHY C69 393	D. Buskulic et al.	(ALEPH Collab.)
ABREU 95B	PL B345 598	P. Abreu et al.	(DELPHI Collab.)
AKERS 95E	ZPHY C66 19	R. Akers et al.	(OPAL Collab.)

 **$B_1(5721)^0$** 

$$I(J^P) = \frac{1}{2}(1^+) \text{ Status: } ***$$

$I, J, P$  need confirmation.

Quantum numbers shown are quark-model predictions.

 **$B_1(5721)^0$  MASS**

OUR FIT uses  $m_{B^+}$  and  $m_{B_1^0} - m_{B^+}$  to determine  $m_{B_1(5721)^0}$ .

VALUE (MeV)	DOCUMENT ID
<b>5723.5 ± 2.0 OUR FIT</b>	Error includes scale factor of 1.1.

 **$m_{B_1^0} - m_{B^+}$** 

VALUE (MeV)	DOCUMENT ID	TECN	COMMENT
<b>444.3 ± 2.0 OUR FIT</b>			Error includes scale factor of 1.1.
<b>444.2 ± 2.3 OUR AVERAGE</b>			Error includes scale factor of 1.3.
446.2 <sup>+1.9</sup> <sub>-2.1</sub> ± 1.2	<sup>1</sup> AALTONEN 09D	CDF	$p\bar{p}$ at 1.96 TeV
441.5 ± 2.4 ± 1.3	ABAZOV 07T	D0	$p\bar{p}$ at 1.96 TeV
<sup>1</sup> Observed in $B_1^0 \rightarrow B^{*+}\pi^-$ .			

 **$B_1(5721)^0$  DECAY MODES**

Mode	Fraction ( $\Gamma_i/\Gamma$ )
$\Gamma_1$ $B^{*+}\pi^-$	dominant

See key on page 457

## Meson Particle Listings

 $B_1(5721)^0, B_2^*(5747)^0$  $B_1(5721)^0$  BRANCHING RATIOS

$\Gamma(B^{*+}\pi^-)/\Gamma_{\text{total}}$	DOCUMENT ID	TECN	COMMENT	$\Gamma_1/\Gamma$
dominant	AALTONEN 09D	CDF	$\rho\bar{p}$ at 1.96 TeV	
dominant	<sup>2</sup> ABAZOV 07T	D0	$\rho\bar{p}$ at 1.96 TeV	

<sup>2</sup> Observed in  $B_1^0 \rightarrow B^{*+}\pi^-$  with  $B^{*+} \rightarrow B^+\gamma$  and  $B^+ \rightarrow J/\psi\pi^+$ .

 $B_1(5721)^0$  REFERENCES

AALTONEN 09D	PRL 102 102003	T. Aaltonen et al.	(CDF Collab.)
ABAZOV 07T	PRL 99 172001	V.M. Abazov et al.	(D0 Collab.)

 $B_2^*(5747)^0$  $I(J^P) = \frac{1}{2}(2^+)$  Status: \*\*\*  
 $I, J, P$  need confirmation.

Quantum numbers shown are quark-model predictions.

 $B_2^*(5747)^0$  MASS

OUR FIT uses  $m_{B^{*+}}, m_{B_1^0} - m_{B^{*+}}$ , and  $m_{B_2^{*0}} - m_{B_1^0}$  to determine  $m_{B_2^*(5747)^0}$ . The  $-0.659$  correlation between statistical uncertainties of  $m_{B_1^0} - m_{B^{*+}}$  and  $m_{B_2^{*0}} - m_{B_1^0}$  measurements reported by ABAZOV 07T is taken into account.

VALUE (MeV)	DOCUMENT ID
<b>5743 ± 5 OUR FIT</b>	Error includes scale factor of 2.9.

 $B_2^*(5747)^0$  WIDTH

VALUE (MeV)	DOCUMENT ID	TECN	COMMENT
<b>22.7<sup>+3.8+3.2</sup><sub>-3.2-10.2</sub></b>	AALTONEN 09D	CDF	$\rho\bar{p}$ at 1.96 TeV

 $m_{B_2^{*0}} - m_{B_1^0}$ 

VALUE (MeV)	DOCUMENT ID	TECN	COMMENT
<b>19 ± 6 OUR FIT</b>	Error includes scale factor of 3.0.		
<b>19 ± 6 OUR AVERAGE</b>	Error includes scale factor of 2.8.		
14.9 <sup>+2.2+1.2</sup> <sub>-2.5-1.4</sub>	<sup>1</sup> AALTONEN 09D	CDF	$\rho\bar{p}$ at 1.96 TeV
26.2 ± 3.1 ± 0.9	<sup>1</sup> ABAZOV 07T	D0	$\rho\bar{p}$ at 1.96 TeV

<sup>1</sup> Observed in  $B_2^{*0} \rightarrow B^{*+}\pi^-$  and  $B_2^{*0} \rightarrow B^+\pi^-$ .

 $B_2^*(5747)^0$  DECAY MODES

Mode	Fraction ( $\Gamma_i/\Gamma$ )
$\Gamma_1 B^+\pi^-$	dominant
$\Gamma_2 B^{*+}\pi^-$	dominant

 $B_2^*(5747)^0$  BRANCHING RATIOS

$\Gamma(B^+\pi^-)/\Gamma_{\text{total}}$	DOCUMENT ID	TECN	COMMENT	$\Gamma_1/\Gamma$
dominant	AALTONEN 09D	CDF	$\rho\bar{p}$ at 1.96 TeV	
dominant	ABAZOV 07T	D0	$\rho\bar{p}$ at 1.96 TeV	

$\Gamma(B^{*+}\pi^-)/\Gamma_{\text{total}}$	DOCUMENT ID	TECN	COMMENT	$\Gamma_2/\Gamma$
dominant	AALTONEN 09D	CDF	$\rho\bar{p}$ at 1.96 TeV	
dominant	ABAZOV 07T	D0	$\rho\bar{p}$ at 1.96 TeV	

$\Gamma(B^{*+}\pi^-)/\Gamma(B^+\pi^-)$	DOCUMENT ID	TECN	COMMENT	$\Gamma_2/\Gamma_1$
<b>1.10 ± 0.42 ± 0.31</b>	<sup>2</sup> ABAZOV 07T	D0	$\rho\bar{p}$ at 1.96 TeV	

<sup>2</sup> Converted from measured ratio of  $R = B(B_2^{*0} \rightarrow B^{*+}\pi^-) / B(B_2^{*0} \rightarrow B^+\pi^-) = 0.475 \pm 0.095 \pm 0.069$ .

 $B_2^*(5747)^0$  REFERENCES

AALTONEN 09D	PRL 102 102003	T. Aaltonen et al.	(CDF Collab.)
ABAZOV 07T	PRL 99 172001	V.M. Abazov et al.	(D0 Collab.)

# Meson Particle Listings

$B_s^0$

## BOTTOM, STRANGE MESONS

### ( $B = \pm 1, S = \mp 1$ )

$B_s^0 = s\bar{b}, \bar{B}_s^0 = \bar{s}b$ , similarly for  $B_s^{*\pm}$

$B_s^0$

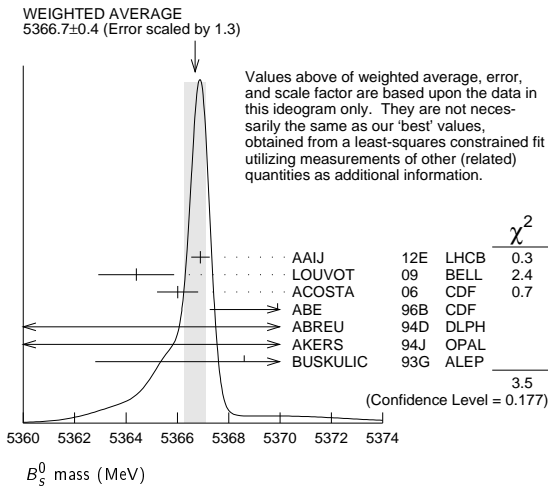
$$I(J^P) = 0(0^-)$$

$I, J, P$  need confirmation. Quantum numbers shown are quark-model predictions.

### $B_s^0$ MASS

VALUE (MeV)	EVTs	DOCUMENT ID	TECN	COMMENT
<b>5366.77 ± 0.24 OUR FIT</b>				
<b>5366.7 ± 0.4 OUR AVERAGE</b>				Error includes scale factor of 1.3. See the ideogram below.
5366.90 ± 0.28 ± 0.23		<sup>1</sup> AAIJ	12E LHCb	$pp$ at 7 TeV
5364.4 ± 1.3 ± 0.7		LOUVOT	09 BELL	$e^+e^- \rightarrow \Upsilon(5S)$
5366.01 ± 0.73 ± 0.33		<sup>2</sup> ACOSTA	06 CDF	$p\bar{p}$ at 1.96 TeV
5369.9 ± 2.3 ± 1.3	32	<sup>3</sup> ABE	96B CDF	$p\bar{p}$ at 1.8 TeV
5374 ± 16 ± 2	3	ABREU	94D DLPH	$e^+e^- \rightarrow Z$
5359 ± 19 ± 7	1	<sup>3</sup> AKERS	94J OPAL	$e^+e^- \rightarrow Z$
5368.6 ± 5.6 ± 1.5	2	BUSKULIC	93G ALEP	$e^+e^- \rightarrow Z$
••• We do not use the following data for averages, fits, limits, etc. •••				
5370 ± 1 ± 3		DRUTSKOY	07A BELL	Repl. by LOUVOT 09
5370 ± 4.0 ± 5.0	6	<sup>4</sup> AKERS	94J OPAL	$e^+e^- \rightarrow Z$
5383.3 ± 4.5 ± 5.0	14	ABE	93F CDF	Repl. by ABE 96B

- <sup>1</sup> Uses  $B_s^0 \rightarrow J/\psi\phi$  fully reconstructed decays.
- <sup>2</sup> Uses exclusively reconstructed final states containing a  $J/\psi \rightarrow \mu^+\mu^-$  decays.
- <sup>3</sup> From the decay  $B_s \rightarrow J/\psi(1S)\phi$ .
- <sup>4</sup> From the decay  $B_s \rightarrow D_s^-\pi^+$ .



$$m_{B_s^0} - m_B$$

$m_B$  is the average of our  $B$  masses ( $m_{B^\pm} + m_{B^0}$ )/2.

VALUE (MeV)	CL%	DOCUMENT ID	TECN	COMMENT
<b>87.35 ± 0.23 OUR FIT</b>				
<b>87.34 ± 0.29 OUR AVERAGE</b>				
87.42 ± 0.30 ± 0.09		<sup>1</sup> AAIJ	12E LHCb	$pp$ at 7 TeV
86.64 ± 0.80 ± 0.08		<sup>2</sup> ACOSTA	06 CDF	$p\bar{p}$ at 1.96 TeV
••• We use the following data for averages but not for fits. •••				
89.7 ± 2.7 ± 1.2		ABE	96B CDF	$p\bar{p}$ at 1.8 TeV
••• We do not use the following data for averages, fits, limits, etc. •••				
80 to 130	68	LEE-FRANZINI	90 CSB2	$e^+e^- \rightarrow \Upsilon(5S)$

- <sup>1</sup> The reported result is  $m_{B_s^0} - m_{B^+} = 87.52 \pm 0.30 \pm 0.12$  MeV. We convert it to the mass difference with respect to the average of ( $m_{B^\pm} + m_{B^0}$ )/2.
- <sup>2</sup> The reported result is  $m_{B_s^0} - m_{B^0} = 86.38 \pm 0.90 \pm 0.06$  MeV. We convert it to the mass difference with respect to the average of ( $m_{B^\pm} + m_{B^0}$ )/2.

$$m_{B_{SH}^0} - m_{B_{SL}^0}$$

See the  $B_s^0 - \bar{B}_s^0$  MIXING section near the end of these  $B_s^0$  Listings.

### $B_s^0$ MEAN LIFE

"OUR EVALUATION" is an average using rescaled values of the data listed below. The average and rescaling were performed by the Heavy Flavor Averaging Group (HFAG) and are described at <http://www.slac.stanford.edu/xorg/hfag/>. The averaging/rescaling procedure takes into account correlations between the measurements and asymmetric lifetime errors.

The

First "OUR EVALUATION" is an average of  $1 / [\Gamma_{B_s^0} + \Gamma_{B_s^{*L}}]$ .  
The Second "OUR EVALUATION" is the average of  $B_s \rightarrow D_s X$  data listed below.

VALUE ( $10^{-12}$ s)	EVTs	DOCUMENT ID	TECN	COMMENT
<b>1.497 ± 0.015 OUR EVALUATION</b>				First
<b>1.466 ± 0.031 OUR EVALUATION</b>				Second
1.518 ± 0.041 ± 0.027		<sup>1</sup> AALTONEN	11AP CDF	$p\bar{p}$ at 1.96 TeV
1.398 ± 0.044 $^{+0.028}_{-0.025}$		<sup>2</sup> ABAZOV	06V D0	$p\bar{p}$ at 1.96 TeV
1.42 $^{+0.14}_{-0.13}$ ± 0.03		<sup>3</sup> ABREU	00Y DLPH	$e^+e^- \rightarrow Z$
1.53 $^{+0.16}_{-0.15}$ ± 0.07		<sup>4</sup> ABREU,P	00G DLPH	$e^+e^- \rightarrow Z$
1.36 ± 0.09 $^{+0.06}_{-0.05}$		<sup>5</sup> ABE	99D CDF	$p\bar{p}$ at 1.8 TeV
1.72 $^{+0.20}_{-0.19}$ $^{+0.18}_{-0.17}$		<sup>6</sup> ACKERSTAFF	98F OPAL	$e^+e^- \rightarrow Z$
1.50 $^{+0.16}_{-0.15}$ ± 0.04		<sup>5</sup> ACKERSTAFF	98G OPAL	$e^+e^- \rightarrow Z$
1.47 ± 0.14 ± 0.08		<sup>4</sup> BARATE	98C ALEP	$e^+e^- \rightarrow Z$
1.54 $^{+0.14}_{-0.13}$ ± 0.04		<sup>5</sup> BUSKULIC	96M ALEP	$e^+e^- \rightarrow Z$
••• We do not use the following data for averages, fits, limits, etc. •••				
1.51 ± 0.11		<sup>7</sup> BARATE	98C ALEP	$e^+e^- \rightarrow Z$
1.56 $^{+0.29}_{-0.26}$ $^{+0.08}_{-0.07}$		<sup>5</sup> ABREU	96F DLPH	Repl. by ABREU 00y
1.65 $^{+0.34}_{-0.31}$ ± 0.12		<sup>4</sup> ABREU	96F DLPH	Repl. by ABREU 00y
1.76 ± 0.20 $^{+0.15}_{-0.10}$		<sup>8</sup> ABREU	96F DLPH	Repl. by ABREU 00y
1.60 ± 0.26 $^{+0.13}_{-0.15}$		<sup>9</sup> ABREU	96F DLPH	Repl. by ABREU,P 00g
1.67 ± 0.14		<sup>10</sup> ABREU	96F DLPH	$e^+e^- \rightarrow Z$
1.61 $^{+0.30}_{-0.29}$ $^{+0.18}_{-0.16}$	90	<sup>4</sup> BUSKULIC	96E ALEP	Repl. by BARATE 98c
1.42 $^{+0.27}_{-0.23}$ ± 0.11	76	<sup>5</sup> ABE	95R CDF	Repl. by ABE 99D
1.74 $^{+1.08}_{-0.69}$ ± 0.07	8	<sup>11</sup> ABE	95R CDF	Sup. by ABE 96N
1.54 $^{+0.25}_{-0.21}$ ± 0.06	79	<sup>5</sup> AKERS	95G OPAL	Repl. by ACKERSTAFF 98g
1.59 $^{+0.17}_{-0.15}$ ± 0.03	134	<sup>5</sup> BUSKULIC	95O ALEP	Sup. by BUSKULIC 96M
0.96 ± 0.37	41	<sup>12</sup> ABREU	94E DLPH	Sup. by ABREU 96F
1.92 $^{+0.45}_{-0.35}$ ± 0.04	31	<sup>5</sup> BUSKULIC	94C ALEP	Sup. by BUSKULIC 95O
1.13 $^{+0.35}_{-0.26}$ ± 0.09	22	<sup>5</sup> ACTON	93H OPAL	Sup. by AKERS 95G

- <sup>1</sup> AALTONEN 11AP combines the fully reconstructed  $B_s^0 \rightarrow D_s^-\pi^+$  decays and partially reconstructed  $B_s^0 \rightarrow D_s X$  decays.
- <sup>2</sup> Measured using  $D_s \mu^+$  vertices.
- <sup>3</sup> Uses  $D_s^- \ell^+$ , and  $\phi \ell^+$  vertices.
- <sup>4</sup> Measured using  $D_s$  hadron vertices.
- <sup>5</sup> Measured using  $D_s^- \ell^+$  vertices.
- <sup>6</sup> ACKERSTAFF 98F use fully reconstructed  $D_s^- \rightarrow \phi\pi^-$  and  $D_s^- \rightarrow K^{*0}K^-$  in the inclusive  $B_s^0$  decay.
- <sup>7</sup> Combined results from  $D_s^- \ell^+$  and  $D_s$  hadron.
- <sup>8</sup> Measured using  $\phi \ell$  vertices.
- <sup>9</sup> Measured using inclusive  $D_s$  vertices.
- <sup>10</sup> Combined result for the four ABREU 96F methods.
- <sup>11</sup> Exclusive reconstruction of  $B_s \rightarrow \psi\phi$ .
- <sup>12</sup> ABREU 94E uses the flight-distance distribution of  $D_s$  vertices,  $\phi$ -lepton vertices, and  $D_s \mu$  vertices.

### $B_s^0$ MEAN LIFE (Flavor specific)

VALUE ( $10^{-12}$ s)	DOCUMENT ID	TECN	COMMENT
<b>1.463 ± 0.032 OUR EVALUATION</b>			
<b>1.456 ± 0.031 OUR AVERAGE</b>			
1.518 ± 0.041 ± 0.027	<sup>1</sup> AALTONEN	11AP CDF	$p\bar{p}$ at 1.96 TeV
1.398 ± 0.044 $^{+0.028}_{-0.025}$	<sup>2</sup> ABAZOV	06V D0	$p\bar{p}$ at 1.96 TeV
1.42 $^{+0.14}_{-0.13}$ ± 0.03	<sup>3</sup> ABREU	00Y DLPH	$e^+e^- \rightarrow Z$

See key on page 457

## Meson Particle Listings

 $B_S^0$ 

$1.36 \pm 0.09 \pm^{+0.06}_{-0.05}$	<sup>4</sup> ABE	99D	CDF	$p\bar{p}$ at 1.8 TeV
$1.50 \pm^{+0.16}_{-0.15} \pm 0.04$	<sup>4</sup> ACKERSTAFF	98G	OPAL	$e^+e^- \rightarrow Z$
$1.54 \pm^{+0.14}_{-0.13} \pm 0.04$	<sup>4</sup> BUSKULIC	96M	ALEP	$e^+e^- \rightarrow Z$

<sup>1</sup> AALTONEN 11AP combines the fully reconstructed  $B_S^0 \rightarrow D_S^- \pi^+$  decays and partially reconstructed  $B_S^0 \rightarrow D_S X$  decays.  
<sup>2</sup> Measured using  $D_S^- \mu^+$  vertices.  
<sup>3</sup> Uses  $D_S^- \ell^+$ , and  $\phi \ell^+$  vertices.  
<sup>4</sup> Measured using  $D_S^- \ell^+$  vertices.

 $B_S^0$  MEAN LIFE ( $B_S \rightarrow J/\psi\phi$ )

VALUE ( $10^{-12}$ s)	DOCUMENT ID	TECN	COMMENT	
<b><math>1.429 \pm 0.088</math> OUR EVALUATION</b>				
<b><math>1.42 \pm^{+0.08}_{-0.07}</math> OUR AVERAGE</b>				
$1.444 \pm^{+0.098}_{-0.090} \pm 0.020$	<sup>1</sup> ABAZOV	05B	D0	$p\bar{p}$ at 1.96 TeV
$1.40 \pm^{+0.15}_{-0.13} \pm 0.02$	<sup>2</sup> ACOSTA	05	CDF	$p\bar{p}$ at 1.96 TeV
$1.34 \pm^{+0.23}_{-0.19} \pm 0.05$	<sup>2</sup> ABE	98B	CDF	$p\bar{p}$ at 1.8 TeV
• • • We do not use the following data for averages, fits, limits, etc. • • •				
$1.39 \pm^{+0.13}_{-0.16} \pm^{+0.01}_{-0.02}$	<sup>2</sup> ABAZOV	05W	D0	$p\bar{p}$ at 1.96 TeV
$1.34 \pm^{+0.23}_{-0.19} \pm 0.05$	<sup>3</sup> ABE	96N	CDF	Repl. by ABE 98B

<sup>1</sup> Measured using fully reconstructed  $B_S \rightarrow J/\psi(1S)\phi$  decays.  
<sup>2</sup> Measured using the time-dependent angular analysis of  $B_S^0 \rightarrow J/\psi\phi$  decays.  
<sup>3</sup> ABE 96N uses  $58 \pm 12$  exclusive  $B_S \rightarrow J/\psi(1S)\phi$  events.

 $\tau_{B_S^0}/\tau_{B^0}$  MEAN LIFE RATIO $\tau_{B_S^0}/\tau_{B^0}$  (direct measurements)

VALUE	DOCUMENT ID	TECN	COMMENT	
<b><math>1.052 \pm 0.061 \pm 0.015</math></b>	<sup>1</sup> ABAZOV	09E	D0	$p\bar{p}$ at 1.96 TeV
• • • We do not use the following data for averages, fits, limits, etc. • • •				
$0.980 \pm^{+0.076}_{-0.071} \pm 0.003$	<sup>2</sup> ABAZOV	05B	D0	Repl. by ABAZOV 05W
$0.91 \pm 0.09 \pm 0.003$	<sup>3</sup> ABAZOV	05W	D0	Repl. by ABAZOV 09E

<sup>1</sup> Measured the angular and lifetime parameters for the time-dependent angular untagged decays  $B_d^0 \rightarrow J/\psi K^{*0}$  and  $B_S^0 \rightarrow J/\psi\phi$ .  
<sup>2</sup> Measured mean life ratio using fully reconstructed decays.  
<sup>3</sup> Measured using the time-dependent angular analysis of  $B_S^0 \rightarrow J/\psi\phi$  decays.

 $B_{SH}^0$  MEAN LIFE $B_{SH}^0$  is the heavy mass state of two  $B_S^0$  CP eigenstates.

“OUR EVALUATION” has been obtained by the Heavy Flavor Averaging Group (HFAG) using the constraint of the flavor-specific lifetime average in a way similar to  $\Delta\Gamma_{B_S^0}/\Gamma_{B_S^0}$ .

VALUE ( $10^{-12}$ s)	DOCUMENT ID	TECN	COMMENT	
<b><math>1.618 \pm 0.024</math> OUR EVALUATION</b>				
<b><math>1.70 \pm^{+0.12}_{-0.11} \pm 0.03</math></b>				
$1.613 \pm^{+0.123}_{-0.113}$	<sup>3,4</sup> AALTONEN	08J	CDF	Repl. by AALTONEN 12D
$1.58 \pm^{+0.39}_{-0.42} \pm^{+0.01}_{-0.02}$	<sup>4</sup> ABAZOV	05W	D0	Repl. by ABAZOV 08AM
$2.07 \pm^{+0.58}_{-0.46} \pm 0.03$	<sup>4</sup> ACOSTA	05	CDF	Repl. by AALTONEN 08J

<sup>1</sup> Uses the time-dependent angular analysis of  $B_S^0 \rightarrow J/\psi\phi$  decays and assuming CP-violating angle  $\beta_S(B^0 \rightarrow J/\psi\phi) = 0.02$ .  
<sup>2</sup> Measured using  $J/\psi f_0(980)$ , a pure CP odd final state.  
<sup>3</sup> Obtained from  $\Delta\Gamma_S$  and  $\Gamma_S$  fit with a correlation of 0.6.  
<sup>4</sup> Measured using the time-dependent angular analysis of  $B_S^0 \rightarrow J/\psi\phi$  decays.

 $B_{SL}^0$  MEAN LIFE $B_{SL}^0$  is the light mass state of two  $B_S^0$  CP eigenstates.

“OUR EVALUATION” has been obtained by the Heavy Flavor Averaging Group (HFAG) using the constraint of the flavor-specific lifetime average in a way similar to  $\Delta\Gamma_{B_S^0}/\Gamma_{B_S^0}$ .

VALUE ( $10^{-12}$ s)	DOCUMENT ID	TECN	COMMENT	
<b><math>1.393 \pm 0.019</math> OUR EVALUATION</b>				
<b><math>1.440 \pm 0.096 \pm 0.009</math></b>				
$1.123 \pm 0.029 \pm 0.011$	<sup>1</sup> AAIJ	12D	LHCB	$pp$ at 7 TeV
$0.075 \pm 0.035 \pm 0.006$	<sup>2</sup> AALTONEN	12D	CDF	$p\bar{p}$ at 1.96 TeV
$0.163 \pm^{+0.065}_{-0.064}$	<sup>3,4</sup> ABAZOV	12D	D0	$p\bar{p}$ at 1.96 TeV

<sup>1</sup> Measured using fully reconstructed  $B_S \rightarrow J/\psi\phi$  decays.  
<sup>2</sup> Measured using the time-dependent angular analysis of  $B_S^0 \rightarrow J/\psi\phi$  decays and assuming CP-violating angle  $\beta_S(B^0 \rightarrow J/\psi\phi) = 0.02$ .  
<sup>3</sup> Obtained from  $\Delta\Gamma_S$  and  $\Gamma_S$  fit with a correlation of 0.6.  
<sup>4</sup> Measured using the time-dependent angular analysis of  $B_S^0 \rightarrow J/\psi\phi$  decays.

• • • We do not use the following data for averages, fits, limits, etc. • • •

$1.437 \pm^{+0.054}_{-0.047}$	<sup>3,4</sup> AALTONEN	08J	CDF	Repl. by AALTONEN 12D
$1.24 \pm^{+0.14}_{-0.11} \pm^{+0.01}_{-0.02}$	<sup>4</sup> ABAZOV	05W	D0	Repl. by ABAZOV 08AM
$1.05 \pm^{+0.16}_{-0.13} \pm 0.02$	<sup>4</sup> ACOSTA	05	CDF	Repl. by AALTONEN 08J
$1.27 \pm 0.33 \pm 0.08$	<sup>5</sup> BARATE	00K	ALEP	$e^+e^- \rightarrow Z$

<sup>1</sup> Measured using decays  $B_S^0 \rightarrow K^+K^-$ .  
<sup>2</sup> Uses the time-dependent angular analysis of  $B_S^0 \rightarrow J/\psi\phi$  decays and assuming CP-violating angle  $\beta_S(B^0 \rightarrow J/\psi\phi) = 0.02$ .  
<sup>3</sup> Obtained from  $\Delta\Gamma_S$  and  $\Gamma_S$  fit with a correlation of 0.6.  
<sup>4</sup> Measured using the time-dependent angular analysis of  $B_S^0 \rightarrow J/\psi\phi$  decays.  
<sup>5</sup> Uses  $\phi\phi$  correlations from  $B_S^0 \rightarrow D_S^{(*)+}D_S^{(*)-}$ .

 $\Delta\Gamma_{B_S^0}/\Gamma_{B_S^0}$ 

$\Gamma_{B_S^0}$  and  $\Delta\Gamma_{B_S^0}$  are the decay rate average and difference between two  $B_S^0$  CP eigenstates (light – heavy).

“OUR EVALUATION” is an average of all available  $B_S$  flavor-specific lifetime measurements with the  $\Delta\Gamma_{B_S^0}/\Gamma_S$  analyses performed by the Heavy Flavor Averaging Group (HFAG) as described in our “Review on  $B$ - $\bar{B}$  Mixing” in the  $B^0$  Section of these Listings.

VALUE	CL%	DOCUMENT ID	TECN	COMMENT	
<b><math>0.150 \pm 0.020</math> OUR EVALUATION</b>					
$0.147 \pm^{+0.036}_{-0.030} \pm^{+0.042}_{-0.041}$		<sup>1</sup> AAIJ	12D	LHCB	$pp$ at 7 TeV
$0.116 \pm^{+0.09}_{-0.10} \pm 0.010$		<sup>2</sup> AALTONEN	12D	CDF	$p\bar{p}$ at 1.96 TeV
$0.24 \pm^{+0.28}_{-0.38} \pm^{+0.03}_{-0.04}$		<sup>3</sup> ABAZOV	12D	D0	$p\bar{p}$ at 1.96 TeV
$0.65 \pm^{+0.25}_{-0.33} \pm 0.01$		<sup>4</sup> ESEN	10	BELL	$e^+e^- \rightarrow \Upsilon(5S)$
$<0.46$	95	<sup>5,6</sup> AALTONEN	08J	CDF	Repl. by AALTONEN 12D
$<0.69$	95	<sup>7</sup> ABREU	00Y	DLPH	$e^+e^- \rightarrow Z$
$<0.83$	95	<sup>8</sup> ABREU,P	00G	DLPH	$e^+e^- \rightarrow Z$
$<0.67$	95	<sup>9</sup> ABE	99D	CDF	$p\bar{p}$ at 1.8 TeV
	95	<sup>10</sup> ACCIARRI	98S	L3	$e^+e^- \rightarrow Z$

• • • We do not use the following data for averages, fits, limits, etc. • • •

<sup>1</sup> Measured using the time-dependent angular analysis of  $B_S^0 \rightarrow J/\psi\phi$  decays.  
<sup>2</sup> Uses the time-dependent angular analysis of  $B_S^0 \rightarrow J/\psi\phi$  decays and assuming CP-violating angle  $\beta_S(B^0 \rightarrow J/\psi\phi) = 0.02$ .  
<sup>3</sup> Measured using fully reconstructed  $B_S \rightarrow J/\psi\phi$  decays.  
<sup>4</sup> Assumes CP violation is negligible.  
<sup>5</sup> Measured using the time-dependent angular analysis of  $B_S^0 \rightarrow J/\psi\phi$  decays.  
<sup>6</sup> Uses  $|A_0|^2 - |A_1|^2 = 0.355 \pm 0.066$  from ACOSTA 05.  
<sup>7</sup> Uses  $D_S^- \ell^+$ , and  $\phi \ell^+$  vertices.  
<sup>8</sup> Measured using  $D_S$  hadron vertices.  
<sup>9</sup> ABE 99D assumes  $\tau_{B_S^0} = 1.55 \pm 0.05$  ps.  
<sup>10</sup> ACCIARRI 98S assumes  $\tau_{B_S^0} = 1.49 \pm 0.06$  ps and PDG 98 values of  $b$  production fraction.

 $\Delta\Gamma_{B_S^0}$ 

“OUR EVALUATION” has been obtained by the Heavy Flavor Averaging Group (HFAG) using the constraint of the flavor-specific lifetime average in a way similar to  $\Delta\Gamma_{B_S^0}/\Gamma_{B_S^0}$ .

VALUE ( $10^{12}$ s $^{-1}$ )	DOCUMENT ID	TECN	COMMENT	
<b><math>0.100 \pm 0.013</math> OUR EVALUATION</b>				
<b><math>0.109 \pm 0.022</math> OUR AVERAGE</b>				
$0.123 \pm 0.029 \pm 0.011$	<sup>1</sup> AAIJ	12D	LHCB	$pp$ at 7 TeV
$0.075 \pm 0.035 \pm 0.006$	<sup>2</sup> AALTONEN	12D	CDF	$p\bar{p}$ at 1.96 TeV
$0.163 \pm^{+0.065}_{-0.064}$	<sup>3,4</sup> ABAZOV	12D	D0	$p\bar{p}$ at 1.96 TeV
$0.085 \pm^{+0.072}_{-0.078} \pm 0.001$	<sup>5</sup> ABAZOV	09E	D0	Repl. by ABAZOV 08AM
$0.076 \pm^{+0.059}_{-0.063} \pm 0.006$	<sup>6</sup> AALTONEN	08J	CDF	Repl. by AALTONEN 12D
$0.19 \pm 0.07 \pm^{+0.02}_{-0.01}$	<sup>4,7</sup> ABAZOV	08AM	D0	Repl. by ABAZOV 12D
$0.12 \pm^{+0.08}_{-0.10} \pm 0.02$	<sup>6,8</sup> ABAZOV	07	D0	Repl. by ABAZOV 07N
$0.13 \pm 0.09$	<sup>9</sup> ABAZOV	07N	D0	Repl. by ABAZOV 09E
$0.47 \pm^{+0.19}_{-0.24} \pm 0.01$	<sup>6</sup> ACOSTA	05	CDF	Repl. by AALTONEN 08J

• • • We do not use the following data for averages, fits, limits, etc. • • •

# Meson Particle Listings

## $B_s^0$

- <sup>1</sup> Measured using the time-dependent angular analysis of  $B_s^0 \rightarrow J/\psi\phi$  decays.
- <sup>2</sup> Uses the time-dependent angular analysis of  $B_s^0 \rightarrow J/\psi\phi$  decays and assuming  $CP$ -violating angle  $\beta_s(B^0 \rightarrow J/\psi\phi) = 0.02$ .
- <sup>3</sup> The error includes both statistical and systematic uncertainties.
- <sup>4</sup> Measured using fully reconstructed  $B_s \rightarrow J/\psi\phi$  decays.
- <sup>5</sup> Measured the angular and lifetime parameters for the time-dependent angular untagged decays  $B_d^0 \rightarrow J/\psi K^{*0}$  and  $B_s^0 \rightarrow J/\psi\phi$ .
- <sup>6</sup> Measured using the time-dependent angular analysis of  $B_s^0 \rightarrow J/\psi\phi$  decays and assuming  $CP$ -violating phase  $\phi_s = 0$ .
- <sup>7</sup> Obtains 90% CL interval  $-0.06 < \Delta\Gamma_s < 0.30$ .
- <sup>8</sup> ABAZOV 07 reports  $0.17 \pm 0.09 \pm 0.02$  with  $CP$ -violating phase  $\phi_s$  as a free parameter.
- <sup>9</sup> Combines  $D^0$  measurements of time-dependent angular distributions in  $B_s^0 \rightarrow J/\psi\phi$  and charge asymmetry in semileptonic decays. There is a 4-fold ambiguity in the solution.

### $\Delta\Gamma_s^{CP} / \Gamma_s$

$\Gamma_s$  and  $\Delta\Gamma_s^{CP}$  are the decay rate average and difference between even,  $\Gamma_s^{CP-even}$ , and odd,  $\Gamma_s^{CP-odd}$ ,  $CP$  eigenstates.

VALUE	CL%	DOCUMENT ID	TECN	COMMENT
• • • We do not use the following data for averages, fits, limits, etc. • • •				
$0.072 \pm 0.021 \pm 0.022$		<sup>1</sup> ABAZOV 09I	D0	$p\bar{p}$ at 1.96 TeV
$>0.012$	95	<sup>1</sup> AALTONEN 08F	CDF	$p\bar{p}$ at 1.96 TeV
$0.079^{+0.038+0.031}_{-0.035-0.030}$		<sup>1</sup> ABAZOV 07Y	D0	Repl. by ABAZOV 09I
$0.25^{+0.21}_{-0.14}$		<sup>2</sup> BARATE 00k	ALEP	$e^+e^- \rightarrow Z$

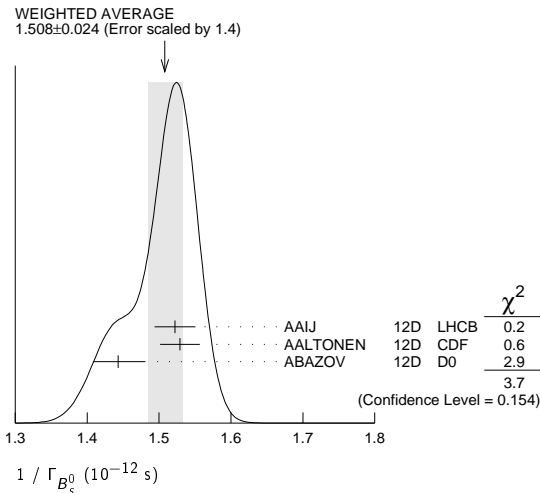
- <sup>1</sup> Assumes  $2 B(B_s^0 \rightarrow D_s^{(*)} D_s^{(*)}) \approx \Delta\Gamma_s^{CP} / \Gamma_s$ .
- <sup>2</sup> Uses  $\phi\phi$  correlations from  $B_s^0 \rightarrow D_s^{(*)+} D_s^{(*)-}$ .

### $1 / \Gamma_{B_s^0}$

"OUR EVALUATION" has been obtained by the Heavy Flavor Averaging Group (HFAG) using the constraint of the flavor-specific lifetime average in a way similar to  $\Delta\Gamma_{B_s^0} / \Gamma_{B_s^0}$ .

VALUE ( $10^{-12}$ s)	DOCUMENT ID	TECN	COMMENT
<b><math>1.497 \pm 0.015</math> OUR EVALUATION</b>			
<b><math>1.508 \pm 0.024</math> OUR AVERAGE</b>			Error includes scale factor of 1.4. See the ideogram below.
$1.522 \pm 0.021 \pm 0.019$	<sup>1</sup> AAIJ 12d	LHCB	$p\bar{p}$ at 7 TeV
$1.529 \pm 0.025 \pm 0.012$	<sup>2</sup> AALTONEN 12D	CDF	$p\bar{p}$ at 1.96 TeV
$1.443^{+0.038}_{-0.035}$	<sup>2,3</sup> ABAZOV 12d	D0	$p\bar{p}$ at 1.96 TeV
• • • We do not use the following data for averages, fits, limits, etc. • • •			
$1.487 \pm 0.060 \pm 0.028$	<sup>2</sup> ABAZOV 09E	D0	Repl. by ABAZOV 08AM
$1.52 \pm 0.04 \pm 0.02$	<sup>2</sup> AALTONEN 08J	CDF	Repl. by AALTONEN 12D
$1.52 \pm 0.05 \pm 0.01$	<sup>2</sup> ABAZOV 08AMD0	D0	Repl. by ABAZOV 12D

- <sup>1</sup> AAIJ 12d reports average decay width of  $B_s^0$ ,  $\Gamma_{B_s^0} = 0.657 \pm 0.009 \pm 0.008 \text{ ps}^{-1}$  that we converted to  $1/\Gamma_{B_s^0}$ .
- <sup>2</sup> Measured using the time-dependent angular analysis of  $B_s^0 \rightarrow J/\psi\phi$  decays.
- <sup>3</sup> The error includes both statistical and systematic uncertainties.



## $B_s^0$ DECAY MODES

These branching fractions all scale with  $B(\bar{B} \rightarrow B_s^0)$ .

The branching fraction  $B(B_s^0 \rightarrow D_s^- \ell^+ \nu_\ell \text{ anything})$  is not a pure measurement since the measured product branching fraction  $B(\bar{B} \rightarrow B_s^0) \times B(B_s^0 \rightarrow D_s^- \ell^+ \nu_\ell \text{ anything})$  was used to determine  $B(\bar{B} \rightarrow B_s^0)$ , as described in the note on " $B^0$ - $\bar{B}^0$  Mixing"

For inclusive branching fractions, e.g.,  $B \rightarrow D^\pm \text{ anything}$ , the values usually are multiplicities, not branching fractions. They can be greater than one.

Mode	Fraction ( $\Gamma_i / \Gamma$ )	Confidence level
$\Gamma_1 D_s^- \text{ anything}$	$(93 \pm 25) \%$	
$\Gamma_2 \ell \nu_\ell X$	$(9.5 \pm 2.7) \%$	
$\Gamma_3 D_s^- \ell^+ \nu_\ell \text{ anything}$	[a] $(7.9 \pm 2.4) \%$	
$\Gamma_4 D_{s1}^-(2536)^- \mu^+ \nu_\mu$	$(2.5 \pm 0.7) \times 10^{-3}$	
$\Gamma_5 D_{s1}^-(2536)^- \rightarrow D^{*-} K_s^0$		
$D_{s1}^- \rightarrow \bar{D}^0 K^+$	$(4.3 \pm 1.7) \times 10^{-3}$	
$\Gamma_6 D_{s2}^-(2573)^- X \mu^+ \nu$		
$D_{s2}^- \rightarrow \bar{D}^0 K^+$	$(2.6 \pm 1.2) \times 10^{-3}$	
$\Gamma_7 D_s^- \pi^+$	$(3.2 \pm 0.4) \times 10^{-3}$	
$\Gamma_8 D_s^- \rho^+$	$(7.4 \pm 1.7) \times 10^{-3}$	
$\Gamma_9 D_s^- \pi^+ \pi^+ \pi^-$	$(6.5 \pm 1.2) \times 10^{-3}$	
$\Gamma_{10} D_s^\mp K^\pm$	$(2.9 \pm 0.6) \times 10^{-4}$	
$\Gamma_{11} D_s^+ D_s^-$	$(5.3 \pm 0.9) \times 10^{-3}$	
$\Gamma_{12} D_s^{*-} \pi^+$	$(2.1 \pm 0.6) \times 10^{-3}$	
$\Gamma_{13} D_s^{*-} \rho^+$	$(1.03 \pm 0.26) \%$	
$\Gamma_{14} D_s^{*+} D_s^- + D_s^{*-} D_s^+$	$(1.24 \pm 0.21) \%$	
$\Gamma_{15} D_s^{*+} D_s^{*-}$	$(1.88 \pm 0.34) \%$	
$\Gamma_{16} D_s^{(*)+} D_s^{(*)-}$	$(4.5 \pm 1.4) \%$	
$\Gamma_{17} \bar{D}^0 \bar{K}^*(892)^0$	$(4.7 \pm 1.4) \times 10^{-4}$	
$\Gamma_{18} J/\psi(1S)\phi$	$(1.09 \pm \frac{0.28}{0.23}) \times 10^{-3}$	
$\Gamma_{19} J/\psi(1S)\pi^0$	$< 1.2 \times 10^{-3}$	90%
$\Gamma_{20} J/\psi(1S)\eta$	$(5.1 \pm \frac{1.3}{1.0}) \times 10^{-4}$	
$\Gamma_{21} J/\psi(1S)K^0$	$(3.6 \pm 0.8) \times 10^{-5}$	
$\Gamma_{22} J/\psi(1S)K^{*0}$	$(9 \pm 4) \times 10^{-5}$	
$\Gamma_{23} J/\psi(1S)\eta'$	$(3.7 \pm \frac{1.0}{0.9}) \times 10^{-4}$	
$\Gamma_{24} J/\psi(1S)f_0(980), f_0 \rightarrow \pi^+ \pi^-$	$(1.36 \pm \frac{0.35}{0.28}) \times 10^{-4}$	
$\Gamma_{25} J/\psi(1S)f_0(1370), f_0 \rightarrow \pi^+ \pi^-$	$(3.4 \pm 1.4) \times 10^{-5}$	
$\Gamma_{26} \psi(2S)\phi$	$(5.7 \pm \frac{1.8}{1.6}) \times 10^{-4}$	
$\Gamma_{27} \pi^+ \pi^-$	$< 1.2 \times 10^{-6}$	90%
$\Gamma_{28} \pi^0 \pi^0$	$< 2.1 \times 10^{-4}$	90%
$\Gamma_{29} \eta \pi^0$	$< 1.0 \times 10^{-3}$	90%
$\Gamma_{30} \eta \eta$	$< 1.5 \times 10^{-3}$	90%
$\Gamma_{31} \rho^0 \rho^0$	$< 3.20 \times 10^{-4}$	90%
$\Gamma_{32} \phi \rho^0$	$< 6.17 \times 10^{-4}$	90%
$\Gamma_{33} \phi \phi$	$(1.9 \pm \frac{0.6}{0.5}) \times 10^{-5}$	
$\Gamma_{34} \pi^+ K^-$	$(5.3 \pm 1.0) \times 10^{-6}$	
$\Gamma_{35} K^+ K^-$	$(2.64 \pm 0.28) \times 10^{-5}$	
$\Gamma_{36} K^0 \bar{K}^0$	$< 6.6 \times 10^{-5}$	90%
$\Gamma_{37} \bar{K}^*(892)^0 \rho^0$	$< 7.67 \times 10^{-4}$	90%
$\Gamma_{38} \bar{K}^*(892)^0 K^*(892)^0$	$(2.8 \pm 0.7) \times 10^{-5}$	
$\Gamma_{39} \phi K^*(892)^0$	$< 1.013 \times 10^{-3}$	90%
$\Gamma_{40} p\bar{p}$	$< 5.9 \times 10^{-5}$	90%
$\Gamma_{41} \gamma \gamma$	$< 8.7 \times 10^{-6}$	90%
$\Gamma_{42} \phi \gamma$	$(5.7 \pm \frac{2.2}{1.9}) \times 10^{-5}$	

### Lepton Family number (LF) violating modes or $\Delta B = 1$ weak neutral current (B1) modes

$\Gamma_{43} \mu^+ \mu^-$	B1	$< 6.4 \times 10^{-9}$	90%
$\Gamma_{44} e^+ e^-$	B1	$< 2.8 \times 10^{-7}$	90%
$\Gamma_{45} e^\pm \mu^\mp$	LF [b]	$< 2.0 \times 10^{-7}$	90%
$\Gamma_{46} \phi(1020) \mu^+ \mu^-$	B1	$(1.23 \pm \frac{0.40}{0.34}) \times 10^{-6}$	
$\Gamma_{47} \phi \nu \bar{\nu}$	B1	$< 5.4 \times 10^{-3}$	90%



See key on page 457

## Meson Particle Listings

 $B_s^0$ [a] Not a pure measurement. See note at head of  $B_s^0$  Decay Modes.

[b] The value is for the sum of the charge states or particle/antiparticle states indicated.

## CONSTRAINED FIT INFORMATION

An overall fit to 8 branching ratios uses 11 measurements and one constraint to determine 6 parameters. The overall fit has a  $\chi^2 = 1.5$  for 6 degrees of freedom.

The following *off-diagonal* array elements are the correlation coefficients  $\langle \delta x_i \delta x_j \rangle / (\delta x_i \delta x_j)$ , in percent, from the fit to the branching fractions,  $x_i \equiv \Gamma_i / \Gamma_{\text{total}}$ . The fit constrains the  $x_i$  whose labels appear in this array to sum to one.

$x_9$	46			
$x_{10}$	48	22		
$x_{18}$	0	0	0	
$x_{24}$	0	0	0	94
	$x_7$	$x_9$	$x_{10}$	$x_{18}$

 $B_s^0$  BRANCHING RATIOS $\Gamma(D_s^- \text{ anything}) / \Gamma_{\text{total}}$   $\Gamma_1 / \Gamma$ 

VALUE	EVTS	DOCUMENT ID	TECN	COMMENT
<b>0.93 ± 0.25 OUR AVERAGE</b>				
0.91 ± 0.18 ± 0.41		<sup>1</sup> DRUTSKOY 07	BELL	$e^+ e^- \rightarrow \Upsilon(4S)$
0.81 ± 0.24 ± 0.22	90	<sup>2</sup> BUSKULIC 96E	ALEP	$e^+ e^- \rightarrow Z$
1.56 ± 0.58 ± 0.44	147	<sup>3</sup> ACTON 92N	OPAL	$e^+ e^- \rightarrow Z$

<sup>1</sup> The extraction of this result takes into account the correlation between the measurements of  $B(\Upsilon(5S) \rightarrow D_s X)$  and  $B(\Upsilon(5S) \rightarrow D^0 X)$ .

<sup>2</sup> BUSKULIC 96E separate  $c\bar{c}$  and  $b\bar{b}$  sources of  $D_s^+$  mesons using a lifetime tag, subtract generic  $\bar{b} \rightarrow W^+ \rightarrow D_s^+$  events, and obtain  $B(\bar{b} \rightarrow B_s^0) \times B(B_s^0 \rightarrow D_s^- \text{ anything}) = 0.088 \pm 0.020 \pm 0.020$  assuming  $B(D_s \rightarrow \phi\pi) = (3.5 \pm 0.4) \times 10^{-2}$  and PDG 1994 values for the relative partial widths to other  $D_s$  channels. We evaluate using our current values  $B(\bar{b} \rightarrow B_s^0) = 0.107 \pm 0.014$  and  $B(D_s \rightarrow \phi\pi) = 0.036 \pm 0.009$ . Our first error is their experiment's and our second error is that due to  $B(\bar{b} \rightarrow B_s^0)$  and  $B(D_s \rightarrow \phi\pi)$ .

<sup>3</sup> ACTON 92N assume that excess of 147 ± 48  $D_s^0$  events over that expected from  $B^0$ ,  $B^+$ , and  $c\bar{c}$  is all from  $B_s^0$  decay. The product branching fraction is measured to be  $B(\bar{b} \rightarrow B_s^0)B(B_s^0 \rightarrow D_s^- \text{ anything}) \times B(D_s^- \rightarrow \phi\pi^-) = (5.9 \pm 1.9 \pm 1.1) \times 10^{-3}$ . We evaluate using our current values  $B(\bar{b} \rightarrow B_s^0) = 0.107 \pm 0.014$  and  $B(D_s \rightarrow \phi\pi) = 0.036 \pm 0.009$ . Our first error is their experiment's and our second error is that due to  $B(\bar{b} \rightarrow B_s^0)$  and  $B(D_s \rightarrow \phi\pi)$ .

 $\Gamma(\ell\nu_\ell X) / \Gamma_{\text{total}}$   $\Gamma_2 / \Gamma$ 

VALUE (units $10^{-2}$ )	DOCUMENT ID	TECN	COMMENT
<b>9.5 ± 2.5 ± 1.1</b> <b>-2.0 - 1.9</b>	<sup>1</sup> LEES	12A	BABR $e^+ e^-$

<sup>1</sup> The measurement corresponds to a branching fraction where the lepton originates from bottom decay and is the average between the electron and muon branching fractions. LEES 12A uses the correlation of the production of  $\phi$  mesons in association with a lepton in  $e^+ e^-$  data taken at center-of-mass energies between 10.54 and 11.2 GeV.

 $\Gamma(D_s^- \ell^+ \nu_\ell \text{ anything}) / \Gamma_{\text{total}}$   $\Gamma_3 / \Gamma$ 

The values and averages in this section serve only to show what values result if one assumes our  $B(\bar{b} \rightarrow B_s^0)$ . They cannot be thought of as measurements since the underlying product branching fractions were also used to determine  $B(\bar{b} \rightarrow B_s^0)$  as described in the note on "Production and Decay of  $b$ -Flavored Hadrons."

VALUE	EVTS	DOCUMENT ID	TECN	COMMENT
<b>0.079 ± 0.024 OUR AVERAGE</b>				
0.076 ± 0.012 ± 0.021	134	<sup>1</sup> BUSKULIC 95o	ALEP	$e^+ e^- \rightarrow Z$
0.107 ± 0.043 ± 0.029		<sup>2</sup> ABREU 92M	DLPH	$e^+ e^- \rightarrow Z$
0.103 ± 0.036 ± 0.028	18	<sup>3</sup> ACTON 92N	OPAL	$e^+ e^- \rightarrow Z$

• • • We do not use the following data for averages, fits, limits, etc. • • •

0.13 ± 0.04 ± 0.04 <sup>27</sup> <sup>4</sup> BUSKULIC 92E ALEP  $e^+ e^- \rightarrow Z$

<sup>1</sup> BUSKULIC 95o use  $D_s \ell$  correlations. The measured product branching ratio is  $B(\bar{b} \rightarrow B_s) \times B(B_s \rightarrow D_s^- \ell^+ \nu_\ell \text{ anything}) = (0.82 \pm 0.09_{-0.13}^{+0.13})\%$  assuming  $B(D_s \rightarrow \phi\pi) = (3.5 \pm 0.4) \times 10^{-2}$  and PDG 1994 values for the relative partial widths to the six other  $D_s$  channels used in this analysis. Combined with results from  $\Upsilon(4S)$  experiments this can be used to extract  $B(\bar{b} \rightarrow B_s) = (11.0 \pm 1.2_{-2.6}^{+2.5})\%$ . We evaluate using our current values  $B(\bar{b} \rightarrow B_s^0) = 0.107 \pm 0.014$  and  $B(D_s \rightarrow \phi\pi) = 0.036 \pm 0.009$ . Our first error is their experiment's and our second error is that due to  $B(\bar{b} \rightarrow B_s^0)$  and  $B(D_s \rightarrow \phi\pi)$ .

<sup>2</sup> ABREU 92M measured muons only and obtained product branching ratio  $B(Z \rightarrow b\bar{b}) \times B(\bar{b} \rightarrow B_s) \times B(B_s \rightarrow D_s \mu^+ \nu_\mu \text{ anything}) \times B(D_s \rightarrow \phi\pi) = (18 \pm 8) \times 10^{-5}$ . We evaluate using our current values  $B(\bar{b} \rightarrow B_s^0) = 0.107 \pm 0.014$  and  $B(D_s \rightarrow \phi\pi) = 0.036 \pm 0.009$ . Our first error is their experiment's and our second error is that due

to  $B(\bar{b} \rightarrow B_s^0)$  and  $B(D_s \rightarrow \phi\pi)$ . We use  $B(Z \rightarrow b\bar{b}) = 2B(Z \rightarrow b\bar{b}) = 2 \times (0.2212 \pm 0.0019)$ .

<sup>3</sup> ACTON 92N is measured using  $D_s \rightarrow \phi\pi^+$  and  $K^*(892)^0 K^+$  events. The product branching fraction measured is measured to be  $B(\bar{b} \rightarrow B_s^0)B(B_s^0 \rightarrow D_s^- \ell^+ \nu_\ell \text{ anything}) \times B(D_s^- \rightarrow \phi\pi^-) = (3.9 \pm 1.1 \pm 0.8) \times 10^{-4}$ . We evaluate using our current values  $B(\bar{b} \rightarrow B_s^0) = 0.107 \pm 0.014$  and  $B(D_s \rightarrow \phi\pi) = 0.036 \pm 0.009$ . Our first error is their experiment's and our second error is that due to  $B(\bar{b} \rightarrow B_s^0)$  and  $B(D_s \rightarrow \phi\pi)$ .

<sup>4</sup> BUSKULIC 92E is measured using  $D_s \rightarrow \phi\pi^+$  and  $K^*(892)^0 K^+$  events. They use  $2.7 \pm 0.7\%$  for the  $\phi\pi^+$  branching fraction. The average product branching fraction is measured to be  $B(\bar{b} \rightarrow B_s^0)B(B_s^0 \rightarrow D_s^- \ell^+ \nu_\ell \text{ anything}) = 0.020 \pm 0.0055_{-0.006}^{+0.005}$ .

We evaluate using our current values  $B(\bar{b} \rightarrow B_s^0) = 0.107 \pm 0.014$  and  $B(D_s \rightarrow \phi\pi) = 0.036 \pm 0.009$ . Our first error is their experiment's and our second error is that due to  $B(\bar{b} \rightarrow B_s^0)$  and  $B(D_s \rightarrow \phi\pi)$ . Superseded by BUSKULIC 95o.

 $\Gamma(D_{s1}(2536)^- \mu^+ \nu_\mu, D_{s1}^- \rightarrow D^{*-} K_S^0) / \Gamma_{\text{total}}$   $\Gamma_4 / \Gamma$ 

VALUE (units $10^{-3}$ )	DOCUMENT ID	TECN	COMMENT
<b>2.5 ± 0.7 ± 0.1</b>	<sup>1</sup> ABAZOV 09G	D0	$p\bar{p}$ at 1.96 TeV

<sup>1</sup> ABAZOV 09G reports  $[\Gamma(B_s^0 \rightarrow D_{s1}(2536)^- \mu^+ \nu_\mu, D_{s1}^- \rightarrow D^{*-} K_S^0) / \Gamma_{\text{total}}] \times [B(\bar{b} \rightarrow B_s^0)] = (2.66 \pm 0.52 \pm 0.45) \times 10^{-4}$  which we divide by our best value  $B(\bar{b} \rightarrow B_s^0) = (10.5 \pm 0.6) \times 10^{-2}$ . Our first error is their experiment's error and our second error is the systematic error from using our best value.

 $\Gamma(D_{s1}(2536)^- X \mu^+ \nu, D_{s1}^- \rightarrow \bar{D}^0 K^+) / \Gamma(D_s^- \ell^+ \nu_\ell \text{ anything})$   $\Gamma_5 / \Gamma_3$ 

VALUE (units $10^{-2}$ )	DOCUMENT ID	TECN	COMMENT
<b>5.4 ± 1.2 ± 0.5</b>	AAIJ	11A	LHCB $pp$ at 7 TeV

 $\Gamma(D_{s2}(2573)^- X \mu^+ \nu, D_{s2}^- \rightarrow \bar{D}^0 K^+) / \Gamma(D_s^- \ell^+ \nu_\ell \text{ anything})$   $\Gamma_6 / \Gamma_3$ 

VALUE (units $10^{-2}$ )	DOCUMENT ID	TECN	COMMENT
<b>3.3 ± 1.0 ± 0.4</b>	AAIJ	11A	LHCB $pp$ at 7 TeV

 $\Gamma(D_{s1}(2536)^- X \mu^+ \nu, D_{s1}^- \rightarrow \bar{D}^0 K^+) / \Gamma(D_{s2}(2573)^- X \mu^+ \nu, D_{s2}^- \rightarrow \bar{D}^0 K^+)$   $\Gamma_5 / \Gamma_6$ 

VALUE	DOCUMENT ID	TECN	COMMENT
• • •			We do not use the following data for averages, fits, limits, etc. • • •
0.61 ± 0.14 ± 0.05	<sup>1</sup> AAIJ	11A	LHCB $pp$ at 7 TeV

<sup>1</sup> Not independent of other AAIJ 11A measurements.

 $\Gamma(D_s^- \pi^+) / \Gamma_{\text{total}}$   $\Gamma_7 / \Gamma$ 

VALUE (units $10^{-3}$ )	EVTS	DOCUMENT ID	TECN	COMMENT
<b>3.2 ± 0.4 OUR FIT</b>				
<b>3.3 ± 0.5 OUR AVERAGE</b>				
3.6 ± 0.5 ± 0.5		<sup>1</sup> LOUVOT 09	BELL	$e^+ e^- \rightarrow \Upsilon(5S)$
3.0 ± 0.7 ± 0.1		<sup>2</sup> ABULENCIA 07c	CDF	$p\bar{p}$ at 1.96 TeV
6.8 ± 2.2 ± 1.6		DRUTSKOY 07A	BELL	Repl. by LOUVOT 09
3.5 ± 1.1 ± 0.2		<sup>3</sup> ABULENCIA 06j	CDF	Repl. by ABULENCIA 07c
<130	6	<sup>4</sup> AKERS 94j	OPAL	$e^+ e^- \rightarrow Z$
seen	1	BUSKULIC 93G	ALEP	$e^+ e^- \rightarrow Z$

<sup>1</sup> LOUVOT 09 reports  $(3.67_{-0.33}^{+0.35+0.65} - 0.645) \times 10^{-3}$  from a measurement of  $[\Gamma(B_s^0 \rightarrow D_s^- \pi^+) / \Gamma_{\text{total}}] \times [B(\Upsilon(10860) \rightarrow B_s^{(*)} \bar{B}_s^{(*)})]$  assuming  $B(\Upsilon(10860) \rightarrow B_s^{(*)} \bar{B}_s^{(*)}) = (19.5 \pm 2.6) \times 10^{-2}$ , which we rescale to our best value  $B(\Upsilon(10860) \rightarrow B_s^{(*)} \bar{B}_s^{(*)}) = (19.9 \pm 3.0) \times 10^{-2}$ . Our first error is their experiment's error and our second error is the systematic error from using our best value.

<sup>2</sup> ABULENCIA 07c reports  $[\Gamma(B_s^0 \rightarrow D_s^- \pi^+) / \Gamma_{\text{total}}] / [B(B^0 \rightarrow D^- \pi^+)] = 1.13 \pm 0.08 \pm 0.23$  which we multiply by our best value  $B(B^0 \rightarrow D^- \pi^+) = (2.68 \pm 0.13) \times 10^{-3}$ . Our first error is their experiment's error and our second error is the systematic error from using our best value.

<sup>3</sup> ABULENCIA 06j reports  $[\Gamma(B_s^0 \rightarrow D_s^- \pi^+) / \Gamma_{\text{total}}] / [B(B^0 \rightarrow D^- \pi^+)] = 1.32 \pm 0.18 \pm 0.38$  which we multiply by our best value  $B(B^0 \rightarrow D^- \pi^+) = (2.68 \pm 0.13) \times 10^{-3}$ . Our first error is their experiment's error and our second error is the systematic error from using our best value.

<sup>4</sup> AKERS 94j sees  $\leq 6$  events and measures the limit on the product branching fraction  $f(\bar{b} \rightarrow B_s^0) \cdot B(B_s^0 \rightarrow D_s^- \pi^+) < 1.3\%$  at CL = 90%. We divide by our current value  $B(\bar{b} \rightarrow B_s^0) = 0.105$ .

 $\Gamma(D_s^- \rho^+) / \Gamma_{\text{total}}$   $\Gamma_8 / \Gamma$ 

VALUE (units $10^{-3}$ )	DOCUMENT ID	TECN	COMMENT
<b>7.4 ± 1.4 ± 1.0</b>	<sup>1</sup> LOUVOT 10	BELL	$e^+ e^- \rightarrow \Upsilon(5S)$

<sup>1</sup> LOUVOT 10 reports  $[\Gamma(B_s^0 \rightarrow D_s^- \rho^+) / \Gamma_{\text{total}}] / [B(B_s^0 \rightarrow D_s^- \pi^+)] = 2.3 \pm 0.4 \pm 0.2$  which we multiply by our best value  $B(B_s^0 \rightarrow D_s^- \pi^+) = (3.2 \pm 0.4) \times 10^{-3}$ . Our first error is their experiment's error and our second error is the systematic error from using our best value.

# Meson Particle Listings

$B_S^0$

$\Gamma(D_S^- \pi^+ \pi^+ \pi^-) / \Gamma_{\text{total}}$	$\Gamma_9 / \Gamma$
VALUE (units $10^{-3}$ )	DOCUMENT ID TECN COMMENT
<b>6.5 ± 1.2 OUR FIT</b>	
<b>6.7 ± 1.5 ± 0.7</b>	<sup>1</sup> ABULENCIA 07c CDF $p\bar{p}$ at 1.96 TeV

<sup>1</sup> ABULENCIA 07c reports  $[\Gamma(B_S^0 \rightarrow D_S^- \pi^+ \pi^+ \pi^-) / \Gamma_{\text{total}}] / [B(B^0 \rightarrow D^- \pi^+ \pi^+ \pi^-)] = 1.05 \pm 0.10 \pm 0.22$  which we multiply by our best value  $B(B^0 \rightarrow D^- \pi^+ \pi^+ \pi^-) = (6.4 \pm 0.7) \times 10^{-3}$ . Our first error is their experiment's error and our second error is the systematic error from using our best value.

$\Gamma(D_S^- \pi^+ \pi^+ \pi^-) / \Gamma(D_S^- \pi^+)$	$\Gamma_9 / \Gamma_7$
VALUE	DOCUMENT ID TECN COMMENT
<b>2.04 ± 0.35 OUR FIT</b>	
<b>2.01 ± 0.37 ± 0.20</b>	AAIJ 11e LHCb $p\bar{p}$ at 7 TeV

$\Gamma(D_S^+ K^\pm) / \Gamma_{\text{total}}$	$\Gamma_{10} / \Gamma$
VALUE (units $10^{-4}$ )	DOCUMENT ID TECN COMMENT
<b>2.9 ± 0.6 OUR FIT</b>	
<b>2.4 ± 1.2 ± 1.0 ± 0.4</b>	<sup>1</sup> LOUVOT 09 BELL $e^+e^- \rightarrow \Upsilon(5S)$

<sup>1</sup> LOUVOT 09 reports  $(2.4 \pm 1.2 \pm 1.0 \pm 0.4) \times 10^{-4}$  from a measurement of  $[\Gamma(B_S^0 \rightarrow D_S^+ K^\pm) / \Gamma_{\text{total}}] \times [B(\Upsilon(10860) \rightarrow B_S^{(*)} \bar{B}_S^{(*)})]$  assuming  $B(\Upsilon(10860) \rightarrow B_S^{(*)} \bar{B}_S^{(*)}) = (19.5 \pm 2.6) \times 10^{-2}$ , which we rescale to our best value  $B(\Upsilon(10860) \rightarrow B_S^{(*)} \bar{B}_S^{(*)}) = (19.9 \pm 3.0) \times 10^{-2}$ . Our first error is their experiment's error and our second error is the systematic error from using our best value.

$\Gamma(D_S^+ K^\pm) / \Gamma(D_S^+ \pi^+)$	$\Gamma_{10} / \Gamma_7$
VALUE	DOCUMENT ID TECN COMMENT
<b>0.92 ± 0.018 OUR FIT</b>	
<b>0.97 ± 0.018 ± 0.009</b>	AALTONEN 09Aq CDF $p\bar{p}$ at 1.96 TeV

$\Gamma(D_S^+ D_S^-) / \Gamma_{\text{total}}$	$\Gamma_{11} / \Gamma$
VALUE (units $10^{-3}$ ) CL%	DOCUMENT ID TECN COMMENT
<b>5.3 ± 0.9 OUR AVERAGE</b>	
5.1 ± 0.7 ± 0.6	<sup>1</sup> AALTONEN 12c CDF $p\bar{p}$ at 1.96 TeV
10.3 ± 3.9 ± 2.6 ± 3.2 ± 2.5	<sup>2</sup> ESEN 10 BELL $e^+e^- \rightarrow \Upsilon(5S)$

**• • •** We do not use the following data for averages, fits, limits, etc. **• • •**  
 10.4 ± 3.5 ± 3.2 ± 1.1 <sup>3</sup> AALTONEN 08F CDF Repl. by AALTONEN 12c  
 <67 90 DRUTSKOY 07A BELL Repl. by ESEN 10

<sup>1</sup> AALTONEN 12c reports  $(f_S/f_d) (B(B_S^0 \rightarrow D_S^+ D_S^-) / B(B^0 \rightarrow D^- D_S^+)) = 0.183 \pm 0.021 \pm 0.017$ . We multiply this result by our best value of  $B(B^0 \rightarrow D^- D_S^+) = (7.2 \pm 0.8) \times 10^{-3}$  and divide by our best value of  $f_S/f_d$ , where  $1/2 f_S/f_d = 0.131 \pm 0.008$ . Our first quoted uncertainty is the combined experiment's uncertainty and our second is the systematic uncertainty from using our best values.  
<sup>2</sup> Uses  $\Upsilon(10860) \rightarrow B_S^* \bar{B}_S^*$  assuming  $B(\Upsilon(10860) \rightarrow B_S^{(*)} \bar{B}_S^{(*)}) = (19.3 \pm 2.9)\%$  and  $\Gamma(\Upsilon(10860) \rightarrow B_S^* \bar{B}_S^*) / \Gamma(\Upsilon(10860) \rightarrow B_S^{(*)} \bar{B}_S^{(*)}) = (90.1 \pm 3.8)\%$ .  
<sup>3</sup> AALTONEN 08F reports  $[\Gamma(B_S^0 \rightarrow D_S^+ D_S^-) / \Gamma_{\text{total}}] / [B(B^0 \rightarrow D^- D_S^+)] = 1.44 \pm 0.48$  which we multiply by our best value  $B(B^0 \rightarrow D^- D_S^+) = (7.2 \pm 0.8) \times 10^{-3}$ . Our first error is their experiment's error and our second error is the systematic error from using our best value.

$\Gamma(D_S^{*-} \pi^+) / \Gamma_{\text{total}}$	$\Gamma_{12} / \Gamma$
VALUE (units $10^{-3}$ )	DOCUMENT ID TECN COMMENT
<b>2.1 ± 0.5 ± 0.3</b>	<sup>1</sup> LOUVOT 10 BELL $e^+e^- \rightarrow \Upsilon(5S)$

<sup>1</sup> LOUVOT 10 reports  $[\Gamma(B_S^0 \rightarrow D_S^{*-} \pi^+) / \Gamma_{\text{total}}] / [B(B_S^0 \rightarrow D_S^- \pi^+)] = 0.65 \pm 0.15 \pm 0.07$  which we multiply by our best value  $B(B_S^0 \rightarrow D_S^- \pi^+) = (3.2 \pm 0.4) \times 10^{-3}$ . Our first error is their experiment's error and our second error is the systematic error from using our best value.

$\Gamma(D_S^{*-} \rho^+) / \Gamma_{\text{total}}$	$\Gamma_{13} / \Gamma$
VALUE (units $10^{-3}$ )	DOCUMENT ID TECN COMMENT
<b>10.3 ± 2.2 ± 1.4</b>	<sup>1</sup> LOUVOT 10 BELL $e^+e^- \rightarrow \Upsilon(5S)$

<sup>1</sup> LOUVOT 10 reports  $[\Gamma(B_S^0 \rightarrow D_S^{*-} \rho^+) / \Gamma_{\text{total}}] / [B(B_S^0 \rightarrow D_S^- \pi^+)] = 3.2 \pm 0.6 \pm 0.3$  which we multiply by our best value  $B(B_S^0 \rightarrow D_S^- \pi^+) = (3.2 \pm 0.4) \times 10^{-3}$ . Our first error is their experiment's error and our second error is the systematic error from using our best value.

$\Gamma(D_S^{*-} \rho^+) / \Gamma(D_S^- \rho^+)$	$\Gamma_{13} / \Gamma_8$
VALUE	DOCUMENT ID TECN COMMENT
<b>• • •</b> We do not use the following data for averages, fits, limits, etc. <b>• • •</b>	
1.4 ± 0.3 ± 0.1	LOUVOT 10 BELL $e^+e^- \rightarrow \Upsilon(5S)$

$[\Gamma(D_S^{*+} D_S^-) + \Gamma(D_S^{*-} D_S^+)] / \Gamma_{\text{total}}$	$\Gamma_{14} / \Gamma$
VALUE (units $10^{-3}$ ) CL%	DOCUMENT ID TECN COMMENT
<b>12.4 ± 2.1 OUR AVERAGE</b>	
11.7 ± 1.6 ± 1.4	<sup>1</sup> AALTONEN 12c CDF $p\bar{p}$ at 1.96 TeV
27.5 ± 8.3 ± 6.9 ± 7.1	<sup>2</sup> ESEN 10 BELL $e^+e^- \rightarrow \Upsilon(5S)$

**• • •** We do not use the following data for averages, fits, limits, etc. **• • •**  
 <121 90 DRUTSKOY 07A BELL Repl. by ESEN 10

<sup>1</sup> AALTONEN 12c reports  $(f_S/f_d) (B(B_S^0 \rightarrow D_S^{*+} D_S^- + D_S^{*-} D_S^+) / B(B^0 \rightarrow D^- D_S^+)) = 0.424 \pm 0.046 \pm 0.035$ . We multiply this result by our best value of  $B(B^0 \rightarrow D^- D_S^+) = (7.2 \pm 0.8) \times 10^{-3}$  and divide by our best value of  $f_S/f_d$ , where  $1/2 f_S/f_d = 0.131 \pm 0.008$ . Our first quoted uncertainty is the combined experiment's uncertainty and our second is the systematic uncertainty from using our best values.

<sup>2</sup> Uses  $\Upsilon(10860) \rightarrow B_S^* \bar{B}_S^*$  assuming  $B(\Upsilon(10860) \rightarrow B_S^{(*)} \bar{B}_S^{(*)}) = (19.3 \pm 2.9)\%$  and  $\Gamma(\Upsilon(10860) \rightarrow B_S^* \bar{B}_S^*) / \Gamma(\Upsilon(10860) \rightarrow B_S^{(*)} \bar{B}_S^{(*)}) = (90.1 \pm 3.8)\%$ .

$\Gamma(D_S^{*+} D_S^-) / \Gamma_{\text{total}}$	$\Gamma_{15} / \Gamma$
VALUE (units $10^{-3}$ ) CL%	DOCUMENT ID TECN COMMENT
<b>18.8 ± 3.4 OUR AVERAGE</b>	
18.1 ± 2.7 ± 2.2	<sup>1</sup> AALTONEN 12c CDF $p\bar{p}$ at 1.96 TeV
30.8 ± 12.2 ± 8.5 ± 10.4 ± 8.6	<sup>2</sup> ESEN 10 BELL $e^+e^- \rightarrow \Upsilon(5S)$

**• • •** We do not use the following data for averages, fits, limits, etc. **• • •**  
 <257 90 DRUTSKOY 07A BELL Repl. by ESEN 10

<sup>1</sup> AALTONEN 12c reports  $(f_S/f_d) (B(B_S^0 \rightarrow D_S^{*+} D_S^-) / B(B^0 \rightarrow D^- D_S^+)) = 0.654 \pm 0.072 \pm 0.065$ . We multiply this result by our best value of  $B(B^0 \rightarrow D^- D_S^+) = (7.2 \pm 0.8) \times 10^{-3}$  and divide by our best value of  $f_S/f_d$ , where  $1/2 f_S/f_d = 0.131 \pm 0.008$ . Our first quoted uncertainty is the combined experiment's uncertainty and our second is the systematic uncertainty from using our best values.

<sup>2</sup> Uses  $\Upsilon(10860) \rightarrow B_S^* \bar{B}_S^*$  assuming  $B(\Upsilon(10860) \rightarrow B_S^{(*)} \bar{B}_S^{(*)}) = (19.3 \pm 2.9)\%$  and  $\Gamma(\Upsilon(10860) \rightarrow B_S^* \bar{B}_S^*) / \Gamma(\Upsilon(10860) \rightarrow B_S^{(*)} \bar{B}_S^{(*)}) = (90.1 \pm 3.8)\%$ .

$\Gamma(D_S^{*+} D_S^-) / \Gamma_{\text{total}}$	$\Gamma_{16} / \Gamma$
VALUE (%) CL%	DOCUMENT ID TECN COMMENT
<b>4.5 ± 1.4 OUR EVALUATION</b>	
<b>3.7 ± 0.6 OUR AVERAGE</b>	
3.5 ± 0.4 ± 0.4	<sup>1</sup> AALTONEN 12c CDF $p\bar{p}$ at 1.96 TeV
6.85 ± 1.53 ± 1.79 ± 1.30 ± 1.80	<sup>2,3</sup> ESEN 10 BELL $e^+e^- \rightarrow \Upsilon(5S)$
3.5 ± 1.0 ± 1.1	<sup>4</sup> ABAZOV 09i D0 $p\bar{p}$ at 1.96 TeV
14 ± 6 ± 3	<sup>5,6</sup> BARATE 00k ALEP $e^+e^- \rightarrow Z$

**• • •** We do not use the following data for averages, fits, limits, etc. **• • •**  
 3.9 ± 1.9 ± 1.6 ± 1.7 ± 1.5 <sup>4</sup> ABAZOV 07Y D0 Repl. by ABAZOV 09i  
 <0.218 90 BARATE 98q ALEP  $e^+e^- \rightarrow Z$

<sup>1</sup> AALTONEN 12c reports  $(f_S/f_d) (B(B_S^0 \rightarrow D_S^{*+} D_S^-) / B(B^0 \rightarrow D^- D_S^+)) = 1.261 \pm 0.095 \pm 0.112$ . We multiply this result by our best value of  $B(B^0 \rightarrow D^- D_S^+) = (7.2 \pm 0.8) \times 10^{-3}$  and divide by our best value of  $f_S/f_d$ , where  $1/2 f_S/f_d = 0.131 \pm 0.008$ . Our first quoted uncertainty is the combined experiment's uncertainty and our second is the systematic uncertainty from using our best values.

<sup>2</sup> Sum of exclusive  $B_S \rightarrow D_S^+ D_S^-$ ,  $B_S \rightarrow D_S^{*+} D_S^-$  and  $B_S \rightarrow D_S^+ D_S^{*-}$ .

<sup>3</sup> Uses  $\Upsilon(10860) \rightarrow B_S^* \bar{B}_S^*$  assuming  $B(\Upsilon(10860) \rightarrow B_S^{(*)} \bar{B}_S^{(*)}) = (19.3 \pm 2.9)\%$  and  $\Gamma(\Upsilon(10860) \rightarrow B_S^* \bar{B}_S^*) / \Gamma(\Upsilon(10860) \rightarrow B_S^{(*)} \bar{B}_S^{(*)}) = (90.1 \pm 3.8)\%$ .

<sup>4</sup> Uses the final states where  $D_S^+ \rightarrow \phi \pi^+$  and  $D_S^- \rightarrow \phi \mu^- \bar{\nu}_\mu$ .

<sup>5</sup> Reports  $B(B_S^0(\text{short}) \rightarrow D_S^{(*)} D_S^{(*)}) = (0.23 \pm 0.10 \pm 0.05) \cdot [0.17/B(D_S \rightarrow \phi \chi)]^2$  assuming  $B(B_S^0 \rightarrow B_S^0(\text{short})) = 50\%$ . We use our best value of  $B(D_S \rightarrow \phi \chi) = 15.7 \pm 1.0\%$  to obtain the quoted result.

<sup>6</sup> Uses  $\phi\phi$  correlations from  $B_S^0(\text{short}) \rightarrow D_S^{(*)+} D_S^{(*)-}$ .

$\Gamma(\bar{D}^0 \bar{K}^*(892^0) / \Gamma_{\text{total}}$	$\Gamma_{17} / \Gamma$
VALUE (units $10^{-4}$ )	DOCUMENT ID TECN COMMENT
<b>4.7 ± 1.2 ± 0.7</b>	<sup>1</sup> AAIJ 11d LHCb $p\bar{p}$ at 7 TeV

<sup>1</sup> AAIJ 11d reports  $[\Gamma(B_S^0 \rightarrow \bar{D}^0 \bar{K}^*(892^0)) / \Gamma_{\text{total}}] / [B(B^0 \rightarrow \bar{D}^0 \rho^0)] = 1.48 \pm 0.34 \pm 0.19$  which we multiply by our best value  $B(B^0 \rightarrow \bar{D}^0 \rho^0) = (3.2 \pm 0.5) \times 10^{-4}$ . Our first error is their experiment's error and our second error is the systematic error from using our best value.

$\Gamma(J/\psi(1S) \phi) / \Gamma_{\text{total}}$	$\Gamma_{18} / \Gamma$
VALUE (units $10^{-3}$ ) EVTS	DOCUMENT ID TECN COMMENT
<b>1.09 ± 0.28 ± 0.23 OUR FIT</b>	
<b>1.4 ± 0.4 ± 0.1</b>	<sup>1</sup> ABE 96q CDF $p\bar{p}$
<b>• • •</b> We do not use the following data for averages, fits, limits, etc. <b>• • •</b>	
<6	<sup>1</sup> AKERS 94J OPAL $e^+e^- \rightarrow Z$
seen	<sup>14</sup> ABE 93F CDF $p\bar{p}$ at 1.8 TeV
seen	<sup>1</sup> ACTON 92N OPAL Sup. by AKERS 94J

- <sup>1</sup> ABE 96q reports  $[\Gamma(B_s^0 \rightarrow J/\psi(1S)\phi)/\Gamma_{\text{total}}] \times [\Gamma(\bar{B} \rightarrow B_s^0)/[\Gamma(\bar{B} \rightarrow B^+) + \Gamma(\bar{B} \rightarrow B^0)]] = (0.185 \pm 0.055 \pm 0.020) \times 10^{-3}$  which we divide by our best value  $\Gamma(\bar{B} \rightarrow B_s^0)/[\Gamma(\bar{B} \rightarrow B^+) + \Gamma(\bar{B} \rightarrow B^0)] = 0.131 \pm 0.008$ . Our first error is their experiment's error and our second error is the systematic error from using our best value.
- <sup>2</sup> AKERS 94J sees one event and measures the limit on the product branching fraction  $f(\bar{B} \rightarrow B_s^0) \cdot B(B_s^0 \rightarrow J/\psi(1S)\phi) < 7 \times 10^{-4}$  at CL = 90%. We divide by  $\Gamma(\bar{B} \rightarrow B_s^0) = 0.112$ .
- <sup>3</sup> ABE 93F measured using  $J/\psi(1S) \rightarrow \mu^+ \mu^-$  and  $\phi \rightarrow K^+ K^-$ .
- <sup>4</sup> IN ACTON 92N a limit on the product branching fraction is measured to be  $f(\bar{B} \rightarrow B_s^0) \cdot B(B_s^0 \rightarrow J/\psi(1S)\phi) \leq 0.22 \times 10^{-2}$ .

VALUE	CL%	DOCUMENT ID	TECN	COMMENT
$<1.2 \times 10^{-3}$	90	1 ACCIARRI	97c L3	

<sup>1</sup> ACCIARRI 97c assumes  $B^0$  production fraction  $(39.5 \pm 4.0\%)$  and  $B_s$   $(12.0 \pm 3.0\%)$ .

VALUE (units $10^{-4}$ )	CL%	DOCUMENT ID	TECN	COMMENT
$5.10 \pm 0.50 \pm 1.17$ $-0.83$		1 LI	12 BELL	$e^+ e^- \rightarrow \Upsilon(4S)$

• • • We do not use the following data for averages, fits, limits, etc. • • •

VALUE (units $10^{-4}$ )	CL%	DOCUMENT ID	TECN	COMMENT
<38	90	2 ACCIARRI	97c L3	

<sup>1</sup> Observed for the first time with significances over  $10 \sigma$ . The second error are total systematic uncertainties including the error on  $N(B_s^{(*)} \bar{B}_s^{(*)})$ .

<sup>2</sup> ACCIARRI 97c assumes  $B^0$  production fraction  $(39.5 \pm 4.0\%)$  and  $B_s$   $(12.0 \pm 3.0\%)$ .

VALUE (units $10^{-5}$ )	DOCUMENT ID	TECN	COMMENT
$3.6 \pm 0.7 \pm 0.3$	1 AALTONEN 11A	CDF	$p\bar{p}$ at 1.96 TeV

<sup>1</sup> AALTONEN 11A reports  $[\Gamma(B_s^0 \rightarrow J/\psi(1S) K^0)/\Gamma_{\text{total}}] \times [B(\bar{B} \rightarrow B_s^0)] / [B(\bar{B} \rightarrow B^0)] / [B(B^0 \rightarrow J/\psi(1S) K^0)] = 0.0109 \pm 0.0019 \pm 0.0011$  which we multiply or divide by our best values  $B(\bar{B} \rightarrow B_s^0) = (10.5 \pm 0.6) \times 10^{-2}$ ,  $B(\bar{B} \rightarrow B^0) = (40.1 \pm 0.8) \times 10^{-2}$ ,  $B(B^0 \rightarrow J/\psi(1S) K^0) = (8.74 \pm 0.32) \times 10^{-4}$ . Our first error is their experiment's error and our second error is the systematic error from using our best values.

VALUE (units $10^{-5}$ )	DOCUMENT ID	TECN	COMMENT
$9 \pm 4 \pm 1$	1 AALTONEN 11A	CDF	$p\bar{p}$ at 1.96 TeV

<sup>1</sup> AALTONEN 11A reports  $[\Gamma(B_s^0 \rightarrow J/\psi(1S) K^{*0})/\Gamma_{\text{total}}] \times [B(\bar{B} \rightarrow B_s^0)] / [B(\bar{B} \rightarrow B^0)] / [B(B^0 \rightarrow J/\psi(1S) K^{*0})] = 0.0168 \pm 0.0024 \pm 0.0068$  which we multiply or divide by our best values  $B(\bar{B} \rightarrow B_s^0) = (10.5 \pm 0.6) \times 10^{-2}$ ,  $B(\bar{B} \rightarrow B^0) = (40.1 \pm 0.8) \times 10^{-2}$ ,  $B(B^0 \rightarrow J/\psi(1S) K^{*0}) = (1.34 \pm 0.06) \times 10^{-3}$ . Our first error is their experiment's error and our second error is the systematic error from using our best values.

VALUE (units $10^{-4}$ )	DOCUMENT ID	TECN	COMMENT
$3.71 \pm 0.61 \pm 0.85$ $-0.60$	1 LI	12 BELL	$e^+ e^- \rightarrow \Upsilon(4S)$

<sup>1</sup> Observed for the first time with significances over  $10 \sigma$ . The second error are total systematic uncertainties including the error on  $N(B_s^{(*)} \bar{B}_s^{(*)})$ .

VALUE	DOCUMENT ID	TECN	COMMENT
$0.73 \pm 0.14 \pm 0.02$	LI	12 BELL	$e^+ e^- \rightarrow \Upsilon(4S)$

VALUE (units $10^{-4}$ )	DOCUMENT ID	TECN	COMMENT
$1.36 \pm 0.35$ $-0.28$ OUR FIT			

VALUE	DOCUMENT ID	TECN	COMMENT
$1.16 \pm 0.31 \pm 0.30$ $-0.19 - 0.25$	1 LI	11 BELL	$e^+ e^- \rightarrow \Upsilon(5S)$

<sup>1</sup> The second error includes both the detector systematic and the uncertainty in the number of produced  $\Upsilon(5S) \rightarrow B_s^{(*)} \bar{B}_s^{(*)}$  pairs.

VALUE	DOCUMENT ID	TECN	COMMENT
$0.125 \pm 0.010$ OUR FIT $0.126 \pm 0.010$ OUR AVERAGE			

VALUE	DOCUMENT ID	TECN	COMMENT
$0.135 \pm 0.036 \pm 0.001$	1 ABAZOV 12c	D0	$p\bar{p}$ at 1.96 TeV
$0.123 \pm 0.025 \pm 0.001$ $-0.022$	2 AAIJ 11	LHCB	$pp$ at 7 TeV
$0.126 \pm 0.012 \pm 0.001$	3 AALTONEN 11AB	CDF	$p\bar{p}$ at 1.96 TeV

<sup>1</sup> ABAZOV 12c reports  $[\Gamma(B_s^0 \rightarrow J/\psi(1S) \phi_0(980), \phi_0 \rightarrow \pi^+ \pi^-)/\Gamma(B_s^0 \rightarrow J/\psi(1S) \phi)] / [B(\phi(1020) \rightarrow K^+ K^-)] = 0.275 \pm 0.041 \pm 0.061$  which we multiply by our best value  $B(\phi(1020) \rightarrow K^+ K^-) = (48.9 \pm 0.5) \times 10^{-2}$ . Our first error is their experiment's error and our second error is the systematic error from using our best value.

<sup>2</sup> AAIJ 11 reports  $[\Gamma(B_s^0 \rightarrow J/\psi(1S) \phi_0(980), \phi_0 \rightarrow \pi^+ \pi^-)/\Gamma(B_s^0 \rightarrow J/\psi(1S) \phi)] / [B(\phi(1020) \rightarrow K^+ K^-)] = 0.252 \pm 0.046 \pm 0.027$   
 $-0.032 - 0.033$  which we multiply by our best value  $B(\phi(1020) \rightarrow K^+ K^-) = (48.9 \pm 0.5) \times 10^{-2}$ . Our first error is their experiment's error and our second error is the systematic error from using our best value.

<sup>3</sup> AALTONEN 11AB reports  $[\Gamma(B_s^0 \rightarrow J/\psi(1S) \phi_0(980), \phi_0 \rightarrow \pi^+ \pi^-)/\Gamma(B_s^0 \rightarrow J/\psi(1S) \phi)] / [B(\phi(1020) \rightarrow K^+ K^-)] = 0.257 \pm 0.020 \pm 0.014$  which we multiply by our best value  $B(\phi(1020) \rightarrow K^+ K^-) = (48.9 \pm 0.5) \times 10^{-2}$ . Our first error is their experiment's error and our second error is the systematic error from using our best value.

VALUE (units $10^{-4}$ )	DOCUMENT ID	TECN	COMMENT
$0.34 \pm 0.11 \pm 0.085$ $-0.14 - 0.054$	1 LI	11 BELL	$e^+ e^- \rightarrow \Upsilon(5S)$

<sup>1</sup> The second error includes both the detector systematic and the uncertainty in the number of produced  $\Upsilon(5S) \rightarrow B_s^{(*)} \bar{B}_s^{(*)}$  pairs.

VALUE (units $10^{-4}$ )	EVTS	DOCUMENT ID	TECN	COMMENT
< 12		1 LI	11 BELL	$e^+ e^- \rightarrow \Upsilon(5S)$

• • • We do not use the following data for averages, fits, limits, etc. • • •

VALUE	DOCUMENT ID	TECN	COMMENT
seen	1 BUSKULIC 93G	ALEP	$e^+ e^- \rightarrow Z$

VALUE	DOCUMENT ID	TECN	COMMENT
$0.53 \pm 0.10$ OUR AVERAGE			

VALUE	DOCUMENT ID	TECN	COMMENT
$0.53 \pm 0.10 \pm 0.09$	ABAZOV 09Y	D0	$p\bar{p}$ at 1.96 TeV
$0.52 \pm 0.13 \pm 0.07$	ABULENCIA 06W	CDF	$p\bar{p}$ at 1.96 TeV

VALUE (units $10^{-6}$ )	CL%	DOCUMENT ID	TECN	COMMENT
< 1.2	90	1 AALTONEN 09c	CDF	$p\bar{p}$ at 1.96 TeV

• • • We do not use the following data for averages, fits, limits, etc. • • •

VALUE	DOCUMENT ID	TECN	COMMENT
< 12	90	2 PENG 10	BELL $e^+ e^- \rightarrow \Upsilon(5S)$
< 1.7	90	3 ABULENCIA,A 06D	CDF Repl. by AALTONEN 09c
< 232	90	4 ABE 00c	SLD $e^+ e^- \rightarrow Z$
< 170	90	5 BUSKULIC 96V	ALEP $e^+ e^- \rightarrow Z$

<sup>1</sup> Obtains this result from  $(f_s/f_d) \cdot B(B_s \rightarrow \pi^+ \pi^-)/B(B^0 \rightarrow K^+ \pi^-) = 0.007 \pm 0.004 \pm 0.005$ , assuming  $f_s/f_d = 0.276 \pm 0.034$  and  $B(B^0 \rightarrow K^+ \pi^-) = (19.4 \pm 0.6) \times 10^{-6}$ .

<sup>2</sup> Uses  $\Upsilon(10860) \rightarrow B_s^* \bar{B}_s^*$  and assumes  $B(\Upsilon(10860) \rightarrow B_s^{(*)} \bar{B}_s^{(*)}) = (19.3 \pm 2.9)\%$  and  $\Gamma(\Upsilon(10860) \rightarrow B_s^{(*)} \bar{B}_s^{(*)}) / \Gamma(\Upsilon(10860) \rightarrow B_s^{(*)} \bar{B}_s^{(*)}) = (90.1 \pm 3.8)\%$ .

<sup>3</sup> ABULENCIA,A 06D obtains this from  $B(B_s \rightarrow \pi^+ \pi^-) / B(B_s \rightarrow K^+ K^-) < 0.05$  at 90% CL, assuming  $B(B_s \rightarrow K^+ K^-) = (33 \pm 6 \pm 7) \times 10^{-6}$ .

<sup>4</sup> ABE 00c assumes  $B(Z \rightarrow b\bar{b}) = (21.7 \pm 0.1)\%$  and the  $B$  fractions  $f_{B^0} = f_{B^+} = (39.7 \pm 1.8)\%$  and  $f_{B_s} = (10.5 \pm 1.8)\%$ .

<sup>5</sup> BUSKULIC 96V assumes PDG 96 production fractions for  $B^0, B^+, B_s, b$  baryons.

VALUE	CL%	DOCUMENT ID	TECN	COMMENT
$<2.1 \times 10^{-4}$	90	1 ACCIARRI 95H	L3	$e^+ e^- \rightarrow Z$

<sup>1</sup> ACCIARRI 95H assumes  $f_{B^0} = 39.5 \pm 4.0$  and  $f_{B_s} = 12.0 \pm 3.0\%$ .

VALUE	CL%	DOCUMENT ID	TECN	COMMENT
$<1.0 \times 10^{-3}$	90	1 ACCIARRI 95H	L3	$e^+ e^- \rightarrow Z$

<sup>1</sup> ACCIARRI 95H assumes  $f_{B^0} = 39.5 \pm 4.0$  and  $f_{B_s} = 12.0 \pm 3.0\%$ .

VALUE	CL%	DOCUMENT ID	TECN	COMMENT
$<1.5 \times 10^{-3}$	90	1 ACCIARRI 95H	L3	$e^+ e^- \rightarrow Z$

<sup>1</sup> ACCIARRI 95H assumes  $f_{B^0} = 39.5 \pm 4.0$  and  $f_{B_s} = 12.0 \pm 3.0\%$ .

VALUE	CL%	DOCUMENT ID	TECN	COMMENT
$<3.20 \times 10^{-4}$	90	1 ABE 00c	SLD	$e^+ e^- \rightarrow Z$

<sup>1</sup> ABE 00c assumes  $B(Z \rightarrow b\bar{b}) = (21.7 \pm 0.1)\%$  and the  $B$  fractions  $f_{B^0} = f_{B^+} = (39.7 \pm 1.8)\%$  and  $f_{B_s} = (10.5 \pm 1.8)\%$ .

VALUE	CL%	DOCUMENT ID	TECN	COMMENT
$<6.17 \times 10^{-4}$	90	1 ABE 00c	SLD	$e^+ e^- \rightarrow Z$

<sup>1</sup> ABE 00c assumes  $B(Z \rightarrow b\bar{b}) = (21.7 \pm 0.1)\%$  and the  $B$  fractions  $f_{B^0} = f_{B^+} = (39.7 \pm 1.8)\%$  and  $f_{B_s} = (10.5 \pm 1.8)\%$ .



- <sup>6</sup> Uses  $B$  production ratio  $f(\bar{B} \rightarrow B^+)/f(\bar{B} \rightarrow B_s^0) = 3.86 \pm 0.59$ , and the number of  $B^+ \rightarrow J/\psi K^+$  decays.  
<sup>7</sup> Uses  $B$  production ratio  $f(\bar{B} \rightarrow B^+)/f(\bar{B} \rightarrow B_s^0) = 3.86 \pm 0.54$  and the number of  $B^+ \rightarrow J/\psi K^+$  decays.  
<sup>8</sup> Assumes production cross-section  $\sigma(B_s)/\sigma(B^+) = 0.270 \pm 0.034$ .  
<sup>9</sup> Assumes production cross section  $\sigma(B^+)/\sigma(B_s) = 3.71 \pm 0.41$  and  $B(B^+ \rightarrow J/\psi K^+ \rightarrow \mu^+ \mu^- K^+) = (5.88 \pm 0.26) \times 10^{-5}$ .  
<sup>10</sup> Assumes production cross-section  $\sigma(B_s)/\sigma(B^+) = 0.100/0.391$  and the CDF measured value of  $\sigma(B^+) = 3.6 \pm 0.6 \mu\text{b}$ .  
<sup>11</sup> ABE 98 assumes production of  $\sigma(B^0) = \sigma(B^+)$  and  $\sigma(B_s)/\sigma(B^0) = 1/3$ . They normalize to their measured  $\sigma(B^0, \rho_T(B) > 6, |y| < 1.0) = 2.39 \pm 0.32 \pm 0.44 \mu\text{b}$ .  
<sup>12</sup> ACCIARRI 97B assume PDG 96 production fractions for  $B^+, B^0, B_s$ , and  $\Lambda_b$ .  
<sup>13</sup> ABE 96L assumes  $B^+/B_s$  production ratio 3/1. They normalize to their measured  $\sigma(B^+, \rho_T(B) > 6 \text{ GeV}/c, |y| < 1) = 2.39 \pm 0.54 \mu\text{b}$ .

**$\Gamma(e^+e^-)/\Gamma_{\text{total}}$**   **$\Gamma_{44}/\Gamma$**   
 Test for  $\Delta B = 1$  weak neutral current.

VALUE	CL%	DOCUMENT ID	TECN	COMMENT
$<2.8 \times 10^{-7}$	90	AALTONEN 09P	CDF	$p\bar{p}$ at 1.96 TeV
• • • We do not use the following data for averages, fits, limits, etc. • • •				
$<5.4 \times 10^{-5}$	90	<sup>1</sup> ACCIARRI 97B	L3	$e^+e^- \rightarrow Z$
<sup>1</sup> ACCIARRI 97B assume PDG 96 production fractions for $B^+, B^0, B_s$ , and $\Lambda_b$ .				

**$\Gamma(e^\pm \mu^\mp)/\Gamma_{\text{total}}$**   **$\Gamma_{45}/\Gamma$**   
 Test of lepton family number conservation.

VALUE	CL%	DOCUMENT ID	TECN	COMMENT
$<2.0 \times 10^{-7}$	90	AALTONEN 09P	CDF	$p\bar{p}$ at 1.96 TeV
• • • We do not use the following data for averages, fits, limits, etc. • • •				
$<6.1 \times 10^{-6}$	90	ABE 98v	CDF	Repl. by AALTONEN 09P
$<4.1 \times 10^{-5}$	90	<sup>1</sup> ACCIARRI 97B	L3	$e^+e^- \rightarrow Z$
<sup>1</sup> ACCIARRI 97B assume PDG 96 production fractions for $B^+, B^0, B_s$ , and $\Lambda_b$ .				

**$\Gamma(\phi(1020)\mu^+\mu^-)/\Gamma_{\text{total}}$**   **$\Gamma_{46}/\Gamma$**   
 Test for  $\Delta B = 1$  weak neutral current.

VALUE	CL%	DOCUMENT ID	TECN	COMMENT
• • • We do not use the following data for averages, fits, limits, etc. • • •				
$<3.2 \times 10^{-6}$	90	<sup>1</sup> ABAZOV 06G	D0	$p\bar{p}$ at 1.96 TeV
$<4.7 \times 10^{-5}$	90	ACOSTA 02D	CDF	$p\bar{p}$ at 1.8 TeV
<sup>1</sup> Uses $B(B_s^0 \rightarrow J/\psi\phi) = 9.3 \times 10^{-4}$ .				

**$\Gamma(\phi(1020)\mu^+\mu^-)/\Gamma(J/\psi(1S)\phi)$**   **$\Gamma_{46}/\Gamma_{18}$**

VALUE (units $10^{-3}$ )	CL%	DOCUMENT ID	TECN	COMMENT
$1.13 \pm 0.19 \pm 0.07$		AALTONEN 11AI	CDF	$p\bar{p}$ at 1.96 TeV
• • • We do not use the following data for averages, fits, limits, etc. • • •				
$1.11 \pm 0.25 \pm 0.09$		AALTONEN 11L	CDF	Repl. by AALTONEN 11AI
$<2.3$	90	AALTONEN 09B	CDF	Repl. by AALTONEN 11L

**$\Gamma(\phi\nu\bar{\nu})/\Gamma_{\text{total}}$**   **$\Gamma_{47}/\Gamma$**   
 Test for  $\Delta B = 1$  weak neutral current.

VALUE	CL%	DOCUMENT ID	TECN	COMMENT
$<5.4 \times 10^{-3}$	90	<sup>1</sup> ADAM 96D	DLPH	$e^+e^- \rightarrow Z$
<sup>1</sup> ADAM 96D assumes $f_{B^0} = f_{B^-} = 0.39$ and $f_{B_s} = 0.12$ .				

**POLARIZATION IN  $B_s^0$  DECAY**

**$\Gamma_L/\Gamma$  in  $B_s^0 \rightarrow D_s^* \rho^+$**

VALUE	DOCUMENT ID	TECN	COMMENT
$1.05 \pm 0.08 + 0.03 - 0.10 - 0.04$	LOUVOT 10	BELL	$e^+e^- \rightarrow \Upsilon(5S)$

**$\Gamma_L/\Gamma$  in  $B_s^0 \rightarrow J/\psi(1S)\phi$**

VALUE	EVTS	DOCUMENT ID	TECN	COMMENT
<b><math>0.543 \pm 0.016</math> OUR AVERAGE</b>				Error includes scale factor of 1.2.
$0.524 \pm 0.013 \pm 0.015$		<sup>1</sup> AALTONEN 12D	CDF	$p\bar{p}$ at 1.96 TeV
$0.558 + 0.017 - 0.019$		<sup>1,2</sup> ABAZOV 12D	D0	$p\bar{p}$ at 1.96 TeV
$0.61 \pm 0.14 \pm 0.02$		<sup>3</sup> AFFOLDER 00N	CDF	$p\bar{p}$ at 1.8 TeV
$0.56 \pm 0.21 + 0.02 - 0.04$	19	ABE 95Z	CDF	$p\bar{p}$ at 1.8 TeV
• • • We do not use the following data for averages, fits, limits, etc. • • •				
$0.555 \pm 0.027 \pm 0.006$		<sup>4</sup> ABAZOV 09E	D0	Repl. by ABAZOV 12D
$0.531 \pm 0.020 \pm 0.007$		<sup>1</sup> AALTONEN 08J	CDF	Repl. by AALTONEN 12D
$0.62 \pm 0.06 \pm 0.01$		ACOSTA 05	CDF	Repl. by AALTONEN 08J

- <sup>1</sup> Measured using the time-dependent angular analysis of  $B_s^0 \rightarrow J/\psi\phi$  decays.  
<sup>2</sup> The error includes both statistical and systematic uncertainties.  
<sup>3</sup> AFFOLDER 00N measurements are based on 40  $B_s^0$  candidates obtained from a data sample of 89 pb<sup>-1</sup>. The  $P$ -wave fraction is found to be  $0.23 \pm 0.19 \pm 0.04$ .  
<sup>4</sup> Measured the angular and lifetime parameters for the time-dependent angular untagged decays  $B_d^0 \rightarrow J/\psi K^{*0}$  and  $B_s^0 \rightarrow J/\psi\phi$ .

**$\Gamma_{\perp}/\Gamma$  in  $B_s^0 \rightarrow J/\psi(1S)\phi$**

VALUE	DOCUMENT ID	TECN	COMMENT
<b><math>0.231 \pm 0.016</math> OUR AVERAGE</b>			
$0.231 \pm 0.014 \pm 0.015$	<sup>1</sup> AALTONEN 12D	CDF	$p\bar{p}$ at 1.96 TeV
$0.231 + 0.024 - 0.030$	<sup>1,2</sup> ABAZOV 12D	D0	$p\bar{p}$ at 1.96 TeV
• • • We do not use the following data for averages, fits, limits, etc. • • •			
$0.244 \pm 0.032 \pm 0.014$	<sup>3</sup> ABAZOV 09E	D0	Repl. by ABAZOV 12D
$0.239 \pm 0.029 \pm 0.011$	<sup>1</sup> AALTONEN 08J	CDF	Repl. by AALTONEN 12D
$0.125 \pm 0.069 \pm 0.002$	ACOSTA 05	CDF	Repl. by AALTONEN 08J
<sup>1</sup> Measured using the time-dependent angular analysis of $B_s^0 \rightarrow J/\psi\phi$ decays.			
<sup>2</sup> The error includes both statistical and systematic uncertainties.			
<sup>3</sup> Measured the angular and lifetime parameters for the time-dependent angular untagged decays $B_d^0 \rightarrow J/\psi K^{*0}$ and $B_s^0 \rightarrow J/\psi\phi$ .			

**$\phi_{\parallel}$  in  $B_s^0 \rightarrow J/\psi(1S)\phi$**

VALUE (rad)	DOCUMENT ID	TECN	COMMENT
<b><math>3.15 \pm 0.22</math></b>	<sup>1</sup> ABAZOV 12D	D0	$p\bar{p}$ at 1.96 TeV
• • • We do not use the following data for averages, fits, limits, etc. • • •			
$2.72 + 1.12 - 0.27 \pm 0.26$	ABAZOV 09E	D0	Repl. by ABAZOV 12D
<sup>1</sup> The error includes both statistical and systematic uncertainties.			

**$\Gamma_L/\Gamma$  in  $B_s^0 \rightarrow \phi\phi$**

VALUE	DOCUMENT ID	TECN	COMMENT
<b><math>0.348 \pm 0.041 \pm 0.021</math></b>	AALTONEN 11AN	CDF	$p\bar{p}$ at 1.96 TeV

**$\Gamma_{\perp}/\Gamma$  in  $B_s^0 \rightarrow \phi\phi$**

VALUE	DOCUMENT ID	TECN	COMMENT
<b><math>0.365 \pm 0.044 \pm 0.027</math></b>	AALTONEN 11AN	CDF	$p\bar{p}$ at 1.96 TeV

**$\phi_{\parallel}$  in  $B_s^0 \rightarrow \phi\phi$**

VALUE (rad)	DOCUMENT ID	TECN	COMMENT
$2.71 + 0.31 - 0.36 \pm 0.22$	<sup>1</sup> AALTONEN 11AN	CDF	$p\bar{p}$ at 1.96 TeV
<sup>1</sup> AALTONEN 11AN quotes $\cos\phi_{\parallel} = -0.91 + 0.15 - 0.13 \pm 0.09$ which we convert to $\phi_{\parallel}$ taking the smaller solution.			

**$\Gamma_L/\Gamma$  in  $B_s^0 \rightarrow K^{*0}\bar{K}^{*0}$**

VALUE	DOCUMENT ID	TECN	COMMENT
<b><math>0.31 \pm 0.12 \pm 0.04</math></b>	AAIJ 12F	LHCB	$p\bar{p}$ at 7 TeV

**$\Gamma_{\perp}/\Gamma$  in  $B_s^0 \rightarrow K^{*0}\bar{K}^{*0}$**

VALUE	DOCUMENT ID	TECN	COMMENT
<b><math>0.38 \pm 0.11 \pm 0.04</math></b>	AAIJ 12F	LHCB	$p\bar{p}$ at 7 TeV

**$B_s^0\bar{B}_s^0$  MIXING**

For a discussion of  $B_s^0\bar{B}_s^0$  mixing see the note on " $B^0\bar{B}^0$  Mixing" in the  $B^0$  Particle Listings above.

$\chi_s$  is a measure of the time-integrated  $B_s^0\bar{B}_s^0$  mixing probability that produced  $B_s^0(\bar{B}_s^0)$  decays as a  $\bar{B}_s^0(B_s^0)$ . Mixing violates  $\Delta B \neq 2$  rule.

$$\chi_s = \frac{x_s^2}{2(1+x_s^2)}$$

$$\chi_s = \frac{\Delta m_{B_s^0}}{\Gamma_{B_s^0}} = (m_{B_{sH}^0} - m_{B_{sL}^0}) \tau_{B_s^0}$$

where  $H, L$  stand for heavy and light states of two  $B_s^0$  CP eigenstates and

$$\tau_{B_s^0} = \frac{1}{0.5(\Gamma_{B_{sH}^0} + \Gamma_{B_{sL}^0})}$$

**$\Delta m_{B_s^0} = m_{B_{sH}^0} - m_{B_{sL}^0}$**

$\Delta m_{B_s^0}$  is a measure of  $2\pi$  times the  $B_s^0\bar{B}_s^0$  oscillation frequency in time-dependent mixing experiments.

"OUR EVALUATION" is provided by the Heavy Flavor Averaging Group (HFAG) by taking into account correlations between measurements.

**$\chi_s$  in  $B_s^0$**

VALUE ( $10^{12} \text{ fs}^{-1}$ )	CL%	DOCUMENT ID	TECN	COMMENT
<b><math>17.69 \pm 0.08</math> OUR EVALUATION</b>				
<b><math>17.69 \pm 0.08</math> OUR AVERAGE</b>				
$17.63 \pm 0.11 \pm 0.02$		<sup>1</sup> AAIJ 12I	LHCB	$p\bar{p}$ at 7 TeV
$17.77 \pm 0.10 \pm 0.07$		<sup>2</sup> ABULENCIA,A 06G	CDF	$p\bar{p}$ at 1.96 TeV

## Meson Particle Listings

 $B_S^0$ 

• • • We do not use the following data for averages, fits, limits, etc. • • •

17-21	90	<sup>3</sup> ABAZOV	06B D0	$p\bar{p}$ at 1.96 TeV
$17.31^{+0.33}_{-0.18} \pm 0.07$		<sup>4</sup> ABULENCIA	06Q CDF	Repl. by ABULENCIA, A 06G
> 8.0	95	<sup>5</sup> ABDALLAH	04J DLPH	$e^+e^- \rightarrow Z^0$
> 4.9	95	<sup>6</sup> ABDALLAH	04J DLPH	$e^+e^- \rightarrow Z^0$
> 8.5	95	<sup>7</sup> ABDALLAH	04J DLPH	$e^+e^- \rightarrow Z^0$
> 5.0	95	<sup>8</sup> ABDALLAH	03B DLPH	$e^+e^- \rightarrow Z$
>10.3	95	<sup>9</sup> ABE	03 SLD	$e^+e^- \rightarrow Z$
>10.9	95	<sup>10</sup> HEISTER	03E ALEP	$e^+e^- \rightarrow Z$
> 5.3	95	<sup>11</sup> ABE	02V SLD	$e^+e^- \rightarrow Z$
> 1.0	95	<sup>12</sup> ABBIENDI	01D OPAL	$e^+e^- \rightarrow Z$
> 7.4	95	<sup>13</sup> ABREU	00Y DLPH	Repl. by ABDALLAH 04J
> 4.0	95	<sup>14</sup> ABREU,P	00G DLPH	$e^+e^- \rightarrow Z$
> 5.2	95	<sup>15</sup> ABBIENDI	99S OPAL	$e^+e^- \rightarrow Z$
<96	95	<sup>16</sup> ABE	99D CDF	$p\bar{p}$ at 1.8 TeV
> 5.8	95	<sup>17</sup> ABE	99J CDF	$p\bar{p}$ at 1.8 TeV
> 9.6	95	<sup>18</sup> BARATE	99J ALEP	$e^+e^- \rightarrow Z$
> 7.9	95	<sup>19</sup> BARATE	98C ALEP	Repl. by BARATE 99J
> 3.1	95	<sup>20</sup> ACKERSTAFF	97U OPAL	Repl. by ABBIENDI 99S
> 2.2	95	<sup>21</sup> ACKERSTAFF	97V OPAL	Repl. by ABBIENDI 99S
> 6.5	95	<sup>22</sup> ADAM	97 DLPH	Repl. by ABREU 00Y
> 6.6	95	<sup>23</sup> BUSKULIC	96M ALEP	Repl. by BARATE 98C
> 2.2	95	<sup>21</sup> AKERS	95J OPAL	Sup. by ACKERSTAFF 97V
> 5.7	95	<sup>24</sup> BUSKULIC	95J ALEP	$e^+e^- \rightarrow Z$
> 1.8	95	<sup>21</sup> BUSKULIC	94B ALEP	$e^+e^- \rightarrow Z$

- Measured using  $B_S^0 \rightarrow D_S^- \pi^+ + D_S^- \pi^+ \pi^- \pi^+$  decays.
- Significance of oscillation signal is  $5.4 \sigma$ . Also reports  $|V_{td} / V_{ts}| = 0.2060 \pm 0.0007^{+0.0081}_{-0.0060}$ .
- A likelihood scan over the oscillation frequency,  $\Delta m_s$ , gives a most probable value of  $19 \text{ ps}^{-1}$  and a range of  $17 < \Delta m_s < 21 (\text{ps}^{-1})$  at 90% C.L. assuming Gaussian uncertainties. Also excludes  $\Delta m_s < 14.8 \text{ ps}^{-1}$  at 95% C.L.
- Significance of oscillation signal is 0.2%. Also reported the value  $|V_{td} / V_{ts}| = 0.208^{+0.001+0.008}_{-0.002-0.006}$ .
- Uses leptons emitted with large momentum transverse to a jet and improved techniques for vertexing and flavor-tagging.
- Updates of  $D_S$ -lepton analysis.
- Combined results from all Delphi analyses.
- Events with a high transverse momentum lepton were removed and an inclusively reconstructed vertex was required.
- ABE 03 uses the novel "charge dipole" technique to reconstruct separate secondary and tertiary vertices originating from the  $B \rightarrow D$  decay chain. The analysis excludes  $\Delta m_s < 4.9 \text{ ps}^{-1}$  and  $7.9 < \Delta m_s < 10.3 \text{ ps}^{-1}$ .
- Three analyses based on complementary event selections: (1) fully-reconstructed hadronic decays; (2) semileptonic decays with  $D_S$  exclusively reconstructed; (3) inclusive semileptonic decays.
- ABE 02V uses exclusively reconstructed  $D_S^-$  mesons and excludes  $\Delta m_s < 1.4 \text{ ps}^{-1}$  and  $2.4 < \Delta m_s < 5.3 \text{ ps}^{-1}$  at 95% CL.
- Uses fully or partially reconstructed  $D_S \ell$  vertices and a mixing tag as a flavor tagging.
- Replaced by ABDALLAH 04A. Uses  $D_S^- \ell^+$ , and  $\phi \ell^+$  vertices, and a multi-variable discriminant as a flavor tagging.
- Uses inclusive  $D_S$  vertices and fully reconstructed  $B_S$  decays and a multi-variable discriminant as a flavor tagging.
- Uses  $\ell$ - $Q_{\text{hem}}$  and  $\ell$ - $\ell$ .
- ABE 99D assumes  $\tau_{B_S^0} = 1.55 \pm 0.05 \text{ ps}$  and  $\Delta\Gamma/\Delta m = (5.6 \pm 2.6) \times 10^{-3}$ .
- ABE 99J uses  $\phi$   $\ell$ - $\ell$  correlation.
- BARATE 99J uses combination of an inclusive lepton and  $D_S^-$ -based analyses.
- BARATE 98C combines results from  $D_S h\ell/Q_{\text{hem}}$ ,  $D_S hK$  in the same side,  $D_S \ell/Q_{\text{hem}}$  and  $D_S \ell K$  in the same side.
- Uses  $\ell$ - $Q_{\text{hem}}$ .
- Uses  $\ell$ - $\ell$ .
- ADAM 97 combines results from  $D_S \ell$ - $Q_{\text{hem}}$ ,  $\ell$ - $Q_{\text{hem}}$ , and  $\ell$ - $\ell$ .
- BUSKULIC 96M uses  $D_S$  lepton correlations and lepton, kaon, and jet charge tags.
- BUSKULIC 95J uses  $\ell$ - $Q_{\text{hem}}$ . They find  $\Delta m_s > 5.6 [ > 6.1 ]$  for  $f_S = 10\% [12\%]$ . We interpolate to our central value  $f_S = 10.5\%$ .

$$x_s = \Delta m_{B_S^0} / \Gamma_{B_S^0}$$

This is derived by the Heavy Flavor Averaging Group (HFAG) from the results on  $\Delta m_{B_S^0}$  and "OUR EVALUATION" of the  $B_S^0$  mean lifetime.

VALUE	DOCUMENT ID
<b>26.49 ± 0.29 OUR EVALUATION</b>	

 $X_s$ 

This is a  $B_S^0 \bar{B}_S^0$  integrated mixing parameter derived from  $x_s$  above and OUR EVALUATION of  $\Delta\Gamma_{B_S^0}/\Gamma_{B_S^0}$ .

VALUE	DOCUMENT ID
<b>0.499292 ± 0.000016 OUR EVALUATION</b>	

CP VIOLATION PARAMETERS in  $B_S^0$ 

$$\text{Re}(\epsilon_{B_S^0}) / (1 + |\epsilon_{B_S^0}|^2)$$

CP impurity in  $B_S^0$  system.

"OUR EVALUATION" is an average using rescaled values of the data listed below. The average and rescaling were performed by the Heavy Flavor Averaging Group (HFAG) and are described at <http://www.slac.stanford.edu/xorg/hfag/>. The averaging/scaling procedure takes into account correlation between the measurements. The value has been obtained from a 2D fit of the  $B_d$  and  $B_s$  asymmetries, which includes the  $B_s$  measurements listed below and the  $B$  factory average for the  $B_d$ .

VALUE (units $10^{-3}$ )	DOCUMENT ID	TECN	COMMENT
<b>-2.6 ± 1.6 OUR EVALUATION</b>			
<b>-2.2 ± 2.0 OUR AVERAGE</b>			Error includes scale factor of 1.1.
-4.5 ± 2.7	<sup>1</sup> ABAZOV	11U D0	$p\bar{p}$ at 1.96 TeV
-0.4 ± 2.3 ± 0.4	<sup>2</sup> ABAZOV	10E D0	$p\bar{p}$ at 1.96 TeV
• • • We do not use the following data for averages, fits, limits, etc. • • •			
-3.6 ± 1.9	<sup>3</sup> ABAZOV	10H D0	Repl. by ABAZOV 11U
6.1 ± 4.8 ± 0.9	<sup>4</sup> ABAZOV	07A D0	Repl. by ABAZOV 10E

- Uses the dimuon charge asymmetry with different impact parameters from which it reports  $A_{SL}^{\mu\mu} = (-18.1 \pm 10.6) \times 10^{-3}$ .
- ABAZOV 10E reports a measurement of flavor-specific asymmetry in  $B_S^0 \rightarrow \mu^+ D_{(s)}^{*-} X$  decays with a decay-time analysis including initial-state flavor tagging,  $A_{SL}^{\mu\mu} = (-1.7 \pm 9.1^{+1.4}_{-1.5}) \times 10^{-3}$  which is approximately equal to  $4 \times \text{Re}(\epsilon_{B_S^0}) / (1 + |\epsilon_{B_S^0}|^2)$ .
- ABAZOV 10H reports a measurement of like-sign dimuon charge asymmetry of  $A_{SL}^{\mu\mu} = (-9.57 \pm 2.51 \pm 1.46) \times 10^{-3}$  in semileptonic  $b$ -hadron decays. Using the measured production ratio of  $B_d^0$  and  $B_s^0$ , and the asymmetry of  $B_d^0 A_{SL}^{\mu\mu} = (-4.7 \pm 4.6) \times 10^{-3}$  measured from  $B$ -factories, they obtain the asymmetry for  $B_S^0$ .
- The first direct measurement of the time integrated flavor untagged charge asymmetry in semileptonic  $B_S^0$  decays is reported as  $2x A_{SL}^{\mu\mu}(\text{untagged}) = A_{SL}^{\mu\mu} = (2.45 \pm 1.93 \pm 0.35) \times 10^{-2}$ .

CP Violation phase  $\beta_s$ 

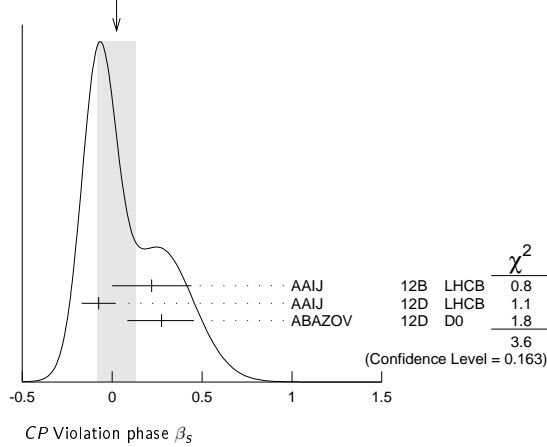
$-2\beta_s$  is the weak phase difference between  $B_S^0$  mixing amplitude and the  $B_S^0 \rightarrow J/\psi \phi$  decay amplitude. The Standard Model value of  $\beta_s$  is  $\arg(-\frac{V_{ts}V_{cb}^*}{V_{cs}V_{cb}^*})$ .

"OUR EVALUATION" is an average using rescaled values of the data listed below. The average and rescaling were performed by the Heavy Flavor Averaging Group (HFAG) and are described at <http://www.slac.stanford.edu/xorg/hfag/>. The averaging/scaling procedure takes into account correlation between the measurements.

VALUE	DOCUMENT ID	TECN	COMMENT
<b>0.08 ± 0.05</b>			
<b>-0.07</b>			
<b>0.02 ± 0.11 OUR AVERAGE</b>			Error includes scale factor of 1.3. See the ideogram below.
0.22 ± 0.22 ± 0.01	<sup>1</sup> AAIJ	12B LHCB	$p\bar{p}$ at 7 TeV
-0.075 ± 0.09 ± 0.03	<sup>2</sup> AAIJ	12D LHCB	$p\bar{p}$ at 7 TeV
	<sup>3</sup> AALTONEN	12D CDF	$p\bar{p}$ at 1.96 TeV
$0.275^{+0.18}_{-0.19}$	<sup>4,5,6</sup> ABAZOV	12D D0	$p\bar{p}$ at 1.96 TeV
• • • We do not use the following data for averages, fits, limits, etc. • • •			
	<sup>7</sup> AALTONEN	08G CDF	Repl. by AALTONEN 12D
0.28 $^{+0.12}_{-0.15} +^{0.04}_{-0.01}$	<sup>5,8</sup> ABAZOV	08AMD0	Repl. by ABAZOV 12D
0.395 ± 0.280 $^{+0.005}_{-0.070}$	<sup>6,9</sup> ABAZOV	07 D0	Repl. by ABAZOV 07N
0.35 $^{+0.20}_{-0.24}$	<sup>6,10</sup> ABAZOV	07N D0	Repl. by ABAZOV 08AM

- Reports  $\phi_s = -2\beta_s = -0.44 \pm 0.44 \pm 0.02$  that was measured using a time-dependent fit to  $B_S^0 \rightarrow J/\psi f_0(980)$  decays.
- Reports  $\phi_s = -2\beta_s = 0.15 \pm 0.18 \pm 0.06$  that was measured using a time-dependent angular analysis of  $B_S^0 \rightarrow J/\psi \phi$  decays.
- Reports  $0.02 < \phi_s < 0.52$  or  $1.08 < \phi_s < 1.55$  at 68% C.L. confidence regions in the two-dimensional space of  $\phi_s$  and  $\Delta\Gamma_{B_S^0}$  from  $B_S^0 \rightarrow J/\psi \phi$  decays.
- The error includes both statistical and systematic uncertainties.
- Measured using fully reconstructed  $B_S \rightarrow J/\psi \phi$  decays.
- Reports  $\phi_s$  which equals to  $-2\beta_s$ .
- Reports  $0.32 < 2\beta_s < 2.82$  at 68% C.L. and confidence regions in the two-dimensional space of  $2\beta_s$  and  $\Delta\Gamma$  from the first measurement of  $B_S^0 \rightarrow J/\psi \phi$  decays using flavor tagging. The probability of a deviation from SM prediction as large as the level of observed data is 15%.
- Reports  $\phi_s = -2\beta_s$  and obtains 90% CL interval  $-0.03 < \beta_s < 0.60$ .
- The first direct measurement of the CP-violating mixing phase is reported from the time-dependent analysis of flavor untagged  $B_S^0 \rightarrow J/\psi \phi$  decays.
- Combines D0 collaboration measurements of time-dependent angular distributions in  $B_S^0 \rightarrow J/\psi \phi$  and charge asymmetry in semileptonic decays. There is a 4-fold ambiguity in the solution.

WEIGHTED AVERAGE 0.02±0.11 (Error scaled by 1.3)



A<sub>CP</sub>(B<sub>s</sub> → π<sup>+</sup>K<sup>-</sup>) A<sub>CP</sub> is defined as

B(B<sub>s</sub><sup>0</sup> → f) - B(B<sub>s</sub><sup>0</sup> → f-bar) / (B(B<sub>s</sub><sup>0</sup> → f) + B(B<sub>s</sub><sup>0</sup> → f-bar))

the CP-violation asymmetry of exclusive B<sub>s</sub><sup>0</sup> and B<sub>s</sub><sup>0</sup> decay.

Table with columns: VALUE, DOCUMENT ID, TECN, COMMENT. Row: 0.39 ± 0.15 ± 0.08, AALTONEN 11N, CDF, p-pbar at 1.96 TeV

PARTIAL BRANCHING FRACTIONS IN B<sub>s</sub> → phi l+ l-

B(B<sub>s</sub> → phi l+ l-) (q^2 < 2.0 GeV^2/c^2)

Table with columns: VALUE (units 10^-7), DOCUMENT ID, TECN, COMMENT. Row: 2.76 ± 0.95 ± 0.89, AALTONEN 11AI, CDF, p-pbar at 1.96 TeV

B(B<sub>s</sub> → phi l+ l-) (2.0 < q^2 < 4.3 GeV^2/c^2)

Table with columns: VALUE (units 10^-7), DOCUMENT ID, TECN, COMMENT. Row: 0.58 ± 0.55 ± 0.19, AALTONEN 11AI, CDF, p-pbar at 1.96 TeV

B(B<sub>s</sub> → phi l+ l-) (4.3 < q^2 < 8.68 GeV^2/c^2)

Table with columns: VALUE (units 10^-7), DOCUMENT ID, TECN, COMMENT. Row: 1.34 ± 0.83 ± 0.43, AALTONEN 11AI, CDF, p-pbar at 1.96 TeV

B(B<sub>s</sub> → phi l+ l-) (10.09 < q^2 < 12.86 GeV^2/c^2)

Table with columns: VALUE (units 10^-7), DOCUMENT ID, TECN, COMMENT. Row: 2.98 ± 0.95 ± 0.95, AALTONEN 11AI, CDF, p-pbar at 1.96 TeV

B(B<sub>s</sub> → phi l+ l-) (14.18 < q^2 < 16.0 GeV^2/c^2)

Table with columns: VALUE (units 10^-7), DOCUMENT ID, TECN, COMMENT. Row: 1.86 ± 0.66 ± 0.59, AALTONEN 11AI, CDF, p-pbar at 1.96 TeV

B(B<sub>s</sub> → phi l+ l-) (16.0 < q^2 GeV^2/c^2)

Table with columns: VALUE (units 10^-7), DOCUMENT ID, TECN, COMMENT. Row: 2.32 ± 0.76 ± 0.74, AALTONEN 11AI, CDF, p-pbar at 1.96 TeV

B(B<sub>s</sub> → phi l+ l-) (1.0 < q^2 < 6.0 GeV^2/c^2)

Table with columns: VALUE (units 10^-7), DOCUMENT ID, TECN, COMMENT. Row: 1.14 ± 0.79 ± 0.36, AALTONEN 11AI, CDF, p-pbar at 1.96 TeV

B(B<sub>s</sub> → phi l+ l-) (0.0 < q^2 < 4.3 GeV^2/c^2)

Table with columns: VALUE (units 10^-7), DOCUMENT ID, TECN, COMMENT. Row: 3.30 ± 1.09 ± 1.05, AALTONEN 11AI, CDF, p-pbar at 1.96 TeV

Main reference table listing authors, document IDs, and techniques for various B meson decays. Includes entries for AALTONEN, ABZOV, CHATRCHYAN, LI, etc.

B<sub>s</sub><sup>0</sup> REFERENCES

Reference table listing authors, document IDs, and techniques for B<sub>s</sub><sup>0</sup> decays. Includes entries for AAIJ, AALTONEN, ABZOV, etc.

## Meson Particle Listings

 $B_s^0, B_s^*, B_{s1}(5830)^0, B_{s2}^*(5840)^0, B_{sJ}^*(5850)$ BUSKULIC 92E PL B294 145  
LEE-FRANZINI 90 PRL 65 2947D. Buskulic et al.  
J. Lee-Franzini et al.(ALEPH Collab.)  
(CUSB II Collab.) $B_s^*$ 

$$I(J^P) = 0(1^-)$$

$I, J, P$  need confirmation. Quantum numbers shown are quark-model predictions.

 $B_s^*$  MASS

From mass difference below and the  $B_s^0$  mass.

VALUE (MeV)	DOCUMENT ID	TECN	COMMENT
<b>5415.4<math>^{+2.4}_{-2.1}</math> OUR FIT</b>			Error includes scale factor of 3.0.
<b>5415.8<math>\pm 1.5</math> OUR AVERAGE</b>			Error includes scale factor of 2.6.
5416.4 $\pm 0.4 \pm 0.5$	LOUVOT 09	BELL	$e^+e^- \rightarrow \Upsilon(5S)$
5411.7 $\pm 1.6 \pm 0.6$	1 AQUINES 06	CLEO	$e^+e^- \rightarrow \Upsilon(5S)$
• • • We do not use the following data for averages, fits, limits, etc. • • •			
5418 $\pm 1 \pm 3$	DRUTSKOY 07A	BELL	Repl. by LOUVOT 09
5414 $\pm 1 \pm 3$	2 BONVICINI 06	CLEO	$e^+e^- \rightarrow \Upsilon(5S)$
1 Utilized the beam constrained invariant mass peak positions for $B_s^*$ and $B_s^*$ to extract the measurement.			
2 Uses 14 candidates consistent with $B_s$ decays into final states with a $J/\psi$ and a $D_s^{(*)-}$ .			

$$m_{B_s^*} - m_{B_s}$$

VALUE (MeV)	DOCUMENT ID	TECN	COMMENT
<b>48.7<math>^{+2.3}_{-2.1}</math> OUR FIT</b>			Error includes scale factor of 2.8.
<b>46.1<math>\pm 1.5</math> OUR AVERAGE</b>			
45.7 $\pm 1.7 \pm 0.7$	3 AQUINES 06	CLEO	$e^+e^- \rightarrow \Upsilon(5S)$
47.0 $\pm 2.6$	4 LEE-FRANZINI 90	CSB2	$e^+e^- \rightarrow \Upsilon(5S)$
• • • We do not use the following data for averages, fits, limits, etc. • • •			
48 $\pm 1 \pm 3$	5 BONVICINI 06	CLEO	Repl. by AQUINES 06
3 Utilized the beam constrained invariant mass peak positions for $B_s^*$ and $B_s^*$ to extract the measurement.			
4 LEE-FRANZINI 90 measure 46.7 $\pm 0.4 \pm 0.2$ MeV for an admixture of $B_s^0, B_s^+$ , and $B_s$ . They use the shape of the photon line to separate the above value for $B_s$ .			
5 Uses 14 candidates consistent with $B_s$ decays into final states with a $J/\psi$ and a $D_s^{(*)-}$ .			

$$|(m_{B_s^*} - m_{B_s}) - (m_{B_s^*} - m_B)|$$

VALUE (MeV)	CL%	DOCUMENT ID	TECN	COMMENT
<6	95	ABREU 95R	DLPH	$E_{cm}^{ee} = 88-94$ GeV

 $B_s^*$  DECAY MODES

Mode	Fraction ( $\Gamma_i/\Gamma$ )
$\Gamma_1 B_s \gamma$	dominant

 $B_s^*$  REFERENCES

LOUVOT 09 PRL 102 021801	R. Louvot et al.	(BELLE Collab.)
DRUTSKOY 07A PR D76 012002	A. Drutskoy et al.	(BELLE Collab.)
AQUINES 06 PRL 96 152001	O. Aquines et al.	(CLEO Collab.)
BONVICINI 06 PRL 96 022002	G. Bonvicini et al.	(CLEO Collab.)
ABREU 95R ZPHY C68 353	P. Abreu et al.	(DELPHI Collab.)
LEE-FRANZINI 90 PRL 65 2947	J. Lee-Franzini et al.	(CUSB II Collab.)

 $B_{s1}(5830)^0$ 

$$I(J^P) = 0(1^+) \text{ Status: } ***$$

$I, J, P$  need confirmation.

Quantum numbers shown are quark-model predictions.

 $B_{s1}(5830)^0$  MASS

VALUE (MeV)	DOCUMENT ID	TECN	COMMENT
<b>5829.4<math>\pm 0.7</math></b>	1 AALTONEN 08k	CDF	$p\bar{p}$ at 1.96 TeV
1 Uses two-body decays into $K^-$ and $B^+$ mesons reconstructed as $B^+ \rightarrow J/\psi K^+$ , $J/\psi \rightarrow \mu^+ \mu^-$ or $B^+ \rightarrow \bar{D}^0 \pi^+, \bar{D}^0 \rightarrow K^+ \pi^-$ .			
$m_{B_{s1}^0} - m_{B^{*+}}$			
VALUE (MeV)	DOCUMENT ID	TECN	COMMENT
<b>504.41<math>\pm 0.21 \pm 0.14</math></b>	2 AALTONEN 08k	CDF	$p\bar{p}$ at 1.96 TeV
2 Uses two-body decays into $K^-$ and $B^+$ mesons reconstructed as $B^+ \rightarrow J/\psi K^+$ , $J/\psi \rightarrow \mu^+ \mu^-$ or $B^+ \rightarrow \bar{D}^0 \pi^+, \bar{D}^0 \rightarrow K^+ \pi^-$ .			

 $B_{s1}(5830)^0$  DECAY MODES

Mode	Fraction ( $\Gamma_i/\Gamma$ )
$\Gamma_1 B^{*+} K^-$	dominant

 $B_{s1}(5830)^0$  BRANCHING RATIOS

$\Gamma(B^{*+} K^-)/\Gamma_{\text{total}}$	DOCUMENT ID	TECN	COMMENT	$\Gamma_1/\Gamma$
dominant	AALTONEN	08k	CDF	$p\bar{p}$ at 1.96 TeV

 $B_{s1}(5830)^0$  REFERENCES

AALTONEN 08k PRL 100 082001	T. Aaltonen et al.	(CDF Collab.)
-----------------------------	--------------------	---------------

 $B_{s2}^*(5840)^0$ 

$$I(J^P) = 0(2^+) \text{ Status: } ***$$

$I, J, P$  need confirmation.

Quantum numbers shown are quark-model predictions.

 $B_{s2}^*(5840)^0$  MASS

VALUE (MeV)	DOCUMENT ID	TECN	COMMENT
<b>5839.7<math>\pm 0.6</math> OUR AVERAGE</b>			
5839.7 $\pm 0.7$	1 AALTONEN 08k	CDF	$p\bar{p}$ at 1.96 TeV
5839.6 $\pm 1.1 \pm 0.7$	2 ABAZOV 08E	D0	$p\bar{p}$ at 1.96 TeV
1 Uses two-body decays into $K^-$ and $B^+$ mesons reconstructed as $B^+ \rightarrow J/\psi K^+$ , $J/\psi \rightarrow \mu^+ \mu^-$ or $B^+ \rightarrow \bar{D}^0 \pi^+, \bar{D}^0 \rightarrow K^+ \pi^-$ .			
2 Observed in $B_{s2}^{*0} \rightarrow B^+ K^-$ . Measured production rate of $B_{s2}^{*0}$ relative to $B^+$ to be (1.15 $\pm 0.23 \pm 0.13$ )%.			

$$m_{B_{s2}^{*0}} - m_{B_{s1}^0}$$

VALUE (MeV)	DOCUMENT ID	TECN	COMMENT
<b>10.5<math>\pm 0.6</math></b>	3 AALTONEN 08k	CDF	$p\bar{p}$ at 1.96 TeV
3 Uses two-body decays into $K^-$ and $B^+$ mesons reconstructed as $B^+ \rightarrow J/\psi K^+$ , $J/\psi \rightarrow \mu^+ \mu^-$ or $B^+ \rightarrow \bar{D}^0 \pi^+, \bar{D}^0 \rightarrow K^+ \pi^-$ .			

 $B_{s2}^*(5840)^0$  DECAY MODES

Mode	Fraction ( $\Gamma_i/\Gamma$ )
$\Gamma_1 B^+ K^-$	dominant

 $B_{s2}^*(5840)^0$  BRANCHING RATIOS

$\Gamma(B^+ K^-)/\Gamma_{\text{total}}$	DOCUMENT ID	TECN	COMMENT	$\Gamma_1/\Gamma$
dominant	AALTONEN 08k	CDF	$p\bar{p}$ at 1.96 TeV	
dominant	4 ABAZOV 08E	D0	$p\bar{p}$ at 1.96 TeV	
4 Measured production rate of $B_{s2}^{*0}$ relative to $B^+$ to be (1.15 $\pm 0.23 \pm 0.13$ )%.				

 $B_{s2}^*(5840)^0$  REFERENCES

AALTONEN 08k PRL 100 082001	T. Aaltonen et al.	(CDF Collab.)
ABAZOV 08E PRL 100 082002	V.M. Abazov et al.	(D0 Collab.)

 $B_{sJ}^*(5850)$ 

$$I(J^P) = ?(?^?)$$

$I, J, P$  need confirmation.

OMITTED FROM SUMMARY TABLE

Signal can be interpreted as coming from  $\bar{b}s$  states. Needs confirmation.

 $B_{sJ}^*(5850)$  MASS

VALUE (MeV)	EVTS	DOCUMENT ID	TECN	COMMENT
<b>5853<math>\pm 15</math></b>	141	AKERS 95E	OPAL	$E_{cm}^{ee} = 88-94$ GeV

 $B_{sJ}^*(5850)$  WIDTH

VALUE (MeV)	EVTS	DOCUMENT ID	TECN	COMMENT
<b>47<math>\pm 22</math></b>	141	AKERS 95E	OPAL	$E_{cm}^{ee} = 88-94$ GeV

 $B_{sJ}^*(5850)$  REFERENCES

AKERS 95E ZPHY C66 19	R. Akers et al.	(OPAL Collab.)
-----------------------	-----------------	----------------



# BOTTOM, CHARMED MESONS ( $B = C = \pm 1$ )

$$B_c^+ = c\bar{b}, B_c^- = \bar{c}b, \text{ similarly for } B_c^{*s}$$

$$B_c^\pm$$

$$I(J^P) = 0(0^-)$$

$I, J, P$  need confirmation.

Quantum numbers shown are quark-model predictions.

### $B_c^\pm$ MASS

VALUE (GeV)	DOCUMENT ID	TECN	COMMENT
<b>6.277 ± 0.006 OUR AVERAGE</b>	Error includes scale factor of 1.6.		
6.2756 ± 0.0029 ± 0.0025	<sup>1</sup> AALTONEN 08M	CDF	$p\bar{p}$ at 1.96 TeV
6.300 ± 0.014 ± 0.005	<sup>1</sup> ABAZOV 08T	D0	$p\bar{p}$ at 1.96 TeV
6.4 ± 0.39 ± 0.13	<sup>2</sup> ABE 98M	CDF	$p\bar{p}$ at 1.8 TeV
••• We do not use the following data for averages, fits, limits, etc. •••			
6.2857 ± 0.0053 ± 0.0012	<sup>1</sup> ABULENCIA 06c	CDF	Repl. by AALTONEN 08M
6.32 ± 0.06	<sup>3</sup> ACKERSTAFF 98o	OPAL	$e^+e^- \rightarrow Z$

- <sup>1</sup> Measured using a fully reconstructed decay mode of  $B_c \rightarrow J/\psi\pi$ .
- <sup>2</sup> ABE 98M observed  $20.4 \pm 6.2$  events in the  $B_c^+ \rightarrow J/\psi(1S)\ell\nu_\ell$  with a significance of  $> 4.8$  standard deviations. The mass value is estimated from  $m(J/\psi(1S)\ell)$ .
- <sup>3</sup> ACKERSTAFF 98o observed 2 candidate events in the  $B_c \rightarrow J/\psi(1S)\pi^+$  channel with an estimated background of 0.63 ± 0.20 events.

### $B_c^\pm$ MEAN LIFE

"OUR EVALUATION" is an average using rescaled values of the data listed below. The average and rescaling were performed by the Heavy Flavor Averaging Group (HFAG) and are described at <http://www.slac.stanford.edu/xorg/hfag/>. The averaging/rescaling procedure takes into account correlations between the measurements.

VALUE ( $10^{-12}$ s)	DOCUMENT ID	TECN	COMMENT
<b>0.453 ± 0.041 OUR EVALUATION</b>			
<b>0.45 ± 0.04 OUR AVERAGE</b>			
$0.448^{+0.038}_{-0.036} \pm 0.032$	<sup>4</sup> ABAZOV 09H	D0	$p\bar{p}$ at 1.96 TeV
$0.463^{+0.073}_{-0.065} \pm 0.036$	<sup>5</sup> ABULENCIA 06o	CDF	$p\bar{p}$ at 1.96 TeV
$0.46^{+0.18}_{-0.16} \pm 0.03$	<sup>5</sup> ABE 98M	CDF	$p\bar{p}$ 1.8 TeV

- <sup>4</sup> The lifetime is measured from the  $J/\psi\mu$  decay vertices.
- <sup>5</sup> The lifetime is measured from the  $J/\psi e$  decay vertices.

### $B_c^\pm$ DECAY MODES × $B(\bar{b} \rightarrow B_c)$

$B_c^-$  modes are charge conjugates of the modes below.

Mode	Fraction ( $\Gamma_i/\Gamma$ )	Confidence level
The following quantities are not pure branching ratios; rather the fraction $\Gamma_i/\Gamma \times B(\bar{b} \rightarrow B_c)$ .		
$\Gamma_1$ $J/\psi(1S)\ell^+\nu_\ell$ anything	$(5.2^{+2.4}_{-2.1}) \times 10^{-5}$	
$\Gamma_2$ $J/\psi(1S)\pi^+$	$< 8.2$	90%
$\Gamma_3$ $J/\psi(1S)\pi^+\pi^+\pi^-$	$< 5.7$	$\times 10^{-4}$
$\Gamma_4$ $J/\psi(1S)a_1(1260)$	$< 1.2$	$\times 10^{-3}$
$\Gamma_5$ $D^*(2010)^+\bar{D}^0$	$< 6.2$	$\times 10^{-3}$

### $B_c^\pm$ BRANCHING RATIOS

$\Gamma(J/\psi(1S)\ell^+\nu_\ell \text{ anything})/\Gamma_{\text{total}} \times B(\bar{b} \rightarrow B_c)$	$\Gamma_i/\Gamma \times B$			
VALUE	CL%	DOCUMENT ID	TECN	COMMENT
<b><math>(5.2^{+2.4}_{-2.1}) \times 10^{-5}</math></b>		<sup>6</sup> ABE 98M	CDF	$p\bar{p}$ 1.8 TeV
••• We do not use the following data for averages, fits, limits, etc. •••				
$< 1.6$	$\times 10^{-4}$	<sup>7</sup> ACKERSTAFF 98o	OPAL	$e^+e^- \rightarrow Z$
$< 1.9$	$\times 10^{-4}$	<sup>8</sup> ABREU 97E	DLPH	$e^+e^- \rightarrow Z$
$< 1.2$	$\times 10^{-4}$	<sup>9</sup> BARATE 97H	ALEP	$e^+e^- \rightarrow Z$

- <sup>6</sup> ABE 98M result is derived from the measurement of  $[\sigma(B_c) \times B(B_c \rightarrow J/\psi(1S)\ell\nu_\ell)] / [\sigma(B^+) \times B(B^+ \rightarrow J/\psi(1S)K^+)] = 0.132 \pm 0.041$  (stat)  $\pm 0.031$  (sys)  $\pm 0.032$  (lifetime) by using PDG 98 values of  $B(b \rightarrow B^+)$  and  $B(B^+ \rightarrow J/\psi(1S)K^+)$ .
- <sup>7</sup> ACKERSTAFF 98o reports  $B(Z \rightarrow B_c X)/B(Z \rightarrow qq) \times B(B_c \rightarrow J/\psi(1S)\ell\nu_\ell) < 6.95 \times 10^{-5}$  at 90%CL. We rescale to our PDG 98 values of  $B(Z \rightarrow b\bar{b})$ .
- <sup>8</sup> ABREU 97E value listed is for an assumed  $\tau_{B_c} = 0.4$  ps and improves to  $1.6 \times 10^{-4}$  for  $\tau_{B_c} = 1.4$  ps.
- <sup>9</sup> BARATE 97H reports  $B(Z \rightarrow B_c X)/B(Z \rightarrow qq) \times B(B_c \rightarrow J/\psi(1S)\ell\nu_\ell) < 5.2 \times 10^{-5}$  at 90%CL. We rescale to our PDG 96 values of  $B(Z \rightarrow b\bar{b})$ . A  $B_c^+ \rightarrow J/\psi(1S)\mu^+\nu_\mu$  candidate event is found, compared to all the known background sources  $2 \times 10^{-3}$ , which gives  $m_{B_c} = 5.96^{+0.25}_{-0.19}$  GeV and  $\tau_{B_c} = 1.77 \pm 0.17$  ps.

### $\Gamma(J/\psi(1S)\pi^+)/\Gamma_{\text{total}} \times B(\bar{b} \rightarrow B_c)$

VALUE	CL%	DOCUMENT ID	TECN	COMMENT
<b><math>&lt; 8.2 \times 10^{-5}</math></b>	90	<sup>10</sup> BARATE 97H	ALEP	$e^+e^- \rightarrow Z$
••• We do not use the following data for averages, fits, limits, etc. •••				
$< 2.4 \times 10^{-4}$	90	<sup>11</sup> ACKERSTAFF 98o	OPAL	$e^+e^- \rightarrow Z$
$< 3.4 \times 10^{-4}$	90	<sup>12</sup> ABREU 97E	DLPH	$e^+e^- \rightarrow Z$
$< 2.0 \times 10^{-5}$	95	<sup>13</sup> ABE 96R	CDF	$p\bar{p}$ 1.8 TeV

- <sup>10</sup> BARATE 97H reports  $B(Z \rightarrow B_c X)/B(Z \rightarrow qq) \times B(B_c \rightarrow J/\psi(1S)\pi) < 3.6 \times 10^{-5}$  at 90%CL. We rescale to our PDG 96 values of  $B(Z \rightarrow b\bar{b})$ .
- <sup>11</sup> ACKERSTAFF 98o reports  $B(Z \rightarrow B_c X)/B(Z \rightarrow qq) \times B(B_c \rightarrow J/\psi(1S)\pi^+) < 1.06 \times 10^{-4}$  at 90%CL. We rescale to our PDG 98 values of  $B(Z \rightarrow b\bar{b})$ .
- <sup>12</sup> ABREU 97E value listed is for an assumed  $\tau_{B_c} = 0.4$  ps and improves to  $2.7 \times 10^{-4}$  for  $\tau_{B_c} = 1.4$  ps.
- <sup>13</sup> ABE 96R reports  $B(b \rightarrow B_c X)/B(b \rightarrow B^+ X) \times B(B_c^+ \rightarrow J/\psi(1S)\pi^+)/B(B^+ \rightarrow J/\psi(1S)K^+) < 0.053$  at 95%CL for  $\tau_{B_c} = 0.8$  ps. It changes from 0.15 to 0.04 for 0.17 ps  $< \tau_{B_c} < 1.6$  ps. We rescale to our PDG 96 values of  $B(b \rightarrow B^+) = 0.378 \pm 0.022$  and  $B(B^+ \rightarrow J/\psi(1S)K^+) = 0.00101 \pm 0.00014$ .

### $\Gamma(J/\psi(1S)\pi^+\pi^+\pi^-)/\Gamma_{\text{total}} \times B(\bar{b} \rightarrow B_c)$

VALUE	CL%	DOCUMENT ID	TECN	COMMENT
<b><math>&lt; 5.7 \times 10^{-4}</math></b>	90	<sup>14</sup> ABREU 97E	DLPH	$e^+e^- \rightarrow Z$

- <sup>14</sup> ABREU 97E value listed is independent of  $0.4 \text{ ps} < \tau_{B_c} < 1.4$  ps.

### $\Gamma(J/\psi(1S)a_1(1260))/\Gamma_{\text{total}} \times B(\bar{b} \rightarrow B_c)$

VALUE	CL%	DOCUMENT ID	TECN	COMMENT
<b><math>&lt; 1.2 \times 10^{-3}</math></b>	90	<sup>15</sup> ACKERSTAFF 98o	OPAL	$e^+e^- \rightarrow Z$

- <sup>15</sup> ACKERSTAFF 98o reports  $B(Z \rightarrow B_c X)/B(Z \rightarrow qq) \times B(B_c \rightarrow J/\psi(1S)a_1(1260)) < 5.29 \times 10^{-4}$  at 90%CL. We rescale to our PDG 98 values of  $B(Z \rightarrow b\bar{b})$ .

### $\Gamma(D^*(2010)^+\bar{D}^0)/\Gamma_{\text{total}} \times B(\bar{b} \rightarrow B_c)$

VALUE	CL%	DOCUMENT ID	TECN	COMMENT
<b><math>&lt; 6.2 \times 10^{-3}</math></b>	90	<sup>16</sup> BARATE 98Q	ALEP	$e^+e^- \rightarrow Z$

- <sup>16</sup> BARATE 98Q reports  $B(Z \rightarrow B_c X) \times B(B_c \rightarrow D^*(2010)^+\bar{D}^0) < 1.9 \times 10^{-3}$  at 90%CL. We rescale to our PDG 98 values of  $B(Z \rightarrow b\bar{b})$ .

### $B_c^\pm$ REFERENCES

ABAZOV 09H	PRL 102 092001	V.M. Abazov et al.	(D0 Collab.)
AALTONEN 08M	PRL 100 182002	T. Aaltonen et al.	(CDF Collab.)
ABAZOV 08T	PRL 101 012001	V.M. Abazov et al.	(D0 Collab.)
ABULENCIA 06C	PRL 96 082002	A. Abulencia et al.	(CDF Collab.)
ABULENCIA 06O	PRL 97 012002	A. Abulencia et al.	(CDF Collab.)
ABE 98M	PRL 81 2432	F. Abe et al.	(CDF Collab.)
Also	PR D58 112004	F. Abe et al.	(CDF Collab.)
ACKERSTAFF 98O	PL B420 157	K. Ackerstaff et al.	(OPAL Collab.)
BARATE 98Q	EPJ C4 387	R. Barate et al.	(ALEPH Collab.)
PDG 98	EPJ C3 1	C. Caso et al.	(DELPHI Collab.)
ABREU 97E	PL B398 207	P. Abreu et al.	(DELPHI Collab.)
BARATE 97H	PL B402 213	R. Barate et al.	(ALEPH Collab.)
ABE 96R	PRL 77 5176	F. Abe et al.	(CDF Collab.)
PDG 96	PR D54 1	R. M. Barnett et al.	(CDF Collab.)

### DEVELOPMENTS IN HEAVY QUARKONIUM SPECTROSCOPY

Written May 2012 by S. Eidelman (Budker Inst. and Novosibirsk State Univ.), B.K. Heltsley (Cornell Univ.), J.J. Hernandez-Rey (Univ. Valencia-CSIC), S. Navas (Univ. Granada), and C. Patrignani (Univ. Genova, INFN).

A golden age for heavy quarkonium physics dawned a decade ago, initiated by the confluence of exciting advances in quantum chromodynamics (QCD) and an explosion of related experimental activity. The subsequent broad spectrum of breakthroughs, surprises, and continuing puzzles had not been anticipated. In that period, the BESII program concluded only

# Meson Particle Listings

## Heavy Quarkonium Spectroscopy

to give birth to BESIII; the  $B$ -factories and CLEO-c flourished; quarkonium production and polarization measurements at HERA and the Tevatron matured; and heavy-ion collisions at RHIC opened a window on the deconfinement regime. For an extensive presentation of the status of heavy quarkonium physics, the reader is referred to several reviews [1–7], the last of which covers developments through the middle of 2010, and which supplies some tabular information and phrasing reproduced here (with kind permission, copyright 2011, Springer). This note focuses solely on experimental developments in heavy quarkonium spectroscopy, and in particular on those too recent to have been included in Ref. 7.

Table 1 lists properties of newly observed conventional heavy quarkonium states, where “newly” is interpreted to mean within the past decade. The  $h_c$  is the  $^1P_1$  state of charmonium, singlet partner of the long-known  $\chi_{cJ}$  triplet  $^3P_J$ . The  $\eta_c(2S)$  is the first excited state of the pseudoscalar ground state  $\eta_c(1S)$ , lying just below the mass of its vector counterpart,  $\psi(2S)$ . The state originally dubbed  $Z(3930)$  is now regarded by many as the first observed  $2P$  state of  $\chi_{cJ}$ , the  $\chi_{c2}(2P)$ . The first  $B$ -meson seen that contains charm is the  $B_c^+$ . The ground state of bottomonium is the  $\eta_b(1S)$ , recently confirmed with a second observation of more than  $5\sigma$  significance. The  $\Upsilon(1D)$  is the lowest-lying  $D$ -wave triplet of the  $b\bar{b}$  system.

**Table 1:** New *conventional* states in the  $c\bar{c}$ ,  $b\bar{c}$ , and  $b\bar{b}$  regions, ordered by mass. Masses  $m$  and widths  $\Gamma$  represent the weighted averages from the listed sources. Quoted uncertainties reflect quadrature summation from individual experiments. In the Process column, the decay mode of the new state claimed is indicated in parentheses. Ellipses (...) indicate inclusively selected event topologies; *i.e.*, additional particles not required by the Experiments to be present. A question mark (?) indicates an unmeasured value. For each Experiment a citation is given, as well as the statistical significance in number of standard deviations ( $\#\sigma$ ), or “(np)” for “not provided”. The Year column gives the date of first measurement cited. The Status column indicates that the state has been observed by at most one (NC!-needs confirmation) or at least two independent experiments with significance of  $>5\sigma$  (OK). The state labelled  $\chi_{c2}(2P)$  has previously been called  $Z(3930)$ . See also the reviews in [1–7]. Adapted from [7] with kind permission, copyright (2011), Springer.

State	$m$ (MeV)	$\Gamma$ (MeV)	$J^{PC}$	Process (mode)	Experiment ( $\#\sigma$ )	Year	Status
$h_c(1P)$	$3525.41 \pm 0.16$	$<1$	$1^{+-}$	$\psi(2S) \rightarrow \pi^0(\gamma\eta_c(1S))$	CLEO [8–10] (13.2)	2004	OK
				$\psi(2S) \rightarrow \pi^0(\gamma\dots)$	CLEO [8–10] (10), BES [11] (19)		
				$p\bar{p} \rightarrow (\gamma\eta_c) \rightarrow (\gamma\gamma\gamma)$	E835 [12] (3.1)		
				$\psi(2S) \rightarrow \pi^0(\dots)$	BESIII [11] (9.5)		
$\eta_c(2S)$	$3638.9 \pm 1.3$	$10 \pm 4$	$0^{-+}$	$B \rightarrow K(K_S^0 K^- \pi^+)$	Belle [13,14] (6.0)	2002	OK
				$e^+e^- \rightarrow e^+e^-(K_S^0 K^- \pi^+)$	BABAR [15,16] (7.8), CLEO [17] (6.5), Belle [18] (6)		
				$e^+e^- \rightarrow J/\psi(\dots)$	BABAR [19] (np), Belle [20] (8.1)		
$\chi_{c2}(2P)$	$3927.2 \pm 2.6$	$24 \pm 6$	$2^{++}$	$e^+e^- \rightarrow e^+e^-(D\bar{D})$	Belle [21] (5.3), BABAR [22,23] (5.8)	2005	OK
$B_c^+$	$6277 \pm 6$	-	$0^-$	$\bar{p}p \rightarrow (\pi^+ J/\psi)\dots$	CDF [24,25] (8.0), D0 [26] (5.2)	2007	OK
$\eta_b(1S)$	$9395.8 \pm 3.0$	$12.4_{-5.7}^{+12.7}$	$0^{-+}$	$\Upsilon(3S) \rightarrow \gamma(\dots)$	BABAR [27] (10), CLEO [28] (4.0)	2008	OK
				$\Upsilon(2S) \rightarrow \gamma(\dots)$	BABAR [29] (3.0)		
				$\Upsilon(5S) \rightarrow \pi^+\pi^-\gamma(\dots)$	Belle [30] (14)		
$h_b(1P)$	$9898.6 \pm 1.4$	?	$1^{+-}$	$\Upsilon(5S) \rightarrow \pi^+\pi^-(\dots)$	Belle [31,30] (5.5)	2011	NC!
				$\Upsilon(3S) \rightarrow \pi^0(\dots)$	BABAR [32] (3.0)		
$\Upsilon(1^3D_2)$	$10163.7 \pm 1.4$	?	$2^{--}$	$\Upsilon(3S) \rightarrow \gamma\gamma(\gamma\gamma\Upsilon(1S))$	CLEO [33] (10.2)	2004	OK
				$\Upsilon(3S) \rightarrow \gamma\gamma(\pi^+\pi^-\Upsilon(1S))$	BABAR [34] (5.8)		
				$\Upsilon(5S) \rightarrow \pi^+\pi^-(\dots)$	Belle [31] (2.4)		
$h_b(2P)$	$10259.8_{-1.2}^{+1.5}$	?	$1^{+-}$	$\Upsilon(5S) \rightarrow \pi^+\pi^-(\dots)$	Belle [31] (11.2)	2011	NC!
$\chi_{bJ}(3P)$	$10530 \pm 10$	?	?	$pp \rightarrow (\gamma\mu^+\mu^-)\dots$	ATLAS [35] ( $>6$ )	2011	NC!

Both the  $h_b(1P)$ , the bottomonium counterpart of  $h_c(1P)$ , and the next excited state,  $h_b(2P)$ , were very recently observed by Belle [31], as described further below, in dipion transitions from either the  $\Upsilon(5S)$  or  $Y_b(10888)$ . All fit into their respective spectroscopies roughly where expected. Their exact masses, production mechanisms, and decay modes provide guidance to their descriptions within QCD. The  $h_b(nP)$  states still need experimental confirmation at the  $5\sigma$  level, as does the  $\chi_{bJ}(3P)$  triplet.

Correspondingly, the menagerie of new, heavy-quarkonium-like *unanticipated* states\* is shown in Table 2; notice that just a handful have been experimentally confirmed. None can unambiguously be assigned a place in the hierarchy of charmonia or bottomonia; neither do any have a universally accepted unconventional origin. The  $X(3872)$  occupies a unique niche among the unexplained states as both the first and the most intriguing. It is, by now, widely studied, yet its interpretation demands much more experimental attention. The  $Y(4260)$  and  $Y(4360)$  are vector states decaying to  $\pi^+\pi^-J/\psi$  and  $\pi^+\pi^-\psi(2S)$ , respectively, yet, unlike most conventional vector charmonia, do not correspond to enhancements in the  $e^+e^-$  hadronic cross section. The three  $Z_c^+$  and two  $Z_b^+$  states, each decaying to a charged pion and conventional heavy quarkonium state, would be manifestly exotic, but remain unconfirmed. Final states of the type  $\Upsilon(nS)\pi^+\pi^-$  from  $e^+e^-$  collisions acquired near the  $\Upsilon(5S)$  have a lineshape differing somewhat from that of multi-hadronic events, which suggested a new state  $Y_b(10888)$ , distinct from  $\Upsilon(5S)$ , which could be analogous to  $Y(4260)$ . The nature of  $Y_b(10888)$ , if it does mimic the behavior of the charmonium-region  $Y$ 's, could help to explain the observed (and otherwise unexpected) high rate of dipion transitions to  $\Upsilon(nS)$  and  $h_b(nP)$  seen in the  $e^+e^-$  collisions near the  $\Upsilon(5S)$ . It could also provide insight into the  $Z_b^+$  states, which appear to be intermediate resonances in the dipion transitions.

BABAR [71,59] has searched for the three  $Z_c^\pm$  states in the charmonium mass region seen by Belle, and failed to observe any significant signals. The approach taken in searching for  $B \rightarrow Z^\pm K \rightarrow (c\bar{c})K\pi$ , where  $(c\bar{c})$  is  $\psi(2S)$  or  $\chi_{c1}$ , is to first fit the data for all reasonable  $K\pi$  mass or angular structure, having demonstrated that the presence of one or more  $Z$ 's cannot be accommodated by this procedure. After doing so, the finding is that some of what might be the Belle excess of events above Belle background gets absorbed into the  $K\pi$  structure of the BABAR background. As shown in Table 2, where Belle observes signals of significances  $5.0\sigma$ ,  $5.0\sigma$ , and  $6.4\sigma$  for  $Z_1(4050)^+$ ,  $Z_2(4250)^+$ , and  $Z(4430)^+$ , respectively, BABAR reports  $1.1\sigma$ ,  $2.0\sigma$ , and  $2.4\sigma$  effects, setting upper limits on product branching fractions that are not inconsistent with Belle's measured rates, leaving the situation unresolved.

\* For consistency with the literature, we preserve the use of  $X$ ,  $Y$ ,  $Z$ , and  $G$ , contrary to the practice of the PDG, which exclusively uses  $X$  for unidentified states.

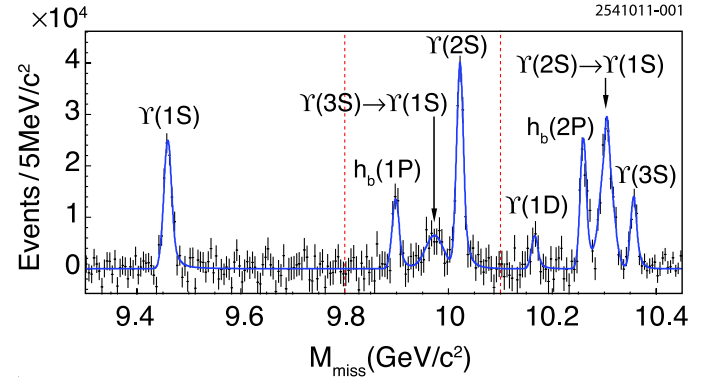


**Figure 1:** From Belle [31], the mass recoiling against  $\pi^+\pi^-$  pairs,  $M_{\text{miss}}$ , in  $e^+e^-$  collision data taken near the peak of the  $\Upsilon(5S)$  (points with error bars). The smooth combinatoric and  $K_S^0 \rightarrow \pi^+\pi^-$  background contributions have already been subtracted. The fit to the various labeled signal contributions overlaid (curve). Adapted from [31] with kind permission, copyright (2011) The American Physical Society.

Although  $\eta_c(2S)$  measurements began to converge on a mass and width nearly a decade ago, refinements are still in progress. In particular, Belle [14] has revisited its analysis of  $B \rightarrow K\eta_c(2S)$ ,  $\eta_c(2S) \rightarrow KK\pi$  decays with more data and methods that account for interference between the above decay chain, an equivalent one with the  $\eta_c(1S)$  instead, and one with no intermediate resonance. The net effect of this interference is far from trivial; it shifts the apparent mass by  $\sim +10$  MeV and blows up the apparent width by a factor of six. The updated  $\eta_c(2S)$  mass and width are in better accordance with other measurements than the previous treatment [13] not including interference. Complementing this measurement in  $B$ -decay, BABAR [15] updated their previous [16]  $\eta_c(2S)$  mass and width measurements in two-photon production, where interference effects, judging from studies of  $\eta_c(1S)$ , appear to be small. In combination, precision on the  $\eta_c(2S)$  mass has improved dramatically.

New results on  $\eta_b$ ,  $h_b$ , and  $Z_b^+$  mostly come from Belle, all from analyses of  $121.4 \text{ fb}^{-1}$  of  $e^+e^-$  collision data collected near the peak of the  $\Upsilon(5S)$  resonance. They also appear in the same types of decay chains:  $\Upsilon(5S) \rightarrow \pi^- Z_b^+ \rightarrow \pi^+(b\bar{b})$ , and, when the  $b\bar{b}$  forms an  $h_b(1P)$ , frequently  $h_b(1P) \rightarrow \gamma\eta_b$ .

Previous unsuccessful searches for  $h_b$  focused on what was considered the most easily detected production mechanism,  $\Upsilon(3S) \rightarrow \pi^0 h_b(1P)$ . In early 2011 BABAR presented marginal evidence for this transition at the  $3\sigma$  level, at a mass near that expected for zero hyperfine splitting.

## Meson Particle Listings

## Heavy Quarkonium Spectroscopy

**Table 2:** As in Table 1, but for new *unconventional* states in the  $c\bar{c}$  and  $b\bar{b}$  regions, ordered by mass. For  $X(3872)$ , the values given are based only upon decays to  $\pi^+\pi^-J/\psi$ .  $X(3945)$  and  $Y(3940)$  have been subsumed under  $X(3915)$  due to compatible properties. The state known as  $Z(3930)$  appears as the  $\chi_{c2}(2P)$  in Table 1. In some cases experiment still allows two  $J^{PC}$  values, in which case both appear. See also the reviews in [1–7]. Adapted from [7] with kind permission, copyright (2011), Springer.

State	$m$ (MeV)	$\Gamma$ (MeV)	$J^{PC}$	Process (mode)	Experiment ( $\#\sigma$ )	Year	Status
$X(3872)$	$3871.68 \pm 0.17$	$< 1.2$	$1^{++}/2^{-+}$	$B \rightarrow K(\pi^+\pi^-J/\psi)$ $p\bar{p} \rightarrow (\pi^+\pi^-J/\psi) + \dots$ $B \rightarrow K(\omega J/\psi)$ $B \rightarrow K(D^{*0}\bar{D}^0)$ $B \rightarrow K(\gamma J/\psi)$ $B \rightarrow K(\gamma\psi(2S))$ $pp \rightarrow (\pi^+\pi^-J/\psi) + \dots$	Belle [36,37] (12.8), BABAR [38] (8.6) CDF [39–41] (np), D0 [42] (5.2) Belle [43] (4.3), BABAR [23] (4.0) Belle [44,45] (6.4), BABAR [46] (4.9) Belle [47] (4.0), BABAR [48,49] (3.6) BABAR [49] (3.5), Belle [47] (0.4) LHCb [50] (np)	2003	OK
$X(3915)$	$3917.4 \pm 2.7$	$28_{-9}^{+10}$	$0/2^{?+}$	$B \rightarrow K(\omega J/\psi)$ $e^+e^- \rightarrow e^+e^-(\omega J/\psi)$	Belle [51] (8.1), BABAR [52] (19) Belle [53] (7.7), BABAR [23] (np)	2004	OK
$X(3940)$	$3942_{-8}^{+9}$	$37_{-17}^{+27}$	$?^{?+}$	$e^+e^- \rightarrow J/\psi(D\bar{D}^*)$ $e^+e^- \rightarrow J/\psi(\dots)$	Belle [54] (6.0) Belle [20] (5.0)	2007	NC!
$G(3900)$	$3943 \pm 21$	$52 \pm 11$	$1^{--}$	$e^+e^- \rightarrow \gamma(D\bar{D})$	BABAR [55] (np), Belle [56] (np)	2007	OK
$Y(4008)$	$4008_{-49}^{+121}$	$226 \pm 97$	$1^{--}$	$e^+e^- \rightarrow \gamma(\pi^+\pi^-J/\psi)$	Belle [57] (7.4)	2007	NC!
$Z_1(4050)^+$	$4051_{-43}^{+24}$	$82_{-55}^{+51}$	$?$	$B \rightarrow K(\pi^+\chi_{c1}(1P))$	Belle [58] (5.0), BABAR [59] (1.1)	2008	NC!
$Y(4140)$	$4143.4 \pm 3.0$	$15_{-7}^{+11}$	$?^{?+}$	$B \rightarrow K(\phi J/\psi)$	CDF [60,61] (5.0)	2009	NC!
$X(4160)$	$4156_{-25}^{+29}$	$139_{-65}^{+113}$	$?^{?+}$	$e^+e^- \rightarrow J/\psi(D\bar{D}^*)$	Belle [54] (5.5)	2007	NC!
$Z_2(4250)^+$	$4248_{-45}^{+135}$	$177_{-72}^{+321}$	$?$	$B \rightarrow K(\pi^+\chi_{c1}(1P))$	Belle [58] (5.0), BABAR [59] (2.0)	2008	NC!
$Y(4260)$	$4263_{-9}^{+8}$	$95 \pm 14$	$1^{--}$	$e^+e^- \rightarrow \gamma(\pi^+\pi^-J/\psi)$ $e^+e^- \rightarrow (\pi^0\pi^0J/\psi)$ $B \rightarrow K(\phi J/\psi)$ $e^+e^- \rightarrow e^+e^-(\phi J/\psi)$	BABAR [62,63] (8.0) CLEO [64] (5.4), Belle [57] (15) CLEO [65] (11) CLEO [65] (5.1) CDF [61] (3.1)	2005	OK
$Y(4274)$	$4274.4_{-6.7}^{+8.4}$	$32_{-15}^{+22}$	$?^{?+}$	$B \rightarrow K(\phi J/\psi)$	CDF [61] (3.1)	2010	NC!
$X(4350)$	$4350.6_{-5.1}^{+4.6}$	$13.3_{-10.0}^{+18.4}$	$0/2^{?+}$	$e^+e^- \rightarrow e^+e^-(\phi J/\psi)$	Belle [66] (3.2)	2009	NC!
$Y(4360)$	$4361 \pm 13$	$74 \pm 18$	$1^{--}$	$e^+e^- \rightarrow \gamma(\pi^+\pi^-J/\psi)$	BABAR [67] (np), Belle [68] (8.0)	2007	OK
$Z(4430)^+$	$4443_{-18}^{+24}$	$107_{-71}^{+113}$	$?$	$B \rightarrow K(\pi^+\psi(2S))$	Belle [69,70] (6.4), BABAR [71] (2.4)	2007	NC!
$X(4630)$	$4634_{-11}^{+9}$	$92_{-32}^{+41}$	$1^{--}$	$e^+e^- \rightarrow \gamma(\Lambda_c^+\Lambda_c^-)$	Belle [72] (8.2)	2007	NC!
$Y(4660)$	$4664 \pm 12$	$48 \pm 15$	$1^{--}$	$e^+e^- \rightarrow \gamma(\pi^+\pi^-\psi(2S))$	Belle [68] (5.8)	2007	NC!
$Z_b(10610)^+$	$10607.2 \pm 2.0$	$18.4 \pm 2.4$	$1^+$	$\Upsilon(5S) \rightarrow \pi^-(\pi^+[b\bar{b}])$	Belle [73,74] (16)	2011	NC!
$Z_b(10650)^+$	$10652.2 \pm 1.5$	$11.5 \pm 2.2$	$1^+$	$\Upsilon(5S) \rightarrow \pi^-(\pi^+[b\bar{b}])$	Belle [73,74] (16)	2011	NC!
$Y_b(10888)$	$10888.4 \pm 3.0$	$30.7_{-7.7}^{+8.9}$	$1^{--}$	$e^+e^- \rightarrow (\pi^+\pi^-\Upsilon(nS))$	Belle [75,76] (2.0)	2010	NC!

The Belle  $h_b$  discovery analysis [31] selects hadronic events and looks for peaks in the mass recoiling against  $\pi^+\pi^-$  pairs, the spectrum for which, after subtraction of smooth combinatoric and  $K_S^0 \rightarrow \pi^+\pi^-$  backgrounds, appears in Fig. 1. Prominent and unmistakable  $h_b(1P)$  and  $h_b(2P)$  peaks are present. This search was directly inspired by a new CLEO result [77], which found the surprisingly copious transitions  $\psi(4160) \rightarrow \pi^+\pi^-h_c(1P)$  and an indication that  $Y(4260) \rightarrow \pi^+\pi^-h_c(1P)$  occurs at a comparable rate as the signature mode,  $Y(4260) \rightarrow \pi^+\pi^-J/\psi$ . The presence of  $\Upsilon(nS)$  peaks in Fig. 1 at rates two orders of magnitude larger than expected for transitions requiring a heavy-quark spin-flip, along with separate studies with exclusive decays  $\Upsilon(nS) \rightarrow \mu^+\mu^-$ , allow precise calibration of the  $\pi^+\pi^-$  recoil mass spectrum and very accurate measurements of  $h_b(1P)$  and  $h_b(2P)$  masses. Both corresponding hyperfine splittings are consistent with zero

within an uncertainty of about 1.5 MeV (lowered to  $\pm 1.1$  MeV for  $h_b(1P)$  in Ref. 30). Belle soon noticed that, for events in the peaks of Fig. 1, there seemed to be two intermediate charged states nearby. For example, Fig. 2 shows a Dalitz plot for events restricted to the  $\Upsilon(2S)$  region of  $\pi^+\pi^-$  recoil mass. The two bands observed in the maximum of the two  $M[\pi^\pm\Upsilon(2S)]^2$  values also appear for  $\Upsilon(1S)$ ,  $\Upsilon(3S)$ ,  $h_b(1P)$ , and  $h_b(2P)$  samples, but do not appear in the respective  $[b\bar{b}]$  sidebands. Belle fits all subsamples to resonant plus non-resonant amplitudes, allowing for interference (notably, between  $\pi^-Z_b^+$  and  $\pi^+Z_b^-$ ), and finds consistent pairs of  $Z_b^+$  masses for all bottomonium transitions, and comparable strengths of the two states. Angular analysis favors a  $J^P = 1^+$  assignment for both  $Z_b^+$  states, which must also have negative  $G$ -parity. Transitions through  $Z_b^+$  to the  $h_b(nP)$  saturate the observed  $\pi^+\pi^-h_b(nP)$  cross sections. The two masses of  $Z_b^+$  states are just a few MeV above the  $B^*\bar{B}$

See key on page 457

## Meson Particle Listings

### Heavy Quarkonium Spectroscopy

and  $B^*\bar{B}^*$  thresholds, respectively. The  $Z_b^+$  cannot be simple mesons because they are charged and have  $b\bar{b}$  content.

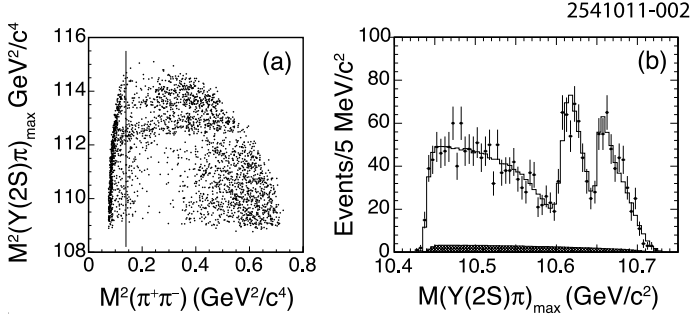


**Figure 2:** From Belle [74]  $e^+e^-$  collision data taken near the peak of the  $\Upsilon(5S)$  for events with a  $\pi^+\pi^-$ -missing mass consistent with a  $\Upsilon(nS)2$ , (a) the maximum of the two possible single  $\pi^\pm$ -missing-mass-squared combinations vs. the  $\pi^+\pi^-$ -mass-squared; and (b) projection of the maximum of the two possible single  $\pi^\pm$ -missing-mass combinations (*points with error bars*) overlaid with a fit (*curve*). Events to the left of the vertical line in (a) are excluded from further analysis. The two horizontal stripes in (a) and two peaks in (b) correspond to the two  $Z_b^+$  states. Adapted from [74] with kind permission, copyright (2011) The American Physical Society.

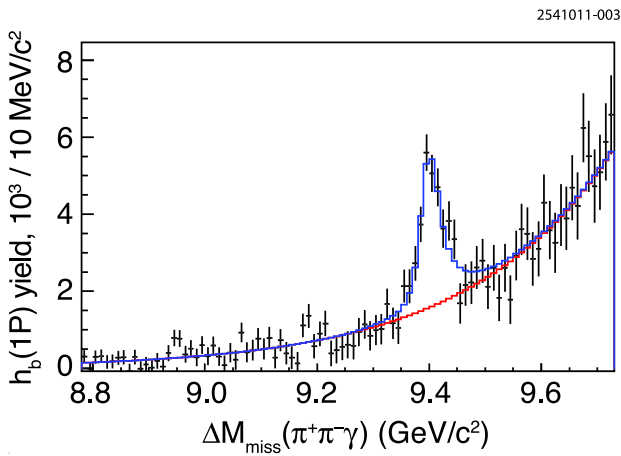


**Figure 3:** From Belle [30]  $e^+e^-$  collision data taken near the peak of the  $\Upsilon(5S)$ , the  $h_b(1P)$  event yield vs. the mass recoiling against the  $\pi^+\pi^-$ -missing mass (corrected for misreconstructed  $\pi^+\pi^-$ ), where the  $h_b(1P)$  yield is obtained by fitting the mass recoiling against the  $\pi^+\pi^-$  (*points with error bars*). The fit results (*solid histograms*) for signal plus background and background alone are superimposed. Adapted from [30] with kind permission, copyright (2011) The American Physical Society.

The third Belle result to flow from these data is confirmation of the  $\eta_b(1S)$  and measurement of the  $h_b(1P) \rightarrow \gamma\eta_b(1S)$  branching fraction, expected to be several tens of percent. To accomplish this, events with the  $\pi^+\pi^-$  recoil mass in the  $h_b(1P)$  mass window and a radiative photon candidate are selected, and the  $\pi^+\pi^-$  recoil mass queried for correlation with non-zero  $h_b(1P)$  population in the  $\pi^+\pi^-$  missing mass spectrum, as shown in Fig. 3. A clear peak is observed, corresponding to the  $\eta_b(1S)$ . A fit is performed to extract the  $\eta_b(1S)$  mass, and first measurements of its width and the branching fraction for  $h_b(1P) \rightarrow \gamma\eta_b(1S)$  (the latter of which is  $(49.8 \pm 6.8_{-5.2}^{+10.9})\%$ ). The mass determination has comparable uncertainty to and a larger central value (by 10 MeV, or  $2.4\sigma$ ) than the average of previous measurements, thereby reducing the new world average hyperfine splitting by nearly 5 MeV, as shown in Table 3.

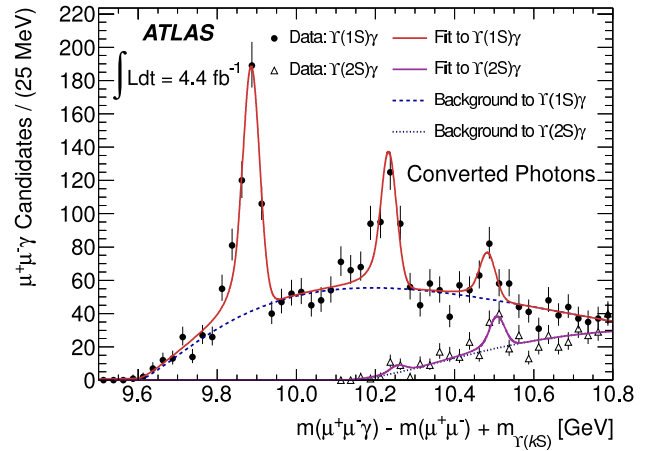


**Figure 4:** From ATLAS [35]  $pp$  collision data (*points with error bars*) taken at  $\sqrt{s} = 7$  TeV, the effective mass of  $\chi_{bJ}(1P, 2P, 3P) \rightarrow \gamma\Upsilon(1S, 2S) \rightarrow \mu^+\mu^-$  and the photon is reconstructed as an  $e^+e^-$  conversion in the tracking system. Fits (*smooth curves*) show significant signals for each triplet (merged- $J$ ) on top of a smooth background. From [35] with kind permission, copyright (2012) The American Physical Society.

The  $\chi_{bJ}(nP)$  states have recently been observed at the LHC by ATLAS [35] for  $n = 1, 2, 3$ , although in each case the three  $J$  states are not distinguished from one another. Events are sought which have both a photon and an  $\Upsilon(1S, 2S) \rightarrow \mu^+\mu^-$  candidate which together form a mass in the  $\chi_b$  region. Observation of all three  $J$ -merged peaks is seen at significance in excess of  $6\sigma$  for both unconverted and converted photons. The mass plot for converted photons, which provide better mass resolution, is shown in Fig. 4. This marks the first observation of the  $\chi_{bJ}(3P)$  triplet, quite near the expected mass.

# Meson Particle Listings

## Heavy Quarkonium Spectroscopy

**Table 3:** Measured  $\eta_b(1S)$  masses and hyperfine splittings, by experiment and production mechanism.

$m(\eta_b)$	$\Delta m_{hf}$	Process	Ref. ( $\chi^2/\text{d.o.f.}$ )
$9394.2^{+4.8}_{-4.9} \pm 2.0$	$66.1^{+4.9}_{-4.8} \pm 2.0$	$\Upsilon(nS)2 \rightarrow \gamma\eta_b$	BABAR [29]
$9388.9^{+3.1}_{-2.3} \pm 2.7$	$71.4^{+2.3}_{-3.1} \pm 2.7$	$\Upsilon(nS)3 \rightarrow \gamma\eta_b$	BABAR [27]
$9391.8 \pm 6.6 \pm 2.0$	$68.5 \pm 6.6 \pm 2.0$	$\Upsilon(nS)3 \rightarrow \gamma\eta_b$	CLEO [28]
$9391.0 \pm 2.8$	$69.3 \pm 2.9$	Above [7]	Avg <sup>a</sup> (0.6/2)
$9401.0 \pm 1.9^{+1.4}_{-2.4}$	$59.3 \pm 1.9^{+2.4}_{-1.4}$	$h_b(1P) \rightarrow \gamma\eta_b$	Belle [30]
$9395.8 \pm 3.0$	$64.5 \pm 3.0$	All	Avg <sup>a</sup> (6.1/3)

<sup>a</sup> An inverse-square-error-weighted average of the individual measurements appearing above, for which all statistical and systematic errors were combined in quadrature without accounting for any possible correlations between them. The uncertainty on this average is inflated by the multiplicative factor  $S$  if  $S^2 \equiv \chi^2/\text{d.o.f.} > 1$ .

### References

- N. Brambilla *et al.*, CERN-2005-005, (CERN, Geneva, 2005), [arXiv:hep-ph/0412158](#).
- E. Eichten *et al.*, Rev. Mod. Phys. **80**, 1161 (2008) [arXiv:hep-ph/0701208](#).
- S. Eidelman, H. Mahlke-Kruger, and C. Patrignani, in C. Amsler *et al.* (Particle Data Group), Phys. Lett. **B667**, 1029 (2008).
- S. Godfrey and S.L. Olsen, Ann. Rev. Nucl. Part. Sci. **58** 51 (2008), [arXiv:0801.3867 \[hep-ph\]](#).
- T. Barnes and S.L. Olsen, Int. J. Mod. Phys. **A24**, 305 (2009).
- G.V. Pakhlova, P.N. Pakhlov, and S.I. Eidelman, Phys. Usp. **53** 219 (2010), [*Usp. Fiz. Nauk* **180** 225 (2010)].
- N. Brambilla *et al.*, Eur. Phys. J. **C71**, 1534 (2011) [arXiv:1010.5827 \[hep-ph\]](#).
- P. Rubin *et al.* (CLEO Collab.), Phys. Rev. **D72**, 092004 (2005) [arXiv:hep-ex/0508037](#).
- J.L. Rosner *et al.* (CLEO Collab.), Phys. Rev. Lett. **95**, 102003 (2005) [arXiv:hep-ex/0505073](#).
- S. Dobbs *et al.* (CLEO Collab.), Phys. Rev. Lett. **101**, 182003 (2008) [arXiv:0805.4599 \[hep-ex\]](#).
- M. Ablikim *et al.* (BESIII Collab.), Phys. Rev. Lett. **104**, 132003 (2010) [arXiv:1002.0501 \[hep-ex\]](#).
- M. Andreotti *et al.* (E835 Collab.), Phys. Rev. **D72**, 032001 (2005).
- S.K. Choi *et al.* (Belle Collab.), Phys. Rev. Lett. **89**, 102001 (2002) [Erratum-ibid. **89** 129901 (2002)], [arXiv:hep-ex/0206002](#).
- A. Vinokurova *et al.* (Belle Collab.), Phys. Lett. **B706**, 139 (2011) [arXiv:1105.0978 \[hep-ex\]](#).
- P. del Amo Sanchez *et al.* (BABAR Collab.), Phys. Rev. **D84**, 021004 (2011) [arXiv:1103.3971 \[hep-ex\]](#).
- B. Aubert *et al.* (BABAR Collab.), Phys. Rev. Lett. **92**, 142002 (2004) [arXiv:hep-ex/0311038](#).
- D.M. Asner *et al.* (CLEO Collab.), Phys. Rev. Lett. **92**, 142001 (2004) [arXiv:hep-ex/0312058](#).
- H. Nakazawa (Belle Collab.), Nucl. Phys. (Proc. Supp.) **184**, 220 (2008).
- B. Aubert *et al.* (BABAR Collab.), Phys. Rev. **D72**, 031101 (2005) [arXiv:hep-ex/0506062](#).
- K. Abe *et al.* (Belle Collab.), Phys. Rev. Lett. **98**, 082001 (2007) [arXiv:hep-ex/0507019](#).
- S. Uehara *et al.* (Belle Collab.), Phys. Rev. Lett. **96**, 082003 (2006) [arXiv:hep-ex/0512035](#).
- B. Aubert *et al.* (BABAR Collab.), Phys. Rev. **D81**, 092003 (2010) [arXiv:1002.0281 \[hep-ex\]](#).
- P. del Amo Sanchez *et al.* (BABAR Collab.), Phys. Rev. **D82**, 011101R (2010) [arXiv:1005.5190 \[hep-ex\]](#).
- F. Abe *et al.* (CDF Collab.), Phys. Rev. Lett. **81**, 2432 (1998) [arXiv:hep-ex/9805034](#).
- T. Aaltonen *et al.* (CDF Collab.), Phys. Rev. Lett. **100**, 182002 (2008) [arXiv:0712.1506 \[hep-ex\]](#).
- V.M. Abazov *et al.* (D0 Collab.), Phys. Rev. Lett. **101**, 012001 (2008) [arXiv:0802.4258 \[hep-ex\]](#).
- B. Aubert *et al.* (BABAR Collab.), Phys. Rev. Lett. **101**, 071801 (2008) [Erratum-ibid. **102**, 029901 (2009)], [arXiv:0807.1086 \[hep-ex\]](#).
- G. Bonvicini *et al.* (CLEO Collab.), Phys. Rev. **D81**, 031104 (2010) [arXiv:0909.5474 \[hep-ex\]](#).
- B. Aubert *et al.* (BABAR Collab.), Phys. Rev. Lett. **103**, 161801 (2009) [arXiv:0903.1124 \[hep-ex\]](#).
- I. Adachi *et al.* (Belle Collab.), [arXiv:1110.3934 \[hep-ex\]](#).
- I. Adachi *et al.* (Belle Collab.), Phys. Rev. Lett. **108**, 032001 (2012) [arXiv:1103.3419 \[hep-ex\]](#).
- J.P. Lees *et al.* (BABAR Collab.), Phys. Rev. **D84**, 091101 (2011) [arXiv:1102.4565 \[hep-ex\]](#).
- G. Bonvicini *et al.* (CLEO Collab.), Phys. Rev. **D70**, 032001 (2004) [arXiv:hep-ex/0404021](#).
- P. del Amo Sanchez *et al.* (BABAR Collab.), Phys. Rev. **D82**, 111102 (2010) [arXiv:1004.0175 \[hep-ex\]](#).
- G. Aad *et al.* (ATLAS Collab.), Phys. Rev. Lett. **108**, 152001 (2012) [arXiv:1112.5154 \[hep-ex\]](#).
- S.K. Choi *et al.* (Belle Collab.), Phys. Rev. Lett. **91**, 262001 (2003) [arXiv:hep-ex/0309032](#).
- S.-K. Choi *et al.* (Belle Collab.), Phys. Rev. **D84**, 052004R (2011) [arXiv:1107.0163 \[hep-ex\]](#).
- B. Aubert *et al.* (BABAR Collab.), Phys. Rev. **D77**, 111101 (2008) [arXiv:0803.2838 \[hep-ex\]](#).
- D.E. Acosta *et al.* (CDF II Collab.), Phys. Rev. Lett. **93**, 072001 (2004) [arXiv:hep-ex/0312021](#).
- A. Abulencia *et al.* (CDF Collab.), Phys. Rev. Lett. **98**, 132002 (2007) [arXiv:hep-ex/0612053](#).
- T. Aaltonen *et al.* (CDF Collab.), Phys. Rev. Lett. **103**, 152001 (2009) [arXiv:0906.5218 \[hep-ex\]](#).
- V.M. Abazov *et al.* (D0 Collab.), Phys. Rev. Lett. **93**, 162002 (2004) [arXiv:hep-ex/0405004](#).
- K. Abe *et al.* (Belle Collab.), [arXiv:hep-ex/0505037](#).
- G. Gokhroo *et al.* (Belle Collab.), Phys. Rev. Lett. **97**, 162002 (2006) [arXiv:hep-ex/0606055](#).
- T. Aushev *et al.*, Phys. Rev. **D81**, 031103R (2010), [arXiv:0810.0358 \[hep-ex\]](#).
- B. Aubert *et al.* (BABAR Collab.), Phys. Rev. **D77**, 011102 (2008) [arXiv:0708.1565 \[hep-ex\]](#).
- V. Bhardwaj *et al.* (Belle Collab.), Phys. Rev. Lett. **107**, 9 (2011) Phys. Rev. Lett. **107** (2011) 9, [arXiv:1105.0177 \[hep-ex\]](#).

See key on page 457

## Meson Particle Listings

### Heavy Quarkonium Spectroscopy

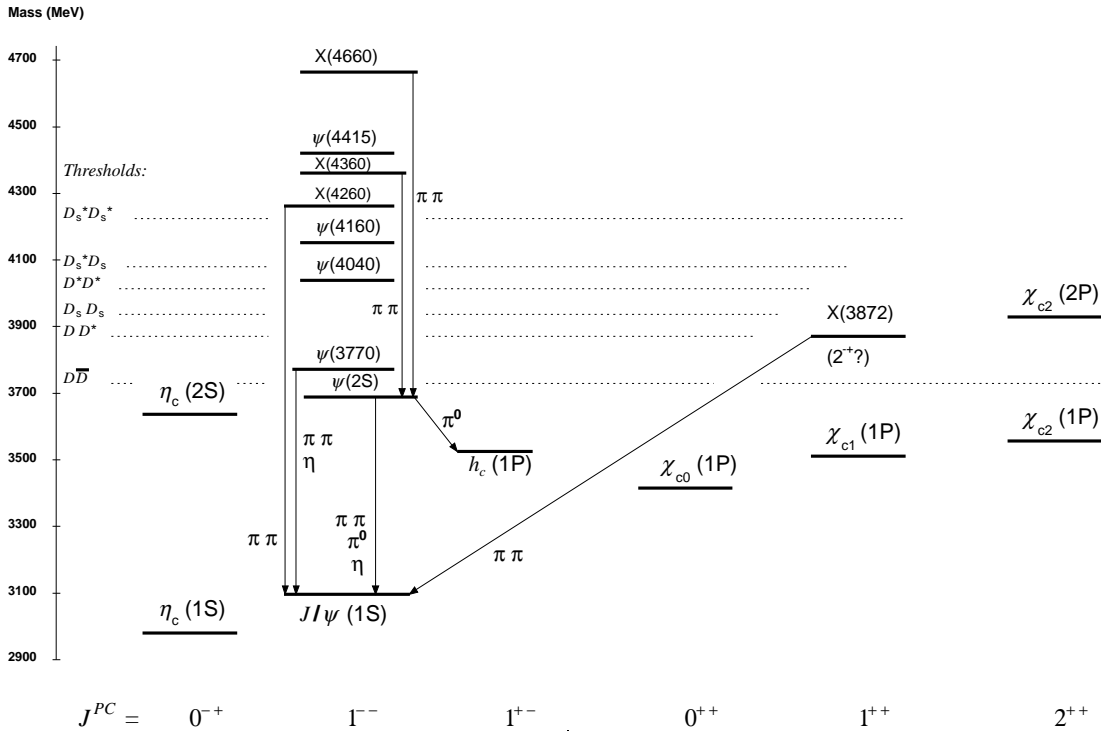
- 
48. B. Aubert *et al.* (BABAR Collab.), Phys. Rev. **D74**, 071101 (2006) arXiv:hep-ex/0607050.
49. B. Aubert *et al.* (BABAR Collab.), Phys. Rev. Lett. **102**, 132001 (2009) arXiv:0809.0042 [hep-ex].
50. R. Aaij *et al.* (LHCb Collab.), Eur. Phys. J. **C72**, 1972 (2012) arXiv:1112.5310 [hep-ex].
51. K. Abe *et al.* (Belle Collab.), Phys. Rev. Lett. **94**, 182002 (2005) arXiv:hep-ex/0408126.
52. B. Aubert *et al.* (BABAR Collab.), Phys. Rev. Lett. **101**, 082001 (2008) arXiv:0711.2047 [hep-ex].
53. S. Uehara *et al.* (Belle Collab.), Phys. Rev. Lett. **104**, 092001 (2010) arXiv:0912.4451 [hep-ex].
54. P. Pakhlov *et al.* (Belle Collab.), Phys. Rev. Lett. **100**, 202001 (2008) arXiv:0708.3812 [hep-ex].
55. B. Aubert *et al.* (BABAR Collab.), arXiv:hep-ex/0607083.
56. G. Pakhlova *et al.* (Belle Collab.), Phys. Rev. **D77**, 011103R (2008) arXiv:0708.0082 [hep-ex].
57. C.Z. Yuan *et al.* (Belle Collab.), Phys. Rev. Lett. **99**, 182004 (2007) arXiv:0707.2541 [hep-ex].
58. R. Mizuk *et al.* (Belle Collab.), Phys. Rev. **D78**, 072004 (2008) arXiv:0806.4098 [hep-ex].
59. J.P. Lees *et al.* (BABAR Collab.), arXiv:1111.5919 [hep-ex].
60. T. Aaltonen *et al.* (CDF Collab.), Phys. Rev. Lett. **102**, 242002 (2009) arXiv:0903.2229 [hep-ex].
61. T. Aaltonen *et al.* (CDF Collab.), arXiv:1101.6058 [hep-ex].
62. B. Aubert *et al.* (BABAR Collab.), Phys. Rev. Lett. **95**, 142001 (2005) arXiv:hep-ex/0506081.
63. B. Aubert *et al.* (BABAR Collab.), arXiv:0808.1543v2 [hep-ex].
64. Q. He *et al.* (CLEO Collab.), Phys. Rev. **D74**, 091104 (2006) arXiv:hep-ex/0611021.
65. T.E. Coan *et al.* (CLEO Collab.), Phys. Rev. Lett. **96**, 162003 (2006) arXiv:hep-ex/0602034.
66. C.P. Shen *et al.* (Belle Collab.), Phys. Rev. Lett. **104**, 112004 (2010) arXiv:0912.2383 [hep-ex].
67. B. Aubert *et al.* (BABAR Collab.), Phys. Rev. Lett. **98**, 212001 (2007) arXiv:hep-ex/0610057.
68. X.L. Wang *et al.* (Belle Collab.), Phys. Rev. Lett. **99**, 142002 (2007) arXiv:0707.3699 [hep-ex].
69. S.K. Choi *et al.* (Belle Collab.), Phys. Rev. Lett. **100**, 142001 (2008) arXiv:0708.1790 [hep-ex].
70. R. Mizuk *et al.* (Belle Collab.), Phys. Rev. **D80**, 031104 (2009) arXiv:0905.2869 [hep-ex].
71. B. Aubert *et al.* (BABAR Collab.), Phys. Rev. **D79**, 112001 (2009) arXiv:0811.0564 [hep-ex].
72. G. Pakhlova *et al.* (Belle Collab.), Phys. Rev. Lett. **101**, 172001 (2008) arXiv:0807.4458 [hep-ex].
73. I. Adachi *et al.* (Belle Collab.), arXiv:1105.4583 [hep-ex].
74. A. Bondar *et al.* (Belle Collab.), Phys. Rev. Lett. **108**, 122001 (2012) arXiv:1110.2251 [hep-ex].
75. K.-F. Chen *et al.* (Belle Collab.), Phys. Rev. **D82**, 091106R (2010) arXiv:0808.2445 [hep-ex].
76. K.F. Chen *et al.* (Belle Collab.), Phys. Rev. Lett. **100**, 112001 (2008) arXiv:0710.2577 [hep-ex].
77. T.K. Pedlar *et al.* (CLEO Collab.), Phys. Rev. Lett. **107**, 041803 (2011) arXiv:1104.2025 [hep-ex].
-

# Meson Particle Listings

## Charmonium, $\eta_c(1S)$

### c $\bar{c}$ MESONS

THE CHARMONIUM SYSTEM



The level scheme of the  $c\bar{c}$  states showing experimentally established states with solid lines. Singlet states are called  $\eta_c$  and  $h_c$ , triplet states  $\psi$  and  $\chi_{cJ}$ , and unassigned charmonium-like states  $X$ . In parentheses it is sufficient to give the radial quantum number and the orbital angular momentum to specify the states with all their quantum numbers. Only observed hadronic transitions are shown; the single photon transitions  $\psi(nS) \rightarrow \gamma\eta_c(mP)$ ,  $\psi(nS) \rightarrow \gamma\chi_{cJ}(mP)$ , and  $\chi_{cJ}(1P) \rightarrow \gamma J/\psi$  are omitted for clarity.

### $\eta_c(1S)$

$$I^G(J^{PC}) = 0^+(0^{-+})$$

**$\eta_c(1S)$  MASS**

VALUE (MeV)	EVTS	DOCUMENT ID	TECN	COMMENT
<b>2981.0 ± 1.1 OUR AVERAGE</b>		Error includes scale factor of 1.7. See the ideogram below.		
2984.5 ± 0.8 ± 3.1	11k	DEL-AMO-SA..11M	BABR	$\gamma\gamma \rightarrow K^+ K^- \pi^+ \pi^- \pi^0$
2985.4 ± 1.5 ± 0.5 ± 2.0	920	1 VINOKUROVA	11 BELL	$B^\pm \rightarrow K^\pm(K_S^0 K^\pm \pi^\mp)$
2982.2 ± 0.4 ± 1.6	14k	2 LEES	10 BABR	$10.6 e^+ e^- \rightarrow K_S^0 K^\pm \pi^\mp$
2985.8 ± 1.5 ± 3.1	0.9k	AUBERT	08AB BABR	$B \rightarrow \eta_c(1S) K^{(*)} \rightarrow K\bar{K}\pi K^{(*)}$
2986.1 ± 1.0 ± 2.5	7.5k	UEHARA	08 BELL	$\gamma\gamma \rightarrow \eta_c \rightarrow \text{hadrons}$
2970 ± 5 ± 6	501	3 ABE	07 BELL	$e^+ e^- \rightarrow J/\psi(c\bar{c})$
2971 ± 3 ± 2 ± 1	195	WU	06 BELL	$B^+ \rightarrow p\bar{p}K^+$
2974 ± 7 ± 2 ± 1	20	WU	06 BELL	$B^+ \rightarrow \Lambda\bar{\Lambda}K^+$
2981.8 ± 1.3 ± 1.5	592	ASNER	04 CLEO	$\gamma\gamma \rightarrow \eta_c \rightarrow K_S^0 K^\pm \pi^\mp$
2984.1 ± 2.1 ± 1.0	190	4 AMBROGIANI	03 E835	$\bar{p}p \rightarrow \eta_c \rightarrow \gamma\gamma$
2977.5 ± 1.0 ± 1.2		5,6 BAI	03 BES	$J/\psi \rightarrow \gamma\eta_c$
2976.3 ± 2.3 ± 1.2		6,7,8 BAI	00F BES	$J/\psi \rightarrow \gamma\eta_c$ and $\psi(2S) \rightarrow \gamma\eta_c$
2969 ± 4 ± 4	80	6 BAI	90B MRK3	$J/\psi \rightarrow \gamma K^+ K^- K^+ K^-$
2984 ± 2.3 ± 4.0		6 GAISER	86 CBAL	$J/\psi \rightarrow \gamma X, \psi(2S) \rightarrow \gamma X$

• • • We do not use the following data for averages, fits, limits, etc. • • •

2982.5 ± 0.4 ± 1.4	12k	9 DEL-AMO-SA..11M	BABR	$\gamma\gamma \rightarrow K_S^0 K^\pm \pi^\mp$
2982.2 ± 0.6		6 MITCHELL	09 CLEO	$e^+ e^- \rightarrow \gamma X$
2982 ± 5	270	10 AUBERT	06E BABR	$B^\pm \rightarrow K^\pm X_c \bar{c}$
2982.5 ± 1.1 ± 0.9	2.5k	11 AUBERT	04B BABR	$\gamma\gamma \rightarrow \eta_c(1S) \rightarrow K\bar{K}\pi$
2979.6 ± 2.3 ± 1.6	180	12 FANG	03 BELL	$B \rightarrow \eta_c K$
2976.6 ± 2.9 ± 1.3	140 <sup>6,7,13</sup>	BAI	00F BES	$J/\psi \rightarrow \gamma\eta_c$
2980.4 ± 2.3 ± 0.6		14 BRANDENB...	00B CLE2	$\gamma\gamma \rightarrow \eta_c \rightarrow K^\pm K_S^0 \pi^\mp$
2975.8 ± 3.9 ± 1.2	7,13	BAI	99B BES	Sup. by BAI 00F
2999 ± 8	25	ABREU	98a DLPH	$e^+ e^- \rightarrow e^+ e^- + \text{hadrons}$
2988.3 ± 3.3 ± 3.1		ARMSTRONG	95F E760	$\bar{p}p \rightarrow \gamma\gamma$
2974.4 ± 1.9	6,13	BISELLO	91 DM2	$J/\psi \rightarrow \eta_c \gamma$
2956 ± 12 ± 12	6	BAI	90B MRK3	$J/\psi \rightarrow \gamma K^+ K^- K_S^0 K_L^0$
2982.6 ± 2.7 ± 2.3	12	BAGLIN	87B SPEC	$\bar{p}p \rightarrow \gamma\gamma$
2980.2 ± 1.6	6,13	BALTRUSAIT..86	MRK3	$J/\psi \rightarrow \eta_c \gamma$
2976 ± 8	6,15	BALTRUSAIT..84	MRK3	$J/\psi \rightarrow 2\phi\gamma$
2982 ± 8	18	16 HIMEL	80B MRK2	$e^+ e^-$
2980 ± 9		16 PARTRIDGE	80B CBAL	$e^+ e^-$

1 Accounts for interference with non-resonant continuum.  
 2 Taking into account interference with the non-resonant  $J^P = 0^-$  amplitude.  
 3 From a fit of the  $J/\psi$  recoil mass spectrum. Supersedes ABE,K 02 and ABE 04c.  
 4 Using mass of  $\psi(2S) = 3686.00$  MeV.  
 5 From a simultaneous fit of five decay modes of the  $\eta_c$ .  
 6 MITCHELL 09 observes a significant asymmetry in the lineshapes of  $\psi(2S) \rightarrow \gamma\eta_c$  and  $J/\psi \rightarrow \gamma\eta_c$  transitions. If ignored, this asymmetry could lead to significant bias whenever the mass and width are measured in  $\psi(2S)$  or  $J/\psi$  radiative decays.  
 7 Using an  $\eta_c$  width of 13.2 MeV.  
 8 Weighted average of the  $\psi(2S)$  and  $J/\psi(1S)$  samples.  
 9 Not independent from the measurements reported by LEES 10.  
 10 From the fit of the kaon momentum spectrum. Systematic errors not evaluated.  
 11 Superseded by LEES 10.

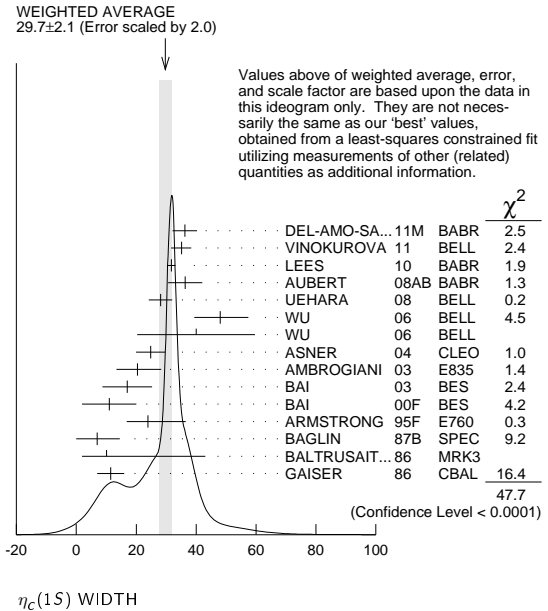
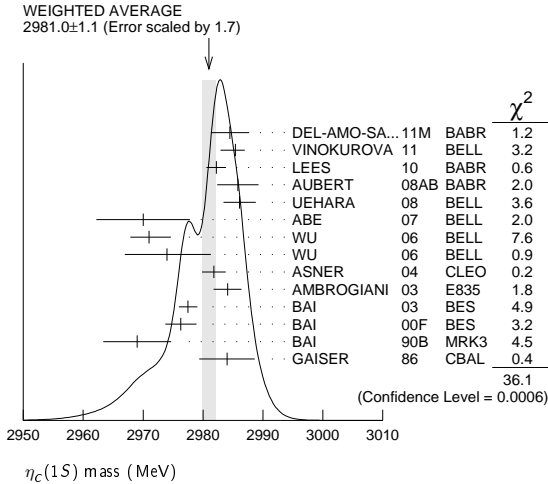


See key on page 457

Meson Particle Listings

$\eta_c(1S)$

- 12 Superseded by VINOKUROVA 11.
- 13 Average of several decay modes.
- 14 Superseded by ASNER 04.
- 15  $\eta_c \rightarrow \phi\phi$ .
- 16 Mass adjusted by us to correspond to  $J/\psi(1S)$  mass = 3097 MeV.



$\eta_c(1S)$  WIDTH

VALUE (MeV)	CL%	EVTS	DOCUMENT ID	TECN	COMMENT
<b>29.7 ± 2.1 OUR AVERAGE</b>					Error includes scale factor of 2.0. See the ideogram below.
36.2 ± 2.8 ± 3.0		11k	DEL-AMO-SA...11M	BABR	$\gamma\gamma \rightarrow K^+K^-\pi^+\pi^-\pi^0$
35.1 ± 3.1 ± 1.0		920	17 VINOKUROVA 11	BELL	$B^{\pm} \rightarrow K_S^0 K^{\pm}\pi^{\mp}$
31.7 ± 1.2 ± 0.8		14k	18 LEES 10	BABR	$10.6 e^+e^- \rightarrow e^+e^-K_S^0 K^{\pm}\pi^{\mp}$
36.3 ± 3.7 ± 4.4		921 ± 32	AUBERT 08AB	BABR	$B \rightarrow \eta_c(1S) K^{(*)} \rightarrow K\bar{K}\pi K^{(*)}$
28.1 ± 3.2 ± 2.2		7.5k	UEHARA 08	BELL	$\gamma\gamma \rightarrow \eta_c \rightarrow \text{hadrons}$
48 ± 8 ± 5		195	WU 06	BELL	$B^+ \rightarrow p\bar{p}K^+$
40 ± 19 ± 5		20	WU 06	BELL	$B^+ \rightarrow \Lambda\bar{\Lambda}K^+$
24.8 ± 3.4 ± 3.5		592	ASNER 04	CLEO	$\gamma\gamma \rightarrow \eta_c \rightarrow K_S^0 K^{\pm}\pi^{\mp}$
20.4 ± 7.7 ± 2.0		190	AMBROGIANI 03	E835	$\bar{p}p \rightarrow \eta_c \rightarrow \gamma\gamma$
17.0 ± 3.7 ± 7.4		19	BAI 03	BES	$J/\psi \rightarrow \gamma\eta_c$
11.0 ± 8.1 ± 4.1		20	BAI 00F	BES	$J/\psi \rightarrow \gamma\eta_c \text{ and } \psi(2S) \rightarrow \gamma\eta_c$
23.9 ± 12.6 ± 7.1			ARMSTRONG 95F	E760	$\bar{p}p \rightarrow \gamma\gamma$
7.0 ± 7.5 ± 7.0		12	BAGLIN 87B	SPEC	$\bar{p}p \rightarrow \gamma\gamma$
10.1 ± 33.0 ± 8.2		23	21 BALTRUSAIT...86	MRK3	$J/\psi \rightarrow \gamma\rho\bar{p}$
11.5 ± 4.5			GAISER 86	CBAL	$J/\psi \rightarrow \gamma X, \psi(2S) \rightarrow \gamma X$
32.1 ± 1.1 ± 1.3		12k	22 DEL-AMO-SA...11M	BABR	$\gamma\gamma \rightarrow K_S^0 K^{\pm}\pi^{\mp}$
34.3 ± 2.3 ± 0.9		2547 ± 90	23 AUBERT 04D	BABR	$\gamma\gamma \rightarrow \eta_c(1S) \rightarrow K\bar{K}\pi$
29 ± 8 ± 6		182 ± 25	24 FANG 03	BELL	$B \rightarrow \eta_c K$
27.0 ± 5.8 ± 1.4			25 BRANDENB...00B	CLE2	$\gamma\gamma \rightarrow \eta_c \rightarrow K^{\pm}K_S^0\pi^{\mp}$
< 40	90	18	HIMEL 80B	MRK2	$e^+e^-$
< 20	90		PARTRIDGE 80B	CBAL	$e^+e^-$

- • • We do not use the following data for averages, fits, limits, etc. • • •
- 17 Accounts for interference with non-resonant continuum.
- 18 Taking into account interference with the non-resonant  $J^P = 0^-$  amplitude.
- 19 From a simultaneous fit of five decay modes of the  $\eta_c$ .
- 20 From a fit to the 4-prong invariant mass in  $\psi(2S) \rightarrow \gamma\eta_c$  and  $J/\psi(1S) \rightarrow \gamma\eta_c$  decays.
- 21 Positive and negative errors correspond to 90% confidence level.
- 22 Not independent from the measurements reported by LEES 10.
- 23 Superseded by LEES 10.
- 24 Superseded by VINOKUROVA 11.
- 25 Superseded by ASNER 04.

$\eta_c(1S)$  DECAY MODES

Mode	Fraction ( $\Gamma_i/\Gamma$ )	Confidence level
<b>Decays involving hadronic resonances</b>		
$\Gamma_1$	$\eta'(958)\pi\pi$	(4.1 ± 1.7) %
$\Gamma_2$	$\rho\rho$	(1.8 ± 0.5) %
$\Gamma_3$	$K^*(892)^0 K^-\pi^+ + c.c.$	(2.0 ± 0.7) %
$\Gamma_4$	$K^*(892)\bar{K}^*(892)$	(6.8 ± 1.3) × 10 <sup>-3</sup>
$\Gamma_5$	$K^{*0}\bar{K}^{*0}\pi^+\pi^-$	(1.1 ± 0.5) %
$\Gamma_6$	$\phi K^+ K^-$	(2.9 ± 1.4) × 10 <sup>-3</sup>
$\Gamma_7$	$\phi\phi$	(1.94 ± 0.30) × 10 <sup>-3</sup>
$\Gamma_8$	$\phi 2(\pi^+\pi^-)$	< 3.5 × 10 <sup>-3</sup>
$\Gamma_9$	$a_0(980)\pi$	< 2 %
$\Gamma_{10}$	$a_2(1320)\pi$	< 2 %
$\Gamma_{11}$	$K^*(892)\bar{K} + c.c.$	< 1.28 %
$\Gamma_{12}$	$f_2(1270)\eta$	< 1.1 %
$\Gamma_{13}$	$\omega\omega$	< 3.1 × 10 <sup>-3</sup>
$\Gamma_{14}$	$\omega\phi$	< 1.7 × 10 <sup>-3</sup>
$\Gamma_{15}$	$f_2(1270)f_2(1270)$	(9.7 ± 2.5) × 10 <sup>-3</sup>
$\Gamma_{16}$	$f_2(1270)f_2'(1525)$	(9.3 ± 3.1) × 10 <sup>-3</sup>
<b>Decays into stable hadrons</b>		
$\Gamma_{17}$	$K\bar{K}\pi$	(7.2 ± 0.6) %
$\Gamma_{18}$	$\eta\pi^+\pi^-$	(4.9 ± 1.8) %
$\Gamma_{19}$	$K^+K^-\pi^+\pi^-$	(6.1 ± 1.2) × 10 <sup>-3</sup>
$\Gamma_{20}$	$K^+K^-\pi^+\pi^-\pi^0$	(3.4 ± 0.6) %
$\Gamma_{21}$	$K^+K^-2(\pi^+\pi^-)$	(7.1 ± 2.9) × 10 <sup>-3</sup>
$\Gamma_{22}$	$2(K^+K^-)$	(1.34 ± 0.32) × 10 <sup>-3</sup>
$\Gamma_{23}$	$2(\pi^+\pi^-)$	(8.6 ± 1.3) × 10 <sup>-3</sup>
$\Gamma_{24}$	$3(\pi^+\pi^-)$	(1.5 ± 0.5) %
$\Gamma_{25}$	$\rho\bar{\rho}$	(1.41 ± 0.17) × 10 <sup>-3</sup>
$\Gamma_{26}$	$\Lambda\bar{\Lambda}$	(9.4 ± 3.2) × 10 <sup>-4</sup>
$\Gamma_{27}$	$K\bar{K}\eta$	< 3.1 %
$\Gamma_{28}$	$\pi^+\pi^-\rho\bar{\rho}$	< 1.2 %
<b>Radiative decays</b>		
$\Gamma_{29}$	$\gamma\gamma$	(1.78 ± 0.16) × 10 <sup>-4</sup>
<b>Charge conjugation (C), Parity (P), Lepton family number (LF) violating modes</b>		
$\Gamma_{30}$	$\pi^+\pi^-$	P, CP < 1.1 × 10 <sup>-4</sup>
$\Gamma_{31}$	$\pi^0\pi^0$	P, CP < 3.5 × 10 <sup>-5</sup>
$\Gamma_{32}$	$K^+K^-$	P, CP < 6 × 10 <sup>-4</sup>
$\Gamma_{33}$	$K_S^0 K_S^0$	P, CP < 3.1 × 10 <sup>-4</sup>



Meson Particle Listings
ηc(1S)

Table with 6 columns: VALUE (eV), CL%, EVTS, DOCUMENT ID, TECN, COMMENT. Includes branching ratios like Γ(ρρ) × Γ(γγ)/Γtotal and Γ(φ2(π+π-))/Γtotal.

Table with 6 columns: VALUE (units 10^-4), CL%, DOCUMENT ID, TECN, COMMENT. Includes branching ratios like Γ(φ2(π+π-))/Γtotal and Γ(a0(980)π)/Γtotal.

ηc(1S) BRANCHING RATIOS

HADRONIC DECAYS

Table with 6 columns: VALUE, EVTS, DOCUMENT ID, TECN, COMMENT. Includes branching ratios like Γ(η'(958)ππ)/Γtotal, Γ(ρρ)/Γtotal, Γ(K\*(892)0 K- π+ + c.c.)/Γtotal, etc.

Table with 6 columns: VALUE, CL%, DOCUMENT ID, TECN, COMMENT. Includes branching ratios like Γ(ωω)/Γtotal, Γ(ωφ)/Γtotal, Γ(φ2(1270)φ2(1270))/Γtotal, etc.



See key on page 457

Meson Particle Listings

$\eta_c(1S), J/\psi(1S)$

Table with 5 columns: VALUE (units 10^-6), EVTS, DOCUMENT ID, TECN, COMMENT. Row 1: 0.250 ± 0.026 OUR FIT. Row 2: 0.26 ± 0.05 OUR AVERAGE Error includes scale factor of 1.4. Row 3: 0.224 +0.038 -0.037 ± 0.020 190 AMBROGIANI 03 E835 p-bar p -> eta\_c -> gamma gamma. Row 4: 0.336 +0.080 -0.070 ARMSTRONG 95F E760 p-bar p -> gamma gamma. Row 5: 0.68 +0.42 -0.31 12 BAGLIN 87B SPEC p-bar p -> gamma gamma.

Charge conjugation (C), Parity (P), Lepton family number (LF) violating modes

Table with 5 columns: VALUE (units 10^-9), CL%, DOCUMENT ID, TECN, COMMENT. Row 1: <11 90 71 ABLIKIM 11G BES3 J/psi -> gamma pi+ pi-. Row 2: <60 90 72 ABLIKIM 06B BES2 J/psi -> pi+ pi- gamma. Row 3: 71 ABLIKIM 11G reports [Gamma(eta\_c(1S) -> pi+ pi-)/Gamma\_total] x [B(J/psi(1S) -> gamma eta\_c(1S))] < 1.82 x 10^-6 which we divide by our best value B(J/psi(1S) -> gamma eta\_c(1S)) = 1.7 x 10^-2. Row 4: 72 ABLIKIM 06B reports [Gamma(eta\_c(1S) -> pi+ pi-)/Gamma\_total] x [B(J/psi(1S) -> gamma eta\_c(1S))] < 1.1 x 10^-5 which we divide by our best value B(J/psi(1S) -> gamma eta\_c(1S)) = 1.7 x 10^-2.

Table with 5 columns: VALUE (units 10^-5), CL%, DOCUMENT ID, TECN, COMMENT. Row 1: < 3.5 90 73 ABLIKIM 11G BES3 J/psi -> gamma pi0 pi0. Row 2: <40 90 74 ABLIKIM 06B BES2 J/psi -> pi0 pi0 gamma. Row 3: 73 ABLIKIM 11G reports [Gamma(eta\_c(1S) -> pi0 pi0)/Gamma\_total] x [B(J/psi(1S) -> gamma eta\_c(1S))] < 6.0 x 10^-7 which we divide by our best value B(J/psi(1S) -> gamma eta\_c(1S)) = 1.7 x 10^-2. Row 4: 74 ABLIKIM 06B reports [Gamma(eta\_c(1S) -> pi0 pi0)/Gamma\_total] x [B(J/psi(1S) -> gamma eta\_c(1S))] < 0.71 x 10^-5 which we divide by our best value B(J/psi(1S) -> gamma eta\_c(1S)) = 1.7 x 10^-2.

Table with 5 columns: VALUE (units 10^-5), CL%, DOCUMENT ID, TECN, COMMENT. Row 1: <60 90 75 ABLIKIM 06B BES2 J/psi -> K+ K- gamma. Row 2: 75 ABLIKIM 06B reports [Gamma(eta\_c(1S) -> K+ K-)/Gamma\_total] x [B(J/psi(1S) -> gamma eta\_c(1S))] < 0.96 x 10^-5 which we divide by our best value B(J/psi(1S) -> gamma eta\_c(1S)) = 1.7 x 10^-2.

Table with 5 columns: VALUE (units 10^-5), CL%, DOCUMENT ID, TECN, COMMENT. Row 1: <31 90 76 ABLIKIM 06B BES2 J/psi -> K\_S^0 K\_S^0 gamma. Row 2: 76 ABLIKIM 06B reports [Gamma(eta\_c(1S) -> K\_S^0 K\_S^0)/Gamma\_total] x [B(J/psi(1S) -> gamma eta\_c(1S))] < 0.53 x 10^-5 which we divide by our best value B(J/psi(1S) -> gamma eta\_c(1S)) = 1.7 x 10^-2.

eta\_c(1S) REFERENCES

Table with 4 columns: ABLIKIM, DEL-AMO-SA., VINOBUROVA, LEES, MITCHELL, ADAMS, AUBERT, UEHARA, WICHT, ABE, ABLIKIM, ABLIKIM, ABLIKIM, PDG, WU, ABLIKIM, KUO, ABE, ABLIKIM, ASNER, AUBERT, AUBERT, BAI, ABDALLAH, AMBROGIANI, BAI, FANG, HUANG, ABE, BAI, BRANDENB..., ACCIARRI, BAI, ABREU, SHIRAI, ARMSTRONG, ALBRECHT, ADRIANI, BISELLO, BAI, CHEN, BAGLIN, BEHREND, BRAUNSCH..., AIHARA. Includes document IDs, techniques, and comments.

Table with 4 columns: BAGLIN, BALTRUSAITIS..., BERGER, GAISER, ALTHOFF, BALTRUSAITIS..., BLOOM, HIMEL, PARTRIDGE. Includes document IDs, techniques, and comments.

J/psi(1S)

I^G(J^PC) = 0^-(1^--)

J/psi(1S) MASS

Table with 5 columns: VALUE (MeV), EVTS, DOCUMENT ID, TECN, COMMENT. Row 1: 3096.916 ± 0.011 OUR AVERAGE. Row 2: 3096.917 ± 0.010 ± 0.007 AULCHENKO 03 KEDR e+ e- -> hadrons. Row 3: 3096.89 ± 0.09 502 1 ARTAMONOV 00 OLYA e+ e- -> hadrons. Row 4: 3096.91 ± 0.03 ± 0.01 2 ARMSTRONG 93B E760 p-bar p -> e+ e-. Row 5: 3096.95 ± 0.1 ± 0.3 193 BAGLIN 87 SPEC p-bar p -> e+ e- X. Row 6: 3097.5 ± 0.3 38k GRIBUSHIN 96 FMPS 515 pi- Be -> 2 mu X. Row 7: 3098.4 ± 2.0 82 LEMOIGNE 82 GOLI 185 pi- Be -> gamma mu+ mu- A. Row 8: 3096.93 ± 0.09 502 3 ZHOLENTZ 80 REDE e+ e- -> mu+ mu-. Row 9: 3097.0 ± 1 4 BRANDELIK 79C DASP e+ e-.

- 1 Reanalysis of ZHOLENTZ 80 using new electron mass (COHEN 87) and radiative corrections (KURAEV 85).
2 Mass central value and systematic error recalculated by us according to Eq. (16) in ARMSTRONG 93B, using the value for the psi(2S) mass from AULCHENKO 03.
3 Superseded by ARTAMONOV 00.
4 From a simultaneous fit to e+ e-, mu+ mu- and hadronic channels assuming Gamma(e+ e-) = Gamma(mu+ mu-).

J/psi(1S) WIDTH

Table with 5 columns: VALUE (keV), EVTS, DOCUMENT ID, TECN, COMMENT. Row 1: 92.9 ± 2.8 OUR AVERAGE Error includes scale factor of 1.1. Row 2: 96.1 ± 3.2 13k 5 ADAMS 06A CLEO e+ e- -> mu+ mu- gamma. Row 3: 84.4 ± 8.9 BAI 95B BES e+ e-. Row 4: 91 ± 11 ± 6 6 ARMSTRONG 93B E760 p-bar p -> e+ e-. Row 5: 85.5 ± 6.1 5.8 7 HSUEH 92 RVUE See T mini-review. Row 6: 94.1 ± 2.7 8 ANASHIN 10 KEDR 3.097 e+ e- -> e+ e-, mu+ mu-. Row 7: 93.7 ± 3.5 7.8k 5 AUBERT 04 BABR e+ e- -> mu+ mu- gamma.

- 5 Calculated by us from the reported values of Gamma(e+ e-) x B(mu+ mu-) using B(e+ e-) = (5.94 ± 0.06)% and B(mu+ mu-) = (5.93 ± 0.06)%.
6 The initial-state radiation correction reevaluated by ANDREOTTI 07 in its Ref. [4].
7 Using data from COFFMAN 92, BALDINI-CELIO 75, BOYARSKI 75, ESPOSITO 75B, BRANDELIK 79C.
8 Assuming Gamma(e+ e-) = Gamma(mu+ mu-) and using Gamma(e+ e-)/Gamma\_total = (5.94 ± 0.06)%.

J/psi(1S) DECAY MODES

Table with 4 columns: Mode, Fraction (Gamma\_i/Gamma), Scale factor/Confidence level. Row 1: Gamma\_1 hadrons (87.7 ± 0.5 %) %
Row 2: Gamma\_2 virtual gamma -> hadrons (13.50 ± 0.30) %
Row 3: Gamma\_3 g g g (64.1 ± 1.0) %
Row 4: Gamma\_4 gamma g g (8.8 ± 1.1) %
Row 5: Gamma\_5 e+ e- (5.94 ± 0.06) %
Row 6: Gamma\_6 e+ e- gamma [a] (8.8 ± 1.4) x 10^-3
Row 7: Gamma\_7 mu+ mu- (5.93 ± 0.06) %

Decays involving hadronic resonances

Table with 4 columns: Gamma\_i, Mode, Fraction (Gamma\_i/Gamma), Scale factor/Confidence level. Row 8: Gamma\_8 rho pi (1.69 ± 0.15) % S=2.4
Row 9: Gamma\_9 rho^0 pi^0 (5.6 ± 0.7) x 10^-3
Row 10: Gamma\_10 a\_2(1320) rho (1.09 ± 0.22) %
Row 11: Gamma\_11 omega pi+ pi+ pi- pi- (8.5 ± 3.4) x 10^-3
Row 12: Gamma\_12 omega pi+ pi- pi^0 (4.0 ± 0.7) x 10^-3
Row 13: Gamma\_13 omega pi+ pi- (8.6 ± 0.7) x 10^-3 S=1.1
Row 14: Gamma\_14 omega f\_2(1270) (4.3 ± 0.6) x 10^-3
Row 15: Gamma\_15 K\*(892)^0 K\*(892)^0 (2.3 ± 0.7) x 10^-4
Row 16: Gamma\_16 K\*(892)^+ K\*(892)^- (1.00 ± 0.22 -0.40) x 10^-3
Row 17: Gamma\_17 K\*(892)^+ K\*(800)^- (1.1 ± 1.0 -0.6) x 10^-3
Row 18: Gamma\_18 eta K\*(892)^0 K\*(892)^0 (1.15 ± 0.26) x 10^-3
Row 19: Gamma\_19 K\*(892)^0 K\*(1430)^0 + c.c. (6.0 ± 0.6) x 10^-3
Row 20: Gamma\_20 K\*(892)^0 K\*(1770)^0 + c.c. -> K\*(892)^0 K- pi+ + c.c. (6.9 ± 0.9) x 10^-4
Row 21: Gamma\_21 omega K\*(892)^0 K + c.c. (6.1 ± 0.9) x 10^-3









$\Gamma(\Sigma^0 \bar{\Sigma}^0) \times \Gamma(e^+ e^-)/\Gamma_{\text{total}}$					$\Gamma_{111} \Gamma_5/\Gamma$
VALUE (eV)	DOCUMENT ID	TECN	COMMENT		
<b>6.4 ± 1.2 ± 0.6</b>	AUBERT	07bD BABR	10.6 $e^+ e^- \rightarrow \Sigma^0 \bar{\Sigma}^0 \gamma$		

$\Gamma(2(\pi^+ \pi^-) K^+ K^-) \times \Gamma(e^+ e^-)/\Gamma_{\text{total}}$					$\Gamma_{112} \Gamma_5/\Gamma$
VALUE (10 <sup>-2</sup> keV)	EVTS	DOCUMENT ID	TECN	COMMENT	
<b>2.75 ± 0.23 ± 0.17</b>	205	AUBERT	06D BABR	10.6 $e^+ e^- \rightarrow K^+ K^- 2(\pi^+ \pi^-) \gamma$	

$\Gamma(\Lambda \bar{\Lambda}) \times \Gamma(e^+ e^-)/\Gamma_{\text{total}}$					$\Gamma_{118} \Gamma_5/\Gamma$
VALUE (eV)	DOCUMENT ID	TECN	COMMENT		
<b>10.7 ± 0.9 ± 0.7</b>	AUBERT	07bD BABR	10.6 $e^+ e^- \rightarrow \Lambda \bar{\Lambda} \gamma$		

$\Gamma(2(K^+ K^-)) \times \Gamma(e^+ e^-)/\Gamma_{\text{total}}$					$\Gamma_{121} \Gamma_5/\Gamma$
VALUE (eV)	EVTS	DOCUMENT ID	TECN	COMMENT	
<b>4.11 ± 0.39 ± 0.30</b>	156 ± 15	AUBERT	07AK BABR	10.6 $e^+ e^- \rightarrow 2(K^+ K^-) \gamma$	
4.0 ± 0.7 ± 0.6	38	<sup>36</sup> AUBERT	05D BABR	10.6 $e^+ e^- \rightarrow 2(K^+ K^-) \gamma$	
		<sup>36</sup>		Superseded by AUBERT 07AK.	

**$J/\psi(1S)$  BRANCHING RATIOS**

For the first four branching ratios, see also the partial widths, and (partial widths)  $\times \Gamma(e^+ e^-)/\Gamma_{\text{total}}$  above.

$\Gamma(\text{hadrons})/\Gamma_{\text{total}}$					$\Gamma_1/\Gamma$
VALUE	DOCUMENT ID	TECN	COMMENT		
<b>0.877 ± 0.005 OUR AVERAGE</b>					
0.878 ± 0.005	BAI	95B BES	$e^+ e^-$		
0.86 ± 0.02	BOYARSKI	75 MRK1	$e^+ e^-$		

$\Gamma(\text{virtual } \gamma \rightarrow \text{hadrons})/\Gamma_{\text{total}}$					$\Gamma_2/\Gamma$
VALUE	DOCUMENT ID	TECN	COMMENT		
<b>0.135 ± 0.003</b>	37,38	SETH	04 RVUE	$e^+ e^-$	
0.17 ± 0.02	<sup>37</sup>	BOYARSKI	75 MRK1	$e^+ e^-$	
				<sup>37</sup> Included in $\Gamma(\text{hadrons})/\Gamma_{\text{total}}$ .	
				<sup>38</sup> Using $B(J/\psi \rightarrow \ell^+ \ell^-) = (5.90 \pm 0.09)\%$ from RPP-2002 and $R = 2.28 \pm 0.04$ determined by a fit to data from BAI 00 and BAI 02c.	

$\Gamma(g g g)/\Gamma_{\text{total}}$					$\Gamma_3/\Gamma$
VALUE (units 10 <sup>-2</sup> )	EVTS	DOCUMENT ID	TECN	COMMENT	
<b>64.1 ± 1.0</b>	6 M	<sup>39</sup> BESSON	08 CLEO	$\psi(2S) \rightarrow \pi^+ \pi^- + \text{hadrons}$	
				<sup>39</sup> Calculated using the value $\Gamma(\gamma g g)/\Gamma(g g g) = 0.137 \pm 0.001 \pm 0.016 \pm 0.004$ from BESSON 08 and the PDG 08 values of $B(\ell^+ \ell^-)$ , $B(\text{virtual } \gamma \rightarrow \text{hadrons})$ , and $B(\gamma \eta_c)$ . The statistical error is negligible and the systematic error is partially correlated with that of $\Gamma(\gamma g g)/\Gamma_{\text{total}}$ measurement of BESSON 08.	

$\Gamma(\gamma g g)/\Gamma_{\text{total}}$					$\Gamma_4/\Gamma$
VALUE (units 10 <sup>-2</sup> )	EVTS	DOCUMENT ID	TECN	COMMENT	
<b>8.79 ± 1.05</b>	200 k	<sup>40</sup> BESSON	08 CLEO	$\psi(2S) \rightarrow \pi^+ \pi^- \gamma + \text{hadrons}$	
				<sup>40</sup> Calculated using the value $\Gamma(\gamma g g)/\Gamma(g g g) = 0.137 \pm 0.001 \pm 0.016 \pm 0.004$ from BESSON 08 and the value of $\Gamma(g g g)/\Gamma_{\text{total}}$ . The statistical error is negligible and the systematic error is partially correlated with that of $\Gamma(g g g)/\Gamma_{\text{total}}$ measurement of BESSON 08.	

$\Gamma(\gamma g g)/\Gamma(g g g)$					$\Gamma_4/\Gamma_3$
VALUE (units 10 <sup>-2</sup> )	EVTS	DOCUMENT ID	TECN	COMMENT	
<b>13.7 ± 0.1 ± 0.7</b>	6 M	BESSON	08 CLEO	$\psi(2S) \rightarrow \pi^+ \pi^- J/\psi$	

$\Gamma(e^+ e^-)/\Gamma_{\text{total}}$					$\Gamma_5/\Gamma$
VALUE (units 10 <sup>-2</sup> )	EVTS	DOCUMENT ID	TECN	COMMENT	
<b>5.94 ± 0.06 OUR AVERAGE</b>					
5.945 ± 0.067 ± 0.042	15 k	LI	05c CLEO	$\psi(2S) \rightarrow J/\psi \pi^+ \pi^-$	
5.90 ± 0.05 ± 0.10		BAI	98D BES	$\psi(2S) \rightarrow J/\psi \pi^+ \pi^-$	
6.09 ± 0.33		BAI	95B BES	$e^+ e^-$	
5.92 ± 0.15 ± 0.20		COFFMAN	92 MRK3	$\psi(2S) \rightarrow J/\psi \pi^+ \pi^-$	
6.9 ± 0.9		BOYARSKI	75 MRK1	$e^+ e^-$	

$\Gamma(e^+ e^- \gamma)/\Gamma_{\text{total}}$					$\Gamma_6/\Gamma$
VALUE (units 10 <sup>-3</sup> )	DOCUMENT ID	TECN	COMMENT		
<b>8.8 ± 1.3 ± 0.4</b>	<sup>41</sup> ARMSTRONG	96 E760	$\bar{p} p \rightarrow e^+ e^- \gamma$		
				<sup>41</sup> For $E_\gamma > 100$ MeV.	

$\Gamma(\mu^+ \mu^-)/\Gamma_{\text{total}}$					$\Gamma_7/\Gamma$
VALUE (units 10 <sup>-2</sup> )	EVTS	DOCUMENT ID	TECN	COMMENT	
<b>5.93 ± 0.06 OUR AVERAGE</b>					
5.960 ± 0.065 ± 0.050	17k	LI	05c CLEO	$\psi(2S) \rightarrow J/\psi \pi^+ \pi^-$	
5.84 ± 0.06 ± 0.10		BAI	98D BES	$\psi(2S) \rightarrow J/\psi \pi^+ \pi^-$	
6.08 ± 0.33		BAI	95B BES	$e^+ e^-$	
5.90 ± 0.15 ± 0.19		COFFMAN	92 MRK3	$\psi(2S) \rightarrow J/\psi \pi^+ \pi^-$	
6.9 ± 0.9		BOYARSKI	75 MRK1	$e^+ e^-$	

$\Gamma(e^+ e^-)/\Gamma(\mu^+ \mu^-)$					$\Gamma_5/\Gamma_7$
VALUE	DOCUMENT ID	TECN	COMMENT		
<b>0.998 ± 0.012 OUR AVERAGE</b>					
1.002 ± 0.021 ± 0.013	<sup>42</sup> ANASHIN	10 KEDR	3.097 $e^+ e^- \rightarrow e^+ e^-$ , $\mu^+ \mu^-$		
0.997 ± 0.012 ± 0.006	LI	05c CLEO	$\psi(2S) \rightarrow J/\psi \pi^+ \pi^-$		
				• • • We do not use the following data for averages, fits, limits, etc. • • •	
1.00 ± 0.07	BAI	95B BES	$e^+ e^-$		
1.00 ± 0.05	BOYARSKI	75 MRK1	$e^+ e^-$		
0.91 ± 0.15	ESPOSITO	75B FRAM	$e^+ e^-$		
0.93 ± 0.10	FORD	75 SPEC	$e^+ e^-$		

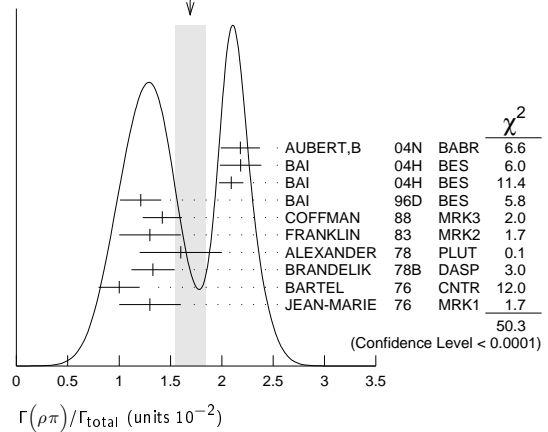
<sup>42</sup> Not independent of the corresponding measurements of  $\Gamma(e^+ e^-) \times \Gamma(e^+ e^-)/\Gamma_{\text{total}}$  and  $\Gamma(\mu^+ \mu^-) \times \Gamma(e^+ e^-)/\Gamma_{\text{total}}$ .

**HADRONIC DECAYS**

$\Gamma(\rho \pi)/\Gamma_{\text{total}}$					$\Gamma_8/\Gamma$
VALUE (units 10 <sup>-2</sup> )	EVTS	DOCUMENT ID	TECN	COMMENT	
<b>1.69 ± 0.15 OUR AVERAGE</b>				Error includes scale factor of 2.4. See the ideogram below.	
2.18 ± 0.19	43,44	AUBERT,B	04N BABR	10.6 $e^+ e^- \rightarrow \pi^+ \pi^- \pi^0 \gamma$	
2.184 ± 0.005 ± 0.201	220k	<sup>44,45</sup> BAI	04H BES	$e^+ e^- \rightarrow J/\psi \rightarrow \pi^+ \pi^- \pi^0$	
2.091 ± 0.021 ± 0.116	44,46	BAI	04H BES	$\psi(2S) \rightarrow \pi^+ \pi^- J/\psi$	
1.21 ± 0.20		BAI	96D BES	$e^+ e^- \rightarrow \rho \pi$	
1.42 ± 0.01 ± 0.19		COFFMAN	88 MRK3	$e^+ e^-$	
1.3 ± 0.3	150	FRANKLIN	83 MRK2	$e^+ e^-$	
1.6 ± 0.4	183	ALEXANDER	78 PLUT	$e^+ e^-$	
1.33 ± 0.21		BRANDELIK	78B DASP	$e^+ e^-$	
1.0 ± 0.2	543	BARTEL	76 CNTR	$e^+ e^-$	
1.3 ± 0.3	153	JEAN-MARIE	76 MRK1	$e^+ e^-$	

<sup>43</sup> From the ratio of  $\Gamma(e^+ e^-) B(\pi^+ \pi^- \pi^0)$  and  $\Gamma(e^+ e^-) B(\mu^+ \mu^-)$  (AUBERT 04).  
<sup>44</sup> Not independent of their  $B(\pi^+ \pi^- \pi^0)$ .  
<sup>45</sup> From  $J/\psi \rightarrow \pi^+ \pi^- \pi^0$  events directly.  
<sup>46</sup> Obtained comparing the rates for  $\pi^+ \pi^- \pi^0$  and  $\mu^+ \mu^-$ , using  $J/\psi$  events produced via  $\psi(2S) \rightarrow \pi^+ \pi^- J/\psi$  and with  $B(J/\psi \rightarrow \mu^+ \mu^-) = 5.88 \pm 0.10\%$ .

WEIGHTED AVERAGE  
1.69 ± 0.15 (Error scaled by 2.4)



$\Gamma(\rho^0 \pi^0)/\Gamma(\rho \pi)$					$\Gamma_9/\Gamma_8$
VALUE	DOCUMENT ID	TECN	COMMENT		
<b>0.328 ± 0.005 ± 0.027</b>	COFFMAN	88 MRK3	$e^+ e^-$		
				• • • We do not use the following data for averages, fits, limits, etc. • • •	
0.35 ± 0.08	ALEXANDER	78 PLUT	$e^+ e^-$		
0.32 ± 0.08	BRANDELIK	78B DASP	$e^+ e^-$		
0.39 ± 0.11	BARTEL	76 CNTR	$e^+ e^-$		
0.37 ± 0.09	JEAN-MARIE	76 MRK1	$e^+ e^-$		

$\Gamma(a_2(1320) \rho)/\Gamma_{\text{total}}$					$\Gamma_{10}/\Gamma$
VALUE (units 10 <sup>-3</sup> )	EVTS	DOCUMENT ID	TECN	COMMENT	
<b>10.9 ± 2.2 OUR AVERAGE</b>					
11.7 ± 0.7 ± 2.5	7584	AUGUSTIN	89 DM2	$J/\psi \rightarrow \rho^0 \rho^\pm \pi^\mp$	
8.4 ± 4.5	36	VANNUCCI	77 MRK1	$e^+ e^- \rightarrow 2(\pi^+ \pi^-) \pi^0$	

$\Gamma(\omega \pi^+ \pi^+ \pi^- \pi^-)/\Gamma_{\text{total}}$					$\Gamma_{11}/\Gamma$
VALUE (units 10 <sup>-4</sup> )	EVTS	DOCUMENT ID	TECN	COMMENT	
<b>85 ± 34</b>	140	VANNUCCI	77 MRK1	$e^+ e^- \rightarrow 3(\pi^+ \pi^-) \pi^0$	

$\Gamma(\omega \pi^+ \pi^- \pi^0)/\Gamma_{\text{total}}$					$\Gamma_{12}/\Gamma$
VALUE (units 10 <sup>-2</sup> )	EVTS	DOCUMENT ID	TECN	COMMENT	
<b>0.40 ± 0.06 ± 0.04</b>	170	<sup>47</sup> AUBERT	06D BABR	10.6 $e^+ e^- \rightarrow \omega \pi^+ \pi^- \pi^0 \gamma$	
				<sup>47</sup> Using $\Gamma(J/\psi \rightarrow e^+ e^-) = 5.52 \pm 0.14 \pm 0.04$ keV.	

## Meson Particle Listings

 $J/\psi(1S)$  $\Gamma(\omega\pi^+\pi^-)/\Gamma_{\text{total}}$   $\Gamma_{13}/\Gamma$ 

VALUE (units $10^{-3}$ )	EVTS	DOCUMENT ID	TECN	COMMENT
<b><math>8.6 \pm 0.7</math> OUR AVERAGE</b>	Error	includes scale factor of 1.1.		
$9.7 \pm 0.6 \pm 0.6$	788	<sup>48</sup> AUBERT	07AU BABR	$10.6 e^+e^- \rightarrow \omega\pi^+\pi^-\gamma$
$7.0 \pm 1.6$	18058	AUGUSTIN	89 DM2	$J/\psi \rightarrow 2(\pi^+\pi^-)\pi^0$
$7.8 \pm 1.6$	215	BURMESTER	77D PLUT	$e^+e^-$
$6.8 \pm 1.9$	348	VANNUCCI	77 MRK1	$e^+e^- \rightarrow 2(\pi^+\pi^-)\pi^0$
<sup>48</sup> AUBERT 07AU quotes $\Gamma_{ee}^{J/\psi} \cdot B(J/\psi \rightarrow \omega\pi^+\pi^-) \cdot B(\omega \rightarrow 3\pi) = 47.8 \pm 3.1 \pm 3.2$ eV.				

 $\Gamma(\omega f_2(1270))/\Gamma_{\text{total}}$   $\Gamma_{14}/\Gamma$ 

VALUE (units $10^{-3}$ )	EVTS	DOCUMENT ID	TECN	COMMENT
<b><math>4.3 \pm 0.6</math> OUR AVERAGE</b>				
$4.3 \pm 0.2 \pm 0.6$	5860	AUGUSTIN	89 DM2	$e^+e^-$
$4.0 \pm 1.6$	70	BURMESTER	77D PLUT	$e^+e^-$
• • • We do not use the following data for averages, fits, limits, etc. • • •				
$1.9 \pm 0.8$	81	VANNUCCI	77 MRK1	$e^+e^- \rightarrow 2(\pi^+\pi^-)\pi^0$

 $\Gamma(K^*(892)^0\bar{K}^*(892)^0)/\Gamma_{\text{total}}$   $\Gamma_{15}/\Gamma$ 

VALUE (units $10^{-4}$ )	CL%	EVTS	DOCUMENT ID	TECN	COMMENT
<b><math>2.3 \pm 0.7 \pm 0.1</math></b>		$25 \pm 8$	<sup>49</sup> AUBERT	07AK BABR	$10.6 e^+e^- \rightarrow \pi^+\pi^-K^+K^- \gamma$
• • • We do not use the following data for averages, fits, limits, etc. • • •					
<5	90		VANNUCCI	77 MRK1	$e^+e^- \rightarrow \pi^+\pi^-K^+K^-$
<sup>49</sup> AUBERT 07AK reports $[\Gamma(J/\psi(1S) \rightarrow K^*(892)^0\bar{K}^*(892)^0)/\Gamma_{\text{total}}] \times [\Gamma(J/\psi(1S) \rightarrow e^+e^-)] = (1.28 \pm 0.40 \pm 0.11) \times 10^{-3}$ keV which we divide by our best value $\Gamma(J/\psi(1S) \rightarrow e^+e^-) = 5.55 \pm 0.14 \pm 0.02$ keV. Our first error is their experiment's error and our second error is the systematic error from using our best value.					

 $\Gamma(K^*(892)^\pm\bar{K}^*(892)^\mp)/\Gamma_{\text{total}}$   $\Gamma_{16}/\Gamma$ 

VALUE (units $10^{-3}$ )	EVTS	DOCUMENT ID	TECN	COMMENT
<b><math>1.00 \pm 0.19 \pm 0.11</math></b>	323	ABLIKIM	10E BES2	$J/\psi \rightarrow K^\pm K_S^0 \pi^\mp \pi^0$

 $\Gamma(K^*(892)^\pm\bar{K}^*(800)^\mp)/\Gamma_{\text{total}}$   $\Gamma_{17}/\Gamma$ 

VALUE (units $10^{-3}$ )	EVTS	DOCUMENT ID	TECN	COMMENT
<b><math>1.09 \pm 0.18 \pm 0.94</math></b>	655	ABLIKIM	10E BES2	$J/\psi \rightarrow K^\pm K_S^0 \pi^\mp \pi^0$

 $\Gamma(\eta K^*(892)^0\bar{K}^*(892)^0)/\Gamma_{\text{total}}$   $\Gamma_{18}/\Gamma$ 

VALUE (units $10^{-3}$ )	EVTS	DOCUMENT ID	TECN	COMMENT
<b><math>1.15 \pm 0.13 \pm 0.22</math></b>	209	ABLIKIM	10c BES2	$J/\psi \rightarrow \eta K^+\pi^- K^-\pi^+$

 $\Gamma(K^*(892)^0\bar{K}_2^*(1430)^0 + c.c.)/\Gamma_{\text{total}}$   $\Gamma_{19}/\Gamma$ 

VALUE (units $10^{-3}$ )	EVTS	DOCUMENT ID	TECN	COMMENT
<b><math>6.0 \pm 0.6</math> OUR AVERAGE</b>				
$5.9 \pm 0.6 \pm 0.2$	$317 \pm 23$	<sup>50,51</sup> AUBERT	07AK BABR	$10.6 e^+e^- \rightarrow \pi^+\pi^-K^+K^- \gamma$
$6.7 \pm 2.6$	40	VANNUCCI	77 MRK1	$e^+e^- \rightarrow \pi^+\pi^-K^+K^-$
<sup>50</sup> Using $B(K_2^*(1430)^0 \rightarrow K\pi) = (49.9 \pm 1.2)\%$ .				
<sup>51</sup> AUBERT 07AK reports $[\Gamma(J/\psi(1S) \rightarrow K^*(892)^0\bar{K}_2^*(1430)^0 + c.c.)/\Gamma_{\text{total}}] \times [\Gamma(J/\psi(1S) \rightarrow e^+e^-)] = (32.9 \pm 2.3 \pm 2.7) \times 10^{-3}$ keV which we divide by our best value $\Gamma(J/\psi(1S) \rightarrow e^+e^-) = 5.55 \pm 0.14 \pm 0.02$ keV. Our first error is their experiment's error and our second error is the systematic error from using our best value.				

 $\Gamma(\omega K^*(892)\bar{K} + c.c.)/\Gamma_{\text{total}}$   $\Gamma_{21}/\Gamma$ 

VALUE (units $10^{-4}$ )	EVTS	DOCUMENT ID	TECN	COMMENT
<b><math>61 \pm 9</math> OUR AVERAGE</b>				
$62.0 \pm 6.8 \pm 10.6$	$899 \pm 98$	ABLIKIM	08E BES2	$J/\psi \rightarrow \omega K_S^0 K^\pm \pi^\mp$
$65.3 \pm 10.2 \pm 13.5$	$176 \pm 28$	ABLIKIM	08E BES2	$J/\psi \rightarrow \omega K^+ K^- \pi^0$
$53 \pm 14 \pm 14$	$530 \pm 140$	BECKER	87 MRK3	$e^+e^- \rightarrow \text{hadrons}$

 $\Gamma(K^+\bar{K}^*(892)^- + c.c.)/\Gamma_{\text{total}}$   $\Gamma_{22}/\Gamma$ 

VALUE (units $10^{-3}$ )	EVTS	DOCUMENT ID	TECN	COMMENT
<b><math>5.12 \pm 0.30</math> OUR AVERAGE</b>				
$5.2 \pm 0.4 \pm 0.1$		<sup>52</sup> AUBERT	08s BABR	$10.6 e^+e^- \rightarrow K^+\bar{K}^*(892)^-\gamma$
$4.57 \pm 0.17 \pm 0.70$	2285	JOUSSET	90 DM2	$J/\psi \rightarrow \text{hadrons}$
$5.26 \pm 0.13 \pm 0.53$		COFFMAN	88 MRK3	$J/\psi \rightarrow K^\pm K_S^0 \pi^\mp, K^+K^- \pi^0$
• • • We do not use the following data for averages, fits, limits, etc. • • •				
$2.6 \pm 0.6$	24	FRANKLIN	83 MRK2	$J/\psi \rightarrow K^+K^- \pi^0$
$3.2 \pm 0.6$	48	VANNUCCI	77 MRK1	$J/\psi \rightarrow K^\pm K_S^0 \pi^\mp$
$4.1 \pm 1.2$	39	BRAUNSCHE...	76 DASP	$J/\psi \rightarrow K^\pm X$

<sup>52</sup>AUBERT 08s reports  $[\Gamma(J/\psi(1S) \rightarrow K^+\bar{K}^*(892)^- + c.c.)/\Gamma_{\text{total}}] \times [\Gamma(J/\psi(1S) \rightarrow e^+e^-)] = (29.0 \pm 1.7 \pm 1.3) \times 10^{-3}$  keV which we divide by our best value  $\Gamma(J/\psi(1S) \rightarrow e^+e^-) = 5.55 \pm 0.14 \pm 0.02$  keV. Our first error is their experiment's error and our second error is the systematic error from using our best value.

 $\Gamma(K^+\bar{K}^*(892)^- + c.c. \rightarrow K^+K^-\pi^0)/\Gamma_{\text{total}}$   $\Gamma_{23}/\Gamma$ 

VALUE (units $10^{-3}$ )	EVTS	DOCUMENT ID	TECN	COMMENT
<b><math>1.97 \pm 0.20 \pm 0.05</math></b>	155	<sup>53</sup> AUBERT	08s BABR	$10.6 e^+e^- \rightarrow K^+K^-\pi^0 \gamma$
<sup>53</sup> AUBERT 08s reports $[\Gamma(J/\psi(1S) \rightarrow K^+\bar{K}^*(892)^- + c.c. \rightarrow K^+K^-\pi^0)/\Gamma_{\text{total}}] \times [\Gamma(J/\psi(1S) \rightarrow e^+e^-)] = (10.96 \pm 0.85 \pm 0.70) \times 10^{-3}$ keV which we divide by our best value $\Gamma(J/\psi(1S) \rightarrow e^+e^-) = 5.55 \pm 0.14 \pm 0.02$ keV. Our first error is their experiment's error and our second error is the systematic error from using our best value.				

 $\Gamma(K^+\bar{K}^*(892)^- + c.c. \rightarrow K^0 K^\pm \pi^\mp)/\Gamma_{\text{total}}$   $\Gamma_{24}/\Gamma$ 

VALUE (units $10^{-3}$ )	EVTS	DOCUMENT ID	TECN	COMMENT
<b><math>3.0 \pm 0.4 \pm 0.1</math></b>	89	<sup>54</sup> AUBERT	08s BABR	$10.6 e^+e^- \rightarrow K_S^0 K^\pm \pi^\mp \gamma$
<sup>54</sup> AUBERT 08s reports $[\Gamma(J/\psi(1S) \rightarrow K^+\bar{K}^*(892)^- + c.c. \rightarrow K^0 K^\pm \pi^\mp)/\Gamma_{\text{total}}] \times [\Gamma(J/\psi(1S) \rightarrow e^+e^-)] = (16.76 \pm 1.70 \pm 1.00) \times 10^{-3}$ keV which we divide by our best value $\Gamma(J/\psi(1S) \rightarrow e^+e^-) = 5.55 \pm 0.14 \pm 0.02$ keV. Our first error is their experiment's error and our second error is the systematic error from using our best value.				

 $\Gamma(K^0\bar{K}^*(892)^0 + c.c.)/\Gamma_{\text{total}}$   $\Gamma_{25}/\Gamma$ 

VALUE (units $10^{-3}$ )	EVTS	DOCUMENT ID	TECN	COMMENT
<b><math>4.39 \pm 0.31</math> OUR AVERAGE</b>				
$4.8 \pm 0.5 \pm 0.1$		<sup>55</sup> AUBERT	08s BABR	$10.6 e^+e^- \rightarrow K^0\bar{K}^*(892)^0 \gamma$
$3.96 \pm 0.15 \pm 0.60$	1192	JOUSSET	90 DM2	$J/\psi \rightarrow \text{hadrons}$
$4.33 \pm 0.12 \pm 0.45$		COFFMAN	88 MRK3	$J/\psi \rightarrow K^\pm K_S^0 \pi^\mp$
• • • We do not use the following data for averages, fits, limits, etc. • • •				
$2.7 \pm 0.6$	45	VANNUCCI	77 MRK1	$J/\psi \rightarrow K^\pm K_S^0 \pi^\mp$
<sup>55</sup> AUBERT 08s reports $[\Gamma(J/\psi(1S) \rightarrow K^0\bar{K}^*(892)^0 + c.c.)/\Gamma_{\text{total}}] \times [\Gamma(J/\psi(1S) \rightarrow e^+e^-)] = (26.6 \pm 2.5 \pm 1.5) \times 10^{-3}$ keV which we divide by our best value $\Gamma(J/\psi(1S) \rightarrow e^+e^-) = 5.55 \pm 0.14 \pm 0.02$ keV. Our first error is their experiment's error and our second error is the systematic error from using our best value.				

 $\Gamma(K^0\bar{K}^*(892)^0 + c.c.)/\Gamma(K^+\bar{K}^*(892)^- + c.c.)$   $\Gamma_{25}/\Gamma_{22}$ 

VALUE	DOCUMENT ID	TECN	COMMENT
<b><math>0.82 \pm 0.05 \pm 0.09</math></b>	COFFMAN	88 MRK3	$J/\psi \rightarrow K\bar{K}^*(892) + c.c.$

 $\Gamma(K^0\bar{K}^*(892)^0 + c.c. \rightarrow K^0 K^\pm \pi^\mp)/\Gamma_{\text{total}}$   $\Gamma_{26}/\Gamma$ 

VALUE (units $10^{-3}$ )	EVTS	DOCUMENT ID	TECN	COMMENT
<b><math>3.2 \pm 0.4 \pm 0.1</math></b>	94	<sup>56</sup> AUBERT	08s BABR	$10.6 e^+e^- \rightarrow K_S^0 K^\pm \pi^\mp \gamma$
<sup>56</sup> AUBERT 08s reports $[\Gamma(J/\psi(1S) \rightarrow K^0\bar{K}^*(892)^0 + c.c. \rightarrow K^0 K^\pm \pi^\mp)/\Gamma_{\text{total}}] \times [\Gamma(J/\psi(1S) \rightarrow e^+e^-)] = (17.70 \pm 1.70 \pm 1.00) \times 10^{-3}$ keV which we divide by our best value $\Gamma(J/\psi(1S) \rightarrow e^+e^-) = 5.55 \pm 0.14 \pm 0.02$ keV. Our first error is their experiment's error and our second error is the systematic error from using our best value.				

 $\Gamma(K_1(1400)^\pm K^\mp)/\Gamma_{\text{total}}$   $\Gamma_{27}/\Gamma$ 

VALUE (units $10^{-3}$ )	DOCUMENT ID	TECN	COMMENT
<b><math>3.8 \pm 0.8 \pm 1.2</math></b>	<sup>57</sup> BAI	99c BES	$e^+e^-$
<sup>57</sup> Assuming $B(K_1(1400) \rightarrow K^*\pi) = 0.94 \pm 0.06$			

 $\Gamma(\bar{K}^*(892)^0 K^+\pi^- + c.c.)/\Gamma_{\text{total}}$   $\Gamma_{28}/\Gamma$ 

VALUE	DOCUMENT ID	TECN	COMMENT
<b>seen</b>	<sup>58</sup> ABLIKIM	06c BES2	$J/\psi \rightarrow \bar{K}^*(892)^0 K^+\pi^-$
<sup>58</sup> A $K_0^*(800)$ is observed by ABLIKIM 06c in the $K^+\pi^-$ mass spectrum of the $\bar{K}^*(892)^0 K^+\pi^-$ final state against the $\bar{K}^*(892)$ . A corresponding branching fraction of the $J/\psi(1S)$ is not presented.			

 $\Gamma(\omega\pi^0\pi^0)/\Gamma_{\text{total}}$   $\Gamma_{29}/\Gamma$ 

VALUE (units $10^{-3}$ )	EVTS	DOCUMENT ID	TECN	COMMENT
<b><math>3.4 \pm 0.3 \pm 0.7</math></b>	509	AUGUSTIN	89 DM2	$J/\psi \rightarrow \pi^+\pi^-\pi^0$

 $\Gamma(b_1(1235)^\pm \pi^\mp)/\Gamma_{\text{total}}$   $\Gamma_{30}/\Gamma$ 

VALUE (units $10^{-4}$ )	EVTS	DOCUMENT ID	TECN	COMMENT
<b><math>30 \pm 5</math> OUR AVERAGE</b>				
$31 \pm 6$	4600	AUGUSTIN	89 DM2	$J/\psi \rightarrow 2(\pi^+\pi^-)\pi^0$
$29 \pm 7$	87	BURMESTER	77D PLUT	$e^+e^-$

 $\Gamma(\omega K^\pm K_S^0 \pi^\mp)/\Gamma_{\text{total}}$   $\Gamma_{31}/\Gamma$ 

VALUE (units $10^{-4}$ )	EVTS	DOCUMENT ID	TECN	COMMENT
<b><math>34 \pm 5</math> OUR AVERAGE</b>				
$37.7 \pm 0.8 \pm 5.8$	1972 $\pm$ 41	ABLIKIM	08E BES2	$e^+e^- \rightarrow J/\psi$
$29.5 \pm 1.4 \pm 7.0$	879 $\pm$ 41	BECKER	87 MRK3	$e^+e^- \rightarrow \text{hadrons}$

 $\Gamma(b_1(1235)^0\pi^0)/\Gamma_{\text{total}}$   $\Gamma_{32}/\Gamma$ 

VALUE (units $10^{-4}$ )	EVTS	DOCUMENT ID	TECN	COMMENT
<b><math>23 \pm 3 \pm 5</math></b>	229	AUGUSTIN	89 DM2	$e^+e^-$

 $\Gamma(\eta K^\pm K_S^0 \pi^\mp)/\Gamma_{\text{total}}$   $\Gamma_{33}/\Gamma$ 

VALUE (units $10^{-4}$ )	EVTS	DOCUMENT ID	TECN	COMMENT
<b><math>21.8 \pm 2.2 \pm 3.4</math></b>	232 $\pm$ 23	ABLIKIM	08E BES2	$e^+e^- \rightarrow J/\psi$

$\Gamma(\phi K^*(892)\bar{K} + c.c.)/\Gamma_{total}$   $\Gamma_{34}/\Gamma$

VALUE (units $10^{-4}$ )	EVTS	DOCUMENT ID	TECN	COMMENT
<b>21.8 ± 2.3 OUR AVERAGE</b>				
20.8 ± 2.7 ± 3.9	195 ± 25	ABLIKIM	08E BES2	$J/\psi \rightarrow \phi K_2^0 K^\pm \pi^\mp$
29.6 ± 3.7 ± 4.7	238 ± 30	ABLIKIM	08E BES2	$J/\psi \rightarrow \phi K^+ K^- \pi^0$
20.7 ± 2.4 ± 3.0		FALVARD	88 DM2	$J/\psi \rightarrow$ hadrons
20 ± 3 ± 3	155 ± 20	BECKER	87 MRK3	$e^+ e^- \rightarrow$ hadrons

$\Gamma(\omega K\bar{K})/\Gamma_{total}$   $\Gamma_{35}/\Gamma$

VALUE (units $10^{-4}$ )	EVTS	DOCUMENT ID	TECN	COMMENT
<b>17.0 ± 3.2 OUR AVERAGE</b>				
13.6 ± 5.0 ± 1.0	24	<sup>59</sup> AUBERT	07AU BABR	$10.6 e^+ e^- \rightarrow \omega K^+ K^- \gamma$
19.8 ± 2.1 ± 3.9		<sup>60</sup> FALVARD	88 DM2	$J/\psi \rightarrow$ hadrons
16 ± 10	22	FELDMAN	77 MRK1	$e^+ e^-$

<sup>59</sup>AUBERT 07AU quotes  $\Gamma_{ee}^{J/\psi} \cdot B(J/\psi \rightarrow \omega K^+ K^-) \cdot B(\eta \rightarrow 3\pi) = 3.3 \pm 1.3 \pm 0.2$  eV.  
<sup>60</sup>Addition of  $\omega K^+ K^-$  and  $\omega K^0 \bar{K}^0$  branching ratios.

$\Gamma(\omega f_0(1710) \rightarrow \omega K\bar{K})/\Gamma_{total}$   $\Gamma_{36}/\Gamma$

VALUE (units $10^{-4}$ )	DOCUMENT ID	TECN	COMMENT
<b>4.8 ± 1.1 ± 0.3</b>	<sup>61,62</sup> FALVARD	88 DM2	$J/\psi \rightarrow$ hadrons

<sup>61</sup>Includes unknown branching fraction  $f_0(1710) \rightarrow K\bar{K}$ .  
<sup>62</sup>Addition of  $f_0(1710) \rightarrow K^+ K^-$  and  $f_0(1710) \rightarrow K^0 \bar{K}^0$  branching ratios.

$\Gamma(\phi 2(\pi^+ \pi^-))/\Gamma_{total}$   $\Gamma_{37}/\Gamma$

VALUE (units $10^{-4}$ )	EVTS	DOCUMENT ID	TECN	COMMENT
<b>16.6 ± 2.3 OUR AVERAGE</b>				
17.3 ± 3.3 ± 1.2	35	<sup>63</sup> AUBERT	06D BABR	$10.6 e^+ e^- \rightarrow \phi 2(\pi^+ \pi^-) \gamma$
16.0 ± 1.0 ± 3.0		FALVARD	88 DM2	$J/\psi \rightarrow$ hadrons

<sup>63</sup>Using  $\Gamma(J/\psi \rightarrow e^+ e^-) = 5.52 \pm 0.14 \pm 0.04$  keV.

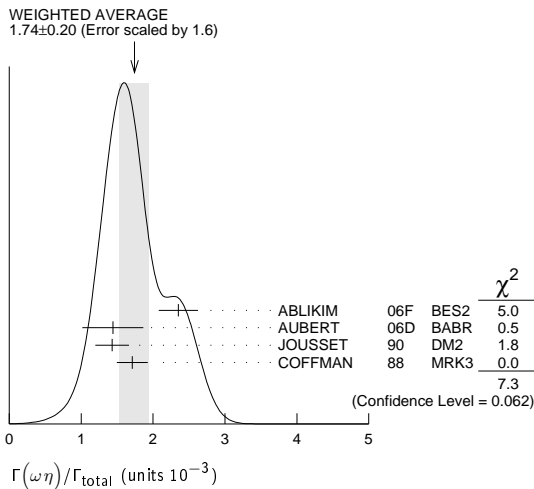
$\Gamma(\Delta(1232)^+ \bar{p} \pi^-)/\Gamma_{total}$   $\Gamma_{38}/\Gamma$

VALUE (units $10^{-3}$ )	EVTS	DOCUMENT ID	TECN	COMMENT
<b>1.58 ± 0.23 ± 0.40</b>	332	EATON	84 MRK2	$e^+ e^-$

$\Gamma(\omega \eta)/\Gamma_{total}$   $\Gamma_{39}/\Gamma$

VALUE (units $10^{-3}$ )	EVTS	DOCUMENT ID	TECN	COMMENT
<b>1.74 ± 0.20 OUR AVERAGE</b>				Error includes scale factor of 1.6. See the ideogram below.
2.352 ± 0.273	5k	<sup>64</sup> ABLIKIM	06F BES2	$J/\psi \rightarrow \omega \eta$
1.44 ± 0.40 ± 0.14	13	<sup>65</sup> AUBERT	06D BABR	$10.6 e^+ e^- \rightarrow \omega \eta \gamma$
1.43 ± 0.10 ± 0.21	378	JOUSSET	90 DM2	$J/\psi \rightarrow$ hadrons
1.71 ± 0.08 ± 0.20		COFFMAN	88 MRK3	$e^+ e^- \rightarrow 3\pi \eta$

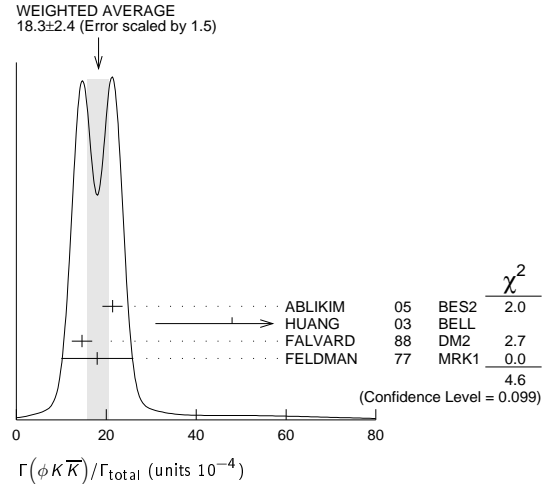
<sup>64</sup>Using  $B(\eta \rightarrow 2\gamma) = (39.43 \pm 0.26)\%$ ,  $B(\eta \rightarrow \pi^+ \pi^- \pi^0) = 22.6 \pm 0.4\%$ ,  $B(\eta \rightarrow \pi^+ \pi^- \gamma) = 4.68 \pm 0.11\%$ , and  $B(\omega \rightarrow \pi^+ \pi^- \pi^0) = (89.1 \pm 0.7)\%$ .  
<sup>65</sup>Using  $\Gamma(J/\psi \rightarrow e^+ e^-) = 5.52 \pm 0.14 \pm 0.04$  keV.



$\Gamma(\phi K\bar{K})/\Gamma_{total}$   $\Gamma_{40}/\Gamma$

VALUE (units $10^{-4}$ )	EVTS	DOCUMENT ID	TECN	COMMENT
<b>18.3 ± 2.4 OUR AVERAGE</b>				Error includes scale factor of 1.5. See the ideogram below.
21.4 ± 0.4 ± 2.2		ABLIKIM	05 BES2	$J/\psi \rightarrow \phi \pi^+ \pi^-$
48 ± 20 ± 6	9.0 ± 3.7 ± 3.0	<sup>66,67</sup> HUANG	03 BELL	$B^+ \rightarrow (\phi K^+ K^-) K^+$
14.6 ± 0.8 ± 2.1		<sup>68</sup> FALVARD	88 DM2	$J/\psi \rightarrow$ hadrons
18 ± 8	14	FELDMAN	77 MRK1	$e^+ e^-$

<sup>66</sup>We have multiplied  $K^+ K^-$  measurement by 2 to obtain  $K\bar{K}$ .  
<sup>67</sup>Using  $B(B^+ \rightarrow J/\psi K^+) = (1.01 \pm 0.05) \times 10^{-3}$ .  
<sup>68</sup>Addition of  $\phi K^+ K^-$  and  $\phi K^0 \bar{K}^0$  branching ratios.



$\Gamma(\phi f_0(1710) \rightarrow \phi K\bar{K})/\Gamma_{total}$   $\Gamma_{41}/\Gamma$

VALUE (units $10^{-4}$ )	DOCUMENT ID	TECN	COMMENT
<b>3.6 ± 0.2 ± 0.6</b>	<sup>69,70</sup> FALVARD	88 DM2	$J/\psi \rightarrow$ hadrons

<sup>69</sup>Including interference with  $f_2'(1525)$ .  
<sup>70</sup>Includes unknown branching fraction  $f_0(1710) \rightarrow K\bar{K}$ .

$\Gamma(\phi f_2(1270))/\Gamma_{total}$   $\Gamma_{42}/\Gamma$

VALUE (units $10^{-3}$ )	CL%	EVTS	DOCUMENT ID	TECN	COMMENT
<b>0.72 ± 0.13 ± 0.02</b>		44 ± 7	<sup>71,72</sup> AUBERT	07AK BABR	$10.6 e^+ e^- \rightarrow \pi^+ \pi^- K^+ K^- \gamma$

• • • We do not use the following data for averages, fits, limits, etc. • • •  
 < 0.45 90 FALVARD 88 DM2  $J/\psi \rightarrow$  hadrons  
 < 0.37 90 VANNUCCI 77 MRK1  $e^+ e^- \rightarrow \pi^+ \pi^- K^+ K^-$

<sup>71</sup>Using  $B(f_2(1270) \rightarrow \pi\pi) = (84.8 \pm 2.4)_{-1.2}^{\pm 2.4}\%$   
<sup>72</sup>AUBERT 07AK reports  $[\Gamma(J/\psi(1S) \rightarrow \phi f_2(1270))/\Gamma_{total}] \times [\Gamma(J/\psi(1S) \rightarrow e^+ e^-)] = (4.02 \pm 0.65 \pm 0.33) \times 10^{-3}$  keV which we divide by our best value  $\Gamma(J/\psi(1S) \rightarrow e^+ e^-) = 5.55 \pm 0.14 \pm 0.02$  keV. Our first error is their experiment's error and our second error is the systematic error from using our best value.

$\Gamma(\Delta(1232)^+ \bar{\Delta}(1232)^-)/\Gamma_{total}$   $\Gamma_{43}/\Gamma$

VALUE (units $10^{-3}$ )	EVTS	DOCUMENT ID	TECN	COMMENT
<b>1.10 ± 0.09 ± 0.28</b>	233	EATON	84 MRK2	$e^+ e^-$

$\Gamma(\Sigma(1385)^+ \bar{\Sigma}(1385)^- (\text{or c.c.}))/\Gamma_{total}$   $\Gamma_{44}/\Gamma$

VALUE (units $10^{-3}$ )	EVTS	DOCUMENT ID	TECN	COMMENT
<b>1.03 ± 0.13 OUR AVERAGE</b>				
1.00 ± 0.04 ± 0.21	631 ± 25	HENRARD	87 DM2	$e^+ e^- \rightarrow \Sigma^{*-}$
1.19 ± 0.04 ± 0.25	754 ± 27	HENRARD	87 DM2	$e^+ e^- \rightarrow \Sigma^{*+}$
0.86 ± 0.18 ± 0.22	56	EATON	84 MRK2	$e^+ e^- \rightarrow \Sigma^{*-}$
1.03 ± 0.24 ± 0.25	68	EATON	84 MRK2	$e^+ e^- \rightarrow \Sigma^{*+}$

$\Gamma(\phi f_2'(1525))/\Gamma_{total}$   $\Gamma_{45}/\Gamma$

VALUE (units $10^{-4}$ )	EVTS	DOCUMENT ID	TECN	COMMENT
<b>8 ± 4 OUR AVERAGE</b>				Error includes scale factor of 2.7.
12.3 ± 0.6 ± 2.0		<sup>73,74</sup> FALVARD	88 DM2	$J/\psi \rightarrow$ hadrons
4.8 ± 1.8	46	<sup>73</sup> GIDAL	81 MRK2	$J/\psi \rightarrow K^+ K^- K^+ K^-$

<sup>73</sup>Re-evaluated using  $B(f_2'(1525) \rightarrow K\bar{K}) = 0.713$ .  
<sup>74</sup>Including interference with  $f_0(1710)$ .

$\Gamma(\phi \pi^+ \pi^-)/\Gamma_{total}$   $\Gamma_{46}/\Gamma$

VALUE (units $10^{-3}$ )	EVTS	DOCUMENT ID	TECN	COMMENT
<b>0.94 ± 0.09 OUR AVERAGE</b>				Error includes scale factor of 1.2.
0.96 ± 0.13	103	<sup>75</sup> AUBERT, BE	06D BABR	$10.6 e^+ e^- \rightarrow K^+ K^- \pi^+ \pi^- \gamma$
1.09 ± 0.02 ± 0.13		ABLIKIM	05 BES2	$J/\psi \rightarrow \phi \pi^+ \pi^-$
0.78 ± 0.03 ± 0.12		FALVARD	88 DM2	$J/\psi \rightarrow$ hadrons
2.1 ± 0.9	23	FELDMAN	77 MRK1	$e^+ e^-$

<sup>75</sup>Derived by us. AUBERT, BE 06D measures  $\Gamma(J/\psi \rightarrow e^+ e^-) \times B(J/\psi \rightarrow \phi \pi^+ \pi^-) \times B(\phi \rightarrow K^+ K^-) = (2.61 \pm 0.30 \pm 0.18)$  eV

$\Gamma(\phi \pi^0 \pi^0)/\Gamma_{total}$   $\Gamma_{47}/\Gamma$

VALUE (units $10^{-3}$ )	EVTS	DOCUMENT ID	TECN	COMMENT
<b>0.56 ± 0.16</b>	23	<sup>76</sup> AUBERT, BE	06D BABR	$10.6 e^+ e^- \rightarrow K^+ K^- \pi^0 \pi^0 \gamma$

<sup>76</sup>Derived by us. AUBERT, BE 06D measures  $\Gamma(J/\psi \rightarrow e^+ e^-) \times B(J/\psi \rightarrow \phi \pi^0 \pi^0) \times B(\phi \rightarrow K^+ K^-) = (1.54 \pm 0.40 \pm 0.16)$  eV

## Meson Particle Listings

 $J/\psi(1S)$  $\Gamma(\phi K^\pm K_S^0 \pi^\mp)/\Gamma_{\text{total}}$   $\Gamma_{48}/\Gamma$ 

VALUE (units $10^{-4}$ )	EVTS	DOCUMENT ID	TECN	COMMENT
<b><math>7.2 \pm 0.8</math></b>	<b>OUR AVERAGE</b>			
$7.4 \pm 0.6 \pm 1.4$	$227 \pm 19$	ABLIKIM	08E BES2	$e^+e^- \rightarrow J/\psi$
$7.4 \pm 0.9 \pm 1.1$		FALVARD	88 DM2	$J/\psi \rightarrow \text{hadrons}$
$7 \pm 0.6 \pm 1.0$	$163 \pm 15$	BECKER	87 MRK3	$e^+e^- \rightarrow \text{hadrons}$

 $\Gamma(\omega f_1(1420))/\Gamma_{\text{total}}$   $\Gamma_{49}/\Gamma$ 

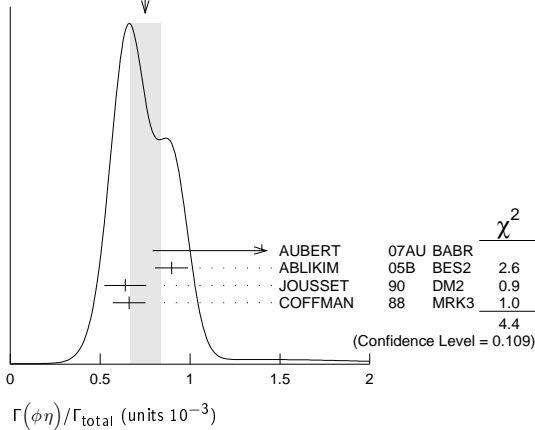
VALUE (units $10^{-4}$ )	EVTS	DOCUMENT ID	TECN	COMMENT
<b><math>6.8 \pm 1.9</math></b>	<b><math>111 \pm 31</math></b>	<b>OUR AVERAGE</b>		
		BECKER	87 MRK3	$e^+e^- \rightarrow \text{hadrons}$

 $\Gamma(\phi\eta)/\Gamma_{\text{total}}$   $\Gamma_{50}/\Gamma$ 

VALUE (units $10^{-3}$ )	EVTS	DOCUMENT ID	TECN	COMMENT
<b><math>0.75 \pm 0.08</math></b>	<b>OUR AVERAGE</b>			
$1.4 \pm 0.6 \pm 0.1$	6	<sup>77</sup> AUBERT	07AU BABR	$10.6 e^+e^- \rightarrow \phi\eta\gamma$
$0.898 \pm 0.024 \pm 0.089$		ABLIKIM	05B BES2	$e^+e^- \rightarrow J/\psi \rightarrow \text{hadr}$
$0.64 \pm 0.04 \pm 0.11$	346	JOUSSET	90 DM2	$J/\psi \rightarrow \text{hadrons}$
$0.661 \pm 0.045 \pm 0.078$		COFFMAN	88 MRK3	$e^+e^- \rightarrow K^+K^-\eta$

<sup>77</sup>AUBERT 07AU quotes  $\Gamma_{ee}^{J/\psi} \cdot B(J/\psi \rightarrow \phi\eta) \cdot B(\phi \rightarrow K^+K^-) \cdot B(\eta \rightarrow \gamma\gamma) = 0.84 \pm 0.37 \pm 0.05$  eV.

WEIGHTED AVERAGE  
0.75±0.08 (Error scaled by 1.5)

 $\Gamma(\Xi^0 \Xi^0)/\Gamma_{\text{total}}$   $\Gamma_{51}/\Gamma$ 

VALUE (units $10^{-3}$ )	EVTS	DOCUMENT ID	TECN	COMMENT
<b><math>1.20 \pm 0.12 \pm 0.21</math></b>	206	OUR AVERAGE		
		ABLIKIM	08o BES2	$e^+e^- \rightarrow J/\psi$

 $\Gamma(\Xi(1530)^-\Xi^+)/\Gamma_{\text{total}}$   $\Gamma_{52}/\Gamma$ 

VALUE (units $10^{-3}$ )	EVTS	DOCUMENT ID	TECN	COMMENT
<b><math>0.59 \pm 0.09 \pm 0.12</math></b>	$75 \pm 11$	OUR AVERAGE		
		HENRARD	87 DM2	$e^+e^-$

 $\Gamma(\rho K^- \bar{\Sigma}(1385)^0)/\Gamma_{\text{total}}$   $\Gamma_{53}/\Gamma$ 

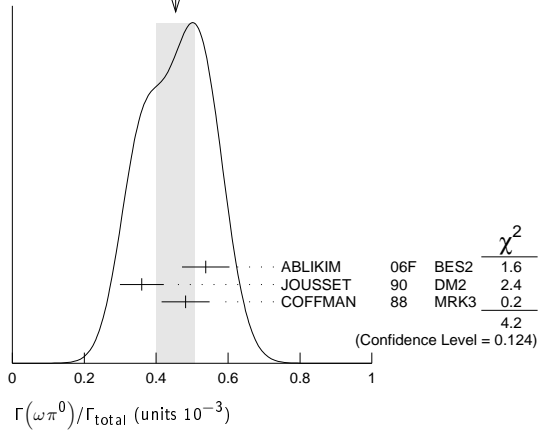
VALUE (units $10^{-3}$ )	EVTS	DOCUMENT ID	TECN	COMMENT
<b><math>0.51 \pm 0.26 \pm 0.18</math></b>	89	OUR AVERAGE		
		EATON	84 MRK2	$e^+e^-$

 $\Gamma(\omega\pi^0)/\Gamma_{\text{total}}$   $\Gamma_{54}/\Gamma$ 

VALUE (units $10^{-3}$ )	EVTS	DOCUMENT ID	TECN	COMMENT
<b><math>0.45 \pm 0.05</math></b>	<b>OUR AVERAGE</b>			
$0.538 \pm 0.012 \pm 0.065$	2090	<sup>78</sup> ABLIKIM	06F BES2	$J/\psi \rightarrow \omega\pi^0$
$0.360 \pm 0.028 \pm 0.054$	222	JOUSSET	90 DM2	$J/\psi \rightarrow \text{hadrons}$
$0.482 \pm 0.019 \pm 0.064$		COFFMAN	88 MRK3	$e^+e^- \rightarrow \pi^0\pi^+\pi^-\pi^0$

<sup>78</sup>Using  $B(\omega \rightarrow \pi^+\pi^-\pi^0) = (89.1 \pm 0.7)\%$ .

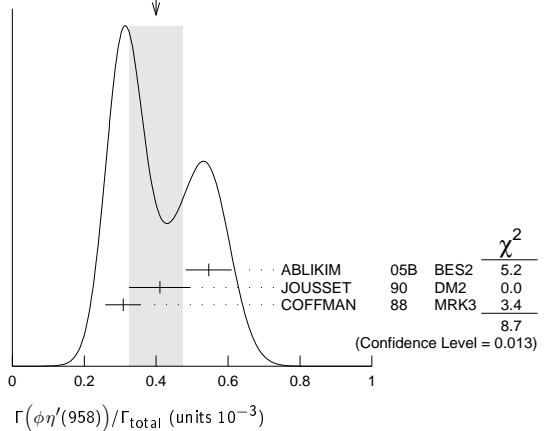
WEIGHTED AVERAGE  
0.45±0.05 (Error scaled by 1.4)

 $\Gamma(\phi\eta'(958))/\Gamma_{\text{total}}$   $\Gamma_{55}/\Gamma$ 

VALUE (units $10^{-3}$ )	CL%	EVTS	DOCUMENT ID	TECN	COMMENT
<b><math>0.40 \pm 0.07</math></b>	<b>OUR AVERAGE</b>				Error includes scale factor of 2.1. See the ideogram below.
$0.546 \pm 0.031 \pm 0.056$			ABLIKIM	05B BES2	$e^+e^- \rightarrow J/\psi \rightarrow \text{hadr}$
$0.41 \pm 0.03 \pm 0.08$		167	JOUSSET	90 DM2	$J/\psi \rightarrow \text{hadrons}$
$0.308 \pm 0.034 \pm 0.036$			COFFMAN	88 MRK3	$e^+e^- \rightarrow K^+K^-\eta'$
$< 1.3$		90	VANNUCCI	77 MRK1	$e^+e^-$

••• We do not use the following data for averages, fits, limits, etc. •••

WEIGHTED AVERAGE  
0.40±0.07 (Error scaled by 2.1)

 $\Gamma(\phi f_0(980))/\Gamma_{\text{total}}$   $\Gamma_{56}/\Gamma$ 

VALUE (units $10^{-4}$ )	EVTS	DOCUMENT ID	TECN	COMMENT
<b><math>3.2 \pm 0.9</math></b>	<b>OUR AVERAGE</b>			Error includes scale factor of 1.9.
$4.6 \pm 0.4 \pm 0.8$		<sup>79</sup> FALVARD	88 DM2	$J/\psi \rightarrow \text{hadrons}$
$2.6 \pm 0.6$	50	<sup>79</sup> GIDAL	81 MRK2	$J/\psi \rightarrow K^+K^-K^+K^-$

<sup>79</sup>Assuming  $B(f_0(980) \rightarrow \pi\pi) = 0.78$ .

 $\Gamma(\phi f_0(980) \rightarrow \phi\pi^+\pi^-)/\Gamma_{\text{total}}$   $\Gamma_{57}/\Gamma$ 

VALUE (units $10^{-3}$ )	EVTS	DOCUMENT ID	TECN	COMMENT
<b><math>0.182 \pm 0.042 \pm 0.005</math></b>	$19.5 \pm 4.5$	<sup>80,81</sup> AUBERT	07AK BABR	$10.6 e^+e^- \rightarrow \pi^+\pi^-K^+K^-\gamma$

<sup>80</sup>Using  $B(\phi \rightarrow K^+K^-) = (49.3 \pm 0.6)\%$ .

<sup>81</sup>AUBERT 07AK reports  $[\Gamma(J/\psi(1S) \rightarrow \phi f_0(980) \rightarrow \phi\pi^+\pi^-)/\Gamma_{\text{total}}] \times [\Gamma(J/\psi(1S) \rightarrow e^+e^-)] = (1.01 \pm 0.22 \pm 0.08) \times 10^{-3}$  keV which we divide by our best value  $\Gamma(J/\psi(1S) \rightarrow e^+e^-) = 5.55 \pm 0.14 \pm 0.02$  keV. Our first error is their experiment's error and our second error is the systematic error from using our best value.

 $\Gamma(\phi f_0(980) \rightarrow \phi\pi^0\pi^0)/\Gamma_{\text{total}}$   $\Gamma_{58}/\Gamma$ 

VALUE (units $10^{-3}$ )	EVTS	DOCUMENT ID	TECN	COMMENT
<b><math>0.171 \pm 0.073 \pm 0.004</math></b>	$7.0 \pm 2.8$	<sup>82,83</sup> AUBERT	07AK BABR	$10.6 e^+e^- \rightarrow \pi^0\pi^0K^+K^-\gamma$

<sup>82</sup>Using  $B(\phi \rightarrow K^+K^-) = (49.3 \pm 0.6)\%$ .

<sup>83</sup>AUBERT 07AK reports  $[\Gamma(J/\psi(1S) \rightarrow \phi f_0(980) \rightarrow \phi\pi^0\pi^0)/\Gamma_{\text{total}}] \times [\Gamma(J/\psi(1S) \rightarrow e^+e^-)] = (0.95 \pm 0.39 \pm 0.10) \times 10^{-3}$  keV which we divide by our best value  $\Gamma(J/\psi(1S) \rightarrow e^+e^-) = 5.55 \pm 0.14 \pm 0.02$  keV. Our first error is their experiment's error and our second error is the systematic error from using our best value.

See key on page 457

## Meson Particle Listings

 $J/\psi(1S)$ 

$\Gamma(\eta\phi f_0(980) \rightarrow \eta\phi\pi^+\pi^-)/\Gamma_{\text{total}}$					$\Gamma_{59}/\Gamma$
VALUE (units $10^{-4}$ )	EVTS	DOCUMENT ID	TECN	COMMENT	
<b>3.23 ± 0.75 ± 0.73</b>	52	ABLIKIM	08F BES	$J/\psi \rightarrow \eta\phi f_0(980)$	

$\Gamma(\phi a_0(980)^0 \rightarrow \phi\eta\pi^0)/\Gamma_{\text{total}}$					$\Gamma_{60}/\Gamma$
VALUE (units $10^{-6}$ )		DOCUMENT ID	TECN	COMMENT	
<b>5.0 ± 2.7 ± 2.5</b>		84 ABLIKIM	11D BES3	$J/\psi \rightarrow \phi\eta\pi^0$	
84 Assuming $a_0(980) - f_0(980)$ mixing and isospin breaking via $\gamma^*$ and $K^*K$ loops.					

$\Gamma(\Xi(1530)^0 \Xi^0)/\Gamma_{\text{total}}$					$\Gamma_{61}/\Gamma$
VALUE (units $10^{-3}$ )	EVTS	DOCUMENT ID	TECN	COMMENT	
<b>0.32 ± 0.12 ± 0.07</b>	24 ± 9	HENRRARD	87 DM2	$e^+e^-$	

$\Gamma(\Sigma(1385)^- \Sigma^+ \text{ (or c.c.)})/\Gamma_{\text{total}}$					$\Gamma_{62}/\Gamma$
VALUE (units $10^{-3}$ )	EVTS	DOCUMENT ID	TECN	COMMENT	
<b>0.31 ± 0.05 OUR AVERAGE</b>					
0.30 ± 0.03 ± 0.07	74 ± 8	HENRRARD	87 DM2	$e^+e^- \rightarrow \Sigma^{*-}$	
0.34 ± 0.04 ± 0.07	77 ± 9	HENRRARD	87 DM2	$e^+e^- \rightarrow \Sigma^{*+}$	
0.29 ± 0.11 ± 0.10	26	EATON	84 MRK2	$e^+e^- \rightarrow \Sigma^{*-}$	
0.31 ± 0.11 ± 0.11	28	EATON	84 MRK2	$e^+e^- \rightarrow \Sigma^{*+}$	

$\Gamma(\phi f_1(1285))/\Gamma_{\text{total}}$					$\Gamma_{63}/\Gamma$
VALUE (units $10^{-4}$ )	EVTS	DOCUMENT ID	TECN	COMMENT	
<b>2.6 ± 0.5 OUR AVERAGE</b>				Error includes scale factor of 1.1.	
3.2 ± 0.6 ± 0.4		JOUSSET	90 DM2	$J/\psi \rightarrow \phi 2(\pi^+\pi^-)$	
2.1 ± 0.5 ± 0.4	25	85 JOUSSET	90 DM2	$J/\psi \rightarrow \phi\eta\pi^+\pi^-$	
••• We do not use the following data for averages, fits, limits, etc. •••					
0.6 ± 0.2 ± 0.1	16 ± 6	BECKER	87 MRK3	$J/\psi \rightarrow \phi K\bar{K}\pi$	
85 We attribute to the $f_1(1285)$ the signal observed in the $\pi^+\pi^-\eta$ invariant mass distribution at 1297 MeV.					

$\Gamma(\eta\pi^+\pi^-)/\Gamma_{\text{total}}$					$\Gamma_{64}/\Gamma$
VALUE (units $10^{-3}$ )	EVTS	DOCUMENT ID	TECN	COMMENT	
<b>0.40 ± 0.17 ± 0.03</b>	9	86 AUBERT	07AU BABR	10.6 $e^+e^- \rightarrow \eta\pi^+\pi^-\gamma$	
86 AUBERT 07AU quotes $\Gamma_{ee}^{J/\psi} \cdot B(J/\psi \rightarrow \eta\pi^+\pi^-) \cdot B(\eta \rightarrow 3\pi) = 0.51 \pm 0.22 \pm 0.03 \text{ eV}$ .					

$\Gamma(\rho\eta)/\Gamma_{\text{total}}$					$\Gamma_{65}/\Gamma$
VALUE (units $10^{-3}$ )	EVTS	DOCUMENT ID	TECN	COMMENT	
<b>0.193 ± 0.023 OUR AVERAGE</b>					
0.194 ± 0.017 ± 0.029	299	JOUSSET	90 DM2	$J/\psi \rightarrow \text{hadrons}$	
0.193 ± 0.013 ± 0.029		COFFMAN	88 MRK3	$e^+e^- \rightarrow \pi^+\pi^-\eta$	

$\Gamma(\omega\eta'(958))/\Gamma_{\text{total}}$					$\Gamma_{66}/\Gamma$
VALUE (units $10^{-3}$ )	EVTS	DOCUMENT ID	TECN	COMMENT	
<b>0.182 ± 0.021 OUR AVERAGE</b>					
0.226 ± 0.043	218	87 ABLIKIM	06F BES2	$J/\psi \rightarrow \omega\eta'$	
0.18 $^{+0.10}_{-0.08} \pm 0.03$	6	JOUSSET	90 DM2	$J/\psi \rightarrow \text{hadrons}$	
0.166 ± 0.017 ± 0.019		COFFMAN	88 MRK3	$e^+e^- \rightarrow 3\pi\eta'$	
87 Using $B(\eta' \rightarrow \pi^+\pi^-\eta) = (44.3 \pm 1.5)\%$ , $B(\eta' \rightarrow \pi^+\pi^-\gamma) = 29.5 \pm 1.0\%$ , $B(\eta \rightarrow 2\gamma) = 39.43 \pm 0.26\%$ , and $B(\omega \rightarrow \pi^+\pi^-\pi^0) = (89.1 \pm 0.7)\%$ .					

$\Gamma(\omega f_0(980))/\Gamma_{\text{total}}$					$\Gamma_{67}/\Gamma$
VALUE (units $10^{-4}$ )		DOCUMENT ID	TECN	COMMENT	
<b>1.41 ± 0.27 ± 0.47</b>		88 AUGUSTIN	89 DM2	$J/\psi \rightarrow 2(\pi^+\pi^-)\pi^0$	
88 Assuming $B(f_0(980) \rightarrow \pi\pi) = 0.78$ .					

$\Gamma(\rho\eta'(958))/\Gamma_{\text{total}}$					$\Gamma_{68}/\Gamma$
VALUE (units $10^{-3}$ )	EVTS	DOCUMENT ID	TECN	COMMENT	
<b>0.105 ± 0.018 OUR AVERAGE</b>					
0.083 ± 0.030 ± 0.012	19	JOUSSET	90 DM2	$J/\psi \rightarrow \text{hadrons}$	
0.114 ± 0.014 ± 0.016		COFFMAN	88 MRK3	$J/\psi \rightarrow \pi^+\pi^-\eta'$	

$\Gamma(a_2(1320)^\pm \pi^\mp)/\Gamma_{\text{total}}$					$\Gamma_{69}/\Gamma$
VALUE (units $10^{-4}$ )	CL%	DOCUMENT ID	TECN	COMMENT	
<b>&lt;43</b>	90	BRAUNSCH...	76 DASP	$e^+e^-$	

$\Gamma(K\bar{K}_2^*(1430) + \text{c.c.})/\Gamma_{\text{total}}$					$\Gamma_{70}/\Gamma$
VALUE (units $10^{-4}$ )	CL%	DOCUMENT ID	TECN	COMMENT	
<b>&lt;40</b>	90	VANNUCCI	77 MRK1	$e^+e^- \rightarrow K^0\bar{K}_2^{*0}$	
••• We do not use the following data for averages, fits, limits, etc. •••					
<66	90	BRAUNSCH...	76 DASP	$e^+e^- \rightarrow K^\pm\bar{K}_2^{*\mp}$	

$\Gamma(K_1(1270)^\pm K^\mp)/\Gamma_{\text{total}}$					$\Gamma_{71}/\Gamma$
VALUE (units $10^{-3}$ )	CL%	DOCUMENT ID	TECN	COMMENT	
<b>&lt;3.0</b>	90	89 BAI	99c BES	$e^+e^-$	
89 Assuming $B(K_1(1270) \rightarrow K\rho) = 0.42 \pm 0.06$					

$\Gamma(K_2^*(1430)^0\bar{K}_2^*(1430)^0)/\Gamma_{\text{total}}$					$\Gamma_{72}/\Gamma$
VALUE (units $10^{-4}$ )	CL%	DOCUMENT ID	TECN	COMMENT	
<b>&lt;29</b>	90	VANNUCCI	77 MRK1	$e^+e^- \rightarrow \pi^+\pi^-K^+K^-$	

$\Gamma(\phi\pi^0)/\Gamma_{\text{total}}$					$\Gamma_{73}/\Gamma$
VALUE (units $10^{-6}$ )	CL%	DOCUMENT ID	TECN	COMMENT	
<b>&lt;6.4</b>	90	ABLIKIM	05B BES2	$e^+e^- \rightarrow J/\psi \rightarrow \phi\gamma\gamma$	
••• We do not use the following data for averages, fits, limits, etc. •••					
<6.8	90	COFFMAN	88 MRK3	$e^+e^- \rightarrow K^+K^-\pi^0$	

$\Gamma(\phi\eta(1405) \rightarrow \phi\eta\pi\pi)/\Gamma_{\text{total}}$					$\Gamma_{74}/\Gamma$
VALUE (units $10^{-4}$ )	CL%	DOCUMENT ID	TECN	COMMENT	
<b>&lt;2.5</b>	90	90 FALVARD	88 DM2	$J/\psi \rightarrow \text{hadrons}$	
90 Includes unknown branching fraction $\eta(1405) \rightarrow \eta\pi\pi$ .					

$\Gamma(\omega f_2'(1525))/\Gamma_{\text{total}}$					$\Gamma_{75}/\Gamma$
VALUE (units $10^{-4}$ )	CL%	DOCUMENT ID	TECN	COMMENT	
<b>&lt;2.2</b>	90	91 VANNUCCI	77 MRK1	$e^+e^- \rightarrow \pi^+\pi^-\pi^0 K^+K^-$	
••• We do not use the following data for averages, fits, limits, etc. •••					
<2.8	90	91 FALVARD	88 DM2	$J/\psi \rightarrow \text{hadrons}$	
91 Re-evaluated assuming $B(f_2'(1525) \rightarrow K\bar{K}) = 0.713$ .					

$\Gamma(\eta\phi(2170) \rightarrow \eta K^*(892)^0\bar{K}^*(892)^0)/\Gamma_{\text{total}}$					$\Gamma_{76}/\Gamma$
VALUE (units $10^{-4}$ )	CL%	DOCUMENT ID	TECN	COMMENT	
<b>&lt;2.52</b>	90	ABLIKIM	10c BES2	$J/\psi \rightarrow \eta K^+\pi^- K^-\pi^+$	

$\Gamma(\Sigma(1385)^0\bar{\Lambda})/\Gamma_{\text{total}}$					$\Gamma_{77}/\Gamma$
VALUE (units $10^{-3}$ )	CL%	DOCUMENT ID	TECN	COMMENT	
<b>&lt;0.2</b>	90	HENRRARD	87 DM2	$e^+e^-$	

$\Gamma(\Delta(1232)^+\bar{p})/\Gamma_{\text{total}}$					$\Gamma_{78}/\Gamma$
VALUE (units $10^{-3}$ )	CL%	DOCUMENT ID	TECN	COMMENT	
<b>&lt;0.1</b>	90	HENRRARD	87 DM2	$e^+e^-$	

$\Gamma(\Theta(1540)\bar{\Theta}(1540) \rightarrow K_S^0\rho K^-\bar{\pi} + \text{c.c.})/\Gamma_{\text{total}}$					$\Gamma_{79}/\Gamma$
VALUE (units $10^{-5}$ )	CL%	DOCUMENT ID	TECN	COMMENT	
<b>&lt;1.1</b>	90	BAI	04G BES2	$e^+e^-$	

$\Gamma(\Theta(1540)K^-\bar{\pi} \rightarrow K_S^0\rho K^-\bar{\pi})/\Gamma_{\text{total}}$					$\Gamma_{80}/\Gamma$
VALUE (units $10^{-5}$ )	CL%	DOCUMENT ID	TECN	COMMENT	
<b>&lt;2.1</b>	90	BAI	04G BES2	$e^+e^-$	

$\Gamma(\Theta(1540)K_S^0\bar{p} \rightarrow K_S^0\bar{p}K^+n)/\Gamma_{\text{total}}$					$\Gamma_{81}/\Gamma$
VALUE (units $10^{-5}$ )	CL%	DOCUMENT ID	TECN	COMMENT	
<b>&lt;1.6</b>	90	BAI	04G BES2	$e^+e^-$	

$\Gamma(\bar{\Theta}(1540)K^+n \rightarrow K_S^0\bar{p}K^+n)/\Gamma_{\text{total}}$					$\Gamma_{82}/\Gamma$
VALUE (units $10^{-5}$ )	CL%	DOCUMENT ID	TECN	COMMENT	
<b>&lt;5.6</b>	90	BAI	04G BES2	$e^+e^-$	

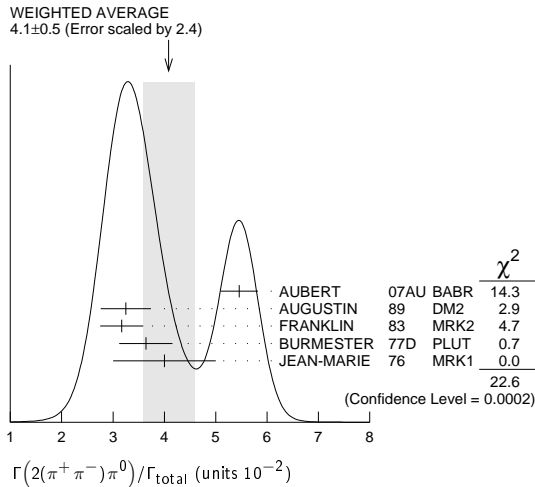
$\Gamma(\bar{\Theta}(1540)K_S^0\rho \rightarrow K_S^0\rho K^-\bar{\pi})/\Gamma_{\text{total}}$					$\Gamma_{83}/\Gamma$
VALUE (units $10^{-5}$ )	CL%	DOCUMENT ID	TECN	COMMENT	
<b>&lt;1.1</b>	90	BAI	04G BES2	$e^+e^-$	

$\Gamma(\Sigma^0\bar{\Lambda})/\Gamma_{\text{total}}$					$\Gamma_{84}/\Gamma$
VALUE (units $10^{-4}$ )	CL%	DOCUMENT ID	TECN	COMMENT	
<b>&lt;0.9</b>	90	HENRRARD	87 DM2	$e^+e^-$	

## STABLE HADRONS

$\Gamma(2(\pi^+\pi^-)\pi^0)/\Gamma_{\text{total}}$					$\Gamma_{85}/\Gamma$
VALUE (units $10^{-2}$ )	EVTS	DOCUMENT ID	TECN	COMMENT	
<b>4.1 ± 0.5 OUR AVERAGE</b>				Error includes scale factor of 2.4. See the ideogram below.	
5.46 ± 0.34 ± 0.14	4990	92 AUBERT	07AU BABR	10.6 $e^+e^- \rightarrow 2(\pi^+\pi^-)\pi^0\gamma$	
3.25 ± 0.49	46055	AUGUSTIN	89 DM2	$J/\psi \rightarrow 2(\pi^+\pi^-)\pi^0$	
3.17 ± 0.42	147	FRANKLIN	83 MRK2	$e^+e^- \rightarrow \text{hadrons}$	
3.64 ± 0.52	1500	BURMESTER	77D PLUT	$e^+e^-$	
4 ± 1	675	JEAN-MARIE	76 MRK1	$e^+e^-$	
92 AUBERT 07AU reports $[\Gamma(J/\psi(1S) \rightarrow 2(\pi^+\pi^-)\pi^0)/\Gamma_{\text{total}}] \times [\Gamma(J/\psi(1S) \rightarrow e^+e^-)] = 0.303 \pm 0.005 \pm 0.018 \text{ keV}$ which we divide by our best value $\Gamma(J/\psi(1S) \rightarrow e^+e^-) = 5.55 \pm 0.14 \pm 0.02 \text{ keV}$ . Our first error is their experiment's error and our second error is the systematic error from using our best value.					

## Meson Particle Listings

 $J/\psi(1S)$  $\Gamma(\omega\pi^+\pi^-)/\Gamma(2\pi^+\pi^-\pi^0)$  $\Gamma_{13}/\Gamma_{85}$ 

VALUE	DOCUMENT ID	TECN	COMMENT
0.3	93 JEAN-MARIE 76	MRK1	$e^+e^-$

• • • We do not use the following data for averages, fits, limits, etc. • • •

<sup>93</sup> Final state  $(\pi^+\pi^-\pi^0)$  under the assumption that  $\pi\pi$  is isospin 0.

 $\Gamma(3\pi^+\pi^-\pi^0)/\Gamma_{total}$  $\Gamma_{86}/\Gamma$ 

VALUE	EVTS	DOCUMENT ID	TECN	COMMENT
<b>0.029±0.006 OUR AVERAGE</b>				
0.028±0.009	11	FRANKLIN 83	MRK2	$e^+e^- \rightarrow$ hadrons
0.029±0.007	181	JEAN-MARIE 76	MRK1	$e^+e^-$

 $\Gamma(\pi^+\pi^-\pi^0)/\Gamma_{total}$  $\Gamma_{87}/\Gamma$ 

VALUE (units $10^{-3}$ )	EVTS	DOCUMENT ID	TECN	COMMENT
<b>20.7 ± 1.2 OUR AVERAGE</b>				Error includes scale factor of 1.6. See the ideogram below.
23.6 ± 2.1 ± 0.5	256	<sup>94</sup> AUBERT 07AU BABR		$10.6 e^+e^- \rightarrow J/\psi\pi^+\pi^-\gamma$
21.8 ± 1.9		<sup>95,96</sup> AUBERT,B 04N BABR		$10.6 e^+e^- \rightarrow \pi^+\pi^-\pi^0\gamma$
21.84±0.05±2.01	220k	<sup>96,97</sup> BAI 04H BES		$e^+e^-$
20.91±0.21±1.16		<sup>96,98</sup> BAI 04H BES		$e^+e^-$
15 ± 2	168	FRANKLIN 83	MRK2	$e^+e^-$

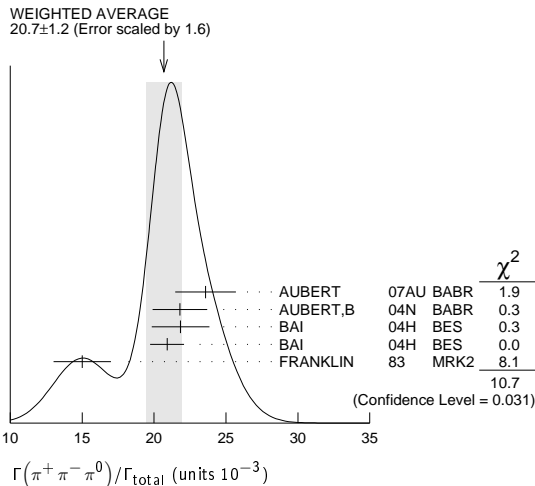
<sup>94</sup>AUBERT 07AU reports  $[\Gamma(J/\psi(1S) \rightarrow \pi^+\pi^-\pi^0)/\Gamma_{total}] \times [\Gamma(\psi(2S) \rightarrow J/\psi(1S)\pi^+\pi^-) \times \Gamma(\psi(2S) \rightarrow e^+e^-)/\Gamma_{total}] = (18.6 \pm 1.2 \pm 1.1) \times 10^{-3}$  keV which we divide by our best value  $\Gamma(\psi(2S) \rightarrow J/\psi(1S)\pi^+\pi^-) \times \Gamma(\psi(2S) \rightarrow e^+e^-)/\Gamma_{total} = 0.789 \pm 0.015$  keV. Our first error is their experiment's error and our second error is the systematic error from using our best value.

<sup>95</sup> From the ratio of  $\Gamma(e^+e^-)B(\pi^+\pi^-\pi^0)$  and  $\Gamma(e^+e^-)B(\mu^+\mu^-)$  (AUBERT 04).

<sup>96</sup> Mostly  $\rho\pi$ , see also  $\rho\pi$  subsection.

<sup>97</sup> From  $J/\psi \rightarrow \pi^+\pi^-\pi^0$  events directly.

<sup>98</sup> Obtained comparing the rates for  $\pi^+\pi^-\pi^0$  and  $\mu^+\mu^-$ , using  $J/\psi$  events produced via  $\psi(2S) \rightarrow \pi^+\pi^-J/\psi$  and with  $B(J/\psi \rightarrow \mu^+\mu^-) = 5.88 \pm 0.10\%$ .

 $\Gamma(\pi^+\pi^-\pi^0 K^+ K^-)/\Gamma_{total}$  $\Gamma_{88}/\Gamma$ 

VALUE (units $10^{-2}$ )	EVTS	DOCUMENT ID	TECN	COMMENT
<b>1.79±0.29 OUR AVERAGE</b>				Error includes scale factor of 2.2.
1.93±0.14±0.05	768	<sup>99</sup> AUBERT 07AU BABR		$10.6 e^+e^- \rightarrow K^+K^-\pi^+\pi^-\pi^0\gamma$
1.2 ± 0.3	309	VANNUCCI 77	MRK1	$e^+e^-$

<sup>99</sup>AUBERT 07AU reports  $[\Gamma(J/\psi(1S) \rightarrow \pi^+\pi^-\pi^0 K^+ K^-)/\Gamma_{total}] \times [\Gamma(J/\psi(1S) \rightarrow e^+e^-)] = 0.1070 \pm 0.0043 \pm 0.0064$  keV which we divide by our best value  $\Gamma(J/\psi(1S) \rightarrow e^+e^-) = 5.55 \pm 0.14 \pm 0.02$  keV. Our first error is their experiment's error and our second error is the systematic error from using our best value.

 $\Gamma(4\pi^+\pi^-\pi^0)/\Gamma_{total}$  $\Gamma_{89}/\Gamma$ 

VALUE (units $10^{-4}$ )	EVTS	DOCUMENT ID	TECN	COMMENT
<b>90±30</b>	13	JEAN-MARIE 76	MRK1	$e^+e^-$

 $\Gamma(\pi^+\pi^- K^+ K^-)/\Gamma_{total}$  $\Gamma_{90}/\Gamma$ 

VALUE (units $10^{-3}$ )	EVTS	DOCUMENT ID	TECN	COMMENT
<b>6.6±0.5 OUR AVERAGE</b>				
6.5±0.4±0.2	1.6k	<sup>100</sup> AUBERT 07AK BABR		$10.6 e^+e^- \rightarrow \pi^+\pi^- K^+ K^- \gamma$
7.2±2.3	205	VANNUCCI 77	MRK1	$e^+e^-$

• • • We do not use the following data for averages, fits, limits, etc. • • •

6.1±0.7±0.2 233 <sup>101</sup>AUBERT 05D BABR  $10.6 e^+e^- \rightarrow K^+K^-\pi^+\pi^- \gamma$

<sup>100</sup>AUBERT 07AK reports  $[\Gamma(J/\psi(1S) \rightarrow \pi^+\pi^- K^+ K^-)/\Gamma_{total}] \times [\Gamma(J/\psi(1S) \rightarrow e^+e^-)] = (36.3 \pm 1.3 \pm 2.1) \times 10^{-3}$  keV which we divide by our best value  $\Gamma(J/\psi(1S) \rightarrow e^+e^-) = 5.55 \pm 0.14 \pm 0.02$  keV. Our first error is their experiment's error and our second error is the systematic error from using our best value.

<sup>101</sup> Superseded by AUBERT 07AK. AUBERT 05D reports  $[\Gamma(J/\psi(1S) \rightarrow \pi^+\pi^- K^+ K^-)/\Gamma_{total}] \times [\Gamma(J/\psi(1S) \rightarrow e^+e^-)] = (33.6 \pm 2.7 \pm 2.7) \times 10^{-3}$  keV which we divide by our best value  $\Gamma(J/\psi(1S) \rightarrow e^+e^-) = 5.55 \pm 0.14 \pm 0.02$  keV. Our first error is their experiment's error and our second error is the systematic error from using our best value.

 $\Gamma(\pi^+\pi^- K^+ K^- \eta)/\Gamma_{total}$  $\Gamma_{91}/\Gamma$ 

VALUE (units $10^{-3}$ )	EVTS	DOCUMENT ID	TECN	COMMENT
<b>1.84±0.28±0.05</b>	73	<sup>102</sup> AUBERT 07AU BABR		$10.6 e^+e^- \rightarrow K^+K^-\pi^+\pi^-\eta\gamma$

<sup>102</sup>AUBERT 07AU reports  $[\Gamma(J/\psi(1S) \rightarrow \pi^+\pi^- K^+ K^- \eta)/\Gamma_{total}] \times [\Gamma(J/\psi(1S) \rightarrow e^+e^-)] = (10.2 \pm 1.3 \pm 0.8) \times 10^{-3}$  keV which we divide by our best value  $\Gamma(J/\psi(1S) \rightarrow e^+e^-) = 5.55 \pm 0.14 \pm 0.02$  keV. Our first error is their experiment's error and our second error is the systematic error from using our best value.

 $\Gamma(\pi^0\pi^0 K^+ K^-)/\Gamma_{total}$  $\Gamma_{92}/\Gamma$ 

VALUE (units $10^{-3}$ )	EVTS	DOCUMENT ID	TECN	COMMENT
<b>2.45±0.31±0.06</b>	203 ± 16	<sup>103</sup> AUBERT 07AK BABR		$10.6 e^+e^- \rightarrow \pi^0\pi^0 K^+ K^- \gamma$

<sup>103</sup>AUBERT 07AK reports  $[\Gamma(J/\psi(1S) \rightarrow \pi^0\pi^0 K^+ K^-)/\Gamma_{total}] \times [\Gamma(J/\psi(1S) \rightarrow e^+e^-)] = (13.6 \pm 1.1 \pm 1.3) \times 10^{-3}$  keV which we divide by our best value  $\Gamma(J/\psi(1S) \rightarrow e^+e^-) = 5.55 \pm 0.14 \pm 0.02$  keV. Our first error is their experiment's error and our second error is the systematic error from using our best value.

 $\Gamma(K\bar{K}\pi)/\Gamma_{total}$  $\Gamma_{93}/\Gamma$ 

VALUE (units $10^{-4}$ )	EVTS	DOCUMENT ID	TECN	COMMENT
<b>61 ± 10 OUR AVERAGE</b>				
55.2±12.0	25	FRANKLIN 83	MRK2	$e^+e^- \rightarrow K^+K^-\pi^0$
78.0±21.0	126	VANNUCCI 77	MRK1	$e^+e^- \rightarrow K_S^0 K^\pm \pi^\mp$

 $\Gamma(2\pi^+\pi^-)/\Gamma_{total}$  $\Gamma_{94}/\Gamma$ 

VALUE (units $10^{-3}$ )	EVTS	DOCUMENT ID	TECN	COMMENT
<b>3.55±0.23 OUR AVERAGE</b>				
3.53±0.12±0.29	1107	<sup>104</sup> ABLIKIM 05H BES2		$e^+e^- \rightarrow \psi(2S) \rightarrow J/\psi\pi^+\pi^-, J/\psi \rightarrow 2(\pi^+\pi^-)$

3.51±0.34±0.09 270 <sup>105</sup>AUBERT 05D BABR  $10.6 e^+e^- \rightarrow 2(\pi^+\pi^-)\gamma$

4.0 ± 1.0 76 JEAN-MARIE 76 MRK1  $e^+e^-$

<sup>104</sup> Computed using  $B(J/\psi \rightarrow \mu^+\mu^-) = 0.0588 \pm 0.0010$ .

<sup>105</sup>AUBERT 05D reports  $[\Gamma(J/\psi(1S) \rightarrow 2(\pi^+\pi^-))/\Gamma_{total}] \times [\Gamma(J/\psi(1S) \rightarrow e^+e^-)] = (19.5 \pm 1.4 \pm 1.3) \times 10^{-3}$  keV which we divide by our best value  $\Gamma(J/\psi(1S) \rightarrow e^+e^-) = 5.55 \pm 0.14 \pm 0.02$  keV. Our first error is their experiment's error and our second error is the systematic error from using our best value.

 $\Gamma(3\pi^+\pi^-)/\Gamma_{total}$  $\Gamma_{95}/\Gamma$ 

VALUE (units $10^{-4}$ )	EVTS	DOCUMENT ID	TECN	COMMENT
<b>43 ± 4 OUR AVERAGE</b>				
43.0 ± 2.9 ± 2.8	496	<sup>106</sup> AUBERT 06D BABR		$10.6 e^+e^- \rightarrow 3(\pi^+\pi^-)\gamma$
40 ± 20	32	JEAN-MARIE 76	MRK1	$e^+e^-$

<sup>106</sup> Using  $\Gamma(J/\psi \rightarrow e^+e^-) = 5.52 \pm 0.14 \pm 0.04$  keV.

 $\Gamma(2\pi^+\pi^-\pi^0)/\Gamma_{total}$  $\Gamma_{96}/\Gamma$ 

VALUE (units $10^{-2}$ )	EVTS	DOCUMENT ID	TECN	COMMENT
<b>1.62±0.09±0.19</b>	761	<sup>107</sup> AUBERT 06D BABR		$10.6 e^+e^- \rightarrow 2(\pi^+\pi^-\pi^0)\gamma$

<sup>107</sup> Using  $\Gamma(J/\psi \rightarrow e^+e^-) = 5.52 \pm 0.14 \pm 0.04$  keV.

See key on page 457

# Meson Particle Listings

## $J/\psi(1S)$

$\Gamma(2(\pi^+\pi^-\eta))/\Gamma_{total}$					$\Gamma_{97}/\Gamma$
VALUE (units $10^{-3}$ )	EVTS	DOCUMENT ID	TECN	COMMENT	
<b>2.29 ± 0.24 OUR AVERAGE</b>					
2.35 ± 0.39 ± 0.20	85	108 AUBERT	07AU BABR	10.6 $e^+e^- \rightarrow 2(\pi^+\pi^-\eta)\gamma\gamma$	
2.26 ± 0.08 ± 0.27	4839	ABLIKIM	05c BES2	$e^+e^- \rightarrow 2(\pi^+\pi^-\eta)$	

108 AUBERT 07AU quotes  $\Gamma_{ec}^{J/\psi} \cdot B(J/\psi \rightarrow 2(\pi^+\pi^-\eta)) \cdot B(\eta \rightarrow \gamma\gamma) = 5.16 \pm 0.85 \pm 0.39$  eV.

$\Gamma(3(\pi^+\pi^-\eta))/\Gamma_{total}$					$\Gamma_{98}/\Gamma$
VALUE (units $10^{-4}$ )	EVTS	DOCUMENT ID	TECN	COMMENT	
<b>7.24 ± 0.96 ± 1.11</b>	616	ABLIKIM	05c BES2	$e^+e^- \rightarrow 3(\pi^+\pi^-\eta)$	

$\Gamma(p\bar{p})/\Gamma_{total}$					$\Gamma_{99}/\Gamma$
VALUE (units $10^{-3}$ )	EVTS	DOCUMENT ID	TECN	COMMENT	
<b>2.17 ± 0.07 OUR AVERAGE</b>					
2.18 ± 0.16 ± 0.07	317	109 WU	06 BELL	$B^+ \rightarrow p\bar{p}K^+$	
2.26 ± 0.01 ± 0.14	63316	BAI	04E BES2	$e^+e^- \rightarrow J/\psi$	
1.97 ± 0.22	99	BALDINI	98 FENI	$e^+e^-$	
1.91 ± 0.04 ± 0.30		PALLIN	87 DM2	$e^+e^-$	
2.16 ± 0.07 ± 0.15	1420	EATON	84 MRK2	$e^+e^-$	
2.5 ± 0.4	133	BRANDELIK	79c DASP	$e^+e^-$	
2.0 ± 0.5		BESCH	78 BONA	$e^+e^-$	
2.2 ± 0.2	331	110 PERUZZI	78 MRK1	$e^+e^-$	

• • • We do not use the following data for averages, fits, limits, etc. • • •

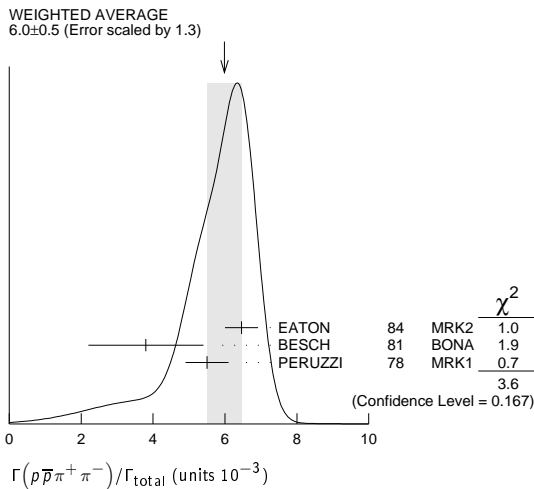
2.0 ± 0.3 48 ANTONELLI 93 SPEC  $e^+e^-$

109 WU 06 reports  $[\Gamma(J/\psi(1S) \rightarrow p\bar{p})/\Gamma_{total}] \times [B(B^+ \rightarrow J/\psi(1S)K^+)] = (2.21 \pm 0.13 \pm 0.10) \times 10^{-6}$  which we divide by our best value  $B(B^+ \rightarrow J/\psi(1S)K^+) = (1.016 \pm 0.033) \times 10^{-3}$ . Our first error is their experiment's error and our second error is the systematic error from using our best value.

110 Assuming angular distribution  $(1+\cos^2\theta)$ .

$\Gamma(p\bar{p}\pi^0)/\Gamma_{total}$					$\Gamma_{100}/\Gamma$
VALUE (units $10^{-3}$ )	EVTS	DOCUMENT ID	TECN	COMMENT	
<b>1.19 ± 0.08 OUR AVERAGE</b>					
1.33 ± 0.02 ± 0.11	11k	ABLIKIM	09b BES2	$e^+e^-$	
1.13 ± 0.09 ± 0.09	685	EATON	84 MRK2	$e^+e^-$	
1.4 ± 0.4		BRANDELIK	79c DASP	$e^+e^-$	
1.00 ± 0.15	109	PERUZZI	78 MRK1	$e^+e^-$	

$\Gamma(p\bar{p}\pi^+\pi^-)/\Gamma_{total}$					$\Gamma_{101}/\Gamma$
VALUE (units $10^{-3}$ )	EVTS	DOCUMENT ID	TECN	COMMENT	
<b>6.0 ± 0.5 OUR AVERAGE</b>					
6.46 ± 0.17 ± 0.43	1435	EATON	84 MRK2	$e^+e^-$	
3.8 ± 1.6	48	BESCH	81 BONA	$e^+e^-$	
5.5 ± 0.6	533	PERUZZI	78 MRK1	$e^+e^-$	



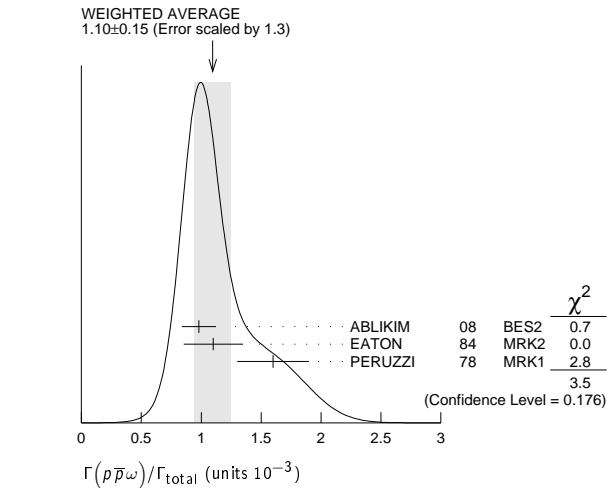
$\Gamma(p\bar{p}\pi^+\pi^-\pi^0)/\Gamma_{total}$					$\Gamma_{102}/\Gamma$
VALUE (units $10^{-3}$ )	EVTS	DOCUMENT ID	TECN	COMMENT	
<b>2.3 ± 0.9 OUR AVERAGE</b>					
3.36 ± 0.65 ± 0.28	364	EATON	84 MRK2	$e^+e^-$	
1.6 ± 0.6	39	PERUZZI	78 MRK1	$e^+e^-$	

Including  $p\bar{p}\pi^+\pi^-\gamma$  and excluding  $\omega, \eta, \eta'$

$\Gamma(p\bar{p}\eta)/\Gamma_{total}$					$\Gamma_{103}/\Gamma$
VALUE (units $10^{-3}$ )	EVTS	DOCUMENT ID	TECN	COMMENT	
<b>2.00 ± 0.12 OUR AVERAGE</b>					
1.91 ± 0.02 ± 0.17	13k	111 ABLIKIM	09 BES2	$e^+e^-$	
2.03 ± 0.13 ± 0.15	826	EATON	84 MRK2	$e^+e^-$	
2.5 ± 1.2		BRANDELIK	79c DASP	$e^+e^-$	
2.3 ± 0.4	197	PERUZZI	78 MRK1	$e^+e^-$	

$\Gamma(p\bar{p}\rho)/\Gamma_{total}$					$\Gamma_{104}/\Gamma$
VALUE (units $10^{-3}$ )	CL%	DOCUMENT ID	TECN	COMMENT	
<b>&lt; 0.31</b>	90	EATON	84 MRK2	$e^+e^- \rightarrow \text{hadrons}\gamma$	

$\Gamma(p\bar{p}\omega)/\Gamma_{total}$					$\Gamma_{105}/\Gamma$
VALUE (units $10^{-3}$ )	EVTS	DOCUMENT ID	TECN	COMMENT	
<b>1.10 ± 0.15 OUR AVERAGE</b>					
0.98 ± 0.03 ± 0.14	2449	ABLIKIM	08 BES2	$e^+e^-$	
1.10 ± 0.17 ± 0.18	486	EATON	84 MRK2	$e^+e^-$	
1.6 ± 0.3	77	PERUZZI	78 MRK1	$e^+e^-$	



$\Gamma(p\bar{p}\eta'(958))/\Gamma_{total}$					$\Gamma_{106}/\Gamma$
VALUE (units $10^{-3}$ )	EVTS	DOCUMENT ID	TECN	COMMENT	
<b>0.21 ± 0.04 OUR AVERAGE</b>					
0.200 ± 0.023 ± 0.028	265 ± 31	112 ABLIKIM	09 BES2	$e^+e^-$	
0.68 ± 0.23 ± 0.17	19	EATON	84 MRK2	$e^+e^-$	
1.8 ± 0.6	19	PERUZZI	78 MRK1	$e^+e^-$	

$\Gamma(p\bar{p}\phi)/\Gamma_{total}$					$\Gamma_{107}/\Gamma$
VALUE (units $10^{-4}$ )	DOCUMENT ID	TECN	COMMENT		
<b>0.45 ± 0.13 ± 0.07</b>	FALVARD 88	DM2	$J/\psi \rightarrow \text{hadrons}$		

$\Gamma(n\bar{n})/\Gamma_{total}$					$\Gamma_{108}/\Gamma$
VALUE (units $10^{-2}$ )	EVTS	DOCUMENT ID	TECN	COMMENT	
<b>0.22 ± 0.04 OUR AVERAGE</b>					
0.231 ± 0.049	79	BALDINI	98 FENI	$e^+e^-$	
0.18 ± 0.09		BESCH	78 BONA	$e^+e^-$	
0.190 ± 0.055	40	ANTONELLI	93 SPEC	$e^+e^-$	

$\Gamma(n\bar{n}\pi^+\pi^-)/\Gamma_{total}$					$\Gamma_{109}/\Gamma$
VALUE (units $10^{-3}$ )	EVTS	DOCUMENT ID	TECN	COMMENT	
<b>3.8 ± 3.6</b>	5	BESCH	81 BONA	$e^+e^-$	

$\Gamma(\Sigma^+\Sigma^-)/\Gamma_{total}$					$\Gamma_{110}/\Gamma$
VALUE (units $10^{-3}$ )	EVTS	DOCUMENT ID	TECN	COMMENT	
<b>1.50 ± 0.10 ± 0.22</b>	399	ABLIKIM	08o BES2	$e^+e^- \rightarrow J/\psi$	

$\Gamma(\Sigma^0\bar{\Sigma}^0)/\Gamma_{total}$					$\Gamma_{111}/\Gamma$
VALUE (units $10^{-3}$ )	EVTS	DOCUMENT ID	TECN	COMMENT	
<b>1.29 ± 0.09 OUR AVERAGE</b>					
1.15 ± 0.24 ± 0.03		113 AUBERT	07bD BABR	10.6 $e^+e^- \rightarrow \Sigma^0\bar{\Sigma}^0\gamma$	
1.33 ± 0.04 ± 0.11	1779	ABLIKIM	06 BES2	$J/\psi \rightarrow \Sigma^0\bar{\Sigma}^0$	
1.06 ± 0.04 ± 0.23	884 ± 30	PALLIN	87 DM2	$e^+e^- \rightarrow \Sigma^0\bar{\Sigma}^0$	
1.58 ± 0.16 ± 0.25	90	EATON	84 MRK2	$e^+e^- \rightarrow \Sigma^0\bar{\Sigma}^0$	
1.3 ± 0.4	52	PERUZZI	78 MRK1	$e^+e^- \rightarrow \Sigma^0\bar{\Sigma}^0$	
2.4 ± 2.6	3	BESCH	81 BONA	$e^+e^- \rightarrow \Sigma^+\Sigma^-$	

## Meson Particle Listings

 $J/\psi(1S)$ 

<sup>113</sup>AUBERT 07bD reports  $[\Gamma(J/\psi(1S) \rightarrow \Sigma^0 \bar{\Sigma}^0)/\Gamma_{\text{total}}] \times [\Gamma(J/\psi(1S) \rightarrow e^+ e^-)] = (6.4 \pm 1.2 \pm 0.6) \times 10^{-3}$  keV which we divide by our best value  $\Gamma(J/\psi(1S) \rightarrow e^+ e^-) = 5.55 \pm 0.14 \pm 0.02$  keV. Our first error is their experiment's error and our second error is the systematic error from using our best value.

$$\Gamma(2(\pi^+ \pi^-) K^+ K^-)/\Gamma_{\text{total}} \quad \Gamma_{112}/\Gamma$$

VALUE (units $10^{-4}$ )	EVTS	DOCUMENT ID	TECN	COMMENT
<b><math>47 \pm 7</math> OUR AVERAGE</b>				Error includes scale factor of 1.3.
$49.8 \pm 4.2 \pm 3.4$	205	<sup>114</sup> AUBERT	06D BABR	$10.6 e^+ e^- \rightarrow \omega K^+ K^- 2(\pi^+ \pi^-) \gamma$
$31 \pm 13$	30	VANNUCCI	77 MRK1	$e^+ e^-$

<sup>114</sup>Using  $\Gamma(J/\psi \rightarrow e^+ e^-) = 5.52 \pm 0.14 \pm 0.04$  keV.

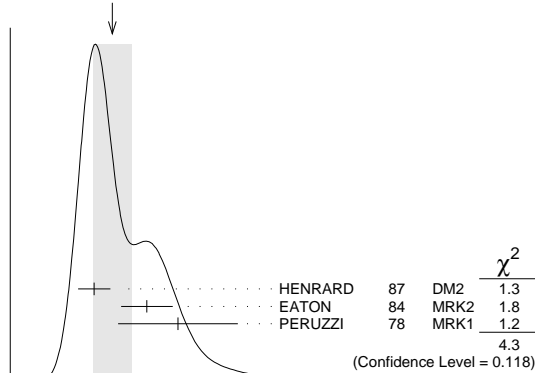
$$\Gamma(p \bar{n} \pi^-)/\Gamma_{\text{total}} \quad \Gamma_{113}/\Gamma$$

VALUE (units $10^{-3}$ )	EVTS	DOCUMENT ID	TECN	COMMENT
<b><math>2.12 \pm 0.09</math> OUR AVERAGE</b>				
$2.36 \pm 0.02 \pm 0.21$	59k	ABLIKIM	06K BES2	$J/\psi \rightarrow p \pi^- \bar{n}$
$2.47 \pm 0.02 \pm 0.24$	55k	ABLIKIM	06K BES2	$J/\psi \rightarrow \bar{p} \pi^+ n$
$2.02 \pm 0.07 \pm 0.16$	1288	EATON	84 MRK2	$e^+ e^- \rightarrow p \pi^-$
$1.93 \pm 0.07 \pm 0.16$	1191	EATON	84 MRK2	$e^+ e^- \rightarrow \bar{p} \pi^+$
$1.7 \pm 0.7$	32	BESCH	81 BONA	$e^+ e^- \rightarrow p \pi^-$
$1.6 \pm 1.2$	5	BESCH	81 BONA	$e^+ e^- \rightarrow \bar{p} \pi^+$
$2.16 \pm 0.29$	194	PERUZZI	78 MRK1	$e^+ e^- \rightarrow p \pi^-$
$2.04 \pm 0.27$	204	PERUZZI	78 MRK1	$e^+ e^- \rightarrow \bar{p} \pi^+$

$$\Gamma(\Xi^- \bar{\Xi}^+)/\Gamma_{\text{total}} \quad \Gamma_{117}/\Gamma$$

VALUE (units $10^{-3}$ )	EVTS	DOCUMENT ID	TECN	COMMENT
<b><math>0.85 \pm 0.16</math> OUR AVERAGE</b>				Error includes scale factor of 1.5. See the ideogram below.
$0.70 \pm 0.06 \pm 0.12$	132 ± 11	HENRARD	87 DM2	$e^+ e^- \rightarrow \Xi^- \bar{\Xi}^+$
$1.14 \pm 0.08 \pm 0.20$	194	EATON	84 MRK2	$e^+ e^- \rightarrow \Xi^- \bar{\Xi}^+$
$1.4 \pm 0.5$	51	PERUZZI	78 MRK1	$e^+ e^- \rightarrow \Xi^- \bar{\Xi}^+$

WEIGHTED AVERAGE  
 $0.85 \pm 0.16$  (Error scaled by 1.5)



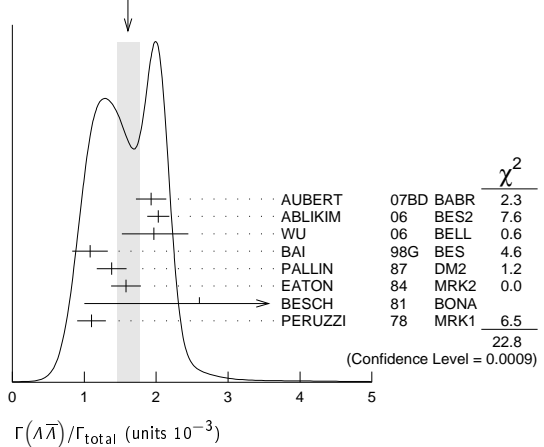
$$\Gamma(\Lambda \bar{\Lambda})/\Gamma_{\text{total}} \quad \Gamma_{118}/\Gamma$$

VALUE (units $10^{-3}$ )	EVTS	DOCUMENT ID	TECN	COMMENT
<b><math>1.61 \pm 0.15</math> OUR AVERAGE</b>				Error includes scale factor of 1.9. See the ideogram below.
$1.93 \pm 0.21 \pm 0.05$		<sup>115</sup> AUBERT	07bD BABR	$10.6 e^+ e^- \rightarrow \Lambda \bar{\Lambda} \gamma$
$2.03 \pm 0.03 \pm 0.15$	8887	ABLIKIM	06 BES2	$J/\psi \rightarrow \Lambda \bar{\Lambda}$
$2.0 \pm 0.5 \pm 0.1$	46	<sup>116</sup> WU	06 BELL	$B^+ \rightarrow \Lambda \bar{\Lambda} K^+$
$1.08 \pm 0.06 \pm 0.24$	631	BAI	98G BES	$e^+ e^-$
$1.38 \pm 0.05 \pm 0.20$	1847	PALLIN	87 DM2	$e^+ e^-$
$1.58 \pm 0.08 \pm 0.19$	365	EATON	84 MRK2	$e^+ e^-$
$2.6 \pm 1.6$	5	BESCH	81 BONA	$e^+ e^-$
$1.1 \pm 0.2$	196	PERUZZI	78 MRK1	$e^+ e^-$

<sup>115</sup>AUBERT 07bD reports  $[\Gamma(J/\psi(1S) \rightarrow \Lambda \bar{\Lambda})/\Gamma_{\text{total}}] \times [\Gamma(J/\psi(1S) \rightarrow e^+ e^-)] = (10.7 \pm 0.9 \pm 0.7) \times 10^{-3}$  keV which we divide by our best value  $\Gamma(J/\psi(1S) \rightarrow e^+ e^-) = 5.55 \pm 0.14 \pm 0.02$  keV. Our first error is their experiment's error and our second error is the systematic error from using our best value.

<sup>116</sup>WU 06 reports  $[\Gamma(J/\psi(1S) \rightarrow \Lambda \bar{\Lambda})/\Gamma_{\text{total}}] \times [B(B^+ \rightarrow J/\psi(1S) K^+)] = (2.00 \pm 0.34 \pm 0.29 \pm 0.34) \times 10^{-6}$  which we divide by our best value  $B(B^+ \rightarrow J/\psi(1S) K^+) = (1.016 \pm 0.033) \times 10^{-3}$ . Our first error is their experiment's error and our second error is the systematic error from using our best value.

WEIGHTED AVERAGE  
 $1.61 \pm 0.15$  (Error scaled by 1.9)



$$\Gamma(\Lambda \bar{\Lambda})/\Gamma(p \bar{p}) \quad \Gamma_{118}/\Gamma_{99}$$

VALUE	DOCUMENT ID	TECN	COMMENT
<b><math>0.90 \pm 0.15</math> <math>-0.14 \pm 0.10</math></b>	<sup>117</sup> WU	06 BELL	$B^+ \rightarrow p \bar{p} K^+, \Lambda \bar{\Lambda} K^+$

<sup>117</sup>Not independent of other  $J/\psi \rightarrow \Lambda \bar{\Lambda}, p \bar{p}$  branching ratios reported by WU 06.

$$\Gamma(\Lambda \Sigma^- \pi^+ \text{ (or c.c.)})/\Gamma_{\text{total}} \quad \Gamma_{119}/\Gamma$$

VALUE (units $10^{-3}$ )	EVTS	DOCUMENT ID	TECN	COMMENT
<b><math>0.83 \pm 0.07</math> OUR AVERAGE</b>				Error includes scale factor of 1.2.
$0.770 \pm 0.051 \pm 0.083$	335	<sup>118</sup> ABLIKIM	07H BES2	$e^+ e^- \rightarrow \Lambda \Sigma^+ \pi^-$
$0.747 \pm 0.056 \pm 0.076$	254	<sup>118</sup> ABLIKIM	07H BES2	$e^+ e^- \rightarrow \Lambda \Sigma^- \pi^+$
$0.90 \pm 0.06 \pm 0.16$	225 ± 15	HENRARD	87 DM2	$e^+ e^- \rightarrow \Lambda \Sigma^+ \pi^-$
$1.11 \pm 0.06 \pm 0.20$	342 ± 18	HENRARD	87 DM2	$e^+ e^- \rightarrow \Lambda \Sigma^- \pi^+$
$1.53 \pm 0.17 \pm 0.38$	135	EATON	84 MRK2	$e^+ e^- \rightarrow \Lambda \Sigma^+ \pi^-$
$1.38 \pm 0.21 \pm 0.35$	118	EATON	84 MRK2	$e^+ e^- \rightarrow \Lambda \Sigma^- \pi^+$

<sup>118</sup>Using  $B(\Lambda \rightarrow \pi^- p) = 63.9\%$  and  $B(\Sigma^+ \rightarrow \pi^0 p) = 51.6\%$ .

$$\Gamma(p K^- \bar{\Lambda})/\Gamma_{\text{total}} \quad \Gamma_{120}/\Gamma$$

VALUE (units $10^{-3}$ )	EVTS	DOCUMENT ID	TECN	COMMENT
<b><math>0.89 \pm 0.07 \pm 0.14</math></b>	307	EATON	84 MRK2	$e^+ e^-$

$$\Gamma(2(K^+ K^-))/\Gamma_{\text{total}} \quad \Gamma_{121}/\Gamma$$

VALUE (units $10^{-3}$ )	EVTS	DOCUMENT ID	TECN	COMMENT
<b><math>0.76 \pm 0.09</math> OUR AVERAGE</b>				
$0.74 \pm 0.09 \pm 0.02$	156 ± 15	<sup>119</sup> AUBERT	07AK BABR	$10.6 e^+ e^- \rightarrow 2(K^+ K^-) \gamma$
$1.4 \pm 0.5 \pm 0.2$	$11.0 \pm 4.3$ $-3.5$	<sup>120</sup> HUANG	03 BELL	$B^+ \rightarrow 2(K^+ K^-) K^+$
$0.7 \pm 0.3$		VANNUCCI	77 MRK1	$e^+ e^-$

• • • We do not use the following data for averages, fits, limits, etc. • • •

$0.72 \pm 0.17 \pm 0.02$  <sup>38</sup> <sup>121</sup>AUBERT 05D BABR  $10.6 e^+ e^- \rightarrow 2(K^+ K^-) \gamma$

<sup>119</sup>AUBERT 07AK reports  $[\Gamma(J/\psi(1S) \rightarrow 2(K^+ K^-))/\Gamma_{\text{total}}] \times [\Gamma(J/\psi(1S) \rightarrow e^+ e^-)] = (4.11 \pm 0.39 \pm 0.30) \times 10^{-3}$  keV which we divide by our best value  $\Gamma(J/\psi(1S) \rightarrow e^+ e^-) = 5.55 \pm 0.14 \pm 0.02$  keV. Our first error is their experiment's error and our second error is the systematic error from using our best value.

<sup>120</sup>Using  $B(B^+ \rightarrow J/\psi K^+) = (1.01 \pm 0.05) \times 10^{-3}$ .

<sup>121</sup>Superseded by AUBERT 07AK. AUBERT 05D reports  $[\Gamma(J/\psi(1S) \rightarrow 2(K^+ K^-))/\Gamma_{\text{total}}] \times [\Gamma(J/\psi(1S) \rightarrow e^+ e^-)] = (4.0 \pm 0.7 \pm 0.6) \times 10^{-3}$  keV which we divide by our best value  $\Gamma(J/\psi(1S) \rightarrow e^+ e^-) = 5.55 \pm 0.14 \pm 0.02$  keV. Our first error is their experiment's error and our second error is the systematic error from using our best value.

$$\Gamma(p K^- \bar{\Sigma}^0)/\Gamma_{\text{total}} \quad \Gamma_{122}/\Gamma$$

VALUE (units $10^{-3}$ )	EVTS	DOCUMENT ID	TECN	COMMENT
<b><math>0.29 \pm 0.06 \pm 0.05</math></b>	90	EATON	84 MRK2	$e^+ e^-$

$$\Gamma(K^+ K^-)/\Gamma_{\text{total}} \quad \Gamma_{123}/\Gamma$$

VALUE (units $10^{-4}$ )	EVTS	DOCUMENT ID	TECN	COMMENT
<b><math>2.37 \pm 0.31</math> OUR AVERAGE</b>				
$2.39 \pm 0.24 \pm 0.22$	107	BALTRUSAIT...85D	MRK3	$e^+ e^-$
$2.2 \pm 0.9$	6	BRANDELIK	79c DASP	$e^+ e^-$

$$\Gamma(K_S^0 K_L^0)/\Gamma_{\text{total}} \quad \Gamma_{124}/\Gamma$$

VALUE (units $10^{-4}$ )	EVTS	DOCUMENT ID	TECN	COMMENT
<b><math>1.46 \pm 0.26</math> OUR AVERAGE</b>				Error includes scale factor of 2.7. See the ideogram below.
$1.82 \pm 0.04 \pm 0.13$	2155 ± 45	<sup>122</sup> BAI	04A BES2	$J/\psi \rightarrow K_S^0 K_L^0 \rightarrow \pi^+ \pi^- X$
$1.18 \pm 0.12 \pm 0.18$		JOUSSET	90 DM2	$J/\psi \rightarrow \text{hadrons}$
$1.01 \pm 0.16 \pm 0.09$	74	BALTRUSAIT...85D	MRK3	$e^+ e^-$

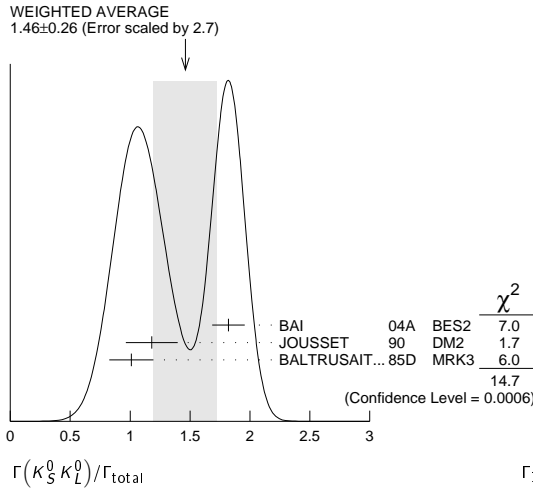


See key on page 457

Meson Particle Listings

$J/\psi(1S)$

<sup>122</sup> Using  $B(K_S^0 \rightarrow \pi^+\pi^-) = 0.6868 \pm 0.0027$ .



$\Gamma(\Lambda\bar{\Lambda}\eta)/\Gamma_{total}$   $\Gamma_{124}/\Gamma$   
 $\Gamma_{125}/\Gamma$

VALUE (units $10^{-4}$ )	EVTS	DOCUMENT ID	TECN	COMMENT
<b>2.62 ± 0.60 ± 0.44</b>	44	123 ABLIKIM	07H BES2	$e^+e^- \rightarrow \psi(2S)$

<sup>123</sup> Using  $B(\Lambda \rightarrow \pi^-p) = 63.9\%$  and  $B(\eta \rightarrow \gamma\gamma) = 39.4\%$ .

$\Gamma(\Lambda\bar{\Lambda}\pi^0)/\Gamma_{total}$   $\Gamma_{126}/\Gamma$

VALUE (units $10^{-4}$ )	CL%	EVTS	DOCUMENT ID	TECN	COMMENT
<b>&lt;0.64</b>		90	124 ABLIKIM	07H BES2	$e^+e^- \rightarrow \psi(2S)$
• • • We do not use the following data for averages, fits, limits, etc. • • •					
2.3 ± 0.7 ± 0.8		11	BAI	98G BES	$e^+e^-$
2.2 ± 0.5 ± 0.5		19 ± 4	HENRARD	87 DM2	$e^+e^-$

<sup>124</sup> Using  $B(\Lambda \rightarrow \pi^-p) = 63.9\%$ .

$\Gamma(\Lambda\bar{\Lambda}\eta K_S^0 + c.c.)/\Gamma_{total}$   $\Gamma_{127}/\Gamma$

VALUE (units $10^{-4}$ )	EVTS	DOCUMENT ID	TECN	COMMENT
<b>6.46 ± 0.20 ± 1.07</b>	1058	125 ABLIKIM	08c BES2	$e^+e^- \rightarrow J/\psi$

<sup>125</sup> Using  $B(\bar{\Lambda} \rightarrow \bar{p}\pi^+) = 63.9\%$  and  $B(K_S^0 \rightarrow \pi^+\pi^-) = 69.2\%$ .

$\Gamma(\pi^+\pi^-)/\Gamma_{total}$   $\Gamma_{128}/\Gamma$

VALUE (units $10^{-4}$ )	EVTS	DOCUMENT ID	TECN	COMMENT
<b>1.47 ± 0.23 OUR AVERAGE</b>				
1.58 ± 0.20 ± 0.15	84	BALTRUSAIT...85D	MRK3	$e^+e^-$
1.0 ± 0.5	5	BRANDELIK	78B DASP	$e^+e^-$
1.6 ± 1.6	1	VANNUCCI	77 MRK1	$e^+e^-$

$\Gamma(\Lambda\bar{\Lambda} + c.c.)/\Gamma_{total}$   $\Gamma_{129}/\Gamma$

VALUE (units $10^{-3}$ )	CL%	DOCUMENT ID	TECN	COMMENT
<b>&lt;0.15</b>		90	PERUZZI	78 MRK1 $e^+e^- \rightarrow AX$

$\Gamma(K_S^0 K_S^0)/\Gamma_{total}$   $\Gamma_{130}/\Gamma$

VALUE (units $10^{-4}$ )	CL%	DOCUMENT ID	TECN	COMMENT
<b>&lt;0.01</b>		95	126 BAI	04D BES $e^+e^-$
• • • We do not use the following data for averages, fits, limits, etc. • • •				
<0.052		90	126 BALTRUSAIT...85c	MRK3 $e^+e^-$

<sup>126</sup> Forbidden by CP.

RADIATIVE DECAYS

$\Gamma(3\gamma)/\Gamma_{total}$   $\Gamma_{131}/\Gamma$

VALUE (units $10^{-6}$ )	CL%	EVTS	DOCUMENT ID	TECN	COMMENT
<b>12 ± 3 ± 2</b>		24.2 ± 7.2 / 6.0	ADAMS	08 CLEO	$\psi(2S) \rightarrow \pi^+\pi^- J/\psi$
• • • We do not use the following data for averages, fits, limits, etc. • • •					
<55		90	PARTRIDGE	80 CBAL	$e^+e^-$

$\Gamma(4\gamma)/\Gamma_{total}$   $\Gamma_{132}/\Gamma$

VALUE (units $10^{-6}$ )	CL%	DOCUMENT ID	TECN	COMMENT	
<b>&lt;9</b>		90	ADAMS	08 CLEO	$\psi(2S) \rightarrow \pi^+\pi^- J/\psi$

$\Gamma(5\gamma)/\Gamma_{total}$   $\Gamma_{133}/\Gamma$

VALUE (units $10^{-6}$ )	CL%	DOCUMENT ID	TECN	COMMENT	
<b>&lt;15</b>		90	ADAMS	08 CLEO	$\psi(2S) \rightarrow \pi^+\pi^- J/\psi$

$\Gamma(\gamma\eta_c(1S))/\Gamma_{total}$   $\Gamma_{134}/\Gamma$

VALUE (units $10^{-2}$ )	EVTS	DOCUMENT ID	TECN	COMMENT
<b>1.7 ± 0.4 OUR AVERAGE</b>				Error includes scale factor of 1.6.
2.06 ± 0.32 ± 0.03		127 MITCHELL	09 CLEO	$e^+e^- \rightarrow \gamma X$
1.27 ± 0.36		GAISER	86 CBAL	$J/\psi \rightarrow \gamma X$

• • • We do not use the following data for averages, fits, limits, etc. • • •

0.79 ± 0.20	273 ± 43	128 AUBERT	06E BABR	$B^\pm \rightarrow K^\pm X_c \bar{c}$
seen	16	BALTRUSAIT...84	MRK3	$J/\psi \rightarrow 2\phi\gamma$

<sup>127</sup> MITCHELL 09 reports  $(1.98 \pm 0.09 \pm 0.30) \times 10^{-2}$  from a measurement of  $[\Gamma(J/\psi(1S) \rightarrow \gamma\eta_c(1S))/\Gamma_{total}] \times [B(\psi(2S) \rightarrow J/\psi(1S)\pi^+\pi^-)]$  assuming  $B(\psi(2S) \rightarrow J/\psi(1S)\pi^+\pi^-) = (35.04 \pm 0.07 \pm 0.77) \times 10^{-2}$ , which we rescale to our best value  $B(\psi(2S) \rightarrow J/\psi(1S)\pi^+\pi^-) = (33.6 \pm 0.4) \times 10^{-2}$ . Our first error is their experiment's error and our second error is the systematic error from using our best value.

<sup>128</sup> Calculated by the authors using an average of  $B(J/\psi \rightarrow \gamma\eta_c) \times B(\eta_c \rightarrow K\bar{K}\pi)$  from BALTRUSAITIS 86, BISELLO 91, BAI 04 and  $B(\eta_c \rightarrow K\bar{K}\pi) = (8.5 \pm 1.8)\%$  from AUBERT 06E.

$\Gamma(\gamma\eta_c(1S) \rightarrow 3\gamma)/\Gamma_{total}$   $\Gamma_{135}/\Gamma$

VALUE (units $10^{-6}$ )	EVTS	DOCUMENT ID	TECN	COMMENT
<b>1.2 ± 2.7 ± 1.1 ± 0.3</b>	1.2 ± 2.8 / 1.1	ADAMS	08 CLEO	$\psi(2S) \rightarrow \pi^+\pi^- J/\psi$

$\Gamma(\gamma\pi^+\pi^-\pi^0)/\Gamma_{total}$   $\Gamma_{136}/\Gamma$

VALUE (units $10^{-3}$ )	DOCUMENT ID	TECN	COMMENT
<b>8.3 ± 0.2 ± 3.1</b>	129 BALTRUSAIT...86B	MRK3	$J/\psi \rightarrow 4\pi\gamma$

<sup>129</sup>  $4\pi$  mass less than 2.0 GeV.

$\Gamma(\gamma\eta\pi\pi)/\Gamma_{total}$   $\Gamma_{137}/\Gamma$

VALUE (units $10^{-3}$ )	DOCUMENT ID	TECN	COMMENT
<b>6.1 ± 1.0 OUR AVERAGE</b>			
5.85 ± 0.3 ± 1.05	130 EDWARDS	83B CBAL	$J/\psi \rightarrow \eta\pi^+\pi^-$
7.8 ± 1.2 ± 2.4	130 EDWARDS	83B CBAL	$J/\psi \rightarrow \eta 2\pi^0$

<sup>130</sup> Broad enhancement at 1700 MeV.

$\Gamma(\gamma\eta_2(1870) \rightarrow \gamma\eta\pi^+\pi^-)/\Gamma_{total}$   $\Gamma_{138}/\Gamma$

VALUE (units $10^{-4}$ )	DOCUMENT ID	TECN	COMMENT
<b>6.2 ± 2.2 ± 0.9</b>	BAI	99 BES	$J/\psi \rightarrow \gamma\eta\pi^+\pi^-$

$\Gamma(\gamma\eta(1405/1475) \rightarrow \gamma K\bar{K}\pi)/\Gamma_{total}$   $\Gamma_{139}/\Gamma$

VALUE (units $10^{-3}$ )	DOCUMENT ID	TECN	COMMENT
<b>2.8 ± 0.6 OUR AVERAGE</b>			Error includes scale factor of 1.6. See the ideogram below.
1.66 ± 0.1 ± 0.58	131,132 BAI	00D BES	$J/\psi \rightarrow \gamma K^\pm K_S^0 \pi^\mp$
3.8 ± 0.3 ± 0.6	133 AUGUSTIN	90 DM2	$J/\psi \rightarrow \gamma K\bar{K}\pi$
4.0 ± 0.7 ± 1.0	133 EDWARDS	82E CBAL	$J/\psi \rightarrow K^+ K^- \pi^0 \gamma$
4.3 ± 1.7	133,134 SCHARRE	80 MRK2	$e^+e^-$

• • • We do not use the following data for averages, fits, limits, etc. • • •

1.78 ± 0.21 ± 0.33	133,135,136 AUGUSTIN	92 DM2	$J/\psi \rightarrow \gamma K\bar{K}\pi$
0.83 ± 0.13 ± 0.18	133,137,138 AUGUSTIN	92 DM2	$J/\psi \rightarrow \gamma K\bar{K}\pi$
0.66 ± 0.17 ± 0.24 / -0.16 - 0.15	133,136,139 BAI	90c MRK3	$J/\psi \rightarrow \gamma K_S^0 K^\pm \pi^\mp$
1.03 ± 0.21 ± 0.26 / -0.18 - 0.19	133,138,140 BAI	90c MRK3	$J/\psi \rightarrow \gamma K_S^0 K^\pm \pi^\mp$

<sup>131</sup> Interference with the  $J/\psi(1S)$  radiative transition to the broad  $K\bar{K}\pi$  pseudoscalar state around 1800 is  $(0.15 \pm 0.01 \pm 0.05) \times 10^{-3}$ .

<sup>132</sup> Interference with  $J/\psi \rightarrow \gamma f_1(1420)$  is  $(-0.03 \pm 0.01 \pm 0.01) \times 10^{-3}$ .

<sup>133</sup> Includes unknown branching fraction for  $\eta(1405) \rightarrow K\bar{K}\pi$ .

<sup>134</sup> Corrected for spin-zero hypothesis for  $\eta(1405)$ .

<sup>135</sup> From fit to the  $a_0(980)\pi 0^-+$  partial wave.

<sup>136</sup>  $a_0(980)\pi$  mode.

<sup>137</sup> From fit to the  $K^*(892)K 0^-+$  partial wave.

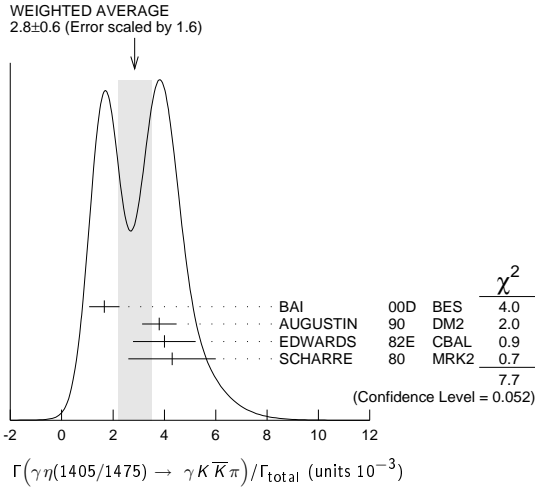
<sup>138</sup>  $K^*K$  mode.

<sup>139</sup> From  $a_0(980)\pi$  final state.

<sup>140</sup> From  $K^*(890)K$  final state.

# Meson Particle Listings

## $J/\psi(1S)$



$\Gamma(\gamma\eta(1405/1475) \rightarrow \gamma\gamma\rho^0) / \Gamma_{\text{total}}$   $\Gamma_{140} / \Gamma$

VALUE (units $10^{-4}$ )	DOCUMENT ID	TECN	COMMENT
<b>0.7±0.20 OUR AVERAGE</b>	Error includes scale factor of 1.8.		
1.07±0.17±0.11	141 BAI	04J	BES2 $J/\psi \rightarrow \gamma\gamma\pi^+\pi^-$
0.64±0.12±0.07	141 COFFMAN	90	MRK3 $J/\psi \rightarrow \gamma\gamma\pi^+\pi^-$

141 Includes unknown branching fraction  $\eta(1405) \rightarrow \gamma\rho^0$ .

$\Gamma(\gamma\eta(1405/1475) \rightarrow \gamma\eta\pi^+\pi^-) / \Gamma_{\text{total}}$   $\Gamma_{141} / \Gamma$

VALUE (units $10^{-4}$ )	EVTS	DOCUMENT ID	TECN	COMMENT
<b>3.0 ±0.5 OUR AVERAGE</b>				
2.6 ±0.7 ±0.4		BAI	99	BES $J/\psi \rightarrow \gamma\eta\pi^+\pi^-$
3.38±0.33±0.64		142 BOLTON	92B	MRK3 $J/\psi \rightarrow \gamma\eta\pi^+\pi^-$

• • • We do not use the following data for averages, fits, limits, etc. • • •

7.0 ±0.6 ±1.1	261	143 AUGUSTIN	90	DM2 $J/\psi \rightarrow \gamma\eta\pi^+\pi^-$
---------------	-----	--------------	----	---

142  $\text{Via } \rho_0(980)\pi$ .  
143 Includes unknown branching fraction to  $\eta\pi^+\pi^-$ .

$\Gamma(\gamma\eta(1405/1475) \rightarrow \gamma\gamma\phi) / \Gamma_{\text{total}}$   $\Gamma_{142} / \Gamma$

VALUE (units $10^{-4}$ )	CL%	DOCUMENT ID	TECN	COMMENT
<b>&lt;0.82</b>	95	BAI	04J	BES2 $J/\psi \rightarrow \gamma\gamma K^+ K^-$

$\Gamma(\gamma\rho\rho) / \Gamma_{\text{total}}$   $\Gamma_{143} / \Gamma$

VALUE (units $10^{-3}$ )	CL%	DOCUMENT ID	TECN	COMMENT
<b>4.5 ±0.8 OUR AVERAGE</b>				
4.7 ±0.3 ±0.9		144 BALTRUSAIT...86B	MRK3	$J/\psi \rightarrow 4\pi\gamma$
3.75±1.05±1.20		145 BURKE	82	MRK2 $J/\psi \rightarrow 4\pi\gamma$

• • • We do not use the following data for averages, fits, limits, etc. • • •

<0.09	90	146 BISELLO	89B	$J/\psi \rightarrow 4\pi\gamma$
-------	----	-------------	-----	---------------------------------

144  $4\pi$  mass less than 2.0 GeV.  
145  $4\pi$  mass less than 2.0 GeV. We have multiplied  $2\rho^0$  measurement by 3 to obtain  $2\rho$ .  
146  $4\pi$  mass in the range 2.0–25 GeV.

$\Gamma(\gamma\rho\omega) / \Gamma_{\text{total}}$   $\Gamma_{144} / \Gamma$

VALUE (units $10^{-4}$ )	CL%	DOCUMENT ID	TECN	COMMENT
<b>&lt;5.4</b>	90	ABLIKIM	08A	BES2 $e^+e^- \rightarrow J/\psi$

$\Gamma(\gamma\rho\phi) / \Gamma_{\text{total}}$   $\Gamma_{145} / \Gamma$

VALUE (units $10^{-3}$ )	CL%	DOCUMENT ID	TECN	COMMENT
<b>&lt;8.8</b>	90	ABLIKIM	08A	BES2 $e^+e^- \rightarrow J/\psi$

$\Gamma(\gamma\eta(958)) / \Gamma_{\text{total}}$   $\Gamma_{146} / \Gamma$

VALUE (units $10^{-3}$ )	EVTS	DOCUMENT ID	TECN	COMMENT
<b>5.16±0.15 OUR AVERAGE</b>		Error includes scale factor of 1.1.		
4.86±0.23±0.08		147 ABLIKIM	11	BES3 $J/\psi \rightarrow \eta'\gamma$
5.24±0.12±0.11		PEDLAR	09	CLE3 $J/\psi \rightarrow \eta'\gamma$
5.55±0.44	35k	ABLIKIM	06E	BES2 $J/\psi \rightarrow \eta'\gamma$

• • • We do not use the following data for averages, fits, limits, etc. • • •

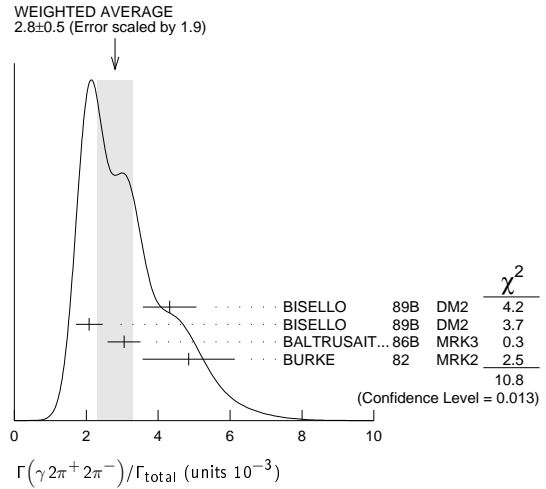
4.50±0.14±0.53		BOLTON	92B	MRK3 $J/\psi \rightarrow \gamma\pi^+\pi^-\eta, \eta \rightarrow \gamma\gamma$
4.30±0.31±0.71		BOLTON	92B	MRK3 $J/\psi \rightarrow \gamma\pi^+\pi^-\eta, \eta \rightarrow \pi^+\pi^-\pi^0$
4.04±0.16±0.85	622	AUGUSTIN	90	DM2 $J/\psi \rightarrow \gamma\eta\pi^+\pi^-$
4.39±0.09±0.66	2420	AUGUSTIN	90	DM2 $J/\psi \rightarrow \gamma\gamma\pi^+\pi^-$
4.1 ±0.3 ±0.6		BLOOM	83	CBAL $e^+e^- \rightarrow 3\gamma + \text{hadrons}$
2.9 ±1.1	6	BRANDELIK	79c	DASP $e^+e^- \rightarrow 3\gamma$
2.4 ±0.7	57	BARTEL	76	CNTR $e^+e^- \rightarrow 2\gamma\rho$

147 ABLIKIM 11 reports  $(4.84 \pm 0.03 \pm 0.24) \times 10^{-3}$  from a measurement of  $[\Gamma(J/\psi(1S) \rightarrow \gamma\eta(958))/\Gamma_{\text{total}}] / [B(\eta'(958) \rightarrow \pi^+\pi^-\eta)] / [B(\eta \rightarrow 2\gamma)]$  assuming  $B(\eta'(958) \rightarrow \pi^+\pi^-\eta) = (43.2 \pm 0.7) \times 10^{-2}$ ,  $B(\eta \rightarrow 2\gamma) = (39.31 \pm 0.20) \times 10^{-2}$ , which we rescale to our best values  $B(\eta'(958) \rightarrow \pi^+\pi^-\eta) = (43.4 \pm 0.7) \times 10^{-2}$ ,  $B(\eta \rightarrow 2\gamma) = (39.31 \pm 0.20) \times 10^{-2}$ . Our first error is their experiment's error and our second error is the systematic error from using our best values.

$\Gamma(\gamma 2\pi^+ 2\pi^-) / \Gamma_{\text{total}}$   $\Gamma_{147} / \Gamma$

VALUE (units $10^{-3}$ )	DOCUMENT ID	TECN	COMMENT
<b>2.8 ±0.5 OUR AVERAGE</b>	Error includes scale factor of 1.9. See the ideogram below.		
4.32±0.14±0.73	148 BISELLO	89B	DM2 $J/\psi \rightarrow 4\pi\gamma$
2.08±0.13±0.35	149 BISELLO	89B	DM2 $J/\psi \rightarrow 4\pi\gamma$
3.05±0.08±0.45	149 BALTRUSAIT...86B	MRK3	$J/\psi \rightarrow 4\pi\gamma$
4.85±0.45±1.20	150 BURKE	82	MRK2 $e^+e^-$

148  $4\pi$  mass less than 3.0 GeV.  
149  $4\pi$  mass less than 2.0 GeV.  
150  $4\pi$  mass less than 2.5 GeV.



$\Gamma(\gamma f_2(1270) f_2(1270)) / \Gamma_{\text{total}}$   $\Gamma_{148} / \Gamma$

VALUE (units $10^{-4}$ )	EVTS	DOCUMENT ID	TECN	COMMENT
<b>9.5 ±0.7 ±1.6</b>	646 ± 45	ABLIKIM	04M	BES $J/\psi \rightarrow \gamma 2\pi^+ 2\pi^-$

$\Gamma(\gamma f_2(1270) f_2(1270) (\text{non resonant})) / \Gamma_{\text{total}}$   $\Gamma_{149} / \Gamma$

VALUE (units $10^{-3}$ )	DOCUMENT ID	TECN	COMMENT
<b>8.2 ±0.8 ±1.7</b>	151 ABLIKIM	04M	BES $J/\psi \rightarrow \gamma 2\pi^+ 2\pi^-$

151 Subtracting contribution from intermediate  $\eta_c(1S)$  decays.

$\Gamma(\gamma K^+ K^- \pi^+ \pi^-) / \Gamma_{\text{total}}$   $\Gamma_{150} / \Gamma$

VALUE (units $10^{-3}$ )	EVTS	DOCUMENT ID	TECN	COMMENT
<b>2.1 ±0.1 ±0.6</b>	1516	BAI	00B	BES $J/\psi \rightarrow \gamma K^+ K^0 \pi^+ \pi^-$

$\Gamma(\gamma f_4(2050)) / \Gamma_{\text{total}}$   $\Gamma_{151} / \Gamma$

VALUE (units $10^{-3}$ )	DOCUMENT ID	TECN	COMMENT
<b>2.7 ±0.5 ±0.5</b>	152 BALTRUSAIT...87	MRK3	$J/\psi \rightarrow \gamma\pi^+\pi^-$

152 Assuming branching fraction  $f_4(2050) \rightarrow \pi\pi / \text{total} = 0.167$ .

$\Gamma(\gamma\omega\omega) / \Gamma_{\text{total}}$   $\Gamma_{152} / \Gamma$

VALUE (units $10^{-3}$ )	EVTS	DOCUMENT ID	TECN	COMMENT
<b>1.61 ±0.33 OUR AVERAGE</b>				
6.0 ±4.8 ±1.8		ABLIKIM	08A	BES2 $J/\psi \rightarrow \gamma\omega\pi^+\pi^-$
1.41±0.2 ±0.42	120 ± 17	BISELLO	87	SPEC $e^+e^-$ , hadrons $\gamma$
1.76±0.09±0.45		BALTRUSAIT...85c	MRK3	$e^+e^- \rightarrow \text{hadrons}\gamma$

$\Gamma(\gamma\eta(1405/1475) \rightarrow \gamma\rho^0\rho^0) / \Gamma_{\text{total}}$   $\Gamma_{153} / \Gamma$

VALUE (units $10^{-3}$ )	DOCUMENT ID	TECN	COMMENT	
<b>1.7 ±0.4 OUR AVERAGE</b>	Error includes scale factor of 1.3.			
2.1 ±0.4	BUGG	95	MRK3 $J/\psi \rightarrow \gamma\pi^+\pi^-\pi^+\pi^-$	
1.36±0.38	153,154	BISELLO	89B	DM2 $J/\psi \rightarrow 4\pi\gamma$

153 Estimated by us from various fits.  
154 Includes unknown branching fraction to  $\rho^0\rho^0$ .

See key on page 457

## Meson Particle Listings

 $J/\psi(1S)$  $\Gamma(\gamma f_2(1270))/\Gamma_{total}$   $\Gamma_{154}/\Gamma$ 

VALUE (units $10^{-3}$ )	EVTS	DOCUMENT ID	TECN	COMMENT
<b>1.43 ± 0.11 OUR AVERAGE</b>				
$1.62 \pm 0.26^{+0.02}_{-0.05}$		155 ABLIKIM	06v BES2	$e^+e^- \rightarrow J/\psi \rightarrow \gamma\pi^+\pi^-$
$1.42 \pm 0.21^{+0.02}_{-0.04}$		156 ABLIKIM	06v BES2	$e^+e^- \rightarrow J/\psi \rightarrow \gamma\pi^0\pi^0$
$1.33 \pm 0.05 \pm 0.20$		157 AUGUSTIN	87 DM2	$J/\psi \rightarrow \gamma\pi^+\pi^-$
$1.36 \pm 0.09 \pm 0.23$		157 BALTRUSAIT...87	MRK3	$J/\psi \rightarrow \gamma\pi^+\pi^-$
$1.48 \pm 0.25 \pm 0.30$	178	EDWARDS	82B CBAL	$e^+e^- \rightarrow 2\pi^0\gamma$
$2.0 \pm 0.7$	35	ALEXANDER	78 PLUT	$e^+e^-$
$1.2 \pm 0.6$	30	158 BRANDELIK	78B DASP	$e^+e^- \rightarrow \pi^+\pi^-\gamma$
155 ABLIKIM 06v reports $[\Gamma(J/\psi(1S) \rightarrow \gamma f_2(1270))/\Gamma_{total}] \times [B(f_2(1270) \rightarrow \pi\pi)] = (1.371 \pm 0.010 \pm 0.222) \times 10^{-3}$ which we divide by our best value $B(f_2(1270) \rightarrow \pi\pi) = (84.8^{+2.4}_{-1.2}) \times 10^{-2}$ . Our first error is their experiment's error and our second error is the systematic error from using our best value.				
156 ABLIKIM 06v reports $[\Gamma(J/\psi(1S) \rightarrow \gamma f_2(1270))/\Gamma_{total}] \times [B(f_2(1270) \rightarrow \pi\pi)] = (1.200 \pm 0.027 \pm 0.174) \times 10^{-3}$ which we divide by our best value $B(f_2(1270) \rightarrow \pi\pi) = (84.8^{+2.4}_{-1.2}) \times 10^{-2}$ . Our first error is their experiment's error and our second error is the systematic error from using our best value.				
157 Estimated using $B(f_2(1270) \rightarrow \pi\pi) = 0.843 \pm 0.012$ . The errors do not contain the uncertainty in the $f_2(1270)$ decay.				
158 Restated by us to take account of spread of E1, M2, E3 transitions.				

 $\Gamma(\gamma f_0(1710) \rightarrow \gamma K\bar{K})/\Gamma_{total}$   $\Gamma_{155}/\Gamma$ 

VALUE (units $10^{-4}$ )	CL%	DOCUMENT ID	TECN	COMMENT
<b>8.5 <math>\pm</math> 1.2 <math>\pm</math> 0.9 OUR AVERAGE</b> Error includes scale factor of 1.2.				
$9.62 \pm 0.29^{+3.51}_{-1.86}$		159 BAI	03G BES	$J/\psi \rightarrow \gamma K\bar{K}$
$5.0 \pm 0.8^{+1.8}_{-0.4}$		160,161 BAI	96C BES	$J/\psi \rightarrow \gamma K^+K^-$
$9.2 \pm 1.4 \pm 1.4$		161 AUGUSTIN	88 DM2	$J/\psi \rightarrow \gamma K^+K^-$
$10.4 \pm 1.2 \pm 1.6$		161 AUGUSTIN	88 DM2	$J/\psi \rightarrow \gamma K_S^0 K_S^0$
$9.6 \pm 1.2 \pm 1.8$		161 BALTRUSAIT...87	MRK3	$J/\psi \rightarrow \gamma K^+K^-$
••• We do not use the following data for averages, fits, limits, etc. •••				
$1.6 \pm 0.2^{+0.6}_{-0.2}$		161,162 BAI	96C BES	$J/\psi \rightarrow \gamma K^+K^-$
$< 0.8$	90	163 BISELLO	89B	$J/\psi \rightarrow 4\pi\gamma$
$1.6 \pm 0.4 \pm 0.3$		164 BALTRUSAIT...87	MRK3	$J/\psi \rightarrow \gamma\pi^+\pi^-$
$3.8 \pm 1.6$		165 EDWARDS	82D CBAL	$e^+e^- \rightarrow \eta\eta\gamma$

159 Includes unknown branching ratio to  $K^+K^-$  or  $K_S^0 K_S^0$ .  
 160 Assuming  $J^P = 2^+$  for  $f_0(1710)$ .  
 161 Includes unknown branching fraction to  $K^+K^-$  or  $K_S^0 K_S^0$ . We have multiplied  $K^+K^-$  measurement by 2, and  $K_S^0 K_S^0$  by 4 to obtain  $K\bar{K}$  result.  
 162 Assuming  $J^P = 0^+$  for  $f_0(1710)$ .  
 163 Includes unknown branching fraction to  $\rho^0\rho^0$ .  
 164 Includes unknown branching fraction to  $\pi^+\pi^-$ .  
 165 Includes unknown branching fraction to  $\eta\eta$ .

 $\Gamma(\gamma f_0(1710) \rightarrow \gamma\pi\pi)/\Gamma_{total}$   $\Gamma_{156}/\Gamma$ 

VALUE (units $10^{-4}$ )	DOCUMENT ID	TECN	COMMENT
<b>4.0 ± 1.0 OUR AVERAGE</b>			
$3.96 \pm 0.06 \pm 1.12$	166 ABLIKIM	06v BES2	$e^+e^- \rightarrow J/\psi \rightarrow \gamma\pi^+\pi^-$
$3.99 \pm 0.15 \pm 2.64$	166 ABLIKIM	06v BES2	$e^+e^- \rightarrow J/\psi \rightarrow \gamma\pi^0\pi^0$
••• We do not use the following data for averages, fits, limits, etc. •••			
$2.5 \pm 1.6 \pm 0.8$	BAI	98H BES	$J/\psi \rightarrow \gamma\pi^0\pi^0$
166 Including unknown branching fraction to $\pi\pi$ .			

 $\Gamma(\gamma f_0(1710) \rightarrow \gamma\omega)/\Gamma_{total}$   $\Gamma_{157}/\Gamma$ 

VALUE (units $10^{-3}$ )	EVTS	DOCUMENT ID	TECN	COMMENT
<b>0.31 ± 0.06 ± 0.08</b>	180	ABLIKIM	06H BES	$J/\psi \rightarrow \gamma\omega$

 $\Gamma(\gamma\eta)/\Gamma_{total}$   $\Gamma_{158}/\Gamma$ 

VALUE (units $10^{-3}$ )	EVTS	DOCUMENT ID	TECN	COMMENT
<b>1.104 ± 0.034 OUR AVERAGE</b>				
$1.101 \pm 0.029 \pm 0.022$		PEDLAR	09 CLE3	$J/\psi \rightarrow \eta\gamma$
$1.123 \pm 0.089$	11k	ABLIKIM	06E BES2	$J/\psi \rightarrow \eta\gamma$
••• We do not use the following data for averages, fits, limits, etc. •••				
$0.88 \pm 0.08 \pm 0.11$		BLOOM	83 CBAL	$e^+e^-$
$0.82 \pm 0.10$		BRANDELIK	79C DASP	$e^+e^-$
$1.3 \pm 0.4$	21	BARTEL	77 CNTR	$e^+e^-$

 $\Gamma(\gamma f_1(1420) \rightarrow \gamma K\bar{K}\pi)/\Gamma_{total}$   $\Gamma_{159}/\Gamma$ 

VALUE (units $10^{-3}$ )	DOCUMENT ID	TECN	COMMENT
<b>0.79 ± 0.13 OUR AVERAGE</b>			
$0.68 \pm 0.04 \pm 0.24$	BAI	00D BES	$J/\psi \rightarrow \gamma K^\pm K_S^0 \pi^\mp$
$0.76 \pm 0.15 \pm 0.21$	167,168 AUGUSTIN	92 DM2	$J/\psi \rightarrow \gamma K\bar{K}\pi$
$0.87 \pm 0.14^{+0.14}_{-0.11}$	167 BAI	90C MRK3	$J/\psi \rightarrow \gamma K_S^0 K^\pm \pi^\mp$

167 Included unknown branching fraction  $f_1(1420) \rightarrow K\bar{K}\pi$ .

168 From fit to the  $K^*(892)K1^{++}$  partial wave.

 $\Gamma(\gamma f_1(1285))/\Gamma_{total}$   $\Gamma_{160}/\Gamma$ 

VALUE (units $10^{-3}$ )	DOCUMENT ID	TECN	COMMENT
<b>0.61 ± 0.08 OUR AVERAGE</b>			
$0.69 \pm 0.16 \pm 0.20$	169 BAI	04J BES2	$J/\psi \rightarrow \gamma\gamma\rho^0$
$0.61 \pm 0.04 \pm 0.21$	170 BAI	00D BES	$J/\psi \rightarrow \gamma K^\pm K_S^0 \pi^\mp$
$0.45 \pm 0.09 \pm 0.17$	171 BAI	99 BES	$J/\psi \rightarrow \gamma\eta\pi^+\pi^-$
$0.625 \pm 0.063 \pm 0.103$	172 BOLTON	92 MRK3	$J/\psi \rightarrow \gamma f_1(1285)$
$0.70 \pm 0.08 \pm 0.16$	173 BOLTON	92B MRK3	$J/\psi \rightarrow \gamma\eta\pi^+\pi^-$
169 Assuming $B(f_1(1285) \rightarrow \rho^0\gamma) = 0.055 \pm 0.013$ .			
170 Assuming $\Gamma(f_1(1285) \rightarrow K\bar{K}\pi)/\Gamma_{total} = 0.090 \pm 0.004$ .			
171 Assuming $\Gamma(f_1(1285) \rightarrow \eta\pi\pi)/\Gamma_{total} = 0.5 \pm 0.18$ .			
172 Obtained summing the sequential decay channels $B(J/\psi \rightarrow \gamma f_1(1285), f_1(1285) \rightarrow \pi\pi\pi) = (1.44 \pm 0.39 \pm 0.27) \times 10^{-4}$ ; $B(J/\psi \rightarrow \gamma f_1(1285), f_1(1285) \rightarrow a_0(980)\pi, a_0(980) \rightarrow \eta\pi) = (3.90 \pm 0.42 \pm 0.87) \times 10^{-4}$ ; $B(J/\psi \rightarrow \gamma f_1(1285), f_1(1285) \rightarrow a_0(980)\pi, a_0(980) \rightarrow K\bar{K}) = (0.66 \pm 0.26 \pm 0.29) \times 10^{-4}$ ; $B(J/\psi \rightarrow \gamma f_1(1285), f_1(1285) \rightarrow \gamma\rho^0) = (0.25 \pm 0.07 \pm 0.03) \times 10^{-4}$ .			
173 Using $B(f_1(1285) \rightarrow a_0(980)\pi) = 0.37$ , and including unknown branching ratio for $a_0(980) \rightarrow \eta\pi$ .			

 $\Gamma(\gamma f_1(1510) \rightarrow \gamma\eta\pi^+\pi^-)/\Gamma_{total}$   $\Gamma_{161}/\Gamma$ 

VALUE (units $10^{-4}$ )	DOCUMENT ID	TECN	COMMENT
<b>4.5 ± 1.0 ± 0.7</b>	BAI	99 BES	$J/\psi \rightarrow \gamma\eta\pi^+\pi^-$

 $\Gamma(\gamma f_2'(1525))/\Gamma_{total}$   $\Gamma_{162}/\Gamma$ 

VALUE (units $10^{-4}$ )	CL%	EVTS	DOCUMENT ID	TECN	COMMENT
<b>4.5 <math>\pm</math> 0.7 <math>\pm</math> 0.4 OUR AVERAGE</b>					
$3.85 \pm 0.17^{+1.91}_{-0.73}$			174 BAI	03G BES	$J/\psi \rightarrow \gamma K\bar{K}$
$3.6 \pm 0.4^{+1.4}_{-0.4}$			174 BAI	96C BES	$J/\psi \rightarrow \gamma K^+K^-$
$5.6 \pm 1.4 \pm 0.9$			174 AUGUSTIN	88 DM2	$J/\psi \rightarrow \gamma K^+K^-$
$4.5 \pm 0.4 \pm 0.9$			174 AUGUSTIN	88 DM2	$J/\psi \rightarrow \gamma K_S^0 K_S^0$
$6.8 \pm 1.6 \pm 1.4$			174 BALTRUSAIT...87	MRK3	$J/\psi \rightarrow \gamma K^+K^-$

••• We do not use the following data for averages, fits, limits, etc. •••  
 $< 3.4$  90 4 175 BRANDELIK 79C DASP  $e^+e^- \rightarrow \pi^+\pi^-\gamma$   
 $< 2.3$  90 3 ALEXANDER 78 PLUT  $e^+e^- \rightarrow K^+K^-\gamma$

174 Using  $B(f_2'(1525) \rightarrow K\bar{K}) = 0.888$ .

175 Assuming isotropic production and decay of the  $f_2'(1525)$  and isospin.

 $\Gamma(\gamma f_2(1640) \rightarrow \gamma\omega)/\Gamma_{total}$   $\Gamma_{163}/\Gamma$ 

VALUE (units $10^{-3}$ )	EVTS	DOCUMENT ID	TECN	COMMENT
<b>0.28 ± 0.05 ± 0.17</b>	141	ABLIKIM	06H BES	$J/\psi \rightarrow \gamma\omega$

 $\Gamma(\gamma f_2(1910) \rightarrow \gamma\omega)/\Gamma_{total}$   $\Gamma_{164}/\Gamma$ 

VALUE (units $10^{-3}$ )	EVTS	DOCUMENT ID	TECN	COMMENT
<b>0.20 ± 0.04 ± 0.13</b>	151	ABLIKIM	06H BES	$J/\psi \rightarrow \gamma\omega$

 $\Gamma(\gamma f_2(1950) \rightarrow \gamma K^*(892)\bar{K}^*(892))/\Gamma_{total}$   $\Gamma_{165}/\Gamma$ 

VALUE (units $10^{-3}$ )	DOCUMENT ID	TECN	COMMENT
<b>0.7 ± 0.1 ± 0.2</b>	BAI	00B BES	$J/\psi \rightarrow \gamma K^+ K^0 \pi^+ \pi^-$

 $\Gamma(\gamma K^*(892)\bar{K}^*(892))/\Gamma_{total}$   $\Gamma_{166}/\Gamma$ 

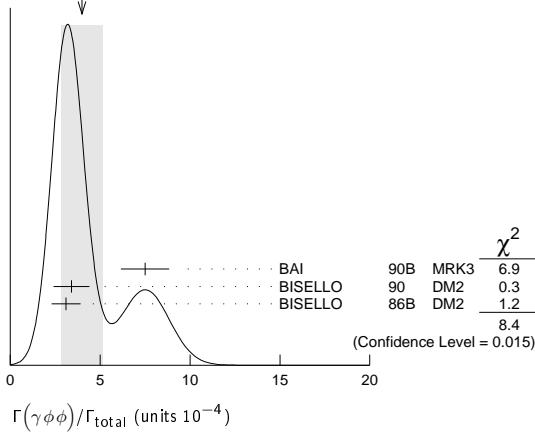
VALUE (units $10^{-3}$ )	EVTS	DOCUMENT ID	TECN	COMMENT
<b>4.0 ± 0.3 ± 1.3</b>	320	176 BAI	00B BES	$J/\psi \rightarrow \gamma K^+ K^0 \pi^+ \pi^-$

176 Summed over all charges.

 $\Gamma(\gamma\phi\phi)/\Gamma_{total}$   $\Gamma_{167}/\Gamma$ 

VALUE (units $10^{-4}$ )	EVTS	DOCUMENT ID	TECN	COMMENT
<b>4.0 ± 1.2 OUR AVERAGE</b> Error includes scale factor of 2.1. See the ideogram below.				
$7.5 \pm 0.6 \pm 1.2$	168	BAI	90B MRK3	$J/\psi \rightarrow \gamma 4K$
$3.4 \pm 0.8 \pm 0.6$	$33 \pm 7$	177 BISELLO	90 DM2	$J/\psi \rightarrow \gamma K^+ K^- K_S^0 K_L^0$
$3.1 \pm 0.7 \pm 0.4$		177 BISELLO	86B DM2	$J/\psi \rightarrow \gamma K^+ K^- K^+ K^-$
177 $\phi\phi$ mass less than 2.9 GeV, $\eta_c$ excluded.				

## Meson Particle Listings

 $J/\psi(1S)$ WEIGHTED AVERAGE  
4.0±1.2 (Error scaled by 2.1)

$\Gamma(\gamma\rho\rho)/\Gamma_{\text{total}}$			$\Gamma_{168}/\Gamma$		
VALUE (units $10^{-3}$ )	CL%	EVTS	DOCUMENT ID	TECN	COMMENT
<b>0.38±0.07±0.07</b>		49	EATON	84	MRK2 $e^+e^-$
••• We do not use the following data for averages, fits, limits, etc. •••					
<0.11	90		PERUZZI	78	MRK1 $e^+e^-$

$\Gamma(\gamma\eta(2225))/\Gamma_{\text{total}}$			$\Gamma_{169}/\Gamma$		
VALUE (units $10^{-3}$ )	EVTS	DOCUMENT ID	TECN	COMMENT	
<b>0.33±0.05 OUR AVERAGE</b>					
0.44±0.04±0.08	196 ± 19	178	ABLIKIM	08i	BES $J/\psi \rightarrow \gamma K^+ K^- K_S^0 K_L^0$
0.33±0.08±0.05		178	BAI	90B	MRK3 $J/\psi \rightarrow \gamma K^+ K^- K^+ K^-$
0.27±0.06±0.06		178	BAI	90B	MRK3 $J/\psi \rightarrow \gamma K^+ K^- K_S^0 K_L^0$
0.24 <sup>+0.15</sup> <sub>-0.10</sub>	179,180	BISELLO	89B	DM2	$J/\psi \rightarrow 4\pi\gamma$
178 Includes unknown branching fraction to $\phi\phi$ .					
179 Estimated by us from various fits.					
180 Includes unknown branching fraction to $\rho^0\rho^0$ .					

$\Gamma(\gamma\eta(1760) \rightarrow \gamma\rho^0\rho^0)/\Gamma_{\text{total}}$			$\Gamma_{170}/\Gamma$		
VALUE (units $10^{-3}$ )	DOCUMENT ID	TECN	COMMENT		
<b>0.13±0.09</b>	181,182	BISELLO	89B	DM2	$J/\psi \rightarrow 4\pi\gamma$
181 Estimated by us from various fits.					
182 Includes unknown branching fraction to $\rho^0\rho^0$ .					

$\Gamma(\gamma\eta(1760) \rightarrow \gamma\omega\omega)/\Gamma_{\text{total}}$			$\Gamma_{171}/\Gamma$		
VALUE (units $10^{-3}$ )	EVTS	DOCUMENT ID	TECN	COMMENT	
<b>1.98±0.08±0.32</b>	1045	ABLIKIM	06H	BES	$J/\psi \rightarrow \gamma\omega\omega$

$\Gamma(\gamma X(1835) \rightarrow \gamma\pi^+\pi^-\eta')/\Gamma_{\text{total}}$			$\Gamma_{172}/\Gamma$		
VALUE (units $10^{-4}$ )	EVTS	DOCUMENT ID	TECN	COMMENT	
<b>2.6 ± 0.4 OUR AVERAGE</b>					
2.87±0.09 <sup>+0.49</sup> <sub>-0.52</sub>	4265	183	ABLIKIM	11c	BES3 $J/\psi \rightarrow \gamma\pi^+\pi^-\eta'$
2.2 ± 0.4 ± 0.4	264	ABLIKIM	05R	BES2	$J/\psi \rightarrow \gamma\pi^+\pi^-\eta'$

183 From a fit of the  $\pi^+\pi^-\eta'$  mass distribution to a combination of  $\gamma f_1(1510)$ ,  $\gamma X(1835)$ , and two unconfirmed states  $\gamma X(2120)$ , and  $\gamma X(2370)$ , for  $M(p\bar{p}) < 2.8$  GeV, and accounting for backgrounds from non- $\eta'$  events and  $J/\psi \rightarrow \pi^0\pi^+\pi^-\eta'$ .

$\Gamma(\gamma X(1835) \rightarrow \gamma\rho\rho)/\Gamma_{\text{total}}$			$\Gamma_{173}/\Gamma$		
VALUE (units $10^{-4}$ )	EVTS	DOCUMENT ID	TECN	COMMENT	
<b>0.75<sup>+0.19</sup><sub>-0.09</sub> OUR AVERAGE</b>					
1.14 <sup>+0.43+0.42</sup> <sub>-0.30-0.26</sub>	231	184	ALEXANDER	10	CLEO $J/\psi \rightarrow \gamma\rho\rho$
0.70±0.04 <sup>+0.19</sup> <sub>-0.08</sub>			BAI	03F	BES2 $J/\psi \rightarrow \gamma\rho\rho$

184 From a fit of the  $p\bar{p}$  mass distribution to a combination of  $\gamma X(1835)$ ,  $\gamma R$  with  $M(R) = 2100$  MeV and  $\Gamma(R) = 160$  MeV, and  $\gamma\rho\rho$  phase space, for  $M(p\bar{p}) < 2.85$  GeV.

$\Gamma(\gamma(K\bar{K}\pi) [P^C = 0^-])/ \Gamma_{\text{total}}$			$\Gamma_{174}/\Gamma$		
VALUE (units $10^{-3}$ )	DOCUMENT ID	TECN	COMMENT		
<b>0.7 ± 0.4 OUR AVERAGE</b>	Error includes scale factor of 2.1.				
0.58±0.03±0.20	185	BAI	00D	BES	$J/\psi \rightarrow \gamma K^\pm K_S^0 \pi^\mp$
2.1 ± 0.1 ± 0.7	186	BAI	00D	BES	$J/\psi \rightarrow \gamma K^\pm K_S^0 \pi^\mp$

185 For a broad structure around 1800 MeV.

186 For a broad structure around 2040 MeV.

$\Gamma(\gamma\pi^0)/\Gamma_{\text{total}}$			$\Gamma_{175}/\Gamma$		
VALUE (units $10^{-5}$ )	EVTS	DOCUMENT ID	TECN	COMMENT	

**3.49<sup>+0.33</sup><sub>-0.30</sub> OUR AVERAGE**

3.63±0.36±0.13		PEDLAR	09	CLE3	$J/\psi \rightarrow \pi^0\gamma$
3.13 <sup>+0.65</sup> <sub>-0.47</sub>	586	ABLIKIM	06E	BES2	$J/\psi \rightarrow \pi^0\gamma$
••• We do not use the following data for averages, fits, limits, etc. •••					
3.6 ± 1.1 ± 0.7		BLOOM	83	CBAL	$e^+e^-$
7.3 ± 4.7	10	BRANDELIK	79c	DASP	$e^+e^-$

$\Gamma(\gamma\rho\rho\pi^+\pi^-)/\Gamma_{\text{total}}$			$\Gamma_{176}/\Gamma$		
VALUE (units $10^{-3}$ )	CL%	DOCUMENT ID	TECN	COMMENT	
<b>&lt;0.79</b>	90	EATON	84	MRK2	$e^+e^-$

$\Gamma(\gamma A\bar{A})/\Gamma_{\text{total}}$			$\Gamma_{177}/\Gamma$		
VALUE (units $10^{-3}$ )	CL%	DOCUMENT ID	TECN	COMMENT	
<b>&lt;0.13</b>	90	HENRARD	87	DM2	$e^+e^-$
••• We do not use the following data for averages, fits, limits, etc. •••					
<0.16	90	BAI	98G	BES	$e^+e^-$

$\Gamma(\gamma f_0(2200))/\Gamma_{\text{total}}$			$\Gamma_{178}/\Gamma$		
VALUE (units $10^{-4}$ )	DOCUMENT ID	TECN	COMMENT		
••• We do not use the following data for averages, fits, limits, etc. •••					
1.5	187	AUGUSTIN	88	DM2	$J/\psi \rightarrow \gamma K_S^0 K_S^0$
187 Includes unknown branching fraction to $K_S^0 K_S^0$ .					

$\Gamma(\gamma f_J(2220))/\Gamma_{\text{total}}$			$\Gamma_{179}/\Gamma$			
VALUE (units $10^{-5}$ )	CL%	EVTS	DOCUMENT ID	TECN	COMMENT	
<b>&gt;250</b>	99.9		188	HASAN	96	SPEC $\bar{p}p \rightarrow \pi^+\pi^-$
••• We do not use the following data for averages, fits, limits, etc. •••						
>300			189	BAI	96B	BES $e^+e^- \rightarrow \gamma\bar{p}p, K\bar{K}$
> 2.3	95		190	AUGUSTIN	88	DM2 $J/\psi \rightarrow \gamma K^+ K^-$
< 1.6	95		190	AUGUSTIN	88	DM2 $J/\psi \rightarrow \gamma K_S^0 K_S^0$
12.4 <sup>+6.4</sup> <sub>-5.2</sub> ± 2.8		23	190	BALTRUSAIT...86D	MRK3	$J/\psi \rightarrow \gamma K_S^0 K_S^0$
8.4 <sup>+3.4</sup> <sub>-2.8</sub> ± 1.6		93	190	BALTRUSAIT...86D	MRK3	$J/\psi \rightarrow \gamma K^+ K^-$
188 Using BAI 96B.						
189 Using BARNES 93.						
190 Includes unknown branching fraction to $K^+ K^-$ or $K_S^0 K_S^0$ .						

$\Gamma(\gamma f_J(2220) \rightarrow \gamma\pi\pi)/\Gamma_{\text{total}}$			$\Gamma_{180}/\Gamma$		
VALUE (units $10^{-4}$ )	DOCUMENT ID	TECN	COMMENT		
<b>0.84±0.26±0.30</b>	BAI	96B	BES	$e^+e^- \rightarrow J/\psi \rightarrow \gamma\pi^+\pi^-$	
••• We do not use the following data for averages, fits, limits, etc. •••					
1.4 ± 0.8 ± 0.4	BAI	98H	BES	$J/\psi \rightarrow \gamma\pi^0\pi^0$	

$\Gamma(\gamma f_J(2220) \rightarrow \gamma K\bar{K})/\Gamma_{\text{total}}$			$\Gamma_{181}/\Gamma$		
VALUE (units $10^{-5}$ )	DOCUMENT ID	TECN	COMMENT		
<b>&lt; 3.6</b>	191	DEL-AMO-SA...10c	BABR	$e^+e^- \rightarrow J/\psi \rightarrow \gamma K^+ K^-$	
••• We do not use the following data for averages, fits, limits, etc. •••					
< 2.9	191	DEL-AMO-SA...10c	BABR	$e^+e^- \rightarrow J/\psi \rightarrow \gamma K_S^0 K_S^0$	
6.6±2.9±2.4	BAI	96B	BES	$e^+e^- \rightarrow J/\psi \rightarrow \gamma K^+ K^-$	
10.8±4.0±3.2	BAI	96B	BES	$e^+e^- \rightarrow J/\psi \rightarrow \gamma K_S^0 K_S^0$	
191 For spin 2 and helicity 0; other combinations lead to more stringent upper limits.					

$\Gamma(\gamma f_J(2220) \rightarrow \gamma\rho\rho)/\Gamma_{\text{total}}$			$\Gamma_{182}/\Gamma$		
VALUE (units $10^{-5}$ )	DOCUMENT ID	TECN	COMMENT		
<b>1.5 ± 0.6 ± 0.5</b>	BAI	96B	BES	$e^+e^- \rightarrow J/\psi \rightarrow \gamma\rho\rho$	

$\Gamma(\gamma f_0(1500))/\Gamma_{\text{total}}$			$\Gamma_{183}/\Gamma$		
VALUE (units $10^{-4}$ )	DOCUMENT ID	TECN	COMMENT		
<b>1.01 ± 0.32 OUR AVERAGE</b>					
1.00±0.03±0.45	192	ABLIKIM	06v	BES2	$e^+e^- \rightarrow J/\psi \rightarrow \gamma\pi^+\pi^-$
1.02±0.09±0.45	192	ABLIKIM	06v	BES2	$e^+e^- \rightarrow J/\psi \rightarrow \gamma\pi^0\pi^0$
••• We do not use the following data for averages, fits, limits, etc. •••					
>5.7 ± 0.8	193,194	BUGG	95	MRK3	$J/\psi \rightarrow \gamma\pi^+\pi^-\pi^+\pi^-$
192 Including unknown branching fraction to $\pi\pi$ .					
193 Including unknown branching ratio for $f_0(1500) \rightarrow \pi^+\pi^-\pi^+\pi^-$ .					
194 Assuming that $f_0(1500)$ decays only to two S-wave dipions.					

$\Gamma(\gamma A \rightarrow \gamma \text{invisible})/\Gamma_{\text{total}}$			$\Gamma_{184}/\Gamma$		
(narrow state A with $m_A < 960$ MeV)					
VALUE (units $10^{-6}$ )	CL%	DOCUMENT ID	TECN	COMMENT	
<b>&lt;6.3</b>	90	195	INSLER	10	CLEO $e^+e^- \rightarrow \pi^+\pi^- J/\psi$
195 The limit varies with mass $m_A$ of a narrow state A and is $4.3 \times 10^{-6}$ for $m_A = 0$ MeV, reaches its largest value of $6.3 \times 10^{-6}$ at $m_A = 500$ MeV, and is $3.6 \times 10^{-6}$ at $m_A = 960$ MeV.					

WEAK DECAYS

Table with 5 columns: VALUE (units 10^-5), CL%, DOCUMENT ID, TECN, COMMENT. Row 1: <1.2, 90, ABLIKIM 06M BES2, e+ e- -> J/psi, Gamma\_185/Gamma\_total

Table with 5 columns: VALUE (units 10^-5), CL%, DOCUMENT ID, TECN, COMMENT. Row 1: <1.1, 90, ABLIKIM 06M BES2, e+ e- -> J/psi, Gamma\_186/Gamma\_total

Table with 5 columns: VALUE (units 10^-5), CL%, DOCUMENT ID, TECN, COMMENT. Row 1: <3.6, 90, 196 ABLIKIM 06M BES2, e+ e- -> J/psi, Gamma\_187/Gamma\_total. Includes note: 196 Using B(Ds- -> phi pi-) = 4.4 +/- 0.5 %.

Table with 5 columns: VALUE, CL%, DOCUMENT ID, TECN, COMMENT. Row 1: <7.5 x 10^-5, 90, ABLIKIM 08J BES2, e+ e- -> J/psi, Gamma\_188/Gamma\_total

Table with 5 columns: VALUE, CL%, DOCUMENT ID, TECN, COMMENT. Row 1: <1.7 x 10^-4, 90, ABLIKIM 08J BES2, e+ e- -> J/psi, Gamma\_189/Gamma\_total

Table with 5 columns: VALUE, CL%, DOCUMENT ID, TECN, COMMENT. Row 1: <1.3 x 10^-4, 90, ABLIKIM 08J BES2, e+ e- -> J/psi, Gamma\_190/Gamma\_total

Table with 5 columns: VALUE (units 10^-5), CL%, DOCUMENT ID, TECN, COMMENT. Row 1: < 0.5, 90, ADAMS 08 CLEO, psi(2S) -> pi+ pi- J/psi, Gamma\_191/Gamma\_total. Includes note: We do not use the following data for averages, fits, limits, etc.

197 WICHT 08 reports [Gamma(J/psi(1S) -> gamma gamma)/Gamma\_total] x [B(B+ -> J/psi(1S) K+)] < 0.16 x 10^-6 which we divide by our best value B(B+ -> J/psi(1S) K+) = 1.016 x 10^-3.

LEPTON FAMILY NUMBER (LF) VIOLATING MODES

Table with 5 columns: VALUE (units 10^-6), CL%, DOCUMENT ID, TECN, COMMENT. Row 1: <1.1, 90, BAI 03D BES, e+ e- -> J/psi, Gamma\_192/Gamma\_total

Table with 5 columns: VALUE (units 10^-6), CL%, DOCUMENT ID, TECN, COMMENT. Row 1: <8.3, 90, ABLIKIM 04 BES, e+ e- -> J/psi, Gamma\_193/Gamma\_total

Table with 5 columns: VALUE (units 10^-6), CL%, DOCUMENT ID, TECN, COMMENT. Row 1: <2.0, 90, ABLIKIM 04 BES, e+ e- -> J/psi, Gamma\_194/Gamma\_total

OTHER DECAYS

Table with 5 columns: VALUE, CL%, DOCUMENT ID, TECN, COMMENT. Row 1: <1.2 x 10^-2, 90, ABLIKIM 08G BES2, psi(2S) -> pi+ pi- J/psi, Gamma\_195/Gamma\_gamma

J/psi(1S) REFERENCES

List of references for J/psi(1S) decays, including ABLIKIM 11 PR D83 012003, AUBERT 07AU PR D76 092005, etc.

Continuation of references for J/psi(1S) decays, including AUBERT 07BD PR D76 092006, ABLIKIM 06 PL B632 181, etc.

## Meson Particle Listings

 $J/\psi(1S)$ , Branching Ratios of  $\psi$ 's and  $\chi$ 's,  $\chi_{c0}(1P)$ 

BURMESTER	77D	PL 72B 135	J. Burmester <i>et al.</i>	(DESY, HAMB, SIEG+)
FELDMAN	77	PRPL 33C 285	G.J. Feldman, M.L. Perl	(LBL, SLAC)
VANNUCCI	77	PR D15 1814	F. Vannucci <i>et al.</i>	(SLAC, LBL)
BARTEL	76	PL 64B 483	W. Bartel <i>et al.</i>	(DESY, HEIDP)
BRAUNSCH...	76	PL 63B 487	W. Braunschweig <i>et al.</i>	(DASP Collab.)
JEAN-MARIE	76	PRL 36 291	B. Jean-Marie <i>et al.</i>	(SLAC, LBL) IG
BALDINI...	75	PL 58B 471	R. Baldini-Celio <i>et al.</i>	(FRAS, ROMA)
BOYARSKI	75	PRL 34 1357	A.M. Boyarski <i>et al.</i>	(SLAC, LBL) JPC
DASP	75	PL 56B 491	W. Braunschweig <i>et al.</i>	(DASP Collab.)
ESPOSITO	75B	LNC 14 73	B. Esposito <i>et al.</i>	(FRAS, NAPL, PADO+)
FORD	75	PRL 34 604	R.L. Ford <i>et al.</i>	(SLAC, PENN)

BRANCHING RATIOS OF  $\psi(2S)$  AND  $\chi_{c0,1,2}$ 

Updated May 2012 by J.J. Hernández-Rey (IFIC, Valencia), S. Navas (University of Granada), and C. Patrignani (INFN, Genova)

Since 2002, the treatment of the branching ratios of the  $\psi(2S)$  and  $\chi_{c0,1,2}$  has undergone an important restructuring.

When measuring a branching ratio experimentally, it is not always possible to normalize the number of events observed in the corresponding decay mode to the total number of particles produced. Therefore, the experimenters sometimes report the number of observed decays with respect to another decay mode of the same or another particle in the relevant decay chain. This is actually equivalent to measuring combinations of branching fractions of several decay modes.

To extract the branching ratio of a given decay mode, the collaborations use some previously reported measurements of the required branching ratios. However, the values are frequently taken from the *Review of Particle Physics* (RPP), which in turn uses the branching ratio reported by the experiment in the following edition, giving rise either to correlations or to plain vicious circles Ref. 1, Ref. 2 as discussed in more detail in earlier editions of this mini-review.

The way to avoid these dependencies and correlations is to extract the branching ratios through a fit that uses the truly measured combinations of branching fractions and partial widths. This fit, in fact, should involve decays from the four concerned particles,  $\psi(2S)$ ,  $\chi_{c0}$ ,  $\chi_{c1}$ , and  $\chi_{c2}$ , and occasionally some combinations of branching ratios of more than one of them. This is what is done since the 2002 edition [3].

The PDG policy is to quote the results of the collaborations in a manner as close as possible to what appears in their original publications. However, in order to avoid the problems mentioned above, we had in some cases to work out the values originally measured, using the number of events and detection efficiencies given by the collaborations, or rescaling back the published results. The information was sometimes spread over several articles, and some articles referred to papers still unpublished, which in turn contained the relevant numbers in footnotes.

Even though the experimental collaborations are entitled to extract whatever branching ratios they consider appropriate by using other published results, we would like to encourage them to also quote explicitly in their articles the actual quantities measured, so that they can be used directly in averages and fits of different experimental determinations.

To inform the reader how we computed some of the values used in this edition of RPP, we use footnotes to indicate the branching ratios actually given by the experiments and the

quantities they use to derive them from the true combination of branching ratios actually measured.

None of the branching ratios of the  $\chi_{c0,1,2}$  are measured independently of the  $\psi(2S)$  radiative decays. We tried to identify those branching ratios which can be correlated in a non-trivial way, and although we cannot preclude the existence of other cases, we are confident that the most relevant correlations have already been removed. Nevertheless, correlations in the errors of different quantities measured by the same experiment have not been taken into account.

## FIT INFORMATION

This is an overall fit to 4 total widths, 1 partial width, 25 combinations of partial widths, 7 branching ratios, and 77 combinations of branching ratios. Of the latter 57 involve decays of more than one particle.

The overall fit uses 223 measurements to determine 49 parameters and has a  $\chi^2$  of 312.2 for 174 degrees of freedom.

The relatively high  $\chi^2$  of the fit, 1.8 per d.o.f., can be traced back to a few specific discrepancies in the data. No rescaling of errors has been applied.

In the listing we provide the correlation coefficients  $< \delta x_i \delta x_j > / (\delta x_i \cdot \delta x_j)$ , in percent, from the fit to the corresponding parameter  $x_i$ .

## References

1. Y.F. Gu and X.H. Li, Phys. Lett. **B449**, 361 (1999).
2. C. Patrignani, Phys. Rev. **D64**, 034017 (2001).
3. Particle Data Group, K.Hagiwara *et al.*, Phys. Rev. **D68**, 010001 (2002).

 $\chi_{c0}(1P)$  $I^G(J^{PC}) = 0^+(0^{++})$  $\chi_{c0}(1P)$  MASS

VALUE (MeV)	EVTs	DOCUMENT ID	TECN	COMMENT
<b>3414.75 ± 0.31 OUR AVERAGE</b>				
3414.2 ± 0.5 ± 2.3	5.4k	UEHARA	08 BELL	$\gamma\gamma \rightarrow \chi_{c0} \rightarrow \text{hadrons}$
3406 ± 7 ± 6	230	<sup>1</sup> ABE	07 BELL	$e^+e^- \rightarrow J/\psi(c\bar{c})$
3414.21 ± 0.39 ± 0.27		ABLIKIM	05G BES2	$\psi(2S) \rightarrow \gamma\chi_{c0}$
3414.7 ± 0.7 ± 0.2		<sup>2</sup> ANDREOTTI	03 E835	$\bar{p}p \rightarrow \chi_{c0} \rightarrow \pi^0\pi^0$
3415.5 ± 0.4 ± 0.4	392	<sup>3</sup> BAGNASCO	02 E835	$\bar{p}p \rightarrow \chi_{c0} \rightarrow J/\psi\gamma$
3417.4 ± 1.8 ± 1.9 ± 0.2		<sup>2</sup> AMBROGIANI	99B E835	$\bar{p}p \rightarrow e^+e^-\gamma$
3414.1 ± 0.6 ± 0.8		BAI	99B BES	$\psi(2S) \rightarrow \gamma X$
3417.8 ± 0.4 ± 4		<sup>2</sup> GAISER	86 CBAL	$\psi(2S) \rightarrow \gamma X$
3416 ± 3 ± 4		<sup>4</sup> TANENBAUM	78 MRK1	$e^+e^-$
••• We do not use the following data for averages, fits, limits, etc. •••				
3416.5 ± 3.0		EISENSTEIN	01 CLE2	$e^+e^- \rightarrow e^+e^-\chi_{c0}$
3422 ± 10		<sup>4</sup> BARTEL	78B CNTR	$e^+e^- \rightarrow J/\psi 2\gamma$
3415 ± 9		<sup>4</sup> BIDDICK	77 CNTR	$e^+e^- \rightarrow \gamma X$

<sup>1</sup> From a fit of the  $J/\psi$  recoil mass spectrum. Supersedes ABE,K 02 and ABE 04G.

<sup>2</sup> Using mass of  $\psi(2S) = 3686.0$  MeV.

<sup>3</sup> Recalculated by ANDREOTTI 05A, using the value of  $\psi(2S)$  mass from AULCHENKO 03.

<sup>4</sup> Mass value shifted by us by amount appropriate for  $\psi(2S)$  mass = 3686 MeV and  $J/\psi(1S)$  mass = 3097 MeV.

 $\chi_{c0}(1P)$  WIDTH

VALUE (MeV)	EVTs	DOCUMENT ID	TECN	COMMENT
<b>10.4 ± 0.6 OUR FIT</b>				
<b>10.5 ± 0.8 OUR AVERAGE</b>	Error includes scale factor of 1.1.			
10.6 ± 1.9 ± 2.6	5.4k	UEHARA	08 BELL	$\gamma\gamma \rightarrow \chi_{c0} \rightarrow \text{hadrons}$
12.6 <sup>+1.5+0.9</sup> <sub>-1.6-1.1</sub>		ABLIKIM	05G BES2	$\psi(2S) \rightarrow \gamma\chi_{c0}$
8.6 <sup>+1.7</sup> <sub>-1.3 ± 0.1</sub>		ANDREOTTI	03 E835	$\bar{p}p \rightarrow \chi_{c0} \rightarrow \pi^0\pi^0$







**$\Gamma(f_0(980) f_0(980))/\Gamma_{\text{total}}$**   **$\Gamma_{13}/\Gamma$**   

VALUE (units 10 <sup>-5</sup> )	EVTs	DOCUMENT ID	TECN	COMMENT
<b>16<sup>+11</sup><sub>-9</sub> ± 1</b>	28	<sup>20</sup> ABLIKIM	05Q	BES2 $\psi(2S) \rightarrow \gamma \pi^+ \pi^- K^+ K^-$

<sup>20</sup> ABLIKIM 05Q reports  $[(\chi_{c0}(1P) \rightarrow f_0(980) f_0(980))/\Gamma_{\text{total}}] \times [B(\psi(2S) \rightarrow \gamma \chi_{c0}(1P))] = (1.59 \pm 0.50^{+0.89}_{-0.72}) \times 10^{-5}$  which we divide by our best value  $B(\psi(2S) \rightarrow \gamma \chi_{c0}(1P)) = (9.68 \pm 0.31) \times 10^{-2}$ . Our first error is their experiment's error and our second error is the systematic error from using our best value. One of the  $f_0(980)$  mesons is identified via decay to  $\pi^+ \pi^-$  while the other via  $K^+ K^-$  decay.

**$\Gamma(f_0(980) f_0(2200))/\Gamma_{\text{total}}$**   **$\Gamma_{14}/\Gamma$**   

VALUE (units 10 <sup>-4</sup> )	EVTs	DOCUMENT ID	TECN	COMMENT
<b>8.0<sup>+2.9</sup><sub>-2.5</sub> ± 0.3</b>	77	<sup>21</sup> ABLIKIM	05Q	BES2 $\psi(2S) \rightarrow \gamma \pi^+ \pi^- K^+ K^-$

<sup>21</sup> ABLIKIM 05Q reports  $(8.42 \pm 1.42^{+1.65}_{-2.29}) \times 10^{-4}$  from a measurement of  $[(\chi_{c0}(1P) \rightarrow f_0(980) f_0(2200))/\Gamma_{\text{total}}] \times [B(\psi(2S) \rightarrow \gamma \chi_{c0}(1P))]$  assuming  $B(\psi(2S) \rightarrow \gamma \chi_{c0}(1P)) = (9.22 \pm 0.11 \pm 0.46) \times 10^{-2}$ , which we rescale to our best value  $B(\psi(2S) \rightarrow \gamma \chi_{c0}(1P)) = (9.68 \pm 0.31) \times 10^{-2}$ . Our first error is their experiment's error and our second error is the systematic error from using our best value. The  $f_0$  mesons are identified via  $f_0(980) \rightarrow \pi^+ \pi^-$  and  $f_0(2200) \rightarrow K^+ K^-$  decays.

**$\Gamma(f_0(1370) f_0(1370))/\Gamma_{\text{total}}$**   **$\Gamma_{15}/\Gamma$**   

VALUE (units 10 <sup>-4</sup> )	CL%	DOCUMENT ID	TECN	COMMENT
<b>&lt;2.8</b>	90	<sup>22</sup> ABLIKIM	05Q	BES2 $\psi(2S) \rightarrow \gamma \pi^+ \pi^- K^+ K^-$

<sup>22</sup> ABLIKIM 05Q reports  $< 2.9 \times 10^{-4}$  from a measurement of  $[(\chi_{c0}(1P) \rightarrow f_0(1370) f_0(1370))/\Gamma_{\text{total}}] \times [B(\psi(2S) \rightarrow \gamma \chi_{c0}(1P))]$  assuming  $B(\psi(2S) \rightarrow \gamma \chi_{c0}(1P)) = (9.22 \pm 0.11 \pm 0.46) \times 10^{-2}$ , which we rescale to our best value  $B(\psi(2S) \rightarrow \gamma \chi_{c0}(1P)) = 9.68 \times 10^{-2}$ . One of the  $f_0(1370)$  mesons is identified via decay to  $\pi^+ \pi^-$  while the other via  $K^+ K^-$  decay. Both branching fractions for these  $f_0$  decays are implicitly included in the quoted result.

**$\Gamma(f_0(1370) f_0(1500))/\Gamma_{\text{total}}$**   **$\Gamma_{16}/\Gamma$**   

VALUE (units 10 <sup>-4</sup> )	CL%	DOCUMENT ID	TECN	COMMENT
<b>&lt;1.7</b>	90	<sup>23</sup> ABLIKIM	05Q	BES2 $\psi(2S) \rightarrow \gamma \pi^+ \pi^- K^+ K^-$

<sup>23</sup> ABLIKIM 05Q reports  $< 1.8 \times 10^{-4}$  from a measurement of  $[(\chi_{c0}(1P) \rightarrow f_0(1370) f_0(1500))/\Gamma_{\text{total}}] \times [B(\psi(2S) \rightarrow \gamma \chi_{c0}(1P))]$  assuming  $B(\psi(2S) \rightarrow \gamma \chi_{c0}(1P)) = (9.22 \pm 0.11 \pm 0.46) \times 10^{-2}$ , which we rescale to our best value  $B(\psi(2S) \rightarrow \gamma \chi_{c0}(1P)) = 9.68 \times 10^{-2}$ . The  $f_0$  mesons are identified via  $f_0(1370) \rightarrow \pi^+ \pi^-$  and  $f_0(1500) \rightarrow K^+ K^-$  decays. Both branching fractions for these  $f_0$  decays are implicitly included in the quoted result.

**$\Gamma(f_0(1370) f_0(1710))/\Gamma_{\text{total}}$**   **$\Gamma_{17}/\Gamma$**   

VALUE (units 10 <sup>-4</sup> )	EVTs	DOCUMENT ID	TECN	COMMENT
<b>6.8<sup>+3.6</sup><sub>-2.4</sub> ± 0.2</b>	61	<sup>24</sup> ABLIKIM	05Q	BES2 $\psi(2S) \rightarrow \gamma \pi^+ \pi^- K^+ K^-$

<sup>24</sup> ABLIKIM 05Q reports  $(7.12 \pm 1.85^{+3.28}_{-1.68}) \times 10^{-4}$  from a measurement of  $[(\chi_{c0}(1P) \rightarrow f_0(1370) f_0(1710))/\Gamma_{\text{total}}] \times [B(\psi(2S) \rightarrow \gamma \chi_{c0}(1P))]$  assuming  $B(\psi(2S) \rightarrow \gamma \chi_{c0}(1P)) = (9.22 \pm 0.11 \pm 0.46) \times 10^{-2}$ , which we rescale to our best value  $B(\psi(2S) \rightarrow \gamma \chi_{c0}(1P)) = (9.68 \pm 0.31) \times 10^{-2}$ . Our first error is their experiment's error and our second error is the systematic error from using our best value. The  $f_0$  mesons are identified via  $f_0(1370) \rightarrow \pi^+ \pi^-$  and  $f_0(1710) \rightarrow K^+ K^-$  decays. Both branching fractions for these  $f_0$  decays are implicitly included in the quoted result.

**$\Gamma(f_0(1500) f_0(1370))/\Gamma_{\text{total}}$**   **$\Gamma_{18}/\Gamma$**   

VALUE (units 10 <sup>-4</sup> )	CL%	DOCUMENT ID	TECN	COMMENT
<b>&lt;1.3</b>	90	<sup>25</sup> ABLIKIM	05Q	BES2 $\psi(2S) \rightarrow \gamma \pi^+ \pi^- K^+ K^-$

<sup>25</sup> ABLIKIM 05Q reports  $< 1.4 \times 10^{-4}$  from a measurement of  $[(\chi_{c0}(1P) \rightarrow f_0(1500) f_0(1370))/\Gamma_{\text{total}}] \times [B(\psi(2S) \rightarrow \gamma \chi_{c0}(1P))]$  assuming  $B(\psi(2S) \rightarrow \gamma \chi_{c0}(1P)) = (9.22 \pm 0.11 \pm 0.46) \times 10^{-2}$ , which we rescale to our best value  $B(\psi(2S) \rightarrow \gamma \chi_{c0}(1P)) = 9.68 \times 10^{-2}$ . The  $f_0$  mesons are identified via  $f_0(1500) \rightarrow \pi^+ \pi^-$  and  $f_0(1370) \rightarrow K^+ K^-$  decays. Both branching fractions for these  $f_0$  decays are implicitly included in the quoted result.

**$\Gamma(f_0(1500) f_0(1500))/\Gamma_{\text{total}}$**   **$\Gamma_{19}/\Gamma$**   

VALUE (units 10 <sup>-4</sup> )	CL%	DOCUMENT ID	TECN	COMMENT
<b>&lt;0.5</b>	90	<sup>26</sup> ABLIKIM	05Q	BES2 $\psi(2S) \rightarrow \gamma \pi^+ \pi^- K^+ K^-$

<sup>26</sup> ABLIKIM 05Q reports  $< 0.55 \times 10^{-4}$  from a measurement of  $[(\chi_{c0}(1P) \rightarrow f_0(1500) f_0(1500))/\Gamma_{\text{total}}] \times [B(\psi(2S) \rightarrow \gamma \chi_{c0}(1P))]$  assuming  $B(\psi(2S) \rightarrow \gamma \chi_{c0}(1P)) = (9.22 \pm 0.11 \pm 0.46) \times 10^{-2}$ , which we rescale to our best value  $B(\psi(2S) \rightarrow \gamma \chi_{c0}(1P)) = 9.68 \times 10^{-2}$ . One of the  $f_0(1500)$  is identified via decay to  $\pi^+ \pi^-$  while the other via  $K^+ K^-$  decay. Both branching fractions for these  $f_0$  decays are implicitly included in the quoted result.

**$\Gamma(f_0(1500) f_0(1710))/\Gamma_{\text{total}}$**   **$\Gamma_{20}/\Gamma$**   

VALUE (units 10 <sup>-4</sup> )	CL%	DOCUMENT ID	TECN	COMMENT
<b>&lt;0.7</b>	90	<sup>27</sup> ABLIKIM	05Q	BES2 $\psi(2S) \rightarrow \gamma \pi^+ \pi^- K^+ K^-$

<sup>27</sup> ABLIKIM 05Q reports  $< 0.73 \times 10^{-4}$  from a measurement of  $[(\chi_{c0}(1P) \rightarrow f_0(1500) f_0(1710))/\Gamma_{\text{total}}] \times [B(\psi(2S) \rightarrow \gamma \chi_{c0}(1P))]$  assuming  $B(\psi(2S) \rightarrow \gamma \chi_{c0}(1P)) = (9.22 \pm 0.11 \pm 0.46) \times 10^{-2}$ , which we rescale to our best value  $B(\psi(2S) \rightarrow \gamma \chi_{c0}(1P)) = 9.68 \times 10^{-2}$ . The  $f_0$  mesons are identified via  $f_0(1500) \rightarrow \pi^+ \pi^-$  and  $f_0(1710) \rightarrow K^+ K^-$  decays. Both branching fractions for these  $f_0$  decays are implicitly included in the quoted result.

**$\Gamma(K^+ K^- \pi^0 \pi^0)/\Gamma_{\text{total}}$**   **$\Gamma_{22}/\Gamma$**   

VALUE (%)	EVTs	DOCUMENT ID	TECN	COMMENT
<b>0.56 ± 0.09 ± 0.02</b>	213.5	<sup>28</sup> HE	08B	CLEO $e^+ e^- \rightarrow \gamma h^+ h^- h^0 h^0$

<sup>28</sup> HE 08B reports  $0.59 \pm 0.05 \pm 0.08 \pm 0.03$  % from a measurement of  $[(\chi_{c0}(1P) \rightarrow K^+ K^- \pi^0 \pi^0)/\Gamma_{\text{total}}] \times [B(\psi(2S) \rightarrow \gamma \chi_{c0}(1P))]$  assuming  $B(\psi(2S) \rightarrow \gamma \chi_{c0}(1P)) = (9.22 \pm 0.11 \pm 0.46) \times 10^{-2}$ , which we rescale to our best value  $B(\psi(2S) \rightarrow \gamma \chi_{c0}(1P)) = (9.68 \pm 0.31) \times 10^{-2}$ . Our first error is their experiment's error and our second error is the systematic error from using our best value.

**$\Gamma(K^+ \pi^- K^0 \pi^0 + c.c.)/\Gamma_{\text{total}}$**   **$\Gamma_{23}/\Gamma$**   

VALUE (%)	EVTs	DOCUMENT ID	TECN	COMMENT
<b>2.52 ± 0.33 ± 0.08</b>	401.7	<sup>29</sup> HE	08B	CLEO $e^+ e^- \rightarrow \gamma h^+ h^- h^0 h^0$

<sup>29</sup> HE 08B reports  $2.64 \pm 0.15 \pm 0.31 \pm 0.14$  % from a measurement of  $[(\chi_{c0}(1P) \rightarrow K^+ \pi^- K^0 \pi^0 + c.c.)/\Gamma_{\text{total}}] \times [B(\psi(2S) \rightarrow \gamma \chi_{c0}(1P))]$  assuming  $B(\psi(2S) \rightarrow \gamma \chi_{c0}(1P)) = (9.22 \pm 0.11 \pm 0.46) \times 10^{-2}$ , which we rescale to our best value  $B(\psi(2S) \rightarrow \gamma \chi_{c0}(1P)) = (9.68 \pm 0.31) \times 10^{-2}$ . Our first error is their experiment's error and our second error is the systematic error from using our best value.

**$\Gamma(\rho^+ K^- K^0 + c.c.)/\Gamma_{\text{total}}$**   **$\Gamma_{24}/\Gamma$**   

VALUE (%)	EVTs	DOCUMENT ID	TECN	COMMENT
<b>1.22 ± 0.21 ± 0.04</b>	179.7	<sup>30</sup> HE	08B	CLEO $e^+ e^- \rightarrow \gamma h^+ h^- h^0 h^0$

<sup>30</sup> HE 08B reports  $1.28 \pm 0.16 \pm 0.15 \pm 0.07$  % from a measurement of  $[(\chi_{c0}(1P) \rightarrow \rho^+ K^- K^0 + c.c.)/\Gamma_{\text{total}}] \times [B(\psi(2S) \rightarrow \gamma \chi_{c0}(1P))]$  assuming  $B(\psi(2S) \rightarrow \gamma \chi_{c0}(1P)) = (9.22 \pm 0.11 \pm 0.46) \times 10^{-2}$ , which we rescale to our best value  $B(\psi(2S) \rightarrow \gamma \chi_{c0}(1P)) = (9.68 \pm 0.31) \times 10^{-2}$ . Our first error is their experiment's error and our second error is the systematic error from using our best value.

**$\Gamma(K^*(892)^- K^+ \pi^0 \rightarrow K^+ \pi^- K^0 \pi^0 + c.c.)/\Gamma_{\text{total}}$**   **$\Gamma_{25}/\Gamma$**   

VALUE (%)	EVTs	DOCUMENT ID	TECN	COMMENT
<b>0.47 ± 0.12 ± 0.01</b>	64.1	<sup>31</sup> HE	08B	CLEO $e^+ e^- \rightarrow \gamma h^+ h^- h^0 h^0$

<sup>31</sup> HE 08B reports  $0.49 \pm 0.10 \pm 0.07 \pm 0.03$  % from a measurement of  $[(\chi_{c0}(1P) \rightarrow K^*(892)^- K^+ \pi^0 \rightarrow K^+ \pi^- K^0 \pi^0 + c.c.)/\Gamma_{\text{total}}] \times [B(\psi(2S) \rightarrow \gamma \chi_{c0}(1P))]$  assuming  $B(\psi(2S) \rightarrow \gamma \chi_{c0}(1P)) = (9.22 \pm 0.11 \pm 0.46) \times 10^{-2}$ , which we rescale to our best value  $B(\psi(2S) \rightarrow \gamma \chi_{c0}(1P)) = (9.68 \pm 0.31) \times 10^{-2}$ . Our first error is their experiment's error and our second error is the systematic error from using our best value.

**$\Gamma(K_S^0 K_S^0 \pi^+ \pi^-)/\Gamma_{\text{total}}$**   **$\Gamma_{26}/\Gamma$**   

VALUE (units 10 <sup>-3</sup> )	EVTs	DOCUMENT ID	TECN	COMMENT
<b>5.8 ± 1.1 ± 0.2</b>	152 ± 14	<sup>32</sup> ABLIKIM	05Q	BES2 $\psi(2S) \rightarrow \gamma \chi_{c0}$

<sup>32</sup> ABLIKIM 05Q reports  $[(\chi_{c0}(1P) \rightarrow K_S^0 K_S^0 \pi^+ \pi^-)/\Gamma_{\text{total}}] \times [B(\psi(2S) \rightarrow \gamma \chi_{c0}(1P))]$  =  $(0.558 \pm 0.051 \pm 0.089) \times 10^{-3}$  which we divide by our best value  $B(\psi(2S) \rightarrow \gamma \chi_{c0}(1P)) = (9.68 \pm 0.31) \times 10^{-2}$ . Our first error is their experiment's error and our second error is the systematic error from using our best value.

**$\Gamma(K^+ K^- \eta \pi^0)/\Gamma_{\text{total}}$**   **$\Gamma_{27}/\Gamma$**   

VALUE (%)	EVTs	DOCUMENT ID	TECN	COMMENT
<b>0.30 ± 0.07 ± 0.01</b>	56.4	<sup>33</sup> HE	08B	CLEO $e^+ e^- \rightarrow \gamma h^+ h^- h^0 h^0$

<sup>33</sup> HE 08B reports  $0.32 \pm 0.05 \pm 0.05 \pm 0.02$  % from a measurement of  $[(\chi_{c0}(1P) \rightarrow K^+ K^- \eta \pi^0)/\Gamma_{\text{total}}] \times [B(\psi(2S) \rightarrow \gamma \chi_{c0}(1P))]$  assuming  $B(\psi(2S) \rightarrow \gamma \chi_{c0}(1P)) = (9.22 \pm 0.11 \pm 0.46) \times 10^{-2}$ , which we rescale to our best value  $B(\psi(2S) \rightarrow \gamma \chi_{c0}(1P)) = (9.68 \pm 0.31) \times 10^{-2}$ . Our first error is their experiment's error and our second error is the systematic error from using our best value.

**$\Gamma(3(\pi^+ \pi^-))/\Gamma_{\text{total}}$**   **$\Gamma_{28}/\Gamma$**   

VALUE (units 10 <sup>-3</sup> )	DOCUMENT ID	TECN	COMMENT
<b>12.0 ± 1.8 OUR EVALUATION</b>	Treating systematic error as correlated.		
<b>12.0 ± 1.7 OUR AVERAGE</b>			
11.7 ± 1.0 ± 1.9	<sup>34</sup> BAI	99B	BES $\psi(2S) \rightarrow \gamma \chi_{c0}$
12.5 ± 2.9 ± 0.5	<sup>34</sup> TANENBAUM	78	MRK1 $\psi(2S) \rightarrow \gamma \chi_{c0}$

<sup>34</sup> Rescaled by us using  $B(\psi(2S) \rightarrow \gamma \chi_{c0}) = (9.4 \pm 0.4)\%$  and  $B(\psi(2S) \rightarrow J/\psi(1S) \pi^+ \pi^-) = (32.6 \pm 0.5)\%$ .

**$\Gamma(K^+ \bar{K}^*(892)^0 \pi^- + c.c.)/\Gamma_{\text{total}}$**   **$\Gamma_{29}/\Gamma$**   

VALUE	DOCUMENT ID
<b>0.0073 ± 0.0016 OUR FIT</b>	

**$\Gamma(K^*(892)^0 \bar{K}^*(892)^0)/\Gamma_{\text{total}}$**   **$\Gamma_{30}/\Gamma$**   

VALUE (units 10 <sup>-3</sup> )	EVTs	DOCUMENT ID	TECN	COMMENT
<b>1.7<sup>+0.6</sup><sub>-0.5</sub> ± 0.1</b>	64	<sup>35</sup> ABLIKIM	05Q	BES2 $\psi(2S) \rightarrow \gamma \pi^+ \pi^- K^+ K^-$

• • • We do not use the following data for averages, fits, limits, etc. • • •

VALUE	DOCUMENT ID	TECN	COMMENT
$1.6 \pm 0.4 \pm 0.1$	<sup>36,37</sup> ABLIKIM	04H	BES Repl. by ABLIKIM 05Q

<sup>35</sup> ABLIKIM 05Q reports  $[(\chi_{c0}(1P) \rightarrow K^*(892)^0 \bar{K}^*(892)^0)/\Gamma_{\text{total}}] \times [B(\psi(2S) \rightarrow \gamma \chi_{c0}(1P))] = (0.168 \pm 0.035^{+0.047}_{-0.040}) \times 10^{-3}$  which we divide by our best value  $B(\psi(2S) \rightarrow \gamma \chi_{c0}(1P)) = (9.68 \pm 0.31) \times 10^{-2}$ . Our first error is their experiment's error and our second error is the systematic error from using our best value.

<sup>36</sup> Assumes  $B(K^*(892)^0 \rightarrow K^- \pi^+) = 2/3$ .

<sup>37</sup> ABLIKIM 04H reports  $[(\chi_{c0}(1P) \rightarrow K^*(892)^0 \bar{K}^*(892)^0)/\Gamma_{\text{total}}] \times [B(\psi(2S) \rightarrow \gamma \chi_{c0}(1P))] = (1.53 \pm 0.29 \pm 0.26) \times 10^{-4}$  which we divide by our best value  $B(\psi(2S) \rightarrow \gamma \chi_{c0}(1P)) = (9.68 \pm 0.31) \times 10^{-2}$ . Our first error is their experiment's error and our second error is the systematic error from using our best value.

## Meson Particle Listings

 $\chi_{c0}(1P)$ 

$\Gamma(\pi\pi)/\Gamma_{\text{total}}$	$\Gamma_{31}/\Gamma$
VALUE (units $10^{-3}$ )	DOCUMENT ID
<b><math>8.5 \pm 0.4</math> OUR FIT</b>	

$\Gamma(\eta\eta)/\Gamma_{\text{total}}$	$\Gamma_{34}/\Gamma$
VALUE (units $10^{-3}$ )	DOCUMENT ID
<b><math>3.03 \pm 0.21</math> OUR FIT</b>	

$\Gamma(\eta\eta)/\Gamma(\pi\pi)$	$\Gamma_{34}/\Gamma_{31}$
VALUE	DOCUMENT ID TECN COMMENT
<b><math>0.356 \pm 0.025</math> OUR FIT</b>	
• • • We do not use the following data for averages, fits, limits, etc. • • •	
$0.26 \pm 0.09 \pm 0.03$	38 ANDREOTTI 05c E835 $\bar{p}p \rightarrow 2$ mesons
$0.24 \pm 0.10 \pm 0.08$	38 BAI 03c BES $\psi(2S) \rightarrow 5\gamma$
38 We have multiplied $\pi^0\pi^0$ measurement by 3 to obtain $\pi\pi$ .	

$\Gamma(\eta\eta')/\Gamma_{\text{total}}$	$\Gamma_{35}/\Gamma$
VALUE (units $10^{-3}$ )	CL% EVTS DOCUMENT ID TECN COMMENT
<b><math>&lt;0.2</math></b>	90 35 $\pm 13$ 39 ASNER 09 CLEO $\psi(2S) \rightarrow \gamma\eta'\eta$
• • • We do not use the following data for averages, fits, limits, etc. • • •	
$<0.5$	90 40 ADAMS 07 CLEO $\psi(2S) \rightarrow \gamma\chi_{c0}$
39 ASNER 09 reports $< 0.25 \times 10^{-3}$ from a measurement of $[\Gamma(\chi_{c0}(1P) \rightarrow \eta\eta')/\Gamma_{\text{total}}] \times [B(\psi(2S) \rightarrow \gamma\chi_{c0}(1P))]$ assuming $B(\psi(2S) \rightarrow \gamma\chi_{c0}(1P)) = (9.22 \pm 0.11 \pm 0.46) \times 10^{-2}$ , which we rescale to our best value $B(\psi(2S) \rightarrow \gamma\chi_{c0}(1P)) = 9.68 \times 10^{-2}$ .	
40 Superseded by ASNER 09. ADAMS 07 reports $< 0.5 \times 10^{-3}$ from a measurement of $[\Gamma(\chi_{c0}(1P) \rightarrow \eta\eta')/\Gamma_{\text{total}}] \times [B(\psi(2S) \rightarrow \gamma\chi_{c0}(1P))]$ assuming $B(\psi(2S) \rightarrow \gamma\chi_{c0}(1P)) = (9.22 \pm 0.11 \pm 0.46) \times 10^{-2}$ , which we rescale to our best value $B(\psi(2S) \rightarrow \gamma\chi_{c0}(1P)) = 9.68 \times 10^{-2}$ .	

$\Gamma(\eta'\eta')/\Gamma_{\text{total}}$	$\Gamma_{36}/\Gamma$
VALUE (units $10^{-3}$ )	EVTS DOCUMENT ID TECN COMMENT
<b><math>2.02 \pm 0.21 \pm 0.06</math></b>	0.4k 41 ASNER 09 CLEO $\psi(2S) \rightarrow \gamma\eta'\eta'$
• • • We do not use the following data for averages, fits, limits, etc. • • •	
$1.6 \pm 0.4 \pm 0.1$	23 42 ADAMS 07 CLEO $\psi(2S) \rightarrow \gamma\chi_{c0}$
41 ASNER 09 reports $(2.12 \pm 0.13 \pm 0.21) \times 10^{-3}$ from a measurement of $[\Gamma(\chi_{c0}(1P) \rightarrow \eta'\eta')/\Gamma_{\text{total}}] \times [B(\psi(2S) \rightarrow \gamma\chi_{c0}(1P))]$ assuming $B(\psi(2S) \rightarrow \gamma\chi_{c0}(1P)) = (9.22 \pm 0.11 \pm 0.46) \times 10^{-2}$ , which we rescale to our best value $B(\psi(2S) \rightarrow \gamma\chi_{c0}(1P)) = (9.68 \pm 0.31) \times 10^{-2}$ . Our first error is their experiment's error and our second error is the systematic error from using our best value.	
42 Superseded by ASNER 09. ADAMS 07 reports $(1.7 \pm 0.4 \pm 0.2) \times 10^{-3}$ from a measurement of $[\Gamma(\chi_{c0}(1P) \rightarrow \eta'\eta')/\Gamma_{\text{total}}] \times [B(\psi(2S) \rightarrow \gamma\chi_{c0}(1P))]$ assuming $B(\psi(2S) \rightarrow \gamma\chi_{c0}(1P)) = 0.0922 \pm 0.0011 \pm 0.0046$ , which we rescale to our best value $B(\psi(2S) \rightarrow \gamma\chi_{c0}(1P)) = (9.68 \pm 0.31) \times 10^{-2}$ . Our first error is their experiment's error and our second error is the systematic error from using our best value.	

$\Gamma(\omega\omega)/\Gamma_{\text{total}}$	$\Gamma_{37}/\Gamma$
VALUE (units $10^{-3}$ )	EVTS DOCUMENT ID TECN COMMENT
<b><math>0.98 \pm 0.11</math> OUR AVERAGE</b>	
$0.94 \pm 0.11 \pm 0.03$	991 43 ABLIKIM 11k BES3 $\psi(2S) \rightarrow \gamma$ hadrons
$2.2 \pm 0.7 \pm 0.1$	38.1 $\pm 9.6$ 44 ABLIKIM 05n BES2 $\psi(2S) \rightarrow \gamma\chi_{c0} \rightarrow \gamma 6\pi$
43 ABLIKIM 11k reports $(0.95 \pm 0.03 \pm 0.11) \times 10^{-3}$ from a measurement of $[\Gamma(\chi_{c0}(1P) \rightarrow \omega\omega)/\Gamma_{\text{total}}] \times [B(\psi(2S) \rightarrow \gamma\chi_{c0}(1P))]$ assuming $B(\psi(2S) \rightarrow \gamma\chi_{c0}(1P)) = (9.62 \pm 0.31) \times 10^{-2}$ , which we rescale to our best value $B(\psi(2S) \rightarrow \gamma\chi_{c0}(1P)) = (9.68 \pm 0.31) \times 10^{-2}$ . Our first error is their experiment's error and our second error is the systematic error from using our best value.	
44 ABLIKIM 05n reports $[\Gamma(\chi_{c0}(1P) \rightarrow \omega\omega)/\Gamma_{\text{total}}] \times [B(\psi(2S) \rightarrow \gamma\chi_{c0}(1P))]$ = $(0.212 \pm 0.053 \pm 0.037) \times 10^{-3}$ which we divide by our best value $B(\psi(2S) \rightarrow \gamma\chi_{c0}(1P)) = (9.68 \pm 0.31) \times 10^{-2}$ . Our first error is their experiment's error and our second error is the systematic error from using our best value.	

$\Gamma(\omega\phi)/\Gamma_{\text{total}}$	$\Gamma_{38}/\Gamma$
VALUE (units $10^{-4}$ )	EVTS DOCUMENT ID TECN COMMENT
<b><math>1.19 \pm 0.22 \pm 0.04</math></b>	76 45 ABLIKIM 11k BES3 $\psi(2S) \rightarrow \gamma$ hadrons
45 ABLIKIM 11k reports $(1.2 \pm 0.1 \pm 0.2) \times 10^{-4}$ from a measurement of $[\Gamma(\chi_{c0}(1P) \rightarrow \omega\phi)/\Gamma_{\text{total}}] \times [B(\psi(2S) \rightarrow \gamma\chi_{c0}(1P))]$ assuming $B(\psi(2S) \rightarrow \gamma\chi_{c0}(1P)) = (9.62 \pm 0.31) \times 10^{-2}$ , which we rescale to our best value $B(\psi(2S) \rightarrow \gamma\chi_{c0}(1P)) = (9.68 \pm 0.31) \times 10^{-2}$ . Our first error is their experiment's error and our second error is the systematic error from using our best value.	

$\Gamma(K^+K^-)/\Gamma_{\text{total}}$	$\Gamma_{39}/\Gamma$
VALUE (units $10^{-3}$ )	DOCUMENT ID
<b><math>6.06 \pm 0.35</math> OUR FIT</b>	

$\Gamma(K_S^0 K_S^0)/\Gamma_{\text{total}}$	$\Gamma_{40}/\Gamma$
VALUE (units $10^{-3}$ )	DOCUMENT ID
<b><math>3.14 \pm 0.18</math> OUR FIT</b>	

$\Gamma(K_S^0 K_S^0)/\Gamma(\pi\pi)$	$\Gamma_{40}/\Gamma_{31}$
VALUE	DOCUMENT ID TECN COMMENT
<b><math>0.369 \pm 0.022</math> OUR FIT</b>	
• • • We do not use the following data for averages, fits, limits, etc. • • •	
$0.31 \pm 0.05 \pm 0.05$	46,47 CHEN 07B BELL $e^+e^- \rightarrow e^+e^-\chi_{c0}$
46 Using $\Gamma(\pi\pi) \times \Gamma(\gamma\gamma)/\Gamma_{\text{total}}$ from the $\pi^+\pi^-$ measurement of NAKAZAWA 05 rescaled by 3/2 to convert to $\pi\pi$ .	
47 Not independent from other measurements.	

$\Gamma(K_S^0 K_S^0)/\Gamma(K^+K^-)$	$\Gamma_{40}/\Gamma_{39}$
VALUE	DOCUMENT ID TECN COMMENT
<b><math>0.519 \pm 0.035</math> OUR FIT</b>	
• • • We do not use the following data for averages, fits, limits, etc. • • •	
$0.49 \pm 0.07 \pm 0.08$	48,49 CHEN 07B BELL $e^+e^- \rightarrow e^+e^-\chi_{c0}$
48 Using $\Gamma(K^+K^-) \times \Gamma(\gamma\gamma)/\Gamma_{\text{total}}$ from NAKAZAWA 05.	
49 Not independent from other measurements.	

$\Gamma(\pi^+\pi^-\eta)/\Gamma_{\text{total}}$	$\Gamma_{41}/\Gamma$
VALUE (units $10^{-3}$ )	CL% DOCUMENT ID TECN COMMENT
<b><math>&lt;0.20</math></b>	90 50 ATHAR 07 CLEO $\psi(2S) \rightarrow \gamma h^+ h^- h^0$
• • • We do not use the following data for averages, fits, limits, etc. • • •	
$<1.0$	90 51 ABLIKIM 06R BES2 $\psi(2S) \rightarrow \gamma\chi_{c0}$
50 ATHAR 07 reports $< 0.21 \times 10^{-3}$ from a measurement of $[\Gamma(\chi_{c0}(1P) \rightarrow \pi^+\pi^-\eta)/\Gamma_{\text{total}}] \times [B(\psi(2S) \rightarrow \gamma\chi_{c0}(1P))]$ assuming $B(\psi(2S) \rightarrow \gamma\chi_{c0}(1P)) = (9.22 \pm 0.11 \pm 0.46) \times 10^{-2}$ , which we rescale to our best value $B(\psi(2S) \rightarrow \gamma\chi_{c0}(1P)) = 9.68 \times 10^{-2}$ .	
51 ABLIKIM 06R reports $< 1.1 \times 10^{-3}$ from a measurement of $[\Gamma(\chi_{c0}(1P) \rightarrow \pi^+\pi^-\eta)/\Gamma_{\text{total}}] \times [B(\psi(2S) \rightarrow \gamma\chi_{c0}(1P))]$ assuming $B(\psi(2S) \rightarrow \gamma\chi_{c0}(1P)) = (9.2 \pm 0.4) \times 10^{-2}$ , which we rescale to our best value $B(\psi(2S) \rightarrow \gamma\chi_{c0}(1P)) = 9.68 \times 10^{-2}$ .	

$\Gamma(\pi^+\pi^-\eta')/\Gamma_{\text{total}}$	$\Gamma_{42}/\Gamma$
VALUE (units $10^{-3}$ )	CL% DOCUMENT ID TECN COMMENT
<b><math>&lt;0.4</math></b>	90 52 ATHAR 07 CLEO $\psi(2S) \rightarrow \gamma h^+ h^- h^0$
• • • We do not use the following data for averages, fits, limits, etc. • • •	
$<0.7$	90 54,55 ABLIKIM 06R BES2 $\psi(2S) \rightarrow \gamma\chi_{c0}$
$<0.7$	90 55,56 BAI 99B BES $\psi(2S) \rightarrow \gamma\chi_{c0}$
52 ATHAR 07 reports $< 0.38 \times 10^{-3}$ from a measurement of $[\Gamma(\chi_{c0}(1P) \rightarrow \pi^+\pi^-\eta')/\Gamma_{\text{total}}] \times [B(\psi(2S) \rightarrow \gamma\chi_{c0}(1P))]$ assuming $B(\psi(2S) \rightarrow \gamma\chi_{c0}(1P)) = (9.22 \pm 0.11 \pm 0.46) \times 10^{-2}$ , which we rescale to our best value $B(\psi(2S) \rightarrow \gamma\chi_{c0}(1P)) = 9.68 \times 10^{-2}$ .	

$\Gamma(\bar{K}^0 K^+ \pi^- + \text{c.c.})/\Gamma_{\text{total}}$	$\Gamma_{43}/\Gamma$
VALUE (units $10^{-3}$ )	CL% DOCUMENT ID TECN COMMENT
<b><math>&lt;0.10</math></b>	90 53 ATHAR 07 CLEO $\psi(2S) \rightarrow \gamma h^+ h^- h^0$
• • • We do not use the following data for averages, fits, limits, etc. • • •	
$<0.7$	90 54,55 ABLIKIM 06R BES2 $\psi(2S) \rightarrow \gamma\chi_{c0}$
$<0.7$	90 55,56 BAI 99B BES $\psi(2S) \rightarrow \gamma\chi_{c0}$
53 ATHAR 07 reports $< 0.10 \times 10^{-3}$ from a measurement of $[\Gamma(\chi_{c0}(1P) \rightarrow \bar{K}^0 K^+ \pi^- + \text{c.c.})/\Gamma_{\text{total}}] \times [B(\psi(2S) \rightarrow \gamma\chi_{c0}(1P))]$ assuming $B(\psi(2S) \rightarrow \gamma\chi_{c0}(1P)) = (9.22 \pm 0.11 \pm 0.46) \times 10^{-2}$ , which we rescale to our best value $B(\psi(2S) \rightarrow \gamma\chi_{c0}(1P)) = 9.68 \times 10^{-2}$ .	
54 ABLIKIM 06R reports $< 0.70 \times 10^{-3}$ from a measurement of $[\Gamma(\chi_{c0}(1P) \rightarrow \bar{K}^0 K^+ \pi^- + \text{c.c.})/\Gamma_{\text{total}}] \times [B(\psi(2S) \rightarrow \gamma\chi_{c0}(1P))]$ assuming $B(\psi(2S) \rightarrow \gamma\chi_{c0}(1P)) = (9.2 \pm 0.4) \times 10^{-2}$ , which we rescale to our best value $B(\psi(2S) \rightarrow \gamma\chi_{c0}(1P)) = 9.68 \times 10^{-2}$ .	

$\Gamma(K^+K^-\pi^0)/\Gamma_{\text{total}}$	$\Gamma_{44}/\Gamma$
VALUE (units $10^{-3}$ )	CL% DOCUMENT ID TECN COMMENT
<b><math>&lt;0.06</math></b>	90 57 ATHAR 07 CLEO $\psi(2S) \rightarrow \gamma h^+ h^- h^0$
• • • We do not use the following data for averages, fits, limits, etc. • • •	
$<0.7$	90 54,55 ABLIKIM 06R BES2 $\psi(2S) \rightarrow \gamma\chi_{c0}$
$<0.7$	90 55,56 BAI 99B BES $\psi(2S) \rightarrow \gamma\chi_{c0}$
57 ATHAR 07 reports $< 0.06 \times 10^{-3}$ from a measurement of $[\Gamma(\chi_{c0}(1P) \rightarrow K^+K^-\pi^0)/\Gamma_{\text{total}}] \times [B(\psi(2S) \rightarrow \gamma\chi_{c0}(1P))]$ assuming $B(\psi(2S) \rightarrow \gamma\chi_{c0}(1P)) = (9.22 \pm 0.11 \pm 0.46) \times 10^{-2}$ , which we rescale to our best value $B(\psi(2S) \rightarrow \gamma\chi_{c0}(1P)) = 9.68 \times 10^{-2}$ .	
55 We have multiplied the $K_S^0 K^+ \pi^-$ measurement by a factor of 2 to convert to $K^0 K^+ \pi^-$ .	
56 Rescaled by us using $B(\psi(2S) \rightarrow \gamma\chi_{c0}) = (9.4 \pm 0.4)\%$ and $B(\psi(2S) \rightarrow J/\psi(1S)\pi^+\pi^-) = (32.6 \pm 0.5)\%$ .	

$\Gamma(K^+K^-\eta)/\Gamma_{\text{total}}$	$\Gamma_{45}/\Gamma$
VALUE (units $10^{-3}$ )	CL% DOCUMENT ID TECN COMMENT
<b><math>&lt;0.23</math></b>	90 58 ATHAR 07 CLEO $\psi(2S) \rightarrow \gamma h^+ h^- h^0$
• • • We do not use the following data for averages, fits, limits, etc. • • •	
$<0.7$	90 54,55 ABLIKIM 06R BES2 $\psi(2S) \rightarrow \gamma\chi_{c0}$
$<0.7$	90 55,56 BAI 99B BES $\psi(2S) \rightarrow \gamma\chi_{c0}$
58 ATHAR 07 reports $< 0.24 \times 10^{-3}$ from a measurement of $[\Gamma(\chi_{c0}(1P) \rightarrow K^+K^-\eta)/\Gamma_{\text{total}}] \times [B(\psi(2S) \rightarrow \gamma\chi_{c0}(1P))]$ assuming $B(\psi(2S) \rightarrow \gamma\chi_{c0}(1P)) = (9.22 \pm 0.11 \pm 0.46) \times 10^{-2}$ , which we rescale to our best value $B(\psi(2S) \rightarrow \gamma\chi_{c0}(1P)) = 9.68 \times 10^{-2}$ .	

$\Gamma(K^+K^-\eta')/\Gamma_{\text{total}}$	$\Gamma_{46}/\Gamma$
VALUE (units $10^{-3}$ )	EVTS DOCUMENT ID TECN COMMENT
<b><math>1.43 \pm 0.48 \pm 0.05</math></b>	16.8 $\pm 4.8$ 59 ABLIKIM 05o BES2 $\psi(2S) \rightarrow \gamma\chi_{c0}$
59 ABLIKIM 05o reports $[\Gamma(\chi_{c0}(1P) \rightarrow K^+K^-\eta')/\Gamma_{\text{total}}] \times [B(\psi(2S) \rightarrow \gamma\chi_{c0}(1P))]$ = $(0.138 \pm 0.039 \pm 0.025) \times 10^{-3}$ which we divide by our best value $B(\psi(2S) \rightarrow \gamma\chi_{c0}(1P)) = (9.68 \pm 0.31) \times 10^{-2}$ . Our first error is their experiment's error and our second error is the systematic error from using our best value.	

See key on page 457

## Meson Particle Listings

 $\chi_{c0}(1P)$ 

$\Gamma(K^+ K^- K^+ K^-)/\Gamma_{\text{total}}$	$\Gamma_{47}/\Gamma$
VALUE (units $10^{-3}$ )	DOCUMENT ID
<b>2.79 ± 0.29 OUR FIT</b>	

$\Gamma(K^+ K^- \phi)/\Gamma_{\text{total}}$	$\Gamma_{48}/\Gamma$			
VALUE (units $10^{-3}$ )	EVTS	DOCUMENT ID	TECN	COMMENT
<b>0.98 ± 0.25 ± 0.03</b>	38	60 ABLIKIM	06T BES2	$\psi(2S) \rightarrow \gamma 2K^+ 2K^-$
60 ABLIKIM 06T reports $(1.03 \pm 0.22 \pm 0.15) \times 10^{-3}$ from a measurement of $[\Gamma(\chi_{c0}(1P) \rightarrow K^+ K^- \phi)/\Gamma_{\text{total}}] \times [B(\psi(2S) \rightarrow \gamma \chi_{c0}(1P))]$ assuming $B(\psi(2S) \rightarrow \gamma \chi_{c0}(1P)) = (9.2 \pm 0.4) \times 10^{-2}$ , which we rescale to our best value $B(\psi(2S) \rightarrow \gamma \chi_{c0}(1P)) = (9.68 \pm 0.31) \times 10^{-2}$ . Our first error is their experiment's error and our second error is the systematic error from using our best value.				

$\Gamma(\phi\phi)/\Gamma_{\text{total}}$	$\Gamma_{49}/\Gamma$
VALUE (units $10^{-3}$ )	DOCUMENT ID
<b>0.82 ± 0.08 OUR FIT</b>	

$\Gamma(p\bar{p})/\Gamma_{\text{total}}$	$\Gamma_{50}/\Gamma$
VALUE (units $10^{-4}$ )	DOCUMENT ID
<b>2.23 ± 0.13 OUR FIT</b>	

$\Gamma(p\bar{p}\pi^0)/\Gamma_{\text{total}}$	$\Gamma_{51}/\Gamma$		
VALUE (units $10^{-3}$ )	DOCUMENT ID	TECN	COMMENT
<b>0.70 ± 0.07 OUR AVERAGE</b>	Error includes scale factor of 1.2.		
0.74 ± 0.06 ± 0.02	61 ONYISI	10 CLE3	$\psi(2S) \rightarrow \gamma p\bar{p}X$
0.56 ± 0.12 ± 0.02	62 ATHAR	07 CLEO	$\psi(2S) \rightarrow \gamma h^+ h^- h^0$

61 ONYISI 10 reports  $(7.76 \pm 0.37 \pm 0.51 \pm 0.39) \times 10^{-4}$  from a measurement of  $[\Gamma(\chi_{c0}(1P) \rightarrow p\bar{p}\pi^0)/\Gamma_{\text{total}}] \times [B(\psi(2S) \rightarrow \gamma \chi_{c0}(1P))]$  assuming  $B(\psi(2S) \rightarrow \gamma \chi_{c0}(1P)) = (9.22 \pm 0.11 \pm 0.46) \times 10^{-2}$ , which we rescale to our best value  $B(\psi(2S) \rightarrow \gamma \chi_{c0}(1P)) = (9.68 \pm 0.31) \times 10^{-2}$ . Our first error is their experiment's error and our second error is the systematic error from using our best value.

62 ATHAR 07 reports  $(0.59 \pm 0.10 \pm 0.08) \times 10^{-3}$  from a measurement of  $[\Gamma(\chi_{c0}(1P) \rightarrow p\bar{p}\pi^0)/\Gamma_{\text{total}}] \times [B(\psi(2S) \rightarrow \gamma \chi_{c0}(1P))]$  assuming  $B(\psi(2S) \rightarrow \gamma \chi_{c0}(1P)) = (9.22 \pm 0.11 \pm 0.46) \times 10^{-2}$ , which we rescale to our best value  $B(\psi(2S) \rightarrow \gamma \chi_{c0}(1P)) = (9.68 \pm 0.31) \times 10^{-2}$ . Our first error is their experiment's error and our second error is the systematic error from using our best value.

$\Gamma(p\bar{p}\eta)/\Gamma_{\text{total}}$	$\Gamma_{52}/\Gamma$		
VALUE (units $10^{-3}$ )	DOCUMENT ID	TECN	COMMENT
<b>0.36 ± 0.04 OUR AVERAGE</b>			
0.36 ± 0.04 ± 0.01	63 ONYISI	10 CLE3	$\psi(2S) \rightarrow \gamma p\bar{p}X$
0.37 ± 0.11 ± 0.01	64 ATHAR	07 CLEO	$\psi(2S) \rightarrow \gamma h^+ h^- h^0$

63 ONYISI 10 reports  $(3.73 \pm 0.38 \pm 0.28 \pm 0.19) \times 10^{-4}$  from a measurement of  $[\Gamma(\chi_{c0}(1P) \rightarrow p\bar{p}\eta)/\Gamma_{\text{total}}] \times [B(\psi(2S) \rightarrow \gamma \chi_{c0}(1P))]$  assuming  $B(\psi(2S) \rightarrow \gamma \chi_{c0}(1P)) = (9.22 \pm 0.11 \pm 0.46) \times 10^{-2}$ , which we rescale to our best value  $B(\psi(2S) \rightarrow \gamma \chi_{c0}(1P)) = (9.68 \pm 0.31) \times 10^{-2}$ . Our first error is their experiment's error and our second error is the systematic error from using our best value.

64 ATHAR 07 reports  $(0.39 \pm 0.11 \pm 0.04) \times 10^{-3}$  from a measurement of  $[\Gamma(\chi_{c0}(1P) \rightarrow p\bar{p}\eta)/\Gamma_{\text{total}}] \times [B(\psi(2S) \rightarrow \gamma \chi_{c0}(1P))]$  assuming  $B(\psi(2S) \rightarrow \gamma \chi_{c0}(1P)) = (9.22 \pm 0.11 \pm 0.46) \times 10^{-2}$ , which we rescale to our best value  $B(\psi(2S) \rightarrow \gamma \chi_{c0}(1P)) = (9.68 \pm 0.31) \times 10^{-2}$ . Our first error is their experiment's error and our second error is the systematic error from using our best value.

$\Gamma(p\bar{p}\omega)/\Gamma_{\text{total}}$	$\Gamma_{53}/\Gamma$		
VALUE (units $10^{-3}$ )	DOCUMENT ID	TECN	COMMENT
<b>0.53 ± 0.06 ± 0.02</b>	65 ONYISI	10 CLE3	$\psi(2S) \rightarrow \gamma p\bar{p}X$
65 ONYISI 10 reports $(5.57 \pm 0.48 \pm 0.42 \pm 0.14) \times 10^{-4}$ from a measurement of $[\Gamma(\chi_{c0}(1P) \rightarrow p\bar{p}\omega)/\Gamma_{\text{total}}] \times [B(\psi(2S) \rightarrow \gamma \chi_{c0}(1P))]$ assuming $B(\psi(2S) \rightarrow \gamma \chi_{c0}(1P)) = (9.22 \pm 0.11 \pm 0.46) \times 10^{-2}$ , which we rescale to our best value $B(\psi(2S) \rightarrow \gamma \chi_{c0}(1P)) = (9.68 \pm 0.31) \times 10^{-2}$ . Our first error is their experiment's error and our second error is the systematic error from using our best value.			

$\Gamma(p\bar{p}\phi)/\Gamma_{\text{total}}$	$\Gamma_{54}/\Gamma$			
VALUE (units $10^{-5}$ )	EVTS	DOCUMENT ID	TECN	COMMENT
<b>6.1 ± 1.4 ± 0.2</b>	42 ± 8	66 ABLIKIM	11F BES3	$\psi(2S) \rightarrow \gamma p\bar{p}K^+ K^-$
66 ABLIKIM 11F reports $(6.12 \pm 1.18 \pm 0.86) \times 10^{-5}$ from a measurement of $[\Gamma(\chi_{c0}(1P) \rightarrow p\bar{p}\phi)/\Gamma_{\text{total}}] \times [B(\psi(2S) \rightarrow \gamma \chi_{c0}(1P))]$ assuming $B(\psi(2S) \rightarrow \gamma \chi_{c0}(1P)) = (9.62 \pm 0.31) \times 10^{-2}$ , which we rescale to our best value $B(\psi(2S) \rightarrow \gamma \chi_{c0}(1P)) = (9.68 \pm 0.31) \times 10^{-2}$ . Our first error is their experiment's error and our second error is the systematic error from using our best value.				

$\Gamma(p\bar{p}\pi^+\pi^-)/\Gamma_{\text{total}}$	$\Gamma_{55}/\Gamma$		
VALUE (units $10^{-3}$ )	DOCUMENT ID	TECN	COMMENT
<b>2.1 ± 0.7 OUR EVALUATION</b>	Error includes scale factor of 1.4. Treating systematic error as correlated.		
<b>2.1 ± 1.0 OUR AVERAGE</b>	Error includes scale factor of 2.0.		
1.57 ± 0.21 ± 0.53	67 BAI	99B BES	$\psi(2S) \rightarrow \gamma \chi_{c0}$
4.20 ± 1.15 ± 0.18	67 TANENBAUM	78 MRK1	$\psi(2S) \rightarrow \gamma \chi_{c0}$
67 Rescaled by us using $B(\psi(2S) \rightarrow \gamma \chi_{c0}) = (9.4 \pm 0.4)\%$ and $B(\psi(2S) \rightarrow J/\psi(1S)\pi^+\pi^-) = (32.6 \pm 0.5)\%$ .			

$\Gamma(p\bar{p}\pi^0\pi^0)/\Gamma_{\text{total}}$	$\Gamma_{56}/\Gamma$			
VALUE (%)	EVTS	DOCUMENT ID	TECN	COMMENT
<b>0.105 ± 0.028 ± 0.003</b>	39.5	68 HE	08B CLEO	$e^+e^- \rightarrow \gamma h^+ h^- h^0 h^0$
68 HE 08B reports $0.11 \pm 0.02 \pm 0.02 \pm 0.01\%$ from a measurement of $[\Gamma(\chi_{c0}(1P) \rightarrow p\bar{p}\pi^0\pi^0)/\Gamma_{\text{total}}] \times [B(\psi(2S) \rightarrow \gamma \chi_{c0}(1P))]$ assuming $B(\psi(2S) \rightarrow \gamma \chi_{c0}(1P)) = (9.22 \pm 0.11 \pm 0.46) \times 10^{-2}$ , which we rescale to our best value $B(\psi(2S) \rightarrow \gamma \chi_{c0}(1P)) = (9.68 \pm 0.31) \times 10^{-2}$ . Our first error is their experiment's error and our second error is the systematic error from using our best value.				

$\Gamma(p\bar{p}K^+ K^- \text{ (non-resonant)})/\Gamma_{\text{total}}$	$\Gamma_{57}/\Gamma$			
VALUE (units $10^{-4}$ )	EVTS	DOCUMENT ID	TECN	COMMENT
<b>1.23 ± 0.26 ± 0.04</b>	48 ± 8	69 ABLIKIM	11F BES3	$\psi(2S) \rightarrow \gamma p\bar{p}K^+ K^-$
69 ABLIKIM 11F reports $(1.24 \pm 0.20 \pm 0.18) \times 10^{-4}$ from a measurement of $[\Gamma(\chi_{c0}(1P) \rightarrow p\bar{p}K^+ K^- \text{ (non-resonant)})/\Gamma_{\text{total}}] \times [B(\psi(2S) \rightarrow \gamma \chi_{c0}(1P))]$ assuming $B(\psi(2S) \rightarrow \gamma \chi_{c0}(1P)) = (9.62 \pm 0.31) \times 10^{-2}$ , which we rescale to our best value $B(\psi(2S) \rightarrow \gamma \chi_{c0}(1P)) = (9.68 \pm 0.31) \times 10^{-2}$ . Our first error is their experiment's error and our second error is the systematic error from using our best value.				

$\Gamma(p\bar{p}K_S^0 K_S^0)/\Gamma_{\text{total}}$	$\Gamma_{58}/\Gamma$			
VALUE (units $10^{-4}$ )	CL%	DOCUMENT ID	TECN	COMMENT
<b>&lt; 8.8</b>	90	70 ABLIKIM	06D BES2	$\psi(2S) \rightarrow \chi_{c0}\gamma$
70 Using $B(\psi(2S) \rightarrow \chi_{c0}\gamma) = (9.2 \pm 0.5)\%$				

$\Gamma(p\bar{p}\pi^-)/\Gamma_{\text{total}}$	$\Gamma_{59}/\Gamma$		
VALUE (units $10^{-4}$ )	DOCUMENT ID	TECN	COMMENT
<b>11.4 ± 3.1 ± 0.4</b>	71 ABLIKIM	06I BES2	$\psi(2S) \rightarrow \gamma p\pi^- X$
71 ABLIKIM 06I reports $[\Gamma(\chi_{c0}(1P) \rightarrow p\bar{p}\pi^-)/\Gamma_{\text{total}}] \times [B(\psi(2S) \rightarrow \gamma \chi_{c0}(1P))]$ = $(1.10 \pm 0.24 \pm 0.18) \times 10^{-4}$ which we divide by our best value $B(\psi(2S) \rightarrow \gamma \chi_{c0}(1P)) = (9.68 \pm 0.31) \times 10^{-2}$ . Our first error is their experiment's error and our second error is the systematic error from using our best value.			

$\Gamma(\Lambda\bar{\Lambda})/\Gamma_{\text{total}}$	$\Gamma_{60}/\Gamma$
VALUE (units $10^{-4}$ )	DOCUMENT ID
<b>3.3 ± 0.4 OUR FIT</b>	

$\Gamma(\Lambda\bar{\Lambda}\pi^+\pi^-)/\Gamma_{\text{total}}$	$\Gamma_{61}/\Gamma$			
VALUE (units $10^{-3}$ )	CL%	DOCUMENT ID	TECN	COMMENT
<b>&lt; 4.0</b>	90	72 ABLIKIM	06D BES2	$\psi(2S) \rightarrow \chi_{c0}\gamma$
72 Using $B(\psi(2S) \rightarrow \chi_{c0}\gamma) = (9.2 \pm 0.5)\%$				

$\Gamma(K^+ \bar{p} \Lambda + \text{c.c.})/\Gamma_{\text{total}}$	$\Gamma_{62}/\Gamma$		
VALUE (units $10^{-3}$ )	DOCUMENT ID	TECN	COMMENT
<b>1.02 ± 0.19 ± 0.03</b>	73 ATHAR	07 CLEO	$\psi(2S) \rightarrow \gamma h^+ h^- h^0$
73 ATHAR 07 reports $(1.07 \pm 0.17 \pm 0.12) \times 10^{-3}$ from a measurement of $[\Gamma(\chi_{c0}(1P) \rightarrow K^+ \bar{p} \Lambda + \text{c.c.})/\Gamma_{\text{total}}] \times [B(\psi(2S) \rightarrow \gamma \chi_{c0}(1P))]$ assuming $B(\psi(2S) \rightarrow \gamma \chi_{c0}(1P)) = (9.22 \pm 0.11 \pm 0.46) \times 10^{-2}$ , which we rescale to our best value $B(\psi(2S) \rightarrow \gamma \chi_{c0}(1P)) = (9.68 \pm 0.31) \times 10^{-2}$ . Our first error is their experiment's error and our second error is the systematic error from using our best value.			

$\Gamma(K^+ \rho \Lambda(1520) + \text{c.c.})/\Gamma_{\text{total}}$	$\Gamma_{63}/\Gamma$			
VALUE (units $10^{-4}$ )	EVTS	DOCUMENT ID	TECN	COMMENT
<b>3.0 ± 0.8 ± 0.1</b>	62 ± 12	74 ABLIKIM	11F BES3	$\psi(2S) \rightarrow \gamma p\bar{p}K^+ K^-$
74 ABLIKIM 11F reports $(3.00 \pm 0.58 \pm 0.50) \times 10^{-4}$ from a measurement of $[\Gamma(\chi_{c0}(1P) \rightarrow K^+ \rho \Lambda(1520) + \text{c.c.})/\Gamma_{\text{total}}] \times [B(\psi(2S) \rightarrow \gamma \chi_{c0}(1P))]$ assuming $B(\psi(2S) \rightarrow \gamma \chi_{c0}(1P)) = (9.62 \pm 0.31) \times 10^{-2}$ , which we rescale to our best value $B(\psi(2S) \rightarrow \gamma \chi_{c0}(1P)) = (9.68 \pm 0.31) \times 10^{-2}$ . Our first error is their experiment's error and our second error is the systematic error from using our best value.				

$\Gamma(\Lambda(1520)\bar{\Lambda}(1520))/\Gamma_{\text{total}}$	$\Gamma_{64}/\Gamma$			
VALUE (units $10^{-4}$ )	EVTS	DOCUMENT ID	TECN	COMMENT
<b>3.2 ± 1.2 ± 0.1</b>	28 ± 10	75 ABLIKIM	11F BES3	$\psi(2S) \rightarrow \gamma p\bar{p}K^+ K^-$
75 ABLIKIM 11F reports $(3.18 \pm 1.11 \pm 0.53) \times 10^{-4}$ from a measurement of $[\Gamma(\chi_{c0}(1P) \rightarrow \Lambda(1520)\bar{\Lambda}(1520))/\Gamma_{\text{total}}] \times [B(\psi(2S) \rightarrow \gamma \chi_{c0}(1P))]$ assuming $B(\psi(2S) \rightarrow \gamma \chi_{c0}(1P)) = (9.62 \pm 0.31) \times 10^{-2}$ , which we rescale to our best value $B(\psi(2S) \rightarrow \gamma \chi_{c0}(1P)) = (9.68 \pm 0.31) \times 10^{-2}$ . Our first error is their experiment's error and our second error is the systematic error from using our best value.				

$\Gamma(\Sigma^0 \bar{\Sigma}^0)/\Gamma_{\text{total}}$	$\Gamma_{65}/\Gamma$			
VALUE (units $10^{-4}$ )	EVTS	DOCUMENT ID	TECN	COMMENT
<b>4.2 ± 0.7 ± 0.1</b>	78 ± 10	76 NAIK	08 CLEO	$\psi(2S) \rightarrow \gamma \Sigma^0 \bar{\Sigma}^0$
76 NAIK 08 reports $(4.41 \pm 0.56 \pm 0.47) \times 10^{-4}$ from a measurement of $[\Gamma(\chi_{c0}(1P) \rightarrow \Sigma^0 \bar{\Sigma}^0)/\Gamma_{\text{total}}] \times [B(\psi(2S) \rightarrow \gamma \chi_{c0}(1P))]$ assuming $B(\psi(2S) \rightarrow \gamma \chi_{c0}(1P)) = (9.22 \pm 0.11 \pm 0.46) \times 10^{-2}$ , which we rescale to our best value $B(\psi(2S) \rightarrow \gamma \chi_{c0}(1P)) = (9.68 \pm 0.31) \times 10^{-2}$ . Our first error is their experiment's error and our second error is the systematic error from using our best value.				

## Meson Particle Listings

 $\chi_{c0}(1P)$  $\Gamma(\Sigma^+\bar{\Sigma}^-)/\Gamma_{total}$   $\Gamma_{66}/\Gamma$ 

VALUE (units $10^{-4}$ )	EVTs	DOCUMENT ID	TECN	COMMENT
<b>3.1 ± 0.7 ± 0.1</b>	39 ± 7	77 NAIK	08	CLEO $\psi(2S) \rightarrow \gamma \Sigma^+ \bar{\Sigma}^-$
77 NAIK 08 reports $(3.25 \pm 0.57 \pm 0.43) \times 10^{-4}$ from a measurement of $[\Gamma(\chi_{c0}(1P) \rightarrow \Sigma^+ \bar{\Sigma}^-)/\Gamma_{total}] \times [B(\psi(2S) \rightarrow \gamma \chi_{c0}(1P))]$ assuming $B(\psi(2S) \rightarrow \gamma \chi_{c0}(1P)) = (9.22 \pm 0.11 \pm 0.46) \times 10^{-2}$ , which we rescale to our best value $B(\psi(2S) \rightarrow \gamma \chi_{c0}(1P)) = (9.68 \pm 0.31) \times 10^{-2}$ . Our first error is their experiment's error and our second error is the systematic error from using our best value.				

 $\Gamma(\Xi^0\bar{\Xi}^0)/\Gamma_{total}$   $\Gamma_{67}/\Gamma$ 

VALUE (units $10^{-4}$ )	EVTs	DOCUMENT ID	TECN	COMMENT
<b>3.2 ± 0.9 ± 0.1</b>	23.3 ± 4.9	78 NAIK	08	CLEO $\psi(2S) \rightarrow \gamma \Xi^0 \bar{\Xi}^0$
78 NAIK 08 reports $(3.34 \pm 0.70 \pm 0.48) \times 10^{-4}$ from a measurement of $[\Gamma(\chi_{c0}(1P) \rightarrow \Xi^0 \bar{\Xi}^0)/\Gamma_{total}] \times [B(\psi(2S) \rightarrow \gamma \chi_{c0}(1P))]$ assuming $B(\psi(2S) \rightarrow \gamma \chi_{c0}(1P)) = (9.22 \pm 0.11 \pm 0.46) \times 10^{-2}$ , which we rescale to our best value $B(\psi(2S) \rightarrow \gamma \chi_{c0}(1P)) = (9.68 \pm 0.31) \times 10^{-2}$ . Our first error is their experiment's error and our second error is the systematic error from using our best value.				

 $\Gamma(\Xi^- \bar{\Xi}^+)/\Gamma_{total}$   $\Gamma_{68}/\Gamma$ 

VALUE (units $10^{-4}$ )	CL%	EVTs	DOCUMENT ID	TECN	COMMENT
<b>4.9 ± 0.7 ± 0.2</b>		95 ± 11	79 NAIK	08	CLEO $\psi(2S) \rightarrow \gamma \Xi^- \bar{\Xi}^+$
• • • We do not use the following data for averages, fits, limits, etc. • • •					
<10.3	90		80 ABLIKIM	06D	BES2 $\psi(2S) \rightarrow \chi_{c0} \gamma$
79 NAIK 08 reports $(5.14 \pm 0.60 \pm 0.47) \times 10^{-4}$ from a measurement of $[\Gamma(\chi_{c0}(1P) \rightarrow \Xi^- \bar{\Xi}^+)/\Gamma_{total}] \times [B(\psi(2S) \rightarrow \gamma \chi_{c0}(1P))]$ assuming $B(\psi(2S) \rightarrow \gamma \chi_{c0}(1P)) = (9.22 \pm 0.11 \pm 0.46) \times 10^{-2}$ , which we rescale to our best value $B(\psi(2S) \rightarrow \gamma \chi_{c0}(1P)) = (9.68 \pm 0.31) \times 10^{-2}$ . Our first error is their experiment's error and our second error is the systematic error from using our best value.					
80 Using $B(\psi(2S) \rightarrow \chi_{c0} \gamma) = (9.2 \pm 0.5)\%$					

 $\Gamma(\rho\bar{\rho})/\Gamma_{total} \times \Gamma(\pi\pi)/\Gamma_{total}$   $\Gamma_{50}/\Gamma \times \Gamma_{31}/\Gamma$ 

VALUE (units $10^{-7}$ )	DOCUMENT ID	TECN	COMMENT
<b>19.0 ± 1.4 OUR FIT</b>			
<b>15.3 ± 2.4 ± 0.8</b>	81 ANDREOTTI 03	E835	$\bar{p}p \rightarrow \chi_{c0} \rightarrow \pi^0 \pi^0$
81 We have multiplied $B(\rho\bar{\rho})B(\pi^0 \pi^0)$ measurement by 3 to obtain $B(\rho\bar{\rho})B(\pi\pi)$ .			

 $\Gamma(\rho\bar{\rho})/\Gamma_{total} \times \Gamma(\pi^0 \eta)/\Gamma_{total}$   $\Gamma_{50}/\Gamma \times \Gamma_{32}/\Gamma$ 

VALUE (units $10^{-7}$ )	DOCUMENT ID	TECN	COMMENT
<b>&lt;0.4</b>	ANDREOTTI 05c	E835	$\bar{p}p \rightarrow \pi^0 \eta$

 $\Gamma(\rho\bar{\rho})/\Gamma_{total} \times \Gamma(\pi^0 \eta')/\Gamma_{total}$   $\Gamma_{50}/\Gamma \times \Gamma_{33}/\Gamma$ 

VALUE (units $10^{-7}$ )	DOCUMENT ID	TECN	COMMENT
<b>&lt;2.5</b>	ANDREOTTI 05c	E835	$\bar{p}p \rightarrow \pi^0 \eta'$

 $\Gamma(\rho\bar{\rho})/\Gamma_{total} \times \Gamma(\eta\eta)/\Gamma_{total}$   $\Gamma_{50}/\Gamma \times \Gamma_{34}/\Gamma$ 

VALUE (units $10^{-7}$ )	DOCUMENT ID	TECN	COMMENT
<b>6.8 ± 0.6 OUR FIT</b>			
<b>4.0 ± 1.2<sup>+0.5</sup><sub>-0.3</sub></b>	ANDREOTTI 05c	E835	$\bar{p}p \rightarrow \eta \eta$

 $\Gamma(\rho\bar{\rho})/\Gamma_{total} \times \Gamma(\eta\eta')/\Gamma_{total}$   $\Gamma_{50}/\Gamma \times \Gamma_{35}/\Gamma$ 

VALUE (units $10^{-6}$ )	DOCUMENT ID	TECN	COMMENT
• • • We do not use the following data for averages, fits, limits, etc. • • •			
<b>2.1<sup>+2.3</sup><sub>-1.5</sub></b>	ANDREOTTI 05c	E835	$\bar{p}p \rightarrow \pi^0 \eta'$

## RADIATIVE DECAYS

 $\Gamma(\gamma J/\psi(1S))/\Gamma_{total}$   $\Gamma_{69}/\Gamma$ 

VALUE (units $10^{-4}$ )	DOCUMENT ID	TECN	COMMENT
<b>117 ± 8 OUR FIT</b>			
• • • We do not use the following data for averages, fits, limits, etc. • • •			
200 ± 20 ± 20	82 ADAM	05A	CLEO $e^+ e^- \rightarrow \psi(2S) \rightarrow \gamma \chi_{c0}$
82 Uses $B(\psi(2S) \rightarrow \gamma \chi_{c0} \rightarrow \gamma \gamma J/\psi)$ from ADAM 05A and $B(\psi(2S) \rightarrow \gamma \chi_{c0})$ from ATHAR 04.			

 $\Gamma(\gamma \rho^0)/\Gamma_{total}$   $\Gamma_{70}/\Gamma$ 

VALUE (units $10^{-6}$ )	CL%	EVTs	DOCUMENT ID	TECN	COMMENT
<b>&lt; 9</b>	90	1.2 ± 4.5	83 BENNETT	08A	CLEO $\psi(2S) \rightarrow \gamma \gamma \rho^0$
• • • We do not use the following data for averages, fits, limits, etc. • • •					
<10	90	6 ± 12	84 ABLIKIM	11E	BES3 $\psi(2S) \rightarrow \gamma \gamma \rho^0$
83 BENNETT 08A reports $< 9.6 \times 10^{-6}$ from a measurement of $[\Gamma(\chi_{c0}(1P) \rightarrow \gamma \rho^0)/\Gamma_{total}] \times [B(\psi(2S) \rightarrow \gamma \chi_{c0}(1P))]$ assuming $B(\psi(2S) \rightarrow \gamma \chi_{c0}(1P)) = (9.2 \pm 0.4) \times 10^{-2}$ , which we rescale to our best value $B(\psi(2S) \rightarrow \gamma \chi_{c0}(1P)) = 9.68 \times 10^{-2}$ .					
84 ABLIKIM 11E reports $< 10.5 \times 10^{-6}$ from a measurement of $[\Gamma(\chi_{c0}(1P) \rightarrow \gamma \rho^0)/\Gamma_{total}] \times [B(\psi(2S) \rightarrow \gamma \chi_{c0}(1P))]$ assuming $B(\psi(2S) \rightarrow \gamma \chi_{c0}(1P)) = (9.62 \pm 0.31) \times 10^{-2}$ , which we rescale to our best value $B(\psi(2S) \rightarrow \gamma \chi_{c0}(1P)) = 9.68 \times 10^{-2}$ .					

 $\Gamma(\gamma\omega)/\Gamma_{total}$   $\Gamma_{71}/\Gamma$ 

VALUE (units $10^{-6}$ )	CL%	EVTs	DOCUMENT ID	TECN	COMMENT
<b>&lt; 8</b>	90	0.0 ± 2.8	85 BENNETT	08A	CLEO $\psi(2S) \rightarrow \gamma \gamma \omega$
• • • We do not use the following data for averages, fits, limits, etc. • • •					
<13	90	5 ± 11	86 ABLIKIM	11E	BES3 $\psi(2S) \rightarrow \gamma \gamma \omega$
85 BENNETT 08A reports $< 8.8 \times 10^{-6}$ from a measurement of $[\Gamma(\chi_{c0}(1P) \rightarrow \gamma \omega)/\Gamma_{total}] \times [B(\psi(2S) \rightarrow \gamma \chi_{c0}(1P))]$ assuming $B(\psi(2S) \rightarrow \gamma \chi_{c0}(1P)) = (9.2 \pm 0.4) \times 10^{-2}$ , which we rescale to our best value $B(\psi(2S) \rightarrow \gamma \chi_{c0}(1P)) = 9.68 \times 10^{-2}$ .					
86 ABLIKIM 11E reports $< 12.9 \times 10^{-6}$ from a measurement of $[\Gamma(\chi_{c0}(1P) \rightarrow \gamma \omega)/\Gamma_{total}] \times [B(\psi(2S) \rightarrow \gamma \chi_{c0}(1P))]$ assuming $B(\psi(2S) \rightarrow \gamma \chi_{c0}(1P)) = (9.62 \pm 0.31) \times 10^{-2}$ , which we rescale to our best value $B(\psi(2S) \rightarrow \gamma \chi_{c0}(1P)) = 9.68 \times 10^{-2}$ .					

 $\Gamma(\gamma\phi)/\Gamma_{total}$   $\Gamma_{72}/\Gamma$ 

VALUE (units $10^{-6}$ )	CL%	EVTs	DOCUMENT ID	TECN	COMMENT
<b>&lt; 6</b>	90	0.1 ± 1.6	87 BENNETT	08A	CLEO $\psi(2S) \rightarrow \gamma \gamma \phi$
• • • We do not use the following data for averages, fits, limits, etc. • • •					
<16	90	15 ± 7	88 ABLIKIM	11E	BES3 $\psi(2S) \rightarrow \gamma \gamma \phi$
87 BENNETT 08A reports $< 6.4 \times 10^{-6}$ from a measurement of $[\Gamma(\chi_{c0}(1P) \rightarrow \gamma \phi)/\Gamma_{total}] \times [B(\psi(2S) \rightarrow \gamma \chi_{c0}(1P))]$ assuming $B(\psi(2S) \rightarrow \gamma \chi_{c0}(1P)) = (9.2 \pm 0.4) \times 10^{-2}$ , which we rescale to our best value $B(\psi(2S) \rightarrow \gamma \chi_{c0}(1P)) = 9.68 \times 10^{-2}$ .					
88 ABLIKIM 11E reports $< 16.2 \times 10^{-6}$ from a measurement of $[\Gamma(\chi_{c0}(1P) \rightarrow \gamma \phi)/\Gamma_{total}] \times [B(\psi(2S) \rightarrow \gamma \chi_{c0}(1P))]$ assuming $B(\psi(2S) \rightarrow \gamma \chi_{c0}(1P)) = (9.62 \pm 0.31) \times 10^{-2}$ , which we rescale to our best value $B(\psi(2S) \rightarrow \gamma \chi_{c0}(1P)) = 9.68 \times 10^{-2}$ .					

 $\Gamma(\gamma\eta)/\Gamma_{total}$   $\Gamma_{73}/\Gamma$ 

VALUE (units $10^{-4}$ )	CL%	DOCUMENT ID	TECN	COMMENT
<b>2.23 ± 0.17 OUR FIT</b>				
• • • We do not use the following data for averages, fits, limits, etc. • • •				
<8	90	89 WICHT	08	BELL $B^\pm \rightarrow K^\pm \gamma \eta$
89 WICHT 08 reports $[\Gamma(\chi_{c0}(1P) \rightarrow \gamma \eta)/\Gamma_{total}] \times [B(B^\pm \rightarrow \chi_{c0}(1P) K^\pm)] < 0.11 \times 10^{-6}$ which we divide by our best value $B(B^\pm \rightarrow \chi_{c0}(1P) K^\pm) = 1.34 \times 10^{-4}$ .				

 $\Gamma(\gamma\gamma)/\Gamma(\gamma J/\psi(1S))$   $\Gamma_{73}/\Gamma_{69}$ 

VALUE (units $10^{-2}$ )	DOCUMENT ID	TECN	COMMENT
<b>1.90 ± 0.19 OUR FIT</b>			
<b>2.0 ± 0.4 OUR AVERAGE</b>			
2.2 ± 0.4 <sup>+0.1</sup> <sub>-0.2</sub>	90 ANDREOTTI 04	E835	$\rho\bar{\rho} \rightarrow \chi_{c0} \rightarrow \gamma \gamma$
1.45 ± 0.74	91 AMBROGIANI 00B	E835	$\bar{p}p \rightarrow \chi_{c2} \rightarrow \gamma \gamma, \gamma J/\psi$
90 The values of $B(\rho\bar{\rho})B(\gamma\gamma)$ and $B(\gamma\gamma)B(\gamma J/\psi)$ measured by ANDREOTTI 04 are not independent. The latter is used in the fit because of smaller systematics.			
91 Calculated by us using $B(J/\psi(1S) \rightarrow e^+ e^-) = 0.0593 \pm 0.0010$ .			

 $\Gamma(\rho\bar{\rho})/\Gamma_{total} \times \Gamma(\gamma J/\psi(1S))/\Gamma_{total}$   $\Gamma_{50}/\Gamma \times \Gamma_{69}/\Gamma$ 

VALUE (units $10^{-7}$ )	EVTs	DOCUMENT ID	TECN	COMMENT
<b>26.2 ± 1.7 OUR FIT</b>				
<b>28.2 ± 2.1 OUR AVERAGE</b>				
28.0 ± 1.9 ± 1.3	392, 92, 93, 94	BAGNASCO 02	E835	$\bar{p}p \rightarrow \chi_{c0} \rightarrow J/\psi \gamma$
29.3 <sup>+5.7</sup> <sub>-4.7</sub> ± 1.5	89	92, 93	AMBROGIANI 99B	$\bar{p}p \rightarrow \chi_{c0} \rightarrow J/\psi \gamma$
92 Values in $(\Gamma(\rho\bar{\rho}) \times \Gamma(\gamma J/\psi(1S))/\Gamma_{total})$ and $(\Gamma(\rho\bar{\rho})/\Gamma_{total} \times \Gamma(\gamma J/\psi(1S))/\Gamma_{total})$ are not independent. The latter is used in the fit since it is less correlated to the total width.				
93 Calculated by us using $B(J/\psi(1S) \rightarrow e^+ e^-) = 0.0593 \pm 0.0010$ .				
94 Recalculated by ANDREOTTI 05A.				

 $\Gamma(\rho\bar{\rho})/\Gamma_{total} \times \Gamma(\gamma\gamma)/\Gamma_{total}$   $\Gamma_{50}/\Gamma \times \Gamma_{73}/\Gamma$ 

VALUE (units $10^{-8}$ )	DOCUMENT ID	TECN	COMMENT
<b>5.0 ± 0.5 OUR FIT</b>			
• • • We do not use the following data for averages, fits, limits, etc. • • •			
6.52 ± 1.18 <sup>+0.48</sup> <sub>-0.72</sub>	95 ANDREOTTI 04	E835	$\rho\bar{\rho} \rightarrow \chi_{c0} \rightarrow \gamma \gamma$
95 The values of $B(\rho\bar{\rho})B(\gamma\gamma)$ and $B(\gamma\gamma)B(\gamma J/\psi)$ measured by ANDREOTTI 04 are not independent. The latter is used in the fit because of smaller systematics.			

 $\chi_{c0}(1P)$  CROSS-PARTICLE BRANCHING RATIOS $\Gamma(\chi_{c0}(1P) \rightarrow \rho\bar{\rho})/\Gamma_{total} \times \Gamma(\psi(2S) \rightarrow \gamma \chi_{c0}(1P))/\Gamma_{total}$ 

VALUE (units $10^{-6}$ )	EVTs	DOCUMENT ID	TECN	COMMENT
<b>21.6 ± 1.4 OUR FIT</b>				
<b>23.7 ± 1.8 OUR AVERAGE</b>				
23.7 ± 1.4 ± 1.4	383 ± 22	96 NAIK	08	CLEO $\psi(2S) \rightarrow \gamma \rho\bar{\rho}$
23.6 <sup>+3.7</sup> <sub>-3.4</sub> ± 3.4	89.5 <sup>+14</sup> <sub>-13</sub>	BAI	04F	BES $\psi(2S) \rightarrow \gamma \chi_{c0}(1P) \rightarrow \gamma \rho\bar{\rho}$
96 Calculated by us. NAIK 08 reports $B(\chi_{c0}^0 \rightarrow \rho\bar{\rho}) = (25.7 \pm 1.5 \pm 1.5 \pm 1.3) \times 10^{-5}$ using $B(\psi(2S) \rightarrow \gamma \chi_{c0}^0) = (9.22 \pm 0.11 \pm 0.46)\%$ .				

 $\Gamma_{50}/\Gamma \times \Gamma_{109}^{\psi(2S)}/\Gamma_{\psi(2S)}$

$$\Gamma(\chi_{c0}(1P) \rightarrow p\bar{p})/\Gamma_{\text{total}} \times \Gamma(\psi(2S) \rightarrow \gamma\chi_{c0}(1P))/\Gamma(\psi(2S) \rightarrow J/\psi(1S)\pi^+\pi^-)$$

VALUE (units $10^{-5}$ )	DOCUMENT ID	TECN	COMMENT
<b>6.4 ± 0.4 OUR FIT</b>			
4.6 ± 1.9	97 BAI	98i BES	$\psi(2S) \rightarrow \gamma\chi_{c0} \rightarrow \gamma\bar{p}p$
97 Calculated by us. The value for $B(\chi_{c0} \rightarrow p\bar{p})$ reported in BAI 98i is derived using $B(\psi(2S) \rightarrow \gamma\chi_{c0}) = (9.3 \pm 0.8)\%$ and $B(\psi(2S) \rightarrow J/\psi(1S)\pi^+\pi^-) = (32.4 \pm 2.6)\%$ [BAI 98d].			

$$\Gamma(\chi_{c0}(1P) \rightarrow \Lambda\bar{\Lambda})/\Gamma_{\text{total}} \times \Gamma(\psi(2S) \rightarrow \gamma\chi_{c0}(1P))/\Gamma_{\text{total}}$$

VALUE (units $10^{-6}$ )	EVTS	DOCUMENT ID	TECN	COMMENT
<b>32 ± 4 OUR FIT</b>				
31.2 ± 3.3 ± 2.0	131 ± 12	98 NAIK	08 CLEO	$\psi(2S) \rightarrow \gamma\Lambda\bar{\Lambda}$
98 Calculated by us. NAIK 08 reports $B(\chi_{c0} \rightarrow \Lambda\bar{\Lambda}) = (33.8 \pm 3.6 \pm 2.2 \pm 1.7) \times 10^{-5}$ using $B(\psi(2S) \rightarrow \gamma\chi_{c0}) = (9.22 \pm 0.11 \pm 0.46)\%$ .				

$$\Gamma(\chi_{c0}(1P) \rightarrow \Lambda\bar{\Lambda})/\Gamma_{\text{total}} \times \Gamma(\psi(2S) \rightarrow \gamma\chi_{c0}(1P))/\Gamma(\psi(2S) \rightarrow J/\psi(1S)\pi^+\pi^-)$$

VALUE (units $10^{-5}$ )	EVTS	DOCUMENT ID	TECN	COMMENT
<b>9.5 ± 1.1 OUR FIT</b>				
13.0 ± 3.6 ± 2.5	15.2 +4.2 -4.0	99 BAI	03E BES	$\psi(2S) \rightarrow \gamma\Lambda\bar{\Lambda}$
99 BAI 03E reports $[B(\chi_{c0} \rightarrow \Lambda\bar{\Lambda})/B(\psi(2S) \rightarrow \gamma\chi_{c0})/B(\psi(2S) \rightarrow J/\psi\pi^+\pi^-)] \times [B^2(\Lambda \rightarrow \pi^-p)/B(J/\psi \rightarrow p\bar{p})] = (2.45 +0.68 -0.65 \pm 0.46)\%$ . We calculate from this measurement the presented value using $B(\Lambda \rightarrow \pi^-p) = (63.9 \pm 0.5)\%$ and $B(J/\psi \rightarrow p\bar{p}) = (2.17 \pm 0.07) \times 10^{-3}$ .				

$$\Gamma(\chi_{c0}(1P) \rightarrow \gamma J/\psi(1S))/\Gamma_{\text{total}} \times \Gamma(\psi(2S) \rightarrow \gamma\chi_{c0}(1P))/\Gamma_{\text{total}}$$

VALUE (units $10^{-2}$ )	EVTS	DOCUMENT ID	TECN	COMMENT
<b>0.113 ± 0.008 OUR FIT</b>				
<b>0.073 ± 0.018 OUR AVERAGE</b>				
0.069 ± 0.018		100 OREGLIA	82 CBAL	$\psi(2S) \rightarrow \gamma\chi_{c0}$
0.4 ± 0.3		101 BRA NDELIK	79B DASP	$\psi(2S) \rightarrow \gamma\chi_{c0}$
0.16 ± 0.11		101 BARTEL	78B CNTR	$\psi(2S) \rightarrow \gamma\chi_{c0}$
3.3 ± 1.7		102 BIDDICK	77 CNTR	$e^+e^- \rightarrow \gamma X$
••• We do not use the following data for averages, fits, limits, etc. •••				
0.125 ± 0.007 ± 0.013	560	103 MENDEZ	08 CLEO	$\psi(2S) \rightarrow \gamma\chi_{c0}$
0.18 ± 0.01 ± 0.02	172	104 ADAM	05A CLEO	Repl. by MENDEZ 08
100 Recalculated by us using $B(J/\psi(1S) \rightarrow \ell^+\ell^-) = 0.1181 \pm 0.0020$ . 101 Recalculated by us using $B(J/\psi(1S) \rightarrow \mu^+\mu^-) = 0.0588 \pm 0.0010$ . 102 Assumes isotropic gamma distribution. 103 Not independent from other measurements of MENDEZ 08. 104 Not independent from other values reported by ADAM 05A.				

$$\Gamma(\chi_{c0}(1P) \rightarrow \gamma J/\psi(1S))/\Gamma_{\text{total}} \times \Gamma(\psi(2S) \rightarrow \gamma\chi_{c0}(1P))/\Gamma(\psi(2S) \rightarrow J/\psi(1S)\text{anything})$$

VALUE (units $10^{-2}$ )	EVTS	DOCUMENT ID	TECN	COMMENT
<b>0.191 ± 0.014 OUR FIT</b>				
••• We do not use the following data for averages, fits, limits, etc. •••				
0.201 ± 0.011 ± 0.021	560	105 MENDEZ	08 CLEO	$\psi(2S) \rightarrow \gamma\chi_{c0}$
0.31 ± 0.02 ± 0.03	172	ADAM	05A CLEO	Repl. by MENDEZ 08
105 Not independent from other measurements of MENDEZ 08.				
$\Gamma_{69}/\Gamma \times \frac{\Gamma(\psi(2S) \rightarrow \gamma\chi_{c0}(1P))}{\Gamma(\psi(2S) \rightarrow J/\psi(1S)\text{anything})} = \Gamma_{69}/\Gamma \times \frac{\Gamma(\psi(2S) \rightarrow \gamma\chi_{c0}(1P))}{\Gamma(\psi(2S) \rightarrow J/\psi(1S)\text{anything})} + \frac{\Gamma_{12}}{\Gamma_{11}} + \frac{\Gamma_{13}}{\Gamma_{11}}$				

$$\Gamma(\chi_{c0}(1P) \rightarrow \gamma J/\psi(1S))/\Gamma_{\text{total}} \times \Gamma(\psi(2S) \rightarrow \gamma\chi_{c0}(1P))/\Gamma(\psi(2S) \rightarrow J/\psi(1S)\pi^+\pi^-)$$

VALUE (units $10^{-2}$ )	EVTS	DOCUMENT ID	TECN	COMMENT
<b>0.338 ± 0.024 OUR FIT</b>				
0.358 ± 0.020 ± 0.037	560	MENDEZ	08 CLEO	$\psi(2S) \rightarrow \gamma\chi_{c0}$
••• We do not use the following data for averages, fits, limits, etc. •••				
0.55 ± 0.04 ± 0.06	172	106 ADAM	05A CLEO	Repl. by MENDEZ 08
106 Not independent from other values reported by ADAM 05A.				

$$\Gamma(\chi_{c0}(1P) \rightarrow \gamma\gamma)/\Gamma_{\text{total}} \times \Gamma(\psi(2S) \rightarrow \gamma\chi_{c0}(1P))/\Gamma_{\text{total}}$$

VALUE (units $10^{-5}$ )	EVTS	DOCUMENT ID	TECN	COMMENT
<b>2.16 ± 0.19 OUR FIT</b>				
<b>2.21 ± 0.33 OUR AVERAGE</b>				
2.17 ± 0.32 ± 0.10	207 ± 31	ECKLUND	08A CLEO	$\psi(2S) \rightarrow \gamma\chi_{c0} \rightarrow 3\gamma$
3.7 ± 1.8 ± 1.0		LEE	85 CBAL	$\psi(2S) \rightarrow \gamma\chi_{c0}$

$$\Gamma(\chi_{c0}(1P) \rightarrow \pi\pi)/\Gamma_{\text{total}} \times \Gamma(\psi(2S) \rightarrow \gamma\chi_{c0}(1P))/\Gamma_{\text{total}}$$

VALUE (units $10^{-4}$ )	EVTS	DOCUMENT ID	TECN	COMMENT
<b>8.25 ± 0.29 OUR FIT</b>				
<b>8.80 ± 0.34 OUR AVERAGE</b>				
9.11 ± 0.08 ± 0.65	17k	107 ABLIKIM	10A BES3	$e^+e^- \rightarrow \psi(2S) \rightarrow \gamma\chi_{c0}$
8.81 ± 0.11 ± 0.43	8.9k	108 ASNER	09 CLEO	$\psi(2S) \rightarrow \gamma\pi^+\pi^-$
8.13 ± 0.19 ± 0.89	2.8k	109 ASNER	09 CLEO	$\psi(2S) \rightarrow \gamma\pi^0\pi^0$
107 Calculated by us. ABLIKIM 10A reports $B(\chi_{c0} \rightarrow \pi^0\pi^0) = (3.23 \pm 0.03 \pm 0.23 \pm 0.14) \times 10^{-3}$ using $B(\psi(2S) \rightarrow \gamma\chi_{c0}) = (9.4 \pm 0.4)\%$ . We have multiplied the $\pi^0\pi^0$ measurement by 3 to obtain $\pi\pi$ . 108 Calculated by us. ASNER 09 reports $B(\chi_{c0} \rightarrow \pi^+\pi^-) = (6.37 \pm 0.08 \pm 0.31 \pm 0.32) \times 10^{-3}$ using $B(\psi(2S) \rightarrow \gamma\chi_{c0}) = (9.22 \pm 0.11 \pm 0.46)\%$ . We have multiplied the $\pi^+\pi^-$ measurement by 3/2 to obtain $\pi\pi$ . 109 Calculated by us. ASNER 09 reports $B(\chi_{c0} \rightarrow \pi^0\pi^0) = (2.94 \pm 0.07 \pm 0.32 \pm 0.15) \times 10^{-3}$ using $B(\psi(2S) \rightarrow \gamma\chi_{c0}) = (9.22 \pm 0.11 \pm 0.46)\%$ . We have multiplied the $\pi^0\pi^0$ measurement by 3 to obtain $\pi\pi$ .				

$$\Gamma(\chi_{c0}(1P) \rightarrow \pi\pi)/\Gamma_{\text{total}} \times \Gamma(\psi(2S) \rightarrow \gamma\chi_{c0}(1P))/\Gamma(\psi(2S) \rightarrow J/\psi(1S)\pi^+\pi^-)$$

VALUE (units $10^{-4}$ )	EVTS	DOCUMENT ID	TECN	COMMENT
<b>24.5 ± 0.9 OUR FIT</b>				
<b>20.7 ± 1.7 OUR AVERAGE</b>				
23.9 ± 2.7 ± 4.1	97 ± 11	110 BAI	03c BES	$\psi(2S) \rightarrow \gamma\chi_{c0} \rightarrow \gamma\pi^0\pi^0$
20.2 ± 1.1 ± 1.5	720 ± 32	111 BAI	98i BES	$\psi(2S) \rightarrow \gamma\chi_{c0} \rightarrow \gamma\pi^+\pi^-$
110 We have multiplied $\pi^0\pi^0$ measurement by 3 to obtain $\pi\pi$ . 111 Calculated by us. The value for $B(\chi_{c0} \rightarrow \pi^+\pi^-)$ reported in BAI 98i is derived using $B(\psi' \rightarrow \gamma\chi_{c0}) = (9.3 \pm 0.8)\%$ and $B(\psi' \rightarrow J/\psi\pi^+\pi^-) = (32.4 \pm 2.6)\%$ [BAI 98d]. We have multiplied $\pi^+\pi^-$ measurement by 3/2 to obtain $\pi\pi$ .				

$$\Gamma(\chi_{c0}(1P) \rightarrow \eta\eta)/\Gamma_{\text{total}} \times \Gamma(\psi(2S) \rightarrow \gamma\chi_{c0}(1P))/\Gamma_{\text{total}}$$

VALUE (units $10^{-4}$ )	EVTS	DOCUMENT ID	TECN	COMMENT
<b>2.93 ± 0.18 OUR FIT</b>				
<b>3.12 ± 0.19 OUR AVERAGE</b>				
3.23 ± 0.09 ± 0.23	2132	112 ABLIKIM	10A BES3	$e^+e^- \rightarrow \psi(2S) \rightarrow \gamma\chi_{c0}$
2.93 ± 0.12 ± 0.29	0.9k	113 ASNER	09 CLEO	$\psi(2S) \rightarrow \gamma\eta\eta$
••• We do not use the following data for averages, fits, limits, etc. •••				
2.86 ± 0.46 ± 0.37	48	114 ADAMS	07 CLEO	$\psi(2S) \rightarrow \gamma\chi_{c0}$
112 Calculated by us. ABLIKIM 10A reports $B(\chi_{c0} \rightarrow \eta\eta) = (3.44 \pm 0.10 \pm 0.24 \pm 0.13) \times 10^{-3}$ using $B(\psi(2S) \rightarrow \gamma\chi_{c0}) = (9.4 \pm 0.4)\%$ . 113 Calculated by us. ASNER 09 reports $B(\chi_{c0} \rightarrow \eta\eta) = (3.18 \pm 0.13 \pm 0.31 \pm 0.16) \times 10^{-3}$ using $B(\psi(2S) \rightarrow \gamma\chi_{c0}) = (9.22 \pm 0.11 \pm 0.46)\%$ . 114 Superseded by ASNER 09. Calculated by us. The value of $B(\chi_{c0}(1P) \rightarrow \eta\eta)$ reported by ADAMS 07 was derived using $B(\psi(2S) \rightarrow \gamma\chi_{c0}(1P)) = (9.22 \pm 0.11 \pm 0.46)\%$ [ATHAR 04].				

$$\Gamma(\chi_{c0}(1P) \rightarrow \eta\eta)/\Gamma_{\text{total}} \times \Gamma(\psi(2S) \rightarrow \gamma\chi_{c0}(1P))/\Gamma(\psi(2S) \rightarrow J/\psi(1S)\pi^+\pi^-)$$

VALUE (units $10^{-3}$ )	DOCUMENT ID	TECN	COMMENT
<b>0.87 ± 0.05 OUR FIT</b>			
0.578 ± 0.241 ± 0.158	BAI	03c BES	$\psi(2S) \rightarrow \gamma\eta\eta$

$$\Gamma(\chi_{c0}(1P) \rightarrow K^+K^-)/\Gamma_{\text{total}} \times \Gamma(\psi(2S) \rightarrow \gamma\chi_{c0}(1P))/\Gamma_{\text{total}}$$

VALUE (units $10^{-4}$ )	EVTS	DOCUMENT ID	TECN	COMMENT
<b>5.87 ± 0.28 OUR FIT</b>				
5.97 ± 0.07 ± 0.32	8.1k	115 ASNER	09 CLEO	$\psi(2S) \rightarrow \gamma K^+K^-$
115 Calculated by us. ASNER 09 reports $B(\chi_{c0} \rightarrow K^+K^-) = (6.47 \pm 0.08 \pm 0.35 \pm 0.32) \times 10^{-3}$ using $B(\psi(2S) \rightarrow \gamma\chi_{c0}) = (9.22 \pm 0.11 \pm 0.46)\%$ .				

$$\Gamma(\chi_{c0}(1P) \rightarrow K^+K^-)/\Gamma_{\text{total}} \times \Gamma(\psi(2S) \rightarrow \gamma\chi_{c0}(1P))/\Gamma(\psi(2S) \rightarrow J/\psi(1S)\pi^+\pi^-)$$

VALUE (units $10^{-3}$ )	EVTS	DOCUMENT ID	TECN	COMMENT
<b>1.75 ± 0.09 OUR FIT</b>				
1.63 ± 0.10 ± 0.15	774 ± 38	116 BAI	98i BES	$\psi(2S) \rightarrow \gamma K^+K^-$
116 Calculated by us. The value for $B(\chi_{c0} \rightarrow K^+K^-)$ reported by BAI 98i is derived using $B(\psi(2S) \rightarrow \gamma\chi_{c0}) = (9.3 \pm 0.8)\%$ and $B(\psi(2S) \rightarrow J/\psi\pi^+\pi^-) = (32.4 \pm 2.6)\%$ [BAI 98d].				

$$\Gamma(\chi_{c0}(1P) \rightarrow K_S^0 K_S^0)/\Gamma_{\text{total}} \times \Gamma(\psi(2S) \rightarrow \gamma\chi_{c0}(1P))/\Gamma_{\text{total}}$$

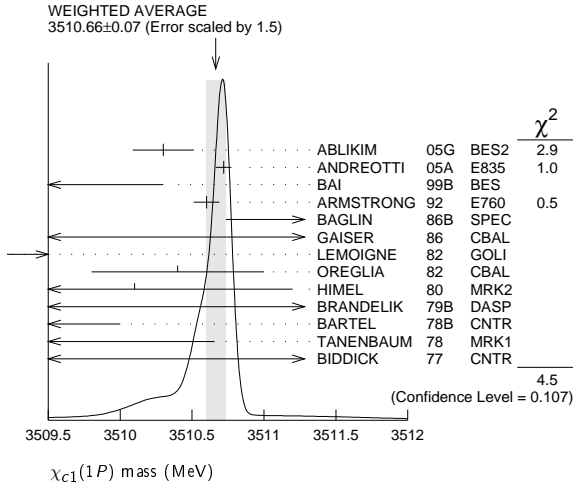
VALUE (units $10^{-4}$ )	EVTS	DOCUMENT ID	TECN	COMMENT
<b>3.04 ± 0.15 OUR FIT</b>				
<b>3.18 ± 0.17 OUR AVERAGE</b>				
3.22 ± 0.07 ± 0.17	2.1k	117 ASNER	09 CLEO	$\psi(2S) \rightarrow \gamma K_S^0 K_S^0$
3.02 ± 0.19 ± 0.33	322	ABLIKIM	05o BES2	$\psi(2S) \rightarrow \gamma K_S^0 K_S^0$
117 Calculated by us. ASNER 09 reports $B(\chi_{c0} \rightarrow K_S^0 K_S^0) = (3.49 \pm 0.08 \pm 0.18 \pm 0.17) \times 10^{-3}$ using $B(\psi(2S) \rightarrow \gamma\chi_{c0}) = (9.22 \pm 0.11 \pm 0.46)\%$ .				



See key on page 457

Meson Particle Listings

$\chi_{c1}(1P)$



$\Gamma_{34}$	$\rho\bar{\rho}$	$(7.3 \pm 0.4) \times 10^{-5}$	
$\Gamma_{35}$	$\rho\bar{\rho}\pi^0$	$(1.64 \pm 0.20) \times 10^{-4}$	
$\Gamma_{36}$	$\rho\bar{\rho}\eta$	$(1.53 \pm 0.26) \times 10^{-4}$	
$\Gamma_{37}$	$\rho\bar{\rho}\omega$	$(2.24 \pm 0.33) \times 10^{-4}$	
$\Gamma_{38}$	$\rho\bar{\rho}\phi$	$< 1.8 \times 10^{-5}$	CL=90%
$\Gamma_{39}$	$\rho\bar{\rho}\pi^+\pi^-$	$(5.0 \pm 1.9) \times 10^{-4}$	
$\Gamma_{40}$	$\rho\bar{\rho}\pi^0\pi^0$		
$\Gamma_{41}$	$\rho\bar{\rho}K^+K^-$ (non-resonant)	$(1.34 \pm 0.24) \times 10^{-4}$	
$\Gamma_{42}$	$\rho\bar{\rho}K_S^0 K_S^0$	$< 4.5 \times 10^{-4}$	CL=90%
$\Gamma_{43}$	$\Lambda\bar{\Lambda}$	$(1.18 \pm 0.19) \times 10^{-4}$	
$\Gamma_{44}$	$\Lambda\bar{\Lambda}\pi^+\pi^-$	$< 1.5 \times 10^{-3}$	CL=90%
$\Gamma_{45}$	$K^+\bar{p}\Lambda$	$(3.2 \pm 1.0) \times 10^{-4}$	
$\Gamma_{46}$	$K^+\rho\Lambda(1520) + c.c.$	$(1.8 \pm 0.5) \times 10^{-4}$	
$\Gamma_{47}$	$\Lambda(1520)\bar{\Lambda}(1520)$	$< 1.0 \times 10^{-4}$	CL=90%
$\Gamma_{48}$	$\Sigma^0\bar{\Sigma}^0$	$< 4 \times 10^{-5}$	CL=90%
$\Gamma_{49}$	$\Sigma^+\bar{\Sigma}^-$	$< 6 \times 10^{-5}$	CL=90%
$\Gamma_{50}$	$\Xi^0\bar{\Xi}^0$	$< 6 \times 10^{-5}$	CL=90%
$\Gamma_{51}$	$\Xi^-\bar{\Xi}^+$	$(8.4 \pm 2.3) \times 10^{-5}$	
$\Gamma_{52}$	$\pi^+\pi^-\pi^+K^+K^-$	$< 2.1 \times 10^{-3}$	
$\Gamma_{53}$	$K_S^0 K_S^0$	$< 6 \times 10^{-5}$	CL=90%

**$\chi_{c1}(1P)$  WIDTH**

VALUE (MeV)	CL%	EVTS	DOCUMENT ID	TECN	COMMENT
<b>0.86 ± 0.05 OUR FIT</b>					
<b>0.88 ± 0.05 OUR AVERAGE</b>					
1.39 +0.40 +0.26 -0.38 -0.77			ABLIKIM 05G BES2		$\psi(2S) \rightarrow \gamma\chi_{c1}$
0.876 ± 0.045 ± 0.026			ANDREOTTI 05A E835		$\rho\bar{\rho} \rightarrow e^+e^-\gamma$
0.87 ± 0.11 ± 0.08		513	6 ARMSTRONG 92 E760		$\bar{p}p \rightarrow e^+e^-\gamma$
<1.3	95		BAGLIN 86B SPEC		$\bar{p}p \rightarrow e^+e^-X$
<3.8	90		GAISER 86 CBAL		$\psi(2S) \rightarrow \gamma X$

• • • We do not use the following data for averages, fits, limits, etc. • • •

<sup>6</sup> Recalculated by ANDREOTTI 05A.

**$\chi_{c1}(1P)$  DECAY MODES**

Mode	Fraction ( $\Gamma_i/\Gamma$ )	Scale factor/ Confidence level
<b>Hadronic decays</b>		
$\Gamma_1$	$3(\pi^+\pi^-)$	$(5.8 \pm 1.4) \times 10^{-3}$ S=1.2
$\Gamma_2$	$2(\pi^+\pi^-\pi^0)$	$(7.6 \pm 2.6) \times 10^{-3}$
$\Gamma_3$	$\pi^+\pi^-\pi^0\pi^0$	$(1.26 \pm 0.17) \%$
$\Gamma_4$	$\rho^+\pi^-\pi^0 + c.c.$	$(1.53 \pm 0.26) \%$
$\Gamma_5$	$\rho^0\pi^+\pi^-$	$(3.9 \pm 3.5) \times 10^{-3}$
$\Gamma_6$	$4\pi^0$	$(5.7 \pm 0.8) \times 10^{-4}$
$\Gamma_7$	$\pi^+\pi^-K^+K^-$	$(4.5 \pm 1.0) \times 10^{-3}$
$\Gamma_8$	$K^+K^-\pi^0\pi^0$	$(1.18 \pm 0.29) \times 10^{-3}$
$\Gamma_9$	$K^+\pi^-K^0\pi^0 + c.c.$	$(9.0 \pm 1.5) \times 10^{-3}$
$\Gamma_{10}$	$\rho^+K^-K^0 + c.c.$	$(5.3 \pm 1.3) \times 10^{-3}$
$\Gamma_{11}$	$K^*(892)^0 K^0\pi^0 \rightarrow K^+\pi^-K^0\pi^0 + c.c.$	$(2.5 \pm 0.7) \times 10^{-3}$
$\Gamma_{12}$	$K^+K^-\eta\pi^0$	$(1.2 \pm 0.4) \times 10^{-3}$
$\Gamma_{13}$	$\pi^+\pi^-K_S^0 K_S^0$	$(7.2 \pm 3.1) \times 10^{-4}$
$\Gamma_{14}$	$K^+K^-\eta$	$(3.3 \pm 1.0) \times 10^{-4}$
$\Gamma_{15}$	$K^0 K^+\pi^- + c.c.$	$(7.3 \pm 0.6) \times 10^{-3}$
$\Gamma_{16}$	$K^*(892)^0 \bar{K}^0 + c.c.$	$(1.0 \pm 0.4) \times 10^{-3}$
$\Gamma_{17}$	$K^*(892)^+ K^- + c.c.$	$(1.5 \pm 0.7) \times 10^{-3}$
$\Gamma_{18}$	$K_S^*(1430)^0 \bar{K}^0 + c.c. \rightarrow K_S^0 K^+\pi^- + c.c.$	$< 8 \times 10^{-4}$ CL=90%
$\Gamma_{19}$	$K_S^*(1430)^+ K^- + c.c. \rightarrow K_S^0 K^+\pi^- + c.c.$	$< 2.3 \times 10^{-3}$ CL=90%
$\Gamma_{20}$	$K^+K^-\pi^0$	$(1.91 \pm 0.26) \times 10^{-3}$
$\Gamma_{21}$	$\eta\pi^+\pi^-$	$(5.0 \pm 0.5) \times 10^{-3}$
$\Gamma_{22}$	$a_0(980)^+\pi^-\pi^0 + c.c. \rightarrow \eta\pi^+\pi^-$	$(1.9 \pm 0.7) \times 10^{-3}$
$\Gamma_{23}$	$f_2(1270)\eta$	$(2.8 \pm 0.8) \times 10^{-3}$
$\Gamma_{24}$	$\pi^+\pi^-\eta'$	$(2.4 \pm 0.5) \times 10^{-3}$
$\Gamma_{25}$	$\pi^0 f_0(980) \rightarrow \pi^0\pi^+\pi^-$	$< 6 \times 10^{-6}$ CL=90%
$\Gamma_{26}$	$K^+\bar{K}^*(892)^0\pi^- + c.c.$	$(3.2 \pm 2.1) \times 10^{-3}$
$\Gamma_{27}$	$K^*(892)^0 \bar{K}^*(892)^0$	$(1.5 \pm 0.4) \times 10^{-3}$
$\Gamma_{28}$	$K^+K^-K_S^0 K_S^0$	$< 5 \times 10^{-4}$ CL=90%
$\Gamma_{29}$	$K^+K^-K^+K^-$	$(5.6 \pm 1.2) \times 10^{-4}$
$\Gamma_{30}$	$K^+K^-\phi$	$(4.3 \pm 1.6) \times 10^{-4}$
$\Gamma_{31}$	$\omega\omega$	$(6.0 \pm 0.7) \times 10^{-4}$
$\Gamma_{32}$	$\omega\phi$	$(2.2 \pm 0.6) \times 10^{-5}$
$\Gamma_{33}$	$\phi\phi$	$(4.4 \pm 0.6) \times 10^{-4}$

**Radiative decays**

$\Gamma_{54}$	$\gamma J/\psi(1S)$	$(34.4 \pm 1.5) \%$
$\Gamma_{55}$	$\gamma\rho^0$	$(2.28 \pm 0.19) \times 10^{-4}$
$\Gamma_{56}$	$\gamma\omega$	$(7.1 \pm 0.9) \times 10^{-5}$
$\Gamma_{57}$	$\gamma\phi$	$(2.6 \pm 0.6) \times 10^{-5}$
$\Gamma_{58}$	$\gamma\gamma$	

**CONSTRAINED FIT INFORMATION**

A multiparticle fit to  $\chi_{c1}(1P)$ ,  $\chi_{c0}(1P)$ ,  $\chi_{c2}(1P)$ , and  $\psi(2S)$  with 4 total widths, a partial width, 25 combinations of partial widths obtained from integrated cross section, and 84 branching ratios uses 223 measurements to determine 49 parameters. The overall fit has a  $\chi^2 = 312.2$  for 174 degrees of freedom.

The following *off-diagonal* array elements are the correlation coefficients  $\langle \delta p_i \delta p_j \rangle / (\delta p_i \delta p_j)$ , in percent, from the fit to parameters  $p_i$ , including the branching fractions,  $x_i \equiv \Gamma_i/\Gamma_{total}$ .

$x_{29}$	8				
$x_{34}$	-9	-4			
$x_{43}$	11	5	-5		
$x_{54}$	36	16	-32	20	
$\Gamma$	-13	-5	-59	-7	-30
	$x_{15}$	$x_{29}$	$x_{34}$	$x_{43}$	$x_{54}$

**$\chi_{c1}(1P)$  PARTIAL WIDTHS**

**$\chi_{c1}(1P) \Gamma(i)\Gamma(\gamma J/\psi(1S))/\Gamma_{total}$**

$\Gamma(\rho\bar{\rho}) \times \Gamma(\gamma J/\psi(1S))/\Gamma_{total}$	DOCUMENT ID	TECN	COMMENT
<b>21.7 ± 0.8 OUR FIT</b>			
<b>21.4 ± 0.9 OUR AVERAGE</b>			
21.5 ± 0.5 ± 0.8	<sup>7</sup> ANDREOTTI 05A E835		$\rho\bar{\rho} \rightarrow e^+e^-\gamma$
21.4 ± 1.5 ± 2.2	<sup>7,8</sup> ARMSTRONG 92 E760		$\bar{p}p \rightarrow e^+e^-\gamma$
19.9 ± 4.4 -4.0	<sup>7</sup> BAGLIN 86B SPEC		$\bar{p}p \rightarrow e^+e^-X$

<sup>7</sup> Calculated by us using  $B(J/\psi(1S) \rightarrow e^+e^-) = 0.0593 \pm 0.0010$ .  
<sup>8</sup> Recalculated by ANDREOTTI 05A.

**$\chi_{c1}(1P)$  BRANCHING RATIOS**

**HADRONIC DECAYS**

$\Gamma(3(\pi^+\pi^-))/\Gamma_{total}$	DOCUMENT ID	TECN	COMMENT
<b>5.8 ± 1.4 OUR EVALUATION</b>			Error includes scale factor of 1.2. Treating systematic error as correlated.
<b>5.8 ± 1.1 OUR AVERAGE</b>			
5.4 ± 0.7 ± 0.9	<sup>9</sup> BAI 99B BES		$\psi(2S) \rightarrow \gamma\chi_{c1}$
16.0 ± 5.9 ± 0.8	<sup>9</sup> TANENBAUM 78 MRK1		$\psi(2S) \rightarrow \gamma\chi_{c1}$

<sup>9</sup> Rescaled by us using  $B(\psi(2S) \rightarrow \gamma\chi_{c1}) = (8.8 \pm 0.4)\%$  and  $B(\psi(2S) \rightarrow J/\psi(1S)\pi^+\pi^-) = (32.6 \pm 0.5)\%$ .

## Meson Particle Listings

 $\chi_{c1}(1P)$  $\Gamma(2(\pi^+\pi^-))/\Gamma_{\text{total}}$   $\Gamma_2/\Gamma$ 

VALUE (units $10^{-3}$ )	DOCUMENT ID	TECN	COMMENT
<b>7.6<math>\pm</math>2.6 OUR EVALUATION</b>	Treating systematic error as correlated.		
<b>8 <math>\pm</math>4 OUR AVERAGE</b>	Error includes scale factor of 1.5.		
4.6 $\pm$ 2.1 $\pm$ 2.6	10 BAI	99B	BES $\psi(2S) \rightarrow \gamma\chi_{c1}$
12.5 $\pm$ 4.2 $\pm$ 0.6	10 TANENBAUM	78	MRK1 $\psi(2S) \rightarrow \gamma\chi_{c1}$
10 Rescaled by us using $B(\psi(2S) \rightarrow \gamma\chi_{c1}) = (8.8 \pm 0.4)\%$ and $B(\psi(2S) \rightarrow J/\psi(1S)\pi^+\pi^-) = (32.6 \pm 0.5)\%$ .			

 $\Gamma(\pi^+\pi^-\pi^0)/\Gamma_{\text{total}}$   $\Gamma_3/\Gamma$ 

VALUE (%)	EVTS	DOCUMENT ID	TECN	COMMENT
<b>1.26<math>\pm</math>0.16<math>\pm</math>0.05</b>	604.7	11 HE	08B	CLEO $e^+e^- \rightarrow \gamma h^+ h^- h^0 h^0$
11 HE 08B reports $1.28 \pm 0.06 \pm 0.15 \pm 0.08\%$ from a measurement of $[\Gamma(\chi_{c1}(1P) \rightarrow \pi^+\pi^-\pi^0)/\Gamma_{\text{total}}] \times [B(\psi(2S) \rightarrow \gamma\chi_{c1}(1P))]$ assuming $B(\psi(2S) \rightarrow \gamma\chi_{c1}(1P)) = (9.07 \pm 0.11 \pm 0.54) \times 10^{-2}$ , which we rescale to our best value $B(\psi(2S) \rightarrow \gamma\chi_{c1}(1P)) = (9.2 \pm 0.4) \times 10^{-2}$ . Our first error is their experiment's error and our second error is the systematic error from using our best value.				

 $\Gamma(\rho^+\pi^-\pi^0 + c.c.)/\Gamma_{\text{total}}$   $\Gamma_4/\Gamma$ 

VALUE (%)	EVTS	DOCUMENT ID	TECN	COMMENT
<b>1.53<math>\pm</math>0.25<math>\pm</math>0.06</b>	712.3	12,13 HE	08B	CLEO $e^+e^- \rightarrow \gamma h^+ h^- h^0 h^0$
12 HE 08B reports $1.56 \pm 0.13 \pm 0.22 \pm 0.10\%$ from a measurement of $[\Gamma(\chi_{c1}(1P) \rightarrow \rho^+\pi^-\pi^0 + c.c.)/\Gamma_{\text{total}}] \times [B(\psi(2S) \rightarrow \gamma\chi_{c1}(1P))]$ assuming $B(\psi(2S) \rightarrow \gamma\chi_{c1}(1P)) = (9.07 \pm 0.11 \pm 0.54) \times 10^{-2}$ , which we rescale to our best value $B(\psi(2S) \rightarrow \gamma\chi_{c1}(1P)) = (9.2 \pm 0.4) \times 10^{-2}$ . Our first error is their experiment's error and our second error is the systematic error from using our best value.				
13 Calculated by us. We have added the values from HE 08B for $\rho^+\pi^-\pi^0$ and $\rho^-\pi^+\pi^0$ decays assuming uncorrelated statistical and fully correlated systematic uncertainties.				

 $\Gamma(\rho^0\pi^+\pi^-)/\Gamma_{\text{total}}$   $\Gamma_5/\Gamma$ 

VALUE (units $10^{-4}$ )	DOCUMENT ID	TECN	COMMENT
<b>39<math>\pm</math>35</b>	14 TANENBAUM	78	MRK1 $\psi(2S) \rightarrow \gamma\chi_{c1}$
14 Estimated using $B(\psi(2S) \rightarrow \gamma\chi_{c1}(1P)) = 0.087$ . The errors do not contain the uncertainty in the $\psi(2S)$ decay.			

 $\Gamma(4\pi^0)/\Gamma_{\text{total}}$   $\Gamma_6/\Gamma$ 

VALUE (units $10^{-3}$ )	EVTS	DOCUMENT ID	TECN	COMMENT
<b>0.57<math>\pm</math>0.03<math>\pm</math>0.08</b>	608	15 ABLIKIM	11A	BES3 $e^+e^- \rightarrow \psi(2S) \rightarrow \gamma\chi_{c1}$
15 ABLIKIM 11A reports $(0.57 \pm 0.03 \pm 0.08) \times 10^{-3}$ from a measurement of $[\Gamma(\chi_{c1}(1P) \rightarrow 4\pi^0)/\Gamma_{\text{total}}] \times [B(\psi(2S) \rightarrow \gamma\chi_{c1}(1P))]$ assuming $B(\psi(2S) \rightarrow \gamma\chi_{c1}(1P)) = (9.2 \pm 0.4) \times 10^{-2}$ .				

 $\Gamma(\pi^+\pi^-K^+K^-)/\Gamma_{\text{total}}$   $\Gamma_7/\Gamma$ 

VALUE (units $10^{-3}$ )	DOCUMENT ID	TECN	COMMENT
<b>4.5<math>\pm</math>1.0 OUR EVALUATION</b>	Treating systematic error as correlated.		
<b>4.5<math>\pm</math>0.9 OUR AVERAGE</b>			
4.2 $\pm$ 0.4 $\pm$ 0.9	16 BAI	99B	BES $\psi(2S) \rightarrow \gamma\chi_{c1}$
7.3 $\pm$ 3.0 $\pm$ 0.4	16 TANENBAUM	78	MRK1 $\psi(2S) \rightarrow \gamma\chi_{c1}$
16 Rescaled by us using $B(\psi(2S) \rightarrow \gamma\chi_{c1}) = (8.8 \pm 0.4)\%$ and $B(\psi(2S) \rightarrow J/\psi(1S)\pi^+\pi^-) = (32.6 \pm 0.5)\%$ .			

 $\Gamma(K^+K^-\pi^0\pi^0)/\Gamma_{\text{total}}$   $\Gamma_8/\Gamma$ 

VALUE (%)	EVTS	DOCUMENT ID	TECN	COMMENT
<b>0.118<math>\pm</math>0.029<math>\pm</math>0.005</b>	45.1	17 HE	08B	CLEO $e^+e^- \rightarrow \gamma h^+ h^- h^0 h^0$
17 HE 08B reports $0.12 \pm 0.02 \pm 0.02 \pm 0.01\%$ from a measurement of $[\Gamma(\chi_{c1}(1P) \rightarrow K^+K^-\pi^0\pi^0)/\Gamma_{\text{total}}] \times [B(\psi(2S) \rightarrow \gamma\chi_{c1}(1P))]$ assuming $B(\psi(2S) \rightarrow \gamma\chi_{c1}(1P)) = (9.07 \pm 0.11 \pm 0.54) \times 10^{-2}$ , which we rescale to our best value $B(\psi(2S) \rightarrow \gamma\chi_{c1}(1P)) = (9.2 \pm 0.4) \times 10^{-2}$ . Our first error is their experiment's error and our second error is the systematic error from using our best value.				

 $\Gamma(K^+\pi^-K^0\pi^0 + c.c.)/\Gamma_{\text{total}}$   $\Gamma_9/\Gamma$ 

VALUE (%)	EVTS	DOCUMENT ID	TECN	COMMENT
<b>0.90<math>\pm</math>0.14<math>\pm</math>0.03</b>	141.3	18 HE	08B	CLEO $e^+e^- \rightarrow \gamma h^+ h^- h^0 h^0$
18 HE 08B reports $0.92 \pm 0.09 \pm 0.11 \pm 0.06\%$ from a measurement of $[\Gamma(\chi_{c1}(1P) \rightarrow K^+\pi^-K^0\pi^0 + c.c.)/\Gamma_{\text{total}}] \times [B(\psi(2S) \rightarrow \gamma\chi_{c1}(1P))]$ assuming $B(\psi(2S) \rightarrow \gamma\chi_{c1}(1P)) = (9.07 \pm 0.11 \pm 0.54) \times 10^{-2}$ , which we rescale to our best value $B(\psi(2S) \rightarrow \gamma\chi_{c1}(1P)) = (9.2 \pm 0.4) \times 10^{-2}$ . Our first error is their experiment's error and our second error is the systematic error from using our best value.				

 $\Gamma(\rho^+K^-K^0 + c.c.)/\Gamma_{\text{total}}$   $\Gamma_{10}/\Gamma$ 

VALUE (%)	EVTS	DOCUMENT ID	TECN	COMMENT
<b>0.53<math>\pm</math>0.13<math>\pm</math>0.02</b>	141.3	19 HE	08B	CLEO $e^+e^- \rightarrow \gamma h^+ h^- h^0 h^0$
19 HE 08B reports $0.54 \pm 0.11 \pm 0.07 \pm 0.03\%$ from a measurement of $[\Gamma(\chi_{c1}(1P) \rightarrow \rho^+K^-K^0 + c.c.)/\Gamma_{\text{total}}] \times [B(\psi(2S) \rightarrow \gamma\chi_{c1}(1P))]$ assuming $B(\psi(2S) \rightarrow \gamma\chi_{c1}(1P)) = (9.07 \pm 0.11 \pm 0.54) \times 10^{-2}$ , which we rescale to our best value $B(\psi(2S) \rightarrow \gamma\chi_{c1}(1P)) = (9.2 \pm 0.4) \times 10^{-2}$ . Our first error is their experiment's error and our second error is the systematic error from using our best value.				

 $\Gamma(K^*(892)^0K^0\pi^0 \rightarrow K^+\pi^-K^0\pi^0 + c.c.)/\Gamma_{\text{total}}$   $\Gamma_{11}/\Gamma$ 

VALUE (%)	EVTS	DOCUMENT ID	TECN	COMMENT
<b>0.25<math>\pm</math>0.07<math>\pm</math>0.01</b>	141.3	20 HE	08B	CLEO $e^+e^- \rightarrow \gamma h^+ h^- h^0 h^0$
20 HE 08B reports $0.25 \pm 0.06 \pm 0.03 \pm 0.02\%$ from a measurement of $[\Gamma(\chi_{c1}(1P) \rightarrow K^*(892)^0K^0\pi^0 \rightarrow K^+\pi^-K^0\pi^0 + c.c.)/\Gamma_{\text{total}}] \times [B(\psi(2S) \rightarrow \gamma\chi_{c1}(1P))]$ assuming $B(\psi(2S) \rightarrow \gamma\chi_{c1}(1P)) = (9.07 \pm 0.11 \pm 0.54) \times 10^{-2}$ , which we rescale to our best value $B(\psi(2S) \rightarrow \gamma\chi_{c1}(1P)) = (9.2 \pm 0.4) \times 10^{-2}$ . Our first error is their experiment's error and our second error is the systematic error from using our best value.				

 $\Gamma(K^+K^-\eta\pi^0)/\Gamma_{\text{total}}$   $\Gamma_{12}/\Gamma$ 

VALUE (%)	EVTS	DOCUMENT ID	TECN	COMMENT
<b>0.118<math>\pm</math>0.036<math>\pm</math>0.005</b>	141.3	21 HE	08B	CLEO $e^+e^- \rightarrow \gamma h^+ h^- h^0 h^0$
21 HE 08B reports $0.12 \pm 0.03 \pm 0.02 \pm 0.01\%$ from a measurement of $[\Gamma(\chi_{c1}(1P) \rightarrow K^+K^-\eta\pi^0)/\Gamma_{\text{total}}] \times [B(\psi(2S) \rightarrow \gamma\chi_{c1}(1P))]$ assuming $B(\psi(2S) \rightarrow \gamma\chi_{c1}(1P)) = (9.07 \pm 0.11 \pm 0.54) \times 10^{-2}$ , which we rescale to our best value $B(\psi(2S) \rightarrow \gamma\chi_{c1}(1P)) = (9.2 \pm 0.4) \times 10^{-2}$ . Our first error is their experiment's error and our second error is the systematic error from using our best value.				

 $\Gamma(\pi^+\pi^-K_S^0K_S^0)/\Gamma_{\text{total}}$   $\Gamma_{13}/\Gamma$ 

VALUE (units $10^{-4}$ )	EVTS	DOCUMENT ID	TECN	COMMENT
<b>7.2<math>\pm</math>3.1<math>\pm</math>0.3</b>	19.8 $\pm$ 7.7	22 ABLIKIM	05o	BES2 $\psi(2S) \rightarrow \chi_{c1}\gamma$
22 ABLIKIM 05o reports $[\Gamma(\chi_{c1}(1P) \rightarrow \pi^+\pi^-K_S^0K_S^0)/\Gamma_{\text{total}}] \times [B(\psi(2S) \rightarrow \gamma\chi_{c1}(1P))]$ = $(0.67 \pm 0.26 \pm 0.11) \times 10^{-4}$ which we divide by our best value $B(\psi(2S) \rightarrow \gamma\chi_{c1}(1P)) = (9.2 \pm 0.4) \times 10^{-2}$ . Our first error is their experiment's error and our second error is the systematic error from using our best value.				

 $\Gamma(K^+K^-\eta)/\Gamma_{\text{total}}$   $\Gamma_{14}/\Gamma$ 

VALUE (units $10^{-3}$ )	DOCUMENT ID	TECN	COMMENT
<b>0.33<math>\pm</math>0.10<math>\pm</math>0.01</b>	23 ATHAR	07	CLEO $\psi(2S) \rightarrow \gamma h^+ h^- h^0$
23 ATHAR 07 reports $(0.34 \pm 0.10 \pm 0.04) \times 10^{-3}$ from a measurement of $[\Gamma(\chi_{c1}(1P) \rightarrow K^+K^-\eta)/\Gamma_{\text{total}}] \times [B(\psi(2S) \rightarrow \gamma\chi_{c1}(1P))]$ assuming $B(\psi(2S) \rightarrow \gamma\chi_{c1}(1P)) = 0.0907 \pm 0.0011 \pm 0.0054$ , which we rescale to our best value $B(\psi(2S) \rightarrow \gamma\chi_{c1}(1P)) = (9.2 \pm 0.4) \times 10^{-2}$ . Our first error is their experiment's error and our second error is the systematic error from using our best value.			

 $\Gamma(K^0K^+\pi^- + c.c.)/\Gamma_{\text{total}}$   $\Gamma_{15}/\Gamma$ 

VALUE (units $10^{-3}$ )	DOCUMENT ID
<b>7.3<math>\pm</math>0.6 OUR FIT</b>	

 $\Gamma(K^*(892)^0\bar{K}^0 + c.c.)/\Gamma_{\text{total}}$   $\Gamma_{16}/\Gamma$ 

VALUE (units $10^{-3}$ )	EVTS	DOCUMENT ID	TECN	COMMENT
<b>1.03<math>\pm</math>0.38<math>\pm</math>0.04</b>	22	24 ABLIKIM	06R	BES2 $\psi(2S) \rightarrow \gamma\chi_{c1}$
24 ABLIKIM 06R reports $(1.1 \pm 0.4 \pm 0.1) \times 10^{-3}$ from a measurement of $[\Gamma(\chi_{c1}(1P) \rightarrow K^*(892)^0\bar{K}^0 + c.c.)/\Gamma_{\text{total}}] \times [B(\psi(2S) \rightarrow \gamma\chi_{c1}(1P))]$ assuming $B(\psi(2S) \rightarrow \gamma\chi_{c1}(1P)) = (8.7 \pm 0.4) \times 10^{-2}$ , which we rescale to our best value $B(\psi(2S) \rightarrow \gamma\chi_{c1}(1P)) = (9.2 \pm 0.4) \times 10^{-2}$ . Our first error is their experiment's error and our second error is the systematic error from using our best value.				

 $\Gamma(K^*(892)^+K^- + c.c.)/\Gamma_{\text{total}}$   $\Gamma_{17}/\Gamma$ 

VALUE (units $10^{-3}$ )	EVTS	DOCUMENT ID	TECN	COMMENT
<b>1.5<math>\pm</math>0.7<math>\pm</math>0.1</b>	27	25 ABLIKIM	06R	BES2 $\psi(2S) \rightarrow \gamma\chi_{c1}$
25 ABLIKIM 06R reports $(1.6 \pm 0.7 \pm 0.2) \times 10^{-3}$ from a measurement of $[\Gamma(\chi_{c1}(1P) \rightarrow K^*(892)^+K^- + c.c.)/\Gamma_{\text{total}}] \times [B(\psi(2S) \rightarrow \gamma\chi_{c1}(1P))]$ assuming $B(\psi(2S) \rightarrow \gamma\chi_{c1}(1P)) = (8.7 \pm 0.4) \times 10^{-2}$ , which we rescale to our best value $B(\psi(2S) \rightarrow \gamma\chi_{c1}(1P)) = (9.2 \pm 0.4) \times 10^{-2}$ . Our first error is their experiment's error and our second error is the systematic error from using our best value.				

 $\Gamma(K_S^*(1430)^0\bar{K}^0 + c.c. \rightarrow K_S^0K^+\pi^- + c.c.)/\Gamma_{\text{total}}$   $\Gamma_{18}/\Gamma$ 

VALUE (units $10^{-3}$ )	CL%	DOCUMENT ID	TECN	COMMENT
<b>&lt;0.8</b>	90	26 ABLIKIM	06R	BES2 $\psi(2S) \rightarrow \gamma\chi_{c1}$
26 ABLIKIM 06R reports $< 0.9 \times 10^{-3}$ from a measurement of $[\Gamma(\chi_{c1}(1P) \rightarrow K_S^*(1430)^0\bar{K}^0 + c.c. \rightarrow K_S^0K^+\pi^- + c.c.)/\Gamma_{\text{total}}] \times [B(\psi(2S) \rightarrow \gamma\chi_{c1}(1P))]$ assuming $B(\psi(2S) \rightarrow \gamma\chi_{c1}(1P)) = (8.7 \pm 0.4) \times 10^{-2}$ , which we rescale to our best value $B(\psi(2S) \rightarrow \gamma\chi_{c1}(1P)) = 9.2 \times 10^{-2}$ .				

 $\Gamma(K_S^*(1430)^+K^- + c.c. \rightarrow K_S^0K^+\pi^- + c.c.)/\Gamma_{\text{total}}$   $\Gamma_{19}/\Gamma$ 

VALUE (units $10^{-3}$ )	CL%	DOCUMENT ID	TECN	COMMENT
<b>&lt;2.3</b>	90	27 ABLIKIM	06R	BES2 $\psi(2S) \rightarrow \gamma\chi_{c1}$
27 ABLIKIM 06R reports $< 2.4 \times 10^{-3}$ from a measurement of $[\Gamma(\chi_{c1}(1P) \rightarrow K_S^*(1430)^+K^- + c.c. \rightarrow K_S^0K^+\pi^- + c.c.)/\Gamma_{\text{total}}] \times [B(\psi(2S) \rightarrow \gamma\chi_{c1}(1P))]$ assuming $B(\psi(2S) \rightarrow \gamma\chi_{c1}(1P)) = (8.7 \pm 0.4) \times 10^{-2}$ , which we rescale to our best value $B(\psi(2S) \rightarrow \gamma\chi_{c1}(1P)) = 9.2 \times 10^{-2}$ .				

 $\Gamma(K^+K^-\pi^0)/\Gamma_{\text{total}}$   $\Gamma_{20}/\Gamma$ 

VALUE (units $10^{-3}$ )	DOCUMENT ID	TECN	COMMENT
<b>1.91<math>\pm</math>0.25<math>\pm</math>0.07</b>	28 ATHAR	07	CLEO $\psi(2S) \rightarrow \gamma h^+ h^- h^0$
28 ATHAR 07 reports $(1.95 \pm 0.16 \pm 0.23) \times 10^{-3}$ from a measurement of $[\Gamma(\chi_{c1}(1P) \rightarrow K^+K^-\pi^0)/\Gamma_{\text{total}}] \times [B(\psi(2S) \rightarrow \gamma\chi_{c1}(1P))]$ assuming $B(\psi(2S) \rightarrow \gamma\chi_{c1}(1P)) = 0.0907 \pm 0.0011 \pm 0.0054$ , which we rescale to our best value $B(\psi(2S) \rightarrow \gamma\chi_{c1}(1P)) = (9.2 \pm 0.4) \times 10^{-2}$ . Our first error is their experiment's error and our second error is the systematic error from using our best value.			



$\Gamma(\eta\pi^+\pi^-)/\Gamma_{\text{total}}$   $\Gamma_{21}/\Gamma$ 

VALUE (units $10^{-3}$ )	EVTS	DOCUMENT ID	TECN	COMMENT
<b>5.0 ± 0.5 OUR AVERAGE</b>				
4.9 ± 0.5 ± 0.2		29 ATHAR	07 CLEO	$\psi(2S) \rightarrow \gamma h^+ h^- h^0$
5.5 ± 1.0 ± 0.2	222	30 ABLIKIM	06R BES2	$\psi(2S) \rightarrow \gamma \chi_{c1}$
29 ATHAR 07 reports $(5.0 \pm 0.3 \pm 0.5) \times 10^{-3}$ from a measurement of $[\Gamma(\chi_{c1}(1P) \rightarrow \eta\pi^+\pi^-)/\Gamma_{\text{total}}] \times [B(\psi(2S) \rightarrow \gamma\chi_{c1}(1P))]$ assuming $B(\psi(2S) \rightarrow \gamma\chi_{c1}(1P)) = 0.0907 \pm 0.0011 \pm 0.0054$ , which we rescale to our best value $B(\psi(2S) \rightarrow \gamma\chi_{c1}(1P)) = (9.2 \pm 0.4) \times 10^{-2}$ . Our first error is their experiment's error and our second error is the systematic error from using our best value.				
30 ABLIKIM 06R reports $(5.9 \pm 0.7 \pm 0.8) \times 10^{-3}$ from a measurement of $[\Gamma(\chi_{c1}(1P) \rightarrow \eta\pi^+\pi^-)/\Gamma_{\text{total}}] \times [B(\psi(2S) \rightarrow \gamma\chi_{c1}(1P))]$ assuming $B(\psi(2S) \rightarrow \gamma\chi_{c1}(1P)) = (8.7 \pm 0.4) \times 10^{-2}$ , which we rescale to our best value $B(\psi(2S) \rightarrow \gamma\chi_{c1}(1P)) = (9.2 \pm 0.4) \times 10^{-2}$ . Our first error is their experiment's error and our second error is the systematic error from using our best value.				

 $\Gamma(a_0(980)^+\pi^-\pi^+ \text{ c.c.} \rightarrow \eta\pi^+\pi^-)/\Gamma_{\text{total}}$   $\Gamma_{22}/\Gamma$ 

VALUE (units $10^{-3}$ )	EVTS	DOCUMENT ID	TECN	COMMENT
<b>1.9 ± 0.7 ± 0.1</b>	58	31 ABLIKIM	06R BES2	$\psi(2S) \rightarrow \gamma \chi_{c1}$
31 ABLIKIM 06R reports $(2.0 \pm 0.5 \pm 0.5) \times 10^{-3}$ from a measurement of $[\Gamma(\chi_{c1}(1P) \rightarrow a_0(980)^+\pi^-\pi^+ \text{ c.c.} \rightarrow \eta\pi^+\pi^-)/\Gamma_{\text{total}}] \times [B(\psi(2S) \rightarrow \gamma\chi_{c1}(1P))]$ assuming $B(\psi(2S) \rightarrow \gamma\chi_{c1}(1P)) = (8.7 \pm 0.4) \times 10^{-2}$ , which we rescale to our best value $B(\psi(2S) \rightarrow \gamma\chi_{c1}(1P)) = (9.2 \pm 0.4) \times 10^{-2}$ . Our first error is their experiment's error and our second error is the systematic error from using our best value.				

 $\Gamma(f_2(1270)\eta)/\Gamma_{\text{total}}$   $\Gamma_{23}/\Gamma$ 

VALUE (units $10^{-3}$ )	EVTS	DOCUMENT ID	TECN	COMMENT
<b>2.8 ± 0.8 ± 0.1</b>	53	32 ABLIKIM	06R BES2	$\psi(2S) \rightarrow \gamma \chi_{c1}$
32 ABLIKIM 06R reports $(3.0 \pm 0.7 \pm 0.5) \times 10^{-3}$ from a measurement of $[\Gamma(\chi_{c1}(1P) \rightarrow f_2(1270)\eta)/\Gamma_{\text{total}}] \times [B(\psi(2S) \rightarrow \gamma\chi_{c1}(1P))]$ assuming $B(\psi(2S) \rightarrow \gamma\chi_{c1}(1P)) = (8.7 \pm 0.4) \times 10^{-2}$ , which we rescale to our best value $B(\psi(2S) \rightarrow \gamma\chi_{c1}(1P)) = (9.2 \pm 0.4) \times 10^{-2}$ . Our first error is their experiment's error and our second error is the systematic error from using our best value.				

 $\Gamma(\pi^+\pi^-\eta)/\Gamma_{\text{total}}$   $\Gamma_{24}/\Gamma$ 

VALUE (units $10^{-3}$ )	DOCUMENT ID	TECN	COMMENT
<b>2.4 ± 0.5 ± 0.1</b>	33 ATHAR	07 CLEO	$\psi(2S) \rightarrow \gamma h^+ h^- h^0$
33 ATHAR 07 reports $(2.4 \pm 0.4 \pm 0.3) \times 10^{-3}$ from a measurement of $[\Gamma(\chi_{c1}(1P) \rightarrow \pi^+\pi^-\eta)/\Gamma_{\text{total}}] \times [B(\psi(2S) \rightarrow \gamma\chi_{c1}(1P))]$ assuming $B(\psi(2S) \rightarrow \gamma\chi_{c1}(1P)) = 0.0907 \pm 0.0011 \pm 0.0054$ , which we rescale to our best value $B(\psi(2S) \rightarrow \gamma\chi_{c1}(1P)) = (9.2 \pm 0.4) \times 10^{-2}$ . Our first error is their experiment's error and our second error is the systematic error from using our best value.			

 $\Gamma(\pi^0 f_0(980) \rightarrow \pi^0\pi^+\pi^-)/\Gamma_{\text{total}}$   $\Gamma_{25}/\Gamma$ 

VALUE	CL%	DOCUMENT ID	TECN	COMMENT
<b>&lt; 6 × 10<sup>-6</sup></b>	90	34 ABLIKIM	11D BES3	$\psi(2S) \rightarrow \gamma\pi^0\pi^+\pi^-$
34 ABLIKIM 11D reports $[\Gamma(\chi_{c1}(1P) \rightarrow \pi^0 f_0(980) \rightarrow \pi^0\pi^+\pi^-)/\Gamma_{\text{total}}] \times [B(\psi(2S) \rightarrow \gamma\chi_{c1}(1P))] < 6.0 \times 10^{-7}$ which we divide by our best value $B(\psi(2S) \rightarrow \gamma\chi_{c1}(1P)) = 9.2 \times 10^{-2}$ .				

 $\Gamma(K^+ \bar{K}^*(892)^0 \pi^- \text{ c.c.})/\Gamma_{\text{total}}$   $\Gamma_{26}/\Gamma$ 

VALUE (units $10^{-4}$ )	DOCUMENT ID	TECN	COMMENT
<b>32 ± 21</b>	35 TANENBAUM	78 MRK1	$\psi(2S) \rightarrow \gamma \chi_{c1}$
35 Estimated using $B(\psi(2S) \rightarrow \gamma\chi_{c1}(1P)) = 0.087$ . The errors do not contain the uncertainty in the $\psi(2S)$ decay.			

 $\Gamma(K^*(892)^0 \bar{K}^*(892)^0)/\Gamma_{\text{total}}$   $\Gamma_{27}/\Gamma$ 

VALUE (units $10^{-3}$ )	EVTS	DOCUMENT ID	TECN	COMMENT
<b>1.5 ± 0.4 ± 0.1</b>	28.4 ± 5.5	36,37 ABLIKIM	04H BES	$\psi(2S) \rightarrow \gamma K^+ K^- \pi^+ \pi^-$
36 ABLIKIM 04H reports $[\Gamma(\chi_{c1}(1P) \rightarrow K^*(892)^0 \bar{K}^*(892)^0)/\Gamma_{\text{total}}] \times [B(\psi(2S) \rightarrow \gamma\chi_{c1}(1P))] = (1.40 \pm 0.27 \pm 0.22) \times 10^{-4}$ which we divide by our best value $B(\psi(2S) \rightarrow \gamma\chi_{c1}(1P)) = (9.2 \pm 0.4) \times 10^{-2}$ . Our first error is their experiment's error and our second error is the systematic error from using our best value.				
37 Assumes $B(K^*(892)^0 \rightarrow K^- \pi^+) = 2/3$ .				

 $\Gamma(K^+ K^- K_S^0 K_S^0)/\Gamma_{\text{total}}$   $\Gamma_{28}/\Gamma$ 

VALUE (units $10^{-4}$ )	CL%	EVTS	DOCUMENT ID	TECN	COMMENT
<b>&lt; 5</b>	90	3.2 ± 2.4	38 ABLIKIM	05o BES2	$\psi(2S) \rightarrow \chi_{c1}\gamma$
38 ABLIKIM 05o reports $[\Gamma(\chi_{c1}(1P) \rightarrow K^+ K^- K_S^0 K_S^0)/\Gamma_{\text{total}}] \times [B(\psi(2S) \rightarrow \gamma\chi_{c1}(1P))] < 4.2 \times 10^{-5}$ which we divide by our best value $B(\psi(2S) \rightarrow \gamma\chi_{c1}(1P)) = 9.2 \times 10^{-2}$ .					

 $\Gamma(K^+ K^- K^+ K^-)/\Gamma_{\text{total}}$   $\Gamma_{29}/\Gamma$ 

VALUE (units $10^{-3}$ )	DOCUMENT ID
<b>0.56 ± 0.12 OUR FIT</b>	

 $\Gamma(K^+ K^- \phi)/\Gamma_{\text{total}}$   $\Gamma_{30}/\Gamma$ 

VALUE (units $10^{-3}$ )	EVTS	DOCUMENT ID	TECN	COMMENT
<b>0.43 ± 0.16 ± 0.02</b>	17	39 ABLIKIM	06T BES2	$\psi(2S) \rightarrow \gamma 2K^+ 2K^-$
39 ABLIKIM 06T reports $(0.46 \pm 0.16 \pm 0.06) \times 10^{-3}$ from a measurement of $[\Gamma(\chi_{c1}(1P) \rightarrow K^+ K^- \phi)/\Gamma_{\text{total}}] \times [B(\psi(2S) \rightarrow \gamma\chi_{c1}(1P))]$ assuming $B(\psi(2S) \rightarrow \gamma\chi_{c1}(1P)) = (8.7 \pm 0.4) \times 10^{-2}$ , which we rescale to our best value $B(\psi(2S) \rightarrow \gamma\chi_{c1}(1P)) = (9.2 \pm 0.4) \times 10^{-2}$ . Our first error is their experiment's error and our second error is the systematic error from using our best value.				

 $\Gamma(\omega\omega)/\Gamma_{\text{total}}$   $\Gamma_{31}/\Gamma$ 

VALUE (units $10^{-4}$ )	EVTS	DOCUMENT ID	TECN	COMMENT
<b>6.0 ± 0.3 ± 0.7</b>	597	40 ABLIKIM	11K BES3	$\psi(2S) \rightarrow \gamma$ hadrons
40 ABLIKIM 11K reports $(6.0 \pm 0.3 \pm 0.7) \times 10^{-4}$ from a measurement of $[\Gamma(\chi_{c1}(1P) \rightarrow \omega\omega)/\Gamma_{\text{total}}] \times [B(\psi(2S) \rightarrow \gamma\chi_{c1}(1P))]$ assuming $B(\psi(2S) \rightarrow \gamma\chi_{c1}(1P)) = (9.2 \pm 0.4) \times 10^{-2}$ .				

 $\Gamma(\omega\phi)/\Gamma_{\text{total}}$   $\Gamma_{32}/\Gamma$ 

VALUE (units $10^{-4}$ )	EVTS	DOCUMENT ID	TECN	COMMENT
<b>0.22 ± 0.06 ± 0.02</b>	15	41 ABLIKIM	11K BES3	$\psi(2S) \rightarrow \gamma$ hadrons
41 ABLIKIM 11K reports $(0.22 \pm 0.06 \pm 0.02) \times 10^{-4}$ from a measurement of $[\Gamma(\chi_{c1}(1P) \rightarrow \omega\phi)/\Gamma_{\text{total}}] \times [B(\psi(2S) \rightarrow \gamma\chi_{c1}(1P))]$ assuming $B(\psi(2S) \rightarrow \gamma\chi_{c1}(1P)) = (9.2 \pm 0.4) \times 10^{-2}$ .				

 $\Gamma(\phi\phi)/\Gamma_{\text{total}}$   $\Gamma_{33}/\Gamma$ 

VALUE (units $10^{-4}$ )	EVTS	DOCUMENT ID	TECN	COMMENT
<b>4.4 ± 0.3 ± 0.5</b>	366	42 ABLIKIM	11K BES3	$\psi(2S) \rightarrow \gamma$ hadrons
42 ABLIKIM 11K reports $(4.4 \pm 0.3 \pm 0.5) \times 10^{-4}$ from a measurement of $[\Gamma(\chi_{c1}(1P) \rightarrow \phi\phi)/\Gamma_{\text{total}}] \times [B(\psi(2S) \rightarrow \gamma\chi_{c1}(1P))]$ assuming $B(\psi(2S) \rightarrow \gamma\chi_{c1}(1P)) = (9.2 \pm 0.4) \times 10^{-2}$ .				

 $\Gamma(\rho\bar{\rho})/\Gamma_{\text{total}}$   $\Gamma_{34}/\Gamma$ 

VALUE (units $10^{-4}$ )	DOCUMENT ID
<b>0.73 ± 0.04 OUR FIT</b>	

 $\Gamma(\rho\bar{\rho}\pi^0)/\Gamma_{\text{total}}$   $\Gamma_{35}/\Gamma$ 

VALUE (units $10^{-3}$ )	DOCUMENT ID	TECN	COMMENT
<b>0.164 ± 0.020 OUR AVERAGE</b>			
0.172 ± 0.020 ± 0.007	43 ONYISI	10 CLE3	$\psi(2S) \rightarrow \gamma\rho\bar{\rho}X$
0.118 ± 0.049 ± 0.005	44 ATHAR	07 CLEO	$\psi(2S) \rightarrow \gamma h^+ h^- h^0$
43 ONYISI 10 reports $(1.75 \pm 0.16 \pm 0.13 \pm 0.11) \times 10^{-4}$ from a measurement of $[\Gamma(\chi_{c1}(1P) \rightarrow \rho\bar{\rho}\pi^0)/\Gamma_{\text{total}}] \times [B(\psi(2S) \rightarrow \gamma\chi_{c1}(1P))]$ assuming $B(\psi(2S) \rightarrow \gamma\chi_{c1}(1P)) = (9.07 \pm 0.11 \pm 0.54) \times 10^{-2}$ , which we rescale to our best value $B(\psi(2S) \rightarrow \gamma\chi_{c1}(1P)) = (9.2 \pm 0.4) \times 10^{-2}$ . Our first error is their experiment's error and our second error is the systematic error from using our best value.			
44 ATHAR 07 reports $(1.2 \pm 0.5 \pm 0.1) \times 10^{-4}$ from a measurement of $[\Gamma(\chi_{c1}(1P) \rightarrow \rho\bar{\rho}\pi^0)/\Gamma_{\text{total}}] \times [B(\psi(2S) \rightarrow \gamma\chi_{c1}(1P))]$ assuming $B(\psi(2S) \rightarrow \gamma\chi_{c1}(1P)) = (9.07 \pm 0.11 \pm 0.54) \times 10^{-2}$ , which we rescale to our best value $B(\psi(2S) \rightarrow \gamma\chi_{c1}(1P)) = (9.2 \pm 0.4) \times 10^{-2}$ . Our first error is their experiment's error and our second error is the systematic error from using our best value.			

 $\Gamma(\rho\bar{\rho}\eta)/\Gamma_{\text{total}}$   $\Gamma_{36}/\Gamma$ 

VALUE (units $10^{-3}$ )	CL%	DOCUMENT ID	TECN	COMMENT
<b>0.153 ± 0.026 ± 0.006</b>		45 ONYISI	10 CLE3	$\psi(2S) \rightarrow \gamma\rho\bar{\rho}X$
• • • We do not use the following data for averages, fits, limits, etc. • • •				
< 0.16	90	46 ATHAR	07 CLEO	$\psi(2S) \rightarrow \gamma h^+ h^- h^0$
45 ONYISI 10 reports $(1.56 \pm 0.22 \pm 0.14 \pm 0.10) \times 10^{-4}$ from a measurement of $[\Gamma(\chi_{c1}(1P) \rightarrow \rho\bar{\rho}\eta)/\Gamma_{\text{total}}] \times [B(\psi(2S) \rightarrow \gamma\chi_{c1}(1P))]$ assuming $B(\psi(2S) \rightarrow \gamma\chi_{c1}(1P)) = (9.07 \pm 0.11 \pm 0.54) \times 10^{-2}$ , which we rescale to our best value $B(\psi(2S) \rightarrow \gamma\chi_{c1}(1P)) = (9.2 \pm 0.4) \times 10^{-2}$ . Our first error is their experiment's error and our second error is the systematic error from using our best value.				
46 ATHAR 07 reports $< 0.16 \times 10^{-3}$ from a measurement of $[\Gamma(\chi_{c1}(1P) \rightarrow \rho\bar{\rho}\eta)/\Gamma_{\text{total}}] \times [B(\psi(2S) \rightarrow \gamma\chi_{c1}(1P))]$ assuming $B(\psi(2S) \rightarrow \gamma\chi_{c1}(1P)) = (9.07 \pm 0.11 \pm 0.54) \times 10^{-2}$ , which we rescale to our best value $B(\psi(2S) \rightarrow \gamma\chi_{c1}(1P)) = 9.2 \times 10^{-2}$ .				

 $\Gamma(\rho\bar{\rho}\omega)/\Gamma_{\text{total}}$   $\Gamma_{37}/\Gamma$ 

VALUE (units $10^{-3}$ )	DOCUMENT ID	TECN	COMMENT
<b>0.224 ± 0.032 ± 0.009</b>	47 ONYISI	10 CLE3	$\psi(2S) \rightarrow \gamma\rho\bar{\rho}X$
47 ONYISI 10 reports $(2.28 \pm 0.28 \pm 0.16 \pm 0.14) \times 10^{-4}$ from a measurement of $[\Gamma(\chi_{c1}(1P) \rightarrow \rho\bar{\rho}\omega)/\Gamma_{\text{total}}] \times [B(\psi(2S) \rightarrow \gamma\chi_{c1}(1P))]$ assuming $B(\psi(2S) \rightarrow \gamma\chi_{c1}(1P)) = (9.07 \pm 0.11 \pm 0.54) \times 10^{-2}$ , which we rescale to our best value $B(\psi(2S) \rightarrow \gamma\chi_{c1}(1P)) = (9.2 \pm 0.4) \times 10^{-2}$ . Our first error is their experiment's error and our second error is the systematic error from using our best value.			

 $\Gamma(\rho\bar{\rho}\phi)/\Gamma_{\text{total}}$   $\Gamma_{38}/\Gamma$ 

VALUE (units $10^{-5}$ )	CL%	DOCUMENT ID	TECN	COMMENT
<b>&lt; 1.8</b>	90	48 ABLIKIM	11F BES3	$\psi(2S) \rightarrow \gamma\rho\bar{\rho}K^+ K^-$
48 ABLIKIM 11F reports $< 1.82 \times 10^{-5}$ from a measurement of $[\Gamma(\chi_{c1}(1P) \rightarrow \rho\bar{\rho}\phi)/\Gamma_{\text{total}}] \times [B(\psi(2S) \rightarrow \gamma\chi_{c1}(1P))]$ assuming $B(\psi(2S) \rightarrow \gamma\chi_{c1}(1P)) = (9.2 \pm 0.4) \times 10^{-2}$ .				

# Meson Particle Listings

## $\chi_{c1}(1P)$

### $\Gamma(p\bar{p}\pi^+\pi^-)/\Gamma_{total}$ $\Gamma_{39}/\Gamma$

VALUE (units $10^{-3}$ )	CL%	DOCUMENT ID	TECN	COMMENT
<b>0.50±0.19 OUR EVALUATION</b>		Treating systematic error as correlated.		
<b>0.50±0.19 OUR AVERAGE</b>				
0.46±0.12±0.15		49 BAI	99B BES	$\psi(2S) \rightarrow \gamma\chi_{c1}$
1.08±0.77±0.05		49 TANENBAUM	78 MRK1	$\psi(2S) \rightarrow \gamma\chi_{c1}$
49 Rescaled by us using $B(\psi(2S) \rightarrow \gamma\chi_{c1}) = (8.8 \pm 0.4)\%$ and $B(\psi(2S) \rightarrow J/\psi(1S)\pi^+\pi^-) = (32.6 \pm 0.5)\%$ .				

### $\Gamma(p\bar{p}\pi^0\pi^0)/\Gamma_{total}$ $\Gamma_{40}/\Gamma$

VALUE (%)	CL%	DOCUMENT ID	TECN	COMMENT
<0.05	90	50 HE	08B CLEO	$e^+e^- \rightarrow \gamma h^+h^-h^0h^0$
50 HE 08B reports < 0.05 % from a measurement of $[\Gamma(\chi_{c1}(1P) \rightarrow p\bar{p}\pi^0\pi^0)/\Gamma_{total}] \times [B(\psi(2S) \rightarrow \gamma\chi_{c1}(1P))]$ assuming $B(\psi(2S) \rightarrow \gamma\chi_{c1}(1P)) = (9.07 \pm 0.11 \pm 0.54) \times 10^{-2}$ , which we rescale to our best value $B(\psi(2S) \rightarrow \gamma\chi_{c1}(1P)) = 9.2 \times 10^{-2}$ .				

### $\Gamma(p\bar{p}K^+K^- \text{ (non-resonant)})/\Gamma_{total}$ $\Gamma_{41}/\Gamma$

VALUE (units $10^{-4}$ )	EVTS	DOCUMENT ID	TECN	COMMENT
<b>1.35±0.15±0.19</b>	82 ± 9	51 ABLIKIM	11F BES3	$\psi(2S) \rightarrow \gamma p\bar{p}K^+K^-$
51 ABLIKIM 11F reports $(1.35 \pm 0.15 \pm 0.19) \times 10^{-4}$ from a measurement of $[\Gamma(\chi_{c1}(1P) \rightarrow p\bar{p}K^+K^- \text{ (non-resonant)})/\Gamma_{total}] \times [B(\psi(2S) \rightarrow \gamma\chi_{c1}(1P))]$ assuming $B(\psi(2S) \rightarrow \gamma\chi_{c1}(1P)) = (9.2 \pm 0.4) \times 10^{-2}$ .				

### $\Gamma(p\bar{p}K_S^0K_S^0)/\Gamma_{total}$ $\Gamma_{42}/\Gamma$

VALUE (units $10^{-4}$ )	CL%	DOCUMENT ID	TECN	COMMENT
<b>&lt;4.5</b>	90	52 ABLIKIM	06D BES2	$\psi(2S) \rightarrow \gamma\chi_{c1}$
52 Using $B(\psi(2S) \rightarrow \chi_{c1}\gamma) (9.1 \pm 0.6)\%$ .				

### $\Gamma(\Lambda\bar{\Lambda})/\Gamma_{total}$ $\Gamma_{43}/\Gamma$

VALUE (units $10^{-4}$ )	DOCUMENT ID
<b>1.18±0.19 OUR FIT</b>	

### $\Gamma(\Lambda\bar{\Lambda}\pi^+\pi^-)/\Gamma_{total}$ $\Gamma_{44}/\Gamma$

VALUE (units $10^{-3}$ )	CL%	DOCUMENT ID	TECN	COMMENT
<b>&lt;1.5</b>	90	53 ABLIKIM	06D BES2	$\psi(2S) \rightarrow \gamma\chi_{c1}$
53 Using $B(\psi(2S) \rightarrow \chi_{c1}\gamma) (9.1 \pm 0.6)\%$ .				

### $\Gamma(K^+\bar{p}\Lambda)/\Gamma_{total}$ $\Gamma_{45}/\Gamma$

VALUE (units $10^{-3}$ )	DOCUMENT ID	TECN	COMMENT
<b>0.32±0.09±0.01</b>	54 ATHAR	07 CLEO	$\psi(2S) \rightarrow \gamma h^+h^-h^0$
54 ATHAR 07 reports $(0.33 \pm 0.09 \pm 0.04) \times 10^{-3}$ from a measurement of $[\Gamma(\chi_{c1}(1P) \rightarrow K^+\bar{p}\Lambda)/\Gamma_{total}] \times [B(\psi(2S) \rightarrow \gamma\chi_{c1}(1P))]$ assuming $B(\psi(2S) \rightarrow \gamma\chi_{c1}(1P)) = 0.0907 \pm 0.0011 \pm 0.0054$ , which we rescale to our best value $B(\psi(2S) \rightarrow \gamma\chi_{c1}(1P)) = (9.2 \pm 0.4) \times 10^{-2}$ . Our first error is their experiment's error and our second error is the systematic error from using our best value.			

### $\Gamma(K^+\rho\Lambda(1520) + c.c.)/\Gamma_{total}$ $\Gamma_{46}/\Gamma$

VALUE (units $10^{-4}$ )	EVTS	DOCUMENT ID	TECN	COMMENT
<b>1.18±0.4±0.3</b>	48 ± 10	55 ABLIKIM	11F BES3	$\psi(2S) \rightarrow \gamma p\bar{p}K^+K^-$
55 ABLIKIM 11F reports $(1.81 \pm 0.38 \pm 0.28) \times 10^{-4}$ from a measurement of $[\Gamma(\chi_{c1}(1P) \rightarrow K^+\rho\Lambda(1520) + c.c.)/\Gamma_{total}] \times [B(\psi(2S) \rightarrow \gamma\chi_{c1}(1P))]$ assuming $B(\psi(2S) \rightarrow \gamma\chi_{c1}(1P)) = (9.2 \pm 0.4) \times 10^{-2}$ .				

### $\Gamma(\Lambda(1520)\bar{\Lambda}(1520))/\Gamma_{total}$ $\Gamma_{47}/\Gamma$

VALUE (units $10^{-4}$ )	CL%	DOCUMENT ID	TECN	COMMENT
<b>&lt;1.0</b>	90	56 ABLIKIM	11F BES3	$\psi(2S) \rightarrow \gamma p\bar{p}K^+K^-$
56 ABLIKIM 11F reports < $1.00 \times 10^{-4}$ from a measurement of $[\Gamma(\chi_{c1}(1P) \rightarrow \Lambda(1520)\bar{\Lambda}(1520))/\Gamma_{total}] \times [B(\psi(2S) \rightarrow \gamma\chi_{c1}(1P))]$ assuming $B(\psi(2S) \rightarrow \gamma\chi_{c1}(1P)) = (9.2 \pm 0.4) \times 10^{-2}$ .				

### $\Gamma(\Sigma^0\bar{\Sigma}^0)/\Gamma_{total}$ $\Gamma_{48}/\Gamma$

VALUE (units $10^{-4}$ )	CL%	EVTS	DOCUMENT ID	TECN	COMMENT
<b>&lt;0.4</b>	90	3.8 ± 2.5	57 NAIK	08 CLEO	$\psi(2S) \rightarrow \gamma\Sigma^0\bar{\Sigma}^0$
57 NAIK 08 reports < $0.44 \times 10^{-4}$ from a measurement of $[\Gamma(\chi_{c1}(1P) \rightarrow \Sigma^0\bar{\Sigma}^0)/\Gamma_{total}] \times [B(\psi(2S) \rightarrow \gamma\chi_{c1}(1P))]$ assuming $B(\psi(2S) \rightarrow \gamma\chi_{c1}(1P)) = (9.07 \pm 0.11 \pm 0.54) \times 10^{-2}$ , which we rescale to our best value $B(\psi(2S) \rightarrow \gamma\chi_{c1}(1P)) = 9.2 \times 10^{-2}$ .					

### $\Gamma(\Sigma^+\bar{\Sigma}^-)/\Gamma_{total}$ $\Gamma_{49}/\Gamma$

VALUE (units $10^{-4}$ )	CL%	EVTS	DOCUMENT ID	TECN	COMMENT
<b>&lt;0.6</b>	90	4.3 ± 2.3	58 NAIK	08 CLEO	$\psi(2S) \rightarrow \gamma\Sigma^+\bar{\Sigma}^-$
58 NAIK 08 reports < $0.65 \times 10^{-4}$ from a measurement of $[\Gamma(\chi_{c1}(1P) \rightarrow \Sigma^+\bar{\Sigma}^-)/\Gamma_{total}] \times [B(\psi(2S) \rightarrow \gamma\chi_{c1}(1P))]$ assuming $B(\psi(2S) \rightarrow \gamma\chi_{c1}(1P)) = (9.07 \pm 0.11 \pm 0.54) \times 10^{-2}$ , which we rescale to our best value $B(\psi(2S) \rightarrow \gamma\chi_{c1}(1P)) = 9.2 \times 10^{-2}$ .					

### $\Gamma(\Xi^0\bar{\Xi}^0)/\Gamma_{total}$ $\Gamma_{50}/\Gamma$

VALUE (units $10^{-4}$ )	CL%	EVTS	DOCUMENT ID	TECN	COMMENT
<b>&lt;0.6</b>	90	1.7 ± 2.4	59 NAIK	08 CLEO	$\psi(2S) \rightarrow \gamma\Xi^0\bar{\Xi}^0$
59 NAIK 08 reports < $0.60 \times 10^{-4}$ from a measurement of $[\Gamma(\chi_{c1}(1P) \rightarrow \Xi^0\bar{\Xi}^0)/\Gamma_{total}] \times [B(\psi(2S) \rightarrow \gamma\chi_{c1}(1P))]$ assuming $B(\psi(2S) \rightarrow \gamma\chi_{c1}(1P)) = (9.07 \pm 0.11 \pm 0.54) \times 10^{-2}$ , which we rescale to our best value $B(\psi(2S) \rightarrow \gamma\chi_{c1}(1P)) = 9.2 \times 10^{-2}$ .					

### $\Gamma(\Xi^- \bar{\Xi}^+)/\Gamma_{total}$ $\Gamma_{51}/\Gamma$

VALUE (units $10^{-4}$ )	CL%	EVTS	DOCUMENT ID	TECN	COMMENT
<b>0.84±0.22±0.03</b>		16.4 ± 4.3	60 NAIK	08 CLEO	$\psi(2S) \rightarrow \gamma\Xi^+\bar{\Xi}^-$
••• We do not use the following data for averages, fits, limits, etc. •••					
< 3.4	90		61 ABLIKIM	06D BES2	$\psi(2S) \rightarrow \gamma\chi_{c1}$
60 NAIK 08 reports $(0.86 \pm 0.22 \pm 0.08) \times 10^{-4}$ from a measurement of $[\Gamma(\chi_{c1}(1P) \rightarrow \Xi^- \bar{\Xi}^+)/\Gamma_{total}] \times [B(\psi(2S) \rightarrow \gamma\chi_{c1}(1P))]$ assuming $B(\psi(2S) \rightarrow \gamma\chi_{c1}(1P)) = (9.07 \pm 0.11 \pm 0.54) \times 10^{-2}$ , which we rescale to our best value $B(\psi(2S) \rightarrow \gamma\chi_{c1}(1P)) = (9.2 \pm 0.4) \times 10^{-2}$ . Our first error is their experiment's error and our second error is the systematic error from using our best value.					
61 Using $B(\psi(2S) \rightarrow \chi_{c1}\gamma) (9.1 \pm 0.6)\%$ .					

### $[\Gamma(\pi^+\pi^-) + \Gamma(K^+K^-)]/\Gamma_{total}$ $\Gamma_{52}/\Gamma$

VALUE (units $10^{-4}$ )	CL%	DOCUMENT ID	TECN	COMMENT
<b>&lt;21</b>		62 FELDMAN	77 MRK1	$\psi(2S) \rightarrow \gamma\chi_{c1}$
••• We do not use the following data for averages, fits, limits, etc. •••				
<38	90	62 BRANDELIK	79B DASP	$\psi(2S) \rightarrow \gamma\chi_{c1}$
62 Estimated using $B(\psi(2S) \rightarrow \gamma\chi_{c1}(1P)) = 0.087$ . The errors do not contain the uncertainty in the $\psi(2S)$ decay.				

### $\Gamma(K_S^0K_S^0)/\Gamma_{total}$ $\Gamma_{53}/\Gamma$

VALUE (units $10^{-4}$ )	CL%	DOCUMENT ID	TECN	COMMENT
<b>&lt;0.6</b>	90	63 ABLIKIM	05o BES2	$\psi(2S) \rightarrow \chi_{c1}\gamma$
63 ABLIKIM 05o reports $[\Gamma(\chi_{c1}(1P) \rightarrow K_S^0K_S^0)/\Gamma_{total}] \times [B(\psi(2S) \rightarrow \gamma\chi_{c1}(1P))]$ < $0.6 \times 10^{-5}$ which we divide by our best value $B(\psi(2S) \rightarrow \gamma\chi_{c1}(1P)) = 9.2 \times 10^{-2}$ .				

## RADIATIVE DECAYS

### $\Gamma(\gamma J/\psi(1S))/\Gamma_{total}$ $\Gamma_{54}/\Gamma$

VALUE	DOCUMENT ID	TECN	COMMENT
<b>0.344±0.015 OUR FIT</b>			
••• We do not use the following data for averages, fits, limits, etc. •••			
0.379±0.008±0.021	64 ADAM	05A CLEO	$e^+e^- \rightarrow \psi(2S) \rightarrow \gamma\chi_{c1}$
64 Uses $B(\psi(2S) \rightarrow \gamma\chi_{c1}) \rightarrow \gamma J/\psi$ from ADAM 05A and $B(\psi(2S) \rightarrow \gamma\chi_{c1})$ from ATHAR 04.			

### $\Gamma(\gamma\rho^0)/\Gamma_{total}$ $\Gamma_{55}/\Gamma$

VALUE (units $10^{-6}$ )	EVTS	DOCUMENT ID	TECN	COMMENT
<b>228±19 OUR AVERAGE</b>				
228±13±22	432 ± 25	65 ABLIKIM	11E BES3	$\psi(2S) \rightarrow \gamma\gamma\rho^0$
229±25 ± 9	186 ± 15	66 BENNETT	08A CLEO	$\psi(2S) \rightarrow \gamma\gamma\rho^0$
65 ABLIKIM 11E reports $(228 \pm 13 \pm 22) \times 10^{-6}$ from a measurement of $[\Gamma(\chi_{c1}(1P) \rightarrow \gamma\rho^0)/\Gamma_{total}] \times [B(\psi(2S) \rightarrow \gamma\chi_{c1}(1P))]$ assuming $B(\psi(2S) \rightarrow \gamma\chi_{c1}(1P)) = (9.2 \pm 0.4) \times 10^{-2}$ .				
66 BENNETT 08A reports $(243 \pm 19 \pm 22) \times 10^{-6}$ from a measurement of $[\Gamma(\chi_{c1}(1P) \rightarrow \gamma\rho^0)/\Gamma_{total}] \times [B(\psi(2S) \rightarrow \gamma\chi_{c1}(1P))]$ assuming $B(\psi(2S) \rightarrow \gamma\chi_{c1}(1P)) = (8.7 \pm 0.4) \times 10^{-2}$ , which we rescale to our best value $B(\psi(2S) \rightarrow \gamma\chi_{c1}(1P)) = (9.2 \pm 0.4) \times 10^{-2}$ . Our first error is their experiment's error and our second error is the systematic error from using our best value.				

### $\Gamma(\gamma\omega)/\Gamma_{total}$ $\Gamma_{56}/\Gamma$

VALUE (units $10^{-6}$ )	EVTS	DOCUMENT ID	TECN	COMMENT
<b>71± 9 OUR AVERAGE</b>				
70± 7± 7	136 ± 14	67 ABLIKIM	11E BES3	$\psi(2S) \rightarrow \gamma\gamma\omega$
78±18± 3	39 ± 7	68 BENNETT	08A CLEO	$\psi(2S) \rightarrow \gamma\gamma\omega$
67 ABLIKIM 11E reports $(69.7 \pm 7.2 \pm 6.6) \times 10^{-6}$ from a measurement of $[\Gamma(\chi_{c1}(1P) \rightarrow \gamma\omega)/\Gamma_{total}] \times [B(\psi(2S) \rightarrow \gamma\chi_{c1}(1P))]$ assuming $B(\psi(2S) \rightarrow \gamma\chi_{c1}(1P)) = (9.2 \pm 0.4) \times 10^{-2}$ .				
68 BENNETT 08A reports $(83 \pm 15 \pm 12) \times 10^{-6}$ from a measurement of $[\Gamma(\chi_{c1}(1P) \rightarrow \gamma\omega)/\Gamma_{total}] \times [B(\psi(2S) \rightarrow \gamma\chi_{c1}(1P))]$ assuming $B(\psi(2S) \rightarrow \gamma\chi_{c1}(1P)) = (8.7 \pm 0.4) \times 10^{-2}$ , which we rescale to our best value $B(\psi(2S) \rightarrow \gamma\chi_{c1}(1P)) = (9.2 \pm 0.4) \times 10^{-2}$ . Our first error is their experiment's error and our second error is the systematic error from using our best value.				

### $\Gamma(\gamma\phi)/\Gamma_{total}$ $\Gamma_{57}/\Gamma$

VALUE (units $10^{-6}$ )	CL%	EVTS	DOCUMENT ID	TECN	COMMENT
<b>26±5±2</b>		43 ± 9	69 ABLIKIM	11E BES3	$\psi(2S) \rightarrow \gamma\gamma\phi$
••• We do not use the following data for averages, fits, limits, etc. •••					
<24	90	5.2 ± 3.1	70 BENNETT	08A CLEO	$\psi(2S) \rightarrow \gamma\gamma\phi$
69 ABLIKIM 11E reports $(25.8 \pm 5.2 \pm 2.3) \times 10^{-6}$ from a measurement of $[\Gamma(\chi_{c1}(1P) \rightarrow \gamma\phi)/\Gamma_{total}] \times [B(\psi(2S) \rightarrow \gamma\chi_{c1}(1P))]$ assuming $B(\psi(2S) \rightarrow \gamma\chi_{c1}(1P)) = (9.2 \pm 0.4) \times 10^{-2}$ .					
70 BENNETT 08A reports < $26 \times 10^{-6}$ from a measurement of $[\Gamma(\chi_{c1}(1P) \rightarrow \gamma\phi)/\Gamma_{total}] \times [B(\psi(2S) \rightarrow \gamma\chi_{c1}(1P))]$ assuming $B(\psi(2S) \rightarrow \gamma\chi_{c1}(1P)) = (8.7 \pm 0.4) \times 10^{-2}$ , which we rescale to our best value $B(\psi(2S) \rightarrow \gamma\chi_{c1}(1P)) = 9.2 \times 10^{-2}$ .					

$\Gamma(\gamma\gamma)/\Gamma_{total}$	CL%	DOCUMENT ID	TECN	COMMENT	$\Gamma_{58}/\Gamma$
VALUE (units $10^{-5}$ )					
••• We do not use the following data for averages, fits, limits, etc. •••					
< 3.5	90	ECKLUND	08A	CLEO $\psi(2S) \rightarrow \gamma\chi_{c1} \rightarrow 3\gamma$	
<150	90	71 YAMADA	77	DASP $e^+e^- \rightarrow 3\gamma$	
71 Estimated using $B(\psi(2S) \rightarrow \gamma\chi_{c1}(1P)) = 0.087$ . The errors do not contain the uncertainty in the $\psi(2S)$ decay.					

$\chi_{c1}(1P)$  CROSS-PARTICLE BRANCHING RATIOS

$\Gamma(\chi_{c1}(1P) \rightarrow p\bar{p})/\Gamma_{total} \times \Gamma(\psi(2S) \rightarrow \gamma\chi_{c1}(1P))/\Gamma(\psi(2S) \rightarrow J/\psi(1S)\pi^+\pi^-)$   
 $\Gamma_{34}/\Gamma \times \Gamma_{110}^{\psi(2S)}/\Gamma_{11}^{\psi(2S)}$

VALUE (units $10^{-5}$ )	DOCUMENT ID	TECN	COMMENT
<b>2.02±0.16 OUR FIT</b>			
<b>1.1 ±1.0</b>	72 BAI	98I	BES $\psi(2S) \rightarrow \gamma\chi_{c1} \rightarrow \gamma\bar{p}p$
72 Calculated by us. The value for $B(\chi_{c1} \rightarrow p\bar{p})$ reported in BAI 98I is derived using $B(\psi(2S) \rightarrow \gamma\chi_{c1}) = (8.7 \pm 0.8)\%$ and $B(\psi(2S) \rightarrow J/\psi(1S)\pi^+\pi^-) = (32.4 \pm 2.6)\%$ [BAI 98d].			

$\Gamma(\chi_{c1}(1P) \rightarrow \Lambda\bar{\Lambda})/\Gamma_{total} \times \Gamma(\psi(2S) \rightarrow \gamma\chi_{c1}(1P))/\Gamma_{total}$   
 $\Gamma_{43}/\Gamma \times \Gamma_{110}^{\psi(2S)}/\Gamma_{11}^{\psi(2S)}$

VALUE (units $10^{-6}$ )	EVTS	DOCUMENT ID	TECN	COMMENT
<b>10.9±1.7 OUR FIT</b>				
<b>10.5±1.6±0.6</b>	46 ± 7	73 NAIK	08	CLEO $\psi(2S) \rightarrow \gamma\Lambda\bar{\Lambda}$
73 Calculated by us. NAIK 08 reports $B(\chi_{c1} \rightarrow \Lambda\bar{\Lambda}) = (11.6 \pm 1.8 \pm 0.7 \pm 0.7) \times 10^{-5}$ using $B(\psi(2S) \rightarrow \gamma\chi_{c1}) = (9.07 \pm 0.11 \pm 0.54)\%$ .				

$\Gamma(\chi_{c1}(1P) \rightarrow \Lambda\bar{\Lambda})/\Gamma_{total} \times \Gamma(\psi(2S) \rightarrow \gamma\chi_{c1}(1P))/\Gamma(\psi(2S) \rightarrow J/\psi(1S)\pi^+\pi^-)$   
 $\Gamma_{43}/\Gamma \times \Gamma_{110}^{\psi(2S)}/\Gamma_{11}^{\psi(2S)}$

VALUE (units $10^{-5}$ )	EVTS	DOCUMENT ID	TECN	COMMENT
<b>3.3±0.5 OUR FIT</b>				
<b>7.1±2.9±1.3</b>	9.0±3.5 -3.1	74 BAI	03E	BES $\psi(2S) \rightarrow \gamma\Lambda\bar{\Lambda}$
74 BAI 03E reports $[B(\chi_{c1} \rightarrow \Lambda\bar{\Lambda})/B(\psi(2S) \rightarrow \gamma\chi_{c1})] / [B(\psi(2S) \rightarrow J/\psi\pi^+\pi^-)] \times [B^2(\Lambda \rightarrow \pi^-p) / B(J/\psi \rightarrow p\bar{p})] = (1.33 \pm 0.52 \pm 0.25)\%$ . We calculate from this measurement the presented value using $B(\Lambda \rightarrow \pi^-p) = (63.9 \pm 0.5)\%$ and $B(J/\psi \rightarrow p\bar{p}) = (2.17 \pm 0.07) \times 10^{-3}$ .				

$\Gamma(\chi_{c1}(1P) \rightarrow \gamma J/\psi(1S))/\Gamma_{total} \times \Gamma(\psi(2S) \rightarrow \gamma\chi_{c1}(1P))/\Gamma_{total}$   
 $\Gamma_{54}/\Gamma \times \Gamma_{110}^{\psi(2S)}/\Gamma_{11}^{\psi(2S)}$

VALUE (units $10^{-2}$ )	EVTS	DOCUMENT ID	TECN	COMMENT
<b>3.18±0.08 OUR FIT</b>				
<b>2.70±0.13 OUR AVERAGE</b>				
2.81±0.05±0.23	13k	BAI	04I	BES2 $\psi(2S) \rightarrow J/\psi\gamma\gamma$
2.56±0.12±0.20		75 GAISER	86	CBAL $\psi(2S) \rightarrow \gamma X$
2.78±0.30		76 OREGLIA	82	CBAL $\psi(2S) \rightarrow \gamma\chi_{c1}$
2.2 ±0.5		76 BRANDELIK	79B	DASP $\psi(2S) \rightarrow \gamma\chi_{c1}$
2.9 ±0.5		76 BARTEL	78B	CNTR $\psi(2S) \rightarrow \gamma\chi_{c1}$
5.0 ±1.5		77 BIDDICK	77	CNTR $e^+e^- \rightarrow \gamma X$
2.8 ±0.9		75 WHITAKER	76	MRK1 $e^+e^-$
••• We do not use the following data for averages, fits, limits, etc. •••				
3.56±0.03±0.12	24.9k	78 MENDEZ	08	CLEO $\psi(2S) \rightarrow \gamma\chi_{c1}$
3.44±0.06±0.13	3.7k	79 ADAM	05A	CLEO Repl. by MENDEZ 08
75 Recalculated by us using $B(J/\psi(1S) \rightarrow \ell^+\ell^-) = 0.1181 \pm 0.0020$ .				
76 Recalculated by us using $B(J/\psi(1S) \rightarrow \mu^+\mu^-) = 0.0588 \pm 0.0010$ .				
77 Assumes isotropic gamma distribution.				
78 Not independent from other measurements of MENDEZ 08.				
79 Not independent from other values reported by ADAM 05A.				

$\Gamma(\chi_{c1}(1P) \rightarrow \gamma J/\psi(1S))/\Gamma_{total} \times \Gamma(\psi(2S) \rightarrow \gamma\chi_{c1}(1P))/\Gamma(\psi(2S) \rightarrow J/\psi(1S)\text{anything})$   
 $\Gamma_{54}/\Gamma \times \Gamma_{110}^{\psi(2S)}/\Gamma_{9}^{\psi(2S)}$

VALUE (units $10^{-2}$ )	EVTS	DOCUMENT ID	TECN	COMMENT
<b>5.34±0.12 OUR FIT</b>				
••• We do not use the following data for averages, fits, limits, etc. •••				
5.70±0.04±0.15	24.9k	80 MENDEZ	08	CLEO $\psi(2S) \rightarrow \gamma\chi_{c1}$
5.77±0.10±0.12	3.7k	ADAM	05A	CLEO Repl. by MENDEZ 08
80 Not independent from other measurements of MENDEZ 08.				

$\Gamma(\chi_{c1}(1P) \rightarrow \gamma J/\psi(1S))/\Gamma_{total} \times \Gamma(\psi(2S) \rightarrow \gamma\chi_{c1}(1P))/\Gamma(\psi(2S) \rightarrow J/\psi(1S)\pi^+\pi^-)$   
 $\Gamma_{54}/\Gamma \times \Gamma_{110}^{\psi(2S)}/\Gamma_{11}^{\psi(2S)}$

VALUE (units $10^{-2}$ )	EVTS	DOCUMENT ID	TECN	COMMENT
<b>9.46±0.23 OUR FIT</b>				
<b>10.15±0.28 OUR AVERAGE</b>				
10.17±0.07±0.27	24.9k	MENDEZ	08	CLEO $\psi(2S) \rightarrow \gamma\chi_{c1}$
12.6 ±0.3 ±3.8	3k	81 ABLIKIM	04B	BES $\psi(2S) \rightarrow J/\psi X$
8.5 ±2.1		82 HIMEL	80	MRK2 $\psi(2S) \rightarrow \gamma\chi_{c1}$
••• We do not use the following data for averages, fits, limits, etc. •••				
10.24±0.17±0.23	3.7k	83 ADAM	05A	CLEO Repl. by MENDEZ 08

81 From a fit to the  $J/\psi$  recoil mass spectra.  
 82 The value for  $B(\psi(2S) \rightarrow \gamma\chi_{c1}) \times B(\chi_{c1} \rightarrow \gamma J/\psi(1S))$  quoted in HIMEL 80 is derived using  $B(\psi(2S) \rightarrow J/\psi(1S)\pi^+\pi^-) = (33 \pm 3)\%$  and  $B(J/\psi(1S) \rightarrow \ell^+\ell^-) = 0.138 \pm 0.018$ . Calculated by us using  $B(J/\psi(1S) \rightarrow \ell^+\ell^-) = 0.1181 \pm 0.0020$ .  
 83 Not independent from other values reported by ADAM 05A.

$\Gamma(\chi_{c1}(1P) \rightarrow K^0 K^+ \pi^- + c.c.)/\Gamma_{total} \times \Gamma(\psi(2S) \rightarrow \gamma\chi_{c1}(1P))/\Gamma_{total}$   
 $\Gamma_{15}/\Gamma \times \Gamma_{110}^{\psi(2S)}/\Gamma_{11}^{\psi(2S)}$

VALUE (units $10^{-4}$ )	DOCUMENT ID	TECN	COMMENT
<b>6.8±0.5 OUR FIT</b>			
<b>7.2±0.6 OUR AVERAGE</b>			
7.3±0.5±0.5	84 ATHAR	07	CLEO $\psi(2S) \rightarrow \gamma K_S^0 K^+ \pi^-$
7.0±0.5±0.9	85 ABLIKIM	06R	BES2 $\psi(2S) \rightarrow \gamma\chi_{c1}$
84 Calculated by us. The value of $B(\chi_{c1} \rightarrow K^0 K^+ \pi^- + c.c.)$ reported by ATHAR 07 was derived using $B(\psi(2S) \rightarrow \gamma\chi_{c1}(1P)) = (9.07 \pm 0.11 \pm 0.54)\%$ .			
85 Calculated by us. ABLIKIM 06R reports $B(\chi_{c1} \rightarrow K_S^0 K^+ \pi^-) = (4.0 \pm 0.3 \pm 0.5) \times 10^{-3}$ . We use $B(\psi(2S) \rightarrow \gamma\chi_{c1}) = (8.7 \pm 0.4) \times 10^{-2}$ .			

$\Gamma(\chi_{c1}(1P) \rightarrow K^0 K^+ \pi^- + c.c.)/\Gamma_{total} \times \Gamma(\psi(2S) \rightarrow \gamma\chi_{c1}(1P))/\Gamma(\psi(2S) \rightarrow J/\psi(1S)\pi^+\pi^-)$   
 $\Gamma_{15}/\Gamma \times \Gamma_{110}^{\psi(2S)}/\Gamma_{11}^{\psi(2S)}$

VALUE (units $10^{-4}$ )	DOCUMENT ID	TECN	COMMENT
<b>20.1±1.6 OUR FIT</b>			
<b>13.2±2.4±3.2</b>	86 BAI	99B	BES $\psi(2S) \rightarrow \gamma K_S^0 K^+ \pi^-$
86 Calculated by us. The value of $B(\chi_{c1} \rightarrow K_S^0 K^+ \pi^-)$ reported by BAI 99B was derived using $B(\psi(2S) \rightarrow \gamma\chi_{c1}(1P)) = (8.7 \pm 0.8)\%$ and $B(\psi(2S) \rightarrow J/\psi\pi^+\pi^-) = (32.4 \pm 2.6)\%$ [BAI 98d].			

$\Gamma(\chi_{c1}(1P) \rightarrow K^+ K^- K^+ K^-)/\Gamma_{total} \times \Gamma(\psi(2S) \rightarrow \gamma\chi_{c1}(1P))/\Gamma_{total}$   
 $\Gamma_{29}/\Gamma \times \Gamma_{110}^{\psi(2S)}/\Gamma_{11}^{\psi(2S)}$

VALUE (units $10^{-4}$ )	EVTS	DOCUMENT ID	TECN	COMMENT
<b>0.52±0.11 OUR FIT</b>				
<b>0.61±0.11±0.08</b>	54	87 ABLIKIM	06T	BES2 $\psi(2S) \rightarrow \gamma K^+ K^+ K^- K^-$
87 Calculated by us. The value of $B(\chi_{c1} \rightarrow 2K^+ 2K^-)$ reported by ABLIKIM 06T was derived using $B(\psi(2S) \rightarrow \gamma\chi_{c1}(1P)) = (8.7 \pm 0.8)\%$ .				

$\Gamma(\chi_{c1}(1P) \rightarrow K^+ K^- K^+ K^-)/\Gamma_{total} \times \Gamma(\psi(2S) \rightarrow \gamma\chi_{c1}(1P))/\Gamma(\psi(2S) \rightarrow J/\psi(1S)\pi^+\pi^-)$   
 $\Gamma_{29}/\Gamma \times \Gamma_{110}^{\psi(2S)}/\Gamma_{11}^{\psi(2S)}$

VALUE (units $10^{-4}$ )	DOCUMENT ID	TECN	COMMENT
<b>1.54±0.31 OUR FIT</b>			
<b>1.13±0.40±0.29</b>	88 BAI	99B	BES $\psi(2S) \rightarrow \gamma K^+ K^+ K^- K^-$
88 Calculated by us. The value of $B(\chi_{c1} \rightarrow 2K^+ 2K^-)$ reported by BAI 99B was derived using $B(\psi(2S) \rightarrow \gamma\chi_{c1}(1P)) = (8.7 \pm 0.8)\%$ and $B(\psi(2S) \rightarrow J/\psi\pi^+\pi^-) = (32.4 \pm 2.6)\%$ [BAI 98d].			

$\Gamma(\chi_{c1}(1P) \rightarrow p\bar{p})/\Gamma_{total} \times \Gamma(\psi(2S) \rightarrow \gamma\chi_{c1}(1P))/\Gamma_{total}$   
 $\Gamma_{34}/\Gamma \times \Gamma_{110}^{\psi(2S)}/\Gamma_{11}^{\psi(2S)}$

VALUE (units $10^{-6}$ )	EVTS	DOCUMENT ID	TECN	COMMENT
<b>6.8±0.5 OUR FIT</b>				
<b>7.5±1.4 OUR AVERAGE</b>				Error includes scale factor of 2.0.
8.2±0.7±0.4	141 ± 13	89 NAIK	08	CLEO $\psi(2S) \rightarrow \gamma\bar{p}p$
4.8±1.4±0.6	18.2±5.5 -4.9	BAI	04F	BES $\psi(2S) \rightarrow \gamma\chi_{c1}(1P) \rightarrow \gamma\bar{p}p$
89 Calculated by us. NAIK 08 reports $B(\chi_{c1} \rightarrow p\bar{p}) = (9.0 \pm 0.8 \pm 0.4 \pm 0.5) \times 10^{-5}$ using $B(\psi(2S) \rightarrow \gamma\chi_{c1}) = (9.07 \pm 0.11 \pm 0.54)\%$ .				

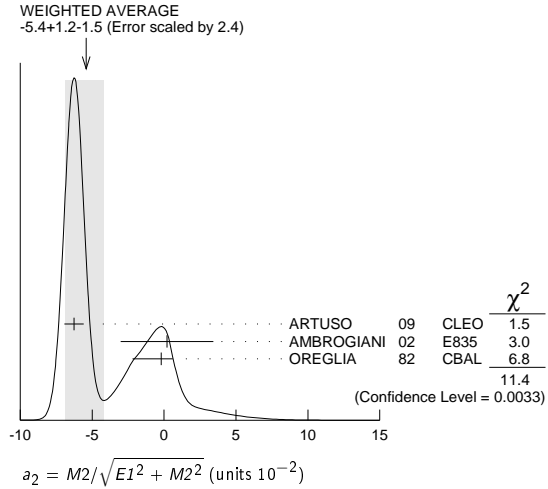
MULTIPOLE AMPLITUDES IN  $\chi_{c1}(1P) \rightarrow \gamma J/\psi(1S)$

$a_2 = M2/\sqrt{E1^2 + M2^2}$  Magnetic quadrupole fractional transition amplitude

VALUE (units $10^{-2}$ )	EVTS	DOCUMENT ID	TECN	COMMENT
<b>-5.4 ±1.2 ±1.5 OUR AVERAGE</b>				Error includes scale factor of 2.4. See the ideogram below.
-6.26±0.63±0.24	39k	ARTUSO	09	CLEO $\psi(2S) \rightarrow \gamma\gamma\ell^+\ell^-$
0.2 ±3.2 ±0.4	2090	AMBROGIANI	02	E835 $p\bar{p} \rightarrow \chi_{c1} \rightarrow J/\psi\gamma$
-0.2 ±0.8 ±2.0	921	OREGLIA	82	CBAL $\psi(2S) \rightarrow \chi_{c1}\gamma \rightarrow J/\psi\gamma\gamma$

# Meson Particle Listings

## $\chi_{c1}(1P), h_c(1P)$



### MULTIPOLE AMPLITUDES IN $\psi(2S) \rightarrow \gamma \chi_{c1}(1S)$ RADIATIVE DECAY

$b_2 = M_2/\sqrt{E1^2 + M^2}$  Magnetic quadrupole fractional transition amplitude

VALUE (units $10^{-2}$ )	EVTS	DOCUMENT ID	TECN	COMMENT
<b>2.9 ± 0.8 OUR AVERAGE</b>				
2.76 ± 0.73 ± 0.23	39k	ARTUSO	09 CLEO	$\psi(2S) \rightarrow \gamma \gamma \ell^+ \ell^-$
7.7 +5.0 -4.5	921	OREGLIA	82 CBAL	$\psi(2S) \rightarrow \gamma \gamma \ell^+ \ell^-$

### MULTIPOLE AMPLITUDE RATIOS IN RADIATIVE DECAYS

$\psi(2S) \rightarrow \gamma \chi_{c1}(1S)$  and  $\chi_{c1} \rightarrow \gamma J/\psi(1S)$

$a_2/b_2$  Magnetic quadrupole transition amplitude ratio

VALUE	EVTS	DOCUMENT ID	TECN	COMMENT
<b>-2.27 ± 0.57 -0.99</b>	39k	<sup>90</sup> ARTUSO	09 CLEO	$\psi(2S) \rightarrow \gamma \gamma \ell^+ \ell^-$

<sup>90</sup> Statistical and systematic errors combined. Not independent of  $a_2(\chi_{c1})$  and  $b_2(\chi_{c1})$  values from ARTUSO 09.

### $\chi_{c1}(1P)$ REFERENCES

ABLIKIM 11A PR D83 012006	M. Ablikim et al.	(BES III Collab.)
ABLIKIM 11D PR D83 032003	M. Ablikim et al.	(BES III Collab.)
ABLIKIM 11E PR D83 112005	M. Ablikim et al.	(BES III Collab.)
ABLIKIM 11F PR D83 112009	M. Ablikim et al.	(BES III Collab.)
ABLIKIM 11K PRL 107 092001	M. Ablikim et al.	(BES III Collab.)
ONYISI 10 PR D82 011103R	P.U.E. Onyisi et al.	(CLEO Collab.)
ARTUSO 09 PR D80 112003	M. Artuso et al.	(CLEO Collab.)
BENNETT 08A PRL 101 151801	J.V. Bennett et al.	(CLEO Collab.)
ECKLUND 08A PR D78 091501R	K.M. Ecklund et al.	(CLEO Collab.)
HE 08B PR D78 092004	Q. He et al.	(CLEO Collab.)
MENDEZ 08 PR D78 011102R	H. Mendez et al.	(CLEO Collab.)
NAIK 08 PR D78 031101R	P. Naik et al.	(CLEO Collab.)
ATHAR 07 PR D75 032002	S.B. Athar et al.	(CLEO Collab.)
ABLIKIM 06D PR D73 052006	M. Ablikim et al.	(BES Collab.)
ABLIKIM 06R PR D74 072001	M. Ablikim et al.	(BES Collab.)
ABLIKIM 06T PL B642 197	M. Ablikim et al.	(BES Collab.)
ABLIKIM 05G PR D71 092002	M. Ablikim et al.	(BES Collab.)
ABLIKIM 05O PL B630 21	M. Ablikim et al.	(BES Collab.)
ADAM 05A PRL 94 232002	M.E. Adam et al.	(CLEO Collab.)
ANDREOTTI 05A NP B717 34	M. Andreotti et al.	(FNAL E835 Collab.)
ABLIKIM 04B PR D70 012003	M. Ablikim et al.	(BES Collab.)
ABLIKIM 04H PR D70 092003	M. Ablikim et al.	(BES Collab.)
ATHAR 04 PR D70 112002	S.B. Athar et al.	(CLEO Collab.)
BAI 04 PR D69 092001	J.Z. Bai et al.	(BES Collab.)
BAI 04 PR D70 012006	J.Z. Bai et al.	(BES Collab.)
AULCHENKO 03 PL B573 63	V.M. Aulchenko et al.	(KEDR Collab.)
BAI 03E PR D67 112001	J.Z. Bai et al.	(BES Collab.)
AMBROGIANI 02 PR D65 052002	M. Ambrogiani et al.	(FNAL E835 Collab.)
BAI 99B PR D60 072001	J.Z. Bai et al.	(BES Collab.)
BAI 98D PR D58 092006	J.Z. Bai et al.	(BES Collab.)
BAI 98I PRL 81 3091	J.Z. Bai et al.	(BES Collab.)
ARMSTRONG 92 NP B373 35	T.A. Armstrong et al.	(FNAL, FERR, GENO+)
Also PRL 68 1468	T.A. Armstrong et al.	(FNAL, FERR, GENO+)
BAGLIN 86B PL B172 455	C. Baglin	(LAPP, CERN, GENO, LYON, OSLO+)
GAISER 86 PR D34 711	J. Gaiser et al.	(Crystal Ball Collab.)
LEMOIGNE 82 PL 113B 509	Y. Lemoigne et al.	(SACL, LOIC, SHMP+)
OREGLIA 82 PR D25 2259	M.J. Oreglia et al.	(SLAC, CIT, HARV+)
Also Private Comm.	M.J. Oreglia	(EFI)
HIMEL 80 PRL 44 920	T. Himel et al.	(LBL, SLAC)
Also Private Comm.	G. Trilling	(LBL, UC)
BRANDELIC 79B NP B160 426	R. Brandelik et al.	(DASP Collab.)
BARTEL 78B PL 79B 492	W. Bartel et al.	(DESY, HEIDP)
TANENBAUM 78 PR D17 1731	W.M. Tanenbaum et al.	(SLAC, LBL)
Also Private Comm.	G. Trilling	(LBL, UC)
BIDDICK 77 PRL 38 1324	C.J. Biddick et al.	(UCSD, UMD, PAVI+)
FELDMAN 77 PRPL 33C 285	G.J. Feldman, M.L. Perl	(LBL, SLAC)
YAMADA 77 Hamburg Conf. 69	S. Yamada et al.	(DASP Collab.)
WHITAKER 76 PRL 37 1596	J.S. Whitaker et al.	(SLAC, LBL)
TANENBAUM 75 PRL 35 1323	W.M. Tanenbaum et al.	(LBL, SLAC)

## $h_c(1P)$

$$I^G(J^{PC}) = ?^?(1+ -)$$

Quantum numbers are quark model prediction,  $C = -$  established by  $\eta_c \gamma$  decay.

### $h_c(1P)$ MASS

VALUE (MeV)	EVTS	DOCUMENT ID	TECN	COMMENT
<b>3525.41 ± 0.16 OUR AVERAGE</b>				Error includes scale factor of 1.2.
3525.40 ± 0.13 ± 0.18	3679	ABLIKIM	10B BES3	$\psi(2S) \rightarrow \pi^0 \gamma \eta_c$
3525.20 ± 0.18 ± 0.12	1282	<sup>1</sup> DOBBS	08A CLEO	$\psi(2S) \rightarrow \pi^0 \eta_c \gamma$
3525.8 ± 0.2 ± 0.2	13	ANDREOTTI	05B E835	$\bar{p}p \rightarrow \eta_c \gamma$
• • • We do not use the following data for averages, fits, limits, etc. • • •				
3525.6 ± 0.5	92 +23 -22	ADAMS	09 CLEO	$\psi(2S) \rightarrow 2(\pi^+ \pi^- \pi^0)$
3524.4 ± 0.6 ± 0.4	168 ± 40	<sup>2</sup> ROSNER	05 CLEO	$\psi(2S) \rightarrow \pi^0 \eta_c \gamma$
3527 ± 8	42	ANTONIAZZI	94 E705	$300 \pi^\pm, pLi \rightarrow J/\psi \pi^0 X$
3526.28 ± 0.18 ± 0.19	59	<sup>3</sup> ARMSTRONG	92D E760	$\bar{p}p \rightarrow J/\psi \pi^0$
3525.4 ± 0.8 ± 0.4	5	BAGLIN	86 SPEC	$\bar{p}p \rightarrow J/\psi X$

<sup>1</sup> Combination of exclusive and inclusive analyses for the reaction  $\psi(2S) \rightarrow \pi^0 \eta_c \rightarrow \pi^0 \eta_c \gamma$ . This result is the average of DOBBS 08A and ROSNER 05.  
<sup>2</sup> Superseded by DOBBS 08A.  
<sup>3</sup> Mass central value and systematic error recalculated by us according to Eq.(16) in ARMSTRONG 93B, using the value for the  $\psi(2S)$  mass from AULCHENKO 03.

### $h_c(1P)$ WIDTH

VALUE (MeV)	CL%	EVTS	DOCUMENT ID	TECN	COMMENT
<b>&lt;1</b>		13	ANDREOTTI	05B E835	$\bar{p}p \rightarrow \eta_c \gamma$
• • • We do not use the following data for averages, fits, limits, etc. • • •					
<1.44	90	3679	<sup>4</sup> ABLIKIM	10B BES3	$\psi(2S) \rightarrow \pi^0 \eta_c$
<1.1	90	59	ARMSTRONG	92D E760	$\bar{p}p \rightarrow J/\psi \pi^0$

<sup>4</sup> The central value is  $\Gamma = 0.73 \pm 0.45 \pm 0.28$  MeV.

### $h_c(1P)$ DECAY MODES

Mode	Fraction ( $\Gamma_i/\Gamma$ )
$\Gamma_1$ $J/\psi(1S)\pi^0$	
$\Gamma_2$ $J/\psi(1S)\pi\pi$	not seen
$\Gamma_3$ $p\bar{p}$	
$\Gamma_4$ $\eta_c(1S)\gamma$	(51 ± 6) %
$\Gamma_5$ $\pi^+ \pi^- \pi^0$	< 2.2 × 10 <sup>-3</sup>
$\Gamma_6$ $2\pi^+ 2\pi^- \pi^0$	(2.2 +0.8 -0.7) %
$\Gamma_7$ $3\pi^+ 3\pi^- \pi^0$	< 2.9 %

### $h_c(1P)$ PARTIAL WIDTHS

$h_c(1P) \Gamma(i)\Gamma(\bar{p}p)/\Gamma(\text{total})$

$\Gamma(\eta_c(1S)\gamma) \times \Gamma(\bar{p}p)/\Gamma_{\text{total}}$	$\Gamma_4 \Gamma_3/\Gamma$			
VALUE (eV)	EVTS	DOCUMENT ID	TECN	COMMENT
• • • We do not use the following data for averages, fits, limits, etc. • • •				
12.0 ± 4.5	13	<sup>5</sup> ANDREOTTI	05B E835	$\bar{p}p \rightarrow \eta_c \gamma$

<sup>5</sup> Assuming  $\Gamma = 1$  MeV.

### $h_c(1P)$ BRANCHING RATIOS

$\Gamma(J/\psi(1S)\pi\pi)/\Gamma(J/\psi(1S)\pi^0)$	$\Gamma_2/\Gamma_1$			
VALUE	CL%	DOCUMENT ID	TECN	COMMENT
<b>&lt;0.18</b>	90	ARMSTRONG	92D E760	$\bar{p}p \rightarrow J/\psi \pi^0$

$\Gamma(\eta_c(1S)\gamma)/\Gamma_{\text{total}}$	$\Gamma_4/\Gamma$			
VALUE (units $10^{-2}$ )	EVTS	DOCUMENT ID	TECN	COMMENT
<b>51 ± 6 OUR AVERAGE</b>				

54.3 ± 6.7 ± 5.2	3679	ABLIKIM	10B BES3	$\psi(2S) \rightarrow \pi^0 \gamma \eta_c$
48 ± 6 ± 7		<sup>6</sup> DOBBS	08A CLEO	$\psi(2S) \rightarrow \pi^0 \eta_c \gamma$
• • • We do not use the following data for averages, fits, limits, etc. • • •				
48 ± 6 ± 7	1282	<sup>7</sup> DOBBS	08A CLEO	$\psi(2S) \rightarrow \pi^0 \eta_c \gamma$
46 ± 12 ± 7	168	<sup>8</sup> ROSNER	05 CLEO	$\psi(2S) \rightarrow \pi^0 \eta_c \gamma$

<sup>6</sup> Average of DOBBS 08A and ROSNER 05. DOBBS 08A reports  $[\Gamma(h_c(1P) \rightarrow \eta_c(1S)\gamma)/\Gamma_{\text{total}}] \times [B(\psi(2S) \rightarrow \pi^0 h_c(1P))] = (4.16 \pm 0.30 \pm 0.37) \times 10^{-4}$  which we divide by our best value  $B(\psi(2S) \rightarrow \pi^0 h_c(1P)) = (8.6 \pm 1.3) \times 10^{-4}$ . Our first error is their experiment's error and our second error is the systematic error from using our best value.  
<sup>7</sup> DOBBS 08A reports  $[\Gamma(h_c(1P) \rightarrow \eta_c(1S)\gamma)/\Gamma_{\text{total}}] \times [B(\psi(2S) \rightarrow \pi^0 h_c(1P))] = (4.19 \pm 0.32 \pm 0.45) \times 10^{-4}$  which we divide by our best value  $B(\psi(2S) \rightarrow \pi^0 h_c(1P)) = (8.6 \pm 1.3) \times 10^{-4}$ . Our first error is their experiment's error and our second error is the systematic error from using our best value.  
<sup>8</sup> ROSNER 05 reports  $[\Gamma(h_c(1P) \rightarrow \eta_c(1S)\gamma)/\Gamma_{\text{total}}] \times [B(\psi(2S) \rightarrow \pi^0 h_c(1P))] = (4.0 \pm 0.8 \pm 0.7) \times 10^{-4}$  which we divide by our best value  $B(\psi(2S) \rightarrow \pi^0 h_c(1P)) = (8.6 \pm 1.3) \times 10^{-4}$ . Our first error is their experiment's error and our second error is the systematic error from using our best value.

See key on page 457

# Meson Particle Listings

## $h_c(1P), \chi_{c2}(1P)$

### $\Gamma(\pi^+\pi^-\pi^0)/\Gamma_{total}$ $\Gamma_5/\Gamma$

VALUE (units $10^{-3}$ )	DOCUMENT ID	TECN	COMMENT
<b>&lt;2.2</b>	<sup>9</sup> ADAMS	09	CLEO $\psi(2S) \rightarrow \pi^0 \gamma \eta_c$
<sup>9</sup> ADAMS 09 reports $[\Gamma(h_c(1P) \rightarrow \pi^+\pi^-\pi^0)/\Gamma_{total}] \times [B(\psi(2S) \rightarrow \pi^0 h_c(1P))]$ < $0.19 \times 10^{-5}$ which we divide by our best value $B(\psi(2S) \rightarrow \pi^0 h_c(1P)) = 8.6 \times 10^{-4}$ .			

### $\Gamma(2\pi^+2\pi^-\pi^0)/\Gamma_{total}$ $\Gamma_6/\Gamma$

VALUE (units $10^{-2}$ )	EVTS	DOCUMENT ID	TECN	COMMENT
<b><math>2.2 \pm 0.8 \pm 0.3</math></b>	92	<sup>10</sup> ADAMS	09	CLEO $\psi(2S) \rightarrow \pi^0 \gamma \eta_c$
<sup>10</sup> ADAMS 09 reports $[\Gamma(h_c(1P) \rightarrow 2\pi^+2\pi^-\pi^0)/\Gamma_{total}] \times [B(\psi(2S) \rightarrow \pi^0 h_c(1P))]$ = $(1.88 \pm 0.48 \pm 0.47) \times 10^{-5}$ which we divide by our best value $B(\psi(2S) \rightarrow \pi^0 h_c(1P))$ = $(8.6 \pm 1.3) \times 10^{-4}$ . Our first error is their experiment's error and our second error is the systematic error from using our best value.				

### $\Gamma(3\pi^+3\pi^-\pi^0)/\Gamma_{total}$ $\Gamma_7/\Gamma$

VALUE (units $10^{-2}$ )	DOCUMENT ID	TECN	COMMENT
<b>&lt;2.9</b>	<sup>11</sup> ADAMS	09	CLEO $\psi(2S) \rightarrow \pi^0 \gamma \eta_c$
<sup>11</sup> ADAMS 09 reports $[\Gamma(h_c(1P) \rightarrow 3\pi^+3\pi^-\pi^0)/\Gamma_{total}] \times [B(\psi(2S) \rightarrow \pi^0 h_c(1P))]$ < $2.5 \times 10^{-5}$ which we divide by our best value $B(\psi(2S) \rightarrow \pi^0 h_c(1P)) = 8.6 \times 10^{-4}$ .			

### $\Gamma(h_c(1P) \rightarrow \eta_c(1S)\gamma)/\Gamma_{total} \times \Gamma(\psi(2S) \rightarrow \pi^0 h_c(1P))/\Gamma_{total}$ $\Gamma_4/\Gamma \times \Gamma_{15}^{\psi(2S)}/\Gamma_{\psi(2S)}$

VALUE (units $10^{-4}$ )	EVTS	DOCUMENT ID	TECN	COMMENT
<b><math>4.3 \pm 0.4</math> OUR AVERAGE</b>				
$4.58 \pm 0.40 \pm 0.50$	3679	<sup>12</sup> ABLIKIM	10B	BES3 $\psi(2S) \rightarrow \pi^0 \gamma X$
$4.16 \pm 0.30 \pm 0.37$	1430	<sup>13</sup> DOBBS	08A	CLEO $\psi(2S) \rightarrow \pi^0 \gamma \eta_c$
<sup>12</sup> Not independent of other branching fractions in ABLIKIM 10B. <sup>13</sup> Not independent of other branching fractions in DOBBS 08A.				

### $h_c(1P)$ REFERENCES

ABLIKIM	10B	PRL 104 132002	M. Ablikim et al.	(BES III Collab.)
ADAMS	09	PR D80 051106	G.S. Adams et al.	(CLEO Collab.)
DOBBS	08A	PRL 101 182003	S. Dobbs et al.	(CLEO Collab.)
ANDREOTTI	05B	PR D72 032001	M. Andreotti et al.	(FNAL E835 Collab.)
ROSNER	05	PRL 95 102003	J.L. Rosner et al.	(CLEO Collab.)
AULCHENKO	03	PL B573 63	V.M. Aulchenko et al.	(KEDR Collab.)
ANTONIAZZI	94	PR D50 4258	L. Antoniazzi et al.	(E705 Collab.)
ARMSTRONG	93B	PR D47 772	T.A. Armstrong et al.	(FNAL E760 Collab.)
ARMSTRONG	92D	PRL 69 2337	T.A. Armstrong et al.	(FNAL, FERR, GENO+)
BAGLIN	86	PL B171 135	C. Baglin et al.	(LAPP, CERN, TORI, STRB+)

### $\chi_{c2}(1P)$

$$J^{PC} = 0^+(2^{++})$$

See the Review on " $\psi(2S)$  and  $\chi_c$  branching ratios" before the  $\chi_{c0}(1P)$  Listings.

### $\chi_{c2}(1P)$ MASS

VALUE (MeV)	EVTS	DOCUMENT ID	TECN	COMMENT
<b><math>3556.20 \pm 0.09</math> OUR AVERAGE</b>				
$3555.3 \pm 0.6 \pm 2.2$	2.5k	UEHARA	08	BELL $\gamma\gamma \rightarrow$ hadrons
$3555.70 \pm 0.59 \pm 0.39$		ABLIKIM	05G	BES2 $\psi(2S) \rightarrow \gamma \chi_{c2}$
$3556.173 \pm 0.123 \pm 0.020$		ANDREOTTI	05A	E835 $p\bar{p} \rightarrow e^+e^-\gamma$
$3559.9 \pm 2.9$		EISENSTEIN	01	CLE2 $e^+e^- \rightarrow e^+e^-\chi_{c2}$
$3556.4 \pm 0.7$		BAI	99B	BES $\psi(2S) \rightarrow \gamma X$
$3556.22 \pm 0.131 \pm 0.020$	585	<sup>1</sup> ARMSTRONG	92	E760 $\bar{p}p \rightarrow e^+e^-\gamma$
$3556.9 \pm 0.4 \pm 0.5$	50	BAGLIN	86B	SPEC $\bar{p}p \rightarrow e^+e^-\gamma$
$3557.8 \pm 0.2 \pm 4$		<sup>2</sup> GAISER	86	CBAL $\psi(2S) \rightarrow \gamma X$
$3553.4 \pm 2.2$	66	<sup>3</sup> LEMOIGNE	82	GOLI $185 \pi^- \text{Be} \rightarrow \gamma \mu^+ \mu^- A$
$3555.9 \pm 0.7$		<sup>4</sup> OREGLIA	82	CBAL $e^+e^- \rightarrow J/\psi 2\gamma$
$3557 \pm 1.5$	69	<sup>5</sup> HIMEL	80	MRK2 $e^+e^- \rightarrow J/\psi 2\gamma$
$3551 \pm 11$	15	BRANDELIK	79B	DASP $e^+e^- \rightarrow J/\psi 2\gamma$
$3553 \pm 4$		<sup>5</sup> BARTEL	78B	CNTR $e^+e^- \rightarrow J/\psi 2\gamma$
$3553 \pm 4 \pm 4$		<sup>5,6</sup> TANENBAUM	78	MRK1 $e^+e^-$
$3563 \pm 7$	360	<sup>5</sup> BIDDICK	77	CNTR $e^+e^- \rightarrow \gamma X$
$3543 \pm 10$	4	WHITAKER	76	MRK1 $e^+e^- \rightarrow J/\psi 2\gamma$

••• We do not use the following data for averages, fits, limits, etc. •••  
<sup>1</sup> Recalculated by ANDREOTTI 05A, using the value of  $\psi(2S)$  mass from AULCHENKO 03.  
<sup>2</sup> Using mass of  $\psi(2S) = 3686.0$  MeV.  
<sup>3</sup>  $J/\psi(1S)$  mass constrained to 3097 MeV.  
<sup>4</sup> Assuming  $\psi(2S)$  mass = 3686 MeV and  $J/\psi(1S)$  mass = 3097 MeV.  
<sup>5</sup> Mass value shifted by us by amount appropriate for  $\psi(2S)$  mass = 3686 MeV and  $J/\psi(1S)$  mass = 3097 MeV.  
<sup>6</sup> From a simultaneous fit to radiative and hadronic decay channels.

### $\chi_{c2}(1P)$ WIDTH

VALUE (MeV)	EVTS	DOCUMENT ID	TECN	COMMENT
<b><math>1.98 \pm 0.11</math> OUR FIT</b>				
<b><math>1.95 \pm 0.13</math> OUR AVERAGE</b>				
$1.915 \pm 0.188 \pm 0.013$		ANDREOTTI	05A	E835 $p\bar{p} \rightarrow e^+e^-\gamma$
$1.96 \pm 0.17 \pm 0.07$	585	<sup>7</sup> ARMSTRONG	92	E760 $\bar{p}p \rightarrow e^+e^-\gamma$
$2.6 \pm 1.4 \pm 1.0$	50	BAGLIN	86B	SPEC $\bar{p}p \rightarrow e^+e^-\gamma$
$2.8 \pm 2.1 \pm 2.0$		<sup>8</sup> GAISER	86	CBAL $\psi(2S) \rightarrow \gamma X$
<sup>7</sup> Recalculated by ANDREOTTI 05A. <sup>8</sup> Errors correspond to 90% confidence level; authors give only width range.				

### $\chi_{c2}(1P)$ DECAY MODES

Mode	Fraction ( $\Gamma_i/\Gamma$ )	Confidence level
<b>Hadronic decays</b>		
$\Gamma_1$ $2(\pi^+\pi^-)$	(1.10±0.11) %	
$\Gamma_2$ $\rho\rho$		
$\Gamma_3$ $\pi^+\pi^-\pi^0\pi^0$	(2.00±0.26) %	
$\Gamma_4$ $\rho^+\pi^-\pi^0 + \text{c.c.}$	(2.4 ± 0.4) %	
$\Gamma_5$ $4\pi^0$	(1.21±0.17) × 10 <sup>-3</sup>	
$\Gamma_6$ $K^+K^-\pi^0\pi^0$	(2.2 ± 0.5) × 10 <sup>-3</sup>	
$\Gamma_7$ $K^+\pi^-K^0\pi^0 + \text{c.c.}$	(1.51±0.22) %	
$\Gamma_8$ $\rho^+K^-K^0 + \text{c.c.}$	(4.5 ± 1.4) × 10 <sup>-3</sup>	
$\Gamma_9$ $K^*(892)^0K^+\pi^- \rightarrow K^+\pi^-K^0\pi^0 + \text{c.c.}$	(3.2 ± 0.9) × 10 <sup>-3</sup>	
$\Gamma_{10}$ $K^*(892)^0K^0\pi^0 \rightarrow K^+\pi^-K^0\pi^0 + \text{c.c.}$	(4.2 ± 0.9) × 10 <sup>-3</sup>	
$\Gamma_{11}$ $K^*(892)^-K^+\pi^0 \rightarrow K^+\pi^-K^0\pi^0 + \text{c.c.}$	(4.1 ± 0.9) × 10 <sup>-3</sup>	
$\Gamma_{12}$ $K^*(892)^+K^0\pi^- \rightarrow K^+\pi^-K^0\pi^0 + \text{c.c.}$	(3.2 ± 0.9) × 10 <sup>-3</sup>	
$\Gamma_{13}$ $K^+K^-\eta\pi^0$	(1.4 ± 0.5) × 10 <sup>-3</sup>	
$\Gamma_{14}$ $K^+K^-\pi^+\pi^-$	(9.1 ± 1.1) × 10 <sup>-3</sup>	
$\Gamma_{15}$ $K^+K^-\pi^+\pi^-\pi^0$	(1.3 ± 0.4) %	
$\Gamma_{16}$ $K^+K^*(892)^0\pi^-\pi^0 + \text{c.c.}$	(2.3 ± 1.2) × 10 <sup>-3</sup>	
$\Gamma_{17}$ $K^*(892)^0K^*(892)^0$	(2.5 ± 0.5) × 10 <sup>-3</sup>	
$\Gamma_{18}$ $3(\pi^+\pi^-)$	(8.6 ± 1.8) × 10 <sup>-3</sup>	
$\Gamma_{19}$ $\phi\phi$	(1.14±0.12) × 10 <sup>-3</sup>	
$\Gamma_{20}$ $\omega\omega$	(9.2 ± 1.1) × 10 <sup>-4</sup>	
$\Gamma_{21}$ $\omega\phi$		
$\Gamma_{22}$ $\pi\pi$	(2.43±0.13) × 10 <sup>-3</sup>	
$\Gamma_{23}$ $\rho^0\pi^+\pi^-$	(4.0 ± 1.7) × 10 <sup>-3</sup>	
$\Gamma_{24}$ $\pi^+\pi^-\eta$	(5.2 ± 1.4) × 10 <sup>-4</sup>	
$\Gamma_{25}$ $\pi^+\pi^-\eta'$	(5.5 ± 2.0) × 10 <sup>-4</sup>	
$\Gamma_{26}$ $\eta\eta$	(5.9 ± 0.5) × 10 <sup>-4</sup>	
$\Gamma_{27}$ $K^+K^-$	(1.09±0.08) × 10 <sup>-3</sup>	
$\Gamma_{28}$ $K_S^0K_S^0$	(5.8 ± 0.5) × 10 <sup>-4</sup>	
$\Gamma_{29}$ $\bar{K}^0K^+\pi^- + \text{c.c.}$	(1.40±0.20) × 10 <sup>-3</sup>	
$\Gamma_{30}$ $K^+K^-\pi^0$	(3.3 ± 0.8) × 10 <sup>-4</sup>	
$\Gamma_{31}$ $K^+K^-\eta$	< 3.5 × 10 <sup>-4</sup>	90%
$\Gamma_{32}$ $\eta\eta'$	< 6 × 10 <sup>-5</sup>	90%
$\Gamma_{33}$ $\eta'\eta'$	< 1.1 × 10 <sup>-4</sup>	90%
$\Gamma_{34}$ $\pi^+\pi^-K_S^0K_S^0$	(2.4 ± 0.6) × 10 <sup>-3</sup>	
$\Gamma_{35}$ $K^+K^-K_S^0K_S^0$	< 4 × 10 <sup>-4</sup>	90%
$\Gamma_{36}$ $K^+K^-K^+K^-$	(1.78±0.22) × 10 <sup>-3</sup>	
$\Gamma_{37}$ $K^+K^-\phi$	(1.55±0.33) × 10 <sup>-3</sup>	
$\Gamma_{38}$ $p\bar{p}$	(7.2 ± 0.4) × 10 <sup>-5</sup>	
$\Gamma_{39}$ $p\bar{p}\pi^0$	(5.1 ± 0.5) × 10 <sup>-4</sup>	
$\Gamma_{40}$ $p\bar{p}\eta$	(1.90±0.28) × 10 <sup>-4</sup>	
$\Gamma_{41}$ $p\bar{p}\omega$	(3.9 ± 0.5) × 10 <sup>-4</sup>	
$\Gamma_{42}$ $p\bar{p}\phi$	(3.0 ± 1.0) × 10 <sup>-5</sup>	
$\Gamma_{43}$ $p\bar{p}\pi^+\pi^-$	(1.32±0.34) × 10 <sup>-3</sup>	
$\Gamma_{44}$ $p\bar{p}\pi^0\pi^0$	(8.6 ± 2.6) × 10 <sup>-4</sup>	
$\Gamma_{45}$ $p\bar{p}K^+K^-$ (non-resonant)	(2.1 ± 0.4) × 10 <sup>-4</sup>	
$\Gamma_{46}$ $p\bar{p}K_S^0K_S^0$	< 7.9 × 10 <sup>-4</sup>	90%
$\Gamma_{47}$ $p\bar{p}\pi^-$	(1.1 ± 0.4) × 10 <sup>-3</sup>	
$\Gamma_{48}$ $\Lambda\bar{\Lambda}$	(1.86±0.27) × 10 <sup>-4</sup>	
$\Gamma_{49}$ $\Lambda\bar{\Lambda}\pi^+\pi^-$	< 3.5 × 10 <sup>-3</sup>	90%
$\Gamma_{50}$ $K^+\bar{p}\Lambda + \text{c.c.}$	(9.1 ± 1.8) × 10 <sup>-4</sup>	
$\Gamma_{51}$ $K^+p\Lambda(1520) + \text{c.c.}$	(3.1 ± 0.7) × 10 <sup>-4</sup>	
$\Gamma_{52}$ $\Lambda(1520)\bar{\Lambda}(1520)$	(5.1 ± 1.6) × 10 <sup>-4</sup>	
$\Gamma_{53}$ $\Sigma^0\bar{\Sigma}^0$	< 8 × 10 <sup>-5</sup>	90%
$\Gamma_{54}$ $\Sigma^+\bar{\Sigma}^-$	< 7 × 10 <sup>-5</sup>	90%



See key on page 457

## Meson Particle Listings

 $\chi_{c2}(1P)$ 

$\Gamma(\phi\phi) \times \Gamma(\gamma\gamma)/\Gamma_{\text{total}}$	$\Gamma_{19}\Gamma_{62}/\Gamma$			
VALUE (eV)	EVTS	DOCUMENT ID	TECN	COMMENT
<b>0.58±0.06 OUR FIT</b>				
<b>0.58±0.18±0.16</b>	26.5 ± 8.1	UEHARA	08	BELL $\gamma\gamma \rightarrow \chi_{c2} \rightarrow 2(K^+K^-)$

 $\chi_{c2}(1P)$  BRANCHING RATIOS

## HADRONIC DECAYS

$\Gamma(2(\pi^+\pi^-))/\Gamma_{\text{total}}$	$\Gamma_1/\Gamma$
VALUE	DOCUMENT ID
<b>0.0110±0.0011 OUR FIT</b>	

$\Gamma(\rho^0\pi^+\pi^-)/\Gamma(2(\pi^+\pi^-))$	$\Gamma_{23}/\Gamma_1$		
VALUE	DOCUMENT ID	TECN	COMMENT
<b>0.36±0.15 OUR FIT</b>			
<b>0.31±0.17</b>	TANENBAUM	78	MRK1 $\psi(2S) \rightarrow \gamma\chi_{c2}$

$\Gamma(\pi^+\pi^-\pi^0\pi^0)/\Gamma_{\text{total}}$	$\Gamma_3/\Gamma$			
VALUE (%)	EVTS	DOCUMENT ID	TECN	COMMENT
<b>2.00±0.25±0.08</b>		21	HE	08B CLEO $e^+e^- \rightarrow \gamma h^+ h^- h^0 h^0$

<sup>21</sup>HE 08B reports  $1.87 \pm 0.07 \pm 0.22 \pm 0.13$  % from a measurement of  $[\Gamma(\chi_{c2}(1P) \rightarrow \pi^+\pi^-\pi^0\pi^0)/\Gamma_{\text{total}}] \times [B(\psi(2S) \rightarrow \gamma\chi_{c2}(1P))]$  assuming  $B(\psi(2S) \rightarrow \gamma\chi_{c2}(1P)) = (9.33 \pm 0.14 \pm 0.61) \times 10^{-2}$ , which we rescale to our best value  $B(\psi(2S) \rightarrow \gamma\chi_{c2}(1P)) = (8.72 \pm 0.34) \times 10^{-2}$ . Our first error is their experiment's error and our second error is the systematic error from using our best value.

$\Gamma(\rho^+\pi^-\pi^0 + \text{c.c.})/\Gamma_{\text{total}}$	$\Gamma_4/\Gamma$			
VALUE (%)	EVTS	DOCUMENT ID	TECN	COMMENT
<b>2.4±0.4±0.1</b>		1031.9	22,23	HE 08B CLEO $e^+e^- \rightarrow \gamma h^+ h^- h^0 h^0$

<sup>22</sup>HE 08B reports  $2.23 \pm 0.11 \pm 0.32 \pm 0.16$  % from a measurement of  $[\Gamma(\chi_{c2}(1P) \rightarrow \rho^+\pi^-\pi^0 + \text{c.c.})/\Gamma_{\text{total}}] \times [B(\psi(2S) \rightarrow \gamma\chi_{c2}(1P))]$  assuming  $B(\psi(2S) \rightarrow \gamma\chi_{c2}(1P)) = (9.33 \pm 0.14 \pm 0.61) \times 10^{-2}$ , which we rescale to our best value  $B(\psi(2S) \rightarrow \gamma\chi_{c2}(1P)) = (8.72 \pm 0.34) \times 10^{-2}$ . Our first error is their experiment's error and our second error is the systematic error from using our best value.

<sup>23</sup>Calculated by us. We have added the values from HE 08B for  $\rho^+\pi^-\pi^0$  and  $\rho^-\pi^+\pi^0$  decays assuming uncorrelated statistical and fully correlated systematic uncertainties.

$\Gamma(4\pi^0)/\Gamma_{\text{total}}$	$\Gamma_5/\Gamma$			
VALUE (units $10^{-3}$ )	EVTS	DOCUMENT ID	TECN	COMMENT
<b>1.21±0.16±0.05</b>		1164	24	ABLIKIM 11A BES3 $e^+e^- \rightarrow \psi(2S) \rightarrow \gamma\chi_{c2}$

<sup>24</sup>ABLIKIM 11A reports  $(1.21 \pm 0.05 \pm 0.16) \times 10^{-3}$  from a measurement of  $[\Gamma(\chi_{c2}(1P) \rightarrow 4\pi^0)/\Gamma_{\text{total}}] \times [B(\psi(2S) \rightarrow \gamma\chi_{c2}(1P))]$  assuming  $B(\psi(2S) \rightarrow \gamma\chi_{c2}(1P)) = (8.74 \pm 0.35) \times 10^{-2}$ , which we rescale to our best value  $B(\psi(2S) \rightarrow \gamma\chi_{c2}(1P)) = (8.72 \pm 0.34) \times 10^{-2}$ . Our first error is their experiment's error and our second error is the systematic error from using our best value.

$\Gamma(K^+K^-\pi^0\pi^0)/\Gamma_{\text{total}}$	$\Gamma_6/\Gamma$			
VALUE (%)	EVTS	DOCUMENT ID	TECN	COMMENT
<b>0.22±0.04±0.01</b>		76.9	25	HE 08B CLEO $e^+e^- \rightarrow \gamma h^+ h^- h^0 h^0$

<sup>25</sup>HE 08B reports  $0.21 \pm 0.03 \pm 0.03 \pm 0.01$  % from a measurement of  $[\Gamma(\chi_{c2}(1P) \rightarrow K^+K^-\pi^0\pi^0)/\Gamma_{\text{total}}] \times [B(\psi(2S) \rightarrow \gamma\chi_{c2}(1P))]$  assuming  $B(\psi(2S) \rightarrow \gamma\chi_{c2}(1P)) = (9.33 \pm 0.14 \pm 0.61) \times 10^{-2}$ , which we rescale to our best value  $B(\psi(2S) \rightarrow \gamma\chi_{c2}(1P)) = (8.72 \pm 0.34) \times 10^{-2}$ . Our first error is their experiment's error and our second error is the systematic error from using our best value.

$\Gamma(K^+\pi^-\pi^0\pi^0 + \text{c.c.})/\Gamma_{\text{total}}$	$\Gamma_7/\Gamma$			
VALUE (%)	EVTS	DOCUMENT ID	TECN	COMMENT
<b>1.51±0.21±0.06</b>		211.6	26	HE 08B CLEO $e^+e^- \rightarrow \gamma h^+ h^- h^0 h^0$

<sup>26</sup>HE 08B reports  $1.41 \pm 0.11 \pm 0.16 \pm 0.10$  % from a measurement of  $[\Gamma(\chi_{c2}(1P) \rightarrow K^+\pi^-\pi^0\pi^0 + \text{c.c.})/\Gamma_{\text{total}}] \times [B(\psi(2S) \rightarrow \gamma\chi_{c2}(1P))]$  assuming  $B(\psi(2S) \rightarrow \gamma\chi_{c2}(1P)) = (9.33 \pm 0.14 \pm 0.61) \times 10^{-2}$ , which we rescale to our best value  $B(\psi(2S) \rightarrow \gamma\chi_{c2}(1P)) = (8.72 \pm 0.34) \times 10^{-2}$ . Our first error is their experiment's error and our second error is the systematic error from using our best value.

$\Gamma(\rho^+K^-K^0 + \text{c.c.})/\Gamma_{\text{total}}$	$\Gamma_8/\Gamma$			
VALUE (%)	EVTS	DOCUMENT ID	TECN	COMMENT
<b>0.45±0.13±0.02</b>		62.9	27	HE 08B CLEO $e^+e^- \rightarrow \gamma h^+ h^- h^0 h^0$

<sup>27</sup>HE 08B reports  $0.42 \pm 0.11 \pm 0.06 \pm 0.03$  % from a measurement of  $[\Gamma(\chi_{c2}(1P) \rightarrow \rho^+K^-K^0 + \text{c.c.})/\Gamma_{\text{total}}] \times [B(\psi(2S) \rightarrow \gamma\chi_{c2}(1P))]$  assuming  $B(\psi(2S) \rightarrow \gamma\chi_{c2}(1P)) = (9.33 \pm 0.14 \pm 0.61) \times 10^{-2}$ , which we rescale to our best value  $B(\psi(2S) \rightarrow \gamma\chi_{c2}(1P)) = (8.72 \pm 0.34) \times 10^{-2}$ . Our first error is their experiment's error and our second error is the systematic error from using our best value.

$\Gamma(K^*(892)^0 K^+\pi^- \rightarrow K^+\pi^- K^0\pi^0 + \text{c.c.})/\Gamma_{\text{total}}$	$\Gamma_9/\Gamma$			
VALUE (%)	EVTS	DOCUMENT ID	TECN	COMMENT
<b>0.32±0.09±0.01</b>		38.7	28	HE 08B CLEO $e^+e^- \rightarrow \gamma h^+ h^- h^0 h^0$

<sup>28</sup>HE 08B reports  $0.30 \pm 0.07 \pm 0.04 \pm 0.02$  % from a measurement of  $[\Gamma(\chi_{c2}(1P) \rightarrow K^*(892)^0 K^+\pi^- \rightarrow K^+\pi^- K^0\pi^0 + \text{c.c.})/\Gamma_{\text{total}}] \times [B(\psi(2S) \rightarrow \gamma\chi_{c2}(1P))]$  assuming  $B(\psi(2S) \rightarrow \gamma\chi_{c2}(1P)) = (9.33 \pm 0.14 \pm 0.61) \times 10^{-2}$ , which we rescale to our best value  $B(\psi(2S) \rightarrow \gamma\chi_{c2}(1P)) = (8.72 \pm 0.34) \times 10^{-2}$ . Our first error is their experiment's error and our second error is the systematic error from using our best value.

$\Gamma(K^*(892)^0 K^0\pi^0 \rightarrow K^+\pi^- K^0\pi^0 + \text{c.c.})/\Gamma_{\text{total}}$	$\Gamma_{10}/\Gamma$			
VALUE (%)	EVTS	DOCUMENT ID	TECN	COMMENT
<b>0.42±0.09±0.02</b>		63.0	29	HE 08B CLEO $e^+e^- \rightarrow \gamma h^+ h^- h^0 h^0$

<sup>29</sup>HE 08B reports  $0.39 \pm 0.07 \pm 0.05 \pm 0.03$  % from a measurement of  $[\Gamma(\chi_{c2}(1P) \rightarrow K^*(892)^0 K^0\pi^0 \rightarrow K^+\pi^- K^0\pi^0 + \text{c.c.})/\Gamma_{\text{total}}] \times [B(\psi(2S) \rightarrow \gamma\chi_{c2}(1P))]$  assuming  $B(\psi(2S) \rightarrow \gamma\chi_{c2}(1P)) = (9.33 \pm 0.14 \pm 0.61) \times 10^{-2}$ , which we rescale to our best value  $B(\psi(2S) \rightarrow \gamma\chi_{c2}(1P)) = (8.72 \pm 0.34) \times 10^{-2}$ . Our first error is their experiment's error and our second error is the systematic error from using our best value.

$\Gamma(K^*(892)^- K^+\pi^0 \rightarrow K^+\pi^- K^0\pi^0 + \text{c.c.})/\Gamma_{\text{total}}$	$\Gamma_{11}/\Gamma$			
VALUE (%)	EVTS	DOCUMENT ID	TECN	COMMENT
<b>0.41±0.09±0.02</b>		51.1	30	HE 08B CLEO $e^+e^- \rightarrow \gamma h^+ h^- h^0 h^0$

<sup>30</sup>HE 08B reports  $0.38 \pm 0.07 \pm 0.04 \pm 0.03$  % from a measurement of  $[\Gamma(\chi_{c2}(1P) \rightarrow K^*(892)^- K^+\pi^0 \rightarrow K^+\pi^- K^0\pi^0 + \text{c.c.})/\Gamma_{\text{total}}] \times [B(\psi(2S) \rightarrow \gamma\chi_{c2}(1P))]$  assuming  $B(\psi(2S) \rightarrow \gamma\chi_{c2}(1P)) = (9.33 \pm 0.14 \pm 0.61) \times 10^{-2}$ , which we rescale to our best value  $B(\psi(2S) \rightarrow \gamma\chi_{c2}(1P)) = (8.72 \pm 0.34) \times 10^{-2}$ . Our first error is their experiment's error and our second error is the systematic error from using our best value.

$\Gamma(K^*(892)^+ K^0\pi^- \rightarrow K^+\pi^- K^0\pi^0 + \text{c.c.})/\Gamma_{\text{total}}$	$\Gamma_{12}/\Gamma$			
VALUE (%)	EVTS	DOCUMENT ID	TECN	COMMENT
<b>0.32±0.09±0.01</b>		39.3	31	HE 08B CLEO $e^+e^- \rightarrow \gamma h^+ h^- h^0 h^0$

<sup>31</sup>HE 08B reports  $0.30 \pm 0.07 \pm 0.04 \pm 0.02$  % from a measurement of  $[\Gamma(\chi_{c2}(1P) \rightarrow K^*(892)^+ K^0\pi^- \rightarrow K^+\pi^- K^0\pi^0 + \text{c.c.})/\Gamma_{\text{total}}] \times [B(\psi(2S) \rightarrow \gamma\chi_{c2}(1P))]$  assuming  $B(\psi(2S) \rightarrow \gamma\chi_{c2}(1P)) = (9.33 \pm 0.14 \pm 0.61) \times 10^{-2}$ , which we rescale to our best value  $B(\psi(2S) \rightarrow \gamma\chi_{c2}(1P)) = (8.72 \pm 0.34) \times 10^{-2}$ . Our first error is their experiment's error and our second error is the systematic error from using our best value.

$\Gamma(K^+K^-\eta\pi^0)/\Gamma_{\text{total}}$	$\Gamma_{13}/\Gamma$			
VALUE (%)	EVTS	DOCUMENT ID	TECN	COMMENT
<b>0.14±0.05±0.01</b>		22.9	32	HE 08B CLEO $e^+e^- \rightarrow \gamma h^+ h^- h^0 h^0$

<sup>32</sup>HE 08B reports  $0.13 \pm 0.04 \pm 0.02 \pm 0.01$  % from a measurement of  $[\Gamma(\chi_{c2}(1P) \rightarrow K^+K^-\eta\pi^0)/\Gamma_{\text{total}}] \times [B(\psi(2S) \rightarrow \gamma\chi_{c2}(1P))]$  assuming  $B(\psi(2S) \rightarrow \gamma\chi_{c2}(1P)) = (9.33 \pm 0.14 \pm 0.61) \times 10^{-2}$ , which we rescale to our best value  $B(\psi(2S) \rightarrow \gamma\chi_{c2}(1P)) = (8.72 \pm 0.34) \times 10^{-2}$ . Our first error is their experiment's error and our second error is the systematic error from using our best value.

$\Gamma(K^+K^-\pi^+\pi^-)/\Gamma_{\text{total}}$	$\Gamma_{14}/\Gamma$
VALUE (units $10^{-3}$ )	DOCUMENT ID
<b>9.1±1.1 OUR FIT</b>	

$\Gamma(K^+K^*(892)^0\pi^- + \text{c.c.})/\Gamma(K^+K^-\pi^+\pi^-)$	$\Gamma_{16}/\Gamma_{14}$		
VALUE	DOCUMENT ID	TECN	COMMENT
<b>0.25±0.13 OUR FIT</b>			
<b>0.25±0.13</b>	TANENBAUM	78	MRK1 $\psi(2S) \rightarrow \gamma\chi_{c2}$

$\Gamma(K^+K^*(892)^0\pi^- + \text{c.c.})/\Gamma_{\text{total}}$	$\Gamma_{16}/\Gamma$
VALUE (units $10^{-4}$ )	DOCUMENT ID
<b>23±12 OUR FIT</b>	

$\Gamma(K^*(892)^0 K^*(892)^0)/\Gamma_{\text{total}}$	$\Gamma_{17}/\Gamma$
VALUE (units $10^{-3}$ )	DOCUMENT ID
<b>2.5±0.5 OUR FIT</b>	

$\Gamma(3(\pi^+\pi^-))/\Gamma_{\text{total}}$	$\Gamma_{18}/\Gamma$		
VALUE (units $10^{-3}$ )	DOCUMENT ID	TECN	COMMENT
<b>8.6±1.8 OUR EVALUATION</b>			Treating systematic error as correlated.
<b>8.6±1.8 OUR AVERAGE</b>			

<sup>33</sup>BAI 99B BES  $\psi(2S) \rightarrow \gamma\chi_{c2}$   
<sup>33</sup>TANENBAUM 78 MRK1  $\psi(2S) \rightarrow \gamma\chi_{c2}$   
<sup>33</sup>Rescaled by us using  $B(\psi(2S) \rightarrow \gamma\chi_{c2}) = (8.3 \pm 0.4)\%$  and  $B(\psi(2S) \rightarrow J/\psi(1S)\pi^+\pi^-) = (32.6 \pm 0.5)\%$ . Multiplied by a factor of 2 to convert from  $K_S^0 K^+\pi^-$  to  $K^0 K^+\pi^-$  decay.

$\Gamma(\phi\phi)/\Gamma_{\text{total}}$	$\Gamma_{19}/\Gamma$
VALUE (units $10^{-3}$ )	DOCUMENT ID
<b>1.14±0.12 OUR FIT</b>	

$\Gamma(\omega\omega)/\Gamma_{\text{total}}$	$\Gamma_{20}/\Gamma$			
VALUE (units $10^{-3}$ )	EVTS	DOCUMENT ID	TECN	COMMENT
<b>0.92±0.11 OUR AVERAGE</b>				

<sup>34</sup>ABLIKIM 11K reports  $(8.9 \pm 0.3 \pm 1.1) \times 10^{-4}$  from a measurement of  $[\Gamma(\chi_{c2}(1P) \rightarrow \omega\omega)/\Gamma_{\text{total}}] \times [B(\psi(2S) \rightarrow \gamma\chi_{c2}(1P))]$  assuming  $B(\psi(2S) \rightarrow \gamma\chi_{c2}(1P)) = (8.74 \pm 0.35) \times 10^{-2}$ , which we rescale to our best value  $B(\psi(2S) \rightarrow \gamma\chi_{c2}(1P)) = (8.72 \pm 0.34) \times 10^{-2}$ . Our first error is their experiment's error and our second error is the systematic error from using our best value.

<sup>35</sup>ABLIKIM 05N reports  $[\Gamma(\chi_{c2}(1P) \rightarrow \omega\omega)/\Gamma_{\text{total}}] \times [B(\psi(2S) \rightarrow \gamma\chi_{c2}(1P))] = (0.165 \pm 0.044 \pm 0.032) \times 10^{-3}$  which we divide by our best value  $B(\psi(2S) \rightarrow \gamma\chi_{c2}(1P)) = (8.72 \pm 0.34) \times 10^{-2}$ . Our first error is their experiment's error and our second error is the systematic error from using our best value.

## Meson Particle Listings

 $\chi_{c2}(1P)$ 

$\Gamma(\omega\phi)/\Gamma_{total}$	CL%	DOCUMENT ID	TECN	COMMENT	$\Gamma_{21}/\Gamma$
<u>VALUE (units <math>10^{-5}</math>)</u>					
<2.0	90	<sup>36</sup> ABLIKIM	11K BES3	$\psi(2S) \rightarrow \gamma$ hadrons	

<sup>36</sup> ABLIKIM 11K reports  $< 2 \times 10^{-5}$  from a measurement of  $[\Gamma(\chi_{c2}(1P) \rightarrow \omega\phi)/\Gamma_{total}] \times [B(\psi(2S) \rightarrow \gamma\chi_{c2}(1P))]$  assuming  $B(\psi(2S) \rightarrow \gamma\chi_{c2}(1P)) = (8.74 \pm 0.35) \times 10^{-2}$ , which we rescale to our best value  $B(\psi(2S) \rightarrow \gamma\chi_{c2}(1P)) = 8.72 \times 10^{-2}$ .

$\Gamma(\pi\pi)/\Gamma_{total}$	DOCUMENT ID	$\Gamma_{22}/\Gamma$
<u>VALUE (units <math>10^{-3}</math>)</u>		
<b>2.43±0.13 OUR FIT</b>		

$\Gamma(\rho^0\pi^+\pi^-)/\Gamma_{total}$	DOCUMENT ID	$\Gamma_{23}/\Gamma$
<u>VALUE (units <math>10^{-4}</math>)</u>		
<b>40±17 OUR FIT</b>		

$\Gamma(\pi^+\pi^-\eta)/\Gamma_{total}$	DOCUMENT ID	TECN	COMMENT	$\Gamma_{24}/\Gamma$
<u>VALUE (units <math>10^{-3}</math>)</u>				
<b>0.52±0.14±0.02</b>	<sup>37</sup> ATHAR	07 CLEO	$\psi(2S) \rightarrow \gamma h^+ h^- h^0$	

• • • We do not use the following data for averages, fits, limits, etc. • • •  
 <1.6 90 <sup>38</sup> ABLIKIM 06R BES2  $\psi(2S) \rightarrow \gamma\chi_{c2}$   
<sup>37</sup> ATHAR 07 reports  $(0.49 \pm 0.12 \pm 0.06) \times 10^{-3}$  from a measurement of  $[\Gamma(\chi_{c2}(1P) \rightarrow \pi^+\pi^-\eta)/\Gamma_{total}] \times [B(\psi(2S) \rightarrow \gamma\chi_{c2}(1P))]$  assuming  $B(\psi(2S) \rightarrow \gamma\chi_{c2}(1P)) = (9.33 \pm 0.14 \pm 0.61) \times 10^{-2}$ , which we rescale to our best value  $B(\psi(2S) \rightarrow \gamma\chi_{c2}(1P)) = (8.72 \pm 0.34) \times 10^{-2}$ . Our first error is their experiment's error and our second error is the systematic error from using our best value.

<sup>38</sup> ABLIKIM 06R reports  $< 1.7 \times 10^{-3}$  from a measurement of  $[\Gamma(\chi_{c2}(1P) \rightarrow \pi^+\pi^-\eta)/\Gamma_{total}] \times [B(\psi(2S) \rightarrow \gamma\chi_{c2}(1P))]$  assuming  $B(\psi(2S) \rightarrow \gamma\chi_{c2}(1P)) = (8.1 \pm 0.4) \times 10^{-2}$ , which we rescale to our best value  $B(\psi(2S) \rightarrow \gamma\chi_{c2}(1P)) = 8.72 \times 10^{-2}$ .

$\Gamma(\pi^+\pi^-\eta')/\Gamma_{total}$	DOCUMENT ID	TECN	COMMENT	$\Gamma_{25}/\Gamma$
<u>VALUE (units <math>10^{-3}</math>)</u>				
<b>0.55±0.20±0.02</b>	<sup>39</sup> ATHAR	07 CLEO	$\psi(2S) \rightarrow \gamma h^+ h^- h^0$	

<sup>39</sup> ATHAR 07 reports  $(0.51 \pm 0.18 \pm 0.06) \times 10^{-3}$  from a measurement of  $[\Gamma(\chi_{c2}(1P) \rightarrow \pi^+\pi^-\eta')/\Gamma_{total}] \times [B(\psi(2S) \rightarrow \gamma\chi_{c2}(1P))]$  assuming  $B(\psi(2S) \rightarrow \gamma\chi_{c2}(1P)) = (9.33 \pm 0.14 \pm 0.61) \times 10^{-2}$ , which we rescale to our best value  $B(\psi(2S) \rightarrow \gamma\chi_{c2}(1P)) = (8.72 \pm 0.34) \times 10^{-2}$ . Our first error is their experiment's error and our second error is the systematic error from using our best value.

$\Gamma(\eta\eta)/\Gamma_{total}$	DOCUMENT ID	$\Gamma_{26}/\Gamma$
<u>VALUE (units <math>10^{-4}</math>)</u>		
<b>5.9±0.5 OUR FIT</b>		

$\Gamma(K^+K^-)/\Gamma_{total}$	DOCUMENT ID	$\Gamma_{27}/\Gamma$
<u>VALUE (units <math>10^{-3}</math>)</u>		
<b>1.09±0.08 OUR FIT</b>		

$\Gamma(K_S^0 K_S^0)/\Gamma_{total}$	DOCUMENT ID	$\Gamma_{28}/\Gamma$
<u>VALUE (units <math>10^{-3}</math>)</u>		
<b>0.58±0.05 OUR FIT</b>		

$\Gamma(K_S^0 K_S^0)/\Gamma(\pi\pi)$	DOCUMENT ID	TECN	COMMENT	$\Gamma_{28}/\Gamma_{22}$
<u>VALUE</u>				
<b>0.239±0.019 OUR FIT</b>				

• • • We do not use the following data for averages, fits, limits, etc. • • •  
 0.27 ± 0.07 ± 0.04 <sup>40,41</sup> CHEN 07B BELL  $e^+e^- \rightarrow e^+e^-\chi_{c2}$

<sup>40</sup> Using  $\Gamma(\pi\pi) \times \Gamma(\gamma\gamma)/\Gamma_{total}$  from the  $\pi^+\pi^-$  measurement of NAKAZAWA 05 rescaled by 3/2 to convert to  $\pi\pi$ .

<sup>41</sup> Not independent from other measurements.

$\Gamma(K_S^0 K_S^0)/\Gamma(K^+K^-)$	DOCUMENT ID	TECN	COMMENT	$\Gamma_{28}/\Gamma_{27}$
<u>VALUE</u>				
<b>0.53±0.05 OUR FIT</b>				

• • • We do not use the following data for averages, fits, limits, etc. • • •  
 0.70 ± 0.21 ± 0.12 <sup>42,43</sup> CHEN 07B BELL  $e^+e^- \rightarrow e^+e^-\chi_{c2}$

<sup>42</sup> Using  $\Gamma(K^+K^-) \times \Gamma(\gamma\gamma)/\Gamma_{total}$  from NAKAZAWA 05.

<sup>43</sup> Not independent from other measurements.

$\Gamma(K^+K^-\pi^0)/\Gamma_{total}$	DOCUMENT ID	TECN	COMMENT	$\Gamma_{30}/\Gamma$
<u>VALUE (units <math>10^{-3}</math>)</u>				
<b>0.33±0.08±0.01</b>	<sup>44</sup> ATHAR	07 CLEO	$\psi(2S) \rightarrow \gamma h^+ h^- h^0$	

<sup>44</sup> ATHAR 07 reports  $(0.31 \pm 0.07 \pm 0.04) \times 10^{-3}$  from a measurement of  $[\Gamma(\chi_{c2}(1P) \rightarrow K^+K^-\pi^0)/\Gamma_{total}] \times [B(\psi(2S) \rightarrow \gamma\chi_{c2}(1P))]$  assuming  $B(\psi(2S) \rightarrow \gamma\chi_{c2}(1P)) = (9.33 \pm 0.14 \pm 0.61) \times 10^{-2}$ , which we rescale to our best value  $B(\psi(2S) \rightarrow \gamma\chi_{c2}(1P)) = (8.72 \pm 0.34) \times 10^{-2}$ . Our first error is their experiment's error and our second error is the systematic error from using our best value.

$\Gamma(K^+K^-\eta)/\Gamma_{total}$	CL%	DOCUMENT ID	TECN	COMMENT	$\Gamma_{31}/\Gamma$
<u>VALUE (units <math>10^{-3}</math>)</u>					
<b>&lt;0.35</b>	90	<sup>45</sup> ATHAR	07 CLEO	$\psi(2S) \rightarrow \gamma h^+ h^- h^0$	

<sup>45</sup> ATHAR 07 reports  $< 0.33 \times 10^{-3}$  from a measurement of  $[\Gamma(\chi_{c2}(1P) \rightarrow K^+K^-\eta)/\Gamma_{total}] \times [B(\psi(2S) \rightarrow \gamma\chi_{c2}(1P))]$  assuming  $B(\psi(2S) \rightarrow \gamma\chi_{c2}(1P)) = (9.33 \pm 0.14 \pm 0.61) \times 10^{-2}$ , which we rescale to our best value  $B(\psi(2S) \rightarrow \gamma\chi_{c2}(1P)) = 8.72 \times 10^{-2}$ .

$\Gamma(\eta\eta')/\Gamma_{total}$	CL%	EVTS	DOCUMENT ID	TECN	COMMENT	$\Gamma_{32}/\Gamma$
<u>VALUE (units <math>10^{-4}</math>)</u>						
<b>&lt;0.6</b>	90	3.3 ± 8.0	<sup>46</sup> ASNER	09 CLEO	$\psi(2S) \rightarrow \gamma\eta\eta'$	

• • • We do not use the following data for averages, fits, limits, etc. • • •  
 <2.5 90 <sup>47</sup> ADAMS 07 CLEO  $\psi(2S) \rightarrow \gamma\chi_{c2}$

<sup>46</sup> ASNER 09 reports  $< 0.6 \times 10^{-4}$  from a measurement of  $[\Gamma(\chi_{c2}(1P) \rightarrow \eta\eta')/\Gamma_{total}] \times [B(\psi(2S) \rightarrow \gamma\chi_{c2}(1P))]$  assuming  $B(\psi(2S) \rightarrow \gamma\chi_{c2}(1P)) = (9.33 \pm 0.14 \pm 0.61) \times 10^{-2}$ , which we rescale to our best value  $B(\psi(2S) \rightarrow \gamma\chi_{c2}(1P)) = 8.72 \times 10^{-2}$ .

<sup>47</sup> Superseded by ASNER 09. ADAMS 07 reports  $< 2.3 \times 10^{-4}$  from a measurement of  $[\Gamma(\chi_{c2}(1P) \rightarrow \eta\eta')/\Gamma_{total}] \times [B(\psi(2S) \rightarrow \gamma\chi_{c2}(1P))]$  assuming  $B(\psi(2S) \rightarrow \gamma\chi_{c2}(1P)) = 0.0933 \pm 0.0014 \pm 0.0061$ , which we rescale to our best value  $B(\psi(2S) \rightarrow \gamma\chi_{c2}(1P)) = 8.72 \times 10^{-2}$ .

$\Gamma(\eta'\eta')/\Gamma_{total}$	CL%	EVTS	DOCUMENT ID	TECN	COMMENT	$\Gamma_{33}/\Gamma$
<u>VALUE (units <math>10^{-4}</math>)</u>						
<b>&lt;1.1</b>	90	12 ± 7	<sup>48</sup> ASNER	09 CLEO	$\psi(2S) \rightarrow \gamma\eta'\eta'$	

• • • We do not use the following data for averages, fits, limits, etc. • • •  
 <3.3 90 <sup>49</sup> ADAMS 07 CLEO  $\psi(2S) \rightarrow \gamma\chi_{c2}$

<sup>48</sup> ASNER 09 reports  $< 1.0 \times 10^{-4}$  from a measurement of  $[\Gamma(\chi_{c2}(1P) \rightarrow \eta'\eta')/\Gamma_{total}] \times [B(\psi(2S) \rightarrow \gamma\chi_{c2}(1P))]$  assuming  $B(\psi(2S) \rightarrow \gamma\chi_{c2}(1P)) = (9.33 \pm 0.14 \pm 0.61) \times 10^{-2}$ , which we rescale to our best value  $B(\psi(2S) \rightarrow \gamma\chi_{c2}(1P)) = 8.72 \times 10^{-2}$ .

<sup>49</sup> Superseded by ASNER 09. ADAMS 07 reports  $< 3.1 \times 10^{-4}$  from a measurement of  $[\Gamma(\chi_{c2}(1P) \rightarrow \eta'\eta')/\Gamma_{total}] \times [B(\psi(2S) \rightarrow \gamma\chi_{c2}(1P))]$  assuming  $B(\psi(2S) \rightarrow \gamma\chi_{c2}(1P)) = 0.0933 \pm 0.0014 \pm 0.0061$ , which we rescale to our best value  $B(\psi(2S) \rightarrow \gamma\chi_{c2}(1P)) = 8.72 \times 10^{-2}$ .

$\Gamma(\pi^+\pi^-K_S^0 K_S^0)/\Gamma_{total}$	EVTS	DOCUMENT ID	TECN	COMMENT	$\Gamma_{34}/\Gamma$
<u>VALUE (units <math>10^{-3}</math>)</u>					
<b>2.4±0.6±0.1</b>	57 ± 11	<sup>50</sup> ABLIKIM	05o BES2	$\psi(2S) \rightarrow \gamma\chi_{c2}$	

<sup>50</sup> ABLIKIM 05o reports  $[\Gamma(\chi_{c2}(1P) \rightarrow \pi^+\pi^-K_S^0 K_S^0)/\Gamma_{total}] \times [B(\psi(2S) \rightarrow \gamma\chi_{c2}(1P))] = (0.207 \pm 0.039 \pm 0.033) \times 10^{-3}$  which we divide by our best value  $B(\psi(2S) \rightarrow \gamma\chi_{c2}(1P)) = (8.72 \pm 0.34) \times 10^{-2}$ . Our first error is their experiment's error and our second error is the systematic error from using our best value.

$\Gamma(K^+K^-K_S^0 K_S^0)/\Gamma_{total}$	CL%	EVTS	DOCUMENT ID	TECN	COMMENT	$\Gamma_{35}/\Gamma$
<u>VALUE (units <math>10^{-4}</math>)</u>						
<b>&lt;4</b>	90	2.3 ± 2.2	<sup>51</sup> ABLIKIM	05o BES2	$e^+e^- \rightarrow \chi_{c2}\gamma$	

<sup>51</sup> ABLIKIM 05o reports  $[\Gamma(\chi_{c2}(1P) \rightarrow K^+K^-K_S^0 K_S^0)/\Gamma_{total}] \times [B(\psi(2S) \rightarrow \gamma\chi_{c2}(1P))] < 3.5 \times 10^{-5}$  which we divide by our best value  $B(\psi(2S) \rightarrow \gamma\chi_{c2}(1P)) = 8.72 \times 10^{-2}$ .

$\Gamma(K^+K^-K^+K^-)/\Gamma_{total}$	DOCUMENT ID	$\Gamma_{36}/\Gamma$
<u>VALUE (units <math>10^{-3}</math>)</u>		
<b>1.78±0.22 OUR FIT</b>		

$\Gamma(K^+K^-\phi)/\Gamma_{total}$	EVTS	DOCUMENT ID	TECN	COMMENT	$\Gamma_{37}/\Gamma$
<u>VALUE (units <math>10^{-3}</math>)</u>					
<b>1.55±0.32±0.06</b>	52	<sup>52</sup> ABLIKIM	06T BES2	$\psi(2S) \rightarrow \gamma 2K^+ 2K^-$	

<sup>52</sup> ABLIKIM 06T reports  $(1.67 \pm 0.26 \pm 0.24) \times 10^{-3}$  from a measurement of  $[\Gamma(\chi_{c2}(1P) \rightarrow K^+K^-\phi)/\Gamma_{total}] \times [B(\psi(2S) \rightarrow \gamma\chi_{c2}(1P))]$  assuming  $B(\psi(2S) \rightarrow \gamma\chi_{c2}(1P)) = (8.1 \pm 0.4) \times 10^{-2}$ , which we rescale to our best value  $B(\psi(2S) \rightarrow \gamma\chi_{c2}(1P)) = (8.72 \pm 0.34) \times 10^{-2}$ . Our first error is their experiment's error and our second error is the systematic error from using our best value.

$\Gamma(\rho\bar{\rho})/\Gamma_{total}$	DOCUMENT ID	$\Gamma_{38}/\Gamma$
<u>VALUE (units <math>10^{-4}</math>)</u>		
<b>0.72±0.04 OUR FIT</b>		

$\Gamma(\rho\bar{\rho}\pi^0)/\Gamma_{total}$	DOCUMENT ID	TECN	COMMENT	$\Gamma_{39}/\Gamma$
<u>VALUE (units <math>10^{-3}</math>)</u>				
<b>0.51±0.05 OUR AVERAGE</b>				

0.52 ± 0.04 ± 0.02 <sup>53</sup> ONYISI 10 CLE3  $\psi(2S) \rightarrow \gamma\rho\bar{\rho}\chi$   
 0.47 ± 0.10 ± 0.02 <sup>54</sup> ATHAR 07 CLEO  $\psi(2S) \rightarrow \gamma h^+ h^- h^0$

<sup>53</sup> ONYISI 10 reports  $(4.83 \pm 0.25 \pm 0.35 \pm 0.31) \times 10^{-4}$  from a measurement of  $[\Gamma(\chi_{c2}(1P) \rightarrow \rho\bar{\rho}\pi^0)/\Gamma_{total}] \times [B(\psi(2S) \rightarrow \gamma\chi_{c2}(1P))]$  assuming  $B(\psi(2S) \rightarrow \gamma\chi_{c2}(1P)) = (9.33 \pm 0.14 \pm 0.61) \times 10^{-2}$ , which we rescale to our best value  $B(\psi(2S) \rightarrow \gamma\chi_{c2}(1P)) = (8.72 \pm 0.34) \times 10^{-2}$ . Our first error is their experiment's error and our second error is the systematic error from using our best value.

<sup>54</sup> ATHAR 07 reports  $(0.44 \pm 0.08 \pm 0.05) \times 10^{-3}$  from a measurement of  $[\Gamma(\chi_{c2}(1P) \rightarrow \rho\bar{\rho}\pi^0)/\Gamma_{total}] \times [B(\psi(2S) \rightarrow \gamma\chi_{c2}(1P))]$  assuming  $B(\psi(2S) \rightarrow \gamma\chi_{c2}(1P)) = (9.33 \pm 0.14 \pm 0.61) \times 10^{-2}$ , which we rescale to our best value  $B(\psi(2S) \rightarrow \gamma\chi_{c2}(1P)) = (8.72 \pm 0.34) \times 10^{-2}$ . Our first error is their experiment's error and our second error is the systematic error from using our best value.



$\Gamma(p\bar{p}\eta)/\Gamma_{total}$	$\Gamma_{40}/\Gamma$
VALUE (units $10^{-3}$ )	DOCUMENT ID TECN COMMENT
<b>0.190±0.028 OUR AVERAGE</b>	
0.188±0.028±0.007	55 ONYISI 10 CLE3 $\psi(2S) \rightarrow \gamma p\bar{p}X$
0.20±0.08±0.01	56 ATHAR 07 CLEO $\psi(2S) \rightarrow \gamma h^+h^-h^0$

55 ONYISI 10 reports  $(1.76 \pm 0.23 \pm 0.14 \pm 0.11) \times 10^{-4}$  from a measurement of  $[\Gamma(\chi_{c2}(1P) \rightarrow p\bar{p}\eta)/\Gamma_{total}] \times [B(\psi(2S) \rightarrow \gamma\chi_{c2}(1P))]$  assuming  $B(\psi(2S) \rightarrow \gamma\chi_{c2}(1P)) = (9.33 \pm 0.14 \pm 0.61) \times 10^{-2}$ , which we rescale to our best value  $B(\psi(2S) \rightarrow \gamma\chi_{c2}(1P)) = (8.72 \pm 0.34) \times 10^{-2}$ . Our first error is their experiment's error and our second error is the systematic error from using our best value.

56 ATHAR 07 reports  $(0.19 \pm 0.07 \pm 0.02) \times 10^{-3}$  from a measurement of  $[\Gamma(\chi_{c2}(1P) \rightarrow p\bar{p}\eta)/\Gamma_{total}] \times [B(\psi(2S) \rightarrow \gamma\chi_{c2}(1P))]$  assuming  $B(\psi(2S) \rightarrow \gamma\chi_{c2}(1P)) = (9.33 \pm 0.14 \pm 0.61) \times 10^{-2}$ , which we rescale to our best value  $B(\psi(2S) \rightarrow \gamma\chi_{c2}(1P)) = (8.72 \pm 0.34) \times 10^{-2}$ . Our first error is their experiment's error and our second error is the systematic error from using our best value.

$\Gamma(p\bar{p}\omega)/\Gamma_{total}$	$\Gamma_{41}/\Gamma$
VALUE (units $10^{-3}$ )	DOCUMENT ID TECN COMMENT
<b>0.39±0.05±0.02</b>	
	57 ONYISI 10 CLE3 $\psi(2S) \rightarrow \gamma p\bar{p}X$

57 ONYISI 10 reports  $(3.68 \pm 0.35 \pm 0.26 \pm 0.24) \times 10^{-4}$  from a measurement of  $[\Gamma(\chi_{c2}(1P) \rightarrow p\bar{p}\omega)/\Gamma_{total}] \times [B(\psi(2S) \rightarrow \gamma\chi_{c2}(1P))]$  assuming  $B(\psi(2S) \rightarrow \gamma\chi_{c2}(1P)) = (9.33 \pm 0.14 \pm 0.61) \times 10^{-2}$ , which we rescale to our best value  $B(\psi(2S) \rightarrow \gamma\chi_{c2}(1P)) = (8.72 \pm 0.34) \times 10^{-2}$ . Our first error is their experiment's error and our second error is the systematic error from using our best value.

$\Gamma(p\bar{p}\phi)/\Gamma_{total}$	$\Gamma_{42}/\Gamma$
VALUE (units $10^{-5}$ )	EVTS DOCUMENT ID TECN COMMENT
<b>3.0±0.9±0.1</b>	24 ± 7 58 ABLIKIM 11F BES3 $\psi(2S) \rightarrow \gamma p\bar{p}K^+K^-$

58 ABLIKIM 11F reports  $(3.04 \pm 0.85 \pm 0.43) \times 10^{-5}$  from a measurement of  $[\Gamma(\chi_{c2}(1P) \rightarrow p\bar{p}\phi)/\Gamma_{total}] \times [B(\psi(2S) \rightarrow \gamma\chi_{c2}(1P))]$  assuming  $B(\psi(2S) \rightarrow \gamma\chi_{c2}(1P)) = (8.74 \pm 0.35) \times 10^{-2}$ , which we rescale to our best value  $B(\psi(2S) \rightarrow \gamma\chi_{c2}(1P)) = (8.72 \pm 0.34) \times 10^{-2}$ . Our first error is their experiment's error and our second error is the systematic error from using our best value.

$\Gamma(p\bar{p}\pi^+\pi^-)/\Gamma_{total}$	$\Gamma_{43}/\Gamma$
VALUE (units $10^{-3}$ )	DOCUMENT ID TECN COMMENT
<b>1.32±0.34 OUR EVALUATION</b>	Treating systematic error as correlated.
<b>1.3 ± 0.4 OUR AVERAGE</b>	Error includes scale factor of 1.3.
1.17±0.19±0.30	59 BAI 99B BES $\psi(2S) \rightarrow \gamma\chi_{c2}$
2.64±1.03±0.14	59 TANENBAUM 78 MRK1 $\psi(2S) \rightarrow \gamma\chi_{c2}$

59 Rescaled by us using  $B(\psi(2S) \rightarrow \gamma\chi_{c2}) = (8.3 \pm 0.4)\%$  and  $B(\psi(2S) \rightarrow J/\psi(1S)\pi^+\pi^-) = (32.6 \pm 0.5)\%$ . Multiplied by a factor of 2 to convert from  $K_S^0 K^+\pi^-$  to  $K^0 K^+\pi^-$  decay.

$\Gamma(p\bar{p}\pi^0\pi^0)/\Gamma_{total}$	$\Gamma_{44}/\Gamma$
VALUE (%)	EVTS DOCUMENT ID TECN COMMENT
<b>0.086±0.026±0.003</b>	29.2 60 HE 08B CLEO $e^+e^- \rightarrow \gamma h^+h^-h^0h^0$

60 HE 08B reports  $0.08 \pm 0.02 \pm 0.01 \pm 0.01\%$  from a measurement of  $[\Gamma(\chi_{c2}(1P) \rightarrow p\bar{p}\pi^0\pi^0)/\Gamma_{total}] \times [B(\psi(2S) \rightarrow \gamma\chi_{c2}(1P))]$  assuming  $B(\psi(2S) \rightarrow \gamma\chi_{c2}(1P)) = (9.33 \pm 0.14 \pm 0.61) \times 10^{-2}$ , which we rescale to our best value  $B(\psi(2S) \rightarrow \gamma\chi_{c2}(1P)) = (8.72 \pm 0.34) \times 10^{-2}$ . Our first error is their experiment's error and our second error is the systematic error from using our best value.

$\Gamma(p\bar{p}K^+K^- \text{ (non-resonant)})/\Gamma_{total}$	$\Gamma_{45}/\Gamma$
VALUE (units $10^{-4}$ )	EVTS DOCUMENT ID TECN COMMENT
<b>2.09±0.35±0.08</b>	131 ± 12 61 ABLIKIM 11F BES3 $\psi(2S) \rightarrow \gamma p\bar{p}K^+K^-$

61 ABLIKIM 11F reports  $(2.08 \pm 0.19 \pm 0.30) \times 10^{-4}$  from a measurement of  $[\Gamma(\chi_{c2}(1P) \rightarrow p\bar{p}K^+K^- \text{ (non-resonant)})/\Gamma_{total}] \times [B(\psi(2S) \rightarrow \gamma\chi_{c2}(1P))]$  assuming  $B(\psi(2S) \rightarrow \gamma\chi_{c2}(1P)) = (8.74 \pm 0.35) \times 10^{-2}$ , which we rescale to our best value  $B(\psi(2S) \rightarrow \gamma\chi_{c2}(1P)) = (8.72 \pm 0.34) \times 10^{-2}$ . Our first error is their experiment's error and our second error is the systematic error from using our best value.

$\Gamma(p\bar{p}K_S^0K_S^0)/\Gamma_{total}$	$\Gamma_{46}/\Gamma$
VALUE (units $10^{-4}$ )	CL% DOCUMENT ID TECN COMMENT
<b>&lt;7.9</b>	90 62 ABLIKIM 06D BES2 $\psi(2S) \rightarrow \chi_{c2}\gamma$

62 Using  $B(\psi(2S) \rightarrow \chi_{c2}\gamma) = (9.3 \pm 0.6)\%$ .

$\Gamma(p\bar{p}\pi^-)/\Gamma_{total}$	$\Gamma_{47}/\Gamma$
VALUE (units $10^{-4}$ )	DOCUMENT ID TECN COMMENT
<b>11.1±3.8±0.4</b>	63 ABLIKIM 06i BES2 $\psi(2S) \rightarrow \gamma p\pi^-X$

63 ABLIKIM 06i reports  $[\Gamma(\chi_{c2}(1P) \rightarrow p\bar{p}\pi^-)/\Gamma_{total}] \times [B(\psi(2S) \rightarrow \gamma\chi_{c2}(1P))]$  =  $(0.97 \pm 0.20 \pm 0.26) \times 10^{-4}$  which we divide by our best value  $B(\psi(2S) \rightarrow \gamma\chi_{c2}(1P)) = (8.72 \pm 0.34) \times 10^{-2}$ . Our first error is their experiment's error and our second error is the systematic error from using our best value.

$\Gamma(\Lambda\bar{\Lambda})/\Gamma_{total}$	$\Gamma_{48}/\Gamma$
VALUE (units $10^{-4}$ )	DOCUMENT ID
<b>1.86±0.27 OUR FIT</b>	

$\Gamma(\Lambda\bar{\Lambda}\pi^+\pi^-)/\Gamma_{total}$	$\Gamma_{49}/\Gamma$
VALUE (units $10^{-3}$ )	CL% DOCUMENT ID TECN COMMENT
<b>&lt;3.5</b>	90 64 ABLIKIM 06D BES2 $\psi(2S) \rightarrow \chi_{c2}\gamma$

64 Using  $B(\psi(2S) \rightarrow \chi_{c2}\gamma) = (9.3 \pm 0.6)\%$ .

$\Gamma(K^+\bar{p}\Lambda + c.c.)/\Gamma_{total}$	$\Gamma_{50}/\Gamma$
VALUE (units $10^{-3}$ )	DOCUMENT ID TECN COMMENT
<b>0.91±0.17±0.04</b>	65 ATHAR 07 CLEO $\psi(2S) \rightarrow \gamma h^+h^-h^0$

65 ATHAR 07 reports  $(0.85 \pm 0.14 \pm 0.10) \times 10^{-3}$  from a measurement of  $[\Gamma(\chi_{c2}(1P) \rightarrow K^+\bar{p}\Lambda + c.c.)/\Gamma_{total}] \times [B(\psi(2S) \rightarrow \gamma\chi_{c2}(1P))]$  assuming  $B(\psi(2S) \rightarrow \gamma\chi_{c2}(1P)) = (9.33 \pm 0.14 \pm 0.61) \times 10^{-2}$ , which we rescale to our best value  $B(\psi(2S) \rightarrow \gamma\chi_{c2}(1P)) = (8.72 \pm 0.34) \times 10^{-2}$ . Our first error is their experiment's error and our second error is the systematic error from using our best value.

$\Gamma(K^+\rho\Lambda(1520) + c.c.)/\Gamma_{total}$	$\Gamma_{51}/\Gamma$
VALUE (units $10^{-4}$ )	EVTS DOCUMENT ID TECN COMMENT
<b>3.1±0.7±0.1</b>	79 ± 13 66 ABLIKIM 11F BES3 $\psi(2S) \rightarrow \gamma p\bar{p}K^+K^-$

66 ABLIKIM 11F reports  $(3.06 \pm 0.50 \pm 0.54) \times 10^{-4}$  from a measurement of  $[\Gamma(\chi_{c2}(1P) \rightarrow K^+\rho\Lambda(1520) + c.c.)/\Gamma_{total}] \times [B(\psi(2S) \rightarrow \gamma\chi_{c2}(1P))]$  assuming  $B(\psi(2S) \rightarrow \gamma\chi_{c2}(1P)) = (8.74 \pm 0.35) \times 10^{-2}$ , which we rescale to our best value  $B(\psi(2S) \rightarrow \gamma\chi_{c2}(1P)) = (8.72 \pm 0.34) \times 10^{-2}$ . Our first error is their experiment's error and our second error is the systematic error from using our best value.

$\Gamma(\Lambda(1520)\bar{\Lambda}(1520))/\Gamma_{total}$	$\Gamma_{52}/\Gamma$
VALUE (units $10^{-4}$ )	EVTS DOCUMENT ID TECN COMMENT
<b>5.1±1.6±0.2</b>	29 ± 7 67 ABLIKIM 11F BES3 $\psi(2S) \rightarrow \gamma p\bar{p}K^+K^-$

67 ABLIKIM 11F reports  $(5.05 \pm 1.29 \pm 0.93) \times 10^{-4}$  from a measurement of  $[\Gamma(\chi_{c2}(1P) \rightarrow \Lambda(1520)\bar{\Lambda}(1520))/\Gamma_{total}] \times [B(\psi(2S) \rightarrow \gamma\chi_{c2}(1P))]$  assuming  $B(\psi(2S) \rightarrow \gamma\chi_{c2}(1P)) = (8.74 \pm 0.35) \times 10^{-2}$ , which we rescale to our best value  $B(\psi(2S) \rightarrow \gamma\chi_{c2}(1P)) = (8.72 \pm 0.34) \times 10^{-2}$ . Our first error is their experiment's error and our second error is the systematic error from using our best value.

$\Gamma(\Sigma^0\Sigma^0)/\Gamma_{total}$	$\Gamma_{53}/\Gamma$
VALUE (units $10^{-4}$ )	CL% EVTS DOCUMENT ID TECN COMMENT
<b>&lt;0.8</b>	90 7.5 ± 3.4 68 NAIK 08 CLEO $\psi(2S) \rightarrow \gamma\Sigma^0\Sigma^0$

68 NAIK 08 reports  $< 0.75 \times 10^{-4}$  from a measurement of  $[\Gamma(\chi_{c2}(1P) \rightarrow \Sigma^0\Sigma^0)/\Gamma_{total}] \times [B(\psi(2S) \rightarrow \gamma\chi_{c2}(1P))]$  assuming  $B(\psi(2S) \rightarrow \gamma\chi_{c2}(1P)) = (9.33 \pm 0.14 \pm 0.61) \times 10^{-2}$ , which we rescale to our best value  $B(\psi(2S) \rightarrow \gamma\chi_{c2}(1P)) = 8.72 \times 10^{-2}$ .

$\Gamma(\Sigma^+\Sigma^-)/\Gamma_{total}$	$\Gamma_{54}/\Gamma$
VALUE (units $10^{-4}$ )	CL% EVTS DOCUMENT ID TECN COMMENT
<b>&lt;0.7</b>	90 4.0 ± 3.5 69 NAIK 08 CLEO $\psi(2S) \rightarrow \gamma\Sigma^+\Sigma^-$

69 NAIK 08 reports  $< 0.67 \times 10^{-4}$  from a measurement of  $[\Gamma(\chi_{c2}(1P) \rightarrow \Sigma^+\Sigma^-)/\Gamma_{total}] \times [B(\psi(2S) \rightarrow \gamma\chi_{c2}(1P))]$  assuming  $B(\psi(2S) \rightarrow \gamma\chi_{c2}(1P)) = (9.33 \pm 0.14 \pm 0.61) \times 10^{-2}$ , which we rescale to our best value  $B(\psi(2S) \rightarrow \gamma\chi_{c2}(1P)) = 8.72 \times 10^{-2}$ .

$\Gamma(\Xi^0\Xi^0)/\Gamma_{total}$	$\Gamma_{55}/\Gamma$
VALUE (units $10^{-4}$ )	CL% EVTS DOCUMENT ID TECN COMMENT
<b>&lt;1.1</b>	90 2.9 ± 1.7 70 NAIK 08 CLEO $\psi(2S) \rightarrow \gamma\Xi^0\Xi^0$

70 NAIK 08 reports  $< 1.06 \times 10^{-4}$  from a measurement of  $[\Gamma(\chi_{c2}(1P) \rightarrow \Xi^0\Xi^0)/\Gamma_{total}] \times [B(\psi(2S) \rightarrow \gamma\chi_{c2}(1P))]$  assuming  $B(\psi(2S) \rightarrow \gamma\chi_{c2}(1P)) = (9.33 \pm 0.14 \pm 0.61) \times 10^{-2}$ , which we rescale to our best value  $B(\psi(2S) \rightarrow \gamma\chi_{c2}(1P)) = 8.72 \times 10^{-2}$ .

$\Gamma(\Xi^-\Xi^+)/\Gamma_{total}$	$\Gamma_{56}/\Gamma$
VALUE (units $10^{-4}$ )	CL% EVTS DOCUMENT ID TECN COMMENT
<b>1.55±0.34±0.06</b>	29 ± 5 71 NAIK 08 CLEO $\psi(2S) \rightarrow \gamma\Xi^-\Xi^+$

• • • We do not use the following data for averages, fits, limits, etc. • • •  
 < 3.7 90 72 ABLIKIM 06D BES2  $\psi(2S) \rightarrow \chi_{c2}\gamma$

71 NAIK 08 reports  $(1.45 \pm 0.30 \pm 0.15) \times 10^{-4}$  from a measurement of  $[\Gamma(\chi_{c2}(1P) \rightarrow \Xi^-\Xi^+)/\Gamma_{total}] \times [B(\psi(2S) \rightarrow \gamma\chi_{c2}(1P))]$  assuming  $B(\psi(2S) \rightarrow \gamma\chi_{c2}(1P)) = (9.33 \pm 0.14 \pm 0.61) \times 10^{-2}$ , which we rescale to our best value  $B(\psi(2S) \rightarrow \gamma\chi_{c2}(1P)) = (8.72 \pm 0.34) \times 10^{-2}$ . Our first error is their experiment's error and our second error is the systematic error from using our best value.

72 Using  $B(\psi(2S) \rightarrow \chi_{c2}\gamma) = (9.3 \pm 0.6)\%$ .

$\Gamma(J/\psi(1S)\pi^+\pi^-\pi^0)/\Gamma_{total}$	$\Gamma_{57}/\Gamma$
VALUE	CL% DOCUMENT ID TECN COMMENT
<b>&lt;0.015</b>	90 BARATE 81 SPEC 190 GeV $\pi^-\pi^-\text{Be} \rightarrow 2\pi 2\mu$

RADIATIVE DECAYS

$\Gamma(\gamma J/\psi(1S))/\Gamma_{total}$	$\Gamma_{58}/\Gamma$
VALUE	DOCUMENT ID TECN COMMENT
<b>0.195±0.008 OUR FIT</b>	

• • • We do not use the following data for averages, fits, limits, etc. • • •  
 0.199±0.005±0.012 73 ADAM 05A CLEO  $e^+e^- \rightarrow \psi(2S) \rightarrow \gamma\chi_{c2}$   
 73 Uses  $B(\psi(2S) \rightarrow \gamma\chi_{c2}) \rightarrow \gamma J/\psi$  from ADAM 05A and  $B(\psi(2S) \rightarrow \gamma\chi_{c2})$  from ATHAR 04.



See key on page 457

Meson Particle Listings

$\chi_{c2}(1P)$

$$\Gamma(\chi_{c2}(1P) \rightarrow K^+ K^-) / \Gamma_{\text{total}} \times \Gamma(\psi(2S) \rightarrow \gamma \chi_{c2}(1P)) / \Gamma_{\text{total}} \times \Gamma_{27} / \Gamma \times \Gamma_{111}^{\psi(2S)} / \Gamma_{\psi(2S)}$$

VALUE (units 10 <sup>-5</sup> )	EVTS	DOCUMENT ID	TECN	COMMENT
<b>9.5 ± 0.6 OUR FIT</b>				
<b>10.5 ± 0.3 ± 0.6</b>	1.6k	93 ASNER	09 CLEO	$\psi(2S) \rightarrow \gamma K^+ K^-$
93 Calculated by us. ASNER 09 reports $B(\chi_{c2} \rightarrow K^+ K^-) = (1.13 \pm 0.03 \pm 0.06 \pm 0.07) \times 10^{-3}$ using $B(\psi(2S) \rightarrow \gamma \chi_{c2}) = (9.33 \pm 0.14 \pm 0.61)\%$ .				

$$\Gamma(\chi_{c2}(1P) \rightarrow K^+ K^-) / \Gamma_{\text{total}} \times \Gamma(\psi(2S) \rightarrow \gamma \chi_{c2}(1P)) / \Gamma(\psi(2S) \rightarrow J/\psi(1S) \pi^+ \pi^-) \times \Gamma_{27} / \Gamma \times \Gamma_{111}^{\psi(2S)} / \Gamma_{11}^{\psi(2S)}$$

VALUE (units 10 <sup>-3</sup> )	EVTS	DOCUMENT ID	TECN	COMMENT
<b>0.283 ± 0.017 OUR FIT</b>				
<b>0.190 ± 0.034 ± 0.019</b>	115 ± 13	94 BAI	98i BES	$\psi(2S) \rightarrow \gamma K^+ K^-$
94 Calculated by us. The value for $B(\chi_{c2} \rightarrow K^+ K^-)$ reported by BAI 98i is derived using $B(\psi(2S) \rightarrow \gamma \chi_{c2}) = (7.8 \pm 0.8)\%$ and $B(\psi(2S) \rightarrow J/\psi \pi^+ \pi^-) = (32.4 \pm 2.6)\%$ [BAI 98d].				

$$\Gamma(\chi_{c2}(1P) \rightarrow K_S^0 K_S^0) / \Gamma_{\text{total}} \times \Gamma(\psi(2S) \rightarrow \gamma \chi_{c2}(1P)) / \Gamma_{\text{total}} \times \Gamma_{28} / \Gamma \times \Gamma_{111}^{\psi(2S)} / \Gamma_{\psi(2S)}$$

VALUE (units 10 <sup>-5</sup> )	EVTS	DOCUMENT ID	TECN	COMMENT
<b>5.1 ± 0.4 OUR FIT</b>				
<b>5.0 ± 0.4 OUR AVERAGE</b>				
4.9 ± 0.3 ± 0.3	373 ± 20	95 ASNER	09 CLEO	$\psi(2S) \rightarrow \gamma K_S^0 K_S^0$
5.72 ± 0.76 ± 0.63	65	ABLIKIM	05o BES2	$\psi(2S) \rightarrow \gamma K_S^0 K_S^0$
95 Calculated by us. ASNER 09 reports $B(\chi_{c2} \rightarrow K_S^0 K_S^0) = (0.53 \pm 0.03 \pm 0.03 \pm 0.03) \times 10^{-3}$ using $B(\psi(2S) \rightarrow \gamma \chi_{c2}) = (9.33 \pm 0.14 \pm 0.61)\%$ .				

$$\Gamma(\chi_{c2}(1P) \rightarrow K_S^0 K_S^0) / \Gamma_{\text{total}} \times \Gamma(\psi(2S) \rightarrow \gamma \chi_{c2}(1P)) / \Gamma(\psi(2S) \rightarrow J/\psi(1S) \pi^+ \pi^-) \times \Gamma_{28} / \Gamma \times \Gamma_{111}^{\psi(2S)} / \Gamma_{11}^{\psi(2S)}$$

VALUE (units 10 <sup>-5</sup> )	DOCUMENT ID	TECN	COMMENT
<b>15.0 ± 1.1 OUR FIT</b>			
<b>14.7 ± 4.1 ± 3.3</b>	96 BAI	99b BES	$\psi(2S) \rightarrow \gamma K_S^0 K_S^0$
96 Calculated by us. The value of $B(\chi_{c2} \rightarrow K_S^0 K_S^0)$ reported by BAI 99b was derived using $B(\psi(2S) \rightarrow \gamma \chi_{c2}(1P)) = (7.8 \pm 0.8)\%$ and $B(\psi(2S) \rightarrow J/\psi \pi^+ \pi^-) = (32.4 \pm 2.6)\%$ [BAI 98d].			

$$\Gamma(\chi_{c2}(1P) \rightarrow \bar{K}^0 K^+ \pi^- + \text{c.c.}) / \Gamma_{\text{total}} \times \Gamma(\psi(2S) \rightarrow \gamma \chi_{c2}(1P)) / \Gamma_{\text{total}} \times \Gamma_{29} / \Gamma \times \Gamma_{111}^{\psi(2S)} / \Gamma_{\psi(2S)}$$

VALUE (units 10 <sup>-4</sup> )	EVTS	DOCUMENT ID	TECN	COMMENT
<b>1.22 ± 0.17 OUR FIT</b>				
<b>1.15 ± 0.18 OUR AVERAGE</b>				
1.21 ± 0.19 ± 0.09	37	97 ATHAR	07 CLEO	$\psi(2S) \rightarrow \gamma K_S^0 K^\pm \pi^\mp$
0.97 ± 0.32 ± 0.13	28	98 ABLIKIM	06r BES2	$\psi(2S) \rightarrow \gamma K_S^0 K^\pm \pi^\mp$
97 Calculated by us. ATHAR 07 reports $B(\chi_{c2} \rightarrow \bar{K}^0 K^+ \pi^- + \text{c.c.}) = (1.3 \pm 0.2 \pm 0.1 \pm 0.1) \times 10^{-3}$ using $B(\psi(2S) \rightarrow \gamma \chi_{c2}) = (9.33 \pm 0.14 \pm 0.61)\%$ .				
98 Calculated by us. ABLIKIM 06r reports $B(\chi_{c2} \rightarrow K_S^0 K^\pm \pi^\mp) = (0.6 \pm 0.2 \pm 0.1) \times 10^{-3}$ using $B(\psi(2S) \rightarrow \gamma \chi_{c2}) = (8.1 \pm 0.6)\%$ . We have multiplied by 2 to obtain $\bar{K}^0 K^+ \pi^- + \text{c.c.}$ from $K_S^0 K^\pm \pi^\mp$ .				

$$\Gamma(\chi_{c2}(1P) \rightarrow 2(\pi^+ \pi^-)) / \Gamma_{\text{total}} \times \Gamma(\psi(2S) \rightarrow \gamma \chi_{c2}(1P)) / \Gamma(\psi(2S) \rightarrow J/\psi(1S) \pi^+ \pi^-) \times \Gamma_1 / \Gamma \times \Gamma_{111}^{\psi(2S)} / \Gamma_{11}^{\psi(2S)}$$

VALUE (units 10 <sup>-3</sup> )	DOCUMENT ID	TECN	COMMENT
<b>2.86 ± 0.27 OUR FIT</b>			
<b>3.1 ± 1.0 OUR AVERAGE</b>			Error includes scale factor of 2.5.
2.3 ± 0.1 ± 0.5	99 BAI	99b BES	$\psi(2S) \rightarrow \gamma \chi_{c2}$
4.3 ± 0.6	100 TANENBAUM	78 MRK1	$\psi(2S) \rightarrow \gamma \chi_{c2}$
99 Calculated by us. The value for $B(\chi_{c2} \rightarrow 2\pi^+ 2\pi^-)$ reported in BAI 99b is derived using $B(\psi(2S) \rightarrow \gamma \chi_{c2}) = (7.8 \pm 0.8)\%$ and $B(\psi(2S) \rightarrow J/\psi(1S) \pi^+ \pi^-) = (32.4 \pm 2.6)\%$ [BAI 98d].			
100 The value for $B(\psi(2S) \rightarrow \gamma \chi_{c2}) \times B(\chi_{c2} \rightarrow 2\pi^+ 2\pi^-)$ reported in TANENBAUM 78 is derived using $B(\psi(2S) \rightarrow J/\psi(1S) \pi^+ \pi^-) \times B(J/\psi(1S) \ell^+ \ell^-) = (4.6 \pm 0.7)\%$ . Calculated by us using $B(J/\psi(1S) \rightarrow \ell^+ \ell^-) = 0.1181 \pm 0.0020$ .			

$$\Gamma(\chi_{c2}(1P) \rightarrow K^+ K^- K^+ K^-) / \Gamma_{\text{total}} \times \Gamma(\psi(2S) \rightarrow \gamma \chi_{c2}(1P)) / \Gamma_{\text{total}} \times \Gamma_{36} / \Gamma \times \Gamma_{111}^{\psi(2S)} / \Gamma_{\psi(2S)}$$

VALUE (units 10 <sup>-4</sup> )	EVTS	DOCUMENT ID	TECN	COMMENT
<b>1.55 ± 0.19 OUR FIT</b>				
<b>1.76 ± 0.16 ± 0.24</b>	160	101 ABLIKIM	06t BES2	$\psi(2S) \rightarrow \gamma 2K^+ 2K^-$
101 Calculated by us. The value of $B(\chi_{c2} \rightarrow 2K^+ 2K^-)$ reported by ABLIKIM 06t was derived using $B(\psi(2S) \rightarrow \gamma \chi_{c2}(1P)) = (8.1 \pm 0.4)\%$ .				

$$\Gamma(\chi_{c2}(1P) \rightarrow K^+ K^- K^+ K^-) / \Gamma_{\text{total}} \times \Gamma(\psi(2S) \rightarrow \gamma \chi_{c2}(1P)) / \Gamma(\psi(2S) \rightarrow J/\psi(1S) \pi^+ \pi^-) \times \Gamma_{36} / \Gamma \times \Gamma_{111}^{\psi(2S)} / \Gamma_{11}^{\psi(2S)}$$

VALUE (units 10 <sup>-4</sup> )	DOCUMENT ID	TECN	COMMENT
<b>4.6 ± 0.6 OUR FIT</b>			
<b>3.6 ± 0.6 ± 0.6</b>	102 BAI	99b BES	$\psi(2S) \rightarrow \gamma 2K^+ 2K^-$
102 Calculated by us. The value of $B(\chi_{c2} \rightarrow 2K^+ 2K^-)$ reported by BAI 99b was derived using $B(\psi(2S) \rightarrow \gamma \chi_{c2}(1P)) = (7.8 \pm 0.8)\%$ and $B(\psi(2S) \rightarrow J/\psi \pi^+ \pi^-) = (32.4 \pm 2.6)\%$ [BAI 98d].			

$$\Gamma(\chi_{c2}(1P) \rightarrow \phi \phi) / \Gamma_{\text{total}} \times \Gamma(\psi(2S) \rightarrow \gamma \chi_{c2}(1P)) / \Gamma_{\text{total}} \times \Gamma_{19} / \Gamma \times \Gamma_{111}^{\psi(2S)} / \Gamma_{\psi(2S)}$$

VALUE (units 10 <sup>-4</sup> )	EVTS	DOCUMENT ID	TECN	COMMENT
<b>1.00 ± 0.10 OUR FIT</b>				
<b>0.98 ± 0.13 OUR AVERAGE</b>				Error includes scale factor of 1.3.
0.94 ± 0.03 ± 0.10	849	103 ABLIKIM	11k BES3	$\psi(2S) \rightarrow \gamma$ hadrons
1.38 ± 0.24 ± 0.23	41	104 ABLIKIM	06t BES2	$\psi(2S) \rightarrow \gamma 2K^+ 2K^-$
103 Calculated by us. The value of $B(\chi_{c2} \rightarrow \phi \phi)$ reported by ABLIKIM 11k was derived using $B(\psi(2S) \rightarrow \gamma \chi_{c2}(1P)) = (8.74 \pm 0.35)\%$ .				
104 Calculated by us. The value of $B(\chi_{c2} \rightarrow \phi \phi)$ reported by ABLIKIM 06t was derived using $B(\psi(2S) \rightarrow \gamma \chi_{c2}(1P)) = (8.1 \pm 0.4)\%$ .				

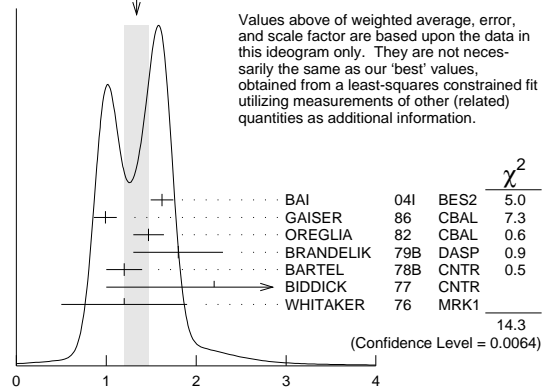
$$\Gamma(\chi_{c2}(1P) \rightarrow \phi \phi) / \Gamma_{\text{total}} \times \Gamma(\psi(2S) \rightarrow \gamma \chi_{c2}(1P)) / \Gamma(\psi(2S) \rightarrow J/\psi(1S) \pi^+ \pi^-) \times \Gamma_{19} / \Gamma \times \Gamma_{111}^{\psi(2S)} / \Gamma_{11}^{\psi(2S)}$$

VALUE (units 10 <sup>-4</sup> )	DOCUMENT ID	TECN	COMMENT
<b>2.96 ± 0.29 OUR FIT</b>			
<b>4.8 ± 1.3 ± 1.3</b>	105 BAI	99b BES	$\psi(2S) \rightarrow \gamma 2K^+ 2K^-$
105 Calculated by us. The value of $B(\chi_{c2} \rightarrow \phi \phi)$ reported by BAI 99b was derived using $B(\psi(2S) \rightarrow \gamma \chi_{c2}(1P)) = (7.8 \pm 0.8)\%$ and $B(\psi(2S) \rightarrow J/\psi \pi^+ \pi^-) = (32.4 \pm 2.6)\%$ [BAI 98d].			

$$\Gamma(\chi_{c2}(1P) \rightarrow \gamma J/\psi(1S)) / \Gamma_{\text{total}} \times \Gamma(\psi(2S) \rightarrow \gamma \chi_{c2}(1P)) / \Gamma_{\text{total}} \times \Gamma_{58} / \Gamma \times \Gamma_{111}^{\psi(2S)} / \Gamma_{\psi(2S)}$$

VALUE (units 10 <sup>-2</sup> )	EVTS	DOCUMENT ID	TECN	COMMENT
<b>1.70 ± 0.04 OUR FIT</b>				
<b>1.34 ± 0.14 OUR AVERAGE</b>				Error includes scale factor of 1.9. See the ideogram below.
1.62 ± 0.04 ± 0.12	5.8k	BAI	04i BES2	$\psi(2S) \rightarrow J/\psi \gamma \gamma$
0.99 ± 0.10 ± 0.08		GAISER	86 CBAL	$\psi(2S) \rightarrow \gamma X$
1.47 ± 0.17		106 OREGLIA	82 CBAL	$\psi(2S) \rightarrow \gamma \chi_{c2}$
1.8 ± 0.5		107 BRANDELNIK	79b DASP	$\psi(2S) \rightarrow \gamma \chi_{c2}$
1.2 ± 0.2		107 BARTEL	78b CNTR	$\psi(2S) \rightarrow \gamma \chi_{c2}$
2.2 ± 1.2		108 BIDDICK	77 CNTR	$e^+ e^- \rightarrow \gamma X$
1.2 ± 0.7		106 WHITAKER	76 MRK1	$e^+ e^-$
• • • We do not use the following data for averages, fits, limits, etc. • • •				
1.95 ± 0.02 ± 0.07	12.4k	109 MENDEZ	08 CLEO	$\psi(2S) \rightarrow \gamma \chi_{c2}$
1.85 ± 0.04 ± 0.07	1.9k	110 ADAM	05a CLEO	Repl. by MENDEZ 08
106 Recalculated by us using $B(J/\psi(1S) \rightarrow \ell^+ \ell^-) = 0.1181 \pm 0.0020$ .				
107 Recalculated by us using $B(J/\psi(1S) \rightarrow \mu^+ \mu^-) = 0.0588 \pm 0.0010$ .				
108 Assumes isotropic gamma distribution.				
109 Not independent from other measurements of MENDEZ 08.				
110 Not independent from other values reported by ADAM 05a.				

WEIGHTED AVERAGE  
1.34 ± 0.14 (Error scaled by 1.9)



$$\Gamma(\chi_{c2}(1P) \rightarrow \gamma J/\psi(1S)) / \Gamma_{\text{total}} \times \Gamma(\psi(2S) \rightarrow \gamma \chi_{c2}(1P)) / \Gamma_{\text{total}} \text{ (units } 10^{-2})$$

$$\Gamma(\chi_{c2}(1P) \rightarrow \gamma J/\psi(1S)) / \Gamma_{\text{total}} \times \Gamma(\psi(2S) \rightarrow \gamma \chi_{c2}(1P)) / \Gamma(\psi(2S) \rightarrow J/\psi(1S) \text{ anything}) \times \Gamma_{58} / \Gamma \times \Gamma_{111}^{\psi(2S)} / \Gamma_{11}^{\psi(2S)}$$

$$\Gamma_{58} / \Gamma \times \Gamma_{111}^{\psi(2S)} / \Gamma_{11}^{\psi(2S)} = \Gamma_{58} / \Gamma \times \Gamma_{111}^{\psi(2S)} / (\Gamma_{11}^{\psi(2S)} + \Gamma_{12}^{\psi(2S)} + \Gamma_{13}^{\psi(2S)} + 0.344 \Gamma_{110}^{\psi(2S)} + 0.195 \Gamma_{111}^{\psi(2S)})$$

VALUE (units 10 <sup>-2</sup> )	EVTS	DOCUMENT ID	TECN	COMMENT
<b>2.86 ± 0.07 OUR FIT</b>				
• • • We do not use the following data for averages, fits, limits, etc. • • •				
3.12 ± 0.03 ± 0.09	12.4k	111 MENDEZ	08 CLEO	$\psi(2S) \rightarrow \gamma \chi_{c2}$
3.11 ± 0.07 ± 0.07	1.9k	ADAM	05a CLEO	Repl. by MENDEZ 08
111 Not independent from other measurements of MENDEZ 08.				



Table listing authors and document IDs for various experiments (ARMSTRONG, BAUER, BAGLIN, etc.)

$\eta_c(2S)$

$I^G(J^{PC}) = 0^+(0^-)$

Quantum numbers are quark model predictions.

$\eta_c(2S)$  MASS

Table of mass measurements for  $\eta_c(2S)$  with columns for VALUE (MeV), EVTS, DOCUMENT ID, TECN, and COMMENT.

Notes for mass measurements: 1 Ignoring possible interference with continuum. 2 Accounts for interference with non-resonant continuum. 3 From a fit of the J/psi recoil mass spectrum. Supersedes ABE, K 02 and ABE 04g.

$\eta_c(2S)$  WIDTH

Table of width measurements for  $\eta_c(2S)$  with columns for VALUE (MeV), CL%, EVTS, DOCUMENT ID, TECN, and COMMENT.

Notes for width measurements: 8 Ignoring possible interference with continuum. 9 Accounts for interference with non-resonant continuum. 10 From the fit of the kaon momentum spectrum. Systematic errors not evaluated.

$\eta_c(2S)$  DECAY MODES

Table of decay modes for  $\eta_c(2S)$  with columns for Mode, Fraction (Gamma\_i/Gamma), and Confidence level.

Table of partial widths for  $\eta_c(2S)$  with columns for Gamma\_i, VALUE (keV), DOCUMENT ID, TECN, and COMMENT.

$\eta_c(2S)$  PARTIAL WIDTHS

Table of branching ratios for  $\eta_c(2S)$  with columns for Gamma(i)Gamma(gamma)/Gamma(total), VALUE (eV), CL%, DOCUMENT ID, TECN, and COMMENT.

$\eta_c(2S)$  Gamma(i)Gamma(gamma)/Gamma(total)

Table of branching ratios for  $\eta_c(2S)$  with columns for Gamma(2pi+2pi-), VALUE (eV), CL%, DOCUMENT ID, TECN, and COMMENT.

Table of branching ratios for  $\eta_c(2S)$  with columns for Gamma(KKpi), VALUE (eV), EVTS, DOCUMENT ID, TECN, and COMMENT.

Table of branching ratios for  $\eta_c(2S)$  with columns for Gamma(K+K-pi+pi-), VALUE (eV), CL%, DOCUMENT ID, TECN, and COMMENT.

Table of branching ratios for  $\eta_c(2S)$  with columns for Gamma(K+K-pi+pi-pi0), VALUE (eV), EVTS, DOCUMENT ID, TECN, and COMMENT.

Table of branching ratios for  $\eta_c(2S)$  with columns for Gamma(2K+2K-), VALUE (eV), CL%, DOCUMENT ID, TECN, and COMMENT.

$\eta_c(2S)$  Gamma(i)Gamma(gamma)/Gamma^2(total)

Table of branching ratios for  $\eta_c(2S)$  with columns for Gamma(rho0)/Gamma(total) \* Gamma(gamma)/Gamma(total), VALUE (units 10^-8), CL%, DOCUMENT ID, TECN, and COMMENT.

Notes for branching ratios: 17 Including the measurements of ARMSTRONG 95f in the AMBROGIANI 01 analysis. 18 For a total width Gamma=5 MeV. 19 For the resonance mass region 3589-3599 MeV/c^2. 20 For the resonance mass region 3575-3660 MeV/c^2.

$\eta_c(2S)$  BRANCHING RATIOS

Table of branching ratios for  $\eta_c(2S)$  with columns for Gamma(hadrons)/Gamma(total), VALUE, CL%, DOCUMENT ID, TECN, and COMMENT.

Table of branching ratios for  $\eta_c(2S)$  with columns for Gamma(KKpi)/Gamma(total), VALUE (units 10^-2), EVTS, DOCUMENT ID, TECN, and COMMENT.

Notes for branching ratios: 22 Derived from a measurement of [B(B+ -> eta\_c(2S)K+) \* B(eta\_c(2S) -> K-Kpi)] / [B(B+ -> eta\_c K+) \* B(eta\_c -> K-Kpi)] = (9.6+2.0/-1.9 +/- 2.5)% and using B(B+ -> eta\_c(2S)K+) = (3.4 +/- 1.8) \* 10^-4, and [B(B+ -> eta\_c K+) \* B(eta\_c -> K-Kpi)] = (6.88 +/- 0.77 +/- 0.55/-0.66) \* 10^-5. 23 For a mass value of 3654 +/- 6 MeV

## Meson Particle Listings

 $\eta_c(2S), \psi(2S)$ 

$\Gamma(2\pi^+2\pi^-)/\Gamma_{\text{total}}$		$\Gamma_3/\Gamma$		
VALUE	DOCUMENT ID	TECN	COMMENT	
not seen	UEHARA	08	BELL $\gamma\gamma \rightarrow \eta_c(2S)$	
$\Gamma(\rho^0\rho^0)/\Gamma_{\text{total}}$		$\Gamma_4/\Gamma$		
VALUE	DOCUMENT ID	TECN	COMMENT	
not seen	ABLIKIM	11H	BES3 $\psi(2S) \rightarrow \gamma 2\pi^+ 2\pi^-$	
$\Gamma(K^+K^-\pi^+\pi^-)/\Gamma_{\text{total}}$		$\Gamma_6/\Gamma$		
VALUE	DOCUMENT ID	TECN	COMMENT	
not seen	UEHARA	08	BELL $\gamma\gamma \rightarrow \eta_c(2S)$	
$\Gamma(K^+K^-\pi^+\pi^0)/\Gamma(K\bar{K}\pi)$		$\Gamma_8/\Gamma_2$		
VALUE	EVTS	DOCUMENT ID	TECN	COMMENT
$0.73 \pm 0.17 \pm 0.17$	1201	24	DEL-AMO-SA...11M	BABR $\gamma\gamma \rightarrow K^+K^-\pi^+\pi^0$
24 We have multiplied the value of $\Gamma(K^+K^-\pi^+\pi^0)/\Gamma(K_S^0K^+\pi^-)$ reported in DEL-AMO-SANCHEZ 11M by a factor 1/3 to obtain $\Gamma(K^+K^-\pi^+\pi^0)/\Gamma(K\bar{K}\pi)$ . Not independent from other measurements reported in DEL-AMO-SANCHEZ 11M.				
$\Gamma(K^{*0}\bar{K}^{*0})/\Gamma_{\text{total}}$		$\Gamma_7/\Gamma$		
VALUE	DOCUMENT ID	TECN	COMMENT	
not seen	ABLIKIM	11H	BES3 $\psi(2S) \rightarrow \gamma K^+K^-\pi^+\pi^-$	
$\Gamma(2K^+2K^-)/\Gamma_{\text{total}}$		$\Gamma_{11}/\Gamma$		
VALUE	DOCUMENT ID	TECN	COMMENT	
not seen	UEHARA	08	BELL $\gamma\gamma \rightarrow \eta_c(2S)$	
$\Gamma(\phi\phi)/\Gamma_{\text{total}}$		$\Gamma_{12}/\Gamma$		
VALUE	DOCUMENT ID	TECN	COMMENT	
not seen	ABLIKIM	11H	BES3 $\psi(2S) \rightarrow \gamma K^+K^-K^+K^-$	
$\Gamma(\gamma\gamma)/\Gamma_{\text{total}}$		$\Gamma_{14}/\Gamma$		
VALUE	CL%	DOCUMENT ID	TECN	COMMENT
$<5 \times 10^{-4}$	90	25	WICHT	08 BELL $B^\pm \rightarrow K^\pm \gamma\gamma$
• • • We do not use the following data for averages, fits, limits, etc. • • •				
not seen		AMBROGIANI	01	E835 $\bar{p}p \rightarrow \gamma\gamma$
$<0.01$	90	LEE	85	CBAL $\psi' \rightarrow \text{photons}$
25 WICHT 08 reports $[\Gamma(\eta_c(2S) \rightarrow \gamma\gamma)/\Gamma_{\text{total}}] \times [B(B^+ \rightarrow \eta_c(2S)K^+)] < 0.18 \times 10^{-6}$ which we divide by our best value $B(B^+ \rightarrow \eta_c(2S)K^+) = 3.4 \times 10^{-4}$ .				

 $\eta_c(2S)$  CROSS-PARTICLE BRANCHING RATIOS

$\Gamma(\eta_c(2S) \rightarrow 2\pi^+2\pi^-)/\Gamma_{\text{total}} \times \Gamma(\psi(2S) \rightarrow \gamma\eta_c(2S))/\Gamma_{\text{total}}$		$\Gamma_3/\Gamma \times \Gamma_{113}^{\psi(2S)}/\Gamma\psi(2S)$		
VALUE	CL%	DOCUMENT ID	TECN	COMMENT
$<14.6 \times 10^{-6}$	90	26	CRONIN-HEN..10	CLEO $\psi(2S) \rightarrow \gamma 2\pi^+ 2\pi^-$
26 Assuming $\Gamma(\eta_c(2S)) = 14$ MeV. CRONIN-HENNESSY 10 gives the analytic dependence of limits on width.				
$\Gamma(\eta_c(2S) \rightarrow \rho^0\rho^0)/\Gamma_{\text{total}} \times \Gamma(\psi(2S) \rightarrow \gamma\eta_c(2S))/\Gamma_{\text{total}}$		$\Gamma_4/\Gamma \times \Gamma_{113}^{\psi(2S)}/\Gamma\psi(2S)$		
VALUE	CL%	DOCUMENT ID	TECN	COMMENT
$<12.7 \times 10^{-7}$	90	ABLIKIM	11H	BES3 $\psi(2S) \rightarrow \gamma 2\pi^+ 2\pi^-$
$\Gamma(\eta_c(2S) \rightarrow 3\pi^+3\pi^-)/\Gamma_{\text{total}} \times \Gamma(\psi(2S) \rightarrow \gamma\eta_c(2S))/\Gamma_{\text{total}}$		$\Gamma_5/\Gamma \times \Gamma_{113}^{\psi(2S)}/\Gamma\psi(2S)$		
VALUE	CL%	DOCUMENT ID	TECN	COMMENT
$<13.2 \times 10^{-6}$	90	27	CRONIN-HEN..10	CLEO $\psi(2S) \rightarrow \gamma 3\pi^+ 3\pi^-$
27 Assuming $\Gamma(\eta_c(2S)) = 14$ MeV. CRONIN-HENNESSY 10 gives the analytic dependence of limits on width.				
$\Gamma(\eta_c(2S) \rightarrow K^+K^-\pi^+\pi^-)/\Gamma_{\text{total}} \times \Gamma(\psi(2S) \rightarrow \gamma\eta_c(2S))/\Gamma_{\text{total}}$		$\Gamma_6/\Gamma \times \Gamma_{113}^{\psi(2S)}/\Gamma\psi(2S)$		
VALUE	CL%	DOCUMENT ID	TECN	COMMENT
$<9.6 \times 10^{-6}$	90	28	CRONIN-HEN..10	CLEO $\psi(2S) \rightarrow \gamma K^+K^-\pi^+\pi^-$
28 Assuming $\Gamma(\eta_c(2S)) = 14$ MeV. CRONIN-HENNESSY 10 gives the analytic dependence of limits on width.				

$\Gamma(\eta_c(2S) \rightarrow K^{*0}\bar{K}^{*0})/\Gamma_{\text{total}} \times \Gamma(\psi(2S) \rightarrow \gamma\eta_c(2S))/\Gamma_{\text{total}}$		$\Gamma_7/\Gamma \times \Gamma_{113}^{\psi(2S)}/\Gamma\psi(2S)$		
VALUE	CL%	DOCUMENT ID	TECN	COMMENT
$<19.6 \times 10^{-7}$	90	ABLIKIM	11H	BES3 $\psi(2S) \rightarrow \gamma K^+K^-\pi^+\pi^-$
$\Gamma(\eta_c(2S) \rightarrow K^+K^-\pi^+\pi^0)/\Gamma_{\text{total}} \times \Gamma(\psi(2S) \rightarrow \gamma\eta_c(2S))/\Gamma_{\text{total}}$		$\Gamma_8/\Gamma \times \Gamma_{113}^{\psi(2S)}/\Gamma\psi(2S)$		
VALUE	CL%	DOCUMENT ID	TECN	COMMENT
$<43.0 \times 10^{-6}$	90	29	CRONIN-HEN..10	CLEO $\psi(2S) \rightarrow \gamma K^+K^-\pi^+\pi^0$
29 Assuming $\Gamma(\eta_c(2S)) = 14$ MeV. CRONIN-HENNESSY 10 gives the analytic dependence of limits on width.				

$\Gamma(\eta_c(2S) \rightarrow K^+K^-2\pi^+2\pi^-)/\Gamma_{\text{total}} \times \Gamma(\psi(2S) \rightarrow \gamma\eta_c(2S))/\Gamma_{\text{total}}$		$\Gamma_9/\Gamma \times \Gamma_{113}^{\psi(2S)}/\Gamma\psi(2S)$		
VALUE	CL%	DOCUMENT ID	TECN	COMMENT
$<9.7 \times 10^{-6}$	90	30	CRONIN-HEN..10	CLEO $\psi(2S) \rightarrow \gamma K^+K^-2\pi^+2\pi^-$
30 Assuming $\Gamma(\eta_c(2S)) = 14$ MeV. CRONIN-HENNESSY 10 gives the analytic dependence of limits on width.				
$\Gamma(\eta_c(2S) \rightarrow K_S^0K^-2\pi^+\pi^- + \text{c.c.})/\Gamma_{\text{total}} \times \Gamma(\psi(2S) \rightarrow \gamma\eta_c(2S))/\Gamma_{\text{total}}$		$\Gamma_{10}/\Gamma \times \Gamma_{113}^{\psi(2S)}/\Gamma\psi(2S)$		
VALUE	CL%	DOCUMENT ID	TECN	COMMENT
$<15.2 \times 10^{-6}$	90	31	CRONIN-HEN..10	CLEO $\psi(2S) \rightarrow \gamma K_S^0K^-2\pi^+\pi^- + \text{c.c.}$
31 Assuming $\Gamma(\eta_c(2S)) = 14$ MeV. CRONIN-HENNESSY 10 gives the analytic dependence of limits on width.				
$\Gamma(\eta_c(2S) \rightarrow \phi\phi)/\Gamma_{\text{total}} \times \Gamma(\psi(2S) \rightarrow \gamma\eta_c(2S))/\Gamma_{\text{total}}$		$\Gamma_{12}/\Gamma \times \Gamma_{113}^{\psi(2S)}/\Gamma\psi(2S)$		
VALUE	CL%	DOCUMENT ID	TECN	COMMENT
$<7.8 \times 10^{-7}$	90	ABLIKIM	11H	BES3 $\psi(2S) \rightarrow \gamma K^+K^-K^+K^-$
$\Gamma(\eta_c(2S) \rightarrow \pi^+\pi^-\eta)/\Gamma_{\text{total}} \times \Gamma(\psi(2S) \rightarrow \gamma\eta_c(2S))/\Gamma_{\text{total}}$		$\Gamma_{15}/\Gamma \times \Gamma_{113}^{\psi(2S)}/\Gamma\psi(2S)$		
VALUE	CL%	DOCUMENT ID	TECN	COMMENT
$<4.3 \times 10^{-6}$	90	32	CRONIN-HEN..10	CLEO $\psi(2S) \rightarrow \gamma \pi^+\pi^-\eta$
32 Assuming $\Gamma(\eta_c(2S)) = 14$ MeV. CRONIN-HENNESSY 10 gives the analytic dependence of limits on width.				
$\Gamma(\eta_c(2S) \rightarrow \pi^+\pi^-\eta')/\Gamma_{\text{total}} \times \Gamma(\psi(2S) \rightarrow \gamma\eta_c(2S))/\Gamma_{\text{total}}$		$\Gamma_{16}/\Gamma \times \Gamma_{113}^{\psi(2S)}/\Gamma\psi(2S)$		
VALUE	CL%	DOCUMENT ID	TECN	COMMENT
$<14.2 \times 10^{-6}$	90	33	CRONIN-HEN..10	CLEO $\psi(2S) \rightarrow \gamma \pi^+\pi^-\eta'$
33 Assuming $\Gamma(\eta_c(2S)) = 14$ MeV. CRONIN-HENNESSY 10 gives the analytic dependence of limits on width.				
$\Gamma(\eta_c(2S) \rightarrow K^+K^-\eta)/\Gamma_{\text{total}} \times \Gamma(\psi(2S) \rightarrow \gamma\eta_c(2S))/\Gamma_{\text{total}}$		$\Gamma_{17}/\Gamma \times \Gamma_{113}^{\psi(2S)}/\Gamma\psi(2S)$		
VALUE	CL%	DOCUMENT ID	TECN	COMMENT
$<5.9 \times 10^{-6}$	90	34	CRONIN-HEN..10	CLEO $\psi(2S) \rightarrow \gamma K^+K^-\eta$
34 Assuming $\Gamma(\eta_c(2S)) = 14$ MeV. CRONIN-HENNESSY 10 gives the analytic dependence of limits on width.				
$\Gamma(\eta_c(2S) \rightarrow \pi^+\pi^-\eta_c(1S))/\Gamma_{\text{total}} \times \Gamma(\psi(2S) \rightarrow \gamma\eta_c(2S))/\Gamma_{\text{total}}$		$\Gamma_{18}/\Gamma \times \Gamma_{113}^{\psi(2S)}/\Gamma\psi(2S)$		
VALUE	CL%	DOCUMENT ID	TECN	COMMENT
$<1.7 \times 10^{-4}$	90	35	CRONIN-HEN..10	CLEO $\psi(2S) \rightarrow \gamma \pi^+\pi^-\eta_c(1S)$
35 Assuming $\Gamma(\eta_c(2S)) = 14$ MeV. CRONIN-HENNESSY 10 gives the analytic dependence of limits on width.				

 $\eta_c(2S)$  REFERENCES

ABLIKIM	11H	PR D84 091102	M. Ablikim et al.	(BES III Collab.)
DEL-AMO-SA...	11M	PR D84 012004	P. del Amo Sanchez et al.	(BABAR Collab.)
VINOKUROVA	11	PL B706 139	A. Vinokurova et al.	(BELLE Collab.)
CRONIN-HEN..	10	PR D81 052002	D. Cronin-Hennessey et al.	(CLEO Collab.)
AUBERT	08AB	PR D78 012006	B. Aubert et al.	(BABAR Collab.)
UEHARA	08	EPJ C53 1	S. Uehara et al.	(BELLE Collab.)
WICHT	08	PL B662 323	J. Wicht et al.	(BELLE Collab.)
ABE	07	PRL 98 082001	K. Abe et al.	(BELLE Collab.)
AUBERT	06E	PRL 96 052002	B. Aubert et al.	(BABAR Collab.)
AUBERT	05C	PR D72 031101R	B. Aubert et al.	(BABAR Collab.)
ABE	04G	PR D70 071102	K. Abe et al.	(BELLE Collab.)
ASNER	04	PRL 92 142001	D.M. Asner et al.	(CLEO Collab.)
AUBERT	04D	PRL 92 142002	B. Aubert et al.	(BABAR Collab.)
ABE,K	02	PRL 89 142001	K. Abe et al.	(BELLE Collab.)
CHOI	02	PRL 89 102001	S.-K. Choi et al.	(BELLE Collab.)
AMBROGIANI	01	PR D64 052003	M. Ambrogiani et al.	(FNAL E835 Collab.)
ABREU	98O	PL B441 479	P. Abreu et al.	(DELPHI Collab.)
ARMSTRONG	95F	PR D52 4839	T.A. Armstrong et al.	(FNAL, FERR, GENO+)
LEE	85	SLAC 282	R.A. Lee	(SLAC)
EDWARDS	82C	PRL 48 70	C. Edwards et al.	(CIT, HARV, PRIN+)

 $\psi(2S)$ 

$$I^G(J^{PC}) = 0^-(1^{--})$$

See the Review on " $\psi(2S)$  and  $\chi_c$  branching ratios" before the  $\chi_{c0}(1P)$  Listings.

 $\psi(2S)$  MASS

OUR FIT includes measurements of  $m_{\psi(2S)}$ ,  $m_{\psi(3770)}$ , and  $m_{\psi(3770)} - m_{\psi(2S)}$ .

VALUE (MeV)	EVTS	DOCUMENT ID	TECN	COMMENT
$3686.109 \pm 0.012$				OUR FIT
$-0.014$				
$3686.108 \pm 0.011$				OUR AVERAGE
$-0.014$				
$3686.12 \pm 0.06 \pm 0.10$	4k	AAIJ	12H	LHCB $pp \rightarrow J/\psi \pi^+\pi^- X$



# Meson Particle Listings

## $\psi(2S)$

$\Gamma_{102}$	$\phi f_2'(1525)$	$(4.4 \pm 1.6) \times 10^{-5}$	
$\Gamma_{103}$	$\Theta(1540)\bar{\Theta}(1540) \rightarrow K_S^0 p K^- \bar{\pi}^+ \text{ c.c.}$	$< 8.8 \times 10^{-6}$	CL=90%
$\Gamma_{104}$	$\Theta(1540)K^- \bar{\pi}^+ \rightarrow K_S^0 p K^- \bar{\pi}^+$	$< 1.0 \times 10^{-5}$	CL=90%
$\Gamma_{105}$	$\Theta(1540)K_S^0 \bar{p} \rightarrow K_S^0 \bar{p} K^+ n$	$< 7.0 \times 10^{-6}$	CL=90%
$\Gamma_{106}$	$\bar{\Theta}(1540)K^+ n \rightarrow K_S^0 \bar{p} K^+ n$	$< 2.6 \times 10^{-5}$	CL=90%
$\Gamma_{107}$	$\bar{\Theta}(1540)K_S^0 p \rightarrow K_S^0 p K^- \bar{\pi}^+$	$< 6.0 \times 10^{-6}$	CL=90%
$\Gamma_{108}$	$K_S^0 K_S^0$	$< 4.6 \times 10^{-6}$	

### Radiative decays

$\Gamma_{109}$	$\gamma \chi_{c0}(1P)$	$(9.68 \pm 0.31) \%$	
$\Gamma_{110}$	$\gamma \chi_{c1}(1P)$	$(9.2 \pm 0.4) \%$	
$\Gamma_{111}$	$\gamma \chi_{c2}(1P)$	$(8.72 \pm 0.34) \%$	
$\Gamma_{112}$	$\gamma \eta_c(1S)$	$(3.4 \pm 0.5) \times 10^{-3}$	S=1.3
$\Gamma_{113}$	$\gamma \eta_c(2S)$	$< 8 \times 10^{-4}$	CL=90%
$\Gamma_{114}$	$\gamma \pi^0$	$(1.6 \pm 0.4) \times 10^{-6}$	
$\Gamma_{115}$	$\gamma \eta'(958)$	$(1.23 \pm 0.06) \times 10^{-4}$	
$\Gamma_{116}$	$\gamma f_2'(1270)$	$(2.1 \pm 0.4) \times 10^{-4}$	
$\Gamma_{117}$	$\gamma f_0(1710)$	$(3.0 \pm 1.3) \times 10^{-5}$	
$\Gamma_{118}$	$\gamma f_0(1710) \rightarrow \gamma \pi^+ \pi^-$	$(6.0 \pm 1.6) \times 10^{-5}$	
$\Gamma_{119}$	$\gamma f_0(1710) \rightarrow \gamma K \bar{K}$	$< 1.4 \times 10^{-4}$	CL=90%
$\Gamma_{120}$	$\gamma \gamma$	$(1.4 \pm 0.5) \times 10^{-6}$	
$\Gamma_{121}$	$\gamma \eta$	$(8.7 \pm 2.1) \times 10^{-4}$	
$\Gamma_{122}$	$\gamma \eta \pi^+ \pi^-$	$< 9 \times 10^{-5}$	CL=90%
$\Gamma_{123}$	$\gamma \eta(1405)$	$(3.6 \pm 2.5) \times 10^{-5}$	
$\Gamma_{124}$	$\gamma \eta(1405) \rightarrow \gamma K \bar{K} \pi$	$< 1.4 \times 10^{-4}$	CL=90%
$\Gamma_{125}$	$\gamma \eta(1405) \rightarrow \eta \pi^+ \pi^-$	$< 8.8 \times 10^{-5}$	CL=90%
$\Gamma_{126}$	$\gamma \eta(1475)$	$(4.0 \pm 0.6) \times 10^{-4}$	
$\Gamma_{127}$	$\gamma \eta(1475) \rightarrow K \bar{K} \pi$	$(3.7 \pm 0.9) \times 10^{-4}$	
$\Gamma_{128}$	$\gamma \eta(1475) \rightarrow \eta \pi^+ \pi^-$	$(2.4 \pm 0.7) \times 10^{-4}$	
$\Gamma_{129}$	$\gamma 2(\pi^+ \pi^-)$	$(2.6 \pm 0.5) \times 10^{-4}$	
$\Gamma_{130}$	$\gamma K^{*0} K^+ \pi^- \text{ c.c.}$	$(1.9 \pm 0.5) \times 10^{-4}$	
$\Gamma_{131}$	$\gamma K^{*0} \bar{K}^{*0}$	$(3.9 \pm 0.5) \times 10^{-5}$	S=2.0
$\Gamma_{132}$	$\gamma K_S^0 K^+ \pi^- \text{ c.c.}$	$(1.20 \pm 0.22) \times 10^{-5}$	
$\Gamma_{133}$	$\gamma K^+ K^- \pi^+ \pi^-$	$(7.2 \pm 1.8) \times 10^{-6}$	
$\Gamma_{134}$	$\gamma \rho \bar{\rho}$	$< 1.6 \times 10^{-6}$	CL=90%
$\Gamma_{135}$	$\gamma f_2(1950) \rightarrow \gamma \rho \bar{\rho}$	$< 2 \times 10^{-6}$	CL=90%
$\Gamma_{136}$	$\gamma f_2(2150) \rightarrow \gamma \rho \bar{\rho}$	$[a] < 1.6 \times 10^{-6}$	
$\Gamma_{137}$	$\gamma X(1835) \rightarrow \gamma \rho \bar{\rho}$	$(2.8 \pm 1.4) \times 10^{-5}$	
$\Gamma_{138}$	$\gamma X \rightarrow \gamma \rho \bar{\rho}$	$< 2.2 \times 10^{-4}$	CL=90%
$\Gamma_{139}$	$\gamma \pi^+ \pi^- \rho \bar{\rho}$	$< 1.7 \times 10^{-4}$	CL=90%
$\Gamma_{140}$	$\gamma 2(\pi^+ \pi^-) K^+ K^-$	$< 4 \times 10^{-5}$	CL=90%
$\Gamma_{141}$	$\gamma 3(\pi^+ \pi^-)$		
$\Gamma_{142}$	$\gamma K^+ K^- K^+ K^-$		

[a] For a narrow resonance in the range  $2.2 < M(X) < 2.8$  GeV.

### CONSTRAINED FIT INFORMATION

A multiparticle fit to  $\chi_{c1}(1P)$ ,  $\chi_{c0}(1P)$ ,  $\chi_{c2}(1P)$ , and  $\psi(2S)$  with 4 total widths, a partial width, 25 combinations of partial widths obtained from integrated cross section, and 84 branching ratios uses 223 measurements to determine 49 parameters. The overall fit has a  $\chi^2 = 312.2$  for 174 degrees of freedom.

The following *off-diagonal* array elements are the correlation coefficients  $\langle \delta p_i \delta p_j \rangle / (\delta p_i \delta p_j)$ , in percent, from the fit to parameters  $p_i$ , including the branching fractions,  $x_i \equiv \Gamma_i / \Gamma_{\text{total}}$ .

$x_7$	5									
$x_8$	1	0								
$x_{11}$	44	12	3							
$x_{12}$	39	8	2	64						
$x_{13}$	27	7	2	57	35					
$x_{19}$	2	1	0	7	5	4				
$x_{109}$	2	1	0	4	3	2	0			
$x_{110}$	2	1	0	5	2	3	0	0		
$x_{111}$	3	1	0	6	4	4	0	0	0	
$\Gamma$	-79	-6	-2	-52	-46	-32	-10	-2	-3	-3
	$x_6$	$x_7$	$x_8$	$x_{11}$	$x_{12}$	$x_{13}$	$x_{19}$	$x_{109}$	$x_{110}$	$x_{111}$

### $\psi(2S)$ PARTIAL WIDTHS

$\Gamma(\text{hadrons})$		$\Gamma_1$			
VALUE (keV)	DOCUMENT ID	TECN	COMMENT		
••• We do not use the following data for averages, fits, limits, etc. •••					
$258 \pm 26$	BAI	02B	BES2	$e^+ e^-$	
$224 \pm 56$	LUTH	75	MRK1	$e^+ e^-$	
$\Gamma(e^+ e^-)$		$\Gamma_6$			
VALUE (keV)	DOCUMENT ID	TECN	COMMENT		
<b>2.35 <math>\pm</math> 0.04 OUR FIT</b>					
<b>2.33 <math>\pm</math> 0.07 OUR AVERAGE</b>					
$2.338 \pm 0.037 \pm 0.096$	ABLIKIM	08B	BES2	$e^+ e^- \rightarrow \text{hadrons}$	
$2.330 \pm 0.036 \pm 0.110$	ABLIKIM	06L	BES2	$e^+ e^- \rightarrow \text{hadrons}$	
$2.44 \pm 0.21$	9 BAI	02B	BES2	$e^+ e^-$	
$2.14 \pm 0.21$	ALEXANDER	89	RVUE	See $\Upsilon$ mini-review	
••• We do not use the following data for averages, fits, limits, etc. •••					
$2.0 \pm 0.3$	BRANDELIK	79C	DASP	$e^+ e^-$	
$2.1 \pm 0.3$	10 LUTH	75	MRK1	$e^+ e^-$	
9 From a simultaneous fit to $e^+ e^-$ , $\mu^+ \mu^-$ , and hadronic channel, assuming $\Gamma_e = \Gamma_\mu = \Gamma_\tau / 0.38847$ .					
10 From a simultaneous fit to $e^+ e^-$ , $\mu^+ \mu^-$ , and hadronic channels assuming $\Gamma(e^+ e^-) = \Gamma(\mu^+ \mu^-)$ .					
$\Gamma(\gamma\gamma)$		$\Gamma_{120}$			
VALUE (eV)	CL%	DOCUMENT ID	TECN	COMMENT	
<b>&lt;43</b>	90	BRANDELIK	79C	DASP	$e^+ e^-$

### $\psi(2S)$ $\Gamma(i)\Gamma(e^+ e^-)/\Gamma(\text{total})$

This combination of a partial width with the partial width into  $e^+ e^-$  and with the total width is obtained from the integrated cross section into channel(i) in the  $e^+ e^-$  annihilation. We list only data that have not been used to determine the partial width  $\Gamma(i)$  or the branching ratio  $\Gamma(i)/\text{total}$ .

$\Gamma(\text{hadrons}) \times \Gamma(e^+ e^-)/\Gamma_{\text{total}}$		$\Gamma_1 \Gamma_6/\Gamma$			
VALUE (keV)	DOCUMENT ID	TECN	COMMENT		
<b>2.233 <math>\pm</math> 0.015 <math>\pm</math> 0.042</b>					
11 ANASHIN 12 KEDR $e^+ e^- \rightarrow \text{hadrons}$					
••• We do not use the following data for averages, fits, limits, etc. •••					
$2.2 \pm 0.4$	ABRAMS	75	MRK1	$e^+ e^-$	
11 ANASHIN 12 reports the value $2.233 \pm 0.015 \pm 0.037 \pm 0.020$ keV, where the third uncertainty is due to assumptions on the interference between the resonance and hadronic continuum. We combined the two systematic uncertainties.					
$\Gamma(\tau^+ \tau^-) \times \Gamma(e^+ e^-)/\Gamma_{\text{total}}$		$\Gamma_8 \Gamma_6/\Gamma$			
VALUE (eV)	EVTs	DOCUMENT ID	TECN	COMMENT	
$9.0 \pm 2.6$	79	12 ANASHIN	07	KEDR	$e^+ e^- \rightarrow \psi(2S) \rightarrow \tau^+ \tau^-$
12 Using $\psi(2S)$ total width of $337 \pm 13$ keV. Systematic errors not evaluated.					
$\Gamma(J/\psi(1S)\pi^+\pi^-) \times \Gamma(e^+ e^-)/\Gamma_{\text{total}}$		$\Gamma_{11} \Gamma_6/\Gamma$			
VALUE (keV)	EVTs	DOCUMENT ID	TECN	COMMENT	
<b>0.789 <math>\pm</math> 0.015 OUR FIT</b>					
<b>0.82 <math>\pm</math> 0.04 OUR AVERAGE</b> Error includes scale factor of 1.6. See the ideogram below.					
$0.852 \pm 0.010 \pm 0.026$	19.5k $\pm$ 243	ADAM	06	CLEO	$3.773 e^+ e^- \rightarrow \gamma \psi(2S)$
$0.76 \pm 0.05 \pm 0.01$	544	13 AUBERT	05D	BABR	$10.6 e^+ e^- \rightarrow \pi^+ \pi^- \mu^+ \mu^- \gamma$
$0.68 \pm 0.09$		14 BAI	98E	BES	$e^+ e^-$
••• We do not use the following data for averages, fits, limits, etc. •••					
$0.90 \pm 0.08 \pm 0.05$	256	15 AUBERT	07Au	BABR	$10.6 e^+ e^- \rightarrow J/\psi \pi^+ \pi^- \gamma$
13 AUBERT 05D reports $[\Gamma(\psi(2S) \rightarrow J/\psi(1S)\pi^+\pi^-) \times \Gamma(\psi(2S) \rightarrow e^+ e^-)/\Gamma_{\text{total}}] \times [B(J/\psi(1S) \rightarrow \mu^+ \mu^-)] = 0.0450 \pm 0.0018 \pm 0.0022$ keV which we divide by our best value $B(J/\psi(1S) \rightarrow \mu^+ \mu^-) = (5.93 \pm 0.06) \times 10^{-2}$ . Our first error is their experiment's error and our second error is the systematic error from using our best value.					
14 The value of $\Gamma(e^+ e^-)$ quoted in BAI 98E is derived using $B(\psi(2S) \rightarrow J/\psi(1S)\pi^+\pi^-) = (32.4 \pm 2.6) \times 10^{-2}$ and $B(J/\psi(1S) \rightarrow \ell^+ \ell^-) = 0.1203 \pm 0.0038$ . Recalculated by us using $B(J/\psi(1S) \rightarrow \ell^+ \ell^-) = 0.1181 \pm 0.0020$ .					
15 AUBERT 07Au reports $[\Gamma(\psi(2S) \rightarrow J/\psi(1S)\pi^+\pi^-) \times \Gamma(\psi(2S) \rightarrow e^+ e^-)/\Gamma_{\text{total}}] \times [B(J/\psi(1S) \rightarrow \pi^+ \pi^- \pi^0)] = 0.0186 \pm 0.0012 \pm 0.0011$ keV which we divide by our best value $B(J/\psi(1S) \rightarrow \pi^+ \pi^- \pi^0) = (2.07 \pm 0.12) \times 10^{-2}$ . Our first error is their experiment's error and our second error is the systematic error from using our best value.					





# Meson Particle Listings

## $\psi(2S)$

$\Gamma(e^+e^-)/\Gamma_{total}$   $\Gamma_6/\Gamma$

VALUE (units $10^{-4}$ )	DOCUMENT ID	TECN	COMMENT
<b>77.3 ± 1.7 OUR FIT</b>			

• • • We do not use the following data for averages, fits, limits, etc. • • •  
 88 ± 13 <sup>29</sup>FELDMAN 77 RVUE  $e^+e^-$   
<sup>29</sup>From an overall fit assuming equal partial widths for  $e^+e^-$  and  $\mu^+\mu^-$ . For a measurement of the ratio see the entry  $\Gamma(\mu^+\mu^-)/\Gamma(e^+e^-)$  below. Includes LUTH 75, HILGER 75, BURMESTER 77.

$\Gamma(\mu^+\mu^-)/\Gamma_{total}$   $\Gamma_7/\Gamma$

VALUE (units $10^{-4}$ )	DOCUMENT ID	TECN	COMMENT
<b>77 ± 8 OUR FIT</b>			

$\Gamma(\mu^+\mu^-)/\Gamma(e^+e^-)$   $\Gamma_7/\Gamma_6$

VALUE	DOCUMENT ID	TECN	COMMENT
<b>1.00 ± 0.11 OUR FIT</b>			

• • • We do not use the following data for averages, fits, limits, etc. • • •  
 0.89 ± 0.16 BOYARSKI 75c MRK1  $e^+e^-$

$\Gamma(\tau^+\tau^-)/\Gamma_{total}$   $\Gamma_8/\Gamma$

VALUE (units $10^{-4}$ )	DOCUMENT ID	TECN	COMMENT
<b>30 ± 4 OUR FIT</b>			
<b>30.8 ± 2.1 ± 3.8</b>			

<sup>30</sup>Computed using PDG 02 value of  $B(\psi(2S) \rightarrow \text{hadrons}) = 0.9810 \pm 0.0030$  to estimate the total number of  $\psi(2S)$  events.  
 30 ABLIKIM 06W BES  $e^+e^- \rightarrow \psi(2S)$

### DECAYS INTO $J/\psi(1S)$ AND ANYTHING

$\Gamma(J/\psi(1S) \text{ anything})/\Gamma_{total}$   $\Gamma_9/\Gamma$

VALUE	EVTS	DOCUMENT ID	TECN	COMMENT
<b>0.595 ± 0.008 OUR FIT</b>				
<b>0.55 ± 0.07 OUR AVERAGE</b>				

0.51 ± 0.12 BRANDELIK 79c DASP  $e^+e^- \rightarrow \mu^+\mu^-X$   
 0.57 ± 0.08 ABRAMS 75B MRK1  $e^+e^- \rightarrow \mu^+\mu^-X$   
 • • • We do not use the following data for averages, fits, limits, etc. • • •  
 0.6254 ± 0.0016 ± 0.0155 1.1M <sup>31</sup>MENDEZ 08 CLEO  $\psi(2S) \rightarrow \ell^+\ell^-X$   
 0.5950 ± 0.0015 ± 0.0190 151k ADAM 05A CLEO Repl. by MENDEZ 08

<sup>31</sup>Not independent from other measurements of MENDEZ 08.

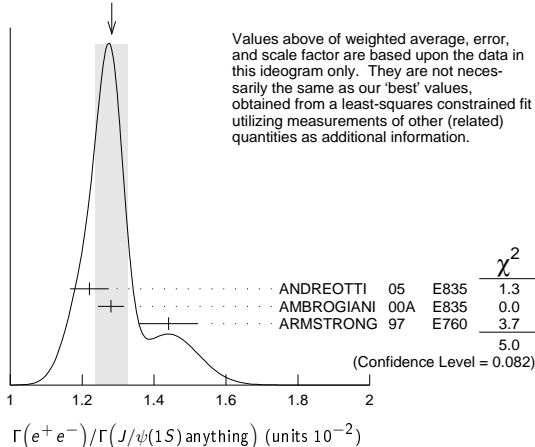
$\Gamma(e^+e^-)/\Gamma(J/\psi(1S) \text{ anything})$   $\Gamma_6/\Gamma_9 = \Gamma_6/(\Gamma_{11} + \Gamma_{12} + \Gamma_{13} + 0.344\Gamma_{110} + 0.195\Gamma_{111})$

VALUE (units $10^{-2}$ )	EVTS	DOCUMENT ID	TECN	COMMENT
<b>1.299 ± 0.026 OUR FIT</b>				

**1.28 ± 0.04 OUR AVERAGE** Error includes scale factor of 1.6. See the ideogram below.  
 1.22 ± 0.02 ± 0.05 5097 ± 73 <sup>32</sup>ANDREOTTI 05 E835  $p\bar{p} \rightarrow \psi(2S) \rightarrow e^+e^-$   
 1.28 ± 0.03 ± 0.02 <sup>32</sup>AMBROGIANI 00A E835  $p\bar{p} \rightarrow \psi(2S)$   
 1.44 ± 0.08 ± 0.02 <sup>32</sup>ARMSTRONG 97 E760  $\bar{p}p \rightarrow \psi(2S)$

<sup>32</sup>Using  $B(J/\psi(1S) \rightarrow e^+e^-) = 0.0593 \pm 0.0010$ .

WEIGHTED AVERAGE  
 1.28 ± 0.04 (Error scaled by 1.6)



$\Gamma(\mu^+\mu^-)/\Gamma(J/\psi(1S) \text{ anything})$   $\Gamma_7/\Gamma_9 = \Gamma_7/(\Gamma_{11} + \Gamma_{12} + \Gamma_{13} + 0.344\Gamma_{110} + 0.195\Gamma_{111})$

VALUE	DOCUMENT ID	TECN	COMMENT
<b>0.0130 ± 0.0014 OUR FIT</b>			
<b>0.014 ± 0.003</b>			

0.014 ± 0.003 HILGER 75 SPEC  $e^+e^-$

$\Gamma(J/\psi(1S) \text{ neutrals})/\Gamma_{total}$   $\Gamma_{10}/\Gamma$

VALUE	DOCUMENT ID	TECN	COMMENT
<b>0.246 ± 0.004 OUR FIT</b>			

$\Gamma(J/\psi(1S)\pi^+\pi^-)/\Gamma_{total}$   $\Gamma_{11}/\Gamma$

VALUE	EVTS	DOCUMENT ID	TECN	COMMENT
<b>0.336 ± 0.004 OUR FIT</b>				
<b>0.343 ± 0.011 OUR AVERAGE</b>				

Error includes scale factor of 1.7.  
 0.3504 ± 0.0007 ± 0.0077 565k MENDEZ 08 CLEO  $\psi(2S) \rightarrow \ell^+\ell^-\pi^+\pi^-$   
 0.323 ± 0.014 BAI 02B BES2  $e^+e^-$   
 0.32 ± 0.04 ABRAMS 75B MRK1  $e^+e^- \rightarrow J/\psi\pi^+\pi^-$   
 • • • We do not use the following data for averages, fits, limits, etc. • • •  
 0.3354 ± 0.0014 ± 0.0110 60k <sup>33</sup>ADAM 05A CLEO Repl. by MENDEZ 08  
<sup>33</sup>Not independent from other values reported by ADAM 05A.

$\Gamma(e^+e^-)/\Gamma(J/\psi(1S)\pi^+\pi^-)$   $\Gamma_6/\Gamma_{11}$

VALUE	DOCUMENT ID	TECN	COMMENT
<b>0.0230 ± 0.0005 OUR FIT</b>			
<b>0.0252 ± 0.0028 ± 0.0011</b>			

<sup>34</sup>AUBERT 02B BABR  $e^+e^-$   
<sup>34</sup>Using  $B(J/\psi(1S) \rightarrow e^+e^-) = 0.0593 \pm 0.0010$ .

$\Gamma(\mu^+\mu^-)/\Gamma(J/\psi(1S)\pi^+\pi^-)$   $\Gamma_7/\Gamma_{11}$

VALUE	DOCUMENT ID	TECN	COMMENT
<b>0.0229 ± 0.0025 OUR FIT</b>			
<b>0.0224 ± 0.0029 OUR AVERAGE</b>			

0.0216 ± 0.0026 ± 0.0014 <sup>35</sup>AUBERT 02B BABR  $e^+e^-$   
 0.0327 ± 0.0077 ± 0.0072 <sup>35</sup>GRIBUSHIN 96 FMPS 515  $\pi^-Be \rightarrow 2\mu X$   
<sup>35</sup>Using  $B(J/\psi(1S) \rightarrow \mu^+\mu^-) = 0.0588 \pm 0.0010$ .

$\Gamma(\tau^+\tau^-)/\Gamma(J/\psi(1S)\pi^+\pi^-)$   $\Gamma_8/\Gamma_{11}$

VALUE (units $10^{-3}$ )	DOCUMENT ID	TECN	COMMENT
<b>9.0 ± 1.1 OUR FIT</b>			
<b>8.73 ± 1.39 ± 1.57</b>			

BAI 02 BES  $e^+e^-$

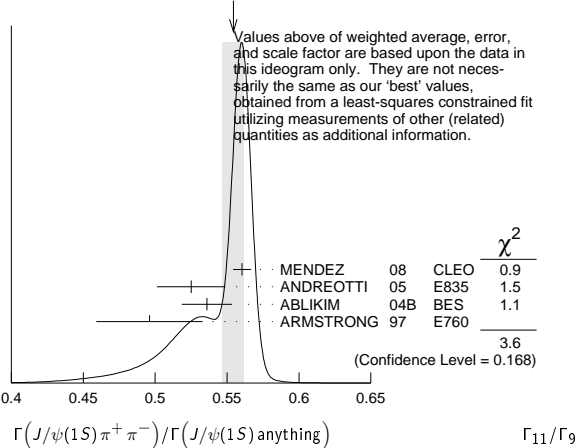
$\Gamma(J/\psi(1S)\pi^+\pi^-)/\Gamma(J/\psi(1S) \text{ anything})$   $\Gamma_{11}/\Gamma_9$

VALUE	EVTS	DOCUMENT ID	TECN	COMMENT
<b>0.5646 ± 0.0026 OUR FIT</b>				
<b>0.554 ± 0.008 OUR AVERAGE</b>				

Error includes scale factor of 1.3. See the ideogram below.  
 0.5604 ± 0.0009 ± 0.0062 565k MENDEZ 08 CLEO  $\psi(2S) \rightarrow \ell^+\ell^-\pi^+\pi^-$   
 0.525 ± 0.009 ± 0.022 4k ANDREOTTI 05 E835  $\psi(2S) \rightarrow J/\psi X$   
 0.536 ± 0.007 ± 0.016 20k <sup>36,37</sup>ABLIKIM 04B BES  $\psi(2S) \rightarrow J/\psi X$   
 0.496 ± 0.037 ARMSTRONG 97 E760  $\bar{p}p \rightarrow \psi(2S)$   
 • • • We do not use the following data for averages, fits, limits, etc. • • •  
 0.5637 ± 0.0027 ± 0.0046 60k ADAM 05A CLEO Repl. by MENDEZ 08

<sup>36</sup>From a fit to the  $J/\psi$  recoil mass spectra.  
<sup>37</sup>ABLIKIM 04B quotes  $B(\psi(2S) \rightarrow J/\psi X) / B(\psi(2S) \rightarrow J/\psi\pi^+\pi^-)$ .

WEIGHTED AVERAGE  
 0.554 ± 0.008 (Error scaled by 1.3)



$\Gamma(J/\psi(1S) \text{ neutrals})/\Gamma(J/\psi(1S)\pi^+\pi^-)$   $\Gamma_{10}/\Gamma_{11} = (0.9761\Gamma_{12} + 0.719\Gamma_{13} + 0.344\Gamma_{110} + 0.195\Gamma_{111})/\Gamma_{11}$

VALUE	DOCUMENT ID	TECN	COMMENT
<b>0.731 ± 0.008 OUR FIT</b>			
<b>0.73 ± 0.09</b>			

TANENBAUM 76 MRK1  $e^+e^-$

$\Gamma(J/\psi(1S)\pi^0\pi^0)/\Gamma_{total}$   $\Gamma_{12}/\Gamma$

VALUE	EVTS	DOCUMENT ID	TECN	COMMENT
<b>0.1775 ± 0.0034 OUR FIT</b>				

• • • We do not use the following data for averages, fits, limits, etc. • • •  
 0.1769 ± 0.0008 ± 0.0053 61k <sup>38</sup>MENDEZ 08 CLEO  $\psi(2S) \rightarrow \ell^+\ell^-2\pi^0$   
 0.1652 ± 0.0014 ± 0.0058 13.4k <sup>39</sup>ADAM 05A CLEO Repl. by MENDEZ 08

<sup>38</sup>Not independent from other measurements of MENDEZ 08.  
<sup>39</sup>Not independent from other values reported by ADAM 05A.

See key on page 457

Meson Particle Listings

$\psi(2S)$

$\Gamma(J/\psi(1S)\pi^0\pi^0)/\Gamma(J/\psi(1S)\text{anything})$   $\Gamma_{12}/\Gamma_9$

VALUE	EVTS	DOCUMENT ID	TECN	COMMENT
<b>0.2982 ± 0.0032 OUR FIT</b>				
<b>0.320 ± 0.012 OUR AVERAGE</b>				
0.300 ± 0.008 ± 0.022	1655 ± 44	ANDREOTTI 05	E835	$\psi(2S) \rightarrow J/\psi X$
0.328 ± 0.013 ± 0.008		AMBROGIANI 00A	E835	$p\bar{p} \rightarrow \psi(2S)$
0.323 ± 0.033		ARMSTRONG 97	E760	$\bar{p}p \rightarrow \psi(2S)$
• • • We do not use the following data for averages, fits, limits, etc. • • •				
0.2829 ± 0.0012 ± 0.0056	61k	MENDEZ 08	CLEO	$\psi(2S) \rightarrow \ell^+ \ell^- 2\pi^0$
0.2776 ± 0.0025 ± 0.0043	13.4k	ADAM 05A	CLEO	Repl. by MENDEZ 08

$\Gamma(J/\psi(1S)\pi^0\pi^0)/\Gamma(J/\psi(1S)\pi^+\pi^-)$   $\Gamma_{12}/\Gamma_{11}$

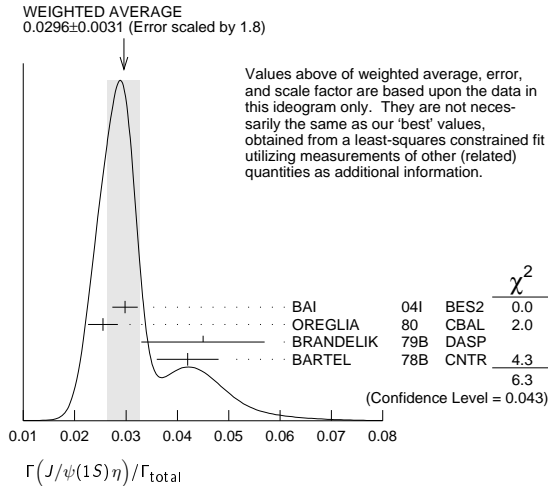
VALUE	EVTS	DOCUMENT ID	TECN	COMMENT
<b>0.528 ± 0.008 OUR FIT</b>				
<b>0.513 ± 0.022 OUR AVERAGE</b>				Error includes scale factor of 2.2.
0.5047 ± 0.0022 ± 0.0102	61k	MENDEZ 08	CLEO	$\psi(2S) \rightarrow \ell^+ \ell^- 2\pi^0$
0.570 ± 0.009 ± 0.026	14k	40 ABLIKIM 04B	BES	$\psi(2S) \rightarrow J/\psi X$
• • • We do not use the following data for averages, fits, limits, etc. • • •				
0.4924 ± 0.0047 ± 0.0086	73k	41,42 ADAM 05A	CLEO	Repl. by MENDEZ 08
0.571 ± 0.018 ± 0.044		43 ANDREOTTI 05	E835	$\psi(2S) \rightarrow J/\psi X$
0.53 ± 0.06		TANENBAUM 76	MRK1	$e^+ e^-$
0.64 ± 0.15		44 HILGER 75	SPEC	$e^+ e^-$

40 From a fit to the  $J/\psi$  recoil mass spectra.  
 41 Not independent from other values reported by ADAM 05A.  
 42 Using 13,217  $J/\psi\pi^0\pi^0$  and 60,010  $J/\psi\pi^+\pi^-$  events.  
 43 Not independent from other values reported by ANDREOTTI 05.  
 44 Ignoring the  $J/\psi(1S)\eta$  and  $J/\psi(1S)\gamma\gamma$  decays.

$\Gamma(J/\psi(1S)\eta)/\Gamma_{\text{total}}$   $\Gamma_{13}/\Gamma$

VALUE	EVTS	DOCUMENT ID	TECN	COMMENT
<b>0.0328 ± 0.0007 OUR FIT</b>				
<b>0.0296 ± 0.0031 OUR AVERAGE</b>				Error includes scale factor of 1.8. See the ideogram below.
0.0298 ± 0.0009 ± 0.0023	5.7k	BAI 04I	BES2	$\psi(2S) \rightarrow J/\psi\gamma\gamma$
0.0255 ± 0.0029	386	45 OREGLIA 80	CBAL	$e^+ e^- \rightarrow J/\psi 2\gamma$
0.045 ± 0.012	17	46 BRANDELIK 79B	DASP	$e^+ e^- \rightarrow J/\psi 2\gamma$
0.042 ± 0.006	164	46 BARTEL 78B	CNTR	$e^+ e^-$
• • • We do not use the following data for averages, fits, limits, etc. • • •				
0.0343 ± 0.0004 ± 0.0009	18.4k	47 MENDEZ 08	CLEO	$\psi(2S) \rightarrow \ell^+ \ell^- \eta$
0.0325 ± 0.0006 ± 0.0011	2.8k	48 ADAM 05A	CLEO	Repl. by MENDEZ 08
0.043 ± 0.008	44	TANENBAUM 76	MRK1	$e^+ e^-$

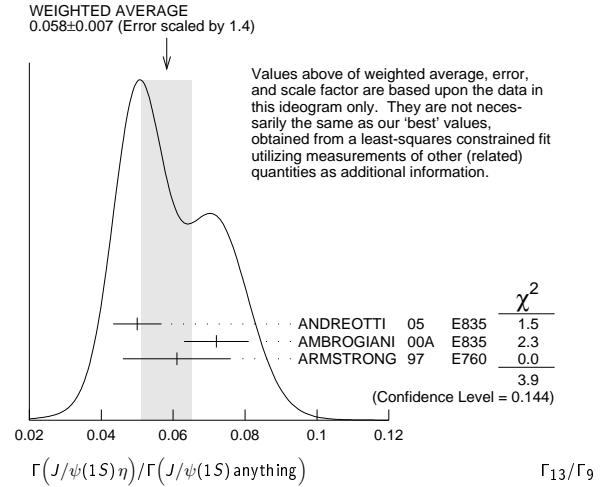
45 Recalculated by us using  $B(J/\psi(1S) \rightarrow \ell^+ \ell^-) = 0.1181 \pm 0.0020$ .  
 46 Recalculated by us using  $B(J/\psi(1S) \rightarrow \mu^+ \mu^-) = 0.0588 \pm 0.0010$ .  
 47 Not independent from other measurements of MENDEZ 08.  
 48 Not independent from other values reported by ADAM 05A.



$\Gamma(J/\psi(1S)\eta)/\Gamma(J/\psi(1S)\text{anything})$   $\Gamma_{13}/\Gamma_9$

VALUE	EVTS	DOCUMENT ID	TECN	COMMENT
<b>0.0551 ± 0.0009 OUR FIT</b>				
<b>0.058 ± 0.007 OUR AVERAGE</b>				Error includes scale factor of 1.4. See the ideogram below.
0.050 ± 0.006 ± 0.003	298 ± 20	ANDREOTTI 05	E835	$\psi(2S) \rightarrow J/\psi X$
0.072 ± 0.009		AMBROGIANI 00A	E835	$p\bar{p} \rightarrow \psi(2S)$
0.061 ± 0.015		ARMSTRONG 97	E760	$\bar{p}p \rightarrow \psi(2S)$
• • • We do not use the following data for averages, fits, limits, etc. • • •				
0.0549 ± 0.0006 ± 0.0009	18.4k	49 MENDEZ 08	CLEO	$\psi(2S) \rightarrow \ell^+ \ell^- \eta$
0.0546 ± 0.0010 ± 0.0007	2.8k	ADAM 05A	CLEO	Repl. by MENDEZ 08

49 Not independent from other measurements of MENDEZ 08.

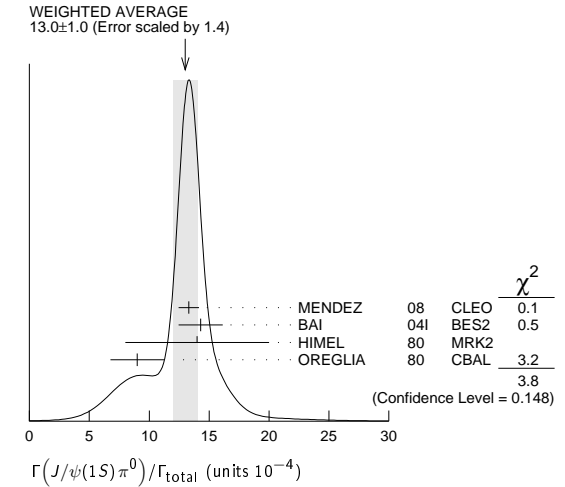


$\Gamma(J/\psi(1S)\eta)/\Gamma(J/\psi(1S)\pi^+\pi^-)$   $\Gamma_{13}/\Gamma_{11}$

VALUE	EVTS	DOCUMENT ID	TECN	COMMENT
<b>0.0976 ± 0.0016 OUR FIT</b>				
<b>0.0979 ± 0.0018 OUR AVERAGE</b>				
0.0979 ± 0.0010 ± 0.0015	18.4k	MENDEZ 08	CLEO	$\psi(2S) \rightarrow \ell^+ \ell^- \eta$
0.098 ± 0.005 ± 0.010	2k	50 ABLIKIM 04B	BES	$\psi(2S) \rightarrow J/\psi X$
0.091 ± 0.021		51 HIMEL 80	MRK2	$e^+ e^- \rightarrow \psi(2S) X$
• • • We do not use the following data for averages, fits, limits, etc. • • •				
0.0968 ± 0.0019 ± 0.0013	2.8k	52 ADAM 05A	CLEO	Repl. by MENDEZ 08
0.095 ± 0.007 ± 0.007		53 ANDREOTTI 05	E835	$\psi(2S) \rightarrow J/\psi X$
50 From a fit to the $J/\psi$ recoil mass spectra. 51 The value for $B(\psi(2S) \rightarrow J/\psi(1S)\eta)$ reported in HIMEL 80 is derived using $B(\psi(2S) \rightarrow J/\psi(1S)\pi^+\pi^-) = (33 \pm 3)\%$ and $B(J/\psi(1S) \rightarrow \ell^+ \ell^-) = 0.138 \pm 0.018$ . Calculated by us using $B(J/\psi(1S) \rightarrow \ell^+ \ell^-) = (0.1181 \pm 0.0020)$ . 52 Not independent from other values reported by ADAM 05A. 53 Not independent from other values reported by ANDREOTTI 05.				

$\Gamma(J/\psi(1S)\pi^0)/\Gamma_{\text{total}}$   $\Gamma_{14}/\Gamma$

VALUE (units $10^{-4}$ )	EVTS	DOCUMENT ID	TECN	COMMENT
<b>13.0 ± 1.0 OUR AVERAGE</b>				Error includes scale factor of 1.4. See the ideogram below.
13.3 ± 0.8 ± 0.3	530	MENDEZ 08	CLEO	$\psi(2S) \rightarrow \ell^+ \ell^- 2\gamma$
14.3 ± 1.4 ± 1.2	280	BAI 04I	BES2	$\psi(2S) \rightarrow J/\psi\gamma\gamma$
14 ± 6	7	HIMEL 80	MRK2	$e^+ e^-$
9 ± 2 ± 1	23	54 OREGLIA 80	CBAL	$\psi(2S) \rightarrow J/\psi 2\gamma$
• • • We do not use the following data for averages, fits, limits, etc. • • •				
13 ± 1 ± 1	88	ADAM 05A	CLEO	Repl. by MENDEZ 08
54 Recalculated by us using $B(J/\psi(1S) \rightarrow \ell^+ \ell^-) = 0.1181 \pm 0.0020$ .				



$\Gamma(J/\psi(1S)\pi^0)/\Gamma(J/\psi(1S)\text{anything})$   $\Gamma_{14}/\Gamma_9 = \Gamma_{14}/(\Gamma_{11} + \Gamma_{12} + \Gamma_{13} + 0.344\Gamma_{110} + 0.195\Gamma_{111})$

VALUE (units $10^{-2}$ )	EVTS	DOCUMENT ID	TECN	COMMENT
<b>0.213 ± 0.012 ± 0.003</b>	527	55 MENDEZ 08	CLEO	$e^+ e^- \rightarrow J/\psi\gamma\gamma$
0.22 ± 0.02 ± 0.01		56 ADAM 05A	CLEO	$e^+ e^- \rightarrow \psi(2S) \rightarrow J/\psi\gamma\gamma$

# Meson Particle Listings

## $\psi(2S)$

<sup>55</sup> Not independent from other values reported by MENDEZ 08. Supersedes ADAM 05A.  
<sup>56</sup> Not independent from other values reported by ADAM 05A.

### $\Gamma(J/\psi(1S)\pi^0)/\Gamma(J/\psi(1S)\pi^+\pi^-)$ $\Gamma_{14}/\Gamma_{11}$

VALUE (units $10^{-2}$ )	EVTS	DOCUMENT ID	TECN	COMMENT
• • • We do not use the following data for averages, fits, limits, etc. • • •				
$0.380 \pm 0.022 \pm 0.005$	527	57 MENDEZ	08	CLEO $e^+e^- \rightarrow J/\psi\gamma\gamma$
$0.39 \pm 0.04 \pm 0.01$		58 ADAM	05A	CLEO $e^+e^- \rightarrow \psi(2S) \rightarrow J/\psi\gamma\gamma$

<sup>57</sup> Not independent from other values reported by MENDEZ 08. Supersedes ADAM 05A.  
<sup>58</sup> Not independent from other values reported by ADAM 05A.

### HADRONIC DECAYS

### $\Gamma(\pi^0 h_c(1P))/\Gamma_{total}$ $\Gamma_{15}/\Gamma$

VALUE (units $10^{-4}$ )	EVTS	DOCUMENT ID	TECN	COMMENT
<b>8.6 ± 1.3 OUR AVERAGE</b>				
$9.0 \pm 1.5 \pm 1.3$	3k	<sup>59</sup> GE	11	CLEO $\Upsilon(2S) \rightarrow \pi^0$ anything
$8.4 \pm 1.3 \pm 1.0$	11k	ABLIKIM	10B	BES3 $\psi(2S) \rightarrow \pi^0 h_c$
• • • We do not use the following data for averages, fits, limits, etc. • • •				
seen	$92^{+23}_{-22}$	ADAMS	09	CLEO $\psi(2S) \rightarrow 2\pi^+ 2\pi^- 2\pi^0$
seen	1282	DOBBS	08A	CLEO $\psi(2S) \rightarrow \pi^0 \eta_c \gamma$
seen	$168 \pm 40$	ROSNER	05	CLEO $\psi(2S) \rightarrow \pi^0 \eta_c \gamma$

<sup>59</sup> Assuming a width  $\Gamma(h_c(1P)) = 0.86 \text{ MeV} \equiv \Gamma_0$ , a measured dependence of the central value of  $B = (7.6 \pm 1.4 \times \Gamma(h_c(1P)/\Gamma_0) \times 10^{-4}$ , and with a systematic error that accounts for the width variation range 0.43–1.29 MeV.

### $\Gamma(3(\pi^+\pi^-)\pi^0)/\Gamma_{total}$ $\Gamma_{16}/\Gamma$

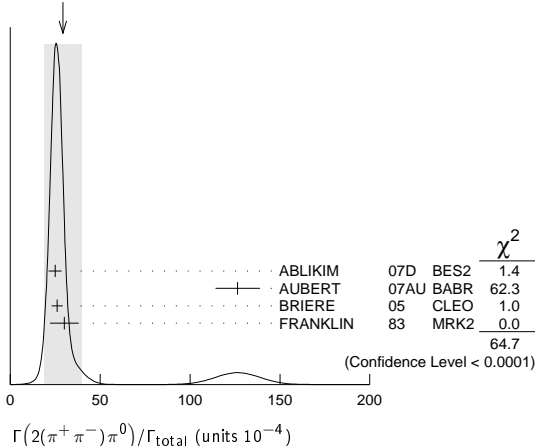
VALUE (units $10^{-4}$ )	EVTS	DOCUMENT ID	TECN	COMMENT
<b>35 ± 16</b>	6	FRANKLIN	83	MRK2 $e^+e^- \rightarrow$ hadrons

### $\Gamma(2(\pi^+\pi^-)\pi^0)/\Gamma_{total}$ $\Gamma_{17}/\Gamma$

VALUE (units $10^{-4}$ )	EVTS	DOCUMENT ID	TECN	COMMENT
<b>29 ± 10 OUR AVERAGE</b>				
Error includes scale factor of 4.6. See the ideogram below.				
$24.9 \pm 0.7 \pm 3.6$	2173	ABLIKIM	07D	BES2 $e^+e^- \rightarrow \psi(2S)$
$127 \pm 12 \pm 2$	410	<sup>60</sup> AUBERT	07AU	BABR $10.6 e^+e^- \rightarrow 2(\pi^+\pi^-)\pi^0\gamma$
$26.1 \pm 0.7 \pm 3.0$	1703	BRIERE	05	CLEO $e^+e^- \rightarrow \psi(2S) \rightarrow 2(\pi^+\pi^-)\pi^0$
$30 \pm 8$	42	FRANKLIN	83	MRK2 $e^+e^-$

<sup>60</sup> AUBERT 07AU reports  $[\Gamma(\psi(2S) \rightarrow 2(\pi^+\pi^-)\pi^0)/\Gamma_{total}] \times [\Gamma(\psi(2S) \rightarrow e^+e^-)] = (297 \pm 22 \pm 18) \times 10^{-4} \text{ keV}$  which we divide by our best value  $\Gamma(\psi(2S) \rightarrow e^+e^-) = 2.35 \pm 0.04 \text{ keV}$ . Our first error is their experiment's error and our second error is the systematic error from using our best value.

WEIGHTED AVERAGE  
 $29 \pm 10$  (Error scaled by 4.6)



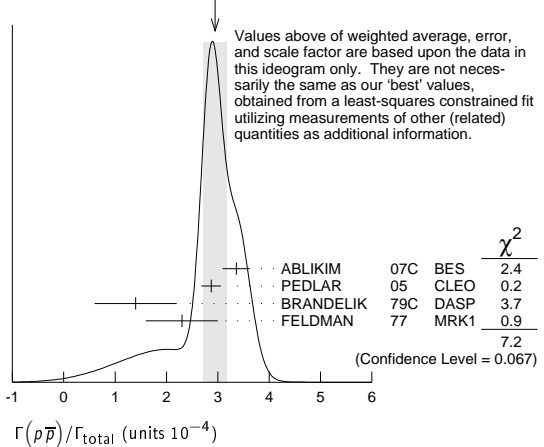
### $\Gamma(\rho\pi_2(1320))/\Gamma_{total}$ $\Gamma_{18}/\Gamma$

VALUE (units $10^{-4}$ )	CL%	EVTS	DOCUMENT ID	TECN	COMMENT
<b>2.55 ± 0.73 ± 0.47</b>		112 ± 31	BAI	04C	BES2 $\psi(2S) \rightarrow 2(\pi^+\pi^-)\pi^0$
• • • We do not use the following data for averages, fits, limits, etc. • • •					
<2.3		90	BAI	98J	BES $e^+e^-$

### $\Gamma(p\bar{p})/\Gamma_{total}$ $\Gamma_{19}/\Gamma$

VALUE (units $10^{-4}$ )	EVTS	DOCUMENT ID	TECN	COMMENT
<b>2.76 ± 0.12 OUR FIT</b>				
<b>2.95 ± 0.23 OUR AVERAGE</b>				
Error includes scale factor of 1.5. See the ideogram below.				
$3.36 \pm 0.09 \pm 0.25$	1618	ABLIKIM	07c	BES $e^+e^- \rightarrow \psi(2S) \rightarrow p\bar{p}$
$2.87 \pm 0.12 \pm 0.15$	557	PEDLAR	05	CLEO $e^+e^- \rightarrow \psi(2S) \rightarrow p\bar{p}$
$1.4 \pm 0.8$	4	BRANDELIK	79c	DASP $e^+e^- \rightarrow \psi(2S) \rightarrow p\bar{p}$
$2.3 \pm 0.7$		FELDMAN	77	MRK1 $e^+e^- \rightarrow \psi(2S) \rightarrow p\bar{p}$

WEIGHTED AVERAGE  
 $2.95 \pm 0.23$  (Error scaled by 1.5)



### $\Gamma(p\bar{p})/\Gamma(J/\psi(1S)\pi^+\pi^-)$ $\Gamma_{19}/\Gamma_{11}$

VALUE (units $10^{-4}$ )	DOCUMENT ID	TECN	COMMENT
<b>8.2 ± 0.4 OUR FIT</b>			
<b>6.98 ± 0.49 ± 0.97</b>	BAI	01	BES $e^+e^- \rightarrow \psi(2S) \rightarrow p\bar{p}$

### $\Gamma(\Delta^+\Delta^-)/\Gamma_{total}$ $\Gamma_{20}/\Gamma$

VALUE (units $10^{-5}$ )	EVTS	DOCUMENT ID	TECN	COMMENT
<b>12.8 ± 1.0 ± 3.4</b>	157	<sup>61</sup> BAI	01	BES $e^+e^- \rightarrow \psi(2S) \rightarrow$ hadrons

<sup>61</sup> Estimated using  $B(\psi(2S) \rightarrow J/\psi\pi^+\pi^-) = 0.310 \pm 0.028$ .

### $\Gamma(\Lambda\bar{\Lambda}\pi^0)/\Gamma_{total}$ $\Gamma_{21}/\Gamma$

VALUE (units $10^{-4}$ )	CL%	DOCUMENT ID	TECN	COMMENT
<b>&lt;1.2</b>	90	<sup>62</sup> ABLIKIM	07H	BES2 $e^+e^- \rightarrow \psi(2S)$

<sup>62</sup> Using  $B(\Lambda \rightarrow \pi^- p) = 63.9\%$  and  $B(\eta \rightarrow \gamma\gamma) = 39.4\%$ .

### $\Gamma(\Lambda\bar{\Lambda}\eta)/\Gamma_{total}$ $\Gamma_{22}/\Gamma$

VALUE (units $10^{-4}$ )	CL%	DOCUMENT ID	TECN	COMMENT
<b>&lt;0.49</b>	90	<sup>63</sup> ABLIKIM	07H	BES2 $e^+e^- \rightarrow \psi(2S)$

<sup>63</sup> Using  $B(\Lambda \rightarrow \pi^- p) = 63.9\%$ .

### $\Gamma(\Lambda\bar{p}K^+)/\Gamma_{total}$ $\Gamma_{23}/\Gamma$

VALUE (units $10^{-4}$ )	EVTS	DOCUMENT ID	TECN	COMMENT
<b>1.0 ± 0.1 ± 0.1</b>	74.0	BRIERE	05	CLEO $e^+e^- \rightarrow \psi(2S) \rightarrow p\bar{p}K^+\pi^-$

### $\Gamma(\Lambda\bar{p}K^+\pi^+\pi^-)/\Gamma_{total}$ $\Gamma_{24}/\Gamma$

VALUE (units $10^{-4}$ )	EVTS	DOCUMENT ID	TECN	COMMENT
<b>1.8 ± 0.3 ± 0.3</b>	45.8	BRIERE	05	CLEO $e^+e^- \rightarrow \psi(2S) \rightarrow p\bar{p}K^+\pi^+\pi^-$

### $\Gamma(\Lambda\bar{\Lambda}\pi^+\pi^-)/\Gamma_{total}$ $\Gamma_{25}/\Gamma$

VALUE (units $10^{-4}$ )	EVTS	DOCUMENT ID	TECN	COMMENT
<b>2.8 ± 0.4 ± 0.5</b>	73.4	BRIERE	05	CLEO $e^+e^- \rightarrow \psi(2S) \rightarrow p\bar{p}2(\pi^+\pi^-)$

### $\Gamma(\Lambda\bar{\Lambda})/\Gamma_{total}$ $\Gamma_{26}/\Gamma$

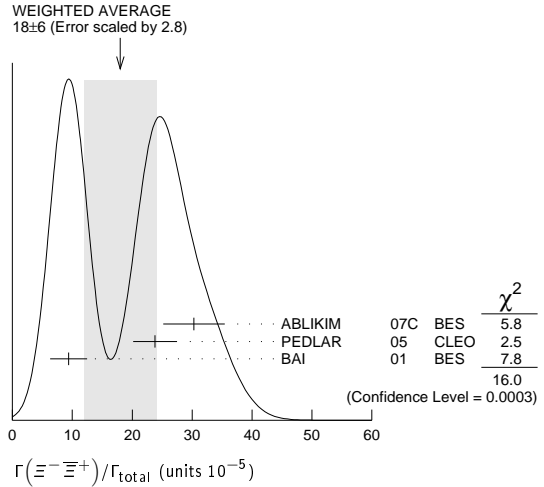
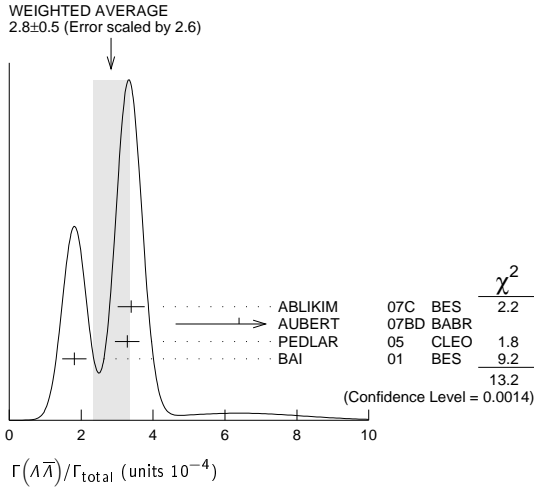
VALUE (units $10^{-4}$ )	CL%	EVTS	DOCUMENT ID	TECN	COMMENT
<b>2.8 ± 0.5 OUR AVERAGE</b>					
Error includes scale factor of 2.6. See the ideogram below.					
$3.39 \pm 0.20 \pm 0.32$		337	ABLIKIM	07c	BES $e^+e^- \rightarrow \psi(2S) \rightarrow$ hadrons
$6.4 \pm 1.8 \pm 0.1$			<sup>64</sup> AUBERT	07BD	BABR $10.6 e^+e^- \rightarrow \Lambda\bar{\Lambda}\gamma$
$3.28 \pm 0.23 \pm 0.25$		208	PEDLAR	05	CLEO $e^+e^- \rightarrow \psi(2S) \rightarrow$ hadrons
$1.81 \pm 0.20 \pm 0.27$		80	<sup>65</sup> BAI	01	BES $e^+e^- \rightarrow \psi(2S) \rightarrow$ hadrons

• • • We do not use the following data for averages, fits, limits, etc. • • •

< 4 90 FELDMAN 77 MRK1  $e^+e^- \rightarrow \psi(2S) \rightarrow$  hadrons

<sup>64</sup> AUBERT 07BD reports  $[\Gamma(\psi(2S) \rightarrow \Lambda\bar{\Lambda})/\Gamma_{total}] \times [\Gamma(\psi(2S) \rightarrow e^+e^-)] = (15 \pm 4 \pm 1) \times 10^{-4} \text{ keV}$  which we divide by our best value  $\Gamma(\psi(2S) \rightarrow e^+e^-) = 2.35 \pm 0.04 \text{ keV}$ . Our first error is their experiment's error and our second error is the systematic error from using our best value.

<sup>65</sup> Estimated using  $B(\psi(2S) \rightarrow J/\psi\pi^+\pi^-) = 0.310 \pm 0.028$ .



$\Gamma(\Sigma^+\bar{\Sigma}^-)/\Gamma_{total}$   $\Gamma_{27}/\Gamma$

VALUE (units $10^{-5}$ )	EVTS	DOCUMENT ID	TECN	COMMENT
<b>25.7 ± 4.4 ± 6.8</b>	35	PEDLAR 05	CLEO	$e^+e^- \rightarrow \psi(2S) \rightarrow \text{hadrons}$

$\Gamma(\Xi^0\bar{\Xi}^0)/\Gamma_{total}$   $\Gamma_{31}/\Gamma$

VALUE (units $10^{-5}$ )	EVTS	DOCUMENT ID	TECN	COMMENT
<b>27.5 ± 6.4 ± 6.1</b>	19	PEDLAR 05	CLEO	$e^+e^- \rightarrow \psi(2S) \rightarrow \text{hadrons}$

$\Gamma(\Sigma^0\bar{\Sigma}^0)/\Gamma_{total}$   $\Gamma_{28}/\Gamma$

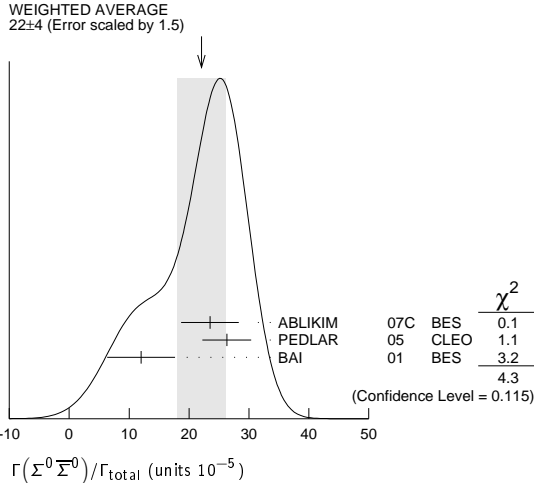
VALUE (units $10^{-5}$ )	EVTS	DOCUMENT ID	TECN	COMMENT
<b>22 ± 4 OUR AVERAGE</b>		Error includes scale factor of 1.5. See the ideogram below.		
23.5 ± 3.6 ± 3.2	59	ABLIKIM 07C	BES	$e^+e^- \rightarrow \psi(2S) \rightarrow \text{hadrons}$
26.3 ± 3.5 ± 2.1	58	PEDLAR 05	CLEO	$e^+e^- \rightarrow \psi(2S) \rightarrow \text{hadrons}$
12 ± 4 ± 4	8	<sup>66</sup> BAI 01	BES	$e^+e^- \rightarrow \psi(2S) \rightarrow \text{hadrons}$

<sup>66</sup> Estimated using  $B(\psi(2S) \rightarrow J/\psi\pi^+\pi^-) = 0.310 \pm 0.028$ .

$\Gamma(\Xi(1530)^0\bar{\Xi}(1530)^0)/\Gamma_{total}$   $\Gamma_{32}/\Gamma$

VALUE (units $10^{-5}$ )	CL%	DOCUMENT ID	TECN	COMMENT
<b>&lt; 8.1</b>	90	<sup>69</sup> BAI 01	BES	$e^+e^- \rightarrow \psi(2S) \rightarrow \text{hadrons}$
••• We do not use the following data for averages, fits, limits, etc. •••				
<32	90	PEDLAR 05	CLEO	$e^+e^- \rightarrow \psi(2S) \rightarrow \text{hadrons}$

<sup>69</sup> Estimated using  $B(\psi(2S) \rightarrow J/\psi\pi^+\pi^-) = 0.310 \pm 0.028$ .



$\Gamma(\Omega^-\bar{\Omega}^+)/\Gamma_{total}$   $\Gamma_{33}/\Gamma$

VALUE (units $10^{-5}$ )	CL%	DOCUMENT ID	TECN	COMMENT
<b>&lt; 7.3</b>	90	<sup>70</sup> BAI 01	BES	$e^+e^- \rightarrow \psi(2S) \rightarrow \text{hadrons}$
••• We do not use the following data for averages, fits, limits, etc. •••				
<16	90	PEDLAR 05	CLEO	$e^+e^- \rightarrow \psi(2S) \rightarrow \text{hadrons}$

<sup>70</sup> Estimated using  $B(\psi(2S) \rightarrow J/\psi\pi^+\pi^-) = 0.310 \pm 0.028$ .

$\Gamma(\Sigma(1385)^+\bar{\Sigma}(1385)^-)/\Gamma_{total}$   $\Gamma_{29}/\Gamma$

VALUE (units $10^{-5}$ )	EVTS	DOCUMENT ID	TECN	COMMENT
<b>11 ± 3 ± 3</b>	14	<sup>67</sup> BAI 01	BES	$e^+e^- \rightarrow \psi(2S) \rightarrow \text{hadrons}$

<sup>67</sup> Estimated using  $B(\psi(2S) \rightarrow J/\psi\pi^+\pi^-) = 0.310 \pm 0.028$ .

$\Gamma(\pi^0\rho\bar{\rho})/\Gamma_{total}$   $\Gamma_{34}/\Gamma$

VALUE (units $10^{-4}$ )	EVTS	DOCUMENT ID	TECN	COMMENT
<b>1.50 ± 0.08 OUR AVERAGE</b>		Error includes scale factor of 1.1.		
1.54 ± 0.06 ± 0.06	948	ALEXANDER 10	CLEO	$\psi(2S) \rightarrow \pi^0\rho\bar{\rho}$
1.32 ± 0.10 ± 0.15	256 ± 18	<sup>71</sup> ABLIKIM 05E	BES2	$e^+e^- \rightarrow \psi(2S) \rightarrow \rho\bar{\rho}\gamma\gamma$
1.4 ± 0.5	9	FRANKLIN 83	MRK2	$e^+e^-$

<sup>71</sup> Computed using  $B(\pi^0 \rightarrow \gamma\gamma) = (98.80 \pm 0.03)\%$ .

$\Gamma(N_1^*(1440)\bar{p} \rightarrow \pi^0\rho\bar{\rho})/\Gamma_{total}$   $\Gamma_{35}/\Gamma$

VALUE (units $10^{-5}$ )	EVTS	DOCUMENT ID	TECN	COMMENT
<b>8.1 ± 0.7 ± 0.3</b>	474	<sup>72</sup> ALEXANDER 10	CLEO	$\psi(2S) \rightarrow \pi^0\rho\bar{\rho}$

<sup>72</sup> From a fit of the  $p\bar{p}$  and  $p\pi^0$  mass distributions to a combination of  $N_1^*(1440)\bar{p}$ ,  $\pi^0 f_0(2100)$ , and two other broad, unestablished resonances.

$\Gamma(\Xi^-\bar{\Xi}^+)/\Gamma_{total}$   $\Gamma_{30}/\Gamma$

VALUE (units $10^{-5}$ )	CL%	EVTS	DOCUMENT ID	TECN	COMMENT
<b>18 ± 6 OUR AVERAGE</b>			Error includes scale factor of 2.8. See the ideogram below.		
30.3 ± 4.0 ± 3.2	67	ABLIKIM 07C	BES	$e^+e^- \rightarrow \psi(2S) \rightarrow \text{hadrons}$	
23.8 ± 3.0 ± 2.1	63	PEDLAR 05	CLEO	$e^+e^- \rightarrow \psi(2S) \rightarrow \text{hadrons}$	
9.4 ± 2.7 ± 1.5	12	<sup>68</sup> BAI 01	BES	$e^+e^- \rightarrow \psi(2S) \rightarrow \text{hadrons}$	

••• We do not use the following data for averages, fits, limits, etc. •••

<20 90 FELDMAN 77 MRK1  $e^+e^- \rightarrow \psi(2S) \rightarrow \text{hadrons}$

<sup>68</sup> Estimated using  $B(\psi(2S) \rightarrow J/\psi\pi^+\pi^-) = 0.310 \pm 0.028$ .

$\Gamma(\pi^0 f_0(2100) \rightarrow \pi^0\rho\bar{\rho})/\Gamma_{total}$   $\Gamma_{36}/\Gamma$

VALUE (units $10^{-5}$ )	EVTS	DOCUMENT ID	TECN	COMMENT
<b>1.1 ± 0.4 ± 0.1</b>	76	<sup>73</sup> ALEXANDER 10	CLEO	$\psi(2S) \rightarrow \pi^0\rho\bar{\rho}$

<sup>73</sup> From a fit of the  $p\bar{p}$  and  $p\pi^0$  mass distributions to a combination of  $N_1^*(1440)\bar{p}$ ,  $\pi^0 f_0(2100)$ , and two other broad, unestablished resonances.

$\Gamma(\eta\rho\bar{\rho})/\Gamma_{total}$   $\Gamma_{37}/\Gamma$

VALUE (units $10^{-5}$ )	EVTS	DOCUMENT ID	TECN	COMMENT
<b>5.7 ± 0.6 OUR AVERAGE</b>				
5.6 ± 0.6 ± 0.3	154	ALEXANDER 10	CLEO	$\psi(2S) \rightarrow \eta\rho\bar{\rho}$
5.8 ± 1.1 ± 0.7	44.8 ± 8.5	<sup>74</sup> ABLIKIM 05E	BES2	$e^+e^- \rightarrow \psi(2S) \rightarrow \rho\bar{\rho}\gamma\gamma$
8 ± 3 ± 3	9.8	BRIERE 05	CLEO	$e^+e^- \rightarrow \psi(2S) \rightarrow \rho\bar{p}\pi^+\pi^-\pi^0$

<sup>74</sup> Computed using  $B(\eta \rightarrow \gamma\gamma) = (39.43 \pm 0.26)\%$ .

$\Gamma(\eta f_0(2100) \rightarrow \eta\rho\bar{\rho})/\Gamma_{total}$   $\Gamma_{38}/\Gamma$

VALUE (units $10^{-5}$ )	EVTS	DOCUMENT ID	TECN	COMMENT
<b>1.2 ± 0.4 ± 0.1</b>	31	<sup>75</sup> ALEXANDER 10	CLEO	$\psi(2S) \rightarrow \eta\rho\bar{\rho}$

<sup>75</sup> From a fit of the  $p\bar{p}$  and  $p\eta$  distributions to a combination of  $N^*(1535)\bar{p}$  and  $\eta f_0(2100)$ .



See key on page 457

# Meson Particle Listings

## $\psi(2S)$

$\Gamma(K^+ K^- 2(\pi^+ \pi^-) \pi^0) / \Gamma_{total}$					$\Gamma_{58} / \Gamma$
VALUE (units $10^{-4}$ )	EVTS	DOCUMENT ID	TECN	COMMENT	
<b>10.0 ± 2.5 ± 1.8</b>	65	ABLIKIM	07D BES2	$e^+ e^- \rightarrow \psi(2S)$	

$\Gamma(K_1(1270)^\pm K^\mp) / \Gamma_{total}$					$\Gamma_{60} / \Gamma$
VALUE (units $10^{-4}$ )		DOCUMENT ID	TECN	COMMENT	
<b>10.0 ± 1.8 ± 2.1</b>	91	BAI	99c BES	$e^+ e^-$	
<sup>91</sup> Assuming $B(K_1(1270) \rightarrow K\rho) = 0.42 \pm 0.06$					

$\Gamma(K_S^0 K_L^0 \pi^+ \pi^-) / \Gamma_{total}$					$\Gamma_{61} / \Gamma$
VALUE (units $10^{-4}$ )	EVTS	DOCUMENT ID	TECN	COMMENT	
<b>2.20 ± 0.25 ± 0.37</b>	83 ± 9	ABLIKIM	05o BES2	$e^+ e^- \rightarrow \psi(2S)$	

$\Gamma(\rho^0 \rho \bar{\rho}) / \Gamma_{total}$					$\Gamma_{62} / \Gamma$
VALUE (units $10^{-4}$ )	EVTS	DOCUMENT ID	TECN	COMMENT	
<b>0.5 ± 0.1 ± 0.2</b>	61.1	BRIERE	05 CLEO	$e^+ e^- \rightarrow \psi(2S) \rightarrow \rho \bar{\rho} \pi^+ \pi^-$	

$\Gamma(K^+ \bar{K}^*(892)^0 \pi^- + c.c.) / \Gamma_{total}$					$\Gamma_{63} / \Gamma$
VALUE (units $10^{-4}$ )		DOCUMENT ID	TECN	COMMENT	
<b>6.7 ± 2.5</b>		TANENBAUM	78 MRK1	$e^+ e^-$	

$\Gamma(2(\pi^+ \pi^-)) / \Gamma_{total}$					$\Gamma_{64} / \Gamma$
VALUE (units $10^{-4}$ )	EVTS	DOCUMENT ID	TECN	COMMENT	
<b>2.4 ± 0.6 OUR AVERAGE</b>	Error includes scale factor of 2.2.				
2.2 ± 0.2 ± 0.2	308	BRIERE	05 CLEO	$e^+ e^- \rightarrow \psi(2S) \rightarrow 2(\pi^+ \pi^-)$	
4.5 ± 1.0		TANENBAUM	78 MRK1	$e^+ e^-$	

$\Gamma(\rho^0 \pi^+ \pi^-) / \Gamma_{total}$					$\Gamma_{65} / \Gamma$
VALUE (units $10^{-4}$ )	EVTS	DOCUMENT ID	TECN	COMMENT	
<b>2.2 ± 0.6 OUR AVERAGE</b>	Error includes scale factor of 1.4.				
2.0 ± 0.2 ± 0.4	285.5	BRIERE	05 CLEO	$e^+ e^- \rightarrow \psi(2S) \rightarrow 2(\pi^+ \pi^-)$	
4.2 ± 1.5		TANENBAUM	78 MRK1	$e^+ e^-$	

$\Gamma(K^+ K^- \pi^+ \pi^- \pi^0) / \Gamma_{total}$					$\Gamma_{66} / \Gamma$
VALUE (units $10^{-4}$ )	EVTS	DOCUMENT ID	TECN	COMMENT	
<b>12.6 ± 0.9 OUR AVERAGE</b>					
18.7 ± 5.7 ± 0.3	32	<sup>92</sup> AUBERT	07AU BABR	10.6 $e^+ e^- \rightarrow K^+ K^- \pi^+ \pi^- \pi^0 \gamma$	
11.7 ± 1.0 ± 1.5	597	ABLIKIM	06G BES2	$\psi(2S) \rightarrow K^+ K^- \pi^+ \pi^- \pi^0$	
12.7 ± 0.5 ± 1.0	711.6	BRIERE	05 CLEO	$e^+ e^- \rightarrow \psi(2S) \rightarrow K^+ K^- \pi^+ \pi^- \pi^0$	
<sup>92</sup> AUBERT 07AU reports $[\Gamma(\psi(2S) \rightarrow K^+ K^- \pi^+ \pi^- \pi^0) / \Gamma_{total}] \times [\Gamma(\psi(2S) \rightarrow e^+ e^-)] = (44 \pm 13 \pm 3) \times 10^{-4}$ keV which we divide by our best value $\Gamma(\psi(2S) \rightarrow e^+ e^-) = 2.35 \pm 0.04$ keV. Our first error is their experiment's error and our second error is the systematic error from using our best value.					

$\Gamma(\omega f_0(1710) \rightarrow \omega K^+ K^-) / \Gamma_{total}$					$\Gamma_{67} / \Gamma$
VALUE (units $10^{-5}$ )	EVTS	DOCUMENT ID	TECN	COMMENT	
<b>5.9 ± 2.0 ± 0.9</b>	19	ABLIKIM	06G BES2	$\psi(2S) \rightarrow K^+ K^- \pi^+ \pi^- \pi^0$	

$\Gamma(K^*(892)^0 K^- \pi^+ \pi^0 + c.c.) / \Gamma_{total}$					$\Gamma_{68} / \Gamma$
VALUE (units $10^{-4}$ )	EVTS	DOCUMENT ID	TECN	COMMENT	
<b>8.6 ± 1.3 ± 1.8</b>	238	ABLIKIM	06G BES2	$\psi(2S) \rightarrow K^+ K^- \pi^+ \pi^- \pi^0$	

$\Gamma(K^*(892)^+ K^- \pi^+ \pi^- + c.c.) / \Gamma_{total}$					$\Gamma_{69} / \Gamma$
VALUE (units $10^{-4}$ )	EVTS	DOCUMENT ID	TECN	COMMENT	
<b>9.6 ± 2.2 ± 1.7</b>	133	ABLIKIM	06G BES2	$\psi(2S) \rightarrow K^+ K^- \pi^+ \pi^- \pi^0$	

$\Gamma(K^*(892)^+ K^- \rho^0 + c.c.) / \Gamma_{total}$					$\Gamma_{70} / \Gamma$
VALUE (units $10^{-4}$ )	EVTS	DOCUMENT ID	TECN	COMMENT	
<b>7.3 ± 2.2 ± 1.4</b>	78	ABLIKIM	06G BES2	$\psi(2S) \rightarrow K^+ K^- \pi^+ \pi^- \pi^0$	

$\Gamma(K^*(892)^0 K^- \rho^+ + c.c.) / \Gamma_{total}$					$\Gamma_{71} / \Gamma$
VALUE (units $10^{-4}$ )	EVTS	DOCUMENT ID	TECN	COMMENT	
<b>6.1 ± 1.3 ± 1.2</b>	125	ABLIKIM	06G BES2	$\psi(2S) \rightarrow K^+ K^- \pi^+ \pi^- \pi^0$	

$\Gamma(\eta K^+ K^-) / \Gamma_{total}$					$\Gamma_{72} / \Gamma$
VALUE (units $10^{-4}$ )	CL%	DOCUMENT ID	TECN	COMMENT	
<b>&lt;1.3</b>	90	BRIERE	05 CLEO	$e^+ e^- \rightarrow \psi(2S) \rightarrow K^+ K^- \pi^+ \pi^- \pi^0$	

$\Gamma(\omega K^+ K^-) / \Gamma_{total}$					$\Gamma_{73} / \Gamma$
VALUE (units $10^{-4}$ )	EVTS	DOCUMENT ID	TECN	COMMENT	
<b>1.85 ± 0.25 OUR AVERAGE</b>	Error includes scale factor of 1.1.				
2.38 ± 0.37 ± 0.29	78	ABLIKIM	06G BES2	$\psi(2S) \rightarrow K^+ K^- \pi^+ \pi^- \pi^0$	
1.9 ± 0.3 ± 0.3	76.8	BRIERE	05 CLEO	$e^+ e^- \rightarrow \psi(2S) \rightarrow K^+ K^- \pi^+ \pi^- \pi^0$	
1.5 ± 0.3 ± 0.2	23.0 ± 5.2	<sup>93</sup> BAI	03B BES	$\psi(2S) \rightarrow K^+ K^- \pi^+ \pi^- \pi^0$	
<sup>93</sup> Normalized to $B(\psi(2S) \rightarrow J/\psi \pi^+ \pi^-) = 0.305 \pm 0.016$ .					

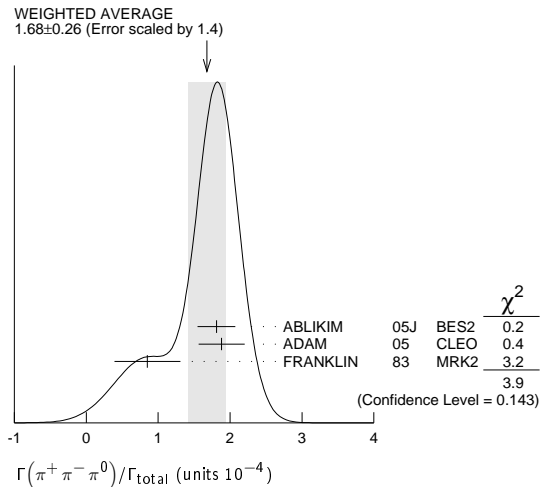
$\Gamma(3(\pi^+ \pi^-)) / \Gamma_{total}$					$\Gamma_{74} / \Gamma$
VALUE (units $10^{-4}$ )	EVTS	DOCUMENT ID	TECN	COMMENT	
<b>3.5 ± 2.0 OUR AVERAGE</b>	Error includes scale factor of 2.8.				
5.45 ± 0.42 ± 0.87	671	ABLIKIM	05H BES2	$e^+ e^- \rightarrow \psi(2S) \rightarrow 3(\pi^+ \pi^-)$	
1.5 ± 1.0		<sup>94</sup> TANENBAUM	78 MRK1	$e^+ e^-$	
<sup>94</sup> Assuming entirely strong decay.					

$\Gamma(\rho \bar{\rho} \pi^+ \pi^- \pi^0) / \Gamma_{total}$					$\Gamma_{75} / \Gamma$
VALUE (units $10^{-4}$ )	EVTS	DOCUMENT ID	TECN	COMMENT	
<b>7.3 ± 0.4 ± 0.6</b>	434.9	BRIERE	05 CLEO	$e^+ e^- \rightarrow \psi(2S) \rightarrow \rho \bar{\rho} \pi^+ \pi^- \pi^0$	

$\Gamma(K^+ K^-) / \Gamma_{total}$					$\Gamma_{76} / \Gamma$
VALUE (units $10^{-5}$ )	CL%	DOCUMENT ID	TECN	COMMENT	
<b>6.3 ± 0.7 OUR AVERAGE</b>					
6.3 ± 0.6 ± 0.3		DOBBS	06A CLEO	$e^+ e^-$	
10 ± 7		BRANDELIK	79c DASP	$e^+ e^-$	
• • • We do not use the following data for averages, fits, limits, etc. • • •					
< 5	90	FELDMAN	77 MRK1	$e^+ e^-$	

$\Gamma(K_S^0 K_L^0) / \Gamma_{total}$					$\Gamma_{77} / \Gamma$
VALUE (units $10^{-5}$ )	EVTS	DOCUMENT ID	TECN	COMMENT	
<b>5.4 ± 0.5 OUR AVERAGE</b>					
5.8 ± 0.8 ± 0.4		DOBBS	06A CLEO	$e^+ e^-$	
5.24 ± 0.47 ± 0.48	156 ± 14	<sup>95</sup> BAI	04B BES2	$\psi(2S) \rightarrow K_S^0 K_L^0 \rightarrow \pi^+ \pi^- X$	
<sup>95</sup> Using $B(K_S^0 \rightarrow \pi^+ \pi^-) = 0.6860 \pm 0.0027$ .					

$\Gamma(\pi^+ \pi^- \pi^0) / \Gamma_{total}$					$\Gamma_{78} / \Gamma$
VALUE (units $10^{-4}$ )	EVTS	DOCUMENT ID	TECN	COMMENT	
<b>1.68 ± 0.26 OUR AVERAGE</b>	Error includes scale factor of 1.4. See the ideogram below.				
1.81 ± 0.18 ± 0.19	260 ± 19	<sup>96</sup> ABLIKIM	05J BES2	$e^+ e^- \rightarrow \psi(2S)$	
1.88 ± 0.16 ± 0.28	194	ADAM	05 CLEO	$e^+ e^- \rightarrow \psi(2S)$	
0.85 ± 0.46	4	FRANKLIN	83 MRK2	$e^+ e^- \rightarrow \text{hadrons}$	
<sup>96</sup> From a PW analysis of $\psi(2S) \rightarrow \pi^+ \pi^- \pi^0$ .					



$\Gamma(\rho(2150) \pi \rightarrow \pi^+ \pi^- \pi^0) / \Gamma_{total}$					$\Gamma_{79} / \Gamma$
VALUE (units $10^{-4}$ )		DOCUMENT ID	TECN	COMMENT	
<b>1.94 ± 0.25 ± 1.15 - 0.34</b>		<sup>97</sup> ABLIKIM	05J BES2	$\psi(2S) \rightarrow \rho(2150) \pi \rightarrow \pi^+ \pi^- \pi^0$	
<sup>97</sup> From a PW analysis of $\psi(2S) \rightarrow \pi^+ \pi^- \pi^0$ .					





See key on page 457

Meson Particle Listings

$\psi(2S)$

$\Gamma(\phi f_2'(1525))/\Gamma_{total}$   $\Gamma_{102}/\Gamma$

VALUE (units $10^{-4}$ )	CL%	EVTS	DOCUMENT ID	TECN	COMMENT
<b>0.44 ± 0.12 ± 0.11</b>		20 ± 6	BAI	04c	$\psi(2S) \rightarrow 2(K^+ K^-)$
••• We do not use the following data for averages, fits, limits, etc. •••					
<0.45	90		BAI	98j	BES $e^+e^- \rightarrow 2(K^+ K^-)$

$\Gamma(\Theta(1540)\bar{\Theta}(1540) \rightarrow K_S^0 p K^- \bar{\pi} + c.c.)/\Gamma_{total}$   $\Gamma_{103}/\Gamma$

VALUE (units $10^{-5}$ )	CL%	DOCUMENT ID	TECN	COMMENT
<b>&lt;0.88</b>	90	BAI	04g	BES2 $e^+e^-$

$\Gamma(\Theta(1540)K^- \bar{\pi} \rightarrow K_S^0 p K^- \bar{\pi})/\Gamma_{total}$   $\Gamma_{104}/\Gamma$

VALUE (units $10^{-5}$ )	CL%	DOCUMENT ID	TECN	COMMENT
<b>&lt;1.0</b>	90	BAI	04g	BES2 $e^+e^-$

$\Gamma(\Theta(1540)K_S^0 \bar{p} \rightarrow K_S^0 \bar{p} K^+ n)/\Gamma_{total}$   $\Gamma_{105}/\Gamma$

VALUE (units $10^{-5}$ )	CL%	DOCUMENT ID	TECN	COMMENT
<b>&lt;0.70</b>	90	BAI	04g	BES2 $e^+e^-$

$\Gamma(\bar{\Theta}(1540)K^+ n \rightarrow K_S^0 \bar{p} K^+ n)/\Gamma_{total}$   $\Gamma_{106}/\Gamma$

VALUE (units $10^{-5}$ )	CL%	DOCUMENT ID	TECN	COMMENT
<b>&lt;2.6</b>	90	BAI	04g	BES2 $e^+e^-$

$\Gamma(\bar{\Theta}(1540)K_S^0 p \rightarrow K_S^0 p K^- \bar{\pi})/\Gamma_{total}$   $\Gamma_{107}/\Gamma$

VALUE (units $10^{-5}$ )	CL%	DOCUMENT ID	TECN	COMMENT
<b>&lt;0.60</b>	90	BAI	04g	BES2 $e^+e^-$

$\Gamma(K_S^0 K_S^0)/\Gamma_{total}$   $\Gamma_{108}/\Gamma$

VALUE (units $10^{-4}$ )	DOCUMENT ID	TECN	COMMENT
<b>&lt;0.046</b>	111 BAI	04D	BES $e^+e^-$

111 Forbidden by CP.

RADIATIVE DECAYS

$\Gamma(\gamma\chi_{c0}(1P))/\Gamma_{total}$   $\Gamma_{109}/\Gamma$

VALUE (units $10^{-2}$ )	EVTS	DOCUMENT ID	TECN	COMMENT
<b>9.68 ± 0.31 OUR FIT</b>				
<b>9.2 ± 0.4 OUR AVERAGE</b>				
9.22 ± 0.11 ± 0.46	72600	ATHAR	04	CLEO $e^+e^- \rightarrow \gamma X$
9.9 ± 0.5 ± 0.8		112 GAISER	86	CBAL $e^+e^- \rightarrow \gamma X$
7.2 ± 2.3		112 BIDDICK	77	CNTR $e^+e^- \rightarrow \gamma X$
7.5 ± 2.6		112 WHITAKER	76	MRK1 $e^+e^-$

112 Angular distribution ( $1+\cos^2\theta$ ) assumed.

$\Gamma(\gamma\chi_{c1}(1P))/\Gamma_{total}$   $\Gamma_{110}/\Gamma$

VALUE (units $10^{-2}$ )	EVTS	DOCUMENT ID	TECN	COMMENT
<b>9.2 ± 0.4 OUR FIT</b>				
<b>8.9 ± 0.5 OUR AVERAGE</b>				
9.07 ± 0.11 ± 0.54	76700	ATHAR	04	CLEO $e^+e^- \rightarrow \gamma X$
9.0 ± 0.5 ± 0.7		113 GAISER	86	CBAL $e^+e^- \rightarrow \gamma X$
7.1 ± 1.9		114 BIDDICK	77	CNTR $e^+e^- \rightarrow \gamma X$

113 Angular distribution ( $1-0.189\cos^2\theta$ ) assumed.  
114 Valid for isotropic distribution of the photon.

$\Gamma(\gamma\chi_{c2}(1P))/\Gamma_{total}$   $\Gamma_{111}/\Gamma$

VALUE (units $10^{-2}$ )	EVTS	DOCUMENT ID	TECN	COMMENT
<b>8.72 ± 0.34 OUR FIT</b>				
<b>8.8 ± 0.5 OUR AVERAGE</b>				Error includes scale factor of 1.1.
9.33 ± 0.14 ± 0.61	79300	ATHAR	04	CLEO $e^+e^- \rightarrow \gamma X$
8.0 ± 0.5 ± 0.7		115 GAISER	86	CBAL $e^+e^- \rightarrow \gamma X$
7.0 ± 2.0		116 BIDDICK	77	CNTR $e^+e^- \rightarrow \gamma X$

115 Angular distribution ( $1-0.052\cos^2\theta$ ) assumed.  
116 Valid for isotropic distribution of the photon.

$[\Gamma(\gamma\chi_{c0}(1P)) + \Gamma(\gamma\chi_{c1}(1P)) + \Gamma(\gamma\chi_{c2}(1P))]/\Gamma_{total}$   $(\Gamma_{109} + \Gamma_{110} + \Gamma_{111})/\Gamma$

VALUE	DOCUMENT ID	TECN	COMMENT
<b>27.6 ± 0.3 ± 2.0</b>	117 ATHAR	04	CLEO $e^+e^- \rightarrow \gamma X$

117 Not independent from ATHAR 04 measurements of  $B(\gamma\chi_{cJ})$ .

$\Gamma(\gamma\chi_{c0}(1P))/\Gamma(\gamma\chi_{c1}(1P))$   $\Gamma_{109}/\Gamma_{110}$

VALUE	DOCUMENT ID	TECN	COMMENT
<b>1.02 ± 0.01 ± 0.07</b>	118 ATHAR	04	CLEO $e^+e^- \rightarrow \gamma X$

118 Not independent from ATHAR 04 measurements of  $B(\gamma\chi_{cJ})$ .

$\Gamma(\gamma\chi_{c2}(1P))/\Gamma(\gamma\chi_{c1}(1P))$   $\Gamma_{111}/\Gamma_{110}$

VALUE	DOCUMENT ID	TECN	COMMENT
<b>1.03 ± 0.02 ± 0.03</b>	119 ATHAR	04	CLEO $e^+e^- \rightarrow \gamma X$

119 Not independent from ATHAR 04 measurements of  $B(\gamma\chi_{cJ})$ .

$\Gamma(\gamma\chi_{c0}(1P))/\Gamma(\gamma\chi_{c2}(1P))$   $\Gamma_{109}/\Gamma_{111}$

VALUE	DOCUMENT ID	TECN	COMMENT
<b>0.99 ± 0.02 ± 0.08</b>	120 ATHAR	04	CLEO $e^+e^- \rightarrow \gamma X$

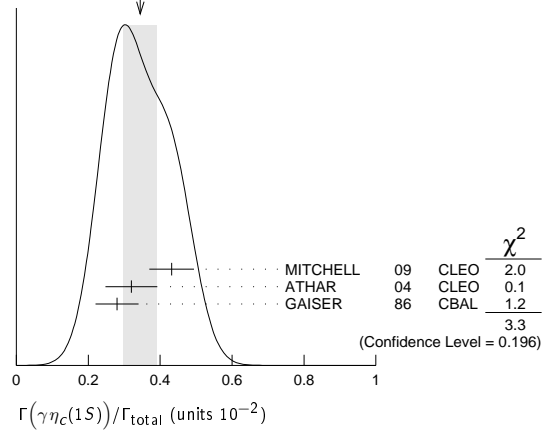
120 Not independent from ATHAR 04 measurements of  $B(\gamma\chi_{cJ})$ .

$\Gamma(\gamma\eta_c(1S))/\Gamma_{total}$   $\Gamma_{112}/\Gamma$

VALUE (units $10^{-2}$ )	EVTS	DOCUMENT ID	TECN	COMMENT
<b>0.34 ± 0.05 OUR AVERAGE</b>				Error includes scale factor of 1.3. See the ideogram below.
0.432 ± 0.016 ± 0.060		MITCHELL	09	CLEO $e^+e^- \rightarrow \gamma X$
0.32 ± 0.04 ± 0.06	2560	121 ATHAR	04	CLEO $e^+e^- \rightarrow \gamma X$
0.28 ± 0.06		122 GAISER	86	CBAL $e^+e^- \rightarrow \gamma X$

121 ATHAR 04 used  $\Gamma_{\eta_c(1S)} = 24.8 \pm 4.9$  MeV to obtain this result.  
122 GAISER 86 used  $\Gamma_{\eta_c(1S)} = 11.5 \pm 4.5$  MeV to obtain this result.

WEIGHTED AVERAGE  
0.34 ± 0.05 (Error scaled by 1.3)



$\Gamma(\gamma\eta_c(2S))/\Gamma_{total}$   $\Gamma_{113}/\Gamma$

VALUE	CL%	EVTS	DOCUMENT ID	TECN	COMMENT
<b>&lt;8 × 10<sup>-4</sup></b>	90	123	CRONIN-HEN..10	CLEO	$\psi(2S) \rightarrow \gamma K \bar{K} \pi$

••• We do not use the following data for averages, fits, limits, etc. •••

VALUE	CL%	EVTS	DOCUMENT ID	TECN	COMMENT
<2 × 10 <sup>-3</sup>	90		ATHAR	04	CLEO $e^+e^- \rightarrow \gamma X$
0.2-1.3 × 10 <sup>-2</sup>	95		EDWARDS	82c	CBAL $e^+e^- \rightarrow \gamma X$

123 CRONIN-HENNESSY 10 reports  $[\Gamma(\psi(2S) \rightarrow \gamma\eta_c(2S))/\Gamma_{total}] \times [B(\eta_c(2S) \rightarrow K \bar{K} \pi)] < 14.5 \times 10^{-6}$  which we divide by our best value  $B(\eta_c(2S) \rightarrow K \bar{K} \pi) = 1.9 \times 10^{-2}$ . This measurement assumes  $\Gamma(\eta_c(2S)) = 14$  MeV. CRONIN-HENNESSY 10 gives the analytic dependence of limits on width.

$\Gamma(\gamma\pi^0)/\Gamma_{total}$   $\Gamma_{114}/\Gamma$

VALUE (units $10^{-6}$ )	CL%	EVTS	DOCUMENT ID	TECN	COMMENT
<b>1.58 ± 0.40 ± 0.13</b>		37	ABLIKIM	10F	BES3 $\psi(2S) \rightarrow \gamma \pi^0$

••• We do not use the following data for averages, fits, limits, etc. •••

VALUE	CL%	EVTS	DOCUMENT ID	TECN	COMMENT
< 5	90		PEDLAR	09	CLE3 $\psi(2S) \rightarrow \gamma X$
<5400	95		124 LIBERMAN	75	SPEC $e^+e^-$
< 1 × 10 <sup>4</sup>	90		WIJK	75	DASP $e^+e^-$

124 Restated by us using  $B(\psi(2S) \rightarrow \mu^+ \mu^-) = 0.0077$ .

$\Gamma(\gamma\eta'(958))/\Gamma_{total}$   $\Gamma_{115}/\Gamma$

VALUE (units $10^{-4}$ )	CL%	EVTS	DOCUMENT ID	TECN	COMMENT
<b>1.23 ± 0.06 OUR AVERAGE</b>					
1.26 ± 0.03 ± 0.08		2226	125 ABLIKIM	10F	BES3 $\psi(2S) \rightarrow 3\gamma \pi^+ \pi^-, 2\gamma \pi^+ \pi^-$
1.19 ± 0.08 ± 0.03			PEDLAR	09	CLE3 $\psi(2S) \rightarrow \gamma X$
1.24 ± 0.27 ± 0.15		23	ABLIKIM	06R	BES2 $e^+e^- \rightarrow \psi(2S)$
1.54 ± 0.31 ± 0.20		~ 43	BAI	98F	BES $\psi(2S) \rightarrow \pi^+ \pi^- 2\gamma, \pi^+ \pi^- 3\gamma$

••• We do not use the following data for averages, fits, limits, etc. •••

VALUE	CL%	EVTS	DOCUMENT ID	TECN	COMMENT
< 60	90		126 BRAUNSCH...	77	DASP $e^+e^-$
< 11	90		127 BARTEL	76	CNTR $e^+e^-$

125 Combining the results from  $\eta' \rightarrow \pi^+ \pi^- \eta$  and  $\eta' \rightarrow \pi^+ \pi^- \gamma$  decay modes.  
126 Restated by us using total decay width 228 keV.  
127 The value is normalized to the branching ratio for  $\Gamma(J/\psi(1S)\eta)/\Gamma_{total}$ .

$\Gamma(\gamma f_2(1270))/\Gamma_{total}$   $\Gamma_{116}/\Gamma$

VALUE (units $10^{-4}$ )	CL%	EVTS	DOCUMENT ID	TECN	COMMENT
<b>2.12 ± 0.19 ± 0.32</b>		128,129	BAI	03c	BES $\psi(2S) \rightarrow \gamma \pi \pi$

••• We do not use the following data for averages, fits, limits, etc. •••

VALUE	CL%	EVTS	DOCUMENT ID	TECN	COMMENT
2.08 ± 0.19 ± 0.33		200.6 ± 18.8	128 BAI	03c	BES $\psi(2S) \rightarrow \gamma \pi^+ \pi^-$
2.90 ± 1.08 ± 1.07		29.9 ± 11.1	128 BAI	03c	BES $\psi(2S) \rightarrow \gamma \pi^0 \pi^0$

128 Normalized to  $B(\psi(2S) \rightarrow J/\psi \pi^+ \pi^-) = 0.305 \pm 0.016$ .  
129 Combining the results from  $\pi^+ \pi^-$  and  $\pi^0 \pi^0$  decay modes.



See key on page 457

Meson Particle Listings

$\psi(2S), \psi(3770)$

Table listing particle decays and sources. Columns include particle name, document ID, year, author(s), and source (e.g., BABAR, CLEO, BES, etc.).

1 Taking into account interference between the resonant and non-resonant D D-bar production.
2 Reanalysis of data presented in BAI 02c. From a global fit over the center-of-mass energy region 3.7-5.0 GeV...
3 Interference between the resonant and non-resonant D D-bar production not taken into account.

Table showing the mass difference m\_psi(3770) - m\_psi(2S) with various fits and measurements. Includes columns for Value (MeV), Document ID, TECN, and Comment.

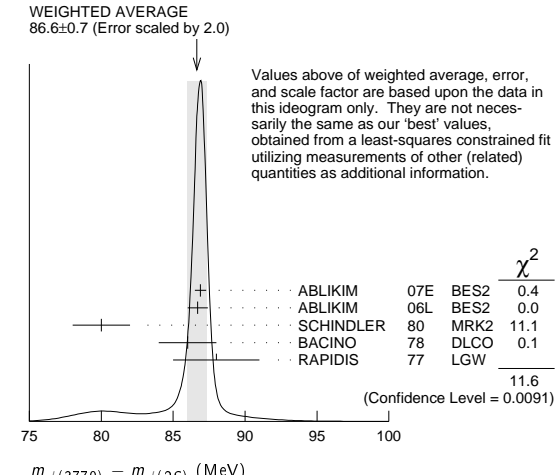


Table titled 'psi(3770) WIDTH' listing width measurements from different experiments. Columns include Value (MeV), EVTS, Document ID, TECN, and Comment.

6 Taking into account interference between the resonant and non-resonant D D-bar production.
7 Reanalysis of data presented in BAI 02c. From a global fit over the center-of-mass energy region 3.7-5.0 GeV...
8 Interference between the resonant and non-resonant D D-bar production not taken into account.

psi(3770) with G-parity JPC = 0^-(1^-^-)

Table titled 'psi(3770) MASS (MeV)' providing the mass measurement from the fit. It includes the fit value, a table of contributing measurements, and a list of data points not used for the fit.

psi(3770) DECAY MODES

In addition to the dominant decay mode to D D-bar, psi(3770) was found to decay into the final states containing the J/psi (BAI 05, ADAM 06). ADAMS 06 and HUANG 06a searched for various decay modes with light hadrons and found a statistically significant signal for the decay to phi eta only (ADAMS 06).

Table listing decay modes for psi(3770). Columns include Mode, Fraction (Gamma\_i/Gamma), Scale factor/Confidence level.

## Meson Particle Listings

 $\psi(3770)$ 

Decays to light hadrons			
$\Gamma_9$	$b_1(1235)\pi$	$< 1.4 \times 10^{-5}$	CL=90%
$\Gamma_{10}$	$\phi\eta'$	$< 7 \times 10^{-4}$	CL=90%
$\Gamma_{11}$	$\omega\eta'$	$< 4 \times 10^{-4}$	CL=90%
$\Gamma_{12}$	$\rho^0\eta'$	$< 6 \times 10^{-4}$	CL=90%
$\Gamma_{13}$	$\phi\eta$	$(3.1 \pm 0.7) \times 10^{-4}$	
$\Gamma_{14}$	$\omega\eta$	$< 1.4 \times 10^{-5}$	CL=90%
$\Gamma_{15}$	$\rho^0\eta$	$< 5 \times 10^{-4}$	CL=90%
$\Gamma_{16}$	$\phi\pi^0$	$< 3 \times 10^{-5}$	CL=90%
$\Gamma_{17}$	$\omega\pi^0$	$< 6 \times 10^{-4}$	CL=90%
$\Gamma_{18}$	$\pi^+\pi^-\pi^0$	$< 5 \times 10^{-6}$	CL=90%
$\Gamma_{19}$	$\rho\pi$	$< 5 \times 10^{-6}$	CL=90%
$\Gamma_{20}$	$K^*(892)^+K^- + \text{c.c.}$	$< 1.4 \times 10^{-5}$	CL=90%
$\Gamma_{21}$	$K^*(892)^0\bar{K}^0 + \text{c.c.}$	$< 1.2 \times 10^{-3}$	CL=90%
$\Gamma_{22}$	$K_S^0 K_L^0$	$< 1.2 \times 10^{-5}$	CL=90%
$\Gamma_{23}$	$2(\pi^+\pi^-)$	$< 1.12 \times 10^{-3}$	CL=90%
$\Gamma_{24}$	$2(\pi^+\pi^-)\pi^0$	$< 1.06 \times 10^{-3}$	CL=90%
$\Gamma_{25}$	$2(\pi^+\pi^-\pi^0)$	$< 5.85\%$	CL=90%
$\Gamma_{26}$	$\omega\pi^+\pi^-$	$< 6.0 \times 10^{-4}$	CL=90%
$\Gamma_{27}$	$3(\pi^+\pi^-)$	$< 9.1 \times 10^{-3}$	
$\Gamma_{28}$	$3(\pi^+\pi^-)\pi^0$	$< 1.37\%$	
$\Gamma_{29}$	$3(\pi^+\pi^-)2\pi^0$	$< 11.74\%$	CL=90%
$\Gamma_{30}$	$\eta\pi^+\pi^-$	$< 1.24 \times 10^{-3}$	CL=90%
$\Gamma_{31}$	$\pi^+\pi^-2\pi^0$	$< 8.9 \times 10^{-3}$	CL=90%
$\Gamma_{32}$	$\rho^0\pi^+\pi^-$	$< 6.9 \times 10^{-3}$	CL=90%
$\Gamma_{33}$	$\eta 3\pi$	$< 1.34 \times 10^{-3}$	CL=90%
$\Gamma_{34}$	$\eta 2(\pi^+\pi^-)$	$< 2.43\%$	
$\Gamma_{35}$	$\eta\rho^0\pi^+\pi^-$	$< 1.45\%$	CL=90%
$\Gamma_{36}$	$\eta' 3\pi$	$< 2.44 \times 10^{-3}$	CL=90%
$\Gamma_{37}$	$K^+K^-\pi^+\pi^-$	$< 9.0 \times 10^{-4}$	CL=90%
$\Gamma_{38}$	$\phi\pi^+\pi^-$	$< 4.1 \times 10^{-4}$	CL=90%
$\Gamma_{39}$	$K^+K^-2\pi^0$	$< 4.2 \times 10^{-3}$	CL=90%
$\Gamma_{40}$	$4(\pi^+\pi^-)$	$< 1.67\%$	CL=90%
$\Gamma_{41}$	$4(\pi^+\pi^-)\pi^0$	$< 3.06\%$	CL=90%
$\Gamma_{42}$	$\phi f_0(980)$	$< 4.5 \times 10^{-4}$	CL=90%
$\Gamma_{43}$	$K^+K^-\pi^+\pi^-\pi^0$	$< 2.36 \times 10^{-3}$	CL=90%
$\Gamma_{44}$	$K^+K^-\rho^0\pi^0$	$< 8 \times 10^{-4}$	CL=90%
$\Gamma_{45}$	$K^+K^-\rho^+\pi^-$	$< 1.46\%$	CL=90%
$\Gamma_{46}$	$\omega K^+K^-$	$< 3.4 \times 10^{-4}$	CL=90%
$\Gamma_{47}$	$\phi\pi^+\pi^-\pi^0$	$< 3.8 \times 10^{-3}$	CL=90%
$\Gamma_{48}$	$K^{*0}K^-\pi^+\pi^0 + \text{c.c.}$	$< 1.62\%$	CL=90%
$\Gamma_{49}$	$K^{*+}K^-\pi^+\pi^0 + \text{c.c.}$	$< 3.23\%$	CL=90%
$\Gamma_{50}$	$K^+K^-\pi^+\pi^-2\pi^0$	$< 2.67\%$	CL=90%
$\Gamma_{51}$	$K^+K^-2(\pi^+\pi^-)$	$< 1.03\%$	CL=90%
$\Gamma_{52}$	$K^+K^-2(\pi^+\pi^-)\pi^0$	$< 3.60\%$	CL=90%
$\Gamma_{53}$	$\eta K^+K^-$	$< 4.1 \times 10^{-4}$	CL=90%
$\Gamma_{54}$	$\eta K^+K^-\pi^+\pi^-$	$< 1.24\%$	CL=90%
$\Gamma_{55}$	$\rho^0 K^+K^-$	$< 5.0 \times 10^{-3}$	CL=90%
$\Gamma_{56}$	$2(K^+K^-)$	$< 6.0 \times 10^{-4}$	CL=90%
$\Gamma_{57}$	$\phi K^+K^-$	$< 7.5 \times 10^{-4}$	CL=90%
$\Gamma_{58}$	$2(K^+K^-)\pi^0$	$< 2.9 \times 10^{-4}$	CL=90%
$\Gamma_{59}$	$2(K^+K^-)\pi^+\pi^-$	$< 3.2 \times 10^{-3}$	CL=90%
$\Gamma_{60}$	$K_S^0 K^-\pi^+$	$< 3.2 \times 10^{-3}$	CL=90%
$\Gamma_{61}$	$K_S^0 K^-\pi^+\pi^0$	$< 1.33\%$	CL=90%
$\Gamma_{62}$	$K_S^0 K^-\rho^+$	$< 6.6 \times 10^{-3}$	CL=90%
$\Gamma_{63}$	$K_S^0 K^-\rho^+\pi^-$	$< 8.7 \times 10^{-3}$	CL=90%
$\Gamma_{64}$	$K_S^0 K^-\pi^+\rho^0$	$< 1.6\%$	CL=90%
$\Gamma_{65}$	$K_S^0 K^-\pi^+\eta$	$< 1.3\%$	CL=90%
$\Gamma_{66}$	$K_S^0 K^-\rho^+\pi^-\pi^0$	$< 4.18\%$	CL=90%
$\Gamma_{67}$	$K_S^0 K^-\rho^+\pi^-\eta$	$< 4.8\%$	CL=90%
$\Gamma_{68}$	$K_S^0 K^-\pi^+2(\pi^+\pi^-)$	$< 1.22\%$	CL=90%
$\Gamma_{69}$	$K_S^0 K^-\pi^+2\pi^0$	$< 2.65\%$	CL=90%
$\Gamma_{70}$	$K_S^0 K^-\rho^+K^-\pi^+$	$< 4.9 \times 10^{-3}$	CL=90%
$\Gamma_{71}$	$K_S^0 K^-\rho^+K^-\pi^+\pi^0$	$< 3.0\%$	CL=90%
$\Gamma_{72}$	$K_S^0 K^-\rho^+K^-\pi^+\eta$	$< 2.2\%$	CL=90%
$\Gamma_{73}$	$K^{*0}K^-\pi^+ + \text{c.c.}$	$< 9.7 \times 10^{-3}$	CL=90%
$\Gamma_{74}$	$\rho\bar{p}\pi^0$	$< 1.2 \times 10^{-3}$	CL=90%
$\Gamma_{75}$	$\rho\bar{p}\pi^+\pi^-$	$< 5.8 \times 10^{-4}$	CL=90%
$\Gamma_{76}$	$\Lambda\bar{\Lambda}$	$< 1.2 \times 10^{-4}$	CL=90%
$\Gamma_{77}$	$\rho\bar{p}\pi^+\pi^-\pi^0$	$< 1.85 \times 10^{-3}$	CL=90%
$\Gamma_{78}$	$\omega\rho\bar{p}$	$< 2.9 \times 10^{-4}$	CL=90%
$\Gamma_{79}$	$\Lambda\bar{\Lambda}\pi^0$	$< 1.2 \times 10^{-3}$	CL=90%
$\Gamma_{80}$	$\rho\bar{p}2(\pi^+\pi^-)$	$< 2.6 \times 10^{-3}$	CL=90%
$\Gamma_{81}$	$\eta\rho\bar{p}$	$< 5.4 \times 10^{-4}$	CL=90%

$\Gamma_{82}$	$\eta\rho\bar{p}\pi^+\pi^-$	$< 3.3 \times 10^{-3}$	CL=90%
$\Gamma_{83}$	$\rho^0\rho\bar{p}$	$< 1.7 \times 10^{-3}$	CL=90%
$\Gamma_{84}$	$\rho\bar{p}K^+K^-$	$< 3.2 \times 10^{-4}$	CL=90%
$\Gamma_{85}$	$\eta\rho\bar{p}K^+K^-$	$< 6.9 \times 10^{-3}$	CL=90%
$\Gamma_{86}$	$\pi^0\rho\bar{p}K^+K^-$	$< 1.2 \times 10^{-3}$	CL=90%
$\Gamma_{87}$	$\phi\rho\bar{p}$	$< 1.3 \times 10^{-4}$	CL=90%
$\Gamma_{88}$	$\Lambda\bar{\Lambda}\pi^+\pi^-$	$< 2.5 \times 10^{-4}$	CL=90%
$\Gamma_{89}$	$\Lambda\bar{p}K^+$	$< 2.8 \times 10^{-4}$	CL=90%
$\Gamma_{90}$	$\Lambda\bar{p}K^+\pi^+\pi^-$	$< 6.3 \times 10^{-4}$	CL=90%

## Radiative decays

$\Gamma_{91}$	$\gamma\chi_{c2}$	$< 9 \times 10^{-4}$	CL=90%
$\Gamma_{92}$	$\gamma\chi_{c1}$	$(2.9 \pm 0.6) \times 10^{-3}$	
$\Gamma_{93}$	$\gamma\chi_{c0}$	$(7.3 \pm 0.9) \times 10^{-3}$	
$\Gamma_{94}$	$\gamma\eta'$	$< 1.8 \times 10^{-4}$	CL=90%
$\Gamma_{95}$	$\gamma\eta$	$< 1.5 \times 10^{-4}$	CL=90%
$\Gamma_{96}$	$\gamma\pi^0$	$< 2 \times 10^{-4}$	CL=90%

## CONSTRAINED FIT INFORMATION

An overall fit to the total width, a partial width, and 3 branching ratios uses 23 measurements and one constraint to determine 5 parameters. The overall fit has a  $\chi^2 = 20.0$  for 19 degrees of freedom.

The following *off-diagonal* array elements are the correlation coefficients  $\langle \delta p_i \delta p_j \rangle / (\delta p_i \delta p_j)$ , in percent, from the fit to parameters  $p_i$ , including the branching fractions,  $x_i \equiv \Gamma_i / \Gamma_{\text{total}}$ . The fit constrains the  $x_i$  whose labels appear in this array to sum to one.

$x_3$	98		
$x_8$	0	0	
$\Gamma$	0	0	-44
	$x_2$	$x_3$	$x_8$

Mode	Rate (MeV)	Scale factor	
$\Gamma_2$	$D^0\bar{D}^0$	$14.1 \pm 1.4$	1.7
$\Gamma_3$	$D^+D^-$	$11.2 \pm 1.1$	1.7
$\Gamma_8$	$e^+e^-$	$(2.62 \pm 0.18) \times 10^{-4}$	1.4

 $\psi(3770)$  PARTIAL WIDTHS

$\Gamma(e^+e^-)$					$\Gamma_8$
VALUE (keV)	EVTS	DOCUMENT ID	TECN	COMMENT	
<b>0.262±0.018 OUR FIT</b>					Error includes scale factor of 1.4.
<b>0.256±0.016 OUR AVERAGE</b>					Error includes scale factor of 1.2.
0.154+0.079+0.021 -0.058-0.027		9,10 ANASHIN	12A	KEDR	$e^+e^- \rightarrow D\bar{D}$
0.22 ± 0.05		11,12 ABLIKIM	08D	BES2	$e^+e^- \rightarrow$ hadrons
0.277 ± 0.011 ± 0.013		12 ABLIKIM	07E	BES2	$e^+e^- \rightarrow$ hadrons
0.203±0.003+0.041 -0.027	1.4M	12,13 BESSON	06	CLEO	$e^+e^- \rightarrow$ hadrons
0.276±0.050		12 SCHINDLER	80	MRK2	$e^+e^-$
0.18 ± 0.06		12 BACINO	78	DLCO	$e^+e^-$
••• We do not use the following data for averages, fits, limits, etc. •••					
0.414+0.072+0.093 -0.080-0.028		10,14 ANASHIN	12A	KEDR	$e^+e^- \rightarrow D\bar{D}$
0.37 ± 0.09		15 RAPIDIS	77	LGW	$e^+e^-$
9 Solution I of the two solutions.					
10 Taking into account interference between the resonant and non-resonant $D\bar{D}$ production.					
11 Reanalysis of data presented in BAI 02c. From a global fit over the center-of-mass energy region 3.7–5.0 GeV covering the $\psi(3770)$ , $\psi(4040)$ , $\psi(4160)$ , and $\psi(4415)$ resonances. Phase angle fixed in the fit to $\delta = 0^\circ$ .					
12 Interference between the resonant and non-resonant $D\bar{D}$ production not taken into account.					
13 BESSON 06 (as corrected in BESSON 10) measure $\sigma(e^+e^- \rightarrow \psi(3770) \rightarrow \text{hadrons}) = 6.36 \pm 0.08^{+0.41}_{-0.30}$ nb at $\sqrt{s} = 3773 \pm 1$ MeV, and obtain $\Gamma_{ee}$ from the Born-level cross section calculated using $\psi(3770)$ mass and width from our 2004 edition, PDG 04.					
14 Solution II of the two solutions.					
15 See also $\Gamma(e^+e^-)/\Gamma_{\text{total}}$ below.					

 $\psi(3770)$  BRANCHING RATIOS

$\Gamma(D\bar{D})/\Gamma_{\text{total}}$					$\Gamma_1/\Gamma = (\Gamma_2+\Gamma_3)/\Gamma$
VALUE	EVTS	DOCUMENT ID	TECN	COMMENT	
<b>0.93 ± 0.08 -0.09 OUR FIT</b>					Error includes scale factor of 2.0.
<b>0.93 ± 0.08 -0.09 OUR AVERAGE</b>					Error includes scale factor of 2.1.
0.849±0.056±0.018		16 ABLIKIM	08B	BES2	$e^+e^- \rightarrow \text{non-}D\bar{D}$
1.033±0.014+0.048 -0.066	1.427M	17 BESSON	06	CLEO	$e^+e^- \rightarrow$ hadrons



## Meson Particle Listings

 $\psi(3770)$ 

$\Gamma(\pi^+\pi^-2\pi^0)/\Gamma_{\text{total}}$			$\Gamma_{31}/\Gamma$			$\Gamma(K^{*+}K^-\pi^+\pi^- + \text{c.c.})/\Gamma_{\text{total}}$			$\Gamma_{49}/\Gamma$							
VALUE (units $10^{-3}$ )	CL%	EVTS	DOCUMENT ID	TECN	COMMENT	VALUE (units $10^{-4}$ )	CL%	EVTS	DOCUMENT ID	TECN	COMMENT					
<8.9	90	218	ABLIKIM	08N	BES2	$e^+e^- \rightarrow \psi(3770)$	<323	90	23	ABLIKIM	07i	BES2	$3.77 e^+e^-$			
$\Gamma(\rho^0\pi^+\pi^-)/\Gamma_{\text{total}}$			$\Gamma_{32}/\Gamma$			$\Gamma(K^+K^-\pi^+\pi^-2\pi^0)/\Gamma_{\text{total}}$			$\Gamma_{50}/\Gamma$							
VALUE (units $10^{-3}$ )	CL%		DOCUMENT ID	TECN	COMMENT	VALUE (units $10^{-3}$ )	CL%	EVTS	DOCUMENT ID	TECN	COMMENT	VALUE (units $10^{-3}$ )	CL%	EVTS		
<6.9	90		23	ABLIKIM	07F	BES2	$e^+e^- \rightarrow \psi(3770)$	24	ABLIKIM	08N	BES2	$e^+e^- \rightarrow \psi(3770)$				
$\Gamma(\eta3\pi)/\Gamma_{\text{total}}$			$\Gamma_{33}/\Gamma$			$\Gamma(K^+K^-2(\pi^+\pi^-))/\Gamma_{\text{total}}$			$\Gamma_{51}/\Gamma$							
VALUE (units $10^{-4}$ )	CL%		DOCUMENT ID	TECN	COMMENT	VALUE (units $10^{-3}$ )	CL%		DOCUMENT ID	TECN	COMMENT	VALUE (units $10^{-3}$ )	CL%			
<13.4	90		27	HUANG	06A	CLEO	$e^+e^- \rightarrow \psi(3770)$		23	ABLIKIM	07F	BES2	$e^+e^- \rightarrow \psi(3770)$			
$\Gamma(\eta2(\pi^+\pi^-))/\Gamma_{\text{total}}$			$\Gamma_{34}/\Gamma$			$\Gamma(K^+K^-2(\pi^+\pi^-)\pi^0)/\Gamma_{\text{total}}$			$\Gamma_{52}/\Gamma$							
VALUE (units $10^{-4}$ )	CL%		DOCUMENT ID	TECN	COMMENT	VALUE (units $10^{-3}$ )	CL%		DOCUMENT ID	TECN	COMMENT	VALUE (units $10^{-3}$ )	CL%			
<243			23	ABLIKIM	07B	BES2	$e^+e^- \rightarrow \psi(3770)$		23	ABLIKIM	07F	BES2	$e^+e^- \rightarrow \psi(3770)$			
$\Gamma(\eta\rho^0\pi^+\pi^-)/\Gamma_{\text{total}}$			$\Gamma_{35}/\Gamma$			$\Gamma(\eta(K^+K^-))/\Gamma_{\text{total}}$			$\Gamma_{53}/\Gamma$							
VALUE (units $10^{-2}$ )	CL%		DOCUMENT ID	TECN	COMMENT	VALUE (units $10^{-4}$ )	CL%		DOCUMENT ID	TECN	COMMENT	VALUE (units $10^{-4}$ )	CL%			
<1.45	90		23	ABLIKIM	10D	BES2	$e^+e^- \rightarrow \psi(3770)$		27	HUANG	06A	CLEO	$e^+e^- \rightarrow \psi(3770)$			
$\Gamma(\eta'3\pi)/\Gamma_{\text{total}}$			$\Gamma_{36}/\Gamma$			$\Gamma(\eta K^+K^-\pi^+\pi^-)/\Gamma_{\text{total}}$			$\Gamma_{54}/\Gamma$							
VALUE (units $10^{-4}$ )	CL%		DOCUMENT ID	TECN	COMMENT	VALUE (units $10^{-2}$ )	CL%		DOCUMENT ID	TECN	COMMENT	VALUE (units $10^{-2}$ )	CL%			
<24.4	90		27	HUANG	06A	CLEO	$e^+e^- \rightarrow \psi(3770)$		23	ABLIKIM	10D	BES2	$e^+e^- \rightarrow \psi(3770)$			
$\Gamma(K^+K^-\pi^+\pi^-)/\Gamma_{\text{total}}$			$\Gamma_{37}/\Gamma$			$\Gamma(\rho^0 K^+K^-)/\Gamma_{\text{total}}$			$\Gamma_{55}/\Gamma$							
VALUE (units $10^{-4}$ )	CL%		DOCUMENT ID	TECN	COMMENT	VALUE (units $10^{-3}$ )	CL%		DOCUMENT ID	TECN	COMMENT	VALUE (units $10^{-3}$ )	CL%			
< 9.0	90		27	HUANG	06A	CLEO	$e^+e^- \rightarrow \psi(3770)$		23	ABLIKIM	07F	BES2	$e^+e^- \rightarrow \psi(3770)$			
••• We do not use the following data for averages, fits, limits, etc. •••																
<48			23	ABLIKIM	07B	BES2	$e^+e^- \rightarrow \psi(3770)$									
$\Gamma(\phi\pi^+\pi^-)/\Gamma_{\text{total}}$			$\Gamma_{38}/\Gamma$			$\Gamma(2(K^+K^-))/\Gamma_{\text{total}}$			$\Gamma_{56}/\Gamma$							
VALUE (units $10^{-4}$ )	CL%		DOCUMENT ID	TECN	COMMENT	VALUE (units $10^{-4}$ )	CL%		DOCUMENT ID	TECN	COMMENT	VALUE (units $10^{-4}$ )	CL%			
< 4.1	90		27	HUANG	06A	CLEO	$e^+e^- \rightarrow \psi(3770)$		27	HUANG	06A	CLEO	$e^+e^- \rightarrow \psi(3770)$			
••• We do not use the following data for averages, fits, limits, etc. •••																
<16			23	ABLIKIM	07B	BES2	$e^+e^- \rightarrow \psi(3770)$		<17			23	ABLIKIM	07B	BES2	$e^+e^- \rightarrow \psi(3770)$
$\Gamma(K^+K^-2\pi^0)/\Gamma_{\text{total}}$			$\Gamma_{39}/\Gamma$			$\Gamma(\phi K^+K^-)/\Gamma_{\text{total}}$			$\Gamma_{57}/\Gamma$							
VALUE (units $10^{-3}$ )	CL%	EVTS	DOCUMENT ID	TECN	COMMENT	VALUE (units $10^{-4}$ )	CL%		DOCUMENT ID	TECN	COMMENT	VALUE (units $10^{-4}$ )	CL%			
<4.2	90	14	ABLIKIM	08N	BES2	$e^+e^- \rightarrow \psi(3770)$	< 7.5	90	27	HUANG	06A	CLEO	$e^+e^- \rightarrow \psi(3770)$			
$\Gamma(4(\pi^+\pi^-))/\Gamma_{\text{total}}$			$\Gamma_{40}/\Gamma$			$\Gamma(2(K^+K^-)\pi^0)/\Gamma_{\text{total}}$			$\Gamma_{58}/\Gamma$							
VALUE (units $10^{-3}$ )	CL%		DOCUMENT ID	TECN	COMMENT	VALUE (units $10^{-4}$ )	CL%		DOCUMENT ID	TECN	COMMENT	VALUE (units $10^{-4}$ )	CL%			
<16.7	90		23	ABLIKIM	07F	BES2	$e^+e^- \rightarrow \psi(3770)$		27	HUANG	06A	CLEO	$e^+e^- \rightarrow \psi(3770)$			
$\Gamma(4(\pi^+\pi^-\pi^0))/\Gamma_{\text{total}}$			$\Gamma_{41}/\Gamma$			$\Gamma(2(K^+K^-)\pi^+\pi^-)/\Gamma_{\text{total}}$			$\Gamma_{59}/\Gamma$							
VALUE (units $10^{-3}$ )	CL%		DOCUMENT ID	TECN	COMMENT	VALUE (units $10^{-3}$ )	CL%		DOCUMENT ID	TECN	COMMENT	VALUE (units $10^{-3}$ )	CL%			
<30.6	90		23	ABLIKIM	07F	BES2	$e^+e^- \rightarrow \psi(3770)$		27	HUANG	06A	CLEO	$e^+e^- \rightarrow \psi(3770)$			
$\Gamma(\phi f_0(980))/\Gamma_{\text{total}}$			$\Gamma_{42}/\Gamma$			$\Gamma(K_S^0 K^-\pi^+)/\Gamma_{\text{total}}$			$\Gamma_{60}/\Gamma$							
VALUE (units $10^{-4}$ )	CL%		DOCUMENT ID	TECN	COMMENT	VALUE (units $10^{-3}$ )	CL%	EVTS	DOCUMENT ID	TECN	COMMENT	VALUE (units $10^{-3}$ )	CL%	EVTS		
<4.5	90		27	HUANG	06A	CLEO	$e^+e^- \rightarrow \psi(3770)$	18	ABLIKIM	08M	BES2	$e^+e^- \rightarrow \psi(3770)$				
$\Gamma(K^+K^-\pi^+\pi^-\pi^0)/\Gamma_{\text{total}}$			$\Gamma_{43}/\Gamma$			$\Gamma(K_S^0 K^-\pi^0)/\Gamma_{\text{total}}$			$\Gamma_{61}/\Gamma$							
VALUE (units $10^{-4}$ )	CL%		DOCUMENT ID	TECN	COMMENT	VALUE (units $10^{-3}$ )	CL%	EVTS	DOCUMENT ID	TECN	COMMENT	VALUE (units $10^{-3}$ )	CL%	EVTS		
< 23.6	90		27	HUANG	06A	CLEO	$e^+e^- \rightarrow \psi(3770)$	40	ABLIKIM	08M	BES2	$e^+e^- \rightarrow \psi(3770)$				
••• We do not use the following data for averages, fits, limits, etc. •••																
<111			23	ABLIKIM	07B	BES2	$e^+e^- \rightarrow \psi(3770)$		<13.3							
$\Gamma(K^+K^-\rho^0\pi^0)/\Gamma_{\text{total}}$			$\Gamma_{44}/\Gamma$			$\Gamma(K_S^0 K^-\rho^+)/\Gamma_{\text{total}}$			$\Gamma_{62}/\Gamma$							
VALUE (units $10^{-4}$ )	CL%		DOCUMENT ID	TECN	COMMENT	VALUE (units $10^{-3}$ )	CL%		DOCUMENT ID	TECN	COMMENT	VALUE (units $10^{-3}$ )	CL%			
<8	90		23	ABLIKIM	07i	BES2	$3.77 e^+e^-$		ABLIKIM	09C	BES2	$e^+e^- \rightarrow \psi(3770)$				
$\Gamma(K^+K^-\rho^+\pi^-)/\Gamma_{\text{total}}$			$\Gamma_{45}/\Gamma$			$\Gamma(K_S^0 K^-2\pi^+\pi^-)/\Gamma_{\text{total}}$			$\Gamma_{63}/\Gamma$							
VALUE (units $10^{-4}$ )	CL%		DOCUMENT ID	TECN	COMMENT	VALUE (units $10^{-3}$ )	CL%	EVTS	DOCUMENT ID	TECN	COMMENT	VALUE (units $10^{-3}$ )	CL%	EVTS		
<146	90		23	ABLIKIM	07i	BES2	$3.77 e^+e^-$	39	ABLIKIM	08M	BES2	$e^+e^- \rightarrow \psi(3770)$				
$\Gamma(\omega K^+K^-)/\Gamma_{\text{total}}$			$\Gamma_{46}/\Gamma$			$\Gamma(K_S^0 K^-\pi^+\rho^0)/\Gamma_{\text{total}}$			$\Gamma_{64}/\Gamma$							
VALUE (units $10^{-4}$ )	CL%		DOCUMENT ID	TECN	COMMENT	VALUE (units $10^{-2}$ )	CL%		DOCUMENT ID	TECN	COMMENT	VALUE (units $10^{-2}$ )	CL%			
< 3.4	90		27	HUANG	06A	CLEO	$e^+e^- \rightarrow \psi(3770)$		ABLIKIM	09C	BES2	$e^+e^- \rightarrow \psi(3770)$				
••• We do not use the following data for averages, fits, limits, etc. •••																
<66	90		23	ABLIKIM	07i	BES2	$3.77 e^+e^-$		<1.6							
$\Gamma(\phi\pi^+\pi^-\pi^0)/\Gamma_{\text{total}}$			$\Gamma_{47}/\Gamma$			$\Gamma(K_S^0 K^-\pi^+\eta)/\Gamma_{\text{total}}$			$\Gamma_{65}/\Gamma$							
VALUE (units $10^{-4}$ )	CL%		DOCUMENT ID	TECN	COMMENT	VALUE (units $10^{-2}$ )	CL%		DOCUMENT ID	TECN	COMMENT	VALUE (units $10^{-2}$ )	CL%			
<38	90		23	ABLIKIM	07i	BES2	$3.77 e^+e^-$		ABLIKIM	09C	BES2	$e^+e^- \rightarrow \psi(3770)$				
$\Gamma(K^{*0}K^-\pi^+\pi^0 + \text{c.c.})/\Gamma_{\text{total}}$			$\Gamma_{48}/\Gamma$			$\Gamma(K_S^0 K^-2\pi^+\pi^-\pi^0)/\Gamma_{\text{total}}$			$\Gamma_{66}/\Gamma$							
VALUE (units $10^{-4}$ )	CL%		DOCUMENT ID	TECN	COMMENT	VALUE (units $10^{-3}$ )	CL%	EVTS	DOCUMENT ID	TECN	COMMENT	VALUE (units $10^{-3}$ )	CL%	EVTS		
<162	90		23	ABLIKIM	07i	BES2	$3.77 e^+e^-$	23	ABLIKIM	08M	BES2	$e^+e^- \rightarrow \psi(3770)$				

$\Gamma(K_S^0 K^- 2\pi^+ \pi^- \eta)/\Gamma_{\text{total}}$	$\Gamma_{67}/\Gamma$
VALUE (units $10^{-2}$ ) CL% <4.8 90	DOCUMENT ID TECN COMMENT ABLIKIM 09C BES2 $e^+ e^- \rightarrow \psi(3770)$

$\Gamma(K_S^0 K^- \pi^+ 2(\pi^+ \pi^-))/\Gamma_{\text{total}}$	$\Gamma_{68}/\Gamma$
VALUE (units $10^{-3}$ ) CL% EVTS <12.2 90 4	DOCUMENT ID TECN COMMENT ABLIKIM 08M BES2 $e^+ e^- \rightarrow \psi(3770)$

$\Gamma(K_S^0 K^- \pi^+ 2\pi^0)/\Gamma_{\text{total}}$	$\Gamma_{69}/\Gamma$
VALUE (units $10^{-3}$ ) CL% EVTS <26.5 90 17	DOCUMENT ID TECN COMMENT ABLIKIM 08M BES2 $e^+ e^- \rightarrow \psi(3770)$

$\Gamma(K_S^0 K^- K^+ K^- \pi^+)/\Gamma_{\text{total}}$	$\Gamma_{70}/\Gamma$
VALUE (units $10^{-3}$ ) CL% <4.9 90	DOCUMENT ID TECN COMMENT ABLIKIM 09C BES2 $e^+ e^- \rightarrow \psi(3770)$

$\Gamma(K_S^0 K^- K^+ K^- \pi^+ \pi^0)/\Gamma_{\text{total}}$	$\Gamma_{71}/\Gamma$
VALUE (units $10^{-2}$ ) CL% <3.0 90	DOCUMENT ID TECN COMMENT ABLIKIM 09C BES2 $e^+ e^- \rightarrow \psi(3770)$

$\Gamma(K_S^0 K^- K^+ K^- \pi^+ \eta)/\Gamma_{\text{total}}$	$\Gamma_{72}/\Gamma$
VALUE (units $10^{-2}$ ) CL% <2.2 90	DOCUMENT ID TECN COMMENT ABLIKIM 09C BES2 $e^+ e^- \rightarrow \psi(3770)$

$\Gamma(K^{*0} K^- \pi^+ + \text{c.c.})/\Gamma_{\text{total}}$	$\Gamma_{73}/\Gamma$
VALUE (units $10^{-3}$ ) CL% <9.7 90	DOCUMENT ID TECN COMMENT 23 ABLIKIM 07F BES2 $e^+ e^- \rightarrow \psi(3770)$

$\Gamma(\rho\bar{\rho}\pi^0)/\Gamma_{\text{total}}$	$\Gamma_{74}/\Gamma$
VALUE (units $10^{-4}$ ) CL% <12	DOCUMENT ID TECN COMMENT 23 ABLIKIM 07B BES2 $e^+ e^- \rightarrow \psi(3770)$

$\Gamma(\rho\bar{\rho}\pi^+ \pi^-)/\Gamma_{\text{total}}$	$\Gamma_{75}/\Gamma$
VALUE (units $10^{-4}$ ) CL% < 5.8 90	DOCUMENT ID TECN COMMENT 27 HUANG 06A CLEO $e^+ e^- \rightarrow \psi(3770)$
••• We do not use the following data for averages, fits, limits, etc. •••	
<16	23 ABLIKIM 07B BES2 $e^+ e^- \rightarrow \psi(3770)$

$\Gamma(\Lambda\bar{\Lambda})/\Gamma_{\text{total}}$	$\Gamma_{76}/\Gamma$
VALUE (units $10^{-4}$ ) CL% <1.2 90	DOCUMENT ID TECN COMMENT 27 HUANG 06A CLEO $e^+ e^- \rightarrow \psi(3770)$
••• We do not use the following data for averages, fits, limits, etc. •••	
<4	23 ABLIKIM 07F BES2 $e^+ e^- \rightarrow \psi(3770)$

$\Gamma(\rho\bar{\rho}\pi^+ \pi^- \pi^0)/\Gamma_{\text{total}}$	$\Gamma_{77}/\Gamma$
VALUE (units $10^{-4}$ ) CL% <18.5 90	DOCUMENT ID TECN COMMENT 27 HUANG 06A CLEO $e^+ e^- \rightarrow \psi(3770)$
••• We do not use the following data for averages, fits, limits, etc. •••	
<73	23 ABLIKIM 07B BES2 $e^+ e^- \rightarrow \psi(3770)$

$\Gamma(\omega\rho\bar{\rho})/\Gamma_{\text{total}}$	$\Gamma_{78}/\Gamma$
VALUE (units $10^{-4}$ ) CL% < 2.9 90	DOCUMENT ID TECN COMMENT 27 HUANG 06A CLEO $e^+ e^- \rightarrow \psi(3770)$
••• We do not use the following data for averages, fits, limits, etc. •••	
<30	28 ABLIKIM 07I BES2 $3.77 e^+ e^-$

$\Gamma(\Lambda\bar{\Lambda}\pi^0)/\Gamma_{\text{total}}$	$\Gamma_{79}/\Gamma$
VALUE (units $10^{-4}$ ) CL% <12 90	DOCUMENT ID TECN COMMENT 23 ABLIKIM 07I BES2 $3.77 e^+ e^-$

$\Gamma(\rho\bar{\rho}2(\pi^+ \pi^-))/\Gamma_{\text{total}}$	$\Gamma_{80}/\Gamma$
VALUE (units $10^{-3}$ ) CL% <2.6 90	DOCUMENT ID TECN COMMENT 23 ABLIKIM 07F BES2 $e^+ e^- \rightarrow \psi(3770)$

$\Gamma(\eta\rho\bar{\rho})/\Gamma_{\text{total}}$	$\Gamma_{81}/\Gamma$
VALUE (units $10^{-4}$ ) CL% < 5.4 90	DOCUMENT ID TECN COMMENT 27 HUANG 06A CLEO $e^+ e^- \rightarrow \psi(3770)$
••• We do not use the following data for averages, fits, limits, etc. •••	
<11	23 ABLIKIM 10D BES2 $e^+ e^- \rightarrow \psi(3770)$

$\Gamma(\eta\rho\bar{\rho}\pi^+ \pi^-)/\Gamma_{\text{total}}$	$\Gamma_{82}/\Gamma$
VALUE (units $10^{-3}$ ) CL% <3.3 90	DOCUMENT ID TECN COMMENT 23 ABLIKIM 10D BES2 $e^+ e^- \rightarrow \psi(3770)$

$\Gamma(\rho^0\rho\bar{\rho})/\Gamma_{\text{total}}$	$\Gamma_{83}/\Gamma$
VALUE (units $10^{-3}$ ) CL% <1.7 90	DOCUMENT ID TECN COMMENT 23 ABLIKIM 07F BES2 $e^+ e^- \rightarrow \psi(3770)$

$\Gamma(\rho\bar{\rho}K^+ K^-)/\Gamma_{\text{total}}$	$\Gamma_{84}/\Gamma$
VALUE (units $10^{-4}$ ) CL% < 3.2 90	DOCUMENT ID TECN COMMENT 27 HUANG 06A CLEO $e^+ e^- \rightarrow \psi(3770)$
••• We do not use the following data for averages, fits, limits, etc. •••	
<11	23 ABLIKIM 07B BES2 $e^+ e^- \rightarrow \psi(3770)$

$\Gamma(\eta\rho\bar{\rho}K^+ K^-)/\Gamma_{\text{total}}$	$\Gamma_{85}/\Gamma$
VALUE (units $10^{-3}$ ) CL% <6.9 90	DOCUMENT ID TECN COMMENT 23 ABLIKIM 10D BES2 $e^+ e^- \rightarrow \psi(3770)$

$\Gamma(\pi^0\rho\bar{\rho}K^+ K^-)/\Gamma_{\text{total}}$	$\Gamma_{86}/\Gamma$
VALUE (units $10^{-3}$ ) CL% <1.2 90	DOCUMENT ID TECN COMMENT 23 ABLIKIM 10D BES2 $e^+ e^- \rightarrow \psi(3770)$

$\Gamma(\phi\rho\bar{\rho})/\Gamma_{\text{total}}$	$\Gamma_{87}/\Gamma$
VALUE (units $10^{-4}$ ) CL% <1.3 90	DOCUMENT ID TECN COMMENT 27 HUANG 06A CLEO $e^+ e^- \rightarrow \psi(3770)$
••• We do not use the following data for averages, fits, limits, etc. •••	
<9	23 ABLIKIM 07B BES2 $e^+ e^- \rightarrow \psi(3770)$

$\Gamma(\Lambda\bar{\Lambda}\pi^+ \pi^-)/\Gamma_{\text{total}}$	$\Gamma_{88}/\Gamma$
VALUE (units $10^{-4}$ ) CL% < 2.5 90	DOCUMENT ID TECN COMMENT 27 HUANG 06A CLEO $e^+ e^- \rightarrow \psi(3770)$
••• We do not use the following data for averages, fits, limits, etc. •••	
<39	23 ABLIKIM 07F BES2 $e^+ e^- \rightarrow \psi(3770)$

$\Gamma(\Lambda\bar{\rho}K^+ \pi^+ \pi^-)/\Gamma_{\text{total}}$	$\Gamma_{89}/\Gamma$
VALUE (units $10^{-4}$ ) CL% <2.8 90	DOCUMENT ID TECN COMMENT 27 HUANG 06A CLEO $e^+ e^- \rightarrow \psi(3770)$

$\Gamma(\Lambda\bar{\rho}K^+ \pi^+ \pi^-)/\Gamma_{\text{total}}$	$\Gamma_{90}/\Gamma$
VALUE (units $10^{-4}$ ) CL% <6.3 90	DOCUMENT ID TECN COMMENT 27 HUANG 06A CLEO $e^+ e^- \rightarrow \psi(3770)$
22 Comparing cross sections at $\sqrt{s} = 3.773$ GeV and $\sqrt{s} = 3.671$ GeV, neglecting interference, and using $\sigma(\psi(3770) \rightarrow D\bar{D}) = 6.39 \pm 0.20$ nb.	
23 Assuming that interference effects between resonance and continuum can be neglected and using $\sigma^{obs}(e^+ e^- \rightarrow \psi(3770)) = 7.15 \pm 0.38$ nb.	
24 Data suggest possible destructive interference with continuum.	
25 Using $\sigma(e^+ e^- \rightarrow \psi(3770) \rightarrow \text{hadrons}) = (6.38 \pm 0.08 \pm 0.41 \pm 0.30)$ nb from BESSON 06 and $B(K_S^0 \rightarrow \pi^+ \pi^-) = 0.6895 \pm 0.0014$ .	
26 Using $B(K_S^0 \rightarrow \pi^+ \pi^-) = 0.6860 \pm 0.0027$ .	
27 Using $\sigma_{tot}(e^+ e^- \rightarrow \psi(3770)) = 7.9 \pm 0.6$ nb at the resonance.	
28 Using $\sigma^{obs} = 7.15 \pm 0.27 \pm 0.27$ nb and neglecting interference.	

## RADIATIVE DECAYS

$\Gamma(\gamma\chi_{c2})/\Gamma_{\text{total}}$	$\Gamma_{91}/\Gamma$
VALUE (units $10^{-3}$ ) CL% <0.9 90	DOCUMENT ID TECN COMMENT 29 COAN 06A CLEO $e^+ e^- \rightarrow \psi(3770) \rightarrow \gamma\gamma J/\psi$
••• We do not use the following data for averages, fits, limits, etc. •••	
<2.0	30 BRIERE 06 CLEO $e^+ e^- \rightarrow \psi(3770) \rightarrow \gamma + \text{hadrons}$

$\Gamma(\gamma\chi_{c1})/\Gamma_{\text{total}}$	$\Gamma_{92}/\Gamma$
VALUE (units $10^{-3}$ ) EVTS $2.9 \pm 0.5 \pm 0.4$	DOCUMENT ID TECN COMMENT 31 BRIERE 06 CLEO $e^+ e^- \rightarrow \psi(3770) \rightarrow \gamma + \text{hadrons}, \gamma\gamma J/\psi$
••• We do not use the following data for averages, fits, limits, etc. •••	
$3.9 \pm 1.4 \pm 0.6$	$54 \pm 17$ 32 BRIERE 06 CLEO $e^+ e^- \rightarrow \psi(3770) \rightarrow \gamma + \text{hadrons}$
$2.8 \pm 0.5 \pm 0.4$	$53 \pm 10$ 29 COAN 06A CLEO $e^+ e^- \rightarrow \psi(3770) \rightarrow \gamma\gamma J/\psi$

$\Gamma(\gamma\chi_{c1})/\Gamma(J/\psi\pi^+ \pi^-)$	$\Gamma_{92}/\Gamma_4$
VALUE EVTS $1.49 \pm 0.31 \pm 0.26$	DOCUMENT ID TECN COMMENT 33 COAN 06A CLEO $e^+ e^- \rightarrow \psi(3770) \rightarrow \gamma\gamma J/\psi$

$\Gamma(\gamma\chi_{c0})/\Gamma_{\text{total}}$	$\Gamma_{93}/\Gamma$
VALUE (units $10^{-3}$ ) CL% EVTS $7.3 \pm 0.7 \pm 0.6$	DOCUMENT ID TECN COMMENT 34 BRIERE 06 CLEO $e^+ e^- \rightarrow \psi(3770) \rightarrow \gamma + \text{hadrons}$
••• We do not use the following data for averages, fits, limits, etc. •••	
< 44	90 29 COAN 06A CLEO $e^+ e^- \rightarrow \psi(3770) \rightarrow \gamma\gamma J/\psi$

$\Gamma(\gamma\chi_{c0})/\Gamma(\gamma\chi_{c2})$	$\Gamma_{93}/\Gamma_{91}$
VALUE CL% >8 90	DOCUMENT ID TECN COMMENT 35 BRIERE 06 CLEO $e^+ e^- \rightarrow \psi(3770)$
••• We do not use the following data for averages, fits, limits, etc. •••	

# Meson Particle Listings

## $\psi(3770)$ , $X(3872)$

### $\Gamma(\gamma\chi_{c0})/\Gamma(\gamma\chi_{c1})$

VALUE	DOCUMENT ID	TECN	COMMENT
• • • We do not use the following data for averages, fits, limits, etc. • • •			
$2.5 \pm 0.6$	35 BRIERE	06	CLEO $e^+e^- \rightarrow \psi(3770)$

### $\Gamma(\gamma\eta)/\Gamma_{total}$

VALUE (units $10^{-4}$ )	CL%	DOCUMENT ID	TECN	COMMENT
<1.8	90	36 PEDLAR	09	CLE3 $\psi(2S) \rightarrow \gamma X$

### $\Gamma(\gamma\pi)/\Gamma_{total}$

VALUE (units $10^{-4}$ )	CL%	DOCUMENT ID	TECN	COMMENT
<1.5	90	36 PEDLAR	09	CLE3 $\psi(2S) \rightarrow \gamma X$

### $\Gamma(\gamma\pi^0)/\Gamma_{total}$

VALUE (units $10^{-4}$ )	CL%	DOCUMENT ID	TECN	COMMENT
<2	90	PEDLAR	09	CLE3 $\psi(2S) \rightarrow \gamma X$

<sup>29</sup>Using  $\Gamma_{ee}(\psi(2S)) = (2.54 \pm 0.03 \pm 0.11)$  keV from ADAM 06 and taking  $\sigma(e^+e^- \rightarrow D\bar{D})$  from HE 05 for  $\sigma(e^+e^- \rightarrow \psi(3770))$ .

<sup>30</sup>Uses  $B(\psi(2S) \rightarrow \gamma\chi_{c2}) = 9.22 \pm 0.11 \pm 0.46\%$  from ATHAR 04,  $\psi(2S)$  mass and width from PDG 04, and  $\Gamma_{ee}(\psi(2S)) = 2.54 \pm 0.03 \pm 0.11$  keV from ADAM 06.

<sup>31</sup>Averages the two measurements from COAN 06A and BRIERE 06.

<sup>32</sup>Uses  $B(\psi(2S) \rightarrow \gamma\chi_{c1}) = 9.07 \pm 0.11 \pm 0.54\%$  from ATHAR 04,  $\psi(2S)$  mass and width from PDG 04, and  $\Gamma_{ee}(\psi(2S)) = 2.54 \pm 0.03 \pm 0.11$  keV from ADAM 06.

<sup>33</sup>Using  $B(\psi(3770) \rightarrow J/\psi\pi^+\pi^-) = (1.89 \pm 0.20 \pm 0.20) \times 10^{-3}$  from ADAM 06.

<sup>34</sup>Uses  $B(\psi(2S) \rightarrow \gamma\chi_{c0}) = 9.33 \pm 0.14 \pm 0.61\%$  from ATHAR 04,  $\psi(2S)$  mass and width from PDG 04, and  $\Gamma_{ee}(\psi(2S)) = 2.54 \pm 0.03 \pm 0.11$  keV from ADAM 06.

<sup>35</sup>Not independent of other results in BRIERE 06.

<sup>36</sup>Assuming maximal destructive interference between  $\psi(3770)$  and continuum sources.

### $\psi(3770)$ REFERENCES

ANASHIN	12A	PL B711 292	V.V. Anashin et al.	(KEDR Collab.)
ABLIKIM	10D	EPJ C66 11	M. Ablikim et al.	(BES II Collab.)
BESSON	10	PR L 104 159901E	D. Besson et al.	(CLEO Collab.)
ABLIKIM	09C	EPJ C64 243	M. Ablikim et al.	(BES Collab.)
PEDLAR	09	PR D79 111101	T.K. Pedlar et al.	(CLEO Collab.)
ABLIKIM	08B	PL B659 74	M. Ablikim et al.	(BES Collab.)
ABLIKIM	08D	PL B660 315	M. Ablikim et al.	(BES Collab.)
ABLIKIM	08M	PL B670 179	M. Ablikim et al.	(BES Collab.)
ABLIKIM	08N	PL B670 184	M. Ablikim et al.	(BES Collab.)
AUBERT	08B	PR D77 011102R	J. Aubert et al.	(BABAR Collab.)
BRODZICKA	08	PR L 100 092001	J. Brodzicka et al.	(BELLE Collab.)
PAKHOLOVA	08	PR D77 011103R	G. Pakhlova et al.	(BELLE Collab.)
ABLIKIM	07B	PL B650 111	M. Ablikim et al.	(BES Collab.)
ABLIKIM	07E	PL B652 238	M. Ablikim et al.	(BES Collab.)
ABLIKIM	07F	PL B656 30	M. Ablikim et al.	(BES Collab.)
ABLIKIM	07I	EPJ C52 305	M. Ablikim et al.	(BES Collab.)
ABLIKIM	07K	PR D76 122002	M. Ablikim et al.	(BES Collab.)
AUBERT	07BE	PR D76 111105R	B. Aubert et al.	(BABAR Collab.)
DOBBS	07	PR D76 112001	S. Dobbs et al.	(CLEO Collab.)
ABLIKIM	06L	PRL 97 121801	M. Ablikim et al.	(BES Collab.)
ABLIKIM	06N	PL B641 145	M. Ablikim et al.	(BES Collab.)
ADAM	06	PRL 96 082004	N.E. Adam et al.	(CLEO Collab.)
ADAMS	06	PR D73 012002	G.S. Adams et al.	(CLEO Collab.)
BESSON	06	PRL 96 092002	D. Besson et al.	(CLEO Collab.)
Also		PRL 104 159901E	D. Besson et al.	(CLEO Collab.)
BRIERE	06	PR D74 031106R	R.A. Briere et al.	(CLEO Collab.)
COAN	06A	PRL 96 102002	T.E. Coan et al.	(CLEO Collab.)
CRONIN-HEN	06	PR D74 012005	D. Cronin-Hennessy et al.	(CLEO Collab.)
HUANG	06A	PRL 96 032003	G.S. Huang et al.	(CLEO Collab.)
BAI	05	PL B605 63	J.Z. Bai et al.	(BES Collab.)
HE	05	PRL 95 121801	Q. He et al.	(CLEO Collab.)
Also		PRL 96 199903 (err.)	Q. He et al.	(CLEO Collab.)
ABLIKIM	04F	PR D70 077101	M. Ablikim et al.	(BES Collab.)
ATHAR	04	PR D70 112002	S.B. Athar et al.	(CLEO Collab.)
CHISTOV	04	PRL 93 051803	R. Chistov et al.	(BELLE Collab.)
PDG	04	PL B592 1	S. Eidelman et al.	(PDG Collab.)
BAI	02C	PRL 88 101802	J.Z. Bai et al.	(BES Collab.)
ADLER	88C	PRL 60 89	J. Adler et al.	(Mark III Collab.)
SCHINDLER	80	PR D21 2716	R.H. Schindler et al.	(Mark II Collab.)
BACINO	78	PRL 40 671	W.J. Bacino et al.	(SLAC, UCLA, UC)
RAPIDIS	77	PRL 39 526	P.A. Rapidis et al.	(LGW Collab.)

## $X(3872)$

$$I^G(J^{PC}) = 0^2(\text{?}^+)$$

Seen by CHOI 03 in  $B \rightarrow K\pi^+\pi^- J/\psi(1S)$  decays as a narrow peak in the invariant mass distribution of the  $\pi^+\pi^- J/\psi(1S)$  final state, but not seen in the  $\gamma\chi_{c1}$  final state of these decays. Possibly absent in the invariant mass spectrum of the final state  $\pi^+\pi^- J/\psi(1S)$  in  $e^+e^-$  collisions. Interpretation as a  $1^{--}$  charmonium state not favored. Isovector hypothesis excluded by AUBERT 05B and CHOI 11. A helicity amplitude analysis of the  $X(3872) \rightarrow J/\psi\pi^+\pi^-$  decay gives two possible  $J^{PC}$  assignments:  $J^{PC} = 1^{++}$  and  $2^{--}$  (ABULENCIA 07E and CHOI 11). A study of the  $3\pi$  invariant mass distribution in  $J/\psi\omega$  decays slightly favors  $J^P = 2^-$  (DEL-AMO-SANCHEZ 10B).

See our note on "Developments in Heavy Quarkonium Spectroscopy".

### $X(3872)$ MASS FROM $J/\psi X$ MODE

VALUE (MeV)	EVTs	DOCUMENT ID	TECN	COMMENT
<b>3871.68 ± 0.17 OUR AVERAGE</b>				
$3871.95 \pm 0.48 \pm 0.12$	0.6k	AAIJ	12H	LHCB $pp \rightarrow J/\psi\pi^+\pi^- X$
$3871.85 \pm 0.27 \pm 0.19$	~ 170	1 CHOI	11	BELL $B \rightarrow K\pi^+\pi^- J/\psi$
$3873 \pm 1.8 \pm 1.3$	27 ± 8	2 DEL-AMO-SA.10B	BABR	$B \rightarrow \omega J/\psi K$
$3871.61 \pm 0.16 \pm 0.19$	6k	2,3 AALTONEN	09AU	CDF2 $p\bar{p} \rightarrow J/\psi\pi^+\pi^- X$
$3871.4 \pm 0.6 \pm 0.1$	93.4	AUBERT	08Y	BABR $B^+ \rightarrow K^+ J/\psi\pi^+\pi^-$
$3868.7 \pm 1.5 \pm 0.4$	9.4	AUBERT	08Y	BABR $B^0 \rightarrow K_S^0 J/\psi\pi^+\pi^-$
$3871.8 \pm 3.1 \pm 3.0$	522	2,4 ABAZOV	04F	D0 $p\bar{p} \rightarrow J/\psi\pi^+\pi^- X$
• • • We do not use the following data for averages, fits, limits, etc. • • •				
$3868.6 \pm 1.2 \pm 0.2$	8	5 AUBERT	06	BABR $B^0 \rightarrow K_S^0 J/\psi\pi^+\pi^-$
$3871.3 \pm 0.6 \pm 0.1$	61	5 AUBERT	06	BABR $B^- \rightarrow K^- J/\psi\pi^+\pi^-$
$3873.4 \pm 1.4$	25	6 AUBERT	05R	BABR $B^+ \rightarrow K^+ J/\psi\pi^+\pi^-$
$3871.3 \pm 0.7 \pm 0.4$	730	2,7 ACOSTA	04	CDF2 $p\bar{p} \rightarrow J/\psi\pi^+\pi^- X$
$3872.0 \pm 0.6 \pm 0.5$	36	8 CHOI	03	BELL $B \rightarrow K\pi^+\pi^- J/\psi$
$3836 \pm 13$	58	2,9 ANTONIAZZI	94	E705 $300\pi^{\pm}\text{Li} \rightarrow J/\psi\pi^+\pi^- X$

- <sup>1</sup> The mass difference for the  $X(3872)$  produced in  $B^+$  and  $B^0$  decays is  $(-0.71 \pm 0.96 \pm 0.19)$  MeV.
- <sup>2</sup> Width consistent with detector resolution.
- <sup>3</sup> A possible equal mixture of two states with a mass difference greater than 3.6 MeV/ $c^2$  is excluded at 95% CL.
- <sup>4</sup> Calculated from the corresponding  $m_{X(3872)} - m_{J/\psi}$  using  $m_{J/\psi}=3096.916$  MeV.
- <sup>5</sup> Calculated from the corresponding  $m_{X(3872)} - m_{\psi(2S)}$  using  $m_{\psi(2S)} = 3686.093$  MeV. Superseded by AUBERT 08Y.
- <sup>6</sup> Calculated from the corresponding  $m_{X(3872)} - m_{\psi(2S)}$  using  $m_{\psi(2S)} = 3685.96$  MeV. Superseded by AUBERT 06.
- <sup>7</sup> Superseded by AALTONEN 09AU.
- <sup>8</sup> Superseded by CHOI 11.
- <sup>9</sup> A lower mass value can be due to an incorrect momentum scale for soft pions.

### $X(3872)$ MASS FROM $\bar{D}^*0 D^0$ MODE

VALUE (MeV)	EVTs	DOCUMENT ID	TECN	COMMENT
• • • We do not use the following data for averages, fits, limits, etc. • • •				
$3872.9 \pm 0.6 \pm 0.4$ $-0.4 - 0.5$	50 <sup>10,11</sup>	AUSHEV	10	BELL $B \rightarrow \bar{D}^*0 D^0 K$
$3875.1 \pm 0.7 \pm 0.5$ $-0.5 \pm 0.5$	33 ± 6	11 AUBERT	08B	BABR $B \rightarrow \bar{D}^*0 D^0 K$
$3875.2 \pm 0.7 \pm 0.9$ $-1.8$	24 ± 6 <sup>11,12</sup>	GOKHROO	06	BELL $B \rightarrow D^0 \bar{D}^*0 \pi^0 K$

- <sup>10</sup> Calculated from the measured  $m_{X(3872)} - m_{D^{*0}} - m_{D^0} = 1.1 \pm 0.6 \pm 0.1$  MeV.
- <sup>11</sup> Experiments report  $D^{*0} \bar{D}^0$  invariant mass above  $D^{*0} \bar{D}^0$  threshold because  $D^{*0}$  decay products are kinematically constrained to the  $D^{*0}$  mass, even though the  $D^{*0}$  may decay off-shell.
- <sup>12</sup> Superseded by AUSHEV 10.

### $m_{X(3872)} - m_{J/\psi}$

VALUE (MeV)	EVTs	DOCUMENT ID	TECN	COMMENT
<b>774.9 ± 3.1 ± 3.0</b>	522	ABAZOV	04F	D0 $p\bar{p} \rightarrow J/\psi\pi^+\pi^- X$

### $m_{X(3872)} - m_{\psi(2S)}$

VALUE (MeV)	EVTs	DOCUMENT ID	TECN	COMMENT
• • • We do not use the following data for averages, fits, limits, etc. • • •				
$187.4 \pm 1.4$	25	13 AUBERT	05R	BABR $B^+ \rightarrow K^+ J/\psi\pi^+\pi^-$

<sup>13</sup> Superseded by AUBERT 06.

### $X(3872)$ WIDTH

VALUE (MeV)	CL%	EVTs	DOCUMENT ID	TECN	COMMENT
<1.2	90		CHOI	11	BELL $B \rightarrow K\pi^+\pi^- J/\psi$
• • • We do not use the following data for averages, fits, limits, etc. • • •					
<3.3	90		AUBERT	08Y	BABR $B^+ \rightarrow K^+ J/\psi\pi^+\pi^-$
<4.1	90	69	AUBERT	06	BABR $B \rightarrow K\pi^+\pi^- J/\psi$
<2.3	90	36	14 CHOI	03	BELL $B \rightarrow K\pi^+\pi^- J/\psi$

<sup>14</sup> Superseded by CHOI 11.

### $X(3872)$ WIDTH FROM $\bar{D}^*0 D^0$ MODE

VALUE (MeV)	EVTs	DOCUMENT ID	TECN	COMMENT
• • • We do not use the following data for averages, fits, limits, etc. • • •				
$3.9 \pm 2.8 \pm 0.2$ $-1.4 - 1.1$	50	15 AUSHEV	10	BELL $B \rightarrow \bar{D}^*0 D^0 K$
$3.0 \pm 1.9 \pm 0.9$ $-1.4$	33 ± 6	AUBERT	08B	BABR $B \rightarrow \bar{D}^*0 D^0 K$

<sup>15</sup> With a measured value of  $B(B \rightarrow X(3872)K) \times B(X(3872) \rightarrow D^{*0} \bar{D}^0) = (0.80 \pm 0.20 \pm 0.10) \times 10^{-4}$ , assumed to be equal for both charged and neutral modes.



X(3872) DECAY MODES

Mode	Fraction ( $\Gamma_i/\Gamma$ )
$\Gamma_1$ $e^+ e^-$	
$\Gamma_2$ $\pi^+ \pi^- J/\psi(1S)$	>2.6%
$\Gamma_3$ $\rho^0 J/\psi(1S)$	
$\Gamma_4$ $\omega J/\psi(1S)$	>1.9%
$\Gamma_5$ $D^0 \bar{D}^0 \pi^0$	> $3.2 \times 10^{-3}$
$\Gamma_6$ $\bar{D}^{*0} D^0$	> $5 \times 10^{-3}$
$\Gamma_7$ $\gamma \gamma$	
$\Gamma_8$ $D^0 \bar{D}^0$	
$\Gamma_9$ $D^+ D^-$	
$\Gamma_{10}$ $\gamma \chi_{c1}$	
$\Gamma_{11}$ $\eta J/\psi$	
$\Gamma_{12}$ $\gamma J/\psi$	> $6 \times 10^{-3}$
$\Gamma_{13}$ $\gamma \psi(2S)$	[a] >3.0%

[a] BHARDWAJ 11 does not observe this decay and presents a stronger 90% CL limit than this value. See measurements listings for details.

X(3872) PARTIAL WIDTHS

$\Gamma(e^+ e^-)$   $\Gamma_1$

VALUE (keV)	CL%	DOCUMENT ID	TECN	COMMENT
<0.28	90	16 YUAN	04	RVUE $e^+ e^- \rightarrow \pi^+ \pi^- J/\psi$

16 Using BAI 98E data on  $e^+ e^- \rightarrow \pi^+ \pi^- \ell^+ \ell^-$ . Assuming that  $\Gamma(\pi^+ \pi^- J/\psi)$  of X(3872) is the same as that of  $\psi(2S)$  (85.4 keV).

X(3872)  $\Gamma(i)\Gamma(e^+ e^-)/\Gamma(\text{total})$

$\Gamma(\pi^+ \pi^- J/\psi(1S)) \times \Gamma(e^+ e^-)/\Gamma_{\text{total}}$   $\Gamma_2 \Gamma_1/\Gamma$

VALUE (eV)	CL%	DOCUMENT ID	TECN	COMMENT
<6.2	90	17,18 AUBERT	05D	BABR $10.6 e^+ e^- \rightarrow K^+ K^- \pi^+ \pi^- \gamma$
<8.3	90	18 DOBBS	05	CLE3 $e^+ e^- \rightarrow \pi^+ \pi^- J/\psi$
<10	90	19 YUAN	04	RVUE $e^+ e^- \rightarrow \pi^+ \pi^- J/\psi$

17 Using  $B(X(3872) \rightarrow J/\psi \pi^+ \pi^-) \cdot B(J/\psi \rightarrow \mu^+ \mu^-) \cdot \Gamma(X(3872) \rightarrow e^+ e^-) < 0.37$  eV from AUBERT 05D and  $B(J/\psi \rightarrow \mu^+ \mu^-) = 0.0588 \pm 0.0010$  from the PDG 04.  
18 Assuming X(3872) has  $J^{PC} = 1^{--}$ .  
19 Using BAI 98E data on  $e^+ e^- \rightarrow \pi^+ \pi^- \ell^+ \ell^-$ . From theoretical calculation of the production cross section and using  $B(J/\psi \rightarrow \mu^+ \mu^-) = (5.88 \pm 0.10)\%$ .

X(3872)  $\Gamma(i)\Gamma(\gamma\gamma)/\Gamma(\text{total})$

$\Gamma(\gamma\gamma) \times \Gamma(\pi^+ \pi^- J/\psi(1S))/\Gamma_{\text{total}}$   $\Gamma_7 \Gamma_2/\Gamma$

VALUE (eV)	CL%	DOCUMENT ID	TECN	COMMENT
<12.9	90	20 DOBBS	05	CLE3 $e^+ e^- \rightarrow \pi^+ \pi^- J/\psi \gamma$

20 Assuming X(3872) has positive C parity and spin 0.

X(3872) BRANCHING RATIOS

$\Gamma(\pi^+ \pi^- J/\psi(1S))/\Gamma_{\text{total}}$   $\Gamma_2/\Gamma$

VALUE	EVTS	DOCUMENT ID	TECN	COMMENT
>0.026	93 ± 17	21 AUBERT	08Y	BABR $B \rightarrow X(3872) K$
>0.04	30	22 AUBERT	05R	BABR $B^+ \rightarrow K^+ J/\psi \pi^+ \pi^-$
>0.04	36 ± 7	23 CHOI	03	BABR $B^+ \rightarrow K^+ J/\psi \pi^+ \pi^-$

21 AUBERT 08Y reports  $[\Gamma(X(3872) \rightarrow \pi^+ \pi^- J/\psi(1S))/\Gamma_{\text{total}}] \times [B(B^+ \rightarrow X(3872) K^+)] = (8.4 \pm 1.5 \pm 0.7) \times 10^{-6}$  which we divide by our best value  $B(B^+ \rightarrow X(3872) K^+) < 3.2 \times 10^{-4}$ .  
22 Superseded by AUBERT 08Y. AUBERT 05R reports  $[\Gamma(X(3872) \rightarrow \pi^+ \pi^- J/\psi(1S))/\Gamma_{\text{total}}] \times [B(B^+ \rightarrow X(3872) K^+)] = (1.28 \pm 0.41) \times 10^{-5}$  which we divide by our best value  $B(B^+ \rightarrow X(3872) K^+) < 3.2 \times 10^{-4}$ .  
23 CHOI 03 reports  $[\Gamma(X(3872) \rightarrow \pi^+ \pi^- J/\psi(1S))/\Gamma_{\text{total}}] \times [B(B^+ \rightarrow X(3872) K^+)] / [B(B^+ \rightarrow \psi(2S) K^+)] / [B(\psi(2S) \rightarrow J/\psi(1S) \pi^+ \pi^-)] = 0.063 \pm 0.012 \pm 0.007$  which we multiply or divide by our best values  $B(B^+ \rightarrow X(3872) K^+) < 3.2 \times 10^{-4}$ ,  $B(B^+ \rightarrow \psi(2S) K^+) = (6.39 \pm 0.33) \times 10^{-4}$ ,  $B(\psi(2S) \rightarrow J/\psi(1S) \pi^+ \pi^-) = (33.6 \pm 0.4) \times 10^{-2}$ .

$\Gamma(\omega J/\psi(1S))/\Gamma_{\text{total}}$   $\Gamma_4/\Gamma$

VALUE	EVTS	DOCUMENT ID	TECN	COMMENT
>0.019	21 ± 7	24 DEL-AMO-SA...	10B	BABR $B^+ \rightarrow \omega J/\psi K^+$

24 DEL-AMO-SANCHEZ 10B reports  $[\Gamma(X(3872) \rightarrow \omega J/\psi(1S))/\Gamma_{\text{total}}] \times [B(B^+ \rightarrow X(3872) K^+)] = (6 \pm 2 \pm 1) \times 10^{-6}$  which we divide by our best value  $B(B^+ \rightarrow X(3872) K^+) < 3.2 \times 10^{-4}$ . DEL-AMO-SANCHEZ 10B also reports  $B(B^0 \rightarrow X(3872) K^0) \times B(X(3872) \rightarrow J/\psi \omega) = (6 \pm 3 \pm 1) \times 10^{-6}$ .

$\Gamma(\omega J/\psi(1S))/\Gamma(\pi^+ \pi^- J/\psi(1S))$

VALUE	DOCUMENT ID	TECN	COMMENT
0.8 ± 0.3	25 DEL-AMO-SA...10B	BABR	$B \rightarrow \omega J/\psi K$

25 Statistical and systematic errors added in quadrature. Uses the values of  $B(B \rightarrow X(3872) K) \times B(X(3872) \rightarrow J/\psi \pi^+ \pi^-)$  reported in AUBERT 08Y, taking into account the common systematics.

$\Gamma(D^0 \bar{D}^0 \pi^0)/\Gamma_{\text{total}}$   $\Gamma_5/\Gamma$

VALUE	EVTS	DOCUMENT ID	TECN	COMMENT
>3.2 × 10 <sup>-3</sup>	17 ± 5	26 GOKHROO	06	BELL $B^+ \rightarrow D^0 \bar{D}^0 \pi^0 K^+$

26 GOKHROO 06 reports  $[\Gamma(X(3872) \rightarrow D^0 \bar{D}^0 \pi^0)/\Gamma_{\text{total}}] \times [B(B^+ \rightarrow X(3872) K^+)] = (1.02 \pm 0.31 \pm 0.21_{-0.29}) \times 10^{-6}$  which we divide by our best value  $B(B^+ \rightarrow X(3872) K^+) < 3.2 \times 10^{-4}$ .

$\Gamma(\bar{D}^{*0} D^0)/\Gamma_{\text{total}}$   $\Gamma_6/\Gamma$

VALUE	EVTS	DOCUMENT ID	TECN	COMMENT
>5 × 10 <sup>-3</sup>	27 ± 6	27 AUBERT	08B	BABR $B^+ \rightarrow \bar{D}^{*0} D^0 K^+$

27 AUBERT 08B reports  $[\Gamma(X(3872) \rightarrow \bar{D}^{*0} D^0)/\Gamma_{\text{total}}] \times [B(B^+ \rightarrow X(3872) K^+)] = (1.67 \pm 0.36 \pm 0.47) \times 10^{-6}$  which we divide by our best value  $B(B^+ \rightarrow X(3872) K^+) < 3.2 \times 10^{-4}$ .

$\Gamma(D^0 \bar{D}^0 \pi^0)/\Gamma(\pi^+ \pi^- J/\psi(1S))$   $\Gamma_5/\Gamma_2$

VALUE	DOCUMENT ID	TECN	COMMENT
seen	28 GOKHROO	06	BELL $B \rightarrow D^0 \bar{D}^0 \pi^0 K$
seen	AUSHEV	10	BELL $B \rightarrow D^0 \bar{D}^0 \pi^0 K$

••• We do not use the following data for averages, fits, limits, etc. •••  
28 May not necessarily be the same state as that observed in the  $J/\psi \pi^+ \pi^-$  mode. Supersedes CHISTOV 04.

$\Gamma(D^0 \bar{D}^0)/\Gamma(\pi^+ \pi^- J/\psi(1S))$   $\Gamma_8/\Gamma_2$

VALUE	DOCUMENT ID	TECN	COMMENT
not seen	CHISTOV	04	BELL $B \rightarrow K D^0 \bar{D}^0$

••• We do not use the following data for averages, fits, limits, etc. •••

$\Gamma(D^+ D^-)/\Gamma(\pi^+ \pi^- J/\psi(1S))$   $\Gamma_9/\Gamma_2$

VALUE	DOCUMENT ID	TECN	COMMENT
not seen	CHISTOV	04	BELL $B \rightarrow K D^+ D^-$

••• We do not use the following data for averages, fits, limits, etc. •••

$\Gamma(\gamma \chi_{c1})/\Gamma(\pi^+ \pi^- J/\psi(1S))$   $\Gamma_{10}/\Gamma_2$

VALUE	CL%	DOCUMENT ID	TECN	COMMENT
<0.89	90	CHOI	03	BELL $B \rightarrow K \pi^+ \pi^- J/\psi$

$\Gamma(\eta J/\psi)/\Gamma(\pi^+ \pi^- J/\psi(1S))$   $\Gamma_{11}/\Gamma_2$

VALUE	CL%	DOCUMENT ID	TECN	COMMENT
<0.6	90	AUBERT	04Y	BABR $B \rightarrow K \eta J/\psi$

••• We do not use the following data for averages, fits, limits, etc. •••

$\Gamma(\eta J/\psi)/\Gamma_{\text{total}}$   $\Gamma_{12}/\Gamma$

VALUE	EVTS	DOCUMENT ID	TECN	COMMENT
>6 × 10 <sup>-3</sup>	29	BHARDWAJ	11	BELL $B^\pm \rightarrow \gamma J/\psi K^\pm$
>9 × 10 <sup>-3</sup>	20	30 AUBERT	09B	BABR $B^+ \rightarrow \gamma J/\psi K^+$
>0.010	19	31 AUBERT, BE	06M	BABR $B^+ \rightarrow \gamma J/\psi K^+$

29 BHARDWAJ 11 reports  $[\Gamma(X(3872) \rightarrow \gamma J/\psi)/\Gamma_{\text{total}}] \times [B(B^+ \rightarrow X(3872) K^+)] = (1.78^{+0.48}_{-0.44} \pm 0.12) \times 10^{-6}$  which we divide by our best value  $B(B^+ \rightarrow X(3872) K^+) < 3.2 \times 10^{-4}$ .  
30 AUBERT 09B reports  $[\Gamma(X(3872) \rightarrow \gamma J/\psi)/\Gamma_{\text{total}}] \times [B(B^+ \rightarrow X(3872) K^+)] = (2.8 \pm 0.8 \pm 0.1) \times 10^{-6}$  which we divide by our best value  $B(B^+ \rightarrow X(3872) K^+) < 3.2 \times 10^{-4}$ .  
31 Superseded by AUBERT 09B. AUBERT, BE 06M reports  $[\Gamma(X(3872) \rightarrow \gamma J/\psi)/\Gamma_{\text{total}}] \times [B(B^+ \rightarrow X(3872) K^+)] = (3.3 \pm 1.0 \pm 0.3) \times 10^{-6}$  which we divide by our best value  $B(B^+ \rightarrow X(3872) K^+) < 3.2 \times 10^{-4}$ .

$\Gamma(\gamma \psi(2S))/\Gamma_{\text{total}}$   $\Gamma_{13}/\Gamma$

VALUE	EVTS	DOCUMENT ID	TECN	COMMENT
not seen		32 BHARDWAJ	11	BELL $B^+ \rightarrow \gamma \psi(2S) K^+$
>0.030	25 ± 7	33 AUBERT	09B	BABR $B^+ \rightarrow \gamma \psi(2S) K^+$

32 BHARDWAJ 11 reports  $B(B^+ \rightarrow K^+ X(3872)) \times B(X \rightarrow \gamma \psi(2S)) < 3.45 \times 10^{-6}$  at 90% CL.  
33 AUBERT 09B reports  $[\Gamma(X(3872) \rightarrow \gamma \psi(2S))/\Gamma_{\text{total}}] \times [B(B^+ \rightarrow X(3872) K^+)] = (9.5 \pm 2.7 \pm 0.6) \times 10^{-6}$  which we divide by our best value  $B(B^+ \rightarrow X(3872) K^+) < 3.2 \times 10^{-4}$ .

$\Gamma(\gamma \psi(2S))/\Gamma(\gamma J/\psi)$   $\Gamma_{13}/\Gamma_{12}$

VALUE	CL%	DOCUMENT ID	TECN	COMMENT
<2.1	90	BHARDWAJ	11	BELL $B^+ \rightarrow K^+ \psi(2S) \gamma$
3.4 ± 1.4		AUBERT	09B	BABR $B^+ \rightarrow \gamma c \bar{c} K^+$

# Meson Particle Listings

## X(3872), X(3915), $\chi_{c2}(2P)$

### X(3872) REFERENCES

AJJ	12H	EPL C72 1972	R. Ajji <i>et al.</i>	(LHCb Collab.)
BHARDWAJ	11	PRL 107 091803	V. Bhardwaj <i>et al.</i>	(BELLE Collab.)
CHOI	11	PR D84 052004	S.-K. Choi <i>et al.</i>	(BELLE Collab.)
AUSHEV	10	PR D81 031103R	T. Aushev <i>et al.</i>	(BELLE Collab.)
DEL-AMO-SA...	10B	PR D82 011101R	P. del Amo Sanchez <i>et al.</i>	(BABAR Collab.)
AALTONEN	09AU	PRL 103 152001	T. Aaltonen <i>et al.</i>	(CDF Collab.)
AUBERT	09B	PRL 102 132001	B. Aubert <i>et al.</i>	(BABAR Collab.)
AUBERT	08B	PR D77 011102R	B. Aubert <i>et al.</i>	(BABAR Collab.)
AUBERT	08Y	PR D77 111101R	B. Aubert <i>et al.</i>	(BABAR Collab.)
ABULENCIA	07E	PRL 98 132002	A. Abulencia <i>et al.</i>	(CDF Collab.)
AUBERT	06	PR D73 011101R	B. Aubert <i>et al.</i>	(BABAR Collab.)
AUBERT BE	06M	PR D74 071101R	B. Aubert <i>et al.</i>	(BABAR Collab.)
GOKHROO	06	PRL 97 162002	G. Gokhroo <i>et al.</i>	(BELLE Collab.)
AUBERT	05B	PR D71 031501R	B. Aubert <i>et al.</i>	(BABAR Collab.)
AUBERT	05D	PR D71 052001	B. Aubert <i>et al.</i>	(BABAR Collab.)
AUBERT	05R	PR D71 071103R	B. Aubert <i>et al.</i>	(BABAR Collab.)
DOBBS	05	PRL 94 032004	S. Dobbs <i>et al.</i>	(CLEO Collab.)
ABAZOV	04F	PRL 93 162002	V.M. Abazov <i>et al.</i>	(DO Collab.)
ACOSTA	04	PRL 93 072001	D. Acosta <i>et al.</i>	(CDF Collab.)
AUBERT	04Y	PRL 93 041801	B. Aubert <i>et al.</i>	(BABAR Collab.)
CHISTOV	04	PRL 93 051803	R. Chistov <i>et al.</i>	(BELLE Collab.)
PDG	04	PL B592 1	S. Eidelman <i>et al.</i>	(PDG Collab.)
YUAN	04	PL B579 74	C.Z. Yuan <i>et al.</i>	(DO Collab.)
CHOI	03	PRL 91 262001	S.-K. Choi <i>et al.</i>	(BELLE Collab.)
BAI	98E	PR D57 3854	J.Z. Bai <i>et al.</i>	(BES Collab.)
ANTONIAZZI	94	PR D50 4258	L. Antoniazzi <i>et al.</i>	(E705 Collab.)

### X(3915) DECAY MODES

Mode	Fraction ( $\Gamma_i/\Gamma$ )
$\Gamma_1$ $\omega J/\psi$	seen
$\Gamma_2$ $\bar{D}^{*0} D^0$	
$\Gamma_3$ $\gamma\gamma$	seen

### X(3915) $\Gamma(i)\Gamma(\gamma\gamma)/\Gamma(\text{total})$

$\Gamma(\omega J/\psi) \times \Gamma(\gamma\gamma)/\Gamma_{\text{total}}$	$\Gamma_1\Gamma_3/\Gamma$			
VALUE (eV)	EVTS	DOCUMENT ID	TECN	COMMENT
$18 \pm 5 \pm 2$	$49 \pm 15$	<sup>5,6</sup> UEHARA	10	BELL $10.6 e^+ e^- \rightarrow e^+ e^- \omega J/\psi$
••• We do not use the following data for averages, fits, limits, etc. •••				
$61 \pm 17 \pm 8$	$49 \pm 15$	<sup>5,7</sup> UEHARA	10	BELL $10.6 e^+ e^- \rightarrow e^+ e^- \omega J/\psi$
<sup>5</sup> May be $\chi_{c2}(2P)$ .				
<sup>6</sup> For $J^P = 2^+$ , helicity-2.				
<sup>7</sup> For $J^P = 0^+$ .				

### X(3915) BRANCHING RATIOS

$\Gamma(\gamma\gamma)/\Gamma_{\text{total}}$	$\Gamma_3/\Gamma$		
VALUE	DOCUMENT ID	TECN	COMMENT
seen	<sup>8</sup> UEHARA	10	BELL $10.6 e^+ e^- \rightarrow e^+ e^- \omega J/\psi$
<sup>8</sup> May be $\chi_{c2}(2P)$ .			

$\Gamma(\omega J/\psi)/\Gamma(\bar{D}^{*0} D^0)$	$\Gamma_1/\Gamma_2$			
VALUE	CL%	DOCUMENT ID	TECN	COMMENT
$>0.71$	90	<sup>9</sup> AUSHEV	10	BELL $B \rightarrow \bar{D}^{*0} D^0 K$

<sup>9</sup> By combining the upper limit  $B(B \rightarrow X(3915) K) \times B(X(3915) \rightarrow D^{*0} \bar{D}^0) < 0.67 \times 10^{-4}$  from AUSHEV 10 with the average of CHOI 05 and AUBERT 08W measurements  $B(B \rightarrow X(3915) K) \times B(X(3915) \rightarrow \omega J/\psi) = (0.51 \pm 0.11) \times 10^{-4}$ .

$\Gamma(\omega J/\psi)/\Gamma_{\text{total}}$	$\Gamma_1/\Gamma$		
VALUE	DOCUMENT ID	TECN	COMMENT
seen	<sup>10</sup> DEL-AMO-SA...10B	BABR	$B \rightarrow \omega J/\psi K$
seen	<sup>11</sup> CHOI	05	BELL $B \rightarrow \omega J/\psi K$
<sup>10</sup> DEL-AMO-SANCHEZ 10B reports $B(B^\pm \rightarrow X(3915) K^\pm) \times B(X(3915) \rightarrow J/\psi\omega) = (3.0^{+0.7+0.5}_{-0.6-0.3}) \times 10^{-5}$ and $B(B^0 \rightarrow X(3915) K^0) \times B(X(3915) \rightarrow J/\psi\omega) = (2.1 \pm 0.9 \pm 0.3) \times 10^{-5}$ .			
<sup>11</sup> CHOI 05 reports $B(B \rightarrow X(3915) K) \times B(X(3915) \rightarrow J/\psi\omega) = (7.1 \pm 1.3 \pm 3.1) \times 10^{-5}$ .			

### X(3915) REFERENCES

AUSHEV	10	PR D81 031103R	T. Aushev <i>et al.</i>	(BELLE Collab.)
DEL-AMO-SA...10B	10B	PR D82 011101R	P. del Amo Sanchez <i>et al.</i>	(BABAR Collab.)
UEHARA	10	PRL 104 092001	S. Uehara <i>et al.</i>	(BELLE Collab.)
AUBERT	08W	PRL 101 082001	B. Aubert <i>et al.</i>	(BABAR Collab.)
CHOI	05	PRL 94 182002	S.-K. Choi <i>et al.</i>	(BELLE Collab.)

## X(3915)

$$I^G(J^{PC}) = 0^+(?^{?+})$$

Observed in  $\omega J/\psi$ , thus  $C = +$ . May be the same state as  $\chi_{c2}(2P)$ .

### X(3915) MASS

VALUE (MeV)	EVTS	DOCUMENT ID	TECN	COMMENT
<b><math>3917.5 \pm 2.7</math> OUR AVERAGE</b>				
$3919.1^{+3.8}_{-3.4} \pm 2.0$		DEL-AMO-SA...10B	BABR	$B \rightarrow \omega J/\psi K$
$3915 \pm 3 \pm 2$	$49 \pm 15$	<sup>1</sup> UEHARA	10	BELL $10.6 e^+ e^- \rightarrow e^+ e^- \omega J/\psi$
$3943 \pm 11 \pm 13$	$58 \pm 11$	<sup>2</sup> CHOI	05	BELL $B \rightarrow \omega J/\psi K$
••• We do not use the following data for averages, fits, limits, etc. •••				
$3914.6^{+3.8}_{-3.4} \pm 2.0$		<sup>2</sup> AUBERT	08W	BABR Superseded by DEL-AMO-SANCHEZ 10B

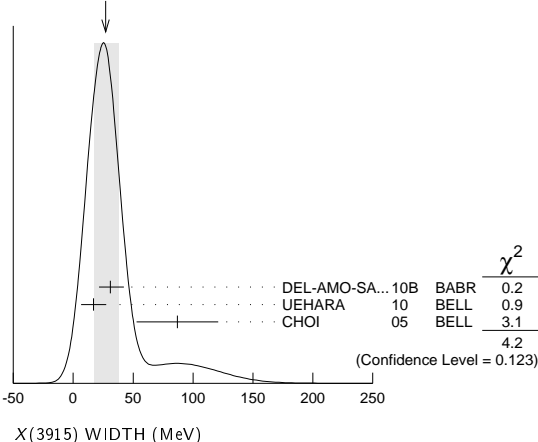
<sup>1</sup> May be  $\chi_{c2}(2P)$ .  
<sup>2</sup>  $\omega J/\psi$  threshold enhancement fitted as an S-wave Breit-Wigner resonance.

### X(3915) WIDTH

VALUE (MeV)	EVTS	DOCUMENT ID	TECN	COMMENT
<b><math>27 \pm 10</math> OUR AVERAGE</b>				Error includes scale factor of 1.4. See the ideogram below.
$31^{+10}_{-8} \pm 5$		DEL-AMO-SA...10B	BABR	$B \rightarrow \omega J/\psi K$
$17 \pm 10 \pm 3$	$49 \pm 15$	<sup>3</sup> UEHARA	10	BELL $10.6 e^+ e^- \rightarrow e^+ e^- \omega J/\psi$
$87 \pm 22 \pm 26$	$58 \pm 11$	<sup>4</sup> CHOI	05	BELL $B \rightarrow \omega J/\psi K$
••• We do not use the following data for averages, fits, limits, etc. •••				
$34^{+12}_{-8} \pm 5$		<sup>4</sup> AUBERT	08W	BABR Superseded by DEL-AMO-SANCHEZ 10B

<sup>3</sup> May be  $\chi_{c2}(2P)$ .  
<sup>4</sup>  $\omega J/\psi$  threshold enhancement fitted as an S-wave Breit-Wigner resonance.

WEIGHTED AVERAGE  
 $27 \pm 10$  (Error scaled by 1.4)



## $\chi_{c2}(2P)$

$$I^G(J^{PC}) = 0^+(2^{++})$$

### $\chi_{c2}(2P)$ MASS

VALUE (MeV)	EVTS	DOCUMENT ID	TECN	COMMENT
<b><math>3927.2 \pm 2.6</math> OUR AVERAGE</b>				
$3926.7 \pm 2.7 \pm 1.1$	$76 \pm 17$	AUBERT	10G	BABR $10.6 e^+ e^- \rightarrow e^+ e^- D\bar{D}$
$3929 \pm 5 \pm 2$	$64$	UEHARA	06	BELL $10.6 e^+ e^- \rightarrow e^+ e^- D\bar{D}$

### $\chi_{c2}(2P)$ WIDTH

VALUE (MeV)	EVTS	DOCUMENT ID	TECN	COMMENT
<b><math>24 \pm 6</math> OUR AVERAGE</b>				
$21.3 \pm 6.8 \pm 3.6$	$76 \pm 17$	AUBERT	10G	BABR $10.6 e^+ e^- \rightarrow e^+ e^- D\bar{D}$
$29 \pm 10 \pm 2$	$64$	UEHARA	06	BELL $10.6 e^+ e^- \rightarrow e^+ e^- D\bar{D}$

### $\chi_{c2}(2P)$ DECAY MODES

Mode	Fraction ( $\Gamma_i/\Gamma$ )
$\Gamma_1$ $\gamma\gamma$	seen
$\Gamma_2$ $K\bar{K}\pi$	
$\Gamma_3$ $K^+ K^- \pi^+ \pi^- \pi^0$	
$\Gamma_4$ $D\bar{D}$	seen
$\Gamma_5$ $D^+ D^-$	seen
$\Gamma_6$ $D^0 \bar{D}^0$	seen

See key on page 457

# Meson Particle Listings

## $\chi_{c2}(2P)$ , $X(3940)$ , $\psi(4040)$

### $\chi_{c2}(2P)$ PARTIAL WIDTHS

#### $\chi_{c2}(2P) \Gamma(i)\Gamma(\gamma\gamma)/\Gamma(\text{total})$

$\Gamma(K\bar{K}\pi) \times \Gamma(\gamma\gamma)/\Gamma_{\text{total}}$	$\Gamma_2/\Gamma$
VALUE (eV) CL% DOCUMENT ID TECN COMMENT	
<b>&lt;2.1</b> 90 DEL-AMO-SA...11M BABR $\gamma\gamma \rightarrow K_S^0 K^\pm \pi^\mp$	

$\Gamma(K^+K^-\pi^+\pi^-\pi^0) \times \Gamma(\gamma\gamma)/\Gamma_{\text{total}}$	$\Gamma_3/\Gamma$
VALUE (eV) CL% DOCUMENT ID TECN COMMENT	
<b>&lt;3.4</b> 90 DEL-AMO-SA...11M BABR $\gamma\gamma \rightarrow K^+K^-\pi^+\pi^-\pi^0$	

$\Gamma(D\bar{D}) \times \Gamma(\gamma\gamma)/\Gamma_{\text{total}}$	$\Gamma_4/\Gamma$
VALUE (keV) EVTS DOCUMENT ID TECN COMMENT	
<b>0.21 ± 0.04 OUR AVERAGE</b>	
0.24 ± 0.05 ± 0.04 76 ± 17 AUBERT 10G BABR 10.6 $e^+e^- \rightarrow e^+e^-D\bar{D}$	
0.18 ± 0.05 ± 0.03 64 <sup>1</sup> UEHARA 06 BELL 10.6 $e^+e^- \rightarrow e^+e^-D\bar{D}$	

<sup>1</sup> Assuming  $B(D^+D^-) = 0.89 B(D^0\bar{D}^0)$ .

### $\chi_{c2}(2P)$ BRANCHING RATIOS

$\Gamma(D^+D^-)/\Gamma(D^0\bar{D}^0)$	$\Gamma_5/\Gamma_6$
VALUE EVTS DOCUMENT ID TECN COMMENT	
<b>0.74 ± 0.43 ± 0.16</b> 64 UEHARA 06 BELL 10.6 $e^+e^- \rightarrow e^+e^-D\bar{D}$	

### $\chi_{c2}(2P)$ REFERENCES

DEL-AMO-SA...11M PR D84 012004 P. del Amo Sanchez et al. (BABAR Collab.)
AUBERT 10G PR D81 092003 B. Aubert et al. (BABAR Collab.)
UEHARA 06 PRL 96 082003 S. Uehara et al. (BELLE Collab.)

## X(3940)

$$J^G(J^{PC}) = ?(???)$$

OMITTED FROM SUMMARY TABLE

Reported by ABE 07, observed in  $e^+e^- \rightarrow J/\psi X$ .

### X(3940) MASS

VALUE (MeV) EVTS DOCUMENT ID TECN COMMENT
<b>3942 ± 7 ± 6</b> 52 PAKHLOV 08 BELL $e^+e^- \rightarrow J/\psi X$
• • • We do not use the following data for averages, fits, limits, etc. • • •
3943 ± 6 ± 6 25 <sup>1</sup> ABE 07 BELL $e^+e^- \rightarrow J/\psi X$
3936 ± 14 266 <sup>2</sup> ABE 07 BELL $e^+e^- \rightarrow J/\psi(c\bar{c})$

<sup>1</sup> From a fit to  $D^{*+}D^-$  and  $D^{*0}\bar{D}^0$  events.  
<sup>2</sup> From the inclusive fit. Not independent of the exclusive measurement by ABE 07.

### X(3940) WIDTH

VALUE (MeV) CL% EVTS DOCUMENT ID TECN COMMENT
<b>37 ± 26 ± 15 ± 8</b> 52 PAKHLOV 08 BELL $e^+e^- \rightarrow J/\psi X$
• • • We do not use the following data for averages, fits, limits, etc. • • •
<52 90 25 ABE 07 BELL $e^+e^- \rightarrow J/\psi X$

### X(3940) DECAY MODES

Mode	Fraction ( $\Gamma_i/\Gamma$ )
$\Gamma_1$ $D\bar{D}^* + c.c.$	seen
$\Gamma_2$ $D\bar{D}$	not seen
$\Gamma_3$ $J/\psi\omega$	not seen

### X(3940) BRANCHING RATIOS

$\Gamma(D\bar{D}^* + c.c.)/\Gamma_{\text{total}}$	$\Gamma_1/\Gamma$
VALUE CL% EVTS DOCUMENT ID TECN COMMENT	
• • • We do not use the following data for averages, fits, limits, etc. • • •	
>0.45 90 25 <sup>3,4</sup> ABE 07 BELL $e^+e^- \rightarrow J/\psi X$	

<sup>3</sup> For  $X(3940)$  decaying to final states with more than two tracks.  
<sup>4</sup> PAKHLOV 08 finds that the inclusive peak near 3940 MeV/ $c^2$  may consist of several states.

$\Gamma(D\bar{D})/\Gamma_{\text{total}}$	$\Gamma_2/\Gamma$
VALUE CL% DOCUMENT ID TECN COMMENT	
• • • We do not use the following data for averages, fits, limits, etc. • • •	
<0.41 90 <sup>5,6</sup> ABE 07 BELL $e^+e^- \rightarrow J/\psi X$	

<sup>5</sup> For  $X(3940)$  decaying to final states with more than two tracks.  
<sup>6</sup> PAKHLOV 08 finds that the inclusive peak near 3940 MeV/ $c^2$  may consist of several states.

### $\Gamma(J/\psi\omega)/\Gamma_{\text{total}}$

VALUE CL% DOCUMENT ID TECN COMMENT
• • • We do not use the following data for averages, fits, limits, etc. • • •
<0.26 90 <sup>7,8</sup> ABE 07 BELL $e^+e^- \rightarrow J/\psi X$

<sup>7</sup> For  $X(3940)$  decaying to final states with more than two tracks.  
<sup>8</sup> PAKHLOV 08 finds that the inclusive peak near 3940 MeV/ $c^2$  may consist of several states.

### X(3940) REFERENCES

PAKHLOV 08 PRL 100 202001 P. Pakhlov et al. (BELLE Collab.)
ABE 07 PRL 98 082001 K. Abe et al. (BELLE Collab.)

## $\psi(4040)$

$$J^G(J^{PC}) = 0^-(1^{--})$$

### $\psi(4040)$ MASS

VALUE (MeV) EVTS DOCUMENT ID TECN COMMENT
<b>4039 ± 1 OUR ESTIMATE</b>
<b>4039.6 ± 4.3</b> 1 ABLIKIM 08D BES2 $e^+e^- \rightarrow$ hadrons
• • • We do not use the following data for averages, fits, limits, etc. • • •
4034 ± 6 2 MO 10 RVUE $e^+e^- \rightarrow$ hadrons
4037 ± 2 3 SETH 05A RVUE $e^+e^- \rightarrow$ hadrons
4040 ± 1 4 SETH 05A RVUE $e^+e^- \rightarrow$ hadrons
4040 ± 10 BRANDELIK 78C DASP $e^+e^-$

<sup>1</sup> Reanalysis of data presented in BAI 02c. From a global fit over the center-of-mass energy region 3.7–5.0 GeV covering the  $\psi(3770)$ ,  $\psi(4040)$ ,  $\psi(4160)$ , and  $\psi(4415)$  resonances. Phase angle fixed in the fit to  $\delta = (130 \pm 46)^\circ$ .  
<sup>2</sup> Reanalysis of data presented in BAI 00 and BAI 02c. From a global fit over the center-of-mass energy 3.8–4.8 GeV covering the  $\psi(4040)$ ,  $\psi(4160)$  and  $\psi(4415)$  resonances and including interference effects.  
<sup>3</sup> From a fit to Crystal Ball (OSTERHELD 86) data.  
<sup>4</sup> From a fit to BES (BAI 02c) data.

### $\psi(4040)$ WIDTH

VALUE (MeV) EVTS DOCUMENT ID TECN COMMENT
<b>80 ± 10 OUR ESTIMATE</b>
<b>84.5 ± 12.3</b> 5 ABLIKIM 08D BES2 $e^+e^- \rightarrow$ hadrons
• • • We do not use the following data for averages, fits, limits, etc. • • •
87 ± 11 6 MO 10 RVUE $e^+e^- \rightarrow$ hadrons
85 ± 10 7 SETH 05A RVUE $e^+e^- \rightarrow$ hadrons
89 ± 6 8 SETH 05A RVUE $e^+e^- \rightarrow$ hadrons
52 ± 10 BRANDELIK 78C DASP $e^+e^-$

<sup>5</sup> Reanalysis of data presented in BAI 02c. From a global fit over the center-of-mass energy region 3.7–5.0 GeV covering the  $\psi(3770)$ ,  $\psi(4040)$ ,  $\psi(4160)$ , and  $\psi(4415)$  resonances. Phase angle fixed in the fit to  $\delta = (130 \pm 46)^\circ$ .  
<sup>6</sup> Reanalysis of data presented in BAI 00 and BAI 02c. From a global fit over the center-of-mass energy 3.8–4.8 GeV covering the  $\psi(4040)$ ,  $\psi(4160)$  and  $\psi(4415)$  resonances and including interference effects.  
<sup>7</sup> From a fit to Crystal Ball (OSTERHELD 86) data.  
<sup>8</sup> From a fit to BES (BAI 02c) data.

### $\psi(4040)$ DECAY MODES

Due to the complexity of the  $c\bar{c}$  threshold region, in this listing, “seen” (“not seen”) means that a cross section for the mode in question has been measured at effective  $\sqrt{s}$  near this particle’s central mass value, more (less) than  $2\sigma$  above zero, without regard to any peaking behavior in  $\sqrt{s}$  or absence thereof. See mode listing(s) for details and references.

Mode	Fraction ( $\Gamma_i/\Gamma$ )	Confidence level
$\Gamma_1$ $e^+e^-$	$(1.07 \pm 0.16) \times 10^{-5}$	
$\Gamma_2$ $D\bar{D}$	seen	
$\Gamma_3$ $D^0\bar{D}^0$	seen	
$\Gamma_4$ $D^+D^-$	seen	
$\Gamma_5$ $D^*D + c.c.$	seen	
$\Gamma_6$ $D^*(2007)^0\bar{D}^0 + c.c.$	seen	
$\Gamma_7$ $D^*(2010)^+D^- + c.c.$	seen	
$\Gamma_8$ $D^*\bar{D}^*$	seen	
$\Gamma_9$ $D^*(2007)^0\bar{D}^*(2007)^0$	seen	
$\Gamma_{10}$ $D^*(2010)^+D^*(2010)^-$	seen	
$\Gamma_{11}$ $D\bar{D}\pi$ (excl. $D^*\bar{D}$ )		
$\Gamma_{12}$ $D^0D^-\pi^+ + c.c.$ (excl. $D^*(2007)^0\bar{D}^0 + c.c.$ , $D^*(2010)^+D^- + c.c.$ )	not seen	
$\Gamma_{13}$ $D\bar{D}^*\pi$ (excl. $D^*\bar{D}^*$ )	not seen	
$\Gamma_{14}$ $D^0\bar{D}^*\pi^+ + c.c.$ (excl. $D^*(2010)^+D^*(2010)^-$ )	seen	

# Meson Particle Listings

## $\psi(4040)$

$\Gamma_{15}$	$D_s^+ D_s^-$		seen					
$\Gamma_{16}$	$J/\psi(1S)$ hadrons							
$\Gamma_{17}$	$J/\psi \pi^+ \pi^-$	$< 4$	$\times 10^{-3}$		90%			
$\Gamma_{18}$	$J/\psi \pi^0 \pi^0$	$< 2$	$\times 10^{-3}$		90%			
$\Gamma_{19}$	$J/\psi \eta$	$< 7$	$\times 10^{-3}$		90%			
$\Gamma_{20}$	$J/\psi \pi^0$	$< 2$	$\times 10^{-3}$		90%			
$\Gamma_{21}$	$J/\psi \pi^+ \pi^- \pi^0$	$< 2$	$\times 10^{-3}$		90%			
$\Gamma_{22}$	$\chi_{c1} \gamma$	$< 1.1$	%		90%			
$\Gamma_{23}$	$\chi_{c2} \gamma$	$< 1.7$	%		90%			
$\Gamma_{24}$	$\chi_{c1} \pi^+ \pi^- \pi^0$	$< 1.1$	%		90%			
$\Gamma_{25}$	$\chi_{c2} \pi^+ \pi^- \pi^0$	$< 3.2$	%		90%			
$\Gamma_{26}$	$h_c(1P) \pi^+ \pi^-$	$< 3$	$\times 10^{-3}$		90%			
$\Gamma_{27}$	$\phi \pi^+ \pi^-$	$< 3$	$\times 10^{-3}$		90%			
$\Gamma_{28}$	$\mu^+ \mu^-$							

### $\psi(4040)$ PARTIAL WIDTHS

$\Gamma(e^+ e^-)$				$\Gamma_1$
VALUE (keV)	DOCUMENT ID	TECN	COMMENT	
<b><math>0.86 \pm 0.07</math></b> OUR ESTIMATE				
<b><math>0.83 \pm 0.20</math></b>	9 ABLIKIM	08D	BES2 $e^+ e^- \rightarrow$ hadrons	
• • • We do not use the following data for averages, fits, limits, etc. • • •				
0.6 to 1.4	10 MO	10	RVUE $e^+ e^- \rightarrow$ hadrons	
$0.88 \pm 0.11$	11 SETH	05A	RVUE $e^+ e^- \rightarrow$ hadrons	
$0.91 \pm 0.13$	12 SETH	05A	RVUE $e^+ e^- \rightarrow$ hadrons	
$0.75 \pm 0.15$	BRADELIK	78C	DASP $e^+ e^-$	

<sup>9</sup> Reanalysis of data presented in BAI 02c. From a global fit over the center-of-mass energy region 3.7–5.0 GeV covering the  $\psi(3770)$ ,  $\psi(4040)$ ,  $\psi(4160)$ , and  $\psi(4415)$  resonances. Phase angle fixed in the fit to  $\delta = (130 \pm 46)^\circ$ .

<sup>10</sup> Reanalysis of data presented in BAI 00 and BAI 02c. From a global fit over the center-of-mass energy 3.8–4.8 GeV covering the  $\psi(4040)$ ,  $\psi(4160)$  and  $\psi(4415)$  resonances and including interference effects. Four sets of solutions are obtained with the same fit quality, mass and total width, but with different  $e^+ e^-$  partial widths. We quote only the range of values.

<sup>11</sup> From a fit to Crystal Ball (OSTERHELD 86) data.

<sup>12</sup> From a fit to BES (BAI 02c) data.

### $\psi(4040)$ BRANCHING RATIOS

$\Gamma(e^+ e^-)/\Gamma_{total}$				$\Gamma_1/\Gamma$
VALUE (units $10^{-5}$ )	DOCUMENT ID	TECN	COMMENT	
• • • We do not use the following data for averages, fits, limits, etc. • • •				
$\sim 1.0$	FELDMAN	77	MRK1 $e^+ e^-$	

$\Gamma(D^0 \bar{D}^0)/\Gamma_{total}$				$\Gamma_3/\Gamma$
VALUE	DOCUMENT ID	TECN	COMMENT	
seen	AUBERT	09M	BABR $e^+ e^- \rightarrow D^0 \bar{D}^0 \gamma$	
seen	CRONIN-HEN..09	CLEO	$e^+ e^- \rightarrow D^0 \bar{D}^0$	
seen	PAKHLOVA	08	BELL $e^+ e^- \rightarrow D^0 \bar{D}^0 \gamma$	

$\Gamma(D^+ D^-)/\Gamma_{total}$				$\Gamma_4/\Gamma$
VALUE	DOCUMENT ID	TECN	COMMENT	
seen	AUBERT	09M	BABR $e^+ e^- \rightarrow D^+ D^- \gamma$	
seen	CRONIN-HEN..09	CLEO	$e^+ e^- \rightarrow D^+ D^-$	
seen	PAKHLOVA	08	BELL $e^+ e^- \rightarrow D^+ D^- \gamma$	

$\Gamma(D \bar{D})/\Gamma(D^* \bar{D} + c.c.)$				$\Gamma_2/\Gamma_5$
VALUE	DOCUMENT ID	TECN	COMMENT	
<b><math>0.24 \pm 0.05 \pm 0.12</math></b>	AUBERT	09M	BABR $e^+ e^- \rightarrow \gamma D^{(*)} \bar{D}$	

$\Gamma(D^0 \bar{D}^0)/\Gamma(D^*(2007)^0 \bar{D}^0 + c.c.)$				$\Gamma_3/\Gamma_6$
VALUE	DOCUMENT ID	TECN	COMMENT	
<b><math>0.05 \pm 0.03</math></b>	13 GOLDHABER	77	MRK1 $e^+ e^-$	

<sup>13</sup> Phase-space factor ( $p^3$ ) explicitly removed.

$\Gamma(D^*(2007)^0 \bar{D}^0 + c.c.)/\Gamma_{total}$				$\Gamma_6/\Gamma$
VALUE	DOCUMENT ID	TECN	COMMENT	
seen	AUBERT	09M	BABR $e^+ e^- \rightarrow D^{*0} \bar{D}^0 \gamma$	
seen	CRONIN-HEN..09	CLEO	$e^+ e^- \rightarrow D^{*0} \bar{D}^0$	

$\Gamma(D^*(2010)^+ D^- + c.c.)/\Gamma_{total}$				$\Gamma_7/\Gamma$
VALUE	DOCUMENT ID	TECN	COMMENT	
seen	AUBERT	09M	BABR $e^+ e^- \rightarrow D^{*+} D^- \gamma$	
seen	CRONIN-HEN..09	CLEO	$e^+ e^- \rightarrow D^{*+} D^-$	
seen	PAKHLOVA	07	BELL $e^+ e^- \rightarrow D^{*+} D^- \gamma$	

$\Gamma(D^*(2010)^+ D^- + c.c.)/\Gamma(D^*(2007)^0 \bar{D}^0 + c.c.)$				$\Gamma_7/\Gamma_6$
VALUE	DOCUMENT ID	TECN	COMMENT	
<b><math>0.95 \pm 0.09 \pm 0.10</math></b>	AUBERT	09M	BABR $e^+ e^- \rightarrow \gamma D^* \bar{D}$	

$\Gamma(D^* \bar{D}^*)/\Gamma(D^* \bar{D} + c.c.)$				$\Gamma_8/\Gamma_5$
VALUE	DOCUMENT ID	TECN	COMMENT	
<b><math>0.18 \pm 0.14 \pm 0.03</math></b>	AUBERT	09M	BABR $e^+ e^- \rightarrow \gamma D^{(*)} \bar{D}^{(*)}$	

$\Gamma(D^*(2007)^0 \bar{D}^*(2007)^0)/\Gamma_{total}$				$\Gamma_9/\Gamma$
VALUE	DOCUMENT ID	TECN	COMMENT	
seen	AUBERT	09M	BABR $e^+ e^- \rightarrow D^{*0} \bar{D}^{*0} \gamma$	
seen	CRONIN-HEN..09	CLEO	$e^+ e^- \rightarrow D^{*0} \bar{D}^{*0}$	

$\Gamma(D^*(2007)^0 \bar{D}^*(2007)^0)/\Gamma(D^*(2007)^0 \bar{D}^0 + c.c.)$				$\Gamma_9/\Gamma_6$
VALUE	DOCUMENT ID	TECN	COMMENT	
<b><math>32.0 \pm 12.0</math></b>	14 GOLDHABER	77	MRK1 $e^+ e^-$	

<sup>14</sup> Phase-space factor ( $p^3$ ) explicitly removed.

$\Gamma(D^*(2010)^+ D^*(2010)^-)/\Gamma_{total}$				$\Gamma_{10}/\Gamma$
VALUE	DOCUMENT ID	TECN	COMMENT	
seen	AUBERT	09M	BABR $e^+ e^- \rightarrow D^{*+} D^{*-} \gamma$	
seen	CRONIN-HEN..09	CLEO	$e^+ e^- \rightarrow D^{*+} D^{*-}$	
seen	PAKHLOVA	07	BELL $e^+ e^- \rightarrow D^{*+} D^{*-} \gamma$	

$\Gamma(D^0 D^- \pi^+ + c.c. (excl. D^*(2007)^0 \bar{D}^0 + c.c., D^*(2010)^+ D^- + c.c.))/\Gamma_{total}$				$\Gamma_{12}/\Gamma$
VALUE	DOCUMENT ID	TECN	COMMENT	
not seen	PAKHLOVA	08A	BELL $e^+ e^- \rightarrow D^0 D^- \pi^+ \gamma$	

$\Gamma(D \bar{D}^* \pi (excl. D^* \bar{D}^*))/\Gamma_{total}$				$\Gamma_{13}/\Gamma$
VALUE	DOCUMENT ID	TECN	COMMENT	
not seen	CRONIN-HEN..09	CLEO	$e^+ e^- \rightarrow D \bar{D}^* \pi$	

$\Gamma(D^0 \bar{D}^* \pi^+ + c.c. (excl. D^*(2010)^+ D^*(2010)^-))/\Gamma_{total}$				$\Gamma_{14}/\Gamma$
VALUE	DOCUMENT ID	TECN	COMMENT	
seen	PAKHLOVA	09	BELL $e^+ e^- \rightarrow D^0 D^{*-} \pi^+ \gamma$	

$\Gamma(D_s^+ D_s^-)/\Gamma_{total}$				$\Gamma_{15}/\Gamma$
VALUE	DOCUMENT ID	TECN	COMMENT	
seen	PAKHLOVA	11	BELL $e^+ e^- \rightarrow D_s^+ D_s^- \gamma$	
seen	DEL-AMO-SA..10N	BABR	$e^+ e^- \rightarrow D_s^+ D_s^- \gamma$	
seen	CRONIN-HEN..09	CLEO	$e^+ e^- \rightarrow D_s^+ D_s^-$	

$\Gamma(J/\psi \pi^+ \pi^-)/\Gamma_{total}$				$\Gamma_{17}/\Gamma$	
VALUE (units $10^{-3}$ )	CL%	DOCUMENT ID	TECN	COMMENT	
$< 4$	90	COAN	06	CLEO 3.97–4.06 $e^+ e^- \rightarrow$ hadrons	

$\Gamma(J/\psi \pi^0 \pi^0)/\Gamma_{total}$				$\Gamma_{18}/\Gamma$	
VALUE (units $10^{-3}$ )	CL%	DOCUMENT ID	TECN	COMMENT	
$< 2$	90	COAN	06	CLEO 3.97–4.06 $e^+ e^- \rightarrow$ hadrons	

$\Gamma(J/\psi \eta)/\Gamma_{total}$				$\Gamma_{19}/\Gamma$	
VALUE (units $10^{-3}$ )	CL%	DOCUMENT ID	TECN	COMMENT	
$< 7$	90	COAN	06	CLEO 3.97–4.06 $e^+ e^- \rightarrow$ hadrons	

$\Gamma(J/\psi \pi^0)/\Gamma_{total}$				$\Gamma_{20}/\Gamma$	
VALUE (units $10^{-3}$ )	CL%	DOCUMENT ID	TECN	COMMENT	
$< 2$	90	COAN	06	CLEO 3.97–4.06 $e^+ e^- \rightarrow$ hadrons	

$\Gamma(J/\psi \pi^+ \pi^- \pi^0)/\Gamma_{total}$				$\Gamma_{21}/\Gamma$	
VALUE (units $10^{-3}$ )	CL%	DOCUMENT ID	TECN	COMMENT	
$< 2$	90	COAN	06	CLEO 3.97–4.06 $e^+ e^- \rightarrow$ hadrons	

$\Gamma(\chi_{c1} \gamma)/\Gamma_{total}$				$\Gamma_{22}/\Gamma$	
VALUE (units $10^{-3}$ )	CL%	DOCUMENT ID	TECN	COMMENT	
$< 11$	90	COAN	06	CLEO 3.97–4.06 $e^+ e^- \rightarrow$ hadrons	

$\Gamma(\chi_{c2} \gamma)/\Gamma_{total}$				$\Gamma_{23}/\Gamma$	
VALUE (units $10^{-3}$ )	CL%	DOCUMENT ID	TECN	COMMENT	
$< 17$	90	COAN	06	CLEO 3.97–4.06 $e^+ e^- \rightarrow$ hadrons	

$\Gamma(\chi_{c1} \pi^+ \pi^- \pi^0)/\Gamma_{total}$				$\Gamma_{24}/\Gamma$	
VALUE (units $10^{-3}$ )	CL%	DOCUMENT ID	TECN	COMMENT	
$< 11$	90	COAN	06	CLEO 3.97–4.06 $e^+ e^- \rightarrow$ hadrons	

$\Gamma(\chi_{c2} \pi^+ \pi^- \pi^0)/\Gamma_{total}$				$\Gamma_{25}/\Gamma$	
VALUE (units $10^{-3}$ )	CL%	DOCUMENT ID	TECN	COMMENT	
$< 32$	90	COAN	06	CLEO 3.97–4.06 $e^+ e^- \rightarrow$ hadrons	

$\Gamma(h_c(1P) \pi^+ \pi^-)/\Gamma_{total}$				$\Gamma_{26}/\Gamma$	
VALUE (units $10^{-3}$ )	CL%	DOCUMENT ID	TECN	COMMENT	
$< 3$	90	15 PEDLAR	11	CLEO $e^+ e^- \rightarrow h_c(1P) \pi^+ \pi^-$	

<sup>15</sup> From several values of  $\sqrt{s}$  near the peak of the  $\psi(4040)$ , PEDLAR 11 measures  $\sigma(e^+ e^- \rightarrow h_c(1P) \pi^+ \pi^-) = 1.0 \pm 8.0 \pm 5.4 \pm 0.2$  pb, where the errors are statistical, systematic, and due to uncertainty in  $B(\psi(2S) \rightarrow \pi^0 h_c(1P))$ , respectively.

See key on page 457

# Meson Particle Listings

## $\psi(4040)$ , $X(4050)^\pm$ , $X(4140)$ , $\psi(4160)$

$\Gamma(\phi\pi^+\pi^-)/\Gamma_{\text{total}}$		$\Gamma_{27}/\Gamma$		
VALUE (units $10^{-3}$ )	CL%	DOCUMENT ID	TECN	COMMENT
<3	90	COAN	06	CLEO 3.97-4.06 $e^+e^- \rightarrow$ hadrons

### $\psi(4040)$ REFERENCES

PAKHOVA	11	PR D83 011101	G. Pakhlova et al.	(BELLE Collab.)
PEDLAR	11	PRL 107 041803	T. Pedlar et al.	(CLEO Collab.)
DEL-AMO-SA...	10N	PR D82 052004	P. del Amo Sanchez et al.	(BABAR Collab.)
MO	10	PR D82 077501	X.H. Mo, C.Z. Yuan, P. Wang	(BHEP)
AUBERT	09M	PR D79 092001	B. Aubert et al.	(BABAR Collab.)
CRONIN-HEN...	09	PR D80 072001	D. Cronin-Hennessy et al.	(CLEO Collab.)
PAKHOVA	09	PR D80 091101R	G. Pakhlova et al.	(BELLE Collab.)
ABLIKIM	08D	PL B660 315	M. Ablikim et al.	(BES Collab.)
PAKHOVA	08	PR D77 011103R	G. Pakhlova et al.	(BELLE Collab.)
PAKHOVA	08A	PRL 100 062001	G. Pakhlova et al.	(BELLE Collab.)
PAKHOVA	07	PRL 98 092001	G. Pakhlova et al.	(BELLE Collab.)
COAN	06	PRL 96 162003	T.E. Coan et al.	(CLEO Collab.)
SETH	05A	PR D72 017501	K.K. Seth	
BAI	02C	PRL 88 101802	J.Z. Bai et al.	(BES Collab.)
BAI	00	PRL 84 594	J.Z. Bai et al.	(BES Collab.)
OSTERHELD	86	SLAC-PUB-4160	A. Osterheld et al.	(SLAC Crystal Ball Collab.)
BRANDELIK	78C	PL 76B 361	R. Brandelik et al.	(DASP Collab.)
		Also ZPHY C1 233	R. Brandelik et al.	(DASP Collab.)
FELDMAN	77	PRPL 33C 285	G.J. Feldman, M.L. Perl	(LBL, SLAC)
GOLDBABER	77	PL 69B 503	G. Goldhaber et al.	(Mark I Collab.)

### $X(4050)^\pm$

$$I(J^P) = ?(??)$$

OMITTED FROM SUMMARY TABLE

Observed by MIZUK 08 in the  $\pi^+\chi_{c1}(1P)$  invariant mass distribution in  $\bar{B}^0 \rightarrow K^-\pi^+\chi_{c1}(1P)$  decays. Not seen by LEES 12B in this same mode after accounting for  $K\pi$  resonant mass and angular structure.

### $X(4050)^\pm$ MASS

VALUE (MeV)	DOCUMENT ID	TECN	COMMENT
$4051 \pm 14^{+20}_{-41}$	1 MIZUK	08	BELL $\bar{B}^0 \rightarrow K^-\pi^+\chi_{c1}(1P)$

<sup>1</sup> From a Dalitz plot analysis with two Breit-Wigner amplitudes.

### $X(4050)^\pm$ WIDTH

VALUE (MeV)	DOCUMENT ID	TECN	COMMENT
$82^{+21+47}_{-17-22}$	2 MIZUK	08	BELL $\bar{B}^0 \rightarrow K^-\pi^+\chi_{c1}(1P)$

<sup>2</sup> From a Dalitz plot analysis with two Breit-Wigner amplitudes.

### $X(4050)^\pm$ DECAY MODES

Mode	Fraction ( $\Gamma_i/\Gamma$ )
$\Gamma_1 \pi^+\chi_{c1}(1P)$	seen

### $X(4050)^\pm$ BRANCHING RATIOS

$\Gamma(\pi^+\chi_{c1}(1P))/\Gamma_{\text{total}}$	DOCUMENT ID	TECN	COMMENT	$\Gamma_1/\Gamma$
seen	3 MIZUK	08	BELL $\bar{B}^0 \rightarrow K^-\pi^+\chi_{c1}(1P)$	

••• We do not use the following data for averages, fits, limits, etc. •••

not seen <sup>4</sup> LEES 12B BABR  $B \rightarrow K\pi\chi_{c1}(1P)$   
<sup>3</sup> With a product branching fraction measurement of  $B(\bar{B}^0 \rightarrow K^-X(4050)^+) \times B(X(4050)^+ \rightarrow \pi^+\chi_{c1}(1P)) = (3.0^{+1.5+3.7}_{-0.8-1.6}) \times 10^{-5}$ .

<sup>4</sup> With a product branching fraction limit of  $B(\bar{B}^0 \rightarrow X(4050)^+K^-) \times B(X(4050)^+ \rightarrow \chi_{c1}\pi^+) < 1.8 \times 10^{-5}$  at 90% CL.

### $X(4050)^\pm$ REFERENCES

LEES	12B	PR D85 052003	J.P. Lees et al.	(BABAR Collab.)
MIZUK	08	PR D78 072004	R. Mizuk et al.	(BELLE Collab.)

### $X(4140)$

$$I^G(J^{PC}) = 0^+(?^{?+})$$

OMITTED FROM SUMMARY TABLE

Needs confirmation.

Seen by AALTONEN 09AH in the  $B^+ \rightarrow XK^+$ ,  $X \rightarrow J/\psi\phi$ . Not seen by SHEN 10 in  $\gamma\gamma \rightarrow J/\psi\phi$ .

### $X(4140)$ MASS

VALUE (MeV)	EVTS	DOCUMENT ID	TECN	COMMENT
$4143.0 \pm 2.9 \pm 1.2$	14 $\pm$ 5	1 AALTONEN	09AH	CDF $B^+ \rightarrow J/\psi\phi K^+$

<sup>1</sup> Statistical significance of 3.8  $\sigma$ .

### $X(4140)$ WIDTH

VALUE (MeV)	EVTS	DOCUMENT ID	TECN	COMMENT
$11.7^{+8.3}_{-5.0} \pm 3.7$	14 $\pm$ 5	2 AALTONEN	09AH	CDF $B^+ \rightarrow J/\psi\phi K^+$

<sup>2</sup> Statistical significance of 3.8  $\sigma$ .

### $X(4140)$ DECAY MODES

Mode	Fraction ( $\Gamma_i/\Gamma$ )
$\Gamma_1 J/\psi\phi$	seen
$\Gamma_2 \gamma\gamma$	not seen

### $X(4140)$ $\Gamma(J/\psi\phi)/\Gamma(\text{total})$

VALUE (eV)	CL%	DOCUMENT ID	TECN	COMMENT	$\Gamma_2\Gamma_1/\Gamma$
<41	90	3 SHEN	10	BELL $10.6 e^+e^- \rightarrow e^+e^- J/\psi\phi$	

••• We do not use the following data for averages, fits, limits, etc. •••  
 < 6 90 <sup>4</sup> SHEN 10 BELL  $10.6 e^+e^- \rightarrow e^+e^- J/\psi\phi$

<sup>3</sup> For  $J^P = 0^+$ .

<sup>4</sup> For  $J^P = 2^+$ .

### $X(4140)$ BRANCHING RATIOS

$\Gamma(J/\psi\phi)/\Gamma_{\text{total}}$	EVTS	DOCUMENT ID	TECN	COMMENT	$\Gamma_1/\Gamma$
seen	14 $\pm$ 5	5 AALTONEN	09AH	CDF $B^+ \rightarrow J/\psi\phi K^+$	

<sup>5</sup> Statistical significance of 3.8  $\sigma$ .

$\Gamma(\gamma\gamma)/\Gamma_{\text{total}}$	DOCUMENT ID	TECN	COMMENT	$\Gamma_2/\Gamma$
not seen	SHEN	10	BELL $10.6 e^+e^- \rightarrow e^+e^- J/\psi\phi$	

### $X(4140)$ REFERENCES

SHEN	10	PRL 104 112004	C.P. Shen et al.	(BELLE Collab.)
AALTONEN	09AH	PRL 102 242002	T. Aaltonen et al.	(CDF Collab.)

### $\psi(4160)$

$$I^G(J^{PC}) = 0^-(1^{--})$$

### $\psi(4160)$ MASS

VALUE (MeV)	DOCUMENT ID	TECN	COMMENT
<b>4191.7 <math>\pm</math> 3 OUR ESTIMATE</b>			
<b>4191.7 <math>\pm</math> 6.5</b>	1 ABLIKIM	08D	BES2 $e^+e^- \rightarrow$ hadrons
••• We do not use the following data for averages, fits, limits, etc. •••			
4193 $\pm$ 7	2 MO	10	RVUE $e^+e^- \rightarrow$ hadrons
4151 $\pm$ 4	3 SETH	05A	RVUE $e^+e^- \rightarrow$ hadrons
4155 $\pm$ 5	4 SETH	05A	RVUE $e^+e^- \rightarrow$ hadrons
4159 $\pm$ 20	BRANDELIK	78C	DASP $e^+e^-$

<sup>1</sup> Reanalysis of data presented in BAI 02c. From a global fit over the center-of-mass energy region 3.7-5.0 GeV covering the  $\psi(3770)$ ,  $\psi(4040)$ ,  $\psi(4160)$ , and  $\psi(4415)$  resonances. Phase angle fixed in the fit to  $\delta = (293 \pm 57)^\circ$ .

<sup>2</sup> Reanalysis of data presented in BAI 00 and BAI 02c. From a global fit over the center-of-mass energy 3.8-4.8 GeV covering the  $\psi(4040)$ ,  $\psi(4160)$  and  $\psi(4415)$  resonances and including interference effects.

<sup>3</sup> From a fit to Crystal Ball (OSTERHELD 86) data.

<sup>4</sup> From a fit to BES (BAI 02c) data.

### $\psi(4160)$ WIDTH

VALUE (MeV)	DOCUMENT ID	TECN	COMMENT
<b>103 <math>\pm</math> 8 OUR ESTIMATE</b>			
<b>71.8 <math>\pm</math> 12.3</b>	5 ABLIKIM	08D	BES2 $e^+e^- \rightarrow$ hadrons
••• We do not use the following data for averages, fits, limits, etc. •••			
79 $\pm$ 14	6 MO	10	RVUE $e^+e^- \rightarrow$ hadrons
107 $\pm$ 10	7 SETH	05A	RVUE $e^+e^- \rightarrow$ hadrons
107 $\pm$ 16	8 SETH	05A	RVUE $e^+e^- \rightarrow$ hadrons
78 $\pm$ 20	BRANDELIK	78C	DASP $e^+e^-$

<sup>5</sup> Reanalysis of data presented in BAI 02c. From a global fit over the center-of-mass energy region 3.7-5.0 GeV covering the  $\psi(3770)$ ,  $\psi(4040)$ ,  $\psi(4160)$ , and  $\psi(4415)$  resonances. Phase angle fixed in the fit to  $\delta = (293 \pm 57)^\circ$ .

<sup>6</sup> Reanalysis of data presented in BAI 00 and BAI 02c. From a global fit over the center-of-mass energy 3.8-4.8 GeV covering the  $\psi(4040)$ ,  $\psi(4160)$  and  $\psi(4415)$  resonances and including interference effects.

<sup>7</sup> From a fit to Crystal Ball (OSTERHELD 86) data.

<sup>8</sup> From a fit to BES (BAI 02c) data.

## Meson Particle Listings

 $\psi(4160)$  $\psi(4160)$  DECAY MODES

Due to the complexity of the  $c\bar{c}$  threshold region, in this listing, "seen" ("not seen") means that a cross section for the mode in question has been measured at effective  $\sqrt{s}$  near this particle's central mass value, more (less) than  $2\sigma$  above zero, without regard to any peaking behavior in  $\sqrt{s}$  or absence thereof. See mode listing(s) for details and references.

Mode	Fraction ( $\Gamma_i/\Gamma$ )	Confidence level
$\Gamma_1$ $e^+e^-$	$(8.1 \pm 0.9) \times 10^{-6}$	
$\Gamma_2$ $D\bar{D}$	seen	
$\Gamma_3$ $D^0\bar{D}^0$	seen	
$\Gamma_4$ $D^+D^-$	seen	
$\Gamma_5$ $D^*\bar{D} + \text{c.c.}$	seen	
$\Gamma_6$ $D^*(2007)^0\bar{D}^0 + \text{c.c.}$	seen	
$\Gamma_7$ $D^*(2010)^+D^- + \text{c.c.}$	seen	
$\Gamma_8$ $D^*\bar{D}^*$	seen	
$\Gamma_9$ $D^*(2007)^0\bar{D}^*(2007)^0$	seen	
$\Gamma_{10}$ $D^*(2010)^+D^*(2010)^-$	seen	
$\Gamma_{11}$ $D^0D^-\pi^+ + \text{c.c. (excl. } D^*(2007)^0\bar{D}^0 + \text{c.c., } D^*(2010)^+D^- + \text{c.c.)}$	not seen	
$\Gamma_{12}$ $D^0\bar{D}^*\pi + \text{c.c. (excl. } D^*\bar{D}^*)$	seen	
$\Gamma_{13}$ $D^0D^*\pi^+ + \text{c.c. (excl. } D^*(2010)^+D^*(2010)^-)$	not seen	
$\Gamma_{14}$ $D_s^+D_s^-$	not seen	
$\Gamma_{15}$ $D_s^{*+}D_s^- + \text{c.c.}$	seen	
$\Gamma_{16}$ $J/\psi\pi^+\pi^-$	$< 3$	$\times 10^{-3}$ 90%
$\Gamma_{17}$ $J/\psi\pi^0\pi^0$	$< 3$	$\times 10^{-3}$ 90%
$\Gamma_{18}$ $J/\psi K^+K^-$	$< 2$	$\times 10^{-3}$ 90%
$\Gamma_{19}$ $J/\psi\eta$	$< 8$	$\times 10^{-3}$ 90%
$\Gamma_{20}$ $J/\psi\pi^0$	$< 1$	$\times 10^{-3}$ 90%
$\Gamma_{21}$ $J/\psi\eta'$	$< 5$	$\times 10^{-3}$ 90%
$\Gamma_{22}$ $J/\psi\pi^+\pi^-\pi^0$	$< 1$	$\times 10^{-3}$ 90%
$\Gamma_{23}$ $\psi(2S)\pi^+\pi^-$	$< 4$	$\times 10^{-3}$ 90%
$\Gamma_{24}$ $\chi_{c1}\gamma$	$< 7$	$\times 10^{-3}$ 90%
$\Gamma_{25}$ $\chi_{c2}\gamma$	$< 1.3$	% 90%
$\Gamma_{26}$ $\chi_{c1}\pi^+\pi^-\pi^0$	$< 2$	$\times 10^{-3}$ 90%
$\Gamma_{27}$ $\chi_{c2}\pi^+\pi^-\pi^0$	$< 8$	$\times 10^{-3}$ 90%
$\Gamma_{28}$ $h_c(1P)\pi^+\pi^-$	$< 5$	$\times 10^{-3}$ 90%
$\Gamma_{29}$ $h_c(1P)\pi^0\pi^0$	$< 2$	$\times 10^{-3}$ 90%
$\Gamma_{30}$ $h_c(1P)\eta$	$< 2$	$\times 10^{-3}$ 90%
$\Gamma_{31}$ $h_c(1P)\pi^0$	$< 4$	$\times 10^{-4}$ 90%
$\Gamma_{32}$ $\phi\pi^+\pi^-$	$< 2$	$\times 10^{-3}$ 90%

 $\psi(4160)$  PARTIAL WIDTHS

$\Gamma(e^+e^-)$	$\Gamma_1$		
VALUE (keV)	DOCUMENT ID	TECN	COMMENT
<b><math>0.83 \pm 0.07</math> OUR ESTIMATE</b>			
<b><math>0.48 \pm 0.22</math></b>	<sup>9</sup> ABLIKIM	08D	BES2 $e^+e^- \rightarrow$ hadrons
••• We do not use the following data for averages, fits, limits, etc. •••			
0.4 to 1.1	<sup>10</sup> MO	10	RVUE $e^+e^- \rightarrow$ hadrons
$0.83 \pm 0.08$	<sup>11</sup> SETH	05A	RVUE $e^+e^- \rightarrow$ hadrons
$0.84 \pm 0.13$	<sup>12</sup> SETH	05A	RVUE $e^+e^- \rightarrow$ hadrons
$0.77 \pm 0.23$	BRANDELIK	78c	DASP $e^+e^-$

<sup>9</sup>Reanalysis of data presented in BAI 02c. From a global fit over the center-of-mass energy region 3.7–5.0 GeV covering the  $\psi(3770)$ ,  $\psi(4040)$ ,  $\psi(4160)$ , and  $\psi(4415)$  resonances. Phase angle fixed in the fit to  $\delta = (293 \pm 57)^\circ$ .

<sup>10</sup>Reanalysis of data presented in BAI 00 and BAI 02c. From a global fit over the center-of-mass energy 3.8–4.8 GeV covering the  $\psi(4040)$ ,  $\psi(4160)$  and  $\psi(4415)$  resonances and including interference effects. Four sets of solutions are obtained with the same fit quality, mass and total width, but with different  $e^+e^-$  partial widths. We quote only the range of values.

<sup>11</sup>From a fit to Crystal Ball (OSTERHELD 86) data.

<sup>12</sup>From a fit to BES (BAI 02c) data.

 $\psi(4160)$  BRANCHING RATIOS

$\Gamma(D\bar{D})/\Gamma(D^*\bar{D}^*)$	$\Gamma_2/\Gamma_8$		
VALUE	DOCUMENT ID	TECN	COMMENT
<b><math>0.02 \pm 0.03 \pm 0.02</math></b>	AUBERT	09M	BABR $e^+e^- \rightarrow \gamma D^{(*)}\bar{D}^{(*)}$
$\Gamma(D^0\bar{D}^0)/\Gamma_{\text{total}}$	$\Gamma_3/\Gamma$		
VALUE	DOCUMENT ID	TECN	COMMENT
seen	CRONIN-HEN..09	CLEO	$e^+e^- \rightarrow D^0\bar{D}^0$
seen	PAKHLOVA	08	BELL $e^+e^- \rightarrow D^0\bar{D}^0\gamma$
••• We do not use the following data for averages, fits, limits, etc. •••			
not seen	AUBERT	09M	BABR $e^+e^- \rightarrow D^0\bar{D}^0\gamma$

$\Gamma(D^+D^-)/\Gamma_{\text{total}}$	$\Gamma_4/\Gamma$		
VALUE	DOCUMENT ID	TECN	COMMENT
seen	CRONIN-HEN..09	CLEO	$e^+e^- \rightarrow D^+D^-$
seen	PAKHLOVA	08	BELL $e^+e^- \rightarrow D^+\bar{D}^-\gamma$
••• We do not use the following data for averages, fits, limits, etc. •••			
not seen	AUBERT	09M	BABR $e^+e^- \rightarrow D^+D^-\gamma$

$\Gamma(D^*(2007)^0\bar{D}^0 + \text{c.c.})/\Gamma_{\text{total}}$	$\Gamma_6/\Gamma$		
VALUE	DOCUMENT ID	TECN	COMMENT
seen	AUBERT	09M	BABR $e^+e^- \rightarrow D^{*0}\bar{D}^0\gamma$
seen	CRONIN-HEN..09	CLEO	$e^+e^- \rightarrow D^{*0}\bar{D}^0$

$\Gamma(D^*(2010)^+D^- + \text{c.c.})/\Gamma_{\text{total}}$	$\Gamma_7/\Gamma$		
VALUE	DOCUMENT ID	TECN	COMMENT
seen	AUBERT	09M	BABR $e^+e^- \rightarrow D^{*+}D^-\gamma$
seen	CRONIN-HEN..09	CLEO	$e^+e^- \rightarrow D^{*+}D^-$
seen	PAKHLOVA	07	BELL $e^+e^- \rightarrow D^{*+}D^-\gamma$

$\Gamma(D^*\bar{D} + \text{c.c.})/\Gamma(D^*\bar{D}^*)$	$\Gamma_5/\Gamma_8$		
VALUE	DOCUMENT ID	TECN	COMMENT
<b><math>0.34 \pm 0.14 \pm 0.05</math></b>	AUBERT	09M	BABR $e^+e^- \rightarrow \gamma D^{(*)}\bar{D}^{(*)}$

$\Gamma(D^*(2007)^0\bar{D}^*(2007)^0)/\Gamma_{\text{total}}$	$\Gamma_9/\Gamma$		
VALUE	DOCUMENT ID	TECN	COMMENT
seen	AUBERT	09M	BABR $e^+e^- \rightarrow D^{*0}\bar{D}^{*0}\gamma$
seen	CRONIN-HEN..09	CLEO	$e^+e^- \rightarrow D^{*0}\bar{D}^{*0}$

$\Gamma(D^*(2010)^+D^*(2010)^-)/\Gamma_{\text{total}}$	$\Gamma_{10}/\Gamma$		
VALUE	DOCUMENT ID	TECN	COMMENT
seen	AUBERT	09M	BABR $e^+e^- \rightarrow D^{*+}D^{*-}\gamma$
seen	CRONIN-HEN..09	CLEO	$e^+e^- \rightarrow D^{*+}D^{*-}$
seen	PAKHLOVA	07	BELL $e^+e^- \rightarrow D^{*+}D^{*-}\gamma$

$\Gamma(D^0D^-\pi^+ + \text{c.c. (excl. } D^*(2007)^0\bar{D}^0 + \text{c.c., } D^*(2010)^+D^- + \text{c.c.})/$	$\Gamma_{11}/\Gamma$			
total	VALUE	DOCUMENT ID	TECN	COMMENT
not seen		PAKHLOVA	08A	BELL $e^+e^- \rightarrow D^0D^-\pi^+\gamma$

$\Gamma(D\bar{D}^*\pi + \text{c.c. (excl. } D^*\bar{D}^*)/$	$\Gamma_{12}/\Gamma$			
total	VALUE	DOCUMENT ID	TECN	COMMENT
seen		CRONIN-HEN..09	CLEO	$e^+e^- \rightarrow D\bar{D}^*\pi$

$\Gamma(D^0D^*\pi^+ + \text{c.c. (excl. } D^*(2010)^+D^*(2010)^-)/$	$\Gamma_{13}/\Gamma$			
total	VALUE	DOCUMENT ID	TECN	COMMENT
not seen		PAKHLOVA	09	BELL $e^+e^- \rightarrow D^0D^*\pi^+\gamma$

$\Gamma(D_s^+D_s^-)/\Gamma_{\text{total}}$	$\Gamma_{14}/\Gamma$			
VALUE	DOCUMENT ID	TECN	COMMENT	
not seen		PAKHLOVA	11	BELL $e^+e^- \rightarrow D_s^+D_s^-\gamma$
not seen		DEL-AMO-SA..10N	BABR	$e^+e^- \rightarrow D_s^+D_s^-\gamma$
not seen		CRONIN-HEN..09	CLEO	$e^+e^- \rightarrow D_s^+D_s^-$

$\Gamma(D_s^{*+}D_s^- + \text{c.c.})/\Gamma_{\text{total}}$	$\Gamma_{15}/\Gamma$			
VALUE	DOCUMENT ID	TECN	COMMENT	
seen		PAKHLOVA	11	BELL $e^+e^- \rightarrow D_s^{*+}D_s^-\gamma$
seen		DEL-AMO-SA..10N	BABR	$e^+e^- \rightarrow D_s^{*+}D_s^-\gamma$
seen		CRONIN-HEN..09	CLEO	$e^+e^- \rightarrow D_s^{*+}D_s^-$

$\Gamma(J/\psi\pi^+\pi^-)/\Gamma_{\text{total}}$	$\Gamma_{16}/\Gamma$			
VALUE (units $10^{-3}$ )	CL%	DOCUMENT ID	TECN	COMMENT
$< 3$	90	COAN	06	CLEO 4.12–4.2 $e^+e^- \rightarrow$ hadrons

$\Gamma(J/\psi\pi^0\pi^0)/\Gamma_{\text{total}}$	$\Gamma_{17}/\Gamma$			
VALUE (units $10^{-3}$ )	CL%	DOCUMENT ID	TECN	COMMENT
$< 3$	90	COAN	06	CLEO 4.12–4.2 $e^+e^- \rightarrow$ hadrons

$\Gamma(J/\psi K^+K^-)/\Gamma_{\text{total}}$	$\Gamma_{18}/\Gamma$			
VALUE (units $10^{-3}$ )	CL%	DOCUMENT ID	TECN	COMMENT
$< 2$	90	COAN	06	CLEO 4.12–4.2 $e^+e^- \rightarrow$ hadrons

$\Gamma(J/\psi\eta)/\Gamma_{\text{total}}$	$\Gamma_{19}/\Gamma$			
VALUE (units $10^{-3}$ )	CL%	DOCUMENT ID	TECN	COMMENT
$< 8$	90	COAN	06	CLEO 4.12–4.2 $e^+e^- \rightarrow$ hadrons

$\Gamma(J/\psi\pi^0)/\Gamma_{\text{total}}$	$\Gamma_{20}/\Gamma$			
VALUE (units $10^{-3}$ )	CL%	DOCUMENT ID	TECN	COMMENT
$< 1$	90	COAN	06	CLEO 4.12–4.2 $e^+e^- \rightarrow$ hadrons

See key on page 457

# Meson Particle Listings

## $\psi(4160)$ , $X(4160)$ , $X(4250)^\pm$

$\Gamma(J/\psi\eta)/\Gamma_{\text{total}}$					$\Gamma_{21}/\Gamma$
VALUE (units $10^{-3}$ )	CL%	DOCUMENT ID	TECN	COMMENT	
<5	90	COAN	06	CLEO 4.12-4.2 $e^+e^- \rightarrow$ hadrons	
$\Gamma(J/\psi\pi^+\pi^-\pi^0)/\Gamma_{\text{total}}$					$\Gamma_{22}/\Gamma$
<1	90	COAN	06	CLEO 4.12-4.2 $e^+e^- \rightarrow$ hadrons	
$\Gamma(\psi(2S)\pi^+\pi^-)/\Gamma_{\text{total}}$					$\Gamma_{23}/\Gamma$
<4	90	COAN	06	CLEO 4.12-4.2 $e^+e^- \rightarrow$ hadrons	
$\Gamma(\chi_{c1}\gamma)/\Gamma_{\text{total}}$					$\Gamma_{24}/\Gamma$
<7	90	COAN	06	CLEO 4.12-4.2 $e^+e^- \rightarrow$ hadrons	
$\Gamma(\chi_{c2}\gamma)/\Gamma_{\text{total}}$					$\Gamma_{25}/\Gamma$
<13	90	COAN	06	CLEO 4.12-4.2 $e^+e^- \rightarrow$ hadrons	
$\Gamma(\chi_{c1}\pi^+\pi^-\pi^0)/\Gamma_{\text{total}}$					$\Gamma_{26}/\Gamma$
<2	90	COAN	06	CLEO 4.12-4.2 $e^+e^- \rightarrow$ hadrons	
$\Gamma(\chi_{c2}\pi^+\pi^-\pi^0)/\Gamma_{\text{total}}$					$\Gamma_{27}/\Gamma$
<8	90	COAN	06	CLEO 4.12-4.2 $e^+e^- \rightarrow$ hadrons	
$\Gamma(h_c(1P)\pi^+\pi^-)/\Gamma_{\text{total}}$					$\Gamma_{28}/\Gamma$
<5	90	13 PEDLAR	11	CLEO $e^+e^- \rightarrow h_c(1P)\pi^+\pi^-$	
<sup>13</sup> At $\sqrt{s} = 4170$ MeV, PEDLAR 11 measures $\sigma(e^+e^- \rightarrow h_c(1P)\pi^+\pi^-) = 15.6 \pm 2.3 \pm 1.9 \pm 3.0$ pb, where the errors are statistical, systematic, and due to uncertainty in $B(\psi(2S) \rightarrow \pi^0 h_c(1P))$ , respectively.					
$\Gamma(h_c(1P)\pi^0\pi^0)/\Gamma_{\text{total}}$					$\Gamma_{29}/\Gamma$
<2	90	14 PEDLAR	11	CLEO $e^+e^- \rightarrow h_c(1P)\pi^0\pi^0$	
<sup>14</sup> At $\sqrt{s} = 4170$ MeV, PEDLAR 11 measures $\sigma(e^+e^- \rightarrow h_c(1P)\pi^0\pi^0) = 3.0 \pm 3.3 \pm 1.1 \pm 0.6$ pb, where the errors are statistical, systematic, and due to uncertainty in $B(\psi(2S) \rightarrow \pi^0 h_c(1P))$ , respectively.					
$\Gamma(h_c(1P)\eta)/\Gamma_{\text{total}}$					$\Gamma_{30}/\Gamma$
<2	90	15 PEDLAR	11	CLEO $e^+e^- \rightarrow h_c(1P)\eta$	
<sup>15</sup> At $\sqrt{s} = 4170$ MeV, PEDLAR 11 measures $\sigma(e^+e^- \rightarrow h_c(1P)\eta) = 4.7 \pm 1.7 \pm 1.0 \pm 0.9$ pb, where the errors are statistical, systematic, and due to uncertainty in $B(\psi(2S) \rightarrow \pi^0 h_c(1P))$ , respectively.					
$\Gamma(h_c(1P)\pi^0)/\Gamma_{\text{total}}$					$\Gamma_{31}/\Gamma$
<0.4	90	16 PEDLAR	11	CLEO $e^+e^- \rightarrow h_c(1P)\pi^0$	
<sup>16</sup> At $\sqrt{s} = 4170$ MeV, PEDLAR 11 measures $\sigma(e^+e^- \rightarrow h_c(1P)\pi^0) = -0.7 \pm 1.8 \pm 0.7 \pm 0.1$ pb, where the errors are statistical, systematic, and due to uncertainty in $B(\psi(2S) \rightarrow \pi^0 h_c(1P))$ , respectively.					
$\Gamma(\phi\pi^+\pi^-)/\Gamma_{\text{total}}$					$\Gamma_{32}/\Gamma$
<2	90	COAN	06	CLEO 4.12-4.2 $e^+e^- \rightarrow$ hadrons	

### $\psi(4160)$ REFERENCES

PAKHOVA	11	PR D83 011101	G. Pakhlova et al.	(BELLE Collab.)
PEDLAR	11	PRL 107 041803	T. Pedlar et al.	(CLEO Collab.)
DEL-AMO-SA...	10N	PR D82 052004	P. del Amo Sanchez et al.	(BABAR Collab.)
MO	10	PR D82 077501	X.H. Mo, C.Z. Yuan, P. Wang	(BHEP)
AUBERT	09M	PR D79 092001	B. Aubert et al.	(BABAR Collab.)
CRONIN-HEN...	09	PR D80 072001	D. Cronin-Hennessy et al.	(CLEO Collab.)
PAKHOVA	09	PR D80 091101R	G. Pakhlova et al.	(BELLE Collab.)
ABLIKIM	08D	PL B660 315	M. Ablikim et al.	(BES Collab.)
PAKHOVA	08	PR D77 011103R	G. Pakhlova et al.	(BELLE Collab.)
PAKHOVA	08A	PRL 100 062001	G. Pakhlova et al.	(BELLE Collab.)
PAKHOVA	07	PRL 98 092001	G. Pakhlova et al.	(BELLE Collab.)
COAN	06	PRL 96 162003	T.E. Coan et al.	(CLEO Collab.)
SETH	05A	PR D72 017501	K.K. Seth	
BAI	02C	PRL 88 101802	J.Z. Bai et al.	(BES Collab.)
BAI	00	PRL 84 594	J.Z. Bai et al.	(BES Collab.)
OSTERHELD	86	SLAC-PUB-4160	A. Osterheld et al.	(SLAC Crystal Ball Collab.)
BRANDELK	78C	PL 76B 361	R. Brandelik et al.	(DASP Collab.)

## $X(4160)$

$$I^G(J^{PC}) = ?^?(?^{??})$$

OMITTED FROM SUMMARY TABLE

Seen by PAKHLOV 08 in  $e^+e^- \rightarrow J/\psi X$ ,  $X \rightarrow D^*\bar{D}^*$

### $X(4160)$ MASS

VALUE (MeV)	EVTS	DOCUMENT ID	TECN	COMMENT
$4156^{+25}_{-20} \pm 15$	24	PAKHOV 08	BELL	$e^+e^- \rightarrow J/\psi X$

### $X(4160)$ WIDTH

VALUE (MeV)	EVTS	DOCUMENT ID	TECN	COMMENT
$139^{+111}_{-61} \pm 21$	24	PAKHOV 08	BELL	$e^+e^- \rightarrow J/\psi X$

### $X(4160)$ DECAY MODES

Mode	Fraction ( $\Gamma_i/\Gamma$ )
$\Gamma_1$ $D\bar{D}$	not seen
$\Gamma_2$ $D^*\bar{D} + \text{c.c.}$	not seen
$\Gamma_3$ $D^*\bar{D}^*$	seen

### $X(4160)$ BRANCHING RATIOS

$\Gamma(D\bar{D})/\Gamma(D^*\bar{D}^*)$					$\Gamma_1/\Gamma_3$
VALUE	CL%	DOCUMENT ID	TECN	COMMENT	
<0.09	90	PAKHOV 08	BELL	$e^+e^- \rightarrow J/\psi X$	
$\Gamma(D^*\bar{D} + \text{c.c.})/\Gamma(D^*\bar{D}^*)$					$\Gamma_2/\Gamma_3$
VALUE	CL%	DOCUMENT ID	TECN	COMMENT	
<0.22	90	PAKHOV 08	BELL	$e^+e^- \rightarrow J/\psi X$	

### $X(4160)$ REFERENCES

PAKHOV	08	PRL 100 202001	P. Pakhlov et al.	(BELLE Collab.)
--------	----	----------------	-------------------	-----------------

## $X(4250)^\pm$

$$I(J^P) = ?^?(?)$$

OMITTED FROM SUMMARY TABLE

Observed by MIZUK 08 in the  $\pi^+\chi_{c1}(1P)$  invariant mass distribution in  $\bar{B}^0 \rightarrow K^-\pi^+\chi_{c1}(1P)$  decays. Not seen by LEES 12B in this same mode after accounting for  $K\pi$  resonant mass and angular structure.

### $X(4250)^\pm$ MASS

VALUE (MeV)	DOCUMENT ID	TECN	COMMENT
$4248^{+44+180}_{-29-35}$	<sup>1</sup> MIZUK 08	BELL	$\bar{B}^0 \rightarrow K^-\pi^+\chi_{c1}(1P)$

<sup>1</sup> From a Dalitz plot analysis with two Breit-Wigner amplitudes.

### $X(4250)^\pm$ WIDTH

VALUE (MeV)	DOCUMENT ID	TECN	COMMENT
$177^{+54+316}_{-39-61}$	<sup>2</sup> MIZUK 08	BELL	$\bar{B}^0 \rightarrow K^-\pi^+\chi_{c1}(1P)$

<sup>2</sup> From a Dalitz plot analysis with two Breit-Wigner amplitudes.

### $X(4250)^\pm$ DECAY MODES

Mode	Fraction ( $\Gamma_i/\Gamma$ )
$\Gamma_1$ $\pi^+\chi_{c1}(1P)$	seen

### $X(4250)^\pm$ BRANCHING RATIOS

$\Gamma(\pi^+\chi_{c1}(1P))/\Gamma_{\text{total}}$					$\Gamma_1/\Gamma$
VALUE	DOCUMENT ID	TECN	COMMENT		
seen	<sup>3</sup> MIZUK 08	BELL	$\bar{B}^0 \rightarrow K^-\pi^+\chi_{c1}(1P)$		
not seen	<sup>4</sup> LEES 12B	BABR	$B \rightarrow K\pi\chi_{c1}(1P)$		

<sup>3</sup> With a product branching fraction measurement of  $B(\bar{B}^0 \rightarrow K^-\chi_{c1}(4250)^+) \times B(X(4250)^+ \rightarrow \pi^+\chi_{c1}(1P)) = (4.0^{+2.3+19.7}_{-0.9-0.5}) \times 10^{-5}$ .

<sup>4</sup> With a product branching fraction limit of  $B(\bar{B}^0 \rightarrow X(4250)^+K^-) \times B(X(4250)^+ \rightarrow \chi_{c1}\pi^+) < 4.0 \times 10^{-5}$  at 90% CL.

## Meson Particle Listings

X(4250)<sup>±</sup>, X(4260)X(4250)<sup>±</sup> REFERENCES

LEES	12B	PR D85 052003	J.P. Lees et al.	(BABAR Collab.)
MIZUK	06	PR D78 072004	R. Mizuk et al.	(BELLE Collab.)

## X(4260)

$$J^G(JPC) = ?^?(1^{--})$$

Seen in radiative return from  $e^+e^-$  collisions at  $\sqrt{s} = 9.54\text{--}10.58$  GeV by AUBERT,B 05i, HE 06B, and YUAN 07, and in  $e^+e^-$  collisions at  $\sqrt{s} \approx 4.26$  GeV by COAN 06. Possibly seen by AUBERT 06 in  $B^- \rightarrow K^- \pi^+ \pi^- J/\psi$ . See also the mini-review under the X(3872). (See the index for the page number.)

## X(4260) MASS

VALUE (MeV)	EVTS	DOCUMENT ID	TECN	COMMENT
<b>4263<sup>+8</sup><sub>-9</sub> OUR AVERAGE</b>		Error includes scale factor of 1.1.		
4247 <sup>+12</sup> <sub>-32</sub>		1 YUAN	07	BELL 10.58 $e^+e^- \rightarrow \gamma \pi^+ \pi^- J/\psi$
4284 <sup>+17</sup> <sub>-16</sub> ± 4	13.6	HE	06B	CLEO 9.4–10.6 $e^+e^- \rightarrow \gamma \pi^+ \pi^- J/\psi$
4259 ± 8 <sup>+2</sup> <sub>-6</sub>	125	2 AUBERT,B	05i	BABR 10.58 $e^+e^- \rightarrow \gamma \pi^+ \pi^- J/\psi$
		1	From a two-resonance fit.	
		2	From a single-resonance fit. Two interfering resonances are not excluded.	

## X(4260) WIDTH

VALUE (MeV)	EVTS	DOCUMENT ID	TECN	COMMENT
<b>95 ± 14 OUR AVERAGE</b>				
108 ± 19 ± 10		3 YUAN	07	BELL 10.58 $e^+e^- \rightarrow \gamma \pi^+ \pi^- J/\psi$
73 <sup>+39</sup> <sub>-25</sub> ± 5	13.6	HE	06B	CLEO 9.4–10.6 $e^+e^- \rightarrow \gamma \pi^+ \pi^- J/\psi$
88 ± 23 <sup>+6</sup> <sub>-4</sub>	125	4 AUBERT,B	05i	BABR 10.58 $e^+e^- \rightarrow \gamma \pi^+ \pi^- J/\psi$
		3	From a two-resonance fit.	
		4	From a single-resonance fit. Two interfering resonances are not excluded.	

## X(4260) DECAY MODES

Mode	Fraction ( $\Gamma_i/\Gamma$ )
$\Gamma_1$ $e^+e^-$	
$\Gamma_2$ $J/\psi \pi^+ \pi^-$	seen
$\Gamma_3$ $J/\psi \pi^0 \pi^0$	seen
$\Gamma_4$ $J/\psi K^+ K^-$	seen
$\Gamma_5$ $J/\psi \eta$	not seen
$\Gamma_6$ $J/\psi \pi^0$	not seen
$\Gamma_7$ $J/\psi \eta'$	not seen
$\Gamma_8$ $J/\psi \pi^+ \pi^- \pi^0$	not seen
$\Gamma_9$ $J/\psi \eta \eta$	not seen
$\Gamma_{10}$ $\psi(2S) \pi^+ \pi^-$	not seen
$\Gamma_{11}$ $\psi(2S) \eta$	not seen
$\Gamma_{12}$ $\chi_{c0} \omega$	not seen
$\Gamma_{13}$ $\chi_{c1} \gamma$	not seen
$\Gamma_{14}$ $\chi_{c2} \gamma$	not seen
$\Gamma_{15}$ $\chi_{c1} \pi^+ \pi^- \pi^0$	not seen
$\Gamma_{16}$ $\chi_{c2} \pi^+ \pi^- \pi^0$	not seen
$\Gamma_{17}$ $h_c(1P) \pi^+ \pi^-$	not seen
$\Gamma_{18}$ $\phi \pi^+ \pi^-$	not seen
$\Gamma_{19}$ $\phi f_0(980) \rightarrow \phi \pi^+ \pi^-$	not seen
$\Gamma_{20}$ $D \bar{D}$	not seen
$\Gamma_{21}$ $D^0 \bar{D}^0$	not seen
$\Gamma_{22}$ $D^+ D^-$	not seen
$\Gamma_{23}$ $D^* \bar{D} + c.c.$	not seen
$\Gamma_{24}$ $D^*(2007)^0 \bar{D}^0 + c.c.$	not seen
$\Gamma_{25}$ $D^*(2010)^+ D^- + c.c.$	not seen
$\Gamma_{26}$ $D^* \bar{D}^*$	not seen
$\Gamma_{27}$ $D^*(2007)^0 \bar{D}^*(2007)^0$	not seen
$\Gamma_{28}$ $D^*(2010)^+ D^*(2010)^-$	not seen
$\Gamma_{29}$ $D \bar{D} \pi + c.c.$	
$\Gamma_{30}$ $D^0 D^- \pi^+ + c.c.$ (excl. $D^*(2007)^0 \bar{D}^{*0} + c.c.$ , $D^*(2010)^+ D^- + c.c.$ )	not seen
$\Gamma_{31}$ $D \bar{D} \pi + c.c.$ (excl. $D^* \bar{D}^*$ )	not seen
$\Gamma_{32}$ $D^0 D^{*-} \pi^+ + c.c.$ (excl. $D^*(2010)^+ D^*(2010)^-$ )	not seen
$\Gamma_{33}$ $D^0 D^*(2010)^- \pi^+ + c.c.$	not seen

$\Gamma_{34}$ $D^* \bar{D}^* \pi$	not seen
$\Gamma_{35}$ $D_s^+ D_s^-$	not seen
$\Gamma_{36}$ $D_s^{*+} D_s^{*-} + c.c.$	not seen
$\Gamma_{37}$ $D_s^{*+} D_s^{*-}$	not seen
$\Gamma_{38}$ $\rho \bar{\rho}$	not seen
$\Gamma_{39}$ $K_S^0 K^\pm \pi^\mp$	not seen
$\Gamma_{40}$ $K^+ K^- \pi^0$	not seen

X(4260)  $\Gamma(i)\Gamma(e^+e^-)/\Gamma(\text{total})$ 

$\Gamma(J/\psi \pi^+ \pi^-) \times \Gamma(e^+e^-)/\Gamma_{\text{total}}$	$\Gamma_2 \Gamma_1/\Gamma$			
VALUE (eV)	EVTS	DOCUMENT ID	TECN	COMMENT
<b>5.9<sup>+1.2</sup><sub>-0.9</sub> OUR AVERAGE</b>				
6.0 ± 1.2 <sup>+4.7</sup> <sub>-0.5</sub>		5 YUAN	07	BELL 10.58 $e^+e^- \rightarrow \gamma \pi^+ \pi^- J/\psi$
8.9 <sup>+3.9</sup> <sub>-3.1</sub> ± 1.8	8.1	HE	06B	CLEO 9.4–10.6 $e^+e^- \rightarrow \gamma \pi^+ \pi^- J/\psi$
5.5 ± 1.0 <sup>+0.8</sup> <sub>-0.7</sub>	125	6 AUBERT,B	05i	BABR 10.58 $e^+e^- \rightarrow \gamma \pi^+ \pi^- J/\psi$
• • • We do not use the following data for averages, fits, limits, etc. • • •				
20.6 ± 2.3 <sup>+9.1</sup> <sub>-1.7</sub>		7 YUAN	07	BELL 10.58 $e^+e^- \rightarrow \gamma \pi^+ \pi^- J/\psi$
		5	Solution I of two equivalent solutions in a fit using two interfering resonances.	
		6	From a single-resonance fit. Two interfering resonances are not excluded.	
		7	Solution II of two equivalent solutions in a fit using two interfering resonances.	

 $\Gamma(J/\psi K^+ K^-) \times \Gamma(e^+e^-)/\Gamma_{\text{total}}$   $\Gamma_4 \Gamma_1/\Gamma$ 

VALUE (eV)	CL%	DOCUMENT ID	TECN	COMMENT
• • • We do not use the following data for averages, fits, limits, etc. • • •				
<1.2	90	8 YUAN	08	BELL $e^+e^- \rightarrow \gamma K^+ K^- J/\psi$
8 From a fit of the broad $K^+ K^- J/\psi$ enhancement including a coherent X(4260) amplitude with mass and width from YUAN 07.				

 $\Gamma(\psi(2S) \pi^+ \pi^-) \times \Gamma(e^+e^-)/\Gamma_{\text{total}}$   $\Gamma_{10} \Gamma_1/\Gamma$ 

VALUE (eV)	CL%	DOCUMENT ID	TECN	COMMENT
• • • We do not use the following data for averages, fits, limits, etc. • • •				
<4.3	90	9 LIU	08H	RVUE 10.58 $e^+e^- \rightarrow \psi(2S) \pi^+ \pi^- \gamma$
7.4 ± 2.1 <sup>+2.1</sup> <sub>-1.7</sub>		10 LIU	08H	RVUE 10.58 $e^+e^- \rightarrow \psi(2S) \pi^+ \pi^- \gamma$
9 For constructive interference with the X(4360) in a combined fit of AUBERT 07s and WANG 07d data with three resonances.				
10 For destructive interference with the X(4360) in a combined fit of AUBERT 07s and WANG 07d data with three resonances.				

 $\Gamma(\phi \pi^+ \pi^-) \times \Gamma(e^+e^-)/\Gamma_{\text{total}}$   $\Gamma_{18} \Gamma_1/\Gamma$ 

VALUE (eV)	CL%	DOCUMENT ID	TECN	COMMENT
<0.4	90	AUBERT,BE	06d	BABR 10.6 $e^+e^- \rightarrow K^+ K^- \pi^+ \pi^- \gamma$

 $\Gamma(\phi f_0(980) \rightarrow \phi \pi^+ \pi^-) \times \Gamma(e^+e^-)/\Gamma_{\text{total}}$   $\Gamma_{19} \Gamma_1/\Gamma$ 

VALUE (eV)	CL%	DOCUMENT ID	TECN	COMMENT
<0.29	90	11 AUBERT	07AK	BABR 10.6 $e^+e^- \rightarrow \pi^+ \pi^- K^+ K^- \gamma$
11 AUBERT 07AK reports $[\Gamma(X(4260) \rightarrow \phi f_0(980) \rightarrow \phi \pi^+ \pi^-) \times \Gamma(X(4260) \rightarrow e^+e^-)/\Gamma_{\text{total}}] \times [B(\phi(1020) \rightarrow K^+ K^-)] < 0.14$ eV which we divide by our best value $B(\phi(1020) \rightarrow K^+ K^-) = 48.9 \times 10^{-2}$ .				

 $\Gamma(K_S^0 K^\pm \pi^\mp) \times \Gamma(e^+e^-)/\Gamma_{\text{total}}$   $\Gamma_{39} \Gamma_1/\Gamma$ 

VALUE (eV)	CL%	DOCUMENT ID	TECN	COMMENT
<0.5	90	AUBERT	08s	BABR 10.6 $e^+e^- \rightarrow K_S^0 K^\pm \pi^\mp \gamma$

 $\Gamma(K^+ K^- \pi^0) \times \Gamma(e^+e^-)/\Gamma_{\text{total}}$   $\Gamma_{40} \Gamma_1/\Gamma$ 

VALUE (eV)	CL%	DOCUMENT ID	TECN	COMMENT
<0.6	90	AUBERT	08s	BABR 10.6 $e^+e^- \rightarrow K^+ K^- \pi^0 \gamma$

## X(4260) BRANCHING RATIOS

 $\Gamma(h_c(1P) \pi^+ \pi^-)/\Gamma(J/\psi \pi^+ \pi^-)$   $\Gamma_{17}/\Gamma_2$ 

VALUE	CL%	DOCUMENT ID	TECN	COMMENT
<1.0	90	12 PEDLAR	11	CLEO $e^+e^- \rightarrow h_c(1P) \pi^+ \pi^-$
12 At $\sqrt{s} = 4260$ MeV, PEDLAR 11 measures $\sigma(e^+e^- \rightarrow h_c(1P) \pi^+ \pi^-) = 32 \pm 17 \pm 6$ pb, where the errors are statistical, systematic, and due to uncertainty in $B(\psi(2S) \rightarrow \pi^0 h_c(1P))$ , respectively.				

 $\Gamma(D \bar{D})/\Gamma(J/\psi \pi^+ \pi^-)$   $\Gamma_{20}/\Gamma_2$ 

VALUE	CL%	DOCUMENT ID	TECN	COMMENT
<1.0	90	13 AUBERT	07BE	BABR $e^+e^- \rightarrow D \bar{D} \gamma$
• • • We do not use the following data for averages, fits, limits, etc. • • •				
<4.0	90	CRONIN-HEN..09	CLEO	$e^+e^-$
13 Using 4259 ± 10 MeV for the mass and 88 ± 24 MeV for the width of X(4260).				



# Meson Particle Listings

## X(4260)

$\Gamma(D^0 \bar{D}^0)/\Gamma_{\text{total}}$			$\Gamma_{21}/\Gamma$
VALUE	DOCUMENT ID	TECN COMMENT	
not seen	CRONIN-HEN..09	CLEO $e^+e^- \rightarrow D^0 \bar{D}^0$	
••• We do not use the following data for averages, fits, limits, etc. •••			
not seen	AUBERT 09M	BABR $e^+e^- \rightarrow D^0 \bar{D}^0 \gamma$	
not seen	PAKHLOVA 08	BELL $e^+e^- \rightarrow D^0 \bar{D}^0 \gamma$	
$\Gamma(D^+ D^-)/\Gamma_{\text{total}}$			$\Gamma_{22}/\Gamma$
VALUE	DOCUMENT ID	TECN COMMENT	
not seen	CRONIN-HEN..09	CLEO $e^+e^- \rightarrow D^+ D^-$	
••• We do not use the following data for averages, fits, limits, etc. •••			
not seen	AUBERT 09M	BABR $e^+e^- \rightarrow D^+ D^- \gamma$	
not seen	PAKHLOVA 08	BELL $e^+e^- \rightarrow D^+ D^- \gamma$	
$\Gamma(D^* \bar{D}^* + c.c.)/\Gamma(J/\psi \pi^+ \pi^-)$			$\Gamma_{23}/\Gamma_2$
VALUE	CL%	DOCUMENT ID	TECN COMMENT
<34	90	AUBERT 09M	BABR $e^+e^- \rightarrow \gamma D^* \bar{D}^*$
••• We do not use the following data for averages, fits, limits, etc. •••			
<45	90	CRONIN-HEN..09	CLEO $e^+e^-$
$\Gamma(D^*(2007)^0 \bar{D}^0 + c.c.)/\Gamma_{\text{total}}$			$\Gamma_{24}/\Gamma$
VALUE	DOCUMENT ID	TECN COMMENT	
not seen	CRONIN-HEN..09	CLEO $e^+e^- \rightarrow D^{*0} \bar{D}^0$	
••• We do not use the following data for averages, fits, limits, etc. •••			
not seen	AUBERT 09M	BABR $e^+e^- \rightarrow D^{*0} \bar{D}^0 \gamma$	
$\Gamma(D^*(2010)^+ D^- + c.c.)/\Gamma_{\text{total}}$			$\Gamma_{25}/\Gamma$
VALUE	DOCUMENT ID	TECN COMMENT	
not seen	CRONIN-HEN..09	CLEO $e^+e^- \rightarrow D^{*+} D^-$	
not seen	PAKHLOVA 07	BELL $e^+e^- \rightarrow D^{*+} D^- \gamma$	
••• We do not use the following data for averages, fits, limits, etc. •••			
not seen	AUBERT 09M	BABR $e^+e^- \rightarrow D^{*+} D^- \gamma$	
$\Gamma(D^* \bar{D}^*)/\Gamma(J/\psi \pi^+ \pi^-)$			$\Gamma_{26}/\Gamma_2$
VALUE	CL%	DOCUMENT ID	TECN COMMENT
<11	90	CRONIN-HEN..09	CLEO $e^+e^-$
••• We do not use the following data for averages, fits, limits, etc. •••			
<40	90	AUBERT 09M	BABR $e^+e^- \rightarrow \gamma D^* \bar{D}^*$
$\Gamma(D^*(2007)^0 \bar{D}^*(2007)^0)/\Gamma_{\text{total}}$			$\Gamma_{27}/\Gamma$
VALUE	DOCUMENT ID	TECN COMMENT	
not seen	CRONIN-HEN..09	CLEO $e^+e^- \rightarrow D^{*0} \bar{D}^{*0}$	
••• We do not use the following data for averages, fits, limits, etc. •••			
not seen	AUBERT 09M	BABR $e^+e^- \rightarrow D^{*0} \bar{D}^{*0} \gamma$	
$\Gamma(D^*(2010)^+ D^*(2010)^-)/\Gamma_{\text{total}}$			$\Gamma_{28}/\Gamma$
VALUE	DOCUMENT ID	TECN COMMENT	
not seen	CRONIN-HEN..09	CLEO $e^+e^- \rightarrow D^{*+} D^{*-}$	
not seen	PAKHLOVA 07	BELL $e^+e^- \rightarrow D^{*+} D^{*-} \gamma$	
••• We do not use the following data for averages, fits, limits, etc. •••			
not seen	AUBERT 09M	BABR $e^+e^- \rightarrow D^{*+} D^{*-} \gamma$	
$\Gamma(D^0 D^- \pi^+ + c.c. (\text{excl. } D^*(2007)^0 \bar{D}^{*0} + c.c., D^*(2010)^+ D^- + c.c.))/\Gamma_{\text{total}}$			$\Gamma_{30}/\Gamma$
VALUE	DOCUMENT ID	TECN COMMENT	
not seen	PAKHLOVA 08A	BELL $10.6 e^+ e^- \rightarrow D^0 D^- \pi^+ \gamma$	
$\Gamma(D \bar{D}^* \pi + c.c. (\text{excl. } D^* \bar{D}^*))/\Gamma_{\text{total}}$			$\Gamma_{31}/\Gamma$
VALUE	DOCUMENT ID	TECN COMMENT	
not seen	CRONIN-HEN..09	CLEO $e^+e^- \rightarrow D^* \bar{D}^* \pi$	
$\Gamma(D \bar{D}^* \pi + c.c. (\text{excl. } D^* \bar{D}^*))/\Gamma(J/\psi \pi^+ \pi^-)$			$\Gamma_{31}/\Gamma_2$
VALUE	CL%	DOCUMENT ID	TECN COMMENT
<15	90	CRONIN-HEN..09	CLEO $e^+e^-$
$\Gamma(D^0 D^{*-} \pi^+ + c.c. (\text{excl. } D^*(2010)^+ D^*(2010)^-))/\Gamma_{\text{total}}$			$\Gamma_{32}/\Gamma$
VALUE	DOCUMENT ID	TECN COMMENT	
not seen	PAKHLOVA 09	BELL $e^+e^- \rightarrow D^0 D^{*-} \pi^+ \gamma$	
$\Gamma(D^0 D^*(2010)^- \pi^+ + c.c.)/\Gamma(J/\psi \pi^+ \pi^-)$			$\Gamma_{33}/\Gamma_2$
VALUE	CL%	DOCUMENT ID	TECN COMMENT
<9	90	PAKHLOVA 09	BELL $e^+e^- \rightarrow D^0 D^{*-} \pi^+$
$\Gamma(D^0 D^*(2010)^- \pi^+ + c.c.)/\Gamma_{\text{total}} \times \Gamma(e^+e^-)/\Gamma_{\text{total}}$			$\Gamma_{33}/\Gamma \times \Gamma_1/\Gamma$
VALUE	CL%	DOCUMENT ID	TECN COMMENT
<0.42 $\times 10^{-6}$	90	14 PAKHLOVA 09	BELL $e^+e^- \rightarrow D^0 D^{*-} \pi^+$

<sup>14</sup> Using  $4263^{+8}_-9$  MeV for the mass of X(4260).

$\Gamma(D^* \bar{D}^* \pi)/\Gamma_{\text{total}}$			$\Gamma_{34}/\Gamma$
VALUE	DOCUMENT ID	TECN COMMENT	
not seen	CRONIN-HEN..09	CLEO $e^+e^- \rightarrow D^* \bar{D}^* \pi$	
$\Gamma(D^* \bar{D}^* \pi)/\Gamma(J/\psi \pi^+ \pi^-)$			$\Gamma_{34}/\Gamma_2$
VALUE	CL%	DOCUMENT ID	TECN COMMENT
<8.2	90	CRONIN-HEN..09	CLEO $e^+e^-$
$\Gamma(D^*_S D^-_S)/\Gamma_{\text{total}}$			$\Gamma_{35}/\Gamma$
VALUE	DOCUMENT ID	TECN COMMENT	
not seen	DEL-AMO-SA...10N	BABR $e^+e^- \rightarrow D^*_S D^-_S \gamma$	
not seen	CRONIN-HEN..09	CLEO $e^+e^- \rightarrow D^*_S D^-_S$	
••• We do not use the following data for averages, fits, limits, etc. •••			
not seen	PAKHLOVA 11	BELL $e^+e^- \rightarrow D^*_S D^-_S \gamma$	
$\Gamma(D^*_S D^-_S)/\Gamma(J/\psi \pi^+ \pi^-)$			$\Gamma_{35}/\Gamma_2$
VALUE	CL%	DOCUMENT ID	TECN COMMENT
<0.7	95	DEL-AMO-SA...10N	BABR $10.6 e^+ e^-$
••• We do not use the following data for averages, fits, limits, etc. •••			
<1.3	90	CRONIN-HEN..09	CLEO $e^+e^-$
$\Gamma(D^*_S D^-_S + c.c.)/\Gamma_{\text{total}}$			$\Gamma_{36}/\Gamma$
VALUE	DOCUMENT ID	TECN COMMENT	
not seen	DEL-AMO-SA...10N	BABR $e^+e^- \rightarrow D^*_S D^-_S \gamma$	
not seen	CRONIN-HEN..09	CLEO $e^+e^- \rightarrow D^*_S D^-_S$	
••• We do not use the following data for averages, fits, limits, etc. •••			
not seen	PAKHLOVA 11	BELL $e^+e^- \rightarrow D^*_S D^-_S \gamma$	
$\Gamma(D^*_S D^-_S + c.c.)/\Gamma(J/\psi \pi^+ \pi^-)$			$\Gamma_{36}/\Gamma_2$
VALUE	CL%	DOCUMENT ID	TECN COMMENT
< 0.8	90	CRONIN-HEN..09	CLEO $e^+e^-$
••• We do not use the following data for averages, fits, limits, etc. •••			
<44	95	DEL-AMO-SA...10N	BABR $10.6 e^+ e^-$
$\Gamma(D^*_S D^-_S)/\Gamma_{\text{total}}$			$\Gamma_{37}/\Gamma$
VALUE	DOCUMENT ID	TECN COMMENT	
not seen	CRONIN-HEN..09	CLEO $e^+e^- \rightarrow D^*_S D^-_S$	
••• We do not use the following data for averages, fits, limits, etc. •••			
not seen	PAKHLOVA 11	BELL $e^+e^- \rightarrow D^*_S D^-_S \gamma$	
not seen	DEL-AMO-SA...10N	BABR $e^+e^- \rightarrow D^*_S D^-_S \gamma$	
$\Gamma(D^*_S D^-_S)/\Gamma(J/\psi \pi^+ \pi^-)$			$\Gamma_{37}/\Gamma_2$
VALUE	CL%	DOCUMENT ID	TECN COMMENT
< 9.5	90	CRONIN-HEN..09	CLEO $e^+e^-$
••• We do not use the following data for averages, fits, limits, etc. •••			
<30	95	DEL-AMO-SA...10N	BABR $10.6 e^+ e^-$
$\Gamma(p \bar{p})/\Gamma(J/\psi \pi^+ \pi^-)$			$\Gamma_{38}/\Gamma_2$
VALUE	CL%	DOCUMENT ID	COMMENT
<0.13	90	15 AUBERT 06B	$e^+e^- \rightarrow p \bar{p} \gamma$

<sup>15</sup> Using  $4259 \pm 10$  MeV for the mass and  $88 \pm 24$  MeV for the width of X(4260).

### X(4260) REFERENCES

PAKHLOVA 11	PR D83 011101	G. Pakhlova et al.	(BELLE Collab.)
PEDLAR 11	PRL 107 041803	T. Pedlar et al.	(CLEO Collab.)
DEL-AMO-SA...10N	PR D82 052004	P. del Amo Sanchez et al.	(BABAR Collab.)
AUBERT 09M	PR D79 092001	B. Aubert et al.	(BABAR Collab.)
CRONIN-HEN...09	PR D80 072001	D. Cronin-Hennessy et al.	(CLEO Collab.)
PAKHLOVA 09	PR D80 091101R	G. Pakhlova et al.	(BELLE Collab.)
AUBERT 08S	PR D77 092002	B. Aubert et al.	(BABAR Collab.)
LIU 08H	PR D78 014032	Z.Q. Liu, X.S. Qin, C.Z. Yuan	
PAKHLOVA 08H	PR D77 011103R	G. Pakhlova et al.	(BELLE Collab.)
PAKHLOVA 08A	PRL 100 062001	G. Pakhlova et al.	(BELLE Collab.)
YUAN 08	PR D77 011105R	C.Z. Yuan et al.	(BELLE Collab.)
AUBERT 07AK	PR D76 012008	B. Aubert et al.	(BABAR Collab.)
AUBERT 07BE	PR D76 111105R	B. Aubert et al.	(BABAR Collab.)
AUBERT 07S	PRL 98 212001	B. Aubert et al.	(BABAR Collab.)
PAKHLOVA 07D	PRL 98 092001	G. Pakhlova et al.	(BELLE Collab.)
WANG 07F	PRL 99 142002	X.L. Wang et al.	(BELLE Collab.)
YUAN 07	PRL 99 182004	C.Z. Yuan et al.	(BELLE Collab.)
AUBERT 06	PR D73 011101R	B. Aubert et al.	(BABAR Collab.)
AUBERT 06B	PR D73 012005	B. Aubert et al.	(BABAR Collab.)
AUBERT,BE	PR D74 091103R	B. Aubert et al.	(BABAR Collab.)
COAN 06	PRL 96 162003	T.E. Coan et al.	(CLEO Collab.)
HE 06B	PR D74 091104R	Q. He et al.	(CLEO Collab.)
AUBERT,B	PRL 95 142001	B. Aubert et al.	(BABAR Collab.)

## Meson Particle Listings

X(4350), X(4360),  $\psi(4415)$ **X(4350)**

$$I^G(J^{PC}) = 0^+(?^{?+})$$

OMITTED FROM SUMMARY TABLE

Seen by SHEN 10 in the  $\gamma\gamma \rightarrow J/\psi\phi$ . Needs confirmation.**X(4350) MASS**

VALUE (MeV)	EVTS	DOCUMENT ID	TECN	COMMENT
$4350.6^{+4.6}_{-5.1} \pm 0.7$	$8.8^{+4.2}_{-3.2}$	<sup>1</sup> SHEN	10	BELL $10.6 e^+ e^- \rightarrow e^+ e^- J/\psi\phi$

<sup>1</sup> Statistical significance of 3.2  $\sigma$ .**X(4350) WIDTH**

VALUE (MeV)	EVTS	DOCUMENT ID	TECN	COMMENT
$13^{+18}_{-9} \pm 4$	$8.8^{+4.2}_{-3.2}$	<sup>2</sup> SHEN	10	BELL $10.6 e^+ e^- \rightarrow e^+ e^- J/\psi\phi$

<sup>2</sup> Statistical significance of 3.2  $\sigma$ .**X(4350) DECAY MODES**

Mode	Fraction ( $\Gamma_i/\Gamma$ )
$\Gamma_1$ $J/\psi\phi$	seen
$\Gamma_2$ $\gamma\gamma$	seen

**X(4350)  $\Gamma(i)\Gamma(\gamma\gamma)/\Gamma(\text{total})$** 

$\Gamma(\gamma\gamma) \times \Gamma(J/\psi\phi)/\Gamma_{\text{total}}$	EVTS	DOCUMENT ID	TECN	COMMENT	$\Gamma_2\Gamma_1/\Gamma$
$6.7^{+3.2}_{-2.4} \pm 1.1$	$8.8^{+4.2}_{-3.2}$	<sup>3</sup> SHEN	10	BELL $10.6 e^+ e^- \rightarrow e^+ e^- J/\psi\phi$	

• • • We do not use the following data for averages, fits, limits, etc. • • •

$1.5^{+0.7}_{-0.6} \pm 0.3$	$8.8^{+4.2}_{-3.2}$	<sup>4</sup> SHEN	10	BELL $10.6 e^+ e^- \rightarrow e^+ e^- J/\psi\phi$	
-----------------------------	---------------------	-------------------	----	--	--

<sup>3</sup> For  $J^P = 0^+$ . Statistical significance of 3.2  $\sigma$ .<sup>4</sup> For  $J^P = 2^+$ . Statistical significance of 3.2  $\sigma$ .**X(4350) BRANCHING RATIOS**

$\Gamma(J/\psi\phi)/\Gamma_{\text{total}}$	DOCUMENT ID	TECN	COMMENT	$\Gamma_1/\Gamma$
seen	<sup>5</sup> SHEN	10	BELL $10.6 e^+ e^- \rightarrow e^+ e^- J/\psi\phi$	

<sup>5</sup> Statistical significance of 3.2  $\sigma$ .

$\Gamma(\gamma\gamma)/\Gamma_{\text{total}}$	DOCUMENT ID	TECN	COMMENT	$\Gamma_2/\Gamma$
seen	<sup>6</sup> SHEN	10	BELL $10.6 e^+ e^- \rightarrow e^+ e^- J/\psi\phi$	

<sup>6</sup> Statistical significance of 3.2  $\sigma$ .**X(4350) REFERENCES**

SHEN 10 PRL 104 112004 C.P. Shen et al. (BELLE Collab.)

**X(4360)**

$$I^G(J^{PC}) = ?^?(1^{--})$$

Seen in radiative return from  $e^+e^-$  collisions at  $\sqrt{s} = 9.54\text{--}10.58$  GeV by AUBERT 07s and WANG 07D. See also the review under the X(3872) particle listings. (See the index for the page number.)**X(4360) MASS**

VALUE (MeV)	DOCUMENT ID	TECN	COMMENT
$4361 \pm 9 \pm 9$	<sup>1</sup> WANG	07D	BELL $10.58 e^+ e^- \rightarrow \gamma\pi^+\pi^-\psi(2S)$

• • • We do not use the following data for averages, fits, limits, etc. • • •

$4355^{+9}_{-10} \pm 9$	<sup>2</sup> LIU	08H	RVUE $10.58 e^+ e^- \rightarrow \psi(2S)\pi^+\pi^-\gamma$
-------------------------	------------------	-----	---

$4324 \pm 24$	<sup>3</sup> AUBERT	07s	BABR $10.58 e^+ e^- \rightarrow \gamma\pi^+\pi^-\psi(2S)$
---------------	---------------------	-----	---

<sup>1</sup> From a two-resonance fit.<sup>2</sup> From a combined fit of AUBERT 07s and WANG 07D data with two resonances.<sup>3</sup> From a single-resonance fit. Systematic errors not estimated.**X(4360) WIDTH**

VALUE (MeV)	DOCUMENT ID	TECN	COMMENT
$74 \pm 15 \pm 10$	<sup>4</sup> WANG	07D	BELL $10.58 e^+ e^- \rightarrow \gamma\pi^+\pi^-\psi(2S)$
$103^{+17}_{-15} \pm 11$	<sup>5</sup> LIU	08H	RVUE $10.58 e^+ e^- \rightarrow \psi(2S)\pi^+\pi^-\gamma$
$172 \pm 33$	<sup>6</sup> AUBERT	07s	BABR $10.58 e^+ e^- \rightarrow \gamma\pi^+\pi^-\psi(2S)$

<sup>4</sup> From a two-resonance fit.<sup>5</sup> From a combined fit of AUBERT 07s and WANG 07D data with two resonances.<sup>6</sup> From a single-resonance fit. Systematic errors not estimated.**X(4360) DECAY MODES**

Mode	Fraction ( $\Gamma_i/\Gamma$ )
$\Gamma_1$ $e^+e^-$	
$\Gamma_2$ $\psi(2S)\pi^+\pi^-$	seen
$\Gamma_3$ $D^0 D^{*-}\pi^+$	

**X(4360)  $\Gamma(i)\Gamma(e^+e^-)/\Gamma(\text{total})$** 

$\Gamma(\psi(2S)\pi^+\pi^-) \times \Gamma(e^+e^-)/\Gamma_{\text{total}}$	DOCUMENT ID	TECN	COMMENT	$\Gamma_2\Gamma_1/\Gamma$
$11.1^{+1.3}_{-1.2}$	<sup>7</sup> LIU	08H	RVUE $10.58 e^+ e^- \rightarrow \psi(2S)\pi^+\pi^-\gamma$	
$12.3 \pm 1.2$	<sup>8</sup> LIU	08H	RVUE $10.58 e^+ e^- \rightarrow \psi(2S)\pi^+\pi^-\gamma$	
$10.4 \pm 1.7 \pm 1.5$	<sup>9</sup> WANG	07D	BELL $10.58 e^+ e^- \rightarrow \gamma\pi^+\pi^-\psi(2S)$	
$11.8 \pm 1.8 \pm 1.4$	<sup>10</sup> WANG	07D	BELL $10.58 e^+ e^- \rightarrow \gamma\pi^+\pi^-\psi(2S)$	

• • • We do not use the following data for averages, fits, limits, etc. • • •

<sup>7</sup> Solution I in a combined fit of AUBERT 07s and WANG 07D data with two resonances.<sup>8</sup> Solution II in a combined fit of AUBERT 07s and WANG 07D data with two resonances.<sup>9</sup> Solution I of two equivalent solutions in a fit using two interfering resonances.<sup>10</sup> Solution II of two equivalent solutions in a fit using two interfering resonances.**X(4360) BRANCHING RATIOS**

$\Gamma(D^0 D^{*-}\pi^+)/\Gamma(\psi(2S)\pi^+\pi^-)$	CL%	DOCUMENT ID	TECN	COMMENT	$\Gamma_3/\Gamma_2$
$< 8$	90	PAKHOVA	09	BELL $e^+e^- \rightarrow X(4360) \rightarrow D^0 D^{*-}\pi^+$	

$\Gamma(D^0 D^{*-}\pi^+)/\Gamma_{\text{total}} \times \Gamma(e^+e^-)/\Gamma_{\text{total}}$	CL%	DOCUMENT ID	TECN	COMMENT	$\Gamma_3/\Gamma \times \Gamma_1/\Gamma$
$< 0.72 \times 10^{-6}$	90	<sup>11</sup> PAKHOVA	09	BELL $e^+e^- \rightarrow X(4360) \rightarrow D^0 D^{*-}\pi^+$	

<sup>11</sup> Using  $4355^{+9}_{-10} \pm 9$  MeV for the mass of X(4360).**X(4360) REFERENCES**PAKHOVA 09 PR D80 091101R G. Pakhlova et al. (BELLE Collab.)  
LIU 08H PR D78 014032 Z.Q. Liu, X.S. Qin, C.Z. Yuan  
AUBERT 07s PRL 98 212001 B. Aubert et al. (BABAR Collab.)  
WANG 07D PRL 99 142002 X.L. Wang et al. (BELLE Collab.) **$\psi(4415)$** 

$$I^G(J^{PC}) = 0^-(1^{--})$$

 **$\psi(4415)$  MASS**

VALUE (MeV)	DOCUMENT ID	TECN	COMMENT
$4415.1 \pm 7.9$	<sup>1</sup> ABLIKIM	08D	BES2 $e^+e^- \rightarrow \text{hadrons}$
$4412 \pm 15$	<sup>2</sup> MO	10	RVUE $e^+e^- \rightarrow \text{hadrons}$
$4411 \pm 7$	<sup>3</sup> PAKHOVA	08A	BELL $10.6 e^+ e^- \rightarrow D^0 D^{*-}\pi^+\gamma$
$4425 \pm 6$	<sup>4</sup> SETH	05A	RVUE $e^+e^- \rightarrow \text{hadrons}$
$4429 \pm 9$	<sup>5</sup> SETH	05A	RVUE $e^+e^- \rightarrow \text{hadrons}$
$4417 \pm 10$	BRANDELIK	78C	DASP $e^+e^-$
$4414 \pm 7$	SIEGRIST	76	MRK1 $e^+e^-$

• • • We do not use the following data for averages, fits, limits, etc. • • •

See key on page 457

Meson Particle Listings

$\psi(4415)$

- <sup>1</sup> Reanalysis of data presented in BAI 02c. From a global fit over the center-of-mass energy region 3.7–5.0 GeV covering the  $\psi(3770)$ ,  $\psi(4040)$ ,  $\psi(4160)$ , and  $\psi(4415)$  resonances. Phase angle fixed in the fit to  $\delta = (234 \pm 88)^\circ$ .
- <sup>2</sup> Reanalysis of data presented in BAI 00 and BAI 02c. From a global fit over the center-of-mass energy 3.8–4.8 GeV covering the  $\psi(4040)$ ,  $\psi(4160)$  and  $\psi(4415)$  resonances and including interference effects.
- <sup>3</sup> Systematic uncertainties not estimated.
- <sup>4</sup> From a fit to Crystal Ball (OSTERHELD 86) data.
- <sup>5</sup> From a fit to BES (BAI 02c) data.

$\psi(4415)$  WIDTH

VALUE (MeV)	DOCUMENT ID	TECN	COMMENT
<b>62 ± 20 OUR ESTIMATE</b>			
<b>71.5 ± 19.0</b>	6 ABLIKIM	08D BES2	$e^+e^- \rightarrow$ hadrons
• • • We do not use the following data for averages, fits, limits, etc. • • •			
118 ± 32	7 MO	10 RVUE	$e^+e^- \rightarrow$ hadrons
77 ± 20	8 PAKHLOVA	08A BELL	$10.6 e^+e^- \rightarrow D^0 D^- \pi^+ \gamma$
119 ± 16	9 SETH	05A RVUE	$e^+e^- \rightarrow$ hadrons
118 ± 35	10 SETH	05A RVUE	$e^+e^- \rightarrow$ hadrons
66 ± 15	BRANDELIK	78C DASP	$e^+e^-$
33 ± 10	SIEGRIST	76 MRK1	$e^+e^-$

- <sup>6</sup> Reanalysis of data presented in BAI 02c. From a global fit over the center-of-mass energy region 3.7–5.0 GeV covering the  $\psi(3770)$ ,  $\psi(4040)$ ,  $\psi(4160)$ , and  $\psi(4415)$  resonances. Phase angle fixed in the fit to  $\delta = (234 \pm 88)^\circ$ .
- <sup>7</sup> Reanalysis of data presented in BAI 00 and BAI 02c. From a global fit over the center-of-mass energy 3.8–4.8 GeV covering the  $\psi(4040)$ ,  $\psi(4160)$  and  $\psi(4415)$  resonances and including interference effects.
- <sup>8</sup> Systematic uncertainties not estimated.
- <sup>9</sup> From a fit to Crystal Ball (OSTERHELD 86) data.
- <sup>10</sup> From a fit to BES (BAI 02c) data.

$\psi(4415)$  DECAY MODES

Due to the complexity of the  $c\bar{c}$  threshold region, in this listing, “seen” (“not seen”) means that a cross section for the mode in question has been measured at effective  $\sqrt{s}$  near this particle’s central mass value, more (less) than  $2\sigma$  above zero, without regard to any peaking behavior in  $\sqrt{s}$  or absence thereof. See mode listing(s) for details and references.

Mode	Fraction ( $\Gamma_j/\Gamma$ )	Confidence level
$\Gamma_1 D\bar{D}$	not seen	
$\Gamma_2 D^0\bar{D}^0$	seen	
$\Gamma_3 D^+D^-$	seen	
$\Gamma_4 D^*\bar{D} + c.c.$	not seen	
$\Gamma_5 D^*(2007)^0\bar{D}^0 + c.c.$	seen	
$\Gamma_6 D^*(2010)^+D^- + c.c.$	seen	
$\Gamma_7 D^*\bar{D}^*$	not seen	
$\Gamma_8 D^*(2007)^0\bar{D}^*(2007)^0 + c.c.$	seen	
$\Gamma_9 D^*(2010)^+D^*(2010)^- + c.c.$	seen	
$\Gamma_{10} D^0D^-\pi^+ (\text{excl. } D^*(2007)^0\bar{D}^0 + c.c., D^*(2010)^+D^- + c.c.)$	< 2.3 %	90%
$\Gamma_{11} D\bar{D}_2^*(2460) \rightarrow D^0D^-\pi^+ + c.c.$	(10 ± 4) %	
$\Gamma_{12} D^0D^*\pi^- + c.c.$	< 11 %	90%
$\Gamma_{13} D_s^+D_s^-$	not seen	
$\Gamma_{14} D_s^{*+}D_s^{*-} + c.c.$	seen	
$\Gamma_{15} D_s^+D_s^{*-}$	not seen	
$\Gamma_{16} e^+e^-$	(9.4 ± 3.2) × 10 <sup>-6</sup>	

$\psi(4415)$  PARTIAL WIDTHS

$\Gamma(e^+e^-)$	DOCUMENT ID	TECN	COMMENT
<b>0.58 ± 0.07 OUR ESTIMATE</b>			
<b>0.35 ± 0.12</b>	11 ABLIKIM	08D BES2	$e^+e^- \rightarrow$ hadrons
• • • We do not use the following data for averages, fits, limits, etc. • • •			
0.4 to 0.8	12 MO	10 RVUE	$e^+e^- \rightarrow$ hadrons
0.72 ± 0.11	13 SETH	05A RVUE	$e^+e^- \rightarrow$ hadrons
0.64 ± 0.23	14 SETH	05A RVUE	$e^+e^- \rightarrow$ hadrons
0.49 ± 0.13	BRANDELIK	78C DASP	$e^+e^-$
0.44 ± 0.14	SIEGRIST	76 MRK1	$e^+e^-$

- <sup>11</sup> Reanalysis of data presented in BAI 02c. From a global fit over the center-of-mass energy region 3.7–5.0 GeV covering the  $\psi(3770)$ ,  $\psi(4040)$ ,  $\psi(4160)$ , and  $\psi(4415)$  resonances. Phase angle fixed in the fit to  $\delta = (234 \pm 88)^\circ$ .
- <sup>12</sup> Reanalysis of data presented in BAI 00 and BAI 02c. From a global fit over the center-of-mass energy 3.8–4.8 GeV covering the  $\psi(4040)$ ,  $\psi(4160)$  and  $\psi(4415)$  resonances and including interference effects. Four sets of solutions are obtained with the same fit quality, mass and total width, but with different  $e^+e^-$  partial widths. We quote only the range of values.
- <sup>13</sup> From a fit to Crystal Ball (OSTERHELD 86) data.
- <sup>14</sup> From a fit to BES (BAI 02c) data.

$\psi(4415)$  BRANCHING RATIOS

$\Gamma(D^0\bar{D}^0)/\Gamma_{\text{total}}$	DOCUMENT ID	TECN	COMMENT
VALUE			
seen	PAKHLOVA	08 BELL	$e^+e^- \rightarrow D^0\bar{D}^0\gamma$
• • • We do not use the following data for averages, fits, limits, etc. • • •			
not seen	AUBERT	09M BABR	$e^+e^- \rightarrow D^0\bar{D}^0\gamma$

$\Gamma(D^+D^-)/\Gamma_{\text{total}}$	DOCUMENT ID	TECN	COMMENT
VALUE			
seen	PAKHLOVA	08 BELL	$e^+e^- \rightarrow D^+D^-\gamma$
• • • We do not use the following data for averages, fits, limits, etc. • • •			
not seen	AUBERT	09M BABR	$e^+e^- \rightarrow D^+D^-\gamma$

$\Gamma(D\bar{D})/\Gamma(D^*\bar{D}^*)$	DOCUMENT ID	TECN	COMMENT
VALUE			
<b>0.14 ± 0.12 ± 0.03</b>	AUBERT	09M BABR	$e^+e^- \rightarrow \gamma D^{(*)}\bar{D}^{(*)}$

$\Gamma(D^*(2007)^0\bar{D}^0 + c.c.)/\Gamma_{\text{total}}$	DOCUMENT ID	TECN	COMMENT
VALUE			
seen	AUBERT	09M BABR	$e^+e^- \rightarrow D^{*0}\bar{D}^0\gamma$

$\Gamma(D^*(2010)^+D^- + c.c.)/\Gamma_{\text{total}}$	DOCUMENT ID	TECN	COMMENT
VALUE			
seen	AUBERT	09M BABR	$e^+e^- \rightarrow D^{*+}D^-\gamma$
seen	PAKHLOVA	07 BELL	$e^+e^- \rightarrow D^{*+}D^-\gamma$

$\Gamma(D^*\bar{D} + c.c.)/\Gamma(D^*\bar{D}^*)$	DOCUMENT ID	TECN	COMMENT
VALUE			
<b>0.17 ± 0.25 ± 0.03</b>	AUBERT	09M BABR	$e^+e^- \rightarrow \gamma D^{(*)}\bar{D}^{(*)}$

$\Gamma(D^*(2007)^0\bar{D}^*(2007)^0 + c.c.)/\Gamma_{\text{total}}$	DOCUMENT ID	TECN	COMMENT
VALUE			
seen	AUBERT	09M BABR	$e^+e^- \rightarrow D^{*0}\bar{D}^{*0}\gamma$

$\Gamma(D^*(2010)^+D^*(2010)^- + c.c.)/\Gamma_{\text{total}}$	DOCUMENT ID	TECN	COMMENT
VALUE			
seen	AUBERT	09M BABR	$e^+e^- \rightarrow D^{*+}D^{*-}\gamma$
seen	PAKHLOVA	07 BELL	$e^+e^- \rightarrow D^{*+}D^{*-}\gamma$

$\Gamma(D\bar{D}_2^*(2460) \rightarrow D^0D^-\pi^+ + c.c.)/\Gamma_{\text{total}}$	DOCUMENT ID	TECN	COMMENT
VALUE (units 10 <sup>-2</sup> )			
<b>10.5 ± 2.4 ± 3.8</b>	15 PAKHLOVA	08A BELL	$10.6 e^+e^- \rightarrow D^0D^-\pi^+ \gamma$
<sup>15</sup> Using 4421 ± 4 MeV for the mass and 62 ± 20 MeV for the width of $\psi(4415)$ .			

$\Gamma(D^0D^-\pi^+ (\text{excl. } D^*(2007)^0\bar{D}^0 + c.c., D^*(2010)^+D^- + c.c.)/\Gamma_{\text{total}}$	DOCUMENT ID	TECN	COMMENT
VALUE			
<b>&lt; 0.22</b>	16 PAKHLOVA	08A BELL	$10.6 e^+e^- \rightarrow D^0D^-\pi^+ \gamma$
<sup>16</sup> Using 4421 ± 4 MeV for the mass and 62 ± 20 MeV for the width of $\psi(4415)$ .			

$\Gamma(D^0D^*\pi^- + c.c.)/\Gamma_{\text{total}} \times \Gamma(e^+e^-)/\Gamma_{\text{total}}$	DOCUMENT ID	TECN	COMMENT
VALUE			
<b>&lt; 0.99 × 10<sup>-6</sup></b>	17 PAKHLOVA	09 BELL	$e^+e^- \rightarrow D^0D^{*-}\pi^+$
<sup>17</sup> Using 4421 ± 4 MeV for the mass of $\psi(4415)$ .			

$\Gamma(D_s^+D_s^-)/\Gamma_{\text{total}}$	DOCUMENT ID	TECN	COMMENT
VALUE			
not seen	PAKHLOVA	11 BELL	$e^+e^- \rightarrow D_s^+D_s^-\gamma$
not seen	DEL-AMO-SA...10N	BABR	$e^+e^- \rightarrow D_s^+D_s^-\gamma$

$\Gamma(D_s^{*+}D_s^- + c.c.)/\Gamma_{\text{total}}$	DOCUMENT ID	TECN	COMMENT
VALUE			
seen	PAKHLOVA	11 BELL	$e^+e^- \rightarrow D_s^{*+}D_s^-\gamma$
seen	DEL-AMO-SA...10N	BABR	$e^+e^- \rightarrow D_s^{*+}D_s^-\gamma$

$\Gamma(D_s^{*+}D_s^{*-})/\Gamma_{\text{total}}$	DOCUMENT ID	TECN	COMMENT
VALUE			
not seen	PAKHLOVA	11 BELL	$e^+e^- \rightarrow D_s^{*+}D_s^{*-}\gamma$
not seen	DEL-AMO-SA...10N	BABR	$e^+e^- \rightarrow D_s^{*+}D_s^{*-}\gamma$

$\psi(4415)$  REFERENCES

PAKHLOVA	11	PR D83 011101	G. Pakhlova et al.	(BELLE Collab.)
DEL-AMO-SA...	10N	PR D82 052004	P. del Amo Sanchez et al.	(BABAR Collab.)
MO	10	PR D82 077501	X.H. Mo, C.Z. Yuan, P. Wang	(BHEP)
AUBERT	09M	PR D79 092001	B. Aubert et al.	(BABAR Collab.)
PAKHLOVA	09M	PR D80 091101R	G. Pakhlova et al.	(BELLE Collab.)
ABLIKIM	08D	PL B660 315	M. Ablikim et al.	(BES Collab.)
PAKHLOVA	08	PR D77 011103R	G. Pakhlova et al.	(BELLE Collab.)
PAKHLOVA	08A	PRL 100 062001	G. Pakhlova et al.	(BELLE Collab.)
PAKHLOVA	07	PRL 98 092001	G. Pakhlova et al.	(BELLE Collab.)
SETH	05A	PR D72 017501	K.K. Seth	
BAI	02C	PRL 88 101802	J.Z. Bai et al.	(BES Collab.)
BAI	00	PRL 84 594	J.Z. Bai et al.	(BES Collab.)
OSTERHELD	86	SLAC-PUB-4160	A. Osterheld et al.	(SLAC Crystal Ball Collab.)
BRANDELIK	78C	PL 76B 361	R. Brandelik et al.	(DASP Collab.)
SIEGRIST	76	PRL 36 700	J.L. Siegrist et al.	(LBL, SLAC)

## Meson Particle Listings

 $X(4430)^\pm, X(4660)$  $X(4430)^\pm$ 

$$I(J^P) = ?(??)$$

OMITTED FROM SUMMARY TABLE

Seen by CHOI 08 in  $B \rightarrow K\pi^+\psi(2S)$  decays and confirmed by reanalysis of the same data sample in MIZUK 09. Not seen by AUBERT 09AA.

 $X(4430)^\pm$  MASS

VALUE (MeV)	DOCUMENT ID	TECN	COMMENT
$4443^{+15+19}_{-43-56}$	1 MIZUK	09	BELL $B \rightarrow K\pi^+\psi(2S)$
••• We do not use the following data for averages, fits, limits, etc. •••			
$4433 \pm 4 \pm 2$	2 CHOI	08	BELL $B \rightarrow K\pi^+\psi(2S)$
<sup>1</sup> From a Dalitz plot analysis.			
<sup>2</sup> Superseded by MIZUK 09.			

 $X(4430)^\pm$  WIDTH

VALUE (MeV)	DOCUMENT ID	TECN	COMMENT
$107^{+86+74}_{-43-56}$	3 MIZUK	09	BELL $B \rightarrow K\pi^+\psi(2S)$
••• We do not use the following data for averages, fits, limits, etc. •••			
$45^{+18+30}_{-13-13}$	4 CHOI	08	BELL $B \rightarrow K\pi^+\psi(2S)$
<sup>3</sup> From a Dalitz plot analysis.			
<sup>4</sup> Superseded by MIZUK 09.			

 $X(4430)^\pm$  DECAY MODES

Mode	Fraction ( $\Gamma_i/\Gamma$ )
$\Gamma_1$ $\pi^+\psi(2S)$	seen
$\Gamma_2$ $\pi^+J/\psi$	not seen

 $X(4430)^\pm$  BRANCHING RATIOS

$\Gamma(\pi^+\psi(2S))/\Gamma_{\text{total}}$	$\Gamma_1/\Gamma$
seen	
not seen	
<sup>5</sup> Measured a product of branching fractions $B(\bar{B}^0 \rightarrow K^- X(4430)^+) \times B(X(4430)^+ \rightarrow \pi^+\psi(2S)) = (3.2^{+1.8+5.3}_{-0.9-1.6}) \times 10^{-5}$ .	
<sup>6</sup> AUBERT 09AA quotes $B(B^+ \rightarrow \bar{K}^0 X(4430)^+) \times B(X(4430)^+ \rightarrow \pi^+\psi(2S)) < 4.7 \times 10^{-5}$ and $B(\bar{B}^0 \rightarrow K^- X(4430)^+) \times B(X(4430)^+ \rightarrow \pi^+\psi(2S)) < 3.1 \times 10^{-5}$ at 95% CL.	
$\Gamma(\pi^+J/\psi)/\Gamma_{\text{total}}$	$\Gamma_2/\Gamma$
not seen	
<sup>7</sup> AUBERT 09AA quotes $B(B^+ \rightarrow \bar{K}^0 X(4430)^+) \times B(X(4430)^+ \rightarrow \pi^+J/\psi) < 1.5 \times 10^{-5}$ and $B(\bar{B}^0 \rightarrow K^- X(4430)^+) \times B(X(4430)^+ \rightarrow \pi^+J/\psi) < 0.4 \times 10^{-5}$ at 95% CL.	

 $X(4430)^\pm$  REFERENCES

AUBERT	09AA	PR D79 112001	B. Aubert <i>et al.</i>	(BABAR Collab.)
MIZUK	09	PR D80 031104R	R. Mizuk <i>et al.</i>	(BELLE Collab.)
CHOI	08	PRL 100 142001	S.-K. Choi <i>et al.</i>	(BELLE Collab.)

 $X(4660)$ 

$$I^G(J^{PC}) = ?^?(1^{--})$$

Seen in radiative return from  $e^+e^-$  collisions at  $\sqrt{s} = 9.54\text{--}10.58$  GeV by WANG 07D. Also obtained in a combined fit of WANG 07D and AUBERT 07S. See also the review under the  $X(3872)$  particle listings. (See the index for the page number.)

 $X(4660)$  MASS

VALUE (MeV)	DOCUMENT ID	TECN	COMMENT
$4664 \pm 11 \pm 5$	WANG	07D	BELL $10.58 e^+e^- \rightarrow \psi(2S)\pi^+\pi^-\gamma$
••• We do not use the following data for averages, fits, limits, etc. •••			
$4661^{+9}_{-8} \pm 6$	<sup>1</sup> LIU	08H	RVUE $10.58 e^+e^- \rightarrow \psi(2S)\pi^+\pi^-\gamma$
<sup>1</sup> From a combined fit of AUBERT 07S and WANG 07D data with two resonances.			

 $X(4660)$  WIDTH

VALUE (MeV)	DOCUMENT ID	TECN	COMMENT
$48 \pm 15 \pm 3$	WANG	07D	BELL $10.58 e^+e^- \rightarrow \psi(2S)\pi^+\pi^-\gamma$
••• We do not use the following data for averages, fits, limits, etc. •••			
$42^{+17}_{-12} \pm 6$	<sup>2</sup> LIU	08H	RVUE $10.58 e^+e^- \rightarrow \psi(2S)\pi^+\pi^-\gamma$
<sup>2</sup> From a combined fit of AUBERT 07S and WANG 07D data with two resonances.			

 $X(4660)$  DECAY MODES

Mode	Fraction ( $\Gamma_i/\Gamma$ )
$\Gamma_1$ $e^+e^-$	
$\Gamma_2$ $\psi(2S)\pi^+\pi^-$	seen
$\Gamma_3$ $D^0 D^{*-}\pi^+$	

 $X(4660)$   $\Gamma(i)\Gamma(e^+e^-)/\Gamma(\text{total})$ 

$\Gamma(\psi(2S)\pi^+\pi^-) \times \Gamma(e^+e^-)/\Gamma_{\text{total}}$	$\Gamma_2\Gamma_1/\Gamma$
seen	
not seen	
<sup>3</sup> Solution I in a combined fit of AUBERT 07S and WANG 07D data with two resonances.	
<sup>4</sup> Solution II in a combined fit of AUBERT 07S and WANG 07D data with two resonances.	
<sup>5</sup> Solution I of two equivalent solutions in a fit using two interfering resonances.	
<sup>6</sup> Solution II of two equivalent solutions in a fit using two interfering resonances.	

 $X(4660)$  BRANCHING RATIOS

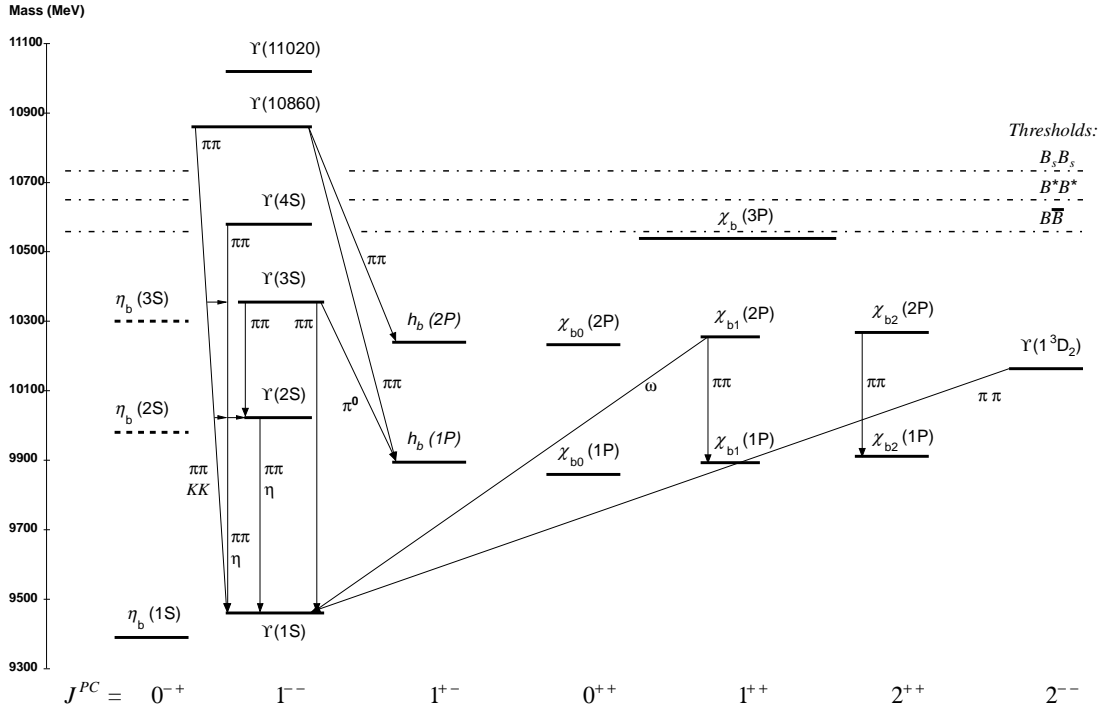
$\Gamma(D^0 D^{*-}\pi^+)/\Gamma(\psi(2S)\pi^+\pi^-)$	$\Gamma_3/\Gamma_2$
$< 10$	
<sup>7</sup> Using $4664 \pm 11 \pm 5$ MeV for the mass of $X(4660)$ .	
$\Gamma(D^0 D^{*-}\pi^+)/\Gamma_{\text{total}} \times \Gamma(e^+e^-)/\Gamma_{\text{total}}$	$\Gamma_3/\Gamma \times \Gamma_1/\Gamma$
$< 0.37 \times 10^{-6}$	

 $X(4660)$  REFERENCES

PAKHLOVA	09	PR D80 091101R	G. Pakhlova <i>et al.</i>	(BELLE Collab.)
LIU	08H	PR D78 014032	Z.Q. Liu, X.S. Qin, C.Z. Yuan	
AUBERT	07S	PRL 98 212001	B. Aubert <i>et al.</i>	(BABAR Collab.)
WANG	07D	PRL 99 142002	X.L. Wang <i>et al.</i>	(BELLE Collab.)

**$b\bar{b}$  MESONS**

## THE BOTTOMONIUM SYSTEM



The level scheme of the  $b\bar{b}$  states showing experimentally established states with solid lines. Singlet states are called  $\eta_b$  and  $h_b$ , triplet states  $Y$  and  $\chi_{bJ}$ . In parentheses it is sufficient to give the radial quantum number and the orbital angular momentum to specify the states with all their quantum numbers. *E.g.*,  $h_b(2P)$  means  $2^1P_1$  with  $n = 2$ ,  $L = 1$ ,  $S = 0$ ,  $J = 1$ ,  $PC = +-$ . The figure shows observed hadronic transitions. The single photon transitions  $Y(nS) \rightarrow \gamma\eta_b(mS)$ ,  $Y(nS) \rightarrow \gamma\chi_{bJ}(mP)$ , and  $\chi_{bJ}(nP) \rightarrow \gamma Y(mS)$  are omitted for clarity.

**WIDTH DETERMINATIONS OF THE  $Y$  STATES**

As is the case for the  $J/\psi(1S)$  and  $\psi(2S)$ , the full widths of the  $b\bar{b}$  states  $Y(1S)$ ,  $Y(2S)$ , and  $Y(3S)$  are not directly measurable, since they are much narrower than the energy resolution of the  $e^+e^-$  storage rings where these states are produced. The common indirect method to determine  $\Gamma$  starts from

$$\Gamma = \Gamma_{\ell\ell}/B_{\ell\ell}, \quad (1)$$

where  $\Gamma_{\ell\ell}$  is one leptonic partial width and  $B_{\ell\ell}$  is the corresponding branching fraction ( $\ell = e, \mu, \text{ or } \tau$ ). One then assumes  $e$ - $\mu$ - $\tau$  universality and uses

$$\Gamma_{\ell\ell} = \Gamma_{ee} \quad (2)$$

$$B_{\ell\ell} = \text{average of } B_{ee}, B_{\mu\mu}, \text{ and } B_{\tau\tau}.$$

The electronic partial width  $\Gamma_{ee}$  is also not directly measurable at  $e^+e^-$  storage rings, only in the combination  $\Gamma_{ee}\Gamma_{\text{had}}/\Gamma$ , where  $\Gamma_{\text{had}}$  is the hadronic partial width and

$$\Gamma_{\text{had}} + 3\Gamma_{ee} = \Gamma. \quad (3)$$

This combination is obtained experimentally from the energy-integrated hadronic cross section

$$\int_{\text{resonance}} \sigma(e^+e^- \rightarrow Y \rightarrow \text{hadrons})dE$$

$$= \frac{6\pi^2 \Gamma_{ee}\Gamma_{\text{had}}}{M^2 \Gamma} C_r = \frac{6\pi^2 \Gamma_{ee}^{(0)}\Gamma_{\text{had}}}{M^2 \Gamma} C_r^{(0)}, \quad (4)$$

where  $M$  is the  $Y$  mass, and  $C_r$  and  $C_r^{(0)}$  are radiative correction factors.  $C_r$  is used for obtaining  $\Gamma_{ee}$  as defined in Eq. (1), and contains corrections from all orders of QED for describing  $(b\bar{b}) \rightarrow e^+e^-$ . The lowest order QED value  $\Gamma_{ee}^{(0)}$ , relevant for comparison with potential-model calculations, is defined by the lowest order QED graph (Born term) alone, and is about 7% lower than  $\Gamma_{ee}$ .

The Listings give experimental results on  $B_{ee}$ ,  $B_{\mu\mu}$ ,  $B_{\tau\tau}$ , and  $\Gamma_{ee}\Gamma_{\text{had}}/\Gamma$ . The entries of the last quantity have been re-evaluated consistently using the correction procedure of KURAEV 85. The partial width  $\Gamma_{ee}$  is obtained from the average values for  $\Gamma_{ee}\Gamma_{\text{had}}/\Gamma$  and  $B_{\ell\ell}$  using

$$\Gamma_{ee} = \frac{\Gamma_{ee}\Gamma_{\text{had}}}{\Gamma(1 - 3B_{\ell\ell})}. \quad (5)$$

## Meson Particle Listings

Bottomonium,  $\eta_b(1S)$ ,  $\Upsilon(1S)$ 

The total width  $\Gamma$  is then obtained from Eq. (1). We do not list  $\Gamma_{ee}$  and  $\Gamma$  values of individual experiments. The  $\Gamma_{ee}$  values in the Meson Summary Table are also those defined in Eq. (1).

 $\eta_b(1S)$ 

$$I^G(J^{PC}) = 0^+(0^{-+})$$

OMITTED FROM SUMMARY TABLE

Quantum numbers shown are quark-model predictions. Observed in radiative decay of the  $\Upsilon(3S)$ , therefore  $C = +$ .

 $\eta_b(1S)$  MASS

VALUE (MeV)	EVTs	DOCUMENT ID	TECN	COMMENT
<b>9391.0 ± 2.8 OUR AVERAGE</b>				
9391.8 ± 6.6 ± 2.0	2.3 ± 0.5k	<sup>1</sup> BONVICINI	10 CLEO	$\Upsilon(3S) \rightarrow \gamma X$
9394.2 <sup>+4.8</sup> <sub>-4.9</sub> ± 2.0	13 ± 5k	<sup>1</sup> AUBERT	09AQ BABR	$\Upsilon(2S) \rightarrow \gamma X$
9388.9 <sup>+3.1</sup> <sub>-2.3</sub> ± 2.7	19 ± 3k	<sup>1</sup> AUBERT	08V BABR	$\Upsilon(3S) \rightarrow \gamma X$

• • • We do not use the following data for averages, fits, limits, etc. • • •

9300 ± 20 ± 20 HEISTER 02D ALEP 181-209 e<sup>+</sup>e<sup>-</sup>

<sup>1</sup> Assuming  $\Gamma_{\eta_b(1S)} = 10$  MeV. Not independent of the corresponding  $\gamma$  energy or mass difference measurements.

 $m_{\Upsilon(1S)} - m_{\eta_b}$ 

VALUE (MeV)	EVTs	DOCUMENT ID	TECN	COMMENT
<b>69.3 ± 2.8 OUR AVERAGE</b>				
68.5 ± 6.6 ± 2.0	2.3 ± 0.5k	<sup>2</sup> BONVICINI	10 CLEO	$\Upsilon(3S) \rightarrow \gamma X$
66.1 <sup>+4.8</sup> <sub>-4.9</sub> ± 2.0	13 ± 5k	<sup>2</sup> AUBERT	09AQ BABR	$\Upsilon(2S) \rightarrow \gamma X$
71.4 <sup>+2.3</sup> <sub>-3.1</sub> ± 2.7	19 ± 3k	<sup>2</sup> AUBERT	08V BABR	$\Upsilon(3S) \rightarrow \gamma X$

<sup>2</sup> Assuming  $\Gamma_{\eta_b(1S)} = 10$  MeV. Not independent of the corresponding  $\gamma$  energy or mass measurements.

 $\gamma$  ENERGY IN  $\Upsilon(3S)$  DECAY

VALUE (MeV)	EVTs	DOCUMENT ID	TECN	COMMENT
<b>920.6<sup>+2.8</sup><sub>-3.2</sub> OUR AVERAGE</b>				
918.6 ± 6.0 ± 1.9	2.3 ± 0.5k	<sup>3</sup> BONVICINI	10 CLEO	$\Upsilon(3S) \rightarrow \gamma X$
921.2 <sup>+2.1</sup> <sub>-2.8</sub> ± 2.4	19 ± 3k	<sup>3</sup> AUBERT	08V BABR	$\Upsilon(3S) \rightarrow \gamma X$

<sup>3</sup> Assuming  $\Gamma_{\eta_b(1S)} = 10$  MeV. Not independent of the corresponding mass or mass difference measurements.

 $\gamma$  ENERGY IN  $\Upsilon(2S)$  DECAY

VALUE (MeV)	EVTs	DOCUMENT ID	TECN	COMMENT
<b>609.3<sup>+4.6</sup><sub>-4.5</sub> ± 1.9</b>	13 ± 5k	<sup>4</sup> AUBERT	09AQ BABR	$\Upsilon(2S) \rightarrow \gamma X$

<sup>4</sup> Assuming  $\Gamma_{\eta_b(1S)} = 10$  MeV. Not independent of the corresponding mass or mass difference measurements.

 $\eta_b(1S)$  DECAY MODES

Mode	Fraction ( $\Gamma_i/\Gamma$ )	Confidence level
$\Gamma_1$ $3h^+3h^-$	not seen	
$\Gamma_2$ $2h^+2h^-$	not seen	
$\Gamma_3$ $4h^+4h^-$		
$\Gamma_4$ $\gamma\gamma$	not seen	
$\Gamma_5$ $\mu^+\mu^-$	$<9 \times 10^{-3}$	90%
$\Gamma_6$ $\tau^+\tau^-$	$<8\%$	90%

 $\eta_b(1S)$   $\Gamma(i)\Gamma(\gamma\gamma)/\Gamma(\text{total})$ 

VALUE (eV)	CL%	DOCUMENT ID	TECN	COMMENT	$\Gamma_1\Gamma_4/\Gamma$
<b><math>\Gamma(3h^+3h^-) \times \Gamma(\gamma\gamma)/\Gamma_{\text{total}}</math></b>					
• • • We do not use the following data for averages, fits, limits, etc. • • •					
$<470$	95	ABDALLAH	06 DLPH	161-209 e <sup>+</sup> e <sup>-</sup>	
$<132$	95	HEISTER	02D ALEP	181-209 e <sup>+</sup> e <sup>-</sup>	

VALUE (eV)	CL%	DOCUMENT ID	TECN	COMMENT	$\Gamma_2\Gamma_4/\Gamma$
<b><math>\Gamma(2h^+2h^-) \times \Gamma(\gamma\gamma)/\Gamma_{\text{total}}</math></b>					
• • • We do not use the following data for averages, fits, limits, etc. • • •					
$<190$	95	ABDALLAH	06 DLPH	161-209 e <sup>+</sup> e <sup>-</sup>	
$<48$	95	HEISTER	02D ALEP	181-209 e <sup>+</sup> e <sup>-</sup>	

 $\Gamma(4h^+4h^-) \times \Gamma(\gamma\gamma)/\Gamma_{\text{total}}$   $\Gamma_3\Gamma_4/\Gamma$ 

VALUE (eV)	CL%	DOCUMENT ID	TECN	COMMENT
• • • We do not use the following data for averages, fits, limits, etc. • • •				
$<660$	95	ABDALLAH	06 DLPH	161-209 e <sup>+</sup> e <sup>-</sup>

 $\eta_b(1S)$  BRANCHING RATIOS

VALUE	CL%	DOCUMENT ID	TECN	COMMENT	$\Gamma_5/\Gamma$
<b><math>&lt;9 \times 10^{-3}</math></b>	90	<sup>5</sup> AUBERT	09Z BABR	$e^+e^- \rightarrow \Upsilon(2S,3S) \rightarrow \gamma\eta_b$	
<sup>5</sup> Obtained using $B(\Upsilon(2S) \rightarrow \gamma\eta_b) = (4.2^{+1.1}_{-1.0} \pm 0.9) \times 10^{-4}$ and $B(\Upsilon(3S) \rightarrow \gamma\eta_b) = (4.8 \pm 0.5 \pm 0.6) \times 10^{-4}$ . This limit is equivalent to $B(\eta_b \rightarrow \mu^+\mu^-) = (-0.25 \pm 0.51 \pm 0.33)\%$ measurement.					

 $\Gamma(\tau^+\tau^-)/\Gamma_{\text{total}}$   $\Gamma_6/\Gamma$ 

VALUE	CL%	DOCUMENT ID	TECN	COMMENT
<b><math>&lt;8 \times 10^{-2}</math></b>	90	AUBERT	09P BABR	$e^+e^- \rightarrow \gamma\tau^+\tau^-$

 $\eta_b(1S)$  REFERENCES

BONVICINI	10	PR D61 031104R	G. Bonvicini et al.	(CLEO Collab.)
AUBERT	09AQ	PRL 103 161801	B. Aubert et al.	(BABAR Collab.)
AUBERT	09P	PRL 103 181801	B. Aubert et al.	(BABAR Collab.)
AUBERT	09Z	PRL 103 081803	B. Aubert et al.	(BABAR Collab.)
AUBERT	08V	PRL 101 071801	B. Aubert et al.	(BABAR Collab.)
ABDALLAH	06	PL B634 340	J.M. Abdallah et al.	(DELPHI Collab.)
HEISTER	02D	PL B530 56	A. Heister et al.	(ALEPH Collab.)

 $\Upsilon(1S)$ 

$$I^G(J^{PC}) = 0^-(1^{--})$$

 $\Upsilon(1S)$  MASS

VALUE (MeV)	DOCUMENT ID	TECN	COMMENT
<b>9460.30 ± 0.26 OUR AVERAGE</b>	Error includes scale factor of 3.3.		
9460.51 ± 0.09 ± 0.05	<sup>1</sup> ARTAMONOV 00	MD1	$e^+e^- \rightarrow \text{hadrons}$
9459.97 ± 0.11 ± 0.07	MACKAY	84 REDE	$e^+e^- \rightarrow \text{hadrons}$
• • • We do not use the following data for averages, fits, limits, etc. • • •			
9460.60 ± 0.09 ± 0.05	<sup>2,3</sup> BARU	92B REDE	$e^+e^- \rightarrow \text{hadrons}$
9460.59 ± 0.12	BARU	86 REDE	$e^+e^- \rightarrow \text{hadrons}$
9460.6 ± 0.4	<sup>3,4</sup> ARTAMONOV 84	REDE	$e^+e^- \rightarrow \text{hadrons}$

<sup>1</sup> Reanalysis of BARU 92B and ARTAMONOV 84 using new electron mass (COHEN 87).

<sup>2</sup> Superseding BARU 86.

<sup>3</sup> Superseded by ARTAMONOV 00.

<sup>4</sup> Value includes data of ARTAMONOV 82.

 $\Upsilon(1S)$  WIDTH

VALUE (keV)	DOCUMENT ID
<b>54.02 ± 1.25 OUR EVALUATION</b>	See the Note on "Width Determinations of the $\Upsilon$ States"

 $\Upsilon(1S)$  DECAY MODES

Mode	Fraction ( $\Gamma_i/\Gamma$ )	Confidence level
$\Gamma_1$ $\tau^+\tau^-$	( 2.60 ± 0.10 ) %	
$\Gamma_2$ $e^+e^-$	( 2.38 ± 0.11 ) %	
$\Gamma_3$ $\mu^+\mu^-$	( 2.48 ± 0.05 ) %	

## Hadronic decays

$\Gamma_4$ $ggg$	(81.7 ± 0.7 ) %	
$\Gamma_5$ $\gamma gg$	( 2.2 ± 0.6 ) %	
$\Gamma_6$ $\eta'(958)$ anything	( 2.94 ± 0.24 ) %	
$\Gamma_7$ $J/\psi(1S)$ anything	( 6.5 ± 0.7 ) × 10 <sup>-4</sup>	
$\Gamma_8$ $\chi_{c0}$ anything	$< 5 \times 10^{-3}$	90%
$\Gamma_9$ $\chi_{c1}$ anything	( 2.3 ± 0.7 ) × 10 <sup>-4</sup>	
$\Gamma_{10}$ $\chi_{c2}$ anything	( 3.4 ± 1.0 ) × 10 <sup>-4</sup>	
$\Gamma_{11}$ $\psi(2S)$ anything	( 2.7 ± 0.9 ) × 10 <sup>-4</sup>	
$\Gamma_{12}$ $\rho\pi$	$< 2 \times 10^{-4}$	90%
$\Gamma_{13}$ $\pi^+\pi^-$	$< 5 \times 10^{-4}$	90%
$\Gamma_{14}$ $K^+K^-$	$< 5 \times 10^{-4}$	90%
$\Gamma_{15}$ $p\bar{p}$	$< 5 \times 10^{-4}$	90%
$\Gamma_{16}$ $\pi^0\pi^+\pi^-$	$< 1.84 \times 10^{-5}$	90%
$\Gamma_{17}$ $D^*(2010)^\pm$ anything	( 2.52 ± 0.20 ) %	
$\Gamma_{18}$ $\bar{d}$ anything	( 2.86 ± 0.28 ) × 10 <sup>-5</sup>	

# Meson Particle Listings

## $\Upsilon(1S)$

### Radiative decays

$\Gamma_{19}$	$\gamma\pi^+\pi^-$	$(6.3 \pm 1.8) \times 10^{-5}$	
$\Gamma_{20}$	$\gamma\pi^0\pi^0$	$(1.7 \pm 0.7) \times 10^{-5}$	
$\Gamma_{21}$	$\gamma\pi^0\eta$	$< 2.4 \times 10^{-6}$	90%
$\Gamma_{22}$	$\gamma K^+K^-$	$[a] \ (1.14 \pm 0.13) \times 10^{-5}$	
$\Gamma_{23}$	$\gamma p\bar{p}$	$[b] < 6 \times 10^{-6}$	90%
$\Gamma_{24}$	$\gamma 2h^+2h^-$	$(7.0 \pm 1.5) \times 10^{-4}$	
$\Gamma_{25}$	$\gamma 3h^+3h^-$	$(5.4 \pm 2.0) \times 10^{-4}$	
$\Gamma_{26}$	$\gamma 4h^+4h^-$	$(7.4 \pm 3.5) \times 10^{-4}$	
$\Gamma_{27}$	$\gamma\pi^+\pi^-K^+K^-$	$(2.9 \pm 0.9) \times 10^{-4}$	
$\Gamma_{28}$	$\gamma 2\pi^+2\pi^-$	$(2.5 \pm 0.9) \times 10^{-4}$	
$\Gamma_{29}$	$\gamma 3\pi^+3\pi^-$	$(2.5 \pm 1.2) \times 10^{-4}$	
$\Gamma_{30}$	$\gamma 2\pi^+2\pi^-K^+K^-$	$(2.4 \pm 1.2) \times 10^{-4}$	
$\Gamma_{31}$	$\gamma\pi^+\pi^-p\bar{p}$	$(1.5 \pm 0.6) \times 10^{-4}$	
$\Gamma_{32}$	$\gamma 2\pi^+2\pi^-p\bar{p}$	$(4 \pm 6) \times 10^{-5}$	
$\Gamma_{33}$	$\gamma 2K^+2K^-$	$(2.0 \pm 2.0) \times 10^{-5}$	
$\Gamma_{34}$	$\gamma \eta'(958)$	$< 1.9 \times 10^{-6}$	90%
$\Gamma_{35}$	$\gamma \eta$	$< 1.0 \times 10^{-6}$	90%
$\Gamma_{36}$	$\gamma f_0(980)$	$< 3 \times 10^{-5}$	90%
$\Gamma_{37}$	$\gamma f_2'(1525)$	$(3.8 \pm 0.9) \times 10^{-5}$	
$\Gamma_{38}$	$\gamma f_2'(1270)$	$(1.01 \pm 0.09) \times 10^{-4}$	
$\Gamma_{39}$	$\gamma \eta(1405)$	$< 8.2 \times 10^{-5}$	90%
$\Gamma_{40}$	$\gamma f_0(1500)$	$< 1.5 \times 10^{-5}$	90%
$\Gamma_{41}$	$\gamma f_0(1710)$	$< 2.6 \times 10^{-4}$	90%
$\Gamma_{42}$	$\gamma f_0(1710) \rightarrow \gamma K^+K^-$	$< 7 \times 10^{-6}$	90%
$\Gamma_{43}$	$\gamma f_0(1710) \rightarrow \gamma \pi^0\pi^0$	$< 1.4 \times 10^{-6}$	90%
$\Gamma_{44}$	$\gamma f_0(1710) \rightarrow \gamma \eta\eta$	$< 1.8 \times 10^{-6}$	90%
$\Gamma_{45}$	$\gamma f_4(2050)$	$< 5.3 \times 10^{-5}$	90%
$\Gamma_{46}$	$\gamma f_0(2200) \rightarrow \gamma K^+K^-$	$< 2 \times 10^{-4}$	90%
$\Gamma_{47}$	$\gamma f_J(2220) \rightarrow \gamma K^+K^-$	$< 8 \times 10^{-7}$	90%
$\Gamma_{48}$	$\gamma f_J(2220) \rightarrow \gamma \pi^+\pi^-$	$< 6 \times 10^{-7}$	90%
$\Gamma_{49}$	$\gamma f_J(2220) \rightarrow \gamma p\bar{p}$	$< 1.1 \times 10^{-6}$	90%
$\Gamma_{50}$	$\gamma \eta(2225) \rightarrow \gamma \phi\phi$	$< 3 \times 10^{-3}$	90%
$\Gamma_{51}$	$\gamma \eta_c(1S)$	$< 5.7 \times 10^{-5}$	90%
$\Gamma_{52}$	$\gamma \chi_{c0}$	$< 6.5 \times 10^{-4}$	90%
$\Gamma_{53}$	$\gamma \chi_{c1}$	$< 2.3 \times 10^{-5}$	90%
$\Gamma_{54}$	$\gamma \chi_{c2}$	$< 7.6 \times 10^{-6}$	90%
$\Gamma_{55}$	$\gamma X(3872) \rightarrow \pi^+\pi^-J/\psi$	$< 1.6 \times 10^{-6}$	90%
$\Gamma_{56}$	$\gamma X(3872) \rightarrow \pi^+\pi^-\pi^0J/\psi$	$< 2.8 \times 10^{-6}$	90%
$\Gamma_{57}$	$\gamma X(3915) \rightarrow \omega J/\psi$	$< 3.0 \times 10^{-6}$	90%
$\Gamma_{58}$	$\gamma X(4140) \rightarrow \phi J/\psi$	$< 2.2 \times 10^{-6}$	90%
$\Gamma_{59}$	$\gamma X$	$[c] < 4.5 \times 10^{-6}$	90%
$\Gamma_{60}$	$\gamma X \bar{X} (m_X < 3.1 \text{ GeV})$	$[d] < 1 \times 10^{-3}$	90%
$\Gamma_{61}$	$\gamma X \bar{X} (m_X < 4.5 \text{ GeV})$	$[e] < 2.4 \times 10^{-4}$	90%
$\Gamma_{62}$	$\gamma X \rightarrow \gamma + \geq 4 \text{ prongs}$	$[f] < 1.78 \times 10^{-4}$	95%
$\Gamma_{63}$	$\gamma a_1^0 \rightarrow \gamma \mu^+\mu^-$	$[g] < 9 \times 10^{-6}$	90%
$\Gamma_{64}$	$\gamma a_1^0 \rightarrow \gamma \tau^+\tau^-$	$[a] < 5.0 \times 10^{-5}$	90%

### Lepton Family number (LF) violating modes

$\Gamma_{65}$	$\mu^\pm \tau^\mp$	$LF < 6.0 \times 10^{-6}$	95%
---------------	--------------------	---------------------------	-----

### Other decays

$\Gamma_{66}$	invisible	$< 3.0 \times 10^{-4}$	90%
---------------	-----------	------------------------	-----

- [a]  $2m_\tau < M(\tau^+\tau^-) < 7500 \text{ MeV}$
- [b]  $2 < m_{K^+K^-} < 3 \text{ GeV}$
- [c]  $X = \text{scalar with } m < 8.0 \text{ GeV}$
- [d]  $X \bar{X} = \text{vectors with } m < 3.1 \text{ GeV}$
- [e]  $X \text{ and } \bar{X} = \text{zero spin with } m < 4.5 \text{ GeV}$
- [f]  $1.5 \text{ GeV} < m_X < 5.0 \text{ GeV}$
- [g]  $201 < M(\mu^+\mu^-) < 3565 \text{ MeV}$

### $\Upsilon(1S) \Gamma(I)\Gamma(e^+e^-)/\Gamma(\text{total})$

$\Gamma(e^+e^-) \times \Gamma(\mu^+\mu^-)/\Gamma(\text{total})$		$\Gamma_2/\Gamma$	
VALUE (eV)	DOCUMENT ID	TECN	COMMENT
<b>31.2 ± 1.6 ± 1.7</b>	KOBEL	92	CBAL $e^+e^- \rightarrow \mu^+\mu^-$
$\Gamma(\text{hadrons}) \times \Gamma(e^+e^-)/\Gamma(\text{total})$		$\Gamma_0/\Gamma$	
VALUE (keV)	DOCUMENT ID	TECN	COMMENT
<b>1.240 ± 0.016 OUR AVERAGE</b>			
1.252 ± 0.004 ± 0.019	5 ROSNER	06	CLEO $9.5 e^+e^- \rightarrow \text{hadrons}$
1.187 ± 0.023 ± 0.031	5 BARU	92B	MD1 $e^+e^- \rightarrow \text{hadrons}$
1.23 ± 0.02 ± 0.05	5 JAKUBOWSKI	88	CBAL $e^+e^- \rightarrow \text{hadrons}$
1.37 ± 0.06 ± 0.09	6 GILES	84B	CLEO $e^+e^- \rightarrow \text{hadrons}$

1.23 ± 0.08 ± 0.04	6 ALBRECHT	82	DASP $e^+e^- \rightarrow \text{hadrons}$
1.13 ± 0.07 ± 0.11	6 NICZYPORUK	82	LENA $e^+e^- \rightarrow \text{hadrons}$
1.09 ± 0.25	6 BOCK	80	CNTR $e^+e^- \rightarrow \text{hadrons}$
1.35 ± 0.14	7 BERGER	79	PLUT $e^+e^- \rightarrow \text{hadrons}$

- <sup>5</sup> Radiative corrections evaluated following KURAEV 85.
- <sup>6</sup> Radiative corrections reevaluated by BUCHMUELLER 88 following KURAEV 85.
- <sup>7</sup> Radiative corrections reevaluated by ALEXANDER 89 using  $B(\mu\mu) = 0.026$ .

### $\Upsilon(1S)$ PARTIAL WIDTHS

$\Gamma(e^+e^-)$		$\Gamma_2$
VALUE (keV)	DOCUMENT ID	
<b>1.340 ± 0.018 OUR EVALUATION</b>		

### $\Upsilon(1S)$ BRANCHING RATIOS

$\Gamma(\tau^+\tau^-)/\Gamma(\text{total})$		$\Gamma_1/\Gamma$		
VALUE (units $10^{-2}$ )	EVTS	DOCUMENT ID	TECN	COMMENT
<b>2.60 ± 0.10 OUR AVERAGE</b>				
2.53 ± 0.13 ± 0.05	60k	8 BESSON	07	CLEO $e^+e^- \rightarrow \Upsilon(1S) \rightarrow \tau^+\tau^-$
2.61 ± 0.12 <sup>+0.09</sup> <sub>-0.13</sub>	25k	CINABRO	94B	CLE2 $e^+e^- \rightarrow \tau^+\tau^-$
2.7 ± 0.4 ± 0.2		9 ALBRECHT	85c	ARG $\Upsilon(2S) \rightarrow \pi^+\pi^-\tau^+\tau^-$
3.4 ± 0.4 ± 0.4		GILES	83	CLEO $e^+e^- \rightarrow \tau^+\tau^-$

<sup>8</sup> BESSON 07 reports  $[\Gamma(\Upsilon(1S) \rightarrow \tau^+\tau^-)/\Gamma(\text{total})] / [B(\Upsilon(1S) \rightarrow \mu^+\mu^-)] = 1.02 \pm 0.02 \pm 0.05$  which we multiply by our best value  $B(\Upsilon(1S) \rightarrow \mu^+\mu^-) = (2.48 \pm 0.05) \times 10^{-2}$ . Our first error is their experiment's error and our second error is the systematic error from using our best value.

<sup>9</sup> Using  $B(\Upsilon(1S) \rightarrow ee) = B(\Upsilon(1S) \rightarrow \mu\mu) = 0.0256$ ; not used for width evaluations.

$\Gamma(e^+e^-)/\Gamma(\text{total})$		$\Gamma_2/\Gamma$		
VALUE (units $10^{-2}$ )	EVTS	DOCUMENT ID	TECN	COMMENT
<b>2.38 ± 0.11 OUR AVERAGE</b>				
2.29 ± 0.08 ± 0.11		ALEXANDER	98	CLE2 $\Upsilon(2S) \rightarrow \pi^+\pi^-e^+e^-$
2.42 ± 0.14 ± 0.14	307	ALBRECHT	87	ARG $\Upsilon(2S) \rightarrow \pi^+\pi^-e^+e^-$
2.8 ± 0.3 ± 0.2	826	BESSON	84	CLEO $\Upsilon(2S) \rightarrow \pi^+\pi^-e^+e^-$
5.1 ± 3.0		BERGER	80c	PLUT $e^+e^- \rightarrow e^+e^-$

$\Gamma(\mu^+\mu^-)/\Gamma(\text{total})$		$\Gamma_3/\Gamma$		
VALUE	EVTS	DOCUMENT ID	TECN	COMMENT
<b>0.0248 ± 0.0005 OUR AVERAGE</b>				
0.0249 ± 0.0002 ± 0.0007	345k	ADAMS	05	CLEO $e^+e^- \rightarrow \mu^+\mu^-$
0.0249 ± 0.0008 ± 0.0013		ALEXANDER	98	CLE2 $\Upsilon(2S) \rightarrow \mu^+\mu^-$
0.0212 ± 0.0020 ± 0.0010		10 BARU	92	MD1 $e^+e^- \rightarrow \mu^+\mu^-$
0.0231 ± 0.0012 ± 0.0010		10 KOBEL	92	CBAL $e^+e^- \rightarrow \mu^+\mu^-$
0.0252 ± 0.0007 ± 0.0007		CHEN	89B	CLEO $e^+e^- \rightarrow \mu^+\mu^-$
0.0261 ± 0.0009 ± 0.0011		KAARSBERG	89	CSB2 $e^+e^- \rightarrow \mu^+\mu^-$
0.0230 ± 0.0025 ± 0.0013	86	ALBRECHT	87	ARG $\Upsilon(2S) \rightarrow \mu^+\mu^-$
0.029 ± 0.003 ± 0.002	864	BESSON	84	CLEO $\Upsilon(2S) \rightarrow \pi^+\pi^-\mu^+\mu^-$
0.027 ± 0.003 ± 0.003		ANDREWS	83	CLEO $e^+e^- \rightarrow \mu^+\mu^-$
0.032 ± 0.013 ± 0.003		ALBRECHT	82	DASP $e^+e^- \rightarrow \mu^+\mu^-$
0.038 ± 0.015 ± 0.002		NICZYPORUK	82	LENA $e^+e^- \rightarrow \mu^+\mu^-$
0.014 <sup>+0.034</sup> <sub>-0.014</sub>		BOCK	80	CNTR $e^+e^- \rightarrow \mu^+\mu^-$
0.022 ± 0.020		BERGER	79	PLUT $e^+e^- \rightarrow \mu^+\mu^-$

<sup>10</sup> Taking into account interference between the resonance and continuum.

$\Gamma(\tau^+\tau^-)/\Gamma(\mu^+\mu^-)$		$\Gamma_1/\Gamma_3$		
VALUE	EVTS	DOCUMENT ID	TECN	COMMENT
<b>1.008 ± 0.023 OUR AVERAGE</b>				
1.005 ± 0.013 ± 0.022	0.7M	11 DEL-AMO-SA...	10c	BABR $\Upsilon(3S) \rightarrow \pi^+\pi^-\Upsilon(1S)$
1.02 ± 0.02 ± 0.05	60k	BESSON	07	CLEO $e^+e^- \rightarrow \Upsilon(1S)$

<sup>11</sup> Allows any number of extra photons with total energy < 500 MeV.

$\Gamma(ggg)/\Gamma(\text{total})$		$\Gamma_4/\Gamma$		
VALUE (units $10^{-2}$ )	EVTS	DOCUMENT ID	TECN	COMMENT
<b>81.7 ± 0.7</b>	20M	12 BESSON	06A	CLEO $\Upsilon(1S) \rightarrow \text{hadrons}$

<sup>12</sup> Calculated using the value  $\Gamma(\gamma gg)/\Gamma(ggg) = (2.70 \pm 0.01 \pm 0.13 \pm 0.24)\%$  from BESSON 06A and PDG 08 values of  $B(\mu^+\mu^-) = (2.48 \pm 0.05)\%$  and  $R_{\text{hadrons}} = 3.51$ . The statistical error is negligible and the systematic error is partially correlated with that of  $\Gamma(\gamma gg)/\Gamma(\text{total})$  measurement of BESSON 06A.

$\Gamma(\gamma gg)/\Gamma(\text{total})$		$\Gamma_5/\Gamma$		
VALUE (units $10^{-2}$ )	EVTS	DOCUMENT ID	TECN	COMMENT
<b>2.20 ± 0.60</b>	400k	13 BESSON	06A	CLEO $\Upsilon(1S) \rightarrow \gamma + \text{hadrons}$

<sup>13</sup> Calculated using BESSON 06A values of  $\Gamma(\gamma gg)/\Gamma(ggg) = (2.70 \pm 0.01 \pm 0.13 \pm 0.24)\%$  and  $\Gamma(ggg)/\Gamma(\text{total})$ . The statistical error is negligible and the systematic error is partially correlated with that of  $\Gamma(ggg)/\Gamma(\text{total})$  measurement of BESSON 06A.





$\Gamma(\gamma f_0(980))/\Gamma_{\text{total}}$   $\Gamma_{36}/\Gamma$

VALUE (units $10^{-9}$ )	CL%	DOCUMENT ID	TECN	COMMENT
<3	90	21 ATHAR	06 CLE3	$\Upsilon(1S) \rightarrow \gamma \pi^+ \pi^-$

<sup>21</sup> Assuming  $B(f_0(980) \rightarrow \pi\pi) = 1$ .

$\Gamma(\gamma f_2'(1525))/\Gamma_{\text{total}}$   $\Gamma_{37}/\Gamma$

VALUE (units $10^{-5}$ )	CL%	EVTS	DOCUMENT ID	TECN	COMMENT
<b>3.8 ± 0.9 OUR AVERAGE</b>					
4.0 ± 1.4 ± 0.1	17 ± 5		22 BESSON	11 CLEO	$\Upsilon(1S) \rightarrow K_S^0 K_S^0$
3.7 ± 0.9 ± 0.8			ATHAR	06 CLE3	$\Upsilon(1S) \rightarrow \gamma K^+ K^-$

- • • We do not use the following data for averages, fits, limits, etc. • • •

<14	90	23 FULTON	90B CLEO	$\Upsilon(1S) \rightarrow \gamma K^+ K^-$
<19.4	90	23 ALBRECHT	89 ARG	$\Upsilon(1S) \rightarrow \gamma K^+ K^-$

<sup>22</sup> BESSON 11 reports  $(4.0 \pm 1.3 \pm 0.6) \times 10^{-5}$  from a measurement of  $[\Gamma(\Upsilon(1S) \rightarrow \gamma f_2'(1525))/\Gamma_{\text{total}}] \times [B(f_2'(1525) \rightarrow K\bar{K})]$  assuming  $B(f_2'(1525) \rightarrow K\bar{K}) = (88.8 \pm 3.1) \times 10^{-2}$ , which we rescale to our best value  $B(f_2'(1525) \rightarrow K\bar{K}) = (88.7 \pm 2.2) \times 10^{-2}$ . Our first error is their experiment's error and our second error is the systematic error from using our best value. The result also assumes  $B(K_S^0 \rightarrow \pi^+ \pi^-) = (69.20 \pm 0.05)\%$  and  $B(f_2'(1525) \rightarrow K\bar{K}) = 4 B(f_2'(1525) \rightarrow K_S^0 K_S^0)$ .

<sup>23</sup> Assuming  $B(f_2'(1525) \rightarrow K\bar{K}) = 0.71$ .

$\Gamma(\gamma f_2(1270))/\Gamma_{\text{total}}$   $\Gamma_{38}/\Gamma$

VALUE (units $10^{-5}$ )	CL%	DOCUMENT ID	TECN	COMMENT
<b>10.1 ± 0.9 OUR AVERAGE</b>				
10.5 ± 1.6 ± 1.9		24 BESSON	07A CLE3	$\Upsilon(1S) \rightarrow \gamma \pi^0 \pi^0$
10.2 ± 0.8 ± 0.7		ATHAR	06 CLE3	$\Upsilon(1S) \rightarrow \gamma \pi^+ \pi^-$
8.1 ± 2.3 ± 2.9		25 ANASTASSOV	99 CLE2	$e^+ e^- \rightarrow \text{hadrons}$

- • • We do not use the following data for averages, fits, limits, etc. • • •

<21	90	25 FULTON	90B CLEO	$\Upsilon(1S) \rightarrow \gamma \pi^+ \pi^-$
<13	90	25 ALBRECHT	89 ARG	$\Upsilon(1S) \rightarrow \gamma \pi^+ \pi^-$
<81	90	SCHMITT	88 CBAL	$\Upsilon(1S) \rightarrow \gamma X$

<sup>24</sup> Using  $B(f_2(1270) \rightarrow \pi^0 \pi^0) = B(f_2(1270) \rightarrow \pi\pi)/3$  and  $B(f_2(1270) \rightarrow \pi\pi) = (0.845 \pm 0.025 - 0.012)_\%$ .

<sup>25</sup> Using  $B(f_2(1270) \rightarrow \pi\pi) = 0.84$ .

$\Gamma(\gamma \eta(1405))/\Gamma_{\text{total}}$   $\Gamma_{39}/\Gamma$

VALUE (units $10^{-5}$ )	CL%	DOCUMENT ID	TECN	COMMENT
<8.2	90	26 FULTON	90B CLEO	$\Upsilon(1S) \rightarrow \gamma K^\pm \pi^\mp K_S^0$

<sup>26</sup> Includes unknown branching ratio of  $\eta(1405) \rightarrow K^\pm \pi^\mp K_S^0$ .

$\Gamma(\gamma f_0(1500))/\Gamma_{\text{total}}$   $\Gamma_{40}/\Gamma$

VALUE (units $10^{-5}$ )	CL%	DOCUMENT ID	TECN	COMMENT
<1.5	90	27 BESSON	07A CLEO	$e^+ e^- \rightarrow \Upsilon(1S) \rightarrow \gamma \pi^0 \pi^0$

- • • We do not use the following data for averages, fits, limits, etc. • • •

<6.1	90	28 BESSON	07A CLEO	$e^+ e^- \rightarrow \Upsilon(1S) \rightarrow \gamma \eta \eta$
------	----	-----------	----------	---

<sup>27</sup> Using  $B(f_0(1500) \rightarrow \pi^0 \pi^0) = B(f_0(1500) \rightarrow \pi\pi)/3$  and  $B(f_0(1500) \rightarrow \pi\pi) = (0.349 \pm 0.023)\%$ .

<sup>28</sup> Calculated by us using  $B(f_0(1500) \rightarrow \eta\eta) = (5.1 \pm 0.9)\%$ .

$\Gamma(\gamma f_0(1710))/\Gamma_{\text{total}}$   $\Gamma_{41}/\Gamma$

VALUE (units $10^{-4}$ )	CL%	DOCUMENT ID	TECN	COMMENT
< 2.6	90	29 ALBRECHT	89 ARG	$\Upsilon(1S) \rightarrow \gamma K^+ K^-$

- • • We do not use the following data for averages, fits, limits, etc. • • •

< 6.3	90	29 FULTON	90B CLEO	$\Upsilon(1S) \rightarrow \gamma K^+ K^-$
<19	90	29 FULTON	90B CLEO	$\Upsilon(1S) \rightarrow \gamma K_S^0 K_S^0$
< 8	90	30 ALBRECHT	89 ARG	$\Upsilon(1S) \rightarrow \gamma \pi^+ \pi^-$
<24	90	31 SCHMITT	88 CBAL	$\Upsilon(1S) \rightarrow \gamma X$

<sup>29</sup> Assuming  $B(f_0(1710) \rightarrow K\bar{K}) = 0.38$ .

<sup>30</sup> Assuming  $B(f_0(1710) \rightarrow \pi\pi) = 0.04$ .

<sup>31</sup> Assuming  $B(f_0(1710) \rightarrow \eta\eta) = 0.18$ .

$\Gamma(\gamma f_0(1710) \rightarrow \gamma K^+ K^-)/\Gamma_{\text{total}}$   $\Gamma_{42}/\Gamma$

VALUE (units $10^{-5}$ )	CL%	DOCUMENT ID	TECN	COMMENT
<0.7	90	ATHAR	06 CLEO	$e^+ e^- \rightarrow \Upsilon(1S) \rightarrow \gamma K^+ K^-$

$\Gamma(\gamma f_0(1710) \rightarrow \gamma \pi^0 \pi^0)/\Gamma_{\text{total}}$   $\Gamma_{43}/\Gamma$

VALUE (units $10^{-6}$ )	CL%	DOCUMENT ID	TECN	COMMENT
<1.4	90	BESSON	07A CLEO	$e^+ e^- \rightarrow \Upsilon(1S) \rightarrow \gamma \pi^0 \pi^0$

$\Gamma(\gamma f_0(1710) \rightarrow \gamma \eta \eta)/\Gamma_{\text{total}}$   $\Gamma_{44}/\Gamma$

VALUE (units $10^{-6}$ )	CL%	DOCUMENT ID	TECN	COMMENT
<1.8	90	BESSON	07A CLEO	$e^+ e^- \rightarrow \Upsilon(1S) \rightarrow \gamma \eta \eta$

$\Gamma(\gamma f_4(2050))/\Gamma_{\text{total}}$   $\Gamma_{45}/\Gamma$

VALUE (units $10^{-9}$ )	CL%	DOCUMENT ID	TECN	COMMENT
<5.3	90	32 ATHAR	06 CLE3	$\Upsilon(1S) \rightarrow \gamma \pi^+ \pi^-$

<sup>32</sup> Assuming  $B(f_4(2050) \rightarrow \pi\pi) = 0.17$ .

$\Gamma(\gamma f_0(2200) \rightarrow \gamma K^+ K^-)/\Gamma_{\text{total}}$   $\Gamma_{46}/\Gamma$

VALUE	CL%	DOCUMENT ID	TECN	COMMENT
<0.0002	90	BARU	89 MD1	$\Upsilon(1S) \rightarrow \gamma K^+ K^-$

$\Gamma(\gamma f_2(2220) \rightarrow \gamma K^+ K^-)/\Gamma_{\text{total}}$   $\Gamma_{47}/\Gamma$

VALUE (units $10^{-7}$ )	CL%	DOCUMENT ID	TECN	COMMENT
< 8	90	ATHAR	06 CLE3	$\Upsilon(1S) \rightarrow \gamma K^+ K^-$

- • • We do not use the following data for averages, fits, limits, etc. • • •

< 160	90	MASEK	02 CLEO	$\Upsilon(1S) \rightarrow \gamma K^+ K^-$
< 150	90	FULTON	90B CLEO	$\Upsilon(1S) \rightarrow \gamma K^+ K^-$
< 290	90	ALBRECHT	89 ARG	$\Upsilon(1S) \rightarrow \gamma K^+ K^-$
<2000	90	BARU	89 MD1	$\Upsilon(1S) \rightarrow \gamma K^+ K^-$

$\Gamma(\gamma f_2(2220) \rightarrow \gamma \pi^+ \pi^-)/\Gamma_{\text{total}}$   $\Gamma_{48}/\Gamma$

VALUE (units $10^{-7}$ )	CL%	DOCUMENT ID	TECN	COMMENT
< 6	90	ATHAR	06 CLE3	$\Upsilon(1S) \rightarrow \gamma \pi^+ \pi^-$

- • • We do not use the following data for averages, fits, limits, etc. • • •

<120	90	MASEK	02 CLEO	$\Upsilon(1S) \rightarrow \gamma \pi^+ \pi^-$
------	----	-------	---------	---

$\Gamma(\gamma f_2(2220) \rightarrow \gamma \rho \bar{\rho})/\Gamma_{\text{total}}$   $\Gamma_{49}/\Gamma$

VALUE (units $10^{-7}$ )	CL%	DOCUMENT ID	TECN	COMMENT
< 11	90	ATHAR	06 CLE3	$\Upsilon(1S) \rightarrow \gamma \rho \bar{\rho}$

- • • We do not use the following data for averages, fits, limits, etc. • • •

<160	90	MASEK	02 CLEO	$\Upsilon(1S) \rightarrow \gamma \rho \bar{\rho}$
------	----	-------	---------	---

$\Gamma(\gamma \eta(2225) \rightarrow \gamma \phi \phi)/\Gamma_{\text{total}}$   $\Gamma_{50}/\Gamma$

VALUE	CL%	DOCUMENT ID	TECN	COMMENT
<0.003	90	BARU	89 MD1	$\Upsilon(1S) \rightarrow \gamma K^+ K^- K^+ K^-$

$\Gamma(\gamma \eta_c(1S))/\Gamma_{\text{total}}$   $\Gamma_{51}/\Gamma$

VALUE (units $10^{-5}$ )	CL%	DOCUMENT ID	TECN	COMMENT
<5.7	90	SHEN	10A BELL	$\Upsilon(1S) \rightarrow \gamma X$

$\Gamma(\gamma \chi_{c0})/\Gamma_{\text{total}}$   $\Gamma_{52}/\Gamma$

VALUE (units $10^{-4}$ )	CL%	DOCUMENT ID	TECN	COMMENT
<6.5	90	SHEN	10A BELL	$\Upsilon(1S) \rightarrow \gamma X$

$\Gamma(\gamma \chi_{c1})/\Gamma_{\text{total}}$   $\Gamma_{53}/\Gamma$

VALUE (units $10^{-5}$ )	CL%	DOCUMENT ID	TECN	COMMENT
<2.3	90	SHEN	10A BELL	$\Upsilon(1S) \rightarrow \gamma X$

$\Gamma(\gamma \chi_{c2})/\Gamma_{\text{total}}$   $\Gamma_{54}/\Gamma$

VALUE (units $10^{-6}$ )	CL%	DOCUMENT ID	TECN	COMMENT
<7.6	90	SHEN	10A BELL	$\Upsilon(1S) \rightarrow \gamma X$

$\Gamma(\gamma X(3872) \rightarrow \pi^+ \pi^- J/\psi)/\Gamma_{\text{total}}$   $\Gamma_{55}/\Gamma$

VALUE (units $10^{-6}$ )	CL%	DOCUMENT ID	TECN	COMMENT
<1.6	90	SHEN	10A BELL	$\Upsilon(1S) \rightarrow \gamma X$

$\Gamma(\gamma X(3872) \rightarrow \pi^+ \pi^- \pi^0 J/\psi)/\Gamma_{\text{total}}$   $\Gamma_{56}/\Gamma$

VALUE (units $10^{-6}$ )	CL%	DOCUMENT ID	TECN	COMMENT
<2.8	90	SHEN	10A BELL	$\Upsilon(1S) \rightarrow \gamma X$

$\Gamma(\gamma X(3915) \rightarrow \omega J/\psi)/\Gamma_{\text{total}}$   $\Gamma_{57}/\Gamma$

VALUE (units $10^{-6}$ )	CL%	DOCUMENT ID	TECN	COMMENT
<3.0	90	SHEN	10A BELL	$\Upsilon(1S) \rightarrow \gamma X$

$\Gamma(\gamma X(4140) \rightarrow \phi J/\psi)/\Gamma_{\text{total}}$   $\Gamma_{58}/\Gamma$

VALUE (units $10^{-6}$ )	CL%	DOCUMENT ID	TECN	COMMENT
<2.2	90	SHEN	10A BELL	$\Upsilon(1S) \rightarrow \gamma X$

$\Gamma(\gamma X)/\Gamma_{\text{total}}$   $\Gamma_{59}/\Gamma$   
( $X = \text{scalar with } m < 8.0 \text{ GeV}$ )

VALUE (units $10^{-6}$ )	CL%	DOCUMENT ID	TECN	COMMENT
< 4.5	90	33 DEL-AMO-SA...11J	BABR	$e^+ e^- \rightarrow \gamma + X$

- • • We do not use the following data for averages, fits, limits, etc. • • •

<30	90	34 BALEST	95 CLEO	$e^+ e^- \rightarrow \gamma + X$
-----	----	-----------	---------	----------------------------------

<sup>33</sup> For a noninteracting scalar  $X$  with mass  $m < 8.0 \text{ GeV}$ .

<sup>34</sup> For a noninteracting pseudoscalar  $X$  with mass  $< 7.2 \text{ GeV}$ .

$\Gamma(\gamma X\bar{X}(m_X < 3.1 \text{ GeV}))/\Gamma_{\text{total}}$   $\Gamma_{60}/\Gamma$   
( $X\bar{X} = \text{vectors with } m < 3.1 \text{ GeV}$ )

VALUE (units $10^{-3}$ )	CL%	DOCUMENT ID	TECN	COMMENT
<1	90	35 BALEST	95 CLEO	$e^+ e^- \rightarrow \gamma + X\bar{X}$

<sup>35</sup> For a noninteracting vector  $X$  with mass  $< 3.1 \text{ GeV}$ .



$\Gamma(\pi^+ \pi^- K^+ K^- \pi^0)/\Gamma_{total}$   $\Gamma_3/\Gamma$ 

VALUE (units $10^{-4}$ )	CL%	DOCUMENT ID	TECN	COMMENT
<1.6	90	6 ASNER	08A CLEO	$\Upsilon(2S) \rightarrow \gamma \pi^+ \pi^- K^+ K^- \pi^0$ 6 ASNER 08A reports $[\Gamma(\chi_{b0}(1P) \rightarrow \pi^+ \pi^- K^+ K^- \pi^0)/\Gamma_{total}] \times [B(\Upsilon(2S) \rightarrow \gamma \chi_{b0}(1P))] < 6 \times 10^{-6}$ which we divide by our best value $B(\Upsilon(2S) \rightarrow \gamma \chi_{b0}(1P)) = 3.8 \times 10^{-2}$ .

 $\Gamma(2\pi^+ \pi^- K^- K_S^0)/\Gamma_{total}$   $\Gamma_4/\Gamma$ 

VALUE (units $10^{-4}$ )	CL%	DOCUMENT ID	TECN	COMMENT
<0.5	90	7 ASNER	08A CLEO	$\Upsilon(2S) \rightarrow \gamma 2\pi^+ \pi^- K^- K_S^0$ 7 ASNER 08A reports $[\Gamma(\chi_{b0}(1P) \rightarrow 2\pi^+ \pi^- K^- K_S^0)/\Gamma_{total}] \times [B(\Upsilon(2S) \rightarrow \gamma \chi_{b0}(1P))] < 2 \times 10^{-6}$ which we divide by our best value $B(\Upsilon(2S) \rightarrow \gamma \chi_{b0}(1P)) = 3.8 \times 10^{-2}$ .

 $\Gamma(2\pi^+ \pi^- K^- K_S^0 2\pi^0)/\Gamma_{total}$   $\Gamma_5/\Gamma$ 

VALUE (units $10^{-4}$ )	CL%	DOCUMENT ID	TECN	COMMENT
<5	90	8 ASNER	08A CLEO	$\Upsilon(2S) \rightarrow \gamma 2\pi^+ \pi^- K^- 2\pi^0$ 8 ASNER 08A reports $[\Gamma(\chi_{b0}(1P) \rightarrow 2\pi^+ \pi^- K^- K_S^0 2\pi^0)/\Gamma_{total}] \times [B(\Upsilon(2S) \rightarrow \gamma \chi_{b0}(1P))] < 18 \times 10^{-6}$ which we divide by our best value $B(\Upsilon(2S) \rightarrow \gamma \chi_{b0}(1P)) = 3.8 \times 10^{-2}$ .

 $\Gamma(2\pi^+ 2\pi^- 2\pi^0)/\Gamma_{total}$   $\Gamma_6/\Gamma$ 

VALUE (units $10^{-4}$ )	CL%	DOCUMENT ID	TECN	COMMENT
<2.1	90	9 ASNER	08A CLEO	$\Upsilon(2S) \rightarrow \gamma 2\pi^+ 2\pi^- 2\pi^0$ 9 ASNER 08A reports $[\Gamma(\chi_{b0}(1P) \rightarrow 2\pi^+ 2\pi^- 2\pi^0)/\Gamma_{total}] \times [B(\Upsilon(2S) \rightarrow \gamma \chi_{b0}(1P))] < 8 \times 10^{-6}$ which we divide by our best value $B(\Upsilon(2S) \rightarrow \gamma \chi_{b0}(1P)) = 3.8 \times 10^{-2}$ .

 $\Gamma(2\pi^+ 2\pi^- K^+ K^-)/\Gamma_{total}$   $\Gamma_7/\Gamma$ 

VALUE (units $10^{-4}$ )	EVTS	DOCUMENT ID	TECN	COMMENT
$1.1 \pm 0.6 \pm 0.1$	7	10 ASNER	08A CLEO	$\Upsilon(2S) \rightarrow \gamma 2\pi^+ 2\pi^- K^+ K^-$ 10 ASNER 08A reports $[\Gamma(\chi_{b0}(1P) \rightarrow 2\pi^+ 2\pi^- K^+ K^-)/\Gamma_{total}] \times [B(\Upsilon(2S) \rightarrow \gamma \chi_{b0}(1P))] = (4 \pm 2 \pm 1) \times 10^{-6}$ which we divide by our best value $B(\Upsilon(2S) \rightarrow \gamma \chi_{b0}(1P)) = (3.8 \pm 0.4) \times 10^{-2}$ . Our first error is their experiment's error and our second error is the systematic error from using our best value.

 $\Gamma(2\pi^+ 2\pi^- K^+ K^- \pi^0)/\Gamma_{total}$   $\Gamma_8/\Gamma$ 

VALUE (units $10^{-4}$ )	CL%	DOCUMENT ID	TECN	COMMENT
<2.7	90	11 ASNER	08A CLEO	$\Upsilon(2S) \rightarrow \gamma 2\pi^+ 2\pi^- K^+ K^- \pi^0$ 11 ASNER 08A reports $[\Gamma(\chi_{b0}(1P) \rightarrow 2\pi^+ 2\pi^- K^+ K^- \pi^0)/\Gamma_{total}] \times [B(\Upsilon(2S) \rightarrow \gamma \chi_{b0}(1P))] < 10 \times 10^{-6}$ which we divide by our best value $B(\Upsilon(2S) \rightarrow \gamma \chi_{b0}(1P)) = 3.8 \times 10^{-2}$ .

 $\Gamma(2\pi^+ 2\pi^- K^+ K^- 2\pi^0)/\Gamma_{total}$   $\Gamma_9/\Gamma$ 

VALUE (units $10^{-4}$ )	CL%	DOCUMENT ID	TECN	COMMENT
<5	90	12 ASNER	08A CLEO	$\Upsilon(2S) \rightarrow \gamma 2\pi^+ 2\pi^- K^+ K^- 2\pi^0$ 12 ASNER 08A reports $[\Gamma(\chi_{b0}(1P) \rightarrow 2\pi^+ 2\pi^- K^+ K^- 2\pi^0)/\Gamma_{total}] \times [B(\Upsilon(2S) \rightarrow \gamma \chi_{b0}(1P))] < 20 \times 10^{-6}$ which we divide by our best value $B(\Upsilon(2S) \rightarrow \gamma \chi_{b0}(1P)) = 3.8 \times 10^{-2}$ .

 $\Gamma(3\pi^+ 2\pi^- K^- K_S^0 \pi^0)/\Gamma_{total}$   $\Gamma_{10}/\Gamma$ 

VALUE (units $10^{-4}$ )	CL%	DOCUMENT ID	TECN	COMMENT
<1.6	90	13 ASNER	08A CLEO	$\Upsilon(2S) \rightarrow \gamma 3\pi^+ 2\pi^- K^- K_S^0 \pi^0$ 13 ASNER 08A reports $[\Gamma(\chi_{b0}(1P) \rightarrow 3\pi^+ 2\pi^- K^- K_S^0 \pi^0)/\Gamma_{total}] \times [B(\Upsilon(2S) \rightarrow \gamma \chi_{b0}(1P))] < 6 \times 10^{-6}$ which we divide by our best value $B(\Upsilon(2S) \rightarrow \gamma \chi_{b0}(1P)) = 3.8 \times 10^{-2}$ .

 $\Gamma(3\pi^+ 3\pi^-)/\Gamma_{total}$   $\Gamma_{11}/\Gamma$ 

VALUE (units $10^{-4}$ )	CL%	DOCUMENT ID	TECN	COMMENT
<0.8	90	14 ASNER	08A CLEO	$\Upsilon(2S) \rightarrow \gamma 3\pi^+ 3\pi^-$ 14 ASNER 08A reports $[\Gamma(\chi_{b0}(1P) \rightarrow 3\pi^+ 3\pi^-)/\Gamma_{total}] \times [B(\Upsilon(2S) \rightarrow \gamma \chi_{b0}(1P))] < 3 \times 10^{-6}$ which we divide by our best value $B(\Upsilon(2S) \rightarrow \gamma \chi_{b0}(1P)) = 3.8 \times 10^{-2}$ .

 $\Gamma(3\pi^+ 3\pi^- 2\pi^0)/\Gamma_{total}$   $\Gamma_{12}/\Gamma$ 

VALUE (units $10^{-4}$ )	CL%	DOCUMENT ID	TECN	COMMENT
<6	90	15 ASNER	08A CLEO	$\Upsilon(2S) \rightarrow \gamma 3\pi^+ 3\pi^- 2\pi^0$ 15 ASNER 08A reports $[\Gamma(\chi_{b0}(1P) \rightarrow 3\pi^+ 3\pi^- 2\pi^0)/\Gamma_{total}] \times [B(\Upsilon(2S) \rightarrow \gamma \chi_{b0}(1P))] < 22 \times 10^{-6}$ which we divide by our best value $B(\Upsilon(2S) \rightarrow \gamma \chi_{b0}(1P)) = 3.8 \times 10^{-2}$ .

 $\Gamma(3\pi^+ 3\pi^- K^+ K^-)/\Gamma_{total}$   $\Gamma_{13}/\Gamma$ 

VALUE (units $10^{-4}$ )	EVTS	DOCUMENT ID	TECN	COMMENT
$2.4 \pm 1.2 \pm 0.2$	9	16 ASNER	08A CLEO	$\Upsilon(2S) \rightarrow \gamma 3\pi^+ 3\pi^- K^+ K^-$ 16 ASNER 08A reports $[\Gamma(\chi_{b0}(1P) \rightarrow 3\pi^+ 3\pi^- K^+ K^-)/\Gamma_{total}] \times [B(\Upsilon(2S) \rightarrow \gamma \chi_{b0}(1P))] = (9 \pm 4 \pm 2) \times 10^{-6}$ which we divide by our best value $B(\Upsilon(2S) \rightarrow \gamma \chi_{b0}(1P)) = (3.8 \pm 0.4) \times 10^{-2}$ . Our first error is their experiment's error and our second error is the systematic error from using our best value.

 $\Gamma(3\pi^+ 3\pi^- K^+ K^- \pi^0)/\Gamma_{total}$   $\Gamma_{14}/\Gamma$ 

VALUE (units $10^{-4}$ )	CL%	DOCUMENT ID	TECN	COMMENT
<10	90	17 ASNER	08A CLEO	$\Upsilon(2S) \rightarrow \gamma 3\pi^+ 3\pi^- K^+ K^- \pi^0$ 17 ASNER 08A reports $[\Gamma(\chi_{b0}(1P) \rightarrow 3\pi^+ 3\pi^- K^+ K^- \pi^0)/\Gamma_{total}] \times [B(\Upsilon(2S) \rightarrow \gamma \chi_{b0}(1P))] < 37 \times 10^{-6}$ which we divide by our best value $B(\Upsilon(2S) \rightarrow \gamma \chi_{b0}(1P)) = 3.8 \times 10^{-2}$ .

 $\Gamma(4\pi^+ 4\pi^-)/\Gamma_{total}$   $\Gamma_{15}/\Gamma$ 

VALUE (units $10^{-4}$ )	CL%	DOCUMENT ID	TECN	COMMENT
<0.8	90	18 ASNER	08A CLEO	$\Upsilon(2S) \rightarrow \gamma 4\pi^+ 4\pi^-$ 18 ASNER 08A reports $[\Gamma(\chi_{b0}(1P) \rightarrow 4\pi^+ 4\pi^-)/\Gamma_{total}] \times [B(\Upsilon(2S) \rightarrow \gamma \chi_{b0}(1P))] < 3 \times 10^{-6}$ which we divide by our best value $B(\Upsilon(2S) \rightarrow \gamma \chi_{b0}(1P)) = 3.8 \times 10^{-2}$ .

 $\Gamma(4\pi^+ 4\pi^- 2\pi^0)/\Gamma_{total}$   $\Gamma_{16}/\Gamma$ 

VALUE (units $10^{-4}$ )	CL%	DOCUMENT ID	TECN	COMMENT
<21	90	19 ASNER	08A CLEO	$\Upsilon(2S) \rightarrow \gamma 4\pi^+ 4\pi^- 2\pi^0$ 19 ASNER 08A reports $[\Gamma(\chi_{b0}(1P) \rightarrow 4\pi^+ 4\pi^- 2\pi^0)/\Gamma_{total}] \times [B(\Upsilon(2S) \rightarrow \gamma \chi_{b0}(1P))] < 77 \times 10^{-6}$ which we divide by our best value $B(\Upsilon(2S) \rightarrow \gamma \chi_{b0}(1P)) = 3.8 \times 10^{-2}$ .

 $\chi_{b0}(1P)$  CROSS-PARTICLE BRANCHING RATIOS $\Gamma(\chi_{b0}(1P) \rightarrow \gamma \Upsilon(1S))/\Gamma_{total} \times \Gamma(\Upsilon(2S) \rightarrow \gamma \chi_{b0}(1P))/\Gamma_{total}$ 

VALUE	CL%	DOCUMENT ID	TECN	COMMENT
<1.7 $\times 10^{-3}$	90	20 LEES	11J BABR	$\Upsilon(2S) \rightarrow X \gamma$ 20 LEES 11J quotes a central value of $\Gamma(\chi_{b0}(1P) \rightarrow \gamma \Upsilon(1S))/\Gamma_{total} \times \Gamma(\Upsilon(2S) \rightarrow \gamma \chi_{b0}(1P))/\Gamma_{total} = (8.3 \pm 5.6 \pm 3.7) \times 10^{-4}$ and derives a 90% CL upper limit of $\Gamma(\gamma \Upsilon(1S))/\Gamma_{total} < 4.6\%$ using $B(\Upsilon(4S) \rightarrow \gamma \chi_{b0}(1P)) = (3.8 \pm 0.4)\%$ .

 $B(\chi_{b0}(1P) \rightarrow \gamma \Upsilon(1S)) \times B(\Upsilon(2S) \rightarrow \gamma \chi_{b0}(1P)) \times B(\Upsilon(1S) \rightarrow \ell^+ \ell^-)$ 

VALUE (units $10^{-5}$ )	EVTS	DOCUMENT ID	TECN	COMMENT
$1.63 \pm 0.24 \pm 0.15$	87	KORNICER	11 CLEO	$e^+ e^- \rightarrow \gamma \gamma \ell^+ \ell^-$

 $\chi_{b0}(1P)$  REFERENCES

KORNICER	11	PR D83 054003	M. Kornicer <i>et al.</i>	(CLEO Collab.)
LEES	11J	PR D84 072002	J.P. Lees <i>et al.</i>	(BABAR Collab.)
ASNER	08A	PR D78 031103	D.M. Asner <i>et al.</i>	(CLEO Collab.)
BRIERE	08	PR D78 092007	R.A. Briere <i>et al.</i>	(CLEO Collab.)
ARTUSO	05	PRL 94 032001	M. Artuso <i>et al.</i>	(CLEO Collab.)
EDWARDS	99	PR D59 032003	K.W. Edwards <i>et al.</i>	(CLEO Collab.)
WALK	86	PR D34 2611	W.S. Walk <i>et al.</i>	(Crystal Ball Collab.)
ALBRECHT	85E	PL 160B 331	H. Albrecht <i>et al.</i>	(ARGUS Collab.)
NERNST	85	PRL 54 2195	R. Nernst <i>et al.</i>	(Crystal Ball Collab.)
HAAS	84	PRL 52 799	J. Haas <i>et al.</i>	(CLEO Collab.)
KLOPFEN...	83	PRL 51 160	C. Klopfenstein <i>et al.</i>	(CUSB Collab.)
PAUSS	83	PL 130B 439	F. Pauss <i>et al.</i>	(MPIM, COLU, CORN, LSU)

 $\chi_{b1}(1P)$ 

$J^{PC} = 0^{+}(1^{+})$

 $J$  needs confirmation.

Observed in radiative decay of the  $\Upsilon(2S)$ , therefore  $C = +$ . Branching ratio requires  $E1$  transition,  $M1$  is strongly disfavored, therefore  $P = +$ .  $J = 1$  from SKWARNICKI 87.

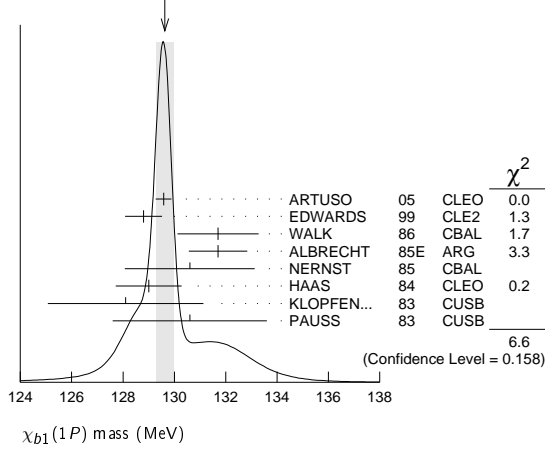
 $\chi_{b1}(1P)$  MASS

VALUE (MeV)	DOCUMENT ID
$9892.78 \pm 0.26 \pm 0.31$ OUR EVALUATION	From average $\gamma$ energy below, using $\Upsilon(2S)$ mass = 10023.26 $\pm$ 0.31 MeV

 $\gamma$  ENERGY IN  $\Upsilon(2S)$  DECAY

VALUE (MeV)	DOCUMENT ID	TECN	COMMENT
$129.63 \pm 0.33$ OUR AVERAGE	Error includes scale factor of 1.3. See the ideogram below.		
129.58 $\pm 0.09 \pm 0.29$	ARTUSO 05	CLEO	$\Upsilon(2S) \rightarrow \gamma X$
128.8 $\pm 0.4 \pm 0.6$	EDWARDS 99	CLE2	$\Upsilon(2S) \rightarrow \gamma \chi(1P)$
131.7 $\pm 0.9 \pm 1.3$	WALK 86	CBAL	$\Upsilon(2S) \rightarrow \gamma \gamma \ell^+ \ell^-$
131.7 $\pm 0.3 \pm 1.1$	ALBRECHT 85E	ARG	$\Upsilon(2S) \rightarrow \text{conv. } \gamma X$
130.6 $\pm 0.8 \pm 2.4$	NERNST 85	CBAL	$\Upsilon(2S) \rightarrow \gamma X$
129 $\pm 0.8 \pm 1$	HAAS 84	CLEO	$\Upsilon(2S) \rightarrow \text{conv. } \gamma X$
128.1 $\pm 0.4 \pm 3.0$	KLOPFEN... 83	CUSB	$\Upsilon(2S) \rightarrow \gamma X$
130.6 $\pm 3.0$	PAUSS 83	CUSB	$\Upsilon(2S) \rightarrow \gamma \gamma \ell^+ \ell^-$

## Meson Particle Listings

 $\chi_{b1}(1P)$ WEIGHTED AVERAGE  
129.63±0.33 (Error scaled by 1.3) $\chi_{b1}(1P)$  DECAY MODES

Mode	Fraction ( $\Gamma_i/\Gamma$ )	Confidence level
$\Gamma_1$ $\gamma \mathcal{T}(1S)$	(33.9±2.2) %	90%
$\Gamma_2$ $D^0 X$	(12.6±2.2) %	
$\Gamma_3$ $\pi^+ \pi^- K^+ K^- \pi^0$	(2.0±0.6) × 10 <sup>-4</sup>	
$\Gamma_4$ $2\pi^+ \pi^- K^- K_S^0$	(1.3±0.5) × 10 <sup>-4</sup>	
$\Gamma_5$ $2\pi^+ \pi^- K^- K_S^0 2\pi^0$	< 6 × 10 <sup>-4</sup>	
$\Gamma_6$ $2\pi^+ 2\pi^- 2\pi^0$	(8.0±2.5) × 10 <sup>-4</sup>	
$\Gamma_7$ $2\pi^+ 2\pi^- K^+ K^-$	(1.5±0.5) × 10 <sup>-4</sup>	
$\Gamma_8$ $2\pi^+ 2\pi^- K^+ K^- \pi^0$	(3.5±1.2) × 10 <sup>-4</sup>	
$\Gamma_9$ $2\pi^+ 2\pi^- K^+ K^- 2\pi^0$	(8.6±3.2) × 10 <sup>-4</sup>	
$\Gamma_{10}$ $3\pi^+ 2\pi^- K^- K_S^0 \pi^0$	(9.3±3.3) × 10 <sup>-4</sup>	
$\Gamma_{11}$ $3\pi^+ 3\pi^-$	(1.9±0.6) × 10 <sup>-4</sup>	
$\Gamma_{12}$ $3\pi^+ 3\pi^- 2\pi^0$	(1.7±0.5) × 10 <sup>-3</sup>	
$\Gamma_{13}$ $3\pi^+ 3\pi^- K^+ K^-$	(2.6±0.8) × 10 <sup>-4</sup>	
$\Gamma_{14}$ $3\pi^+ 3\pi^- K^+ K^- \pi^0$	(7.5±2.6) × 10 <sup>-4</sup>	
$\Gamma_{15}$ $4\pi^+ 4\pi^-$	(2.6±0.9) × 10 <sup>-4</sup>	
$\Gamma_{16}$ $4\pi^+ 4\pi^- 2\pi^0$	(1.4±0.6) × 10 <sup>-3</sup>	

 $\chi_{b1}(1P)$  BRANCHING RATIOS

$\Gamma(\gamma \mathcal{T}(1S))/\Gamma_{total}$	$\Gamma_1/\Gamma$			
VALUE (units 10 <sup>-4</sup> )	EVTS	DOCUMENT ID	TECN	COMMENT
<b>0.339±0.022 OUR AVERAGE</b>				
0.331±0.018±0.017	3222	<sup>1,2</sup> KORNICER 11	CLEO	$e^+e^- \rightarrow \gamma \ell^+ \ell^-$
0.350±0.023±0.018	13k	<sup>3</sup> LEES 11J	BABR	$\mathcal{T}(2S) \rightarrow X \gamma$
0.32 ± 0.06 ± 0.07		WALK 86	CBAL	$\mathcal{T}(2S) \rightarrow \gamma \ell^+ \ell^-$
0.47 ± 0.18		KLOPFEN... 83	CUSB	$\mathcal{T}(2S) \rightarrow \gamma \ell^+ \ell^-$

<sup>1</sup> Assuming  $B(\mathcal{T}(1S) \rightarrow \ell^+ \ell^-) = (2.48 \pm 0.05)\%$ .<sup>2</sup> KORNICER 11 reports  $[\Gamma(\chi_{b1}(1P) \rightarrow \gamma \mathcal{T}(1S))/\Gamma_{total}] \times [B(\mathcal{T}(2S) \rightarrow \gamma \chi_{b1}(1P))] = (22.8 \pm 0.4 \pm 1.2) \times 10^{-3}$  which we divide by our best value  $B(\mathcal{T}(2S) \rightarrow \gamma \chi_{b1}(1P)) = (6.9 \pm 0.4) \times 10^{-2}$ . Our first error is their experiment's error and our second error is the systematic error from using our best value.<sup>3</sup> LEES 11J reports  $[\Gamma(\chi_{b1}(1P) \rightarrow \gamma \mathcal{T}(1S))/\Gamma_{total}] \times [B(\mathcal{T}(2S) \rightarrow \gamma \chi_{b1}(1P))] = (24.1 \pm 0.6 \pm 1.5) \times 10^{-3}$  which we divide by our best value  $B(\mathcal{T}(2S) \rightarrow \gamma \chi_{b1}(1P)) = (6.9 \pm 0.4) \times 10^{-2}$ . Our first error is their experiment's error and our second error is the systematic error from using our best value.

$\Gamma(D^0 X)/\Gamma_{total}$	$\Gamma_2/\Gamma$			
VALUE (units 10 <sup>-2</sup> )	EVTS	DOCUMENT ID	TECN	COMMENT
<b>12.6±1.9±1.1</b>	2310	<sup>4</sup> BRIERE 08	CLEO	$\mathcal{T}(2S) \rightarrow \gamma D^0 X$

<sup>4</sup> For  $p_{D^0} > 2.5$  GeV/c.

$\Gamma(\pi^+ \pi^- K^+ K^- \pi^0)/\Gamma_{total}$	$\Gamma_3/\Gamma$			
VALUE (units 10 <sup>-4</sup> )	EVTS	DOCUMENT ID	TECN	COMMENT
<b>2.0±0.6±0.1</b>	18	<sup>5</sup> ASNER 08A	CLEO	$\mathcal{T}(2S) \rightarrow \gamma \pi^+ \pi^- K^+ K^- \pi^0$

<sup>5</sup> ASNER 08A reports  $[\Gamma(\chi_{b1}(1P) \rightarrow \pi^+ \pi^- K^+ K^- \pi^0)/\Gamma_{total}] \times [B(\mathcal{T}(2S) \rightarrow \gamma \chi_{b1}(1P))] = (14 \pm 3 \pm 3) \times 10^{-6}$  which we divide by our best value  $B(\mathcal{T}(2S) \rightarrow \gamma \chi_{b1}(1P)) = (6.9 \pm 0.4) \times 10^{-2}$ . Our first error is their experiment's error and our second error is the systematic error from using our best value. $\Gamma(2\pi^+ \pi^- K^- K_S^0)/\Gamma_{total}$   $\Gamma_4/\Gamma$ 

VALUE (units 10 <sup>-4</sup> )	EVTS	DOCUMENT ID	TECN	COMMENT
<b>1.3±0.5±0.1</b>	11	<sup>6</sup> ASNER 08A	CLEO	$\mathcal{T}(2S) \rightarrow \gamma 2\pi^+ \pi^- K^- K_S^0$
<sup>6</sup> ASNER 08A reports $[\Gamma(\chi_{b1}(1P) \rightarrow 2\pi^+ \pi^- K^- K_S^0)/\Gamma_{total}] \times [B(\mathcal{T}(2S) \rightarrow \gamma \chi_{b1}(1P))] = (9 \pm 3 \pm 2) \times 10^{-6}$ which we divide by our best value $B(\mathcal{T}(2S) \rightarrow \gamma \chi_{b1}(1P)) = (6.9 \pm 0.4) \times 10^{-2}$ . Our first error is their experiment's error and our second error is the systematic error from using our best value.				

 $\Gamma(2\pi^+ \pi^- K^- K_S^0 2\pi^0)/\Gamma_{total}$   $\Gamma_5/\Gamma$ 

VALUE (units 10 <sup>-4</sup> )	CL%	DOCUMENT ID	TECN	COMMENT
<b>&lt;6</b>	90	<sup>7</sup> ASNER 08A	CLEO	$\mathcal{T}(2S) \rightarrow \gamma 2\pi^+ \pi^- K^- 2\pi^0$
<sup>7</sup> ASNER 08A reports $[\Gamma(\chi_{b1}(1P) \rightarrow 2\pi^+ \pi^- K^- K_S^0 2\pi^0)/\Gamma_{total}] \times [B(\mathcal{T}(2S) \rightarrow \gamma \chi_{b1}(1P))] < 42 \times 10^{-6}$ which we divide by our best value $B(\mathcal{T}(2S) \rightarrow \gamma \chi_{b1}(1P)) = 6.9 \times 10^{-2}$ .				

 $\Gamma(2\pi^+ 2\pi^- 2\pi^0)/\Gamma_{total}$   $\Gamma_6/\Gamma$ 

VALUE (units 10 <sup>-4</sup> )	EVTS	DOCUMENT ID	TECN	COMMENT
<b>8.0±2.4±0.4</b>	46	<sup>8</sup> ASNER 08A	CLEO	$\mathcal{T}(2S) \rightarrow \gamma 2\pi^+ 2\pi^- 2\pi^0$
<sup>8</sup> ASNER 08A reports $[\Gamma(\chi_{b1}(1P) \rightarrow 2\pi^+ 2\pi^- 2\pi^0)/\Gamma_{total}] \times [B(\mathcal{T}(2S) \rightarrow \gamma \chi_{b1}(1P))] = (55 \pm 9 \pm 14) \times 10^{-6}$ which we divide by our best value $B(\mathcal{T}(2S) \rightarrow \gamma \chi_{b1}(1P)) = (6.9 \pm 0.4) \times 10^{-2}$ . Our first error is their experiment's error and our second error is the systematic error from using our best value.				

 $\Gamma(2\pi^+ 2\pi^- K^+ K^-)/\Gamma_{total}$   $\Gamma_7/\Gamma$ 

VALUE (units 10 <sup>-4</sup> )	EVTS	DOCUMENT ID	TECN	COMMENT
<b>1.5±0.5±0.1</b>	18	<sup>9</sup> ASNER 08A	CLEO	$\mathcal{T}(2S) \rightarrow \gamma 2\pi^+ 2\pi^- K^+ K^-$
<sup>9</sup> ASNER 08A reports $[\Gamma(\chi_{b1}(1P) \rightarrow 2\pi^+ 2\pi^- K^+ K^-)/\Gamma_{total}] \times [B(\mathcal{T}(2S) \rightarrow \gamma \chi_{b1}(1P))] = (10 \pm 3 \pm 2) \times 10^{-6}$ which we divide by our best value $B(\mathcal{T}(2S) \rightarrow \gamma \chi_{b1}(1P)) = (6.9 \pm 0.4) \times 10^{-2}$ . Our first error is their experiment's error and our second error is the systematic error from using our best value.				

 $\Gamma(2\pi^+ 2\pi^- K^+ K^- \pi^0)/\Gamma_{total}$   $\Gamma_8/\Gamma$ 

VALUE (units 10 <sup>-4</sup> )	EVTS	DOCUMENT ID	TECN	COMMENT
<b>3.5±1.2±0.2</b>	22	<sup>10</sup> ASNER 08A	CLEO	$\mathcal{T}(2S) \rightarrow \gamma 2\pi^+ 2\pi^- K^+ K^- \pi^0$
<sup>10</sup> ASNER 08A reports $[\Gamma(\chi_{b1}(1P) \rightarrow 2\pi^+ 2\pi^- K^+ K^- \pi^0)/\Gamma_{total}] \times [B(\mathcal{T}(2S) \rightarrow \gamma \chi_{b1}(1P))] = (24 \pm 6 \pm 6) \times 10^{-6}$ which we divide by our best value $B(\mathcal{T}(2S) \rightarrow \gamma \chi_{b1}(1P)) = (6.9 \pm 0.4) \times 10^{-2}$ . Our first error is their experiment's error and our second error is the systematic error from using our best value.				

 $\Gamma(2\pi^+ 2\pi^- K^+ K^- 2\pi^0)/\Gamma_{total}$   $\Gamma_9/\Gamma$ 

VALUE (units 10 <sup>-4</sup> )	EVTS	DOCUMENT ID	TECN	COMMENT
<b>8.6±3.2±0.4</b>	26	<sup>11</sup> ASNER 08A	CLEO	$\mathcal{T}(2S) \rightarrow \gamma 2\pi^+ 2\pi^- K^+ K^- 2\pi^0$
<sup>11</sup> ASNER 08A reports $[\Gamma(\chi_{b1}(1P) \rightarrow 2\pi^+ 2\pi^- K^+ K^- 2\pi^0)/\Gamma_{total}] \times [B(\mathcal{T}(2S) \rightarrow \gamma \chi_{b1}(1P))] = (59 \pm 14 \pm 17) \times 10^{-6}$ which we divide by our best value $B(\mathcal{T}(2S) \rightarrow \gamma \chi_{b1}(1P)) = (6.9 \pm 0.4) \times 10^{-2}$ . Our first error is their experiment's error and our second error is the systematic error from using our best value.				

 $\Gamma(3\pi^+ 2\pi^- K^- K_S^0 \pi^0)/\Gamma_{total}$   $\Gamma_{10}/\Gamma$ 

VALUE (units 10 <sup>-4</sup> )	EVTS	DOCUMENT ID	TECN	COMMENT
<b>9.3±3.3±0.5</b>	21	<sup>12</sup> ASNER 08A	CLEO	$\mathcal{T}(2S) \rightarrow \gamma 3\pi^+ 2\pi^- K^- K_S^0 \pi^0$
<sup>12</sup> ASNER 08A reports $[\Gamma(\chi_{b1}(1P) \rightarrow 3\pi^+ 2\pi^- K^- K_S^0 \pi^0)/\Gamma_{total}] \times [B(\mathcal{T}(2S) \rightarrow \gamma \chi_{b1}(1P))] = (64 \pm 16 \pm 16) \times 10^{-6}$ which we divide by our best value $B(\mathcal{T}(2S) \rightarrow \gamma \chi_{b1}(1P)) = (6.9 \pm 0.4) \times 10^{-2}$ . Our first error is their experiment's error and our second error is the systematic error from using our best value.				

 $\Gamma(3\pi^+ 3\pi^-)/\Gamma_{total}$   $\Gamma_{11}/\Gamma$ 

VALUE (units 10 <sup>-4</sup> )	EVTS	DOCUMENT ID	TECN	COMMENT
<b>1.9±0.6±0.1</b>	25	<sup>13</sup> ASNER 08A	CLEO	$\mathcal{T}(2S) \rightarrow \gamma 3\pi^+ 3\pi^-$
<sup>13</sup> ASNER 08A reports $[\Gamma(\chi_{b1}(1P) \rightarrow 3\pi^+ 3\pi^-)/\Gamma_{total}] \times [B(\mathcal{T}(2S) \rightarrow \gamma \chi_{b1}(1P))] = (13 \pm 3 \pm 3) \times 10^{-6}$ which we divide by our best value $B(\mathcal{T}(2S) \rightarrow \gamma \chi_{b1}(1P)) = (6.9 \pm 0.4) \times 10^{-2}$ . Our first error is their experiment's error and our second error is the systematic error from using our best value.				

 $\Gamma(3\pi^+ 3\pi^- 2\pi^0)/\Gamma_{total}$   $\Gamma_{12}/\Gamma$ 

VALUE (units 10 <sup>-4</sup> )	EVTS	DOCUMENT ID	TECN	COMMENT
<b>17±5±1</b>	56	<sup>14</sup> ASNER 08A	CLEO	$\mathcal{T}(2S) \rightarrow \gamma 3\pi^+ 3\pi^- 2\pi^0$
<sup>14</sup> ASNER 08A reports $[\Gamma(\chi_{b1}(1P) \rightarrow 3\pi^+ 3\pi^- 2\pi^0)/\Gamma_{total}] \times [B(\mathcal{T}(2S) \rightarrow \gamma \chi_{b1}(1P))] = (119 \pm 18 \pm 32) \times 10^{-6}$ which we divide by our best value $B(\mathcal{T}(2S) \rightarrow \gamma \chi_{b1}(1P)) = (6.9 \pm 0.4) \times 10^{-2}$ . Our first error is their experiment's error and our second error is the systematic error from using our best value.				

 $\Gamma(3\pi^+ 3\pi^- K^+ K^-)/\Gamma_{total}$   $\Gamma_{13}/\Gamma$ 

VALUE (units 10 <sup>-4</sup> )	EVTS	DOCUMENT ID	TECN	COMMENT
<b>2.6±0.8±0.1</b>	21	<sup>15</sup> ASNER 08A	CLEO	$\mathcal{T}(2S) \rightarrow \gamma 3\pi^+ 3\pi^- K^+ K^-$
<sup>15</sup> ASNER 08A reports $[\Gamma(\chi_{b1}(1P) \rightarrow 3\pi^+ 3\pi^- K^+ K^-)/\Gamma_{total}] \times [B(\mathcal{T}(2S) \rightarrow \gamma \chi_{b1}(1P))] = (18 \pm 4 \pm 4) \times 10^{-6}$ which we divide by our best value $B(\mathcal{T}(2S) \rightarrow \gamma \chi_{b1}(1P)) = (6.9 \pm 0.4) \times 10^{-2}$ . Our first error is their experiment's error and our second error is the systematic error from using our best value.				

See key on page 457

## Meson Particle Listings

 $\chi_{b1}(1P), h_b(1P), \chi_{b2}(1P)$  $\Gamma(3\pi^+3\pi^-K^+K^-\pi^0)/\Gamma_{total}$   $\Gamma_{14}/\Gamma$ 

VALUE (units $10^{-4}$ )	EVTS	DOCUMENT ID	TECN	COMMENT
<b><math>7.5 \pm 2.6 \pm 0.4</math></b>	28	16 ASNER	08A CLEO	$\Upsilon(2S) \rightarrow \gamma 3\pi^+ 3\pi^- K^+ K^- \pi^0$
<p><sup>16</sup> ASNER 08A reports <math>[\Gamma(\chi_{b1}(1P) \rightarrow 3\pi^+ 3\pi^- K^+ K^- \pi^0)/\Gamma_{total}] \times [B(\Upsilon(2S) \rightarrow \gamma \chi_{b1}(1P))] = (52 \pm 11 \pm 14) \times 10^{-6}</math> which we divide by our best value <math>B(\Upsilon(2S) \rightarrow \gamma \chi_{b1}(1P)) = (6.9 \pm 0.4) \times 10^{-2}</math>. Our first error is their experiment's error and our second error is the systematic error from using our best value.</p>				

 $\Gamma(4\pi^+4\pi^-)/\Gamma_{total}$   $\Gamma_{15}/\Gamma$ 

VALUE (units $10^{-4}$ )	EVTS	DOCUMENT ID	TECN	COMMENT
<b><math>2.6 \pm 0.9 \pm 0.1</math></b>	24	17 ASNER	08A CLEO	$\Upsilon(2S) \rightarrow \gamma 4\pi^+ 4\pi^-$
<p><sup>17</sup> ASNER 08A reports <math>[\Gamma(\chi_{b1}(1P) \rightarrow 4\pi^+ 4\pi^-)/\Gamma_{total}] \times [B(\Upsilon(2S) \rightarrow \gamma \chi_{b1}(1P))] = (18 \pm 4 \pm 5) \times 10^{-6}</math> which we divide by our best value <math>B(\Upsilon(2S) \rightarrow \gamma \chi_{b1}(1P)) = (6.9 \pm 0.4) \times 10^{-2}</math>. Our first error is their experiment's error and our second error is the systematic error from using our best value.</p>				

 $\Gamma(4\pi^+4\pi^-2\pi^0)/\Gamma_{total}$   $\Gamma_{16}/\Gamma$ 

VALUE (units $10^{-4}$ )	EVTS	DOCUMENT ID	TECN	COMMENT
<b><math>14 \pm 5 \pm 1</math></b>	26	18 ASNER	08A CLEO	$\Upsilon(2S) \rightarrow \gamma 4\pi^+ 4\pi^- 2\pi^0$
<p><sup>18</sup> ASNER 08A reports <math>[\Gamma(\chi_{b1}(1P) \rightarrow 4\pi^+ 4\pi^- 2\pi^0)/\Gamma_{total}] \times [B(\Upsilon(2S) \rightarrow \gamma \chi_{b1}(1P))] = (96 \pm 24 \pm 29) \times 10^{-6}</math> which we divide by our best value <math>B(\Upsilon(2S) \rightarrow \gamma \chi_{b1}(1P)) = (6.9 \pm 0.4) \times 10^{-2}</math>. Our first error is their experiment's error and our second error is the systematic error from using our best value.</p>				

 $\chi_{b1}(1P)$  Cross-Particle Branching Ratios $\Gamma(\chi_{b1}(1P) \rightarrow \gamma \Upsilon(1S))/\Gamma_{total} \times \Gamma(\Upsilon(2S) \rightarrow \gamma \chi_{b1}(1P))/\Gamma_{total}$   $\Gamma_1/\Gamma \times \Gamma_{13}^{T(2S)}/\Gamma_{T(2S)}$ 

VALUE (units $10^{-3}$ )	EVTS	DOCUMENT ID	TECN	COMMENT
<b><math>24.1 \pm 0.6 \pm 1.5</math></b>	13k	LEES	11J BABR	$\Upsilon(2S) \rightarrow X \gamma$

 $B(\chi_{b1}(1P) \rightarrow \gamma \Upsilon(1S)) \times B(\Upsilon(2S) \rightarrow \gamma \chi_{b1}(1P)) \times B(\Upsilon(1S) \rightarrow \ell^+ \ell^-)$ 

VALUE (units $10^{-4}$ )	EVTS	DOCUMENT ID	TECN	COMMENT
<b><math>5.65 \pm 0.11 \pm 0.27</math></b>	3222	KORNICER	11 CLEO	$e^+ e^- \rightarrow \gamma \gamma \ell^+ \ell^-$

 $B(\chi_{b1}(1P) \rightarrow \gamma \Upsilon(1S)) \times B(\Upsilon(3S) \rightarrow \gamma \chi_{b1}(1P)) \times B(\Upsilon(1S) \rightarrow \ell^+ \ell^-)$ 

VALUE (units $10^{-5}$ )	EVTS	DOCUMENT ID	TECN	COMMENT
<b><math>1.33 \pm 0.30 \pm 0.23</math></b>	50	KORNICER	11 CLEO	$e^+ e^- \rightarrow \gamma \gamma \ell^+ \ell^-$

 $B(\chi_{b2}(1P) \rightarrow \rho X + \bar{\rho} X)/B(\chi_{b1}(1P) \rightarrow \rho X + \bar{\rho} X)$ 

VALUE	DOCUMENT ID	TECN	COMMENT
<b><math>1.068 \pm 0.010 \pm 0.040</math></b>	BRIERE 07	CLEO	$\Upsilon(2S) \rightarrow \gamma \chi_{bJ}(1P)$

 $B(\chi_{b0}(1P) \rightarrow \rho X + \bar{\rho} X)/B(\chi_{b1}(1P) \rightarrow \rho X + \bar{\rho} X)$ 

VALUE	DOCUMENT ID	TECN	COMMENT
<b><math>1.11 \pm 0.15 \pm 0.20</math></b>	BRIERE 07	CLEO	$\Upsilon(2S) \rightarrow \gamma \chi_{bJ}(1P)$

 $\chi_{b1}(1P)$  REFERENCES

	DOCUMENT ID	TECN	COMMENT
KORNICER 11	PR D83 054003	M. Kornicer et al.	(CLEO Collab.)
LEES 11J	PR D84 072002	J.P. Lees et al.	(BABAR Collab.)
ASNER 08A	PR D78 091103	D.M. Asner et al.	(CLEO Collab.)
BRIERE 08	PR D78 092007	R.A. Briere et al.	(CLEO Collab.)
BRIERE 07	PR D76 012005	R.A. Briere et al.	(CLEO Collab.)
ARTUSO 05	PRL 94 032001	M. Artuso et al.	(CLEO Collab.)
EDWARDS 99	PR D59 032003	K.W. Edwards et al.	(CLEO Collab.)
SKWARNICKI 87	PRL 58 972	T. Skwarnicki et al.	(Crystal Ball Collab.)
WALK 86	PR D34 2611	W.S. Walk et al.	(Crystal Ball Collab.)
ALBRECHT 85E	PL 160B 331	H. Albrecht et al.	(ARGUS Collab.)
NERNST 85	PRL 54 2195	R. Nernst et al.	(Crystal Ball Collab.)
HAAS 84	PRL 52 799	J. Haas et al.	(CLEO Collab.)
KLOPFEN... 83	PRL 51 160	C. Klopffstein et al.	(CUSB Collab.)
PAUSS 83	PL 130B 439	F. Pauss et al.	(MPIM, COLU, CORN, LSU+)

 $h_b(1P)$ 

$$J^G(J^{PC}) = ?^?(1^{+-})$$

Quantum numbers are quark model predictions,  $C = -$  established by  $\eta_b \gamma$  decay.

 $h_b(1P)$  MASS

VALUE (MeV)	EVTS	DOCUMENT ID	TECN	COMMENT
<b><math>9898.6 \pm 1.4</math></b> OUR AVERAGE				
$9898.2_{-1.0}^{+1.1} \pm 1.0$	50.0k	ADACHI	12 BELL	$10.86 e^+ e^- \rightarrow \pi^+ \pi^- \pi^0 \text{MM}$
$9902 \pm 4 \pm 2$	10.8k	LEES	11K BABR	$\Upsilon(3S) \rightarrow \eta_b \gamma \pi^0$

 $h_b(1P)$  DECAY MODES

Mode	Fraction ( $\Gamma_i/\Gamma$ )
$\Gamma_1 \eta_b(1S) \gamma$	seen

 $h_b(1P)$  BRANCHING RATIOS

$\Gamma(\eta_b(1S) \gamma)/\Gamma_{total}$	$\Gamma_1/\Gamma$
seen	10.8k

 $h_b(1P)$  REFERENCES

ADACHI 12	PRL 108 032001	I. Adachi et al.	(BELLE Collab.)
LEES 11K	PR D84 091101	J.P. Lees et al.	(BABAR Collab.)

 $\chi_{b2}(1P)$ 

$$J^G(J^{PC}) = 0^+(2^{+-})$$
  
 $J$  needs confirmation.

Observed in radiative decay of the  $\Upsilon(2S)$ , therefore  $C = +$ . Branching ratio requires E1 transition, M1 is strongly disfavored, therefore  $P = +$ .  $J = 2$  from SKWARNICKI 87.

 $\chi_{b2}(1P)$  MASS

VALUE (MeV)	DOCUMENT ID
<b><math>9912.21 \pm 0.26 \pm 0.31</math></b> OUR EVALUATION	From average $\gamma$ energy below, using $\Upsilon(2S)$ mass = 10023.26 $\pm$ 0.31 MeV

 $\gamma$  ENERGY IN  $\Upsilon(2S)$  DECAY

VALUE (MeV)	DOCUMENT ID	TECN	COMMENT
<b><math>110.44 \pm 0.29</math></b> OUR AVERAGE	Error includes scale factor of 1.1.		
$110.58 \pm 0.08 \pm 0.30$	ARTUSO 05	CLEO	$\Upsilon(2S) \rightarrow \gamma X$
$110.8 \pm 0.3 \pm 0.6$	EDWARDS 99	CLE2	$\Upsilon(2S) \rightarrow \gamma \chi(1P)$
$107.0 \pm 1.1 \pm 1.3$	WALK 86	CBAL	$\Upsilon(2S) \rightarrow \gamma \gamma \ell^+ \ell^-$
$110.6 \pm 0.3 \pm 0.9$	ALBRECHT 85E	ARG	$\Upsilon(2S) \rightarrow \text{conv.} \gamma X$
$110.4 \pm 0.8 \pm 2.2$	NERNST 85	CBAL	$\Upsilon(2S) \rightarrow \gamma X$
$109.5 \pm 0.7 \pm 1.0$	HAA5 84	CLEO	$\Upsilon(2S) \rightarrow \text{conv.} \gamma X$
$108.2 \pm 0.3 \pm 2.0$	KLOPFEN... 83	CUSB	$\Upsilon(2S) \rightarrow \gamma X$
$108.8 \pm 4.0$	PAUSS 83	CUSB	$\Upsilon(2S) \rightarrow \gamma \gamma \ell^+ \ell^-$

 $\chi_{b2}(1P)$  DECAY MODES

Mode	Fraction ( $\Gamma_i/\Gamma$ )	Confidence level
$\Gamma_1 \gamma \Upsilon(1S)$	(19.1 $\pm$ 1.2) %	
$\Gamma_2 D^0 X$	< 7.9 %	90%
$\Gamma_3 \pi^+ \pi^- K^+ K^- \pi^0$	(8 $\pm$ 5) $\times$ 10 <sup>-5</sup>	
$\Gamma_4 2\pi^+ \pi^- K^- K_S^0$	< 1.0 $\times$ 10 <sup>-4</sup>	90%
$\Gamma_5 2\pi^+ \pi^- K^- K_S^0 2\pi^0$	(5.3 $\pm$ 2.4) $\times$ 10 <sup>-4</sup>	
$\Gamma_6 2\pi^+ 2\pi^- 2\pi^0$	(3.5 $\pm$ 1.4) $\times$ 10 <sup>-4</sup>	
$\Gamma_7 2\pi^+ 2\pi^- K^+ K^-$	(1.1 $\pm$ 0.4) $\times$ 10 <sup>-4</sup>	
$\Gamma_8 2\pi^+ 2\pi^- K^+ K^- \pi^0$	(2.1 $\pm$ 0.9) $\times$ 10 <sup>-4</sup>	
$\Gamma_9 2\pi^+ 2\pi^- K^+ K^- 2\pi^0$	(3.9 $\pm$ 1.8) $\times$ 10 <sup>-4</sup>	
$\Gamma_{10} 3\pi^+ 2\pi^- K^- K_S^0 \pi^0$	< 5 $\times$ 10 <sup>-4</sup>	90%
$\Gamma_{11} 3\pi^+ 3\pi^-$	(7.0 $\pm$ 3.1) $\times$ 10 <sup>-5</sup>	
$\Gamma_{12} 3\pi^+ 3\pi^- 2\pi^0$	(1.0 $\pm$ 0.4) $\times$ 10 <sup>-3</sup>	
$\Gamma_{13} 3\pi^+ 3\pi^- K^+ K^-$	< 8 $\times$ 10 <sup>-5</sup>	90%
$\Gamma_{14} 3\pi^+ 3\pi^- K^+ K^- \pi^0$	(3.6 $\pm$ 1.5) $\times$ 10 <sup>-4</sup>	
$\Gamma_{15} 4\pi^+ 4\pi^-$	(8 $\pm$ 4) $\times$ 10 <sup>-5</sup>	
$\Gamma_{16} 4\pi^+ 4\pi^- 2\pi^0$	(1.8 $\pm$ 0.7) $\times$ 10 <sup>-3</sup>	

 $\chi_{b2}(1P)$  BRANCHING RATIOS

$\Gamma(\gamma \Upsilon(1S))/\Gamma_{total}$	$\Gamma_1/\Gamma$
<b><math>0.191 \pm 0.012</math></b> OUR AVERAGE	
$0.186 \pm 0.011 \pm 0.009$	1,2 KORNICER 11
$0.194 \pm 0.014 \pm 0.009$	3 LEES 11J
$0.27 \pm 0.06 \pm 0.06$	WALK 86
$0.20 \pm 0.05$	KLOPFEN... 83

<sup>1</sup> Assuming  $B(\Upsilon(1S) \rightarrow \ell^+ \ell^-) = (2.48 \pm 0.05)\%$ .

<sup>2</sup> KORNICER 11 reports  $[\Gamma(\chi_{b2}(1P) \rightarrow \gamma \Upsilon(1S))/\Gamma_{total}] \times [B(\Upsilon(2S) \rightarrow \gamma \chi_{b2}(1P))] = (1.33 \pm 0.04 \pm 0.07) \times 10^{-2}$  which we divide by our best value  $B(\Upsilon(2S) \rightarrow \gamma \chi_{b2}(1P)) = (7.15 \pm 0.35) \times 10^{-2}$ . Our first error is their experiment's error and our second error is the systematic error from using our best value.

<sup>3</sup> LEES 11J reports  $[\Gamma(\chi_{b2}(1P) \rightarrow \gamma \Upsilon(1S))/\Gamma_{total}] \times [B(\Upsilon(2S) \rightarrow \gamma \chi_{b2}(1P))] = (13.9 \pm 0.5 \pm 0.9)_{-1.1} \times 10^{-3}$  which we divide by our best value  $B(\Upsilon(2S) \rightarrow \gamma \chi_{b2}(1P)) = (7.15 \pm 0.35) \times 10^{-2}$ . Our first error is their experiment's error and our second error is the systematic error from using our best value.

 $\Gamma(D^0 X)/\Gamma_{total}$   $\Gamma_2/\Gamma$ 

VALUE	CL%	DOCUMENT ID	TECN	COMMENT
<b><math>&lt; 7.9 \times 10^{-2}</math></b>	90	4,5 BRIERE 08	CLEO	$\Upsilon(2S) \rightarrow \gamma D^0 X$

<sup>4</sup> For  $p_{D^0} > 2.5$  GeV/c.

<sup>5</sup> The authors also present their result as  $(5.4 \pm 1.9 \pm 0.5) \times 10^{-2}$ .

# Meson Particle Listings

## $\chi_{b2}(1P)$ , $\Upsilon(2S)$

$\Gamma(\pi^+\pi^-K^+K^-\pi^0)/\Gamma_{\text{total}}$					$\Gamma_3/\Gamma$
VALUE (units $10^{-4}$ )	EVTS	DOCUMENT ID	TECN	COMMENT	
<b><math>0.84 \pm 0.50 \pm 0.04</math></b>	8	<sup>6</sup> ASNER	08A CLEO	$\Upsilon(2S) \rightarrow \gamma\pi^+\pi^-K^+K^-\pi^0$	
<sup>6</sup> ASNER 08A reports $[\Gamma(\chi_{b2}(1P) \rightarrow \pi^+\pi^-K^+K^-\pi^0)/\Gamma_{\text{total}}] \times [B(\Upsilon(2S) \rightarrow \gamma\chi_{b2}(1P))]$ = $(6 \pm 3 \pm 2) \times 10^{-6}$ which we divide by our best value $B(\Upsilon(2S) \rightarrow \gamma\chi_{b2}(1P))$ = $(7.15 \pm 0.35) \times 10^{-2}$ . Our first error is their experiment's error and our second error is the systematic error from using our best value.					

$\Gamma(2\pi^+\pi^-K^-K_S^0)/\Gamma_{\text{total}}$					$\Gamma_4/\Gamma$
VALUE (units $10^{-4}$ )	CL%	DOCUMENT ID	TECN	COMMENT	
<b>&lt;1.0</b>	90	<sup>7</sup> ASNER	08A CLEO	$\Upsilon(2S) \rightarrow \gamma 2\pi^+\pi^-K^-K_S^0$	
<sup>7</sup> ASNER 08A reports $[\Gamma(\chi_{b2}(1P) \rightarrow 2\pi^+\pi^-K^-K_S^0)/\Gamma_{\text{total}}] \times [B(\Upsilon(2S) \rightarrow \gamma\chi_{b2}(1P))]$ = $7 \times 10^{-6}$ which we divide by our best value $B(\Upsilon(2S) \rightarrow \gamma\chi_{b2}(1P))$ = $7.15 \times 10^{-2}$ .					

$\Gamma(2\pi^+\pi^-K^-K_S^0 2\pi^0)/\Gamma_{\text{total}}$					$\Gamma_5/\Gamma$
VALUE (units $10^{-4}$ )	EVTS	DOCUMENT ID	TECN	COMMENT	
<b><math>5.3 \pm 2.4 \pm 0.3</math></b>	11	<sup>8</sup> ASNER	08A CLEO	$\Upsilon(2S) \rightarrow \gamma 2\pi^+\pi^-K^-2\pi^0$	
<sup>8</sup> ASNER 08A reports $[\Gamma(\chi_{b2}(1P) \rightarrow 2\pi^+\pi^-K^-K_S^0 2\pi^0)/\Gamma_{\text{total}}] \times [B(\Upsilon(2S) \rightarrow \gamma\chi_{b2}(1P))]$ = $(38 \pm 14 \pm 10) \times 10^{-6}$ which we divide by our best value $B(\Upsilon(2S) \rightarrow \gamma\chi_{b2}(1P))$ = $(7.15 \pm 0.35) \times 10^{-2}$ . Our first error is their experiment's error and our second error is the systematic error from using our best value.					

$\Gamma(2\pi^+2\pi^-2\pi^0)/\Gamma_{\text{total}}$					$\Gamma_6/\Gamma$
VALUE (units $10^{-4}$ )	EVTS	DOCUMENT ID	TECN	COMMENT	
<b><math>3.5 \pm 1.4 \pm 0.2</math></b>	19	<sup>9</sup> ASNER	08A CLEO	$\Upsilon(2S) \rightarrow \gamma 2\pi^+2\pi^-2\pi^0$	
<sup>9</sup> ASNER 08A reports $[\Gamma(\chi_{b2}(1P) \rightarrow 2\pi^+2\pi^-2\pi^0)/\Gamma_{\text{total}}] \times [B(\Upsilon(2S) \rightarrow \gamma\chi_{b2}(1P))]$ = $(25 \pm 8 \pm 6) \times 10^{-6}$ which we divide by our best value $B(\Upsilon(2S) \rightarrow \gamma\chi_{b2}(1P))$ = $(7.15 \pm 0.35) \times 10^{-2}$ . Our first error is their experiment's error and our second error is the systematic error from using our best value.					

$\Gamma(2\pi^+2\pi^-K^+K^-)/\Gamma_{\text{total}}$					$\Gamma_7/\Gamma$
VALUE (units $10^{-4}$ )	EVTS	DOCUMENT ID	TECN	COMMENT	
<b><math>1.1 \pm 0.4 \pm 0.1</math></b>	14	<sup>10</sup> ASNER	08A CLEO	$\Upsilon(2S) \rightarrow \gamma 2\pi^+2\pi^-K^+K^-$	
<sup>10</sup> ASNER 08A reports $[\Gamma(\chi_{b2}(1P) \rightarrow 2\pi^+2\pi^-K^+K^-)/\Gamma_{\text{total}}] \times [B(\Upsilon(2S) \rightarrow \gamma\chi_{b2}(1P))]$ = $(8 \pm 2 \pm 2) \times 10^{-6}$ which we divide by our best value $B(\Upsilon(2S) \rightarrow \gamma\chi_{b2}(1P))$ = $(7.15 \pm 0.35) \times 10^{-2}$ . Our first error is their experiment's error and our second error is the systematic error from using our best value.					

$\Gamma(2\pi^+2\pi^-K^+K^-\pi^0)/\Gamma_{\text{total}}$					$\Gamma_8/\Gamma$
VALUE (units $10^{-4}$ )	EVTS	DOCUMENT ID	TECN	COMMENT	
<b><math>2.1 \pm 0.9 \pm 0.1</math></b>	13	<sup>11</sup> ASNER	08A CLEO	$\Upsilon(2S) \rightarrow \gamma 2\pi^+2\pi^-K^+K^-\pi^0$	
<sup>11</sup> ASNER 08A reports $[\Gamma(\chi_{b2}(1P) \rightarrow 2\pi^+2\pi^-K^+K^-\pi^0)/\Gamma_{\text{total}}] \times [B(\Upsilon(2S) \rightarrow \gamma\chi_{b2}(1P))]$ = $(15 \pm 5 \pm 4) \times 10^{-6}$ which we divide by our best value $B(\Upsilon(2S) \rightarrow \gamma\chi_{b2}(1P))$ = $(7.15 \pm 0.35) \times 10^{-2}$ . Our first error is their experiment's error and our second error is the systematic error from using our best value.					

$\Gamma(2\pi^+2\pi^-K^+K^-2\pi^0)/\Gamma_{\text{total}}$					$\Gamma_9/\Gamma$
VALUE (units $10^{-4}$ )	EVTS	DOCUMENT ID	TECN	COMMENT	
<b><math>3.9 \pm 1.8 \pm 0.2</math></b>	11	<sup>12</sup> ASNER	08A CLEO	$\Upsilon(2S) \rightarrow \gamma 2\pi^+2\pi^-K^+K^-2\pi^0$	
<sup>12</sup> ASNER 08A reports $[\Gamma(\chi_{b2}(1P) \rightarrow 2\pi^+2\pi^-K^+K^-2\pi^0)/\Gamma_{\text{total}}] \times [B(\Upsilon(2S) \rightarrow \gamma\chi_{b2}(1P))]$ = $(28 \pm 11 \pm 7) \times 10^{-6}$ which we divide by our best value $B(\Upsilon(2S) \rightarrow \gamma\chi_{b2}(1P))$ = $(7.15 \pm 0.35) \times 10^{-2}$ . Our first error is their experiment's error and our second error is the systematic error from using our best value.					

$\Gamma(3\pi^+2\pi^-K^-K_S^0\pi^0)/\Gamma_{\text{total}}$					$\Gamma_{10}/\Gamma$
VALUE (units $10^{-4}$ )	CL%	DOCUMENT ID	TECN	COMMENT	
<b>&lt;5</b>	90	<sup>13</sup> ASNER	08A CLEO	$\Upsilon(2S) \rightarrow \gamma 3\pi^+2\pi^-K^-K_S^0\pi^0$	
<sup>13</sup> ASNER 08A reports $[\Gamma(\chi_{b2}(1P) \rightarrow 3\pi^+2\pi^-K^-K_S^0\pi^0)/\Gamma_{\text{total}}] \times [B(\Upsilon(2S) \rightarrow \gamma\chi_{b2}(1P))]$ < $36 \times 10^{-6}$ which we divide by our best value $B(\Upsilon(2S) \rightarrow \gamma\chi_{b2}(1P))$ = $7.15 \times 10^{-2}$ .					

$\Gamma(3\pi^+3\pi^-)/\Gamma_{\text{total}}$					$\Gamma_{11}/\Gamma$
VALUE (units $10^{-4}$ )	EVTS	DOCUMENT ID	TECN	COMMENT	
<b><math>0.70 \pm 0.31 \pm 0.03</math></b>	9	<sup>14</sup> ASNER	08A CLEO	$\Upsilon(2S) \rightarrow \gamma 3\pi^+3\pi^-$	
<sup>14</sup> ASNER 08A reports $[\Gamma(\chi_{b2}(1P) \rightarrow 3\pi^+3\pi^-)/\Gamma_{\text{total}}] \times [B(\Upsilon(2S) \rightarrow \gamma\chi_{b2}(1P))]$ = $(5 \pm 2 \pm 1) \times 10^{-6}$ which we divide by our best value $B(\Upsilon(2S) \rightarrow \gamma\chi_{b2}(1P))$ = $(7.15 \pm 0.35) \times 10^{-2}$ . Our first error is their experiment's error and our second error is the systematic error from using our best value.					

$\Gamma(3\pi^+3\pi^-2\pi^0)/\Gamma_{\text{total}}$					$\Gamma_{12}/\Gamma$
VALUE (units $10^{-4}$ )	EVTS	DOCUMENT ID	TECN	COMMENT	
<b><math>10.2 \pm 3.6 \pm 0.5</math></b>	34	<sup>15</sup> ASNER	08A CLEO	$\Upsilon(2S) \rightarrow \gamma 3\pi^+3\pi^-2\pi^0$	
<sup>15</sup> ASNER 08A reports $[\Gamma(\chi_{b2}(1P) \rightarrow 3\pi^+3\pi^-2\pi^0)/\Gamma_{\text{total}}] \times [B(\Upsilon(2S) \rightarrow \gamma\chi_{b2}(1P))]$ = $(73 \pm 16 \pm 20) \times 10^{-6}$ which we divide by our best value $B(\Upsilon(2S) \rightarrow \gamma\chi_{b2}(1P))$ = $(7.15 \pm 0.35) \times 10^{-2}$ . Our first error is their experiment's error and our second error is the systematic error from using our best value.					

$\Gamma(3\pi^+3\pi^-K^+K^-)/\Gamma_{\text{total}}$					$\Gamma_{13}/\Gamma$
VALUE (units $10^{-4}$ )	CL%	DOCUMENT ID	TECN	COMMENT	
<b>&lt;0.8</b>	90	<sup>16</sup> ASNER	08A CLEO	$\Upsilon(2S) \rightarrow \gamma 3\pi^+3\pi^-K^+K^-$	
<sup>16</sup> ASNER 08A reports $[\Gamma(\chi_{b2}(1P) \rightarrow 3\pi^+3\pi^-K^+K^-)/\Gamma_{\text{total}}] \times [B(\Upsilon(2S) \rightarrow \gamma\chi_{b2}(1P))]$ < $6 \times 10^{-6}$ which we divide by our best value $B(\Upsilon(2S) \rightarrow \gamma\chi_{b2}(1P))$ = $7.15 \times 10^{-2}$ .					

$\Gamma(3\pi^+3\pi^-K^+K^-\pi^0)/\Gamma_{\text{total}}$					$\Gamma_{14}/\Gamma$
VALUE (units $10^{-4}$ )	EVTS	DOCUMENT ID	TECN	COMMENT	
<b><math>3.6 \pm 1.5 \pm 0.2</math></b>	14	<sup>17</sup> ASNER	08A CLEO	$\Upsilon(2S) \rightarrow \gamma 3\pi^+3\pi^-K^+K^-\pi^0$	
<sup>17</sup> ASNER 08A reports $[\Gamma(\chi_{b2}(1P) \rightarrow 3\pi^+3\pi^-K^+K^-\pi^0)/\Gamma_{\text{total}}] \times [B(\Upsilon(2S) \rightarrow \gamma\chi_{b2}(1P))]$ = $(26 \pm 8 \pm 7) \times 10^{-6}$ which we divide by our best value $B(\Upsilon(2S) \rightarrow \gamma\chi_{b2}(1P))$ = $(7.15 \pm 0.35) \times 10^{-2}$ . Our first error is their experiment's error and our second error is the systematic error from using our best value.					

$\Gamma(4\pi^+4\pi^-)/\Gamma_{\text{total}}$					$\Gamma_{15}/\Gamma$
VALUE (units $10^{-4}$ )	EVTS	DOCUMENT ID	TECN	COMMENT	
<b><math>0.84 \pm 0.40 \pm 0.04</math></b>	7	<sup>18</sup> ASNER	08A CLEO	$\Upsilon(2S) \rightarrow \gamma 4\pi^+4\pi^-$	
<sup>18</sup> ASNER 08A reports $[\Gamma(\chi_{b2}(1P) \rightarrow 4\pi^+4\pi^-)/\Gamma_{\text{total}}] \times [B(\Upsilon(2S) \rightarrow \gamma\chi_{b2}(1P))]$ = $(6 \pm 2 \pm 2) \times 10^{-6}$ which we divide by our best value $B(\Upsilon(2S) \rightarrow \gamma\chi_{b2}(1P))$ = $(7.15 \pm 0.35) \times 10^{-2}$ . Our first error is their experiment's error and our second error is the systematic error from using our best value.					

$\Gamma(4\pi^+4\pi^-2\pi^0)/\Gamma_{\text{total}}$					$\Gamma_{16}/\Gamma$
VALUE (units $10^{-4}$ )	EVTS	DOCUMENT ID	TECN	COMMENT	
<b><math>18 \pm 7 \pm 1</math></b>	29	<sup>19</sup> ASNER	08A CLEO	$\Upsilon(2S) \rightarrow \gamma 4\pi^+4\pi^-2\pi^0$	
<sup>19</sup> ASNER 08A reports $[\Gamma(\chi_{b2}(1P) \rightarrow 4\pi^+4\pi^-2\pi^0)/\Gamma_{\text{total}}] \times [B(\Upsilon(2S) \rightarrow \gamma\chi_{b2}(1P))]$ = $(132 \pm 31 \pm 40) \times 10^{-6}$ which we divide by our best value $B(\Upsilon(2S) \rightarrow \gamma\chi_{b2}(1P))$ = $(7.15 \pm 0.35) \times 10^{-2}$ . Our first error is their experiment's error and our second error is the systematic error from using our best value.					

### $\chi_{b2}(1P)$ Cross-Particle Branching Ratios

$\Gamma(\chi_{b2}(1P) \rightarrow \gamma \Upsilon(2S))/\Gamma_{\text{total}} \times \Gamma(\Upsilon(2S) \rightarrow \gamma \chi_{b2}(1P))/\Gamma_{\text{total}}$					$\Gamma_1/\Gamma \times \Gamma_{14}(\Upsilon(2S))/\Gamma \Upsilon(2S)$
VALUE (units $10^{-3}$ )	EVTS	DOCUMENT ID	TECN	COMMENT	
<b><math>13.9 \pm 0.5 \pm 0.9 - 1.1</math></b>	8k	LEES	11J BABR	$\Upsilon(2S) \rightarrow X\gamma$	
<b><math>B(\chi_{b2}(1P) \rightarrow \gamma \Upsilon(1S)) \times B(\Upsilon(2S) \rightarrow \gamma \chi_{b2}(1P)) \times B(\Upsilon(1S) \rightarrow \ell^+\ell^-)</math></b>					
VALUE (units $10^{-4}$ )	EVTS	DOCUMENT ID	TECN	COMMENT	
<b><math>3.29 \pm 0.09 \pm 0.16</math></b>	1770	KORNICER	11 CLEO	$e^+e^- \rightarrow \gamma\gamma\ell^+\ell^-$	
<b><math>B(\chi_{b2}(1P) \rightarrow \gamma \Upsilon(1S)) \times B(\Upsilon(3S) \rightarrow \gamma \chi_{b2}(1P)) \times B(\Upsilon(1S) \rightarrow \ell^+\ell^-)</math></b>					
VALUE (units $10^{-5}$ )	EVTS	DOCUMENT ID	TECN	COMMENT	
<b><math>3.56 \pm 0.40 \pm 0.41</math></b>	126	KORNICER	11 CLEO	$e^+e^- \rightarrow \gamma\gamma\ell^+\ell^-$	

### $\chi_{b2}(1P)$ REFERENCES

KORNICER 11 PR D83 054003	M. Kornicer et al.	(CLEO Collab.)
LEES 11J PR D84 072002	J.P. Lees et al.	(BABAR Collab.)
ASNER 08A PR D78 091103	D.M. Asner et al.	(CLEO Collab.)
BRIERE 08 PR D78 092007	R.A. Briere et al.	(CLEO Collab.)
ARTUSO 05 PRL 94 032001	M. Artuso et al.	(CLEO Collab.)
EDWARDS 99 PR D59 032003	K.W. Edwards et al.	(CLEO Collab.)
SKWARNICKI 87 PRL 58 972	T. Skwarnicki et al.	(Crystal Ball Collab./J)
WALK 86 PR D34 2611	W.S. Walk et al.	(Crystal Ball Collab.)
ALBRECHT 85E PL 160B 331	H. Albrecht et al.	(ARGUS Collab.)
NERNST 85 PRL 54 2195	R. Nernst et al.	(Crystal Ball Collab.)
HAAS 84 PRL 52 799	J. Haas et al.	(CLEO Collab.)
KLOPFEN... 83 PRL 51 160	C. Klopffenstein et al.	(CUSB Collab.)
PAUSS 83 PL 130B 439	F. Pauss et al.	(MPIM, COLU, CORN, LSU+)

### $\Upsilon(2S)$

$I^G(J^{PC}) = 0^-(1^{--})$

### $\Upsilon(2S)$ MASS

VALUE (GeV)	DOCUMENT ID	TECN	COMMENT
<b><math>10.02326 \pm 0.00031</math> OUR AVERAGE</b>			
10.0235 ± 0.0005	<sup>1</sup> ARTAMONOV 00	MD1	$e^+e^- \rightarrow$ hadrons
10.0231 ± 0.0004	BARBER 84	REDE	$e^+e^- \rightarrow$ hadrons
• • • We do not use the following data for averages, fits, limits, etc. • • •			
10.0236 ± 0.0005	<sup>2,3</sup> BARU	86B REDE	$e^+e^- \rightarrow$ hadrons
<sup>1</sup> Reanalysis of BARU 86B using new electron mass (COHEN 87).			
<sup>2</sup> Reanalysis of ARTAMONOV 84.			
<sup>3</sup> Superseded by ARTAMONOV 00.			

### $m\Upsilon(3S) - m\Upsilon(2S)$

VALUE (MeV)	DOCUMENT ID	TECN	COMMENT
<b><math>331.50 \pm 0.02 \pm 0.13</math></b>	LEES	11c BABR	$e^+e^- \rightarrow \pi^+\pi^-X$

See key on page 457

# Meson Particle Listings

## $T(2S)$

### $T(2S)$ WIDTH

VALUE (keV) DOCUMENT ID  
**31.98±2.63 OUR EVALUATION** See the Note on "Width Determinations of the  $T$  States"

### $T(2S)$ DECAY MODES

Mode	Fraction ( $\Gamma_i/\Gamma$ )	Scale factor/ Confidence level
$\Gamma_1$ $\Upsilon(1S)\pi^+\pi^-$	(17.92±0.26) %	
$\Gamma_2$ $\Upsilon(1S)\pi^0\pi^0$	(8.6 ± 0.4) %	
$\Gamma_3$ $\tau^+\tau^-$	(2.00±0.21) %	
$\Gamma_4$ $\mu^+\mu^-$	(1.93±0.17) %	S=2.2
$\Gamma_5$ $e^+e^-$	(1.91±0.16) %	
$\Gamma_6$ $\Upsilon(1S)\pi^0$	< 1.8 $\times 10^{-4}$	CL=90%
$\Gamma_7$ $\Upsilon(1S)\eta$	(2.34±0.31) $\times 10^{-4}$	
$\Gamma_8$ $J/\psi(1S)$ anything	< 6 $\times 10^{-3}$	CL=90%
$\Gamma_9$ $\bar{d}$ anything	(3.4 ± 0.6) $\times 10^{-5}$	
$\Gamma_{10}$ hadrons	(94 ± 11) %	
$\Gamma_{11}$ $ggg$	(58.8 ± 1.2) %	
$\Gamma_{12}$ $\gamma gg$	(8.8 ± 1.1) %	

### Radiative decays

$\Gamma_{13}$ $\gamma\chi_{b1}(1P)$	(6.9 ± 0.4) %	
$\Gamma_{14}$ $\gamma\chi_{b2}(1P)$	(7.15 ± 0.35) %	
$\Gamma_{15}$ $\gamma\chi_{b0}(1P)$	(3.8 ± 0.4) %	
$\Gamma_{16}$ $\gamma f_0(1710)$	< 5.9 $\times 10^{-4}$	CL=90%
$\Gamma_{17}$ $\gamma f_2'(1525)$	< 5.3 $\times 10^{-4}$	CL=90%
$\Gamma_{18}$ $\gamma f_2(1270)$	< 2.41 $\times 10^{-4}$	CL=90%
$\Gamma_{19}$ $\gamma f_J(2220)$		
$\Gamma_{20}$ $\gamma\eta_c(1S)$	< 2.7 $\times 10^{-5}$	CL=90%
$\Gamma_{21}$ $\gamma\chi_{c0}$	< 1.0 $\times 10^{-4}$	CL=90%
$\Gamma_{22}$ $\gamma\chi_{c1}$	< 3.6 $\times 10^{-6}$	CL=90%
$\Gamma_{23}$ $\gamma\chi_{c2}$	< 1.5 $\times 10^{-5}$	CL=90%
$\Gamma_{24}$ $\gamma X(3872) \rightarrow \pi^+\pi^- J/\psi$	< 8 $\times 10^{-7}$	CL=90%
$\Gamma_{25}$ $\gamma X(3872) \rightarrow \pi^+\pi^- \pi^0 J/\psi$	< 2.4 $\times 10^{-6}$	CL=90%
$\Gamma_{26}$ $\gamma X(3915) \rightarrow \omega J/\psi$	< 2.8 $\times 10^{-6}$	CL=90%
$\Gamma_{27}$ $\gamma X(4140) \rightarrow \phi J/\psi$	< 1.2 $\times 10^{-6}$	CL=90%
$\Gamma_{28}$ $\gamma X(4350) \rightarrow \phi J/\psi$	< 1.3 $\times 10^{-6}$	CL=90%
$\Gamma_{29}$ $\gamma\eta_b(1S)$	(3.9 ± 1.5) $\times 10^{-4}$	
$\Gamma_{30}$ $\gamma X \rightarrow \gamma + \geq 4$ prongs	[a] < 1.95 $\times 10^{-4}$	CL=95%
$\Gamma_{31}$ $\gamma A^0 \rightarrow \gamma$ hadrons	< 8 $\times 10^{-5}$	CL=90%

### Lepton Family number (LF) violating modes

$\Gamma_{32}$ $e^\pm\tau^\mp$	LF < 3.2 $\times 10^{-6}$	CL=90%
$\Gamma_{33}$ $\mu^\pm\tau^\mp$	LF < 3.3 $\times 10^{-6}$	CL=90%

[a] 1.5 GeV <  $m_X$  < 5.0 GeV

### $T(2S)$ $\Gamma(i)\Gamma(e^+e^-)/\Gamma(\text{total})$

$\Gamma(\mu^+\mu^-) \times \Gamma(e^+e^-)/\Gamma_{\text{total}}$	$\Gamma_4\Gamma_5/\Gamma$
<u>VALUE (eV)</u> <u>DOCUMENT ID</u> <u>TECN</u> <u>COMMENT</u>	
<b>6.5±1.5±1.0</b>	KOBEL 92 CBAL $e^+e^- \rightarrow \mu^+\mu^-$

$\Gamma(\Upsilon(1S)\pi^+\pi^-) \times \Gamma(e^+e^-)/\Gamma_{\text{total}}$	$\Gamma_1\Gamma_5/\Gamma$
<u>VALUE (eV)</u> <u>EVTS</u> <u>DOCUMENT ID</u> <u>TECN</u> <u>COMMENT</u>	
<b>105.4±1.0±4.2</b>	11.8K <sup>4</sup> AUBERT 08BP BABR 10.58 $e^+e^- \rightarrow \gamma\pi^+\pi^-\ell^+\ell^-$
<sup>4</sup> Using B( $\Upsilon(1S) \rightarrow e^+e^-$ ) = (2.38 ± 0.11)% and B( $\Upsilon(1S) \rightarrow \mu^+\mu^-$ ) = (2.48 ± 0.05)%.	

$\Gamma(\text{hadrons}) \times \Gamma(e^+e^-)/\Gamma_{\text{total}}$	$\Gamma_{10}\Gamma_5/\Gamma$
<u>VALUE (keV)</u> <u>DOCUMENT ID</u> <u>TECN</u> <u>COMMENT</u>	
<b>0.577±0.009 OUR AVERAGE</b>	
0.581±0.004±0.009	<sup>5</sup> ROSNER 06 CLEO 10.0 $e^+e^- \rightarrow$ hadrons
0.552±0.031±0.017	<sup>5</sup> BARU 96 MD1 $e^+e^- \rightarrow$ hadrons
0.54 ± 0.04 ± 0.02	<sup>5</sup> JAKUBOWSKI 88 CBAL $e^+e^- \rightarrow$ hadrons
0.58 ± 0.03 ± 0.04	<sup>6</sup> GILES 84B CLEO $e^+e^- \rightarrow$ hadrons
0.60 ± 0.12 ± 0.07	<sup>6</sup> ALBRECHT 82 DASP $e^+e^- \rightarrow$ hadrons
0.54 ± 0.07 <sup>+0.09</sup> <sub>-0.05</sub>	<sup>6</sup> NICZYPORUK 81C LENA $e^+e^- \rightarrow$ hadrons
0.41 ± 0.18	<sup>6</sup> BOCK 80 CNTR $e^+e^- \rightarrow$ hadrons

<sup>5</sup>Radiative corrections evaluated following KURAEV 85.

<sup>6</sup>Radiative corrections reevaluated by BUCHMUELLER 88 following KURAEV 85.

### $T(2S)$ PARTIAL WIDTHS

$\Gamma(e^+e^-)$   $\Gamma_5$   
VALUE (keV) DOCUMENT ID  
**0.612±0.011 OUR EVALUATION**

### $T(2S)$ BRANCHING RATIOS

$\Gamma(\Upsilon(1S)\pi^+\pi^-)/\Gamma_{\text{total}}$	$\Gamma_1/\Gamma$
Abbreviation MM in the COMMENT field below stands for missing mass.	
<u>VALUE (units <math>10^{-2}</math>)</u> <u>EVTS</u> <u>DOCUMENT ID</u> <u>TECN</u> <u>COMMENT</u>	
<b>17.92±0.26 OUR AVERAGE</b>	
16.8 ± 1.1 ± 1.3	906k <sup>7</sup> LEES 11C BABR $e^+e^- \rightarrow \pi^+\pi^- X$
17.80±0.05±0.37	170k <sup>8</sup> LEES 11L BABR $\Upsilon(2S) \rightarrow \pi^+\pi^-\mu^+\mu^-$
18.02±0.02±0.61	851k <sup>9</sup> BHARI 09 CLEO $e^+e^- \rightarrow \pi^+\pi^- MM$
17.22±0.17±0.75	11.8K <sup>10</sup> AUBERT 08BP BABR $e^+e^- \rightarrow \gamma\pi^+\pi^-\ell^+\ell^-$
19.2 ± 0.2 ± 1.0	52.6k <sup>11</sup> ALEXANDER 98 CLE2 $\pi^+\pi^-\ell^+\ell^-$ , $\pi^+\pi^- MM$
18.1 ± 0.5 ± 1.0	11.6k ALBRECHT 87 ARG $e^+e^- \rightarrow \pi^+\pi^- MM$
16.9 ± 4.0	GELPHMAN 85 CBAL $e^+e^- \rightarrow e^+e^-\pi^+\pi^-$
19.1 ± 1.2 ± 0.6	BESSION 84 CLEO $\pi^+\pi^- MM$
18.9 ± 2.6	FONSECA 84 CUSB $e^+e^- \rightarrow \ell^+\ell^-\pi^+\pi^-$
21 ± 7	7 NICZYPORUK 81B LENA $e^+e^- \rightarrow \ell^+\ell^-\pi^+\pi^-$

<sup>7</sup>LEES 11C reports  $[\Gamma(\Upsilon(2S) \rightarrow \Upsilon(1S)\pi^+\pi^-)/\Gamma_{\text{total}}] \times [B(\Upsilon(3S) \rightarrow \Upsilon(2S)\text{anything})] = (1.78 \pm 0.02 \pm 0.11) \times 10^{-2}$  which we divide by our best value  $B(\Upsilon(3S) \rightarrow \Upsilon(2S)\text{anything}) = (10.6 \pm 0.8) \times 10^{-2}$ . Our first error is their experiment's error and our second error is the systematic error from using our best value.

<sup>8</sup>Using  $B(\Upsilon(1S) \rightarrow \mu^+\mu^-) = (2.48 \pm 0.05)\%$ .

<sup>9</sup>A weighted average of the inclusive and exclusive results.

<sup>10</sup>Using  $B(\Upsilon(2S) \rightarrow e^+e^-) = (1.91 \pm 0.16)\%$ ,  $B(\Upsilon(2S) \rightarrow \mu^+\mu^-) = (1.93 \pm 0.17)\%$  and,  $\Gamma_{ee}(\Upsilon(2S)) = 0.612 \pm 0.011$  keV.

<sup>11</sup>Using  $B(\Upsilon(1S) \rightarrow e^+e^-) = (2.52 \pm 0.17)\%$  and  $B(\Upsilon(1S) \rightarrow \mu^+\mu^-) = (2.48 \pm 0.07)\%$ .

$\Gamma(\Upsilon(1S)\pi^0\pi^0)/\Gamma_{\text{total}}$	$\Gamma_2/\Gamma$
<u>VALUE (units <math>10^{-2}</math>)</u> <u>EVTS</u> <u>DOCUMENT ID</u> <u>TECN</u> <u>COMMENT</u>	
<b>8.6 ± 0.4 OUR AVERAGE</b>	
8.43±0.16±0.42	38k <sup>12</sup> BHARI 09 CLEO $e^+e^- \rightarrow \pi^0\pi^0\ell^+\ell^-$
9.2 ± 0.6 ± 0.8	275 <sup>13</sup> ALEXANDER 98 CLE2 $e^+e^- \rightarrow \pi^0\pi^0\ell^+\ell^-$
9.5 ± 1.9 ± 1.9	25 ALBRECHT 87 ARG $e^+e^- \rightarrow \pi^0\pi^0\ell^+\ell^-$
8.0 ± 1.5	GELPHMAN 85 CBAL $e^+e^- \rightarrow \pi^0\pi^0\ell^+\ell^-$
10.3 ± 2.3	FONSECA 84 CUSB $e^+e^- \rightarrow \pi^0\pi^0\ell^+\ell^-$

<sup>12</sup>Authors assume  $B(\Upsilon(1S) \rightarrow e^+e^-) + B(\Upsilon(1S) \rightarrow \mu^+\mu^-) = 4.96\%$ .

<sup>13</sup>Using  $B(\Upsilon(1S) \rightarrow e^+e^-) = (2.52 \pm 0.17)\%$  and  $B(\Upsilon(1S) \rightarrow \mu^+\mu^-) = (2.48 \pm 0.07)\%$ .

$\Gamma(\Upsilon(1S)\pi^0\pi^0)/\Gamma(\Upsilon(1S)\pi^+\pi^-)$	$\Gamma_2/\Gamma_1$
<u>VALUE</u> <u>DOCUMENT ID</u> <u>TECN</u> <u>COMMENT</u>	
0.462±0.037	<sup>14</sup> BHARI 09 CLEO $e^+e^- \rightarrow \Upsilon(2S)$

• • • We do not use the following data for averages, fits, limits, etc. • • •

<sup>14</sup>Not independent of other values reported by BHARI 09.

$\Gamma(\tau^+\tau^-)/\Gamma_{\text{total}}$	$\Gamma_3/\Gamma$
<u>VALUE (units <math>10^{-2}</math>)</u> <u>EVTS</u> <u>DOCUMENT ID</u> <u>TECN</u> <u>COMMENT</u>	
<b>2.00±0.21 OUR AVERAGE</b>	
2.00±0.12±0.18	22k <sup>15</sup> BESSION 07 CLEO $e^+e^- \rightarrow \Upsilon(2S) \rightarrow \tau^+\tau^-$
1.7 ± 1.5 ± 0.6	HAAS 84B CLEO $e^+e^- \rightarrow \tau^+\tau^-$

<sup>15</sup>BESSION 07 reports  $[\Gamma(\Upsilon(2S) \rightarrow \tau^+\tau^-)/\Gamma_{\text{total}}] / [B(\Upsilon(2S) \rightarrow \mu^+\mu^-)] = 1.04 \pm 0.04 \pm 0.05$  which we multiply by our best value  $B(\Upsilon(2S) \rightarrow \mu^+\mu^-) = (1.93 \pm 0.17) \times 10^{-2}$ . Our first error is their experiment's error and our second error is the systematic error from using our best value.

$\Gamma(\mu^+\mu^-)/\Gamma_{\text{total}}$	$\Gamma_4/\Gamma$
<u>VALUE</u> <u>CL%</u> <u>EVTS</u> <u>DOCUMENT ID</u> <u>TECN</u> <u>COMMENT</u>	
<b>0.0193±0.0017 OUR AVERAGE</b>	Error includes scale factor of 2.2. See the ideogram below.
0.0203±0.0003±0.0008	120k ADAMS 05 CLEO $e^+e^- \rightarrow \mu^+\mu^-$
0.0122±0.0028±0.0019	<sup>16</sup> KOBEL 92 CBAL $e^+e^- \rightarrow \mu^+\mu^-$
0.0138±0.0025±0.0015	KAARSBERG 89 CSB2 $e^+e^- \rightarrow \mu^+\mu^-$
0.009 ± 0.006 ± 0.006	<sup>17</sup> ALBRECHT 85 ARG $e^+e^- \rightarrow \mu^+\mu^-$
0.018 ± 0.008 ± 0.005	HAAS 84B CLEO $e^+e^- \rightarrow \mu^+\mu^-$
< 0.038	90 NICZYPORUK 81C LENA $e^+e^- \rightarrow \mu^+\mu^-$

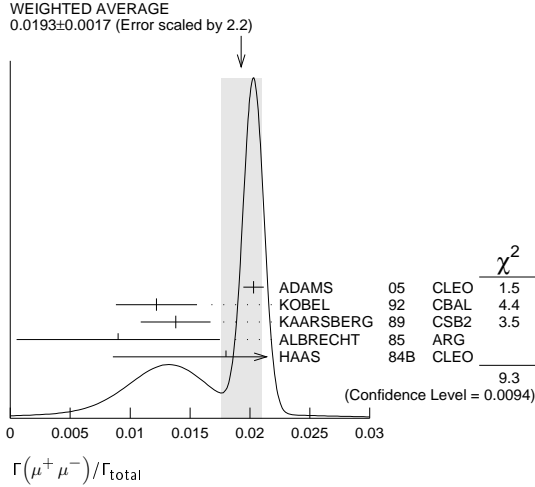
• • • We do not use the following data for averages, fits, limits, etc. • • •

<sup>16</sup>Taking into account interference between the resonance and continuum.

<sup>17</sup>Re-evaluated using  $B(\Upsilon(1S) \rightarrow \mu^+\mu^-) = 0.026$ .

Meson Particle Listings

$\Upsilon(2S)$



$\Gamma(\tau^+\tau^-)/\Gamma(\mu^+\mu^-)$					$\Gamma_3/\Gamma_4$
VALUE	EVTS	DOCUMENT ID	TECN	COMMENT	
$1.04 \pm 0.04 \pm 0.05$	22k	BESSON 07	CLEO	$e^+e^- \rightarrow \Upsilon(2S)$	

$\Gamma(\Upsilon(1S)\pi^0)/\Gamma_{total}$					$\Gamma_6/\Gamma$
VALUE (units $10^{-3}$ )	CL%	DOCUMENT ID	TECN	COMMENT	
$< 0.18$	90	18 HE 08A	CLEO	$e^+e^- \rightarrow \ell^+\ell^-\gamma\gamma$	
• • • We do not use the following data for averages, fits, limits, etc. • • •					
$< 1.1$	90	ALEXANDER 98	CLE2	$e^+e^- \rightarrow \ell^+\ell^-\gamma\gamma$	
$< 8$	90	LURZ 87	CBAL	$e^+e^- \rightarrow \ell^+\ell^-\gamma\gamma$	
18 Authors assume $B(\Upsilon(1S) \rightarrow e^+e^-) + B(\Upsilon(1S) \rightarrow \mu^+\mu^-) = 4.96\%$ .					

$\Gamma(\Upsilon(1S)\eta)/\Gamma_{total}$					$\Gamma_7/\Gamma$
VALUE (units $10^{-4}$ )	CL%	EVTS	DOCUMENT ID	TECN	COMMENT
$2.34 \pm 0.31$	OUR AVERAGE				
$2.39 \pm 0.31 \pm 0.14$		112	19 LEES 11L	BABR	$\Upsilon(2S) \rightarrow \ell^+\ell^-\eta$
$2.1^{+0.7}_{-0.6} \pm 0.3$		14	20 HE 08A	CLEO	$e^+e^- \rightarrow \ell^+\ell^-\eta$
• • • We do not use the following data for averages, fits, limits, etc. • • •					
$< 9$	90	19,21 AUBERT 08BP	BABR	$e^+e^- \rightarrow \gamma\pi^+\pi^-\pi^0\ell^+\ell^-$	
$< 28$	90	ALEXANDER 98	CLE2	$e^+e^- \rightarrow \ell^+\ell^-\eta$	
$< 50$	90	ALBRECHT 87	ARG	$e^+e^- \rightarrow \pi^+\pi^-\ell^+\ell^-MM$	
$< 70$	90	LURZ 87	CBAL	$e^+e^- \rightarrow \ell^+\ell^-(\gamma\gamma, 3\pi^0)$	
$< 100$	90	BESSON 84	CLEO	$e^+e^- \rightarrow \pi^+\pi^-\ell^+\ell^-MM$	
$< 20$	90	FONSECA 84	CUSB	$e^+e^- \rightarrow \ell^+\ell^-(\gamma\gamma, \pi^+\pi^-\pi^0)$	

19 Using  $B(\Upsilon(1S) \rightarrow e^+e^-) = (2.38 \pm 0.11)\%$  and  $B(\Upsilon(1S) \rightarrow \mu^+\mu^-) = (2.48 \pm 0.05)\%$ .  
 20 Authors assume  $B(\Upsilon(1S) \rightarrow e^+e^-) + B(\Upsilon(1S) \rightarrow \mu^+\mu^-) = 4.96\%$ .  
 21 Using  $\Gamma_{ee}(\Upsilon(2S)) = 0.612 \pm 0.011$  keV.

$\Gamma(\Upsilon(1S)\eta)/\Gamma(\Upsilon(1S)\pi^+\pi^-)$					$\Gamma_7/\Gamma_1$
VALUE (units $10^{-3}$ )	CL%	DOCUMENT ID	TECN	COMMENT	
$1.35 \pm 0.17 \pm 0.08$		22 LEES 11L	BABR	$\Upsilon(2S) \rightarrow (\pi^+\pi^-\pi^0)(\gamma\gamma)\mu^+\mu^-$	
$< 5.2$	90	23 AUBERT 08BP	BABR	$e^+e^- \rightarrow \gamma\pi^+\pi^-(\pi^0)\ell^+\ell^-$	
22 Not independent of other values reported by LEES 11L. 23 Not independent of other values reported by AUBERT 08BP.					

$\Gamma(J/\psi(1S) \text{ anything})/\Gamma_{total}$					$\Gamma_8/\Gamma$
VALUE	CL%	DOCUMENT ID	TECN	COMMENT	
$< 0.006$	90	MASCHMANN 90	CBAL	$e^+e^- \rightarrow \text{hadrons}$	

$\Gamma(\bar{d} \text{ anything})/\Gamma_{total}$					$\Gamma_9/\Gamma$
VALUE (units $10^{-5}$ )	EVTS	DOCUMENT ID	TECN	COMMENT	
$3.37 \pm 0.50 \pm 0.25$	58	ASNER 07	CLEO	$e^+e^- \rightarrow \bar{d}X$	

$\Gamma(ggg)/\Gamma_{total}$					$\Gamma_{11}/\Gamma$
VALUE (units $10^{-2}$ )	EVTS	DOCUMENT ID	TECN	COMMENT	
$58.8 \pm 1.2$	6M	24 BESSON 06A	CLEO	$\Upsilon(2S) \rightarrow \text{hadrons}$	
24 Calculated using the value $\Gamma(\gamma gg)/\Gamma(ggg) = (3.18 \pm 0.04 \pm 0.22 \pm 0.41)\%$ from BESSON 06A and PDG 08 values of $B(\pi^+\pi^-\Upsilon(1S)) = (18.1 \pm 0.4)\%$ , $B(\pi^0\pi^0\Upsilon(1S)) = (8.6 \pm 0.4)\%$ , $B(\mu^+\mu^-) = (1.93 \pm 0.17)\%$ , and $R_{\text{hadrons}} = 3.51$ . The statistical error is negligible and the systematic error is partially correlated with that of $\Gamma(\gamma gg)/\Gamma_{total}$ measurement of BESSON 06A.					

$\Gamma(\gamma gg)/\Gamma_{total}$					$\Gamma_{12}/\Gamma$
VALUE (units $10^{-2}$ )	EVTS	DOCUMENT ID	TECN	COMMENT	
$8.79 \pm 1.05$	100k	25 BESSON 06A	CLEO	$\Upsilon(2S) \rightarrow \gamma + \text{hadrons}$	
25 Calculated using BESSON 06A values of $\Gamma(\gamma gg)/\Gamma(ggg) = (3.18 \pm 0.04 \pm 0.22 \pm 0.41)\%$ and $\Gamma(ggg)/\Gamma_{total}$ . The statistical error is negligible and the systematic error is partially correlated with that of $\Gamma(ggg)/\Gamma_{total}$ measurement of BESSON 06A.					

$\Gamma(ggg)/\Gamma(ggg)$					$\Gamma_{12}/\Gamma_{11}$
VALUE (units $10^{-2}$ )	EVTS	DOCUMENT ID	TECN	COMMENT	
$3.18 \pm 0.04 \pm 0.47$	6M	BESSON 06A	CLEO	$\Upsilon(2S) \rightarrow (\gamma +) \text{hadrons}$	

$\Gamma(\gamma\chi_{b1}(1P))/\Gamma_{total}$					$\Gamma_{13}/\Gamma$
VALUE	EVTS	DOCUMENT ID	TECN	COMMENT	
$0.069 \pm 0.004$	OUR AVERAGE				
$0.0693 \pm 0.0012 \pm 0.0041$	407k	ARTUSO 05	CLEO	$e^+e^- \rightarrow \gamma X$	
$0.069 \pm 0.005 \pm 0.009$		EDWARDS 99	CLE2	$\Upsilon(2S) \rightarrow \gamma\chi(1P)$	
$0.091 \pm 0.018 \pm 0.022$		ALBRECHT 85E	ARG	$e^+e^- \rightarrow \gamma \text{conv. } X$	
$0.065 \pm 0.007 \pm 0.012$		NERNST 85	CBAL	$e^+e^- \rightarrow \gamma X$	
$0.080 \pm 0.017 \pm 0.016$		HAAS 84	CLEO	$e^+e^- \rightarrow \gamma \text{conv. } X$	
$0.059 \pm 0.014$		KLOPFEN... 83	CUSB	$e^+e^- \rightarrow \gamma X$	

$\Gamma(\gamma\chi_{b2}(1P))/\Gamma_{total}$					$\Gamma_{14}/\Gamma$
VALUE	EVTS	DOCUMENT ID	TECN	COMMENT	
$0.0715 \pm 0.0035$	OUR AVERAGE				
$0.0724 \pm 0.0011 \pm 0.0040$	410k	ARTUSO 05	CLEO	$e^+e^- \rightarrow \gamma X$	
$0.074 \pm 0.005 \pm 0.008$		EDWARDS 99	CLE2	$\Upsilon(2S) \rightarrow \gamma\chi(1P)$	
$0.098 \pm 0.021 \pm 0.024$		ALBRECHT 85E	ARG	$e^+e^- \rightarrow \gamma \text{conv. } X$	
$0.058 \pm 0.007 \pm 0.010$		NERNST 85	CBAL	$e^+e^- \rightarrow \gamma X$	
$0.102 \pm 0.018 \pm 0.021$		HAAS 84	CLEO	$e^+e^- \rightarrow \gamma \text{conv. } X$	
$0.061 \pm 0.014$		KLOPFEN... 83	CUSB	$e^+e^- \rightarrow \gamma X$	

$\Gamma(\gamma\chi_{b0}(1P))/\Gamma_{total}$					$\Gamma_{15}/\Gamma$
VALUE	EVTS	DOCUMENT ID	TECN	COMMENT	
$0.038 \pm 0.004$	OUR AVERAGE				
$0.0375 \pm 0.0012 \pm 0.0047$	198k	ARTUSO 05	CLEO	$e^+e^- \rightarrow \gamma X$	
$0.034 \pm 0.005 \pm 0.006$		EDWARDS 99	CLE2	$\Upsilon(2S) \rightarrow \gamma\chi(1P)$	
$0.064 \pm 0.014 \pm 0.016$		ALBRECHT 85E	ARG	$e^+e^- \rightarrow \gamma \text{conv. } X$	
$0.036 \pm 0.008 \pm 0.009$		NERNST 85	CBAL	$e^+e^- \rightarrow \gamma X$	
$0.044 \pm 0.023 \pm 0.009$		HAAS 84	CLEO	$e^+e^- \rightarrow \gamma \text{conv. } X$	
• • • We do not use the following data for averages, fits, limits, etc. • • •					
$0.035 \pm 0.014$		KLOPFEN... 83	CUSB	$e^+e^- \rightarrow \gamma X$	

$\Gamma(\gamma f_0(1710))/\Gamma_{total}$					$\Gamma_{16}/\Gamma$
VALUE (units $10^{-5}$ )	CL%	DOCUMENT ID	TECN	COMMENT	
$< 59$	90	26 ALBRECHT 89	ARG	$\Upsilon(2S) \rightarrow \gamma K^+K^-$	
• • • We do not use the following data for averages, fits, limits, etc. • • •					
$< 5.9$	90	27 ALBRECHT 89	ARG	$\Upsilon(2S) \rightarrow \gamma\pi^+\pi^-$	
26 Re-evaluated assuming $B(f_0(1710) \rightarrow K^+K^-) = 0.19$ . 27 Includes unknown branching ratio of $f_0(1710) \rightarrow \pi^+\pi^-$ .					

$\Gamma(\gamma f'_2(1525))/\Gamma_{total}$					$\Gamma_{17}/\Gamma$
VALUE (units $10^{-5}$ )	CL%	DOCUMENT ID	TECN	COMMENT	
$< 53$	90	28 ALBRECHT 89	ARG	$\Upsilon(2S) \rightarrow \gamma K^+K^-$	
28 Re-evaluated assuming $B(f'_2(1525) \rightarrow K\bar{K}) = 0.71$ .					

$\Gamma(\gamma f_2(1270))/\Gamma_{total}$					$\Gamma_{18}/\Gamma$
VALUE (units $10^{-5}$ )	CL%	DOCUMENT ID	TECN	COMMENT	
$< 24.1$	90	29 ALBRECHT 89	ARG	$\Upsilon(2S) \rightarrow \gamma\pi^+\pi^-$	
29 Using $B(f_2(1270) \rightarrow \pi\pi) = 0.84$ .					

$\Gamma(\gamma f_J(2220))/\Gamma_{total}$					$\Gamma_{19}/\Gamma$
VALUE (units $10^{-5}$ )	CL%	DOCUMENT ID	TECN	COMMENT	
$< 6.8$	90	30 ALBRECHT 89	ARG	$\Upsilon(2S) \rightarrow \gamma K^+K^-$	
30 Includes unknown branching ratio of $f_J(2220) \rightarrow K^+K^-$ .					

$\Gamma(\gamma\eta_b(1S))/\Gamma_{total}$					$\Gamma_{29}/\Gamma$
VALUE (units $10^{-4}$ )	CL%	EVTS	DOCUMENT ID	TECN	COMMENT
$3.9 \pm 1.1^{+1.1}_{-0.9}$		13 $\pm$ 5k	31 AUBERT 09Aq	BABR	$\Upsilon(2S) \rightarrow \gamma X$
• • • We do not use the following data for averages, fits, limits, etc. • • •					
$< 21$	90		LEES 11J	BABR	$\Upsilon(2S) \rightarrow \gamma X$
$< 8.4$	90		31 BONVICINI 10	CLEO	$\Upsilon(2S) \rightarrow \gamma X$
$< 5.1$	90		32 ARTUSO 05	CLEO	$e^+e^- \rightarrow \gamma X$

31 Assuming  $\Gamma_{\eta_b(1S)} = 10$  MeV.  
 32 Superseded by BONVICINI 10.

$\Gamma(\gamma\eta_c(1S))/\Gamma_{total}$					$\Gamma_{20}/\Gamma$
VALUE	CL%	DOCUMENT ID	TECN	COMMENT	
$< 2.7 \times 10^{-5}$	90	WANG 11B	BELL	$\Upsilon(2S) \rightarrow \gamma X$	



See key on page 457

Meson Particle Listings
T(2S), T(1D), chi\_b0(2P)

Table with 5 columns: VALUE, CL%, DOCUMENT ID, TECN, COMMENT. Row 1: <1.0 x 10^-4, 90, WANG, 11B, BELL, T(2S) -> gamma X

Table with 5 columns: VALUE, CL%, DOCUMENT ID, TECN, COMMENT. Row 1: <3.6 x 10^-6, 90, WANG, 11B, BELL, T(2S) -> gamma X

Table with 5 columns: VALUE, CL%, DOCUMENT ID, TECN, COMMENT. Row 1: <1.5 x 10^-5, 90, WANG, 11B, BELL, T(2S) -> gamma X

Table with 5 columns: VALUE, CL%, DOCUMENT ID, TECN, COMMENT. Row 1: <0.8 x 10^-6, 90, WANG, 11B, BELL, T(2S) -> gamma X

Table with 5 columns: VALUE, CL%, DOCUMENT ID, TECN, COMMENT. Row 1: <2.4 x 10^-6, 90, WANG, 11B, BELL, T(2S) -> gamma X

Table with 5 columns: VALUE, CL%, DOCUMENT ID, TECN, COMMENT. Row 1: <2.8 x 10^-6, 90, WANG, 11B, BELL, T(2S) -> gamma X

Table with 5 columns: VALUE, CL%, DOCUMENT ID, TECN, COMMENT. Row 1: <1.2 x 10^-6, 90, WANG, 11B, BELL, T(2S) -> gamma X

Table with 5 columns: VALUE, CL%, DOCUMENT ID, TECN, COMMENT. Row 1: <1.3 x 10^-6, 90, WANG, 11B, BELL, T(2S) -> gamma X

Table with 5 columns: VALUE, CL%, DOCUMENT ID, TECN, COMMENT. Row 1: <1.95, 95, ROSNER, 07A, CLEO, e+e- -> gamma X

Table with 5 columns: VALUE, CL%, DOCUMENT ID, TECN, COMMENT. Row 1: <8 x 10^-5, 90, 33 LEES, 11H, BABR, T(2S) -> gamma hadrons

LEPTON FAMILY NUMBER (LF) VIOLATING MODES

Table with 5 columns: VALUE, CL%, DOCUMENT ID, TECN, COMMENT. Row 1: <3.2, 90, LEES, 10B, BABR, e+e- -> e+tau tau-

Table with 5 columns: VALUE, CL%, DOCUMENT ID, TECN, COMMENT. Row 1: <3.3, 90, LEES, 10B, BABR, e+e- -> mu+tau tau-

T(2S) Cross-Particle Branching Ratios

Table with 5 columns: VALUE, EVTS, DOCUMENT ID, TECN, COMMENT. Row 1: 1.78 +/- 0.02 +/- 0.11, 906k, LEES, 11c, BABR, e+e- -> pi+pi-X

T(2S) REFERENCES

Large table of references for T(2S) with columns for author, document ID, year, and affiliation.

Large table of references for T(2S), T(1D), and chi\_b0(2P) with columns for author, document ID, year, and affiliation.

T(1D)

J^PC = 0^-(2^-)

First observed by BONVICINI 04 in the decay to gamma gamma T(1S) and confirmed by DEL-AMO-SANCHEZ 10R in the decay to pi+ pi- T(1S). Data consistent with J^P = 2^-. The states with J = 1 and 3 also possibly seen, but need confirmation.

T(1D) MASS

Table with 5 columns: VALUE, EVTS, DOCUMENT ID, TECN, COMMENT. Row 1: 10163.7 +/- 1.4 OUR AVERAGE

T(1D) DECAY MODES

Table with 3 columns: Mode, Fraction, Gamma\_i/Gamma. Row 1: gamma gamma T(1S), seen

T(1D) BRANCHING RATIOS

Table with 5 columns: VALUE, CL%, DOCUMENT ID, TECN, COMMENT. Row 1: <0.25, 90, BONVICINI, 04, CLE3, T(3S) -> 4 gamma e+ l-

Table with 5 columns: VALUE, CL%, DOCUMENT ID, TECN, COMMENT. Row 1: 0.66 +/- 0.15 +/- 0.06

Using theoretical predictions for B(chi\_bJ(2P) -> gamma T(1D)).

Table with 5 columns: VALUE, CL%, DOCUMENT ID, TECN, COMMENT. Row 1: <1.2, 90, 2 BONVICINI, 04, CLE3, T(3S) -> 4 gamma e+ l-

Assuming J = 2.

T(1D) REFERENCES

Table with 5 columns: DEL-AMO-SA...10R, PR D82 111102, P. del Amo Sanchez et al., (BABAR Collab.)

chi\_b0(2P)

J^PC = 0^+(0^+)

J needs confirmation.

Observed in radiative decay of the T(3S), therefore C = +. Branching ratio requires E1 transition, M1 is strongly disfavored, therefore P = +.

chi\_b0(2P) MASS

Table with 5 columns: VALUE, EVTS, DOCUMENT ID, TECN, COMMENT. Row 1: 10.2325 +/- 0.0004 +/- 0.0005 OUR EVALUATION

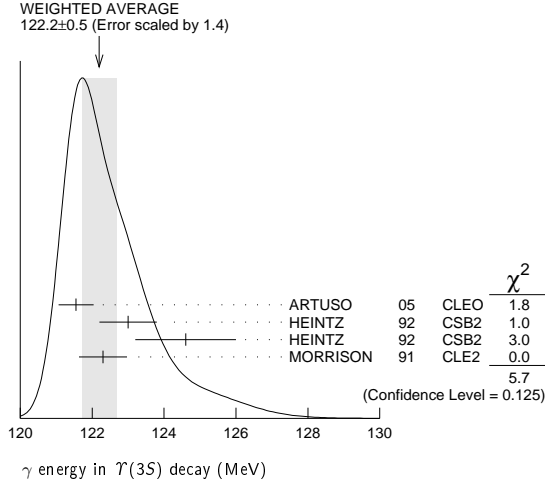
# Meson Particle Listings

## $\chi_{b0}(2P)$

### $\gamma$ ENERGY IN $T(3S)$ DECAY

VALUE (MeV)	EVTS	DOCUMENT ID	TECN	COMMENT
<b>121.9 ± 0.4 OUR EVALUATION</b>				Treating systematic errors as correlated
<b>122.2 ± 0.5 OUR AVERAGE</b>				Error includes scale factor of 1.4. See the ideogram below.
121.55 ± 0.16 ± 0.46		ARTUSO 05	CLEO	$T(3S) \rightarrow \gamma X$
123.0 ± 0.8	4959	1 HEINTZ 92	CSB2	$e^+e^- \rightarrow \gamma X$
124.6 ± 1.4	17	2 HEINTZ 92	CSB2	$e^+e^- \rightarrow \ell^+\ell^-\gamma\gamma$
122.3 ± 0.3 ± 0.6	9903	MORRISON 91	CLE2	$e^+e^- \rightarrow \gamma X$

<sup>1</sup> A systematic uncertainty on the energy scale of 0.9% not included. Supersedes NARAIN 91.  
<sup>2</sup> A systematic uncertainty on the energy scale of 0.9% not included. Supersedes HEINTZ 91.



### $\chi_{b0}(2P)$ DECAY MODES

Mode	Fraction ( $\Gamma_i/\Gamma$ )	Confidence level
$\Gamma_1 \gamma T(2S)$	$(4.6 \pm 2.1) \%$	
$\Gamma_2 \gamma T(1S)$	$(9 \pm 6) \times 10^{-3}$	
$\Gamma_3 D^0 X$	$< 8.2 \%$	90%
$\Gamma_4 \pi^+ \pi^- K^+ K^- \pi^0$	$< 3.4 \times 10^{-5}$	90%
$\Gamma_5 2\pi^+ \pi^- K^- K_S^0$	$< 5 \times 10^{-5}$	90%
$\Gamma_6 2\pi^+ \pi^- K^- K_S^0 2\pi^0$	$< 2.2 \times 10^{-4}$	90%
$\Gamma_7 2\pi^+ 2\pi^- 2\pi^0$	$< 2.4 \times 10^{-4}$	90%
$\Gamma_8 2\pi^+ 2\pi^- K^+ K^-$	$< 1.5 \times 10^{-4}$	90%
$\Gamma_9 2\pi^+ 2\pi^- K^+ K^- \pi^0$	$< 2.2 \times 10^{-4}$	90%
$\Gamma_{10} 2\pi^+ 2\pi^- K^+ K^- 2\pi^0$	$< 1.1 \times 10^{-3}$	90%
$\Gamma_{11} 3\pi^+ 2\pi^- K^- K_S^0 \pi^0$	$< 7 \times 10^{-4}$	90%
$\Gamma_{12} 3\pi^+ 3\pi^-$	$< 7 \times 10^{-5}$	90%
$\Gamma_{13} 3\pi^+ 3\pi^- 2\pi^0$	$< 1.2 \times 10^{-3}$	90%
$\Gamma_{14} 3\pi^+ 3\pi^- K^+ K^-$	$< 1.5 \times 10^{-4}$	90%
$\Gamma_{15} 3\pi^+ 3\pi^- K^+ K^- \pi^0$	$< 7 \times 10^{-4}$	90%
$\Gamma_{16} 4\pi^+ 4\pi^-$	$< 1.7 \times 10^{-4}$	90%
$\Gamma_{17} 4\pi^+ 4\pi^- 2\pi^0$	$< 6 \times 10^{-4}$	90%

### $\chi_{b0}(2P)$ BRANCHING RATIOS

$\Gamma(\gamma T(2S))/\Gamma_{total}$	CL%	DOCUMENT ID	TECN	COMMENT	$\Gamma_1/\Gamma$
<b>0.046 ± 0.020 ± 0.007</b>		3 HEINTZ 92	CSB2	$e^+e^- \rightarrow \ell^+\ell^-\gamma\gamma$	
••• We do not use the following data for averages, fits, limits, etc. •••					
<0.028	90	4 LEES 11J	BABR	$T(3S) \rightarrow X\gamma$	
<0.089	90	5 CRAWFORD 92B	CLE2	$e^+e^- \rightarrow \ell^+\ell^-\gamma\gamma$	
<sup>3</sup> Using $B(T(2S) \rightarrow \mu^+\mu^-) = (1.44 \pm 0.10)\%$ , $B(T(3S) \rightarrow \gamma\chi_{b0}(2P)) = (6.0 \pm 0.4 \pm 0.6)\%$ and assuming $e\mu$ universality. Supersedes HEINTZ 91.					
<sup>4</sup> LEES 11J quotes a central value of $\Gamma(\chi_{b0}(2P) \rightarrow \gamma T(2S))/\Gamma_{total} \times \Gamma(T(3S) \rightarrow \gamma\chi_{b0}(2P))/\Gamma_{total} = (-0.3 \pm 0.2 \pm 0.5) \times 10^{-4}$ .					
<sup>5</sup> Using $B(T(2S) \rightarrow \mu^+\mu^-) = (1.37 \pm 0.26)\%$ , $B(T(3S) \rightarrow \gamma\gamma T(2S)) \times 2 B(T(2S) \rightarrow \mu^+\mu^-) < 1.19 \times 10^{-4}$ , and $B(T(3S) \rightarrow \chi_{b0}(2P)\gamma) = 0.049$ .					
$\Gamma(\gamma T(1S))/\Gamma_{total}$	CL%	DOCUMENT ID	TECN	COMMENT	$\Gamma_2/\Gamma$
<b>0.009 ± 0.006 ± 0.001</b>		6 HEINTZ 92	CSB2	$e^+e^- \rightarrow \ell^+\ell^-\gamma\gamma$	
••• We do not use the following data for averages, fits, limits, etc. •••					
<0.012	90	7 LEES 11J	BABR	$T(3S) \rightarrow X\gamma$	
<0.025	90	8 CRAWFORD 92B	CLE2	$e^+e^- \rightarrow \ell^+\ell^-\gamma\gamma$	

<sup>6</sup> Using  $B(T(1S) \rightarrow \mu^+\mu^-) = (2.57 \pm 0.07)\%$ ,  $B(T(3S) \rightarrow \gamma\chi_{b0}(2P)) = (6.0 \pm 0.4 \pm 0.6)\%$  and assuming  $e\mu$  universality. Supersedes HEINTZ 91.  
<sup>7</sup> LEES 11J quotes a central value of  $\Gamma(\chi_{b0}(2P) \rightarrow \gamma T(1S))/\Gamma_{total} \times \Gamma(T(3S) \rightarrow \gamma\chi_{b0}(2P))/\Gamma_{total} = (3.9 \pm 2.2 \pm 1.2) \times 10^{-4}$ .  
<sup>8</sup> Using  $B(T(1S) \rightarrow \mu^+\mu^-) = (2.57 \pm 0.07)\%$ ,  $B(T(3S) \rightarrow \gamma\gamma T(1S)) \times 2 B(T(1S) \rightarrow \mu^+\mu^-) < 0.63 \times 10^{-4}$ , and  $B(T(3S) \rightarrow \chi_{b0}(2P)\gamma) = 0.049$ .

$\Gamma(D^0 X)/\Gamma_{total}$	CL%	DOCUMENT ID	TECN	COMMENT	$\Gamma_3/\Gamma$
<b>&lt; 8.2 × 10<sup>-2</sup></b>	90	9,10 BRIERE 08	CLEO	$T(3S) \rightarrow \gamma D^0 X$	

<sup>9</sup> For  $p_{D^0} > 2.5$  GeV/c.  
<sup>10</sup> The authors also present their result as  $(4.1 \pm 3.0 \pm 0.4) \times 10^{-2}$ .

$\Gamma(\pi^+ \pi^- K^+ K^- \pi^0)/\Gamma_{total}$	CL%	DOCUMENT ID	TECN	COMMENT	$\Gamma_4/\Gamma$
<b>&lt; 0.34</b>	90	11 ASNER 08A	CLEO	$T(3S) \rightarrow \gamma\pi^+ \pi^- K^+ K^- \pi^0$	

<sup>11</sup> ASNER 08A reports  $[\Gamma(\chi_{b0}(2P) \rightarrow \pi^+ \pi^- K^+ K^- \pi^0)/\Gamma_{total}] \times [B(T(3S) \rightarrow \gamma\chi_{b0}(2P))] < 2 \times 10^{-6}$  which we divide by our best value  $B(T(3S) \rightarrow \gamma\chi_{b0}(2P)) = 5.9 \times 10^{-2}$ .

$\Gamma(2\pi^+ \pi^- K^- K_S^0)/\Gamma_{total}$	CL%	DOCUMENT ID	TECN	COMMENT	$\Gamma_5/\Gamma$
<b>&lt; 0.5</b>	90	12 ASNER 08A	CLEO	$T(3S) \rightarrow \gamma 2\pi^+ \pi^- K^- K_S^0$	

<sup>12</sup> ASNER 08A reports  $[\Gamma(\chi_{b0}(2P) \rightarrow 2\pi^+ \pi^- K^- K_S^0)/\Gamma_{total}] \times [B(T(3S) \rightarrow \gamma\chi_{b0}(2P))] < 3 \times 10^{-6}$  which we divide by our best value  $B(T(3S) \rightarrow \gamma\chi_{b0}(2P)) = 5.9 \times 10^{-2}$ .

$\Gamma(2\pi^+ \pi^- K^- K_S^0 2\pi^0)/\Gamma_{total}$	CL%	DOCUMENT ID	TECN	COMMENT	$\Gamma_6/\Gamma$
<b>&lt; 2.2</b>	90	13 ASNER 08A	CLEO	$T(3S) \rightarrow \gamma 2\pi^+ \pi^- K^- 2\pi^0$	

<sup>13</sup> ASNER 08A reports  $[\Gamma(\chi_{b0}(2P) \rightarrow 2\pi^+ \pi^- K^- K_S^0 2\pi^0)/\Gamma_{total}] \times [B(T(3S) \rightarrow \gamma\chi_{b0}(2P))] < 13 \times 10^{-6}$  which we divide by our best value  $B(T(3S) \rightarrow \gamma\chi_{b0}(2P)) = 5.9 \times 10^{-2}$ .

$\Gamma(2\pi^+ 2\pi^- 2\pi^0)/\Gamma_{total}$	CL%	DOCUMENT ID	TECN	COMMENT	$\Gamma_7/\Gamma$
<b>&lt; 2.4</b>	90	14 ASNER 08A	CLEO	$T(3S) \rightarrow \gamma 2\pi^+ 2\pi^- 2\pi^0$	

<sup>14</sup> ASNER 08A reports  $[\Gamma(\chi_{b0}(2P) \rightarrow 2\pi^+ 2\pi^- 2\pi^0)/\Gamma_{total}] \times [B(T(3S) \rightarrow \gamma\chi_{b0}(2P))] < 14 \times 10^{-6}$  which we divide by our best value  $B(T(3S) \rightarrow \gamma\chi_{b0}(2P)) = 5.9 \times 10^{-2}$ .

$\Gamma(2\pi^+ 2\pi^- K^+ K^-)/\Gamma_{total}$	CL%	DOCUMENT ID	TECN	COMMENT	$\Gamma_8/\Gamma$
<b>&lt; 1.5</b>	90	15 ASNER 08A	CLEO	$T(3S) \rightarrow \gamma 2\pi^+ 2\pi^- K^+ K^-$	

<sup>15</sup> ASNER 08A reports  $[\Gamma(\chi_{b0}(2P) \rightarrow 2\pi^+ 2\pi^- K^+ K^-)/\Gamma_{total}] \times [B(T(3S) \rightarrow \gamma\chi_{b0}(2P))] < 9 \times 10^{-6}$  which we divide by our best value  $B(T(3S) \rightarrow \gamma\chi_{b0}(2P)) = 5.9 \times 10^{-2}$ .

$\Gamma(2\pi^+ 2\pi^- K^+ K^- \pi^0)/\Gamma_{total}$	CL%	DOCUMENT ID	TECN	COMMENT	$\Gamma_9/\Gamma$
<b>&lt; 2.2</b>	90	16 ASNER 08A	CLEO	$T(3S) \rightarrow \gamma 2\pi^+ 2\pi^- K^+ K^- \pi^0$	

<sup>16</sup> ASNER 08A reports  $[\Gamma(\chi_{b0}(2P) \rightarrow 2\pi^+ 2\pi^- K^+ K^- \pi^0)/\Gamma_{total}] \times [B(T(3S) \rightarrow \gamma\chi_{b0}(2P))] < 13 \times 10^{-6}$  which we divide by our best value  $B(T(3S) \rightarrow \gamma\chi_{b0}(2P)) = 5.9 \times 10^{-2}$ .

$\Gamma(2\pi^+ 2\pi^- K^+ K^- 2\pi^0)/\Gamma_{total}$	CL%	DOCUMENT ID	TECN	COMMENT	$\Gamma_{10}/\Gamma$
<b>&lt; 11</b>	90	17 ASNER 08A	CLEO	$T(3S) \rightarrow \gamma 2\pi^+ 2\pi^- K^+ K^- 2\pi^0$	

<sup>17</sup> ASNER 08A reports  $[\Gamma(\chi_{b0}(2P) \rightarrow 2\pi^+ 2\pi^- K^+ K^- 2\pi^0)/\Gamma_{total}] \times [B(T(3S) \rightarrow \gamma\chi_{b0}(2P))] < 63 \times 10^{-6}$  which we divide by our best value  $B(T(3S) \rightarrow \gamma\chi_{b0}(2P)) = 5.9 \times 10^{-2}$ .

$\Gamma(3\pi^+ 2\pi^- K^- K_S^0 \pi^0)/\Gamma_{total}$	CL%	DOCUMENT ID	TECN	COMMENT	$\Gamma_{11}/\Gamma$
<b>&lt; 7</b>	90	18 ASNER 08A	CLEO	$T(3S) \rightarrow \gamma 3\pi^+ 2\pi^- K^- K_S^0 \pi^0$	

<sup>18</sup> ASNER 08A reports  $[\Gamma(\chi_{b0}(2P) \rightarrow 3\pi^+ 2\pi^- K^- K_S^0 \pi^0)/\Gamma_{total}] \times [B(T(3S) \rightarrow \gamma\chi_{b0}(2P))] < 39 \times 10^{-6}$  which we divide by our best value  $B(T(3S) \rightarrow \gamma\chi_{b0}(2P)) = 5.9 \times 10^{-2}$ .

$\Gamma(3\pi^+ 3\pi^-)/\Gamma_{total}$	CL%	DOCUMENT ID	TECN	COMMENT	$\Gamma_{12}/\Gamma$
<b>&lt; 0.7</b>	90	19 ASNER 08A	CLEO	$T(3S) \rightarrow \gamma 3\pi^+ 3\pi^-$	

<sup>19</sup> ASNER 08A reports  $[\Gamma(\chi_{b0}(2P) \rightarrow 3\pi^+ 3\pi^-)/\Gamma_{total}] \times [B(T(3S) \rightarrow \gamma\chi_{b0}(2P))] < 4 \times 10^{-6}$  which we divide by our best value  $B(T(3S) \rightarrow \gamma\chi_{b0}(2P)) = 5.9 \times 10^{-2}$ .

See key on page 457

# Meson Particle Listings

## $\chi_{b0}(2P), \chi_{b1}(2P)$

### $\Gamma(3\pi^+3\pi^-2\pi^0)/\Gamma_{total}$ $\Gamma_{13}/\Gamma$

VALUE (units $10^{-4}$ )	CL%	DOCUMENT ID	TECN	COMMENT
<12	90	20 ASNER	08A CLEO	$\Upsilon(3S) \rightarrow \gamma 3\pi^+3\pi^-2\pi^0$
20 ASNER 08A reports $[\Gamma(\chi_{b0}(2P) \rightarrow 3\pi^+3\pi^-2\pi^0)/\Gamma_{total}] \times [B(\Upsilon(3S) \rightarrow \gamma\chi_{b0}(2P))]$ < $72 \times 10^{-6}$ which we divide by our best value $B(\Upsilon(3S) \rightarrow \gamma\chi_{b0}(2P)) = 5.9 \times 10^{-2}$ .				

### $\Gamma(3\pi^+3\pi^-K^+K^-)/\Gamma_{total}$ $\Gamma_{14}/\Gamma$

VALUE (units $10^{-4}$ )	CL%	DOCUMENT ID	TECN	COMMENT
<1.5	90	21 ASNER	08A CLEO	$\Upsilon(3S) \rightarrow \gamma 3\pi^+3\pi^-K^+K^-$
21 ASNER 08A reports $[\Gamma(\chi_{b0}(2P) \rightarrow 3\pi^+3\pi^-K^+K^-)/\Gamma_{total}] \times [B(\Upsilon(3S) \rightarrow \gamma\chi_{b0}(2P))]$ < $9 \times 10^{-6}$ which we divide by our best value $B(\Upsilon(3S) \rightarrow \gamma\chi_{b0}(2P)) = 5.9 \times 10^{-2}$ .				

### $\Gamma(3\pi^+3\pi^-K^+K^-\pi^0)/\Gamma_{total}$ $\Gamma_{15}/\Gamma$

VALUE (units $10^{-4}$ )	CL%	DOCUMENT ID	TECN	COMMENT
<7	90	22 ASNER	08A CLEO	$\Upsilon(3S) \rightarrow \gamma 3\pi^+3\pi^-K^+K^-\pi^0$
22 ASNER 08A reports $[\Gamma(\chi_{b0}(2P) \rightarrow 3\pi^+3\pi^-K^+K^-\pi^0)/\Gamma_{total}] \times [B(\Upsilon(3S) \rightarrow \gamma\chi_{b0}(2P))]$ < $43 \times 10^{-6}$ which we divide by our best value $B(\Upsilon(3S) \rightarrow \gamma\chi_{b0}(2P)) = 5.9 \times 10^{-2}$ .				

### $\Gamma(4\pi^+4\pi^-)/\Gamma_{total}$ $\Gamma_{16}/\Gamma$

VALUE (units $10^{-4}$ )	CL%	DOCUMENT ID	TECN	COMMENT
<1.7	90	23 ASNER	08A CLEO	$\Upsilon(3S) \rightarrow \gamma 4\pi^+4\pi^-$
23 ASNER 08A reports $[\Gamma(\chi_{b0}(2P) \rightarrow 4\pi^+4\pi^-)/\Gamma_{total}] \times [B(\Upsilon(3S) \rightarrow \gamma\chi_{b0}(2P))]$ < $10 \times 10^{-6}$ which we divide by our best value $B(\Upsilon(3S) \rightarrow \gamma\chi_{b0}(2P)) = 5.9 \times 10^{-2}$ .				

### $\Gamma(4\pi^+4\pi^-2\pi^0)/\Gamma_{total}$ $\Gamma_{17}/\Gamma$

VALUE (units $10^{-4}$ )	CL%	DOCUMENT ID	TECN	COMMENT
<6	90	24 ASNER	08A CLEO	$\Upsilon(3S) \rightarrow \gamma 4\pi^+4\pi^-2\pi^0$
24 ASNER 08A reports $[\Gamma(\chi_{b0}(2P) \rightarrow 4\pi^+4\pi^-2\pi^0)/\Gamma_{total}] \times [B(\Upsilon(3S) \rightarrow \gamma\chi_{b0}(2P))]$ < $38 \times 10^{-6}$ which we divide by our best value $B(\Upsilon(3S) \rightarrow \gamma\chi_{b0}(2P)) = 5.9 \times 10^{-2}$ .				

### $\Gamma(\chi_{b0}(2P) \rightarrow \gamma \Upsilon(1S))/\Gamma_{total} \times \Gamma(\Upsilon(3S) \rightarrow \gamma\chi_{b0}(2P))/\Gamma_{total}$ $\Gamma_2/\Gamma \times \Gamma_{21}^{(\Upsilon(3S))}/\Gamma(\Upsilon(3S))$

VALUE (units $10^{-4}$ )	CL%	DOCUMENT ID	TECN	COMMENT
<8.2	90	25 LEES	11J BABR	$\Upsilon(3S) \rightarrow X \gamma$
25 LEES 11J quotes a central value of $\Gamma(\chi_{b0}(2P) \rightarrow \gamma \Upsilon(1S))/\Gamma_{total} \times \Gamma(\Upsilon(3S) \rightarrow \gamma\chi_{b0}(2P))/\Gamma_{total} = (3.9 \pm 2.2 \pm 1.2 \pm 0.6) \times 10^{-4}$ and derives a 90% CL upper limit of $B(\chi_{b0}(2P) \rightarrow \gamma \Upsilon(1S)) < 1.2\%$ using $B(\Upsilon(3S) \rightarrow \gamma\chi_{b0}(2P)) = (5.9 \pm 0.6)\%$ .				

### $\Gamma(\chi_{b0}(2P) \rightarrow \gamma \Upsilon(2S))/\Gamma_{total} \times \Gamma(\Upsilon(3S) \rightarrow \gamma\chi_{b0}(2P))/\Gamma_{total}$ $\Gamma_1/\Gamma \times \Gamma_{21}^{(\Upsilon(3S))}/\Gamma(\Upsilon(3S))$

VALUE (units $10^{-3}$ )	CL%	DOCUMENT ID	TECN	COMMENT
<1.6	90	26 LEES	11J BABR	$\Upsilon(3S) \rightarrow X \gamma$
26 LEES 11J quotes a central value of $\Gamma(\chi_{b0}(2P) \rightarrow \gamma \Upsilon(2S))/\Gamma_{total} \times \Gamma(\Upsilon(3S) \rightarrow \gamma\chi_{b0}(2P))/\Gamma_{total} = (-0.3 \pm 0.2 \pm 0.5 \pm 0.4)\%$ and derives a 90% CL upper limit of $B(\chi_{b0}(2P) \rightarrow \gamma \Upsilon(2S)) < 2.8\%$ using $B(\Upsilon(3S) \rightarrow \gamma\chi_{b0}(2P)) = (5.9 \pm 0.6)\%$ .				

### $\chi_{b0}(2P)$ REFERENCES

LEES	11J	PR D84 072002	J.P. Lees et al.	(BABAR Collab.)
ASNER	08A	PR D78 091103	D.M. Asner et al.	(CLEO Collab.)
BRIERE	08	PR D78 092007	R.A. Briere et al.	(CLEO Collab.)
ARTUSO	05	PRL 94 032001	M. Artuso et al.	(CLEO Collab.)
CRAWFORD	92B	PL B294 139	G. Crawford, R. Fulton	(CLEO Collab.)
HEINTZ	92	PR D46 1928	U. Heintz et al.	(CUSB II Collab.)
HEINTZ	91	PRL 66 1563	U. Heintz et al.	(CUSB Collab.)
MORRISON	91	PRL 67 1696	R.J. Morrison et al.	(CLEO Collab.)
NARAIN	91	PRL 66 3113	M. Narain et al.	(CUSB Collab.)

### $\chi_{b1}(2P)$

$$J^G(J^{PC}) = 0^+(1^{++})$$

J needs confirmation.

Observed in radiative decay of the  $\Upsilon(3S)$ , therefore  $C = +$ . Branching ratio requires E1 transition, M1 is strongly disfavored, therefore  $P = +$ .

### $\chi_{b1}(2P)$ MASS

VALUE (GeV)	DOCUMENT ID	COMMENT
$10.25546 \pm 0.00022 \pm 0.00050$ OUR EVALUATION		From $\gamma$ energy below, using $\Upsilon(3S)$ mass = 10355.2 $\pm$ 0.5 MeV

### $m_{\chi_{b1}(2P)} - m_{\chi_{b0}(2P)}$

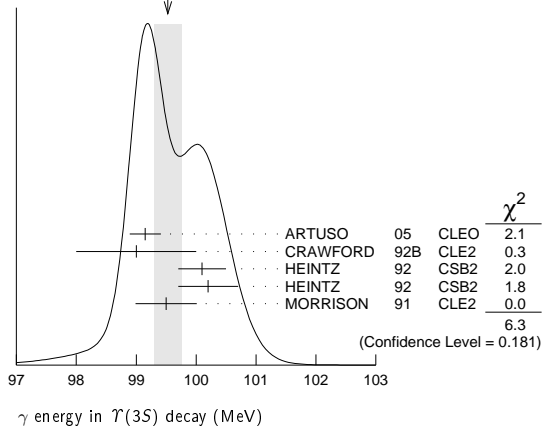
VALUE (MeV)	DOCUMENT ID	TECN	COMMENT
$23.5 \pm 0.7 \pm 0.7$	<sup>1</sup> HEINTZ	92 CSB2	$e^+e^- \rightarrow \gamma X, \ell^+\ell^-\gamma\gamma$

<sup>1</sup> From the average photon energy for inclusive and exclusive events. Supersedes NARAIN 91.

### $\gamma$ ENERGY IN $\Upsilon(3S)$ DECAY

VALUE (MeV)	EVTS	DOCUMENT ID	TECN	COMMENT
<b><math>99.26 \pm 0.22</math> OUR EVALUATION</b>		Treating systematic errors as correlated		
<b><math>99.53 \pm 0.23</math> OUR AVERAGE</b>		Error includes scale factor of 1.3. See the ideogram below.		
$99.15 \pm 0.07 \pm 0.25$		ARTUSO	05 CLEO	$\Upsilon(3S) \rightarrow \gamma X$
$99 \pm 1$	169	CRAWFORD	92B CLE2	$e^+e^- \rightarrow \ell^+\ell^-\gamma\gamma$
$100.1 \pm 0.4$	11147	<sup>2</sup> HEINTZ	92 CSB2	$e^+e^- \rightarrow \gamma X$
$100.2 \pm 0.5$	223	<sup>3</sup> HEINTZ	92 CSB2	$e^+e^- \rightarrow \ell^+\ell^-\gamma\gamma$
$99.5 \pm 0.1 \pm 0.5$	25759	MORRISON	91 CLE2	$e^+e^- \rightarrow \gamma X$
<sup>2</sup> A systematic uncertainty on the energy scale of 0.9% not included. Supersedes NARAIN 91.				
<sup>3</sup> A systematic uncertainty on the energy scale of 0.9% not included. Supersedes HEINTZ 91.				

WEIGHTED AVERAGE  
99.53±0.23 (Error scaled by 1.3)



### $\chi_{b1}(2P)$ DECAY MODES

Mode	Fraction ( $\Gamma_i/\Gamma$ )	Scale factor
$\Gamma_1 \omega \Upsilon(1S)$	$(1.63 \pm 0.40) \%$	
$\Gamma_2 \gamma \Upsilon(2S)$	$(19.9 \pm 1.9) \%$	
$\Gamma_3 \gamma \Upsilon(1S)$	$(9.2 \pm 0.8) \%$	1.1
$\Gamma_4 \pi^+\pi^-\chi_{b1}(1P)$	$(9.1 \pm 1.3) \times 10^{-3}$	
$\Gamma_5 D^0 X$	$(8.8 \pm 1.7) \%$	
$\Gamma_6 \pi^+\pi^-K^+K^-\pi^0$	$(3.1 \pm 1.0) \times 10^{-4}$	
$\Gamma_7 2\pi^+\pi^-K^-K_S^0$	$(1.1 \pm 0.5) \times 10^{-4}$	
$\Gamma_8 2\pi^+\pi^-K^-K_S^0 2\pi^0$	$(7.7 \pm 3.2) \times 10^{-4}$	
$\Gamma_9 2\pi^+2\pi^-2\pi^0$	$(5.9 \pm 2.0) \times 10^{-4}$	
$\Gamma_{10} 2\pi^+2\pi^-K^+K^-$	$(10 \pm 4) \times 10^{-5}$	
$\Gamma_{11} 2\pi^+2\pi^-K^+K^-\pi^0$	$(5.5 \pm 1.8) \times 10^{-4}$	
$\Gamma_{12} 2\pi^+2\pi^-K^+K^-2\pi^0$	$(10 \pm 4) \times 10^{-4}$	
$\Gamma_{13} 3\pi^+2\pi^-K^-K_S^0\pi^0$	$(6.7 \pm 2.6) \times 10^{-4}$	
$\Gamma_{14} 3\pi^+3\pi^-$	$(1.2 \pm 0.4) \times 10^{-4}$	
$\Gamma_{15} 3\pi^+3\pi^-2\pi^0$	$(1.2 \pm 0.4) \times 10^{-3}$	
$\Gamma_{16} 3\pi^+3\pi^-K^+K^-$	$(2.0 \pm 0.8) \times 10^{-4}$	
$\Gamma_{17} 3\pi^+3\pi^-K^+K^-\pi^0$	$(6.1 \pm 2.2) \times 10^{-4}$	
$\Gamma_{18} 4\pi^+4\pi^-$	$(1.7 \pm 0.6) \times 10^{-4}$	
$\Gamma_{19} 4\pi^+4\pi^-2\pi^0$	$(1.9 \pm 0.7) \times 10^{-3}$	

### $\chi_{b1}(2P)$ BRANCHING RATIOS

$\Gamma(\omega \Upsilon(1S))/\Gamma_{total}$	$\Gamma_1/\Gamma$		
VALUE (units $10^{-2}$ )	DOCUMENT ID	TECN	COMMENT
$1.63 \pm 0.35 \pm 0.16$ $-0.31 - 0.15$	<sup>4</sup> CRONIN-HEN..04	CLE3	$\Upsilon(3S) \rightarrow \gamma\omega \Upsilon(1S)$
<sup>4</sup> Using $B(\Upsilon(3S) \rightarrow \gamma\chi_{b1}(2P)) = (11.3 \pm 0.6)\%$ and $B(\Upsilon(1S) \rightarrow \ell^+\ell^-) = 2 B(\Upsilon(1S) \rightarrow \mu^+\mu^-) = 2(2.48 \pm 0.06)\%$ .			

$\Gamma(\gamma \Upsilon(2S))/\Gamma_{total}$	$\Gamma_2/\Gamma$		
VALUE	DOCUMENT ID	TECN	COMMENT
<b><math>0.199 \pm 0.019</math> OUR AVERAGE</b>			
$0.190 \pm 0.018 \pm 0.017$	<sup>5</sup> LEES	11J BABR	$\Upsilon(3S) \rightarrow X \gamma$
$0.356 \pm 0.042 \pm 0.092$	<sup>6</sup> CRAWFORD	92B CLE2	$e^+e^- \rightarrow \ell^+\ell^-\gamma\gamma$
$0.199 \pm 0.020 \pm 0.022$	<sup>7</sup> HEINTZ	92 CSB2	$e^+e^- \rightarrow \ell^+\ell^-\gamma\gamma$



See key on page 457

Meson Particle Listings

$\chi_{b1}(2P)$ ,  $h_b(2P)$ ,  $\chi_{b2}(2P)$

$$\frac{\Gamma(\chi_{b1}(2P) \rightarrow \gamma \Upsilon(2S)) / \Gamma_{\text{total}} \times \Gamma(\Upsilon(3S) \rightarrow \gamma \chi_{b1}(2P)) / \Gamma_{\text{total}}}{\Gamma_2 / \Gamma \times \Gamma_{\Upsilon(3S)} / \Gamma \Upsilon(3S)}$$

VALUE (units $10^{-2}$ )	EVTS	DOCUMENT ID	TECN	COMMENT
<b>2.4 ± 0.1 ± 0.2</b>	4.3k	LEES	11j	BABR $\Upsilon(3S) \rightarrow X \gamma$

$$B(\chi_{b1}(2P) \rightarrow \chi_{b1}(1P) \pi^+ \pi^-) \times B(\Upsilon(3S) \rightarrow \chi_{b1}(2P) X)$$

VALUE (units $10^{-3}$ )	EVTS	DOCUMENT ID	TECN	COMMENT
<b>1.16 ± 0.07 ± 0.12</b>	31k	LEES	11c	BABR $e^+ e^- \rightarrow \pi^+ \pi^- X$

$$B(\chi_{b2}(2P) \rightarrow \rho X + \bar{\rho} X) / B(\chi_{b1}(2P) \rightarrow \rho X + \bar{\rho} X)$$

VALUE	DOCUMENT ID	TECN	COMMENT
<b>1.109 ± 0.007 ± 0.040</b>	BRIERE 07	CLEO	$\Upsilon(3S) \rightarrow \gamma \chi_{bJ}(2P)$

$$B(\chi_{b0}(2P) \rightarrow \rho X + \bar{\rho} X) / B(\chi_{b1}(2P) \rightarrow \rho X + \bar{\rho} X)$$

VALUE	DOCUMENT ID	TECN	COMMENT
<b>1.082 ± 0.025 ± 0.060</b>	BRIERE 07	CLEO	$\Upsilon(3S) \rightarrow \gamma \chi_{bJ}(2P)$

$\chi_{b1}(2P)$  REFERENCES

LEES	11C	PR D84 011104	J.P. Lees et al.	(BABAR Collab.)
LEES	11J	PR D84 072002	J.P. Lees et al.	(BABAR Collab.)
ASNER	08A	PR D78 091103	D.M. Asner et al.	(CLEO Collab.)
BRIERE	08	PR D78 092007	R.A. Briere et al.	(CLEO Collab.)
BRIERE	07	PR D76 012005	R.A. Briere et al.	(CLEO Collab.)
CRAWFIELD	06	PR D73 012003	C. Crawford et al.	(CLEO Collab.)
ARTUSO	05	PRL 94 032001	M. Artuso et al.	(CLEO Collab.)
CRONIN-HEN..	04	PRL 92 222002	D. Cronin-Hennessy et al.	(CLEO Collab.)
CRAWFORD	92B	PL B294 139	G. Crawford, R. Fulton	(CLEO Collab.)
HEINTZ	92	PR D46 1928	U. Heintz et al.	(CUSB II Collab.)
HEINTZ	91	PRL 66 1563	U. Heintz et al.	(CUSB Collab.)
MORRISON	91	PRL 67 1696	R.J. Morrison et al.	(CLEO Collab.)
NARAIN	91	PRL 66 3113	M. Narain et al.	(CUSB Collab.)

$h_b(2P)$

$$J^G(J^{PC}) = ?^?(1^{+-})$$

OMITTED FROM SUMMARY TABLE

Quantum numbers are quark model predictions.

$h_b(2P)$  MASS

VALUE (GeV)	EVTS	DOCUMENT ID	TECN	COMMENT
<b>10.2598 ± 0.0006 +0.0014 -0.0010</b>	83.9k	ADACHI	12	BELL 10.86 $e^+ e^- \rightarrow \pi^+ \pi^-$ MM

$h_b(2P)$  DECAY MODES

Mode	Fraction ( $\Gamma_i/\Gamma$ )
$\Gamma_1$ hadrons	not seen

$h_b(2P)$  BRANCHING RATIOS

$\Gamma(\text{hadrons})/\Gamma_{\text{total}}$	$\Gamma_1/\Gamma$
<b>not seen</b>	83.9k

$h_b(2P)$  REFERENCES

ADACHI	12	PRL 108 032001	I. Adachi et al.	(BELLE Collab.)
--------	----	----------------	------------------	-----------------

$\chi_{b2}(2P)$

$$J^G(J^{PC}) = 0^+(2^{++})$$

J needs confirmation.

Observed in radiative decay of the  $\Upsilon(3S)$ , therefore  $C = +$ . Branching ratio requires E1 transition, M1 is strongly disfavored, therefore  $P = +$ .

$\chi_{b2}(2P)$  MASS

VALUE (GeV)	DOCUMENT ID
<b>10.26865 ± 0.00022 ± 0.00050</b>	OUR EVALUATION

From  $\gamma$  energy below, using  $\Upsilon(3S)$  mass = 10355.2 ± 0.5 MeV

$m_{\chi_{b2}(2P)} - m_{\chi_{b1}(2P)}$

VALUE (MeV)	DOCUMENT ID	TECN	COMMENT
<b>13.5 ± 0.4 ± 0.5</b>	<sup>1</sup> HEINTZ	92	CSB2 $e^+ e^- \rightarrow \gamma X, \ell^+ \ell^- \gamma \gamma$

<sup>1</sup> From the average photon energy for inclusive and exclusive events. Supersedes NARAIN 91.

$\gamma$  ENERGY IN  $\Upsilon(3S)$  DECAY

VALUE (MeV)	EVTS	DOCUMENT ID	TECN	COMMENT
<b>86.19 ± 0.22</b>	OUR EVALUATION	Treating systematic errors as correlated		
<b>86.40 ± 0.18</b>	OUR AVERAGE			
86.04 ± 0.06 ± 0.27		ARTUSO	05	CLEO $\Upsilon(3S) \rightarrow \gamma X$
86 ± 1	101	CRAWFORD	92B	CLE2 $e^+ e^- \rightarrow \ell^+ \ell^- \gamma \gamma$
86.7 ± 0.4	10319	<sup>2</sup> HEINTZ	92	CSB2 $e^+ e^- \rightarrow \gamma X$
86.9 ± 0.4	157	<sup>3</sup> HEINTZ	92	CSB2 $e^+ e^- \rightarrow \ell^+ \ell^- \gamma \gamma$
86.4 ± 0.1 ± 0.4	30741	MORRISON	91	CLE2 $e^+ e^- \rightarrow \gamma X$

<sup>2</sup> A systematic uncertainty on the energy scale of 0.9% not included. Supersedes NARAIN 91.

<sup>3</sup> A systematic uncertainty on the energy scale of 0.9% not included. Supersedes HEINTZ 91.

$\chi_{b2}(2P)$  DECAY MODES

Mode	Fraction ( $\Gamma_i/\Gamma$ )	Scale factor/Confidence level
$\Gamma_1$ $\omega \Upsilon(1S)$	( 1.10 +0.34 -0.30 ) %	
$\Gamma_2$ $\gamma \Upsilon(2S)$	( 10.6 ± 2.6 ) %	S=2.0
$\Gamma_3$ $\gamma \Upsilon(1S)$	( 7.0 ± 0.7 ) %	
$\Gamma_4$ $\pi \pi \chi_{b2}(1P)$	( 5.1 ± 0.9 ) × 10 <sup>-3</sup>	
$\Gamma_5$ $D^0 X$	< 2.4 %	CL=90%
$\Gamma_6$ $\pi^+ \pi^- K^+ K^- \pi^0$	< 1.1 × 10 <sup>-4</sup>	CL=90%
$\Gamma_7$ $2\pi^+ \pi^- K^- K_S^0$	< 9 × 10 <sup>-5</sup>	CL=90%
$\Gamma_8$ $2\pi^+ \pi^- K^- K_S^0 2\pi^0$	< 7 × 10 <sup>-4</sup>	CL=90%
$\Gamma_9$ $2\pi^+ 2\pi^- 2\pi^0$	( 3.9 ± 1.6 ) × 10 <sup>-4</sup>	
$\Gamma_{10}$ $2\pi^+ 2\pi^- K^+ K^-$	( 9 ± 4 ) × 10 <sup>-5</sup>	
$\Gamma_{11}$ $2\pi^+ 2\pi^- K^+ K^- \pi^0$	( 2.4 ± 1.1 ) × 10 <sup>-4</sup>	
$\Gamma_{12}$ $2\pi^+ 2\pi^- K^+ K^- 2\pi^0$	( 4.7 ± 2.3 ) × 10 <sup>-4</sup>	
$\Gamma_{13}$ $3\pi^+ 2\pi^- K^- K_S^0 \pi^0$	< 4 × 10 <sup>-4</sup>	CL=90%
$\Gamma_{14}$ $3\pi^+ 3\pi^-$	( 9 ± 4 ) × 10 <sup>-5</sup>	
$\Gamma_{15}$ $3\pi^+ 3\pi^- 2\pi^0$	( 1.2 ± 0.4 ) × 10 <sup>-3</sup>	
$\Gamma_{16}$ $3\pi^+ 3\pi^- K^+ K^-$	( 1.4 ± 0.7 ) × 10 <sup>-4</sup>	
$\Gamma_{17}$ $3\pi^+ 3\pi^- K^+ K^- \pi^0$	( 4.2 ± 1.7 ) × 10 <sup>-4</sup>	
$\Gamma_{18}$ $4\pi^+ 4\pi^-$	( 9 ± 5 ) × 10 <sup>-5</sup>	
$\Gamma_{19}$ $4\pi^+ 4\pi^- 2\pi^0$	( 1.3 ± 0.5 ) × 10 <sup>-3</sup>	

$\chi_{b2}(2P)$  BRANCHING RATIOS

$\Gamma(\omega \Upsilon(1S)) / \Gamma_{\text{total}}$	$\Gamma_1/\Gamma$
<b>1.10 +0.32 +0.11 -0.28 -0.10</b>	20.1 +5.8 -5.1 <sup>4</sup> CRONIN-HEN..04

<sup>4</sup> Using  $B(\Upsilon(3S) \rightarrow \gamma \chi_{b2}(2P)) = (11.4 \pm 0.8)\%$  and  $B(\Upsilon(1S) \rightarrow \ell^+ \ell^-) = 2$   $B(\Upsilon(1S) \rightarrow \mu^+ \mu^-) = 2(2.48 \pm 0.06)\%$ .

$\Gamma(\gamma \Upsilon(2S)) / \Gamma_{\text{total}}$

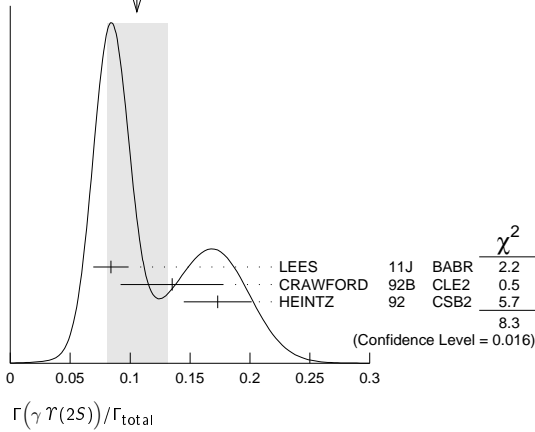
VALUE	EVTS	DOCUMENT ID	TECN	COMMENT
<b>0.106 ± 0.026</b>	OUR AVERAGE	Error includes scale factor of 2.0. See the ideogram below.		
0.084 ± 0.011 ± 0.010	2.5k	<sup>5</sup> LEES	11j	BABR $\Upsilon(3S) \rightarrow X \gamma$
0.135 ± 0.025 ± 0.035		<sup>6</sup> CRAWFORD	92B	CLE2 $e^+ e^- \rightarrow \ell^+ \ell^- \gamma \gamma$
0.173 ± 0.021 ± 0.019		<sup>7</sup> HEINTZ	92	CSB2 $e^+ e^- \rightarrow \ell^+ \ell^- \gamma \gamma$

<sup>5</sup> LEES 11j reports  $[\Gamma(\chi_{b2}(2P) \rightarrow \gamma \Upsilon(2S)) / \Gamma_{\text{total}}] \times [B(\Upsilon(3S) \rightarrow \gamma \chi_{b2}(2P))] = (1.1 \pm 0.1 \pm 0.1) \times 10^{-2}$  which we divide by our best value  $B(\Upsilon(3S) \rightarrow \gamma \chi_{b2}(2P)) = (13.1 \pm 1.6) \times 10^{-2}$ . Our first error is their experiment's error and our second error is the systematic error from using our best value.

<sup>6</sup> Using  $B(\Upsilon(2S) \rightarrow \mu^+ \mu^-) = (1.37 \pm 0.26)\%$ ,  $B(\Upsilon(3S) \rightarrow \gamma \gamma \Upsilon(2S)) \times 2 B(\Upsilon(2S) \rightarrow \mu^+ \mu^-) = (4.98 \pm 0.94 \pm 0.62) \times 10^{-4}$ , and  $B(\Upsilon(3S) \rightarrow \gamma \chi_{b2}(2P)) = 0.135 \pm 0.003 \pm 0.017$ .

<sup>7</sup> Using  $B(\Upsilon(2S) \rightarrow \mu^+ \mu^-) = (1.44 \pm 0.10)\%$ ,  $B(\Upsilon(3S) \rightarrow \gamma \chi_{b2}(2P)) = (11.1 \pm 0.5 \pm 0.4)\%$  and assuming  $e\mu$  universality. Supersedes HEINTZ 91.

## Meson Particle Listings

 $\chi_{b2}(2P)$ WEIGHTED AVERAGE  
0.106±0.026 (Error scaled by 2.0) $\Gamma(\gamma\Upsilon(1S))/\Gamma_{\text{total}}$   $\Gamma_3/\Gamma$ 

VALUE (units 10 <sup>-4</sup> )	EVTS	DOCUMENT ID	TECN	COMMENT
<b>0.070±0.007 OUR AVERAGE</b>				
0.070±0.004±0.008	11k	8 LEES	11J BABR	$\Upsilon(3S) \rightarrow X\gamma$
0.072±0.014±0.013		9 CRAWFORD	92B CLE2	$e^+e^- \rightarrow \ell^+\ell^-\gamma\gamma$
0.070±0.010±0.006		10 HEINTZ	92 CSB2	$e^+e^- \rightarrow \ell^+\ell^-\gamma\gamma$

<sup>8</sup>LEES 11J reports  $[\Gamma(\chi_{b2}(2P) \rightarrow \gamma\Upsilon(1S))/\Gamma_{\text{total}}] \times [B(\Upsilon(3S) \rightarrow \gamma\chi_{b2}(2P))] = (9.2 \pm 0.3 \pm 0.4) \times 10^{-3}$  which we divide by our best value  $B(\Upsilon(3S) \rightarrow \gamma\chi_{b2}(2P)) = (13.1 \pm 1.6) \times 10^{-2}$ . Our first error is their experiment's error and our second error is the systematic error from using our best value.

<sup>9</sup>Using  $B(\Upsilon(1S) \rightarrow \mu^+\mu^-) = (2.57 \pm 0.07)\%$ ,  $B(\Upsilon(3S) \rightarrow \gamma\gamma\Upsilon(2S)) \times 2B(\Upsilon(1S) \rightarrow \mu^+\mu^-) = (5.03 \pm 0.94 \pm 0.63) \times 10^{-4}$ , and  $B(\Upsilon(3S) \rightarrow \gamma\chi_{b2}(2P)) = 0.135 \pm 0.003 \pm 0.017$ .

<sup>10</sup>Using  $B(\Upsilon(1S) \rightarrow \mu^+\mu^-) = (2.57 \pm 0.07)\%$ ,  $B(\Upsilon(3S) \rightarrow \gamma\chi_{b2}(2P)) = (11.1 \pm 0.5 \pm 0.4)\%$  and assuming  $e\mu$  universality. Supersedes HEINTZ 91.

 $\Gamma(\pi\pi\chi_{b2}(1P))/\Gamma_{\text{total}}$   $\Gamma_4/\Gamma$ 

VALUE (units 10 <sup>-3</sup> )	EVTS	DOCUMENT ID	TECN	COMMENT
<b>5.1±0.9 OUR AVERAGE</b>				
4.9±0.7±0.6	17k	11 LEES	11c BABR	$e^+e^- \rightarrow \pi^+\pi^-X$
6.0±1.6±1.4		12 CAWLFIELD	06 CLE3	$\Upsilon(3S) \rightarrow 2(\gamma\pi\ell)$

<sup>11</sup> $(0.64 \pm 0.05 \pm 0.08) \times 10^{-3}$ . We derive the value assuming  $B(\Upsilon(3S) \rightarrow \chi_{b2}(2P)X) = B(\Upsilon(3S) \rightarrow \chi_{b2}(2P)\gamma) = (13.1 \pm 1.6) \times 10^{-2}$ .

<sup>12</sup>CAWLFIELD 06 quote  $\Gamma(\chi_{b2}(2P) \rightarrow \pi\pi\chi_{b2}(1P)) = 0.83 \pm 0.22 \pm 0.08 \pm 0.19$  keV assuming l-spin conservation, no D-wave contribution,  $\Gamma(\chi_{b1}(2P)) = 96 \pm 16$  keV, and  $\Gamma(\chi_{b2}(2P)) = 138 \pm 19$  keV.

 $\Gamma(D^0X)/\Gamma_{\text{total}}$   $\Gamma_5/\Gamma$ 

VALUE	CL%	DOCUMENT ID	TECN	COMMENT
<b>&lt;2.4 × 10<sup>-2</sup></b>	90	13,14 BRIERE	08 CLEO	$\Upsilon(3S) \rightarrow \gamma D^0 X$

<sup>13</sup>For  $p_{D^0} > 2.5$  GeV/c.

<sup>14</sup>The authors also present their result as  $(0.2 \pm 1.4 \pm 0.1) \times 10^{-2}$ .

 $\Gamma(\pi^+\pi^-K^+K^-\pi^0)/\Gamma_{\text{total}}$   $\Gamma_6/\Gamma$ 

VALUE (units 10 <sup>-4</sup> )	CL%	DOCUMENT ID	TECN	COMMENT
<b>&lt;1.1</b>	90	15 ASNER	08A CLEO	$\Upsilon(3S) \rightarrow \gamma\pi^+\pi^-K^+K^-\pi^0$

<sup>15</sup>ASNER 08A reports  $[\Gamma(\chi_{b2}(2P) \rightarrow \pi^+\pi^-K^+K^-\pi^0)/\Gamma_{\text{total}}] \times [B(\Upsilon(3S) \rightarrow \gamma\chi_{b2}(2P))] < 14 \times 10^{-6}$  which we divide by our best value  $B(\Upsilon(3S) \rightarrow \gamma\chi_{b2}(2P)) = 13.1 \times 10^{-2}$ .

 $\Gamma(2\pi^+\pi^-K^-K_S^0)/\Gamma_{\text{total}}$   $\Gamma_7/\Gamma$ 

VALUE (units 10 <sup>-4</sup> )	CL%	DOCUMENT ID	TECN	COMMENT
<b>&lt;0.9</b>	90	16 ASNER	08A CLEO	$\Upsilon(3S) \rightarrow \gamma 2\pi^+\pi^-K^-K_S^0$

<sup>16</sup>ASNER 08A reports  $[\Gamma(\chi_{b2}(2P) \rightarrow 2\pi^+\pi^-K^-K_S^0)/\Gamma_{\text{total}}] \times [B(\Upsilon(3S) \rightarrow \gamma\chi_{b2}(2P))] < 12 \times 10^{-6}$  which we divide by our best value  $B(\Upsilon(3S) \rightarrow \gamma\chi_{b2}(2P)) = 13.1 \times 10^{-2}$ .

 $\Gamma(2\pi^+\pi^-K^-K_S^0 2\pi^0)/\Gamma_{\text{total}}$   $\Gamma_8/\Gamma$ 

VALUE (units 10 <sup>-4</sup> )	CL%	DOCUMENT ID	TECN	COMMENT
<b>&lt;7</b>	90	17 ASNER	08A CLEO	$\Upsilon(3S) \rightarrow \gamma 2\pi^+\pi^-K^-2\pi^0$

<sup>17</sup>ASNER 08A reports  $[\Gamma(\chi_{b2}(2P) \rightarrow 2\pi^+\pi^-K^-K_S^0 2\pi^0)/\Gamma_{\text{total}}] \times [B(\Upsilon(3S) \rightarrow \gamma\chi_{b2}(2P))] < 87 \times 10^{-6}$  which we divide by our best value  $B(\Upsilon(3S) \rightarrow \gamma\chi_{b2}(2P)) = 13.1 \times 10^{-2}$ .

 $\Gamma(2\pi^+2\pi^-2\pi^0)/\Gamma_{\text{total}}$   $\Gamma_9/\Gamma$ 

VALUE (units 10 <sup>-4</sup> )	EVTS	DOCUMENT ID	TECN	COMMENT
<b>3.9±1.6±0.5</b>	23	18 ASNER	08A CLEO	$\Upsilon(3S) \rightarrow \gamma 2\pi^+2\pi^-2\pi^0$

<sup>18</sup>ASNER 08A reports  $[\Gamma(\chi_{b2}(2P) \rightarrow 2\pi^+2\pi^-2\pi^0)/\Gamma_{\text{total}}] \times [B(\Upsilon(3S) \rightarrow \gamma\chi_{b2}(2P))] = (51 \pm 16 \pm 13) \times 10^{-6}$  which we divide by our best value  $B(\Upsilon(3S) \rightarrow \gamma\chi_{b2}(2P)) = (13.1 \pm 1.6) \times 10^{-2}$ . Our first error is their experiment's error and our second error is the systematic error from using our best value.

 $\Gamma(2\pi^+2\pi^-K^+K^-)/\Gamma_{\text{total}}$   $\Gamma_{10}/\Gamma$ 

VALUE (units 10 <sup>-4</sup> )	EVTS	DOCUMENT ID	TECN	COMMENT
<b>0.9±0.4±0.1</b>	11	19 ASNER	08A CLEO	$\Upsilon(3S) \rightarrow \gamma 2\pi^+2\pi^-K^+K^-$

<sup>19</sup>ASNER 08A reports  $[\Gamma(\chi_{b2}(2P) \rightarrow 2\pi^+2\pi^-K^+K^-)/\Gamma_{\text{total}}] \times [B(\Upsilon(3S) \rightarrow \gamma\chi_{b2}(2P))] = (12 \pm 4 \pm 3) \times 10^{-6}$  which we divide by our best value  $B(\Upsilon(3S) \rightarrow \gamma\chi_{b2}(2P)) = (13.1 \pm 1.6) \times 10^{-2}$ . Our first error is their experiment's error and our second error is the systematic error from using our best value.

 $\Gamma(2\pi^+2\pi^-K^+K^-\pi^0)/\Gamma_{\text{total}}$   $\Gamma_{11}/\Gamma$ 

VALUE (units 10 <sup>-4</sup> )	EVTS	DOCUMENT ID	TECN	COMMENT
<b>2.4±1.0±0.3</b>	16	20 ASNER	08A CLEO	$\Upsilon(3S) \rightarrow \gamma 2\pi^+2\pi^-K^+K^-\pi^0$

<sup>20</sup>ASNER 08A reports  $[\Gamma(\chi_{b2}(2P) \rightarrow 2\pi^+2\pi^-K^+K^-\pi^0)/\Gamma_{\text{total}}] \times [B(\Upsilon(3S) \rightarrow \gamma\chi_{b2}(2P))] = (32 \pm 11 \pm 8) \times 10^{-6}$  which we divide by our best value  $B(\Upsilon(3S) \rightarrow \gamma\chi_{b2}(2P)) = (13.1 \pm 1.6) \times 10^{-2}$ . Our first error is their experiment's error and our second error is the systematic error from using our best value.

 $\Gamma(2\pi^+2\pi^-K^+K^-2\pi^0)/\Gamma_{\text{total}}$   $\Gamma_{12}/\Gamma$ 

VALUE (units 10 <sup>-4</sup> )	EVTS	DOCUMENT ID	TECN	COMMENT
<b>4.7±2.2±0.6</b>	14	21 ASNER	08A CLEO	$\Upsilon(3S) \rightarrow \gamma 2\pi^+2\pi^-K^+K^-2\pi^0$

<sup>21</sup>ASNER 08A reports  $[\Gamma(\chi_{b2}(2P) \rightarrow 2\pi^+2\pi^-K^+K^-2\pi^0)/\Gamma_{\text{total}}] \times [B(\Upsilon(3S) \rightarrow \gamma\chi_{b2}(2P))] = (62 \pm 23 \pm 17) \times 10^{-6}$  which we divide by our best value  $B(\Upsilon(3S) \rightarrow \gamma\chi_{b2}(2P)) = (13.1 \pm 1.6) \times 10^{-2}$ . Our first error is their experiment's error and our second error is the systematic error from using our best value.

 $\Gamma(3\pi^+2\pi^-K^-K_S^0\pi^0)/\Gamma_{\text{total}}$   $\Gamma_{13}/\Gamma$ 

VALUE (units 10 <sup>-4</sup> )	CL%	DOCUMENT ID	TECN	COMMENT
<b>&lt;4</b>	90	22 ASNER	08A CLEO	$\Upsilon(3S) \rightarrow \gamma 3\pi^+2\pi^-K^-K_S^0\pi^0$

<sup>22</sup>ASNER 08A reports  $[\Gamma(\chi_{b2}(2P) \rightarrow 3\pi^+2\pi^-K^-K_S^0\pi^0)/\Gamma_{\text{total}}] \times [B(\Upsilon(3S) \rightarrow \gamma\chi_{b2}(2P))] < 58 \times 10^{-6}$  which we divide by our best value  $B(\Upsilon(3S) \rightarrow \gamma\chi_{b2}(2P)) = 13.1 \times 10^{-2}$ .

 $\Gamma(3\pi^+3\pi^-)/\Gamma_{\text{total}}$   $\Gamma_{14}/\Gamma$ 

VALUE (units 10 <sup>-4</sup> )	EVTS	DOCUMENT ID	TECN	COMMENT
<b>0.9±0.4±0.1</b>	14	23 ASNER	08A CLEO	$\Upsilon(3S) \rightarrow \gamma 3\pi^+3\pi^-$

<sup>23</sup>ASNER 08A reports  $[\Gamma(\chi_{b2}(2P) \rightarrow 3\pi^+3\pi^-)/\Gamma_{\text{total}}] \times [B(\Upsilon(3S) \rightarrow \gamma\chi_{b2}(2P))] = (12 \pm 4 \pm 3) \times 10^{-6}$  which we divide by our best value  $B(\Upsilon(3S) \rightarrow \gamma\chi_{b2}(2P)) = (13.1 \pm 1.6) \times 10^{-2}$ . Our first error is their experiment's error and our second error is the systematic error from using our best value.

 $\Gamma(3\pi^+3\pi^-2\pi^0)/\Gamma_{\text{total}}$   $\Gamma_{15}/\Gamma$ 

VALUE (units 10 <sup>-4</sup> )	EVTS	DOCUMENT ID	TECN	COMMENT
<b>12±4±1</b>	45	24 ASNER	08A CLEO	$\Upsilon(3S) \rightarrow \gamma 3\pi^+3\pi^-2\pi^0$

<sup>24</sup>ASNER 08A reports  $[\Gamma(\chi_{b2}(2P) \rightarrow 3\pi^+3\pi^-2\pi^0)/\Gamma_{\text{total}}] \times [B(\Upsilon(3S) \rightarrow \gamma\chi_{b2}(2P))] = (159 \pm 33 \pm 43) \times 10^{-6}$  which we divide by our best value  $B(\Upsilon(3S) \rightarrow \gamma\chi_{b2}(2P)) = (13.1 \pm 1.6) \times 10^{-2}$ . Our first error is their experiment's error and our second error is the systematic error from using our best value.

 $\Gamma(3\pi^+3\pi^-K^+K^-)/\Gamma_{\text{total}}$   $\Gamma_{16}/\Gamma$ 

VALUE (units 10 <sup>-4</sup> )	EVTS	DOCUMENT ID	TECN	COMMENT
<b>1.4±0.7±0.2</b>	12	25 ASNER	08A CLEO	$\Upsilon(3S) \rightarrow \gamma 3\pi^+3\pi^-K^+K^-$

<sup>25</sup>ASNER 08A reports  $[\Gamma(\chi_{b2}(2P) \rightarrow 3\pi^+3\pi^-K^+K^-)/\Gamma_{\text{total}}] \times [B(\Upsilon(3S) \rightarrow \gamma\chi_{b2}(2P))] = (19 \pm 7 \pm 5) \times 10^{-6}$  which we divide by our best value  $B(\Upsilon(3S) \rightarrow \gamma\chi_{b2}(2P)) = (13.1 \pm 1.6) \times 10^{-2}$ . Our first error is their experiment's error and our second error is the systematic error from using our best value.

 $\Gamma(3\pi^+3\pi^-K^+K^-\pi^0)/\Gamma_{\text{total}}$   $\Gamma_{17}/\Gamma$ 

VALUE (units 10 <sup>-4</sup> )	EVTS	DOCUMENT ID	TECN	COMMENT
<b>4.2±1.7±0.5</b>	16	26 ASNER	08A CLEO	$\Upsilon(3S) \rightarrow \gamma 3\pi^+3\pi^-K^+K^-\pi^0$

<sup>26</sup>ASNER 08A reports  $[\Gamma(\chi_{b2}(2P) \rightarrow 3\pi^+3\pi^-K^+K^-\pi^0)/\Gamma_{\text{total}}] \times [B(\Upsilon(3S) \rightarrow \gamma\chi_{b2}(2P))] = (55 \pm 16 \pm 15) \times 10^{-6}$  which we divide by our best value  $B(\Upsilon(3S) \rightarrow \gamma\chi_{b2}(2P)) = (13.1 \pm 1.6) \times 10^{-2}$ . Our first error is their experiment's error and our second error is the systematic error from using our best value.

 $\Gamma(4\pi^+4\pi^-)/\Gamma_{\text{total}}$   $\Gamma_{18}/\Gamma$ 

VALUE (units 10 <sup>-4</sup> )	EVTS	DOCUMENT ID	TECN	COMMENT
<b>0.9±0.4±0.1</b>	9	27 ASNER	08A CLEO	$\Upsilon(3S) \rightarrow \gamma 4\pi^+4\pi^-$

<sup>27</sup>ASNER 08A reports  $[\Gamma(\chi_{b2}(2P) \rightarrow 4\pi^+4\pi^-)/\Gamma_{\text{total}}] \times [B(\Upsilon(3S) \rightarrow \gamma\chi_{b2}(2P))] = (12 \pm 5 \pm 3) \times 10^{-6}$  which we divide by our best value  $B(\Upsilon(3S) \rightarrow \gamma\chi_{b2}(2P)) = (13.1 \pm 1.6) \times 10^{-2}$ . Our first error is their experiment's error and our second error is the systematic error from using our best value.

See key on page 457

Meson Particle Listings

$\chi_{b2}(2P), \Upsilon(3S)$

$\Gamma(4\pi^+4\pi^-2\pi^0)/\Gamma_{total}$		$\Gamma_{19}/\Gamma$	
VALUE (units $10^{-4}$ )	EVTs	DOCUMENT ID	TECN COMMENT
<b>13±5±2</b>	27	28 ASNER	08A CLEO $\Upsilon(3S) \rightarrow \gamma 4\pi^+ 4\pi^- 2\pi^0$
<sup>28</sup> ASNER 08A reports $[\Gamma(\chi_{b2}(2P) \rightarrow 4\pi^+ 4\pi^- 2\pi^0)/\Gamma_{total}] \times [B(\Upsilon(3S) \rightarrow \gamma \chi_{b2}(2P))]$ $= (165 \pm 46 \pm 50) \times 10^{-6}$ which we divide by our best value $B(\Upsilon(3S) \rightarrow \gamma \chi_{b2}(2P))$ $= (13.1 \pm 1.6) \times 10^{-2}$ . Our first error is their experiment's error and our second error is the systematic error from using our best value.			

$\chi_{b2}(2P)$  Cross-Particle Branching Ratios

$\Gamma(\chi_{b2}(2P) \rightarrow \gamma \Upsilon(1S))/\Gamma_{total} \times \Gamma(\Upsilon(3S) \rightarrow \gamma \chi_{b2}(2P))/\Gamma_{total}$		$\Gamma_3/\Gamma \times \Gamma_{19}^{\Upsilon(3S)}/\Gamma \Upsilon(3S)$	
VALUE (units $10^{-3}$ )	EVTs	DOCUMENT ID	TECN COMMENT
<b>9.2±0.3±0.4</b>	11k	LEES	11J BABR $\Upsilon(3S) \rightarrow X \gamma$

$\Gamma(\chi_{b2}(2P) \rightarrow \gamma \Upsilon(2S))/\Gamma_{total} \times \Gamma(\Upsilon(3S) \rightarrow \gamma \chi_{b2}(2P))/\Gamma_{total}$		$\Gamma_2/\Gamma \times \Gamma_{19}^{\Upsilon(3S)}/\Gamma \Upsilon(3S)$	
VALUE (units $10^{-2}$ )	EVTs	DOCUMENT ID	TECN COMMENT
<b>1.1±0.1±0.1</b>	2.5k	LEES	11J BABR $\Upsilon(3S) \rightarrow X \gamma$

$B(\chi_{b2}(2P) \rightarrow \chi_{b2}(1P)\pi^+\pi^-) \times B(\Upsilon(3S) \rightarrow \chi_{b2}(2P)X)$			
VALUE (units $10^{-3}$ )	EVTs	DOCUMENT ID	TECN COMMENT
<b>0.64±0.05±0.08</b>	17k	LEES	11C BABR $e^+e^- \rightarrow \pi^+\pi^-X$

$\chi_{b2}(2P)$  REFERENCES

LEES	11C	PR D84 011104	J.P. Lees et al.	(BABAR Collab.)
LEES	11J	PR D84 072002	J.P. Lees et al.	(BABAR Collab.)
ASNER	08A	PR D78 091103	D.M. Asner et al.	(CLEO Collab.)
BRIERE	08	PR D78 092007	R.A. Briere et al.	(CLEO Collab.)
CAWFIELD	06	PR D73 012003	C. Cawfield et al.	(CLEO Collab.)
ARTUSO	05	PRL 94 032001	M. Artuso et al.	(CLEO Collab.)
CRONIN-HEN...	04	PRL 92 222002	D. Cronin-Hennessy et al.	(CLEO Collab.)
CRAWFORD	92B	PL B294 139	G. Crawford, R. Fulton	(CLEO Collab.)
HEINTZ	92	PR D46 1928	U. Heintz et al.	(CUSB II Collab.)
HEINTZ	91	PRL 66 1563	U. Heintz et al.	(CUSB Collab.)
MORRISON	91	PRL 67 1696	R.J. Morrison et al.	(CLEO Collab.)
NARAIN	91	PRL 66 3113	M. Narain et al.	(CUSB Collab.)

$\Upsilon(3S)$

$J^{PC} = 0^-(1^{--})$

$\Upsilon(3S)$  MASS

VALUE (GeV)	DOCUMENT ID	TECN	COMMENT
<b>10.3552±0.0005</b>	1 ARTAMONOV 00	MD1	$e^+e^- \rightarrow$ hadrons
• • • We do not use the following data for averages, fits, limits, etc. • • •			
10.3553±0.0005	2,3 BARU	86B	REDE $e^+e^- \rightarrow$ hadrons
<sup>1</sup> Reanalysis of BARU 86B using new electron mass (COHEN 87).			
<sup>2</sup> Reanalysis of ARTAMONOV 84.			
<sup>3</sup> Superseded by ARTAMONOV 00.			

$m\Upsilon(3S) - m\Upsilon(2S)$

VALUE (MeV)	DOCUMENT ID	TECN	COMMENT
<b>331.50±0.02±0.13</b>	LEES	11C	BABR $e^+e^- \rightarrow \pi^+\pi^-X$

$\Upsilon(3S)$  WIDTH

VALUE (keV)	DOCUMENT ID
<b>20.32±1.85 OUR EVALUATION</b>	See the Note on "Width Determinations of the $\Upsilon$ States"

$\Upsilon(3S)$  DECAY MODES

Mode	Fraction ( $\Gamma_i/\Gamma$ )	Scale factor/ Confidence level
$\Gamma_1$ $\Upsilon(2S)$ anything	(10.6 ± 0.8) %	
$\Gamma_2$ $\Upsilon(2S)\pi^+\pi^-$	(2.82 ± 0.18) %	S=1.6
$\Gamma_3$ $\Upsilon(2S)\pi^0\pi^0$	(1.85 ± 0.14) %	
$\Gamma_4$ $\Upsilon(2S)\gamma\gamma$	(5.0 ± 0.7) %	
$\Gamma_5$ $\Upsilon(2S)\pi^0$	< 5.1 × 10 <sup>-4</sup>	CL=90%
$\Gamma_6$ $\Upsilon(1S)\pi^+\pi^-$	(4.37 ± 0.08) %	
$\Gamma_7$ $\Upsilon(1S)\pi^0\pi^0$	(2.20 ± 0.13) %	
$\Gamma_8$ $\Upsilon(1S)\eta$	< 1 × 10 <sup>-4</sup>	CL=90%
$\Gamma_9$ $\Upsilon(1S)\pi^0$	< 7 × 10 <sup>-5</sup>	CL=90%
$\Gamma_{10}$ $h_b(1P)\pi^0$	< 1.2 × 10 <sup>-3</sup>	CL=90%
$\Gamma_{11}$ $h_b(1P)\pi^0 \rightarrow \gamma\eta_b(1S)\pi^0$	(4.3 ± 1.4) × 10 <sup>-4</sup>	

$\Gamma_{12}$ $h_b(1P)\pi^+\pi^-$	< 1.2 × 10 <sup>-4</sup>	CL=90%
$\Gamma_{13}$ $\tau^+\tau^-$	(2.29 ± 0.30) %	
$\Gamma_{14}$ $\mu^+\mu^-$	(2.18 ± 0.21) %	S=2.1
$\Gamma_{15}$ $e^+e^-$	seen	
$\Gamma_{16}$ hadrons		
$\Gamma_{17}$ $ggg$	(35.7 ± 2.6) %	
$\Gamma_{18}$ $\gamma gg$	(9.7 ± 1.8) × 10 <sup>-3</sup>	

Radiative decays

$\Gamma_{19}$ $\gamma\chi_{b2}(2P)$	(13.1 ± 1.6) %	S=3.4
$\Gamma_{20}$ $\gamma\chi_{b1}(2P)$	(12.6 ± 1.2) %	S=2.4
$\Gamma_{21}$ $\gamma\chi_{b0}(2P)$	(5.9 ± 0.6) %	S=1.4
$\Gamma_{22}$ $\gamma\chi_{b2}(1P)$	(9.9 ± 1.3) × 10 <sup>-3</sup>	S=2.0
$\Gamma_{23}$ $\gamma A^0 \rightarrow \gamma$ hadrons	< 8 × 10 <sup>-5</sup>	CL=90%
$\Gamma_{24}$ $\gamma\chi_{b1}(1P)$	(9 ± 5) × 10 <sup>-4</sup>	S=1.9
$\Gamma_{25}$ $\gamma\chi_{b0}(1P)$	(2.7 ± 0.4) × 10 <sup>-3</sup>	
$\Gamma_{26}$ $\gamma\eta_b(2S)$	< 6.2 × 10 <sup>-4</sup>	CL=90%
$\Gamma_{27}$ $\gamma\eta_b(1S)$	(5.1 ± 0.7) × 10 <sup>-4</sup>	
$\Gamma_{28}$ $\gamma X \rightarrow \gamma + \geq 4$ prongs	[a] < 2.2 × 10 <sup>-4</sup>	CL=95%
$\Gamma_{29}$ $\gamma a_1^0 \rightarrow \gamma\tau^+\tau^-$	[b] < 1.6 × 10 <sup>-4</sup>	CL=90%

Lepton Family number (LF) violating modes

$\Gamma_{30}$ $e^\pm\tau^\mp$	LF	< 4.2 × 10 <sup>-6</sup>	CL=90%
$\Gamma_{31}$ $\mu^\pm\tau^\mp$	LF	< 3.1 × 10 <sup>-6</sup>	CL=90%

[a] 1.5 GeV <  $m_X$  < 5.0 GeV

[b] For  $m_{\tau^+\tau^-}$  in the ranges 4.03–9.52 and 9.61–10.10 GeV.

$\Upsilon(3S) \Gamma(i)\Gamma(e^+e^-)/\Gamma_{total}$

$\Gamma(\text{hadrons}) \times \Gamma(e^+e^-)/\Gamma_{total}$	DOCUMENT ID	TECN	COMMENT	$\Gamma_{16}\Gamma_{15}/\Gamma$
<b>0.413±0.007 OUR AVERAGE</b>				
0.413 ± 0.004 ± 0.006	ROSNER	06	CLEO $10.4 e^+e^- \rightarrow$ hadrons	
0.45 ± 0.03 ± 0.03	<sup>4</sup> GILES	84B	CLEO $e^+e^- \rightarrow$ hadrons	
<sup>4</sup> Radiative corrections reevaluated by BUCHMUELLER 88 following KURAEV 85.				

$\Gamma(\Upsilon(1S)\pi^+\pi^-) \times \Gamma(e^+e^-)/\Gamma_{total}$	DOCUMENT ID	TECN	COMMENT	$\Gamma_6\Gamma_{15}/\Gamma$
<b>18.46±0.27±0.77</b>	6.4K	<sup>5</sup> AUBERT	08BP BABR $e^+e^- \rightarrow \gamma\pi^+\pi^-\ell^+\ell^-$	
<sup>5</sup> Using $B(\Upsilon(1S) \rightarrow e^+e^-) = (2.38 \pm 0.11)\%$ and $B(\Upsilon(1S) \rightarrow \mu^+\mu^-) = (2.48 \pm 0.05)\%$ .				

$\Upsilon(3S)$  PARTIAL WIDTHS

$\Gamma(e^+e^-)$	DOCUMENT ID
<b>0.443±0.008 OUR EVALUATION</b>	

$\Upsilon(3S)$  BRANCHING RATIOS

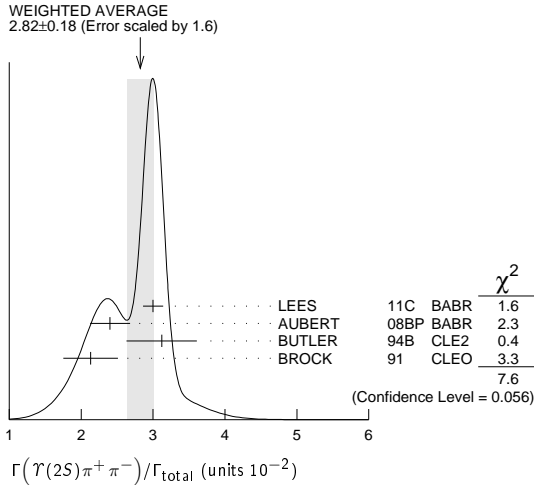
$\Gamma(\Upsilon(2S) \text{ anything})/\Gamma_{total}$	DOCUMENT ID	TECN	COMMENT	$\Gamma_1/\Gamma$
<b>0.106 ± 0.008 OUR AVERAGE</b>				
0.1023 ± 0.0105	4625	<sup>6,7,8</sup> BUTLER	94B CLE2 $e^+e^- \rightarrow \ell^+\ell^-X$	
0.111 ± 0.012	4891	<sup>7,8,9</sup> BROCK	91 CLEO $e^+e^- \rightarrow \pi^+\pi^-X, \pi^+\pi^-\ell^+\ell^-$	
<sup>6</sup> Using $B(\Upsilon(2S) \rightarrow \Upsilon(1S)\gamma\gamma) = (0.038 \pm 0.007)\%$ , and $B(\Upsilon(2S) \rightarrow \Upsilon(1S)\pi^0\pi^0) = (1/2)B(\Upsilon(2S) \rightarrow \Upsilon(1S)\pi^+\pi^-)$ .				
<sup>7</sup> Using $B(\Upsilon(1S) \rightarrow \mu^+\mu^-) = (2.48 \pm 0.06)\%$ . With the assumption of $e\mu$ universality.				
<sup>8</sup> Using $B(\Upsilon(2S) \rightarrow \Upsilon(1S)\pi^+\pi^-) = (18.5 \pm 0.8)\%$ .				
<sup>9</sup> Using $B(\Upsilon(2S) \rightarrow \mu^+\mu^-) = (1.31 \pm 0.21)\%$ , $B(\Upsilon(2S) \rightarrow \Upsilon(1S)\gamma\gamma) \times 2B(\Upsilon(1S) \rightarrow \mu^+\mu^-) = (0.188 \pm 0.035)\%$ , and $B(\Upsilon(2S) \rightarrow \Upsilon(1S)\pi^0\pi^0) \times 2B(\Upsilon(1S) \rightarrow \mu^+\mu^-) = (0.436 \pm 0.056)\%$ . With the assumption of $e\mu$ universality.				

$\Gamma(\Upsilon(2S)\pi^+\pi^-)/\Gamma_{total}$	DOCUMENT ID	TECN	COMMENT	$\Gamma_2/\Gamma$
<b>2.82±0.18 OUR AVERAGE</b>	Error	includes scale factor of 1.6.	See the ideogram below.	
3.00 ± 0.02 ± 0.14	543k	LEES	11C BABR $e^+e^- \rightarrow \pi^+\pi^-X$	
2.40 ± 0.10 ± 0.26	800	<sup>10</sup> AUBERT	08BP BABR $e^+e^- \rightarrow \gamma\pi^+\pi^-e^+e^-$	
3.12 ± 0.49	980	<sup>11,12</sup> BUTLER	94B CLE2 $e^+e^- \rightarrow \pi^+\pi^-\ell^+\ell^-$	
2.13 ± 0.38	974	<sup>13</sup> BROCK	91 CLEO $e^+e^- \rightarrow \pi^+\pi^-X, \pi^+\pi^-\ell^+\ell^-$	
• • • We do not use the following data for averages, fits, limits, etc. • • •				
4.82 ± 0.65 ± 0.53	138	<sup>13</sup> WU	93 CUSB $\Upsilon(3S) \rightarrow \pi^+\pi^-\ell^+\ell^-$	
3.1 ± 2.0	5	MAGERAS	82 CUSB $\Upsilon(3S) \rightarrow \pi^+\pi^-\ell^+\ell^-$	

# Meson Particle Listings

## $\Upsilon(3S)$

- <sup>10</sup> Using  $B(\Upsilon(1S) \rightarrow e^+e^-) = (2.38 \pm 0.11)\%$ ,  $B(\Upsilon(1S) \rightarrow \mu^+\mu^-) = (2.48 \pm 0.05)\%$ , and  $\Gamma_{ee}(\Upsilon(3S)) = 0.443 \pm 0.008$  keV.  
<sup>11</sup> From the exclusive mode.  
<sup>12</sup> Using  $B(\Upsilon(2S) \rightarrow \Upsilon(1S)\gamma\gamma) = (0.038 \pm 0.007)\%$ , and  $B(\Upsilon(2S) \rightarrow \Upsilon(1S)\pi^0\pi^0) = (1/2)B(\Upsilon(2S) \rightarrow \Upsilon(1S)\pi^+\pi^-)$ .  
<sup>13</sup> Using  $B(\Upsilon(2S) \rightarrow \mu^+\mu^-) = (1.31 \pm 0.21)\%$ ,  $B(\Upsilon(2S) \rightarrow \Upsilon(1S)\gamma\gamma) \times 2B(\Upsilon(1S) \rightarrow \mu^+\mu^-) = (0.188 \pm 0.035)\%$ , and  $B(\Upsilon(2S) \rightarrow \Upsilon(1S)\pi^0\pi^0) \times 2B(\Upsilon(1S) \rightarrow \mu^+\mu^-) = (0.436 \pm 0.056)\%$ . With the assumption of  $e\mu$  universality.



**$\Gamma(\Upsilon(2S)\pi^0\pi^0)/\Gamma_{total}$   $\Gamma_3/\Gamma$**

VALUE (units $10^{-2}$ )	EVTS	DOCUMENT ID	TECN	COMMENT
<b><math>1.85 \pm 0.14</math> OUR AVERAGE</b>				
$1.82 \pm 0.09 \pm 0.12$	4391	14 BHARI	09 CLEO	$e^+e^- \rightarrow \pi^0\pi^0\ell^+\ell^-$
$2.16 \pm 0.39$	15,16	BUTLER	94B CLE2	$e^+e^- \rightarrow \pi^0\pi^0\ell^+\ell^-$
$1.7 \pm 0.5 \pm 0.2$	10	17 HEINTZ	92 CSB2	$e^+e^- \rightarrow \pi^0\pi^0\ell^+\ell^-$

<sup>14</sup> Authors assume  $B(\Upsilon(1S) \rightarrow e^+e^-) + B(\Upsilon(1S) \rightarrow \mu^+\mu^-) = 4.06\%$ .  
<sup>15</sup>  $B(\Upsilon(2S) \rightarrow \mu^+\mu^-) = (1.31 \pm 0.21)\%$  and assuming  $e\mu$  universality.  
<sup>16</sup> From the exclusive mode.  
<sup>17</sup>  $B(\Upsilon(2S) \rightarrow \mu^+\mu^-) = (1.44 \pm 0.10)\%$  and assuming  $e\mu$  universality. Supersedes HEINTZ 91.

**$\Gamma(\Upsilon(2S)\gamma\gamma)/\Gamma_{total}$   $\Gamma_4/\Gamma$**

VALUE	DOCUMENT ID	TECN	COMMENT
<b><math>0.0502 \pm 0.0069</math></b>	18 BUTLER	94B CLE2	$e^+e^- \rightarrow \ell^+\ell^-\gamma\gamma$

<sup>18</sup> From the exclusive mode.

**$\Gamma(\Upsilon(2S)\pi^0)/\Gamma_{total}$   $\Gamma_5/\Gamma$**

VALUE (units $10^{-3}$ )	CL%	DOCUMENT ID	TECN	COMMENT
<b>&lt;0.51</b>	90	19 HE	08A CLEO	$e^+e^- \rightarrow \ell^+\ell^-\gamma\gamma$

<sup>19</sup> Authors assume  $B(\Upsilon(2S) \rightarrow e^+e^-) + B(\Upsilon(1S) \rightarrow \mu^+\mu^-) = 4.06\%$ .

**$\Gamma(\Upsilon(1S)\pi^+\pi^-)/\Gamma_{total}$   $\Gamma_6/\Gamma$**   
 Abbreviation MM in the COMMENT field below stands for missing mass.

VALUE (units $10^{-2}$ )	EVTS	DOCUMENT ID	TECN	COMMENT
<b><math>4.37 \pm 0.08</math> OUR AVERAGE</b>				
$4.32 \pm 0.07 \pm 0.13$	90k	20 LEES	11L BABR	$\Upsilon(3S) \rightarrow \pi^+\pi^-\ell^+\ell^-$
$4.46 \pm 0.01 \pm 0.13$	190k	21 BHARI	09 CLEO	$e^+e^- \rightarrow \pi^+\pi^-$ MM
$4.17 \pm 0.06 \pm 0.19$	6.4K	22 AUBERT	08BP BABR	$10.58 e^+e^- \rightarrow \gamma\pi^+\pi^-\ell^+\ell^-$
$4.52 \pm 0.35$	11830	23 BUTLER	94B CLE2	$e^+e^- \rightarrow \pi^+\pi^-X$ , $\pi^+\pi^-\ell^+\ell^-$
$4.46 \pm 0.34 \pm 0.50$	451	23 WU	93 CUSB	$\Upsilon(3S) \rightarrow \pi^+\pi^-\ell^+\ell^-$
$4.46 \pm 0.30$	11221	23 BROCK	91 CLEO	$e^+e^- \rightarrow \pi^+\pi^-X$ , $\pi^+\pi^-\ell^+\ell^-$

• • • We do not use the following data for averages, fits, limits, etc. • • •  
 $4.9 \pm 1.0$  22 GREEN 82 CLEO  $\Upsilon(3S) \rightarrow \pi^+\pi^-\ell^+\ell^-$   
 $3.9 \pm 1.3$  26 MAGERAS 82 CUSB  $\Upsilon(3S) \rightarrow \pi^+\pi^-\ell^+\ell^-$

<sup>20</sup> Using  $B(\Upsilon(1S) \rightarrow e^+e^-) = (2.38 \pm 0.11)\%$  and  $B(\Upsilon(1S) \rightarrow \mu^+\mu^-) = (2.48 \pm 0.05)\%$ .  
<sup>21</sup> A weighted average of the inclusive and exclusive results.  
<sup>22</sup> Using  $B(\Upsilon(2S) \rightarrow e^+e^-) = (1.91 \pm 0.16)\%$ ,  $B(\Upsilon(2S) \rightarrow \mu^+\mu^-) = (1.93 \pm 0.17)\%$ , and  $\Gamma_{ee}(\Upsilon(3S)) = 0.443 \pm 0.008$  keV.  
<sup>23</sup> Using  $B(\Upsilon(1S) \rightarrow \mu^+\mu^-) = (2.48 \pm 0.06)\%$ . With the assumption of  $e\mu$  universality.

**$\Gamma(\Upsilon(2S)\pi^+\pi^-)/\Gamma(\Upsilon(1S)\pi^+\pi^-)$   $\Gamma_2/\Gamma_6$**

VALUE	EVTS	DOCUMENT ID	TECN	COMMENT
<b><math>0.577 \pm 0.026 \pm 0.060</math></b>	800	24 AUBERT	08BP BABR	$e^+e^- \rightarrow \gamma\pi^+\pi^-\ell^+\ell^-$

<sup>24</sup> Using  $B(\Upsilon(1S) \rightarrow e^+e^-) = (2.38 \pm 0.11)\%$ ,  $B(\Upsilon(1S) \rightarrow \mu^+\mu^-) = (2.48 \pm 0.05)\%$ ,  $B(\Upsilon(2S) \rightarrow e^+e^-) = (1.91 \pm 0.16)\%$ , and  $B(\Upsilon(2S) \rightarrow \mu^+\mu^-) = (1.93 \pm 0.17)\%$ . Not independent of other values reported by AUBERT 08BP.

**$\Gamma(\Upsilon(1S)\pi^0\pi^0)/\Gamma_{total}$   $\Gamma_7/\Gamma$**

VALUE (units $10^{-2}$ )	EVTS	DOCUMENT ID	TECN	COMMENT
<b><math>2.20 \pm 0.13</math> OUR AVERAGE</b>				
$2.24 \pm 0.09 \pm 0.11$	6584	25 BHARI	09 CLEO	$e^+e^- \rightarrow \pi^0\pi^0\ell^+\ell^-$
$1.99 \pm 0.34$	56	26 BUTLER	94B CLE2	$e^+e^- \rightarrow \pi^0\pi^0\ell^+\ell^-$
$2.2 \pm 0.4 \pm 0.3$	33	27 HEINTZ	92 CSB2	$e^+e^- \rightarrow \pi^0\pi^0\ell^+\ell^-$

<sup>25</sup> Authors assume  $B(\Upsilon(1S) \rightarrow e^+e^-) + B(\Upsilon(1S) \rightarrow \mu^+\mu^-) = 4.96\%$ .  
<sup>26</sup> Using  $B(\Upsilon(1S) \rightarrow \mu^+\mu^-) = (2.48 \pm 0.06)\%$  and assuming  $e\mu$  universality.  
<sup>27</sup> Using  $B(\Upsilon(1S) \rightarrow \mu^+\mu^-) = (2.57 \pm 0.07)\%$  and assuming  $e\mu$  universality. Supersedes HEINTZ 91.

**$\Gamma(\Upsilon(1S)\pi^0\pi^0)/\Gamma(\Upsilon(1S)\pi^+\pi^-)$   $\Gamma_7/\Gamma_6$**

VALUE	DOCUMENT ID	TECN	COMMENT
$0.501 \pm 0.043$	28 BHARI	09 CLEO	$e^+e^- \rightarrow \Upsilon(3S)$

<sup>28</sup> Not independent of other values reported by BHARI 09.

**$\Gamma(\Upsilon(1S)\eta)/\Gamma_{total}$   $\Gamma_8/\Gamma$**

VALUE (units $10^{-3}$ )	CL%	DOCUMENT ID	TECN	COMMENT
<b>&lt;0.1</b>	90	29 LEES	11L BABR	$\Upsilon(3S) \rightarrow (\pi^+\pi^-)(\gamma\gamma)\ell^+\ell^-$

• • • We do not use the following data for averages, fits, limits, etc. • • •  
 $<0.8$  90 29,30 AUBERT 08BP BABR  $e^+e^- \rightarrow \gamma\pi^+\pi^-\pi^0\ell^+\ell^-$   
 $<0.18$  90 31 HE 08A CLEO  $e^+e^- \rightarrow \ell^+\ell^-\eta$   
 $<2.2$  90 BROCK 91 CLEO  $e^+e^- \rightarrow \ell^+\ell^-\eta$

<sup>29</sup> Using  $B(\Upsilon(1S) \rightarrow e^+e^-) = (2.38 \pm 0.11)\%$ ,  $B(\Upsilon(1S) \rightarrow \mu^+\mu^-) = (2.48 \pm 0.05)\%$ .  
<sup>30</sup> Using  $\Gamma_{ee}(\Upsilon(3S)) = 0.443 \pm 0.008$  keV.  
<sup>31</sup> Authors assume  $B(\Upsilon(1S) \rightarrow e^+e^-) + B(\Upsilon(1S) \rightarrow \mu^+\mu^-) = 4.96\%$ .

**$\Gamma(\Upsilon(1S)\eta)/\Gamma(\Upsilon(1S)\pi^+\pi^-)$   $\Gamma_8/\Gamma_6$**

VALUE (units $10^{-2}$ )	CL%	DOCUMENT ID	TECN	COMMENT
<b>&lt;0.23</b>	90	32 LEES	11L BABR	$\Upsilon(3S) \rightarrow (\pi^+\pi^-)(\gamma\gamma)\ell^+\ell^-$

• • • We do not use the following data for averages, fits, limits, etc. • • •  
 $<1.9$  90 33 AUBERT 08BP BABR  $e^+e^- \rightarrow \gamma\pi^+\pi^-(\pi^0)\ell^+\ell^-$

<sup>32</sup> Not independent of other values reported by LEES 11L.  
<sup>33</sup> Not independent of other values reported by AUBERT 08BP.

**$\Gamma(\Upsilon(1S)\pi^0)/\Gamma_{total}$   $\Gamma_9/\Gamma$**

VALUE (units $10^{-3}$ )	CL%	DOCUMENT ID	TECN	COMMENT
<b>&lt;0.07</b>	90	34 HE	08A CLEO	$e^+e^- \rightarrow \ell^+\ell^-\gamma\gamma$

<sup>34</sup> Authors assume  $B(\Upsilon(1S) \rightarrow e^+e^-) + B(\Upsilon(1S) \rightarrow \mu^+\mu^-) = 4.96\%$ .

**$\Gamma(h_b(1P)\pi^0)/\Gamma_{total}$   $\Gamma_{10}/\Gamma$**

VALUE	CL%	DOCUMENT ID	TECN	COMMENT
<b><math>&lt;1.2 \times 10^{-3}</math></b>	90	35 GE	11 CLEO	$\Upsilon(3S) \rightarrow \pi^0$ anything

<sup>35</sup> Assuming  $M(h_b(1P)) = 9900$  MeV and  $\Gamma(h_b(1P)) = 0$  MeV, and allowing  $B(h_b(1P) \rightarrow \gamma\eta_b(1S))$  to vary from 0-100%.

**$\Gamma(h_b(1P)\pi^0 \rightarrow \gamma\eta_b(1S)\pi^0)/\Gamma_{total}$   $\Gamma_{11}/\Gamma$**

VALUE (units $10^{-4}$ )	DOCUMENT ID	TECN	COMMENT
<b><math>4.3 \pm 1.1 \pm 0.9</math></b>	LEES	11K BABR	$\Upsilon(3S) \rightarrow \eta_b\gamma\pi^0$

**$\Gamma(h_b(1P)\pi^+\pi^-)/\Gamma_{total}$   $\Gamma_{12}/\Gamma$**

VALUE (units $10^{-4}$ )	CL%	DOCUMENT ID	TECN	COMMENT
<b>&lt; 1.2</b>	90	36 LEES	11C BABR	$e^+e^- \rightarrow \pi^+\pi^-X$

• • • We do not use the following data for averages, fits, limits, etc. • • •  
 $<18$  36 BUTLER 94B CLE2  $e^+e^- \rightarrow \pi^+\pi^-X$   
 $<15$  36 BROCK 91 CLEO  $e^+e^- \rightarrow \pi^+\pi^-X$

<sup>36</sup> For  $M(h_b(1P)) = 9900$  MeV.

**$\Gamma(\tau^+\tau^-)/\Gamma_{total}$   $\Gamma_{13}/\Gamma$**

VALUE (units $10^{-2}$ )	EVTS	DOCUMENT ID	TECN	COMMENT
<b><math>2.29 \pm 0.21 \pm 0.22</math></b>	15k	37 BESSON	07 CLEO	$e^+e^- \rightarrow \Upsilon(3S) \rightarrow \tau^+\tau^-$

<sup>37</sup> BESSON 07 reports  $[\Gamma(\Upsilon(3S) \rightarrow \tau^+\tau^-)/\Gamma_{total}] / [B(\Upsilon(3S) \rightarrow \mu^+\mu^-)] = 1.05 \pm 0.08 \pm 0.05$  which we multiply by our best value  $B(\Upsilon(3S) \rightarrow \mu^+\mu^-) = (2.18 \pm 0.21) \times 10^{-2}$ . Our first error is their experiment's error and our second error is the systematic error from using our best value.

**$\Gamma(\tau^+\tau^-)/\Gamma(\mu^+\mu^-)$   $\Gamma_{13}/\Gamma_{14}$**

VALUE	EVTS	DOCUMENT ID	TECN	COMMENT
<b><math>1.05 \pm 0.08 \pm 0.05</math></b>	15k	BESSON	07 CLEO	$e^+e^- \rightarrow \Upsilon(3S)$

**$\Gamma(\mu^+\mu^-)/\Gamma_{total}$   $\Gamma_{14}/\Gamma$**

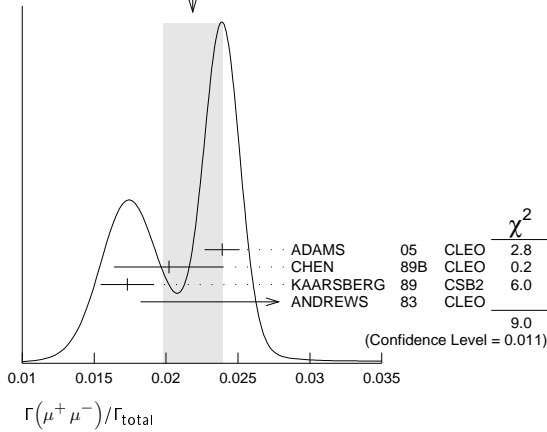
VALUE	EVTS	DOCUMENT ID	TECN	COMMENT
<b><math>0.0218 \pm 0.0021</math> OUR AVERAGE</b>				Error includes scale factor of 2.1. See the ideogram below.
$0.0239 \pm 0.0007 \pm 0.0010$	81k	ADAMS	05 CLEO	$e^+e^- \rightarrow \mu^+\mu^-$
$0.0202 \pm 0.0019 \pm 0.0033$		CHEN	89B CLEO	$e^+e^- \rightarrow \mu^+\mu^-$
$0.0173 \pm 0.0015 \pm 0.0011$		KAARSBERG	89 CSB2	$e^+e^- \rightarrow \mu^+\mu^-$
$0.033 \pm 0.013 \pm 0.007$	1096	ANDREWS	83 CLEO	$e^+e^- \rightarrow \mu^+\mu^-$



See key on page 457

Meson Particle Listings  
 $\Upsilon(3S)$

WEIGHTED AVERAGE  
0.0218±0.0021 (Error scaled by 2.1)



$\Gamma(ggg)/\Gamma_{total}$   $\Gamma_{17}/\Gamma$

VALUE (units $10^{-2}$ )	EVTS	DOCUMENT ID	TECN	COMMENT
<b>35.7±2.6</b>	3M	<sup>38</sup> BESSON	06A	CLEO $\Upsilon(3S) \rightarrow$ hadrons

<sup>38</sup> Calculated using BESSON 06A value of  $\Gamma(\gamma gg)/\Gamma(ggg) = (2.72 \pm 0.06 \pm 0.32 \pm 0.37)\%$  and the PDG 08 values of  $B(\Upsilon(2S) + \text{anything}) = (10.6 \pm 0.8)\%$ ,  $B(\pi^+ \pi^- \Upsilon(1S)) = (4.40 \pm 0.10)\%$ ,  $B(\pi^0 \pi^0 \Upsilon(1S)) = (2.20 \pm 0.13)\%$ ,  $B(\gamma \chi_{b2}(2P)) = (13.1 \pm 1.6)\%$ ,  $B(\gamma \chi_{b1}(2P)) = (12.6 \pm 1.2)\%$ ,  $B(\gamma \chi_{b0}(2P)) = (5.9 \pm 0.6)\%$ ,  $B(\gamma \chi_{b0}(1P)) = (0.30 \pm 0.11)\%$ ,  $B(\mu^+ \mu^-) = (2.18 \pm 0.21)\%$ , and  $R_{\text{hadrons}} = 3.51$ . The statistical error is negligible and the systematic error is partially correlated with  $\Gamma(\gamma gg)/\Gamma_{total}$  BESSON 06A value.

$\Gamma(\gamma gg)/\Gamma_{total}$   $\Gamma_{18}/\Gamma$

VALUE (units $10^{-2}$ )	EVTS	DOCUMENT ID	TECN	COMMENT
<b>0.97±0.18</b>	60k	<sup>39</sup> BESSON	06A	CLEO $\Upsilon(3S) \rightarrow \gamma +$ hadrons

<sup>39</sup> Calculated using BESSON 06A values of  $\Gamma(\gamma gg)/\Gamma(ggg) = (2.72 \pm 0.06 \pm 0.32 \pm 0.37)\%$  and  $\Gamma(ggg)/\Gamma_{total}$ . The statistical error is negligible and the systematic error is partially correlated with  $\Gamma(ggg)/\Gamma_{total}$  BESSON 06A value.

$\Gamma(\gamma gg)/\Gamma(ggg)$   $\Gamma_{18}/\Gamma_{17}$

VALUE (units $10^{-2}$ )	EVTS	DOCUMENT ID	TECN	COMMENT
<b>2.72±0.06±0.49</b>	3M	BESSON	06A	CLEO $\Upsilon(3S) \rightarrow (\gamma +)$ hadrons

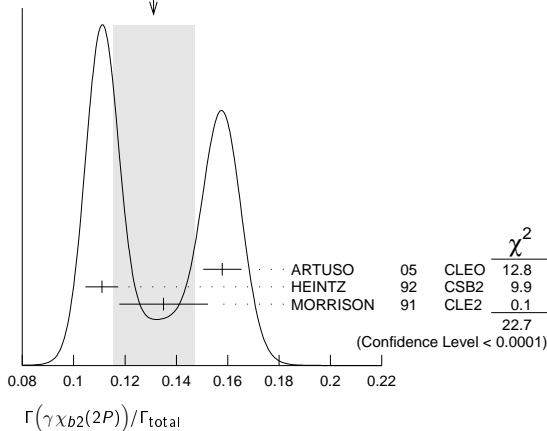
$\Gamma(\gamma \chi_{b2}(2P))/\Gamma_{total}$   $\Gamma_{19}/\Gamma$

VALUE	EVTS	DOCUMENT ID	TECN	COMMENT
<b>0.131 ± 0.016 OUR AVERAGE</b>				Error includes scale factor of 3.4. See the ideogram below.

0.1579±0.0017±0.0073	568k	ARTUSO	05	CLEO $e^+ e^- \rightarrow \gamma X$
0.111 ± 0.005 ± 0.004	10319	<sup>40</sup> HEINTZ	92	CSB2 $e^+ e^- \rightarrow \gamma X$
0.135 ± 0.003 ± 0.017	30741	MORRISON	91	CLE2 $e^+ e^- \rightarrow \gamma X$

<sup>40</sup> Supersedes NARAIN 91.

WEIGHTED AVERAGE  
0.131±0.016 (Error scaled by 3.4)



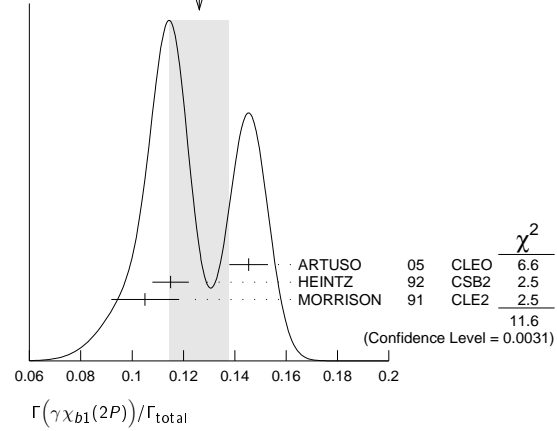
$\Gamma(\gamma \chi_{b1}(2P))/\Gamma_{total}$   $\Gamma_{20}/\Gamma$

VALUE	EVTS	DOCUMENT ID	TECN	COMMENT
<b>0.126 ± 0.012 OUR AVERAGE</b>				Error includes scale factor of 2.4. See the ideogram below.

0.1454±0.0018±0.0073	537k	ARTUSO	05	CLEO $e^+ e^- \rightarrow \gamma X$
0.115 ± 0.005 ± 0.005	11147	<sup>41</sup> HEINTZ	92	CSB2 $e^+ e^- \rightarrow \gamma X$
0.105 +0.003 -0.002 ± 0.013	25759	MORRISON	91	CLE2 $e^+ e^- \rightarrow \gamma X$

<sup>41</sup> Supersedes NARAIN 91.

WEIGHTED AVERAGE  
0.126±0.012 (Error scaled by 2.4)



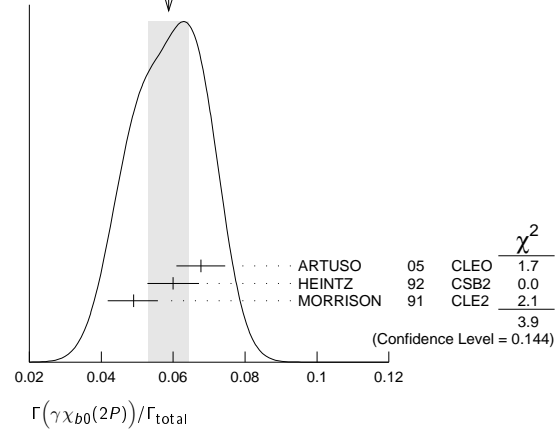
$\Gamma(\gamma \chi_{b0}(2P))/\Gamma_{total}$   $\Gamma_{21}/\Gamma$

VALUE	EVTS	DOCUMENT ID	TECN	COMMENT
<b>0.059 ± 0.006 OUR AVERAGE</b>				Error includes scale factor of 1.4. See the ideogram below.

0.0677±0.0020±0.0065	225k	ARTUSO	05	CLEO $e^+ e^- \rightarrow \gamma X$
0.060 ± 0.004 ± 0.006	4959	<sup>42</sup> HEINTZ	92	CSB2 $e^+ e^- \rightarrow \gamma X$
0.049 +0.003 -0.004 ± 0.006	9903	MORRISON	91	CLE2 $e^+ e^- \rightarrow \gamma X$

<sup>42</sup> Supersedes NARAIN 91.

WEIGHTED AVERAGE  
0.059±0.006 (Error scaled by 1.4)



$\Gamma(\gamma \chi_{b2}(1P))/\Gamma_{total}$   $\Gamma_{22}/\Gamma$

VALUE (units $10^{-3}$ )	CL%	EVTS	DOCUMENT ID	TECN	COMMENT
<b>9.9±1.3 OUR AVERAGE</b>					Error includes scale factor of 2.0.

7.5±1.2±0.5	126	<sup>43,44</sup> KORNICER	11	CLEO $e^+ e^- \rightarrow \gamma \gamma \ell^+ \ell^-$
10.5±0.3±0.7 -0.6	9.7k	LEES	11J	BABR $\Upsilon(3S) \rightarrow X \gamma$

• • • We do not use the following data for averages, fits, limits, etc. • • •

<19	90	<sup>45</sup> ASNER	08A	CLEO $\Upsilon(3S) \rightarrow \gamma +$ hadrons
seen		<sup>46</sup> HEINTZ	92	CSB2 $e^+ e^- \rightarrow \gamma \gamma \ell^+ \ell^-$

<sup>43</sup> Assuming  $B(\Upsilon(1S) \rightarrow \ell^+ \ell^-) = (2.48 \pm 0.05)\%$ .

<sup>44</sup> KORNICER 11 reports  $[\Gamma(\Upsilon(3S) \rightarrow \gamma \chi_{b2}(1P))/\Gamma_{total}] \times [B(\chi_{b2}(1P) \rightarrow \gamma \Upsilon(1S))] = (1.435 \pm 0.162 \pm 0.169) \times 10^{-3}$  which we divide by our best value  $B(\chi_{b2}(1P) \rightarrow \gamma \Upsilon(1S)) = (19.1 \pm 1.2) \times 10^{-2}$ . Our first error is their experiment's error and our second error is the systematic error from using our best value.

<sup>45</sup> ASNER 08A reports  $[\Gamma(\Upsilon(3S) \rightarrow \gamma \chi_{b2}(1P))/\Gamma_{total}] / [B(\Upsilon(2S) \rightarrow \gamma \chi_{b2}(1P))] < 27.1 \times 10^{-2}$  which we multiply by our best value  $B(\Upsilon(2S) \rightarrow \gamma \chi_{b2}(1P)) = 7.15 \times 10^{-2}$ .

## Meson Particle Listings

### $\Upsilon(3S)$ , $\chi_b(3P)$ , $\Upsilon(4S)$

<sup>46</sup> HEINTZ 92, while unable to distinguish between different  $J$  states, measures  $\sum J B(\Upsilon(3S) \rightarrow \gamma \chi_{bJ}) \times B(\chi_{bJ} \rightarrow \gamma \Upsilon(1S)) = (1.7 \pm 0.4 \pm 0.6) \times 10^{-3}$  for  $J = 0, 1, 2$  using inclusive  $\Upsilon(1S)$  decays and  $(1.2_{-0.3}^{+0.4} \pm 0.09) \times 10^{-3}$  for  $J = 1, 2$  using  $\Upsilon(1S) \rightarrow \ell^+ \ell^-$ .

$\Gamma(\gamma \chi_{b1}(1P))/\Gamma_{total}$						$\Gamma_{24}/\Gamma$	
VALUE (units $10^{-3}$ )	CL%	EVTS	DOCUMENT ID	TECN	COMMENT		
<b>0.9 ± 0.5 OUR AVERAGE</b>							
1.6 ± 0.5 ± 0.1	50	47,48	KORNICER	11	CLEO	$e^+ e^- \rightarrow \gamma \gamma \ell^+ \ell^-$	
0.5 ± 0.3 ± 0.2	-		LEES	11J	BABR	$\Upsilon(3S) \rightarrow X \gamma$	

• • • We do not use the following data for averages, fits, limits, etc. • • •  
 <1.7 90 <sup>49</sup> ASNER 08A CLEO  $\Upsilon(3S) \rightarrow \gamma +$  hadrons  
 seen <sup>50</sup> HEINTZ 92 CSB2  $e^+ e^- \rightarrow \gamma \gamma \ell^+ \ell^-$

<sup>47</sup> Assuming  $B(\Upsilon(1S) \rightarrow \ell^+ \ell^-) = (2.48 \pm 0.05)\%$ .  
<sup>48</sup> KORNICER 11 reports  $[\Gamma(\Upsilon(3S) \rightarrow \gamma \chi_{b1}(1P))/\Gamma_{total}] \times [B(\chi_{b1}(1P) \rightarrow \gamma \Upsilon(1S))] = (5.38 \pm 1.20 \pm 0.95) \times 10^{-4}$  which we divide by our best value  $B(\chi_{b1}(1P) \rightarrow \gamma \Upsilon(1S)) = (33.9 \pm 2.2) \times 10^{-2}$ . Our first error is their experiment's error and our second error is the systematic error from using our best value.

<sup>49</sup> ASNER 08A reports  $[\Gamma(\Upsilon(3S) \rightarrow \gamma \chi_{b1}(1P))/\Gamma_{total}] / [B(\Upsilon(2S) \rightarrow \gamma \chi_{b1}(1P))] < 2.5 \times 10^{-2}$  which we multiply by our best value  $B(\Upsilon(2S) \rightarrow \gamma \chi_{b1}(1P)) = 6.9 \times 10^{-2}$ .

<sup>50</sup> HEINTZ 92, while unable to distinguish between different  $J$  states, measures  $\sum J B(\Upsilon(3S) \rightarrow \gamma \chi_{bJ}) \times B(\chi_{bJ} \rightarrow \gamma \Upsilon(1S)) = (1.7 \pm 0.4 \pm 0.6) \times 10^{-3}$  for  $J = 0, 1, 2$  using inclusive  $\Upsilon(1S)$  decays and  $(1.2_{-0.3}^{+0.4} \pm 0.09) \times 10^{-3}$  for  $J = 1, 2$  using  $\Upsilon(1S) \rightarrow \ell^+ \ell^-$ .

$\Gamma(\gamma \chi_{b0}(1P))/\Gamma_{total}$						$\Gamma_{25}/\Gamma$	
VALUE (units $10^{-2}$ )	CL%	EVTS	DOCUMENT ID	TECN	COMMENT		
<b>0.27 ± 0.04 OUR AVERAGE</b>							
0.27 ± 0.04 ± 0.02		2.3k	LEES	11J	BABR	$\Upsilon(3S) \rightarrow X \gamma$	
0.30 ± 0.04 ± 0.10	8.7k		ARTUSO	05	CLEO	$e^+ e^- \rightarrow \gamma X$	

• • • We do not use the following data for averages, fits, limits, etc. • • •  
 <0.8 90 <sup>51</sup> ASNER 08A CLEO  $\Upsilon(3S) \rightarrow \gamma +$  hadrons  
<sup>51</sup> ASNER 08A reports  $[\Gamma(\Upsilon(3S) \rightarrow \gamma \chi_{b0}(1P))/\Gamma_{total}] / [B(\Upsilon(2S) \rightarrow \gamma \chi_{b0}(1P))] < 21.9 \times 10^{-2}$  which we multiply by our best value  $B(\Upsilon(2S) \rightarrow \gamma \chi_{b0}(1P)) = 3.8 \times 10^{-2}$ .

$\Gamma(\gamma \eta_b(2S))/\Gamma_{total}$						$\Gamma_{26}/\Gamma$	
VALUE (units $10^{-4}$ )	CL%	DOCUMENT ID	TECN	COMMENT			
<b>&lt; 6.2</b>							
< 6.2	90		ARTUSO	05	CLEO	$e^+ e^- \rightarrow \gamma X$	
<b>• • • We do not use the following data for averages, fits, limits, etc. • • •</b>							
<19	90		LEES	11J	BABR	$\Upsilon(3S) \rightarrow X \gamma$	

$\Gamma(\gamma \eta_b(1S))/\Gamma_{total}$						$\Gamma_{27}/\Gamma$	
VALUE (units $10^{-4}$ )	CL%	EVTS	DOCUMENT ID	TECN	COMMENT		
<b>5.1 ± 0.7 OUR AVERAGE</b>							
7.1 ± 1.8 ± 1.3	2.3 ± 0.5k	52	BONVICINI	10	CLEO	$\Upsilon(3S) \rightarrow \gamma X$	
4.8 ± 0.5 ± 0.6	19 ± 3k	52	AUBERT	09Aq	BABR	$\Upsilon(3S) \rightarrow \gamma X$	

• • • We do not use the following data for averages, fits, limits, etc. • • •  
 <8.5 90 LEES 11J BABR  $\Upsilon(3S) \rightarrow X \gamma$   
 4.8 ± 0.5 ± 1.2 19 ± 3k <sup>52,53</sup> AUBERT 08v BABR  $\Upsilon(3S) \rightarrow \gamma X$   
 <4.3 90 <sup>54</sup> ARTUSO 05 CLEO  $e^+ e^- \rightarrow \gamma X$

<sup>52</sup> Assuming  $\Gamma_{\eta_b(1S)} = 10$  MeV.  
<sup>53</sup> Systematic error re-evaluated by AUBERT 09Aq.  
<sup>54</sup> Superseded by BONVICINI 10.

$\Gamma(\gamma X \rightarrow \gamma + \geq 4 \text{ prongs})/\Gamma_{total}$						$\Gamma_{28}/\Gamma$	
(1.5 GeV < $m_X$ < 5.0 GeV)							
VALUE (units $10^{-4}$ )	CL%	DOCUMENT ID	TECN	COMMENT			
<b>&lt; 2.2</b>							
< 2.2	95		ROSNER	07A	CLEO	$e^+ e^- \rightarrow \gamma X$	

$\Gamma(\gamma a_1^0 \rightarrow \gamma \tau^+ \tau^-)/\Gamma_{total}$						$\Gamma_{29}/\Gamma$	
VALUE	CL%	DOCUMENT ID	TECN	COMMENT			
<b>&lt; 1.6 × 10<sup>-4</sup></b>							
< 1.6 × 10 <sup>-4</sup>	90	55	AUBERT	09p	BABR	$e^+ e^- \rightarrow \gamma a_1^0 \rightarrow \gamma \tau^+ \tau^-$	

<sup>55</sup> For a narrow scalar or pseudoscalar  $a_1^0$  with  $M(\tau^+ \tau^-)$  in the ranges 4.03–9.52 and 9.61–10.10 GeV. Measured 90% CL limits as a function of  $M(\tau^+ \tau^-)$  range from 1.5–16 × 10<sup>-5</sup>.

$\Gamma(\gamma A^0 \rightarrow \gamma \text{hadrons})/\Gamma_{total}$						$\Gamma_{23}/\Gamma$	
(0.3 GeV < $m_{A^0}$ < 7 GeV)							
VALUE	CL%	DOCUMENT ID	TECN	COMMENT			
<b>&lt; 8 × 10<sup>-5</sup></b>							
< 8 × 10 <sup>-5</sup>	90	56	LEES	11H	BABR	$\Upsilon(3S) \rightarrow \gamma$ hadrons	

<sup>56</sup> For a narrow scalar or pseudoscalar  $A^0$ , excluding known resonances, with mass in the range 0.3–7 GeV. Measured 90% CL limits as a function of  $m_{A^0}$  range from 1 × 10<sup>-6</sup> to 8 × 10<sup>-5</sup>.

LEPTON FAMILY NUMBER (LF) VIOLATING MODES

$\Gamma(e^\pm \tau^\mp)/\Gamma_{total}$						$\Gamma_{30}/\Gamma$	
VALUE (units $10^{-6}$ )	CL%	DOCUMENT ID	TECN	COMMENT			
<b>&lt; 4.2</b>							
< 4.2	90		LEES	10b	BABR	$e^+ e^- \rightarrow e^\pm \tau^\mp$	

$\Gamma(\mu^\pm \tau^\mp)/\Gamma_{total}$						$\Gamma_{31}/\Gamma$	
VALUE (units $10^{-6}$ )	CL%	DOCUMENT ID	TECN	COMMENT			
<b>&lt; 3.1</b>							
< 3.1	90		LEES	10b	BABR	$e^+ e^- \rightarrow \mu^\pm \tau^\mp$	
<b>• • • We do not use the following data for averages, fits, limits, etc. • • •</b>							
< 20.3	95		LOVE	08A	CLEO	$e^+ e^- \rightarrow \mu^\pm \tau^\mp$	

### $\Upsilon(3S)$ REFERENCES

GE	11	PR D84 032008	J.Y. Ge et al.	(CLEO Collab.)			
KORNICER	11	PR D83 054003	M. Koricner et al.	(CLEO Collab.)			
LEES	11C	PR D84 011104	J.P. Lees et al.	(BABAR Collab.)			
LEES	11H	PRL 107 221803	J.P. Lees et al.	(BABAR Collab.)			
LEES	11J	PR D84 072002	J.P. Lees et al.	(BABAR Collab.)			
LEES	11K	PR D84 091101	J.P. Lees et al.	(BABAR Collab.)			
LEES	11L	PR D84 092003	J.P. Lees et al.	(BABAR Collab.)			
BONVICINI	10	PR D81 031104R	G. Bonvicini et al.	(CLEO Collab.)			
LEES	10B	PRL 104 151802	J.P. Lees et al.	(BABAR Collab.)			
AUBERT	09Aq	PRL 103 161801	B. Aubert et al.	(BABAR Collab.)			
AUBERT	09P	PRL 103 181801	B. Aubert et al.	(BABAR Collab.)			
BHARI	09	PR D79 011103	S.R. Bhari et al.	(CLEO Collab.)			
ASNER	08A	PR D78 091103	D.M. Asner et al.	(CLEO Collab.)			
AUBERT	08BP	PR D78 122002	B. Aubert et al.	(BABAR Collab.)			
AUBERT	08V	PRL 101 071801	B. Aubert et al.	(BABAR Collab.)			
HE	08A	PRL 101 192001	Q. He et al.	(CLEO Collab.)			
LOVE	08A	PRL 101 201601	W. Love et al.	(CLEO Collab.)			
PDG	08	PL B667 1	C. Amsler et al.	(PDG Collab.)			
BESSION	07	PRL 98 052002	D. Besson et al.	(CLEO Collab.)			
ROSNER	07A	PR D76 117102	J.L. Rosner et al.	(CLEO Collab.)			
BESSION	06A	PR D74 012003	D. Besson et al.	(CLEO Collab.)			
ROSNER	06	PRL 96 092003	J.L. Rosner et al.	(CLEO Collab.)			
ADAMS	05	PRL 94 012001	G.S. Adams et al.	(CLEO Collab.)			
ARTUSO	05	PRL 94 032001	M. Artuso et al.	(CLEO Collab.)			
ARTAMONOV	00	PL B474 427	A.S. Artamonov et al.	(CLEO Collab.)			
BUTLER	94B	PR D49 40	F. Butler et al.	(CLEO Collab.)			
WU	93	PL B301 307	Q.W. Wu et al.	(CLEO Collab.)			
HEINTZ	92	PR D46 1928	U. Heintz et al.	(CUSB II Collab.)			
BROCK	91	PR D43 1448	I.C. Brock et al.	(CLEO Collab.)			
HEINTZ	91	PRL 66 1563	U. Heintz et al.	(CLEO Collab.)			
MORRISON	91	PRL 67 1696	R.J. Morrison et al.	(CLEO Collab.)			
NARAIN	91	PRL 66 3113	M. Narain et al.	(CLEO Collab.)			
CHEN	89B	PR D39 3528	W.Y. Chen et al.	(CLEO Collab.)			
KAAERSBERG	89	PRL 62 2077	T.M. Kaarsberg et al.	(CUSB Collab.)			
BUCHMUELLER	88	HE e+e- Physics 412	W. Buchmueller, S. Cooper	(HANN, DESY, MIT)			
Editors: A. Ali and P. Soeding, World Scientific, Singapore							
COHEN	87	RMP 59 1121	E.R. Cohen, B.N. Taylor	(RIS, NBS)			
BARU	86B	ZPHY C32 622 (erratum)	S.E. Baru et al.	(NOVO)			
KURAEV	85	SJNP 41 466	E.A. Kuraev, V.S. Fadin	(NOVO)			
Translated from YAF 41 733.							
ARTAMONOV	84	PL 137B 272	A.S. Artamonov et al.	(NOVO)			
GILES	84B	PR D29 1285	R. Giles et al.	(CLEO Collab.)			
ANDREWS	83	PRL 50 807	D.E. Andrews et al.	(CLEO Collab.)			
GREEN	82	PRL 49 617	J. Green et al.	(CLEO Collab.)			
MAGERAS	82	PL 118B 453	G. Mageras et al.	(COLU, CORN, LSU+)			

### $\chi_b(3P)$

$$I^G(J^{PC}) = ??(??^+)$$

OMITTED FROM SUMMARY TABLE  
 A mixture of  $J = 0, 1,$  and  $2$  spin components observed in the radiative decay to  $\Upsilon(1S)$  and  $\Upsilon(2S)$ , therefore  $C = +$ .

### $\chi_b(3P)$ MASS

VALUE (GeV)	DOCUMENT ID	TECN	COMMENT
<b>10.530 ± 0.005 ± 0.009</b>			
10.530 ± 0.005 ± 0.009	<sup>1</sup> AAD	12A	ATLS $pp \rightarrow \gamma \mu^+ \mu^- + X$

<sup>1</sup> The mass barycenter of the merged lineshapes from the  $J = 1$  and  $2$  states.

### $\chi_b(3P)$ DECAY MODES

Mode	Fraction ( $\Gamma_i/\Gamma$ )
$\Gamma_1 \Upsilon(1S) \gamma$	seen
$\Gamma_2 \Upsilon(2S) \gamma$	seen

### $\chi_b(3P)$ BRANCHING RATIOS

$\Gamma(\Upsilon(1S) \gamma)/\Gamma_{total}$						$\Gamma_1/\Gamma$	
VALUE	DOCUMENT ID	TECN	COMMENT				
<b>seen</b>							
seen	AAD	12A	ATLS	$pp \rightarrow \gamma \mu^+ \mu^- + X$			

$\Gamma(\Upsilon(2S) \gamma)/\Gamma_{total}$						$\Gamma_2/\Gamma$	
VALUE	DOCUMENT ID	TECN	COMMENT				
<b>seen</b>							
seen	AAD	12A	ATLS	$pp \rightarrow \gamma \mu^+ \mu^- + X$			

### $\chi_b(3P)$ REFERENCES

AAD	12A	PRL 108 152001	G. Aad et al.	(ATLAS Collab.)
-----	-----	----------------	---------------	-----------------

### $\Upsilon(4S)$ or $\Upsilon(10580)$

$$I^G(J^{PC}) = 0^-(1^{-}-)$$

$\Upsilon(4S)$  MASS

VALUE (GeV)	DOCUMENT ID	TECN	COMMENT
<b>10.5794 ± 0.0012 OUR AVERAGE</b>			
10.5793 ± 0.0004 ± 0.0012	AUBERT	05Q	BABR $e^+e^- \rightarrow$ hadrons
10.5800 ± 0.0035	<sup>1</sup> BEBEK	87	CLEO $e^+e^- \rightarrow$ hadrons
••• We do not use the following data for averages, fits, limits, etc. •••			
10.5774 ± 0.0010	<sup>2</sup> LOVELOCK	85	CUSB $e^+e^- \rightarrow$ hadrons
<sup>1</sup> Reanalysis of BESSON 85.			
<sup>2</sup> No systematic error given.			

$\Upsilon(4S)$  WIDTH

VALUE (MeV)	DOCUMENT ID	TECN	COMMENT
<b>20.5 ± 2.5 OUR AVERAGE</b>			
20.7 ± 1.6 ± 2.5	AUBERT	05Q	BABR $e^+e^- \rightarrow$ hadrons
20 ± 2 ± 4	BESSON	85	CLEO $e^+e^- \rightarrow$ hadrons
••• We do not use the following data for averages, fits, limits, etc. •••			
25 ± 2.5	LOVELOCK	85	CUSB $e^+e^- \rightarrow$ hadrons

$\Upsilon(4S)$  DECAY MODES

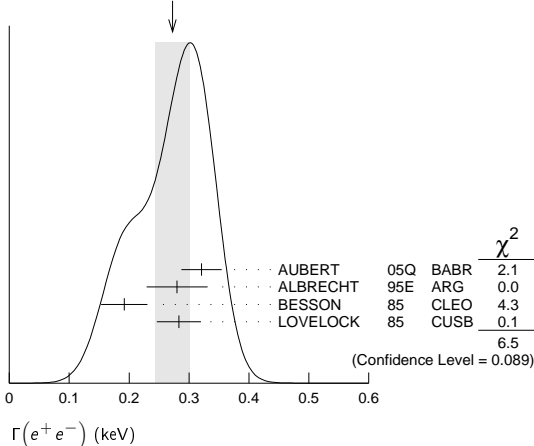
Mode	Fraction ( $\Gamma_i/\Gamma$ )	Confidence level
$\Gamma_1$ $B\bar{B}$	> 96 %	95%
$\Gamma_2$ $B^+B^-$	(51.3 ± 0.6) %	
$\Gamma_3$ $D_S^+$ anything + c.c.	(17.8 ± 2.6) %	
$\Gamma_4$ $B^0\bar{B}^0$	(48.7 ± 0.6) %	
$\Gamma_5$ $J/\psi K_S^0(J/\psi, \eta_c) K_S^0$	< 4 × 10 <sup>-7</sup>	90%
$\Gamma_6$ non- $B\bar{B}$	< 4 %	95%
$\Gamma_7$ $e^+e^-$	(1.57 ± 0.08) × 10 <sup>-5</sup>	
$\Gamma_8$ $\rho^+\rho^-$	< 5.7 × 10 <sup>-6</sup>	90%
$\Gamma_9$ $J/\psi(1S)$ anything	< 1.9 × 10 <sup>-4</sup>	95%
$\Gamma_{10}$ $D^{*+}$ anything + c.c.	< 7.4 %	90%
$\Gamma_{11}$ $\phi$ anything	(7.1 ± 0.6) %	
$\Gamma_{12}$ $\phi\eta$	< 1.8 × 10 <sup>-6</sup>	90%
$\Gamma_{13}$ $\phi\eta'$	< 4.3 × 10 <sup>-6</sup>	90%
$\Gamma_{14}$ $\rho\eta$	< 1.3 × 10 <sup>-6</sup>	90%
$\Gamma_{15}$ $\rho\eta'$	< 2.5 × 10 <sup>-6</sup>	90%
$\Gamma_{16}$ $\Upsilon(1S)$ anything	< 4 × 10 <sup>-3</sup>	90%
$\Gamma_{17}$ $\Upsilon(1S)\pi^+\pi^-$	(8.1 ± 0.6) × 10 <sup>-5</sup>	
$\Gamma_{18}$ $\Upsilon(1S)\eta$	(1.96 ± 0.11) × 10 <sup>-4</sup>	
$\Gamma_{19}$ $\Upsilon(2S)\pi^+\pi^-$	(8.6 ± 1.3) × 10 <sup>-5</sup>	
$\Gamma_{20}$ $h_p(1P)\pi^+\pi^-$	not seen	
$\Gamma_{21}$ $\bar{d}$ anything	< 1.3 × 10 <sup>-5</sup>	90%

$\Upsilon(4S)$  PARTIAL WIDTHS

$\Gamma(e^+e^-)$	DOCUMENT ID	TECN	COMMENT
<b>0.272 ± 0.029 OUR AVERAGE</b>			
0.321 ± 0.017 ± 0.029	AUBERT	05Q	BABR $e^+e^- \rightarrow$ hadrons
0.28 ± 0.05 ± 0.01	<sup>3</sup> ALBRECHT	95E	ARG $e^+e^- \rightarrow$ hadrons
0.192 ± 0.007 ± 0.038	BESSON	85	CLEO $e^+e^- \rightarrow$ hadrons
0.283 ± 0.037	LOVELOCK	85	CUSB $e^+e^- \rightarrow$ hadrons

<sup>3</sup> Using LEYAOUANC 77 parametrization of  $\Gamma(s)$ .

WEIGHTED AVERAGE  
0.272 ± 0.029 (Error scaled by 1.5)



$\Upsilon(4S)$  BRANCHING RATIOS

$B\bar{B}$  DECAYS

The ratio of branching fraction to charged and neutral B mesons is often derived assuming isospin invariance in the decays, and relies on the knowledge of the  $B^+/B^0$  lifetime ratio. "OUR EVALUATION" is obtained based on averages of rescaled data listed below. The average and rescaling were performed by the Heavy Flavor Averaging Group (HFAG) and are described at <http://www.slac.stanford.edu/xorg/hfag/>. The averaging/rescaling procedure takes into account the common dependence of the measurement on the value of the lifetime ratio.

$\Gamma(B^+B^-)/\Gamma_{total}$	DOCUMENT ID	TECN	COMMENT
<b>0.513 ± 0.006 OUR EVALUATION</b>			
Assuming $B(\Upsilon(4S) \rightarrow B\bar{B}) = 1$			

$\Gamma(D_S^+ \text{ anything + c.c.})/\Gamma_{total}$	DOCUMENT ID	TECN	COMMENT
<b>0.178 ± 0.021 ± 0.016</b>	<sup>4</sup> ARTUSO	05B	CLE3 $e^+e^- \rightarrow D_X X$
<sup>4</sup> ARTUSO 05B reports $[\Gamma(\Upsilon(4S) \rightarrow D_S^+ \text{ anything + c.c.})/\Gamma_{total}] \times [B(D_S^+ \rightarrow \phi\pi^+)] = (8.0 \pm 0.2 \pm 0.9) \times 10^{-3}$ which we divide by our best value $B(D_S^+ \rightarrow \phi\pi^+) = (4.5 \pm 0.4) \times 10^{-2}$ . Our first error is their experiment's error and our second error is the systematic error from using our best value.			

$\Gamma(B^0\bar{B}^0)/\Gamma_{total}$	DOCUMENT ID	TECN	COMMENT
<b>0.487 ± 0.006 OUR EVALUATION</b>			
Assuming $B(\Upsilon(4S) \rightarrow B\bar{B}) = 1$			
••• We do not use the following data for averages, fits, limits, etc. •••			
0.487 ± 0.010 ± 0.008	<sup>5</sup> AUBERT,B	05H	BABR $\Upsilon(4S) \rightarrow \bar{B}B \rightarrow D^*\ell\nu_\ell$
<sup>5</sup> Direct measurement. This value is averaged with the value extracted from the $\Gamma(B^+B^-)/\Gamma(B^0\bar{B}^0)$ measurements.			

$\Gamma(B^+B^-)/\Gamma(B^0\bar{B}^0)$	DOCUMENT ID	TECN	COMMENT
<b>1.055 ± 0.025 OUR EVALUATION</b>			
1.006 ± 0.036 ± 0.031	<sup>6</sup> AUBERT	04F	BABR $\Upsilon(4S) \rightarrow B\bar{B} \rightarrow J/\psi K$
1.01 ± 0.03 ± 0.09	<sup>6</sup> HASTINGS	03	BELL $\Upsilon(4S) \rightarrow B\bar{B} \rightarrow$ dileptons
1.058 ± 0.084 ± 0.136	<sup>7</sup> ATHAR	02	CLEO $\Upsilon(4S) \rightarrow B\bar{B} \rightarrow D^*\ell\nu$
1.10 ± 0.06 ± 0.05	<sup>8</sup> AUBERT	02	BABR $\Upsilon(4S) \rightarrow B\bar{B} \rightarrow (c\bar{c})K^*$
1.04 ± 0.07 ± 0.04	<sup>9</sup> ALEXANDER	01	CLEO $\Upsilon(4S) \rightarrow B\bar{B} \rightarrow J/\psi K^*$
<sup>6</sup> HASTINGS 03 and AUBERT 04F assume $\tau(B^+)/\tau(B^0) = 1.083 \pm 0.017$ .			
<sup>7</sup> ATHAR 02 assumes $\tau(B^+)/\tau(B^0) = 1.074 \pm 0.028$ . Supersedes BARIISH 95.			
<sup>8</sup> AUBERT 02 assumes $\tau(B^+)/\tau(B^0) = 1.062 \pm 0.029$ .			
<sup>9</sup> ALEXANDER 01 assumes $\tau(B^+)/\tau(B^0) = 1.066 \pm 0.024$ .			

$\Gamma(J/\psi K_S^0(J/\psi, \eta_c) K_S^0)/\Gamma_{total}$	DOCUMENT ID	TECN	COMMENT
<b>&lt; 4</b>	<sup>10</sup> TAJIMA	07A	BELL $\Upsilon(4S) \rightarrow B^0\bar{B}^0$
<sup>10</sup> $\Upsilon(4S)$ with $CP = +1$ decays to the final state with $CP = -1$ .			

non- $B\bar{B}$  DECAYS

$\Gamma(\text{non-}B\bar{B})/\Gamma_{total}$	DOCUMENT ID	TECN	COMMENT
<b>&lt; 0.04</b>	BARISH	96B	CLEO $e^+e^-$

$\Gamma(e^+e^-)/\Gamma_{total}$	DOCUMENT ID	TECN	COMMENT
<b>1.57 ± 0.08 OUR AVERAGE</b>			
1.55 ± 0.04 ± 0.07	AUBERT	05Q	BABR $e^+e^- \rightarrow$ hadrons
2.77 ± 0.50 ± 0.49	<sup>11</sup> ALBRECHT	95E	ARG $e^+e^- \rightarrow$ hadrons
<sup>11</sup> Using LEYAOUANC 77 parametrization of $\Gamma(s)$ .			

$\Gamma(\rho^+\rho^-)/\Gamma_{total}$	DOCUMENT ID	TECN	COMMENT
<b>&lt; 5.7 × 10<sup>-6</sup></b>	AUBERT	08B0	BABR $e^+e^- \rightarrow \pi^+\pi^-\pi^0$

$\Gamma(J/\psi(1S) \text{ anything})/\Gamma_{total}$	DOCUMENT ID	TECN	COMMENT
<b>&lt; 1.9</b>	<sup>12</sup> ABE	02D	BELL $e^+e^- \rightarrow J/\psi X \rightarrow \ell^+\ell^-X$
< 4.7	<sup>12</sup> AUBERT	01c	BABR $e^+e^- \rightarrow J/\psi X \rightarrow \ell^+\ell^-X$
<sup>12</sup> Uses $B(J/\psi \rightarrow e^+e^-) = 0.0593 \pm 0.0010$ and $B(J/\psi \rightarrow \mu^+\mu^-) = 0.0588 \pm 0.0010$ .			

$\Gamma(D^{*+} \text{ anything + c.c.})/\Gamma_{total}$	DOCUMENT ID	TECN	COMMENT
<b>&lt; 0.074</b>	<sup>13</sup> ALEXANDER	90c	CLEO $e^+e^-$
<sup>13</sup> For $x > 0.473$ .			

## Meson Particle Listings

 $\Upsilon(4S)$ ,  $X(10610)^\pm$  $\Gamma(\phi \text{ anything})/\Gamma_{\text{total}}$   $\Gamma_{11}/\Gamma$ 

VALUE (units $10^{-2}$ )	CL%	DOCUMENT ID	TECN	COMMENT
<b><math>7.1 \pm 0.1 \pm 0.6</math></b>		HUANG 07	CLEO	$\Upsilon(4S) \rightarrow \phi X$

• • • We do not use the following data for averages, fits, limits, etc. • • •

<0.23	90	14 ALEXANDER 90c	CLEO	$e^+e^-$
-------	----	------------------	------	----------

<sup>14</sup> For  $x > 0.52$ .

 $\Gamma(\phi\eta)/\Gamma_{\text{total}}$   $\Gamma_{12}/\Gamma$ 

VALUE (units $10^{-6}$ )	CL%	DOCUMENT ID	TECN	COMMENT
<b>&lt;1.8</b>	90	15 BELOUS 09	BELL	$e^+e^- \rightarrow \phi\eta$

• • • We do not use the following data for averages, fits, limits, etc. • • •

<2.5	90	AUBERT,BE 06f	BABR	$e^+e^- \rightarrow \phi\eta$
------	----	---------------	------	-------------------------------

<sup>15</sup> Using all intermedite branching fraction values from PDG 08.

 $\Gamma(\phi\pi')/\Gamma_{\text{total}}$   $\Gamma_{13}/\Gamma$ 

VALUE (units $10^{-6}$ )	CL%	DOCUMENT ID	TECN	COMMENT
<b>&lt;4.3</b>	90	16 BELOUS 09	BELL	$e^+e^- \rightarrow \phi\pi'$

<sup>16</sup> Using all intermedite branching fraction values from PDG 08.

 $\Gamma(\rho\eta)/\Gamma_{\text{total}}$   $\Gamma_{14}/\Gamma$ 

VALUE (units $10^{-6}$ )	CL%	DOCUMENT ID	TECN	COMMENT
<b>&lt;1.3</b>	90	17 BELOUS 09	BELL	$e^+e^- \rightarrow \rho\eta$

<sup>17</sup> Using all intermedite branching fraction values from PDG 08.

 $\Gamma(\rho\pi')/\Gamma_{\text{total}}$   $\Gamma_{15}/\Gamma$ 

VALUE (units $10^{-6}$ )	CL%	DOCUMENT ID	TECN	COMMENT
<b>&lt;2.5</b>	90	18 BELOUS 09	BELL	$e^+e^- \rightarrow \rho\pi'$

<sup>18</sup> Using all intermedite branching fraction values from PDG 08.

 $\Gamma(\Upsilon(1S) \text{ anything})/\Gamma_{\text{total}}$   $\Gamma_{16}/\Gamma$ 

VALUE	CL%	DOCUMENT ID	TECN	COMMENT
<b>&lt;0.004</b>	90	ALEXANDER 90c	CLEO	$e^+e^-$

 $\Gamma(\Upsilon(1S)\pi^+\pi^-)/\Gamma_{\text{total}}$   $\Gamma_{17}/\Gamma$ 

VALUE (units $10^{-5}$ )	CL%	EVTs	DOCUMENT ID	TECN	COMMENT
<b><math>8.1 \pm 0.6</math> OUR AVERAGE</b>					
8.5 ± 1.3 ± 0.2		113 ± 16	19 SOKOLOV 09	BELL	$e^+e^- \rightarrow \pi^+\pi^-\mu^+\mu^-$
8.00 ± 0.64 ± 0.27		430	20 AUBERT 08BP	BABR	$\Upsilon(4S) \rightarrow \pi^+\pi^-\ell^+\ell^-$

• • • We do not use the following data for averages, fits, limits, etc. • • •

17.8 ± 4.0 ± 0.3			21,22 SOKOLOV 07	BELL	$e^+e^- \rightarrow \pi^+\pi^-\mu^+\mu^-$
9.0 ± 1.5 ± 0.2		167 ± 19	23 AUBERT 06R	BABR	$e^+e^- \rightarrow \pi^+\pi^-\mu^+\mu^-$
<12		90	GLENN 99	CLE2	$e^+e^-$

<sup>19</sup> SOKOLOV 09 reports  $[\Gamma(\Upsilon(4S) \rightarrow \Upsilon(1S)\pi^+\pi^-)/\Gamma_{\text{total}}] \times [\text{B}(\Upsilon(1S) \rightarrow \mu^+\mu^-)] = (0.221 \pm 0.030 \pm 0.014) \times 10^{-5}$  which we divide by our best value  $\text{B}(\Upsilon(1S) \rightarrow \mu^+\mu^-) = (2.48 \pm 0.05) \times 10^{-2}$ . Our first error is their experiment's error and our second error is the systematic error from using our best value.

<sup>20</sup> Using  $\text{B}(\Upsilon(1S) \rightarrow e^+e^-) = (2.38 \pm 0.11)\%$  and  $\text{B}(\Upsilon(1S) \rightarrow \mu^+\mu^-) = (2.48 \pm 0.05)\%$ .

<sup>21</sup> SOKOLOV 07 reports  $[\Gamma(\Upsilon(4S) \rightarrow \Upsilon(1S)\pi^+\pi^-)/\Gamma_{\text{total}}] \times [\text{B}(\Upsilon(1S) \rightarrow \mu^+\mu^-)] = (4.42 \pm 0.81 \pm 0.56) \times 10^{-6}$  which we divide by our best value  $\text{B}(\Upsilon(1S) \rightarrow \mu^+\mu^-) = (2.48 \pm 0.05) \times 10^{-2}$ . Our first error is their experiment's error and our second error is the systematic error from using our best value.

<sup>22</sup> According to the authors, systematic errors were underestimated.

<sup>23</sup> Superseded by AUBERT 08BP. AUBERT 06R reports  $[\Gamma(\Upsilon(4S) \rightarrow \Upsilon(1S)\pi^+\pi^-)/\Gamma_{\text{total}}] \times [\text{B}(\Upsilon(1S) \rightarrow \mu^+\mu^-)] = (2.23 \pm 0.25 \pm 0.27) \times 10^{-6}$  which we divide by our best value  $\text{B}(\Upsilon(1S) \rightarrow \mu^+\mu^-) = (2.48 \pm 0.05) \times 10^{-2}$ . Our first error is their experiment's error and our second error is the systematic error from using our best value.

<sup>24</sup> Using  $\text{B}(\Upsilon(1S) \rightarrow e^+e^-) = (2.38 \pm 0.11)\%$  and  $\text{B}(\Upsilon(1S) \rightarrow \mu^+\mu^-) = (2.48 \pm 0.05)\%$ .

<sup>25</sup> Not independent of other values reported by AUBERT 08BP.

 $\Gamma(\Upsilon(1S)\eta)/\Gamma_{\text{total}}$   $\Gamma_{18}/\Gamma$ 

VALUE (units $10^{-4}$ )	EVTs	DOCUMENT ID	TECN	COMMENT
<b><math>1.96 \pm 0.06 \pm 0.09</math></b>	56	24 AUBERT 08BP	BABR	$\Upsilon(4S) \rightarrow \pi^+\pi^-\pi^0\ell^+\ell^-$

<sup>24</sup> Using  $\text{B}(\Upsilon(1S) \rightarrow e^+e^-) = (2.38 \pm 0.11)\%$  and  $\text{B}(\Upsilon(1S) \rightarrow \mu^+\mu^-) = (2.48 \pm 0.05)\%$ .

 $\Gamma(\Upsilon(1S)\eta)/\Gamma(\Upsilon(1S)\pi^+\pi^-)$   $\Gamma_{18}/\Gamma_{17}$ 

VALUE	EVTs	DOCUMENT ID	TECN	COMMENT
<b><math>2.41 \pm 0.40 \pm 0.12</math></b>	56	25 AUBERT 08BP	BABR	$\Upsilon(4S) \rightarrow \pi^+\pi^-(\pi^0)\ell^+\ell^-$

• • • We do not use the following data for averages, fits, limits, etc. • • •

<sup>25</sup> Not independent of other values reported by AUBERT 08BP.

 $\Gamma(\Upsilon(2S)\pi^+\pi^-)/\Gamma_{\text{total}}$   $\Gamma_{19}/\Gamma$ 

VALUE (units $10^{-4}$ )	CL%	EVTs	DOCUMENT ID	TECN	COMMENT
<b><math>0.86 \pm 0.11 \pm 0.07</math></b>		220	26 AUBERT 08BP	BABR	$\Upsilon(4S) \rightarrow \pi^+\pi^-\ell^+\ell^-$

• • • We do not use the following data for averages, fits, limits, etc. • • •

0.8 ± 0.17 ± 0.08		97 ± 15	27 AUBERT 06R	BABR	$e^+e^- \rightarrow \pi^+\pi^-\mu^+\mu^-$
<3.9		90	GLENN 99	CLE2	$e^+e^-$

<sup>26</sup> Using  $\text{B}(\Upsilon(2S) \rightarrow e^+e^-) = (1.91 \pm 0.16)\%$  and  $\text{B}(\Upsilon(2S) \rightarrow \mu^+\mu^-) = (1.93 \pm 0.17)\%$ .

<sup>27</sup> Superseded by AUBERT 08BP. AUBERT 06R reports  $[\Gamma(\Upsilon(4S) \rightarrow \Upsilon(2S)\pi^+\pi^-)/\Gamma_{\text{total}}] \times [\text{B}(\Upsilon(2S) \rightarrow \mu^+\mu^-)] = (1.69 \pm 0.26 \pm 0.20) \times 10^{-6}$  which we divide by our best value  $\text{B}(\Upsilon(2S) \rightarrow \mu^+\mu^-) = (1.93 \pm 0.17) \times 10^{-2}$ . Our first error is their experiment's error and our second error is the systematic error from using our best value.

 $\Gamma(\Upsilon(2S)\pi^+\pi^-)/\Gamma(\Upsilon(1S)\pi^+\pi^-)$   $\Gamma_{19}/\Gamma_{17}$ 

VALUE	EVTs	DOCUMENT ID	TECN	COMMENT
<b>• • •</b>				We do not use the following data for averages, fits, limits, etc. • • •
1.16 ± 0.16 ± 0.14	220	28 AUBERT 08BP	BABR	$\Upsilon(4S) \rightarrow \pi^+\pi^-\ell^+\ell^-$

<sup>28</sup> Using  $\text{B}(\Upsilon(1S) \rightarrow e^+e^-) = (2.38 \pm 0.11)\%$ ,  $\text{B}(\Upsilon(1S) \rightarrow \mu^+\mu^-) = (2.48 \pm 0.05)\%$ ,  $\text{B}(\Upsilon(2S) \rightarrow e^+e^-) = (1.91 \pm 0.16)\%$ , and  $\text{B}(\Upsilon(2S) \rightarrow \mu^+\mu^-) = (1.93 \pm 0.17)\%$ . Not independent of other values reported by AUBERT 08BP.

 $\Gamma(h_b(1P)\pi^+\pi^-)/\Gamma_{\text{total}}$   $\Gamma_{20}/\Gamma$ 

VALUE	EVTs	DOCUMENT ID	TECN	COMMENT
<b>not seen</b>	35 ± 21k	29 ADACHI 12	BELL	10.58 $e^+e^- \rightarrow h_b(1P)\pi^+\pi^-$

<sup>29</sup> From the upper limit on the ratio of  $\sigma(e^+e^- \rightarrow h_b(1P)\pi^+\pi^-)$  at the  $\Upsilon(4S)$  to that at the  $\Upsilon(5S)$  of 0.27.

 $\Gamma(\bar{d} \text{ anything})/\Gamma_{\text{total}}$   $\Gamma_{21}/\Gamma$ 

VALUE (units $10^{-5}$ )	CL%	DOCUMENT ID	TECN	COMMENT
<b>&lt;1.3</b>	90	ASNEN 07	CLEO	$e^+e^- \rightarrow \bar{d}X$

 $\Upsilon(4S)$  REFERENCES

ADACHI 12	PRL 108 032001	I. Adachi <i>et al.</i>	(BELLE Collab.)
BELOUS 09	PL B681 400	K. Belous <i>et al.</i>	(BELLE Collab.)
SOKOLOV 09	PR D79 051103R	A. Sokolov <i>et al.</i>	(BELLE Collab.)
AUBERT 08BP	PR D78 071103	B. Aubert <i>et al.</i>	(BABAR Collab.)
AUBERT 08BP	PR D78 112002	B. Aubert <i>et al.</i>	(BABAR Collab.)
PDG 08	B667 1	C. Amisber <i>et al.</i>	(PDG Collab.)
ASNEN 07	PL D75 012009	D.M. Asnen <i>et al.</i>	(CLEO Collab.)
HUANG 07	PR D75 012002	G.S. Huang <i>et al.</i>	(CLEO Collab.)
SOKOLOV 07	PR D75 071103R	A. Sokolov <i>et al.</i>	(BELLE Collab.)
TAJIMA 07A	PRL 99 211601	O. Tajima <i>et al.</i>	(BELLE Collab.)
AUBERT 06R	PRL 96 232001	B. Aubert <i>et al.</i>	(BABAR Collab.)
AUBERT,BE 06F	PR D74 111103R	B. Aubert <i>et al.</i>	(BABAR Collab.)
ARTUSO 05B	PRL 95 261801	M. Artuso <i>et al.</i>	(CLEO Collab.)
AUBERT 05Q	PR D72 032005	B. Aubert <i>et al.</i>	(BABAR Collab.)
AUBERT,B 05H	PRL 95 042001	B. Aubert <i>et al.</i>	(BABAR Collab.)
AUBERT 04F	PR D69 071101	B. Aubert <i>et al.</i>	(BABAR Collab.)
HASTINGS 03	PR D67 052004	N.C. Hastings <i>et al.</i>	(BELLE Collab.)
ABE 02D	PRL 88 092001	K. ABE <i>et al.</i>	(BELLE Collab.)
ATHAR 02	PR D66 052003	S.B. Athar <i>et al.</i>	(CLEO Collab.)
AUBERT 02	PR D65 032001	B. Aubert <i>et al.</i>	(BABAR Collab.)
ALEXANDER 01	PRL 86 2737	J.P. Alexander <i>et al.</i>	(CLEO Collab.)
AUBERT 01C	PRL 87 162002	B. Aubert <i>et al.</i>	(BABAR Collab.)
GLENN 99	PR D59 052003	S. Glenn <i>et al.</i>	(CLEO Collab.)
BARISH 96B	PRL 76 1570	B.C. Barish <i>et al.</i>	(CLEO Collab.)
ALBRECHT 95E	ZPHY C65 619	H. Albrecht <i>et al.</i>	(ARGUS Collab.)
BARISH 95	PR D51 1014	B.C. Barish <i>et al.</i>	(CLEO Collab.)
ALEXANDER 90C	PRL 64 2226	J. Alexander <i>et al.</i>	(CLEO Collab.)
BEBEK 87	PR D36 1289	C. Bebek <i>et al.</i>	(CLEO Collab.)
BESSON 85	PRL 54 3811	D. Besson <i>et al.</i>	(CLEO Collab.)
LOVELOCK 85	PRL 54 377	D.M.J. Lovelock <i>et al.</i>	(CUSB Collab.)
LEYAOUANC 77	PL B71 397	A. Le Yaouanc <i>et al.</i>	(ORSAY)

 **$X(10610)^\pm$** 

$$J^P(J^P) = ?^+(1^+)$$

OMITTED FROM SUMMARY TABLE

Observed by BONDAR 12 in  $\Upsilon(5S)$  decays to  $\Upsilon(nS)\pi^+\pi^-$  ( $n = 1, 2, 3$ ) and  $h_b(mP)\pi^+\pi^-$  ( $m = 1, 2$ ).  $J^P = 1^+$  is favored from angular analyses.

 $X(10610)^\pm$  MASS

VALUE (MeV)	DOCUMENT ID	TECN	COMMENT
<b><math>10607.2 \pm 2.0</math></b>	1 BONDAR 12	BELL	$e^+e^- \rightarrow \text{hadrons}$

• • • We do not use the following data for averages, fits, limits, etc. • • •

10611 ± 4 ± 3	2 BONDAR 12	BELL	$e^+e^- \rightarrow \Upsilon(1S)\pi^+\pi^-$
10609 ± 2 ± 3	2 BONDAR 12	BELL	$e^+e^- \rightarrow \Upsilon(2S)\pi^+\pi^-$
10608 ± 2 ± 3	2 BONDAR 12	BELL	$e^+e^- \rightarrow \Upsilon(3S)\pi^+\pi^-$
10605 ± 2 ± 3	2 BONDAR 12	BELL	$e^+e^- \rightarrow h_b(1P)\pi^+\pi^-$
10599 ± 6 ± 5	2 BONDAR 12	BELL	$e^+e^- \rightarrow h_b(2P)\pi^+\pi^-$

<sup>1</sup> Average of the BONDAR 12 measurements in separate channels.

<sup>2</sup> Superseded by the average measurement of BONDAR 12.

 $X(10610)^\pm$  WIDTH

VALUE (MeV)	DOCUMENT ID	TECN	COMMENT
<b><math>18.4 \pm 2.4</math></b>	3 BONDAR 12	BELL	$e^+e^- \rightarrow \text{hadrons}$

• • • We do not use the following data for averages, fits, limits, etc. • • •

22.3 ± 7.7 <sub>-3.0</sub> ± 4.0	4 BONDAR 12	BELL	$e^+e^- \rightarrow \Upsilon(1S)\pi^+\pi^-$
24.2 ± 3.1 <sub>-3.0</sub> ± 2.0	4 BONDAR 12	BELL	$e^+e^- \rightarrow \Upsilon(2S)\pi^+\pi^-$
17.6 ± 3.0 ± 3.0	4 BONDAR 12	BELL	$e^+e^- \rightarrow \Upsilon(3S)\pi^+\pi^-$
11.4 ± 4.5 <sub>-2.1</sub> ± 1.2	4 BONDAR 12	BELL	$e^+e^- \rightarrow h_b(1P)\pi^+\pi^-$
13 ± 10 <sub>-8</sub> ± 9 <sub>-7</sub>	4 BONDAR 12	BELL	$e^+e^- \rightarrow h_b(2P)\pi^+\pi^-$

<sup>3</sup> Average of the BONDAR 12 measurements in separate channels.

<sup>4</sup> Superseded by the average measurement of BONDAR 12.

See key on page 457

# Meson Particle Listings

## $X(10610)^\pm$ , $X(10650)^\pm$ , $\Upsilon(10860)$

 **$X(10610)^+$  DECAY MODES** $X(10610)^-$  decay modes are charge conjugates of the modes below.

Mode	Fraction ( $\Gamma_i/\Gamma$ )
$\Gamma_1$ $\Upsilon(1S)\pi^+$	seen
$\Gamma_2$ $\Upsilon(2S)\pi^+$	seen
$\Gamma_3$ $\Upsilon(3S)\pi^+$	seen
$\Gamma_4$ $h_b(1P)\pi^+$	seen
$\Gamma_5$ $h_b(2P)\pi^+$	seen

 **$X(10610)^\pm$  BRANCHING RATIOS**

$\Gamma(\Upsilon(1S)\pi^+)/\Gamma_{\text{total}}$	VALUE	DOCUMENT ID	TECN	COMMENT	$\Gamma_1/\Gamma$
seen		BONDAR	12	BELL	$e^+e^- \rightarrow \Upsilon(1S)\pi^+\pi^-$
$\Gamma(\Upsilon(2S)\pi^+)/\Gamma_{\text{total}}$	VALUE	DOCUMENT ID	TECN	COMMENT	$\Gamma_2/\Gamma$
seen		BONDAR	12	BELL	$e^+e^- \rightarrow \Upsilon(2S)\pi^+\pi^-$
$\Gamma(\Upsilon(3S)\pi^+)/\Gamma_{\text{total}}$	VALUE	DOCUMENT ID	TECN	COMMENT	$\Gamma_3/\Gamma$
seen		BONDAR	12	BELL	$e^+e^- \rightarrow \Upsilon(3S)\pi^+\pi^-$
$\Gamma(h_b(1P)\pi^+)/\Gamma_{\text{total}}$	VALUE	DOCUMENT ID	TECN	COMMENT	$\Gamma_4/\Gamma$
seen		BONDAR	12	BELL	$e^+e^- \rightarrow h_b(1P)\pi^+\pi^-$
$\Gamma(h_b(2P)\pi^+)/\Gamma_{\text{total}}$	VALUE	DOCUMENT ID	TECN	COMMENT	$\Gamma_5/\Gamma$
seen		BONDAR	12	BELL	$e^+e^- \rightarrow h_b(2P)\pi^+\pi^-$

 **$X(10610)^\pm$  REFERENCES**BONDAR 12 PRL 108 122001 A. Bondar *et al.* (BELLE Collab.)

$$X(10650)^\pm \quad I^G(J^P) = ?^+(1^+)$$

OMITTED FROM SUMMARY TABLE

Observed by BONDAR 12 in  $\Upsilon(nS)$  decays to  $\Upsilon(nS)\pi^+\pi^-$  ( $n = 1, 2, 3$ ) and  $h_b(mP)\pi^+\pi^-$  ( $m = 1, 2$ ).  $J^P = 1^+$  is favored from angular analyses.

 **$X(10650)^\pm$  MASS**

VALUE (MeV)	DOCUMENT ID	TECN	COMMENT
<b><math>10652.2 \pm 1.5</math></b>	<sup>1</sup> BONDAR	12	BELL $e^+e^- \rightarrow$ hadrons
$10657 \pm 6 \pm 3$	<sup>2</sup> BONDAR	12	BELL $e^+e^- \rightarrow \Upsilon(1S)\pi^+\pi^-$
$10651 \pm 2 \pm 3$	<sup>2</sup> BONDAR	12	BELL $e^+e^- \rightarrow \Upsilon(2S)\pi^+\pi^-$
$10652 \pm 1 \pm 2$	<sup>2</sup> BONDAR	12	BELL $e^+e^- \rightarrow \Upsilon(3S)\pi^+\pi^-$
$10654 \pm 3 \pm 1$	<sup>2</sup> BONDAR	12	BELL $e^+e^- \rightarrow h_b(1P)\pi^+\pi^-$
$10651 \pm 2 \pm 3$	<sup>2</sup> BONDAR	12	BELL $e^+e^- \rightarrow h_b(2P)\pi^+\pi^-$

<sup>1</sup> Average of the BONDAR 12 measurements in separate channels.<sup>2</sup> Superseded by the average measurement of BONDAR 12. **$X(10650)^\pm$  WIDTH**

VALUE (MeV)	DOCUMENT ID	TECN	COMMENT
<b><math>11.5 \pm 2.2</math></b>	<sup>3</sup> BONDAR	12	BELL $e^+e^- \rightarrow$ hadrons
$16.3 \pm 9.8 \pm 6.0$	<sup>4</sup> BONDAR	12	BELL $e^+e^- \rightarrow \Upsilon(1S)\pi^+\pi^-$
$13.3 \pm 3.3 \pm 4.0$	<sup>4</sup> BONDAR	12	BELL $e^+e^- \rightarrow \Upsilon(2S)\pi^+\pi^-$
$8.4 \pm 2.0 \pm 2.0$	<sup>4</sup> BONDAR	12	BELL $e^+e^- \rightarrow \Upsilon(3S)\pi^+\pi^-$
$20.9 \pm 5.4 \pm 2.1$	<sup>4</sup> BONDAR	12	BELL $e^+e^- \rightarrow h_b(1P)\pi^+\pi^-$
$19 \pm 7 \pm 11$	<sup>4</sup> BONDAR	12	BELL $e^+e^- \rightarrow h_b(2P)\pi^+\pi^-$

<sup>3</sup> Average of the BONDAR 12 measurements in separate channels.<sup>4</sup> Superseded by the average measurement of BONDAR 12. **$X(10650)^+$  DECAY MODES** $X(10650)^-$  decay modes are charge conjugates of the modes below.

Mode	Fraction ( $\Gamma_i/\Gamma$ )
$\Gamma_1$ $\Upsilon(1S)\pi^+$	seen
$\Gamma_2$ $\Upsilon(2S)\pi^+$	seen
$\Gamma_3$ $\Upsilon(3S)\pi^+$	seen
$\Gamma_4$ $h_b(1P)\pi^+$	seen
$\Gamma_5$ $h_b(2P)\pi^+$	seen

 **$X(10650)^\pm$  BRANCHING RATIOS**

$\Gamma(\Upsilon(1S)\pi^+)/\Gamma_{\text{total}}$	VALUE	DOCUMENT ID	TECN	COMMENT	$\Gamma_1/\Gamma$
seen		BONDAR	12	BELL	$e^+e^- \rightarrow \Upsilon(1S)\pi^+\pi^-$
$\Gamma(\Upsilon(2S)\pi^+)/\Gamma_{\text{total}}$	VALUE	DOCUMENT ID	TECN	COMMENT	$\Gamma_2/\Gamma$
seen		BONDAR	12	BELL	$e^+e^- \rightarrow \Upsilon(2S)\pi^+\pi^-$
$\Gamma(\Upsilon(3S)\pi^+)/\Gamma_{\text{total}}$	VALUE	DOCUMENT ID	TECN	COMMENT	$\Gamma_3/\Gamma$
seen		BONDAR	12	BELL	$e^+e^- \rightarrow \Upsilon(3S)\pi^+\pi^-$
$\Gamma(h_b(1P)\pi^+)/\Gamma_{\text{total}}$	VALUE	DOCUMENT ID	TECN	COMMENT	$\Gamma_4/\Gamma$
seen		BONDAR	12	BELL	$e^+e^- \rightarrow h_b(1P)\pi^+\pi^-$
$\Gamma(h_b(2P)\pi^+)/\Gamma_{\text{total}}$	VALUE	DOCUMENT ID	TECN	COMMENT	$\Gamma_5/\Gamma$
seen		BONDAR	12	BELL	$e^+e^- \rightarrow h_b(2P)\pi^+\pi^-$

 **$X(10650)^\pm$  REFERENCES**BONDAR 12 PRL 108 122001 A. Bondar *et al.* (BELLE Collab.)

$$\Upsilon(10860) \quad I^G(J^PC) = 0^-(1^{--})$$

 **$\Upsilon(10860)$  MASS**

VALUE (MeV) DOCUMENT ID TECN COMMENT  
 **$10876 \pm 11$  OUR EVALUATION** Weighted-average of Belle and BaBar results, but tripling the scaling  $S$ -factors applied to the uncertainties to account for model-dependence, handling of radiative corrections, and interference effects.

• • • We do not use the following data for averages, fits, limits, etc. • • •

$10879 \pm 3$	<sup>1,2</sup> CHEN	10	BELL $e^+e^- \rightarrow$ hadrons
$10888.4 \pm 2.7$	<sup>3</sup> CHEN	10	BELL $e^+e^- \rightarrow \Upsilon(1S, 2S, 3S)\pi^+\pi^-$
$10876 \pm 2$	<sup>1</sup> AUBERT	09E	BABR $e^+e^- \rightarrow$ hadrons
$10869 \pm 2$	<sup>4</sup> AUBERT	09E	BABR $e^+e^- \rightarrow$ hadrons
$10868 \pm 6 \pm 5$	<sup>5</sup> BESSON	85	CLEO $e^+e^- \rightarrow$ hadrons
$10845 \pm 20$	<sup>6</sup> LOVELOCK	85	CUSB $e^+e^- \rightarrow$ hadrons

<sup>1</sup> In a model where a flat non-resonant  $b\bar{b}$ -continuum is incoherently added to a second flat component interfering with two Breit-Wigner resonances. Systematic uncertainties not estimated.<sup>2</sup> The parameters of the  $\Upsilon(11020)$  are fixed to those in AUBERT 09E.<sup>3</sup> In a model where a flat nonresonant  $\Upsilon(1S, 2S, 3S)\pi^+\pi^-$  continuum interferes with a single Breit-Wigner resonance.<sup>4</sup> In a model where a non-resonant  $b\bar{b}$ -continuum represented by a threshold function at  $\sqrt{s} = 2m_B$  is incoherently added to a flat component interfering with two Breit-Wigner resonances. Not independent of other AUBERT 09E results. Systematic uncertainties not estimated.<sup>5</sup> Assuming four Gaussians with radiative tails and a single step in  $R$ .<sup>6</sup> In a coupled-channel model with three resonances and a smooth step in  $R$ . **$\Upsilon(10860)$  WIDTH**

VALUE (MeV)	DOCUMENT ID	TECN	COMMENT
<b><math>55 \pm 28</math> OUR EVALUATION</b>			Weighted-average of Belle and BaBar results, but tripling the scaling $S$ -factors applied to the uncertainties to account for model-dependence, handling of radiative corrections, and interference effects.
$46 \pm 9$	<sup>7,8</sup> CHEN	10	BELL $e^+e^- \rightarrow$ hadrons
$30.7 \pm 8.3$	<sup>9</sup> CHEN	10	BELL $e^+e^- \rightarrow \Upsilon(1S, 2S, 3S)\pi^+\pi^-$
$43 \pm 4$	<sup>7</sup> AUBERT	09E	BABR $e^+e^- \rightarrow$ hadrons
$74 \pm 4$	<sup>10</sup> AUBERT	09E	BABR $e^+e^- \rightarrow$ hadrons
$112 \pm 17 \pm 23$	<sup>11</sup> BESSON	85	CLEO $e^+e^- \rightarrow$ hadrons
$110 \pm 15$	<sup>12</sup> LOVELOCK	85	CUSB $e^+e^- \rightarrow$ hadrons

• • • We do not use the following data for averages, fits, limits, etc. • • •

## Meson Particle Listings

 $\Upsilon(10860)$ 

- <sup>7</sup>In a model where a flat non-resonant  $b\bar{b}$ -continuum is incoherently added to a second flat component interfering with two Breit-Wigner resonances. Systematic uncertainties not estimated.
- <sup>8</sup>The parameters of the  $\Upsilon(11020)$  are fixed to those in AUBERT 09E.
- <sup>9</sup>In a model where a flat nonresonant  $\Upsilon(1S, 2S, 3S)\pi^+\pi^-$  continuum interferes with a single Breit-Wigner resonance.
- <sup>10</sup>In a model where a non-resonant  $b\bar{b}$ -continuum represented by a threshold function at  $\sqrt{s}=2m_B$  is incoherently added to a flat component interfering with two Breit-Wigner resonances. Not independent of other AUBERT 09E results. Systematic uncertainties not estimated.
- <sup>11</sup>Assuming four Gaussians with radiative tails and a single step in  $R$ .
- <sup>12</sup>In a coupled-channel model with three resonances and a smooth step in  $R$ .

 $\Upsilon(10860)$  DECAY MODES

Mode	Fraction ( $\Gamma_i/\Gamma$ )	Confidence level
$\Gamma_1$ $B\bar{B}X$	( 75.9 $\pm$ 2.7 $\overline{-4.0}$ ) %	
$\Gamma_2$ $B\bar{B}$	( 5.5 $\pm$ 1.0 ) %	
$\Gamma_3$ $B\bar{B}^* + \text{c.c.}$	( 13.7 $\pm$ 1.6 ) %	
$\Gamma_4$ $B^*\bar{B}^*$	( 38.1 $\pm$ 3.4 ) %	
$\Gamma_5$ $B\bar{B}^*(*)\pi$	< 19.7 %	90%
$\Gamma_6$ $B\bar{B}\pi$	( 0.0 $\pm$ 1.2 ) %	
$\Gamma_7$ $B^*\bar{B}\pi + B\bar{B}^*\pi$	( 7.3 $\pm$ 2.3 ) %	
$\Gamma_8$ $B^*\bar{B}^*\pi$	( 1.0 $\pm$ 1.4 ) %	
$\Gamma_9$ $B\bar{B}\pi\pi$	< 8.9 %	90%
$\Gamma_{10}$ $B_s^{(*)}\bar{B}_s^{(*)}$	( 19.9 $\pm$ 3.0 ) %	
$\Gamma_{11}$ $B_s\bar{B}_s$	( 5 $\pm$ 5 ) $\times 10^{-3}$	
$\Gamma_{12}$ $B_s\bar{B}_s^* + \text{c.c.}$	( 1.5 $\pm$ 0.7 ) %	
$\Gamma_{13}$ $B_s^*\bar{B}_s^*$	( 17.9 $\pm$ 2.8 ) %	
$\Gamma_{14}$ no open-bottom	( 4.2 $\pm$ 5.0 $\overline{-0.6}$ ) %	
$\Gamma_{15}$ $e^+e^-$	( 5.6 $\pm$ 3.1 ) $\times 10^{-6}$	
$\Gamma_{16}$ $\Upsilon(1S)\pi^+\pi^-$	( 5.3 $\pm$ 0.6 ) $\times 10^{-3}$	
$\Gamma_{17}$ $\Upsilon(2S)\pi^+\pi^-$	( 7.8 $\pm$ 1.3 ) $\times 10^{-3}$	
$\Gamma_{18}$ $\Upsilon(3S)\pi^+\pi^-$	( 4.8 $\pm$ 1.9 $\overline{-1.7}$ ) $\times 10^{-3}$	
$\Gamma_{19}$ $\Upsilon(1S)K^+K^-$	( 6.1 $\pm$ 1.8 ) $\times 10^{-4}$	
$\Gamma_{20}$ $h_b(1P)\pi^+\pi^-$	( 3.5 $\pm$ 1.0 $\overline{-1.3}$ ) $\times 10^{-3}$	
$\Gamma_{21}$ $h_b(2P)\pi^+\pi^-$	( 6.0 $\pm$ 2.1 $\overline{-1.8}$ ) $\times 10^{-3}$	

## Inclusive Decays.

These decay modes are submodes of one or more of the decay modes above.

$\Gamma_{22}$ $\phi$ anything	( 13.8 $\pm$ 2.4 $\overline{-1.7}$ ) %	
$\Gamma_{23}$ $D^0$ anything + c.c.	( 108 $\pm$ 8 ) %	
$\Gamma_{24}$ $D_s$ anything + c.c.	( 46 $\pm$ 6 ) %	
$\Gamma_{25}$ $J/\psi$ anything	( 2.06 $\pm$ 0.21 ) %	
$\Gamma_{26}$ $B^0$ anything + c.c.	( 77 $\pm$ 8 ) %	
$\Gamma_{27}$ $B^+$ anything + c.c.	( 72 $\pm$ 6 ) %	

 $\Upsilon(10860)$  PARTIAL WIDTHS

$\Gamma(e^+e^-)$	$\Gamma_{15}$
VALUE (keV)	DOCUMENT ID TECN COMMENT
<b>0.31 <math>\pm</math> 0.07 OUR AVERAGE</b>	Error includes scale factor of 1.3.
0.22 $\pm$ 0.05 $\pm$ 0.07	BESSON 85 CLEO $e^+e^- \rightarrow$ hadrons
0.365 $\pm$ 0.070	LOVELOCK 85 CUSB $e^+e^- \rightarrow$ hadrons

 $\Upsilon(10860)$  BRANCHING RATIOS

"OUR EVALUATION" is obtained based on averages of rescaled data listed below. The averages and rescaling were performed by the Heavy Flavor Averaging Group (HFAG) and are described at <http://www.slac.stanford.edu/xorg/hfag/>.

$\Gamma(B\bar{B}X)/\Gamma_{\text{total}}$	$\Gamma_1/\Gamma$
VALUE EVTS DOCUMENT ID TECN COMMENT	
<b>0.759 <math>\pm</math> 0.027 <math>\overline{0.040}</math> OUR EVALUATION</b>	
<b>0.71 <math>\pm</math> 0.06 OUR AVERAGE</b>	
0.737 $\pm$ 0.032 $\pm$ 0.051	1063 <sup>13</sup> DRUTSKOY 10 BELL $\Upsilon(5S) \rightarrow B^+X, B^0X$
0.589 $\pm$ 0.100 $\pm$ 0.092	<sup>14</sup> HUANG 07 CLEO $\Upsilon(5S) \rightarrow$ hadrons
$\Gamma(B\bar{B})/\Gamma_{\text{total}}$	$\Gamma_2/\Gamma$
VALUE (units $10^{-2}$ ) CL% DOCUMENT ID TECN COMMENT	
<b>5.5 <math>\pm</math> 1.0 <math>\overline{0.9 \pm 0.4}</math></b>	<sup>15</sup> DRUTSKOY 10 BELL $\Upsilon(5S) \rightarrow B^+X, B^0X$

••• We do not use the following data for averages, fits, limits, etc. •••

<13.8 90 <sup>14</sup> HUANG 07 CLEO  $\Upsilon(5S) \rightarrow$  hadrons

$\Gamma(B\bar{B})/\Gamma(B\bar{B}X)$	$\Gamma_2/\Gamma_1$
VALUE CL% DOCUMENT ID TECN COMMENT	
<b>&lt;0.22</b>	90
AQUINES 06 CLE3 $\Upsilon(5S) \rightarrow$ hadrons	

$\Gamma(B\bar{B}^* + \text{c.c.})/\Gamma_{\text{total}}$	$\Gamma_3/\Gamma$
VALUE DOCUMENT ID TECN COMMENT	
<b>0.137 <math>\pm</math> 0.016 OUR AVERAGE</b>	
0.137 $\pm$ 0.013 $\pm$ 0.011	<sup>15</sup> DRUTSKOY 10 BELL $\Upsilon(5S) \rightarrow B^+X, B^0X$
0.143 $\pm$ 0.053 $\pm$ 0.027	<sup>14</sup> HUANG 07 CLEO $\Upsilon(5S) \rightarrow$ hadrons

$\Gamma(B\bar{B}^* + \text{c.c.})/\Gamma(B\bar{B}X)$	$\Gamma_3/\Gamma_1$
VALUE EVTS DOCUMENT ID TECN COMMENT	
<b>0.24 <math>\pm</math> 0.09 <math>\pm</math> 0.03</b>	
AQUINES 06 CLE3 $\Upsilon(5S) \rightarrow$ hadrons	

$\Gamma(B^*\bar{B}^*)/\Gamma_{\text{total}}$	$\Gamma_4/\Gamma$
VALUE DOCUMENT ID TECN COMMENT	
<b>0.381 <math>\pm</math> 0.034 OUR AVERAGE</b>	
0.375 $\pm$ 0.021 $\overline{-0.019}$ $\pm$ 0.030	<sup>15</sup> DRUTSKOY 10 BELL $\Upsilon(5S) \rightarrow B^+X, B^0X$
0.436 $\pm$ 0.083 $\pm$ 0.072	<sup>14</sup> HUANG 07 CLEO $\Upsilon(5S) \rightarrow$ hadrons

$\Gamma(B^*\bar{B}^*)/\Gamma(B\bar{B}X)$	$\Gamma_4/\Gamma_1$
VALUE EVTS DOCUMENT ID TECN COMMENT	
<b>0.74 <math>\pm</math> 0.15 <math>\pm</math> 0.08</b>	
AQUINES 06 CLE3 $\Upsilon(5S) \rightarrow$ hadrons	

$\Gamma(B\bar{B}^*(*)\pi)/\Gamma_{\text{total}}$	$\Gamma_5/\Gamma$
VALUE CL% DOCUMENT ID TECN COMMENT	
<b>&lt;0.197</b>	
<sup>14</sup> HUANG 07 CLEO $\Upsilon(5S) \rightarrow$ hadrons	

$\Gamma(B\bar{B}^*(*)\pi)/\Gamma(B\bar{B}X)$	$\Gamma_5/\Gamma_1$
VALUE CL% DOCUMENT ID TECN COMMENT	
<b>&lt;0.32</b>	
AQUINES 06 CLE3 $\Upsilon(5S) \rightarrow$ hadrons	

$\Gamma(B\bar{B}\pi\pi)/\Gamma_{\text{total}}$	$\Gamma_6/\Gamma$
VALUE (units $10^{-2}$ ) EVTS DOCUMENT ID TECN COMMENT	
<b>0.0 <math>\pm</math> 1.2 <math>\pm</math> 0.3</b>	
0	<sup>15</sup> DRUTSKOY 10 BELL $\Upsilon(5S) \rightarrow B^+,^0\pi^-\pi^-\pi^+$

$[\Gamma(B^*\bar{B}\pi) + \Gamma(B\bar{B}^*\pi)]/\Gamma_{\text{total}}$	$\Gamma_7/\Gamma$
VALUE (units $10^{-2}$ ) EVTS DOCUMENT ID TECN COMMENT	
<b>7.3 <math>\pm</math> 2.3 <math>\overline{-2.1}</math> <math>\pm</math> 0.8</b>	
38	<sup>15</sup> DRUTSKOY 10 BELL $\Upsilon(5S) \rightarrow B^+,^0\pi^-\pi^+$

$\Gamma(B^*\bar{B}^*\pi)/\Gamma_{\text{total}}$	$\Gamma_8/\Gamma$
VALUE (units $10^{-2}$ ) EVTS DOCUMENT ID TECN COMMENT	
<b>1.0 <math>\pm</math> 1.4 <math>\overline{-1.3}</math> <math>\pm</math> 0.4</b>	
5	<sup>15</sup> DRUTSKOY 10 BELL $\Upsilon(5S) \rightarrow B^+,^0\pi^-\pi^+$

$\Gamma(B\bar{B}\pi\pi)/\Gamma_{\text{total}}$	$\Gamma_9/\Gamma$
VALUE CL% DOCUMENT ID TECN COMMENT	
<b>&lt;0.089</b>	
<sup>14</sup> HUANG 07 CLEO $\Upsilon(5S) \rightarrow$ hadrons	

$\Gamma(B\bar{B}\pi\pi)/\Gamma(B\bar{B}X)$	$\Gamma_9/\Gamma_1$
VALUE CL% DOCUMENT ID TECN COMMENT	
<b>&lt;0.14</b>	
AQUINES 06 CLE3 $\Upsilon(5S) \rightarrow$ hadrons	

$\Gamma(B_s^{(*)}\bar{B}_s^{(*)})/\Gamma_{\text{total}}$	$\Gamma_{10}/\Gamma = (\Gamma_{11} + \Gamma_{12} + \Gamma_{13})/\Gamma$
VALUE DOCUMENT ID TECN COMMENT	
<b>0.199 <math>\pm</math> 0.030 OUR EVALUATION</b>	
<b>0.195 <math>\pm</math> 0.030 <math>\overline{-0.023}</math> OUR AVERAGE</b>	
0.180 $\pm$ 0.013 $\pm$ 0.032	<sup>16</sup> DRUTSKOY 07 BELL $\Upsilon(5S) \rightarrow D^0X, D_sX$
0.21 $\pm$ 0.06 $\overline{-0.03}$	<sup>17</sup> HUANG 07 CLEO $\Upsilon(5S) \rightarrow D_sX$

••• We do not use the following data for averages, fits, limits, etc. •••

0.160  $\pm$  0.026  $\pm$  0.058 <sup>18</sup> ARTUSO 05B CLEO  $e^+e^- \rightarrow D_X X$

$\Gamma(B_s^{(*)}\bar{B}_s^{(*)})/\Gamma(B\bar{B}X)$	$\Gamma_{10}/\Gamma_1$
VALUE DOCUMENT ID TECN COMMENT	
<b>0.262 <math>\pm</math> 0.051 <math>\overline{-0.043}</math> OUR EVALUATION</b>	

$\Gamma(B_s^*\bar{B}_s^*)/\Gamma(B_s^{(*)}\bar{B}_s^{(*)})$	$\Gamma_{13}/\Gamma_{10} = \Gamma_{13}/(\Gamma_{11} + \Gamma_{12} + \Gamma_{13})$
VALUE (units $10^{-2}$ ) DOCUMENT ID TECN COMMENT	
<b>90.1 <math>\pm</math> 3.8 <math>\overline{4.0 \pm 0.2}</math></b>	
<sup>19</sup> LOUVOT 09 BELL 10.86 $e^+e^- \rightarrow B_s^{(*)}\bar{B}_s^{(*)}$	
••• We do not use the following data for averages, fits, limits, etc. •••	
93 $\pm$ 7 $\overline{-9}$ $\pm$ 1	<sup>19</sup> DRUTSKOY 07A BELL Superseded by LOUVOT 09

$\Gamma(B_s\bar{B}_s)/\Gamma(B_s^{(*)}\bar{B}_s^{(*)})$	$\Gamma_{11}/\Gamma_{10} = \Gamma_{11}/(\Gamma_{11} + \Gamma_{12} + \Gamma_{13})$
VALUE (units $10^{-2}$ ) DOCUMENT ID TECN COMMENT	
<b>2.6 <math>\pm</math> 2.6 <math>\overline{-2.5}</math></b>	
<sup>19</sup> LOUVOT 09 BELL 10.86 $e^+e^- \rightarrow B_s^{(*)}\bar{B}_s^{(*)}$	

See key on page 457

# Meson Particle Listings

## $\Upsilon(10860)$

$\Gamma(B_s \bar{B}_s^*)/\Gamma(B_s^* \bar{B}_s^*)$		$\Gamma_{11}/\Gamma_{13}$	
VALUE	CL%	DOCUMENT ID	TECN COMMENT
$<0.16$	90	BONVICINI 06	CLE3 $e^+e^-$

$\Gamma(B_s \bar{B}_s^* + c.c.)/\Gamma(B_s^{(*)} \bar{B}_s^{(*)})$		$\Gamma_{12}/\Gamma_{10} = \Gamma_{12}/(\Gamma_{11} + \Gamma_{12} + \Gamma_{13})$	
VALUE (units $10^{-2}$ )		DOCUMENT ID	TECN COMMENT
$7.3^{+3.3}_{-3.0} \pm 0.1$		LOUVOT 09	BELL 10.86 $e^+e^- \rightarrow B_s^{(*)} \bar{B}_s^{(*)}$

$\Gamma(B_s \bar{B}_s^* + c.c.)/\Gamma(B_s^* \bar{B}_s^*)$		$\Gamma_{12}/\Gamma_{13}$	
VALUE	CL%	DOCUMENT ID	TECN COMMENT
$<0.16$	90	BONVICINI 06	CLE3 $e^+e^-$

$\Gamma(\text{no open-bottom})/\Gamma_{\text{total}}$		$\Gamma_{14}/\Gamma$	
VALUE		DOCUMENT ID	
$0.042^{+0.046}_{-0.006}$		<b>OUR EVALUATION</b>	

$\Gamma(\Upsilon(1S)\pi^+\pi^-)/\Gamma_{\text{total}}$		$\Gamma_{16}/\Gamma$	
VALUE (units $10^{-3}$ )	EVTS	DOCUMENT ID	TECN COMMENT
$5.3 \pm 0.3 \pm 0.5$	325	20 CHEN 08	BELL 10.87 $e^+e^- \rightarrow \Upsilon(1S)\pi^+\pi^-$

$\Gamma(\Upsilon(2S)\pi^+\pi^-)/\Gamma_{\text{total}}$		$\Gamma_{17}/\Gamma$	
VALUE (units $10^{-3}$ )	EVTS	DOCUMENT ID	TECN COMMENT
$7.8 \pm 0.6 \pm 1.1$	186	20 CHEN 08	BELL 10.87 $e^+e^- \rightarrow \Upsilon(2S)\pi^+\pi^-$

$\Gamma(\Upsilon(3S)\pi^+\pi^-)/\Gamma_{\text{total}}$		$\Gamma_{18}/\Gamma$	
VALUE (units $10^{-3}$ )	EVTS	DOCUMENT ID	TECN COMMENT
$4.8^{+1.9}_{-1.5} \pm 0.7$	10	20 CHEN 08	BELL 10.87 $e^+e^- \rightarrow \Upsilon(3S)\pi^+\pi^-$

$\Gamma(\Upsilon(1S)K^+K^-)/\Gamma_{\text{total}}$		$\Gamma_{19}/\Gamma$	
VALUE (units $10^{-4}$ )	EVTS	DOCUMENT ID	TECN COMMENT
$6.1^{+1.6}_{-1.4} \pm 1.0$	20	20 CHEN 08	BELL 10.87 $e^+e^- \rightarrow \Upsilon(1S)K^+K^-$

$\Gamma(h_b(1P)\pi^+\pi^-)/\Gamma(\Upsilon(2S)\pi^+\pi^-)$		$\Gamma_{20}/\Gamma_{17}$	
VALUE		DOCUMENT ID	TECN COMMENT
$0.45 \pm 0.08^{+0.07}_{-0.12}$		ADACHI 12	BELL 10.86 $e^+e^- \rightarrow \text{hadrons}$

$\Gamma(h_b(2P)\pi^+\pi^-)/\Gamma(\Upsilon(2S)\pi^+\pi^-)$		$\Gamma_{21}/\Gamma_{17}$	
VALUE		DOCUMENT ID	TECN COMMENT
$0.77 \pm 0.08^{+0.22}_{-0.17}$		ADACHI 12	BELL 10.86 $e^+e^- \rightarrow \text{hadrons}$

$\Gamma(\phi \text{ anything})/\Gamma_{\text{total}}$		$\Gamma_{22}/\Gamma$	
VALUE		DOCUMENT ID	TECN COMMENT
$0.138 \pm 0.007^{+0.023}_{-0.015}$		HUANG 07	CLEO $\Upsilon(5S) \rightarrow \phi X$

$\Gamma(D^0 \text{ anything} + c.c.)/\Gamma_{\text{total}}$		$\Gamma_{23}/\Gamma$	
VALUE		DOCUMENT ID	TECN COMMENT
$1.076 \pm 0.040 \pm 0.068$		DRUTSKOY 07	BELL $\Upsilon(5S) \rightarrow D^0 X$

$\Gamma(D_s \text{ anything} + c.c.)/\Gamma_{\text{total}}$		$\Gamma_{24}/\Gamma$	
VALUE		DOCUMENT ID	TECN COMMENT
$0.46 \pm 0.06$		<b>OUR AVERAGE</b>	
$0.472 \pm 0.024 \pm 0.072$		16 DRUTSKOY 07	BELL $\Upsilon(5S) \rightarrow D_s X$
$0.44 \pm 0.09 \pm 0.04$		21 ARTUSO 05B	CLE3 $e^+e^- \rightarrow D_X X$

$\Gamma(J/\psi \text{ anything})/\Gamma_{\text{total}}$		$\Gamma_{25}/\Gamma$	
VALUE (units $10^{-2}$ )		DOCUMENT ID	TECN COMMENT
$2.060 \pm 0.160 \pm 0.134$		DRUTSKOY 07	BELL $\Upsilon(5S) \rightarrow J/\psi X$

$\Gamma(B^0 \text{ anything} + c.c.)/\Gamma_{\text{total}}$		$\Gamma_{26}/\Gamma$	
VALUE	EVTS	DOCUMENT ID	TECN COMMENT
$0.770^{+0.058}_{-0.056} \pm 0.061$	352	DRUTSKOY 10	BELL $\Upsilon(5S) \rightarrow B^0 X$

$\Gamma(B^+ \text{ anything} + c.c.)/\Gamma_{\text{total}}$		$\Gamma_{27}/\Gamma$	
VALUE	EVTS	DOCUMENT ID	TECN COMMENT
$0.721^{+0.039}_{-0.038} \pm 0.050$	711	DRUTSKOY 10	BELL $\Upsilon(5S) \rightarrow B^+ X$

<sup>21</sup> ARTUSO 05B reports  $[\Gamma(\Upsilon(10860) \rightarrow D_s \text{ anything} + c.c.)/\Gamma_{\text{total}}] \times [B(D_s^+ \rightarrow \phi\pi^+)] = 0.0198 \pm 0.0019 \pm 0.0038$  which we divide by our best value  $B(D_s^+ \rightarrow \phi\pi^+) = (4.5 \pm 0.4) \times 10^{-2}$ . Our first error is their experiment's error and our second error is the systematic error from using our best value.

### $\Upsilon(10860)$ REFERENCES

ADACHI 12	PRL 108 032001	I. Adachi <i>et al.</i>	(BELLE Collab.)
CHEN 10	PR D82 091106R	K.-F. Chen <i>et al.</i>	(BELLE Collab.)
DRUTSKOY 10	PR D81 112003	A. Drutskoy <i>et al.</i>	(BELLE Collab.)
AUBERT 09E	PRL 102 012001	B. Aubert <i>et al.</i>	(BABAR Collab.)
LOUVOT 09	PRL 102 021801	R. Louvot <i>et al.</i>	(BELLE Collab.)
CHEN 08	PRL 100 112001	K.-F. Chen <i>et al.</i>	(BELLE Collab.)
DRUTSKOY 07	PRL 98 052001	A. Drutskoy <i>et al.</i>	(BELLE Collab.)
DRUTSKOY 07A	PR D76 012002	A. Drutskoy <i>et al.</i>	(BELLE Collab.)
HUANG 07	PR D75 012002	G.S. Huang <i>et al.</i>	(CLEO Collab.)
AQUINES 06	PRL 96 152001	O. Aquines <i>et al.</i>	(CLEO Collab.)
BONVICINI 06	PRL 96 022002	G. Bonvicini <i>et al.</i>	(CLEO Collab.)
PDG 06	JPG 33 1	W.-M. Yao <i>et al.</i>	(PDG Collab.)
ARTUSO 05B	PRL 95 261801	M. Artuso <i>et al.</i>	(CLEO Collab.)
BESSION 85	PRL 54 381	D. Besson <i>et al.</i>	(CLEO Collab.)
LOVELOCK 85	PRL 54 377	D.M.J. Lovelock <i>et al.</i>	(CUSB Collab.)

## $\Upsilon(11020)$

$$I^G(J^{PC}) = 0^-(1^{--})$$

### $\Upsilon(11020)$ MASS

VALUE (GeV)	DOCUMENT ID	TECN	COMMENT
$11.019 \pm 0.008$	<b>OUR AVERAGE</b>		
$11.019 \pm 0.005 \pm 0.007$	BESSION 85	CLEO	$e^+e^- \rightarrow \text{hadrons}$
$11.020 \pm 0.030$	LOVELOCK 85	CUSB	$e^+e^- \rightarrow \text{hadrons}$
• • • We do not use the following data for averages, fits, limits, etc. • • •			
$10.996 \pm 0.002$	<sup>1</sup> AUBERT 09E	BABR	$e^+e^- \rightarrow \text{hadrons}$

<sup>1</sup> In a model where a flat non-resonant  $b\bar{b}$ -continuum is incoherently added to a second flat component interfering with two Breit-Wigner resonances. Systematic uncertainties not estimated.

### $\Upsilon(11020)$ WIDTH

VALUE (MeV)	DOCUMENT ID	TECN	COMMENT
$79 \pm 16$	<b>OUR AVERAGE</b>		
$61 \pm 13 \pm 22$	BESSION 85	CLEO	$e^+e^- \rightarrow \text{hadrons}$
$90 \pm 20$	LOVELOCK 85	CUSB	$e^+e^- \rightarrow \text{hadrons}$
• • • We do not use the following data for averages, fits, limits, etc. • • •			
$37 \pm 3$	<sup>2</sup> AUBERT 09E	BABR	$e^+e^- \rightarrow \text{hadrons}$

<sup>2</sup> In a model where a flat non-resonant  $b\bar{b}$ -continuum is incoherently added to a second flat component interfering with two Breit-Wigner resonances. Systematic uncertainties not estimated.

### $\Upsilon(11020)$ DECAY MODES

Mode	Fraction ( $\Gamma_i/\Gamma$ )
$\Gamma_1 e^+e^-$	$(1.6 \pm 0.5) \times 10^{-6}$

### $\Upsilon(11020)$ PARTIAL WIDTHS

$\Gamma(e^+e^-)$	DOCUMENT ID	TECN	COMMENT	$\Gamma_1$
VALUE (keV)				
$0.130 \pm 0.030$	<b>OUR AVERAGE</b>			
$0.095 \pm 0.03 \pm 0.035$	BESSION 85	CLEO	$e^+e^- \rightarrow \text{hadrons}$	
$0.156 \pm 0.040$	LOVELOCK 85	CUSB	$e^+e^- \rightarrow \text{hadrons}$	

### $\Upsilon(11020)$ REFERENCES

AUBERT 09E	PRL 102 012001	B. Aubert <i>et al.</i>	(BABAR Collab.)
BESSION 85	PRL 54 381	D. Besson <i>et al.</i>	(CLEO Collab.)
LOVELOCK 85	PRL 54 377	D.M.J. Lovelock <i>et al.</i>	(CUSB Collab.)

<sup>13</sup> Not independent of DRUTSKOY 10 values for  $\Upsilon(5S) \rightarrow B^{\pm,0} \text{ anything}$ .  
<sup>14</sup> Using measurements or limits from AQUINES 06.  
<sup>15</sup> Assuming isospin conservation.  
<sup>16</sup> Using  $B(D_s^+ \rightarrow \phi\pi^+) = (4.4 \pm 0.6)\%$  from PDG 06.  
<sup>17</sup> Supersedes ARTUSO 05B. Combining inclusive  $\phi$ ,  $D_s$ , and  $B$  measurements. Using  $B(D_s^+ \rightarrow \phi\pi^+) = 4.4 \pm 0.6\%$  from PDG 06.  
<sup>18</sup> Uses a model-dependent estimate  $B(B_s \rightarrow D_s X) = (92 \pm 11)\%$ .  
<sup>19</sup> From a measurement of  $\sigma(e^+e^- \rightarrow B_s^* \bar{B}_s^*) / \sigma(e^+e^- \rightarrow B_s^{(*)} \bar{B}_s^{(*)})$  at  $\sqrt{s} = 10.86$  GeV.  
<sup>20</sup> Assuming that the observed events are solely due to the  $\Upsilon(5S)$  resonance.





<b><i>N</i> BARYONS (<i>S</i> = 0, <i>I</i> = 1/2)</b>	
<i>p</i> . . . . .	1253
<i>n</i> . . . . .	1262
<i>N</i> resonances . . . . .	1271

<b><math>\Delta</math> BARYONS (<i>S</i> = 0, <i>I</i> = 3/2)</b>	
$\Delta$ resonances . . . . .	1305

<b><math>\Lambda</math> BARYONS (<i>S</i> = -1, <i>I</i> = 0)</b>	
$\Lambda$ . . . . .	1327
$\Lambda$ resonances . . . . .	1331

<b><math>\Sigma</math> BARYONS (<i>S</i> = -1, <i>I</i> = 1)</b>	
$\Sigma^+$ . . . . .	1343
$\Sigma^0$ . . . . .	1345
$\Sigma^-$ . . . . .	1346
$\Sigma$ resonances . . . . .	1348

<b><math>\Xi</math> BARYONS (<i>S</i> = -2, <i>I</i> = 1/2)</b>	
$\Xi^0$ . . . . .	1367
$\Xi^-$ . . . . .	1369
$\Xi$ resonances . . . . .	1372

<b><math>\Omega</math> BARYONS (<i>S</i> = -3, <i>I</i> = 0)</b>	
$\Omega^-$ . . . . .	1380
$\Omega$ resonances . . . . .	1381

<b>CHARMED BARYONS (<i>C</i> = +1)</b>	
$\Lambda_c^+$ . . . . .	1385
$\Lambda_c(2595)^+$ . . . . .	1391
$\Lambda_c(2625)^+$ . . . . .	1392
$\Lambda_c(2765)^+$ . . . . .	1393
$\Lambda_c(2880)^+$ . . . . .	1393
$\Lambda_c(2940)^+$ . . . . .	1393
$\Sigma_c(2455)$ . . . . .	1394
$\Sigma_c(2520)$ . . . . .	1395
$\Sigma_c(2800)$ . . . . .	1396
$\Xi_c^+$ . . . . .	1396
$\Xi_c^0$ . . . . .	1398
$\Xi_c^{\prime+}$ . . . . .	1399
$\Xi_c^{\prime0}$ . . . . .	1399
$\Xi_c(2645)$ . . . . .	1399
$\Xi_c(2790)$ . . . . .	1400
$\Xi_c(2815)$ . . . . .	1400
$\Xi_c(2930)$ . . . . .	1400
$\Xi_c(2980)$ . . . . .	1400
$\Xi_c(3055)$ . . . . .	1401
$\Xi_c(3080)$ . . . . .	1401
$\Xi_c(3123)$ . . . . .	1402
$\Omega_c^0$ . . . . .	1402
$\Omega_c(2770)^0$ . . . . .	1403

<b>DOUBLY-CHARMED BARYONS (<i>C</i> = +2)</b>	
$\Xi_{cc}^+$ . . . . .	1404

<b>BOTTOM (BEAUTY) BARYONS (<i>B</i> = -1)</b>	
$\Lambda_b^0$ . . . . .	1405
$\Sigma_b$ . . . . .	1407
$\Sigma_b^*$ . . . . .	1408
$\Xi_b^0, \Xi_b^-$ . . . . .	1408
$\Omega_b^-$ . . . . .	1409
<i>b</i> -baryon ADMIXTURE ( $\Lambda_b, \Xi_b, \Sigma_b, \Omega_b$ ) . . . . .	1409

**Notes in the Baryon Listings**

Baryon Decay Parameters . . . . .	1264
<i>N</i> and $\Delta$ Resonances (rev.) . . . . .	1268
Baryon Magnetic Moments . . . . .	1327
$\Lambda$ and $\Sigma$ Resonances . . . . .	1330
The $\Sigma(1670)$ Region . . . . .	1353
Radiative Hyperon Decays . . . . .	1368
$\Xi$ Resonances . . . . .	1372
Charmed Baryons (rev.) . . . . .	1383
$\Lambda_c^+$ Branching Fractions . . . . .	1386



**N BARYONS**  
**(S = 0, I = 1/2)**  
*p, N<sup>+</sup> = uud; n, N<sup>0</sup> = udd*

**p**  $I(J^P) = \frac{1}{2}(\frac{1}{2}^+)$  Status: \*\*\*\*

**p MASS (atomic mass units u)**

The mass is known much more precisely in u (atomic mass units) than in MeV. See the next data block.

VALUE (u)	DOCUMENT ID	TECN	COMMENT
<b>1.007276466812 ± 0.00000000090</b>	MOHR	12	RVUE 2010 CODATA value
• • • We do not use the following data for averages, fits, limits, etc. • • •			
1.00727646677 ± 0.00000000010	MOHR	08	RVUE 2006 CODATA value
1.00727646688 ± 0.00000000013	MOHR	05	RVUE 2002 CODATA value
1.00727646688 ± 0.00000000013	MOHR	99	RVUE 1998 CODATA value
1.007276470 ± 0.000000012	COHEN	87	RVUE 1986 CODATA value

**p MASS (MeV)**

The mass is known much more precisely in u (atomic mass units) than in MeV. The conversion from u to MeV, 1 u = 931.494 061(21) MeV/c<sup>2</sup> (MOHR 12, the 2010 CODATA value), involves the relatively poorly known electronic charge.

VALUE (MeV)	DOCUMENT ID	TECN	COMMENT
<b>938.272046 ± 0.000021</b>	MOHR	12	RVUE 2010 CODATA value
• • • We do not use the following data for averages, fits, limits, etc. • • •			
938.272013 ± 0.000023	MOHR	08	RVUE 2006 CODATA value
938.272029 ± 0.000080	MOHR	05	RVUE 2002 CODATA value
938.271998 ± 0.000038	MOHR	99	RVUE 1998 CODATA value
938.27231 ± 0.00028	COHEN	87	RVUE 1986 CODATA value
938.2796 ± 0.0027	COHEN	73	RVUE 1973 CODATA value

**|m<sub>p</sub> - m<sub>p̄</sub>| / m<sub>p</sub>**

A test of CPT invariance. Note that the comparison of the p̄ and p charge-to-mass ratio, given in the next data block, is much better determined.

VALUE	CL%	DOCUMENT ID	TECN	COMMENT
<b>&lt; 2 × 10<sup>-9</sup></b>	90	<sup>1</sup> HORI	06	SPEC p̄e <sup>-</sup> He atom
• • • We do not use the following data for averages, fits, limits, etc. • • •				
< 1.0 × 10 <sup>-8</sup>	90	<sup>1</sup> HORI	03	SPEC p̄e <sup>-</sup> <sup>4</sup> He, p̄e <sup>-</sup> <sup>3</sup> He
< 6 × 10 <sup>-8</sup>	90	<sup>1</sup> HORI	01	SPEC p̄e <sup>-</sup> He atom
< 5 × 10 <sup>-7</sup>		<sup>2</sup> TORII	99	SPEC p̄e <sup>-</sup> He atom

<sup>1</sup>HORI 01, HORI 03, and HORI 06 use the more-precisely-known constraint on the p̄ charge-to-mass ratio of GABRIELSE 99 (see below) to get their results. Their results are not independent of the HORI 01, HORI 03, and HORI 06 values for |q<sub>p</sub> + q<sub>p̄</sub>|/e, below.  
<sup>2</sup>TORII 99 uses the more-precisely-known constraint on the p̄ charge-to-mass ratio of GABRIELSE 95 (see below) to get this result. This is not independent of the TORII 99 value for |q<sub>p</sub> + q<sub>p̄</sub>|/e, below.

**p̄/p CHARGE-TO-MASS RATIO, |(q<sub>p̄</sub> - q<sub>p</sub>)/m<sub>p̄</sub>| / (q<sub>p</sub>/m<sub>p</sub>)**

A test of CPT invariance. Listed here are measurements involving the inertial masses. For a discussion of what may be inferred about the ratio of p̄ and p gravitational masses, see ERICSON 90; they obtain an upper bound of 10<sup>-6</sup>-10<sup>-7</sup> for violation of the equivalence principle for p̄'s.

VALUE	DOCUMENT ID	TECN	COMMENT
<b>0.99999999991 ± 0.0000000009</b>	GABRIELSE	99	TRAP Penning trap
• • • We do not use the following data for averages, fits, limits, etc. • • •			
1.0000000015 ± 0.0000000011	<sup>3</sup> GABRIELSE	95	TRAP Penning trap
1.000000023 ± 0.000000042	<sup>4</sup> GABRIELSE	90	TRAP Penning trap

<sup>3</sup>Equation (2) of GABRIELSE 95 should read M(p̄)/M(p) = 0.999 999 9985 (11) (G. Gabrielse, private communication).  
<sup>4</sup>GABRIELSE 90 also measures m<sub>p̄</sub>/m<sub>e</sub> = 1836.152660 ± 0.000083 and m<sub>p</sub>/m<sub>e</sub> = 1836.152680 ± 0.000088. Both are completely consistent with the 1986 CODATA (COHEN 87) value for m<sub>p</sub>/m<sub>e</sub> = 1836.152701 ± 0.000037.

**(|q<sub>p̄</sub> - q<sub>p</sub>)/m<sub>p̄</sub>| / (q<sub>p</sub>/m<sub>p</sub>)**

A test of CPT invariance. Taken from the p̄/p charge-to-mass ratio, above.

VALUE	DOCUMENT ID
<b>(-9 ± 9) × 10<sup>-11</sup> OUR EVALUATION</b>	

**|q<sub>p</sub> + q<sub>p̄</sub>|/e**

A test of CPT invariance. Note that the comparison of the p̄ and p charge-to-mass ratios given above is much better determined. See also a similar test involving the electron.

VALUE	CL%	DOCUMENT ID	TECN	COMMENT
<b>&lt; 2 × 10<sup>-9</sup></b>	90	<sup>5</sup> HORI	06	SPEC p̄e <sup>-</sup> He atom
• • • We do not use the following data for averages, fits, limits, etc. • • •				
< 1.0 × 10 <sup>-8</sup>	90	<sup>5</sup> HORI	03	SPEC p̄e <sup>-</sup> <sup>4</sup> He, p̄e <sup>-</sup> <sup>3</sup> He
< 6 × 10 <sup>-8</sup>	90	<sup>5</sup> HORI	01	SPEC p̄e <sup>-</sup> He atom
< 5 × 10 <sup>-7</sup>		<sup>6</sup> TORII	99	SPEC p̄e <sup>-</sup> He atom
< 2 × 10 <sup>-5</sup>		<sup>7</sup> HUGHES	92	RVUE

<sup>5</sup>HORI 01, HORI 03, and HORI 06 use the more-precisely-known constraint on the p̄ charge-to-mass ratio of GABRIELSE 99 (see above) to get their results. Their results are not independent of the HORI 01, HORI 03, and HORI 06 values for |m<sub>p</sub> - m<sub>p̄</sub>|/m<sub>p</sub>, above.  
<sup>6</sup>TORII 99 uses the more-precisely-known constraint on the p̄ charge-to-mass ratio of GABRIELSE 95 (see above) to get this result. This is not independent of the TORII 99 value for |m<sub>p</sub> - m<sub>p̄</sub>|/m<sub>p</sub>, above.  
<sup>7</sup>HUGHES 92 uses recent measurements of Rydberg-energy and cyclotron-frequency ratios.

**|q<sub>p</sub> + q<sub>e</sub>|/e**

See BRESSI 11 for a summary of experiments on the neutrality of matter. See also "n CHARGE" in the neutron Listings.

VALUE	DOCUMENT ID	COMMENT
<b>&lt; 1 × 10<sup>-21</sup></b>	<sup>8</sup> BRESSI	11 Neutrality of SF <sub>6</sub>
• • • We do not use the following data for averages, fits, limits, etc. • • •		
< 3.2 × 10 <sup>-20</sup>	<sup>9</sup> SENGUPTA	00 binary pulsar
< 0.8 × 10 <sup>-21</sup>	MARINELLI	84 Magnetic levitation
< 1.0 × 10 <sup>-21</sup>	<sup>8</sup> DYLLA	73 Neutrality of SF <sub>6</sub>

<sup>8</sup>BRESSI 11 uses the method of DYLLA 73 but finds serious errors in that experiment that greatly reduce its accuracy. The BRESSI 11 limit assumes that n → p e<sup>-</sup> ν<sub>e</sub> conserves charge. Thus the limit applies equally to the charge of the neutron.  
<sup>9</sup>SENGUPTA 00 uses the difference between the observed rate of rotational energy loss by the binary pulsar PSR B1913+16 and the rate predicted by general relativity to set this limit. See the paper for assumptions.

**p MAGNETIC MOMENT**

See the "Note on Baryon Magnetic Moments" in the A Listings.

VALUE (μ <sub>N</sub> )	DOCUMENT ID	TECN	COMMENT
<b>2.792847356 ± 0.000000023</b>	MOHR	12	RVUE 2010 CODATA value
• • • We do not use the following data for averages, fits, limits, etc. • • •			
2.792847356 ± 0.000000023	MOHR	08	RVUE 2006 CODATA value
2.792847351 ± 0.000000028	MOHR	05	RVUE 2002 CODATA value
2.792847337 ± 0.000000029	MOHR	99	RVUE 1998 CODATA value
2.792847386 ± 0.000000063	COHEN	87	RVUE 1986 CODATA value
2.7928456 ± 0.0000011	COHEN	73	RVUE 1973 CODATA value

**p̄ MAGNETIC MOMENT**

A few early results have been omitted.

VALUE (μ <sub>N</sub> )	DOCUMENT ID	TECN	COMMENT
<b>-2.793 ± 0.006 OUR AVERAGE</b>			
-2.7862 ± 0.0083	PASK	09	CNTR p̄ He <sup>+</sup> hyperfine structure
-2.8005 ± 0.0090	KREISSL	88	CNTR p̄ <sup>208</sup> Pb 11 → 10 X-ray
-2.817 ± 0.048	ROBERTS	78	CNTR
-2.791 ± 0.021	HU	75	CNTR Exotic atoms

**(μ<sub>p</sub> + μ<sub>p̄</sub>) / μ<sub>p</sub>**

A test of CPT invariance. Calculated from the p and p̄ magnetic moments, above.

VALUE	DOCUMENT ID
<b>(-0.1 ± 2.1) × 10<sup>-3</sup> OUR EVALUATION</b>	

**p ELECTRIC DIPOLE MOMENT**

A nonzero value is forbidden by both T invariance and P invariance.

VALUE (10 <sup>-23</sup> ecm)	EVTS	DOCUMENT ID	TECN	COMMENT
<b>&lt; 0.54</b>		<sup>10</sup> DMITRIEV	03	Uses <sup>199</sup> Hg atom EDM
• • • We do not use the following data for averages, fits, limits, etc. • • •				
- 3.7 ± 6.3		CHO	89	NMR TI F molecules
< 400		DZUBA	85	THEO Uses <sup>129</sup> Xe moment
130 ± 200		<sup>11</sup> WILKENING	84	
900 ± 1400		<sup>12</sup> WILKENING	84	
700 ± 900	1G	HARRISON	69	MBR Molecular beam

## Baryon Particle Listings

 $\rho$ 

<sup>10</sup>DMITRIEV 03 calculates this limit from the limit on the electric dipole moment of the <sup>199</sup>Hg atom.

<sup>11</sup>This WILKENING 84 value includes a finite-size effect and a magnetic effect.

<sup>12</sup>This WILKENING 84 value is more cautious than the other and excludes the finite-size effect, which relies on uncertain nuclear integrals.

 $\rho$  ELECTRIC POLARIZABILITY  $\alpha_p$ 

For a very complete review of the "polarizability of the nucleon and Compton scattering," see SCHUMACHER 05. His recommended values for the proton are  $\alpha_p = (12.0 \pm 0.6) \times 10^{-4} \text{ fm}^3$  and  $\beta_p = (1.9 \pm 0.6) \times 10^{-4} \text{ fm}^3$ , almost exactly our averages.

VALUE ( $10^{-4} \text{ fm}^3$ )	DOCUMENT ID	TECN	COMMENT
<b>12.0 ± 0.6 OUR AVERAGE</b>			
12.1 ± 1.1 ± 0.5	<sup>13</sup> BEANE 03	03	EFT + $\gamma p$
11.82 ± 0.98 ± 0.52 -0.98	<sup>14</sup> BLANPIED 01	01	LEGS $p(\vec{\gamma}, \gamma), p(\vec{\gamma}, \pi^0), p(\vec{\gamma}, \pi^+)$
11.9 ± 0.5 ± 1.3	<sup>15</sup> OLMOSDEL... 01	CNTR	$\gamma p$ Compton scattering
12.1 ± 0.8 ± 0.5	<sup>16</sup> MACGIBBON 95	RVUE	global average
••• We do not use the following data for averages, fits, limits, etc. •••			
11.7 ± 0.8 ± 0.7	<sup>17</sup> BARANOV 01	RVUE	Global average
12.5 ± 0.6 ± 0.9	MACGIBBON 95	CNTR	$\gamma p$ Compton scattering
9.8 ± 0.4 ± 1.1	HALLIN 93	CNTR	$\gamma p$ Compton scattering
10.62 ± 1.25 ± 1.07 -1.19 -1.03	ZIEGER 92	CNTR	$\gamma p$ Compton scattering
10.9 ± 2.2 ± 1.3	<sup>18</sup> FEDERSPIEL 91	CNTR	$\gamma p$ Compton scattering
<sup>13</sup> BEANE 03 uses effective field theory and low-energy $\gamma p$ and $\gamma d$ Compton-scattering data. It also gets for the isoscalar polarizabilities (see the erratum) $\alpha_N = (13.0 \pm 1.9 \pm 3.9) \times 10^{-4} \text{ fm}^3$ and $\beta_N = (-1.8 \pm 1.9 \pm 2.1) \times 10^{-4} \text{ fm}^3$ .			
<sup>14</sup> BLANPIED 01 gives $\alpha_p + \beta_p$ and $\alpha_p - \beta_p$ . The separate $\alpha_p$ and $\beta_p$ are provided to us by A. Sandorfi. The first error above is statistics plus systematics; the second is from the model.			
<sup>15</sup> This OLMOSDELEON 01 result uses the TAPS data alone, and does not use the (re-evaluated) sum-rule constraint that $\alpha + \beta = (13.8 \pm 0.4) \times 10^{-4} \text{ fm}^3$ . See the paper for a discussion.			
<sup>16</sup> MACGIBBON 95 combine the results of ZIEGER 92, FEDERSPIEL 91, and their own experiment to get a "global average" in which model errors and systematic errors are treated in a consistent way. See MACGIBBON 95 for a discussion.			
<sup>17</sup> BARANOV 01 combines the results of 10 experiments from 1958 through 1995 to get a global average that takes into account both systematic and model errors and does not use the theoretical constraint on the sum $\alpha_p + \beta_p$ .			
<sup>18</sup> FEDERSPIEL 91 obtains for the (static) electric polarizability $\alpha_p$ , defined in terms of the induced electric dipole moment by $\mathbf{D} = 4\pi\epsilon_0\alpha_p\mathbf{E}$ , the value $(7.0 \pm 2.2 \pm 1.3) \times 10^{-4} \text{ fm}^3$ .			

 $\rho$  MAGNETIC POLARIZABILITY  $\beta_p$ 

The electric and magnetic polarizabilities are subject to a dispersion sum-rule constraint  $\bar{\alpha} + \bar{\beta} = (14.2 \pm 0.5) \times 10^{-4} \text{ fm}^3$ . Errors here are anticorrelated with those on  $\bar{\alpha}_p$  due to this constraint.

VALUE ( $10^{-4} \text{ fm}^3$ )	DOCUMENT ID	TECN	COMMENT
<b>1.9 ± 0.5 OUR AVERAGE</b>			
3.4 ± 1.1 ± 0.1	<sup>19</sup> BEANE 03	03	EFT + $\gamma p$
1.43 ± 0.98 ± 0.52 -0.98	<sup>20</sup> BLANPIED 01	01	LEGS $p(\vec{\gamma}, \gamma), p(\vec{\gamma}, \pi^0), p(\vec{\gamma}, \pi^+)$
1.2 ± 0.7 ± 0.5	<sup>21</sup> OLMOSDEL... 01	CNTR	$\gamma p$ Compton scattering
2.1 ± 0.8 ± 0.5	<sup>22</sup> MACGIBBON 95	RVUE	global average
••• We do not use the following data for averages, fits, limits, etc. •••			
2.3 ± 0.9 ± 0.7	<sup>23</sup> BARANOV 01	RVUE	Global average
1.7 ± 0.6 ± 0.9	MACGIBBON 95	CNTR	$\gamma p$ Compton scattering
4.4 ± 0.4 ± 1.1	HALLIN 93	CNTR	$\gamma p$ Compton scattering
3.58 ± 1.19 ± 1.03 -1.25 -1.07	ZIEGER 92	CNTR	$\gamma p$ Compton scattering
3.3 ± 2.2 ± 1.3	FEDERSPIEL 91	CNTR	$\gamma p$ Compton scattering
<sup>19</sup> BEANE 03 uses effective field theory and low-energy $\gamma p$ and $\gamma d$ Compton-scattering data. It also gets for the isoscalar polarizabilities (see the erratum) $\alpha_N = (13.0 \pm 1.9 \pm 3.9) \times 10^{-4} \text{ fm}^3$ and $\beta_N = (-1.8 \pm 1.9 \pm 2.1) \times 10^{-4} \text{ fm}^3$ .			
<sup>20</sup> BLANPIED 01 gives $\alpha_p + \beta_p$ and $\alpha_p - \beta_p$ . The separate $\alpha_p$ and $\beta_p$ are provided to us by A. Sandorfi. The first error above is statistics plus systematics; the second is from the model.			
<sup>21</sup> This OLMOSDELEON 01 result uses the TAPS data alone, and does not use the (re-evaluated) sum-rule constraint that $\alpha + \beta = (13.8 \pm 0.4) \times 10^{-4} \text{ fm}^3$ . See the paper for a discussion.			
<sup>22</sup> MACGIBBON 95 combine the results of ZIEGER 92, FEDERSPIEL 91, and their own experiment to get a "global average" in which model errors and systematic errors are treated in a consistent way. See MACGIBBON 95 for a discussion.			
<sup>23</sup> BARANOV 01 combines the results of 10 experiments from 1958 through 1995 to get a global average that takes into account both systematic and model errors and does not use the theoretical constraint on the sum $\alpha_p + \beta_p$ .			

 $\rho$  CHARGE RADIUS

This is the rms electric charge radius,  $\sqrt{\langle r_E^2 \rangle}$ .

Most measurements of the radius of the proton involve electron-proton interactions, and most of the more recent values agree with one another. The most precise of these is  $r_p = 0.879(8) \text{ fm}$  (BERNAUER 10). The

CODATA 10 value (MOHR 12), obtained from the electronic results, is  $0.8775(51)$ . However, a measurement using muonic hydrogen finds  $r_p = 0.84184(67) \text{ fm}$  (POHL 10), which is eight times more precise and seven standard deviations (using the CODATA 10 error) from the electronic results.

Since POHL 10, there has been a lot of discussion about the disagreement, especially concerning the modeling of muonic hydrogen. Here is an incomplete list of papers: DERUJULA 10, CLOET 11, DISTLER 11, DERUJULA 11, ARRINGTON 11, BERNAUER 11, and HILL 11.

Until the difference between the  $ep$  and  $\mu p$  values is understood, it does not make much sense to average all the values together. For the present, we stick with the less precise (and provisionally suspect) CODATA 2010 value (MOHR 12). It is up to workers in this field to solve this puzzle.

VALUE (fm)	DOCUMENT ID	TECN	COMMENT
<b>0.8775 ± 0.0051</b>	MOHR 12	RVUE	2010 CODATA value
••• We do not use the following data for averages, fits, limits, etc. •••			
0.879 ± 0.005 ± 0.006	BERNAUER 10	SPEC	$ep \rightarrow ep$ form factor
0.912 ± 0.009 ± 0.007	BORISYUK 10		reanalyzes old $ep$ data
0.871 ± 0.009 ± 0.003	HILL 10		z-expansion reanalysis
0.84184 ± 0.00036 ± 0.00056	POHL 10		$\mu p$ -atom Lamb shift
0.8768 ± 0.0069	MOHR 08	RVUE	2006 CODATA value
0.844 ± 0.008 -0.004	BELUSHKIN 07		Dispersion analysis
0.897 ± 0.018	BLUNDEN 05		SICK 03 + $2\gamma$ correction
0.8750 ± 0.0068	MOHR 05	RVUE	2002 CODATA value
0.895 ± 0.010 ± 0.013	SICK 03		$ep \rightarrow ep$ reanalysis
0.830 ± 0.040 ± 0.040	<sup>24</sup> ESCHRICH 01		$ep \rightarrow ep$
0.883 ± 0.014	MELNIKOV 00		1S Lamb Shift in H
0.880 ± 0.015	ROSENFELDR.00		$ep + \text{Coul. corrections}$
0.847 ± 0.008	MERGELL 96		$ep + \text{disp. relations}$
0.877 ± 0.024	WONG 94		reanalysis of Mainz $ep$ data
0.865 ± 0.020	MCCORD 91		$ep \rightarrow ep$
0.862 ± 0.012	SIMON 80		$ep \rightarrow ep$
0.880 ± 0.030	BORKOWSKI 74		$ep \rightarrow ep$
0.810 ± 0.020	AKIMOV 72		$ep \rightarrow ep$
0.800 ± 0.025	FREREJACQ... 66		$ep \rightarrow ep$ ( $\text{CH}_2$ tgt.)
0.805 ± 0.011	HAND 63		$ep \rightarrow ep$

<sup>24</sup>ESCHRICH 01 actually gives  $\langle r^2 \rangle = (0.69 \pm 0.06 \pm 0.06) \text{ fm}^2$ .

 $\rho$  MAGNETIC RADIUS

This is the rms magnetic radius,  $\sqrt{\langle r_M^2 \rangle}$ .

VALUE (fm)	DOCUMENT ID	TECN	COMMENT
<b>0.777 ± 0.013 ± 0.010</b>	BERNAUER 10	SPEC	$ep \rightarrow ep$ form factor
••• We do not use the following data for averages, fits, limits, etc. •••			
0.876 ± 0.010 ± 0.016	BORISYUK 10		reanalyzes old $ep \rightarrow ep$ data
0.854 ± 0.005	BELUSHKIN 07		Dispersion analysis

 $\rho$  MEAN LIFE

A test of baryon conservation. See the " $\rho$  Partial Mean Lives" section below for limits for identified final states. The limits here are to "anything" or are for "disappearance" modes of a bound proton ( $p$ ) or ( $n$ ). See also the  $3\nu$  modes in the "Partial Mean Lives" section. Table 1 of BACK 03 is a nice summary.

LIMIT (years)	PARTICLE	CL%	DOCUMENT ID	TECN	COMMENT
<b>&gt;5.8 × 10<sup>29</sup></b>	$n$	90	<sup>25</sup> ARAKI	06	KLND $n \rightarrow$ invisible
<b>&gt;2.1 × 10<sup>29</sup></b>	$p$	90	<sup>26</sup> AHMED	04	SNO $p \rightarrow$ invisible
••• We do not use the following data for averages, fits, limits, etc. •••					
>1.9 × 10 <sup>29</sup>	$n$	90	<sup>26</sup> AHMED	04	SNO $n \rightarrow$ invisible
>1.8 × 10 <sup>25</sup>	$n$	90	<sup>27</sup> BACK	03	BORX
>1.1 × 10 <sup>26</sup>	$p$	90	<sup>27</sup> BACK	03	BORX
>3.5 × 10 <sup>28</sup>	$p$	90	<sup>28</sup> ZDESENKO	03	$p \rightarrow$ invisible
>1 × 10 <sup>28</sup>	$p$	90	<sup>29</sup> AHMAD	02	SNO $p \rightarrow$ invisible
>4 × 10 <sup>23</sup>	$p$	95	TRETYAK	01	$d \rightarrow n + ?$
>1.9 × 10 <sup>24</sup>	$p$	90	<sup>30</sup> BERNABEI	00B	DAMA
>1.6 × 10 <sup>25</sup>	$p, n$		<sup>31,32</sup> EVANS	77	
>3 × 10 <sup>23</sup>	$p$		<sup>32</sup> DIX	70	CNTR
>3 × 10 <sup>23</sup>	$p, n$		<sup>32,33</sup> FLEROV	58	

<sup>25</sup>ARAKI 06 looks for signs of de-excitation of the residual nucleus after disappearance of a neutron from the  $s$  shell of <sup>12</sup>C.

<sup>26</sup>AHMED 04 looks for the de-excitation of a residual <sup>15</sup>O\* or <sup>15</sup>N\* following the disappearance of a neutron or proton in <sup>16</sup>O.

<sup>27</sup>BACK 03 looks for decays of unstable nuclides left after  $N$  decays of parent <sup>12</sup>C, <sup>13</sup>C, <sup>16</sup>O nuclei. These are "invisible channel" limits.

<sup>28</sup>ZDESENKO 03 gets this limit on proton disappearance in deuterium by analyzing SNO data in AHMAD 02.

<sup>29</sup>AHMAD 02 (see its footnote 7) looks for neutrons left behind after the disappearance of the proton in deuterons.

<sup>30</sup>BERNABEI 00B looks for the decay of a <sup>128</sup><sub>53</sub>I nucleus following the disappearance of a proton in the otherwise-stable <sup>129</sup>Xe nucleus.

<sup>31</sup>EVANS 77 looks for the daughter nuclide <sup>129</sup>Xe from possible <sup>130</sup>Te decays in ancient Te ore samples.

See key on page 457

Baryon Particle Listings

p

<sup>32</sup>This mean-life limit has been obtained from a half-life limit by dividing the latter by  $\ln(2) = 0.693$ .  
<sup>33</sup>FLEROV 58 looks for the spontaneous fission of a <sup>232</sup>Th nucleus after the disappearance of one of its nucleons.

**$\bar{p}$  MEAN LIFE**

Of the two astrophysical limits here, that of GEER 00d involves considerably more refinements in its modeling. The other limits come from direct observations of stored antiprotons. See also "p Partial Mean Lives" after "p Partial Mean Lives," below, for exclusive-mode limits. The best (lifetime/branching fraction) limit there is  $7 \times 10^5$  years, for  $\bar{p} \rightarrow e^- \gamma$ . We advance only the exclusive-mode limits to our Summary Tables.

LIMIT (years)	CL%	EVTs	DOCUMENT ID	TECN	COMMENT
$>8 \times 10^5$	90		<sup>34</sup> GEER	00D	$\bar{p}/p$ ratio, cosmic rays
$>0.28$			GABRIELSE	90	TRAP Penning trap
$>0.08$	90	1	BELL	79	CNTR Storage ring
$>1 \times 10^7$			GOLDEN	79	SPEC $\bar{p}/p$ ratio, cosmic rays
$>3.7 \times 10^{-3}$			BREGMAN	78	CNTR Storage ring

<sup>34</sup>GEER 00D uses agreement between a model of galactic  $\bar{p}$  production and propagation and the observed  $\bar{p}/p$  cosmic-ray spectrum to set this limit.

**p DECAY MODES**

See the "Note on Nucleon Decay" in our 1994 edition (Phys. Rev. **D50**, 1173) for a short review.

The "partial mean life" limits tabulated here are the limits on  $\tau/B_j$ , where  $\tau$  is the total mean life and  $B_j$  is the branching fraction for the mode in question. For  $N$  decays,  $p$  and  $n$  indicate proton and neutron partial lifetimes.

Mode	Partial mean life (10 <sup>30</sup> years)	Confidence level
<b>Antilepton + meson</b>		
$\tau_1 N \rightarrow e^+ \pi$	$> 158 (n), > 8200 (p)$	90%
$\tau_2 N \rightarrow \mu^+ \pi$	$> 100 (n), > 6600 (p)$	90%
$\tau_3 N \rightarrow \nu \pi$	$> 112 (n), > 25 (p)$	90%
$\tau_4 p \rightarrow e^+ \eta$	$> 313$	90%
$\tau_5 p \rightarrow \mu^+ \eta$	$> 126$	90%
$\tau_6 n \rightarrow \nu \eta$	$> 158$	90%
$\tau_7 N \rightarrow e^+ \rho$	$> 217 (n), > 75 (p)$	90%
$\tau_8 N \rightarrow \mu^+ \rho$	$> 228 (n), > 110 (p)$	90%
$\tau_9 N \rightarrow \nu \rho$	$> 19 (n), > 162 (p)$	90%
$\tau_{10} p \rightarrow e^+ \omega$	$> 107$	90%
$\tau_{11} p \rightarrow \mu^+ \omega$	$> 117$	90%
$\tau_{12} n \rightarrow \nu \omega$	$> 108$	90%
$\tau_{13} N \rightarrow e^+ K$	$> 17 (n), > 150 (p)$	90%
$\tau_{14} p \rightarrow e^+ K_S^0$	$> 120$	90%
$\tau_{15} p \rightarrow e^+ K_L^0$	$> 51$	90%
$\tau_{16} N \rightarrow \mu^+ K$	$> 26 (n), > 120 (p)$	90%
$\tau_{17} p \rightarrow \mu^+ K_S^0$	$> 150$	90%
$\tau_{18} p \rightarrow \mu^+ K_L^0$	$> 83$	90%
$\tau_{19} N \rightarrow \nu K$	$> 86 (n), > 670 (p)$	90%
$\tau_{20} n \rightarrow \nu K_S^0$	$> 51$	90%
$\tau_{21} p \rightarrow e^+ K^*(892)^0$	$> 84$	90%
$\tau_{22} N \rightarrow \nu K^*(892)$	$> 78 (n), > 51 (p)$	90%
<b>Antilepton + mesons</b>		
$\tau_{23} p \rightarrow e^+ \pi^+ \pi^-$	$> 82$	90%
$\tau_{24} p \rightarrow e^+ \pi^0 \pi^0$	$> 147$	90%
$\tau_{25} n \rightarrow e^+ \pi^- \pi^0$	$> 52$	90%
$\tau_{26} p \rightarrow \mu^+ \pi^+ \pi^-$	$> 133$	90%
$\tau_{27} p \rightarrow \mu^+ \pi^0 \pi^0$	$> 101$	90%
$\tau_{28} n \rightarrow \mu^+ \pi^- \pi^0$	$> 74$	90%
$\tau_{29} n \rightarrow e^+ K^0 \pi^-$	$> 18$	90%
<b>Lepton + meson</b>		
$\tau_{30} n \rightarrow e^- \pi^+$	$> 65$	90%
$\tau_{31} n \rightarrow \mu^- \pi^+$	$> 49$	90%
$\tau_{32} n \rightarrow e^- \rho^+$	$> 62$	90%
$\tau_{33} n \rightarrow \mu^- \rho^+$	$> 7$	90%
$\tau_{34} n \rightarrow e^- K^+$	$> 32$	90%
$\tau_{35} n \rightarrow \mu^- K^+$	$> 57$	90%

**Lepton + mesons**

$\tau_{36} p \rightarrow e^- \pi^+ \pi^+$	$> 30$	90%
$\tau_{37} n \rightarrow e^- \pi^+ \pi^0$	$> 29$	90%
$\tau_{38} p \rightarrow \mu^- \pi^+ \pi^+$	$> 17$	90%
$\tau_{39} n \rightarrow \mu^- \pi^+ \pi^0$	$> 34$	90%
$\tau_{40} p \rightarrow e^- \pi^+ K^+$	$> 75$	90%
$\tau_{41} p \rightarrow \mu^- \pi^+ K^+$	$> 245$	90%

**Antilepton + photon(s)**

$\tau_{42} p \rightarrow e^+ \gamma$	$> 670$	90%
$\tau_{43} p \rightarrow \mu^+ \gamma$	$> 478$	90%
$\tau_{44} n \rightarrow \nu \gamma$	$> 28$	90%
$\tau_{45} p \rightarrow e^+ \gamma \gamma$	$> 100$	90%
$\tau_{46} n \rightarrow \nu \gamma \gamma$	$> 219$	90%

**Three (or more) leptons**

$\tau_{47} p \rightarrow e^+ e^+ e^-$	$> 793$	90%
$\tau_{48} p \rightarrow e^+ \mu^+ \mu^-$	$> 359$	90%
$\tau_{49} p \rightarrow e^+ \nu \nu$	$> 17$	90%
$\tau_{50} n \rightarrow e^+ e^- \nu$	$> 257$	90%
$\tau_{51} n \rightarrow \mu^+ e^- \nu$	$> 83$	90%
$\tau_{52} n \rightarrow \mu^+ \mu^- \nu$	$> 79$	90%
$\tau_{53} p \rightarrow \mu^+ e^+ e^-$	$> 529$	90%
$\tau_{54} p \rightarrow \mu^+ \mu^+ \mu^-$	$> 675$	90%
$\tau_{55} p \rightarrow \mu^+ \nu \nu$	$> 21$	90%
$\tau_{56} p \rightarrow e^- \mu^+ \mu^+$	$> 6$	90%
$\tau_{57} n \rightarrow 3\nu$	$> 0.0005$	90%
$\tau_{58} n \rightarrow 5\nu$		

**Inclusive modes**

$\tau_{59} N \rightarrow e^+ \text{anything}$	$> 0.6 (n, p)$	90%
$\tau_{60} N \rightarrow \mu^+ \text{anything}$	$> 12 (n, p)$	90%
$\tau_{61} N \rightarrow \nu \text{anything}$		
$\tau_{62} N \rightarrow e^+ \pi^0 \text{anything}$	$> 0.6 (n, p)$	90%
$\tau_{63} N \rightarrow 2 \text{ bodies, } \nu\text{-free}$		

**$\Delta B = 2$  dinucleon modes**

The following are lifetime limits per iron nucleus.

$\tau_{64} pp \rightarrow \pi^+ \pi^+$	$> 0.7$	90%
$\tau_{65} pn \rightarrow \pi^+ \pi^0$	$> 2$	90%
$\tau_{66} nn \rightarrow \pi^+ \pi^-$	$> 0.7$	90%
$\tau_{67} nn \rightarrow \pi^0 \pi^0$	$> 3.4$	90%
$\tau_{68} pp \rightarrow e^+ e^+$	$> 5.8$	90%
$\tau_{69} pp \rightarrow e^+ \mu^+$	$> 3.6$	90%
$\tau_{70} pp \rightarrow \mu^+ \mu^+$	$> 1.7$	90%
$\tau_{71} pn \rightarrow e^+ \bar{\nu}$	$> 2.8$	90%
$\tau_{72} pn \rightarrow \mu^+ \bar{\nu}$	$> 1.6$	90%
$\tau_{73} nn \rightarrow \nu_e \bar{\nu}_e$	$> 0.000049$	90%
$\tau_{74} nn \rightarrow \nu_\mu \bar{\nu}_\mu$		
$\tau_{75} pn \rightarrow \text{invisible}$	$> 2.10 \times 10^{25}$	90%
$\tau_{76} pp \rightarrow \text{invisible}$	$> 0.00005$	90%

**$\bar{p}$  DECAY MODES**

@	Mode	Partial mean life (years)	Confidence level
$\tau_{77}$	$\bar{p} \rightarrow e^- \gamma$	$> 7 \times 10^5$	90%
$\tau_{78}$	$\bar{p} \rightarrow \mu^- \gamma$	$> 5 \times 10^4$	90%
$\tau_{79}$	$\bar{p} \rightarrow e^- \pi^0$	$> 4 \times 10^5$	90%
$\tau_{80}$	$\bar{p} \rightarrow \mu^- \pi^0$	$> 5 \times 10^4$	90%
$\tau_{81}$	$\bar{p} \rightarrow e^- \eta$	$> 2 \times 10^4$	90%
$\tau_{82}$	$\bar{p} \rightarrow \mu^- \eta$	$> 8 \times 10^3$	90%
$\tau_{83}$	$\bar{p} \rightarrow e^- K_S^0$	$> 900$	90%
$\tau_{84}$	$\bar{p} \rightarrow \mu^- K_S^0$	$> 4 \times 10^3$	90%
$\tau_{85}$	$\bar{p} \rightarrow e^- K_L^0$	$> 9 \times 10^3$	90%
$\tau_{86}$	$\bar{p} \rightarrow \mu^- K_L^0$	$> 7 \times 10^3$	90%
$\tau_{87}$	$\bar{p} \rightarrow e^- \gamma \gamma$	$> 2 \times 10^4$	90%
$\tau_{88}$	$\bar{p} \rightarrow \mu^- \gamma \gamma$	$> 2 \times 10^4$	90%
$\tau_{89}$	$\bar{p} \rightarrow e^- \rho$		
$\tau_{90}$	$\bar{p} \rightarrow e^- \omega$	$> 200$	90%
$\tau_{91}$	$\bar{p} \rightarrow e^- K^*(892)^0$		

# Baryon Particle Listings

p

### p PARTIAL MEAN LIVES

The "partial mean life" limits tabulated here are the limits on  $\tau/B_j$ , where  $\tau$  is the total mean life for the proton and  $B_j$  is the branching fraction for the mode in question.

Decaying particle:  $p$  = proton,  $n$  = bound neutron. The same event may appear under more than one partial decay mode. Background estimates may be accurate to a factor of two.

### Antilepton + meson

#### $\tau(N \rightarrow e^+ \pi)$

$\tau_1$

LIMIT (10 <sup>30</sup> years)	PARTICLE	CL%	EVTs	BKGD EST	DOCUMENT ID	TECN
>8200	p	90	0	0.3	NISHINO 09	SKAM
>158	n	90	3	5	MCGREW 99	IMB3
• • • We do not use the following data for averages, fits, limits, etc. • • •						
>540	p	90	0	0.2	MCGREW 99	IMB3
>1600	p	90	0	0.1	SHIOZAWA 98	SKAM
>70	p	90	0	0.5	BERGER 91	FREJ
>70	n	90	0	$\leq 0.1$	BERGER 91	FREJ
>550	p	90	0	0.7	<sup>35</sup> BECKER-SZ... 90	IMB3
>260	p	90	0	<0.04	HIRATA 89c	KAMI
>130	n	90	0	<0.2	HIRATA 89c	KAMI
>310	p	90	0	0.6	SEIDEL 88	IMB
>100	n	90	0	1.6	SEIDEL 88	IMB
>1.3	n	90	0		BARTELT 87	SOUD
>1.3	p	90	0		BARTELT 87	SOUD
>250	p	90	0	0.3	HAINES 86	IMB
>31	n	90	8	9	HAINES 86	IMB
>64	p	90	0	<0.4	ARISAKA 85	KAMI
>26	n	90	0	<0.7	ARISAKA 85	KAMI
>82	p (free)	90	0	0.2	BLEWITT 85	IMB
>250	p	90	0	0.2	BLEWITT 85	IMB
>25	n	90	4	4	PARK 85	IMB
>15	p, n	90	0		BATTISTONI 84	NUSX
>0.5	p	90	1	0.3	<sup>36</sup> BARTELT 83	SOUD
>0.5	n	90	1	0.3	<sup>36</sup> BARTELT 83	SOUD
>5.8	p	90	2		<sup>37</sup> KRISHNA... 82	KOLR
>5.8	n	90	2		<sup>37</sup> KRISHNA... 82	KOLR
>0.1	n	90			<sup>38</sup> GURR 67	CNTR

<sup>35</sup> This BECKER-SZENDY 90 result includes data from SEIDEL 88.

<sup>36</sup> Limit based on zero events.

<sup>37</sup> We have calculated 90% CL limit from 1 confined event.

<sup>38</sup> We have converted half-life to 90% CL mean life.

#### $\tau(N \rightarrow \mu^+ \pi)$

$\tau_2$

LIMIT (10 <sup>30</sup> years)	PARTICLE	CL%	EVTs	BKGD EST	DOCUMENT ID	TECN
>6600	p	90	0	0.3	NISHINO 09	SKAM
>100	n	90	0	<0.2	HIRATA 89c	KAMI
• • • We do not use the following data for averages, fits, limits, etc. • • •						
>473	p	90	0	0.6	MCGREW 99	IMB3
>90	n	90	1	1.9	MCGREW 99	IMB3
>81	p	90	0	0.2	BERGER 91	FREJ
>35	n	90	1	1.0	BERGER 91	FREJ
>230	p	90	0	<0.07	HIRATA 89c	KAMI
>270	p	90	0	0.5	SEIDEL 88	IMB
>63	n	90	0	0.5	SEIDEL 88	IMB
>76	p	90	2	1	HAINES 86	IMB
>23	n	90	8	7	HAINES 86	IMB
>46	p	90	0	<0.7	ARISAKA 85	KAMI
>20	n	90	0	<0.4	ARISAKA 85	KAMI
>59	p (free)	90	0	0.2	BLEWITT 85	IMB
>100	p	90	1	0.4	BLEWITT 85	IMB
>38	n	90	1	4	PARK 85	IMB
>10	p, n	90	0		BATTISTONI 84	NUSX
>1.3	p, n	90	0		ALEKSEEV 81	BAKS

#### $\tau(N \rightarrow \nu \pi)$

$\tau_3$

LIMIT (10 <sup>30</sup> years)	PARTICLE	CL%	EVTs	BKGD EST	DOCUMENT ID	TECN
>16	p	90	6	6.7	WALL 00b	SOU2
>112	n	90	6	6.6	MCGREW 99	IMB3
• • • We do not use the following data for averages, fits, limits, etc. • • •						
>39	n	90	4	3.8	WALL 00b	SOU2
>10	p	90	15	20.3	MCGREW 99	IMB3
>13	n	90	1	1.2	BERGER 89	FREJ
>10	p	90	11	14	BERGER 89	FREJ
>25	p	90	32	32.8	<sup>39</sup> HIRATA 89c	KAMI
>100	n	90	1	3	HIRATA 89c	KAMI
>6	n	90	73	60	HAINES 86	IMB
>2	p	90	16	13	KAJITA 86	KAMI

>40	n	90	0	1	KAJITA 86	KAMI
>7	n	90	28	19	PARK 85	IMB
>7	n	90	0		BATTISTONI 84	NUSX
>2	p	90	$\leq 3$		BATTISTONI 84	NUSX
>5.8	p	90	1		<sup>40</sup> KRISHNA... 82	KOLR
>0.3	p	90	2		<sup>41</sup> CHERRY 81	HOME
>0.1	p	90			<sup>42</sup> GURR 67	CNTR

<sup>39</sup> In estimating the background, this HIRATA 89c limit (as opposed to the later limits of WALL 00b and MCGREW 99) does not take into account present understanding that the flux of  $\nu_\mu$  originating in the upper atmosphere is depleted. Doing so would reduce the background and thus also would reduce the limit here.

<sup>40</sup> We have calculated 90% CL limit from 1 confined event.

<sup>41</sup> We have converted 2 possible events to 90% CL limit.

<sup>42</sup> We have converted half-life to 90% CL mean life.

#### $\tau(p \rightarrow e^+ \eta)$

$\tau_4$

LIMIT (10 <sup>30</sup> years)	PARTICLE	CL%	EVTs	BKGD EST	DOCUMENT ID	TECN
>313	p	90	0	0.2	MCGREW 99	IMB3
• • • We do not use the following data for averages, fits, limits, etc. • • •						
>81	p	90	1	1.7	WALL 00b	SOU2
>44	p	90	0	0.1	BERGER 91	FREJ
>140	p	90	0	<0.04	HIRATA 89c	KAMI
>100	p	90	0	0.6	SEIDEL 88	IMB
>200	p	90	5	3.3	HAINES 86	IMB
>64	p	90	0	<0.8	ARISAKA 85	KAMI
>64	p (free)	90	5	6.5	BLEWITT 85	IMB
>200	p	90	5	4.7	BLEWITT 85	IMB
>1.2	p	90	2		<sup>43</sup> CHERRY 81	HOME

<sup>43</sup> We have converted 2 possible events to 90% CL limit.

#### $\tau(p \rightarrow \mu^+ \eta)$

$\tau_5$

LIMIT (10 <sup>30</sup> years)	PARTICLE	CL%	EVTs	BKGD EST	DOCUMENT ID	TECN
>126	p	90	3	2.8	MCGREW 99	IMB3
• • • We do not use the following data for averages, fits, limits, etc. • • •						
>89	p	90	0	1.6	WALL 00b	SOU2
>26	p	90	1	0.8	BERGER 91	FREJ
>69	p	90	1	<0.08	HIRATA 89c	KAMI
>1.3	p	90	0	0.7	PHILLIPS 89	HPW
>34	p	90	1	1.5	SEIDEL 88	IMB
>46	p	90	7	6	HAINES 86	IMB
>26	p	90	1	<0.8	ARISAKA 85	KAMI
>17	p (free)	90	6	6	BLEWITT 85	IMB
>46	p	90	7	8	BLEWITT 85	IMB

#### $\tau(n \rightarrow \nu \eta)$

$\tau_6$

LIMIT (10 <sup>30</sup> years)	PARTICLE	CL%	EVTs	BKGD EST	DOCUMENT ID	TECN
>158	n	90	0	1.2	MCGREW 99	IMB3
• • • We do not use the following data for averages, fits, limits, etc. • • •						
>71	n	90	2	3.7	WALL 00b	SOU2
>29	n	90	0	0.9	BERGER 89	FREJ
>54	n	90	2	0.9	HIRATA 89c	KAMI
>16	n	90	3	2.1	SEIDEL 88	IMB
>25	n	90	7	6	HAINES 86	IMB
>30	n	90	0	0.4	KAJITA 86	KAMI
>18	n	90	4	3	PARK 85	IMB
>0.6	n	90	2		<sup>44</sup> CHERRY 81	HOME

<sup>44</sup> We have converted 2 possible events to 90% CL limit.

#### $\tau(N \rightarrow e^+ \rho)$

$\tau_7$

LIMIT (10 <sup>30</sup> years)	PARTICLE	CL%	EVTs	BKGD EST	DOCUMENT ID	TECN
>217	n	90	4	4.8	MCGREW 99	IMB3
>75	p	90	2	2.7	HIRATA 89c	KAMI
• • • We do not use the following data for averages, fits, limits, etc. • • •						
>29	p	90	0	2.2	BERGER 91	FREJ
>41	n	90	0	1.4	BERGER 91	FREJ
>58	n	90	0	1.9	HIRATA 89c	KAMI
>38	n	90	2	4.1	SEIDEL 88	IMB
>1.2	p	90	0		BARTELT 87	SOUD
>1.5	n	90	0		BARTELT 87	SOUD
>17	p	90	7	7	HAINES 86	IMB
>14	n	90	9	4	HAINES 86	IMB
>12	p	90	0	<1.2	ARISAKA 85	KAMI
>6	p	90	2	<1	ARISAKA 85	KAMI
>6.7	p (free)	90	6	6	BLEWITT 85	IMB
>17	p	90	7	7	BLEWITT 85	IMB
>12	n	90	4	2	PARK 85	IMB
>0.6	n	90	1	0.3	<sup>45</sup> BARTELT 83	SOUD
>0.5	p	90	1	0.3	<sup>45</sup> BARTELT 83	SOUD
>9.8	p	90	1		<sup>46</sup> KRISHNA... 82	KOLR
>0.8	p	90	2		<sup>47</sup> CHERRY 81	HOME

<sup>45</sup> Limit based on zero events.

<sup>46</sup> We have calculated 90% CL limit from 0 confined events.

<sup>47</sup> We have converted 2 possible events to 90% CL limit.

$\tau(N \rightarrow \mu^+ \rho)$  78

Table with columns: LIMIT (10^30 years), PARTICLE, CL%, EVTS, BKGD EST, DOCUMENT ID, TECN. Rows include >228 n, >110 p, and various p particles with associated event counts and document references.

$\tau(N \rightarrow \nu \rho)$  79

Table with columns: LIMIT (10^30 years), PARTICLE, CL%, EVTS, BKGD EST, DOCUMENT ID, TECN. Rows include >162 p, >19 n, and various p particles with associated event counts and document references.

$\tau(p \rightarrow e^+ \omega)$  710

Table with columns: LIMIT (10^30 years), PARTICLE, CL%, EVTS, BKGD EST, DOCUMENT ID, TECN. Rows include >107 p, >17 p, >45 p, >26 p, >1.5 p, >37 p, >25 p, >12 p (free), >37 p, >0.6 p, >9.8 p, >2.8 p, and various p particles with associated event counts and document references.

$\tau(p \rightarrow \mu^+ \omega)$  711

Table with columns: LIMIT (10^30 years), PARTICLE, CL%, EVTS, BKGD EST, DOCUMENT ID, TECN. Rows include >117 p, >11 p, >57 p, >4.4 p, >10 p, >23 p, >6.5 p (free), >23 p, and various p particles with associated event counts and document references.

$\tau(n \rightarrow \nu \omega)$  712

Table with columns: LIMIT (10^30 years), PARTICLE, CL%, EVTS, BKGD EST, DOCUMENT ID, TECN. Rows include >108 n, >17 n, >43 n, >6 n, >12 n, >18 n, >16 n, >2.0 n, and various n particles with associated event counts and document references.

$\tau(N \rightarrow e^+ K)$  713

Table with columns: LIMIT (10^30 years), PARTICLE, CL%, EVTS, BKGD EST, DOCUMENT ID, TECN. Rows include >17 n, >150 p, and various p particles with associated event counts and document references.

$\tau(p \rightarrow e^+ K_S^0)$  714

Table with columns: LIMIT (10^30 years), PARTICLE, CL%, EVTS, BKGD EST, DOCUMENT ID, TECN. Rows include >2000 p, >120 p, >76 p, and various p particles with associated event counts and document references.

$\tau(p \rightarrow e^+ K_L^0)$  715

Table with columns: LIMIT (10^30 years), PARTICLE, CL%, EVTS, BKGD EST, DOCUMENT ID, TECN. Rows include >51 p, >44 p, and various p particles with associated event counts and document references.

$\tau(N \rightarrow \mu^+ K)$  716

Table with columns: LIMIT (10^30 years), PARTICLE, CL%, EVTS, BKGD EST, DOCUMENT ID, TECN. Rows include >120 p, >120 p, >26 n, >120 p, >54 p, >3.0 p, >19 p, >1.5 p, >1.1 p, >40 p, >19 p, >6.7 p (free), >40 p, >6 p, >0.6 p, >0.4 n, >5.8 p, >2.0 p, >0.2 n, and various p particles with associated event counts and document references.

$\tau(p \rightarrow \mu^+ K_S^0)$  717

Table with columns: LIMIT (10^30 years), PARTICLE, CL%, EVTS, BKGD EST, DOCUMENT ID, TECN. Rows include >2600 p, >150 p, >64 p, and various p particles with associated event counts and document references.

$\tau(p \rightarrow \mu^+ K_L^0)$  718

Table with columns: LIMIT (10^30 years), PARTICLE, CL%, EVTS, BKGD EST, DOCUMENT ID, TECN. Rows include >83 p, >44 p, and various p particles with associated event counts and document references.

52 We have converted 2 possible events to 90% CL limit.

54 BARTELT 87 limit applies to  $p \rightarrow \mu^+ K_S^0$ .

55 Limit based on zero events.

56 We have calculated 90% CL limit from 1 confined event.

57 We have converted half-life to 90% CL mean life.

58 We have doubled the  $p \rightarrow \mu^+ K^0$  limit given in KOBAYASHI 05 to obtain this  $p \rightarrow \mu^+ K_S^0$  limit.

## Baryon Particle Listings

 $\rho$  $\tau(N \rightarrow \nu K)$  719

LIMIT ( $10^{30}$ years)	PARTICLE	CL%	EVS	BKGD EST	DOCUMENT ID	TECN
>2300	$p$	90	0	1.3	KOBAYASHI 05	SKAM
> 86	$n$	90	0	2.4	HIRATA 89c	KAMI
••• We do not use the following data for averages, fits, limits, etc. •••						
> 26	$n$	90	16	9.1	WALL 00	SOU2
> 670	$p$	90			HAYATO 99	SKAM
> 151	$p$	90	15	21.4	MCGREW 99	IMB3
> 30	$n$	90	34	34.1	MCGREW 99	IMB3
> 43	$p$	90	1	1.54	59 ALLISON 98	SOU2
> 15	$n$	90	1	1.8	BERGER 89	FREJ
> 15	$p$	90	1	1.8	BERGER 89	FREJ
> 100	$p$	90	9	7.3	HIRATA 89c	KAMI
> 0.28	$p$	90	0	0.7	PHILLIPS 89	HPW
> 0.3	$p$	90	0		BARTELT 87	SOUND
> 0.75	$n$	90	0		60 BARTELT 87	SOUND
> 10	$p$	90	6	5	HAINES 86	IMB
> 15	$n$	90	3	5	HAINES 86	IMB
> 28	$p$	90	3	3	KAJITA 86	KAMI
> 32	$n$	90	0	1.4	KAJITA 86	KAMI
> 1.8	$p$ (free)	90	6	11	BLEWITT 85	IMB
> 9.6	$p$	90	6	5	BLEWITT 85	IMB
> 10	$n$	90	2	2	PARK 85	IMB
> 5	$n$	90	0		BATTISTONI 84	NUSX
> 2	$p$	90	0		BATTISTONI 84	NUSX
> 0.3	$n$	90	0		61 BARTELT 83	SOUND
> 0.1	$p$	90	0		61 BARTELT 83	SOUND
> 5.8	$p$	90	1		62 KRISHNA... 82	KOLR
> 0.3	$n$	90	2		63 CHERRY 81	HOME

<sup>59</sup>This ALLISON 98 limit is with no background subtraction; with subtraction the limit becomes  $> 46 \times 10^{30}$  years.

<sup>60</sup>BARTELT 87 limit applies to  $n \rightarrow \nu K_S^0$ .

<sup>61</sup>Limit based on zero events.

<sup>62</sup>We have calculated 90% CL limit from 1 confined event.

<sup>63</sup>We have converted 2 possible events to 90% CL limit.

 $\tau(n \rightarrow \nu K_S^0)$  720

LIMIT ( $10^{30}$ years)	PARTICLE	CL%	EVS	BKGD EST	DOCUMENT ID	TECN
>260	$n$	90	34	30	64 KOBAYASHI 05	SKAM
••• We do not use the following data for averages, fits, limits, etc. •••						
> 51	$n$	90	16	9.1	WALL 00	SOU2
<sup>64</sup> We have doubled the $n \rightarrow \nu K_S^0$ limit given in KOBAYASHI 05 to obtain this $n \rightarrow \nu K_S^0$ limit.						

 $\tau(p \rightarrow e^+ K^*(892)^0)$  721

LIMIT ( $10^{30}$ years)	PARTICLE	CL%	EVS	BKGD EST	DOCUMENT ID	TECN
>84	$p$	90	38	52.0	MCGREW 99	IMB3
••• We do not use the following data for averages, fits, limits, etc. •••						
>10	$p$	90	0	0.8	BERGER 91	FREJ
>52	$p$	90	2	1.55	HIRATA 89c	KAMI
>10	$p$	90	1	<1	ARISAKA 85	KAMI

 $\tau(N \rightarrow \nu K^*(892)^0)$  722

LIMIT ( $10^{30}$ years)	PARTICLE	CL%	EVS	BKGD EST	DOCUMENT ID	TECN
>51	$p$	90	7	9.1	MCGREW 99	IMB3
>78	$n$	90	40	50	MCGREW 99	IMB3
••• We do not use the following data for averages, fits, limits, etc. •••						
>22	$n$	90	0	2.1	BERGER 89	FREJ
>17	$p$	90	0	2.4	BERGER 89	FREJ
>20	$p$	90	5	2.1	HIRATA 89c	KAMI
>21	$n$	90	4	2.4	HIRATA 89c	KAMI
>10	$p$	90	7	6	HAINES 86	IMB
> 5	$n$	90	8	7	HAINES 86	IMB
> 8	$p$	90	3	2	KAJITA 86	KAMI
> 6	$n$	90	2	1.6	KAJITA 86	KAMI
> 5.8	$p$ (free)	90	10	16	BLEWITT 85	IMB
> 9.6	$p$	90	7	6	BLEWITT 85	IMB
> 7	$n$	90	1	4	PARK 85	IMB
> 2.1	$p$	90	1		65 BATTISTONI 82	NUSX

<sup>65</sup>We have converted 1 possible event to 90% CL limit.

## Antilepton + mesons

 $\tau(p \rightarrow e^+ \pi^+ \pi^-)$  723

LIMIT ( $10^{30}$ years)	PARTICLE	CL%	EVS	BKGD EST	DOCUMENT ID	TECN
>82	$p$	90	16	23.1	MCGREW 99	IMB3
••• We do not use the following data for averages, fits, limits, etc. •••						
>21	$p$	90	0	2.2	BERGER 91	FREJ

 $\tau(p \rightarrow e^+ \pi^0 \pi^0)$  724

LIMIT ( $10^{30}$ years)	PARTICLE	CL%	EVS	BKGD EST	DOCUMENT ID	TECN
>147	$p$	90	2	0.8	MCGREW 99	IMB3
••• We do not use the following data for averages, fits, limits, etc. •••						
> 38	$p$	90	1	0.5	BERGER 91	FREJ

 $\tau(n \rightarrow e^+ \pi^- \pi^0)$  725

LIMIT ( $10^{30}$ years)	PARTICLE	CL%	EVS	BKGD EST	DOCUMENT ID	TECN
>52	$n$	90	38	34.2	MCGREW 99	IMB3
••• We do not use the following data for averages, fits, limits, etc. •••						
>32	$n$	90	1	0.8	BERGER 91	FREJ

 $\tau(p \rightarrow \mu^+ \pi^+ \pi^-)$  726

LIMIT ( $10^{30}$ years)	PARTICLE	CL%	EVS	BKGD EST	DOCUMENT ID	TECN
>133	$p$	90	25	38.0	MCGREW 99	IMB3
••• We do not use the following data for averages, fits, limits, etc. •••						
> 17	$p$	90	1	2.6	BERGER 91	FREJ
> 3.3	$p$	90	0	0.7	PHILLIPS 89	HPW

 $\tau(p \rightarrow \mu^+ \pi^0 \pi^0)$  727

LIMIT ( $10^{30}$ years)	PARTICLE	CL%	EVS	BKGD EST	DOCUMENT ID	TECN
>101	$p$	90	3	1.6	MCGREW 99	IMB3
••• We do not use the following data for averages, fits, limits, etc. •••						
> 33	$p$	90	1	0.9	BERGER 91	FREJ

 $\tau(n \rightarrow \mu^+ \pi^- \pi^0)$  728

LIMIT ( $10^{30}$ years)	PARTICLE	CL%	EVS	BKGD EST	DOCUMENT ID	TECN
>74	$n$	90	17	20.8	MCGREW 99	IMB3
••• We do not use the following data for averages, fits, limits, etc. •••						
>33	$n$	90	0	1.1	BERGER 91	FREJ

 $\tau(n \rightarrow e^+ K^0 \pi^-)$  729

LIMIT ( $10^{30}$ years)	PARTICLE	CL%	EVS	BKGD EST	DOCUMENT ID	TECN
>18	$n$	90	1	0.2	BERGER 91	FREJ

## Lepton + meson

 $\tau(n \rightarrow e^- \pi^+)$  730

LIMIT ( $10^{30}$ years)	PARTICLE	CL%	EVS	BKGD EST	DOCUMENT ID	TECN
>65	$n$	90	0	1.6	SEIDEL 88	IMB
••• We do not use the following data for averages, fits, limits, etc. •••						
>55	$n$	90	0	1.09	BERGER 91B	FREJ
>16	$n$	90	9	7	HAINES 86	IMB
>25	$n$	90	2	4	PARK 85	IMB

 $\tau(n \rightarrow \mu^- \pi^+)$  731

LIMIT ( $10^{30}$ years)	PARTICLE	CL%	EVS	BKGD EST	DOCUMENT ID	TECN
>49	$n$	90	0	0.5	SEIDEL 88	IMB
••• We do not use the following data for averages, fits, limits, etc. •••						
>33	$n$	90	0	1.40	BERGER 91B	FREJ
> 2.7	$n$	90	0	0.7	PHILLIPS 89	HPW
>25	$n$	90	7	6	HAINES 86	IMB
>27	$n$	90	2	3	PARK 85	IMB

 $\tau(n \rightarrow e^- \rho^+)$  732

LIMIT ( $10^{30}$ years)	PARTICLE	CL%	EVS	BKGD EST	DOCUMENT ID	TECN
>62	$n$	90	2	4.1	SEIDEL 88	IMB
••• We do not use the following data for averages, fits, limits, etc. •••						
>12	$n$	90	13	6	HAINES 86	IMB
>12	$n$	90	5	3	PARK 85	IMB

 $\tau(n \rightarrow \mu^- \rho^+)$  733

LIMIT ( $10^{30}$ years)	PARTICLE	CL%	EVS	BKGD EST	DOCUMENT ID	TECN
>7	$n$	90	1	1.1	SEIDEL 88	IMB
••• We do not use the following data for averages, fits, limits, etc. •••						
>2.6	$n$	90	0	0.7	PHILLIPS 89	HPW
>9	$n$	90	7	5	HAINES 86	IMB
>9	$n$	90	2	2	PARK 85	IMB

 $\tau(n \rightarrow e^- K^+)$  734

LIMIT ( $10^{30}$ years)	PARTICLE	CL%	EVS	BKGD EST	DOCUMENT ID	TECN
>32	$n$	90	3	2.96	BERGER 91B	FREJ
••• We do not use the following data for averages, fits, limits, etc. •••						
> 0.23	$n$	90	0	0.7	PHILLIPS 89	HPW



$\tau(n \rightarrow \mu^- K^+)$  **735**

LIMIT ( $10^{30}$ years)	PARTICLE	CL%	EVTs	BKGD EST	DOCUMENT ID	TECN
>57	n	90	0	2.18	BERGER 91B	FREJ
••• We do not use the following data for averages, fits, limits, etc. •••						
> 4.7	n	90	0	0.7	PHILLIPS 89	HPW

Lepton + mesons

$\tau(p \rightarrow e^- \pi^+ \pi^+)$  **736**

LIMIT ( $10^{30}$ years)	PARTICLE	CL%	EVTs	BKGD EST	DOCUMENT ID	TECN
>30	p	90	1	2.50	BERGER 91B	FREJ
••• We do not use the following data for averages, fits, limits, etc. •••						
> 2.0	p	90	0	0.7	PHILLIPS 89	HPW

$\tau(n \rightarrow e^- \pi^+ \pi^0)$  **737**

LIMIT ( $10^{30}$ years)	PARTICLE	CL%	EVTs	BKGD EST	DOCUMENT ID	TECN
>29	n	90	1	0.78	BERGER 91B	FREJ

$\tau(p \rightarrow \mu^- \pi^+ \pi^+)$  **738**

LIMIT ( $10^{30}$ years)	PARTICLE	CL%	EVTs	BKGD EST	DOCUMENT ID	TECN
>17	p	90	1	1.72	BERGER 91B	FREJ
••• We do not use the following data for averages, fits, limits, etc. •••						
> 7.8	p	90	0	0.7	PHILLIPS 89	HPW

$\tau(n \rightarrow \mu^- \pi^+ \pi^0)$  **739**

LIMIT ( $10^{30}$ years)	PARTICLE	CL%	EVTs	BKGD EST	DOCUMENT ID	TECN
>34	n	90	0	0.78	BERGER 91B	FREJ

$\tau(p \rightarrow e^- \pi^+ K^+)$  **740**

LIMIT ( $10^{30}$ years)	PARTICLE	CL%	EVTs	BKGD EST	DOCUMENT ID	TECN
>75	p	90	81	127.2	MCGREW 99	IMB3
••• We do not use the following data for averages, fits, limits, etc. •••						
>20	p	90	3	2.50	BERGER 91B	FREJ

$\tau(p \rightarrow \mu^- \pi^+ K^+)$  **741**

LIMIT ( $10^{30}$ years)	PARTICLE	CL%	EVTs	BKGD EST	DOCUMENT ID	TECN
>245	p	90	3	4.0	MCGREW 99	IMB3
••• We do not use the following data for averages, fits, limits, etc. •••						
> 5	p	90	2	0.78	BERGER 91B	FREJ

Antilepton + photon(s)

$\tau(p \rightarrow e^+ \gamma)$  **742**

LIMIT ( $10^{30}$ years)	PARTICLE	CL%	EVTs	BKGD EST	DOCUMENT ID	TECN
>670	p	90	0	0.1	MCGREW 99	IMB3
••• We do not use the following data for averages, fits, limits, etc. •••						
>133	p	90	0	0.3	BERGER 91	FREJ
>460	p	90	0	0.6	SEIDEL 88	IMB
>360	p	90	0	0.3	HAINES 86	IMB
> 87	p (free)	90	0	0.2	BLEWITT 85	IMB
>360	p	90	0	0.2	BLEWITT 85	IMB
> 0.1	p	90			66 GURR 67	CNTR

<sup>66</sup>We have converted half-life to 90% CL mean life.

$\tau(p \rightarrow \mu^+ \gamma)$  **743**

LIMIT ( $10^{30}$ years)	PARTICLE	CL%	EVTs	BKGD EST	DOCUMENT ID	TECN
>478	p	90	0	0.1	MCGREW 99	IMB3
••• We do not use the following data for averages, fits, limits, etc. •••						
>155	p	90	0	0.1	BERGER 91	FREJ
>380	p	90	0	0.5	SEIDEL 88	IMB
> 97	p	90	3	2	HAINES 86	IMB
> 61	p (free)	90	0	0.2	BLEWITT 85	IMB
>280	p	90	0	0.6	BLEWITT 85	IMB
> 0.3	p	90			67 GURR 67	CNTR

<sup>67</sup>We have converted half-life to 90% CL mean life.

$\tau(n \rightarrow \nu \gamma)$  **744**

LIMIT ( $10^{30}$ years)	PARTICLE	CL%	EVTs	BKGD EST	DOCUMENT ID	TECN
>28	n	90	163	144.7	MCGREW 99	IMB3
••• We do not use the following data for averages, fits, limits, etc. •••						
>24	n	90	10	6.86	BERGER 91B	FREJ
> 9	n	90	73	60	HAINES 86	IMB
>11	n	90	28	19	PARK 85	IMB

$\tau(p \rightarrow e^+ \gamma \gamma)$  **745**

LIMIT ( $10^{30}$ years)	PARTICLE	CL%	EVTs	BKGD EST	DOCUMENT ID	TECN
>100	p	90	1	0.8	BERGER 91	FREJ

$\tau(n \rightarrow \nu \gamma \gamma)$  **746**

LIMIT ( $10^{30}$ years)	PARTICLE	CL%	EVTs	BKGD EST	DOCUMENT ID	TECN
>219	n	90	5	7.5	MCGREW 99	IMB3

Three (or more) leptons

$\tau(p \rightarrow e^+ e^+ e^-)$  **747**

LIMIT ( $10^{30}$ years)	PARTICLE	CL%	EVTs	BKGD EST	DOCUMENT ID	TECN
>793	p	90	0	0.5	MCGREW 99	IMB3
••• We do not use the following data for averages, fits, limits, etc. •••						
>147	p	90	0	0.1	BERGER 91	FREJ
>510	p	90	0	0.3	HAINES 86	IMB
> 89	p (free)	90	0	0.5	BLEWITT 85	IMB
>510	p	90	0	0.7	BLEWITT 85	IMB

$\tau(p \rightarrow e^+ \mu^+ \mu^-)$  **748**

LIMIT ( $10^{30}$ years)	PARTICLE	CL%	EVTs	BKGD EST	DOCUMENT ID	TECN
>359	p	90	1	0.9	MCGREW 99	IMB3
••• We do not use the following data for averages, fits, limits, etc. •••						
> 81	p	90	0	0.16	BERGER 91	FREJ
> 5.0	p	90	0	0.7	PHILLIPS 89	HPW

$\tau(p \rightarrow e^+ \nu \nu)$  **749**

LIMIT ( $10^{30}$ years)	PARTICLE	CL%	EVTs	BKGD EST	DOCUMENT ID	TECN
>17	p	90	152	153.7	MCGREW 99	IMB3
••• We do not use the following data for averages, fits, limits, etc. •••						
>11	p	90	11	6.08	BERGER 91B	FREJ

$\tau(n \rightarrow e^+ e^- \nu)$  **750**

LIMIT ( $10^{30}$ years)	PARTICLE	CL%	EVTs	BKGD EST	DOCUMENT ID	TECN
>257	n	90	5	7.5	MCGREW 99	IMB3
••• We do not use the following data for averages, fits, limits, etc. •••						
> 74	n	90	0	< 0.1	BERGER 91B	FREJ
> 45	n	90	5	5	HAINES 86	IMB
> 26	n	90	4	3	PARK 85	IMB

$\tau(n \rightarrow \mu^+ e^- \nu)$  **751**

LIMIT ( $10^{30}$ years)	PARTICLE	CL%	EVTs	BKGD EST	DOCUMENT ID	TECN
>83	n	90	25	29.4	MCGREW 99	IMB3
••• We do not use the following data for averages, fits, limits, etc. •••						
>47	n	90	0	< 0.1	BERGER 91B	FREJ

$\tau(n \rightarrow \mu^+ \mu^- \nu)$  **752**

LIMIT ( $10^{30}$ years)	PARTICLE	CL%	EVTs	BKGD EST	DOCUMENT ID	TECN
>79	n	90	100	145	MCGREW 99	IMB3
••• We do not use the following data for averages, fits, limits, etc. •••						
>42	n	90	0	1.4	BERGER 91B	FREJ
> 5.1	n	90	0	0.7	PHILLIPS 89	HPW
>16	n	90	14	7	HAINES 86	IMB
>19	n	90	4	7	PARK 85	IMB

$\tau(p \rightarrow \mu^+ e^+ e^-)$  **753**

LIMIT ( $10^{30}$ years)	PARTICLE	CL%	EVTs	BKGD EST	DOCUMENT ID	TECN
>529	p	90	0	1.0	MCGREW 99	IMB3
••• We do not use the following data for averages, fits, limits, etc. •••						
> 91	p	90	0	≤ 0.1	BERGER 91	FREJ

$\tau(p \rightarrow \mu^+ \mu^+ \mu^-)$  **754**

LIMIT ( $10^{30}$ years)	PARTICLE	CL%	EVTs	BKGD EST	DOCUMENT ID	TECN
>675	p	90	0	0.3	MCGREW 99	IMB3
••• We do not use the following data for averages, fits, limits, etc. •••						
>119	p	90	0	0.2	BERGER 91	FREJ
> 10.5	p	90	0	0.7	PHILLIPS 89	HPW
>190	p	90	1	0.1	HAINES 86	IMB
> 44	p (free)	90	1	0.7	BLEWITT 85	IMB
>190	p	90	1	0.9	BLEWITT 85	IMB
> 2.1	p	90	1		68 BATTISTONI 82	NUSX

<sup>68</sup>We have converted 1 possible event to 90% CL limit.

$\tau(p \rightarrow \mu^+ \nu \nu)$  **755**

LIMIT ( $10^{30}$ years)	PARTICLE	CL%	EVTs	BKGD EST	DOCUMENT ID	TECN
>21	p	90	7	11.23	BERGER 91B	FREJ

# Baryon Particle Listings

## $p$

$\tau(p \rightarrow e^- \mu^+ \mu^+)$  **756**

LIMIT (10 <sup>30</sup> years)	PARTICLE	CL%	EVTs	BKGD EST	DOCUMENT ID	TECN
>6.0	$p$	90	0	0.7	PHILLIPS 89	HPW

$\tau(n \rightarrow 3\nu)$  **757**  
See also the "to anything" and "disappearance" limits for bound nucleons in the "p Mean Life" data block just in front of the list of possible  $p$  decay modes. Such modes could of course be to three (or five) neutrinos, and the limits are stronger, but we do not repeat them here.

LIMIT (10 <sup>30</sup> years)	PARTICLE	CL%	EVTs	BKGD EST	DOCUMENT ID	TECN
>0.00049	$n$	90	2	2	69 SUZUKI 93B	KAMI
• • • We do not use the following data for averages, fits, limits, etc. • • •						
>0.0023	$n$	90			70 GLICENSTEIN 97	KAMI
>0.00003	$n$	90	11	6.1	71 BERGER 91B	FREJ
>0.00012	$n$	90	7	11.2	71 BERGER 91B	FREJ
>0.0005	$n$	90	0		LEARNED 79	RVUE

69 The SUZUKI 93B limit applies to any of  $\nu_e \nu_e \bar{\nu}_e$ ,  $\nu_\mu \nu_\mu \bar{\nu}_\mu$ , or  $\nu_\tau \nu_\tau \bar{\nu}_\tau$ .  
70 GLICENSTEIN 97 uses Kamioka data and the idea that the disappearance of the neutron's magnetic moment should produce radiation.  
71 The first BERGER 91B limit is for  $n \rightarrow \nu_e \nu_e \bar{\nu}_e$ , the second is for  $n \rightarrow \nu_\mu \nu_\mu \bar{\nu}_\mu$ .

$\tau(n \rightarrow 5\nu)$  **758**  
See the note on  $\tau(n \rightarrow 3\nu)$  on the previous data block.

LIMIT (10 <sup>30</sup> years)	PARTICLE	CL%	EVTs	BKGD EST	DOCUMENT ID	TECN
• • • We do not use the following data for averages, fits, limits, etc. • • •						
>0.0017	$n$	90			72 GLICENSTEIN 97	KAMI

72 GLICENSTEIN 97 uses Kamioka data and the idea that the disappearance of the neutron's magnetic moment should produce radiation.

**Inclusive modes**

$\tau(N \rightarrow e^+$  anything) **759**

LIMIT (10 <sup>30</sup> years)	PARTICLE	CL%	EVTs	BKGD EST	DOCUMENT ID	TECN
>0.6	$p, n$	90			73 LEARNED 79	RVUE

73 The electron may be primary or secondary.

$\tau(N \rightarrow \mu^+$  anything) **760**

LIMIT (10 <sup>30</sup> years)	PARTICLE	CL%	EVTs	BKGD EST	DOCUMENT ID	TECN
>12	$p, n$	90	2		74,75 CHERRY 81	HOME
• • • We do not use the following data for averages, fits, limits, etc. • • •						
>1.8	$p, n$	90			75 COWSIK 80	CNTR
>6	$p, n$	90			75 LEARNED 79	RVUE

74 We have converted 2 possible events to 90% CL limit.  
75 The muon may be primary or secondary.

$\tau(N \rightarrow \nu$  anything) **761**  
Anything =  $\pi, \rho, K$ , etc.

LIMIT (10 <sup>30</sup> years)	PARTICLE	CL%	EVTs	BKGD EST	DOCUMENT ID	TECN
• • • We do not use the following data for averages, fits, limits, etc. • • •						
>0.0002	$p, n$	90	0		LEARNED 79	RVUE

$\tau(N \rightarrow e^+ \pi^0$  anything) **762**

LIMIT (10 <sup>30</sup> years)	PARTICLE	CL%	EVTs	BKGD EST	DOCUMENT ID	TECN
>0.6	$p, n$	90	0		LEARNED 79	RVUE

$\tau(N \rightarrow 2$  bodies,  $\nu$ -free) **763**

LIMIT (10 <sup>30</sup> years)	PARTICLE	CL%	EVTs	BKGD EST	DOCUMENT ID	TECN
• • • We do not use the following data for averages, fits, limits, etc. • • •						
>1.3	$p, n$	90	0		ALEKSEEV 81	BAKS

**$\Delta B = 2$  dinucleon modes**

$\tau(pp \rightarrow \pi^+ \pi^+)$  **764**

LIMIT (10 <sup>30</sup> years)	CL%	EVTs	BKGD EST	DOCUMENT ID	TECN	COMMENT
>0.7	90	4	2.34	BERGER 91B	FREJ	$\tau$ per iron nucleus

$\tau(pn \rightarrow \pi^+ \pi^0)$  **765**

LIMIT (10 <sup>30</sup> years)	CL%	EVTs	BKGD EST	DOCUMENT ID	TECN	COMMENT
>2.0	90	0	0.31	BERGER 91B	FREJ	$\tau$ per iron nucleus

$\tau(nn \rightarrow \pi^+ \pi^-)$  **766**

LIMIT (10 <sup>30</sup> years)	CL%	EVTs	BKGD EST	DOCUMENT ID	TECN	COMMENT
>0.7	90	4	2.18	BERGER 91B	FREJ	$\tau$ per iron nucleus

$\tau(nn \rightarrow \pi^0 \pi^0)$  **767**

LIMIT (10 <sup>30</sup> years)	CL%	EVTs	BKGD EST	DOCUMENT ID	TECN	COMMENT
>3.4	90	0	0.78	BERGER 91B	FREJ	$\tau$ per iron nucleus

$\tau(pp \rightarrow e^+ e^+)$  **768**

LIMIT (10 <sup>30</sup> years)	CL%	EVTs	BKGD EST	DOCUMENT ID	TECN	COMMENT
>5.8	90	0	<0.1	BERGER 91B	FREJ	$\tau$ per iron nucleus

$\tau(pp \rightarrow e^+ \mu^+)$  **769**

LIMIT (10 <sup>30</sup> years)	CL%	EVTs	BKGD EST	DOCUMENT ID	TECN	COMMENT
>3.6	90	0	<0.1	BERGER 91B	FREJ	$\tau$ per iron nucleus

$\tau(pp \rightarrow \mu^+ \mu^+)$  **770**

LIMIT (10 <sup>30</sup> years)	CL%	EVTs	BKGD EST	DOCUMENT ID	TECN	COMMENT
>1.7	90	0	0.62	BERGER 91B	FREJ	$\tau$ per iron nucleus

$\tau(pn \rightarrow e^+ \bar{\nu})$  **771**

LIMIT (10 <sup>30</sup> years)	CL%	EVTs	BKGD EST	DOCUMENT ID	TECN	COMMENT
>2.8	90	5	9.67	BERGER 91B	FREJ	$\tau$ per iron nucleus

$\tau(pn \rightarrow \mu^+ \bar{\nu})$  **772**

LIMIT (10 <sup>30</sup> years)	CL%	EVTs	BKGD EST	DOCUMENT ID	TECN	COMMENT
>1.6	90	4	4.37	BERGER 91B	FREJ	$\tau$ per iron nucleus

$\tau(nn \rightarrow \nu_e \bar{\nu}_e)$  **773**  
We include "invisible" modes here.

LIMIT (10 <sup>30</sup> years)	CL%	EVTs	BKGD EST	DOCUMENT ID	TECN	COMMENT
>1.4	90			76 ARAKI 06	KLND	$nn \rightarrow$ invisible
• • • We do not use the following data for averages, fits, limits, etc. • • •						
>0.000042	90			77 TRETAYAK 04	CNTR	
>0.000049	90			78 BACK 03	BORX	
>0.000012	90			79 BERNABEI 00b	DAMA	
>0.000012	90	5	9.7	BERGER 91B	FREJ	$\tau$ per iron nucleus

76 ARAKI 06 looks for signs of de-excitation of the residual nucleus after disappearance of two neutrons from the  $s$  shell of  $^{12}\text{C}$ .  
77 TRETAYAK 04 uses data from an old Homestake-mine radiochemical experiment on limits for invisible decays of  $^{39}\text{K}$  to  $^{37}\text{Ar}$ .  
78 BACK 03 looks for decays of unstable nuclides left after  $NN$  decays of parent  $^{12}\text{C}$ ,  $^{13}\text{C}$ ,  $^{16}\text{O}$  nuclei. These are "invisible channel" limits.  
79 BERNABEI 00b looks for the decay of a  $^{127}\text{Xe}$  nucleus following the disappearance of an  $nn$  pair in the otherwise-stable  $^{129}\text{Xe}$  nucleus. The limit here applies as well to  $nn \rightarrow \nu_\mu \bar{\nu}_\mu$ ,  $nn \rightarrow \nu_\tau \bar{\nu}_\tau$ , or any "disappearance" mode.

$\tau(nn \rightarrow \nu_\mu \bar{\nu}_\mu)$  **774**

LIMIT (10 <sup>30</sup> years)	CL%	EVTs	BKGD EST	DOCUMENT ID	TECN	COMMENT
• • • We do not use the following data for averages, fits, limits, etc. • • •						
>0.000006	90	4	4.4	BERGER 91B	FREJ	$\tau$ per iron nucleus

$\tau(pn \rightarrow$  invisible) **775**  
This violates charge conservation as well as baryon number conservation.

VALUE (10 <sup>30</sup> years)	CL%	DOCUMENT ID	TECN
>0.000021	90	80 TRETAYAK 04	CNTR

80 TRETAYAK 04 uses data from an old Homestake-mine radiochemical experiment on limits for invisible decays of  $^{39}\text{K}$  to  $^{37}\text{Ar}$ .

$\tau(pp \rightarrow$  invisible) **776**  
This violates charge conservation as well as baryon number conservation.

LIMIT (10 <sup>30</sup> years)	CL%	EVTs	BKGD EST	CL%	DOCUMENT ID	TECN
>0.00005	90				81 BACK 03	BORX
• • • We do not use the following data for averages, fits, limits, etc. • • •						
>0.00000055	90				82 BERNABEI 00b	DAMA

81 BACK 03 looks for decays of unstable nuclides left after  $NN$  decays of parent  $^{12}\text{C}$ ,  $^{13}\text{C}$ ,  $^{16}\text{O}$  nuclei. These are "invisible channel" limits.  
82 BERNABEI 00b looks for the decay of a  $^{127}\text{Xe}$  nucleus following the disappearance of a  $pp$  pair in the otherwise-stable  $^{129}\text{Xe}$  nucleus.

**$\bar{p}$  PARTIAL MEAN LIVES**

The "partial mean life" limits tabulated here are the limits on  $\bar{\tau}/B_i$ , where  $\bar{\tau}$  is the total mean life for the antiproton and  $B_i$  is the branching fraction for the mode in question.

$\tau(\bar{p} \rightarrow e^- \gamma)$  **777**

VALUE (years)	CL%	DOCUMENT ID	TECN	COMMENT
> $7 \times 10^5$	90	GEER 00	APEX	8.9 GeV/c $\bar{p}$ beam
• • • We do not use the following data for averages, fits, limits, etc. • • •				
>1848	95	GEER 94	CALO	8.9 GeV/c $\bar{p}$ beam

$\tau(\bar{p} \rightarrow \mu^- \gamma)$  778

Table with columns: VALUE (years), CL%, DOCUMENT ID, TECN, COMMENT. Row 1: >5 x 10^4, 90, GEER 00, APEX, 8.9 GeV/c p-bar beam. Row 2: >5.0 x 10^4, 90, HU 98B, APEX, 8.9 GeV/c p-bar beam.

$\tau(\bar{p} \rightarrow e^- \pi^0)$  779

Table with columns: VALUE (years), CL%, DOCUMENT ID, TECN, COMMENT. Row 1: > 4 x 10^5, 90, GEER 00, APEX, 8.9 GeV/c p-bar beam. Row 2: >554, 95, GEER 94, CALO, 8.9 GeV/c p-bar beam.

$\tau(\bar{p} \rightarrow \mu^- \pi^0)$  780

Table with columns: VALUE (years), CL%, DOCUMENT ID, TECN, COMMENT. Row 1: >5 x 10^4, 90, GEER 00, APEX, 8.9 GeV/c p-bar beam. Row 2: >4.8 x 10^4, 90, HU 98B, APEX, 8.9 GeV/c p-bar beam.

$\tau(\bar{p} \rightarrow e^- \eta)$  781

Table with columns: VALUE (years), CL%, DOCUMENT ID, TECN, COMMENT. Row 1: > 2 x 10^4, 90, GEER 00, APEX, 8.9 GeV/c p-bar beam. Row 2: >171, 95, GEER 94, CALO, 8.9 GeV/c p-bar beam.

$\tau(\bar{p} \rightarrow \mu^- \eta)$  782

Table with columns: VALUE (years), CL%, DOCUMENT ID, TECN, COMMENT. Row 1: >8 x 10^3, 90, GEER 00, APEX, 8.9 GeV/c p-bar beam. Row 2: >7.9 x 10^3, 90, HU 98B, APEX, 8.9 GeV/c p-bar beam.

$\tau(\bar{p} \rightarrow e^- K_S^0)$  783

Table with columns: VALUE (years), CL%, DOCUMENT ID, TECN, COMMENT. Row 1: >900, 90, GEER 00, APEX, 8.9 GeV/c p-bar beam. Row 2: > 29, 95, GEER 94, CALO, 8.9 GeV/c p-bar beam.

$\tau(\bar{p} \rightarrow \mu^- K_S^0)$  784

Table with columns: VALUE (years), CL%, DOCUMENT ID, TECN, COMMENT. Row 1: >4 x 10^3, 90, GEER 00, APEX, 8.9 GeV/c p-bar beam. Row 2: >4.3 x 10^3, 90, HU 98B, APEX, 8.9 GeV/c p-bar beam.

$\tau(\bar{p} \rightarrow e^- K_L^0)$  785

Table with columns: VALUE (years), CL%, DOCUMENT ID, TECN, COMMENT. Row 1: >9 x 10^3, 90, GEER 00, APEX, 8.9 GeV/c p-bar beam. Row 2: >9, 95, GEER 94, CALO, 8.9 GeV/c p-bar beam.

$\tau(\bar{p} \rightarrow \mu^- K_L^0)$  786

Table with columns: VALUE (years), CL%, DOCUMENT ID, TECN, COMMENT. Row 1: >7 x 10^3, 90, GEER 00, APEX, 8.9 GeV/c p-bar beam. Row 2: >6.5 x 10^3, 90, HU 98B, APEX, 8.9 GeV/c p-bar beam.

$\tau(\bar{p} \rightarrow e^- \gamma \gamma)$  787

Table with columns: VALUE (years), CL%, DOCUMENT ID, TECN, COMMENT. Row 1: >2 x 10^4, 90, GEER 00, APEX, 8.9 GeV/c p-bar beam.

$\tau(\bar{p} \rightarrow \mu^- \gamma \gamma)$  788

Table with columns: VALUE (years), CL%, DOCUMENT ID, TECN, COMMENT. Row 1: >2 x 10^4, 90, GEER 00, APEX, 8.9 GeV/c p-bar beam. Row 2: >2.3 x 10^4, 90, HU 98B, APEX, 8.9 GeV/c p-bar beam.

$\tau(\bar{p} \rightarrow e^- \rho)$  789

Table with columns: VALUE (years), CL%, DOCUMENT ID, TECN, COMMENT. Row 1: >200, 90, GEER 83, APEX, 8.9 GeV/c p-bar beam. Row 2: >1 x 10^3, 90, GEER 84, APEX, 8.9 GeV/c p-bar beam.

$\tau(\bar{p} \rightarrow e^- \omega)$  790

Table with columns: VALUE (years), CL%, DOCUMENT ID, TECN, COMMENT. Row 1: >200, 90, GEER 00, APEX, 8.9 GeV/c p-bar beam.

$\tau(\bar{p} \rightarrow e^- K^*(892)^0)$  791

Table with columns: VALUE (years), CL%, DOCUMENT ID, TECN, COMMENT. Row 1: >1 x 10^3, 90, GEER 84, APEX, 8.9 GeV/c p-bar beam.

p REFERENCES

Mohr, B.N. Taylor, D.B. Newell (NIST)
ARRINGTON, J.C. Bernauer et al. (ANL)
BERNAUER, J.C. Bernauer et al. (MAMI A1 Collab.)
BRESSI, G. Bressi et al. (LEGN, PAVII, PADO, TRST+)
CLOET, I.C. Cloet, G.A. Miller (WASH)
DERUJULA, A. de Rujula (MADE, BOST, CERN)
DISTLER, M.O. Distler, J.C. Bernauer, T. Walcher (MANZ)
HILL, R.J. Hill, G. Paz (EFI)
BERNAUER, J.C. Bernauer et al. (MAMI A1 Collab.)
BORISYUK, D. Borisjuk (KIEV)
DERUJULA, A. De Rujula (MADU, CERN)
HILL, R.J. Hill, G. Paz (CHIC)
POHL, R. Pohl et al. (MPIQ, ENSP, COIM, +)
NISHINO, H. Nishino et al. (Super-Kamiokande Collab.)
PASK, T. Pask et al. (Stefan Meyer Inst., Vienna, TOKY+)
MOHR, P.J. Mohr, B.N. Taylor, D.B. Newell (NIST)
BELUSHKIN, M.A. Belushkin, H.W. Hammer, U.-G. Meissner (BONN+)
ARAKI, T. Araki et al. (CERN, TOKYO+)
HORI, M. Hori et al. (MAMI, BASL)
BLUNDEN, P.G. Blunden, I. Sick (MAMI, BASL)
KOBAYASHI, K. Kobayashi et al. (Super-Kamiokande Collab.)
MOHR, P.J. Mohr, B.N. Taylor (NIST)
SCHUMACHER, M. Schumacher (GOET)
AHMED, S.N. Ahmed et al. (SNO Collab.)
TRET'YAK, V.I. Tret'yak, V.Yu. Denisov, Yu.G. Zdesenko (KIEV)
Translated from ZETFP 79 136.
BACK, H.O. Back et al. (BOREXINO Collab.)
BEANE, S.R. Beane et al.
Also: PL B607 320 (erratum)
DMITRIEV, V.F. Dmitriev, R.A. Senkov (NOVO)
HORI, M. Hori et al. (CERN ASACUSA Collab.)
SICK, I. Sick (BASL)
ZDESENKO, Yu.G. Zdesenko, V.I. Tret'yak (KIEV)
AHMAD, Q.R. Ahmad et al. (SNO Collab.)
BARANOV, P.S. Baranov et al.
Translated from FECAV 32 699.
BLANPIED, G. Blanpied et al. (BNL LEGS Collab.)
ESCHRICH, I. Eschrich et al. (FNAL SELEX Collab.)
HORI, M. Hori et al. (CERN ASACUSA Collab.)
OLMOSDEL, V. Olmos de Leon et al. (MAMI TAPS Collab.)
TRET'YAK, V.I. Tret'yak, Yu.G. Zdesenko (KIEV)
BERNABEI, R. Bernabei et al. (Gran Sasso DAMA Collab.)
GEER, S. Geer et al. (FNAL APEX Collab.)
Also: PR D62 052004
Also: PRL 85 3546 (erratum)
GEER, S. Geer et al. (FNAL APEX Collab.)
GEER, S. Geer et al. (FNAL APEX Collab.)
GEER, S. Geer et al. (FNAL APEX Collab.)
GEER, S. Geer et al. (FNAL APEX Collab.)
MELNIKOV, K. Melnikov et al. (SLAC, KARL)
ROSENFELDR., R. Rosenfelder
SENGUPTA, S. Sengupta
WALL, D. Wall et al. (Soudan-2 Collab.)
WALL, D. Wall et al. (Soudan-2 Collab.)
GABRIELSE, G. Gabrielse et al.
HAYATO, Y. Hayato et al. (Super-Kamiokande Collab.)
MCGREW, C. McGrew et al. (IMB-3 Collab.)
MOHR, P.J. Mohr, B.N. Taylor (NIST)
Also: RMP 72 351
TORII, H.A. Torii et al. (CERN PS-205 Collab.)
ALLISON, W.W.M. Allison et al. (Soudan-2 Collab.)
HU, M. Hu et al. (FNAL APEX Collab.)
SHIOZAWA, M. Shiozawa et al. (Super-Kamiokande Collab.)
GILCENSTEIN, J.F. Gilcenstein (SACL)
MERGELL, P. Mergell et al. (MANZ, BONN)
GABRIELSE, G. Gabrielse et al. (HARV, MANZ, SEOUL)
MACGIBBON, B.E. MacGibbon et al. (ILL, SASK, INRM)
GEER, S. Geer et al. (FNAL, UCLA, PSU)
WONG, C.W. Wong (UCLA)
HALLIN, E.L. Hallin et al. (SASK, BOST, ILL)
SUZUKI, Y. Suzuki et al. (KAMIOKANDE Collab.)
HUGHES, R.J. Hughes, B.I. Deutch (LANL, AARH)
ZIEGER, A. Zieger et al. (MPCM)
Also: PL B281 417 (erratum)
BERGER, C. Berger et al. (FREJUS Collab.)
BERGER, C. Berger et al. (FREJUS Collab.)
FEDERSPIEL, F.J. Federspiel et al. (ILL)
MCCORD, M. McCord et al.
BECKER-SZ., R.A. Becker-Szendy et al. (IMB-3 Collab.)
ERICSON, T.E.O. Ericson, A. Richter (CERN, DARM)
GABRIELSE, G. Gabrielse et al. (HARV, MANZ, WASH+)
BERGER, C. Berger et al. (FREJUS Collab.)
CHO, D. Cho, K. Sangster, E.A. Hinds (YALE)
HIRATA, K.S. Hirata et al. (Kamiokande Collab.)
PHILLIPS, T.J. Phillips et al. (HPW Collab.)
KREISSL, A. Kreissl et al. (CERN PS176 Collab.)
SEIDEL, S. Seidel et al. (IMB Collab.)
BARTELT, J.E. Bartelt et al. (Soudan Collab.)
Also: PR D40 1701 (erratum)
COHEN, E.R. Cohen, B.N. Taylor (RISC, NBS)
HAINES, T.J. Haines et al. (IMB Collab.)
KAJITA, T. Kajita et al. (Kamiokande Collab.)
ARISAKA, K. Arisaka et al. (Kamiokande Collab.)
BLEWITT, G.B. Blewitt et al. (IMB Collab.)
DZUBA, V.A. Dzuba, V.V. Flambaum, P.G. Silvestrov (NOVO)
PARK, H.S. Park et al. (IMB Collab.)
BATTISTONI, G. Battistoni et al. (NUSEX Collab.)
MARINELLI, M. Marinelli, G. Maripurgo (GENO)
WILKENING, D.A. Wilkening, N.F. Ramsey, D.J. Larson (HARV+)
BARTELT, J.E. Bartelt et al. (MINN, ANL)
BATTISTONI, G. Battistoni et al. (NUSEX Collab.)
KRISHNA..., M.R. Krishnaswamy et al. (TATA, OSKK+)
ALEKSEEV, E.N. Alekseev et al. (PNPI)
Translated from ZETFP 33 664.
CHERRY, M.L. Cherry et al. (PENN, BNL)
COWSIK, R. Cowisik, V.S. Narasimham (TATA)
SIMON, G.G. Simon et al.
BELL, M. Bell et al. (CERN)
GOLDEN, R.L. Golden et al. (NASA, PSSLL)
LEARNED, J.G. Learned, F. Reines, A. Soni (UCI)
BREGMAN, M. Bregman et al. (CERN)
ROBERTS, B.L. Roberts (WILL, RHEL)
EVANS, J.C. Evans Jr., R.I. Steinberg (BNL, PENN)
HU, E. Hu et al. (COLU, YALE)
BORKOWSKI, F. Borkowski et al.
COHEN, E.R. Cohen, B.N. Taylor (RISC, NBS)
DYLLA, H.F. Dylla, J.G. King (MIT)
AKIMOV, Yu.K. Akimov et al. (YERE)
Translated from ZETF 62 1231.

## Baryon Particle Listings

 $\rho, n$ 

DIX	70	Thesis Case	F.W. Dix	(CASE)
HARRISON	69	PRL 22 1263	G.E. Harrison, P.G.H. Sanders, S.J. Wright	(OXF)
GURR	67	PR 158 1321	H.S. Gurr <i>et al.</i>	(CASE, WITW)
FREREJACQ...	66	PR 141 1308	D. Frerejacque <i>et al.</i>	
HAND	63	RMP 35 335	L.N. Hand <i>et al.</i>	
FLEROV	58	DOKL 3 79	G.N. Flerov <i>et al.</i>	(ASCI)

**n**

$$I(J^P) = \frac{1}{2}(\frac{1}{2}^+) \text{ Status: } ***$$

We have omitted some results that have been superseded by later experiments. See our earlier editions.

Anyone interested in the neutron should look at these two new review articles: D. Dubbers and M.G. Schmidt, "The neutron and its role in cosmology and particle physics," *Reviews of Modern Physics* **83** 1111 (2011); and F.E. Wietfeldt and G.L. Greene, "The neutron lifetime," *Reviews of Modern Physics* **83** 1173 (2011).

**n MASS (atomic mass units u)**

The mass is known much more precisely in u (atomic mass units) than in MeV. See the next data block.

VALUE (u)	DOCUMENT ID	TECN	COMMENT
<b>1.00866491600 ± 0.0000000043</b>	MOHR 12	RVUE	2010 CODATA value
• • • We do not use the following data for averages, fits, limits, etc. • • •			
1.00866491597 ± 0.00000000043	MOHR 08	RVUE	2006 CODATA value
1.00866491560 ± 0.00000000055	MOHR 05	RVUE	2002 CODATA value
1.00866491578 ± 0.00000000055	MOHR 99	RVUE	1998 CODATA value
1.008665904 ± 0.000000014	COHEN 87	RVUE	1986 CODATA value

**n MASS (MeV)**

The mass is known much more precisely in u (atomic mass units) than in MeV. The conversion from u to MeV,  $1 u = 931.494 061(21) \text{ MeV}/c^2$  (MOHR 12, the 2010 CODATA value), involves the relatively poorly known electronic charge.

VALUE (MeV)	DOCUMENT ID	TECN	COMMENT
<b>939.565379 ± 0.000021</b>	MOHR 12	RVUE	2010 CODATA value
• • • We do not use the following data for averages, fits, limits, etc. • • •			
939.565346 ± 0.000023	MOHR 08	RVUE	2006 CODATA value
939.565360 ± 0.000081	MOHR 05	RVUE	2002 CODATA value
939.565331 ± 0.000037	1 KESSLER 99	SPEC	$np \rightarrow d\gamma$
939.565330 ± 0.000038	MOHR 99	RVUE	1998 CODATA value
939.56565 ± 0.00028	2,3 DIFILIPPO 94	TRAP	Penning trap
939.56563 ± 0.00028	COHEN 87	RVUE	1986 CODATA value
939.56564 ± 0.00028	3,4 GREENE 86	SPEC	$np \rightarrow d\gamma$
939.5731 ± 0.0027	3 COHEN 73	RVUE	1973 CODATA value

<sup>1</sup> We use the 1998 CODATA u-to-MeV conversion factor (see the heading above) to get this mass in MeV from the much more precisely measured KESSLER 99 value of  $1.00866491637 \pm 0.00000000082 u$ .

<sup>2</sup> The mass is known much more precisely in u:  $m = 1.0086649235 \pm 0.0000000023 u$ . We use the 1986 CODATA conversion factor to get the mass in MeV.

<sup>3</sup> These determinations are not independent of the  $m_n - m_p$  measurements below.

<sup>4</sup> The mass is known much more precisely in u:  $m = 1.008664919 \pm 0.000000014 u$ .

 **$\pi$  MASS**

VALUE (MeV)	EVTS	DOCUMENT ID	TECN	COMMENT
<b>939.485 ± 0.051</b>	59	5 CRESTI 86	HBC	$\bar{p}p \rightarrow \pi n$

<sup>5</sup> This is a corrected result (see the erratum). The error is statistical. The maximum systematic error is 0.029 MeV.

$$(m_n - m_{\pi}) / m_n$$

A test of CPT invariance. Calculated from the  $n$  and  $\pi$  masses, above.

VALUE	DOCUMENT ID
<b>(9 ± 6) × 10<sup>-5</sup> OUR EVALUATION</b>	

$$m_n - m_p$$

VALUE (MeV)	DOCUMENT ID	TECN	COMMENT
<b>1.29333217 ± 0.00000042</b>	6 MOHR 12	RVUE	2010 CODATA value
• • • We do not use the following data for averages, fits, limits, etc. • • •			
1.29333214 ± 0.00000043	7 MOHR 08	RVUE	2006 CODATA value
1.2933317 ± 0.00000005	8 MOHR 05	RVUE	2002 CODATA value
1.2933318 ± 0.00000005	9 MOHR 99	RVUE	1998 CODATA value
1.293318 ± 0.000009	10 COHEN 87	RVUE	1986 CODATA value
1.2933328 ± 0.0000072	GREENE 86	SPEC	$np \rightarrow d\gamma$
1.293429 ± 0.000036	COHEN 73	RVUE	1973 CODATA value

<sup>6</sup> The 2010 CODATA mass difference in u is  $m_n - m_p = 1.38844919(45) \times 10^{-3} u$ .

<sup>7</sup> Calculated by us from the MOHR 08 ratio  $m_n/m_p = 1.00137841918(46)$ . In u,  $m_n - m_p = 1.38844920(46) \times 10^{-3} u$ .

<sup>8</sup> Calculated by us from the MOHR 05 ratio  $m_n/m_p = 1.00137841870 \pm 0.00000000058$ . In u,  $m_n - m_p = (1.3884487 \pm 0.0000006) \times 10^{-3} u$ .

<sup>9</sup> Calculated by us from the MOHR 99 ratio  $m_n/m_p = 1.00137841887 \pm 0.00000000058$ . In u,  $m_n - m_p = (1.3884489 \pm 0.0000006) \times 10^{-3} u$ .

<sup>10</sup> Calculated by us from the COHEN 87 ratio  $m_n/m_p = 1.001378404 \pm 0.000000009$ . In u,  $m_n - m_p = 0.001388434 \pm 0.000000009 u$ .

**n MEAN LIFE**

Limits on lifetimes for *bound* neutrons are given in the section "p PARTIAL MEAN LIVES."

The mean life of the neutron,  $878.5 \pm 0.8$  s, obtained by SEREBROV 05 (for a more detailed account, see SEREBROV 08a) was so far from our average of seven other measurements,  $885.7 \pm 0.8$  s, that it made no sense to include it in our average. Thus our 2006, 2008, and 2010 *Reviews* stayed with  $885.7 \pm 0.8$  s; but we noted that in light of SEREBROV 05 our value should be regarded as suspect until further experiments clarified matters.

However, after our 2010 *Review*, PICHLMAIER 10 obtained a mean life of  $880.7 \pm 1.8$  s, and we averaged the best seven results to get  $881.5 \pm 1.5$  s for our 2011 off-year web update. And since then, ARZUMANOV 12, responding to comments of SEREBROV 10b, recalculated the systematic corrections to its 2000 measurement (ARZUMANOV 00) and lowered its value from  $885.4 \pm 0.9 \pm 0.4$  s to  $881.6 \pm 0.8 \pm 1.9$  s. Thus the trend is definitely toward a shorter lifetime.

There seems little better to do than to again average the best seven measurements. The result,  $880.1 \pm 1.1$  s (including a scale factor of 1.8), is 5.6 s lower than the value we gave in 2010—a drop of 7.0 old and 5.1 new standard deviations.

For a full review of all matters concerning the neutron lifetime, see F.E. Wietfeldt and G.L. Greene, "The neutron lifetime," *Reviews of Modern Physics* **83** 1173 (2011). In particular, there is a full discussion of the experimental methods and results; and an average lifetime is obtained making several different selections of those results. (The revised ARZUMANOV 12 mean life was not yet available.)

VALUE (s)	DOCUMENT ID	TECN	COMMENT
<b>880.1 ± 1.1 OUR AVERAGE</b>	Error includes scale factor of 1.8. See the ideogram below.		
881.6 ± 0.8 ± 1.9	11 ARZUMANOV 12	CNTR	UCN double bottle
880.7 ± 1.3 ± 1.2	PICHLMAIER 10	CNTR	UCN material bottle
886.3 ± 1.2 ± 3.2	NICO 05	CNTR	In-beam $n$ , trapped $p$
878.5 ± 0.7 ± 0.3	SEREBROV 05	CNTR	UCN gravitational trap
889.2 ± 3.0 ± 3.8	BYRNE 96	CNTR	Penning trap
882.6 ± 2.7	12 MAMPE 93	CNTR	UCN material bottle
887.6 ± 3.0	MAMPE 89	CNTR	UCN material bottle
• • • We do not use the following data for averages, fits, limits, etc. • • •			
886.8 ± 1.2 ± 3.2	DEWEY 03	CNTR	See NICO 05
885.4 ± 0.9 ± 0.4	ARZUMANOV 00	CNTR	See ARZUMANOV 12
888.4 ± 3.1 ± 1.1	13 NESVIZHEV... 92	CNTR	UCN material bottle
888.4 ± 2.9	ALFIMENKOV 90	CNTR	See NESVIZHEVSKII 92
893.6 ± 3.8 ± 3.7	BYRNE 90	CNTR	See BYRNE 96
878 ± 27 ± 14	KOSSAKOW... 89	TPC	Pulsed beam
877 ± 10	PAUL 89	CNTR	Magnetic storage ring
876 ± 10 ± 19	LAST 88	SPEC	Pulsed beam
891 ± 9	SPIVAK 88	CNTR	Beam
903 ± 13	KOSVINTSEV 86	CNTR	UCN material bottle
937 ± 18	14 BYRNE 80	CNTR	
875 ± 95	KOSVINTSEV 80	CNTR	
881 ± 8	BONDAREN... 78	CNTR	See SPIVAK 88
918 ± 14	CHRISTENSEN72	CNTR	

<sup>11</sup> ARZUMANOV 12 reanalyzes its systematic corrections in ARZUMANOV 00 and obtains this corrected value.

<sup>12</sup> IGNATOVICH 95 calls into question some of the corrections and averaging procedures used by MAMPE 93. The response, BONDARENKO 96, denies the validity of the criticisms.

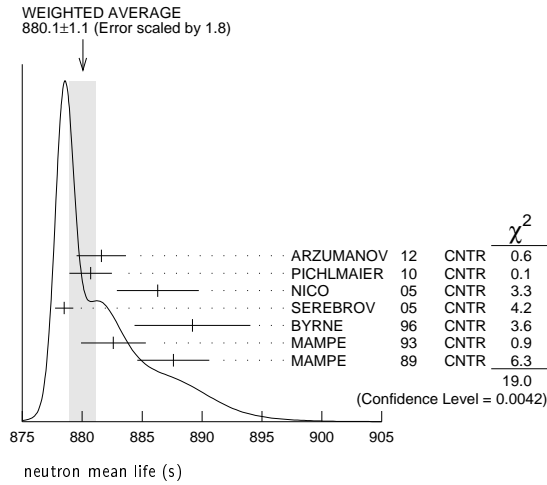
<sup>13</sup> The NESVIZHEVSKII 92 measurement has been withdrawn by A. Serebrov.

<sup>14</sup> The BYRNE 80 measurement has been withdrawn (J. Byrne, private communication, 1990).

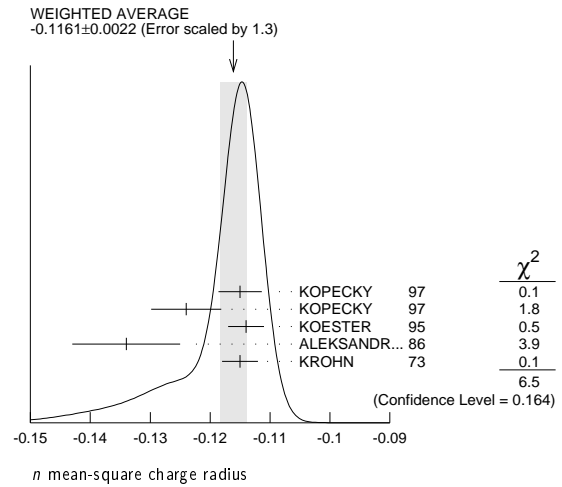
See key on page 457

# Baryon Particle Listings

*n*



<sup>18</sup> This value is as corrected by KOESTER 76.



## *n* MAGNETIC MOMENT

See the "Note on Baryon Magnetic Moments" in the *A* Listings.

VALUE ( $\mu_N$ )	DOCUMENT ID	TECN	COMMENT
<b>-1.91304272 ± 0.00000045</b>	MOHR 12	RVUE	2010 CODATA value
••• We do not use the following data for averages, fits, limits, etc. •••			
-1.91304273 ± 0.00000045	MOHR 08	RVUE	2006 CODATA value
-1.91304273 ± 0.00000045	MOHR 05	RVUE	2002 CODATA value
-1.91304272 ± 0.00000045	MOHR 99	RVUE	1998 CODATA value
-1.91304275 ± 0.00000045	COHEN 87	RVUE	1986 CODATA value
-1.91304277 ± 0.00000048	<sup>15</sup> GREENE 82	MRS	

<sup>15</sup> GREENE 82 measures the moment to be  $(1.04187564 \pm 0.00000026) \times 10^{-3}$  Bohr magnetons. The value above is obtained by multiplying this by  $m_p/m_e = 1836.152701 \pm 0.000037$  (the 1986 CODATA value from COHEN 87).

## *n* ELECTRIC DIPOLE MOMENT

A nonzero value is forbidden by both *T* invariance and *P* invariance. A number of early results have been omitted. See RAMSEY 90, GOLUB 94, and LAMOREAUX 09 for reviews.

VALUE ( $10^{-25}$ ecm)	CL%	DOCUMENT ID	TECN	COMMENT
<b>&lt; 0.29</b>	90	<sup>16</sup> BAKER 06	MRS	UCN's, $h\nu = 2\mu_n B \pm 2d_n E$
••• We do not use the following data for averages, fits, limits, etc. •••				
< 0.63	90	<sup>17</sup> HARRIS 99	MRS	$d = (-0.1 \pm 0.36) \times 10^{-25}$
< 0.97	90	ALTAREV 96	MRS	$(+0.26 \pm 0.40 \pm 0.16) \times 10^{-25}$
< 1.1	95	ALTAREV 92	MRS	See ALTAREV 96
< 1.2	95	SMITH 90	MRS	See HARRIS 99
< 2.6	95	ALTAREV 86	MRS	$d = (-1.4 \pm 0.6) \times 10^{-25}$
0.3 ± 4.8		PENDLEBURY 84	MRS	Ultracold neutrons
< 6	90	ALTAREV 81	MRS	$d = (2.1 \pm 2.4) \times 10^{-25}$
< 16	90	ALTAREV 79	MRS	$d = (4.0 \pm 7.5) \times 10^{-25}$

<sup>16</sup> LAMOREAUX 07 faults BAKER 06 for not including in the estimate of systematic error an effect due to the Earth's rotation. BAKER 07 replies (1) that the effect was included implicitly in the analysis and (2) that further analysis confirms that the BAKER 06 limit is correct as is. See also SILENKO 07.

<sup>17</sup> This HARRIS 99 result includes the result of SMITH 90. However, the averaging of the results of these two experiments has been criticized by LAMOREAUX 00.

## *n* MEAN-SQUARE CHARGE RADIUS

The mean-square charge radius of the neutron,  $\langle r_n^2 \rangle$ , is related to the neutron-electron scattering length  $b_{ne}$  by  $\langle r_n^2 \rangle = 3(m_e a_0 / m_n) b_{ne}$ , where  $m_e$  and  $m_n$  are the masses of the electron and neutron, and  $a_0$  is the Bohr radius. Numerically,  $\langle r_n^2 \rangle = 86.34 b_{ne}$ , if we use  $a_0$  for a nucleus with infinite mass.

VALUE ( $\text{fm}^2$ )	DOCUMENT ID	COMMENT
<b>-0.1161 ± 0.0022 OUR AVERAGE</b>		Error includes scale factor of 1.3. See the ideogram below.
-0.115 ± 0.002 ± 0.003	KOPECKY 97	<i>ne</i> scattering (Pb)
-0.124 ± 0.003 ± 0.005	KOPECKY 97	<i>ne</i> scattering (Bi)
-0.114 ± 0.003	KOESTER 95	<i>ne</i> scattering (Pb, Bi)
-0.134 ± 0.009	ALEKSANDR... 86	<i>ne</i> scattering (Bi)
-0.115 ± 0.003	<sup>18</sup> KROHN 73	<i>ne</i> scattering (Ne, Ar, Kr, Xe)
••• We do not use the following data for averages, fits, limits, etc. •••		
-0.117 <sup>+0.007</sup> / <sub>-0.011</sub>	BELUSHKIN 07	Dispersion analysis
-0.113 ± 0.003 ± 0.004	KOPECKY 95	<i>ne</i> scattering (Pb)
-0.114 ± 0.003	KOESTER 86	<i>ne</i> scattering (Pb, Bi)
-0.118 ± 0.002	KOESTER 76	<i>ne</i> scattering (Pb)
-0.120 ± 0.002	KOESTER 76	<i>ne</i> scattering (Bi)
-0.116 ± 0.003	KROHN 66	<i>ne</i> scattering (Ne, Ar, Kr, Xe)

## *n* MAGNETIC RADIUS

This is the rms magnetic radius,  $\sqrt{\langle r_M^2 \rangle}$ .

VALUE (fm)	DOCUMENT ID	COMMENT
<b>0.862 ± 0.009</b>	BELUSHKIN 07	Dispersion analysis
<b>-0.008</b>		

## *n* ELECTRIC POLARIZABILITY $\alpha_n$

Following is the electric polarizability  $\alpha_n$  defined in terms of the induced electric dipole moment by  $\mathbf{D} = 4\pi\epsilon_0\alpha_n\mathbf{E}$ . For a review, see SCHMIED-MAYER 89.

For a very complete review of the "polarizability of the nucleon and Compton scattering," see SCHUMACHER 05. His recommended values for the neutron are  $\alpha_n = (12.5 \pm 1.7) \times 10^{-4} \text{ fm}^3$  and  $\beta_n = (2.7 \mp 1.8) \times 10^{-4} \text{ fm}^3$ , which agree with our averages within errors.

VALUE ( $10^{-4} \text{ fm}^3$ )	DOCUMENT ID	TECN	COMMENT
<b>11.6 ± 1.5 OUR AVERAGE</b>			
12.5 ± 1.8 <sup>+1.6</sup> / <sub>-1.3</sub>	<sup>19</sup> KOSSERT 03	CNTR	$\gamma d \rightarrow \gamma pn$
8.8 ± 2.4 ± 3.0	<sup>20</sup> LUNDIN 03	CNTR	$\gamma d \rightarrow \gamma d$
12.0 ± 1.5 ± 2.0	SCHMIEDM... 91	CNTR	<i>n</i> Pb transmission
10.7 <sup>+3.3</sup> / <sub>-10.7</sub>	ROSE 90b	CNTR	$\gamma d \rightarrow \gamma np$
••• We do not use the following data for averages, fits, limits, etc. •••			
13.6	<sup>21</sup> KOLB 00	CNTR	$\gamma d \rightarrow \gamma np$
0.0 ± 5.0	<sup>22</sup> KOESTER 95	CNTR	<i>n</i> Pb, <i>n</i> Bi transmission
11.7 <sup>+4.3</sup> / <sub>-11.7</sub>	ROSE 90	CNTR	See ROSE 90b
8 ± 10	KOESTER 88	CNTR	<i>n</i> Pb, <i>n</i> Bi transmission
12 ± 10	SCHMIEDM... 88	CNTR	<i>n</i> Pb, <i>n</i> C transmission

<sup>19</sup> KOSSERT 03 gets  $\alpha_n - \beta_n = (9.8 \pm 3.6 <sup>+2.1</sup>/<sub>-1.1</sub> \pm 2.2) \times 10^{-4} \text{ fm}^3$ , and uses  $\alpha_n + \beta_n = (15.2 \pm 0.5) \times 10^{-4} \text{ fm}^3$  from LEVCHUK 00. Thus the errors on  $\alpha_n$  and  $\beta_n$  are anti-correlated.

<sup>20</sup> LUNDIN 03 measures  $\alpha_n - \beta_n = (6.4 \pm 2.4) \times 10^{-4} \text{ fm}^3$  and uses accurate values for  $\alpha_p$  and  $\alpha_n$  and a precise sum-rule result for  $\alpha_n + \beta_n$ . The second error is a model uncertainty, and errors on  $\alpha_n$  and  $\beta_n$  are anticorrelated.

<sup>21</sup> KOLB 00 obtains this value with a lower limit of  $7.6 \times 10^{-4} \text{ fm}^3$  but no upper limit from this experiment alone. Combined with results of ROSE 90, the 1- $\sigma$  range is  $(7.6-14.0) \times 10^{-4} \text{ fm}^3$ .

<sup>22</sup> KOESTER 95 uses natural Pb and the isotopes 208, 207, and 206. See this paper for a discussion of methods used by various groups to extract  $\alpha_n$  from data.

## *n* MAGNETIC POLARIZABILITY $\beta_n$

VALUE ( $10^{-4} \text{ fm}^3$ )	DOCUMENT ID	TECN	COMMENT
<b>3.7 ± 2.0 OUR AVERAGE</b>			
2.7 ± 1.8 <sup>+1.3</sup> / <sub>-1.6</sub>	<sup>23</sup> KOSSERT 03	CNTR	$\gamma d \rightarrow \gamma pn$
6.5 ± 2.4 ± 3.0	<sup>24</sup> LUNDIN 03	CNTR	$\gamma d \rightarrow \gamma d$
••• We do not use the following data for averages, fits, limits, etc. •••			
1.6	<sup>25</sup> KOLB 00	CNTR	$\gamma d \rightarrow \gamma np$

## Baryon Particle Listings

 $n$ 

- <sup>23</sup> KOSSERT 03 gets  $\alpha_n - \beta_n = (9.8 \pm 3.6^{+2.1}_{-1.1} \pm 2.2) \times 10^{-4} \text{ fm}^3$ , and uses  $\alpha_n + \beta_n = (15.2 \pm 0.5) \times 10^{-4} \text{ fm}^3$  from LEVCHUK 00. Thus the errors on  $\alpha_n$  and  $\beta_n$  are anti-correlated.
- <sup>24</sup> LUNDIN 03 measures  $\alpha_n - \beta_n = (6.4 \pm 2.4) \times 10^{-4} \text{ fm}^3$  and uses accurate values for  $\alpha_p$  and  $\beta_p$  and a precise sum-rule result for  $\alpha_n + \beta_n$ . The second error is a model uncertainty, and errors on  $\alpha_n$  and  $\beta_n$  are anticorrelated.
- <sup>25</sup> KOLB 00 obtains this value with an upper limit of  $7.6 \times 10^{-4} \text{ fm}^3$  but no lower limit from this experiment alone. Combined with results of ROSE 90, the  $1\text{-}\sigma$  range is  $(1.2\text{--}7.6) \times 10^{-4} \text{ fm}^3$ .

 $n$  CHARGESee also " $|q_p + q_e|/e$ " in the proton Listings.

VALUE ( $10^{-21} e$ )	DOCUMENT ID	TECN	COMMENT
<b><math>-0.2 \pm 0.8</math> OUR AVERAGE</b>			
$-0.1 \pm 1.1$	26 BRESSI	11	Neutrality of SF <sub>6</sub>
$-0.4 \pm 1.1$	27 BAUMANN	88	Cold $n$ deflection
• • • We do not use the following data for averages, fits, limits, etc. • • •			
$-15 \pm 22$	28 GAEHLER	82 CNTR	Cold $n$ deflection
<sup>26</sup> As a limit, this BRESSI 11 value is $< 1 \times 10^{-21} e$ .			
<sup>27</sup> The BAUMANN 88 error $\pm 1.1$ gives the 68% CL limits about the the value $-0.4$ .			
<sup>28</sup> The GAEHLER 82 error $\pm 22$ gives the 90% CL limits about the the value $-15$ .			

LIMIT ON  $n\pi$  OSCILLATIONSMean Time for  $n\pi$  Transition in Vacuum

A test of  $\Delta B=2$  baryon number nonconservation. MOHAPATRA 80 and MOHAPATRA 89 discuss the theoretical motivations for looking for  $n\pi$  oscillations. DOVER 83 and DOVER 85 give phenomenological analyses. The best limits come from looking for the decay of neutrons bound in nuclei. However, these analyses require model-dependent corrections for nuclear effects. See KABIR 83, DOVER 89, ALBERICO 91, and GAL 00 for discussions. Direct searches for  $n \rightarrow \pi$  transitions using reactor neutrons are cleaner but give somewhat poorer limits. We include limits for both free and bound neutrons in the Summary Table. See MOHAPATRA 09 for a recent review.

VALUE (s)	CL%	DOCUMENT ID	TECN	COMMENT
<b><math>&gt;1.3 \times 10^8</math></b>	90	CHUNG	02B SOU2	$n$ bound in iron
<b><math>&gt;8.6 \times 10^7</math></b>	90	BALDO...	94 CNTR	Reactor (free) neutrons
• • • We do not use the following data for averages, fits, limits, etc. • • •				
$>1 \times 10^7$	90	BALDO...	90 CNTR	See BALDO-CEOLIN 94
$>1.2 \times 10^8$	90	BERGER	90 FREJ	$n$ bound in iron
$>4.9 \times 10^5$	90	BRESSI	90 CNTR	Reactor neutrons
$>4.7 \times 10^5$	90	BRESSI	89 CNTR	See BRESSI 90
$>1.2 \times 10^8$	90	TAKITA	86 CNTR	$n$ bound in oxygen
$>1 \times 10^6$	90	FIDECARO	85 CNTR	Reactor neutrons
$>8.8 \times 10^7$	90	PARK	85B CNTR	
$>3 \times 10^7$		BATTISTONI	84 NUSX	
$>2.7 \times 10^7\text{--}1.1 \times 10^8$		JONES	84 CNTR	
$>2 \times 10^7$		CHERRY	83 CNTR	

LIMIT ON  $nn'$  OSCILLATIONS

Lee and Yang (LEE 56) proposed the existence of mirror world in an attempt to restore global parity symmetry. See BEREZHIANI 06 for a recent discussion.

VALUE (s)	CL%	DOCUMENT ID	TECN	COMMENT
<b><math>&gt;414</math></b>	90	SEREBROV	08 CNTR	UCN, B field on & off
• • • We do not use the following data for averages, fits, limits, etc. • • •				
$>12$	95	<sup>29</sup> ALTAREV	09A CNTR	UCN, scan $0 \leq B \leq 12.5 \mu\text{T}$
$>103$	95	BAN	07 CNTR	UCN, B field on & off
<sup>29</sup> Losses of neutrons due to oscillations to mirror neutrons would be maximal when the magnetic fields $B$ and $B'$ in the two worlds were equal. Hence the scan over $B$ by ALTAREV 09A: the limit applies for any $B'$ over the given range. At $B' = 0$ , the limit is 141 s (95% CL).				

 $n$  DECAY MODES

Mode	Fraction ( $\Gamma_i/\Gamma$ )	Confidence level
$\Gamma_1$ $p e^- \bar{\nu}_e$	100	%
$\Gamma_2$ $p e^- \bar{\nu}_e \gamma$	[a] $(3.09 \pm 0.32) \times 10^{-3}$	
$\Gamma_3$ hydrogen-atom $\bar{\nu}_e$		
<b>Charge conservation (Q) violating mode</b>		
$\Gamma_4$ $p \nu_e \bar{\nu}_e$	Q $< 8$	$\times 10^{-27}$ 68%

[a] This limit is for  $\gamma$  energies between 15 and 340 keV. $n$  BRANCHING RATIOS

$\Gamma(p e^- \bar{\nu}_e \gamma)/\Gamma_{\text{total}}$	CL%	DOCUMENT ID	TECN	COMMENT	$\Gamma_2/\Gamma$
<b><math>3.09 \pm 0.11 \pm 0.30</math></b>		30 COOPER	10 CNTR	$\gamma, p, e^-$ coincidence	
• • • We do not use the following data for averages, fits, limits, etc. • • •					
$3.13 \pm 0.11 \pm 0.33$		NICO	06 CNTR	See COOPER 10	
$< 6.9$	90	31 BECK	02 CNTR	$\gamma, p, e^-$ coincidence	
<sup>30</sup> This COOPER 10 result is for $\gamma$ energies between 15 and 340 keV.					
<sup>31</sup> This BECK 02 limit is for $\gamma$ energies between 35 and 100 keV.					

$\Gamma(\text{hydrogen-atom } \bar{\nu}_e)/\Gamma_{\text{total}}$	CL%	DOCUMENT ID	TECN	COMMENT	$\Gamma_3/\Gamma$
• • • We do not use the following data for averages, fits, limits, etc. • • •					
$< 3 \times 10^{-2}$	95	32 GREEN	90 RVUE		
<sup>32</sup> GREEN 90 infers that $\tau(\text{hydrogen-atom } \bar{\nu}_e) > 3 \times 10^4$ s by comparing neutron lifetime measurements made in storage experiments with those made in $\beta$ -decay experiments. However, the result depends sensitively on the lifetime measurements, and does not of course take into account more recent measurements of same.					

$\Gamma(p \nu_e \bar{\nu}_e)/\Gamma_{\text{total}}$	CL%	DOCUMENT ID	TECN	COMMENT	$\Gamma_4/\Gamma$
Forbidden by charge conservation.					
<b><math>&lt; 8 \times 10^{-27}</math></b>	68	33 NORMAN	96 RVUE	$^{71}\text{Ga} \rightarrow ^{71}\text{Ge}$ neutrals	
• • • We do not use the following data for averages, fits, limits, etc. • • •					
$< 9.7 \times 10^{-18}$	90	ROY	83 CNTR	$^{113}\text{Cd} \rightarrow ^{113m}\text{In}$ neut.	
$< 7.9 \times 10^{-21}$		VAIDYA	83 CNTR	$^{87}\text{Rb} \rightarrow ^{87m}\text{Sr}$ neut.	
$< 9 \times 10^{-24}$	90	BARABANOV	80 CNTR	$^{71}\text{Ga} \rightarrow ^{71}\text{GeX}$	
$< 3 \times 10^{-19}$		NORMAN	79 CNTR	$^{87}\text{Rb} \rightarrow ^{87m}\text{Sr}$ neut.	
<sup>33</sup> NORMAN 96 gets this limit by attributing SAGE and GALLEX counting rates to the charge-nonconserving transition $^{71}\text{Ga} \rightarrow ^{71}\text{Ge} + \text{neutrals}$ rather than to solar-neutrino reactions.					

## BARYON DECAY PARAMETERS

Written 1996 by E.D. Commins (University of California, Berkeley).

*Baryon semileptonic decays*

The typical spin-1/2 baryon semileptonic decay is described by a matrix element, the hadronic part of which may be written as:

$$\bar{B}_f [ f_1(q^2)\gamma_\lambda + i f_2(q^2)\sigma_{\lambda\mu}q^\mu + g_1(q^2)\gamma_\lambda\gamma_5 + g_3(q^2)\gamma_5q_\lambda ] B_i. \quad (1)$$

Here  $B_i$  and  $\bar{B}_f$  are spinors describing the initial and final baryons, and  $q = p_i - p_f$ , while the terms in  $f_1$ ,  $f_2$ ,  $g_1$ , and  $g_3$  account for vector, induced tensor ("weak magnetism"), axial vector, and induced pseudoscalar contributions [1]. Second-class current contributions are ignored here. In the limit of zero momentum transfer,  $f_1$  reduces to the vector coupling constant  $g_V$ , and  $g_1$  reduces to the axial-vector coupling constant  $g_A$ . The latter coefficients are related by Cabibbo's theory [2], generalized to six quarks (and three mixing angles) by Kobayashi and Maskawa [3]. The  $g_3$  term is negligible for transitions in which an  $e^\pm$  is emitted, and gives a very small correction, which can be estimated by PCAC [4], for  $\mu^\pm$  modes. Recoil effects include weak magnetism, and are taken into account adequately by considering terms of first order in

$$\delta = \frac{m_i - m_f}{m_i + m_f}, \quad (2)$$

where  $m_i$  and  $m_f$  are the masses of the initial and final baryons.

The experimental quantities of interest are the total decay rate, the lepton-neutrino angular correlation, the asymmetry coefficients in the decay of a polarized initial baryon, and the polarization of the decay baryon in its own rest frame for an unpolarized initial baryon. Formulae for these quantities are

derived by standard means [5] and are analogous to formulae for nuclear beta decay [6]. We use the notation of Ref. 6 in the Listings for neutron beta decay. For comparison with experiments at higher  $q^2$ , it is necessary to modify the form factors at  $q^2 = 0$  by a “dipole”  $q^2$  dependence, and for high-precision comparisons to apply appropriate radiative corrections [7].

The ratio  $g_A/g_V$  may be written as

$$g_A/g_V = |g_A/g_V| e^{i\phi_{AV}} . \quad (3)$$

The presence of a “triple correlation” term in the transition probability, proportional to  $\text{Im}(g_A/g_V)$  and of the form

$$\sigma_i \cdot (\mathbf{p}_\ell \times \mathbf{p}_\nu) \quad (4)$$

for initial baryon polarization or

$$\sigma_f \cdot (\mathbf{p}_\ell \times \mathbf{p}_\nu) \quad (5)$$

for final baryon polarization, would indicate failure of time-reversal invariance. The phase angle  $\phi$  has been measured precisely only in neutron decay (and in  $^{19}\text{Ne}$  nuclear beta decay), and the results are consistent with  $T$  invariance.

### Hyperon nonleptonic decays

The amplitude for a spin-1/2 hyperon decaying into a spin-1/2 baryon and a spin-0 meson may be written in the form

$$M = G_F m_\pi^2 \cdot \bar{B}_f (A - B\gamma_5) B_i , \quad (6)$$

where  $A$  and  $B$  are constants [1]. The transition rate is proportional to

$$R = 1 + \gamma \hat{\omega}_f \cdot \hat{\omega}_i + (1 - \gamma)(\hat{\omega}_f \cdot \hat{\mathbf{n}})(\hat{\omega}_i \cdot \hat{\mathbf{n}}) + \alpha(\hat{\omega}_f \cdot \hat{\mathbf{n}} + \hat{\omega}_i \cdot \hat{\mathbf{n}}) + \beta \hat{\mathbf{n}} \cdot (\hat{\omega}_f \times \hat{\omega}_i) , \quad (7)$$

where  $\hat{\mathbf{n}}$  is a unit vector in the direction of the final baryon momentum, and  $\hat{\omega}_i$  and  $\hat{\omega}_f$  are unit vectors in the directions of the initial and final baryon spins. (The sign of the last term in the above equation was incorrect in our 1988 and 1990 editions.)

The parameters  $\alpha$ ,  $\beta$ , and  $\gamma$  are defined as

$$\begin{aligned} \alpha &= 2 \text{Re}(s^*p) / (|s|^2 + |p|^2) , \\ \beta &= 2 \text{Im}(s^*p) / (|s|^2 + |p|^2) , \\ \gamma &= (|s|^2 - |p|^2) / (|s|^2 + |p|^2) , \end{aligned} \quad (8)$$

where  $s = A$  and  $p = |\mathbf{p}_f| B / (E_f + m_f)$ ; here  $E_f$  and  $\mathbf{p}_f$  are the energy and momentum of the final baryon. The parameters  $\alpha$ ,  $\beta$ , and  $\gamma$  satisfy

$$\alpha^2 + \beta^2 + \gamma^2 = 1 . \quad (9)$$

If the hyperon polarization is  $\mathbf{P}_Y$ , the polarization  $\mathbf{P}_B$  of the decay baryons is

$$\mathbf{P}_B = \frac{(\alpha + \mathbf{P}_Y \cdot \hat{\mathbf{n}})\hat{\mathbf{n}} + \beta(\mathbf{P}_Y \times \hat{\mathbf{n}}) + \gamma\hat{\mathbf{n}} \times (\mathbf{P}_Y \times \hat{\mathbf{n}})}{1 + \alpha\mathbf{P}_Y \cdot \hat{\mathbf{n}}} . \quad (10)$$

Here  $\mathbf{P}_B$  is defined in the rest system of the baryon, obtained by a Lorentz transformation along  $\hat{\mathbf{n}}$  from the hyperon rest frame, in which  $\hat{\mathbf{n}}$  and  $\mathbf{P}_Y$  are defined.

An additional useful parameter  $\phi$  is defined by

$$\beta = (1 - \alpha^2)^{1/2} \sin\phi . \quad (11)$$

In the Listings, we compile  $\alpha$  and  $\phi$  for each decay, since these quantities are most closely related to experiment and are essentially uncorrelated. When necessary, we have changed the signs of reported values to agree with our sign conventions. In the Baryon Summary Table, we give  $\alpha$ ,  $\phi$ , and  $\Delta$  (defined below) with errors, and also give the value of  $\gamma$  without error.

Time-reversal invariance requires, in the absence of final-state interactions, that  $s$  and  $p$  be relatively real, and therefore that  $\beta = 0$ . However, for the decays discussed here, the final-state interaction is strong. Thus

$$s = |s| e^{i\delta_s} \text{ and } p = |p| e^{i\delta_p} , \quad (12)$$

where  $\delta_s$  and  $\delta_p$  are the pion-baryon  $s$ - and  $p$ -wave strong interaction phase shifts. We then have

$$\beta = \frac{-2|s||p|}{|s|^2 + |p|^2} \sin(\delta_s - \delta_p) . \quad (13)$$

One also defines  $\Delta = -\tan^{-1}(\beta/\alpha)$ . If  $T$  invariance holds,  $\Delta = \delta_s - \delta_p$ . For  $\Lambda \rightarrow p\pi^-$  decay, the value of  $\Delta$  may be compared with the  $s$ - and  $p$ -wave phase shifts in low-energy  $\pi^-p$  scattering, and the results are consistent with  $T$  invariance.

See also the note on “Radiative Hyperon Decays” in the  $\Xi^0$  Listings in this *Review*.

### References

1. E.D. Commins and P.H. Bucksbaum, *Weak Interactions of Leptons and Quarks* (Cambridge University Press, Cambridge, England, 1983).
2. N. Cabibbo, Phys. Rev. Lett. **10**, 531 (1963).
3. M. Kobayashi and T. Maskawa, Prog. Theor. Phys. **49**, 652 (1973).
4. M.L. Goldberger and S.B. Treiman, Phys. Rev. **111**, 354 (1958).
5. P.H. Frampton and W.K. Tung, Phys. Rev. **D3**, 1114 (1971).
6. J.D. Jackson, S.B. Treiman, and H.W. Wyld, Jr., Phys. Rev. **106**, 517 (1957), and Nucl. Phys. **4**, 206 (1957).
7. Y. Yokoo, S. Suzuki, and M. Morita, Prog. Theor. Phys. **50**, 1894 (1973).

### $n \rightarrow p e^- \bar{\nu}_e$ DECAY PARAMETERS

See the above “Note on Baryon Decay Parameters.” For discussions of recent results, see the references cited at the beginning of the section on the neutron mean life. For discussions of the values of the weak coupling constants  $g_A$  and  $g_V$  obtained using the neutron lifetime and asymmetry parameter  $A$ , comparisons with other methods of obtaining these constants, and implications for particle physics and for astrophysics, see DUBBERS 91 and WOOLCOCK 91. For tests of the  $V-A$  theory of

# Baryon Particle Listings

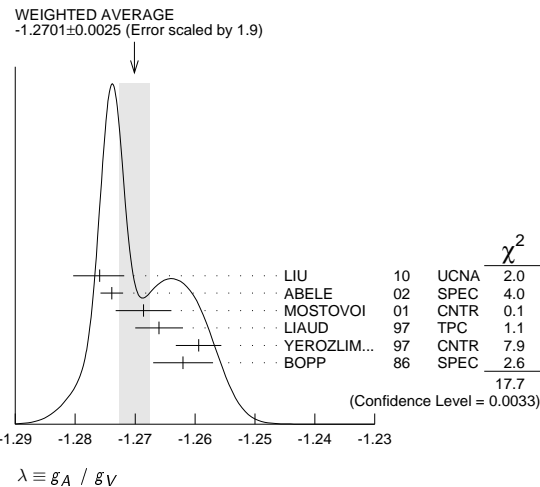
*n*

neutron decay, see EROZOLIMSKII 91B, MOSTOVOI 96, NICO 05, SEV-ERIJNS 06, and ABELE 08.

## $\lambda \equiv g_A / g_V$

VALUE	DOCUMENT ID	TECN	COMMENT
<b>-1.2701 ± 0.0025 OUR AVERAGE</b>			Error includes scale factor of 1.9. See the ideogram below.
-1.27590 ± 0.00409 -0.00445	LIU	10	UCNA Ultracold <i>n</i> , polarized
-1.2739 ± 0.0019	34 ABELE	02	SPEC Cold <i>n</i> , polarized, A
-1.2686 ± 0.0046 ± 0.0007	35 MOSTOVOI	01	CNTR A and B × polarizations
-1.266 ± 0.004	LIAUD	97	TPC Cold <i>n</i> , polarized, A
-1.2594 ± 0.0038	36 YEROZLIM...	97	CNTR Cold <i>n</i> , polarized, A
-1.262 ± 0.005	BOPP	86	SPEC Cold <i>n</i> , polarized, A
• • • We do not use the following data for averages, fits, limits, etc. • • •			
-1.275 ± 0.006 ± 0.015	SCHUMANN	08	CNTR Cold <i>n</i> , polarized
-1.274 ± 0.003	ABELE	97D	SPEC Cold <i>n</i> , polarized, A
-1.266 ± 0.004	SCHRECK...	95	TPC See LIAUD 97
-1.2544 ± 0.0036	EROZOLIM...	91	CNTR See YEROZOLIMSKY 97
-1.226 ± 0.042	MOSTOVOY	83	RVUE
-1.261 ± 0.012	EROZOLIM...	79	CNTR Cold <i>n</i> , polarized, A
-1.259 ± 0.017	37 STRATOWA	78	CNTR <i>p</i> recoil spectrum, a
-1.263 ± 0.015	EROZOLIM...	77	CNTR See EROZOLIMSKII 79
-1.250 ± 0.036	37 DOBROZE...	75	CNTR See STRATOWA 78
-1.258 ± 0.015	38 KROHN	75	CNTR Cold <i>n</i> , polarized, A
-1.263 ± 0.016	39 KROPF	74	RVUE <i>n</i> decay alone
-1.250 ± 0.009	39 KROPF	74	RVUE <i>n</i> decay + nuclear ft

34 This is the combined result of ABELE 02 and ABELE 97D.  
 35 MOSTOVOI 01 measures the two *P*-odd correlations *A* and *B*, or rather *SA* and *SB*, where *S* is the *n* polarization, in free neutron decay.  
 36 YEROZOLIMSKY 97 makes a correction to the EROZOLIMSKII 91 value.  
 37 These experiments measure the absolute value of  $g_A/g_V$  only.  
 38 KROHN 75 includes events of CHRISTENSEN 70.  
 39 KROPF 74 reviews all data through 1972.

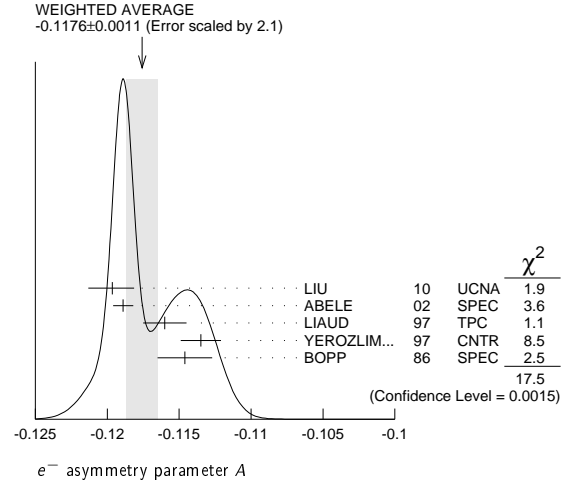


## $e^-$ ASYMMETRY PARAMETER *A*

This is the neutron-spin electron-momentum correlation coefficient. Unless otherwise noted, the values are corrected for radiative effects and weak magnetism. In the Standard Model, *A* is related to  $\lambda \equiv g_A/g_V$  by  $A = -2(\lambda^2 - |\lambda|) / (1 + 3\lambda^2)$ ; this assumes that  $g_A$  and  $g_V$  are real.

VALUE	DOCUMENT ID	TECN	COMMENT
<b>-0.1176 ± 0.0011 OUR AVERAGE</b>			Error includes scale factor of 2.1. See the ideogram below.
-0.11966 ± 0.00089 ± 0.00123 -0.00140	LIU	10	UCNA Ultracold <i>n</i> , polarized
-0.1189 ± 0.0007	40 ABELE	02	SPEC Cold <i>n</i> , polarized
-0.1160 ± 0.0009 ± 0.0012	LIAUD	97	TPC Cold <i>n</i> , polarized
-0.1135 ± 0.0014	41 YEROZLIM...	97	CNTR Cold <i>n</i> , polarized
-0.1146 ± 0.0019	BOPP	86	SPEC Cold <i>n</i> , polarized
• • • We do not use the following data for averages, fits, limits, etc. • • •			
-0.1138 ± 0.0046 ± 0.0021	PATTIE	09	SPEC Ultracold <i>n</i> , polarized
-0.1168 ± 0.0017	42 MOSTOVOI	01	CNTR Inferred
-0.1189 ± 0.0012	ABELE	97D	SPEC Cold <i>n</i> , polarized
-0.1160 ± 0.0009 ± 0.0011	SCHRECK...	95	TPC See LIAUD 97
-0.1116 ± 0.0014	EROZOLIM...	91	CNTR See YEROZOLIMSKY 97
-0.114 ± 0.005	43 EROZOLIM...	79	CNTR Cold <i>n</i> , polarized
-0.113 ± 0.006	43 KROHN	75	CNTR Cold <i>n</i> , polarized

40 This is the combined result of ABELE 02 and ABELE 97D.  
 41 YEROZOLIMSKY 97 makes a correction to the EROZOLIMSKII 91 value.  
 42 MOSTOVOI 01 calculates this from its measurement of  $\lambda = g_A/g_V$  above.  
 43 These results are not corrected for radiative effects and weak magnetism, but the corrections are small compared to the errors.



## $\nu_e$ ASYMMETRY PARAMETER *B*

This is the neutron-spin antineutrino-momentum correlation coefficient. In the Standard Model, *B* is related to  $\lambda \equiv g_A/g_V$  by  $B = 2\lambda(\lambda - 1) / (1 + 3\lambda^2)$ ; this assumes that  $g_A$  and  $g_V$  are real.

VALUE	DOCUMENT ID	TECN	COMMENT
<b>0.9807 ± 0.0030 OUR AVERAGE</b>			
0.9802 ± 0.0034 ± 0.0036	SCHUMANN	07	CNTR Cold <i>n</i> , polarized
0.967 ± 0.006 ± 0.010	KREUZ	05	CNTR Cold <i>n</i> , polarized
0.9801 ± 0.0046	SEREBROV	98	CNTR Cold <i>n</i> , polarized
0.9894 ± 0.0083	KUZNETSOV	95	CNTR Cold <i>n</i> , polarized
1.00 ± 0.05	CHRISTENSEN70	CNTR	Cold <i>n</i> , polarized
0.995 ± 0.034	EROZOLIM...	70C	CNTR Cold <i>n</i> , polarized
• • • We do not use the following data for averages, fits, limits, etc. • • •			
0.9876 ± 0.0004	44 MOSTOVOI	01	CNTR Inferred

## PROTON ASYMMETRY PARAMETER *C*

Describes the correlation between the neutron spin and the proton momentum. In the Standard Model, *C* is related to  $\lambda \equiv g_A/g_V$  by  $C = -x_c(A + B) = x_c 4\lambda / (1 + 3\lambda^2)$ , where  $x_c = 0.27484$  is a kinematic factor; this assumes that  $g_A$  and  $g_V$  are real.

VALUE	DOCUMENT ID	TECN	COMMENT
<b>-0.2377 ± 0.0010 ± 0.0024</b>	SCHUMANN	08	CNTR Cold <i>n</i> , polarized

## $e^- \nu_e$ ANGULAR CORRELATION COEFFICIENT *a*

For a review of past experiments and plans for future measurements of the *a* parameter, see WIETFELDT 05. In the Standard Model, *a* is related to  $\lambda \equiv g_A/g_V$  by  $a = (1 - \lambda^2) / (1 + 3\lambda^2)$ ; this assumes that  $g_A$  and  $g_V$  are real.

VALUE	DOCUMENT ID	TECN	COMMENT
<b>-0.103 ± 0.004 OUR AVERAGE</b>			
-0.1054 ± 0.0055	BYRNE	02	SPEC Proton recoil spectrum
-0.1017 ± 0.0051	STRATOWA	78	CNTR Proton recoil spectrum
-0.091 ± 0.039	GRIGOREV	68	SPEC Proton recoil spectrum
• • • We do not use the following data for averages, fits, limits, etc. • • •			
-0.1045 ± 0.0014	45 MOSTOVOI	01	CNTR Inferred
45 MOSTOVOI 01 calculates this from its measurement of $\lambda = g_A/g_V$ above.			

## $\phi_{AV}$ , PHASE OF $g_A$ RELATIVE TO $g_V$

Time reversal invariance requires this to be 0 or 180°. This is related to *D* given in the next data block and  $\lambda \equiv g_A/g_V$  by  $\sin(\phi_{AV}) \equiv D(1 + 3\lambda^2) / 2|\lambda|$ ; this assumes that  $g_A$  and  $g_V$  are real.

VALUE (°)	DOCUMENT ID	TECN	COMMENT
<b>180.018 ± 0.026 OUR AVERAGE</b>			
180.013 ± 0.028	MUMM	11	CNTR Cold <i>n</i> , polarized > 91%
180.04 ± 0.09	SOLDNER	04	CNTR Cold <i>n</i> , polarized
180.08 ± 0.13	LISING	00	CNTR Polarized > 93%
• • • We do not use the following data for averages, fits, limits, etc. • • •			
179.71 ± 0.39	EROZOLIM...	78	CNTR Cold <i>n</i> , polarized
180.35 ± 0.43	EROZOLIM...	74	CNTR Cold <i>n</i> , polarized
181.1 ± 1.3	46 KROPF	74	RVUE <i>n</i> decay
180.14 ± 0.22	STEINBERG	74	CNTR Cold <i>n</i> , polarized

46 KROPF 74 reviews all data through 1972.



See key on page 457

Baryon Particle Listings

n

TRIPLE CORRELATION COEFFICIENT D

These are measurements of the component of n spin perpendicular to the decay plane in beta decay. Should be zero if T invariance is not violated.

Table with columns: VALUE (units 10^-4), DOCUMENT ID, TECN, COMMENT. Includes entries for MUMM, SOLDNER, LISING, EROZOLIM..., and STEINBERG.

TRIPLE CORRELATION COEFFICIENT R

Another test of time-reversal invariance. R measures the polarization of the electron in the direction perpendicular to the plane defined by the neutron spin and the electron momentum. R = 0 for T invariance.

Table with columns: VALUE, DOCUMENT ID, TECN, COMMENT. Includes entry for KOZELA.

n REFERENCES

We have omitted some papers that have been superseded by later experiments. See our earlier editions.

Large table of references for the 'n' section, listing authors, document IDs, and technical details.

Large table of references for the 'Baryon Particle Listings' section, listing authors, document IDs, and technical details.

# Baryon Particle Listings

## $N$ 's and $\Delta$ 's

### $N$ AND $\Delta$ RESONANCES

Written April 2012 by E. Klempt (University of Bonn) and R.L. Workman (George Washington University).

#### I. Introduction

The excited states of the nucleon have been studied in a large number of formation and production experiments. The Breit-Wigner masses and widths, the pole positions, and the elasticities of the  $N$  and  $\Delta$  resonances in the Baryon Summary Table come largely from partial-wave analyses of  $\pi N$  total, elastic, and charge-exchange scattering data. The most comprehensive analyses were carried out by the Karlsruhe-Helsinki (KH80) [1], Carnegie Mellon-Berkeley (CMB80) [2], and George Washington U (GWU) [3] groups. Partial-wave analyses have also been performed on much smaller  $\pi N$  reaction data sets to get  $N\eta$ ,  $\Lambda K$ , and  $\Sigma K$  branching fractions. Other branching fractions come from analyses of  $\pi N \rightarrow N\pi\pi$  data. A number of groups have undertaken multichannel analyses of these and associated photo-induced reactions (see Sec. VI).

Table 1. The status of the  $N$  resonances. Only those with an overall status of \*\*\* or \*\*\*\* are included in the main Baryon Summary Table.

Particle	$J^P$	Status		Status as seen in —									
		overall	$\pi N$	$\gamma N$	$N\eta$	$N\sigma$	$N\omega$	$\Lambda K$	$\Sigma K$	$N\rho$	$\Delta\pi$		
$N$	$1/2^+$	****											
$N(1440)$	$1/2^+$	****	****	****		***				*	***		
$N(1520)$	$3/2^-$	****	****	****	***					***	***		
$N(1535)$	$1/2^-$	****	****	****	****					**	*		
$N(1650)$	$1/2^-$	****	****	***	***		***	**	**	**	***		
$N(1675)$	$5/2^-$	****	****	***	*		*		*	*	***		
$N(1680)$	$5/2^+$	****	****	****	*	**				***	***		
$N(1685)$	? <sup>?</sup>	*											
$N(1700)$	$3/2^-$	***	***	**	*		*	*	*	*	***		
$N(1710)$	$1/2^+$	***	***	***	***	**	***	**	*	**			
$N(1720)$	$3/2^+$	****	****	***	***		**	**	**	*			
$N(1860)$	$5/2^+$	**	**							*	*		
$N(1875)$	$3/2^-$	***	*	***		**	***	**			***		
$N(1880)$	$1/2^+$	**	*	*	**		*						
$N(1895)$	$1/2^-$	**	*	**	**		**	*					
$N(1900)$	$3/2^+$	***	**	***	**	**	***	**	*	**			
$N(1990)$	$7/2^+$	**	**	**					*				
$N(2000)$	$5/2^+$	**	*	**	**		**	*	**				
$N(2040)$	$3/2^+$	*											
$N(2060)$	$5/2^-$	**	**	**	*			**					
$N(2100)$	$1/2^+$	*											
$N(2150)$	$3/2^-$	**	**	**			**			**			
$N(2190)$	$7/2^-$	****	****	***		*	**		*				
$N(2220)$	$9/2^+$	****	****										
$N(2250)$	$9/2^-$	****	****										
$N(2600)$	$11/2^-$	***	***										
$N(2700)$	$13/2^+$	**	**										

\*\*\*\* Existence is certain, and properties are at least fairly well explored.  
 \*\*\* Existence is very likely but further confirmation of quantum numbers and branching fractions is required.  
 \*\* Evidence of existence is only fair.  
 \* Evidence of existence is poor.

In recent years, a large amount of data on photoproduction of many final states has been accumulated, and these data are beginning to make a significant impact on the properties of

baryon resonances. A survey of data on photoproduction can be found in the proceedings of recent conferences [4] and workshops [5], and in a recent review [6].

#### II. Naming scheme for baryon resonances

In the past, when nearly all resonance information came from elastic  $\pi N$  scattering, it was common to label resonances with the incoming partial wave  $L_{2I,2J}$ , as in  $\Delta(1232)P_{33}$  and  $N(1680)F_{15}$ . However, most recent information has come from  $\gamma N$  experiments. Therefore, we have replaced  $L_{2I,2J}$  with the spin-parity  $J^P$  of the state, as in  $\Delta(1232) 3/2^+$  and  $N(1680) 5/2^+$ . This applies to all baryons, including those such as the  $\Xi$  resonances and charm baryons that are not produced in formation experiments. Names of the stable baryons ( $N, \Lambda, \Sigma, \Xi, \Omega, \Lambda_c, \dots$ ) have no spin, parity, or mass attached.

Table 2. The status of the  $\Delta$  resonances. Only those with an overall status of \*\*\* or \*\*\*\* are included in the main Baryon Summary Table.

Particle	$J^P$	Status		Status as seen in —									
		overall	$\pi N$	$\gamma N$	$N\eta$	$N\sigma$	$N\omega$	$\Lambda K$	$\Sigma K$	$N\rho$	$\Delta\pi$		
$\Delta(1232)$	$3/2^+$	****	****	****	F								
$\Delta(1600)$	$3/2^+$	***	***	***	o						*	***	
$\Delta(1620)$	$1/2^-$	****	****	***	r						***	***	
$\Delta(1700)$	$3/2^-$	****	****	****		b					**	***	
$\Delta(1750)$	$1/2^+$	*	*			i							
$\Delta(1900)$	$1/2^-$	**	**	**		d					**	**	**
$\Delta(1905)$	$5/2^+$	****	****	****		d					***	**	**
$\Delta(1910)$	$1/2^+$	****	****	**		e				*	*	**	
$\Delta(1920)$	$3/2^+$	***	***	**		n				***		**	
$\Delta(1930)$	$5/2^-$	***	***										
$\Delta(1940)$	$3/2^-$	**	*	**	F						(seen in $\Delta\eta$ )		
$\Delta(1950)$	$7/2^+$	****	****	****	o					***	*	***	
$\Delta(2000)$	$5/2^+$	**			r							**	
$\Delta(2150)$	$1/2^-$	*	*		b								
$\Delta(2200)$	$7/2^-$	*	*			i							
$\Delta(2300)$	$9/2^+$	**	**			d							
$\Delta(2350)$	$5/2^-$	*	*			d							
$\Delta(2390)$	$7/2^+$	*	*			e							
$\Delta(2400)$	$9/2^-$	**	**			n							
$\Delta(2420)$	$11/2^+$	****	****	*									
$\Delta(2750)$	$13/2^-$	**	**										
$\Delta(2950)$	$15/2^+$	**	**										

\*\*\*\* Existence is certain, and properties are at least fairly well explored.  
 \*\*\* Existence is very likely but further confirmation of quantum numbers and branching fractions is required.  
 \*\* Evidence of existence is only fair.  
 \* Evidence of existence is poor.

#### III. Using the $N$ and $\Delta$ listings

Tables 1 and 2 list all the  $N$  and  $\Delta$  entries in the Baryon Listings and give our evaluation of the overall status, the status from  $\pi N \rightarrow N\pi$  scattering data and from photoproduction experiments, and the status channel by channel. Only the established resonances (overall status 3 or 4 stars) are promoted to the Baryon Summary Table. We have omitted from the Listings information from old analyses, prior to KH80 and CMB80 which can be found in earlier editions. A rather complete survey of older results was given in our 1982 edition [7].

The star rating assigned to a resonance depends on the data base and the analysis. As a rule, we award an overall status \*\*\* or \*\*\*\* only to those resonances which are confirmed by independent analyses and which are derived from analyses based on complete information, *i.e.*, for analyses based on three observables in  $\pi N$  scattering or eight properly chosen observables in photoproduction. Use of dispersion relations (as in the KH80, CMB80, and GWU analyses) may lift these requirements. Three and four-star resonances should be observed in one of their strongest decay modes. Weak signals or signals emerging in analyses with incomplete experimental information are given \*\* or \* status. We do not consider new results without proper error evaluation.

In the Data Listings, we give first the Breit-Wigner mass and width but warn the reader that Breit-Wigner parameters depend on the formalism used, such as for angular momentum barrier factors or cut-off parameters, and the assumed or modeled background. Then we give pole-related quantities, such as the position of the pole and its elastic residue. For the first time, we give residues and phases of hadronic transition amplitudes and helicity amplitudes. Branching ratios and photoproduction amplitudes follow.

#### IV. Properties of resonances

Resonances are defined by poles of the scattering amplitude in the complex energy  $w = \sqrt{s}$  plane [8]. In contrast to other quantities related to resonance phenomena, such as the Breit-Wigner mass or the K-matrix pole, a pole of the scattering amplitude does not depend on the chosen field parameterization, and production and decay properties factorize. It is the pole position which should be compared to eigenvalues of the Hamiltonian of full QCD.

Examining the Listings, one finds a much larger spread in Breit-Wigner parameters compared to pole parameters. In his *pole-emic* against Breit-Wigner parameters, Hohler [9] concluded: “*In contrast to the conventional (Breit-Wigner) parameters, the pole positions and speed plots have a well-defined relation to S-matrix theory. They also give more information on the resonances and thresholds and can be used for the prediction on other reactions that couple to the excited states [italics in original].*”

In scattering theory, the amplitude for the scattering process leading from the initial state  $a$  to the final state  $b$  is given by the  $S$  matrix, which can be decomposed as follows:

$$S_{ab} = I_{ab} + 2i\sqrt{\rho_a}T_{ab}\sqrt{\rho_b}. \quad (1)$$

Here  $I_{ab}$  is the identity operator, and  $T_{ab}$  describes the transition from the initial state to the final state (e.g.  $\pi N$  to  $\Sigma K$ ).  $T_{ab}$  contains coupling constants, the decay momenta  $k$  to the power  $L$  to yield the correct threshold behavior when angular momenta are involved, and a correction  $F(L, r^2, k^2)$ , e.g. in Blatt-Weisskopf form, with a range parameter  $r$ . The two-body phase-space  $\rho$  is given (see Eq. 39.17 in Sec. 39) by

$$\rho(s) = \frac{1}{16\pi} \frac{2|\vec{k}|}{\sqrt{s}}. \quad (2)$$

The transition amplitude  $T$  contains poles due to resonances and background terms. Above the threshold for inelastic reactions, a resonance is associated with a cluster of poles in different Riemann sheets. The pole closest to the real axis has the strongest impact on the data. It is situated on the second Riemann sheet, starting at the highest threshold below the pole position. If the threshold is close to the pole position, poles in other sheets may have an important impact as well.

Other complications may occur: Broad resonances are difficult to disentangle from background amplitudes, *e.g.*, due to left-hand cuts originating from meson and baryon exchange forces. A two-particle subsystem generates a square-root singularity at its threshold; poles in a two-body subsystem, *e.g.*, the  $\rho$  meson in the  $\pi\pi$  system, lead to branch points in the complex energy plane. Neglecting some of these aspects leads to a model dependence of the pole position. These uncertainties increase with the particle width.

Several particle properties are related to poles. First, poles exist on multiple Riemann sheets. In the Listings, we give for each resonance the position of the most relevant pole. The poles of the scattering amplitude can be found by analytic continuation of the amplitude. The real part of the pole position in the complex energy plane defines the particle mass, the imaginary part its half width:  $w_{\text{pole}} = m_{\text{pole}} - i\Gamma_{\text{pole}}/2$ . Residues of transition amplitudes are the first term in a Laurent expansion and can be calculated through a contour integral of the amplitude  $T_{ab}$  around the pole position in the energy plane:

$$\begin{aligned} \text{Res}(a \rightarrow b) &= \oint \frac{d\sqrt{s}}{2\pi i} \sqrt{\rho_a} T_{ab}(s) \sqrt{\rho_b} \\ &= \frac{1}{2w_{\text{pole}}} \sqrt{\rho_a(s_{\text{pole}})} g_a g_b \sqrt{\rho_b(s_{\text{pole}})}, \end{aligned} \quad (4)$$

where  $g_a$  and  $g_b$  are coupling constants. In the Listings, we give normalized residues,  $2 \text{Res}(a \rightarrow b)/\Gamma_{\text{pole}}$ . For elastic scattering, *e.g.*, for  $\pi N \rightarrow N\pi$ , this gives the elastic residue:

$$\text{Res}(a \rightarrow a) = \frac{1}{2w_{\text{pole}}} \rho_a(s_{\text{pole}}) g_a^2. \quad (5)$$

Branching ratios of a pole can be defined by

$$BR_{\text{pole}}(\text{channel } b) = \frac{|\text{Res}(\pi N \rightarrow b)|^2}{|\text{Res}(\pi N \rightarrow N\pi)| \cdot (\Gamma_{\text{pole}}/2)}. \quad (6)$$

This information is, however, not given in the literature.

Within models, background amplitudes can be parameterized using an effective Lagrangian approach (as in dynamical coupled-channel approaches), or by low-order polynomial functions. In the latter case, resonances are then added, sometimes in the form of Breit-Wigner amplitudes. In the Listings, particle properties related to fits to data using Breit-Wigner amplitudes are given as well. These are the Breit-Wigner mass and width, the partial decay widths, and the branching ratios. It should be noted that Breit-Wigner parameters depend on the background parameterization.

# Baryon Particle Listings

## $N$ 's and $\Delta$ 's

The multichannel relativistic Breit-Wigner amplitude is given by

$$A_{ab} = \sqrt{\rho_a} T_{ab} \sqrt{\rho_b} = \frac{-g_a g_b \sqrt{\rho_a \rho_b}}{s - m_{\text{BW}}^2 + i \sum_a g_a^2 \rho_a}, \quad (7)$$

where  $m_{\text{BW}}$  is called the Breit-Wigner mass. In the case of two channels, Eq. (7) is known as the Flatté formula. The inclusion of angular momenta leads to additional factors. The energy-dependent partial decay widths, defined by  $\sqrt{s} \Gamma_a(s) = g_a^2 \rho_a(s)$ , can be used to bring Eq. (7) into the form of Eq. (39.57). Evaluated at the Breit-Wigner mass, it gives the partial decay width  $\Gamma_a$  at the resonance position

$$m_{\text{BW}} \Gamma_a = g_a^2 \rho_a(m_{\text{BW}}^2). \quad (8)$$

The branching ratio for the decay of a resonance into channel  $a$ ,

$$BR_a = \Gamma_a / \Gamma_{\text{BW}}, \quad (9)$$

vanishes by definition for decay modes with thresholds above the Breit-Wigner mass. That the sum  $\sum_a BR_a$  equals one follows from the definition. Unobserved decay modes lead to the inequality  $\sum_a BR_a \leq 1$ . In the case of broad resonances, definitions (8) and (9) may be counter-intuitive. Branching ratios can also be defined as

$$BR'_a = \int_{\text{threshold}}^{\infty} \frac{ds}{\pi} \frac{g_a^2 \rho_a(s)}{(m_{\text{BW}}^2 - s)^2 + (\sum_a g_a^2 \rho_a(s))^2}. \quad (10)$$

Here  $\rho(s)$  should not be continued below threshold. These branching ratios include decays of resonances into channels with thresholds above their nominal masses. The relation  $\sum_a BR'_a = 1$  is needed for normalization.

### V. Electromagnetic interactions

A new approach to the nucleon excitation spectrum is provided by dedicated facilities at the Universities of Bonn and Mainz, and at the national laboratories Jefferson Lab in the US and SPring-8 in Japan. High-precision cross sections and polarization observables in photoproduction of pseudoscalar mesons provide a data set that is nearly a “complete experiment,” one that fully constrains the four complex amplitudes describing the spin-structure of the reaction. A large number of photoproduction reactions has been studied.

In photoproduction, the spins of the photon and nucleon can be parallel or anti-parallel, and there are spin-flip and non-flip transitions. Four independent amplitudes can be defined using the photon polarization and the hadronic current [10]. The amplitudes can be expanded in a series of electric and magnetic multipoles. In general, two amplitudes, one electric and one magnetic, contribute to one  $J^P$  combination. For a given resonance, these two amplitudes are related to the helicity amplitudes  $A_{1/2}$  and  $A_{3/2}$ . The final state may have isospin  $I = 1/2$  or  $I = 3/2$ .

If a Breit-Wigner parametrization is used, the  $N\gamma$  partial width,  $\Gamma_\gamma$ , is given in terms of the helicity amplitudes  $A_{1/2}$  and  $A_{3/2}$  by

$$\Gamma_\gamma = \frac{k_{\text{BW}}^2}{\pi} \frac{2m_N}{(2J+1)m_{\text{BW}}} (|A_{1/2}|^2 + |A_{3/2}|^2). \quad (11)$$

Here  $m_N$  and  $m_{\text{BW}}$  are the nucleon and resonance masses,  $J$  is the resonance spin, and  $k_{\text{BW}}$  is the photon c.m. decay momentum. Most earlier analyses have quoted the real quantities  $A_{1/2}$  and  $A_{3/2}$ .

Other more recent studies have quoted related complex quantities, evaluated at the T-matrix pole. The complex helicity amplitudes for photoproduction of the final state  $b$ ,  $\tilde{A}_{1/2}$  and  $\tilde{A}_{3/2}$ , are given by

$$\text{Res}((\gamma N)_h \rightarrow b) = \frac{\tilde{A}_b^h g_b}{2w_{\text{pole}}} |k_{\text{pole}}| \sqrt{\frac{2m_N}{(2J+1)\pi} \cdot \rho_b(w_{\text{pole}}^2)}. \quad (12)$$

$\tilde{A}_{1/2}$  and  $\tilde{A}_{3/2}$  are defined at the pole position, and are normalized to reproduce Eq. (11) when the pole position is replaced by the Breit-Wigner mass.

The amplitudes  $\tilde{A}_{1/2}$  and  $\tilde{A}_{3/2}$ , the elastic residues, and the residues of the transition amplitudes are complex numbers. Eq. (8) defines  $g_{N\pi}$  up to a sign. (Here,  $g_{N\pi}$  is the  $N\pi$  decay constant of a resonance, not the  $\pi N$  coupling constant!) Due to Eq. (12), the phase of the helicity amplitude depends on this definition. We define the phase of  $g_{N\pi}$  clockwise.

The determination of eight real numbers from four complex amplitudes (with one overall phase undetermined) requires at least seven independent data points. At least one further measurement is required to resolve discrete ambiguities that result from the fact that data are proportional to squared amplitudes. Photon beams and nucleon targets can be polarized (with linear or circular polarization  $P_\perp$ ,  $P_\odot$ , and  $\vec{T}$ , respectively); and the recoil polarization of the outgoing nucleon  $\vec{R}$  can be measured. Experiments can be divided into three classes: those with polarized photons and a polarized target (BT); and those measuring the baryon recoil polarization and using either a polarized photon (BR) or a polarized target (TR). Different sign conventions are used in the literature, as summarized in Ref. 12.

A large number of polarization observables has been determined that constrain energy-dependent partial-wave solutions. One of the best studied reactions is  $\gamma p \rightarrow \Lambda K^+$ . Published data include differential cross sections, the beam asymmetry  $\Sigma$ , the target asymmetry  $T$ , the recoil polarization  $P$ , and the BR double-polarization variables  $C_x, C_z, O_x$ , and  $O_z$ . For  $\gamma p \rightarrow p\pi^0$ ,  $\gamma p \rightarrow n\pi^+$ , and  $\gamma p \rightarrow p\eta$ , differential cross sections and beam asymmetries have been published; BT data for  $E, F, G$ , and  $H$  have been presented at conferences [13].

Electroproduction of mesons provides information on the internal structure of resonances. The helicity amplitudes become functions of the momentum transfer, and a third amplitude,  $S_{1/2}$ , contributes to the process. Recent experimental results and their interpretation are reviewed by I.G. Aznauryan and

V.D. Burkert [14] and by L. Tiator, D. Drechsel, S.S. Kamalov, and M. Vanderhaeghen [15].

## VI. Partial wave analyses

Several PWA groups are now actively involved in the analysis of the new data. Of the three “classical” analysis groups at KH, CMB, and GWU, only the GWU group is still active. This group maintains a nearly complete database, covering reactions from  $\pi N$  and  $KN$  elastic scattering to  $\gamma N \rightarrow N\pi$ ,  $N\eta$ , and  $N\eta'$ . It is presently the only group determining energy-independent  $\pi N$  elastic amplitudes from scattering data. Given the high-precision of photoproduction data already collected and to be taken in the near future, we estimate that an improved spectrum of  $N$  and  $\Delta$  resonances should become available in the forthcoming years.

Energy-dependent fits are performed by various groups with the aim to understand the reaction dynamics and to identify  $N$  and  $\Delta$  resonances. Ideally, the Bethe-Salpeter equation should be solved to describe the data. For practical reasons, approximations have to be made. We mention here: (1) The Mainz unitary isobar model [16] focusses on the correct treatment of the low-energy domain; resonances are added to the unitary amplitude as a sum of Breit-Wigner amplitudes. (2) Multichannel analyses using K-matrix parameterizations derive background terms from a chiral Lagrangian—providing a microscopical description of the background—(Giessen [17,18]), or from phenomenology (Bonn-Gatchina [19]). (3) Several groups (Argonne-Osaka [20], Bonn-Jülich [22,23], Dubna-Mainz-Taipeh [21], EBAC-Jlab [24], Valencia [25]) use dynamical reaction models, driven by chiral Lagrangians, which take dispersive parts of intermediate states into account. The Giessen group pioneered multichannel analyses of large data sets on pion- and photo-induced reactions [17,18]. The Bonn-Gatchina group included recent high-statistics data and reported systematic searches for new baryon resonances in all relevant partial waves. A summary of their results can be found in Ref. 19.

## References

- G. Höhler, *Pion-Nucleon Scattering*, Landolt-Börnstein, Vol. I/9b2 (1983), ed. H. Schopper, Springer Verlag.
- R.E. Cutkosky *et al.*, Baryon 1980, *IV International Conference on Baryon Resonances*, Toronto, ed. N. Isgur, p. 19.
- R.A. Arndt *et al.*, Phys. Rev. **C74**, 045205 (2006).
- Hadron 2011: 14th International Conference on Hadron Spectroscopy*, München, Germany, June 13-17, 2011, published in eConf.
- NSTAR 2011: 8th International Workshop on the Physics of Excited Nucleons*, May 17-20, 2011, Newport News, Virginia, USA.
- E. Klempt and J.M. Richard, Rev. Mod. Phys. **82**, 1095 (2010).
- M. Roos *et al.*, Phys. Lett. **B111**, 1 (1982).
- R.H. Dalitz and R.G. Moorhouse, Proc. Roy. Soc. Lond. **A318**, 279 (1970).
- C. Caso *et al.*, Eur. Phys. J. **C3**, 1 (1998).
- G.F. Chew *et al.*, Phys. Rev. **106**, 1345 (1957).
- C.G. Fasano *et al.*, Phys. Rev. **C46**, 2430 (1992).
- A.M. Sandorfi *et al.*, “A Rosetta Stone relating conventions in photo-meson partial wave analyses,” arXiv:1108.5411 [nucl-th].
- R. Beck, “Light baryon spectroscopy: recent results,” presented at *Hadron2011*, op.cit.
- I.G. Aznauryan and V.D. Burkert, Prog. Part. Nucl. Phys. **67**, 1 (2012).
- L. Tiator *et al.*, Eur. Phys. J. ST **198**, 141 (2011).
- D. Drechsel, S.S. Kamalov, and L. Tiator, Eur. Phys. J. A **34**, 69 (2007).
- G. Penner and U. Mosel, Phys. Rev. C **66**, 055211 (2002).
- G. Penner and U. Mosel, Phys. Rev. C **66**, 055212 (2002).
- A.V. Anisovich *et al.*, EPJ **A48**, 15 (2012).
- T. Sato and T.-S. H. Lee, J. Phys. G **36**, 073001 (2009).
- G.Y. Chen *et al.*, Phys. Rev. C **76**, 035206 (2007).
- M. Döring *et al.*, Phys. Lett. B **681**, 26 (2009).
- M. Döring *et al.*, Nucl. Phys. A **829**, 170 (2009).
- A. Matsuyama, T. Sato, and T.-S.H. Lee, Phys. Rept. **439**, 193 (2007).
- S. Sarkar, E. Oset, and M.J. Vicente Vacas, Nucl. Phys. A **750**, 294 (2005) [Erratum-ibid. A **780**, 78 (2006)].

**N(1440) 1/2<sup>+</sup>**

$I(J^P) = \frac{1}{2}(\frac{1}{2}^+)$  Status: \* \* \* \*

Most of the results published before 1975 were last included in our 1982 edition, Physics Letters **111B** 1 (1982). Some further obsolete results published before 1984 were last included in our 2006 edition, Journal of Physics, G **33** 1 (2006).

## N(1440) BREIT-WIGNER MASS

VALUE (MeV)	DOCUMENT ID	TECN	COMMENT
<b>1420 to 1470 (≈ 1440) OUR ESTIMATE</b>			
1430 ± 8	ANISOVICH	12A	DPWA Multichannel
1485.0 ± 1.2	ARNDT	06	DPWA $\pi N \rightarrow \pi N, \eta N$
1462 ± 10	MANLEY	92	IPWA $\pi N \rightarrow \pi N \& N\pi\pi$
1440 ± 30	CUTKOSKY	80	IPWA $\pi N \rightarrow \pi N$
1410 ± 12	HOEHLER	79	IPWA $\pi N \rightarrow \pi N$
• • • We do not use the following data for averages, fits, limits, etc. • • •			
1440 ± 12	ANISOVICH	10	DPWA Multichannel
1439 ± 19	BATINIC	10	DPWA $\pi N \rightarrow N\pi, N\eta$
1436 ± 15	SARANTSEV	08	DPWA Multichannel
1468.0 ± 4.5	ARNDT	04	DPWA $\pi N \rightarrow \pi N, \eta N$
1518 ± 5	PENNER	02c	DPWA Multichannel
1479 ± 80	VRANA	00	DPWA Multichannel
1463 ± 7	ARNDT	96	IPWA $\gamma N \rightarrow \pi N$
1467	ARNDT	95	DPWA $\pi N \rightarrow N\pi$
1465	LI	93	IPWA $\gamma N \rightarrow \pi N$
1471	CUTKOSKY	90	IPWA $\pi N \rightarrow \pi N$
1380	<sup>1</sup> LONGACRE	77	IPWA $\pi N \rightarrow N\pi\pi$
1390	<sup>2</sup> LONGACRE	75	IPWA $\pi N \rightarrow N\pi\pi$

## N(1440) BREIT-WIGNER WIDTH

VALUE (MeV)	DOCUMENT ID	TECN	COMMENT
<b>200 to 450 (≈ 300) OUR ESTIMATE</b>			
365 ± 35	ANISOVICH	12A	DPWA Multichannel
284 ± 18	ARNDT	06	DPWA $\pi N \rightarrow \pi N, \eta N$
391 ± 34	MANLEY	92	IPWA $\pi N \rightarrow \pi N \& N\pi\pi$
340 ± 70	CUTKOSKY	80	IPWA $\pi N \rightarrow \pi N$
135 ± 10	HOEHLER	79	IPWA $\pi N \rightarrow \pi N$

## Baryon Particle Listings

 $N(1440)$ 

• • • We do not use the following data for averages, fits, limits, etc. • • •

335 ± 50	ANISOVICH	10	DPWA	Multichannel
437 ± 141	BATINIC	10	DPWA	$\pi N \rightarrow N\pi, N\eta$
335 ± 40	SARANTSEV	08	DPWA	Multichannel
360 ± 26	ARNDT	04	DPWA	$\pi N \rightarrow \pi N, \eta N$
668 ± 41	PENNER	02c	DPWA	Multichannel
490 ± 120	VRANA	00	DPWA	Multichannel
360 ± 20	ARNDT	96	IPWA	$\gamma N \rightarrow \pi N$
440	ARNDT	95	DPWA	$\pi N \rightarrow N\pi$
315	LI	93	IPWA	$\gamma N \rightarrow \pi N$
545 ± 170	CUTKOSKY	90	IPWA	$\pi N \rightarrow \pi N$
200	<sup>1</sup> LONGACRE	77	IPWA	$\pi N \rightarrow N\pi\pi$
200	<sup>2</sup> LONGACRE	75	IPWA	$\pi N \rightarrow N\pi\pi$

 $N(1440)$  POLE POSITION

## REAL PART

VALUE (MeV)	DOCUMENT ID	TECN	COMMENT
<b>1350 to 1380 (<math>\approx 1365</math>) OUR ESTIMATE</b>			
1370 ± 4	ANISOVICH	12A	DPWA Multichannel
1359	<sup>3</sup> ARNDT	06	DPWA $\pi N \rightarrow \pi N, \eta N$
1385	<sup>4</sup> HOEHLER	93	SPED $\pi N \rightarrow \pi N$
1375 ± 30	CUTKOSKY	80	IPWA $\pi N \rightarrow \pi N$
• • • We do not use the following data for averages, fits, limits, etc. • • •			
1370 ± 4	ANISOVICH	10	DPWA Multichannel
1363 ± 11	BATINIC	10	DPWA $\pi N \rightarrow N\pi, N\eta$
1371 ± 7	SARANTSEV	08	DPWA Multichannel
1357	<sup>5</sup> ARNDT	04	DPWA $\pi N \rightarrow \pi N, \eta N$
1383	VRANA	00	DPWA Multichannel
1346	<sup>6</sup> ARNDT	95	DPWA $\pi N \rightarrow N\pi$
1360	<sup>7</sup> ARNDT	91	DPWA $\pi N \rightarrow \pi N$ Soln SM90
1370	CUTKOSKY	90	IPWA $\pi N \rightarrow \pi N$
1381 or 1379	<sup>8</sup> LONGACRE	78	IPWA $\pi N \rightarrow N\pi\pi$
1360 or 1333	<sup>1</sup> LONGACRE	77	IPWA $\pi N \rightarrow N\pi\pi$

## -2xIMAGINARY PART

VALUE (MeV)	DOCUMENT ID	TECN	COMMENT
<b>160 to 220 (<math>\approx 190</math>) OUR ESTIMATE</b>			
190 ± 7	ANISOVICH	12A	DPWA Multichannel
162	<sup>3</sup> ARNDT	06	DPWA $\pi N \rightarrow \pi N, \eta N$
164	<sup>4</sup> HOEHLER	93	SPED $\pi N \rightarrow \pi N$
180 ± 40	CUTKOSKY	80	IPWA $\pi N \rightarrow \pi N$
• • • We do not use the following data for averages, fits, limits, etc. • • •			
193 ± 7	ANISOVICH	10	DPWA Multichannel
151 ± 13	BATINIC	10	DPWA $\pi N \rightarrow N\pi, N\eta$
192 ± 20	SARANTSEV	08	DPWA Multichannel
160	<sup>5</sup> ARNDT	04	DPWA $\pi N \rightarrow \pi N, \eta N$
316	VRANA	00	DPWA Multichannel
176	<sup>6</sup> ARNDT	95	DPWA $\pi N \rightarrow N\pi$
252	<sup>7</sup> ARNDT	91	DPWA $\pi N \rightarrow \pi N$ Soln SM90
228	CUTKOSKY	90	IPWA $\pi N \rightarrow \pi N$
209 or 210	<sup>8</sup> LONGACRE	78	IPWA $\pi N \rightarrow N\pi\pi$
167 or 234	<sup>1</sup> LONGACRE	77	IPWA $\pi N \rightarrow N\pi\pi$

 $N(1440)$  ELASTIC POLE RESIDUEMODULUS  $|r|$ 

VALUE (MeV)	DOCUMENT ID	TECN	COMMENT
<b>40 to 52 (<math>\approx 46</math>) OUR ESTIMATE</b>			
48 ± 3	ANISOVICH	12A	DPWA Multichannel
38	<sup>3</sup> ARNDT	06	DPWA $\pi N \rightarrow \pi N, \eta N$
40	HOEHLER	93	SPED $\pi N \rightarrow \pi N$
52 ± 5	CUTKOSKY	80	IPWA $\pi N \rightarrow \pi N$
• • • We do not use the following data for averages, fits, limits, etc. • • •			
44	BATINIC	10	DPWA $\pi N \rightarrow N\pi, N\eta$
36	<sup>5</sup> ARNDT	04	DPWA $\pi N \rightarrow \pi N, \eta N$
42	<sup>6</sup> ARNDT	95	DPWA $\pi N \rightarrow N\pi$
109	<sup>7</sup> ARNDT	91	DPWA $\pi N \rightarrow \pi N$ Soln SM90
74	CUTKOSKY	90	IPWA $\pi N \rightarrow \pi N$

PHASE  $\theta$ 

VALUE (°)	DOCUMENT ID	TECN	COMMENT
<b>75 to 100 (<math>\approx 85</math>) OUR ESTIMATE</b>			
- 78 ± 4	ANISOVICH	12A	DPWA Multichannel
- 98	<sup>3</sup> ARNDT	06	DPWA $\pi N \rightarrow \pi N, \eta N$
-100 ± 35	CUTKOSKY	80	IPWA $\pi N \rightarrow \pi N$
• • • We do not use the following data for averages, fits, limits, etc. • • •			
- 88	BATINIC	10	DPWA $\pi N \rightarrow N\pi, N\eta$
-102	<sup>5</sup> ARNDT	04	DPWA $\pi N \rightarrow \pi N, \eta N$
-101	<sup>6</sup> ARNDT	95	DPWA $\pi N \rightarrow N\pi$
- 93	<sup>7</sup> ARNDT	91	DPWA $\pi N \rightarrow \pi N$ Soln SM90
- 84	CUTKOSKY	90	IPWA $\pi N \rightarrow \pi N$

 $N(1440)$  INELASTIC POLE RESIDUE

The "normalized residue" is the residue divided by  $\Gamma_{pole}$ .

Normalized residue in  $N\pi \rightarrow N(1440) \rightarrow \Delta\pi, P\text{-wave}$ 

MODULUS (%)	PHASE (°)	DOCUMENT ID	TECN	COMMENT
<b>27 ± 2</b>	<b>40 ± 5</b>	ANISOVICH	12A	DPWA Multichannel

Normalized residue in  $N\pi \rightarrow N(1440) \rightarrow N(\pi\pi)_{S\text{-wave}}^{I=0}$ 

MODULUS (%)	PHASE (°)	DOCUMENT ID	TECN	COMMENT
<b>21 ± 5</b>	<b>-135 ± 7</b>	ANISOVICH	12A	DPWA Multichannel

 $N(1440)$  DECAY MODES

The following branching fractions are our estimates, not fits or averages.

Mode	Fraction ( $\Gamma_i/\Gamma$ )
$\Gamma_1$ $N\pi$	55-75 %
$\Gamma_2$ $N\eta$	(0.0 ± 1.0) %
$\Gamma_3$ $N\pi\pi$	30-40 %
$\Gamma_4$ $\Delta\pi$	20-30 %
$\Gamma_5$ $\Delta(1232)\pi, P\text{-wave}$	15-30 %
$\Gamma_6$ $N\rho$	< 8 %
$\Gamma_7$ $N\rho, S=1/2, P\text{-wave}$	(0.0 ± 1.0) %
$\Gamma_8$ $N\rho, S=3/2, P\text{-wave}$	
$\Gamma_9$ $N(\pi\pi)_{S\text{-wave}}^{I=0}$	10-20 %
$\Gamma_{10}$ $p\gamma$	0.035-0.048 %
$\Gamma_{11}$ $p\gamma, \text{helicity}=1/2$	0.035-0.048 %
$\Gamma_{12}$ $n\gamma$	0.02-0.04 %
$\Gamma_{13}$ $n\gamma, \text{helicity}=1/2$	0.02-0.04 %

 $N(1440)$  BRANCHING RATIOS

$\Gamma(N\pi)/\Gamma_{total}$	DOCUMENT ID	TECN	COMMENT	$\Gamma_1/\Gamma$
<b>VALUE (%)</b>				
<b>55 to 75 OUR ESTIMATE</b>				
62 ± 3	ANISOVICH	12A	DPWA Multichannel	
78.7 ± 1.6	ARNDT	06	DPWA $\pi N \rightarrow \pi N, \eta N$	
69 ± 3	MANLEY	92	IPWA $\pi N \rightarrow \pi N \& N\pi\pi$	
68 ± 4	CUTKOSKY	80	IPWA $\pi N \rightarrow \pi N$	
51 ± 5	HOEHLER	79	IPWA $\pi N \rightarrow \pi N$	
• • • We do not use the following data for averages, fits, limits, etc. • • •				
60 ± 6	ANISOVICH	10	DPWA Multichannel	
62 ± 4	BATINIC	10	DPWA $\pi N \rightarrow N\pi, N\eta$	
75.0 ± 2.4	ARNDT	04	DPWA $\pi N \rightarrow \pi N, \eta N$	
57 ± 1	PENNER	02c	DPWA Multichannel	
72 ± 5	VRANA	00	DPWA Multichannel	
68	ARNDT	95	DPWA $\pi N \rightarrow N\pi$	

$\Gamma(N\eta)/\Gamma_{total}$	DOCUMENT ID	TECN	COMMENT	$\Gamma_2/\Gamma$
<b>VALUE (%)</b>				
<b>0 ± 1</b>	VRANA	00	DPWA Multichannel	

Note: Signs of couplings from  $\pi N \rightarrow N\pi\pi$  analyses were changed in the 1986 edition to agree with the baryon-first convention; the overall phase ambiguity is resolved by choosing a negative sign for the  $\Delta(1620) S_{31}$  coupling to  $\Delta(1232)\pi$ .

$(\Gamma_i\Gamma_j)^{1/2}/\Gamma_{total}$ in $N\pi \rightarrow N(1440) \rightarrow \Delta(1232)\pi, P\text{-wave}$	DOCUMENT ID	TECN	COMMENT	$(\Gamma_1\Gamma_5)^{1/2}/\Gamma$
<b>VALUE</b>				
<b>+0.37 to +0.41 OUR ESTIMATE</b>				
+0.39 ± 0.02	MANLEY	92	IPWA $\pi N \rightarrow \pi N \& N\pi\pi$	
+0.41	<sup>1,9</sup> LONGACRE	77	IPWA $\pi N \rightarrow N\pi\pi$	
+0.37	<sup>2</sup> LONGACRE	75	IPWA $\pi N \rightarrow N\pi\pi$	

$\Gamma(\Delta(1232)\pi, P\text{-wave})/\Gamma_{total}$	DOCUMENT ID	TECN	COMMENT	$\Gamma_5/\Gamma$
<b>VALUE (%)</b>				
<b>15 to 30 (<math>\approx 20</math>) OUR ESTIMATE</b>				
21 ± 8	ANISOVICH	12A	DPWA Multichannel	
16 ± 1	VRANA	00	DPWA Multichannel	

$(\Gamma_i\Gamma_j)^{1/2}/\Gamma_{total}$ in $N\pi \rightarrow N(1440) \rightarrow N\rho, S=1/2, P\text{-wave}$	DOCUMENT ID	TECN	COMMENT	$(\Gamma_1\Gamma_7)^{1/2}/\Gamma$
<b>VALUE</b>				
<b>±0.07 to ±0.25 OUR ESTIMATE</b>				
-0.11	<sup>1,9</sup> LONGACRE	77	IPWA $\pi N \rightarrow N\pi\pi$	
+0.23	<sup>2</sup> LONGACRE	75	IPWA $\pi N \rightarrow N\pi\pi$	

$\Gamma(N\rho, S=1/2, P\text{-wave})/\Gamma_{total}$	DOCUMENT ID	TECN	COMMENT	$\Gamma_7/\Gamma$
<b>VALUE (%)</b>				
<b>0 ± 1</b>	VRANA	00	DPWA Multichannel	

Baryon Particle Listings  
N(1440), N(1520)

$(\Gamma_1 \Gamma_2)^{1/2} / \Gamma_{\text{total}}$ in $N\pi \rightarrow N(1440) \rightarrow N\rho, S=3/2, P\text{-wave}$	$(\Gamma_1 \Gamma_8)^{1/2} / \Gamma$		
VALUE	DOCUMENT ID	TECN	COMMENT
+0.18	1.9 LONGACRE 77	IPWA	$\pi N \rightarrow N\pi\pi$

$(\Gamma_1 \Gamma_2)^{1/2} / \Gamma_{\text{total}}$ in $N\pi \rightarrow N(1440) \rightarrow N(\pi\pi)_{S=0}^1$	$(\Gamma_1 \Gamma_9)^{1/2} / \Gamma$		
VALUE	DOCUMENT ID	TECN	COMMENT
$\pm 0.17$ to $\pm 0.25$ OUR ESTIMATE			
+0.24 ± 0.03	MANLEY 92	IPWA	$\pi N \rightarrow \pi N \& N\pi\pi$
-0.18	1.9 LONGACRE 77	IPWA	$\pi N \rightarrow N\pi\pi$
-0.23	2 LONGACRE 75	IPWA	$\pi N \rightarrow N\pi\pi$

$\Gamma(N(\pi\pi)_{S=0}^1) / \Gamma_{\text{total}}$	$\Gamma_9 / \Gamma$		
VALUE (%)	DOCUMENT ID	TECN	COMMENT
$10$ to $20$ ( $\approx 15$ ) OUR ESTIMATE			
17 ± 7	ANISOVICH 12A	DPWA	Multichannel
12 ± 1	VRANA 00	DPWA	Multichannel

N(1440) PHOTON DECAY AMPLITUDES

Papers on  $\gamma N$  amplitudes predating 1981 may be found in our 2006 edition, Journal of Physics, G **33** 1 (2006).

N(1440) →  $\rho\gamma$ , helicity-1/2 amplitude  $A_{1/2}$

VALUE (GeV <sup>-1/2</sup> )	DOCUMENT ID	TECN	COMMENT
$-0.060 \pm 0.004$ OUR ESTIMATE			
-0.061 ± 0.008	ANISOVICH 12A	DPWA	Multichannel
-0.051 ± 0.002	DUGGER 07	DPWA	$\gamma N \rightarrow \pi N$
-0.063 ± 0.005	ARNDT 96	IPWA	$\gamma N \rightarrow \pi N$
-0.069 ± 0.018	CRAWFORD 83	IPWA	$\gamma N \rightarrow \pi N$
-0.063 ± 0.008	AWAJI 81	DPWA	$\gamma N \rightarrow \pi N$
• • • We do not use the following data for averages, fits, limits, etc. • • •			
-0.052 ± 0.010	ANISOVICH 10	DPWA	Multichannel
-0.061	DRECHSEL 07	DPWA	$\gamma N \rightarrow \pi N$
-0.087	PENNER 02D	DPWA	Multichannel
-0.085 ± 0.003	LI 93	IPWA	$\gamma N \rightarrow \pi N$
-0.129	10 WADA 84	DPWA	Compton scattering

N(1440) →  $n\gamma$ , helicity-1/2 amplitude  $A_{1/2}$

VALUE (GeV <sup>-1/2</sup> )	DOCUMENT ID	TECN	COMMENT
$+0.040 \pm 0.010$ OUR ESTIMATE			
0.045 ± 0.015	ARNDT 96	IPWA	$\gamma N \rightarrow \pi N$
0.037 ± 0.010	AWAJI 81	DPWA	$\gamma N \rightarrow \pi N$
0.030 ± 0.003	FUJII 81	DPWA	$\gamma N \rightarrow \pi N$
• • • We do not use the following data for averages, fits, limits, etc. • • •			
0.054	DRECHSEL 07	DPWA	$\gamma N \rightarrow \pi N$
0.121	PENNER 02D	DPWA	Multichannel
0.085 ± 0.006	LI 93	IPWA	$\gamma N \rightarrow \pi N$

N(1440) FOOTNOTES

- LONGACRE 77 pole positions are from a search for poles in the unitarized T-matrix; the first (second) value uses, in addition to  $\pi N \rightarrow N\pi\pi$  data, elastic amplitudes from a Saclay (CERN) partial-wave analysis. The other LONGACRE 77 values are from eyeball fits with Breit-Wigner circles to the T-matrix amplitudes.
- From method II of LONGACRE 75: eyeball fits with Breit-Wigner circles to the T-matrix amplitudes.
- ARNDT 06 also finds a second-sheet pole with real part = 1388 MeV,  $-2 \times$  imaginary part = 165 MeV, and residue with modulus 86 MeV and phase =  $-46$  degrees.
- See HOEHLER 93 for a detailed discussion of the evidence for and the pole parameters of N and  $\Delta$  resonances as determined from Argand diagrams of  $\pi N$  elastic partial-wave amplitudes and from plots of the speeds with which the amplitudes traverse the diagrams.
- ARNDT 04 also finds a second-sheet pole with real part = 1385 MeV,  $-2 \times$  imaginary part = 166 MeV, and residue with modulus 82 MeV and phase =  $-51^\circ$ .
- ARNDT 95 also finds a second-sheet pole with real part = 1383 MeV,  $-2 \times$  imaginary part = 210 MeV, and residue with modulus 92 MeV and phase =  $-54^\circ$ .
- ARNDT 91 (Soln SM90) also finds a second-sheet pole with real part = 1413 MeV,  $-2 \times$  imaginary part = 256 MeV, and residue = (78-153i) MeV.
- LONGACRE 78 values are from a search for poles in the unitarized T-matrix. The first (second) value uses, in addition to  $\pi N \rightarrow N\pi\pi$  data, elastic amplitudes from a Saclay (CERN) partial-wave analysis.
- LONGACRE 77 considers this coupling to be well determined.
- WADA 84 is inconsistent with other analyses; see the Note on N and  $\Delta$  Resonances.

N(1440) REFERENCES

For early references, see Physics Letters **111B** 1 (1982).

ANISOVICH 12A	EPJ A48 15	A.V. Anisovich et al.	(BONN, PNPI)
ANISOVICH 10	EPJ A44 203	A.V. Anisovich et al.	(BONN, PNPI)
BATINIC 10	PR C82 038203	M. Batinic et al.	(ZAGR)
SARANTSEV 08	PL B659 94	A.V. Sarantsev et al.	(CB-ELSA/A2-TAPS Collab.)
DRECHSEL 07	EPJ A34 69	D. Drechsel, S.S. Kamalov, L. Tiator	(MAINZ, JHR)
DUGGER 07	PR C76 025211	M. Dugger et al.	(Jefferson Lab CLAS Collab.)
ARNDT 06	PR C74 045205	R.A. Arndt et al.	(GWU)
PDG 06	JPG 33 1	W.-M. Yao et al.	(PDG Collab.)
ARNDT 04	PR C69 035213	R.A. Arndt et al.	(GWU, TRIU)
PENNER 02C	PR C66 055211	G. Penner, U. Mosel	(GIES)
PENNER 02D	PR C66 055212	G. Penner, U. Mosel	(GIES)
VRANA 00	PRPL 328 181	T.P. Vrana, S.A. Dytman., T.-S.H. Lee	(PITT+)
ARNDT 96	PR C53 430	R.A. Arndt, I.I. Strakovsky, R.L. Workman	(VPI)
ARNDT 95	PR C52 2120	R.A. Arndt et al.	(VPI, BRCO)
HOEHLER 93	$\pi N$ Newsletter 9 1	G. Hoehler	(KARL)

LI 93	PR C47 2759	Z.J. Li et al.	(VPI)
MANLEY 92	PR D45 4002	D.M. Manley, E.M. Saleski	(KENT) IJP
Also	PR D30 904	D.M. Manley et al.	(VPI)
ARNDT 91	PR D43 2131	R.A. Arndt et al.	(VPI, TELE) IJP
CUTKOSKY 90	PR D42 235	R.E. Cutkosky, S. Wang	(CMU)
WADA 84	NP B247 313	Y. Wada et al.	(INUS)
CRAWFORD 83	NP B211 1	R.L. Crawford, W.T. Morton	(GLAS)
PDG 82	PL 111B 1	M. Roos et al.	(HELS, CIT, CERN)
AWAJI 81	Bonn Conf. 352	N. Awaji, R. Kajikawa	(NAGO)
Also	NP B197 365	K. Fujii et al.	(NAGO)
FUJII 81	NP B187 53	K. Fujii et al.	(NAGO, OSAK)
CUTKOSKY 80	Toronto Conf. 19	R.E. Cutkosky et al.	(CMU, LBL) IJP
Also	PR D20 2839	R.E. Cutkosky et al.	(CMU, LBL) IJP
HOEHLER 79	PDAT 12-1	G. Hoehler et al.	(KARLT) IJP
Also	Toronto Conf. 3	R. Koch	(KARLT) IJP
LONGACRE 78	PR D17 1795	R.S. Longacre et al.	(LBL, SLAC)
LONGACRE 77	NP B122 493	R.S. Longacre, J. Dolbeau	(SACL) IJP
Also	NP B108 365	J. Dolbeau et al.	(SACL) IJP
LONGACRE 75	PL 55B 415	R.S. Longacre et al.	(LBL, SLAC) IJP

N(1520)  $3/2^-$

$I(J^P) = \frac{1}{2}(3/2^-)$  Status: \* \* \* \*

Most of the results published before 1975 were last included in our 1982 edition, Physics Letters **111B** 1 (1982). Some further obsolete results published before 1984 were last included in our 2006 edition, Journal of Physics, G **33** 1 (2006).

N(1520) BREIT-WIGNER MASS

VALUE (MeV)	DOCUMENT ID	TECN	COMMENT
$1515$ to $1525$ ( $\approx 1520$ ) OUR ESTIMATE			
1517 ± 3	ANISOVICH 12A	DPWA	Multichannel
1514.5 ± 0.2	ARNDT 06	DPWA	$\pi N \rightarrow \pi N, \eta N$
1524 ± 4	MANLEY 92	IPWA	$\pi N \rightarrow \pi N \& N\pi\pi$
1525 ± 10	CUTKOSKY 80	IPWA	$\pi N \rightarrow \pi N$
1519 ± 4	HOEHLER 79	IPWA	$\pi N \rightarrow \pi N$
• • • We do not use the following data for averages, fits, limits, etc. • • •			
1524 ± 4	ANISOVICH 10	DPWA	Multichannel
1522 ± 8	BATINIC 10	DPWA	$\pi N \rightarrow N\pi, N\eta$
1520 ± 10	THOMA 08	DPWA	Multichannel
1516.3 ± 0.8	ARNDT 04	DPWA	$\pi N \rightarrow \pi N, \eta N$
1509 ± 1	PENNER 02C	DPWA	Multichannel
1518 ± 3	VRANA 00	DPWA	Multichannel
1516 ± 10	ARNDT 96	IPWA	$\gamma N \rightarrow \pi N$
1515	ARNDT 95	DPWA	$\pi N \rightarrow N\pi$
1510	LI 93	IPWA	$\gamma N \rightarrow \pi N$
1510	1 LONGACRE 77	IPWA	$\pi N \rightarrow N\pi\pi$
1520	2 LONGACRE 75	IPWA	$\pi N \rightarrow N\pi\pi$

N(1520) BREIT-WIGNER WIDTH

VALUE (MeV)	DOCUMENT ID	TECN	COMMENT
$100$ to $125$ ( $\approx 115$ ) OUR ESTIMATE			
114 ± 5	ANISOVICH 12A	DPWA	Multichannel
103.6 ± 0.4	ARNDT 06	DPWA	$\pi N \rightarrow \pi N, \eta N$
124 ± 8	MANLEY 92	IPWA	$\pi N \rightarrow \pi N \& N\pi\pi$
120 ± 15	CUTKOSKY 80	IPWA	$\pi N \rightarrow \pi N$
114 ± 7	HOEHLER 79	IPWA	$\pi N \rightarrow \pi N$
• • • We do not use the following data for averages, fits, limits, etc. • • •			
117 ± 6	ANISOVICH 10	DPWA	Multichannel
132 ± 11	BATINIC 10	DPWA	$\pi N \rightarrow N\pi, N\eta$
125 ± 15	THOMA 08	DPWA	Multichannel
98.6 ± 2.6	ARNDT 04	DPWA	$\pi N \rightarrow \pi N, \eta N$
100 ± 2	PENNER 02C	DPWA	Multichannel
124 ± 4	VRANA 00	DPWA	Multichannel
106 ± 4	ARNDT 96	IPWA	$\gamma N \rightarrow \pi N$
106	ARNDT 95	DPWA	$\pi N \rightarrow N\pi$
120	LI 93	IPWA	$\gamma N \rightarrow \pi N$
110	1 LONGACRE 77	IPWA	$\pi N \rightarrow N\pi\pi$
150	2 LONGACRE 75	IPWA	$\pi N \rightarrow N\pi\pi$

N(1520) POLE POSITION

REAL PART

VALUE (MeV)	DOCUMENT ID	TECN	COMMENT
$1505$ to $1515$ ( $\approx 1510$ ) OUR ESTIMATE			
1507 ± 3	ANISOVICH 12A	DPWA	Multichannel
1515	ARNDT 06	DPWA	$\pi N \rightarrow \pi N, \eta N$
1510	3 HOEHLER 93	ARGD	$\pi N \rightarrow \pi N$
1510 ± 5	CUTKOSKY 80	IPWA	$\pi N \rightarrow \pi N$
• • • We do not use the following data for averages, fits, limits, etc. • • •			
1512 ± 3	ANISOVICH 10	DPWA	Multichannel
1506 ± 9	BATINIC 10	DPWA	$\pi N \rightarrow N\pi, N\eta$
1509 ± 7	THOMA 08	DPWA	Multichannel
1514	ARNDT 04	DPWA	$\pi N \rightarrow \pi N, \eta N$
1504	VRANA 00	DPWA	Multichannel
1515	ARNDT 95	DPWA	$\pi N \rightarrow N\pi$
1511	ARNDT 91	DPWA	$\pi N \rightarrow \pi N$ Soln SM90
1514 or 1511	4 LONGACRE 78	IPWA	$\pi N \rightarrow N\pi\pi$
1508 or 1505	1 LONGACRE 77	IPWA	$\pi N \rightarrow N\pi\pi$

## Baryon Particle Listings

 $N(1520)$  $-2 \times$ IMAGINARY PART

VALUE (MeV)	DOCUMENT ID	TECN	COMMENT
<b>105 to 120 (<math>\approx 110</math>) OUR ESTIMATE</b>			
111 $\pm$ 5	ANISOVICH 12A	DPWA	Multichannel
113	ARNDT 06	DPWA	$\pi N \rightarrow \pi N, \eta N$
120	<sup>3</sup> HOEHLER 93	ARGD	$\pi N \rightarrow \pi N$
114 $\pm$ 10	CUTKOSKY 80	IPWA	$\pi N \rightarrow \pi N$
• • • We do not use the following data for averages, fits, limits, etc. • • •			
110 $\pm$ 6	ANISOVICH 10	DPWA	Multichannel
122 $\pm$ 9	BATINIC 10	DPWA	$\pi N \rightarrow N\pi, N\eta$
113 $\pm$ 12	THOMA 08	DPWA	Multichannel
102	ARNDT 04	DPWA	$\pi N \rightarrow \pi N, \eta N$
112	VRANA 00	DPWA	Multichannel
110	ARNDT 95	DPWA	$\pi N \rightarrow N\pi$
108	ARNDT 91	DPWA	$\pi N \rightarrow \pi N$ Soln SM90
146 or 137	<sup>4</sup> LONGACRE 78	IPWA	$\pi N \rightarrow N\pi\pi$
109 or 107	<sup>1</sup> LONGACRE 77	IPWA	$\pi N \rightarrow N\pi\pi$

 $N(1520)$  ELASTIC POLE RESIDUEMODULUS  $|r|$ 

VALUE (MeV)	DOCUMENT ID	TECN	COMMENT
<b>35 <math>\pm</math> 3 OUR ESTIMATE</b>			
36 $\pm$ 3	ANISOVICH 12A	DPWA	Multichannel
38	ARNDT 06	DPWA	$\pi N \rightarrow \pi N, \eta N$
32	HOEHLER 93	ARGD	$\pi N \rightarrow \pi N$
35 $\pm$ 2	CUTKOSKY 80	IPWA	$\pi N \rightarrow \pi N$
• • • We do not use the following data for averages, fits, limits, etc. • • •			
35	BATINIC 10	DPWA	$\pi N \rightarrow N\pi, N\eta$
35	ARNDT 04	DPWA	$\pi N \rightarrow \pi N, \eta N$
34	ARNDT 95	DPWA	$\pi N \rightarrow N\pi$
33	ARNDT 91	DPWA	$\pi N \rightarrow \pi N$ Soln SM90

PHASE  $\theta$ 

VALUE ( $^\circ$ )	DOCUMENT ID	TECN	COMMENT
<b><math>-10 \pm 5</math> OUR ESTIMATE</b>			
$-14 \pm 3$	ANISOVICH 12A	DPWA	Multichannel
$-5$	ARNDT 06	DPWA	$\pi N \rightarrow \pi N, \eta N$
$-8$	HOEHLER 93	ARGD	$\pi N \rightarrow \pi N$
$-12 \pm 5$	CUTKOSKY 80	IPWA	$\pi N \rightarrow \pi N$
• • • We do not use the following data for averages, fits, limits, etc. • • •			
$-7$	BATINIC 10	DPWA	$\pi N \rightarrow N\pi, N\eta$
$-6$	ARNDT 04	DPWA	$\pi N \rightarrow \pi N, \eta N$
$7$	ARNDT 95	DPWA	$\pi N \rightarrow N\pi$
$-10$	ARNDT 91	DPWA	$\pi N \rightarrow \pi N$ Soln SM90

 $N(1520)$  INELASTIC POLE RESIDUE

The "normalized residue" is the residue divided by  $\Gamma_{pole}$ .

Normalized residue in  $N\pi \rightarrow N(1520) \rightarrow \Delta\pi, S$ -wave

MODULUS (%)	PHASE ( $^\circ$ )	DOCUMENT ID	TECN	COMMENT
<b>33 <math>\pm</math> 5</b>	<b>150 <math>\pm</math> 20</b>	ANISOVICH 12A	DPWA	Multichannel

Normalized residue in  $N\pi \rightarrow N(1520) \rightarrow \Delta\pi, D$ -wave

MODULUS (%)	PHASE ( $^\circ$ )	DOCUMENT ID	TECN	COMMENT
<b>25 <math>\pm</math> 3</b>	<b>100 <math>\pm</math> 20</b>	ANISOVICH 12A	DPWA	Multichannel

 $N(1520)$  DECAY MODES

The following branching fractions are our estimates, not fits or averages.

Mode	Fraction ( $\Gamma_i/\Gamma$ )
$\Gamma_1$ $N\pi$	55–65 %
$\Gamma_2$ $N\eta$	$(2.3 \pm 0.4) \times 10^{-3}$
$\Gamma_3$ $N\pi\pi$	20–30 %
$\Gamma_4$ $\Delta\pi$	15–25 %
$\Gamma_5$ $\Delta(1232)\pi, S$ -wave	10–20 %
$\Gamma_6$ $\Delta(1232)\pi, D$ -wave	10–15 %
$\Gamma_7$ $N\rho$	15–25 %
$\Gamma_8$ $N\rho, S=3/2, S$ -wave	$(9.0 \pm 1.0) \%$
$\Gamma_9$ $N(\pi\pi)_{S=0}^0$	$< 8 \%$
$\Gamma_{10}$ $p\gamma$	0.31–0.52 %
$\Gamma_{11}$ $p\gamma, \text{helicity}=1/2$	0.01–0.02 %
$\Gamma_{12}$ $p\gamma, \text{helicity}=3/2$	0.30–0.50 %
$\Gamma_{13}$ $n\gamma$	0.30–0.53 %
$\Gamma_{14}$ $n\gamma, \text{helicity}=1/2$	0.04–0.10 %
$\Gamma_{15}$ $n\gamma, \text{helicity}=3/2$	0.25–0.45 %

 $N(1520)$  BRANCHING RATIOS

$\Gamma(N\pi)/\Gamma_{total}$	DOCUMENT ID	TECN	COMMENT	$\Gamma_1/\Gamma$
<b>55 to 65 OUR ESTIMATE</b>				
62 $\pm$ 3	ANISOVICH 12A	DPWA	Multichannel	
63.2 $\pm$ 0.1	ARNDT 06	DPWA	$\pi N \rightarrow \pi N, \eta N$	
59 $\pm$ 3	MANLEY 92	IPWA	$\pi N \rightarrow \pi N \& N\pi\pi$	
58 $\pm$ 3	CUTKOSKY 80	IPWA	$\pi N \rightarrow \pi N$	
54 $\pm$ 3	HOEHLER 79	IPWA	$\pi N \rightarrow \pi N$	
• • • We do not use the following data for averages, fits, limits, etc. • • •				
57 $\pm$ 5	ANISOVICH 10	DPWA	Multichannel	
55 $\pm$ 5	BATINIC 10	DPWA	$\pi N \rightarrow N\pi, N\eta$	
58 $\pm$ 8	THOMA 08	DPWA	Multichannel	
64.0 $\pm$ 0.5	ARNDT 04	DPWA	$\pi N \rightarrow \pi N, \eta N$	
56 $\pm$ 1	PENNER 02c	DPWA	Multichannel	
63 $\pm$ 2	VRANA 00	DPWA	Multichannel	
61	ARNDT 95	DPWA	$\pi N \rightarrow N\pi$	

$\Gamma(N\eta)/\Gamma_{total}$	DOCUMENT ID	TECN	COMMENT	$\Gamma_2/\Gamma$
<b>0.23 <math>\pm</math> 0.04 OUR AVERAGE</b>				
0.23 $\pm$ 0.04	PENNER 02c	DPWA	Multichannel	
0 $\pm$ 1	VRANA 00	DPWA	Multichannel	
• • • We do not use the following data for averages, fits, limits, etc. • • •				
0.1 $\pm$ 0.1	BATINIC 10	DPWA	$\pi N \rightarrow N\pi, N\eta$	
0.2 $\pm$ 0.1	THOMA 08	DPWA	Multichannel	
0.08 to 0.12	ARNDT 05	DPWA	Multichannel	
0.08 $\pm$ 0.01	TIATOR 99	DPWA	$\gamma p \rightarrow p\eta$	

Note: Signs of couplings from  $\pi N \rightarrow N\pi\pi$  analyses were changed in the 1986 edition to agree with the baryon-first convention; the overall phase ambiguity is resolved by choosing a negative sign for the  $\Delta(1620) S_{31}$  coupling to  $\Delta(1232)\pi$ .

$(\Gamma_i\Gamma_j)^{1/2}/\Gamma_{total}$ in $N\pi \rightarrow N(1520) \rightarrow \Delta(1232)\pi, S$ -wave	DOCUMENT ID	TECN	COMMENT	$(\Gamma_1\Gamma_5)^{1/2}/\Gamma$
<b><math>-0.26</math> to <math>-0.20</math> OUR ESTIMATE</b>				
$-0.18 \pm 0.05$	MANLEY 92	IPWA	$\pi N \rightarrow \pi N \& N\pi\pi$	
$-0.26$	<sup>1,5</sup> LONGACRE 77	IPWA	$\pi N \rightarrow N\pi\pi$	
$-0.24$	<sup>2</sup> LONGACRE 75	IPWA	$\pi N \rightarrow N\pi\pi$	

$\Gamma(\Delta(1232)\pi, S\text{-wave})/\Gamma_{total}$	DOCUMENT ID	TECN	COMMENT	$\Gamma_5/\Gamma$
<b>10 to 20 OUR ESTIMATE</b>				
19 $\pm$ 4	ANISOVICH 12A	DPWA	Multichannel	
15 $\pm$ 2	VRANA 00	DPWA	Multichannel	
• • • We do not use the following data for averages, fits, limits, etc. • • •				
12 $\pm$ 4	THOMA 08	DPWA	Multichannel	

$(\Gamma_i\Gamma_j)^{1/2}/\Gamma_{total}$ in $N\pi \rightarrow N(1520) \rightarrow \Delta(1232)\pi, D$ -wave	DOCUMENT ID	TECN	COMMENT	$(\Gamma_1\Gamma_6)^{1/2}/\Gamma$
<b><math>-0.28</math> to <math>-0.24</math> OUR ESTIMATE</b>				
$-0.29 \pm 0.03$	MANLEY 92	IPWA	$\pi N \rightarrow \pi N \& N\pi\pi$	
$-0.21$	<sup>1,5</sup> LONGACRE 77	IPWA	$\pi N \rightarrow N\pi\pi$	
$-0.30$	<sup>2</sup> LONGACRE 75	IPWA	$\pi N \rightarrow N\pi\pi$	

$\Gamma(\Delta(1232)\pi, D\text{-wave})/\Gamma_{total}$	DOCUMENT ID	TECN	COMMENT	$\Gamma_6/\Gamma$
<b>10 to 15 OUR ESTIMATE</b>				
9 $\pm$ 2	ANISOVICH 12A	DPWA	Multichannel	
11 $\pm$ 2	VRANA 00	DPWA	Multichannel	
• • • We do not use the following data for averages, fits, limits, etc. • • •				
14 $\pm$ 5	THOMA 08	DPWA	Multichannel	

$(\Gamma_i\Gamma_j)^{1/2}/\Gamma_{total}$ in $N\pi \rightarrow N(1520) \rightarrow N\rho, S=3/2, S$ -wave	DOCUMENT ID	TECN	COMMENT	$(\Gamma_1\Gamma_8)^{1/2}/\Gamma$
<b><math>-0.35</math> to <math>-0.31</math> OUR ESTIMATE</b>				
$-0.35 \pm 0.03$	MANLEY 92	IPWA	$\pi N \rightarrow \pi N \& N\pi\pi$	
$-0.35$	<sup>1,5</sup> LONGACRE 77	IPWA	$\pi N \rightarrow N\pi\pi$	
$-0.24$	<sup>2</sup> LONGACRE 75	IPWA	$\pi N \rightarrow N\pi\pi$	

$\Gamma(N\rho, S=3/2, S\text{-wave})/\Gamma_{total}$	DOCUMENT ID	TECN	COMMENT	$\Gamma_8/\Gamma$
<b>9 <math>\pm</math> 1</b>				
	VRANA 00	DPWA	Multichannel	

$(\Gamma_i\Gamma_j)^{1/2}/\Gamma_{total}$ in $N\pi \rightarrow N(1520) \rightarrow N(\pi\pi)_{S=0}^0$	DOCUMENT ID	TECN	COMMENT	$(\Gamma_1\Gamma_9)^{1/2}/\Gamma$
<b><math>-0.22</math> to <math>-0.06</math> OUR ESTIMATE</b>				
$-0.13$	<sup>1,5</sup> LONGACRE 77	IPWA	$\pi N \rightarrow N\pi\pi$	
$-0.17$	<sup>2</sup> LONGACRE 75	IPWA	$\pi N \rightarrow N\pi\pi$	



# Baryon Particle Listings

## $N(1520)$ , $N(1535)$

$\Gamma(N(\pi\pi)_{S=0}^{\pi=0})/\Gamma_{\text{total}}$	DOCUMENT ID	TECN	COMMENT
VALUE (%)			
<b>1±1</b>	VRANA	00	DPWA Multichannel
••• We do not use the following data for averages, fits, limits, etc. •••			
<4	THOMA	08	DPWA Multichannel

### $N(1520)$ PHOTON DECAY AMPLITUDES

Papers on  $\gamma N$  amplitudes predating 1981 may be found in our 2006 edition, Journal of Physics, G **33** 1 (2006).

#### $N(1520) \rightarrow \rho\gamma$ , helicity-1/2 amplitude $A_{1/2}$

VALUE (GeV <sup>-1/2</sup> )	DOCUMENT ID	TECN	COMMENT
<b>-0.024±0.009 OUR ESTIMATE</b>			
-0.022±0.004	ANISOVICH	12A	DPWA Multichannel
-0.028±0.002	DUGGER	07	DPWA $\gamma N \rightarrow \pi N$
-0.038±0.003	AHRENS	02	DPWA $\gamma N \rightarrow \pi N$
-0.020±0.007	ARNDT	96	IPWA $\gamma N \rightarrow \pi N$
-0.028±0.014	CRAWFORD	83	IPWA $\gamma N \rightarrow \pi N$
-0.007±0.004	AWAJI	81	DPWA $\gamma N \rightarrow \pi N$
••• We do not use the following data for averages, fits, limits, etc. •••			
-0.032±0.006	ANISOVICH	10	DPWA Multichannel
-0.027	DRECHSEL	07	DPWA $\gamma N \rightarrow \pi N$
-0.003	PENNER	02D	DPWA Multichannel
-0.052±0.010±0.007	<sup>6</sup> MUKHOPAD... 98		$\gamma p \rightarrow \eta p$
-0.020±0.002	LI	93	IPWA $\gamma N \rightarrow \pi N$
-0.012	WADA	84	DPWA Compton scattering

#### $N(1520) \rightarrow \rho\gamma$ , helicity-3/2 amplitude $A_{3/2}$

VALUE (GeV <sup>-1/2</sup> )	DOCUMENT ID	TECN	COMMENT
<b>0.150±0.015 OUR ESTIMATE</b>			
0.131±0.010	ANISOVICH	12A	DPWA Multichannel
0.143±0.002	DUGGER	07	DPWA $\gamma N \rightarrow \pi N$
0.147±0.010	AHRENS	02	DPWA $\gamma N \rightarrow \pi N$
0.167±0.005	ARNDT	96	IPWA $\gamma N \rightarrow \pi N$
0.156±0.022	CRAWFORD	83	IPWA $\gamma N \rightarrow \pi N$
0.168±0.013	AWAJI	81	DPWA $\gamma N \rightarrow \pi N$
••• We do not use the following data for averages, fits, limits, etc. •••			
0.138±0.008	ANISOVICH	10	DPWA Multichannel
0.161	DRECHSEL	07	DPWA $\gamma N \rightarrow \pi N$
0.151	PENNER	02D	DPWA Multichannel
0.130±0.020±0.015	<sup>6</sup> MUKHOPAD... 98		$\gamma p \rightarrow \eta p$
0.167±0.002	LI	93	IPWA $\gamma N \rightarrow \pi N$
0.168	WADA	84	DPWA Compton scattering

#### $N(1520) \rightarrow n\gamma$ , helicity-1/2 amplitude $A_{1/2}$

VALUE (GeV <sup>-1/2</sup> )	DOCUMENT ID	TECN	COMMENT
<b>-0.059±0.009 OUR ESTIMATE</b>			
-0.048±0.008	ARNDT	96	IPWA $\gamma N \rightarrow \pi N$
-0.066±0.013	AWAJI	81	DPWA $\gamma N \rightarrow \pi N$
-0.067±0.004	FUJII	81	DPWA $\gamma N \rightarrow \pi N$
••• We do not use the following data for averages, fits, limits, etc. •••			
-0.077	DRECHSEL	07	DPWA $\gamma N \rightarrow \pi N$
-0.084	PENNER	02D	DPWA Multichannel
-0.058±0.003	LI	93	IPWA $\gamma N \rightarrow \pi N$

#### $N(1520) \rightarrow n\gamma$ , helicity-3/2 amplitude $A_{3/2}$

VALUE (GeV <sup>-1/2</sup> )	DOCUMENT ID	TECN	COMMENT
<b>-0.139±0.011 OUR ESTIMATE</b>			
-0.140±0.010	ARNDT	96	IPWA $\gamma N \rightarrow \pi N$
-0.124±0.009	AWAJI	81	DPWA $\gamma N \rightarrow \pi N$
-0.158±0.003	FUJII	81	DPWA $\gamma N \rightarrow \pi N$
••• We do not use the following data for averages, fits, limits, etc. •••			
-0.154	DRECHSEL	07	DPWA $\gamma N \rightarrow \pi N$
-0.159	PENNER	02D	DPWA Multichannel
-0.131±0.003	LI	93	IPWA $\gamma N \rightarrow \pi N$

### $N(1520)$ FOOTNOTES

- <sup>1</sup> LONGACRE 77 pole positions are from a search for poles in the unitarized T-matrix; the first (second) value uses, in addition to  $\pi N \rightarrow N\pi\pi$  data, elastic amplitudes from a Saclay (CERN) partial-wave analysis. The other LONGACRE 77 values are from eyeball fits with Breit-Wigner circles to the T-matrix amplitudes.
- <sup>2</sup> From method II of LONGACRE 75: eyeball fits with Breit-Wigner circles to the T-matrix amplitudes.
- <sup>3</sup> See HOEHLER 93 for a detailed discussion of the evidence for and the pole parameters of  $N$  and  $\Delta$  resonances as determined from Argand diagrams of  $\pi N$  elastic partial-wave amplitudes and from plots of the speeds with which the amplitudes traverse the diagrams.
- <sup>4</sup> LONGACRE 78 values are from a search for poles in the unitarized T-matrix. The first (second) value uses, in addition to  $\pi N \rightarrow N\pi\pi$  data, elastic amplitudes from a Saclay (CERN) partial-wave analysis.
- <sup>5</sup> LONGACRE 77 considers this coupling to be well determined.
- <sup>6</sup> MUKHOPADHYAY 98 uses an effective Lagrangian approach to analyze  $\eta$  photoproduction data. The ratio of the  $A_{3/2}$  and  $A_{1/2}$  amplitudes is determined, with less model dependence than the amplitudes themselves, to be  $A_{3/2}/A_{1/2} = -2.5 \pm 0.5 \pm 0.4$ .

### $N(1520)$ REFERENCES

For early references, see Physics Letters **111B** 1 (1982). For very early references, see Reviews of Modern Physics **37** 633 (1965).

ANISOVICH	12A	EPJ A48 15	A.V. Anisovich et al.	(BONN, PNPI)
ANISOVICH	10	EPJ A44 203	A.V. Anisovich et al.	(BONN, PNPI)
BATINIC	10	PR C82 038203	M. Batinic et al.	(ZAGR)
THOMA	08	PL B659 87	U. Thoma et al.	(CB-ELSA Collab.)
DRECHSEL	07	EPJ A34 69	D. Drechsel, S.S. Kamalov, L. Tiator	(MAINZ, JINR)
DUGGER	07	PR C76 025211	M. Dugger et al.	(Jefferson Lab CLAS Collab.)
ARNDT	06	PR C74 045205	R.A. Arndt et al.	(GWU)
PDG	06	JPG 33 1	W.-M. Yao et al.	(PDG Collab.)
ARNDT	05	PR C72 045202	R.A. Arndt et al.	(GWU, PNPI)
ARNDT	04	PR C69 035213	R.A. Arndt et al.	(GWU, TRIU)
AHRENS	02	PRL 88 232002	J. Ahrens et al.	(Mainz MAMI GDH/A2 Collab.)
PENNER	02C	PR C66 055211	G. Penner, U. Mosel	(GIES)
PENNER	02D	PR C66 055212	G. Penner, U. Mosel	(GIES)
VRANA	00	PRPL 328 181	T.P. Vrana, S.A. Dytman, T.-S.H. Lee	(PITT+)
TIATOR	99	PR C60 035210	L. Tiator et al.	
MUKHOPAD... 98		PL B444 77	N.C. Mukhopadhyay, N. Mathur	(VPI)
ARNDT	96	PR C53 4300	R.A. Arndt, I.I. Strakovsky, R.L. Workman	(VPI, BRCC)
ARNDT	95	PR C52 2120	R.A. Arndt et al.	(VPI, KARL)
HOEHLER	93	$\pi N$ Newsletter 9 1	G. Hoehler	(KARL)
LI	93	PR C47 2759	Z.J. Li et al.	(VPI)
MANLEY	92	PR D45 4002	D.M. Manley, E.M. Saleski	(KENT) IUP
Also		PR D30 904	D.M. Manley et al.	(VPI)
ARNDT	91	PR D43 2131	R.A. Arndt et al.	(VPI, TELE) IUP
WADA	84	NP B247 313	Y. Wada et al.	(INUS)
CRAWFORD	83	NP B211 1	R.L. Crawford, W.T. Morton	(GLAS)
PDG	82	PL 111B 1	M. Roos et al.	(HELS, CIT, CERN)
AWAJI	81	Bonn Conf. 352	N. Awaji, R. Kajikawa	(NAGO)
Also		NP B197 365	K. Fujii et al.	(NAGO)
FUJII	81	NP B187 53	K. Fujii et al.	(NAGO, OSAK)
CUTKOSKY	80	Toronto Conf. 19	R.E. Cutkosky et al.	(CMU, LBL) IUP
Also		PR D20 2839	R.E. Cutkosky et al.	(CMU, LBL) IUP
HOEHLER	79	PDAT 12-1	G. Hoehler et al.	(KARLT) IUP
Also		Toronto Conf. 3	R. Koch	(KARLT) IUP
LONGACRE	78	PR D17 1795	R.S. Longacre et al.	(LBL, SLAC)
LONGACRE	77	NP B122 493	R.S. Longacre, J. Dolbeau	(SACL) IUP
Also		NP B108 365	J. Dolbeau et al.	(SACL) IUP
LONGACRE	75	PL 55B 415	R.S. Longacre et al.	(LBL, SLAC) IUP

### $N(1535) 1/2^-$

$$I(J^P) = \frac{1}{2}(\frac{1}{2}^-) \text{ Status: } ***$$

Most of the results published before 1975 were last included in our 1982 edition, Physics Letters **111B** 1 (1982). Some further obsolete results published before 1984 were last included in our 2006 edition, Journal of Physics, G **33** 1 (2006).

### $N(1535)$ BREIT-WIGNER MASS

VALUE (MeV)	DOCUMENT ID	TECN	COMMENT
<b>1525 to 1545 (<math>\approx 1535</math>) OUR ESTIMATE</b>			
1519 ± 5	ANISOVICH	12A	DPWA Multichannel
1547.0 ± 0.7	ARNDT	06	DPWA $\pi N \rightarrow \pi N, \eta N$
1534 ± 7	MANLEY	92	IPWA $\pi N \rightarrow \pi N$ & $N\pi\pi$
1550 ± 40	CUTKOSKY	80	IPWA $\pi N \rightarrow \pi N$
1526 ± 7	HOEHLER	79	IPWA $\pi N \rightarrow \pi N$
••• We do not use the following data for averages, fits, limits, etc. •••			
1535 ± 20	ANISOVICH	10	DPWA Multichannel
1553 ± 8	BATINIC	10	DPWA $\pi N \rightarrow N\pi, N\eta$
1548 ± 15	THOMA	08	DPWA Multichannel
1546.7 ± 2.2	ARNDT	04	DPWA $\pi N \rightarrow \pi N, \eta N$
1526 ± 2	PENNER	02C	DPWA Multichannel
1530 ± 10	BAI	01B	BES $J/\psi \rightarrow p\bar{p}\eta$
1522 ± 11	THOMPSON	01	CLAS $\gamma^* p \rightarrow p\eta$
1542 ± 3	VRANA	00	DPWA Multichannel
1532 ± 5	ARMSTRONG	99B	DPWA $\gamma^* p \rightarrow p\eta$
1549.0 ± 2.1	ABAEV	96	DPWA $\pi^- p \rightarrow \eta n$
1525 ± 10	ARNDT	96	IPWA $\gamma N \rightarrow \pi N$
1535	ARNDT	95	DPWA $\pi N \rightarrow N\pi$
1544 ± 13	KRUSCHE	95	DPWA $\gamma p \rightarrow p\eta$
1518	LI	93	IPWA $\gamma N \rightarrow \pi N$
1520	<sup>1</sup> LONGACRE	77	IPWA $\pi N \rightarrow N\pi\pi$
1510	<sup>2</sup> LONGACRE	75	IPWA $\pi N \rightarrow N\pi\pi$

### $N(1535)$ BREIT-WIGNER WIDTH

VALUE (MeV)	DOCUMENT ID	TECN	COMMENT
<b>125 to 175 (<math>\approx 150</math>) OUR ESTIMATE</b>			
128 ± 14	ANISOVICH	12A	DPWA Multichannel
188.4 ± 3.8	ARNDT	06	DPWA $\pi N \rightarrow \pi N, \eta N$
148.2 ± 8.1	GREEN	97	DPWA $\pi N \rightarrow \pi N, \eta N$
151 ± 27	MANLEY	92	IPWA $\pi N \rightarrow \pi N$ & $N\pi\pi$
240 ± 80	CUTKOSKY	80	IPWA $\pi N \rightarrow \pi N$
120 ± 20	HOEHLER	79	IPWA $\pi N \rightarrow \pi N$
••• We do not use the following data for averages, fits, limits, etc. •••			
170 ± 35	ANISOVICH	10	DPWA Multichannel
182 ± 25	BATINIC	10	DPWA $\pi N \rightarrow N\pi, N\eta$
170 ± 20	THOMA	08	DPWA Multichannel
178.0 ± 11.6	ARNDT	04	DPWA $\pi N \rightarrow \pi N, \eta N$
129 ± 8	PENNER	02C	DPWA Multichannel
95 ± 25	BAI	01B	BES $J/\psi \rightarrow p\bar{p}\eta$
143 ± 18	THOMPSON	01	CLAS $\gamma^* p \rightarrow p\eta$

## Baryon Particle Listings

 $N(1535)$ 

112 ± 19	VRANA	00	DPWA	Multichannel
154 ± 20	ARMSTRONG	99B	DPWA	$\gamma^* p \rightarrow p\eta$
212 ± 20	3 KRUSCHE	97	DPWA	$\gamma N \rightarrow \eta N$
168.8 ± 11.6	ABAEV	96	DPWA	$\pi^- p \rightarrow \eta n$
103 ± 5	ARNDT	96	IPWA	$\gamma N \rightarrow \pi N$
66	ARNDT	95	DPWA	$\pi N \rightarrow N\pi$
200 ± 40	KRUSCHE	95	DPWA	$\gamma p \rightarrow p\eta$
84	LI	93	IPWA	$\gamma N \rightarrow \pi N$
135	1 LONGACRE	77	IPWA	$\pi N \rightarrow N\pi\pi$
100	2 LONGACRE	75	IPWA	$\pi N \rightarrow N\pi\pi$

 $N(1535)$  POLE POSITION

## REAL PART

VALUE (MeV)	DOCUMENT ID	TECN	COMMENT
<b>1490 to 1530 (<math>\approx 1510</math>) OUR ESTIMATE</b>			
1501 ± 4	ANISOVICH	12A	DPWA Multichannel
1502	ARNDT	06	DPWA $\pi N \rightarrow \pi N, \eta N$
1487	4 HOEHLER	93	SPED $\pi N \rightarrow \pi N$
1510 ± 50	CUTKOSKY	80	IPWA $\pi N \rightarrow \pi N$
• • • We do not use the following data for averages, fits, limits, etc. • • •			
1510 ± 25	ANISOVICH	10	DPWA Multichannel
1521 ± 14	BATINIC	10	DPWA $\pi N \rightarrow N\pi, N\eta$
1508 $^{+10}_{-30}$	THOMA	08	DPWA Multichannel
1526	ARNDT	04	DPWA $\pi N \rightarrow \pi N, \eta N$
1525	VRANA	00	DPWA Multichannel
1510 ± 10	5 ARNDT	98	DPWA $\pi N \rightarrow \pi N, \eta N$
1501	ARNDT	95	DPWA $\pi N \rightarrow N\pi$
1499	ARNDT	91	DPWA $\pi N \rightarrow \pi N$ Soln SM90
1496 or 1499	6 LONGACRE	78	IPWA $\pi N \rightarrow N\pi\pi$
1525 or 1527	1 LONGACRE	77	IPWA $\pi N \rightarrow N\pi\pi$

## -2xIMAGINARY PART

VALUE (MeV)	DOCUMENT ID	TECN	COMMENT
<b>90 to 250 (<math>\approx 170</math>) OUR ESTIMATE</b>			
134 ± 11	ANISOVICH	12A	DPWA Multichannel
95	ARNDT	06	DPWA $\pi N \rightarrow \pi N, \eta N$
260 ± 80	CUTKOSKY	80	IPWA $\pi N \rightarrow \pi N$
• • • We do not use the following data for averages, fits, limits, etc. • • •			
140 ± 30	ANISOVICH	10	DPWA Multichannel
190 ± 28	BATINIC	10	DPWA $\pi N \rightarrow N\pi, N\eta$
165 ± 15	THOMA	08	DPWA Multichannel
130	ARNDT	04	DPWA $\pi N \rightarrow \pi N, \eta N$
102	VRANA	00	DPWA Multichannel
170 ± 30	5 ARNDT	98	DPWA $\pi N \rightarrow \pi N, \eta N$
124	ARNDT	95	DPWA $\pi N \rightarrow N\pi$
110	ARNDT	91	DPWA $\pi N \rightarrow \pi N$ Soln SM90
103 or 105	6 LONGACRE	78	IPWA $\pi N \rightarrow N\pi\pi$
135 or 123	1 LONGACRE	77	IPWA $\pi N \rightarrow N\pi\pi$

 $N(1535)$  ELASTIC POLE RESIDUEMODULUS  $|r|$ 

VALUE (MeV)	DOCUMENT ID	TECN	COMMENT
<b>50 ± 20 OUR ESTIMATE</b>			
31 ± 4	ANISOVICH	12A	DPWA Multichannel
16	ARNDT	06	DPWA $\pi N \rightarrow \pi N, \eta N$
120 ± 40	CUTKOSKY	80	IPWA $\pi N \rightarrow \pi N$
• • • We do not use the following data for averages, fits, limits, etc. • • •			
68	BATINIC	10	DPWA $\pi N \rightarrow N\pi, N\eta$
33	ARNDT	04	DPWA $\pi N \rightarrow \pi N, \eta N$
31	ARNDT	95	DPWA $\pi N \rightarrow N\pi$
23	ARNDT	91	DPWA $\pi N \rightarrow \pi N$ Soln SM90

PHASE  $\theta$ 

VALUE ( $^\circ$ )	DOCUMENT ID	TECN	COMMENT
<b>-15 ± 15 OUR ESTIMATE</b>			
-29 ± 5	ANISOVICH	12A	DPWA Multichannel
-16	ARNDT	06	DPWA $\pi N \rightarrow \pi N, \eta N$
+15 ± 45	CUTKOSKY	80	IPWA $\pi N \rightarrow \pi N$
• • • We do not use the following data for averages, fits, limits, etc. • • •			
12	BATINIC	10	DPWA $\pi N \rightarrow N\pi, N\eta$
14	ARNDT	04	DPWA $\pi N \rightarrow \pi N, \eta N$
-12	ARNDT	95	DPWA $\pi N \rightarrow N\pi$
-13	ARNDT	91	DPWA $\pi N \rightarrow \pi N$ Soln SM90

 $N(1535)$  INELASTIC POLE RESIDUEThe "normalized residue" is the residue divided by  $\Gamma_{pole}$ .Normalized residue in  $N\pi \rightarrow N(1535) \rightarrow N\eta$ 

MODULUS (%)	PHASE ( $^\circ$ )	DOCUMENT ID	TECN	COMMENT
<b>43 ± 3</b>	<b>-76 ± 5</b>	ANISOVICH	12A	DPWA Multichannel

Normalized residue in  $N\pi \rightarrow N(1535) \rightarrow \Delta\pi, D$ -wave

MODULUS (%)	PHASE ( $^\circ$ )	DOCUMENT ID	TECN	COMMENT
<b>12 ± 3</b>	<b>145 ± 17</b>	ANISOVICH	12A	DPWA Multichannel

 $N(1535)$  DECAY MODES

The following branching fractions are our estimates, not fits or averages.

Mode	Fraction ( $\Gamma_i/\Gamma$ )
$\Gamma_1$ $N\pi$	35-55 %
$\Gamma_2$ $N\eta$	(42 ± 10) %
$\Gamma_3$ $N\pi\pi$	1-10 %
$\Gamma_4$ $\Delta\pi$	< 1 %
$\Gamma_5$ $\Delta(1232)\pi, D$ -wave	0-4 %
$\Gamma_6$ $N\rho$	< 4 %
$\Gamma_7$ $N\rho, S=1/2, S$ -wave	( 2.0 ± 1.0) %
$\Gamma_8$ $N\rho, S=3/2, D$ -wave	( 0.0 ± 1.0) %
$\Gamma_9$ $N(\pi\pi)_{S=0}^{J=0}$	( 2 ± 1 ) %
$\Gamma_{10}$ $N(1440)\pi$	( 8 ± 3 ) %
$\Gamma_{11}$ $p\gamma$	0.15-0.30 %
$\Gamma_{12}$ $p\gamma, \text{helicity}=1/2$	0.15-0.30 %
$\Gamma_{13}$ $n\gamma$	0.01-0.25 %
$\Gamma_{14}$ $n\gamma, \text{helicity}=1/2$	0.01-0.25 %

 $N(1535)$  BRANCHING RATIOS $\Gamma(N\pi)/\Gamma_{total}$ 

VALUE (%)	DOCUMENT ID	TECN	COMMENT	$\Gamma_1/\Gamma$
<b>35 to 55 OUR ESTIMATE</b>				
54 ± 5	ANISOVICH	12A	DPWA Multichannel	
35.5 ± 0.2	ARNDT	06	DPWA $\pi N \rightarrow \pi N, \eta N$	
39.4 ± 0.9	GREEN	97	DPWA $\pi N \rightarrow \pi N, \eta N$	
51 ± 5	MANLEY	92	IPWA $\pi N \rightarrow \pi N \& N\pi\pi$	
50 ± 10	CUTKOSKY	80	IPWA $\pi N \rightarrow \pi N$	
38 ± 4	HOEHLER	79	IPWA $\pi N \rightarrow \pi N$	
• • • We do not use the following data for averages, fits, limits, etc. • • •				
35 ± 15	ANISOVICH	10	DPWA Multichannel	
46 ± 7	BATINIC	10	DPWA $\pi N \rightarrow N\pi, N\eta$	
37 ± 9	THOMA	08	DPWA Multichannel	
36.0 ± 0.9	ARNDT	04	DPWA $\pi N \rightarrow \pi N, \eta N$	
36 ± 1	PENNER	02c	DPWA Multichannel	
35 ± 8	VRANA	00	DPWA Multichannel	
33.0 ± 1.1	ABAEV	96	DPWA $\pi^- p \rightarrow \eta n$	
31	ARNDT	95	DPWA $\pi N \rightarrow N\pi$	

 $\Gamma(N\eta)/\Gamma_{total}$ 

VALUE (%)	CL%	DOCUMENT ID	TECN	COMMENT	$\Gamma_2/\Gamma$
<b>42 ± 10 OUR ESTIMATE</b>					
33 ± 5		ANISOVICH	12A	DPWA Multichannel	
53 ± 1		PENNER	02c	DPWA Multichannel	
51 ± 5		VRANA	00	DPWA Multichannel	
• • • We do not use the following data for averages, fits, limits, etc. • • •					
50 ± 7		BATINIC	10	DPWA $\pi N \rightarrow N\pi, N\eta$	
40 ± 10		THOMA	08	DPWA Multichannel	
>45	95	7 ARMSTRONG	99B	DPWA $p(e, e'p)\eta$	
56.8 ± 1.1		GREEN	97	DPWA $\pi N \rightarrow \pi N, \eta N$	
59.1 ± 1.7		ABAEV	96	DPWA $\pi^- p \rightarrow \eta n$	

 $\Gamma(N\eta)/\Gamma(N\pi)$ 

VALUE	DOCUMENT ID	TECN	COMMENT	$\Gamma_2/\Gamma_1$
0.95 ± 0.03	AZNAURYAN	09	CLAS $\pi, \eta$ electroproduction	

 $(\Gamma_1\Gamma_7)^{1/2}/\Gamma_{total}$  in  $N\pi \rightarrow N(1535) \rightarrow N\eta$ 

VALUE	DOCUMENT ID	TECN	COMMENT	$(\Gamma_1\Gamma_2)^{1/2}/\Gamma$
<b>+0.44 to +0.50 OUR ESTIMATE</b>				
+0.47 ± 0.02	MANLEY	92	IPWA $\pi N \rightarrow \pi N \& N\pi\pi$	

Note: Signs of couplings from  $\pi N \rightarrow N\pi\pi$  analyses were changed in the 1986 edition to agree with the baryon-first convention; the overall phase ambiguity is resolved by choosing a negative sign for the  $\Delta(1620) S_{31}$  coupling to  $\Delta(1232)\pi$ . $(\Gamma_1\Gamma_7)^{1/2}/\Gamma_{total}$  in  $N\pi \rightarrow N(1535) \rightarrow \Delta(1232)\pi, D$ -wave

VALUE	DOCUMENT ID	TECN	COMMENT	$(\Gamma_1\Gamma_5)^{1/2}/\Gamma$
<b>-0.04 to +0.06 OUR ESTIMATE</b>				
+0.00 ± 0.04	MANLEY	92	IPWA $\pi N \rightarrow \pi N \& N\pi\pi$	
0.00	1 LONGACRE	77	IPWA $\pi N \rightarrow N\pi\pi$	
+0.06	2 LONGACRE	75	IPWA $\pi N \rightarrow N\pi\pi$	

$\Gamma(\Delta(1232)\pi, D\text{-wave})/\Gamma_{\text{total}}$				$\Gamma_5/\Gamma$
VALUE (%)	DOCUMENT ID	TECN	COMMENT	
<b>0 to 4 OUR ESTIMATE</b>				
2.5 ± 1.5	ANISOVICH	12A	DPWA	Multichannel
1 ± 1	VRANA	00	DPWA	Multichannel
• • • We do not use the following data for averages, fits, limits, etc. • • •				
23 ± 8	THOMA	08	DPWA	Multichannel

$(\Gamma_1\Gamma_2)^{1/2}/\Gamma_{\text{total}}$ in $N\pi \rightarrow N(1535) \rightarrow N\rho, S=1/2, S\text{-wave}$				$(\Gamma_1\Gamma_7)^{1/2}/\Gamma$
VALUE	DOCUMENT ID	TECN	COMMENT	
<b>-0.14 to -0.06 OUR ESTIMATE</b>				
-0.10 ± 0.03	MANLEY	92	IPWA	$\pi N \rightarrow \pi N$ & $N\pi\pi$
-0.10	<sup>1</sup> LONGACRE	77	IPWA	$\pi N \rightarrow N\pi\pi$
-0.09	<sup>2</sup> LONGACRE	75	IPWA	$\pi N \rightarrow N\pi\pi$

$\Gamma(N\rho, S=1/2, S\text{-wave})/\Gamma_{\text{total}}$				$\Gamma_7/\Gamma$
VALUE (%)	DOCUMENT ID	TECN	COMMENT	
<b>2 ± 1</b>	VRANA	00	DPWA	Multichannel

$\Gamma(N\rho, S=3/2, D\text{-wave})/\Gamma_{\text{total}}$				$\Gamma_8/\Gamma$
VALUE (%)	DOCUMENT ID	TECN	COMMENT	
<b>0 ± 1</b>	VRANA	00	DPWA	Multichannel

$(\Gamma_1\Gamma_9)^{1/2}/\Gamma_{\text{total}}$ in $N\pi \rightarrow N(1535) \rightarrow N(\pi\pi)_{S=0}^{J=0}$				$(\Gamma_1\Gamma_9)^{1/2}/\Gamma$
VALUE	DOCUMENT ID	TECN	COMMENT	
<b>+0.03 to +0.13 OUR ESTIMATE</b>				
+0.07 ± 0.04	MANLEY	92	IPWA	$\pi N \rightarrow \pi N$ & $N\pi\pi$
+0.08	<sup>1</sup> LONGACRE	77	IPWA	$\pi N \rightarrow N\pi\pi$
+0.09	<sup>2</sup> LONGACRE	75	IPWA	$\pi N \rightarrow N\pi\pi$

$\Gamma(N(\pi\pi)_{S=0}^{J=0})/\Gamma_{\text{total}}$				$\Gamma_9/\Gamma$
VALUE (%)	DOCUMENT ID	TECN	COMMENT	
<b>2 ± 1</b>	VRANA	00	DPWA	Multichannel

$(\Gamma_1\Gamma_7)^{1/2}/\Gamma_{\text{total}}$ in $N\pi \rightarrow N(1535) \rightarrow N(1440)\pi$				$(\Gamma_1\Gamma_{10})^{1/2}/\Gamma$
VALUE	DOCUMENT ID	TECN	COMMENT	
<b>+0.10 ± 0.05</b>	MANLEY	92	IPWA	$\pi N \rightarrow \pi N$ & $N\pi\pi$

$\Gamma(N(1440)\pi)/\Gamma_{\text{total}}$				$\Gamma_{10}/\Gamma$
VALUE (%)	DOCUMENT ID	TECN	COMMENT	
<b>8 ± 3 OUR ESTIMATE</b>				
8 ± 2	<sup>8</sup> STAROSTIN	03		$\pi^- p \rightarrow n3\pi^0$
10 ± 9	VRANA	00	DPWA	Multichannel

**N(1535) PHOTON DECAY AMPLITUDES**

Papers on  $\gamma N$  amplitudes predating 1981 may be found in our 2006 edition, Journal of Physics, G **33** 1 (2006).

**N(1535) → pγ, helicity-1/2 amplitude A<sub>1/2</sub>**

VALUE (GeV <sup>-1/2</sup> )	DOCUMENT ID	TECN	COMMENT
<b>+0.090 ± 0.030 OUR ESTIMATE</b>			
0.105 ± 0.010	ANISOVICH	12A	DPWA Multichannel
0.091 ± 0.002	DUGGER	07	DPWA $\gamma N \rightarrow \pi N$
0.120 ± 0.011 ± 0.015	<sup>3</sup> KRUSCHE	97	DPWA $\gamma N \rightarrow \eta N$
0.060 ± 0.015	ARNDT	96	IPWA $\gamma N \rightarrow \pi N$
0.097 ± 0.006	BENMERROU..95	DPWA	$\gamma N \rightarrow N\eta$
0.095 ± 0.011	<sup>9</sup> BENMERROU..91		$\gamma p \rightarrow p\eta$
0.053 ± 0.015	CRAWFORD	83	IPWA $\gamma N \rightarrow \pi N$
0.077 ± 0.021	AWAJI	81	DPWA $\gamma N \rightarrow \pi N$
• • • We do not use the following data for averages, fits, limits, etc. • • •			
0.090 ± 0.015	ANISOVICH	10	DPWA Multichannel
0.090 ± 0.025	<sup>10</sup> ANISOVICH	09A	DPWA $\gamma d \rightarrow \eta N(N)$
0.066	DRECHSEL	07	DPWA $\gamma N \rightarrow \pi N$
0.090	PENNER	02D	DPWA Multichannel
0.110 to 0.140	KRUSCHE	95	DPWA $\gamma p \rightarrow p\eta$
0.125 ± 0.025	KRUSCHE	95C	IPWA $\gamma d \rightarrow \eta N(N)$
0.061 ± 0.003	LI	93	IPWA $\gamma N \rightarrow \pi N$
0.055	WADA	84	DPWA Compton scattering

**N(1535) → nγ, helicity-1/2 amplitude A<sub>1/2</sub>**

VALUE (GeV <sup>-1/2</sup> )	DOCUMENT ID	TECN	COMMENT
<b>-0.046 ± 0.027 OUR ESTIMATE</b>			
-0.080 ± 0.020	<sup>11</sup> ANISOVICH	09A	DPWA $\gamma d \rightarrow \eta N(N)$
-0.020 ± 0.035	ARNDT	96	IPWA $\gamma N \rightarrow \pi N$
0.035 ± 0.014	AWAJI	81	DPWA $\gamma N \rightarrow \pi N$
-0.062 ± 0.003	FUJII	81	DPWA $\gamma N \rightarrow \pi N$
• • • We do not use the following data for averages, fits, limits, etc. • • •			
-0.051	DRECHSEL	07	DPWA $\gamma N \rightarrow \pi N$
-0.024	PENNER	02D	DPWA Multichannel
-0.100 ± 0.030	KRUSCHE	95C	IPWA $\gamma d \rightarrow \eta N(N)$
-0.046 ± 0.005	LI	93	IPWA $\gamma N \rightarrow \pi N$

<b>N(1535) → Nγ, ratio A<sub>1/2</sub><sup>0</sup>/A<sub>1/2</sub><sup>P</sup></b>			
VALUE (GeV <sup>-1/2</sup> )	DOCUMENT ID	TECN	
• • • We do not use the following data for averages, fits, limits, etc. • • •			
-0.84 ± 0.15	MUKHOPAD...	95B	IPWA

**N(1535) FOOTNOTES**

- <sup>1</sup> LONGACRE 77 pole positions are from a search for poles in the unitarized T-matrix; the first (second) value uses, in addition to  $\pi N \rightarrow N\pi\pi$  data, elastic amplitudes from a Saclay (CERN) partial-wave analysis. The other LONGACRE 77 values are from eyeball fits with Breit-Wigner circles to the T-matrix amplitudes.
- <sup>2</sup> From method II of LONGACRE 75: eyeball fits with Breit-Wigner circles to the T-matrix amplitudes.
- <sup>3</sup> KRUSCHE 97 fits with the mass fixed at 1544 MeV.
- <sup>4</sup> See HOEHLER 93 for a detailed discussion of the evidence for and the pole parameters of  $N$  and  $\Delta$  resonances as determined from Argand diagrams of  $\pi N$  elastic partial-wave amplitudes and from plots of the speeds with which the amplitudes traverse the diagrams.
- <sup>5</sup> ARNDT 98 also lists pole residues, which display more model dependence than do the associated pole positions.
- <sup>6</sup> LONGACRE 78 values are from a search for poles in the unitarized T-matrix. The first (second) value uses, in addition to  $\pi N \rightarrow N\pi\pi$  data, elastic amplitudes from a Saclay (CERN) partial-wave analysis.
- <sup>7</sup> The best value ARMSTRONG 99B obtains is  $\approx 0.55$ ; this assumes  $S_{11}$  dominance in the reaction  $p(e, e'p)\eta$  at  $Q^2 = 4$  (GeV/c)<sup>2</sup>.
- <sup>8</sup> This STAROSTIN 03 value is an estimate made using simplest assumptions.
- <sup>9</sup> BENMERROUCHE 91 uses an effective Lagrangian approach to analyze  $\eta$  photoproduction data.
- <sup>10</sup> This ANISOVICH 09A amplitude is evaluated at the pole position; the phase is  $(20 \pm 15)^\circ$ .
- <sup>11</sup> This ANISOVICH 09A amplitude is evaluated at the pole position; the phase is  $(20 \pm 20)^\circ$ .

**N(1535) REFERENCES**

For early references, see Physics Letters **111B** 1 (1982).

ANISOVICH 12A	EPJ A48 15	A.V. Anisovich <i>et al.</i>	(BONN, PNPI)
ANISOVICH 10	EPJ A44 203	A.V. Anisovich <i>et al.</i>	(BONN, PNPI)
BATINIC 10	PR C82 038203	M. Batinic <i>et al.</i>	(ZAGR)
ANISOVICH 09A	EPJ A41 13	A.V. Anisovich <i>et al.</i>	(BONN, PNPI, BASL)
AZNAURYAN 09	PR C80 055203	I.G. Aznauryan <i>et al.</i>	(JLAB CLAS Collab.)
THOMA 08	PL B659 87	U. Thoma <i>et al.</i>	(CB-ELSA Collab.)
DRECHSEL 07	EPJ A34 69	D. Drechsel, S.S. Kamalov, L. Tiator	(MAINZ, JINR)
DUGGER 07	PR C76 025211	M. Dugger <i>et al.</i>	(Jefferson Lab CLAS Collab.)
ARNDT 06	PR C74 045205	R.A. Arndt <i>et al.</i>	(GWU)
PDG 06	JPG 33 1	W.-M. Yao <i>et al.</i>	(PDG Collab.)
ARNDT 04	PR C69 035213	R.A. Arndt <i>et al.</i>	(GWU, TRIU)
STAROSTIN 03	PR C67 068201	A. Starostin <i>et al.</i>	(BNL Crystal Ball Collab.)
PENNER 02C	PR C66 055211	G. Penner, U. Mosel	(GIES)
PENNER 02D	PR C66 055212	G. Penner, U. Mosel	(GIES)
BAI 01B	PL B510 75	J.Z. Bai <i>et al.</i>	(BES Collab.)
THOMPSON 01	PRL 86 1702	R. Thompson <i>et al.</i>	(Jefferson Lab CLAS Collab.)
VRANA 00	PRPL 328 181	T.P. Vrana, S.A. Dytman, T.-S.H. Lee	(PITT+)
ARMSTRONG 99B	PR D60 052004	C.S. Armstrong <i>et al.</i>	
ARNDT 98	PR C58 3636	R.A. Arndt <i>et al.</i>	
GREEN 97	PR C55 R2167	A.M. Green, S. Wycech	(HELS, WINR)
KRUSCHE 97	PL B397 171	B. Krusche <i>et al.</i>	(GIES, RPI, SASK)
ABAEV 96	PR C53 385	V.V. Aboev, B.M.K. Nefkens	(UCLA)
ARNDT 96	PR C53 430	R.A. Arndt, I.I. Strakovsky, R.L. Workman	(VPI)
ARNDT 95	PR C52 2120	R.A. Arndt <i>et al.</i>	(VPI, BRCO)
BENMERROU...95	PR D51 3237	M. Benmerrouche, N.C. Mukhopadhyay, J.F. Zhang	
KRUSCHE 95	PRL 74 3736	B. Krusche <i>et al.</i>	(GIES, MANZ, GLAS+)
KRUSCHE 95C	PL B358 40	B. Krusche <i>et al.</i>	(GIES, MANZ, GLAS+)
MUKHOPAD...95B	PL B364 1	N.C. Mukhopadhyay, J.F. Zhang, M. Benmerrouche	
HOEHLER 93	$\pi N$ Newsletter 9 1	G. Hohler	(KARL)
LI 93	PR C47 2759	Z.J. Li <i>et al.</i>	(VPI)
MANLEY 92	PR D45 4002	D.M. Manley, E.M. Saleski	(KENT) IJP
Also	PR D30 904	D.M. Manley <i>et al.</i>	(VPI)
ARNDT 91	PR D43 2131	R.A. Arndt <i>et al.</i>	(VPI, TELE) IJP
BENMERROU...91	PRL 67 1070	M. Benmerrouche, N.C. Mukhopadhyay	(RPI)
WADA 84	NP B247 313	Y. Wada <i>et al.</i>	(INUS)
CRAWFORD 83	NP B211 1	R.L. Crawford, W.T. Morton	(GLAS)
PDG 82	PL 111B 1	M. Roos <i>et al.</i>	(HELS, CIT, CERN)
AWAJI 81	Bonn Conf. 352	N. Awaji, R. Kajikawa	(NAGO)
Also	NP B197 365	K. Fujii <i>et al.</i>	(NAGO)
FUJII 81	NP B187 53	K. Fujii <i>et al.</i>	(NAGO, OSAK)
CUTKOSKY 80	Toronto Conf. 19	R.E. Cutkosky <i>et al.</i>	(CMU, LBL) IJP
Also	PR D20 2839	R.E. Cutkosky <i>et al.</i>	(CMU, LBL) IJP
HOEHLER 79	PDAT 12-1	G. Hohler <i>et al.</i>	(KARLT) IJP
Also	Toronto Conf. 3	R. Koch	(KARLT) IJP
LONGACRE 78	PR D17 1795	R.S. Longacre <i>et al.</i>	(LBL, SLAC)
LONGACRE 77	NP B122 493	R.S. Longacre, J. Dolbeau	(SACL) IJP
Also	NP B108 365	J. Dolbeau <i>et al.</i>	(SACL) IJP
LONGACRE 75	PL 55B 415	R.S. Longacre <i>et al.</i>	(LBL, SLAC) IJP

## Baryon Particle Listings

 $N(1650)$  $N(1650) 1/2^-$ 

$$I(J^P) = \frac{1}{2}(\frac{1}{2}^-) \text{ Status: } ****$$

Most of the results published before 1975 were last included in our 1982 edition, Physics Letters **111B** 1 (1982). Some further obsolete results published before 1984 were last included in our 2006 edition, Journal of Physics, G **33** 1 (2006).

 $N(1650)$  BREIT-WIGNER MASS

VALUE (MeV)	DOCUMENT ID	TECN	COMMENT
<b>1645 to 1670 (<math>\approx 1655</math>) OUR ESTIMATE</b>			
1651 $\pm$ 6	ANISOVICH 12A	DPWA	Multichannel
1634.7 $\pm$ 1.1	ARNDT 06	DPWA	$\pi N \rightarrow \pi N, \eta N$
1659 $\pm$ 9	MANLEY 92	IPWA	$\pi N \rightarrow \pi N$ & $N\pi\pi$
1650 $\pm$ 30	CUTKOSKY 80	IPWA	$\pi N \rightarrow \pi N$
1670 $\pm$ 8	HOEHLER 79	IPWA	$\pi N \rightarrow \pi N$
• • • We do not use the following data for averages, fits, limits, etc. • • •			
1680 $\pm$ 40	ANISOVICH 10	DPWA	Multichannel
1652 $\pm$ 9	BATINIC 10	DPWA	$\pi N \rightarrow N\pi, N\eta$
1655 $\pm$ 15	THOMA 08	DPWA	Multichannel
1651.2 $\pm$ 4.7	ARNDT 04	DPWA	$\pi N \rightarrow \pi N, \eta N$
1665 $\pm$ 2	PENNER 02c	DPWA	Multichannel
1647 $\pm$ 20	BAI 01B	BES	$J/\psi \rightarrow p\bar{p}\eta$
1689 $\pm$ 12	VRANA 00	DPWA	Multichannel
1677 $\pm$ 8	ARNDT 96	IPWA	$\gamma N \rightarrow \pi N$
1667	ARNDT 95	DPWA	$\pi N \rightarrow N\pi$
1712	<sup>1</sup> ARNDT 95	DPWA	$\pi N \rightarrow N\pi$
1674	LI 93	IPWA	$\gamma N \rightarrow \pi N$
1672	MUSETTE 80	IPWA	$\pi^- p \rightarrow \Lambda K^0$
1680	SAXON 80	DPWA	$\pi^- p \rightarrow \Lambda K^0$
1700	<sup>2</sup> LONGACRE 77	IPWA	$\pi N \rightarrow N\pi\pi$
1660	<sup>3</sup> LONGACRE 75	IPWA	$\pi N \rightarrow N\pi\pi$

 $N(1650)$  BREIT-WIGNER WIDTH

VALUE (MeV)	DOCUMENT ID	TECN	COMMENT
<b>120 to 180 (<math>\approx 150</math>) OUR ESTIMATE</b>			
104 $\pm$ 10	ANISOVICH 12A	DPWA	Multichannel
115.4 $\pm$ 2.8	ARNDT 06	DPWA	$\pi N \rightarrow \pi N, \eta N$
167.9 $\pm$ 9.4	GREEN 97	DPWA	$\pi N \rightarrow \pi N, \eta N$
173 $\pm$ 12	MANLEY 92	IPWA	$\pi N \rightarrow \pi N$ & $N\pi\pi$
150 $\pm$ 40	CUTKOSKY 80	IPWA	$\pi N \rightarrow \pi N$
180 $\pm$ 20	HOEHLER 79	IPWA	$\pi N \rightarrow \pi N$
• • • We do not use the following data for averages, fits, limits, etc. • • •			
170 $\pm$ 45	ANISOVICH 10	DPWA	Multichannel
202 $\pm$ 16	BATINIC 10	DPWA	$\pi N \rightarrow N\pi, N\eta$
180 $\pm$ 20	THOMA 08	DPWA	Multichannel
130.6 $\pm$ 7.0	ARNDT 04	DPWA	$\pi N \rightarrow \pi N, \eta N$
138 $\pm$ 7	PENNER 02c	DPWA	Multichannel
145 $\pm$ 80 -45	BAI 01B	BES	$J/\psi \rightarrow p\bar{p}\eta$
202 $\pm$ 40	VRANA 00	DPWA	Multichannel
160 $\pm$ 12	ARNDT 96	IPWA	$\gamma N \rightarrow \pi N$
90	ARNDT 95	DPWA	$\pi N \rightarrow N\pi$
184	<sup>1</sup> ARNDT 95	DPWA	$\pi N \rightarrow N\pi$
225	LI 93	IPWA	$\gamma N \rightarrow \pi N$
179	MUSETTE 80	IPWA	$\pi^- p \rightarrow \Lambda K^0$
120	SAXON 80	DPWA	$\pi^- p \rightarrow \Lambda K^0$
170	<sup>2</sup> LONGACRE 77	IPWA	$\pi N \rightarrow N\pi\pi$
130	<sup>3</sup> LONGACRE 75	IPWA	$\pi N \rightarrow N\pi\pi$

 $N(1650)$  POLE POSITION

## REAL PART

VALUE (MeV)	DOCUMENT ID	TECN	COMMENT
<b>1640 to 1670 (<math>\approx 1655</math>) OUR ESTIMATE</b>			
1647 $\pm$ 6	ANISOVICH 12A	DPWA	Multichannel
1648	ARNDT 06	DPWA	$\pi N \rightarrow \pi N, \eta N$
1670	<sup>4</sup> HOEHLER 93	ARGD	$\pi N \rightarrow \pi N$
1640 $\pm$ 20	CUTKOSKY 80	IPWA	$\pi N \rightarrow \pi N$
• • • We do not use the following data for averages, fits, limits, etc. • • •			
1670 $\pm$ 35	ANISOVICH 10	DPWA	Multichannel
1646 $\pm$ 8	BATINIC 10	DPWA	$\pi N \rightarrow N\pi, N\eta$
1645 $\pm$ 15	THOMA 08	DPWA	Multichannel
1653	ARNDT 04	DPWA	$\pi N \rightarrow \pi N, \eta N$
1663	VRANA 00	DPWA	Multichannel
1660 $\pm$ 10	<sup>5</sup> ARNDT 98	DPWA	$\pi N \rightarrow \pi N, \eta N$
1673	ARNDT 95	DPWA	$\pi N \rightarrow N\pi$
1689	<sup>1</sup> ARNDT 95	DPWA	$\pi N \rightarrow N\pi$
1657	ARNDT 91	DPWA	$\pi N \rightarrow \pi N$ Soln SM90
1648 or 1651	<sup>6</sup> LONGACRE 78	IPWA	$\pi N \rightarrow N\pi\pi$
1699 or 1698	<sup>2</sup> LONGACRE 77	IPWA	$\pi N \rightarrow N\pi\pi$

## -2xIMAGINARY PART

VALUE (MeV)	DOCUMENT ID	TECN	COMMENT
<b>100 to 170 (<math>\approx 135</math>) OUR ESTIMATE</b>			
103 $\pm$ 8	ANISOVICH 12A	DPWA	Multichannel
80	ARNDT 06	DPWA	$\pi N \rightarrow \pi N, \eta N$
163	<sup>4</sup> HOEHLER 93	ARGD	$\pi N \rightarrow \pi N$
150 $\pm$ 30	CUTKOSKY 80	IPWA	$\pi N \rightarrow \pi N$
• • • We do not use the following data for averages, fits, limits, etc. • • •			
170 $\pm$ 40	ANISOVICH 10	DPWA	Multichannel
204 $\pm$ 17	BATINIC 10	DPWA	$\pi N \rightarrow N\pi, N\eta$
187 $\pm$ 20	THOMA 08	DPWA	Multichannel
182	ARNDT 04	DPWA	$\pi N \rightarrow \pi N, \eta N$
240	VRANA 00	DPWA	Multichannel
140 $\pm$ 20	<sup>5</sup> ARNDT 98	DPWA	$\pi N \rightarrow \pi N, \eta N$
82	ARNDT 95	DPWA	$\pi N \rightarrow N\pi$
192	<sup>1</sup> ARNDT 95	DPWA	$\pi N \rightarrow N\pi$
160	ARNDT 91	DPWA	$\pi N \rightarrow \pi N$ Soln SM90
117 or 119	<sup>6</sup> LONGACRE 78	IPWA	$\pi N \rightarrow N\pi\pi$
174 or 173	<sup>2</sup> LONGACRE 77	IPWA	$\pi N \rightarrow N\pi\pi$

 $N(1650)$  ELASTIC POLE RESIDUEMODULUS  $|r|$ 

VALUE (MeV)	DOCUMENT ID	TECN	COMMENT
<b>20 to 50 (<math>\approx 35</math>) OUR ESTIMATE</b>			
24 $\pm$ 3	ANISOVICH 12A	DPWA	Multichannel
14	ARNDT 06	DPWA	$\pi N \rightarrow \pi N, \eta N$
39	HOEHLER 93	ARGD	$\pi N \rightarrow \pi N$
60 $\pm$ 10	CUTKOSKY 80	IPWA	$\pi N \rightarrow \pi N$
• • • We do not use the following data for averages, fits, limits, etc. • • •			
100	BATINIC 10	DPWA	$\pi N \rightarrow N\pi, N\eta$
69	ARNDT 04	DPWA	$\pi N \rightarrow \pi N, \eta N$
22	ARNDT 95	DPWA	$\pi N \rightarrow N\pi$
72	<sup>1</sup> ARNDT 95	DPWA	$\pi N \rightarrow N\pi$
54	ARNDT 91	DPWA	$\pi N \rightarrow \pi N$ Soln SM90

PHASE  $\theta$ 

VALUE ( $^\circ$ )	DOCUMENT ID	TECN	COMMENT
<b>50 to 80 (<math>\approx 70</math>) OUR ESTIMATE</b>			
-75 $\pm$ 12	ANISOVICH 12A	DPWA	Multichannel
-69	ARNDT 06	DPWA	$\pi N \rightarrow \pi N, \eta N$
-37	HOEHLER 93	ARGD	$\pi N \rightarrow \pi N$
-75 $\pm$ 25	CUTKOSKY 80	IPWA	$\pi N \rightarrow \pi N$
• • • We do not use the following data for averages, fits, limits, etc. • • •			
-65	BATINIC 10	DPWA	$\pi N \rightarrow N\pi, N\eta$
-55	ARNDT 04	DPWA	$\pi N \rightarrow \pi N, \eta N$
-29	ARNDT 95	DPWA	$\pi N \rightarrow N\pi$
-85	<sup>1</sup> ARNDT 95	DPWA	$\pi N \rightarrow N\pi$
-38	ARNDT 91	DPWA	$\pi N \rightarrow \pi N$ Soln SM90

 $N(1650)$  INELASTIC POLE RESIDUE

The "normalized residue" is the residue divided by  $\Gamma_{pole}$ .

Normalized residue in  $N\pi \rightarrow N(1650) \rightarrow N\eta$ 

MODULUS (%)	PHASE ( $^\circ$ )	DOCUMENT ID	TECN	COMMENT
<b>29 <math>\pm</math> 3</b>	<b>134 <math>\pm</math> 10</b>	ANISOVICH 12A	DPWA	Multichannel

Normalized residue in  $N\pi \rightarrow N(1650) \rightarrow \Lambda K$ 

MODULUS (%)	PHASE ( $^\circ$ )	DOCUMENT ID	TECN	COMMENT
<b>23 <math>\pm</math> 9</b>	<b>85 <math>\pm</math> 9</b>	ANISOVICH 12A	DPWA	Multichannel

Normalized residue in  $N\pi \rightarrow N(1650) \rightarrow \Delta\pi, D$ -wave

MODULUS (%)	PHASE ( $^\circ$ )	DOCUMENT ID	TECN	COMMENT
<b>23 <math>\pm</math> 4</b>	<b>-30 <math>\pm</math> 20</b>	ANISOVICH 12A	DPWA	Multichannel

 $N(1650)$  DECAY MODES

The following branching fractions are our estimates, not fits or averages.

Mode	Fraction ( $\Gamma_i/\Gamma$ )
$\Gamma_1$ $N\pi$	50-90 %
$\Gamma_2$ $N\eta$	5-15 %
$\Gamma_3$ $\Lambda K$	3-11 %
$\Gamma_4$ $\Sigma K$	
$\Gamma_5$ $N\pi\pi$	10-20 %
$\Gamma_6$ $\Delta\pi$	0-25 %
$\Gamma_7$ $\Delta(1232)\pi, D$ -wave	0-25 %
$\Gamma_8$ $N\rho$	4-12 %

$\Gamma_9$	$N\rho, S=1/2, S\text{-wave}$	(1.0±1.0) %
$\Gamma_{10}$	$N\rho, S=3/2, D\text{-wave}$	(13.0±3.0) %
$\Gamma_{11}$	$N(\pi\pi)_{S\text{-wave}}^{J=0}$	<4 %
$\Gamma_{12}$	$N(1440)\pi$	<5 %
$\Gamma_{13}$	$p\gamma$	0.04–0.20 %
$\Gamma_{14}$	$p\gamma, \text{helicity}=1/2$	0.04–0.20 %
$\Gamma_{15}$	$n\gamma$	0.003–0.17 %
$\Gamma_{16}$	$n\gamma, \text{helicity}=1/2$	0.003–0.17 %

## N(1650) BRANCHING RATIOS

$\Gamma(N\pi)/\Gamma_{\text{total}}$	DOCUMENT ID	TECN	COMMENT	$\Gamma_1/\Gamma$
<b>50 to 90 (≈ 70) OUR ESTIMATE</b>				
51 ± 4	ANISOVICH	12A	DPWA Multichannel	
100	ARNDT	06	DPWA $\pi N \rightarrow \pi N, \eta N$	
73.5 ± 1.1	GREEN	97	DPWA $\pi N \rightarrow \pi N, \eta N$	
89 ± 7	MANLEY	92	IPWA $\pi N \rightarrow \pi N \& N\pi\pi$	
65 ± 10	CUTKOSKY	80	IPWA $\pi N \rightarrow \pi N$	
61 ± 4	HOEHLER	79	IPWA $\pi N \rightarrow \pi N$	
• • • We do not use the following data for averages, fits, limits, etc. • • •				
50 ± 25	ANISOVICH	10	DPWA Multichannel	
79 ± 6	BATINIC	10	DPWA $\pi N \rightarrow N\pi, N\eta$	
70 ± 15	THOMA	08	DPWA Multichannel	
100.0	ARNDT	04	DPWA $\pi N \rightarrow \pi N, \eta N$	
65 ± 4	PENNER	02c	DPWA Multichannel	
74 ± 2	VRANA	00	DPWA Multichannel	
99	ARNDT	95	DPWA $\pi N \rightarrow N\pi$	
27	<sup>1</sup> ARNDT	95	DPWA $\pi N \rightarrow N\pi$	

$\Gamma(N\eta)/\Gamma_{\text{total}}$	DOCUMENT ID	TECN	COMMENT	$\Gamma_2/\Gamma$
<b>5 to 15 OUR ESTIMATE</b>				
18 ± 4	ANISOVICH	12A	DPWA Multichannel	
1.0±0.6	PENNER	02c	DPWA Multichannel	
6 ± 1	VRANA	00	DPWA Multichannel	
• • • We do not use the following data for averages, fits, limits, etc. • • •				
13 ± 5	BATINIC	10	DPWA $\pi N \rightarrow N\pi, N\eta$	
15 ± 6	THOMA	08	DPWA Multichannel	

$\Gamma(\Lambda K)/\Gamma_{\text{total}}$	DOCUMENT ID	TECN	COMMENT	$\Gamma_3/\Gamma$
<b>2.9±0.4 OUR AVERAGE</b> Error includes scale factor of 1.2.				
10 ± 5	ANISOVICH	12A	DPWA Multichannel	
4 ± 1	SHKLYAR	05	DPWA Multichannel	
2.7±0.4	PENNER	02c	DPWA Multichannel	

$(\Gamma_i\Gamma_f)^{1/2}/\Gamma_{\text{total}}$ in $N\pi \rightarrow N(1650) \rightarrow \Lambda K$	DOCUMENT ID	TECN	COMMENT	$(\Gamma_1\Gamma_3)^{1/2}/\Gamma$
<b>−0.27 to −0.17 OUR ESTIMATE</b>				
−0.22	BELL	83	DPWA $\pi^- p \rightarrow \Lambda K^0$	
−0.22	SAXON	80	DPWA $\pi^- p \rightarrow \Lambda K^0$	

$(\Gamma_i\Gamma_f)^{1/2}/\Gamma_{\text{total}}$ in $N\pi \rightarrow N(1650) \rightarrow \Sigma K$	DOCUMENT ID	TECN	COMMENT	$(\Gamma_1\Gamma_4)^{1/2}/\Gamma$
<b>−0.254</b>				
−0.254	LIVANOS	80	DPWA $\pi p \rightarrow \Sigma K$	

Note: Signs of couplings from  $\pi N \rightarrow N\pi\pi$  analyses were changed in the 1986 edition to agree with the baryon-first convention; the overall phase ambiguity is resolved by choosing a negative sign for the  $\Delta(1620) S_{31}$  coupling to  $\Delta(1232)\pi$ .

$(\Gamma_i\Gamma_f)^{1/2}/\Gamma_{\text{total}}$ in $N\pi \rightarrow N(1650) \rightarrow \Delta(1232)\pi, D\text{-wave}$	DOCUMENT ID	TECN	COMMENT	$(\Gamma_1\Gamma_7)^{1/2}/\Gamma$
<b>+0.15 to 0.23 OUR ESTIMATE</b>				
+0.12±0.04	MANLEY	92	IPWA $\pi N \rightarrow \pi N \& N\pi\pi$	
+0.29	<sup>2,7</sup> LONGACRE	77	IPWA $\pi N \rightarrow N\pi\pi$	
+0.15	<sup>3</sup> LONGACRE	75	IPWA $\pi N \rightarrow N\pi\pi$	
• • • We do not use the following data for averages, fits, limits, etc. • • •				
+0.26±0.14	THOMA	08	DPWA Multichannel	

$\Gamma(\Delta(1232)\pi, D\text{-wave})/\Gamma_{\text{total}}$	DOCUMENT ID	TECN	COMMENT	$\Gamma_7/\Gamma$
<b>0 to 25 OUR ESTIMATE</b>				
19±9	ANISOVICH	12A	DPWA Multichannel	
2±1	VRANA	00	DPWA Multichannel	
• • • We do not use the following data for averages, fits, limits, etc. • • •				
10±5	THOMA	08	DPWA Multichannel	

$(\Gamma_i\Gamma_f)^{1/2}/\Gamma_{\text{total}}$ in $N\pi \rightarrow N(1650) \rightarrow N\rho, S=1/2, S\text{-wave}$	DOCUMENT ID	TECN	COMMENT	$(\Gamma_1\Gamma_9)^{1/2}/\Gamma$
<b>±0.03 to ±0.19 OUR ESTIMATE</b>				
−0.01±0.09	MANLEY	92	IPWA $\pi N \rightarrow \pi N \& N\pi\pi$	
+0.17	<sup>2,7</sup> LONGACRE	77	IPWA $\pi N \rightarrow N\pi\pi$	
−0.16	<sup>3</sup> LONGACRE	75	IPWA $\pi N \rightarrow N\pi\pi$	

$\Gamma(N\rho, S=1/2, S\text{-wave})/\Gamma_{\text{total}}$	DOCUMENT ID	TECN	COMMENT	$\Gamma_9/\Gamma$
<b>1±1</b>				
	VRANA	00	DPWA Multichannel	

$(\Gamma_i\Gamma_f)^{1/2}/\Gamma_{\text{total}}$ in $N\pi \rightarrow N(1650) \rightarrow N\rho, S=3/2, D\text{-wave}$	DOCUMENT ID	TECN	COMMENT	$(\Gamma_1\Gamma_{10})^{1/2}/\Gamma$
<b>+0.17 to +0.29 OUR ESTIMATE</b>				
+0.16±0.06	MANLEY	92	IPWA $\pi N \rightarrow \pi N \& N\pi\pi$	
+0.29	<sup>2,7</sup> LONGACRE	77	IPWA $\pi N \rightarrow N\pi\pi$	

$\Gamma(N\rho, S=3/2, D\text{-wave})/\Gamma_{\text{total}}$	DOCUMENT ID	TECN	COMMENT	$\Gamma_{10}/\Gamma$
<b>13±3</b>				
	VRANA	00	DPWA Multichannel	

$(\Gamma_i\Gamma_f)^{1/2}/\Gamma_{\text{total}}$ in $N\pi \rightarrow N(1650) \rightarrow N(\pi\pi)_{S\text{-wave}}^{J=0}$	DOCUMENT ID	TECN	COMMENT	$(\Gamma_1\Gamma_{11})^{1/2}/\Gamma$
<b>+0.04 to +0.18 OUR ESTIMATE</b>				
+0.12±0.08	MANLEY	92	IPWA $\pi N \rightarrow \pi N \& N\pi\pi$	
0.00	<sup>2,7</sup> LONGACRE	77	IPWA $\pi N \rightarrow N\pi\pi$	
+0.25	<sup>3</sup> LONGACRE	75	IPWA $\pi N \rightarrow N\pi\pi$	

$\Gamma(N(\pi\pi)_{S\text{-wave}}^{J=0})/\Gamma_{\text{total}}$	DOCUMENT ID	TECN	COMMENT	$\Gamma_{11}/\Gamma$
<b>1±1</b>				
	VRANA	00	DPWA Multichannel	

$(\Gamma_i\Gamma_f)^{1/2}/\Gamma_{\text{total}}$ in $N\pi \rightarrow N(1650) \rightarrow N(1440)\pi$	DOCUMENT ID	TECN	COMMENT	$(\Gamma_1\Gamma_{12})^{1/2}/\Gamma$
<b>+0.11±0.06</b>				
	MANLEY	92	IPWA $\pi N \rightarrow \pi N \& N\pi\pi$	

$\Gamma(N(1440)\pi)/\Gamma_{\text{total}}$	DOCUMENT ID	TECN	COMMENT	$\Gamma_{12}/\Gamma$
<b>3±1</b>				
	VRANA	00	DPWA Multichannel	

## N(1650) PHOTON DECAY AMPLITUDES

Papers on  $\gamma N$  amplitudes predating 1981 may be found in our 2006 edition, Journal of Physics, G **33** 1 (2006).

N(1650) → pγ, helicity-1/2 amplitude A<sub>1/2</sub>

VALUE (GeV <sup>−1/2</sup> )	DOCUMENT ID	TECN	COMMENT
<b>+0.053±0.016 OUR ESTIMATE</b>			
0.033±0.007	ANISOVICH	12A	DPWA Multichannel
0.022±0.007	DUGGER	07	DPWA $\gamma N \rightarrow \pi N$
0.069±0.005	ARNDT	96	IPWA $\gamma N \rightarrow \pi N$
0.033±0.015	CRAWFORD	83	IPWA $\gamma N \rightarrow \pi N$
0.050±0.010	AWAJI	81	DPWA $\gamma N \rightarrow \pi N$
• • • We do not use the following data for averages, fits, limits, etc. • • •			
0.060±0.020	ANISOVICH	10	DPWA Multichannel
0.100±0.035	<sup>8</sup> ANISOVICH	09A	DPWA $\gamma d \rightarrow \eta N(N)$
0.033	DRECHSEL	07	DPWA $\gamma N \rightarrow \pi N$
0.049	PENNER	02D	DPWA Multichannel
0.068±0.003	LI	93	IPWA $\gamma N \rightarrow \pi N$
0.091	WADA	84	DPWA Compton scattering

N(1650) → nγ, helicity-1/2 amplitude A<sub>1/2</sub>

VALUE (GeV <sup>−1/2</sup> )	DOCUMENT ID	TECN	COMMENT
<b>−0.015±0.021 OUR ESTIMATE</b>			
−0.055±0.020	<sup>9</sup> ANISOVICH	09A	DPWA $\gamma d \rightarrow \eta N(N)$
−0.015±0.005	ARNDT	96	IPWA $\gamma N \rightarrow \pi N$
−0.008±0.004	AWAJI	81	DPWA $\gamma N \rightarrow \pi N$
0.004±0.004	FUJII	81	DPWA $\gamma N \rightarrow \pi N$
• • • We do not use the following data for averages, fits, limits, etc. • • •			
0.009	DRECHSEL	07	DPWA $\gamma N \rightarrow \pi N$
−0.011	PENNER	02D	DPWA Multichannel
−0.002±0.002	LI	93	IPWA $\gamma N \rightarrow \pi N$

N(1650) γp → ΛK<sup>+</sup> AMPLITUDES

$(\Gamma_i\Gamma_f)^{1/2}/\Gamma_{\text{total}}$ in $p\gamma \rightarrow N(1650) \rightarrow \Lambda K^+$	DOCUMENT ID	TECN	COMMENT	$(E_{0+} \text{ amplitude})$
<b>7.8 ± 0.3</b>				
7.8 ± 0.3	WORKMAN	90	DPWA	
8.13	TANABE	89	DPWA	

## Baryon Particle Listings

 $N(1650)$ ,  $N(1675)$  $p\gamma \rightarrow N(1650) \rightarrow \Lambda K^+$  phase angle  $\theta$  ( $E_{0+}$  amplitude)

VALUE (degrees)	DOCUMENT ID	TECN
• • • We do not use the following data for averages, fits, limits, etc. • • •		
-107 ± 3	WORKMAN 90	DPWA
-107.8	TANABE 89	DPWA

 $N(1650)$  FOOTNOTES

- <sup>1</sup> ARNDT 95 finds two distinct states.  
<sup>2</sup> LONGACRE 77 pole positions are from a search for poles in the unitarized T-matrix; the first (second) value uses, in addition to  $\pi N \rightarrow N\pi\pi$  data, elastic amplitudes from a Saclay (CERN) partial-wave analysis. The other LONGACRE 77 values are from eyeball fits with Breit-Wigner circles to the T-matrix amplitudes.  
<sup>3</sup> From method II of LONGACRE 75: eyeball fits with Breit-Wigner circles to the T-matrix amplitudes.  
<sup>4</sup> See HOEHLER 93 for a detailed discussion of the evidence for and the pole parameters of  $N$  and  $\Delta$  resonances as determined from Argand diagrams of  $\pi N$  elastic partial-wave amplitudes and from plots of the speeds with which the amplitudes traverse the diagrams.  
<sup>5</sup> ARNDT 98 also lists pole residues, which display more model dependence than do the associated pole positions.  
<sup>6</sup> LONGACRE 78 values are from a search for poles in the unitarized T-matrix. The first (second) value uses, in addition to  $\pi N \rightarrow N\pi\pi$  data, elastic amplitudes from a Saclay (CERN) partial-wave analysis.  
<sup>7</sup> LONGACRE 77 considers this coupling to be well determined.  
<sup>8</sup> This ANISOVICH 09A amplitude is evaluated at the pole position; the phase is  $(25 \pm 20)^\circ$ .  
<sup>9</sup> This ANISOVICH 09A amplitude is evaluated at the pole position; the phase is  $(30 \pm 25)^\circ$ .

 $N(1650)$  REFERENCES

For early references, see Physics Letters **111B** 1 (1982).

ANISOVICH 12A	EPJ A48 15	A.V. Anisovich et al.	(BONN, PNPI)
ANISOVICH 10	EPJ A44 203	A.V. Anisovich et al.	(BONN, PNPI)
BATINIC 10	PR C82 038203	M. Batinic et al.	(ZAGR)
ANISOVICH 09A	EPJ A41 13	A.V. Anisovich et al.	(BONN, PNPI, BASL)
THOMA 08	PL B659 87	U. Thoma et al.	(CB-ELSA Collab.)
DRECHSEL 07	EPJ A34 69	D. Drechsel, S.S. Kamalov, L. Tiator	(MAINZ, JINR)
DUGGER 07	PR C76 025211	M. Dugger et al.	(Jefferson Lab CLAS Collab.)
ARNDT 06	PR C74 045205	R.A. Arndt et al.	(GWU)
PDG 06	JPG 33 1	W.-M. Yao et al.	(PDG Collab.)
SHKLYAR 05	PR C72 015210	V. Shklyar, H. Lenske, U. Mosel	(GIES)
ARNDT 04	PR C69 035213	R.A. Arndt et al.	(GWU, TRIU)
PENNER 02C	PR C66 055211	G. Penner, U. Mosel	(GIES)
PENNER 02D	PR C66 055212	G. Penner, U. Mosel	(GIES)
BAI 01B	PL B510 75	J.Z. Bai et al.	(BES Collab.)
VRANA 00	PRPL 328 181	T.P. Vrana, S.A. Dytman, T.-S.H. Lee	(PITT+)
ARNDT 98	PR C58 3636	R.A. Arndt et al.	
GREEN 97	PR C55 R2167	A.M. Green, S. Wycech	(HELZ, WINR)
ARNDT 96	PR C53 430	R.A. Arndt, I.I. Strakovsky, R.L. Workman	(VPI)
ARNDT 95	PR C52 2120	R.A. Arndt et al.	(VPI, BRCO)
HOEHLER 93	$\pi N$ Newsletter 9 1	G. Hoehler	(KARL)
LI 93	PR C47 2759	Z.J. Li et al.	(VPI)
MANLEY 92	PR D45 4002	D.M. Manley, E.M. Saleski	(KENT IUP)
Also	PR D30 904	D.M. Manley et al.	(VPI)
ARNDT 91	PR D43 2131	R.A. Arndt et al.	(VPI, TELE) IUP
WORKMAN 90	PR C42 781	R.L. Workman	(VPI)
TANABE 89	PR C39 741	H. Tanabe, M. Kohno, C. Bennhold	(MANZ)
Also	NC 102A 193	M. Kohno, H. Tanabe, C. Bennhold	(MANZ)
WADA 84	NP B247 313	Y. Wada et al.	(INUS)
BELL 83	NP B222 389	K.W. Bell et al.	(RL) IUP
CRAWFORD 83	NP B211 1	R.L. Crawford, W.T. Morton	(GLAS)
PDG 82	PL 111B 1	M. Roos et al.	(HELZ, CIT, CERN)
AWAJI 81	Bonn Conf. 352	N. Awaji, R. Kajikawa	(NAGO)
Also	NP B197 365	K. Fujii et al.	(NAGO)
FUJII 81	NP B187 53	K. Fujii et al.	(NAGO, OSAK)
CUTKOSKY 80	Toronto Conf. 19	R.E. Cutkosky et al.	(CMU, LBL) IUP
Also	PR D20 2839	R.E. Cutkosky et al.	(CMU, LBL) IUP
LIVANOS 80	Toronto Conf. 35	P. Livanos et al.	(SACL) IUP
MUSETTE 80	NC 57A 37	M. Musette	(BRUX) IUP
SAXON 80	NP B162 522	D.H. Saxon et al.	(RHEL, BRIS) IUP
HOEHLER 79	PDAT 12-1	G. Hoehler et al.	(KARLT) IUP
Also	Toronto Conf. 3	R. Koch	(KARLT) IUP
LONGACRE 78	PR D17 1795	R.S. Longacre et al.	(LBL, SLAC)
LONGACRE 77	NP B122 493	R.S. Longacre, J. Dolbeau	(SACL) IUP
Also	NP B108 365	J. Dolbeau et al.	(SACL) IUP
LONGACRE 75	PL 55B 415	R.S. Longacre et al.	(LBL, SLAC) IUP

 $N(1675) 5/2^-$ 

$$I(J^P) = \frac{1}{2}(\frac{5}{2}^-) \text{ Status: } ***$$

Most of the results published before 1975 were last included in our 1982 edition, Physics Letters **111B** 1 (1982). Some further obsolete results published before 1984 were last included in our 2006 edition, Journal of Physics, **G 33** 1 (2006).

 $N(1675)$  BREIT-WIGNER MASS

VALUE (MeV)	DOCUMENT ID	TECN	COMMENT
<b>1670 to 1680 (<math>\approx 1675</math>) OUR ESTIMATE</b>			
1664 ± 5	ANISOVICH 12A	DPWA	Multichannel
1674.1 ± 0.2	ARNDT 06	DPWA	$\pi N \rightarrow \pi N, \eta N$
1676 ± 2	MANLEY 92	IPWA	$\pi N \rightarrow \pi N$ & $N\pi\pi$
1675 ± 10	CUTKOSKY 80	IPWA	$\pi N \rightarrow \pi N$
1679 ± 8	HOEHLER 79	IPWA	$\pi N \rightarrow \pi N$

• • • We do not use the following data for averages, fits, limits, etc. • • •

1678 ± 5	ANISOVICH 10	DPWA	Multichannel
1679 ± 9	BATINIC 10	DPWA	$\pi N \rightarrow N\pi, N\eta$
1678 ± 15	THOMA 08	DPWA	Multichannel
1676.2 ± 0.6	ARNDT 04	DPWA	$\pi N \rightarrow \pi N, \eta N$
1685 ± 4	VRANA 00	DPWA	Multichannel
1673 ± 5	ARNDT 96	IPWA	$\gamma N \rightarrow \pi N$
1673	ARNDT 95	DPWA	$\pi N \rightarrow N\pi$
1666	LI 93	IPWA	$\gamma N \rightarrow \pi N$
1670	SAXON 80	DPWA	$\pi^- p \rightarrow \Lambda K^0$
1650	<sup>1</sup> LONGACRE 77	IPWA	$\pi N \rightarrow N\pi\pi$
1660	<sup>2</sup> LONGACRE 75	IPWA	$\pi N \rightarrow N\pi\pi$

 $N(1675)$  BREIT-WIGNER WIDTH

VALUE (MeV)	DOCUMENT ID	TECN	COMMENT
<b>130 to 165 (<math>\approx 150</math>) OUR ESTIMATE</b>			
152 ± 7	ANISOVICH 12A	DPWA	Multichannel
146.5 ± 1.0	ARNDT 06	DPWA	$\pi N \rightarrow \pi N, \eta N$
159 ± 7	MANLEY 92	IPWA	$\pi N \rightarrow \pi N$ & $N\pi\pi$
160 ± 20	CUTKOSKY 80	IPWA	$\pi N \rightarrow \pi N$
120 ± 15	HOEHLER 79	IPWA	$\pi N \rightarrow \pi N$
• • • We do not use the following data for averages, fits, limits, etc. • • •			
177 ± 15	ANISOVICH 10	DPWA	Multichannel
152 ± 8	BATINIC 10	DPWA	$\pi N \rightarrow N\pi, N\eta$
220 ± 25	THOMA 08	DPWA	Multichannel
151.8 ± 3.0	ARNDT 04	DPWA	$\pi N \rightarrow \pi N, \eta N$
131 ± 10	VRANA 00	DPWA	Multichannel
154 ± 7	ARNDT 96	IPWA	$\gamma N \rightarrow \pi N$
154	ARNDT 95	DPWA	$\pi N \rightarrow N\pi$
136	LI 93	IPWA	$\gamma N \rightarrow \pi N$
40	SAXON 80	DPWA	$\pi^- p \rightarrow \Lambda K^0$
130	<sup>1</sup> LONGACRE 77	IPWA	$\pi N \rightarrow N\pi\pi$
150	<sup>2</sup> LONGACRE 75	IPWA	$\pi N \rightarrow N\pi\pi$

 $N(1675)$  POLE POSITION

## REAL PART

VALUE (MeV)	DOCUMENT ID	TECN	COMMENT
<b>1655 to 1665 (<math>\approx 1660</math>) OUR ESTIMATE</b>			
1654 ± 4	ANISOVICH 12A	DPWA	Multichannel
1657	ARNDT 06	DPWA	$\pi N \rightarrow \pi N, \eta N$
1656	<sup>3</sup> HOEHLER 93	ARGD	$\pi N \rightarrow \pi N$
1660 ± 10	CUTKOSKY 80	IPWA	$\pi N \rightarrow \pi N$
• • • We do not use the following data for averages, fits, limits, etc. • • •			
1650 ± 5	ANISOVICH 10	DPWA	Multichannel
1658 ± 9	BATINIC 10	DPWA	$\pi N \rightarrow N\pi, N\eta$
1639 ± 10	THOMA 08	DPWA	Multichannel
1659	ARNDT 04	DPWA	$\pi N \rightarrow \pi N, \eta N$
1674	VRANA 00	DPWA	Multichannel
1663	ARNDT 95	DPWA	$\pi N \rightarrow N\pi$
1655	ARNDT 91	DPWA	$\pi N \rightarrow \pi N$ Soln SM90
1663 or 1668	<sup>4</sup> LONGACRE 78	IPWA	$\pi N \rightarrow N\pi\pi$
1649 or 1650	<sup>1</sup> LONGACRE 77	IPWA	$\pi N \rightarrow N\pi\pi$

-2*x*IMAGINARY PART

VALUE (MeV)	DOCUMENT ID	TECN	COMMENT
<b>125 to 150 (<math>\approx 135</math>) OUR ESTIMATE</b>			
151 ± 5	ANISOVICH 12A	DPWA	Multichannel
139	ARNDT 06	DPWA	$\pi N \rightarrow \pi N, \eta N$
126	<sup>3</sup> HOEHLER 93	ARGD	$\pi N \rightarrow \pi N$
140 ± 10	CUTKOSKY 80	IPWA	$\pi N \rightarrow \pi N$
• • • We do not use the following data for averages, fits, limits, etc. • • •			
143 ± 7	ANISOVICH 10	DPWA	Multichannel
137 ± 7	BATINIC 10	DPWA	$\pi N \rightarrow N\pi, N\eta$
180 ± 20	THOMA 08	DPWA	Multichannel
146	ARNDT 04	DPWA	$\pi N \rightarrow \pi N, \eta N$
120	VRANA 00	DPWA	Multichannel
152	ARNDT 95	DPWA	$\pi N \rightarrow N\pi$
124	ARNDT 91	DPWA	$\pi N \rightarrow \pi N$ Soln SM90
146 or 171	<sup>4</sup> LONGACRE 78	IPWA	$\pi N \rightarrow N\pi\pi$
127 or 127	<sup>1</sup> LONGACRE 77	IPWA	$\pi N \rightarrow N\pi\pi$

 $N(1675)$  ELASTIC POLE RESIDUEMODULUS  $|r|$ 

VALUE (MeV)	DOCUMENT ID	TECN	COMMENT
<b>27 ± 5 OUR ESTIMATE</b>			
28 ± 1	ANISOVICH 12A	DPWA	Multichannel
27	ARNDT 06	DPWA	$\pi N \rightarrow \pi N, \eta N$
23	HOEHLER 93	ARGD	$\pi N \rightarrow \pi N$
31 ± 5	CUTKOSKY 80	IPWA	$\pi N \rightarrow \pi N$
• • • We do not use the following data for averages, fits, limits, etc. • • •			
25	BATINIC 10	DPWA	$\pi N \rightarrow N\pi, N\eta$
29	ARNDT 04	DPWA	$\pi N \rightarrow \pi N, \eta N$
29	ARNDT 95	DPWA	$\pi N \rightarrow N\pi$
28	ARNDT 91	DPWA	$\pi N \rightarrow \pi N$ Soln SM90

PHASE  $\theta$

VALUE (°)	DOCUMENT ID	TECN	COMMENT
<b>-25 ± 6 OUR ESTIMATE</b>			
-26 ± 4	ANISOVICH 12A	DPWA	Multichannel
-21	ARNDT 06	DPWA	$\pi N \rightarrow \pi N, \eta N$
-22	HOEHLER 93	ARGD	$\pi N \rightarrow \pi N$
-30 ± 10	CUTKOSKY 80	IPWA	$\pi N \rightarrow \pi N$
• • • We do not use the following data for averages, fits, limits, etc. • • •			
-16	BATINIC 10	DPWA	$\pi N \rightarrow N\pi, N\eta$
-22	ARNDT 04	DPWA	$\pi N \rightarrow \pi N, \eta N$
-6	ARNDT 95	DPWA	$\pi N \rightarrow N\pi$
-17	ARNDT 91	DPWA	$\pi N \rightarrow \pi N$ Soln SM90

N(1675) INELASTIC POLE RESIDUE

The "normalized residue" is the residue divided by  $\Gamma_{pole}$ .

Normalized residue in  $N\pi \rightarrow N(1675) \rightarrow \Delta\pi, D\text{-wave}$

MODULUS (%)	PHASE (°)	DOCUMENT ID	TECN	COMMENT
<b>33 ± 5</b>	<b>82 ± 10</b>	ANISOVICH 12A	DPWA	Multichannel

Normalized residue in  $N\pi \rightarrow N(1675) \rightarrow N\sigma$

MODULUS (%)	PHASE (°)	DOCUMENT ID	TECN	COMMENT
<b>15 ± 4</b>	<b>132 ± 18</b>	ANISOVICH 12A	DPWA	Multichannel

N(1675) DECAY MODES

The following branching fractions are our estimates, not fits or averages.

Mode	Fraction ( $\Gamma_i/\Gamma$ )
$\Gamma_1$ $N\pi$	35-45 %
$\Gamma_2$ $N\eta$	( 0.0 ± 1.0 ) %
$\Gamma_3$ $\Lambda K$	< 1 %
$\Gamma_4$ $\Sigma K$	
$\Gamma_5$ $N\pi\pi$	50-60 %
$\Gamma_6$ $\Delta\pi$	50-60 %
$\Gamma_7$ $\Delta(1232)\pi, D\text{-wave}$	( 50 ± 15 ) %
$\Gamma_8$ $\Delta(1232)\pi, G\text{-wave}$	
$\Gamma_9$ $N\rho$	< 1-3 %
$\Gamma_{10}$ $N\rho, S=1/2, D\text{-wave}$	( 0.0 ± 1.0 ) %
$\Gamma_{11}$ $N\rho, S=3/2, D\text{-wave}$	( 1.0 ± 1.0 ) %
$\Gamma_{12}$ $N\rho, S=3/2, G\text{-wave}$	
$\Gamma_{13}$ $N(\pi\pi)_{S\text{-wave}}^{J=0}$	( 7.0 ± 3.0 ) %
$\Gamma_{14}$ $p\gamma$	0-0.02 %
$\Gamma_{15}$ $p\gamma, \text{helicity}=1/2$	0-0.01 %
$\Gamma_{16}$ $p\gamma, \text{helicity}=3/2$	0-0.01 %
$\Gamma_{17}$ $n\gamma$	0-0.15 %
$\Gamma_{18}$ $n\gamma, \text{helicity}=1/2$	0-0.05 %
$\Gamma_{19}$ $n\gamma, \text{helicity}=3/2$	0-0.10 %

N(1675) BRANCHING RATIOS

$\Gamma(N\pi)/\Gamma_{total}$

VALUE (%)	DOCUMENT ID	TECN	COMMENT	$\Gamma_1/\Gamma$
<b>35 to 45 OUR ESTIMATE</b>				
40 ± 3	ANISOVICH 12A	DPWA	Multichannel	
39.3 ± 0.1	ARNDT 06	DPWA	$\pi N \rightarrow \pi N, \eta N$	
47 ± 2	MANLEY 92	IPWA	$\pi N \rightarrow \pi N \& N\pi\pi$	
38 ± 5	CUTKOSKY 80	IPWA	$\pi N \rightarrow \pi N$	
38 ± 3	HOEHLER 79	IPWA	$\pi N \rightarrow \pi N$	
• • • We do not use the following data for averages, fits, limits, etc. • • •				
37 ± 5	ANISOVICH 10	DPWA	Multichannel	
35 ± 4	BATINIC 10	DPWA	$\pi N \rightarrow N\pi, N\eta$	
30 ± 8	THOMA 08	DPWA	Multichannel	
40.0 ± 0.2	ARNDT 04	DPWA	$\pi N \rightarrow \pi N, \eta N$	
35 ± 1	VRANA 00	DPWA	Multichannel	
38	ARNDT 95	DPWA	$\pi N \rightarrow N\pi$	

$\Gamma(N\eta)/\Gamma_{total}$

VALUE (%)	DOCUMENT ID	TECN	COMMENT	$\Gamma_2/\Gamma$
<b>0 ± 1</b>	VRANA 00	DPWA	Multichannel	
• • • We do not use the following data for averages, fits, limits, etc. • • •				
0.1 ± 0.1	BATINIC 10	DPWA	$\pi N \rightarrow N\pi, N\eta$	
3 ± 3	THOMA 08	DPWA	Multichannel	

$(\Gamma_i\Gamma_f)^{1/2}/\Gamma_{total}$  in  $N\pi \rightarrow N(1675) \rightarrow \Lambda K$

VALUE	DOCUMENT ID	TECN	COMMENT	$(\Gamma_1\Gamma_3)^{1/2}/\Gamma$
<b>±0.04 to ±0.08 OUR ESTIMATE</b>				
-0.01	BELL 83	DPWA	$\pi^- p \rightarrow \Lambda K^0$	
+0.036	5 SAXON 80	DPWA	$\pi^- p \rightarrow \Lambda K^0$	

Note: Signs of couplings from  $\pi N \rightarrow N\pi\pi$  analyses were changed in the 1986 edition to agree with the baryon-first convention; the overall phase ambiguity is resolved by choosing a negative sign for the  $\Delta(1620) S_{31}$  coupling to  $\Delta(1232)\pi$ .

$(\Gamma_i\Gamma_f)^{1/2}/\Gamma_{total}$  in  $N\pi \rightarrow N(1675) \rightarrow \Delta(1232)\pi, D\text{-wave}$

VALUE	DOCUMENT ID	TECN	COMMENT	$(\Gamma_1\Gamma_7)^{1/2}/\Gamma$
<b>+0.46 to +0.50 OUR ESTIMATE</b>				
+0.496 ± 0.003	MANLEY 92	IPWA	$\pi N \rightarrow \pi N \& N\pi\pi$	
+0.46	1,6 LONGACRE 77	IPWA	$\pi N \rightarrow N\pi\pi$	
+0.50	2 LONGACRE 75	IPWA	$\pi N \rightarrow N\pi\pi$	

$\Gamma(\Delta(1232)\pi, D\text{-wave})/\Gamma_{total}$

VALUE (%)	DOCUMENT ID	TECN	COMMENT	$\Gamma_7/\Gamma$
<b>50 ± 15 OUR ESTIMATE</b>				
33 ± 8	ANISOVICH 12A	DPWA	Multichannel	
63 ± 2	VRANA 00	DPWA	Multichannel	
• • • We do not use the following data for averages, fits, limits, etc. • • •				
24 ± 8	THOMA 08	DPWA	Multichannel	

$(\Gamma_i\Gamma_f)^{1/2}/\Gamma_{total}$  in  $N\pi \rightarrow N(1675) \rightarrow N\rho, S=1/2, D\text{-wave}$

VALUE	DOCUMENT ID	TECN	COMMENT	$(\Gamma_1\Gamma_{10})^{1/2}/\Gamma$
<b>+0.04 ± 0.02</b>				
	MANLEY 92	IPWA	$\pi N \rightarrow \pi N \& N\pi\pi$	

$\Gamma(N\rho, S=1/2, D\text{-wave})/\Gamma_{total}$

VALUE (%)	DOCUMENT ID	TECN	COMMENT	$\Gamma_{10}/\Gamma$
<b>0 ± 1</b>				
	VRANA 00	DPWA	Multichannel	

$(\Gamma_i\Gamma_f)^{1/2}/\Gamma_{total}$  in  $N\pi \rightarrow N(1675) \rightarrow N\rho, S=3/2, D\text{-wave}$

VALUE	DOCUMENT ID	TECN	COMMENT	$(\Gamma_1\Gamma_{11})^{1/2}/\Gamma$
<b>-0.12 to -0.06 OUR ESTIMATE</b>				
-0.03 ± 0.02	MANLEY 92	IPWA	$\pi N \rightarrow \pi N \& N\pi\pi$	
-0.15	1,6 LONGACRE 77	IPWA	$\pi N \rightarrow N\pi\pi$	

$\Gamma(N\rho, S=3/2, D\text{-wave})/\Gamma_{total}$

VALUE (%)	DOCUMENT ID	TECN	COMMENT	$\Gamma_{11}/\Gamma$
<b>1 ± 1</b>				
	VRANA 00	DPWA	Multichannel	

$(\Gamma_i\Gamma_f)^{1/2}/\Gamma_{total}$  in  $N\pi \rightarrow N(1675) \rightarrow N(\pi\pi)_{S\text{-wave}}^{J=0}$

VALUE	DOCUMENT ID	TECN	COMMENT	$(\Gamma_1\Gamma_{13})^{1/2}/\Gamma$
<b>+0.03</b>				
	1,6 LONGACRE 77	IPWA	$\pi N \rightarrow N\pi\pi$	

$\Gamma(N(\pi\pi)_{S\text{-wave}}^{J=0})/\Gamma_{total}$

VALUE (%)	DOCUMENT ID	TECN	COMMENT	$\Gamma_{13}/\Gamma$
<b>7 ± 3</b>				
	ANISOVICH 12A	DPWA	Multichannel	

N(1675) PHOTON DECAY AMPLITUDES

Papers on  $\gamma N$  amplitudes predating 1981 may be found in our 2006 edition, Journal of Physics, G 33 1 (2006).

N(1675)  $\rightarrow p\gamma, \text{helicity-1/2}$  amplitude  $A_{1/2}$

VALUE (GeV <sup>-1/2</sup> )	DOCUMENT ID	TECN	COMMENT
<b>+0.019 ± 0.008 OUR ESTIMATE</b>			
0.024 ± 0.003	ANISOVICH 12A	DPWA	Multichannel
0.018 ± 0.002	DUGGER 07	DPWA	$\gamma N \rightarrow \pi N$
0.015 ± 0.010	ARNDT 96	IPWA	$\gamma N \rightarrow \pi N$
0.021 ± 0.011	CRAWFORD 83	IPWA	$\gamma N \rightarrow \pi N$
0.034 ± 0.005	AWAJI 81	DPWA	$\gamma N \rightarrow \pi N$
• • • We do not use the following data for averages, fits, limits, etc. • • •			
0.021 ± 0.004	ANISOVICH 10	DPWA	Multichannel
0.015	DRECHSEL 07	DPWA	$\gamma N \rightarrow \pi N$
0.012 ± 0.002	LI 93	IPWA	$\gamma N \rightarrow \pi N$

N(1675)  $\rightarrow p\gamma, \text{helicity-3/2}$  amplitude  $A_{3/2}$

VALUE (GeV <sup>-1/2</sup> )	DOCUMENT ID	TECN	COMMENT
<b>+0.015 ± 0.009 OUR ESTIMATE</b>			
0.025 ± 0.007	ANISOVICH 12A	DPWA	Multichannel
0.021 ± 0.001	DUGGER 07	DPWA	$\gamma N \rightarrow \pi N$
0.010 ± 0.007	ARNDT 96	IPWA	$\gamma N \rightarrow \pi N$
0.015 ± 0.009	CRAWFORD 83	IPWA	$\gamma N \rightarrow \pi N$
0.024 ± 0.008	AWAJI 81	DPWA	$\gamma N \rightarrow \pi N$
• • • We do not use the following data for averages, fits, limits, etc. • • •			
0.024 ± 0.008	ANISOVICH 10	DPWA	Multichannel
0.022	DRECHSEL 07	DPWA	$\gamma N \rightarrow \pi N$
0.021 ± 0.002	LI 93	IPWA	$\gamma N \rightarrow \pi N$

# Baryon Particle Listings

## $N(1675)$ , $N(1680)$

### $N(1675) \rightarrow n\gamma$ , helicity-1/2 amplitude $A_{1/2}$

VALUE (GeV <sup>-1/2</sup> )	DOCUMENT ID	TECN	COMMENT
<b>-0.043 ± 0.012 OUR ESTIMATE</b>			
-0.049 ± 0.010	ARNDT 96	IPWA	$\gamma N \rightarrow \pi N$
-0.057 ± 0.024	AWAJI 81	DPWA	$\gamma N \rightarrow \pi N$
-0.033 ± 0.004	FUJII 81	DPWA	$\gamma N \rightarrow \pi N$
••• We do not use the following data for averages, fits, limits, etc. •••			
-0.062	DRECHSEL 07	DPWA	$\gamma N \rightarrow \pi N$
-0.060 ± 0.003	LI 93	IPWA	$\gamma N \rightarrow \pi N$

### $N(1675) \rightarrow n\gamma$ , helicity-3/2 amplitude $A_{3/2}$

VALUE (GeV <sup>-1/2</sup> )	DOCUMENT ID	TECN	COMMENT
<b>-0.058 ± 0.013 OUR ESTIMATE</b>			
-0.051 ± 0.010	ARNDT 96	IPWA	$\gamma N \rightarrow \pi N$
-0.077 ± 0.018	AWAJI 81	DPWA	$\gamma N \rightarrow \pi N$
-0.069 ± 0.004	FUJII 81	DPWA	$\gamma N \rightarrow \pi N$
••• We do not use the following data for averages, fits, limits, etc. •••			
-0.084	DRECHSEL 07	DPWA	$\gamma N \rightarrow \pi N$
-0.074 ± 0.003	LI 93	IPWA	$\gamma N \rightarrow \pi N$

### $N(1675)$ FOOTNOTES

- LONGACRE 77 pole positions are from a search for poles in the unitarized T-matrix; the first (second) value uses, in addition to  $\pi N \rightarrow N\pi\pi$  data, elastic amplitudes from a Saclay (CERN) partial-wave analysis. The other LONGACRE 77 values are from eyeball fits with Breit-Wigner circles to the T-matrix amplitudes.
- From method II of LONGACRE 75: eyeball fits with Breit-Wigner circles to the T-matrix amplitudes.
- See HOEHLER 93 for a detailed discussion of the evidence for and the pole parameters of  $N$  and  $\Delta$  resonances as determined from Argand diagrams of  $\pi N$  elastic partial-wave amplitudes and from plots of the speeds with which the amplitudes traverse the diagrams.
- LONGACRE 78 values are from a search for poles in the unitarized T-matrix. The first (second) value uses, in addition to  $\pi N \rightarrow N\pi\pi$  data, elastic amplitudes from a Saclay (CERN) partial-wave analysis.
- SAXON 80 finds the coupling phase is near 90°.
- LONGACRE 77 considers this coupling to be well determined.

### $N(1675)$ REFERENCES

For early references, see Physics Letters **111B** 1 (1982).

ANISOVICH 12A	EPJ A48 15	A.V. Anisovich et al.	(BONN, PNPI)
ANISOVICH 10	EPJ A44 203	A.V. Anisovich et al.	(BONN, PNPI)
BATINIC 10	PR C82 038203	M. Batinic et al.	(ZAGR)
THOMA 08	PL B659 87	U. Thoma et al.	(CB-ELSA Collab.)
DRECHSEL 07	EPJ A34 69	D. Drechsel, S.S. Kamalov, L. Tiator	(MAINZ, JINR)
DUGGER 07	PR C76 025211	M. Dugger et al.	(Jefferson Lab CLAS Collab.)
ARNDT 06	PR C74 045205	R.A. Arndt et al.	(GWU)
PDG 06	JPG 33 1	W.-M. Yao et al.	(PDG Collab.)
ARNDT 04	PR C69 035213	R.A. Arndt et al.	(GWU, TRIU)
VRANA 00	PRPL 328 181	T.P. Vrana, S.A. Dytman, T.-S.H. Lee	(PITT+)
ARNDT 96	PR C53 430	R.A. Arndt, I.I. Strakovsky, R.L. Workman	(VPI)
ARNDT 95	PR C52 2120	R.A. Arndt et al.	(VPI, BRCO)
HOEHLER 93	$\pi N$ Newsletter 9 1	G. Hoehler	(KARL)
LI 93	PR C47 2759	Z.J. Li et al.	(VPI)
MANLEY 92	PR D45 4002	D.M. Manley, E.M. Saleski	(KENT) IJP
Also	PR D30 904	D.M. Manley et al.	(VPI)
ARNDT 91	PR D43 2131	R.A. Arndt et al.	(VPI, TELE) IJP
BELL 83	NP B222 389	K.W. Bell et al.	(RL) IJP
CRAWFORD 83	NP B211 1	R.L. Crawford, W.T. Morton	(GLAS)
PDG 82	PL 111B 1	M. Roos et al.	(HELS, CIT, CERN)
AWAJI 81	Bonn Conf. 352	N. Awaji, R. Kajikawa	(NAGO)
Also	NP B197 365	K. Fujii et al.	(NAGO)
FUJII 81	NP B187 53	K. Fujii et al.	(NAGO, OSAK)
CUTKOSKY 80	Toronto Conf. 19	R.E. Cutkosky et al.	(CMU, LBL) IJP
Also	PR D20 2839	R.E. Cutkosky et al.	(CMU, LBL) IJP
SAXON 80	NP B162 522	D.H. Saxon et al.	(RHEL, BRIS) IJP
HOEHLER 79	PDAT 12-1	G. Hoehler et al.	(KARLT) IJP
Also	Toronto Conf. 3	R. Koch	(KARLT) IJP
LONGACRE 78	PR D17 1795	R.S. Longacre et al.	(LBL, SLAC)
LONGACRE 77	NP B122 493	R.S. Longacre, J. Dolbeau	(SACL) IJP
Also	NP B109 345	J. Dolbeau et al.	(SACL) IJP
LONGACRE 75	PL 95B 415	R.S. Longacre et al.	(LBL, SLAC) IJP

## $N(1680) 5/2^+$

$$I(J^P) = \frac{1}{2}(\frac{5}{2}^+) \text{ Status: } ***$$

Most of the results published before 1975 were last included in our 1982 edition, Physics Letters **111B** 1 (1982). Some further obsolete results published before 1984 were last included in our 2006 edition, Journal of Physics, **G 33** 1 (2006).

### $N(1680)$ BREIT-WIGNER MASS

VALUE (MeV)	DOCUMENT ID	TECN	COMMENT
<b>1680 to 1690 (<math>\approx 1685</math>) OUR ESTIMATE</b>			
1689 ± 6	ANISOVICH 12A	DPWA	Multichannel
1680.1 ± 0.2	ARNDT 06	DPWA	$\pi N \rightarrow \pi N, \eta N$
1684 ± 4	MANLEY 92	IPWA	$\pi N \rightarrow \pi N \& N\pi\pi$
1680 ± 10	CUTKOSKY 80	IPWA	$\pi N \rightarrow \pi N$
1684 ± 3	HOEHLER 79	IPWA	$\pi N \rightarrow \pi N$

••• We do not use the following data for averages, fits, limits, etc. •••

1685 ± 5	ANISOVICH 10	DPWA	Multichannel
1680 ± 7	BATINIC 10	DPWA	$\pi N \rightarrow N\pi, \eta N$
1684 ± 8	THOMA 08	DPWA	Multichannel
1683.2 ± 0.7	ARNDT 04	DPWA	$\pi N \rightarrow \pi N, \eta N$
1679 ± 3	VRANA 00	DPWA	Multichannel
1679 ± 5	IPWA 96	IPWA	$\gamma N \rightarrow \pi N$
1678	ARNDT 95	DPWA	$\pi N \rightarrow N\pi$
1660	<sup>1</sup> LONGACRE 77	IPWA	$\pi N \rightarrow N\pi\pi$
1670	<sup>2</sup> LONGACRE 75	IPWA	$\pi N \rightarrow N\pi\pi$

### $N(1680)$ BREIT-WIGNER WIDTH

VALUE (MeV)	DOCUMENT ID	TECN	COMMENT
<b>120 to 140 (<math>\approx 130</math>) OUR ESTIMATE</b>			
118 ± 6	ANISOVICH 12A	DPWA	Multichannel
128.0 ± 1.1	ARNDT 06	DPWA	$\pi N \rightarrow \pi N, \eta N$
139 ± 8	MANLEY 92	IPWA	$\pi N \rightarrow \pi N \& N\pi\pi$
120 ± 10	CUTKOSKY 80	IPWA	$\pi N \rightarrow \pi N$
128 ± 8	HOEHLER 79	IPWA	$\pi N \rightarrow \pi N$
••• We do not use the following data for averages, fits, limits, etc. •••			
117 ± 12	ANISOVICH 10	DPWA	Multichannel
142 ± 7	BATINIC 10	DPWA	$\pi N \rightarrow N\pi, \eta N$
105 ± 8	THOMA 08	DPWA	Multichannel
134.4 ± 3.8	ARNDT 04	DPWA	$\pi N \rightarrow \pi N, \eta N$
128 ± 9	VRANA 00	DPWA	Multichannel
124 ± 4	ARNDT 96	IPWA	$\gamma N \rightarrow \pi N$
126	ARNDT 95	DPWA	$\pi N \rightarrow N\pi$
150	<sup>1</sup> LONGACRE 77	IPWA	$\pi N \rightarrow N\pi\pi$
130	<sup>2</sup> LONGACRE 75	IPWA	$\pi N \rightarrow N\pi\pi$

### $N(1680)$ POLE POSITION

#### REAL PART

VALUE (MeV)	DOCUMENT ID	TECN	COMMENT
<b>1665 to 1680 (<math>\approx 1675</math>) OUR ESTIMATE</b>			
1676 ± 6	ANISOVICH 12A	DPWA	Multichannel
1674	ARNDT 06	DPWA	$\pi N \rightarrow \pi N, \eta N$
1673	<sup>3</sup> HOEHLER 93	ARGD	$\pi N \rightarrow \pi N$
1667 ± 5	CUTKOSKY 80	IPWA	$\pi N \rightarrow \pi N$
••• We do not use the following data for averages, fits, limits, etc. •••			
1672 ± 4	ANISOVICH 10	DPWA	Multichannel
1672 ± 4	BATINIC 10	DPWA	$\pi N \rightarrow N\pi, \eta N$
1674 ± 5	THOMA 08	DPWA	Multichannel
1678	ARNDT 04	DPWA	$\pi N \rightarrow \pi N, \eta N$
1667	VRANA 00	DPWA	Multichannel
1670	ARNDT 95	DPWA	$\pi N \rightarrow N\pi$
1670	ARNDT 91	DPWA	$\pi N \rightarrow \pi N$ Soln SM90
1668 or 1674	<sup>4</sup> LONGACRE 78	IPWA	$\pi N \rightarrow N\pi\pi$
1656 or 1653	<sup>1</sup> LONGACRE 77	IPWA	$\pi N \rightarrow N\pi\pi$

#### -2xIMAGINARY PART

VALUE (MeV)	DOCUMENT ID	TECN	COMMENT
<b>110 to 135 (<math>\approx 120</math>) OUR ESTIMATE</b>			
113 ± 4	ANISOVICH 12A	DPWA	Multichannel
115	ARNDT 06	DPWA	$\pi N \rightarrow \pi N, \eta N$
135	<sup>3</sup> HOEHLER 93	ARGD	$\pi N \rightarrow \pi N$
110 ± 10	CUTKOSKY 80	IPWA	$\pi N \rightarrow \pi N$
••• We do not use the following data for averages, fits, limits, etc. •••			
114 ± 12	ANISOVICH 10	DPWA	Multichannel
135 ± 6	BATINIC 10	DPWA	$\pi N \rightarrow N\pi, \eta N$
95 ± 10	THOMA 08	DPWA	Multichannel
120	ARNDT 04	DPWA	$\pi N \rightarrow \pi N, \eta N$
122	VRANA 00	DPWA	Multichannel
120	ARNDT 95	DPWA	$\pi N \rightarrow N\pi$
116	ARNDT 91	DPWA	$\pi N \rightarrow \pi N$ Soln SM90
132 or 137	<sup>4</sup> LONGACRE 78	IPWA	$\pi N \rightarrow N\pi\pi$
145 or 143	<sup>1</sup> LONGACRE 77	IPWA	$\pi N \rightarrow N\pi\pi$

### $N(1680)$ ELASTIC POLE RESIDUE

#### MODULUS |r|

VALUE (MeV)	DOCUMENT ID	TECN	COMMENT
<b>40 ± 5 OUR ESTIMATE</b>			
43 ± 4	ANISOVICH 12A	DPWA	Multichannel
42	ARNDT 06	DPWA	$\pi N \rightarrow \pi N, \eta N$
44	HOEHLER 93	ARGD	$\pi N \rightarrow \pi N$
34 ± 2	CUTKOSKY 80	IPWA	$\pi N \rightarrow \pi N$
••• We do not use the following data for averages, fits, limits, etc. •••			
44	BATINIC 10	DPWA	$\pi N \rightarrow N\pi, \eta N$
43	ARNDT 04	DPWA	$\pi N \rightarrow \pi N, \eta N$
40	ARNDT 95	DPWA	$\pi N \rightarrow N\pi$
37	ARNDT 91	DPWA	$\pi N \rightarrow \pi N$ Soln SM90



# Baryon Particle Listings

## $N(1680)$

**PHASE  $\theta$** 

VALUE (°)	DOCUMENT ID	TECN	COMMENT
<b>-10±10 OUR ESTIMATE</b>			
-2±10	ANISOVICH 12A	DPWA	Multichannel
-4	ARNDT 06	DPWA	$\pi N \rightarrow \pi N, \eta N$
-17	HOEHLER 93	ARGD	$\pi N \rightarrow \pi N$
-25±5	CUTKOSKY 80	IPWA	$\pi N \rightarrow \pi N$
••• We do not use the following data for averages, fits, limits, etc. •••			
-19	BATINIC 10	DPWA	$\pi N \rightarrow N\pi, N\eta$
1	ARNDT 04	DPWA	$\pi N \rightarrow \pi N, \eta N$
+1	ARNDT 95	DPWA	$\pi N \rightarrow \pi N$
-14	ARNDT 91	DPWA	$\pi N \rightarrow \pi N$ Soln SM90

 **$N(1680)$  INELASTIC POLE RESIDUE**

The "normalized residue" is the residue divided by  $\Gamma_{pole}$ .

**Normalized residue in  $N\pi \rightarrow N(1680) \rightarrow \Delta\pi, P$ -wave**

MODULUS (%)	PHASE (°)	DOCUMENT ID	TECN	COMMENT
15±3	-70±45	ANISOVICH 12A	DPWA	Multichannel

**Normalized residue in  $N\pi \rightarrow N(1680) \rightarrow \Delta\pi, F$ -wave**

MODULUS (%)	PHASE (°)	DOCUMENT ID	TECN	COMMENT
23±4	85±15	ANISOVICH 12A	DPWA	Multichannel

**Normalized residue in  $N\pi \rightarrow N(1680) \rightarrow N(\pi\pi)_{S=0}^{I=0}$** 

MODULUS (%)	PHASE (°)	DOCUMENT ID	TECN	COMMENT
26±4	-56±15	ANISOVICH 12A	DPWA	Multichannel

 **$N(1680)$  DECAY MODES**

The following branching fractions are our estimates, not fits or averages.

Mode	Fraction ( $\Gamma_i/\Gamma$ )
$\Gamma_1$ $N\pi$	65-70 %
$\Gamma_2$ $N\eta$	( 0.0±1.0 ) %
$\Gamma_3$ $\Lambda K$	
$\Gamma_4$ $\Sigma K$	
$\Gamma_5$ $N\pi\pi$	30-40 %
$\Gamma_6$ $\Delta\pi$	5-15 %
$\Gamma_7$ $\Delta(1232)\pi, P$ -wave	(10 ±5 ) %
$\Gamma_8$ $\Delta(1232)\pi, F$ -wave	0-12 %
$\Gamma_9$ $N\rho$	3-15 %
$\Gamma_{10}$ $N\rho, S=1/2, F$ -wave	
$\Gamma_{11}$ $N\rho, S=3/2, P$ -wave	
$\Gamma_{12}$ $N\rho, S=3/2, F$ -wave	1-5 %
$\Gamma_{13}$ $N(\pi\pi)_{S=0}^{I=0}$	(11 ±5 ) %
$\Gamma_{14}$ $p\gamma$	0.21-0.32 %
$\Gamma_{15}$ $p\gamma, \text{ helicity}=1/2$	0.001-0.011 %
$\Gamma_{16}$ $p\gamma, \text{ helicity}=3/2$	0.20-0.32 %
$\Gamma_{17}$ $n\gamma$	0.021-0.046 %
$\Gamma_{18}$ $n\gamma, \text{ helicity}=1/2$	0.004-0.029 %
$\Gamma_{19}$ $n\gamma, \text{ helicity}=3/2$	0.01-0.024 %

 **$N(1680)$  BRANCHING RATIOS**

$\Gamma(N\pi)/\Gamma_{total}$	DOCUMENT ID	TECN	COMMENT	$\Gamma_1/\Gamma$
<b>VALUE (%)</b>				
<b>65 to 70 OUR ESTIMATE</b>				
64 ± 5	ANISOVICH 12A	DPWA	Multichannel	
70.1± 0.1	ARNDT 06	DPWA	$\pi N \rightarrow \pi N, \eta N$	
70 ± 3	MANLEY 92	IPWA	$\pi N \rightarrow \pi N \& N\pi\pi$	
62 ± 5	CUTKOSKY 80	IPWA	$\pi N \rightarrow \pi N$	
65 ± 2	HOEHLER 79	IPWA	$\pi N \rightarrow \pi N$	
••• We do not use the following data for averages, fits, limits, etc. •••				
66 ± 8	ANISOVICH 10	DPWA	Multichannel	
67 ± 3	BATINIC 10	DPWA	$\pi N \rightarrow N\pi, N\eta$	
72 ± 15	THOMA 08	DPWA	Multichannel	
67.0± 0.4	ARNDT 04	DPWA	$\pi N \rightarrow \pi N, \eta N$	
69 ± 2	VRANA 00	DPWA	Multichannel	
68	ARNDT 95	DPWA	$\pi N \rightarrow \pi N$	

$(\Gamma_i\Gamma_j)^{1/2}/\Gamma_{total}$ in $N\pi \rightarrow N(1680) \rightarrow N\eta$	DOCUMENT ID	TECN	COMMENT	$(\Gamma_1\Gamma_2)^{1/2}/\Gamma$
<b>VALUE (%)</b>				
••• We do not use the following data for averages, fits, limits, etc. •••				
not seen	BAKER 79	DPWA	$\pi^- p \rightarrow n\eta$	

 **$\Gamma(N\eta)/\Gamma_{total}$** 

VALUE (%)	DOCUMENT ID	TECN	COMMENT	$\Gamma_2/\Gamma$
<b>0 ± 1</b>				
••• We do not use the following data for averages, fits, limits, etc. •••				
0.4 ± 0.2	BATINIC 10	DPWA	$\pi N \rightarrow N\pi, N\eta$	
<1	THOMA 08	DPWA	Multichannel	
0.15 <sup>+0.35</sup> <sub>-0.10</sub>	TIATOR 99	DPWA	$\gamma p \rightarrow p\eta$	

$(\Gamma_i\Gamma_j)^{1/2}/\Gamma_{total}$  in  $N\pi \rightarrow N(1680) \rightarrow \Lambda K$   $(\Gamma_1\Gamma_3)^{1/2}/\Gamma$   
Coupling to  $\Lambda K$  not required in the analyses of SAXON 80 or BELL 83.

Note: Signs of couplings from  $\pi N \rightarrow N\pi\pi$  analyses were changed in the 1986 edition to agree with the baryon-first convention; the overall phase ambiguity is resolved by choosing a negative sign for the  $\Delta(1620) S_{31}$  coupling to  $\Delta(1232)\pi$ .

 **$(\Gamma_i\Gamma_j)^{1/2}/\Gamma_{total}$  in  $N\pi \rightarrow N(1680) \rightarrow \Delta(1232)\pi, P$ -wave**

VALUE (%)	DOCUMENT ID	TECN	COMMENT	$(\Gamma_1\Gamma_7)^{1/2}/\Gamma$
<b>-0.31 to -0.21 OUR ESTIMATE</b>				
-0.26 ± 0.04	MANLEY 92	IPWA	$\pi N \rightarrow \pi N \& N\pi\pi$	
-0.27	1,5 LONGACRE 77	IPWA	$\pi N \rightarrow N\pi\pi$	
-0.25	2 LONGACRE 75	IPWA	$\pi N \rightarrow N\pi\pi$	

 **$\Gamma(\Delta(1232)\pi, P\text{-wave})/\Gamma_{total}$** 

VALUE (%)	DOCUMENT ID	TECN	COMMENT	$\Gamma_7/\Gamma$
<b>10±5 OUR ESTIMATE</b>				
5±3	ANISOVICH 12A	DPWA	Multichannel	
14±3	VRANA 00	DPWA	Multichannel	
••• We do not use the following data for averages, fits, limits, etc. •••				
8±3	THOMA 08	DPWA	Multichannel	

 **$(\Gamma_i\Gamma_j)^{1/2}/\Gamma_{total}$  in  $N\pi \rightarrow N(1680) \rightarrow \Delta(1232)\pi, F$ -wave**

VALUE (%)	DOCUMENT ID	TECN	COMMENT	$(\Gamma_1\Gamma_8)^{1/2}/\Gamma$
<b>+0.03 to +0.11 OUR ESTIMATE</b>				
+0.07 ± 0.03	MANLEY 92	IPWA	$\pi N \rightarrow \pi N \& N\pi\pi$	
+0.07	1,5 LONGACRE 77	IPWA	$\pi N \rightarrow N\pi\pi$	
+0.08	2 LONGACRE 75	IPWA	$\pi N \rightarrow N\pi\pi$	

 **$\Gamma(\Delta(1232)\pi, F\text{-wave})/\Gamma_{total}$** 

VALUE (%)	DOCUMENT ID	TECN	COMMENT	$\Gamma_8/\Gamma$
<b>0 to 12 (<math>\approx 5</math>) OUR ESTIMATE</b>				
10±3	ANISOVICH 12A	DPWA	Multichannel	
1±1	VRANA 00	DPWA	Multichannel	
••• We do not use the following data for averages, fits, limits, etc. •••				
4±3	THOMA 08	DPWA	Multichannel	

 **$(\Gamma_i\Gamma_j)^{1/2}/\Gamma_{total}$  in  $N\pi \rightarrow N(1680) \rightarrow N\rho, S=3/2, P$ -wave**

VALUE (%)	DOCUMENT ID	TECN	COMMENT	$(\Gamma_1\Gamma_{11})^{1/2}/\Gamma$
<b>-0.30 to -0.10 OUR ESTIMATE</b>				
-0.20 ± 0.05	MANLEY 92	IPWA	$\pi N \rightarrow \pi N \& N\pi\pi$	
-0.23	1,5 LONGACRE 77	IPWA	$\pi N \rightarrow N\pi\pi$	
-0.30	2 LONGACRE 75	IPWA	$\pi N \rightarrow N\pi\pi$	

 **$\Gamma(N\rho, S=3/2, P\text{-wave})/\Gamma_{total}$** 

VALUE (%)	DOCUMENT ID	TECN	COMMENT	$\Gamma_{11}/\Gamma$
<b>5±1</b>				
	VRANA 00	DPWA	Multichannel	

 **$(\Gamma_i\Gamma_j)^{1/2}/\Gamma_{total}$  in  $N\pi \rightarrow N(1680) \rightarrow N\rho, S=3/2, F$ -wave**

VALUE (%)	DOCUMENT ID	TECN	COMMENT	$(\Gamma_1\Gamma_{12})^{1/2}/\Gamma$
<b>-0.18 to -0.10 OUR ESTIMATE</b>				
-0.13 ± 0.03	MANLEY 92	IPWA	$\pi N \rightarrow \pi N \& N\pi\pi$	
-0.15	1,5 LONGACRE 77	IPWA	$\pi N \rightarrow N\pi\pi$	

 **$\Gamma(N\rho, S=3/2, F\text{-wave})/\Gamma_{total}$** 

VALUE (%)	DOCUMENT ID	TECN	COMMENT	$\Gamma_{12}/\Gamma$
<b>3±1</b>				
	VRANA 00	DPWA	Multichannel	

 **$(\Gamma_i\Gamma_j)^{1/2}/\Gamma_{total}$  in  $N\pi \rightarrow N(1680) \rightarrow N(\pi\pi)_{S=0}^{I=0}$** 

VALUE (%)	DOCUMENT ID	TECN	COMMENT	$(\Gamma_1\Gamma_{13})^{1/2}/\Gamma$
<b>+0.25 to +0.35 OUR ESTIMATE</b>				
+0.29 ± 0.04	MANLEY 92	IPWA	$\pi N \rightarrow \pi N \& N\pi\pi$	
+0.31	1,5 LONGACRE 77	IPWA	$\pi N \rightarrow N\pi\pi$	
+0.30	2 LONGACRE 75	IPWA	$\pi N \rightarrow N\pi\pi$	

 **$\Gamma(N(\pi\pi)_{S=0}^{I=0})/\Gamma_{total}$** 

VALUE (%)	DOCUMENT ID	TECN	COMMENT	$\Gamma_{13}/\Gamma$
<b>11±5 OUR ESTIMATE</b>				
14±7	ANISOVICH 12A	DPWA	Multichannel	
9±1	VRANA 00	DPWA	Multichannel	
••• We do not use the following data for averages, fits, limits, etc. •••				
11±5	THOMA 08	DPWA	Multichannel	

# Baryon Particle Listings

## $N(1680)$ , $N(1685)$ , $N(1700)$

### $N(1680)$ PHOTON DECAY AMPLITUDES

Papers on  $\gamma N$  amplitudes predating 1981 may be found in our 2006 edition, Journal of Physics, G **33** 1 (2006).

#### $N(1680) \rightarrow \rho\gamma$ , helicity-1/2 amplitude $A_{1/2}$

VALUE (GeV <sup>-1/2</sup> )	DOCUMENT ID	TECN	COMMENT
<b>-0.015 ± 0.006 OUR ESTIMATE</b>			
-0.013 ± 0.003	ANISOVICH 12A	DPWA	Multichannel
-0.017 ± 0.001	DUGGER 07	DPWA	$\gamma N \rightarrow \pi N$
-0.010 ± 0.004	ARNDT 96	IPWA	$\gamma N \rightarrow \pi N$
-0.017 ± 0.018	CRAWFORD 83	IPWA	$\gamma N \rightarrow \pi N$
-0.009 ± 0.006	AWAJI 81	DPWA	$\gamma N \rightarrow \pi N$
••• We do not use the following data for averages, fits, limits, etc. •••			
-0.012 ± 0.006	ANISOVICH 10	DPWA	Multichannel
-0.025	DRECHSEL 07	DPWA	$\gamma N \rightarrow \pi N$
-0.006 ± 0.002	LI 93	IPWA	$\gamma N \rightarrow \pi N$

#### $N(1680) \rightarrow \rho\gamma$ , helicity-3/2 amplitude $A_{3/2}$

VALUE (GeV <sup>-1/2</sup> )	DOCUMENT ID	TECN	COMMENT
<b>+0.133 ± 0.012 OUR ESTIMATE</b>			
0.135 ± 0.006	ANISOVICH 12A	DPWA	Multichannel
0.134 ± 0.002	DUGGER 07	DPWA	$\gamma N \rightarrow \pi N$
0.145 ± 0.005	ARNDT 96	IPWA	$\gamma N \rightarrow \pi N$
0.132 ± 0.010	CRAWFORD 83	IPWA	$\gamma N \rightarrow \pi N$
0.115 ± 0.008	AWAJI 81	DPWA	$\gamma N \rightarrow \pi N$
••• We do not use the following data for averages, fits, limits, etc. •••			
0.136 ± 0.012	ANISOVICH 10	DPWA	Multichannel
0.134	DRECHSEL 07	DPWA	$\gamma N \rightarrow \pi N$
0.154 ± 0.002	LI 93	IPWA	$\gamma N \rightarrow \pi N$

#### $N(1680) \rightarrow n\gamma$ , helicity-1/2 amplitude $A_{1/2}$

VALUE (GeV <sup>-1/2</sup> )	DOCUMENT ID	TECN	COMMENT
<b>+0.029 ± 0.010 OUR ESTIMATE</b>			
0.030 ± 0.005	ARNDT 96	IPWA	$\gamma N \rightarrow \pi N$
0.017 ± 0.014	AWAJI 81	DPWA	$\gamma N \rightarrow \pi N$
0.032 ± 0.003	FUJII 81	DPWA	$\gamma N \rightarrow \pi N$
••• We do not use the following data for averages, fits, limits, etc. •••			
0.028	DRECHSEL 07	DPWA	$\gamma N \rightarrow \pi N$
0.022 ± 0.002	LI 93	IPWA	$\gamma N \rightarrow \pi N$

#### $N(1680) \rightarrow n\gamma$ , helicity-3/2 amplitude $A_{3/2}$

VALUE (GeV <sup>-1/2</sup> )	DOCUMENT ID	TECN	COMMENT
<b>-0.033 ± 0.009 OUR ESTIMATE</b>			
-0.040 ± 0.015	ARNDT 96	IPWA	$\gamma N \rightarrow \pi N$
-0.033 ± 0.013	AWAJI 81	DPWA	$\gamma N \rightarrow \pi N$
-0.023 ± 0.005	FUJII 81	DPWA	$\gamma N \rightarrow \pi N$
••• We do not use the following data for averages, fits, limits, etc. •••			
-0.038	DRECHSEL 07	DPWA	$\gamma N \rightarrow \pi N$
-0.048 ± 0.002	LI 93	IPWA	$\gamma N \rightarrow \pi N$

### $N(1680)$ FOOTNOTES

- LONGACRE 77 pole positions are from a search for poles in the unitarized T-matrix; the first (second) value uses, in addition to  $\pi N \rightarrow N\pi\pi$  data, elastic amplitudes from a Saclay (CERN) partial-wave analysis. The other LONGACRE 77 values are from eyeball fits with Breit-Wigner circles to the T-matrix amplitudes.
- From method II of LONGACRE 75: eyeball fits with Breit-Wigner circles to the T-matrix amplitudes.
- See HOEHLER 93 for a detailed discussion of the evidence for and the pole parameters of  $N$  and  $\Delta$  resonances as determined from Argand diagrams of  $\pi N$  elastic partial-wave amplitudes and from plots of the speeds with which the amplitudes traverse the diagrams.
- LONGACRE 78 values are from a search for poles in the unitarized T-matrix. The first (second) value uses, in addition to  $\pi N \rightarrow N\pi\pi$  data, elastic amplitudes from a Saclay (CERN) partial-wave analysis.
- LONGACRE 77 considers this coupling to be well determined.

### $N(1680)$ REFERENCES

For early references, see Physics Letters **111B** 1 (1982). For very early references, see Reviews of Modern Physics **37** 633 (1965).

ANISOVICH 12A	EPJ A48 15	A.V. Anisovich <i>et al.</i>	(BONN, PNPI)
ANISOVICH 10	EPJ A44 203	A.V. Anisovich <i>et al.</i>	(BONN, PNPI)
BATINIC 10	PR C82 038203	M. Batinic <i>et al.</i>	(ZAGR)
THOMA 08	PL B659 87	U. Thoma <i>et al.</i>	(CB-ELSA Collab.)
DRECHSEL 07	EPJ A34 69	D. Drechsel, S.S. Kamalov, L. Tiator	(MAINZ, JINR)
DUGGER 07	PR C76 025211	M. Dugger <i>et al.</i>	(Jefferson Lab CLAS Collab.)
ARNDT 06	PR C74 045205	R.A. Arndt <i>et al.</i>	(GWU)
PDG 06	JPG 33 1	W.-M. Yao <i>et al.</i>	(PDG Collab.)
ARNDT 04	PR C69 035213	R.A. Arndt <i>et al.</i>	(GWU, TRIU)
VRANA 00	PRPL 328 181	T.P. Vrana, S.A. Dytman, T.-S.H. Lee	(PITT+)
TIATOR 99	PR C60 035210	L. Tiator <i>et al.</i>	
ARNDT 96	PR C53 490	R.A. Arndt, I.L. Strakovsky, R.L. Workman	(VPI)
ARNDT 95	PR C52 2120	R.A. Arndt <i>et al.</i>	(VPI, BRCCO)
HOEHLER 93	$\pi N$ Newsletter 9 1	G. Höhler	(KARL)
LI 93	PR C47 2759	Z.J. Li <i>et al.</i>	(VPI)
MANLEY 92	PR D45 4002	D.M. Manley, E.M. Saleski	(KENT) IJP
Also	PR D30 904	D.M. Manley <i>et al.</i>	(VPI)

ARNDT 91	PR D43 2131	R.A. Arndt <i>et al.</i>	(VPI, TELE) IJP
BELL 83	NP B222 389	K.W. Bell <i>et al.</i>	(RL) IJP
CRAWFORD 83	NP B211 1	R.L. Crawford, W.T. Morton	(GLAS)
PDG 82	PL 111B 1	M. Roos <i>et al.</i>	(HELS, CIT, CERN)
AWAJI 81	Bonn Conf. 352	N. Awaji, R. Kajikawa	(NAGO)
Also	NP B197 365	K. Fujii <i>et al.</i>	(NAGO)
FUJII 81	NP B187 53	K. Fujii <i>et al.</i>	(NAGO, OSAK)
CUTKOSKY 80	Toronto Conf. 19	R.E. Cutkosky <i>et al.</i>	(CMU, LBL) IJP
Also	PR D20 2839	R.E. Cutkosky <i>et al.</i>	(CMU, LBL) IJP
SAXON 80	NP B152 522	D.H. Saxon <i>et al.</i>	(RHEL, BRIS) IJP
BAKER 79	NP B156 93	R.D. Baker <i>et al.</i>	(RHEL) IJP
HOEHLER 79	PDAT 12-1	G. Höhler <i>et al.</i>	(KARLT) IJP
Also	Toronto Conf. 3	R. Koch	(KARLT) IJP
LONGACRE 78	PR D17 1795	R.S. Longacre <i>et al.</i>	(LBL, SLAC)
LONGACRE 77	NP B122 493	R.S. Longacre, J. Dolbeau	(SACL) IJP
Also	NP B108 365	J. Dolbeau <i>et al.</i>	(SACL) IJP
LONGACRE 75	PL 55B 415	R.S. Longacre <i>et al.</i>	(LBL, SLAC) IJP

### $N(1685) \text{ ? ?}$

$$I(J^P) = \frac{1}{2}(?)^? \text{ Status: *}$$

#### OMITTED FROM SUMMARY TABLE

There is a small literature (which we do not try to cover) on this possible narrow state. See KUZNETSOV 11A, MART 11, and the other papers for further references. This state does not gain status by being a sought-after member of a baryon anti-decuplet.

### $N(1685)$ MASS

VALUE (MeV)	DOCUMENT ID	TECN	COMMENT
~ 1670	JAEGLE 11	CBTP	$\gamma d \rightarrow \eta n (p)$
~ 1685	KUZNETSOV 11	GRAL	$\gamma d \rightarrow \gamma n (p)$
~ 1680	KUZNETSOV 07	GRAL	$\gamma d \rightarrow \eta n (p)$

### $N(1685)$ WIDTH

VALUE (MeV)	DOCUMENT ID	TECN	COMMENT
~ 25	JAEGLE 11	CBTP	$\gamma d \rightarrow \eta n (p)$
••• We do not use the following data for averages, fits, limits, etc. •••			
< 30	KUZNETSOV 11	GRAL	$\gamma d \rightarrow \gamma n (p)$
< 30	KUZNETSOV 07	GRAL	$\gamma d \rightarrow \eta n (p)$

### $N(1685)$ REFERENCES

JAEGLE 11	EPJ A47 89	I. Jaegle <i>et al.</i>	(CBELSA/TAPS Collab.)
Also	PR L100 252002	I. Jaegle <i>et al.</i>	(CBELSA/TAPS Collab.)
KUZNETSOV 11	PR C83 022201	V. Kuznetsov <i>et al.</i>	(GRAAL Collab.)
KUZNETSOV 11A	JETPL 94 503	V. Kuznetsov, M.V. Polyakov, M. Thumann	(INRM+)
MART 11	PR D83 094015	T. Mart	(U. Indonesia)
KUZNETSOV 07	PL B647 23	V. Kuznetsov <i>et al.</i>	(GRAAL Collab.)

### $N(1700) 3/2^-$

$$I(J^P) = \frac{1}{2}(\frac{3}{2}^-) \text{ Status: ***}$$

Most of the results published before 1975 are now obsolete and have been omitted. They may be found in our 1982 edition, Physics Letters **111B** 1 (1982). Some further obsolete results published before 1984 were last included in our 2006 edition, Journal of Physics, G **33** 1 (2006).

The various partial-wave analyses do not agree very well.

The latest GWU analysis (ARNDT 06) finds no evidence for this resonance.

### $N(1700)$ BREIT-WIGNER MASS

VALUE (MeV)	DOCUMENT ID	TECN	COMMENT
<b>1650 to 1750 (<math>\approx 1700</math>) OUR ESTIMATE</b>			
1790 ± 40	ANISOVICH 12A	DPWA	Multichannel
1737 ± 44	MANLEY 92	IPWA	$\pi N \rightarrow \pi N$ & $N\pi\pi$
1675 ± 25	CUTKOSKY 80	IPWA	$\pi N \rightarrow \pi N$
1731 ± 15	HOEHLER 79	IPWA	$\pi N \rightarrow \pi N$
••• We do not use the following data for averages, fits, limits, etc. •••			
1817 ± 22	BATINIC 10	DPWA	$\pi N \rightarrow N\pi, N\eta$
1740 ± 20	THOMA 08	DPWA	Multichannel
1736 ± 33	VRANA 00	DPWA	Multichannel
1650	SAXON 80	DPWA	$\pi^- p \rightarrow \Lambda K^0$
1690 to 1710	BAKER 78	DPWA	$\pi^- p \rightarrow \Lambda K^0$
1719	BARBOUR 78	DPWA	$\gamma N \rightarrow \pi N$
1670 ± 10	<sup>1</sup> BAKER 77	IPWA	$\pi^- p \rightarrow \Lambda K^0$
1690	<sup>1</sup> BAKER 77	DPWA	$\pi^- p \rightarrow \Lambda K^0$
1660	<sup>2</sup> LONGACRE 77	IPWA	$\pi N \rightarrow N\pi\pi$
1710	<sup>3</sup> LONGACRE 75	IPWA	$\pi N \rightarrow N\pi\pi$

## N(1700) BREIT-WIGNER WIDTH

VALUE (MeV)	DOCUMENT ID	TECN	COMMENT
<b>100 to 250 (≈ 150) OUR ESTIMATE</b>			
390 ± 140	ANISOVICH 12A	DPWA	Multichannel
250 ± 220	MANLEY 92	IPWA	$\pi N \rightarrow \pi N$ & $N\pi\pi$
90 ± 40	CUTKOSKY 80	IPWA	$\pi N \rightarrow \pi N$
110 ± 30	HOEHLER 79	IPWA	$\pi N \rightarrow \pi N$
• • • We do not use the following data for averages, fits, limits, etc. • • •			
134 ± 37	BATINIC 10	DPWA	$\pi N \rightarrow N\pi, N\eta$
180 ± 30	THOMA 08	DPWA	Multichannel
175 ± 133	VRANA 00	DPWA	Multichannel
70	SAXON 80	DPWA	$\pi^- p \rightarrow \Lambda K^0$
70 to 100	BAKER 78	DPWA	$\pi^- p \rightarrow \Lambda K^0$
126	BARBOUR 78	DPWA	$\gamma N \rightarrow \pi N$
90 ± 25	<sup>1</sup> BAKER 77	IPWA	$\pi^- p \rightarrow \Lambda K^0$
100	<sup>1</sup> BAKER 77	DPWA	$\pi^- p \rightarrow \Lambda K^0$
600	<sup>2</sup> LONGACRE 77	IPWA	$\pi N \rightarrow N\pi\pi$
300	<sup>3</sup> LONGACRE 75	IPWA	$\pi N \rightarrow N\pi\pi$

## N(1700) POLE POSITION

VALUE (MeV)	DOCUMENT ID	TECN	COMMENT
<b>REAL PART</b>			
<b>1650 to 1750 (≈ 1700) OUR ESTIMATE</b>			
1770 ± 40	ANISOVICH 12A	DPWA	Multichannel
1700	<sup>4</sup> HOEHLER 93	SPED	$\pi N \rightarrow \pi N$
1660 ± 30	CUTKOSKY 80	IPWA	$\pi N \rightarrow \pi N$
• • • We do not use the following data for averages, fits, limits, etc. • • •			
1806 ± 23	BATINIC 10	DPWA	$\pi N \rightarrow N\pi, N\eta$
1710 ± 15	THOMA 08	DPWA	Multichannel
1704	VRANA 00	DPWA	Multichannel
not seen	ARNDT 91	DPWA	$\pi N \rightarrow \pi N$ Soln SM90
1710 or 1678	<sup>5</sup> LONGACRE 78	IPWA	$\pi N \rightarrow N\pi\pi$
1616 or 1613	<sup>2</sup> LONGACRE 77	IPWA	$\pi N \rightarrow N\pi\pi$

## -2xIMAGINARY PART

VALUE (MeV)	DOCUMENT ID	TECN	COMMENT
<b>100 to 300 OUR ESTIMATE</b>			
420 ± 180	ANISOVICH 12A	DPWA	Multichannel
120	<sup>4</sup> HOEHLER 93	SPED	$\pi N \rightarrow \pi N$
90 ± 40	CUTKOSKY 80	IPWA	$\pi N \rightarrow \pi N$
• • • We do not use the following data for averages, fits, limits, etc. • • •			
129 ± 33	BATINIC 10	DPWA	$\pi N \rightarrow N\pi, N\eta$
155 ± 25	THOMA 08	DPWA	Multichannel
156	VRANA 00	DPWA	Multichannel
not seen	ARNDT 91	DPWA	$\pi N \rightarrow \pi N$ Soln SM90
607 or 567	<sup>5</sup> LONGACRE 78	IPWA	$\pi N \rightarrow N\pi\pi$
577 or 575	<sup>2</sup> LONGACRE 77	IPWA	$\pi N \rightarrow N\pi\pi$

## N(1700) ELASTIC POLE RESIDUE

## MODULUS |r|

VALUE (MeV)	DOCUMENT ID	TECN	COMMENT
<b>5 to 50 OUR ESTIMATE</b>			
50 ± 40	ANISOVICH 12A	DPWA	Multichannel
5	HOEHLER 93	SPED	$\pi N \rightarrow \pi N$
6 ± 3	CUTKOSKY 80	IPWA	$\pi N \rightarrow \pi N$
• • • We do not use the following data for averages, fits, limits, etc. • • •			
7	BATINIC 10	DPWA	$\pi N \rightarrow N\pi, N\eta$

PHASE  $\theta$ 

VALUE (°)	DOCUMENT ID	TECN	COMMENT
<b>-120 to 20 OUR ESTIMATE</b>			
-100 ± 40	ANISOVICH 12A	DPWA	Multichannel
0 ± 50	CUTKOSKY 80	IPWA	$\pi N \rightarrow \pi N$
• • • We do not use the following data for averages, fits, limits, etc. • • •			
-34	BATINIC 10	DPWA	$\pi N \rightarrow N\pi, N\eta$

## N(1700) INELASTIC POLE RESIDUE

The "normalized residue" is the residue divided by  $\Gamma_{pole}$ .

Normalized residue in  $N\pi \rightarrow N(1700) \rightarrow \Delta\pi, S\text{-wave}$ 

MODULUS (%)	PHASE (°)	DOCUMENT ID	TECN	COMMENT
34 ± 21	-60 ± 40	ANISOVICH 12A	DPWA	Multichannel

Normalized residue in  $N\pi \rightarrow N(1700) \rightarrow \Delta\pi, D\text{-wave}$ 

MODULUS (%)	PHASE (°)	DOCUMENT ID	TECN	COMMENT
8 ± 6	90 ± 35	ANISOVICH 12A	DPWA	Multichannel

## N(1700) DECAY MODES

The following branching fractions are our estimates, not fits or averages.

Mode	Fraction ( $\Gamma_i/\Gamma$ )
$\Gamma_1$ $N\pi$	(12 ± 5) %
$\Gamma_2$ $N\eta$	(0.0 ± 1.0) %
$\Gamma_3$ $\Lambda K$	< 3 %
$\Gamma_4$ $\Sigma K$	
$\Gamma_5$ $N\pi\pi$	85-95 %
$\Gamma_6$ $\Delta\pi$	
$\Gamma_7$ $\Delta(1232)\pi, S\text{-wave}$	10-90 %
$\Gamma_8$ $\Delta(1232)\pi, D\text{-wave}$	< 20 %
$\Gamma_9$ $N\rho$	< 35 %
$\Gamma_{10}$ $N\rho, S=1/2, D\text{-wave}$	
$\Gamma_{11}$ $N\rho, S=3/2, S\text{-wave}$	(7.0 ± 1.0) %
$\Gamma_{12}$ $N\rho, S=3/2, D\text{-wave}$	
$\Gamma_{13}$ $N(\pi\pi)_{S\text{-wave}}^{J=0}$	
$\Gamma_{14}$ $p\gamma$	0.01-0.05 %
$\Gamma_{15}$ $p\gamma, \text{helicity}=1/2$	0.0-0.024 %
$\Gamma_{16}$ $p\gamma, \text{helicity}=3/2$	0.002-0.026 %
$\Gamma_{17}$ $n\gamma$	0.01-0.13 %
$\Gamma_{18}$ $n\gamma, \text{helicity}=1/2$	0.0-0.09 %
$\Gamma_{19}$ $n\gamma, \text{helicity}=3/2$	0.01-0.05 %

## N(1700) BRANCHING RATIOS

$\Gamma(N\pi)/\Gamma_{total}$	DOCUMENT ID	TECN	COMMENT	$\Gamma_1/\Gamma$
<b>VALUE (%)</b>				
<b>12 ± 5 OUR ESTIMATE</b>				
12 ± 5	ANISOVICH 12A	DPWA	Multichannel	
1 ± 2	MANLEY 92	IPWA	$\pi N \rightarrow \pi N$ & $N\pi\pi$	
11 ± 5	CUTKOSKY 80	IPWA	$\pi N \rightarrow \pi N$	
8 ± 3	HOEHLER 79	IPWA	$\pi N \rightarrow \pi N$	
• • • We do not use the following data for averages, fits, limits, etc. • • •				
9 ± 6	BATINIC 10	DPWA	$\pi N \rightarrow N\pi, N\eta$	
8 ± 4	THOMA 08	DPWA	Multichannel	
4 ± 2	VRANA 00	DPWA	Multichannel	
<b><math>\Gamma(N\eta)/\Gamma_{total}</math></b>				
<b>VALUE (%)</b>				
0 ± 1	VRANA 00	DPWA	Multichannel	
• • • We do not use the following data for averages, fits, limits, etc. • • •				
14 ± 5	BATINIC 10	DPWA	$\pi N \rightarrow N\pi, N\eta$	
10 ± 5	THOMA 08	DPWA	Multichannel	

$(\Gamma_i\Gamma_f)^{1/2}/\Gamma_{total}$ in $N\pi \rightarrow N(1700) \rightarrow \Lambda K$	DOCUMENT ID	TECN	COMMENT	$(\Gamma_1\Gamma_3)^{1/2}/\Gamma$
<b>VALUE</b>				
<b>-0.06 to +0.04 OUR ESTIMATE</b>				
-0.012	BELL 83	DPWA	$\pi^- p \rightarrow \Lambda K^0$	
-0.012	SAXON 80	DPWA	$\pi^- p \rightarrow \Lambda K^0$	
• • • We do not use the following data for averages, fits, limits, etc. • • •				
-0.04	<sup>6</sup> BAKER 78	DPWA	See SAXON 80	
-0.03 ± 0.004	<sup>1</sup> BAKER 77	IPWA	$\pi^- p \rightarrow \Lambda K^0$	
-0.03	<sup>1</sup> BAKER 77	DPWA	$\pi^- p \rightarrow \Lambda K^0$	
+0.026 ± 0.019	DEVENISH 74B		Fixed-t dispersion rel.	

$(\Gamma_i\Gamma_f)^{1/2}/\Gamma_{total}$ in $N\pi \rightarrow N(1700) \rightarrow \Sigma K$	DOCUMENT ID	TECN	COMMENT	$(\Gamma_1\Gamma_4)^{1/2}/\Gamma$
<b>VALUE</b>				
• • • We do not use the following data for averages, fits, limits, etc. • • •				
not seen	LIVANOS 80	DPWA	$\pi p \rightarrow \Sigma K$	
<0.017	<sup>7</sup> DEANS 75	DPWA	$\pi N \rightarrow \Sigma K$	

Note: Signs of couplings from  $\pi N \rightarrow N\pi\pi$  analyses were changed in the 1986 edition to agree with the baryon-first convention; the overall phase ambiguity is resolved by choosing a negative sign for the  $\Delta(1620) S_{31}$  coupling to  $\Delta(1232)\pi$ .

$(\Gamma_i\Gamma_f)^{1/2}/\Gamma_{total}$ in $N\pi \rightarrow N(1700) \rightarrow \Delta(1232)\pi, S\text{-wave}$	DOCUMENT ID	TECN	COMMENT	$(\Gamma_1\Gamma_7)^{1/2}/\Gamma$
<b>VALUE</b>				
+0.02 ± 0.03	MANLEY 92	IPWA	$\pi N \rightarrow \pi N$ & $N\pi\pi$	
0.00	<sup>2</sup> LONGACRE 77	IPWA	$\pi N \rightarrow N\pi\pi$	
-0.16	<sup>3</sup> LONGACRE 75	IPWA	$\pi N \rightarrow N\pi\pi$	

$\Gamma(\Delta(1232)\pi, S\text{-wave})/\Gamma_{total}$	DOCUMENT ID	TECN	COMMENT	$\Gamma_7/\Gamma$
<b>VALUE (%)</b>				
<b>10 to 90 OUR ESTIMATE</b>				
72 ± 23	ANISOVICH 12A	DPWA	Multichannel	
11 ± 1	VRANA 00	DPWA	Multichannel	
• • • We do not use the following data for averages, fits, limits, etc. • • •				
10 ± 5	THOMA 08	DPWA	Multichannel	

# Baryon Particle Listings

## $N(1700)$ , $N(1710)$

$(\Gamma_1 \Gamma_f)^{1/2} / \Gamma_{\text{total}}$  in  $N\pi \rightarrow N(1700) \rightarrow \Delta(1232)\pi$ , D-wave  $(\Gamma_1 \Gamma_8)^{1/2} / \Gamma$

VALUE	DOCUMENT ID	TECN	COMMENT
+0.10 ± 0.09	MANLEY 92	IPWA	$\pi N \rightarrow \pi N$ & $N\pi\pi$
-0.12	2 LONGACRE 77	IPWA	$\pi N \rightarrow N\pi\pi$
+0.14	3 LONGACRE 75	IPWA	$\pi N \rightarrow N\pi\pi$

$\Gamma(\Delta(1232)\pi, \text{D-wave}) / \Gamma_{\text{total}}$   $\Gamma_8 / \Gamma$

VALUE (%)	DOCUMENT ID	TECN	COMMENT
<b>&lt;20 OUR ESTIMATE</b>			
<10	ANISOVICH 12A	DPWA	Multichannel
79 ± 56	VRANA 00	DPWA	Multichannel
••• We do not use the following data for averages, fits, limits, etc. •••			
20 ± 11	THOMA 08	DPWA	Multichannel

$(\Gamma_1 \Gamma_f)^{1/2} / \Gamma_{\text{total}}$  in  $N\pi \rightarrow N(1700) \rightarrow N\rho, S=3/2, S\text{-wave}$   $(\Gamma_1 \Gamma_{11})^{1/2} / \Gamma$

VALUE	DOCUMENT ID	TECN	COMMENT
<b>±0.01 to ±0.13 OUR ESTIMATE</b>			
-0.04 ± 0.06	MANLEY 92	IPWA	$\pi N \rightarrow \pi N$ & $N\pi\pi$
-0.07	2 LONGACRE 77	IPWA	$\pi N \rightarrow N\pi\pi$
+0.07	3 LONGACRE 75	IPWA	$\pi N \rightarrow N\pi\pi$

$\Gamma(N\rho, S=3/2, S\text{-wave}) / \Gamma_{\text{total}}$   $\Gamma_{11} / \Gamma$

VALUE (%)	DOCUMENT ID	TECN	COMMENT
7 ± 1	VRANA 00	DPWA	Multichannel

$(\Gamma_1 \Gamma_f)^{1/2} / \Gamma_{\text{total}}$  in  $N\pi \rightarrow N(1700) \rightarrow N(\pi\pi)_{S=0}^0$   $(\Gamma_1 \Gamma_{13})^{1/2} / \Gamma$

VALUE	DOCUMENT ID	TECN	COMMENT
<b>±0.02 to ±0.28 OUR ESTIMATE</b>			
+0.02 ± 0.02	MANLEY 92	IPWA	$\pi N \rightarrow \pi N$ & $N\pi\pi$
0.00	2 LONGACRE 77	IPWA	$\pi N \rightarrow N\pi\pi$
+0.2	3 LONGACRE 75	IPWA	$\pi N \rightarrow N\pi\pi$

$\Gamma(N(\pi\pi)_{S=0}^0) / \Gamma_{\text{total}}$   $\Gamma_{13} / \Gamma$

VALUE (%)	DOCUMENT ID	TECN	COMMENT
0 ± 1	VRANA 00	DPWA	Multichannel
••• We do not use the following data for averages, fits, limits, etc. •••			
18 ± 12	THOMA 08	DPWA	Multichannel

### $N(1700)$ PHOTON DECAY AMPLITUDES

Papers on  $\gamma N$  amplitudes predating 1981 may be found in our 2006 edition, Journal of Physics, G **33** 1 (2006).

#### $N(1700) \rightarrow \rho\gamma$ , helicity-1/2 amplitude $A_{1/2}$

VALUE ( $\text{GeV}^{-1/2}$ )	DOCUMENT ID	TECN	COMMENT
<b>-0.018 ± 0.013 OUR ESTIMATE</b>			
0.041 ± 0.017	ANISOVICH 12A	DPWA	Multichannel
-0.016 ± 0.014	CRAWFORD 83	IPWA	$\gamma N \rightarrow \pi N$
-0.002 ± 0.013	AWAJI 81	DPWA	$\gamma N \rightarrow \pi N$
••• We do not use the following data for averages, fits, limits, etc. •••			
-0.033 ± 0.021	BARBOUR 78	DPWA	$\gamma N \rightarrow \pi N$

#### $N(1700) \rightarrow \rho\gamma$ , helicity-3/2 amplitude $A_{3/2}$

VALUE ( $\text{GeV}^{-1/2}$ )	DOCUMENT ID	TECN	COMMENT
<b>-0.002 ± 0.024 OUR ESTIMATE</b>			
-0.034 ± 0.013	ANISOVICH 12A	DPWA	Multichannel
-0.009 ± 0.012	CRAWFORD 83	IPWA	$\gamma N \rightarrow \pi N$
0.029 ± 0.014	AWAJI 81	DPWA	$\gamma N \rightarrow \pi N$
••• We do not use the following data for averages, fits, limits, etc. •••			
-0.014 ± 0.025	BARBOUR 78	DPWA	$\gamma N \rightarrow \pi N$

#### $N(1700) \rightarrow n\gamma$ , helicity-1/2 amplitude $A_{1/2}$

VALUE ( $\text{GeV}^{-1/2}$ )	DOCUMENT ID	TECN	COMMENT
<b>0.000 ± 0.050 OUR ESTIMATE</b>			
0.006 ± 0.024	AWAJI 81	DPWA	$\gamma N \rightarrow \pi N$
-0.002 ± 0.013	FUJII 81	DPWA	$\gamma N \rightarrow \pi N$
••• We do not use the following data for averages, fits, limits, etc. •••			
+0.050 ± 0.042	BARBOUR 78	DPWA	$\gamma N \rightarrow \pi N$

#### $N(1700) \rightarrow n\gamma$ , helicity-3/2 amplitude $A_{3/2}$

VALUE ( $\text{GeV}^{-1/2}$ )	DOCUMENT ID	TECN	COMMENT
<b>-0.003 ± 0.044 OUR ESTIMATE</b>			
-0.033 ± 0.017	AWAJI 81	DPWA	$\gamma N \rightarrow \pi N$
0.018 ± 0.018	FUJII 81	DPWA	$\gamma N \rightarrow \pi N$
••• We do not use the following data for averages, fits, limits, etc. •••			
+0.035 ± 0.030	BARBOUR 78	DPWA	$\gamma N \rightarrow \pi N$

### $N(1700) \gamma p \rightarrow \Lambda K^+$ AMPLITUDES

$(\Gamma_1 \Gamma_f)^{1/2} / \Gamma_{\text{total}}$  in  $p\gamma \rightarrow N(1700) \rightarrow \Lambda K^+$  ( $E_2-$  amplitude)

VALUE (units $10^{-3}$ )	DOCUMENT ID	TECN	COMMENT
••• We do not use the following data for averages, fits, limits, etc. •••			
4.09	TANABE 89	DPWA	

$(\Gamma_1 \Gamma_f)^{1/2} / \Gamma_{\text{total}}$  in  $p\gamma \rightarrow N(1700) \rightarrow \Lambda K^+$  ( $M_{2-}$  amplitude)

VALUE (units $10^{-3}$ )	DOCUMENT ID	TECN	COMMENT
••• We do not use the following data for averages, fits, limits, etc. •••			
-7.09	TANABE 89	DPWA	

$p\gamma \rightarrow N(1700) \rightarrow \Lambda K^+$  phase angle  $\theta$  ( $E_2-$  amplitude)

VALUE (degrees)	DOCUMENT ID	TECN	COMMENT
••• We do not use the following data for averages, fits, limits, etc. •••			
-35.9	TANABE 89	DPWA	

### $N(1700)$ FOOTNOTES

- The two BAKER 77 entries are from an IPWA using the Barrelet-zero method and from a conventional energy-dependent analysis.
- LONGACRE 77 pole positions are from a search for poles in the unitarized T-matrix; the first (second) value uses, in addition to  $\pi N \rightarrow N\pi\pi$  data, elastic amplitudes from a Saclay (CERN) partial-wave analysis. The other LONGACRE 77 values are from eyeball fits with Breit-Wigner circles to the T-matrix amplitudes.
- From method II of LONGACRE 75: eyeball fits with Breit-Wigner circles to the T-matrix amplitudes.
- See HOEHLER 93 for a detailed discussion of the evidence for and the pole parameters of  $N$  and  $\Delta$  resonances as determined from Argand diagrams of  $\pi N$  elastic partial-wave amplitudes and from plots of the speeds with which the amplitudes traverse the diagrams.
- LONGACRE 78 values are from a search for poles in the unitarized T-matrix. The first (second) value uses, in addition to  $\pi N \rightarrow N\pi\pi$  data, elastic amplitudes from a Saclay (CERN) partial-wave analysis.
- The overall phase of BAKER 78 couplings has been changed to agree with previous conventions.
- The range given is from the four best solutions.

### $N(1700)$ REFERENCES

For early references, see Physics Letters **111B** 1 (1982).

ANISOVICH 12A	EPJ A48 15	A.V. Anisovich et al.	(BONN, PNPI)
BATINIC 10	PR C82 038203	M. Batinic et al.	(ZAGR)
THOMA 08	PL B659 87	U. Thoma et al.	(CB-ELSA Collab.)
ARNDT 06	PR C74 045205	R.A. Arndt et al.	(GWU)
PDG 06	JPG 33 1	W.-M. Yao et al.	(PDG Collab.)
VRANA 00	PRPL 328 181	T.P. Vrana, S.A. Dytman, T.-S.H. Lee	(PITT+)
HOEHLER 93	$\pi N$ Newsletter 9 1	G. Hohlner	(KARL)
MANLEY 92	PR D45 4002	D.M. Manley, E.M. Saleski	(KENT) IJP
Also	PR D30 904	D.M. Manley et al.	(VPI)
ARNDT 91	PR D43 2131	R.A. Arndt et al.	(VPI, TELE) IJP
TANABE 89	PR C39 741	H. Tanabe, M. Kohno, C. Bennhold	(MANZ)
Also	NC 102A 193	M. Kohno, H. Tanabe, C. Bennhold	(MANZ)
BELL 83	NP B222 389	K.W. Bell et al.	(RL) IJP
CRAWFORD 83	NP B211 1	R.L. Crawford, W.T. Morton	(GLAS)
PDG 82	PL 111B 1	M. Roos et al.	(HELS, CIT, CERN)
AWAJI 81	Bonn Conf. 352	N. Awaji, R. Kajikawa	(NAGO)
Also	NP B197 365	K. Fujii et al.	(NAGO)
FUJII 81	NP B187 53	K. Fujii et al.	(NAGO, OSAK)
CUTKOSKY 80	Toronto Conf. 19	R.E. Cutkosky et al.	(CMU, LBL) IJP
Also	PR D20 2839	R.E. Cutkosky et al.	(CMU, LBL) IJP
LIVANOS 80	Toronto Conf. 35	P. Livanos et al.	(SACL) IJP
SAXON 80	NP B162 522	D.H. Saxon et al.	(RHEL, BRIS) IJP
HOEHLER 79	PDAT 12-1	G. Hohlner et al.	(KARL) IJP
Also	Toronto Conf. 3	R. Koch	(KARL) IJP
BAKER 78	NP B141 29	R.D. Baker et al.	(RL, CAVE) IJP
BARBOUR 78	NP B141 253	I.M. Barbour, R.L. Crawford, N.H. Parsons	(GLAS)
LONGACRE 78	PR D17 1795	R.S. Longacre et al.	(LBL, SLAC)
BAKER 77	NP B126 365	R.D. Baker et al.	(RHEL) IJP
LONGACRE 77	NP B122 493	R.S. Longacre, J. Dolbeau	(SACL) IJP
Also	NP B108 365	J. Dolbeau et al.	(SACL) IJP
DEANS 75	NP B96 90	S.R. Deans et al.	(SFLA, ALAH) IJP
LONGACRE 75	PL 55B 415	R.S. Longacre et al.	(LBL, SLAC) IJP
DEVENISH 74B	NP B81 330	R.C.E. Devenish, C.D. Froggatt, B.R. Martin	(DESY+)

### $N(1710) 1/2^+$

$$I(J^P) = \frac{1}{2}(\frac{1}{2}^+) \text{ Status: } ** *$$

Most of the results published before 1975 were last included in our 1982 edition, Physics Letters **111B** 1 (1982). Some further obsolete results published before 1984 were last included in our 2006 edition, Journal of Physics, G **33** 1 (2006).

The latest GWU analysis (ARNDT 06) finds no evidence for this resonance.

### $N(1710)$ BREIT-WIGNER MASS

VALUE (MeV)	DOCUMENT ID	TECN	COMMENT
<b>1680 to 1740 (<math>\approx 1710</math>) OUR ESTIMATE</b>			
1710 ± 20	ANISOVICH 12A	DPWA	Multichannel
1717 ± 28	MANLEY 92	IPWA	$\pi N \rightarrow \pi N$ & $N\pi\pi$
1700 ± 50	CUTKOSKY 80	IPWA	$\pi N \rightarrow \pi N$
1723 ± 9	HOEHLER 79	IPWA	$\pi N \rightarrow \pi N$
••• We do not use the following data for averages, fits, limits, etc. •••			
1725 ± 25	ANISOVICH 10	DPWA	Multichannel
1729 ± 16	1 BATINIC 10	DPWA	$\pi N \rightarrow \pi N, N\eta$
1752 ± 3	PENNER 02c	DPWA	Multichannel
1699 ± 65	VRANA 00	DPWA	Multichannel
1720 ± 10	ARNDT 96	IPWA	$\gamma N \rightarrow \pi N$
1706	CUTKOSKY 90	IPWA	$\pi N \rightarrow \pi N$
1730	SAXON 80	DPWA	$\pi^- p \rightarrow \Lambda K^0$
1720	2 LONGACRE 77	IPWA	$\pi N \rightarrow N\pi\pi$
1710	3 LONGACRE 75	IPWA	$\pi N \rightarrow N\pi\pi$

See key on page 457

# Baryon Particle Listings

## $N(1710)$

### $N(1710)$ BREIT-WIGNER WIDTH

VALUE (MeV)	DOCUMENT ID	TECN	COMMENT
<b>50 to 250 (<math>\approx 100</math>) OUR ESTIMATE</b>			
200 $\pm$ 18	ANISOVICH	12A	DPWA Multichannel
480 $\pm$ 230	MANLEY	92	IPWA $\pi N \rightarrow \pi N$ & $N\pi\pi$
93 $\pm$ 30	CUTKOSKY	90	IPWA $\pi N \rightarrow \pi N$
90 $\pm$ 30	CUTKOSKY	80	IPWA $\pi N \rightarrow \pi N$
120 $\pm$ 15	HOEHLER	79	IPWA $\pi N \rightarrow \pi N$
• • • We do not use the following data for averages, fits, limits, etc. • • •			
200 $\pm$ 35	ANISOVICH	10	DPWA Multichannel
180 $\pm$ 17	<sup>1</sup> BATINIC	10	DPWA $\pi N \rightarrow N\pi, N\eta$
386 $\pm$ 59	PENNER	02c	DPWA Multichannel
143 $\pm$ 100	VRANA	00	DPWA Multichannel
105 $\pm$ 10	ARNDT	96	IPWA $\gamma N \rightarrow \pi N$
540	BELL	83	DPWA $\pi^- p \rightarrow \Lambda K^0$
550	SAXON	80	DPWA $\pi^- p \rightarrow \Lambda K^0$
120	<sup>2</sup> LONGACRE	77	IPWA $\pi N \rightarrow N\pi\pi$
75	<sup>3</sup> LONGACRE	75	IPWA $\pi N \rightarrow N\pi\pi$

### $N(1710)$ POLE POSITION

#### REAL PART

VALUE (MeV)	DOCUMENT ID	TECN	COMMENT
<b>1670 to 1770 (<math>\approx 1720</math>) OUR ESTIMATE</b>			
1687 $\pm$ 17	ANISOVICH	12A	DPWA Multichannel
1690	<sup>4</sup> HOEHLER	93	SPED $\pi N \rightarrow \pi N$
1698	CUTKOSKY	90	IPWA $\pi N \rightarrow \pi N$
1690 $\pm$ 20	CUTKOSKY	80	IPWA $\pi N \rightarrow \pi N$
• • • We do not use the following data for averages, fits, limits, etc. • • •			
1708 $\pm$ 18	ANISOVICH	10	DPWA Multichannel
1711 $\pm$ 15	<sup>1</sup> BATINIC	10	DPWA $\pi N \rightarrow N\pi, N\eta$
1679	VRANA	00	DPWA Multichannel
1770	ARNDT	95	DPWA $\pi N \rightarrow \pi N$
1636	ARNDT	91	DPWA $\pi N \rightarrow \pi N$ Soln SM90
1708 or 1712	<sup>5</sup> LONGACRE	78	IPWA $\pi N \rightarrow N\pi\pi$
1720 or 1711	<sup>2</sup> LONGACRE	77	IPWA $\pi N \rightarrow N\pi\pi$

#### -2xIMAGINARY PART

VALUE (MeV)	DOCUMENT ID	TECN	COMMENT
<b>80 to 380 (<math>\approx 230</math>) OUR ESTIMATE</b>			
200 $\pm$ 25	ANISOVICH	12A	DPWA Multichannel
200	<sup>4</sup> HOEHLER	93	SPED $\pi N \rightarrow \pi N$
88	CUTKOSKY	90	IPWA $\pi N \rightarrow \pi N$
80 $\pm$ 20	CUTKOSKY	80	IPWA $\pi N \rightarrow \pi N$
• • • We do not use the following data for averages, fits, limits, etc. • • •			
200 $\pm$ 20	ANISOVICH	10	DPWA Multichannel
174 $\pm$ 16	<sup>1</sup> BATINIC	10	DPWA $\pi N \rightarrow N\pi, N\eta$
132	VRANA	00	DPWA Multichannel
378	ARNDT	95	DPWA $\pi N \rightarrow \pi N$
544	ARNDT	91	DPWA $\pi N \rightarrow \pi N$ Soln SM90
17 or 22	<sup>5</sup> LONGACRE	78	IPWA $\pi N \rightarrow N\pi\pi$
123 or 115	<sup>2</sup> LONGACRE	77	IPWA $\pi N \rightarrow N\pi\pi$

### $N(1710)$ ELASTIC POLE RESIDUE

#### MODULUS $|r|$

VALUE (MeV)	DOCUMENT ID	TECN	COMMENT
6 $\pm$ 4	ANISOVICH	12A	DPWA Multichannel
15	HOEHLER	93	SPED $\pi N \rightarrow \pi N$
9	CUTKOSKY	90	IPWA $\pi N \rightarrow \pi N$
8 $\pm$ 2	CUTKOSKY	80	IPWA $\pi N \rightarrow \pi N$
• • • We do not use the following data for averages, fits, limits, etc. • • •			
24	<sup>1</sup> BATINIC	10	DPWA $\pi N \rightarrow N\pi, N\eta$
37	ARNDT	95	DPWA $\pi N \rightarrow \pi N$
149	ARNDT	91	DPWA $\pi N \rightarrow \pi N$ Soln SM90

#### PHASE $\theta$

VALUE ( $^\circ$ )	DOCUMENT ID	TECN	COMMENT
120 $\pm$ 70	ANISOVICH	12A	DPWA Multichannel
-167	CUTKOSKY	90	IPWA $\pi N \rightarrow \pi N$
175 $\pm$ 35	CUTKOSKY	80	IPWA $\pi N \rightarrow \pi N$
• • • We do not use the following data for averages, fits, limits, etc. • • •			
20	<sup>1</sup> BATINIC	10	DPWA $\pi N \rightarrow N\pi, N\eta$
-167	ARNDT	95	DPWA $\pi N \rightarrow \pi N$
149	ARNDT	91	DPWA $\pi N \rightarrow \pi N$ Soln SM90

### $N(1710)$ INELASTIC POLE RESIDUE

The "normalized residue" is the residue divided by  $\Gamma_{pole}$ .

#### Normalized residue in $N\pi \rightarrow N(1710) \rightarrow N\eta$

MODULUS (%)	PHASE ( $^\circ$ )	DOCUMENT ID	TECN	COMMENT
12 $\pm$ 4	0 $\pm$ 45	ANISOVICH	12A	DPWA Multichannel

### Normalized residue in $N\pi \rightarrow N(1710) \rightarrow \Lambda K$

MODULUS (%)	PHASE ( $^\circ$ )	DOCUMENT ID	TECN	COMMENT
17 $\pm$ 6	-110 $\pm$ 20	ANISOVICH	12A	DPWA Multichannel

### $N(1710)$ DECAY MODES

The following branching fractions are our estimates, not fits or averages.

Mode	Fraction ( $\Gamma_i/\Gamma$ )
$\Gamma_1$ $N\pi$	5-20 %
$\Gamma_2$ $N\eta$	10-30 %
$\Gamma_3$ $N\omega$	(13.0 $\pm$ 2.0) %
$\Gamma_4$ $\Lambda K$	5-25 %
$\Gamma_5$ $\Sigma K$	
$\Gamma_6$ $N\pi\pi$	40-90 %
$\Gamma_7$ $\Delta\pi$	15-40 %
$\Gamma_8$ $\Delta(1232)\pi, P$ -wave	
$\Gamma_9$ $N\rho$	5-25 %
$\Gamma_{10}$ $N\rho, S=1/2, P$ -wave	
$\Gamma_{11}$ $N\rho, S=3/2, P$ -wave	
$\Gamma_{12}$ $N(\pi\pi)_{S=0}^{L=0}$	10-40 %
$\Gamma_{13}$ $p\gamma$	0.002-0.08 %
$\Gamma_{14}$ $p\gamma, \text{helicity}=1/2$	0.002-0.08 %
$\Gamma_{15}$ $n\gamma$	0.0-0.02%
$\Gamma_{16}$ $n\gamma, \text{helicity}=1/2$	0.0-0.02%

### $N(1710)$ BRANCHING RATIOS

$\Gamma(N\pi)/\Gamma_{total}$	$\Gamma_1/\Gamma$		
VALUE (%)	DOCUMENT ID	TECN	COMMENT
<b>5 to 20 OUR ESTIMATE</b>			
5 $\pm$ 4	ANISOVICH	12A	DPWA Multichannel
9 $\pm$ 4	MANLEY	92	IPWA $\pi N \rightarrow \pi N$ & $N\pi\pi$
20 $\pm$ 4	CUTKOSKY	80	IPWA $\pi N \rightarrow \pi N$
12 $\pm$ 4	HOEHLER	79	IPWA $\pi N \rightarrow \pi N$
• • • We do not use the following data for averages, fits, limits, etc. • • •			
12 $\pm$ 6	ANISOVICH	10	DPWA Multichannel
22 $\pm$ 24	<sup>1</sup> BATINIC	10	DPWA $\pi N \rightarrow N\pi, N\eta$
14 $\pm$ 8	PENNER	02c	DPWA Multichannel
27 $\pm$ 13	VRANA	00	DPWA Multichannel

$\Gamma(N\eta)/\Gamma_{total}$	$\Gamma_2/\Gamma$		
VALUE (%)	DOCUMENT ID	TECN	COMMENT
<b>10 to 30 OUR ESTIMATE</b>			
17 $\pm$ 10	ANISOVICH	12A	DPWA Multichannel
36 $\pm$ 11	PENNER	02c	DPWA Multichannel
6 $\pm$ 1	VRANA	00	DPWA Multichannel
• • • We do not use the following data for averages, fits, limits, etc. • • •			
6 $\pm$ 8	<sup>1</sup> BATINIC	10	DPWA $\pi N \rightarrow N\pi, N\eta$

$\Gamma(N\omega)/\Gamma_{total}$	$\Gamma_3/\Gamma$		
VALUE (%)	DOCUMENT ID	TECN	COMMENT
13 $\pm$ 2	PENNER	02c	DPWA Multichannel

$(\Gamma_i\Gamma_f)^{1/2}/\Gamma_{total}$ in $N\pi \rightarrow N(1710) \rightarrow \Lambda K$	$(\Gamma_1\Gamma_4)^{1/2}/\Gamma$		
VALUE	DOCUMENT ID	TECN	COMMENT
<b>+0.12 to +0.18 OUR ESTIMATE</b>			
+0.16	BELL	83	DPWA $\pi^- p \rightarrow \Lambda K^0$
+0.14	SAXON	80	DPWA $\pi^- p \rightarrow \Lambda K^0$

$\Gamma(\Lambda K)/\Gamma_{total}$	$\Gamma_4/\Gamma$		
VALUE (%)	DOCUMENT ID	TECN	COMMENT
<b>5 to 25 OUR ESTIMATE</b>			
23 $\pm$ 7	ANISOVICH	12A	DPWA Multichannel
5 $\pm$ 3	SHKLYAR	05	DPWA Multichannel
5 $\pm$ 2	PENNER	02c	DPWA Multichannel
10 $\pm$ 10	VRANA	00	DPWA Multichannel

$\Gamma(\Sigma K)/\Gamma_{total}$	$\Gamma_5/\Gamma$		
VALUE (%)	DOCUMENT ID	TECN	COMMENT
• • • We do not use the following data for averages, fits, limits, etc. • • •			
7 $\pm$ 7	PENNER	02c	DPWA Multichannel

## Baryon Particle Listings

 $N(1710)$ ,  $N(1720)$  $(\Gamma_1 \Gamma_f)^{1/2} / \Gamma_{\text{total}}$  in  $N\pi \rightarrow N(1710) \rightarrow \Sigma K$   $(\Gamma_1 \Gamma_8)^{1/2} / \Gamma$ 

VALUE	DOCUMENT ID	TECN	COMMENT
-0.034	LIVANOS	80	DPWA $\pi p \rightarrow \Sigma K$

Note: Signs of couplings from  $\pi N \rightarrow N\pi\pi$  analyses were changed in the 1986 edition to agree with the baryon-first convention; the overall phase ambiguity is resolved by choosing a negative sign for the  $\Delta(1620) S_{31}$  coupling to  $\Delta(1232)\pi$ .

 $(\Gamma_1 \Gamma_f)^{1/2} / \Gamma_{\text{total}}$  in  $N\pi \rightarrow N(1710) \rightarrow \Delta(1232)\pi$ ,  $P$ -wave  $(\Gamma_1 \Gamma_8)^{1/2} / \Gamma$ 

VALUE	DOCUMENT ID	TECN	COMMENT
<b><math>\pm 0.16</math> to <math>\pm 0.22</math> OUR ESTIMATE</b>			
-0.21 $\pm$ 0.04	MANLEY	92	IPWA $\pi N \rightarrow \pi N$ & $N\pi\pi$
-0.17	2 LONGACRE	77	IPWA $\pi N \rightarrow N\pi\pi$
+0.20	3 LONGACRE	75	IPWA $\pi N \rightarrow N\pi\pi$

 $\Gamma(\Delta(1232)\pi, P\text{-wave}) / \Gamma_{\text{total}}$   $\Gamma_8 / \Gamma$ 

VALUE (%)	DOCUMENT ID	TECN	COMMENT
39 $\pm$ 8	VRANA	00	DPWA Multichannel

 $(\Gamma_1 \Gamma_f)^{1/2} / \Gamma_{\text{total}}$  in  $N\pi \rightarrow N(1710) \rightarrow N\rho, S=1/2$ ,  $P$ -wave  $(\Gamma_1 \Gamma_{10})^{1/2} / \Gamma$ 

VALUE	DOCUMENT ID	TECN	COMMENT
<b><math>\pm 0.09</math> to <math>\pm 0.19</math> OUR ESTIMATE</b>			
+0.05 $\pm$ 0.06	MANLEY	92	IPWA $\pi N \rightarrow \pi N$ & $N\pi\pi$
+0.19	2 LONGACRE	77	IPWA $\pi N \rightarrow N\pi\pi$
-0.20	3 LONGACRE	75	IPWA $\pi N \rightarrow N\pi\pi$

 $\Gamma(N\rho, S=1/2, P\text{-wave}) / \Gamma_{\text{total}}$   $\Gamma_{10} / \Gamma$ 

VALUE (%)	DOCUMENT ID	TECN	COMMENT
17 $\pm$ 1	VRANA	00	DPWA Multichannel

 $(\Gamma_1 \Gamma_f)^{1/2} / \Gamma_{\text{total}}$  in  $N\pi \rightarrow N(1710) \rightarrow N\rho, S=3/2$ ,  $P$ -wave  $(\Gamma_1 \Gamma_{11})^{1/2} / \Gamma$ 

VALUE	DOCUMENT ID	TECN	COMMENT
+0.31	2 LONGACRE	77	IPWA $\pi N \rightarrow N\pi\pi$

 $(\Gamma_1 \Gamma_f)^{1/2} / \Gamma_{\text{total}}$  in  $N\pi \rightarrow N(1710) \rightarrow N(\pi\pi)_{S\text{-wave}}^{J=0}$   $(\Gamma_1 \Gamma_{12})^{1/2} / \Gamma$ 

VALUE	DOCUMENT ID	TECN	COMMENT
<b><math>\pm 0.14</math> to <math>\pm 0.22</math> OUR ESTIMATE</b>			
+0.04 $\pm$ 0.05	MANLEY	92	IPWA $\pi N \rightarrow \pi N$ & $N\pi\pi$
-0.26	2 LONGACRE	77	IPWA $\pi N \rightarrow N\pi\pi$
-0.28	3 LONGACRE	75	IPWA $\pi N \rightarrow N\pi\pi$

 $\Gamma(N(\pi\pi)_{S\text{-wave}}^{J=0}) / \Gamma_{\text{total}}$   $\Gamma_{12} / \Gamma$ 

VALUE (%)	DOCUMENT ID	TECN	COMMENT
1 $\pm$ 1	VRANA	00	DPWA Multichannel

 $N(1710)$  PHOTON DECAY AMPLITUDES

Papers on  $\gamma N$  amplitudes predating 1981 may be found in our 2006 edition, Journal of Physics, G **33** 1 (2006).

 $N(1710) \rightarrow \rho\gamma$ , helicity-1/2 amplitude  $A_{1/2}$ 

VALUE (GeV <sup>-1/2</sup> )	DOCUMENT ID	TECN	COMMENT
<b><math>0.024 \pm 0.010</math> OUR ESTIMATE</b>			
0.052 $\pm$ 0.015	ANISOVICH	12A	DPWA Multichannel
0.007 $\pm$ 0.015	ARNDT	96	IPWA $\gamma N \rightarrow \pi N$
0.006 $\pm$ 0.018	CRAWFORD	83	IPWA $\gamma N \rightarrow \pi N$
0.028 $\pm$ 0.009	AWAJI	81	DPWA $\gamma N \rightarrow \pi N$
••• We do not use the following data for averages, fits, limits, etc. •••			
0.025 $\pm$ 0.010	ANISOVICH	10	DPWA Multichannel
0.044	PENNER	02D	DPWA Multichannel
-0.037 $\pm$ 0.002	LI	93	IPWA $\gamma N \rightarrow \pi N$

 $N(1710) \rightarrow n\gamma$ , helicity-1/2 amplitude  $A_{1/2}$ 

VALUE (GeV <sup>-1/2</sup> )	DOCUMENT ID	TECN	COMMENT
<b><math>-0.002 \pm 0.014</math> OUR ESTIMATE</b>			
-0.002 $\pm$ 0.015	ARNDT	96	IPWA $\gamma N \rightarrow \pi N$
0.000 $\pm$ 0.018	AWAJI	81	DPWA $\gamma N \rightarrow \pi N$
-0.001 $\pm$ 0.003	FUJII	81	DPWA $\gamma N \rightarrow \pi N$
••• We do not use the following data for averages, fits, limits, etc. •••			
-0.024	PENNER	02D	DPWA Multichannel
0.052 $\pm$ 0.003	LI	93	IPWA $\gamma N \rightarrow \pi N$

 $N(1710) \gamma p \rightarrow \Lambda K^+$  AMPLITUDES $(\Gamma_1 \Gamma_f)^{1/2} / \Gamma_{\text{total}}$  in  $p\gamma \rightarrow N(1710) \rightarrow \Lambda K^+$  ( $M_{1-}$  amplitude)

VALUE (units 10 <sup>-3</sup> )	DOCUMENT ID	TECN	COMMENT
••• We do not use the following data for averages, fits, limits, etc. •••			
-10.6 $\pm$ 0.4	WORKMAN	90	DPWA
-7.21	TANABE	89	DPWA

 $p\gamma \rightarrow N(1710) \rightarrow \Lambda K^+$  phase angle  $\theta$  ( $M_{1-}$  amplitude)

VALUE (degrees)	DOCUMENT ID	TECN	COMMENT
••• We do not use the following data for averages, fits, limits, etc. •••			
215 $\pm$ 3	WORKMAN	90	DPWA
176.3	TANABE	89	DPWA

 $N(1710)$  FOOTNOTES

- BATINIC 10 finds evidence for a second  $P_{11}$  state with all parameters except for the phase of the pole residue very similar to the parameters we give here.
- LONGACRE 77 pole positions are from a search for poles in the unitarized T-matrix; the first (second) value uses, in addition to  $\pi N \rightarrow N\pi\pi$  data, elastic amplitudes from a Saclay (CERN) partial-wave analysis. The other LONGACRE 77 values are from eyeball fits with Breit-Wigner circles to the T-matrix amplitudes.
- From method II of LONGACRE 75: eyeball fits with Breit-Wigner circles to the T-matrix amplitudes.
- See HOEHLER 93 for a detailed discussion of the evidence for and the pole parameters of  $N$  and  $\Delta$  resonances as determined from Argand diagrams of  $\pi N$  elastic partial-wave amplitudes and from plots of the speeds with which the amplitudes traverse the diagrams.
- LONGACRE 78 values are from a search for poles in the unitarized T-matrix. The first (second) value uses, in addition to  $\pi N \rightarrow N\pi\pi$  data, elastic amplitudes from a Saclay (CERN) partial-wave analysis.

 $N(1710)$  REFERENCES

For early references, see Physics Letters **111B** 1 (1982).

ANISOVICH 12A	EPJ A48 15	A.V. Anisovich et al.	(BONN, PNPI)
ANISOVICH 10	EPJ A44 203	A.V. Anisovich et al.	(BONN, PNPI)
BATINIC 10	PR C82 038203	M. Batinic et al.	(ZAGR)
ARNDT 06	PR C74 045205	R.A. Arndt et al.	(GWU)
PDG 06	JPG 33 1	W.-M. Yao et al.	(PDG Collab.)
SHKLYAR 05	PR C72 015210	V. Shklyar, H. Lenske, U. Mosel	(GIES)
PENNER 02D	PR C66 055211	G. Penner, U. Mosel	(GIES)
PENNER 02C	PR C66 055212	G. Penner, U. Mosel	(GIES)
VRANA 00	PRPL 329 181	T.P. Vrana, S.A. Dylman, T.-S.H. Lee	(PITT+)
ARNDT 96	PR C53 430	R.A. Arndt, I.I. Strakovsky, R.L. Workman	(VPI)
ARNDT 95	PR C52 2120	R.A. Arndt et al.	(VPI, BRCC)
HOEHLER 93	$\pi N$ Newsletter 9 1	G. Hoehler	(KARL)
LI 93	PR C47 2759	Z.J. Li et al.	(VPI)
MANLEY 92	PR D45 4002	D.M. Manley, E.M. Saleski	(KENT) IUP
Also	PR D30 904	D.M. Manley et al.	(VPI)
ARNDT 91	PR D43 2131	R.A. Arndt et al.	(VPI, TELE) IUP
CUTKOSKY 90	PR D42 235	R.E. Cutkosky, S. Wang	(VPI)
WORKMAN 90	PR C42 781	R.L. Workman	(VPI)
TANABE 89	PR C39 741	H. Tanabe, M. Kohno, C. Bennhold	(MANZ)
Also	NC 102A 193	M. Kohno, H. Tanabe, C. Bennhold	(MANZ)
BELL 83	NP B222 389	K.W. Bell et al.	(RL) IUP
CRAWFORD 83	NP B211 1	R.L. Crawford, W.T. Morton	(GLAS)
PDG 82	PL 111B 1	M. Roos et al.	(HELS, CIT, CERN)
AWAJI 81	Bonn Conf. 352	N. Awaji, R. Kajikawa	(NAGO)
Also	NP B197 365	K. Fujii et al.	(NAGO)
FUJII 81	NP B187 53	K. Fujii et al.	(NAGO, OSAK)
CUTKOSKY 80	Toronto Conf. 19	R.E. Cutkosky et al.	(CMU, LBL) IUP
Also	PR D20 2839	R.E. Cutkosky et al.	(CMU)
LIVANOS 80	Toronto Conf. 35	P. Livanos et al.	(SACL) IUP
SAXON 80	NP B162 522	D.H. Saxon et al.	(RHEL, BRIS) IUP
HOEHLER 79	PDAT 12-1	G. Hoehler et al.	(KARL) IUP
Also	Toronto Conf. 3	R. Koch	(KARL) IUP
LONGACRE 78	PR D17 1795	R.S. Longacre et al.	(LBL, SLAC)
LONGACRE 77	NP B122 493	R.S. Longacre, J. Dolbeau	(SACL) IUP
Also	NP B108 365	J. Dolbeau et al.	(SACL) IUP
LONGACRE 75	PL 55B 415	R.S. Longacre et al.	(LBL, SLAC) IUP

 $N(1720) 3/2^+$ 

$$I(J^P) = \frac{1}{2}(\frac{3}{2}^+) \text{ Status: } ***$$

Most of the results published before 1975 were last included in our 1982 edition, Physics Letters **111B** 1 (1982). Some further obsolete results published before 1984 were last included in our 2006 edition, Journal of Physics, G **33** 1 (2006).

 $N(1720)$  BREIT-WIGNER MASS

VALUE (MeV)	DOCUMENT ID	TECN	COMMENT
<b>1700 to 1750 (<math>\approx 1720</math>) OUR ESTIMATE</b>			
1690 $\pm$ 70	ANISOVICH 12A	DPWA	Multichannel
-35			
1763.8 $\pm$ 4.6	ARNDT 06	DPWA	$\pi N \rightarrow \pi N, \eta N$
1717 $\pm$ 31	MANLEY 92	IPWA	$\pi N \rightarrow \pi N$ & $N\pi\pi$
1700 $\pm$ 50	CUTKOSKY 80	IPWA	$\pi N \rightarrow \pi N$
1710 $\pm$ 20	HOEHLER 79	IPWA	$\pi N \rightarrow \pi N$
••• We do not use the following data for averages, fits, limits, etc. •••			
1770 $\pm$ 100	ANISOVICH 10	DPWA	Multichannel
1720 $\pm$ 18	BATINIC 10	DPWA	$\pi N \rightarrow N\pi, N\eta$
1790 $\pm$ 100	THOMA 08	DPWA	Multichannel
1749.6 $\pm$ 4.5	ARNDT 04	DPWA	$\pi N \rightarrow \pi N, \eta N$
1705 $\pm$ 10	PENNER 02C	DPWA	Multichannel
1716 $\pm$ 112	VRANA 00	DPWA	Multichannel
1713 $\pm$ 10	ARNDT 96	IPWA	$\gamma N \rightarrow \pi N$
1820	ARNDT 95	DPWA	$\pi N \rightarrow N\pi$
1720	LI 93	IPWA	$\gamma N \rightarrow \pi N$
1690	SAXON 80	DPWA	$\pi^- p \rightarrow \Lambda K^0$
1750	1 LONGACRE 77	IPWA	$\pi N \rightarrow N\pi\pi$
1720	2 LONGACRE 75	IPWA	$\pi N \rightarrow N\pi\pi$

See key on page 457

Baryon Particle Listings  
N(1720)

## N(1720) BREIT-WIGNER WIDTH

VALUE (MeV)	DOCUMENT ID	TECN	COMMENT
<b>150 to 400 (≈ 250) OUR ESTIMATE</b>			
420 ± 100	ANISOVICH	12A	DPWA Multichannel
210 ± 22	ARNDT	06	DPWA $\pi N \rightarrow \pi N, \eta N$
380 ± 180	MANLEY	92	IPWA $\pi N \rightarrow \pi N \& N\pi\pi$
125 ± 70	CUTKOSKY	80	IPWA $\pi N \rightarrow \pi N$
190 ± 30	HOEHLER	79	IPWA $\pi N \rightarrow \pi N$
• • • We do not use the following data for averages, fits, limits, etc. • • •			
650 ± 120	ANISOVICH	10	DPWA Multichannel
244 ± 28	BATINIC	10	DPWA $\pi N \rightarrow N\pi, N\eta$
690 ± 100	THOMA	08	DPWA Multichannel
256 ± 22	ARNDT	04	DPWA $\pi N \rightarrow \pi N, \eta N$
237 ± 73	PENNER	02c	DPWA Multichannel
121 ± 39	VRANA	00	DPWA Multichannel
153 ± 15	ARNDT	96	IPWA $\gamma N \rightarrow \pi N$
354	ARNDT	95	DPWA $\pi N \rightarrow N\pi$
200	LI	93	IPWA $\gamma N \rightarrow \pi N$
120	SAXON	80	DPWA $\pi^- \rho \rightarrow \Lambda K^0$
130	<sup>1</sup> LONGACRE	77	IPWA $\pi N \rightarrow N\pi\pi$
150	<sup>2</sup> LONGACRE	75	IPWA $\pi N \rightarrow N\pi\pi$

## N(1720) POLE POSITION

REAL PART VALUE (MeV)	DOCUMENT ID	TECN	COMMENT
<b>1660 to 1690 (≈ 1675) OUR ESTIMATE</b>			
1660 ± 30	ANISOVICH	12A	DPWA Multichannel
1666	ARNDT	06	DPWA $\pi N \rightarrow \pi N, \eta N$
1686	<sup>3</sup> HOEHLER	93	SPED $\pi N \rightarrow \pi N$
1680 ± 30	CUTKOSKY	80	IPWA $\pi N \rightarrow \pi N$
• • • We do not use the following data for averages, fits, limits, etc. • • •			
1660 ± 35	ANISOVICH	10	DPWA Multichannel
1691 ± 23	BATINIC	10	DPWA $\pi N \rightarrow N\pi, N\eta$
1630 ± 90	THOMA	08	DPWA Multichannel
1655	ARNDT	04	DPWA $\pi N \rightarrow \pi N, \eta N$
1692	VRANA	00	DPWA Multichannel
1717	ARNDT	95	DPWA $\pi N \rightarrow N\pi$
1675	ARNDT	91	DPWA $\pi N \rightarrow \pi N$ Soln SM90
1716 or 1716	<sup>4</sup> LONGACRE	78	IPWA $\pi N \rightarrow N\pi\pi$
1745 or 1748	<sup>1</sup> LONGACRE	77	IPWA $\pi N \rightarrow N\pi\pi$

## -2xIMAGINARY PART

VALUE (MeV)	DOCUMENT ID	TECN	COMMENT
<b>150 to 400 (≈ 250) OUR ESTIMATE</b>			
450 ± 100	ANISOVICH	12A	DPWA Multichannel
355	ARNDT	06	DPWA $\pi N \rightarrow \pi N, \eta N$
187	<sup>3</sup> HOEHLER	93	SPED $\pi N \rightarrow \pi N$
120 ± 40	CUTKOSKY	80	IPWA $\pi N \rightarrow \pi N$
• • • We do not use the following data for averages, fits, limits, etc. • • •			
360 ± 80	ANISOVICH	10	DPWA Multichannel
233 ± 23	BATINIC	10	DPWA $\pi N \rightarrow N\pi, N\eta$
460 ± 80	THOMA	08	DPWA Multichannel
278	ARNDT	04	DPWA $\pi N \rightarrow \pi N, \eta N$
94	VRANA	00	DPWA Multichannel
388	ARNDT	95	DPWA $\pi N \rightarrow N\pi$
114	ARNDT	91	DPWA $\pi N \rightarrow \pi N$ Soln SM90
124 or 126	<sup>4</sup> LONGACRE	78	IPWA $\pi N \rightarrow N\pi\pi$
135 or 123	<sup>1</sup> LONGACRE	77	IPWA $\pi N \rightarrow N\pi\pi$

## N(1720) ELASTIC POLE RESIDUE

MODULUS  r  VALUE (MeV)	DOCUMENT ID	TECN	COMMENT
<b>15 ± 8 OUR ESTIMATE</b>			
22 ± 8	ANISOVICH	12A	DPWA Multichannel
25	ARNDT	06	DPWA $\pi N \rightarrow \pi N, \eta N$
15	HOEHLER	93	SPED $\pi N \rightarrow \pi N$
8 ± 2	CUTKOSKY	80	IPWA $\pi N \rightarrow \pi N$
• • • We do not use the following data for averages, fits, limits, etc. • • •			
20	BATINIC	10	DPWA $\pi N \rightarrow N\pi, N\eta$
20	ARNDT	04	DPWA $\pi N \rightarrow \pi N, \eta N$
39	ARNDT	95	DPWA $\pi N \rightarrow N\pi$
11	ARNDT	91	DPWA $\pi N \rightarrow \pi N$ Soln SM90

PHASE  $\theta$ 

VALUE (°)	DOCUMENT ID	TECN	COMMENT
<b>-130 ± 30 OUR ESTIMATE</b>			
-115 ± 30	ANISOVICH	12A	DPWA Multichannel
-94	ARNDT	06	DPWA $\pi N \rightarrow \pi N, \eta N$
-160 ± 30	CUTKOSKY	80	IPWA $\pi N \rightarrow \pi N$
• • • We do not use the following data for averages, fits, limits, etc. • • •			
-109	BATINIC	10	DPWA $\pi N \rightarrow N\pi, N\eta$
-88	ARNDT	04	DPWA $\pi N \rightarrow \pi N, \eta N$
-70	ARNDT	95	DPWA $\pi N \rightarrow N\pi$
-130	ARNDT	91	DPWA $\pi N \rightarrow \pi N$ Soln SM90

## N(1720) INELASTIC POLE RESIDUE

The "normalized residue" is the residue divided by  $\Gamma_{pole}$ .Normalized residue in  $N\pi \rightarrow N(1720) \rightarrow N\eta$ 

MODULUS (%)	DOCUMENT ID	TECN	COMMENT
<b>3 ± 2</b>	ANISOVICH	12A	DPWA Multichannel

Normalized residue in  $N\pi \rightarrow N(1720) \rightarrow \Lambda K$ 

MODULUS (%)	PHASE (°)	DOCUMENT ID	TECN	COMMENT
<b>6 ± 4</b>	<b>-150 ± 45</b>	ANISOVICH	12A	DPWA Multichannel

Normalized residue in  $N\pi \rightarrow N(1720) \rightarrow \Delta\pi, P\text{-wave}$ 

MODULUS (%)	PHASE (°)	DOCUMENT ID	TECN	COMMENT
<b>29 ± 8</b>	<b>80 ± 40</b>	ANISOVICH	12A	DPWA Multichannel

Normalized residue in  $N\pi \rightarrow N(1720) \rightarrow \Delta\pi, F\text{-wave}$ 

MODULUS (%)	DOCUMENT ID	TECN	COMMENT
<b>3 ± 3</b>	ANISOVICH	12A	DPWA Multichannel

## N(1720) DECAY MODES

The following branching fractions are our estimates, not fits or averages.

Mode	Fraction ( $\Gamma_i/\Gamma$ )
$\Gamma_1$ $N\pi$	(11 ± 3) %
$\Gamma_2$ $N\eta$	(4 ± 1) %
$\Gamma_3$ $\Lambda K$	1-15 %
$\Gamma_4$ $\Sigma K$	
$\Gamma_5$ $N\pi\pi$	>70 %
$\Gamma_6$ $\Delta\pi$	
$\Gamma_7$ $\Delta(1232)\pi, P\text{-wave}$	(75 ± 15) %
$\Gamma_8$ $N\rho$	70-85 %
$\Gamma_9$ $N\rho, S=1/2, P\text{-wave}$	large
$\Gamma_{10}$ $N\rho, S=3/2, P\text{-wave}$	
$\Gamma_{11}$ $N(\pi\pi)_{S\text{-wave}}^{L=0}$	
$\Gamma_{12}$ $\rho\gamma$	0.05-0.25 %
$\Gamma_{13}$ $\rho\gamma, \text{helicity}=1/2$	0.05-0.15 %
$\Gamma_{14}$ $\rho\gamma, \text{helicity}=3/2$	0.002-0.16 %
$\Gamma_{15}$ $n\gamma$	0.0-0.016 %
$\Gamma_{16}$ $n\gamma, \text{helicity}=1/2$	0.0-0.01 %
$\Gamma_{17}$ $n\gamma, \text{helicity}=3/2$	0.0-0.015 %

## N(1720) BRANCHING RATIOS

$\Gamma(N\pi)/\Gamma_{total}$ VALUE (%)	DOCUMENT ID	TECN	COMMENT	$\Gamma_1/\Gamma$
<b>11 ± 3 OUR ESTIMATE</b>				
10 ± 5	ANISOVICH	12A	DPWA Multichannel	
9.4 ± 0.5	ARNDT	06	DPWA $\pi N \rightarrow \pi N, \eta N$	
13 ± 5	MANLEY	92	IPWA $\pi N \rightarrow \pi N \& N\pi\pi$	
10 ± 4	CUTKOSKY	80	IPWA $\pi N \rightarrow \pi N$	
14 ± 3	HOEHLER	79	IPWA $\pi N \rightarrow \pi N$	
• • • We do not use the following data for averages, fits, limits, etc. • • •				
14 ± 5	ANISOVICH	10	DPWA Multichannel	
18 ± 3	BATINIC	10	DPWA $\pi N \rightarrow N\pi, N\eta$	
9 ± 6	THOMA	08	DPWA Multichannel	
19.0 ± 0.4	ARNDT	04	DPWA $\pi N \rightarrow \pi N, \eta N$	
17 ± 2	PENNER	02c	DPWA Multichannel	
5 ± 5	VRANA	00	DPWA Multichannel	
16	ARNDT	95	DPWA $\pi N \rightarrow N\pi$	

$\Gamma(N\eta)/\Gamma_{total}$ VALUE (%)	DOCUMENT ID	TECN	COMMENT	$\Gamma_2/\Gamma$
<b>3.8 ± 0.9 OUR AVERAGE</b>				
3 ± 2	ANISOVICH	12A	DPWA Multichannel	
4 ± 1	VRANA	00	DPWA Multichannel	
• • • We do not use the following data for averages, fits, limits, etc. • • •				
0 ± 1	BATINIC	10	DPWA $\pi N \rightarrow N\pi, N\eta$	
10 ± 7	THOMA	08	DPWA Multichannel	
0.2 ± 0.2	PENNER	02c	DPWA Multichannel	

$\Gamma(\Lambda K)/\Gamma_{total}$ VALUE (%)	DOCUMENT ID	TECN	COMMENT	$\Gamma_3/\Gamma$
<b>4.4 ± 0.4 OUR AVERAGE</b>				
4.3 ± 0.4	SHKLYAR	05	DPWA Multichannel	
9 ± 3	PENNER	02c	DPWA Multichannel	
• • • We do not use the following data for averages, fits, limits, etc. • • •				
12 ± 9	THOMA	08	DPWA Multichannel	

$\Gamma(\Delta(1232)\pi, P\text{-wave})/\Gamma_{total}$ VALUE (%)	DOCUMENT ID	TECN	COMMENT	$\Gamma_7/\Gamma$
<b>75 ± 15</b>	ANISOVICH	12A	DPWA Multichannel	

## Baryon Particle Listings

## N(1720)

$(\Gamma_1 \Gamma_7)^{1/2} / \Gamma_{\text{total}}$ in $N\pi \rightarrow N(1720) \rightarrow \Lambda K$		$(\Gamma_1 \Gamma_3)^{1/2} / \Gamma$	
VALUE	DOCUMENT ID	TECN	COMMENT
<b>-0.14 to -0.06 OUR ESTIMATE</b>			
-0.09	BELL 83	DPWA	$\pi^- p \rightarrow \Lambda K^0$
-0.11	SAXON 80	DPWA	$\pi^- p \rightarrow \Lambda K^0$

Note: Signs of couplings from  $\pi N \rightarrow N\pi\pi$  analyses were changed in the 1986 edition to agree with the baryon-first convention; the overall phase ambiguity is resolved by choosing a negative sign for the  $\Delta(1620) S_{31}$  coupling to  $\Delta(1232)\pi$ .

$(\Gamma_1 \Gamma_7)^{1/2} / \Gamma_{\text{total}}$ in $N\pi \rightarrow N(1720) \rightarrow \Delta(1232)\pi$ , P-wave		$(\Gamma_1 \Gamma_7)^{1/2} / \Gamma$	
VALUE	DOCUMENT ID	TECN	COMMENT
-0.17	<sup>1</sup> LONGACRE 77	IPWA	$\pi N \rightarrow N\pi\pi$

$(\Gamma_1 \Gamma_7)^{1/2} / \Gamma_{\text{total}}$ in $N\pi \rightarrow N(1720) \rightarrow N\rho$ , S=1/2, P-wave		$(\Gamma_1 \Gamma_9)^{1/2} / \Gamma$	
VALUE	DOCUMENT ID	TECN	COMMENT
<b>-0.30 to +0.40 OUR ESTIMATE</b>			
+0.34 ± 0.05	MANLEY 92	IPWA	$\pi N \rightarrow \pi N$ & $N\pi\pi$
-0.26	<sup>1</sup> LONGACRE 77	IPWA	$\pi N \rightarrow N\pi\pi$
+0.40	<sup>2</sup> LONGACRE 75	IPWA	$\pi N \rightarrow N\pi\pi$

$\Gamma(N\rho, S=1/2, P\text{-wave}) / \Gamma_{\text{total}}$		$\Gamma_9 / \Gamma$	
VALUE (%)	DOCUMENT ID	TECN	COMMENT
91 ± 1	VRA NA 00	DPWA	Multichannel

$(\Gamma_1 \Gamma_7)^{1/2} / \Gamma_{\text{total}}$ in $N\pi \rightarrow N(1720) \rightarrow N\rho$ , S=3/2, P-wave		$(\Gamma_1 \Gamma_{10})^{1/2} / \Gamma$	
VALUE	DOCUMENT ID	TECN	COMMENT
+0.15	<sup>1</sup> LONGACRE 77	IPWA	$\pi N \rightarrow N\pi\pi$

$(\Gamma_1 \Gamma_7)^{1/2} / \Gamma_{\text{total}}$ in $N\pi \rightarrow N(1720) \rightarrow N(\pi\pi)_{S\text{-wave}}^{I=0}$		$(\Gamma_1 \Gamma_{11})^{1/2} / \Gamma$	
VALUE	DOCUMENT ID	TECN	COMMENT
-0.19	<sup>1</sup> LONGACRE 77	IPWA	$\pi N \rightarrow N\pi\pi$

## N(1720) PHOTON DECAY AMPLITUDES

Papers on  $\gamma N$  amplitudes predating 1981 may be found in our 2006 edition, Journal of Physics, G **33** 1 (2006).

N(1720) → pγ, helicity-1/2 amplitude A<sub>1/2</sub>

VALUE (GeV <sup>-1/2</sup> )		DOCUMENT ID		TECN		COMMENT	
<b>-0.01 to +0.11 OUR ESTIMATE</b>							
0.110 ± 0.045	ANISOVICH 12A	DPWA	Multichannel				
0.097 ± 0.003	DUGGER 07	DPWA	$\gamma N \rightarrow \pi N$				
-0.015 ± 0.015	ARNDT 96	IPWA	$\gamma N \rightarrow \pi N$				
0.044 ± 0.066	CRAWFORD 83	IPWA	$\gamma N \rightarrow \pi N$				
-0.004 ± 0.007	AWAJI 81	DPWA	$\gamma N \rightarrow \pi N$				
• • • We do not use the following data for averages, fits, limits, etc. • • •							
0.130 ± 0.050	ANISOVICH 10	DPWA	Multichannel				
0.073	DRECHSEL 07	DPWA	$\gamma N \rightarrow \pi N$				
-0.053	PENNER 02D	DPWA	Multichannel				
0.012 ± 0.003	LI 93	IPWA	$\gamma N \rightarrow \pi N$				

N(1720) → pγ, helicity-3/2 amplitude A<sub>3/2</sub>

VALUE (GeV <sup>-1/2</sup> )		DOCUMENT ID		TECN		COMMENT	
<b>-0.019 ± 0.020 OUR ESTIMATE</b>							
0.150 ± 0.030	ANISOVICH 12A	DPWA	Multichannel				
-0.039 ± 0.003	DUGGER 07	DPWA	$\gamma N \rightarrow \pi N$				
0.007 ± 0.010	ARNDT 96	IPWA	$\gamma N \rightarrow \pi N$				
-0.024 ± 0.006	CRAWFORD 83	IPWA	$\gamma N \rightarrow \pi N$				
-0.040 ± 0.016	AWAJI 81	DPWA	$\gamma N \rightarrow \pi N$				
• • • We do not use the following data for averages, fits, limits, etc. • • •							
0.100 ± 0.050	ANISOVICH 10	DPWA	Multichannel				
-0.011	DRECHSEL 07	DPWA	$\gamma N \rightarrow \pi N$				
0.027	PENNER 02D	DPWA	Multichannel				
-0.022 ± 0.003	LI 93	IPWA	$\gamma N \rightarrow \pi N$				

N(1720) → nγ, helicity-1/2 amplitude A<sub>1/2</sub>

VALUE (GeV <sup>-1/2</sup> )		DOCUMENT ID		TECN		COMMENT	
<b>+0.004 ± 0.015 OUR ESTIMATE</b>							
0.007 ± 0.015	ARNDT 96	IPWA	$\gamma N \rightarrow \pi N$				
0.002 ± 0.005	AWAJI 81	DPWA	$\gamma N \rightarrow \pi N$				
• • • We do not use the following data for averages, fits, limits, etc. • • •							
-0.003	DRECHSEL 07	DPWA	$\gamma N \rightarrow \pi N$				
-0.004	PENNER 02D	DPWA	Multichannel				
0.050 ± 0.004	LI 93	IPWA	$\gamma N \rightarrow \pi N$				

N(1720) → nγ, helicity-3/2 amplitude A<sub>3/2</sub>

VALUE (GeV <sup>-1/2</sup> )		DOCUMENT ID		TECN		COMMENT	
<b>-0.010 to +0.020 OUR ESTIMATE</b>							
-0.005 ± 0.025	ARNDT 96	IPWA	$\gamma N \rightarrow \pi N$				
-0.015 ± 0.019	AWAJI 81	DPWA	$\gamma N \rightarrow \pi N$				
• • • We do not use the following data for averages, fits, limits, etc. • • •							
-0.031	DRECHSEL 07	DPWA	$\gamma N \rightarrow \pi N$				
0.003	PENNER 02D	DPWA	Multichannel				
-0.017 ± 0.004	LI 93	IPWA	$\gamma N \rightarrow \pi N$				

N(1720) γρ → ΛK<sup>+</sup> AMPLITUDES

$(\Gamma_1 \Gamma_7)^{1/2} / \Gamma_{\text{total}}$ in $p\gamma \rightarrow N(1720) \rightarrow \Lambda K^+$		$(E_{1+}$ amplitude)	
VALUE (units 10 <sup>-3</sup> )	DOCUMENT ID	TECN	COMMENT
• • • We do not use the following data for averages, fits, limits, etc. • • •			
10.2 ± 0.2	WORKMAN 90	DPWA	
9.52	TANABE 89	DPWA	

$p\gamma \rightarrow N(1720) \rightarrow \Lambda K^+$ phase angle θ		$(E_{1+}$ amplitude)	
VALUE (degrees)	DOCUMENT ID	TECN	COMMENT
• • • We do not use the following data for averages, fits, limits, etc. • • •			
-124 ± 2	WORKMAN 90	DPWA	
-103.4	TANABE 89	DPWA	

$(\Gamma_1 \Gamma_7)^{1/2} / \Gamma_{\text{total}}$ in $p\gamma \rightarrow N(1720) \rightarrow \Lambda K^+$		$(M_{1+}$ amplitude)	
VALUE (units 10 <sup>-3</sup> )	DOCUMENT ID	TECN	COMMENT
• • • We do not use the following data for averages, fits, limits, etc. • • •			
-4.5 ± 0.2	WORKMAN 90	DPWA	
3.18	TANABE 89	DPWA	

## N(1720) FOOTNOTES

- <sup>1</sup> LONGACRE 77 pole positions are from a search for poles in the unitarized T-matrix; the first (second) value uses, in addition to  $\pi N \rightarrow N\pi\pi$  data, elastic amplitudes from a Saclay (CERN) partial-wave analysis. The other LONGACRE 77 values are from eyeball fits with Breit-Wigner circles to the T-matrix amplitudes.
- <sup>2</sup> From method II of LONGACRE 75: eyeball fits with Breit-Wigner circles to the T-matrix amplitudes.
- <sup>3</sup> See HOEHLER 93 for a detailed discussion of the evidence for and the pole parameters of  $N$  and  $\Delta$  resonances as determined from Argand diagrams of  $\pi N$  elastic partial-wave amplitudes and from plots of the speeds with which the amplitudes traverse the diagrams.
- <sup>4</sup> LONGACRE 78 values are from a search for poles in the unitarized T-matrix. The first (second) value uses, in addition to  $\pi N \rightarrow N\pi\pi$  data, elastic amplitudes from a Saclay (CERN) partial-wave analysis.

## N(1720) REFERENCES

For early references, see Physics Letters **111B** 1 (1982).

ANISOVICH 12A	EPJ A48 15	A.V. Anisovich et al.	(BONN, PNPI)
ANISOVICH 10	EPJ A44 203	A.V. Anisovich et al.	(BONN, PNPI)
BATINIC 10	PR C82 039203	M. Batinic et al.	(ZAGR)
THOMA 08	PL B659 87	U. Thoma et al.	(CB-ELSA Collab.)
DRECHSEL 07	EPJ A34 69	D. Drechsel, S.S. Kamalov, L. Tiator	(MAINZ, JINR)
DUGGER 07	PR C76 025211	M. Dugger et al.	(Jefferson Lab CLAS Collab.)
ARNDT 06	PR C74 045205	R.A. Arndt et al.	(GWU)
PDG 06	JPG 33 1	W.-M. Yao et al.	(PDG Collab.)
SHKLYAR 05	PR C72 015210	V. Shklyar, H. Lenske, U. Mosel	(GIES)
ARNDT 04	PR C69 035213	R.A. Arndt et al.	(GWU, TRIU)
PENNER 02C	PR C66 055211	G. Penner, U. Mosel	(GIES)
PENNER 02D	PR C66 055212	G. Penner, U. Mosel	(GIES)
VRA NA 00	PRPL 329 181	T.P. Vrana, S.A. Dytman, T.-S.H. Lee	(PITT-)
ARNDT 96	PR C53 430	R.A. Arndt, I.I. Strakovsky, R.L. Workman	(VPI)
ARNDT 95	PR C52 2120	R.A. Arndt et al.	(VPI, BRCC)
HOEHLER 93	π N Newsletter 9 1	G. Hohlner	(KARL)
LI 93	PR C47 2759	Z.J. Li et al.	(VPI)
MANLEY 92	PR D45 4002	D.M. Manley, E.M. Saleski	(KENT) IJP
Also	PR D30 904	D.M. Manley et al.	(VPI)
ARNDT 91	PR D43 2131	R.A. Arndt et al.	(VPI, TELE) IJP
WORKMAN 90	PR C42 781	R.L. Workman	(VPI)
TANABE 89	PR C39 741	H. Tanabe, M. Kohno, C. Bennhold	(MANZ)
Also	NC 102A 193	M. Kohno, H. Tanabe, C. Bennhold	(MANZ)
BELL 83	NP B222 389	K.W. Bell et al.	(RL) IJP
CRAWFORD 83	NP B211 1	R.L. Crawford, W.T. Morton	(GLAS)
PDG 82	PL 111B 1	M. Roos et al.	(HELS, CIT, CERN)
AWAJI 81	Bonn Conf. 352	N. Awaji, R. Kajikawa	(NAGO)
Also	NP B197 365	K. Fujii et al.	(NAGO)
CUTKOSKY 80	Toronto Conf. 19	R.E. Cutkosky et al.	(CMU, LBL) IJP
Also	PR D20 2839	R.E. Cutkosky et al.	(CMU, LBL) IJP
SAXON 80	NP B162 522	D.H. Saxon et al.	(RHEL, BRIS) IJP
HOEHLER 79	PDAT 12-1	G. Hohlner et al.	(KARLT) IJP
Also	Toronto Conf. 3	R. Koch	(KARLT) IJP
LONGACRE 78	PR D17 1795	R.S. Longacre et al.	(LBL, SLAC)
LONGACRE 77	NP B122 493	R.S. Longacre, J. Dolbeau	(SACL) IJP
Also	NP B108 365	J. Dolbeau et al.	(SACL) IJP
LONGACRE 75	PL 55B 415	R.S. Longacre et al.	(LBL, SLAC) IJP



Baryon Particle Listings  
N(1860), N(1875)

**N(1860) 5/2<sup>+</sup>**

$I(J^P) = \frac{1}{2}(\frac{5}{2}^+)$  Status: \*\*

OMITTED FROM SUMMARY TABLE

Before the 2012 Review, all the evidence for a  $J^P = 5/2^+$  state with a mass above 1800 MeV was filed under a two-star N(2000). There is now some evidence from ANISOVICH 12A for two  $5/2^+$  states in this region, so we have split the older data (according to mass) between two two-star  $5/2^+$  states, an N(1860) and an N(2000).

**N(1860) BREIT-WIGNER MASS**

VALUE (MeV)	DOCUMENT ID	TECN	COMMENT
<b>1820 to 1960 (≈ 1860) OUR ESTIMATE</b>			
1860 +120 - 60	ANISOVICH 12A	DPWA	Multichannel
1817.7	ARNDT 06	DPWA	$\pi N \rightarrow \pi N, \eta N$
1903 ± 87	MANLEY 92	IPWA	$\pi N \rightarrow \pi N & N\pi\pi$
1882 ± 10	HOEHLER 79	IPWA	$\pi N \rightarrow \pi N$
• • • We do not use the following data for averages, fits, limits, etc. • • •			
1814	ARNDT 95	DPWA	$\pi N \rightarrow N\pi$

**N(1860) BREIT-WIGNER WIDTH**

VALUE (MeV)	DOCUMENT ID	TECN	COMMENT
270 +140 - 50	ANISOVICH 12A	DPWA	Multichannel
117.6	ARNDT 06	DPWA	$\pi N \rightarrow \pi N, \eta N$
490 ± 310	MANLEY 92	IPWA	$\pi N \rightarrow \pi N & N\pi\pi$
95 ± 20	HOEHLER 79	IPWA	$\pi N \rightarrow \pi N$
• • • We do not use the following data for averages, fits, limits, etc. • • •			
176	ARNDT 95	DPWA	$\pi N \rightarrow N\pi$

**N(1860) POLE POSITION**

**REAL PART**

VALUE (MeV)	DOCUMENT ID	TECN	COMMENT
1830 +120 - 60	ANISOVICH 12A	DPWA	Multichannel
1807	ARNDT 06	DPWA	$\pi N \rightarrow \pi N, \eta N$

**-2xIMAGINARY PART**

VALUE (MeV)	DOCUMENT ID	TECN	COMMENT
250 +150 - 50	ANISOVICH 12A	DPWA	Multichannel
109	ARNDT 06	DPWA	$\pi N \rightarrow \pi N, \eta N$

**N(1860) ELASTIC POLE RESIDUE**

**MODULUS |r|**

VALUE (MeV)	DOCUMENT ID	TECN	COMMENT
50 ± 20	ANISOVICH 12A	DPWA	Multichannel
60	ARNDT 06	DPWA	$\pi N \rightarrow \pi N, \eta N$

**PHASE  $\theta$**

VALUE (°)	DOCUMENT ID	TECN	COMMENT
-80 ± 40	ANISOVICH 12A	DPWA	Multichannel
-67	ARNDT 06	DPWA	$\pi N \rightarrow \pi N, \eta N$

**N(1860) DECAY MODES**

Mode
$\Gamma_1$ $N\pi$
$\Gamma_2$ $N\pi\pi$
$\Gamma_3$ $\Delta(1232)\pi, P$ -wave
$\Gamma_4$ $N\rho, S=3/2, P$ -wave
$\Gamma_5$ $N\rho, S=3/2, F$ -wave

**N(1860) BRANCHING RATIOS**

$\Gamma(N\pi)/\Gamma_{total}$	DOCUMENT ID	TECN	COMMENT	$\Gamma_1/\Gamma$
20 ± 6	ANISOVICH 12A	DPWA	Multichannel	
12.7	ARNDT 06	DPWA	$\pi N \rightarrow \pi N, \eta N$	
8 ± 5	MANLEY 92	IPWA	$\pi N \rightarrow \pi N & N\pi\pi$	
4 ± 2	HOEHLER 79	IPWA	$\pi N \rightarrow \pi N$	
• • • We do not use the following data for averages, fits, limits, etc. • • •				
10	ARNDT 95	DPWA	$\pi N \rightarrow N\pi$	

$(\Gamma_1\Gamma_2)/\Gamma_{total}$ in $N\pi \rightarrow N(1860) \rightarrow \Delta(1232)\pi, P$ -wave	DOCUMENT ID	TECN	COMMENT	$(\Gamma_1\Gamma_3)/\Gamma$
+0.10 ± 0.06	MANLEY 92	IPWA	$\pi N \rightarrow \pi N & N\pi\pi$	

$(\Gamma_1\Gamma_2)/\Gamma_{total}$ in $N\pi \rightarrow N(1860) \rightarrow N\rho, S=3/2, P$ -wave	DOCUMENT ID	TECN	COMMENT	$(\Gamma_1\Gamma_4)/\Gamma$
-0.22 ± 0.08	MANLEY 92	IPWA	$\pi N \rightarrow \pi N & N\pi\pi$	

$(\Gamma_1\Gamma_2)/\Gamma_{total}$ in $N\pi \rightarrow N(1860) \rightarrow N\rho, S=3/2, F$ -wave	DOCUMENT ID	TECN	COMMENT	$(\Gamma_1\Gamma_5)/\Gamma$
+0.11 ± 0.06	MANLEY 92	IPWA	$\pi N \rightarrow \pi N & N\pi\pi$	

**N(1860) PHOTON DECAY AMPLITUDES**

N(1860) $\rightarrow \rho\gamma$ , helicity-1/2 amplitude $A_{1/2}$	DOCUMENT ID	TECN	COMMENT
0.020 ± 0.012	<sup>1</sup> ANISOVICH 12A	DPWA	Phase = (120 ± 50)°

N(1860) $\rightarrow \rho\gamma$ , helicity-3/2 amplitude $A_{3/2}$	DOCUMENT ID	TECN	COMMENT
0.050 ± 0.020	<sup>1</sup> ANISOVICH 12A	DPWA	Phase = (-80 ± 60)°

**N(1860) FOOTNOTES**

<sup>1</sup> This ANISOVICH 12A value is the complex helicity amplitude at the pole position.

**N(1860) REFERENCES**

ANISOVICH 12A	EPJ A48 15	A.V. Anisovich et al.	(BONN, PNPI)
ARNDT 06	PR C74 045205	R.A. Arndt et al.	(GWU)
ARNDT 95	PR C52 2120	R.A. Arndt et al.	(VPI, BRCO)
MANLEY 92	PR D45 4002	D.M. Manley, E.M. Saleski	(KENT)
	Also PR D30 904	D.M. Manley et al.	(VPI)
HOEHLER 79	PDAT 12-1	G. Hohler et al.	(KARLT)

**N(1875) 3/2<sup>-</sup>**

$I(J^P) = \frac{1}{2}(\frac{3}{2}^-)$  Status: \*\*\*

Before the 2012 Review, all the evidence for a  $J^P = 3/2^-$  state with a mass above 1800 MeV was filed under a two-star N(2080).

There is now evidence from ANISOVICH 12A for two  $3/2^-$  states in this region, so we have split the older data (according to mass) between a three-star N(1875) and a two-star N(2120).

The latest GWU analysis (ARNDT 06) finds no evidence for this resonance.

**N(1875) BREIT-WIGNER MASS**

VALUE (MeV)	DOCUMENT ID	TECN	COMMENT
<b>1820 to 1920 (≈ 1875) OUR ESTIMATE</b>			
1880 ± 20	ANISOVICH 12A	DPWA	Multichannel
1804 ± 55	MANLEY 92	IPWA	$\pi N \rightarrow \pi N & N\pi\pi$
1920	BELL 83	DPWA	$\pi^- p \rightarrow \Lambda K^0$
1880 ± 100	<sup>1</sup> CUTKOSKY 80	IPWA	$\pi N \rightarrow \pi N$
1900	SAXON 80	DPWA	$\pi^- p \rightarrow \Lambda K^0$
• • • We do not use the following data for averages, fits, limits, etc. • • •			
2048 ± 65	BATINIC 10	DPWA	$\pi N \rightarrow N\pi, N\eta$
1946 ± 1	PENNER 02c	DPWA	Multichannel
1895	MART 00	DPWA	$\gamma p \rightarrow \Lambda K^+$
2003 ± 18	VRANA 00	DPWA	Multichannel
1880	BAKER 79	DPWA	$\pi^- p \rightarrow n\eta$

**N(1875) BREIT-WIGNER WIDTH**

VALUE (MeV)	DOCUMENT ID	TECN	COMMENT
<b>160 to 320 (≈ 220) OUR ESTIMATE</b>			
200 ± 25	ANISOVICH 12A	DPWA	Multichannel
450 ± 185	MANLEY 92	IPWA	$\pi N \rightarrow \pi N & N\pi\pi$
320	BELL 83	DPWA	$\pi^- p \rightarrow \Lambda K^0$
180 ± 60	<sup>1</sup> CUTKOSKY 80	IPWA	$\pi N \rightarrow \pi N$ (lower m)
240	SAXON 80	DPWA	$\pi^- p \rightarrow \Lambda K^0$
• • • We do not use the following data for averages, fits, limits, etc. • • •			
529 ± 128	BATINIC 10	DPWA	$\pi N \rightarrow N\pi, N\eta$
859 ± 7	PENNER 02c	DPWA	Multichannel
372	MART 00	DPWA	$\gamma p \rightarrow \Lambda K^+$
1070 ± 858	VRANA 00	DPWA	Multichannel
87	BAKER 79	DPWA	$\pi^- p \rightarrow n\eta$

**N(1875) POLE POSITION**

**REAL PART**

VALUE (MeV)	DOCUMENT ID	TECN	COMMENT
<b>1800 to 1950 OUR ESTIMATE</b>			
1860 ± 25	ANISOVICH 12A	DPWA	Multichannel
1880 ± 100	<sup>1</sup> CUTKOSKY 80	IPWA	$\pi N \rightarrow \pi N$ (lower m)
• • • We do not use the following data for averages, fits, limits, etc. • • •			
1957 ± 49	BATINIC 10	DPWA	$\pi N \rightarrow N\pi, N\eta$
1824	VRANA 00	DPWA	Multichannel
not seen	ARNDT 91	DPWA	$\pi N \rightarrow \pi N$ Soln SM90

## Baryon Particle Listings

 $N(1875)$  $-2 \times \text{IMAGINARY PART}$ 

VALUE (MeV)	DOCUMENT ID	TECN	COMMENT
<b>150 to 250 OUR ESTIMATE</b>			
200 ± 20	ANISOVICH 12A	DPWA	Multichannel
160 ± 80	<sup>1</sup> CUTKOSKY 80	IPWA	$\pi N \rightarrow \pi N$ (lower $m$ )
••• We do not use the following data for averages, fits, limits, etc. •••			
467 ± 106	BATINIC 10	DPWA	$\pi N \rightarrow N\pi, N\eta$
614	VRANA 00	DPWA	Multichannel
not seen	ARNDT 91	DPWA	$\pi N \rightarrow \pi N$ Soln SM90

 $N(1875)$  ELASTIC POLE RESIDUEMODULUS  $|r|$ 

VALUE (MeV)	DOCUMENT ID	TECN	COMMENT
<b>2 to 10 OUR ESTIMATE</b>			
2.5 ± 1.0	ANISOVICH 12A	DPWA	Multichannel
10 ± 5	<sup>1</sup> CUTKOSKY 80	IPWA	$\pi N \rightarrow \pi N$ (lower $m$ )
••• We do not use the following data for averages, fits, limits, etc. •••			
53	BATINIC 10	DPWA	$\pi N \rightarrow N\pi, N\eta$

PHASE  $\theta$ 

VALUE (°)	DOCUMENT ID	TECN	COMMENT
100 ± 80	<sup>1</sup> CUTKOSKY 80	IPWA	$\pi N \rightarrow \pi N$ (lower $m$ )
••• We do not use the following data for averages, fits, limits, etc. •••			
-65	BATINIC 10	DPWA	$\pi N \rightarrow N\pi, N\eta$

 $N(1875)$  INELASTIC POLE RESIDUE

The "normalized residue" is the residue divided by  $\Gamma_{pole}$ .

Normalized residue in  $N\pi \rightarrow N(1875) \rightarrow \Lambda K$ 

MODULUS (%)	DOCUMENT ID	TECN	COMMENT
<b>1.5 ± 0.5</b>	ANISOVICH 12A	DPWA	Multichannel

Normalized residue in  $N\pi \rightarrow N(1875) \rightarrow \Sigma K$ 

MODULUS (%)	DOCUMENT ID	TECN	COMMENT
<b>4 ± 2</b>	ANISOVICH 12A	DPWA	Multichannel

Normalized residue in  $N\pi \rightarrow N(1875) \rightarrow N\sigma$ 

MODULUS (%)	PHASE (°)	DOCUMENT ID	TECN	COMMENT
<b>8 ± 3</b>	<b>-170 ± 65</b>	ANISOVICH 12A	DPWA	Multichannel

 $N(1875)$  DECAY MODES

Mode	Fraction ( $\Gamma_i/\Gamma$ )	Scale factor
$\Gamma_1$ $N\pi$	(12 ± 10) %	2.5
$\Gamma_2$ $N\eta$	(3.5 ± 3.5) %	
$\Gamma_3$ $N\omega$	(21 ± 7) %	
$\Gamma_4$ $\Lambda K$		
$\Gamma_5$ $\Sigma K$		
$\Gamma_6$ $N\pi\pi$	(7 ± 4) × 10 <sup>-3</sup>	
$\Gamma_7$ $\Delta(1232)\pi, S\text{-wave}$	(40 ± 10) %	
$\Gamma_8$ $\Delta(1232)\pi, D\text{-wave}$	(17 ± 10) %	
$\Gamma_9$ $N\rho, S=3/2, S\text{-wave}$	(6 ± 6) %	
$\Gamma_{10}$ $N(\pi\pi)_{S\text{-wave}}^{J=0}$	(24 ± 24) %	
$\Gamma_{11}$ $n\gamma, \text{helicity}=1/2$		
$\Gamma_{12}$ $n\gamma, \text{helicity}=3/2$		
$\Gamma_{13}$ $p\gamma$	0.008–0.016 %	
$\Gamma_{14}$ $p\gamma, \text{helicity}=1/2$	0.006–0.010 %	
$\Gamma_{15}$ $p\gamma, \text{helicity}=3/2$	0.002–0.006 %	

 $N(1875)$  BRANCHING RATIOS

$\Gamma(N\pi)/\Gamma_{total}$	DOCUMENT ID	TECN	COMMENT	$\Gamma_1/\Gamma$
<b>12 ± 10 OUR ESTIMATE</b>				
3 ± 2	ANISOVICH 12A	DPWA	Multichannel	
23 ± 3	MANLEY 92	IPWA	$\pi N \rightarrow \pi N \& N\pi\pi$	
10 ± 4	<sup>1</sup> CUTKOSKY 80	IPWA	$\pi N \rightarrow \pi N$ (lower $m$ )	
••• We do not use the following data for averages, fits, limits, etc. •••				
17 ± 7	BATINIC 10	DPWA	$\pi N \rightarrow N\pi, N\eta$	
12 ± 2	PENNER 02c	DPWA	Multichannel	
13 ± 3	VRANA 00	DPWA	Multichannel	

 $\Gamma(N\eta)/\Gamma_{total}$ 

VALUE (%)	DOCUMENT ID	TECN	COMMENT	$\Gamma_2/\Gamma$
<b>3.5 ± 3.5 OUR AVERAGE</b>			Error includes scale factor of 2.5.	
7 ± 2	PENNER 02c	DPWA	Multichannel	
0 ± 2	VRANA 00	DPWA	Multichannel	
••• We do not use the following data for averages, fits, limits, etc. •••				
8 ± 3	BATINIC 10	DPWA	$\pi N \rightarrow N\pi, N\eta$	

 $(\Gamma_i\Gamma_j)^{1/2}/\Gamma_{total}$  in  $N\pi \rightarrow N(1875) \rightarrow N\eta$ 

VALUE (%)	DOCUMENT ID	TECN	COMMENT	$(\Gamma_1\Gamma_2)^{1/2}/\Gamma$
<b>6 ± 4 OUR ESTIMATE</b>				
5 ± 2	ANISOVICH 12A	DPWA	Multichannel	
6.5	BAKER 79	DPWA	$\pi^- p \rightarrow n\eta$	

 $\Gamma(N\omega)/\Gamma_{total}$ 

VALUE (%)	DOCUMENT ID	TECN	COMMENT	$\Gamma_3/\Gamma$
<b>21 ± 7</b>	PENNER 02c	DPWA	Multichannel	

 $\Gamma(\Lambda K)/\Gamma_{total}$ 

VALUE (%)	DOCUMENT ID	TECN	COMMENT	$\Gamma_4/\Gamma$
0.2 ± 0.2	PENNER 02c	DPWA	Multichannel	
••• We do not use the following data for averages, fits, limits, etc. •••				

 $(\Gamma_i\Gamma_j)^{1/2}/\Gamma_{total}$  in  $N\pi \rightarrow N(1875) \rightarrow \Lambda K$ 

VALUE (%)	DOCUMENT ID	TECN	COMMENT	$(\Gamma_1\Gamma_4)^{1/2}/\Gamma$
<b>4 ± 2 OUR ESTIMATE</b>				
4 ± 2	ANISOVICH 12A	DPWA	Multichannel	
4	BELL 83	DPWA	$\pi^- p \rightarrow \Lambda K^0$	
3	SAXON 80	DPWA	$\pi^- p \rightarrow \Lambda K^0$	

 $\Gamma(\Sigma K)/\Gamma_{total}$ 

VALUE (%)	DOCUMENT ID	TECN	COMMENT	$\Gamma_5/\Gamma$
<b>0.7 ± 0.4</b>	PENNER 02c	DPWA	Multichannel	

 $(\Gamma_i\Gamma_j)^{1/2}/\Gamma_{total}$  in  $N\pi \rightarrow N(1875) \rightarrow \Sigma K$ 

VALUE (%)	DOCUMENT ID	TECN	COMMENT	$(\Gamma_1\Gamma_5)^{1/2}/\Gamma$
<b>1 to 10 OUR ESTIMATE</b>				
15 ± 8	ANISOVICH 12A	DPWA	Multichannel	
1.4 to 3.7	<sup>2</sup> DEANS 75	DPWA	$\pi N \rightarrow \Sigma K$	

 $(\Gamma_i\Gamma_j)^{1/2}/\Gamma_{total}$  in  $N\pi \rightarrow N(1875) \rightarrow \Delta(1232)\pi, S\text{-wave}$ 

VALUE (%)	DOCUMENT ID	TECN	COMMENT	$(\Gamma_1\Gamma_7)^{1/2}/\Gamma$
-0.09 ± 0.09	MANLEY 92	IPWA	$\pi N \rightarrow \pi N \& N\pi\pi$	

 $\Gamma(\Delta(1232)\pi, S\text{-wave})/\Gamma_{total}$ 

VALUE (%)	DOCUMENT ID	TECN	COMMENT	$\Gamma_7/\Gamma$
<b>40 ± 10</b>	VRANA 00	DPWA	Multichannel	

 $(\Gamma_i\Gamma_j)^{1/2}/\Gamma_{total}$  in  $N\pi \rightarrow N(1875) \rightarrow \Delta(1232)\pi, D\text{-wave}$ 

VALUE (%)	DOCUMENT ID	TECN	COMMENT	$(\Gamma_1\Gamma_8)^{1/2}/\Gamma$
+0.22 ± 0.07	MANLEY 92	IPWA	$\pi N \rightarrow \pi N \& N\pi\pi$	

 $\Gamma(\Delta(1232)\pi, D\text{-wave})/\Gamma_{total}$ 

VALUE (%)	DOCUMENT ID	TECN	COMMENT	$\Gamma_8/\Gamma$
<b>17 ± 10</b>	VRANA 00	DPWA	Multichannel	

 $(\Gamma_i\Gamma_j)^{1/2}/\Gamma_{total}$  in  $N\pi \rightarrow N(1875) \rightarrow N\rho, S=3/2, S\text{-wave}$ 

VALUE (%)	DOCUMENT ID	TECN	COMMENT	$(\Gamma_1\Gamma_9)^{1/2}/\Gamma$
-0.24 ± 0.06	MANLEY 92	IPWA	$\pi N \rightarrow \pi N \& N\pi\pi$	

 $\Gamma(N\rho, S=3/2, S\text{-wave})/\Gamma_{total}$ 

VALUE (%)	DOCUMENT ID	TECN	COMMENT	$\Gamma_9/\Gamma$
<b>6 ± 6</b>	VRANA 00	DPWA	Multichannel	

 $(\Gamma_i\Gamma_j)^{1/2}/\Gamma_{total}$  in  $N\pi \rightarrow N(1875) \rightarrow N(\pi\pi)_{S\text{-wave}}^{J=0}$ 

VALUE (%)	DOCUMENT ID	TECN	COMMENT	$(\Gamma_1\Gamma_{10})^{1/2}/\Gamma$
+0.25 ± 0.06	MANLEY 92	IPWA	$\pi N \rightarrow \pi N \& N\pi\pi$	

 $\Gamma(N(\pi\pi)_{S\text{-wave}}^{J=0})/\Gamma_{total}$ 

VALUE (%)	DOCUMENT ID	TECN	COMMENT	$\Gamma_{10}/\Gamma$
<b>24 ± 24</b>	VRANA 00	DPWA	Multichannel	

 $(\Gamma_i\Gamma_j)^{1/2}/\Gamma_{total}$  in  $p\gamma \rightarrow N(1875) \rightarrow N\eta$ 

VALUE (%)	DOCUMENT ID	TECN	COMMENT	$(\Gamma_{13}\Gamma_2)^{1/2}/\Gamma$
60 ± 12	ANISOVICH 12A	DPWA	Multichannel	
0.37	HICKS 73	MPWA	$\gamma p \rightarrow p\eta$	

 $N(1875)$  PHOTON DECAY AMPLITUDES

Papers on  $\gamma N$  amplitudes predating 1981 may be found in our 2006 edition, Journal of Physics, G **33** 1 (2006).

 $N(1875) \rightarrow p\gamma, \text{helicity}=1/2$  amplitude  $A_{1/2}$ 

VALUE (GeV <sup>-1/2</sup> )	DOCUMENT ID	TECN	COMMENT
0.018 ± 0.010	ANISOVICH 12A	DPWA	Multichannel
-0.020 ± 0.008	AWAJI 81	DPWA	$\gamma N \rightarrow \pi N$
••• We do not use the following data for averages, fits, limits, etc. •••			
0.012	PENNER 02d	DPWA	Multichannel
0.026 ± 0.052	DEVENISH 74	DPWA	$\gamma N \rightarrow \pi N$

See key on page 457

Baryon Particle Listings  
 $N(1875)$ ,  $N(1880)$

$N(1875) \rightarrow p\gamma$ , helicity-3/2 amplitude  $A_{3/2}$

VALUE (GeV <sup>-1/2</sup> )	DOCUMENT ID	TECN	COMMENT
-0.009 ± 0.005	ANISOVICH 12A	DPWA	Multichannel
0.017 ± 0.011	AWAJI 81	DPWA	$\gamma N \rightarrow \pi N$
••• We do not use the following data for averages, fits, limits, etc. •••			
-0.010	PENNER 02D	DPWA	Multichannel
0.128 ± 0.057	DEVENISH 74	DPWA	$\gamma N \rightarrow \pi N$

$N(1875) \rightarrow n\gamma$ , helicity-1/2 amplitude  $A_{1/2}$

VALUE (GeV <sup>-1/2</sup> )	DOCUMENT ID	TECN	COMMENT
<b>0.007 ± 0.013</b>	AWAJI 81	DPWA	$\gamma N \rightarrow \pi N$
••• We do not use the following data for averages, fits, limits, etc. •••			
0.023	PENNER 02D	DPWA	Multichannel
0.053 ± 0.083	DEVENISH 74	DPWA	$\gamma N \rightarrow \pi N$

$N(1875) \rightarrow n\gamma$ , helicity-3/2 amplitude  $A_{3/2}$

VALUE (GeV <sup>-1/2</sup> )	DOCUMENT ID	TECN	COMMENT
<b>-0.053 ± 0.034</b>	AWAJI 81	DPWA	$\gamma N \rightarrow \pi N$
••• We do not use the following data for averages, fits, limits, etc. •••			
-0.009	PENNER 02D	DPWA	Multichannel
0.100 ± 0.141	DEVENISH 74	DPWA	$\gamma N \rightarrow \pi N$

$N(1875) \gamma p \rightarrow \Lambda K^+$  AMPLITUDES

$(\Gamma_1 \Gamma_2)^{1/2} / \Gamma_{\text{total}}$  in  $p\gamma \rightarrow N(1875) \rightarrow \Lambda K^+$  ( $E_2-$  amplitude)

VALUE (units 10 <sup>-3</sup> )	DOCUMENT ID	TECN	COMMENT
••• We do not use the following data for averages, fits, limits, etc. •••			
2.29 <sup>+0.7</sup> <sub>-0.2</sub>	MART 00	DPWA	$\gamma p \rightarrow \Lambda K^+$
5.5 ± 0.3	WORKMAN 90	DPWA	
4.09	TANABE 89	DPWA	

$p\gamma \rightarrow N(1875) \rightarrow \Lambda K^+$  phase angle  $\theta$  ( $E_2-$  amplitude)

VALUE (degrees)	DOCUMENT ID	TECN	COMMENT
••• We do not use the following data for averages, fits, limits, etc. •••			
-48 ± 5	WORKMAN 90	DPWA	
-35.9	TANABE 89	DPWA	

$(\Gamma_1 \Gamma_2)^{1/2} / \Gamma_{\text{total}}$  in  $p\gamma \rightarrow N(1875) \rightarrow \Lambda K^+$  ( $M_2-$  amplitude)

VALUE (units 10 <sup>-3</sup> )	DOCUMENT ID	TECN	COMMENT
••• We do not use the following data for averages, fits, limits, etc. •••			
-6.7 ± 0.2	WORKMAN 90	DPWA	
-4.09	TANABE 89	DPWA	

**$N(1875)$  FOOTNOTES**

- CUTKOSKY 80 finds a lower mass  $D_{13}$  resonance, as well as one in this region. Both are listed here.
- The range given for DEANS 75 is from the four best solutions. Disagrees with  $\pi^+ p \rightarrow \Sigma^+ K^+$  data of WINNIK 77 around 1920 MeV.

**$N(1875)$  REFERENCES**

For early references, see Physics Letters **111B** 1 (1982).

ANISOVICH 12A	EPJ A48 15	A.V. Anisovich <i>et al.</i>	(BONN, PNPI)
BATINIC 10	PR C82 038203	M. Batinic <i>et al.</i>	(ZAGR)
ARNDT 06	PR C74 045205	R.A. Arndt <i>et al.</i>	(GWU)
PDG 06	JPG 33 1	W.-M. Yao <i>et al.</i>	(PDG Collab.)
PENNER 02C	PR C66 055211	G. Penner, U. Mosel	(GIES)
PENNER 02D	PR C66 055212	G. Penner, U. Mosel	(GIES)
MART 00	PR C61 012201	T. Mart, C. Bennhold	
VRANA 00	PRPL 328 181	T.P. Vrana, S.A. Dytman, T.-S.H. Lee	(PITT+)
MANLEY 92	PR D45 4002	D.M. Manley, E.M. Saleski	(KENT) IJP
Also	PR D30 904	D.M. Manley <i>et al.</i>	(VPI)
ARNDT 91	PR D43 2131	R.A. Arndt <i>et al.</i>	(VPI, TELE) IJP
WORKMAN 90	PR C42 781	R.L. Workman	(VPI)
TANABE 89	PR C39 741	H. Tanabe, M. Kohno, C. Bennhold	(MANZ)
Also	NC 102A 193	M. Kohno, H. Tanabe, C. Bennhold	(MANZ)
BELL 83	NP B22 389	K.W. Bell <i>et al.</i>	(RL) IJP
AWAJI 81	Bonn Conf. 352	N. Awaji, R. Kajikawa	(NAGO)
Also	NP B197 365	K. Fujii <i>et al.</i>	(NAGO)
CUTKOSKY 80	Tomonto Conf. 19	R.E. Cutkosky <i>et al.</i>	(CMU, LBL) IJP
Also	PR D20 2839	R.E. Cutkosky <i>et al.</i>	(CMU, LBL) IJP
SAXON 80	NP B162 522	D.H. Saxon <i>et al.</i>	(RHEL, BRIS) IJP
BAKER 79	NP B156 93	R.D. Baker <i>et al.</i>	(RHEL) IJP
WINNIK 77	NP B128 66	M. Winnik <i>et al.</i>	(HAIF) I
DEANS 75	NP B96 90	S.R. Deans <i>et al.</i>	(SFLA, ALAH) IJP
DEVENISH 74	PL 52B 227	R.C.E. Devenish, D.H. Lyth, W.A. Rankin	(DESY+) IJP
HICKS 73	PR D7 2614	H.R. Hicks <i>et al.</i>	(CMU, ORNL, SFLA) IJP

$N(1880) 1/2^+$

$I(J^P) = \frac{1}{2}(\frac{1}{2}^+)$  Status: \*\*

OMITTED FROM SUMMARY TABLE

**$N(1880)$  BREIT-WIGNER MASS**

VALUE (MeV)	DOCUMENT ID	TECN	COMMENT
1870 ± 35	ANISOVICH 12A	DPWA	Multichannel
1885 ± 30	MANLEY 92	IPWA	$\pi N \rightarrow \pi N$ & $N\pi\pi$

**$N(1880)$  BREIT-WIGNER WIDTH**

VALUE (MeV)	DOCUMENT ID	TECN	COMMENT
235 ± 65	ANISOVICH 12A	DPWA	Multichannel
113 ± 44	MANLEY 92	IPWA	$\pi N \rightarrow \pi N$ & $N\pi\pi$

**$N(1880)$  POLE POSITION**

**REAL PART**

VALUE (MeV)	DOCUMENT ID	TECN	COMMENT
1860 ± 35	ANISOVICH 12A	DPWA	Multichannel

**-2xIMAGINARY PART**

VALUE (MeV)	DOCUMENT ID	TECN	COMMENT
250 ± 70	ANISOVICH 12A	DPWA	Multichannel

**$N(1880)$  ELASTIC POLE RESIDUE**

**MODULUS  $|r|$**

VALUE (MeV)	DOCUMENT ID	TECN	COMMENT
6 ± 4	ANISOVICH 12A	DPWA	Multichannel

**PHASE  $\theta$**

VALUE (°)	DOCUMENT ID	TECN	COMMENT
80 ± 65	ANISOVICH 12A	DPWA	Multichannel

**$N(1880)$  INELASTIC POLE RESIDUE**

The "normalized residue" is the residue divided by  $\Gamma_{\text{pole}}$ .

**Normalized residue in  $N\pi \rightarrow N(1880) \rightarrow N\eta$**

MODULUS (%)	PHASE (°)	DOCUMENT ID	TECN	COMMENT
11 ± 7	-75 ± 55	ANISOVICH 12A	DPWA	Multichannel

**Normalized residue in  $N\pi \rightarrow N(1880) \rightarrow \Lambda K$**

MODULUS (%)	PHASE (°)	DOCUMENT ID	TECN	COMMENT
3 ± 2	40 ± 40	ANISOVICH 12A	DPWA	Multichannel

**Normalized residue in  $N\pi \rightarrow N(1880) \rightarrow \Sigma K$**

MODULUS (%)	PHASE (°)	DOCUMENT ID	TECN	COMMENT
11 ± 6	95 ± 40	ANISOVICH 12A	DPWA	Multichannel

**Normalized residue in  $N\pi \rightarrow N(1880) \rightarrow \Delta\pi, P$ -wave**

MODULUS (%)	PHASE (°)	DOCUMENT ID	TECN	COMMENT
20 ± 8	-150 ± 50	ANISOVICH 12A	DPWA	Multichannel

**$N(1880)$  DECAY MODES**

Mode
$\Gamma_1 N\pi$
$\Gamma_2 N\eta$
$\Gamma_3 \Lambda K$
$\Gamma_4 \Sigma K$
$\Gamma_5 \Delta(1232)\pi$

**$N(1880)$  BRANCHING RATIOS**

$\Gamma(N\pi)/\Gamma_{\text{total}}$	VALUE (%)	DOCUMENT ID	TECN	COMMENT	$\Gamma_1/\Gamma$
	5 ± 3	ANISOVICH 12A	DPWA	Multichannel	
	15 ± 6	MANLEY 92	IPWA	$\pi N \rightarrow \pi N$ & $N\pi\pi$	

$\Gamma(N\eta)/\Gamma_{\text{total}}$	VALUE (%)	DOCUMENT ID	TECN	COMMENT	$\Gamma_2/\Gamma$
	25 <sup>+30</sup> <sub>-20</sub>	ANISOVICH 12A	DPWA	Multichannel	
	-19 ± 8	MANLEY 92	IPWA	$\pi N \rightarrow \pi N$ & $N\pi\pi$	

$\Gamma(\Lambda K)/\Gamma_{\text{total}}$	VALUE (%)	DOCUMENT ID	TECN	COMMENT	$\Gamma_3/\Gamma$
	2 ± 1	ANISOVICH 12A	DPWA	Multichannel	

## Baryon Particle Listings

 $N(1880)$ ,  $N(1895)$ 

$\Gamma(\Sigma K)/\Gamma_{\text{total}}$	DOCUMENT ID	TECN	COMMENT	$\Gamma_4/\Gamma$
VALUE (%)				
17±7	ANISOVICH	12A	DPWA	Multichannel

$\Gamma(\Delta(1232)\pi)/\Gamma_{\text{total}}$	DOCUMENT ID	TECN	COMMENT	$\Gamma_5/\Gamma$
VALUE (%)				
29±12	ANISOVICH	12A	DPWA	Multichannel

 **$N(1880)$  PHOTON DECAY AMPLITUDES** **$N(1880) \rightarrow p\gamma$ , helicity-1/2 amplitude  $A_{1/2}$** 

VALUE	DOCUMENT ID	TECN	COMMENT
0.014±0.003	<sup>1</sup> ANISOVICH	12A	DPWA Phase = (-130 ± 60) <sup>o</sup>

 **$N(1880)$  FOOTNOTES**

<sup>1</sup> This ANISOVICH 12A value is the complex helicity amplitude at the pole position.

 **$N(1880)$  REFERENCES**

ANISOVICH	12A	EPJ A48 15	A.V. Anisovich et al.	(BONN, PNPI)
MANLEY	92	PR D45 4002	D.M. Manley, E.M. Saleski	(KENT)
Also		PR D30 904	D.M. Manley et al.	(VPI)

 **$N(1895) 1/2^-$** 

$$I(J^P) = \frac{1}{2}(1/2^-) \text{ Status: } **$$

OMITTED FROM SUMMARY TABLE

Before our 2012 *Review*, this state appeared in our Listings as the  $N(2090)$ . Any structure in the  $S_{11}$  wave above 1800 MeV is listed here. A few early results that are now obsolete have been omitted.

The latest GWU analysis (ARNDT 06) finds no evidence for this resonance.

 **$N(1895)$  BREIT-WIGNER MASS**

VALUE (MeV)	DOCUMENT ID	TECN	COMMENT
<b>≈ 2090 OUR ESTIMATE</b>			
1895 ± 15	ANISOVICH	12A	DPWA Multichannel
1928 ± 59	MANLEY	92	IPWA $\pi N \rightarrow \pi N$ & $N\pi\pi$
2180 ± 80	CUTKOSKY	80	IPWA $\pi N \rightarrow \pi N$
1880 ± 20	HOEHLER	79	IPWA $\pi N \rightarrow \pi N$
••• We do not use the following data for averages, fits, limits, etc. •••			
1812 ± 25	BATINIC	10	DPWA $\pi N \rightarrow N\pi, N\eta$
1822 ± 43	VRANA	00	DPWA Multichannel
1897 ± 50 <sup>+30</sup> / <sub>-2</sub>	PLOETZKE	98	SPEC $\gamma\rho \rightarrow \rho\eta'(958)$

 **$N(1895)$  BREIT-WIGNER WIDTH**

VALUE (MeV)	DOCUMENT ID	TECN	COMMENT
90 <sup>+30</sup> / <sub>-15</sub>	ANISOVICH	12A	DPWA Multichannel
414 ± 157	MANLEY	92	IPWA $\pi N \rightarrow \pi N$ & $N\pi\pi$
350 ± 100	CUTKOSKY	80	IPWA $\pi N \rightarrow \pi N$
95 ± 30	HOEHLER	79	IPWA $\pi N \rightarrow \pi N$
••• We do not use the following data for averages, fits, limits, etc. •••			
405 ± 40	BATINIC	10	DPWA $\pi N \rightarrow N\pi, N\eta$
248 ± 185	VRANA	00	DPWA Multichannel
396 ± 155 <sup>+35</sup> / <sub>-45</sub>	PLOETZKE	98	SPEC $\gamma\rho \rightarrow \rho\eta'(958)$

 **$N(1895)$  POLE POSITION****REAL PART**

VALUE (MeV)	DOCUMENT ID	TECN	COMMENT
1900 ± 15	ANISOVICH	12A	DPWA Multichannel
2150 ± 70	CUTKOSKY	80	IPWA $\pi N \rightarrow \pi N$
1937 or 1949	<sup>1</sup> LONGACRE	78	IPWA $\pi N \rightarrow N\pi\pi$
••• We do not use the following data for averages, fits, limits, etc. •••			
1797 ± 26	BATINIC	10	DPWA $\pi N \rightarrow N\pi, N\eta$
1795	VRANA	00	DPWA Multichannel

**-2×IMAGINARY PART**

VALUE (MeV)	DOCUMENT ID	TECN	COMMENT
90 <sup>+30</sup> / <sub>-15</sub>	ANISOVICH	12A	DPWA Multichannel
350 ± 100	CUTKOSKY	80	IPWA $\pi N \rightarrow \pi N$
139 or 131	<sup>1</sup> LONGACRE	78	IPWA $\pi N \rightarrow N\pi\pi$
••• We do not use the following data for averages, fits, limits, etc. •••			
420 ± 45	BATINIC	10	DPWA $\pi N \rightarrow N\pi, N\eta$
220	VRANA	00	DPWA Multichannel

 **$N(1895)$  ELASTIC POLE RESIDUE****MODULUS  $|r|$** 

VALUE (MeV)	DOCUMENT ID	TECN	COMMENT
1 ± 1	ANISOVICH	12A	DPWA Multichannel
40 ± 20	CUTKOSKY	80	IPWA $\pi N \rightarrow \pi N$
••• We do not use the following data for averages, fits, limits, etc. •••			
60	BATINIC	10	DPWA $\pi N \rightarrow N\pi, N\eta$

**PHASE  $\theta$** 

VALUE (°)	DOCUMENT ID	TECN	COMMENT
0 ± 90	CUTKOSKY	80	IPWA $\pi N \rightarrow \pi N$
••• We do not use the following data for averages, fits, limits, etc. •••			
-164	BATINIC	10	DPWA $\pi N \rightarrow N\pi, N\eta$

 **$N(1895)$  INELASTIC POLE RESIDUE**

The "normalized residue" is the residue divided by  $\Gamma_{\text{pole}}$ .

**Normalized residue in  $N\pi \rightarrow N(1895) \rightarrow N\eta$** 

MODULUS (%)	PHASE (°)	DOCUMENT ID	TECN	COMMENT
6 ± 2	40 ± 20	ANISOVICH	12A	DPWA Multichannel

**Normalized residue in  $N\pi \rightarrow N(1895) \rightarrow \Lambda K$** 

MODULUS (%)	PHASE (°)	DOCUMENT ID	TECN	COMMENT
5 ± 2	-90 ± 30	ANISOVICH	12A	DPWA Multichannel

**Normalized residue in  $N\pi \rightarrow N(1895) \rightarrow \Sigma K$** 

MODULUS (%)	PHASE (°)	DOCUMENT ID	TECN	COMMENT
6 ± 2	40 ± 30	ANISOVICH	12A	DPWA Multichannel

 **$N(1895)$  DECAY MODES**

Mode
$\Gamma_1$ $N\pi$
$\Gamma_2$ $N\eta$
$\Gamma_3$ $\Lambda K$
$\Gamma_4$ $\Sigma K$
$\Gamma_5$ $N\pi\pi$
$\Gamma_6$ $\Delta\pi$
$\Gamma_7$ $\Delta(1232)\pi$ , $D$ -wave
$\Gamma_8$ $N\rho$
$\Gamma_9$ $N\rho$ , $S=1/2$ , $S$ -wave
$\Gamma_{10}$ $N\rho$ , $S=3/2$ , $D$ -wave
$\Gamma_{11}$ $N(\pi\pi)_{S=0}^{I=0}$
$\Gamma_{12}$ $N(1440)\pi$

 **$N(1895)$  BRANCHING RATIOS**

$\Gamma(N\pi)/\Gamma_{\text{total}}$	DOCUMENT ID	TECN	COMMENT	$\Gamma_1/\Gamma$
VALUE (%)				
2 ± 1	ANISOVICH	12A	DPWA Multichannel	
10 ± 10	MANLEY	92	IPWA $\pi N \rightarrow \pi N$ & $N\pi\pi$	
18 ± 8	CUTKOSKY	80	IPWA $\pi N \rightarrow \pi N$	
9 ± 5	HOEHLER	79	IPWA $\pi N \rightarrow \pi N$	
••• We do not use the following data for averages, fits, limits, etc. •••				
32 ± 6	BATINIC	10	DPWA $\pi N \rightarrow N\pi, N\eta$	
17 ± 3	VRANA	00	DPWA Multichannel	

$\Gamma(N\eta)/\Gamma_{\text{total}}$	DOCUMENT ID	TECN	COMMENT	$\Gamma_2/\Gamma$
VALUE (%)				
21 ± 6	ANISOVICH	12A	DPWA Multichannel	
41 ± 4	VRANA	00	DPWA Multichannel	
••• We do not use the following data for averages, fits, limits, etc. •••				
22 ± 10	BATINIC	10	DPWA $\pi N \rightarrow N\pi, N\eta$	

$\Gamma(\Lambda K)/\Gamma_{\text{total}}$	DOCUMENT ID	TECN	COMMENT	$\Gamma_3/\Gamma$
VALUE (%)				
18 ± 5	ANISOVICH	12A	DPWA Multichannel	

$\Gamma(\Sigma K)/\Gamma_{\text{total}}$	DOCUMENT ID	TECN	COMMENT	$\Gamma_4/\Gamma$
VALUE (%)				
13 ± 7	ANISOVICH	12A	DPWA Multichannel	

$(\Gamma_1\Gamma_7)^{1/2}/\Gamma_{\text{total}}$ in $N\pi \rightarrow N(1895) \rightarrow \Lambda K$	DOCUMENT ID	TECN	COMMENT	$(\Gamma_1\Gamma_3)^{1/2}/\Gamma$
VALUE				
not seen	SAXON	80	DPWA $\pi^- p \rightarrow \Lambda K^0$	

$\Gamma(\Delta(1232)\pi, D\text{-wave})/\Gamma_{\text{total}}$	DOCUMENT ID	TECN	COMMENT	$\Gamma_7/\Gamma$
VALUE (%)				
1 ± 1	VRANA	00	DPWA Multichannel	

See key on page 457

# Baryon Particle Listings

## $N(1895)$ , $N(1900)$

$\Gamma(N\rho, S=1/2, S\text{-wave})/\Gamma_{\text{total}}$	DOCUMENT ID	TECN	COMMENT	$\Gamma_9/\Gamma$
VALUE (%)				
36±1	VRANA	00	DPWA	Multichannel

$\Gamma(N\rho, S=3/2, D\text{-wave})/\Gamma_{\text{total}}$	DOCUMENT ID	TECN	COMMENT	$\Gamma_{10}/\Gamma$
VALUE (%)				
1±1	VRANA	00	DPWA	Multichannel

$\Gamma(N(\pi\pi)_{S=0}^{J=0})/\Gamma_{\text{total}}$	DOCUMENT ID	TECN	COMMENT	$\Gamma_{11}/\Gamma$
VALUE (%)				
2±1	VRANA	00	DPWA	Multichannel

$\Gamma(N(1440)\pi)/\Gamma_{\text{total}}$	DOCUMENT ID	TECN	COMMENT	$\Gamma_{12}/\Gamma$
VALUE (%)				
2±1	VRANA	00	DPWA	Multichannel

### N(1895) PHOTON DECAY AMPLITUDES

$N(1895) \rightarrow \rho\gamma$ , helicity-1/2 amplitude  $A_{1/2}$

VALUE	DOCUMENT ID	TECN	COMMENT
0.012±0.006	2 ANISOVICH	12A	DPWA Phase = (120 ± 50)°

### N(1895) FOOTNOTES

- <sup>1</sup> LONGACRE 78 values are from a search for poles in the unitarized T-matrix. The first (second) value uses, in addition to  $\pi N \rightarrow N\pi\pi$  data, elastic amplitudes from a Saclay (CERN) partial-wave analysis.
- <sup>2</sup> This ANISOVICH 12A value is the complex helicity amplitude at the pole position.

### N(1895) REFERENCES

ANISOVICH 12A	EPJ A48 15	A.V. Anisovich et al.	(BONN, PNPI)
BATINIC 10	PR C82 038203	M. Batinic et al.	(ZAGR)
ARNDT 06	PR C74 045205	R.A. Arndt et al.	(GWU)
VRANA 00	PRPL 328 181	T.P. Vrana, S.A. Dytman., T.-S.H. Lee	(PITT+)
PLOETZKE 98	PL B444 555	R. Ploetzke et al.	(Bonn SAPHIR Collab.)
MANLEY 92	PR D45 4002	D.M. Manley, E.M. Saleski	(KEPT) IJP
	PR D30 904	D.M. Manley et al.	(VPI)
CUTKOSKY 80	Toronto Conf. 19	R.E. Cutkosky et al.	(CMU, LBL) IJP
	PR D20 2839	R.E. Cutkosky et al.	(CMU, LBL)
SAXON 80	NP B162 522	D.H. Saxon et al.	(RHEL, BRIS) IJP
HOEHLER 79	PDAT 12-1	G. Hohlner et al.	(KARLT) IJP
	Toronto Conf. 3	R. Koch	(KARLT) IJP
LONGACRE 78	PR D17 1795	R.S. Longacre et al.	(LBL, SLAC)

## N(1900) 3/2<sup>+</sup>

$$I(J^P) = \frac{1}{2}(\frac{3}{2}^+)$$
 Status: \*\*\*

The latest GWU analysis (ARNDT 06) finds no evidence for this resonance.

### N(1900) BREIT-WIGNER MASS

VALUE (MeV)	DOCUMENT ID	TECN	COMMENT
<b>~ 1900 OUR ESTIMATE</b>			
1905 ± 30	ANISOVICH	12A	DPWA Multichannel
1915 ± 60	NIKONOV	08	DPWA Multichannel
1879 ± 17	MANLEY	92	IPWA $\pi N \rightarrow \pi N$ & $N\pi\pi$
• • • We do not use the following data for averages, fits, limits, etc. • • •			
1951 ± 53	PENNER	02c	DPWA Multichannel

### N(1900) BREIT-WIGNER WIDTH

VALUE (MeV)	DOCUMENT ID	TECN	COMMENT
<b>~ 250 OUR ESTIMATE</b>			
250 <sup>+120</sup> <sub>-50</sub>	ANISOVICH	12A	DPWA Multichannel
180 ± 40	NIKONOV	08	DPWA Multichannel
498 ± 78	MANLEY	92	IPWA $\pi N \rightarrow \pi N$ & $N\pi\pi$
• • • We do not use the following data for averages, fits, limits, etc. • • •			
622 ± 42	PENNER	02c	DPWA Multichannel

### N(1900) POLE POSITION

**REAL PART**

VALUE (MeV)	DOCUMENT ID	TECN	COMMENT
1900 ± 30	ANISOVICH	12A	DPWA Multichannel

**-2×IMAGINARY PART**

VALUE (MeV)	DOCUMENT ID	TECN	COMMENT
200 <sup>+100</sup> <sub>-60</sub>	ANISOVICH	12A	DPWA Multichannel

### N(1900) ELASTIC POLE RESIDUE

MODULUS  r	DOCUMENT ID	TECN	COMMENT
VALUE (MeV)			
3±2	ANISOVICH	12A	DPWA Multichannel

PHASE $\theta$	DOCUMENT ID	TECN	COMMENT
VALUE (°)			
10±35	ANISOVICH	12A	DPWA Multichannel

### N(1900) INELASTIC POLE RESIDUE

The "normalized residue" is the residue divided by  $\Gamma_{\text{pole}}$ .

**Normalized residue in  $N\pi \rightarrow N(1900) \rightarrow N\eta$**

MODULUS (%)	PHASE (°)	DOCUMENT ID	TECN	COMMENT
5±2	70 ± 60	ANISOVICH	12A	DPWA Multichannel

**Normalized residue in  $N\pi \rightarrow N(1900) \rightarrow \Lambda K$**

MODULUS (%)	PHASE (°)	DOCUMENT ID	TECN	COMMENT
7±3	135 ± 25	ANISOVICH	12A	DPWA Multichannel

**Normalized residue in  $N\pi \rightarrow N(1900) \rightarrow \Sigma K$**

MODULUS (%)	PHASE (°)	DOCUMENT ID	TECN	COMMENT
4±2	110 ± 30	ANISOVICH	12A	DPWA Multichannel

### N(1900) DECAY MODES

Mode	Fraction ( $\Gamma_i/\Gamma$ )
$\Gamma_1$ $N\pi$	~ 10 %
$\Gamma_2$ $N\pi\pi$	
$\Gamma_3$ $N\rho, S=1/2, P\text{-wave}$	
$\Gamma_4$ $N\eta$	~ 12 %
$\Gamma_5$ $N\omega$	(39 ± 9) %
$\Gamma_6$ $\Lambda K$	0-10 %
$\Gamma_7$ $\Sigma K$	( 5.0 ± 2.0) %

### N(1900) BRANCHING RATIOS

$\Gamma(N\pi)/\Gamma_{\text{total}}$	DOCUMENT ID	TECN	COMMENT
VALUE (%)			
<b>~ 10 OUR ESTIMATE</b>			
3 ± 2	ANISOVICH	12A	DPWA Multichannel
26 ± 6	MANLEY	92	IPWA $\pi N \rightarrow \pi N$ & $N\pi\pi$
• • • We do not use the following data for averages, fits, limits, etc. • • •			
2 to 9	NIKONOV	08	DPWA Multichannel
16 ± 2	PENNER	02c	DPWA Multichannel

$\Gamma(N\eta)/\Gamma_{\text{total}}$	DOCUMENT ID	TECN	COMMENT
VALUE (%)			
<b>~ 12 OUR ESTIMATE</b>			
10 ± 4	ANISOVICH	12A	DPWA Multichannel
14 ± 5	PENNER	02c	DPWA Multichannel

$\Gamma(N\omega)/\Gamma_{\text{total}}$	DOCUMENT ID	TECN	COMMENT
VALUE (%)			
<b>39 ± 9</b>	PENNER	02c	DPWA Multichannel

$(\Gamma_i/\Gamma_f)^{1/2}/\Gamma_{\text{total}}$ in $N\pi \rightarrow N(1900) \rightarrow N\rho, S=1/2, P\text{-wave}$	DOCUMENT ID	TECN	COMMENT
VALUE			
-0.34 ± 0.03	MANLEY	92	IPWA $\pi N \rightarrow \pi N$ & $N\pi\pi$

$\Gamma(\Lambda K)/\Gamma_{\text{total}}$	DOCUMENT ID	TECN	COMMENT
VALUE (%)			
<b>0 to 10 OUR ESTIMATE</b>			
16 ± 5	ANISOVICH	12A	DPWA Multichannel
2.4 ± 0.3	SHKLYAR	05	DPWA Multichannel
• • • We do not use the following data for averages, fits, limits, etc. • • •			
5 to 15	NIKONOV	08	DPWA Multichannel
0.1 ± 0.1	PENNER	02c	DPWA Multichannel

$\Gamma(\Sigma K)/\Gamma_{\text{total}}$	DOCUMENT ID	TECN	COMMENT
VALUE (%)			
<b>5 ± 2</b>	ANISOVICH	12A	DPWA Multichannel
• • • We do not use the following data for averages, fits, limits, etc. • • •			
1 ± 1	PENNER	02c	DPWA Multichannel

### N(1900) PHOTON DECAY AMPLITUDES

Papers on  $\gamma N$  amplitudes predating 1981 may be found in our 2006 edition, Journal of Physics, G **33** 1 (2006).

$N(1900) \rightarrow \rho\gamma$ , helicity-1/2 amplitude  $A_{1/2}$

VALUE (GeV <sup>-1/2</sup> )	DOCUMENT ID	TECN	COMMENT
0.026 ± 0.015	ANISOVICH	12A	DPWA Multichannel
• • • We do not use the following data for averages, fits, limits, etc. • • •			
-0.017	PENNER	02d	DPWA Multichannel

## Baryon Particle Listings

 $N(1900)$ ,  $N(1990)$  $N(1900) \rightarrow p\gamma$ , helicity-3/2 amplitude  $A_{3/2}$ 

VALUE (GeV <sup>-1/2</sup> )	DOCUMENT ID	TECN	COMMENT
-0.065 ± 0.030	ANISOVICH 12A	DPWA	Multichannel
••• We do not use the following data for averages, fits, limits, etc. •••			
0.031	PENNER 02D	DPWA	Multichannel

 $N(1900) \rightarrow n\gamma$ , helicity-1/2 amplitude  $A_{1/2}$ 

VALUE (GeV <sup>-1/2</sup> )	DOCUMENT ID	TECN	COMMENT
••• We do not use the following data for averages, fits, limits, etc. •••			
-0.016	PENNER 02D	DPWA	Multichannel

 $N(1900) \rightarrow n\gamma$ , helicity-3/2 amplitude  $A_{3/2}$ 

VALUE (GeV <sup>-1/2</sup> )	DOCUMENT ID	TECN	COMMENT
••• We do not use the following data for averages, fits, limits, etc. •••			
-0.002	PENNER 02D	DPWA	Multichannel

## N(1900) REFERENCES

ANISOVICH 12A	EPJ A48 15	A.V. Anisovich et al.	(BONN, PNPI)
NIKONOV 08	PL B662 245	V.A. Nikonov et al.	(Bonn, Gatchina)
ARNDT 06	PR C74 045205	R.A. Arndt et al.	(GWU)
PDG 06	JPG 33 1	W.-M. Yao et al.	(PDG Collab.)
SHKLYAR 05	PR C72 015210	V. Shklyar, H. Lenske, U. Mosel	(GIES)
PENNER 02C	PR C66 055211	G. Penner, U. Mosel	(GIES)
PENNER 02D	PR C66 055212	G. Penner, U. Mosel	(GIES)
MANLEY 92	PR D45 4002	D.M. Manley, E.M. Sleski	(KENT)
Also	PR D30 904	D.M. Manley et al.	(VPI)

 $N(1990) 7/2^+$ 

$$I(J^P) = \frac{1}{2}(\frac{7}{2}^+) \text{ Status: } **$$

OMITTED FROM SUMMARY TABLE

Most of the results published before 1975 are now obsolete and have been omitted. They may be found in our 1982 edition, Physics Letters **111B** 1 (1982). Some further obsolete results published before 1984 were last included in our 2006 edition, Journal of Physics, G **33** 1 (2006).

The various analyses do not agree very well with one another.

The latest GWU analysis (ARNDT 06) finds no evidence for this resonance.

## N(1990) BREIT-WIGNER MASS

VALUE (MeV)	DOCUMENT ID	TECN	COMMENT
<b>≈ 1990 OUR ESTIMATE</b>			
2060 ± 65	ANISOVICH 12A	DPWA	Multichannel
2086 ± 28	MANLEY 92	IPWA	$\pi N \rightarrow \pi N$ & $N\pi\pi$
1970 ± 50	CUTKOSKY 80	IPWA	$\pi N \rightarrow \pi N$
2005 ± 150	HOEHLER 79	IPWA	$\pi N \rightarrow \pi N$
1999	BARBOUR 78	DPWA	$\gamma N \rightarrow \pi N$
••• We do not use the following data for averages, fits, limits, etc. •••			
2311 ± 16	VRANA 00	DPWA	Multichannel

## N(1990) BREIT-WIGNER WIDTH

VALUE (MeV)	DOCUMENT ID	TECN	COMMENT
240 ± 50	ANISOVICH 12A	DPWA	Multichannel
535 ± 120	MANLEY 92	IPWA	$\pi N \rightarrow \pi N$ & $N\pi\pi$
350 ± 120	CUTKOSKY 80	IPWA	$\pi N \rightarrow \pi N$
350 ± 100	HOEHLER 79	IPWA	$\pi N \rightarrow \pi N$
216	BARBOUR 78	DPWA	$\gamma N \rightarrow \pi N$
••• We do not use the following data for averages, fits, limits, etc. •••			
205 ± 72	VRANA 00	DPWA	Multichannel

## N(1990) POLE POSITION

## REAL PART

VALUE (MeV)	DOCUMENT ID	TECN	COMMENT
2030 ± 65	ANISOVICH 12A	DPWA	Multichannel
1900 ± 30	CUTKOSKY 80	IPWA	$\pi N \rightarrow \pi N$
••• We do not use the following data for averages, fits, limits, etc. •••			
2301	VRANA 00	DPWA	Multichannel
not seen	ARNDT 91	DPWA	$\pi N \rightarrow \pi N$ Soln SM90

## -2xIMAGINARY PART

VALUE (MeV)	DOCUMENT ID	TECN	COMMENT
240 ± 60	ANISOVICH 12A	DPWA	Multichannel
260 ± 60	CUTKOSKY 80	IPWA	$\pi N \rightarrow \pi N$
••• We do not use the following data for averages, fits, limits, etc. •••			
202	VRANA 00	DPWA	Multichannel
not seen	ARNDT 91	DPWA	$\pi N \rightarrow \pi N$ Soln SM90

## N(1990) ELASTIC POLE RESIDUE

MODULUS  $|r|$ 

VALUE (MeV)	DOCUMENT ID	TECN	COMMENT
2 ± 1	ANISOVICH 12A	DPWA	Multichannel
9 ± 3	CUTKOSKY 80	IPWA	$\pi N \rightarrow \pi N$

PHASE  $\theta$ 

VALUE (°)	DOCUMENT ID	TECN	COMMENT
125 ± 65	ANISOVICH 12A	DPWA	Multichannel
-60 ± 30	CUTKOSKY 80	IPWA	$\pi N \rightarrow \pi N$

## N(1990) DECAY MODES

Mode	
$\Gamma_1$	$N\pi$
$\Gamma_2$	$N\eta$
$\Gamma_3$	$\Lambda K$
$\Gamma_4$	$\Sigma K$
$\Gamma_5$	$N\pi\pi$
$\Gamma_6$	$p\gamma$ , helicity=1/2
$\Gamma_7$	$p\gamma$ , helicity=3/2
$\Gamma_8$	$n\gamma$ , helicity=1/2
$\Gamma_9$	$n\gamma$ , helicity=3/2

## N(1990) BRANCHING RATIOS

$\Gamma(N\pi)/\Gamma_{\text{total}}$	VALUE (%)	DOCUMENT ID	TECN	COMMENT	$\Gamma_1/\Gamma$
2 ± 1	ANISOVICH 12A	DPWA	Multichannel		
6 ± 2	MANLEY 92	IPWA	$\pi N \rightarrow \pi N$ & $N\pi\pi$		
6 ± 2	CUTKOSKY 80	IPWA	$\pi N \rightarrow \pi N$		
4 ± 2	HOEHLER 79	IPWA	$\pi N \rightarrow \pi N$		
••• We do not use the following data for averages, fits, limits, etc. •••					
22 ± 11	VRANA 00	DPWA	Multichannel		

$(\Gamma_1\Gamma_7)^{1/2}/\Gamma_{\text{total}}$ in $N\pi \rightarrow N(1990) \rightarrow N\eta$	VALUE	DOCUMENT ID	TECN	COMMENT	$(\Gamma_1\Gamma_2)^{1/2}/\Gamma$
-0.043	BAKER 79	DPWA	$\pi^- p \rightarrow n\eta$		

$\Gamma(N\eta)/\Gamma_{\text{total}}$	VALUE (%)	DOCUMENT ID	TECN	COMMENT	$\Gamma_2/\Gamma$
0 ± 1	VRANA 00	DPWA	Multichannel		

$(\Gamma_1\Gamma_7)^{1/2}/\Gamma_{\text{total}}$ in $N\pi \rightarrow N(1990) \rightarrow \Lambda K$	VALUE	DOCUMENT ID	TECN	COMMENT	$(\Gamma_1\Gamma_3)^{1/2}/\Gamma$
+0.01	BELL 83	DPWA	$\pi^- p \rightarrow \Lambda K^0$		
not seen	SAXON 80	DPWA	$\pi^- p \rightarrow \Lambda K^0$		
-0.021 ± 0.033	DEVENISH 74B		Fixed-t dispersion rel.		

$(\Gamma_1\Gamma_7)^{1/2}/\Gamma_{\text{total}}$ in $N\pi \rightarrow N(1990) \rightarrow \Sigma K$	VALUE	DOCUMENT ID	TECN	COMMENT	$(\Gamma_1\Gamma_4)^{1/2}/\Gamma$
0.010 to 0.023	<sup>1</sup> DEANS 75	DPWA	$\pi N \rightarrow \Sigma K$		
0.06	LANGBEIN 73	IPWA	$\pi N \rightarrow \Sigma K$ (sol. 1)		

$(\Gamma_1\Gamma_7)^{1/2}/\Gamma_{\text{total}}$ in $N\pi \rightarrow N(1990) \rightarrow N\pi\pi$	VALUE	DOCUMENT ID	TECN	COMMENT	$(\Gamma_1\Gamma_5)^{1/2}/\Gamma$
not seen	LONGACRE 75	IPWA	$\pi N \rightarrow N\pi\pi$		

## N(1990) PHOTON DECAY AMPLITUDES

Papers on  $\gamma N$  amplitudes predating 1981 may be found in our 2006 edition, Journal of Physics, G **33** 1 (2006).

 $N(1990) \rightarrow p\gamma$ , helicity-1/2 amplitude  $A_{1/2}$ 

VALUE (GeV <sup>-1/2</sup> )	DOCUMENT ID	TECN	COMMENT
0.042 ± 0.014	<sup>2</sup> ANISOVICH 12A	DPWA	Phase = (-30 ± 20)°
0.030 ± 0.029	AWAJI 81	DPWA	$\gamma N \rightarrow \pi N$
••• We do not use the following data for averages, fits, limits, etc. •••			
0.040	BARBOUR 78	DPWA	$\gamma N \rightarrow \pi N$

 $N(1990) \rightarrow p\gamma$ , helicity-3/2 amplitude  $A_{3/2}$ 

VALUE (GeV <sup>-1/2</sup> )	DOCUMENT ID	TECN	COMMENT
0.058 ± 0.012	<sup>2</sup> ANISOVICH 12A	DPWA	Phase = (-35 ± 25)°
0.086 ± 0.060	AWAJI 81	DPWA	$\gamma N \rightarrow \pi N$
••• We do not use the following data for averages, fits, limits, etc. •••			
+0.004	BARBOUR 78	DPWA	$\gamma N \rightarrow \pi N$

**N(1990) → nγ, helicity-1/2 amplitude A<sub>1/2</sub>**

VALUE (GeV <sup>-1/2</sup> )	DOCUMENT ID	TECN	COMMENT
-0.001	AWAJI 81	DPWA	γN → πN
••• We do not use the following data for averages, fits, limits, etc. •••			
-0.069	BARBOUR 78	DPWA	γN → πN

**N(1990) → nγ, helicity-3/2 amplitude A<sub>3/2</sub>**

VALUE (GeV <sup>-1/2</sup> )	DOCUMENT ID	TECN	COMMENT
-0.178	AWAJI 81	DPWA	γN → πN
••• We do not use the following data for averages, fits, limits, etc. •••			
-0.072	BARBOUR 78	DPWA	γN → πN

**N(1990) FOOTNOTES**

- The range given for DEANS 75 is from the four best solutions.
- This ANISOVICH 12A value is the complex helicity amplitude at the pole position.

**N(1990) REFERENCES**

For early references, see Physics Letters **111B 1** (1982).

ANISOVICH 12A	EPJ A48 15	A.V. Anisovich <i>et al.</i>	(BONN, PNPI)
ARNDT 06	PR C74 045205	R.A. Arndt <i>et al.</i>	(GWU)
PDG 06	JPG 33 1	W.-M. Yao <i>et al.</i>	(PDG Collab.)
VRANA 00	PRPL 328 181	T.P. Vrana, S.A. Dytman, T.-S.H. Lee	(PITT+)
MANLEY 92	PR D45 4002	D.M. Manley, E.M. Saleski	(KENT) IJP
Also	PR D30 904	D.M. Manley <i>et al.</i>	(VPI)
ARNDT 91	PR D43 2131	R.A. Arndt <i>et al.</i>	(VPI, TELE) IJP
BELL 83	NP B222 389	K.W. Bell <i>et al.</i>	(RL) IJP
PDG 82	PL 111B 1	M. Roos <i>et al.</i>	(HELS, CIT, CERN)
AWAJI 81	Bonn Conf. 352	N. Awaji, R. Kajikawa	(NAGO)
Also	NP B197 365	K. Fujii <i>et al.</i>	(NAGO)
CUTKOSKY 80	Toronto Conf. 19	R.E. Cutkosky <i>et al.</i>	(CMU, LBL) IJP
Also	PR D20 2839	R.E. Cutkosky <i>et al.</i>	(CMU, LBL) IJP
SAXON 80	NP B162 522	D.H. Saxon <i>et al.</i>	(RHEL, BRIS) IJP
BAKER 79	NP B156 93	R.D. Baker <i>et al.</i>	(RHEL) IJP
HOEHLER 79	PDAT 12-1	G. Hoehler <i>et al.</i>	(KARLT) IJP
Also	Toronto Conf. 3	R. Koch	(KARLT) IJP
BARBOUR 78	NP B141 253	I.M. Barbour, R.L. Crawford, N.H. Parsons	(GLAS)
DEANS 75	NP B96 90	S.R. Deans <i>et al.</i>	(SFLA, ALAH) IJP
LONGACRE 75	PL 55B 415	R.S. Longacre <i>et al.</i>	(LBL, SLAC) IJP
DEVENISH 74B	NP B81 330	R.C.E. Devenish, C.D. Froggatt, B.R. Martin	(DESY+) IJP
LANGBEIN 73	NP B53 251	W. Langbein, F. Wagner	(MUNI) IJP

**N(2000) 5/2<sup>+</sup>**

$I(J^P) = \frac{1}{2}(5/2^+)$  Status: \*\*

OMITTED FROM SUMMARY TABLE

Before the 2012 Review, all the evidence for a  $J^P = 5/2^+$  state with a mass above 1800 MeV was filed under a two-star N(2000). There is now some evidence from ANISOVICH 12A for two 5/2<sup>+</sup> states in this region, so we have split the older data (according to mass) between two two-star 5/2<sup>+</sup> states, an N(1860) and an N(2000).

**N(2000) BREIT-WIGNER MASS**

VALUE (MeV)	DOCUMENT ID	TECN	COMMENT
<b>1950 to 2150 (≈ 2050) OUR ESTIMATE</b>			
2090 ± 120	ANISOVICH 12A	DPWA	Multichannel
2025	AYED 76	IPWA	πN → πN
1970	<sup>1</sup> LANGBEIN 73	IPWA	πN → ΣK (sol. 2)
2175	ALMEHED 72	IPWA	πN → πN
1930	DEANS 72	MPWA	γp → ΛK (sol. D)

**N(2000) BREIT-WIGNER WIDTH**

VALUE (MeV)	DOCUMENT ID	TECN	COMMENT
460 ± 100	ANISOVICH 12A	DPWA	Multichannel
157	AYED 76	IPWA	πN → πN
170	<sup>1</sup> LANGBEIN 73	IPWA	πN → ΣK (sol. 2)
150	ALMEHED 72	IPWA	πN → πN
112	DEANS 72	MPWA	γp → ΛK (sol. D)

**N(2000) POLE POSITION**

**REAL PART**

VALUE (MeV)	DOCUMENT ID	TECN	COMMENT
2030 ± 110	ANISOVICH 12A	DPWA	Multichannel
••• We do not use the following data for averages, fits, limits, etc. •••			
1779	ARNDT 04	DPWA	πN → πN, ηN

**-2xIMAGINARY PART**

VALUE (MeV)	DOCUMENT ID	TECN	COMMENT
480 ± 100	ANISOVICH 12A	DPWA	Multichannel
••• We do not use the following data for averages, fits, limits, etc. •••			
248	ARNDT 04	DPWA	πN → πN, ηN

**N(2000) ELASTIC POLE RESIDUE**

**MODULUS |r|**

VALUE (MeV)	DOCUMENT ID	TECN	COMMENT
35 ± 80 -15	ANISOVICH 12A	DPWA	Multichannel
••• We do not use the following data for averages, fits, limits, etc. •••			
47	ARNDT 04	DPWA	πN → πN, ηN

**PHASE θ**

VALUE (°)	DOCUMENT ID	TECN	COMMENT
-100 ± 40	ANISOVICH 12A	DPWA	Multichannel
••• We do not use the following data for averages, fits, limits, etc. •••			
-61	ARNDT 04	DPWA	πN → πN, ηN

**N(2000) DECAY MODES**

Mode	Γ <sub>1</sub>	Γ <sub>2</sub>	Γ <sub>3</sub>	Γ <sub>4</sub>	Γ <sub>5</sub>
	Nπ	Nη	ΛK	ΣK	pγ

**N(2000) BRANCHING RATIOS**

Γ(Nπ)/Γ <sub>total</sub>	DOCUMENT ID	TECN	COMMENT	Γ <sub>1</sub> /Γ
9 ± 4	ANISOVICH 12A	DPWA	Multichannel	
8	AYED 76	IPWA	πN → πN	
25	ALMEHED 72	IPWA	πN → πN	

(Γ <sub>1</sub> Γ <sub>2</sub> ) <sup>1/2</sup> /Γ <sub>total</sub> in Nπ → N(2000) → Nη	DOCUMENT ID	TECN	COMMENT	(Γ <sub>1</sub> Γ <sub>2</sub> ) <sup>1/2</sup> /Γ
+0.03	BAKER 79	DPWA	π <sup>-</sup> p → nη	

(Γ <sub>1</sub> Γ <sub>3</sub> ) <sup>1/2</sup> /Γ <sub>total</sub> in Nπ → N(2000) → ΛK	DOCUMENT ID	TECN	COMMENT	(Γ <sub>1</sub> Γ <sub>3</sub> ) <sup>1/2</sup> /Γ
not seen	SAXON 80	DPWA	π <sup>-</sup> p → ΛK <sup>0</sup>	

(Γ <sub>1</sub> Γ <sub>4</sub> ) <sup>1/2</sup> /Γ <sub>total</sub> in Nπ → N(2000) → ΣK	DOCUMENT ID	TECN	COMMENT	(Γ <sub>1</sub> Γ <sub>4</sub> ) <sup>1/2</sup> /Γ
0.022	<sup>2</sup> DEANS 75	DPWA	πN → ΣK	
0.05	<sup>1</sup> LANGBEIN 73	IPWA	πN → ΣK (sol. 2)	

(Γ <sub>1</sub> Γ <sub>5</sub> ) <sup>1/2</sup> /Γ <sub>total</sub> in pγ → N(2000) → ΛK	DOCUMENT ID	TECN	COMMENT	(Γ <sub>5</sub> Γ <sub>3</sub> ) <sup>1/2</sup> /Γ
0.0022	DEANS 72	MPWA	γp → ΛK (sol. D)	

**N(2000) PHOTON DECAY AMPLITUDES**

Papers on γN amplitudes predating 1981 may be found in our 2006 edition, Journal of Physics, G **33 1** (2006).

**N(2000) → pγ, helicity-1/2 amplitude A<sub>1/2</sub>**

VALUE (GeV <sup>-1/2</sup> )	DOCUMENT ID	TECN	COMMENT
0.035 ± 0.015	<sup>3</sup> ANISOVICH 12A	DPWA	Phase = (15 ± 40)°

**N(2000) → pγ, helicity-3/2 amplitude A<sub>3/2</sub>**

VALUE (GeV <sup>-1/2</sup> )	DOCUMENT ID	TECN	COMMENT
0.050 ± 0.014	<sup>3</sup> ANISOVICH 12A	DPWA	Phase = (-130 ± 40)°

**N(2000) FOOTNOTES**

- Not seen in solution 1 of LANGBEIN 73.
- Value given is from solution 1 of DEANS 75; not present in solutions 2, 3, or 4.
- This ANISOVICH 12A value is the complex helicity amplitude at the pole position.

**N(2000) REFERENCES**

ANISOVICH 12A	EPJ A48 15	A.V. Anisovich <i>et al.</i>	(BONN, PNPI)
PDG 06	JPG 33 1	W.-M. Yao <i>et al.</i>	(PDG Collab.)
ARNDT 04	PR C69 035213	R.A. Arndt <i>et al.</i>	(GWU, TRIU)
SAXON 80	NP B162 522	D.H. Saxon <i>et al.</i>	(RHEL, BRIS) IJP
BAKER 79	NP B156 93	R.D. Baker <i>et al.</i>	(RHEL) IJP
AYED 76	Thesis CEA-N-1921	R. Ayed	(SACL) IJP
DEANS 75	NP B96 90	S.R. Deans <i>et al.</i>	(SFLA, ALAH) IJP
LANGBEIN 73	NP B53 251	W. Langbein, F. Wagner	(MUNI) IJP
ALMEHED 72	NP B40 157	S. Almeded, C. Lovelace	(LUND, RUTG) IJP
DEANS 72	PR D6 1906	S.R. Deans <i>et al.</i>	(SFLA) IJP

## Baryon Particle Listings

 $N(2040), N(2060)$ 

$$N(2040) \ 3/2^+ \quad J^P = \frac{3}{2}^+ \quad \text{Status: } *$$

OMITTED FROM SUMMARY TABLE

 $N(2040)$  MASS

VALUE (MeV)	DOCUMENT ID	TECN	COMMENT
<b>2052<math>\pm</math>13<sub>21</sub> OUR AVERAGE</b>			
2040 $\pm$ 4 $\pm$ 25	ABLIKIM	09B	BES2 $J/\psi \rightarrow p\bar{p}\pi^0$
2068 $\pm$ 3 $\pm$ 15 <sub>40</sub>	ABLIKIM	06K	BES2 $J/\psi \rightarrow p\bar{p}\pi^-, n\bar{p}\pi^+$

 $N(2040)$  WIDTH

VALUE (MeV)	DOCUMENT ID	TECN	COMMENT
<b>191<math>\pm</math>33 OUR AVERAGE</b>			
230 $\pm$ 8 $\pm$ 52	ABLIKIM	09B	BES2 $J/\psi \rightarrow p\bar{p}\pi^0$
165 $\pm$ 14 $\pm$ 40	ABLIKIM	06K	BES2 $J/\psi \rightarrow p\bar{p}\pi^-, n\bar{p}\pi^+$

 $N(2040)$  REFERENCES

ABLIKIM	09B	PR D80 052004	M. Ablikim et al.	(BES2 Collab.)
ABLIKIM	06K	PRL 97 062001	M. Ablikim et al.	(BES2 Collab.)

$$N(2060) \ 5/2^- \quad I(J^P) = \frac{1}{2}(\frac{5}{2}^-) \quad \text{Status: } **$$

OMITTED FROM SUMMARY TABLE

Before our 2012 *Review*, this state appeared in our Listings as the  $N(2200)$ .

The latest GWU analysis (ARNDT 06) finds no evidence for this resonance.

 $N(2060)$  BREIT-WIGNER MASS

VALUE (MeV)	DOCUMENT ID	TECN	COMMENT
<b><math>\approx</math> 2060 OUR ESTIMATE</b>			
2060 $\pm$ 15	ANISOVICH	12A	DPWA Multichannel
1900	BELL	83	DPWA $\pi^-p \rightarrow \Lambda K^0$
2180 $\pm$ 80	CUTKOSKY	80	IPWA $\pi N \rightarrow \pi N$
1920	SAXON	80	DPWA $\pi^-p \rightarrow \Lambda K^0$
2228 $\pm$ 30	HOEHLER	79	IPWA $\pi N \rightarrow \pi N$
••• We do not use the following data for averages, fits, limits, etc. •••			
2217 $\pm$ 27	BATINIC	10	DPWA $\pi N \rightarrow N\pi, N\eta$

 $N(2060)$  BREIT-WIGNER WIDTH

VALUE (MeV)	DOCUMENT ID	TECN	COMMENT
375 $\pm$ 25	ANISOVICH	12A	DPWA Multichannel
130	BELL	83	DPWA $\pi^-p \rightarrow \Lambda K^0$
400 $\pm$ 100	CUTKOSKY	80	IPWA $\pi N \rightarrow \pi N$
220	SAXON	80	DPWA $\pi^-p \rightarrow \Lambda K^0$
310 $\pm$ 50	HOEHLER	79	IPWA $\pi N \rightarrow \pi N$
••• We do not use the following data for averages, fits, limits, etc. •••			
481 $\pm$ 17	BATINIC	10	DPWA $\pi N \rightarrow N\pi, N\eta$

 $N(2060)$  POLE POSITION

## REAL PART

VALUE (MeV)	DOCUMENT ID	TECN	COMMENT
2040 $\pm$ 15	ANISOVICH	12A	DPWA Multichannel
2100 $\pm$ 60	CUTKOSKY	80	IPWA $\pi N \rightarrow \pi N$
••• We do not use the following data for averages, fits, limits, etc. •••			
2144 $\pm$ 31	BATINIC	10	DPWA $\pi N \rightarrow N\pi, N\eta$

## -2xIMAGINARY PART

VALUE (MeV)	DOCUMENT ID	TECN	COMMENT
390 $\pm$ 25	ANISOVICH	12A	DPWA Multichannel
360 $\pm$ 80	CUTKOSKY	80	IPWA $\pi N \rightarrow \pi N$
••• We do not use the following data for averages, fits, limits, etc. •••			
438 $\pm$ 13	BATINIC	10	DPWA $\pi N \rightarrow N\pi, N\eta$

 $N(2060)$  ELASTIC POLE RESIDUEMODULUS  $|r|$ 

VALUE (MeV)	DOCUMENT ID	TECN	COMMENT
19 $\pm$ 5	ANISOVICH	12A	DPWA Multichannel
20 $\pm$ 10	CUTKOSKY	80	IPWA $\pi N \rightarrow \pi N$
••• We do not use the following data for averages, fits, limits, etc. •••			
26	BATINIC	10	DPWA $\pi N \rightarrow N\pi, N\eta$

PHASE  $\theta$ 

VALUE ( $^\circ$ )	DOCUMENT ID	TECN	COMMENT
-125 $\pm$ 20	ANISOVICH	12A	DPWA Multichannel
-90 $\pm$ 50	CUTKOSKY	80	IPWA $\pi N \rightarrow \pi N$
••• We do not use the following data for averages, fits, limits, etc. •••			
-71	BATINIC	10	DPWA $\pi N \rightarrow N\pi, N\eta$

 $N(2060)$  INELASTIC POLE RESIDUE

The "normalized residue" is the residue divided by  $\Gamma_{pole}$ .

Normalized residue in  $N\pi \rightarrow N(2060) \rightarrow N\eta$ 

MODULUS (%)	PHASE ( $^\circ$ )	DOCUMENT ID	TECN	COMMENT
5 $\pm$ 3	40 $\pm$ 25	ANISOVICH	12A	DPWA Multichannel

Normalized residue in  $N\pi \rightarrow N(2060) \rightarrow \Lambda K$ 

MODULUS (%)	DOCUMENT ID	TECN	COMMENT
1 $\pm$ 0.5	ANISOVICH	12A	DPWA Multichannel

Normalized residue in  $N\pi \rightarrow N(2060) \rightarrow \Sigma K$ 

MODULUS (%)	PHASE ( $^\circ$ )	DOCUMENT ID	TECN	COMMENT
4 $\pm$ 2	-70 $\pm$ 30	ANISOVICH	12A	DPWA Multichannel

 $N(2060)$  DECAY MODES

Mode
$\Gamma_1$ $N\pi$
$\Gamma_2$ $N\eta$
$\Gamma_3$ $\Lambda K$
$\Gamma_4$ $\Sigma K$

 $N(2060)$  BRANCHING RATIOS

$\Gamma(N\pi)/\Gamma_{total}$	DOCUMENT ID	TECN	COMMENT	$\Gamma_1/\Gamma$
8 $\pm$ 2	ANISOVICH	12A	DPWA Multichannel	
10 $\pm$ 3	CUTKOSKY	80	IPWA $\pi N \rightarrow \pi N$	
7 $\pm$ 2	HOEHLER	79	IPWA $\pi N \rightarrow \pi N$	
••• We do not use the following data for averages, fits, limits, etc. •••				
13 $\pm$ 4	BATINIC	10	DPWA $\pi N \rightarrow N\pi, N\eta$	

$\Gamma(N\eta)/\Gamma_{total}$	DOCUMENT ID	TECN	COMMENT	$\Gamma_2/\Gamma$
4 $\pm$ 2	ANISOVICH	12A	DPWA Multichannel	
••• We do not use the following data for averages, fits, limits, etc. •••				
0.2 $\pm$ 1.0	BATINIC	10	DPWA $\pi N \rightarrow N\pi, N\eta$	

$(\Gamma_1\Gamma_2)^{1/2}/\Gamma_{total}$ in $N\pi \rightarrow N(2060) \rightarrow N\eta$	DOCUMENT ID	TECN	COMMENT	$(\Gamma_1\Gamma_2)^{1/2}/\Gamma$
0.066	BAKER	79	DPWA $\pi^-p \rightarrow n\eta$	

$(\Gamma_1\Gamma_3)^{1/2}/\Gamma_{total}$ in $N\pi \rightarrow N(2060) \rightarrow \Lambda K$	DOCUMENT ID	TECN	COMMENT	$(\Gamma_1\Gamma_3)^{1/2}/\Gamma$
-0.03	BELL	83	DPWA $\pi^-p \rightarrow \Lambda K^0$	
-0.05	SAXON	80	DPWA $\pi^-p \rightarrow \Lambda K^0$	

$\Gamma(\Sigma K)/\Gamma_{total}$	DOCUMENT ID	TECN	COMMENT	$\Gamma_4/\Gamma$
3 $\pm$ 2	ANISOVICH	12A	DPWA Multichannel	

 $N(2060)$  PHOTON DECAY AMPLITUDES

Papers on  $\gamma N$  amplitudes predating 1981 may be found in our 2006 edition, *Journal of Physics, G* **33** 1 (2006).

 $N(2060) \rightarrow p\gamma$ , helicity-1/2 amplitude  $A_{1/2}$ 

VALUE ( $\text{GeV}^{-1/2}$ )	DOCUMENT ID	TECN	COMMENT
0.065 $\pm$ 0.012	<sup>1</sup> ANISOVICH	12A	DPWA Phase = (15 $\pm$ 8) $^\circ$

 $N(2060) \rightarrow p\gamma$ , helicity-3/2 amplitude  $A_{3/2}$ 

VALUE ( $\text{GeV}^{-1/2}$ )	DOCUMENT ID	TECN	COMMENT
0.055 $\pm$ 15 <sub>-35</sub>	<sup>1</sup> ANISOVICH	12A	DPWA Phase = (15 $\pm$ 10) $^\circ$

 $N(2060)$  FOOTNOTES

<sup>1</sup> This ANISOVICH 12A value is the complex helicity amplitude at the pole position.



**$N(2060)$  REFERENCES**

ANISOVICH	12A	EPJ A40 15	A.V. Anisovich et al.	(BONN, PNPI)
BATINIC	10	PR C82 038203	M. Batinic et al.	(ZAGR)
ARNDT	06	PR C74 045205	R.A. Arndt et al.	(GWU)
PDG	06	JPG 33 1	W.-M. Yao et al.	(PDG Collab.)
BELL	83	NP B222 389	K.W. Bell et al.	(RL) IJP
CUTKOSKY	80	Toronto Conf. 19	R.E. Cutkosky et al.	(CMU, LBL) IJP
Also		PR D20 2839	R.E. Cutkosky et al.	(CMU, LBL)
SAXON	80	NP B162 522	D.H. Saxon et al.	(RHEL, BRIS) IJP
BAKER	79	NP B156 93	R.D. Baker et al.	(RHEL) IJP
HOEHLER	79	PDAT 12-1	G. Hoehler et al.	(KARLT) IJP
Also		Toronto Conf. 3	R. Koch	(KARLT) IJP

**$N(2100)$  DECAY MODES**

Mode	Fraction ( $\Gamma_i/\Gamma$ )
$\Gamma_1$ $N\pi$	(61±60) %
$\Gamma_2$ $N\eta$	
$\Gamma_3$ $\Lambda K$	
$\Gamma_4$ $N\pi\pi$	
$\Gamma_5$ $\Delta(1232)\pi$ , $P$ -wave	
$\Gamma_6$ $N\rho$ , $S=1/2$ , $P$ -wave	
$\Gamma_7$ $N(\pi\pi)_{S=0}^{J=0}$ $S$ -wave	

**$N(2100) 1/2^+$**

$I(J^P) = \frac{1}{2}(\frac{1}{2}^+)$  Status: \*

OMITTED FROM SUMMARY TABLE

The latest GWU analysis (ARNDT 06) finds no evidence for this resonance.

**$N(2100)$  BRANCHING RATIOS**

$\Gamma(N\pi)/\Gamma_{total}$	$\Gamma_1/\Gamma$		
VALUE (%)	DOCUMENT ID	TECN	COMMENT
12±3	CUTKOSKY	80	IPWA $\pi N \rightarrow \pi N$
10±4	HOEHLER	79	IPWA $\pi N \rightarrow \pi N$
••• We do not use the following data for averages, fits, limits, etc. •••			
16±5	BATINIC	10	DPWA $\pi N \rightarrow N\pi, N\eta$
2±5	VRANA	00	DPWA Multichannel

$\Gamma(N\eta)/\Gamma_{total}$	$\Gamma_2/\Gamma$		
VALUE (%)	DOCUMENT ID	TECN	COMMENT
61±61	VRANA	00	DPWA Multichannel
••• We do not use the following data for averages, fits, limits, etc. •••			
83±5	BATINIC	10	DPWA $\pi N \rightarrow N\pi, N\eta$

$\Gamma(\Lambda K)/\Gamma_{total}$	$\Gamma_3/\Gamma$		
VALUE (%)	DOCUMENT ID	TECN	COMMENT
21±20	VRANA	00	DPWA Multichannel

$(\Gamma_1\Gamma_7)^{1/2}/\Gamma_{total}$  in  $N\pi \rightarrow N(2100) \rightarrow \Delta(1232)\pi$ ,  $P$ -wave  $(\Gamma_1\Gamma_5)^{1/2}/\Gamma$

$\Gamma(\Delta(1232)\pi, P\text{-wave})/\Gamma_{total}$	$\Gamma_5/\Gamma$		
VALUE (%)	DOCUMENT ID	TECN	COMMENT
2±1	VRANA	00	DPWA Multichannel

$\Gamma(N\rho, S=1/2, P\text{-wave})/\Gamma_{total}$	$\Gamma_6/\Gamma$		
VALUE (%)	DOCUMENT ID	TECN	COMMENT
4±1	VRANA	00	DPWA Multichannel

$\Gamma(N(\pi\pi)_{S=0}^{J=0})/\Gamma_{total}$	$\Gamma_7/\Gamma$		
VALUE (%)	DOCUMENT ID	TECN	COMMENT
10±1	VRANA	00	DPWA Multichannel

**$N(2100)$  REFERENCES**

BATINIC	10	PR C82 038203	M. Batinic et al.	(ZAGR)
ABLKIM	06K	PRL 97 062001	M. Ablikim et al.	(BES2 Collab.)
ARNDT	06	PR C74 045205	R.A. Arndt et al.	(GWU)
VRANA	00	PRPL 328 181	T.P. Vrana, S.A. Dytman, T.-S.H. Lee	(PITT+)
PLOETZKE	98	PL B444 555	R. Ploetzke et al.	(Bonn SAPHIR Collab.)
ARNDT	91	PR D43 2131	R.A. Arndt et al.	(VPI, TELE) IJP
CUTKOSKY	80	Toronto Conf. 19	R.E. Cutkosky et al.	(CMU, LBL) IJP
Also		PR D20 2839	R.E. Cutkosky et al.	(CMU, LBL)
HOEHLER	79	PDAT 12-1	G. Hoehler et al.	(KARLT) IJP
Also		Toronto Conf. 3	R. Koch	(KARLT) IJP

**$N(2120) 3/2^-$**

$I(J^P) = \frac{1}{2}(\frac{3}{2}^-)$  Status: \*\*

OMITTED FROM SUMMARY TABLE

Before the 2012 Review, all the evidence for a  $J^P = 3/2^-$  state with a mass above 1800 MeV was filed under a two-star  $N(2080)$ .

There is now evidence from ANISOVICH 12A for two  $3/2^-$  states in this region, so we have split the older data (according to mass) between a three-star  $N(1875)$  and a two-star  $N(2120)$ .

**$N(2120)$  BREIT-WIGNER MASS**

VALUE (MeV)	DOCUMENT ID	TECN	COMMENT
<b>2120 OUR ESTIMATE</b>			
2150±60	ANISOVICH	12A	DPWA Multichannel
2060±80	CUTKOSKY	80	IPWA $\pi N \rightarrow \pi N$
2081±20	HOEHLER	79	IPWA $\pi N \rightarrow \pi N$

**$N(2120)$  BREIT-WIGNER WIDTH**

VALUE (MeV)	DOCUMENT ID	TECN	COMMENT
330±45	ANISOVICH	12A	DPWA Multichannel
300±100	CUTKOSKY	80	IPWA $\pi N \rightarrow \pi N$ (higher $m$ )
265±40	HOEHLER	79	IPWA $\pi N \rightarrow \pi N$

**$N(2100)$  BREIT-WIGNER MASS**

VALUE (MeV)	DOCUMENT ID	TECN	COMMENT
<b>≈ 2100 OUR ESTIMATE</b>			
2125±75	CUTKOSKY	80	IPWA $\pi N \rightarrow \pi N$
2050±20	HOEHLER	79	IPWA $\pi N \rightarrow \pi N$
••• We do not use the following data for averages, fits, limits, etc. •••			
2157±42	BATINIC	10	DPWA $\pi N \rightarrow N\pi, N\eta$
2068±3 <sup>+15</sup> <sub>-40</sub>	ABLKIM	06K	BES2 $J/\psi \rightarrow (p\pi^-)\bar{p}$
2084±93	VRANA	00	DPWA Multichannel
1986±26 <sup>+10</sup> <sub>-30</sub>	PLOETZKE	98	SPEC $\gamma p \rightarrow p\eta$ (958)

**$N(2100)$  BREIT-WIGNER WIDTH**

VALUE (MeV)	DOCUMENT ID	TECN	COMMENT
260±100	CUTKOSKY	80	IPWA $\pi N \rightarrow \pi N$
200±30	HOEHLER	79	IPWA $\pi N \rightarrow \pi N$
••• We do not use the following data for averages, fits, limits, etc. •••			
355±88	BATINIC	10	DPWA $\pi N \rightarrow N\pi, N\eta$
165±14±40	ABLKIM	06K	BES2 $J/\psi \rightarrow (p\pi^-)\bar{p}$
1077±643	VRANA	00	DPWA Multichannel
296±100 <sup>+60</sup> <sub>-10</sub>	PLOETZKE	98	SPEC $\gamma p \rightarrow p\eta$ (958)

**$N(2100)$  POLE POSITION**

**REAL PART**

VALUE (MeV)	DOCUMENT ID	TECN	COMMENT
2120±40	CUTKOSKY	80	IPWA $\pi N \rightarrow \pi N$
••• We do not use the following data for averages, fits, limits, etc. •••			
2120±47	BATINIC	10	DPWA $\pi N \rightarrow N\pi, N\eta$
1810	VRANA	00	DPWA Multichannel
not seen	ARNDT	91	DPWA $\pi N \rightarrow \pi N$ Soln SM90

**-2xIMAGINARY PART**

VALUE (MeV)	DOCUMENT ID	TECN	COMMENT
240±80	CUTKOSKY	80	IPWA $\pi N \rightarrow \pi N$
••• We do not use the following data for averages, fits, limits, etc. •••			
346±80	BATINIC	10	DPWA $\pi N \rightarrow N\pi, N\eta$
622	VRANA	00	DPWA Multichannel
not seen	ARNDT	91	DPWA $\pi N \rightarrow \pi N$ Soln SM90

**$N(2100)$  ELASTIC POLE RESIDUE**

**MODULUS  $|r|$**

VALUE (MeV)	DOCUMENT ID	TECN	COMMENT
14±7	CUTKOSKY	80	IPWA $\pi N \rightarrow \pi N$
••• We do not use the following data for averages, fits, limits, etc. •••			
33	BATINIC	10	DPWA $\pi N \rightarrow N\pi, N\eta$

**PHASE  $\theta$**

VALUE (°)	DOCUMENT ID	TECN	COMMENT
35±25	CUTKOSKY	80	IPWA $\pi N \rightarrow \pi N$
••• We do not use the following data for averages, fits, limits, etc. •••			
-59	BATINIC	10	DPWA $\pi N \rightarrow N\pi, N\eta$

## Baryon Particle Listings

 $N(2120)$ ,  $N(2190)$  $N(2120)$  POLE POSITION

## REAL PART

VALUE (MeV)	DOCUMENT ID	TECN	COMMENT
2110 ± 50	ANISOVICH 12A	DPWA	Multichannel
2050 ± 70	CUTKOSKY 80	IPWA	$\pi N \rightarrow \pi N$ (higher $m$ )

## -2×IMAGINARY PART

VALUE (MeV)	DOCUMENT ID	TECN	COMMENT
340 ± 45	ANISOVICH 12A	DPWA	Multichannel
200 ± 80	CUTKOSKY 80	IPWA	$\pi N \rightarrow \pi N$ (higher $m$ )

 $N(2120)$  ELASTIC POLE RESIDUEMODULUS  $|r|$ 

VALUE (MeV)	DOCUMENT ID	TECN	COMMENT
13 ± 3	ANISOVICH 12A	DPWA	Multichannel
30 ± 20	CUTKOSKY 80	IPWA	$\pi N \rightarrow \pi N$ (higher $m$ )

PHASE  $\theta$ 

VALUE (°)	DOCUMENT ID	TECN	COMMENT
-20 ± 10	ANISOVICH 12A	DPWA	Multichannel
0 ± 100	CUTKOSKY 80	IPWA	$\pi N \rightarrow \pi N$ (higher $m$ )

 $N(2120)$  INELASTIC POLE RESIDUE

The "normalized residue" is the residue divided by  $\Gamma_{pole}$ .

Normalized residue in  $N\pi \rightarrow N(2120) \rightarrow \Lambda K$ 

MODULUS (%)	PHASE (°)	DOCUMENT ID	TECN	COMMENT
3 ± 1	100 ± 30	ANISOVICH 12A	DPWA	Multichannel

Normalized residue in  $N\pi \rightarrow N(2120) \rightarrow \Sigma K$ 

MODULUS (%)	PHASE (°)	DOCUMENT ID	TECN	COMMENT
2 ± 1.5	-50 ± 40	ANISOVICH 12A	DPWA	Multichannel

 $N(2120)$  DECAY MODES

Mode	$\Gamma_1$	$N\pi$
	$\Gamma_1$	$N\pi$

 $N(2120)$  BRANCHING RATIOS

$\Gamma(N\pi)/\Gamma_{total}$	DOCUMENT ID	TECN	COMMENT	$\Gamma_1/\Gamma$
6 ± 2	ANISOVICH 12A	DPWA	Multichannel	
14 ± 7	CUTKOSKY 80	IPWA	$\pi N \rightarrow \pi N$ (higher $m$ )	
6 ± 2	HOEHLER 79	IPWA	$\pi N \rightarrow \pi N$	

 $N(2120)$  PHOTON DECAY AMPLITUDES $N(2120) \rightarrow p\gamma$ , helicity-1/2 amplitude  $A_{1/2}$ 

VALUE	DOCUMENT ID	TECN	COMMENT
0.125 ± 0.045	<sup>2</sup> ANISOVICH 12A	DPWA	Phase = (-55 ± 20)°

 $N(2120) \rightarrow p\gamma$ , helicity-3/2 amplitude  $A_{3/2}$ 

VALUE	DOCUMENT ID	TECN	COMMENT
0.150 ± 0.060	<sup>2</sup> ANISOVICH 12A	DPWA	Phase = (-35 ± 15)°

 $N(2120)$  FOOTNOTES

- <sup>1</sup> CUTKOSKY 80 finds a lower mass  $D_{13}$  resonance, as well as one in this region. Both are listed here.  
<sup>2</sup> This ANISOVICH 12A value is the complex helicity amplitude at the pole position.

 $N(2120)$  REFERENCES

ANISOVICH 12A	EPJ A48 15	A.V. Anisovich et al.	(BONN, PNPI)
CUTKOSKY 80	Toronto Conf. 19	R.E. Cutkosky et al.	(CMU, LBL)
HOEHLER 79	PDAT 12-1	G. Hohler et al.	(KARLT)

 $N(2190) 7/2^-$ 

$$I(J^P) = \frac{1}{2}(7/2^-) \text{ Status: } ***$$

Most of the results published before 1975 were last included in our 1982 edition, Physics Letters **111B** 1 (1982). Some further obsolete results published before 1984 were last included in our 2006 edition, Journal of Physics, G **33** 1 (2006).

 $N(2190)$  BREIT-WIGNER MASS

## VALUE (MeV)

DOCUMENT ID	TECN	COMMENT
<b>2100 to 2200 (≈ 2190) OUR ESTIMATE</b>		
2180 ± 20	ANISOVICH 12A	DPWA Multichannel
2152.4 ± 1.4	ARNDT 06	DPWA $\pi N \rightarrow \pi N, \eta N$
2127 ± 9	MANLEY 92	IPWA $\pi N \rightarrow \pi N \& N\pi\pi$
2200 ± 70	CUTKOSKY 80	IPWA $\pi N \rightarrow \pi N$
2140 ± 12	HOEHLER 79	IPWA $\pi N \rightarrow \pi N$
2140 ± 40	HENDRY 78	MPWA $\pi N \rightarrow \pi N$
••• We do not use the following data for averages, fits, limits, etc. •••		
2125 ± 61	BATINIC 10	DPWA $\pi N \rightarrow N\pi, N\eta$
2192.1 ± 8.7	ARNDT 04	DPWA $\pi N \rightarrow \pi N, \eta N$
2168 ± 18	VRANA 00	DPWA Multichannel
2131	ARNDT 95	DPWA $\pi N \rightarrow N\pi$
2180	SAXON 80	DPWA $\pi^- p \rightarrow \Lambda K^0$

 $N(2190)$  BREIT-WIGNER WIDTH

## VALUE (MeV)

DOCUMENT ID	TECN	COMMENT
<b>300 to 700 (≈ 500) OUR ESTIMATE</b>		
335 ± 40	ANISOVICH 12A	DPWA Multichannel
484 ± 13	ARNDT 06	DPWA $\pi N \rightarrow \pi N, \eta N$
550 ± 50	MANLEY 92	IPWA $\pi N \rightarrow \pi N \& N\pi\pi$
500 ± 150	CUTKOSKY 80	IPWA $\pi N \rightarrow \pi N$
390 ± 30	HOEHLER 79	IPWA $\pi N \rightarrow \pi N$
270 ± 50	HENDRY 78	MPWA $\pi N \rightarrow \pi N$
••• We do not use the following data for averages, fits, limits, etc. •••		
381 ± 160	BATINIC 10	DPWA $\pi N \rightarrow N\pi, N\eta$
726 ± 62	ARNDT 04	DPWA $\pi N \rightarrow \pi N, \eta N$
453 ± 101	VRANA 00	DPWA Multichannel
476	ARNDT 95	DPWA $\pi N \rightarrow N\pi$
80	SAXON 80	DPWA $\pi^- p \rightarrow \Lambda K^0$

 $N(2190)$  POLE POSITION

## REAL PART

VALUE (MeV)	DOCUMENT ID	TECN	COMMENT
<b>2050 to 2100 (≈ 2075) OUR ESTIMATE</b>			
2150 ± 25	ANISOVICH 12A	DPWA	Multichannel
2070	ARNDT 06	DPWA	$\pi N \rightarrow \pi N, \eta N$
2042	<sup>1</sup> HOEHLER 93	SPED	$\pi N \rightarrow \pi N$
2100 ± 50	CUTKOSKY 80	IPWA	$\pi N \rightarrow \pi N$
••• We do not use the following data for averages, fits, limits, etc. •••			
2063 ± 32	BATINIC 10	DPWA	$\pi N \rightarrow N\pi, N\eta$
2076	ARNDT 04	DPWA	$\pi N \rightarrow \pi N, \eta N$
2107	VRANA 00	DPWA	Multichannel
2030	ARNDT 95	DPWA	$\pi N \rightarrow N\pi$
2060	ARNDT 91	DPWA	$\pi N \rightarrow \pi N$ Soln SM90

## -2×IMAGINARY PART

VALUE (MeV)	DOCUMENT ID	TECN	COMMENT
<b>400 to 520 (≈ 450) OUR ESTIMATE</b>			
330 ± 30	ANISOVICH 12A	DPWA	Multichannel
520	ARNDT 06	DPWA	$\pi N \rightarrow \pi N, \eta N$
482	<sup>1</sup> HOEHLER 93	SPED	$\pi N \rightarrow \pi N$
400 ± 160	CUTKOSKY 80	IPWA	$\pi N \rightarrow \pi N$
••• We do not use the following data for averages, fits, limits, etc. •••			
330 ± 101	BATINIC 10	DPWA	$\pi N \rightarrow N\pi, N\eta$
502	ARNDT 04	DPWA	$\pi N \rightarrow \pi N, \eta N$
380	VRANA 00	DPWA	Multichannel
460	ARNDT 95	DPWA	$\pi N \rightarrow N\pi$
464	ARNDT 91	DPWA	$\pi N \rightarrow \pi N$ Soln SM90

 $N(2190)$  ELASTIC POLE RESIDUEMODULUS  $|r|$ 

VALUE (MeV)	DOCUMENT ID	TECN	COMMENT
30 ± 5	ANISOVICH 12A	DPWA	Multichannel
72	ARNDT 06	DPWA	$\pi N \rightarrow \pi N, \eta N$
45	HOEHLER 93	SPED	$\pi N \rightarrow \pi N$
25 ± 10	CUTKOSKY 80	IPWA	$\pi N \rightarrow \pi N$
••• We do not use the following data for averages, fits, limits, etc. •••			
34	BATINIC 10	DPWA	$\pi N \rightarrow N\pi, N\eta$
68	ARNDT 04	DPWA	$\pi N \rightarrow \pi N, \eta N$
46	ARNDT 95	DPWA	$\pi N \rightarrow N\pi$
54	ARNDT 91	DPWA	$\pi N \rightarrow \pi N$ Soln SM90

Baryon Particle Listings  
N(2190), N(2220)

PHASE  $\theta$

VALUE (°)	DOCUMENT ID	TECN	COMMENT
30 ± 10	ANISOVICH 12A	DPWA	Multichannel
-32	ARNDT 06	DPWA	$\pi N \rightarrow \pi N, \eta N$
-30 ± 50	CUTKOSKY 80	IPWA	$\pi N \rightarrow \pi N$
• • • We do not use the following data for averages, fits, limits, etc. • • •			
-19	BATINIC 10	DPWA	$\pi N \rightarrow N\pi, N\eta$
-32	ARNDT 04	DPWA	$\pi N \rightarrow \pi N, \eta N$
-23	ARNDT 95	DPWA	$\pi N \rightarrow N\pi$
-44	ARNDT 91	DPWA	$\pi N \rightarrow \pi N$ Soln SM90

N(2190) INELASTIC POLE RESIDUE

The "normalized residue" is the residue divided by  $\Gamma_{pole}$ .

Normalized residue in  $N\pi \rightarrow N(2190) \rightarrow \Lambda K$

MODULUS (%)	PHASE (°)	DOCUMENT ID	TECN	COMMENT
3 ± 1	20 ± 15	ANISOVICH 12A	DPWA	Multichannel

N(2190) DECAY MODES

The following branching fractions are our estimates, not fits or averages.

Mode	Fraction ( $\Gamma_i/\Gamma$ )
$\Gamma_1$ $N\pi$	10-20 %
$\Gamma_2$ $N\eta$	(0.0 ± 1.0) %
$\Gamma_3$ $N\omega$	seen
$\Gamma_4$ $\Lambda K$	seen
$\Gamma_5$ $\Sigma K$	
$\Gamma_6$ $N\pi\pi$	seen
$\Gamma_7$ $N\rho$	seen
$\Gamma_8$ $p\gamma$	0.02-0.06 %
$\Gamma_9$ $p\gamma$ , helicity=1/2	0.02-0.04 %
$\Gamma_{10}$ $p\gamma$ , helicity=3/2	0.002-0.02 %

N(2190) BRANCHING RATIOS

$\Gamma(N\pi)/\Gamma_{total}$	DOCUMENT ID	TECN	COMMENT	$\Gamma_1/\Gamma$
VALUE (%)				
<b>10 to 20 OUR ESTIMATE</b>				
16 ± 2	ANISOVICH 12A	DPWA	Multichannel	
23.8 ± 0.1	ARNDT 06	DPWA	$\pi N \rightarrow \pi N, \eta N$	
22 ± 1	MANLEY 92	IPWA	$\pi N \rightarrow \pi N \& N\pi\pi$	
12 ± 6	CUTKOSKY 80	IPWA	$\pi N \rightarrow \pi N$	
14 ± 2	HOEHLER 79	IPWA	$\pi N \rightarrow \pi N$	
16 ± 4	HENDRY 78	MPWA	$\pi N \rightarrow \pi N$	
• • • We do not use the following data for averages, fits, limits, etc. • • •				
18 ± 12	BATINIC 10	DPWA	$\pi N \rightarrow N\pi, N\eta$	
23.0 ± 0.2	ARNDT 04	DPWA	$\pi N \rightarrow \pi N, \eta N$	
20 ± 4	VRANA 00	DPWA	Multichannel	
23	ARNDT 95	DPWA	$\pi N \rightarrow \pi N$	

$\Gamma(N\eta)/\Gamma_{total}$	DOCUMENT ID	TECN	COMMENT	$\Gamma_2/\Gamma$
VALUE (%)				
<b>0 ± 1</b>	VRANA 00	DPWA	Multichannel	
• • • We do not use the following data for averages, fits, limits, etc. • • •				
0.1 ± 0.3	BATINIC 10	DPWA	$\pi N \rightarrow N\pi, N\eta$	

$\Gamma(N\omega)/\Gamma_{total}$	DOCUMENT ID	TECN	COMMENT	$\Gamma_3/\Gamma$
VALUE (%)				
seen	WILLIAMS 09	IPWA	$\gamma p \rightarrow p\omega$	

$\Gamma(\Lambda K)/\Gamma_{total}$	DOCUMENT ID	TECN	COMMENT	$\Gamma_4/\Gamma$
VALUE (%)				
<b>0.5 ± 0.3</b>	ANISOVICH 12A	DPWA	Multichannel	

$(\Gamma_i\Gamma_f)^{1/2}/\Gamma_{total}$ in $N\pi \rightarrow N(2190) \rightarrow \Lambda K$	DOCUMENT ID	TECN	COMMENT	$(\Gamma_1\Gamma_4)^{1/2}/\Gamma$
VALUE				
-0.02	BELL 83	DPWA	$\pi^- p \rightarrow \Lambda K^0$	
-0.02	SAXON 80	DPWA	$\pi^- p \rightarrow \Lambda K^0$	

$(\Gamma_i\Gamma_f)^{1/2}/\Gamma_{total}$ in $N\pi \rightarrow N(2190) \rightarrow N\rho, S=3/2, D\text{-wave}$	DOCUMENT ID	TECN	COMMENT	$(\Gamma_1\Gamma_0)^{1/2}/\Gamma$
VALUE				
-0.25 ± 0.03	MANLEY 92	IPWA	$\pi N \rightarrow \pi N \& N\pi\pi$	

$\Gamma(N\rho, S=3/2, D\text{-wave})/\Gamma_{total}$	DOCUMENT ID	TECN	COMMENT	$\Gamma_0/\Gamma$
VALUE (%)				
29 ± 28	VRANA 00	DPWA	Multichannel	

N(2190) PHOTON DECAY AMPLITUDES

Papers on  $\gamma N$  amplitudes predating 1981 may be found in our 2006 edition, Journal of Physics, G **33** 1 (2006).

N(2190)  $\rightarrow p\gamma$ , helicity-1/2 amplitude  $A_{1/2}$

VALUE (GeV <sup>-1/2</sup> )	DOCUMENT ID	TECN	COMMENT
-0.065 ± 0.008	ANISOVICH 12A	DPWA	Multichannel

N(2190)  $\rightarrow p\gamma$ , helicity-3/2 amplitude  $A_{3/2}$

VALUE (GeV <sup>-1/2</sup> )	DOCUMENT ID	TECN	COMMENT
0.035 ± 0.017	ANISOVICH 12A	DPWA	Multichannel

N(2190)  $\rightarrow p\gamma$ , ratio of helicity amplitudes  $A_{3/2}/A_{1/2}$

VALUE	DOCUMENT ID	TECN	COMMENT
-0.17 ± 0.15	WILLIAMS 09	IPWA	$\gamma p \rightarrow p\omega$

N(2190)  $\gamma p \rightarrow \Lambda K^+$  AMPLITUDES

$(\Gamma_i\Gamma_f)^{1/2}/\Gamma_{total}$  in  $p\gamma \rightarrow N(2190) \rightarrow \Lambda K^+$  ( $E_{4-}$  amplitude)

VALUE (units 10 <sup>-3</sup> )	DOCUMENT ID	TECN
2.5 ± 1.0	WORKMAN 90	DPWA
2.04	TANABE 89	DPWA

$p\gamma \rightarrow N(2190) \rightarrow \Lambda K^+$  phase angle  $\theta$  ( $E_{4-}$  amplitude)

VALUE (degrees)	DOCUMENT ID	TECN
-4 ± 9	WORKMAN 90	DPWA
-27.5	TANABE 89	DPWA

$(\Gamma_i\Gamma_f)^{1/2}/\Gamma_{total}$  in  $p\gamma \rightarrow N(2190) \rightarrow \Lambda K^+$  ( $M_{4-}$  amplitude)

VALUE (units 10 <sup>-3</sup> )	DOCUMENT ID	TECN
-7.0 ± 0.7	WORKMAN 90	DPWA
-5.78	TANABE 89	DPWA

N(2190) FOOTNOTES

<sup>1</sup> See HOEHLER 93 for a detailed discussion of the evidence for and the pole parameters of  $N$  and  $\Delta$  resonances as determined from Argand diagrams of  $\pi N$  elastic partial-wave amplitudes and from plots of the speeds with which the amplitudes traverse the diagrams.

N(2190) REFERENCES

For early references, see Physics Letters **111B** 1 (1982).

ANISOVICH 12A	EPJ A48 15	A.V. Anisovich et al.	(BONN, PNPI)
BATINIC 10	PR C82 038203	M. Batinić et al.	(ZAGR)
WILLIAMS 09	PR C80 065209	M. Williams et al.	(CEBAF CLAS Collab.)
ARNDT 06	PR C74 045205	R.A. Arndt et al.	(GWU)
PDG 06	JPG 33 1	W.-M. Yao et al.	(PDG Collab.)
ARNDT 04	PR C69 035213	R.A. Arndt et al.	(GWU, TRIU)
VRANA 00	PRPL 328 181	T.P. Vrana, S.A. Dytman, T.-S.H. Lee	(PITT+)
ARNDT 95	PR C52 2120	R.A. Arndt et al.	(VPI, BRCO)
HOEHLER 93	$\pi N$ Newsletter 9 1	G. Høhler	(KARL)
MANLEY 92	PR D45 4002	D.M. Manley, E.M. Saleski	(KENT) IJP
Also	PR D30 904	D.M. Manley et al.	(VPI)
ARNDT 91	PR D43 2131	R.A. Arndt et al.	(VPI, TELE) IJP
WORKMAN 90	PR C42 781	R.L. Workman	(VPI)
TANABE 89	PR C39 741	H. Tanabe, M. Kohno, C. Bennhold	(MANZ)
Also	NC 102A 193	M. Kohno, H. Tanabe, C. Bennhold	(MANZ)
BELL 83	NP B222 389	K.W. Bell et al.	(RL) IJP
PDG 82	PL 111B 1	M. Roos et al.	(HELS, CIT, CERN)
CUTKOSKY 80	Toronto Conf. 19	R.E. Cutkosky et al.	(CMU, LBL) IJP
Also	PR D20 2839	R.E. Cutkosky et al.	(CMU, LBL) IJP
SAXON 80	NP B162 522	D.H. Saxon et al.	(RHEL, BRIS) IJP
HOEHLER 79	PDAT 12-1	G. Høhler et al.	(KARLT) IJP
Also	Toronto Conf. 3	R. Koch	(KARLT) IJP
HENDRY 78	PRL 41 222	A.W. Hendry	(IND, LBL) IJP
Also	ANP 136 1	A.W. Hendry	(IND)

**N(2220) 9/2<sup>+</sup>**

$I(J^P) = \frac{1}{2}(9^+)$  Status: \*\*\*

Most of the results published before 1975 were last included in our 1982 edition, Physics Letters **111B** 1 (1982). Some further obsolete results published before 1980 were last included in our 2006 edition, Journal of Physics, G **33** 1 (2006).

N(2220) BREIT-WIGNER MASS

VALUE (MeV)	DOCUMENT ID	TECN	COMMENT
<b>2200 to 2300 (≈ 2250) OUR ESTIMATE</b>			
2316.3 ± 2.9	ARNDT 06	DPWA	$\pi N \rightarrow \pi N, \eta N$
2230 ± 80	CUTKOSKY 80	IPWA	$\pi N \rightarrow \pi N$
2205 ± 10	HOEHLER 79	IPWA	$\pi N \rightarrow \pi N$
2300 ± 100	HENDRY 78	MPWA	$\pi N \rightarrow \pi N$
• • • We do not use the following data for averages, fits, limits, etc. • • •			

# Baryon Particle Listings

## $N(2220)$ , $N(2250)$

2270 ± 11	ARNDT	04	DPWA	$\pi N \rightarrow \pi N, \eta N$
2258	ARNDT	95	DPWA	$\pi N \rightarrow N\pi$

### $N(2220)$ BREIT-WIGNER WIDTH

VALUE (MeV)	DOCUMENT ID	TECN	COMMENT
<b>350 to 500 (≈ 400) OUR ESTIMATE</b>			
633 ± 17	ARNDT	06	DPWA $\pi N \rightarrow \pi N, \eta N$
500 ± 150	CUTKOSKY	80	IPWA $\pi N \rightarrow \pi N$
365 ± 30	HOEHLER	79	IPWA $\pi N \rightarrow \pi N$
450 ± 150	HENDRY	78	MPWA $\pi N \rightarrow \pi N$
• • • We do not use the following data for averages, fits, limits, etc. • • •			
366 ± 42	ARNDT	04	DPWA $\pi N \rightarrow \pi N, \eta N$
334	ARNDT	95	DPWA $\pi N \rightarrow N\pi$

### $N(2220)$ POLE POSITION

#### REAL PART

VALUE (MeV)	DOCUMENT ID	TECN	COMMENT
<b>2130 to 2200 (≈ 2170) OUR ESTIMATE</b>			
2150 ± 35	ANISOVICH	12A	DPWA Multichannel
2199	ARNDT	06	DPWA $\pi N \rightarrow \pi N, \eta N$
2135	<sup>1</sup> HOEHLER	93	ARGD $\pi N \rightarrow \pi N$
2160 ± 80	CUTKOSKY	80	IPWA $\pi N \rightarrow \pi N$
• • • We do not use the following data for averages, fits, limits, etc. • • •			
2209	ARNDT	04	DPWA $\pi N \rightarrow \pi N, \eta N$
2203	ARNDT	95	DPWA $\pi N \rightarrow N\pi$
2253	ARNDT	91	DPWA $\pi N \rightarrow \pi N$ Soln SM90

#### -2xIMAGINARY PART

VALUE (MeV)	DOCUMENT ID	TECN	COMMENT
<b>400 to 560 (≈ 480) OUR ESTIMATE</b>			
440 ± 40	ANISOVICH	12A	DPWA Multichannel
372	ARNDT	06	DPWA $\pi N \rightarrow \pi N, \eta N$
400	<sup>2</sup> HOEHLER	93	ARGD $\pi N \rightarrow \pi N$
480 ± 100	CUTKOSKY	80	IPWA $\pi N \rightarrow \pi N$
• • • We do not use the following data for averages, fits, limits, etc. • • •			
564	ARNDT	04	DPWA $\pi N \rightarrow \pi N, \eta N$
536	ARNDT	95	DPWA $\pi N \rightarrow N\pi$
640	ARNDT	91	DPWA $\pi N \rightarrow \pi N$ Soln SM90

### $N(2220)$ ELASTIC POLE RESIDUE

#### MODULUS $|r|$

VALUE (MeV)	DOCUMENT ID	TECN	COMMENT
60 ± 12	ANISOVICH	12A	DPWA Multichannel
33	ARNDT	06	DPWA $\pi N \rightarrow \pi N, \eta N$
40	HOEHLER	93	ARGD $\pi N \rightarrow \pi N$
45 ± 20	CUTKOSKY	80	IPWA $\pi N \rightarrow \pi N$
• • • We do not use the following data for averages, fits, limits, etc. • • •			
96	ARNDT	04	DPWA $\pi N \rightarrow \pi N, \eta N$
68	ARNDT	95	DPWA $\pi N \rightarrow N\pi$
85	ARNDT	91	DPWA $\pi N \rightarrow \pi N$ Soln SM90

#### PHASE $\theta$

VALUE (°)	DOCUMENT ID	TECN	COMMENT
-58 ± 12	ANISOVICH	12A	DPWA Multichannel
-33	ARNDT	06	DPWA $\pi N \rightarrow \pi N, \eta N$
-50	HOEHLER	93	ARGD $\pi N \rightarrow \pi N$
-45 ± 25	CUTKOSKY	80	IPWA $\pi N \rightarrow \pi N$
• • • We do not use the following data for averages, fits, limits, etc. • • •			
-71	ARNDT	04	DPWA $\pi N \rightarrow \pi N, \eta N$
-43	ARNDT	95	DPWA $\pi N \rightarrow N\pi$
-62	ARNDT	91	DPWA $\pi N \rightarrow \pi N$ Soln SM90

### $N(2220)$ DECAY MODES

The following branching fractions are our estimates, not fits or averages.

Mode	Fraction ( $\Gamma_i/\Gamma$ )
$\Gamma_1$ $N\pi$	15-25 %
$\Gamma_2$ $N\eta$	
$\Gamma_3$ $\Lambda K$	

### $N(2220)$ BRANCHING RATIOS

$\Gamma(N\pi)/\Gamma_{\text{total}}$	DOCUMENT ID	TECN	COMMENT	$\Gamma_1/\Gamma$
<b>15 to 25 OUR ESTIMATE</b>				
24 ± 5	ANISOVICH	12A	DPWA Multichannel	
24.6 ± 0.1	ARNDT	06	DPWA $\pi N \rightarrow \pi N, \eta N$	
15 ± 3	CUTKOSKY	80	IPWA $\pi N \rightarrow \pi N$	
18.0 ± 1.5	HOEHLER	79	IPWA $\pi N \rightarrow \pi N$	
12 ± 4	HENDRY	78	MPWA $\pi N \rightarrow \pi N$	
• • • We do not use the following data for averages, fits, limits, etc. • • •				
20.0 ± 0.6	ARNDT	04	DPWA $\pi N \rightarrow \pi N, \eta N$	
26	ARNDT	95	DPWA $\pi N \rightarrow N\pi$	

### $(\Gamma_1\Gamma_2)^{1/2}/\Gamma_{\text{total}}$ in $N\pi \rightarrow N(2220) \rightarrow \Lambda K$ $(\Gamma_1\Gamma_3)^{1/2}/\Gamma$

VALUE	DOCUMENT ID	TECN	COMMENT
not required	BELL	83	DPWA $\pi^- p \rightarrow \Lambda K^0$
not seen	SAXON	80	DPWA $\pi^- p \rightarrow \Lambda K^0$

### $N(2220)$ PHOTON DECAY AMPLITUDES

Papers on  $\gamma N$  amplitudes predating 1981 may be found in our 2006 edition, Journal of Physics, G **33** 1 (2006).

### $N(2220) \rightarrow p\gamma$ , helicity-1/2 amplitude $A_{1/2}$

VALUE (GeV <sup>-1/2</sup> )	DOCUMENT ID	TECN	COMMENT
< 0.01	<sup>3</sup> ANISOVICH	12A	DPWA Multichannel

### $N(2220) \rightarrow p\gamma$ , helicity-3/2 amplitude $A_{3/2}$

VALUE (GeV <sup>-1/2</sup> )	DOCUMENT ID	TECN	COMMENT
< 0.01	<sup>3</sup> ANISOVICH	12A	DPWA Multichannel

### $N(2220)$ FOOTNOTES

- See HOEHLER 93 for a detailed discussion of the evidence for and the pole parameters of  $N$  and  $\Delta$  resonances as determined from Argand diagrams of  $\pi N$  elastic partial-wave amplitudes and from plots of the speeds with which the amplitudes traverse the diagrams.
- See HOEHLER 93 for a detailed discussion of the evidence for and the pole parameters of  $N$  and  $\Delta$  resonances as determined from Argand diagrams of  $\pi N$  elastic partial-wave amplitudes and from plots of the speeds with which the amplitudes traverse the diagrams.
- This ANISOVICH 12A value is the complex helicity amplitude at the pole position.

### $N(2220)$ REFERENCES

For early references, see Physics Letters **111B** 1 (1982).

ANISOVICH	12A	EPJ A48 15	A.V. Anisovich et al.	(BONN, PNPI)
ARNDT	06	PR C74 045205	R.A. Arndt et al.	(GWU)
PDG	06	JPG 33 1	W.-M. Yao et al.	(PDG Collab.)
ARNDT	04	PR C69 035213	R.A. Arndt et al.	(GWU, TRIU)
ARNDT	95	PR C52 2120	R.A. Arndt et al.	(VPI, BRCC)
HOEHLER	93	$\pi N$ Newsletter 9 1	G. Hohlner	(KARL)
ARNDT	91	PR D43 2131	R.A. Arndt et al.	(VPI, TELE) IJP
BELL	83	NP B222 389	K.W. Bell et al.	(RL) IJP
PDG	82	PL 111B 1	M. Roos et al.	(HELS, CIT, CERN)
CUTKOSKY	80	Toronto Conf. 19	R.E. Cutkosky et al.	(CMU, LBL) IJP
Also		PR D20 2839	R.E. Cutkosky et al.	(CMU, LBL) IJP
SAXON	80	NP B162 522	D.H. Saxon et al.	(RHEL, BRIS) IJP
HOEHLER	79	PDAT 12-1	G. Hohlner et al.	(KARL) IJP
Also		Toronto Conf. 3	R. Koch	(KARL) IJP
HENDRY	78	PRL 41 222	A.W. Hendry	(IND, LBL) IJP
Also		ANP 136 1	A.W. Hendry	(IND)

### $N(2250)$ 9/2<sup>-</sup>

$$I(J^P) = \frac{1}{2}(\frac{9}{2}^-) \text{ Status: } ***$$

Some obsolete results published before 1980 were last included in our 2006 edition, Journal of Physics, G **33** 1 (2006).

### $N(2250)$ BREIT-WIGNER MASS

VALUE (MeV)	DOCUMENT ID	TECN	COMMENT
<b>2200 to 2350 (≈ 2275) OUR ESTIMATE</b>			
2280 ± 40	ANISOVICH	12A	DPWA Multichannel
2302 ± 6	ARNDT	06	DPWA $\pi N \rightarrow \pi N, \eta N$
2250 ± 80	CUTKOSKY	80	IPWA $\pi N \rightarrow \pi N$
2268 ± 15	HOEHLER	79	IPWA $\pi N \rightarrow \pi N$
2200 ± 100	HENDRY	78	MPWA $\pi N \rightarrow \pi N$
• • • We do not use the following data for averages, fits, limits, etc. • • •			
2376 ± 43	ARNDT	04	DPWA $\pi N \rightarrow \pi N, \eta N$
2291	ARNDT	95	DPWA $\pi N \rightarrow N\pi$

### $N(2250)$ BREIT-WIGNER WIDTH

VALUE (MeV)	DOCUMENT ID	TECN	COMMENT
<b>230 to 800 (≈ 500) OUR ESTIMATE</b>			
520 ± 50	ANISOVICH	12A	DPWA Multichannel
628 ± 28	ARNDT	06	DPWA $\pi N \rightarrow \pi N, \eta N$
480 ± 120	CUTKOSKY	80	IPWA $\pi N \rightarrow \pi N$
300 ± 40	HOEHLER	79	IPWA $\pi N \rightarrow \pi N$
350 ± 100	HENDRY	78	MPWA $\pi N \rightarrow \pi N$
• • • We do not use the following data for averages, fits, limits, etc. • • •			
924 ± 178	ARNDT	04	DPWA $\pi N \rightarrow \pi N, \eta N$
772	ARNDT	95	DPWA $\pi N \rightarrow N\pi$

See key on page 457

# Baryon Particle Listings

## $N(2250)$ , $N(2600)$ , $N(2700)$

### $N(2250)$ POLE POSITION

#### REAL PART

VALUE (MeV)	DOCUMENT ID	TECN	COMMENT
<b>2150 to 2250 (<math>\approx 2200</math>) OUR ESTIMATE</b>			
2195 $\pm$ 45	ANISOVICH 12A	DPWA	Multichannel
2217	ARNDT 06	DPWA	$\pi N \rightarrow \pi N, \eta N$
2187	1 HOEHLER 93	SPED	$\pi N \rightarrow \pi N$
2150 $\pm$ 50	CUTKOSKY 80	IPWA	$\pi N \rightarrow \pi N$
• • • We do not use the following data for averages, fits, limits, etc. • • •			
2238	ARNDT 04	DPWA	$\pi N \rightarrow \pi N, \eta N$
2087	ARNDT 95	DPWA	$\pi N \rightarrow N\pi$
2243	ARNDT 91	DPWA	$\pi N \rightarrow \pi N$ Soln SM90

#### -2xIMAGINARY PART

VALUE (MeV)	DOCUMENT ID	TECN	COMMENT
<b>350 to 550 (<math>\approx 450</math>) OUR ESTIMATE</b>			
470 $\pm$ 50	ANISOVICH 12A	DPWA	Multichannel
431	ARNDT 06	DPWA	$\pi N \rightarrow \pi N, \eta N$
388	1 HOEHLER 93	SPED	$\pi N \rightarrow \pi N$
360 $\pm$ 100	CUTKOSKY 80	IPWA	$\pi N \rightarrow \pi N$
• • • We do not use the following data for averages, fits, limits, etc. • • •			
536	ARNDT 04	DPWA	$\pi N \rightarrow \pi N, \eta N$
680	ARNDT 95	DPWA	$\pi N \rightarrow N\pi$
650	ARNDT 91	DPWA	$\pi N \rightarrow \pi N$ Soln SM90

### $N(2250)$ ELASTIC POLE RESIDUE

#### MODULUS $|r|$

VALUE (MeV)	DOCUMENT ID	TECN	COMMENT
26 $\pm$ 5	ANISOVICH 12A	DPWA	Multichannel
21	ARNDT 06	DPWA	$\pi N \rightarrow \pi N, \eta N$
21	HOEHLER 93	SPED	$\pi N \rightarrow \pi N$
20 $\pm$ 6	CUTKOSKY 80	IPWA	$\pi N \rightarrow \pi N$
• • • We do not use the following data for averages, fits, limits, etc. • • •			
33	ARNDT 04	DPWA	$\pi N \rightarrow \pi N, \eta N$
24	ARNDT 95	DPWA	$\pi N \rightarrow N\pi$
47	ARNDT 91	DPWA	$\pi N \rightarrow \pi N$ Soln SM90

#### PHASE $\theta$

VALUE ( $^\circ$ )	DOCUMENT ID	TECN	COMMENT
-38 $\pm$ 25	ANISOVICH 12A	DPWA	Multichannel
-20	ARNDT 06	DPWA	$\pi N \rightarrow \pi N, \eta N$
-50 $\pm$ 20	CUTKOSKY 80	IPWA	$\pi N \rightarrow \pi N$
• • • We do not use the following data for averages, fits, limits, etc. • • •			
-25	ARNDT 04	DPWA	$\pi N \rightarrow \pi N, \eta N$
-44	ARNDT 95	DPWA	$\pi N \rightarrow N\pi$
-37	ARNDT 91	DPWA	$\pi N \rightarrow \pi N$ Soln SM90

### $N(2250)$ DECAY MODES

The following branching fractions are our estimates, not fits or averages.

Mode	Fraction ( $\Gamma_i/\Gamma$ )
$\Gamma_1$ $N\pi$	5-15 %
$\Gamma_2$ $N\eta$	
$\Gamma_3$ $\Lambda K$	

### $N(2250)$ BRANCHING RATIOS

$\Gamma(N\pi)/\Gamma_{total}$	DOCUMENT ID	TECN	COMMENT	$\Gamma_1/\Gamma$
<b>5 to 15 OUR ESTIMATE</b>				
12 $\pm$ 4	ANISOVICH 12A	DPWA	Multichannel	
8.9 $\pm$ 0.1	ARNDT 06	DPWA	$\pi N \rightarrow \pi N, \eta N$	
10 $\pm$ 2	CUTKOSKY 80	IPWA	$\pi N \rightarrow \pi N$	
10 $\pm$ 2	HOEHLER 79	IPWA	$\pi N \rightarrow \pi N$	
9 $\pm$ 2	HENDRY 78	MPWA	$\pi N \rightarrow \pi N$	
• • • We do not use the following data for averages, fits, limits, etc. • • •				
11.0 $\pm$ 0.4	ARNDT 04	DPWA	$\pi N \rightarrow \pi N, \eta N$	
10	ARNDT 95	DPWA	$\pi N \rightarrow N\pi$	

$(\Gamma_1\Gamma_2)^{1/2}/\Gamma_{total}$ in $N\pi \rightarrow N(2250) \rightarrow \Lambda K$	DOCUMENT ID	TECN	COMMENT	$(\Gamma_1\Gamma_3)^{1/2}/\Gamma$
-0.02	BELL 83	DPWA	$\pi^- p \rightarrow \Lambda K^0$	
not seen	SAXON 80	DPWA	$\pi^- p \rightarrow \Lambda K^0$	

### $N(2250)$ PHOTON DECAY AMPLITUDES

Papers on  $\gamma N$  amplitudes predating 1981 may be found in our 2006 edition, Journal of Physics, G **33** 1 (2006).

### $N(2250) \rightarrow p\gamma$ , helicity-1/2 amplitude $A_{1/2}$

VALUE ( $\text{GeV}^{-1/2}$ )	DOCUMENT ID	TECN	COMMENT
<0.01	2 ANISOVICH 12A	DPWA	Multichannel

### $N(2250) \rightarrow p\gamma$ , helicity-3/2 amplitude $A_{3/2}$

VALUE ( $\text{GeV}^{-1/2}$ )	DOCUMENT ID	TECN	COMMENT
<0.01	2 ANISOVICH 12A	DPWA	Multichannel

### $N(2250)$ FOOTNOTES

- See HOEHLER 93 for a detailed discussion of the evidence for and the pole parameters of  $N$  and  $\Delta$  resonances as determined from Argand diagrams of  $\pi N$  elastic partial-wave amplitudes and from plots of the speeds with which the amplitudes traverse the diagrams.
- This ANISOVICH 12A value is the complex helicity amplitude at the pole position.

### $N(2250)$ REFERENCES

ANISOVICH 12A	EPJ A48 15	A.V. Anisovich et al.	(BONN, PNPI)
ARNDT 06	PR C74 045205	R.A. Arndt et al.	(GWU)
PDG 06	JPG 33 1	W.-M. Yao et al.	(PDG Collab.)
ARNDT 04	PR C69 035213	R.A. Arndt et al.	(GWU, TRIU)
ARNDT 95	PR C52 2120	R.A. Arndt et al.	(VPI, BRCO)
HOEHLER 93	$\pi N$ Newsletter 9 1	G. Hohlner	(KARL)
ARNDT 91	PR D43 2131	R.A. Arndt et al.	(VPI, TELE) IJP
BELL 83	NP B222 389	K.W. Bell et al.	(RL) IJP
CUTKOSKY 80	Toronto Conf. 19	R.E. Cutkosky et al.	(CMU, LBL) IJP
Also	PR D20 2839	R.E. Cutkosky et al.	(CMU, LBL) IJP
SAXON 80	NP B162 522	D.H. Saxon et al.	(RHEL, BRIS) IJP
HOEHLER 79	PDAT 12-1	G. Hohlner et al.	(KARLT) IJP
Also	Toronto Conf. 3	R. Koch	(KARLT) IJP
HENDRY 78	PRL 41 222	A.W. Hendry	(IND, LBL) IJP
Also	ANP 136 1	A.W. Hendry	(IND)

### $N(2600)$ $11/2^-$

$$I(J^P) = \frac{1}{2}(\frac{1}{2}^-) \text{Status: } ***$$

### $N(2600)$ BREIT-WIGNER MASS

VALUE (MeV)	DOCUMENT ID	TECN	COMMENT
<b>2550 to 2750 (<math>\approx 2600</math>) OUR ESTIMATE</b>			
2623 $\pm$ 197	ARNDT 06	DPWA	$\pi N \rightarrow \pi N, \eta N$
2577 $\pm$ 50	HOEHLER 79	IPWA	$\pi N \rightarrow \pi N$
2700 $\pm$ 100	HENDRY 78	MPWA	$\pi N \rightarrow \pi N$

### $N(2600)$ BREIT-WIGNER WIDTH

VALUE (MeV)	DOCUMENT ID	TECN	COMMENT
<b>500 to 800 (<math>\approx 650</math>) OUR ESTIMATE</b>			
1311 $\pm$ 996	ARNDT 06	DPWA	$\pi N \rightarrow \pi N, \eta N$
400 $\pm$ 100	HOEHLER 79	IPWA	$\pi N \rightarrow \pi N$
900 $\pm$ 100	HENDRY 78	MPWA	$\pi N \rightarrow \pi N$

### $N(2600)$ DECAY MODES

Mode	Fraction ( $\Gamma_i/\Gamma$ )
$\Gamma_1$ $N\pi$	5-10 %

### $N(2600)$ BRANCHING RATIOS

$\Gamma(N\pi)/\Gamma_{total}$	DOCUMENT ID	TECN	COMMENT	$\Gamma_1/\Gamma$
<b>5 to 10 OUR ESTIMATE</b>				
5.0 $\pm$ 1.8	ARNDT 06	DPWA	$\pi N \rightarrow \pi N, \eta N$	
5 $\pm$ 1	HOEHLER 79	IPWA	$\pi N \rightarrow \pi N$	
8 $\pm$ 2	HENDRY 78	MPWA	$\pi N \rightarrow \pi N$	

### $N(2600)$ REFERENCES

ARNDT 06	PR C74 045205	R.A. Arndt et al.	(GWU)
HOEHLER 79	PDAT 12-1	G. Hohlner et al.	(KARLT) IJP
Also	Toronto Conf. 3	R. Koch	(KARLT) IJP
HENDRY 78	PRL 41 222	A.W. Hendry	(IND, LBL) IJP
Also	ANP 136 1	A.W. Hendry	(IND)

### $N(2700)$ $13/2^+$

$$I(J^P) = \frac{1}{2}(\frac{1}{2}^+) \text{Status: } **$$

OMITTED FROM SUMMARY TABLE

The latest GWU analysis (ARNDT 06) finds no evidence for this resonance.

### $N(2700)$ BREIT-WIGNER MASS

VALUE (MeV)	DOCUMENT ID	TECN	COMMENT
<b><math>\approx 2700</math> OUR ESTIMATE</b>			
2612 $\pm$ 45	HOEHLER 79	IPWA	$\pi N \rightarrow \pi N$
3000 $\pm$ 100	HENDRY 78	MPWA	$\pi N \rightarrow \pi N$

### $N(2700)$ BREIT-WIGNER WIDTH

VALUE (MeV)	DOCUMENT ID	TECN	COMMENT
350 $\pm$ 50	HOEHLER 79	IPWA	$\pi N \rightarrow \pi N$
900 $\pm$ 150	HENDRY 78	MPWA	$\pi N \rightarrow \pi N$

## Baryon Particle Listings

 $N(2700)$ ,  $N(\sim 3000)$  $N(2700)$  DECAY MODES

Mode
$\Gamma_1 \quad N \pi$

 $N(2700)$  BRANCHING RATIOS

$\Gamma(N\pi)/\Gamma_{\text{total}}$	DOCUMENT ID	TECN	COMMENT	$\Gamma_1/\Gamma$
4 $\pm$ 1	HOEHLER 79	IPWA	$\pi N \rightarrow \pi N$	
7 $\pm$ 2	HENDRY 78	MPWA	$\pi N \rightarrow \pi N$	

 $N(2700)$  REFERENCES

ARNDT 06	PR C74 045205	R.A. Arndt <i>et al.</i>	(GWU)
HOEHLER 79	PDAT 12-1	G. Hohlner <i>et al.</i>	(KARLT) IJP
Also	Toronto Conf. 3	R. Koch	(KARLT) IJP
HENDRY 78	PRL 41 222	A.W. Hendry	(IND, LBL) IJP
Also	ANP 136 1	A.W. Hendry	(IND)

$N(\sim 3000)$  Region  
 Partial-Wave Analyses

## OMITTED FROM SUMMARY TABLE

We list here miscellaneous high-mass candidates for isospin-1/2 resonances found in partial-wave analyses.

Our 1982 edition had an  $N(3245)$ , an  $N(3690)$ , and an  $N(3755)$ , each a narrow peak seen in a production experiment. Since nothing has been heard from them since the 1960's, we declare them to be dead. There was also an  $N(3030)$ , deduced from total cross-section and  $180^\circ$  elastic cross-section measurements; it is the KOCH 80  $L_{1,15}$  state below.

 $N(\sim 3000)$  BREIT-WIGNER MASS

VALUE (MeV)	DOCUMENT ID	TECN	COMMENT
$\approx 3000$ OUR ESTIMATE			
2600	KOCH 80	IPWA	$\pi N \rightarrow \pi N D_{13}$
3100	KOCH 80	IPWA	$\pi N \rightarrow \pi N L_{1,15}$ wave
3500	KOCH 80	IPWA	$\pi N \rightarrow \pi N M_{1,17}$ wave
3500 to 4000	KOCH 80	IPWA	$\pi N \rightarrow \pi N N_{1,19}$ wave
3500 $\pm$ 200	HENDRY 78	MPWA	$\pi N \rightarrow \pi N L_{1,15}$ wave
3800 $\pm$ 200	HENDRY 78	MPWA	$\pi N \rightarrow \pi N M_{1,17}$ wave
4100 $\pm$ 200	HENDRY 78	MPWA	$\pi N \rightarrow \pi N N_{1,19}$ wave

 $N(\sim 3000)$  BREIT-WIGNER WIDTH

VALUE (MeV)	DOCUMENT ID	TECN	COMMENT
1300 $\pm$ 200	HENDRY 78	MPWA	$\pi N \rightarrow \pi N L_{1,15}$ wave
1600 $\pm$ 200	HENDRY 78	MPWA	$\pi N \rightarrow \pi N M_{1,17}$ wave
1900 $\pm$ 300	HENDRY 78	MPWA	$\pi N \rightarrow \pi N N_{1,19}$ wave

 $N(\sim 3000)$  DECAY MODES

Mode
$\Gamma_1 \quad N \pi$

 $N(\sim 3000)$  BRANCHING RATIOS

$\Gamma(N\pi)/\Gamma_{\text{total}}$	DOCUMENT ID	TECN	COMMENT	$\Gamma_1/\Gamma$
6 $\pm$ 2	HENDRY 78	MPWA	$\pi N \rightarrow \pi N L_{1,15}$ wave	
4.0 $\pm$ 1.5	HENDRY 78	MPWA	$\pi N \rightarrow \pi N M_{1,17}$ wave	
3.0 $\pm$ 1.5	HENDRY 78	MPWA	$\pi N \rightarrow \pi N N_{1,19}$ wave	

 $N(\sim 3000)$  REFERENCES

KOCH 80	Toronto Conf. 3	R. Koch	(KARLT) IJP
HENDRY 78	PRL 41 222	A.W. Hendry	(IND, LBL) IJP
Also	ANP 136 1	A.W. Hendry	(IND) IJP

$\Delta(1232)$

## $\Delta$ BARYONS

### ( $S = 0, I = 3/2$ )

$\Delta^{++} = uuu, \Delta^+ = uud, \Delta^0 = udd, \Delta^- = ddd$

$\Delta(1232) 3/2^+$

$I(J^P) = \frac{3}{2}(\frac{3}{2}^+)$  Status: \*\*\*\*

Most of the results published before 1975 were last included in our 1982 edition, Physics Letters **111B** 1 (1982). Some further obsolete results published before 1984 were last included in our 2006 edition, Journal of Physics, G **33** 1 (2006).

$\Delta(1232)$  BREIT-WIGNER MASSES

MIXED CHARGES

VALUE (MeV)	DOCUMENT ID	TECN	COMMENT
<b>1230 to 1234 (<math>\approx 1232</math>) OUR ESTIMATE</b>			
1228 $\pm 2$	ANISOVICH	12A	DPWA Multichannel
1233.4 $\pm 0.4$	ARNDT	06	DPWA $\pi N \rightarrow \pi N, \eta N$
1231 $\pm 1$	MANLEY	92	IPWA $\pi N \rightarrow \pi N \& N\pi\pi$
1232 $\pm 3$	CUTKOSKY	80	IPWA $\pi N \rightarrow \pi N$
1233 $\pm 2$	HOEHLER	79	IPWA $\pi N \rightarrow \pi N$
••• We do not use the following data for averages, fits, limits, etc. •••			
1230 $\pm 2$	ANISOVICH	10	DPWA Multichannel
1232.9 $\pm 1.2$	ARNDT	04	DPWA $\pi N \rightarrow \pi N, \eta N$
1228 $\pm 1$	PENNER	02c	DPWA Multichannel
1234 $\pm 5$	VRANA	00	DPWA Multichannel
1233	ARNDT	95	DPWA $\pi N \rightarrow N\pi$

$\Delta(1232)^{++}$  MASS

VALUE (MeV)	DOCUMENT ID	TECN	COMMENT
••• We do not use the following data for averages, fits, limits, etc. •••			
1230.55 $\pm 0.20$	GRIDNEV	06	DPWA $\pi N \rightarrow \pi N$
1231.88 $\pm 0.29$	BERNICHIA	96	Fit to PEDRONI 78
1230.5 $\pm 0.2$	ABAEV	95	IPWA $\pi N \rightarrow \pi N$
1230.9 $\pm 0.3$	KOCH	80b	IPWA $\pi N \rightarrow \pi N$
1231.1 $\pm 0.2$	PEDRONI	78	$\pi N \rightarrow \pi N$ 70-370 MeV

$\Delta(1232)^+$  MASS

VALUE (MeV)	DOCUMENT ID	COMMENT
••• We do not use the following data for averages, fits, limits, etc. •••		
1234.9 $\pm 1.4$	MIROSHNIC...	79 Fit photoproduction

$\Delta(1232)^0$  MASS

VALUE (MeV)	DOCUMENT ID	TECN	COMMENT
••• We do not use the following data for averages, fits, limits, etc. •••			
1231.3 $\pm 0.6$	BREITSCHOP..06	CNTR	Using new CHEX data
1233.40 $\pm 0.22$	GRIDNEV	06	DPWA $\pi N \rightarrow \pi N$
1234.35 $\pm 0.75$	BERNICHIA	96	Fit to PEDRONI 78
1233.1 $\pm 0.3$	ABAEV	95	IPWA $\pi N \rightarrow \pi N$
1233.6 $\pm 0.5$	KOCH	80b	IPWA $\pi N \rightarrow \pi N$
1233.8 $\pm 0.2$	PEDRONI	78	$\pi N \rightarrow \pi N$ 70-370 MeV

$m_{\Delta^0} - m_{\Delta^{++}}$

VALUE (MeV)	DOCUMENT ID	TECN	COMMENT
••• We do not use the following data for averages, fits, limits, etc. •••			
2.86 $\pm 0.30$	GRIDNEV	06	DPWA $\pi N \rightarrow \pi N$
2.25 $\pm 0.68$	BERNICHIA	96	Fit to PEDRONI 78
2.6 $\pm 0.4$	ABAEV	95	IPWA $\pi N \rightarrow \pi N$
2.7 $\pm 0.3$	1 PEDRONI	78	See the masses
1 Using $\pi^\pm d$ as well, PEDRONI 78 determine $(M^- - M^{++}) + (M^0 - M^+)/3 = 4.6 \pm 0.2$ MeV.			

$\Delta(1232)$  BREIT-WIGNER WIDTHS

MIXED CHARGES

VALUE (MeV)	DOCUMENT ID	TECN	COMMENT
<b>114 to 120 (<math>\approx 117</math>) OUR ESTIMATE</b>			
110 $\pm 3$	ANISOVICH	12A	DPWA Multichannel
118.7 $\pm 0.6$	ARNDT	06	DPWA $\pi N \rightarrow \pi N, \eta N$
118 $\pm 4$	MANLEY	92	IPWA $\pi N \rightarrow \pi N \& N\pi\pi$
120 $\pm 5$	CUTKOSKY	80	IPWA $\pi N \rightarrow \pi N$
116 $\pm 5$	HOEHLER	79	IPWA $\pi N \rightarrow \pi N$
••• We do not use the following data for averages, fits, limits, etc. •••			
112 $\pm 4$	ANISOVICH	10	DPWA Multichannel
118.0 $\pm 2.2$	ARNDT	04	DPWA $\pi N \rightarrow \pi N, \eta N$
106 $\pm 1$	PENNER	02c	DPWA Multichannel
112 $\pm 1.8$	VRANA	00	DPWA Multichannel
114	ARNDT	95	DPWA $\pi N \rightarrow N\pi$

$\Delta(1232)^{++}$  WIDTH

VALUE (MeV)	DOCUMENT ID	TECN	COMMENT
••• We do not use the following data for averages, fits, limits, etc. •••			
112.2 $\pm 0.7$	GRIDNEV	06	DPWA $\pi N \rightarrow \pi N$
109.07 $\pm 0.48$	BERNICHIA	96	Fit to PEDRONI 78
111.0 $\pm 1.0$	KOCH	80b	IPWA $\pi N \rightarrow \pi N$
111.3 $\pm 0.5$	PEDRONI	78	$\pi N \rightarrow \pi N$ 70-370 MeV

$\Delta(1232)^+$  WIDTH

VALUE (MeV)	DOCUMENT ID	COMMENT
••• We do not use the following data for averages, fits, limits, etc. •••		
131.1 $\pm 2.4$	MIROSHNIC...	79 Fit photoproduction

$\Delta(1232)^0$  WIDTH

VALUE (MeV)	DOCUMENT ID	TECN	COMMENT
••• We do not use the following data for averages, fits, limits, etc. •••			
112.5 $\pm 1.9$	BREITSCHOP..06	CNTR	Using new CHEX data
116.9 $\pm 0.7$	GRIDNEV	06	DPWA $\pi N \rightarrow \pi N$
117.58 $\pm 1.16$	BERNICHIA	96	Fit to PEDRONI 78
113.0 $\pm 1.5$	KOCH	80b	IPWA $\pi N \rightarrow \pi N$
117.9 $\pm 0.9$	PEDRONI	78	$\pi N \rightarrow \pi N$ 70-370 MeV

$\Delta^0 - \Delta^{++}$  WIDTH DIFFERENCE

VALUE (MeV)	DOCUMENT ID	TECN	COMMENT
••• We do not use the following data for averages, fits, limits, etc. •••			
4.66 $\pm 1.0$	GRIDNEV	06	DPWA $\pi N \rightarrow \pi N$
8.45 $\pm 1.11$	BERNICHIA	96	Fit to PEDRONI 78
5.1 $\pm 1.0$	ABAEV	95	IPWA $\pi N \rightarrow \pi N$
6.6 $\pm 1.0$	PEDRONI	78	See the widths

$\Delta(1232)$  POLE POSITIONS

REAL PART, MIXED CHARGES

VALUE (MeV)	DOCUMENT ID	TECN	COMMENT
<b>1209 to 1211 (<math>\approx 1210</math>) OUR ESTIMATE</b>			
1210.5 $\pm 1.0$	ANISOVICH	12A	DPWA Multichannel
1211	ARNDT	06	DPWA $\pi N \rightarrow \pi N, \eta N$
1209	2 HOEHLER	93	ARGD $\pi N \rightarrow \pi N$
1210 $\pm 1$	CUTKOSKY	80	IPWA $\pi N \rightarrow \pi N$
••• We do not use the following data for averages, fits, limits, etc. •••			
1211 $\pm 1$	ANISOVICH	10	DPWA Multichannel
1210	ARNDT	04	DPWA $\pi N \rightarrow \pi N, \eta N$
1217	VRANA	00	DPWA Multichannel
1211	ARNDT	95	DPWA $\pi N \rightarrow N\pi$
1210	ARNDT	91	DPWA $\pi N \rightarrow \pi N$ Soln SM90

-2xIMAGINARY PART, MIXED CHARGES

VALUE (MeV)	DOCUMENT ID	TECN	COMMENT
<b>98 to 102 (<math>\approx 100</math>) OUR ESTIMATE</b>			
99 $\pm 2$	ANISOVICH	12A	DPWA Multichannel
99	ARNDT	06	DPWA $\pi N \rightarrow \pi N, \eta N$
100	2 HOEHLER	93	ARGD $\pi N \rightarrow \pi N$
100 $\pm 2$	CUTKOSKY	80	IPWA $\pi N \rightarrow \pi N$
••• We do not use the following data for averages, fits, limits, etc. •••			
100 $\pm 2$	ANISOVICH	10	DPWA Multichannel
100	ARNDT	04	DPWA $\pi N \rightarrow \pi N, \eta N$
96	VRANA	00	DPWA Multichannel
100	ARNDT	95	DPWA $\pi N \rightarrow N\pi$
100	ARNDT	91	DPWA $\pi N \rightarrow \pi N$ Soln SM90

REAL PART,  $\Delta(1232)^{++}$

VALUE (MeV)	DOCUMENT ID	COMMENT
••• We do not use the following data for averages, fits, limits, etc. •••		
1212.50 $\pm 0.24$	BERNICHIA	96 Fit to PEDRONI 78

-2xIMAGINARY PART,  $\Delta(1232)^{++}$

VALUE (MeV)	DOCUMENT ID	COMMENT
••• We do not use the following data for averages, fits, limits, etc. •••		
97.37 $\pm 0.42$	BERNICHIA	96 Fit to PEDRONI 78

REAL PART,  $\Delta(1232)^+$

VALUE (MeV)	DOCUMENT ID	TECN	COMMENT
••• We do not use the following data for averages, fits, limits, etc. •••			
1211 $\pm 1$ to 1212 $\pm 1$	HANSTEIN	96	DPWA $\gamma N \rightarrow \pi N$
1206.9 $\pm 0.9$ to 1210.5 $\pm 1.8$	MIROSHNIC...	79	Fit photoproduction

-2xIMAGINARY PART,  $\Delta(1232)^+$

VALUE (MeV)	DOCUMENT ID	TECN	COMMENT
••• We do not use the following data for averages, fits, limits, etc. •••			
102 $\pm 2$ to 99 $\pm 2$	3 HANSTEIN	96	DPWA $\gamma N \rightarrow \pi N$
111.2 $\pm 2.0$ to 116.6 $\pm 2.2$	MIROSHNIC...	79	Fit photoproduction

## Baryon Particle Listings

 $\Delta(1232)$ **REAL PART,  $\Delta(1232)^0$** 

VALUE (MeV)	DOCUMENT ID	COMMENT
••• We do not use the following data for averages, fits, limits, etc. •••		
1213.20 ± 0.66	BERNICHIA 96	Fit to PEDRONI 78

**-2xIMAGINARY PART,  $\Delta(1232)^0$** 

VALUE (MeV)	DOCUMENT ID	COMMENT
••• We do not use the following data for averages, fits, limits, etc. •••		
104.10 ± 1.01	BERNICHIA 96	Fit to PEDRONI 78

<sup>2</sup> See HOEHLER 93 for a detailed discussion of the evidence for and the pole parameters of  $N$  and  $\Delta$  resonances as determined from Argand diagrams of  $\pi N$  elastic partial-wave amplitudes and from plots of the speeds with which the amplitudes traverse the diagrams.

<sup>3</sup> The second (lower) value of HANSTEIN 96 here goes with the second (higher) value of the real part in the preceding data block.

 **$\Delta(1232)$  ELASTIC POLE RESIDUES****ABSOLUTE VALUE, MIXED CHARGES**

VALUE (MeV)	DOCUMENT ID	TECN	COMMENT
51.6 ± 0.6	ANISOVICH 12A	DPWA	Multichannel
52	ARNDT 06	DPWA	$\pi N \rightarrow \pi N, \eta N$
50	HOEHLER 93	ARGD	$\pi N \rightarrow \pi N$
53 ± 2	CUTKOSKY 80	IPWA	$\pi N \rightarrow \pi N$
••• We do not use the following data for averages, fits, limits, etc. •••			
53	ARNDT 04	DPWA	$\pi N \rightarrow \pi N, \eta N$
38	<sup>4</sup> ARNDT 95	DPWA	$\pi N \rightarrow N\pi$
52	ARNDT 91	DPWA	$\pi N \rightarrow \pi N$ Soln SM90

**PHASE, MIXED CHARGES**

VALUE (°)	DOCUMENT ID	TECN	COMMENT
-46 ± 1	ANISOVICH 12A	DPWA	Multichannel
-47	ARNDT 06	DPWA	$\pi N \rightarrow \pi N, \eta N$
-48	HOEHLER 93	ARGD	$\pi N \rightarrow \pi N$
-47 ± 1	CUTKOSKY 80	IPWA	$\pi N \rightarrow \pi N$
••• We do not use the following data for averages, fits, limits, etc. •••			
-47	ARNDT 04	DPWA	$\pi N \rightarrow \pi N, \eta N$
-22	<sup>4</sup> ARNDT 95	DPWA	$\pi N \rightarrow N\pi$
-31	ARNDT 91	DPWA	$\pi N \rightarrow \pi N$ Soln SM90

<sup>4</sup> This ARNDT 95 value is in error, as pointed out by HOEHLER 01. The corrected value is in line with the ARNDT 91 value (R.A. Arndt, private communication).

 **$\Delta(1232)$  DECAY MODES**

The following branching fractions are our estimates, not fits or averages.

Mode	Fraction ( $\Gamma_j/\Gamma$ )
$\Gamma_1$ $N\pi$	100 %
$\Gamma_2$ $N\gamma$	0.55-0.65 %
$\Gamma_3$ $N\gamma$ , helicity=1/2	0.11-0.13 %
$\Gamma_4$ $N\gamma$ , helicity=3/2	0.44-0.52 %

 **$\Delta(1232)$  BRANCHING RATIOS**

$\Gamma(N\pi)/\Gamma_{\text{total}}$	DOCUMENT ID	TECN	COMMENT	$\Gamma_1/\Gamma$
<b>1.0 OUR ESTIMATE</b>				
1.00	ARNDT 06	DPWA	$\pi N \rightarrow \pi N, \eta N$	
1.0	MANLEY 92	IPWA	$\pi N \rightarrow \pi N$ & $N\pi\pi$	
1.0	CUTKOSKY 80	IPWA	$\pi N \rightarrow \pi N$	
1.0	HOEHLER 79	IPWA	$\pi N \rightarrow \pi N$	
••• We do not use the following data for averages, fits, limits, etc. •••				
1.0	ANISOVICH 10	DPWA	Multichannel	
1.000	ARNDT 04	DPWA	$\pi N \rightarrow \pi N, \eta N$	
1.00	PENNER 02c	DPWA	Multichannel	
1.00 ± 0.01	VRANA 00	DPWA	Multichannel	
1.0	ARNDT 95	DPWA	$\pi N \rightarrow N\pi$	

 **$\Delta(1232)$  PHOTON DECAY AMPLITUDES**

Papers on  $\gamma N$  amplitudes predating 1981 may be found in our 2006 edition, Journal of Physics, G 33 1 (2006).

 **$\Delta(1232) \rightarrow N\gamma$ , helicity-1/2 amplitude  $A_{1/2}$** 

VALUE (GeV <sup>-1/2</sup> )	DOCUMENT ID	TECN	COMMENT
<b>-0.135 ± 0.006 OUR ESTIMATE</b>			
-0.131 ± 0.004	ANISOVICH 12A	DPWA	Multichannel
-0.139 ± 0.004	DUGGER 07	DPWA	$\gamma N \rightarrow \pi N$
-0.137 ± 0.005	AHRENS 04A	DPWA	$\bar{\gamma}p \rightarrow N\pi$
-0.129 ± 0.001	ARNDT 02	DPWA	$\gamma p \rightarrow N\pi$
-0.1357 ± 0.0013 ± 0.0037	BLANPIED 01	LEGS	$\gamma p \rightarrow p\gamma, p\pi^0, n\pi^+$
-0.131 ± 0.001	BECK 00	IPWA	$\bar{\gamma}p \rightarrow p\pi^0, n\pi^+$
-0.140 ± 0.005	KAMALOV 99	DPWA	$\gamma N \rightarrow \pi N$

-0.1294 ± 0.0013	HANSTEIN 98	IPWA	$\gamma N \rightarrow \pi N$
-0.135 ± 0.005	ARNDT 97	IPWA	$\gamma N \rightarrow \pi N$
-0.1278 ± 0.0012	DAVIDSON 97	DPWA	$\gamma N \rightarrow \pi N$
-0.141 ± 0.005	ARNDT 96	IPWA	$\gamma N \rightarrow \pi N$
-0.135 ± 0.016	DAVIDSON 91B	FIT	$\gamma N \rightarrow \pi N$
-0.145 ± 0.015	CRAWFORD 83	IPWA	$\gamma N \rightarrow \pi N$
-0.138 ± 0.004	AWAJI 81	DPWA	$\gamma N \rightarrow \pi N$
••• We do not use the following data for averages, fits, limits, etc. •••			
-0.136 ± 0.005	ANISOVICH 10	DPWA	Multichannel
-0.140	DRECHSEL 07	DPWA	$\gamma N \rightarrow \pi N$
-0.128	PENNER 02D	DPWA	Multichannel
-0.1312	HANSTEIN 98	DPWA	$\gamma N \rightarrow \pi N$
-0.143 ± 0.004	LI 93	IPWA	$\gamma N \rightarrow \pi N$
-0.140 ± 0.007	DAVIDSON 90	FIT	See DAVIDSON 91B

 **$\Delta(1232) \rightarrow N\gamma$ , helicity-3/2 amplitude  $A_{3/2}$** 

VALUE (GeV <sup>-1/2</sup> )	DOCUMENT ID	TECN	COMMENT
<b>-0.250 ± 0.008 OUR ESTIMATE</b>			
-0.254 ± 0.005	ANISOVICH 12A	DPWA	Multichannel
-0.258 ± 0.005	DUGGER 07	DPWA	$\gamma N \rightarrow \pi N$
-0.256 ± 0.003	AHRENS 04A	DPWA	$\bar{\gamma}p \rightarrow N\pi$
-0.243 ± 0.001	ARNDT 02	DPWA	$\gamma p \rightarrow N\pi$
-0.2669 ± 0.0016 ± 0.0078	BLANPIED 01	LEGS	$\gamma p \rightarrow p\gamma, p\pi^0, n\pi^+$
-0.251 ± 0.001	BECK 00	IPWA	$\bar{\gamma}p \rightarrow p\pi^0, n\pi^+$
-0.258 ± 0.006	KAMALOV 99	DPWA	$\gamma N \rightarrow \pi N$
-0.2466 ± 0.0013	HANSTEIN 98	IPWA	$\gamma N \rightarrow \pi N$
-0.250 ± 0.008	ARNDT 97	IPWA	$\gamma N \rightarrow \pi N$
-0.2524 ± 0.0013	DAVIDSON 97	DPWA	$\gamma N \rightarrow \pi N$
-0.261 ± 0.005	ARNDT 96	IPWA	$\gamma N \rightarrow \pi N$
-0.251 ± 0.033	DAVIDSON 91B	FIT	$\gamma N \rightarrow \pi N$
-0.263 ± 0.026	CRAWFORD 83	IPWA	$\gamma N \rightarrow \pi N$
-0.259 ± 0.006	AWAJI 81	DPWA	$\gamma N \rightarrow \pi N$
••• We do not use the following data for averages, fits, limits, etc. •••			
-0.267 ± 0.008	ANISOVICH 10	DPWA	Multichannel
-0.265	DRECHSEL 07	DPWA	$\gamma N \rightarrow \pi N$
-0.247	PENNER 02D	DPWA	Multichannel
-0.2522	HANSTEIN 98	DPWA	$\gamma N \rightarrow \pi N$
-0.262 ± 0.004	LI 93	IPWA	$\gamma N \rightarrow \pi N$
-0.254 ± 0.011	DAVIDSON 90	FIT	See DAVIDSON 91B

 **$\Delta(1232) \rightarrow N\gamma$ ,  $E_2/M_1$  ratio**

VALUE	DOCUMENT ID	TECN	COMMENT
<b>-0.025 ± 0.005 OUR ESTIMATE</b>			
-0.0274 ± 0.0003 ± 0.0030	AHRENS 04A	DPWA	$\bar{\gamma}p \rightarrow N\pi$
-0.020 ± 0.002	ARNDT 02	DPWA	$\gamma p \rightarrow N\pi$
-0.0307 ± 0.0026 ± 0.0024	BLANPIED 01	LEGS	$\gamma p \rightarrow p\gamma, p\pi^0, n\pi^+$
-0.016 ± 0.004 ± 0.002	GALLER 01	DPWA	$\gamma p \rightarrow \gamma p$
-0.025 ± 0.001 ± 0.002	BECK 00	IPWA	$\bar{\gamma}p \rightarrow p\pi^0, n\pi^+$
-0.0233 ± 0.0017	HANSTEIN 98	IPWA	$\gamma N \rightarrow \pi N$
-0.015 ± 0.005	<sup>5</sup> ARNDT 97	IPWA	$\gamma N \rightarrow \pi N$
-0.0319 ± 0.0024	DAVIDSON 97	DPWA	$\gamma N \rightarrow \pi N$
••• We do not use the following data for averages, fits, limits, etc. •••			
-0.022	DRECHSEL 07	DPWA	$\gamma N \rightarrow \pi N$
-0.026	PENNER 02D	DPWA	Multichannel
-0.0254 ± 0.0010	HANSTEIN 98	DPWA	$\gamma N \rightarrow \pi N$
-0.025 ± 0.002 ± 0.002	BECK 97	IPWA	$\gamma N \rightarrow \pi N$
-0.030 ± 0.003 ± 0.002	BLANPIED 97	DPWA	$\gamma N \rightarrow \pi N, \gamma N$
-0.027 ± 0.003 ± 0.001	KHANDAKER 95	DPWA	$\gamma N \rightarrow \pi N$
-0.015 ± 0.005	WORKMAN 92	IPWA	$\gamma N \rightarrow \pi N$
-0.0157 ± 0.0072	DAVIDSON 91B	FIT	$\gamma N \rightarrow \pi N$
-0.0107 ± 0.0037	DAVIDSON 90	FIT	$\gamma N \rightarrow \pi N$
-0.015 ± 0.002	DAVIDSON 86	FIT	$\gamma N \rightarrow \pi N$
+0.037 ± 0.004	TANABE 85	FIT	$\gamma N \rightarrow \pi N$

 **$\Delta(1232) \rightarrow N\gamma$ , absolute value of  $E_2/M_1$  ratio at pole**

VALUE	DOCUMENT ID	TECN	COMMENT
••• We do not use the following data for averages, fits, limits, etc. •••			
0.065 ± 0.007	ARNDT 97	DPWA	$\gamma N \rightarrow \pi N$
0.058	HANSTEIN 96	DPWA	$\gamma N \rightarrow \pi N$

 **$\Delta(1232) \rightarrow N\gamma$ , phase of  $E_2/M_1$  ratio at pole**

VALUE	DOCUMENT ID	TECN	COMMENT
••• We do not use the following data for averages, fits, limits, etc. •••			
-122 ± 5	ARNDT 97	DPWA	$\gamma N \rightarrow \pi N$
-127.2	HANSTEIN 96	DPWA	$\gamma N \rightarrow \pi N$

<sup>5</sup> This ARNDT 97 value is very sensitive to the database being fitted. The result is from a fit to the full pion photoproduction database, apart from the BLANPIED 97 cross-section measurements.



$\Delta(1232)$  MAGNETIC MOMENTS

$\Delta(1232)^{++}$  MAGNETIC MOMENT

The values are extracted from UCLA and SIN data on  $\pi^+ p$  bremsstrahlung using a variety of different theoretical approximations and methods. Our estimate is *only* a rough guess of the range we expect the moment to lie within.

VALUE ( $\mu_N$ )	DOCUMENT ID	TECN	COMMENT
<b>3.7 to 7.5 OUR ESTIMATE</b>			
6.14 ± 0.51	LOPEZCAST...01	DPWA	$\pi^+ p \rightarrow \pi^+ p \gamma$
4.52 ± 0.50 ± 0.45	BOSSHARD 91		$\pi^+ p \rightarrow \pi^+ p \gamma$ (SIN data)
3.7 to 4.2	LIN 91B		$\pi^+ p \rightarrow \pi^+ p \gamma$ (from UCLA data)
4.6 to 4.9	LIN 91B		$\pi^+ p \rightarrow \pi^+ p \gamma$ (from SIN data)
5.6 to 7.5	WITTMAN 88		$\pi^+ p \rightarrow \pi^+ p \gamma$ (from UCLA data)
6.9 to 9.8	HELLER 87		$\pi^+ p \rightarrow \pi^+ p \gamma$ (from UCLA data)
4.7 to 6.7	NEFKENS 78		$\pi^+ p \rightarrow \pi^+ p \gamma$ (UCLA data)

$\Delta(1232)^+$  MAGNETIC MOMENT

VALUE ( $\mu_N$ )	DOCUMENT ID	COMMENT
2.7 <sup>+1.0</sup> <sub>-1.3</sub> ± 1.5 ± 3	<sup>6</sup> KOTULLA 02	$\gamma p \rightarrow p \pi^0 \gamma'$

<sup>6</sup>The second error is systematic, the third is an estimate of theoretical uncertainties.

$\Delta(1232)$  REFERENCES

For early references, see Physics Letters **111B** 1 (1982).

ANISOVICH 12A	EPJ A48 15	A.V. Anisovich <i>et al.</i>	(BONN, PNPI)
ANISOVICH 10	EPJ A44 203	A.V. Anisovich <i>et al.</i>	(BONN, PNPI)
DRECHSEL 07	EPJ A34 69	D. Drechsel, S.S. Kamalov, L. Tiator	(MAINZ, JINR)
DUGGER 07	PR C76 025211	M. Dugger <i>et al.</i>	(Jefferson Lab CLAS Collab.)
ARNDT 06	PR C74 045205	R.A. Arndt <i>et al.</i>	(GWU)
BREITSCHOP...06	PL B639 424	J. Breitschopf <i>et al.</i>	(TUBIN, HEBR, CSUS)
GRIDNEV 06	PAN 69 1542	A.B. Gridnev <i>et al.</i>	(PNPI, BONN, GWU)
PDG 06	JPG 33 1	W.-M. Yao <i>et al.</i>	(PDG Collab.)
AHRENS 04A	EPJ A21 323	J. Ahrens <i>et al.</i>	(Mainz GDH, A2 Collab.)
ARNDT 04	PR C69 035213	R.A. Arndt <i>et al.</i>	(GWU, TRIU)
ARNDT 02	PR C66 055213	R.A. Arndt <i>et al.</i>	(GWU)
KOTULLA 02	PRL 89 272001	M. Kotulla <i>et al.</i>	(MAMI TAPS Collab.)
PENNER 02C	PR C66 055211	G. Penner, U. Mosel	(GIES)
PENNER 02D	PR C66 055212	G. Penner, U. Mosel	(GIES)
BLANPIED 01	PR C64 025203	G. Blanpied <i>et al.</i>	(BNL LEGS Collab.)
GALLER 01	PL B503 245	G. Galler <i>et al.</i>	(Mainz LARA Collab.)
HOHLER 01	NSTAR 2001 185	G. Hohler	(KARL)
LOPEZCAST...01	PL B517 339	G. Lopez Castro, A. Mariano	
Also	NP A697 440	G. Lopez Castro, A. Mariano	
BECK 00	PR C61 035204	R. Beck <i>et al.</i>	(Mainz Microtron DAPHNE Col.)
VRANA 00	PRPL 328 181	T.P. Vrana, S.A. Dytman, T.-S.H. Lee	(PITT+)
KAMALOV 99	PRL 83 4494	S.S. Kamalov, S.N. Yang	(Taiwan U.)
HANSTEIN 98	NP A632 561	O. Hanstein, D. Drechsel, L. Tiator	(VPI)
ARNDT 97	PR C56 577	R.A. Arndt, I.I. Strakovsky, R.L. Workman	(VPI)
BECK 97	PRL 78 606	R. Beck <i>et al.</i>	(MANZ, SACL, PAVI, GLAS)
Also	PRL 79 4510	R.L. Beck, H.P. Krahn	(MANZ)
Also	PRL 79 4512	R.L. Beck, H.P. Krahn	(MANZ)
Also	PRL 79 4515 (erratum)	R.L. Beck <i>et al.</i>	(MANZ, SACL, PAVI, GLAS)
BLANPIED 97	PRL 79 4337	G.S. Blanpied <i>et al.</i>	(LEGS Collab.)
DAVIDSON 97	PRL 79 4509	R.M. Davidson, N.C.A. Mukhopadhyay	(RPI)
ARNDT 96	PR C53 430	R.A. Arndt, I.I. Strakovsky, R.L. Workman	(VPI)
BERNICHIA 96	NP A597 623	A. Bernicha, G. Lopez Castro, J. Pestieau	(LOUV+)
HANSTEIN 96	PL B385 45	O. Hanstein, D. Drechsel, L. Tiator	(MANZ)
ABAEV 95	ZPHY A352 85	V.V. Abaev, S.P. Kruglov	(PNPI)
ARNDT 95	PR C52 2120	R.A. Arndt <i>et al.</i>	(VPI, BRCO)
KHANDAKER 95	PR D51 3946	M. Khandaker, A.M. Sandorff	(BNL, VPI)
HOEHLER 93	$\pi N$ Newsletter 9 1	G. Hoehler	(KARL)
LI 93	PR C47 2759	Z.J. Li <i>et al.</i>	(VPI)
MANLEY 92	PR D45 4002	D.M. Manley, E.M. Saleski	(KENT) IJP
Also	PR D30 904	D.M. Manley <i>et al.</i>	(VPI)
WORKMAN 92	PR C46 1546	R.L. Workman, R.A. Arndt, Z.J. Li	(VPI)
ARNDT 91	PR D43 2131	R.A. Arndt <i>et al.</i>	(VPI, TELE) IJP
BOSSHARD 91	PR D44 1962	A. Bosshard <i>et al.</i>	(ZURI, LBL, VILL+)
Also	PRL 64 2619	A. Bosshard <i>et al.</i>	(CATH, LAUS, LBL+)
DAVIDSON 91B	PR D43 71	R.M. Davidson, N.C. Mukhopadhyay, R.S. Wittman	(CUNY)
LIN 91B	PR C44 1819	D.H. Lin, M.K. Liou, Z.M. Ding	(CUNY, CSOK)
Also	PR C43 8930	D. Lin, M.K. Liou	(CUNY)
DAVIDSON 90	PR D42 20	R.M. Davidson, N.C. Mukhopadhyay	(RPI)
WITTMAN 88	PR C37 2075	R. Wittman	(TRIU)
HELLER 87	PR C35 718	L. Heller <i>et al.</i>	(LANL, MIT, ILL)
DAVIDSON 86	PRL 56 804	R.M. Davidson, N.C. Mukhopadhyay, R. Wittman	(RPI)
TANABE 85	PR C31 1876	H. Tanabe, K. Ohta	(KOMAB)
CRAWFORD 83	NP B211 1	R.L. Crawford, W.T. Morton	(GLAS)
PDG 82	PL 111B 1	M. Roos <i>et al.</i>	(HELS, CIT, CERN)
AWAJI 81	Bonn Conf. 352	N. Awaji, R. Kajikawa	(NAGO)
Also	NP B197 365	K. Fujii <i>et al.</i>	(NAGO)
CUTKOSKY 80	Toronto Conf. 19	R.E. Cutkosky <i>et al.</i>	(CMU, LBL) IJP
Also	PR D20 2839	R.E. Cutkosky <i>et al.</i>	(CMU, LBL)
KOCH 80B	NP A336 331	R. Koch, E. Pietarinen	(KARLT) IJP
HOEHLER 79	PDAT 12-1	G. Hoehler <i>et al.</i>	(KARLT) IJP
Also	Toronto Conf. 3	R. Koch	(KARLT) IJP
MIROSHNICH... 79	SJNP 29 94	I.I. Miroshnichenko <i>et al.</i>	(KFTI) IJP
Also	Translated from YAF 29 188.		
NEFKENS 78	PR D18 3911	B.M.K. Nefkens <i>et al.</i>	(UCLA, CATH) IJP
PEDRONI 78	NP A300 321	E. Pedroni <i>et al.</i>	(SIN, ISNG, KARLE+) IJP

$\Delta(1600) 3/2^+$

$I(J^P) = \frac{3}{2}(\frac{3}{2}^+)$  Status: \*\*\*

Most of the results published before 1975 are now obsolete and have been omitted. They may be found in our 1982 edition, Physics Letters **111B** 1 (1982). Some further obsolete results published before 1984 were last included in our 2006 edition, Journal of Physics, G **33** 1 (2006).

The various analyses are not in good agreement.

$\Delta(1600)$  BREIT-WIGNER MASS

VALUE (MeV)	DOCUMENT ID	TECN	COMMENT
<b>1500 to 1700 (<math>\approx 1600</math>) OUR ESTIMATE</b>			
1510 ± 20	ANISOVICH 12A	DPWA	Multichannel
1706 ± 10	MANLEY 92	IPWA	$\pi N \rightarrow \pi N$ & $N \pi \pi$
1600 ± 50	CUTKOSKY 80	IPWA	$\pi N \rightarrow \pi N$
1522 ± 13	HOEHLER 79	IPWA	$\pi N \rightarrow \pi N$
••• We do not use the following data for averages, fits, limits, etc. •••			
1650 ± 40	HORN 08A	DPWA	Multichannel
1667 ± 1	PENNER 02C	DPWA	Multichannel
1687 ± 44	VRANA 00	DPWA	Multichannel
1672 ± 15	ARNDT 96	IPWA	$\gamma N \rightarrow \pi N$
1706	LI 93	IPWA	$\gamma N \rightarrow \pi N$
1690	BARNHAM 80	IPWA	$\pi N \rightarrow N \pi \pi$
1560	<sup>1</sup> LONGACRE 77	IPWA	$\pi N \rightarrow N \pi \pi$
1640	<sup>2</sup> LONGACRE 75	IPWA	$\pi N \rightarrow N \pi \pi$

$\Delta(1600)$  BREIT-WIGNER WIDTH

VALUE (MeV)	DOCUMENT ID	TECN	COMMENT
<b>220 to 420 (<math>\approx 320</math>) OUR ESTIMATE</b>			
220 ± 45	ANISOVICH 12A	DPWA	Multichannel
430 ± 73	MANLEY 92	IPWA	$\pi N \rightarrow \pi N$ & $N \pi \pi$
300 ± 100	CUTKOSKY 80	IPWA	$\pi N \rightarrow \pi N$
220 ± 40	HOEHLER 79	IPWA	$\pi N \rightarrow \pi N$
••• We do not use the following data for averages, fits, limits, etc. •••			
530 ± 60	HORN 08A	DPWA	Multichannel
397 ± 10	PENNER 02C	DPWA	Multichannel
493 ± 75	VRANA 00	DPWA	Multichannel
315 ± 20	ARNDT 96	IPWA	$\gamma N \rightarrow \pi N$
215	LI 93	IPWA	$\gamma N \rightarrow \pi N$
250	BARNHAM 80	IPWA	$\pi N \rightarrow N \pi \pi$
180	<sup>1</sup> LONGACRE 77	IPWA	$\pi N \rightarrow N \pi \pi$
300	<sup>2</sup> LONGACRE 75	IPWA	$\pi N \rightarrow N \pi \pi$

$\Delta(1600)$  POLE POSITION

REAL PART VALUE (MeV)	DOCUMENT ID	TECN	COMMENT
<b>1460 to 1560 (<math>\approx 1510</math>) OUR ESTIMATE</b>			
1498 ± 25	ANISOVICH 12A	DPWA	Multichannel
1457	ARNDT 06	DPWA	$\pi N \rightarrow \pi N, \eta N$
1550	<sup>3</sup> HOEHLER 93	SPED	$\pi N \rightarrow \pi N$
1550 ± 40	CUTKOSKY 80	IPWA	$\pi N \rightarrow \pi N$
••• We do not use the following data for averages, fits, limits, etc. •••			
1510 <sup>+20</sup> <sub>-50</sub>	HORN 08A	DPWA	Multichannel
1599	VRANA 00	DPWA	Multichannel
1675	ARNDT 95	DPWA	$\pi N \rightarrow N \pi$
1612	ARNDT 91	DPWA	$\pi N \rightarrow \pi N$ Soln SM90
1609 or 1610	<sup>4</sup> LONGACRE 78	IPWA	$\pi N \rightarrow N \pi \pi$
1541 or 1542	<sup>1</sup> LONGACRE 77	IPWA	$\pi N \rightarrow N \pi \pi$

−2×IMAGINARY PART

VALUE (MeV)	DOCUMENT ID	TECN	COMMENT
<b>200 to 350 (<math>\approx 275</math>) OUR ESTIMATE</b>			
230 ± 50	ANISOVICH 12A	DPWA	Multichannel
400	ARNDT 06	DPWA	$\pi N \rightarrow \pi N, \eta N$
200 ± 60	CUTKOSKY 80	IPWA	$\pi N \rightarrow \pi N$
••• We do not use the following data for averages, fits, limits, etc. •••			
230 ± 40	HORN 08A	DPWA	Multichannel
312	VRANA 00	DPWA	Multichannel
386	ARNDT 95	DPWA	$\pi N \rightarrow N \pi$
230	ARNDT 91	DPWA	$\pi N \rightarrow \pi N$ Soln SM90
323 or 325	<sup>4</sup> LONGACRE 78	IPWA	$\pi N \rightarrow N \pi \pi$
178 or 178	<sup>1</sup> LONGACRE 77	IPWA	$\pi N \rightarrow N \pi \pi$

## Baryon Particle Listings

 $\Delta(1600)$  $\Delta(1600)$  ELASTIC POLE RESIDUEMODULUS  $|r|$ 

VALUE (MeV)	DOCUMENT ID	TECN	COMMENT
11±6	ANISOVICH 12A	DPWA	Multichannel
44	ARNDT 06	DPWA	$\pi N \rightarrow \pi N, \eta N$
17±4	CUTKOSKY 80	IPWA	$\pi N \rightarrow \pi N$
••• We do not use the following data for averages, fits, limits, etc. •••			
52	ARNDT 95	DPWA	$\pi N \rightarrow N\pi$
16	ARNDT 91	DPWA	$\pi N \rightarrow \pi N$ Soln SM90

PHASE  $\theta$ 

VALUE (°)	DOCUMENT ID	TECN	COMMENT
-160±33	ANISOVICH 12A	DPWA	Multichannel
+147	ARNDT 06	DPWA	$\pi N \rightarrow \pi N, \eta N$
-150±30	CUTKOSKY 80	IPWA	$\pi N \rightarrow \pi N$
••• We do not use the following data for averages, fits, limits, etc. •••			
+14	ARNDT 95	DPWA	$\pi N \rightarrow N\pi$
-73	ARNDT 91	DPWA	$\pi N \rightarrow \pi N$ Soln SM90

 $\Delta(1600)$  INELASTIC POLE RESIDUE

The "normalized residue" is the residue divided by  $\Gamma_{pole}$ .

Normalized residue in  $N\pi \rightarrow \Delta(1600) \rightarrow \Delta\pi, P$ -wave

MODULUS (%)	PHASE (°)	DOCUMENT ID	TECN	COMMENT
14±10	154±40	ANISOVICH 12A	DPWA	Multichannel

Normalized residue in  $N\pi \rightarrow \Delta(1600) \rightarrow \Delta\pi, F$ -wave

MODULUS (%)	DOCUMENT ID	TECN	COMMENT
1.0±0.5	ANISOVICH 12A	DPWA	Multichannel

 $\Delta(1600)$  DECAY MODES

The following branching fractions are our estimates, not fits or averages.

Mode	Fraction ( $\Gamma_i/\Gamma$ )
$\Gamma_1$ $N\pi$	10–25 %
$\Gamma_2$ $\Sigma K$	
$\Gamma_3$ $N\pi\pi$	75–90 %
$\Gamma_4$ $\Delta\pi$	40–70 %
$\Gamma_5$ $\Delta(1232)\pi, P$ -wave	
$\Gamma_6$ $\Delta(1232)\pi, F$ -wave	
$\Gamma_7$ $N\rho$	<25 %
$\Gamma_8$ $N\rho, S=1/2, P$ -wave	
$\Gamma_9$ $N\rho, S=3/2, P$ -wave	
$\Gamma_{10}$ $N\rho, S=3/2, F$ -wave	
$\Gamma_{11}$ $N(1440)\pi$	10–35 %
$\Gamma_{12}$ $N(1440)\pi, P$ -wave	
$\Gamma_{13}$ $N\gamma$	0.001–0.035 %
$\Gamma_{14}$ $N\gamma, \text{helicity}=1/2$	0.0–0.02 %
$\Gamma_{15}$ $N\gamma, \text{helicity}=3/2$	0.001–0.015 %

 $\Delta(1600)$  BRANCHING RATIOS

$\Gamma(N\pi)/\Gamma_{total}$	DOCUMENT ID	TECN	COMMENT	$\Gamma_1/\Gamma$
10 to 25 OUR ESTIMATE				
12±5	ANISOVICH 12A	DPWA	Multichannel	
12±2	MANLEY 92	IPWA	$\pi N \rightarrow \pi N$ & $N\pi\pi$	
18±4	CUTKOSKY 80	IPWA	$\pi N \rightarrow \pi N$	
21±6	HOEHLER 79	IPWA	$\pi N \rightarrow \pi N$	
••• We do not use the following data for averages, fits, limits, etc. •••				
10±3	HORN 08A	DPWA	Multichannel	
13±1	PENNER 02C	DPWA	Multichannel	
28±5	VRANA 00	DPWA	Multichannel	

$(\Gamma_i\Gamma_f)^{1/2}/\Gamma_{total}$ in $N\pi \rightarrow \Delta(1600) \rightarrow \Sigma K$	DOCUMENT ID	TECN	COMMENT	$(\Gamma_1\Gamma_5)^{1/2}/\Gamma$
-0.36 to -0.28 OUR ESTIMATE				
0.006 to 0.042	<sup>5</sup> DEANS 75	DPWA	$\pi N \rightarrow \Sigma K$	

Note: Signs of couplings from  $\pi N \rightarrow N\pi\pi$  analyses were changed in the 1986 edition to agree with the baryon-first convention; the overall phase ambiguity is resolved by choosing a negative sign for the  $\Delta(1620) S_{31}$  coupling to  $\Delta(1232)\pi$ .

$(\Gamma_i\Gamma_f)^{1/2}/\Gamma_{total}$ in $N\pi \rightarrow \Delta(1600) \rightarrow \Delta(1232)\pi, P$ -wave	DOCUMENT ID	TECN	COMMENT	$(\Gamma_1\Gamma_5)^{1/2}/\Gamma$
+0.27 to +0.33 OUR ESTIMATE				
+0.29±0.02	MANLEY 92	IPWA	$\pi N \rightarrow \pi N$ & $N\pi\pi$	
+0.24±0.05	BARNHAM 80	IPWA	$\pi N \rightarrow N\pi\pi$	
+0.34	<sup>1,6</sup> LONGACRE 77	IPWA	$\pi N \rightarrow N\pi\pi$	
+0.30	<sup>2</sup> LONGACRE 75	IPWA	$\pi N \rightarrow N\pi\pi$	

 $\Gamma(\Delta(1232)\pi, P$ -wave) $/\Gamma_{total}$ 

VALUE (%)	DOCUMENT ID	TECN	COMMENT	$\Gamma_5/\Gamma$
78±6	ANISOVICH 12A	DPWA	Multichannel	
59±10	VRANA 00	DPWA	Multichannel	

$(\Gamma_i\Gamma_f)^{1/2}/\Gamma_{total}$ in $N\pi \rightarrow \Delta(1600) \rightarrow \Delta(1232)\pi, F$ -wave	DOCUMENT ID	TECN	COMMENT	$(\Gamma_1\Gamma_6)^{1/2}/\Gamma$
-0.15 to -0.03 OUR ESTIMATE				
-0.07	<sup>1,6</sup> LONGACRE 77	IPWA	$\pi N \rightarrow N\pi\pi$	

$(\Gamma_i\Gamma_f)^{1/2}/\Gamma_{total}$ in $N\pi \rightarrow \Delta(1600) \rightarrow N\rho, S=1/2, P$ -wave	DOCUMENT ID	TECN	COMMENT	$(\Gamma_1\Gamma_8)^{1/2}/\Gamma$
+0.10	<sup>1,6</sup> LONGACRE 77	IPWA	$\pi N \rightarrow N\pi\pi$	

$(\Gamma_i\Gamma_f)^{1/2}/\Gamma_{total}$ in $N\pi \rightarrow \Delta(1600) \rightarrow N\rho, S=3/2, P$ -wave	DOCUMENT ID	TECN	COMMENT	$(\Gamma_1\Gamma_9)^{1/2}/\Gamma$
+0.10	<sup>1,6</sup> LONGACRE 77	IPWA	$\pi N \rightarrow N\pi\pi$	

$(\Gamma_i\Gamma_f)^{1/2}/\Gamma_{total}$ in $N\pi \rightarrow \Delta(1600) \rightarrow N(1440)\pi, P$ -wave	DOCUMENT ID	TECN	COMMENT	$(\Gamma_1\Gamma_{12})^{1/2}/\Gamma$
+0.15 to +0.23 OUR ESTIMATE				
+0.16±0.02	MANLEY 92	IPWA	$\pi N \rightarrow \pi N$ & $N\pi\pi$	
+0.23±0.04	BARNHAM 80	IPWA	$\pi N \rightarrow N\pi\pi$	

$\Gamma(N(1440)\pi)/\Gamma_{total}$	DOCUMENT ID	TECN	COMMENT	$\Gamma_{11}/\Gamma$
13±4	VRANA 00	DPWA	Multichannel	

 $\Delta(1600)$  PHOTON DECAY AMPLITUDES

Papers on  $\gamma N$  amplitudes predating 1981 may be found in our 2006 edition, Journal of Physics, G 33 1 (2006).

 $\Delta(1600) \rightarrow N\gamma, \text{helicity-1/2}$  amplitude  $A_{1/2}$ 

VALUE ( $\text{GeV}^{-1/2}$ )	DOCUMENT ID	TECN	COMMENT
-0.023±0.020 OUR ESTIMATE			
-0.050±0.009	ANISOVICH 12A	DPWA	Multichannel
-0.018±0.015	ARNDT 96	IPWA	$\gamma N \rightarrow \pi N$
-0.039±0.030	CRAWFORD 83	IPWA	$\gamma N \rightarrow \pi N$
-0.046±0.013	AWAJI 81	DPWA	$\gamma N \rightarrow \pi N$
••• We do not use the following data for averages, fits, limits, etc. •••			
0.0	PENNER 02D	DPWA	Multichannel
-0.026±0.002	LI 93	IPWA	$\gamma N \rightarrow \pi N$
-0.200	<sup>7</sup> WADA 84	DPWA	Compton scattering
0.000±0.030	BARBOUR 78	DPWA	$\gamma N \rightarrow \pi N$

 $\Delta(1600) \rightarrow N\gamma, \text{helicity-3/2}$  amplitude  $A_{3/2}$ 

VALUE ( $\text{GeV}^{-1/2}$ )	DOCUMENT ID	TECN	COMMENT
-0.009±0.021 OUR ESTIMATE			
-0.040±0.012	ANISOVICH 12A	DPWA	Multichannel
-0.025±0.015	ARNDT 96	IPWA	$\gamma N \rightarrow \pi N$
-0.013±0.014	CRAWFORD 83	IPWA	$\gamma N \rightarrow \pi N$
0.025±0.031	AWAJI 81	DPWA	$\gamma N \rightarrow \pi N$
••• We do not use the following data for averages, fits, limits, etc. •••			
-0.024	PENNER 02D	DPWA	Multichannel
-0.016±0.002	LI 93	IPWA	$\gamma N \rightarrow \pi N$
0.023	WADA 84	DPWA	Compton scattering
0.000±0.045	BARBOUR 78	DPWA	$\gamma N \rightarrow \pi N$

 $\Delta(1600)$  FOOTNOTES

<sup>1</sup> LONGACRE 77 pole positions are from a search for poles in the unitarized T-matrix; the first (second) value uses, in addition to  $\pi N \rightarrow N\pi\pi$  data, elastic amplitudes from a Saclay (CERN) partial-wave analysis. The other LONGACRE 77 values are from eyeball fits with Breit-Wigner circles to the T-matrix amplitudes.

<sup>2</sup> From method II of LONGACRE 75: eyeball fits with Breit-Wigner circles to the T-matrix amplitudes.

<sup>3</sup> See HOEHLER 93 for a detailed discussion of the evidence for and the pole parameters of  $N$  and  $\Delta$  resonances as determined from Argand diagrams of  $\pi N$  elastic partial-wave amplitudes and from plots of the speeds with which the amplitudes traverse the diagrams.

<sup>4</sup> LONGACRE 78 values are from a search for poles in the unitarized T-matrix. The first (second) value uses, in addition to  $\pi N \rightarrow N\pi\pi$  data, elastic amplitudes from a Saclay (CERN) partial-wave analysis.

<sup>5</sup> The range given is from the four best solutions. DEANS 75 disagrees with  $\pi^+ p \rightarrow \Sigma^+ K^+$  data of WINNIK 77 around 1920 MeV.

<sup>6</sup> LONGACRE 77 considers this coupling to be well determined.

<sup>7</sup> WADA 84 is inconsistent with other analyses — see the Note on  $N$  and  $\Delta$  Resonances.

See key on page 457

# Baryon Particle Listings

## $\Delta(1600)$ , $\Delta(1620)$

### $\Delta(1600)$ REFERENCES

For early references, see Physics Letters **111B** 1 (1982).

ANISOVICH	12A	EPJ A48 15	A.V. Anisovich <i>et al.</i>	(BONN, PNPI)
HORN	08A	EPJ A38 173	I. Horn <i>et al.</i>	(CB-ELSA Collab.)
Also		PRL 101 202002	I. Horn <i>et al.</i>	(CB-ELSA Collab.)
ARNDT	06	PR C74 045205	R.A. Arndt <i>et al.</i>	(GVU)
PDG	06	JPG 33 1	W.-M. Yao <i>et al.</i>	(PDG Collab.)
PENNER	02C	PR C66 055211	G. Penner, U. Mosel	(GIES)
PENNER	02D	PR C66 055212	G. Penner, U. Mosel	(GIES)
VRANA	00	PRPL 328 181	T.P. Vrana, S.A. Dytman, T.-S.H. Lee	(PITT+)
ARNDT	96	PR C53 430	R.A. Arndt, I.I. Strakovsky, R.L. Workman	(VPI)
ARNDT	95	PR C52 2120	R.A. Arndt <i>et al.</i>	(VPI, BRCO)
HOEHLER	93	$\pi$ N Newsletter 9 1	G. Hohler	(KARL)
LI	93	PR C47 2759	Z.J. Li <i>et al.</i>	(VPI)
MANLEY	92	PR D45 4002	D.M. Manley, E.M. Saleski	(KENT) IJP
Also		PR D30 904	D.M. Manley <i>et al.</i>	(VPI)
ARNDT	91	PR D43 2131	R.A. Arndt <i>et al.</i>	(VPI, TELE) IJP
WADA	84	NP B247 313	Y. Wada <i>et al.</i>	(INUS)
CRAWFORD	83	NP B211 1	R.L. Crawford, W.T. Morton	(GLAS)
PDG	82	PL 111B 1	M. Roos <i>et al.</i>	(HELS, CIT, CERN)
AWAJI	81	Bonn Conf. 352	N. Awaji, R. Kajikawa	(NAGO)
Also		NP B197 365	K. Fujii <i>et al.</i>	(NAGO)
BARNHAM	80	NP B168 243	K.W.J. Barnham <i>et al.</i>	(LOIC)
CUTKOSKY	80	Toronto Conf. 19	R.E. Cutkosky <i>et al.</i>	(CMU, LBL) IJP
Also		PR D20 2839	R.E. Cutkosky <i>et al.</i>	(CMU, LBL) IJP
HOEHLER	79	PDAT 12-1	G. Hohler <i>et al.</i>	(KARLT) IJP
Also		Toronto Conf. 3	R. Koch	(KARLT) IJP
BARBOUR	78	NP B141 253	I.M. Barbour, R.L. Crawford, N.H. Parsons	(GLAS)
LONGACRE	78	PR D17 1735	R.S. Longacre <i>et al.</i>	(LBL, SLAC)
LONGACRE	77	NP B122 493	R.S. Longacre, J. Dolbeau	(SACL) IJP
Also		NP B108 365	J. Dolbeau <i>et al.</i>	(SACL) IJP
WINNIK	77	NP B128 66	M. Winnik <i>et al.</i>	(HAIF) I
DEANS	75	NP B96 90	S.R. Deans <i>et al.</i>	(SFLA, ALAH) IJP
LONGACRE	75	PL 55B 415	R.S. Longacre <i>et al.</i>	(LBL, SLAC) IJP

### $\Delta(1620)$ POLE POSITION

#### REAL PART

VALUE (MeV)	DOCUMENT ID	TECN	COMMENT
<b>1590 to 1610 (<math>\approx</math> 1600) OUR ESTIMATE</b>			
1597 $\pm$ 4	ANISOVICH 12A	DPWA	Multichannel
1595	ARNDT 06	DPWA	$\pi N \rightarrow \pi N, \eta N$
1608	4 HOEHLER 93	SPED	$\pi N \rightarrow \pi N$
1600 $\pm$ 15	CUTKOSKY 80	IPWA	$\pi N \rightarrow \pi N$
• • • We do not use the following data for averages, fits, limits, etc. • • •			
1596 $\pm$ 7	ANISOVICH 10	DPWA	Multichannel
1615 $\pm$ 25	THOMA 08	DPWA	Multichannel
1594	ARNDT 04	DPWA	$\pi N \rightarrow \pi N, \eta N$
1607	VRANA 00	DPWA	Multichannel
1585	ARNDT 95	DPWA	$\pi N \rightarrow N\pi$
1587	ARNDT 91	DPWA	$\pi N \rightarrow \pi N$ Soln SM90
1583 or 1583	5 LONGACRE 78	IPWA	$\pi N \rightarrow N\pi\pi$
1575 or 1572	2 LONGACRE 77	IPWA	$\pi N \rightarrow N\pi\pi$

#### –2xIMAGINARY PART

VALUE (MeV)	DOCUMENT ID	TECN	COMMENT
<b>120 to 140 (<math>\approx</math> 130) OUR ESTIMATE</b>			
130 $\pm$ 9	ANISOVICH 12A	DPWA	Multichannel
135	ARNDT 06	DPWA	$\pi N \rightarrow \pi N, \eta N$
116	4 HOEHLER 93	SPED	$\pi N \rightarrow \pi N$
120 $\pm$ 20	CUTKOSKY 80	IPWA	$\pi N \rightarrow \pi N$
• • • We do not use the following data for averages, fits, limits, etc. • • •			
130 $\pm$ 10	ANISOVICH 10	DPWA	Multichannel
180 $\pm$ 35	THOMA 08	DPWA	Multichannel
118	ARNDT 04	DPWA	$\pi N \rightarrow \pi N, \eta N$
148	VRANA 00	DPWA	Multichannel
104	ARNDT 95	DPWA	$\pi N \rightarrow N\pi$
120	ARNDT 91	DPWA	$\pi N \rightarrow \pi N$ Soln SM90
143 or 149	5 LONGACRE 78	IPWA	$\pi N \rightarrow N\pi\pi$
119 or 128	2 LONGACRE 77	IPWA	$\pi N \rightarrow N\pi\pi$

### $\Delta(1620)$ ELASTIC POLE RESIDUE

#### MODULUS $|r|$

VALUE (MeV)	DOCUMENT ID	TECN	COMMENT
18 $\pm$ 2	ANISOVICH 12A	DPWA	Multichannel
15	ARNDT 06	DPWA	$\pi N \rightarrow \pi N, \eta N$
19	HOEHLER 93	SPED	$\pi N \rightarrow \pi N$
15 $\pm$ 2	CUTKOSKY 80	IPWA	$\pi N \rightarrow \pi N$
• • • We do not use the following data for averages, fits, limits, etc. • • •			
17	ARNDT 04	DPWA	$\pi N \rightarrow \pi N, \eta N$
14	ARNDT 95	DPWA	$\pi N \rightarrow N\pi$
15	ARNDT 91	DPWA	$\pi N \rightarrow \pi N$ Soln SM90

#### PHASE $\theta$

VALUE (°)	DOCUMENT ID	TECN	COMMENT
–100 $\pm$ 5	ANISOVICH 12A	DPWA	Multichannel
–92	ARNDT 06	DPWA	$\pi N \rightarrow \pi N, \eta N$
–95	HOEHLER 93	SPED	$\pi N \rightarrow \pi N$
–110 $\pm$ 20	CUTKOSKY 80	IPWA	$\pi N \rightarrow \pi N$
• • • We do not use the following data for averages, fits, limits, etc. • • •			
–104	ARNDT 04	DPWA	$\pi N \rightarrow \pi N, \eta N$
–121	ARNDT 95	DPWA	$\pi N \rightarrow N\pi$
–125	ARNDT 91	DPWA	$\pi N \rightarrow \pi N$ Soln SM90

### $\Delta(1620)$ INELASTIC POLE RESIDUE

The “normalized residue” is the residue divided by  $\Gamma_{pole}$ .

#### Normalized residue in $N\pi \rightarrow \Delta(1620) \rightarrow \Delta\pi, D$ -wave

MODULUS (%)	PHASE (°)	DOCUMENT ID	TECN	COMMENT
38 $\pm$ 9	–85 $\pm$ 30	ANISOVICH 12A	DPWA	Multichannel

### $\Delta(1620)$ DECAY MODES

The following branching fractions are our estimates, not fits or averages.

Mode	Fraction ( $\Gamma_i/\Gamma$ )
$\Gamma_1$ $N\pi$	20–30 %
$\Gamma_2$ $N\pi\pi$	70–80 %
$\Gamma_3$ $\Delta\pi$	30–60 %
$\Gamma_4$ $\Delta(1232)\pi, D$ -wave	
$\Gamma_5$ $N\rho$	7–25 %
$\Gamma_6$ $N\rho, S=1/2, S$ -wave	
$\Gamma_7$ $N\rho, S=3/2, D$ -wave	
$\Gamma_8$ $N(1440)\pi$	
$\Gamma_9$ $N\gamma$	0.03–0.10 %
$\Gamma_{10}$ $N\gamma, \text{helicity}=1/2$	0.03–0.10 %

## $\Delta(1620) 1/2^-$

$$I(J^P) = \frac{3}{2}(\frac{1}{2}^-) \text{ Status: } ***$$

Most of the results published before 1975 were last included in our 1982 edition, Physics Letters **111B** 1 (1982). Some further obsolete results published before 1984 were last included in our 2006 edition, Journal of Physics, G **33** 1 (2006).

### $\Delta(1620)$ BREIT-WIGNER MASS

VALUE (MeV)	DOCUMENT ID	TECN	COMMENT
<b>1600 to 1660 (<math>\approx</math> 1630) OUR ESTIMATE</b>			
1600 $\pm$ 8	ANISOVICH 12A	DPWA	Multichannel
1615.2 $\pm$ 0.4	ARNDT 06	DPWA	$\pi N \rightarrow \pi N, \eta N$
1672 $\pm$ 7	MANLEY 92	IPWA	$\pi N \rightarrow \pi N \& N\pi\pi$
1620 $\pm$ 20	CUTKOSKY 80	IPWA	$\pi N \rightarrow \pi N$
1610 $\pm$ 7	HOEHLER 79	IPWA	$\pi N \rightarrow \pi N$
• • • We do not use the following data for averages, fits, limits, etc. • • •			
1625 $\pm$ 10	ANISOVICH 10	DPWA	Multichannel
1650 $\pm$ 25	THOMA 08	DPWA	Multichannel
1614.1 $\pm$ 1.1	ARNDT 04	DPWA	$\pi N \rightarrow \pi N, \eta N$
1612 $\pm$ 2	PENNER 02C	DPWA	Multichannel
1617 $\pm$ 15	VRANA 00	DPWA	Multichannel
1672 $\pm$ 5	ARNDT 96	IPWA	$\gamma N \rightarrow \pi N$
1617	ARNDT 95	DPWA	$\pi N \rightarrow N\pi$
1669	LI 93	IPWA	$\gamma N \rightarrow \pi N$
1620	BARNHAM 80	IPWA	$\pi N \rightarrow N\pi\pi$
1712.8 $\pm$ 6.0	1 CHEW 80	BPWA	$\pi^+ p \rightarrow \pi^+ p$
1786.7 $\pm$ 2.0	1 CHEW 80	BPWA	$\pi^+ p \rightarrow \pi^+ p$
1580	2 LONGACRE 77	IPWA	$\pi N \rightarrow N\pi\pi$
1600	3 LONGACRE 75	IPWA	$\pi N \rightarrow N\pi\pi$

### $\Delta(1620)$ BREIT-WIGNER WIDTH

VALUE (MeV)	DOCUMENT ID	TECN	COMMENT
<b>130 to 150 (<math>\approx</math> 140) OUR ESTIMATE</b>			
130 $\pm$ 11	ANISOVICH 12A	DPWA	Multichannel
146.9 $\pm$ 1.9	ARNDT 06	DPWA	$\pi N \rightarrow \pi N, \eta N$
154 $\pm$ 37	MANLEY 92	IPWA	$\pi N \rightarrow \pi N \& N\pi\pi$
140 $\pm$ 20	CUTKOSKY 80	IPWA	$\pi N \rightarrow \pi N$
139 $\pm$ 18	HOEHLER 79	IPWA	$\pi N \rightarrow \pi N$
• • • We do not use the following data for averages, fits, limits, etc. • • •			
148 $\pm$ 15	ANISOVICH 10	DPWA	Multichannel
250 $\pm$ 60	THOMA 08	DPWA	Multichannel
141.0 $\pm$ 6.0	ARNDT 04	DPWA	$\pi N \rightarrow \pi N, \eta N$
202 $\pm$ 7	PENNER 02C	DPWA	Multichannel
143 $\pm$ 42	VRANA 00	DPWA	Multichannel
147 $\pm$ 8	ARNDT 96	IPWA	$\gamma N \rightarrow \pi N$
108	ARNDT 95	DPWA	$\pi N \rightarrow N\pi$
184	LI 93	IPWA	$\gamma N \rightarrow \pi N$
120	BARNHAM 80	IPWA	$\pi N \rightarrow N\pi\pi$
228.3 $\pm$ 18.0	1 CHEW 80	BPWA	$\pi^+ p \rightarrow \pi^+ p$ (lower mass)
30.0 $\pm$ 6.4	1 CHEW 80	BPWA	$\pi^+ p \rightarrow \pi^+ p$ (higher mass)
120	2 LONGACRE 77	IPWA	$\pi N \rightarrow N\pi\pi$
150	3 LONGACRE 75	IPWA	$\pi N \rightarrow N\pi\pi$

## Baryon Particle Listings

 $\Delta(1620)$ ,  $\Delta(1700)$  $\Delta(1620)$  BRANCHING RATIOS

$\Gamma(N\pi)/\Gamma_{\text{total}}$		DOCUMENT ID	TECN	COMMENT	$\Gamma_1/\Gamma$
VALUE (%)					
<b>20 to 30 OUR ESTIMATE</b>					
28 $\pm$ 3		ANISOVICH	12A	DPWA Multichannel	
31.5 $\pm$ 0.1		ARNDT	06	DPWA $\pi N \rightarrow \pi N, \eta N$	
9 $\pm$ 2		MANLEY	92	IPWA $\pi N \rightarrow \pi N \& N\pi\pi$	
25 $\pm$ 3		CUTKOSKY	80	IPWA $\pi N \rightarrow \pi N$	
35 $\pm$ 6		HOEHLER	79	IPWA $\pi N \rightarrow \pi N$	
••• We do not use the following data for averages, fits, limits, etc. •••					
23 $\pm$ 5		ANISOVICH	10	DPWA Multichannel	
22 $\pm$ 12		THOMA	08	DPWA Multichannel	
31.0 $\pm$ 0.4		ARNDT	04	DPWA $\pi N \rightarrow \pi N, \eta N$	
34 $\pm$ 1		PENNER	02C	DPWA Multichannel	
45 $\pm$ 5		VRANA	00	DPWA Multichannel	
29		ARNDT	95	DPWA $\pi N \rightarrow N\pi$	
60		<sup>1</sup> CHEW	80	BPWA $\pi^+ p \rightarrow \pi^+ p$ (lower mass)	
36		<sup>1</sup> CHEW	80	BPWA $\pi^+ p \rightarrow \pi^+ p$ (higher mass)	

Note: Signs of couplings from  $\pi N \rightarrow N\pi\pi$  analyses were changed in the 1986 edition to agree with the baryon-first convention; the overall phase ambiguity is resolved by choosing a negative sign for the  $\Delta(1620)$   $S_{31}$  coupling to  $\Delta(1232)\pi$ .

$(\Gamma_1\Gamma_2)^{1/2}/\Gamma_{\text{total}}$ in $N\pi \rightarrow \Delta(1620) \rightarrow \Delta(1232)\pi$ , D-wave		DOCUMENT ID	TECN	COMMENT	$(\Gamma_1\Gamma_4)^{1/2}/\Gamma$
VALUE					
<b>-0.36 to -0.28 OUR ESTIMATE</b>					
-0.24 $\pm$ 0.03		MANLEY	92	IPWA $\pi N \rightarrow \pi N \& N\pi\pi$	
-0.33 $\pm$ 0.06		BARNHAM	80	IPWA $\pi N \rightarrow N\pi\pi$	
-0.39		<sup>2,6</sup> LONGACRE	77	IPWA $\pi N \rightarrow N\pi\pi$	
-0.40		<sup>3</sup> LONGACRE	75	IPWA $\pi N \rightarrow N\pi\pi$	

$\Gamma(\Delta(1232)\pi, D\text{-wave})/\Gamma_{\text{total}}$		DOCUMENT ID	TECN	COMMENT	$\Gamma_4/\Gamma$
VALUE (%)					
60 $\pm$ 17		ANISOVICH	12A	DPWA Multichannel	
39 $\pm$ 2		VRANA	00	DPWA Multichannel	
••• We do not use the following data for averages, fits, limits, etc. •••					
48 $\pm$ 25		THOMA	08	DPWA Multichannel	

$(\Gamma_1\Gamma_2)^{1/2}/\Gamma_{\text{total}}$ in $N\pi \rightarrow \Delta(1620) \rightarrow N\rho, S=1/2, S\text{-wave}$		DOCUMENT ID	TECN	COMMENT	$(\Gamma_1\Gamma_6)^{1/2}/\Gamma$
VALUE					
<b>+0.12 to +0.22 OUR ESTIMATE</b>					
+0.15 $\pm$ 0.02		MANLEY	92	IPWA $\pi N \rightarrow \pi N \& N\pi\pi$	
+0.40 $\pm$ 0.10		BARNHAM	80	IPWA $\pi N \rightarrow N\pi\pi$	
+0.08		<sup>2,6</sup> LONGACRE	77	IPWA $\pi N \rightarrow N\pi\pi$	
+0.28		<sup>3</sup> LONGACRE	75	IPWA $\pi N \rightarrow N\pi\pi$	

$\Gamma(N\rho, S=1/2, S\text{-wave})/\Gamma_{\text{total}}$		DOCUMENT ID	TECN	COMMENT	$\Gamma_6/\Gamma$
VALUE (%)					
14 $\pm$ 3		VRANA	00	DPWA Multichannel	

$(\Gamma_1\Gamma_2)^{1/2}/\Gamma_{\text{total}}$ in $N\pi \rightarrow \Delta(1620) \rightarrow N\rho, S=3/2, D\text{-wave}$		DOCUMENT ID	TECN	COMMENT	$(\Gamma_1\Gamma_7)^{1/2}/\Gamma$
VALUE					
<b>-0.15 to -0.03 OUR ESTIMATE</b>					
-0.06 $\pm$ 0.02		MANLEY	92	IPWA $\pi N \rightarrow \pi N \& N\pi\pi$	
-0.13		<sup>2,6</sup> LONGACRE	77	IPWA $\pi N \rightarrow N\pi\pi$	

$\Gamma(N\rho, S=3/2, D\text{-wave})/\Gamma_{\text{total}}$		DOCUMENT ID	TECN	COMMENT	$\Gamma_7/\Gamma$
VALUE (%)					
2 $\pm$ 1		VRANA	00	DPWA Multichannel	

$(\Gamma_1\Gamma_2)^{1/2}/\Gamma_{\text{total}}$ in $N\pi \rightarrow \Delta(1620) \rightarrow N(1440)\pi$		DOCUMENT ID	TECN	COMMENT	$(\Gamma_1\Gamma_8)^{1/2}/\Gamma$
VALUE					
0.11 $\pm$ 0.05		BARNHAM	80	IPWA $\pi N \rightarrow N\pi\pi$	

$\Gamma(N(1440)\pi)/\Gamma_{\text{total}}$		DOCUMENT ID	TECN	COMMENT	$\Gamma_8/\Gamma$
VALUE (%)					
0 $\pm$ 1		VRANA	00	DPWA Multichannel	
••• We do not use the following data for averages, fits, limits, etc. •••					
19 $\pm$ 12		THOMA	08	DPWA Multichannel	

 $\Delta(1620)$  PHOTON DECAY AMPLITUDES

Papers on  $\gamma N$  amplitudes predating 1981 may be found in our 2006 edition, Journal of Physics, G **33** 1 (2006).

 $\Delta(1620) \rightarrow N\gamma$ , helicity-1/2 amplitude  $A_{1/2}$ 

VALUE (GeV <sup>-1/2</sup> )	DOCUMENT ID	TECN	COMMENT
<b>+0.027 <math>\pm</math> 0.011 OUR ESTIMATE</b>			
0.052 $\pm$ 0.005	ANISOVICH	12A	DPWA Multichannel
0.050 $\pm$ 0.002	DUGGER	07	DPWA $\gamma N \rightarrow \pi N$
0.035 $\pm$ 0.020	ARNDT	96	IPWA $\gamma N \rightarrow \pi N$
0.035 $\pm$ 0.010	CRAWFORD	83	IPWA $\gamma N \rightarrow \pi N$
0.010 $\pm$ 0.015	AWAJI	81	DPWA $\gamma N \rightarrow \pi N$

••• We do not use the following data for averages, fits, limits, etc. •••

0.063 $\pm$ 0.012	ANISOVICH	10	DPWA Multichannel
0.066	DRECHSEL	07	DPWA $\gamma N \rightarrow \pi N$
-0.050	PENNER	02D	DPWA Multichannel
0.042 $\pm$ 0.003	LI	93	IPWA $\gamma N \rightarrow \pi N$
0.066	WADA	84	DPWA Compton scattering

 $\Delta(1620)$  FOOTNOTES

- <sup>1</sup> CHEW 80 reports two  $S_{31}$  resonances at somewhat higher masses than other analyses. Problems with this analysis are discussed in section 2.1.11 of HOEHLER 83.
- <sup>2</sup> LONGACRE 77 pole positions are from a search for poles in the unitarized T-matrix; the first (second) value uses, in addition to  $\pi N \rightarrow N\pi\pi$  data, elastic amplitudes from a Saclay (CERN) partial-wave analysis. The other LONGACRE 77 values are from eyeball fits with Breit-Wigner circles to the T-matrix amplitudes.
- <sup>3</sup> From method II of LONGACRE 75: eyeball fits with Breit-Wigner circles to the T-matrix amplitudes.
- <sup>4</sup> See HOEHLER 93 for a detailed discussion of the evidence for and the pole parameters of  $N$  and  $\Delta$  resonances as determined from Argand diagrams of  $\pi N$  elastic partial-wave amplitudes and from plots of the speeds with which the amplitudes traverse the diagrams.
- <sup>5</sup> LONGACRE 78 values are from a search for poles in the unitarized T-matrix. The first (second) value uses, in addition to  $\pi N \rightarrow N\pi\pi$  data, elastic amplitudes from a Saclay (CERN) partial-wave analysis.
- <sup>6</sup> LONGACRE 77 considers this coupling to be well determined.

 $\Delta(1620)$  REFERENCES

For early references, see Physics Letters **111B** 1 (1982).

ANISOVICH	12A	EPJ A48 15	A.V. Anisovich et al.	(BONN, PNPI)
ANISOVICH	10	EPJ A44 203	A.V. Anisovich et al.	(BONN, PNPI)
THOMA	08	PL B659 87	U. Thoma et al.	(CB-ELSA Collab.)
DRECHSEL	07	EPJ A34 69	D. Drechsel, S.S. Kamalov, L. Tiator	(MAINZ, JINR)
DUGGER	07	PR C76 025211	M. Dugger et al.	(Jefferson Lab CLAS Collab.)
ARNDT	06	PR C74 045205	R.A. Arndt et al.	(GWU)
PDG	06	JPG 33 1	W.-M. Yao et al.	(PDG Collab.)
ARNDT	04	PR C69 035213	R.A. Arndt et al.	(GWU, TRIU)
PENNER	02C	PR C66 055211	G. Penner, U. Mosel	(GIES)
PENNER	02D	PR C66 055212	G. Penner, U. Mosel	(GIES)
VRANA	00	PRPL 328 181	T.P. Vrana, S.A. Dytman, T.-S.H. Lee	(PITT+)
ARNDT	96	PR C53 430	R.A. Arndt, I.I. Strakovsky, R.L. Workman	(VPI)
ARNDT	95	PR C52 2120	R.A. Arndt et al.	(VPI)
HOEHLER	93	$\pi N$ Newsletter 9 1	G. Hohler	(KARL)
LI	93	PR C47 2759	Z.J. Li et al.	(VPI)
MANLEY	92	PR D45 4002	D.M. Manley, E.M. Saleski	(KEINT) IJP
Also		PR D30 304	D.M. Manley et al.	(VPI)
ARNDT	91	PR D43 2131	R.A. Arndt et al.	(VPI, TELE) IJP
WADA	84	NP B247 313	Y. Wada et al.	(INUS)
CRAWFORD	83	NP B211 1	R.L. Crawford, W.T. Morton	(GLAS)
HOEHLER	83	Landolt-Boernstein 1/9B2	G. Hohler	(KARLT)
PDG	82	PL 111B 1	M. Roos et al.	(HEL5, CIT, CERN)
AWAJI	81	Bonn Conf. 352	N. Awaji, R. Kajikawa	(NAGO)
Also		NP B197 365	K. Fujii et al.	(NAGO)
BARNHAM	80	NP B168 243	K.W.J. Barnham et al.	(LOIC)
CHEW	80	Toronto Conf. 123	D.M. Chew	(LBL) IJP
CUTKOSKY	80	Toronto Conf. 19	R.E. Cutkosky et al.	(CMU, LBL) IJP
Also		PR D20 2839	R.E. Cutkosky et al.	(CMU, LBL) IJP
HOEHLER	79	PDAT 12-1	G. Hohler et al.	(KARLT) IJP
Also		Toronto Conf. 3	R. Koch	(KARLT) IJP
LONGACRE	78	PR D17 1795	R.S. Longacre et al.	(LBL, SLAC)
LONGACRE	77	NP B122 493	R.S. Longacre, J. Dolbeau	(SACL) IJP
Also		NP B108 365	J. Dolbeau et al.	(SACL) IJP
LONGACRE	75	PL 55B 415	R.S. Longacre et al.	(LBL, SLAC) IJP

 $\Delta(1700) 3/2^-$ 

$$I(J^P) = \frac{3}{2}(\frac{3}{2}^-) \text{ Status: } ***$$

Most of the results published before 1975 were last included in our 1982 edition, Physics Letters **111B** 1 (1982). Some further obsolete results published before 1984 were last included in our 2006 edition, Journal of Physics, G **33** 1 (2006).

 $\Delta(1700)$  BREIT-WIGNER MASS

VALUE (MeV)	DOCUMENT ID	TECN	COMMENT
<b>1670 to 1750 (<math>\approx</math> 1700) OUR ESTIMATE</b>			
1715 $^{+30}_{-15}$	ANISOVICH	12A	DPWA Multichannel
1695.0 $\pm$ 1.3	ARNDT	06	DPWA $\pi N \rightarrow \pi N, \eta N$
1762 $\pm$ 44	MANLEY	92	IPWA $\pi N \rightarrow \pi N \& N\pi\pi$
1710 $\pm$ 30	CUTKOSKY	80	IPWA $\pi N \rightarrow \pi N$
1680 $\pm$ 70	HOEHLER	79	IPWA $\pi N \rightarrow \pi N$
••• We do not use the following data for averages, fits, limits, etc. •••			
1780 $\pm$ 40	ANISOVICH	10	DPWA Multichannel
1790 $\pm$ 30	HORN	08A	DPWA Multichannel
1770 $\pm$ 40	THOMA	08	DPWA Multichannel
1687.9 $\pm$ 2.5	ARNDT	04	DPWA $\pi N \rightarrow \pi N, \eta N$
1678 $\pm$ 1	PENNER	02C	DPWA Multichannel
1732 $\pm$ 23	VRANA	00	DPWA Multichannel
1690 $\pm$ 15	ARNDT	96	IPWA $\gamma N \rightarrow \pi N$
1680	ARNDT	95	DPWA $\pi N \rightarrow N\pi$
1655	LI	93	IPWA $\gamma N \rightarrow \pi N$
1650	BARNHAM	80	IPWA $\pi N \rightarrow N\pi\pi$
1718.4 $^{+13.1}_{-13.0}$	<sup>1</sup> CHEW	80	BPWA $\pi^+ p \rightarrow \pi^+ p$
1600	<sup>2</sup> LONGACRE	77	IPWA $\pi N \rightarrow N\pi\pi$
1680	<sup>3</sup> LONGACRE	75	IPWA $\pi N \rightarrow N\pi\pi$

See key on page 457

## Baryon Particle Listings

 $\Delta(1700)$  $\Delta(1700)$  BREIT-WIGNER WIDTH

VALUE (MeV)	DOCUMENT ID	TECN	COMMENT
<b>200 to 400 (<math>\approx 300</math>) OUR ESTIMATE</b>			
310 $\pm$ 40	ANISOVICH	12A	DPWA Multichannel
375.5 $\pm$ 7.0	ARNDT	06	DPWA $\pi N \rightarrow \pi N, \eta N$
600 $\pm$ 250	MANLEY	92	IPWA $\pi N \rightarrow \pi N$ & $N\pi\pi$
280 $\pm$ 80	CUTKOSKY	80	IPWA $\pi N \rightarrow \pi N$
230 $\pm$ 80	HOEHLER	79	IPWA $\pi N \rightarrow \pi N$
••• We do not use the following data for averages, fits, limits, etc. •••			
580 $\pm$ 120	ANISOVICH	10	DPWA Multichannel
580 $\pm$ 60	HORN	08A	DPWA Multichannel
630 $\pm$ 150	THOMA	08	DPWA Multichannel
364.8 $\pm$ 16.6	ARNDT	04	DPWA $\pi N \rightarrow \pi N, \eta N$
606 $\pm$ 15	PENNER	02C	DPWA Multichannel
119 $\pm$ 70	VRANA	00	DPWA Multichannel
285 $\pm$ 20	ARNDT	96	IPWA $\gamma N \rightarrow \pi N$
272	ARNDT	95	DPWA $\pi N \rightarrow N\pi$
348	LI	93	IPWA $\gamma N \rightarrow \pi N$
160	BARNHAM	80	IPWA $\pi N \rightarrow N\pi\pi$
193.3 $\pm$ 26.0	<sup>1</sup> CHEW	80	BPWA $\pi^+ p \rightarrow \pi^+ p$
200	<sup>2</sup> LONGACRE	77	IPWA $\pi N \rightarrow N\pi\pi$
240	<sup>3</sup> LONGACRE	75	IPWA $\pi N \rightarrow N\pi\pi$

 $\Delta(1700)$  POLE POSITION

VALUE (MeV)	DOCUMENT ID	TECN	COMMENT
<b>REAL PART</b>			
<b>1620 to 1680 (<math>\approx 1650</math>) OUR ESTIMATE</b>			
1680 $\pm$ 10	ANISOVICH	12A	DPWA Multichannel
1632	ARNDT	06	DPWA $\pi N \rightarrow \pi N, \eta N$
1651	<sup>4</sup> HOEHLER	93	SPED $\pi N \rightarrow \pi N$
1675 $\pm$ 25	CUTKOSKY	80	IPWA $\pi N \rightarrow \pi N$
••• We do not use the following data for averages, fits, limits, etc. •••			
1650 $\pm$ 30	ANISOVICH	10	DPWA Multichannel
1640 $\pm$ 25	HORN	08A	DPWA Multichannel
1610 $\pm$ 35	THOMA	08	DPWA Multichannel
1617	ARNDT	04	DPWA $\pi N \rightarrow \pi N, \eta N$
1726	VRANA	00	DPWA Multichannel
1655	ARNDT	95	DPWA $\pi N \rightarrow N\pi$
1646	ARNDT	91	DPWA $\pi N \rightarrow \pi N$ Soln SM90
1681 or 1672	<sup>5</sup> LONGACRE	78	IPWA $\pi N \rightarrow N\pi\pi$
1600 or 1594	<sup>2</sup> LONGACRE	77	IPWA $\pi N \rightarrow N\pi\pi$

 $-2 \times$  IMAGINARY PART

VALUE (MeV)	DOCUMENT ID	TECN	COMMENT
<b>160 to 300 (<math>\approx 230</math>) OUR ESTIMATE</b>			
305 $\pm$ 15	ANISOVICH	12A	DPWA Multichannel
253	ARNDT	06	DPWA $\pi N \rightarrow \pi N, \eta N$
159	<sup>4</sup> HOEHLER	93	SPED $\pi N \rightarrow \pi N$
220 $\pm$ 40	CUTKOSKY	80	IPWA $\pi N \rightarrow \pi N$
••• We do not use the following data for averages, fits, limits, etc. •••			
275 $\pm$ 35	ANISOVICH	10	DPWA Multichannel
325 $\pm$ 35	HORN	08A	DPWA Multichannel
320 $\pm$ 60	THOMA	08	DPWA Multichannel
226	ARNDT	04	DPWA $\pi N \rightarrow \pi N, \eta N$
118	VRANA	00	DPWA Multichannel
242	ARNDT	95	DPWA $\pi N \rightarrow N\pi$
208	ARNDT	91	DPWA $\pi N \rightarrow \pi N$ Soln SM90
245 or 241	<sup>5</sup> LONGACRE	78	IPWA $\pi N \rightarrow N\pi\pi$
208 or 201	<sup>2</sup> LONGACRE	77	IPWA $\pi N \rightarrow N\pi\pi$

 $\Delta(1700)$  ELASTIC POLE RESIDUEMODULUS  $|r|$ 

VALUE (MeV)	DOCUMENT ID	TECN	COMMENT
42 $\pm$ 7	ANISOVICH	12A	DPWA Multichannel
18	ARNDT	06	DPWA $\pi N \rightarrow \pi N, \eta N$
10	HOEHLER	93	SPED $\pi N \rightarrow \pi N$
13 $\pm$ 3	CUTKOSKY	80	IPWA $\pi N \rightarrow \pi N$
••• We do not use the following data for averages, fits, limits, etc. •••			
16	ARNDT	04	DPWA $\pi N \rightarrow \pi N, \eta N$
16	ARNDT	95	DPWA $\pi N \rightarrow N\pi$
13	ARNDT	91	DPWA $\pi N \rightarrow \pi N$ Soln SM90

PHASE  $\theta$ 

VALUE ( $^\circ$ )	DOCUMENT ID	TECN	COMMENT
-3 $\pm$ 15	ANISOVICH	12A	DPWA Multichannel
-40	ARNDT	06	DPWA $\pi N \rightarrow \pi N, \eta N$
-20 $\pm$ 25	CUTKOSKY	80	IPWA $\pi N \rightarrow \pi N$
••• We do not use the following data for averages, fits, limits, etc. •••			
-47	ARNDT	04	DPWA $\pi N \rightarrow \pi N, \eta N$
-12	ARNDT	95	DPWA $\pi N \rightarrow N\pi$
-22	ARNDT	91	DPWA $\pi N \rightarrow \pi N$ Soln SM90

 $\Delta(1700)$  INELASTIC POLE RESIDUEThe "normalized residue" is the residue divided by  $\Gamma_{pole}$ .Normalized residue in  $N\pi \rightarrow \Delta(1700) \rightarrow \Delta\eta$ 

MODULUS (%)	PHASE ( $^\circ$ )	DOCUMENT ID	TECN	COMMENT
<b>12 <math>\pm</math> 3</b>	<b>-60 <math>\pm</math> 15</b>	ANISOVICH	12A	DPWA Multichannel

 $\Delta(1700)$  DECAY MODES

The following branching fractions are our estimates, not fits or averages.

Mode	Fraction ( $\Gamma_i/\Gamma$ )
$\Gamma_1$ $N\pi$	10-20 %
$\Gamma_2$ $\Sigma K$	
$\Gamma_3$ $N\pi\pi$	80-90 %
$\Gamma_4$ $\Delta\pi$	30-60 %
$\Gamma_5$ $\Delta(1232)\pi$ , S-wave	25-50 %
$\Gamma_6$ $\Delta(1232)\pi$ , D-wave	5-15 %
$\Gamma_7$ $N\rho$	30-55 %
$\Gamma_8$ $N\rho$ , S=1/2, D-wave	
$\Gamma_9$ $N\rho$ , S=3/2, S-wave	5-20 %
$\Gamma_{10}$ $N\rho$ , S=3/2, D-wave	
$\Gamma_{11}$ $N(1535)\pi$	
$\Gamma_{12}$ $\Delta(1232)\eta$	(5.0 $\pm$ 2.0) %
$\Gamma_{13}$ $N\gamma$	0.22-0.60 %
$\Gamma_{14}$ $N\gamma$ , helicity=1/2	0.12-0.30 %
$\Gamma_{15}$ $N\gamma$ , helicity=3/2	0.10-0.30 %

 $\Delta(1700)$  BRANCHING RATIOS

$\Gamma(N\pi)/\Gamma_{total}$	VALUE (%)	DOCUMENT ID	TECN	COMMENT	$\Gamma_1/\Gamma$
<b>10 to 20 OUR ESTIMATE</b>					
	22 $\pm$ 4	ANISOVICH	12A	DPWA Multichannel	
	15.6 $\pm$ 0.1	ARNDT	06	DPWA $\pi N \rightarrow \pi N, \eta N$	
	14 $\pm$ 6	MANLEY	92	IPWA $\pi N \rightarrow \pi N$ & $N\pi\pi$	
	12 $\pm$ 3	CUTKOSKY	80	IPWA $\pi N \rightarrow \pi N$	
	20 $\pm$ 3	HOEHLER	79	IPWA $\pi N \rightarrow \pi N$	
••• We do not use the following data for averages, fits, limits, etc. •••					
	16 $\pm$ 7	ANISOVICH	10	DPWA Multichannel	
	20 $\pm$ 7	HORN	08A	DPWA Multichannel	
	15 $\pm$ 8	THOMA	08	DPWA Multichannel	
	15.0 $\pm$ 0.1	ARNDT	04	DPWA $\pi N \rightarrow \pi N, \eta N$	
	14 $\pm$ 1	PENNER	02C	DPWA Multichannel	
	5 $\pm$ 1	VRANA	00	DPWA Multichannel	
	16	ARNDT	95	DPWA $\pi N \rightarrow N\pi$	
	16	<sup>1</sup> CHEW	80	BPWA $\pi^+ p \rightarrow \pi^+ p$	

Note: Signs of couplings from  $\pi N \rightarrow N\pi\pi$  analyses were changed in the 1986 edition to agree with the baryon-first convention; the overall phase ambiguity is resolved by choosing a negative sign for the  $\Delta(1620)$   $S_{31}$  coupling to  $\Delta(1232)\pi$ .

$(\Gamma_i/\Gamma_{total})^{1/2}$ in $N\pi \rightarrow \Delta(1700) \rightarrow \Delta(1232)\pi$ , S-wave	VALUE	DOCUMENT ID	TECN	COMMENT	$(\Gamma_1/\Gamma_5)^{1/2}/\Gamma$
<b>+0.21 to +0.29 OUR ESTIMATE</b>					
	+0.32 $\pm$ 0.06	MANLEY	92	IPWA $\pi N \rightarrow \pi N$ & $N\pi\pi$	
	+0.18 $\pm$ 0.04	BARNHAM	80	IPWA $\pi N \rightarrow N\pi\pi$	
	+0.30	<sup>2,6</sup> LONGACRE	77	IPWA $\pi N \rightarrow N\pi\pi$	
	+0.24	<sup>3</sup> LONGACRE	75	IPWA $\pi N \rightarrow N\pi\pi$	

$\Gamma(\Delta(1232)\pi, S\text{-wave})/\Gamma_{total}$	VALUE (%)	DOCUMENT ID	TECN	COMMENT	$\Gamma_5/\Gamma$
	20 $\pm$ 25	ANISOVICH	12A	DPWA Multichannel	
	-13	VRANA	00	DPWA Multichannel	
	90 $\pm$ 2				

$(\Gamma_i/\Gamma_{total})^{1/2}$ in $N\pi \rightarrow \Delta(1700) \rightarrow \Delta(1232)\pi$ , D-wave	VALUE	DOCUMENT ID	TECN	COMMENT	$(\Gamma_1/\Gamma_6)^{1/2}/\Gamma$
<b>+0.05 to +0.11 OUR ESTIMATE</b>					
	+0.08 $\pm$ 0.03	MANLEY	92	IPWA $\pi N \rightarrow \pi N$ & $N\pi\pi$	
	0.14 $\pm$ 0.04	BARNHAM	80	IPWA $\pi N \rightarrow N\pi\pi$	
	+0.05	<sup>2,6</sup> LONGACRE	77	IPWA $\pi N \rightarrow N\pi\pi$	
	+0.10	<sup>3</sup> LONGACRE	75	IPWA $\pi N \rightarrow N\pi\pi$	

$\Gamma(\Delta(1232)\pi, D\text{-wave})/\Gamma_{total}$	VALUE (%)	DOCUMENT ID	TECN	COMMENT	$\Gamma_6/\Gamma$
<b>5 to 15 OUR ESTIMATE</b>					
	12 $\pm$ 14	ANISOVICH	12A	DPWA Multichannel	
	-7	VRANA	00	DPWA Multichannel	
	4 $\pm$ 1				

## Baryon Particle Listings

 $\Delta(1700)$ ,  $\Delta(1750)$ 

$(\Gamma_1 \Gamma_f)^{1/2} / \Gamma_{\text{total}}$ in $N\pi \rightarrow \Delta(1700) \rightarrow N\rho, S=1/2, D\text{-wave}$	$(\Gamma_1 \Gamma_g)^{1/2} / \Gamma$		
VALUE	DOCUMENT ID	TECN	COMMENT
$+0.17 \pm 0.05$	BARNHAM	80	IPWA $\pi N \rightarrow N\pi\pi$

$(\Gamma_1 \Gamma_f)^{1/2} / \Gamma_{\text{total}}$ in $N\pi \rightarrow \Delta(1700) \rightarrow N\rho, S=3/2, S\text{-wave}$	$(\Gamma_1 \Gamma_g)^{1/2} / \Gamma$		
VALUE	DOCUMENT ID	TECN	COMMENT
$\pm 0.11$ to $\pm 0.19$ OUR ESTIMATE			
$+0.10 \pm 0.03$	MANLEY	92	IPWA $\pi N \rightarrow \pi N$ & $N\pi\pi$
$+0.04$	<sup>2,6</sup> LONGACRE	77	IPWA $\pi N \rightarrow N\pi\pi$
$-0.30$	<sup>3</sup> LONGACRE	75	IPWA $\pi N \rightarrow N\pi\pi$

$\Gamma(N\rho, S=3/2, S\text{-wave}) / \Gamma_{\text{total}}$	$\Gamma_9 / \Gamma$		
VALUE (%)	DOCUMENT ID	TECN	COMMENT
$1 \pm 1$	VRANA	00	DPWA Multichannel

$(\Gamma_1 \Gamma_f)^{1/2} / \Gamma_{\text{total}}$ in $N\pi \rightarrow \Delta(1700) \rightarrow N\rho, S=3/2, D\text{-wave}$	$(\Gamma_1 \Gamma_{10})^{1/2} / \Gamma$		
VALUE	DOCUMENT ID	TECN	COMMENT
$0.18 \pm 0.07$	BARNHAM	80	IPWA $\pi N \rightarrow N\pi\pi$

$\Gamma(N(1535)\pi) / \Gamma_{\text{total}}$	$\Gamma_{11} / \Gamma$		
VALUE (%)	DOCUMENT ID	TECN	COMMENT
• • • We do not use the following data for averages, fits, limits, etc. • • •			
$4 \pm 2$	HORN	08A	DPWA Multichannel

$\Gamma(\Delta(1232)\eta) / \Gamma_{\text{total}}$	$\Gamma_{12} / \Gamma$		
VALUE (%)	DOCUMENT ID	TECN	COMMENT
• • • We do not use the following data for averages, fits, limits, etc. • • •			
$5 \pm 2$	ANISOVICH	12A	DPWA Multichannel
$2 \pm 1$	HORN	08A	DPWA Multichannel

$\Gamma(N(1535)\pi) / \Gamma(\Delta(1232)\eta)$	$\Gamma_{11} / \Gamma_{12}$		
VALUE	DOCUMENT ID	TECN	COMMENT
• • • We do not use the following data for averages, fits, limits, etc. • • •			
0.67	KASHEVAROV	09	CBAL $\gamma\rho \rightarrow \rho\pi^0\eta$

 $\Delta(1700)$  PHOTON DECAY AMPLITUDES

Papers on  $\gamma N$  amplitudes predating 1981 may be found in our 2006 edition, Journal of Physics, G **33** 1 (2006).

$\Delta(1700) \rightarrow N\gamma$ , helicity-1/2 amplitude $A_{1/2}$			
VALUE (GeV <sup>-1/2</sup> )	DOCUMENT ID	TECN	COMMENT
$\pm 0.104 \pm 0.015$ OUR ESTIMATE			
0.160 $\pm$ 0.020	ANISOVICH	12A	DPWA Multichannel
0.125 $\pm$ 0.003	DUGGER	07	DPWA $\gamma N \rightarrow \pi N$
0.090 $\pm$ 0.025	ARNDT	96	IPWA $\gamma N \rightarrow \pi N$
0.111 $\pm$ 0.017	CRAWFORD	83	IPWA $\gamma N \rightarrow \pi N$
0.089 $\pm$ 0.033	AWAJI	81	DPWA $\gamma N \rightarrow \pi N$
• • • We do not use the following data for averages, fits, limits, etc. • • •			
0.160 $\pm$ 0.045	ANISOVICH	10	DPWA Multichannel
0.160 $\pm$ 0.040	HORN	08A	DPWA Multichannel
0.226	DRECHSEL	07	DPWA $\gamma N \rightarrow \pi N$
0.096	PENNER	02D	DPWA Multichannel
0.121 $\pm$ 0.004	LI	93	IPWA $\gamma N \rightarrow \pi N$

$\Delta(1700) \rightarrow N\gamma$ , helicity-3/2 amplitude $A_{3/2}$			
VALUE (GeV <sup>-1/2</sup> )	DOCUMENT ID	TECN	COMMENT
$\pm 0.085 \pm 0.022$ OUR ESTIMATE			
0.165 $\pm$ 0.025	ANISOVICH	12A	DPWA Multichannel
0.105 $\pm$ 0.003	DUGGER	07	DPWA $\gamma N \rightarrow \pi N$
0.097 $\pm$ 0.020	ARNDT	96	IPWA $\gamma N \rightarrow \pi N$
0.107 $\pm$ 0.015	CRAWFORD	83	IPWA $\gamma N \rightarrow \pi N$
0.060 $\pm$ 0.015	AWAJI	81	DPWA $\gamma N \rightarrow \pi N$
• • • We do not use the following data for averages, fits, limits, etc. • • •			
0.160 $\pm$ 0.040	ANISOVICH	10	DPWA Multichannel
0.150 $\pm$ 0.030	HORN	08A	DPWA Multichannel
0.210	DRECHSEL	07	DPWA $\gamma N \rightarrow \pi N$
0.154	PENNER	02D	DPWA Multichannel
0.115 $\pm$ 0.004	LI	93	IPWA $\gamma N \rightarrow \pi N$

 $\Delta(1700)$  FOOTNOTES

- Problems with CHEW 80 are discussed in section 2.1.11 of HOEHLER 83.
- LONGACRE 77 pole positions are from a search for poles in the unitarized T-matrix; the first (second) value uses, in addition to  $\pi N \rightarrow N\pi\pi$  data, elastic amplitudes from a Saclay (CERN) partial-wave analysis. The other LONGACRE 77 values are from eyeball fits with Breit-Wigner circles to the T-matrix amplitudes.
- From method II of LONGACRE 75: eyeball fits with Breit-Wigner circles to the T-matrix amplitudes.
- See HOEHLER 93 for a detailed discussion of the evidence for and the pole parameters of  $N$  and  $\Delta$  resonances as determined from Argand diagrams of  $\pi N$  elastic partial-wave amplitudes and from plots of the speeds with which the amplitudes traverse the diagrams.
- LONGACRE 78 values are from a search for poles in the unitarized T-matrix. The first (second) value uses, in addition to  $\pi N \rightarrow N\pi\pi$  data, elastic amplitudes from a Saclay (CERN) partial-wave analysis.
- LONGACRE 77 considers this coupling to be well determined.

 $\Delta(1700)$  REFERENCES

For early references, see Physics Letters **111B** 1 (1982).

ANISOVICH 12A	EPJ A48 15	A.V. Anisovich <i>et al.</i>	(BONN, PNPI)
ANISOVICH 10	EPJ A44 203	A.V. Anisovich <i>et al.</i>	(BONN, PNPI)
KASHEVAROV 08A	EPJ A42 141	V.L. Kashevarov <i>et al.</i>	(MAMI Crystal Ball/TAPS)
HORN 08A	EPJ A38 173	I. Horn <i>et al.</i>	(CB-ELSA Collab.)
	PRL 101 202002	I. Horn <i>et al.</i>	(CB-ELSA Collab.)
THOMA 08	PL B659 87	U. Thoma <i>et al.</i>	(CB-ELSA Collab.)
DRECHSEL 07	EPJ A34 69	D. Drechsel, S.S. Kamalov, L. Tiator	(MAINZ, JINR)
DUGGER 07	PR C76 025211	M. Dugger <i>et al.</i>	(Jefferson Lab CLAS Collab.)
ARNDT 06	PR C74 045205	R.A. Arndt <i>et al.</i>	(GWU)
PDG 06	JPG 33 1	W.-M. Yao <i>et al.</i>	(PDG Collab.)
ARNDT 04	PR C69 035213	R.A. Arndt <i>et al.</i>	(GWU, TRIU)
PENNER 02C	PR C66 055211	G. Penner, U. Mosel	(GIES)
PENNER 02D	PR C66 055212	G. Penner, U. Mosel	(GIES)
VRANA 00	PRPL 328 181	T.P. Vrana, S.A. Dytman, T.-S.H. Lee	(PITT+)
ARNDT 96	PR C53 430	R.A. Arndt, I.I. Strakovsky, R.L. Workman	(VPI)
ARNDT 95	PR C52 2120	R.A. Arndt <i>et al.</i>	(VPI, BRCO)
HOEHLER 93	$\pi N$ Newsletter 9 1	G. Hohlner	(KARL)
LI 93	PR C47 2759	Z.J. Li <i>et al.</i>	(VPI)
MANLEY 92	PR D45 4002	D.M. Manley, E.M. Saleski	(KENT IJP)
	Also PR D30 904	D.M. Manley <i>et al.</i>	(VPI)
ARNDT 91	PR D43 2131	R.A. Arndt <i>et al.</i>	(VPI, TELE IJP)
CRAWFORD 83	NP B211 1	R.L. Crawford, W.T. Morton	(GLAS)
HOEHLER 83	Landolt-Boernstein 1/9B2	G. Hohlner	(KARL)
PDG 82	PL 111B 1	M. Roos <i>et al.</i>	(HELS, CIT, CERN)
AWAJI 81	Bonn Conf. 352	N. Awaji, R. Kajikawa	(NAGO)
	Also NP B197 365	K. Fujii <i>et al.</i>	(NAGO)
BARNHAM 80	NP B168 243	K.W.J. Barnham <i>et al.</i>	(LOIC)
CHEW 80	Toronto Conf. 123	D.M. Chew	(LBL IJP)
CUTKOSKY 80	Toronto Conf. 19	R.E. Cutkosky <i>et al.</i>	(CMU, LBL IJP)
	Also PR D20 2839	R.E. Cutkosky <i>et al.</i>	(CMU, LBL IJP)
HOEHLER 79	PDAT 12-1	G. Hohlner <i>et al.</i>	(KARL) IJP
	Also Toronto Conf. 3	R. Koch	(KARL) IJP
LONGACRE 78	PR D17 1795	R.S. Longacre <i>et al.</i>	(LBL, SLAC)
LONGACRE 77	NP B122 493	R.S. Longacre, J. Dolbeau	(SACL) IJP
	Also NP B108 365	J. Dolbeau <i>et al.</i>	(SACL) IJP
LONGACRE 75	PL 55B 415	R.S. Longacre <i>et al.</i>	(LBL, SLAC) IJP

 $\Delta(1750) 1/2^+$ 

$$I(J^P) = \frac{3}{2}(\frac{1}{2}^+) \text{ Status: } *$$

OMITTED FROM SUMMARY TABLE

Neither ARNDT 06 nor ANISOVICH 12A finds any evidence for this resonance.

 $\Delta(1750)$  BREIT-WIGNER MASS

VALUE (MeV)	DOCUMENT ID	TECN	COMMENT
$\approx 1750$ OUR ESTIMATE			
1744 $\pm$ 36	MANLEY	92	IPWA $\pi N \rightarrow \pi N$ & $N\pi\pi$
• • • We do not use the following data for averages, fits, limits, etc. • • •			
1712 $\pm$ 1	PENNER	02C	DPWA Multichannel
1721 $\pm$ 61	VRANA	00	DPWA Multichannel
1715.2 $\pm$ 21.0	<sup>1</sup> CHEW	80	BPWA $\pi^+ p \rightarrow \pi^+ p$
1778.4 $\pm$ 9.0	<sup>1</sup> CHEW	80	BPWA $\pi^+ p \rightarrow \pi^+ p$

 $\Delta(1750)$  BREIT-WIGNER WIDTH

VALUE (MeV)	DOCUMENT ID	TECN	COMMENT
• • • We do not use the following data for averages, fits, limits, etc. • • •			
300 $\pm$ 120	MANLEY	92	IPWA $\pi N \rightarrow \pi N$ & $N\pi\pi$
• • • We do not use the following data for averages, fits, limits, etc. • • •			
643 $\pm$ 17	PENNER	02C	DPWA Multichannel
70 $\pm$ 50	VRANA	00	DPWA Multichannel
93.3 $\pm$ 55.0	<sup>1</sup> CHEW	80	BPWA $\pi^+ p \rightarrow \pi^+ p$
23.0 $\pm$ 29.0	<sup>1</sup> CHEW	80	BPWA $\pi^+ p \rightarrow \pi^+ p$

 $\Delta(1750)$  POLE POSITION

REAL PART	DOCUMENT ID	TECN	COMMENT
VALUE (MeV)			
1748	<sup>2</sup> ARNDT	04	DPWA $\pi N \rightarrow \pi N, \eta N$
• • • We do not use the following data for averages, fits, limits, etc. • • •			
1714	VRANA	00	DPWA Multichannel
−2 <i>x</i> IMAGINARY PART	DOCUMENT ID	TECN	COMMENT
VALUE (MeV)			
524	<sup>2</sup> ARNDT	04	DPWA $\pi N \rightarrow \pi N, \eta N$
• • • We do not use the following data for averages, fits, limits, etc. • • •			
68	VRANA	00	DPWA Multichannel

 $\Delta(1750)$  ELASTIC POLE RESIDUE

MODULUS $ r $	DOCUMENT ID	TECN	COMMENT
VALUE (MeV)			
48	<sup>2</sup> ARNDT	04	DPWA $\pi N \rightarrow \pi N, \eta N$
PHASE $\theta$	DOCUMENT ID	TECN	COMMENT
VALUE (°)			
158	<sup>2</sup> ARNDT	04	DPWA $\pi N \rightarrow \pi N, \eta N$

See key on page 457

# Baryon Particle Listings

## $\Delta(1750), \Delta(1900)$

### $\Delta(1750)$ DECAY MODES

Mode	
$\Gamma_1$	$N\pi$
$\Gamma_2$	$N\pi\pi$
$\Gamma_3$	$N(1440)\pi$
$\Gamma_4$	$\Sigma K$

### $\Delta(1750)$ BRANCHING RATIOS

$\Gamma(N\pi)/\Gamma_{total}$	DOCUMENT ID	TECN	COMMENT	$\Gamma_1/\Gamma$
8±3	MANLEY	92	IPWA $\pi N \rightarrow \pi N$ & $N\pi\pi$	
••• We do not use the following data for averages, fits, limits, etc. •••				
1±1	PENNER	02c	DPWA Multichannel	
6±9	VRANA	00	DPWA Multichannel	
18	<sup>1</sup> CHEW	80	BPWA $\pi^+ p \rightarrow \pi^+ p$	
20	<sup>1</sup> CHEW	80	BPWA $\pi^+ p \rightarrow \pi^+ p$	

$(\Gamma_1\Gamma_3)^{1/2}/\Gamma_{total}$ in $N\pi \rightarrow \Delta(1700) \rightarrow N(1440)\pi$	DOCUMENT ID	TECN	COMMENT	$(\Gamma_1\Gamma_3)^{1/2}/\Gamma$
+0.15±0.03	MANLEY	92	IPWA $\pi N \rightarrow \pi N$	

$\Gamma(N(1440)\pi)/\Gamma_{total}$	DOCUMENT ID	TECN	COMMENT	$\Gamma_3/\Gamma$
83±1	VRANA	00	DPWA Multichannel	

$\Gamma(\Sigma K)/\Gamma_{total}$	DOCUMENT ID	TECN	COMMENT	$\Gamma_4/\Gamma$
0.1±0.1	PENNER	02c	DPWA Multichannel	

### $\Delta(1750)$ PHOTON DECAY AMPLITUDES

Papers on  $\gamma N$  amplitudes predating 1981 may be found in our 2006 edition, Journal of Physics, G **33** 1 (2006).

$\Delta(1750) \rightarrow N\gamma$ , helicity-1/2 amplitude $A_{1/2}$	DOCUMENT ID	TECN	COMMENT
0.053	PENNER	02d	DPWA Multichannel

### $\Delta(1750)$ FOOTNOTES

- <sup>1</sup> CHEW 80 reports four resonances in the  $P_{31}$  wave — see also the  $\Delta(1910)$ . Problems with this analysis are discussed in section 2.1.11 of HOEHLER 83.
- <sup>2</sup> ARNDT 04 gives no corresponding Breit-Wigner parameters for this state, because the mass so obtained is about 500 MeV higher than that suggested by the position of the pole.

### $\Delta(1750)$ REFERENCES

ANISOVICH	12A	EPJ A48 15	A.V. Anisovich et al.	(BONN, PNPI)
ARNDT	06	PR C74 045205	R.A. Arndt et al.	(GWU)
PDG	06	JPG 33 1	W.-M. Yao et al.	(PDG Collab.)
ARNDT	04	PR C69 035213	R.A. Arndt et al.	(GWU, TRIU)
PENNER	02c	PR C66 055211	G. Penner, U. Mosel	(GIES)
PENNER	02d	PR C66 055212	G. Penner, U. Mosel	(GIES)
VRANA	00	PRPL 328 181	T.P. Vrana, S.A. Dytman., T.-S.H. Lee	(PITT+)
MANLEY	92	PR D45 4002	D.M. Manley, E.M. Saleski	(KENT)
		Also	PR D30 904	(VPI)
HOEHLER	83	Landolt-Boernstein 1/9B2	G. Hohler	(KARLT)
CHEW	80	Toronto Conf. 123	D.M. Chew	(LBL)

**$\Delta(1900) 1/2^-$**   $I(J^P) = \frac{3}{2}(\frac{1}{2}^-)$  Status: \*\*  
 OMITTED FROM SUMMARY TABLE

Some obsolete results published before 1980 were last included in our 2006 edition, Journal of Physics, G **33** 1 (2006). Some further obsolete results published before 1984 were last included in our 2006 edition, Journal of Physics, G **33** 1 (2006).

The latest GWU analysis (ARNDT 06) finds no evidence for this resonance.

### $\Delta(1900)$ BREIT-WIGNER MASS

VALUE (MeV)	DOCUMENT ID	TECN	COMMENT
<b>1840 to 1920 (≈ 1860) OUR ESTIMATE</b>			
1840 ± 30	ANISOVICH	12A	DPWA Multichannel
1920 ± 24	MANLEY	92	IPWA $\pi N \rightarrow \pi N$ & $N\pi\pi$
1890 ± 50	CUTKOSKY	80	IPWA $\pi N \rightarrow \pi N$
1908 ± 30	HOEHLER	79	IPWA $\pi N \rightarrow \pi N$
••• We do not use the following data for averages, fits, limits, etc. •••			

1802 ± 87	VRANA	00	DPWA Multichannel
1918.5 ± 23.0	CHEW	80	BPWA $\pi^+ p \rightarrow \pi^+ p$

### $\Delta(1900)$ BREIT-WIGNER WIDTH

VALUE (MeV)	DOCUMENT ID	TECN	COMMENT
300 ± 45	ANISOVICH	12A	DPWA Multichannel
263 ± 39	MANLEY	92	IPWA $\pi N \rightarrow \pi N$ & $N\pi\pi$
170 ± 50	CUTKOSKY	80	IPWA $\pi N \rightarrow \pi N$
140 ± 40	HOEHLER	79	IPWA $\pi N \rightarrow \pi N$
••• We do not use the following data for averages, fits, limits, etc. •••			
48 ± 45	VRANA	00	DPWA Multichannel
93.5 ± 54.0	CHEW	80	BPWA $\pi^+ p \rightarrow \pi^+ p$

### $\Delta(1900)$ POLE POSITION

#### REAL PART

VALUE (MeV)	DOCUMENT ID	TECN	COMMENT
1845 ± 25	ANISOVICH	12A	DPWA Multichannel
1780	<sup>1</sup> HOEHLER	93	SPED $\pi N \rightarrow \pi N$
1870 ± 40	CUTKOSKY	80	IPWA $\pi N \rightarrow \pi N$
••• We do not use the following data for averages, fits, limits, etc. •••			
1795	VRANA	00	DPWA Multichannel
not seen	ARNDT	91	DPWA $\pi N \rightarrow \pi N$ Soln SM90
2029 or 2025	<sup>2</sup> LONGACRE	78	IPWA $\pi N \rightarrow N\pi\pi$

#### -2xIMAGINARY PART

VALUE (MeV)	DOCUMENT ID	TECN	COMMENT
300 ± 45	ANISOVICH	12A	DPWA Multichannel
180 ± 50	CUTKOSKY	80	IPWA $\pi N \rightarrow \pi N$
••• We do not use the following data for averages, fits, limits, etc. •••			
58	VRANA	00	DPWA Multichannel
not seen	ARNDT	91	DPWA $\pi N \rightarrow \pi N$ Soln SM90
164 or 163	<sup>2</sup> LONGACRE	78	IPWA $\pi N \rightarrow N\pi\pi$

### $\Delta(1900)$ ELASTIC POLE RESIDUE

#### MODULUS $|r|$

VALUE (MeV)	DOCUMENT ID	TECN	COMMENT
10 ± 3	ANISOVICH	12A	DPWA Multichannel
10 ± 3	CUTKOSKY	80	IPWA $\pi N \rightarrow \pi N$

#### PHASE $\theta$

VALUE (°)	DOCUMENT ID	TECN	COMMENT
-125 ± 20	ANISOVICH	12A	DPWA Multichannel
+ 20 ± 40	CUTKOSKY	80	IPWA $\pi N \rightarrow \pi N$

### $\Delta(1900)$ INELASTIC POLE RESIDUE

The "normalized residue" is the residue divided by  $\Gamma_{pole}$ .

#### Normalized residue in $N\pi \rightarrow \Delta(1900) \rightarrow \Sigma K$

MODULUS (%)	PHASE (°)	DOCUMENT ID	TECN	COMMENT
7 ± 2	-50 ± 30	ANISOVICH	12A	DPWA Multichannel

#### Normalized residue in $N\pi \rightarrow \Delta(1900) \rightarrow \Delta\pi, D$ -wave

MODULUS (%)	PHASE (°)	DOCUMENT ID	TECN	COMMENT
12 <sup>+8</sup> <sub>-5</sub>	110 ± 20	ANISOVICH	12A	DPWA Multichannel

### $\Delta(1900)$ DECAY MODES

The following branching fractions are our estimates, not fits or averages.

Mode	Fraction ( $\Gamma_i/\Gamma$ )	
$\Gamma_1$	$N\pi$	10-30 %
$\Gamma_2$	$\Sigma K$	
$\Gamma_3$	$N\pi\pi$	
$\Gamma_4$	$\Delta\pi$	
$\Gamma_5$	$\Delta(1232)\pi, D$ -wave	
$\Gamma_6$	$N\rho$	
$\Gamma_7$	$N\rho, S=1/2, S$ -wave	
$\Gamma_8$	$N\rho, S=3/2, D$ -wave	
$\Gamma_9$	$N(1440)\pi, S$ -wave	
$\Gamma_{10}$	$N\gamma, \text{ helicity}=1/2$	

## Baryon Particle Listings

 $\Delta(1900)$ ,  $\Delta(1905)$  $\Delta(1900)$  BRANCHING RATIOS

$\Gamma(N\pi)/\Gamma_{\text{total}}$	DOCUMENT ID	TECN	COMMENT	$\Gamma_1/\Gamma$
7 ± 3	ANISOVICH 12A	DPWA	Multichannel	
41 ± 4	MANLEY 92	IPWA	$\pi N \rightarrow \pi N$ & $N\pi\pi$	
10 ± 3	CUTKOSKY 80	IPWA	$\pi N \rightarrow \pi N$	
8 ± 4	HOEHLER 79	IPWA	$\pi N \rightarrow \pi N$	
33 ± 10	VRANA 00	DPWA	Multichannel	
28	CHEW 80	BPWA	$\pi^+ p \rightarrow \pi^+ p$	

• • • We do not use the following data for averages, fits, limits, etc. • • •

$(\Gamma_1\Gamma_2)^{1/2}/\Gamma_{\text{total}}$ in $N\pi \rightarrow \Delta(1900) \rightarrow \Sigma K$	DOCUMENT ID	TECN	COMMENT	$(\Gamma_1\Gamma_2)^{1/2}/\Gamma$
<0.03	CANDLIN 84	DPWA	$\pi^+ p \rightarrow \Sigma^+ K^+$	

$(\Gamma_1\Gamma_2)^{1/2}/\Gamma_{\text{total}}$ in $N\pi \rightarrow \Delta(1900) \rightarrow \Delta(1232)\pi$ , D-wave	DOCUMENT ID	TECN	COMMENT	$(\Gamma_1\Gamma_2)^{1/2}/\Gamma$
+0.25 ± 0.07	MANLEY 92	IPWA	$\pi N \rightarrow \pi N$ & $N\pi\pi$	

$\Gamma(\Delta(1232)\pi, D\text{-wave})/\Gamma_{\text{total}}$	DOCUMENT ID	TECN	COMMENT	$\Gamma_5/\Gamma$
15 <sup>+50</sup> <sub>-10</sub>	ANISOVICH 12A	DPWA	Multichannel	
28 ± 1	VRANA 00	DPWA	Multichannel	

$(\Gamma_1\Gamma_2)^{1/2}/\Gamma_{\text{total}}$ in $N\pi \rightarrow \Delta(1900) \rightarrow N\rho$ , S=1/2, S-wave	DOCUMENT ID	TECN	COMMENT	$(\Gamma_1\Gamma_2)^{1/2}/\Gamma$
-0.14 ± 0.11	MANLEY 92	IPWA	$\pi N \rightarrow \pi N$ & $N\pi\pi$	

$\Gamma(N\rho, S=1/2, S\text{-wave})/\Gamma_{\text{total}}$	DOCUMENT ID	TECN	COMMENT	$\Gamma_7/\Gamma$
30 ± 2	VRANA 00	DPWA	Multichannel	

$(\Gamma_1\Gamma_2)^{1/2}/\Gamma_{\text{total}}$ in $N\pi \rightarrow \Delta(1900) \rightarrow N\rho$ , S=3/2, D-wave	DOCUMENT ID	TECN	COMMENT	$(\Gamma_1\Gamma_2)^{1/2}/\Gamma$
-0.37 ± 0.07	MANLEY 92	IPWA	$\pi N \rightarrow \pi N$ & $N\pi\pi$	

$\Gamma(N\rho, S=3/2, D\text{-wave})/\Gamma_{\text{total}}$	DOCUMENT ID	TECN	COMMENT	$\Gamma_8/\Gamma$
5 ± 1	VRANA 00	DPWA	Multichannel	

$(\Gamma_1\Gamma_2)^{1/2}/\Gamma_{\text{total}}$ in $N\pi \rightarrow \Delta(1900) \rightarrow N(1440)\pi$ , S-wave	DOCUMENT ID	TECN	COMMENT	$(\Gamma_1\Gamma_2)^{1/2}/\Gamma$
-0.16 ± 0.11	MANLEY 92	IPWA	$\pi N \rightarrow \pi N$ & $N\pi\pi$	

$\Gamma(N(1440)\pi, S\text{-wave})/\Gamma_{\text{total}}$	DOCUMENT ID	TECN	COMMENT	$\Gamma_9/\Gamma$
4 ± 1	VRANA 00	DPWA	Multichannel	

 $\Delta(1900)$  PHOTON DECAY AMPLITUDES

Papers on  $\gamma N$  amplitudes predating 1981 may be found in our 2006 edition, Journal of Physics, G **33** 1 (2006).

$\Delta(1900) \rightarrow N\gamma$ , helicity-1/2 amplitude $A_{1/2}$	DOCUMENT ID	TECN	COMMENT
0.059 ± 0.016	<sup>3</sup> ANISOVICH 12A	DPWA	Phase = (60 ± 25)°
-0.004 ± 0.016	CRAWFORD 83	IPWA	$\gamma N \rightarrow \pi N$
0.029 ± 0.008	AWAJI 81	DPWA	$\gamma N \rightarrow \pi N$

 $\Delta(1900)$  FOOTNOTES

- See HOEHLER 93 for a detailed discussion of the evidence for and the pole parameters of  $N$  and  $\Delta$  resonances as determined from Argand diagrams of  $\pi N$  elastic partial-wave amplitudes and from plots of the speeds with which the amplitudes traverse the diagrams.
- LONGACRE 78 values are from a search for poles in the unitarized T-matrix. The first (second) value uses, in addition to  $\pi N \rightarrow N\pi\pi$  data, elastic amplitudes from a Saclay (CERN) partial-wave analysis.
- This ANISOVICH 12A value is the complex helicity amplitude at the pole position.

 $\Delta(1900)$  REFERENCES

For early references, see Physics Letters **111B** 1 (1982).

ANISOVICH 12A	EPJ A48 15	A.V. Anisovich et al.	(BONN, PNPI)
ARNDT 06	PR C74 045205	R.A. Arndt et al.	(GWU)
PDG 06	JPG 33 1	W.-M. Yao et al.	(PDG Collab.)
VRANA 00	PRPL 328 181	T.P. Vrana, S.A. Dytman, T.-S.H. Lee	(PITT+)
HOEHLER 93	$\pi N$ Newsletter 9 1	G. Höhler	(KARL)
MANLEY 92	PR D45 4002	D.M. Manley, E.M. Saleski	(KENT) IJP
Also	PR D30 904	D.M. Manley et al.	(VPI)
ARNDT 91	PR D43 2131	R.A. Arndt et al.	(VPI, TELE) IJP

CANDLIN 84	NP B238 477	D.J. Candlin et al.	(EDIN, RAL, LOWC)
CRAWFORD 83	NP B211 1	R.L. Crawford, W.T. Morton	(GLAS)
AWAJI 81	Bonn Conf. 352	N. Awaji, R. Kajikawa	(NAGO)
Also	NP B197 365	K. Fujii et al.	(NAGO)
CHEW 80	Toronto Conf. 123	D.M. Chew	(LBL) IJP
CUTKOSKY 80	Toronto Conf. 19	R.E. Cutkosky et al.	(CMU, LBL) IJP
Also	PR D20 2839	R.E. Cutkosky et al.	(CMU, LBL) IJP
HOEHLER 79	PDAT 12-1	G. Höhler et al.	(KARL) IJP
Also	Toronto Conf. 3	R. Koch	(KARL) IJP
LONGACRE 78	PR D17 1795	R.S. Longacre et al.	(LBL, SLAC)

 $\Delta(1905) 5/2^+$ 

$$I(J^P) = \frac{3}{2}(\frac{5}{2}^+) \text{ Status: } ***$$

Most of the results published before 1975 were last included in our 1982 edition, Physics Letters **111B** 1 (1982). Some further obsolete results published before 1984 were last included in our 2006 edition, Journal of Physics, G **33** 1 (2006).

 $\Delta(1905)$  BREIT-WIGNER MASS

VALUE (MeV)	DOCUMENT ID	TECN	COMMENT
<b>1855 to 1910 (<math>\approx</math> 1880) OUR ESTIMATE</b>			
1861 ± 6	ANISOVICH 12A	DPWA	Multichannel
1857.8 ± 1.6	ARNDT 06	DPWA	$\pi N \rightarrow \pi N, \eta N$
1881 ± 18	MANLEY 92	IPWA	$\pi N \rightarrow \pi N$ & $N\pi\pi$
1910 ± 30	CUTKOSKY 80	IPWA	$\pi N \rightarrow \pi N$
1905 ± 20	HOEHLER 79	IPWA	$\pi N \rightarrow \pi N$
• • • We do not use the following data for averages, fits, limits, etc. • • •			
1890 ± 25	<sup>1</sup> ANISOVICH 10	DPWA	Multichannel
1855.7 ± 4.2	ARNDT 04	DPWA	$\pi N \rightarrow \pi N, \eta N$
1873 ± 77	VRANA 00	DPWA	Multichannel
1895 ± 8	ARNDT 96	IPWA	$\gamma N \rightarrow \pi N$
1850	ARNDT 95	DPWA	$\pi N \rightarrow N\pi$
1960 ± 40	CANDLIN 84	DPWA	$\pi^+ p \rightarrow \Sigma^+ K^+$
1787.0 <sup>+6.0</sup> <sub>-5.7</sub>	CHEW 80	BPWA	$\pi^+ p \rightarrow \pi^+ p$
1830	<sup>2</sup> LONGACRE 75	IPWA	$\pi N \rightarrow N\pi\pi$

 $\Delta(1905)$  BREIT-WIGNER WIDTH

VALUE (MeV)	DOCUMENT ID	TECN	COMMENT
<b>270 to 400 (<math>\approx</math> 330) OUR ESTIMATE</b>			
335 ± 18	ANISOVICH 12A	DPWA	Multichannel
320.6 ± 8.6	ARNDT 06	DPWA	$\pi N \rightarrow \pi N, \eta N$
327 ± 51	MANLEY 92	IPWA	$\pi N \rightarrow \pi N$ & $N\pi\pi$
400 ± 100	CUTKOSKY 80	IPWA	$\pi N \rightarrow \pi N$
260 ± 20	HOEHLER 79	IPWA	$\pi N \rightarrow \pi N$
• • • We do not use the following data for averages, fits, limits, etc. • • •			
335 ± 30	ANISOVICH 10	DPWA	Multichannel
334 ± 22	ARNDT 04	DPWA	$\pi N \rightarrow \pi N, \eta N$
461 ± 111	VRANA 00	DPWA	Multichannel
354 ± 10	ARNDT 96	IPWA	$\gamma N \rightarrow \pi N$
294	ARNDT 95	DPWA	$\pi N \rightarrow N\pi$
270 ± 40	CANDLIN 84	DPWA	$\pi^+ p \rightarrow \Sigma^+ K^+$
66.0 <sup>+24.0</sup> <sub>-16.0</sub>	CHEW 80	BPWA	$\pi^+ p \rightarrow \pi^+ p$
220	<sup>2</sup> LONGACRE 75	IPWA	$\pi N \rightarrow N\pi\pi$

 $\Delta(1905)$  POLE POSITION

REAL PART	DOCUMENT ID	TECN	COMMENT
<b>1805 to 1835 (<math>\approx</math> 1820) OUR ESTIMATE</b>			
1805 ± 10	ANISOVICH 12A	DPWA	Multichannel
1819	ARNDT 06	DPWA	$\pi N \rightarrow \pi N, \eta N$
1829	<sup>3</sup> HOEHLER 93	SPED	$\pi N \rightarrow \pi N$
1830 ± 40	CUTKOSKY 80	IPWA	$\pi N \rightarrow \pi N$
• • • We do not use the following data for averages, fits, limits, etc. • • •			
1800 ± 15	ANISOVICH 10	DPWA	Multichannel
1825	ARNDT 04	DPWA	$\pi N \rightarrow \pi N, \eta N$
1793	VRANA 00	DPWA	Multichannel
1832	ARNDT 95	DPWA	$\pi N \rightarrow N\pi$
1794	ARNDT 91	DPWA	$\pi N \rightarrow \pi N$ Soln SM90
1813 or 1808	<sup>4</sup> LONGACRE 78	IPWA	$\pi N \rightarrow N\pi\pi$

-2*x*IMAGINARY PART

VALUE (MeV)	DOCUMENT ID	TECN	COMMENT
<b>265 to 300 (<math>\approx</math> 280) OUR ESTIMATE</b>			
300 ± 15	ANISOVICH 12A	DPWA	Multichannel
247	ARNDT 06	DPWA	$\pi N \rightarrow \pi N, \eta N$
303	<sup>3</sup> HOEHLER 93	SPED	$\pi N \rightarrow \pi N$
280 ± 60	CUTKOSKY 80	IPWA	$\pi N \rightarrow \pi N$
• • • We do not use the following data for averages, fits, limits, etc. • • •			
300 ± 20	ANISOVICH 10	DPWA	Multichannel
270	ARNDT 04	DPWA	$\pi N \rightarrow \pi N, \eta N$
302	VRANA 00	DPWA	Multichannel
254	ARNDT 95	DPWA	$\pi N \rightarrow N\pi$
230	ARNDT 91	DPWA	$\pi N \rightarrow \pi N$ Soln SM90
193 or 187	<sup>4</sup> LONGACRE 78	IPWA	$\pi N \rightarrow N\pi\pi$



See key on page 457

# Baryon Particle Listings

## $\Delta(1905)$

### $\Delta(1905)$ ELASTIC POLE RESIDUE

#### MODULUS $|r|$

VALUE (MeV)	DOCUMENT ID	TECN	COMMENT
20 ± 2	ANISOVICH 12A	DPWA	Multichannel
15	ARNDT 06	DPWA	$\pi N \rightarrow \pi N, \eta N$
25	HOEHLER 93	SPED	$\pi N \rightarrow \pi N$
25 ± 8	CUTKOSKY 80	IPWA	$\pi N \rightarrow \pi N$
• • • We do not use the following data for averages, fits, limits, etc. • • •			
16	ARNDT 04	DPWA	$\pi N \rightarrow \pi N, \eta N$
12	ARNDT 95	DPWA	$\pi N \rightarrow N\pi$
14	ARNDT 91	DPWA	$\pi N \rightarrow \pi N$ Soln SM90

#### PHASE $\theta$

VALUE (°)	DOCUMENT ID	TECN	COMMENT
-44 ± 5	ANISOVICH 12A	DPWA	Multichannel
-30	ARNDT 06	DPWA	$\pi N \rightarrow \pi N, \eta N$
-50 ± 20	CUTKOSKY 80	IPWA	$\pi N \rightarrow \pi N$
• • • We do not use the following data for averages, fits, limits, etc. • • •			
-25	ARNDT 04	DPWA	$\pi N \rightarrow \pi N, \eta N$
-4	ARNDT 95	DPWA	$\pi N \rightarrow N\pi$
-40	ARNDT 91	DPWA	$\pi N \rightarrow \pi N$ Soln SM90

### $\Delta(1905)$ INELASTIC POLE RESIDUE

The "normalized residue" is the residue divided by  $\Gamma_{pole}$ .

#### Normalized residue in $N\pi \rightarrow \Delta(1905) \rightarrow \Delta\pi, P$ -wave

MODULUS (%)	PHASE (°)	DOCUMENT ID	TECN	COMMENT
25 ± 6	0 ± 15	ANISOVICH 12A	DPWA	Multichannel

### $\Delta(1905)$ DECAY MODES

The following branching fractions are our estimates, not fits or averages.

Mode	Fraction ( $\Gamma_i/\Gamma$ )
$\Gamma_1$ $N\pi$	9-15 %
$\Gamma_2$ $\Sigma K$	
$\Gamma_3$ $N\pi\pi$	85-95 %
$\Gamma_4$ $\Delta\pi$	<25 %
$\Gamma_5$ $\Delta(1232)\pi, P$ -wave	
$\Gamma_6$ $\Delta(1232)\pi, F$ -wave	
$\Gamma_7$ $N\rho$	>60 %
$\Gamma_8$ $N\rho, S=3/2, P$ -wave	
$\Gamma_9$ $N\rho, S=3/2, F$ -wave	
$\Gamma_{10}$ $N\rho, S=1/2, F$ -wave	
$\Gamma_{11}$ $N\gamma$	0.012-0.036 %
$\Gamma_{12}$ $N\gamma, \text{ helicity}=1/2$	0.002-0.006 %
$\Gamma_{13}$ $N\gamma, \text{ helicity}=3/2$	0.01-0.03 %

### $\Delta(1905)$ BRANCHING RATIOS

#### $\Gamma(N\pi)/\Gamma_{total}$

VALUE (%)	DOCUMENT ID	TECN	COMMENT	$\Gamma_1/\Gamma$
<b>9 to 15 OUR ESTIMATE</b>				
13 ± 2	ANISOVICH 12A	DPWA	Multichannel	
12.2 ± 0.1	ARNDT 06	DPWA	$\pi N \rightarrow \pi N, \eta N$	
12 ± 3	MANLEY 92	IPWA	$\pi N \rightarrow \pi N \& N\pi\pi$	
8 ± 3	CUTKOSKY 80	IPWA	$\pi N \rightarrow \pi N$	
15 ± 2	HOEHLER 79	IPWA	$\pi N \rightarrow \pi N$	
• • • We do not use the following data for averages, fits, limits, etc. • • •				
12 ± 3	ANISOVICH 10	DPWA	Multichannel	
12.0 ± 0.2	ARNDT 04	DPWA	$\pi N \rightarrow \pi N, \eta N$	
9 ± 1	VRANA 00	DPWA	Multichannel	
12	ARNDT 95	DPWA	$\pi N \rightarrow N\pi$	
11	CHEW 80	BPWA	$\pi^+\rho \rightarrow \pi^+\rho$	

#### $(\Gamma_i\Gamma_f)^{1/2}/\Gamma_{total}$ in $N\pi \rightarrow \Delta(1905) \rightarrow \Sigma K$ $(\Gamma_1\Gamma_2)^{1/2}/\Gamma$

VALUE	DOCUMENT ID	TECN	COMMENT
-0.015 ± 0.003	CANDLIN 84	DPWA	$\pi^+\rho \rightarrow \Sigma^+ K^+$

Note: Signs of couplings from  $\pi N \rightarrow N\pi\pi$  analyses were changed in the 1986 edition to agree with the baryon-first convention; the overall phase ambiguity is resolved by choosing a negative sign for the  $\Delta(1620) S_{31}$  coupling to  $\Delta(1232)\pi$ .

#### $(\Gamma_i\Gamma_f)^{1/2}/\Gamma_{total}$ in $N\pi \rightarrow \Delta(1905) \rightarrow \Delta(1232)\pi, P$ -wave $(\Gamma_1\Gamma_5)^{1/2}/\Gamma$

VALUE	DOCUMENT ID	TECN	COMMENT
-0.04 ± 0.05	MANLEY 92	IPWA	$\pi N \rightarrow \pi N \& N\pi\pi$

#### $\Gamma(\Delta(1232)\pi, P\text{-wave})/\Gamma_{total}$

VALUE (%)	DOCUMENT ID	TECN	COMMENT	$\Gamma_5/\Gamma$
45 ± 14	ANISOVICH 12A	DPWA	Multichannel	
23 ± 1	VRANA 00	DPWA	Multichannel	

#### $(\Gamma_i\Gamma_f)^{1/2}/\Gamma_{total}$ in $N\pi \rightarrow \Delta(1905) \rightarrow \Delta(1232)\pi, F$ -wave $(\Gamma_1\Gamma_6)^{1/2}/\Gamma$

VALUE	DOCUMENT ID	TECN	COMMENT
+0.02 ± 0.03	MANLEY 92	IPWA	$\pi N \rightarrow \pi N \& N\pi\pi$
+0.20	<sup>2</sup> LONGACRE 75	IPWA	$\pi N \rightarrow N\pi\pi$

#### $\Gamma(\Delta(1232)\pi, F\text{-wave})/\Gamma_{total}$

VALUE (%)	DOCUMENT ID	TECN	COMMENT	$\Gamma_6/\Gamma$
44 ± 1	VRANA 00	DPWA	Multichannel	

#### $(\Gamma_i\Gamma_f)^{1/2}/\Gamma_{total}$ in $N\pi \rightarrow \Delta(1905) \rightarrow N\rho, S=3/2, P$ -wave $(\Gamma_1\Gamma_8)^{1/2}/\Gamma$

VALUE	DOCUMENT ID	TECN	COMMENT
<b>+0.30 to +0.36 OUR ESTIMATE</b>			
+0.33 ± 0.03	MANLEY 92	IPWA	$\pi N \rightarrow \pi N \& N\pi\pi$
+0.33	<sup>2</sup> LONGACRE 75	IPWA	$\pi N \rightarrow N\pi\pi$

#### $\Gamma(N\rho, S=3/2, P\text{-wave})/\Gamma_{total}$

VALUE (%)	DOCUMENT ID	TECN	COMMENT	$\Gamma_8/\Gamma$
24 ± 1	VRANA 00	DPWA	Multichannel	

### $\Delta(1905)$ PHOTON DECAY AMPLITUDES

Papers on  $\gamma N$  amplitudes predating 1981 may be found in our 2006 edition, Journal of Physics, G **33** 1 (2006).

#### $\Delta(1905) \rightarrow N\gamma, \text{ helicity-1/2 amplitude } A_{1/2}$

VALUE (GeV <sup>-1/2</sup> )	DOCUMENT ID	TECN	COMMENT
<b>+0.026 ± 0.011 OUR ESTIMATE</b>			
0.025 ± 0.004	ANISOVICH 12A	DPWA	Multichannel
0.021 ± 0.004	DUGGER 07	DPWA	$\gamma N \rightarrow \pi N$
0.022 ± 0.005	ARNDT 96	IPWA	$\gamma N \rightarrow \pi N$
0.021 ± 0.010	CRAWFORD 83	IPWA	$\gamma N \rightarrow \pi N$
0.043 ± 0.020	AWAJI 81	DPWA	$\gamma N \rightarrow \pi N$
• • • We do not use the following data for averages, fits, limits, etc. • • •			
0.028 ± 0.012	<sup>1</sup> ANISOVICH 10	DPWA	Multichannel
0.018	DRECHSEL 07	DPWA	$\gamma N \rightarrow \pi N$
0.055 ± 0.004	LI 93	IPWA	$\gamma N \rightarrow \pi N$

#### $\Delta(1905) \rightarrow N\gamma, \text{ helicity-3/2 amplitude } A_{3/2}$

VALUE (GeV <sup>-1/2</sup> )	DOCUMENT ID	TECN	COMMENT
<b>-0.045 ± 0.020 OUR ESTIMATE</b>			
-0.049 ± 0.004	ANISOVICH 12A	DPWA	Multichannel
-0.046 ± 0.005	DUGGER 07	DPWA	$\gamma N \rightarrow \pi N$
-0.045 ± 0.005	ARNDT 96	IPWA	$\gamma N \rightarrow \pi N$
-0.056 ± 0.028	CRAWFORD 83	IPWA	$\gamma N \rightarrow \pi N$
-0.025 ± 0.023	AWAJI 81	DPWA	$\gamma N \rightarrow \pi N$
• • • We do not use the following data for averages, fits, limits, etc. • • •			
-0.042 ± 0.015	<sup>1</sup> ANISOVICH 10	DPWA	Multichannel
-0.028	DRECHSEL 07	DPWA	$\gamma N \rightarrow \pi N$
0.002 ± 0.003	LI 93	IPWA	$\gamma N \rightarrow \pi N$

### $\Delta(1905)$ FOOTNOTES

- ANISOVICH 10 finds an alternate solution for this resonance. The only statistically significant differences are in the Breit-Wigner mass and  $\gamma\rho$  couplings.
- From method II of LONGACRE 75: eyeball fits with Breit-Wigner circles to the T-matrix amplitudes.
- See HOEHLER 93 for a detailed discussion of the evidence for and the pole parameters of  $N$  and  $\Delta$  resonances as determined from Argand diagrams of  $\pi N$  elastic partial-wave amplitudes and from plots of the speeds with which the amplitudes traverse the diagrams.
- LONGACRE 78 values are from a search for poles in the unitarized T-matrix. The first (second) value uses, in addition to  $\pi N \rightarrow N\pi\pi$  data, elastic amplitudes from a Saclay (CERN) partial-wave analysis.

### $\Delta(1905)$ REFERENCES

For early references, see Physics Letters **111B** 1 (1982).

ANISOVICH 12A	EPJ A48 15	A.V. Anisovich et al.	(BONN, PNPI)
ANISOVICH 10	EPJ A44 203	A.V. Anisovich et al.	(BONN, PNPI)
DRECHSEL 07	EPJ A34 69	D. Drechsel, S.S. Kamalov, L. Tiator	(MAINZ, JINR)
DUGGER 07	PR C76 025211	M. Dugger et al.	(Jefferson Lab CLAS Collab.)
ARNDT 06	PR C74 045205	R.A. Arndt et al.	(GWU)
PDG 06	JPG 33 1	W.-M. Yao et al.	(PDG Collab.)
ARNDT 04	PR C69 035213	R.A. Arndt et al.	(GWU, TRIU)
VRANA 00	PRPL 328 181	T.P. Vrana, S.A. Dytman, T.-S.H. Lee	(PITT+)
ARNDT 96	PR C53 430	R.A. Arndt, I.I. Strakovsky, R.L. Workman	(VPI)
ARNDT 95	PR C52 2120	R.A. Arndt et al.	(VPI, BRCO)
HOEHLER 93	$\pi N$ Newsletter 9 1	G. Hohler	(KARL)
LI 93	PR C47 2759	Z.J. Li et al.	(VPI)
MANLEY 92	PR D45 4002	D.M. Manley, E.M. Saleski	(KENT) IJP
Also	PR D30 904	D.M. Manley et al.	(VPI)

## Baryon Particle Listings

 $\Delta(1905), \Delta(1910)$ 

ARNDT	91	PR D43 2131	R.A. Arndt <i>et al.</i>	(VPI, TELE) IJP
CANDLIN	84	NP B238 477	D.J. Candlin <i>et al.</i>	(EDIN, RAL, LOWC)
CRAWFORD	83	NP B211 1	R.L. Crawford, W.T. Morton	(GLAS)
PDG	82	PL 111B 1	M. Roos <i>et al.</i>	(HELS, CIT, CERN)
AWAJI	81	Bonn Conf. 352	N. Awaji, R. Kajikawa	(NAGO)
Also		NP B197 365	K. Fujii <i>et al.</i>	(NAGO)
CHEW	80	Toronto Conf. 123	D.M. Chew	(LBL) IJP
CUTKOSKY	80	Toronto Conf. 19	R.E. Cutkosky <i>et al.</i>	(CMU, LBL) IJP
Also		PR D20 2839	R.E. Cutkosky <i>et al.</i>	(CMU, LBL) IJP
HOEHLER	79	PDAT 12-1	G. Hoehler <i>et al.</i>	(KARLT) IJP
Also		Toronto Conf. 3	R. Koch	(KARLT) IJP
LONGACRE	78	PR D17 1795	R.S. Longacre <i>et al.</i>	(LBL, SLAC)
LONGACRE	75	PL 55B 415	R.S. Longacre <i>et al.</i>	(LBL, SLAC) IJP

 $\Delta(1910) 1/2^+$ 

$$I(J^P) = \frac{3}{2}(\frac{1}{2}^+) \text{ Status: } ***$$

Most of the results published before 1975 were last included in our 1982 edition, Physics Letters **111B** 1 (1982). Some further obsolete results published before 1984 were last included in our 2006 edition, Journal of Physics, G **33** 1 (2006).

 $\Delta(1910)$  BREIT-WIGNER MASS

VALUE (MeV)	DOCUMENT ID	TECN	COMMENT
<b>1860 to 1910 (<math>\approx 1890</math>) OUR ESTIMATE</b>			
1860 $\pm 40$	ANISOVICH 12A	DPWA	Multichannel
2067.9 $\pm 1.7$	ARNDT 06	DPWA	$\pi N \rightarrow \pi N, \eta N$
1882 $\pm 10$	MANLEY 92	IPWA	$\pi N \rightarrow \pi N \& N\pi\pi$
1910 $\pm 40$	CUTKOSKY 80	IPWA	$\pi N \rightarrow \pi N$
1888 $\pm 20$	HOEHLER 79	IPWA	$\pi N \rightarrow \pi N$
••• We do not use the following data for averages, fits, limits, etc. •••			
1995 $\pm 12$	VRANA 00	DPWA	Multichannel
2152	ARNDT 95	DPWA	$\pi N \rightarrow N\pi$
1960.1 $\pm 21.0$	<sup>1</sup> CHEW 80	BPWA	$\pi^+ p \rightarrow \pi^+ p$
2121.4 $^{+13.0}_{-14.3}$	<sup>1</sup> CHEW 80	BPWA	$\pi^+ p \rightarrow \pi^+ p$
1790	<sup>2</sup> LONGACRE 77	IPWA	$\pi N \rightarrow N\pi\pi$

 $\Delta(1910)$  BREIT-WIGNER WIDTH

VALUE (MeV)	DOCUMENT ID	TECN	COMMENT
<b>220 to 340 (<math>\approx 280</math>) OUR ESTIMATE</b>			
350 $\pm 55$	ANISOVICH 12A	DPWA	Multichannel
543 $\pm 10$	ARNDT 06	DPWA	$\pi N \rightarrow \pi N, \eta N$
239 $\pm 25$	MANLEY 92	IPWA	$\pi N \rightarrow \pi N \& N\pi\pi$
225 $\pm 50$	CUTKOSKY 80	IPWA	$\pi N \rightarrow \pi N$
280 $\pm 50$	HOEHLER 79	IPWA	$\pi N \rightarrow \pi N$
••• We do not use the following data for averages, fits, limits, etc. •••			
713 $\pm 465$	VRANA 00	DPWA	Multichannel
760	ARNDT 95	DPWA	$\pi N \rightarrow N\pi$
152.9 $\pm 60.0$	<sup>1</sup> CHEW 80	BPWA	$\pi^+ p \rightarrow \pi^+ p$
172.2 $\pm 37.0$	<sup>1</sup> CHEW 80	BPWA	$\pi^+ p \rightarrow \pi^+ p$
170	<sup>2</sup> LONGACRE 77	IPWA	$\pi N \rightarrow N\pi\pi$

 $\Delta(1910)$  POLE POSITION

## REAL PART

VALUE (MeV)	DOCUMENT ID	TECN	COMMENT
<b>1830 to 1880 (<math>\approx 1855</math>) OUR ESTIMATE</b>			
1850 $\pm 40$	ANISOVICH 12A	DPWA	Multichannel
1771	ARNDT 06	DPWA	$\pi N \rightarrow \pi N, \eta N$
1874	<sup>3</sup> HOEHLER 93	SPED	$\pi N \rightarrow \pi N$
1880 $\pm 30$	CUTKOSKY 80	IPWA	$\pi N \rightarrow \pi N$
••• We do not use the following data for averages, fits, limits, etc. •••			
1880	VRANA 00	DPWA	Multichannel
1810	ARNDT 95	DPWA	$\pi N \rightarrow N\pi$
1950	ARNDT 91	DPWA	$\pi N \rightarrow \pi N$ Soln SM90
1792 or 1801	<sup>2</sup> LONGACRE 77	IPWA	$\pi N \rightarrow N\pi\pi$

 $-2 \times$  IMAGINARY PART

VALUE (MeV)	DOCUMENT ID	TECN	COMMENT
<b>200 to 500 (<math>\approx 350</math>) OUR ESTIMATE</b>			
350 $\pm 45$	ANISOVICH 12A	DPWA	Multichannel
479	ARNDT 06	DPWA	$\pi N \rightarrow \pi N, \eta N$
283	<sup>3</sup> HOEHLER 93	SPED	$\pi N \rightarrow \pi N$
200 $\pm 40$	CUTKOSKY 80	IPWA	$\pi N \rightarrow \pi N$
••• We do not use the following data for averages, fits, limits, etc. •••			
496	VRANA 00	DPWA	Multichannel
494	ARNDT 95	DPWA	$\pi N \rightarrow N\pi$
398	ARNDT 91	DPWA	$\pi N \rightarrow \pi N$ Soln SM90
172 or 165	<sup>2</sup> LONGACRE 77	IPWA	$\pi N \rightarrow N\pi\pi$

 $\Delta(1910)$  ELASTIC POLE RESIDUEMODULUS  $|r|$ 

VALUE (MeV)	DOCUMENT ID	TECN	COMMENT
24 $\pm 6$	ANISOVICH 12A	DPWA	Multichannel
45	ARNDT 06	DPWA	$\pi N \rightarrow \pi N, \eta N$
38	HOEHLER 93	SPED	$\pi N \rightarrow \pi N$
20 $\pm 4$	CUTKOSKY 80	IPWA	$\pi N \rightarrow \pi N$
••• We do not use the following data for averages, fits, limits, etc. •••			
53	ARNDT 95	DPWA	$\pi N \rightarrow N\pi$
37	ARNDT 91	DPWA	$\pi N \rightarrow \pi N$ Soln SM90

PHASE  $\theta$ 

VALUE ( $^\circ$ )	DOCUMENT ID	TECN	COMMENT
-145 $\pm 30$	ANISOVICH 12A	DPWA	Multichannel
+172	ARNDT 06	DPWA	$\pi N \rightarrow \pi N, \eta N$
-90 $\pm 30$	CUTKOSKY 80	IPWA	$\pi N \rightarrow \pi N$
••• We do not use the following data for averages, fits, limits, etc. •••			
-176	ARNDT 95	DPWA	$\pi N \rightarrow N\pi$
-91	ARNDT 91	DPWA	$\pi N \rightarrow \pi N$ Soln SM90

 $\Delta(1910)$  INELASTIC POLE RESIDUE

The "normalized residue" is the residue divided by  $\Gamma_{pole}$ .

Normalized residue in  $N\pi \rightarrow \Delta(1910) \rightarrow \Sigma K$ 

MODULUS (%)	PHASE ( $^\circ$ )	DOCUMENT ID	TECN	COMMENT
<b>7 <math>\pm 2</math></b>	<b>-110 <math>\pm 30</math></b>	ANISOVICH 12A	DPWA	Multichannel

Normalized residue in  $N\pi \rightarrow \Delta(1910) \rightarrow \Delta\pi, P$ -wave

MODULUS (%)	PHASE ( $^\circ$ )	DOCUMENT ID	TECN	COMMENT
<b>16 <math>\pm 9</math></b>	<b>95 <math>\pm 40</math></b>	ANISOVICH 12A	DPWA	Multichannel

 $\Delta(1910)$  DECAY MODES

The following branching fractions are our estimates, not fits or averages.

Mode	Fraction ( $\Gamma_i/\Gamma$ )
$\Gamma_1$ $N\pi$	15-30 %
$\Gamma_2$ $\Sigma K$	(9 $\pm 5$ ) %
$\Gamma_3$ $N\pi\pi$	
$\Gamma_4$ $\Delta\pi$	(60 $\pm 28$ ) %
$\Gamma_5$ $\Delta(1232)\pi, P$ -wave	
$\Gamma_6$ $N\rho$	
$\Gamma_7$ $N\rho, S=3/2, P$ -wave	
$\Gamma_8$ $N(1440)\pi$	
$\Gamma_9$ $N(1440)\pi, P$ -wave	
$\Gamma_{10}$ $N\gamma$	0.0-0.02 %
$\Gamma_{11}$ $N\gamma, \text{ helicity}=1/2$	0.0-0.02 %

 $\Delta(1910)$  BRANCHING RATIOS

$\Gamma(N\pi)/\Gamma_{total}$	DOCUMENT ID	TECN	COMMENT	$\Gamma_1/\Gamma$
<b>15 to 30 OUR ESTIMATE</b>				
12 $\pm 3$	ANISOVICH 12A	DPWA	Multichannel	
23.9 $\pm 0.1$	ARNDT 06	DPWA	$\pi N \rightarrow \pi N, \eta N$	
23 $\pm 8$	MANLEY 92	IPWA	$\pi N \rightarrow \pi N \& N\pi\pi$	
19 $\pm 3$	CUTKOSKY 80	IPWA	$\pi N \rightarrow \pi N$	
24 $\pm 6$	HOEHLER 79	IPWA	$\pi N \rightarrow \pi N$	
••• We do not use the following data for averages, fits, limits, etc. •••				
29 $\pm 21$	VRANA 00	DPWA	Multichannel	
26	ARNDT 95	DPWA	$\pi N \rightarrow N\pi$	
17	<sup>1</sup> CHEW 80	BPWA	$\pi^+ p \rightarrow \pi^+ p$	
40	<sup>1</sup> CHEW 80	BPWA	$\pi^+ p \rightarrow \pi^+ p$	

 $(\Gamma_1\Gamma_2)^{1/2}/\Gamma_{total}$  in  $N\pi \rightarrow \Delta(1910) \rightarrow \Sigma K$ 

VALUE	DOCUMENT ID	TECN	COMMENT
< 0.03	CANDLIN 84	DPWA	$\pi^+ p \rightarrow \Sigma^+ K^+$
••• We do not use the following data for averages, fits, limits, etc. •••			
-0.019	LIVANOS 80	DPWA	$\pi p \rightarrow \Sigma K$

 $\Gamma(\Sigma K)/\Gamma_{total}$ 

VALUE (%)	DOCUMENT ID	TECN	COMMENT
<b>9 <math>\pm 5</math></b>	ANISOVICH 12A	DPWA	Multichannel

Note: Signs of couplings from  $\pi N \rightarrow N\pi\pi$  analyses were changed in the 1986 edition to agree with the baryon-first convention; the overall phase ambiguity is resolved by choosing a negative sign for the  $\Delta(1620) S_{31}$  coupling to  $\Delta(1232)\pi$ .

 $(\Gamma_1\Gamma_2)^{1/2}/\Gamma_{total}$  in  $N\pi \rightarrow \Delta(1910) \rightarrow \Delta(1232)\pi, P$ -wave

VALUE	DOCUMENT ID	TECN	COMMENT
+0.06	<sup>2</sup> LONGACRE 77	IPWA	$\pi N \rightarrow N\pi\pi$

See key on page 457

# Baryon Particle Listings

## $\Delta(1910)$ , $\Delta(1920)$

$\Gamma(\Delta\pi)/\Gamma_{total}$	DOCUMENT ID	TECN	COMMENT	$\Gamma_4/\Gamma$
VALUE (%)				
<b>60±28</b>	ANISOVICH	12A	DPWA	Multichannel

$(\Gamma_1\Gamma_7)^{1/2}/\Gamma_{total}$ in $N\pi \rightarrow \Delta(1910) \rightarrow N\rho, S=3/2, P\text{-wave}$	DOCUMENT ID	TECN	COMMENT	$(\Gamma_1\Gamma_7)^{1/2}/\Gamma$
VALUE				
+0.29	2 LONGACRE	77	IPWA	$\pi N \rightarrow N\pi\pi$

$(\Gamma_1\Gamma_7)^{1/2}/\Gamma_{total}$ in $N\pi \rightarrow \Delta(1910) \rightarrow N(1440)\pi, P\text{-wave}$	DOCUMENT ID	TECN	COMMENT	$(\Gamma_1\Gamma_7)^{1/2}/\Gamma$
VALUE				
-0.39±0.04	MANLEY	92	IPWA	$\pi N \rightarrow \pi N \& N\pi\pi$

$\Gamma(N(1440)\pi)/\Gamma_{total}$	DOCUMENT ID	TECN	COMMENT	$\Gamma_8/\Gamma$
VALUE (%)				
56±7	VRANA	00	DPWA	Multichannel

### $\Delta(1910)$ PHOTON DECAY AMPLITUDES

Papers on  $\gamma N$  amplitudes predating 1981 may be found in our 2006 edition, Journal of Physics, G **33** 1 (2006).

### $\Delta(1910) \rightarrow N\gamma$ , helicity-1/2 amplitude $A_{1/2}$

VALUE (GeV <sup>-1/2</sup> )	DOCUMENT ID	TECN	COMMENT
<b>+0.003±0.014 OUR ESTIMATE</b>			
0.022±0.009	ANISOVICH	12A	DPWA Multichannel
-0.002±0.008	ARNDT	96	IPWA $\gamma N \rightarrow \pi N$
0.014±0.030	CRAWFORD	83	IPWA $\gamma N \rightarrow \pi N$
0.025±0.011	AWAJI	81	DPWA $\gamma N \rightarrow \pi N$
• • • We do not use the following data for averages, fits, limits, etc. • • •			
0.032±0.003	LI	93	IPWA $\gamma N \rightarrow \pi N$

### $\Delta(1910)$ FOOTNOTES

- 1 CHEW 80 reports four resonances in the  $P_{31}$  wave — see also the  $\Delta(1750)$ . Problems with this analysis are discussed in section 2.1.11 of HOEHLER 83.
- 2 LONGACRE 77 pole positions are from a search for poles in the unitarized T-matrix; the first (second) value uses, in addition to  $\pi N \rightarrow N\pi\pi$  data, elastic amplitudes from a Saclay (CERN) partial-wave analysis. The other LONGACRE 77 values are from eyeball fits with Breit-Wigner circles to the T-matrix amplitudes.
- 3 See HOEHLER 93 for a detailed discussion of the evidence for and the pole parameters of  $N$  and  $\Delta$  resonances as determined from Argand diagrams of  $\pi N$  elastic partial-wave amplitudes and from plots of the speeds with which the amplitudes traverse the diagrams.

### $\Delta(1910)$ REFERENCES

For early references, see Physics Letters **111B** 1 (1982).

ANISOVICH 12A	EPJ A48 15	A.V. Anisovich et al.	(BONN, PNPI)
ARNDT 06	PR C74 045205	R.A. Arndt et al.	(GWU)
PDG 06	JPG 33 1	W.-M. Yao et al.	(PDG Collab.)
VRANA 00	PRPL 328 181	T.P. Vrana, S.A. Dytman, T.-S.H. Lee	(PITT+)
ARNDT 96	PR C53 430	R.A. Arndt, I.I. Strakovsky, R.L. Workman	(VPI)
ARNDT 95	PR C52 2120	R.A. Arndt et al.	(VPI, BRCO)
HOEHLER 93	$\pi N$ Newsletter 9 1	G. Höhler	(KARL)
LI 93	PR C47 2759	Z.J. Li et al.	(VPI)
MANLEY 92	PR D45 4002	D.M. Manley, E.M. Saleski	(KENT) IJP
Also	PR D30 904	D.M. Manley et al.	(VPI)
ARNDT 91	PR D43 2131	R.A. Arndt et al.	(VPI, TELE) IJP
CANDLIN 84	NP B238 477	D.J. Candlin et al.	(EDIN, RAL, LOWC)
CRAWFORD 83	NP B211 1	R.L. Crawford, W.T. Morton	(GLAS)
HOEHLER 83	Landoil-Boerstein 1/982	G. Höhler	(KARL)
PDG 82	PL 111B 1	M. Roos et al.	(HELS, CIT, CERN)
AWAJI 81	Bonn Conf. 352	N. Awaji, R. Kajikawa	(NAGO)
Also	NP B197 365	K. Fujii et al.	(NAGO)
CHEW 80	Toronto Conf. 123	D.M. Chew	(LBL) IJP
CUTKOSKY 80	Toronto Conf. 19	R.E. Cutkosky et al.	(CMU, LBL) IJP
Also	PR D20 2839	R.E. Cutkosky et al.	(CMU, LBL) IJP
LIVANOS 80	Toronto Conf. 35	P. Livanos et al.	(SACL) IJP
HOEHLER 79	PDAT 12-1	G. Höhler et al.	(KARL) IJP
Also	Toronto Conf. 3	R. Koch	(KARL) IJP
LONGACRE 77	NP B122 493	R.S. Longacre, J. Dolbeau	(SACL) IJP
Also	NP B108 365	J. Dolbeau et al.	(SACL) IJP

$\Delta(1920) 3/2^+$

 $I(J^P) = \frac{3}{2}(\frac{3}{2}^+)$  Status: \*\*\*

Most of the results published before 1975 were last included in our 1982 edition, Physics Letters **111B** 1 (1982). Some further obsolete results published before 1984 were last included in our 2006 edition, Journal of Physics, G **33** 1 (2006).

The latest GWU analysis (ARNDT 06) finds no evidence for this resonance.

### $\Delta(1920)$ BREIT-WIGNER MASS

VALUE (MeV)	DOCUMENT ID	TECN	COMMENT
<b>1900 to 1920 (<math>\approx</math> 1920) OUR ESTIMATE</b>			
1900 ± 30	ANISOVICH	12A	DPWA Multichannel
2014 ± 16	MANLEY	92	IPWA $\pi N \rightarrow \pi N \& N\pi\pi$
1920 ± 80	CUTKOSKY	80	IPWA $\pi N \rightarrow \pi N$
1868 ± 10	HOEHLER	79	IPWA $\pi N \rightarrow \pi N$

• • • We do not use the following data for averages, fits, limits, etc. • • •

1990 ± 35	HORN	08A	DPWA Multichannel
2057 ± 1	PENNER	02C	DPWA Multichannel
1889 ± 100	VRANA	00	DPWA Multichannel
1840 ± 40	CANDLIN	84	DPWA $\pi^+ p \rightarrow \Sigma^+ K^+$
1955.0 ± 13.0	1 CHEW	80	BPWA $\pi^+ p \rightarrow \pi^+ p$
2065.0 ± 13.6 12.9	1 CHEW	80	BPWA $\pi^+ p \rightarrow \pi^+ p$

### $\Delta(1920)$ BREIT-WIGNER WIDTH

VALUE (MeV)	DOCUMENT ID	TECN	COMMENT
<b>180 to 300 (<math>\approx</math> 260) OUR ESTIMATE</b>			
310 ± 60	ANISOVICH	12A	DPWA Multichannel
152 ± 55	MANLEY	92	IPWA $\pi N \rightarrow \pi N \& N\pi\pi$
300 ± 100	CUTKOSKY	80	IPWA $\pi N \rightarrow \pi N$
220 ± 80	HOEHLER	79	IPWA $\pi N \rightarrow \pi N$
• • • We do not use the following data for averages, fits, limits, etc. • • •			
330 ± 60	HORN	08A	DPWA Multichannel
525 ± 32	PENNER	02C	DPWA Multichannel
123 ± 53	VRANA	00	DPWA Multichannel
200 ± 40	CANDLIN	84	DPWA $\pi^+ p \rightarrow \Sigma^+ K^+$
88.3 ± 35.0	1 CHEW	80	BPWA $\pi^+ p \rightarrow \pi^+ p$
62.0 ± 44.0	1 CHEW	80	BPWA $\pi^+ p \rightarrow \pi^+ p$

### $\Delta(1920)$ POLE POSITION

#### REAL PART

VALUE (MeV)	DOCUMENT ID	TECN	COMMENT
<b>1850 to 1950 (<math>\approx</math> 1900) OUR ESTIMATE</b>			
1890 ± 30	ANISOVICH	12A	DPWA Multichannel
1900	2 HOEHLER	93	SPED $\pi N \rightarrow \pi N$
1900 ± 80	CUTKOSKY	80	IPWA $\pi N \rightarrow \pi N$
• • • We do not use the following data for averages, fits, limits, etc. • • •			
1980 ± 25	HORN	08A	DPWA Multichannel
1880	VRANA	00	DPWA Multichannel
not seen	ARNDT	91	DPWA $\pi N \rightarrow \pi N$ Soln SM90

#### -2xIMAGINARY PART

VALUE (MeV)	DOCUMENT ID	TECN	COMMENT
<b>200 to 400 (<math>\approx</math> 300) OUR ESTIMATE</b>			
300 ± 60	ANISOVICH	12A	DPWA Multichannel
300 ± 100	CUTKOSKY	80	IPWA $\pi N \rightarrow \pi N$
• • • We do not use the following data for averages, fits, limits, etc. • • •			
310 ± 40 60	HORN	08A	DPWA Multichannel
120	VRANA	00	DPWA Multichannel
not seen	ARNDT	91	DPWA $\pi N \rightarrow \pi N$ Soln SM90

### $\Delta(1920)$ ELASTIC POLE RESIDUE

#### MODULUS $|r|$

VALUE (MeV)	DOCUMENT ID	TECN	COMMENT
17 ± 8	ANISOVICH	12A	DPWA Multichannel
24 ± 4	CUTKOSKY	80	IPWA $\pi N \rightarrow \pi N$

#### PHASE $\theta$

VALUE (°)	DOCUMENT ID	TECN	COMMENT
-40 ± 20	ANISOVICH	12A	DPWA Multichannel
-150 ± 30	CUTKOSKY	80	IPWA $\pi N \rightarrow \pi N$

### $\Delta(1920)$ INELASTIC POLE RESIDUE

The "normalized residue" is the residue divided by  $\Gamma_{pole}$ .

#### Normalized residue in $N\pi \rightarrow \Delta(1920) \rightarrow \Delta\eta$

MODULUS (%)	PHASE (°)	DOCUMENT ID	TECN	COMMENT
<b>17 ± 8</b>	<b>70 ± 20</b>	ANISOVICH	12A	DPWA Multichannel

#### Normalized residue in $N\pi \rightarrow \Delta(1920) \rightarrow \Sigma K$

MODULUS (%)	PHASE (°)	DOCUMENT ID	TECN	COMMENT
<b>9 ± 3</b>	<b>80 ± 40</b>	ANISOVICH	12A	DPWA Multichannel

#### Normalized residue in $N\pi \rightarrow \Delta(1920) \rightarrow \Delta\pi, P\text{-wave}$

MODULUS (%)	PHASE (°)	DOCUMENT ID	TECN	COMMENT
<b>20 ± 12</b>	<b>-120 ± 30</b>	ANISOVICH	12A	DPWA Multichannel

#### Normalized residue in $N\pi \rightarrow \Delta(1920) \rightarrow \Delta\pi, F\text{-wave}$

MODULUS (%)	PHASE (°)	DOCUMENT ID	TECN	COMMENT
<b>28 ± 7</b>	<b>-95 ± 35</b>	ANISOVICH	12A	DPWA Multichannel

## Baryon Particle Listings

 $\Delta(1920)$ ,  $\Delta(1930)$  $\Delta(1920)$  DECAY MODES

The following branching fractions are our estimates, not fits or averages.

Mode	Fraction ( $\Gamma_i/\Gamma$ )
$\Gamma_1$ $N\pi$	5–20 %
$\Gamma_2$ $\Sigma K$	( 2.14 ± 0.30 ) %
$\Gamma_3$ $N\pi\pi$	
$\Gamma_4$ $\Delta(1232)\pi$ , $P$ -wave	
$\Gamma_5$ $\Delta(1232)\pi$ , $F$ -wave	
$\Gamma_6$ $N(1440)\pi$ , $P$ -wave	
$\Gamma_7$ $N(1535)\pi$	
$\Gamma_8$ $N a_0(980)$	
$\Gamma_9$ $\Delta(1232)\eta$	(15 ± 8) %
$\Gamma_{10}$ $N\gamma$	0.0–0.4 %
$\Gamma_{11}$ $N\gamma$ , helicity=1/2	0.0–0.2 %
$\Gamma_{12}$ $N\gamma$ , helicity=3/2	0.0–0.2 %

 $\Delta(1920)$  BRANCHING RATIOS

$\Gamma(N\pi)/\Gamma_{\text{total}}$	DOCUMENT ID	TECN	COMMENT	$\Gamma_1/\Gamma$
<b>5 to 20 OUR ESTIMATE</b>				
8 ± 4	ANISOVICH	12A	DPWA Multichannel	
2 ± 2	MANLEY	92	IPWA $\pi N \rightarrow \pi N$ & $N\pi\pi$	
20 ± 5	CUTKOSKY	80	IPWA $\pi N \rightarrow \pi N$	
14 ± 4	HOEHLER	79	IPWA $\pi N \rightarrow \pi N$	
••• We do not use the following data for averages, fits, limits, etc. •••				
15 ± 8	HORN	08A	DPWA Multichannel	
15 ± 1	PENNER	02C	DPWA Multichannel	
5 ± 4	VRANA	00	DPWA Multichannel	
24	<sup>1</sup> CHEW	80	BPWA $\pi^+ p \rightarrow \pi^+ p$	
18	<sup>1</sup> CHEW	80	BPWA $\pi^+ p \rightarrow \pi^+ p$	

$(\Gamma_1\Gamma_2)^{1/2}/\Gamma_{\text{total}}$ in $N\pi \rightarrow \Delta(1920) \rightarrow \Sigma K$	DOCUMENT ID	TECN	COMMENT	$(\Gamma_1\Gamma_2)^{1/2}/\Gamma$
VALUE (%)				
–0.052 ± 0.015	CANDLIN	84	DPWA $\pi^+ p \rightarrow \Sigma^+ K^+$	
••• We do not use the following data for averages, fits, limits, etc. •••				
–0.049	LIVANOS	80	DPWA $\pi p \rightarrow \Sigma K$	

$\Gamma(\Sigma K)/\Gamma_{\text{total}}$	DOCUMENT ID	TECN	COMMENT	$\Gamma_2/\Gamma$
VALUE (%)				
<b>2.14 ± 0.30 OUR AVERAGE</b>				
4 ± 2	ANISOVICH	12A	DPWA Multichannel	
2.1 ± 0.3	PENNER	02C	DPWA Multichannel	

$(\Gamma_1\Gamma_4)^{1/2}/\Gamma_{\text{total}}$ in $N\pi \rightarrow \Delta(1920) \rightarrow \Delta(1232)\pi$ , $P$ -wave	DOCUMENT ID	TECN	COMMENT	$(\Gamma_1\Gamma_4)^{1/2}/\Gamma$
VALUE (%)				
–0.13 ± 0.04	MANLEY	92	IPWA $\pi N \rightarrow \pi N$ & $N\pi\pi$	

$\Gamma(\Delta(1232)\pi, P\text{-wave})/\Gamma_{\text{total}}$	DOCUMENT ID	TECN	COMMENT	$\Gamma_4/\Gamma$
VALUE (%)				
22 ± 12	ANISOVICH	12A	DPWA Multichannel	
41 ± 3	VRANA	00	DPWA Multichannel	

$\Gamma(\Delta(1232)\pi, F\text{-wave})/\Gamma_{\text{total}}$	DOCUMENT ID	TECN	COMMENT	$\Gamma_5/\Gamma$
VALUE (%)				
45 ± 20	ANISOVICH	12A	DPWA Multichannel	

$(\Gamma_1\Gamma_6)^{1/2}/\Gamma_{\text{total}}$ in $N\pi \rightarrow \Delta(1920) \rightarrow N(1440)\pi$ , $P$ -wave	DOCUMENT ID	TECN	COMMENT	$(\Gamma_1\Gamma_6)^{1/2}/\Gamma$
VALUE (%)				
+0.06 ± 0.07	MANLEY	92	IPWA $\pi N \rightarrow \pi N$ & $N\pi\pi$	

$\Gamma(N(1440)\pi, P\text{-wave})/\Gamma_{\text{total}}$	DOCUMENT ID	TECN	COMMENT	$\Gamma_6/\Gamma$
VALUE (%)				
53 ± 8	VRANA	00	DPWA Multichannel	

$\Gamma(N(1535)\pi)/\Gamma_{\text{total}}$	DOCUMENT ID	TECN	COMMENT	$\Gamma_7/\Gamma$
VALUE (%)				
••• We do not use the following data for averages, fits, limits, etc. •••				
6 ± 4	HORN	08A	DPWA Multichannel	

$\Gamma(N a_0(980))/\Gamma_{\text{total}}$	DOCUMENT ID	TECN	COMMENT	$\Gamma_8/\Gamma$
VALUE (%)				
••• We do not use the following data for averages, fits, limits, etc. •••				
4 ± 2	HORN	08A	DPWA Multichannel	

$\Gamma(\Delta(1232)\eta)/\Gamma_{\text{total}}$	DOCUMENT ID	TECN	COMMENT	$\Gamma_9/\Gamma$
VALUE (%)				
<b>15 ± 8</b>	ANISOVICH	12A	DPWA Multichannel	
••• We do not use the following data for averages, fits, limits, etc. •••				
10 ± 5	HORN	08A	DPWA Multichannel	

 $\Delta(1920)$  PHOTON DECAY AMPLITUDES

Papers on  $\gamma N$  amplitudes predating 1981 may be found in our 2006 edition, Journal of Physics, G **33** 1 (2006).

 $\Delta(1920) \rightarrow N\gamma$ , helicity-1/2 amplitude  $A_{1/2}$ 

VALUE ( $\text{GeV}^{-1/2}$ )	DOCUMENT ID	TECN	COMMENT
0.130 + 0.030 – 0.060	ANISOVICH	12A	DPWA Multichannel
0.040 ± 0.014	AWAJI	81	DPWA $\gamma N \rightarrow \pi N$
••• We do not use the following data for averages, fits, limits, etc. •••			
0.022 ± 0.008	HORN	08A	DPWA Multichannel
–0.007	PENNER	02D	DPWA Multichannel

 $\Delta(1920) \rightarrow N\gamma$ , helicity-3/2 amplitude  $A_{3/2}$ 

VALUE ( $\text{GeV}^{-1/2}$ )	DOCUMENT ID	TECN	COMMENT
–0.115 + 0.025 – 0.050	ANISOVICH	12A	DPWA Multichannel
0.023 ± 0.017	AWAJI	81	DPWA $\gamma N \rightarrow \pi N$
••• We do not use the following data for averages, fits, limits, etc. •••			
0.042 ± 0.012	HORN	08A	DPWA Multichannel
–0.001	PENNER	02D	DPWA Multichannel

 $\Delta(1920)$  FOOTNOTES

- <sup>1</sup> CHEW 80 reports two  $P_{33}$  resonances in this mass region. Problems with this analysis are discussed in section 2.1.11 of HOEHLER 83.
- <sup>2</sup> See HOEHLER 93 for a detailed discussion of the evidence for and the pole parameters of  $N$  and  $\Delta$  resonances as determined from Argand diagrams of  $\pi N$  elastic partial-wave amplitudes and from plots of the speeds with which the amplitudes traverse the diagrams.

 $\Delta(1920)$  REFERENCES

For early references, see Physics Letters **111B** 1 (1982).

ANISOVICH 12A	EPJ A48 15	A.V. Anisovich et al.	(BONN, PNPI)
HORN 08A	EPJ A38 173	I. Horn et al.	(CB-ELSA Collab.)
Also	PRL 101 202002	I. Horn et al.	(CB-ELSA Collab.)
ARNDT 06	PR C74 045205	R.A. Arndt et al.	(GWU)
PDG 06	JPG 33 1	W.-M. Yao et al.	(PDG Collab.)
PENNER 02C	PR C66 055211	G. Penner, U. Mosel	(GIES)
PENNER 02D	PR C66 055212	G. Penner, U. Mosel	(GIES)
VRANA 00	PRPL 328 181	T.P. Vrana, S.A. Dytman, T.-S.H. Lee	(PITT+)
HOEHLER 93	$\pi N$ Newsletter 9 1	G. Hohlner	(KARL)
MANLEY 92	PR D45 4002	D.M. Manley, E.M. Saleski	(KENT) IJP
Also	PR D30 304	D.M. Manley et al.	(VPI)
ARNDT 91	PR D43 2131	R.A. Arndt et al.	(VPI, TELE) IJP
CANDLIN 84	NP B238 477	D.J. Candlin et al.	(EDIN, RAL, LOWC)
HOEHLER 83	Landolt-Boernstein 1/9B2	G. Hohlner	(KARL)
PDG 82	PL 111B 1	M. Roos et al.	(HELS, CIT, CERN)
AWAJI 81	Bonn Conf. 352	N. Awaji, R. Kajikawa	(NAGO)
Also	NP B197 365	K. Fujii et al.	(NAGO)
CHEW 80	Toronto Conf. 123	D.M. Chew	(LBL) IJP
CUTKOSKY 80	Toronto Conf. 19	R.E. Cutkosky et al.	(CMU, LBL) IJP
Also	PR D20 2839	R.E. Cutkosky et al.	(CMU, LBL) IJP
LIVANOS 80	Toronto Conf. 35	P. Livanos et al.	(SACL) IJP
HOEHLER 79	PDAT 12-1	G. Hohlner et al.	(KARL) IJP
Also	Toronto Conf. 3	R. Koch	(KARL) IJP

 $\Delta(1930)$  5/2<sup>-</sup>

$$I(J^P) = \frac{3}{2}(5/2^-) \text{ Status: } ***$$

Most of the results published before 1975 were last included in our 1982 edition, Physics Letters **111B** 1 (1982). Some further obsolete results published before 1984 were last included in our 2006 edition, Journal of Physics, G **33** 1 (2006).

 $\Delta(1930)$  BREIT-WIGNER MASS

VALUE (MeV)	DOCUMENT ID	TECN	COMMENT
<b>1900 to 2000 (<math>\approx</math> 1950) OUR ESTIMATE</b>			
2233 ± 53	ARNDT	06	DPWA $\pi N \rightarrow \pi N, \eta N$
1956 ± 22	MANLEY	92	IPWA $\pi N \rightarrow \pi N$ & $N\pi\pi$
1940 ± 30	CUTKOSKY	80	IPWA $\pi N \rightarrow \pi N$
1901 ± 15	HOEHLER	79	IPWA $\pi N \rightarrow \pi N$
••• We do not use the following data for averages, fits, limits, etc. •••			
2046 ± 45	ARNDT	04	DPWA $\pi N \rightarrow \pi N, \eta N$
1932 ± 100	VRANA	00	DPWA Multichannel
1955 ± 15	ARNDT	96	IPWA $\gamma N \rightarrow \pi N$
2056	ARNDT	95	DPWA $\pi N \rightarrow \pi N$
1963	LI	93	IPWA $\gamma N \rightarrow \pi N$
1910.0 <sup>+</sup> ± 15.0 – 17.2	CHEW	80	BPWA $\pi^+ p \rightarrow \pi^+ p$

 $\Delta(1930)$  BREIT-WIGNER WIDTH

VALUE (MeV)	DOCUMENT ID	TECN	COMMENT
<b>220 to 500 (<math>\approx</math> 360) OUR ESTIMATE</b>			
773 ± 187	ARNDT	06	DPWA $\pi N \rightarrow \pi N, \eta N$
530 ± 140	MANLEY	92	IPWA $\pi N \rightarrow \pi N$ & $N\pi\pi$
320 ± 60	CUTKOSKY	80	IPWA $\pi N \rightarrow \pi N$
195 ± 60	HOEHLER	79	IPWA $\pi N \rightarrow \pi N$

See key on page 457

# Baryon Particle Listings

## $\Delta(1930), \Delta(1940)$

••• We do not use the following data for averages, fits, limits, etc. •••

402 ± 198	ARNDT	04	DPWA	$\pi N \rightarrow \pi N, \eta N$
316 ± 237	VRANA	00	DPWA	Multichannel
350 ± 20	ARNDT	96	IPWA	$\gamma N \rightarrow \pi N$
590	ARNDT	95	DPWA	$\pi N \rightarrow N\pi$
260	LI	93	IPWA	$\gamma N \rightarrow \pi N$
74.8 <sup>+</sup> <sub>-</sub> 17.0 16.0	CHEW	80	BPWA	$\pi^+ p \rightarrow \pi^+ p$

### $\Delta(1930)$ POLE POSITION

#### REAL PART

VALUE (MeV)	DOCUMENT ID	TECN	COMMENT
<b>1840 to 1960 (≈ 1900) OUR ESTIMATE</b>			
2001	ARNDT	06	DPWA $\pi N \rightarrow \pi N, \eta N$
1850	<sup>1</sup> HOEHLER	93	SPED $\pi N \rightarrow \pi N$
1890 ± 50	CUTKOSKY	80	IPWA $\pi N \rightarrow \pi N$

••• We do not use the following data for averages, fits, limits, etc. •••

1966	ARNDT	04	DPWA $\pi N \rightarrow \pi N, \eta N$
1883	VRANA	00	DPWA Multichannel
1913	ARNDT	95	DPWA $\pi N \rightarrow N\pi$
2018	ARNDT	91	DPWA $\pi N \rightarrow \pi N$ Soln SM90

#### -2xIMAGINARY PART

VALUE (MeV)	DOCUMENT ID	TECN	COMMENT
<b>175 to 360 (≈ 270) OUR ESTIMATE</b>			
387	ARNDT	06	DPWA $\pi N \rightarrow \pi N, \eta N$
180	<sup>1</sup> HOEHLER	93	SPED $\pi N \rightarrow \pi N$
260 ± 60	CUTKOSKY	80	IPWA $\pi N \rightarrow \pi N$
••• We do not use the following data for averages, fits, limits, etc. •••			
364	ARNDT	04	DPWA $\pi N \rightarrow \pi N, \eta N$
250	VRANA	00	DPWA Multichannel
246	ARNDT	95	DPWA $\pi N \rightarrow N\pi$
398	ARNDT	91	DPWA $\pi N \rightarrow \pi N$ Soln SM90

### $\Delta(1930)$ ELASTIC POLE RESIDUE

#### MODULUS |r|

VALUE (MeV)	DOCUMENT ID	TECN	COMMENT
7	ARNDT	06	DPWA $\pi N \rightarrow \pi N, \eta N$
20	HOEHLER	93	SPED $\pi N \rightarrow \pi N$
18 ± 6	CUTKOSKY	80	IPWA $\pi N \rightarrow \pi N$
••• We do not use the following data for averages, fits, limits, etc. •••			
16	ARNDT	04	DPWA $\pi N \rightarrow \pi N, \eta N$
8	ARNDT	95	DPWA $\pi N \rightarrow N\pi$
15	ARNDT	91	DPWA $\pi N \rightarrow \pi N$ Soln SM90

#### PHASE $\theta$

VALUE (°)	DOCUMENT ID	TECN	COMMENT
-12	ARNDT	06	DPWA $\pi N \rightarrow \pi N, \eta N$
-20 ± 40	CUTKOSKY	80	IPWA $\pi N \rightarrow \pi N$
••• We do not use the following data for averages, fits, limits, etc. •••			
-21	ARNDT	04	DPWA $\pi N \rightarrow \pi N, \eta N$
-47	ARNDT	95	DPWA $\pi N \rightarrow N\pi$
-24	ARNDT	91	DPWA $\pi N \rightarrow \pi N$ Soln SM90

### $\Delta(1930)$ DECAY MODES

The following branching fractions are our estimates, not fits or averages.

Mode	Fraction ( $\Gamma_i/\Gamma$ )
$\Gamma_1$ $N\pi$	5-15 %
$\Gamma_2$ $\Sigma K$	
$\Gamma_3$ $N\pi\pi$	
$\Gamma_4$ $N\gamma$	0.0-0.02 %
$\Gamma_5$ $N\gamma$ , helicity=1/2	0.0-0.01 %
$\Gamma_6$ $N\gamma$ , helicity=3/2	0.0-0.01 %

### $\Delta(1930)$ BRANCHING RATIOS

$\Gamma(N\pi)/\Gamma_{total}$	DOCUMENT ID	TECN	COMMENT
<b>5 to 15 OUR ESTIMATE</b>			
8.1 ± 1.2	ARNDT	06	DPWA $\pi N \rightarrow \pi N, \eta N$
18 ± 2	MANLEY	92	IPWA $\pi N \rightarrow \pi N$ & $N\pi\pi$
14 ± 4	CUTKOSKY	80	IPWA $\pi N \rightarrow \pi N$
4 ± 3	HOEHLER	79	IPWA $\pi N \rightarrow \pi N$
••• We do not use the following data for averages, fits, limits, etc. •••			
4.0 ± 1.4	ARNDT	04	DPWA $\pi N \rightarrow \pi N, \eta N$
9 ± 8	VRANA	00	DPWA Multichannel
11	ARNDT	95	DPWA $\pi N \rightarrow N\pi$
11	CHEW	80	BPWA $\pi^+ p \rightarrow \pi^+ p$

$(\Gamma_i\Gamma_j)^{1/2}/\Gamma_{total}$ in $N\pi \rightarrow \Delta(1930) \rightarrow \Sigma K$	DOCUMENT ID	TECN	COMMENT
VALUE			
< 0.015	CANDLIN	84	DPWA $\pi^+ p \rightarrow \Sigma^+ K^+$

••• We do not use the following data for averages, fits, limits, etc. •••  
-0.031 LIVANOS 80 DPWA  $\pi p \rightarrow \Sigma K$

$(\Gamma_i\Gamma_j)^{1/2}/\Gamma_{total}$ in $N\pi \rightarrow \Delta(1930) \rightarrow N\pi\pi$	DOCUMENT ID	TECN	COMMENT
VALUE			
not seen	LONGACRE	75	IPWA $\pi N \rightarrow N\pi\pi$

### $\Delta(1930)$ PHOTON DECAY AMPLITUDES

Papers on  $\gamma N$  amplitudes predating 1981 may be found in our 2006 edition, Journal of Physics, G **33** 1 (2006).

#### $\Delta(1930) \rightarrow N\gamma$ , helicity-1/2 amplitude $A_{1/2}$

VALUE (GeV <sup>-1/2</sup> )	DOCUMENT ID	TECN	COMMENT
<b>-0.009 ± 0.028 OUR ESTIMATE</b>			
-0.007 ± 0.010	ARNDT	96	IPWA $\gamma N \rightarrow \pi N$
0.009 ± 0.009	AWAJI	81	DPWA $\gamma N \rightarrow \pi N$
••• We do not use the following data for averages, fits, limits, etc. •••			
-0.019 ± 0.001	LI	93	IPWA $\gamma N \rightarrow \pi N$

#### $\Delta(1930) \rightarrow N\gamma$ , helicity-3/2 amplitude $A_{3/2}$

VALUE (GeV <sup>-1/2</sup> )	DOCUMENT ID	TECN	COMMENT
<b>-0.018 ± 0.028 OUR ESTIMATE</b>			
0.005 ± 0.010	ARNDT	96	IPWA $\gamma N \rightarrow \pi N$
-0.025 ± 0.011	AWAJI	81	DPWA $\gamma N \rightarrow \pi N$
••• We do not use the following data for averages, fits, limits, etc. •••			
0.009 ± 0.001	LI	93	IPWA $\gamma N \rightarrow \pi N$

### $\Delta(1930)$ FOOTNOTES

<sup>1</sup> See HOEHLER 93 for a detailed discussion of the evidence for and the pole parameters of  $N$  and  $\Delta$  resonances as determined from Argand diagrams of  $\pi N$  elastic partial-wave amplitudes and from plots of the speeds with which the amplitudes traverse the diagrams.

### $\Delta(1930)$ REFERENCES

For early references, see Physics Letters **111B** 1 (1982).

ARNDT 06	PR C74 045205	R.A. Arndt et al.	(GWU)
PDG 06	JPG 33 1	W.-M. Yao et al.	(PDG Collab.)
ARNDT 04	PR C69 035213	R.A. Arndt et al.	(GWU, TRIU)
VRANA 00	PRPL 328 181	T.P. Vrana, S.A. Dytman, T.-S.H. Lee	(PITT+)
ARNDT 96	PR C53 430	R.A. Arndt, I.I. Strakovsky, R.L. Workman	(VPI)
ARNDT 95	PR C52 2120	R.A. Arndt et al.	(VPI, BRCC)
HOEHLER 93	$\pi N$ Newsletter 9 1	G. Hoehler	(KARL)
LI 93	PR C47 2759	Z.J. Li et al.	(VPI)
MANLEY 92	PR D45 4002	D.M. Manley, E.M. Saleski	(KENT) IUP
Also	PR D30 904	D.M. Manley et al.	(VPI)
ARNDT 91	PR D43 2131	R.A. Arndt et al.	(VPI, TELE) IUP
CANDLIN 84	NP B238 477	D.J. Candlin et al.	(EDIN, RAL, LOWC)
PDG 82	PL 111B 1	M. Roos et al.	(HELS, CIT, CERN)
AWAJI 81	Bonn Conf. 352	N. Awaji, R. Kajikawa	(NAGO)
Also	NP B197 365	K. Fujii et al.	(NAGO)
CHEW 80	Toronto Conf. 123	D.M. Chew	(LBL) IUP
CUTKOSKY 80	Toronto Conf. 19	R.E. Cutkosky et al.	(CMU, LBL) IUP
Also	PR D20 2839	R.E. Cutkosky et al.	(CMU, LBL) IUP
LIVANOS 80	Toronto Conf. 35	P. Livanos et al.	(SACL) IUP
HOEHLER 79	PDAT 12-1	G. Hoehler et al.	(KARL) IUP
Also	Toronto Conf. 3	R. Koch	(KARL) IUP
LONGACRE 75	PL 55B 415	R.S. Longacre et al.	(LBL, SLAC) IUP

### $\Delta(1940) 3/2^-$

$$I(J^P) = \frac{3}{2}(\frac{3}{2}^-) \text{ Status: } * *$$

OMITTED FROM SUMMARY TABLE

The latest GWU analysis (ARNDT 06) finds no evidence for this resonance.

### $\Delta(1940)$ BREIT-WIGNER MASS

VALUE (MeV)	DOCUMENT ID	TECN	COMMENT
<b>1940 to 2060 (≈ 2000) OUR ESTIMATE</b>			
1995 <sup>+</sup> <sub>-</sub> 105 60	ANISOVICH	12A	DPWA Multichannel
2057 ± 110	MANLEY	92	IPWA $\pi N \rightarrow \pi N$ & $N\pi\pi$
2058.1 ± 34.5	CHEW	80	BPWA $\pi^+ p \rightarrow \pi^+ p$
1940 ± 100	CUTKOSKY	80	IPWA $\pi N \rightarrow \pi N$
••• We do not use the following data for averages, fits, limits, etc. •••			
1990 ± 40	HORN	08A	DPWA Multichannel

### $\Delta(1940)$ BREIT-WIGNER WIDTH

VALUE (MeV)	DOCUMENT ID	TECN	COMMENT
450 ± 100	ANISOVICH	12A	DPWA Multichannel
460 ± 320	MANLEY	92	IPWA $\pi N \rightarrow \pi N$ & $N\pi\pi$
198.4 ± 45.5	CHEW	80	BPWA $\pi^+ p \rightarrow \pi^+ p$
200 ± 100	CUTKOSKY	80	IPWA $\pi N \rightarrow \pi N$
••• We do not use the following data for averages, fits, limits, etc. •••			
410 ± 70	HORN	08A	DPWA Multichannel

# Baryon Particle Listings

## $\Delta(1940), \Delta(1950)$

### $\Delta(1940)$ POLE POSITION

#### REAL PART

VALUE (MeV)	DOCUMENT ID	TECN	COMMENT
$1990^{+100}_{-50}$	ANISOVICH	12A	DPWA Multichannel
$1900 \pm 100$	CUTKOSKY	80	IPWA $\pi N \rightarrow \pi N$
1915 or 1926	<sup>1</sup> LONGACRE	78	IPWA $\pi N \rightarrow N\pi\pi$
••• We do not use the following data for averages, fits, limits, etc. •••			
$1985 \pm 30$	HORN	08A	DPWA Multichannel

#### -2xIMAGINARY PART

VALUE (MeV)	DOCUMENT ID	TECN	COMMENT
$450 \pm 90$	ANISOVICH	12A	DPWA Multichannel
$200 \pm 60$	CUTKOSKY	80	IPWA $\pi N \rightarrow \pi N$
190 or 186	<sup>1</sup> LONGACRE	78	IPWA $\pi N \rightarrow N\pi\pi$
••• We do not use the following data for averages, fits, limits, etc. •••			
$390 \pm 50$	HORN	08A	DPWA Multichannel

### $\Delta(1940)$ ELASTIC POLE RESIDUE

#### MODULUS |r|

VALUE (MeV)	DOCUMENT ID	TECN	COMMENT
$4 \pm 4$	ANISOVICH	12A	DPWA Multichannel
$8 \pm 3$	CUTKOSKY	80	IPWA $\pi N \rightarrow \pi N$

#### PHASE $\theta$

VALUE (°)	DOCUMENT ID	TECN	COMMENT
$135 \pm 45$	CUTKOSKY	80	IPWA $\pi N \rightarrow \pi N$

### $\Delta(1940)$ DECAY MODES

Mode	
$\Gamma_1$	$N\pi$
$\Gamma_2$	$\Sigma K$
$\Gamma_3$	$N\pi\pi$
$\Gamma_4$	$\Delta(1232)\pi, S\text{-wave}$
$\Gamma_5$	$\Delta(1232)\pi, D\text{-wave}$
$\Gamma_6$	$N\rho, S=3/2, S\text{-wave}$
$\Gamma_7$	$N(1535)\pi$
$\Gamma_8$	$N a_0(980)$
$\Gamma_9$	$\Delta(1232)\eta$
$\Gamma_{10}$	$N\gamma, \text{helicity}=1/2$
$\Gamma_{11}$	$N\gamma, \text{helicity}=3/2$

### $\Delta(1940)$ BRANCHING RATIOS

$\Gamma(N\pi)/\Gamma_{\text{total}}$	DOCUMENT ID	TECN	COMMENT	$\Gamma_1/\Gamma$
$18 \pm 12$	MANLEY	92	IPWA $\pi N \rightarrow \pi N \text{ \& } N\pi\pi$	
18	CHEW	80	BPWA $\pi^+ p \rightarrow \pi^+ p$	
$5 \pm 2$	CUTKOSKY	80	IPWA $\pi N \rightarrow \pi N$	
••• We do not use the following data for averages, fits, limits, etc. •••				
$9 \pm 4$	HORN	08A	DPWA Multichannel	

$(\Gamma_i \Gamma_j)^{1/2} / \Gamma_{\text{total}}$ in $N\pi \rightarrow \Delta(1940) \rightarrow \Sigma K$	DOCUMENT ID	TECN	COMMENT	$(\Gamma_1 \Gamma_2)^{1/2} / \Gamma$
$<0.015$	CANDLIN	84	DPWA $\pi^+ p \rightarrow \Sigma^+ K^+$	

$(\Gamma_i \Gamma_j)^{1/2} / \Gamma_{\text{total}}$ in $N\pi \rightarrow \Delta(1940) \rightarrow \Delta(1232)\pi, S\text{-wave}$	DOCUMENT ID	TECN	COMMENT	$(\Gamma_1 \Gamma_4)^{1/2} / \Gamma$
$+0.11 \pm 0.10$	MANLEY	92	IPWA $\pi N \rightarrow \pi N \text{ \& } N\pi\pi$	

$(\Gamma_i \Gamma_j)^{1/2} / \Gamma_{\text{total}}$ in $N\pi \rightarrow \Delta(1940) \rightarrow \Delta(1232)\pi, D\text{-wave}$	DOCUMENT ID	TECN	COMMENT	$(\Gamma_1 \Gamma_5)^{1/2} / \Gamma$
$+0.27 \pm 0.16$	MANLEY	92	IPWA $\pi N \rightarrow \pi N \text{ \& } N\pi\pi$	

$(\Gamma_i \Gamma_j)^{1/2} / \Gamma_{\text{total}}$ in $N\pi \rightarrow \Delta(1940) \rightarrow N\rho, S=3/2, S\text{-wave}$	DOCUMENT ID	TECN	COMMENT	$(\Gamma_1 \Gamma_6)^{1/2} / \Gamma$
$+0.25 \pm 0.10$	MANLEY	92	IPWA $\pi N \rightarrow \pi N \text{ \& } N\pi\pi$	

$\Gamma(N(1535)\pi)/\Gamma_{\text{total}}$	DOCUMENT ID	TECN	COMMENT	$\Gamma_7/\Gamma$
$2 \pm 1$	HORN	08A	DPWA Multichannel	
••• We do not use the following data for averages, fits, limits, etc. •••				

$\Gamma(N a_0(980))/\Gamma_{\text{total}}$	DOCUMENT ID	TECN	COMMENT	$\Gamma_8/\Gamma$
$2 \pm 1$	HORN	08A	DPWA Multichannel	
••• We do not use the following data for averages, fits, limits, etc. •••				

### $\Gamma(\Delta(1232)\eta)/\Gamma_{\text{total}}$

VALUE (%)	DOCUMENT ID	TECN	COMMENT	$\Gamma_9/\Gamma$
$4 \pm 2$	HORN	08A	DPWA Multichannel	
••• We do not use the following data for averages, fits, limits, etc. •••				

### $\Delta(1940)$ PHOTON DECAY AMPLITUDES

Papers on  $\gamma N$  amplitudes predating 1981 may be found in our 2006 edition, Journal of Physics, G **33** 1 (2006).

#### $\Delta(1940) \rightarrow N\gamma, \text{helicity-1/2 amplitude } A_{1/2}$

VALUE ( $\text{GeV}^{-1/2}$ )	DOCUMENT ID	TECN	COMMENT
$-0.036 \pm 0.058$	AWAJI	81	DPWA $\gamma N \rightarrow \pi N$
••• We do not use the following data for averages, fits, limits, etc. •••			
$0.160 \pm 0.040$	HORN	08A	DPWA Multichannel

#### $\Delta(1940) \rightarrow N\gamma, \text{helicity-3/2 amplitude } A_{3/2}$

VALUE ( $\text{GeV}^{-1/2}$ )	DOCUMENT ID	TECN	COMMENT
$-0.031 \pm 0.012$	AWAJI	81	DPWA $\gamma N \rightarrow \pi N$
••• We do not use the following data for averages, fits, limits, etc. •••			
$0.110 \pm 0.030$	HORN	08A	DPWA Multichannel

### $\Delta(1940)$ FOOTNOTES

<sup>1</sup> LONGACRE 78 values are from a search for poles in the unitarized T-matrix. The first (second) value uses, in addition to  $\pi N \rightarrow N\pi\pi$  data, elastic amplitudes from a Saclay (CERN) partial-wave analysis.

### $\Delta(1940)$ REFERENCES

ANISOVICH	12A	EPJ A48 15	A.V. Anisovich <i>et al.</i>	(BONN, PNPI)
HORN	08A	EPJ A38 173	I. Horn <i>et al.</i>	(CB-ELSA Collab.)
		Also PRL 101 202002	I. Horn <i>et al.</i>	(CB-ELSA Collab.)
ARNDT	06	PR C74 045205	R.A. Arndt <i>et al.</i>	(GWU)
PDG	06	JPG 33 1	W.-M. Yao <i>et al.</i>	(PDG Collab.)
MANLEY	92	PR D45 4002	D.M. Manley, E.M. Saleski	(KENT) IUP
		Also PR D30 904	D.M. Manley <i>et al.</i>	(VPI)
CANDLIN	84	NP B238 477	D.J. Candlin <i>et al.</i>	(EDIN, RAL, LOWC)
AWAJI	81	Bonn Conf. 352	N. Awaji, R. Kajikawa	(NAGO)
		Also NP B197 365	K. Fujii <i>et al.</i>	(NAGO)
CHEW	80	Toronto Conf. 123	D.M. Chew	(LBL) IUP
CUTKOSKY	80	Toronto Conf. 19	R.E. Cutkosky <i>et al.</i>	(CMU, LBL) IUP
		Also PR D20 2839	R.E. Cutkosky <i>et al.</i>	(CMU, LBL)
LONGACRE	78	PR D17 1795	R.S. Longacre <i>et al.</i>	(LBL, SLAC)

## $\Delta(1950) 7/2^+$

$$I(J^P) = \frac{3}{2}(\frac{7}{2}^+) \text{ Status: } ***$$

Most of the results published before 1975 were last included in our 1982 edition, Physics Letters **111B** 1 (1982). Some further obsolete results published before 1984 were last included in our 2006 edition, Journal of Physics, G **33** 1 (2006).

### $\Delta(1950)$ BREIT-WIGNER MASS

VALUE (MeV)	DOCUMENT ID	TECN	COMMENT
<b>1915 to 1950 (<math>\approx</math> 1930) OUR ESTIMATE</b>			
$1915 \pm 6$	ANISOVICH	12A	DPWA Multichannel
$1921.3 \pm 0.2$	ARNDT	06	DPWA $\pi N \rightarrow \pi N, \eta N$
$1945 \pm 2$	MANLEY	92	IPWA $\pi N \rightarrow \pi N \text{ \& } N\pi\pi$
$1950 \pm 15$	CUTKOSKY	80	IPWA $\pi N \rightarrow \pi N$
$1913 \pm 8$	HOEHLER	79	IPWA $\pi^+ p \rightarrow \pi^+ p$
••• We do not use the following data for averages, fits, limits, etc. •••			
$1928 \pm 8$	ANISOVICH	10	DPWA Multichannel
$1923.3 \pm 0.5$	ARNDT	04	DPWA $\pi N \rightarrow \pi N, \eta N$
$1936 \pm 5$	VRANA	00	DPWA Multichannel
$1947 \pm 9$	ARNDT	96	IPWA $\gamma N \rightarrow \pi N$
1921	ARNDT	95	DPWA $\pi N \rightarrow N\pi$
1940	LI	93	IPWA $\gamma N \rightarrow \pi N$
$1925 \pm 20$	CANDLIN	84	DPWA $\pi^+ p \rightarrow \Sigma^+ K^+$
$1855.0^{+11.0}_{-10.0}$	CHEW	80	BPWA $\pi^+ p \rightarrow \pi^+ p$
1925	<sup>1</sup> LONGACRE	75	IPWA $\pi N \rightarrow N\pi\pi$

### $\Delta(1950)$ BREIT-WIGNER WIDTH

VALUE (MeV)	DOCUMENT ID	TECN	COMMENT
<b>235 to 335 (<math>\approx</math> 285) OUR ESTIMATE</b>			
$246 \pm 10$	ANISOVICH	12A	DPWA Multichannel
$271.1 \pm 1.1$	ARNDT	06	DPWA $\pi N \rightarrow \pi N, \eta N$
$300 \pm 7$	MANLEY	92	IPWA $\pi N \rightarrow \pi N \text{ \& } N\pi\pi$
$340 \pm 50$	CUTKOSKY	80	IPWA $\pi N \rightarrow \pi N$
$224 \pm 10$	HOEHLER	79	IPWA $\pi N \rightarrow \pi N$

••• We do not use the following data for averages, fits, limits, etc. •••

290 ± 14	ANISOVICH	10	DPWA	Multichannel
278.2 ± 3.0	ARNDT	04	DPWA	$\pi N \rightarrow \pi N, \eta N$
245 ± 12	VRANA	00	DPWA	Multichannel
302 ± 9	ARNDT	96	IPWA	$\gamma N \rightarrow \pi N$
232	ARNDT	95	DPWA	$\pi N \rightarrow N\pi$
306	LI	93	IPWA	$\gamma N \rightarrow \pi N$
330 ± 4.0	CANDLIN	84	DPWA	$\pi^+ p \rightarrow \Sigma^+ K^+$
157.2 +22.0 -19.0	CHEW	80	BPWA	$\pi^+ p \rightarrow \pi^+ p$
240	<sup>1</sup> LONGACRE	75	IPWA	$\pi N \rightarrow N\pi\pi$

$\Delta(1950)$  POLE POSITION

REAL PART

VALUE (MeV)	DOCUMENT ID	TECN	COMMENT
<b>1870 to 1890 (≈ 1880) OUR ESTIMATE</b>			
1890 ± 4	ANISOVICH	12A	DPWA Multichannel
1876	ARNDT	06	DPWA $\pi N \rightarrow \pi N, \eta N$
1878	<sup>2</sup> HOEHLER	93	ARGD $\pi N \rightarrow \pi N$
1890 ± 15	CUTKOSKY	80	IPWA $\pi N \rightarrow \pi N$
••• We do not use the following data for averages, fits, limits, etc. •••			
1882 ± 8	ANISOVICH	10	DPWA Multichannel
1874	ARNDT	04	DPWA $\pi N \rightarrow \pi N, \eta N$
1910	VRANA	00	DPWA Multichannel
1880	ARNDT	95	DPWA $\pi N \rightarrow N\pi$
1884	ARNDT	91	DPWA $\pi N \rightarrow \pi N$ Soln SM90
1924 or 1924	<sup>3</sup> LONGACRE	78	IPWA $\pi N \rightarrow N\pi\pi$

-2×IMAGINARY PART

VALUE (MeV)	DOCUMENT ID	TECN	COMMENT
<b>220 to 260 (≈ 240) OUR ESTIMATE</b>			
243 ± 8	ANISOVICH	12A	DPWA Multichannel
227	ARNDT	06	DPWA $\pi N \rightarrow \pi N, \eta N$
230	<sup>2</sup> HOEHLER	93	ARGD $\pi N \rightarrow \pi N$
260 ± 4.0	CUTKOSKY	80	IPWA $\pi N \rightarrow \pi N$
••• We do not use the following data for averages, fits, limits, etc. •••			
262 ± 12	ANISOVICH	10	DPWA Multichannel
236	ARNDT	04	DPWA $\pi N \rightarrow \pi N, \eta N$
230	VRANA	00	DPWA Multichannel
236	ARNDT	95	DPWA $\pi N \rightarrow N\pi$
238	ARNDT	91	DPWA $\pi N \rightarrow \pi N$ Soln SM90
258 or 258	<sup>3</sup> LONGACRE	78	IPWA $\pi N \rightarrow N\pi\pi$

$\Delta(1950)$  ELASTIC POLE RESIDUE

MODULUS |r|

VALUE (MeV)	DOCUMENT ID	TECN	COMMENT
58 ± 2	ANISOVICH	12A	DPWA Multichannel
53	ARNDT	06	DPWA $\pi N \rightarrow \pi N, \eta N$
47	HOEHLER	93	ARGD $\pi N \rightarrow \pi N$
50 ± 7	CUTKOSKY	80	IPWA $\pi N \rightarrow \pi N$
••• We do not use the following data for averages, fits, limits, etc. •••			
57	ARNDT	04	DPWA $\pi N \rightarrow \pi N, \eta N$
54	ARNDT	95	DPWA $\pi N \rightarrow N\pi$
61	ARNDT	91	DPWA $\pi N \rightarrow \pi N$ Soln SM90

PHASE  $\theta$

VALUE (°)	DOCUMENT ID	TECN	COMMENT
-24 ± 3	ANISOVICH	12A	DPWA Multichannel
-31	ARNDT	06	DPWA $\pi N \rightarrow \pi N, \eta N$
-32	HOEHLER	93	ARGD $\pi N \rightarrow \pi N$
-33 ± 8	CUTKOSKY	80	IPWA $\pi N \rightarrow \pi N$
••• We do not use the following data for averages, fits, limits, etc. •••			
-34	ARNDT	04	DPWA $\pi N \rightarrow \pi N, \eta N$
-17	ARNDT	95	DPWA $\pi N \rightarrow N\pi$
-23	ARNDT	91	DPWA $\pi N \rightarrow \pi N$ Soln SM90

$\Delta(1950)$  INELASTIC POLE RESIDUE

The "normalized residue" is the residue divided by  $\Gamma_{pole}$ .

Normalized residue in  $N\pi \rightarrow \Delta(1950) \rightarrow \Sigma K$

MODULUS (%)	PHASE (°)	DOCUMENT ID	TECN	COMMENT
5 ± 1	-65 ± 25	ANISOVICH	12A	DPWA Multichannel

Normalized residue in  $N\pi \rightarrow \Delta(1950) \rightarrow \Delta\pi, F\text{-wave}$

MODULUS (%)	PHASE (°)	DOCUMENT ID	TECN	COMMENT
12 ± 4	12 ± 10	ANISOVICH	12A	DPWA Multichannel

$\Delta(1950)$  DECAY MODES

The following branching fractions are our estimates, not fits or averages.

Mode	Fraction ( $\Gamma_i/\Gamma$ )
$\Gamma_1$ $N\pi$	35-45 %
$\Gamma_2$ $\Sigma K$	
$\Gamma_3$ $N\pi\pi$	
$\Gamma_4$ $\Delta\pi$	20-30 %
$\Gamma_5$ $\Delta(1232)\pi, F\text{-wave}$	
$\Gamma_6$ $\Delta(1232)\pi, H\text{-wave}$	<10 %
$\Gamma_7$ $N\rho$	
$\Gamma_8$ $N\rho, S=1/2, F\text{-wave}$	
$\Gamma_9$ $N\rho, S=3/2, F\text{-wave}$	
$\Gamma_{10}$ $N\gamma$	
$\Gamma_{11}$ $N\gamma, \text{helicity}=1/2$	0.03-0.055 %
$\Gamma_{12}$ $N\gamma, \text{helicity}=3/2$	0.05-0.075 %

$\Delta(1950)$  BRANCHING RATIOS

$\Gamma(N\pi)/\Gamma_{total}$	VALUE (%)	DOCUMENT ID	TECN	COMMENT	$\Gamma_1/\Gamma$	
<b>35 to 45 OUR ESTIMATE</b>						
45 ± 2	ANISOVICH	12A	DPWA	Multichannel		
47.1 ± 0.1	ARNDT	06	DPWA	$\pi N \rightarrow \pi N, \eta N$		
38 ± 1	MANLEY	92	IPWA	$\pi N \rightarrow \pi N \& N\pi\pi$		
39 ± 4	CUTKOSKY	80	IPWA	$\pi N \rightarrow \pi N$		
38 ± 2	HOEHLER	79	IPWA	$\pi N \rightarrow \pi N$		
••• We do not use the following data for averages, fits, limits, etc. •••						
44 ± 8	ANISOVICH	10	DPWA	Multichannel		
48.0 ± 0.2	ARNDT	04	DPWA	$\pi N \rightarrow \pi N, \eta N$		
44 ± 1	VRANA	00	DPWA	Multichannel		
49	ARNDT	95	DPWA	$\pi N \rightarrow N\pi$		
44	CHEW	80	BPWA	$\pi^+ p \rightarrow \pi^+ p$		

$(\Gamma_i\Gamma_f)^{1/2}/\Gamma_{total}$ in $N\pi \rightarrow \Delta(1950) \rightarrow \Sigma K$	VALUE	DOCUMENT ID	TECN	COMMENT	$(\Gamma_1\Gamma_2)^{1/2}/\Gamma$
-0.053 ± 0.005	CANDLIN	84	DPWA	$\pi^+ p \rightarrow \Sigma^+ K^+$	

$\Gamma(\Sigma K)/\Gamma_{total}$	VALUE (%)	DOCUMENT ID	TECN	COMMENT	$\Gamma_2/\Gamma$
0.4 ± 0.1	ANISOVICH	12A	DPWA	Multichannel	

Note: Signs of couplings from  $\pi N \rightarrow N\pi\pi$  analyses were changed in the 1986 edition to agree with the baryon-first convention; the overall phase ambiguity is resolved by choosing a negative sign for the  $\Delta(1620) S_{31}$  coupling to  $\Delta(1232)\pi$ .

$(\Gamma_i\Gamma_f)^{1/2}/\Gamma_{total}$ in $N\pi \rightarrow \Delta(1950) \rightarrow \Delta(1232)\pi, F\text{-wave}$	VALUE	DOCUMENT ID	TECN	COMMENT	$(\Gamma_1\Gamma_5)^{1/2}/\Gamma$
<b>+0.28 to +0.32 OUR ESTIMATE</b>					
+0.27 ± 0.02	MANLEY	92	IPWA	$\pi N \rightarrow \pi N \& N\pi\pi$	
+0.32	<sup>1</sup> LONGACRE	75	IPWA	$\pi N \rightarrow N\pi\pi$	

$\Gamma(\Delta(1232)\pi, F\text{-wave})/\Gamma_{total}$	VALUE (%)	DOCUMENT ID	TECN	COMMENT	$\Gamma_5/\Gamma$
2.8 ± 1.4	ANISOVICH	12A	DPWA	Multichannel	
36 ± 1	VRANA	00	DPWA	Multichannel	

$(\Gamma_i\Gamma_f)^{1/2}/\Gamma_{total}$ in $N\pi \rightarrow \Delta(1950) \rightarrow N\rho, S=3/2, F\text{-wave}$	VALUE	DOCUMENT ID	TECN	COMMENT	$(\Gamma_1\Gamma_9)^{1/2}/\Gamma$
+0.24	<sup>1</sup> LONGACRE	75	IPWA	$\pi N \rightarrow N\pi\pi$	

$\Delta(1950)$  PHOTON DECAY AMPLITUDES

Papers on  $\gamma N$  amplitudes predating 1981 may be found in our 2006 edition, Journal of Physics, G **33** 1 (2006).

$\Delta(1950) \rightarrow N\gamma, \text{helicity}=1/2$  amplitude  $A_{1/2}$

VALUE ( $\text{GeV}^{-1/2}$ )	DOCUMENT ID	TECN	COMMENT
<b>-0.076 ± 0.012 OUR ESTIMATE</b>			
0.071 ± 0.004	ANISOVICH	12A	DPWA Multichannel
-0.079 ± 0.006	ARNDT	96	IPWA $\gamma N \rightarrow \pi N$
-0.068 ± 0.007	AWAJI	81	DPWA $\gamma N \rightarrow \pi N$
••• We do not use the following data for averages, fits, limits, etc. •••			
-0.083 ± 0.008	ANISOVICH	10	DPWA Multichannel
-0.094	DRECHSEL	07	DPWA $\gamma N \rightarrow \pi N$
-0.102 ± 0.003	LI	93	IPWA $\gamma N \rightarrow \pi N$

## Baryon Particle Listings

 $\Delta(1950)$ ,  $\Delta(2000)$ ,  $\Delta(2150)$  $\Delta(1950) \rightarrow N\gamma$ , helicity-3/2 amplitude  $A_{3/2}$ 

VALUE (GeV <sup>-1/2</sup> )	DOCUMENT ID	TECN	COMMENT
<b>-0.097 ± 0.010 OUR ESTIMATE</b>			
-0.094 ± 0.005	ANISOVICH	12A	DPWA Multichannel
-0.103 ± 0.006	ARNDT	96	IPWA $\gamma N \rightarrow \pi N$
-0.094 ± 0.016	AWAJI	81	DPWA $\gamma N \rightarrow \pi N$
••• We do not use the following data for averages, fits, limits, etc. •••			
-0.092 ± 0.008	ANISOVICH	10	DPWA Multichannel
-0.121	DRECHSEL	07	DPWA $\gamma N \rightarrow \pi N$
-0.115 ± 0.003	LI	93	IPWA $\gamma N \rightarrow \pi N$

 $\Delta(1950)$  FOOTNOTES

- From method II of LONGACRE 75: eyeball fits with Breit-Wigner circles to the T-matrix amplitudes.
- See HOEHLER 93 for a detailed discussion of the evidence for and the pole parameters of  $N$  and  $\Delta$  resonances as determined from Argand diagrams of  $\pi N$  elastic partial-wave amplitudes and from plots of the speeds with which the amplitudes traverse the diagrams.
- LONGACRE 78 values are from a search for poles in the unitarized T-matrix. The first (second) value uses, in addition to  $\pi N \rightarrow N\pi\pi$  data, elastic amplitudes from a Saclay (CERN) partial-wave analysis.

 $\Delta(1950)$  REFERENCES

ANISOVICH	12A	EPJ A48 15	A.V. Anisovich et al.	(BONN, PNPI)
ANISOVICH	10	EPJ A44 203	A.V. Anisovich et al.	(BONN, PNPI)
DRECHSEL	07	EPJ A34 49	D. Drechsel, S.S. Kamalov, L. Tiator	(MAINZ, JINR)
ARNDT	06	PR C74 045205	R.A. Arndt et al.	(GWU)
PDG	06	JPG 33 1	W.-M. Yao et al.	(PDG Collab.)
ARNDT	04	PR C69 035213	R.A. Arndt et al.	(GWU, TRIU)
VRANA	00	PRPL 328 181	T.P. Vrana, S.A. Dytman., T.-S.H. Lee	(PITT+)
ARNDT	96	PR C53 430	R.A. Arndt, I.I. Strakovsky, R.L. Workman	(VPI)
ARNDT	95	PR C52 2120	R.A. Arndt et al.	(VPI, BRCO)
HOEHLER	93	$\pi N$ Newsletter 9 1	G. Hoehler	(KARL)
LI	93	PR C47 2759	Z.J. Li et al.	(VPI)
MANLEY	92	PR D45 4002	D.M. Manley, E.M. Saleski	(KENT) IJP
Also		PR D30 904	D.M. Manley et al.	(VPI)
ARNDT	91	PR D43 2131	R.A. Arndt et al.	(VPI, TELE) IJP
CANDLIN	84	NP B238 477	D.J. Candlin et al.	(EDIN, RAL, LOWC)
PDG	82	PL 111B 1	M. Roos et al.	(HEL5, CIT, CERN)
AWAJI	81	Bonn Conf. 352	N. Awaji, R. Kajikawa	(NAGO)
Also		NP B197 365	K. Fujii et al.	(NAGO)
CHEW	80	Toronto Conf. 123	D.M. Chew	(LBL) IJP
CUTKOSKY	80	Toronto Conf. 19	R.E. Cutkosky et al.	(CMU, LBL) IJP
Also		PR D20 2839	R.E. Cutkosky et al.	(CMU, LBL) IJP
HOEHLER	79	PDAT 12-1	G. Hoehler et al.	(KARL) IJP
Also		Toronto Conf. 3	R. Koch	(KARL) IJP
LONGACRE	78	PR D17 1795	R.S. Longacre et al.	(LBL, SLAC)
LONGACRE	75	PL 95B 415	R.S. Longacre et al.	(LBL, SLAC) IJP

 $\Delta(2000) 5/2^+$ 

$$J(P) = \frac{3}{2}(\frac{5}{2}^+) \text{ Status: } **$$

OMITTED FROM SUMMARY TABLE

The latest GWU analysis (ARNDT 06) finds no evidence for this resonance.

 $\Delta(2000)$  BREIT-WIGNER MASS

VALUE (MeV)	DOCUMENT ID	TECN	COMMENT
<b>≈ 2000 OUR ESTIMATE</b>			
1724 ± 61	VRANA	00	DPWA Multichannel
1752 ± 32	MANLEY	92	IPWA $\pi N \rightarrow \pi N$ & $N\pi\pi$
2200 ± 125	CUTKOSKY	80	IPWA $\pi N \rightarrow \pi N$

 $\Delta(2000)$  BREIT-WIGNER WIDTH

VALUE (MeV)	DOCUMENT ID	TECN	COMMENT
138 ± 68	VRANA	00	DPWA Multichannel
251 ± 93	MANLEY	92	IPWA $\pi N \rightarrow \pi N$ & $N\pi\pi$
400 ± 125	CUTKOSKY	80	IPWA $\pi N \rightarrow \pi N$

 $\Delta(2000)$  POLE POSITION

REAL PART			
VALUE (MeV)	DOCUMENT ID	TECN	COMMENT
1697	VRANA	00	DPWA Multichannel
2150 ± 100	CUTKOSKY	80	IPWA $\pi N \rightarrow \pi N$
-2×IMAGINARY PART			
VALUE (MeV)	DOCUMENT ID	TECN	COMMENT
112	VRANA	00	DPWA Multichannel
350 ± 100	CUTKOSKY	80	IPWA $\pi N \rightarrow \pi N$

 $\Delta(2000)$  ELASTIC POLE RESIDUE

MODULUS  r			
VALUE (MeV)	DOCUMENT ID	TECN	COMMENT
16 ± 5	CUTKOSKY	80	IPWA $\pi N \rightarrow \pi N$

PHASE  $\theta$ 

VALUE (°)	DOCUMENT ID	TECN	COMMENT
150 ± 90	CUTKOSKY	80	IPWA $\pi N \rightarrow \pi N$

 $\Delta(2000)$  DECAY MODES

Mode
$\Gamma_1$ $N\pi$
$\Gamma_2$ $N\pi\pi$
$\Gamma_3$ $\Delta(1232)\pi$ , P-wave
$\Gamma_4$ $\Delta(1232)\pi$ , F-wave
$\Gamma_5$ $N\rho$ , S=3/2, P-wave

 $\Delta(2000)$  BRANCHING RATIOS

$\Gamma(N\pi)/\Gamma_{\text{total}}$	DOCUMENT ID	TECN	COMMENT	$\Gamma_1/\Gamma$
0 ± 1	VRANA	00	DPWA Multichannel	
2 ± 1	MANLEY	92	IPWA $\pi N \rightarrow \pi N$ & $N\pi\pi$	
7 ± 4	CUTKOSKY	80	IPWA $\pi N \rightarrow \pi N$	

$(\Gamma_1\Gamma_2)^{1/2}/\Gamma_{\text{total}}$ in $N\pi \rightarrow \Delta(2000) \rightarrow \Delta(1232)\pi$ , P-wave	DOCUMENT ID	TECN	COMMENT	$(\Gamma_1\Gamma_3)^{1/2}/\Gamma$
VALUE				
+0.07 ± 0.03	MANLEY	92	IPWA $\pi N \rightarrow \pi N$ & $N\pi\pi$	

$\Gamma(\Delta(1232)\pi, P\text{-wave})/\Gamma_{\text{total}}$	DOCUMENT ID	TECN	COMMENT	$\Gamma_3/\Gamma$
VALUE				
0 ± 1	VRANA	00	DPWA Multichannel	

$(\Gamma_1\Gamma_4)^{1/2}/\Gamma_{\text{total}}$ in $N\pi \rightarrow \Delta(2000) \rightarrow \Delta(1232)\pi$ , F-wave	DOCUMENT ID	TECN	COMMENT	$(\Gamma_1\Gamma_4)^{1/2}/\Gamma$
VALUE				
+0.09 ± 0.04	MANLEY	92	IPWA $\pi N \rightarrow \pi N$ & $N\pi\pi$	

$\Gamma(\Delta(1232)\pi, F\text{-wave})/\Gamma_{\text{total}}$	DOCUMENT ID	TECN	COMMENT	$\Gamma_4/\Gamma$
VALUE				
40 ± 1	VRANA	00	DPWA Multichannel	

$(\Gamma_1\Gamma_5)^{1/2}/\Gamma_{\text{total}}$ in $N\pi \rightarrow \Delta(2000) \rightarrow N\rho$ , S=3/2, P-wave	DOCUMENT ID	TECN	COMMENT	$(\Gamma_1\Gamma_5)^{1/2}/\Gamma$
VALUE				
-0.06 ± 0.01	MANLEY	92	IPWA $\pi N \rightarrow \pi N$ & $N\pi\pi$	

$\Gamma(N\rho, S=3/2, P\text{-wave})/\Gamma_{\text{total}}$	DOCUMENT ID	TECN	COMMENT	$\Gamma_5/\Gamma$
VALUE				
60 ± 60	VRANA	00	DPWA Multichannel	

 $\Delta(2000)$  REFERENCES

ARNDT	06	PR C74 045205	R.A. Arndt et al.	(GWU)
VRANA	00	PRPL 328 181	T.P. Vrana, S.A. Dytman., T.-S.H. Lee	(PITT+)
MANLEY	92	PR D45 4002	D.M. Manley, E.M. Saleski	(KENT) IJP
Also		PR D30 904	D.M. Manley et al.	(VPI)
CUTKOSKY	80	Toronto Conf. 19	R.E. Cutkosky et al.	(CMU, LBL)
Also		PR D20 2839	R.E. Cutkosky et al.	(CMU, LBL)

 $\Delta(2150) 1/2^-$ 

$$J(P) = \frac{3}{2}(\frac{1}{2}^-) \text{ Status: } *$$

OMITTED FROM SUMMARY TABLE

The latest GWU analysis (ARNDT 06) finds no evidence for this resonance.

 $\Delta(2150)$  BREIT-WIGNER MASS

VALUE (MeV)	DOCUMENT ID	TECN	COMMENT
<b>≈ 2150 OUR ESTIMATE</b>			
2047.4 ± 27.0	<sup>1</sup> CHEW	80	BPWA $\pi^+ p \rightarrow \pi^+ p$
2203.2 ± 8.4	<sup>1</sup> CHEW	80	BPWA $\pi^+ p \rightarrow \pi^+ p$
2150 ± 100	CUTKOSKY	80	IPWA $\pi N \rightarrow \pi N$

 $\Delta(2150)$  BREIT-WIGNER WIDTH

VALUE (MeV)	DOCUMENT ID	TECN	COMMENT
121.6 ± 62.0	<sup>1</sup> CHEW	80	BPWA $\pi^+ p \rightarrow \pi^+ p$
120.5 ± 45.0	<sup>1</sup> CHEW	80	BPWA $\pi^+ p \rightarrow \pi^+ p$
200 ± 100	CUTKOSKY	80	IPWA $\pi N \rightarrow \pi N$

 $\Delta(2150)$  POLE POSITION

REAL PART			
VALUE (MeV)	DOCUMENT ID	TECN	COMMENT
2140 ± 80	CUTKOSKY	80	IPWA $\pi N \rightarrow \pi N$



See key on page 457

# Baryon Particle Listings

## $\Delta(2150)$ , $\Delta(2200)$ , $\Delta(2300)$

**-2xIMAGINARY PART**

VALUE (MeV)	DOCUMENT ID	TECN	COMMENT
200±80	CUTKOSKY 80	IPWA	$\pi N \rightarrow \pi N$

**$\Delta(2150)$  ELASTIC POLE RESIDUE**

**MODULUS  $|r|$**

VALUE (MeV)	DOCUMENT ID	TECN	COMMENT
7±2	CUTKOSKY 80	IPWA	$\pi N \rightarrow \pi N$

**PHASE  $\theta$**

VALUE (°)	DOCUMENT ID	TECN	COMMENT
-60±90	CUTKOSKY 80	IPWA	$\pi N \rightarrow \pi N$

**$\Delta(2150)$  DECAY MODES**

Mode	$\Gamma_1$	$\Gamma_2$
$N\pi$		
$\Sigma K$		

**$\Delta(2150)$  BRANCHING RATIOS**

$\Gamma(N\pi)/\Gamma_{total}$	DOCUMENT ID	TECN	COMMENT	$\Gamma_1/\Gamma$
41	1 CHEW 80	BPWA	$\pi^+ p \rightarrow \pi^+ p$	
37	1 CHEW 80	BPWA	$\pi^+ p \rightarrow \pi^+ p$	
8±2	CUTKOSKY 80	IPWA	$\pi N \rightarrow \pi N$	

$(\Gamma_1\Gamma_2)^{1/2}/\Gamma_{total}$ in $N\pi \rightarrow \Delta(2150) \rightarrow \Sigma K$	DOCUMENT ID	TECN	COMMENT	$(\Gamma_1\Gamma_2)^{1/2}/\Gamma$
<0.03	CANDLIN 84	DPWA	$\pi^+ p \rightarrow \Sigma^+ K^+$	

**$\Delta(2150)$  FOOTNOTES**

<sup>1</sup> CHEW 80 reports two  $S_{31}$  resonances in this mass region. Problems with this analysis are discussed in section 2.1.11 of HOEHLER 83.

**$\Delta(2150)$  REFERENCES**

ARNDT 06	PR C74 045205	R.A. Arndt et al.	(GWU)
CANDLIN 84	NP B238 477	D.J. Candlin et al.	(EDIN, RAL, LOWC)
HOEHLER 83	Landolt-Boernstein 1/9B2 6	G. Hahler	(KARLT)
CHEW 80	Toronto Conf. 123	D.M. Chew	(LBL) IJP
CUTKOSKY 80	Toronto Conf. 19	R.E. Cutkosky et al.	(CMU, LBL) IJP
Also	PR D20 2839	R.E. Cutkosky et al.	(CMU, LBL)

$\Delta(2200)$ $7/2^-$	$I(J^P) = \frac{3}{2}(\frac{7}{2}^-)$ Status: *
------------------------	---

OMITTED FROM SUMMARY TABLE

The various analyses are not in good agreement.

The latest GWU analysis (ARNDT 06) finds no evidence for this resonance.

**$\Delta(2200)$  BREIT-WIGNER MASS**

VALUE (MeV)	DOCUMENT ID	TECN	COMMENT
<b><math>\approx 2200</math> OUR ESTIMATE</b>			
2200±80	CUTKOSKY 80	IPWA	$\pi N \rightarrow \pi N$
2215±60	HOEHLER 79	IPWA	$\pi N \rightarrow \pi N$
2280±80	HENDRY 78	MPWA	$\pi N \rightarrow \pi N$
••• We do not use the following data for averages, fits, limits, etc. •••			
2280±40	CANDLIN 84	DPWA	$\pi^+ p \rightarrow \Sigma^+ K^+$

**$\Delta(2200)$  BREIT-WIGNER WIDTH**

VALUE (MeV)	DOCUMENT ID	TECN	COMMENT
450±100	CUTKOSKY 80	IPWA	$\pi N \rightarrow \pi N$
400±100	HOEHLER 79	IPWA	$\pi N \rightarrow \pi N$
400±150	HENDRY 78	MPWA	$\pi N \rightarrow \pi N$
••• We do not use the following data for averages, fits, limits, etc. •••			
400± 50	CANDLIN 84	DPWA	$\pi^+ p \rightarrow \Sigma^+ K^+$

**$\Delta(2200)$  POLE POSITION**

REAL PART	DOCUMENT ID	TECN	COMMENT
2100±50	CUTKOSKY 80	IPWA	$\pi N \rightarrow \pi N$

**-2xIMAGINARY PART**

VALUE (MeV)	DOCUMENT ID	TECN	COMMENT
340±80	CUTKOSKY 80	IPWA	$\pi N \rightarrow \pi N$

**$\Delta(2200)$  ELASTIC POLE RESIDUE**

**MODULUS  $|r|$**

VALUE (MeV)	DOCUMENT ID	TECN	COMMENT
8±3	CUTKOSKY 80	IPWA	$\pi N \rightarrow \pi N$

**PHASE  $\theta$**

VALUE (°)	DOCUMENT ID	TECN	COMMENT
-70±40	CUTKOSKY 80	IPWA	$\pi N \rightarrow \pi N$

**$\Delta(2200)$  DECAY MODES**

Mode	$\Gamma_1$	$\Gamma_2$
$N\pi$		
$\Sigma K$		

**$\Delta(2200)$  BRANCHING RATIOS**

$\Gamma(N\pi)/\Gamma_{total}$	DOCUMENT ID	TECN	COMMENT	$\Gamma_1/\Gamma$
6±2	CUTKOSKY 80	IPWA	$\pi N \rightarrow \pi N$	
5±2	HOEHLER 79	IPWA	$\pi N \rightarrow \pi N$	
9±2	HENDRY 78	MPWA	$\pi N \rightarrow \pi N$	

$(\Gamma_1\Gamma_2)^{1/2}/\Gamma_{total}$ in $N\pi \rightarrow \Delta(2200) \rightarrow \Sigma K$	DOCUMENT ID	TECN	COMMENT	$(\Gamma_1\Gamma_2)^{1/2}/\Gamma$
-0.014±0.005	CANDLIN 84	DPWA	$\pi^+ p \rightarrow \Sigma^+ K^+$	

**$\Delta(2200)$  REFERENCES**

ARNDT 06	PR C74 045205	R.A. Arndt et al.	(GWU)
CANDLIN 84	NP B238 477	D.J. Candlin et al.	(EDIN, RAL, LOWC)
CUTKOSKY 80	Toronto Conf. 19	R.E. Cutkosky et al.	(CMU, LBL) IJP
Also	PR D20 2839	R.E. Cutkosky et al.	(CMU, LBL) IJP
HOEHLER 79	PDAT 12-1	G. Hahler et al.	(KARLT) IJP
Also	Toronto Conf. 3	R. Koch	(KARLT) IJP
HENDRY 78	PRL 41 222	A.W. Hendry	(IND, LBL) IJP
Also	ANP 136 1	A.W. Hendry	(IND)

$\Delta(2300)$ $9/2^+$	$I(J^P) = \frac{3}{2}(\frac{9}{2}^+)$ Status: **
------------------------	--

OMITTED FROM SUMMARY TABLE

The latest GWU analysis (ARNDT 06) finds no evidence for this resonance.

**$\Delta(2300)$  BREIT-WIGNER MASS**

VALUE (MeV)	DOCUMENT ID	TECN	COMMENT
<b><math>\approx 2300</math> OUR ESTIMATE</b>			
2204.5± 3.4	CHEW 80	BPWA	$\pi^+ p \rightarrow \pi^+ p$
2400 ±125	CUTKOSKY 80	IPWA	$\pi N \rightarrow \pi N$
2217 ± 80	HOEHLER 79	IPWA	$\pi N \rightarrow \pi N$
2450 ±100	HENDRY 78	MPWA	$\pi N \rightarrow \pi N$
••• We do not use the following data for averages, fits, limits, etc. •••			
2400	CANDLIN 84	DPWA	$\pi^+ p \rightarrow \Sigma^+ K^+$

**$\Delta(2300)$  BREIT-WIGNER WIDTH**

VALUE (MeV)	DOCUMENT ID	TECN	COMMENT
32.3± 1.0	CHEW 80	BPWA	$\pi^+ p \rightarrow \pi^+ p$
425 ±150	CUTKOSKY 80	IPWA	$\pi N \rightarrow \pi N$
300 ±100	HOEHLER 79	IPWA	$\pi N \rightarrow \pi N$
500 ±200	HENDRY 78	MPWA	$\pi N \rightarrow \pi N$
••• We do not use the following data for averages, fits, limits, etc. •••			
200	CANDLIN 84	DPWA	$\pi^+ p \rightarrow \Sigma^+ K^+$

**$\Delta(2300)$  POLE POSITION**

REAL PART	DOCUMENT ID	TECN	COMMENT
2370±80	CUTKOSKY 80	IPWA	$\pi N \rightarrow \pi N$

**-2xIMAGINARY PART**

VALUE (MeV)	DOCUMENT ID	TECN	COMMENT
420±160	CUTKOSKY 80	IPWA	$\pi N \rightarrow \pi N$

**$\Delta(2300)$  ELASTIC POLE RESIDUE**

**MODULUS  $|r|$**

VALUE (MeV)	DOCUMENT ID	TECN	COMMENT
10±4	CUTKOSKY 80	IPWA	$\pi N \rightarrow \pi N$

## Baryon Particle Listings

 $\Delta(2300)$ ,  $\Delta(2350)$ ,  $\Delta(2390)$ PHASE  $\theta$ 

VALUE ( $^\circ$ )	DOCUMENT ID	TECN	COMMENT
$-20 \pm 30$	CUTKOSKY 80	IPWA	$\pi N \rightarrow \pi N$

 $\Delta(2300)$  DECAY MODES

Mode
$\Gamma_1$ $N\pi$
$\Gamma_2$ $\Sigma K$

 $\Delta(2300)$  BRANCHING RATIOS

$\Gamma(N\pi)/\Gamma_{\text{total}}$	DOCUMENT ID	TECN	COMMENT	$\Gamma_1/\Gamma$
5	CHEW 80	BPWA	$\pi^+ p \rightarrow \pi^+ p$	
$6 \pm 2$	CUTKOSKY 80	IPWA	$\pi N \rightarrow \pi N$	
$3 \pm 2$	HOEHLER 79	IPWA	$\pi N \rightarrow \pi N$	
$8 \pm 2$	HENDRY 78	MPWA	$\pi N \rightarrow \pi N$	

$(\Gamma_1\Gamma_2)^{1/2}/\Gamma_{\text{total}}$ in $N\pi \rightarrow \Delta(2300) \rightarrow \Sigma K$	DOCUMENT ID	TECN	COMMENT	$(\Gamma_1\Gamma_2)^{1/2}/\Gamma$
$-0.017$	CANDLIN 84	DPWA	$\pi^+ p \rightarrow \Sigma^+ K^+$	

 $\Delta(2300)$  REFERENCES

ARNDT 06	PR C74 045205	R.A. Arndt <i>et al.</i>	(GWU)
CANDLIN 84	NP B238 477	D.J. Candlin <i>et al.</i>	(EDIN, RAL, LOWC)
CHEW 80	Toronto Conf. 123	D.M. Chew	(LBL) IJP
CUTKOSKY 80	Toronto Conf. 19	R.E. Cutkosky <i>et al.</i>	(CMU, LBL) IJP
Also	PR D20 2839	R.E. Cutkosky <i>et al.</i>	(CMU, LBL)
HOEHLER 79	PDAT 12-1	G. Hoehler <i>et al.</i>	(KARLT) IJP
Also	Toronto Conf. 3	R. Koch	(KARLT) IJP
HENDRY 78	PRL 41 222	A.W. Hendry	(IND, LBL) IJP
Also	ANP 136 1	A.W. Hendry	(IND)

 $\Delta(2350)$   $5/2^-$ 

$$I(J^P) = \frac{3}{2}(\frac{5}{2}^-) \text{ Status: } *$$

OMITTED FROM SUMMARY TABLE

The latest GWU analysis (ARNDT 06) finds no evidence for this resonance.

 $\Delta(2350)$  BREIT-WIGNER MASS

VALUE (MeV)	DOCUMENT ID	TECN	COMMENT
$\approx 2350$ OUR ESTIMATE			
$2171 \pm 18$	MANLEY 92	IPWA	$\pi N \rightarrow \pi N$ & $N\pi\pi$
$2400 \pm 125$	CUTKOSKY 80	IPWA	$\pi N \rightarrow \pi N$
$2305 \pm 26$	HOEHLER 79	IPWA	$\pi N \rightarrow \pi N$
••• We do not use the following data for averages, fits, limits, etc. •••			
$2459 \pm 100$	VRANA 00	DPWA	Multichannel

 $\Delta(2350)$  BREIT-WIGNER WIDTH

VALUE (MeV)	DOCUMENT ID	TECN	COMMENT
$264 \pm 51$	MANLEY 92	IPWA	$\pi N \rightarrow \pi N$ & $N\pi\pi$
$400 \pm 150$	CUTKOSKY 80	IPWA	$\pi N \rightarrow \pi N$
$300 \pm 70$	HOEHLER 79	IPWA	$\pi N \rightarrow \pi N$
••• We do not use the following data for averages, fits, limits, etc. •••			
$480 \pm 360$	VRANA 00	DPWA	Multichannel

 $\Delta(2350)$  POLE POSITION

REAL PART	DOCUMENT ID	TECN	COMMENT
$2400 \pm 125$	CUTKOSKY 80	IPWA	$\pi N \rightarrow \pi N$
••• We do not use the following data for averages, fits, limits, etc. •••			
2427	VRANA 00	DPWA	Multichannel

 $-2 \times$ IMAGINARY PART

VALUE (MeV)	DOCUMENT ID	TECN	COMMENT
$400 \pm 150$	CUTKOSKY 80	IPWA	$\pi N \rightarrow \pi N$
••• We do not use the following data for averages, fits, limits, etc. •••			
458	VRANA 00	DPWA	Multichannel

 $\Delta(2350)$  ELASTIC POLE RESIDUE

MODULUS $ r $	DOCUMENT ID	TECN	COMMENT
$15 \pm 8$	CUTKOSKY 80	IPWA	$\pi N \rightarrow \pi N$

PHASE  $\theta$ 

VALUE ( $^\circ$ )	DOCUMENT ID	TECN	COMMENT
$-70 \pm 70$	CUTKOSKY 80	IPWA	$\pi N \rightarrow \pi N$

 $\Delta(2350)$  DECAY MODES

Mode
$\Gamma_1$ $N\pi$
$\Gamma_2$ $\Sigma K$

 $\Delta(2350)$  BRANCHING RATIOS

$\Gamma(N\pi)/\Gamma_{\text{total}}$	DOCUMENT ID	TECN	COMMENT	$\Gamma_1/\Gamma$
$2.0 \pm 0.3$	MANLEY 92	IPWA	$\pi N \rightarrow \pi N$ & $N\pi\pi$	
$20 \pm 10$	CUTKOSKY 80	IPWA	$\pi N \rightarrow \pi N$	
$4 \pm 2$	HOEHLER 79	IPWA	$\pi N \rightarrow \pi N$	
••• We do not use the following data for averages, fits, limits, etc. •••				
$7 \pm 14$	VRANA 00	DPWA	Multichannel	

$(\Gamma_1\Gamma_2)^{1/2}/\Gamma_{\text{total}}$ in $N\pi \rightarrow \Delta(2350) \rightarrow \Sigma K$	DOCUMENT ID	TECN	COMMENT	$(\Gamma_1\Gamma_2)^{1/2}/\Gamma$
$< 0.015$	CANDLIN 84	DPWA	$\pi^+ p \rightarrow \Sigma^+ K^+$	

 $\Delta(2350)$  REFERENCES

ARNDT 06	PR C74 045205	R.A. Arndt <i>et al.</i>	(GWU)
VRANA 00	PRPL 328 181	T.P. Vrana, S.A. Dytman., T.-S.H. Lee	(PITT+)
MANLEY 92	PR D45 4002	D.M. Manley, E.M. Salewski	(KENT) IJP
Also	PR D30 904	D.M. Manley <i>et al.</i>	(VPI)
CANDLIN 84	NP B238 477	D.J. Candlin <i>et al.</i>	(EDIN, RAL, LOWC)
CUTKOSKY 80	Toronto Conf. 19	R.E. Cutkosky <i>et al.</i>	(CMU, LBL) IJP
Also	PR D20 2839	R.E. Cutkosky <i>et al.</i>	(CMU, LBL)
HOEHLER 79	PDAT 12-1	G. Hoehler <i>et al.</i>	(KARLT) IJP
Also	Toronto Conf. 3	R. Koch	(KARLT) IJP

 $\Delta(2390)$   $7/2^+$ 

$$I(J^P) = \frac{3}{2}(\frac{7}{2}^+) \text{ Status: } *$$

OMITTED FROM SUMMARY TABLE

The latest GWU analysis (ARNDT 06) finds no evidence for this resonance.

 $\Delta(2390)$  BREIT-WIGNER MASS

VALUE (MeV)	DOCUMENT ID	TECN	COMMENT
$\approx 2390$ OUR ESTIMATE			
$2350 \pm 100$	CUTKOSKY 80	IPWA	$\pi N \rightarrow \pi N$
$2425 \pm 60$	HOEHLER 79	IPWA	$\pi N \rightarrow \pi N$

 $\Delta(2390)$  BREIT-WIGNER WIDTH

VALUE (MeV)	DOCUMENT ID	TECN	COMMENT
$300 \pm 100$	CUTKOSKY 80	IPWA	$\pi N \rightarrow \pi N$
$300 \pm 80$	HOEHLER 79	IPWA	$\pi N \rightarrow \pi N$

 $\Delta(2390)$  POLE POSITION

REAL PART	DOCUMENT ID	TECN	COMMENT
$2350 \pm 100$	CUTKOSKY 80	IPWA	$\pi N \rightarrow \pi N$

 $-2 \times$ IMAGINARY PART

VALUE (MeV)	DOCUMENT ID	TECN	COMMENT
$260 \pm 100$	CUTKOSKY 80	IPWA	$\pi N \rightarrow \pi N$

 $\Delta(2390)$  ELASTIC POLE RESIDUE

MODULUS $ r $	DOCUMENT ID	TECN	COMMENT
$12 \pm 6$	CUTKOSKY 80	IPWA	$\pi N \rightarrow \pi N$

PHASE  $\theta$ 

VALUE ( $^\circ$ )	DOCUMENT ID	TECN	COMMENT
$-90 \pm 60$	CUTKOSKY 80	IPWA	$\pi N \rightarrow \pi N$

 $\Delta(2390)$  DECAY MODES

Mode
$\Gamma_1$ $N\pi$
$\Gamma_2$ $\Sigma K$

 $\Delta(2390)$  BRANCHING RATIOS

$\Gamma(N\pi)/\Gamma_{\text{total}}$	DOCUMENT ID	TECN	COMMENT	$\Gamma_1/\Gamma$
$8 \pm 4$	CUTKOSKY 80	IPWA	$\pi N \rightarrow \pi N$	
$7 \pm 4$	HOEHLER 79	IPWA	$\pi N \rightarrow \pi N$	

See key on page 457

# Baryon Particle Listings

## $\Delta(2390)$ , $\Delta(2400)$ , $\Delta(2420)$

$(\Gamma_1\Gamma_2)^{1/2}/\Gamma_{\text{total}}$ in $N\pi \rightarrow \Delta(2390) \rightarrow \Sigma K$	DOCUMENT ID	TECN	COMMENT	$(\Gamma_1\Gamma_2)^{1/2}/\Gamma$
<0.015	CANDLIN	84	DPWA $\pi^+ p \rightarrow \Sigma^+ K^+$	

### $\Delta(2390)$ REFERENCES

ARNDT 06	PR C74 045205	R.A. Arndt et al.	(GWU)
CANDLIN 84	NP B238 477	D.J. Candlin et al.	(EDIN, RAL, LOWC)
CUTKOSKY 80	Toronto Conf. 19	R.E. Cutkosky et al.	(CMU, LBL) IJP
Also	PR D20 2839	R.E. Cutkosky et al.	(CMU, LBL)
HOEHLER 79	PDAT 12-1	G. Hoehler et al.	(KARLT) IJP
Also	Toronto Conf. 3	R. Koch	(KARLT) IJP

$\Delta(2400) 9/2^-$	$I(J^P) = \frac{3}{2}(\frac{9}{2}^-)$ Status: **
----------------------	--

OMITTED FROM SUMMARY TABLE

### $\Delta(2400)$ BREIT-WIGNER MASS

VALUE (MeV)	DOCUMENT ID	TECN	COMMENT
$\approx 2400$ OUR ESTIMATE			
2643 $\pm$ 141	ARNDT 06	DPWA	$\pi N \rightarrow \pi N, \eta N$
2300 $\pm$ 100	CUTKOSKY 80	IPWA	$\pi N \rightarrow \pi N$
2468 $\pm$ 50	HOEHLER 79	IPWA	$\pi N \rightarrow \pi N$
2200 $\pm$ 100	HENDRY 78	MPWA	$\pi N \rightarrow \pi N$

### $\Delta(2400)$ BREIT-WIGNER WIDTH

VALUE (MeV)	DOCUMENT ID	TECN	COMMENT
895 $\pm$ 432	ARNDT 06	DPWA	$\pi N \rightarrow \pi N, \eta N$
330 $\pm$ 100	CUTKOSKY 80	IPWA	$\pi N \rightarrow \pi N$
480 $\pm$ 100	HOEHLER 79	IPWA	$\pi N \rightarrow \pi N$
450 $\pm$ 200	HENDRY 78	MPWA	$\pi N \rightarrow \pi N$

### $\Delta(2400)$ POLE POSITION

REAL PART			
VALUE (MeV)	DOCUMENT ID	TECN	COMMENT
1983	ARNDT 06	DPWA	$\pi N \rightarrow \pi N, \eta N$
2260 $\pm$ 60	CUTKOSKY 80	IPWA	$\pi N \rightarrow \pi N$
-2xIMAGINARY PART			
VALUE (MeV)	DOCUMENT ID	TECN	COMMENT
878	ARNDT 06	DPWA	$\pi N \rightarrow \pi N, \eta N$
320 $\pm$ 160	CUTKOSKY 80	IPWA	$\pi N \rightarrow \pi N$

### $\Delta(2400)$ ELASTIC POLE RESIDUE

MODULUS $ r $			
VALUE (MeV)	DOCUMENT ID	TECN	COMMENT
24	ARNDT 06	DPWA	$\pi N \rightarrow \pi N, \eta N$
8 $\pm$ 4	CUTKOSKY 80	IPWA	$\pi N \rightarrow \pi N$

PHASE $\theta$			
VALUE ( $^\circ$ )	DOCUMENT ID	TECN	COMMENT
-139	ARNDT 06	DPWA	$\pi N \rightarrow \pi N, \eta N$
-25 $\pm$ 15	CUTKOSKY 80	IPWA	$\pi N \rightarrow \pi N$

### $\Delta(2400)$ DECAY MODES

Mode	Fraction ( $\Gamma_i/\Gamma$ )
$\Gamma_1 N\pi$	
$\Gamma_2 \Sigma K$	

### $\Delta(2400)$ BRANCHING RATIOS

$\Gamma(N\pi)/\Gamma_{\text{total}}$	DOCUMENT ID	TECN	COMMENT	$\Gamma_1/\Gamma$
6.4 $\pm$ 2.2	ARNDT 06	DPWA	$\pi N \rightarrow \pi N, \eta N$	
5 $\pm$ 2	CUTKOSKY 80	IPWA	$\pi N \rightarrow \pi N$	
6 $\pm$ 3	HOEHLER 79	IPWA	$\pi N \rightarrow \pi N$	
10 $\pm$ 3	HENDRY 78	MPWA	$\pi N \rightarrow \pi N$	

$(\Gamma_1\Gamma_2)^{1/2}/\Gamma_{\text{total}}$ in $N\pi \rightarrow \Delta(2400) \rightarrow \Sigma K$	DOCUMENT ID	TECN	COMMENT	$(\Gamma_1\Gamma_2)^{1/2}/\Gamma$
<0.015	CANDLIN	84	DPWA $\pi^+ p \rightarrow \Sigma^+ K^+$	

### $\Delta(2400)$ REFERENCES

ARNDT 06	PR C74 045205	R.A. Arndt et al.	(GWU)
CANDLIN 84	NP B238 477	D.J. Candlin et al.	(EDIN, RAL, LOWC)
CUTKOSKY 80	Toronto Conf. 19	R.E. Cutkosky et al.	(CMU, LBL) IJP
Also	PR D20 2839	R.E. Cutkosky et al.	(CMU, LBL)
HOEHLER 79	PDAT 12-1	G. Hoehler et al.	(KARLT) IJP
Also	Toronto Conf. 3	R. Koch	(KARLT) IJP
HENDRY 78	PRL 41 222	A.W. Hendry	(IND, LBL) IJP
Also	ANP 136 1	A.W. Hendry	(IND)

## $\Delta(2420) 11/2^+$

$$I(J^P) = \frac{3}{2}(\frac{11}{2}^+) \text{ Status: } ***$$

Most of the results published before 1975 are now obsolete and have been omitted. They may be found in our 1982 edition, Physics Letters **111B** 1 (1982).

### $\Delta(2420)$ BREIT-WIGNER MASS

VALUE (MeV)	DOCUMENT ID	TECN	COMMENT
$\approx 2400$ to $\approx 2500$ ( $\approx 2420$ ) OUR ESTIMATE			
2633 $\pm$ 29	ARNDT 06	DPWA	$\pi N \rightarrow \pi N, \eta N$
2400 $\pm$ 125	CUTKOSKY 80	IPWA	$\pi N \rightarrow \pi N$
2416 $\pm$ 17	HOEHLER 79	IPWA	$\pi N \rightarrow \pi N$
2400 $\pm$ 60	HENDRY 78	MPWA	$\pi N \rightarrow \pi N$
••• We do not use the following data for averages, fits, limits, etc. •••			
2400	CANDLIN 84	DPWA	$\pi^+ p \rightarrow \Sigma^+ K^+$
2358.0 $\pm$ 9.0	CHEW 80	BPWA	$\pi^+ p \rightarrow \pi^+ p$

### $\Delta(2420)$ BREIT-WIGNER WIDTH

VALUE (MeV)	DOCUMENT ID	TECN	COMMENT
$\approx 300$ to $\approx 500$ ( $\approx 400$ ) OUR ESTIMATE			
692 $\pm$ 47	ARNDT 06	DPWA	$\pi N \rightarrow \pi N, \eta N$
450 $\pm$ 150	CUTKOSKY 80	IPWA	$\pi N \rightarrow \pi N$
340 $\pm$ 28	HOEHLER 79	IPWA	$\pi N \rightarrow \pi N$
460 $\pm$ 100	HENDRY 78	MPWA	$\pi N \rightarrow \pi N$
••• We do not use the following data for averages, fits, limits, etc. •••			
400	CANDLIN 84	DPWA	$\pi^+ p \rightarrow \Sigma^+ K^+$
202.2 $\pm$ 45.0	CHEW 80	BPWA	$\pi^+ p \rightarrow \pi^+ p$

### $\Delta(2420)$ POLE POSITION

REAL PART			
VALUE (MeV)	DOCUMENT ID	TECN	COMMENT
$\approx 2260$ to $\approx 2400$ ( $\approx 2330$ ) OUR ESTIMATE			
2529	ARNDT 06	DPWA	$\pi N \rightarrow \pi N, \eta N$
2300	<sup>1</sup> HOEHLER 93	ARGD	$\pi N \rightarrow \pi N$
2360 $\pm$ 100	CUTKOSKY 80	IPWA	$\pi N \rightarrow \pi N$

-2xIMAGINARY PART			
VALUE (MeV)	DOCUMENT ID	TECN	COMMENT
$\approx 350$ to $\approx 750$ ( $\approx 550$ ) OUR ESTIMATE			
621	ARNDT 06	DPWA	$\pi N \rightarrow \pi N, \eta N$
620	<sup>1</sup> HOEHLER 93	ARGD	$\pi N \rightarrow \pi N$
420 $\pm$ 100	CUTKOSKY 80	IPWA	$\pi N \rightarrow \pi N$

### $\Delta(2420)$ ELASTIC POLE RESIDUE

MODULUS $ r $			
VALUE (MeV)	DOCUMENT ID	TECN	COMMENT
33	ARNDT 06	DPWA	$\pi N \rightarrow \pi N, \eta N$
39	HOEHLER 93	ARGD	$\pi N \rightarrow \pi N$
18 $\pm$ 6	CUTKOSKY 80	IPWA	$\pi N \rightarrow \pi N$

PHASE $\theta$			
VALUE ( $^\circ$ )	DOCUMENT ID	TECN	COMMENT
-45	ARNDT 06	DPWA	$\pi N \rightarrow \pi N, \eta N$
-60	HOEHLER 93	ARGD	$\pi N \rightarrow \pi N$
-30 $\pm$ 40	CUTKOSKY 80	IPWA	$\pi N \rightarrow \pi N$

### $\Delta(2420)$ DECAY MODES

The following branching fractions are our estimates, not fits or averages.

Mode	Fraction ( $\Gamma_i/\Gamma$ )
$\Gamma_1 N\pi$	5-15 %
$\Gamma_2 \Sigma K$	

### $\Delta(2420)$ BRANCHING RATIOS

$\Gamma(N\pi)/\Gamma_{\text{total}}$	DOCUMENT ID	TECN	COMMENT	$\Gamma_1/\Gamma$
$\approx 5$ to $\approx 15$ OUR ESTIMATE				
8.5 $\pm$ 0.8	ARNDT 06	DPWA	$\pi N \rightarrow \pi N, \eta N$	
8 $\pm$ 3	CUTKOSKY 80	IPWA	$\pi N \rightarrow \pi N$	
8.0 $\pm$ 1.5	HOEHLER 79	IPWA	$\pi N \rightarrow \pi N$	
11 $\pm$ 2	HENDRY 78	MPWA	$\pi N \rightarrow \pi N$	
••• We do not use the following data for averages, fits, limits, etc. •••				
22	CHEW 80	BPWA	$\pi^+ p \rightarrow \pi^+ p$	

## Baryon Particle Listings

 $\Delta(2420)$ ,  $\Delta(2750)$ ,  $\Delta(2950)$ ,  $\Delta(\sim 3000)$ 

$(\Gamma_1 \Gamma_2)^{J^P} / \Gamma_{\text{total}}$ in $N\pi \rightarrow \Delta(2420) \rightarrow \Sigma K$	$(\Gamma_1 \Gamma_2)^{J^P} / \Gamma$		
VALUE	DOCUMENT ID	TECN	COMMENT
-0.016	CANDLIN 84	DPWA	$\pi^+ p \rightarrow \Sigma^+ K^+$

 $\Delta(2420)$  FOOTNOTES

<sup>1</sup> See HOEHLER 93 for a detailed discussion of the evidence for and the pole parameters of  $N$  and  $\Delta$  resonances as determined from Argand diagrams of  $\pi N$  elastic partial-wave amplitudes and from plots of the speeds with which the amplitudes traverse the diagrams.

 $\Delta(2420)$  REFERENCES

ARNDT 06	PR C74 045205	R.A. Arndt et al.	(GWU)
HOEHLER 93	$\pi N$ Newsletter 9 1	G. Hohler	(KARL)
CANDLIN 84	NP B238 477	D.J. Candlin et al.	(EDIN, RAL, LOWC)
PDG 82	PL 111B 1	M. Roos et al.	(HELS, CIT, CERN)
CHEW 80	Toronto Conf. 123	D.M. Chew	(LBL) IJP
CUTKOSKY 80	Toronto Conf. 19	R.E. Cutkosky et al.	(CMU, LBL) IJP
Also	PR D20 2839	R.E. Cutkosky et al.	(CMU, LBL)
HOEHLER 79	PDAT 12-1	G. Hohler et al.	(KARL) IJP
Also	Toronto Conf. 3	R. Koch	(KARL) IJP
HENDRY 78	PRL 41 222	A.W. Hendry	(IND, LBL) IJP
Also	ANP 136 1	A.W. Hendry	(IND)

$\Delta(2750) 13/2^-$   $I(J^P) = \frac{3}{2}(13^-)$  Status: \*\*

OMITTED FROM SUMMARY TABLE

The latest GWU analysis (ARNDT 06) finds no evidence for this resonance.

 $\Delta(2750)$  BREIT-WIGNER MASS

VALUE (MeV)	DOCUMENT ID	TECN	COMMENT
$\approx 2750$ OUR ESTIMATE			
2794 $\pm$ 80	HOEHLER 79	IPWA	$\pi N \rightarrow \pi N$
2650 $\pm$ 100	HENDRY 78	MPWA	$\pi N \rightarrow \pi N$

 $\Delta(2750)$  BREIT-WIGNER WIDTH

VALUE (MeV)	DOCUMENT ID	TECN	COMMENT
350 $\pm$ 100	HOEHLER 79	IPWA	$\pi N \rightarrow \pi N$
500 $\pm$ 100	HENDRY 78	MPWA	$\pi N \rightarrow \pi N$

 $\Delta(2750)$  DECAY MODES

Mode
$\Gamma_1 N \pi$

 $\Delta(2750)$  BRANCHING RATIOS

$\Gamma(N\pi) / \Gamma_{\text{total}}$	$\Gamma_1 / \Gamma$		
VALUE (%)			
4.0 $\pm$ 1.5	HOEHLER 79	IPWA	$\pi N \rightarrow \pi N$
5 $\pm$ 1	HENDRY 78	MPWA	$\pi N \rightarrow \pi N$

 $\Delta(2750)$  REFERENCES

ARNDT 06	PR C74 045205	R.A. Arndt et al.	(GWU)
HOEHLER 79	PDAT 12-1	G. Hohler et al.	(KARL) IJP
Also	Toronto Conf. 3	R. Koch	(KARL) IJP
HENDRY 78	PRL 41 222	A.W. Hendry	(IND, LBL) IJP
Also	ANP 136 1	A.W. Hendry	(IND)

$\Delta(2950) 15/2^+$   $I(J^P) = \frac{3}{2}(15^+)$  Status: \*\*

OMITTED FROM SUMMARY TABLE

 $\Delta(2950)$  BREIT-WIGNER MASS

VALUE (MeV)	DOCUMENT ID	TECN	COMMENT
$\approx 2950$ OUR ESTIMATE			
2990 $\pm$ 100	HOEHLER 79	IPWA	$\pi N \rightarrow \pi N$
2850 $\pm$ 100	HENDRY 78	MPWA	$\pi N \rightarrow \pi N$

 $\Delta(2950)$  BREIT-WIGNER WIDTH

VALUE (MeV)	DOCUMENT ID	TECN	COMMENT
330 $\pm$ 100	HOEHLER 79	IPWA	$\pi N \rightarrow \pi N$
700 $\pm$ 200	HENDRY 78	MPWA	$\pi N \rightarrow \pi N$

 $\Delta(2950)$  DECAY MODES

Mode
$\Gamma_1 N \pi$

 $\Delta(2950)$  BRANCHING RATIOS

$\Gamma(N\pi) / \Gamma_{\text{total}}$	$\Gamma_1 / \Gamma$		
VALUE (%)			
4 $\pm$ 2	HOEHLER 79	IPWA	$\pi N \rightarrow \pi N$
3 $\pm$ 1	HENDRY 78	MPWA	$\pi N \rightarrow \pi N$

 $\Delta(2950)$  REFERENCES

HOEHLER 79	PDAT 12-1	G. Hohler et al.	(KARL) IJP
Also	Toronto Conf. 3	R. Koch	(KARL) IJP
HENDRY 78	PRL 41 222	A.W. Hendry	(IND, LBL) IJP
Also	ANP 136 1	A.W. Hendry	(IND)

 $\Delta(\sim 3000)$  Region  
Partial-Wave Analyses

OMITTED FROM SUMMARY TABLE

We list here miscellaneous high-mass candidates for isospin-3/2 resonances found in partial-wave analyses.

Our 1982 edition also had a  $\Delta(2850)$  and a  $\Delta(3230)$ . The evidence for them was deduced from total cross-section and  $180^\circ$  elastic cross-section measurements. The  $\Delta(2850)$  has been resolved into the  $\Delta(2750) 13_{13}$  and  $\Delta(2950) K_{3,15}$ . The  $\Delta(3230)$  is perhaps related to the  $K_{3,13}$  of HENDRY 78 and to the  $L_{3,17}$  of KOCH 80.

 $\Delta(\sim 3000)$  BREIT-WIGNER MASS

VALUE (MeV)	DOCUMENT ID	TECN	COMMENT
$\approx 3000$ OUR ESTIMATE			
3300	<sup>1</sup> KOCH 80	IPWA	$\pi N \rightarrow \pi N L_{3,17}$ wave
3500	<sup>1</sup> KOCH 80	IPWA	$\pi N \rightarrow \pi N M_{3,19}$ wave
2850 $\pm$ 150	HENDRY 78	MPWA	$\pi N \rightarrow \pi N 1_{3,11}$ wave
3200 $\pm$ 200	HENDRY 78	MPWA	$\pi N \rightarrow \pi N K_{3,13}$ wave
3300 $\pm$ 200	HENDRY 78	MPWA	$\pi N \rightarrow \pi N L_{3,17}$ wave
3700 $\pm$ 200	HENDRY 78	MPWA	$\pi N \rightarrow \pi N M_{3,19}$ wave
4100 $\pm$ 300	HENDRY 78	MPWA	$\pi N \rightarrow \pi N N_{3,21}$ wave

 $\Delta(\sim 3000)$  BREIT-WIGNER WIDTH

VALUE (MeV)	DOCUMENT ID	TECN	COMMENT
700 $\pm$ 200	HENDRY 78	MPWA	$\pi N \rightarrow \pi N 1_{3,11}$ wave
1000 $\pm$ 300	HENDRY 78	MPWA	$\pi N \rightarrow \pi N K_{3,13}$ wave
1100 $\pm$ 300	HENDRY 78	MPWA	$\pi N \rightarrow \pi N L_{3,17}$ wave
1300 $\pm$ 400	HENDRY 78	MPWA	$\pi N \rightarrow \pi N M_{3,19}$ wave
1600 $\pm$ 500	HENDRY 78	MPWA	$\pi N \rightarrow \pi N N_{3,21}$ wave

 $\Delta(\sim 3000)$  DECAY MODES

Mode
$\Gamma_1 N \pi$

 $\Delta(\sim 3000)$  BRANCHING RATIOS

$\Gamma(N\pi) / \Gamma_{\text{total}}$	$\Gamma_1 / \Gamma$		
VALUE (%)			
6 $\pm$ 2	HENDRY 78	MPWA	$\pi N \rightarrow \pi N 1_{3,11}$ wave
5 $\pm$ 2	HENDRY 78	MPWA	$\pi N \rightarrow \pi N K_{3,13}$ wave
3 $\pm$ 1	HENDRY 78	MPWA	$\pi N \rightarrow \pi N L_{3,17}$ wave
3 $\pm$ 1	HENDRY 78	MPWA	$\pi N \rightarrow \pi N M_{3,19}$ wave
2 $\pm$ 1	HENDRY 78	MPWA	$\pi N \rightarrow \pi N N_{3,21}$ wave

 $\Delta(\sim 3000)$  FOOTNOTES

<sup>1</sup> In addition, KOCH 80 reports some evidence for an  $S_{31}$   $\Delta(2700)$  and a  $P_{33}$   $\Delta(2800)$ .

 $\Delta(\sim 3000)$  REFERENCES

KOCH 80	Toronto Conf. 3	R. Koch	(KARL) IJP
HENDRY 78	PRL 41 222	A.W. Hendry	(IND, LBL) IJP
Also	ANP 136 1	A.W. Hendry	(IND)

# Λ BARYONS

$(S = -1, I = 0)$

$\Lambda^0 = uds$

Λ  $I(J^P) = 0(\frac{1}{2}^+)$  Status: \*\*\*\*

We have omitted some results that have been superseded by later experiments. See our earlier editions.

**Λ MASS**

The fit uses Λ, Σ<sup>+</sup>, Σ<sup>0</sup>, Σ<sup>-</sup> mass and mass-difference measurements.

VALUE (MeV)	EVTS	DOCUMENT ID	TECN	COMMENT
<b>1115.683 ± 0.006 OUR FIT</b>				
<b>1115.683 ± 0.006 OUR AVERAGE</b>				
1115.678 ± 0.006 ± 0.006	20k	HARTOUNI 94	SPEC	pp 27.5 GeV/c
1115.690 ± 0.008 ± 0.006	18k	<sup>1</sup> HARTOUNI 94	SPEC	pp 27.5 GeV/c
••• We do not use the following data for averages, fits, limits, etc. •••				
1115.59 ± 0.08	935	HYMAN 72	HEBC	
1115.39 ± 0.12	195	MAYEUR 67	EMUL	
1115.6 ± 0.4		LONDON 66	HBC	
1115.65 ± 0.07	488	<sup>2</sup> SCHMIDT 65	HBC	
1115.44 ± 0.12		<sup>3</sup> BHOWMIK 63	RVUE	

<sup>1</sup>We assume CPT invariance: this is the  $\bar{\Lambda}$  mass as measured by HARTOUNI 94. See below for the fractional mass difference, testing CPT.  
<sup>2</sup>The SCHMIDT 65 masses have been reevaluated using our April 1973 proton and  $K^\pm$  and  $\pi^\pm$  masses. P. Schmidt, private communication (1974).  
<sup>3</sup>The mass has been raised 35 keV to take into account a 46 keV increase in the proton mass and an 11 keV decrease in the  $\pi^\pm$  mass (note added Reviews of Modern Physics **39** 1 (1967)).

$(m_\Lambda - m_{\bar{\Lambda}}) / m_\Lambda$

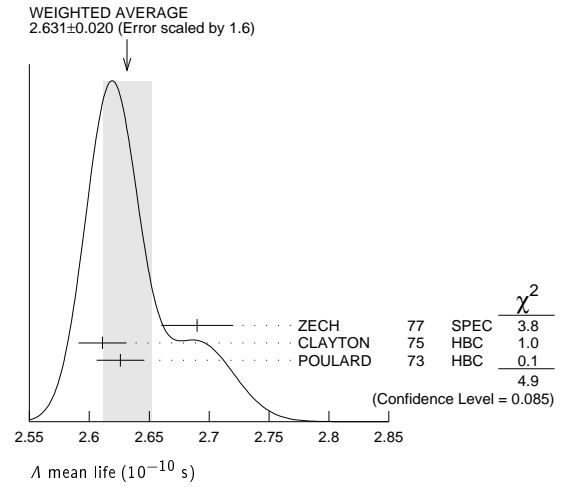
A test of CPT invariance.

VALUE (units 10 <sup>-5</sup> )	EVTS	DOCUMENT ID	TECN	COMMENT
<b>- 0.1 ± 1.1 OUR AVERAGE</b>				Error includes scale factor of 1.6.
+ 1.3 ± 1.2	31k	<sup>4</sup> RYBICKI 96	NA32	$\pi^-$ Cu, 230 GeV
- 1.08 ± 0.90		HARTOUNI 94	SPEC	pp 27.5 GeV/c
4.5 ± 5.4		CHIEN 66	HBC	6.9 GeV/c $\bar{p}p$
••• We do not use the following data for averages, fits, limits, etc. •••				
-26 ± 13		BADIER 67	HBC	2.4 GeV/c $\bar{p}p$
<sup>4</sup> RYBICKI 96 is an analysis of old ACCMOR (NA32) data.				

**Λ MEAN LIFE**

Measurements with an error  $\geq 0.1 \times 10^{-10}$  s have been omitted altogether, and only the latest high-statistics measurements are used for the average.

VALUE (10 <sup>-10</sup> s)	EVTS	DOCUMENT ID	TECN	COMMENT
<b>2.632 ± 0.020 OUR AVERAGE</b>				Error includes scale factor of 1.6. See the ideogram below.
2.69 ± 0.03	53k	ZECH 77	SPEC	Neutral hyperon beam
2.611 ± 0.020	34k	CLAYTON 75	HBC	0.96-1.4 GeV/c $K^- p$
2.626 ± 0.020	36k	POULARD 73	HBC	0.4-2.3 GeV/c $K^- p$
••• We do not use the following data for averages, fits, limits, etc. •••				
2.69 ± 0.05	6582	ALTHOFF 73B	OSPK	$\pi^+ n \rightarrow \Lambda K^+$
2.54 ± 0.04	4572	BALTAY 71B	HBC	$K^- p$ at rest
2.535 ± 0.035	8342	GRIMM 68	HBC	
2.47 ± 0.08	2600	HEPP 68	HBC	
2.35 ± 0.09	916	BURAN 66	HLBC	
2.452 <sup>+0.056</sup> <sub>-0.054</sub>	2213	ENGELMANN 66	HBC	
2.59 ± 0.09	794	HUBBARD 64	HBC	
2.59 ± 0.07	1378	SCHWARTZ 64	HBC	
2.36 ± 0.06	2239	BLOCK 63	HEBC	



$(\tau_\Lambda - \tau_{\bar{\Lambda}}) / \tau_\Lambda$

A test of CPT invariance.

VALUE	DOCUMENT ID	TECN	COMMENT
<b>-0.001 ± 0.009 OUR AVERAGE</b>			
-0.0018 ± 0.0066 ± 0.0056	BARNES 96	CNTR	LEAR $\bar{p}p \rightarrow \bar{\Lambda}\Lambda$
0.044 ± 0.085	BADIER 67	HBC	2.4 GeV/c $\bar{p}p$

**BARYON MAGNETIC MOMENTS**

Written 1994 by C.G. Wohl (LBNL).

The figure below shows the measured magnetic moments of the stable baryons. It also shows the predictions of the simplest quark model, using the measured  $p$ ,  $n$ , and  $\Lambda$  moments as input. In this model, the moments are [1]

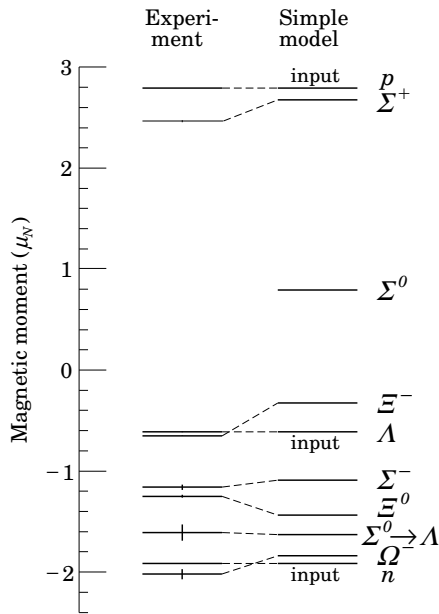
$$\begin{aligned} \mu_p &= (4\mu_u - \mu_d)/3 & \mu_n &= (4\mu_d - \mu_u)/3 \\ \mu_{\Sigma^+} &= (4\mu_u - \mu_s)/3 & \mu_{\Sigma^-} &= (4\mu_d - \mu_s)/3 \\ \mu_{\Xi^0} &= (4\mu_s - \mu_u)/3 & \mu_{\Xi^-} &= (4\mu_s - \mu_d)/3 \\ \mu_\Lambda &= \mu_s & \mu_{\Sigma^0} &= (2\mu_u + 2\mu_d - \mu_s)/3 \\ \mu_{\Omega^-} &= 3\mu_s \end{aligned}$$

and the  $\Sigma^0 \rightarrow \Lambda$  transition moment is

$$\mu_{\Sigma^0\Lambda} = (\mu_d - \mu_u)/\sqrt{3}.$$

The quark moments that result from this model are  $\mu_u = +1.852 \mu_N$ ,  $\mu_d = -0.972 \mu_N$ , and  $\mu_s = -0.613 \mu_N$ . The corresponding effective quark masses, taking the quarks to be Dirac point particles, where  $\mu = q\hbar/2m$ , are 338, 322, and 510 MeV. As the figure shows, the model gives a good first approximation to the experimental moments. For efforts to make a better model, we refer to the literature [2].

## Baryon Particle Listings

 $\Lambda$ 

## References

- See, for example, D.H. Perkins, *Introduction to High Energy Physics* (Addison-Wesley, Reading, MA, 1987), or D. Griffiths, *Introduction to Elementary Particles* (Harper & Row, New York, 1987).
- See, for example, J. Franklin, Phys. Rev. **D29**, 2648 (1984); H.J. Lipkin, Nucl. Phys. **B241**, 477 (1984); K. Suzuki, H. Kumagai, and Y. Tanaka, Europhys. Lett. **2**, 109 (1986); S.K. Gupta and S.B. Khadkikar, Phys. Rev. **D36**, 307 (1987); M.I. Krivoruchenko, Sov. J. Nucl. Phys. **45**, 109 (1987); L. Brekke and J.L. Rosner, Comm. Nucl. Part. Phys. **18**, 83 (1988); K.-T. Chao, Phys. Rev. **D41**, 920 (1990) and references cited therein. Also, see references cited in discussions of results in the experimental papers..

 $\Lambda$  MAGNETIC MOMENT

See the "Note on Baryon Magnetic Moments" above. Measurements with an error  $\geq 0.15 \mu_N$  have been omitted.

VALUE ( $\mu_N$ )	EVTS	DOCUMENT ID	TECN	COMMENT
<b>-0.613 ± 0.004 OUR AVERAGE</b>				
-0.606 ± 0.015	200k	COX	81	SPEC
-0.6138 ± 0.0047	3M	SCHACHIN...	78	SPEC
-0.59 ± 0.07	350k	HELLER	77	SPEC
-0.57 ± 0.05	1.2M	BUNCE	76	SPEC
-0.66 ± 0.07	1300	DAHL-JENSEN	71	EMUL 200 KG field

 $\Lambda$  ELECTRIC DIPOLE MOMENT

A nonzero value is forbidden by both  $T$  invariance and  $P$  invariance.

VALUE ( $10^{-16} e\text{-cm}$ )	CL%	DOCUMENT ID	TECN
<b>&lt; 1.5</b>	95	<sup>5</sup> PONDROM	81 SPEC
• • • We do not use the following data for averages, fits, limits, etc. • • •			
<100	95	<sup>6</sup> BARONI	71 EMUL
<500	95	GIBSON	66 EMUL

<sup>5</sup> PONDROM 81 measures  $(-3.0 \pm 7.4) \times 10^{-17} e\text{-cm}$ .

<sup>6</sup> BARONI 71 measures  $(-5.9 \pm 2.9) \times 10^{-15} e\text{-cm}$ .

 $\Lambda$  DECAY MODES

Mode	Fraction ( $\Gamma_i/\Gamma$ )
$\Gamma_1$ $p\pi^-$	$(63.9 \pm 0.5) \%$
$\Gamma_2$ $n\pi^0$	$(35.8 \pm 0.5) \%$
$\Gamma_3$ $n\gamma$	$(1.75 \pm 0.15) \times 10^{-3}$
$\Gamma_4$ $p\pi^- \gamma$	[a] $(8.4 \pm 1.4) \times 10^{-4}$
$\Gamma_5$ $p e^- \bar{\nu}_e$	$(8.32 \pm 0.14) \times 10^{-4}$
$\Gamma_6$ $p\mu^- \bar{\nu}_\mu$	$(1.57 \pm 0.35) \times 10^{-4}$

[a] See the Listings below for the pion momentum range used in this measurement.

## CONSTRAINED FIT INFORMATION

An overall fit to 5 branching ratios uses 20 measurements and one constraint to determine 5 parameters. The overall fit has a  $\chi^2 = 10.5$  for 16 degrees of freedom.

The following *off-diagonal* array elements are the correlation coefficients  $\langle \delta x_i \delta x_j \rangle / (\delta x_i \delta x_j)$ , in percent, from the fit to the branching fractions,  $x_i \equiv \Gamma_i/\Gamma_{\text{total}}$ . The fit constrains the  $x_i$  whose labels appear in this array to sum to one.

$x_2$	-100			
$x_3$	-2	-1		
$x_5$	46	-46	-1	
$x_6$	0	0	0	0
	$x_1$	$x_2$	$x_3$	$x_5$

 $\Lambda$  BRANCHING RATIOS

$\Gamma(p\pi^-)/\Gamma(N\pi)$				$\Gamma_1/(\Gamma_1+\Gamma_2)$
VALUE	EVTS	DOCUMENT ID	TECN	COMMENT
<b>0.641 ± 0.005 OUR FIT</b>				
<b>0.640 ± 0.005 OUR AVERAGE</b>				
0.646 ± 0.008	4572	BALTAY	71B HBC	$K^- p$ at rest
0.635 ± 0.007	6736	DOYLE	69 HBC	$\pi^- p \rightarrow \Lambda K^0$
0.643 ± 0.016	903	HUMPHREY	62 HBC	
0.624 ± 0.030		CRAWFORD	59B HBC	$\pi^- p \rightarrow \Lambda K^0$

$\Gamma(n\pi^0)/\Gamma(N\pi)$				$\Gamma_2/(\Gamma_1+\Gamma_2)$
VALUE	EVTS	DOCUMENT ID	TECN	COMMENT
<b>0.359 ± 0.005 OUR FIT</b>				
<b>0.310 ± 0.028 OUR AVERAGE</b>				
0.35 ± 0.05		BROWN	63 HLBC	
0.291 ± 0.034	75	CHRETIEN	63 HLBC	

$\Gamma(n\gamma)/\Gamma_{\text{total}}$				$\Gamma_3/\Gamma$
VALUE (units $10^{-3}$ )	EVTS	DOCUMENT ID	TECN	COMMENT
<b>1.75 ± 0.15 OUR FIT</b>				
<b>1.75 ± 0.15</b>	1816	LARSON	93 SPEC	$K^- p$ at rest
• • • We do not use the following data for averages, fits, limits, etc. • • •				
$1.78 \pm 0.24^{+0.14}_{-0.16}$	287	NOBLE	92 SPEC	See LARSON 93

$\Gamma(n\gamma)/\Gamma(n\pi^0)$				$\Gamma_3/\Gamma_2$
VALUE (units $10^{-3}$ )	EVTS	DOCUMENT ID	TECN	COMMENT
• • • We do not use the following data for averages, fits, limits, etc. • • •				
$2.86 \pm 0.74 \pm 0.57$	24	BIAGI	86 SPEC	SPS hyperon beam

$\Gamma(p\pi^- \gamma)/\Gamma(p\pi^-)$				$\Gamma_4/\Gamma_1$
VALUE (units $10^{-3}$ )	EVTS	DOCUMENT ID	TECN	COMMENT
<b>1.32 ± 0.22</b>	72	BAGGETT	72c HBC	$\pi^- < 95 \text{ MeV}/c$

$\Gamma(p e^- \bar{\nu}_e)/\Gamma(p\pi^-)$				$\Gamma_5/\Gamma_1$
VALUE (units $10^{-3}$ )	EVTS	DOCUMENT ID	TECN	COMMENT
<b>1.301 ± 0.019 OUR FIT</b>				
<b>1.301 ± 0.019 OUR AVERAGE</b>				
1.335 ± 0.056	7111	BOURQUIN	83 SPEC	SPS hyperon beam
1.313 ± 0.024	10k	WISE	80 SPEC	
1.23 ± 0.11	544	LINDQUIST	77 SPEC	$\pi^- p \rightarrow K^0 \Lambda$
1.27 ± 0.07	1089	KATZ	73 HBC	
1.31 ± 0.06	1078	ALTHOFF	71 OSPK	
1.17 ± 0.13	86	<sup>7</sup> CANTER	71 HBC	$K^- p$ at rest
1.20 ± 0.12	143	<sup>8</sup> MALONEY	69 HBC	
1.17 ± 0.18	120	<sup>8</sup> BAGLIN	64 FBC	$K^-$ freon 1.45 GeV/c
1.23 ± 0.20	150	<sup>8</sup> ELY	63 FBC	
• • • We do not use the following data for averages, fits, limits, etc. • • •				
1.32 ± 0.15	218	<sup>7</sup> LINDQUIST	71 OSPK	See LINDQUIST 77

<sup>7</sup> Changed by us from  $\Gamma(p e^- \bar{\nu}_e)/\Gamma(N\pi)$  assuming the authors used  $\Gamma(p\pi^-)/\Gamma_{\text{total}} = 2/3$ .

<sup>8</sup> Changed by us from  $\Gamma(p e^- \bar{\nu}_e)/\Gamma(N\pi)$  because  $\Gamma(p e^- \nu)/\Gamma(p\pi^-)$  is the directly measured quantity.

$\Gamma(\rho\mu^- \bar{\nu}_\mu)/\Gamma(N\pi^-)$		$\Gamma_6/(\Gamma_1+\Gamma_2)$		
VALUE (units 10 <sup>-4</sup> )	EVTS	DOCUMENT ID	TECN	COMMENT
<b>1.57 ± 0.35 OUR FIT</b>				
<b>1.57 ± 0.35 OUR AVERAGE</b>				
1.4 ± 0.5	14	BAGGETT	72B	HBC $K^- p$ at rest
2.4 ± 0.8	9	CANTER	71B	HBC $K^- p$ at rest
1.3 ± 0.7	3	LIND	64	RVUE
1.5 ± 1.2	2	RONNE	64	FBC

Λ DECAY PARAMETERS

See the "Note on Baryon Decay Parameters" in the neutron Listings. Some early results have been omitted.

α<sub>-</sub> FOR Λ → pπ<sup>-</sup>

VALUE	EVTS	DOCUMENT ID	TECN	COMMENT
<b>0.642 ± 0.013 OUR AVERAGE</b>				
0.584 ± 0.046	8500	ASTBURY	75	SPEC
0.649 ± 0.023	10325	CLELAND	72	OSPK
0.67 ± 0.06	3520	DAUBER	69	HBC From $\Xi$ decay
0.645 ± 0.017	10130	OVERSETH	67	OSPK Λ from $\pi^- p$
0.62 ± 0.07	1156	CRONIN	63	CNTR Λ from $\pi^- p$

α<sub>+</sub> FOR Λ →  $\bar{p}\pi^+$

VALUE	EVTS	DOCUMENT ID	TECN	COMMENT
<b>-0.71 ± 0.08 OUR AVERAGE</b>				
-0.755 ± 0.083 ± 0.063	≈ 8.7k	ABLIKIM	10	BES $J/\psi \rightarrow \Lambda \bar{\Lambda}$
-0.63 ± 0.13	770	TIXIER	88	DM2 $J/\psi \rightarrow \Lambda \bar{\Lambda}$

φ ANGLE FOR Λ → pπ<sup>-</sup>

(tanφ = β / γ)

VALUE (°)	EVTS	DOCUMENT ID	TECN	COMMENT
<b>-6.5 ± 3.5 OUR AVERAGE</b>				
-7.0 ± 4.5	10325	CLELAND	72	OSPK Λ from $\pi^- p$
-8.0 ± 6.0	10130	OVERSETH	67	OSPK Λ from $\pi^- p$
13.0 ± 17.0	1156	CRONIN	63	OSPK Λ from $\pi^- p$

α<sub>0</sub> / α<sub>-</sub> = α(Λ → nπ<sup>0</sup>) / α(Λ → pπ<sup>-</sup>)

VALUE	EVTS	DOCUMENT ID	TECN	COMMENT
<b>1.01 ± 0.07 OUR AVERAGE</b>				
1.000 ± 0.068	4760	<sup>9</sup> OLSEN	70	OSPK $\pi^+ n \rightarrow \Lambda K^+$
1.10 ± 0.27		CORK	60	CNTR

<sup>9</sup> OLSEN 70 compares proton and neutron distributions from Λ decay.

(α + α<sub>-</sub>) / (α - α<sub>-</sub>) in Λ → pπ<sup>-</sup>, Λ →  $\bar{p}\pi^+$

Zero if CP is conserved; α<sub>-</sub> and α<sub>+</sub> are the asymmetry parameters for Λ → pπ<sup>-</sup> and Λ →  $\bar{p}\pi^+$  decay. See also the Ξ<sup>-</sup> for a similar test involving the decay chain Ξ<sup>-</sup> → Λπ<sup>-</sup>, Λ → pπ<sup>-</sup> and the corresponding antiparticle chain.

VALUE	EVTS	DOCUMENT ID	TECN	COMMENT
<b>0.006 ± 0.021 OUR AVERAGE</b>				
-0.081 ± 0.055 ± 0.059	≈ 8.7k	ABLIKIM	10	BES $J/\psi \rightarrow \Lambda \bar{\Lambda}$
+0.013 ± 0.022	96k	BARNES	96	CNTR LEAR $\bar{p}p \rightarrow \Lambda \bar{\Lambda}$
+0.01 ± 0.10	770	TIXIER	88	DM2 $J/\psi \rightarrow \Lambda \bar{\Lambda}$
-0.02 ± 0.14	10k	<sup>10</sup> CHAUVAT	85	CNTR $p\bar{p}, \bar{p}p$ ISR

••• We do not use the following data for averages, fits, limits, etc. •••

-0.07 ± 0.09 4063 BARNES 87 CNTR See BARNES 96

<sup>10</sup> CHAUVAT 85 actually gives α<sub>+</sub>(Λ)/α<sub>-</sub>(Λ) = -1.04 ± 0.29. Assumes polarization is same in  $\bar{p}p \rightarrow \Lambda \bar{X}$  and  $p\bar{p} \rightarrow \Lambda X$ . Tests of this assumption, based on C-invariance and fragmentation, are satisfied by the data.

g<sub>A</sub> / g<sub>V</sub> FOR Λ → pe<sup>-</sup>ν<sub>e</sub>

Measurements with fewer than 500 events have been omitted. Where necessary, signs have been changed to agree with our conventions, which are given in the "Note on Baryon Decay Parameters" in the neutron Listings. The measurements all assume that the form factor g<sub>2</sub> = 0. See also the footnote on DWORKIN 90.

VALUE	EVTS	DOCUMENT ID	TECN	COMMENT
<b>-0.718 ± 0.015 OUR AVERAGE</b>				
-0.719 ± 0.016 ± 0.012	37k	<sup>11</sup> DWORKIN	90	SPEC eν angular corr.
-0.70 ± 0.03	7111	BOURQUIN	83	SPEC Ξ → Λπ <sup>-</sup>
-0.734 ± 0.031	10k	<sup>12</sup> WISE	81	SPEC eν angular correl.
-0.63 ± 0.06	817	ALTHOFF	73	OSPK Polarized Λ

<sup>11</sup> The tabulated result assumes the weak-magnetism coupling  $w \equiv g_w(0)/g_v(0)$  to be 0.97, as given by the CVC hypothesis and as assumed by the other listed measurements. However, DWORKIN 90 measures w to be 0.15 ± 0.30, and then  $g_A/g_V = -0.731 \pm 0.016$ .

<sup>12</sup> This experiment measures only the absolute value of g<sub>A</sub>/g<sub>V</sub>.

Λ REFERENCES

We have omitted some papers that have been superseded by later experiments. See our earlier editions.

ABLIKIM	10	PR D81 012003	M. Ablikim et al.	(BES Collab.)
BARNES	96	PR C54 1877	P.D. Barnes et al.	(CERN PS-185 Collab.)
RYBICKI	96	APP B27 2155	K. Rybicki	
HARTOUNI	94	PRL 72 1322	E.P. Hartouni et al.	(BNL E766 Collab.)
Also		PRL 72 2821 (erratum)	E.P. Hartouni et al.	(BNL E766 Collab.)
LARSON	93	PR D47 799	K.D. Larson et al.	(BNL-811 Collab.)
NOBLE	92	PRL 69 414	A.J. Noble et al.	(BIRM, BOST, BRCO+)
DWORKIN	90	PR D41 780	J. Dworkin et al.	(BRIS, GEVA, HEIDP+)
TIXIER	88	PL B212 523	M.H. Tixier et al.	(DM2 Collab.)
BARNES	87	PL B199 147	P.D. Barnes et al.	(CMU, SAFL, LANL+)
BIAGI	86	ZPHY C30 201	S.F. Biagi et al.	(BRIS, CERN, GEVA+)
CHAUVAT	85	PL 163B 273	P. Chauvat et al.	(CERN, CLER, UCLA+)
BOURQUIN	83	ZPHY C21 1	M.H. Bourquin et al.	(BRIS, GEVA, HEIDP+)
COX	81	PRL 46 877	P.T. Cox et al.	(MICH, WISC, RUTG, MINV+)
PONDROM	81	PR D23 814	L. Pondrom et al.	(WISC, MICH, RUTG+)
WISE	81	PL 98B 123	J.E. Wise et al.	(MASA, BNL)
WISE	80	PL 91B 165	J.E. Wise et al.	(MASA, BNL)
SCHACHIN...	78	PRL 41 1348	L. Schachinger et al.	(MICH, RUTG, WISC)
HELLER	77	PL 68B 480	K. Heller et al.	(MICH, WISC, HEIDH)
LINDQUIST	77	PR D16 2104	J. Lindquist et al.	(EFI, OSU, ANL)
Also		JPG 2 L211	J. Lindquist et al.	(EFI, WUSL, OSU+)
ZECH	77	NP B124 413	G. Zech et al.	(SIEG, CERN, DORT, HEIDH)
BUNCE	76	PRL 36 1113	G.R.M. Bunce et al.	(WISC, MICH, RUTG)
ASTBURY	75	NP B99 30	P. Astbury et al.	(LOIC, CERN, ET+)
CLAYTON	75	NP B95 130	E.F. Clayton et al.	(LOIC, RHEL)
ALTHOFF	73	PL 43B 237	K.H. Althoff et al.	(CERN, HEID)
ALTHOFF	73B	NP B66 29	K.H. Althoff et al.	(CERN, HEID)
KATZ	73	Thesis MDDP-TR-74-044	C.N. Katz	(UMD)
POULARD	73	PL 46B 135	G. Poulard, A. Givernaud, A.C. Borg	(SAFL)
BAGGETT	72B	ZPHY 252 362	M.J. Baggett et al.	(HEID)
BAGGETT	72C	PL 42B 379	M.J. Baggett et al.	(HEID)
CLELAND	72	NP B40 221	W.E. Cleland et al.	(CERN, GEVA, LUND)
HYMAN	72	PR D5 1063	L.G. Hyman et al.	(ANL, CMU)
ALTHOFF	71	PL 37B 531	K.H. Althoff et al.	(CERN, HEID)
BALTAY	71B	PR D4 670	C. Baltay et al.	(COLU, BING)
BARONI	71	UNC 2 1256	C. Baroni, S. Petrega, G. Romano	(ROMA)
CANTER	71	PRL 26 868	J. Canter et al.	(STON, COLU)
CANTER	71B	PR 27 59	J. Canter et al.	(STON, COLU)
DAHL-JENSEN	71	NC 3A 1	E. Dahl-Jensen et al.	(CERN, ANKA, LAUS+)
LINDQUIST	71	PRL 27 612	J. Lindquist et al.	(EFI, WUSL, OSU+)
OLSEN	70	PRL 24 843	S.L. Olsen et al.	(WISC, MICH)
DAUBER	69	PR 179 1262	P.M. Dauber et al.	(LRL)
DOYLE	69	Thesis UCLR 18139	J.C. Doyle	(LRL)
MALONEY	69	PRL 23 425	J.E. Maloney, B. Sechi-Zorn	(UMD)
GRIMM	68	NC 54A 187	H.J. Grimm	(HEID)
HEPP	68	ZPHY 214 71	V. Hepp, H. Schleich	(HEID)
BADIER	67	PL 25B 152	J. Badier et al.	(EPOL)
MAYEUR	67	U.Libr.BruX.Bul. 32	C. Mayeur, E. Tompa, J.H. Wickens	(BELG, LOUC)
OVERSETH	67	PRL 19 391	O.E. Overseth, R.F. Roth	(MICH, PRIN)
PDG	67	RMP 39 1	A.H. Rosenfeld et al.	(LRL, CERN, YALE)
BURAN	66	PL 20 318	T. Buran et al.	(OSLO)
CHIEN	66	PR 152 1171	C.Y. Chien et al.	(YALE, BNL)
ENGELMANN	66	NC 45A 1038	R. Engelmann et al.	(HEID, REHO)
GIBSON	66	NC 45A 882	W.M. Gibson, K. Green	(BRIS)
LONDON	66	PR 143 1034	G.W. London et al.	(BNL, SYRA)
SCHMIDT	65	PR 140B 1328	P. Schmidt	(COLU)
BAGLIN	64	NC 35 977	C. Baglin et al.	(EPOL, CERN, LOUC, RHEL+)
HUBBARD	64	PR 135 B183	J.R. Hubbard et al.	(LRL)
LIND	64	PR 135 B1483	V.G. Lind et al.	(WISC)
RONNE	64	PL 11 357	B.E. Ronne et al.	(CERN, EPOL, LOUC+)
SCHWARTZ	64	Thesis UCLR 11360	J.A. Schwartz	(LRL)
BHOWMIK	63	NC 28 1494	B. Bhowmik, D.P. Goyal	(DELH)
BLOCK	63	PR 130 766	M.M. Block et al.	(NWES, BGNA, SYRA+)
BROWN	63	PR 130 769	J.L. Brown et al.	(LRL, MICH)
CHRETIEN	63	PR 131 2208	M. Chretien et al.	(BRAN, BROW, HARV+)
CRONIN	63	PR 129 1795	J.W. Cronin, O.E. Overseth	(PRIN)
ELY	63	PR 131 868	R.P. Ely et al.	(LRL)
HUMPHREY	62	PR 127 1305	W.E. Humphrey, R.R. Ross	(LRL)
CORK	60	PR 120 1000	B. Cork et al.	(LRL, PRIN, BNL)
CRAWFORD	59B	PRL 2 266	F.S. Crawford et al.	(LRL)

# Baryon Particle Listings

## $\Lambda$ , $\Lambda$ 's and $\Sigma$ 's

### $\Lambda$ AND $\Sigma$ RESONANCES

**Introduction:** Since our last edition, there have been a few measurements of properties of the lowest  $\Lambda$  and  $\Sigma$  resonances—mostly of masses and widths. But the field remains at a standstill. What follows is a much abbreviated version of the note on  $\Lambda$  and  $\Sigma$  Resonances from our 1990 edition [1]. In particular, see that edition for some representative Argand plots from partial-wave analyses.

Table 1 is an attempt to evaluate the status, both overall and channel by channel, of each  $\Lambda$  and  $\Sigma$  resonance in the Particle Listings. The evaluations are of course partly subjective. A blank indicates there is no evidence at all: either the relevant couplings are small or the resonance does not really exist. The main Baryon Summary Table includes only the established resonances (overall status 3 or 4 stars). A number of the 1- and 2-star entries may eventually disappear, but there are certainly many resonances yet to be discovered underlying the established ones.

**Sign conventions for resonance couplings:** In terms of the isospin-0 and -1 elastic scattering amplitudes  $A_0$  and  $A_1$ , the amplitude for  $K^-p \rightarrow \bar{K}^0 n$  scattering is  $\pm(A_1 - A_0)/2$ , where the sign depends on conventions used in conjunction with the Clebsch-Gordan coefficients (such as, is the baryon or the meson the “first” particle). If this reaction is partial-wave analyzed and if the overall phase is chosen so that, say, the  $\Sigma(1775)D_{15}$  amplitude at resonance points along the positive imaginary axis (points “up”), then any  $\Sigma$  at resonance will point “up” and any  $\Lambda$  at resonance will point “down” (along the negative imaginary axis). Thus the phase at resonance determines the isospin. The above ignores background amplitudes in the resonating partial waves.

That is the basic idea. In a similar but somewhat more complicated way, the phases of the  $\bar{K}N \rightarrow \Lambda\pi$  and  $\bar{K}N \rightarrow \Sigma\pi$  amplitudes for a resonating wave help determine the SU(3) multiplet to which the resonance belongs. Again, a convention has to be adopted for some overall arbitrary phases: which way is “up”? Our convention is that of Levi-Setti [2] and is shown in Fig. 1, which also compares experimental results with theoretical predictions for the signs of several resonances. In the Listings, a + or – sign in front of a measurement of an inelastic resonance coupling indicates the sign (the *absence* of a sign means that the sign is not determined, *not* that it is positive). For more details, see Appendix II of our 1982 edition [3].

**Errors on masses and widths:** The errors quoted on resonance parameters from partial-wave analyses are often only statistical, and the parameters can change by more than these errors when a different parametrization of the waves is used.

Furthermore, the different analyses use more or less the same data, so it is not really appropriate to treat the different determinations of the resonance parameters as independent or to average them together. In any case, the spread of the masses, widths, and branching fractions from the different analyses is certainly a better indication of the uncertainties than are the quoted errors. In the Baryon Summary Table, we usually give a range reflecting the spread of the values rather than a particular value with error.

For three states, the  $\Lambda(1520)$ , the  $\Lambda(1820)$ , and the  $\Sigma(1775)$ , there is enough information to make an overall fit to the various branching fractions. It is then necessary to use the quoted errors, but the errors obtained from the fit should not be taken seriously.

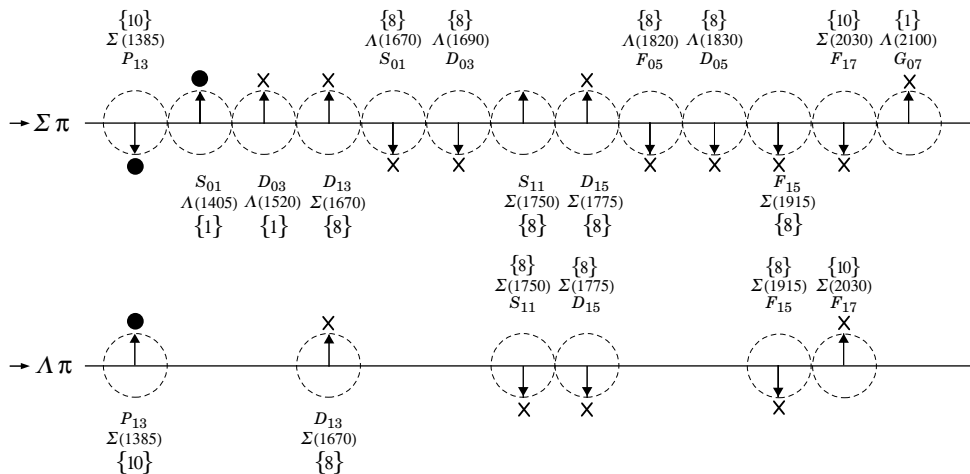


Figure 1. The signs of the imaginary parts of resonating amplitudes in the  $\bar{K}N \rightarrow \Lambda\pi$  and  $\Sigma\pi$  channels. The signs of the  $\Sigma(1385)$  and  $\Lambda(1405)$ , marked with a •, are set by convention, and then the others are determined relative to them. The signs required by the SU(3) assignments of the resonances are shown with an arrow, and the experimentally determined signs are shown with an x.



Table 1. The status of the Λ and Σ resonances. Only those with an overall status of \*\*\* or \*\*\*\* are included in the main Baryon Summary Table.

Particle	J <sup>P</sup>	Overall status	Status as seen in —			
			N $\bar{K}$	Λπ	Σπ	Other channels
Λ(1116)	1/2+	****		F		Nπ(weakly)
Λ(1405)	1/2-	****	****	o	****	
Λ(1520)	3/2-	****	****	r	****	Λππ, Λγ
Λ(1600)	1/2+	***	***	b	**	
Λ(1670)	1/2-	****	****	i	****	Λη
Λ(1690)	3/2-	****	****	d	****	Λππ, Σππ
Λ(1800)	1/2-	***	***	d	**	N $\bar{K}^*$ , Σ(1385)π
Λ(1810)	1/2+	***	***	e	**	N $\bar{K}^*$
Λ(1820)	5/2+	****	****	n	****	Σ(1385)π
Λ(1830)	5/2-	****	***	F	****	Σ(1385)π
Λ(1890)	3/2+	****	****	o	**	N $\bar{K}^*$ , Σ(1385)π
Λ(2000)	*	*	*	r	*	Λω, N $\bar{K}^*$
Λ(2020)	7/2+	*	*	b	*	
Λ(2100)	7/2-	****	****	i	***	Λω, N $\bar{K}^*$
Λ(2110)	5/2+	***	**	d	*	Λω, N $\bar{K}^*$
Λ(2325)	3/2-	*	*	d	*	Λω
Λ(2350)	***	***	*	e	*	
Λ(2585)	**	**	*	n	*	
Σ(1193)	1/2+	****				Nπ(weakly)
Σ(1385)	3/2+	****		****	****	
Σ(1480)	*	*	*	*	*	
Σ(1560)	**	**	**	**	**	
Σ(1580)	3/2-	*	*	*	*	
Σ(1620)	1/2-	**	**	*	*	
Σ(1660)	1/2+	***	***	*	**	
Σ(1670)	3/2-	****	****	****	****	several others
Σ(1690)	**	**	**	*	*	Λππ
Σ(1750)	1/2-	***	***	**	*	Ση
Σ(1770)	1/2+	*	*	*	*	
Σ(1775)	5/2-	****	****	****	***	several others
Σ(1840)	3/2+	*	*	**	*	
Σ(1880)	1/2+	**	**	**	*	N $\bar{K}^*$
Σ(1915)	5/2+	****	***	****	***	Σ(1385)π
Σ(1940)	3/2-	***	*	***	**	quasi-2-body
Σ(2000)	1/2-	*	*	*	*	N $\bar{K}^*$ , Λ(1520)π
Σ(2030)	7/2+	****	****	****	**	several others
Σ(2070)	5/2+	*	*	*	*	
Σ(2080)	3/2+	**	**	**	*	
Σ(2100)	7/2-	*	*	*	*	
Σ(2250)	****	***	*	*	*	
Σ(2455)	**	*	*	*	*	
Σ(2620)	**	*	*	*	*	
Σ(3000)	*	*	*	*	*	
Σ(3170)	*	*	*	*	*	multi-body

**Production experiments:** Partial-wave analyses of course separate partial waves, whereas a peak in a cross section or an invariant mass distribution usually cannot be disentangled from background and analyzed for its quantum numbers; and more than one resonance may be contributing to the peak. Results from partial-wave analyses and from production experiments are generally kept separate in the Listings, and in the Baryon Summary Table results from production experiments are used only for the low-mass states. The Σ(1385) and Λ(1405) of course lie below the  $\bar{K}N$  threshold and nearly everything about them is learned from production experiments; and production and formation experiments agree quite well in the case

of Λ(1520) and results have been combined. There is some disagreement between production and formation experiments in the 1600–1700 MeV region: see the note on the Σ(1670).

**References**

1. Particle Data Group, Phys. Lett. **B239**, VIII.64 (1990).
2. R. Levi-Setti, in *Proceedings of the Lund International Conference on Elementary Particles* (Lund, 1969), p. 339.
3. Particle Data Group, Phys. Lett. **111B** (1982).

**Λ(1405) 1/2<sup>-</sup>**  $I(J^P) = 0(\frac{1}{2}^-)$  Status: \*\*\*

The nature of the Λ(1405) has been a puzzle for decades: three-quark state or hybrid; two poles or one. We cannot here survey the rather extensive literature. See, for example, CIEPLY 10, KISSLINGER 11, and SEKIYARA 11, for discussions and earlier references.

It seems to be the universal opinion of the chiral-unitary community that there are two poles in the 1400-MeV region. ZYCHOR 08 presents experimental evidence against the two-pole model, but this is disputed by GENG 07A. See also REVA 09, which finds little basis for choosing between one- and two-pole models.

A single, ordinary three-quark Λ(1405) fits nicely into a  $J^P = 1/2^-$  SU(4)  $\bar{7}$  multiplet, whose other members are the  $\Lambda_c(2595)^+$ ,  $\Xi_c(2790)^+$ , and  $\Xi_c(2790)^0$ ; see Fig. 1 of our note on “Charmed Baryons.”

**Λ(1405) MASS**

VALUE (MeV)	EVTS	DOCUMENT ID	TECN	COMMENT
<b>1405.1<sup>+1.3</sup><sub>-1.0</sub> OUR AVERAGE</b>				
1405 <sup>+1.4</sup> <sub>-1.0</sub>		ESMAILI	10	RVUE <sup>4</sup> He K <sup>-</sup> → Σ <sup>±</sup> π <sup>∓</sup> X at rest
1406.5 ± 4.0		<sup>1</sup> DALITZ	91	M-matrix fit
• • • We do not use the following data for averages, fits, limits, etc. • • •				
1391 ± 1	700	<sup>1</sup> HEMINGWAY	85	HBC K <sup>-</sup> p 4.2 GeV/c
~ 1405	400	<sup>2</sup> THOMAS	73	HBC π <sup>-</sup> p 1.69 GeV/c
1405	120	BARBARO...	68B	DBC K <sup>-</sup> d 2.1–2.7 GeV/c
1400 ± 5	67	BIRMINGHAM	66	HBC K <sup>-</sup> p 3.5 GeV/c
1382 ± 8		ENGLER	65	HDDB π <sup>-</sup> p, π <sup>+</sup> d 1.68 GeV/c
1400 ± 24		MUSGRAVE	65	HBC $\bar{p}p$ 3–4 GeV/c
1410		ALEXANDER	62	HBC π <sup>-</sup> p 2.1 GeV/c
1405		ALSTON	62	HBC K <sup>-</sup> p 1.2–0.5 GeV/c
1405		ALSTON	61B	HBC K <sup>-</sup> p 1.15 GeV/c

**EXTRAPOLATIONS BELOW N $\bar{K}$  THRESHOLD**

VALUE (MeV)	EVTS	DOCUMENT ID	TECN	COMMENT
• • • We do not use the following data for averages, fits, limits, etc. • • •				
1407.56 or 1407.50		<sup>3</sup> KIMURA	00	potential model
1411		<sup>4</sup> MARTIN	81	K-matrix fit
1406		<sup>5</sup> CHAO	73	DPWA 0-range fit (sol. B)
1421		MARTIN	70	RVUE Constant K-matrix
1416 ± 4		MARTIN	69	HBC Constant K-matrix
1403 ± 3		KIM	67	HBC K-matrix fit
1407.5 ± 1.2		<sup>6</sup> KITTEL	66	HBC 0-effective-range fit
1410.7 ± 1.0		KIM	65	HBC 0-effective-range fit
1409.6 ± 1.7		<sup>6</sup> SAKITT	65	HBC 0-effective-range fit

**Λ(1405) WIDTH**

VALUE (MeV)	EVTS	DOCUMENT ID	TECN	COMMENT
<b>50 ± 2</b>				
		<sup>1</sup> DALITZ	91	M-matrix fit
• • • We do not use the following data for averages, fits, limits, etc. • • •				
24 <sup>+4</sup> <sub>-3</sub>		ESMAILI	10	RVUE <sup>4</sup> He K <sup>-</sup> → Σ <sup>±</sup> π <sup>∓</sup> X at rest
32 ± 1	700	<sup>1</sup> HEMINGWAY	85	HBC K <sup>-</sup> p 4.2 GeV/c
45 to 55	400	<sup>2</sup> THOMAS	73	HBC π <sup>-</sup> p 1.69 GeV/c
35	120	BARBARO...	68B	DBC K <sup>-</sup> d 2.1–2.7 GeV/c
50 ± 10	67	BIRMINGHAM	66	HBC K <sup>-</sup> p 3.5 GeV/c
89 ± 20		ENGLER	65	HDDB
60 ± 20		MUSGRAVE	65	HBC
35 ± 5		ALEXANDER	62	HBC
50		ALSTON	62	HBC
20		ALSTON	61B	HBC

## Baryon Particle Listings

 $\Lambda(1405)$ ,  $\Lambda(1520)$ EXTRAPOLATIONS BELOW  $N\bar{K}$  THRESHOLD

VALUE (MeV)	DOCUMENT ID	TECN	COMMENT
••• We do not use the following data for averages, fits, limits, etc. •••			
50.24 or 50.26	3 KIMURA	00	potential model
30	4 MARTIN	81	K-matrix fit
55	5,7 CHAO	73 DPWA	0-range fit (sol. B)
20	MARTIN	70 RVUE	Constant K-matrix
29 ± 6	MARTIN	69 HBC	Constant K-matrix
50 ± 5	KIM	67 HBC	K-matrix fit
34.1 ± 4.1	6 KITTEL	66 HBC	
37.0 ± 3.2	KIM	65 HBC	
28.2 ± 4.1	6 SAKITT	65 HBC	

 $\Lambda(1405)$  DECAY MODES

Mode	Fraction ( $\Gamma_i/\Gamma$ )
$\Gamma_1$ $\Sigma \pi$	100 %
$\Gamma_2$ $\Lambda \gamma$	
$\Gamma_3$ $\Sigma^0 \gamma$	
$\Gamma_4$ $N\bar{K}$	

 $\Lambda(1405)$  PARTIAL WIDTHS

$\Gamma(\Lambda \gamma)$	$\Gamma_2$	
VALUE (keV)	DOCUMENT ID	COMMENT
••• We do not use the following data for averages, fits, limits, etc. •••		
27 ± 8	BURKHARDT 91	Isobar model fit

$\Gamma(\Sigma^0 \gamma)$	$\Gamma_3$	
VALUE (keV)	DOCUMENT ID	COMMENT
••• We do not use the following data for averages, fits, limits, etc. •••		
10 ± 4 or 23 ± 7	BURKHARDT 91	Isobar model fit

 $\Lambda(1405)$  BRANCHING RATIOS

$\Gamma(N\bar{K})/\Gamma(\Sigma \pi)$	$\Gamma_4/\Gamma_1$			
VALUE	CL%	DOCUMENT ID	TECN	COMMENT
••• We do not use the following data for averages, fits, limits, etc. •••				
<3	95	HEMINGWAY 85	HBC	$K^- p$ 4.2 GeV/c

 $\Lambda(1405)$  FOOTNOTES

- DALITZ 91 fits the HEMINGWAY 85 data.
- THOMAS 73 data is fit by CHAO 73 (see next section).
- The KIMURA 00 values are from fits A and B from a coupled-channel potential model using low-energy  $\bar{K}N$  and  $\Sigma \pi$  data, kaonic-hydrogen x-ray measurements, and our  $\Lambda(1405)$  mass and width. The results bear mainly on the nature of the  $\Lambda(1405)$ : three-quark state or  $\bar{K}N$  bound state.
- The MARTIN 81 fit includes the  $K^\pm p$  forward scattering amplitudes and the dispersion relations they must satisfy.
- See also the accompanying paper of THOMAS 73.
- Data of SAKITT 65 are used in the fit by KITTEL 66.
- An asymmetric shape, with  $\Gamma/2 = 41$  MeV below resonance, 14 MeV above.

 $\Lambda(1405)$  REFERENCES

KISSLINGER 11	EPJ A47 8	L.S. Kisslinger, E.M. Henley (CMU, WASH)
SEKHARA 11	PR C83 055202	T. Sekhara, T. Hyodo, D. Jido (KYOT, KYOTU+)
CIEPLY 10	EPJ A43 191	A. Cieply, J. Smekjal (NPI, Tech. U, Czech Rep.)
ESMAILI 10	PL B686 23	J. Esmaili, Y. Akaishi, T. Yamazaki (RIKEN, ISUT+)
REVAL 09	PR C79 035202	J. Reval, N.V. Shevchenko (BUDA, NPI, Czech Rep.)
ZYCHOR 08	PL B660 167	I. Zychor et al. (COSY ANKE Collab.)
GENG 07A	EPJ A34 405	L.S. Geng, E. Oset (YALE)
KIMURA 00	PR C62 015206	M. Kimura et al. (CERN, UNM, BIRM)
BURKHARDT 91	PR C44 607	H. Burkhardt, J. Lowe (NOTT, UNM, BIRM)
DALITZ 91	JPG 17 289	R.H. Dalitz, A. Deloff (OXFT, WINR)
HEMINGWAY 85	NP B253 742	R.L. Hemingway (CERN, J)
MARTIN 81	NP B179 33	A.D. Martin (DURH)
CHAO 73	NP B56 46	Y.A. Chao et al. (RHEL, CMU, LOUC)
THOMAS 73	NP B56 15	D.W. Thomas et al. (CMU, J)
MARTIN 70	NP B16 479	A.D. Martin, G.G. Ross (DURH)
MARTIN 69	PR 183 1352	B.R. Martin, M. Sakitt (LOUC, BNL)
Also	PR 183 1345	B.R. Martin, M. Sakitt (LOUC, BNL)
BARBARO... 68B	PRL 21 573	A. Barbaro-Galtri et al. (LRL, SLAC)
KIM 67	PRL 19 1074	J.K. Kim (YALE)
BIRMINGHAM 66	PR 152 1148	M. Haque et al. (BIRM, GLAS, LOIC, OXF+)
KITTEL 66	PL 21 349	W. Kittel, G. Otter, I. Wacek (VIEN)
ENGLER 65	PRL 15 224	A. Engler et al. (CMU, BNL, IJ)
KIM 65	PRL 14 29	J.K. Kim (COLU)
MUSGRAVE 65	NC 35 735	B. Musgrave et al. (BIRM, CERN, EPOL+)
SAKITT 65	PR 139 8719	M. Sakitt et al. (UMD, LRL)
ALEXANDER 62	PRL 8 447	G. Alexander et al. (LRL, I)
ALSTON 62	CERN Conf. 311	M.H. Alston et al. (LRL, I)
ALSTON 61B	PRL 6 698	M.H. Alston et al. (LRL, I)

## OTHER RELATED PAPERS

IWASAKI 97	PRL 78 3067	M. Iwasaki et al. (KEK 228 Collab.)
FINK 90	PR C41 2720	P.J.Jr. Fink et al. (IBM, ORST, ANSM)
LEINWEBER 90	ANP 198 203	D.B. Leinweber (MCM)
MUELLER-GR... 90	NP A513 557	A. Mueller-Groeling, K. Holinde, J. Speth (JULI)
BARRETT 89	NC 102A 179	R.C. Barrett (SURR)
BATTY 89	NC 102A 255	C.J. Batty, A. Gal (RAL, HEBR)
CAPSTICK 89	Excited Baryons 88, p.32	S. Capstick (GUEL)
LOWE 89	NC 102A 167	J. Lowe (BIRM)
WHITEHOUSE 89	PRL 63 1352	D.A. Whitehouse et al. (BIRM, BOST, BRCO+)
SIEGEL 88	PR C38 2221	P.B. Siegel, W. Weise (REGG)
WORKMAN 88	PR D37 3117	R.L. Workman, H.W. Fearing (TRIU)
SCHNICK 87	PRL 58 1719	J. Schnick, R.H. Landau (ORST)
CAPSTICK 86	PR D34 2809	S. Capstick, N. Isgur (TNTO)
JENNINGS 86	PL B176 229	B.K. Jennings (TRIU)
MALTMAN 86	PR D34 1372	K. Maltman, N. Isgur (LANL, TNTO)
ZHONG 86	PL B171 471	Y.S. Zhong et al. (ADLD, TRIU, SURR)
BURKHARDT 85	NP A440 653	H. Burkhardt, J. Lowe, A.S. Rosenthal (NOTT+)
DAREWYCH 85	PR D32 1765	J.W. Darewych, R. Konik, N. Isgur (YORKC, TNTO)
VEIT 85	PR D31 1033	E.A. Veit et al. (TRIU, ADLD, SURR)
KIANG 84	PR C30 1638	D. Kiang et al. (DALH, MCM)
MILLER 84	Conference paper	D.J. Miller (LOUC)
Conf. Intersections between Particle and Nuclear Physics, p. 783		
VANDIJK 84	PR D30 937	W. van Dijk (MCM)
VEIT 84	PL 137B 415	E.A. Veit et al. (TRIU, SURR, CERN)
DALITZ 82	Heid. Conf.	R.H. Dalitz et al. (OXFT)
Heidelberg Conf., p. 201		
DALITZ 81	Kaon Conf.	R.H. Dalitz, J.G. McGinley (OXFT)
Low and Intermediate Energy Kaon-Nucleon Physics, p.381		
MARTIN 81B	Kaon Conf.	A.D. Martin (DURH)
Low and Intermediate Energy Kaon-Nucleon Physics, p. 97		
OADES 77	NC 42A 462	G.C. Oades, G. Rasche (AARH, ZURI)
SHAW 73	Purdue Conf. 417	G.L. Shaw (UCI)
BARBARO... 72	LBL-555	A. Barbaro-Galtri (LBL)
DOBSON 72	PR D6 3256	P.N. Dobson, R. McEhane (HAWA)
RAJASEKA... 72	PR D5 610	G. Rajasekaran (TATA)
Earlier papers also cited in RAJASEKARAN 72.		
CLINE 71	PRL 26 1194	D. Cline, R. Laumann, J. Mapp (WISC)
MARTIN 71	PL 35B 62	A.D. Martin, A.D. Martin, G.G. Ross (DURH, LOUC+)
DALITZ 67	PL 153 1617	R.H. Dalitz, T.C. Wong, G. Rajasekaran (OXFT+)
DONALD 66	PL 22 711	R.A. Donald et al. (LVP)
KADYK 66	PRL 17 599	J.A. Kadyk et al. (LRL)
ABRAMS 65	PR 139 B454	G.S. Abrams, B. Sechi-Zorn (UMD)

 $\Lambda(1520) 3/2^-$ 

$$I(J^P) = 0(\frac{3}{2}^-) \text{ Status: } ***$$

Discovered by FERRO-LUZZI 62; the elaboration in WATSON 63 is the classic paper on the Breit-Wigner analysis of a multichannel resonance.

The measurements of the mass, width, and elasticity published before 1975 are now obsolete and have been omitted. They were last listed in our 1982 edition Physics Letters **111B** 1 (1982).

Production and formation experiments agree quite well, so they are listed together here.

 $\Lambda(1520)$  MASS

VALUE (MeV)	EVTS	DOCUMENT ID	TECN	COMMENT
<b>1519.5 ± 1.0 OUR ESTIMATE</b>				
<b>1519.53 ± 0.19 OUR AVERAGE</b>				
1520.4 ± 0.6 ± 1.5		<sup>1</sup> QIANG	10 SPEC	$e p \rightarrow e' K^+ X$ (fit to X)
1517.3 ± 1.5	300	BARBER	80D SPEC	$\gamma p \rightarrow \Lambda(1520) K^+$
1517.8 ± 1.2	5k	BARLAG	79 HBC	$K^- p$ 4.2 GeV/c
1520.0 ± 0.5		ALSTON... 78	DPWA	$\bar{K}N \rightarrow \bar{K}N$
1519.7 ± 0.3	4k	CAMERON	77 HBC	$K^- p$ 0.96-1.36 GeV/c
1519 ± 1		GOPAL	77 DPWA	$\bar{K}N$ multichannel
1519.4 ± 0.3	2000	CORDEN	75 DBC	$K^- d$ 1.4-1.8 GeV/c
<sup>1</sup> QIANG 10 gets 1518.8 MeV for the pole mass (no errors given).				

 $\Lambda(1520)$  WIDTH

VALUE (MeV)	EVTS	DOCUMENT ID	TECN	COMMENT
<b>15.6 ± 1.0 OUR ESTIMATE</b>				
<b>15.64 ± 0.29 OUR AVERAGE</b>				
Error includes scale factor of 1.1.				
18.6 ± 1.9 ± 1.0		<sup>2</sup> QIANG	10 SPEC	$e p \rightarrow e' K^+ X$ (fit to X)
16.3 ± 3.3	300	BARBER	80D SPEC	$\gamma p \rightarrow \Lambda(1520) K^+$
16 ± 1		GOPAL	80 DPWA	$\bar{K}N \rightarrow \bar{K}N$
14 ± 3	677	<sup>3</sup> BARLAG	79 HBC	$K^- p$ 4.2 GeV/c
15.4 ± 0.5		ALSTON... 78	DPWA	$\bar{K}N \rightarrow \bar{K}N$
16.3 ± 0.5	4k	CAMERON	77 HBC	$K^- p$ 0.96-1.36 GeV/c
15.0 ± 0.5		GOPAL	77 DPWA	$\bar{K}N$ multichannel
15.5 ± 1.6	2000	CORDEN	75 DBC	$K^- d$ 1.4-1.8 GeV/c
<sup>2</sup> QIANG 10 gets 17.2 MeV for the pole width (no errors given).				
<sup>3</sup> From the best-resolution sample of $\Lambda \pi \pi$ events only.				

$\Lambda(1520)$  DECAY MODES

Mode	Fraction ( $\Gamma_i/\Gamma$ )
$\Gamma_1$ $N\bar{K}$	45 ± 1%
$\Gamma_2$ $\Sigma\pi$	42 ± 1%
$\Gamma_3$ $\Lambda\pi\pi$	10 ± 1%
$\Gamma_4$ $\Sigma(1385)\pi$	
$\Gamma_5$ $\Sigma(1385)\pi(\rightarrow\Lambda\pi\pi)$	
$\Gamma_6$ $\Lambda(\pi\pi)_{S\text{-wave}}$	
$\Gamma_7$ $\Sigma\pi\pi$	0.9 ± 0.1%
$\Gamma_8$ $\Lambda\gamma$	0.85 ± 0.15%
$\Gamma_9$ $\Sigma^0\gamma$	

CONSTRAINED FIT INFORMATION

An overall fit to 9 branching ratios uses 26 measurements and one constraint to determine 6 parameters. The overall fit has a  $\chi^2 = 17.6$  for 21 degrees of freedom.

The following *off-diagonal* array elements are the correlation coefficients  $\langle\delta x_i\delta x_j\rangle/(\delta x_i\delta x_j)$ , in percent, from the fit to the branching fractions,  $x_i \equiv \Gamma_i/\Gamma_{\text{total}}$ . The fit constrains the  $x_i$  whose labels appear in this array to sum to one.

$x_2$	-64				
$x_3$	-32	-34			
$x_7$	-4	-3	-1		
$x_8$	-8	-7	-3	0	
$x_9$	-24	-21	-10	-1	-1
	$x_1$	$x_2$	$x_3$	$x_7$	$x_8$

$\Lambda(1520)$  BRANCHING RATIOS

See "Sign conventions for resonance couplings" in the Note on  $\Lambda$  and  $\Sigma$  Resonances.

$\Gamma(N\bar{K})/\Gamma_{\text{total}}$	DOCUMENT ID	TECN	COMMENT	$\Gamma_1/\Gamma$
<b>0.45 ± 0.01 OUR ESTIMATE</b>				
<b>0.447 ± 0.007 OUR FIT</b>			Error includes scale factor of 1.2.	
<b>0.455 ± 0.011 OUR AVERAGE</b>				

0.47 ± 0.02	GOPAL	80	DPWA	$\bar{K}N \rightarrow \bar{K}N$
0.45 ± 0.03	ALSTON...	78	DPWA	$\bar{K}N \rightarrow \bar{K}N$
0.448 ± 0.014	CORDEN	75	DBC	$K^-d$ 1.4-1.8 GeV/c
• • • We do not use the following data for averages, fits, limits, etc. • • •				
0.47 ± 0.01	GOPAL	77	DPWA	See GOPAL 80
0.42	MAST	76	HBC	$K^-p \rightarrow \bar{K}^0n$

$\Gamma(\Sigma\pi)/\Gamma_{\text{total}}$	DOCUMENT ID	TECN	COMMENT	$\Gamma_2/\Gamma$
<b>0.42 ± 0.01 OUR ESTIMATE</b>				
<b>0.420 ± 0.007 OUR FIT</b>			Error includes scale factor of 1.2.	
<b>0.423 ± 0.011 OUR AVERAGE</b>				

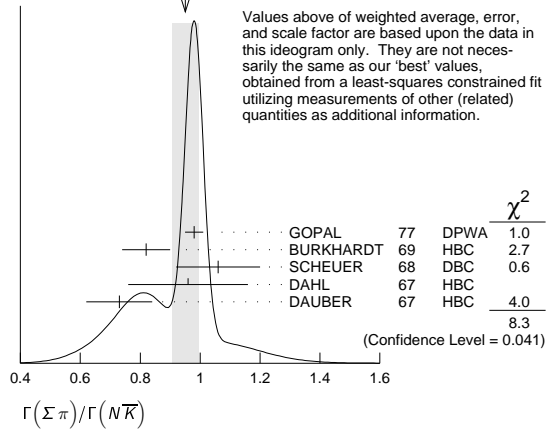
0.426 ± 0.014	CORDEN	75	DBC	$K^-d$ 1.4-1.8 GeV/c
0.418 ± 0.017	BARBARO...	69B	HBC	$K^-p$ 0.28-0.45 GeV/c
• • • We do not use the following data for averages, fits, limits, etc. • • •				
0.46	KIM	71	DPWA	K-matrix analysis

$\Gamma(\Sigma\pi)/\Gamma(N\bar{K})$	DOCUMENT ID	TECN	COMMENT	$\Gamma_2/\Gamma_1$
<b>0.940 ± 0.026 OUR FIT</b>			Error includes scale factor of 1.3.	
<b>0.95 ± 0.04 OUR AVERAGE</b>			Error includes scale factor of 1.7. See the ideogram below.	

0.98 ± 0.03	4	GOPAL	77	DPWA	$\bar{K}N$ multichannel
0.82 ± 0.08		BURKHARDT	69	HBC	$K^-p$ 0.8-1.2 GeV/c
1.06 ± 0.14		SCHEUER	68	DBC	$K^-N$ 3 GeV/c
0.96 ± 0.20		DAHL	67	HBC	$\pi^-p$ 1.6-4 GeV/c
0.73 ± 0.11		DAUBER	67	HBC	$K^-p$ 2 GeV/c
• • • We do not use the following data for averages, fits, limits, etc. • • •					
1.06 ± 0.12		BERTHON	74	HBC	Quasi-2-body $\sigma$
1.72 ± 0.78		MUSGRAVE	65	HBC	

<sup>4</sup> The  $\bar{K}N \rightarrow \Sigma\pi$  amplitude at resonance is +0.46 ± 0.01.

WEIGHTED AVERAGE  
 0.95 ± 0.04 (Error scaled by 1.7)



Values above of weighted average, error, and scale factor are based upon the data in this ideogram only. They are not necessarily the same as our 'best' values, obtained from a least-squares constrained fit utilizing measurements of other (related) quantities as additional information.

DOCUMENT ID	TECN	COMMENT	$\chi^2$
GOPAL 77	DPWA		1.0
BURKHARDT 69	HBC		2.7
SCHEUER 68	DBC		0.6
DAHL 67	HBC		4.0
DAUBER 67	HBC		4.0
			8.3
			(Confidence Level = 0.041)

$\Gamma(\Lambda\pi\pi)/\Gamma_{\text{total}}$	DOCUMENT ID	TECN	COMMENT	$\Gamma_3/\Gamma$	
<b>0.10 ± 0.01 OUR ESTIMATE</b>					
<b>0.095 ± 0.005 OUR FIT</b>			Error includes scale factor of 1.2.		
<b>0.096 ± 0.008 OUR AVERAGE</b>			Error includes scale factor of 1.6.		
0.091 ± 0.006	CORDEN	75	DBC	$K^-d$ 1.4-1.8 GeV/c	
0.11 ± 0.01	5	MAST	73B	IPWA	$K^-p \rightarrow \Lambda\pi\pi$
• • • Assumes $\Gamma(N\bar{K})/\Gamma_{\text{total}} = 0.46 \pm 0.02$ .					

$\Gamma(\Lambda\pi\pi)/\Gamma(N\bar{K})$	DOCUMENT ID	TECN	COMMENT	$\Gamma_3/\Gamma_1$
<b>0.213 ± 0.012 OUR FIT</b>			Error includes scale factor of 1.2.	
<b>0.202 ± 0.021 OUR AVERAGE</b>				
0.22 ± 0.03	BURKHARDT	69	HBC	$K^-p$ 0.8-1.2 GeV/c
0.19 ± 0.04	SCHEUER	68	DBC	$K^-N$ 3 GeV/c
0.17 ± 0.05	DAHL	67	HBC	$\pi^-p$ 1.6-4 GeV/c
0.21 ± 0.18	DAUBER	67	HBC	$K^-p$ 2 GeV/c
• • • We do not use the following data for averages, fits, limits, etc. • • •				
0.27 ± 0.13	BERTHON	74	HBC	Quasi-2-body $\sigma$
0.2	KIM	71	DPWA	K-matrix analysis

$\Gamma(\Sigma\pi)/\Gamma(\Lambda\pi\pi)$	DOCUMENT ID	TECN	COMMENT	$\Gamma_2/\Gamma_3$
<b>4.42 ± 0.25 OUR FIT</b>			Error includes scale factor of 1.2.	
<b>3.9 ± 0.6 OUR AVERAGE</b>				
3.9 ± 1.0	UHLIG	67	HBC	$K^-p$ 0.9-1.0 GeV/c
3.3 ± 1.1	BIRMINGHAM	66	HBC	$K^-p$ 3.5 GeV/c
4.5 ± 1.0	ARMENTEROS	65C	HBC	

$\Gamma(\Sigma(1385)\pi)/\Gamma_{\text{total}}$	DOCUMENT ID	TECN	COMMENT	$\Gamma_4/\Gamma$
<b>0.041 ± 0.005</b>				
	CHAN	72	HBC	$K^-p \rightarrow \Lambda\pi\pi$

$\Gamma(\Sigma(1385)\pi(\rightarrow\Lambda\pi\pi))/\Gamma(\Lambda\pi\pi)$	DOCUMENT ID	TECN	COMMENT	$\Gamma_5/\Gamma_3$	
<b>0.58 ± 0.22</b>					
<b>0.82 ± 0.10</b>					
0.58 ± 0.22	CORDEN	75	DBC	$K^-d$ 1.4-1.8 GeV/c	
0.82 ± 0.10	6	MAST	73B	IPWA	$K^-p \rightarrow \Lambda\pi\pi$
• • • We do not use the following data for averages, fits, limits, etc. • • •					
< 0.44	90	WIELAND	11	SPHR	$\gamma p \rightarrow K^+\Lambda(1520)$
0.39 ± 0.10	7	BURKHARDT	71	HBC	$K^-p \rightarrow (\Lambda\pi\pi)\pi$

<sup>6</sup> Both  $\Sigma(1385)\pi$   $DS_{03}$  and  $\Sigma(\pi\pi)$   $DP_{03}$  contribute.  
<sup>7</sup> The central bin (1514-1524 MeV) gives 0.74 ± 0.10; other bins are lower by 2-to-5 standard deviations.

$\Gamma(\Lambda(\pi\pi)_{S\text{-wave}})/\Gamma(\Lambda\pi\pi)$	DOCUMENT ID	TECN	COMMENT	$\Gamma_6/\Gamma_3$
<b>0.20 ± 0.08</b>				
	CORDEN	75	DBC	$K^-d$ 1.4-1.8 GeV/c

$\Gamma(\Sigma\pi\pi)/\Gamma_{\text{total}}$	DOCUMENT ID	TECN	COMMENT	$\Gamma_7/\Gamma$	
<b>0.009 ± 0.001 OUR ESTIMATE</b>					
<b>0.0086 ± 0.0005 OUR FIT</b>					
<b>0.0086 ± 0.0005 OUR AVERAGE</b>					
0.007 ± 0.002	8	CORDEN	75	DBC	$K^-d$ 1.4-1.8 GeV/c
0.0085 ± 0.0006	9	MAST	73	MPWA	$K^-p \rightarrow \Sigma\pi\pi$
0.010 ± 0.0015		BARBARO...	69B	HBC	$K^-p$ 0.28-0.45 GeV/c

<sup>8</sup> Much of the  $\Sigma\pi\pi$  decay proceeds via  $\Sigma(1385)\pi$ .

<sup>9</sup> Assumes  $\Gamma(N\bar{K})/\Gamma_{\text{total}} = 0.46$ .

## Baryon Particle Listings

 $\Lambda(1520)$ ,  $\Lambda(1600)$ ,  $\Lambda(1670)$ 

$\Gamma(\Lambda\gamma)/\Gamma_{\text{total}}$						$\Gamma_8/\Gamma$	
VALUE (units $10^{-3}$ )	EVTS	DOCUMENT ID	TECN	COMMENT			
<b>8.5±1.5 OUR ESTIMATE</b>							
<b>8.8±1.1 OUR FIT</b>							
<b>8.8±1.1 OUR AVERAGE</b>							
10.7±2.9 <sup>+1.5</sup> <sub>-0.4</sub>	32	TAYLOR	05	CLAS	$\gamma p \rightarrow K^+ \Lambda \gamma$		
10.2±2.1±1.5	290	ANTIPOV	04A	SPNX	$p N(C) \rightarrow \Lambda(1520) K^+ N(C)$		
8.0±1.4	238	MAST	68B	HBC	Using $\Gamma(N\bar{K})/\Gamma_{\text{total}} = 0.45$		

$\Gamma(\Sigma^0\gamma)/\Gamma_{\text{total}}$						$\Gamma_9/\Gamma$	
VALUE		DOCUMENT ID	TECN	COMMENT			
<b>0.0195±0.0034 OUR FIT</b>							
<b>0.02 ±0.0035</b>							
	10	MAST	68B	HBC	Not measured; see note		
10 Calculated from $\Gamma(\Lambda\gamma)/\Gamma_{\text{total}}$ , assuming SU(3). Needed to constrain the sum of all the branching ratios to be unity.							

 **$\Lambda(1520)$  REFERENCES**

WIELAND	11	EPJ A47 47	F. Wieland <i>et al.</i>	(ELSA SAPHIR Collab.)
QIANG	10	PL B694 123	Y. Qiang <i>et al.</i>	(DUKE, JEFF, PNPI, GWU+)
TAYLOR	05	PR C71 054609	S. Taylor <i>et al.</i>	(JLab CLAS Collab.)
Also		PR C72 039902 (errat.)	S. Taylor <i>et al.</i>	(JLab CLAS Collab.)
ANTIPOV	04A	PL B604 22	Yu.M. Antipov <i>et al.</i>	(IHEP SPHINX Collab.)
PDC	82	PL 111B 1	M. Roos <i>et al.</i>	(HELS, CIT, CERN)
BARBER	80D	ZPHY C7 17	D.P. Barber <i>et al.</i>	(DARE, LANC, SHEF)
GOPAL	80	Toronto Conf. 159	G.P. Gopal	(RHEL) IJP
BARLAG	79	NP B149 220	S.J.M. Barlag <i>et al.</i>	(AMST, CERN, NIJM+)
ALSTON-...	78	PR D18 182	M. Alston-Garnjost <i>et al.</i>	(LBL, MTHO+) IJP
Also		PRL 38 1007	M. Alston-Garnjost <i>et al.</i>	(LBL, MTHO+) IJP
CAMERON	77	NP B131 399	W. Cameron <i>et al.</i>	(RHEL, LOIC) IJP
GOPAL	77	NP B119 362	G.P. Gopal <i>et al.</i>	(LOIC, RHEL) IJP
MAST	76	PR D14 13	T.S. Mast <i>et al.</i>	(LBL)
CORDEN	75	NP B84 306	M.J. Corden <i>et al.</i>	(BIRM)
BERTHON	74	NC 21A 146	A. Berthon <i>et al.</i>	(CDEF, RHEL, SACL+)
MAST	73	PR D7 3212	T.S. Mast <i>et al.</i>	(LBL) IJP
MAST	73B	PR D7 5	T.S. Mast <i>et al.</i>	(LBL) IJP
CHAN	72	PRL 28 256	S.B. Chan <i>et al.</i>	(MASA, YALE)
BURKHARDT	71	NP B27 64	E. Burkhardt <i>et al.</i>	(HEID, CERN, SACL)
KIM	71	PRL 27 356	J.K. Kim	(HARV) IJP
Also		Duke Conf. 161	J.K. Kim	(HARV) IJP
Hyperon Resonances, 1970				
BARBARO-...	69B	Lund Conf. 352	A. Barbaro-Galieri <i>et al.</i>	(LRL)
Also		Duke Conf. 95	R.D. Tripp	(LRL)
Hyperon Resonances 1970				
BURKHARDT	69	NP B14 106	E. Burkhardt <i>et al.</i>	(HEID, EFL, CERN+)
MAST	68B	PRL 21 1715	T.S. Mast <i>et al.</i>	(LRL)
SCHUEUR	68	NP B8 503	J.C. Scheuer <i>et al.</i>	(SABRE Collab.)
DAHL	67	PR 163 1377	O.I. Dahl <i>et al.</i>	(LRL)
DAUBER	67	PL 24B 525	M. Haque <i>et al.</i>	(UCLA)
UHLIG	67	PR 155 1448	R.P. Uhlig <i>et al.</i>	(UMD, NRL)
BIRMINGHAM	66	PR 152 1148	M. Haque <i>et al.</i>	(BIRM, GLAS, LOIC, OXF+)
ARMENTEROS	65C	PL 19 338	R. Armenteros <i>et al.</i>	(CERN, HEID, SACL)
MUSGRAVE	65	NC 35 735	B. Musgrave <i>et al.</i>	(BIRM, CERN, EPOL+)
WATSON	63	PR 131 2248	M.B. Watson, M. Ferro-Luzzi, R.D. Tripp	(LRL) IJP
FERRO-LUZZI	62	PRL 8 28	M. Ferro-Luzzi, R.D. Tripp, M.B. Watson	(LRL) IJP

 **$\Lambda(1600)$   $1/2^+$** 

$$I(J^P) = 0(\frac{1}{2}^+) \text{ Status: } ***$$

See also the  $\Lambda(1810)$   $P_{01}$ . There are quite possibly two  $P_{01}$  states in this region.

 **$\Lambda(1600)$  MASS**

VALUE (MeV)	DOCUMENT ID	TECN	COMMENT
<b>1560 to 1700 (<math>\approx 1600</math>) OUR ESTIMATE</b>			
1568±20	GOPAL	80	DPWA $\bar{K}N \rightarrow \bar{K}N$
1703±100	ALSTON-...	78	DPWA $\bar{K}N \rightarrow \bar{K}N$
1573±25	GOPAL	77	DPWA $\bar{K}N$ multichannel
1596±6	KANE	74	DPWA $K^- p \rightarrow \Sigma\pi$
1620±10	LANGBEIN	72	IPWA $\bar{K}N$ multichannel
••• We do not use the following data for averages, fits, limits, etc. •••			
1572 or 1617	1 MARTIN	77	DPWA $\bar{K}N$ multichannel
1646±7	2 CARROLL	76	DPWA $ls_{\text{spin}}=0$ total $\sigma$
1570	KIM	71	DPWA K-matrix analysis

 **$\Lambda(1600)$  WIDTH**

VALUE (MeV)	DOCUMENT ID	TECN	COMMENT
<b>50 to 250 (<math>\approx 150</math>) OUR ESTIMATE</b>			
116±20	GOPAL	80	DPWA $\bar{K}N \rightarrow \bar{K}N$
593±200	ALSTON-...	78	DPWA $\bar{K}N \rightarrow \bar{K}N$
147±50	GOPAL	77	DPWA $\bar{K}N$ multichannel
175±20	KANE	74	DPWA $K^- p \rightarrow \Sigma\pi$
60±10	LANGBEIN	72	IPWA $\bar{K}N$ multichannel
••• We do not use the following data for averages, fits, limits, etc. •••			
247 or 271	1 MARTIN	77	DPWA $\bar{K}N$ multichannel
20	2 CARROLL	76	DPWA $ls_{\text{spin}}=0$ total $\sigma$
50	KIM	71	DPWA K-matrix analysis

 **$\Lambda(1600)$  DECAY MODES**

Mode	Fraction ( $\Gamma_i/\Gamma$ )
$\Gamma_1$ $N\bar{K}$	15–30 %
$\Gamma_2$ $\Sigma\pi$	10–60 %

The above branching fractions are our estimates, not fits or averages.

 **$\Lambda(1600)$  BRANCHING RATIOS**

See "Sign conventions for resonance couplings" in the Note on  $\Lambda$  and  $\Sigma$  Resonances.

$\Gamma(N\bar{K})/\Gamma_{\text{total}}$	DOCUMENT ID	TECN	COMMENT	$\Gamma_1/\Gamma$
<b>0.15 to 0.30 OUR ESTIMATE</b>				
0.23±0.04	GOPAL	80	DPWA $\bar{K}N \rightarrow \bar{K}N$	
0.14±0.05	ALSTON-...	78	DPWA $\bar{K}N \rightarrow \bar{K}N$	
0.25±0.15	LANGBEIN	72	IPWA $\bar{K}N$ multichannel	
••• We do not use the following data for averages, fits, limits, etc. •••				
0.24±0.04	GOPAL	77	DPWA See GOPAL 80	
0.30 or 0.29	1 MARTIN	77	DPWA $\bar{K}N$ multichannel	

$(\Gamma_1\Gamma_2)^{1/2}/\Gamma_{\text{total}}$ in $N\bar{K} \rightarrow \Lambda(1600) \rightarrow \Sigma\pi$	DOCUMENT ID	TECN	COMMENT	$(\Gamma_1\Gamma_2)^{1/2}/\Gamma$
<b>0.15 to 0.30 OUR ESTIMATE</b>				
−0.16±0.04	GOPAL	77	DPWA $\bar{K}N$ multichannel	
−0.33±0.11	KANE	74	DPWA $K^- p \rightarrow \Sigma\pi$	
0.28±0.09	LANGBEIN	72	IPWA $\bar{K}N$ multichannel	
••• We do not use the following data for averages, fits, limits, etc. •••				
−0.39 or −0.39	1 MARTIN	77	DPWA $\bar{K}N$ multichannel	
not seen	HEPP	76B	DPWA $K^- N \rightarrow \Sigma\pi$	

 **$\Lambda(1600)$  FOOTNOTES**

<sup>1</sup> The two MARTIN 77 values are from a T-matrix pole and from a Breit-Wigner fit.

<sup>2</sup> A total cross-section bump with  $(J+1/2)\Gamma_{\text{el}}/\Gamma_{\text{total}} = 0.04$ .

 **$\Lambda(1600)$  REFERENCES**

GOPAL	80	Toronto Conf. 159	G.P. Gopal	(RHEL) IJP
ALSTON-...	78	PR D18 182	M. Alston-Garnjost <i>et al.</i>	(LBL, MTHO+) IJP
Also		PRL 38 1007	M. Alston-Garnjost <i>et al.</i>	(LBL, MTHO+) IJP
GOPAL	77	NP B119 362	G.P. Gopal <i>et al.</i>	(LOIC, RHEL) IJP
MARTIN	77	NP B127 349	B.R. Martin, M.K. Pidcock, R.G. Moorhouse	(LOUC+) IJP
Also		NP B126 266	B.R. Martin, M.K. Pidcock	(LOUC) IJP
Also		NP B126 285	B.R. Martin, M.K. Pidcock	(LOUC) IJP
CARROLL	76	PRL 37 806	A.S. Carroll <i>et al.</i>	(BNL) I
HEPP	76B	PL 65B 487	V. Hepp <i>et al.</i>	(CERN, HEIDH, MPIM) IJP
KANE	74	LBL-2452	D.F. Kane	(LBL) IJP
LANGBEIN	72	NP B47 477	W. Langbein, F. Wagner	(MPIM) IJP
KIM	71	PRL 27 356	J.K. Kim	(HARV) IJP

 **$\Lambda(1670)$   $1/2^-$** 

$$I(J^P) = 0(\frac{1}{2}^-) \text{ Status: } ***$$

The measurements of the mass, width, and elasticity published before 1974 are now obsolete and have been omitted. They were last listed in our 1982 edition Physics Letters **111B** 1 (1982).

 **$\Lambda(1670)$  MASS**

VALUE (MeV)	DOCUMENT ID	TECN	COMMENT
<b>1660 to 1680 (<math>\approx 1670</math>) OUR ESTIMATE</b>			
1677.5±0.8	1 GARCIA-REC-...	03	DPWA $\bar{K}N$ multichannel
1673 ±2	MANLEY	02	DPWA $\bar{K}N$ multichannel
1670.8±1.7	KOISO	85	DPWA $K^- p \rightarrow \Sigma\pi$
1667 ±5	GOPAL	80	DPWA $\bar{K}N \rightarrow \bar{K}N$
1671 ±3	ALSTON-...	78	DPWA $\bar{K}N \rightarrow \bar{K}N$
1670 ±5	GOPAL	77	DPWA $\bar{K}N$ multichannel
1675 ±2	HEPP	76B	DPWA $K^- N \rightarrow \Sigma\pi$
1679 ±1	KANE	74	DPWA $K^- p \rightarrow \Sigma\pi$
1665 ±5	PREVOST	74	DPWA $K^- N \rightarrow \Sigma(1385)\pi$
••• We do not use the following data for averages, fits, limits, etc. •••			
1668.9±2.0	ABAEV	96	DPWA $K^- p \rightarrow \Lambda\eta$
1664	2 MARTIN	77	DPWA $\bar{K}N$ multichannel

 **$\Lambda(1670)$  WIDTH**

VALUE (MeV)	DOCUMENT ID	TECN	COMMENT
<b>25 to 50 (<math>\approx 35</math>) OUR ESTIMATE</b>			
29.2±1.4	1 GARCIA-REC-...	03	DPWA $\bar{K}N$ multichannel
23 ±6	MANLEY	02	DPWA $\bar{K}N$ multichannel
34.1±3.7	KOISO	85	DPWA $K^- p \rightarrow \Sigma\pi$
29 ±5	GOPAL	80	DPWA $\bar{K}N \rightarrow \bar{K}N$
29 ±5	ALSTON-...	78	DPWA $\bar{K}N \rightarrow \bar{K}N$

See key on page 457

# Baryon Particle Listings

## $\Lambda(1670), \Lambda(1690)$

45 ± 10	GOPAL	77	DPWA	$\bar{K}N$ multichannel
46 ± 5	HEPP	76B	DPWA	$K^-N \rightarrow \Sigma\pi$
40 ± 3	KANE	74	DPWA	$K^-p \rightarrow \Sigma\pi$
19 ± 5	PREVOST	74	DPWA	$K^-N \rightarrow \Sigma(1385)\pi$
••• We do not use the following data for averages, fits, limits, etc. •••				
21.1 ± 3.6	ABAEV	96	DPWA	$K^-p \rightarrow \Lambda\eta$
12	<sup>2</sup> MARTIN	77	DPWA	$\bar{K}N$ multichannel

### $\Lambda(1670)$ DECAY MODES

Mode	Fraction ( $\Gamma_i/\Gamma$ )
$\Gamma_1$ $N\bar{K}$	20–30 %
$\Gamma_2$ $\Sigma\pi$	25–55 %
$\Gamma_3$ $\Lambda\eta$	10–25 %
$\Gamma_4$ $\Sigma(1385)\pi$	

The above branching fractions are our estimates, not fits or averages.

### $\Lambda(1670)$ BRANCHING RATIOS

See “Sign conventions for resonance couplings” in the Note on  $\Lambda$  and  $\Sigma$  Resonances.

$\Gamma(N\bar{K})/\Gamma_{\text{total}}$	DOCUMENT ID	TECN	COMMENT	$\Gamma_1/\Gamma$
<b>0.20 to 0.30 OUR ESTIMATE</b>				
0.37 ± 0.07	MANLEY	02	DPWA $\bar{K}N$ multichannel	
0.18 ± 0.03	GOPAL	80	DPWA $\bar{K}N \rightarrow \bar{K}N$	
0.17 ± 0.03	ALSTON-...	78	DPWA $\bar{K}N \rightarrow \bar{K}N$	
••• We do not use the following data for averages, fits, limits, etc. •••				
0.20 ± 0.03	GOPAL	77	DPWA See GOPAL 80	
0.15	<sup>2</sup> MARTIN	77	DPWA $\bar{K}N$ multichannel	

$\Gamma(\Lambda\eta)/\Gamma_{\text{total}}$	DOCUMENT ID	TECN	COMMENT	$\Gamma_3/\Gamma$
<b>0.30 ± 0.08</b>				
	ABAEV	96	DPWA $K^-p \rightarrow \Lambda\eta$	

$(\Gamma_1\Gamma_2)^{1/2}/\Gamma_{\text{total}}$ in $N\bar{K} \rightarrow \Lambda(1670) \rightarrow \Sigma\pi$	DOCUMENT ID	TECN	COMMENT	$(\Gamma_1\Gamma_2)^{1/2}/\Gamma$
-0.38 ± 0.03	MANLEY	02	DPWA $\bar{K}N$ multichannel	
-0.26 ± 0.02	KOISO	85	DPWA $K^-p \rightarrow \Sigma\pi$	
-0.31 ± 0.03	GOPAL	77	DPWA $\bar{K}N$ multichannel	
-0.29 ± 0.03	HEPP	76B	DPWA $K^-N \rightarrow \Sigma\pi$	
-0.23 ± 0.03	LONDON	75	HLBC $K^-p \rightarrow \Sigma^0\pi^0$	
-0.27 ± 0.02	KANE	74	DPWA $K^-p \rightarrow \Sigma\pi$	
••• We do not use the following data for averages, fits, limits, etc. •••				
-0.13	<sup>2</sup> MARTIN	77	DPWA $\bar{K}N$ multichannel	

$(\Gamma_1\Gamma_2)^{1/2}/\Gamma_{\text{total}}$ in $N\bar{K} \rightarrow \Lambda(1670) \rightarrow \Lambda\eta$	DOCUMENT ID	TECN	COMMENT	$(\Gamma_1\Gamma_3)^{1/2}/\Gamma$
+0.24 ± 0.04	MANLEY	02	DPWA $\bar{K}N$ multichannel	
+0.20 ± 0.05	BAXTER	73	DPWA $K^-p \rightarrow$ neutrals	
••• We do not use the following data for averages, fits, limits, etc. •••				
0.24	KIM	71	DPWA K-matrix analysis	
0.26	ARMENTEROS69c	HBC		
0.20 or 0.23	BERLEY	65	HBC	

$(\Gamma_1\Gamma_2)^{1/2}/\Gamma_{\text{total}}$ in $N\bar{K} \rightarrow \Lambda(1670) \rightarrow \Sigma(1385)\pi$	DOCUMENT ID	TECN	COMMENT	$(\Gamma_1\Gamma_4)^{1/2}/\Gamma$
-0.17 ± 0.06	MANLEY	02	DPWA $\bar{K}N$ multichannel	
-0.18 ± 0.05	PREVOST	74	DPWA $K^-N \rightarrow \Sigma(1385)\pi$	

### $\Lambda(1670)$ FOOTNOTES

- GARCIA-RECIO 03 gives pole, not Breit-Wigner, parameters, but the narrow width of the  $\Lambda(1670)$  means there will be little difference.
- MARTIN 77 obtains identical resonance parameters from a T-matrix pole and from a Breit-Wigner fit.

### $\Lambda(1670)$ REFERENCES

GARCIA-RECIO... 03	PR D67 076009	C. Garcia-Recio et al.	(GRAN, VALE)
MANLEY 02	PRL 88 012002	D.M. Manley et al.	(BNL Crystal Ball Collab.)
ABAEV 96	PR C53 385	V.V. Abaev, B.M.K. Nefkens	(UCLA)
KOISO 85	NP A433 619	H. Koiso et al.	(TOKYU, MASA)
PDG 82	PL 111B 1	M. Roos et al.	(HEL5, CIT, CERN)
GOPAL 80	Toronto Conf. 159	G.P. Gopal	(RHEL) IJP
ALSTON-... 78	PR D18 182	M. Alston-Garnjost et al.	(LBL, MTHO+) IJP
Also	PRL 38 1007	M. Alston-Garnjost et al.	(LBL, MTHO+) IJP
GOPAL 77	NP B119 362	G.P. Gopal et al.	(LOIC, RHEL) IJP
MARTIN 77	NP B127 349	B.R. Martin, M.K. Pidcock, R.G. Moorhouse	(LOUC+) IJP
Also	NP B126 266	B.R. Martin, M.K. Pidcock	(LOUC)
Also	NP B126 285	B.R. Martin, M.K. Pidcock	(LOUC) IJP

HEPP 76B	PL 65B 487	V. Hepp et al.	(CERN, HEIDH, MPIM) IJP
LONDON 75	NP B85 289	G.W. London et al.	(BNL, CERN, EPOL+) IJP
KANE 74	LBL-2452	D.F. Kane	(LBL) IJP
PREVOST 74	NP B69 246	J. Prevost et al.	(SACL, CERN, HEID) IJP
BAXTER 73	NP B67 125	D.F. Baxter et al.	(OXF) IJP
KIM 71	PRL 27 356	J.K. Kim	(HARV) IJP
Also	Duke Conf. 161	J.K. Kim	(HARV) IJP
ARMENTEROS 69c	Hyperon Resonances, 1970	R. Armenteros et al.	(CERN, HEID, SACL) IJP
Values are quoted in LEVI-SETTI 69.	Lund Paper 229		
BERLEY 65	PRL 15 641	D. Berley et al.	(BNL) IJP

## $\Lambda(1690) 3/2^-$

$I(J^P) = 0(\frac{3}{2}^-)$  Status: \*\*\*

The measurements of the mass, width, and elasticity published before 1974 are now obsolete and have been omitted. They were last listed in our 1982 edition Physics Letters **111B 1** (1982).

### $\Lambda(1690)$ MASS

VALUE (MeV)	DOCUMENT ID	TECN	COMMENT
<b>1685 to 1695 (<math>\approx 1690</math>) OUR ESTIMATE</b>			
1695.7 ± 2.6	KOISO	85	DPWA $K^-p \rightarrow \Sigma\pi$
1690 ± 5	GOPAL	80	DPWA $\bar{K}N \rightarrow \bar{K}N$
1692 ± 5	ALSTON-...	78	DPWA $\bar{K}N \rightarrow \bar{K}N$
1690 ± 5	GOPAL	77	DPWA $\bar{K}N$ multichannel
1690 ± 3	HEPP	76B	DPWA $K^-N \rightarrow \Sigma\pi$
1689 ± 1	KANE	74	DPWA $K^-p \rightarrow \Sigma\pi$
••• We do not use the following data for averages, fits, limits, etc. •••			
1687 or 1689	<sup>1</sup> MARTIN	77	DPWA $\bar{K}N$ multichannel
1692 ± 4	CARROLL	76	DPWA Isospin-0 total $\sigma$

### $\Lambda(1690)$ WIDTH

VALUE (MeV)	DOCUMENT ID	TECN	COMMENT
<b>50 to 70 (<math>\approx 60</math>) OUR ESTIMATE</b>			
67.2 ± 5.6	KOISO	85	DPWA $K^-p \rightarrow \Sigma\pi$
61 ± 5	GOPAL	80	DPWA $\bar{K}N \rightarrow \bar{K}N$
64 ± 10	ALSTON-...	78	DPWA $\bar{K}N \rightarrow \bar{K}N$
60 ± 5	GOPAL	77	DPWA $\bar{K}N$ multichannel
82 ± 8	HEPP	76B	DPWA $K^-N \rightarrow \Sigma\pi$
60 ± 4	KANE	74	DPWA $K^-p \rightarrow \Sigma\pi$
••• We do not use the following data for averages, fits, limits, etc. •••			
62 or 62	<sup>1</sup> MARTIN	77	DPWA $\bar{K}N$ multichannel
38	CARROLL	76	DPWA Isospin-0 total $\sigma$

### $\Lambda(1690)$ DECAY MODES

Mode	Fraction ( $\Gamma_i/\Gamma$ )
$\Gamma_1$ $N\bar{K}$	20–30 %
$\Gamma_2$ $\Sigma\pi$	20–40 %
$\Gamma_3$ $\Lambda\pi\pi$	~ 25 %
$\Gamma_4$ $\Sigma\pi\pi$	~ 20 %
$\Gamma_5$ $\Lambda\eta$	
$\Gamma_6$ $\Sigma(1385)\pi, S$ -wave	

The above branching fractions are our estimates, not fits or averages.

### $\Lambda(1690)$ BRANCHING RATIOS

The sum of all the quoted branching ratios is more than 1.0. The two-body ratios are from partial-wave analyses, and thus probably are more reliable than the three-body ratios, which are determined from bumps in cross sections. Of the latter, the  $\Sigma\pi\pi$  bump looks more significant. (The error given for the  $\Lambda\pi\pi$  ratio looks unreasonably small.) Hardly any of the  $\Sigma\pi\pi$  decay can be via  $\Sigma(1385)$ , for then seven times as much  $\Lambda\pi\pi$  decay would be required. See “Sign conventions for resonance couplings” in the Note on  $\Lambda$  and  $\Sigma$  Resonances.

$\Gamma(N\bar{K})/\Gamma_{\text{total}}$	DOCUMENT ID	TECN	COMMENT	$\Gamma_1/\Gamma$
<b>0.2 to 0.3 OUR ESTIMATE</b>				
0.23 ± 0.03	GOPAL	80	DPWA $\bar{K}N \rightarrow \bar{K}N$	
0.22 ± 0.03	ALSTON-...	78	DPWA $\bar{K}N \rightarrow \bar{K}N$	
••• We do not use the following data for averages, fits, limits, etc. •••				
0.24 ± 0.03	GOPAL	77	DPWA See GOPAL 80	
0.28 or 0.26	<sup>1</sup> MARTIN	77	DPWA $\bar{K}N$ multichannel	

$(\Gamma_1\Gamma_2)^{1/2}/\Gamma_{\text{total}}$ in $N\bar{K} \rightarrow \Lambda(1690) \rightarrow \Sigma\pi$	DOCUMENT ID	TECN	COMMENT	$(\Gamma_1\Gamma_2)^{1/2}/\Gamma$
-0.34 ± 0.02	KOISO	85	DPWA $K^-p \rightarrow \Sigma\pi$	
-0.25 ± 0.03	GOPAL	77	DPWA $\bar{K}N$ multichannel	
-0.29 ± 0.03	HEPP	76B	DPWA $K^-N \rightarrow \Sigma\pi$	
-0.28 ± 0.03	LONDON	75	HLBC $K^-p \rightarrow \Sigma^0\pi^0$	
-0.28 ± 0.02	KANE	74	DPWA $K^-p \rightarrow \Sigma\pi$	
••• We do not use the following data for averages, fits, limits, etc. •••				
-0.30 or -0.28	<sup>1</sup> MARTIN	77	DPWA $\bar{K}N$ multichannel	

## Baryon Particle Listings

 $\Lambda(1690), \Lambda(1800)$ 

$(\Gamma_i \Gamma_f)^{1/2} / \Gamma_{\text{total}}$ in $N\bar{K} \rightarrow \Lambda(1690) \rightarrow \Lambda \eta$	$(\Gamma_1 \Gamma_5)^{1/2} / \Gamma$		
VALUE	DOCUMENT ID	TECN	COMMENT
0.00 ± 0.03	BAXTER 73	DPWA	$K^- p \rightarrow$ neutrals

$(\Gamma_i \Gamma_f)^{1/2} / \Gamma_{\text{total}}$ in $N\bar{K} \rightarrow \Lambda(1690) \rightarrow \Lambda \pi \pi$	$(\Gamma_1 \Gamma_3)^{1/2} / \Gamma$		
VALUE	DOCUMENT ID	TECN	COMMENT
0.25 ± 0.02	<sup>2</sup> BARTLEY 68	HDBC	$K^- p \rightarrow \Lambda \pi \pi$

$(\Gamma_i \Gamma_f)^{1/2} / \Gamma_{\text{total}}$ in $N\bar{K} \rightarrow \Lambda(1690) \rightarrow \Sigma \pi \pi$	$(\Gamma_1 \Gamma_4)^{1/2} / \Gamma$		
VALUE	DOCUMENT ID	TECN	COMMENT
0.21	ARMENTEROS68C	HDBC	$K^- N \rightarrow \Sigma \pi \pi$

$(\Gamma_i \Gamma_f)^{1/2} / \Gamma_{\text{total}}$ in $N\bar{K} \rightarrow \Lambda(1690) \rightarrow \Sigma(1385) \pi, S\text{-wave}$	$(\Gamma_1 \Gamma_6)^{1/2} / \Gamma$		
VALUE	DOCUMENT ID	TECN	COMMENT
+0.27 ± 0.04	PREVOST 74	DPWA	$K^- N \rightarrow \Sigma(1385) \pi$

 $\Lambda(1690)$  FOOTNOTES

- <sup>1</sup> The two MARTIN 77 values are from a T-matrix pole and from a Breit-Wigner fit. Another  $D_{03} \Lambda$  at 1966 MeV is also suggested by MARTIN 77, but is very uncertain.  
<sup>2</sup> BARTLEY 68 uses only cross-section data. The enhancement is not seen by PREVOST 71.

 $\Lambda(1690)$  REFERENCES

KOISO 85	NP A433 619	H. Koiso <i>et al.</i>	(TOKY, MASA)
PDC 82	PL 111B 1	M. Roos <i>et al.</i>	(HELS, CIT, CERN)
GOPAL 80	Toronto Conf. 159	G.P. Gopal	(RHEL) IJP
ALSTON... 78	PR D18 182	M. Alston-Garnjost <i>et al.</i>	(LBL, MTHO+) IJP
Also	PRL 38 1007	M. Alston-Garnjost <i>et al.</i>	(LBL, MTHO+) IJP
GOPAL 77	NP B119 362	G.P. Gopal <i>et al.</i>	(LOIC, RHEL) IJP
MARTIN 77	NP B127 349	B.R. Martin, M.K. Pidcock, R.G. Moorhouse	(LOUC+) IJP
Also	NP B126 266	B.R. Martin, M.K. Pidcock	(LOUC) IJP
Also	NP B126 285	B.R. Martin, M.K. Pidcock	(LOUC) IJP
CARROLL 76	PRL 37 806	A.S. Carroll <i>et al.</i>	(BNL) I
HEPP 76B	PL 65B 487	V. Hepp <i>et al.</i>	(CERN, HEIDH, MPIM) IJP
LONDON 75	NP B85 289	G.W. London <i>et al.</i>	(BNL, CERN, EPOL+) IJP
KANE 74	LBL-2452	D.F. Kane	(LBL) IJP
PREVOST 74	NP B69 246	J. Prevost <i>et al.</i>	(SACL, CERN, HEID) IJP
BAXTER 73	NP B67 125	D.F. Baxter <i>et al.</i>	(OXF) IJP
PREVOST 71	Amsterdam Conf.	J. Prevost	(CERN, HEID, SACL) IJP
ARMENTEROS 68C	NP B8 216	R. Armenteros <i>et al.</i>	(CERN, HEID, SACL) I
BARTLEY 68	PRL 21 1111	J.H. Bartley <i>et al.</i>	(TUFTS, FSU, BRAN) I

$$\Lambda(1800) 1/2^- \quad I(J^P) = 0(\frac{1}{2}^-) \text{ Status: } ***$$

This is the second resonance in the  $S_{01}$  wave, the first being the  $\Lambda(1670)$ .

 $\Lambda(1800)$  MASS

VALUE (MeV)	DOCUMENT ID	TECN	COMMENT
<b>1720 to 1850 (<math>\approx 1800</math>) OUR ESTIMATE</b>			
1845 ± 10	MANLEY 02	DPWA	$\bar{K} N$ multichannel
1841 ± 10	GOPAL 80	DPWA	$\bar{K} N \rightarrow \bar{K} N$
1725 ± 20	ALSTON... 78	DPWA	$\bar{K} N \rightarrow \bar{K} N$
1825 ± 20	GOPAL 77	DPWA	$\bar{K} N$ multichannel
1830 ± 20	LANGBEIN 72	IPWA	$\bar{K} N$ multichannel
• • • We do not use the following data for averages, fits, limits, etc. • • •			
1767 or 1842	<sup>1</sup> MARTIN 77	DPWA	$\bar{K} N$ multichannel
1780	KIM 71	DPWA	K-matrix analysis
1872 ± 10	BRICMAN 70B	DPWA	$\bar{K} N \rightarrow \bar{K} N$

 $\Lambda(1800)$  WIDTH

VALUE (MeV)	DOCUMENT ID	TECN	COMMENT
<b>200 to 400 (<math>\approx 300</math>) OUR ESTIMATE</b>			
518 ± 84	MANLEY 02	DPWA	$\bar{K} N$ multichannel
228 ± 20	GOPAL 80	DPWA	$\bar{K} N \rightarrow \bar{K} N$
185 ± 20	ALSTON... 78	DPWA	$\bar{K} N \rightarrow \bar{K} N$
230 ± 20	GOPAL 77	DPWA	$\bar{K} N$ multichannel
70 ± 15	LANGBEIN 72	IPWA	$\bar{K} N$ multichannel
• • • We do not use the following data for averages, fits, limits, etc. • • •			
435 or 473	<sup>1</sup> MARTIN 77	DPWA	$\bar{K} N$ multichannel
40	KIM 71	DPWA	K-matrix analysis
100 ± 20	BRICMAN 70B	DPWA	$\bar{K} N \rightarrow \bar{K} N$

 $\Lambda(1800)$  DECAY MODES

Mode	Fraction ( $\Gamma_i / \Gamma$ )
$\Gamma_1 \quad N\bar{K}$	25–40 %
$\Gamma_2 \quad \Sigma \pi$	seen
$\Gamma_3 \quad \Sigma(1385) \pi$	seen
$\Gamma_4 \quad N\bar{K}^*(892)$	seen
$\Gamma_5 \quad N\bar{K}^*(892), S=1/2, S\text{-wave}$	
$\Gamma_6 \quad N\bar{K}^*(892), S=3/2, D\text{-wave}$	

The above branching fractions are our estimates, not fits or averages.

 $\Lambda(1800)$  BRANCHING RATIOS

See "Sign conventions for resonance couplings" in the Note on  $\Lambda$  and  $\Sigma$  Resonances.

$\Gamma(N\bar{K}) / \Gamma_{\text{total}}$	DOCUMENT ID	TECN	COMMENT	$\Gamma_1 / \Gamma$
<b>0.25 to 0.40 OUR ESTIMATE</b>				
0.24 ± 0.10	MANLEY 02	DPWA	$\bar{K} N$ multichannel	
0.36 ± 0.04	GOPAL 80	DPWA	$\bar{K} N \rightarrow \bar{K} N$	
0.28 ± 0.05	ALSTON... 78	DPWA	$\bar{K} N \rightarrow \bar{K} N$	
0.35 ± 0.15	LANGBEIN 72	IPWA	$\bar{K} N$ multichannel	
• • • We do not use the following data for averages, fits, limits, etc. • • •				
0.37 ± 0.05	GOPAL 77	DPWA	See GOPAL 80	
1.21 or 0.70	<sup>1</sup> MARTIN 77	DPWA	$\bar{K} N$ multichannel	
0.80	KIM 71	DPWA	K-matrix analysis	
0.18 ± 0.02	BRICMAN 70B	DPWA	$\bar{K} N \rightarrow \bar{K} N$	

$(\Gamma_i \Gamma_f)^{1/2} / \Gamma_{\text{total}}$ in $N\bar{K} \rightarrow \Lambda(1800) \rightarrow \Sigma \pi$	$(\Gamma_1 \Gamma_2)^{1/2} / \Gamma$		
VALUE	DOCUMENT ID	TECN	COMMENT
−0.08 ± 0.05	GOPAL 77	DPWA	$\bar{K} N$ multichannel
• • • We do not use the following data for averages, fits, limits, etc. • • •			
−0.74 or −0.43	<sup>1</sup> MARTIN 77	DPWA	$\bar{K} N$ multichannel
0.24	KIM 71	DPWA	K-matrix analysis

$(\Gamma_i \Gamma_f)^{1/2} / \Gamma_{\text{total}}$ in $N\bar{K} \rightarrow \Lambda(1800) \rightarrow \Sigma(1385) \pi$	$(\Gamma_1 \Gamma_3)^{1/2} / \Gamma$		
VALUE	DOCUMENT ID	TECN	COMMENT
+0.056 ± 0.028	<sup>2</sup> CAMERON 78	DPWA	$K^- p \rightarrow \Sigma(1385) \pi$

$(\Gamma_i \Gamma_f)^{1/2} / \Gamma_{\text{total}}$ in $N\bar{K} \rightarrow \Lambda(1800) \rightarrow N\bar{K}^*(892), S=1/2, S\text{-wave}$	$(\Gamma_1 \Gamma_5)^{1/2} / \Gamma$		
VALUE	DOCUMENT ID	TECN	COMMENT
−0.17 ± 0.03	<sup>2</sup> CAMERON 78B	DPWA	$K^- p \rightarrow N\bar{K}^*$

$(\Gamma_i \Gamma_f)^{1/2} / \Gamma_{\text{total}}$ in $N\bar{K} \rightarrow \Lambda(1800) \rightarrow N\bar{K}^*(892), S=3/2, D\text{-wave}$	$(\Gamma_1 \Gamma_6)^{1/2} / \Gamma$		
VALUE	DOCUMENT ID	TECN	COMMENT
−0.13 ± 0.04	CAMERON 78B	DPWA	$K^- p \rightarrow N\bar{K}^*$

 $\Lambda(1800)$  FOOTNOTES

- <sup>1</sup> The two MARTIN 77 values are from a T-matrix pole and from a Breit-Wigner fit.  
<sup>2</sup> The published sign has been changed to be in accord with the baryon-first convention.

 $\Lambda(1800)$  REFERENCES

MANLEY 02	PRL 88 012002	D.M. Manley <i>et al.</i>	(BNL Crystal Ball Collab.)
GOPAL 80	Toronto Conf. 159	G.P. Gopal	(RHEL) IJP
ALSTON... 78	PR D18 182	M. Alston-Garnjost <i>et al.</i>	(LBL, MTHO+) IJP
Also	PRL 38 1007	M. Alston-Garnjost <i>et al.</i>	(LBL, MTHO+) IJP
CAMERON 78	NP B343 189	W. Cameron <i>et al.</i>	(RHEL, LOIC) IJP
CAMERON 78B	NP B146 327	W. Cameron <i>et al.</i>	(RHEL, LOIC) IJP
GOPAL 77	NP B119 362	G.P. Gopal <i>et al.</i>	(LOIC, RHEL) IJP
MARTIN 77	NP B127 349	B.R. Martin, M.K. Pidcock, R.G. Moorhouse	(LOUC+) IJP
Also	NP B126 266	B.R. Martin, M.K. Pidcock	(LOUC) IJP
Also	NP B126 285	B.R. Martin, M.K. Pidcock	(LOUC) IJP
LANGBEIN 72	NP B47 477	W. Langbein, F. Wagner	(MPIM) IJP
KIM 71	PRL 27 356	J.K. Kim	(HARV) IJP
Also	Duke Conf. 161	J.K. Kim	(HARV) IJP
BRICMAN 70B	PL 33B 511	C. Bricman, M. Ferro-Luzzi, J.P. Lagnaux	(CERN) IJP

See key on page 457

# Baryon Particle Listings

## $\Lambda(1810), \Lambda(1820)$

### $\Lambda(1810) 1/2^+$

$$I(J^P) = 0(\frac{1}{2}^+) \text{ Status: } ***$$

Almost all the recent analyses contain a  $P_{01}$  state, and sometimes two of them, but the masses, widths, and branching ratios vary greatly. See also the  $\Lambda(1600) P_{01}$ .

#### $\Lambda(1810)$ MASS

VALUE (MeV)	DOCUMENT ID	TECN	COMMENT
<b>1750 to 1850 (<math>\approx 1810</math>) OUR ESTIMATE</b>			
1841 $\pm$ 20	GOPAL 80	DPWA	$\bar{K}N \rightarrow \bar{K}N$
1853 $\pm$ 20	GOPAL 77	DPWA	$\bar{K}N$ multichannel
1735 $\pm$ 5	CARROLL 76	DPWA	Isospin-0 total $\sigma$
1746 $\pm$ 10	PREVOST 74	DPWA	$K^-N \rightarrow \Sigma(1385)\pi$
1780 $\pm$ 20	LANGBEIN 72	IPWA	$\bar{K}N$ multichannel
••• We do not use the following data for averages, fits, limits, etc. •••			
1861 or 1953	<sup>1</sup> MARTIN 77	DPWA	$\bar{K}N$ multichannel
1755	KIM 71	DPWA	K-matrix analysis
1800	ARMENTEROS70	HBC	$\bar{K}N \rightarrow \bar{K}N$
1750	ARMENTEROS70	HBC	$\bar{K}N \rightarrow \Sigma\pi$
1690 $\pm$ 10	BARBARO... 70	HBC	$\bar{K}N \rightarrow \Sigma\pi$
1740	BAILEY 69	DPWA	$\bar{K}N \rightarrow \bar{K}N$
1745	ARMENTEROS68B	HBC	$\bar{K}N \rightarrow \bar{K}N$

#### $\Lambda(1810)$ WIDTH

VALUE (MeV)	DOCUMENT ID	TECN	COMMENT
<b>50 to 250 (<math>\approx 150</math>) OUR ESTIMATE</b>			
164 $\pm$ 20	GOPAL 80	DPWA	$\bar{K}N \rightarrow \bar{K}N$
90 $\pm$ 20	CAMERON 78B	DPWA	$K^-p \rightarrow N\bar{K}^*$
166 $\pm$ 20	GOPAL 77	DPWA	$\bar{K}N$ multichannel
46 $\pm$ 20	PREVOST 74	DPWA	$K^-N \rightarrow \Sigma(1385)\pi$
120 $\pm$ 10	LANGBEIN 72	IPWA	$\bar{K}N$ multichannel
••• We do not use the following data for averages, fits, limits, etc. •••			
535 or 585	<sup>1</sup> MARTIN 77	DPWA	$\bar{K}N$ multichannel
28	CARROLL 76	DPWA	Isospin-0 total $\sigma$
35	KIM 71	DPWA	K-matrix analysis
30	ARMENTEROS70	HBC	$\bar{K}N \rightarrow \bar{K}N$
70	ARMENTEROS70	HBC	$\bar{K}N \rightarrow \Sigma\pi$
22	BARBARO... 70	HBC	$\bar{K}N \rightarrow \Sigma\pi$
300	BAILEY 69	DPWA	$\bar{K}N \rightarrow \bar{K}N$
147	ARMENTEROS68B	HBC	

#### $\Lambda(1810)$ DECAY MODES

Mode	Fraction ( $\Gamma_i/\Gamma$ )
$\Gamma_1$ $N\bar{K}$	20-50 %
$\Gamma_2$ $\Sigma\pi$	10-40 %
$\Gamma_3$ $\Sigma(1385)\pi$	seen
$\Gamma_4$ $N\bar{K}^*(892)$	30-60 %
$\Gamma_5$ $N\bar{K}^*(892), S=1/2, P\text{-wave}$	
$\Gamma_6$ $N\bar{K}^*(892), S=3/2, P\text{-wave}$	

The above branching fractions are our estimates, not fits or averages.

#### $\Lambda(1810)$ BRANCHING RATIOS

See "Sign conventions for resonance couplings" in the Note on  $\Lambda$  and  $\Sigma$  Resonances.

$\Gamma(N\bar{K})/\Gamma_{\text{total}}$	DOCUMENT ID	TECN	COMMENT	$\Gamma_1/\Gamma$
<b>0.2 to 0.5 OUR ESTIMATE</b>				
0.24 $\pm$ 0.04	GOPAL 80	DPWA	$\bar{K}N \rightarrow \bar{K}N$	
0.36 $\pm$ 0.05	LANGBEIN 72	IPWA	$\bar{K}N$ multichannel	
••• We do not use the following data for averages, fits, limits, etc. •••				
0.21 $\pm$ 0.04	GOPAL 77	DPWA	See GOPAL 80	
0.52 or 0.49	<sup>1</sup> MARTIN 77	DPWA	$\bar{K}N$ multichannel	
0.30	KIM 71	DPWA	K-matrix analysis	
0.15	ARMENTEROS70	DPWA	$\bar{K}N \rightarrow \bar{K}N$	
0.55	BAILEY 69	DPWA	$\bar{K}N \rightarrow \bar{K}N$	
0.4	ARMENTEROS68B	DPWA	$\bar{K}N \rightarrow \bar{K}N$	

$(\Gamma_1/\Gamma)_{\text{total}}$ in $N\bar{K} \rightarrow \Lambda(1810) \rightarrow \Sigma\pi$	DOCUMENT ID	TECN	COMMENT	$(\Gamma_1/\Gamma_2)_{\text{total}}$
<b>0.2 to 0.5 OUR ESTIMATE</b>				
-0.24 $\pm$ 0.04	GOPAL 77	DPWA	$\bar{K}N$ multichannel	
••• We do not use the following data for averages, fits, limits, etc. •••				
+0.25 or +0.23	<sup>1</sup> MARTIN 77	DPWA	$\bar{K}N$ multichannel	
< 0.01	LANGBEIN 72	IPWA	$\bar{K}N$ multichannel	
0.17	KIM 71	DPWA	K-matrix analysis	
+0.20	<sup>2</sup> ARMENTEROS70	DPWA	$\bar{K}N \rightarrow \Sigma\pi$	
-0.13 $\pm$ 0.03	BARBARO... 70	DPWA	$\bar{K}N \rightarrow \Sigma\pi$	

$(\Gamma_1/\Gamma)_{\text{total}}$ in $N\bar{K} \rightarrow \Lambda(1810) \rightarrow \Sigma(1385)\pi$	DOCUMENT ID	TECN	COMMENT	$(\Gamma_1/\Gamma_3)_{\text{total}}$
<b>0.2 to 0.5 OUR ESTIMATE</b>				
+0.18 $\pm$ 0.10	PREVOST 74	DPWA	$K^-N \rightarrow \Sigma(1385)\pi$	

$(\Gamma_1/\Gamma)_{\text{total}}$ in $N\bar{K} \rightarrow \Lambda(1810) \rightarrow N\bar{K}^*(892), S=1/2, P\text{-wave}$	DOCUMENT ID	TECN	COMMENT	$(\Gamma_1/\Gamma_5)_{\text{total}}$
<b>0.2 to 0.5 OUR ESTIMATE</b>				
-0.14 $\pm$ 0.03	<sup>2</sup> CAMERON 78B	DPWA	$K^-p \rightarrow N\bar{K}^*$	

$(\Gamma_1/\Gamma)_{\text{total}}$ in $N\bar{K} \rightarrow \Lambda(1810) \rightarrow N\bar{K}^*(892), S=3/2, P\text{-wave}$	DOCUMENT ID	TECN	COMMENT	$(\Gamma_1/\Gamma_6)_{\text{total}}$
<b>0.2 to 0.5 OUR ESTIMATE</b>				
+0.35 $\pm$ 0.06	CAMERON 78B	DPWA	$K^-p \rightarrow N\bar{K}^*$	

#### $\Lambda(1810)$ FOOTNOTES

- The two MARTIN 77 values are from a T-matrix pole and from a Breit-Wigner fit.
- The published sign has been changed to be in accord with the baryon-first convention.

#### $\Lambda(1810)$ REFERENCES

GOPAL 80	Toronto Conf. 159	G.P. Gopal	(RHEL) IJP
CAMERON 78B	NP B146 327	W. Cameron et al.	(RHEL, LOIC) IJP
GOPAL 77	NP B119 362	G.P. Gopal et al.	(LOIC, RHEL) IJP
MARTIN 77	NP B127 349	B.R. Martin, M.K. Pidcock, R.G. Moorhouse	(LOUC+) IJP
Also	NP B126 266	B.R. Martin, M.K. Pidcock	(LOUC) IJP
Also	NP B126 285	B.R. Martin, M.K. Pidcock	(LOUC) IJP
CARROLL 76	PRL 37 806	A.S. Carroll et al.	(BNL) I
PREVOST 74	NP B69 246	J. Prevost et al.	(SACL, CERN, HEID)
LANGBEIN 72	NP B47 477	W. Langbein, F. Wagner	(MPIM) IJP
KIM 71	PRL 27 356	J.K. Kim	(HARV) IJP
Also	Duke Conf. 161	J.K. Kim	(HARV) IJP
Hyperon Resonances, 1970			
ARMENTEROS 70	Duke Conf. 123	R. Armenteros et al.	(CERN, HEID, SACL) IJP
Hyperon Resonances, 1970			
BARBARO... 70	Duke Conf. 173	A. Barbaro-Galtheri	(LRL) IJP
Hyperon Resonances, 1970			
BAILEY 69	Thesis UCRL 50617	J.M. Bailey	(LLL) IJP
ARMENTEROS 68B	NP B8 195	R. Armenteros et al.	(CERN, HEID, SACL) IJP

### $\Lambda(1820) 5/2^+$

$$I(J^P) = 0(\frac{5}{2}^+) \text{ Status: } ****$$

This resonance is the cornerstone of all partial-wave analyses in this region. Most of the results published before 1973 are now obsolete and have been omitted. They may be found in our 1982 edition Physics Letters **111B** 1 (1982).

Most of the quoted errors are statistical only; the systematic errors due to the particular parametrizations used in the partial-wave analyses are not included. For this reason we do not calculate weighted averages for the mass and width.

#### $\Lambda(1820)$ MASS

VALUE (MeV)	DOCUMENT ID	TECN	COMMENT
<b>1815 to 1825 (<math>\approx 1820</math>) OUR ESTIMATE</b>			
1823 $\pm$ 3	GOPAL 80	DPWA	$\bar{K}N \rightarrow \bar{K}N$
1819 $\pm$ 2	ALSTON... 78	DPWA	$\bar{K}N \rightarrow \bar{K}N$
1822 $\pm$ 2	GOPAL 77	DPWA	$\bar{K}N$ multichannel
1821 $\pm$ 2	KANE 74	DPWA	$K^-p \rightarrow \Sigma\pi$
••• We do not use the following data for averages, fits, limits, etc. •••			
1830	DECLAIS 77	DPWA	$\bar{K}N \rightarrow \bar{K}N$
1817 or 1819	<sup>1</sup> MARTIN 77	DPWA	$\bar{K}N$ multichannel

#### $\Lambda(1820)$ WIDTH

VALUE (MeV)	DOCUMENT ID	TECN	COMMENT
<b>70 to 90 (<math>\approx 80</math>) OUR ESTIMATE</b>			
77 $\pm$ 5	GOPAL 80	DPWA	$\bar{K}N \rightarrow \bar{K}N$
72 $\pm$ 5	ALSTON... 78	DPWA	$\bar{K}N \rightarrow \bar{K}N$
81 $\pm$ 5	GOPAL 77	DPWA	$\bar{K}N$ multichannel
87 $\pm$ 3	KANE 74	DPWA	$K^-p \rightarrow \Sigma\pi$
••• We do not use the following data for averages, fits, limits, etc. •••			
82	DECLAIS 77	DPWA	$\bar{K}N \rightarrow \bar{K}N$
76 or 76	<sup>1</sup> MARTIN 77	DPWA	$\bar{K}N$ multichannel

#### $\Lambda(1820)$ DECAY MODES

Mode	Fraction ( $\Gamma_i/\Gamma$ )
$\Gamma_1$ $N\bar{K}$	55-65 %
$\Gamma_2$ $\Sigma\pi$	8-14 %
$\Gamma_3$ $\Sigma(1385)\pi$	5-10 %
$\Gamma_4$ $\Sigma(1385)\pi, P\text{-wave}$	
$\Gamma_5$ $\Sigma(1385)\pi, F\text{-wave}$	
$\Gamma_6$ $\Lambda\eta$	
$\Gamma_7$ $\Sigma\pi\pi$	

The above branching fractions are our estimates, not fits or averages.

## Baryon Particle Listings

 $\Lambda(1820), \Lambda(1830)$  $\Lambda(1820)$  BRANCHING RATIOS

Errors quoted do not include uncertainties in the parametrizations used in the partial-wave analyses and are thus too small. See also "Sign conventions for resonance couplings" in the Note on  $\Lambda$  and  $\Sigma$  Resonances.

$\Gamma(N\bar{K})/\Gamma_{\text{total}}$	DOCUMENT ID	TECN	COMMENT	$\Gamma_1/\Gamma$
<b>0.55 to 0.65 OUR ESTIMATE</b>				
0.58 ± 0.02	GOPAL	80	DPWA $\bar{K}N \rightarrow \bar{K}N$	
0.60 ± 0.03	ALSTON...	78	DPWA $\bar{K}N \rightarrow \bar{K}N$	
••• We do not use the following data for averages, fits, limits, etc. •••				
0.51	DECLAIS	77	DPWA $\bar{K}N \rightarrow \bar{K}N$	
0.57 ± 0.02	GOPAL	77	DPWA See GOPAL 80	
0.59 or 0.58	<sup>1</sup> MARTIN	77	DPWA $\bar{K}N$ multichannel	

$(\Gamma_1\Gamma_2)^{1/2}/\Gamma_{\text{total}}$ in $N\bar{K} \rightarrow \Lambda(1820) \rightarrow \Sigma\pi$	DOCUMENT ID	TECN	COMMENT	$(\Gamma_1\Gamma_2)^{1/2}/\Gamma$
<b>0.03 to 0.10 OUR ESTIMATE</b>				
-0.28 ± 0.03	GOPAL	77	DPWA $\bar{K}N$ multichannel	
-0.28 ± 0.01	KANE	74	DPWA $K^-p \rightarrow \Sigma\pi$	
••• We do not use the following data for averages, fits, limits, etc. •••				
-0.25 or -0.25	<sup>1</sup> MARTIN	77	DPWA $\bar{K}N$ multichannel	

$(\Gamma_1\Gamma_2)^{1/2}/\Gamma_{\text{total}}$ in $N\bar{K} \rightarrow \Lambda(1820) \rightarrow \Lambda\eta$	DOCUMENT ID	TECN	COMMENT	$(\Gamma_1\Gamma_2)^{1/2}/\Gamma$
-0.096 <sup>+0.040</sup> <sub>-0.020</sub>	RADER	73	MPWA	

$\Gamma(\Sigma\pi\pi)/\Gamma_{\text{total}}$	DOCUMENT ID	TECN	COMMENT	$\Gamma_7/\Gamma$
no clear signal	<sup>2</sup> ARMENTEROS68C	HDBC	$K^-N \rightarrow \Sigma\pi\pi$	

$(\Gamma_1\Gamma_2)^{1/2}/\Gamma_{\text{total}}$ in $N\bar{K} \rightarrow \Lambda(1820) \rightarrow \Sigma(1385)\pi, P\text{-wave}$	DOCUMENT ID	TECN	COMMENT	$(\Gamma_1\Gamma_2)^{1/2}/\Gamma$
-0.167 ± 0.054	<sup>3</sup> CAMERON	78	DPWA $K^-p \rightarrow \Sigma(1385)\pi$	
+0.27 ± 0.03	PREVOST	74	DPWA $K^-N \rightarrow \Sigma(1385)\pi$	

$(\Gamma_1\Gamma_2)^{1/2}/\Gamma_{\text{total}}$ in $N\bar{K} \rightarrow \Lambda(1820) \rightarrow \Sigma(1385)\pi, F\text{-wave}$	DOCUMENT ID	TECN	COMMENT	$(\Gamma_1\Gamma_2)^{1/2}/\Gamma$
+0.065 ± 0.029	<sup>3</sup> CAMERON	78	DPWA $K^-p \rightarrow \Sigma(1385)\pi$	

 $\Lambda(1820)$  FOOTNOTES

- <sup>1</sup> The two MARTIN 77 values are from a T-matrix pole and from a Breit-Wigner fit.  
<sup>2</sup> There is a suggestion of a bump, enough to be consistent with what is expected from  $\Sigma(1385) \rightarrow \Sigma\pi$  decay.  
<sup>3</sup> The published sign has been changed to be in accord with the baryon-first convention.

 $\Lambda(1820)$  REFERENCES

PDG	82	PL 111B 1	M. Roos <i>et al.</i>	(HELS, CIT, CERN)
GOPAL	80	Toronto Conf. 159	G.P. Gopal	(RHEL) IJP
ALSTON...	78	PR D18 182	M. Alston-Garnjost <i>et al.</i>	(LBL, MTHO+) IJP
Also		PRL 38 1007	M. Alston-Garnjost <i>et al.</i>	(LBL, MTHO+) IJP
CAMERON	78	NP B143 189	W. Cameron <i>et al.</i>	(RHEL, LOIC) IJP
DECLAIS	77	CERN 77-16	Y. Declais <i>et al.</i>	(CAEN, CERN) IJP
GOPAL	77	NP B119 362	G.P. Gopal <i>et al.</i>	(LOIC, RHEL) IJP
MARTIN	77	NP B127 349	B.R. Martin, M.K. Pidcock, R.G. Moorhouse	(LOUC+) IJP
Also		NP B126 266	B.R. Martin, M.K. Pidcock	(LOUC) IJP
Also		NP B126 285	B.R. Martin, M.K. Pidcock	(LOUC) IJP
KANE	74	LBL-2452	D.F. Kane	(LBL) IJP
PREVOST	74	NP B69 246	J. Prevost <i>et al.</i>	(SACL, CERN, HEID)
RADER	73	NC 16A 178	R.K. Rader <i>et al.</i>	(SACL, HEID, CERN+)
ARMENTEROS 68C	68C	NP B8 216	R. Armenteros <i>et al.</i>	(CERN, HEID, SACL)

 $\Lambda(1830) 5/2^-$ 

$$I(J^P) = 0(\frac{5}{2}^-) \text{ Status: } ***$$

For results published before 1973 (they are now obsolete), see our 1982 edition Physics Letters **111B** 1 (1982).

The best evidence for this resonance is in the  $\Sigma\pi$  channel.

 $\Lambda(1830)$  MASS

VALUE (MeV)	DOCUMENT ID	TECN	COMMENT
<b>1810 to 1830 (<math>\approx 1830</math>) OUR ESTIMATE</b>			
1831 ± 10	GOPAL	80	DPWA $\bar{K}N \rightarrow \bar{K}N$
1825 ± 10	GOPAL	77	DPWA $\bar{K}N$ multichannel
1825 ± 1	KANE	74	DPWA $K^-p \rightarrow \Sigma\pi$
••• We do not use the following data for averages, fits, limits, etc. •••			
1817 or 1818	<sup>1</sup> MARTIN	77	DPWA $\bar{K}N$ multichannel

 $\Lambda(1830)$  WIDTH

VALUE (MeV)	DOCUMENT ID	TECN	COMMENT
<b>60 to 110 (<math>\approx 95</math>) OUR ESTIMATE</b>			
100 ± 10	GOPAL	80	DPWA $\bar{K}N \rightarrow \bar{K}N$
94 ± 10	GOPAL	77	DPWA $\bar{K}N$ multichannel
119 ± 3	KANE	74	DPWA $K^-p \rightarrow \Sigma\pi$
••• We do not use the following data for averages, fits, limits, etc. •••			
56 or 56	<sup>1</sup> MARTIN	77	DPWA $\bar{K}N$ multichannel

 $\Lambda(1830)$  DECAY MODES

Mode	Fraction ( $\Gamma_i/\Gamma$ )
$\Gamma_1$ $N\bar{K}$	3-10 %
$\Gamma_2$ $\Sigma\pi$	35-75 %
$\Gamma_3$ $\Sigma(1385)\pi$	>15 %
$\Gamma_4$ $\Sigma(1385)\pi, D\text{-wave}$	
$\Gamma_5$ $\Lambda\eta$	

The above branching fractions are our estimates, not fits or averages.

 $\Lambda(1830)$  BRANCHING RATIOS

See "Sign conventions for resonance couplings" in the Note on  $\Lambda$  and  $\Sigma$  Resonances.

$\Gamma(N\bar{K})/\Gamma_{\text{total}}$	DOCUMENT ID	TECN	COMMENT	$\Gamma_1/\Gamma$
<b>0.03 to 0.10 OUR ESTIMATE</b>				
0.08 ± 0.03	GOPAL	80	DPWA $\bar{K}N \rightarrow \bar{K}N$	
0.02 ± 0.02	ALSTON...	78	DPWA $\bar{K}N \rightarrow \bar{K}N$	
••• We do not use the following data for averages, fits, limits, etc. •••				
0.04 ± 0.03	GOPAL	77	DPWA See GOPAL 80	
0.04 or 0.04	<sup>1</sup> MARTIN	77	DPWA $\bar{K}N$ multichannel	

$(\Gamma_1\Gamma_2)^{1/2}/\Gamma_{\text{total}}$ in $N\bar{K} \rightarrow \Lambda(1830) \rightarrow \Sigma\pi$	DOCUMENT ID	TECN	COMMENT	$(\Gamma_1\Gamma_2)^{1/2}/\Gamma$
-0.17 ± 0.03	GOPAL	77	DPWA $\bar{K}N$ multichannel	
-0.15 ± 0.01	KANE	74	DPWA $K^-p \rightarrow \Sigma\pi$	
••• We do not use the following data for averages, fits, limits, etc. •••				
-0.17 or -0.17	<sup>1</sup> MARTIN	77	DPWA $\bar{K}N$ multichannel	

$(\Gamma_1\Gamma_2)^{1/2}/\Gamma_{\text{total}}$ in $N\bar{K} \rightarrow \Lambda(1830) \rightarrow \Lambda\eta$	DOCUMENT ID	TECN	COMMENT	$(\Gamma_1\Gamma_2)^{1/2}/\Gamma$
-0.044 ± 0.020	RADER	73	MPWA	

$(\Gamma_1\Gamma_2)^{1/2}/\Gamma_{\text{total}}$ in $N\bar{K} \rightarrow \Lambda(1830) \rightarrow \Sigma(1385)\pi$	DOCUMENT ID	TECN	COMMENT	$(\Gamma_1\Gamma_2)^{1/2}/\Gamma$
+0.141 ± 0.014	<sup>2</sup> CAMERON	78	DPWA $K^-p \rightarrow \Sigma(1385)\pi$	
+0.13 ± 0.03	PREVOST	74	DPWA $K^-N \rightarrow \Sigma(1385)\pi$	

 $\Lambda(1830)$  FOOTNOTES

- <sup>1</sup> The two MARTIN 77 values are from a T-matrix pole and from a Breit-Wigner fit.  
<sup>2</sup> The CAMERON 78 upper limit on G-wave decay is 0.03. The published sign has been changed to be in accord with the baryon-first convention.

 $\Lambda(1830)$  REFERENCES

PDG	82	PL 111B 1	M. Roos <i>et al.</i>	(HELS, CIT, CERN)
GOPAL	80	Toronto Conf. 159	G.P. Gopal	(RHEL) IJP
ALSTON...	78	PR D18 182	M. Alston-Garnjost <i>et al.</i>	(LBL, MTHO+) IJP
Also		PRL 38 1007	M. Alston-Garnjost <i>et al.</i>	(LBL, MTHO+) IJP
CAMERON	78	NP B143 189	W. Cameron <i>et al.</i>	(RHEL, LOIC) IJP
GOPAL	77	NP B119 362	G.P. Gopal <i>et al.</i>	(LOIC, RHEL) IJP
MARTIN	77	NP B127 349	B.R. Martin, M.K. Pidcock, R.G. Moorhouse	(LOUC+) IJP
Also		NP B126 266	B.R. Martin, M.K. Pidcock	(LOUC) IJP
Also		NP B126 285	B.R. Martin, M.K. Pidcock	(LOUC) IJP
KANE	74	LBL-2452	D.F. Kane	(LBL) IJP
PREVOST	74	NP B69 246	J. Prevost <i>et al.</i>	(SACL, CERN, HEID)
RADER	73	NC 16A 178	R.K. Rader <i>et al.</i>	(SACL, HEID, CERN+)



See key on page 457

Baryon Particle Listings  
 $\Lambda(1890)$ ,  $\Lambda(2000)$  $\Lambda(1890) 3/2^+$  $I(J^P) = 0(\frac{3}{2}^+)$  Status: \*\*\*\*For results published before 1974 (they are now obsolete), see our 1982 edition Physics Letters **111B** 1 (1982).The  $J^P = 3/2^+$  assignment is consistent with all available data (including polarization) and recent partial-wave analyses. The dominant inelastic modes remain unknown. $\Lambda(1890)$  MASS

VALUE (MeV)	DOCUMENT ID	TECN	COMMENT
<b>1850 to 1910 (<math>\approx 1890</math>) OUR ESTIMATE</b>			
1897 $\pm$ 5	GOPAL 80	DPWA	$\bar{K}N \rightarrow \bar{K}N$
1908 $\pm$ 10	ALSTON... 78	DPWA	$\bar{K}N \rightarrow \bar{K}N$
1900 $\pm$ 5	GOPAL 77	DPWA	$\bar{K}N$ multichannel
1894 $\pm$ 10	HEMINGWAY 75	DPWA	$K^-p \rightarrow \bar{K}N$
••• We do not use the following data for averages, fits, limits, etc. •••			
1856 or 1868	<sup>1</sup> MARTIN 77	DPWA	$\bar{K}N$ multichannel
1900	<sup>2</sup> NAKKASYAN 75	DPWA	$K^-p \rightarrow \Lambda\omega$

 $\Lambda(1890)$  WIDTH

VALUE (MeV)	DOCUMENT ID	TECN	COMMENT
<b>60 to 200 (<math>\approx 100</math>) OUR ESTIMATE</b>			
74 $\pm$ 10	GOPAL 80	DPWA	$\bar{K}N \rightarrow \bar{K}N$
119 $\pm$ 20	ALSTON... 78	DPWA	$\bar{K}N \rightarrow \bar{K}N$
72 $\pm$ 10	GOPAL 77	DPWA	$\bar{K}N$ multichannel
107 $\pm$ 10	HEMINGWAY 75	DPWA	$K^-p \rightarrow \bar{K}N$
••• We do not use the following data for averages, fits, limits, etc. •••			
191 or 193	<sup>1</sup> MARTIN 77	DPWA	$\bar{K}N$ multichannel
100	<sup>2</sup> NAKKASYAN 75	DPWA	$K^-p \rightarrow \Lambda\omega$

 $\Lambda(1890)$  DECAY MODES

Mode	Fraction ( $\Gamma_i/\Gamma$ )
$\Gamma_1$ $N\bar{K}$	20–35 %
$\Gamma_2$ $\Sigma\pi$	3–10 %
$\Gamma_3$ $\Sigma(1385)\pi$	seen
$\Gamma_4$ $\Sigma(1385)\pi$ , $P$ -wave	
$\Gamma_5$ $\Sigma(1385)\pi$ , $F$ -wave	
$\Gamma_6$ $N\bar{K}^*(892)$	seen
$\Gamma_7$ $N\bar{K}^*(892)$ , $S=1/2$ , $P$ -wave	
$\Gamma_8$ $\Lambda\omega$	

The above branching fractions are our estimates, not fits or averages.

 $\Lambda(1890)$  BRANCHING RATIOSSee "Sign conventions for resonance couplings" in the Note on  $\Lambda$  and  $\Sigma$  Resonances.

$\Gamma(N\bar{K})/\Gamma_{\text{total}}$	DOCUMENT ID	TECN	COMMENT	$\Gamma_1/\Gamma$
<b>0.20 to 0.35 OUR ESTIMATE</b>				
0.20 $\pm$ 0.02	GOPAL 80	DPWA	$\bar{K}N \rightarrow \bar{K}N$	
0.34 $\pm$ 0.05	ALSTON... 78	DPWA	$\bar{K}N \rightarrow \bar{K}N$	
0.24 $\pm$ 0.04	HEMINGWAY 75	DPWA	$K^-p \rightarrow \bar{K}N$	
••• We do not use the following data for averages, fits, limits, etc. •••				
0.18 $\pm$ 0.02	GOPAL 77	DPWA	See GOPAL 80	
0.36 or 0.34	<sup>1</sup> MARTIN 77	DPWA	$\bar{K}N$ multichannel	

$(\Gamma_i/\Gamma_f)^{1/2}/\Gamma_{\text{total}}$ in $N\bar{K} \rightarrow \Lambda(1890) \rightarrow \Sigma\pi$	DOCUMENT ID	TECN	COMMENT	$(\Gamma_1\Gamma_2)^{1/2}/\Gamma$
<b>VALUE</b>				
-0.09 $\pm$ 0.03	GOPAL 77	DPWA	$\bar{K}N$ multichannel	
••• We do not use the following data for averages, fits, limits, etc. •••				
+0.15 or +0.14	<sup>1</sup> MARTIN 77	DPWA	$\bar{K}N$ multichannel	

$(\Gamma_i/\Gamma_f)^{1/2}/\Gamma_{\text{total}}$ in $N\bar{K} \rightarrow \Lambda(1890) \rightarrow \Lambda\omega$	DOCUMENT ID	TECN	COMMENT	$(\Gamma_1\Gamma_8)^{1/2}/\Gamma$
<b>VALUE</b>				
seen	BACCARI 77	IPWA	$K^-p \rightarrow \Lambda\omega$	
0.032	<sup>2</sup> NAKKASYAN 75	DPWA	$K^-p \rightarrow \Lambda\omega$	

$(\Gamma_i/\Gamma_f)^{1/2}/\Gamma_{\text{total}}$ in $N\bar{K} \rightarrow \Lambda(1890) \rightarrow \Sigma(1385)\pi$ , $P$ -wave	DOCUMENT ID	TECN	COMMENT	$(\Gamma_1\Gamma_4)^{1/2}/\Gamma$
<b>VALUE</b>				
<0.03	CAMERON 78	DPWA	$K^-p \rightarrow \Sigma(1385)\pi$	

$(\Gamma_i/\Gamma_f)^{1/2}/\Gamma_{\text{total}}$ in $N\bar{K} \rightarrow \Lambda(1890) \rightarrow \Sigma(1385)\pi$ , $F$ -wave	DOCUMENT ID	TECN	COMMENT	$(\Gamma_1\Gamma_5)^{1/2}/\Gamma$
<b>VALUE</b>				
-0.126 $\pm$ 0.055	<sup>3</sup> CAMERON 78	DPWA	$K^-p \rightarrow \Sigma(1385)\pi$	

$(\Gamma_i/\Gamma_f)^{1/2}/\Gamma_{\text{total}}$ in $N\bar{K} \rightarrow \Lambda(1890) \rightarrow N\bar{K}^*(892)$	DOCUMENT ID	TECN	COMMENT	$(\Gamma_1\Gamma_6)^{1/2}/\Gamma$
<b>VALUE</b>				
-0.07 $\pm$ 0.03	<sup>3,4</sup> CAMERON 78B	DPWA	$K^-p \rightarrow N\bar{K}^*$	

 $\Lambda(1890)$  FOOTNOTES

- The two MARTIN 77 values are from a T-matrix pole and from a Breit-Wigner fit.
- Found in one of two best solutions.
- The published sign has been changed to be in accord with the baryon-first convention.
- Upper limits on the  $P_3$  and  $F_3$  waves are each 0.03.

 $\Lambda(1890)$  REFERENCES

PDG 82	PL 111B 1	M. Roos <i>et al.</i>	(HELS, CIT, CERN)
GOPAL 80	Toronto Conf. 159	G.P. Gopal	(RHEL) IJP
ALSTON... 78	PR D18 182	M. Alston-Garnjost <i>et al.</i>	(LBL, MTHO+) IJP
Also	PR L 38 1007	M. Alston-Garnjost <i>et al.</i>	(LBL, MTHO+) IJP
CAMERON 78	NP B143 189	W. Cameron <i>et al.</i>	(RHEL, LOIC) IJP
CAMERON 78B	NP B146 327	W. Cameron <i>et al.</i>	(RHEL, LOIC) IJP
BACCARI 77	NC 41A 96	B. Baccari <i>et al.</i>	(SACL, CDEF) IJP
GOPAL 77	NP B119 362	G.P. Gopal <i>et al.</i>	(LOIC, RHEL) IJP
MARTIN 77	NP B127 349	B.R. Martin, M.K. Pidcock, R.G. Moorhouse	(LOUC+) IJP
Also	NP B126 266	B.R. Martin, M.K. Pidcock	(LOUC) IJP
Also	NP B126 285	B.R. Martin, M.K. Pidcock	(LOUC) IJP
HEMINGWAY 75	NP B91 12	R.J. Hemingway <i>et al.</i>	(CERN, HEIDH, MPIM) IJP
NAKKASYAN 75	NP B93 85	A. Nakkasyan	(CERN) IJP

 $\Lambda(2000)$  $I(J^P) = 0(?^?)$  Status: \*

OMITTED FROM SUMMARY TABLE

We list here all the ambiguous resonance possibilities with a mass around 2 GeV. The proposed quantum numbers are  $D_3$  (BARBARO-GALTIERI 70 in  $\Sigma\pi$ ),  $D_3+F_5$ ,  $P_3+D_5$ , or  $P_1+D_3$  (BRANDSTETTER 72 in  $\Lambda\omega$ ), and  $S_1$  (CAMERON 78B in  $N\bar{K}^*$ ). The first two of the above analyses should now be considered obsolete. See also NAKKASYAN 75. $\Lambda(2000)$  MASS

VALUE (MeV)	DOCUMENT ID	TECN	COMMENT
<b><math>\approx 2000</math> OUR ESTIMATE</b>			
2030 $\pm$ 30			
1935 to 1971	CAMERON 78B	DPWA	$K^-p \rightarrow N\bar{K}^*$
1951 to 2034	<sup>1</sup> BRANDSTET...72	DPWA	$K^-p \rightarrow \Lambda\omega$
	<sup>1</sup> BRANDSTET...72	DPWA	$K^-p \rightarrow \Lambda\omega$
2010 $\pm$ 30	BARBARO... 70	DPWA	$K^-p \rightarrow \Sigma\pi$

 $\Lambda(2000)$  WIDTH

VALUE (MeV)	DOCUMENT ID	TECN	COMMENT
125 $\pm$ 25	CAMERON 78B	DPWA	$K^-p \rightarrow N\bar{K}^*$
180 to 240	<sup>1</sup> BRANDSTET...72	DPWA	(lower mass)
73 to 154	<sup>1</sup> BRANDSTET...72	DPWA	(higher mass)
130 $\pm$ 50	BARBARO... 70	DPWA	$K^-p \rightarrow \Sigma\pi$

 $\Lambda(2000)$  DECAY MODES

Mode
$\Gamma_1$ $N\bar{K}$
$\Gamma_2$ $\Sigma\pi$
$\Gamma_3$ $\Lambda\omega$
$\Gamma_4$ $N\bar{K}^*(892)$ , $S=1/2$ , $S$ -wave
$\Gamma_5$ $N\bar{K}^*(892)$ , $S=3/2$ , $D$ -wave

 $\Lambda(2000)$  BRANCHING RATIOSSee "Sign conventions for resonance couplings" in the Note on  $\Lambda$  and  $\Sigma$  Resonances.

$(\Gamma_i/\Gamma_f)^{1/2}/\Gamma_{\text{total}}$ in $N\bar{K} \rightarrow \Lambda(2000) \rightarrow \Sigma\pi$	DOCUMENT ID	TECN	COMMENT	$(\Gamma_1\Gamma_2)^{1/2}/\Gamma$
<b>VALUE</b>				
-0.20 $\pm$ 0.04	BARBARO... 70	DPWA	$K^-p \rightarrow \Sigma\pi$	

$(\Gamma_i/\Gamma_f)^{1/2}/\Gamma_{\text{total}}$ in $N\bar{K} \rightarrow \Lambda(2000) \rightarrow \Lambda\omega$	DOCUMENT ID	TECN	COMMENT	$(\Gamma_1\Gamma_3)^{1/2}/\Gamma$
<b>VALUE</b>				
0.17 to 0.25	<sup>1</sup> BRANDSTET...72	DPWA	(lower mass)	
0.04 to 0.15	<sup>1</sup> BRANDSTET...72	DPWA	(higher mass)	

$(\Gamma_i/\Gamma_f)^{1/2}/\Gamma_{\text{total}}$ in $N\bar{K} \rightarrow \Lambda(2000) \rightarrow N\bar{K}^*(892)$ , $S=1/2$ , $S$ -wave	DOCUMENT ID	TECN	COMMENT	$(\Gamma_1\Gamma_4)^{1/2}/\Gamma$
<b>VALUE</b>				
-0.12 $\pm$ 0.03	<sup>2</sup> CAMERON 78B	DPWA	$K^-p \rightarrow N\bar{K}^*$	

$(\Gamma_i/\Gamma_f)^{1/2}/\Gamma_{\text{total}}$ in $N\bar{K} \rightarrow \Lambda(2000) \rightarrow N\bar{K}^*(892)$ , $S=3/2$ , $D$ -wave	DOCUMENT ID	TECN	COMMENT	$(\Gamma_1\Gamma_5)^{1/2}/\Gamma$
<b>VALUE</b>				
+0.09 $\pm$ 0.03	CAMERON 78B	DPWA	$K^-p \rightarrow N\bar{K}^*$	

## Baryon Particle Listings

 $\Lambda(2000)$ ,  $\Lambda(2020)$ ,  $\Lambda(2100)$  $\Lambda(2000)$  FOOTNOTES

<sup>1</sup> The parameters quoted here are ranges from the three best fits; the lower state probably has  $J \leq 3/2$ , and the higher one probably has  $J \leq 5/2$ .

<sup>2</sup> The published sign has been changed to be in accord with the baryon-first convention.

 $\Lambda(2000)$  REFERENCES

CAMERON 78B NP B146 327	W. Cameron et al.	(RHEL, LOIC) IJP
NAKKASYAN 75 NP B93 95	A. Nakkasyan	(CERN) IJP
BRANDSTET... 72 NP B39 13	A.A. Brandstetter et al.	(RHEL, CDEF+)
BARBARO... 70 Duke Conf. 173	A. Barbaro-Galteri	(LRL) IJP

Hyperon Resonances, 1970

 $\Lambda(2020)$  7/2<sup>+</sup>

$$I(J^P) = 0(\frac{7}{2}^+) \text{ Status: } *$$

## OMITTED FROM SUMMARY TABLE

In LITCHFIELD 71, need for the state rests solely on a possibly inconsistent polarization measurement at 1.784 GeV/c. HEMINGWAY 75 does not require this state. GOPAL 77 does not need it in either  $N\bar{K}$  or  $\Sigma\pi$ . With new  $K^-n$  angular distributions included, DECLAIS 77 sees it. However, this and other new data are included in GOPAL 80 and the state is not required. BACCARI 77 weakly supports it.

 $\Lambda(2020)$  MASS

VALUE (MeV)	DOCUMENT ID	TECN	COMMENT
<b><math>\approx 2020</math> OUR ESTIMATE</b>			
2140	BACCARI 77	DPWA	$K^-p \rightarrow \Lambda\omega$
2117	DECLAIS 77	DPWA	$\bar{K}N \rightarrow \bar{K}N$
2100 $\pm$ 30	LITCHFIELD 71	DPWA	$K^-p \rightarrow \bar{K}N$
2020 $\pm$ 20	BARBARO... 70	DPWA	$K^-p \rightarrow \Sigma\pi$

 $\Lambda(2020)$  WIDTH

VALUE (MeV)	DOCUMENT ID	TECN	COMMENT
128	BACCARI 77	DPWA	$K^-p \rightarrow \Lambda\omega$
167	DECLAIS 77	DPWA	$\bar{K}N \rightarrow \bar{K}N$
120 $\pm$ 30	LITCHFIELD 71	DPWA	$K^-p \rightarrow \bar{K}N$
160 $\pm$ 30	BARBARO... 70	DPWA	$K^-p \rightarrow \Sigma\pi$

 $\Lambda(2020)$  DECAY MODES

Mode	Fraction ( $\Gamma_i/\Gamma$ )
$\Gamma_1$ $N\bar{K}$	25–35 %
$\Gamma_2$ $\Sigma\pi$	$\sim 5$ %
$\Gamma_3$ $\Lambda\eta$	$<3$ %
$\Gamma_4$ $\Xi K$	$<3$ %
$\Gamma_5$ $\Lambda\omega$	$<8$ %
$\Gamma_6$ $N\bar{K}^*(892)$	10–20 %
$\Gamma_7$ $N\bar{K}^*(892)$ , $S=1/2$ , G-wave	
$\Gamma_8$ $N\bar{K}^*(892)$ , $S=3/2$ , D-wave	

 $\Lambda(2020)$  BRANCHING RATIOS

See "Sign conventions for resonance couplings" in the Note on  $\Lambda$  and  $\Sigma$  Resonances.

$\Gamma(N\bar{K})/\Gamma_{\text{total}}$	DOCUMENT ID	TECN	COMMENT	$\Gamma_1/\Gamma$
0.05	DECLAIS 77	DPWA	$\bar{K}N \rightarrow \bar{K}N$	
0.05 $\pm$ 0.02	LITCHFIELD 71	DPWA	$K^-p \rightarrow \bar{K}N$	

$(\Gamma_1\Gamma_2)^{1/2}/\Gamma_{\text{total}}$ in $N\bar{K} \rightarrow \Lambda(2020) \rightarrow \Sigma\pi$	DOCUMENT ID	TECN	COMMENT	$(\Gamma_1\Gamma_2)^{1/2}/\Gamma$
-0.15 $\pm$ 0.02	BARBARO... 70	DPWA	$K^-p \rightarrow \Sigma\pi$	

$(\Gamma_1\Gamma_3)^{1/2}/\Gamma_{\text{total}}$ in $N\bar{K} \rightarrow \Lambda(2020) \rightarrow \Lambda\omega$	DOCUMENT ID	TECN	COMMENT	$(\Gamma_1\Gamma_3)^{1/2}/\Gamma$
$<0.05$	BACCARI 77	DPWA	$K^-p \rightarrow \Lambda\omega$	

 $\Lambda(2020)$  REFERENCES

GOPAL 80 Toronto Conf. 159	G.P. Gopal	(RHEL)
BACCARI 77 NC 41A 96	B. Bacchari et al.	(SACL, CDEF) IJP
DECLAIS 77 CERN 77-16	Y. Declais et al.	(CAEN, CERN) IJP
GOPAL 77 NP B119 362	G.P. Gopal et al.	(LOIC, RHEL)
HEMINGWAY 75 NP B91 12	R.J. Hemingway et al.	(CERN, HEIDH, MPIM) IJP
LITCHFIELD 71 NP B30 125	P.J. Litchfield et al.	(RHEL, CDEF, SACL) IJP
BARBARO... 70 Duke Conf. 173	A. Barbaro-Galteri	(LRL) IJP

Hyperon Resonances, 1970

 $\Lambda(2100)$  7/2<sup>-</sup>

$$I(J^P) = 0(\frac{7}{2}^-) \text{ Status: } ***$$

Discovered by COOL 66 and by WOHL 66. Most of the results published before 1973 are now obsolete and have been omitted. They may be found in our 1982 edition Physics Letters **111B** 1 (1982).

This entry only includes results from partial-wave analyses. Parameters of peaks seen in cross sections and in invariant-mass distributions around 2100 MeV used to be listed in a separate entry immediately following. It may be found in our 1986 edition Physics Letters **170B** 1 (1986).

 $\Lambda(2100)$  MASS

VALUE (MeV)	DOCUMENT ID	TECN	COMMENT
<b>2090 to 2110 (<math>\approx 2100</math>) OUR ESTIMATE</b>			
2104 $\pm$ 10	GOPAL 80	DPWA	$\bar{K}N \rightarrow \bar{K}N$
2106 $\pm$ 30	DEBELLEFON 78	DPWA	$\bar{K}N \rightarrow \bar{K}N$
2110 $\pm$ 10	GOPAL 77	DPWA	$\bar{K}N$ multichannel
2105 $\pm$ 10	HEMINGWAY 75	DPWA	$K^-p \rightarrow \bar{K}N$
2115 $\pm$ 10	KANE 74	DPWA	$K^-p \rightarrow \Sigma\pi$
••• We do not use the following data for averages, fits, limits, etc. •••			
2094	BACCARI 77	DPWA	$K^-p \rightarrow \Lambda\omega$
2094	DECLAIS 77	DPWA	$\bar{K}N \rightarrow \bar{K}N$
2110 or 2089	<sup>1</sup> NAKKASYAN 75	DPWA	$K^-p \rightarrow \Lambda\omega$

 $\Lambda(2100)$  WIDTH

VALUE (MeV)	DOCUMENT ID	TECN	COMMENT
<b>100 to 250 (<math>\approx 200</math>) OUR ESTIMATE</b>			
157 $\pm$ 40	DEBELLEFON 78	DPWA	$\bar{K}N \rightarrow \bar{K}N$
250 $\pm$ 30	GOPAL 77	DPWA	$\bar{K}N$ multichannel
241 $\pm$ 30	HEMINGWAY 75	DPWA	$K^-p \rightarrow \bar{K}N$
152 $\pm$ 15	KANE 74	DPWA	$K^-p \rightarrow \Sigma\pi$
••• We do not use the following data for averages, fits, limits, etc. •••			
98	BACCARI 77	DPWA	$K^-p \rightarrow \Lambda\omega$
250	DECLAIS 77	DPWA	$\bar{K}N \rightarrow \bar{K}N$
244 or 302	<sup>1</sup> NAKKASYAN 75	DPWA	$K^-p \rightarrow \Lambda\omega$

 $\Lambda(2100)$  DECAY MODES

Mode	Fraction ( $\Gamma_i/\Gamma$ )
$\Gamma_1$ $N\bar{K}$	25–35 %
$\Gamma_2$ $\Sigma\pi$	$\sim 5$ %
$\Gamma_3$ $\Lambda\eta$	$<3$ %
$\Gamma_4$ $\Xi K$	$<3$ %
$\Gamma_5$ $\Lambda\omega$	$<8$ %
$\Gamma_6$ $N\bar{K}^*(892)$	10–20 %
$\Gamma_7$ $N\bar{K}^*(892)$ , $S=1/2$ , G-wave	
$\Gamma_8$ $N\bar{K}^*(892)$ , $S=3/2$ , D-wave	

The above branching fractions are our estimates, not fits or averages.

 $\Lambda(2100)$  BRANCHING RATIOS

See "Sign conventions for resonance couplings" in the Note on  $\Lambda$  and  $\Sigma$  Resonances.

$\Gamma(N\bar{K})/\Gamma_{\text{total}}$	DOCUMENT ID	TECN	COMMENT	$\Gamma_1/\Gamma$
<b>0.25 to 0.35 OUR ESTIMATE</b>				
0.34 $\pm$ 0.03	GOPAL 80	DPWA	$\bar{K}N \rightarrow \bar{K}N$	
0.24 $\pm$ 0.06	DEBELLEFON 78	DPWA	$\bar{K}N \rightarrow \bar{K}N$	
0.31 $\pm$ 0.03	HEMINGWAY 75	DPWA	$K^-p \rightarrow \bar{K}N$	
••• We do not use the following data for averages, fits, limits, etc. •••				
0.29	DECLAIS 77	DPWA	$\bar{K}N \rightarrow \bar{K}N$	
0.30 $\pm$ 0.03	GOPAL 77	DPWA	See GOPAL 80	

$(\Gamma_1\Gamma_2)^{1/2}/\Gamma_{\text{total}}$ in $N\bar{K} \rightarrow \Lambda(2100) \rightarrow \Sigma\pi$	DOCUMENT ID	TECN	COMMENT	$(\Gamma_1\Gamma_2)^{1/2}/\Gamma$
+0.12 $\pm$ 0.04	GOPAL 77	DPWA	$\bar{K}N$ multichannel	
+0.11 $\pm$ 0.01	KANE 74	DPWA	$K^-p \rightarrow \Sigma\pi$	

$(\Gamma_1\Gamma_3)^{1/2}/\Gamma_{\text{total}}$ in $N\bar{K} \rightarrow \Lambda(2100) \rightarrow \Lambda\eta$	DOCUMENT ID	TECN	COMMENT	$(\Gamma_1\Gamma_3)^{1/2}/\Gamma$
-0.050 $\pm$ 0.020	RADER 73	MPWA	$K^-p \rightarrow \Lambda\eta$	

See key on page 457

# Baryon Particle Listings

## $\Lambda(2100)$ , $\Lambda(2110)$ , $\Lambda(2325)$

$(\Gamma_i \Gamma_f)^{1/2} / \Gamma_{\text{total}}$  in  $N\bar{K} \rightarrow \Lambda(2100) \rightarrow \Xi K$   $(\Gamma_1 \Gamma_4)^{1/2} / \Gamma$

VALUE	DOCUMENT ID	TECN	COMMENT
0.035 ± 0.018	LITCHFIELD 71	DPWA	$K^- p \rightarrow \Xi K$
• • • We do not use the following data for averages, fits, limits, etc. • • •			
0.003	MULLER 69B	DPWA	$K^- p \rightarrow \Xi K$
0.05	TRIPP 67	RVUE	$K^- p \rightarrow \Xi K$

$(\Gamma_i \Gamma_f)^{1/2} / \Gamma_{\text{total}}$  in  $N\bar{K} \rightarrow \Lambda(2100) \rightarrow \Lambda\omega$   $(\Gamma_1 \Gamma_5)^{1/2} / \Gamma$

VALUE	DOCUMENT ID	TECN	COMMENT
-0.070	<sup>2</sup> BACCARI 77	DPWA	$GD_{37}$ wave
+0.011	<sup>2</sup> BACCARI 77	DPWA	$GG_{17}$ wave
+0.008	<sup>2</sup> BACCARI 77	DPWA	$GG_{37}$ wave
0.122 or 0.154	<sup>1</sup> NAKKASYAN 75	DPWA	$K^- p \rightarrow \Lambda\omega$

$(\Gamma_i \Gamma_f)^{1/2} / \Gamma_{\text{total}}$  in  $N\bar{K} \rightarrow \Lambda(2100) \rightarrow N\bar{K}^*(892), S=3/2, D\text{-wave}$   $(\Gamma_1 \Gamma_6)^{1/2} / \Gamma$

VALUE	DOCUMENT ID	TECN	COMMENT
+0.21 ± 0.04	CAMERON 78B	DPWA	$K^- p \rightarrow N\bar{K}^*$

$(\Gamma_i \Gamma_f)^{1/2} / \Gamma_{\text{total}}$  in  $N\bar{K} \rightarrow \Lambda(2100) \rightarrow N\bar{K}^*(892), S=1/2, G\text{-wave}$   $(\Gamma_1 \Gamma_7)^{1/2} / \Gamma$

VALUE	DOCUMENT ID	TECN	COMMENT
-0.04 ± 0.03	<sup>3</sup> CAMERON 78B	DPWA	$K^- p \rightarrow N\bar{K}^*$

### $\Lambda(2100)$ FOOTNOTES

- <sup>1</sup> The NAKKASYAN 75 values are from the two best solutions found. Each has the  $\Lambda(2100)$  and one additional resonance ( $P_3$  or  $F_5$ ).
- <sup>2</sup> Note that the three for BACCARI 77 entries are for three different waves.
- <sup>3</sup> The published sign has been changed to be in accord with the baryon-first convention. The upper limit on the  $G_3$  wave is 0.03.

### $\Lambda(2100)$ REFERENCES

PDG 86	PL 170B 1	M. Aguilar-Benitez et al.	(CERN, CIT+)
PDG 82	PL 111B 1	M. Roos et al.	(HELS, CIT, CERN)
GOPAL 80	Toronto Conf. 159	G.P. Gopal	(RHEL) IJP
CAMERON 78B	NP B146 327	W. Cameron et al.	(RHEL, LOIC) IJP
DEBELLEFON 78	NC 42A 403	A. de Bellefon et al.	(CDEF, SACL) IJP
BACCARI 77	NC 41A 96	B. Baccari et al.	(SACL, CDEF) IJP
DECLAIS 77	CERN 77-16	Y. Declais et al.	(CAEN, CERN) IJP
GOPAL 77	NP B119 362	G.P. Gopal et al.	(LOIC, RHEL) IJP
HEMINGWAY 75	NP B91 12	R.J. Hemingway et al.	(CERN, HEIDH, MPIM) IJP
NAKKASYAN 75	NP B93 85	A. Nakkasyan	(CERN) IJP
KANE 74	LBL-2452	D.F. Kane	(LBL) IJP
RADER 73	NC 16A 178	R.K. Rader et al.	(SACL, HEID, CERN+) IJP
LITCHFIELD 71	NP B30 125	P.J. Litchfield et al.	(RHEL, CDEF, SACL) IJP
MULLER 69B	Thesis UCRL 19372	R.A. Muller	(LRL)
TRIPP 67	NP B3 10	R.D. Tripp et al.	(LRL, SLAC, CERN+) IJP
COOL 66	PRL 16 1228	R.L. Cool et al.	(BNL)
WOHL 66	PRL 17 107	C.G. Wohl, F.T. Solmitz, M.L. Stevenson	(LRL) IJP

$\Lambda(2110) 5/2^+$   $I(J^P) = 0(\frac{5}{2}^+)$  Status: \*\*\*

For results published before 1974 (they are now obsolete), see our 1982 edition Physics Letters **111B** 1 (1982). All the references have been retained.

This resonance is in the Baryon Summary Table, but the evidence for it could be better.

### $\Lambda(2110)$ MASS

VALUE (MeV)	DOCUMENT ID	TECN	COMMENT
<b>2090 to 2140 (<math>\approx 2110</math>) OUR ESTIMATE</b>			
2092 ± 25	GOPAL 80	DPWA	$\bar{K}N \rightarrow \bar{K}N$
2125 ± 25	CAMERON 78B	DPWA	$K^- p \rightarrow N\bar{K}^*$
2106 ± 50	DEBELLEFON 78	DPWA	$\bar{K}N \rightarrow \bar{K}N$
2140 ± 20	DEBELLEFON 77	DPWA	$K^- p \rightarrow \Sigma\pi$
2100 ± 50	GOPAL 77	DPWA	$\bar{K}N$ multichannel
2112 ± 7	KANE 74	DPWA	$K^- p \rightarrow \Sigma\pi$
• • • We do not use the following data for averages, fits, limits, etc. • • •			
2137	BACCARI 77	DPWA	$K^- p \rightarrow \Lambda\omega$
2103	<sup>1</sup> NAKKASYAN 75	DPWA	$K^- p \rightarrow \Lambda\omega$

### $\Lambda(2110)$ WIDTH

VALUE (MeV)	DOCUMENT ID	TECN	COMMENT
<b>150 to 250 (<math>\approx 200</math>) OUR ESTIMATE</b>			
245 ± 25	GOPAL 80	DPWA	$\bar{K}N \rightarrow \bar{K}N$
160 ± 30	CAMERON 78B	DPWA	$K^- p \rightarrow N\bar{K}^*$
251 ± 50	DEBELLEFON 78	DPWA	$\bar{K}N \rightarrow \bar{K}N$
140 ± 20	DEBELLEFON 77	DPWA	$K^- p \rightarrow \Sigma\pi$
200 ± 50	GOPAL 77	DPWA	$\bar{K}N$ multichannel
190 ± 30	KANE 74	DPWA	$K^- p \rightarrow \Sigma\pi$
• • • We do not use the following data for averages, fits, limits, etc. • • •			
132	BACCARI 77	DPWA	$K^- p \rightarrow \Lambda\omega$
391	<sup>1</sup> NAKKASYAN 75	DPWA	$K^- p \rightarrow \Lambda\omega$

### $\Lambda(2110)$ DECAY MODES

Mode	Fraction ( $\Gamma_i/\Gamma$ )
$\Gamma_1$ $N\bar{K}$	5–25 %
$\Gamma_2$ $\Sigma\pi$	10–40 %
$\Gamma_3$ $\Lambda\omega$	seen
$\Gamma_4$ $\Sigma(1385)\pi$	seen
$\Gamma_5$ $\Sigma(1385)\pi, P\text{-wave}$	
$\Gamma_6$ $N\bar{K}^*(892)$	10–60 %
$\Gamma_7$ $N\bar{K}^*(892), S=1/2, F\text{-wave}$	

The above branching fractions are our estimates, not fits or averages.

### $\Lambda(2110)$ BRANCHING RATIOS

See "Sign conventions for resonance couplings" in the Note on  $\Lambda$  and  $\Sigma$  Resonances.

$\Gamma(N\bar{K})/\Gamma_{\text{total}}$   $\Gamma_1/\Gamma$

VALUE	DOCUMENT ID	TECN	COMMENT
<b>0.05 to 0.25 OUR ESTIMATE</b>			
0.07 ± 0.03	GOPAL 80	DPWA	$\bar{K}N \rightarrow \bar{K}N$
0.27 ± 0.06	<sup>2</sup> DEBELLEFON 78	DPWA	$\bar{K}N \rightarrow \bar{K}N$
• • • We do not use the following data for averages, fits, limits, etc. • • •			
0.07 ± 0.03	GOPAL 77	DPWA	See GOPAL 80

$(\Gamma_i \Gamma_f)^{1/2} / \Gamma_{\text{total}}$  in  $N\bar{K} \rightarrow \Lambda(2110) \rightarrow \Sigma\pi$   $(\Gamma_1 \Gamma_2)^{1/2} / \Gamma$

VALUE	DOCUMENT ID	TECN	COMMENT
+0.14 ± 0.01	DEBELLEFON 77	DPWA	$K^- p \rightarrow \Sigma\pi$
+0.20 ± 0.03	KANE 74	DPWA	$K^- p \rightarrow \Sigma\pi$
• • • We do not use the following data for averages, fits, limits, etc. • • •			
+0.10 ± 0.03	GOPAL 77	DPWA	$\bar{K}N$ multichannel

$(\Gamma_i \Gamma_f)^{1/2} / \Gamma_{\text{total}}$  in  $N\bar{K} \rightarrow \Lambda(2110) \rightarrow \Lambda\omega$   $(\Gamma_1 \Gamma_3)^{1/2} / \Gamma$

VALUE	DOCUMENT ID	TECN	COMMENT
<0.05	BACCARI 77	DPWA	$K^- p \rightarrow \Lambda\omega$
0.112	<sup>1</sup> NAKKASYAN 75	DPWA	$K^- p \rightarrow \Lambda\omega$

$(\Gamma_i \Gamma_f)^{1/2} / \Gamma_{\text{total}}$  in  $N\bar{K} \rightarrow \Lambda(2110) \rightarrow \Sigma(1385)\pi$   $(\Gamma_1 \Gamma_4)^{1/2} / \Gamma$

VALUE	DOCUMENT ID	TECN	COMMENT
+0.071 ± 0.025	<sup>3</sup> CAMERON 78	DPWA	$K^- p \rightarrow \Sigma(1385)\pi$

$(\Gamma_i \Gamma_f)^{1/2} / \Gamma_{\text{total}}$  in  $N\bar{K} \rightarrow \Lambda(2110) \rightarrow N\bar{K}^*(892)$   $(\Gamma_1 \Gamma_6)^{1/2} / \Gamma$

VALUE	DOCUMENT ID	TECN	COMMENT
-0.17 ± 0.04	<sup>4</sup> CAMERON 78B	DPWA	$K^- p \rightarrow N\bar{K}^*$

### $\Lambda(2110)$ FOOTNOTES

- <sup>1</sup> Found in one of two best solutions.
- <sup>2</sup> The published error of 0.6 was a misprint.
- <sup>3</sup> The CAMERON 78 upper limit on  $F$ -wave decay is 0.03. The sign here has been changed to be in accord with the baryon-first convention.
- <sup>4</sup> The published sign has been changed to be in accord with the baryon-first convention. The CAMERON 78B upper limits on the  $P_3$  and  $F_3$  waves are each 0.03.

### $\Lambda(2110)$ REFERENCES

PDG 82	PL 111B 1	M. Roos et al.	(HELS, CIT, CERN)
GOPAL 80	Toronto Conf. 159	G.P. Gopal	(RHEL) IJP
CAMERON 78	NP B143 189	W. Cameron et al.	(RHEL, LOIC) IJP
CAMERON 78B	NP B146 327	W. Cameron et al.	(RHEL, LOIC) IJP
DEBELLEFON 78	NC 42A 403	A. de Bellefon et al.	(CDEF, SACL) IJP
BACCARI 77	NC 41A 96	B. Baccari et al.	(SACL, CDEF) IJP
DEBELLEFON 77	NC 37A 175	A. de Bellefon et al.	(CDEF, SACL) IJP
GOPAL 77	NP B119 362	G.P. Gopal et al.	(LOIC, RHEL) IJP
NAKKASYAN 75	NP B93 85	A. Nakkasyan	(CERN) IJP
KANE 74	LBL-2452	D.F. Kane	(LBL) IJP

$\Lambda(2325) 3/2^-$   $I(J^P) = 0(\frac{3}{2}^-)$  Status: \*

OMITTED FROM SUMMARY TABLE

BACCARI 77 finds this state with either  $J^P = 3/2^-$  or  $3/2^+$  in a energy-dependent partial-wave analysis of  $K^- p \rightarrow \Lambda\omega$  from 2070 to 2436 MeV. A subsequent semi-energy-independent analysis from threshold to 2436 MeV selects  $3/2^-$ . DEBELLEFON 78 (same group) also sees this state in an energy-dependent partial-wave analysis of  $K^- p \rightarrow \bar{K}N$  data, and finds  $J^P = 3/2^-$  or  $3/2^+$ . They again prefer  $J^P = 3/2^-$ , but only on the basis of model-dependent considerations.

## Baryon Particle Listings

 $\Lambda(2325)$ ,  $\Lambda(2350)$ ,  $\Lambda(2585)$  Bumps $\Lambda(2325)$  MASS

VALUE (MeV)	DOCUMENT ID	TECN	COMMENT
$\approx 2325$ OUR ESTIMATE			
2342 ± 30	DEBELLEFON 78	DPWA	$\bar{K}N \rightarrow \bar{K}N$
2327 ± 20	BACCARI 77	DPWA	$K^-p \rightarrow \Lambda\omega$

 $\Lambda(2325)$  WIDTH

VALUE (MeV)	DOCUMENT ID	TECN	COMMENT
177 ± 40	DEBELLEFON 78	DPWA	$\bar{K}N \rightarrow \bar{K}N$
160 ± 40	BACCARI 77	IPWA	$K^-p \rightarrow \Lambda\omega$

 $\Lambda(2325)$  DECAY MODES

Mode	$\Gamma_1/\Gamma$
$\Gamma_1$ $N\bar{K}$	
$\Gamma_2$ $\Lambda\omega$	

 $\Lambda(2325)$  BRANCHING RATIOS

$\Gamma(N\bar{K})/\Gamma_{\text{total}}$	DOCUMENT ID	TECN	COMMENT	$\Gamma_1/\Gamma$
0.19 ± 0.06	DEBELLEFON 78	DPWA	$\bar{K}N \rightarrow \bar{K}N$	

$(\Gamma_1\Gamma_2)^{1/2}/\Gamma_{\text{total}}$ in $N\bar{K} \rightarrow \Lambda(2325) \rightarrow \Lambda\omega$	DOCUMENT ID	TECN	COMMENT	$(\Gamma_1\Gamma_2)^{1/2}/\Gamma$
0.06 ± 0.02	<sup>1</sup> BACCARI 77	IPWA	$DS_{33}$ wave	
0.05 ± 0.02	<sup>1</sup> BACCARI 77	DPWA	$DD_{13}$ wave	
0.08 ± 0.03	<sup>1</sup> BACCARI 77	DPWA	$DD_{33}$ wave	

 $\Lambda(2325)$  FOOTNOTES

<sup>1</sup> Note that the three BACCARI 77 entries are for three different waves.

 $\Lambda(2325)$  REFERENCES

DEBELLEFON 78	NC 42A 403	A. de Bellefon et al.	(CDEF, SACL) IJP
BACCARI 77	NC 41A 96	B. Baccari et al.	(SACL, CDEF) IJP

$\Lambda(2350)$   $9/2^+$   $I(J^P) = 0(\frac{9}{2}^+)$  Status: \*\*\*

DAUM 68 favors  $J^P = 7/2^-$  or  $9/2^+$ . BRICMAN 70 favors  $9/2^+$ . LASINSKI 71 suggests three states in this region using a Pomeron + resonances model. There are now also three formation experiments from the College de France-Saclay group, DEBELLEFON 77, BACCARI 77, and DEBELLEFON 78, which find  $9/2^+$  in energy-dependent partial-wave analyses of  $\bar{K}N \rightarrow \Sigma\pi$ ,  $\Lambda\omega$ , and  $N\bar{K}$ .

 $\Lambda(2350)$  MASS

VALUE (MeV)	DOCUMENT ID	TECN	COMMENT
<b>2340 to 2370 (<math>\approx 2350</math>) OUR ESTIMATE</b>			
2370 ± 50	DEBELLEFON 78	DPWA	$\bar{K}N \rightarrow \bar{K}N$
2365 ± 20	DEBELLEFON 77	DPWA	$K^-p \rightarrow \Sigma\pi$
2358 ± 6	BRICMAN 70	CNTR	Total, charge exchange
••• We do not use the following data for averages, fits, limits, etc. •••			
2372	BACCARI 77	DPWA	$K^-p \rightarrow \Lambda\omega$
2344 ± 15	COOL 70	CNTR	$K^-p$ , $K^-d$ total
2360 ± 20	LU 70	CNTR	$\gamma p \rightarrow K^+Y^*$
2340 ± 7	BUGG 68	CNTR	$K^-p$ , $K^-d$ total

 $\Lambda(2350)$  WIDTH

VALUE (MeV)	DOCUMENT ID	TECN	COMMENT
<b>100 to 250 (<math>\approx 150</math>) OUR ESTIMATE</b>			
204 ± 50	DEBELLEFON 78	DPWA	$\bar{K}N \rightarrow \bar{K}N$
110 ± 20	DEBELLEFON 77	DPWA	$K^-p \rightarrow \Sigma\pi$
324 ± 30	BRICMAN 70	CNTR	Total, charge exchange
••• We do not use the following data for averages, fits, limits, etc. •••			
257	BACCARI 77	DPWA	$K^-p \rightarrow \Lambda\omega$
190	COOL 70	CNTR	$K^-p$ , $K^-d$ total
55	LU 70	CNTR	$\gamma p \rightarrow K^+Y^*$
140 ± 20	BUGG 68	CNTR	$K^-p$ , $K^-d$ total

 $\Lambda(2350)$  DECAY MODES

Mode	Fraction ( $\Gamma_i/\Gamma$ )
$\Gamma_1$ $N\bar{K}$	$\sim 12\%$
$\Gamma_2$ $\Sigma\pi$	$\sim 10\%$
$\Gamma_3$ $\Lambda\omega$	

The above branching fractions are our estimates, not fits or averages.

 $\Lambda(2350)$  BRANCHING RATIOS

See "Sign conventions for resonance couplings" in the Note on  $\Lambda$  and  $\Sigma$  Resonances.

$\Gamma(N\bar{K})/\Gamma_{\text{total}}$	DOCUMENT ID	TECN	COMMENT	$\Gamma_1/\Gamma$
$\sim 0.12$ OUR ESTIMATE				
0.12 ± 0.04	DEBELLEFON 78	DPWA	$\bar{K}N \rightarrow \bar{K}N$	

$(\Gamma_1\Gamma_2)^{1/2}/\Gamma_{\text{total}}$ in $N\bar{K} \rightarrow \Lambda(2350) \rightarrow \Sigma\pi$	DOCUMENT ID	TECN	COMMENT	$(\Gamma_1\Gamma_2)^{1/2}/\Gamma$
−0.11 ± 0.02	DEBELLEFON 77	DPWA	$K^-p \rightarrow \Sigma\pi$	

$(\Gamma_1\Gamma_3)^{1/2}/\Gamma_{\text{total}}$ in $N\bar{K} \rightarrow \Lambda(2350) \rightarrow \Lambda\omega$	DOCUMENT ID	TECN	COMMENT	$(\Gamma_1\Gamma_3)^{1/2}/\Gamma$
<0.05	BACCARI 77	DPWA	$K^-p \rightarrow \Lambda\omega$	

 $\Lambda(2350)$  REFERENCES

DEBELLEFON 78	NC 42A 403	A. de Bellefon et al.	(CDEF, SACL) IJP
BACCARI 77	NC 41A 96	B. Baccari et al.	(SACL, CDEF) IJP
DEBELLEFON 77	NC 37A 175	A. de Bellefon et al.	(CDEF, SACL) IJP
LASINSKI 71	NP B29 125	T.A. Lasinski	(EFI) IJP
BRICMAN 70	PL 31B 152	C. Bricman et al.	(CERN, CAEN, SACL)
COOL 70	PR D1 1887	R.L. Cool et al.	(BNL) I
Also	PRL 16 1228	R.L. Cool et al.	(BNL) I
LU 70	PR D2 1846	D.C. Lu et al.	(YALE)
BUGG 68	PR 168 1456	D.V. Bugg et al.	(RHEL, BIRM, CAVE) I
DAUM 68	NP B7 19	C. Daum et al.	(CERN) JP

 $\Lambda(2585)$  Bumps

$I(J^P) = 0(?^?)$  Status: \*\*

OMITTED FROM SUMMARY TABLE

 $\Lambda(2585)$  MASS (BUMPS)

VALUE (MeV)	DOCUMENT ID	TECN	COMMENT
$\approx 2585$ OUR ESTIMATE			
2585 ± 45	ABRAMS 70	CNTR	$K^-p$ , $K^-d$ total
2530 ± 25	LU 70	CNTR	$\gamma p \rightarrow K^+Y^*$

 $\Lambda(2585)$  WIDTH (BUMPS)

VALUE (MeV)	DOCUMENT ID	TECN	COMMENT
300	ABRAMS 70	CNTR	$K^-p$ , $K^-d$ total
150	LU 70	CNTR	$\gamma p \rightarrow K^+Y^*$

 $\Lambda(2585)$  DECAY MODES (BUMPS)

Mode	$\Gamma_1/\Gamma$
$\Gamma_1$ $N\bar{K}$	

 $\Lambda(2585)$  BRANCHING RATIOS (BUMPS)

$(J+\frac{1}{2}) \times \Gamma(N\bar{K})/\Gamma_{\text{total}}$	DOCUMENT ID	TECN	COMMENT	$\Gamma_1/\Gamma$
$J$ is not known, so only $(J+\frac{1}{2}) \times \Gamma(N\bar{K})/\Gamma_{\text{total}}$ can be given.				
0.12 ± 0.12	<sup>1</sup> BRICMAN 70	CNTR	Total, charge exchange	

 $\Lambda(2585)$  FOOTNOTES (BUMPS)

<sup>1</sup> The resonance is at the end of the region analyzed — no clear signal.

 $\Lambda(2585)$  REFERENCES (BUMPS)

ABRAMS 70	PR D1 1917	R.J. Abrams et al.	(BNL) I
Also	PRL 16 1228	R.L. Cool et al.	(BNL) I
BRICMAN 70	PL 31B 152	C. Bricman et al.	(CERN, CAEN, SACL)
LU 70	PR D2 1846	D.C. Lu et al.	(YALE)

## $\Sigma$ BARYONS

### ( $S = -1, I = 1$ )

$\Sigma^+ = uus, \Sigma^0 = uds, \Sigma^- = dds$



$I(J^P) = 1(\frac{1}{2}^+)$  Status: \*\*\*\*

We have omitted some results that have been superseded by later experiments. See our earlier editions.

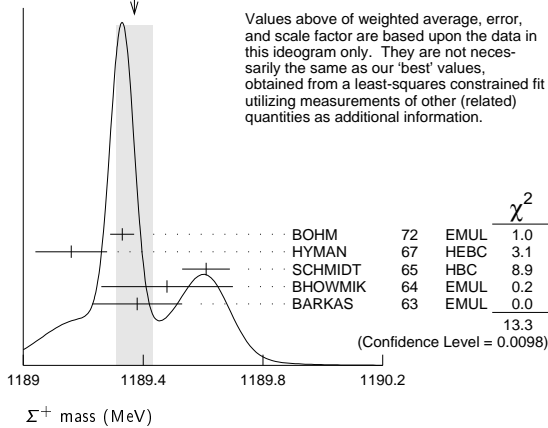
### $\Sigma^+$ MASS

The fit uses  $\Sigma^+, \Sigma^0, \Sigma^-$ , and  $\Lambda$  mass and mass-difference measurements.

VALUE (MeV)	EVTS	DOCUMENT ID	TECN	COMMENT
<b>1189.37 ± 0.07 OUR FIT</b>				Error includes scale factor of 2.2.
<b>1189.37 ± 0.06 OUR AVERAGE</b>				Error includes scale factor of 1.8. See the ideogram below.
1189.33 ± 0.04	607	<sup>1</sup> BOHM	72	EMUL
1189.16 ± 0.12		HYMAN	67	HEBC
1189.61 ± 0.08	4205	SCHMIDT	65	HBC See note with $\Lambda$ mass
1189.48 ± 0.22	58	<sup>2</sup> BHOWMIK	64	EMUL
1189.38 ± 0.15	144	<sup>2</sup> BARKAS	63	EMUL

<sup>1</sup> BOHM 72 is updated with our 1973  $K^-, \pi^-,$  and  $\pi^0$  masses (Reviews of Modern Physics **45** S1 (1973)).  
<sup>2</sup> These masses have been raised 30 keV to take into account a 46 keV increase in the proton mass and a 21 keV decrease in the  $\pi^0$  mass (note added 1967 edition, Reviews of Modern Physics **39** 1 (1967)).

WEIGHTED AVERAGE  
1189.37 ± 0.06 (Error scaled by 1.8)



### $\Sigma^+$ MEAN LIFE

Measurements with fewer than 1000 events have been omitted.

VALUE ( $10^{-10}$ s)	EVTS	DOCUMENT ID	TECN	COMMENT
<b>0.8018 ± 0.0026 OUR AVERAGE</b>				
0.8038 ± 0.0040 ± 0.0014		BARBOSA	00	E761 hyperons, 375 GeV
0.8043 ± 0.0080 ± 0.0014		<sup>3</sup> BARBOSA	00	E761 hyperons, 375 GeV
0.798 ± 0.005	30k	MARRAFFINO	80	HBC $K^- p$ 0.42-0.5 GeV/c
0.807 ± 0.013	5719	CONFORTO	76	HBC $K^- p$ 1-1.4 GeV/c
0.795 ± 0.010	20k	EISELE	70	HBC $K^- p$ at rest
0.803 ± 0.008	10664	BARLOUTAUD	69	HBC $K^- p$ 0.4-1.2 GeV/c
0.83 ± 0.032	1300	<sup>4</sup> CHANG	66	HBC

<sup>3</sup> This is a measurement of the  $\Sigma^-$  lifetime. Here we assume  $CPT$  invariance; see below for the fractional  $\Sigma^+ - \Sigma^-$  lifetime difference obtained by BARBOSA 00.  
<sup>4</sup> We have increased the CHANG 66 error of 0.018; see our 1970 edition, Reviews of Modern Physics **42** 87 (1970).

$(\tau_{\Sigma^+} - \tau_{\Sigma^-}) / \tau_{\Sigma^+}$

A test of  $CPT$  invariance.

VALUE	DOCUMENT ID	TECN	COMMENT
<b><math>(-6 \pm 12) \times 10^{-4}</math></b>	BARBOSA	00	E761 hyperons, 375 GeV

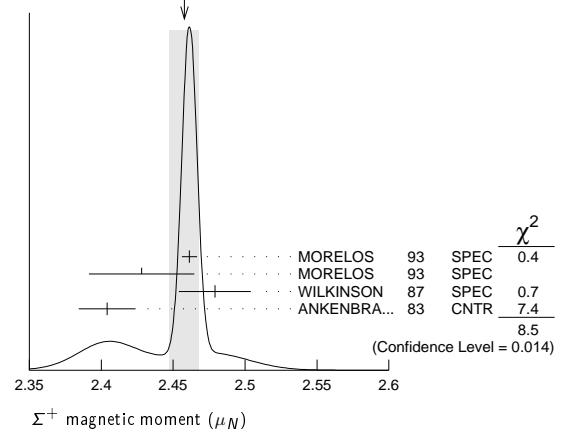
### $\Sigma^+$ MAGNETIC MOMENT

See the "Note on Baryon Magnetic Moments" in the  $\Lambda$  Listings. Measurements with an error  $\geq 0.1 \mu_N$  have been omitted.

VALUE ( $\mu_N$ )	EVTS	DOCUMENT ID	TECN	COMMENT
<b>2.458 ± 0.010 OUR AVERAGE</b>				Error includes scale factor of 2.1. See the ideogram below.
2.4613 ± 0.0034 ± 0.0040	250k	MORELOS	93	SPEC $p$ Cu 800 GeV
2.428 ± 0.036 ± 0.007	12k	<sup>5</sup> MORELOS	93	SPEC $p$ Cu 800 GeV
2.479 ± 0.012 ± 0.022	137k	WILKINSON	87	SPEC $p$ Be 400 GeV
2.4040 ± 0.0198	44k	<sup>6</sup> ANKENBRA...	83	CNTR $p$ Cu 400 GeV

<sup>5</sup> We assume  $CPT$  invariance: this is (minus) the  $\Sigma^-$  magnetic moment as measured by MORELOS 93. See below for the moment difference testing  $CPT$ .  
<sup>6</sup> ANKENBRANDT 83 gives the value  $2.38 \pm 0.02 \mu_N$ . MORELOS 93 uses the same hyperon magnet and channel and claims to determine the field integral better, leading to the revised value given here.

WEIGHTED AVERAGE  
2.458 ± 0.010 (Error scaled by 2.1)



$(\mu_{\Sigma^+} + \mu_{\Sigma^-}) / \mu_{\Sigma^+}$

A test of  $CPT$  invariance.

VALUE	DOCUMENT ID	TECN	COMMENT
<b>0.014 ± 0.015</b>	<sup>7</sup> MORELOS	93	SPEC $p$ Cu 800 GeV

<sup>7</sup> This is our calculation from the MORELOS 93 measurements of the  $\Sigma^+$  and  $\Sigma^-$  magnetic moments given above. The statistical error on  $\mu_{\Sigma^-}$  dominates the error here.

### $\Sigma^+$ DECAY MODES

Mode	Fraction ( $\Gamma_i / \Gamma$ )	Confidence level
$\Gamma_1$ $p \pi^0$	$(51.57 \pm 0.30) \%$	
$\Gamma_2$ $n \pi^+$	$(48.31 \pm 0.30) \%$	
$\Gamma_3$ $p \gamma$	$(1.23 \pm 0.05) \times 10^{-3}$	
$\Gamma_4$ $n \pi^+ \gamma$	[a] $(4.5 \pm 0.5) \times 10^{-4}$	
$\Gamma_5$ $\Lambda e^+ \nu_e$	$(2.0 \pm 0.5) \times 10^{-5}$	

### $\Delta S = \Delta Q$ ( $SQ$ ) violating modes or $\Delta S = 1$ weak neutral current ( $S1$ ) modes

Mode	Fraction	Confidence level
$\Gamma_6$ $n e^+ \nu_e$	$SQ < 5 \times 10^{-6}$	90%
$\Gamma_7$ $n \mu^+ \nu_\mu$	$SQ < 3.0 \times 10^{-5}$	90%
$\Gamma_8$ $p e^+ e^-$	$S1 < 7 \times 10^{-6}$	
$\Gamma_9$ $p \mu^+ \mu^-$	$S1 (9 \pm \frac{9}{-8}) \times 10^{-8}$	

[a] See the Listings below for the pion momentum range used in this measurement.

### CONSTRAINED FIT INFORMATION

An overall fit to 2 branching ratios uses 14 measurements and one constraint to determine 3 parameters. The overall fit has a  $\chi^2 = 7.7$  for 12 degrees of freedom.

The following off-diagonal array elements are the correlation coefficients  $\langle \delta x_i \delta x_j \rangle / (\delta x_i \delta x_j)$ , in percent, from the fit to the branching fractions,  $x_i \equiv \Gamma_i / \Gamma_{total}$ . The fit constrains the  $x_i$  whose labels appear in this array to sum to one.

$x_2$	-100	
$x_3$	12	-14
	$x_1$	$x_2$

# Baryon Particle Listings

Σ<sup>+</sup>

### Σ<sup>+</sup> BRANCHING RATIOS

**Γ( $n\pi^+$ )/Γ( $N\pi$ )** **Γ<sub>2</sub>/(Γ<sub>1</sub>+Γ<sub>2</sub>)**

VALUE	EVTS	DOCUMENT ID	TECN	COMMENT
<b>0.4836±0.0030 OUR FIT</b>				
<b>0.4836±0.0030 OUR AVERAGE</b>				
0.4828±0.0036	10k	<sup>8</sup> MARRAFFINO 80	HBC	$K^-p$ 0.42-0.5 GeV/c
0.488 ±0.008	1861	NOWAK 78	HBC	
0.484 ±0.015	537	TOVEE 71	EMUL	
0.488 ±0.010	1331	BARLOUTAUD 69	HBC	$K^-p$ 0.4-1.2 GeV/c
0.46 ±0.02	534	CHANG 66	HBC	
0.490 ±0.024	308	HUMPHREY 62	HBC	

<sup>8</sup> MARRAFFINO 80 actually gives Γ( $p\pi^0$ )/Γ(total) = 0.5172 ± 0.0036.

**Γ( $p\gamma$ )/Γ( $p\pi^0$ )** **Γ<sub>3</sub>/Γ<sub>1</sub>**

VALUE (units $10^{-3}$ )	EVTS	DOCUMENT ID	TECN	COMMENT
<b>2.38±0.10 OUR FIT</b>				
<b>2.38±0.10 OUR AVERAGE</b>				
2.32±0.11±0.10	32k	TIMM 95	E761	$\Sigma^+$ 375 GeV
2.81±0.39 <sup>+0.21</sup> / <sub>-0.43</sub>	408	HESSEY 89	CNTR	$K^-p \rightarrow \Sigma^+\pi^-$ at rest
2.52±0.28	190	<sup>9</sup> KOBAYASHI 87	CNTR	$\pi^+p \rightarrow \Sigma^+K^+$
2.46 <sup>+0.30</sup> / <sub>-0.35</sub>	155	BIAGI 85	CNTR	CERN hyperon beam
2.11±0.38	46	MANZ 80	HBC	$K^-p \rightarrow \Sigma^+\pi^-$
2.1 ±0.3	45	ANG 69B	HBC	$K^-p$ at rest
2.76±0.51	31	GERSHWIN 69B	HBC	$K^-p \rightarrow \Sigma^+\pi^-$
3.7 ±0.8	24	BAZIN 65	HBC	$K^-p$ at rest

<sup>9</sup> KOBAYASHI 87 actually gives Γ( $p\gamma$ )/Γ(total) = (1.30 ± 0.15) × 10<sup>-3</sup>.

**Γ( $n\pi^+\gamma$ )/Γ( $n\pi^+$ )** **Γ<sub>4</sub>/Γ<sub>2</sub>**

The  $\pi^+$  momentum cuts differ, so we do not average the results but simply use the latest value in the Summary Table.

VALUE (units $10^{-3}$ )	EVTS	DOCUMENT ID	TECN	COMMENT
<b>0.93±0.10</b>				
0.27±0.05	29	ANG 69B	HBC	$\pi^+$ < 110 MeV/c
~1.8		BAZIN 65B	HBC	$\pi^+$ < 116 MeV/c

**Γ( $\Lambda e^+ \nu_e$ )/Γ<sub>total</sub>** **Γ<sub>5</sub>/Γ**

VALUE (units $10^{-5}$ )	EVTS	DOCUMENT ID	TECN	COMMENT
<b>2.0±0.5 OUR AVERAGE</b>				
1.6±0.7	5	BALTAY 69	HBC	$K^-p$ at rest
2.9±1.0	10	EISELE 69	HBC	$K^-p$ at rest
2.0±0.8	6	BARASH 67	HBC	$K^-p$ at rest

**Γ( $n e^+ \nu_e$ )/Γ( $n\pi^+$ )** **Γ<sub>6</sub>/Γ<sub>2</sub>**

Test of ΔS = ΔQ rule. Experiments with an effective denominator less than 100,000 have been omitted.

EFFECTIVE DENOM.	EVTS	DOCUMENT ID	TECN	COMMENT
<b>&lt; 1.1 × 10<sup>-5</sup> OUR LIMIT</b> Our 90% CL limit = (2.3 events)/(effective denominator sum). [Number of events increased to 2.3 for a 90% confidence level.]				
111000	0	<sup>10</sup> EBENHOH 74	HBC	$K^-p$ at rest
105000	0	<sup>10</sup> SECHI-ZORN 73	HBC	$K^-p$ at rest

<sup>10</sup> Effective denominator calculated by us.

**Γ( $n\mu^+ \nu_\mu$ )/Γ( $n\pi^+$ )** **Γ<sub>7</sub>/Γ<sub>2</sub>**

Test of ΔS = ΔQ rule.

EFFECTIVE DENOM.	EVTS	DOCUMENT ID	TECN	COMMENT
<b>&lt; 6.2 × 10<sup>-5</sup> OUR LIMIT</b> Our 90% CL limit = (6.7 events)/(effective denominator sum). [Number of events increased to 6.7 for a 90% confidence level.]				
33800	0	BAGGETT 69B	HBC	
62000	2	<sup>11</sup> EISELE 69B	HBC	
10150	0	<sup>12</sup> COURANT 64	HBC	
1710	0	<sup>12</sup> NAUENBERG 64	HBC	
120	1	GALTIERI 62	EMUL	

<sup>11</sup> Effective denominator calculated by us.  
<sup>12</sup> Effective denominator taken from EISELE 67.

**Γ( $p e^+ e^-$ )/Γ<sub>total</sub>** **Γ<sub>8</sub>/Γ**

VALUE (units $10^{-6}$ )	DOCUMENT ID	TECN	COMMENT
<b>&lt; 7</b>			
	<sup>13</sup> ANG 69B	HBC	$K^-p$ at rest

<sup>13</sup> ANG 69B found three  $p e^+ e^-$  events in agreement with  $\gamma \rightarrow e^+ e^-$  conversion from  $\Sigma^+ \rightarrow p\gamma$ . The limit given here is for neutral currents.

**Γ( $p\mu^+ \mu^-$ )/Γ<sub>total</sub>** **Γ<sub>9</sub>/Γ**

A test for a ΔS = 1 weak neutral current, but also allowed by higher-order electroweak interactions.

VALUE (units $10^{-8}$ )	EVTS	DOCUMENT ID	TECN	COMMENT
<b>8.6<sup>+6.6</sup>/<sub>-5.4</sub> ± 5.5</b>				
	3	<sup>14</sup> PARK 05	HYCP	$p$ Cu, 800 GeV

<sup>14</sup> The masses of the three dimuons of PARK 05 are within 1 MeV of one another, perhaps indicating the existence of a new state  $P^0$  with mass 214.3 ± 0.5 MeV. In that case, the decay is  $\Sigma^+ \rightarrow pP^0$ ,  $P^0 \rightarrow \mu^+ \mu^-$ , with a branching fraction of (3.1<sup>+2.4</sup>/<sub>-1.9</sub> ± 1.5) × 10<sup>-8</sup>.

**Γ( $\Sigma^+ \rightarrow n e^+ \nu_e$ )/Γ( $\Sigma^- \rightarrow n e^- \bar{\nu}_e$ )** **Γ<sub>6</sub>/Γ<sub>3</sub><sup>-</sup>**

VALUE	CL%	EVTS	DOCUMENT ID	TECN	COMMENT
<b>&lt; 0.009 OUR LIMIT</b> Our 90% CL limit, using Γ( $n e^+ \nu_e$ )/Γ( $n\pi^+$ ) above.					
••• We do not use the following data for averages, fits, limits, etc. •••					
<0.019	90	0	EBENHOH 74	HBC	$K^-p$ at rest
<0.018	90	0	SECHI-ZORN 73	HBC	$K^-p$ at rest
<0.12	95	0	COLE 71	HBC	$K^-p$ at rest
<0.03	90	0	EISELE 69B	HBC	See EBENHOH 74

**Γ( $\Sigma^+ \rightarrow n\mu^+ \nu_\mu$ )/Γ( $\Sigma^- \rightarrow n\mu^- \bar{\nu}_\mu$ )** **Γ<sub>7</sub>/Γ<sub>4</sub><sup>-</sup>**

VALUE	CL%	EVTS	DOCUMENT ID	TECN	COMMENT
<b>&lt; 0.12 OUR LIMIT</b> Our 90% CL limit, using Γ( $n\mu^+ \nu_\mu$ )/Γ( $n\pi^+$ ) above.					
••• We do not use the following data for averages, fits, limits, etc. •••					
0.06 <sup>+0.045</sup> / <sub>-0.03</sub>		2	EISELE 69B	HBC	$K^-p$ at rest

**Γ( $\Sigma^+ \rightarrow n\ell^+ \nu$ )/Γ( $\Sigma^- \rightarrow n\ell^- \bar{\nu}$ )** **(Γ<sub>6</sub>+Γ<sub>7</sub>)/(Γ<sub>3</sub><sup>-</sup>+Γ<sub>4</sub><sup>-</sup>)**

Test of ΔS = ΔQ rule.

VALUE	CL%	EVTS	DOCUMENT ID	TECN	COMMENT
<b>&lt; 0.043 OUR LIMIT</b> Our 90% CL limit, using [Γ( $n e^+ \nu_e$ ) + Γ( $n\mu^+ \nu_\mu$ )]/Γ( $n\pi^+$ ).					
••• We do not use the following data for averages, fits, limits, etc. •••					
<0.08		1	NORTON 69	HBC	
<0.034		0	BAGGETT 67	HBC	

### Σ<sup>+</sup> DECAY PARAMETERS

See the "Note on Baryon Decay Parameters" in the neutron Listings. A few early results have been omitted.

**α<sub>0</sub> FOR Σ<sup>+</sup> → ρπ<sup>0</sup>**

VALUE	EVTS	DOCUMENT ID	TECN	COMMENT
<b>-0.980<sup>+0.017</sup>/<sub>-0.015</sub> OUR FIT</b>				
<b>-0.980<sup>+0.017</sup>/<sub>-0.013</sub> OUR AVERAGE</b>				
-0.945 <sup>+0.055</sup> / <sub>-0.042</sub>	1259	<sup>15</sup> LIPMAN 73	OSPK	$\pi^+p \rightarrow \Sigma^+$
-0.940±0.045	16k	BELLA MY 72	ASPK	$\pi^+p \rightarrow \Sigma^+K^+$
-0.98 <sup>+0.05</sup> / <sub>-0.02</sub>	1335	<sup>16</sup> HARRIS 70	OSPK	$\pi^+p \rightarrow \Sigma^+K^+$
-0.999±0.022	32k	BANGERTER 69	HBC	$K^-p$ 0.4 GeV/c

<sup>15</sup> Decay protons scattered off aluminum.  
<sup>16</sup> Decay protons scattered off carbon.

**φ<sub>0</sub> ANGLE FOR Σ<sup>+</sup> → ρπ<sup>0</sup>** **(tan φ<sub>0</sub> = β/γ)**

VALUE (°)	EVTS	DOCUMENT ID	TECN	COMMENT
<b>36 ± 34 OUR AVERAGE</b>				
38.1 <sup>+35.7</sup> / <sub>-37.1</sub>	1259	<sup>17</sup> LIPMAN 73	OSPK	$\pi^+p \rightarrow \Sigma^+K^+$
22 ± 90		<sup>18</sup> HARRIS 70	OSPK	$\pi^+p \rightarrow \Sigma^+K^+$

<sup>17</sup> Decay proton scattered off aluminum.  
<sup>18</sup> Decay protons scattered off carbon.

**α<sub>+</sub> / α<sub>0</sub>**

Older results have been omitted.

VALUE	EVTS	DOCUMENT ID	TECN	COMMENT
<b>-0.069±0.013 OUR FIT</b>				
<b>-0.073±0.021</b>				
	23k	MARRAFFINO 80	HBC	$K^-p$ 0.42-0.5 GeV/c

**α<sub>+</sub> FOR Σ<sup>+</sup> → nπ<sup>+</sup>**

VALUE	EVTS	DOCUMENT ID	TECN	COMMENT
<b>0.068±0.013 OUR FIT</b>				
<b>0.066±0.016 OUR AVERAGE</b>				
0.037±0.049	4101	BERLEY 70B	HBC	
0.069±0.017	35k	BANGERTER 69	HBC	$K^-p$ 0.4 GeV/c

**φ<sub>+</sub> ANGLE FOR Σ<sup>+</sup> → nπ<sup>+</sup>** **(tan φ<sub>+</sub> = β/γ)**

VALUE (°)	EVTS	DOCUMENT ID	TECN	COMMENT
<b>167±20 OUR AVERAGE</b> Error includes scale factor of 1.1.				
184±24	1054	<sup>19</sup> BERLEY 70B	HBC	
143±29	560	BANGERTER 69B	HBC	$K^-p$ 0.4 GeV/c

<sup>19</sup> Changed from 176 to 184° to agree with our sign convention.

**α<sub>γ</sub> FOR Σ<sup>+</sup> → pγ**

VALUE	EVTS	DOCUMENT ID	TECN	COMMENT
<b>-0.76 ± 0.08 OUR AVERAGE</b>				
-0.720±0.086±0.045	35k	<sup>20</sup> FOUCHER 92	SPEC	$\Sigma^+$ 375 GeV
-0.86 ±0.13 ±0.04	190	KOBAYASHI 87	CNTR	$\pi^+p \rightarrow \Sigma^+K^+$
-0.53 <sup>+0.38</sup> / <sub>-0.36</sub>	46	MANZ 80	HBC	$K^-p \rightarrow \Sigma^+\pi^-$
-1.03 <sup>+0.52</sup> / <sub>-0.42</sub>	61	GERSHWIN 69B	HBC	$K^-p \rightarrow \Sigma^+\pi^-$

<sup>20</sup> See TIMM 95 for a detailed description of the analysis.

**$\Sigma^+$  REFERENCES**

We have omitted some papers that have been superseded by later experiments. See our earlier editions.

PARK	05	PRL 94 021801	H.K. Park <i>et al.</i>	(FNAL HyperCP Collab.)
BARBOSA	00	PR D61 031101R	R.F. Barbosa <i>et al.</i>	(FNAL E761 Collab.)
TIMM	95	PR D51 4638	S. Timm <i>et al.</i>	(FNAL E761 Collab.)
MORELOS	93	PRL 71 3417	A. Morelos <i>et al.</i>	(FNAL E761 Collab.)
FOUCHER	92	PRL 68 3004	M. Foucher <i>et al.</i>	(FNAL E761 Collab.)
HESSEY	89	ZPHY C42 175	N.P. Hessey <i>et al.</i>	(BNL-811 Collab.)
KOBAYASHI	87	PRL 59 868	M. Kobayashi <i>et al.</i>	(KYOT)
WILKINSON	87	PRL 58 855	C.A. Wilkinson <i>et al.</i>	(WISC, MICH, RUTG+)
BIAGI	85	ZPHY C28 495	S.F. Biagi <i>et al.</i>	(CERN WA62 Collab.)
ANKENBRANDT	83	PRL 51 863	C.M. Ankenbrandt <i>et al.</i>	(FNAL, IOWA, ISU+)
MANZ	80	PL 96B 217	A. Manz <i>et al.</i>	(MPIM, VAND)
MARRAFFINO	80	PR D21 2501	J. Marraffino <i>et al.</i>	(VAND, MPIM)
NOWAK	78	NP B139 61	R.J. Nowak <i>et al.</i>	(LOUC, BELG, DURH+)
CONFORTO	76	NP B105 189	B. Conforto <i>et al.</i>	(RHEL, LOUC)
EBENHOH	74	ZPHY 264 367	H. Ebenhoh <i>et al.</i>	(HEIDT)
EBENHOH	73	ZPHY 264 413	W. Ebenhoh <i>et al.</i>	(HEIDT)
LIPMAN	73	PL 43B 89	N.H. Lipman <i>et al.</i>	(RHEL, SUSS, LOWC)
PDG	73	RMP 45 51	T.A. Sechinski <i>et al.</i>	(LBL, BRAN, CERN+)
SECHI-ZORN	73	PR D8 12	B. Sechi-Zorn, G.A. Snow	(UMD)
BELLAMY	72	PL 39B 299	E.H. Bellamy <i>et al.</i>	(LOWC, RHEL, SUSS)
BOHM	72	NP B48 1	G. Bohm <i>et al.</i>	(BERL, KIDR, BRUX, IASD+)
Also		IJHE-73-2 Nov	G. Bohm	(BERL, KIDR, BRUX, IASD, DUUC+)
COLE	71	PR D4 631	J. Cole <i>et al.</i>	(STON, COLU)
TOVEE	71	NP B33 493	D.W. Tovee <i>et al.</i>	(LOUC, KIDR, BERL+)
BERLEY	70B	PR D1 2015	D. Berley <i>et al.</i>	(BNL, MASA, YALE)
EISELE	70	ZPHY 238 372	F. Eisele <i>et al.</i>	(HEID)
HARRIS	70	PRL 24 165	F. Harris <i>et al.</i>	(MICH, WISC)
PDG	70	RMP 42 87	A. Barbaro-Gatti <i>et al.</i>	(LRL, BRAN+)
ANG	69B	ZPHY 228 151	G. Ang <i>et al.</i>	(HEID)
BAGGETT	69B	Thesis MDDP-TR-973	N.V. Baggett	(UMD)
BALTAY	69	PRL 22 615	C. Baltay <i>et al.</i>	(COLU, STON)
BANGERTER	69	Thesis UCRL 19244	R.O. Bangerter	(LRL)
BANGERTER	69B	PR 187 1821	R.O. Bangerter <i>et al.</i>	(LRL)
BARLOUTAUD	69	NP B14 153	R. Barloutaud <i>et al.</i>	(SACL, CERN, HEID)
EISELE	69	ZPHY 221 1	F. Eisele <i>et al.</i>	(HEID)
Also		PRL 13 291	W. Willis <i>et al.</i>	(BNL, CERN, HEID, UMD)
EISELE	69B	ZPHY 221 401	F. Eisele <i>et al.</i>	(HEID)
GERSHWIN	69B	PR 188 2077	L.K. Gershwin <i>et al.</i>	(LRL)
Also		Thesis UCRL 19246	L.K. Gershwin	(LRL)
NORTON	69	Thesis Nevis 175	H. Norton	(COLU)
BAGGETT	67	PRL 19 1458	N. Baggett <i>et al.</i>	(UMD)
Also		Vienna Abs. 374	N.V. Baggett, B. Kehoe	(UMD)
Also		Private Comm.	N.V. Baggett	(UMD)
BARASH	67	PRL 19 181	N. Barash <i>et al.</i>	(HEID)
EISELE	67	ZPHY 205 409	F. Eisele <i>et al.</i>	(HEID)
HYMAN	67	PL 25B 376	L.G. Hyman <i>et al.</i>	(ANL, CMU, NWES)
PDG	67	RMP 39 1	A.H. Rosenfeld <i>et al.</i>	(LRL, CERN, YALE)
CHANG	66	PR 151 1081	C.Y. Chang	(COLU)
Also		Thesis Nevis 145	C.Y. Chang	(COLU)
BAZIN	65	PRL 14 154	M. Bazin <i>et al.</i>	(PRIN, COLU)
BAZIN	65B	PR 140B 1358	M. Bazin <i>et al.</i>	(PRIN, RUTG, COLU)
SCHMIDT	65	PR 140B 1328	P. Schmidt	(COLU)
BHOWMIK	64	NP 53 22	B. Bhowmik <i>et al.</i>	(DELH)
COURANT	64	PR 136 B1791	H. Courant <i>et al.</i>	(CERN, HEID, UMD+)
NAUENBERG	64	PRL 12 679	U. Nauenberg <i>et al.</i>	(COLU, RUTG, PRIN)
BARKAS	63	PRL 11 26	W.H. Barkas, J.N. Dyer, H.H. Heckman	(LRL)
Also		Thesis UCRL 9450	J.N. Dyer	(LRL)
GALTIERI	62	PRL 9 26	A. Barbaro-Gatti <i>et al.</i>	(LRL)
HUMPHREY	62	PR 127 1305	W.E. Humphrey, R.R. Ross	(LRL)

76.23 ± 0.55	109	COLAS	75	HLBC	$\Sigma^0 \rightarrow \Lambda \gamma$
76.63 ± 0.28	208	SCHMIDT	65	HBC	See note with $\Lambda$ mass

**$\Sigma^0$  MEAN LIFE**

These lifetimes are deduced from measurements of the cross sections for the Primakoff process  $\Lambda \rightarrow \Sigma^0$  in nuclear Coulomb fields. An alternative expression of the same information is the  $\Sigma^0$ - $\Lambda$  transition magnetic moment given in the following section. The relation is  $(\mu_{\Sigma^0 \Lambda} / \mu_N)^2 \tau = 1.92951 \times 10^{-19}$  s (see DEVLIN 86).

VALUE ( $10^{-20}$ s)	DOCUMENT ID	TECN	COMMENT
<b>7.4 ± 0.7 OUR EVALUATION</b>	Using $\mu_{\Sigma^0 \Lambda}$ (see the above note).		
6.5 <sup>+1.7</sup> <sub>-1.1</sub>	<sup>2</sup> DEVLIN	86	SPEC Primakoff effect
7.6 ± 0.5 ± 0.7	<sup>3</sup> PETERSEN	86	SPEC Primakoff effect
• • • We do not use the following data for averages, fits, limits, etc. • • •			
5.8 ± 1.3	<sup>2</sup> DYDAK	77	SPEC See DEVLIN 86
<sup>2</sup> DEVLIN 86 is a recalculation of the results of DYDAK 77 removing a numerical approximation made in that work.			
<sup>3</sup> An additional uncertainty of the Primakoff formalism is estimated to be < 5%.			

**$|\mu(\Sigma^0 \rightarrow \Lambda)|$  TRANSITION MAGNETIC MOMENT**

See the note in the  $\Sigma^0$  mean-life section above. Also, see the "Note on Baryon Magnetic Moments" in the  $\Lambda$  Listings.

VALUE ( $\mu_N$ )	DOCUMENT ID	TECN	COMMENT
<b>1.61 ± 0.08 OUR AVERAGE</b>			
1.72 <sup>+0.17</sup> <sub>-0.19</sub>	<sup>4</sup> DEVLIN	86	SPEC Primakoff effect
1.59 ± 0.05 ± 0.07	<sup>5</sup> PETERSEN	86	SPEC Primakoff effect
• • • We do not use the following data for averages, fits, limits, etc. • • •			
1.82 <sup>+0.25</sup> <sub>-0.18</sub>	<sup>4</sup> DYDAK	77	SPEC See DEVLIN 86
<sup>4</sup> DEVLIN 86 is a recalculation of the results of DYDAK 77 removing a numerical approximation made in that work.			
<sup>5</sup> An additional uncertainty of the Primakoff formalism is estimated to be < 2.5%.			

**$\Sigma^0$  DECAY MODES**

Mode	Fraction ( $\Gamma_i/\Gamma$ )	Confidence level
$\Gamma_1 \Lambda \gamma$	100 %	
$\Gamma_2 \Lambda \gamma \gamma$	< 3 %	90%
$\Gamma_3 \Lambda e^+ e^-$	[a] 5 × 10 <sup>-3</sup>	

[a] A theoretical value using QED.

**$\Sigma^0$  BRANCHING RATIOS**

$\Gamma(\Lambda \gamma \gamma) / \Gamma_{total}$	CL%	DOCUMENT ID	TECN	$\Gamma_2/\Gamma$
< 0.03	90	COLAS	75	HLBC
$\Gamma(\Lambda e^+ e^-) / \Gamma_{total}$		DOCUMENT ID	COMMENT	$\Gamma_3/\Gamma$
0.00545		FEINBERG	58	Theoretical QED calculation

See COURANT 63 and ALFF 65 for measurements of the invariant-mass spectrum of the Dalitz pairs.

**$\Sigma^0$  REFERENCES**

WANG	97	PR D56 2544	M.H.L.S. Wang <i>et al.</i>	(BNL-E766 Collab.)
DEVLIN	86	PR D34 1626	T. Devlin, P.C. Petersen, A. Beretvas	(RUTG)
PETERSEN	86	PRL 57 949	P.C. Petersen <i>et al.</i>	(RUTG, WISC, MICH+)
DYDAK	77	NP B118 1	F. Dydak <i>et al.</i>	(CERN, DORT, HEIDH)
COLAS	75	NP B91 253	J. Colas <i>et al.</i>	(ORSAY)
ALFF	65	PR 137 B1105	C. Alff <i>et al.</i>	(COLU, RUTG, BNL) P
DOSCH	65	PL 14 239	H.C. Dosch <i>et al.</i>	(HEID)
SCHMIDT	65	PR 140B 1328	P. Schmidt	(COLU)
BURNSTEIN	64	PRL 13 66	R.A. Burnstein <i>et al.</i>	(UMD)
COURANT	63	PRL 10 409	H. Courant <i>et al.</i>	(CERN, UMD) P
FEINBERG	58	PR 109 1019	G. Feinberg	(BNL)



$I(J^P) = 1(\frac{1}{2}^+)$  Status: \* \* \* \*

COURANT 63 and ALFF 65, using  $\Sigma^0 \rightarrow \Lambda e^+ e^-$  decays (Dalitz decays), determined the  $\Sigma^0$  parity to be positive, given that  $J = 1/2$  and that certain very reasonable assumptions about form factors are true. The results of experiments involving the Primakoff effect, from which the  $\Sigma^0$  mean life and  $\Sigma^0 \rightarrow \Lambda$  transition magnetic moment come (see below), strongly support  $J = 1/2$ .

**$\Sigma^0$  MASS**

The fit uses  $\Sigma^+$ ,  $\Sigma^0$ ,  $\Sigma^-$ , and  $\Lambda$  mass and mass-difference measurements.

VALUE (MeV)	EVTS	DOCUMENT ID	TECN	COMMENT
<b>1192.642 ± 0.024 OUR FIT</b>				
• • • We do not use the following data for averages, fits, limits, etc. • • •				
1192.65 ± 0.020 ± 0.014	3327	<sup>1</sup> WANG	97	SPEC $\Sigma^0 \rightarrow \Lambda \gamma \rightarrow (p\pi^-)(e^+ e^-)$
<sup>1</sup> This WANG 97 result is redundant with the $\Sigma^0$ - $\Lambda$ mass-difference measurement below.				
$m_{\Sigma^-} - m_{\Sigma^0}$				
VALUE (MeV)	EVTS	DOCUMENT ID	TECN	COMMENT
<b>4.807 ± 0.035 OUR FIT</b>				Error includes scale factor of 1.1.
<b>4.86 ± 0.08 OUR AVERAGE</b>				Error includes scale factor of 1.2.
4.87 ± 0.12	37	DOSCH	65	HBC
5.01 ± 0.12	12	SCHMIDT	65	HBC See note with $\Lambda$ mass
4.75 ± 0.1	18	BURNSTEIN	64	HBC

**$m_{\Sigma^0} - m_{\Lambda}$**

VALUE (MeV)	EVTS	DOCUMENT ID	TECN	COMMENT
<b>76.959 ± 0.023 OUR FIT</b>				
<b>76.966 ± 0.020 ± 0.013</b>	3327	WANG	97	SPEC $\Sigma^0 \rightarrow \Lambda \gamma \rightarrow (p\pi^-)(e^+ e^-)$
• • • We do not use the following data for averages, fits, limits, etc. • • •				

# Baryon Particle Listings

$\Sigma^-$



$$I(J^P) = 1(\frac{1}{2}^+) \text{ Status: } ****$$

We have omitted some results that have been superseded by later experiments. See our earlier editions.

## $\Sigma^-$ MASS

The fit uses  $\Sigma^+$ ,  $\Sigma^0$ ,  $\Sigma^-$ , and  $\Lambda$  mass and mass-difference measurements.

VALUE (MeV)	EVTS	DOCUMENT ID	TECN	COMMENT
<b>1197.449 ± 0.030 OUR FIT</b>				Error includes scale factor of 1.2.
<b>1197.45 ± 0.04 OUR AVERAGE</b>				Error includes scale factor of 1.2.
1197.417 ± 0.040		GUREV 93	SPEC	$\Sigma^-$ C atom, crystal diff.
1197.532 ± 0.057		GALL 88	CNTR	$\Sigma^-$ Pb, $\Sigma^-$ W atoms
1197.43 ± 0.08	3000	SCHMIDT 65	HBC	See note with $\Lambda$ mass
• • • We do not use the following data for averages, fits, limits, etc. • • •				
1197.24 ± 0.15		<sup>1</sup> DUGAN 75	CNTR	Exotic atoms
<sup>1</sup> GALL 88 concludes that the DUGAN 75 mass needs to be reevaluated.				

## $m_{\Sigma^-} - m_{\Sigma^+}$

VALUE (MeV)	EVTS	DOCUMENT ID	TECN	COMMENT
<b>8.08 ± 0.08 OUR FIT</b>				Error includes scale factor of 1.9.
<b>8.09 ± 0.16 OUR AVERAGE</b>				
7.91 ± 0.23	86	BOHM 72	EMUL	
8.25 ± 0.25	2500	DOSCH 65	HBC	
8.25 ± 0.40	87	BARKAS 63	EMUL	

## $m_{\Sigma^-} - m_{\Lambda}$

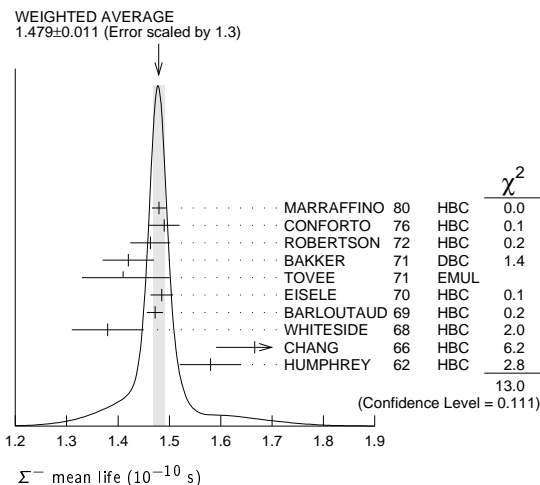
VALUE (MeV)	EVTS	DOCUMENT ID	TECN	COMMENT
<b>81.766 ± 0.030 OUR FIT</b>				Error includes scale factor of 1.2.
<b>81.69 ± 0.07 OUR AVERAGE</b>				
81.64 ± 0.09	2279	HEPP 68	HBC	
81.80 ± 0.13	85	SCHMIDT 65	HBC	See note with $\Lambda$ mass
81.70 ± 0.19		BURNSTEIN 64	HBC	

## $\Sigma^-$ MEAN LIFE

Measurements with an error  $\geq 0.2 \times 10^{-10}$  s have been omitted.

VALUE ( $10^{-10}$ s)	EVTS	DOCUMENT ID	TECN	COMMENT
<b>1.479 ± 0.011 OUR AVERAGE</b>				Error includes scale factor of 1.3. See the ideogram below.
1.480 ± 0.014	16k	MARRAFFINO 80	HBC	$K^- p$ 0.42–0.5 GeV/c
1.49 ± 0.03	8437	CONFORTO 76	HBC	$K^- p$ 1–1.4 GeV/c
1.463 ± 0.039	2400	ROBERTSON 72	HBC	$K^- p$ 0.25 GeV/c
1.42 ± 0.05	1383	BAKKER 71	DBC	$K^- N \rightarrow \Sigma^- \pi \pi$
1.41 ± 0.09		TOVEE 71	EMUL	
1.485 ± 0.022	100k	EISELE 70	HBC	$K^- p$ at rest
1.472 ± 0.016	10k	BARLOUTAUD 69	HBC	$K^- p$ 0.4–1.2 GeV/c
1.38 ± 0.07	506	WHITESIDE 68	HBC	$K^- p$ at rest
1.666 ± 0.075	3267	<sup>2</sup> CHANG 66	HBC	$K^- p$ at rest
1.58 ± 0.06	1208	HUMPHREY 62	HBC	$K^- p$ at rest

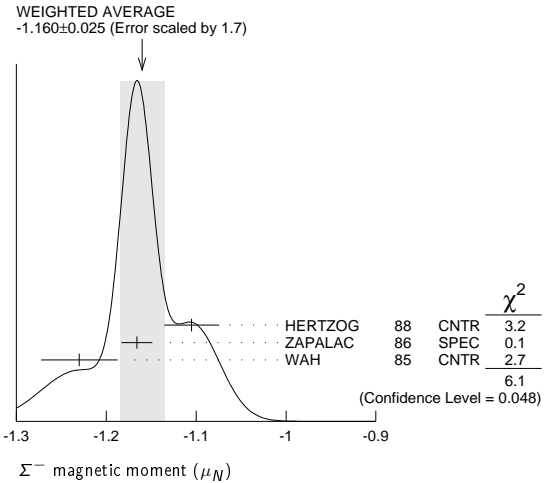
<sup>2</sup>We have increased the CHANG 66 error of 0.026; see our 1970 edition, Reviews of Modern Physics **42** 87 (1970).



## $\Sigma^-$ MAGNETIC MOMENT

See the "Note on Baryon Magnetic Moments" in the  $\Lambda$  Listings. Measurements with an error  $\geq 0.3 \mu_N$  have been omitted.

VALUE ( $\mu_N$ )	EVTS	DOCUMENT ID	TECN	COMMENT
<b>-1.160 ± 0.025 OUR AVERAGE</b>				Error includes scale factor of 1.7. See the ideogram below.
-1.105 ± 0.029 ± 0.010		HERTZOG 88	CNTR	$\Sigma^-$ Pb, $\Sigma^-$ W atoms
-1.166 ± 0.014 ± 0.010	671k	ZAPALAC 86	SPEC	$n e^- \nu, n \pi^-$ decays
-1.23 ± 0.03 ± 0.03		WAH 85	CNTR	$p Cu \rightarrow \Sigma^- X$
• • • We do not use the following data for averages, fits, limits, etc. • • •				
-0.89 ± 0.14	516k	DECK 83	SPEC	$p Be \rightarrow \Sigma^- X$



## $\Sigma^-$ CHARGE RADIUS

VALUE (fm)	DOCUMENT ID	TECN	COMMENT
<b>0.780 ± 0.080 ± 0.060</b>	<sup>3</sup> ESCHRICH 01	SELX	$\Sigma^- e \rightarrow \Sigma^- e$
<sup>3</sup> ESCHRICH 01 actually gives $\langle r^2 \rangle = (0.61 \pm 0.12 \pm 0.09) \text{ fm}^2$ .			

## $\Sigma^-$ DECAY MODES

Mode	Fraction ( $\Gamma_i/\Gamma$ )
$\Gamma_1$ $n \pi^-$	(99.848 ± 0.005) %
$\Gamma_2$ $n \pi^- \gamma$	[a] (4.6 ± 0.6) × 10 <sup>-4</sup>
$\Gamma_3$ $n e^- \bar{\nu}_e$	(1.017 ± 0.034) × 10 <sup>-3</sup>
$\Gamma_4$ $n \mu^- \bar{\nu}_\mu$	(4.5 ± 0.4) × 10 <sup>-4</sup>
$\Gamma_5$ $\Lambda e^- \bar{\nu}_e$	(5.73 ± 0.27) × 10 <sup>-5</sup>

[a] See the Listings below for the pion momentum range used in this measurement.

## CONSTRAINED FIT INFORMATION

An overall fit to 3 branching ratios uses 16 measurements and one constraint to determine 4 parameters. The overall fit has a  $\chi^2 = 8.7$  for 13 degrees of freedom.

The following *off-diagonal* array elements are the correlation coefficients  $\langle \delta x_i \delta x_j \rangle / (\delta x_i \delta x_j)$ , in percent, from the fit to the branching fractions,  $x_i \equiv \Gamma_i/\Gamma_{\text{total}}$ . The fit constrains the  $x_i$  whose labels appear in this array to sum to one.

$x_3$	-64		
$x_4$	-77	0	
$x_5$	-5	0	0
	$x_1$	$x_3$	$x_4$

## $\Sigma^-$ BRANCHING RATIOS

$\Gamma(n \pi^- \gamma) / \Gamma(n \pi^-)$   $\Gamma_2 / \Gamma_1$   
 The  $\pi^+$  momentum cuts differ, so we do not average the results but simply use the latest value for the Summary Table.

VALUE (units 10 <sup>-3</sup> )	EVTS	DOCUMENT ID	TECN	COMMENT
<b>0.46 ± 0.06</b>	292	EBENHOH 73	HBC	$\pi^+ < 150 \text{ MeV/c}$
• • • We do not use the following data for averages, fits, limits, etc. • • •				
0.10 ± 0.02	23	ANG 69B	HBC	$\pi^- < 110 \text{ MeV/c}$
~ 1.1		BAZIN 65B	HBC	$\pi^- < 166 \text{ MeV/c}$



See key on page 457

Baryon Particle Listings

$\Sigma^-$

$\Gamma(n e \bar{\nu}_e) / \Gamma(n \pi^-)$   $\Gamma_3 / \Gamma_1$

Measurements with an error  $\geq 0.2 \times 10^{-3}$  have been omitted.

VALUE (units $10^{-3}$ )	EVTS	DOCUMENT ID	TECN	COMMENT
<b>1.019 ± 0.035 OUR FIT</b>				
<b>1.019 ± 0.031 OUR AVERAGE</b>				
0.96 ± 0.05	2847	BOURQUIN	83c	SPEC SPS hyperon beam
1.09 <sup>+0.06</sup> <sub>-0.08</sub>	601	<sup>4</sup> EBENHOH	74	HBC $K^- p$ at rest
1.05 <sup>+0.07</sup> <sub>-0.13</sub>	455	<sup>4</sup> SECHI-ZORN	73	HBC $K^- p$ at rest
0.97 ± 0.15	57	COLE	71	HBC $K^- p$ at rest
1.11 ± 0.09	180	BIERMAN	68	HBC

<sup>4</sup> An additional negative systematic error is included for internal radiative corrections and latest form factors; see BOURQUIN 83c.

$\Gamma(n \mu^- \bar{\nu}_\mu) / \Gamma(n \pi^-)$   $\Gamma_4 / \Gamma_1$

VALUE (units $10^{-3}$ )	EVTS	DOCUMENT ID	TECN	COMMENT
<b>0.45 ± 0.04 OUR FIT</b>				
<b>0.45 ± 0.04 OUR AVERAGE</b>				
0.38 ± 0.11	13	COLE	71	HBC $K^- p$ at rest
0.43 ± 0.06	72	ANG	69	HBC $K^- p$ at rest
0.43 ± 0.09	56	BAGGETT	69	HBC $K^- p$ at rest
0.56 ± 0.20	11	BAZIN	65B	HBC $K^- p$ at rest
0.66 ± 0.15	22	COURANT	64	HBC

$\Gamma(\Lambda e^- \bar{\nu}_e) / \Gamma(n \pi^-)$   $\Gamma_5 / \Gamma_1$

VALUE (units $10^{-4}$ )	EVTS	DOCUMENT ID	TECN	COMMENT
<b>0.574 ± 0.027 OUR FIT</b>				
<b>0.574 ± 0.027 OUR AVERAGE</b>				
0.561 ± 0.031	1620	<sup>5</sup> BOURQUIN	82	SPEC SPS hyperon beam
0.63 ± 0.11	114	THOMPSON	80	ASPK Hyperon beam
0.52 ± 0.09	31	BALTAY	69	HBC $K^- p$ at rest
0.69 ± 0.12	31	EISELE	69	HBC $K^- p$ at rest
0.64 ± 0.12	35	BARASH	67	HBC $K^- p$ at rest
0.75 ± 0.28	11	COURANT	64	HBC $K^- p$ at rest

<sup>5</sup> The value is from BOURQUIN 83B, and includes radiation corrections and new acceptance.

$\Sigma^-$  DECAY PARAMETERS

See the "Note on Baryon Decay Parameters" in the neutron Listings. Older, outdated results have been omitted.

$\alpha_-$  FOR  $\Sigma^- \rightarrow \pi \pi^-$

VALUE	EVTS	DOCUMENT ID	TECN	COMMENT
<b>-0.068 ± 0.008 OUR AVERAGE</b>				
-0.062 ± 0.024	28k	HANSL	78	HBC $K^- p \rightarrow \Sigma^- \pi^+$
-0.067 ± 0.011	60k	BOGERT	70	HBC $K^- p$ 0.4 GeV/c
-0.071 ± 0.012	51k	BANGERTER	69	HBC $K^- p$ 0.4 GeV/c

$\phi$  ANGLE FOR  $\Sigma^- \rightarrow \pi \pi^-$

( $\tan \phi = \beta / \gamma$ )

VALUE (°)	EVTS	DOCUMENT ID	TECN	COMMENT
<b>10 ± 15 OUR AVERAGE</b>				
+ 5 ± 23	1092	<sup>6</sup> BERLEY	70B	HBC $n$ rescattering
14 ± 19	1385	BANGERTER	69B	HBC $K^- p$ 0.4 GeV/c

<sup>6</sup> BERLEY 70B changed from -5 to +5° to agree with our sign convention.

$g_A/g_V$  FOR  $\Sigma^- \rightarrow n e^- \bar{\nu}_e$

Measurements with fewer than 500 events have been omitted. Where necessary, signs have been changed to agree with our conventions, which are given in the "Note on Baryon Decay Parameters" in the neutron Listings. What is actually listed is  $|g_1/f_1 - 0.237g_2/f_1|$ . This reduces to  $g_A/g_V \equiv g_1(0)/f_1(0)$  on making the usual assumption that  $g_2 = 0$ . See also the note on HSUEH 88.

VALUE	EVTS	DOCUMENT ID	TECN	COMMENT
<b>0.340 ± 0.017 OUR AVERAGE</b>				
+0.327 ± 0.007 ± 0.019	50k	<sup>7</sup> HSUEH	88	SPEC $\Sigma^-$ 250 GeV
+0.34 ± 0.05	4456	<sup>8</sup> BOURQUIN	83c	SPEC SPS hyperon beam
0.385 ± 0.037	3507	<sup>9</sup> TANENBAUM	74	ASPK

• • • We do not use the following data for averages, fits, limits, etc. • • •

0.29 ± 0.07 25k HSUEH 85 SPEC See HSUEH 88  
 0.17 <sup>+0.07</sup> <sub>-0.09</sub> 519 DECAMP 77 ELEEC Hyperon beam

<sup>7</sup> The sign is, with our conventions, unambiguously positive. The value assumes, as usual, that  $g_2 = 0$ . If  $g_2$  is included in the fit, than (with our sign convention)  $g_2 = -0.56 \pm 0.37$ , with a corresponding reduction of  $g_A/g_V$  to  $+0.20 \pm 0.08$ .

<sup>8</sup> BOURQUIN 83c favors the positive sign by at least 2.6 standard deviations.

<sup>9</sup> TANENBAUM 74 gives  $0.435 \pm 0.035$ , assuming no  $q^2$  dependence in  $g_A$  and  $g_V$ . The listed result allows  $q^2$  dependence, and is taken from HSUEH 88.

$f_2(0)/f_1(0)$  FOR  $\Sigma^- \rightarrow n e^- \bar{\nu}_e$

The signs have been changed to be in accord with our conventions, given in the "Note on Baryon Decay Parameters" in the neutron Listings.

VALUE	EVTS	DOCUMENT ID	TECN	COMMENT
<b>0.97 ± 0.14 OUR AVERAGE</b>				
+0.96 ± 0.07 ± 0.13	50k	HSUEH	88	SPEC $\Sigma^-$ 250 GeV
+1.02 ± 0.34	4456	BOURQUIN	83c	SPEC SPS hyperon beam

TRIPLE CORRELATION COEFFICIENT  $D$  FOR  $\Sigma^- \rightarrow n e^- \bar{\nu}_e$

The coefficient  $D$  of the term  $D \mathbf{P}(\hat{p}_e \times \hat{p}_\nu)$  in the  $\Sigma^- \rightarrow n e^- \bar{\nu}_e$  decay angular distribution. A nonzero value would indicate a violation of time-reversal invariance.

VALUE	EVTS	DOCUMENT ID	TECN	COMMENT
<b>0.11 ± 0.10</b>	50k	HSUEH	88	SPEC $\Sigma^-$ 250 GeV

$g_V/g_A$  FOR  $\Sigma^- \rightarrow \Lambda e^- \bar{\nu}_e$

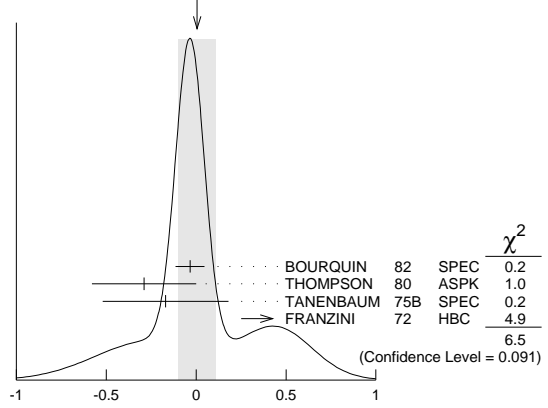
For the sign convention, see the "Note on Baryon Decay Parameters" in the neutron Listings. The value is predicted to be zero by conserved vector current theory. The values averaged assume CVC-SU(3) weak magnetism term.

VALUE	EVTS	DOCUMENT ID	TECN	COMMENT
<b>0.01 ± 0.10 OUR AVERAGE</b>				
Error includes scale factor of 1.5. See the ideogram below.				
-0.034 ± 0.080	1620	<sup>10</sup> BOURQUIN	82	SPEC SPS hyperon beam
-0.29 ± 0.29	114	THOMPSON	80	ASPK BNL hyperon beam
-0.17 ± 0.35	55	TANENBAUM	75B	SPEC BNL hyperon beam
+0.45 ± 0.20	186	<sup>10,11</sup> FRANZINI	72	HBC

<sup>10</sup> The sign has been changed to agree with our convention.

<sup>11</sup> The FRANZINI 72 value includes the events of earlier papers.

WEIGHTED AVERAGE  
 0.01 ± 0.10 (Error scaled by 1.5)



$g_{WM}/g_A$  FOR  $\Sigma^- \rightarrow \Lambda e^- \bar{\nu}_e$

The values quoted assume the CVC prediction  $g_V = 0$ .

VALUE	EVTS	DOCUMENT ID	TECN	COMMENT
<b>2.4 ± 1.7 OUR AVERAGE</b>				
1.75 ± 3.5	114	THOMPSON	80	ASPK BNL hyperon beam
3.5 ± 4.5	55	TANENBAUM	75B	SPEC BNL hyperon beam
2.4 ± 2.1	186	FRANZINI	72	HBC

$\Sigma^-$  REFERENCES

We have omitted some papers that have been superseded by later experiments. See our earlier editions.

ESCHRICH	01	PL B522 233	I. Eschrich et al.	(FNAL SELEX Collab.)
GUREV	93	JETPL 57 400	M. P. Gurev et al.	(PNPI)
Translated from ZETFP 57 383.				
GALL	88	PRL 60 186	K.P. Gall et al.	(BOST, MIT, WILL, CIT+)
HERTZOG	88	PR D37 1142	D.W. Hertzog et al.	(WILL, BOST, MIT+)
HSUEH	88	PR D38 2056	S.-Y. Hsueh et al.	(CHIC, ELMT, FNAL+)
ZAPALAC	86	PRL 57 1526	G. Zapalac et al.	(EFI, ELMT, FNAL+)
HSUEH	85	PRL 54 2399	S.-Y. Hsueh et al.	(CHIC, ELMT, FNAL+)
WAH	85	PRL 55 2551	Y.-W. Wah et al.	(FNAL, IOWA, ISU)
BOURQUIN	83B	ZPHY C21 27	M.H. Bourquin et al.	(BRIS, GEVA, HEIDP+)
BOURQUIN	83C	ZPHY C21 17	M.H. Bourquin et al.	(BRIS, GEVA, HEIDP+)
DECK	83	PR D28 1	L. Deck et al.	(RUTG, WISC, MICH, MINN)
BOURQUIN	82	ZPHY C12 307	M.H. Bourquin et al.	(BRIS, GEVA, HEIDP+)
MARRAFFINO	80	PR D21 2501	J. Marraffino et al.	(VAND, MFM)
THOMPSON	80	PR D21 25	J.A. Thompson et al.	(PITT, BNL)
HANSL	78	NP B132 45	T. Hansl et al.	(MPIM, VAND)
DECAMP	77	PL 66B 295	D. Decamp et al.	(LALO, EPOL)
CONFORTO	76	NP B105 189	B. Conforto et al.	(RHEL, LOIC)
DUGAN	75	NP A254 396	G. Dugan et al.	(COLU, YALE)
TANENBAUM	75B	PR D12 1871	W. Tanenbaum et al.	(YALE, FNAL, BNL)
EBENHOH	74	ZPHY 266 367	H. Ebenhoeh et al.	(HEIDT)
TANENBAUM	74	PRL 33 175	W. Tanenbaum et al.	(YALE, FNAL, BNL)
EBENHOH	73	ZPHY 264 413	W. Ebenhoeh et al.	(HEIDT)
SECHI-ZORN	73	PR D8 12	B. Sechi-Zorn, G.A. Snow	(UNID)
BOHM	72	NP B48 1	G. Bohm et al.	(BERL, KIDR, BRUX, IASD+)
FRANZINI	72	PR D6 2417	P. Franzini et al.	(COLU, HEID, UMD+)
ROBERTSON	72	Thesis UMI 78-00877	R.M. Robertson	(IIT)
BAKKER	71	LCN 1 37	A.M. Bakker et al.	(SABRE Collab.)
COLE	71	PR D4 631	J. Cole et al.	(STON, COLU)
Also Thesis Nevis 175				
TOVEE	71	NP B33 493	D.N. Tovee et al.	(LOUC, KIDR, BERL+)
BERLEY	70B	PR D1 2015	D. Berley et al.	(BNL, MASA, YALE)
BOGERT	70	PR D2 6	D.V. Bogert et al.	(BNL, MASA, YALE)
EISELE	70	ZPHY 238 372	F. Eisele et al.	(HEID)
PDG	70	RMP 42 87	A. Barbaro-Gatti et al.	(LRL, BRAN+)
ANG	69	ZPHY 223 103	G. Ang et al.	(HEID)
ANG	69B	ZPHY 228 151	G. Ang et al.	(HEID)

# Baryon Particle Listings

## $\Sigma^-, \Sigma(1385)$

BAGGETT 69	PRL 23 249	N.V. Baggett, B. Kehoe, G.A. Snow	(UMD)
BALTAY 69	PRL 22 615	C. Baltay et al.	(COLU, STON)
BANGERTER 69	Thesis UCRL 19244	R.O. Bangertter	(LRL)
BANGERTER 69B	PR 187 1821	R.O. Bangertter et al.	(LRL)
BARLOUTAUD 69	NP B14 153	R. Barloutaud et al.	(SACL, CERN, HEID)
EISELE 69	ZPHY 221 1	F. Eisele et al.	(HEID)
BIERMAN 68	PRL 20 1459	E. Bierman et al.	(PRIN)
HEPP 68	ZPHY 214 71	V. Hepp, H. Schleich	(HEID)
WHITESIDE 68	NC 94A 537	H. Whiteside, J. Gollub	(OBER)
BARASH 67	PRL 19 181	N. Barash et al.	(UMD)
CHANG 66	PR 151 1081	C.Y. Chang	(COLU)
BAZIN 65B	PR 140B 1358	M. Bazin et al.	(PRIN, RUTG, COLU)
DOSCH 65	PL 14 239	H.C. Dosch et al.	(HEID)
Also	PR 151 1081	C.Y. Chang	(COLU)
SCHMIDT 65	PR 140B 1328	P. Schmidt	(COLU)
BURNSTEIN 64	PRL 13 66	R.A. Burnstein et al.	(UMD)
COURANT 64	PR 136 B1791	H. Courant et al.	(CERN, HEID, UMD+)
BARKAS 63	PRL 11 26	W.H. Barkas, J.N. Dyer, H.H. Heckman	(LRL)
HUMPHREY 62	PR 127 1305	W.E. Humphrey, R.R. Ross	(LRL)

### $\Sigma(1385) 3/2^+$

$I(J^P) = 1(\frac{3}{2}^+)$  Status: \* \* \* \*

Discovered by ALSTON 60. Early measurements of the mass and width for combined charge states have been omitted. They may be found in our 1984 edition Reviews of Modern Physics 56 S1 (1984).

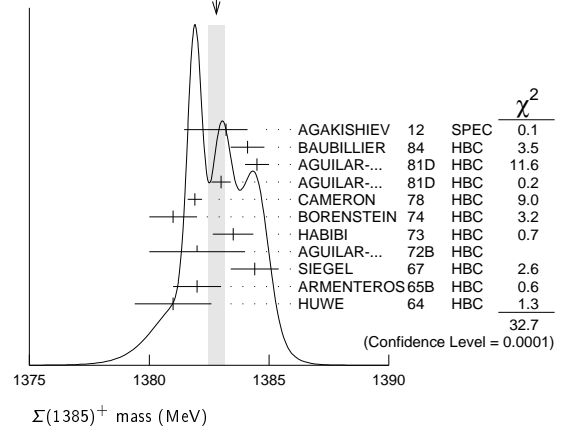
We average only the most significant determinations. We do not average results from inclusive experiments with large backgrounds or results which are not accompanied by some discussion of experimental resolution. Nevertheless systematic differences between experiments remain. (See the ideograms in the Listings below.) These differences could arise from interference effects that change with production mechanism and/or beam momentum. They can also be accounted for in part by differences in the parametrizations employed. (See BORENSTEIN 74 for a discussion on this point.) Thus BORENSTEIN 74 uses a Breit-Wigner with energy-independent width, since a *P*-wave was found to give unsatisfactory fits. CAMERON 78 uses the same form. On the other hand HOLMGREN 77 obtains a good fit to their  $\Lambda\pi$  spectrum with a *P*-wave Breit-Wigner, but includes the partial width for the  $\Sigma\pi$  decay mode in the parametrization. AGUILAR-BENITEZ 81D gives masses and widths for five different Breit-Wigner shapes. The results vary considerably. Only the best-fit *S*-wave results are given here.

### $\Sigma(1385)$ MASSES

#### $\Sigma(1385)^+$ MASS

VALUE (MeV)	EVTS	DOCUMENT ID	TECN	COMMENT
<b>1382.80 ± 0.35 OUR AVERAGE</b>		Error includes scale factor of 1.9. See the ideogram below.		
1383.2 ± 0.9 <sup>+0.1</sup> / <sub>-1.5</sub>		AGAKISHIEV 12	SPEC	$pp \rightarrow \Sigma(1385)^+ K^+ n$ , 3.5 GeV
1384.1 ± 0.7	1897	BAUBILLIER 84	HBC	$K^-p \rightarrow 8.25$ GeV/ <i>c</i>
1384.5 ± 0.5	5256	AGUILAR-... 81D	HBC	$K^-p \rightarrow \Lambda\pi\pi$ 4.2 GeV/ <i>c</i>
1383.0 ± 0.4	9361	AGUILAR-... 81D	HBC	$K^-p \rightarrow \Lambda 3\pi$ 4.2 GeV/ <i>c</i>
1381.9 ± 0.3	6900	CAMERON 78	HBC	$K^-p$ 0.96-1.36 GeV/ <i>c</i>
1381 ± 1	6846	BORENSTEIN 74	HBC	$K^-p$ 2.18 GeV/ <i>c</i>
1383.5 ± 0.85	2300	HABIBI 73	HBC	$K^-p \rightarrow \Lambda\pi\pi$
1382 ± 2	400	AGUILAR-... 72B	HBC	$K^-p \rightarrow \Lambda\pi$ 's
1384.4 ± 1.0	1260	SIEGEL 67	HBC	$K^-p$ 2.1 GeV/ <i>c</i>
1382 ± 1	750	ARMENTEROS65B	HBC	$K^-p$ 0.9-1.2 GeV/ <i>c</i>
1381.0 ± 1.6	859	HUWE 64	HBC	$K^-p$ 1.22 GeV/ <i>c</i>
• • • We do not use the following data for averages, fits, limits, etc. • • •				
1385.1 ± 1.2	600	BAKER 80	HYBR	$\pi^+p$ 7 GeV/ <i>c</i>
1383.2 ± 1.0	750	BAKER 80	HYBR	$K^-p$ 7 GeV/ <i>c</i>
1381 ± 2	7k	<sup>1</sup> BAUBILLIER 79B	HBC	$K^-p$ 8.25 GeV/ <i>c</i>
1391 ± 2	2k	CAUTIS 79	HYBR	$\pi^+p/K^-p$ 11.5 GeV
1390 ± 2	100	<sup>1</sup> SUGAHARA 79B	HBC	$\pi^-p$ 6 GeV/ <i>c</i>
1385 ± 3	22k	<sup>1,2</sup> BARREIRO 77B	HBC	$K^-p$ 4.2 GeV/ <i>c</i>
1385 ± 1	2594	HOLMGREN 77	HBC	See AGUILAR-BENITEZ 81D
1380 ± 2		<sup>1</sup> BARDADIN-... 75	HBC	$K^-p$ 14.3 GeV/ <i>c</i>
1382 ± 1	3740	<sup>3</sup> BERTHON 74	HBC	$K^-p$ 1263-1843 MeV/ <i>c</i>
1390 ± 6	46	AGUILAR-... 70B	HBC	$K^-p \rightarrow \Sigma\pi$ 's 4 GeV/ <i>c</i>
1383 ± 8	62	<sup>4</sup> BIRMINGHAM 66	HBC	$K^-p$ 3.5 GeV/ <i>c</i>
1378 ± 5	135	LONDON 66	HBC	$K^-p$ 2.24 GeV/ <i>c</i>
1384.3 ± 1.9	250	<sup>4</sup> SMITH 65	HBC	$K^-p$ 1.8 GeV/ <i>c</i>
1382.6 ± 2.1	250	<sup>4</sup> SMITH 65	HBC	$K^-p$ 1.95 GeV/ <i>c</i>
1375.0 ± 3.9	170	COOPER 64	HBC	$K^-p$ 1.45 GeV/ <i>c</i>
1376.0 ± 3.9	154	<sup>4</sup> ELY 61	HLBC	$K^-p$ 1.11 GeV/ <i>c</i>

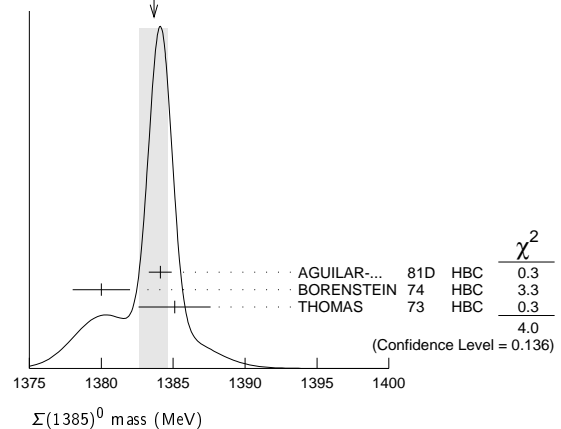
WEIGHTED AVERAGE  
1382.80±0.35 (Error scaled by 1.9)



#### $\Sigma(1385)^0$ MASS

VALUE (MeV)	EVTS	DOCUMENT ID	TECN	COMMENT
<b>1383.7 ± 1.0 OUR AVERAGE</b>		Error includes scale factor of 1.4. See the ideogram below.		
1384.1 ± 0.8	5722	AGUILAR-... 81D	HBC	$K^-p \rightarrow \Lambda 3\pi$ 4.2 GeV/ <i>c</i>
1380 ± 2	3100	<sup>5</sup> BORENSTEIN 74	HBC	$K^-p \rightarrow \Lambda 3\pi$ 2.18 GeV/ <i>c</i>
1385.1 ± 2.5	240	<sup>4</sup> THOMAS 73	HBC	$\pi^-p \rightarrow \Lambda\pi^0 K^0$
• • • We do not use the following data for averages, fits, limits, etc. • • •				
1389 ± 3	500	<sup>6</sup> BAUBILLIER 79B	HBC	$K^-p$ 8.25 GeV/ <i>c</i>

WEIGHTED AVERAGE  
1383.7±1.0 (Error scaled by 1.4)



#### $\Sigma(1385)^-$ MASS

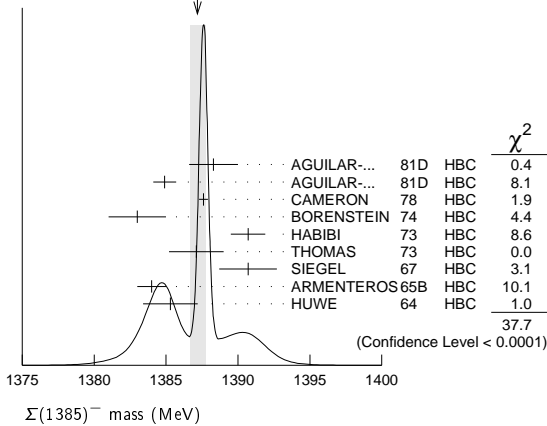
VALUE (MeV)	EVTS	DOCUMENT ID	TECN	COMMENT
<b>1387.2 ± 0.5 OUR AVERAGE</b>		Error includes scale factor of 2.2. See the ideogram below.		
1388.3 ± 1.7	620	AGUILAR-... 81D	HBC	$K^-p \rightarrow \Lambda\pi\pi$ 4.2 GeV/ <i>c</i>
1384.9 ± 0.8	3346	AGUILAR-... 81D	HBC	$K^-p \rightarrow \Lambda 3\pi$ 4.2 GeV/ <i>c</i>
1387.6 ± 0.3	9720	CAMERON 78	HBC	$K^-p$ 0.96-1.36 GeV/ <i>c</i>
1383 ± 2	2303	BORENSTEIN 74	HBC	$K^-p$ 2.18 GeV/ <i>c</i>
1390.7 ± 1.2	1900	HABIBI 73	HBC	$K^-p \rightarrow \Lambda\pi\pi$
1387.1 ± 1.9	630	<sup>4</sup> THOMAS 73	HBC	$\pi^-p \rightarrow \Lambda\pi^- K^+$
1390.7 ± 2.0	370	SIEGEL 67	HBC	$K^-p$ 2.1 GeV/ <i>c</i>
1384 ± 1	1380	ARMENTEROS65B	HBC	$K^-p$ 0.9-1.2 GeV/ <i>c</i>
1385.3 ± 1.9	1086	<sup>4</sup> HUWE 64	HBC	$K^-p$ 1.15-1.30 GeV/ <i>c</i>
• • • We do not use the following data for averages, fits, limits, etc. • • •				
1383 ± 1	4.5k	<sup>1</sup> BAUBILLIER 79B	HBC	$K^-p$ 8.25 GeV/ <i>c</i>
1380 ± 6	150	<sup>1</sup> SUGAHARA 79B	HBC	$\pi^-p$ 6 GeV/ <i>c</i>
1387 ± 3	12k	<sup>1,2</sup> BARREIRO 77B	HBC	$K^-p$ 4.2 GeV/ <i>c</i>
1391 ± 3	193	HOLMGREN 77	HBC	See AGUILAR-BENITEZ 81D
1383 ± 2		<sup>1</sup> BARDADIN-... 75	HBC	$K^-p$ 14.3 GeV/ <i>c</i>
1389 ± 1	3060	<sup>3</sup> BERTHON 74	HBC	$K^-p$ 1263-1843 MeV/ <i>c</i>
1389 ± 9	15	LONDON 66	HBC	$K^-p$ 2.24 GeV/ <i>c</i>
1391.5 ± 2.6	120	<sup>4</sup> SMITH 65	HBC	$K^-p$ 1.8 GeV/ <i>c</i>
1399.8 ± 2.2	58	<sup>4</sup> SMITH 65	HBC	$K^-p$ 1.95 GeV/ <i>c</i>
1392.0 ± 6.2	200	COOPER 64	HBC	$K^-p$ 1.45 GeV/ <i>c</i>
1382 ± 3	93	DAHL 61	DBC	$K^-d$ 0.45 GeV/ <i>c</i>
1376.0 ± 4.4	224	<sup>4</sup> ELY 61	HLBC	$K^-p$ 1.11 GeV/ <i>c</i>

See key on page 457

Baryon Particle Listings

$\Sigma(1385)$

WEIGHTED AVERAGE  
1387.2±0.5 (Error scaled by 2.2)



$m_{\Sigma(1385)^-} - m_{\Sigma(1385)^+}$

VALUE (MeV)	CL%	DOCUMENT ID	TECN	COMMENT
••• We do not use the following data for averages, fits, limits, etc. •••				
- 2 to +6	95	7 BORENSTEIN 74	HBC	$K^- p \rightarrow 2.18 \text{ GeV}/c$
7.2±1.4		7 HABIBI 73	HBC	$K^- p \rightarrow \Lambda \pi \pi$
6.3±2.0		7 SIEGEL 67	HBC	$K^- p \rightarrow 2.1 \text{ GeV}/c$
11 ±9		7 LONDON 66	HBC	$K^- p \rightarrow 2.24 \text{ GeV}/c$
9 ±6		LONDON 66	HBC	$\Lambda 3\pi$ events
2.0±1.5		7 ARMENTEROS65B	HBC	$K^- p \rightarrow 0.9-1.2 \text{ GeV}/c$
7.2±2.1		7 SMITH 65	HBC	$K^- p \rightarrow 1.8 \text{ GeV}/c$
17.2±2.0		7 SMITH 65	HBC	$K^- p \rightarrow 1.95 \text{ GeV}/c$
17 ±7		7 COOPER 64	HBC	$K^- p \rightarrow 1.45 \text{ GeV}/c$
4.3±2.2		7 HUWE 64	HBC	$K^- p \rightarrow 1.22 \text{ GeV}/c$
0.0±4.2		7 ELY 61	HLBC	$K^- p \rightarrow 1.11 \text{ GeV}/c$

$m_{\Sigma(1385)^0} - m_{\Sigma(1385)^+}$

VALUE (MeV)	CL%	DOCUMENT ID	TECN	COMMENT
••• We do not use the following data for averages, fits, limits, etc. •••				
-4 to +4	95	7 BORENSTEIN 74	HBC	$K^- p \rightarrow 2.18 \text{ GeV}/c$

$m_{\Sigma(1385)^-} - m_{\Sigma(1385)^0}$

VALUE (MeV)	DOCUMENT ID	TECN	COMMENT
••• We do not use the following data for averages, fits, limits, etc. •••			
2.0±2.4	7 THOMAS 73	HBC	$\pi^- p \rightarrow \Lambda \pi^- K^+$

$\Sigma(1385)$  WIDTHS

$\Sigma(1385)^+$  WIDTH

VALUE (MeV)	EVTS	DOCUMENT ID	TECN	COMMENT
<b>36.0± 0.7 OUR AVERAGE</b>				
40.2± 2.1 <sup>+1.2</sup> <sub>-2.8</sub>		AGAKISHIEV 12	SPEC	$pp \rightarrow \Sigma(1385)^+ K^+ n$ , 3.5 GeV
37.2± 2.0	1897	BAUBILLIER 84	HBC	$K^- p \rightarrow 8.25 \text{ GeV}/c$
35.1± 1.7	5256	AGUILAR-... 81D	HBC	$K^- p \rightarrow \Lambda \pi \pi \rightarrow 4.2 \text{ GeV}/c$
37.5± 2.0	9361	AGUILAR-... 81D	HBC	$K^- p \rightarrow \Lambda 3\pi \rightarrow 4.2 \text{ GeV}/c$
35.5± 1.9	6900	CAMERON 78	HBC	$K^- p \rightarrow 0.96-1.36 \text{ GeV}/c$
34.0± 1.6	6846	8 BORENSTEIN 74	HBC	$K^- p \rightarrow 2.18 \text{ GeV}/c$
38.3± 3.2	2300	9 HABIBI 73	HBC	$K^- p \rightarrow \Lambda \pi \pi$
32.5± 6.0	400	AGUILAR-... 72B	HBC	$K^- p \rightarrow \Lambda \pi^s$
36 ± 4	1260	9 SIEGEL 67	HBC	$K^- p \rightarrow 2.1 \text{ GeV}/c$
32.0± 4.7	750	9 ARMENTEROS65B	HBC	$K^- p \rightarrow 0.95-1.20 \text{ GeV}/c$
46.5± 6.4	859	9 HUWE 64	HBC	$K^- p \rightarrow 1.15-1.30 \text{ GeV}/c$
••• We do not use the following data for averages, fits, limits, etc. •••				
40 ± 3	600	BAKER 80	HYBR	$\pi^+ p \rightarrow 7 \text{ GeV}/c$
37 ± 2	750	BAKER 80	HYBR	$K^- p \rightarrow 7 \text{ GeV}/c$
37 ± 2	7k	1 BAUBILLIER 79B	HBC	$K^- p \rightarrow 8.25 \text{ GeV}/c$
30 ± 4	2k	CAUTIS 79	HYBR	$\pi^+ p / K^- p \rightarrow 11.5 \text{ GeV}$
30 ± 6	100	1 SUGAHARA 79B	HBC	$\pi^- p \rightarrow 6 \text{ GeV}/c$
43 ± 5	22k	1,2 BARREIRO 77B	HBC	$K^- p \rightarrow 4.2 \text{ GeV}/c$
34 ± 2	2594	HOLMGREN 77	HBC	See AGUILAR-BENITEZ 81D
40.0± 3.2		1 BARDADIN-... 75	HBC	$K^- p \rightarrow 14.3 \text{ GeV}/c$
48 ± 3	3740	3 BERTHON 74	HBC	$K^- p \rightarrow 1263-1843 \text{ MeV}/c$
33 ± 20	46	9 AGUILAR-... 70B	HBC	$K^- p \rightarrow \Sigma \pi^s \rightarrow 4 \text{ GeV}/c$
25 ± 32	62	9 BIRMINGHAM 66	HBC	$K^- p \rightarrow 3.5 \text{ GeV}/c$
30.3± 7.5	250	9 SMITH 65	HBC	$K^- p \rightarrow 1.8 \text{ GeV}/c$
33.1± 8.3	250	9 SMITH 65	HBC	$K^- p \rightarrow 1.95 \text{ GeV}/c$
51 ± 16	170	9 COOPER 64	HBC	$K^- p \rightarrow 1.45 \text{ GeV}/c$
48 ± 16	154	9 ELY 61	HLBC	$K^- p \rightarrow 1.11 \text{ GeV}/c$

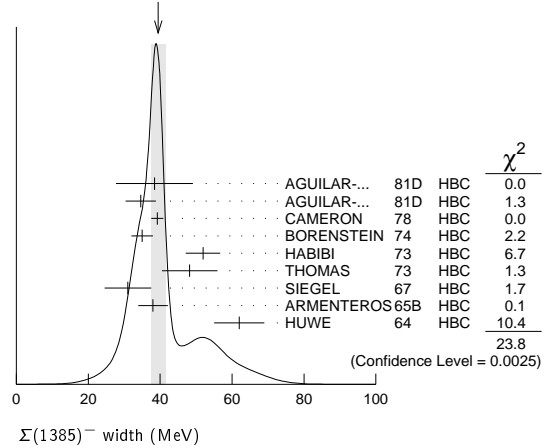
$\Sigma(1385)^0$  WIDTH

VALUE (MeV)	EVTS	DOCUMENT ID	TECN	COMMENT
<b>36 ± 5 OUR AVERAGE</b>				
34.8± 5.6	5722	AGUILAR-... 81D	HBC	$K^- p \rightarrow \Lambda 3\pi \rightarrow 4.2 \text{ GeV}/c$
39.3± 10.2	240	9 THOMAS 73	HBC	$\pi^- p \rightarrow \Lambda \pi^0 K^0$
••• We do not use the following data for averages, fits, limits, etc. •••				
53 ± 8	3100	10 BORENSTEIN 74	HBC	$K^- p \rightarrow \Lambda 3\pi \rightarrow 2.18 \text{ GeV}/c$
30 ± 9	106	CURTIS 63	OSPK	$\pi^- p \rightarrow 1.5 \text{ GeV}/c$

$\Sigma(1385)^-$  WIDTH

VALUE (MeV)	EVTS	DOCUMENT ID	TECN	COMMENT
<b>39.4± 2.1 OUR AVERAGE</b>				
Error includes scale factor of 1.7. See the ideogram below.				
38.4± 10.7	620	AGUILAR-... 81D	HBC	$K^- p \rightarrow \Lambda \pi \pi \rightarrow 4.2 \text{ GeV}/c$
34.6± 4.2	3346	AGUILAR-... 81D	HBC	$K^- p \rightarrow \Lambda 3\pi \rightarrow 4.2 \text{ GeV}/c$
39.2± 1.7	9720	CAMERON 78	HBC	$K^- p \rightarrow 0.96-1.36 \text{ GeV}/c$
35 ± 3	2303	8 BORENSTEIN 74	HBC	$K^- p \rightarrow 2.18 \text{ GeV}/c$
51.9± 4.8	1900	9 HABIBI 73	HBC	$K^- p \rightarrow \Lambda \pi \pi$
48.2± 7.7	630	9 THOMAS 73	HBC	$\pi^- p \rightarrow \Lambda \pi^- K^0$
31.0± 6.5	370	9 SIEGEL 67	HBC	$K^- p \rightarrow 2.1 \text{ GeV}/c$
38.0± 4.1	1382	9 ARMENTEROS65B	HBC	$K^- p \rightarrow 0.95-1.20 \text{ GeV}/c$
62 ± 7	1086	HUWE 64	HBC	$K^- p \rightarrow 1.15-1.30 \text{ GeV}/c$
••• We do not use the following data for averages, fits, limits, etc. •••				
44 ± 4	4.5k	1 BAUBILLIER 79B	HBC	$K^- p \rightarrow 8.25 \text{ GeV}/c$
58 ± 4	150	1 SUGAHARA 79B	HBC	$\pi^- p \rightarrow 6 \text{ GeV}/c$
45 ± 5	12k	1,2 BARREIRO 77B	HBC	$K^- p \rightarrow 4.2 \text{ GeV}/c$
35 ± 10	193	HOLMGREN 77	HBC	See AGUILAR-BENITEZ 81D
47 ± 6		1 BARDADIN-... 75	HBC	$K^- p \rightarrow 14.3 \text{ GeV}/c$
40 ± 3	3060	3 BERTHON 74	HBC	$K^- p \rightarrow 1263-1843 \text{ MeV}/c$
29.2± 10.6	120	9 SMITH 65	HBC	$K^- p \rightarrow 1.80 \text{ GeV}/c$
17.1± 8.9	58	9 SMITH 65	HBC	$K^- p \rightarrow 1.95 \text{ GeV}/c$
88 ± 24	200	9 COOPER 64	HBC	$K^- p \rightarrow 1.45 \text{ GeV}/c$
40		DAHL 61	DBC	$K^- d \rightarrow 0.45 \text{ GeV}/c$
66 ± 18	224	9 ELY 61	HLBC	$K^- p \rightarrow 1.11 \text{ GeV}/c$

WEIGHTED AVERAGE  
39.4±2.1 (Error scaled by 1.7)



$\Sigma(1385)$  POLE POSITIONS

$\Sigma(1385)^+$  REAL PART

VALUE	DOCUMENT ID	COMMENT
1379±1	LICHTENBERG74	Extrapolates HABIBI 73

$\Sigma(1385)^+$  -IMAGINARY PART

VALUE	DOCUMENT ID	COMMENT
17.5±1.5	LICHTENBERG74	Extrapolates HABIBI 73

$\Sigma(1385)^-$  REAL PART

VALUE	DOCUMENT ID	COMMENT
1383±1	LICHTENBERG74	Extrapolates HABIBI 73

$\Sigma(1385)^-$  -IMAGINARY PART

VALUE	DOCUMENT ID	COMMENT
22.5±1.5	LICHTENBERG74	Extrapolates HABIBI 73

## Baryon Particle Listings

 $\Sigma(1385)$ ,  $\Sigma(1480)$  Bumps $\Sigma(1385)$  DECAY MODES

Mode	Fraction ( $\Gamma_i/\Gamma$ )	Confidence level
$\Gamma_1 \Lambda\pi$	(87.0 $\pm$ 1.5 ) %	
$\Gamma_2 \Sigma\pi$	(11.7 $\pm$ 1.5 ) %	
$\Gamma_3 \Lambda\gamma$	( 1.25 $^{+0.13}_{-0.12}$ ) %	
$\Gamma_4 \Sigma^-\gamma$	< 2.4	$\times 10^{-4}$ 90%
$\Gamma_5 N\bar{K}$		

The above branching fractions are our estimates, not fits or averages.

 $\Sigma(1385)$  BRANCHING RATIOS

$\Gamma(\Sigma\pi)/\Gamma(\Lambda\pi)$	VALUE	DOCUMENT ID	TECN	CHG	COMMENT	$\Gamma_2/\Gamma_1$
<b>0.135 <math>\pm</math> 0.011 OUR AVERAGE</b>						
0.20 $\pm$ 0.06	DIONISI	78b	HBC	$\pm$	$K^-p \rightarrow Y^* K\bar{K}$	
0.16 $\pm$ 0.03	BERTHON	74	HBC	$-$	$K^-p$ 1.26-1.84 GeV/c	
0.11 $\pm$ 0.02	BERTHON	74	HBC	$-$	$K^-p$ 1.26-1.84 GeV/c	
0.21 $\pm$ 0.05	BORENSTEIN	74	HBC	$+$	$K^-p \rightarrow \Lambda\pi^+\pi^-$ , $\Sigma^0\pi^+\pi^-$	
0.18 $\pm$ 0.04	MAST	73	MPWA	$\pm$	$K^-p \rightarrow \Lambda\pi^+\pi^-$ , $\Sigma^0\pi^+\pi^-$	
0.10 $\pm$ 0.05	THOMAS	73	HBC	$-$	$\pi^-p \rightarrow \Lambda K\pi, \Sigma K\pi$	
0.16 $\pm$ 0.07	AGUILAR...	72b	HBC	$+$	$K^-p$ 3.9, 4.6 GeV/c	
0.13 $\pm$ 0.04	COLLEY	71b	DBC	$-0$	$K^-N$ 1.5 GeV/c	
0.13 $\pm$ 0.04	PAN	69	HBC	$+$	$\pi^+p \rightarrow \Lambda K\pi, \Sigma K\pi$	
0.08 $\pm$ 0.06	LONDON	66	HBC	$+$	$K^-p$ 2.24 GeV/c	
0.163 $\pm$ 0.041	ARMENTEROS65b	HBC	$\pm$	$K^-p$ 0.95-1.20 GeV/c		
0.09 $\pm$ 0.04	HUWE	64	HBC	$\pm$	$K^-p$ 1.2-1.7 GeV	
• • • We do not use the following data for averages, fits, limits, etc. • • •						
<0.04	ALSTON	62	HBC	$\pm$	$K^-p$ 1.15 GeV/c	
0.04 $\pm$ 0.04	BASTIEN	61	HBC	$\pm$		

$\Gamma(\Lambda\gamma)/\Gamma(\Lambda\pi)$	VALUE (units $10^{-2}$ )	EVTs	DOCUMENT ID	TECN	COMMENT	$\Gamma_3/\Gamma_1$
<b>1.43<math>^{+0.15}_{-0.13}</math> OUR AVERAGE</b>						
1.42 $\pm$ 0.12 $^{+0.11}_{-0.07}$	624 $\pm$ 25	KELLER	11	CLAS	$\gamma p \rightarrow K^+\Lambda\gamma, E_\gamma$ 1.6-3.8 GeV	
1.53 $\pm$ 0.39 $^{+0.15}_{-0.24}$	61	TAYLOR	05	CLAS	$\gamma p \rightarrow K^+\Lambda\gamma$	

$\Gamma(\Sigma^-\gamma)/\Gamma_{total}$	VALUE	CL%	DOCUMENT ID	TECN	CHG	COMMENT	$\Gamma_4/\Gamma$
<b>&lt;2.4 <math>\times 10^{-4}</math></b>	90	11	MOLCHANOV	04	SELX	$\Sigma^-\text{Pb} \rightarrow \Sigma(1385)^-\text{Pb}, 600 \text{ GeV}$	
• • • We do not use the following data for averages, fits, limits, etc. • • •							
<6.1 $\times 10^{-4}$	90	12	ARIK	77	SPEC	$\Sigma^-\text{Pb} \rightarrow \Sigma(1385)^-\text{Pb}, 23 \text{ GeV}$	

$(\Gamma_i/\Gamma_j)^{1/2}/\Gamma_{total}$ in $N\bar{K} \rightarrow \Sigma(1385) \rightarrow \Lambda\pi$	VALUE	DOCUMENT ID	CHG	COMMENT	$(\Gamma_5/\Gamma_1)^{1/2}/\Gamma$
+0.586 $\pm$ 0.319	13	DEVENISH	74b	0	Fixed-t dispersion rel.

 $\Sigma(1385)$  FOOTNOTES

- From fit to inclusive  $\Lambda\pi$  spectrum.
- Includes data of HOLMGREN 77.
- The errors are statistical only. The resolution is not unfolded.
- The error is enlarged to  $\Gamma/\sqrt{N}$ . See the note on the  $K^*(892)$  mass in the 1984 edition.
- From a fit to  $\Lambda\pi^0$  with the width fixed at 34 MeV.
- From fit to inclusive  $\Lambda\pi^0$  spectrum with the width fixed at 40 MeV.
- Redundant with data in the mass Listings.
- Results from  $\Lambda\pi^+\pi^-$  and  $\Lambda\pi^+\pi^-\pi^0$  combined by us.
- The error is enlarged to  $4\Gamma/\sqrt{N}$ . See the note on the  $K^*(892)$  mass in the 1984 edition.
- Consistent with +, 0, and - widths equal.
- We calculate this from the MOLCHANOV 04 upper limit of 9.5 keV on the  $\Sigma^-\gamma$  width.
- We calculate this from the ARIK 77 upper limit of 24 keV on the  $\Sigma^-\gamma$  width.
- An extrapolation of the parametrized amplitude below threshold.

 $\Sigma(1385)$  REFERENCES

AGAKISHIEV	12	PR C85 035203	G. Agakishiev et al.	(HADES Collab.)
KELLER	11	PR D83 072004	D. Keller et al.	(CLAS Collab.)
TAYLOR	05	PR C71 054609	S. Taylor et al.	(JLab CLAS Collab.)
Also		PR C72 039902 (errat.)	S. Taylor et al.	(JLab CLAS Collab.)
MOLCHANOV	04	PL B590 161	V.V. Molchanov et al.	(FNAL SELEX Collab.)
BAUBILLIER	84	ZPHY C23 213	M. Baubillier et al.	(BIRM, CERN, GLAS+)
PDG	84	RMP 56 51	C.G. Wohl et al.	(LBL, CIT, CERN)
AGUILAR...	81D	AFIS A77 144	M. Aguilar-Benitez, J. Salicio	(MADR)
BAKER	80	NP B146 207	P.A. Baker et al.	(LOIC)
BAUBILLIER	79b	NP B148 18	M. Baubillier et al.	(BIRM, CERN, GLAS+)
CAUTIS	79	NP B156 507	C.V. Cautis et al.	(SLAC)
SUGAHARA	79b	NP B156 237	R. Sugahara et al.	(KEK, OSK, KINK)
CAMERON	78	NP B143 189	W. Cameron et al.	(RHEL, LOIC)
DIONISI	78b	PL 78B 154	C. Dionisi, R. Armenteros, J. Diaz	(CERN, AMST+)
ARIK	77	PRL 38 1000	E. Arik et al.	(PITT, BNL, MASA)
BARREIRO	77b	NP B126 319	F. Barreiro et al.	(CERN, AMST, NIJM)
HOLMGREN	77	NP B119 261	S.O. Holmgren et al.	(CERN, AMST, NIJM)

BARDADIN...	75	NP B98 418	M. Bardadin-Otwinowska et al.	(SACL, EPOL+)
BERTHON	74	NC 21A 146	A. Berthon et al.	(CDEF, RHEL, SACL+)
BORENSTEIN	74	PR D9 3006	S.R. Borenstein et al.	(BNL, MICH)
DEVENISH	74b	NP B81 330	R.C.E. Devenish, C.D. Froggatt, B.R. Martin	(DESY+)
LICHTENBERG	74	PR D10 3865	D.B. Lichtenberg	(IND)
Also		Private Comm.	D.B. Lichtenberg	(IND)
HABIBI	73	Thesis Nevis 199	M. Habibi	(COLU)
Also		Purdue Conf. 387	C. Ballay et al.	(COLU, BING)
MAST	73	PR D7 3212	T.S. Mast et al.	(LBL) JJP
Also		PR D7 5	T.S. Mast et al.	(LBL) JJP
THOMAS	73	NP B56 15	D.W. Thomas et al.	(CNL) JJP
AGUILAR...	72b	PR D6 29	M. Aguilar-Benitez et al.	(BIRM)
COLLEY	71b	NP B31 61	D.C. Colley et al.	(BIRM, EDIN, GLAS+)
AGUILAR...	70b	PL 8 365	M. Aguilar-Benitez et al.	(BNL, SYR)
PAN	69	PRL 23 808	Y.L. Pan, F.L. Forman	(PENN) I
SIEGEL	67	Thesis UCRL 18041	D.M. Siegel	(LRL)
BIRMINGHAM	66	PR 152 1148	M. Haque et al.	(BIRM, GLAS, LOIC, OXF+)
LONDON	66	PR 143 1034	G.W. London et al.	(BNL, SYR) J
ARMENTEROS	65b	PL 19 75	R. Armenteros et al.	(CERN, HEID, SACL)
SMITH	65	Thesis UCLA	L.T. Smith	(UCLA)
COOPER	64	PL 8 365	N.W.A. Cooper et al.	(CERN, AMST)
HUWE	64	Thesis UCRL 11291	D.O. Huwe	(LRL) JJP
Also		PR 181 1824	D.O. Huwe	(LRL)
CURTIS	63	PR 132 1771	L.J. Curtis et al.	(MICH) J
ALSTON	62	CERN Conf. 311	M.H. Alston et al.	(LRL)
BASTIEN	61	PRL 6 702	P.L. Bastien, M. Ferro-Luzzi, A.H. Rosenfeld	(LRL)
DAHL	61	PRL 6 142	O.I. Dahl et al.	(LRL)
ELY	61	PRL 7 461	R.P. Ely et al.	(LRL) J
ALSTON	60	PRL 5 520	M.H. Alston et al.	(LRL) J

 $\Sigma(1480)$  Bumps

$$I(J^P) = 1(?)^? \quad \text{Status: *}$$

## OMITTED FROM SUMMARY TABLE

These are peaks seen in  $\Lambda\pi$  and  $\Sigma\pi$  spectra in the reaction  $\pi^+p \rightarrow (\gamma\pi)K^+$  at 1.7 GeV/c. Also, the  $Y$  polarization oscillates in the same region.

MILLER 70 suggests a possible alternate explanation in terms of a reflection of  $N(1675) \rightarrow \Lambda K$  decay. However, such an explanation for the  $(\Sigma^+\pi^0)K^+$  channel in terms of  $\Delta(1650) \rightarrow \Sigma K$  decay seems unlikely (see PAN 70). In addition such reflections would also have to account for the oscillation of the  $Y$  polarization in the 1480 MeV region.

HANSON 71, with less data than PAN 70, can neither confirm nor deny the existence of this state. MAST 75 sees no structure in this region in  $K^-p \rightarrow \Lambda\pi^0$ .

ENGELEN 80 performs a multichannel analysis of  $K^-p \rightarrow p\bar{K}^0\pi^-$  at 4.2 GeV/c. They observe a 3.5 standard-deviation signal at 1480 MeV in  $p\bar{K}^0$  which cannot be explained as a reflection of any competing channel.

PRAKHOV 04 sees no evidence for this or other light  $\Sigma$  resonances, aside from the  $\Sigma(1385)$ , in  $K^-p \rightarrow \Lambda\pi^0\pi^0$ .

ZYCHOR 06 finds peaks in  $pp \rightarrow pK^+(\pi^\pm X^\mp)$  at  $p_{beam} = 3.65 \text{ GeV}/c$ .

 $\Sigma(1480)$  MASS (PRODUCTION EXPERIMENTS)

VALUE (MeV)	EVTs	DOCUMENT ID	TECN	COMMENT
<b><math>\approx 1480</math> OUR ESTIMATE</b>				
1480 $\pm$ 15	365 $\pm$ 60	ZYCHOR	06	SPEC $pp \rightarrow pK^+(\pi^\pm X^\mp)$
1480	120	ENGELEN	80	HBC $K^-p \rightarrow (p\bar{K}^0)\pi^-$
1485 $\pm$ 10		CLINE	73	MPWA $K^-d \rightarrow (\Lambda\pi^-)p$
1479 $\pm$ 10		PAN	70	HBC $\pi^+p \rightarrow (\Lambda\pi^+)K^+$
1465 $\pm$ 15		PAN	70	HBC $\pi^+p \rightarrow (\Sigma\pi)K^+$

 $\Sigma(1480)$  WIDTH (PRODUCTION EXPERIMENTS)

VALUE (MeV)	EVTs	DOCUMENT ID	TECN	COMMENT
60 $\pm$ 15	365 $\pm$ 60	ZYCHOR	06	SPEC $pp \rightarrow pK^+(\pi^\pm X^\mp)$
80 $\pm$ 20	120	ENGELEN	80	HBC $K^-p \rightarrow (p\bar{K}^0)\pi^-$
40 $\pm$ 20		CLINE	73	MPWA $K^-d \rightarrow (\Lambda\pi^-)p$
31 $\pm$ 15		PAN	70	HBC $\pi^+p \rightarrow (\Lambda\pi^+)K^+$
30 $\pm$ 20		PAN	70	HBC $\pi^+p \rightarrow (\Sigma\pi)K^+$

 $\Sigma(1480)$  DECAY MODES (PRODUCTION EXPERIMENTS)

Mode	$\Gamma_i/\Gamma_j$
$N\bar{K}$	$\Gamma_1$
$\Lambda\pi$	$\Gamma_2$
$\Sigma\pi$	$\Gamma_3$

See key on page 457

Baryon Particle Listings

$\Sigma(1480)$  Bumps,  $\Sigma(1560)$  Bumps,  $\Sigma(1580)$

$\Sigma(1480)$  BRANCHING RATIOS  
(PRODUCTION EXPERIMENTS)

$\Gamma(\Sigma\pi)/\Gamma(\Lambda\pi)$				$\Gamma_3/\Gamma_2$
VALUE	DOCUMENT ID	TECN	CHG	
0.82±0.51	PAN	70	HBC +	

$\Gamma(N\bar{K})/\Gamma(\Lambda\pi)$				$\Gamma_1/\Gamma_2$
VALUE	DOCUMENT ID	TECN	CHG	
0.72±0.50	PAN	70	HBC +	

$\Gamma(N\bar{K})/\Gamma_{total}$				$\Gamma_1/\Gamma$
VALUE	DOCUMENT ID	TECN	COMMENT	
small	CLINE	73	MPWA $K^- d \rightarrow (\Lambda\pi^-) p$	

$\Sigma(1480)$  REFERENCES  
(PRODUCTION EXPERIMENTS)

ZYCHOR 06	PRL 96 012002	I. Zychor <i>et al.</i>	(ANKE Collab.)
PRAKHOV 04	PR C69 042202	S. Prakhov <i>et al.</i>	(BNL Crystal Ball Collab.)
ENGELN 80	NP B167 61	J.J. Engelen <i>et al.</i>	(NIJM, AMST, CERN+)
MAST 75	PR D11 3078	T.S. Mast <i>et al.</i>	(LBL)
CLINE 73	LNC 6 205	D. Cline, R. Laumann, J. Mapp	(WISC) JUP
HANSON 71	PR D4 1296	P. Hanson, G.E. Kalmus, J. Louie	(LBL) I
MILLER 70	Duke Conf. 229	D.H. Miller	(PURD)
Hyperon Resonances, 1970			
PAN 70	PR D2 449	Y.L. Pan <i>et al.</i>	(PENN)
Also	PRL 23 808	Y.L. Pan, F.L. Forman	(PENN) I
Also	PRL 23 806	Y.L. Pan, F.L. Forman	(PENN) I

$\Sigma(1560)$  Bumps  $I(J^P) = 1(??)$  Status: \*\*

OMITTED FROM SUMMARY TABLE

This entry lists peaks reported in mass spectra around 1560 MeV without implying that they are necessarily related.

DIONISI 78B observes a 6 standard-deviation enhancement at 1553 MeV in the charged  $\Lambda/\Sigma\pi$  mass spectra from  $K^- p \rightarrow (\Lambda/\Sigma)\pi K\bar{K}$  at 4.2 GeV/c. In a CERN ISR experiment, LOCKMAN 78 reports a narrow 6 standard-deviation enhancement at 1572 MeV in  $\Lambda\pi^\pm$  from the reaction  $pp \rightarrow \Lambda\pi^+\pi^-X$ . These enhancements are unlikely to be associated with the  $\Sigma(1580)$  (which has not been confirmed by several recent experiments – see the next entry in the Listings).

CARROLL 76 observes a bump at 1550 MeV (as well as one at 1580 MeV) in the isospin-1  $\bar{K}N$  total cross section, but uncertainties in cross section measurements outside the mass range of the experiment preclude estimating its significance.

See also MEADOWS 80 for a review of this state.

$\Sigma(1560)$  MASS  
(PRODUCTION EXPERIMENTS)

VALUE (MeV)	EVTS	DOCUMENT ID	TECN	CHG	COMMENT
$\approx 1560$ OUR ESTIMATE					
1553±7	121	DIONISI	78B	HBC ±	$K^- p \rightarrow (Y\pi) K\bar{K}$
1572±4	40	LOCKMAN	78	SPEC ±	$pp \rightarrow \Lambda\pi^+\pi^-X$

$\Sigma(1560)$  WIDTH  
(PRODUCTION EXPERIMENTS)

VALUE (MeV)	EVTS	DOCUMENT ID	TECN	CHG	COMMENT
79±30	121	DIONISI	78B	HBC ±	$K^- p \rightarrow (Y\pi) K\bar{K}$
15±6	40	1 LOCKMAN	78	SPEC ±	$pp \rightarrow \Lambda\pi^+\pi^-X$

$\Sigma(1560)$  DECAY MODES  
(PRODUCTION EXPERIMENTS)

Mode	Fraction ( $\Gamma_i/\Gamma$ )
$\Gamma_1 \Lambda\pi$	seen
$\Gamma_2 \Sigma\pi$	

$\Sigma(1560)$  BRANCHING RATIOS  
(PRODUCTION EXPERIMENTS)

$\Gamma(\Sigma\pi)/[\Gamma(\Lambda\pi) + \Gamma(\Sigma\pi)]$					$\Gamma_2/(\Gamma_1+\Gamma_2)$
VALUE	DOCUMENT ID	TECN	CHG	COMMENT	
0.35±0.12	DIONISI	78B	HBC ±	$K^- p \rightarrow (Y\pi) K\bar{K}$	

$\Gamma(\Lambda\pi)/\Gamma_{total}$					$\Gamma_1/\Gamma$
VALUE	DOCUMENT ID	TECN	CHG	COMMENT	
seen	LOCKMAN	78	SPEC ±	$pp \rightarrow \Lambda\pi^+\pi^-X$	

$\Sigma(1560)$  FOOTNOTES  
(PRODUCTION EXPERIMENTS)

<sup>1</sup> The width observed by LOCKMAN 78 is consistent with experimental resolution.

$\Sigma(1560)$  REFERENCES  
(PRODUCTION EXPERIMENTS)

MEADOWS 80	Toronto Conf. 283	B.T. Meadows	(CINC)
DIONISI 78B	PL 78B 154	C. Dionisi, R. Armenteros, J. Diaz	(CERN, AMST+)
LOCKMAN 78	Saclay DPHPE 78-01	W. Lockman <i>et al.</i>	(UCLA, SACL)
CARROLL 76	PRL 37 806	A.S. Carroll <i>et al.</i>	(BNL) I

$\Sigma(1580) 3/2^-$   $I(J^P) = 1(3/2^-)$  Status: \*

OMITTED FROM SUMMARY TABLE

Seen in the isospin-1  $\bar{K}N$  cross section at BNL (LI 73, CARROLL 76) and in a partial-wave analysis of  $K^- p \rightarrow \Lambda\pi^0$  for c.m. energies 1560–1600 MeV by LITCHFIELD 74. LITCHFIELD 74 finds  $J^P = 3/2^-$ . Not seen by ENGLER 78 or by CAMERON 78C (with larger statistics in  $K_L^0 p \rightarrow \Lambda\pi^+$  and  $\Sigma^0\pi^+$ ).

Neither OLMSTED 04 (in  $K^- p \rightarrow \Lambda\pi^0$ ) nor PRAKHOV 04 (in  $K^- p \rightarrow \Lambda\pi^0\pi^0$ ) see any evidence for this state.

$\Sigma(1580)$  MASS

VALUE (MeV)	DOCUMENT ID	TECN	COMMENT
$\approx 1580$ OUR ESTIMATE			
1583±4	1 CARROLL	76	DPWA Isospin-1 total $\sigma$
1582±4	2 LITCHFIELD	74	DPWA $K^- p \rightarrow \Lambda\pi^0$

$\Sigma(1580)$  WIDTH

VALUE (MeV)	DOCUMENT ID	TECN	COMMENT
15	1 CARROLL	76	DPWA Isospin-1 total $\sigma$
11±4	2 LITCHFIELD	74	DPWA $K^- p \rightarrow \Lambda\pi^0$

$\Sigma(1580)$  DECAY MODES

Mode
$\Gamma_1 N\bar{K}$
$\Gamma_2 \Lambda\pi$
$\Gamma_3 \Sigma\pi$

$\Sigma(1580)$  BRANCHING RATIOS

See "Sign conventions for resonance couplings" in the Note on  $\Lambda$  and  $\Sigma$  Resonances.

$\Gamma(N\bar{K})/\Gamma_{total}$					$\Gamma_1/\Gamma$
VALUE	DOCUMENT ID	TECN	COMMENT		
+0.03±0.01	2 LITCHFIELD	74	DPWA $\bar{K}N$ multichannel		

$(\Gamma_1\Gamma_2)^{1/2}/\Gamma_{total}$ in $N\bar{K} \rightarrow \Sigma(1580) \rightarrow \Lambda\pi$					$(\Gamma_1\Gamma_2)^{1/2}/\Gamma$
VALUE	DOCUMENT ID	TECN	COMMENT		
not seen	CAMERON	78c	HBC $K_L^0 p \rightarrow \Lambda\pi^+$		
not seen	ENGLER	78	HBC $K_L^0 p \rightarrow \Lambda\pi^+$		
+0.10±0.02	2 LITCHFIELD	74	DPWA $K^- p \rightarrow \Lambda\pi^0$		

$(\Gamma_1\Gamma_3)^{1/2}/\Gamma_{total}$ in $N\bar{K} \rightarrow \Sigma(1580) \rightarrow \Sigma\pi$					$(\Gamma_1\Gamma_3)^{1/2}/\Gamma$
VALUE	DOCUMENT ID	TECN	COMMENT		
not seen	CAMERON	78c	HBC $K_L^0 p \rightarrow \Sigma^0\pi^+$		
not seen	ENGLER	78	HBC $K_L^0 p \rightarrow \Sigma^0\pi^+$		
+0.03±0.04	2 LITCHFIELD	74	DPWA $\bar{K}N$ multichannel		

$\Sigma(1580)$  FOOTNOTES

<sup>1</sup> CARROLL 76 sees a total-cross-section bump with  $(J+1/2) \Gamma_{el} / \Gamma_{total} = 0.06$ .

<sup>2</sup> The main effect observed by LITCHFIELD 74 is in the  $\Lambda\pi$  final state; the  $\bar{K}N$  and  $\Sigma\pi$  couplings are estimated from a multichannel fit including total-cross-section data of LI 73.

## Baryon Particle Listings

 $\Sigma(1580)$ ,  $\Sigma(1620)$ ,  $\Sigma(1620)$  Production Experiments $\Sigma(1580)$  REFERENCES

OLMSTED	04	PL B580 29	J. Olmsted et al.	(BNL Crystal Ball Collab.)
PRAKHOV	04	PR C69 042202	S. Prakhov et al.	(BNL Crystal Ball Collab.)
CAMERON	78C	NP B132 189	W. Cameron et al.	(BGNA, EDIN, GLAS-)
ENGLER	78	PR D18 3061	A. Engler et al.	(CMU, ANL)
CARROLL	76	PRL 37 806	A.S. Carroll et al.	(BNL)I
LITCHFIELD	74	PL 51B 509	P.J. Litchfield	(CERN)IJP
LI	73	Purdue Conf. 283	K.K. Li	(BNL)I

 $\Sigma(1620) 1/2^-$ 

$$I(J^P) = 1(\frac{1}{2}^-) \text{ Status: } **$$

OMITTED FROM SUMMARY TABLE

The  $S_{11}$  state at 1697 MeV reported by VANHORN 75 is tentatively listed under the  $\Sigma(1750)$ . CARROLL 76 sees two bumps in the isospin-1 total cross section near this mass.

Production experiments are listed separately in the next entry.

 $\Sigma(1620)$  MASS

VALUE (MeV)	DOCUMENT ID	TECN	COMMENT
$\approx 1620$ OUR ESTIMATE			
1600 $\pm$ 6	1 MORRIS	78	DPWA $K^- n \rightarrow \Lambda \pi^-$
1608 $\pm$ 5	2 CARROLL	76	DPWA Isospin-1 total $\sigma$
1633 $\pm$ 10	3 CARROLL	76	DPWA Isospin-1 total $\sigma$
1630 $\pm$ 10	LANGBEIN	72	IPWA $\bar{K} N$ multichannel
1620	KIM	71	DPWA K-matrix analysis

 $\Sigma(1620)$  WIDTH

VALUE (MeV)	DOCUMENT ID	TECN	COMMENT
87 $\pm$ 19	1 MORRIS	78	DPWA $K^- n \rightarrow \Lambda \pi^-$
15	2 CARROLL	76	DPWA Isospin-1 total $\sigma$
10	3 CARROLL	76	DPWA Isospin-1 total $\sigma$
65 $\pm$ 20	LANGBEIN	72	IPWA $\bar{K} N$ multichannel
40	KIM	71	DPWA K-matrix analysis

 $\Sigma(1620)$  DECAY MODES

Mode
$\Gamma_1$ $N\bar{K}$
$\Gamma_2$ $\Lambda\pi$
$\Gamma_3$ $\Sigma\pi$

 $\Sigma(1620)$  BRANCHING RATIOS

$\Gamma(N\bar{K})/\Gamma_{\text{total}}$	DOCUMENT ID	TECN	COMMENT	$\Gamma_1/\Gamma$
0.22 $\pm$ 0.02	LANGBEIN	72	IPWA $\bar{K} N$ multichannel	
0.05	KIM	71	DPWA K-matrix analysis	

$(\Gamma_1\Gamma_2)^{1/2}/\Gamma_{\text{total}}$ in $N\bar{K} \rightarrow \Sigma(1620) \rightarrow \Lambda\pi$	DOCUMENT ID	TECN	COMMENT	$(\Gamma_1\Gamma_2)^{1/2}/\Gamma$
0.12 $\pm$ 0.02	1 MORRIS	78	DPWA $K^- n \rightarrow \Lambda \pi^-$	
not seen	BAILLON	75	IPWA $\bar{K} N \rightarrow \Lambda \pi$	
0.15	KIM	71	DPWA K-matrix analysis	

$(\Gamma_1\Gamma_3)^{1/2}/\Gamma_{\text{total}}$ in $N\bar{K} \rightarrow \Sigma(1620) \rightarrow \Sigma\pi$	DOCUMENT ID	TECN	COMMENT	$(\Gamma_1\Gamma_3)^{1/2}/\Gamma$
not seen	HEPP	76B	DPWA $K^- N \rightarrow \Sigma\pi$	
0.40 $\pm$ 0.06	LANGBEIN	72	IPWA $\bar{K} N$ multichannel	
0.08	KIM	71	DPWA K-matrix analysis	

 $\Sigma(1620)$  FOOTNOTES

- <sup>1</sup> MORRIS 78 obtains an equally good fit without including this resonance.  
<sup>2</sup> Total cross-section bump with  $(J+1/2) \Gamma_{\text{el}} / \Gamma_{\text{total}}$  is 0.06 seen by CARROLL 76.  
<sup>3</sup> Total cross-section bump with  $(J+1/2) \Gamma_{\text{el}} / \Gamma_{\text{total}}$  is 0.04 seen by CARROLL 76.

 $\Sigma(1620)$  REFERENCES

MORRIS	78	PR D17 55	W.A. Morris et al.	(FSU)IJP
CARROLL	76	PRL 37 806	A.S. Carroll et al.	(BNL)I
HEPP	76B	PL 65B 487	V. Hepp et al.	(CERN, HEIDH, MPIM)IJP
BAILLON	75	NP B94 39	P.H. Baillon, P.J. Litchfield	(CERN, RHEL)IJP
VANHORN	75	NP B87 145	A.J. van Horn	(LBL)IJP
Also	NP B87 157	A.J. van Horn		(LBL)IJP
LANGBEIN	72	NP B47 477	W. Langbein, F. Wagner	(MPIM)IJP
KIM	71	PRL 27 356	J.K. Kim	(HARV)IJP
Also	Duke Conf. 161	J.K. Kim		(HARV)IJP
		Hyperon Resonances, 1970		

 $\Sigma(1620)$  Production Experiments

$$I(J^P) = 1(?^?)$$

OMITTED FROM SUMMARY TABLE

Formation experiments are listed separately in the previous entry.

The results of CRENNELL 69B at 3.9 GeV/c are not confirmed by SABRE 70 at 3.0 GeV/c. However, at 4.5 GeV/c, AMMANN 70 sees a peak at 1642 MeV which on the basis of branching ratios they do not associate with the  $\Sigma(1670)$ . See MILLER 70 for a review of these conflicts.

 $\Sigma(1620)$  MASS (PRODUCTION EXPERIMENTS)

VALUE (MeV)	EVTS	DOCUMENT ID	TECN	CHG	COMMENT
$\approx 1620$ OUR ESTIMATE					
1642 $\pm$ 12		AMMANN	70	DBC	$K^- N$ 4.5 GeV/c
1618 $\pm$ 3	20	BLUMENFELD	69	HBC +	$K_L^0 p$
1619 $\pm$ 8		CRENNELL	69B	DBC $\pm$	$K^- N \rightarrow \Lambda \pi \pi$
		••• We do not use the following data for averages, fits, limits, etc. •••			
1616 $\pm$ 8		CRENNELL	68	DBC $\pm$	See CRENNELL 69B

 $\Sigma(1620)$  WIDTH (PRODUCTION EXPERIMENTS)

VALUE (MeV)	EVTS	DOCUMENT ID	TECN	CHG	COMMENT
55 $\pm$ 24		AMMANN	70	DBC	$K^- N$ 4.5 GeV/c
30 $\pm$ 10	20	BLUMENFELD	69	HBC +	
72 $\pm$ 22 15		CRENNELL	69B	DBC $\pm$	
		••• We do not use the following data for averages, fits, limits, etc. •••			
66 $\pm$ 16		CRENNELL	68	DBC $\pm$	See CRENNELL 69B

 $\Sigma(1620)$  DECAY MODES (PRODUCTION EXPERIMENTS)

Mode
$\Gamma_1$ $N\bar{K}$
$\Gamma_2$ $\Lambda\pi$
$\Gamma_3$ $\Sigma\pi$
$\Gamma_4$ $\Lambda\pi\pi$
$\Gamma_5$ $\Sigma(1385)\pi$
$\Gamma_6$ $\Lambda(1405)\pi$

 $\Sigma(1620)$  BRANCHING RATIOS (PRODUCTION EXPERIMENTS)

$\Gamma(\Lambda\pi\pi)/\Gamma(\Lambda\pi)$	DOCUMENT ID	TECN	CHG	$\Gamma_4/\Gamma_2$
$\sim 2.5$	BLUMENFELD	69	HBC +	

$\Gamma(N\bar{K})/\Gamma(\Lambda\pi)$	DOCUMENT ID	TECN	CHG	COMMENT	$\Gamma_1/\Gamma_2$
0.4 $\pm$ 0.4	AMMANN	70	DBC	$K^- p$ 4.5 GeV/c	
0.0 $\pm$ 0.1	CRENNELL	68	DBC +	See CRENNELL 69B	

$\Gamma(\Lambda\pi)/\Gamma_{\text{total}}$	DOCUMENT ID	TECN	CHG	$\Gamma_2/\Gamma$
large	CRENNELL	68	DBC $\pm$	

$\Gamma(\Sigma(1385)\pi)/\Gamma(\Lambda\pi)$	DOCUMENT ID	TECN	CHG	COMMENT	$\Gamma_5/\Gamma_2$
< 0.3	AMMANN	70	DBC	$K^- p$ 4.5 GeV/c	
0.2 $\pm$ 0.1	CRENNELL	68	DBC $\pm$		

$\Gamma(\Sigma\pi)/\Gamma(\Lambda\pi)$	DOCUMENT ID	TECN	CHG	COMMENT	$\Gamma_3/\Gamma_2$
< 1.1	AMMANN	70	DBC	$K^- N$ 4.5 GeV/c	

$\Gamma(\Lambda(1405)\pi)/\Gamma(\Lambda\pi)$	DOCUMENT ID	TECN	CHG	COMMENT	$\Gamma_6/\Gamma_2$
0.7 $\pm$ 0.4	AMMANN	70	DBC	$K^- p$ 4.5 GeV/c	

See key on page 457

Baryon Particle Listings

$\Sigma(1620)$  Production Experiments,  $\Sigma(1660)$ ,  $\Sigma(1670)$

$\Sigma(1620)$  REFERENCES  
(PRODUCTION EXPERIMENTS)

AMMANN 70 PRL 24 327	A.C. Ammann <i>et al.</i>	(PURD, IND)
Also PR D7 1345	A.C. Ammann <i>et al.</i>	(PURD, IUPU)
MILLER 70 Duke Conf. 229	D.H. Miller	(PURD)
Hyperon Resonances, 1970		
SABRE 70 NP B16 201	R. Barloutaud <i>et al.</i>	(SABRE Collab.)
BLUMENFELD 69 PL 29B 58	B.J. Blumenfeld, G.R. Kalbfleisch	(BNL)1
CRENNELL 69B Lund Paper 183	D.J. Crennell <i>et al.</i>	(BNL, CUNY)1
Results are quoted in LEVI-SETTI 69C.		
Also Lund Conf.	R. Levi-Setti	(EFI)
CRENNELL 68 PRL 21 648	D.J. Crennell <i>et al.</i>	(BNL, CUNY)1

$\Sigma(1660) 1/2^+$   $I(J^P) = 1(\frac{1}{2}^+)$  Status: \*\*\*

For results published before 1974 (they are now obsolete), see our 1982 edition Physics Letters **111B** 1 (1982).

$\Sigma(1660)$  MASS

VALUE (MeV)	DOCUMENT ID	TECN	COMMENT
<b>1630 to 1690 (<math>\approx 1660</math>) OUR ESTIMATE</b>			
1634.8 $\pm$ 2.7 - 4.5	GAO	11	DPWA $K^-p \rightarrow \Lambda\pi^0$
1665.1 $\pm$ 11.2	1 KOISO	85	DPWA $K^-p \rightarrow \Sigma\pi$
1670 $\pm$ 10	GOPAL	80	DPWA $\bar{K}N \rightarrow \bar{K}N$
1679 $\pm$ 10	ALSTON-...	78	DPWA $\bar{K}N \rightarrow \bar{K}N$
1676 $\pm$ 15	GOPAL	77	DPWA $\bar{K}N$ multichannel
1668 $\pm$ 25	VANHORN	75	DPWA $K^-p \rightarrow \Lambda\pi^0$
1670 $\pm$ 20	KANE	74	DPWA $K^-p \rightarrow \Sigma\pi$
• • • We do not use the following data for averages, fits, limits, etc. • • •			
1565 or 1597	2 MARTIN	77	DPWA $\bar{K}N$ multichannel
1660 $\pm$ 30	3 BAILLON	75	IPWA $\bar{K}N \rightarrow \Lambda\pi$
1671 $\pm$ 2	4 PONTE	75	DPWA $K^-p \rightarrow \Lambda\pi^0$

$\Sigma(1660)$  WIDTH

VALUE (MeV)	DOCUMENT ID	TECN	COMMENT
<b>40 to 200 (<math>\approx 100</math>) OUR ESTIMATE</b>			
120 $\pm$ 12	GAO	11	DPWA $K^-p \rightarrow \Lambda\pi^0$
81.5 $\pm$ 22.2	1 KOISO	85	DPWA $K^-p \rightarrow \Sigma\pi$
152 $\pm$ 20	GOPAL	80	DPWA $\bar{K}N \rightarrow \bar{K}N$
38 $\pm$ 10	ALSTON-...	78	DPWA $\bar{K}N \rightarrow \bar{K}N$
120 $\pm$ 20	GOPAL	77	DPWA $\bar{K}N$ multichannel
230 $\pm$ 165 - 60	VANHORN	75	DPWA $K^-p \rightarrow \Lambda\pi^0$
250 $\pm$ 110	KANE	74	DPWA $K^-p \rightarrow \Sigma\pi$
• • • We do not use the following data for averages, fits, limits, etc. • • •			
202 or 217	2 MARTIN	77	DPWA $\bar{K}N$ multichannel
80 $\pm$ 40	3 BAILLON	75	IPWA $\bar{K}N \rightarrow \Lambda\pi$
81 $\pm$ 10	4 PONTE	75	DPWA $K^-p \rightarrow \Lambda\pi^0$

$\Sigma(1660)$  DECAY MODES

Mode	Fraction ( $\Gamma_i/\Gamma$ )
$\Gamma_1$ $N\bar{K}$	10-30 %
$\Gamma_2$ $\Lambda\pi$	seen
$\Gamma_3$ $\Sigma\pi$	seen

$\Sigma(1660)$  BRANCHING RATIOS

See "Sign conventions for resonance couplings" in the Note on  $\Lambda$  and  $\Sigma$  Resonances.

$\Gamma(N\bar{K})/\Gamma_{total}$	DOCUMENT ID	TECN	COMMENT	$\Gamma_1/\Gamma$
<b>0.1 to 0.3 OUR ESTIMATE</b>				
0.12 $\pm$ 0.03	GOPAL	80	DPWA $\bar{K}N \rightarrow \bar{K}N$	
0.10 $\pm$ 0.05	ALSTON-...	78	DPWA $\bar{K}N \rightarrow \bar{K}N$	
• • • We do not use the following data for averages, fits, limits, etc. • • •				
<0.04	GOPAL	77	DPWA See GOPAL 80	
0.27 or 0.29	2 MARTIN	77	DPWA $\bar{K}N$ multichannel	

$(\Gamma_1\Gamma_2)^{1/2}/\Gamma_{total}$ in $N\bar{K} \rightarrow \Sigma(1660) \rightarrow \Lambda\pi$	DOCUMENT ID	TECN	COMMENT	$(\Gamma_1\Gamma_2)^{1/2}/\Gamma$
<b>0.1 to 0.3 OUR ESTIMATE</b>				
-0.065 $\pm$ 0.015 -0.017	GAO	11	DPWA $K^-p \rightarrow \Lambda\pi^0$	
< 0.04	GOPAL	77	DPWA $\bar{K}N$ multichannel	
0.12 $\pm$ 0.12 -0.04	VANHORN	75	DPWA $K^-p \rightarrow \Lambda\pi^0$	
• • • We do not use the following data for averages, fits, limits, etc. • • •				
-0.10 or -0.11	2 MARTIN	77	DPWA $\bar{K}N$ multichannel	
-0.04 $\pm$ 0.02	3 BAILLON	75	IPWA $\bar{K}N \rightarrow \Lambda\pi$	
+0.16 $\pm$ 0.01	4 PONTE	75	DPWA $K^-p \rightarrow \Lambda\pi^0$	

$(\Gamma_1\Gamma_2)^{1/2}/\Gamma_{total}$ in $N\bar{K} \rightarrow \Sigma(1660) \rightarrow \Sigma\pi$	DOCUMENT ID	TECN	COMMENT	$(\Gamma_1\Gamma_3)^{1/2}/\Gamma$
-0.13 $\pm$ 0.04	1 KOISO	85	DPWA $K^-p \rightarrow \Sigma\pi$	
-0.16 $\pm$ 0.03	GOPAL	77	DPWA $\bar{K}N$ multichannel	
-0.11 $\pm$ 0.01	KANE	74	DPWA $K^-p \rightarrow \Sigma\pi$	
• • • We do not use the following data for averages, fits, limits, etc. • • •				
-0.34 or -0.37	2 MARTIN	77	DPWA $\bar{K}N$ multichannel	
not seen	HEPP	76B	DPWA $K^-N \rightarrow \Sigma\pi$	

$\Sigma(1660)$  FOOTNOTES

- The evidence of KOISO 85 is weak.
- The two MARTIN 77 values are from a T-matrix pole and from a Breit-Wigner fit.
- From solution 1 of BAILLON 75; not present in solution 2.
- From solution 2 of PONTE 75; not present in solution 1.

$\Sigma(1660)$  REFERENCES

GAO 11 NP A867 41	P. Gao, B.S. Zou, A. Sibirtsev	(BHEP, BEJT+)
KOISO 85 NP A433 619	H. Koiso <i>et al.</i>	(TOKY, MASA)
PDG 82 PL 111B 1	M. Roos <i>et al.</i>	(HELS, CIT, CERN)
GOPAL 80 Toronto Conf. 159	G.P. Gopal	(RHEL) IJP
ALSTON-... 78 PR D18 182	M. Alston-Garnjost <i>et al.</i>	(LBL, MTHO+) IJP
Also PRL 38 1007	M. Alston-Garnjost <i>et al.</i>	(LBL, MTHO+) IJP
GOPAL 77 NP B119 362	G.P. Gopal <i>et al.</i>	(LOIC, RHEL) IJP
MARTIN 77 NP B127 349	B.R. Martin, M.K. Pidcock, R.G. Moorhouse	(LOUC+) IJP
Also NP B126 266	B.R. Martin, M.K. Pidcock	(LOUC) IJP
Also NP B126 285	B.R. Martin, M.K. Pidcock	(LOUC) IJP
HEPP 76B PL 65B 487	V. Hepp <i>et al.</i>	(CERN, HEIDH, MPIM) IJP
BAILLON 75 NP B94 39	P.H. Baillon, P.J. Litchfield	(CERN, RHEL) IJP
PONTE 75 PR D12 2597	R.A. Ponte <i>et al.</i>	(MASA, TENN, UCR) IJP
VANHORN 75 NP B87 145	A.J. van Horn	(CERN, RHEL) IJP
Also NP B87 157	A.J. van Horn	(LBL) IJP
KANE 74 LBL-2452	D.F. Kane	(LBL) IJP

THE  $\Sigma(1670)$  REGION

**Production experiments:** The measured  $\Sigma\pi/\Sigma\pi\pi$  branching ratio for the  $\Sigma(1670)$  produced in the reaction  $K^-p \rightarrow \pi^-\Sigma(1670)^+$  is strongly dependent on momentum transfer. This was first discovered by EBERHARD 69, who suggested that there exist two  $\Sigma$  resonances with the same mass and quantum numbers: one with a large  $\Sigma\pi\pi$  (mainly  $\Lambda(1405)\pi$ ) branching fraction produced peripherally, and the other with a large  $\Sigma\pi$  branching fraction produced at larger angles. The experimental results have been confirmed by AGUILAR-BENITEZ 70, ASPELL 74, ESTES 74, and TIMMERMANS 76. If, in fact, there are two resonances, the most likely quantum numbers for both the  $\Sigma\pi$  and the  $\Lambda(1405)\pi$  states are  $D_{13}$ . There is also possibly a third  $\Sigma$  in this region, the  $\Sigma(1690)$  in the Listings, the main evidence for which is a large  $\Lambda\pi/\Sigma\pi\pi$  branching ratio. These topics have been reviewed by EBERHARD 73 and by MILLER 70.

**Formation experiments:** Two states are also observed near this mass in formation experiments. One of these, the  $\Sigma(1670)D_{13}$ , has the same quantum numbers as those observed in production and has a large  $\Sigma\pi/\Sigma\pi\pi$  branching ratio; it may well be the  $\Sigma(1670)$  produced at larger angles (see TIMMERMANS 76). The other state, the  $\Sigma(1660)P_{11}$ , has different quantum numbers, its  $\Sigma\pi/\Sigma\pi\pi$  branching ratio is unknown, and its relation to the produced  $\Sigma(1670)$  states is obscure.

## Baryon Particle Listings

 $\Sigma(1670)$ 

$$\Sigma(1670) \frac{3}{2}^-$$

$$J(P) = 1(\frac{3}{2}^-) \text{ Status: } ****$$

For most results published before 1974 (they are now obsolete), see our 1982 edition Physics Letters **111B** 1 (1982).

Results from production experiments are listed separately in the next entry.

 $\Sigma(1670)$  MASS

VALUE (MeV)	DOCUMENT ID	TECN	COMMENT
<b>1665 to 1685 (<math>\approx 1670</math>) OUR ESTIMATE</b>			
1673.1 <sup>+1.4</sup> <sub>-1.6</sub>	GAO	11	DPWA $K^-p \rightarrow \Lambda\pi^0$
1665.1 $\pm$ 4.1	KOISO	85	DPWA $K^-p \rightarrow \Sigma\pi$
1682 $\pm$ 5	GOPAL	80	DPWA $\bar{K}N \rightarrow \bar{K}N$
1679 $\pm 10$	ALSTON-...	78	DPWA $\bar{K}N \rightarrow \bar{K}N$
1670 $\pm 5$	GOPAL	77	DPWA $\bar{K}N$ multichannel
1670 $\pm 6$	HEPP	76B	DPWA $K^-N \rightarrow \Sigma\pi$
1685 $\pm 20$	BAILLON	75	IPWA $\bar{K}N \rightarrow \Lambda\pi$
1659 <sup>+12</sup> <sub>-5</sub>	VANHORN	75	DPWA $K^-p \rightarrow \Lambda\pi^0$
1670 $\pm 2$	KANE	74	DPWA $K^-p \rightarrow \Sigma\pi$
• • • We do not use the following data for averages, fits, limits, etc. • • •			
1667 or 1668	<sup>1</sup> MARTIN	77	DPWA $\bar{K}N$ multichannel
1650	DEBELLEFON	76	IPWA $K^-p \rightarrow \Lambda\pi^0$
1671 $\pm 3$	PONTE	75	DPWA $K^-p \rightarrow \Lambda\pi^0$ (sol. 1)
1655 $\pm 2$	PONTE	75	DPWA $K^-p \rightarrow \Lambda\pi^0$ (sol. 2)

 $\Sigma(1670)$  WIDTH

VALUE (MeV)	DOCUMENT ID	TECN	COMMENT
<b>40 to 80 (<math>\approx 60</math>) OUR ESTIMATE</b>			
53 <sup>+7</sup> <sub>-5.5</sub>	GAO	11	DPWA $K^-p \rightarrow \Lambda\pi^0$
65.0 $\pm$ 7.3	KOISO	85	DPWA $K^-p \rightarrow \Sigma\pi$
79 $\pm 10$	GOPAL	80	DPWA $\bar{K}N \rightarrow \bar{K}N$
56 $\pm 20$	ALSTON-...	78	DPWA $\bar{K}N \rightarrow \bar{K}N$
50 $\pm 5$	GOPAL	77	DPWA $\bar{K}N$ multichannel
56 $\pm 3$	HEPP	76B	DPWA $K^-N \rightarrow \Sigma\pi$
85 $\pm 25$	BAILLON	75	IPWA $\bar{K}N \rightarrow \Lambda\pi$
32 $\pm 11$	VANHORN	75	DPWA $K^-p \rightarrow \Lambda\pi^0$
79 $\pm 6$	KANE	74	DPWA $K^-p \rightarrow \Sigma\pi$
• • • We do not use the following data for averages, fits, limits, etc. • • •			
46 or 46	<sup>1</sup> MARTIN	77	DPWA $\bar{K}N$ multichannel
80	DEBELLEFON	76	IPWA $K^-p \rightarrow \Lambda\pi^0$
44 $\pm 11$	PONTE	75	DPWA $K^-p \rightarrow \Lambda\pi^0$ (sol. 1)
76 $\pm 5$	PONTE	75	DPWA $K^-p \rightarrow \Lambda\pi^0$ (sol. 2)

 $\Sigma(1670)$  DECAY MODES

Mode	Fraction ( $\Gamma_i/\Gamma$ )
$\Gamma_1$ $N\bar{K}$	7-13 %
$\Gamma_2$ $\Lambda\pi$	5-15 %
$\Gamma_3$ $\Sigma\pi$	30-60 %
$\Gamma_4$ $\Lambda\pi\pi$	
$\Gamma_5$ $\Sigma\pi\pi$	
$\Gamma_6$ $\Sigma(1385)\pi$	
$\Gamma_7$ $\Sigma(1385)\pi, S$ -wave	
$\Gamma_8$ $\Lambda(1405)\pi$	
$\Gamma_9$ $\Lambda(1520)\pi$	

The above branching fractions are our estimates, not fits or averages.

 $\Sigma(1670)$  BRANCHING RATIOS

See "Sign conventions for resonance couplings" in the Note on  $\Lambda$  and  $\Sigma$  Resonances.

$\Gamma(N\bar{K})/\Gamma_{\text{total}}$	DOCUMENT ID	TECN	COMMENT
<b>0.07 to 0.13 OUR ESTIMATE</b>			
0.10 $\pm$ 0.03	GOPAL	80	DPWA $\bar{K}N \rightarrow \bar{K}N$
0.11 $\pm$ 0.03	ALSTON-...	78	DPWA $\bar{K}N \rightarrow \bar{K}N$
• • • We do not use the following data for averages, fits, limits, etc. • • •			
0.08 $\pm$ 0.03	GOPAL	77	DPWA See GOPAL 80
0.07 or 0.07	<sup>1</sup> MARTIN	77	DPWA $\bar{K}N$ multichannel

$(\Gamma_i\Gamma_f)^{1/2}/\Gamma_{\text{total}}$ in $N\bar{K} \rightarrow \Sigma(1670) \rightarrow \Lambda\pi$	DOCUMENT ID	TECN	COMMENT
VALUE			
+0.08 <sup>+0.022</sup> <sub>-0.018</sub>	GAO	11	DPWA $K^-p \rightarrow \Lambda\pi^0$
0.17 $\pm$ 0.03	<sup>2</sup> MORRIS	78	DPWA $K^-n \rightarrow \Lambda\pi^-$
0.13 $\pm$ 0.02	<sup>2</sup> MORRIS	78	DPWA $K^-n \rightarrow \Lambda\pi^-$
+0.10 $\pm$ 0.02	GOPAL	77	DPWA $\bar{K}N$ multichannel
+0.06 $\pm$ 0.02	BAILLON	75	IPWA $\bar{K}N \rightarrow \Lambda\pi$
+0.09 $\pm$ 0.02	VANHORN	75	DPWA $K^-p \rightarrow \Lambda\pi^0$
+0.018 $\pm$ 0.060	DEVENISH	74B	Fixed-t dispersion rel.
• • • We do not use the following data for averages, fits, limits, etc. • • •			
+0.08 or +0.08	<sup>1</sup> MARTIN	77	DPWA $\bar{K}N$ multichannel
+0.05	DEBELLEFON	76	IPWA $K^-p \rightarrow \Lambda\pi^0$
0.08 $\pm$ 0.01	PONTE	75	DPWA $K^-p \rightarrow \Lambda\pi^0$ (sol. 1)
0.17 $\pm$ 0.01	PONTE	75	DPWA $K^-p \rightarrow \Lambda\pi^0$ (sol. 2)

$(\Gamma_i\Gamma_f)^{1/2}/\Gamma_{\text{total}}$ in $N\bar{K} \rightarrow \Sigma(1670) \rightarrow \Sigma\pi$	DOCUMENT ID	TECN	COMMENT
VALUE			
+0.20 $\pm$ 0.02	KOISO	85	DPWA $K^-p \rightarrow \Sigma\pi$
+0.21 $\pm$ 0.02	GOPAL	77	DPWA $\bar{K}N$ multichannel
+0.20 $\pm$ 0.01	HEPP	76B	DPWA $K^-N \rightarrow \Sigma\pi$
+0.21 $\pm$ 0.03	KANE	74	DPWA $K^-p \rightarrow \Sigma\pi$
• • • We do not use the following data for averages, fits, limits, etc. • • •			
+0.18 or +0.17	<sup>1</sup> MARTIN	77	DPWA $\bar{K}N$ multichannel

$\Gamma(\Lambda\pi\pi)/\Gamma_{\text{total}}$	DOCUMENT ID	TECN	COMMENT
VALUE			
• • • We do not use the following data for averages, fits, limits, etc. • • •			
<0.11	ARMENTEROS68E	HBC	$K^-p$ ( $\Gamma_1=0.09$ )

$(\Gamma_i\Gamma_f)^{1/2}/\Gamma_{\text{total}}$ in $N\bar{K} \rightarrow \Sigma(1670) \rightarrow \Sigma(1385)\pi, S$ -wave	DOCUMENT ID	TECN	COMMENT
VALUE			
+0.11 $\pm$ 0.03	PREVOST	74	DPWA $K^-N \rightarrow \Sigma(1385)\pi$
• • • We do not use the following data for averages, fits, limits, etc. • • •			
0.17 $\pm$ 0.02	<sup>3</sup> SIMS	68	DBC $K^-N \rightarrow \Lambda\pi\pi$

$\Gamma(\Sigma\pi\pi)/\Gamma_{\text{total}}$	DOCUMENT ID	TECN	COMMENT
VALUE			
• • • We do not use the following data for averages, fits, limits, etc. • • •			
<0.14	<sup>4</sup> ARMENTEROS68E	HBC	$K^-p, K^-d$ ( $\Gamma_1=0.09$ )

$\Gamma(\Lambda(1405)\pi)/\Gamma_{\text{total}}$	DOCUMENT ID	TECN	COMMENT
VALUE			
• • • We do not use the following data for averages, fits, limits, etc. • • •			
<0.06	ARMENTEROS68E	HBC	$K^-p, K^-d$ ( $\Gamma_1=0.09$ )

$\Gamma_i\Gamma_f/\Gamma_{\text{total}}^2$ in $N\bar{K} \rightarrow \Sigma(1670) \rightarrow \Lambda(1405)\pi$	DOCUMENT ID	TECN	COMMENT
VALUE			
0.007 $\pm$ 0.002	<sup>5</sup> BRUCKER	70	DBC $K^-N \rightarrow \Sigma\pi\pi$
• • • We do not use the following data for averages, fits, limits, etc. • • •			
<0.03	BERLEY	69	HBC $K^-p$ 0.6-0.82 GeV/c

$\Gamma(\Lambda(1405)\pi)/\Gamma(\Sigma(1385)\pi)$	DOCUMENT ID	TECN	COMMENT
VALUE			
0.23 $\pm$ 0.08	BRUCKER	70	DBC $K^-N \rightarrow \Sigma\pi\pi$

$(\Gamma_i\Gamma_f)^{1/2}/\Gamma_{\text{total}}$ in $N\bar{K} \rightarrow \Sigma(1670) \rightarrow \Lambda(1520)\pi$	DOCUMENT ID	TECN	COMMENT
VALUE			
0.081 $\pm$ 0.016	<sup>6</sup> CAMERON	77	DPWA $P$ -wave decay

 $\Sigma(1670)$  FOOTNOTES

- The two MARTIN 77 values are from a T-matrix pole and from a Breit-Wigner fit.
- Results are with and without an  $S_{11}$   $\Sigma(1620)$  in the fit.
- SIMS 68 uses only cross-section data. Result used as upper limit only.
- Ratio only for  $\Sigma 2\pi$  system in  $l=1$ , which cannot be  $\Sigma(1385)$ .
- Assuming the  $\Lambda(1405)\pi$  cross-section bump is due only to  $3/2^-$  resonance.
- The CAMERON 77 upper limit on  $F$ -wave decay is 0.03.

 $\Sigma(1670)$  REFERENCES

GAO	11	NP A867 41	P. Gao, B.S. Zou, A. Sibirtsev	(BHEP, BEIJ+)
KOISO	85	NP A433 619	H. Koiso et al.	(TOKY, MASA)
PDG	82	PL 111B 1	M. Roos et al.	(HEL5, CIT, CERN)
GOPAL	80	Toronto Conf. 159	G.P. Gopal	(RHEL) IJP
ALSTON-...	78	PR D18 182	M. Alston-Garnjost et al.	(LBL, MTHO+) IJP
		PRL 38 1007	M. Alston-Garnjost et al.	(LBL, MTHO+) IJP
MORRIS	78	PR D17 55	W.A. Morris et al.	(FSU) IJP
CAMERON	77	NP B131 399	W. Cameron et al.	(RHEL, LOIC) IJP
GOPAL	77	NP B119 362	G.P. Gopal et al.	(LOIC, RHEL) IJP
MARTIN	77	NP B127 349	B.R. Martin, M.K. Pidcock, R.G. Moorhouse	(LOUC+) IJP
		Also	B.R. Martin, M.K. Pidcock	(LOUC)
		Also	B.R. Martin, M.K. Pidcock	(LOUC) IJP
DEBELLEFON	76	NP B109 129	A. de Bellefon, A. Berthon	(CDEF) IJP
HEPP	76B	PL 65B 487	V. Hepp et al.	(CERN, HEIDH, MPM) IJP



See key on page 457

## Baryon Particle Listings

### $\Sigma(1670), \Sigma(1670)$ Bumps

BAILLON	75	NP B94 39	P.H. Baillon, P.J. Litchfield	(CERN, RHEL) IJP
PONTE	75	PR D12 2597	R.A. Ponte et al.	(MASA, TENN, UCR) IJP
VANHORN	75	NP B87 145	A.J. van Horn	(LBL) IJP
	Also	NP B87 157	A.J. van Horn	(LBL) IJP
DEVENISH	74B	NP B81 330	R.C.E. Devenish, C.D. Froggatt, B.R. Martin	(DESY+) IJP
KANE	74	LBL-2452	D.F. Kane	(LBL) IJP
PREVOST	74	NP B69 246	J. Prevost et al.	(SACL, CERN, HEID) IJP
BRUCKER	70	Duke Conf. 195	E.B. Brucker et al.	(FSU) I
		Hyperon Resonances, 1970		
BERLEY	69	PL 30B 430	D. Berley et al.	(BNL)
ARMENTEROS	68E	PL 28B 521	R. Armenteros et al.	(CERN, HEID, SACL) I
SIMS	68	PRL 21 1413	W.H. Sims et al.	(FSU, TUFTS, BRAN)

<0.24	0	PRIMER	68	HBC	+	$K^- p$ 4.6-5 GeV/c
<0.6		LONDON	66	HBC	+	$K^- p$ 2.25 GeV/c
<0.19	0	ALVAREZ	63	HBC	+	$K^- p$ 1.15 GeV/c
$\geq 0.5 \pm 0.25$		SMITH	63	HBC	-0	

### $\Sigma(1670)$ Bumps

$$I(J^P) = 1(?)^?$$

OMITTED FROM SUMMARY TABLE  
Formation experiments are listed separately in the preceding entry.

Probably there are two states at the same mass with the same quantum numbers, one decaying to  $\Sigma\pi$  and  $\Lambda\pi$ , the other to  $\Lambda(1405)\pi$ . See the note in front of the preceding entry.

### $\Sigma(1670)$ MASS (PRODUCTION EXPERIMENTS)

VALUE (MeV)	EVTS	DOCUMENT ID	TECN	CHG	COMMENT	
$\approx 1670$ OUR ESTIMATE						
$1670 \pm 4$		<sup>1</sup> CARROLL	76	DPWA	Isospin-1 total $\sigma$	
$1675 \pm 10$		<sup>2</sup> HEPP	76	DBC	$K^- N$ 1.6-1.75 GeV/c	
$1665 \pm 1$		APSELL	74	HBC	$K^- p$ 2.87 GeV/c	
$1688 \pm 2$ or $1683 \pm 5$ 1.2k		BERTHON	74	HBC	0 Quasi-2-body $\sigma$	
$1670 \pm 6$		AGUILAR-...	70B	HBC	$K^- p \rightarrow \Sigma\pi\pi$ 4 GeV	
$1668 \pm 10$		AGUILAR-...	70B	HBC	$K^- p \rightarrow \Sigma 3\pi$ 4 GeV	
$1660 \pm 10$		ALVAREZ	63	HBC	+	$K^- p$ 1.51 GeV/c
● ● ● We do not use the following data for averages, fits, limits, etc. ● ● ●						
$1668 \pm 10$	150	<sup>3</sup> FERRERSORIA	81	OMEG	$-\pi^- p$ 9,12 GeV/c	
$1655$ to $1677$		TIMMERMAN	576	HBC	+	$K^- p$ 4.2 GeV/c
$1665 \pm 5$		BUGG	68	CNTR	$K^- p$ , $d$ total $\sigma$	
$1661 \pm 9$	70	PRIMER	68	HBC	+	See BARNES 69E
$1685$		ALEXANDER	62c	HBC	-0	$\pi^- p$ 2-2.2 GeV/c

### $\Sigma(1670)$ WIDTH (PRODUCTION EXPERIMENTS)

VALUE (MeV)	EVTS	DOCUMENT ID	TECN	CHG	COMMENT	
$67.0 \pm 2.4$		APSELL	74	HBC	$K^- p$ 2.87 GeV/c	
$110 \pm 12$		AGUILAR-...	70B	HBC	$K^- p \rightarrow \Sigma\pi\pi$ 4 GeV	
$135^{+40}_{-30}$		AGUILAR-...	70B	HBC	$K^- p \rightarrow \Sigma 3\pi$ 4 GeV	
$40 \pm 10$		ALVAREZ	63	HBC	+	
● ● ● We do not use the following data for averages, fits, limits, etc. ● ● ●						
$90 \pm 20$	150	<sup>3</sup> FERRERSORIA	81	OMEG	$-\pi^- p$ 9,12 GeV/c	
$52$		<sup>1</sup> CARROLL	76	DPWA	Isospin-1 total $\sigma$	
$48$ to $63$		TIMMERMAN	576	HBC	+	$K^- p$ 4.2 GeV/c
$30 \pm 15$		BUGG	68	CNTR		
$60 \pm 20$	70	PRIMER	68	HBC	+	See BARNES 69E
$45$		ALEXANDER	62c	HBC	-0	

### $\Sigma(1670)$ DECAY MODES (PRODUCTION EXPERIMENTS)

Mode	
$\Gamma_1$	$N\bar{K}$
$\Gamma_2$	$\Lambda\pi$
$\Gamma_3$	$\Sigma\pi$
$\Gamma_4$	$\Lambda\pi\pi$
$\Gamma_5$	$\Sigma\pi\pi$
$\Gamma_6$	$\Sigma(1385)\pi$
$\Gamma_7$	$\Lambda(1405)\pi$

### $\Sigma(1670)$ BRANCHING RATIOS (PRODUCTION EXPERIMENTS)

$\Gamma(N\bar{K})/\Gamma(\Sigma\pi)$		$\Gamma_1/\Gamma_3$				
VALUE	EVTS	DOCUMENT ID	TECN	CHG	COMMENT	
<0.03		TIMMERMAN	576	HBC	+	$K^- p$ 4.2 GeV/c
<0.10		BERTHON	74	HBC	0	Quasi-2-body $\sigma$
<0.2		AGUILAR-...	70B	HBC		
<0.26		BARNES	69E	HBC	+	$K^- p$ 3.9-5 GeV/c
0.025		BUGG	68	CNTR	0	Assuming $J = 3/2$

### $\Gamma(\Lambda\pi)/\Gamma(\Sigma\pi)$

VALUE	EVTS	DOCUMENT ID	TECN	CHG	COMMENT	
$0.76 \pm 0.09$		ESTES	74	HBC	0	$K^- p$ 2.1,2.6 GeV/c
$0.45 \pm 0.15$		BARNES	69E	HBC	+	$K^- p$ 3.9-5 GeV/c
$0.15 \pm 0.07$		HUWE	69	HBC	+	
$0.11 \pm 0.06$	33	BUTTON-...	68	HBC	+	$K^- p$ 1.7 GeV/c
● ● ● We do not use the following data for averages, fits, limits, etc. ● ● ●						
$\leq 0.45 \pm 0.07$		TIMMERMAN	576	HBC	+	$K^- p$ 4.2 GeV/c
$0.55 \pm 0.11$		BERTHON	74	HBC	0	Quasi-2-body $\sigma$
0	0	PRIMER	68	HBC	+	See BARNES 69E
<0.6		LONDON	66	HBC	+	$K^- p$ 2.25 GeV/c
1.2	130	ALVAREZ	63	HBC	+	$K^- p$ 1.15 GeV/c
1.2		SMITH	63	HBC	-0	

### $\Gamma(\Lambda\pi\pi)/\Gamma(\Sigma\pi)$

VALUE	EVTS	DOCUMENT ID	TECN	CHG	COMMENT	
<0.6		LONDON	66	HBC	+	$K^- p$ 2.25 GeV/c
0.56	90	ALVAREZ	63	HBC	+	$K^- p$ 1.15 GeV/c
0.17		SMITH	63	HBC	-0	

### $\Gamma(\Sigma\pi\pi)/\Gamma(\Sigma\pi)$

VALUE	EVTS	DOCUMENT ID	TECN	CHG	COMMENT	
largest at small angles		ESTES	74	HBC	0	$K^- p$ 2.1,2.6 GeV/c
● ● ● We do not use the following data for averages, fits, limits, etc. ● ● ●						
<0.2		<sup>2</sup> HEPP	76	DBC	-	$K^- N$ 1.6-1.75 GeV/c
0.56	180	ALVAREZ	63	HBC	+	$K^- p$ 1.15 GeV/c

### $\Gamma(\Lambda(1405)\pi)/\Gamma(\Sigma\pi)$

VALUE	EVTS	DOCUMENT ID	TECN	CHG	COMMENT	
$1.8 \pm 0.3$ to $0.02 \pm 0.07$	3.4	TIMMERMAN	576	HBC	+	$K^- p$ 4.2 GeV/c
largest at small angles		ESTES	74	HBC	$\pm$	$K^- p$ 2.1,2.6 GeV/c
$3.0 \pm 1.6$	50	LONDON	66	HBC	+	$K^- p$ 2.25 GeV/c
● ● ● We do not use the following data for averages, fits, limits, etc. ● ● ●						
$0.58 \pm 0.20$	17	PRIMER	68	HBC	+	See BARNES 69E

### $\Gamma(\Sigma\pi)/\Gamma(\Sigma\pi\pi)$

VALUE	EVTS	DOCUMENT ID	TECN	CHG	COMMENT	
varies with prod. angle		<sup>5</sup> APSELL	74	HBC	+	$K^- p$ 2.87 GeV/c
$1.39 \pm 0.16$		BERTHON	74	HBC	0	Quasi-2-body $\sigma$
$2.5$ to $0.24$		EBERHARD	69	HBC	+	$K^- p$ 2.6 GeV/c
<0.4		BIRMINGHAM	66	HBC	+	$K^- p$ 3.5 GeV/c
$0.30 \pm 0.15$		LONDON	66	HBC	+	$K^- p$ 2.25 GeV/c

### $\Gamma(\Lambda(1405)\pi)/\Gamma(\Sigma\pi\pi)$

VALUE	EVTS	DOCUMENT ID	TECN	CHG	COMMENT	
$0.97 \pm 0.08$		TIMMERMAN	576	HBC		$K^- p$ 4.2 GeV/c
$1.00 \pm 0.02$		APSELL	74	HBC		$K^- p$ 2.87 GeV/c
$0.90^{+0.10}_{-0.16}$		EBERHARD	65	HBC	+	$K^- p$ 2.45 GeV/c

### $\Gamma(\Lambda(1405)\pi)/\Gamma(\Sigma(1385)\pi)$

VALUE	EVTS	DOCUMENT ID	TECN	CHG	COMMENT	
<0.8		EBERHARD	65	HBC	+	$K^- p$ 2.45 GeV/c

### $\Gamma(\Lambda\pi\pi)/\Gamma(\Sigma\pi\pi)$

VALUE	EVTS	DOCUMENT ID	TECN	CHG	COMMENT	
$0.35 \pm 0.2$		BIRMINGHAM	66	HBC	+	$K^- p$ 3.5 GeV/c

### $\Gamma(\Lambda\pi)/\Gamma(\Sigma\pi\pi)$

VALUE	EVTS	DOCUMENT ID	TECN	CHG	COMMENT	
<0.2		BIRMINGHAM	66	HBC	+	$K^- p$ 3.5 GeV/c

### $\Gamma(\Lambda\pi)/[\Gamma(\Lambda\pi) + \Gamma(\Sigma\pi)]$

VALUE	EVTS	DOCUMENT ID	TECN	CHG	COMMENT	
<0.6		AGUILAR-...	70B	HBC		

### $\Gamma_2/\Gamma_3$

### $\Gamma_4/\Gamma_3$

### $\Gamma_5/\Gamma_3$

### $\Gamma_7/\Gamma_3$

### $\Gamma_3/\Gamma_5$

### $\Gamma_7/\Gamma_5$

### $\Gamma_7/\Gamma_6$

### $\Gamma_4/\Gamma_5$

### $\Gamma_2/\Gamma_5$

### $\Gamma_2/(\Gamma_2 + \Gamma_3)$

## Baryon Particle Listings

 $\Sigma(1670)$  Bumps,  $\Sigma(1690)$  Bumps,  $\Sigma(1750)$  $\Gamma(\Sigma(1385)\pi)/\Gamma(\Sigma\pi)$ 

VALUE	DOCUMENT ID	TECN	COMMENT	$\Gamma_6/\Gamma_3$
$\leq 0.21 \pm 0.05$	TIMMERMANS76	HBC	$K^- p$ 4.2 GeV/c	

 $\Sigma(1670)$  QUANTUM NUMBERS  
(PRODUCTION EXPERIMENTS)

VALUE	EVTS	DOCUMENT ID	TECN	CHG	COMMENT
$J^P = 3/2^-$	400	BUTTON...	68	HBC	$\pm \Sigma^0 \pi$
$J^P = 3/2^-$		EBERHARD	67	HBC	$+$ $\Lambda(1405)\pi$
$J^P = 3/2^+$		LEVEQUE	65	HBC	$\Lambda(1405)\pi$

 $\Sigma(1670)$  FOOTNOTES

- Total cross-section bump with  $(J+1/2) \Gamma_{el} / \Gamma_{total} = 0.23$ .
- Enhancements in  $\Sigma\pi$  and  $\Sigma\pi\pi$  cross sections.
- Backward production in the  $\Lambda\pi^- K^+$  final state.
- Depending on production angle.
- APSELL 74, ESTES 74, and TIMMERMANS 76 find strong branching ratio dependence on production angle, as in earlier production experiments.

 $\Sigma(1670)$  REFERENCES  
(PRODUCTION EXPERIMENTS)

FERRERSORIA 81	NP B178 373	A. Ferrer Soria et al.	(CERN, CDEF, EPOL+)
CARROLL 76	PRL 37 806	A.S. Carroll et al.	(BNL)
HEPP 76	NP B115 82	V. Hepp et al.	(CERN, HEID, MPIM)
TIMMERMANS 76	NP B112 77	J.J.M. Timmermans et al.	(NIJM, CERN+)
APSELL 74	PR D10 1419	S.P. Apsell et al.	(BRAN, UMD, SYRA+)
BERTHON 74	NC 21A 146	A. Berthon et al.	(CDEF, RHEL, SACL+)
ESTES 74	Thesis LBL-3827	R.D. Estes	(LBL)
AGUILAR-... 70B	PRL 25 58	M. Aguilar-Benitez et al.	(BNL, SYRA)
BARNES 69E	BNL 13823	V.E. Barnes et al.	(BNL, SYRA)
EBERHARD 69	PRL 22 200	P.H. Eberhard et al.	(LRL)
HUVE 69	PR 181 1824	D.O. Huve	(LRL)
BUGG 68	PR 168 1466	D.V. Bugg et al.	(RHEL, BIRM, CAVE)
BUTTON... 68	PRL 21 1123	J. Button-Shafer	(MASA, LRL) JP
PRIMER 68	PRL 20 610	M. Primer et al.	(SYRA, BNL)
EBERHARD 67	PR 163 1446	P. Eberhard et al.	(LRL, ILL) JP
BIRMINGHAM 66	PR 152 1148	M. Hogue et al.	(BIRM, GLAS, LOIC, OXF+)
LONDON 66	PR 143 1034	G.W. London et al.	(BNL, SYRA) IJ
EBERHARD 65	PRL 14 466	P.H. Eberhard et al.	(LRL, ILL) I
LEVEQUE 65	PL 18 69	A. Leveque et al.	(SACL, EPOL, GLAS+)
ALVAREZ 63	PRL 10 184	L.W. Alvarez et al.	(LRL) I
SMITH 63	Athens Conf. 67	G.A. Smith	(LRL)
ALEXANDER 62C	CERN Conf. 320	G. Alexander et al.	(LRL) I

 $\Sigma(1690)$  Bumps

$I(J^P) = 1(??) \text{ Status: } **$

OMITTED FROM SUMMARY TABLE

See the note preceding the  $\Sigma(1670)$  Listings. Seen in production experiments only, mainly in  $\Lambda\pi$ . $\Sigma(1690)$  MASS  
(PRODUCTION EXPERIMENTS)

VALUE (MeV)	EVTS	DOCUMENT ID	TECN	CHG	COMMENT
$\approx 1690$ OUR ESTIMATE					
$1698 \pm 20$	70	1 GODDARD	79	HBC	$+$ $\pi^+ p$ 10.3 GeV/c
$1707 \pm 20$	40	2 GODDARD	79	HBC	$+$ $\pi^+ p$ 10.3 GeV/c
$1698 \pm 20$	15	ADERHOLZ	69	HBC	$+$ $\pi^+ p$ 8 GeV/c
$1682 \pm 2$	46	BLUMENFELD	69	HBC	$+$ $K_L^0 p$
$1700 \pm 20$		MOTT	69	HBC	$+$ $K^- p$ 5.5 GeV/c
$1694 \pm 24$	60	3 PRIMER	68	HBC	$+$ $K^- p$ 4.6-5 GeV/c
$1700 \pm 6$		4 SIMS	68	HBC	$-$ $K^- N \rightarrow \Lambda\pi\pi$
$1715 \pm 12$	30	COLLEY	67	HBC	$+$ $K^- p$ 6 GeV/c

 $\Sigma(1690)$  WIDTH  
(PRODUCTION EXPERIMENTS)

VALUE (MeV)	EVTS	DOCUMENT ID	TECN	CHG	COMMENT
$240 \pm 60$	70	1 GODDARD	79	HBC	$+$ $\pi^+ p$ 10.3 GeV/c
$130^{+100}_{-60}$	40	2 GODDARD	79	HBC	$+$ $\pi^+ p$ 10.3 GeV/c
$142 \pm 40$	15	ADERHOLZ	69	HBC	$+$ $\pi^+ p$ 8 GeV/c
$25 \pm 10$	46	BLUMENFELD	69	HBC	$+$ $K_L^0 p$
$130 \pm 25$		MOTT	69	HBC	$+$ $K^- p$ 5.5 GeV/c
$105 \pm 35$	60	3 PRIMER	68	HBC	$+$ $K^- p$ 4.6-5 GeV/c
$62 \pm 14$		4 SIMS	68	HBC	$-$ $K^- N \rightarrow \Lambda\pi\pi$
$100 \pm 35$	30	COLLEY	67	HBC	$+$ $K^- p$ 6 GeV/c

 $\Sigma(1690)$  DECAY MODES  
(PRODUCTION EXPERIMENTS)

Mode	$\Gamma_1/\Gamma_2$
$\Gamma_1 \quad N\bar{K}$	
$\Gamma_2 \quad \Lambda\pi$	
$\Gamma_3 \quad \Sigma\pi$	
$\Gamma_4 \quad \Sigma(1385)\pi$	
$\Gamma_5 \quad \Lambda\pi\pi$ (including $\Sigma(1385)\pi$ )	

 $\Sigma(1690)$  BRANCHING RATIOS  
(PRODUCTION EXPERIMENTS)

$\Gamma(N\bar{K})/\Gamma(\Lambda\pi)$	VALUE	EVTS	DOCUMENT ID	TECN	CHG	COMMENT	$\Gamma_1/\Gamma_2$
	small		GODDARD	79	HBC	$+$ $\pi^+ p$ 10.2 GeV/c	
	$< 0.2$		MOTT	69	HBC	$+$ $K^- p$ 5.5 GeV/c	
	$0.4 \pm 0.25$	18	COLLEY	67	HBC	$+$ 6/30 events	

$\Gamma(\Sigma\pi)/\Gamma(\Lambda\pi)$	VALUE	CL%	DOCUMENT ID	TECN	CHG	COMMENT	$\Gamma_3/\Gamma_2$
	small		GODDARD	79	HBC	$+$ $\pi^+ p$ 10.2 GeV/c	
	$< 0.4$	90	MOTT	69	HBC	$+$ $K^- p$ 5.5 GeV/c	
	$0.3 \pm 0.3$		COLLEY	67	HBC	$+$ 4/30 events	

$\Gamma(\Sigma(1385)\pi)/\Gamma(\Lambda\pi)$	VALUE	DOCUMENT ID	TECN	CHG	COMMENT	$\Gamma_4/\Gamma_2$
	$< 0.5$	MOTT	69	HBC	$+$ $K^- p$ 5.5 GeV/c	

$\Gamma(\Lambda\pi\pi \text{ (including } \Sigma(1385)\pi)) / \Gamma(\Lambda\pi)$	VALUE	DOCUMENT ID	TECN	CHG	COMMENT	$\Gamma_5/\Gamma_2$
	$2.0 \pm 0.6$	BLUMENFELD	69	HBC	$+$ 31/15 events	
	$0.5 \pm 0.25$	COLLEY	67	HBC	$+$ 15/30 events	

$\Gamma(\Sigma(1385)\pi)/\Gamma(\Lambda\pi\pi \text{ (including } \Sigma(1385)\pi))$	VALUE	DOCUMENT ID	TECN	CHG	COMMENT	$\Gamma_4/\Gamma_5$
	large	SIMS	68	HBC	$-$ $K^- N \rightarrow \Lambda\pi\pi$	
	small	COLLEY	67	HBC	$+$ $K^- p$ 6 GeV/c	

 $\Sigma(1690)$  FOOTNOTES  
(PRODUCTION EXPERIMENTS)

- From  $\pi^+ p \rightarrow (\Lambda\pi^+) K^+$ ,  $J > 1/2$  is not required by the data.
- From  $\pi^+ p \rightarrow (\Lambda\pi^+) (K\pi)^+$ ,  $J > 1/2$  is indicated, but large background precludes a definite conclusion.
- See the  $\Sigma(1670)$  Listings. AGUILAR-BENITEZ 70B with three times the data of PRIMER 68 find no evidence for the  $\Sigma(1690)$ .
- This analysis, which is difficult and requires several assumptions and shows no unambiguous  $\Sigma(1690)$  signal, suggests  $J^P = 5/2^+$ . Such a state would lead all previously known  $Y^*$  trajectories.

 $\Sigma(1690)$  REFERENCES  
(PRODUCTION EXPERIMENTS)

GODDARD 79	PR D19 1350	M.C. Goddard et al.	(TNT0, BNL) IJ
AGUILAR-... 70B	PRL 25 58	M. Aguilar-Benitez et al.	(BNL, SYRA)
ADERHOLZ 69	NP B11 259	M. Aderholz et al.	(AACH3, BERL, CERN+) I
BLUMENFELD 69	PL 29B 58	B.J. Blumenfeld, G.R. Kalbfleisch	(BNL) I
MOTT 69	PR 177 1966	J. Mott et al.	(NWES, ANL) I
Also	PRL 18 266	M. Derrick et al.	(ANL, NWES) I
PRIMER 68	PRL 20 610	M. Primer et al.	(SYRA, BNL) I
SIMS 68	PRL 21 1413	W.H. Sims et al.	(FSU, TUFTS, BRAN) I
COLLEY 67	PL 24B 489	D.C. Colley	(BIRM, GLAS, LOIC, MUNI, OXF+) I

 $\Sigma(1750)$   $1/2^-$ 

$I(J^P) = 1(\frac{1}{2}^-) \text{ Status: } ***$

For most results published before 1974 (they are now obsolete), see our 1982 edition Physics Letters **111B** 1 (1982).There is evidence for this state in many partial-wave analyses, but with wide variations in the mass, width, and couplings. The latest analyses indicated significant couplings to  $N\bar{K}$  and  $\Lambda\pi$ , as well as to  $\Sigma\eta$  whose threshold is at 1746 MeV (JONES 74). $\Sigma(1750)$  MASS

VALUE (MeV)	DOCUMENT ID	TECN	COMMENT
$1730$ to $1800$ ( $\approx 1750$ ) OUR ESTIMATE			
$1756 \pm 10$	GOPAL 80	DPWA	$\bar{K}N \rightarrow \bar{K}N$
$1770 \pm 10$	ALSTON-... 78	DPWA	$\bar{K}N \rightarrow \bar{K}N$
$1770 \pm 15$	GOPAL 77	DPWA	$\bar{K}N$ multichannel

See key on page 457

# Baryon Particle Listings

## $\Sigma(1750), \Sigma(1770)$

••• We do not use the following data for averages, fits, limits, etc. •••

1800 or 1813	1 MARTIN	77	DPWA	$\bar{K}N$ multichannel
1715±10	2 CARROLL	76	DPWA	Isospin-1 total $\sigma$
1730	DEBELLEFON	76	IPWA	$K^-p \rightarrow \Lambda\pi^0$
1780±30	BAILLON	75	IPWA	$\bar{K}N \rightarrow \Lambda\pi$ (sol. 1)
1700±30	BAILLON	75	IPWA	$\bar{K}N \rightarrow \Lambda\pi$ (sol. 2)
1697 <sup>+20</sup> <sub>-10</sub>	VANHORN	75	DPWA	$K^-p \rightarrow \Lambda\pi^0$
1785±12	CHU	74	DBC	Fits $\sigma(K^-n \rightarrow \Sigma^-\eta)$
1760±5	3 JONES	74	HBC	Fits $\sigma(K^-p \rightarrow \Sigma^0\eta)$
1739±10	PREVOST	74	DPWA	$K^-N \rightarrow \Sigma(1385)\pi$

### $\Sigma(1750)$ WIDTH

VALUE (MeV)	DOCUMENT ID	TECN	COMMENT
<b>60 to 160 (≈ 90) OUR ESTIMATE</b>			
64±10	GOPAL	80	DPWA $\bar{K}N \rightarrow \bar{K}N$
161±20	ALSTON-...	78	DPWA $\bar{K}N \rightarrow \bar{K}N$
60±10	GOPAL	77	DPWA $\bar{K}N$ multichannel
••• We do not use the following data for averages, fits, limits, etc. •••			
117 or 119	1 MARTIN	77	DPWA $\bar{K}N$ multichannel
10	2 CARROLL	76	DPWA Isospin-1 total $\sigma$
110	DEBELLEFON	76	IPWA $K^-p \rightarrow \Lambda\pi^0$
140±30	BAILLON	75	IPWA $\bar{K}N \rightarrow \Lambda\pi$ (sol. 1)
160±50	BAILLON	75	IPWA $\bar{K}N \rightarrow \Lambda\pi$ (sol. 2)
66 <sup>+14</sup> <sub>-12</sub>	VANHORN	75	DPWA $K^-p \rightarrow \Lambda\pi^0$
89±33	CHU	74	DBC Fits $\sigma(K^-n \rightarrow \Sigma^-\eta)$
92±7	3 JONES	74	HBC Fits $\sigma(K^-p \rightarrow \Sigma^0\eta)$
108±20	PREVOST	74	DPWA $K^-N \rightarrow \Sigma(1385)\pi$

### $\Sigma(1750)$ DECAY MODES

Mode	Fraction ( $\Gamma_i/\Gamma$ )
$\Gamma_1$ $N\bar{K}$	10–40 %
$\Gamma_2$ $\Lambda\pi$	seen
$\Gamma_3$ $\Sigma\pi$	<8 %
$\Gamma_4$ $\Sigma\eta$	15–55 %
$\Gamma_5$ $\Sigma(1385)\pi$	
$\Gamma_6$ $\Lambda(1520)\pi$	

The above branching fractions are our estimates, not fits or averages.

### $\Sigma(1750)$ BRANCHING RATIOS

See “Sign conventions for resonance couplings” in the Note on  $\Lambda$  and  $\Sigma$  Resonances.

$\Gamma(N\bar{K})/\Gamma_{\text{total}}$	$\Gamma_1/\Gamma$
0.1 to 0.4 OUR ESTIMATE	
0.14±0.03	
0.33±0.05	

VALUE	DOCUMENT ID	TECN	COMMENT
0.14±0.03	GOPAL	80	DPWA $\bar{K}N \rightarrow \bar{K}N$
0.33±0.05	ALSTON-...	78	DPWA $\bar{K}N \rightarrow \bar{K}N$

••• We do not use the following data for averages, fits, limits, etc. •••

0.15±0.03	GOPAL	77	DPWA See GOPAL 80
0.06 or 0.05	1 MARTIN	77	DPWA $\bar{K}N$ multichannel

$(\Gamma_i/\Gamma)^{1/2}/\Gamma_{\text{total}}$ in $N\bar{K} \rightarrow \Sigma(1750) \rightarrow \Lambda\pi$	$(\Gamma_1\Gamma_3)^{1/2}/\Gamma$		
0.04 ± 0.03	GOPAL	77	DPWA $\bar{K}N$ multichannel

••• We do not use the following data for averages, fits, limits, etc. •••

-0.10 or -0.09	1 MARTIN	77	DPWA $\bar{K}N$ multichannel
-0.12	DEBELLEFON	76	IPWA $K^-p \rightarrow \Lambda\pi^0$
-0.12 ± 0.02	BAILLON	75	IPWA $\bar{K}N \rightarrow \Lambda\pi$ (sol. 1)
-0.13 ± 0.03	BAILLON	75	IPWA $\bar{K}N \rightarrow \Lambda\pi$ (sol. 2)
-0.13 ± 0.04	VANHORN	75	DPWA $K^-p \rightarrow \Lambda\pi^0$
-0.120 ± 0.077	DEVENISH	74B	Fixed- $t$ dispersion rel.

$(\Gamma_i/\Gamma)^{1/2}/\Gamma_{\text{total}}$ in $N\bar{K} \rightarrow \Sigma(1750) \rightarrow \Sigma\pi$	$(\Gamma_1\Gamma_3)^{1/2}/\Gamma$		
-0.09±0.05	GOPAL	77	DPWA $\bar{K}N$ multichannel

••• We do not use the following data for averages, fits, limits, etc. •••

+0.06 or +0.06	1 MARTIN	77	DPWA $\bar{K}N$ multichannel
0.13±0.02	LANGBEIN	72	IPWA $\bar{K}N$ multichannel

$(\Gamma_i/\Gamma)^{1/2}/\Gamma_{\text{total}}$ in $N\bar{K} \rightarrow \Sigma(1750) \rightarrow \Sigma\eta$	$(\Gamma_1\Gamma_4)^{1/2}/\Gamma$		
0.23±0.01	3 JONES	74	HBC Fits $\sigma(K^-p \rightarrow \Sigma^0\eta)$

••• We do not use the following data for averages, fits, limits, etc. •••

seen	CLINE	69	DBC Threshold bump
------	-------	----	--------------------

$(\Gamma_i/\Gamma)^{1/2}/\Gamma_{\text{total}}$ in $N\bar{K} \rightarrow \Sigma(1750) \rightarrow \Sigma(1385)\pi$	$(\Gamma_1\Gamma_5)^{1/2}/\Gamma$		
0.18±0.15	PREVOST	74	DPWA $K^-N \rightarrow \Sigma(1385)\pi$

$(\Gamma_i/\Gamma)^{1/2}/\Gamma_{\text{total}}$ in $N\bar{K} \rightarrow \Sigma(1750) \rightarrow \Lambda(1520)\pi$	$(\Gamma_1\Gamma_6)^{1/2}/\Gamma$		
0.032±0.021	CAMERON	77	DPWA $P$ -wave decay

### $\Sigma(1750)$ FOOTNOTES

- <sup>1</sup> The two MARTIN 77 values are from a T-matrix pole and from a Breit-Wigner fit.
- <sup>2</sup> A total cross-section bump with  $(J+1/2)\Gamma_{\text{el}}/\Gamma_{\text{total}} = 0.30$ .
- <sup>3</sup> An S-wave Breit-Wigner fit to the threshold cross section with no background and errors statistical only.

### $\Sigma(1750)$ REFERENCES

PDG	82	PL 111B 1	M. Roos et al.	(HELS, CIT, CERN)
GOPAL	80	Toronto Conf. 159	G.P. Gopal	(RHEL) IJP
ALSTON-...	78	PR D18 182	M. Alston-Garnjost et al.	(LBL, MTHO+) IJP
Also		PRL 38 1007	M. Alston-Garnjost et al.	(LBL, MTHO+) IJP
CAMERON	77	NP B131 399	W. Cameron et al.	(RHEL, LOIC) IJP
GOPAL	77	NP B119 362	G.P. Gopal et al.	(LOIC, RHEL) IJP
MARTIN	77	NP B127 349	B.R. Martin, M.K. Pidcock, R.G. Moorhouse	(LOUC+) IJP
Also		NP B126 266	B.R. Martin, M.K. Pidcock	(LOUC) IJP
Also		NP B126 285	B.R. Martin, M.K. Pidcock	(LOUC) IJP
CARROLL	76	PRL 37 806	A.S. Carroll et al.	(BNL) I
DEBELLEFON	76	NP B109 129	A. de Bellefon, A. Berthon	(CDEF) IJP
BAILLON	75	NP B94 39	P.H. Baillon, P.J. Litchfield	(CERN, RHEL) IJP
VANHORN	75	NP B87 145	A.J. van Horn	(LBL) IJP
Also		NP B87 157	A.J. van Horn	(LBL) IJP
CHU	74	NC 20A 35	R.Y.L. Chu et al.	(PLAT, TUFTS, BRAN) IJP
DEVENISH	74B	NP B81 330	R.C.E. Devenish, C.D. Froggatt, B.R. Martin	(DSY+) IJP
JONES	74	NP B73 141	M.D. Jones	(CHIC) IJP
PREVOST	74	NP B69 246	J. Prevost et al.	(SACL, CERN, HEID)
LANGBEIN	72	NP B47 477	W. Langbein, F. Wagner	(MPIM) IJP
CLINE	69	LCN 2 407	D. Cline, R. Laumann, J. Mapp	(WISC)

### $\Sigma(1770) 1/2^+$

$I(J^P) = 1(\frac{1}{2}^+)$  Status: \*

OMITTED FROM SUMMARY TABLE

Evidence for this state now rests solely on solution 1 of BAILLON 75, (see the footnotes) but the  $\Lambda\pi$  partial-wave amplitudes of this solution are in disagreement with amplitudes from most other  $\Lambda\pi$  analyses.

### $\Sigma(1770)$ MASS

VALUE (MeV)	DOCUMENT ID	TECN	COMMENT
<b>≈ 1770 OUR ESTIMATE</b>			
1738±10	1 GOPAL	77	DPWA $\bar{K}N$ multichannel
1770±20	2 BAILLON	75	IPWA $\bar{K}N \rightarrow \Lambda\pi$
1772	3 KANE	72	DPWA $K^-p \rightarrow \Sigma\pi$

### $\Sigma(1770)$ WIDTH

VALUE (MeV)	DOCUMENT ID	TECN	COMMENT
72±10	1 GOPAL	77	DPWA $\bar{K}N$ multichannel
80±30	2 BAILLON	75	IPWA $\bar{K}N \rightarrow \Lambda\pi$
80	3 KANE	72	DPWA $K^-p \rightarrow \Sigma\pi$

### $\Sigma(1770)$ DECAY MODES

Mode	
$\Gamma_1$ $N\bar{K}$	
$\Gamma_2$ $\Lambda\pi$	
$\Gamma_3$ $\Sigma\pi$	

### $\Sigma(1770)$ BRANCHING RATIOS

See “Sign conventions for resonance couplings” in the Note on  $\Lambda$  and  $\Sigma$  Resonances.

$\Gamma(N\bar{K})/\Gamma_{\text{total}}$	$\Gamma_1/\Gamma$		
0.14±0.04	1 GOPAL	77	DPWA $\bar{K}N$ multichannel

$(\Gamma_i/\Gamma)^{1/2}/\Gamma_{\text{total}}$ in $N\bar{K} \rightarrow \Sigma(1770) \rightarrow \Lambda\pi$	$(\Gamma_1\Gamma_2)^{1/2}/\Gamma$		
< 0.04	GOPAL	77	DPWA $\bar{K}N$ multichannel
-0.08±0.02	2 BAILLON	75	IPWA $\bar{K}N \rightarrow \Lambda\pi$

$(\Gamma_i/\Gamma)^{1/2}/\Gamma_{\text{total}}$ in $N\bar{K} \rightarrow \Sigma(1770) \rightarrow \Sigma\pi$	$(\Gamma_1\Gamma_3)^{1/2}/\Gamma$		
< 0.04	GOPAL	77	DPWA $\bar{K}N$ multichannel
-0.108	3 KANE	72	DPWA $K^-p \rightarrow \Sigma\pi$

# Baryon Particle Listings

## $\Sigma(1770), \Sigma(1775)$

### $\Sigma(1770)$ FOOTNOTES

- <sup>1</sup> Required to fit the isospin-1 total cross section of CARROLL 76 in the  $\bar{K}N$  channel. The addition of new  $K^-p$  polarization and  $K^-n$  differential cross-section data in GOPAL 80 find it to be more consistent with the  $\Sigma(1660) P_{11}$ .
- <sup>2</sup> From solution 1 of BAILLON 75; not present in solution 2.
- <sup>3</sup> Not required in KANE 74, which supersedes KANE 72.

### $\Sigma(1770)$ REFERENCES

GOPAL	80	Toronto Conf. 159	G.P. Gopal	(RHEL)
GOPAL	77	NP B119 362	G.P. Gopal et al.	(LOIC, RHEL) IJP
CARROLL	76	PRL 37 806	A.S. Carroll et al.	(BNL) I
BAILLON	75	NP B94 39	P.H. Baillon, P.J. Litchfield	(CERN, RHEL) IJP
KANE	74	LBL-2452	D.F. Kane	(LBL) IJP
KANE	72	PR D5 1583	D.F.J. Kane	(LBL)

$\Sigma(1775) 5/2^-$

$$J(J^P) = 1(\frac{5}{2}^-) \text{ Status: } ***$$

Discovered by GALTIERI 63, this resonance plays the same role as cornerstone for isospin-1 analyses in this region as the  $\Lambda(1820) F_{05}$  does in the isospin-0 channel.

For most results published before 1974 (they are now obsolete), see our 1982 edition Physics Letters **111B** 1 (1982).

### $\Sigma(1775)$ MASS

VALUE (MeV)	DOCUMENT ID	TECN	COMMENT
<b>1770 to 1780 (<math>\approx 1775</math>) OUR ESTIMATE</b>			
1778 ± 5	GOPAL 80	DPWA	$\bar{K}N \rightarrow \bar{K}N$
1777 ± 5	ALSTON-... 78	DPWA	$\bar{K}N \rightarrow \bar{K}N$
1774 ± 5	GOPAL 77	DPWA	$\bar{K}N$ multichannel
1775 ± 10	BAILLON 75	IPWA	$\bar{K}N \rightarrow \Lambda\pi$
1774 ± 10	VANHORN 75	DPWA	$K^-p \rightarrow \Lambda\pi^0$
1772 ± 6	KANE 74	DPWA	$K^-p \rightarrow \Sigma\pi$
••• We do not use the following data for averages, fits, limits, etc. •••			
1772 or 1777	<sup>1</sup> MARTIN 77	DPWA	$\bar{K}N$ multichannel
1765	DEBELLEFON 76	IPWA	$K^-p \rightarrow \Lambda\pi^0$

### $\Sigma(1775)$ WIDTH

VALUE (MeV)	DOCUMENT ID	TECN	COMMENT
<b>105 to 135 (<math>\approx 120</math>) OUR ESTIMATE</b>			
137 ± 10	GOPAL 80	DPWA	$\bar{K}N \rightarrow \bar{K}N$
116 ± 10	ALSTON-... 78	DPWA	$\bar{K}N \rightarrow \bar{K}N$
130 ± 10	GOPAL 77	DPWA	$\bar{K}N$ multichannel
125 ± 15	BAILLON 75	IPWA	$\bar{K}N \rightarrow \Lambda\pi$
146 ± 18	VANHORN 75	DPWA	$K^-p \rightarrow \Lambda\pi^0$
154 ± 10	KANE 74	DPWA	$K^-p \rightarrow \Sigma\pi$
••• We do not use the following data for averages, fits, limits, etc. •••			
102 or 103	<sup>1</sup> MARTIN 77	DPWA	$\bar{K}N$ multichannel
120	DEBELLEFON 76	IPWA	$K^-p \rightarrow \Lambda\pi^0$

### $\Sigma(1775)$ DECAY MODES

Mode	Fraction ( $\Gamma_i/\Gamma$ )
$\Gamma_1$ $N\bar{K}$	37–43%
$\Gamma_2$ $\Lambda\pi$	14–20%
$\Gamma_3$ $\Sigma\pi$	2–5%
$\Gamma_4$ $\Sigma(1385)\pi$	8–12%
$\Gamma_5$ $\Sigma(1385)\pi, D$ -wave	
$\Gamma_6$ $\Lambda(1520)\pi$	17–23%
$\Gamma_7$ $\Sigma\pi\pi$	

The above branching fractions are our estimates, not fits or averages.

### CONSTRAINED FIT INFORMATION

An overall fit to 8 branching ratios uses 16 measurements and one constraint to determine 5 parameters. The overall fit has a  $\chi^2 = 63.9$  for 12 degrees of freedom.

The following *off-diagonal* array elements are the correlation coefficients  $\langle \delta x_i \delta x_j \rangle / (\delta x_i \delta x_j)$ , in percent, from the fit to the branching fractions,  $x_i \equiv \Gamma_i/\Gamma_{\text{total}}$ . The fit constrains the  $x_i$  whose labels appear in this array to sum to one.

$x_2$	–30			
$x_3$	–17	–21		
$x_4$	–37	–49	–14	
$x_6$	–81	6	8	16
	$x_1$	$x_2$	$x_3$	$x_4$

### $\Sigma(1775)$ BRANCHING RATIOS

See “Sign conventions for resonance couplings” in the Note on  $\Lambda$  and  $\Sigma$  Resonances. Also, the errors quoted do not include uncertainties due to the parametrization used in the partial-wave analyses and are thus too small.

#### $\Gamma(N\bar{K})/\Gamma_{\text{total}}$ $\Gamma_1/\Gamma$

VALUE	DOCUMENT ID	TECN	COMMENT
<b>0.37 to 0.43 OUR ESTIMATE</b>			
<b>0.45 ± 0.04 OUR FIT</b>	Error includes scale factor of 3.1.		
<b>0.391 ± 0.017 OUR AVERAGE</b>			
0.40 ± 0.02	GOPAL 80	DPWA	$\bar{K}N \rightarrow \bar{K}N$
0.37 ± 0.03	ALSTON-... 78	DPWA	$\bar{K}N \rightarrow \bar{K}N$
••• We do not use the following data for averages, fits, limits, etc. •••			
0.41 ± 0.03	GOPAL 77	DPWA	See GOPAL 80
0.37 or 0.36	<sup>1</sup> MARTIN 77	DPWA	$\bar{K}N$ multichannel

#### $(\Gamma_1\Gamma_f)^{1/2}/\Gamma_{\text{total}}$ in $N\bar{K} \rightarrow \Sigma(1775) \rightarrow \Lambda\pi$ $(\Gamma_1\Gamma_2)^{1/2}/\Gamma$

VALUE	DOCUMENT ID	TECN	COMMENT
<b>0.305 ± 0.018 OUR FIT</b> Error includes scale factor of 2.4.			
<b>–0.262 ± 0.015 OUR AVERAGE</b>			
–0.28 ± 0.03	GOPAL 77	DPWA	$\bar{K}N$ multichannel
–0.25 ± 0.02	BAILLON 75	IPWA	$\bar{K}N \rightarrow \Lambda\pi$
–0.28 ± 0.04	VANHORN 75	DPWA	$K^-p \rightarrow \Lambda\pi^0$
–0.259 ± 0.048	DEVENISH 74B		Fixed- $t$ dispersion rel.
••• We do not use the following data for averages, fits, limits, etc. •••			
–0.29 or –0.28	<sup>1</sup> MARTIN 77	DPWA	$\bar{K}N$ multichannel
–0.30	DEBELLEFON 76	IPWA	$K^-p \rightarrow \Lambda\pi^0$

#### $(\Gamma_1\Gamma_f)^{1/2}/\Gamma_{\text{total}}$ in $N\bar{K} \rightarrow \Sigma(1775) \rightarrow \Sigma\pi$ $(\Gamma_1\Gamma_3)^{1/2}/\Gamma$

VALUE	DOCUMENT ID	TECN	COMMENT
<b>0.105 ± 0.025 OUR FIT</b> Error includes scale factor of 3.1.			
<b>0.098 ± 0.016 OUR AVERAGE</b> Error includes scale factor of 1.8.			
+0.13 ± 0.02	GOPAL 77	DPWA	$\bar{K}N$ multichannel
0.09 ± 0.01	KANE 74	DPWA	$K^-p \rightarrow \Sigma\pi$
••• We do not use the following data for averages, fits, limits, etc. •••			
+0.08 or +0.08	<sup>1</sup> MARTIN 77	DPWA	$\bar{K}N$ multichannel

#### $(\Gamma_1\Gamma_f)^{1/2}/\Gamma_{\text{total}}$ in $N\bar{K} \rightarrow \Sigma(1775) \rightarrow \Lambda(1520)\pi$ $(\Gamma_1\Gamma_6)^{1/2}/\Gamma$

VALUE	DOCUMENT ID	TECN	COMMENT
<b>0.315 ± 0.010 OUR FIT</b> Error includes scale factor of 1.5.			
<b>0.303 ± 0.009 OUR AVERAGE</b> Signs on measurements were ignored.			
–0.305 ± 0.010	<sup>2</sup> CAMERON 77	DPWA	$K^-p \rightarrow \Lambda(1520)\pi^0$
0.31 ± 0.02	BARLETTA 72	DPWA	$K^-p \rightarrow \Lambda(1520)\pi^0$
0.27 ± 0.03	ARMENTEROS65c	HBC	$K^-p \rightarrow \Lambda(1520)\pi^0$

#### $(\Gamma_1\Gamma_f)^{1/2}/\Gamma_{\text{total}}$ in $N\bar{K} \rightarrow \Sigma(1775) \rightarrow \Sigma(1385)\pi$ $(\Gamma_1\Gamma_4)^{1/2}/\Gamma$

VALUE	DOCUMENT ID	TECN	COMMENT
<b>0.211 ± 0.022 OUR FIT</b> Error includes scale factor of 2.8.			
<b>0.188 ± 0.010 OUR AVERAGE</b> Signs on measurements were ignored.			
–0.184 ± 0.011	<sup>3</sup> CAMERON 78	DPWA	$K^-p \rightarrow \Sigma(1385)\pi$
+0.20 ± 0.02	PREVOST 74	DPWA	$K^-n \rightarrow \Sigma(1385)\pi$
••• We do not use the following data for averages, fits, limits, etc. •••			
0.32 ± 0.06	SIMS 68	DBC	$K^-n \rightarrow \Lambda\pi\pi$
0.24 ± 0.03	ARMENTEROS67c	HBC	$K^-p \rightarrow \Lambda\pi\pi$

#### $\Gamma(\Lambda\pi)/\Gamma(N\bar{K})$ $\Gamma_2/\Gamma_1$

VALUE	DOCUMENT ID	TECN	COMMENT
<b>0.46 ± 0.09 OUR FIT</b> Error includes scale factor of 2.9.			
<b>0.33 ± 0.05</b>	UHLIG 67	HBC	$K^-p$ 0.9 GeV/c

#### $\Gamma(\Sigma\pi\pi)/\Gamma_{\text{total}}$ $\Gamma_7/\Gamma$

VALUE	DOCUMENT ID	TECN	COMMENT
••• We do not use the following data for averages, fits, limits, etc. •••			
0.12	<sup>4</sup> ARMENTEROS68c	HDBC	$K^-n \rightarrow \Sigma\pi\pi$

#### $\Gamma(\Sigma(1385)\pi)/\Gamma(N\bar{K})$ $\Gamma_4/\Gamma_1$

VALUE	DOCUMENT ID	TECN	COMMENT
<b>0.22 ± 0.07 OUR FIT</b> Error includes scale factor of 3.6.			
<b>0.25 ± 0.09</b>	UHLIG 67	HBC	$K^-p$ 0.9 GeV/c

#### $\Gamma(\Lambda(1520)\pi)/\Gamma(N\bar{K})$ $\Gamma_6/\Gamma_1$

VALUE	DOCUMENT ID	TECN	COMMENT
<b>0.49 ± 0.11 OUR FIT</b> Error includes scale factor of 3.5.			
<b>0.28 ± 0.05</b>	UHLIG 67	HBC	$K^-p$ 0.9 GeV/c

### $\Sigma(1775)$ FOOTNOTES

- <sup>1</sup> The two MARTIN 77 values are from a T-matrix pole and from a Breit-Wigner fit.
- <sup>2</sup> This rate combines  $P$ -wave- and  $F$ -wave decays. The CAMERON 77 results for the separate  $P$ -wave- and  $F$ -wave decays are  $-0.303 \pm 0.010$  and  $-0.037 \pm 0.014$ . The published signs have been changed here to be in accord with the baryon-first convention.
- <sup>3</sup> The CAMERON 78 upper limit on  $G$ -wave decay is 0.03.
- <sup>4</sup> For about 3/4 of this, the  $\Sigma\pi$  system has  $l = 0$  and is almost entirely  $\Lambda(1520)$ . For the rest, the  $\Sigma\pi$  has  $l = 1$ , which is about what is expected from the known  $\Sigma(1775) \rightarrow \Sigma(1385)\pi$  rate, as seen in  $\Lambda\pi\pi$ .

# Baryon Particle Listings

## $\Sigma(1775)$ , $\Sigma(1840)$ , $\Sigma(1880)$

 **$\Sigma(1775)$  REFERENCES**

PDG	82	PL 111B 1	M. Roos <i>et al.</i>	(HEL5, CIT, CERN)
GOPAL	80	Toronto Conf. 159	G.P. Gopal	(RHEL) IJP
ALSTON-...	78	PR D18 182	M. Alston-Garnjost <i>et al.</i>	(LBL, MTHO+) IJP
Also		PRL 38 1007	M. Alston-Garnjost <i>et al.</i>	(LBL, MTHO+) IJP
CAMERON	78	NP B143 189	W. Cameron <i>et al.</i>	(RHEL, LOIC) IJP
CAMERON	77	NP B131 399	W. Cameron <i>et al.</i>	(RHEL, LOIC) IJP
GOPAL	77	NP B119 362	G.P. Gopal <i>et al.</i>	(LOIC, RHEL) IJP
MARTIN	77	NP B127 349	B.R. Martin, M.K. Pidcock, R.G. Moorhouse	(LOUC+) IJP
Also		NP B126 266	B.R. Martin, M.K. Pidcock	(LOUC) IJP
Also		NP B126 285	B.R. Martin, M.K. Pidcock	(LOUC) IJP
DEBELLEFON	76	NP B109 129	A. de Bellefon, A. Berthon	(CDEF) IJP
BAILLON	75	NP B94 39	P.H. Baillon, P.J. Litchfield	(CERN, RHEL) IJP
VANHORN	75	NP B87 145	A.J. van Horn	(LBL) IJP
Also		NP B87 157	A.J. van Horn	(LBL) IJP
DEVENISH	74B	NP B81 330	R.C.E. Devenish, C.D. Froggatt, B.R. Martin	(DESY+) IJP
KANE	74	LBL-2452	D.F. Kane	(LBL) IJP
PREVOST	74	NP B69 246	J. Prevost <i>et al.</i>	(SACL, CERN, HEID) IJP
BARLETTA	72	NP B40 45	W.A. Barletta	(EFI) IJP
Also		PRL 17 841	S. Fenster <i>et al.</i>	(CHIC, ANL, CERN) IJP
ARMENTEROS	68C	NP B8 216	R. Armenteros <i>et al.</i>	(CERN, HEID, SAACL) I
SIMS	68	PRL 21 1413	W.H. Sims <i>et al.</i>	(FSU, TUFTS, BRAN)
ARMENTEROS	67C	ZPHY 202 486	R. Armenteros <i>et al.</i>	(CERN, HEID, SAACL)
UHLIG	67	PR 155 1448	R.P. Uhlig <i>et al.</i>	(UMD, NRL)
ARMENTEROS	65C	PL 19 338	R. Armenteros <i>et al.</i>	(CERN, HEID, SAACL) IJP
GALTIERI	63	PL 6 296	A. Galtieri, A. Hussain, R. Tripp	(LRL) IJ

 **$\Sigma(1840)$  REFERENCES**

MARTIN	77	NP B127 349	B.R. Martin, M.K. Pidcock, R.G. Moorhouse	(LOUC+) IJP
Also		NP B126 266	B.R. Martin, M.K. Pidcock	(LOUC) IJP
Also		NP B126 285	B.R. Martin, M.K. Pidcock	(LOUC) IJP
BAILLON	75	NP B94 39	P.H. Baillon, P.J. Litchfield	(CERN, RHEL) IJP
VANHORN	75	NP B87 145	A.J. van Horn	(LBL) IJP
Also		NP B87 157	A.J. van Horn	(LBL) IJP
DEVENISH	74B	NP B81 330	R.C.E. Devenish, C.D. Froggatt, B.R. Martin	(DESY+) IJP
LANGBEIN	72	NP B47 477	W. Langbein, F. Wagner	(MFM) IJP

 **$\Sigma(1880) 1/2^+$** 

$$I(J^P) = 1(\frac{1}{2}^+) \text{ Status: } **$$

OMITTED FROM SUMMARY TABLE

A  $P_{11}$  resonance is suggested by several partial-wave analyses, but with wide variations in the mass and other parameters. We list here all claims which lie well above the  $P_{11}$   $\Sigma(1770)$ .

 **$\Sigma(1880)$  MASS**

VALUE (MeV)	DOCUMENT ID	TECN	COMMENT
$\approx 1880$ OUR ESTIMATE			
$1826 \pm 20$	GOPAL	80	DPWA $\bar{K}N \rightarrow \bar{K}N$
$1870 \pm 10$	CAMERON	78B	DPWA $K^-p \rightarrow N\bar{K}^*$
$1847$ or $1863$	1 MARTIN	77	DPWA $\bar{K}N$ multichannel
$1960 \pm 30$	2 BAILLON	75	IPWA $\bar{K}N \rightarrow \Lambda\pi$
$1985 \pm 50$	VANHORN	75	DPWA $K^-p \rightarrow \Lambda\pi^0$
$1898$	3 LEA	73	DPWA Multichannel K-matrix
$\sim 1850$	ARMENTEROS70		IPWA $\bar{K}N \rightarrow \bar{K}N$
$1950 \pm 50$	BARBARO...	70	DPWA $K^-N \rightarrow \Lambda\pi$
$1920 \pm 30$	LITCHFIELD	70	DPWA $K^-N \rightarrow \Lambda\pi$
$1850$	BAILEY	69	DPWA $\bar{K}N \rightarrow \bar{K}N$
$1882 \pm 40$	SMART	68	DPWA $K^-N \rightarrow \Lambda\pi$

 **$\Sigma(1880)$  WIDTH**

VALUE (MeV)	DOCUMENT ID	TECN	COMMENT
$86 \pm 15$	GOPAL	80	DPWA $\bar{K}N \rightarrow \bar{K}N$
$80 \pm 10$	CAMERON	78B	DPWA $K^-p \rightarrow N\bar{K}^*$
$216$ or $220$	1 MARTIN	77	DPWA $\bar{K}N$ multichannel
$260 \pm 40$	2 BAILLON	75	IPWA $\bar{K}N \rightarrow \Lambda\pi$
$220 \pm 140$	VANHORN	75	DPWA $K^-p \rightarrow \Lambda\pi^0$
$222$	3 LEA	73	DPWA Multichannel K-matrix
$\sim 30$	ARMENTEROS70		IPWA $\bar{K}N \rightarrow \bar{K}N$
$200 \pm 50$	BARBARO...	70	DPWA $K^-N \rightarrow \Lambda\pi$
$170 \pm 40$	LITCHFIELD	70	DPWA $K^-N \rightarrow \Lambda\pi$
$200$	BAILEY	69	DPWA $\bar{K}N \rightarrow \bar{K}N$
$222 \pm 150$	SMART	68	DPWA $K^-N \rightarrow \Lambda\pi$

 **$\Sigma(1880)$  DECAY MODES**

Mode
$\Gamma_1$ $N\bar{K}$
$\Gamma_2$ $\Lambda\pi$
$\Gamma_3$ $\Sigma\pi$
$\Gamma_4$ $N\bar{K}^*(892)$ , $S=1/2$ , $P$ -wave
$\Gamma_5$ $N\bar{K}^*(892)$ , $S=3/2$ , $P$ -wave

 **$\Sigma(1880)$  BRANCHING RATIOS**

See "Sign conventions for resonance couplings" in the Note on  $\Lambda$  and  $\Sigma$  Resonances.

$\Gamma_i/\Gamma_{\text{total}}$	DOCUMENT ID	TECN	COMMENT
VALUE			
$0.06 \pm 0.02$	GOPAL	80	DPWA $\bar{K}N \rightarrow \bar{K}N$
$0.27$ or $0.27$	1 MARTIN	77	DPWA $\bar{K}N$ multichannel
$0.31$	3 LEA	73	DPWA Multichannel K-matrix
$0.20$	ARMENTEROS70		IPWA $\bar{K}N \rightarrow \bar{K}N$
$0.22$	BAILEY	69	DPWA $\bar{K}N \rightarrow \bar{K}N$

$(\Gamma_i/\Gamma_{\text{total}})^{1/2}$ in $N\bar{K} \rightarrow \Sigma(1880) \rightarrow \Lambda\pi$	DOCUMENT ID	TECN	COMMENT	$(\Gamma_1/\Gamma_2)^{1/2}$
VALUE				
$-0.24$ or $-0.24$	1 MARTIN	77	DPWA $\bar{K}N$ multichannel	
$-0.12 \pm 0.02$	2 BAILLON	75	IPWA $\bar{K}N \rightarrow \Lambda\pi$	
$+0.05$ or $+0.07$ $-0.02$	VANHORN	75	DPWA $K^-p \rightarrow \Lambda\pi^0$	
$-0.169 \pm 0.119$ $-0.30$	DEVENISH	74B	Fixed- $t$ dispersion rel.	
$-0.09 \pm 0.04$	3 LEA	73	DPWA Multichannel K-matrix	
$-0.14 \pm 0.03$	BARBARO...	70	DPWA $K^-N \rightarrow \Lambda\pi$	
$-0.11 \pm 0.03$	LITCHFIELD	70	DPWA $K^-N \rightarrow \Lambda\pi$	
	SMART	68	DPWA $K^-N \rightarrow \Lambda\pi$	

 **$\Sigma(1840)$  FOOTNOTES**

- 1 The two MARTIN 77 values are from a T-matrix pole and from a Breit-Wigner fit.  
2 From solution 1 of BAILLON 75; not present in solution 2.

 **$\Sigma(1840) 3/2^+$** 

$$I(J^P) = 1(\frac{3}{2}^+) \text{ Status: } *$$

OMITTED FROM SUMMARY TABLE

For the time being, we list together here all resonance claims in the  $P_{13}$  wave between 1700 and 1900 MeV.

 **$\Sigma(1840)$  MASS**

VALUE (MeV)	DOCUMENT ID	TECN	COMMENT
$\approx 1840$ OUR ESTIMATE			
$1798$ or $1802$	1 MARTIN	77	DPWA $\bar{K}N$ multichannel
$1720 \pm 30$	2 BAILLON	75	IPWA $\bar{K}N \rightarrow \Lambda\pi$
$1925 \pm 200$	VANHORN	75	DPWA $K^-p \rightarrow \Lambda\pi^0$
$1840 \pm 10$	LANGBEIN	72	IPWA $\bar{K}N$ multichannel

 **$\Sigma(1840)$  WIDTH**

VALUE (MeV)	DOCUMENT ID	TECN	COMMENT
$93$ or $93$	1 MARTIN	77	DPWA $\bar{K}N$ multichannel
$120 \pm 30$	2 BAILLON	75	IPWA $\bar{K}N \rightarrow \Lambda\pi$
$65$ or $65$ $\pm 20$	VANHORN	75	DPWA $K^-p \rightarrow \Lambda\pi^0$
$120 \pm 10$	LANGBEIN	72	IPWA $\bar{K}N$ multichannel

 **$\Sigma(1840)$  DECAY MODES**

Mode
$\Gamma_1$ $N\bar{K}$
$\Gamma_2$ $\Lambda\pi$
$\Gamma_3$ $\Sigma\pi$

 **$\Sigma(1840)$  BRANCHING RATIOS**

See "Sign conventions for resonance couplings" in the Note on  $\Lambda$  and  $\Sigma$  Resonances.

$\Gamma_i/\Gamma_{\text{total}}$	DOCUMENT ID	TECN	COMMENT
VALUE			
$0$ or $0$	1 MARTIN	77	DPWA $\bar{K}N$ multichannel
$0.37 \pm 0.13$	LANGBEIN	72	IPWA $\bar{K}N$ multichannel

$(\Gamma_i/\Gamma_{\text{total}})^{1/2}$ in $N\bar{K} \rightarrow \Sigma(1840) \rightarrow \Lambda\pi$	DOCUMENT ID	TECN	COMMENT	$(\Gamma_1/\Gamma_2)^{1/2}$
VALUE				
$+0.03$ or $+0.03$	1 MARTIN	77	DPWA $\bar{K}N$ multichannel	
$+0.11 \pm 0.02$	2 BAILLON	75	IPWA $\bar{K}N \rightarrow \Lambda\pi$	
$+0.06 \pm 0.04$	VANHORN	75	DPWA $K^-p \rightarrow \Lambda\pi^0$	
$+0.122 \pm 0.078$ $0.20 \pm 0.04$	DEVENISH	74B	Fixed- $t$ dispersion rel.	
	LANGBEIN	72	IPWA $\bar{K}N$ multichannel	

$(\Gamma_i/\Gamma_{\text{total}})^{1/2}$ in $N\bar{K} \rightarrow \Sigma(1840) \rightarrow \Sigma\pi$	DOCUMENT ID	TECN	COMMENT	$(\Gamma_1/\Gamma_3)^{1/2}$
VALUE				
$-0.04$ or $-0.04$	1 MARTIN	77	DPWA $\bar{K}N$ multichannel	
$0.15 \pm 0.04$	LANGBEIN	72	IPWA $\bar{K}N$ multichannel	

# Baryon Particle Listings

## $\Sigma(1880), \Sigma(1915)$

$(\Gamma_i \Gamma_f)^{1/2} / \Gamma_{total}$  in  $N\bar{K} \rightarrow \Sigma(1880) \rightarrow \Sigma\pi$   $(\Gamma_1 \Gamma_3)^{1/2} / \Gamma$

VALUE	DOCUMENT ID	TECN	COMMENT
+0.30 or +0.29 not seen	1 MARTIN 77 3 LEA 73	DPWA	$\bar{K}N$ multichannel Multichannel K-matrix

$(\Gamma_i \Gamma_f)^{1/2} / \Gamma_{total}$  in  $N\bar{K} \rightarrow \Sigma(1880) \rightarrow N\bar{K}^*(892), S=1/2, P\text{-wave } (\Gamma_1 \Gamma_4)^{1/2} / \Gamma$

VALUE	DOCUMENT ID	TECN	COMMENT
-0.05 ± 0.03	4 CAMERON 78B	DPWA	$K^- p \rightarrow N\bar{K}^*$

$(\Gamma_i \Gamma_f)^{1/2} / \Gamma_{total}$  in  $N\bar{K} \rightarrow \Sigma(1880) \rightarrow N\bar{K}^*(892), S=3/2, P\text{-wave } (\Gamma_1 \Gamma_5)^{1/2} / \Gamma$

VALUE	DOCUMENT ID	TECN	COMMENT
+0.11 ± 0.03	CAMERON 78B	DPWA	$K^- p \rightarrow N\bar{K}^*$

### $\Sigma(1880)$ FOOTNOTES

- The two MARTIN 77 values are from a T-matrix pole and from a Breit-Wigner fit.
- From solution 1 of BAILLON 75; not present in solution 2.
- Only unconstrained states from table 1 of LEA 73 are listed.
- The published sign has been changed to be in accord with the baryon-first convention.

### $\Sigma(1880)$ REFERENCES

GOPAL 80	Toronto Conf. 159	G.P. Gopal	(RHEL) IJP
CAMERON 78B	NP B146 327	W. Cameron et al.	(RHEL, LOIC) IJP
MARTIN 77	NP B127 349	B.R. Martin, M.K. Pidcock, R.G. Moorhouse	(LOUC+) IJP
	Also NP B126 266	B.R. Martin, M.K. Pidcock	(LOUC) IJP
	Also NP B126 285	B.R. Martin, M.K. Pidcock	(LOUC) IJP
BAILLON 75	NP B94 39	P.H. Baillon, P.J. Litchfield	(CERN, RHEL) IJP
VANHORN 75	NP B87 145	A.J. van Horn	(LBL) IJP
	Also NP B87 157	A.J. van Horn	(LBL) IJP
DEVENISH 74B	NP B81 330	R.C.E. Devenish, C.D. Froggatt, B.R. Martin	(DESY+) IJP
LEA 73	NP B56 77	A.T. Lea et al.	(RHEL, LOUC, GLAS, AARH) IJP
ARMENTEROS 70	Duke Conf. 123	R. Armenteros et al.	(CERN, HEID, SACL) IJP
	Hyperon Resonances, 1970		
BARBARO... 70	Duke Conf. 173	A. Barbaro-Galiteri	(LRL) IJP
	Hyperon Resonances, 1970		
LITCHFIELD 70	NP B22 269	P.J. Litchfield	(RHEL) IJP
BAILEY 69	Thesis UCRL 50617	J.M. Bailey	(LLL) IJP
SMART 68	PR 169 1330	W.M. Smart	(LRL) IJP

## $\Sigma(1915) 5/2^+$

$$I(J^P) = 1(\frac{5}{2}^+) \text{ Status: } ***$$

Discovered by COOL 66. For results published before 1974 (they are now obsolete), see our 1982 edition Physics Letters **111B** 1 (1982).

This entry only includes results from partial-wave analyses. Parameters of peaks seen in cross sections and invariant-mass distributions in this region used to be listed in a separate entry immediately following. They may be found in our 1986 edition Physics Letters **170B** 1 (1986).

### $\Sigma(1915)$ MASS

VALUE (MeV)	DOCUMENT ID	TECN	COMMENT
<b>1900 to 1935 (<math>\approx 1915</math>) OUR ESTIMATE</b>			
1937 ± 20	ALSTON-...	78	DPWA $\bar{K}N \rightarrow \bar{K}N$
1894 ± 5	1 CORDEN	77c	$K^- n \rightarrow \Sigma\pi$
1909 ± 5	1 CORDEN	77c	$K^- n \rightarrow \Sigma\pi$
1920 ± 10	GOPAL	77	DPWA $\bar{K}N$ multichannel
1900 ± 4	2 CORDEN	76	DPWA $K^- n \rightarrow \Lambda\pi^-$
1920 ± 30	BAILLON	75	IPWA $\bar{K}N \rightarrow \Lambda\pi$
1914 ± 10	HEMINGWAY	75	DPWA $K^- p \rightarrow \bar{K}N$
1920 ± 15 -20	VANHORN	75	DPWA $K^- p \rightarrow \Lambda\pi^0$
1920 ± 5	KANE	74	DPWA $K^- p \rightarrow \Sigma\pi$
••• We do not use the following data for averages, fits, limits, etc. •••			
not seen	DECLAIS	77	DPWA $\bar{K}N \rightarrow \bar{K}N$
1925 or 1933	3 MARTIN	77	DPWA $\bar{K}N$ multichannel
1915	DEBELLEFON	76	IPWA $K^- p \rightarrow \Lambda\pi^0$

### $\Sigma(1915)$ WIDTH

VALUE (MeV)	DOCUMENT ID	TECN	COMMENT
<b>80 to 160 (<math>\approx 120</math>) OUR ESTIMATE</b>			
161 ± 20	ALSTON-...	78	DPWA $\bar{K}N \rightarrow \bar{K}N$
107 ± 14	1 CORDEN	77c	$K^- n \rightarrow \Sigma\pi$
85 ± 13	1 CORDEN	77c	$K^- n \rightarrow \Sigma\pi$
130 ± 10	GOPAL	77	DPWA $\bar{K}N$ multichannel
75 ± 14	2 CORDEN	76	DPWA $K^- n \rightarrow \Lambda\pi^-$
70 ± 20	BAILLON	75	IPWA $\bar{K}N \rightarrow \Lambda\pi$
85 ± 15	HEMINGWAY	75	DPWA $K^- p \rightarrow \bar{K}N$
102 ± 18	VANHORN	75	DPWA $K^- p \rightarrow \Lambda\pi^0$
162 ± 25	KANE	74	DPWA $K^- p \rightarrow \Sigma\pi$
••• We do not use the following data for averages, fits, limits, etc. •••			
171 or 173	3 MARTIN	77	DPWA $\bar{K}N$ multichannel
60	DEBELLEFON	76	IPWA $K^- p \rightarrow \Lambda\pi^0$

### $\Sigma(1915)$ DECAY MODES

Mode	Fraction ( $\Gamma_i / \Gamma$ )
$\Gamma_1 \ N\bar{K}$	5-15 %
$\Gamma_2 \ \Lambda\pi$	seen
$\Gamma_3 \ \Sigma\pi$	seen
$\Gamma_4 \ \Sigma(1385)\pi$	<5 %
$\Gamma_5 \ \Sigma(1385)\pi, P\text{-wave}$	
$\Gamma_6 \ \Sigma(1385)\pi, F\text{-wave}$	

The above branching fractions are our estimates, not fits or averages.

### $\Sigma(1915)$ BRANCHING RATIOS

See "Sign conventions for resonance couplings" in the Note on  $\Lambda$  and  $\Sigma$  Resonances.

$\Gamma(N\bar{K}) / \Gamma_{total}$   $\Gamma_1 / \Gamma$

VALUE	DOCUMENT ID	TECN	COMMENT
<b>0.05 to 0.15 OUR ESTIMATE</b>			
0.03 ± 0.02	4 GOPAL 80	DPWA	$\bar{K}N \rightarrow \bar{K}N$
0.14 ± 0.05	ALSTON-...	78	DPWA $\bar{K}N \rightarrow \bar{K}N$
0.11 ± 0.04	HEMINGWAY 75	DPWA	$K^- p \rightarrow \bar{K}N$
••• We do not use the following data for averages, fits, limits, etc. •••			
0.05 ± 0.03	GOPAL 77	DPWA	See GOPAL 80
0.08 or 0.08	3 MARTIN 77	DPWA	$\bar{K}N$ multichannel

$(\Gamma_i \Gamma_f)^{1/2} / \Gamma_{total}$  in  $N\bar{K} \rightarrow \Sigma(1915) \rightarrow \Lambda\pi$   $(\Gamma_1 \Gamma_2)^{1/2} / \Gamma$

VALUE	DOCUMENT ID	TECN	COMMENT
-0.09 ± 0.03	GOPAL 77	DPWA	$\bar{K}N$ multichannel
-0.10 ± 0.01	2 CORDEN 76	DPWA	$K^- n \rightarrow \Lambda\pi^-$
-0.06 ± 0.02	BAILLON 75	IPWA	$\bar{K}N \rightarrow \Lambda\pi$
-0.09 ± 0.02	VANHORN 75	DPWA	$K^- p \rightarrow \Lambda\pi^0$
-0.087 ± 0.056	DEVENISH 74B		Fixed- $t$ dispersion rel.
••• We do not use the following data for averages, fits, limits, etc. •••			
-0.09 or -0.09	3 MARTIN 77	DPWA	$\bar{K}N$ multichannel
-0.10	DEBELLEFON 76	IPWA	$K^- p \rightarrow \Lambda\pi^0$

$(\Gamma_i \Gamma_f)^{1/2} / \Gamma_{total}$  in  $N\bar{K} \rightarrow \Sigma(1915) \rightarrow \Sigma\pi$   $(\Gamma_1 \Gamma_3)^{1/2} / \Gamma$

VALUE	DOCUMENT ID	TECN	COMMENT
-0.17 ± 0.01	1 CORDEN 77c		$K^- n \rightarrow \Sigma\pi$
-0.15 ± 0.02	1 CORDEN 77c		$K^- n \rightarrow \Sigma\pi$
-0.19 ± 0.03	GOPAL 77	DPWA	$\bar{K}N$ multichannel
-0.16 ± 0.03	KANE 74	DPWA	$K^- p \rightarrow \Sigma\pi$
••• We do not use the following data for averages, fits, limits, etc. •••			
-0.05 or -0.05	3 MARTIN 77	DPWA	$\bar{K}N$ multichannel

$(\Gamma_i \Gamma_f)^{1/2} / \Gamma_{total}$  in  $N\bar{K} \rightarrow \Sigma(1915) \rightarrow \Sigma(1385)\pi, P\text{-wave } (\Gamma_1 \Gamma_5)^{1/2} / \Gamma$

VALUE	DOCUMENT ID	TECN	COMMENT
<0.01	CAMERON 78	DPWA	$K^- p \rightarrow \Sigma(1385)\pi$

$(\Gamma_i \Gamma_f)^{1/2} / \Gamma_{total}$  in  $N\bar{K} \rightarrow \Sigma(1915) \rightarrow \Sigma(1385)\pi, F\text{-wave } (\Gamma_1 \Gamma_6)^{1/2} / \Gamma$

VALUE	DOCUMENT ID	TECN	COMMENT
+0.039 ± 0.009	5 CAMERON 78	DPWA	$K^- p \rightarrow \Sigma(1385)\pi$

### $\Sigma(1915)$ FOOTNOTES

- The two entries for CORDEN 77c are from two different acceptable solutions.
- Preferred solution 3; see CORDEN 76 for other possibilities.
- The two MARTIN 77 values are from a T-matrix pole and from a Breit-Wigner fit.
- The mass and width are fixed to the GOPAL 77 values due to the low elasticity.
- The published sign has been changed to be in accord with the baryon-first convention.

### $\Sigma(1915)$ REFERENCES

PDG 86	PL 170B 1	M. Aguilar-Benitez et al.	(CERN, CIT+)
PDG 82	PL 111B 1	M. Roos et al.	(HELS, CIT, CERN)
GOPAL 80	Toronto Conf. 159	G.P. Gopal	(RHEL) IJP
ALSTON-...	PR D18 182	M. Alston-Garnjost et al.	(LBL, MTHO+) IJP
	Also PRL 38 1007	M. Alston-Garnjost et al.	(LBL, MTHO+) IJP
CAMERON 78	NP B143 189	W. Cameron et al.	(RHEL, LOIC) IJP
CORDEN 77c	NP B125 61	M.J. Corden et al.	(BIRM) IJP
DECLAIS 77	CERN 77-16	Y. Declais et al.	(CAEN, CERN) IJP
GOPAL 77	NP B119 362	G.P. Gopal et al.	(LOIC, RHEL) IJP
MARTIN 77	NP B127 349	B.R. Martin, M.K. Pidcock, R.G. Moorhouse	(LOUC+) IJP
	Also NP B126 266	B.R. Martin, M.K. Pidcock	(LOUC) IJP
	Also NP B126 285	B.R. Martin, M.K. Pidcock	(LOUC) IJP
CORDEN 76	NP B104 382	M.J. Corden et al.	(BIRM) IJP
DEBELLEFON 76	NP B109 129	A. de Bellefon, A. Berthon	(CDF) IJP
BAILLON 75	NP B94 39	P.H. Baillon, P.J. Litchfield	(CERN, RHEL) IJP
HEMINGWAY 75	NP B91 12	R.J. Hemingway et al.	(CERN, HEIDH, MPIM) IJP
VANHORN 75	NP B87 145	A.J. van Horn	(LBL) IJP
	Also NP B87 157	A.J. van Horn	(LBL) IJP
DEVENISH 74B	NP B81 330	R.C.E. Devenish, C.D. Froggatt, B.R. Martin	(DESY+) IJP
KANE 74	LBL-2452	D.F. Kane	(LBL) IJP
COOL 66	PRL 16 1228	R.L. Cool et al.	(BNL)

See key on page 457

Baryon Particle Listings  
 $\Sigma(1940), \Sigma(2000)$

$\Sigma(1940) 3/2^-$

$I(J^P) = 1(\frac{3}{2}^-)$  Status: \*\*\*

For results published before 1974 (they are now obsolete), see our 1982 edition Physics Letters **111B** 1 (1982).

Not all analyses require this state. It is not required by the GOYAL 77 analysis of  $K^- n \rightarrow (\Sigma\pi)^-$  nor by the GOPAL 80 analysis of  $K^- n \rightarrow K^- n$ . See also HEMINGWAY 75.

$\Sigma(1940)$  MASS

VALUE (MeV)	DOCUMENT ID	TECN	COMMENT
<b>1900 to 1950 (<math>\approx 1940</math>) OUR ESTIMATE</b>			
1920 ± 50	GOPAL 77	DPWA	$\bar{K}N$ multichannel
1950 ± 30	BAILLON 75	IPWA	$\bar{K}N \rightarrow \Lambda\pi$
1949 <sup>+40</sup> <sub>-60</sub>	VANHORN 75	DPWA	$K^- p \rightarrow \Lambda\pi^0$
1935 ± 80	KANE 74	DPWA	$K^- p \rightarrow \Sigma\pi$
1940 ± 20	LITCHFIELD 74B	DPWA	$K^- p \rightarrow \Lambda(1520)\pi^0$
1950 ± 20	LITCHFIELD 74C	DPWA	$K^- p \rightarrow \Delta(1232)\bar{K}$
••• We do not use the following data for averages, fits, limits, etc. •••			
1886 or 1893	<sup>1</sup> MARTIN 77	DPWA	$\bar{K}N$ multichannel
1940	DEBELLEFON 76	IPWA	$K^- p \rightarrow \Lambda\pi^0, F_{17}$ wave

$\Sigma(1940)$  WIDTH

VALUE (MeV)	DOCUMENT ID	TECN	COMMENT
<b>150 to 300 (<math>\approx 220</math>) OUR ESTIMATE</b>			
170 ± 25	CAMERON 78B	DPWA	$K^- p \rightarrow N\bar{K}^*$
300 ± 80	GOPAL 77	DPWA	$\bar{K}N$ multichannel
150 ± 75	BAILLON 75	IPWA	$\bar{K}N \rightarrow \Lambda\pi$
160 <sup>+70</sup> <sub>-40</sub>	VANHORN 75	DPWA	$K^- p \rightarrow \Lambda\pi^0$
330 ± 80	KANE 74	DPWA	$K^- p \rightarrow \Sigma\pi$
60 ± 20	LITCHFIELD 74B	DPWA	$K^- p \rightarrow \Lambda(1520)\pi^0$
70 <sup>+30</sup> <sub>-20</sub>	LITCHFIELD 74C	DPWA	$K^- p \rightarrow \Delta(1232)\bar{K}$
••• We do not use the following data for averages, fits, limits, etc. •••			
157 or 159	<sup>1</sup> MARTIN 77	DPWA	$\bar{K}N$ multichannel

$\Sigma(1940)$  DECAY MODES

Mode	Fraction ( $\Gamma_i/\Gamma$ )
$\Gamma_1 N\bar{K}$	<20 %
$\Gamma_2 \Lambda\pi$	seen
$\Gamma_3 \Sigma\pi$	seen
$\Gamma_4 \Sigma(1385)\pi$	seen
$\Gamma_5 \Sigma(1385)\pi, S$ -wave	
$\Gamma_6 \Lambda(1520)\pi$	seen
$\Gamma_7 \Lambda(1520)\pi, P$ -wave	
$\Gamma_8 \Lambda(1520)\pi, F$ -wave	
$\Gamma_9 \Delta(1232)\bar{K}$	seen
$\Gamma_{10} \Delta(1232)\bar{K}, S$ -wave	
$\Gamma_{11} \Delta(1232)\bar{K}, D$ -wave	
$\Gamma_{12} N\bar{K}^*(892)$	seen
$\Gamma_{13} N\bar{K}^*(892), S=3/2, S$ -wave	

$\Sigma(1940)$  BRANCHING RATIOS

See "Sign conventions for resonance couplings" in the Note on  $\Lambda$  and  $\Sigma$  Resonances.

$\Gamma(N\bar{K})/\Gamma_{total}$	$\Gamma_i/\Gamma$		
<b>&lt;0.2 OUR ESTIMATE</b>			
<0.04			
0.14 or 0.13	<sup>1</sup> MARTIN 77 DPWA $\bar{K}N$ multichannel		
<b><math>(\Gamma_i/\Gamma)^{1/2}/\Gamma_{total}</math> in <math>N\bar{K} \rightarrow \Sigma(1940) \rightarrow \Lambda\pi</math></b>			
VALUE	DOCUMENT ID	TECN	COMMENT
-0.06 ± 0.03	GOPAL 77	DPWA	$\bar{K}N$ multichannel
-0.04 ± 0.02	BAILLON 75	IPWA	$\bar{K}N \rightarrow \Lambda\pi$
-0.05 ± 0.03 -0.02	VANHORN 75	DPWA	$K^- p \rightarrow \Lambda\pi^0$
-0.153 ± 0.070	DEVENISH 74B		Fixed- $t$ dispersion rel.
••• We do not use the following data for averages, fits, limits, etc. •••			
-0.15 or -0.14	<sup>1</sup> MARTIN 77	DPWA	$\bar{K}N$ multichannel

$(\Gamma_i/\Gamma)^{1/2}/\Gamma_{total}$ in $N\bar{K} \rightarrow \Sigma(1940) \rightarrow \Sigma\pi$	$(\Gamma_i/\Gamma_3)^{1/2}/\Gamma$		
VALUE	DOCUMENT ID	TECN	COMMENT
-0.08 ± 0.04	GOPAL 77	DPWA	$\bar{K}N$ multichannel
-0.14 ± 0.04	KANE 74	DPWA	$K^- p \rightarrow \Sigma\pi$
••• We do not use the following data for averages, fits, limits, etc. •••			
+0.16 or +0.16	<sup>1</sup> MARTIN 77	DPWA	$\bar{K}N$ multichannel

$(\Gamma_i/\Gamma)^{1/2}/\Gamma_{total}$ in $N\bar{K} \rightarrow \Sigma(1940) \rightarrow \Lambda(1520)\pi, P$ -wave	$(\Gamma_i/\Gamma_7)^{1/2}/\Gamma$		
VALUE	DOCUMENT ID	TECN	COMMENT
< 0.03	CAMERON 77	DPWA	$K^- p \rightarrow \Lambda(1520)\pi^0$
-0.11 ± 0.04	LITCHFIELD 74B	DPWA	$K^- p \rightarrow \Lambda(1520)\pi^0$

$(\Gamma_i/\Gamma)^{1/2}/\Gamma_{total}$ in $N\bar{K} \rightarrow \Sigma(1940) \rightarrow \Lambda(1520)\pi, F$ -wave	$(\Gamma_i/\Gamma_8)^{1/2}/\Gamma$		
VALUE	DOCUMENT ID	TECN	COMMENT
0.062 ± 0.021	CAMERON 77	DPWA	$K^- p \rightarrow \Lambda(1520)\pi^0$
-0.08 ± 0.04	LITCHFIELD 74B	DPWA	$K^- p \rightarrow \Lambda(1520)\pi^0$

$(\Gamma_i/\Gamma)^{1/2}/\Gamma_{total}$ in $N\bar{K} \rightarrow \Sigma(1940) \rightarrow \Delta(1232)\bar{K}, S$ -wave	$(\Gamma_i/\Gamma_{10})^{1/2}/\Gamma$		
VALUE	DOCUMENT ID	TECN	COMMENT
-0.16 ± 0.05	LITCHFIELD 74C	DPWA	$K^- p \rightarrow \Delta(1232)\bar{K}$

$(\Gamma_i/\Gamma)^{1/2}/\Gamma_{total}$ in $N\bar{K} \rightarrow \Sigma(1940) \rightarrow \Delta(1232)\bar{K}, D$ -wave	$(\Gamma_i/\Gamma_{11})^{1/2}/\Gamma$		
VALUE	DOCUMENT ID	TECN	COMMENT
-0.14 ± 0.05	LITCHFIELD 74C	DPWA	$K^- p \rightarrow \Delta(1232)\bar{K}$

$(\Gamma_i/\Gamma)^{1/2}/\Gamma_{total}$ in $N\bar{K} \rightarrow \Sigma(1940) \rightarrow \Sigma(1385)\pi$	$(\Gamma_i/\Gamma_4)^{1/2}/\Gamma$		
VALUE	DOCUMENT ID	TECN	COMMENT
+0.066 ± 0.025	<sup>2</sup> CAMERON 78	DPWA	$K^- p \rightarrow \Sigma(1385)\pi$

$(\Gamma_i/\Gamma)^{1/2}/\Gamma_{total}$ in $N\bar{K} \rightarrow \Sigma(1940) \rightarrow N\bar{K}^*(892)$	$(\Gamma_i/\Gamma_{12})^{1/2}/\Gamma$		
VALUE	DOCUMENT ID	TECN	COMMENT
-0.09 ± 0.02	<sup>3</sup> CAMERON 78B	DPWA	$K^- p \rightarrow N\bar{K}^*$

$\Sigma(1940)$  FOOTNOTES

- <sup>1</sup> The two MARTIN 77 values are from a T-matrix pole and from a Breit-Wigner fit.
- <sup>2</sup> The published sign has been changed to be in accord with the baryon-first convention.
- <sup>3</sup> Upper limits on the  $D_1$  and  $D_3$  waves are each 0.03.

$\Sigma(1940)$  REFERENCES

PDG 82	PL 111B 1	M. Roos et al.	(HELS, CIT, CERN)
GOPAL 80	Toronto Conf. 159	G.P. Gopal	(RHEL)
CAMERON 78	NP B143 189	W. Cameron et al.	(RHEL, LOIC) IJP
CAMERON 78B	NP B146 327	W. Cameron et al.	(RHEL, LOIC) IJP
CAMERON 77	NP B131 399	W. Cameron et al.	(RHEL, LOIC) IJP
GOPAL 77	NP B119 362	G.P. Gopal et al.	(LOIC, RHEL) IJP
GOPAL 77	PR D16 2746	D.P. Goyal, A.V. Sodhi	(DELH)
MARTIN 77	NP B127 349	B.R. Martin, M.K. Piddcock, R.G. Moorhouse	(LOUC+) IJP
Also	NP B126 266	B.R. Martin, M.K. Piddcock	(LOUC)
Also	NP B126 285	B.R. Martin, M.K. Piddcock	(LOUC) IJP
DEBELLEFON 76	NP B109 129	A. de Bellefon, A. Berthon	(CDEF) IJP
BAILLON 75	NP B94 39	P.H. Baillon, P.J. Litchfield	(CERN, RHEL) IJP
HEMINGWAY 75	NP B91 12	R.J. Hemingway et al.	(CERN, HEIDH, MPIM) IJP
VANHORN 75	NP B87 145	A.J. van Horn	(LBL) IJP
Also	NP B87 157	A.J. van Horn	(LBL) IJP
DEVENISH 74B	NP B81 330	R.C.E. Devenish, C.D. Froggatt, B.R. Martin	(DESY+) IJP
KANE 74	LBL-2452	D.F. Kane	(LBL) IJP
LITCHFIELD 74B	NP B74 19	P.J. Litchfield et al.	(CERN, HEIDH) IJP
LITCHFIELD 74C	NP B74 39	P.J. Litchfield et al.	(CERN, HEIDH) IJP

$\Sigma(2000) 1/2^-$

$I(J^P) = 1(\frac{1}{2}^-)$  Status: \*

OMITTED FROM SUMMARY TABLE

We list here all reported  $S_{11}$  states lying above the  $\Sigma(1750) S_{11}$ .

$\Sigma(2000)$  MASS

VALUE (MeV)	DOCUMENT ID	TECN	COMMENT
<b><math>\approx 2000</math> OUR ESTIMATE</b>			
1944 ± 15	GOPAL 80	DPWA	$\bar{K}N \rightarrow \bar{K}N$
1955 ± 15	GOPAL 77	DPWA	$\bar{K}N$ multichannel
1755 or 1834	<sup>1</sup> MARTIN 77	DPWA	$\bar{K}N$ multichannel
2004 ± 40	VANHORN 75	DPWA	$K^- p \rightarrow \Lambda\pi^0$

$\Sigma(2000)$  WIDTH

VALUE (MeV)	DOCUMENT ID	TECN	COMMENT
215 ± 25	GOPAL 80	DPWA	$\bar{K}N \rightarrow \bar{K}N$
170 ± 40	GOPAL 77	DPWA	$\bar{K}N$ multichannel
413 or 450	<sup>1</sup> MARTIN 77	DPWA	$\bar{K}N$ multichannel
116 ± 40	VANHORN 75	DPWA	$K^- p \rightarrow \Lambda\pi^0$

# Baryon Particle Listings

## $\Sigma(2000), \Sigma(2030)$

### $\Sigma(2000)$ DECAY MODES

Mode	
$\Gamma_1$	$N\bar{K}$
$\Gamma_2$	$\Lambda\pi$
$\Gamma_3$	$\Sigma\pi$
$\Gamma_4$	$\Lambda(1520)\pi$
$\Gamma_5$	$N\bar{K}^*(892), S=1/2, S\text{-wave}$
$\Gamma_6$	$N\bar{K}^*(892), S=3/2, D\text{-wave}$

### $\Sigma(2000)$ BRANCHING RATIOS

See "Sign conventions for resonance couplings" in the Note on  $\Lambda$  and  $\Sigma$  Resonances.

$\Gamma(N\bar{K})/\Gamma_{\text{total}}$	DOCUMENT ID	TECN	COMMENT	$\Gamma_1/\Gamma$
0.51 ± 0.05	GOPAL	80	DPWA $\bar{K}N \rightarrow \bar{K}N$	
0.44 ± 0.05	GOPAL	77	DPWA See GOPAL 80	
0.62 or 0.57	<sup>1</sup> MARTIN	77	DPWA $\bar{K}N$ multichannel	

$(\Gamma_i\Gamma_f)^{1/2}/\Gamma_{\text{total}}$ in $N\bar{K} \rightarrow \Sigma(2000) \rightarrow \Lambda\pi$	DOCUMENT ID	TECN	COMMENT	$(\Gamma_1\Gamma_2)^{1/2}/\Gamma$
0.08 ± 0.03	GOPAL	77	DPWA $\bar{K}N$ multichannel	
-0.19 or -0.18	<sup>1</sup> MARTIN	77	DPWA $\bar{K}N$ multichannel	
not seen	BAILLON	75	IPWA $\bar{K}N \rightarrow \Lambda\pi$	
+0.07 ± 0.02 -0.01	VANHORN	75	DPWA $K^-p \rightarrow \Lambda\pi^0$	

$(\Gamma_i\Gamma_f)^{1/2}/\Gamma_{\text{total}}$ in $N\bar{K} \rightarrow \Sigma(2000) \rightarrow \Sigma\pi$	DOCUMENT ID	TECN	COMMENT	$(\Gamma_1\Gamma_3)^{1/2}/\Gamma$
+0.20 ± 0.04	GOPAL	77	DPWA $\bar{K}N$ multichannel	
+0.26 or +0.24	<sup>1</sup> MARTIN	77	DPWA $\bar{K}N$ multichannel	

$(\Gamma_i\Gamma_f)^{1/2}/\Gamma_{\text{total}}$ in $N\bar{K} \rightarrow \Sigma(2000) \rightarrow \Lambda(1520)\pi$	DOCUMENT ID	TECN	COMMENT	$(\Gamma_1\Gamma_4)^{1/2}/\Gamma$
+0.081 ± 0.021	<sup>2</sup> CAMERON	77	DPWA $P\text{-wave decay}$	

$(\Gamma_i\Gamma_f)^{1/2}/\Gamma_{\text{total}}$ in $N\bar{K} \rightarrow \Sigma(2000) \rightarrow N\bar{K}^*(892), S=1/2, S\text{-wave}$	DOCUMENT ID	TECN	COMMENT	$(\Gamma_1\Gamma_5)^{1/2}/\Gamma$
+0.10 ± 0.02	<sup>2</sup> CAMERON	78B	DPWA $K^-p \rightarrow N\bar{K}^*$	

$(\Gamma_i\Gamma_f)^{1/2}/\Gamma_{\text{total}}$ in $N\bar{K} \rightarrow \Sigma(2000) \rightarrow N\bar{K}^*(892), S=3/2, D\text{-wave}$	DOCUMENT ID	TECN	COMMENT	$(\Gamma_1\Gamma_6)^{1/2}/\Gamma$
-0.07 ± 0.03	CAMERON	78B	DPWA $K^-p \rightarrow N\bar{K}^*$	

### $\Sigma(2000)$ FOOTNOTES

- The two MARTIN 77 values are from a T-matrix pole and from a Breit-Wigner fit.
- The published sign has been changed to be in accord with the baryon-first convention.

### $\Sigma(2000)$ REFERENCES

GOPAL	80	Toronto Conf. 159	G.P. Gopal	(RHEL) IJP
CAMERON	78B	NP B146 327	W. Cameron et al.	(RHEL, LOIC) IJP
CAMERON	77	NP B131 399	W. Cameron et al.	(RHEL, LOIC) IJP
GOPAL	77	NP B119 362	G.P. Gopal et al.	(RHEL, RHEL) IJP
MARTIN	77	NP B127 349	B.R. Martin, M.K. Pidcock, R.G. Moorhouse	(LOIC, RHEL) IJP
Also		NP B126 266	B.R. Martin, M.K. Pidcock	(LOUC) IJP
Also		NP B126 285	B.R. Martin, M.K. Pidcock	(LOUC) IJP
BAILLON	75	NP B94 39	P.H. Baillon, P.J. Litchfield	(CERN, RHEL) IJP
VANHORN	75	NP B87 145	A.J. van Horn	(LBL) IJP
Also		NP B87 157	A.J. van Horn	(LBL) IJP

$\Sigma(2030) 7/2^+$

 $I(J^P) = 1(\frac{7}{2}^+)$  Status: \*\*\*

Discovered by COOL 66 and by WOHL 66. For most results published before 1974 (they are now obsolete), see our 1982 edition Physics Letters **111B** 1 (1982).

This entry only includes results from partial-wave analyses. Parameters of peaks seen in cross sections and invariant-mass distributions around 2030 MeV may be found in our 1984 edition, Reviews of Modern Physics **56** S1 (1984).

### $\Sigma(2030)$ MASS

VALUE (MeV)	DOCUMENT ID	TECN	COMMENT
<b>2025 to 2040 (<math>\approx</math> 2030) OUR ESTIMATE</b>			
2036 ± 5	GOPAL	80	DPWA $\bar{K}N \rightarrow \bar{K}N$
2038 ± 10	CORDEN	77B	$K^-N \rightarrow N\bar{K}^*$
2040 ± 5	GOPAL	77	DPWA $\bar{K}N$ multichannel
2030 ± 3	<sup>1</sup> CORDEN	76	DPWA $K^-n \rightarrow \Lambda\pi^-$
2035 ± 15	BAILLON	75	IPWA $\bar{K}N \rightarrow \Lambda\pi$

2038 ± 10	HEMINGWAY	75	DPWA $K^-p \rightarrow \bar{K}N$
2042 ± 11	VANHORN	75	DPWA $K^-p \rightarrow \Lambda\pi^0$
2020 ± 6	KANE	74	DPWA $K^-p \rightarrow \Sigma\pi$
2035 ± 10	LITCHFIELD	74B	DPWA $K^-p \rightarrow \Lambda(1520)\pi^0$
2020 ± 30	LITCHFIELD	74C	DPWA $K^-p \rightarrow \Delta(1232)\bar{K}$
2025 ± 10	LITCHFIELD	74D	DPWA $K^-p \rightarrow \Lambda(1820)\pi^0$
• • • We do not use the following data for averages, fits, limits, etc. • • •			
2027 to 2057	GOYAL	77	DPWA $K^-N \rightarrow \Sigma\pi$
2030	DEBELLEFON	76	IPWA $K^-p \rightarrow \Lambda\pi^0$

### $\Sigma(2030)$ WIDTH

VALUE (MeV)	DOCUMENT ID	TECN	COMMENT
<b>150 to 200 (<math>\approx</math> 180) OUR ESTIMATE</b>			
172 ± 10	GOPAL	80	DPWA $\bar{K}N \rightarrow \bar{K}N$
137 ± 40	CORDEN	77B	$K^-N \rightarrow N\bar{K}^*$
190 ± 10	GOPAL	77	DPWA $\bar{K}N$ multichannel
201 ± 9	<sup>1</sup> CORDEN	76	DPWA $K^-n \rightarrow \Lambda\pi^-$
180 ± 20	BAILLON	75	IPWA $\bar{K}N \rightarrow \Lambda\pi$
172 ± 15	HEMINGWAY	75	DPWA $K^-p \rightarrow \bar{K}N$
178 ± 13	VANHORN	75	DPWA $K^-p \rightarrow \Lambda\pi^0$
111 ± 5	KANE	74	DPWA $K^-p \rightarrow \Sigma\pi$
160 ± 20	LITCHFIELD	74B	DPWA $K^-p \rightarrow \Lambda(1520)\pi^0$
200 ± 30	LITCHFIELD	74C	DPWA $K^-p \rightarrow \Delta(1232)\bar{K}$
• • • We do not use the following data for averages, fits, limits, etc. • • •			
260	DECLAIS	77	DPWA $\bar{K}N \rightarrow \bar{K}N$
126 to 195	GOYAL	77	DPWA $K^-N \rightarrow \Sigma\pi$
160	DEBELLEFON	76	IPWA $K^-p \rightarrow \Lambda\pi^0$
70 to 125	LITCHFIELD	74D	DPWA $K^-p \rightarrow \Lambda(1820)\pi^0$

### $\Sigma(2030)$ DECAY MODES

Mode	Fraction ( $\Gamma_i/\Gamma$ )
$\Gamma_1$	$N\bar{K}$ 17-23 %
$\Gamma_2$	$\Lambda\pi$ 17-23 %
$\Gamma_3$	$\Sigma\pi$ 5-10 %
$\Gamma_4$	$\Xi K$ <2 %
$\Gamma_5$	$\Sigma(1385)\pi$ 5-15 %
$\Gamma_6$	$\Sigma(1385)\pi, F\text{-wave}$
$\Gamma_7$	$\Lambda(1520)\pi$ 10-20 %
$\Gamma_8$	$\Lambda(1520)\pi, D\text{-wave}$
$\Gamma_9$	$\Lambda(1520)\pi, G\text{-wave}$
$\Gamma_{10}$	$\Delta(1232)\bar{K}$ 10-20 %
$\Gamma_{11}$	$\Delta(1232)\bar{K}, F\text{-wave}$
$\Gamma_{12}$	$\Delta(1232)\bar{K}, H\text{-wave}$
$\Gamma_{13}$	$N\bar{K}^*(892)$ <5 %
$\Gamma_{14}$	$N\bar{K}^*(892), S=1/2, F\text{-wave}$
$\Gamma_{15}$	$N\bar{K}^*(892), S=3/2, F\text{-wave}$
$\Gamma_{16}$	$\Lambda(1820)\pi, P\text{-wave}$

The above branching fractions are our estimates, not fits or averages.

### $\Sigma(2030)$ BRANCHING RATIOS

See "Sign conventions for resonance couplings" in the Note on  $\Lambda$  and  $\Sigma$  Resonances.

$\Gamma(N\bar{K})/\Gamma_{\text{total}}$	DOCUMENT ID	TECN	COMMENT	$\Gamma_1/\Gamma$
<b>0.17 to 0.23 OUR ESTIMATE</b>				
0.19 ± 0.03	GOPAL	80	DPWA $\bar{K}N \rightarrow \bar{K}N$	
0.18 ± 0.03	HEMINGWAY	75	DPWA $K^-p \rightarrow \bar{K}N$	
• • • We do not use the following data for averages, fits, limits, etc. • • •				
0.15	DECLAIS	77	DPWA $\bar{K}N \rightarrow \bar{K}N$	
0.24 ± 0.02	GOPAL	77	DPWA See GOPAL 80	

$(\Gamma_i\Gamma_f)^{1/2}/\Gamma_{\text{total}}$ in $N\bar{K} \rightarrow \Sigma(2030) \rightarrow \Lambda\pi$	DOCUMENT ID	TECN	COMMENT	$(\Gamma_1\Gamma_2)^{1/2}/\Gamma$
+0.18 ± 0.02	GOPAL	77	DPWA $\bar{K}N$ multichannel	
+0.20 ± 0.01	<sup>1</sup> CORDEN	76	DPWA $K^-n \rightarrow \Lambda\pi^-$	
+0.18 ± 0.02	BAILLON	75	IPWA $\bar{K}N \rightarrow \Lambda\pi$	
+0.20 ± 0.01	VANHORN	75	DPWA $K^-p \rightarrow \Lambda\pi^0$	
+0.195 ± 0.053	DEVENISH	74B	Fixed- $t$ dispersion rel.	
• • • We do not use the following data for averages, fits, limits, etc. • • •				
0.20	DEBELLEFON	76	IPWA $K^-p \rightarrow \Lambda\pi^0$	



See key on page 457

# Baryon Particle Listings

## $\Sigma(2030)$ , $\Sigma(2070)$ , $\Sigma(2080)$

$(\Gamma_1 \Gamma_2)^{1/2} / \Gamma_{\text{total}}$ in $N\bar{K} \rightarrow \Sigma(2030) \rightarrow \Sigma\pi$	DOCUMENT ID	TECN	COMMENT	$(\Gamma_1 \Gamma_3)^{1/2} / \Gamma$
$-0.09 \pm 0.01$	2 CORDEN	77c	$K^- n \rightarrow \Sigma\pi$	
$-0.06 \pm 0.01$	2 CORDEN	77c	$K^- n \rightarrow \Sigma\pi$	
$-0.15 \pm 0.03$	GOPAL	77	DPWA $\bar{K}N$ multichannel	
$-0.10 \pm 0.01$	KANE	74	DPWA $K^- p \rightarrow \Sigma\pi$	
• • • We do not use the following data for averages, fits, limits, etc. • • •				
$-0.085 \pm 0.02$	3 GOYAL	77	DPWA $K^- N \rightarrow \Sigma\pi$	

$(\Gamma_1 \Gamma_2)^{1/2} / \Gamma_{\text{total}}$ in $N\bar{K} \rightarrow \Sigma(2030) \rightarrow \Xi K$	DOCUMENT ID	TECN	COMMENT	$(\Gamma_1 \Gamma_4)^{1/2} / \Gamma$
0.023	MULLER	69B	DPWA $K^- p \rightarrow \Xi K$	
<0.05	BURGUN	68	DPWA $K^- p \rightarrow \Xi K$	
<0.05	TRIPP	67	RVUE $K^- p \rightarrow \Xi K$	

$(\Gamma_1 \Gamma_2)^{1/2} / \Gamma_{\text{total}}$ in $N\bar{K} \rightarrow \Sigma(2030) \rightarrow \Lambda(1820)\pi$ , P-wave	DOCUMENT ID	TECN	COMMENT	$(\Gamma_1 \Gamma_{16})^{1/2} / \Gamma$
0.14 ± 0.02	CORDEN	75B	DBC $K^- n \rightarrow N\bar{K}\pi^-$	
0.18 ± 0.04	LITCHFIELD	74D	DPWA $K^- p \rightarrow \Lambda(1820)\pi^0$	

$(\Gamma_1 \Gamma_2)^{1/2} / \Gamma_{\text{total}}$ in $N\bar{K} \rightarrow \Sigma(2030) \rightarrow \Lambda(1520)\pi$ , D-wave	DOCUMENT ID	TECN	COMMENT	$(\Gamma_1 \Gamma_8)^{1/2} / \Gamma$
+0.114 ± 0.010	4 CAMERON	77	DPWA $K^- p \rightarrow \Lambda(1520)\pi^0$	
0.14 ± 0.03	LITCHFIELD	74B	DPWA $K^- p \rightarrow \Lambda(1520)\pi^0$	
• • • We do not use the following data for averages, fits, limits, etc. • • •				
0.10 ± 0.03	5 CORDEN	75B	DBC $K^- n \rightarrow N\bar{K}\pi^-$	

$(\Gamma_1 \Gamma_2)^{1/2} / \Gamma_{\text{total}}$ in $N\bar{K} \rightarrow \Sigma(2030) \rightarrow \Lambda(1520)\pi$ , G-wave	DOCUMENT ID	TECN	COMMENT	$(\Gamma_1 \Gamma_9)^{1/2} / \Gamma$
+0.146 ± 0.010	4 CAMERON	77	DPWA $K^- p \rightarrow \Lambda(1520)\pi^0$	
0.02 ± 0.02	LITCHFIELD	74B	DPWA $K^- p \rightarrow \Lambda(1520)\pi^0$	

$(\Gamma_1 \Gamma_2)^{1/2} / \Gamma_{\text{total}}$ in $N\bar{K} \rightarrow \Sigma(2030) \rightarrow \Delta(1232)\bar{K}$ , F-wave	DOCUMENT ID	TECN	COMMENT	$(\Gamma_1 \Gamma_{11})^{1/2} / \Gamma$
0.16 ± 0.03	LITCHFIELD	74c	DPWA $K^- p \rightarrow \Delta(1232)\bar{K}$	
• • • We do not use the following data for averages, fits, limits, etc. • • •				
0.17 ± 0.03	5 CORDEN	75B	DBC $K^- n \rightarrow N\bar{K}\pi^-$	

$(\Gamma_1 \Gamma_2)^{1/2} / \Gamma_{\text{total}}$ in $N\bar{K} \rightarrow \Sigma(2030) \rightarrow \Delta(1232)\bar{K}$ , H-wave	DOCUMENT ID	TECN	COMMENT	$(\Gamma_1 \Gamma_{12})^{1/2} / \Gamma$
0.00 ± 0.02	LITCHFIELD	74c	DPWA $K^- p \rightarrow \Delta(1232)\bar{K}$	

$(\Gamma_1 \Gamma_2)^{1/2} / \Gamma_{\text{total}}$ in $N\bar{K} \rightarrow \Sigma(2030) \rightarrow \Sigma(1385)\pi$	DOCUMENT ID	TECN	COMMENT	$(\Gamma_1 \Gamma_5)^{1/2} / \Gamma$
+0.153 ± 0.026	4 CAMERON	78	DPWA $K^- p \rightarrow \Sigma(1385)\pi$	

$(\Gamma_1 \Gamma_2)^{1/2} / \Gamma_{\text{total}}$ in $N\bar{K} \rightarrow \Sigma(2030) \rightarrow N\bar{K}^*(892)$ , S=1/2, F-wave	DOCUMENT ID	TECN	COMMENT	$(\Gamma_1 \Gamma_{14})^{1/2} / \Gamma$
+0.06 ± 0.03	4 CAMERON	78B	DPWA $K^- p \rightarrow N\bar{K}^*$	
-0.02 ± 0.01	CORDEN	77B	$K^- d \rightarrow NN\bar{K}^*$	

$(\Gamma_1 \Gamma_2)^{1/2} / \Gamma_{\text{total}}$ in $N\bar{K} \rightarrow \Sigma(2030) \rightarrow N\bar{K}^*(892)$ , S=3/2, F-wave	DOCUMENT ID	TECN	COMMENT	$(\Gamma_1 \Gamma_{15})^{1/2} / \Gamma$
+0.04 ± 0.03	6 CAMERON	78B	DPWA $K^- p \rightarrow N\bar{K}^*$	
-0.12 ± 0.02	CORDEN	77B	$K^- d \rightarrow NN\bar{K}^*$	

### $\Sigma(2030)$ FOOTNOTES

- 1 Preferred solution 3; see CORDEN 76 for other possibilities.
- 2 The two entries for CORDEN 77c are from two different acceptable solutions.
- 3 This coupling is extracted from unnormalized data.
- 4 The published sign has been changed to be in accord with the baryon-first convention.
- 5 An upper limit.
- 6 The upper limit on the  $G_3$  wave is 0.03.

### $\Sigma(2030)$ REFERENCES

PDG	84	RMP 56 51	C.G. Wohl et al.	(LBL, CIT, CERN)
PDG	82	PL 111B 1	M. Roos et al.	(HEL5, CIT, CERN)
GOPAL	80	Toronto Conf. 159	G.P. Gopal	(RHEL) IJP
CAMERON	78	NP B143 189	W. Cameron et al.	(RHEL, LOIC) IJP
CAMERON	78B	NP B146 327	W. Cameron et al.	(RHEL, LOIC) IJP
CAMERON	77	NP B131 399	W. Cameron et al.	(RHEL, LOIC) IJP
CORDEN	77B	NP B121 365	M.J. Corden et al.	(BIRM) IJP
CORDEN	77C	NP B125 61	M.J. Corden et al.	(BIRM) IJP
DECLAIS	77	CERN 77-16	Y. Declais et al.	(CAEN, CERN) IJP
GOPAL	77	NP B119 362	G.P. Gopal et al.	(LOIC, RHEL) IJP
GOYAL	77	PR D16 2746	D.P. Goyal, A.V. Sodhi	(DELH) IJP
CORDEN	76	NP B104 382	M.J. Corden et al.	(BIRM) IJP
DEBELLEFON	76	NP B109 129	A. de Bellefon, A. Berthon	(CDEF) IJP
BAILLON	75	NP B94 39	P.H. Baillon, P.J. Litchfield	(CERN, RHEL) IJP

CORDEN	75B	NP B92 365	M.J. Corden et al.	(BIRM) IJP
HEMINGWAY	75	NP B91 12	R.J. Hemingway et al.	(CERN, HEIDH, MPIM) IJP
VANHORN	75	NP B87 145	A.J. van Horn	(LBL) IJP
Also		NP B87 157	A.J. van Horn	(LBL) IJP
DEVENISH	74B	NP B81 330	R.C.E. Devenish, C.D. Froggatt, B.R. Martin	(DESY+) IJP
KANE	74	LBL-2452	D.F. Kane	(LBL) IJP
LITCHFIELD	74B	NP B74 19	P.J. Litchfield et al.	(CERN, HEIDH) IJP
LITCHFIELD	74C	NP B74 39	P.J. Litchfield et al.	(CERN, HEIDH) IJP
LITCHFIELD	74D	NP B74 12	P.J. Litchfield et al.	(CERN, HEIDH) IJP
MULLER	69B	Thesis UCRL 19372	R.A. Muller	(LRL) IJP
BURGUN	68	NP B8 447	G. Burgun et al.	(SACL, CDEF, RHEL) IJP
TRIPP	67	NP B3 10	R.D. Tripp et al.	(LRL, SLAC, CERN+) IJP
COOL	66	PRL 16 1228	R.L. Cool et al.	(BNL) IJP
WOHL	66	PRL 17 107	C.G. Wohl, F.T. Solmitz, M.L. Stevenson	(LRL) IJP

$\Sigma(2070) 5/2^+$

$$I(J^P) = 1(\frac{5}{2}^+) \text{ Status: } *$$

### OMITTED FROM SUMMARY TABLE

This state suggested by BERTHON 70B finds support in GOPAL 80 with new  $K^- p$  polarization and  $K^- n$  angular distributions. The very broad state seen in KANE 72 is not required in the later (KANE 74) analysis of  $\bar{K}N \rightarrow \Sigma\pi$ .

### $\Sigma(2070)$ MASS

VALUE (MeV)	DOCUMENT ID	TECN	COMMENT
$\approx 2070$ OUR ESTIMATE			
2051 ± 25	GOPAL	80	DPWA $\bar{K}N \rightarrow \bar{K}N$
2057	KANE	72	DPWA $K^- p \rightarrow \Sigma\pi$
2070 ± 10	BERTHON	70B	DPWA $K^- p \rightarrow \Sigma\pi$

### $\Sigma(2070)$ WIDTH

VALUE (MeV)	DOCUMENT ID	TECN	COMMENT
300 ± 30	GOPAL	80	DPWA $\bar{K}N \rightarrow \bar{K}N$
906	KANE	72	DPWA $K^- p \rightarrow \Sigma\pi$
140 ± 20	BERTHON	70B	DPWA $K^- p \rightarrow \Sigma\pi$

### $\Sigma(2070)$ DECAY MODES

Mode	
$\Gamma_1$	$N\bar{K}$
$\Gamma_2$	$\Sigma\pi$

### $\Sigma(2070)$ BRANCHING RATIOS

See "Sign conventions for resonance couplings" in the Note on  $\Lambda$  and  $\Sigma$  Resonances.

$\Gamma(N\bar{K}) / \Gamma_{\text{total}}$	DOCUMENT ID	TECN	COMMENT	$\Gamma_1 / \Gamma$
0.08 ± 0.03	GOPAL	80	DPWA $\bar{K}N \rightarrow \bar{K}N$	

$(\Gamma_1 \Gamma_2)^{1/2} / \Gamma_{\text{total}}$ in $N\bar{K} \rightarrow \Sigma(2070) \rightarrow \Sigma\pi$	DOCUMENT ID	TECN	COMMENT	$(\Gamma_1 \Gamma_2)^{1/2} / \Gamma$
+0.104	KANE	72	DPWA $K^- p \rightarrow \Sigma\pi$	
+0.12 ± 0.02	BERTHON	70B	DPWA $K^- p \rightarrow \Sigma\pi$	

### $\Sigma(2070)$ REFERENCES

GOPAL	80	Toronto Conf. 159	G.P. Gopal	(RHEL) IJP
KANE	74	LBL-2452	D.F. Kane	(LBL) IJP
KANE	72	PR D5 1583	D.F.J. Kane	(LBL) IJP
BERTHON	70B	NP B24 417	A. Berthon et al.	(CDEF, RHEL, SACL) IJP

$\Sigma(2080) 3/2^+$

$$I(J^P) = 1(\frac{3}{2}^+) \text{ Status: } **$$

### OMITTED FROM SUMMARY TABLE

Suggested by some but not all partial-wave analyses across this region.

### $\Sigma(2080)$ MASS

VALUE (MeV)	DOCUMENT ID	TECN	COMMENT
$\approx 2080$ OUR ESTIMATE			
2091 ± 7	<sup>1</sup> CORDEN	76	DPWA $K^- n \rightarrow \Lambda\pi^-$
2070 to 2120	DEBELLEFON	76	IPWA $K^- p \rightarrow \Lambda\pi^0$
2120 ± 40	BAILLON	75	IPWA $\bar{K}N \rightarrow \Lambda\pi$ (sol. 1)
2140 ± 40	BAILLON	75	IPWA $\bar{K}N \rightarrow \Lambda\pi$ (sol. 2)
2082 ± 4	COX	70	DPWA See CORDEN 76
2070 ± 30	LITCHFIELD	70	DPWA $K^- N \rightarrow \Lambda\pi$

## Baryon Particle Listings

 $\Sigma(2080)$ ,  $\Sigma(2100)$ ,  $\Sigma(2250)$  $\Sigma(2080)$  WIDTH

VALUE (MeV)	DOCUMENT ID	TECN	COMMENT
186±48	<sup>1</sup> CORDEN 76	DPWA	$K^- n \rightarrow \Lambda \pi^-$
100	DEBELLEFON 76	IPWA	$K^- p \rightarrow \Lambda \pi^0$
240±5.0	BAILLON 75	IPWA	$\bar{K} N \rightarrow \Lambda \pi$ (sol. 1)
200±5.0	BAILLON 75	IPWA	$\bar{K} N \rightarrow \Lambda \pi$ (sol. 2)
87±2.0	COX 70	DPWA	See CORDEN 76
250±4.0	LITCHFIELD 70	DPWA	$K^- N \rightarrow \Lambda \pi$

 $\Sigma(2080)$  DECAY MODES

Mode	
$\Gamma_1$	$N\bar{K}$
$\Gamma_2$	$\Lambda\pi$

 $\Sigma(2080)$  BRANCHING RATIOS

See "Sign conventions for resonance couplings" in the Note on  $\Lambda$  and  $\Sigma$  Resonances.

$(\Gamma_1\Gamma_2)^{1/2}/\Gamma_{\text{total}}$ in $N\bar{K} \rightarrow \Sigma(2080) \rightarrow \Lambda\pi$	DOCUMENT ID	TECN	COMMENT	$(\Gamma_1\Gamma_2)^{1/2}/\Gamma$
-0.10±0.03	<sup>1</sup> CORDEN 76	DPWA	$K^- n \rightarrow \Lambda \pi^-$	
-0.10	DEBELLEFON 76	IPWA	$K^- p \rightarrow \Lambda \pi^0$	
-0.13±0.04	BAILLON 75	IPWA	$\bar{K} N \rightarrow \Lambda \pi$ (sol. 1 and 2)	
-0.16±0.03	COX 70	DPWA	See CORDEN 76	
-0.09±0.03	LITCHFIELD 70	DPWA	$K^- N \rightarrow \Lambda \pi$	

 $\Sigma(2080)$  FOOTNOTES

<sup>1</sup> Preferred solution 3; see CORDEN 76 for other possibilities, including a  $D_{15}$  at this mass.

 $\Sigma(2080)$  REFERENCES

CORDEN 76	NP B104 382	M.J. Corden et al.	(BIRM) IJP
DEBELLEFON 76	NP B109 129	A. de Bellefon, A. Berthon	(CDEF) IJP
	Also NP B90 1	A. de Bellefon et al.	(CDEF, SACL) IJP
BAILLON 75	NP B94 39	P.H. Baillon, P.J. Litchfield	(CERN, RHCL) IJP
COX 70	NP B19 61	G.F. Cox et al.	(BIRM, EDIN, GLAS, LOIC) IJP
LITCHFIELD 70	NP B22 269	P.J. Litchfield	(RHCL) IJP

 $\Sigma(2100) 7/2^-$ 

$$I(J^P) = 1(\frac{7}{2}^-) \text{ Status: } *$$

OMITTED FROM SUMMARY TABLE

 $\Sigma(2100)$  MASS

VALUE (MeV)	DOCUMENT ID	TECN	COMMENT
$\approx 2100$ OUR ESTIMATE			
2060±20	BARBARO... 70	DPWA	$K^- p \rightarrow \Lambda \pi^0$
2120±30	BARBARO... 70	DPWA	$K^- p \rightarrow \Sigma \pi$

 $\Sigma(2100)$  WIDTH

VALUE (MeV)	DOCUMENT ID	TECN	COMMENT
70±30	BARBARO... 70	DPWA	$K^- p \rightarrow \Lambda \pi^0$
135±30	BARBARO... 70	DPWA	$K^- p \rightarrow \Sigma \pi$

 $\Sigma(2100)$  DECAY MODES

Mode	
$\Gamma_1$	$N\bar{K}$
$\Gamma_2$	$\Lambda\pi$
$\Gamma_3$	$\Sigma\pi$

 $\Sigma(2100)$  BRANCHING RATIOS

See "Sign conventions for resonance couplings" in the Note on  $\Lambda$  and  $\Sigma$  Resonances.

$(\Gamma_1\Gamma_2)^{1/2}/\Gamma_{\text{total}}$ in $N\bar{K} \rightarrow \Sigma(2100) \rightarrow \Lambda\pi$	DOCUMENT ID	TECN	COMMENT	$(\Gamma_1\Gamma_2)^{1/2}/\Gamma$
-0.07±0.02	BARBARO... 70	DPWA	$K^- p \rightarrow \Lambda \pi^0$	

$(\Gamma_1\Gamma_3)^{1/2}/\Gamma_{\text{total}}$ in $N\bar{K} \rightarrow \Sigma(2100) \rightarrow \Sigma\pi$	DOCUMENT ID	TECN	COMMENT	$(\Gamma_1\Gamma_3)^{1/2}/\Gamma$
+0.13±0.02	BARBARO... 70	DPWA	$K^- p \rightarrow \Sigma \pi$	

 $\Sigma(2100)$  REFERENCES

BARBARO... 70	Duke Conf. 173	A. Barbaro-Galderi	(LRL) IJP
	Hyperon Resonances, 1970		

 $\Sigma(2250)$ 

$$I(J^P) = 1(?^?) \text{ Status: } ***$$

Results from partial-wave analyses are too weak to warrant separating them from the production and cross-section experiments. LASINSKI 71 in  $\bar{K}N$  using a Pomeron + resonances model, and DEBELLEFON 76, DEBELLEFON 77, and DEBELLEFON 78 in energy-dependent partial-wave analyses of  $\bar{K}N \rightarrow \Lambda\pi$ ,  $\Sigma\pi$ , and  $N\bar{K}$ , respectively, suggest two resonances around this mass.

 $\Sigma(2250)$  MASS

VALUE (MeV)	DOCUMENT ID	TECN	COMMENT
<b>2210 to 2280 (<math>\approx 2250</math>) OUR ESTIMATE</b>			
2270±50	DEBELLEFON 78	DPWA	$D_5$ wave
2210±30	DEBELLEFON 78	DPWA	$G_9$ wave
2275±20	DEBELLEFON 77	DPWA	$D_5$ wave
2215±20	DEBELLEFON 77	DPWA	$G_9$ wave
2300±30	<sup>1</sup> DEBELLEFON 75B	HBC	$K^- p \rightarrow \Xi^*0 K^0$
2251 <sup>+30</sup> <sub>-20</sub>	VANHORN 75	DPWA	$K^- p \rightarrow \Lambda \pi^0, F_5$ wave
2280±14	AGUILAR-... 70B	HBC	$K^- p$ 3.9, 4.6 GeV/c
2237±11	BRICMAN 70	CNTR	Total, charge exchange
2255±10	COOL 70	CNTR	$K^- p, K^- d$ total
2250±7	BUGG 68	CNTR	$K^- p, K^- d$ total
••• We do not use the following data for averages, fits, limits, etc. •••			
2260	DEBELLEFON 76	IPWA	$D_5$ wave
2215	DEBELLEFON 76	IPWA	$G_9$ wave
2250±20	LU 70	CNTR	$\gamma p \rightarrow K^+ Y^*$
2245	BLANPIED 65	CNTR	$\gamma p \rightarrow K^+ Y^*$
2299±6	BOCK 65	HBC	$\bar{p}p$ 5.7 GeV/c

 $\Sigma(2250)$  WIDTH

VALUE (MeV)	DOCUMENT ID	TECN	COMMENT
<b>60 to 150 (<math>\approx 100</math>) OUR ESTIMATE</b>			
120±40	DEBELLEFON 78	DPWA	$D_5$ wave
80±20	DEBELLEFON 78	DPWA	$G_9$ wave
70±20	DEBELLEFON 77	DPWA	$D_5$ wave
60±20	DEBELLEFON 77	DPWA	$G_9$ wave
130±20	<sup>1</sup> DEBELLEFON 75B	HBC	$K^- p \rightarrow \Xi^*0 K^0$
192±30	VANHORN 75	DPWA	$K^- p \rightarrow \Lambda \pi^0, F_5$ wave
100±20	AGUILAR-... 70B	HBC	$K^- p$ 3.9, 4.6 GeV/c
164±50	BRICMAN 70	CNTR	Total, charge exchange
230±20	BUGG 68	CNTR	$K^- p, K^- d$ total
••• We do not use the following data for averages, fits, limits, etc. •••			
100	DEBELLEFON 76	IPWA	$D_5$ wave
140	DEBELLEFON 76	IPWA	$G_9$ wave
170	COOL 70	CNTR	$K^- p, K^- d$ total
125	LU 70	CNTR	$\gamma p \rightarrow K^+ Y^*$
150	BLANPIED 65	CNTR	$\gamma p \rightarrow K^+ Y^*$
21 <sup>+17</sup> <sub>-21</sub>	BOCK 65	HBC	$\bar{p}p$ 5.7 GeV/c

 $\Sigma(2250)$  DECAY MODES

Mode	Fraction ( $\Gamma_i/\Gamma$ )	
$\Gamma_1$	$N\bar{K}$	<10 %
$\Gamma_2$	$\Lambda\pi$	seen
$\Gamma_3$	$\Sigma\pi$	seen
$\Gamma_4$	$N\bar{K}\pi$	
$\Gamma_5$	$\Xi(1530)K$	

The above branching fractions are our estimates, not fits or averages.

 $\Sigma(2250)$  BRANCHING RATIOS

See "Sign conventions for resonance couplings" in the Note on  $\Lambda$  and  $\Sigma$  Resonances.

$\Gamma(N\bar{K})/\Gamma_{\text{total}}$	DOCUMENT ID	TECN	COMMENT	$\Gamma_1/\Gamma$
<b>&lt;0.1 OUR ESTIMATE</b>				
0.08±0.02	DEBELLEFON 78	DPWA	$D_5$ wave	
0.02±0.01	DEBELLEFON 78	DPWA	$G_9$ wave	

$(J+\frac{1}{2}) \times \Gamma(N\bar{K})/\Gamma_{\text{total}}$	DOCUMENT ID	TECN	COMMENT	$\Gamma_1/\Gamma$
0.16±0.12	BRICMAN 70	CNTR	Total, charge exchange	
0.42	COOL 70	CNTR	$K^- p, K^- d$ total	
0.47	BUGG 68	CNTR		

••• We do not use the following data for averages, fits, limits, etc. •••

See key on page 457

Baryon Particle Listings

$\Sigma(2250)$ ,  $\Sigma(2455)$  Bumps,  $\Sigma(2620)$  Bumps,  $\Sigma(3000)$  Bumps

$(\Gamma_1 \Gamma_f)^{1/2} / \Gamma_{\text{total}}$  in  $N\bar{K} \rightarrow \Sigma(2250) \rightarrow \Lambda\pi$   $(\Gamma_1 \Gamma_2)^{1/2} / \Gamma$

VALUE	DOCUMENT ID	TECN	COMMENT
-0.16 ± 0.03	VANHORN 75	DPWA	$K^- p \rightarrow \Lambda\pi^0, F_5$ wave
••• We do not use the following data for averages, fits, limits, etc. •••			
+0.11	DEBELLEFON 76	IPWA	$D_5$ wave
-0.10	DEBELLEFON 76	IPWA	$G_9$ wave
-0.18	BARBARO... 70	DPWA	$K^- p \rightarrow \Lambda\pi^0, G_9$ wave

$(\Gamma_1 \Gamma_f)^{1/2} / \Gamma_{\text{total}}$  in  $N\bar{K} \rightarrow \Sigma(2250) \rightarrow \Sigma\pi$   $(\Gamma_1 \Gamma_3)^{1/2} / \Gamma$

VALUE	DOCUMENT ID	TECN	COMMENT
+0.06 ± 0.02	DEBELLEFON 77	DPWA	$D_5$ wave
-0.03 ± 0.02	DEBELLEFON 77	DPWA	$G_9$ wave
+0.07	BARBARO... 70	DPWA	$K^- p \rightarrow \Sigma\pi, G_9$ wave

$\Gamma(N\bar{K}) / \Gamma(\Sigma\pi)$   $\Gamma_1 / \Gamma_3$

VALUE	DOCUMENT ID	TECN	COMMENT
<0.18	BARNES 69	HBC	1 standard dev. limit

$\Gamma(\Lambda\pi) / \Gamma(\Sigma\pi)$   $\Gamma_2 / \Gamma_3$

VALUE	DOCUMENT ID	TECN	COMMENT
<0.18	BARNES 69	HBC	1 standard dev. limit

$(\Gamma_1 \Gamma_f)^{1/2} / \Gamma_{\text{total}}$  in  $N\bar{K} \rightarrow \Sigma(2250) \rightarrow \Xi(1530)K$   $(\Gamma_1 \Gamma_5)^{1/2} / \Gamma$

VALUE	DOCUMENT ID	TECN	COMMENT
0.18 ± 0.04	1 DEBELLEFON 75B	HBC	$K^- p \rightarrow \Xi^+ K^0$

$\Sigma(2250)$  FOOTNOTES

<sup>1</sup> Seen in the (initial and final state)  $D_5$  wave. Isospin not determined.

$\Sigma(2250)$  REFERENCES

DEBELLEFON 78	NC 42A 403	A. de Bellefon et al.	(CDEF, SACL) IJP
DEBELLEFON 77	NC 37A 175	A. de Bellefon et al.	(CDEF, SACL) IJP
DEBELLEFON 76	NP B109 129	A. de Bellefon, A. Berthon	(CDEF) IJP
Also	NP B90 1	A. de Bellefon et al.	(CDEF, SACL) IJP
DEBELLEFON 75B	NC 28A 289	A. de Bellefon et al.	(CDEF, SACL) IJP
VANHORN 75	NP B87 145	A.J. van Horn	(LBL) IJP
Also	NP B87 157	A.J. van Horn	(LBL) IJP
LASINSKI 71	NP B29 125	T.A. Lasinski	(EFI) IJP
AGUILAR... 70B	PRL 25 58	M. Aguilar-Benitez et al.	(BNL, SYRA)
BARBARO... 70	Duke Conf. 173	A. Barbaro-Galteri	(LRL) IJP
Hyperon Resonances, 1970			
BRICMAN 70	PL 31B 152	C. Bricman et al.	(CERN, CAEN, SACL)
COOL 70	PR D1 1887	R.L. Cool et al.	(BNL) I
Also	PRL 16 1228	R.L. Cool et al.	(BNL) I
LU 70	PR D2 1846	D.C. Lu et al.	(YALE)
BARNES 69	PRL 22 479	V.E. Barnes et al.	(BNL, SYRA)
BUGG 68	PR 168 1466	D.V. Bugg et al.	(RHEL, BIRM, CAVE) I
BLANPIED 65	PRL 14 741	W.A. Blanpied et al.	(YALE, CEA)
BOCK 65	PL 17 166	R.K. Bock et al.	(CERN, SACL)

**$\Sigma(2455)$  Bumps**  $I(J^P) = 1(?)^?$  Status: \*\*

OMITTED FROM SUMMARY TABLE

There is also some slight evidence for  $Y^*$  states in this mass region from the reaction  $\gamma p \rightarrow K^+ X$  — see GREENBERG 68.

$\Sigma(2455)$  MASS

VALUE (MeV)	DOCUMENT ID	TECN	COMMENT
$\approx 2455$ OUR ESTIMATE			
2455 ± 10	ABRAMS 70	CNTR	$K^- p, K^- d$ total
2455 ± 7	BUGG 68	CNTR	$K^- p, K^- d$ total

$\Sigma(2455)$  WIDTH

VALUE (MeV)	DOCUMENT ID	TECN	COMMENT
140	ABRAMS 70	CNTR	$K^- p, K^- d$ total
100 ± 20	BUGG 68	CNTR	

$\Sigma(2455)$  DECAY MODES

Mode
$\Gamma_1$ $N\bar{K}$

$\Sigma(2455)$  BRANCHING RATIOS

$(J+\frac{1}{2}) \times \Gamma(N\bar{K}) / \Gamma_{\text{total}}$   $\Gamma_1 / \Gamma$

VALUE	DOCUMENT ID	TECN	COMMENT
0.39	ABRAMS 70	CNTR	$K^- p, K^- d$ total
0.05 ± 0.05	<sup>1</sup> BRICMAN 70	CNTR	Total, charge exchange
0.3	BUGG 68	CNTR	

$\Sigma(2455)$  FOOTNOTES

<sup>1</sup> Fit of total cross section given by BRICMAN 70 is poor in this region.

$\Sigma(2455)$  REFERENCES

ABRAMS 70	PR D1 1917	R.J. Abrams et al.	(BNL) I
Also	PRL 19 678	R.J. Abrams et al.	(BNL)
BRICMAN 70	PL 31B 152	C. Bricman et al.	(CERN, CAEN, SACL)
BUGG 68	PR 168 1466	D.V. Bugg et al.	(RHEL, BIRM, CAVE) I
GREENBERG 68	PRL 20 221	J.S. Greenberg et al.	(YALE)

**$\Sigma(2620)$  Bumps**

$I(J^P) = 1(?)^?$  Status: \*\*

OMITTED FROM SUMMARY TABLE

$\Sigma(2620)$  MASS

VALUE (MeV)	DOCUMENT ID	TECN	COMMENT
$\approx 2620$ OUR ESTIMATE			
2542 ± 22	DIBIANCA 75	DBC	$K^- N \rightarrow \Xi K\pi$
2620 ± 15	ABRAMS 70	CNTR	$K^- p, K^- d$ total

$\Sigma(2620)$  WIDTH

VALUE (MeV)	DOCUMENT ID	TECN	COMMENT
221 ± 81	DIBIANCA 75	DBC	$K^- N \rightarrow \Xi K\pi$
175	ABRAMS 70	CNTR	$K^- p, K^- d$ total

$\Sigma(2620)$  DECAY MODES

Mode
$\Gamma_1$ $N\bar{K}$

$\Sigma(2620)$  BRANCHING RATIOS

$(J+\frac{1}{2}) \times \Gamma(N\bar{K}) / \Gamma_{\text{total}}$   $\Gamma_1 / \Gamma$

VALUE	DOCUMENT ID	TECN	COMMENT
0.32	ABRAMS 70	CNTR	$K^- p, K^- d$ total
0.36 ± 0.12	BRICMAN 70	CNTR	Total, charge exchange

$\Sigma(2620)$  REFERENCES

DIBIANCA 75	NP B98 137	F.A. Dibianca, R.J. Endorf	(CMU)
ABRAMS 70	PR D1 1917	R.J. Abrams et al.	(BNL) I
Also	PRL 19 678	R.J. Abrams et al.	(BNL)
BRICMAN 70	PL 31B 152	C. Bricman et al.	(CERN, CAEN, SACL)

**$\Sigma(3000)$  Bumps**

$I(J^P) = 1(?)^?$  Status: \*

OMITTED FROM SUMMARY TABLE

Seen as an enhancement in  $\Lambda\pi$  and  $\bar{K}N$  invariant mass spectra and in the missing mass of neutrals recoiling against a  $K^0$ .

$\Sigma(3000)$  MASS

VALUE (MeV)	DOCUMENT ID	TECN	CHG	COMMENT
$\approx 3000$ OUR ESTIMATE				
3000	EHRlich 66	HBC	0	$\pi^- p$ 7.91 GeV/c

$\Sigma(3000)$  DECAY MODES

Mode
$\Gamma_1$ $N\bar{K}$
$\Gamma_2$ $\Lambda\pi$

$\Sigma(3000)$  REFERENCES

EHRlich 66	PR 152 1194	R. Ehrlich, W. Selove, H. Yuta	(PENN) I
------------	-------------	--------------------------------	----------

## Baryon Particle Listings

 $\Sigma(3170)$  Bumps **$\Sigma(3170)$  Bumps** $I(J^P) = 1(?^?)$  Status: \*

OMITTED FROM SUMMARY TABLE

Seen by AMIRZADEH 79 as a narrow 6.5-standard-deviation enhancement in the reaction  $K^- p \rightarrow Y^{*+} \pi^-$  using data from independent high statistics bubble chamber experiments at 8.25 and 6.5 GeV/c. The dominant decay modes are multibody, multistrange final states and the production is via isospin-3/2 baryon exchange. Isospin 1 is favored.

Not seen in a  $K^- p$  experiment in LASS at 11 GeV/c (ASTON 85B).

 **$\Sigma(3170)$  MASS  
(PRODUCTION EXPERIMENTS)**

VALUE (MeV)	EVTS	DOCUMENT ID	TECN	COMMENT
$\approx 3170$ OUR ESTIMATE				
$3170 \pm 5$	35	AMIRZADEH 79	HBC	$K^- p \rightarrow Y^{*+} \pi^-$

 **$\Sigma(3170)$  WIDTH  
(PRODUCTION EXPERIMENTS)**

VALUE (MeV)	EVTS	DOCUMENT ID	TECN	COMMENT
<20	35	<sup>1</sup> AMIRZADEH 79	HBC	$K^- p \rightarrow Y^{*+} \pi^-$

 **$\Sigma(3170)$  DECAY MODES  
(PRODUCTION EXPERIMENTS)**

Mode	Fraction ( $\Gamma_i/\Gamma$ )
$\Gamma_1$ $\Lambda K \bar{K} \pi$ 's	seen
$\Gamma_2$ $\Sigma K \bar{K} \pi$ 's	seen
$\Gamma_3$ $\Xi K \pi$ 's	seen

 **$\Sigma(3170)$  BRANCHING RATIOS  
(PRODUCTION EXPERIMENTS)** $\Gamma(\Lambda K \bar{K} \pi \text{'s})/\Gamma_{\text{total}}$   $\Gamma_1/\Gamma$ 

VALUE	DOCUMENT ID	TECN	COMMENT
seen	AMIRZADEH 79	HBC	$K^- p \rightarrow Y^{*+} \pi^-$

 $\Gamma(\Sigma K \bar{K} \pi \text{'s})/\Gamma_{\text{total}}$   $\Gamma_2/\Gamma$ 

VALUE	DOCUMENT ID	TECN	COMMENT
seen	AMIRZADEH 79	HBC	$K^- p \rightarrow Y^{*+} \pi^-$

 $\Gamma(\Xi K \pi \text{'s})/\Gamma_{\text{total}}$   $\Gamma_3/\Gamma$ 

VALUE	DOCUMENT ID	TECN	COMMENT
seen	AMIRZADEH 79	HBC	$K^- p \rightarrow Y^{*+} \pi^-$

 **$\Sigma(3170)$  FOOTNOTES  
(PRODUCTION EXPERIMENTS)**

<sup>1</sup> Observed width consistent with experimental resolution.

 **$\Sigma(3170)$  REFERENCES  
(PRODUCTION EXPERIMENTS)**

ASTON 85B	PR D32 2270	D. Aston <i>et al.</i>	(SLAC, CARL, CNRC, CIN C)
AMIRZADEH 79	PL 89B 125	J. Amirzadeh <i>et al.</i>	(BIRM, CERN, GLAS+) <sup>1</sup>
Also	Toronto Conf. 263	J.B. Kinson <i>et al.</i>	(BIRM, CERN, GLAS+) <sup>1</sup>

See key on page 457

Baryon Particle Listings

$\Xi^0$

**$\Xi$  BARYONS**  
 **$(S = -2, I = 1/2)$**   
 $\Xi^0 = uss, \Xi^- = dss$

$\Xi^0$

$I(J^P) = \frac{1}{2}(\frac{1}{2}^+)$  Status: \* \* \* \*

The parity has not actually been measured, but + is of course expected.

**$\Xi^0$  MASS**

The fit uses the  $\Xi^0, \Xi^-,$  and  $\Xi^+$  masses and the  $\Xi^- - \Xi^0$  mass difference. It assumes that the  $\Xi^-$  and  $\Xi^+$  masses are the same.

VALUE (MeV)	EVTS	DOCUMENT ID	TECN	COMMENT
<b>1314.86 ± 0.20 OUR FIT</b>				
<b>1314.82 ± 0.06 ± 0.20</b>	3120	FANTI	00 NA48	p Be, 450 GeV
• • • We do not use the following data for averages, fits, limits, etc. • • •				
1315.2 ± 0.92	49	WILQUET	72 HLBC	
1313.4 ± 1.8	1	PALMER	68 HBC	

**$m_{\Xi^-} - m_{\Xi^0}$**

The fit uses the  $\Xi^0, \Xi^-,$  and  $\Xi^+$  masses and the  $\Xi^- - \Xi^0$  mass difference. It assumes that the  $\Xi^-$  and  $\Xi^+$  masses are the same.

VALUE (MeV)	EVTS	DOCUMENT ID	TECN	COMMENT
<b>6.85 ± 0.21 OUR FIT</b>				
<b>6.3 ± 0.7 OUR AVERAGE</b>				
6.9 ± 2.2	29	LONDON	66 HBC	
6.1 ± 0.9	88	PJERROU	65B HBC	
6.8 ± 1.6	23	JAUNEAU	63 FBC	
• • • We do not use the following data for averages, fits, limits, etc. • • •				
6.1 ± 1.6	45	CARMONY	64B HBC	See PJERROU 65B

**$\Xi^0$  MEAN LIFE**

VALUE ( $10^{-10}$ s)	EVTS	DOCUMENT ID	TECN	COMMENT
<b>2.90 ± 0.09 OUR AVERAGE</b>				
2.83 ± 0.16	6300	1 ZECH	77 SPEC	Neutral hyperon beam
2.86 <sup>+0.21</sup> <sub>-0.19</sub>	652	BALTAY	74 HBC	1.75 GeV/c $K^- p$
2.90 <sup>+0.32</sup> <sub>-0.27</sub>	157	2 MAYEUR	72 HLBC	2.1 GeV/c $K^-$
3.07 <sup>+0.22</sup> <sub>-0.20</sub>	340	DAUBER	69 HBC	
3.0 ± 0.5	80	PJERROU	65B HBC	
2.5 <sup>+0.4</sup> <sub>-0.3</sub>	101	HUBBARD	64 HBC	
3.9 <sup>+1.4</sup> <sub>-0.8</sub>	24	JAUNEAU	63 FBC	
• • • We do not use the following data for averages, fits, limits, etc. • • •				
3.5 <sup>+1.0</sup> <sub>-0.8</sub>	45	CARMONY	64B HBC	See PJERROU 65B

<sup>1</sup>The ZECH 77 result is  $\tau_{\Xi^0} = [2.77 - (\tau_A - 2.69)] \times 10^{-10}$  s, in which we use  $\tau_A = 2.63 \times 10^{-10}$  s.  
<sup>2</sup>The MAYEUR 72 value is modified by the erratum.

**$\Xi^0$  MAGNETIC MOMENT**

See the "Note on Baryon Magnetic Moments" in the  $\Lambda$  Listings.

VALUE ( $\mu_N$ )	EVTS	DOCUMENT ID	TECN	COMMENT
<b>-1.250 ± 0.014 OUR AVERAGE</b>				
-1.253 ± 0.014	270k	COX	81 SPEC	
-1.20 ± 0.06	42k	BUNCE	79 SPEC	

**$\Xi^0$  DECAY MODES**

Mode	Fraction ( $\Gamma_i/\Gamma$ )	Confidence level
$\Gamma_1 \Lambda\pi^0$	(99.525 ± 0.012) %	
$\Gamma_2 \Lambda\gamma$	( 1.17 ± 0.07 ) × 10 <sup>-3</sup>	
$\Gamma_3 \Lambda e^+ e^-$	( 7.6 ± 0.6 ) × 10 <sup>-6</sup>	
$\Gamma_4 \Sigma^0 \gamma$	( 3.33 ± 0.10 ) × 10 <sup>-3</sup>	
$\Gamma_5 \Sigma^+ e^- \bar{\nu}_e$	( 2.53 ± 0.08 ) × 10 <sup>-4</sup>	
$\Gamma_6 \Sigma^+ \mu^- \bar{\nu}_\mu$	( 4.6 <sup>+1.8</sup> <sub>-1.4</sub> ) × 10 <sup>-6</sup>	

**$\Delta S = \Delta Q$  ( $SQ$ ) violating modes or  $\Delta S = 2$  forbidden ( $S2$ ) modes**

$\Gamma_i$	Mode	$SQ$	Value	Confidence level
$\Gamma_7$	$\Sigma^- e^+ \nu_e$	$SQ < 9$	× 10 <sup>-4</sup>	90%
$\Gamma_8$	$\Sigma^- \mu^+ \nu_\mu$	$SQ < 9$	× 10 <sup>-4</sup>	90%
$\Gamma_9$	$p \pi^-$	$S2 < 8$	× 10 <sup>-6</sup>	90%
$\Gamma_{10}$	$p e^- \bar{\nu}_e$	$S2 < 1.3$	× 10 <sup>-3</sup>	
$\Gamma_{11}$	$p \mu^- \bar{\nu}_\mu$	$S2 < 1.3$	× 10 <sup>-3</sup>	

**CONSTRAINED FIT INFORMATION**

An overall fit to 3 branching ratios uses 9 measurements and one constraint to determine 4 parameters. The overall fit has a  $\chi^2 = 4.6$  for 6 degrees of freedom.

The following off-diagonal array elements are the correlation coefficients  $\langle \delta x_i \delta x_j \rangle / (\delta x_i \delta x_j)$ , in percent, from the fit to the branching fractions,  $x_i \equiv \Gamma_i/\Gamma_{total}$ . The fit constrains the  $x_i$  whose labels appear in this array to sum to one.

$x_2$	-57		
$x_4$	-82	0	
$x_5$	-7	0	0
	$x_1$	$x_2$	$x_4$

**$\Xi^0$  BRANCHING RATIOS**

**$\Gamma(\Lambda\gamma)/\Gamma(\Lambda\pi^0)$   $\Gamma_2/\Gamma_1$**

VALUE (units 10 <sup>-3</sup> )	EVTS	DOCUMENT ID	TECN	COMMENT
<b>1.17 ± 0.07 OUR FIT</b>				
<b>1.17 ± 0.07 OUR AVERAGE</b>				
1.17 ± 0.05 ± 0.06	672	<sup>3</sup> LAI	04A NA48	p Be, 450 GeV
1.91 ± 0.34 ± 0.19	31	<sup>4</sup> FANTI	00 NA48	p Be, 450 GeV
1.06 ± 0.12 ± 0.11	116	JAMES	90 SPEC	FNAL hyperons

<sup>3</sup>LAI 04A used our 2002 value of 99.5% for the  $\Xi^0 \rightarrow \Lambda\pi^0$  branching fraction to get  $\Gamma(\Xi^0 \rightarrow \Lambda\gamma)/\Gamma_{total} = (1.16 \pm 0.05 \pm 0.06) \times 10^{-3}$ . We adjust slightly to go back to what was directly measured.

<sup>4</sup>FANTI 00 used our 1998 value of 99.5% for the  $\Xi^0 \rightarrow \Lambda\pi^0$  branching fraction to get  $\Gamma(\Xi^0 \rightarrow \Lambda\gamma)/\Gamma_{total} = (1.90 \pm 0.34 \pm 0.19) \times 10^{-3}$ . We adjust slightly to go back to what was directly measured.

**$\Gamma(\Lambda e^+ e^-)/\Gamma_{total}$   $\Gamma_3/\Gamma$**

VALUE (units 10 <sup>-6</sup> )	EVTS	DOCUMENT ID	TECN	COMMENT
<b>7.6 ± 0.4 ± 0.5</b>	397 ± 21	<sup>5</sup> BATLEY	07C NA48	p Be, 400 GeV

<sup>5</sup>This BATLEY 07C result is consistent with internal bremsstrahlung.

**$\Gamma(\Sigma^0 \gamma)/\Gamma(\Lambda\pi^0)$   $\Gamma_4/\Gamma_1$**

VALUE (units 10 <sup>-3</sup> )	EVTS	DOCUMENT ID	TECN	COMMENT
<b>3.35 ± 0.10 OUR FIT</b>				
<b>3.35 ± 0.10 OUR AVERAGE</b>				
3.34 ± 0.05 ± 0.09	4045	ALAVI-HARATI	01C KTEV	p nucleus, 800 GeV
3.16 ± 0.76 ± 0.32	17	<sup>6</sup> FANTI	00 NA48	p Be, 450 GeV
3.56 ± 0.42 ± 0.10	85	TEIGE	89 SPEC	FNAL hyperons

<sup>6</sup>FANTI 00 used our 1998 value of 99.5% for the  $\Xi^0 \rightarrow \Lambda\pi^0$  branching fraction to get  $\Gamma(\Xi^0 \rightarrow \Sigma^0 \gamma)/\Gamma_{total} = (3.14 \pm 0.76 \pm 0.32) \times 10^{-3}$ . We adjust slightly to go back to what was directly measured.

**$\Gamma(\Sigma^+ e^- \bar{\nu}_e)/\Gamma_{total}$   $\Gamma_5/\Gamma$**

VALUE (units 10 <sup>-4</sup> )	EVTS	DOCUMENT ID	TECN	COMMENT
<b>2.53 ± 0.08 OUR FIT</b>				
<b>2.53 ± 0.08 OUR AVERAGE</b>				
2.51 ± 0.03 ± 0.09	6101	BATLEY	07 NA48	p Be, 400 GeV
2.55 ± 0.14 ± 0.10	419	<sup>7</sup> BATLEY	07 NA48	p Be, 400 GeV
2.71 ± 0.22 ± 0.31	176	AFFOLDER	99 KTEV	p nucleus, 800 GeV

<sup>7</sup>This BATLEY 07 result is for  $\Xi^0 \rightarrow \Sigma^- e^+ \nu_e$  events.

**$\Gamma(\Sigma^+ \mu^- \bar{\nu}_\mu)/\Gamma(\Sigma^+ e^- \bar{\nu}_e)$   $\Gamma_6/\Gamma_5$**

VALUE	EVTS	DOCUMENT ID	TECN	COMMENT
<b>0.018<sup>+0.007</sup><sub>-0.005</sub> ± 0.002</b>	9	ABOUZAID	05 KTEV	p nucleus 800 GeV

**$\Gamma(\Sigma^+ \mu^- \bar{\nu}_\mu)/\Gamma(\Lambda\pi^0)$   $\Gamma_6/\Gamma_1$**

VALUE (units 10 <sup>-3</sup> )	CL%	EVTS	DOCUMENT ID	TECN	COMMENT
• • • We do not use the following data for averages, fits, limits, etc. • • •					
<1.1	90	0	YEH	74 HBC	Effective denom.=2100
<1.5			DAUBER	69 HBC	
<7			HUBBARD	66 HBC	

**$\Gamma(\Sigma^- e^+ \nu_e)/\Gamma(\Lambda\pi^0)$   $\Gamma_7/\Gamma_1$**

VALUE (units 10 <sup>-3</sup> )	CL%	EVTS	DOCUMENT ID	TECN	COMMENT
Test of $\Delta S = \Delta Q$ rule.					
<b>&lt;0.9</b>	90	0	YEH	74 HBC	Effective denom.=2500
• • • We do not use the following data for averages, fits, limits, etc. • • •					
<1.5			DAUBER	69 HBC	
<6			HUBBARD	66 HBC	

## Baryon Particle Listings

=0

 $\Gamma(\Sigma^- \mu^+ \nu_\mu)/\Gamma(\Lambda\pi^0)$   $\Gamma_8/\Gamma_1$ Test of  $\Delta S = \Delta Q$  rule.

VALUE (units $10^{-3}$ )	CL%	EVTS	DOCUMENT ID	TECN	COMMENT
<0.9	90	0	YEH	74	HBC Effective denom.=2500

••• We do not use the following data for averages, fits, limits, etc. •••

<1.5			DAUBER	69	HBC
<6			HUBBARD	66	HBC

 $\Gamma(p\pi^-)/\Gamma(\Lambda\pi^0)$   $\Gamma_9/\Gamma_1$  $\Delta S=2$ . Forbidden in first-order weak interaction.

VALUE (units $10^{-6}$ )	CL%	EVTS	DOCUMENT ID	TECN	COMMENT
< 8.2	90		WHITE	05	HYCP p Cu, 800 GeV

••• We do not use the following data for averages, fits, limits, etc. •••

< 36	90		GEWENIGER	75	SPEC
<1800	90	0	YEH	74	HBC Effective denom.=1300
< 900			DAUBER	69	HBC
<5000			HUBBARD	66	HBC

 $\Gamma(p e^- \bar{\nu}_e)/\Gamma(\Lambda\pi^0)$   $\Gamma_{10}/\Gamma_1$  $\Delta S=2$ . Forbidden in first-order weak interaction.

VALUE (units $10^{-3}$ )	CL%	EVTS	DOCUMENT ID	TECN	COMMENT
<1.3			DAUBER	69	HBC

••• We do not use the following data for averages, fits, limits, etc. •••

<3.4	90	0	YEH	74	HBC Effective denom.=670
<6			HUBBARD	66	HBC

 $\Gamma(p\mu^- \bar{\nu}_\mu)/\Gamma(\Lambda\pi^0)$   $\Gamma_{11}/\Gamma_1$  $\Delta S=2$ . Forbidden in first-order weak interaction.

VALUE (units $10^{-3}$ )	CL%	EVTS	DOCUMENT ID	TECN	COMMENT
<1.3			DAUBER	69	HBC

••• We do not use the following data for averages, fits, limits, etc. •••

<3.5	90	0	YEH	74	HBC Effective denom.=664
<6			HUBBARD	66	HBC

 $\Xi^0$  DECAY PARAMETERS

See the "Note on Baryon Decay Parameters" in the neutron Listings.

 $\alpha(\Xi^0) \alpha_-(\Lambda)$ This is a product of the  $\Xi^0 \rightarrow \Lambda\pi^0$  and  $\Lambda \rightarrow p\pi^-$  asymmetries.

VALUE	EVTS	DOCUMENT ID	TECN	COMMENT
<b>-0.261 ± 0.006 OUR AVERAGE</b>				

-0.276 ± 0.001 ± 0.035	4M	BATLEY	10B	NA48 p Be, 400 GeV
-0.260 ± 0.004 ± 0.005	300k	HANDLER	82	SPEC FNAL hyperons

••• We do not use the following data for averages, fits, limits, etc. •••

-0.317 ± 0.027	6075	BUNCE	78	SPEC FNAL hyperons
-0.35 ± 0.06	505	BALTAY	74	HBC $K^- p$ 1.75 GeV/c
-0.28 ± 0.06	739	DAUBER	69	HBC $K^- p$ 1.7-2.6 GeV/c

 $\alpha$  FOR  $\Xi^0 \rightarrow \Lambda\pi^0$ The above average,  $\alpha(\Xi^0)\alpha_-(\Lambda) = -0.261 \pm 0.006$ , divided by our current average  $\alpha_-(\Lambda) = 0.642 \pm 0.013$ , gives the following value for  $\alpha(\Xi^0)$ .

VALUE	DOCUMENT ID
<b>-0.406 ± 0.013 OUR EVALUATION</b>	

 $\phi$  ANGLE FOR  $\Xi^0 \rightarrow \Lambda\pi^0$  ( $\tan\phi = \beta/\gamma$ )

VALUE (°)	EVTS	DOCUMENT ID	TECN	COMMENT
<b>21 ± 12 OUR AVERAGE</b>				

16 ± 17	652	BALTAY	74	HBC 1.75 GeV/c $K^- p$
38 ± 19	739	8 DAUBER	69	HBC
- 8 ± 30	146	9 BERGE	66	HBC

<sup>8</sup>DAUBER 69 uses  $\alpha_\Lambda = 0.647 \pm 0.020$ .<sup>9</sup>The errors have been multiplied by 1.2 due to approximations used for the  $\Xi$  polarization; see DAUBER 69 for a discussion.

## RADIATIVE HYPERON DECAYS

Revised July 2011 by J.D. Jackson (LBNL).

The weak radiative decays of spin-1/2 hyperons,  $B_i \rightarrow B_f \gamma$ , yield information about matrix elements (form factors) similar to that gained from weak hadronic decays. For a polarized spin-1/2 hyperon decaying radiatively via a  $\Delta Q = 0$ ,  $\Delta S = 1$  transition, the angular distribution of the direction  $\hat{\mathbf{p}}$  of the final spin-1/2 baryon in the hyperon rest frame is

$$\frac{dN}{d\Omega} = \frac{N}{4\pi} (1 + \alpha_\gamma \mathbf{P}_i \cdot \hat{\mathbf{p}}). \quad (1)$$

Here  $\mathbf{P}_i$  is the polarization of the decaying hyperon, and  $\alpha_\gamma$  is the asymmetry parameter. In terms of the form factors  $F_1(q^2)$ ,

$F_2(q^2)$ , and  $G(q^2)$  of the effective hadronic weak electromagnetic vertex,

$$F_1(q^2)\gamma_\lambda + iF_2(q^2)\sigma_{\lambda\mu}q^\mu + G(q^2)\gamma_\lambda\gamma_5,$$

 $\alpha_\gamma$  is

$$\alpha_\gamma = \frac{2 \operatorname{Re}[G(0)F_M^*(0)]}{|G(0)|^2 + |F_M(0)|^2}, \quad (2)$$

where  $F_M = (m_i - m_f)[F_2 - F_1/(m_i + m_f)]$ . If the decaying hyperon is unpolarized, the decay baryon has a longitudinal polarization given by  $P_f = -\alpha_\gamma [1]$ .

The angular distribution for the weak hadronic decay,  $B_i \rightarrow B_f \pi$ , has the same form as Eq. (1), but of course with a different asymmetry parameter,  $\alpha_\pi$ . Now, however, if the decaying hyperon is unpolarized, the decay baryon has a longitudinal polarization given by  $P_f = +\alpha_\pi [2,3]$ . The difference of sign is because the spins of the pion and photon are different.

$\Xi^0 \rightarrow \Lambda \gamma$  decay—The radiative decay  $\Xi^0 \rightarrow \Lambda \gamma$  of an unpolarized  $\Xi^0$  uses the hadronic decay  $\Lambda \rightarrow p\pi^-$  as the analyzer. As noted above, the longitudinal polarization of the  $\Lambda$  will be  $P_\Lambda = -\alpha_{\Xi\Lambda\gamma}$ . Let  $\alpha_-$  be the  $\Lambda \rightarrow p\pi^-$  asymmetry parameter and  $\theta_{\Lambda p}$  be the angle, as seen in the  $\Lambda$  rest frame, between the  $\Lambda$  line of flight and the proton momentum. Then the hadronic version of Eq. (1) applied to the  $\Lambda \rightarrow p\pi^-$  decay gives

$$\frac{dN}{d \cos \theta_{\Lambda p}} = \frac{N}{2} (1 - \alpha_{\Xi\Lambda\gamma} \alpha_- \cos \theta_{\Lambda p}) \quad (3)$$

for the angular distribution of the proton in the  $\Lambda$  frame. Our current value, from the CERN NA48/1 experiment [4], is  $\alpha_{\Xi\Lambda\gamma} = -0.704 \pm 0.019 \pm 0.064$ .

$\Xi^0 \rightarrow \Sigma^0 \gamma$  decay—The asymmetry parameter here,  $\alpha_{\Xi\Sigma\gamma}$ , is measured by following the decay chain  $\Xi^0 \rightarrow \Sigma^0 \gamma$ ,  $\Sigma^0 \rightarrow \Lambda \gamma$ ,  $\Lambda \rightarrow p\pi^-$ . Again, for an unpolarized  $\Xi^0$ , the longitudinal polarization of the  $\Sigma^0$  will be  $P_\Sigma = -\alpha_{\Xi\Sigma\gamma}$ . In the  $\Sigma^0 \rightarrow \Lambda \gamma$  decay, a parity-conserving magnetic-dipole transition, the polarization of the  $\Sigma^0$  is transferred to the  $\Lambda$ , as may be seen as follows. Let  $\theta_{\Sigma\Lambda}$  be the angle seen in the  $\Sigma^0$  rest frame between the  $\Sigma^0$  line of flight and the  $\Lambda$  momentum. For  $\Sigma^0$  helicity  $+1/2$ , the probability amplitudes for positive and negative spin states of the  $\Sigma^0$  along the  $\Lambda$  momentum are  $\cos(\theta_{\Sigma\Lambda}/2)$  and  $\sin(\theta_{\Sigma\Lambda}/2)$ . Then the amplitude for a negative helicity photon and a negative helicity  $\Lambda$  is  $\cos(\theta_{\Sigma\Lambda}/2)$ , while the amplitude for positive helicities for the photon and  $\Lambda$  is  $\sin(\theta_{\Sigma\Lambda}/2)$ . For  $\Sigma^0$  helicity  $-1/2$ , the amplitudes are interchanged. If the  $\Sigma^0$  has longitudinal polarization  $P_\Sigma$ , the probabilities for  $\Lambda$  helicities  $\pm 1/2$  are therefore

$$p(\pm 1/2) = \frac{1}{2}(1 \mp P_\Sigma) \cos^2(\theta_{\Sigma\Lambda}/2) + \frac{1}{2}(1 \pm P_\Sigma) \sin^2(\theta_{\Sigma\Lambda}/2), \quad (4)$$

and the longitudinal polarization of the  $\Lambda$  is

$$P_\Lambda = -P_\Sigma \cos \theta_{\Sigma\Lambda} = +\alpha_{\Xi\Sigma\gamma} \cos \theta_{\Sigma\Lambda}. \quad (5)$$

Using Eq. (1) for the  $\Lambda \rightarrow p\pi^-$  decay again, we get for the joint angular distribution of the  $\Sigma^0 \rightarrow \Lambda\gamma, \Lambda \rightarrow p\pi^-$  chain,

$$\frac{d^2N}{d\cos\theta_{\Sigma\Lambda}d\cos\theta_{\Lambda p}} = \frac{N}{4} (1 + \alpha_{\Xi\Sigma\gamma} \cos\theta_{\Sigma\Lambda} \alpha_- \cos\theta_{\Lambda p}). \quad (6)$$

Our current average for  $\alpha_{\Xi\Sigma\gamma}$  is  $-0.69 \pm 0.06$  [4,5].

## References

- R.E. Behrends, Phys. Rev. **111**, 1691 (1958); see Eq. (7) or (8).
- In ancient times, the signs of the asymmetry term in the angular distributions of radiative and hadronic decays of polarized hyperons were sometimes opposite. For roughly 50 years, however, the overwhelming convention has been to make them the same. The aim, not always achieved, is to remove ambiguities.
- For the definition of  $\alpha_{\pi}$ , see the note on “Baryon Decay Parameters” in the Neutron Listings.
- J.R. Batley *et al.*, Phys. Lett. **B693**, 241 (2010).
- A. Alavi-Harati *et al.*, Phys. Rev. Lett. **86**, 3239 (2001).

## $\alpha$ FOR $\Xi^0 \rightarrow \Lambda\gamma$

See the note above on “Radiative Hyperon Decays.”

VALUE	EVTS	DOCUMENT ID	TECN	COMMENT
$-0.704 \pm 0.019 \pm 0.064$	52k	<sup>10</sup> BATLEY	10B NA48	$p$ Be, 400 GeV
• • • We do not use the following data for averages, fits, limits, etc. • • •				
$-0.78 \pm 0.18 \pm 0.06$	672	LAI	04A NA48	See BATLEY 10b
$-0.43 \pm 0.44$	87	<sup>11</sup> JAMES	90 SPEC	FNAL hyperons

- <sup>10</sup>BATLEY 10b also measured the  $\Xi^0 \rightarrow \bar{\Lambda}\gamma$  asymmetry to be  $-0.798 \pm 0.064$  (no systematic error given) with 4769 events.  
<sup>11</sup>The sign has been changed; see the erratum, JAMES 02.

## $\alpha$ FOR $\Xi^0 \rightarrow \Lambda e^+ e^-$

VALUE	EVTS	DOCUMENT ID	TECN	COMMENT
$-0.8 \pm 0.2$	$397 \pm 21$	<sup>12</sup> BATLEY	07c NA48	$p$ Be, 400 GeV

- <sup>12</sup>This BATLEY 07c result is consistent with the asymmetry  $\alpha$  for  $\Xi^0 \rightarrow \Lambda\gamma$ , as expected if the mechanism is internal bremsstrahlung.

## $\alpha$ FOR $\Xi^0 \rightarrow \Sigma^0\gamma$

See the note above on “Radiative Hyperon Decays.”

VALUE	EVTS	DOCUMENT ID	TECN	COMMENT
$-0.69 \pm 0.06$	<b>OUR AVERAGE</b>			
$-0.729 \pm 0.030 \pm 0.076$	15k	<sup>13</sup> BATLEY	10B NA48	$p$ Be, 400 GeV
$-0.63 \pm 0.08 \pm 0.05$	4045	ALAVI-HARATI01c	KTEV	$p$ nucleus, 800 GeV
• • • We do not use the following data for averages, fits, limits, etc. • • •				
$+0.20 \pm 0.32 \pm 0.05$	85	<sup>14</sup> TEIGE	89 SPEC	FNAL hyperons

- <sup>13</sup>BATLEY 10b also measured the  $\Xi^0 \rightarrow \Sigma^0\gamma$  asymmetry to be  $-0.786 \pm 0.104$  (no systematic error given) with 1404 events.  
<sup>14</sup>This result has been withdrawn, due to an error. See the erratum, TEIGE 02.

## $g_1(0)/f_1(0)$ FOR $\Xi^0 \rightarrow \Sigma^+ e^- \bar{\nu}_e$

VALUE	EVTS	DOCUMENT ID	TECN	COMMENT
$1.21 \pm 0.05$	<b>OUR AVERAGE</b>			
$+1.20 \pm 0.04 \pm 0.03$	6520	<sup>15</sup> BATLEY	07 NA48	$p$ Be, 400 GeV
$+1.32 \pm 0.21 \pm 0.17$	487	<sup>16</sup> ALAVI-HARATI01i	KTEV	$p$ nucleus, 800 GeV

- <sup>15</sup>This BATLEY 07 result uses our 2006 value of  $V_{us}$  from semileptonic kaon decays as input.  
<sup>16</sup>ALAVI-HARATI 01i assumes here that the second-class current is zero and that the weak-magnetism term takes its exact SU(3) value.

## $g_2(0)/f_1(0)$ FOR $\Xi^0 \rightarrow \Sigma^+ e^- \bar{\nu}_e$

VALUE	EVTS	DOCUMENT ID	TECN	COMMENT
$-1.7 \pm 2.1 \pm 0.5$	487	<sup>17</sup> ALAVI-HARATI01i	KTEV	$p$ nucleus, 800 GeV

- <sup>17</sup>ALAVI-HARATI 01i thus assumes that  $g_2 = 0$  in calculating  $g_1/f_1$ , above.

## $f_2(0)/f_1(0)$ FOR $\Xi^0 \rightarrow \Sigma^+ e^- \bar{\nu}_e$

VALUE	EVTS	DOCUMENT ID	TECN	COMMENT
$2.0 \pm 1.2 \pm 0.5$	487	ALAVI-HARATI01i	KTEV	$p$ nucleus, 800 GeV

## $\Xi^0$ REFERENCES

BATLEY	10B	PL B693 241	J.R. Batley <i>et al.</i>	(CERN NA48/1 Collab.)
BATLEY	07	PL B645 36	J.R. Batley <i>et al.</i>	(CERN NA48/1 Collab.)
BATLEY	07C	PL B650 1	J.R. Batley <i>et al.</i>	(CERN NA48 Collab.)
ABOUZAID	05	PRL 95 081801	E. Abouzaid <i>et al.</i>	(FNAL KTeV Collab.)
WHITE	05	PRL 94 101804	C.G. White <i>et al.</i>	(FNAL HyperCP Collab.)
LAI	04A	PL B584 251	A. Lai <i>et al.</i>	(CERN NA48 Collab.)
JAMES	02	PRL 89 169901 (erratum)	C. James <i>et al.</i>	(MINN, MICH, WISC, RUTG)
TEIGE	02	PRL 89 169902 (erratum)	S. Teige <i>et al.</i>	(RUTG, MICH, MINN)
ALAVI-HARATI	01c	PRL 86 3239	A. Alavi-Harati <i>et al.</i>	(FNAL KTeV Collab.)
ALAVI-HARATI	01i	PRL 87 132001	A. Alavi-Harati <i>et al.</i>	(FNAL KTeV Collab.)
FANTI	00	EPJ C12 69	V. Fanti <i>et al.</i>	(CERN NA48 Collab.)
AFFOLDER	99	PRL 82 3751	A. Affolder <i>et al.</i>	(FNAL KTeV Collab.)
JAMES	90	PRL 64 843	C. James <i>et al.</i>	(MINN, MICH, WISC, RUTG)
TEIGE	89	PRL 63 2717	S. Teige <i>et al.</i>	(RUTG, MICH, MINN)
HANDLER	82	PR D25 639	R. Handler <i>et al.</i>	(WISC, MICH, MINN+)
COX	81	PRL 46 877	P.T. Cox <i>et al.</i>	(MICH, WISC, RUTG, MINN+)
BUNCE	79	PL 86B 386	G.R.M. Bunce <i>et al.</i>	(BNL, MICH, RUTG+)
BUNCE	78	PR D18 633	G.R.M. Bunce <i>et al.</i>	(WISC, MICH, RUTG)
ZECH	77	NP B124 413	G. Zech <i>et al.</i>	(SIEG, CERN, DORT, HEIDH)
GEWENIGER	75	PL 57B 193	C. Geweniger <i>et al.</i>	(CERN, HEIDH)
BALTAY	74	PR D9 49	C. Baltay <i>et al.</i>	(COLU, BING, J)
YEH	74	PR D10 3545	N. Yeh <i>et al.</i>	(BING, COLU)
MAYEUR	72	NP B47 333	C. Mayeur <i>et al.</i>	(BRUX, CERN, TUFTS, LOUC)
Also		NP B53 268 (erratum)	C. Mayeur	
WILQUET	72	PL 42B 372	G. Wilquet <i>et al.</i>	(BRUX, CERN, TUFTS+)
DAUBER	69	PR 179 1262	P.M. Dauber <i>et al.</i>	(LRL)
PALMER	68	PL 26B 323	R.B. Palmer <i>et al.</i>	(BNL, SYRA)
BERGE	66	PR 147 945	J.P. Berge <i>et al.</i>	(LRL)
HUBBARD	66	Thesis UCRL 11510	J.R. Hubbard	(LRL)
LONDON	66	PR 143 1034	G.W. London <i>et al.</i>	(BNL, SYRA)
PJERROU	65B	PRL 14 275	G.M. Pjerrou <i>et al.</i>	(UCLA)
Also		Thesis	G.M. Pjerrou	(UCLA)
CARMONY	64B	PRL 12 482	D.D. Carmony <i>et al.</i>	(UCLA)
HUBBARD	64	PR 135 B183	J.R. Hubbard <i>et al.</i>	(LRL)
JAUNEAU	63	PL 4 49	L. Jauneau <i>et al.</i>	(EPOL, CERN, LOUC+)
Also		Siena Conf. 1 1	L. Jauneau <i>et al.</i>	(EPOL, CERN, LOUC+)



$$(J^P) = \frac{1}{2}(\frac{1}{2}^+) \text{ Status: } ***$$

The parity has not actually been measured, but + is of course expected.

We have omitted some results that have been superseded by later experiments. See our earlier editions.

## $\Xi^-$ MASS

The fit uses the  $\Xi^-, \Xi^+$ , and  $\Xi^0$  masses and the  $\Xi^- - \Xi^+$  mass difference. It assumes that the  $\Xi^-$  and  $\Xi^+$  masses are the same.

VALUE (MeV)	EVTS	DOCUMENT ID	TECN	COMMENT
$1321.71 \pm 0.07$	<b>OUR FIT</b>			
$1321.70 \pm 0.08 \pm 0.05$	2478 $\pm$ 68	ABDALLAH	06E DLPH	from Z decays
• • • We do not use the following data for averages, fits, limits, etc. • • •				
$1321.46 \pm 0.34$	632	DIBIANCA	75 DBC	4.9 GeV/c $K^- d$
$1321.12 \pm 0.41$	268	WILQUET	72 HLCB	
$1321.87 \pm 0.51$	195	<sup>1</sup> GOLDWASSER 70	HBC	5.5 GeV/c $K^- p$
$1321.67 \pm 0.52$	6	CHIEN	66 HBC	6.9 GeV/c $\bar{p} p$
$1321.4 \pm 1.1$	299	LONDON	66 HBC	
$1321.3 \pm 0.4$	149	PJERROU	65B HBC	
$1321.1 \pm 0.3$	241	<sup>2</sup> BADIER	64 HBC	
$1321.4 \pm 0.4$	517	<sup>2</sup> JAUNEAU	63D FBC	
$1321.1 \pm 0.65$	62	<sup>2</sup> SCHNEIDER	63 HBC	

<sup>1</sup>GOLDWASSER 70 uses  $m_{\Lambda} = 1115.58$  MeV.

<sup>2</sup>These masses have been increased 0.09 MeV because the  $\Lambda$  mass increased.

## $\Xi^+$ MASS

The fit uses the  $\Xi^-, \Xi^+$ , and  $\Xi^0$  masses and the  $\Xi^- - \Xi^+$  mass difference. It assumes that the  $\Xi^-$  and  $\Xi^+$  masses are the same.

VALUE (MeV)	EVTS	DOCUMENT ID	TECN	COMMENT
$1321.71 \pm 0.07$	<b>OUR FIT</b>			
$1321.73 \pm 0.08 \pm 0.05$	2256 $\pm$ 63	ABDALLAH	06E DLPH	from Z decays
• • • We do not use the following data for averages, fits, limits, etc. • • •				
$1321.6 \pm 0.8$	35	VOTRUBA	72 HBC	10 GeV/c $K^+ p$
$1321.2 \pm 0.4$	34	STONE	70 HBC	
$1320.69 \pm 0.93$	5	CHIEN	66 HBC	6.9 GeV/c $\bar{p} p$

$$(m_{\Xi^-} - m_{\Xi^+}) / m_{\Xi^-}$$

A test of  $CP$  invariance.

VALUE	DOCUMENT ID	TECN	COMMENT
$(-2.5 \pm 8.7) \times 10^{-5}$	ABDALLAH	06E DLPH	from Z decays

# Baryon Particle Listings



## $\Xi^-$ MEAN LIFE

Measurements with an error  $> 0.2 \times 10^{-10}$  s or with systematic errors not included have been omitted.

VALUE ( $10^{-10}$ s)	EVTS	DOCUMENT ID	TECN	COMMENT
<b><math>1.639 \pm 0.015</math> OUR AVERAGE</b>				
$1.65 \pm 0.07 \pm 0.12$	$2478 \pm 68$	ABDALLAH	06E	DLPH from Z decays
$1.652 \pm 0.051$	32k	BOURQUIN	84	SPEC Hyperon beam
$1.665 \pm 0.065$	41k	BOURQUIN	79	SPEC Hyperon beam
$1.609 \pm 0.028$	4286	HEMINGWAY	78	HBC $4.2 \text{ GeV}/c \ K^- p$
$1.67 \pm 0.08$		DIBIANCA	75	DBC $4.9 \text{ GeV}/c \ K^- d$
$1.63 \pm 0.03$	4303	BALTAY	74	HBC $1.75 \text{ GeV}/c \ K^- p$
$1.73 \begin{smallmatrix} +0.08 \\ -0.07 \end{smallmatrix}$	680	MAYEUR	72	HLBC $2.1 \text{ GeV}/c \ K^-$
$1.61 \pm 0.04$	2610	DAUBER	69	HBC
$1.80 \pm 0.16$	299	LONDON	66	HBC
$1.70 \pm 0.12$	246	PJERROU	65B	HBC
$1.69 \pm 0.07$	794	HUBBARD	64	HBC
$1.86 \begin{smallmatrix} +0.15 \\ -0.14 \end{smallmatrix}$	517	JAUNEAU	63D	FBC

## $\Xi^+$ MEAN LIFE

VALUE ( $10^{-10}$ s)	EVTS	DOCUMENT ID	TECN	COMMENT
<b><math>1.70 \pm 0.08 \pm 0.12</math></b>	$2256 \pm 63$	ABDALLAH	06E	DLPH from Z decays
• • • We do not use the following data for averages, fits, limits, etc. • • •				
$1.55 \begin{smallmatrix} +0.35 \\ -0.20 \end{smallmatrix}$	35	$^3$ VOTRUBA	72	HBC $10 \text{ GeV}/c \ K^+ p$
$1.6 \pm 0.3$	34	STONE	70	HBC
$1.9 \begin{smallmatrix} +0.7 \\ -0.5 \end{smallmatrix}$	12	$^3$ SHEN	67	HBC
$1.51 \pm 0.55$	5	$^3$ CHIEN	66	HBC $6.9 \text{ GeV}/c \ \bar{p} p$

$^3$ The error is statistical only.

$$(\tau_{\Xi^-} - \tau_{\Xi^+}) / \tau_{\Xi^-}$$

A test of CPT invariance.

VALUE	DOCUMENT ID	TECN	COMMENT
<b><math>-0.01 \pm 0.07</math></b>	ABDALLAH	06E	DLPH from Z decays

## $\Xi^-$ MAGNETIC MOMENT

See the "Note on Baryon Magnetic Moments" in the  $\Lambda$  Listings.

VALUE ( $\mu_N$ )	EVTS	DOCUMENT ID	TECN	COMMENT
<b><math>-0.6507 \pm 0.0025</math> OUR AVERAGE</b>				
$-0.6505 \pm 0.0025$	4.36M	DURYEA	92	SPEC $800 \text{ GeV } p \text{ Be}$
$-0.661 \pm 0.036 \pm 0.036$	44k	TROST	89	SPEC $\Xi^- \sim 250 \text{ GeV}$
$-0.69 \pm 0.04$	218k	RAMEIKA	84	SPEC $400 \text{ GeV } p \text{ Be}$
• • • We do not use the following data for averages, fits, limits, etc. • • •				
$-0.674 \pm 0.021 \pm 0.020$	122k	HO	90	SPEC See DURYEA 92
$-2.1 \pm 0.8$	2436	COOL	74	OSPK $1.8 \text{ GeV}/c \ K^- p$
$-0.1 \pm 2.1$	2724	BINGHAM	70B	OSPK $1.8 \text{ GeV}/c \ K^- p$

## $\Xi^+$ MAGNETIC MOMENT

See the "Note on Baryon Magnetic Moments" in the  $\Lambda$  Listings.

VALUE ( $\mu_N$ )	EVTS	DOCUMENT ID	TECN	COMMENT
<b><math>+0.657 \pm 0.028 \pm 0.020</math></b>	70k	HO	90	SPEC $800 \text{ GeV } p \text{ Be}$

$$(\mu_{\Xi^-} + \mu_{\Xi^+}) / |\mu_{\Xi^-}|$$

A test of CPT invariance. We calculate this from the  $\Xi^-$  and  $\Xi^+$  magnetic moments above.

VALUE	DOCUMENT ID
<b><math>+0.01 \pm 0.05</math> OUR EVALUATION</b>	

## $\Xi^-$ DECAY MODES

Mode	Fraction ( $\Gamma_i/\Gamma$ )	Confidence level
$\Gamma_1 \Lambda \pi^-$	$(99.887 \pm 0.035) \%$	
$\Gamma_2 \Sigma^- \gamma$	$(1.27 \pm 0.23) \times 10^{-4}$	
$\Gamma_3 \Lambda e^- \bar{\nu}_e$	$(5.63 \pm 0.31) \times 10^{-4}$	
$\Gamma_4 \Lambda \mu^- \bar{\nu}_\mu$	$(3.5 \begin{smallmatrix} +3.5 \\ -2.2 \end{smallmatrix}) \times 10^{-4}$	
$\Gamma_5 \Sigma^0 e^- \bar{\nu}_e$	$(8.7 \pm 1.7) \times 10^{-5}$	
$\Gamma_6 \Sigma^0 \mu^- \bar{\nu}_\mu$	$< 8 \times 10^{-4}$	90%
$\Gamma_7 \Xi^0 e^- \bar{\nu}_e$	$< 2.3 \times 10^{-3}$	90%

## $\Delta S = 2$ forbidden ( $S2$ ) modes

$\Gamma_8 n \pi^-$	$S2 < 1.9$	$\times 10^{-5}$	90%
$\Gamma_9 n e^- \bar{\nu}_e$	$S2 < 3.2$	$\times 10^{-3}$	90%
$\Gamma_{10} n \mu^- \bar{\nu}_\mu$	$S2 < 1.5$	%	90%
$\Gamma_{11} p \pi^- \pi^-$	$S2 < 4$	$\times 10^{-4}$	90%
$\Gamma_{12} p \pi^- e^- \bar{\nu}_e$	$S2 < 4$	$\times 10^{-4}$	90%
$\Gamma_{13} p \pi^- \mu^- \bar{\nu}_\mu$	$S2 < 4$	$\times 10^{-4}$	90%
$\Gamma_{14} p \mu^- \mu^-$	$L < 4$	$\times 10^{-8}$	90%

## CONSTRAINED FIT INFORMATION

An overall fit to 4 branching ratios uses 5 measurements and one constraint to determine 5 parameters. The overall fit has a  $\chi^2 = 1.0$  for 1 degrees of freedom.

The following off-diagonal array elements are the correlation coefficients  $\langle \delta x_i \delta x_j \rangle / (\delta x_i \delta x_j)$ , in percent, from the fit to the branching fractions,  $x_i \equiv \Gamma_i/\Gamma_{\text{total}}$ . The fit constrains the  $x_i$  whose labels appear in this array to sum to one.

$x_2$	-6			
$x_3$	-8	0		
$x_4$	-99	0	-1	
$x_5$	-5	0	0	0
	$x_1$	$x_2$	$x_3$	$x_4$

## $\Xi^-$ BRANCHING RATIOS

A number of early results have been omitted.

$\Gamma(\Sigma^- \gamma)/\Gamma(\Lambda \pi^-)$	VALUE (units $10^{-4}$ )	EVTS	DOCUMENT ID	TECN	COMMENT	$\Gamma_2/\Gamma_1$
<b><math>1.27 \pm 0.24</math> OUR FIT</b>						
<b><math>1.27 \pm 0.23</math> OUR AVERAGE</b>						
$1.22 \pm 0.23 \pm 0.06$	211	$^4$ DUBBS	94	E761	$\Xi^-$ 375 GeV	
$2.27 \pm 1.02$	9	BIAGI	87B	SPEC	SPS hyperon beam	

$^4$ DUBBS 94 also finds weak evidence that the asymmetry parameter  $\alpha_\gamma$  is positive ( $\alpha_\gamma = 1.0 \pm 1.3$ ).

$\Gamma(\Lambda e^- \bar{\nu}_e)/\Gamma(\Lambda \pi^-)$	VALUE (units $10^{-3}$ )	EVTS	DOCUMENT ID	TECN	COMMENT	$\Gamma_3/\Gamma_1$
<b><math>0.564 \pm 0.031</math> OUR FIT</b>						
<b><math>0.564 \pm 0.031</math></b>	2857	BOURQUIN	83	SPEC	SPS hyperon beam	
• • • We do not use the following data for averages, fits, limits, etc. • • •						
$0.30 \pm 0.13$	11	THOMPSON	80	ASPK	Hyperon beam	

$\Gamma(\Lambda \mu^- \bar{\nu}_\mu)/\Gamma(\Lambda \pi^-)$	VALUE (units $10^{-3}$ )	CL%	EVTS	DOCUMENT ID	TECN	COMMENT	$\Gamma_4/\Gamma_1$
<b><math>0.35 \begin{smallmatrix} +0.35 \\ -0.22 \end{smallmatrix}</math> OUR FIT</b>							
<b><math>0.35 \pm 0.35</math></b>	1			YEH	74	HBC	Effective denom.=2859
• • • We do not use the following data for averages, fits, limits, etc. • • •							
$< 2.3$	90	0		THOMPSON	80	ASPK	Effective denom.=1017
$< 1.3$				DAUBER	69	HBC	
$< 12$				BERGE	66	HBC	

$\Gamma(\Sigma^0 e^- \bar{\nu}_e)/\Gamma(\Lambda \pi^-)$	VALUE (units $10^{-3}$ )	EVTS	DOCUMENT ID	TECN	COMMENT	$\Gamma_5/\Gamma_1$
<b><math>0.087 \pm 0.017</math> OUR FIT</b>						
<b><math>0.087 \pm 0.017</math></b>	154	BOURQUIN	83	SPEC	SPS hyperon beam	

$[\Gamma(\Lambda e^- \bar{\nu}_e) + \Gamma(\Sigma^0 e^- \bar{\nu}_e)]/\Gamma(\Lambda \pi^-)$	VALUE (units $10^{-3}$ )	EVTS	DOCUMENT ID	TECN	COMMENT	$(\Gamma_3 + \Gamma_5)/\Gamma_1$
• • • We do not use the following data for averages, fits, limits, etc. • • •						
$0.651 \pm 0.031$	3011	$^5$ BOURQUIN	83	SPEC	SPS hyperon beam	
$0.68 \pm 0.22$	17	$^6$ DUCLOS	71	OSPK		

$^5$  See the separate BOURQUIN 83 values for  $\Gamma(\Lambda e^- \bar{\nu}_e)/\Gamma(\Lambda \pi^-)$  and  $\Gamma(\Sigma^0 e^- \bar{\nu}_e)/\Gamma(\Lambda \pi^-)$  above.

$^6$  DUCLOS 71 cannot distinguish  $\Sigma^0$ s from  $\Lambda$ 's. The Cabibbo theory predicts the  $\Sigma^0$  rate is about a factor 6 smaller than the  $\Lambda$  rate.

$\Gamma(\Sigma^0 \mu^- \bar{\nu}_\mu)/\Gamma(\Lambda \pi^-)$	VALUE (units $10^{-3}$ )	CL%	EVTS	DOCUMENT ID	TECN	COMMENT	$\Gamma_6/\Gamma_1$
<b><math>&lt; 0.76</math></b>	90	0		YEH	74	HBC	Effective denom.=3026
• • • We do not use the following data for averages, fits, limits, etc. • • •							
$< 5$				BERGE	66	HBC	

$\Gamma(\Xi^0 e^- \bar{\nu}_e)/\Gamma(\Lambda \pi^-)$	VALUE (units $10^{-3}$ )	CL%	EVTS	DOCUMENT ID	TECN	COMMENT	$\Gamma_7/\Gamma_1$
<b><math>&lt; 2.3</math></b>	90	0		YEH	74	HBC	Effective denom.=1000



See key on page 457

Baryon Particle Listings



**$\Gamma(n\pi^-)/\Gamma(\Lambda\pi^-)$**   **$\Gamma_8/\Gamma_1$**   
 $\Delta S=2$ . Forbidden in first-order weak interaction.

VALUE (units $10^{-3}$ )	CL%	EVTS	DOCUMENT ID	TECN	COMMENT
<0.019	90		BIAGI 82b	SPEC	SPS hyperon beam
••• We do not use the following data for averages, fits, limits, etc. •••					
<3.0	90	0	YEH 74	HBC	Effective denom.=760
<1.1			DAUBER 69	HBC	
<5.0			FERRO-LUZZI 63	HBC	

**$\Gamma(ne^-\bar{\nu}_e)/\Gamma(\Lambda\pi^-)$**   **$\Gamma_9/\Gamma_1$**   
 $\Delta S=2$ . Forbidden in first-order weak interaction.

VALUE (units $10^{-3}$ )	CL%	EVTS	DOCUMENT ID	TECN	COMMENT
< 3.2	90	0	YEH 74	HBC	Effective denom.=715
••• We do not use the following data for averages, fits, limits, etc. •••					
<10	90		BINGHAM 65	RVUE	

**$\Gamma(n\mu^-\bar{\nu}_\mu)/\Gamma(\Lambda\pi^-)$**   **$\Gamma_{10}/\Gamma_1$**   
 $\Delta S=2$ . Forbidden in first-order weak interaction.

VALUE (units $10^{-3}$ )	CL%	EVTS	DOCUMENT ID	TECN	COMMENT
<15.3	90	0	YEH 74	HBC	Effective denom.=150

**$\Gamma(p\pi^-\pi^-)/\Gamma(\Lambda\pi^-)$**   **$\Gamma_{11}/\Gamma_1$**   
 $\Delta S=2$ . Forbidden in first-order weak interaction.

VALUE (units $10^{-4}$ )	CL%	EVTS	DOCUMENT ID	TECN	COMMENT
<3.7	90	0	YEH 74	HBC	Effective denom.=6200

**$\Gamma(p\pi^-e^-\bar{\nu}_e)/\Gamma(\Lambda\pi^-)$**   **$\Gamma_{12}/\Gamma_1$**   
 $\Delta S=2$ . Forbidden in first-order weak interaction.

VALUE (units $10^{-4}$ )	CL%	EVTS	DOCUMENT ID	TECN	COMMENT
<3.7	90	0	YEH 74	HBC	Effective denom.=6200

**$\Gamma(p\pi^-\mu^-\bar{\nu}_\mu)/\Gamma(\Lambda\pi^-)$**   **$\Gamma_{13}/\Gamma_1$**   
 $\Delta S=2$ . Forbidden in first-order weak interaction.

VALUE (units $10^{-4}$ )	CL%	EVTS	DOCUMENT ID	TECN	COMMENT
<3.7	90	0	YEH 74	HBC	Effective denom.=6200

**$\Gamma(p\mu^-\mu^-)/\Gamma(\Lambda\pi^-)$**   **$\Gamma_{14}/\Gamma_1$**   
 $\Delta L=2$  decay, forbidden by total lepton number conservation.

VALUE (units $10^{-8}$ )	CL%	DOCUMENT ID	TECN	COMMENT
<4.0	90	RAJARAM 05	HYCP	p Cu, 800 GeV
••• We do not use the following data for averages, fits, limits, etc. •••				
<3.7 $\times 10^4$	90	7 LITTENBERG 92b	HBC	Uses YEH 74 data

<sup>7</sup> This LITTENBERG 92b limit and the identical YEH 74 limits for the preceding three modes all result from nonobservance of any 3-prong decays of the  $\Xi^-$ . One could as well apply the limit to the *sum* of the four modes.

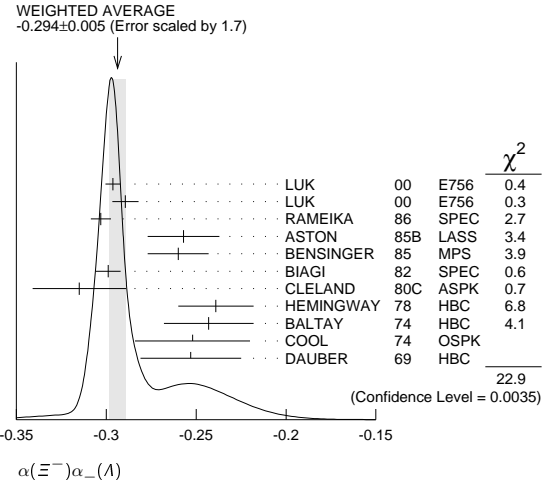
**$\Xi^-$  DECAY PARAMETERS**

See the "Note on Baryon Decay Parameters" in the neutron Listings.

**$\alpha(\Xi^-)\alpha_-(\Lambda)$**

VALUE	EVTS	DOCUMENT ID	TECN	COMMENT
<b>-0.294 ± 0.005 OUR AVERAGE</b>				Error includes scale factor of 1.7. See the ideogram below.
-0.2963 ± 0.0042	189k	LUK	00 E756	p Be, 800 GeV
-0.2894 ± 0.0073	63k	<sup>8</sup> LUK	00 E756	p Be, 800 GeV
-0.303 ± 0.004 ± 0.004	192k	RAMEIKA	86 SPEC	400 GeV pBe
-0.257 ± 0.020	11k	ASTON	85b LASS	11 GeV/c $K^-p$
-0.260 ± 0.017	21k	BENSINGER	85 MPS	5 GeV/c $K^-p$
-0.299 ± 0.007	150k	BIAGI	82 SPEC	SPS hyperon beam
-0.315 ± 0.026	9046	CLELAND	80c ASPK	BNL hyperon beam
-0.239 ± 0.021	6599	HEMINGWAY	78 HBC	4.2 GeV/c $K^-p$
-0.243 ± 0.025	4303	BALTAY	74 HBC	1.75 GeV/c $K^-p$
-0.252 ± 0.032	2436	COOL	74 OSPK	1.8 GeV/c $K^-p$
-0.253 ± 0.028	2781	DAUBER	69 HBC	

<sup>8</sup> This LUK 00 value is for  $\alpha(\Xi^+)\alpha_+(\bar{\Lambda})$ . We assume CP conservation here by including it in the average for  $\alpha(\Xi^-)\alpha_-(\Lambda)$ . But see the second data block below for the CP test.



**$\alpha$  FOR  $\Xi^- \rightarrow \Lambda\pi^-$**   
 The above average,  $\alpha(\Xi^-)\alpha_-(\Lambda) = -0.294 \pm 0.005$ , where the error includes a scale factor of 1.7, divided by our current average  $\alpha_-(\Lambda) = 0.642 \pm 0.013$ , gives the following value for  $\alpha(\Xi^-)$ .

**-0.458 ± 0.012 OUR EVALUATION** Error includes scale factor of 1.8.

**$\frac{[\alpha(\Xi^-)\alpha_-(\Lambda) - \alpha(\Xi^+)\alpha_+(\bar{\Lambda})]}{[\alpha(\Xi^-)\alpha_-(\Lambda) + \alpha(\Xi^+)\alpha_+(\bar{\Lambda})]}$**   
 This is zero if CP is conserved. The  $\alpha$ 's are the decay-asymmetry parameters for  $\Xi^- \rightarrow \Lambda\pi^-$  and  $\Lambda \rightarrow p\pi^-$  and for  $\Xi^+ \rightarrow \bar{\Lambda}\pi^+$  and  $\bar{\Lambda} \rightarrow \bar{p}\pi^+$ .

VALUE (units $10^{-4}$ )	EVTS	DOCUMENT ID	TECN	COMMENT
<b>0.0 ± 5.1 ± 4.4</b>	158M	HOLMSTROM 04	HYCP	p Cu, 800 GeV
••• We do not use the following data for averages, fits, limits, etc. •••				
+120 ± 140	252k	LUK	00 E756	p Be, 800 GeV

**$\phi$  ANGLE FOR  $\Xi^- \rightarrow \Lambda\pi^-$**  ( $\tan\phi = \beta/\gamma$ )

VALUE (°)	EVTS	DOCUMENT ID	TECN	COMMENT
<b>-2.1 ± 0.8 OUR AVERAGE</b>				
-2.39 ± 0.64 ± 0.64	144M	<sup>9</sup> HUANG	04 HYCP	p Cu, 800 GeV
-1.61 ± 2.66 ± 0.37	1.35M	<sup>10</sup> CHAKRAVO...	03 E756	p Be, 800 GeV
5 ± 10	11k	ASTON	85b LASS	$K^-p$
14.7 ± 16.0	21k	<sup>11</sup> BENSINGER	85 MPS	5 GeV/c $K^-p$
11 ± 9	4303	BALTAY	74 HBC	1.75 GeV/c $K^-p$
5 ± 16	2436	COOL	74 OSPK	1.8 GeV/c $K^-p$
-14 ± 11	2781	DAUBER	69 HBC	Uses $\alpha_\Lambda = 0.647 \pm 0.020$
0 ± 12	1004	<sup>12</sup> BERGE	66 HBC	
••• We do not use the following data for averages, fits, limits, etc. •••				
-26 ± 30	2724	BINGHAM	70b OSPK	
0 ± 20.4	364	<sup>12</sup> LONDON	66 HBC	Using $\alpha_\Lambda = 0.62$
54 ± 30	356	<sup>12</sup> CARMONY	64b HBC	

<sup>9</sup> From this result and  $\alpha_\Xi$ , HUANG 04 gets  $\beta_\Xi = -0.037 \pm 0.011 \pm 0.010$  and  $\gamma_\Xi = 0.888 \pm 0.0004 \pm 0.006$ . And the strong p-s phase difference for  $\Lambda\pi^-$  scattering is  $(4.6 \pm 1.4 \pm 1.2)^\circ$ .

<sup>10</sup> From this result and  $\alpha_\Xi$ , CHAKRAVORTY 03 obtains  $\beta_\Xi = -0.025 \pm 0.042 \pm 0.006$  and  $\gamma_\Xi = 0.889 \pm 0.001 \pm 0.007$ . And the strong p-s phase difference for  $\Lambda\pi^-$  scattering is  $(3.17 \pm 5.28 \pm 0.73)^\circ$ .

<sup>11</sup> BENSINGER 85 used  $\alpha_\Lambda = 0.642 \pm 0.013$ .

<sup>12</sup> The errors have been multiplied by 1.2 due to approximations used for the  $\Xi$  polarization; see DAUBER 69 for a discussion.

**$g_A/g_V$  FOR  $\Xi^- \rightarrow \Lambda e^-\bar{\nu}_e$**

VALUE	EVTS	DOCUMENT ID	TECN	COMMENT
<b>-0.25 ± 0.05</b>	1992	<sup>13</sup> BOURQUIN	83 SPEC	SPS hyperon beam

<sup>13</sup> BOURQUIN 83 assumes that  $g_2 = 0$ . Also, the sign has been changed to agree with our conventions, given in the "Note on Baryon Decay Parameters" in the neutron Listings.

**$\Xi^-$  REFERENCES**

We have omitted some papers that have been superseded by later experiments. See our earlier editions.

ABDALLAH 06E	PL B639 179	J. Abdallah et al.	(DELPHI Collab.)
RAJARAM 05	PRL 94 181801	D. Rajaram et al.	(FNAL HyperCP Collab.)
HOLMSTROM 04	PRL 93 262001	T. Holmstrom et al.	(FNAL HyperCP Collab.)
HUANG 04	PRL 93 011802	M. Huang et al.	(FNAL HyperCP Collab.)
CHAKRAVO... 03	PRL 91 031601	A. Chakravorty et al.	(FNAL E756 Collab.)
LUK 00	PRL 85 4860	K.B. Luk et al.	(FNAL E756 Collab.)
DUBBS 94	PRL 72 808	T. Dubbs et al.	(FNAL E761 Collab.)
DURYEA 92	PRL 68 768	J. Duryea et al.	(MINN, FNAL, MICH, RUTG)
LITTENBERG 92B	PR D46 R892	L.S. Littenberg, R.E. Shrock	(BNL, STON)
HO 90	PRL 65 1713	P.M. Ho et al.	(MICH, FNAL, MINN, RUTG)
Also	PR D44 3402	P.M. Ho et al.	(MICH, FNAL, MINN, RUTG)
TROST 89	PR D40 1703	L.H. Trost et al.	(FNAL-715 Collab.)
BIAGI 87B	ZPHY C35 143	S.F. Biagi et al.	(BRIS, CERN, GEVA+)
RAMEIKA 86	PR D33 3172	R. Rameika et al.	(RUTG, MICH, WIS+)

# Baryon Particle Listings

## $\Xi^-, \Xi^0, \Xi(1530)$

ASTON	85B	PR D32 2270	D. Aston <i>et al.</i>	(SLAC, CARL, CNRC, CINC)
BENSINGER	85	NP B252 561	J.R. Bensingier <i>et al.</i>	(CHIC, ELMT, FNAL+)
BOURQUIN	84	NP B241 1	M.H. Bourquin <i>et al.</i>	(BRIS, GEVA, HEIDP+)
RAMEIKA	84	PRL 52 581	R. Rameika <i>et al.</i>	(RUTG, MICH, WISC+)
BOURQUIN	83	ZPHY C21 1	M.H. Bourquin <i>et al.</i>	(BRIS, GEVA, HEIDP+)
BIAGI	82	PL 112B 265	S.F. Biagi <i>et al.</i>	(BRIS, CAVE, GEVA+)
BIAGI	82B	PL 112B 277	S.F. Biagi <i>et al.</i>	(LOQM, GEVA, RL+)
CLELAND	80C	PR D21 12	W.E. Cleland <i>et al.</i>	(PITT, BNL)
THOMPSON	80	PR D21 25	J.A. Thompson <i>et al.</i>	(PITT, BNL)
BOURQUIN	79	PL 07B 297	M.H. Bourquin <i>et al.</i>	(BRIS, GEVA, HEIDP+)
HEMINGWAY	78	NP B142 205	R.J. Hemingway <i>et al.</i>	(CERN, ZEEM, NIJM+)
DIBIANCA	75	NP B98 137	F.A. Dibianca, R.J. Endorf	(CMU)
BALTAY	74	PR D9 49	C. Baltay <i>et al.</i>	(COLU, BING)J
COOL	74	PR D10 792	R.L. Cool <i>et al.</i>	(BNL)
Also	PRL 29 1630		R.L. Cool <i>et al.</i>	(BNL)
YEH	74	PR D10 3545	N. Yeh <i>et al.</i>	(BING, COLU)
MAYEUR	72	NP B47 333	C. Mayeur <i>et al.</i>	(BRUX, CERN, TUFTS, LOUC)
VOTRUBA	72	NP B45 77	M.F. Votruba, A. Saffer, T.M. Ratcliffe	(BIRM+)
WILQUET	72	PL 42B 372	G. Wilquet <i>et al.</i>	(BRUX, CERN, TUFTS+)
DUCLOS	71	NP B32 493	J. Duclos <i>et al.</i>	(CERN)
BINGHAM	70B	PR D1 3010	G.M. Bingham <i>et al.</i>	(UCSD, WASH)
GOLDWASSER	70	PR D1 1960	E.L. Goldwasser, P.F. Schultz	(ILL)
STONE	70	PL 32B 515	S.L. Stone <i>et al.</i>	(ROCH)
DAUBER	69	PR 179 1262	P.M. Dauber <i>et al.</i>	(LRL)J
SHEN	67	PL 25B 443	B.C. Shen, A. Firestone, G. Goldhaber	(UCB+)
BERGE	66	PR 147 945	J.P. Berge <i>et al.</i>	(LRL)
CHIEN	66	PR 152 1171	C.Y. Chien <i>et al.</i>	(YALE, BNL)
LONDON	66	PR 143 1034	G.W. London <i>et al.</i>	(BNL, SYRA)
BINGHAM	65	PRSL 285 202	H.H. Bingham	(CERN)
PJERROU	65B	PRL 14 275	G.M. Pjerrou <i>et al.</i>	(UCLA)
Also	Thesis		G.M. Pjerrou	(UCLA)
BADIER	64	Dubna Conf. 1 593	J. Badier <i>et al.</i>	(EPOL, SACL, ZEEM)
CARMONY	64B	PRL 12 482	D.D. Carmony <i>et al.</i>	(UCLA)J
HUBBARD	64	PR 135 B183	J.R. Hubbard <i>et al.</i>	(LRL)
FERRI-LUZZI	63	PR 130 1568	M. Ferro-Luzzi <i>et al.</i>	(LRL)
JAUNEAU	63D	Siena Conf. 4	L. Jauneau <i>et al.</i>	(EPOL, CERN, LOUC+)
Also	PL 5 261		L. Jauneau <i>et al.</i>	(EPOL, CERN, LOUC+)
SCHNEIDER	63	PL 4 360	J. Schneider	(CERN)

### $\Xi$ RESONANCES

The accompanying table gives our evaluation of the present status of the  $\Xi$  resonances. Not much is known about  $\Xi$  resonances. This is because (1) they can only be produced as a part of a final state, and so the analysis is more complicated than if direct formation were possible, (2) the production cross sections are small (typically a few  $\mu\text{b}$ ), and (3) the final states are topologically complicated and difficult to study with electronic techniques. Thus early information about  $\Xi$  resonances came entirely from bubble chamber experiments, where the numbers of events are small, and only in the 1980's did electronic experiments make any significant contributions. However, nothing of significance on  $\Xi$  resonances has been added since our 1988 edition.

For a detailed earlier review, see Meadows [1].

Table 1. The status of the  $\Xi$  resonances. Only those with an overall status of \*\*\* or \*\*\*\* are included in the Baryon Summary Table.

Particle	$J^P$	Overall status	Status as seen in —				
			$\Xi\pi$	$\Lambda K$	$\Sigma K$	$\Xi(1530)\pi$	Other channels
$\Xi(1318)$	1/2+	****					Decays weakly
$\Xi(1530)$	3/2+	****	****				
$\Xi(1620)$	*	*	*				
$\Xi(1690)$		***		***	**		
$\Xi(1820)$	3/2-	***	**	***	**	**	
$\Xi(1950)$		***	**	**		*	
$\Xi(2030)$		***	**	**	***		
$\Xi(2120)$	*	*		*			
$\Xi(2250)$	**	**					3-body decays
$\Xi(2370)$	**	**					3-body decays
$\Xi(2500)$	*	*		*	*		3-body decays

\*\*\*\* Existence is certain, and properties are at least fairly well explored.  
 \*\*\* Existence ranges from very likely to certain, but further confirmation is desirable and/or quantum numbers, branching fractions, etc. are not well determined.  
 \*\* Evidence of existence is only fair.  
 \* Evidence of existence is poor.

### Reference

- B.T. Meadows, in *Proceedings of the IV<sup>th</sup> International Conference on Baryon Resonances* (Toronto, 1980), ed. N. Isgur, p. 283.

## $\Xi(1530) 3/2^+$

$$I(J^P) = \frac{1}{2}(\frac{3}{2}^+) \text{ Status: } ***$$

This is the only  $\Xi$  resonance whose properties are all reasonably well known. Assuming that the  $\Lambda_c^+$  has  $J^P = 1/2^+$ , AUBERT 08AK, in a study of  $\Lambda_c^+ \rightarrow \Xi^- \pi^+ K^+$ , finds conclusively that the spin of the  $\Xi(1530)^0$  is 3/2. In conjunction with SCHLEIN 63B and BUTTON-SHAFFER 66, this proves also that the parity is +.

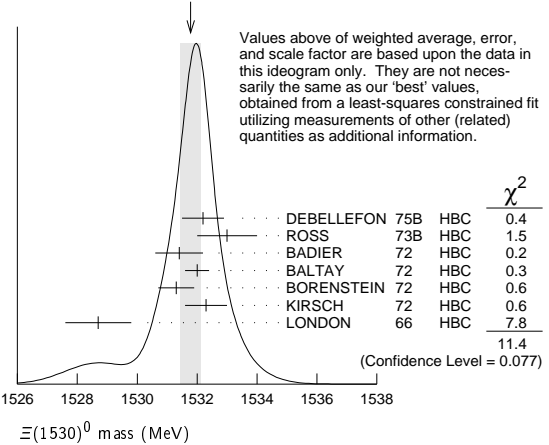
We use only those determinations of the mass and width that are accompanied by some discussion of systematics and resolution.

### $\Xi(1530)$ MASSES

#### $\Xi(1530)^0$ MASS

VALUE (MeV)	EVTS	DOCUMENT ID	TECN	COMMENT
<b>1531.80 ± 0.32 OUR FIT</b>		Error includes scale factor of 1.3.		
<b>1531.78 ± 0.34 OUR AVERAGE</b>		Error includes scale factor of 1.4. See the ideogram below.		
1532.2 ± 0.7		DEBELLEFON	75B HBC	$K^- p \rightarrow \Xi^- \bar{K} \pi$
1533 ± 1		ROSS	73B HBC	$K^- p \rightarrow \Xi \bar{K} \pi(\pi)$
1531.4 ± 0.8	59	BADIER	72 HBC	$K^- p$ 3.95 GeV/c
1532.0 ± 0.4	1262	BALTAY	72 HBC	$K^- p$ 1.75 GeV/c
1531.3 ± 0.6	324	BORENSTEIN	72 HBC	$K^- p$ 2.2 GeV/c
1532.3 ± 0.7	286	KIRSCH	72 HBC	$K^- p$ 2.87 GeV/c
1528.7 ± 1.1	76	LONDON	66 HBC	$K^- p$ 2.24 GeV/c
● ● ● We do not use the following data for averages, fits, limits, etc. ● ● ●				
1532.1 ± 0.4	1244	ASTON	85B LASS	$K^- p$ 11 GeV/c
1532.1 ± 0.6	2700	<sup>1</sup> BAUBILLIER	81B HBC	$K^- p$ 8.25 GeV/c
1530 ± 1	450	BIAGI	81 SPEC	SPS hyperon beam
1527 ± 0.6	80	SIXEL	79 HBC	$K^- p$ 10 GeV/c
1535 ± 0.4	100	SIXEL	79 HBC	$K^- p$ 16 GeV/c
1533.6 ± 1.4	97	BERTHON	74 HBC	Quasi-2-body $\sigma$

WEIGHTED AVERAGE  
1531.78 ± 0.34 (Error scaled by 1.4)



#### $\Xi(1530)^-$ MASS

VALUE (MeV)	EVTS	DOCUMENT ID	TECN	COMMENT
<b>1535.0 ± 0.6 OUR FIT</b>				
<b>1535.2 ± 0.8 OUR AVERAGE</b>				
1534.5 ± 1.2		DEBELLEFON	75B HBC	$K^- p \rightarrow \Xi^- \bar{K} \pi$
1535.3 ± 2.0		ROSS	73B HBC	$K^- p \rightarrow \Xi \bar{K} \pi(\pi)$
1536.2 ± 1.6	185	KIRSCH	72 HBC	$K^- p$ 2.87 GeV/c
1535.7 ± 3.2	38	LONDON	66 HBC	$K^- p$ 2.24 GeV/c
● ● ● We do not use the following data for averages, fits, limits, etc. ● ● ●				
1540 ± 3	48	BERTHON	74 HBC	Quasi-2-body $\sigma$
1534.7 ± 1.1	334	BALTAY	72 HBC	$K^- p$ 1.75 GeV/c

### $m_{\Xi(1530)^-} - m_{\Xi(1530)}$

VALUE (MeV)	DOCUMENT ID	TECN	COMMENT
<b>3.2 ± 0.6 OUR FIT</b>			
<b>2.9 ± 0.9 OUR AVERAGE</b>			
2.7 ± 1.0	BALTAY	72 HBC	$K^- p$ 1.75 GeV/c
2.0 ± 3.2	MERRILL	66 HBC	$K^- p$ 1.7-2.7 GeV/c
5.7 ± 3.0	PJERROU	65B HBC	$K^- p$ 1.8-1.95 GeV/c
● ● ● We do not use the following data for averages, fits, limits, etc. ● ● ●			

See key on page 457

# Baryon Particle Listings

## $\Xi(1530), \Xi(1620), \Xi(1690)$

3.9±1.8	2	KIRSCH	72	HBC	$K^- p$ 2.87 GeV/c
7 ±4	2	LONDON	66	HBC	$K^- p$ 2.24 GeV/c

### $\Xi(1530)$ WIDTHS

#### $\Xi(1530)^0$ WIDTH

VALUE (MeV)	EVTS	DOCUMENT ID	TECN	COMMENT
<b>9.1±0.5 OUR AVERAGE</b>				
9.5±1.2		DEBELLEFON	75B	HBC $K^- p \rightarrow \Xi^- \bar{K} \pi$
9.1±2.4		ROSS	73B	HBC $K^- p \rightarrow \Xi^- \bar{K} \pi(\pi)$
11 ±2		BADIER	72	HBC $K^- p$ 3.95 GeV/c
9.0±0.7		BALTAY	72	HBC $K^- p$ 1.75 GeV/c
8.4±1.4		BORENSTEIN	72	HBC $\Xi^- \pi^+$
11.0±1.8		KIRSCH	72	HBC $\Xi^- \pi^+$
7 ±7		BERGE	66	HBC $K^- p$ 1.5-1.7 GeV/c
8.5±3.5		LONDON	66	HBC $K^- p$ 2.24 GeV/c
7 ±2		SCHLEIN	63B	HBC $K^- p$ 1.8, 1.95 GeV/c
••• We do not use the following data for averages, fits, limits, etc. •••				
12.8±1.0	2700	1 BAUBILLIER	81B	HBC $K^- p$ 8.25 GeV/c
19 ±6	80	3 SIXEL	79	HBC $K^- p$ 10 GeV/c
14 ±5	100	3 SIXEL	79	HBC $K^- p$ 16 GeV/c

#### $\Xi(1530)^-$ WIDTH

VALUE (MeV)	DOCUMENT ID	TECN	COMMENT
<b>9.9±1.7 OUR AVERAGE</b>			
9.6±2.8	DEBELLEFON 75B	HBC	$K^- p \rightarrow \Xi^- \bar{K} \pi$
8.3±3.6	ROSS 73B	HBC	$K^- p \rightarrow \Xi^- \bar{K} \pi(\pi)$
7.8±3.5 7.8	BALTAY 72	HBC	$K^- p$ 1.75 GeV/c
16.2±4.6	KIRSCH 72	HBC	$\Xi^- \pi^0, \Xi^0 \pi^-$

### $\Xi(1530)$ POLE POSITIONS

#### $\Xi(1530)^0$ REAL PART

VALUE	DOCUMENT ID	COMMENT
1531.6±0.4	LICHTENBERG74	Using HABIBI 73

#### $\Xi(1530)^0$ IMAGINARY PART

VALUE	DOCUMENT ID	COMMENT
4.45±0.35	LICHTENBERG74	Using HABIBI 73

#### $\Xi(1530)^-$ REAL PART

VALUE	DOCUMENT ID	COMMENT
1534.4±1.1	LICHTENBERG74	Using HABIBI 73

#### $\Xi(1530)^-$ IMAGINARY PART

VALUE	DOCUMENT ID	COMMENT
3.9 +1.75 -3.9	LICHTENBERG74	Using HABIBI 73

### $\Xi(1530)$ DECAY MODES

Mode	Fraction ( $\Gamma_i/\Gamma$ )	Confidence level
$\Gamma_1 \Xi \pi$	100 %	
$\Gamma_2 \Xi \gamma$	<4 %	90%

### $\Xi(1530)$ BRANCHING RATIOS

$\Gamma(\Xi \gamma)/\Gamma_{\text{total}}$	CL%	DOCUMENT ID	TECN	COMMENT	$\Gamma_2/\Gamma$
<0.04	90	KALBFLEISCH 75	HBC	$K^- p$ 2.18 GeV/c	

### $\Xi(1530)$ FOOTNOTES

- 1 BAUBILLIER 81B is a fit to the inclusive spectrum. The resolution (5 MeV) is not unfolded.
- 2 Redundant with data in the mass Listings.
- 3 SIXEL 79 doesn't unfold the experimental resolution of 15 MeV.

### $\Xi(1530)$ REFERENCES

AUBERT 08AK	PR D78 034008	B. Aubert et al.	(BABAR Collab.)
ASTON 85B	PR D32 2270	D. Aston et al.	(SLAC, CARL, CNRC, CINC)
BAUBILLIER 81B	NP B192 1	M. Baubillier et al.	(BIRM, CERN, GLAS+)
BIAGI 81	ZPHY C9 305	S.F. Biagi et al.	(BRIS, CAVE, GEVA+)
SIXEL 79	NP B159 125	P. Sixel et al.	(AACH3, BERL, CERN, LOIC+)
DEBELLEFON 75B	NC 28A 289	A. de Bellefon et al.	(CDEF, SACL)
KALBFLEISCH 75	PR D11 987	G.R. Kalbfleisch, R.C. Strand, J.W. Chapman	(BNL+)
BERTHON 74	NC 21A 146	A. Berthon et al.	(CDEF, RHEL, SACL+)
LICHTENBERG 74	PR D10 3865	D.B. Lichtenberg	(IND)
	Also	D.B. Lichtenberg	(IND)
HABIBI 73	Thesis Nevis 199	M. Habibi	(COLU)
ROSS 75B	Purdue Conf. 355	R.T. Ross, J.L. Lloyd, D. Radojicic	(OXF)
BADIER 72	NP B37 429	J. Badier et al.	(EPOL)
BALTAY 72	PL 42B 129	C. Baltay et al.	(COLU, BING)
BORENSTEIN 72	PR D5 1559	S.R. Borenstein et al.	(BNL, MICH)1
KIRSCH 72	NP B40 349	L.E. Kirsch et al.	(BRAN, UMD, SYRA+)
BERGE 66	PR 147 945	J.P. Berge et al.	(LRL)1
BUTTON... 66	PR 142 883	J. Button-Shafer et al.	(LRL)JP
LONDON 66	PR 143 1034	G.W. London et al.	(BNL, SYRA)1J
MERRILL 66	Thesis UCRL 16455	D.W. Merrill	(LRL)JP
PJERROU 65B	PRL 14 275	G.M. Pjerrou et al.	(UCLA)
SCHLEIN 63B	PRL 11 167	P.E. Schlein et al.	(UCLA)1JP

### OTHER RELATED PAPERS

MAZZUCATO 81	NP B178 1	M. Mazzucato et al.	(AMST, CERN, NUM+)
BRIEFEL 77	PR D16 2706	E. Briefel et al.	(BRAN, UMD, SYRA+)
BRIEFEL 75	PR D12 1859	E. Briefel et al.	(BRAN, UMD, SYRA+)
HUNGERBU... 74	PR D10 2051	V. Hungerbuehler et al.	(YALE, FNAL, BNL+)
BUTTON... 66	PR 142 883	J. Button-Shafer et al.	(LRL)JP

## $\Xi(1620)$

$I(J^P) = \frac{1}{2}(?)^?$  Status: \*  
J, P need confirmation.

### OMITTED FROM SUMMARY TABLE

What little evidence there is consists of weak signals in the  $\Xi \pi$  channel. A number of other experiments (e.g., BORENSTEIN 72 and HASSALL 81) have looked for but not seen any effect.

### $\Xi(1620)$ MASS

VALUE (MeV)	EVTS	DOCUMENT ID	TECN	COMMENT
<b>≈ 1620 OUR ESTIMATE</b>				
1624±3	31	BRIEFEL 77	HBC	$K^- p$ 2.87 GeV/c
1633±12	34	DEBELLEFON 75B	HBC	$K^- p \rightarrow \Xi^- \bar{K} \pi$
1606±6	29	ROSS 72	HBC	$K^- p$ 3.1-3.7 GeV/c

### $\Xi(1620)$ WIDTH

VALUE (MeV)	EVTS	DOCUMENT ID	TECN	COMMENT
22.5	31	1 BRIEFEL 77	HBC	$K^- p$ 2.87 GeV/c
40 ±15	34	DEBELLEFON 75B	HBC	$K^- p \rightarrow \Xi^- \bar{K} \pi$
21 ±7	29	ROSS 72	HBC	$K^- p \rightarrow \Xi^- \pi^+ K^*0(892)$

### $\Xi(1620)$ DECAY MODES

Mode
$\Gamma_1 \Xi \pi$

### $\Xi(1620)$ FOOTNOTES

- 1 The fit is insensitive to values between 15 and 30 MeV.

### $\Xi(1620)$ REFERENCES

HASSALL 81	NP B189 397	J.K. Hassall et al.	(CAVE, MSU)
BRIEFEL 77	PR D16 2706	E. Briefel et al.	(BRAN, UMD, SYRA+)
	Also	Duke Conf. 317	(BRAN, UMD, SYRA+)
		Hyperon Resonances, 1970	
	Also	PR D12 1859	E. Briefel et al.
DEBELLEFON 75B	NC 28A 289	A. de Bellefon et al.	(BRAN, UMD, SYRA+)
BORENSTEIN 72	PR D5 1559	S.R. Borenstein et al.	(CDEF, SACL)
ROSS 72	PL 38B 177	R.T. Ross et al.	(BNL, MICH)1
			(OXF)1

### OTHER RELATED PAPERS

HUNGERBU... 74	PR D10 2051	V. Hungerbuehler et al.	(YALE, FNAL, BNL+)
SCHMIDT 73	Purdue Conf. 363	P.E. Schmidt	(BRAN)
KALBFLEISCH 70	Duke Conf. 331	G.R. Kalbfleisch	(BNL)1
		Hyperon Resonances 1970	
APSELL 69	PRL 23 884	S.P. Appell et al.	(BRAN, UMD, SYRA+)
BARTSCH 69	PL 28B 439	J. Bartsch et al.	(AACH, BERL, CERN+)

## $\Xi(1690)$

$I(J^P) = \frac{1}{2}(?)^?$  Status: \*\*\*

AUBERT 08AK, in a study of  $\Lambda_c^+ \rightarrow \Xi^- \pi^+ K^+$ , finds some evidence that the  $\Xi(1690)$  has  $J^P = 1/2^-$ .

DIONISI 78 sees a threshold enhancement in both the neutral and negatively charged  $\Sigma \bar{K}$  mass spectra in  $K^- p \rightarrow (\Sigma \bar{K}) K \pi$  at 4.2 GeV/c. The data from the  $\Sigma \bar{K}$  channels alone cannot distinguish between a resonance and a large scattering length. Weaker evidence at the same mass is seen in the corresponding  $\Lambda \bar{K}$  channels, and a coupled-channel analysis yields results consistent with a new  $\Xi$ .

BIAGI 81 sees an enhancement at 1700 MeV in the diffractively produced  $\Lambda K^-$  system. A peak is also observed in the  $\Lambda \bar{K}^0$  mass spectrum at 1660 MeV that is consistent with a 1720 MeV resonance decaying to  $\Sigma^0 \bar{K}^0$ , with the  $\gamma$  from the  $\Sigma^0$  decay not detected.

BIAGI 87 provides further confirmation of this state in diffractive dissociation of  $\Xi^-$  into  $\Lambda K^-$ . The significance claimed is 6.7 standard deviations.

ADAMOVIICH 98 sees a peak of  $1400 \pm 300$  events in the  $\Xi^- \pi^+$  spectrum produced by 345 GeV/c  $\Sigma^-$ -nucleus interactions.

## Baryon Particle Listings

 $\Xi(1690)$ ,  $\Xi(1820)$  $\Xi(1690)$  MASSES

## MIXED CHARGES

VALUE (MeV) DOCUMENT ID  
**1690 ± 10 OUR ESTIMATE** This is only an educated guess; the error given is larger than the error on the average of the published values.

 $\Xi(1690)^0$  MASS

VALUE (MeV)	EVTS	DOCUMENT ID	TECN	COMMENT
1686 ± 4	1400	ADAMOVICH	98 WA89	$\Sigma^-$ nucleus, 345 GeV/c
1699 ± 5	175	<sup>1</sup> DIONISI	78 HBC	$K^- p$ 4.2 GeV/c
1684 ± 5	183	<sup>2</sup> DIONISI	78 HBC	$K^- p$ 4.2 GeV/c

 $\Xi(1690)^-$  MASS

VALUE (MeV)	EVTS	DOCUMENT ID	TECN	COMMENT
1691.1 ± 1.9 ± 2.0	104	BIAGI	87 SPEC	$\Xi^-$ Be 116 GeV
1700 ± 10	150	<sup>3</sup> BIAGI	81 SPEC	$\Xi^-$ H 100, 135 GeV
1694 ± 6	45	<sup>4</sup> DIONISI	78 HBC	$K^- p$ 4.2 GeV/c

 $\Xi(1690)$  WIDTHS

## MIXED CHARGES

VALUE (MeV) DOCUMENT ID  
**<30 OUR ESTIMATE**

 $\Xi(1690)^0$  WIDTH

VALUE (MeV)	EVTS	DOCUMENT ID	TECN	COMMENT
10 ± 6	1400	ADAMOVICH	98 WA89	$\Sigma^-$ nucleus, 345 GeV/c
44 ± 23	175	<sup>1</sup> DIONISI	78 HBC	$K^- p$ 4.2 GeV/c
20 ± 4	183	<sup>2</sup> DIONISI	78 HBC	$K^- p$ 4.2 GeV/c

 $\Xi(1690)^-$  WIDTH

VALUE (MeV)	CL%	EVTS	DOCUMENT ID	TECN	COMMENT
< 8	90	104	BIAGI	87 SPEC	$\Xi^-$ Be 116 GeV
47 ± 14		150	<sup>3</sup> BIAGI	81 SPEC	$\Xi^-$ H 100, 135 GeV
26 ± 6		45	<sup>4</sup> DIONISI	78 HBC	$K^- p$ 4.2 GeV/c

 $\Xi(1690)$  DECAY MODES

Mode	Fraction ( $\Gamma_i/\Gamma$ )
$\Gamma_1$ $\Lambda\bar{K}$	seen
$\Gamma_2$ $\Sigma\bar{K}$	seen
$\Gamma_3$ $\Xi\pi$	seen
$\Gamma_4$ $\Xi^- \pi^+ \pi^0$	
$\Gamma_5$ $\Xi^- \pi^+ \pi^-$	possibly seen
$\Gamma_6$ $\Xi(1530)\pi$	

 $\Xi(1690)$  BRANCHING RATIOS

$\Gamma(\Lambda\bar{K})/\Gamma_{\text{total}}$	$\Gamma_1/\Gamma$
VALUE EVTS DOCUMENT ID TECN CHG COMMENT	
seen 104 BIAGI 87 SPEC - $\Xi^-$ Be 116 GeV	

$\Gamma(\Sigma\bar{K})/\Gamma(\Lambda\bar{K})$	$\Gamma_2/\Gamma_1$
VALUE EVTS DOCUMENT ID TECN CHG COMMENT	
0.75 ± 0.39 75 ABE 02c BELL $e^+e^- \approx \gamma(4S)$	
2.7 ± 0.9 DIONISI 78 HBC 0 $K^- p$ 4.2 GeV/c	
3.1 ± 1.4 DIONISI 78 HBC - $K^- p$ 4.2 GeV/c	

$\Gamma(\Xi\pi)/\Gamma(\Sigma\bar{K})$	$\Gamma_3/\Gamma_2$
VALUE DOCUMENT ID TECN CHG COMMENT	
<0.09 DIONISI 78 HBC 0 $K^- p$ 4.2 GeV/c	

$\Gamma(\Xi\pi)/\Gamma_{\text{total}}$	$\Gamma_3/\Gamma$
VALUE DOCUMENT ID TECN COMMENT	
seen ADAMOVICH 98 WA89 $\Sigma^-$ nucleus, 345 GeV/c	

$\Gamma(\Xi^- \pi^+ \pi^0)/\Gamma(\Sigma\bar{K})$	$\Gamma_4/\Gamma_2$
VALUE DOCUMENT ID TECN CHG COMMENT	
<0.04 DIONISI 78 HBC 0 $K^- p$ 4.2 GeV/c	

$\Gamma(\Xi^- \pi^+ \pi^-)/\Gamma_{\text{total}}$	$\Gamma_5/\Gamma$
VALUE EVTS DOCUMENT ID TECN CHG COMMENT	
possibly seen 4 BIAGI 87 SPEC - $\Xi^-$ Be 116 GeV	

$\Gamma(\Xi^- \pi^+ \pi^-)/\Gamma(\Sigma\bar{K})$	$\Gamma_5/\Gamma_2$
VALUE DOCUMENT ID TECN CHG COMMENT	
<0.03 DIONISI 78 HBC - $K^- p$ 4.2 GeV/c	

 $\Gamma(\Xi(1530)\pi)/\Gamma(\Sigma\bar{K})$ 

VALUE	DOCUMENT ID	TECN	CHG	COMMENT	$\Gamma_6/\Gamma_2$
<0.06	DIONISI	78 HBC	-	$K^- p$ 4.2 GeV/c	

 $\Xi(1690)$  FOOTNOTES

- From a fit to the  $\Sigma^+ K^-$  spectrum.
- From a coupled-channel analysis of the  $\Sigma^+ K^-$  and  $\Lambda\bar{K}^0$  spectra.
- A fit to the inclusive spectrum from  $\Xi^- N \rightarrow \Lambda K^- X$ .
- From a coupled-channel analysis of the  $\Sigma^0 K^-$  and  $\Lambda K^-$  spectra.

 $\Xi(1690)$  REFERENCES

AUBERT	08AK PR D78 034008	B. Aubert et al.	(BABAR Collab.)
ABE	02C PL B524 33	K. Abe et al.	(KEK BELLE Collab.)
ADAMOVICH	98 EPJ C5 621	M.I. Adamovich et al.	(CERN WA89 Collab.)
BIAGI	87 ZPHY C34 15	S.F. Biagi et al.	(BRIS, CERN, GEVA+)
BIAGI	81 ZPHY C3 305	S.F. Biagi et al.	(BRIS, CAVE, GEVA+)
DIONISI	78 PL 80B 145	C. Dionisi et al.	(CERN, AMST, NIJ+)

 $\Xi(1820) 3/2^-$ 

$$I(J^P) = \frac{1}{2}(3/2^-) \text{ Status: } ***$$

The clearest evidence is an 8-standard-deviation peak in  $\Lambda K^-$  seen by GAY 76C. TEODORO 78 favors  $J = 3/2$ , but cannot make a parity discrimination. BIAGI 87C is consistent with  $J = 3/2$  and favors negative parity for this  $J$  value.

 $\Xi(1820)$  MASS

We only average the measurements that appear to us to be most significant and best determined.

VALUE (MeV)	EVTS	DOCUMENT ID	TECN	CHG	COMMENT
<b>1823 ± 5 OUR ESTIMATE</b>					
<b>1823.4 ± 1.4 OUR AVERAGE</b>					
1819.4 ± 3.1 ± 2.0	280	<sup>1</sup> BIAGI	87 SPEC	0	$\Xi^-$ Be $\rightarrow$ ( $\Lambda K^-$ ) X
1826 ± 3 ± 1	54	BIAGI	87c SPEC	0	$\Xi^-$ Be $\rightarrow$ ( $\Lambda\bar{K}^0$ ) X
1822 ± 6		JENKINS	83 MPS	-	$K^- p \rightarrow K^+$ (MM)
1830 ± 6	300	BIAGI	81 SPEC	-	SPS hyperon beam
1823 ± 2	130	GAY	76c HBC	-	$K^- p$ 4.2 GeV/c
••• We do not use the following data for averages, fits, limits, etc. •••					
1817 ± 3		ADAMOVICH	99b WA89		$\Sigma^-$ nucleus, 345 GeV
1797 ± 19	74	BRIEFEL	77 HBC	0	$K^- p$ 2.87 GeV/c
1829 ± 9	68	BRIEFEL	77 HBC	-0	$\Xi(1530)\pi$
1860 ± 14	39	BRIEFEL	77 HBC	-	$\Sigma^- \bar{K}^0$
1870 ± 9	44	BRIEFEL	77 HBC	0	$\Lambda\bar{K}^0$
1813 ± 4	57	BRIEFEL	77 HBC	-	$\Lambda K^-$
1807 ± 27		DIBIANCA	75 DBC	-0	$\Xi\pi\pi, \Xi^*\pi$
1762 ± 8	28	<sup>2</sup> BADIÉ	72 HBC	-0	$\Xi\pi, \Xi\pi\pi, YK$
1838 ± 5	38	<sup>2</sup> BADIÉ	72 HBC	-0	$\Xi\pi, \Xi\pi\pi, YK$
1830 ± 10	25	<sup>3</sup> CRENNELL	70b DBC	-0	3.6, 3.9 GeV/c
1826 ± 12		<sup>4</sup> CRENNELL	70b DBC	-0	3.6, 3.9 GeV/c
1830 ± 10	40	ALITTI	69 HBC	-	$\Lambda, \Sigma\bar{K}$
1814 ± 4	30	BADIÉ	65 HBC	0	$\Lambda\bar{K}^0$
1817 ± 7	29	SMITH	65c HBC	-0	$\Lambda\bar{K}^0, \Lambda K^-$
1770		HALSTEINSLID63	FBC	-0	$K^-$ freon 3.5 GeV/c

 $\Xi(1820)$  WIDTH

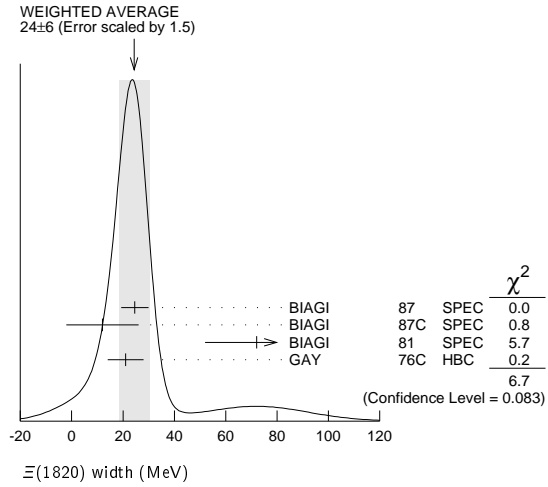
VALUE (MeV)	EVTS	DOCUMENT ID	TECN	CHG	COMMENT
<b>24 +15 -10 OUR ESTIMATE</b>					
<b>24 ± 6 OUR AVERAGE</b>					Error includes scale factor of 1.5. See the ideogram below.
24.6 ± 5.3	280	<sup>1</sup> BIAGI	87 SPEC	0	$\Xi^-$ Be $\rightarrow$ ( $\Lambda K^-$ ) X
12 ± 14 ± 1.7	54	BIAGI	87c SPEC	0	$\Xi^-$ Be $\rightarrow$ ( $\Lambda\bar{K}^0$ ) X
72 ± 20	300	BIAGI	81 SPEC	-	SPS hyperon beam
21 ± 7	130	GAY	76c HBC	-	$K^- p$ 4.2 GeV/c
••• We do not use the following data for averages, fits, limits, etc. •••					
23 ± 13		ADAMOVICH	99b WA89		$\Sigma^-$ nucleus, 345 GeV
99 ± 57	74	BRIEFEL	77 HBC	0	$K^- p$ 2.87 GeV/c
52 ± 34	68	BRIEFEL	77 HBC	-0	$\Xi(1530)\pi$
72 ± 17	39	BRIEFEL	77 HBC	-	$\Sigma^- \bar{K}^0$
44 ± 11	44	BRIEFEL	77 HBC	0	$\Lambda\bar{K}^0$
26 ± 11	57	BRIEFEL	77 HBC	-	$\Lambda K^-$
85 ± 58		DIBIANCA	75 DBC	-0	$\Xi\pi\pi, \Xi^*\pi$
51 ± 13		<sup>2</sup> BADIÉ	72 HBC	-0	Lower mass

See key on page 457

# Baryon Particle Listings

## $\Xi(1820)$

58 ± 13	2	BADIER	72	HBC	-0	Higher mass
103 +38 -24	3	CRENNELL	70B	DBC	-0	3.6, 3.9 GeV/c
48 +36 -19	4	CRENNELL	70B	DBC	-0	3.6, 3.9 GeV/c
55 +40 -20		ALITTI	69	HBC	-	$\Lambda, \Sigma \bar{K}$
12 ± 4		BADIER	65	HBC	0	$\Lambda \bar{K}^0$
30 ± 7		SMITH	65B	HBC	-0	$\Lambda \bar{K}$
< 80		HALSTEINSLID63	FBC	-0	-	$K^-$ from 3.5 GeV/c



### $\Xi(1820)$ DECAY MODES

Mode	Fraction ( $\Gamma_i/\Gamma$ )
$\Gamma_1$ $\Lambda \bar{K}$	large
$\Gamma_2$ $\Sigma \bar{K}$	small
$\Gamma_3$ $\Xi \pi$	small
$\Gamma_4$ $\Xi(1530) \pi$	small
$\Gamma_5$ $\Xi \pi \pi$ (not $\Xi(1530) \pi$ )	

### $\Xi(1820)$ BRANCHING RATIOS

The dominant modes seem to be  $\Lambda \bar{K}$  and (perhaps)  $\Xi(1530) \pi$ , but the branching fractions are very poorly determined.

$\Gamma(\Lambda \bar{K})/\Gamma_{total}$	DOCUMENT ID	TECN	CHG	COMMENT	$\Gamma_1/\Gamma$
VALUE					
<b>0.25 ± 0.05 OUR AVERAGE</b>					
0.24 ± 0.05	ANISOVICH	12A	DPWA	Multichannel	
0.30 ± 0.15	ALITTI	69	HBC	$K^- p$ 3.9-5 GeV/c	

$\Gamma(\Xi \pi)/\Gamma_{total}$	DOCUMENT ID	TECN	CHG	COMMENT	$\Gamma_3/\Gamma$
VALUE					
<b>0.10 ± 0.10</b>					
	ALITTI	69	HBC	$K^- p$ 3.9-5 GeV/c	

$\Gamma(\Xi \pi)/\Gamma(\Lambda \bar{K})$	DOCUMENT ID	TECN	CHG	COMMENT	$\Gamma_3/\Gamma_1$
VALUE					
<b>&lt; 0.36</b>					
0.20 ± 0.20	GAY	76C	HBC	$K^- p$ 4.2 GeV/c	
	BADIER	65	HBC	$K^- p$ 3 GeV/c	

$\Gamma(\Xi \pi)/\Gamma(\Xi(1530) \pi)$	DOCUMENT ID	TECN	CHG	COMMENT	$\Gamma_3/\Gamma_4$
VALUE					
<b>1.5 +0.6 -0.4</b>					
	APSELL	70	HBC	$K^- p$ 2.87 GeV/c	

$\Gamma(\Sigma \bar{K})/\Gamma_{total}$	DOCUMENT ID	TECN	CHG	COMMENT	$\Gamma_2/\Gamma$
VALUE					
<b>0.30 ± 0.15</b>					
	ALITTI	69	HBC	$K^- p$ 3.9-5 GeV/c	

• • • We do not use the following data for averages, fits, limits, etc. • • •  
< 0.02 TRIPP 67 RVUE Use SMITH 65c

$\Gamma(\Sigma \bar{K})/\Gamma(\Lambda \bar{K})$	DOCUMENT ID	TECN	CHG	COMMENT	$\Gamma_2/\Gamma_1$
VALUE					
<b>0.24 ± 0.10</b>					
	GAY	76C	HBC	$K^- p$ 4.2 GeV/c	

$\Gamma(\Xi(1530) \pi)/\Gamma_{total}$	DOCUMENT ID	TECN	CHG	COMMENT	$\Gamma_4/\Gamma$
VALUE					
<b>0.30 ± 0.15</b>					
	ALITTI	69	HBC	$K^- p$ 3.9-5 GeV/c	

• • • We do not use the following data for averages, fits, limits, etc. • • •  
seen ASTON 85B LASS  $K^- p$  11 GeV/c  
not seen 5 HASSALL 81 HBC  $K^- p$  6.5 GeV/c  
< 0.25 6 DAUBER 69 HBC  $K^- p$  2.7 GeV/c

$\Gamma(\Xi(1530) \pi)/\Gamma(\Lambda \bar{K})$	DOCUMENT ID	TECN	CHG	COMMENT	$\Gamma_4/\Gamma_1$
VALUE					
<b>0.38 ± 0.27 OUR AVERAGE</b>					
1.0 ± 0.3	GAY	76C	HBC	$K^- p$ 4.2 GeV/c	
0.26 ± 0.13	SMITH	65C	HBC	$K^- p$ 2.45-2.7 GeV/c	

$\Gamma(\Xi \pi \pi$ (not $\Xi(1530) \pi))/\Gamma(\Lambda \bar{K})$	DOCUMENT ID	TECN	CHG	COMMENT	$\Gamma_5/\Gamma_1$
VALUE					
<b>0.30 ± 0.20</b>					
	BIAGI	87	SPEC	$\Xi^-$ Be 116 GeV	
< 0.14	7 BADIER	65	HBC	0 1 st. dev. limit	
> 0.1	SMITH	65C	HBC	-0 $K^- p$ 2.45-2.7 GeV/c	

$\Gamma(\Xi \pi \pi$ (not $\Xi(1530) \pi))/\Gamma(\Xi(1530) \pi)$	DOCUMENT ID	TECN	CHG	COMMENT	$\Gamma_5/\Gamma_4$
VALUE					
consistent with zero					
	GAY	76C	HBC	$K^- p$ 4.2 GeV/c	
0.3 ± 0.5	8 APSELL	70	HBC	0 $K^- p$ 2.87 GeV/c	

### $\Xi(1820)$ FOOTNOTES

- BIAGI 87 also sees weak signals in the in the  $\Xi^- \pi^+ \pi^-$  channel at 1782.6 ± 1.4 MeV ( $\Gamma = 6.0 ± 1.5$  MeV) and 1831.9 ± 2.8 MeV ( $\Gamma = 9.6 ± 9.9$  MeV).
- BADIER 72 adds all channels and divides the peak into lower and higher mass regions. The data can also be fitted with a single Breit-Wigner of mass 1800 MeV and width 150 MeV.
- From a fit to inclusive  $\Xi \pi$ ,  $\Xi \pi \pi$ , and  $\Lambda K^-$  spectra.
- From a fit to inclusive  $\Xi \pi$  and  $\Xi \pi \pi$  spectra only.
- Including  $\Xi \pi \pi$ .
- DAUBER 69 uses in part the same data as SMITH 65c.
- For the decay mode  $\Xi^- \pi^+ \pi^0$  only. This limit includes  $\Xi(1530) \pi$ .
- Or less. Upper limit for the 3-body decay.

### $\Xi(1820)$ REFERENCES

ANISOVICH 12A	EPJ A48 15	A.V. Anisovich et al.	(BONN, PNPI)
ADAMOVIICH 99B	EPJ C11 271	M.L. Adamovich et al.	(CERN WA89 Collab.)
BIAGI 87	ZPHY C34 15	S.F. Biagi et al.	(BRIS, CERN, GEVA+)
BIAGI 87C	ZPHY C34 175	S.F. Biagi et al.	(BRIS, CERN, GEVA+)
ASTON 85B	PR D32 2270	D. Aston et al.	(SLAC, CARL, CNRC, CINC)
JENKINS 83	PRL 51 951	C.M. Jenkins et al.	(FSU, BRAN, LBL+)
BIAGI 81	ZPHY C9 305	S.F. Biagi et al.	(BRIS, CAVE, GEVA+)
HASSALL 81	NP B189 397	J.K. Hassall et al.	(CAVE, MSU)
TEODORO 78	PL 77B 451	D. Teodoro et al.	(AMST, CERN, NIJM+)
BRIEFEL 77	PR D16 2706	E. Briefel et al.	(BRAN, UMD, SYRA+)
Also	PL 23 384	S.F. Apseil et al.	(BRAN, UMD, SYRA+)
GAY 76C	PL 02B 477	J.B. Gay et al.	(AMST, CERN, NIJM+)
DIBIANCA 75	NP B98 137	F.A. Dibianca, R.J. Endorf	(CMU)
BADIER 72	NP B37 429	J. Badier et al.	(EPOL)
APSELL 70	PRL 24 777	S.P. Apseil et al.	(BRAN, UMD, SYRA+)
CRENNELL 70B	PR D1 847	D.J. Crennell et al.	(BNL)
ALITTI 69	PRL 22 79	J. Alitti et al.	(BNL, SYRA)
DAUBER 69	PR 179 1262	P.M. Dauber et al.	(LRL)
TRIPP 67	NP B3 10	R.D. Tripp et al.	(LRL, SLAC, CERN+)
BADIER 65	PL 16 171	J. Badier et al.	(EPOL, SACL, AMST)
SMITH 65B	Athens Conf. 251	G.A. Smith, J.S. Lindsey	(LRL)
SMITH 65C	PRL 14 25	G.A. Smith et al.	(LRL) IJP
HALSTEINSLID 63	Siena Conf. 1 73	A. Halsteinslid et al.	(BERG, CERN, EPOL+)

### OTHER RELATED PAPERS

TEODORO 78	PL 77B 451	D. Teodoro et al.	(AMST, CERN, NIJM+)
BRIEFEL 75	PR D12 1859	E. Briefel et al.	(BRAN, UMD, SYRA+)
SCHMIDT 73	Purdue Conf. 363	P.E. Schmidt	(BRAN)
MERRILL 68	PR 167 1202	D.W. Merrill, J. Button-Shafer	(LRL)
SMITH 64	PRL 13 61	G.A. Smith et al.	(LRL) IJP

# Baryon Particle Listings

## $\Xi(1950), \Xi(2030)$

### $\Xi(1950)$

$$I(J^P) = \frac{1}{2}(?)^? \text{ Status: } ***$$

We list here everything reported between 1875 and 2000 MeV. The accumulated evidence for a  $\Xi$  near 1950 MeV seems strong enough to include a  $\Xi(1950)$  in the main Baryon Table, but not much can be said about its properties. In fact, there may be more than one  $\Xi$  near this mass.

#### $\Xi(1950)$ MASS

VALUE (MeV)	EVTS	DOCUMENT ID	TECN	COMMENT
<b>1950 ± 15 OUR ESTIMATE</b>				
1955 ± 6		ADAMOVICH 99b	WA89	$\Sigma^-$ nucleus, 345 GeV
1944 ± 9	129	BIAGI 87	SPEC	$\Xi^- \text{Be} \rightarrow (\Xi^- \pi^+) \pi^- X$
1963 ± 5 ± 2	63	BIAGI 87c	SPEC	$\Xi^- \text{Be} \rightarrow (\Lambda \bar{K}^0) X$
1937 ± 7	150	BIAGI 81	SPEC	SPS hyperon beam
1961 ± 18	139	BRIEFEL 77	HBC	$2.87 K^- p \rightarrow \Xi^- \pi^+ X$
1936 ± 22	44	BRIEFEL 77	HBC	$2.87 K^- p \rightarrow \Xi^0 \pi^- X$
1964 ± 10	56	BRIEFEL 77	HBC	$\Xi(1530) \pi$
1900 ± 12		DIBIANCA 75	DBC	$\Xi \pi$
1952 ± 11	25	ROSS 73c		$(\Xi \pi)^-$
1956 ± 6	29	BADIER 72	HBC	$\Xi \pi, \Xi \pi \pi, Y K$
1955 ± 14	21	GOLDWASSER 70	HBC	$\Xi \pi$
1894 ± 18	66	DAUBER 69	HBC	$\Xi \pi$
1930 ± 20	27	ALITTI 68	HBC	$\Xi^- \pi^+$
1933 ± 16	35	BADIER 65	HBC	$\Xi^- \pi^+$

#### $\Xi(1950)$ WIDTH

VALUE (MeV)	EVTS	DOCUMENT ID	TECN	COMMENT
<b>60 ± 20 OUR ESTIMATE</b>				
68 ± 22		ADAMOVICH 99b	WA89	$\Sigma^-$ nucleus, 345 GeV
100 ± 31	129	BIAGI 87	SPEC	$\Xi^- \text{Be} \rightarrow (\Xi^- \pi^+) \pi^- X$
25 ± 15 ± 1.2	63	BIAGI 87c	SPEC	$\Xi^- \text{Be} \rightarrow (\Lambda \bar{K}^0) X$
60 ± 8	150	BIAGI 81	SPEC	SPS hyperon beam
159 ± 5.7	139	BRIEFEL 77	HBC	$2.87 K^- p \rightarrow \Xi^- \pi^+ X$
87 ± 26	44	BRIEFEL 77	HBC	$2.87 K^- p \rightarrow \Xi^0 \pi^- X$
60 ± 39	56	BRIEFEL 77	HBC	$\Xi(1530) \pi$
63 ± 7.8		DIBIANCA 75	DBC	$\Xi \pi$
38 ± 10		ROSS 73c		$(\Xi \pi)^-$
35 ± 11	29	BADIER 72	HBC	$\Xi \pi, \Xi \pi \pi, Y K$
56 ± 26	21	GOLDWASSER 70	HBC	$\Xi \pi$
98 ± 23	66	DAUBER 69	HBC	$\Xi \pi$
80 ± 4.0	27	ALITTI 68	HBC	$\Xi^- \pi^+$
140 ± 35	35	BADIER 65	HBC	$\Xi^- \pi^+$

#### $\Xi(1950)$ DECAY MODES

Mode	Fraction ( $\Gamma_i/\Gamma$ )
$\Gamma_1 \Lambda \bar{K}$	seen
$\Gamma_2 \Sigma \bar{K}$	possibly seen
$\Gamma_3 \Xi \pi$	seen
$\Gamma_4 \Xi(1530) \pi$	
$\Gamma_5 \Xi \pi \pi$ (not $\Xi(1530) \pi$ )	

#### $\Xi(1950)$ BRANCHING RATIOS

$\Gamma(\Sigma \bar{K})/\Gamma(\Lambda \bar{K})$					$\Gamma_2/\Gamma_1$
VALUE	CL%	EVTS	DOCUMENT ID	TECN	COMMENT
<2.3	90	0	BIAGI 87c	SPEC	$\Xi^- \text{Be} 116 \text{ GeV}$
$\Gamma(\Sigma \bar{K})/\Gamma_{\text{total}}$					$\Gamma_2/\Gamma$
VALUE	CL%	EVTS	DOCUMENT ID	TECN	COMMENT
possibly seen		17	HASSALL 81	HBC	$K^- p 6.5 \text{ GeV/c}$
$\Gamma(\Xi \pi)/\Gamma(\Xi(1530) \pi)$					$\Gamma_3/\Gamma_4$
VALUE	CL%	EVTS	DOCUMENT ID	TECN	COMMENT
$2.8^{+0.7}_{-0.6}$			APSELL 70	HBC	
$\Gamma(\Xi \pi \pi \text{ (not } \Xi(1530) \pi))/\Gamma(\Xi(1530) \pi)$					$\Gamma_5/\Gamma_4$
VALUE	CL%	EVTS	DOCUMENT ID	TECN	COMMENT
$0.0 \pm 0.3$			APSELL 70	HBC	

### $\Xi(1950)$ REFERENCES

ADAMOVICH 99b	EPJ C11 271	M.I. Adamovich et al.	(CERN WA89 Collab.)
BIAGI 87	ZPHY C34 15	S.F. Biagi et al.	(BRIS, CERN, GEVA+)
BIAGI 87c	ZPHY C34 175	S.F. Biagi et al.	(BRIS, CERN, GEVA+)
BIAGI 81	ZPHY C9 305	S.F. Biagi et al.	(BRIS, CAVE, GEVA+)
HASSALL 81	NP B189 397	J.K. Hassall et al.	(CAVE, MSU)
BRIEFEL 77	PR D16 2706	E. Briefel et al.	(BRAN, UMD, SYRA+)
Also	Duke Conf. 317	E. Briefel et al.	(BRAN, UMD, SYRA+)
Hyperon Resonances, 1970			
DIBIANCA 75	NP B98 137	F.A. Dibianna, R.J. Endorf	(CMU)
ROSS 73c	Purdue Conf. 345	R.T. Ross, J.L. Lloyd, D. Radojicic	(OXF)
BADIER 72	NP B37 429	J. Badier et al.	(EPOL)
APSELL 70	PRL 24 777	S.P. Apseil et al.	(BRAN, UMD, SYRA+)
GOLDWASSER 70	PR D1 1960	E.L. Goldwasser, P.F. Schultz	(ILL)
DAUBER 69	PR 179 1262	P.M. Dauber et al.	(LRL)
ALITTI 68	PRL 21 1119	J. Alitti et al.	(BNL, SYRA)
BADIER 65	PL 16 171	J. Badier et al.	(EPOL, SACL, AMST)

### $\Xi(2030)$

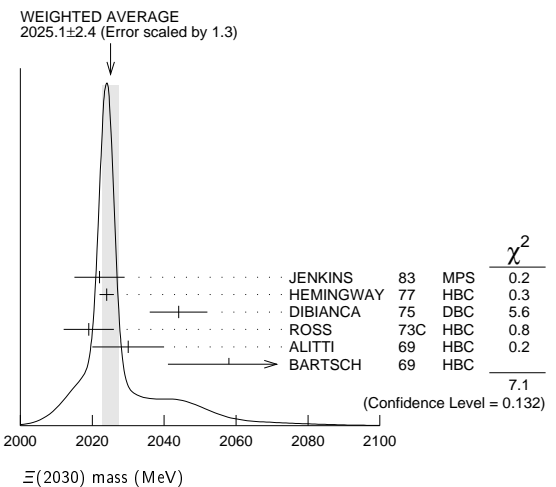
$$I(J^P) = \frac{1}{2}(\geq \frac{5}{2})^? \text{ Status: } ***$$

The evidence for this state has been much improved by HEMINGWAY 77, who see an eight standard deviation enhancement in  $\Sigma \bar{K}$  and a weaker coupling to  $\Lambda \bar{K}$ . ALITTI 68 and HEMINGWAY 77 observe no signals in the  $\Xi \pi \pi$  (or  $\Xi(1530) \pi$ ) channel, in contrast to DIBIANCA 75. The decay  $(\Lambda/\Sigma) \bar{K} \pi$  reported by BARTSCH 69 is also not confirmed by HEMINGWAY 77.

A moments analysis of the HEMINGWAY 77 data indicates at a level of three standard deviations that  $J \geq 5/2$ .

#### $\Xi(2030)$ MASS

VALUE (MeV)	EVTS	DOCUMENT ID	TECN	CHG	COMMENT
<b>2025 ± 5 OUR ESTIMATE</b>					
<b>2025.1 ± 2.4 OUR AVERAGE</b> Error includes scale factor of 1.3. See the ideogram below.					
2022 ± 7		JENKINS 83	MPS	-	$K^- p \rightarrow K^+$
					MM
2024 ± 2	200	HEMINGWAY 77	HBC	-	$K^- p 4.2 \text{ GeV/c}$
2044 ± 8		DIBIANCA 75	DBC	-0	$\Xi \pi \pi, \Xi^* \pi$
2019 ± 7	15	ROSS 73c	HBC	-0	$\Sigma \bar{K}$
2030 ± 10	42	ALITTI 69	HBC	-	$K^- p 3.9-5 \text{ GeV/c}$
2058 ± 17	40	BARTSCH 69	HBC	-0	$K^- p 10 \text{ GeV/c}$

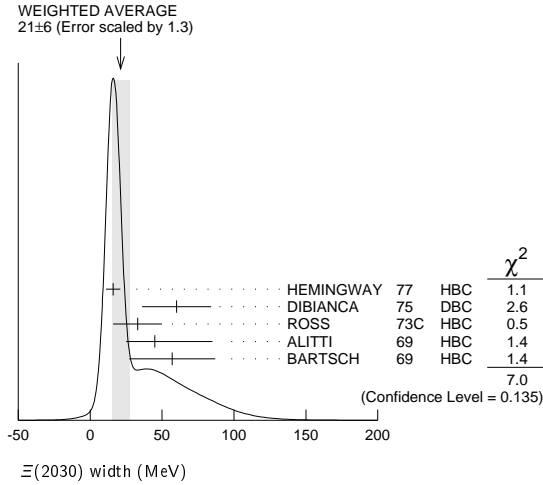


#### $\Xi(2030)$ WIDTH

VALUE (MeV)	EVTS	DOCUMENT ID	TECN	CHG	COMMENT
<b>20 ± 15 OUR ESTIMATE</b>					
<b>21 ± 6 OUR AVERAGE</b> Error includes scale factor of 1.3. See the ideogram below.					
16 ± 5	200	HEMINGWAY 77	HBC	-	$K^- p 4.2 \text{ GeV/c}$
60 ± 24		DIBIANCA 75	DBC	-0	$\Xi \pi \pi, \Xi^* \pi$
33 ± 17	15	ROSS 73c	HBC	-0	$\Sigma \bar{K}$
$45^{+40}_{-20}$		ALITTI 69	HBC	-	$K^- p 3.9-5 \text{ GeV/c}$
57 ± 30		BARTSCH 69	HBC	-0	$K^- p 10 \text{ GeV/c}$

See key on page 457

Baryon Particle Listings  
 $\Xi(2030)$ ,  $\Xi(2120)$



$\Xi(2030)$  DECAY MODES

Mode	Fraction ( $\Gamma_i/\Gamma$ )
$\Gamma_1$ $\Lambda\bar{K}$	~ 20 %
$\Gamma_2$ $\Sigma\bar{K}$	~ 80 %
$\Gamma_3$ $\Xi\pi$	small
$\Gamma_4$ $\Xi(1530)\pi$	small
$\Gamma_5$ $\Xi\pi\pi$ (not $\Xi(1530)\pi$ )	small
$\Gamma_6$ $\Lambda\bar{K}\pi$	small
$\Gamma_7$ $\Sigma\bar{K}\pi$	small

$\Xi(2030)$  BRANCHING RATIOS

$\Gamma(\Xi\pi)/[\Gamma(\Lambda\bar{K}) + \Gamma(\Sigma\bar{K}) + \Gamma(\Xi\pi) + \Gamma(\Xi(1530)\pi)]$	$\Gamma_3/(\Gamma_1+\Gamma_2+\Gamma_3+\Gamma_4)$
VALUE	DOCUMENT ID TECN CHG COMMENT
<0.30	ALITTI 69 HBC - 1 standard dev. limit

$\Gamma(\Xi\pi)/\Gamma(\Sigma\bar{K})$	$\Gamma_3/\Gamma_2$
VALUE	DOCUMENT ID TECN CHG COMMENT
<0.19	95 HEMINGWAY 77 HBC - $K^-p$ 4.2 GeV/c

$\Gamma(\Lambda\bar{K})/[\Gamma(\Lambda\bar{K}) + \Gamma(\Sigma\bar{K}) + \Gamma(\Xi\pi) + \Gamma(\Xi(1530)\pi)]$	$\Gamma_1/(\Gamma_1+\Gamma_2+\Gamma_3+\Gamma_4)$
VALUE	DOCUMENT ID TECN CHG COMMENT
$0.25 \pm 0.15$	ALITTI 69 HBC - $K^-p$ 3.9-5 GeV/c

$\Gamma(\Lambda\bar{K})/\Gamma(\Sigma\bar{K})$	$\Gamma_1/\Gamma_2$
VALUE	DOCUMENT ID TECN CHG COMMENT
$0.22 \pm 0.09$	HEMINGWAY 77 HBC - $K^-p$ 4.2 GeV/c

$\Gamma(\Sigma\bar{K})/[\Gamma(\Lambda\bar{K}) + \Gamma(\Sigma\bar{K}) + \Gamma(\Xi\pi) + \Gamma(\Xi(1530)\pi)]$	$\Gamma_2/(\Gamma_1+\Gamma_2+\Gamma_3+\Gamma_4)$
VALUE	DOCUMENT ID TECN CHG COMMENT
$0.75 \pm 0.20$	ALITTI 69 HBC - $K^-p$ 3.9-5 GeV/c

$\Gamma(\Xi(1530)\pi)/[\Gamma(\Lambda\bar{K}) + \Gamma(\Sigma\bar{K}) + \Gamma(\Xi\pi) + \Gamma(\Xi(1530)\pi)]$	$\Gamma_4/(\Gamma_1+\Gamma_2+\Gamma_3+\Gamma_4)$
VALUE	DOCUMENT ID TECN CHG COMMENT
<0.15	ALITTI 69 HBC - 1 standard dev. limit

$[\Gamma(\Xi(1530)\pi) + \Gamma(\Xi\pi\pi \text{ (not } \Xi(1530)\pi))]/\Gamma(\Sigma\bar{K})$	$(\Gamma_4+\Gamma_5)/\Gamma_2$
VALUE	DOCUMENT ID TECN CHG COMMENT
<0.11	95 HEMINGWAY 77 HBC - $K^-p$ 4.2 GeV/c

$\Gamma(\Lambda\bar{K}\pi)/\Gamma_{\text{total}}$	$\Gamma_6/\Gamma$
VALUE	DOCUMENT ID TECN COMMENT
seen	BARTSCH 69 HBC $K^-p$ 10 GeV

$\Gamma(\Lambda\bar{K}\pi)/\Gamma(\Sigma\bar{K})$	$\Gamma_6/\Gamma_2$
VALUE	DOCUMENT ID TECN CHG COMMENT
<0.32	95 HEMINGWAY 77 HBC - $K^-p$ 4.2 GeV/c

$\Gamma(\Sigma\bar{K}\pi)/\Gamma_{\text{total}}$	$\Gamma_7/\Gamma$
VALUE	DOCUMENT ID TECN COMMENT
seen	BARTSCH 69 HBC $K^-p$ 10 GeV

$\Gamma(\Sigma\bar{K}\pi)/\Gamma(\Sigma\bar{K})$	$\Gamma_7/\Gamma_2$
VALUE	CL% DOCUMENT ID TECN CHG COMMENT
<0.04	95 HEMINGWAY 77 HBC - $K^-p$ 4.2 GeV/c

$\Xi(2030)$  FOOTNOTES

- <sup>1</sup> For the decay mode  $\Xi^- \pi^+ \pi^-$  only.
- <sup>2</sup> For the decay mode  $\Sigma^\pm K^- \pi^\mp$  only.

$\Xi(2030)$  REFERENCES

JENKINS 83	PRL 51 951	C.M. Jenkins et al.	(FSU, BRAN, LBL+)
HEMINGWAY 77	PL 68B 197	R.J. Hemingway et al.	(AMST, CERN, NIJM+)
Also	PL 62B 477	J.B. Gay et al.	(AMST, CERN, NIJM)
DIBIANCA 75	NP B98 137	F.A. Dibianca, R.J. Endorf	(CMU)
ROSS 73C	Purdue Conf. 345	R.T. Ross, J.L. Lloyd, D. Radojicic	(OXF)
ALITTI 69	PRL 22 79	J. Alitti et al.	(BNL, SYRA)
BARTSCH 69	PL 28B 439	J. Bartsch et al.	(AACH, BERL, CERN+)
ALITTI 68	PRL 21 1119	J. Alitti et al.	(BNL, SYRA)

$\Xi(2120)$

$I(J^P) = \frac{1}{2}(?)^?$  Status: \*  
 J, P need confirmation.

OMITTED FROM SUMMARY TABLE

$\Xi(2120)$  MASS

VALUE (MeV)	EVTS	DOCUMENT ID	TECN	COMMENT
$\approx 2120$ OUR ESTIMATE				
$2137 \pm 4$	18	<sup>1</sup> CHLIAPNIK...	79 HBC	$K^+p$ 32 GeV/c
$2123 \pm 7$		<sup>2</sup> GAY	76c HBC	$K^-p$ 4.2 GeV/c

$\Xi(2120)$  WIDTH

VALUE (MeV)	EVTS	DOCUMENT ID	TECN	COMMENT
<20	18	<sup>1</sup> CHLIAPNIK...	79 HBC	$K^+p$ 32 GeV/c
$25 \pm 12$		<sup>2</sup> GAY	76c HBC	$K^-p$ 4.2 GeV/c

$\Xi(2120)$  DECAY MODES

Mode	Fraction ( $\Gamma_i/\Gamma$ )
$\Gamma_1$ $\Lambda\bar{K}$	seen

$\Xi(2120)$  BRANCHING RATIOS

$\Gamma(\Lambda\bar{K})/\Gamma_{\text{total}}$	$\Gamma_1/\Gamma$
VALUE	DOCUMENT ID TECN COMMENT
seen	<sup>1</sup> CHLIAPNIK... 79 HBC $K^+p \rightarrow (\bar{\Lambda} K^+) X$
seen	<sup>2</sup> GAY 76c HBC $K^-p$ 4.2 GeV/c

$\Xi(2120)$  FOOTNOTES

- <sup>1</sup> CHLIAPNIKOV 79 does not uniquely identify the  $K^+$  in the  $(\bar{\Lambda} K^+) X$  final state. It also reports bumps with fewer events at 2240, 2540, and 2830 MeV.
- <sup>2</sup> GAY 76c sees a 4-standard deviation signal. However, HEMINGWAY 77, with more events from the same experiment points out that the signal is greatly reduced if a cut is made on the 4-momentum  $u$ . This suggests an anomalous production mechanism if the  $\Xi(2120)$  is real.

$\Xi(2120)$  REFERENCES

CHLIAPNIK... 79	NP B158 253	P.V. Chliapnikov et al.	(CERN, BELG, MONS)
HEMINGWAY 77	PL 68B 197	R.J. Hemingway et al.	(AMST, CERN, NIJM+)
GAY 76c	PL 62B 477	J.B. Gay et al.	(AMST, CERN, NIJM)

## Baryon Particle Listings

 $\Xi(2250)$ ,  $\Xi(2370)$ ,  $\Xi(2500)$  $\Xi(2250)$ 
 $I(J^P) = \frac{1}{2}(?)$  Status: \*\*  
 $J, P$  need confirmation.

OMITTED FROM SUMMARY TABLE

The evidence for this state is mixed. BARTSCH 69 sees a bump of not much statistical significance in  $\Lambda\bar{K}\pi$ ,  $\Sigma\bar{K}\pi$ , and  $\Xi\pi\pi$  mass spectra. GOLDWASSER 70 sees a narrower bump in  $\Xi\pi\pi$  at a higher mass. Not seen by HASSALL 81 with 45 events/ $\mu\text{b}$  at 6.5 GeV/c. Seen by JENKINS 83. Perhaps seen by BIAGI 87.

 $\Xi(2250)$  MASS

VALUE (MeV)	EVTS	DOCUMENT ID	TECN	CHG	COMMENT
<b><math>\approx 2250</math> OUR ESTIMATE</b>					
2189 $\pm$ 7	66	BIAGI	87	SPEC	$\Xi^- \text{Be} \rightarrow (\Xi^- \pi^+ \pi^-)$ X
2214 $\pm$ 5		JENKINS	83	MPS	$K^- p \rightarrow K^+$ MM
2295 $\pm$ 15	18	GOLDWASSER 70	HBC	-	$K^- p$ 5.5 GeV/c
2244 $\pm$ 52	35	BARTSCH 69	HBC	-	$K^- p$ 10 GeV/c

 $\Xi(2250)$  WIDTH

VALUE (MeV)	EVTS	DOCUMENT ID	TECN	CHG	COMMENT
46 $\pm$ 27	66	BIAGI	87	SPEC	$\Xi^- \text{Be} \rightarrow (\Xi^- \pi^+ \pi^-)$ X
< 30		GOLDWASSER 70	HBC	-	$K^- p$ 5.5 GeV/c
130 $\pm$ 80		BARTSCH 69	HBC	-	

 $\Xi(2250)$  DECAY MODES

Mode	Fraction ( $\Gamma_i/\Gamma$ )
$\Gamma_1$ $\Xi\pi\pi$	
$\Gamma_2$ $\Lambda\bar{K}\pi$	
$\Gamma_3$ $\Sigma\bar{K}\pi$	

 $\Xi(2250)$  REFERENCES

BIAGI 87	ZPHY C34 15	S.F. Biagi <i>et al.</i>	(BRIS, CERN, GEVA+)
JENKINS 83	PRL 51 951	C.M. Jenkins <i>et al.</i>	(FSU, BRAN, LBL+)
HASSALL 81	NP B189 397	J.K. Hassall <i>et al.</i>	(CAVE, MSU)
GOLDWASSER 70	PR D1 1960	E.L. Goldwasser, P.F. Schultz	(ILL)
BARTSCH 69	PL 28B 439	J. Bartsch <i>et al.</i>	(AACH, BERL, CERN+)

 $\Xi(2370)$ 
 $I(J^P) = \frac{1}{2}(?)$  Status: \*\*  
 $J, P$  need confirmation.

OMITTED FROM SUMMARY TABLE

 $\Xi(2370)$  MASS

VALUE (MeV)	EVTS	DOCUMENT ID	TECN	CHG	COMMENT
<b><math>\approx 2370</math> OUR ESTIMATE</b>					
2356 $\pm$ 10		JENKINS	83	MPS	$K^- p \rightarrow K^+$ MM
2370	50	HASSALL 81	HBC	-0	$K^- p$ 6.5 GeV/c
2373 $\pm$ 8	94	AMIRZADEH 80	HBC	-0	$K^- p$ 8.25 GeV/c
2392 $\pm$ 27		DIBIANCA 75	DBC	-	$\Xi 2\pi$

 $\Xi(2370)$  WIDTH

VALUE (MeV)	EVTS	DOCUMENT ID	TECN	CHG	COMMENT
80	50	HASSALL 81	HBC	-0	$K^- p$ 6.5 GeV/c
80 $\pm$ 25	94	AMIRZADEH 80	HBC	-0	$K^- p$ 8.25 GeV/c
75 $\pm$ 69		DIBIANCA 75	DBC	-	$\Xi 2\pi$

 $\Xi(2370)$  DECAY MODES

Mode	Fraction ( $\Gamma_i/\Gamma$ )
$\Gamma_1$ $\Lambda\bar{K}\pi$ Includes $\Gamma_4 + \Gamma_6$ .	seen
$\Gamma_2$ $\Sigma\bar{K}\pi$ Includes $\Gamma_5 + \Gamma_6$ .	seen
$\Gamma_3$ $\Omega^- K$	
$\Gamma_4$ $\Lambda\bar{K}^*(892)$	
$\Gamma_5$ $\Sigma\bar{K}^*(892)$	
$\Gamma_6$ $\Sigma(1385)\bar{K}$	

 $\Xi(2370)$  BRANCHING RATIOS

$\Gamma(\Lambda\bar{K}\pi)/\Gamma_{\text{total}}$	DOCUMENT ID	TECN	CHG	COMMENT	$\Gamma_1/\Gamma$
seen	AMIRZADEH 80	HBC	-0	$K^- p$ 8.25 GeV/c	

$\Gamma(\Sigma\bar{K}\pi)/\Gamma_{\text{total}}$	DOCUMENT ID	TECN	CHG	COMMENT	$\Gamma_2/\Gamma$
seen	AMIRZADEH 80	HBC	-0	$K^- p$ 8.25 GeV/c	

$[\Gamma(\Lambda\bar{K}\pi) + \Gamma(\Sigma\bar{K}\pi)]/\Gamma_{\text{total}}$	DOCUMENT ID	TECN	CHG	COMMENT	$(\Gamma_1 + \Gamma_2)/\Gamma$
seen	HASSALL 81	HBC	-0	$K^- p$ 6.5 GeV/c	

$\Gamma(\Omega^- K)/\Gamma_{\text{total}}$	DOCUMENT ID	TECN	CHG	COMMENT	$\Gamma_3/\Gamma$
0.09 $\pm$ 0.04	<sup>1</sup> KINSON 80	HBC	-	$K^- p$ 8.25 GeV/c	

$[\Gamma(\Lambda\bar{K}^*(892)) + \Gamma(\Sigma\bar{K}^*(892))]/\Gamma_{\text{total}}$	DOCUMENT ID	TECN	CHG	COMMENT	$(\Gamma_4 + \Gamma_5)/\Gamma$
0.22 $\pm$ 0.13	<sup>1</sup> KINSON 80	HBC	-	$K^- p$ 8.25 GeV/c	

$\Gamma(\Sigma(1385)\bar{K})/\Gamma_{\text{total}}$	DOCUMENT ID	TECN	CHG	COMMENT	$\Gamma_6/\Gamma$
0.12 $\pm$ 0.08	<sup>1</sup> KINSON 80	HBC	-	$K^- p$ 8.25 GeV/c	

 $\Xi(2370)$  FOOTNOTES<sup>1</sup> KINSON 80 is a reanalysis of AMIRZADEH 80 with 50% more events. $\Xi(2370)$  REFERENCES

JENKINS 83	PRL 51 951	C.M. Jenkins <i>et al.</i>	(FSU, BRAN, LBL+)
HASSALL 81	NP B189 397	J.K. Hassall <i>et al.</i>	(CAVE, MSU)
AMIRZADEH 80	PL 90B 324	J. Amirzadeh <i>et al.</i>	(BIRM, CERN, GLAS+)
KINSON 80	Toronto Conf. 263	J.B. Kinson <i>et al.</i>	(BIRM, CERN, GLAS+)
DIBIANCA 75	NP B98 137	F.A. Dibianca, R.J. Endorf	(CMU)

 $\Xi(2500)$ 
 $I(J^P) = \frac{1}{2}(?)$  Status: \*  
 $J, P$  need confirmation.

OMITTED FROM SUMMARY TABLE

The ALITTI 69 peak might be instead the  $\Xi(2370)$  or might be neither the  $\Xi(2370)$  nor the  $\Xi(2500)$ .

 $\Xi(2500)$  MASS

VALUE (MeV)	EVTS	DOCUMENT ID	TECN	CHG	COMMENT
<b><math>\approx 2500</math> OUR ESTIMATE</b>					
2505 $\pm$ 10		JENKINS	83	MPS	$K^- p \rightarrow K^+$ MM
2430 $\pm$ 20	30	ALITTI 69	HBC	-	$K^- p$ 4.6-5 GeV/c
2500 $\pm$ 10	45	BARTSCH 69	HBC	-0	$K^- p$ 10 GeV/c

 $\Xi(2500)$  WIDTH

VALUE (MeV)	DOCUMENT ID	TECN	CHG
150 $^{+60}_{-40}$	ALITTI 69	HBC	-
59 $\pm$ 27	BARTSCH 69	HBC	-0

 $\Xi(2500)$  DECAY MODES

Mode	Fraction ( $\Gamma_i/\Gamma$ )
$\Gamma_1$ $\Xi\pi$	
$\Gamma_2$ $\Lambda\bar{K}$	
$\Gamma_3$ $\Sigma\bar{K}$	
$\Gamma_4$ $\Xi\pi\pi$	seen
$\Gamma_5$ $\Xi(1530)\pi$	
$\Gamma_6$ $\Lambda\bar{K}\pi + \Sigma\bar{K}\pi$	seen

 $\Xi(2500)$  BRANCHING RATIOS

$\Gamma(\Xi\pi)/[\Gamma(\Xi\pi) + \Gamma(\Lambda\bar{K}) + \Gamma(\Sigma\bar{K}) + \Gamma(\Xi(1530)\pi)]$	DOCUMENT ID	TECN	CHG	COMMENT	$\Gamma_1/(\Gamma_1 + \Gamma_2 + \Gamma_3 + \Gamma_5)$
< 0.5	ALITTI 69	HBC	-	1 standard dev. limit	

$\Gamma(\Lambda\bar{K})/[\Gamma(\Xi\pi) + \Gamma(\Lambda\bar{K}) + \Gamma(\Sigma\bar{K}) + \Gamma(\Xi(1530)\pi)]$	DOCUMENT ID	TECN	CHG
0.5 $\pm$ 0.2	ALITTI 69	HBC	-



See key on page 457

Baryon Particle Listings  
 $\Xi(2500)$

$\Gamma(\Sigma\bar{K}) / [\Gamma(\Xi\pi) + \Gamma(\Lambda\bar{K}) + \Gamma(\Sigma\bar{K}) + \Gamma(\Xi(1530)\pi)]$				$\Gamma_3 / (\Gamma_1 + \Gamma_2 + \Gamma_3 + \Gamma_5)$
VALUE	DOCUMENT ID	TECN	CHG	
0.5 ± 0.2	ALITTI	69	HBC	-

$\Gamma(\Xi(1530)\pi) / [\Gamma(\Xi\pi) + \Gamma(\Lambda\bar{K}) + \Gamma(\Sigma\bar{K}) + \Gamma(\Xi(1530)\pi)]$				$\Gamma_5 / (\Gamma_1 + \Gamma_2 + \Gamma_3 + \Gamma_5)$
VALUE	DOCUMENT ID	TECN	COMMENT	
<0.2	ALITTI	69	HBC	1 standard dev. limit

$\Gamma(\Xi\pi\pi) / \Gamma_{total}$				$\Gamma_4 / \Gamma$
VALUE	DOCUMENT ID	TECN	CHG	
seen	BARTSCH	69	HBC	-0

$[\Gamma(\Lambda\bar{K}\pi) + \Gamma(\Sigma\bar{K}\pi)] / \Gamma_{total}$				$\Gamma_6 / \Gamma$
VALUE	DOCUMENT ID	TECN	CHG	
seen	BARTSCH	69	HBC	-0

$\Xi(2500)$  REFERENCES

JENKINS	83	PRL 51 951	C.M. Jenkins <i>et al.</i>	(FSU, BRAN, LBL+)
ALITTI	69	PRL 22 79	J. Alitti <i>et al.</i>	(BNL, SYR)1
BARTSCH	69	PL 28B 439	J. Bartsch <i>et al.</i>	(AACH, BERL, CERN+)

## Baryon Particle Listings

 $\Omega^-$  **$\Omega^-$  BARYONS**  
( $S = -3, I = 0$ )

$$\Omega^- = sss$$

 $\Omega^-$ 

$$I(J^P) = 0(\frac{3}{2}^+) \text{ Status: } ****$$

The unambiguous discovery in both production and decay was by BARNES 64. The quantum numbers follow from the assignment of the particle to the baryon decuplet. DEUTSCHMANN 78 and BAUBILLIER 78 rule out  $J = 1/2$  and find consistency with  $J = 3/2$ . AUBERT, BE 06 finds from the decay angular distributions of  $\Xi_c^0 \rightarrow \Omega^- K^+$  and  $\Omega_c^0 \rightarrow \Omega^- K^+$  that  $J = 3/2$ ; this depends on the spins of the  $\Xi_c^0$  and  $\Omega_c^0$  being  $J = 1/2$ , their supposed values.

We have omitted some results that have been superseded by later experiments. See our earlier editions.

 **$\Omega^-$  MASS**

The fit assumes the  $\Omega^-$  and  $\bar{\Omega}^+$  masses are the same, and averages them together.

VALUE (MeV)	EVTS	DOCUMENT ID	TECN	COMMENT
<b>1672.45 ± 0.29 OUR FIT</b>				
<b>1672.43 ± 0.32 OUR AVERAGE</b>				
1673 ± 1	100	HARTOUNI 85	SPEC	80–280 GeV $K_L^0 C$
1673.0 ± 0.8	41	BAUBILLIER 78	HBC	8.25 GeV/c $K^- p$
1671.7 ± 0.6	27	HEMINGWAY 78	HBC	4.2 GeV/c $K^- p$
1673.4 ± 1.7	4	<sup>1</sup> DIBIANCA 75	DBC	4.9 GeV/c $K^- d$
1673.3 ± 1.0	3	PALMER 68	HBC	$K^- p$ 4.6, 5 GeV/c
1671.8 ± 0.8	3	SCHULTZ 68	HBC	$K^- p$ 5.5 GeV/c
1674.2 ± 1.6	5	SCOTTER 68	HBC	$K^- p$ 6 GeV/c
1672.1 ± 1.0	1	<sup>2</sup> FRY 55	EMUL	
• • • We do not use the following data for averages, fits, limits, etc. • • •				
1671.43 ± 0.78	13	<sup>3</sup> DEUTSCH... 73	HBC	$K^- p$ 10 GeV/c
1671.9 ± 1.2	6	<sup>3</sup> SPETH 69	HBC	See DEUTSCHMANN 73
1673.0 ± 8.0	1	ABRAMS 64	HBC	$\rightarrow \Xi^- \pi^0$
1670.6 ± 1.0	1	<sup>2</sup> FRY 55B	EMUL	
1615	1	<sup>4</sup> EISENBERG 54	EMUL	

<sup>1</sup>DIBIANCA 75 gives a mass for each event. We quote the average.

<sup>2</sup>The FRY 55 and FRY 55B events were identified as  $\Omega^-$  by ALVAREZ 73. The masses assume decay to  $\Lambda K^-$  at rest. For FRY 55B, decay from an atomic orbit could Doppler shift the  $K^-$  energy and the resulting  $\Omega^-$  mass by several MeV. This shift is negligible for FRY 55 because the  $\Omega$  decay is approximately perpendicular to its orbital velocity, as is known because the  $\Lambda$  strikes the nucleus (L.Alvarez, private communication 1973). We have calculated the error assuming that the orbital n is 4 or larger.

<sup>3</sup>Excluded from the average; the  $\Omega^-$  lifetimes measured by the experiments differ significantly from other measurements.

<sup>4</sup>The EISENBERG 54 mass was calculated for decay in flight. ALVAREZ 73 has shown that the  $\Omega$  interacted with an Ag nucleus to give  $K^- \Xi Ag$ .

 **$\bar{\Omega}^+$  MASS**

The fit assumes the  $\Omega^-$  and  $\bar{\Omega}^+$  masses are the same, and averages them together.

VALUE (MeV)	EVTS	DOCUMENT ID	TECN	COMMENT
<b>1672.45 ± 0.29 OUR FIT</b>				
<b>1672.5 ± 0.7 OUR AVERAGE</b>				
1672 ± 1	72	HARTOUNI 85	SPEC	80–280 GeV $K_L^0 C$
1673.1 ± 1.0	1	FIRESTONE 71B	HBC	12 GeV/c $K^+ d$

$$(m_{\Omega^-} - m_{\bar{\Omega}^+}) / m_{\Omega^-}$$

A test of  $CPT$  invariance.

VALUE	DOCUMENT ID	TECN	COMMENT
<b>(-1.44 ± 7.98) × 10<sup>-5</sup></b>	CHAN 98	E756	$p$ Be, 800 GeV

 **$\Omega^-$  MEAN LIFE**

Measurements with an error  $> 0.1 \times 10^{-10}$  s have been omitted. The fit assumes the  $\Omega^-$  and  $\bar{\Omega}^+$  mean lives are the same, and averages them together.

VALUE (10 <sup>-10</sup> s)	EVTS	DOCUMENT ID	TECN	COMMENT
<b>0.821 ± 0.011 OUR FIT</b>				
<b>0.821 ± 0.011 OUR AVERAGE</b>				
0.817 ± 0.013 ± 0.018	6934	CHAN 98	E756	$p$ Be, 800 GeV
0.811 ± 0.037	1096	LUK 88	SPEC	$p$ Be 400 GeV
0.823 ± 0.013	12k	BOURQUIN 84	SPEC	SPS hyperon beam
• • • We do not use the following data for averages, fits, limits, etc. • • •				

0.822 ± 0.028 2437 BOURQUIN 79B SPEC See BOURQUIN 84

 **$\bar{\Omega}^+$  MEAN LIFE**

The fit assumes the  $\Omega^-$  and  $\bar{\Omega}^+$  mean lives are the same, and averages them together.

VALUE (10 <sup>-10</sup> s)	EVTS	DOCUMENT ID	TECN	COMMENT
<b>0.821 ± 0.011 OUR FIT</b>				
<b>0.823 ± 0.031 ± 0.022</b>	1801	CHAN 98	E756	$p$ Be, 800 GeV

$$(\tau_{\Omega^-} - \tau_{\bar{\Omega}^+}) / \tau_{\Omega^-}$$

A test of  $CPT$  invariance. Our calculation, from the averages in the preceding two data blocks.

VALUE	DOCUMENT ID
<b>0.00 ± 0.05 OUR ESTIMATE</b>	

 **$\Omega^-$  MAGNETIC MOMENT**

VALUE ( $\mu_N$ )	EVTS	DOCUMENT ID	TECN	COMMENT
<b>-2.02 ± 0.05 OUR AVERAGE</b>				
-2.024 ± 0.056	235k	WALLACE 95	SPEC	$\Omega^-$ 300–550 GeV
-1.94 ± 0.17 ± 0.14	25k	DIEHL 91	SPEC	Spin-transfer production

 **$\Omega^-$  DECAY MODES**

Mode	Fraction ( $\Gamma_i/\Gamma$ )	Confidence level
$\Gamma_1 \Lambda K^-$	(67.8 ± 0.7) %	
$\Gamma_2 \Xi^0 \pi^-$	(23.6 ± 0.7) %	
$\Gamma_3 \Xi^- \pi^0$	(8.6 ± 0.4) %	
$\Gamma_4 \Xi^- \pi^+ \pi^-$	(3.7 <sup>+0.7</sup> <sub>-0.6</sub> ) × 10 <sup>-4</sup>	
$\Gamma_5 \Xi(1530)^0 \pi^-$	< 7 × 10 <sup>-5</sup>	90%
$\Gamma_6 \Xi^0 e^- \bar{\nu}_e$	(5.6 ± 2.8) × 10 <sup>-3</sup>	
$\Gamma_7 \Xi^- \gamma$	< 4.6 × 10 <sup>-4</sup>	90%

 **$\Delta S = 2$  forbidden ( $S_2$ ) modes**

$\Gamma_8 \Lambda \pi^-$	$S_2$	< 2.9 × 10 <sup>-6</sup>	90%
--------------------------	-------	--------------------------	-----

 **$\Omega^-$  BRANCHING RATIOS**

The BOURQUIN 84 values (which include results of BOURQUIN 79B, a separate experiment) are much more accurate than any other results, and so the other results have been omitted.

$\Gamma(\Lambda K^-)/\Gamma_{\text{total}}$	VALUE	EVTS	DOCUMENT ID	TECN	COMMENT	$\Gamma_1/\Gamma$
	<b>0.678 ± 0.007</b>	14k	BOURQUIN 84	SPEC	SPS hyperon beam	
	• • • We do not use the following data for averages, fits, limits, etc. • • •					
	0.686 ± 0.013	1920	BOURQUIN 79B	SPEC	See BOURQUIN 84	

$\Gamma(\Xi^0 \pi^-)/\Gamma_{\text{total}}$	VALUE	EVTS	DOCUMENT ID	TECN	COMMENT	$\Gamma_2/\Gamma$
	<b>0.236 ± 0.007</b>	1947	BOURQUIN 84	SPEC	SPS hyperon beam	
	• • • We do not use the following data for averages, fits, limits, etc. • • •					
	0.234 ± 0.013	317	BOURQUIN 79B	SPEC	See BOURQUIN 84	

$\Gamma(\Xi^- \pi^0)/\Gamma_{\text{total}}$	VALUE	EVTS	DOCUMENT ID	TECN	COMMENT	$\Gamma_3/\Gamma$
	<b>0.086 ± 0.004</b>	759	BOURQUIN 84	SPEC	SPS hyperon beam	
	• • • We do not use the following data for averages, fits, limits, etc. • • •					
	0.080 ± 0.008	145	BOURQUIN 79B	SPEC	See BOURQUIN 84	

$\Gamma(\Xi^- \pi^+ \pi^-)/\Gamma_{\text{total}}$	VALUE (units 10 <sup>-4</sup> )	EVTS	DOCUMENT ID	TECN	COMMENT	$\Gamma_4/\Gamma$
	<b>3.74<sup>+0.67</sup><sub>-0.56</sub></b>	100	<sup>5</sup> KAMAEV 10	HYCP	$p$ Cu, 800 GeV	
	• • • We do not use the following data for averages, fits, limits, etc. • • •					
	4.3 <sup>+3.4</sup> <sub>-1.3</sub>	4	BOURQUIN 84	SPEC	SPS hyperon beam	

<sup>5</sup>This KAMAEV 10 value uses 76  $\Omega^- \rightarrow \Xi^- \pi^+ \pi^-$  and 24  $\bar{\Omega}^+ \rightarrow \Xi^+ \pi^- \pi^+$  decays. The  $\Omega^-$  and  $\bar{\Omega}^+$  branching fractions measurements are statistically equal. The errors given combine statistical and systematic contributions. The  $CP$  branching-fraction asymmetry,  $(\Omega^- - \bar{\Omega}^+)/\text{sum}$ , is  $+0.12 \pm 0.20$ .

See key on page 457

Baryon Particle Listings

$\Omega^-, \Omega(2250)^-, \Omega(2380)^-$

$\Gamma(\Xi(1530)^0 \pi^-)/\Gamma_{total}$   $\Gamma_5/\Gamma$

Table with columns: VALUE (units 10^-4), CL%, EVTS, DOCUMENT ID, TECN, COMMENT. Row 1: <0.7, 90, KAMAEV 10 HYCP p Cu, 800 GeV

• • • We do not use the following data for averages, fits, limits, etc. • • •

6.4 +5.1 -2.0 4 6 BOURQUIN 84 SPEC SPS hyperon beam

6 The same 4 events as in the previous mode, with the isospin factor to take into account  $\Xi(1530)^0 \rightarrow \Xi^0 \pi^0$  decays included. BOURQUIN 84 adopted a theoretical assumption that  $\Xi(1530)^0 \pi^-$  would dominate  $\Xi^- \pi^+ \pi^-$  decay.

$\Gamma(\Xi^0 e^- \bar{\nu}_e)/\Gamma_{total}$   $\Gamma_6/\Gamma$

Table with columns: VALUE (units 10^-3), EVTS, DOCUMENT ID, TECN, COMMENT. Row 1: 5.6 ± 2.8, 14, BOURQUIN 84 SPEC SPS hyperon beam

• • • We do not use the following data for averages, fits, limits, etc. • • •

~10 3 BOURQUIN 79B SPEC See BOURQUIN 84

$\Gamma(\Xi^- \gamma)/\Gamma_{total}$   $\Gamma_7/\Gamma$

Table with columns: VALUE (units 10^-4), CL%, EVTS, DOCUMENT ID, TECN, COMMENT. Row 1: < 4.6, 90, 0, ALBUQUERQ...94 E761  $\Omega^-$  375 GeV

• • • We do not use the following data for averages, fits, limits, etc. • • •

<22 90 9 BOURQUIN 84 SPEC SPS hyperon beam
<31 90 0 BOURQUIN 79B SPEC See BOURQUIN 84

$\Gamma(\Lambda \pi^-)/\Gamma_{total}$   $\Gamma_8/\Gamma$

$\Delta S=2$ . Forbidden in first-order weak interaction.

Table with columns: VALUE (units 10^-6), CL%, DOCUMENT ID, TECN, COMMENT. Row 1: < 2.9, 90, WHITE 05 HYCP p Cu, 800 GeV

• • • We do not use the following data for averages, fits, limits, etc. • • •

< 190 90 BOURQUIN 84 SPEC SPS hyperon beam
<1300 90 BOURQUIN 79B SPEC See BOURQUIN 84

$\Omega^-$  DECAY PARAMETERS

$\alpha$  FOR  $\Omega^- \rightarrow \Lambda K^-$

Some early results have been omitted.

Table with columns: VALUE, EVTS, DOCUMENT ID, TECN, COMMENT. Row 1: 0.0180 ± 0.0024 OUR AVERAGE

+0.0207 ± 0.0051 ± 0.0081 960k 7 CHEN 05 HYCP p Cu, 800 GeV
+0.0178 ± 0.0019 ± 0.0016 4.5M 7 LU 05A HYCP p Cu, 800 GeV

• • • We do not use the following data for averages, fits, limits, etc. • • •

-0.028 ± 0.047 6953 CHAN 98 E756 p Be, 800 GeV
-0.034 ± 0.079 1743 LUK 88 SPEC p Be 400 GeV
-0.025 ± 0.028 12k BOURQUIN 84 SPEC SPS hyperon beam

7 The results of CHEN 05 and LU 05A are from different experimental runs.

$\bar{\alpha}$  FOR  $\bar{\Omega}^+ \rightarrow \bar{\Lambda} K^+$

Table with columns: VALUE, EVTS, DOCUMENT ID, TECN, COMMENT. Row 1: -0.0181 ± 0.0028 ± 0.0026 1.89M LU 06 HYCP p Cu, 800 GeV

• • • We do not use the following data for averages, fits, limits, etc. • • •

+0.017 ± 0.077 1823 CHAN 98 E756 p Be, 800 GeV

$(\alpha + \bar{\alpha})/(\alpha - \bar{\alpha})$  in  $\Omega^- \rightarrow \Lambda K^-, \bar{\Omega}^+ \rightarrow \bar{\Lambda} K^+$

Zero if CP is conserved.

Table with columns: VALUE, DOCUMENT ID, TECN, COMMENT. Row 1: -0.016 ± 0.092 ± 0.089 8 LU 06 HYCP p Cu, 800 GeV

8 This value uses the results of CHEN 05, LU 05A, and LU 06.

$\alpha$  FOR  $\Omega^- \rightarrow \Xi^0 \pi^-$

Table with columns: VALUE, EVTS, DOCUMENT ID, TECN, COMMENT. Row 1: +0.09 ± 0.14 1630 BOURQUIN 84 SPEC SPS hyperon beam

$\alpha$  FOR  $\Omega^- \rightarrow \Xi^- \pi^0$

Table with columns: VALUE, EVTS, DOCUMENT ID, TECN, COMMENT. Row 1: +0.05 ± 0.21 614 BOURQUIN 84 SPEC SPS hyperon beam

$\Omega^-$  REFERENCES

We have omitted some papers that have been superseded by later experiments. See our earlier editions.

Reference list table with columns: AUTHOR, YEAR, DOCUMENT ID, TECN, COMMENT. Includes KAMAEV 10 PL B693 236, AUBERT,BE 06 PRL 97 112001, etc.

Reference list table with columns: AUTHOR, YEAR, DOCUMENT ID, TECN, COMMENT. Includes DEUTSCH... 78 PL 73B 96, HEMINGWAY 78 NP B142 205, etc.

$\Omega(2250)^-$

$I(J^P) = 0(?^?)$  Status: \* \* \*

$\Omega(2250)^-$  MASS

Table with columns: VALUE (MeV), EVTS, DOCUMENT ID, TECN, COMMENT. Row 1: 2252 ± 9 OUR AVERAGE

$\Omega(2250)^-$  WIDTH

Table with columns: VALUE (MeV), EVTS, DOCUMENT ID, TECN, COMMENT. Row 1: 55 ± 18 OUR AVERAGE

$\Omega(2250)^-$  DECAY MODES

Table with columns: Mode, Fraction ( $\Gamma_i/\Gamma$ ). Row 1:  $\Xi^- \pi^+ K^-$ , seen

$\Omega(2250)^-$  BRANCHING RATIOS

Table with columns: VALUE, EVTS, DOCUMENT ID, TECN, COMMENT,  $\Gamma_2/\Gamma_1$ . Row 1:  $\Gamma(\Xi(1530)^0 K^-)/\Gamma(\Xi^- \pi^+ K^-)$

$\Omega(2250)^-$  REFERENCES

Reference list table with columns: AUTHOR, YEAR, DOCUMENT ID, TECN, COMMENT. Includes ASTON 87B PL B194 579, etc.

$\Omega(2380)^-$

Status: \* \* \*

OMITTED FROM SUMMARY TABLE

$\Omega(2380)^-$  MASS

Table with columns: VALUE (MeV), EVTS, DOCUMENT ID, TECN, COMMENT. Row 1:  $\approx 2380$  OUR ESTIMATE

$\Omega(2380)^-$  WIDTH

Table with columns: VALUE (MeV), EVTS, DOCUMENT ID, TECN, COMMENT. Row 1: 26 ± 23 45 BIAGI 86B SPEC SPS  $\Xi^-$  beam

$\Omega(2380)^-$  DECAY MODES

Table with columns: Mode, Fraction ( $\Gamma_i/\Gamma$ ). Row 1:  $\Xi^- \pi^+ K^-$ , seen

$\Omega(2380)^-$  BRANCHING RATIOS

Table with columns: VALUE, CL%, EVTS, DOCUMENT ID, TECN, COMMENT,  $\Gamma_2/\Gamma_1$ . Row 1:  $\Gamma(\Xi(1530)^0 K^-)/\Gamma(\Xi^- \pi^+ K^-)$

## Baryon Particle Listings

 $\Omega(2380)^-$ ,  $\Omega(2470)^-$ 

$\Gamma(\Xi^- \bar{K}^*(892)^0) / \Gamma(\Xi^- \pi^+ K^-)$					$\Gamma_3 / \Gamma_1$
VALUE	EVTS	DOCUMENT ID	TECN	COMMENT	
$0.5 \pm 0.3$	21	BIAGI	86B	SPEC	$\Xi^-$ Be 116 GeV/c

 $\Omega(2380)^-$  REFERENCESBIAGI 86B ZPHY C31 33 S.F. Biagi *et al.* (LOQM, GEVA, RAL+) $\Omega(2470)^-$ 

Status: \*\*

## OMITTED FROM SUMMARY TABLE

A peak in the  $\Omega^- \pi^+ \pi^-$  mass spectrum with a signal significance claimed to be at least 5.5 standard deviations. There is no reason to seriously doubt the existence of this state, but unless the evidence is overwhelming we usually wait for confirmation from a second experiment before elevating peaks to the Summary Table.

 $\Omega(2470)^-$  MASS

VALUE (MeV)	EVTS	DOCUMENT ID	TECN	COMMENT
$2474 \pm 12$	59	ASTON	88G	LASS $K^- p$ 11 GeV/c

 $\Omega(2470)^-$  WIDTH

VALUE (MeV)	EVTS	DOCUMENT ID	TECN	COMMENT
$72 \pm 33$	59	ASTON	88G	LASS $K^- p$ 11 GeV/c

 $\Omega(2470)^-$  DECAY MODES

Mode

 $\Gamma_1 \quad \Omega^- \pi^+ \pi^-$  $\Omega(2470)^-$  REFERENCESASTON 88G PL B215 799 D. Aston *et al.* (SLAC, NAGO, CINC, INUS)

## CHARMED BARYONS

### (C = +1)

$\Lambda_c^+ = udc, \Sigma_c^{++} = uuc, \Sigma_c^+ = udc, \Sigma_c^0 = ddc,$   
 $\Xi_c^+ = usc, \Xi_c^0 = dsc, \Omega_c^0 = ssc$

**CHARMED BARYONS**

Revised March 2012 by C.G. Wohl (LBNL).

There are 17 known charmed baryons, and four other candidates not well enough established to be promoted to the Summary Tables.\* Fig. 1(a) shows the mass spectrum, and for comparison Fig. 1(b) shows the spectrum of the lightest strange baryons. The  $\Lambda_c$  and  $\Sigma_c$  spectra ought to look much like the  $\Lambda$  and  $\Sigma$  spectra, since a  $\Lambda_c$  or a  $\Sigma_c$  differs from a  $\Lambda$  or a  $\Sigma$  only by the replacement of the  $s$  quark with a  $c$  quark. However, a  $\Xi$  or an  $\Omega$  has more than one  $s$  quark, only *one* of which is changed to a  $c$  quark to make a  $\Xi_c$  or an  $\Omega_c$ . Thus the  $\Xi_c$  and  $\Omega_c$  spectra ought to be richer than the  $\Xi$  and  $\Omega$  spectra.\*\*

Before discussing the observed spectra, we review the theory of SU(4) multiplets, which tells what charmed baryons to expect; this is essential, because few of the spin-parity values given in Fig. 1(a) have been measured. Rather, they have been assigned in accord with expectations of the theory. However, they are all very likely as shown (see below).

**SU(4) multiplets**—Baryons made from  $u, d, s,$  and  $c$  quarks belong to SU(4) multiplets. The multiplet numerology, analogous to  $3 \times 3 \times 3 = 10 + 8_1 + 8_2 + 1$  for the subset of baryons made from just  $u, d,$  and  $s$  quarks, is  $4 \times 4 \times 4 = 20 + 20'_1 + 20'_2 + \bar{4}$ . Figure 2(a) shows the 20-plet whose bottom level is an SU(3) decuplet, such as the decuplet that includes the  $\Delta(1232)$ . Figure 2(b) shows the 20'-plet whose bottom level is an SU(3) octet, such as the octet that includes the nucleon. Figure 2(c) shows the  $\bar{4}$  multiplet, an inverted tetrahedron. One level up from the bottom level of each multiplet are the baryons with one  $c$  quark. All the baryons in a given multiplet have the same spin and parity. Each  $N$  or  $\Delta$  or SU(3)-singlet- $\Lambda$  resonance calls for another 20'- or 20- or  $\bar{4}$ -plet, respectively.

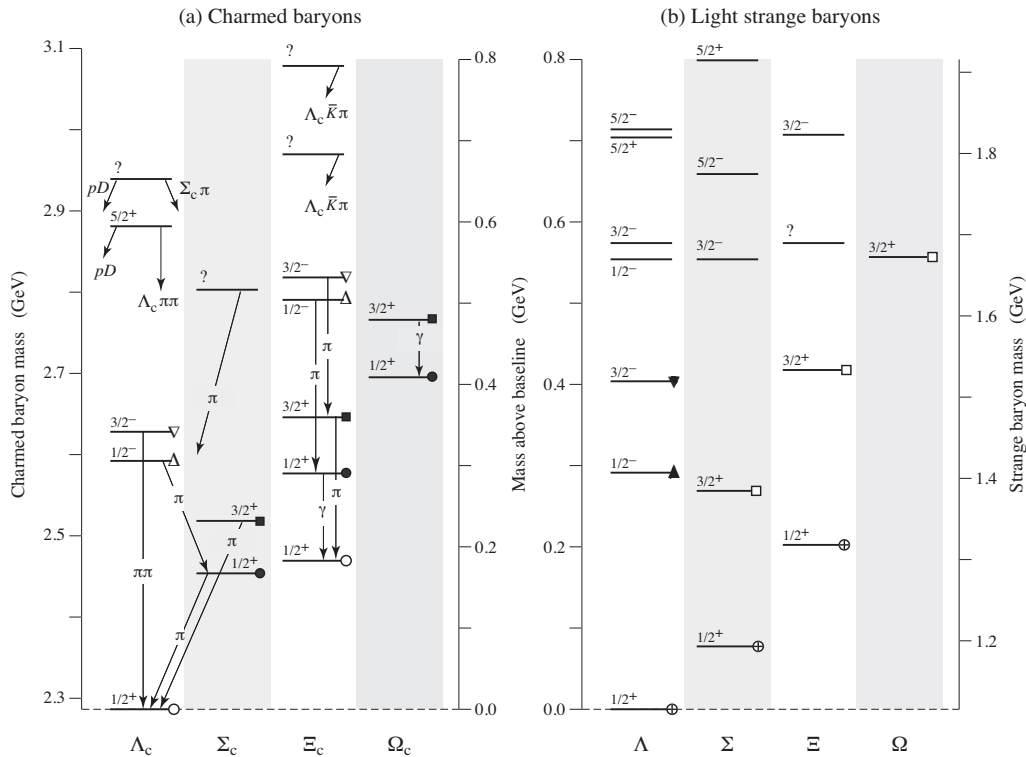


**Fig. 1.** (a) The known charmed baryons, and (b) the lightest “4-star” strange baryons. Note that there are two  $J^P = 1/2^+$   $\Xi_c$  states, and that the lightest  $\Omega_c$  does not have  $J = 3/2$ . The  $J^P = 1/2^+$  states, all tabbed with a circle, belong to the SU(4) multiplet that includes the nucleon; states with a circle with the same fill belong to the same SU(3) multiplet within that SU(4) multiplet. Similar remarks apply to the other states: same shape of tab, same SU(4) multiplet; same fill of that shape, same SU(3) multiplet. The  $J^P = 1/2^-$  and  $3/2^-$  states tabbed with triangles complete two SU(4)  $\bar{4}$  multiplets.

# Baryon Particle Listings

## Charmed Baryons

The flavor symmetries shown in Fig. 2 are of course badly broken, but the figure is the simplest way to see what charmed baryons should exist. For example, from Fig. 2(b), we expect to find, in the same  $J^P = 1/2^+$  20'-plet as the nucleon, a  $\Lambda_c$ , a  $\Sigma_c$ , two  $\Xi_c$ 's, and an  $\Omega_c$ . Note that this  $\Omega_c$  has  $J^P = 1/2^+$  and is not in the same SU(4) multiplet as the famous  $J^P = 3/2^+$   $\Omega^-$ .

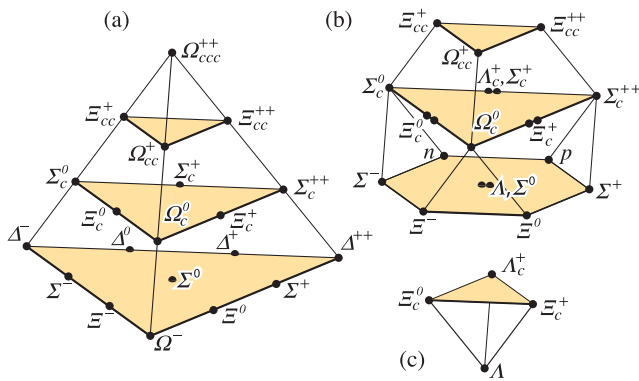


**Figure 2:** SU(4) multiplets of baryons made of  $u$ ,  $d$ ,  $s$ , and  $c$  quarks. (a) The 20-plet with an SU(3) decuplet on the lowest level. (b) The 20'-plet with an SU(3) octet on the lowest level. (c) The  $\bar{4}$ -plet. Note that here and in Fig. 3, but not in Fig. 1, each charge state is shown separately.

Figure 3 shows in more detail the middle level of the 20'-plet of Fig. 2(b); it splits apart into two SU(3) multiplets, a  $\bar{3}$  and a 6. The states of the  $\bar{3}$  are antisymmetric under the interchange of the two light quarks (the  $u$ ,  $d$ , and  $s$  quarks), whereas the states of the 6 are symmetric under this interchange. We use a prime to distinguish the  $\Xi_c$  in the 6 from the one in the  $\bar{3}$ .

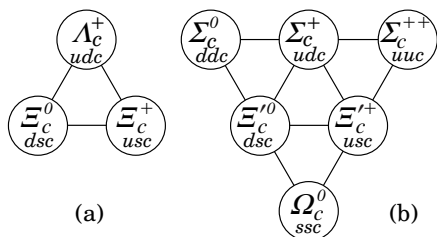


**Figure 3:** The SU(3) multiplets on the second level of the SU(4) multiplet of Fig. 2(b). The  $\Lambda_c$  and  $\Xi_c$  tabbed with open circles in Fig. 1(a) complete a  $J^P = 1/2^+$  SU(3)  $\bar{3}$ -plet, as in (a) here. The  $\Sigma_c$ ,  $\Xi_c$ , and  $\Omega_c$  tabbed with closed circles in Fig. 1(a) complete a  $J^P = 1/2^+$  SU(3) 6-plet, as in (b) here. Together the nine particles complete the charm = +1 level of a  $J^P = 1/2^+$  SU(4) 20'-plet, as in Fig. 2(b).

**The observed spectra**—(1) The parity of the lightest  $\Lambda_c$  is defined to be positive (as are the parities of the  $p$ ,  $n$ , and  $\Lambda$ ); the limited evidence about its spin is consistent with  $J = 1/2$ . However, few of the  $J^P$  quantum numbers given in Fig. 1(a) have been measured. Models using spin-spin and spin-orbit interactions between the quarks, with parameters determined using a few of the masses as input, lead to the  $J^P$  assignments shown.<sup>†</sup> There are no surprises: the  $J^P = 1/2^+$  states come first, then the  $J^P = 3/2^+$  states . . .

(2) There is, however, evidence that many of the  $J^P$  assignments in Fig. 1(a) must be correct. As is well known, the successive mass differences between the  $J^P = 3/2^+$  particles, the  $\Delta(1232)^-$ ,  $\Sigma(1385)^-$ ,  $\Xi(1535)^-$ , and  $\Omega^-$ , which lie along the lower left edge of the 20-plet in Fig. 2(a), should according to SU(3) be about equal; and indeed experimentally they nearly are. In the same way, the mass differences between the  $J^P = 1/2^+$   $\Sigma_c(2455)^0$ ,  $\Xi_c^0$ , and  $\Omega_c^0$ ,<sup>‡</sup> the particles along the left edge of Fig. 3(b), should be about equal—assuming, of course, that they *do* all have the same  $J^P$ . The measured differences are  $125.0 \pm 2.9$  MeV and  $117.3 \pm 3.4$  MeV—not perfect, but close. Similarly, the mass differences between the presumed  $J^P = 3/2^+$   $\Sigma_c(2520)^0$ ,  $\Xi_c(2645)^0$ , and  $\Omega_c(2770)^0$  are  $127.1 \pm 0.8$  MeV and  $120.0 \pm 2.1$  MeV. In Fig. 1(a), these two sets of charm particles are tabbed with solid circles and solid squares.

(3) Other evidence comes from the decay of the  $\Lambda_c(2593)$ . The only allowed strong decay is  $\Lambda_c(2593)^+ \rightarrow \Lambda_c^+ \pi \pi$ , and this appears to be dominated by the submode  $\Sigma_c(2455)\pi$ , despite little available phase space for the latter (the “ $Q$ ” is about 2 MeV, the c.m. decay momentum about 20 MeV/c). Thus the decay is almost certainly  $s$ -wave, which, assuming that the  $\Sigma_c(2455)$  does indeed have  $J^P = 1/2^+$ , makes  $J^P = 1/2^-$  for the  $\Lambda_c(2593)$ .

### Footnotes:

\* The unpromoted states are a  $\Lambda_c(2765)^+$ , a  $\Xi_c(2930)$ , a  $\Xi_c(3055)$ , and a  $\Xi_c(3123)$ . There is also very weak evidence for a baryon with *two*  $c$  quarks, a  $\Xi_{cc}^+$  at 3519 MeV. See the Particle Listings.

\*\* For example, there are three  $\Omega_c^0$  states (properly symmetrized states of  $ssc$ ,  $scs$ , and  $css$ ) corresponding to each  $\Omega^-$  ( $sss$ ) state.

† This is not the place to discuss the details of the models, nor to attempt a guide to the literature. See the discovery papers of the various charmed baryons for references to the models that lead to the quantum-number assignments.

‡ A reminder about the Particle Data Group naming scheme: A particle has its mass as part of its name if and only if it decays strongly. Thus  $\Sigma(1385)$  and  $\Sigma_c(2455)$  but  $\Omega^-$  and  $\Xi_c'$ .



$I(J^P) = 0(\frac{1}{2}^+)$  Status: \*\*\*\*

The parity of the  $\Lambda_c^+$  is defined to be positive (as are the parities of the proton, neutron, and  $\Lambda$ ). The quark content is  $udc$ . Results of an analysis of  $pK^-\pi^+$  decays (JEZABEK 92) are consistent with  $J = 1/2$ . Nobody doubts that the spin is indeed 1/2.

The only new measurements since our 2010 Review are of limits on rare or forbidden  $\Lambda_c^+ \rightarrow p\ell^+\ell^-$  and  $\bar{p}\ell^+\ell^+$  modes.

We have omitted some results that have been superseded by later experiments. The omitted results may be found in earlier editions.

$\Lambda_c^+$  MASS

Our value in 2004,  $2284.9 \pm 0.6$  MeV, was the average of the measurements now filed below as "not used." The BABAR measurement is so much better that we use it alone. Note that it is about 2.6 (old) standard deviations above the 2004 value.

The fit also includes  $\Sigma_c^-\Lambda_c^+$  and  $\Lambda_c^{*+}\Lambda_c^+$  mass-difference measurements, but this doesn't affect the  $\Lambda_c^+$  mass. The new (in 2006)  $\Lambda_c^+$  mass simply pushes all those other masses higher.

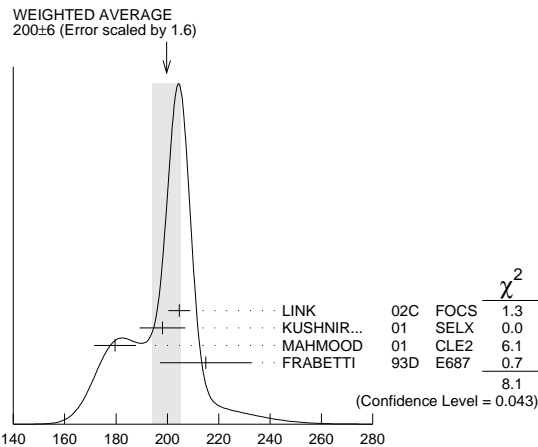
VALUE (MeV)	EVTS	DOCUMENT ID	TECN	COMMENT
<b>2286.46 ± 0.14 OUR FIT</b>				
<b>2286.46 ± 0.14</b>	4891	1 AUBERT,B	05s BABR	$\Lambda_c^0 K^+$ and $\Sigma^0 K_S^0 K^+$
• • • We do not use the following data for averages, fits, limits, etc. • • •				
2284.7 ± 0.6 ± 0.7	1134	AVERY	91 CLEO	Six modes
2281.7 ± 2.7 ± 2.6	29	ALVAREZ	90b NA14	$pK^-\pi^+$
2285.8 ± 0.6 ± 1.2	101	BARLAG	89 NA32	$pK^-\pi^+$
2284.7 ± 2.3 ± 0.5	5	AGUILAR...	88b LEBE	$pK^-\pi^+$
2283.1 ± 1.7 ± 2.0	628	ALBRECHT	88c ARG	$pK^-\pi^+$ , $p\bar{K}^0$ , $\Lambda 3\pi$
2286.2 ± 1.7 ± 0.7	97	ANJOS	88b E691	$pK^-\pi^+$
2281 ± 3	2	JONES	87 HBC	$pK^-\pi^+$
2283 ± 3	3	BOSETTI	82 HBC	$pK^-\pi^+$
2290 ± 3	1	CALICCHIO	80 HYBR	$pK^-\pi^+$

1 AUBERT,B 05s uses low-Q  $\Lambda_c^0 K^+$  and  $\Sigma^0 K_S^0 K^+$  decays to minimize systematic errors. The error above includes systematic as well as statistical errors. Many cross checks and adjustments to properties of the BABAR detector, as well as the large number of clean events, make this by far the best measurement of the  $\Lambda_c^+$  mass.

$\Lambda_c^+$  MEAN LIFE

Measurements with an error  $\geq 100 \times 10^{-15}$  s or with fewer than 20 events have been omitted from the Listings.

VALUE ( $10^{-15}$ s)	EVTS	DOCUMENT ID	TECN	COMMENT
<b>200 ± 6 OUR AVERAGE</b>	Error	includes scale factor of 1.6.	See the ideogram below.	
204.6 ± 3.4 ± 2.5	8034	LINK	02c FOCs	$pK^-\pi^+$
198.1 ± 7.0 ± 5.6	1630	KUSHNIR...	01 SELX	$\Lambda_c^+ \rightarrow pK^-\pi^+$
179.6 ± 6.9 ± 4.4	4749	MAHMOOD	01 CLE2	$e^+e^- \approx \Upsilon(4S)$
215 ± 16 ± 8	1340	FRABETTI	93D E687	$\gamma Be, \Lambda_c^+ \rightarrow pK^-\pi^+$
• • • We do not use the following data for averages, fits, limits, etc. • • •				
180 ± 30 ± 30	29	ALVAREZ	90 NA14	$\gamma, \Lambda_c^+ \rightarrow pK^-\pi^+$
200 ± 30 ± 30	90	FRABETTI	90 E687	$\gamma Be, \Lambda_c^+ \rightarrow pK^-\pi^+$
196 $^{+23}_{-20}$	101	BARLAG	89 NA32	$pK^-\pi^+$ + c.c.
220 ± 30 ± 20	97	ANJOS	88b E691	$pK^-\pi^+$ + c.c.



$\Lambda_c^+$  mean life

$\Lambda_c^+$  DECAY MODES

Nearly all branching fractions of the  $\Lambda_c^+$  are measured relative to the  $pK^-\pi^+$  mode, but there are no model-independent measurements of this branching fraction. We explain how we arrive at our value of  $B(\Lambda_c^+ \rightarrow pK^-\pi^+)$  in a Note at the beginning of the branching-ratio measurements, below. When this branching fraction is eventually well determined, all the other branching fractions will slide up or down proportionally as the true value differs from the value we use here.

Mode	Fraction ( $\Gamma_i/\Gamma$ )	Scale factor/ Confidence level
<b>Hadronic modes with a p: S = -1 final states</b>		
$\Gamma_1$ $p\bar{K}^0$	( 2.3 ± 0.6 ) %	
$\Gamma_2$ $pK^-\pi^+$	[a] ( 5.0 ± 1.3 ) %	
$\Gamma_3$ $p\bar{K}^*(892)^0$	[b] ( 1.6 ± 0.5 ) %	
$\Gamma_4$ $\Delta(1232)^{++}K^-$	( 8.6 ± 3.0 ) $\times 10^{-3}$	
$\Gamma_5$ $\Lambda(1520)\pi^+$	[b] ( 1.8 ± 0.6 ) %	
$\Gamma_6$ $pK^-\pi^+$ nonresonant	( 2.8 ± 0.8 ) %	
$\Gamma_7$ $p\bar{K}^0\pi^0$	( 3.3 ± 1.0 ) %	
$\Gamma_8$ $p\bar{K}^0\eta$	( 1.2 ± 0.4 ) %	
$\Gamma_9$ $p\bar{K}^0\pi^+\pi^-$	( 2.6 ± 0.7 ) %	
$\Gamma_{10}$ $pK^-\pi^+\pi^0$	( 3.4 ± 1.0 ) %	
$\Gamma_{11}$ $pK^*(892)^-\pi^+$	[b] ( 1.1 ± 0.5 ) %	
$\Gamma_{12}$ $p(K^-\pi^+)_{\text{nonresonant}}\pi^0$	( 3.6 ± 1.2 ) %	
$\Gamma_{13}$ $\Delta(1232)K^*(892)$	seen	
$\Gamma_{14}$ $pK^-\pi^+\pi^+\pi^-$	( 1.1 ± 0.8 ) $\times 10^{-3}$	
$\Gamma_{15}$ $pK^-\pi^+\pi^0\pi^0$	( 8 ± 4 ) $\times 10^{-3}$	
$\Gamma_{16}$ $pK^-\pi^+3\pi^0$		
<b>Hadronic modes with a p: S = 0 final states</b>		
$\Gamma_{17}$ $p\pi^+\pi^-$	( 3.5 ± 2.0 ) $\times 10^{-3}$	
$\Gamma_{18}$ $p f_0(980)$	[b] ( 2.8 ± 1.9 ) $\times 10^{-3}$	
$\Gamma_{19}$ $p\pi^+\pi^+\pi^-\pi^-$	( 1.8 ± 1.2 ) $\times 10^{-3}$	
$\Gamma_{20}$ $pK^+K^-$	( 7.7 ± 3.5 ) $\times 10^{-4}$	
$\Gamma_{21}$ $p\phi$	[b] ( 8.2 ± 2.7 ) $\times 10^{-4}$	
$\Gamma_{22}$ $pK^+K^-\text{non-}\phi$	( 3.5 ± 1.7 ) $\times 10^{-4}$	
<b>Hadronic modes with a hyperon: S = -1 final states</b>		
$\Gamma_{23}$ $\Lambda\pi^+$	( 1.07 ± 0.28 ) %	
$\Gamma_{24}$ $\Lambda\pi^+\pi^0$	( 3.6 ± 1.3 ) %	
$\Gamma_{25}$ $\Lambda\rho^+$	< 5 %	CL=95%
$\Gamma_{26}$ $\Lambda\pi^+\pi^+\pi^-$	( 2.6 ± 0.7 ) %	
$\Gamma_{27}$ $\Sigma(1385)^+\pi^+\pi^-, \Sigma^{*+} \rightarrow \Lambda\pi^+$	( 7 ± 4 ) $\times 10^{-3}$	
$\Gamma_{28}$ $\Sigma(1385)^-\pi^+\pi^+, \Sigma^{*-} \rightarrow \Lambda\pi^-\rho^0$	( 5.5 ± 1.7 ) $\times 10^{-3}$	
$\Gamma_{29}$ $\Lambda\pi^+\rho^0$	( 1.1 ± 0.5 ) %	
$\Gamma_{30}$ $\Sigma(1385)^+\rho^0, \Sigma^{*+} \rightarrow \Lambda\pi^+$	( 3.7 ± 3.1 ) $\times 10^{-3}$	
$\Gamma_{31}$ $\Lambda\pi^+\pi^+\pi^-\text{nonresonant}$	< 8 $\times 10^{-3}$	CL=90%
$\Gamma_{32}$ $\Lambda\pi^+\pi^+\pi^-\pi^0\text{total}$	( 1.8 ± 0.8 ) %	
$\Gamma_{33}$ $\Lambda\pi^+\eta$	[b] ( 1.8 ± 0.6 ) %	
$\Gamma_{34}$ $\Sigma(1385)^+\eta$	[b] ( 8.5 ± 3.3 ) $\times 10^{-3}$	
$\Gamma_{35}$ $\Lambda\pi^+\omega$	[b] ( 1.2 ± 0.5 ) %	
$\Gamma_{36}$ $\Lambda\pi^+\pi^+\pi^-\pi^0$ , no $\eta$ or $\omega$	< 7 $\times 10^{-3}$	CL=90%
$\Gamma_{37}$ $\Lambda K^+\bar{K}^0$	( 4.7 ± 1.5 ) $\times 10^{-3}$	S=1.2
$\Gamma_{38}$ $\Xi(1690)^0 K^+, \Xi^{*0} \rightarrow \Lambda\bar{K}^0$	( 1.3 ± 0.5 ) $\times 10^{-3}$	
$\Gamma_{39}$ $\Sigma^0\pi^+$	( 1.05 ± 0.28 ) %	
$\Gamma_{40}$ $\Sigma^+\pi^0$	( 1.00 ± 0.34 ) %	
$\Gamma_{41}$ $\Sigma^+\eta$	( 5.5 ± 2.3 ) $\times 10^{-3}$	
$\Gamma_{42}$ $\Sigma^+\pi^+\pi^-$	( 3.6 ± 1.0 ) %	
$\Gamma_{43}$ $\Sigma^+\rho^0$	< 1.4 %	CL=95%
$\Gamma_{44}$ $\Sigma^-\pi^+\pi^+$	( 1.7 ± 0.5 ) %	
$\Gamma_{45}$ $\Sigma^0\pi^+\pi^0$	( 1.8 ± 0.8 ) %	
$\Gamma_{46}$ $\Sigma^0\pi^+\pi^+\pi^-$	( 8.3 ± 3.1 ) $\times 10^{-3}$	
$\Gamma_{47}$ $\Sigma^+\pi^+\pi^-\pi^0$	—	
$\Gamma_{48}$ $\Sigma^+\omega$	[b] ( 2.7 ± 1.0 ) %	
$\Gamma_{49}$ $\Sigma^+K^+K^-$	( 2.8 ± 0.8 ) $\times 10^{-3}$	
$\Gamma_{50}$ $\Sigma^+\phi$	[b] ( 3.1 ± 0.9 ) $\times 10^{-3}$	
$\Gamma_{51}$ $\Xi(1690)^0 K^+, \Xi^{*0} \rightarrow \Sigma^+K^-$	( 8.1 ± 3.0 ) $\times 10^{-4}$	
$\Gamma_{52}$ $\Sigma^+K^+K^-\text{nonresonant}$	< 6 $\times 10^{-4}$	CL=90%
$\Gamma_{53}$ $\Xi^0 K^+$	( 3.9 ± 1.4 ) $\times 10^{-3}$	
$\Gamma_{54}$ $\Xi^- K^+\pi^+$	( 5.1 ± 1.4 ) $\times 10^{-3}$	
$\Gamma_{55}$ $\Xi(1530)^0 K^+$	[b] ( 2.6 ± 1.0 ) $\times 10^{-3}$	

## Baryon Particle Listings

 $\Lambda_c^+$ Hadronic modes with a hyperon:  $S = 0$  final states

$\Gamma_{56}$	$\Lambda K^+$	$(5.0 \pm 1.6) \times 10^{-4}$	
$\Gamma_{57}$	$\Lambda K^+ \pi^+ \pi^-$	$< 4 \times 10^{-4}$	CL=90%
$\Gamma_{58}$	$\Sigma^0 K^+$	$(4.2 \pm 1.3) \times 10^{-4}$	
$\Gamma_{59}$	$\Sigma^0 K^+ \pi^+ \pi^-$	$< 2.1 \times 10^{-4}$	CL=90%
$\Gamma_{60}$	$\Sigma^+ K^+ \pi^-$	$(1.7 \pm 0.7) \times 10^{-3}$	
$\Gamma_{61}$	$\Sigma^+ K^*(892)^0$	[b] $(2.8 \pm 1.1) \times 10^{-3}$	
$\Gamma_{62}$	$\Sigma^- K^+ \pi^+$	$< 1.0 \times 10^{-3}$	CL=90%

## Doubly Cabibbo-suppressed modes

$\Gamma_{63}$	$\rho K^+ \pi^-$	$< 2.3 \times 10^{-4}$	CL=90%
---------------	------------------	------------------------	--------

## Semileptonic modes

$\Gamma_{64}$	$\Lambda \ell^+ \nu_\ell$	[c] $(2.0 \pm 0.6) \%$	
$\Gamma_{65}$	$\Lambda e^+ \nu_e$	$(2.1 \pm 0.6) \%$	
$\Gamma_{66}$	$\Lambda \mu^+ \nu_\mu$	$(2.0 \pm 0.7) \%$	

## Inclusive modes

$\Gamma_{67}$	$e^+$ anything	$(4.5 \pm 1.7) \%$	
$\Gamma_{68}$	$\rho e^+$ anything	$(1.8 \pm 0.9) \%$	
$\Gamma_{69}$	$\Lambda e^+$ anything		
$\Gamma_{70}$	$\rho$ anything	$(50 \pm 16) \%$	
$\Gamma_{71}$	$p$ anything (no $\Lambda$ )	$(12 \pm 19) \%$	
$\Gamma_{72}$	$\rho$ hadrons		
$\Gamma_{73}$	$n$ anything	$(50 \pm 16) \%$	
$\Gamma_{74}$	$n$ anything (no $\Lambda$ )	$(29 \pm 17) \%$	
$\Gamma_{75}$	$\Lambda$ anything	$(35 \pm 11) \%$	S=1.4
$\Gamma_{76}$	$\Sigma^\pm$ anything	[d] $(10 \pm 5) \%$	
$\Gamma_{77}$	3prongs	$(24 \pm 8) \%$	

 $\Delta C = 1$  weak neutral current (CI) modes, or Lepton Family number (LF), or Lepton number (L), or Baryon number (B) violating modes

$\Gamma_{78}$	$\rho e^+ e^-$	CI	$< 5.5 \times 10^{-6}$	CL=90%
$\Gamma_{79}$	$\rho \mu^+ \mu^-$	CI	$< 4.4 \times 10^{-5}$	CL=90%
$\Gamma_{80}$	$\rho e^+ \mu^-$	LF	$< 9.9 \times 10^{-6}$	CL=90%
$\Gamma_{81}$	$\rho e^- \mu^+$	LF	$< 1.9 \times 10^{-5}$	CL=90%
$\Gamma_{82}$	$\bar{p} 2e^+$	L,B	$< 2.7 \times 10^{-6}$	CL=90%
$\Gamma_{83}$	$\bar{p} 2\mu^+$	L,B	$< 9.4 \times 10^{-6}$	CL=90%
$\Gamma_{84}$	$\bar{p} e^+ \mu^+$	L,B	$< 1.6 \times 10^{-5}$	CL=90%
$\Gamma_{85}$	$\Sigma^- \mu^+ \mu^+$	L	$< 7.0 \times 10^{-4}$	CL=90%

[a] See the note on " $\Lambda_c^+$  Branching Fractions" below.

[b] This branching fraction includes all the decay modes of the final-state resonance.

[c] An  $\ell$  indicates an  $e$  or a  $\mu$  mode, not a sum over these modes.

[d] The value is for the sum of the charge states or particle/antiparticle states indicated.

## CONSTRAINED FIT INFORMATION

An overall fit to 18 branching ratios uses 33 measurements and one constraint to determine 12 parameters. The overall fit has a  $\chi^2 = 15.5$  for 22 degrees of freedom.

The following *off-diagonal* array elements are the correlation coefficients  $\langle \delta x_i \delta x_j \rangle / (\delta x_i \delta x_j)$ , in percent, from the fit to the branching fractions,  $x_i \equiv \Gamma_i / \Gamma_{\text{total}}$ . The fit constrains the  $x_i$  whose labels appear in this array to sum to one.

$x_{23}$	96									
$x_{26}$	97	93								
$x_{37}$	82	83	80							
$x_{39}$	95	98	92	82						
$x_{42}$	93	90	91	77	88					
$x_{44}$	82	79	80	68	78	80				
$x_{46}$	69	66	70	57	66	65	57			
$x_{49}$	88	85	86	72	84	93	75	61		
$x_{50}$	85	82	83	70	81	90	72	59	84	
$x_{54}$	93	96	90	80	94	87	77	64	82	79
	$x_2$	$x_{23}$	$x_{26}$	$x_{37}$	$x_{39}$	$x_{42}$	$x_{44}$	$x_{46}$	$x_{49}$	$x_{50}$

 $\Lambda_c^+$  BRANCHING FRACTIONS

Revised 2002 by P.R. Burchat (Stanford University).

Most  $\Lambda_c^+$  branching fractions are measured relative to the decay mode  $\Lambda_c^+ \rightarrow pK^- \pi^+$ . However, there are no completely model-independent measurements of the absolute branching fraction for  $\Lambda_c^+ \rightarrow pK^- \pi^+$ . Here we describe the measurements that have been used to extract  $B(\Lambda_c^+ \rightarrow pK^- \pi^+)$ , the model-dependence of the results, and the method we have used to average the results.

ARGUS (ALBRECHT 88C) and CLEO (CRAWFORD 92) measure  $B(\bar{B} \rightarrow \Lambda_c^+ X) \cdot B(\Lambda_c^+ \rightarrow pK^- \pi^+)$  to be  $(0.30 \pm 0.12 \pm 0.06) \%$  and  $(0.273 \pm 0.051 \pm 0.039) \%$ . Under the assumptions that decays of  $\bar{B}$  mesons to baryons are dominated by  $\bar{B} \rightarrow \Lambda_c^+ X$  and that  $\Lambda_c^+ X$  final states other than  $\Lambda_c^+ \bar{N} X$  can be neglected, they also measure  $B(\bar{B} \rightarrow \Lambda_c^+ X)$  to be  $(6.8 \pm 0.5 \pm 0.3) \%$  (ALBRECHT 92O) and  $(6.4 \pm 0.8 \pm 0.8) \%$  (CRAWFORD 92). Combining these results, we get  $B(\Lambda_c^+ \rightarrow pK^- \pi^+) = (4.14 \pm 0.91) \%$ . However, the assumption that  $\bar{B}$  decay modes to baryons other than  $\Lambda_c^+ \bar{N} X$  are negligible is not on solid ground experimentally or theoretically [2]. Therefore, the branching fraction for  $\Lambda_c^+ \rightarrow pK^- \pi^+$  given above may be low by some undetermined amount.

A second type of model-dependent determination of  $B(\Lambda_c^+ \rightarrow pK^- \pi^+)$  is based on measurements by ARGUS (ALBRECHT 91G) and CLEO (BERGFELD 94) of  $\sigma(e^+e^- \rightarrow \Lambda_c^+ X) \cdot B(\Lambda_c^+ \rightarrow \Lambda \ell^+ \nu_\ell) = (4.15 \pm 1.03 \pm 1.18) \text{ pb}$  and  $(4.77 \pm 0.25 \pm 0.66) \text{ pb}$ . ARGUS (ALBRECHT 96E) and CLEO (AVERY 91) have also measured  $\sigma(e^+e^- \rightarrow \Lambda_c^+ X) \cdot B(\Lambda_c^+ \rightarrow pK^- \pi^+)$ . The weighted average is  $(11.2 \pm 1.3) \text{ pb}$ .

From these measurements, we extract  $R \equiv B(\Lambda_c^+ \rightarrow pK^- \pi^+) / B(\Lambda_c^+ \rightarrow \Lambda \ell^+ \nu_\ell) = 2.40 \pm 0.43$ . We estimate the  $\Lambda_c^+ \rightarrow pK^- \pi^+$  branching fraction from the equation

$$B(\Lambda_c^+ \rightarrow pK^- \pi^+) = R f F \frac{\Gamma(D \rightarrow X \ell^+ \nu_\ell)}{1 + |V_{cd}/V_{cs}|^2} \cdot \tau(\Lambda_c^+), \quad (1)$$

where  $f = B(\Lambda_c^+ \rightarrow \Lambda \ell^+ \nu_\ell) / B(\Lambda_c^+ \rightarrow X_s \ell^+ \nu_\ell)$  and  $F = \Gamma(\Lambda_c^+ \rightarrow X_s \ell^+ \nu_\ell) / \Gamma(D^0 \rightarrow X_s \ell^+ \nu_\ell)$ . When we use  $1 + |V_{cd}/V_{cs}|^2 = 1.05$  and the world averages  $\Gamma(D \rightarrow X \ell^+ \nu_\ell) = (0.166 \pm 0.006) \times 10^{12} \text{ s}^{-1}$  and  $\tau(\Lambda_c^+) = (0.192 \pm 0.005) \times 10^{-12} \text{ s}$ , we calculate  $B(\Lambda_c^+ \rightarrow pK^- \pi^+) = (7.3 \pm 1.4) \% \cdot f F$ . Theoretical estimates for  $f$  and  $F$  are near 1.0 with significant uncertainties.

So, we have two results with significant model-dependence:  $B(\Lambda_c^+ \rightarrow pK^- \pi^+) = (4.14 \pm 0.91) \%$  from  $\bar{B}$  decays, and  $B(\Lambda_c^+ \rightarrow pK^- \pi^+) = (7.3 \pm 1.4) \% \cdot f F$  from semileptonic  $\Lambda_c^+$  decays. If we set  $f F = 1.0$  in the second result, and assign an uncertainty of 30% to each result to account for the unknown model-dependence, we get the consistent results  $B(\Lambda_c^+ \rightarrow pK^- \pi^+) = (4.14 \pm 0.91 \pm 1.24) \%$  and  $B(\Lambda_c^+ \rightarrow pK^- \pi^+) = (7.3 \pm 1.4 \pm 2.2) \%$ . The weighted average of these two results is  $B(\Lambda_c^+ \rightarrow pK^- \pi^+) = (5.0 \pm 1.3) \%$ , where the uncertainty contains both the experimental uncertainty and the 30% estimate of model dependence in each result. We assigned the value  $(5.0 \pm 1.3) \%$  to the  $\Lambda_c^+ \rightarrow pK^- \pi^+$  branching fraction in our 2000 *Review* [1].



A third type of measurement of  $B(\Lambda_c^+ \rightarrow pK^-\pi^+)$  has been published by CLEO (JAFPE 00). Under the assumption that a  $\bar{D}$  meson and an antiproton in opposite hemispheres is evidence for a  $\Lambda_c^+$  in the hemisphere of the  $\bar{p}$ , the fraction of such  $\bar{D}\bar{p}$  events with a  $\Lambda_c^+ \rightarrow pK^-\pi^+$  decay can be used to determine the  $\Lambda_c^+ \rightarrow pK^-\pi^+$  branching fraction. CLEO measures  $B(\Lambda_c^+ \rightarrow pK^-\pi^+) = (5.0 \pm 1.3)\%$ , which is coincidentally exactly the same value as our PDG 00 average given above. The quoted uncertainty includes significant contributions from model-dependent effects (*e.g.*, differences between the  $\bar{p}$  momentum spectrum in events with a  $\Lambda_c^+$  and  $\bar{p}$  in the same hemisphere, and with a  $\bar{D}$  and  $\bar{p}$  in opposite hemispheres; extrapolation of the  $\Lambda_c^+$  and  $\bar{D}$  momentum spectrum below the minimum value used for rejecting  $B$  decay products; and our limited understanding of backgrounds such as  $D\bar{D}N\bar{p}$  events).

We have chosen to continue to assign the value  $(5.0 \pm 1.3)\%$  to the  $\Lambda_c^+ \rightarrow pK^-\pi^+$  branching fraction (given as PDG 02 below). As was noted earlier, most of the other  $\Lambda_c^+$  decay modes are measured relative to this mode.

New methods for measuring the  $\Lambda_c^+$  absolute branching fractions have been proposed [2,3].

## References

1. D.E. Groom *et al.* (Particle Data Group), *Review of Particle Physics*, Eur. Phys. J. **C15**, 1 (2000).
2. I. Duniety, Phys. Rev. **D58**, 094010 (1998).
3. P. Migliozi *et al.*, Phys. Lett. **B462**, 217 (1999).

## $\Lambda_c^+$ BRANCHING RATIOS

### Hadronic modes with a $p$ : $S = -1$ final states

$\Gamma(p\bar{K}^0)/\Gamma(pK^-\pi^+)$					$\Gamma_1/\Gamma_2$
VALUE	EVTs	DOCUMENT ID	TECN	COMMENT	
<b>0.47 ± 0.04 OUR AVERAGE</b>					
0.46 ± 0.02 ± 0.04	1025	ALAM	98 CLE2	$e^+e^- \approx \Upsilon(4S)$	
0.44 ± 0.07 ± 0.05	133	AVERY	91 CLEO	$e^+e^- 10.5$ GeV	
0.55 ± 0.17 ± 0.14	45	ANJOS	90 E691	$\gamma$ Be 70–260 GeV	
0.62 ± 0.15 ± 0.03	73	ALBRECHT	88c ARG	$e^+e^- 10$ GeV	

$\Gamma(pK^-\pi^+)/\Gamma_{total}$					$\Gamma_2/\Gamma$
See the note on " $\Lambda_c^+$ Branching Fractions" above.					

VALUE	EVTs	DOCUMENT ID	TECN	COMMENT	
<b>0.050 ± 0.013 OUR FIT</b>					
<b>0.050 ± 0.013</b>		PDG	02	See note at top of ratios	
• • • We do not use the following data for averages, fits, limits, etc. • • •					
0.050 ± 0.005 ± 0.012	1205	<sup>2</sup> JAFPE	00 CLE2	$e^+e^- 10.52-10.58$ GeV	
0.041 ± 0.010		<sup>3,4</sup> ALBRECHT	92o ARG	$e^+e^- \approx \Upsilon(4S)$	
0.044 ± 0.012		<sup>3,5</sup> CRAWFORD	92 CLEO	$e^+e^- 10.5$ GeV	

<sup>2</sup>JAFPE 00 assumes that a  $\bar{D}$  meson and an antiproton in opposite hemispheres tags for a  $\Lambda_c^+$  in the hemisphere of the  $\bar{p}$ . The fraction of such  $\bar{D}\bar{p}$  events with a  $\Lambda_c^+ \rightarrow pK^-\pi^+$  decay then gives the  $pK^-\pi^+$  branching fraction. See the paper for assumptions, caveats, etc.

<sup>3</sup>To extract  $\Gamma(pK^-\pi^+)/\Gamma_{total}$ , we use  $B(\bar{B} \rightarrow \Lambda_c^+ X) \cdot B(\Lambda_c^+ \rightarrow pK^-\pi^+) = (0.28 \pm 0.06)\%$ , which is the average of measurements from ARGUS (ALBRECHT 88c) and CLEO (CRAWFORD 92).

<sup>4</sup>ALBRECHT 92o measures  $B(\bar{B} \rightarrow \Lambda_c^+ X) = (6.8 \pm 0.5 \pm 0.3)\%$ .

<sup>5</sup>CRAWFORD 92 measures  $B(\bar{B} \rightarrow \Lambda_c^+ X) = (6.4 \pm 0.8 \pm 0.8)\%$ .

$\Gamma(p\bar{K}^*(892)^0)/\Gamma(pK^-\pi^+)$					$\Gamma_3/\Gamma_2$
Unseen decay modes of the $\bar{K}^*(892)^0$ are included.					
VALUE	EVTs	DOCUMENT ID	TECN	COMMENT	
<b>0.31 ± 0.04 OUR AVERAGE</b>					
0.29 ± 0.04 ± 0.03		<sup>6</sup> AITALA	00 E791	$\pi^- N$ , 500 GeV	
0.35 ± 0.06 ± 0.03	39	BOZEK	93 NA32	$\pi^-$ Cu 230 GeV	
0.42 ± 0.24	12	BASILE	81b CNTR	$pp \rightarrow \Lambda_c^+ e^- X$	
• • • We do not use the following data for averages, fits, limits, etc. • • •					
0.35 ± 0.11		BARLAG	90d NA32	See BOZEK 93	

<sup>6</sup>AITALA 00 makes a coherent 5-dimensional amplitude analysis of  $946 \pm 38 \Lambda_c^+ \rightarrow pK^-\pi^+$  decays.

$\Gamma(\Delta(1232)^{++}K^-)/\Gamma(pK^-\pi^+)$					$\Gamma_4/\Gamma_2$
Unseen decay modes of the $\Delta(1232)^{++}$ are included.					
VALUE	EVTs	DOCUMENT ID	TECN	COMMENT	
<b>0.17 ± 0.04 OUR AVERAGE</b>					
0.18 ± 0.03 ± 0.03		<sup>7</sup> AITALA	00 E791	$\pi^- N$ , 500 GeV	
0.12 ± 0.04 ± 0.05	14	BOZEK	93 NA32	$\pi^-$ Cu 230 GeV	
0.40 ± 0.17	17	BASILE	81b CNTR	$pp \rightarrow \Lambda_c^+ e^- X$	

<sup>7</sup>AITALA 00 makes a coherent 5-dimensional amplitude analysis of  $946 \pm 38 \Lambda_c^+ \rightarrow pK^-\pi^+$  decays.

$\Gamma(\Lambda(1520)\pi^+)/\Gamma(pK^-\pi^+)$					$\Gamma_5/\Gamma_2$
Unseen decay modes of the $\Lambda(1520)$ are included.					
VALUE	EVTs	DOCUMENT ID	TECN	COMMENT	
<b>0.35 ± 0.08 OUR AVERAGE</b>					
0.34 ± 0.08 ± 0.05		<sup>8</sup> AITALA	00 E791	$\pi^- N$ , 500 GeV	
0.40 ± 0.18 ± 0.09	12	BOZEK	93 NA32	$\pi^-$ Cu 230 GeV	

<sup>8</sup>AITALA 00 makes a coherent 5-dimensional amplitude analysis of  $946 \pm 38 \Lambda_c^+ \rightarrow pK^-\pi^+$  decays.

$\Gamma(pK^-\pi^+ \text{ nonresonant})/\Gamma(pK^-\pi^+)$					$\Gamma_6/\Gamma_2$
VALUE	EVTs	DOCUMENT ID	TECN	COMMENT	
<b>0.55 ± 0.06 OUR AVERAGE</b>					
0.55 ± 0.06 ± 0.04		<sup>9</sup> AITALA	00 E791	$\pi^- N$ , 500 GeV	
0.56 ± 0.07 ± 0.05	71	BOZEK	93 NA32	$\pi^-$ Cu 230 GeV	

<sup>9</sup>AITALA 00 makes a coherent 5-dimensional amplitude analysis of  $946 \pm 38 \Lambda_c^+ \rightarrow pK^-\pi^+$  decays.

$\Gamma(p\bar{K}^0\pi^0)/\Gamma(pK^-\pi^+)$					$\Gamma_7/\Gamma_2$
VALUE	EVTs	DOCUMENT ID	TECN	COMMENT	
<b>0.66 ± 0.05 ± 0.07</b>	774	ALAM	98 CLE2	$e^+e^- \approx \Upsilon(4S)$	

$\Gamma(p\bar{K}^0\eta)/\Gamma(pK^-\pi^+)$					$\Gamma_8/\Gamma_2$
Unseen decay modes of the $\eta$ are included.					
VALUE	EVTs	DOCUMENT ID	TECN	COMMENT	
<b>0.25 ± 0.04 ± 0.04</b>	57	AMMAR	95 CLE2	$e^+e^- \approx \Upsilon(4S)$	

$\Gamma(p\bar{K}^0\pi^+\pi^-)/\Gamma(pK^-\pi^+)$					$\Gamma_9/\Gamma_2$
VALUE	EVTs	DOCUMENT ID	TECN	COMMENT	
<b>0.51 ± 0.06 OUR AVERAGE</b>					
0.52 ± 0.04 ± 0.05	985	ALAM	98 CLE2	$e^+e^- \approx \Upsilon(4S)$	
0.43 ± 0.12 ± 0.04	83	AVERY	91 CLEO	$e^+e^- 10.5$ GeV	
0.98 ± 0.36 ± 0.08	12	BARLAG	90d NA32	$\pi^-$ 230 GeV	

$\Gamma(pK^-\pi^+\pi^0)/\Gamma(pK^-\pi^+)$					$\Gamma_{10}/\Gamma_2$
VALUE	EVTs	DOCUMENT ID	TECN	COMMENT	
<b>0.67 ± 0.04 ± 0.11</b>	2606	ALAM	98 CLE2	$e^+e^- \approx \Upsilon(4S)$	

$\Gamma(pK^*(892)^-\pi^+)/\Gamma(p\bar{K}^0\pi^+\pi^-)$					$\Gamma_{11}/\Gamma_9$
Unseen decay modes of the $K^*(892)^-$ are included.					
VALUE	EVTs	DOCUMENT ID	TECN	COMMENT	
<b>0.44 ± 0.14</b>	17	ALEEV	94 BIS2	$n\bar{N}$ 20–70 GeV	

$\Gamma(p(K^-\pi^+)_{\text{nonresonant}}\pi^0)/\Gamma(pK^-\pi^+)$					$\Gamma_{12}/\Gamma_2$
VALUE	EVTs	DOCUMENT ID	TECN	COMMENT	
<b>0.73 ± 0.12 ± 0.05</b>	67	BOZEK	93 NA32	$\pi^-$ Cu 230 GeV	

$\Gamma(\Delta(1232)\bar{K}^*(892))/\Gamma_{total}$					$\Gamma_{13}/\Gamma$
VALUE	EVTs	DOCUMENT ID	TECN	COMMENT	
<b>seen</b>	35	AMENDOLIA	87 SPEC	$\gamma$ Ge-Si	

$\Gamma(pK^-\pi^+\pi^+\pi^-)/\Gamma(pK^-\pi^+)$					$\Gamma_{14}/\Gamma_2$
VALUE	EVTs	DOCUMENT ID	TECN	COMMENT	
<b>0.022 ± 0.015</b>		BARLAG	90d NA32	$\pi^-$ 230 GeV	

$\Gamma(pK^-\pi^+\pi^0\pi^0)/\Gamma(pK^-\pi^+)$					$\Gamma_{15}/\Gamma_2$
VALUE	EVTs	DOCUMENT ID	TECN	COMMENT	
<b>0.16 ± 0.07 ± 0.03</b>	15	BOZEK	93 NA32	$\pi^-$ Cu 230 GeV	

$\Gamma(pK^-\pi^+3\pi^0)/\Gamma(pK^-\pi^+)$					$\Gamma_{16}/\Gamma_2$
VALUE	EVTs	DOCUMENT ID	TECN	COMMENT	
<b>• • •</b>					
0.10 ± 0.06 ± 0.02	8	BOZEK	93 NA32	$\pi^-$ Cu 230 GeV	

### Hadronic modes with a $p$ : $S = 0$ final states

$\Gamma(p\pi^+\pi^-)/\Gamma(pK^-\pi^+)$					$\Gamma_{17}/\Gamma_2$
VALUE	EVTs	DOCUMENT ID	TECN	COMMENT	
<b>0.069 ± 0.036</b>		BARLAG	90d NA32	$\pi^-$ 230 GeV	

## Baryon Particle Listings

 $\Lambda_C^+$  $\Gamma(\rho f_0(980))/\Gamma(\rho K^- \pi^+)$   $\Gamma_{18}/\Gamma_2$ 

Unseen decay modes of the  $f_0(980)$  are included.

VALUE	DOCUMENT ID	TECN	COMMENT
<b>0.055 ± 0.036</b>	BARLAG	90D	NA32 $\pi^-$ 230 GeV

 $\Gamma(\rho \pi^+ \pi^+ \pi^- \pi^-)/\Gamma(\rho K^- \pi^+)$   $\Gamma_{19}/\Gamma_2$ 

VALUE	DOCUMENT ID	TECN	COMMENT
<b>0.036 ± 0.023</b>	BARLAG	90D	NA32 $\pi^-$ 230 GeV

 $\Gamma(\rho K^+ K^-)/\Gamma(\rho K^- \pi^+)$   $\Gamma_{20}/\Gamma_2$ 

VALUE	EVTS	DOCUMENT ID	TECN	COMMENT
<b>0.015 ± 0.006 OUR AVERAGE</b>		Error includes scale factor of 2.1.		
0.014 ± 0.002 ± 0.002	676	ABE	02c	BELL $e^+ e^- \approx \Upsilon(4S)$
0.039 ± 0.009 ± 0.007	214	ALEXANDER	96c	CLE2 $e^+ e^- \approx \Upsilon(4S)$
• • • We do not use the following data for averages, fits, limits, etc. • • •				
0.096 ± 0.029 ± 0.010	30	FRABETTI	93H	E687 $\gamma$ Be, $\bar{E}_\gamma$ 220 GeV
0.048 ± 0.027		BARLAG	90D	NA32 $\pi^-$ 230 GeV

 $\Gamma(\rho \phi)/\Gamma(\rho K^- \pi^+)$   $\Gamma_{21}/\Gamma_2$ 

Unseen decay modes of the  $\phi$  are included.

VALUE	EVTS	DOCUMENT ID	TECN	COMMENT
<b>0.0164 ± 0.0032 OUR AVERAGE</b>		Error includes scale factor of 1.2.		
0.015 ± 0.002 ± 0.002	345	ABE	02c	BELL $e^+ e^- \approx \Upsilon(4S)$
0.024 ± 0.006 ± 0.003	54	ALEXANDER	96c	CLE2 $e^+ e^- \approx \Upsilon(4S)$
• • • We do not use the following data for averages, fits, limits, etc. • • •				
0.040 ± 0.027		BARLAG	90D	NA32 $\pi^-$ 230 GeV

 $\Gamma(\rho K^+ K^- \text{ non-}\phi)/\Gamma(\rho K^- \pi^+)$   $\Gamma_{22}/\Gamma_2$ 

VALUE	EVTS	DOCUMENT ID	TECN	COMMENT
<b>0.007 ± 0.002 ± 0.002</b>	344	ABE	02c	BELL $e^+ e^- \approx \Upsilon(4S)$

Hadronic modes with a hyperon:  $S = -1$  final states $\Gamma(\Lambda \pi^+)/\Gamma(\rho K^- \pi^+)$   $\Gamma_{23}/\Gamma_2$ 

VALUE	CL%	EVTS	DOCUMENT ID	TECN	COMMENT
<b>0.214 ± 0.016 OUR FIT</b>			Error includes scale factor of 1.1.		
<b>0.204 ± 0.019 OUR AVERAGE</b>					
0.217 ± 0.013 ± 0.020		750	LINK	05F	FOCS $\gamma$ nucleus, $\bar{E}_\gamma \approx 180$ GeV
0.18 ± 0.03 ± 0.04			ALBRECHT	92	ARG $e^+ e^- \approx 10.4$ GeV
0.18 ± 0.03 ± 0.03		87	AVERY	91	CLEO $e^+ e^-$ 10.5 GeV
• • • We do not use the following data for averages, fits, limits, etc. • • •					
<0.33		90	ANJOS	90	E691 $\gamma$ Be 70–260 GeV
<0.16		90	ALBRECHT	88c	ARG $e^+ e^-$ 10 GeV

 $\Gamma(\Lambda \pi^+ \pi^0)/\Gamma(\rho K^- \pi^+)$   $\Gamma_{24}/\Gamma_2$ 

VALUE	EVTS	DOCUMENT ID	TECN	COMMENT
<b>0.73 ± 0.09 ± 0.16</b>	464	AVERY	94	CLE2 $e^+ e^- \approx \Upsilon(3S), \Upsilon(4S)$

 $\Gamma(\Lambda \rho^+)/\Gamma(\rho K^- \pi^+)$   $\Gamma_{25}/\Gamma_2$ 

VALUE	CL%	DOCUMENT ID	TECN	COMMENT
<b>&lt;0.95</b>	95	AVERY	94	CLE2 $e^+ e^- \approx \Upsilon(3S), \Upsilon(4S)$

 $\Gamma(\Lambda \pi^+ \pi^+ \pi^-)/\Gamma(\rho K^- \pi^+)$   $\Gamma_{26}/\Gamma_2$ 

VALUE	EVTS	DOCUMENT ID	TECN	COMMENT
<b>0.525 ± 0.032 OUR FIT</b>				
<b>0.522 ± 0.032 OUR AVERAGE</b>				
0.508 ± 0.024 ± 0.024	1356	LINK	05F	FOCS $\gamma$ nucleus, $\bar{E}_\gamma \approx 180$ GeV
0.65 ± 0.11 ± 0.12	289	AVERY	91	CLEO $e^+ e^-$ 10.5 GeV
0.82 ± 0.29 ± 0.27	44	ANJOS	90	E691 $\gamma$ Be 70–260 GeV
0.94 ± 0.41 ± 0.13	10	BARLAG	90D	NA32 $\pi^-$ 230 GeV
0.61 ± 0.16 ± 0.04	105	ALBRECHT	88c	ARG $e^+ e^-$ 10 GeV

 $\Gamma(\Sigma(1385)^+ \pi^+ \pi^-, \Sigma^{*+} \rightarrow \Lambda \pi^+)/\Gamma(\Lambda \pi^+ \pi^+ \pi^-)$   $\Gamma_{27}/\Gamma_{26}$ 

VALUE	DOCUMENT ID	TECN	COMMENT
<b>0.28 ± 0.10 ± 0.08</b>	LINK	05F	FOCS $\gamma$ nucleus, $\bar{E}_\gamma \approx 180$ GeV

 $\Gamma(\Sigma(1385)^- \pi^+ \pi^+, \Sigma^{*-} \rightarrow \Lambda \pi^-)/\Gamma(\Lambda \pi^+ \pi^+ \pi^-)$   $\Gamma_{28}/\Gamma_{26}$ 

VALUE	DOCUMENT ID	TECN	COMMENT
<b>0.21 ± 0.03 ± 0.02</b>	LINK	05F	FOCS $\gamma$ nucleus, $\bar{E}_\gamma \approx 180$ GeV

 $\Gamma(\Lambda \pi^+ \rho^0)/\Gamma(\Lambda \pi^+ \pi^+ \pi^-)$   $\Gamma_{29}/\Gamma_{26}$ 

VALUE	DOCUMENT ID	TECN	COMMENT
<b>0.40 ± 0.12 ± 0.12</b>	LINK	05F	FOCS $\gamma$ nucleus, $\bar{E}_\gamma \approx 180$ GeV

 $\Gamma(\Sigma(1385)^+ \rho^0, \Sigma^{*+} \rightarrow \Lambda \pi^+)/\Gamma(\Lambda \pi^+ \pi^+ \pi^-)$   $\Gamma_{30}/\Gamma_{26}$ 

VALUE	DOCUMENT ID	TECN	COMMENT
<b>0.14 ± 0.09 ± 0.07</b>	LINK	05F	FOCS $\gamma$ nucleus, $\bar{E}_\gamma \approx 180$ GeV

 $\Gamma(\Lambda \pi^+ \pi^+ \pi^- \text{ nonresonant})/\Gamma(\Lambda \pi^+ \pi^+ \pi^-)$   $\Gamma_{31}/\Gamma_{26}$ 

VALUE	CL%	DOCUMENT ID	TECN	COMMENT
<b>&lt;0.3</b>	90	LINK	05F	FOCS $\gamma$ nucleus, $\bar{E}_\gamma \approx 180$ GeV

 $\Gamma(\rho \bar{K}^0 \pi^+ \pi^-)/\Gamma(\Lambda \pi^+ \pi^+ \pi^-)$   $\Gamma_9/\Gamma_{26}$ 

VALUE	EVTS	DOCUMENT ID	TECN	COMMENT
• • • We do not use the following data for averages, fits, limits, etc. • • •				
2.6 ± 1.2		ALEEVE	96	SPEC $n$ nucleus, 50 GeV/c
4.3 ± 1.2	130	ALEEVE	84	BIS2 $n$ C 40–70 GeV

 $\Gamma(\Lambda \pi^+ \pi^+ \pi^- \pi^0 \text{ total})/\Gamma(\rho K^- \pi^+)$   $\Gamma_{32}/\Gamma_2$ 

VALUE	EVTS	DOCUMENT ID	TECN	COMMENT
<b>0.36 ± 0.09 ± 0.09</b>	50	<sup>10</sup> CRONIN-HEN..03	CLE3	$e^+ e^- \approx \Upsilon(4S)$
<sup>10</sup> CRONIN-HENNESSY 03 finds this channel to be dominantly $\Lambda \eta \pi^+$ and $\Lambda \omega \pi^+$ ; see below.				

 $\Gamma(\Lambda \pi^+ \eta)/\Gamma(\rho K^- \pi^+)$   $\Gamma_{33}/\Gamma_2$ 

Unseen decay modes of the  $\eta$  are included.

VALUE	EVTS	DOCUMENT ID	TECN	COMMENT
<b>0.36 ± 0.07 OUR AVERAGE</b>				
0.41 ± 0.17 ± 0.10	11	CRONIN-HEN..03	CLE3	$e^+ e^- \approx \Upsilon(4S)$
0.35 ± 0.05 ± 0.06	116	AMMAR	95	CLE2 $e^+ e^- \approx \Upsilon(4S)$

 $\Gamma(\Sigma(1385)^+ \eta)/\Gamma(\rho K^- \pi^+)$   $\Gamma_{34}/\Gamma_2$ 

Unseen decay modes of the  $\Sigma(1385)^+$  and  $\eta$  are included.

VALUE	EVTS	DOCUMENT ID	TECN	COMMENT
<b>0.17 ± 0.04 ± 0.03</b>	54	AMMAR	95	CLE2 $e^+ e^- \approx \Upsilon(4S)$

 $\Gamma(\Lambda \pi^+ \omega)/\Gamma(\rho K^- \pi^+)$   $\Gamma_{35}/\Gamma_2$ 

Unseen decay modes of the  $\omega$  are included.

VALUE	EVTS	DOCUMENT ID	TECN	COMMENT
<b>0.24 ± 0.06 ± 0.06</b>	32	CRONIN-HEN..03	CLE3	$e^+ e^- \approx \Upsilon(4S)$

 $\Gamma(\Lambda \pi^+ \pi^+ \pi^- \pi^0, \text{ no } \eta \text{ or } \omega)/\Gamma(\rho K^- \pi^+)$   $\Gamma_{36}/\Gamma_2$ 

VALUE	CL%	DOCUMENT ID	TECN	COMMENT
<b>&lt;0.13</b>	90	CRONIN-HEN..03	CLE3	$e^+ e^- \approx \Upsilon(4S)$

 $\Gamma(\Lambda K^+ \bar{K}^0)/\Gamma(\rho K^- \pi^+)$   $\Gamma_{37}/\Gamma_2$ 

VALUE	EVTS	DOCUMENT ID	TECN	COMMENT
<b>0.093 ± 0.018 OUR FIT</b>		Error includes scale factor of 1.7.		
<b>0.131 ± 0.020 OUR AVERAGE</b>				
0.142 ± 0.018 ± 0.022	251	LINK	05F	FOCS $\gamma$ nucleus, $\bar{E}_\gamma \approx 180$ GeV
0.12 ± 0.02 ± 0.02	59	AMMAR	95	CLE2 $e^+ e^- \approx \Upsilon(4S)$

 $\Gamma(\Xi(1690)^0 K^+, \Xi^{*0} \rightarrow \Lambda \bar{K}^0)/\Gamma(\Lambda K^+ \bar{K}^0)$   $\Gamma_{38}/\Gamma_{37}$ 

VALUE	EVTS	DOCUMENT ID	TECN	COMMENT
<b>0.28 ± 0.07 OUR AVERAGE</b>				
0.32 ± 0.10 ± 0.04	84 ± 24	LINK	05F	FOCS $\gamma$ nucleus, $\bar{E}_\gamma \approx 180$ GeV
0.26 ± 0.08 ± 0.03	93	ABE	02c	BELL $e^+ e^- \approx \Upsilon(4S)$

 $\Gamma(\Lambda K^+ \bar{K}^0)/\Gamma(\Lambda \pi^+)$   $\Gamma_{37}/\Gamma_{23}$ 

VALUE	EVTS	DOCUMENT ID	TECN	COMMENT
<b>0.43 ± 0.08 OUR FIT</b>		Error includes scale factor of 2.0.		
<b>0.395 ± 0.026 ± 0.036</b>	460 ± 30	AUBERT	07U	BABR $e^+ e^- \approx \Upsilon(4S)$

 $\Gamma(\Sigma^0 \pi^+)/\Gamma(\rho K^- \pi^+)$   $\Gamma_{39}/\Gamma_2$ 

VALUE	EVTS	DOCUMENT ID	TECN	COMMENT
<b>0.210 ± 0.018 OUR FIT</b>				
<b>0.20 ± 0.04 OUR AVERAGE</b>				
0.21 ± 0.02 ± 0.04	196	AVERY	94	CLE2 $e^+ e^- \approx \Upsilon(3S), \Upsilon(4S)$
0.17 ± 0.06 ± 0.04		ALBRECHT	92	ARG $e^+ e^- \approx 10.4$ GeV

 $\Gamma(\Sigma^0 \pi^+)/\Gamma(\Lambda \pi^+)$   $\Gamma_{39}/\Gamma_{23}$ 

VALUE	EVTS	DOCUMENT ID	TECN	COMMENT
<b>0.98 ± 0.05 OUR FIT</b>				
<b>0.98 ± 0.05 OUR AVERAGE</b>				
0.977 ± 0.015 ± 0.051	33k	AUBERT	07U	BABR $e^+ e^- \approx \Upsilon(4S)$
1.09 ± 0.11 ± 0.19	750	LINK	05F	FOCS $\gamma$ nucleus, $\bar{E}_\gamma \approx 180$ GeV

 $\Gamma(\Sigma^+ \pi^0)/\Gamma(\rho K^- \pi^+)$   $\Gamma_{40}/\Gamma_2$ 

VALUE	EVTS	DOCUMENT ID	TECN	COMMENT
<b>0.20 ± 0.03 ± 0.03</b>	93	KUBOTA	93	CLE2 $e^+ e^- \approx \Upsilon(4S)$

 $\Gamma(\Sigma^+ \eta)/\Gamma(\rho K^- \pi^+)$   $\Gamma_{41}/\Gamma_2$ 

Unseen decay modes of the  $\eta$  are included.

VALUE	EVTS	DOCUMENT ID	TECN	COMMENT
<b>0.11 ± 0.03 ± 0.02</b>	26	AMMAR	95	CLE2 $e^+ e^- \approx \Upsilon(4S)$

 $\Gamma(\Sigma^+ \pi^+ \pi^-)/\Gamma(\rho K^- \pi^+)$   $\Gamma_{42}/\Gamma_2$ 

VALUE	EVTS	DOCUMENT ID	TECN	COMMENT
<b>0.72 ± 0.07 OUR FIT</b>				
<b>0.69 ± 0.08 OUR AVERAGE</b>				
0.72 ± 0.14	47 ± 9	VAZQUEZ-JA...08	SELX	$\Sigma^-$ nucleus, 600 GeV
0.74 ± 0.07 ± 0.09	487	KUBOTA	93	CLE2 $e^+ e^- \approx \Upsilon(4S)$
0.54 $^{+0.18}_{-0.15}$	11	BARLAG	92	NA32 $\pi^-$ Cu 230 GeV

 $\Gamma(\Sigma^+ \rho^0)/\Gamma(\rho K^- \pi^+)$   $\Gamma_{43}/\Gamma_2$ 

VALUE	CL%	DOCUMENT ID	TECN	COMMENT
<b>&lt;0.27</b>	95	KUBOTA	93	CLE2 $e^+ e^- \approx \Upsilon(4S)$

$\Gamma(\Sigma^- \pi^+ \pi^+)/\Gamma(\rho K^- \pi^+)$   $\Gamma_{44}/\Gamma_2$

VALUE	EVTS	DOCUMENT ID	TECN	COMMENT
<b>0.33 ± 0.06 OUR FIT</b>				
0.314 ± 0.067	30 ± 6	VAZQUEZ-JA...08	SELX	$\Sigma^-$ nucleus, 600 GeV

$\Gamma(\Sigma^- \pi^+ \pi^+)/\Gamma(\Sigma^+ \pi^+ \pi^-)$   $\Gamma_{44}/\Gamma_{42}$

VALUE	EVTS	DOCUMENT ID	TECN	COMMENT
<b>0.46 ± 0.09 OUR FIT</b>				
0.53 ± 0.15 ± 0.07	56	FRABETTI 94E	E687	$\gamma$ Be, $\bar{E}_\gamma$ 220 GeV

$\Gamma(\Sigma^0 \pi^+ \pi^0)/\Gamma(\rho K^- \pi^+)$   $\Gamma_{45}/\Gamma_2$

VALUE	EVTS	DOCUMENT ID	TECN	COMMENT
<b>0.36 ± 0.09 ± 0.10</b>				
0.36 ± 0.09 ± 0.10	117	AVERY 94	CLE2	$e^+ e^- \approx \Upsilon(3S), \Upsilon(4S)$

$\Gamma(\Sigma^0 \pi^+ \pi^+ \pi^-)/\Gamma(\rho K^- \pi^+)$   $\Gamma_{46}/\Gamma_2$

VALUE	EVTS	DOCUMENT ID	TECN	COMMENT
<b>0.17 ± 0.04 OUR FIT</b>				
0.21 ± 0.05 ± 0.05	90	AVERY 94	CLE2	$e^+ e^- \approx \Upsilon(3S), \Upsilon(4S)$

$\Gamma(\Sigma^0 \pi^+ \pi^+ \pi^-)/\Gamma(\Lambda \pi^+ \pi^-)$   $\Gamma_{46}/\Gamma_{26}$

VALUE	EVTS	DOCUMENT ID	TECN	COMMENT
<b>0.31 ± 0.08 OUR FIT</b>				
0.26 ± 0.06 ± 0.09	480	LINK 05F	FOCS	$\gamma$ nucleus, $\bar{E}_\gamma \approx 180$ GeV

$\Gamma(\Sigma^+ \omega)/\Gamma(\rho K^- \pi^+)$   $\Gamma_{48}/\Gamma_2$

Unseen decay modes of the  $\omega$  are included.

VALUE	EVTS	DOCUMENT ID	TECN	COMMENT
<b>0.54 ± 0.13 ± 0.06</b>				
0.54 ± 0.13 ± 0.06	107	KUBOTA 93	CLE2	$e^+ e^- \approx \Upsilon(4S)$

$\Gamma(\Sigma^+ K^+ K^-)/\Gamma(\rho K^- \pi^+)$   $\Gamma_{49}/\Gamma_2$

VALUE	EVTS	DOCUMENT ID	TECN	COMMENT
<b>0.056 ± 0.008 OUR FIT</b>				
0.070 ± 0.011 ± 0.011	59	AVERY 93	CLE2	$e^+ e^- \approx 10.5$ GeV

$\Gamma(\Sigma^+ K^+ K^-)/\Gamma(\Sigma^+ \pi^+ \pi^-)$   $\Gamma_{49}/\Gamma_{42}$

VALUE	EVTS	DOCUMENT ID	TECN	COMMENT
<b>0.078 ± 0.009 OUR FIT</b>				
0.074 ± 0.009 OUR AVERAGE				
0.076 ± 0.007 ± 0.009	246	ABE 02c	BELL	$e^+ e^- \approx \Upsilon(4S)$
0.071 ± 0.011 ± 0.011	103	LINK 02G	FOCS	$\gamma$ nucleus, $\approx 180$ GeV

$\Gamma(\Sigma^+ \phi)/\Gamma(\rho K^- \pi^+)$   $\Gamma_{50}/\Gamma_2$

Unseen decay modes of the  $\phi$  are included.

VALUE	EVTS	DOCUMENT ID	TECN	COMMENT
<b>0.062 ± 0.010 OUR FIT</b>				
0.069 ± 0.023 ± 0.016	26	AVERY 93	CLE2	$e^+ e^- \approx 10.5$ GeV

$\Gamma(\Sigma^+ \phi)/\Gamma(\Sigma^+ \pi^+ \pi^-)$   $\Gamma_{50}/\Gamma_{42}$

Unseen decay modes of the  $\phi$  are included.

VALUE	EVTS	DOCUMENT ID	TECN	COMMENT
<b>0.087 ± 0.012 OUR FIT</b>				
0.086 ± 0.012 OUR AVERAGE				
0.085 ± 0.012 ± 0.012	129	ABE 02c	BELL	$e^+ e^- \approx \Upsilon(4S)$
0.087 ± 0.016 ± 0.006	57	LINK 02G	FOCS	$\gamma$ nucleus, $\approx 180$ GeV

$\Gamma(\Xi(1690)^0 K^+, \Xi^{*0} \rightarrow \Sigma^+ K^-)/\Gamma(\Sigma^+ \pi^+ \pi^-)$   $\Gamma_{51}/\Gamma_{42}$

VALUE	EVTS	DOCUMENT ID	TECN	COMMENT
<b>0.023 ± 0.005 OUR AVERAGE</b>				
0.023 ± 0.005 ± 0.005	75	ABE 02c	BELL	$e^+ e^- \approx \Upsilon(4S)$
0.022 ± 0.006 ± 0.006	34	LINK 02G	FOCS	$\gamma$ nucleus, $\approx 180$ GeV

$\Gamma(\Sigma^+ K^+ K^- \text{ nonresonant})/\Gamma(\Sigma^+ \pi^+ \pi^-)$   $\Gamma_{52}/\Gamma_{42}$

VALUE	CL%	DOCUMENT ID	TECN	COMMENT
<b>&lt;0.018</b>				
<0.018	90	ABE 02c	BELL	$e^+ e^- \approx \Upsilon(4S)$
<0.028	90	LINK 02G	FOCS	$\gamma$ nucleus, $\approx 180$ GeV

• • • We do not use the following data for averages, fits, limits, etc. • • •

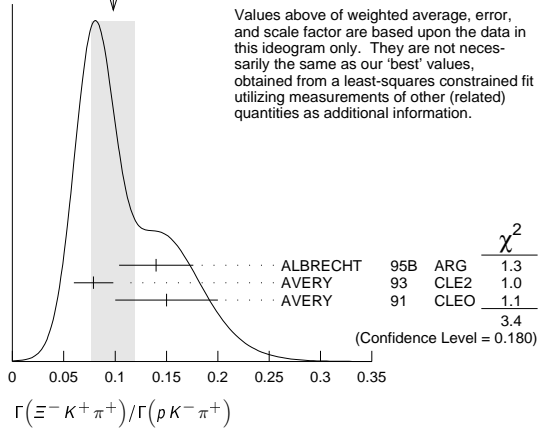
$\Gamma(\Xi^0 K^+)/\Gamma(\rho K^- \pi^+)$   $\Gamma_{53}/\Gamma_2$

VALUE	EVTS	DOCUMENT ID	TECN	COMMENT
<b>0.078 ± 0.013 ± 0.013</b>				
0.078 ± 0.013 ± 0.013	56	AVERY 93	CLE2	$e^+ e^- \approx 10.5$ GeV

$\Gamma(\Xi^- K^+ \pi^+)/\Gamma(\rho K^- \pi^+)$   $\Gamma_{54}/\Gamma_2$

VALUE	EVTS	DOCUMENT ID	TECN	COMMENT
<b>0.102 ± 0.010 OUR FIT</b>				Error includes scale factor of 1.1.
<b>0.098 ± 0.021 OUR AVERAGE</b>				Error includes scale factor of 1.3. See the ideogram below.
0.14 ± 0.03 ± 0.02	34	ALBRECHT 95B	ARG	$e^+ e^- \approx 10.4$ GeV
0.079 ± 0.013 ± 0.014	60	AVERY 93	CLE2	$e^+ e^- \approx 10.5$ GeV
0.15 ± 0.04 ± 0.03	30	AVERY 91	CLEO	$e^+ e^- 10.5$ GeV

WEIGHTED AVERAGE  
0.098±0.021 (Error scaled by 1.3)



$\Gamma(\Xi(1530)^0 K^+)/\Gamma(\rho K^- \pi^+)$   $\Gamma_{55}/\Gamma_2$

Unseen decay modes of the  $\Xi(1530)^0$  are included.

VALUE	EVTS	DOCUMENT ID	TECN	COMMENT
<b>0.052 ± 0.014 OUR AVERAGE</b>				
0.05 ± 0.02 ± 0.01	11	ALBRECHT 95B	ARG	$e^+ e^- \approx 10.4$ GeV
0.053 ± 0.016 ± 0.010	24	AVERY 93	CLE2	$e^+ e^- \approx 10.5$ GeV

$\Gamma(\Xi^- K^+ \pi^+)/\Gamma(\Lambda \pi^+)$   $\Gamma_{54}/\Gamma_{23}$

VALUE	EVTS	DOCUMENT ID	TECN	COMMENT
<b>0.47 ± 0.04 OUR FIT</b>				
0.480 ± 0.016 ± 0.039	2665 ± 84	AUBERT 07u	BABR	$e^+ e^- \approx \Upsilon(4S)$

Hadronic modes with a hyperon: S = 0 final states

$\Gamma(\Lambda K^+)/\Gamma(\Lambda \pi^+)$   $\Gamma_{56}/\Gamma_{23}$

VALUE	EVTS	DOCUMENT ID	TECN	COMMENT
<b>0.047 ± 0.009 OUR AVERAGE</b>				Error includes scale factor of 1.8.
0.044 ± 0.004 ± 0.003	1162 ± 101	AUBERT 07u	BABR	$e^+ e^- \approx \Upsilon(4S)$
0.074 ± 0.010 ± 0.012	265	ABE 02c	BELL	$e^+ e^- \approx \Upsilon(4S)$

$\Gamma(\Lambda K^+ \pi^+ \pi^-)/\Gamma(\Lambda \pi^+)$   $\Gamma_{57}/\Gamma_{23}$

VALUE	CL%	DOCUMENT ID	TECN	COMMENT
<b>&lt;4.1 × 10<sup>-2</sup></b>				
<4.1 × 10 <sup>-2</sup>	90	AUBERT 07u	BABR	$e^+ e^- \approx \Upsilon(4S)$

$\Gamma(\Sigma^0 K^+)/\Gamma(\Sigma^0 \pi^+)$   $\Gamma_{58}/\Gamma_{39}$

VALUE	EVTS	DOCUMENT ID	TECN	COMMENT
<b>0.040 ± 0.006 OUR AVERAGE</b>				
0.038 ± 0.005 ± 0.003	366 ± 52	AUBERT 07u	BABR	$e^+ e^- \approx \Upsilon(4S)$
0.056 ± 0.014 ± 0.008	75	ABE 02c	BELL	$e^+ e^- \approx \Upsilon(4S)$

$\Gamma(\Sigma^0 K^+ \pi^+ \pi^-)/\Gamma(\Sigma^0 \pi^+)$   $\Gamma_{59}/\Gamma_{39}$

VALUE	CL%	DOCUMENT ID	TECN	COMMENT
<b>&lt;2.0 × 10<sup>-2</sup></b>				
<2.0 × 10 <sup>-2</sup>	90	AUBERT 07u	BABR	$e^+ e^- \approx \Upsilon(4S)$

$\Gamma(\Sigma^+ K^+ \pi^-)/\Gamma(\Sigma^+ \pi^+ \pi^-)$   $\Gamma_{60}/\Gamma_{42}$

VALUE	EVTS	DOCUMENT ID	TECN	COMMENT
<b>0.047 ± 0.011 ± 0.008</b>				
0.047 ± 0.011 ± 0.008	105	ABE 02c	BELL	$e^+ e^- \approx \Upsilon(4S)$

$\Gamma(\Sigma^+ K^*(892)^0)/\Gamma(\Sigma^+ \pi^+ \pi^-)$   $\Gamma_{61}/\Gamma_{42}$

Unseen decay modes of the  $K^*(892)^0$  are included.

VALUE	EVTS	DOCUMENT ID	TECN	COMMENT
<b>0.078 ± 0.018 ± 0.013</b>				
0.078 ± 0.018 ± 0.013	49	LINK 02G	FOCS	$\gamma$ nucleus, $\approx 180$ GeV

$\Gamma(\Sigma^- K^+ \pi^+)/\Gamma(\Sigma^+ K^*(892)^0)$   $\Gamma_{62}/\Gamma_{61}$

VALUE	CL%	DOCUMENT ID	TECN	COMMENT
<b>&lt;0.35</b>				
<0.35	90	LINK 02G	FOCS	$\gamma$ nucleus, $\approx 180$ GeV

Doubly Cabibbo-suppressed modes

$\Gamma(\rho K^+ \pi^-)/\Gamma(\rho K^- \pi^+)$   $\Gamma_{63}/\Gamma_2$

VALUE	CL%	DOCUMENT ID	TECN	COMMENT
<b>&lt;0.0046</b>				
<0.0046	90	LINK 05k	FOCS	R = (0.05 ± 0.26 ± 0.02)%

Semileptonic modes

$\Gamma(\Lambda e^+ \nu_e)/\Gamma(\rho K^- \pi^+)$   $\Gamma_{64}/\Gamma_2$

We average here the averages of the next two data blocks.

VALUE	DOCUMENT ID	COMMENT
<b>0.41 ± 0.05 OUR AVERAGE</b>		
0.42 ± 0.07	PDG 02	Our $\Gamma(\Lambda e^+ \nu_e)/\Gamma(\rho K^- \pi^+)$
0.39 ± 0.08	PDG 02	Our $\Gamma(\Lambda \mu^+ \nu_\mu)/\Gamma(\rho K^- \pi^+)$

# Baryon Particle Listings

## $\Lambda_c^+$

### $\Gamma(\Lambda e^+ \nu_e)/\Gamma(pK^- \pi^+)$ $\Gamma_{65}/\Gamma_2$

VALUE	DOCUMENT ID	TECN	COMMENT
<b>0.42 ± 0.07 OUR AVERAGE</b>			
0.43 ± 0.08	11,12 BERGFELD	94	CLE2 $e^+ e^- \approx \gamma(4S)$
0.38 ± 0.14	12,13 ALBRECHT	91G	ARG $e^+ e^- \approx 10.4$ GeV

<sup>11</sup> BERGFELD 94 measures  $\sigma(e^+ e^- \rightarrow \Lambda_c^+ X) \cdot B(\Lambda_c^+ \rightarrow \Lambda e^+ \nu_e) = (4.87 \pm 0.28 \pm 0.69)$  pb.

<sup>12</sup> To extract  $\Gamma(\Lambda_c^+ \rightarrow \Lambda e^+ \nu_e)/\Gamma(\Lambda_c^+ \rightarrow pK^- \pi^+)$ , we use  $\sigma(e^+ e^- \rightarrow \Lambda_c^+ X) \cdot B(\Lambda_c^+ \rightarrow pK^- \pi^+) = (11.2 \pm 1.3)$  pb, which is the weighted average of measurements from ARGUS (ALBRECHT 96E) and CLEO (AVERY 91).

<sup>13</sup> ALBRECHT 91G measures  $\sigma(e^+ e^- \rightarrow \Lambda_c^+ X) \cdot B(\Lambda_c^+ \rightarrow \Lambda e^+ \nu_e) = (4.20 \pm 1.28 \pm 0.71)$  pb.

### $\Gamma(\Lambda \mu^+ \nu_\mu)/\Gamma(pK^- \pi^+)$ $\Gamma_{66}/\Gamma_2$

VALUE	DOCUMENT ID	TECN	COMMENT
<b>0.39 ± 0.08 OUR AVERAGE</b>			
0.40 ± 0.09	14,15 BERGFELD	94	CLE2 $e^+ e^- \approx \gamma(4S)$
0.35 ± 0.20	15,16 ALBRECHT	91G	ARG $e^+ e^- \approx 10.4$ GeV

<sup>14</sup> BERGFELD 94 measures  $\sigma(e^+ e^- \rightarrow \Lambda_c^+ X) \cdot B(\Lambda_c^+ \rightarrow \Lambda \mu^+ \nu_\mu) = (4.43 \pm 0.51 \pm 0.64)$  pb.

<sup>15</sup> To extract  $\Gamma(\Lambda_c^+ \rightarrow \Lambda \mu^+ \nu_\mu)/\Gamma(\Lambda_c^+ \rightarrow pK^- \pi^+)$ , we use  $\sigma(e^+ e^- \rightarrow \Lambda_c^+ X) \cdot B(\Lambda_c^+ \rightarrow pK^- \pi^+) = (11.2 \pm 1.3)$  pb, which is the weighted average of measurements from ARGUS (ALBRECHT 96E) and CLEO (AVERY 91).

<sup>16</sup> ALBRECHT 91G measures  $\sigma(e^+ e^- \rightarrow \Lambda_c^+ X) \cdot B(\Lambda_c^+ \rightarrow \Lambda \mu^+ \nu_\mu) = (3.91 \pm 2.02 \pm 0.90)$  pb.

#### Inclusive modes

### $\Gamma(e^+ \text{ anything})/\Gamma_{\text{total}}$ $\Gamma_{67}/\Gamma$

VALUE	DOCUMENT ID	TECN	COMMENT
<b>0.045 ± 0.017</b>	VELLA	82	MRK2 $e^+ e^-$ 4.5–6.8 GeV

### $\Gamma(p e^+ \text{ anything})/\Gamma_{\text{total}}$ $\Gamma_{68}/\Gamma$

VALUE	DOCUMENT ID	TECN	COMMENT
<b>0.018 ± 0.009</b>	17 VELLA	82	MRK2 $e^+ e^-$ 4.5–6.8 GeV

<sup>17</sup> VELLA 82 includes protons from  $\Lambda$  decay.

### $\Gamma(\Lambda e^+ \text{ anything})/\Gamma_{\text{total}}$ $\Gamma_{69}/\Gamma$

VALUE	DOCUMENT ID	TECN	COMMENT
• • • We do not use the following data for averages, fits, limits, etc. • • •			
0.011 ± 0.008	18 VELLA	82	MRK2 $e^+ e^-$ 4.5–6.8 GeV

<sup>18</sup> VELLA 82 includes  $\Lambda$ 's from  $\Sigma^0$  decay.

### $\Gamma(p \text{ anything})/\Gamma_{\text{total}}$ $\Gamma_{70}/\Gamma$

VALUE	DOCUMENT ID	TECN	COMMENT
<b>0.50 ± 0.08 ± 0.14</b>	19 CRAWFORD	92	CLEO $e^+ e^-$ 10.5 GeV

<sup>19</sup> This CRAWFORD 92 value includes protons from  $\Lambda$  decay. The value is model dependent, but account is taken of this in the systematic error.

### $\Gamma(p \text{ anything (no } \Lambda))/\Gamma_{\text{total}}$ $\Gamma_{71}/\Gamma$

VALUE	DOCUMENT ID	TECN	COMMENT
<b>0.12 ± 0.10 ± 0.16</b>	CRAWFORD	92	CLEO $e^+ e^-$ 10.5 GeV

### $\Gamma(n \text{ anything})/\Gamma_{\text{total}}$ $\Gamma_{73}/\Gamma$

VALUE	DOCUMENT ID	TECN	COMMENT
<b>0.50 ± 0.08 ± 0.14</b>	20 CRAWFORD	92	CLEO $e^+ e^-$ 10.5 GeV

<sup>20</sup> This CRAWFORD 92 value includes neutrons from  $\Lambda$  decay. The value is model dependent, but account is taken of this in the systematic error.

### $\Gamma(n \text{ anything (no } \Lambda))/\Gamma_{\text{total}}$ $\Gamma_{74}/\Gamma$

VALUE	DOCUMENT ID	TECN	COMMENT
<b>0.29 ± 0.09 ± 0.15</b>	CRAWFORD	92	CLEO $e^+ e^-$ 10.5 GeV

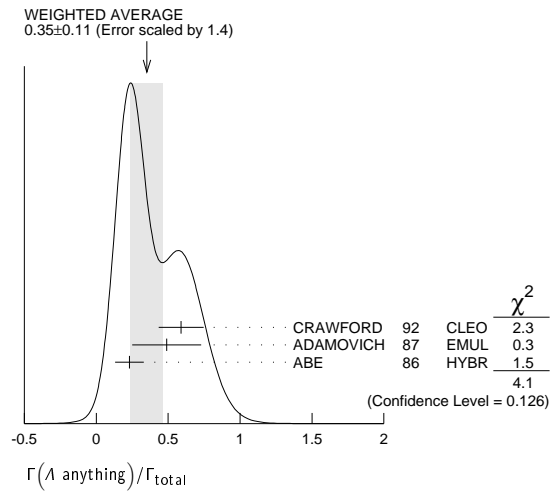
### $\Gamma(p \text{ hadrons})/\Gamma_{\text{total}}$ $\Gamma_{72}/\Gamma$

VALUE	DOCUMENT ID	TECN	COMMENT
• • • We do not use the following data for averages, fits, limits, etc. • • •			
0.41 ± 0.24	ADAMOVICH	87	EMUL $\gamma A$ 20–70 GeV/c

### $\Gamma(\Lambda \text{ anything})/\Gamma_{\text{total}}$ $\Gamma_{75}/\Gamma$

VALUE	EVTS	DOCUMENT ID	TECN	COMMENT
<b>0.35 ± 0.11 OUR AVERAGE</b>	Error	includes scale factor of 1.4. See the ideogram below.		
0.59 ± 0.10 ± 0.12		CRAWFORD	92	CLEO $e^+ e^-$ 10.5 GeV
0.49 ± 0.24		ADAMOVICH	87	EMUL $\gamma A$ 20–70 GeV/c
0.23 ± 0.10	8	21 ABE	86	HYBR 20 GeV $\gamma p$

<sup>21</sup> ABE 86 includes  $\Lambda$ 's from  $\Sigma^0$  decay.



### $\Gamma(\Sigma^\pm \text{ anything})/\Gamma_{\text{total}}$ $\Gamma_{76}/\Gamma$

VALUE	EVTS	DOCUMENT ID	TECN	COMMENT
<b>0.1 ± 0.05</b>	5	ABE	86	HYBR 20 GeV $\gamma p$

### $\Gamma(3\text{prongs})/\Gamma_{\text{total}}$ $\Gamma_{77}/\Gamma$

VALUE	DOCUMENT ID	TECN	COMMENT
<b>0.24 ± 0.07 ± 0.04</b>	KAYIS-TOPAK.03	CHRS	$\nu_\mu$ emulsion, $\bar{E} = 27$ GeV

#### Rare or forbidden modes

### $\Gamma(p e^+ e^-)/\Gamma_{\text{total}}$ $\Gamma_{78}/\Gamma$

A test for the  $\Delta C=1$  weak neutral current. Allowed by higher-order electroweak interactions.

VALUE	CL%	EVTS	DOCUMENT ID	TECN	COMMENT
<b>&lt; 5.5 × 10<sup>-6</sup></b>	90	4.0 ± 7.1	LEES	11G	BABR $e^+ e^- \approx \gamma(4S)$

### $\Gamma(p \mu^+ \mu^-)/\Gamma_{\text{total}}$ $\Gamma_{79}/\Gamma$

A test for the  $\Delta C=1$  weak neutral current. Allowed by higher-order electroweak interactions.

VALUE	CL%	EVTS	DOCUMENT ID	TECN	COMMENT
<b>&lt; 44 × 10<sup>-6</sup></b>	90	11.1 ± 5.6	LEES	11G	BABR $e^+ e^- \approx \gamma(4S)$

• • • We do not use the following data for averages, fits, limits, etc. • • •

VALUE	CL%	EVTS	DOCUMENT ID	TECN	COMMENT
<b>&lt; 3.4 × 10<sup>-4</sup></b>	90	0	KODAMA	95	E653 $\pi^-$ emulsion 600 GeV

### $\Gamma(p e^+ \mu^-)/\Gamma_{\text{total}}$ $\Gamma_{80}/\Gamma$

A test of lepton family-number conservation.

VALUE	CL%	EVTS	DOCUMENT ID	TECN	COMMENT
<b>&lt; 9.9 × 10<sup>-6</sup></b>	90	-0.7 ± 3.0	LEES	11G	BABR $e^+ e^- \approx \gamma(4S)$

### $\Gamma(p e^- \mu^+)/\Gamma_{\text{total}}$ $\Gamma_{81}/\Gamma$

A test of lepton family-number conservation.

VALUE	CL%	EVTS	DOCUMENT ID	TECN	COMMENT
<b>&lt; 19 × 10<sup>-6</sup></b>	90	6.2 ± 4.9	LEES	11G	BABR $e^+ e^- \approx \gamma(4S)$

### $\Gamma(\bar{p} 2e^+)/\Gamma_{\text{total}}$ $\Gamma_{82}/\Gamma$

A test of lepton- and baryon-number conservation.

VALUE	CL%	EVTS	DOCUMENT ID	TECN	COMMENT
<b>&lt; 2.7 × 10<sup>-6</sup></b>	90	-1.5 ± 4.5	LEES	11G	BABR $e^+ e^- \approx \gamma(4S)$

### $\Gamma(\bar{p} 2\mu^+)/\Gamma_{\text{total}}$ $\Gamma_{83}/\Gamma$

A test of lepton- and baryon-number conservation and of lepton family-number conservation.

VALUE	CL%	EVTS	DOCUMENT ID	TECN	COMMENT
<b>&lt; 9.4 × 10<sup>-6</sup></b>	90	0.0 ± 2.2	LEES	11G	BABR $e^+ e^- \approx \gamma(4S)$

### $\Gamma(\bar{p} e^+ \mu^+)/\Gamma_{\text{total}}$ $\Gamma_{84}/\Gamma$

A test of lepton- and baryon-number conservation and of lepton family-number conservation.

VALUE	CL%	EVTS	DOCUMENT ID	TECN	COMMENT
<b>&lt; 16 × 10<sup>-6</sup></b>	90	10.1 ± 6.8	LEES	11G	BABR $e^+ e^- \approx \gamma(4S)$

### $\Gamma(\Sigma^- \mu^+ \mu^+)/\Gamma_{\text{total}}$ $\Gamma_{85}/\Gamma$

A test of lepton-number conservation.

VALUE	CL%	EVTS	DOCUMENT ID	TECN	COMMENT
<b>&lt; 7.0 × 10<sup>-4</sup></b>	90	0	KODAMA	95	E653 $\pi^-$ emulsion 600 GeV

See key on page 457

# Baryon Particle Listings

## $\Lambda_c^+$ , $\Lambda_c(2595)^+$

### $\Lambda_c^+$ DECAY PARAMETERS

See the note on "Baryon Decay Parameters" in the neutron Listings.

#### $\alpha$ FOR $\Lambda_c^+ \rightarrow \Lambda\pi^+$

VALUE	EVTS	DOCUMENT ID	TECN	COMMENT
<b><math>-0.91 \pm 0.15</math> OUR AVERAGE</b>				
$-0.78 \pm 0.16 \pm 0.19$		LINK	06A	FOCS $\gamma A, \bar{E}_\gamma \approx 180$ GeV
$-0.94 \pm 0.21 \pm 0.12$	414	22 BISHAI	95	CLE2 $e^+e^- \approx \gamma(4S)$
$-0.96 \pm 0.42$		ALBRECHT	92	ARG $e^+e^- \approx 10.4$ GeV
$-1.1 \pm 0.4$	86	AVERY	90B	CLEO $e^+e^- \approx 10.6$ GeV

22 BISHAI 95 actually gives  $\alpha = -0.94 \pm 0.21 \pm 0.12$ ,  $0.06 - 0.06$ , chopping the errors at the physical limit  $-1.0$ . However, for  $\alpha \approx -1.0$ , some experiments should get unphysical values ( $\alpha < -1.0$ ), and for averaging with other measurements such values (or errors that extend below  $-1.0$ ) should not be chopped.

#### $\alpha$ FOR $\Lambda_c^+ \rightarrow \Sigma^+\pi^0$

VALUE	EVTS	DOCUMENT ID	TECN	COMMENT
<b><math>-0.45 \pm 0.31 \pm 0.06</math></b>	89	BISHAI	95	CLE2 $e^+e^- \approx \gamma(4S)$

#### $\alpha$ FOR $\Lambda_c^+ \rightarrow \Lambda e^+\nu_e$

The experiments don't cover the complete (or same incomplete)  $M(\Lambda e^+)$  range, but we average them together anyway.

VALUE	EVTS	DOCUMENT ID	TECN	COMMENT
<b><math>-0.86 \pm 0.04</math> OUR AVERAGE</b>				
$-0.86 \pm 0.03 \pm 0.02$	3201	23 HINSON	05	CLEO $e^+e^- \approx \gamma(4S)$
$-0.91 \pm 0.42 \pm 0.25$		24 ALBRECHT	94B	ARG $e^+e^- \approx 10$ GeV
$-0.82 \pm 0.09 \pm 0.06$ $-0.06 - 0.03$	700	25 CRAWFORD	95	CLE2 See HINSON 05
$-0.89 \pm 0.17 \pm 0.09$ $-0.11 - 0.05$	350	26 BERGFELD	94	CLE2 See CRAWFORD 95

- 23 HINSON 05 measures the form-factor ratio  $R \equiv f_2/f_1$  for  $\Lambda_c^+ \rightarrow \Lambda e^+\nu_e$  events to be  $-0.31 \pm 0.05 \pm 0.04$  and the pole mass to be  $2.21 \pm 0.08 \pm 0.14$  GeV/c<sup>2</sup>, and from these calculates  $\alpha$ , averaged over  $q^2$ , where  $\langle q^2 \rangle = 0.67$  (GeV/c)<sup>2</sup>.
- 24 ALBRECHT 94B uses  $\Lambda e^+$  and  $\Lambda\mu^+$  events in the mass range  $1.85 < M(\Lambda e^+) < 2.20$  GeV.
- 25 CRAWFORD 95 measures the form-factor ratio  $R \equiv f_2/f_1$  for  $\Lambda_c^+ \rightarrow \Lambda e^+\nu_e$  events to be  $-0.25 \pm 0.14 \pm 0.08$  and from this calculates  $\alpha$ , averaged over  $q^2$ , to be the above.
- 26 BERGFELD 94 uses  $\Lambda e^+$  events.

### $\Lambda_c^+$ , $\bar{\Lambda}_c^-$ CP-VIOLATING DECAY ASYMMETRIES

#### $(\alpha + \bar{\alpha})/(\alpha - \bar{\alpha})$ in $\Lambda_c^+ \rightarrow \Lambda\pi^+$ , $\bar{\Lambda}_c^- \rightarrow \bar{\Lambda}\pi^-$

This is zero if CP is conserved.

VALUE	DOCUMENT ID	TECN	COMMENT
<b><math>-0.07 \pm 0.19 \pm 0.24</math></b>	LINK	06A	FOCS $\gamma A, \bar{E}_\gamma \approx 180$ GeV

#### $(\alpha + \bar{\alpha})/(\alpha - \bar{\alpha})$ in $\Lambda_c^+ \rightarrow \Lambda e^+\nu_e$ , $\bar{\Lambda}_c^- \rightarrow \bar{\Lambda}e^-\bar{\nu}_e$

This is zero if CP is conserved.

VALUE	DOCUMENT ID	TECN	COMMENT
<b><math>0.00 \pm 0.03 \pm 0.02</math></b>	HINSON	05	CLEO $e^+e^- \approx \gamma(4S)$

### $\Lambda_c^+$ REFERENCES

We have omitted some papers that have been superseded by later experiments. The omitted papers may be found in our 1992 edition (Physical Review D45, 1 June, Part II) or in earlier editions.

LEES	11G	PR D84 072006	J.P. Lees et al.	(BABAR Collab.)
VAZQUEZ-JA...	08	PL B66 6 299	E. Vazquez-Jauregui et al.	(SELEX Collab.)
AUBERT	07U	PR D75 052002	B. Aubert et al.	(BABAR Collab.)
LINK	06A	PL B634 165	J.M. Link et al.	(FNAL FOCUS Collab.)
AUBERT,B	05S	PR D72 052006	B. Aubert et al.	(BABAR Collab.)
HINSON	05	PRL 94 191801	J.W. Hinson et al.	(CLEO Collab.)
LINK	05F	PL B624 22	J.M. Link et al.	(FNAL FOCUS Collab.)
LINK	05K	PL B624 166	J.M. Link et al.	(FNAL FOCUS Collab.)
CRONIN-HEN...	03	PR D67 012001	D. Cronin-Hennessy et al.	(CLEO Collab.)
KAYIS-TOPAK...	03	PL B555 156	A. Kayis-Topkusu et al.	(CERN CHORUS Collab.)
ABE	02C	PL B524 33	K. Abe et al.	(KEK BELLE Collab.)
LINK	02C	PRL 88 161801	J.M. Link et al.	(FNAL FOCUS Collab.)
LINK	02G	PL B540 25	J.M. Link et al.	(FNAL FOCUS Collab.)
PDG	02	PR D66 010001	K. Hagiwara et al.	(FNAL FOCUS Collab.)
KUSHNIR...	01	PRL 86 5243	A. Kushnirko et al.	(FNAL SELEX Collab.)
MAHMOOD	01	PRL 86 2232	A.M. Mahmood et al.	(CLEO Collab.)
AITALA	00	PL B471 449	E.M. Aitala et al.	(FNAL E791 Collab.)
JAFFE	00	PR D62 072005	D.E. Jaffe et al.	(CLEO Collab.)
ALAM	98	PR D57 4467	M.S. Alam et al.	(CLEO Collab.)
ALBRECHT	96E	PRPL 276 223	H. Albrecht et al.	(ARGUS Collab.)
ALEEV	96	JINRRC 3-77 31	A.N. Aleev et al.	(Serpukhov EXCHARM Collab.)
ALEXANDER	96C	PR D53 R1013	J.P. Alexander et al.	(CLEO Collab.)
ALBRECHT	95B	PL B342 397	H. Albrecht et al.	(ARGUS Collab.)
AMMAR	95	PRL 74 3534	R. Ammar et al.	(CLEO Collab.)
BISHAI	95	PL B350 256	M. Bishai et al.	(CLEO Collab.)
CRAWFORD	95	PRL 75 624	G. Crawford et al.	(CLEO Collab.)
KODAMA	95	PL B345 85	K. Kodama et al.	(FNAL E653 Collab.)
ALBRECHT	94B	PL B326 320	H. Albrecht et al.	(ARGUS Collab.)
ALEEV	94	PAN 57 1370	A.N. Aleev et al.	(Serpukhov BIS-2 Collab.)
		Translated from YF 57 1443.		
AVERY	94	PL B325 257	P. Avery et al.	(CLEO Collab.)
BERGFELD	94	PL B323 219	T. Bergfeld et al.	(CLEO Collab.)
FRABETTI	94E	PL B328 193	P.L. Frabetti et al.	(FNAL E687 Collab.)
AVERY	93	PRL 71 2391	P. Avery et al.	(CLEO Collab.)
BOZEK	93	PL B312 247	A. Bozek et al.	(CERN NA32 Collab.)

FRABETTI	93D	PRL 70 1755	P.L. Frabetti et al.	(FNAL E687 Collab.)
FRABETTI	93H	PL B314 477	P.L. Frabetti et al.	(FNAL E687 Collab.)
KUBOTA	93	PRL 71 3255	Y. Kubota et al.	(CLEO Collab.)
ALBRECHT	92	PL B274 239	H. Albrecht et al.	(ARGUS Collab.)
ALBRECHT	92O	ZPHY C56 1	H. Albrecht et al.	(ARGUS Collab.)
BARLAG	92	PL B283 465	S. Barlag et al.	(ACCMOR Collab.)
CRAWFORD	92	PR D45 752	G. Crawford et al.	(CLEO Collab.)
JEZABEK	92	PL B286 175	M. Jezabek, K. Rybicki, R. Rylko	(CRAC)
ALBRECHT	91G	PL B269 234	H. Albrecht et al.	(ARGUS Collab.)
AVERY	91	PR D43 3599	P. Avery et al.	(CLEO Collab.)
ALVAREZ	90	ZPHY C47 539	M.P. Alvarez et al.	(CERN NA14/2 Collab.)
ALVAREZ	90B	PL B246 256	M.P. Alvarez et al.	(CERN NA14/2 Collab.)
ANJOS	90	PR D41 801	J.C. Anjos et al.	(FNAL E691 Collab.)
AVERY	90B	PRL 65 2842	P. Avery et al.	(CLEO Collab.)
BARLAG	90D	ZPHY C48 29	S. Barlag et al.	(ACCMOR Collab.)
FRABETTI	90	PL B251 639	P.L. Frabetti et al.	(FNAL E687 Collab.)
BARLAG	89	PL B218 374	S. Barlag et al.	(ACCMOR Collab.)
AGUILAR...	88B	ZPHY C40 321	M. Aguilar-Benitez et al.	(LEBC-EHS Collab.)
		Also	PL B189 254	M. Aguilar-Benitez et al.
		Also	PL B199 462	M. Aguilar-Benitez et al.
		Also	SJNP 48 833	M. Begalli et al.
			Translated from YAF 48 1310.	
ALBRECHT	88C	PL B207 109	H. Albrecht et al.	(ARGUS Collab.)
ANJOS	88B	EPL 60 1379	J.C. Anjos et al.	(FNAL E691 Collab.)
ADAMOVICH	87	EPL 4 887	M.I. Adamovich et al.	(Photon Emulsion Collab.)
		Also	SJNP 46 447	F. Viaggi et al.
			Translated from YAF 46 799.	
AMENDOLIA	87	ZPHY C36 513	S.R. Amendolia et al.	(CERN NA1 Collab.)
JONES	87	ZPHY C36 593	G.T. Jones et al.	(CERN WA21 Collab.)
ABE	86	PR D33 1	K. Abe et al.	
ALEEV	84	ZPHY C23 333	A.N. Aleev et al.	(BIS-2 Collab.)
BOSETTI	82	PL 109B 234	P.C. Bosetti et al.	(AACH3, BONN, CERN+)
VELLA	82	PRL 48 1515	E. Vella et al.	(SLAC, LBL, UCB)
BASILE	81B	NC 62A 14	M. Basile et al.	(CERN, BGN, PGIA, FRAS)
CALICCHIO	80	PL 93B 521	M. Calicchio et al.	(BARI, BIRM, BRUX+)

### OTHER RELATED PAPERS

MIGLIOZZI	99	PL B462 217	P. Migliozi et al.
DUNIETZ	98	PR D58 094010	I. Dunietz

## $\Lambda_c(2595)^+$

$$I(J^P) = 0(\frac{1}{2}^-) \text{ Status: } ** *$$

The  $\Lambda_c^+ \pi^+ \pi^-$  mode is largely, and perhaps entirely,  $\Sigma_c \pi$ , which is just at threshold; since the  $\Sigma_c$  has  $J^P = 1/2^+$ , the  $J^P$  here is almost certainly  $1/2^-$ . This result is in accord with the theoretical expectation that this is the charm counterpart of the strange  $\Lambda(1405)$ .

### $\Lambda_c(2595)^+$ MASS

The mass is obtained from the  $\Lambda_c(2595)^+ - \Lambda_c^+$  mass-difference measurements below.

VALUE (MeV)	DOCUMENT ID
<b><math>2592.25 \pm 0.28</math> OUR FIT</b>	

### $\Lambda_c(2595)^+ - \Lambda_c^+$ MASS DIFFERENCE

VALUE (MeV)	EVTS	DOCUMENT ID	TECN	COMMENT
<b><math>305.79 \pm 0.24</math> OUR FIT</b>				
<b><math>305.79 \pm 0.14 \pm 0.20</math></b>	3.5k	AALTONEN	11H	CDF $p\bar{p}$ at 1.96 TeV
$305.6 \pm 0.3$		1 BLECHMAN	03	Threshold shift
$309.7 \pm 0.9 \pm 0.4$	19	ALBRECHT	97	ARG $e^+e^- \approx 10$ GeV
$309.2 \pm 0.7 \pm 0.3$	14 ± 4.5	FRABETTI	96	E687 $\gamma Be, \bar{E}_\gamma \approx 220$ GeV
$307.5 \pm 0.4 \pm 1.0$	112 ± 17	EDWARDS	95	CLE2 $e^+e^- \approx 10.5$ GeV

1 BLECHMAN 03 finds that a more sophisticated treatment than a simple Breit-Wigner for the proximity of the threshold of the dominant decay,  $\Sigma_c(2455)\pi$ , lowers the  $\Lambda_c(2595)^+ - \Lambda_c^+$  mass difference by 2 or 3 MeV. The analysis of AALTONEN 11H bears this out.

### $\Lambda_c(2595)^+$ WIDTH

VALUE (MeV)	EVTS	DOCUMENT ID	TECN	COMMENT
<b><math>2.59 \pm 0.30 \pm 0.47</math></b>	3.5k	2 AALTONEN	11H	CDF $p\bar{p}$ at 1.96 TeV
$2.9 \pm 2.9 \pm 1.8$ $-2.1 - 1.4$	19	ALBRECHT	97	ARG $e^+e^- \approx 10$ GeV
$3.9 \pm 1.4 \pm 2.0$ $-1.2 - 1.0$	112 ± 17	EDWARDS	95	CLE2 $e^+e^- \approx 10.5$ GeV

2 AALTONEN 11H treats the three charged modes  $\Lambda_c(2595)^+ \rightarrow \Sigma_c(2455)^+ \pi^-$ ,  $\Sigma_c(2455)^+ \pi^0$ ,  $\Sigma_c(2455)^0 \pi^+$  separately in terms of a common coupling constant  $h_2$  and obtains  $h_2^2 = 0.36 \pm 0.08$ . From this the width is determined.

## Baryon Particle Listings

 $\Lambda_c(2595)^+$ ,  $\Lambda_c(2625)^+$  $\Lambda_c(2595)^+$  DECAY MODES

$\Lambda_c^+ \pi \pi$  and its submode  $\Sigma_c(2455) \pi$  — the latter just barely — are the only strong decays allowed to an excited  $\Lambda_c^+$  having this mass; and the submode seems to dominate.

Mode	Fraction ( $\Gamma_i/\Gamma$ )
$\Gamma_1$ $\Lambda_c^+ \pi^+ \pi^-$	[a] $\approx 67\%$
$\Gamma_2$ $\Sigma_c(2455)^{++} \pi^-$	$24 \pm 7\%$
$\Gamma_3$ $\Sigma_c(2455)^0 \pi^+$	$24 \pm 7\%$
$\Gamma_4$ $\Lambda_c^+ \pi^+ \pi^-$ 3-body	$18 \pm 10\%$
$\Gamma_5$ $\Lambda_c^+ \pi^0$	[b] not seen
$\Gamma_6$ $\Lambda_c^+ \gamma$	not seen

[a] Assuming isospin conservation, so that the other third is  $\Lambda_c^+ \pi^0 \pi^0$ .

[b] A test that the isospin is indeed 0, so that the particle is indeed a  $\Lambda_c^+$ .

 $\Lambda_c(2595)^+$  BRANCHING RATIOS

$\Gamma(\Sigma_c(2455)^{++} \pi^-)/\Gamma(\Lambda_c^+ \pi^+ \pi^-)$				$\Gamma_2/\Gamma_1$
VALUE	DOCUMENT ID	TECN	COMMENT	
<b><math>0.36 \pm 0.10</math> OUR AVERAGE</b>				
$0.37 \pm 0.12 \pm 0.13$	ALBRECHT	97	ARG	$e^+ e^- \approx 10$ GeV
$0.36 \pm 0.09 \pm 0.09$	EDWARDS	95	CLE2	$e^+ e^- \approx 10.5$ GeV

$\Gamma(\Sigma_c(2455)^0 \pi^+)/\Gamma(\Lambda_c^+ \pi^+ \pi^-)$				$\Gamma_3/\Gamma_1$
VALUE	DOCUMENT ID	TECN	COMMENT	
<b><math>0.37 \pm 0.10</math> OUR AVERAGE</b>				
$0.29 \pm 0.10 \pm 0.11$	ALBRECHT	97	ARG	$e^+ e^- \approx 10$ GeV
$0.42 \pm 0.09 \pm 0.09$	EDWARDS	95	CLE2	$e^+ e^- \approx 10.5$ GeV

$[\Gamma(\Sigma_c(2455)^{++} \pi^-) + \Gamma(\Sigma_c(2455)^0 \pi^+)]/\Gamma(\Lambda_c^+ \pi^+ \pi^-)$				$(\Gamma_2 + \Gamma_3)/\Gamma_1$	
VALUE	CL%	DOCUMENT ID	TECN	COMMENT	
<b><math>0.66 \pm 0.13 \pm 0.07</math></b>		ALBRECHT	97	ARG	$e^+ e^- \approx 10$ GeV
$> 0.51$	90	3 FRABETTI	96	E687	$\gamma$ Be, $\overline{E}_\gamma \approx 220$ GeV

• • • We do not use the following data for averages, fits, limits, etc. • • •

<sup>3</sup> The results of FRABETTI 96 are consistent with this ratio being 100%.

$\Gamma(\Lambda_c^+ \pi^0)/\Gamma(\Lambda_c^+ \pi^+ \pi^-)$				$\Gamma_5/\Gamma_1$	
VALUE	CL%	DOCUMENT ID	TECN	COMMENT	
<b><math>&lt; 3.53</math></b>		EDWARDS	95	CLE2	$e^+ e^- \approx 10.5$ GeV

$\Lambda_c^+ \pi^0$  decay is forbidden by isospin conservation if this state is in fact a  $\Lambda_c$ .

$\Gamma(\Lambda_c^+ \gamma)/\Gamma(\Lambda_c^+ \pi^+ \pi^-)$				$\Gamma_6/\Gamma_1$	
VALUE	CL%	DOCUMENT ID	TECN	COMMENT	
<b><math>&lt; 0.98</math></b>		EDWARDS	95	CLE2	$e^+ e^- \approx 10.5$ GeV

 $\Lambda_c(2595)^+$  REFERENCES

AALTONEN	11H	PR D84 012003	T. Aaltonen et al.	(CDF Collab.)
BLECHMAN	03	PR D67 074033	A.E. Blechman et al.	(JHU, FLOR)
ALBRECHT	97	PL B402 207	H. Albrecht et al.	(ARGUS Collab.)
FRABETTI	96	PL B365 461	P.L. Frabetti et al.	(FNAL E687 Collab.)
EDWARDS	95	PRL 74 3331	K.W. Edwards et al.	(CLEO Collab.)

$\Lambda_c(2625)^+$   $J(P) = 0(\frac{3}{2}^-)$  Status: \* \* \*

The spin-parity has not been measured but is expected to be  $3/2^-$ ; this is presumably the charm counterpart of the strange  $\Lambda(1520)$ .

 $\Lambda_c(2625)^+$  MASS

The mass is obtained from the  $\Lambda_c(2625)^+ - \Lambda_c^+$  mass-difference measurements below.

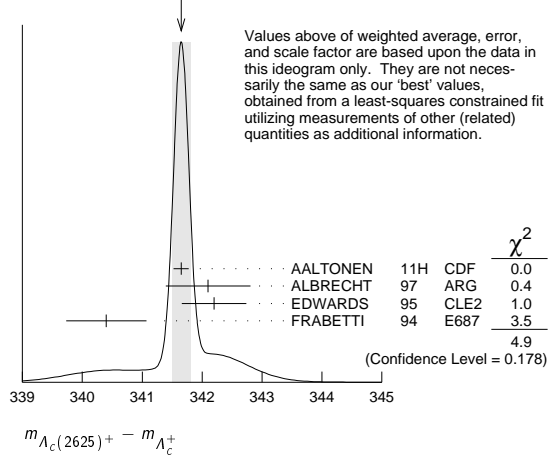
VALUE (MeV)	EVTS	DOCUMENT ID	TECN	COMMENT
<b><math>2628.11 \pm 0.19</math> OUR FIT</b>				Error includes scale factor of 1.1.
$2626.6 \pm 0.5 \pm 1.5$	42 $\pm$ 9	ALBRECHT	93F	ARG See ALBRECHT 97

• • • We do not use the following data for averages, fits, limits, etc. • • •

 $\Lambda_c(2625)^+ - \Lambda_c^+$  MASS DIFFERENCE

VALUE (MeV)	EVTS	DOCUMENT ID	TECN	COMMENT
<b><math>341.65 \pm 0.13</math> OUR FIT</b>				Error includes scale factor of 1.1.
<b><math>341.65 \pm 0.15</math> OUR AVERAGE</b>				Error includes scale factor of 1.3. See the ideogram below.
$341.65 \pm 0.04 \pm 0.12$	6.2k	AALTONEN	11H	CDF $p\overline{p}$ at 1.96 TeV
$342.1 \pm 0.5 \pm 0.5$	51	ALBRECHT	97	ARG $e^+ e^- \approx 10$ GeV
$342.2 \pm 0.2 \pm 0.5$	245 $\pm$ 19	EDWARDS	95	CLE2 $e^+ e^- \approx 10.5$ GeV
$340.4 \pm 0.6 \pm 0.3$	40 $\pm$ 9	FRABETTI	94	E687 $\gamma$ Be, $\overline{E}_\gamma = 220$ GeV

WEIGHTED AVERAGE  
341.65 $\pm$ 0.15 (Error scaled by 1.3)



Values above of weighted average, error, and scale factor are based upon the data in this ideogram only. They are not necessarily the same as our 'best' values, obtained from a least-squares constrained fit utilizing measurements of other (related) quantities as additional information.

 $\Lambda_c(2625)^+$  WIDTH

VALUE (MeV)	CL%	EVTS	DOCUMENT ID	TECN	COMMENT
<b><math>&lt; 0.97</math></b>			AALTONEN	11H	CDF $p\overline{p}$ at 1.96 TeV
$< 1.9$	90	245 $\pm$ 19	EDWARDS	95	CLE2 $e^+ e^- \approx 10.5$ GeV
$< 3.2$	90		ALBRECHT	93F	ARG $e^+ e^- \approx 7(4.5)$

• • • We do not use the following data for averages, fits, limits, etc. • • •

 $\Lambda_c(2625)^+$  DECAY MODES

$\Lambda_c^+ \pi \pi$  and its submode  $\Sigma(2455) \pi$  are the only strong decays allowed to an excited  $\Lambda_c^+$  having this mass.

Mode	Fraction ( $\Gamma_i/\Gamma$ )	Confidence level
$\Gamma_1$ $\Lambda_c^+ \pi^+ \pi^-$	[a] $\approx 67\%$	
$\Gamma_2$ $\Sigma_c(2455)^{++} \pi^-$	$< 5$	90%
$\Gamma_3$ $\Sigma_c(2455)^0 \pi^+$	$< 5$	90%
$\Gamma_4$ $\Lambda_c^+ \pi^+ \pi^-$ 3-body	large	
$\Gamma_5$ $\Lambda_c^+ \pi^0$	[b] not seen	
$\Gamma_6$ $\Lambda_c^+ \gamma$	not seen	

[a] Assuming isospin conservation, so that the other third is  $\Lambda_c^+ \pi^0 \pi^0$ .

[b] A test that the isospin is indeed 0, so that the particle is indeed a  $\Lambda_c^+$ .

 $\Lambda_c(2625)^+$  BRANCHING RATIOS

$\Gamma(\Sigma_c(2455)^{++} \pi^-)/\Gamma(\Lambda_c^+ \pi^+ \pi^-)$				$\Gamma_2/\Gamma_1$
VALUE	CL%	DOCUMENT ID	TECN	COMMENT
<b><math>&lt; 0.08</math></b>		EDWARDS	95	CLE2 $e^+ e^- \approx 10.5$ GeV

$\Gamma(\Sigma_c(2455)^0 \pi^+)/\Gamma(\Lambda_c^+ \pi^+ \pi^-)$				$\Gamma_3/\Gamma_1$
VALUE	CL%	DOCUMENT ID	TECN	COMMENT
<b><math>&lt; 0.07</math></b>		EDWARDS	95	CLE2 $e^+ e^- \approx 10.5$ GeV

$[\Gamma(\Sigma_c(2455)^{++} \pi^-) + \Gamma(\Sigma_c(2455)^0 \pi^+)]/\Gamma(\Lambda_c^+ \pi^+ \pi^-)$				$(\Gamma_2 + \Gamma_3)/\Gamma_1$	
VALUE	CL%	EVTS	DOCUMENT ID	TECN	COMMENT
$< 0.36$	90		FRABETTI	94	E687 $\gamma$ Be, $\overline{E}_\gamma = 220$ GeV
$0.46 \pm 0.14$		21	ALBRECHT	93F	ARG $e^+ e^- \approx 7(4.5)$

$\Gamma(\Lambda_c^+ \pi^+ \pi^- \text{ 3-body})/\Gamma(\Lambda_c^+ \pi^+ \pi^-)$				$\Gamma_4/\Gamma_1$	
VALUE	CL%	EVTS	DOCUMENT ID	TECN	COMMENT
$0.54 \pm 0.14$		16	ALBRECHT	93F	ARG $e^+ e^- \approx 7(4.5)$

• • • We do not use the following data for averages, fits, limits, etc. • • •

$\Gamma(\Lambda_c^+ \pi^0)/\Gamma(\Lambda_c^+ \pi^+ \pi^-)$				$\Gamma_5/\Gamma_1$
VALUE	CL%	DOCUMENT ID	TECN	COMMENT
<b><math>&lt; 0.91</math></b>		EDWARDS	95	CLE2 $e^+ e^- \approx 10.5$ GeV

$\Lambda_c^+ \pi^0$  decay is forbidden by isospin conservation if this state is in fact a  $\Lambda_c$ .

$\Gamma(\Lambda_c^+ \gamma)/\Gamma(\Lambda_c^+ \pi^+ \pi^-)$				$\Gamma_6/\Gamma_1$
VALUE	CL%	DOCUMENT ID	TECN	COMMENT
<b><math>&lt; 0.52</math></b>		EDWARDS	95	CLE2 $e^+ e^- \approx 10.5$ GeV

See key on page 457

## Baryon Particle Listings

 $\Lambda_c(2625)^+$ ,  $\Lambda_c(2765)^+$ ,  $\Lambda_c(2880)^+$ ,  $\Lambda_c(2940)^+$  $\Lambda_c(2625)^+$  REFERENCES

AALTONEN	11H	PR D94 012003	T. Aaltonen et al.	(CDF Collab.)
ALBRECHT	97	PL B402 207	H. Albrecht et al.	(ARGUS Collab.)
EDWARDS	95	PRL 74 3331	K.W. Edwards et al.	(CLEO Collab.)
FRABETTI	94	PRL 72 961	P.L. Frabetti et al.	(FNAL E687 Collab.)
ALBRECHT	93F	PL B317 227	H. Albrecht et al.	(ARGUS Collab.)

$$\Lambda_c(2765)^+ \quad I(J^P) = ?(??) \quad \text{Status: } *$$

or  $\Sigma_c(2765)$

OMITTED FROM SUMMARY TABLE

A broad, statistically significant peak ( $997^{+141}_{-129}$  events) seen in  $\Lambda_c^+ \pi^+ \pi^-$ . However, nothing at all is known about its quantum numbers, including whether it is a  $\Lambda_c^+$  or a  $\Sigma_c$ , or whether the width might be due to overlapping states.

 $\Lambda_c(2765)^+$  MASS

The mass is obtained from the  $\Lambda_c(2765)^+ - \Lambda_c^+$  mass-difference measurement below.

VALUE (MeV)	DOCUMENT ID
<b>2766.6 ± 2.4 OUR FIT</b>	

 $\Lambda_c(2765)^+ - \Lambda_c^+$  MASS DIFFERENCE

VALUE (MeV)	EVTs	DOCUMENT ID	TECN	COMMENT
<b>480.1 ± 2.4 OUR FIT</b>				
480.1 ± 2.4	997 <sup>+141</sup> <sub>-129</sub>	ARTUSO	01	CLE2 $e^+ e^- \approx \mathcal{T}(4S)$

 $\Lambda_c(2765)^+$  WIDTH

VALUE (MeV)	DOCUMENT ID	TECN	COMMENT
<b>50</b>	ARTUSO	01	CLE2 $e^+ e^- \approx \mathcal{T}(4S)$

 $\Lambda_c(2765)^+$  DECAY MODES

Mode	Fraction ( $\Gamma_i/\Gamma$ )
$\Gamma_1$ $\Lambda_c^+ \pi^+ \pi^-$	seen

 $\Lambda_c(2765)^+$  REFERENCES

ARTUSO	01	PRL 86 4479	M. Artuso et al.	(CLEO Collab.)
--------	----	-------------	------------------	----------------

$$\Lambda_c(2880)^+ \quad I(J^P) = 0(\frac{5}{2}^+) \quad \text{Status: } ***$$

A narrow peak seen in  $\Lambda_c^+ \pi^+ \pi^-$  and in  $pD^0$ . It is not seen in  $pD^+$ , and therefore it is probably a  $\Lambda_c^+$  and not a  $\Sigma_c$ . The evidence for spin 5/2 comes from the  $\Sigma_c(2455)\pi$  decay angular distribution, and the evidence for parity + comes from agreement of the  $\Sigma_c(2520)/\Sigma_c(2455)$  branching ratio with a prediction of heavy quark symmetry (see MIZUK 07).

 $\Lambda_c(2880)^+$  MASS

VALUE (MeV)	EVTs	DOCUMENT ID	TECN	COMMENT
<b>2881.53 ± 0.35 OUR FIT</b>				
<b>2881.50 ± 0.35 OUR AVERAGE</b>				
2881.9 ± 0.1 ± 0.5	2.8k ± 190	AUBERT	07	BABR in $pD^0$
2881.2 ± 0.2 ± 0.4	690 ± 50	MIZUK	07	BELL in $\Sigma_c(2455)^{0,++} \pi^\pm$

 $\Lambda_c(2880)^+ - \Lambda_c^+$  MASS DIFFERENCE

VALUE (MeV)	EVTs	DOCUMENT ID	TECN	COMMENT
<b>595.1 ± 0.4 OUR FIT</b>				
596 ± 1 ± 2	350 <sup>+57</sup> <sub>-55</sub>	ARTUSO	01	CLE2 in $\Lambda_c^+ \pi^+ \pi^-$

 $\Lambda_c(2880)^+$  WIDTH

VALUE (MeV)	CL%	EVTs	DOCUMENT ID	TECN	COMMENT
<b>5.8 ± 1.1 OUR AVERAGE</b>					
5.8 ± 1.5 ± 1.1		2.8k ± 190	AUBERT	07	BABR in $pD^0$
5.8 ± 0.7 ± 1.1		690 ± 50	MIZUK	07	BELL in $\Sigma_c(2455)^{0,++} \pi^\pm$
••• We do not use the following data for averages, fits, limits, etc. •••					
<8	90		ARTUSO	01	CLEO in $\Lambda_c^+ \pi^+ \pi^-$

 $\Lambda_c(2880)^+$  DECAY MODES

Mode	Fraction ( $\Gamma_i/\Gamma$ )
$\Gamma_1$ $\Lambda_c^+ \pi^+ \pi^-$	seen
$\Gamma_2$ $\Sigma_c(2455)^{0,++} \pi^\pm$	seen
$\Gamma_3$ $\Sigma_c(2520)^{0,++} \pi^\pm$	seen
$\Gamma_4$ $pD^0$	seen

 $\Lambda_c(2880)^+$  BRANCHING RATIOS

$\Gamma(\Sigma_c(2455)^{0,++} \pi^\pm)/\Gamma(\Lambda_c^+ \pi^+ \pi^-)$	$\Gamma_2/\Gamma_1$
<b>0.392 ± 0.031 OUR AVERAGE</b>	Error includes scale factor of 1.3.
0.404 ± 0.021 ± 0.014	MIZUK 07 BELL in $\Sigma_c(2455)^{0,++} \pi^\pm$
0.31 ± 0.06 ± 0.03	96 ARTUSO 01 CLE2 $e^+ e^- \approx \mathcal{T}(4S)$

$\Gamma(\Sigma_c(2520)^{0,++} \pi^\pm)/\Gamma(\Lambda_c^+ \pi^+ \pi^-)$	$\Gamma_3/\Gamma_1$
<b>0.091 ± 0.025 ± 0.010</b>	
<0.11	90 ARTUSO 01 CLE2 $e^+ e^- \approx \mathcal{T}(4S)$

$\Gamma(\Sigma_c(2520)^{0,++} \pi^\pm)/\Gamma(\Sigma_c(2455)^{0,++} \pi^\pm)$	$\Gamma_3/\Gamma_2$
<b>0.225 ± 0.062 ± 0.025</b>	
••• We do not use the following data for averages, fits, limits, etc. •••	
	<sup>1</sup> MIZUK 07 BELL in $\Sigma_c(2455)^{0,++} \pi^\pm$
<sup>1</sup> This MIZUK 07 ratio is redundant with MIZUK 07 ratios given above.	

 $\Lambda_c(2880)^+$  REFERENCES

AUBERT	07	PRL 98 012001	B. Aubert et al.	(BABAR Collab.)
MIZUK	07	PRL 98 262001	R. Mizuk et al.	(BELLE Collab.)
ARTUSO	01	PRL 86 4479	M. Artuso et al.	(CLEO Collab.)

$$\Lambda_c(2940)^+ \quad I(J^P) = 0(??) \quad \text{Status: } ***$$

A fairly narrow peak of good statistical significance first seen in the  $pD^0$  mass spectrum. It is not seen in  $pD^+$ , and thus it is probably a  $\Lambda_c^+$  and not a  $\Sigma_c$ . It is also seen in  $\Sigma_c(2455)^{0,++} \pi^\pm$ .

 $\Lambda_c(2940)^+$  MASS

VALUE (MeV)	EVTs	DOCUMENT ID	TECN	COMMENT
<b>2939.3<sup>+1.4</sup><sub>-1.5</sub> OUR AVERAGE</b>				
2939.8 ± 1.3 ± 1.0	2280 ± 310	AUBERT	07	BABR in $pD^0$
2938.0 ± 1.3 <sup>+2.0</sup> <sub>-4.0</sub>	220 <sup>+80</sup> <sub>-60</sub>	MIZUK	07	BELL in $\Sigma_c(2455)^{0,++} \pi^\pm$

 $\Lambda_c(2940)^+$  WIDTH

VALUE (MeV)	EVTs	DOCUMENT ID	TECN	COMMENT
<b>17<sup>+8</sup><sub>-6</sub> OUR AVERAGE</b>				
17.5 ± 5.2 ± 5.9	2280 ± 310	AUBERT	07	BABR in $pD^0$
13 <sup>+8</sup> <sub>-5</sub> <sup>+27</sup> <sub>-7</sub>	220 <sup>+80</sup> <sub>-60</sub>	MIZUK	07	BELL in $\Sigma_c(2455)^{0,++} \pi^\pm$

 $\Lambda_c(2940)^+$  DECAY MODES

Mode	Fraction ( $\Gamma_i/\Gamma$ )
$\Gamma_1$ $pD^0$	seen
$\Gamma_2$ $\Sigma_c(2455)^{0,++} \pi^\pm$	seen

 $\Lambda_c(2940)^+$  REFERENCES

AUBERT	07	PRL 98 012001	B. Aubert et al.	(BABAR Collab.)
MIZUK	07	PRL 98 262001	R. Mizuk et al.	(BELLE Collab.)

## Baryon Particle Listings

 $\Sigma_c(2455)$  $\Sigma_c(2455)$ 

$$I(J^P) = 1(\frac{1}{2}^+) \text{ Status: } ****$$

The angular distribution of  $B^- \rightarrow \Sigma_c(2455)^0 \bar{p}$  favors  $J = 1/2$  (as the quark model predicts).  $J = 3/2$  is excluded by more than four  $\sigma$  see AUBERT 08BN.

 $\Sigma_c(2455)$  MASSES

The masses are obtained from the mass-difference measurements that follow.

 $\Sigma_c(2455)^{++}$  MASS

VALUE (MeV)

DOCUMENT ID

**2453.98 ± 0.16 OUR FIT** $\Sigma_c(2455)^+$  MASS

VALUE (MeV)

DOCUMENT ID

**2452.9 ± 0.4 OUR FIT** $\Sigma_c(2455)^0$  MASS

VALUE (MeV)

DOCUMENT ID

**2453.74 ± 0.16 OUR FIT** $\Sigma_c(2455) - \Lambda_c^+$  MASS DIFFERENCES $m_{\Sigma_c^{++}} - m_{\Lambda_c^+}$ 

VALUE (MeV)

EVTS

DOCUMENT ID

TECN

COMMENT

**167.52 ± 0.08 OUR FIT****167.51 ± 0.09 OUR AVERAGE**

Error includes scale factor of 1.1.

167.44 ± 0.04 ± 0.12 13.8k

AALTONEN 11H CDF  $p\bar{p}$  at 1.96 TeV

167.4 ± 0.1 ± 0.2 2k

ARTUSO 02 CLE2  $e^+e^- \approx \mathcal{T}(4S)$ 

167.35 ± 0.19 ± 0.12 461

LINK 00c FOCS  $\gamma$  nucleus,  $\bar{E}_\gamma$  180 GeV

167.76 ± 0.29 ± 0.15 122

AITALA 96B E791  $\pi^- N$ , 500 GeV

167.6 ± 0.6 ± 0.6 56

FRABETTI 96 E687  $\gamma$ Be,  $\bar{E}_\gamma \approx 220$  GeV

168.2 ± 0.3 ± 0.2 126

CRAWFORD 93 CLE2  $e^+e^- \approx \mathcal{T}(4S)$ 

167.8 ± 0.4 ± 0.3 54

BOWCOCK 89 CLEO  $e^+e^-$  10 GeV

168.2 ± 0.5 ± 1.6 92

ALBRECHT 88D ARG  $e^+e^-$  10 GeV

167.4 ± 0.5 ± 2.0 46

DIESBURG 87 SPEC  $nA \sim 600$  GeV

••• We do not use the following data for averages, fits, limits, etc. •••

167 ± 1 2

JONES 87 HBC  $\nu p$  in BEBC

166 ± 1 1

BOSETTI 82 HBC See JONES 87

168 ± 3 6

BALTAY 79 HLBC  $\nu$  Ne-H in 15-ft

166 ± 15 1

CAZZOLI 75 HBC  $\nu p$  in BNL 7-ft $m_{\Sigma_c^+} - m_{\Lambda_c^+}$ 

VALUE (MeV)

EVTS

DOCUMENT ID

TECN

COMMENT

**166.4 ± 0.4 OUR FIT****166.4 ± 0.2 ± 0.3**661 AMMAR 01 CLE2  $e^+e^- \approx \mathcal{T}(4S)$ 

••• We do not use the following data for averages, fits, limits, etc. •••

168.5 ± 0.4 ± 0.2 111

CRAWFORD 93 CLE2 See AMMAR 01

168 ± 3 1

CALICCHIO 80 HBC  $\nu p$  in BEBC-TST $m_{\Sigma_c^0} - m_{\Lambda_c^+}$ 

VALUE (MeV)

EVTS

DOCUMENT ID

TECN

COMMENT

**167.27 ± 0.08 OUR FIT****167.29 ± 0.09 OUR AVERAGE**

167.28 ± 0.03 ± 0.12 15.9k

AALTONEN 11H CDF  $p\bar{p}$  at 1.96 TeV

167.2 ± 0.1 ± 0.2 2k

ARTUSO 02 CLE2  $e^+e^- \approx \mathcal{T}(4S)$ 

167.38 ± 0.21 ± 0.13 362

LINK 00c FOCS  $\gamma$  nucleus,  $\bar{E}_\gamma$  180 GeV

167.38 ± 0.29 ± 0.15 143

AITALA 96B E791  $\pi^- N$ , 500 GeV

167.8 ± 0.6 ± 0.2

ALEEV 96 SPEC  $n$  nucleus, 50 GeV/c

166.6 ± 0.5 ± 0.6 69

FRABETTI 96 E687  $\gamma$ Be,  $\bar{E}_\gamma \approx 220$  GeV

167.1 ± 0.3 ± 0.2 124

CRAWFORD 93 CLE2  $e^+e^- \approx \mathcal{T}(4S)$ 

168.4 ± 1.0 ± 0.3 14

ANJOS 89D E691  $\gamma$ Be 90–260 GeV

••• We do not use the following data for averages, fits, limits, etc. •••

167.9 ± 0.5 ± 0.3 48

<sup>1</sup> BOWCOCK 89 CLEO  $e^+e^-$  10 GeV

167.0 ± 0.5 ± 1.6 70

<sup>1</sup> ALBRECHT 88D ARG  $e^+e^-$  10 GeV

178.2 ± 0.4 ± 2.0 85

<sup>2</sup> DIESBURG 87 SPEC  $nA \sim 600$  GeV

163 ± 2 1

AMMAR 86 EMUL  $\nu A$ 

<sup>1</sup> This result enters the fit through  $m_{\Sigma_c^{++}} - m_{\Sigma_c^0}$  given below.

<sup>2</sup> See the note on DIESBURG 87 in the  $m_{\Sigma_c^{++}} - m_{\Sigma_c^0}$  section below.

 $\Sigma_c(2455)$  MASS DIFFERENCES $m_{\Sigma_c^{++}} - m_{\Sigma_c^0}$ 

VALUE (MeV)

DOCUMENT ID

TECN

COMMENT

**0.24 ± 0.09 OUR FIT** Error includes scale factor of 1.1.**0.26 ± 0.14 OUR AVERAGE** Error includes scale factor of 1.2.

+ 0.2 ± 0.1 ± 0.1

ARTUSO 02 CLE2  $e^+e^- \approx \mathcal{T}(4S)$ 

− 0.03 ± 0.28 ± 0.11

LINK 00c FOCS  $\gamma$  nucleus,  $\bar{E}_\gamma$  180 GeV

+ 0.38 ± 0.40 ± 0.15

AITALA 96B E791  $\pi^- N$ , 500 GeV

+ 1.1 ± 0.4 ± 0.1

CRAWFORD 93 CLE2  $e^+e^- \approx \mathcal{T}(4S)$ 

− 0.1 ± 0.6 ± 0.1

BOWCOCK 89 CLEO  $e^+e^-$  10 GeV

+ 1.2 ± 0.7 ± 0.3

ALBRECHT 88D ARG  $e^+e^- \sim 10$  GeV

••• We do not use the following data for averages, fits, limits, etc. •••

− 10.8 ± 2.9

<sup>3</sup> DIESBURG 87 SPEC  $nA \sim 600$  GeV<sup>3</sup> DIESBURG 87 is completely incompatible with the other experiments, which is surprising since it agrees with them about  $m_{\Sigma_c(2455)^{++}} - m_{\Lambda_c^+}$ . We go with the majority here. $m_{\Sigma_c^+} - m_{\Sigma_c^0}$ 

VALUE (MeV)

DOCUMENT ID

TECN

COMMENT

**− 0.9 ± 0.4 OUR FIT**

••• We do not use the following data for averages, fits, limits, etc. •••

1.4 ± 0.5 ± 0.3

CRAWFORD 93 CLE2 See AMMAR 01

 $\Sigma_c(2455)$  WIDTHS $\Sigma_c(2455)^{++}$  WIDTH

VALUE (MeV)

EVTS

DOCUMENT ID

TECN

COMMENT

**2.26 ± 0.25 OUR AVERAGE**

2.34 ± 0.13 ± 0.45 13.8k

AALTONEN 11H CDF  $p\bar{p}$  at 1.96 TeV

2.3 ± 0.2 ± 0.3 2k

ARTUSO 02 CLE2  $e^+e^- \approx \mathcal{T}(4S)$ 2.05  $^{+0.41}_{-0.38}$  ± 0.38 1110LINK 02 FOCS  $\gamma$  nucleus,  $\bar{E}_\gamma \approx 180$  GeV $\Sigma_c(2455)^+$  WIDTH

VALUE (MeV)

CL%

EVTS

DOCUMENT ID

TECN

COMMENT

**< 4.6**AMMAR 01 CLE2  $e^+e^- \approx \mathcal{T}(4S)$  $\Sigma_c(2455)^0$  WIDTH

VALUE (MeV)

EVTS

DOCUMENT ID

TECN

COMMENT

**2.16 ± 0.26 OUR AVERAGE** Error includes scale factor of 1.1.

1.65 ± 0.11 ± 0.49 15.9k

AALTONEN 11H CDF  $p\bar{p}$  at 1.96 TeV

2.6 ± 0.5 ± 0.3

AUBERT 08BN BABR  $B^- \rightarrow \bar{p}\Lambda_c^+\pi^-$ 

2.5 ± 0.2 ± 0.3 2k

ARTUSO 02 CLE2  $e^+e^- \approx \mathcal{T}(4S)$ 1.55  $^{+0.41}_{-0.37}$  ± 0.38 913LINK 02 FOCS  $\gamma$  nucleus,  $\bar{E}_\gamma \approx 180$  GeV $\Sigma_c(2455)$  DECAY MODES

$\Lambda_c^+ \pi$  is the only strong decay allowed to a  $\Sigma_c$  having this mass.

Mode	Fraction ( $\Gamma_i/\Gamma$ )
$\Gamma_1 \Lambda_c^+ \pi$	$\approx 100\%$

 $\Sigma_c(2455)$  REFERENCES

AALTONEN 11H PR D84 012003	T. Aaltonen <i>et al.</i>	(CDF Collab.)
AUBERT 08BN PR D78 112003	B. Aubert <i>et al.</i>	(BABAR Collab.)
ARTUSO 02 PR D65 071101R	M. Artuso <i>et al.</i>	(CLEO Collab.)
LINK 02 PL B525 205	J.M. Link <i>et al.</i>	(FNAL FOCUS Collab.)
AMMAR 01 PRL 86 1167	R. Ammar <i>et al.</i>	(CLEO Collab.)
LINK 00c PL B488 218	J.M. Link <i>et al.</i>	(FNAL FOCUS Collab.)
AITALA 96B PL B379 292	E.M. Ait'ala <i>et al.</i>	(FNAL E791 Collab.)
ALEEV 96 JINRRC 3-77 31	A.N. Alev <i>et al.</i>	(Serpukhov EXCHARM Collab.)
FRABETTI 96 PL B365 461	P.L. Frabetti <i>et al.</i>	(FNAL E687 Collab.)
CRAWFORD 93 PRL 71 3259	G. Crawford <i>et al.</i>	(CLEO Collab.)
ANJOS 89D PRL 62 1721	J.C. Anjos <i>et al.</i>	(FNAL E691 Collab.)
BOWCOCK 89 PRL 62 1240	T.J.V. Bowcock <i>et al.</i>	(CLEO Collab.)
ALBRECHT 88D PL B211 489	H. Albrecht <i>et al.</i>	(ARGUS Collab.)
DIESBURG 87 PRL 59 2711	M. Diesburg <i>et al.</i>	(FNAL E400 Collab.)
JONES 87 ZPHY C36 593	G.T. Jones <i>et al.</i>	(CERN WA21 Collab.)
AMMAR 86 JETPL 43 515	R. Ammar <i>et al.</i>	(ITEP)
	Translated from ZETFP 43 401.	
BOSETTI 82 PL 109B 234	P.C. Bosetti <i>et al.</i>	(AACH3, BONN, CERN+)
CALICCHIO 80 PL 93B 521	M. Calicchio <i>et al.</i>	(BARI, BIRM, BRUX+)
BALTAY 79 PRL 42 1721	C. Baltay <i>et al.</i>	(COLU, BNL)†
CAZZOLI 75 PRL 34 1125	E.G. Cazzoli <i>et al.</i>	(BNL)



$\Sigma_c(2520)$

$I(J^P) = 1(\frac{3}{2}^+)$  Status: \*\*\*

Seen in the  $\Lambda_c^+ \pi^\pm$  mass spectrum. The natural assignment is that this is the  $J^P = 3/2^+$  excitation of the  $\Sigma_c(2455)$ , the charm counterpart of the  $\Sigma(1385)$ , but neither  $J$  nor  $P$  has been measured.

$\Sigma_c(2520)$  MASSES

The masses are obtained from the mass-difference measurements that follow.

$\Sigma_c(2520)^{++}$  MASS

VALUE (MeV)	EVTS	DOCUMENT ID	TECN	COMMENT
<b>2517.9 ± 0.6 OUR FIT</b>				Error includes scale factor of 1.6.
• • • We do not use the following data for averages, fits, limits, etc. • • •				
2530 ± 5 ± 5	6	<sup>1</sup> AMMO SOV 93	HLBC	$\nu p \rightarrow \mu^- \Sigma_c(2530)^{++}$

<sup>1</sup>AMMO SOV 93 sees a cluster of 6 events and estimates the background to be 1 event.

$\Sigma_c(2520)^+$  MASS

VALUE (MeV)	DOCUMENT ID
<b>2517.5 ± 2.3 OUR FIT</b>	

$\Sigma_c(2520)^0$  MASS

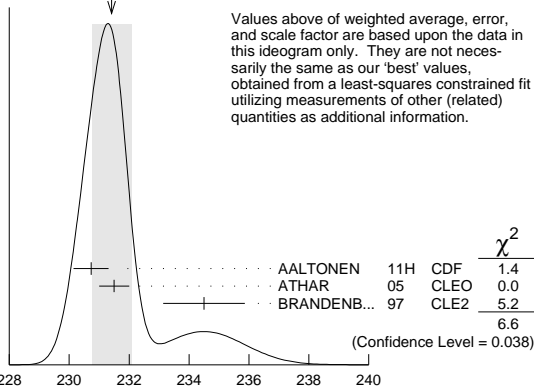
VALUE (MeV)	DOCUMENT ID
<b>2518.8 ± 0.6 OUR FIT</b>	

$\Sigma_c(2520)$  MASS DIFFERENCES

$m_{\Sigma_c(2520)^{++}} - m_{\Lambda_c^+}$

VALUE (MeV)	EVTS	DOCUMENT ID	TECN	COMMENT
<b>231.4 ± 0.6 OUR FIT</b>				Error includes scale factor of 1.6.
<b>231.4 ± 0.7 OUR AVERAGE</b>				Error includes scale factor of 1.8. See the ideogram below.
230.73 ± 0.56 ± 0.16	8.8k	AALTONEN 11H	CDF	$p\bar{p}$ at 1.96 TeV
231.5 ± 0.4 ± 0.3	1330 ± 110	ATHAR 05	CLEO	$e^+ e^-$ , 9.4–11.5 GeV
234.5 ± 1.1 ± 0.8	677	BRANDENB... 97	CLE2	$e^+ e^- \approx \Upsilon(4S)$

WEIGHTED AVERAGE  
231.4 ± 0.7 (Error scaled by 1.8)



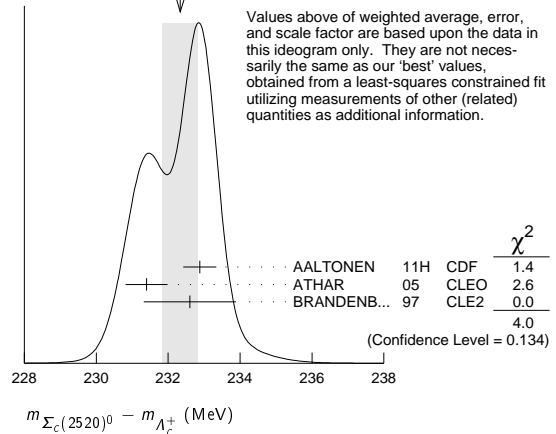
$m_{\Sigma_c(2520)^+} - m_{\Lambda_c^+}$

VALUE (MeV)	EVTS	DOCUMENT ID	TECN	COMMENT
<b>231.0 ± 2.3 OUR FIT</b>				
<b>231.0 ± 1.1 ± 2.0</b>	327	AMMAR 01	CLE2	$e^+ e^- \approx \Upsilon(4S)$

$m_{\Sigma_c(2520)^0} - m_{\Lambda_c^+}$

VALUE (MeV)	EVTS	DOCUMENT ID	TECN	COMMENT
<b>232.3 ± 0.5 OUR FIT</b>				Error includes scale factor of 1.6.
<b>232.3 ± 0.5 OUR AVERAGE</b>				Error includes scale factor of 1.4. See the ideogram below.
232.88 ± 0.43 ± 0.16	9.0k	AALTONEN 11H	CDF	$p\bar{p}$ at 1.96 TeV
231.4 ± 0.5 ± 0.3	1350 ± 120	ATHAR 05	CLEO	$e^+ e^-$ , 9.4–11.5 GeV
232.6 ± 1.0 ± 0.8	504	BRANDENB... 97	CLE2	$e^+ e^- \approx \Upsilon(4S)$

WEIGHTED AVERAGE  
232.3 ± 0.5 (Error scaled by 1.4)



Values above of weighted average, error, and scale factor are based upon the data in this ideogram only. They are not necessarily the same as our 'best' values, obtained from a least-squares constrained fit utilizing measurements of other (related) quantities as additional information.

$m_{\Sigma_c(2520)^{++}} - m_{\Sigma_c(2520)^0}$

VALUE (MeV)	DOCUMENT ID	TECN	COMMENT
<b>0.1 ± 0.8 ± 0.3</b>			
1.9 ± 1.4 ± 1.0	<sup>2</sup> ATHAR 05	CLEO	$e^+ e^-$ , 9.4–11.5 GeV
	<sup>3</sup> BRANDENB... 97	CLE2	$e^+ e^- \approx \Upsilon(4S)$

<sup>2</sup>This ATHAR 05 result is redundant with measurements in earlier entries.  
<sup>3</sup>This BRANDENBURG 97 result is redundant with measurements in earlier entries.

$\Sigma_c(2520)$  WIDTHS

$\Sigma_c(2520)^{++}$  WIDTH

VALUE (MeV)	CL%	EVTS	DOCUMENT ID	TECN	COMMENT
<b>14.9 ± 1.5 OUR AVERAGE</b>					
15.03 ± 2.12 ± 1.36		8.8k	AALTONEN 11H	CDF	$p\bar{p}$ at 1.96 TeV
14.4 <sup>+1.6</sup> <sub>-1.5</sub> ± 1.4		1330 ± 110	ATHAR 05	CLEO	$e^+ e^-$ , 9.4–11.5 GeV
17.9 <sup>+3.8</sup> <sub>-3.2</sub> ± 4.0		677	BRANDENB... 97	CLE2	$e^+ e^- \approx \Upsilon(4S)$

$\Sigma_c(2520)^+$  WIDTH

VALUE (MeV)	CL%	EVTS	DOCUMENT ID	TECN	COMMENT	
<b>&lt;17</b>		90	327	AMMAR 01	CLE2	$e^+ e^- \approx \Upsilon(4S)$

$\Sigma_c(2520)^0$  WIDTH

VALUE (MeV)	CL%	EVTS	DOCUMENT ID	TECN	COMMENT
<b>14.5 ± 1.5 OUR AVERAGE</b>					
12.51 ± 1.82 ± 1.37		9.0k	AALTONEN 11H	CDF	$p\bar{p}$ at 1.96 TeV
16.6 <sup>+1.9</sup> <sub>-1.7</sub> ± 1.4		1350 ± 120	ATHAR 05	CLEO	$e^+ e^-$ , 9.4–11.5 GeV
13.0 <sup>+3.7</sup> <sub>-3.0</sub> ± 4.0		504	BRANDENB... 97	CLE2	$e^+ e^- \approx \Upsilon(4S)$

$\Sigma_c(2520)$  DECAY MODES

$\Lambda_c^+ \pi$  is the only strong decay allowed to a  $\Sigma_c$  having this mass.

Mode	Fraction ( $\Gamma_i/\Gamma$ )
$\Gamma_1 \Lambda_c^+ \pi$	$\approx 100\%$

$\Sigma_c(2520)$  REFERENCES

AALTONEN 11H	PR D84 012003	T. Aaltonen et al.	(CDF Collab.)
ATHAR 05	PR D71 051101R	S.B. Athar et al.	(CLEO Collab.)
AMMAR 01	PRL 86 1167	R. Ammar et al.	(CLEO Collab.)
BRANDENB... 97	PRL 78 2304	G. Brandenburg et al.	(CLEO Collab.)
AMMO SOV 93	JETPL 58 247	V.V. Ammosov et al.	(SERP)
Translated from ZETFP 58 241.			

# Baryon Particle Listings

## $\Sigma_c(2800), \Xi_c^+$

### $\Sigma_c(2800)$

$I(J^P) = 1(?^?)$  Status: \*\*\*

Seen in the  $\Lambda_c^+ \pi^+, \Lambda_c^+ \pi^0,$  and  $\Lambda_c^+ \pi^-$  mass spectra.

#### $\Sigma_c(2800)$ MASSES

The charged ++ and + masses are obtained from the mass-difference measurements that follow. The neutral mass is dominated by the mass-difference measurement, but is pulled up somewhat by the less well-determined but considerably higher direct-mass measurement. It is possible, in fact, that AUBERT 08BN is seeing a different  $\Sigma_c$ .

#### $\Sigma_c(2800)^{++}$ MASS

VALUE (MeV) DOCUMENT ID

2801  $\pm 4$  OUR FIT

#### $\Sigma_c(2800)^+$ MASS

VALUE (MeV) DOCUMENT ID

2792  $\pm 14$  OUR FIT

#### $\Sigma_c(2800)^0$ MASS

VALUE (MeV) DOCUMENT ID TECN COMMENT

2806  $\pm 5$  OUR FIT Error includes scale factor of 1.3.

2846  $\pm 8 \pm 10$  AUBERT 08BN BABR  $B^- \rightarrow \bar{p} \Lambda_c^+ \pi^-$

#### $\Sigma_c(2800)$ MASS DIFFERENCES

##### $m_{\Sigma_c(2800)^{++}} - m_{\Lambda_c^+}$

VALUE (MeV) EVTS DOCUMENT ID TECN COMMENT

514  $\pm 4$  OUR FIT

514.5  $\pm 3.4 \pm 2.8$  2810  $\pm 1090$  MIZUK 05 BELL  $e^+ e^- \approx \Upsilon(4S)$

##### $m_{\Sigma_c(2800)^+} - m_{\Lambda_c^+}$

VALUE (MeV) EVTS DOCUMENT ID TECN COMMENT

505  $\pm 14$  OUR FIT

505.4  $\pm 5.8 \pm 12.4$  1540  $\pm 1750$  MIZUK 05 BELL  $e^+ e^- \approx \Upsilon(4S)$

##### $m_{\Sigma_c(2800)^0} - m_{\Lambda_c^+}$

VALUE (MeV) EVTS DOCUMENT ID TECN COMMENT

519  $\pm 5$  OUR FIT Error includes scale factor of 1.3.

515.4  $\pm 3.2 \pm 2.1$  2240  $\pm 1300$  MIZUK 05 BELL  $e^+ e^- \approx \Upsilon(4S)$

#### $\Sigma_c(2800)$ WIDTHS

##### $\Sigma_c(2800)^{++}$ WIDTH

VALUE (MeV) EVTS DOCUMENT ID TECN COMMENT

75  $\pm 18 \pm 12$  2810  $\pm 1090$  MIZUK 05 BELL  $e^+ e^- \approx \Upsilon(4S)$

##### $\Sigma_c(2800)^+$ WIDTH

VALUE (MeV) EVTS DOCUMENT ID TECN COMMENT

62  $\pm 37 \pm 52$  1540  $\pm 1750$  MIZUK 05 BELL  $e^+ e^- \approx \Upsilon(4S)$

##### $\Sigma_c(2800)^0$ WIDTH

VALUE (MeV) EVTS DOCUMENT ID TECN COMMENT

72  $\pm 22$  OUR AVERAGE

86  $\pm 33$  22 AUBERT 08BN BABR  $B^- \rightarrow \bar{p} \Lambda_c^+ \pi^-$

61  $\pm 18 \pm 22$  2240  $\pm 1300$  MIZUK 05 BELL  $e^+ e^- \approx \Upsilon(4S)$

#### $\Sigma_c(2800)$ DECAY MODES

Mode	Fraction ( $\Gamma_i/\Gamma$ )
$\Gamma_1 \Lambda_c^+ \pi$	seen

#### $\Sigma_c(2800)$ REFERENCES

AUBERT	08BN PR D78 112003	B. Aubert et al.	(BABAR Collab.)
MIZUK	05 PRL 94 122002	R. Mizuk et al.	(BELLE Collab.)

### $\Xi_c^+$

$I(J^P) = \frac{1}{2}(\frac{1}{2}^+)$  Status: \*\*\*

According to the quark model, the  $\Xi_c^+$  (quark content  $usc$ ) and  $\Xi_c^0$  form an isospin doublet, and the spin-parity ought to be  $J^P = 1/2^+$ . None of  $I, J,$  or  $P$  has actually been measured.

#### $\Xi_c^+$ MASS

The fit uses the  $\Xi_c^+$  and  $\Xi_c^0$  mass and mass-difference measurements.

VALUE (MeV) EVTS DOCUMENT ID TECN COMMENT

2467.8  $\pm 0.4$  OUR FIT

2467.6  $\pm 0.4$  OUR AVERAGE

2468.1 $\pm 0.4 \pm 0.2$	4950 $\pm 286$	1 LESIAK	05 BELL	$e^+ e^-, \Upsilon(4S)$
2465.8 $\pm 1.9 \pm 2.5$	90	FRABETTI	98 E687	$\gamma$ Be, $\bar{E}_\gamma = 220$ GeV
2467.0 $\pm 1.6 \pm 2.0$	147	EDWARDS	96 CLE2	$e^+ e^- \approx \Upsilon(4S)$
2465.1 $\pm 3.6 \pm 1.9$	30	ALBRECHT	90F ARG	$e^+ e^-$ at $\Upsilon(4S)$
2467 $\pm 3 \pm 4$	23	ALAM	89 CLEO	$e^+ e^-$ 10.6 GeV
2466.5 $\pm 2.7 \pm 1.2$	5	BARLAG	89c ACCM	$\pi^-$ Cu 230 GeV
2464.4 $\pm 2.0 \pm 1.4$	30	FRABETTI	93B E687	See FRABETTI 98
2459 $\pm 5 \pm 30$	56	2 COTEUS	87 SPEC	$nA \approx 600$ GeV
2460 $\pm 25$	82	BIAGI	83 SPEC	$\Sigma^-$ Be 135 GeV

<sup>1</sup> The systematic error was (wrongly) given the other way round in LESIAK 05; see the erratum.

<sup>2</sup> Although COTEUS 87 claims to agree well with BIAGI 83 on the mass and width, there appears to be a discrepancy between the two experiments. BIAGI 83 sees a single peak (stated significance about 6 standard deviations) in the  $\Lambda K^- \pi^+ \pi^+$  mass spectrum. COTEUS 87 sees two peaks in the same spectrum, one at the  $\Xi_c^+$  mass, the other 75 MeV lower. The latter is attributed to  $\Xi_c^+ \rightarrow \Sigma^0 K^- \pi^+ \pi^+ \rightarrow (\Lambda \gamma) K^- \pi^+ \pi^+$ , with the  $\gamma$  unseen. The combined significance of the double peak is stated to be 5.5 standard deviations. But the absence of any trace of a lower peak in BIAGI 83 seems to us to throw into question the interpretation of the lower peak of COTEUS 87.

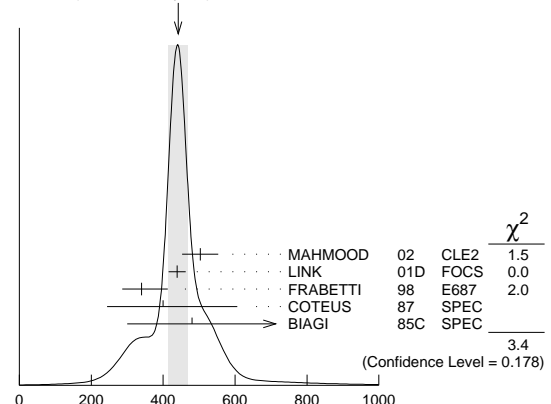
#### $\Xi_c^+$ MEAN LIFE

VALUE ( $10^{-15}$  s) EVTS DOCUMENT ID TECN COMMENT

442  $\pm 26$  OUR AVERAGE Error includes scale factor of 1.3. See the ideogram below.

503 $\pm 47 \pm 18$	250	MAHMOOD	02 CLE2	$e^+ e^- \approx \Upsilon(4S)$
439 $\pm 22 \pm 9$	532	LINK	01D FOCS	$\gamma$ nucleus, $\bar{E}_\gamma \approx 180$ GeV
340 $\pm 70$	56	FRABETTI	98 E687	$\gamma$ Be, $\bar{E}_\gamma = 220$ GeV
400 $\pm 180$	102	COTEUS	87 SPEC	$nA \approx 600$ GeV
480 $\pm 210$	53	BIAGI	85c SPEC	$\Sigma^-$ Be 135 GeV
410 $\pm 110$	30	FRABETTI	93B E687	See FRABETTI 98
200 $\pm 110$	6	BARLAG	89c ACCM	$\pi^- (K^-)$ Cu 230 GeV

WEIGHTED AVERAGE  
442 $\pm$ 26 (Error scaled by 1.3)



$\Xi_c^+$  mean life

#### $\Xi_c^+$ DECAY MODES

Mode	Fraction ( $\Gamma_i/\Gamma$ )	Confidence level
------	--------------------------------	------------------

See key on page 457

Baryon Particle Listings

$\Xi^+$   
 $\Xi^0$   
 $\Xi^-$

No absolute branching fractions have been measured.  
The following are branching ratios relative to  $\Xi^- 2\pi^+$ .

Cabibbo-favored ( $S = -2$ ) decays

$\Gamma$	Decay Mode	Value	Document ID	TECN	Comment
$\Gamma_1$	$\rho 2K_S^0$	[a] 0.087 ± 0.022			
$\Gamma_2$	$\Lambda \bar{K}^0 \pi^+$	—			
$\Gamma_3$	$\Sigma(1385)^+ \bar{K}^0$	[a,b] 1.0 ± 0.5			
$\Gamma_4$	$\Lambda K^- 2\pi^+$	[a] 0.323 ± 0.033			
$\Gamma_5$	$\Lambda \bar{K}^*(892)^0 \pi^+$	[a,b] < 0.2			90%
$\Gamma_6$	$\Sigma(1385)^+ K^- \pi^+$	[a,b] < 0.3			90%
$\Gamma_7$	$\Sigma^+ K^- \pi^+$	[a] 0.94 ± 0.11			
$\Gamma_8$	$\Sigma^+ \bar{K}^*(892)^0$	[a,b] 0.81 ± 0.15			
$\Gamma_9$	$\Sigma^0 K^- 2\pi^+$	[a] 0.29 ± 0.16			
$\Gamma_{10}$	$\Xi^0 \pi^+$	[a] 0.55 ± 0.16			
$\Gamma_{11}$	$\Xi^- 2\pi^+$	[a] DEFINED AS 1			
$\Gamma_{12}$	$\Xi(1530)^0 \pi^+$	[a,b] < 0.1			90%
$\Gamma_{13}$	$\Xi^0 \pi^+ \pi^0$	[a] 2.34 ± 0.68			
$\Gamma_{14}$	$\Xi^0 \pi^- 2\pi^+$	[a] 1.74 ± 0.50			
$\Gamma_{15}$	$\Xi^0 e^+ \nu_e$	[a] 2.3 $\begin{matrix} +0.7 \\ -0.9 \end{matrix}$			
$\Gamma_{16}$	$\Omega^- K^+ \pi^+$	[a] 0.07 ± 0.04			

Cabibbo-suppressed decays

$\Gamma_{17}$	$\rho K^- \pi^+$	[a] 0.21 ± 0.03			
$\Gamma_{18}$	$\rho \bar{K}^*(892)^0$	[a,b] 0.12 ± 0.02			
$\Gamma_{19}$	$\Sigma^+ \pi^+ \pi^-$	[a] 0.48 ± 0.20			
$\Gamma_{20}$	$\Sigma^- 2\pi^+$	[a] 0.18 ± 0.09			
$\Gamma_{21}$	$\Sigma^+ K^+ K^-$	[a] 0.15 ± 0.07			
$\Gamma_{22}$	$\Sigma^+ \phi$	[a,b] < 0.11			90%
$\Gamma_{23}$	$\Xi(1690)^0 K^+, \Xi(1690)^0 \rightarrow \Sigma^+ K^-$	[a] < 0.05			90%

[a] No absolute branching fractions have been measured. The value here is the branching ratio relative to  $\Xi^- 2\pi^+$ .

[b] This branching fraction includes all the decay modes of the final-state resonance.

$\Xi_c^+$  BRANCHING RATIOS

Cabibbo-favored ( $S = -2$ ) decays

$\Gamma(p 2K_S^0)/\Gamma(\Xi^- 2\pi^+)$	$\Gamma_1/\Gamma_{11}$
VALUE EVTS DOCUMENT ID TECN COMMENT	
0.087 ± 0.016 ± 0.014 168 ± 27 LESIAK 05 BELL $e^+ e^-$ , $\Upsilon(4S)$	

$\Gamma(\Sigma(1385)^+ \bar{K}^0)/\Gamma(\Xi^- 2\pi^+)$	$\Gamma_3/\Gamma_{11}$
VALUE EVTS DOCUMENT ID TECN COMMENT	
1.00 ± 0.49 ± 0.24 20 LINK 03E FOCS < 1.72, 90% CL	

$\Gamma(\Lambda K^- 2\pi^+)/\Gamma(\Xi^- 2\pi^+)$	$\Gamma_4/\Gamma_{11}$
VALUE EVTS DOCUMENT ID TECN COMMENT	
0.323 ± 0.033 OUR AVERAGE	
0.32 ± 0.03 ± 0.02 1177 ± 55 LESIAK 05 BELL $e^+ e^-$ , $\Upsilon(4S)$	
0.28 ± 0.06 ± 0.06 58 LINK 03E FOCS $\gamma$ nucleus, $\bar{E}_\gamma \approx 180$ GeV	
0.58 ± 0.16 ± 0.07 61 BERGFELD 96 CLE2 $e^+ e^- \approx \Upsilon(4S)$	

$\Gamma(\Lambda \bar{K}^*(892)^0 \pi^+)/\Gamma(\Lambda K^- 2\pi^+)$	$\Gamma_5/\Gamma_4$
VALUE CL% DOCUMENT ID TECN COMMENT	
< 0.5 90 BERGFELD 96 CLE2 $e^+ e^- \approx \Upsilon(4S)$	

$\Gamma(\Sigma(1385)^+ K^- \pi^+)/\Gamma(\Lambda K^- 2\pi^+)$	$\Gamma_6/\Gamma_4$
VALUE CL% DOCUMENT ID TECN COMMENT	
< 0.7 90 BERGFELD 96 CLE2 $e^+ e^- \approx \Upsilon(4S)$	

$\Gamma(\Sigma^+ K^- \pi^+)/\Gamma(\Xi^- 2\pi^+)$	$\Gamma_7/\Gamma_{11}$
VALUE EVTS DOCUMENT ID TECN COMMENT	
0.94 ± 0.10 OUR AVERAGE	
0.91 ± 0.11 ± 0.04 251 LINK 03E FOCS $\gamma$ nucleus, $\bar{E}_\gamma \approx 180$ GeV	
0.92 ± 0.20 ± 0.07 3 JUN 00 SELX $\Sigma^-$ nucleus, 600 GeV	
1.18 ± 0.26 ± 0.17 119 BERGFELD 96 CLE2 $e^+ e^- \approx \Upsilon(4S)$	

<sup>3</sup>This JUN 00 result is redundant with other results given below.

$\Gamma(\Sigma^+ \bar{K}^*(892)^0)/\Gamma(\Xi^- 2\pi^+)$	$\Gamma_8/\Gamma_{11}$
VALUE EVTS DOCUMENT ID TECN COMMENT	
0.81 ± 0.15 OUR AVERAGE	
0.78 ± 0.16 ± 0.06 119 LINK 03E FOCS $\gamma$ nucleus, $\bar{E}_\gamma \approx 180$ GeV	
0.92 ± 0.27 ± 0.14 61 BERGFELD 96 CLE2 $e^+ e^- \approx \Upsilon(4S)$	

$\Gamma(\Sigma^0 K^- 2\pi^+)/\Gamma(\Lambda K^- 2\pi^+)$	$\Gamma_9/\Gamma_4$
VALUE EVTS DOCUMENT ID TECN COMMENT	
0.84 ± 0.36 47 4 COTEUS 87 SPEC $nA \approx 600$ GeV	

<sup>4</sup> See, however, the note on the COTEUS 87  $\Xi_c^+$  mass measurement.

$\Gamma(\Xi^0 \pi^+)/\Gamma(\Xi^- 2\pi^+)$	$\Gamma_{10}/\Gamma_{11}$
VALUE EVTS DOCUMENT ID TECN COMMENT	
0.55 ± 0.13 ± 0.09 39 EDWARDS 96 CLE2 $e^+ e^- \approx \Upsilon(4S)$	

$\Gamma(\Xi^- 2\pi^+)/\Gamma_{total}$	$\Gamma_{11}/\Gamma$			
VALUE EVTS DOCUMENT ID TECN COMMENT				
• • • We do not use the following data for averages, fits, limits, etc. • • •				
seen 131 BERGFELD 96 CLE2 $e^+ e^- \approx \Upsilon(4S)$				
seen 160 AVERY 95 CLE2 $e^+ e^- \approx \Upsilon(4S)$				
seen 30 FRABETTI 93B E687 $\gamma$ Be, $\bar{E}_\gamma \approx 220$ GeV				
seen 30 ALBRECHT 90F ARG $e^+ e^-$ at $\Upsilon(4S)$				
seen 23 ALAM 89 CLEO $e^+ e^- 10.6$ GeV				

$\Gamma(\Xi(1530)^0 \pi^+)/\Gamma(\Xi^- 2\pi^+)$	$\Gamma_{12}/\Gamma_{11}$
VALUE CL% DOCUMENT ID TECN COMMENT	
< 0.1 90 LINK 03E FOCS $\gamma$ nucleus, $\bar{E}_\gamma \approx 180$ GeV	

Unseen decay modes of the  $\Xi(1530)^0$  are included.

• • • We do not use the following data for averages, fits, limits, etc. • • •				
< 0.2 90 BERGFELD 96 CLE2 $e^+ e^- \approx \Upsilon(4S)$				

$\Gamma(\Xi^0 \pi^+ \pi^0)/\Gamma(\Xi^- 2\pi^+)$	$\Gamma_{13}/\Gamma_{11}$
VALUE EVTS DOCUMENT ID TECN COMMENT	
2.34 ± 0.57 ± 0.37 81 EDWARDS 96 CLE2 $e^+ e^- \approx \Upsilon(4S)$	

$\Gamma(\Xi(1530)^0 \pi^+)/\Gamma(\Xi^0 \pi^+ \pi^0)$	$\Gamma_{12}/\Gamma_{13}$
VALUE CL% DOCUMENT ID TECN COMMENT	
< 0.3 90 EDWARDS 96 CLE2 $e^+ e^- \approx \Upsilon(4S)$	

$\Gamma(\Xi^0 \pi^- 2\pi^+)/\Gamma(\Xi^- 2\pi^+)$	$\Gamma_{14}/\Gamma_{11}$
VALUE EVTS DOCUMENT ID TECN COMMENT	
1.74 ± 0.42 ± 0.27 57 EDWARDS 96 CLE2 $e^+ e^- \approx \Upsilon(4S)$	

$\Gamma(\Xi^0 e^+ \nu_e)/\Gamma(\Xi^- 2\pi^+)$	$\Gamma_{15}/\Gamma_{11}$
VALUE EVTS DOCUMENT ID TECN COMMENT	
2.3 ± 0.6 $\begin{matrix} +0.3 \\ -0.6 \end{matrix}$ 41 ALEXANDER 95B CLE2 $e^+ e^- \approx \Upsilon(4S)$	

$\Gamma(\Omega^- K^+ \pi^+)/\Gamma(\Xi^- 2\pi^+)$	$\Gamma_{16}/\Gamma_{11}$
VALUE EVTS DOCUMENT ID TECN COMMENT	
0.07 ± 0.03 ± 0.03 14 LINK 03E FOCS < 0.12, 90% CL	

Cabibbo-suppressed decays

$\Gamma(\rho K^- \pi^+)/\Gamma(\Xi^- 2\pi^+)$	$\Gamma_{17}/\Gamma_{11}$			
VALUE EVTS DOCUMENT ID TECN COMMENT				
0.21 ± 0.04 OUR AVERAGE				
0.194 ± 0.054 47 ± 11 VAZQUEZ-JA...08 SELX $\Sigma^-$ nucleus, 600 GeV				
0.234 ± 0.047 ± 0.022 202 LINK 01B FOCS $\gamma$ nucleus				
• • • We do not use the following data for averages, fits, limits, etc. • • •				
0.20 ± 0.04 ± 0.02 76 JUN 00 SELX See VAZQUEZ-JAUREGUI 08				

$\Gamma(\rho \bar{K}^*(892)^0)/\Gamma(\rho K^- \pi^+)$	$\Gamma_{18}/\Gamma_{17}$
VALUE DOCUMENT ID TECN COMMENT	
0.54 ± 0.09 ± 0.05 LINK 01B FOCS $\gamma$ nucleus	

$\Gamma(\Sigma^+ \pi^+ \pi^-)/\Gamma(\Xi^- 2\pi^+)$	$\Gamma_{19}/\Gamma_{11}$
VALUE EVTS DOCUMENT ID TECN COMMENT	
0.48 ± 0.20 21 ± 8 VAZQUEZ-JA...08 SELX $\Sigma^-$ nucleus, 600 GeV	

$\Gamma(\Sigma^- 2\pi^+)/\Gamma(\Xi^- 2\pi^+)$	$\Gamma_{20}/\Gamma_{11}$
VALUE EVTS DOCUMENT ID TECN COMMENT	
0.18 ± 0.09 10 ± 4 VAZQUEZ-JA...08 SELX $\Sigma^-$ nucleus, 600 GeV	

$\Gamma(\Sigma^+ K^+ K^-)/\Gamma(\Sigma^+ K^- \pi^+)$	$\Gamma_{21}/\Gamma_7$
VALUE EVTS DOCUMENT ID TECN COMMENT	
0.16 ± 0.06 ± 0.01 17 LINK 03E FOCS $\gamma$ nucleus, $\bar{E}_\gamma \approx 180$ GeV	

$\Gamma(\Sigma^+ \phi)/\Gamma(\Sigma^+ K^- \pi^+)$	$\Gamma_{22}/\Gamma_7$
VALUE CL% DOCUMENT ID TECN COMMENT	
< 0.12 90 LINK 03E FOCS $\gamma$ nucleus, $\bar{E}_\gamma \approx 180$ GeV	

$\Gamma(\Xi(1690)^0 K^+ \times B(\Xi(1690)^0 \rightarrow \Sigma^+ K^-))/\Gamma(\Sigma^+ K^- \pi^+)$	$\Gamma_{23}/\Gamma_7$
VALUE CL% DOCUMENT ID TECN COMMENT	
< 0.05 90 LINK 03E FOCS $\gamma$ nucleus, $\bar{E}_\gamma \approx 180$ GeV	

## Baryon Particle Listings

$$\Xi_c^+, \Xi_c^0$$

 $\Xi_c^+$  REFERENCES

VAZQUEZ-JA...	08	PL B666 299	E. Vazquez-Jauregui <i>et al.</i>	(SLEX Collab.)
LESIAK	05	PL B605 237	T. Lesiak <i>et al.</i>	(BELLE Collab.)
Also		PL B617 198 (erratum)	T. Lesiak <i>et al.</i>	(BELLE Collab.)
LINK	03E	PL B571 139	J.M. Link <i>et al.</i>	(FNAL FOCUS Collab.)
MAHMOOD	02	PR D65 031102	A.H. Mahmood <i>et al.</i>	(CLEO Collab.)
LINK	01B	PL B512 277	J.M. Link <i>et al.</i>	(FNAL FOCUS Collab.)
LINK	01D	PL B523 53	J.M. Link <i>et al.</i>	(FNAL FOCUS Collab.)
JUN	00	PRL 84 1857	S.Y. Jun <i>et al.</i>	(FNAL SLEX Collab.)
FRABETTI	98	PL B427 211	P.L. Frabetti <i>et al.</i>	(FNAL E687 Collab.)
BERGFELD	96	PL B365 431	T. Bergfeld <i>et al.</i>	(CLEO Collab.)
EDWARDS	96	PL B373 261	K.W. Edwards <i>et al.</i>	(CLEO Collab.)
ALEXANDER	95B	PRL 74 3113	J. Alexander <i>et al.</i>	(CLEO Collab.)
Also		PRL 75 4155 (erratum)	J. Alexander <i>et al.</i>	(CLEO Collab.)
AVERY	95	PRL 75 4364	P. Avery <i>et al.</i>	(CLEO Collab.)
FRABETTI	93B	PRL 70 1381	P.L. Frabetti <i>et al.</i>	(FNAL E687 Collab.)
ALBRECHT	90F	PL B247 121	H. Albrecht <i>et al.</i>	(ARGUS Collab.)
ALAM	89	PL B226 401	M.S. Alam <i>et al.</i>	(CLEO Collab.)
BARLAG	89C	PL B233 522	S. Barlag <i>et al.</i>	(ACCMOR Collab.)
COTEUS	87	PRL 59 1530	P. Coteus <i>et al.</i>	(FNAL E400 Collab.)
BIAGI	85C	PL 150B 230	S.F. Biagi <i>et al.</i>	(CERN WA62 Collab.)
BIAGI	83	PL 122B 455	S.F. Biagi <i>et al.</i>	(CERN WA62 Collab.)

$$\Xi_c^0$$

$$I(J^P) = \frac{1}{2}(\frac{1}{2}^+) \text{ Status: } ***$$

According to the quark model, the  $\Xi_c^0$  (quark content  $dsc$ ) and  $\Xi_c^+$  form an isospin doublet, and the spin-parity ought to be  $J^P = 1/2^+$ . None of  $I$ ,  $J$ , or  $P$  has actually been measured.

 $\Xi_c^0$  MASS

The fit uses the  $\Xi_c^0$  and  $\Xi_c^+$  mass and mass-difference measurements.

VALUE (MeV)	EVTS	DOCUMENT ID	TECN	COMMENT
<b>2470.88<math>\pm</math>0.34</b>				<b>OUR FIT</b> Error includes scale factor of 1.1.
<b>-0.80</b>				

**2471.09 $\pm$ 0.35** OUR AVERAGE

2471.0 $\pm$ 0.3 $\pm$ 0.2	8620 $\pm$ 355	<sup>1</sup> LESIAK	05	BELL	$e^+e^-$ , $\Upsilon(4S)$
2470.0 $\pm$ 2.8 $\pm$ 2.6	85	FRABETTI	98B	E687	$\gamma$ Be, $\bar{E}_\gamma = 220$ GeV
2469 $\pm$ 2 $\pm$ 3	9	HENDERSON	92B	CLEO	$\Omega^- K^+$
2472.1 $\pm$ 2.7 $\pm$ 1.6	54	ALBRECHT	90F	ARG	$e^+e^-$ at $\Upsilon(4S)$
2473.3 $\pm$ 1.9 $\pm$ 1.2	4	BARLAG	90	ACCM	$\pi^- (K^-)$ Cu 230 GeV
2472 $\pm$ 3 $\pm$ 4	19	ALAM	89	CLEO	$e^+e^-$ 10.6 GeV
••• We do not use the following data for averages, fits, limits, etc. •••					
2462.1 $\pm$ 3.1 $\pm$ 1.4	42	<sup>2</sup> FRABETTI	93C	E687	See FRABETTI 98B
2471 $\pm$ 3 $\pm$ 4	14	AVERY	89	CLEO	See ALAM 89

<sup>1</sup>The systematic error was (wrongly) given the other way round in LESIAK 05.

<sup>2</sup>The FRABETTI 93C mass is well below the other measurements.

 $\Xi_c^0 - \Xi_c^+$  MASS DIFFERENCE

VALUE (MeV)	DOCUMENT ID	TECN	COMMENT
<b>3.1<math>\pm</math>0.4</b>			<b>OUR FIT</b>
<b>3.1<math>\pm</math>0.5</b>			<b>OUR AVERAGE</b>
+2.9 $\pm$ 0.5	LESIAK	05	BELL $e^+e^-$ , $\Upsilon(4S)$
+7.0 $\pm$ 4.5 $\pm$ 2.2	ALBRECHT	90F	ARG $e^+e^-$ at $\Upsilon(4S)$
+6.8 $\pm$ 3.3 $\pm$ 0.5	BARLAG	90	ACCM $\pi^- (K^-)$ Cu 230 GeV
+5 $\pm$ 4 $\pm$ 1	ALAM	89	CLEO $\Xi_c^0 \rightarrow \Xi^- \pi^+$ , $\Xi_c^+ \rightarrow \Xi^- \pi^+ \pi^+$

 $\Xi_c^0$  MEAN LIFE

VALUE ( $10^{-15}$ s)	EVTS	DOCUMENT ID	TECN	COMMENT
<b>112<math>\pm</math>13</b>				<b>OUR AVERAGE</b>
118 $\pm$ 14	110	LINK	02H	FOCS $\gamma$ nucleus, $\approx 180$ GeV
101 $\pm$ 25	42	FRABETTI	93C	E687 $\gamma$ Be, $\bar{E}_\gamma = 220$ GeV
82 $\pm$ 59	4	BARLAG	90	ACCM $\pi^- (K^-)$ Cu 230 GeV

 $\Xi_c^0$  DECAY MODES

No absolute branching fractions have been measured. Several measurements of ratios of fractions may be found in the Listings that follow.

Mode	Fraction ( $\Gamma_i/\Gamma$ )
$\Gamma_1$ $pK^-K^-\pi^+$	seen
$\Gamma_2$ $pK^-\bar{K}^*(892)^0$	seen
$\Gamma_3$ $pK^-K^-\pi^+$ no $\bar{K}^*(892)^0$	seen
$\Gamma_4$ $\Lambda K_S^0$	seen
$\Gamma_5$ $\Lambda K^-\pi^+$	

$\Gamma_6$ $\Lambda\bar{K}^0\pi^+\pi^-$	seen
$\Gamma_7$ $\Lambda K^-\pi^+\pi^+\pi^-$	seen
$\Gamma_8$ $\Xi^- \pi^+$	seen
$\Gamma_9$ $\Xi^- \pi^+\pi^+\pi^-$	seen
$\Gamma_{10}$ $\Omega^- K^+$	seen
$\Gamma_{11}$ $\Xi^- e^+ \nu_e$	seen
$\Gamma_{12}$ $\Xi^- \ell^+$ anything	seen

 $\Xi_c^0$  BRANCHING RATIOS

$\Gamma(pK^-K^-\pi^+)/\Gamma(\Xi^- \pi^+)$	$\Gamma_1/\Gamma_8$			
VALUE	EVTS	DOCUMENT ID	TECN	COMMENT
<b>0.34<math>\pm</math>0.04</b>				<b>OUR AVERAGE</b>
0.33 $\pm$ 0.03 $\pm$ 0.03	1908 $\pm$ 62	LESIAK	05	BELL $e^+e^-$ , $\Upsilon(4S)$
0.35 $\pm$ 0.06 $\pm$ 0.03	148 $\pm$ 18	DANKO	04	CLEO $e^+e^-$

 $\Gamma(pK^-\bar{K}^*(892)^0)/\Gamma(\Xi^- \pi^+)$   $\Gamma_2/\Gamma_8$ 

VALUE	DOCUMENT ID	TECN	COMMENT
<b>0.210<math>\pm</math>0.045<math>\pm</math>0.015</b>	DANKO	04	CLEO $e^+e^-$
••• We do not use the following data for averages, fits, limits, etc. •••			
seen	BARLAG	90	ACCM $\pi^- (K^-)$ Cu 230 GeV

 $\Gamma(pK^-K^-\pi^+$  no  $\bar{K}^*(892)^0)/\Gamma(\Xi^- \pi^+)$   $\Gamma_3/\Gamma_8$ 

VALUE	DOCUMENT ID	TECN	COMMENT
<b>0.21<math>\pm</math>0.04<math>\pm</math>0.02</b>	DANKO	04	CLEO $e^+e^-$

 $\Gamma(\Lambda K_S^0)/\Gamma(\Xi^- \pi^+)$   $\Gamma_4/\Gamma_8$ 

VALUE	EVTS	DOCUMENT ID	TECN	COMMENT
<b>0.21<math>\pm</math>0.02<math>\pm</math>0.02</b>	465 $\pm$ 37	LESIAK	05	BELL $e^+e^-$ , $\Upsilon(4S)$
••• We do not use the following data for averages, fits, limits, etc. •••				
seen	7	ALBRECHT	95B	ARG $e^+e^- \approx 10.4$ GeV

 $\Gamma(\Lambda K^-\pi^+)/\Gamma(\Xi^- \pi^+)$   $\Gamma_5/\Gamma_8$ 

VALUE	EVTS	DOCUMENT ID	TECN	COMMENT
<b>1.07<math>\pm</math>0.12<math>\pm</math>0.07</b>	2979 $\pm$ 211	LESIAK	05	BELL $e^+e^-$ , $\Upsilon(4S)$

 $\Gamma(\Lambda\bar{K}^0\pi^+\pi^-)/\Gamma_{\text{total}}$   $\Gamma_6/\Gamma$ 

VALUE	DOCUMENT ID	TECN	COMMENT
seen	FRABETTI	98B	E687 $\gamma$ Be, $\bar{E}_\gamma = 220$ GeV

 $\Gamma(\Lambda K^-\pi^+\pi^+\pi^-)/\Gamma_{\text{total}}$   $\Gamma_7/\Gamma$ 

VALUE	DOCUMENT ID	TECN	COMMENT
seen	FRABETTI	98B	E687 $\gamma$ Be, $\bar{E}_\gamma = 220$ GeV

 $\Gamma(\Xi^- \pi^+)/\Gamma(\Xi^- \pi^+\pi^+\pi^-)$   $\Gamma_8/\Gamma_9$ 

VALUE	DOCUMENT ID	TECN	COMMENT
<b>0.30<math>\pm</math>0.12<math>\pm</math>0.05</b>	ALBRECHT	90F	ARG $e^+e^-$ at $\Upsilon(4S)$

 $\Gamma(\Omega^- K^+)/\Gamma(\Xi^- \pi^+)$   $\Gamma_{10}/\Gamma_8$ 

VALUE	EVTS	DOCUMENT ID	TECN	COMMENT
<b>0.297<math>\pm</math>0.024</b>				<b>OUR AVERAGE</b>
0.294 $\pm$ 0.018 $\pm$ 0.016	650	AUBERT,B	05M	BABR $e^+e^- \approx \Upsilon(4S)$
0.50 $\pm$ 0.21 $\pm$ 0.05	9	HENDERSON	92B	CLEO $e^+e^- \approx 10.6$ GeV

 $\Gamma(\Xi^- e^+ \nu_e)/\Gamma(\Xi^- \pi^+)$   $\Gamma_{11}/\Gamma_8$ 

VALUE	EVTS	DOCUMENT ID	TECN	COMMENT
<b>3.1<math>\pm</math>1.0<math>\pm</math>0.3</b>	54	ALEXANDER	95B	CLE2 $e^+e^- \approx \Upsilon(4S)$

 $\Gamma(\Xi^- \ell^+ \text{ anything})/\Gamma(\Xi^- \pi^+)$   $\Gamma_{12}/\Gamma_8$ 

The ratio is for the average (not the sum) of the  $\Xi^- e^+$  anything and  $\Xi^- \mu^+$  anything modes.

VALUE	EVTS	DOCUMENT ID	TECN	COMMENT
<b>0.96<math>\pm</math>0.43<math>\pm</math>0.18</b>	18	ALBRECHT	93B	ARG $e^+e^- \approx 10.4$ GeV

 $\Gamma(\Xi^- \ell^+ \text{ anything})/\Gamma(\Xi^- \pi^+\pi^+\pi^-)$   $\Gamma_{12}/\Gamma_9$ 

The ratio is for the average (not the sum) of the  $\Xi^- e^+$  anything and  $\Xi^- \mu^+$  anything modes.

VALUE	EVTS	DOCUMENT ID	TECN	COMMENT
<b>0.29<math>\pm</math>0.12<math>\pm</math>0.04</b>	18	ALBRECHT	93B	ARG $e^+e^- \approx 10.4$ GeV

 $\Xi_c^0$  DECAY PARAMETERS

See the note on "Baryon Decay Parameters" in the neutron Listings.

 $\alpha$  FOR  $\Xi_c^0 \rightarrow \Xi^- \pi^+$ 

VALUE	EVTS	DOCUMENT ID	TECN	COMMENT
<b>-0.56<math>\pm</math>0.39<math>\pm</math>0.10</b>	138	CHAN	01	CLE2 $e^+e^- \approx \Upsilon(4S)$

See key on page 457

Baryon Particle Listings

$$\Xi_c^0, \Xi_c^{'+}, \Xi_c^{'0}, \Xi_c(2645)$$

$\Xi_c^0$  REFERENCES

AUBERT, B	05M	PRL 95 142003	B. Aubert et al.	(BABAR Collab.)
LESIAK	05	PL B605 237	T. Lesiak et al.	(BELLE Collab.)
Also		PL B617 198 (erratum)	T. Lesiak et al.	(BELLE Collab.)
DANKO	04	PR D69 052004	I. Danko et al.	(CLEO Collab.)
LINK	02H	PL B541 211	J.M. Link et al.	(FNAL FOCUS Collab.)
CHAN	01	PR D63 111102R	S. Chan et al.	(CLEO Collab.)
FRABETTI	98B	PL B426 403	P.L. Frabetti et al.	(FNAL E687 Collab.)
ALBRECHT	95B	PL B342 397	H. Albrecht et al.	(ARGUS Collab.)
ALEXANDER	95B	PRL 74 3113	J. Alexander et al.	(CLEO Collab.)
Also		PRL 75 4155 (erratum)	J. Alexander et al.	(CLEO Collab.)
ALBRECHT	93B	PL B303 368	H. Albrecht et al.	(ARGUS Collab.)
FRABETTI	93C	PRL 70 2058	P.L. Frabetti et al.	(FNAL E687 Collab.)
HENDERSON	92B	PL B283 161	S. Henderson et al.	(CLEO Collab.)
ALBRECHT	90F	PL B247 121	H. Albrecht et al.	(ARGUS Collab.)
BARLAG	90	PL B236 495	S. Barlag et al.	(ACCMOR Collab.)
ALAM	89	PL B226 401	M.S. Alam et al.	(CLEO Collab.)
AVERY	89	PRL 62 863	P. Avery et al.	(CLEO Collab.)

$$\Xi_c^{'+}$$

$$I(J^P) = \frac{1}{2}(\frac{1}{2}^+) \text{ Status: } ***$$

The  $\Xi_c^{'+}$  and  $\Xi_c^{'0}$  presumably complete the SU(3) sextet whose other members are the  $\Sigma_c^{++}$ ,  $\Sigma_c^+$ ,  $\Sigma_c^0$ , and  $\Omega_c^0$ ; see Fig. 3 in the Note on Charmed Baryons just before the  $\Lambda_c^+$  Listings. The quantum numbers given above come from this presumption but have not been measured.

$\Xi_c^{'+}$  MASS

The mass is obtained from the mass-difference measurement that follows.

VALUE (MeV)	DOCUMENT ID
<b>2575.6 ± 3.1 OUR FIT</b>	

$\Xi_c^{'+} - \Xi_c^+$  MASS DIFFERENCE

VALUE (MeV)	EVTS	DOCUMENT ID	TECN	COMMENT
<b>107.8 ± 3.0 OUR FIT</b>				
<b>107.8 ± 1.7 ± 2.5</b>	25	JESSOP	99	CLE2 $e^+e^- \approx \Upsilon(4S)$

$\Xi_c^{'+}$  DECAY MODES

The  $\Xi_c^{'+} - \Xi_c^+$  mass difference is too small for any strong decay to occur.

Mode	Fraction ( $\Gamma_i/\Gamma$ )
$\Gamma_1$ $\Xi_c^+ \gamma$	seen

$\Xi_c^{'0}$  REFERENCES

JESSOP	99	PRL 82 492	C.P. Jessop et al.	(CLEO Collab.)
--------	----	------------	--------------------	----------------

$$\Xi_c^{'0}$$

$$I(J^P) = \frac{1}{2}(\frac{1}{2}^+) \text{ Status: } ***$$

See the note in the Listing for the  $\Xi_c^{'+}$ , above.

$\Xi_c^{'0}$  MASS

The mass is obtained from the mass-difference measurement that follows.

VALUE (MeV)	DOCUMENT ID
<b>2577.9 ± 2.9 OUR FIT</b>	

$\Xi_c^{'0} - \Xi_c^0$  MASS DIFFERENCE

VALUE (MeV)	EVTS	DOCUMENT ID	TECN	COMMENT
<b>107.0 ± 2.9 OUR FIT</b>				
<b>107.0 ± 1.4 ± 2.5</b>	28	JESSOP	99	CLE2 $e^+e^- \approx \Upsilon(4S)$

$\Xi_c^{'0}$  DECAY MODES

The  $\Xi_c^{'0} - \Xi_c^0$  mass difference is too small for any strong decay to occur.

Mode	Fraction ( $\Gamma_i/\Gamma$ )
$\Gamma_1$ $\Xi_c^0 \gamma$	seen

$\Xi_c^{'0}$  REFERENCES

JESSOP	99	PRL 82 492	C.P. Jessop et al.	(CLEO Collab.)
--------	----	------------	--------------------	----------------

$$\Xi_c(2645)$$

$$I(J^P) = \frac{1}{2}(\frac{3}{2}^+) \text{ Status: } ***$$

A narrow peak seen in the  $\Xi_c \pi$  mass spectrum. The natural assignment is that this is the  $J^P = 3/2^+$  excitation of the  $\Xi_c$  in the same SU(4) multiplet as the  $\Delta(1232)$ , but the quantum numbers have not been measured.

$\Xi_c(2645)$  MASSES

The masses are obtained from the mass-difference measurements that follow.

$\Xi_c(2645)^+$  MASS

VALUE (MeV)	EVTS	DOCUMENT ID	TECN	COMMENT
<b>2645.9 ± 0.5 OUR FIT</b>				Error includes scale factor of 1.1.
<b>2645.6 ± 0.2 ± 0.6</b>	578 ± 32	LESIAK	08	BELL $e^+e^- \approx \Upsilon(4S)$

$\Xi_c(2645)^0$  MASS

VALUE (MeV)	EVTS	DOCUMENT ID	TECN	COMMENT
<b>2645.9 ± 0.5 OUR FIT</b>				
<b>2645.7 ± 0.2 ± 0.6</b>	611 ± 32	LESIAK	08	BELL $e^+e^- \approx \Upsilon(4S)$

$\Xi_c(2645) - \Xi_c$  MASS DIFFERENCES

$m_{\Xi_c(2645)^+} - m_{\Xi_c^+}$

VALUE (MeV)	EVTS	DOCUMENT ID	TECN	COMMENT
<b>175.0 ± 0.8 OUR FIT</b>				Error includes scale factor of 1.2.
<b>175.6 ± 1.4 OUR AVERAGE</b>				Error includes scale factor of 1.7.
177.1 ± 0.5 ± 1.1	47	FRABETTI	98B	E687 $\gamma$ Be, $\bar{E}_\gamma = 220$ GeV
174.3 ± 0.5 ± 1.0	34	GIBBONS	96	CLE2 $e^+e^- \approx \Upsilon(4S)$

$m_{\Xi_c(2645)^0} - m_{\Xi_c^0}$

VALUE (MeV)	EVTS	DOCUMENT ID	TECN	COMMENT
<b>178.1 ± 0.6 OUR FIT</b>				
<b>178.2 ± 0.5 ± 1.0</b>	55	AVERY	95	CLE2 $e^+e^- \approx \Upsilon(4S)$

$\Xi_c(2645)^+ - \Xi_c(2645)^0$  MASS DIFFERENCE

$m_{\Xi_c(2645)^+} - m_{\Xi_c(2645)^0}$

VALUE (MeV)	DOCUMENT ID	TECN	COMMENT
<b>0.0 ± 0.5 OUR FIT</b>			
<b>-0.1 ± 0.3 ± 0.6</b>	LESIAK	08	BELL $\approx 600$ evts each

$\Xi_c(2645)$  WIDTHS

$\Xi_c(2645)^+$  WIDTH

VALUE (MeV)	CL%	DOCUMENT ID	TECN	COMMENT
<b>&lt;3.1</b>	90	GIBBONS	96	CLE2 $e^+e^- \approx \Upsilon(4S)$

$\Xi_c(2645)^0$  WIDTH

VALUE (MeV)	CL%	EVTS	DOCUMENT ID	TECN	COMMENT
<b>&lt;5.5</b>	90	55	AVERY	95	CLE2 $e^+e^- \approx \Upsilon(4S)$

$\Xi_c(2645)$  DECAY MODES

$\Xi_c \pi$  is the only strong decay allowed to a  $\Xi_c$  resonance having this mass.

Mode	Fraction ( $\Gamma_i/\Gamma$ )
$\Gamma_1$ $\Xi_c^0 \pi^+$	seen
$\Gamma_2$ $\Xi_c^+ \pi^-$	seen

$\Xi_c(2645)$  REFERENCES

LESIAK	08	PL B665 9	T. Lesiak et al.	(BELLE Collab.)
FRABETTI	98B	PL B426 403	P.L. Frabetti et al.	(FNAL E687 Collab.)
GIBBONS	96	PRL 77 310	L.K. Gibbons et al.	(CLEO Collab.)
AVERY	95	PRL 75 4364	P. Avery et al.	(CLEO Collab.)

## Baryon Particle Listings

 $\Xi_c(2790)$ ,  $\Xi_c(2815)$ ,  $\Xi_c(2930)$ ,  $\Xi_c(2980)$  $\Xi_c(2790)$ 

$$I(J^P) = \frac{1}{2}(\frac{1}{2}^-) \text{ Status: } ***$$

A peak seen in the  $\Xi_c^- \pi$  mass spectrum. The simplest assignment, based on the mass, width, and decay mode, is that this belongs in the same SU(4) multiplet as the  $\Lambda(1405)$  and the  $\Lambda_c(2595)^+$ , but the spin and parity have not been measured.

 $\Xi_c(2790)$  MASSES

The masses are obtained from the mass-difference measurements that follow.

 $\Xi_c(2790)^+$  MASS

VALUE (MeV)	EVTS	DOCUMENT ID	TECN	COMMENT
<b>2789.1 ± 3.2 OUR FIT</b>				

 $\Xi_c(2790)^0$  MASS

VALUE (MeV)	EVTS	DOCUMENT ID	TECN	COMMENT
<b>2791.8 ± 3.3 OUR FIT</b>				

 $\Xi_c(2790) - \Xi_c$  MASS DIFFERENCES $m_{\Xi_c(2790)^+} - m_{\Xi_c^0}$ 

VALUE (MeV)	EVTS	DOCUMENT ID	TECN	COMMENT
<b>318.2 ± 3.2 OUR FIT</b>				
<b>318.2 ± 1.3 ± 2.9</b>	18	CSORNA	01	CLEO $e^+ e^- \approx \Upsilon(4S)$

 $m_{\Xi_c(2790)^0} - m_{\Xi_c^+}$ 

VALUE (MeV)	EVTS	DOCUMENT ID	TECN	COMMENT
<b>324.0 ± 3.3 OUR FIT</b>				
<b>324.0 ± 1.3 ± 3.0</b>	14	CSORNA	01	CLEO $e^+ e^- \approx \Upsilon(4S)$

 $\Xi_c(2790)$  WIDTHS $\Xi_c(2790)^+$  WIDTH

VALUE (MeV)	CL%	DOCUMENT ID	TECN	COMMENT
<b>&lt;15</b>	90	CSORNA	01	CLEO $e^+ e^- \approx \Upsilon(4S)$

 $\Xi_c(2790)^0$  WIDTH

VALUE (MeV)	CL%	DOCUMENT ID	TECN	COMMENT
<b>&lt;12</b>	90	CSORNA	01	CLEO $e^+ e^- \approx \Upsilon(4S)$

 $\Xi_c(2790)$  DECAY MODES

Mode	Fraction ( $\Gamma_i/\Gamma$ )
$\Gamma_1 \Xi_c^- \pi$	seen

 $\Xi_c(2790)$  REFERENCES

CSORNA	01	PRL 86 4243	S.E. Csorna et al.	(CLEO Collab.)
--------	----	-------------	--------------------	----------------

 $\Xi_c(2815)$ 

$$I(J^P) = \frac{1}{2}(\frac{3}{2}^-) \text{ Status: } ***$$

A narrow peak seen in the  $\Xi_c \pi \pi$  mass spectrum. The simplest assignment is that this belongs to the same SU(4) multiplet as the  $\Lambda(1520)$  and the  $\Lambda_c(2625)$ , but the spin and parity have not been measured.

 $\Xi_c(2815)$  MASSES

The masses are obtained from the mass-difference measurements that follow.

 $\Xi_c(2815)^+$  MASS

VALUE (MeV)	EVTS	DOCUMENT ID	TECN	COMMENT
<b>2816.6 ± 0.9 OUR FIT</b>				
<b>2817.0 ± 1.2 ± 0.7 ± 0.8</b>	73 ± 10	LESIAK	08	BELL $e^+ e^- \approx \Upsilon(4S)$

 $\Xi_c(2815)^0$  MASS

VALUE (MeV)	EVTS	DOCUMENT ID	TECN	COMMENT
<b>2819.6 ± 1.2 OUR FIT</b>				
<b>2820.4 ± 1.4 ± 0.9 ± 1.0</b>	48 ± 8	LESIAK	08	BELL $e^+ e^- \approx \Upsilon(4S)$

 $\Xi_c(2815) - \Xi_c$  MASS DIFFERENCES $m_{\Xi_c(2815)^+} - m_{\Xi_c^+}$ 

VALUE (MeV)	EVTS	DOCUMENT ID	TECN	COMMENT
<b>348.8 ± 0.9 OUR FIT</b>				
<b>348.6 ± 0.6 ± 1.0</b>	20	ALEXANDER	99B	CLE2 $e^+ e^- \approx \Upsilon(4S)$

 $m_{\Xi_c(2815)^0} - m_{\Xi_c^0}$ 

VALUE (MeV)	EVTS	DOCUMENT ID	TECN	COMMENT
<b>348.7 ± 1.2 OUR FIT</b>				
<b>347.2 ± 0.7 ± 2.0</b>	9	ALEXANDER	99B	CLE2 $e^+ e^- \approx \Upsilon(4S)$

 $\Xi_c(2815)^+ - \Xi_c(2815)^0$  MASS DIFFERENCE $m_{\Xi_c(2815)^+} - m_{\Xi_c(2815)^0}$ 

VALUE (MeV)	DOCUMENT ID	TECN	COMMENT
<b>-3.1 ± 1.3 OUR FIT</b>			
<b>-3.4 ± 1.9 ± 0.9</b>	LESIAK	08	BELL 73 & 48 events

 $\Xi_c(2815)$  WIDTHS $\Xi_c(2815)^+$  WIDTH

VALUE (MeV)	CL%	DOCUMENT ID	TECN	COMMENT
<b>&lt;3.5</b>	90	ALEXANDER	99B	CLE2 $e^+ e^- \approx \Upsilon(4S)$

 $\Xi_c(2815)^0$  WIDTH

VALUE (MeV)	CL%	DOCUMENT ID	TECN	COMMENT
<b>&lt;6.5</b>	90	ALEXANDER	99B	CLE2 $e^+ e^- \approx \Upsilon(4S)$

 $\Xi_c(2815)$  DECAY MODES

The  $\Xi_c \pi \pi$  modes are consistent with being entirely via  $\Xi_c(2645) \pi$ .

Mode	Fraction ( $\Gamma_i/\Gamma$ )
$\Gamma_1 \Xi_c^+ \pi^+ \pi^-$	seen
$\Gamma_2 \Xi_c^0 \pi^+ \pi^-$	seen

 $\Xi_c(2815)$  REFERENCES

LESIAK	08	PL B665 9	T. Lesiak et al.	(BELLE Collab.)
ALEXANDER	99B	PRL 83 3390	J.P. Alexander et al.	(CLEO Collab.)

 $\Xi_c(2930)$ 

$$I(J^P) = ?(??) \text{ Status: } *$$

OMITTED FROM SUMMARY TABLE

A peak seen in the  $\Lambda_c^+ K^-$  mass projection of  $B^- \rightarrow \Lambda_c^+ \bar{\Lambda}_c^- K^-$  events.

 $\Xi_c(2930)$  MASS

VALUE (MeV)	EVTS	DOCUMENT ID	TECN	COMMENT
<b>2931 ± 3 ± 5</b>	≈ 34	AUBERT	08H	BABR $\Upsilon(4S) \rightarrow B \bar{B}$

 $\Xi_c(2930)$  WIDTH

VALUE (MeV)	EVTS	DOCUMENT ID	TECN	COMMENT
<b>36 ± 7 ± 11</b>	≈ 34	AUBERT	08H	BABR $\Upsilon(4S) \rightarrow B \bar{B}$

 $\Xi_c(2930)$  REFERENCES

AUBERT	08H	PR D77 031101R	B. Aubert et al.	(BABAR Collab.)
--------	-----	----------------	------------------	-----------------

 $\Xi_c(2980)$ 

$$I(J^P) = \frac{1}{2}(??) \text{ Status: } ***$$

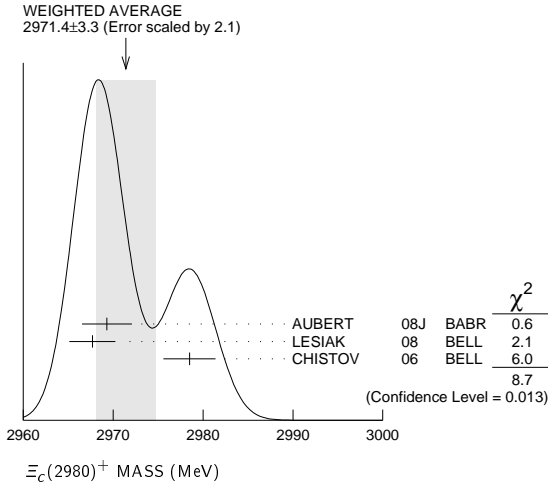
 $\Xi_c(2980)$  MASSES $\Xi_c(2980)^+$  MASS

VALUE (MeV)	EVTS	DOCUMENT ID	TECN	COMMENT
<b>2971.4 ± 3.3 OUR AVERAGE</b>				Error includes scale factor of 2.1. See the ideogram below.
2969.3 ± 2.2 ± 1.7	756 ± 206	AUBERT	08J	BABR $e^+ e^- \approx 10.58 \text{ GeV}$
2967.7 ± 2.3 ± 1.1 ± 1.2	78 ± 13	LESIAK	08	BELL $e^+ e^- \approx \Upsilon(4S)$
2978.5 ± 2.1 ± 2.0	405 ± 51	CHISTOV	06	BELL $e^+ e^- \approx \Upsilon(4S)$

See key on page 457

# Baryon Particle Listings

## $\Xi_c(2980), \Xi_c(3055), \Xi_c(3080)$



### $\Xi_c(2980)^0$ MASS

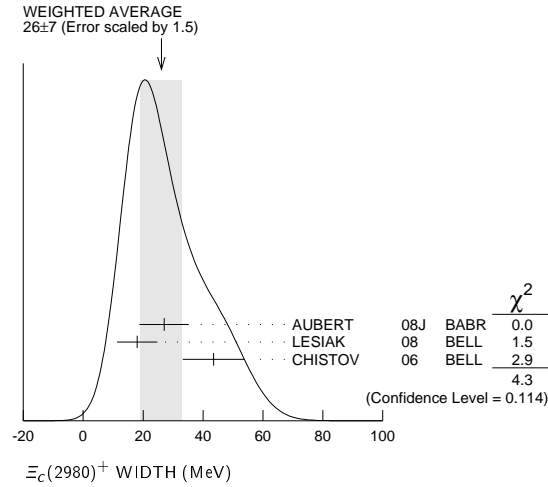
The evidence is statistically weaker for this charge state.

VALUE (MeV)	EVTS	DOCUMENT ID	TECN	COMMENT
<b>2968.0±2.6 OUR AVERAGE</b>		Error includes scale factor of 1.2.		
2972.9±4.4±1.6	67 ± 44	AUBERT 08J BABR	08J	BABR $e^+e^- \approx 10.58$ GeV
2965.7±2.4±1.2	57 ± 13	LESIAK 08 BELL	08	BELL $e^+e^- \approx \Upsilon(4S)$
2977.1±8.8±3.5	42 ± 24	CHISTOV 06 BELL	06	BELL $e^+e^- \approx \Upsilon(4S)$

### $\Xi_c(2980)^+$ WIDTHS

#### $\Xi_c(2980)^+$ WIDTH

VALUE (MeV)	EVTS	DOCUMENT ID	TECN	COMMENT
<b>26 ± 7 OUR AVERAGE</b>		Error includes scale factor of 1.5. See the ideogram below.		
27 ± 8 ± 2	756 ± 206	AUBERT 08J BABR	08J	BABR $e^+e^- \approx 10.58$ GeV
18 ± 6 ± 3	78 ± 13	LESIAK 08 BELL	08	BELL $e^+e^- \approx \Upsilon(4S)$
43.5±7.5±7.0	405 ± 51	CHISTOV 06 BELL	06	BELL $e^+e^- \approx \Upsilon(4S)$



### $\Xi_c(2980)^0$ WIDTH

VALUE (MeV)	EVTS	DOCUMENT ID	TECN	COMMENT
<b>20±7 OUR AVERAGE</b>		Error includes scale factor of 1.3.		
31±7±8	67 ± 44	AUBERT 08J BABR	08J	BABR $e^+e^- \approx 10.58$ GeV
15±6±3	57 ± 13	LESIAK 08 BELL	08	BELL $e^+e^- \approx \Upsilon(4S)$

### $\Xi_c(2980)$ DECAY MODES

Mode	Fraction ( $\Gamma_i/\Gamma$ )
$\Gamma_1$ $\Lambda_c^+ \bar{K} \pi$	seen
$\Gamma_2$ $\Sigma_c(2455) \bar{K}$	seen
$\Gamma_3$ $\Lambda_c^+ \bar{K}$	not seen
$\Gamma_4$ $\Xi_c 2\pi$	seen
$\Gamma_5$ $\Xi_c(2645) \pi$	seen

### $\Xi_c(2980)$ BRANCHING RATIOS

$\Gamma(\Lambda_c^+ \bar{K} \pi)/\Gamma_{total}$	DOCUMENT ID	TECN	COMMENT	$\Gamma_1/\Gamma$
seen	AUBERT 08J BABR	08J	BABR $e^+e^- \approx \Upsilon(4S)$	
seen	CHISTOV 06 BELL	06	BELL $e^+e^- \approx \Upsilon(4S)$	
$\Gamma(\Sigma_c(2455) \bar{K})/\Gamma(\Lambda_c^+ \bar{K} \pi)$	DOCUMENT ID	TECN	COMMENT	$\Gamma_2/\Gamma_1$
<b>0.55±0.07±0.13</b>	AUBERT 08J BABR	08J	BABR $e^+e^- \approx \Upsilon(4S)$	
$\Gamma(\Xi_c(2645) \pi)/\Gamma_{total}$	DOCUMENT ID	TECN	COMMENT	$\Gamma_5/\Gamma$
seen	LESIAK 08 BELL	08	BELL $e^+e^- \approx \Upsilon(4S)$	

### $\Xi_c(2980)$ REFERENCES

AUBERT 08J PR D77 012002	B. Aubert et al.	(BABAR Collab.)
LESIAK 08 PL B665 9	T. Lesiak et al.	(BELLE Collab.)
CHISTOV 06 PRL 97 162001	R. Chistov et al.	(BELLE Collab.)

## $\Xi_c(3055)$

$I(J^P) = ?(??)$  Status: \*\*

OMITTED FROM SUMMARY TABLE

A peak in the  $\Sigma_c(2455)^{++} K^- \rightarrow \Lambda_c^+ K^- \pi^+$  mass spectrum with a claimed significance of 6.4 standard deviations.

### $\Xi_c(3055)$ MASSES

VALUE (MeV)	EVTS	DOCUMENT ID	TECN	COMMENT
<b>3054.2±1.2±0.5</b>	218 ± 95	AUBERT 08J BABR	08J	BABR $e^+e^- \approx 10.58$ GeV

### $\Xi_c(3055)$ WIDTHS

VALUE (MeV)	EVTS	DOCUMENT ID	TECN	COMMENT
<b>17±6±11</b>	218 ± 95	AUBERT 08J BABR	08J	BABR $e^+e^- \approx 10.58$ GeV

### $\Xi_c(3055)$ REFERENCES

AUBERT 08J PR D77 012002	B. Aubert et al.	(BABAR Collab.)
--------------------------	------------------	-----------------

## $\Xi_c(3080)$

$I(J^P) = \frac{1}{2}(??)$  Status: \*\*\*

A narrow peak seen in the  $\Lambda_c^+ K^- \pi^+$  and  $\Lambda_c^+ K_S^0 \pi^-$  mass spectra.

### $\Xi_c(3080)$ MASSES

VALUE (MeV)	EVTS	DOCUMENT ID	TECN	COMMENT
<b>3077.0±0.4 OUR AVERAGE</b>				
3077.0±0.4±0.2	403 ± 60	AUBERT 08J BABR	08J	BABR $e^+e^- \approx 10.58$ GeV
3076.7±0.9±0.5	326 ± 40	CHISTOV 06 BELL	06	BELL $e^+e^- \approx \Upsilon(4S)$

### $\Xi_c(3080)^0$ MASS

VALUE (MeV)	EVTS	DOCUMENT ID	TECN	COMMENT
<b>3079.9±1.4 OUR AVERAGE</b>		Error includes scale factor of 1.3.		
3079.3±1.1±0.2	90 ± 27	AUBERT 08J BABR	08J	BABR $e^+e^- \approx 10.58$ GeV
3082.8±1.8±1.5	67 ± 20	CHISTOV 06 BELL	06	BELL $e^+e^- \approx \Upsilon(4S)$

### $\Xi_c(3080)$ WIDTHS

VALUE (MeV)	EVTS	DOCUMENT ID	TECN	COMMENT
<b>5.8±1.0 OUR AVERAGE</b>				
5.5±1.3±0.6	403 ± 60	AUBERT 08J BABR	08J	BABR $e^+e^- \approx 10.58$ GeV
6.2±1.2±0.8	326 ± 40	CHISTOV 06 BELL	06	BELL $e^+e^- \approx \Upsilon(4S)$

### $\Xi_c(3080)^0$ WIDTH

VALUE (MeV)	EVTS	DOCUMENT ID	TECN	COMMENT
<b>5.6±2.2 OUR AVERAGE</b>				
5.9±2.3±1.5	90 ± 27	AUBERT 08J BABR	08J	BABR $e^+e^- \approx 10.58$ GeV
5.2±3.1±1.8	67 ± 20	CHISTOV 06 BELL	06	BELL $e^+e^- \approx \Upsilon(4S)$

## Baryon Particle Listings

 $\Xi_c(3080), \Xi_c(3123), \Omega_c^0$  $\Xi_c(3080)$  DECAY MODES

Mode	Fraction ( $\Gamma_i/\Gamma$ )
$\Gamma_1 \Lambda_c^+ \bar{K} \pi$	seen
$\Gamma_2 \Sigma_c(2455) \bar{K}$	seen
$\Gamma_3 \Sigma_c(2455) \bar{K} + \Sigma_c(2520) \bar{K}$	seen
$\Gamma_4 \Lambda_c^+ \bar{K}$	not seen
$\Gamma_5 \Lambda_c^+ \bar{K} \pi^+ \pi^-$	not seen

 $\Xi_c(3080)$  BRANCHING RATIOS

$\Gamma(\Sigma_c(2455) \bar{K})/\Gamma(\Lambda_c^+ \bar{K} \pi)$		$\Gamma_2/\Gamma_1$	
VALUE	DOCUMENT ID	TECN	COMMENT
<b>0.45 ± 0.06 OUR AVERAGE</b>			
0.45 ± 0.05 ± 0.05	AUBERT 08J	BABR	in $\Lambda_c^+ K^- \pi^+$
0.44 ± 0.12 ± 0.07	AUBERT 08J	BABR	in $\Lambda_c^+ K_S^0 \pi^-$

$[\Gamma(\Sigma_c(2455) \bar{K}) + \Gamma(\Sigma_c(2520) \bar{K})]/\Gamma(\Lambda_c^+ \bar{K} \pi)$		$\Gamma_3/\Gamma_1$	
VALUE	DOCUMENT ID	TECN	COMMENT
<b>0.89 ± 0.12 OUR AVERAGE</b>			
0.95 ± 0.14 ± 0.06	AUBERT 08J	BABR	in $\Lambda_c^+ K^- \pi^+$
0.78 ± 0.21 ± 0.05	AUBERT 08J	BABR	in $\Lambda_c^+ K_S^0 \pi^-$

 $\Xi_c(3080)$  REFERENCES

AUBERT 08J PR D77 012002	B. Aubert <i>et al.</i>	(BABAR Collab.)
CHRISTOV 06 PRL 97 162001	R. Christov <i>et al.</i>	(BELLE Collab.)

 $\Xi_c(3123)$ 

$$I(J^P) = ?(??) \text{ Status: } *$$

OMITTED FROM SUMMARY TABLE

A peak in the  $\Sigma_c(2520)^+ K^- \rightarrow \Lambda_c^+ K^- \pi^+$  mass spectrum with a significance of 3.6 standard deviations.

 $\Xi_c(3123)$  MASSES

$\Xi_c(3123)^+$ MASS	VALUE (MeV)	EVTS	DOCUMENT ID	TECN	COMMENT
<b>3122.9 ± 1.3 ± 0.3</b>	101 ± 35		AUBERT 08J	BABR	$e^+ e^- \approx 10.58$ GeV

 $\Xi_c(3123)$  WIDTHS

$\Xi_c(3123)^+$ WIDTH	VALUE (MeV)	EVTS	DOCUMENT ID	TECN	COMMENT
<b>4.4 ± 3.4 ± 1.7</b>	101 ± 35		AUBERT 08J	BABR	$e^+ e^- \approx 10.58$ GeV

 $\Xi_c(3123)$  REFERENCES

AUBERT 08J PR D77 012002	B. Aubert <i>et al.</i>	(BABAR Collab.)
--------------------------	-------------------------	-----------------

 $\Omega_c^0$ 

$$I(J^P) = 0(\frac{1}{2}^+) \text{ Status: } ***$$

The quantum numbers have not been measured, but are simply assigned in accord with the quark model, in which the  $\Omega_c^0$  is the ssc ground state.

 $\Omega_c^0$  MASS

VALUE (MeV)	EVTS	DOCUMENT ID	TECN	COMMENT
<b>2695.2 ± 1.7 OUR FIT</b>	Error includes scale factor of 1.3.			
<b>2695.2 ± 1.8 OUR AVERAGE</b>	Error includes scale factor of 1.3. See the ideogram below.			
2693.6 ± 0.3 ± 1.8	725 ± 45	SOLOVIEVA 09 BELL	$\Omega^- \pi^+$ in $e^+ e^- \rightarrow \Upsilon(4S)$	
2694.6 ± 2.6 ± 1.9	40	<sup>1</sup> CRONIN-HEN..01 CLE2	$e^+ e^- \approx 10.6$ GeV	
2699.9 ± 1.5 ± 2.5	42	<sup>2</sup> FRABETTI 94H E687	$\gamma$ Be, $\bar{E}_\gamma = 221$ GeV	
• • • We do not use the following data for averages, fits, limits, etc. • • •				
2705.9 ± 3.3 ± 2.0	10	<sup>3</sup> FRABETTI 93 E687	$\gamma$ Be, $\bar{E}_\gamma = 221$ GeV	
2719.0 ± 7.0 ± 2.5	11	<sup>4</sup> ALBRECHT 92H ARG	$e^+ e^- \approx 10.6$ GeV	
2740 ± 20	3	BIAGI 85B SPEC	$\Sigma^-$ Be 135 GeV/c	

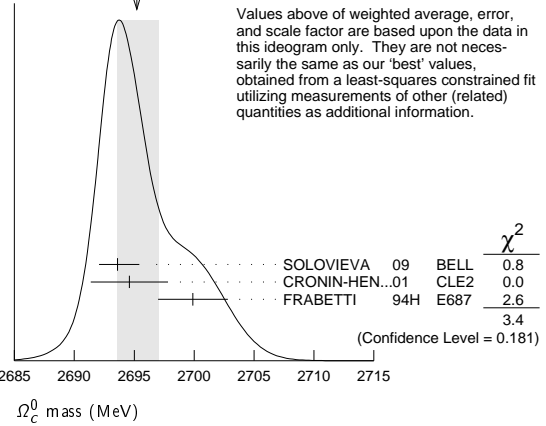
<sup>1</sup> CRONIN-HENNESSY 01 sees  $40.4 \pm 9.0$  events in a sum over five channels.

<sup>2</sup> FRABETTI 94H claims a signal of  $42.5 \pm 8.8$   $\Sigma^+ K^- K^- \pi^+$  events. The background is about 24 events.

<sup>3</sup> FRABETTI 93 claims a signal of  $10.3 \pm 3.9$   $\Omega^- \pi^+$  events above a background of 5.8 events.

<sup>4</sup> ALBRECHT 92H claims a signal of  $11.5 \pm 4.3$   $\Xi^- K^- \pi^+ \pi^+$  events. The background is about 5 events.

WEIGHTED AVERAGE  
2695.2±1.8-1.6 (Error scaled by 1.3)

 $\Omega_c^0$  MEAN LIFE

VALUE ( $10^{-15}$ s)	EVTS	DOCUMENT ID	TECN	COMMENT
<b>69 ± 12 OUR AVERAGE</b>				
72 ± 11 ± 11	64	LINK 03C	FOCS	$\Omega^- \pi^+, \Xi^- K^- \pi^+ \pi^+$
55 $^{+13}_{-11}$ $^{+18}_{-23}$	86	ADAMOVIICH 95B	WA89	$\Omega^- \pi^- \pi^+ \pi^+, \Xi^- K^- \pi^+ \pi^+$
86 $^{+27}_{-20}$ ± 28	25	FRABETTI 95D	E687	$\Sigma^+ K^- K^- \pi^+$

 $\Omega_c^0$  DECAY MODES

No absolute branching fractions have been measured.

Mode	Fraction ( $\Gamma_i/\Gamma$ )
$\Gamma_1 \Sigma^+ K^- K^- \pi^+$	seen
$\Gamma_2 \Xi^0 K^- \pi^+$	seen
$\Gamma_3 \Xi^- K^- \pi^+ \pi^+$	seen
$\Gamma_4 \Omega^- e^+ \nu_e$	seen
$\Gamma_5 \Omega^- \pi^+$	seen
$\Gamma_6 \Omega^- \pi^+ \pi^0$	seen
$\Gamma_7 \Omega^- \pi^- \pi^+ \pi^+$	seen

 $\Omega_c^0$  BRANCHING RATIOS

$\Gamma(\Sigma^+ K^- K^- \pi^+)/\Gamma_{\text{total}}$		$\Gamma_1/\Gamma$		
VALUE	EVTS	DOCUMENT ID	TECN	COMMENT
seen	42	FRABETTI 94H	E687	$\gamma$ Be, $\bar{E}_\gamma = 221$ GeV

$\Gamma(\Sigma^+ K^- K^- \pi^+)/\Gamma(\Omega^- \pi^+)$		$\Gamma_1/\Gamma_5$		
VALUE	CL%	DOCUMENT ID	TECN	COMMENT
• • • We do not use the following data for averages, fits, limits, etc. • • •				
<4.8	90	CRONIN-HEN..01	CLE2	$e^+ e^- \approx 10.6$ GeV

$\Gamma(\Xi^0 K^- \pi^+)/\Gamma(\Omega^- \pi^+)$		$\Gamma_2/\Gamma_5$		
VALUE	EVTS	DOCUMENT ID	TECN	COMMENT
<b>4.0 ± 2.5 ± 0.4</b>	9	CRONIN-HEN..01	CLE2	$e^+ e^- \approx 10.6$ GeV

$\Gamma(\Xi^- K^- \pi^+ \pi^+)/\Gamma_{\text{total}}$		$\Gamma_3/\Gamma$		
VALUE	EVTS	DOCUMENT ID	TECN	COMMENT
seen	11	ALBRECHT 92H	ARG	$e^+ e^- \approx 10.6$ GeV
seen	3	BIAGI 85B	SPEC	$\Sigma^-$ Be 135 GeV/c

$\Gamma(\Xi^- K^- \pi^+ \pi^+)/\Gamma(\Omega^- \pi^+)$		$\Gamma_3/\Gamma_5$			
VALUE	CL%	EVTS	DOCUMENT ID	TECN	COMMENT
<b>0.46 ± 0.13 ± 0.03</b>	45 ± 12		AUBERT 07AH	BABR	$e^+ e^- \approx \Upsilon(4S)$
• • • We do not use the following data for averages, fits, limits, etc. • • •					
1.6 ± 1.1 ± 0.4	7	CRONIN-HEN..01	CLE2	$e^+ e^- \approx 10.6$ GeV	
<2.8	90	FRABETTI 93	E687	$\gamma$ Be, $\bar{E}_\gamma = 221$ GeV	



See key on page 457

## Baryon Particle Listings

$\Omega_c^0, \Omega_c(2770)^0$

$\Gamma(\Omega^- \pi^+)/\Gamma(\Omega^- e^+ \nu_e)$				$\Gamma_5/\Gamma_4$
VALUE	EVTS	DOCUMENT ID	TECN	COMMENT
<b>0.41 ± 0.19 ± 0.04</b>	11	AMMAR 02	CLE2	$e^+ e^- \approx \Upsilon(4S)$

$\Gamma(\Omega^- \pi^+ \pi^0)/\Gamma(\Omega^- \pi^+)$				$\Gamma_6/\Gamma_5$
VALUE	EVTS	DOCUMENT ID	TECN	COMMENT
<b>1.27 ± 0.31 ± 0.11</b>	64 ± 15	AUBERT 07AH	BABR	$e^+ e^- \approx \Upsilon(4S)$
• • • We do not use the following data for averages, fits, limits, etc. • • •				
4.2 ± 2.2 ± 0.9	12	CRONIN-HEN..01	CLE2	$e^+ e^- \approx 10.6$ GeV

$\Gamma(\Omega^- \pi^- \pi^+ \pi^+)/\Gamma(\Omega^- \pi^+)$				$\Gamma_7/\Gamma_5$	
VALUE	CL%	EVTS	DOCUMENT ID	TECN	COMMENT
<b>0.28 ± 0.09 ± 0.01</b>		25 ± 8	AUBERT 07AH	BABR	$e^+ e^- \approx \Upsilon(4S)$
• • • We do not use the following data for averages, fits, limits, etc. • • •					
<0.56	90		CRONIN-HEN..01	CLE2	$e^+ e^- \approx 10.6$ GeV
seen			ADAMOVICH 95B	WA89	$\Sigma^- 340$ GeV
<1.6	90		FRABETTI 93	E687	$\gamma$ Be, $\overline{E}_\gamma = 221$ GeV

 $\Omega_c^0$  REFERENCES

SOLOVIEVA 09	PL B672 1	E. Solovieva <i>et al.</i>	(BELLE Collab.)
AUBERT 07AH	PRL 99 062001	B. Aubert <i>et al.</i>	(BABAR Collab.)
LINK 03C	PL B561 41	J.M. Link <i>et al.</i>	(FNAL FOCUS Collab.)
AMMAR 02	PRL 89 171803	R. Ammar <i>et al.</i>	(CLEO Collab.)
CRONIN-HEN...01	PRL 86 3730	D. Cronin-Hennessy <i>et al.</i>	(CLEO Collab.)
ADAMOVICH 95B	PL B358 151	M.I. Adamovich <i>et al.</i>	(CERN WA89 Collab.)
FRABETTI 95D	PL B357 678	P.L. Frabetti <i>et al.</i>	(FNAL E687 Collab.)
FRABETTI 94H	PL B338 106	P.L. Frabetti <i>et al.</i>	(FNAL E687 Collab.)
FRABETTI 93	PL B300 190	P.L. Frabetti <i>et al.</i>	(FNAL E687 Collab.)
ALBRECHT 92H	PL B208 367	H. Albrecht <i>et al.</i>	(ARGUS Collab.)
BIAGI 85B	ZPHY C28 175	S.F. Biagi <i>et al.</i>	(CERN WA62 Collab.)

 $\Omega_c(2770)^0$ 

$I(J^P) = 0(\frac{3}{2}^+)$  Status: \*\*\*

The natural assignment is that this goes with the  $\Sigma_c(2520)$  and  $\Xi_c(2645)$  to complete the lowest mass  $J^P = \frac{3}{2}^+$  SU(3) sextet, part of the SU(4) 20-plet that includes the  $\Delta(1232)$ . But  $J$  and  $P$  have not been measured.

 $\Omega_c(2770)^0$  MASS

The mass is obtained from the mass-difference measurement that follows.

VALUE (MeV)	DOCUMENT ID
<b>2765.9 ± 2.0 OUR FIT</b>	Error includes scale factor of 1.2.

 $\Omega_c(2770)^0 - \Omega_c^0$  MASS DIFFERENCE

VALUE (MeV)	EVTS	DOCUMENT ID	TECN	COMMENT
-------------	------	-------------	------	---------

**70.7<sup>+0.8</sup><sub>-0.9</sub> OUR FIT**

**70.7<sup>+0.8</sup><sub>-1.0</sub> OUR AVERAGE**

70.7 ± 0.9 <sup>+0.1</sup> <sub>-0.9</sub>	54 ± 9	SOLOVIEVA 09	BELL	$\Omega_c^0 \gamma$ in $e^+ e^- \rightarrow \Upsilon(4S)$
70.8 ± 1.0 ± 1.1	105 ± 22	AUBERT, BE 06i	BABR	$e^+ e^- \approx \Upsilon(4S)$

 $\Omega_c(2770)^0$  DECAY MODES

The  $\Omega_c(2770)^0 - \Omega_c^0$  mass difference is too small for any strong decay to occur.

Mode	Fraction ( $\Gamma_i/\Gamma$ )
$\Gamma_1 \Omega_c^0 \gamma$	presumably 100%

 $\Omega_c(2770)^0$  REFERENCES

SOLOVIEVA 09	PL B672 1	E. Solovieva <i>et al.</i>	(BELLE Collab.)
AUBERT, BE 06i	PRL 97 232001	B. Aubert <i>et al.</i>	(BABAR Collab.)

## Baryon Particle Listings

 $\Xi_{cc}^+$  $\Xi_{cc}^+$ 

## DOUBLY CHARMED BARYONS (C = +2)

$$\Xi_{cc}^{++} = ucc, \Xi_{cc}^+ = dcc, \Omega_{cc}^+ = scc$$

 $\Xi_{cc}^+$ 

$$I(J^P) = ?(?^?) \quad \text{Status: } *$$

OMITTED FROM SUMMARY TABLE

This would presumably be an isospin-1/2 particle, a  $ccu \Xi_{cc}^{++}$  and a  $ccd \Xi_{cc}^+$ . However, opposed to the evidence cited below, the BABAR experiment has found no evidence for a  $\Xi_{cc}^+$  in a search in  $\Lambda_c^+ K^- \pi^+$  and  $\Xi_c^0 \pi^+$  modes, and no evidence of a  $\Xi_{cc}^{++}$  in  $\Lambda_c^+ K^- \pi^+ \pi^+$  and  $\Xi_c^0 \pi^+ \pi^+$  modes (AUBERT,B 06D). Nor has the BELLE experiment found any evidence for a  $\Xi_{cc}^+$  in the  $\Lambda_c^+ K^- \pi^+$  mode (CHISTOV 06).

 $\Xi_{cc}^+$  MASS

VALUE (MeV)	EVTS	DOCUMENT ID	TECN	COMMENT
<b>3518.9 ± 0.9 OUR AVERAGE</b>				
3518 ± 3	6	<sup>1</sup> OCHERASHVI..05	SELX	$\Sigma^-$ nucleus $\approx$ 600 GeV
3519 ± 1	16	<sup>2</sup> MATTSON 02	SELX	$\Sigma^-$ nucleus $\approx$ 600 GeV

<sup>1</sup> OCHERASHVILI 05 claims "an excess of 5.62 events over ...  $1.38 \pm 0.13$  events" for a significance of  $4.8 \sigma$  in  $pD^+ K^-$  events.

<sup>2</sup> MATTSON 02 claims "an excess of 15.9 events over an expected background of  $6.1 \pm 0.5$  events, a statistical significance of  $6.3 \sigma$ " in the  $\Lambda_c^+ K^- \pi^+$  invariant-mass spectrum.

The probability that the peak is a fluctuation increases from  $1.0 \times 10^{-6}$  to  $1.1 \times 10^{-4}$  when the number of bins searched is considered.

 $\Xi_{cc}^+$  MEAN LIFE

VALUE ( $10^{-15}$ s)	CL%	DOCUMENT ID	TECN	COMMENT
<b>&lt;33</b>	90	MATTSON 02	SELX	$\Sigma^-$ nucleus, $\approx$ 600 GeV

 $\Xi_{cc}^+$  DECAY MODES

Mode	$\Gamma_1$	$\Gamma_2$
$\Lambda_c^+ K^- \pi^+$		
$pD^+ K^-$		

$\Gamma(pD^+ K^-)/\Gamma(\Lambda_c^+ K^- \pi^+)$				$\Gamma_2/\Gamma_1$
VALUE	EVTS	DOCUMENT ID	TECN	COMMENT
<b>0.36 ± 0.21</b>	6	OCHERASHVI..05	SELX	$\Sigma^- \approx$ 600 GeV

 $\Xi_{cc}^+$  REFERENCES

AUBERT,B 06D	PR D74 011103R	B. Aubert <i>et al.</i>	(BABAR Collab.)
CHISTOV 06	PRL 97 162001	R. Chistov <i>et al.</i>	(BELLE Collab.)
OCHERASHVI..05	PL B628 18	A. Ocherashvili <i>et al.</i>	(FNAL SELEX Collab.)
MATTSON 02	PRL 89 112001	M. Mattson <i>et al.</i>	(FNAL SELEX Collab.)

# BOTTOM BARYONS

## ( $B = -1$ )

$$\Lambda_b^0 = udb, \Xi_b^0 = usb, \Xi_b^- = dsb, \Omega_b^- = sss$$



$$I(J^P) = 0(\frac{1}{2}^+) \text{ Status: } ***$$

In the quark model, a  $\Lambda_b^0$  is an isospin-0  $u d b$  state. The lowest  $\Lambda_b^0$  ought to have  $J^P = 1/2^+$ . None of  $I, J,$  or  $P$  have actually been measured.

### $\Lambda_b^0$ MASS

$m_{\Lambda_b^0}$	VALUE (MeV)	EVTs	DOCUMENT ID	TECN	COMMENT
<b>5619.4 ± 0.7</b>	<b>OUR AVERAGE</b>				
5619.19 ± 0.70 ± 0.30			1 AAIJ	12E	LHCB $pp$ at 7 TeV
5619.7 ± 1.2 ± 1.2			2 ACOSTA	06	CDF $p\bar{p}$ at 1.96 TeV
5621 ± 4 ± 3			3 ABE	97B	CDF $p\bar{p}$ at 1.8 TeV
5668 ± 16 ± 8		4	4 ABREU	96N	DLPH $e^+e^- \rightarrow Z$
5614 ± 21 ± 4		4	4 BUSKULIC	96L	ALEP $e^+e^- \rightarrow Z$
not seen			5 ABE	93B	CDF Sup. by ABE 97B
5640 ± 50 ± 30		16	6 ALBAJAR	91E	UA1 $p\bar{p}$ 630 GeV
5640 +100 -210		52	BARI	91	SFM $\Lambda_b^0 \rightarrow pD^0\pi^-$
5650 +150 -200		90	BARI	91	SFM $\Lambda_b^0 \rightarrow \Lambda_c^+ \pi^+ \pi^- \pi^-$

- • • We do not use the following data for averages, fits, limits, etc. • • •
- 1 Uses  $\Lambda_b^0 \rightarrow J/\psi\Lambda$  fully reconstructed decays.
- 2 Uses exclusively reconstructed final states containing a  $J/\psi \rightarrow \mu^+\mu^-$  decays.
- 3 ABE 97B observed 38 events with a background of  $18 \pm 1.6$  events in the mass range 5.60–5.65 GeV/ $c^2$ , a significance of  $> 3.4$  standard deviations.
- 4 Uses 4 fully reconstructed  $\Lambda_b$  events.
- 5 ABE 93B states that, based on the signal claimed by ALBAJAR 91E, CDF should have found  $30 \pm 23 \Lambda_b^0 \rightarrow J/\psi(1S)\Lambda$  events. Instead, CDF found not more than 2 events.
- 6 ALBAJAR 91E claims 16 ± 5 events above a background of  $9 \pm 1$  events, a significance of about 5 standard deviations.

### $m_{\Lambda_b^0} - m_{B^0}$

VALUE (MeV)	DOCUMENT ID	TECN	COMMENT
<b>339.2 ± 1.4 ± 0.1</b>	7 ACOSTA	06	CDF $p\bar{p}$ at 1.96 TeV

7 Uses exclusively reconstructed final states containing  $J/\psi \rightarrow \mu^+\mu^-$  decays.

### $m_{\Lambda_b^0} - m_{B^+}$

VALUE (MeV)	DOCUMENT ID	TECN	COMMENT
<b>339.71 ± 0.71 ± 0.09</b>	8 AAIJ	12E	LHCB $pp$ at 7 TeV

8 Uses exclusively reconstructed final states containing  $J/\psi \rightarrow \mu^+\mu^-$  decays.

### $\Lambda_b^0$ MEAN LIFE

See  $b$ -baryon Admixture section for data on  $b$ -baryon mean life average over species of  $b$ -baryon particles.

“OUR EVALUATION” is an average using rescaled values of the data listed below. The average and rescaling were performed by the Heavy Flavor Averaging Group (HFAG) and are described at <http://www.slac.stanford.edu/xorg/hfag/>. The averaging/rescaling procedure takes into account correlations between the measurements and asymmetric lifetime errors.

VALUE ( $10^{-12}$ s)	EVTs	DOCUMENT ID	TECN	COMMENT
<b>1.425 ± 0.032</b>	<b>OUR EVALUATION</b>			
1.537 ± 0.045 ± 0.014		9 AALTONEN	11	CDF $p\bar{p}$ at 1.96 TeV
1.401 ± 0.046 ± 0.035		10 AALTONEN	10B	CDF $p\bar{p}$ at 1.96 TeV
1.218 +0.130 -0.115 ± 0.042		9 ABZOV	07S	D0 $p\bar{p}$ at 1.96 TeV
1.290 +0.119 +0.087 -0.110 -0.091		11 ABZOV	07U	D0 $p\bar{p}$ at 1.96 TeV
1.11 +0.19 -0.18 ± 0.05		12 ABREU	99W	DLPH $e^+e^- \rightarrow Z$
1.29 +0.24 -0.22 ± 0.06		12 ACKERSTAFF	98G	OPAL $e^+e^- \rightarrow Z$
1.21 ± 0.11		12 BARATE	98D	ALEP $e^+e^- \rightarrow Z$
1.32 ± 0.15 ± 0.07		13 ABE	96M	CDF $p\bar{p}$ at 1.8 TeV

• • • We do not use the following data for averages, fits, limits, etc. • • •

1.593 +0.083 -0.078 ± 0.033	9 ABULENCIA	07A	CDF	Repl. by AALTONEN 11
1.22 +0.22 -0.18 ± 0.04	9 ABZOV	05c	D0	Repl. by ABZOV 07S
1.19 +0.21 -0.18 ± 0.07 -0.08	ABREU	96D	DLPH	Repl. by ABREU 99W
1.14 +0.22 -0.19 ± 0.07	69 AKERS	95K	OPAL	Repl. by ACKERSTAFF 98G
1.02 +0.23 -0.18 ± 0.06	44 BUSKULIC	95L	ALEP	Repl. by BARATE 98D

- 9 Measured mean life using fully reconstructed  $\Lambda_b^0 \rightarrow J/\psi\Lambda$  decays.
- 10 Measured mean life using fully reconstructed  $\Lambda_b^0 \rightarrow \Lambda_c^+ \pi^-$  decays.
- 11 Measured using semileptonic decays  $\Lambda_b^0 \rightarrow \Lambda_c^+ \mu^- X$  and  $\Lambda_c^+ \rightarrow K_S^0 p$ .
- 12 Measured using  $\Lambda_c \ell^-$  and  $\Lambda \ell^+ \ell^-$ .
- 13 Excess  $\Lambda_c \ell^-$ , decay lengths.

### $\tau_{\Lambda_b^0}/\tau_{B^0}$ MEAN LIFE RATIO

#### $\tau_{\Lambda_b^0}/\tau_{B^0}$ (direct measurements)

VALUE	DOCUMENT ID	TECN	COMMENT
<b>1.00 ± 0.06</b>	<b>OUR AVERAGE</b>		Error includes scale factor of 2.0.
1.020 ± 0.030 ± 0.008	14 AALTONEN	11	CDF $p\bar{p}$ at 1.96 TeV
0.811 +0.096 -0.087 ± 0.034	14,15 ABZOV	07S	D0 $p\bar{p}$ at 1.96 TeV
1.041 ± 0.057	16 ABULENCIA	07A	CDF Repl. by AALTONEN 11
0.87 +0.17 -0.14 ± 0.03	16 ABZOV	05c	D0 Repl. by ABZOV 07S

• • • We do not use the following data for averages, fits, limits, etc. • • •

- 14 Uses fully reconstructed  $\Lambda_b \rightarrow J/\psi\Lambda$  decays.
- 15 Uses  $B^0 \rightarrow J/\psi K_S^0$  decays for denominator.
- 16 Measured mean life ratio using fully reconstructed decays.

### $\Lambda_b^0$ DECAY MODES

The branching fractions  $B(b\text{-baryon} \rightarrow \Lambda \ell^- \bar{\nu}_\ell \text{ anything})$  and  $B(\Lambda_b^0 \rightarrow \Lambda_c^+ \ell^- \bar{\nu}_\ell \text{ anything})$  are not pure measurements because the underlying measured products of these with  $B(b \rightarrow b\text{-baryon})$  were used to determine  $B(b \rightarrow b\text{-baryon})$ , as described in the note “Production and Decay of  $b$ -Flavored Hadrons.”

For inclusive branching fractions, e.g.,  $\Lambda_b \rightarrow \bar{\Lambda}_c \text{ anything}$ , the values usually are multiplicities, not branching fractions. They can be greater than one.

Mode	Fraction ( $\Gamma_i/\Gamma$ )	Scale factor/ Confidence level
$\Gamma_1$ $J/\psi(1S)\Lambda \times B(b \rightarrow \Lambda_b^0)$	$(5.8 \pm 0.8) \times 10^{-5}$	
$\Gamma_2$ $pD^0\pi^-$		
$\Gamma_3$ $\Lambda_c^+ \pi^-$	$(5.7 +4.0 -2.6) \times 10^{-3}$	S=1.6
$\Gamma_4$ $\Lambda_c^+ a_1(1260)^-$	seen	
$\Gamma_5$ $\Lambda_c^+ \pi^+ \pi^- \pi^-$	$(8 +5 -4) \times 10^{-3}$	S=1.6
$\Gamma_6$ $\Lambda_c(2595)^+ \pi^-, \Lambda_c(2595)^+ \rightarrow \Lambda_c^+ \pi^+ \pi^-$	$(3.7 +2.8 -2.3) \times 10^{-4}$	
$\Gamma_7$ $\Lambda_c(2625)^+ \pi^-, \Lambda_c(2625)^+ \rightarrow \Lambda_c^+ \pi^+ \pi^-$	$(3.6 +2.7 -2.1) \times 10^{-4}$	
$\Gamma_8$ $\Sigma_c(2455)^0 \pi^+ \pi^-, \Sigma_c^0 \rightarrow \Lambda_c^+ \pi^-$	$(6 +5 -4) \times 10^{-4}$	
$\Gamma_9$ $\Sigma_c(2455)^{++} \pi^- \pi^-, \Sigma_c^{++} \rightarrow \Lambda_c^+ \pi^+$	$(3.5 +2.8 -2.3) \times 10^{-4}$	
$\Gamma_{10}$ $\Lambda K^0 2\pi^+ 2\pi^-$		
$\Gamma_{11}$ $\Lambda_c^+ \ell^- \bar{\nu}_\ell \text{ anything}$	[a] $(9.8 \pm 2.3) \%$	
$\Gamma_{12}$ $\Lambda_c^+ \ell^- \bar{\nu}_\ell$	$(6.5 +3.2 -2.5) \%$	S=1.8
$\Gamma_{13}$ $\Lambda_c^+ \pi^+ \pi^- \ell^- \bar{\nu}_\ell$	$(5.6 \pm 3.1) \%$	
$\Gamma_{14}$ $\Lambda_c(2595)^+ \ell^- \bar{\nu}_\ell$	$(8 \pm 5) \times 10^{-3}$	
$\Gamma_{15}$ $\Lambda_c(2625)^+ \ell^- \bar{\nu}_\ell$	$(1.4 +0.9 -0.7) \%$	
$\Gamma_{16}$ $\Sigma_c(2455)^0 \pi^+ \ell^- \bar{\nu}_\ell$		
$\Gamma_{17}$ $\Sigma_c(2455)^{++} \pi^- \ell^- \bar{\nu}_\ell$		
$\Gamma_{18}$ $p h^-$	[b] $< 2.3 \times 10^{-5}$	CL=90%
$\Gamma_{19}$ $p \pi^-$	$(3.5 \pm 1.0) \times 10^{-6}$	
$\Gamma_{20}$ $p K^-$	$(5.5 \pm 1.4) \times 10^{-6}$	
$\Gamma_{21}$ $\Lambda \mu^+ \mu^-$	$(1.7 \pm 0.7) \times 10^{-6}$	
$\Gamma_{22}$ $\Lambda \gamma$	$< 1.3 \times 10^{-3}$	CL=90%

[a] Not a pure measurement. See note at head of  $\Lambda_b^0$  Decay Modes.

[b] Here  $h^-$  means  $\pi^-$  or  $K^-$ .

## Baryon Particle Listings

 $\Lambda_b^0$ 

## CONSTRAINED FIT INFORMATION

An overall fit to 5 branching ratios uses 5 measurements and one constraint to determine 4 parameters. The overall fit has a  $\chi^2 = 3.9$  for 2 degrees of freedom.

The following *off-diagonal* array elements are the correlation coefficients  $\langle \delta x_i \delta x_j \rangle / (\delta x_i \delta x_j)$ , in percent, from the fit to the branching fractions,  $x_i \equiv \Gamma_i / \Gamma_{\text{total}}$ . The fit constrains the  $x_i$  whose labels appear in this array to sum to one.

$x_5$	93	
$x_{12}$	14	13
	$x_3$	$x_5$

 $\Lambda_b^0$  BRANCHING RATIOS $\Gamma(J/\psi(1S)\Lambda \times B(b \rightarrow \Lambda_b^0)) / \Gamma_{\text{total}}$   $\Gamma_1 / \Gamma$ 

VALUE (units $10^{-5}$ )	EVTS	DOCUMENT ID	TECN	COMMENT
--------------------------	------	-------------	------	---------

**5.8 ± 0.8 OUR AVERAGE**  
 6.01 ± 0.60 ± 0.58 ± 0.28 17 ABAZOV 11o D0  $p\bar{p}$  at 1.96 TeV  
 4.7 ± 2.3 ± 0.2 18 ABE 97b CDF  $p\bar{p}$  at 1.8 TeV

• • • We do not use the following data for averages, fits, limits, etc. • • •  
 180 ± 60 ± 90 16 ALBAJAR 91e UA1  $p\bar{p}$  at 630 GeV  
 17 ABAZOV 11o uses  $B(B^0 \rightarrow J/\psi K_S^0) \times B(b \rightarrow B^0) = (1.74 \pm 0.08) \times 10^{-4}$  to obtain the result. The  $(\pm 0.08) \times 10^{-4}$  uncertainty of this product is listed as the last uncertainty of the measurement,  $(\pm 0.28) \times 10^{-5}$ .

18 ABE 97b reports  $[B(\Lambda_b^0 \rightarrow J/\psi \Lambda) \times B(b \rightarrow \Lambda_b^0)] / [B(B^0 \rightarrow J/\psi K_S^0) \times B(b \rightarrow B^0)] = 0.27 \pm 0.12 \pm 0.05$ . We multiply by our best value  $B(B^0 \rightarrow J/\psi K_S^0) \times B(b \rightarrow B^0) = (1.74 \pm 0.08) \times 10^{-4}$ . Our first error is their experiment error and our second error is the systematic error from using our best value.

 $\Gamma(pD^0\pi^-) / \Gamma_{\text{total}}$   $\Gamma_2 / \Gamma$ 

VALUE	EVTS	DOCUMENT ID	TECN	COMMENT
-------	------	-------------	------	---------

• • • We do not use the following data for averages, fits, limits, etc. • • •  
 seen 52 BARI 91 SFM  $D^0 \rightarrow K^-\pi^+$   
 seen BASILE 81 SFM  $D^0 \rightarrow K^-\pi^+$

 $\Gamma(\Lambda_c^+ \pi^-) / \Gamma_{\text{total}}$   $\Gamma_3 / \Gamma$ 

VALUE (units $10^{-3}$ )	EVTS	DOCUMENT ID	TECN	COMMENT
--------------------------	------	-------------	------	---------

**5.7 ± 4.0 OUR FIT** Error includes scale factor of 1.6.

**8.8 ± 2.8 ± 1.5** 19 ABULENCIA 07b CDF  $p\bar{p}$  at 1.96 TeV  
 • • • We do not use the following data for averages, fits, limits, etc. • • •

seen 3 ABREU 96N DLPH  $\Lambda_c^+ \rightarrow pK^-\pi^+$   
 seen 4 BUSKULIC 96L ALEP  $\Lambda_c^+ \rightarrow pK^-\pi^+$ ,  
 $p\bar{K}^0, \Lambda\pi^+\pi^+\pi^-$

19 The result is obtained from  $(f_{\text{baryon}}/f_d) (B(\Lambda_b^0 \rightarrow \Lambda_c^+ \pi^-) / B(\bar{B}^0 \rightarrow D^+\pi^-)) = 0.82 \pm 0.08 \pm 0.11 \pm 0.22$ , assuming  $f_{\text{baryon}}/f_d = 0.25 \pm 0.04$  and  $B(\bar{B}^0 \rightarrow D^+\pi^-) = (2.68 \pm 0.13) \times 10^{-3}$ .

 $\Gamma(\Lambda_c^+ a_1(1260)^-) / \Gamma_{\text{total}}$   $\Gamma_4 / \Gamma$ 

VALUE	EVTS	DOCUMENT ID	TECN	COMMENT
-------	------	-------------	------	---------

seen 1 ABREU 96N DLPH  $\Lambda_c^+ \rightarrow pK^-\pi^+, a_1^- \rightarrow \rho^0\pi^- \rightarrow \pi^+\pi^-\pi^-$

 $\Gamma(\Lambda_c^+ \pi^+\pi^-\pi^-) / \Gamma_{\text{total}}$   $\Gamma_5 / \Gamma$ 

VALUE (units $10^{-3}$ )	EVTS	DOCUMENT ID	TECN	COMMENT
--------------------------	------	-------------	------	---------

**8 ± 5 OUR FIT** Error includes scale factor of 1.6.

**17 ± 4 ± 11** 20 AALTONEN 12A CDF  $p\bar{p}$  at 1.96 TeV

• • • We do not use the following data for averages, fits, limits, etc. • • •  
 seen 90 BARI 91 SFM  $\Lambda_c^+ \rightarrow pK^-\pi^+$

20 AALTONEN 12A reports  $[\Gamma(\Lambda_b^0 \rightarrow \Lambda_c^+ \pi^+\pi^-\pi^-) / \Gamma_{\text{total}}] / [B(\Lambda_b^0 \rightarrow \Lambda_c^+ \pi^-)] = 3.04 \pm 0.33 \pm 0.70 \pm 0.55$  which we multiply by our best value  $B(\Lambda_b^0 \rightarrow \Lambda_c^+ \pi^-) = (5.7 \pm 2.6) \times 10^{-3}$ . Our first error is their experiment's error and our second error is the systematic error from using our best value.

 $\Gamma(\Lambda_c^+ \pi^+\pi^-\pi^-) / \Gamma(\Lambda_c^+ \pi^-)$   $\Gamma_5 / \Gamma_3$ 

VALUE	DOCUMENT ID	TECN	COMMENT
-------	-------------	------	---------

**1.46 ± 0.22 OUR FIT** Error includes scale factor of 1.1.

**1.43 ± 0.16 ± 0.13** AAIJ 11E LHCB  $pp$  at 7 TeV

 $\Gamma(\Lambda_c(2595)^+\pi^-, \Lambda_c(2595)^+ \rightarrow \Lambda_c^+ \pi^+\pi^-) / \Gamma(\Lambda_c^+ \pi^+\pi^-\pi^-)$   $\Gamma_6 / \Gamma_5$ 

VALUE (units $10^{-2}$ )	DOCUMENT ID	TECN	COMMENT
--------------------------	-------------	------	---------

**4.4 ± 1.7 ± 0.6** AAIJ 11E LHCB  $pp$  at 7 TeV

 $\Gamma(\Lambda_c(2625)^+\pi^-, \Lambda_c(2625)^+ \rightarrow \Lambda_c^+ \pi^+\pi^-) / \Gamma(\Lambda_c^+ \pi^+\pi^-\pi^-)$   $\Gamma_7 / \Gamma_5$ 

VALUE (units $10^{-2}$ )	DOCUMENT ID	TECN	COMMENT
--------------------------	-------------	------	---------

**4.3 ± 1.5 ± 0.4** AAIJ 11E LHCB  $pp$  at 7 TeV

 $\Gamma(\Sigma_c(2455)^0 \pi^+\pi^-, \Sigma_c^0 \rightarrow \Lambda_c^+ \pi^-) / \Gamma(\Lambda_c^+ \pi^+\pi^-\pi^-)$   $\Gamma_8 / \Gamma_5$ 

VALUE (units $10^{-2}$ )	DOCUMENT ID	TECN	COMMENT
--------------------------	-------------	------	---------

**7.4 ± 2.4 ± 1.2** AAIJ 11E LHCB  $pp$  at 7 TeV

 $\Gamma(\Sigma_c(2455)^{++} \pi^-\pi^-, \Sigma_c^{++} \rightarrow \Lambda_c^+ \pi^+) / \Gamma(\Lambda_c^+ \pi^+\pi^-\pi^-)$   $\Gamma_9 / \Gamma_5$ 

VALUE (units $10^{-2}$ )	DOCUMENT ID	TECN	COMMENT
--------------------------	-------------	------	---------

**4.2 ± 1.8 ± 0.7** AAIJ 11E LHCB  $pp$  at 7 TeV

 $\Gamma(\Lambda K^0 2\pi^+ 2\pi^-) / \Gamma_{\text{total}}$   $\Gamma_{10} / \Gamma$ 

VALUE	EVTS	DOCUMENT ID	TECN	COMMENT
-------	------	-------------	------	---------

• • • We do not use the following data for averages, fits, limits, etc. • • •  
 seen 4 21 ARENTON 86 FMPS  $\Lambda K_S^0 2\pi^+ 2\pi^-$

21 See the footnote to the ARENTON 86 mass value.

 $\Gamma(\Lambda_c^+ \ell^- \bar{\nu}_\ell \text{anything}) / \Gamma_{\text{total}}$   $\Gamma_{11} / \Gamma$ 

The values and averages in this section serve only to show what values result if one assumes our  $B(b \rightarrow b\text{-baryon})$ . They cannot be thought of as measurements since the underlying product branching fractions were also used to determine  $B(b \rightarrow b\text{-baryon})$  as described in the note on "Production and Decay of  $b$ -Flavored Hadrons."

VALUE	EVTS	DOCUMENT ID	TECN	COMMENT
-------	------	-------------	------	---------

**0.098 ± 0.023 OUR AVERAGE**

0.092 ± 0.017 ± 0.016 22 BARATE 98D ALEP  $e^+e^- \rightarrow Z$

0.13 ± 0.04 ± 0.02 29 23 ABREU 95S DLPH  $e^+e^- \rightarrow Z$

• • • We do not use the following data for averages, fits, limits, etc. • • •

0.081 ± 0.020 ± 0.014 55 24 BUSKULIC 95L ALEP Repl. by BARATE 98D

0.16 ± 0.06 ± 0.03 21 25 BUSKULIC 92E ALEP  $\Lambda_c^+ \rightarrow pK^-\pi^+$

22 BARATE 98D reports  $[\Gamma(\Lambda_b^0 \rightarrow \Lambda_c^+ \ell^- \bar{\nu}_\ell \text{anything}) / \Gamma_{\text{total}}] \times [B(\bar{b} \rightarrow b\text{-baryon})] = 0.0086 \pm 0.0007 \pm 0.0014$  which we divide by our best value  $B(\bar{b} \rightarrow b\text{-baryon}) = (9.3 \pm 1.6) \times 10^{-2}$ . Our first error is their experiment's error and our second error is the systematic error from using our best value. Measured using  $\Lambda_c \ell^- \bar{\nu}_\ell \ell^+$ .

23 ABREU 95s reports  $[\Gamma(\Lambda_b^0 \rightarrow \Lambda_c^+ \ell^- \bar{\nu}_\ell \text{anything}) / \Gamma_{\text{total}}] \times [B(\bar{b} \rightarrow b\text{-baryon})] = 0.0118 \pm 0.0026 \pm 0.0031 \pm 0.0021$  which we divide by our best value  $B(\bar{b} \rightarrow b\text{-baryon}) = (9.3 \pm 1.6) \times 10^{-2}$ . Our first error is their experiment's error and our second error is the systematic error from using our best value.

24 BUSKULIC 95L reports  $[\Gamma(\Lambda_b^0 \rightarrow \Lambda_c^+ \ell^- \bar{\nu}_\ell \text{anything}) / \Gamma_{\text{total}}] \times [B(\bar{b} \rightarrow b\text{-baryon})] = 0.00755 \pm 0.0014 \pm 0.0012$  which we divide by our best value  $B(\bar{b} \rightarrow b\text{-baryon}) = (9.3 \pm 1.6) \times 10^{-2}$ . Our first error is their experiment's error and our second error is the systematic error from using our best value.

25 BUSKULIC 92e reports  $[\Gamma(\Lambda_b^0 \rightarrow \Lambda_c^+ \ell^- \bar{\nu}_\ell \text{anything}) / \Gamma_{\text{total}}] \times [B(\bar{b} \rightarrow b\text{-baryon})] = 0.015 \pm 0.0035 \pm 0.0045$  which we divide by our best value  $B(\bar{b} \rightarrow b\text{-baryon}) = (9.3 \pm 1.6) \times 10^{-2}$ . Our first error is their experiment's error and our second error is the systematic error from using our best value. Superseded by BUSKULIC 95L.

 $\Gamma(\Lambda_c^+ \ell^- \bar{\nu}_\ell) / \Gamma_{\text{total}}$   $\Gamma_{12} / \Gamma$ 

VALUE	DOCUMENT ID	TECN	COMMENT
-------	-------------	------	---------

**0.065 ± 0.032** **OUR FIT** Error includes scale factor of 1.8.

**0.050 ± 0.011 ± 0.016** 26 ABDALLAH 04A DLPH  $e^+e^- \rightarrow Z^0$   
**−0.008 − 0.012**

26 Derived from a combined likelihood and event rate fit to the distribution of the  $I_{\text{sgur}}$ -Wise variable and using HQET. The slope of the form factor is measured to be  $\rho^2 = 2.03 \pm 0.46 \pm 0.72 \pm 1.00$ .

 $\Gamma(\Lambda_c^+ \ell^- \bar{\nu}_\ell) / \Gamma(\Lambda_c^+ \pi^-)$   $\Gamma_{12} / \Gamma_3$ 

VALUE	DOCUMENT ID	TECN	COMMENT
-------	-------------	------	---------

**11 ± 4** **OUR FIT** Error includes scale factor of 1.2.

**16.6 ± 3.0 ± 2.8** AALTONEN 09E CDF  $p\bar{p}$  at 1.96 TeV  
**−3.6**

 $\Gamma(\Lambda_c^+ \pi^+\pi^-\ell^-\bar{\nu}_\ell) / \Gamma_{\text{total}}$   $\Gamma_{13} / \Gamma$ 

VALUE	DOCUMENT ID	TECN	COMMENT
-------	-------------	------	---------

**0.056 ± 0.031** 27 ABDALLAH 04A DLPH  $e^+e^- \rightarrow Z^0$   
**−0.030**

27 Derived from the fraction of  $\Gamma(\Lambda_b^0 \rightarrow \Lambda_c^+ \ell^- \bar{\nu}_\ell) / (\Gamma(\Lambda_b^0 \rightarrow \Lambda_c^+ \ell^- \bar{\nu}_\ell) + \Gamma(\Lambda_b^0 \rightarrow \Lambda_c^+ \pi^+\pi^-\ell^-\bar{\nu}_\ell)) = 0.47 \pm 0.10 \pm 0.07 \pm 0.06 \pm 0.06$ .

 $\Gamma(\Lambda_c^+ \ell^- \bar{\nu}_\ell) / [\Gamma(\Lambda_c^+ \ell^- \bar{\nu}_\ell) + \Gamma(\Lambda_c^+ \pi^+\pi^-\ell^-\bar{\nu}_\ell)]$   $\Gamma_{12} / (\Gamma_{12} + \Gamma_{13})$ 

VALUE	DOCUMENT ID	TECN	COMMENT
-------	-------------	------	---------

**0.47 ± 0.10 ± 0.07** ABDALLAH 04A DLPH  $e^+e^- \rightarrow Z^0$   
**−0.08 − 0.06**

 $\Gamma(\Lambda_c(2595)^+\ell^-\bar{\nu}_\ell) / \Gamma(\Lambda_c^+ \ell^- \bar{\nu}_\ell)$   $\Gamma_{14} / \Gamma_{12}$ 

VALUE	DOCUMENT ID	TECN	COMMENT
-------	-------------	------	---------

**0.126 ± 0.033 ± 0.047** AALTONEN 09E CDF  $p\bar{p}$  at 1.96 TeV  
**−0.038**

See key on page 457

## Baryon Particle Listings

 $\Lambda_b^0, \Sigma_b$ 

$\Gamma(\Lambda_c(2625)^+ \ell^- \bar{\nu}_\ell) / \Gamma(\Lambda_c^+ \ell^- \bar{\nu}_\ell)$		$\Gamma_{15} / \Gamma_{12}$	
VALUE	DOCUMENT ID	TECN	COMMENT
$0.210 \pm 0.042 \pm_{-0.050}^{0.071}$	AALTONEN	09E	CDF $p\bar{p}$ at 1.96 TeV

$[\frac{1}{2}\Gamma(\Sigma_c(2455)^0 \pi^+ \ell^- \bar{\nu}_\ell) + \frac{1}{2}\Gamma(\Sigma_c(2455)^{++} \pi^- \ell^- \bar{\nu}_\ell)] / \Gamma(\Lambda_c^+ \ell^- \bar{\nu}_\ell)$ ( $\frac{1}{2}\Gamma_{16} + \frac{1}{2}\Gamma_{17}$ ) / $\Gamma_{12}$			
VALUE	DOCUMENT ID	TECN	COMMENT
$0.054 \pm 0.022 \pm_{-0.018}^{0.021}$	AALTONEN	09E	CDF $p\bar{p}$ at 1.96 TeV

$\Gamma(\rho h^-) / \Gamma_{\text{total}}$		$\Gamma_{18} / \Gamma$		
VALUE	CL%	DOCUMENT ID	TECN	COMMENT
$< 2.3 \times 10^{-5}$	90	<sup>28</sup> ACOSTA	05o	CDF $p\bar{p}$ at 1.96 TeV
<sup>28</sup> Assumes $f_\Lambda / f_d = 0.25$ , and equal momentum distribution for $\Lambda_b$ and $B$ mesons.				

$\Gamma(\rho \pi^-) / \Gamma_{\text{total}}$		$\Gamma_{19} / \Gamma$		
VALUE (units $10^{-6}$ )	CL%	DOCUMENT ID	TECN	COMMENT
$3.5 \pm 0.8 \pm 0.6$		<sup>29</sup> AALTONEN	09c	CDF $p\bar{p}$ at 1.96 TeV

• • • We do not use the following data for averages, fits, limits, etc. • • •

$< 50$  90 <sup>30</sup> BUSKULIC 96v ALEP  $e^+ e^- \rightarrow Z$

<sup>29</sup> AALTONEN 09c reports  $[\Gamma(\Lambda_b^0 \rightarrow \rho \pi^-) / \Gamma_{\text{total}}] / [B(B^0 \rightarrow K^+ \pi^-)] \times [B(\bar{b} \rightarrow b\text{-baryon})] / [B(\bar{b} \rightarrow B^0)] = 0.042 \pm 0.007 \pm 0.006$  which we multiply or divide by our best values  $B(B^0 \rightarrow K^+ \pi^-) = (1.94 \pm 0.06) \times 10^{-5}$ ,  $B(\bar{b} \rightarrow b\text{-baryon}) = (9.3 \pm 1.6) \times 10^{-2}$ ,  $B(\bar{b} \rightarrow B^0) = (40.1 \pm 0.8) \times 10^{-2}$ . Our first error is their experiment's error and our second error is the systematic error from using our best values.

<sup>30</sup> BUSKULIC 96v assumes PDG 96 production fractions for  $B^0, B^+, B_s, b$  baryons.

$\Gamma(\rho K^-) / \Gamma_{\text{total}}$		$\Gamma_{20} / \Gamma$		
VALUE (units $10^{-6}$ )	CL%	DOCUMENT ID	TECN	COMMENT
$5.5 \pm 1.0 \pm 1.0$		<sup>31</sup> AALTONEN	09c	CDF $p\bar{p}$ at 1.96 TeV

• • • We do not use the following data for averages, fits, limits, etc. • • •

$< 360$  90 <sup>32</sup> ADAM 96d DLPH  $e^+ e^- \rightarrow Z$

$< 50$  90 <sup>33</sup> BUSKULIC 96v ALEP  $e^+ e^- \rightarrow Z$

<sup>31</sup> AALTONEN 09c reports  $[\Gamma(\Lambda_b^0 \rightarrow \rho K^-) / \Gamma_{\text{total}}] / [B(B^0 \rightarrow K^+ \pi^-)] \times [B(\bar{b} \rightarrow b\text{-baryon})] / [B(\bar{b} \rightarrow B^0)] = 0.066 \pm 0.009 \pm 0.008$  which we multiply or divide by our best values  $B(B^0 \rightarrow K^+ \pi^-) = (1.94 \pm 0.06) \times 10^{-5}$ ,  $B(\bar{b} \rightarrow b\text{-baryon}) = (9.3 \pm 1.6) \times 10^{-2}$ ,  $B(\bar{b} \rightarrow B^0) = (40.1 \pm 0.8) \times 10^{-2}$ . Our first error is their experiment's error and our second error is the systematic error from using our best values.

<sup>32</sup> ADAM 96d assumes  $f_{B^0} = f_{B^-} = 0.39$  and  $f_{B_s} = 0.12$ .

<sup>33</sup> BUSKULIC 96v assumes PDG 96 production fractions for  $B^0, B^+, B_s, b$  baryons.

$\Gamma(\Lambda \mu^+ \mu^-) / \Gamma_{\text{total}}$		$\Gamma_{21} / \Gamma$		
VALUE (units $10^{-7}$ )	CL%	DOCUMENT ID	TECN	COMMENT
$17.3 \pm 4.2 \pm 5.5$		AALTONEN	11A1	CDF $p\bar{p}$ at 1.96 TeV

$\Gamma(\Lambda \gamma) / \Gamma_{\text{total}}$		$\Gamma_{22} / \Gamma$		
VALUE	CL%	DOCUMENT ID	TECN	COMMENT
$< 1.3 \times 10^{-3}$	90	ACOSTA	02G	CDF $p\bar{p}$ at 1.8 TeV

PARTIAL BRANCHING FRACTIONS IN  $\Lambda_b \rightarrow \Lambda \mu^+ \mu^-$ 

$B(\Lambda_b \rightarrow \Lambda \mu^+ \mu^-) (q^2 < 2.0 \text{ GeV}^2/c^2)$			
VALUE (units $10^{-7}$ )	DOCUMENT ID	TECN	COMMENT
$0.15 \pm 2.01 \pm 0.05$	AALTONEN	11A1	CDF $p\bar{p}$ at 1.96 TeV

$B(\Lambda_b \rightarrow \Lambda \mu^+ \mu^-) (2.0 < q^2 < 4.3 \text{ GeV}^2/c^2)$			
VALUE (units $10^{-7}$ )	DOCUMENT ID	TECN	COMMENT
$1.8 \pm 1.7 \pm 0.6$	AALTONEN	11A1	CDF $p\bar{p}$ at 1.96 TeV

$B(\Lambda_b \rightarrow \Lambda \mu^+ \mu^-) (4.3 < q^2 < 8.68 \text{ GeV}^2/c^2)$			
VALUE (units $10^{-7}$ )	DOCUMENT ID	TECN	COMMENT
$-0.2 \pm 1.6 \pm 0.1$	AALTONEN	11A1	CDF $p\bar{p}$ at 1.96 TeV

$B(\Lambda_b \rightarrow \Lambda \mu^+ \mu^-) (10.09 < q^2 < 12.86 \text{ GeV}^2/c^2)$			
VALUE (units $10^{-7}$ )	DOCUMENT ID	TECN	COMMENT
$3.0 \pm 1.5 \pm 1.0$	AALTONEN	11A1	CDF $p\bar{p}$ at 1.96 TeV

$B(\Lambda_b \rightarrow \Lambda \mu^+ \mu^-) (14.18 < q^2 < 16.0 \text{ GeV}^2/c^2)$			
VALUE (units $10^{-7}$ )	DOCUMENT ID	TECN	COMMENT
$1.0 \pm 0.7 \pm 0.3$	AALTONEN	11A1	CDF $p\bar{p}$ at 1.96 TeV

$B(\Lambda_b \rightarrow \Lambda \mu^+ \mu^-) (16.0 < q^2 \text{ GeV}^2/c^2)$			
VALUE (units $10^{-7}$ )	DOCUMENT ID	TECN	COMMENT
$7.0 \pm 1.9 \pm 2.2$	AALTONEN	11A1	CDF $p\bar{p}$ at 1.96 TeV

$B(\Lambda_b \rightarrow \Lambda \mu^+ \mu^-) (1.0 < q^2 < 6.0 \text{ GeV}^2/c^2)$			
VALUE (units $10^{-7}$ )	DOCUMENT ID	TECN	COMMENT
$1.3 \pm 2.1 \pm 0.4$	AALTONEN	11A1	CDF $p\bar{p}$ at 1.96 TeV

$B(\Lambda_b \rightarrow \Lambda \mu^+ \mu^-) (0.0 < q^2 < 4.3 \text{ GeV}^2/c^2)$			
VALUE (units $10^{-7}$ )	DOCUMENT ID	TECN	COMMENT
$2.7 \pm 2.5 \pm 0.9$	AALTONEN	11A1	CDF $p\bar{p}$ at 1.96 TeV

## CP VIOLATION

 $A_{CP}$  is defined as

$$A_{CP} = \frac{B(\Lambda_b^0 \rightarrow f) - B(\bar{\Lambda}_b^0 \rightarrow \bar{f})}{B(\Lambda_b^0 \rightarrow f) + B(\bar{\Lambda}_b^0 \rightarrow \bar{f})}$$

the CP-violation asymmetry of exclusive  $\Lambda_b^0$  and  $\bar{\Lambda}_b^0$  decay.

$A_{CP}(\Lambda_b \rightarrow \rho \pi^-)$			
VALUE	DOCUMENT ID	TECN	COMMENT
$0.03 \pm 0.17 \pm 0.05$	AALTONEN	11N	CDF $p\bar{p}$ at 1.96 TeV

$A_{CP}(\Lambda_b \rightarrow \rho K^-)$			
VALUE	DOCUMENT ID	TECN	COMMENT
$0.37 \pm 0.17 \pm 0.03$	AALTONEN	11N	CDF $p\bar{p}$ at 1.96 TeV

 $\Lambda_b^0$  REFERENCES

AALJ	12E	PL B708 241	R. Aaij et al.	(LHCb Collab.)
AALTONEN	12A	PR D85 032003	T. Aaltonen et al.	(CDF Collab.)
AALJ	11E	PR D84 092001	R. Aaij et al.	(LHCb Collab.)
AALTONEN	11	PRL 106 121804	T. Aaltonen et al.	(CDF Collab.)
AALTONEN	11A1	PRL 107 201802	T. Aaltonen et al.	(CDF Collab.)
AALTONEN	11N	PRL 106 181802	T. Aaltonen et al.	(CDF Collab.)
ABAZOV	110	PR D84 031102	V.M. Abazov et al.	(DO Collab.)
AALTONEN	10B	PRL 104 102002	T. Aaltonen et al.	(CDF Collab.)
AALTONEN	09C	PRL 103 031801	T. Aaltonen et al.	(CDF Collab.)
AALTONEN	09E	PR D79 032001	T. Aaltonen et al.	(CDF Collab.)
ABAZOV	07S	PRL 99 142001	V.M. Abazov et al.	(DO Collab.)
ABAZOV	07U	PRL 99 182001	V.M. Abazov et al.	(DO Collab.)
ABULENCIA	07A	PRL 98 122001	A. Abulencia et al.	(FNAL CDF Collab.)
ABULENCIA	07B	PRL 98 122002	A. Abulencia et al.	(FNAL CDF Collab.)
ACOSTA	06E	PRL 96 202001	D. Acosta et al.	(CDF Collab.)
ABAZOV	05C	PRL 94 102001	V.M. Abazov et al.	(DO Collab.)
ACOSTA	05O	PR D72 051104R	D. Acosta et al.	(CDF Collab.)
ABDALLAH	04A	PL B585 63	J. Abdallah et al.	(DELPHI Collab.)
ACOSTA	02G	PR D66 112002	D. Acosta et al.	(CDF Collab.)
ABREU	99W	EPJ C10 185	P. Abreu et al.	(DELPHI Collab.)
ACKERSTAFF	98G	PL B426 161	K. Ackerstaff et al.	(OPAL Collab.)
BARATE	98D	EPJ C2 197	R. Barate et al.	(ALEPH Collab.)
ABE	97B	PR D55 1142	F. Abe et al.	(CDF Collab.)
ABE	96M	PRL 77 1439	F. Abe et al.	(CDF Collab.)
ABREU	96D	ZPHY C71 199	P. Abreu et al.	(DELPHI Collab.)
ABREU	96N	PL B374 351	P. Abreu et al.	(DELPHI Collab.)
ADAM	96D	ZPHY C72 207	W. Adam et al.	(DELPHI Collab.)
BUSKULIC	96L	PL B380 442	D. Buskalic et al.	(ALEPH Collab.)
BUSKULIC	96V	PL B384 471	D. Buskalic et al.	(ALEPH Collab.)
PDG	96	PR D54 1	R. M. Barnett et al.	(ALEPH Collab.)
ABREU	95S	ZPHY C68 375	P. Abreu et al.	(DELPHI Collab.)
AKERS	95K	PL B353 402	R. Akers et al.	(OPAL Collab.)
BUSKULIC	95L	PL B357 685	D. Buskalic et al.	(ALEPH Collab.)
ABE	93B	PR D47 R2639	F. Abe et al.	(CDF Collab.)
BUSKULIC	92E	PL B294 145	D. Buskalic et al.	(ALEPH Collab.)
ALBAJAR	91E	PL B273 540	C. Albajar et al.	(UA1 Collab.)
BARJ	91	NC 104A 1787	G. Bari et al.	(CERN R422 Collab.)
ARENTON	86	NP B274 707	M.W. Arenton et al.	(ARIZ, NDAM, VAND)
BASILE	81	LNC 31 97	M. Basile et al.	(CERN R415 Collab.)

 $\Sigma_b$  $I(J^P) = 1(\frac{1}{2}^+)$  Status: \* \* \* $I, J, P$  need confirmation.

In the quark model  $\Sigma_b^+, \Sigma_b^0, \Sigma_b^-$  are an isotriplet ( $uub, udb, ddb$ ) state. The lowest  $\Sigma_b$  ought to have  $J^P = 1/2^+$ . None of  $I, J, P$  have actually been measured.

 $\Sigma_b$  MASS

$\Sigma_b^+$ MASS			
VALUE (MeV)	DOCUMENT ID	TECN	COMMENT
$5811.3 \pm_{-0.8}^{0.9} \pm 1.7$	<sup>1</sup> AALTONEN	12F	CDF $p\bar{p}$ at 1.96 TeV

• • • We do not use the following data for averages, fits, limits, etc. • • •

$5807.8 \pm_{-2.2}^{2.0} \pm 1.7$	<sup>2</sup> AALTONEN	07k	CDF Repl. by AALTONEN 12F
-----------------------------------	-----------------------	-----	---------------------------

$\Sigma_b^0$ MASS			
VALUE (MeV)	DOCUMENT ID	TECN	COMMENT
$5815.5 \pm_{-0.5}^{0.6} \pm 1.7$	<sup>1</sup> AALTONEN	12F	CDF $p\bar{p}$ at 1.96 TeV

• • • We do not use the following data for averages, fits, limits, etc. • • •

$5815.2 \pm 1.0 \pm 1.7$	<sup>2</sup> AALTONEN	07k	CDF Repl. by AALTONEN 12F
--------------------------	-----------------------	-----	---------------------------

$m_{\Sigma_b^+} - m_{\Sigma_b^-}$			
VALUE (MeV)	DOCUMENT ID	TECN	COMMENT
$-4.2 \pm_{-1.0}^{1.1} \pm 0.1$	<sup>1</sup> AALTONEN	12F	CDF $p\bar{p}$ at 1.96 TeV

<sup>1</sup> Measured using the fully reconstructed  $\Lambda_b^0 \rightarrow \Lambda_c^+ \pi^-$  and  $\Lambda_c^+ \rightarrow K^- \pi^+$  decays.<sup>2</sup> Observed four  $\Lambda_b^0 \pi^\pm$  resonances in the fully reconstructed decay mode  $\Lambda_b^0 \rightarrow \Lambda_c^+ \pi^-$ , where  $\Lambda_c^+ \rightarrow p K^- \pi^+$ .

## Baryon Particle Listings

$$\Sigma_b, \Sigma_b^*, \Xi_b^0, \Xi_b^-$$

 $\Sigma_b$  WIDTH $\Sigma_b^+$  WIDTH

VALUE (MeV)	DOCUMENT ID	TECN	COMMENT
$9.7^{+3.8+1.2}_{-2.8-1.1}$	<sup>3</sup> AALTONEN	12F	CDF $p\bar{p}$ at 1.96 TeV

 $\Sigma_b^-$  WIDTH

VALUE (MeV)	DOCUMENT ID	TECN	COMMENT
$4.9^{+3.1}_{-2.1} \pm 1.1$	<sup>3</sup> AALTONEN	12F	CDF $p\bar{p}$ at 1.96 TeV

<sup>3</sup> Measured using the fully reconstructed  $\Lambda_b^0 \rightarrow \Lambda_c^+ \pi^-$  and  $\Lambda_c^+ \rightarrow K^- \pi^+$  decays.

 $\Sigma_b$  DECAY MODES

Mode	Fraction ( $\Gamma_i/\Gamma$ )
$\Gamma_1 \Lambda_b^0 \pi$	dominant

 $\Sigma_b$  BRANCHING RATIOS

$\Gamma(\Lambda_b^0 \pi)/\Gamma_{\text{total}}$	DOCUMENT ID	TECN	COMMENT	$\Gamma_1/\Gamma$
dominant	AALTONEN	07K	CDF $p\bar{p}$ at 1.96 TeV	

 $\Sigma_b$  REFERENCES

AALTONEN	12F	PR D85 092011	T. Aaltonen et al.	(CDF Collab.)
AALTONEN	07K	PRL 99 202001	T. Aaltonen et al.	(CDF Collab.)

$$\Sigma_b^*$$

$$I(J^P) = 1(\frac{3}{2}^+) \text{ Status: } ***$$

$I, J, P$  need confirmation. Quantum numbers shown are quark-model predictions.

 $\Sigma_b^*$  MASS $\Sigma_b^{*+}$  MASS

VALUE (MeV)	DOCUMENT ID	TECN	COMMENT
$5832.1 \pm 0.7^{+1.7}_{-1.8}$	<sup>1</sup> AALTONEN	12F	CDF $p\bar{p}$ at 1.96 TeV

 $\Sigma_b^{*-}$  MASS

VALUE (MeV)	DOCUMENT ID	TECN	COMMENT
$5835.1 \pm 0.6^{+1.7}_{-1.8}$	<sup>1</sup> AALTONEN	12F	CDF $p\bar{p}$ at 1.96 TeV

 $m_{\Sigma_b^{*+}} - m_{\Sigma_b^{*-}}$ 

VALUE (MeV)	DOCUMENT ID	TECN	COMMENT
$-3.0^{+1.0}_{-0.9} \pm 0.1$	<sup>1</sup> AALTONEN	12F	CDF $p\bar{p}$ at 1.96 TeV

<sup>1</sup> Measured using the fully reconstructed  $\Lambda_b^0 \rightarrow \Lambda_c^+ \pi^-$  and  $\Lambda_c^+ \rightarrow K^- \pi^+$  decays.

 $\Sigma_b^*$  WIDTH $\Sigma_b^{*+}$  WIDTH

VALUE (MeV)	DOCUMENT ID	TECN	COMMENT
$11.5^{+2.7+1.0}_{-2.2-1.5}$	<sup>2</sup> AALTONEN	12F	CDF $p\bar{p}$ at 1.96 TeV

 $\Sigma_b^{*-}$  WIDTH

VALUE (MeV)	DOCUMENT ID	TECN	COMMENT
$7.5^{+2.2+0.9}_{-1.8-1.4}$	<sup>2</sup> AALTONEN	12F	CDF $p\bar{p}$ at 1.96 TeV

<sup>2</sup> Measured using the fully reconstructed  $\Lambda_b^0 \rightarrow \Lambda_c^+ \pi^-$  and  $\Lambda_c^+ \rightarrow K^- \pi^+$  decays.

 $m_{\Sigma_b^{*-}} - m_{\Sigma_b^{*+}}$ 

VALUE (MeV)	DOCUMENT ID	TECN	COMMENT
$21.2^{+2.0+0.4}_{-1.9-0.3}$	<sup>3</sup> AALTONEN	07K	CDF $p\bar{p}$ at 1.96 TeV

<sup>3</sup> Observed four  $\Lambda_b^0 \pi^\pm$  resonances in the fully reconstructed decay mode  $\Lambda_b^0 \rightarrow \Lambda_c^+ \pi^-$ , where  $\Lambda_c^+ \rightarrow p K^- \pi^+$ . Assumes  $m_{\Sigma_b^{*+}} - m_{\Sigma_b^+} = m_{\Sigma_b^{*-}} - m_{\Sigma_b^-}$ .

 $\Sigma_b^*$  DECAY MODES

Mode	Fraction ( $\Gamma_i/\Gamma$ )
$\Gamma_1 \Lambda_b^0 \pi$	dominant

 $\Sigma_b^*$  BRANCHING RATIOS $\Gamma(\Lambda_b^0 \pi)/\Gamma_{\text{total}}$ 

VALUE	DOCUMENT ID	TECN	COMMENT	$\Gamma_1/\Gamma$
dominant	AALTONEN	07K	CDF $p\bar{p}$ at 1.96 TeV	

 $\Sigma_b^*$  REFERENCES

AALTONEN	12F	PR D85 092011	T. Aaltonen et al.	(CDF Collab.)
AALTONEN	07K	PRL 99 202001	T. Aaltonen et al.	(CDF Collab.)

$$\Xi_b^0, \Xi_b^-$$

$$I(J^P) = \frac{1}{2}(\frac{1}{2}^+) \text{ Status: } ***$$

In the quark model,  $\Xi_b^0$  and  $\Xi_b^-$  are an iso doublet ( $usb, dsb$ ) state; the lowest  $\Xi_b^0$  and  $\Xi_b^-$  ought to have  $J^P = 1/2^+$ . None of  $I, J, \text{ or } P$  have actually been measured.

 $\Xi_b$  MASSES $\Xi_b^-$  MASS

VALUE (MeV)	DOCUMENT ID	TECN	COMMENT
<b>5791.1 <math>\pm</math> 2.2 OUR AVERAGE</b>	Includes data from the datablock that follows this one.		
5796.7 $\pm$ 5.1 $\pm$ 1.4	<sup>1</sup> AALTONEN	11X	CDF $p\bar{p}$ at 1.96 TeV
5790.9 $\pm$ 2.6 $\pm$ 0.8	<sup>2</sup> AALTONEN	09AP	CDF $p\bar{p}$ at 1.96 TeV
5774 $\pm$ 11 $\pm$ 15	<sup>3</sup> ABAZOV	07K	D0 $p\bar{p}$ at 1.96 TeV
5792.9 $\pm$ 2.5 $\pm$ 1.7	<sup>4</sup> AALTONEN	07A	CDF Repl. by AALTONEN 09AP

<sup>1</sup> Measured in  $\Xi_b^- \rightarrow \Xi_c^0 \pi^-$  with  $25.8^{+5.5}_{-5.2}$  candidates.

<sup>2</sup> Measured in  $\Xi_b^- \rightarrow J/\psi \Xi^-$  decays with  $66^{+14}_{-9}$  candidates.

<sup>3</sup> Observed in  $\Xi_b^- \rightarrow J/\psi \Xi^-$  decays with  $15.2 \pm 4.4^{+1.9}_{-0.4}$  candidates, a significance of 5.5 sigma.

<sup>4</sup> Observed in  $\Xi_b^- \rightarrow J/\psi \Xi^-$  decays with  $17.5 \pm 4.3$  candidates, a significance of 7.7 sigma.

 $\Xi_b^0$  MASS

VALUE (MeV)	DOCUMENT ID	TECN	COMMENT
<b>5787.8 <math>\pm</math> 5.0 <math>\pm</math> 1.3</b>	<sup>5</sup> AALTONEN	11X	CDF $p\bar{p}$ at 1.96 TeV

The data in this block is included in the average printed for a previous datablock.

<sup>5</sup> Measured in  $\Xi_b^0 \rightarrow \Xi_c^+ \pi^-$  with  $25.3^{+5.6}_{-5.4}$  candidates.

 $m_{\Xi_b^-} - m_{\Xi_b^0}$ 

VALUE (MeV)	DOCUMENT ID	TECN	COMMENT
<b>3.1 <math>\pm</math> 5.6 <math>\pm</math> 1.3</b>	<sup>6</sup> AALTONEN	11X	CDF $p\bar{p}$ at 1.96 TeV

<sup>6</sup> Derived from measurements in  $\Xi_b^0 \rightarrow \Xi_c^+ \pi^-$  and  $\Xi_b^- \rightarrow J/\psi \Xi^-$  from AALTONEN 09AP taking correlated systematic uncertainties into account.

 $\Xi_b^-$  MEAN LIFE

VALUE ( $10^{-12}$ s)	DOCUMENT ID	TECN	COMMENT
<b>1.56 <math>^{+0.27}_{-0.25} \pm 0.02</math></b>	<sup>7</sup> AALTONEN	09AP	CDF $p\bar{p}$ at 1.96 TeV

<sup>7</sup> Measured in  $\Xi_b^- \rightarrow J/\psi \Xi^-$  decays with  $66^{+14}_{-9}$  candidates.

 $\Xi_b$  MEAN LIFE

"OUR EVALUATION" is an average using rescaled values of the data listed below. The average and rescaling were performed by the Heavy Flavor Averaging Group (HFAG) and are described at <http://www.slac.stanford.edu/xorg/hfag/>. The averaging/rescaling procedure takes into account correlations between the measurements and asymmetric lifetime errors.

VALUE ( $10^{-12}$ s)	EVTS	DOCUMENT ID	TECN	COMMENT
<b>1.49 <math>^{+0.19}_{-0.18}</math> OUR EVALUATION</b>				

1.56  $^{+0.27}_{-0.25} \pm 0.02$  <sup>8</sup> AALTONEN 09AP CDF  $p\bar{p}$  at 1.96 TeV

1.48  $^{+0.40}_{-0.31} \pm 0.12$  <sup>9</sup> ABDALLAH 05C DLPH  $e^+ e^- \rightarrow Z^0$

1.35  $^{+0.37+0.15}_{-0.28-0.17}$  <sup>10</sup> BUSKULIC 96T ALEP  $e^+ e^- \rightarrow Z$

••• We do not use the following data for averages, fits, limits, etc. •••

1.5  $^{+0.7}_{-0.4} \pm 0.3$  <sup>8</sup> <sup>11</sup> ABREU 95V DLPH Repl. by ABDALLAH 05C

<sup>8</sup> Measured in  $\Xi_b^- \rightarrow J/\psi \Xi^-$  decays with  $66^{+14}_{-9}$  candidates.

<sup>9</sup> Used the decay length of  $\Xi^-$  accompanied by a lepton of the same sign.

<sup>10</sup> Excess  $\Xi^- \ell^-$ , impact parameters.

<sup>11</sup> Excess  $\Xi^- \ell^-$ , decay lengths.

See key on page 457

## Baryon Particle Listings

 $\Xi_b^0, \Xi_b^-, \Omega_b^-, b$ -baryon ADMIXTURE ( $\Lambda_b, \Xi_b, \Sigma_b, \Omega_b$ ) $\Xi_b$  DECAY MODES

Mode	Fraction ( $\Gamma_i/\Gamma$ )	Scale factor
$\Gamma_1 \quad \Xi_b^- \rightarrow \Xi^- \ell^- \bar{\nu}_\ell X \times B(\bar{b} \rightarrow \Xi_b^-)$	$(3.9 \pm 1.2) \times 10^{-4}$	1.4
$\Gamma_2 \quad \Xi_b^- \rightarrow J/\psi \Xi^- \times B(b \rightarrow \Xi_b^-)$	$(1.02 \pm_{-0.21}^{+0.26}) \times 10^{-5}$	

 $\Xi_b$  BRANCHING RATIOS

$\Gamma(\Xi^- \ell^- \bar{\nu}_\ell X \times B(\bar{b} \rightarrow \Xi_b^-))/\Gamma_{\text{total}}$	$\Gamma_1/\Gamma$
<b><math>3.9 \pm 1.2</math> OUR AVERAGE</b> Error includes scale factor of 1.4.	
$3.0 \pm 1.0 \pm 0.3$	ABDALLAH 05c DLPH $e^+ e^- \rightarrow Z^0$
$5.4 \pm 1.1 \pm 0.8$	BUSKULIC 96T ALEP Excess $\Xi^- \ell^-$ over $\Xi^- \ell^+$
• • • We do not use the following data for averages, fits, limits, etc. • • •	
$5.9 \pm 2.1 \pm 1.0$	ABREU 95V DLPH Repl. by ABDALLAH 05c

 $\Gamma(J/\psi \Xi^- \times B(b \rightarrow \Xi_b^-))/\Gamma_{\text{total}}$ 

VALUE (units $10^{-4}$ )	DOCUMENT ID	TECN	COMMENT
<b><math>0.102 \pm 0.026</math> OUR AVERAGE</b>			
$0.098 \pm_{-0.016}^{+0.023} \pm 0.014$	12 AALTONEN	09AP CDF	$p\bar{p}$ at 1.96 TeV
$0.16 \pm 0.07 \pm 0.02$	13 ABAZOV	07K D0	$p\bar{p}$ at 1.96 TeV

<sup>12</sup>AALTONEN 09AP reports  $[\Gamma(\Xi_b^- \rightarrow J/\psi \Xi^- \times B(b \rightarrow \Xi_b^-))/\Gamma_{\text{total}}] / [B(\Lambda_b^0 \rightarrow J/\psi(1S)\Lambda \times B(b \rightarrow \Lambda_b^0))] = 0.167 \pm_{-0.025}^{+0.037} \pm 0.012$  which we multiply by our best value  $B(\Lambda_b^0 \rightarrow J/\psi(1S)\Lambda \times B(b \rightarrow \Lambda_b^0)) = (5.8 \pm 0.8) \times 10^{-5}$ . Our first error is their experiment's error and our second error is the systematic error from using our best value.

<sup>13</sup>ABAZOV 07K reports  $[\Gamma(\Xi_b^- \rightarrow J/\psi \Xi^- \times B(b \rightarrow \Xi_b^-))/\Gamma_{\text{total}}] / [B(\Lambda_b^0 \rightarrow J/\psi(1S)\Lambda \times B(b \rightarrow \Lambda_b^0))] = 0.28 \pm 0.09 \pm_{-0.08}^{+0.09}$  which we multiply by our best value  $B(\Lambda_b^0 \rightarrow J/\psi(1S)\Lambda \times B(b \rightarrow \Lambda_b^0)) = (5.8 \pm 0.8) \times 10^{-5}$ . Our first error is their experiment's error and our second error is the systematic error from using our best value.

 $\Xi_b$  REFERENCES

AALTONEN 11X PRL 107 102001	T. Aaltonen et al.	(CDF Collab.)
AALTONEN 09AP PR D80 072003	T. Aaltonen et al.	(CDF Collab.)
AALTONEN 07A PRL 99 052002	T. Aaltonen et al.	(CDF Collab.)
ABAZOV 07K PRL 99 052001	V.M. Abazov et al.	(D0 Collab.)
ABDALLAH 05c EPJ C44 299	J. Abdallah et al.	(DELPHI Collab.)
BUSKULIC 96T PL B384 449	D. Buskulic et al.	(ALEPH Collab.)
ABREU 95V ZPHY C68 541	P. Abreu et al.	(DELPHI Collab.)



$I(J^P) = 0(\frac{1}{2}^+)$  Status: \*\*\*  
I, J, P need confirmation.

In the quark model  $\Omega_b^-$  is  $ssb$  ground state. None of its quantum numbers has been measured.

 $\Omega_b$  MASS

VALUE (MeV)	DOCUMENT ID	TECN	COMMENT
<b><math>6071 \pm 40</math> OUR AVERAGE</b> Error includes scale factor of 6.2.			
$6054.4 \pm 6.8 \pm 0.9$	1 AALTONEN	09AP CDF	$p\bar{p}$ at 1.96 TeV
$6165 \pm 10 \pm 13$	2 ABAZOV	08AL D0	$p\bar{p}$ at 1.96 TeV

- <sup>1</sup> Observed in  $\Omega_b^- \rightarrow J/\psi \Omega^-$  decays with  $16 \pm_{-4}^{+6}$  candidates, a significance of 5.5 sigma from a combined mass-lifetime fit.
- <sup>2</sup> Observed in  $\Omega_b^- \rightarrow J/\psi \Omega^-$  decays with  $17.8 \pm 4.9 \pm 0.8$  candidates, a significance of 5.4 sigma.

 $\Omega_b$  MEAN LIFE

VALUE ( $10^{-12}$ s)	DOCUMENT ID	TECN	COMMENT
<b><math>1.13 \pm 0.53</math> OUR AVERAGE</b>			
$1.13 \pm_{-0.40}^{+0.53} \pm 0.02$	3 AALTONEN	09AP CDF	$p\bar{p}$ at 1.96 TeV

- <sup>3</sup> Observed in  $\Omega_b^- \rightarrow J/\psi \Omega^-$  decays with  $16 \pm_{-4}^{+6}$  candidates, a significance of 5.5 sigma from a combined mass-lifetime fit.

 $\Omega_b$  DECAY MODES

Mode	Fraction ( $\Gamma_i/\Gamma$ )
$\Gamma_1 \quad J/\psi \Omega^- \times B(b \rightarrow \Omega_b)$	$(2.9 \pm_{-0.8}^{+1.1}) \times 10^{-6}$

 $\Omega_b$  BRANCHING RATIOS $\Gamma(J/\psi \Omega^- \times B(b \rightarrow \Omega_b))/\Gamma_{\text{total}}$ 

VALUE (units $10^{-4}$ )	DOCUMENT ID	TECN	COMMENT
<b><math>0.029 \pm 0.011</math> OUR AVERAGE</b>			
$0.026 \pm_{-0.007}^{+0.010} \pm 0.004$	4 AALTONEN	09AP CDF	$p\bar{p}$ at 1.96 TeV
$0.08 \pm 0.04 \pm 0.02$	5 ABAZOV	08AL D0	$p\bar{p}$ at 1.96 TeV
<sup>4</sup> AALTONEN 09AP reports $[\Gamma(\Omega_b^- \rightarrow J/\psi \Omega^- \times B(b \rightarrow \Omega_b))/\Gamma_{\text{total}}] / [B(\Lambda_b^0 \rightarrow J/\psi(1S)\Lambda \times B(b \rightarrow \Lambda_b^0))] = 0.045 \pm_{-0.012}^{+0.017} \pm 0.004$ which we multiply by our best value $B(\Lambda_b^0 \rightarrow J/\psi(1S)\Lambda \times B(b \rightarrow \Lambda_b^0)) = (5.8 \pm 0.8) \times 10^{-5}$ . Our first error is their experiment's error and our second error is the systematic error from using our best value.			
<sup>5</sup> ABAZOV 08AL reports $[\Gamma(\Omega_b^- \rightarrow J/\psi \Omega^- \times B(b \rightarrow \Omega_b))/\Gamma_{\text{total}}] / [B(\Xi_b^- \rightarrow J/\psi \Xi^- \times B(b \rightarrow \Xi_b^-))] = 0.80 \pm 0.32 \pm_{-0.22}^{+0.14}$ which we multiply by our best value $B(\Xi_b^- \rightarrow J/\psi \Xi^- \times B(b \rightarrow \Xi_b^-)) = (1.02 \pm_{-0.21}^{+0.26}) \times 10^{-5}$ . Our first error is their experiment's error and our second error is the systematic error from using our best value.			

 $\Omega_b$  REFERENCES

AALTONEN 09AP PR D80 072003	T. Aaltonen et al.	(CDF Collab.)
ABAZOV 08AL PRL 101 232002	V.M. Abazov et al.	(D0 Collab.)

 $b$ -baryon ADMIXTURE ( $\Lambda_b, \Xi_b, \Sigma_b, \Omega_b$ ) $b$ -baryon ADMIXTURE MEAN LIFE

Each measurement of the  $b$ -baryon mean life is an average over an admixture of various  $b$  baryons which decay weakly. Different techniques emphasize different admixtures of produced particles, which could result in a different  $b$ -baryon mean life. More  $b$ -baryon flavor specific channels are not included in the measurement.

"OUR EVALUATION" is an average using rescaled values of the data listed below. The average and rescaling were performed by the Heavy Flavor Averaging Group (HFAG) and are described at <http://www.slac.stanford.edu/xorg/hfag/>. The averaging/rescaling procedure takes into account correlations between the measurements and asymmetric lifetime errors.

 $\Omega_b$  MEAN LIFE

VALUE ( $10^{-12}$ s)	EVTS	DOCUMENT ID	TECN	COMMENT
<b><math>1.382 \pm 0.029</math> OUR EVALUATION</b>				
$1.401 \pm 0.046 \pm 0.035$	1	AALTONEN	10B CDF	$p\bar{p}$ at 1.96 TeV
$1.218 \pm_{-0.115}^{+0.130} \pm 0.042$	2	ABAZOV	07S D0	$p\bar{p}$ at 1.96 TeV
$1.290 \pm_{-0.110}^{+0.119} \pm 0.087$	3	ABAZOV	07U D0	$p\bar{p}$ at 1.96 TeV
$1.593 \pm_{-0.078}^{+0.083} \pm 0.033$	2	ABULENCIA	07A CDF	$p\bar{p}$ at 1.96 TeV
$1.16 \pm 0.20 \pm 0.08$	4	ABREU	99W DLPH	$e^+ e^- \rightarrow Z$
$1.19 \pm 0.14 \pm 0.07$	5	ABREU	99W DLPH	$e^+ e^- \rightarrow Z$
$1.11 \pm_{-0.18}^{+0.19} \pm 0.05$	6	ABREU	99W DLPH	$e^+ e^- \rightarrow Z$
$1.29 \pm_{-0.22}^{+0.24} \pm 0.06$	6	ACKERSTAFF	98G OPAL	$e^+ e^- \rightarrow Z$
$1.20 \pm 0.08 \pm 0.06$	7	BARATE	98D ALEP	$e^+ e^- \rightarrow Z$
$1.21 \pm 0.11$	6	BARATE	98D ALEP	$e^+ e^- \rightarrow Z$
$1.32 \pm 0.15 \pm 0.07$	8	ABE	96M CDF	$p\bar{p}$ at 1.8 TeV
$1.10 \pm_{-0.17}^{+0.19} \pm 0.09$	6	ABREU	96D DLPH	$e^+ e^- \rightarrow Z$
$1.16 \pm 0.11 \pm 0.06$	6	AKERS	96L OPAL	$e^+ e^- \rightarrow Z$
• • • We do not use the following data for averages, fits, limits, etc. • • •				
$1.22 \pm_{-0.18}^{+0.22} \pm 0.04$	2	ABAZOV	05c D0	Repl. by ABAZOV 07S
$1.14 \pm 0.08 \pm 0.04$	9	ABREU	99W DLPH	$e^+ e^- \rightarrow Z$
$1.46 \pm_{-0.21}^{+0.22} \pm 0.07$		ABREU	96D DLPH	Repl. by ABREU 99W
$1.27 \pm_{-0.29}^{+0.35} \pm 0.09$		ABREU	95S DLPH	Repl. by ABREU 99W
$1.05 \pm_{-0.11}^{+0.12} \pm 0.09$	290	BUSKULIC	95L ALEP	Repl. by BARATE 98D
$1.04 \pm_{-0.38}^{+0.48} \pm 0.10$	11	10 ABREU	93F DLPH	Excess $\Lambda \mu^-$ , decay lengths
$1.05 \pm_{-0.20}^{+0.23} \pm 0.08$	157	11 AKERS	93 OPAL	Excess $\Lambda \ell^-$ , decay lengths
$1.12 \pm_{-0.29}^{+0.32} \pm 0.16$	101	12 BUSKULIC	92I ALEP	Excess $\Lambda \ell^-$ , impact parameters

- <sup>1</sup> Measured mean life using fully reconstructed  $\Lambda_b^0 \rightarrow \Lambda^+ \pi^-$  decays.
- <sup>2</sup> Measured mean life using fully reconstructed  $\Lambda_b^0 \rightarrow J/\psi \Lambda$  decays.
- <sup>3</sup> Measured using semileptonic decays  $\Lambda_b(0) \rightarrow \Lambda_c^+ \mu \nu X, \Lambda_c^+ \rightarrow K_S^0 p$ .
- <sup>4</sup> Measured using  $\Lambda \ell^-$  decay length.
- <sup>5</sup> Measured using  $p \ell^-$  decay length.
- <sup>6</sup> Measured using  $\Lambda_c \ell^-$  and  $\Lambda \ell^+ \ell^-$ .
- <sup>7</sup> Measured using the excess of  $\Lambda \ell^-$ , lepton impact parameter.

## Baryon Particle Listings

 $b$ -baryon ADMIXTURE ( $\Lambda_b, \Xi_b, \Sigma_b, \Omega_b$ )

<sup>8</sup> Measured using  $\Lambda_c \ell^-$ .

<sup>9</sup> This ABREU 99w result is the combined result of the  $\Lambda \ell^-, p \ell^-,$  and excess  $\Lambda \mu^-$  impact parameter measurements.

<sup>10</sup> ABREU 93f superseded by ABREU 96d.

<sup>11</sup> AKERS 93 superseded by AKERS 96.

<sup>12</sup> BUSKULIC 92i superseded by BUSKULIC 95L.

### $b$ -baryon ADMIXTURE DECAY MODES ( $\Lambda_b, \Xi_b, \Sigma_b, \Omega_b$ )

These branching fractions are actually an average over weakly decaying  $b$ -baryons weighted by their production rates at the LHC, LEP, and Tevatron, branching ratios, and detection efficiencies. They scale with the  $b$ -baryon production fraction  $B(b \rightarrow b\text{-baryon})$ .

The branching fractions  $B(b\text{-baryon} \rightarrow \Lambda \ell^- \bar{\nu}_\ell \text{ anything})$  and  $B(\Lambda_b^0 \rightarrow \Lambda_c^+ \ell^- \bar{\nu}_\ell \text{ anything})$  are not pure measurements because the underlying measured products of these with  $B(b \rightarrow b\text{-baryon})$  were used to determine  $B(b \rightarrow b\text{-baryon})$ , as described in the note "Production and Decay of  $b$ -Flavored Hadrons."

For inclusive branching fractions, e.g.,  $B \rightarrow D^\pm \text{ anything}$ , the values usually are multiplicities, not branching fractions. They can be greater than one.

Mode	Fraction ( $\Gamma_i/\Gamma$ )
$\Gamma_1$ $p \mu^- \bar{\nu}$ anything	$(5.3^{+2.2}_{-1.9})\%$
$\Gamma_2$ $p \ell \bar{\nu}_\ell$ anything	$(5.1 \pm 1.2)\%$
$\Gamma_3$ $p$ anything	$(63 \pm 21)\%$
$\Gamma_4$ $\Lambda \ell^- \bar{\nu}_\ell$ anything	$(3.4 \pm 0.6)\%$
$\Gamma_5$ $\Lambda \ell^+ \nu_\ell$ anything	
$\Gamma_6$ $\Lambda$ anything	
$\Gamma_7$ $\Lambda_c^+ \ell^- \bar{\nu}_\ell$ anything	
$\Gamma_8$ $\Lambda/\bar{\Lambda}$ anything	$(35 \pm 8)\%$
$\Gamma_9$ $\Xi^- \ell^- \bar{\nu}_\ell$ anything	$(5.9 \pm 1.6) \times 10^{-3}$

### $b$ -baryon ADMIXTURE ( $\Lambda_b, \Xi_b, \Sigma_b, \Omega_b$ ) BRANCHING RATIOS

$\Gamma(p \mu^- \bar{\nu} \text{ anything})/\Gamma_{\text{total}}$					$\Gamma_1/\Gamma$
VALUE	EVTS	DOCUMENT ID	TECN	COMMENT	
<b><math>0.053 \pm 0.020</math></b> <b><math>-0.017 \pm 0.009</math></b>	125	13 ABREU	95s	DLPH $e^+ e^- \rightarrow Z$	

<sup>13</sup> ABREU 95s reports  $[\Gamma(b\text{-baryon} \rightarrow p \mu^- \bar{\nu} \text{ anything})/\Gamma_{\text{total}}] \times [B(\bar{b} \rightarrow b\text{-baryon})] = 0.0049 \pm 0.0011^{+0.0015}_{-0.0011}$  which we divide by our best value  $B(\bar{b} \rightarrow b\text{-baryon}) = (9.3 \pm 1.6) \times 10^{-2}$ . Our first error is their experiment's error and our second error is the systematic error from using our best value.

$\Gamma(p \ell \bar{\nu}_\ell \text{ anything})/\Gamma_{\text{total}}$					$\Gamma_2/\Gamma$
VALUE	DOCUMENT ID	TECN	COMMENT		
<b><math>0.051 \pm 0.009 \pm 0.009</math></b>	14 BARATE	98v	ALEP $e^+ e^- \rightarrow Z$		

<sup>14</sup> BARATE 98v reports  $[\Gamma(b\text{-baryon} \rightarrow p \ell \bar{\nu}_\ell \text{ anything})/\Gamma_{\text{total}}] \times [B(\bar{b} \rightarrow b\text{-baryon})] = (4.72 \pm 0.66 \pm 0.44) \times 10^{-3}$  which we divide by our best value  $B(\bar{b} \rightarrow b\text{-baryon}) = (9.3 \pm 1.6) \times 10^{-2}$ . Our first error is their experiment's error and our second error is the systematic error from using our best value.

$\Gamma(p \ell \bar{\nu}_\ell \text{ anything})/\Gamma(p \text{ anything})$					$\Gamma_2/\Gamma_3$
VALUE	DOCUMENT ID	TECN	COMMENT		
<b><math>0.080 \pm 0.012 \pm 0.014</math></b>	BARATE	98v	ALEP $e^+ e^- \rightarrow Z$		

$\Gamma(\Lambda \ell^- \bar{\nu}_\ell \text{ anything})/\Gamma_{\text{total}}$					$\Gamma_4/\Gamma$
VALUE	EVTS	DOCUMENT ID	TECN	COMMENT	
<b><math>0.034 \pm 0.006</math></b> OUR AVERAGE					
$0.035 \pm 0.005 \pm 0.006$		15 BARATE	98d	ALEP $e^+ e^- \rightarrow Z$	
$0.031 \pm 0.004 \pm 0.005$		16 AKERS	96	OPAL Excess of $\Lambda \ell^-$ over $\Lambda \ell^+$	
$0.032 \pm 0.008 \pm 0.006$	262	17 ABREU	95s	DLPH Excess of $\Lambda \ell^-$ over $\Lambda \ell^+$	
$0.066 \pm 0.013 \pm 0.011$	290	18 BUSKULIC	95L	ALEP Excess of $\Lambda \ell^-$ over $\Lambda \ell^+$	
••• We do not use the following data for averages, fits, limits, etc. •••					
seen	157	19 AKERS	93	OPAL Excess of $\Lambda \ell^-$ over $\Lambda \ell^+$	
$0.075 \pm 0.022 \pm 0.013$	101	20 BUSKULIC	92i	ALEP Excess of $\Lambda \ell^-$ over $\Lambda \ell^+$	

<sup>15</sup> BARATE 98d reports  $[\Gamma(b\text{-baryon} \rightarrow \Lambda \ell^- \bar{\nu}_\ell \text{ anything})/\Gamma_{\text{total}}] \times [B(\bar{b} \rightarrow b\text{-baryon})] = 0.00326 \pm 0.00016 \pm 0.00039$  which we divide by our best value  $B(\bar{b} \rightarrow b\text{-baryon}) = (9.3 \pm 1.6) \times 10^{-2}$ . Our first error is their experiment's error and our second error is the systematic error from using our best value. Measured using the excess of  $\Lambda \ell^-,$  lepton impact parameter.

<sup>16</sup> AKERS 96 reports  $[\Gamma(b\text{-baryon} \rightarrow \Lambda \ell^- \bar{\nu}_\ell \text{ anything})/\Gamma_{\text{total}}] \times [B(\bar{b} \rightarrow b\text{-baryon})] = 0.00291 \pm 0.00023 \pm 0.00025$  which we divide by our best value  $B(\bar{b} \rightarrow b\text{-baryon}) = (9.3 \pm 1.6) \times 10^{-2}$ . Our first error is their experiment's error and our second error is the systematic error from using our best value.

<sup>17</sup> ABREU 95s reports  $[\Gamma(b\text{-baryon} \rightarrow \Lambda \ell^- \bar{\nu}_\ell \text{ anything})/\Gamma_{\text{total}}] \times [B(\bar{b} \rightarrow b\text{-baryon})] = 0.0030 \pm 0.0006 \pm 0.0004$  which we divide by our best value  $B(\bar{b} \rightarrow b\text{-baryon}) = (9.3 \pm 1.6) \times 10^{-2}$ . Our first error is their experiment's error and our second error is the systematic error from using our best value.

<sup>18</sup> BUSKULIC 95L reports  $[\Gamma(b\text{-baryon} \rightarrow \Lambda \ell^- \bar{\nu}_\ell \text{ anything})/\Gamma_{\text{total}}] \times [B(\bar{b} \rightarrow b\text{-baryon})] = 0.0061 \pm 0.0006 \pm 0.0010$  which we divide by our best value  $B(\bar{b} \rightarrow b\text{-baryon}) = (9.3 \pm 1.6) \times 10^{-2}$ . Our first error is their experiment's error and our second error is the systematic error from using our best value.

<sup>19</sup> AKERS 93 superseded by AKERS 96.

<sup>20</sup> BUSKULIC 92i reports  $[\Gamma(b\text{-baryon} \rightarrow \Lambda \ell^- \bar{\nu}_\ell \text{ anything})/\Gamma_{\text{total}}] \times [B(\bar{b} \rightarrow b\text{-baryon})] = 0.0070 \pm 0.0010 \pm 0.0018$  which we divide by our best value  $B(\bar{b} \rightarrow b\text{-baryon}) = (9.3 \pm 1.6) \times 10^{-2}$ . Our first error is their experiment's error and our second error is the systematic error from using our best value. Superseded by BUSKULIC 95L.

$\Gamma(\Lambda \ell^+ \nu_\ell \text{ anything})/\Gamma(\Lambda \text{ anything})$					$\Gamma_5/\Gamma_6$
VALUE	DOCUMENT ID	TECN	COMMENT		
<b><math>0.080 \pm 0.012 \pm 0.008</math></b>	ABBIENDI	99L	OPAL $e^+ e^- \rightarrow Z$		
••• We do not use the following data for averages, fits, limits, etc. •••					
$0.070 \pm 0.012 \pm 0.007$	ACKERSTAFF	97N	OPAL Repl. by ABBIENDI 99L		

$\Gamma(\Lambda/\bar{\Lambda} \text{ anything})/\Gamma_{\text{total}}$					$\Gamma_8/\Gamma$
VALUE	DOCUMENT ID	TECN	COMMENT		
<b><math>0.35 \pm 0.08</math></b> OUR AVERAGE					
$0.38 \pm 0.05 \pm 0.06$	21 ABBIENDI	99L	OPAL $e^+ e^- \rightarrow Z$		
$0.24^{+0.13}_{-0.08} \pm 0.04$	22 ABREU	95c	DLPH $e^+ e^- \rightarrow Z$		
••• We do not use the following data for averages, fits, limits, etc. •••					
$0.42 \pm 0.06 \pm 0.07$	23 ACKERSTAFF	97N	OPAL Repl. by ABBIENDI 99L		

<sup>21</sup> ABBIENDI 99L reports  $[\Gamma(b\text{-baryon} \rightarrow \Lambda/\bar{\Lambda} \text{ anything})/\Gamma_{\text{total}}] \times [B(\bar{b} \rightarrow b\text{-baryon})] = 0.035 \pm 0.0032 \pm 0.0035$  which we divide by our best value  $B(\bar{b} \rightarrow b\text{-baryon}) = (9.3 \pm 1.6) \times 10^{-2}$ . Our first error is their experiment's error and our second error is the systematic error from using our best value.

<sup>22</sup> ABREU 95c reports  $0.28^{+0.17}_{-0.12}$  from a measurement of  $[\Gamma(b\text{-baryon} \rightarrow \Lambda/\bar{\Lambda} \text{ anything})/\Gamma_{\text{total}}] \times [B(\bar{b} \rightarrow b\text{-baryon})]$  assuming  $B(\bar{b} \rightarrow b\text{-baryon}) = 0.08 \pm 0.02$ , which we rescale to our best value  $B(\bar{b} \rightarrow b\text{-baryon}) = (9.3 \pm 1.6) \times 10^{-2}$ . Our first error is their experiment's error and our second error is the systematic error from using our best value.

<sup>23</sup> ACKERSTAFF 97N reports  $[\Gamma(b\text{-baryon} \rightarrow \Lambda/\bar{\Lambda} \text{ anything})/\Gamma_{\text{total}}] \times [B(\bar{b} \rightarrow b\text{-baryon})] = 0.0393 \pm 0.0046 \pm 0.0037$  which we divide by our best value  $B(\bar{b} \rightarrow b\text{-baryon}) = (9.3 \pm 1.6) \times 10^{-2}$ . Our first error is their experiment's error and our second error is the systematic error from using our best value.

$\Gamma(\Xi^- \ell^- \bar{\nu}_\ell \text{ anything})/\Gamma_{\text{total}}$					$\Gamma_9/\Gamma$
VALUE	DOCUMENT ID	TECN	COMMENT		
<b><math>0.0059 \pm 0.0016</math></b> OUR AVERAGE					
$0.0058 \pm 0.0015 \pm 0.0010$	24 BUSKULIC	96T	ALEP Excess $\Xi^- \ell^-$ over $\Xi^- \ell^+$		
$0.0063 \pm 0.0025 \pm 0.0011$	25 ABREU	95v	DLPH Excess $\Xi^- \ell^-$ over $\Xi^- \ell^+$		

<sup>24</sup> BUSKULIC 96T reports  $[\Gamma(b\text{-baryon} \rightarrow \Xi^- \ell^- \bar{\nu}_\ell \text{ anything})/\Gamma_{\text{total}}] \times [B(\bar{b} \rightarrow b\text{-baryon})] = 0.00054 \pm 0.00011 \pm 0.00008$  which we divide by our best value  $B(\bar{b} \rightarrow b\text{-baryon}) = (9.3 \pm 1.6) \times 10^{-2}$ . Our first error is their experiment's error and our second error is the systematic error from using our best value.

<sup>25</sup> ABREU 95v reports  $[\Gamma(b\text{-baryon} \rightarrow \Xi^- \ell^- \bar{\nu}_\ell \text{ anything})/\Gamma_{\text{total}}] \times [B(\bar{b} \rightarrow b\text{-baryon})] = 0.00059 \pm 0.00021 \pm 0.0001$  which we divide by our best value  $B(\bar{b} \rightarrow b\text{-baryon}) = (9.3 \pm 1.6) \times 10^{-2}$ . Our first error is their experiment's error and our second error is the systematic error from using our best value.

### $b$ -baryon ADMIXTURE ( $\Lambda_b, \Xi_b, \Sigma_b, \Omega_b$ ) REFERENCES

AALTONEN	07B	PRL 104 102002	T. Aaltonen et al.	(CDF Collab.)
ABAZOV	07S	PRL 99 142001	V.M. Abazov et al.	(DO Collab.)
ABAZOV	07U	PRL 99 182001	V.M. Abazov et al.	(DO Collab.)
ABULENCIA	07A	PRL 98 122001	A. Abulencia et al.	(FNAL CDF Collab.)
ABAZOV	05C	PRL 94 102001	V.M. Abazov et al.	(DO Collab.)
ABBIENDI	99L	EPJ C9 1	G. Abbiendi et al.	(OPAL Collab.)
ABREU	99W	EPJ C10 185	P. Abreu et al.	(DELPHI Collab.)
ACKERSTAFF	98G	PL B426 161	K. Ackerstaff et al.	(OPAL Collab.)
BARATE	98D	EPJ C2 197	R. Barate et al.	(ALEPH Collab.)
BARATE	98V	EPJ C5 205	R. Barate et al.	(ALEPH Collab.)
ACKERSTAFF	97N	ZPHY C74 423	K. Ackerstaff et al.	(OPAL Collab.)
ABE	96M	PRL 77 1439	F. Abe et al.	(CDF Collab.)
ABREU	96D	ZPHY C71 199	P. Abreu et al.	(DELPHI Collab.)
AKERS	96J	ZPHY C69 195	R. Akers et al.	(OPAL Collab.)
BUSKULIC	96T	PL B384 449	D. Buskulic et al.	(ALEPH Collab.)
ABREU	95C	PL B347 447	P. Abreu et al.	(DELPHI Collab.)
ABREU	95S	ZPHY C68 375	P. Abreu et al.	(DELPHI Collab.)
ABREU	95V	ZPHY C68 541	P. Abreu et al.	(DELPHI Collab.)
BUSKULIC	95L	PL B357 685	D. Buskulic et al.	(ALEPH Collab.)
ABREU	93F	PL B311 379	P. Abreu et al.	(DELPHI Collab.)
AKERS	93	PL B316 435	R. Akers et al.	(OPAL Collab.)
BUSKULIC	92I	PL B297 449	D. Buskulic et al.	(ALEPH Collab.)



## MISCELLANEOUS SEARCHES

Magnetic Monopole Searches . . . . .	1413
Supersymmetric Particle Searches . . . . .	1420
Technicolor . . . . .	1475
Quark and Lepton Compositeness . . . . .	1484
Extra Dimensions . . . . .	1489
WIMPs and Other Particle Searches . . . . .	1500

## Notes in the Search Listings

Magnetic Monopoles (rev.) . . . . .	1413
Supersymmetry (rev.) . . . . .	1420
I. Theory (rev.) . . . . .	1420
II. Experiment (rev.) . . . . .	1437
Dynamical Electroweak Symmetry Breaking (rev.) . . . . .	1475
Searches for Quark and Lepton Compositeness . . . . .	1484
Extra Dimensions (rev.) . . . . .	1489
WIMPs and Other Particle Searches (rev.) . . . . .	1500

## SEARCHES IN OTHER SECTIONS

Higgs Bosons — $H^0$ and $H^\pm$ . . . . .	501
Heavy Bosons Other than Higgs Bosons . . . . .	543
Leptoquarks (rev.) . . . . .	555
Axions ( $A^0$ ) and Other Very Light Bosons . . . . .	562
Heavy Charged Lepton Searches . . . . .	621
Double- $\beta$ Decay . . . . .	631
Heavy Neutral Leptons, Searches for . . . . .	647
$b'$ (Fourth Generation) Quark . . . . .	687
Free Quark Searches . . . . .	688





**SEARCHES FOR  
MONOPOLES,  
SUPERSYMMETRY,  
TECHNICOLOR,  
COMPOSITENESS,  
EXTRA DIMENSIONS, etc.**

**Magnetic Monopole Searches**

**MAGNETIC MONOPOLES**

Updated August 2011 by D. Milstead (Stockholm Univ.) and E.J. Weinberg (Columbia Univ.).

The symmetry between electric and magnetic fields in the sourcefree Maxwell's equations naturally suggests that electric charges might have magnetic counterparts, known as magnetic monopoles. Although the greatest interest has been in the supermassive monopoles that are a firm prediction of all grand unified theories, one cannot exclude the possibility of lighter monopoles, even though there is at present no strong theoretical motivation for these.

In either case, the magnetic charge is constrained by a quantization condition first found by Dirac [1]. Consider a monopole with magnetic charge  $Q_M$  and a Coulomb magnetic field

$$\mathbf{B} = \frac{Q_M}{4\pi} \frac{\hat{\mathbf{r}}}{r^2}. \quad (1)$$

Any vector potential  $\mathbf{A}$  whose curl is equal to  $\mathbf{B}$  must be singular along some line running from the origin to spatial infinity. This Dirac string singularity could potentially be detected through the extra phase that the wavefunction of a particle with electric charge  $Q_E$  would acquire if it moved along a loop encircling the string. For the string to be unobservable, this phase must be a multiple of  $2\pi$ . Requiring that this be the case for any pair of electric and magnetic charges gives the condition that all charges be integer multiples of minimum charges  $Q_E^{\min}$  and  $Q_M^{\min}$  obeying

$$Q_E^{\min} Q_M^{\min} = 2\pi. \quad (2)$$

(For monopoles which also carry an electric charge, called dyons, the quantization conditions on their electric charges can be modified. However, the constraints on magnetic charges, as well as those on all purely electric particles, will be unchanged.)

Another way to understand this result is to note that the conserved orbital angular momentum of a point electric charge moving in the field of a magnetic monopole has an additional component, with

$$\mathbf{L} = m\mathbf{r} \times \mathbf{v} - 4\pi Q_E Q_M \hat{\mathbf{r}} \quad (3)$$

Requiring the radial component of  $\mathbf{L}$  to be quantized in half-integer units yields Eq. (2).

If there are unbroken gauge symmetries in addition to the U(1) of electromagnetism, the above analysis must be modified [2,3]. For example, a monopole could have both a

U(1) magnetic charge and a color magnetic charge. The latter could combine with the color charge of a quark to give an additional contribution to the phase factor associated with a loop around the Dirac string, so that the U(1) charge could be the Dirac charge  $Q_M^D \equiv 2\pi/e$ , the result that would be obtained by substituting the electron charge into Eq. (2). On the other hand, for monopoles without color-magnetic charge, one would simply insert the quark electric charges into Eq. (2) and conclude that  $Q_M$  must be a multiple of  $6\pi/e$ .

The prediction of GUT monopoles arises from the work of 't Hooft [4] and Polyakov [5], who showed that certain spontaneously broken gauge theories have nonsingular classical solutions that lead to magnetic monopoles in the quantum theory. The simplest example occurs in a theory where the vacuum expectation value of a triplet Higgs field  $\phi$  breaks an SU(2) gauge symmetry down to the U(1) of electromagnetism and gives a mass  $M_V$  to two of the gauge bosons. In order to have finite energy,  $\phi$  must approach a vacuum value at infinity. However, there is a continuous family of possible vacua, since the scalar field potential determines only the magnitude  $v$  of  $\langle\phi\rangle$ , but not its orientation in the internal SU(2) space. In the monopole solution, the direction of  $\phi$  in internal space is correlated with the position in physical space; *i.e.*,  $\phi^a \sim v\hat{r}^a$ . The stability of the solution follows from the fact that this twisting Higgs field cannot be smoothly deformed to a spatially uniform vacuum configuration. Reducing the energetic cost of the spatial variation of  $\phi$  requires a nonzero gauge potential, which turns out to yield the magnetic field corresponding to a charge  $Q_M = 4\pi/e$ . Numerical solution of the classical field equations shows that the mass of this monopole is

$$M_{\text{mon}} \sim \frac{4\pi M_V}{e^2}. \quad (4)$$

The essential ingredient here was the fact that the Higgs fields at spatial infinity could be arranged in a topologically nontrivial configuration. A discussion of the general conditions under which this is possible is beyond the scope of this review, so we restrict ourselves to the two phenomenologically most important cases.

The first is the electroweak theory, with SU(2) × U(1) broken to U(1). There are no topologically nontrivial configurations of the Higgs field, and hence no topologically stable monopole solutions.

The second is when any simple Lie group is broken to a subgroup with a U(1) factor, a case that includes all grand unified theories. The monopole mass is determined by the mass scale of the symmetry breaking that allows nontrivial topology. For example, an SU(5) model with

$$\text{SU}(5) \xrightarrow{M_X} \text{SU}(3) \times \text{SU}(2) \times \text{U}(1) \xrightarrow{M_W} \text{SU}(3) \times \text{U}(1) \quad (5)$$

has a monopole [6] with  $Q_M = 2\pi/e$  and mass

$$M_{\text{mon}} \sim \frac{4\pi M_X}{g^2}, \quad (6)$$

## Searches Particle Listings

### Magnetic Monopole Searches

where  $g$  is the SU(5) gauge coupling. For a unification scale of  $10^{16}$  GeV, these monopoles would have a mass  $M_{\text{mon}} \sim 10^{17} - 10^{18}$  GeV.

In theories with several stages of symmetry breaking, monopoles of different mass scales can arise. In an SO(10) theory with

$$\text{SO}(10) \xrightarrow{M_1} \text{SU}(4) \times \text{SU}(2) \times \text{SU}(2) \xrightarrow{M_2} \text{SU}(3) \times \text{SU}(2) \times \text{U}(1) \quad (7)$$

there is monopole with  $Q_M = 2\pi/e$  and mass  $\sim 4\pi M_1/g^2$  and a much lighter monopole with  $Q_M = 4\pi/e$  and mass  $\sim 4\pi M_2/g^2$  [7].

The central core of a GUT monopole contains the fields of the superheavy gauge bosons that mediate baryon number violation, so one might expect that baryon number conservation could be violated in baryon-monopole scattering. The surprising feature, pointed out by Callan [8] and Rubakov [9], is that these processes are not suppressed by powers of the gauge boson mass. Instead, the cross-sections for catalysis processes such as  $p + \text{monopole} \rightarrow e^+ + \pi^0 + \text{monopole}$  are essentially geometric; *i.e.*,  $\sigma_{\Delta B} \sim 10^{-27} \text{ cm}^2$ , where  $\beta = v/c$ . Note, however, that intermediate mass monopoles arising at later stages of symmetry breakings, such as the doubly charged monopoles of the SO(10) theory, do not catalyze baryon number violation.

**Production and Annihilation:** GUT monopoles are far too massive to be produced in any foreseeable accelerator. However, they could have been produced in the early universe as topological defects arising via the Kibble mechanism [10] in a symmetry-breaking phase transition. Estimates of the initial monopole abundance, and of the degree to which it can be reduced by monopole-antimonopole annihilation, predict a present-day monopole abundance that exceeds by many orders of magnitude the astrophysical and experimental bounds described below [11]. Cosmological inflation and other proposed solutions to this primordial monopole problem generically lead to present-day abundances exponentially smaller than could be plausibly detected, although potentially observable abundances can be obtained in scenarios with carefully tuned parameters.

If monopoles light enough to be produced at colliders exist, one would expect that these could be produced by analogs of the electromagnetic processes that produce pairs of electrically charged particles. Because of the large size of the magnetic charge, this is a strong coupling problem for which perturbation theory cannot be trusted. Indeed, the problem of obtaining reliable quantitative estimates of the production cross-sections remains an open one, on which there is no clear consensus.

**Astrophysical and Cosmological Bounds:** If there were no galactic magnetic field, one would expect monopoles in the galaxy to have typical velocities of the order of  $10^{-3}c$ , comparable to the virial velocity in the galaxy (relevant if the monopoles cluster with the galaxy) and the peculiar velocity of the galaxy with respect to the CMB rest frame (relevant if the monopoles are not bound to the galaxy). This situation is modified by the existence of a galactic magnetic field  $B \sim 3\mu\text{G}$ .

A monopole with the Dirac charge and mass  $M$  would be accelerated by this field to a velocity

$$v_{\text{mag}} \sim \begin{cases} c, & M \lesssim 10^{11} \text{ GeV} \\ 10^{-3}c \left( \frac{10^{17} \text{ GeV}}{M} \right)^{1/2}, & M \gtrsim 10^{11} \text{ GeV} \end{cases} \quad (8)$$

Accelerating these monopoles drains energy from the magnetic field. Parker [12] obtained an upper bound on the flux of monopoles in the galaxy by requiring that the rate of this energy loss be small compared to the time scale on which the galactic field can be regenerated. With reasonable choices for the astrophysical parameters (see Ref. 13 for details), this Parker bound is

$$F < \begin{cases} 10^{-15} \text{ cm}^{-2} \text{ sr}^{-1} \text{ sec}^{-1}, & M \lesssim 10^{17} \text{ GeV} \\ 10^{-15} \left( \frac{M}{10^{17} \text{ GeV}} \right) \text{ cm}^{-2} \text{ sr}^{-1} \text{ sec}^{-1}, & M \gtrsim 10^{17} \text{ GeV} \end{cases} \quad (9)$$

Applying similar arguments to an earlier seed field that was the progenitor of the current galactic field leads to a tighter bound [14],

$$F < \left[ \frac{M}{10^{17} \text{ GeV}} + (3 \times 10^{-6}) \right] 10^{-16} \text{ cm}^{-2} \text{ sr}^{-1} \text{ sec}^{-1}. \quad (10)$$

Considering magnetic fields in galactic clusters gives a bound [15] which, although less secure, is about three orders of magnitude lower than the Parker bound.

A flux bound can also be inferred from the total mass of monopoles in the universe. If the monopole mass density is a fraction  $\Omega_M$  of the critical density, and the monopoles were uniformly distributed throughout the universe, there would be a monopole flux

$$F_{\text{uniform}} = 1.3 \times 10^{-16} \Omega_M \left( \frac{10^{17} \text{ GeV}}{M} \right) \left( \frac{v}{10^{-3}c} \right) \text{ cm}^{-2} \text{ sr}^{-1} \text{ sec}^{-1}. \quad (11)$$

If we assume that  $\Omega_M \sim 0.1$ , this gives a stronger constraint than the Parker bound for  $M \sim 10^{15}$  GeV. However, monopoles with masses  $\sim 10^{17}$  GeV are not ejected by the galactic field and can be gravitationally bound to the galaxy. In this case their flux within the galaxy is increased by about five orders of magnitude for a given value of  $\Omega_M$ , and the mass density bound only becomes stronger than the Parker bound for  $M \sim 10^{18}$  GeV.

A much more stringent flux bound applies to GUT monopoles that catalyze baryon number violation. The essential idea is that compact astrophysical objects would capture monopoles at a rate proportional to the galactic flux. These monopoles would then catalyze proton decay, with the energy released in the decay leading to an observable increase in the luminosity of the object. A variety of bounds, based on neutron stars [16–20], white dwarfs [21], and Jovian planets [22] have been obtained. These depend in the obvious manner on the catalysis cross section, but also on the details of the astrophysical scenarios; *e.g.*, on how much the accumulated density is reduced by monopole-antimonopole annihilation, and

on whether monopoles accumulated in the progenitor star survive its collapse to a white dwarf or neutron star. The bounds obtained in this manner lie in the range

$$F\left(\frac{\sigma_{\Delta B}\beta}{10^{-27}\text{cm}^2}\right) \sim (10^{-18} - 10^{-29})\text{cm}^{-2}\text{sr}^{-1}\text{sec}^{-1}. \quad (12)$$

It is important to remember that not all GUT monopoles catalyze baryon number nonconservation. In particular, the intermediate mass monopoles that arise in some GUTs at later stages of symmetry-breaking are examples of theoretically motivated monopoles that are exempt from the bound of Eq. (12).

**Searches for Magnetic Monopoles:** To date there have been no confirmed observations of exotic particles possessing magnetic charge. Precision measurements of the properties of known particles have led to tight limits on the values of magnetic charge they may possess. Using the induction method (see below), the electron's magnetic charge has been found to be  $Q_e^m < 10^{-24}Q_M^D$  [23] (where  $Q_M^D$  is the Dirac charge). Furthermore, measurements of the anomalous magnetic moment of the muon have been used to place a model dependent lower limit of 120 GeV on the monopole mass <sup>1</sup> [24]. Nevertheless, guided mainly by Dirac's argument and the predicted existence of monopoles from spontaneous symmetry breaking mechanisms, searches have been routinely made for monopoles produced at accelerators, in cosmic rays, and bound in matter [25]. Although the resultant limits from such searches are usually made under the assumption of a particle possessing only magnetic charge, most of the searches are also sensitive to dyons.

**Search Techniques:** Search strategies are determined by the expected interactions of monopoles as they pass through matter. These would give rise to a number of striking characteristic signatures. Since a complete description of monopole search techniques falls outside of the scope of this minireview, only the most common methods are described below. More comprehensive descriptions of search techniques can be found in Refs. [26,27].

The induction method exploits the long-ranged electromagnetic interaction of the monopole with the quantum state of a superconducting ring which would lead to a monopole which passes through such a ring inducing a permanent current. The induction technique typically uses Superconducting Quantum Interference Devices (SQUID) technology for detection and is employed for searches for monopoles in cosmic rays and matter. Another approach is to exploit the electromagnetic energy loss of monopoles. Monopoles with Dirac charge would typically lose energy at a rate which is several thousand times larger than that expected from particles possessing the elementary electric charge. Consequently, scintillators, gas chambers and nuclear track detectors (NTDs) have been used in cosmic ray and collider experiments. A further approach, which has

been used at colliders, is to search for particles describing a non-helical path in a uniform magnetic field.

**Searches for Monopoles Bound in Matter:** Monopoles have been sought in a range of bulk materials which it is assumed would have absorbed incident cosmic ray monopoles over a long exposure time of order million years. Materials which have been studied include moon rock, meteorites, manganese modules, and sea water [28]. A stringent upper limit on the monopoles per nucleon ratio of  $\sim 10^{-29}$  has been obtained [28].

**Searches in Cosmic Rays:** Direct searches for monopoles in cosmic rays refer to those experiments in which the passage of the monopole is measured by an active detector. Catalysis processes in which GUT monopoles could induce nucleon decay are discussed in the next section. To interpret the results of the non-catalysis searches, the cross section for the catalysis process is typically either set to zero [29] or assigned a modest value (1mb) [30]. Searches which explicitly exploit the expected catalysed decays are discussed in the next section.

Although early cosmic ray searches using the induction technique [31] and NTDs [32] observed monopole candidates, none of these apparent observations have been confirmed. Recent experiments have typically employed large scale detectors. The MACRO experiment at the Gran Sasso underground laboratory comprised three different types of detector: liquid scintillator, limited stream tubes, and NTDs, which provided a total acceptance of  $\sim 10000\text{m}^2$  for an isotropic flux. As shown in Fig. 1, this experiment has so far provided the most extensive  $\beta$ -dependent flux limits for GUT monopoles with Dirac charge [30]. Also shown are limits from an experiment at the OHYA mine in Japan [29], which used a  $2000\text{m}^2$  array of NTDs.

In Fig. 1, upper flux limits are also shown as a function of mass for monopole speed  $\beta > 0.05$ . In addition to MACRO and OYHA flux limits, results from the SLIM [33] high-altitude experiment are shown. The SLIM experiment provided a good sensitivity to intermediate mass monopoles ( $10^5 \lesssim M \lesssim 10^{12}$  GeV). In addition to the results shown in Fig. 1, a limit of  $\sim 9 \times 10^{-16} \text{cm}^{-2}\text{s}^{-1}\text{sr}^{-1}$  was obtained for monopoles with  $\beta = 0.76$  by The AMANDA-II experiment [34]. This limit extends to  $\sim 4 \times 10^{-17} \text{cm}^{-2}\text{s}^{-1}\text{sr}^{-1}$  for  $\beta \sim 1$ . The most stringent constraints on the flux of ultra-relativistic monopoles have been obtained by the RICE [35] and ANITA-II experiments [36] at the South Pole which were sensitive to monopoles with  $\gamma$  values of  $10^7 \lesssim \gamma \lesssim 10^{12}$  and  $10^9 \lesssim \gamma \lesssim 10^{13}$ , respectively, and which produced flux limits as low as  $10^{-19} \text{cm}^{-2}\text{s}^{-1}\text{sr}^{-1}$ . In addition to the aforementioned flux limits for monopoles with the Dirac charge, the OHYA experiment also presented limits for monopoles with charges up to  $3Q_M^D$ , as did the the SLIM experiment.

<sup>1</sup> Where no ambiguity is likely to arise, a reference to a monopole implies a particle possessing Dirac charge.

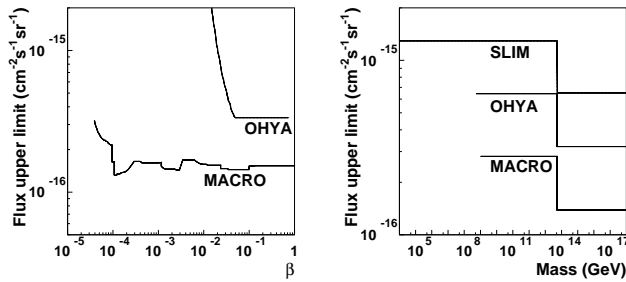


**Figure 1:** Upper flux limits for (a) GUT monopoles as a function of  $\beta$  (b) Monopoles as a function of mass for  $\beta > 0.05$ .

**Searches via the Catalysis of Nucleon-Decay:** Searches have also been performed for evidence of the catalysed decay of a nucleon, as predicted by the Callan-Rubakov mechanism. Searches have been made at a range of experiments which are sensitive to the induced nucleon decay of a passing monopole. For example, searches have been made with the Soudan [37] and Macro [38] experiments, using tracking detectors. Searches at Kamiokande [39], IMB [40] and the underwater Lake Baikal experiment [41] which exploit the Cerenkov effect have also been made. The resulting  $\beta$ -dependent flux limits from these experiments, which typically vary between  $6 \times 10^{-17} - 9 \times 10^{-14} \text{cm}^{-2}\text{sr}^{-1}\text{s}^{-1}$  [25], are sensitive to the assumed values of the catalysis cross sections.

**Searches at Colliders:** Searches have been performed at hadron-hadron, electron-positron and lepton-hadron experiments. Collider searches can be broadly classed as being direct or indirect. In a direct search, evidence of the passage of a monopole through material, such as a charged particle track, is sought. In indirect searches, virtual monopole processes are assumed to influence the production rates of certain final states.

**Direct Searches at Colliders:** Collider experiments typically express their results in terms of upper limits on a production cross section and/or monopole mass. To calculate these limits, ansatzes are used to model the kinematics of monopole-antimonopole pair production processes since perturbative field theory cannot be used to calculate the rate and kinematic properties of produced monopoles. Limits therefore suffer from a degree of model-dependence, implying that a comparison between the results of different experiments can be problematic, in particular when this concerns excluded mass regions. A conservative approach with as little model-dependence as possible is thus to present the upper cross-section limits as a function of one half the centre-of-mass energy of the collisions, as shown in Fig. 2 for recent results from high energy colliders.

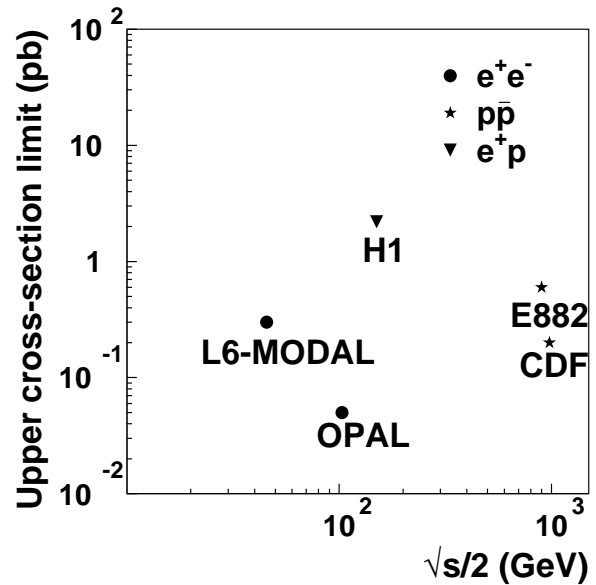


**Figure 2:** Upper limits on the production cross sections of monopoles from various collider-based experiments.

Searches for monopoles produced at the highest available energies in hadron-hadron collisions were made at the Tevatron by the CDF [42] and E882 [43] experiments. Complementary approaches were used; the CDF experiment used a dedicated time-of-flight system whereas the E882 experiment employed the induction technique to search for stopped monopoles in discarded detector material which had been part of the CDF and D0 detectors using periods of luminosity. Considered together, the searches provide a sensitivity to monopoles with charges between  $Q_M^D$  and  $6Q_M^D$  and masses up to around 900 GeV. Earlier searches at the Tevatron, such as Ref. 44, used NTDs and were based on comparatively modest amounts of integrated luminosity. Lower energy hadron-hadron experiments have employed a variety of search techniques including plastic track detectors [45] and searches for trapped monopoles [46].

The only LEP-2 search was made by OPAL [47] which quoted cross section limits for the production of monopoles possessing masses up to around 103 GeV. At LEP-1, searches were made with NTDs deployed around an interaction region. This allowed a range of charges to be sought for masses up to  $\sim 45$  GeV. The L6-MODAL experiment [48] gave limits for monopoles with charges in the range  $0.9Q_M^D$  and  $3.6Q_M^D$ , whilst an earlier search by the MODAL experiment was sensitive to monopoles with charges as low as  $0.1Q_M^D$  [49]. The deployment of NTDs around the beam interaction point was also used at earlier  $e^+e^-$  colliders such as KEK [50] and PETRA [51]. Searches at  $e^+e^-$  facilities have also been made for particles following non-helical trajectories [52,53].

There has so far been one search for monopole production in lepton-hadron scattering. Using the induction method,

monopoles were sought which could have stopped in the aluminium beampipe which had been used by the H1 experiment at HERA [54]. Cross section limits were set for monopoles with charges in the range  $Q_M^D - 6Q_M^D$  for masses up to around 140 GeV.

**Indirect Searches at Colliders:** It has been proposed that virtual monopoles can mediate processes which give rise to multi-photon final-states [55,56]. Photon-based searches were made by the D0 [57] and L3 [58] experiments. The D0 work led to spin-dependent lower mass limits of between 610 and 1580 GeV, while L3 reported a lower mass limit of 510 GeV. However, it should be stressed that uncertainties on the theoretical calculations which were used to derive these limits are difficult to estimate.

### References

1. P.A.M.Dirac, Proc. Roy. Soc. Lond. **A133**, 60 (1931).
2. F. Englert and P. Windey, Phys. Rev. **D14**, 2728 (1976).
3. P. Goddard, J. Nuyts, and D. I. Olive, Nucl. Phys. **B125**, 1 (1977).
4. G.'t Hooft, Nucl. Phys. **B79**, 276 (1974).
5. A.M. Polyakov, JETP Lett. **20**, 194 (1974) [Pisma Zh. Eksp. Teor. Fiz. **20**, 430 (1974)].
6. C.P. Dokos and T.N. Tomaras, Phys. Rev. **D21**, 2940 (1980).
7. G. Lazarides and Q. Shafi, Phys. Lett. **B94**, 149 (1980).
8. C.G. Callan, Phys. Rev. **D26**, 2058 (1982).
9. V.A. Rubakov, Nucl. Phys. **B203**, 311 (1982).
10. T.W.B. Kibble, J. Phys. **A9**, 1387 (1976).
11. J. Preskill, Phys. Rev. Lett. **43**, 1365 (1979).
12. E.N. Parker, Astrophys. J. **160**, 383 (1970).
13. M.S. Turner, E.N. Parker, and T.J. Bogdan, Phys. Rev. **D26**, 1296 (1982).
14. F.C. Adams *et al.*, Phys. Rev. Lett. **70**, 2511 (1993).
15. Y. Rephaeli and M.S. Turner, Phys. Lett. **B121**, 115 (1983).
16. E.W. Kolb, S.A. Colgate, and J.A. Harvey, Phys. Rev. Lett. **49**, 1373 (1982).
17. S. Dimopoulos, J. Preskill, and F. Wilczek, Phys. Lett. **B119**, 320 (1982).
18. K. Freese, M.S. Turner, and D.N. Schramm, Phys. Rev. Lett. **51**, 1625 (1983).
19. E.W. Kolb and M.S. Turner, Astrophys. J. **286**, 702 (1984).
20. J.A. Harvey, Nucl. Phys. **B236**, 255 (1984).
21. K. Freese and E. Krasteva, Phys. Rev. **D59**, 063007 (1999).
22. J. Arafune, M. Fukugita, and S. Yanagita, Phys. Rev. **D32**, 2586 (1985).
23. L.L. Vant-Hull, Phys. Rev. **173**, 1412 (1968).
24. S. Graf, A. Schaefer, and W. Greiner, Phys. Lett. **B262**, 463 (1991).
25. Review of Particle Physics 2012 (*this Review*), listing on *Searches for Magnetic Monopoles*.
26. G. Giacomelli and L. Patrizii, arXiv:hep-ex/0506014.
27. M. Fairbairn *et al.*, Phys. Rept. **438**, 1 (2007).
28. J.M. Kovalik and J.L. Kirschvink, Phys. Rev. **A33**, 1183 (1986) ; H. Jeon and M. J. Longo, Phys. Rev. Lett. **75**, 1443 (1995) [Erratum-ibid. **76**, 159 (1996)].
29. S. Orito *et al.*, Phys. Rev. Lett. **66**, 1951 (1991).
30. M. Ambrosio *et al.*, [MACRO Collab.], Eur. Phys. J. **C25**, 511 (2002).
31. B. Cabrera, Phys. Rev. Lett. **48**, 1378 (1982).
32. P.B. Price *et al.*, Phys. Rev. Lett. **35**, 487 (1975).
33. S. Balestra *et al.*, Eur. Phys. J. **C55**, 57 (2008).
34. R. Abbasi *et al.*, Eur. Phys. J. **C69**, 361-378 (2010).
35. D.P. Hogan *et al.*, Phys. Rev. **D78**, 075031 (2008).
36. M. Detrixhe *et al.*, Phys. Rev. **D83**, 023513 (2011).
37. J.E. Bartelt *et al.*, Phys. Rev. **D36**, 1990 (1987) [Erratum-ibid. **D40**, 1701 (1989)].
38. M. Ambrosio *et al.*, Eur. Phys. J. C **26**, 163 (2002).
39. T. Kajita *et al.*, J. Phys. Soc. Jpn. **54** (1985) 4065.
40. R. Becker-Szendy *et al.*, Phys. Rev. **D49**, 2169 (1994).
41. V. A. Balkanov *et al.*, Prog. Part. Nucl. Phys. **40**, 391 (1998).
42. A. Abulencia *et al.*, [CDF Collab.], Phys. Rev. Lett. **96**, 201801 (2006).
43. G.R. Kalbfleisch *et al.*, Phys. Rev. **D69**, 052002 (2004).
44. P.B. Price, G.X. Ren, and K. Kinoshita, Phys. Rev. Lett. **59**, 2523 (1987).
45. B. Aubert *et al.*, Phys. Lett. **B120**, 465 (1983).
46. R.A. Carrigan, F.A. Nezrick, and B.P. Strauss, Phys. Rev. **D8**, 3717 (1973).
47. G. Abbiendi *et al.*, [OPAL Collab.], Phys. Lett. **B663**, 37 (2008).
48. J.L. Pinfold *et al.*, Phys. Lett. **B316**, 407 (1993).
49. K. Kinoshita *et al.*, Phys. Rev. **D46**, 881 (1992).
50. K. Kinoshita *et al.*, Phys. Lett. **B228**, 543 (1989).
51. P. Musset *et al.*, Phys. Lett. **B128**, 333 (1983).
52. T. Gentile *et al.*, [Cleo Collab.], Phys. Rev. **D35**, 1081 (1987).
53. W. Braunschweig *et al.*, [TASSO Collab.], Z. Phys. **C38**, 543 (1988).
54. A. Aktas *et al.*, [H1 Collab.], Eur. Phys. J. **C41**, 133 (2005).
55. A. De Rujula, Nucl. Phys. **B435**, 257 (1995).
56. I.F. Ginzburg and A. Schiller, Phys. Rev. **D60**, 075016 (1999).
57. B. Abbott *et al.*, [D0 Collab.], Phys. Rev. Lett. **81**, 524 (1998).
58. M. Acciarri *et al.*, [L3 Collab.], Phys. Lett. **B345**, 609 (1995).

### Monopole Production Cross Section — Accelerator Searches

X-SECT (cm <sup>2</sup> )	MASS (GeV)	CHG (g)	ENERGY (GeV)	BEAM	DOCUMENT ID	TECN
<5E-38	45-102	1	206	e <sup>+</sup> e <sup>-</sup>	1 ABBIENDI	08 OPAL
<0.2E-36	200-700	1	1960	p $\bar{p}$	2 ABULENCIA	06K CNTR
< 2.E-36		1	300	e <sup>+</sup> p	3,4 AKTAS	05A INDU
< 0.2 E-36		2	300	e <sup>+</sup> p	3,4 AKTAS	05A INDU
< 0.09E-36		3	300	e <sup>+</sup> p	3,4 AKTAS	05A INDU
< 0.05E-36		≥ 6	300	e <sup>+</sup> p	3,4 AKTAS	05A INDU
< 2.E-36		1	300	e <sup>+</sup> p	3,5 AKTAS	05A INDU
< 0.2E-36		2	300	e <sup>+</sup> p	3,5 AKTAS	05A INDU
< 0.07E-36		3	300	e <sup>+</sup> p	3,5 AKTAS	05A INDU
< 0.06E-36		≥ 6	300	e <sup>+</sup> p	3,5 AKTAS	05A INDU
< 0.6E-36	>265	1	1800	p $\bar{p}$	6 KALBFLEISCH	04 INDU
< 0.2E-36	>355	2	1800	p $\bar{p}$	6 KALBFLEISCH	04 INDU
< 0.07E-36	>410	3	1800	p $\bar{p}$	6 KALBFLEISCH	04 INDU





See key on page 457

Searches Particle Listings
Magnetic Monopole Searches

- 20 AMBROSIO 02c limit for catalysis of nucleon decay with catalysis cross section of ≈ 1 mb. The flux limit increases by ~ 3 at the higher β limit, and increases to 1 × 10−14 cm−2 sr−1 s−1 if the catalysis cross section is 0.01 mb. Based upon 71193 hr of data with the streamer detector, with an acceptance of 4250 m2 sr.
21 AMBROSIO 02d result for "more than two years of data." Ionization search using several subsystems. Limit curve as a function of β not given. Included in AMBROSIO 02b.
22 AMBROSIO 97 global MACRO 90%CL is 0.78 × 10−15 at β=1.1 × 10−4, goes through a minimum at 0.61 × 10−15 near β=(1.1-2.7) × 10−3, then rises to 0.84 × 10−15 at β=0.1. The global limit in this region is below the Parker bound at 10−15. Less stringent limits are established for 4 × 10−5 < β < 1 × 10−4. Limits set by various triggers and different subdetectors are given in the paper. All limits assume a catalysis cross section smaller than a few mb.
23 AHLEN 94 limit for dyons extends down to β=0.9E−4 and a limit of 1.3E−14 extends to β = 0.8E−4. Also see comment by PRICE 94 and reply of BARISH 94. One loophole in the AHLEN 94 result is that in the case of monopoles catalyzing nucleon decay, relativistic particles could veto the events. See AMBROSIO 97 for additional results.
24 Catalysis of nucleon decay; sensitive to assumed catalysis cross section.
25 ORITO 91 limits are functions of velocity. Lowest limits are given here.
26 Used DKMPR mechanism and Penning effect.
27 Assumes monopole attaches fermion nucleus.
28 Limit from combining data of CAPLIN 86, BERMON 85, INCANDELA 84, and CABRERA 83. For a discussion of controversy about CAPLIN 86 observed event, see GUY 87. Also see SCHOUTEN 87.
29 Based on lack of high-energy solar neutrinos from catalysis in the sun.
30 Anomalous long-range α (4He) tracks.
31 CABRERA 82 candidate event has single Dirac charge within ±5%.
32 ALVAREZ 75, FLEISCHER 75, and FRIEDLANDER 75 explain as fragmenting nucleus. EBERHARD 75 and ROSS 76 discuss conflict with other experiments. HAGSTROM 77 reinterprets as antinucleus. PRICE 78 reassesses.

Monopole Flux — Astrophysics

Table with columns: FLUX (cm−2sr−1s−1), MASS (GeV), CHG (g), COMMENTS (β = v/c), EVTS, DOCUMENT ID, TECN. Rows include faint white dwarf, galactic field, Jovian planets, solar trapping, neutron stars, pulsars, intergalactic field, neutron stars, galactic halo, galactic field.

Monopole Density — Matter Searches

Table with columns: DENSITY, CHG (g), MATERIAL, EVTS, DOCUMENT ID, TECN. Rows include Meteorites and other, Fe ore, deep schist, manganese nodules, seawater, iron aerosols, air, seawater, 11 materials, moon rock, seawater, manganese nodules, manganese, magnetite, meteor, meteorite.

Monopole Density — Astrophysics

Table with columns: DENSITY, CHG (g), MATERIAL, EVTS, DOCUMENT ID, TECN. Rows include sun, catalysis, moon wake, earth heat, 42cm absorption, moon wake.

REFERENCES FOR Magnetic Monopole Searches

DETRIXHE 11 PR D83 023513 M. Detrixhe et al. (ANITA Collab.)
ABBASI 10A EPJ C69 361 R. Abbasi et al. (IceCube Collab.)
ABBIENDI 08 PL B663 37 G. Abbiendi et al. (OPAL Collab.)
BALESTRA 08 EPJ C55 57 S. Balestra et al. (SLIM Collab.)
HOGAN 08 PR D78 075031 D.P. Hogan et al. (KANS, NEBR, DELA)
ABULENCIA 06K PRL 96 201801 A. Abulencia et al. (CDF Collab.)
AKTAS 05A EPJ C41 133 A. Aktas et al. (H1 Collab.)
KALBFLEISCH 04 PR D69 052002 G.R. Kalbfleisch et al. (OKLA)
AMBROSIO 02B EPJ C25 511 M. Ambrosio et al. (MACRO Collab.)
AMBROSIO 02C EPJ C26 163 M. Ambrosio et al. (MACRO Collab.)
AMBROSIO 02D ASP 18 27 M. Ambrosio et al. (MACRO Collab.)
KALBFLEISCH 00 PRL 85 5292 G.R. Kalbfleisch et al.
FREESE 99 PR D59 063007 K. Freese, E. Kravtseva
ABBOTT 88 PRL 61 524 B. Abbott et al. (D0 Collab.)
AMBROSIO 97 PL B406 249 M. Ambrosio et al. (MACRO Collab.)
HE 97 PRL 79 3134 Y.D. He (UCB)
ACCIARRI 95C PRL B345 609 M. Acciarrri et al. (L3 Collab.)
JEON 90 PRL 75 1443 H. Jeon, M.J. Longo (MICH)
Also PRL 76 159 (erratum) H. Jeon, M.J. Longo
AHLEN 94 PRL 72 608 S.P. Ahlen et al. (MACRO Collab.)
BARISH 94 PRL 73 1306 B.C. Barish, G. Giacomelli, J.T. Hong (CIT+)
BECKER-SZ... 94 PR D49 2149 R.A. Becker-Szendy et al. (IMB Collab.)
PRICE 94 PRL 73 1305 P.B. Price (PUB)
ADAMS 93 PRL 70 2511 F.C. Adams et al. (MICH, FNAL)
PINFOLD 93 PL B316 407 J.L. Pinfold et al. (ALBE, HARV, MONT+)
KINOSHITA 92 PR D46 R881 K. Kinoshita et al. (HARV, BGN, REHO)
THRON 92 PR D46 4846 J.L. Thron et al. (SOUDAN-2 Collab.)
GARDNER 91 PR D44 622 R.D. Gardner et al. (STAN)
HUBER 91 PR D44 636 M.E. Huber et al. (STAN)
ORITO 91 PRL 66 1951 S. Orto et al. (ICEPP, WASCR, NIHO, ICRR)
BERMON 90 PRL 64 839 S. Bermon et al. (IBM, BNL)
BERTANI 90 EPL 12 613 M. Bertani et al. (BGN, INFN)
BEZRUKOV 90 SJNP 52 54 L.B. Bezrukov et al. (INRM)
Translated from YAF 52 86
BUCKLAND 90 PR D41 2726 K.N. Buckland et al. (UCSD)
GHOSH 90 EPL 12 25 D.C. Ghosh, S. Chatterjea (JADA)
HUBER 90 PRL 64 835 M.E. Huber et al. (STAN)
PRICE 90 PRL 65 149 P.B. Price, J. Guiru, K. Kinoshita (UCB, HARV)
KINOSHITA BRAUNSC... 88B ZPHY C38 543 K. Kinoshita et al. (HARV, TISA, KEK+)
KINOSHITA 88 PRL 60 1610 R. Braunschweig et al. (TASSO Collab.)
BARISH 87 PR D36 2641 K. Kinoshita et al. (HARV, TISA, KEK+)
BARTLETT 87 PR D36 1990 J.E. Bartlett et al. (Soudan Collab.)
Also PR D40 1701 (erratum) J.E. Bartlett et al. (Soudan Collab.)
EBISU 87 PR D36 3359 T. Ebisu, T. Watanabe (KOBE)
Also JPG 11 883 T. Ebisu, T. Watanabe (KOBE)
GENTILE 87 PR D35 1081 T. Gentile et al. (CLEO Collab.)
GUY 87 NAT 325 463 J. Guy (LOIC)
MASEK 87 PR D35 2758 G.E. Masek et al. (UCSD)
NAKAMURA 87 PL B183 395 S. Nakamura et al. (INUS, WASCR, NIHO)
PRICE 87 PRL 59 2523 P.B. Price, R. Guoxiao, K. Kinoshita (UCB, HARV)
SCHOUTEN 87 JPE 20 850 J.C. Schouten et al. (LOIC)
SHEPKO 87 PR D35 2917 M.J. Shepko et al. (TAMU)
TSUKAMOTO 87 EPL 3 39 T. Tsukamoto et al. (ICRR)
CAPLIN 86 NAT 321 402 A.D. Caplin et al. (LOIC)
Also JPE 20 850 J.C. Schouten et al. (LOIC)
Also NAT 325 463 J. Guy (LOIC)
CROMAR 86 PRL 56 2561 M.W. Cromar, A.F. Clark, F.R. Fickett (NBSB)
HARA 86 PRL 56 553 T. Hara et al. (ICRR, KYOT, KEK, KOBE+)
INCANDELA 86 PR D34 2637 J. Incandela et al. (CHIC, FNAL, MICH)
KOVALIK 86 PR A33 1183 J.M. Kovalik, J.L. Kirschvink (CIT)
PRICE 86 PRL 56 1226 P.B. Price, M.H. Salamon (UCB)
ARAFUNE 85 PR D32 2586 J. Arafune, M. Fukugita, S. Yanagita (ICRR, KYOTU+)
BERMON 85 PRL 55 3050 S. Bermon et al. (IBM)
BRACCI 85B NP D58 726 L. Bracci, G. Fiorentini, G. Mezzorani (PISA+)
Also LNC 42 123 L. Bracci, G. Fiorentini (PISA)
CAPLIN 85 NAT 317 234 A.D. Caplin et al. (LOIC)
EBISU 85 JPG 11 883 T. Ebisu, T. Watanabe (KOBE)
KAJITA 85 JPSJ 54 4065 T. Kajita et al. (ICRR, KEK, NIIG)
PARK 85B NP B252 261 H.S. Park et al. (IMB Collab.)
BATTISTONI 84 PL 133B 454 G. Battistoni et al. (NUSEX Collab.)
FRYBERGER 84 PR D29 1524 D. Fryberger et al. (SLAC, UCB)
HARVEY 84 NP B236 295 J.A. Harvey (PRIN)
INCANDELA 84 PRL 53 2067 J. Incandela et al. (CHIC, FNAL, MICH)
KAJINO 84 PRL 52 1373 F. Kajino et al. (ICRR)
KAWAGOE 84 JKG 10 447 K. Kawagoe et al. (ICRR)
KAWAGOE 84 LNC 41 315 K. Kawagoe et al. (TOKY)
KOLB 84 APJ 286 702 E.W. Kolb, M.S. Turner (FNAL, CHIC)
KRISHNA... 84 PL 142B 99 M.R. Krishnaswamy et al. (TATA, OSKC+)
LISS 84 PR D30 884 T.M. Liss, S.P. Ahlen, G. Tarle (UCB, IND+)
PRICE 84 PRL 52 1265 P.B. Price et al. (ROMA, UCB, IND+)
PRICE 84B PL 140B 112 P.B. Price (CERN)
TARLE 84 PRL 52 90 G. Tarle, S.P. Ahlen, T.M. Liss (UCB, MICH+)
ANDERSON 83 PR D28 2308 S.N. Anderson et al. (WASH)
ARAFUNE 83 PL 133B 380 J. Arafune, M. Fukugita (ICRR, KYOTU)
AUBERT 83B PL 120B 465 L. Aubert et al. (CERN, LAPP)
BARTLETT 83B PRL 50 655 J.E. Bartlett et al. (MINN, ANL)
BARWICK 83 PR D28 2338 S.W. Barwick, K. Kinoshita, P.B. Price (UCB)
BONARELLI 83 PL 126B 137 R. Bonarelli, P. Capiluppi, I. d'Antone (BGN)
BOSETTI 83 PL 133B 265 P.C. Bosetti et al. (AACH3, HAWA, TOKY)
CABRERA 83 PRL 51 1933 B. Cabrera et al. (STAN)
DOKE 83 PL 129B 370 T. Doke et al. (WASU, RIKK, TTAM, RIKEN)
ERREDE 83 PRL 51 245 S.M. Errede et al. (IMB Collab.)
FREESE 83B PRL 51 1625 K. Freese, M.S. Turner, D.N. Schramm (CHIC)
GROOM 83 PRL 50 573 D.E. Groom et al. (UTAH, STAN)
MASHIMO 83 PL 128B 327 T. Mashimo et al. (ICEPP)
MIKHAILOV 83 PL 130B 331 V.F. Mikhailov (KAZA)
MUSSET 83 PL 129B 333 P. Musset, M. Price, E. Lohrmann (CERN, HAMB)
REPHELII 83 PL 121B 115 Y. Rephelli, M.S. Turner (CHIC)
SCHATTEN 83 PR D27 1525 K.H. Schatten (CHIC)
ALEXEYEV 82 LNC 35 413 E.N. Alekseev et al. (INRM)
BONARELLI 82 PL 112B 100 R. Bonarelli et al. (BGN)
CABRERA 82 PRL 48 1378 B. Cabrera (STAN)
DELL 82 NP B209 45 G.F. Dell et al. (BNL, ADEL, ROMA)
DIMOPOUL... 82 PL 119B 320 S. Dimopoulos, J. Preskill, F. Wilczek (HARV+)
KINOSHITA 82 PRL 48 77 K. Kinoshita, P.B. Price, D. Fryberger (UCB+)
KOLB 82 PRL 49 1373 E.W. Kolb, S.A. Colgate, J.A. Harvey (LASL, PRIN)
MASHIMO 82 JPSJ 51 3067 T. Mashimo, K. Kawagoe, M. Koshiba (INUS)
SALPETER 82 PRL 49 1114 E.E. Salpeter, S.I. Shapiro, I. Wasserman (COBN)
TURNER 82 PR D26 1296 M.S. Turner, E.W. Parker, T.J. Bogdan (CHIC)
BARTLETT 81 PR D24 612 D.F. Bartlett et al. (COLO, GESC)
KINOSHITA 81B PR D24 1707 K. Kinoshita, P.B. Price (UCB)
ULLMAN 81 PRL 47 289 J.D. Ullman (LEHM, BNL)
CARRIGAN 80 NAT 288 348 R.A. Carrigan (FNAL)
BRODERICK 79 PR D19 1046 J.J. Broderick et al. (VPI)
BARTLETT 78 PR D18 2253 D.F. Bartlett, D. Soo, M.G. White (COLO, PRIN)
CARRIGAN 78 PR D17 1754 R.A. Carrigan, B.P. Strauss, G. Giacomelli (FNAL+)
HOFFMANN 78 LNC 23 357 H. Hoffmann et al. (CERN, ROMA)
PRICE 78 PR D18 1382 P.B. Price et al. (UCB, HOU)

## Searches Particle Listings

## Magnetic Monopole Searches, Supersymmetric Particle Searches

HAGSTROM	77	PRL 38 729	R. Hagstrom	(LBL)
CARRIGAN	76	PR D13 1823	R.A. Carrigan, F.A. Nezrick, B.P. Strauss	(FNAL)
DELL	76	LCN 15 269	G.F. Dell et al.	(CERN, BNL, ROMA, ADEL)
ROSS	76	LBL-4665	R.R. Ross	(LBL)
STEVENS	76B	PR D14 2207	D.M. Stevens et al.	(VPI, BNL)
ZRELOV	76	CZJP B26 1306	V.P. Zrelov et al.	(JINR)
ALVAREZ	75	LBL-4260	L.W. Alvarez	(LBL)
BURKE	75	PL 60B 113	D.L. Burke et al.	(MICH)
CABRERA	75	Thesis	B. Cabrera	(STAN)
CARRIGAN	75	NP B91 279	R.A. Carrigan, F.A. Nezrick	(FNAL)
Also		PR D3 56	R.A. Carrigan, F.A. Nezrick	(FNAL)
EBERHARD	75	PR D11 3099	P.H. Eberhard et al.	(LBL, MPIM)
EBERHARD	75B	LBL-4289	P.H. Eberhard	(LBL)
FLEISCHER	75	PRL 35 1412	R.L. Fleischer, R.N.F. Walker	(GESC, WUSL)
FRIEDLANDER	75	PRL 35 1167	M.W. Friedlander	(WUSL)
GIACOMELLI	75	NC 28A 21	G. Giacomelli et al.	(BGNA, CERN, SAACL+)
PRICE	75	PRL 35 487	P.B. Price et al.	(UCB, HOUS)
CARRIGAN	74	PR D10 3867	R.A. Carrigan, F.A. Nezrick, B.P. Strauss	(FNAL)
CARRIGAN	73	PR D8 3717	R.A. Carrigan, F.A. Nezrick, B.P. Strauss	(FNAL)
ROSS	73	PR D9 698	R.R. Ross et al.	(LBL, SLAC)
Also		PR D4 3260	P.H. Eberhard et al.	(LBL, SLAC)
Also		SCI 167 701	L.W. Alvarez et al.	(LBL, SLAC)
BARTLETT	72	PR D6 1817	D.F. Bartlett, M.D. Lahana	(COLO)
GUREVICH	72	PL 38B 549	I.I. Gurevich et al.	(KIAE, NOVO, SERP)
Also		JETP 34 917	L.M. Barkov, I.I. Gurevich, M.S. Zolotarev	(KIAE+)
Also		Translated from ZETF 61 1721		
Also		PL 31B 394	I.I. Gurevich et al.	(KIAE, NOVO, SERP)
FLEISCHER	71	PR D4 24	R.L. Fleischer et al.	(GESC)
KOLM	71	PR D4 1285	H.H. Kolm, F. Villa, A. Odian	(MIT, SLAC)
PARKER	70	APJ 160 383	E.N. Parker	(CHIC)
SCHATTEN	70	PR D1 2245	K.H. Schatten	(NASA)
FLEISCHER	69	PR 177 2029	R.L. Fleischer et al.	(GESC, FSU)
FLEISCHER	69B	PR 184 1393	R.L. Fleischer et al.	(GESC, UNCS, GSCO)
FLEISCHER	69C	PR 184 1398	R.L. Fleischer, P.B. Price, R.T. Woods	(GESC)
Also		JAP 41 958	R.L. Fleischer et al.	(GESC)
CARTHERS	66	PR 149 1070	W.C.J. Carthers, R.J. Stefanski, R.K. Adair	(ROMA, UCSD, CERN)
AMALDI	63	NC 28 773	E. Amaldi et al.	(ROMA, MIT, BRAN)
GOTO	63	PR 132 387	E. Goto, H.H. Kolm, K.W. Ford	(TOKY, MIT, BRAN)
PETUKHOV	63	NP 49 87	V.A. Petukhov, M.M. Yakimenko	(LEBD)
PURCELL	63	PR 129 2326	E.M. Purcell et al.	(HARV, BNL)
FIDECARO	61	NC 22 657	M. Fidecaro, G. Finocchiaro, G. Giacomelli	(CERN)
BRADNER	59	PR 114 603	H. Bradner, W.M. Isbell	(LBL)
MALKUS	51	PR 83 899	W.V.R. Malkus	(CHIC)

## OTHER RELATED PAPERS

GROOM	86	PRPL 140 323	D.E. Groom	(UTAH)
Review				

## Supersymmetric Particle Searches

## SUPERSYMMETRY, PART I (THEORY)

Revised December 2011 by Howard E. Haber (UC Santa Cruz).

- I.1. Introduction
- I.2. Structure of the MSSM
  - I.2.1. R-parity and the lightest supersymmetric particle
  - I.2.2. The goldstino and gravitino
  - I.2.3. Hidden sectors and the structure of supersymmetry-breaking
  - I.2.4. Supersymmetry and extra dimensions
  - I.2.5. Split-supersymmetry
- I.3. Parameters of the MSSM
  - I.3.1. The supersymmetry-conserving parameters
  - I.3.2. The supersymmetry-breaking parameters
  - I.3.3. MSSM-124
- I.4. The supersymmetric-particle spectrum
  - I.4.1. The charginos and neutralinos
  - I.4.2. The squarks, sleptons and sneutrinos
- I.5. The Higgs sector of the MSSM
  - I.5.1. The tree-level MSSM Higgs sector
  - I.5.2. The radiatively-corrected MSSM Higgs sector
- I.6. Restricting the MSSM parameter freedom
  - I.6.1. Gaugino mass unification
  - I.6.2. The constrained MSSM: mSUGRA, CMSSM, ...
  - I.6.3. Gauge-mediated supersymmetry-breaking
  - I.6.4. The phenomenological MSSM
- I.7. Experimental data confronts the MSSM
  - I.7.1. Naturalness constraints and the little hierarchy
  - I.7.2. Constraints from virtual exchange of supersymmetric particles

## I.8. Massive neutrinos in low-energy supersymmetry

## I.8.1. The supersymmetric seesaw

## I.8.2. R-parity-violating supersymmetry

## I.9. Extensions beyond the MSSM

**I.1. Introduction:** Supersymmetry (SUSY) is a generalization of the space-time symmetries of quantum field theory that transforms fermions into bosons and vice versa. The existence of such a non-trivial extension of the Poincaré symmetry of ordinary quantum field theory was initially surprising, and its form is highly constrained by theoretical principles [1]. Supersymmetry also provides a framework for the unification of particle physics and gravity [2–5], which is governed by the Planck energy scale,  $M_P \approx 10^{19}$  GeV (where the gravitational interactions become comparable in magnitude to the gauge interactions). In particular, it is possible that supersymmetry will ultimately explain the origin of the large hierarchy of energy scales from the  $W$  and  $Z$  masses to the Planck scale [6–10]. This is the so-called *gauge hierarchy*. The stability of the gauge hierarchy in the presence of radiative quantum corrections is not possible to maintain in the Standard Model, but can be maintained in supersymmetric theories.

If supersymmetry were an exact symmetry of nature, then particles and their superpartners (which differ in spin by half a unit) would be degenerate in mass. Since superpartners have not (yet) been observed, supersymmetry must be a broken symmetry. Nevertheless, the stability of the gauge hierarchy can still be maintained if the supersymmetry breaking is *soft* [11,12], and the corresponding supersymmetry-breaking mass parameters are no larger than a few TeV. In particular, soft-supersymmetry-breaking terms of the Lagrangian are either linear, quadratic, or cubic in the fields, with some restrictions elucidated in Ref. 11. The impact of such terms becomes negligible at energy scales much larger than the size of the supersymmetry-breaking masses. The most interesting theories of this type are theories of “low-energy” (or “weak-scale”) supersymmetry, where the effective scale of supersymmetry breaking is tied to the scale of electroweak symmetry breaking [7–10]. The latter is characterized by the Standard Model Higgs vacuum expectation value,  $v \simeq 246$  GeV.

Although there are no unambiguous experimental results (at present) that require the existence of new physics at the TeV-scale, expectations of the latter are primarily based on three theoretical arguments. First, a *natural* explanation (*i.e.*, one that is stable with respect to quantum corrections) of the gauge hierarchy demands new physics at the TeV-scale [10]. Second, the unification of the three Standard Model gauge couplings at a very high energy close to the Planck scale is possible if new physics beyond the Standard Model (which modifies the running of the gauge couplings above the electroweak scale) is present. The minimal supersymmetric extension of the Standard Model, where supersymmetric masses lie below a few TeV, provides simple example of successful gauge coupling unification [13]. Third, the existence of dark matter, which

makes up approximately one quarter of the energy density of the universe, cannot be explained within the Standard Model of particle physics [14]. Remarkably, a stable weakly-interacting massive particle (WIMP) whose mass and interaction rate are governed by new physics associated with the TeV-scale can be consistent with the observed density of dark matter (this is the so-called *WIMP miracle*, which is reviewed in Ref. 15). The lightest supersymmetric particle is a promising (although not the unique) candidate for the dark matter [16,17]. Further aspects of dark matter can be found in Ref. 18.

**I.2. Structure of the MSSM:** The minimal supersymmetric extension of the Standard Model (MSSM) consists of taking the fields of the two-Higgs-doublet extension of the Standard Model and adding the corresponding supersymmetric partners [19,20]. The corresponding field content of the MSSM and their gauge quantum numbers are shown in Table 1. The electric charge  $Q = T_3 + \frac{1}{2}Y$  is determined in terms of the third component of the weak isospin ( $T_3$ ) and the U(1) hypercharge ( $Y$ ).

**Table 1:** The fields of the MSSM and their  $SU(3) \times SU(2) \times U(1)$  quantum numbers are listed. Only one generation of quarks and leptons is exhibited. For each lepton, quark, and Higgs super-multiplet, there is a corresponding anti-particle multiplet of charge-conjugated fermions and their associated scalar partners.

Field Content of the MSSM					
Super-Multiplets	Boson Fields	Fermionic Partners	SU(3)	SU(2)	U(1)
gluon/gluino	$g$	$\tilde{g}$	8	1	0
gauge/	$W^\pm, W^0$	$\tilde{W}^\pm, \tilde{W}^0$	1	3	0
gaugino	$B$	$\tilde{B}$	1	1	0
slepton/	$(\tilde{\nu}, \tilde{e}^-)_L$	$(\nu, e^-)_L$	1	2	-1
lepton	$\tilde{e}_R^-$	$e_R^-$	1	1	-2
squark/	$(\tilde{u}_L, \tilde{d}_L)$	$(u, d)_L$	3	2	1/3
quark	$\tilde{u}_R$	$u_R$	3	1	4/3
	$\tilde{d}_R$	$d_R$	3	1	-2/3
Higgs/	$(H_d^0, H_d^-)$	$(\tilde{H}_d^0, \tilde{H}_d^-)$	1	2	-1
higgsino	$(H_u^+, H_u^0)$	$(\tilde{H}_u^+, \tilde{H}_u^0)$	1	2	1

The gauge super-multiplets consist of the gluons and their *gluino* fermionic superpartners, and the  $SU(2) \times U(1)$  gauge bosons and their *gaugino* fermionic superpartners. The Higgs multiplets consist of two complex doublets of Higgs fields, their *higgsino* fermionic superpartners, and the corresponding antiparticle fields. The matter super-multiplets consist of three generations of left-handed and right-handed quarks and lepton fields, their scalar superpartners (squark and slepton fields), and the corresponding antiparticle fields. The enlarged Higgs sector of the MSSM constitutes the minimal structure needed to guarantee the cancellation of anomalies from the introduction of the higgsino superpartners. Moreover, without a second Higgs doublet, one cannot generate mass for both “up”-type and

“down”-type quarks (and charged leptons) in a way consistent with the supersymmetry [21–23].

A general supersymmetric Lagrangian is determined by three functions of the superfields (composed of the fields of the super-multiplets): the superpotential, the Kähler potential, and the gauge kinetic-energy function [5]. For *renormalizable* globally supersymmetric theories, minimal forms for the latter two functions are required in order to generate canonical kinetic energy terms for all the fields. A renormalizable superpotential, which is at most cubic in the superfields, yields supersymmetric Yukawa couplings and mass terms. A combination of gauge invariance and supersymmetry produces couplings of gaugino fields to matter (or Higgs) fields and their corresponding superpartners. The (renormalizable) MSSM Lagrangian is then constructed by including all possible supersymmetric interaction terms (of dimension four or less) that satisfy  $SU(3) \times SU(2) \times U(1)$  gauge invariance and  $B-L$  conservation (where  $B$  = baryon number and  $L$  = lepton number). Finally, the most general soft-supersymmetry-breaking terms are added [11,12,24]. To generate nonzero neutrino masses, extra structure is needed as discussed in Section I.8.

**I.2.1. R-parity and the lightest supersymmetric particle:** As a consequence of  $B-L$  invariance, the MSSM possesses a multiplicative R-parity invariance, where  $R = (-1)^{3(B-L)+2S}$  for a particle of spin  $S$  [25]. Note that this implies that all the ordinary Standard Model particles have even R parity, whereas the corresponding supersymmetric partners have odd R parity. The conservation of R parity in scattering and decay processes has a crucial impact on supersymmetric phenomenology. For example, starting from an initial state involving ordinary (R-even) particles, it follows that supersymmetric particles must be produced in pairs. In general, these particles are highly unstable and decay into lighter states. However, R-parity invariance also implies that the lightest supersymmetric particle (LSP) is absolutely stable, and must eventually be produced at the end of a decay chain initiated by the decay of a heavy unstable supersymmetric particle.

In order to be consistent with cosmological constraints, a stable LSP is almost certainly electrically and color neutral [26]. (There are some model circumstances in which a colored gluino LSP is allowed [27], but we do not consider this possibility further here.) Consequently, the LSP in an R-parity-conserving theory is weakly interacting with ordinary matter, *i.e.*, it behaves like a stable heavy neutrino and will escape collider detectors without being directly observed. Thus, the canonical signature for conventional R-parity-conserving supersymmetric theories is missing (transverse) energy, due to the escape of the LSP. Moreover, as noted at the end of Section I, the LSP is a promising candidate for dark matter [16,17].

**I.2.2. The goldstino and gravitino:** In the MSSM, supersymmetry breaking is accomplished by including the most general renormalizable soft-supersymmetry-breaking terms consistent with the  $SU(3) \times SU(2) \times U(1)$  gauge symmetry and R-parity invariance. These terms parameterize our ignorance of

## Searches Particle Listings

### Supersymmetric Particle Searches

the fundamental mechanism of supersymmetry breaking. If supersymmetry breaking occurs spontaneously, then a massless Goldstone fermion called the *goldstino* ( $\tilde{G}_{1/2}$ ) must exist. The goldstino would then be the LSP, and could play an important role in supersymmetric phenomenology [28].

However, the goldstino degrees of freedom are physical only in models of spontaneously-broken global supersymmetry. If supersymmetry is a local symmetry, then the theory must incorporate gravity; the resulting theory is called supergravity [29]. In models of spontaneously-broken supergravity, the goldstino is “absorbed” by the *gravitino* ( $\tilde{G}$ ) [sometimes called  $\tilde{g}_{3/2}$  in the older literature], the spin-3/2 superpartner of the graviton [30]. By this super-Higgs mechanism, the goldstino is removed from the physical spectrum and the gravitino acquires a mass ( $m_{3/2}$ ). In processes with center-of-mass energy  $E \gg m_{3/2}$ , the goldstino–gravitino equivalence theorem [31] states that the interactions of the helicity  $\pm\frac{1}{2}$  gravitino (whose properties approximate those of the goldstino) dominate those of the helicity  $\pm\frac{3}{2}$  gravitino. The interactions of gravitinos with other light fields can be described by a low-energy effective Lagrangian that is determined by fundamental principles (see, *e.g.*, Ref. 32).

**I.2.3. Hidden sectors and the structure of supersymmetry breaking [24]:** It is very difficult (perhaps impossible) to construct a realistic model of spontaneously-broken low-energy supersymmetry where the supersymmetry breaking arises solely as a consequence of the interactions of the particles of the MSSM. An alternative scheme posits a theory consisting of at least two distinct sectors: a *hidden* sector consisting of particles that are completely neutral with respect to the Standard Model gauge group, and a *visible* sector consisting of the particles of the MSSM. There are no renormalizable tree-level interactions between particles of the visible and hidden sectors. Supersymmetry breaking is assumed to originate in the hidden sector, and its effects are transmitted to the MSSM by some mechanism (often involving the mediation by particles that comprise an additional *messenger* sector). Two theoretical scenarios have been examined in detail: gravity-mediated and gauge-mediated supersymmetry breaking.

Supergravity models provide a natural mechanism for transmitting the supersymmetry breaking of the hidden sector to the particle spectrum of the MSSM. In models of *gravity-mediated* supersymmetry breaking, gravity is the messenger of supersymmetry breaking [33–35]. More precisely, supersymmetry breaking is mediated by effects of gravitational strength (suppressed by inverse powers of the Planck mass). In this scenario, the gravitino mass is of order the electroweak-symmetry-breaking scale, while its couplings are roughly gravitational in strength [2,36]. Such a gravitino typically plays no role in supersymmetric phenomenology at colliders (except perhaps indirectly in the case where the gravitino is the LSP [37]).

In *gauge-mediated* supersymmetry breaking, gauge forces transmit the supersymmetry breaking to the MSSM. A typical

structure of such models involves a hidden sector where supersymmetry is broken, a messenger sector consisting of particles (messengers) with  $SU(3) \times SU(2) \times U(1)$  quantum numbers, and the visible sector consisting of the fields of the MSSM [38–40]. The direct coupling of the messengers to the hidden sector generates a supersymmetry-breaking spectrum in the messenger sector. Finally, supersymmetry breaking is transmitted to the MSSM via the virtual exchange of the messengers. In models of *direct gauge mediation*, the supersymmetry-breaking sector includes fields that carry Standard Model quantum numbers, in which case no separate messenger sector is required [41].

The gravitino mass in models of gauge-mediated supersymmetry breaking is typically in the eV range (although in some cases it can be as large as a GeV), which implies that  $\tilde{G}$  is the LSP. In particular, the gravitino is a potential dark matter candidate (for a recent review and guide to the literature, see Ref. 17). The couplings of the helicity  $\pm\frac{1}{2}$  components of  $\tilde{G}$  to the particles of the MSSM (which approximate those of the goldstino, cf. Section I.2.3) are significantly stronger than gravitational strength and amenable to experimental collider analyses.

The concept of a hidden sector is more general than supersymmetry. *Hidden valley* models [42] posit the existence of a hidden sector of new particles and interactions that are very weakly coupled to particles of the Standard Model. The impact of a hidden valley on supersymmetric phenomenology at colliders can be significant if the LSP lies in the valley sector [43].

#### I.2.4. Supersymmetry and extra dimensions:

Approaches to supersymmetry breaking have also been developed in the context of theories in which the number of space dimensions is greater than three. In particular, a number of supersymmetry-breaking mechanisms have been proposed that are inherently extra-dimensional [44]. The size of the extra dimensions can be significantly larger than  $M_P^{-1}$ ; in some cases on the order of  $(\text{TeV})^{-1}$  or even larger [45,46].

For example, in one approach, the fields of the MSSM live on some brane (a lower-dimensional manifold embedded in a higher-dimensional spacetime), while the sector of the theory that breaks supersymmetry lives on a second-separated brane. Two examples of this approach are anomaly-mediated supersymmetry breaking of Ref. 47, and gaugino-mediated supersymmetry breaking of Ref. 48; in both cases supersymmetry breaking is transmitted through fields that live in the bulk (the higher-dimensional space between the two branes). This setup has some features in common with both gravity-mediated and gauge-mediated supersymmetry breaking (*e.g.*, a hidden and visible sector and messengers).

Alternatively, one can consider a higher-dimensional theory that is compactified to four spacetime dimensions. In this approach, supersymmetry is broken by boundary conditions on the compactified space that distinguish between fermions and bosons. This is the so-called Scherk-Schwarz mechanism [49]. The phenomenology of such models can be strikingly different

from that of the usual MSSM [50]. All these extra-dimensional ideas clearly deserve further investigation, although they will not be discussed further here.

**I.2.5. Split-supersymmetry:** If supersymmetry is not connected with the origin of the electroweak scale, string theory suggests that supersymmetry still plays a significant role in Planck-scale physics. However, it may still be possible that some remnant of the superparticle spectrum survives down to the TeV-scale or below. This is the idea of *split-supersymmetry* [51], in which supersymmetric scalar partners of the quarks and leptons are significantly heavier (perhaps by many orders of magnitude) than 1 TeV, whereas the fermionic partners of the gauge and Higgs bosons have masses on the order of 1 TeV or below (presumably protected by some chiral symmetry). With the exception of a single light neutral scalar whose properties are indistinguishable from those of the Standard Model Higgs boson, all other Higgs bosons are also taken to be very heavy.

The supersymmetry breaking required to produce such a scenario would destabilize the gauge hierarchy. In particular, split-supersymmetry cannot provide a natural explanation for the existence of the light Standard-Model-like Higgs boson, whose mass lies orders below the mass scale of the heavy scalars. Nevertheless, models of split-supersymmetry can account for the dark matter (which is assumed to be the LSP) and gauge coupling unification. Thus, there is some motivation for pursuing the phenomenology of such approaches [52]. One notable difference from the usual MSSM phenomenology is the existence of a long-lived gluino [53].

**I.3. Parameters of the MSSM:** The parameters of the MSSM are conveniently described by considering separately the supersymmetry-conserving sector and the supersymmetry-breaking sector. A careful discussion of the conventions used in defining the tree-level MSSM parameters can be found in Ref. 54. For simplicity, consider first the case of one generation of quarks, leptons, and their scalar superpartners.

**I.3.1. The supersymmetric-conserving parameters:**

The parameters of the supersymmetry-conserving sector consist of: (i) gauge couplings:  $g_s$ ,  $g$ , and  $g'$ , corresponding to the Standard Model gauge group  $SU(3) \times SU(2) \times U(1)$  respectively; (ii) a supersymmetry-conserving higgsino mass parameter  $\mu$ ; and (iii) Higgs-fermion Yukawa coupling constants:  $\lambda_u$ ,  $\lambda_d$ , and  $\lambda_e$  (corresponding to the coupling of one generation of left- and right-handed quarks and leptons, and their superpartners to the Higgs bosons and higgsinos). Because there is no right-handed neutrino (and its superpartner) in the MSSM as defined here, one cannot introduce a Yukawa coupling  $\lambda_\nu$ .

**I.3.2. The supersymmetric-breaking parameters:**

The supersymmetry-breaking sector contains the following set of parameters: (i) gaugino Majorana masses  $M_3$ ,  $M_2$ , and  $M_1$  associated with the  $SU(3)$ ,  $SU(2)$ , and  $U(1)$  subgroups of the Standard Model; (ii) five scalar squared-mass parameters for the squarks and sleptons,  $M_{\tilde{Q}}^2$ ,  $M_{\tilde{U}}^2$ ,  $M_{\tilde{D}}^2$ ,  $M_{\tilde{L}}^2$ , and  $M_{\tilde{E}}^2$

[corresponding to the five electroweak gauge multiplets, *i.e.*, superpartners of  $(u, d)_L$ ,  $u_L^c$ ,  $d_L^c$ ,  $(\nu, e^-)_L$ , and  $e_L^c$ , where the superscript  $c$  indicates a charge-conjugated fermion and flavor indices are suppressed]; and (iii) Higgs-squark-squark and Higgs-slepton-slepton trilinear interaction terms, with coefficients  $\lambda_u A_U$ ,  $\lambda_d A_D$ , and  $\lambda_e A_E$  (which define the so-called “ $A$ -parameters”). It is traditional to factor out the Yukawa couplings in the definition of the  $A$ -parameters (originally motivated by a simple class of gravity-mediated supersymmetry-breaking models [2,4]). If the  $A$ -parameters defined in this way are parametrically of the same order (or smaller) as compared to other supersymmetry-breaking mass parameters, then only the  $A$ -parameters of the third generation will be phenomenologically relevant. Finally, we add: (iv) three scalar squared-mass parameters—two of which ( $m_1^2$  and  $m_2^2$ ) contribute to the diagonal Higgs squared-masses, given by  $m_1^2 + |\mu|^2$  and  $m_2^2 + |\mu|^2$ , and a third which contributes to the off-diagonal Higgs squared-mass term,  $m_{12}^2 \equiv B\mu$  (which defines the “ $B$ -parameter”).

The breaking of the electroweak symmetry  $SU(2) \times U(1)$  to  $U(1)_{EM}$  is only possible after introducing the supersymmetry-breaking Higgs squared-mass parameters. Minimizing the resulting tree-level Higgs scalar potential, these three squared-mass parameters can be re-expressed in terms of the two Higgs vacuum expectation values,  $v_d$  and  $v_u$  (also called  $v_1$  and  $v_2$ , respectively, in the literature), and the CP-odd Higgs mass  $A^0$  (cf. Section I.5). Here,  $v_d$  [ $v_u$ ] is the vacuum expectation value of the neutral component of the Higgs field  $H_d$  [ $H_u$ ] that couples exclusively to down-type (up-type) quarks and leptons. Note that  $v_d^2 + v_u^2 = 4m_W^2/g^2 \simeq (246 \text{ GeV})^2$  is fixed by the  $W$  mass and the gauge coupling, whereas the ratio

$$\tan \beta = v_u/v_d \quad (1)$$

is a free parameter of the model. By convention, the phases of the Higgs field are chosen such that  $0 \leq \beta \leq \pi/2$ . Equivalently, the tree-level conditions for the scalar potential minimum relate the diagonal and off-diagonal Higgs squared-masses in terms of  $m_Z^2 = \frac{1}{4}(g^2 + g'^2)(v_d^2 + v_u^2)$ , the angle  $\beta$  and the CP-odd Higgs mass  $m_A$ :

$$\sin 2\beta = \frac{2m_{12}^2}{m_1^2 + m_2^2 + 2|\mu|^2} = \frac{2m_{12}^2}{m_A^2}, \quad (2)$$

$$\frac{1}{2}m_Z^2 = -|\mu|^2 + \frac{m_1^2 - m_2^2 \tan^2 \beta}{\tan^2 \beta - 1}. \quad (3)$$

Note that supersymmetry-breaking mass terms for the fermionic superpartners of scalar fields and non-holomorphic trilinear scalar interactions (*i.e.*, interactions that mix scalar fields and their complex conjugates) have not been included above in the soft-supersymmetry-breaking sector. These terms can potentially destabilize the gauge hierarchy [11] in models with a gauge-singlet superfield. The latter is not present in the MSSM; hence as noted in Ref. 12, these so-called non-standard soft-supersymmetry-breaking terms are benign. However, the coefficients of these terms (which have dimensions of mass)

# Searches Particle Listings

## Supersymmetric Particle Searches

are expected to be significantly suppressed compared to the TeV-scale in a fundamental theory of supersymmetry-breaking. Consequently, we follow the usual approach and omit these terms from further consideration.

**I.3.3. MSSM-124:** The total number of independent physical parameters that define the MSSM (in its most general form) is quite large, primarily due to the soft-supersymmetry-breaking sector. In particular, in the case of three generations of quarks, leptons, and their superpartners,  $M_Q^2$ ,  $M_U^2$ ,  $M_D^2$ ,  $M_L^2$ , and  $M_E^2$  are hermitian  $3 \times 3$  matrices, and  $A_U$ ,  $A_D$ , and  $A_E$  are complex  $3 \times 3$  matrices. In addition,  $M_1$ ,  $M_2$ ,  $M_3$ ,  $B$ , and  $\mu$  are, in general, complex. Finally, as in the Standard Model, the Higgs-fermion Yukawa couplings,  $\lambda_f$  ( $f = u, d$ , and  $e$ ), are complex  $3 \times 3$  matrices that are related to the quark and lepton mass matrices via:  $M_f = \lambda_f v_f / \sqrt{2}$ , where  $v_e \equiv v_d$  [with  $v_u$  and  $v_d$  as defined above Eq. (1)].

However, not all these parameters are physical. Some of the MSSM parameters can be eliminated by expressing interaction eigenstates in terms of the mass eigenstates, with an appropriate redefinition of the MSSM fields to remove unphysical degrees of freedom. The analysis of Ref. 55 shows that the MSSM possesses 124 independent parameters. Of these, 18 parameters correspond to Standard Model parameters (including the QCD vacuum angle  $\theta_{\text{QCD}}$ ), one corresponds to a Higgs sector parameter (the analogue of the Standard Model Higgs mass), and 105 are genuinely new parameters of the model. The latter include: five real parameters and three  $CP$ -violating phases in the gaugino/higgsino sector, 21 squark and slepton masses, 36 real mixing angles to define the squark and slepton mass eigenstates, and 40  $CP$ -violating phases that can appear in squark and slepton interactions. The most general  $R$ -parity-conserving minimal supersymmetric extension of the Standard Model (without additional theoretical assumptions) will be denoted henceforth as MSSM-124 [56].

**I.4. The supersymmetric-particle spectrum:** The supersymmetric particles (*sparticles*) differ in spin by half a unit from their Standard Model partners. The supersymmetric partners of the gauge and Higgs bosons are fermions, whose names are obtained by appending “ino” at the end of the corresponding Standard Model particle name. The gluino is the color-octet Majorana fermion partner of the gluon with mass  $M_{\tilde{g}} = |M_3|$ . The supersymmetric partners of the electroweak gauge and Higgs bosons (the gauginos and higgsinos) can mix. As a result, the physical states of definite mass are model-dependent linear combinations of the charged and neutral gauginos and higgsinos, called *charginos* and *neutralinos*, respectively. Like the gluino, the neutralinos are also Majorana fermions, which provide for some distinctive phenomenological signatures [57,58]. The supersymmetric partners of the quarks and leptons are spin-zero bosons: the *squarks*, charged *sleptons*, and *sneutrinos*, respectively. A complete set of Feynman rules for the sparticles of the MSSM can be found in Ref. 59. The MSSM Feynman rules also are implicitly contained in a number of

Feynman diagram and amplitude generation software packages (see *e.g.*, Refs. 60–62).

**I.4.1. The charginos and neutralinos:** The mixing of the charged gauginos ( $\tilde{W}^\pm$ ) and charged higgsinos ( $H_u^\pm$  and  $H_d^\pm$ ) is described (at tree-level) by a  $2 \times 2$  complex mass matrix [63–65]:

$$M_C \equiv \begin{pmatrix} M_2 & \frac{1}{\sqrt{2}} g v_u \\ \frac{1}{\sqrt{2}} g v_d & \mu \end{pmatrix}. \quad (4)$$

To determine the physical chargino states and their masses, one must perform a singular value decomposition [66,67] of the complex matrix  $M_C$ :

$$U^* M_C V^{-1} = \text{diag}(M_{\tilde{\chi}_1^\pm}, M_{\tilde{\chi}_2^\pm}), \quad (5)$$

where  $U$  and  $V$  are unitary matrices, and the right-hand side of Eq. (5) is the diagonal matrix of (non-negative) chargino masses. The physical chargino states are denoted by  $\tilde{\chi}_1^\pm$  and  $\tilde{\chi}_2^\pm$ . These are linear combinations of the charged gaugino and higgsino states determined by the matrix elements of  $U$  and  $V$  [63–65]. The chargino masses correspond to the *singular values* [66] of  $M_C$ , *i.e.*, the positive square roots of the eigenvalues of  $M_C^\dagger M_C$ :

$$M_{\tilde{\chi}_1^\pm, \tilde{\chi}_2^\pm}^2 = \frac{1}{2} \left\{ |\mu|^2 + |M_2|^2 + 2m_W^2 \mp \left[ (|\mu|^2 + |M_2|^2 + 2m_W^2)^2 - 4|\mu|^2|M_2|^2 - 4m_W^4 \sin^2 2\beta + 8m_W^2 \sin 2\beta \text{Re}(\mu M_2) \right]^{1/2} \right\}, \quad (6)$$

where the states are ordered such that  $M_{\tilde{\chi}_1^\pm} \leq M_{\tilde{\chi}_2^\pm}$ .

It is convenient to choose a convention where  $\tan \beta$  and  $M_2$  are real and positive. Note that the relative phase of  $M_2$  and  $\mu$  is meaningful. (If  $CP$ -violating effects are neglected, then  $\mu$  can be chosen real but may be either positive or negative.) The sign of  $\mu$  is convention-dependent; the reader is warned that both sign conventions appear in the literature. The sign convention for  $\mu$  in Eq. (4) is used by the LEP collaborations [68] in their plots of exclusion contours in the  $M_2$  vs.  $\mu$  plane derived from the non-observation of  $e^+e^- \rightarrow \tilde{\chi}_1^+ \tilde{\chi}_1^-$ .

The mixing of the neutral gauginos ( $\tilde{B}$  and  $\tilde{W}^0$ ) and neutral higgsinos ( $\tilde{H}_d^0$  and  $\tilde{H}_u^0$ ) is described (at tree-level) by a  $4 \times 4$  complex symmetric mass matrix [63,64,69,70]:

$$M_N \equiv \begin{pmatrix} M_1 & 0 & -\frac{1}{2} g' v_d & \frac{1}{2} g' v_u \\ 0 & M_2 & \frac{1}{2} g v_d & -\frac{1}{2} g v_u \\ -\frac{1}{2} g' v_d & \frac{1}{2} g v_d & 0 & -\mu \\ \frac{1}{2} g' v_u & -\frac{1}{2} g v_u & -\mu & 0 \end{pmatrix}. \quad (7)$$

To determine the physical neutralino states and their masses, one must perform a Takagi-diagonalization [66,67,71,72] of the complex symmetric matrix  $M_N$ :

$$W^T M_N W = \text{diag}(M_{\tilde{\chi}_1^0}, M_{\tilde{\chi}_2^0}, M_{\tilde{\chi}_3^0}, M_{\tilde{\chi}_4^0}), \quad (8)$$

where  $W$  is a unitary matrix and the right-hand side of Eq. (8) is the diagonal matrix of (non-negative) neutralino masses. The physical neutralino states are denoted by  $\tilde{\chi}_i^0$  ( $i = 1, \dots, 4$ ), where

the states are ordered such that  $M_{\tilde{\chi}_1^0} \leq M_{\tilde{\chi}_2^0} \leq M_{\tilde{\chi}_3^0} \leq M_{\tilde{\chi}_4^0}$ . The  $\tilde{\chi}_i^0$  are the linear combinations of the neutral gaugino and higgsino states determined by the matrix elements of  $W$  (in Ref. 63,  $W = N^{-1}$ ). The neutralino masses correspond to the singular values of  $M_N$  (i.e., the positive square roots of the eigenvalues of  $M_N^\dagger M_N$ ). Exact formulae for these masses can be found in Refs. [69] and [73]. A numerical algorithm for determining the mixing matrix  $W$  has been given by Ref. 74.

If a chargino or neutralino state approximates a particular gaugino or higgsino state, it is convenient to employ the corresponding nomenclature. Specifically, if  $M_1$  and  $M_2$  are small compared to  $m_Z$  and  $|\mu|$ , then the lightest neutralino  $\tilde{\chi}_1^0$  would be nearly a pure *photino*,  $\tilde{\gamma}$ , the supersymmetric partner of the photon. If  $M_1$  and  $m_Z$  are small compared to  $M_2$  and  $|\mu|$ , then the lightest neutralino would be nearly a pure *bin*o,  $\tilde{B}$ , the supersymmetric partner of the weak hypercharge gauge boson. If  $M_2$  and  $m_Z$  are small compared to  $M_1$  and  $|\mu|$ , then the lightest chargino pair and neutralino would constitute a triplet of roughly mass-degenerate pure *wino*s,  $\tilde{W}^\pm$ , and  $\tilde{W}_3^0$ , the supersymmetric partners of the weak SU(2) gauge bosons. Finally, if  $|\mu|$  and  $m_Z$  are small compared to  $M_1$  and  $M_2$ , then the lightest neutralino would be nearly a pure *higgsino*. Each of the above cases leads to a strikingly different phenomenology.

**I.4.2. The squarks, sleptons and sneutrinos:** For a given fermion  $f$ , there are two supersymmetric partners,  $\tilde{f}_L$  and  $\tilde{f}_R$ , which are scalar partners of the corresponding left- and right-handed fermion. (There is no  $\tilde{\nu}_R$  in the MSSM.) However, in general,  $\tilde{f}_L$  and  $\tilde{f}_R$  are not mass eigenstates, since there is  $\tilde{f}_L$ - $\tilde{f}_R$  mixing. For three generations of squarks, one must in general diagonalize  $6 \times 6$  matrices corresponding to the basis  $(\tilde{q}_{iL}, \tilde{q}_{iR})$ , where  $i = 1, 2, 3$  are the generation labels. For simplicity, only the one-generation case is illustrated in detail below. (The effects of second and third generation squark mixing can be significant and is treated in Ref. 75.)

Using the notation of the third family, the one-generation tree-level squark squared-mass matrix is given by [76]

$$M_F^2 = \begin{pmatrix} M_Q^2 + m_q^2 + L_q & m_q X_q^* \\ m_q X_q & M_R^2 + m_q^2 + R_q \end{pmatrix}, \quad (9)$$

where

$$X_q \equiv A_q - \mu^* (\cot \beta)^{2T_{3q}}, \quad (10)$$

and  $T_{3q} = \frac{1}{2} [-\frac{1}{2}]$  for  $q = t [b]$ . The diagonal squared masses are governed by soft-supersymmetry-breaking squared masses  $M_Q^2$  and  $M_R^2 \equiv M_U^2 [M_D^2]$  for  $q = t [b]$ , the corresponding quark masses  $m_t [m_b]$ , and electroweak correction terms:

$$L_q \equiv (T_{3q} - e_q \sin^2 \theta_W) m_Z^2 \cos 2\beta, \quad R_q \equiv e_q \sin^2 \theta_W m_Z^2 \cos 2\beta, \quad (11)$$

where  $e_q = \frac{2}{3} [-\frac{1}{3}]$  for  $q = t [b]$ . The off-diagonal squared squark masses are proportional to the corresponding quark masses and depend on  $\tan \beta$  [Eq. (1)], the soft-supersymmetry-breaking  $A$ -parameters and the higgsino mass parameter  $\mu$ . The signs of the  $A$  and  $\mu$  parameters are convention-dependent;

other choices appear frequently in the literature. Due to the appearance of the *quark* mass in the off-diagonal element of the squark squared-mass matrix, one expects the  $\tilde{q}_L$ - $\tilde{q}_R$  mixing to be small, with the possible exception of the third generation, where mixing can be enhanced by factors of  $m_t$  and  $m_b \tan \beta$ .

In the case of third generation  $\tilde{q}_L$ - $\tilde{q}_R$  mixing, the mass eigenstates (usually denoted by  $\tilde{q}_1$  and  $\tilde{q}_2$ , with  $m_{\tilde{q}_1} < m_{\tilde{q}_2}$ ) are determined by diagonalizing the  $2 \times 2$  matrix  $M_F^2$  given by Eq. (9). The corresponding squared masses and mixing angle are given by [76]:

$$m_{\tilde{q}_{1,2}}^2 = \frac{1}{2} \left[ \text{Tr} M_F^2 \mp \sqrt{(\text{Tr} M_F^2)^2 - 4 \det M_F^2} \right],$$

$$\sin 2\theta_{\tilde{q}} = \frac{2m_q |X_q|}{m_{\tilde{q}_2}^2 - m_{\tilde{q}_1}^2}. \quad (12)$$

The one-generation results above also apply to the charged sleptons, with the obvious substitutions:  $q \rightarrow \tau$  with  $T_{3\tau} = -\frac{1}{2}$  and  $e_\tau = -1$ , and the replacement of the supersymmetry-breaking parameters:  $M_Q^2 \rightarrow M_L^2$ ,  $M_D^2 \rightarrow M_E^2$ , and  $A_q \rightarrow A_\tau$ . For the neutral sleptons,  $\tilde{\nu}_R$  does not exist in the MSSM, so  $\tilde{\nu}_L$  is a mass eigenstate.

In the case of three generations, the supersymmetry-breaking scalar-squared masses  $[M_Q^2, M_U^2, M_D^2, M_L^2, \text{ and } M_E^2]$  and the  $A$ -parameters that parameterize the Higgs couplings to up- and down-type squarks and charged sleptons (henceforth denoted by  $A_U$ ,  $A_D$ , and  $A_E$ , respectively) are now  $3 \times 3$  matrices as noted in Section I.3. The diagonalization of the  $6 \times 6$  squark mass matrices yields  $\tilde{f}_{iL}$ - $\tilde{f}_{jR}$  mixing (for  $i \neq j$ ). In practice, since the  $\tilde{f}_L$ - $\tilde{f}_R$  mixing is appreciable only for the third generation, this additional complication can often be neglected (although see Ref. 75 for examples in which the mixing between the second and third generations is relevant).

Radiative loop corrections will modify all tree-level results for masses quoted in this section. These corrections must be included in any precision study of supersymmetric phenomenology [77]. Beyond tree level, the definition of the supersymmetric parameters becomes convention-dependent. For example, one can define physical couplings or running couplings, which differ beyond the tree level. This provides a challenge to any effort that attempts to extract supersymmetric parameters from data. The Supersymmetry Les Houches Accord (SLHA) [78] has been adopted, which establishes a set of conventions for specifying generic file structures for supersymmetric model specifications and input parameters, supersymmetric mass and coupling spectra, and decay tables. These provide a universal interface between spectrum calculation programs, decay packages, and high energy physics event generators. Ultimately, these efforts will facilitate the reconstruction of the fundamental supersymmetric theory (and its breaking mechanism) from high-precision studies of supersymmetric phenomena at future colliders.

**I.5. The Higgs sector of the MSSM:** Next, consider the MSSM Higgs sector [22,23,79]. Despite the large number

# Searches Particle Listings

## Supersymmetric Particle Searches

of potential  $CP$ -violating phases among the MSSM-124 parameters, the tree-level MSSM Higgs sector is automatically  $CP$ -conserving. That is, unphysical phases can be absorbed into the definition of the Higgs fields such that  $\tan\beta$  is a real parameter (conventionally chosen to be positive). Consequently, the physical neutral Higgs scalars are  $CP$  eigenstates. The MSSM Higgs sector contains five physical spin-zero particles: a charged Higgs boson pair ( $H^\pm$ ), two  $CP$ -even neutral Higgs bosons (denoted by  $h^0$  and  $H^0$  where  $m_h < m_H$ ), and one  $CP$ -odd neutral Higgs boson ( $A^0$ ).

**I.5.1 The Tree-level MSSM Higgs sector:** The properties of the Higgs sector are determined by the Higgs potential, which is made up of quadratic terms [whose squared-mass coefficients were specified above Eq. (1)] and quartic interaction terms governed by dimensionless couplings. The quartic interaction terms are manifestly supersymmetric at tree level (although these are modified by supersymmetry-breaking effects at the loop level). In general, the quartic couplings arise from two sources: (i) the supersymmetric generalization of the scalar potential (the so-called “ $F$ -terms”), and (ii) interaction terms related by supersymmetry to the coupling of the scalar fields and the gauge fields, whose coefficients are proportional to the corresponding gauge couplings (the so-called “ $D$ -terms”).

In the MSSM,  $F$ -term contributions to the quartic couplings are absent (although such terms may be present in extensions of the MSSM, *e.g.*, models with Higgs singlets). As a result, the strengths of the MSSM quartic Higgs interactions are fixed in terms of the gauge couplings. Due to the resulting constraint on the form of the two-Higgs-doublet scalar potential, all the tree-level MSSM Higgs-sector parameters depend only on two quantities:  $\tan\beta$  [defined in Eq. (1)] and one Higgs mass usually taken to be  $m_A$ . From these two quantities, one can predict the values of the remaining Higgs boson masses, an angle  $\alpha$  (which measures the component of the original  $Y = \pm 1$  Higgs doublet states in the physical  $CP$ -even neutral scalars), and the Higgs boson self-couplings.

**I.5.2 The radiatively-corrected MSSM Higgs sector:**

When radiative corrections are incorporated, additional parameters of the supersymmetric model enter via virtual loops. The impact of these corrections can be significant [80]. For example, the tree-level MSSM-124 prediction for the upper bound of the lightest  $CP$ -even Higgs mass,  $m_h \leq m_Z |\cos 2\beta| \leq m_Z$  [22,23], can be substantially modified when radiative corrections are included. The qualitative behavior of these radiative corrections can be most easily seen in the large top-squark mass limit, where in addition, both the splitting of the two diagonal entries and the two off-diagonal entries of the top-squark squared-mass matrix [Eq. (9)] are small in comparison to the average of the two top-squark squared masses,  $M_S^2 \equiv \frac{1}{2}(M_{t_1}^2 + M_{t_2}^2)$ . In this case (assuming  $m_A > m_Z$ ), the predicted upper bound for  $m_h$  (which reaches its maximum at large  $\tan\beta$ ) is approximately given by

$$m_h^2 \lesssim m_Z^2 + \frac{3g^2 m_t^4}{8\pi^2 m_W^2} \left[ \ln(M_S^2/m_t^2) + \frac{X_t^2}{M_S^2} \left( 1 - \frac{X_t^2}{12M_S^2} \right) \right], \quad (13)$$

where  $X_t \equiv A_t - \mu \cot\beta$  is the top-squark mixing factor [see Eq. (9)].

A more complete treatment of the radiative corrections [81] shows that Eq. (13) somewhat overestimates the true upper bound of  $m_h$ . These more refined computations, which incorporate renormalization group improvement and the leading two-loop contributions, yield  $m_h \lesssim 135$  GeV (with an accuracy of a few GeV) for  $m_t = 175$  GeV and  $M_S \lesssim 2$  TeV [81]. This Higgs-mass upper bound can be relaxed somewhat in non-minimal extensions of the MSSM, as noted in Section I.9.

In addition, one-loop radiative corrections can introduce  $CP$ -violating effects in the Higgs sector, which depend on some of the  $CP$ -violating phases among the MSSM-124 parameters [82]. Although these effects are more model-dependent, they can have a non-trivial impact on the Higgs searches at future colliders. A summary of the current MSSM Higgs mass limits can be found in Ref. 83.

**I.6. Restricting the MSSM parameter freedom:** In Sections I.4 and I.5, we surveyed the parameters that comprise the MSSM-124. However, in its most general form, the MSSM-124 is not a phenomenologically-viable theory over most of its parameter space. This conclusion follows from the observation that a generic point in the MSSM-124 parameter space exhibits: (i) no conservation of the separate lepton numbers  $L_e$ ,  $L_\mu$ , and  $L_\tau$ ; (ii) unsuppressed flavor-changing neutral currents (FCNC’s); and (iii) new sources of  $CP$  violation that are inconsistent with the experimental bounds.

For example, the MSSM contains many new sources of  $CP$  violation [84]. In particular, some combinations of the complex phases of the gaugino-mass parameters, the  $A$ -parameters, and  $\mu$  must be less than on the order of  $10^{-2}$ – $10^{-3}$  (for a supersymmetry-breaking scale of 100 GeV) to avoid generating electric dipole moments for the neutron, electron, and atoms in conflict with observed data [85–87]. The non-observation of FCNC’s [88–90] places additional strong constraints on the off-diagonal matrix elements of the squark and slepton soft-supersymmetry-breaking squared masses and  $A$ -parameters (see Section I.3.3). As a result of the phenomenological deficiencies listed above, almost the entire MSSM-124 parameter space is ruled out! This theory is viable only at very special “exceptional” regions of the full parameter space.

The MSSM-124 is also theoretically incomplete as it provides no explanation for the origin of the supersymmetry-breaking parameters (and in particular, why these parameters should conform to the exceptional points of the parameter space mentioned above). Moreover, there is no understanding of the choice of parameters that leads to the breaking of the electroweak symmetry. What is needed ultimately is a fundamental theory of supersymmetry breaking, which would provide a rationale for a set of soft-supersymmetry-breaking terms that is consistent with all phenomenological constraints.

The successful unification of the  $SU(3) \times SU(2) \times U(1)$  gauge couplings in supersymmetric grand unified theories [8,51,91,92]



suggests the possibility that the high-energy structure of the theory may be considerable simpler than its low-energy realization. The desired phenomenological constraints of the low-energy theory can often be implemented by the dynamics which govern the more fundamental theory that resides at the high energy scale.

In this Section, we examine a number of theoretical frameworks that yield phenomenologically viable regions of the the general MSSM parameter space. The resulting supersymmetric particle spectrum is then a function of a relatively small number of input parameters. This is accomplished by imposing a simple structure on the soft-supersymmetry-breaking terms at a common high-energy scale  $M_X$  (typically chosen to be the Planck scale,  $M_P$ , the grand unification scale,  $M_{\text{GUT}}$ , or the messenger scale,  $M_{\text{mess}}$ ). Using the renormalization group equations, one can then derive the low-energy MSSM parameters relevant for collider physics. The initial conditions (at the appropriate high-energy scale) for the renormalization group equations depend on the mechanism by which supersymmetry breaking is communicated to the effective low energy theory.

Examples of this scenario are provided by models of gravity-mediated and gauge-mediated supersymmetry breaking, to be discussed in more detail below. In some of these approaches, one of the diagonal Higgs squared-mass parameters is driven negative by renormalization group evolution [93]. In such models, electroweak symmetry breaking is generated radiatively, and the resulting electroweak symmetry-breaking scale is intimately tied to the scale of low-energy supersymmetry breaking.

### I.6.1. Gaugino mass unification:

One prediction that arises in many grand unified supergravity models and gauge-mediated supersymmetry-breaking models is the unification of the (tree-level) gaugino mass parameters at some high-energy scale  $M_X$ :

$$M_1(M_X) = M_2(M_X) = M_3(M_X) = m_{1/2}. \quad (14)$$

Consequently, the effective low-energy gaugino mass parameters (at the electroweak scale) are related:

$$M_3 = (g_s^2/g^2)M_2 \simeq 3.5M_2, \quad M_1 = (5g'^2/3g^2)M_2 \simeq 0.5M_2. \quad (15)$$

In this case, the chargino and neutralino masses and mixing angles depend only on three unknown parameters: the gluino mass,  $\mu$ , and  $\tan\beta$ . If in addition  $|\mu| \gg M_1 \gtrsim m_Z$ , then the lightest neutralino is nearly a pure bino, an assumption often made in supersymmetric particle searches at colliders.

Although Eqs. (14) and (15) are often assumed in many phenomenological studies, a truly model-independent approach would take the gaugino mass parameters,  $M_i$ , to be independent parameters to be determined by experiment. For example, although LEP data yields a lower bound of 46 GeV on the mass of the lightest neutralino [94], an exactly massless neutralino *cannot* be ruled out today in a model-independent analysis [95].

It is possible that the tree-level masses for the gauginos are absent. In this case, the gaugino mass parameters arise at one-loop and do not satisfy Eq. (15). In supergravity, there exists a model-independent contribution to the gaugino mass whose origin can be traced to the super-conformal (super-Weyl) anomaly, which is common to all supergravity models [47]. Eq. (15) is then replaced (in the one-loop approximation) by:

$$M_i \simeq \frac{b_i g_i^2}{16\pi^2} m_{3/2}, \quad (16)$$

where  $m_{3/2}$  is the gravitino mass (assumed to be on the order of 1 TeV), and  $b_i$  are the coefficients of the MSSM gauge beta-functions corresponding to the corresponding U(1), SU(2), and SU(3) gauge groups:  $(b_1, b_2, b_3) = (\frac{33}{5}, 1, -3)$ . Eq. (16) yields  $M_1 \simeq 2.8M_2$  and  $M_3 \simeq -8.3M_2$ , which implies that the lightest chargino pair and neutralino comprise a nearly mass-degenerate triplet of winos,  $\widetilde{W}^\pm, \widetilde{W}^0$  (c.f. Table 1), over most of the MSSM parameter space. (For example, if  $|\mu| \gg m_Z$ , then Eq. (16) implies that  $M_{\widetilde{X}_1^\pm} \simeq M_{\widetilde{X}_1^0} \simeq M_2$  [96].)

The corresponding supersymmetric phenomenology differs significantly from the standard phenomenology based on Eq. (15), and is explored in detail in Ref. 97. Under certain theoretical assumptions on the structure of the Kähler potential (the so-called sequestered form introduced in Ref. 47), anomaly-mediated supersymmetry breaking also generates (approximate) flavor-diagonal squark and slepton mass matrices. This approach is called *anomaly-mediated* supersymmetry breaking (AMSB). However in its simplest formulation, AMSB yields negative squared-mass contributions for the sleptons in the MSSM. It may be possible to cure this fatal flaw in approaches beyond the minimal supersymmetric model [98]. Alternatively, one can assume that anomaly-mediation is not the sole source of supersymmetry-breaking in the slepton sector.

Finally, it should be noted that the unification of gaugino masses (and scalar masses) can be accidental. In particular, the energy scale where unification takes place may not be directly related to any physical scale. This phenomenon has been called *mirage unification* and can occur in certain theories of fundamental supersymmetry-breaking [99].

**I.6.2. The constrained MSSM: mSUGRA, CMSSM, ...** In the *minimal* supergravity (mSUGRA) framework [2–4], a form of the Kähler potential is employed that yields minimal kinetic energy terms for the MSSM fields [100]. As a result, the soft-supersymmetry-breaking parameters at the high-energy scale  $M_X$  take a particularly simple form in which the scalar squared masses and the  $A$ -parameters are flavor-diagonal and universal [34]:

$$\begin{aligned} M_Q^2(M_X) &= M_U^2(M_X) = M_D^2(M_X) = m_0^2 \mathbf{1}, \\ M_L^2(M_X) &= M_E^2(M_X) = m_0^2 \mathbf{1}, \\ m_1^2(M_X) &= m_2^2(M_X) = m_0^2, \\ A_U(M_X) &= A_D(M_X) = A_E(M_X) = A_0 \mathbf{1}, \end{aligned} \quad (17)$$

# Searches Particle Listings

## Supersymmetric Particle Searches

where  $\mathbf{1}$  is a  $3 \times 3$  identity matrix in generation space. As in the Standard Model, this approach exhibits minimal flavor violation, whose unique source is the nontrivial flavor structure of the Higgs-fermion Yukawa couplings. The gaugino masses are also unified according to Eq. (14).

Renormalization group evolution is then used to derive the values of the supersymmetric parameters at the low-energy (electroweak) scale. For example, to compute squark masses, one must use the *low-energy* values for  $M_Q^2$ ,  $M_U^2$ , and  $M_D^2$  in Eq. (9). Through the renormalization group running with boundary conditions specified in Eqs. (15) and (17), one can show that the low-energy values of  $M_Q^2$ ,  $M_U^2$ , and  $M_D^2$  depend primarily on  $m_0^2$  and  $m_{1/2}^2$ . A number of useful approximate analytic expressions for superpartner masses in terms of the mSUGRA parameters can be found in Ref. 101.

In the mSUGRA approach, one typically finds that four flavors of squarks (with two squark eigenstates per flavor) and  $\tilde{b}_R$  are nearly mass-degenerate. The  $\tilde{b}_L$  mass and the diagonal  $\tilde{t}_L$  and  $\tilde{t}_R$  masses are reduced compared to the common squark mass of the first two generations. In addition, there are six flavors of nearly mass-degenerate sleptons (with two slepton eigenstates per flavor for the charged sleptons and one per flavor for the sneutrinos); the sleptons are expected to be somewhat lighter than the mass-degenerate squarks. Finally, third-generation squark masses and tau-slepton masses are sensitive to the strength of the respective  $\tilde{f}_L$ - $\tilde{f}_R$  mixing, as discussed below Eq. (9). The LSP is typically the lightest neutralino,  $\tilde{\chi}_1^0$ , which is dominated by its bino component. In particular, mSUGRA parameter regimes in which the LSP is a chargino or the  $\tilde{\tau}_1$  (the lightest scalar superpartner of the  $\tau$ -lepton) are not phenomenologically viable.

One can count the number of independent parameters in the mSUGRA framework. In addition to 18 Standard Model parameters (excluding the Higgs mass), one must specify  $m_0$ ,  $m_{1/2}$ ,  $A_0$ , the Planck-scale values for  $\mu$  and  $B$ -parameters (denoted by  $\mu_0$  and  $B_0$ ), and the gravitino mass  $m_{3/2}$ . Without additional model assumptions,  $m_{3/2}$  is independent of the parameters that govern the mass spectrum of the superpartners of the Standard Model [34]. In principle,  $A_0$ ,  $B_0$ ,  $\mu_0$ , and  $m_{3/2}$  can be complex, although in the mSUGRA approach, these parameters are taken (arbitrarily) to be real.

As previously noted, renormalization group evolution is used to compute the low-energy values of the mSUGRA parameters, which then fixes all the parameters of the low-energy MSSM. In particular, the two Higgs vacuum expectation values (or equivalently,  $m_Z$  and  $\tan\beta$ ) can be expressed as a function of the Planck-scale supergravity parameters. The simplest procedure is to remove  $\mu_0$  and  $B_0$  in favor of  $m_Z$  and  $\tan\beta$  [the sign of  $\mu_0$ , denoted  $\text{sgn}(\mu_0)$  below, is not fixed in this process]. In this case, the MSSM spectrum and its interaction strengths are determined by five parameters:

$$m_0, A_0, m_{1/2}, \tan\beta, \text{ and } \text{sgn}(\mu_0), \quad (18)$$

in addition to the 18 parameters of the Standard Model and an independent gravitino mass  $m_{3/2}$ . This framework is conventionally called the *constrained minimal supersymmetric extension of the Standard Model* (CMSSM).

In the early literature, additional conditions were obtained by assuming a simplifying form for the hidden sector that provides the fundamental source of supersymmetry breaking. Two additional relations emerged among the mSUGRA parameters [100]:  $B_0 = A_0 - m_0$  and  $m_{3/2} = m_0$ . These relations characterize a theory that was called minimal supergravity when first proposed. In the more recent literature, it has been more common to omit these extra conditions in defining the mSUGRA model (in which case the mSUGRA model and the CMSSM are synonymous). The authors of Ref. 102 advocate restoring the original nomenclature in which the mSUGRA model is defined with the extra conditions as originally proposed. Additional mSUGRA variations can be considered where different relations among the CMSSM parameters are imposed.

One can also relax the universality of scalar masses by decoupling the squared-masses of the Higgs bosons and the squarks/sleptons. This leads to the non-universal Higgs mass models (NUHM), thereby adding one or two new parameters to the CMSSM depending on whether the diagonal Higgs scalar squared-mass parameters ( $m_1^2$  and  $m_2^2$ ) are set equal (NUHM1) or taken to be independent (NUHM2) at the high energy scale  $M_X^2$ . Clearly, this modification preserves the minimal flavor violation of the mSUGRA approach. Nevertheless, the mSUGRA approach and its NUHM generalizations are probably too simplistic. Theoretical considerations suggest that the universality of Planck-scale soft-supersymmetry-breaking parameters is not generic [103]. In particular, effective operators at the Planck scale exist that do not respect flavor universality, and it is difficult to find a theoretical principle that would forbid them.

**I.6.3. Gauge-mediated supersymmetry breaking:** In contrast to models of gravity-mediated supersymmetry breaking, the universality of the fundamental soft-supersymmetry-breaking squark and slepton squared-mass parameters is guaranteed in gauge-mediated supersymmetry breaking because the supersymmetry breaking is communicated to the sector of MSSM fields via gauge interactions [39,40]. In the minimal gauge-mediated supersymmetry-breaking (GMSB) approach, there is one effective mass scale,  $\Lambda$ , that determines all low-energy scalar and gaugino mass parameters through loop effects (while the resulting  $A$ -parameters are suppressed). In order that the resulting superpartner masses be on the order of 1 TeV or less, one must have  $\Lambda \sim 100$  TeV. The origin of the  $\mu$  and  $B$ -parameters is quite model-dependent, and lies somewhat outside the ansatz of gauge-mediated supersymmetry breaking. The simplest models of this type are even more restrictive than the CMSSM, with two fewer degrees of freedom. Benchmark reference points for GMSB models have been proposed in Ref. 104 to facilitate collider studies.

The minimal GMSB is not a fully realized model. The sector of supersymmetry-breaking dynamics can be very complex,

and no complete model of gauge-mediated supersymmetry yet exists that is both simple and compelling. However, advances in the theory of dynamical supersymmetry breaking (which exploit the existence of metastable supersymmetry-breaking vacua in broad classes of models [105]) have generated new ideas and opportunities for model building. As a result, simpler models of successful gauge mediation of supersymmetry breaking have been achieved with the potential for overcoming a number of long-standing theoretical challenges [106]. In addition, model-independent techniques that encompass all known gauge mediation models have been recently formulated [107]. These methods are well-suited for a comprehensive analysis [108] of the phenomenological profile of gauge-mediated supersymmetry breaking.

It was noted in Section I.2 that the gravitino is the LSP in GMSB models. As a result, the next-to-lightest supersymmetric particle (NLSP) now plays a crucial role in the phenomenology of supersymmetric particle production and decays. Note that unlike the LSP, the NLSP can be charged. In GMSB models, the most likely candidates for the NLSP are  $\tilde{\chi}_1^0$  and  $\tilde{\tau}_R^\pm$ . The NLSP will decay into its superpartner plus a gravitino (*e.g.*,  $\tilde{\chi}_1^0 \rightarrow \gamma\tilde{G}$ ,  $\tilde{\chi}_1^0 \rightarrow Z\tilde{G}$ , or  $\tilde{\tau}_R^\pm \rightarrow \tau^\pm\tilde{G}$ ), with lifetimes and branching ratios that depend on the model parameters.

Different choices for the identity of the NLSP and its decay rate lead to a variety of distinctive supersymmetric phenomenologies [40,109]. For example, a long-lived  $\tilde{\chi}_1^0$ -NLSP that decays outside collider detectors leads to supersymmetric decay chains with missing energy in association with leptons and/or hadronic jets (this case is indistinguishable from the standard phenomenology of the  $\tilde{\chi}_1^0$ -LSP). On the other hand, if  $\tilde{\chi}_1^0 \rightarrow \gamma\tilde{G}$  is the dominant decay mode, and the decay occurs inside the detector, then nearly *all* supersymmetric particle decay chains would contain a photon. In contrast, in the case of a  $\tilde{\tau}_R^\pm$ -NLSP, the  $\tilde{\tau}_R^\pm$  would either be long-lived or would decay inside the detector into a  $\tau$ -lepton plus missing energy.

**I.6.4. The phenomenological MSSM:** Of course, any of the theoretical assumptions described in this Section could be wrong and must eventually be tested experimentally. To facilitate the exploration of MSSM phenomena in a more model-independent way while respecting the constraints noted at the beginning of this Section, the phenomenological MSSM (pMSSM) has been introduced [110].

The pMSSM is governed by 19 independent real parameters beyond the Standard Model, which include the three gaugino masses  $M_1$ ,  $M_2$  and  $M_3$ , the Higgs sector parameters  $m_A$  and  $\tan\beta$ , the Higgsino mass parameter  $\mu$ , five squark and slepton squared-mass parameters for the degenerate first and second generations ( $M_{\tilde{Q}}^2$ ,  $M_{\tilde{U}}^2$ ,  $M_{\tilde{D}}^2$ , ( $M_{\tilde{L}}^2$  and  $M_{\tilde{E}}^2$ ), the five corresponding squark and slepton squared-mass parameters for the third generation, and three third-generation  $A$ -parameters ( $A_t$ ,  $A_b$  and  $A_\tau$ ). Note that the first and second generation  $A$ -parameters can be neglected as their phenomenological consequences are negligible. Search strategies at the LHC for the more general pMSSM have been examined in Ref. 111.

If supersymmetric phenomena are discovered, the measurements of (low-energy) supersymmetric parameters may eventually provide sufficient information to determine the organizing principle governing supersymmetry breaking and yield significant constraints on the values of the fundamental (high-energy) supersymmetric parameters. In particular, a number of sophisticated techniques have been recently developed for analyzing experimental data to test the viability of the particular supersymmetric framework and for measuring the fundamental model parameters and their uncertainties [112].

#### I.7. Experimental data confronts the MSSM:

Suppose some version of the MSSM satisfies the phenomenological constraints addressed in Section I.6. What are the expectations for the magnitude of the parameters that define such a model, and are these expectations consistent with present experimental data? For details on the constraints on supersymmetric particle masses from previous collider studies at LEP and the Tevatron and the most recent constraints from LHC data, see Ref. 94. Additional constraints arise from limits on the contributions of virtual supersymmetric particle exchange to a variety of Standard Model processes [88–90].

Recent LHC data has been especially effective in ruling out the existence of colored supersymmetric particles (primarily the gluino and the first two generations of squarks) with masses below about 1 TeV in the CMSSM [113]. However, such constraints are relaxed, in some cases by as much as a factor of two, in more generic frameworks of the MSSM [114].

#### I.7.1 Naturalness constraints and the little hierarchy:

In Section I, weak-scale supersymmetry was motivated as a natural solution to the hierarchy problem, which could provide an understanding of the origin of the electroweak symmetry-breaking scale without a significant fine-tuning of the fundamental MSSM parameters. In this framework, the soft-supersymmetry-breaking masses must be generally of the order of 1 TeV or below [115]. This requirement is most easily seen in the determination of  $m_Z$  by the scalar potential minimum condition. In light of Eq. (3), to avoid the fine-tuning of MSSM parameters, the soft-supersymmetry breaking squared-masses  $m_1^2$  and  $m_2^2$  and the higgsino squared-mass  $|\mu|^2$  should all be roughly of  $\mathcal{O}(m_Z^2)$ . Many authors have proposed quantitative measures of fine-tuning [115,116]. One of the simplest measures is the one given by Barbieri and Giudice [115],

$$\Delta_i \equiv \left| \frac{\partial \ln m_Z^2}{\partial \ln p_i} \right|, \quad \Delta \equiv \max \Delta_i, \quad (19)$$

where the  $p_i$  are the MSSM parameters at the high-energy scale  $M_X$ , which are set by the fundamental supersymmetry-breaking dynamics. The theory is more fine-tuned as  $\Delta$  becomes larger.

One can apply the fine-tuning measure to any explicit model of supersymmetry-breaking. For example, in the approaches discussed in Section I.6, the  $p_i$  are parameters of the model at the energy scale  $M_X$  where the soft-supersymmetry breaking operators are generated by the dynamics of supersymmetry breaking. Renormalization group evolution then determines the

## Searches Particle Listings

### Supersymmetric Particle Searches

values of the parameters appearing in Eq. (3) at the electroweak scale. In this way,  $\Delta$  is sensitive to all the supersymmetry-breaking parameters of the model (see e.g. Ref. 117).

Consequently, there is a tension between the present experimental lower limits on the masses of colored supersymmetric particles [118] and the expectation that supersymmetry-breaking is associated with the electroweak symmetry-breaking scale. Moreover, this tension is exacerbated [119,120] by the experimental lower Higgs mass bound ( $m_h \gtrsim 115$  GeV) [83], which is not far from the the MSSM upper bound ( $m_h \lesssim 135$  GeV) [the dependence of the latter on the top-squark mass and mixing was noted in Section I.5.2]. If  $M_{\text{SUSY}}$  characterizes the scale of supersymmetric particle masses, then one would expect  $\Delta \sim M_{\text{SUSY}}^2/m_Z^2$ . For example, if  $M_{\text{SUSY}} \sim 1$  TeV then there must be at least a  $\Delta^{-1} \sim 1\%$  fine-tuning of the MSSM parameters to achieve the observed value of the  $Z$  mass. This separation of the electroweak symmetry breaking and supersymmetry breaking scales is an example of the *little hierarchy problem* [119,121].

However, one must be very cautious when drawing conclusions about the viability of weak-scale supersymmetry to explain the origin of electroweak symmetry breaking. First, one must decide the largest tolerable value of  $\Delta$  within the framework of weak-scale supersymmetry (should it be  $\Delta \sim 10?$   $100?$   $1000?$ ). Second, the fine-tuning parameter  $\Delta$  depends quite sensitively on the assumptions of the supersymmetry-breaking dynamics (e.g. the value of  $M_X$  and relations among supersymmetry-breaking parameters in the fundamental high energy theory).

For example, in so-called focus point supersymmetry models [122], all squark masses can be as heavy as 5 TeV *without* significant fine-tuning. This can be attributed to a focusing behavior of the renormalization group evolution when certain relations hold among the high-energy values of the scalar squared-mass supersymmetry-breaking parameters. In this approach, the mass of the light CP-even Higgs boson can naturally be near its maximally allowed MSSM upper bound [123]. A recent reanalysis of focus-point and related models with modest fine-tuning in the context of CMSSM can be found in Ref. 124.

Among the colored superpartners, the third generation squarks generically have the most significant impact on the naturalness constraints [125], whereas their masses are the least constrained by LHC data. Hence, in the absence of any relation between third generation squarks and those of the first two generations, the naturalness constraints due to present LHC data can be considerably weaker than those obtained in the CMSSM. Indeed, models with first and second generation squark masses in the multi-TeV range do not generically require significant fine tuning. Such models have the added benefit that undesirable FCNCs mediated by squark exchange are naturally suppressed [126]. Other MSSM mass spectra that are compatible with moderate fine tuning have been investigated in Ref. 127. Moreover, one can also consider extensions of the MSSM in which the degree of fine-tuning is relaxed [128].

Finally, experimentally reported upper limits for supersymmetric particle masses are rarely model-independent. For example, mass limits for the gluino and the first and second generation squarks obtained under the assumption of the CMSSM can often be evaded in alternative or extended MSSM models, e.g., compressed supersymmetry [129] and stealth supersymmetry [130]. Moreover, experimental limits on the masses for the third generation squarks and color-neutral supersymmetric particles are less constrained than the masses of other colored supersymmetric states. The simplified models approach [131] is sometimes advertised as being more model-independent by focusing narrowly on a specific generic production process and decay chain. However this approach also depends on assumptions of the relative masses of the produced particle and decay products and the lack of interference from competing processes.

Thus, it is certainly premature in the first few years of the LHC era to conclude that weak scale supersymmetry is on the verge of exclusion.

#### ***I.7.2 Constraints from virtual exchange of supersymmetric particles***

There are a number of low-energy measurements that are sensitive to the effects of new physics through supersymmetric loop effects. For example, the virtual exchange of supersymmetric particles can contribute to the muon anomalous magnetic moment,  $a_\mu \equiv \frac{1}{2}(g-2)_\mu$  [132]. The Standard Model prediction for  $a_\mu$  exhibits a  $3.3\sigma$  deviation from the experimentally observed value [133], although a very recent theoretical re-analysis claims that the deviation exceeds  $4\sigma$  [134].

The rare inclusive decay  $b \rightarrow s\gamma$  also provides a sensitive probe to the virtual effects of new physics beyond the Standard Model. Experimental measurements of  $B \rightarrow X_s + \gamma$  by the BELLE collaboration [135] are in very good agreement with the theoretical predictions of Ref. 136. In both cases, supersymmetric corrections can contribute an observable shift from the Standard Model prediction in some regions of the MSSM parameter space [137,138].

The rare decay  $B_s \rightarrow \mu^+\mu^-$  is especially sensitive to supersymmetric loop effects, with some loop contributions that scale as  $\tan^6\beta$  when  $\tan\beta \gg 1$  [139]. Current experimental limits [140] are within about a factor of five of the predicted Standard Model rate. The absence of a *significant* deviation in these and other  $B$ -physics observables from their Standard Model predictions places interesting constraints on the low-energy supersymmetry parameters [141].

#### ***I.8. Massive neutrinos in low-energy supersymmetry:***

In the minimal Standard Model and its supersymmetric extension, there are no right-handed neutrinos, and Majorana mass terms for the left-handed neutrinos are absent. However, given the overwhelming evidence for neutrino masses and mixing [142,143], any viable model of fundamental particles must provide a mechanism for generating neutrino masses [144]. In extended supersymmetric models, various mechanisms exist for producing massive neutrinos [145]. Although one can devise models for generating massive Dirac neutrinos [146], the

most common approaches for incorporating neutrino masses are based on  $L$ -violating supersymmetric extensions of the MSSM, which generate massive Majorana neutrinos. Two classes of  $L$ -violating supersymmetric models will now be considered.

**I.8.1. The supersymmetric seesaw:** Neutrino masses can be incorporated into the Standard Model by introducing  $SU(3) \times SU(2) \times U(1)$  singlet right-handed neutrinos ( $\nu_R$ ) and super-heavy Majorana masses (typically on the order of a grand unified mass) for the  $\nu_R$ . In addition, one must also include a standard Yukawa couplings between the lepton doublets, the Higgs doublet, and the  $\nu_R$ . The Higgs vacuum expectation value then induces an off-diagonal  $\nu_L$ - $\nu_R$  masses on the order of the electroweak scale. Diagonalizing the neutrino mass matrix (in the three-generation model) yields three superheavy neutrino states, and three very light neutrino states that are identified as the light neutrino states observed in nature. This is the seesaw mechanism [147].

The supersymmetric generalization of the seesaw model of neutrino masses is now easily constructed [148,149]. In the seesaw-extended Standard Model, lepton number is broken due to the presence of  $\Delta L = 2$  terms in the Lagrangian (which include the Majorana mass terms for the light and super-heavy neutrinos). Consequently, the seesaw-extended MSSM conserves R-parity. The supersymmetric analogue of the Majorana neutrino mass term in the sneutrino sector leads to sneutrino-antisneutrino mixing phenomena [149,150].

**I.8.2. R-parity-violating supersymmetry:** A second approach to incorporating massive neutrinos in supersymmetric models is to retain the minimal particle content of the MSSM, while removing the assumption of R-parity invariance [152]. The most general R-parity-violating (RPV) model involving the MSSM spectrum introduces many new parameters to both the supersymmetry-conserving and the supersymmetry-breaking sectors. Each new interaction term violates either  $B$  or  $L$  conservation. For example, consider new scalar-fermion Yukawa couplings derived from the following interactions:

$$(\lambda_L)_{pmn} \hat{L}_p \hat{L}_m \hat{E}_n^c + (\lambda'_L)_{pmn} \hat{L}_p \hat{Q}_m \hat{D}_n^c + (\lambda_B)_{pmn} \hat{U}_p^c \hat{D}_m^c \hat{D}_n^c, \quad (20)$$

where  $p$ ,  $m$ , and  $n$  are generation indices, and gauge group indices are suppressed. In the notation above,  $\hat{Q}$ ,  $\hat{U}^c$ ,  $\hat{D}^c$ ,  $\hat{L}$ , and  $\hat{E}^c$  respectively represent  $(u, d)_L$ ,  $u_L^c$ ,  $d_L^c$ ,  $(\nu, e^-)_L$ , and  $e_L^c$  and the corresponding superpartners.

The Yukawa interactions are obtained from Eq. (20) by taking all possible combinations involving two fermions and one scalar superpartner. Note that the term in Eq. (20) proportional to  $\lambda_B$  violates  $B$ , while the other two terms violate  $L$ . Even if all the terms of Eq. (20) are absent, there is one more possible supersymmetric source of R-parity violation. In the notation of Eq. (20), one can add a term of the form  $(\mu_L)_p \hat{H}_u \hat{L}_p$ , where  $\hat{H}_u$  represents the  $Y = 1$  Higgs doublet and its higgsino superpartner. This term is the RPV generalization of the supersymmetry-conserving Higgs mass parameter  $\mu$  of the MSSM, in which the  $Y = -1$  Higgs/higgsino super-multiplet

$\hat{H}_d$  is replaced by the slepton/lepton super-multiplet  $\hat{L}_p$ . The RPV-parameters  $(\mu_L)_p$  also violate  $L$ .

Phenomenological constraints derived from data on various low-energy  $B$ - and  $L$ -violating processes can be used to establish limits on each of the coefficients  $(\lambda_L)_{pmn}$ ,  $(\lambda'_L)_{pmn}$ , and  $(\lambda_B)_{pmn}$  taken one at a time [152,153]. If more than one coefficient is simultaneously non-zero, then the limits are, in general, more complicated [154]. All possible RPV terms cannot be simultaneously present and unsuppressed; otherwise the proton decay rate would be many orders of magnitude larger than the present experimental bound. One way to avoid proton decay is to impose  $B$  or  $L$  invariance (either one alone would suffice). Otherwise, one must accept the requirement that certain RPV coefficients must be extremely suppressed.

One particularly interesting class of RPV models is one in which  $B$  is conserved, but  $L$  is violated. It is possible to enforce baryon number conservation, while allowing for lepton-number-violating interactions by imposing a discrete  $\mathbf{Z}_3$  baryon *triality* symmetry on the low-energy theory [155], in place of the standard  $\mathbf{Z}_2$  R-parity. Since the distinction between the Higgs and matter super-multiplets is lost in RPV models, R-parity violation permits the mixing of sleptons and Higgs bosons, the mixing of neutrinos and neutralinos, and the mixing of charged leptons and charginos, leading to more complicated mass matrices and mass eigenstates than in the MSSM. Recent attempts to fit neutrino masses and mixing in this framework can be found in Ref. 151.

The supersymmetric phenomenology of the RPV models exhibits features that are quite distinct from that of the MSSM [152]. The LSP is no longer stable, which implies that not all supersymmetric decay chains must yield missing-energy events at colliders. Nevertheless, the loss of the missing-energy signature is often compensated by other striking signals (which depend on which R-parity-violating parameters are dominant). For example, supersymmetric particles in RPV models can be singly produced (in contrast to R-parity-conserving models where supersymmetric particles are produced in pairs). The phenomenology of pair-produced supersymmetric particles is also modified in RPV models due to new decay chains not present in R-parity-conserving supersymmetry [152].

In RPV models with lepton number violation (these include low-energy supersymmetry models with baryon triality mentioned above), both  $\Delta L = 1$  and  $\Delta L = 2$  phenomena are allowed, leading to neutrino masses and mixing [156], neutrinoless double-beta decay [157], sneutrino-antisneutrino mixing [158],  $s$ -channel resonant production of sneutrinos in  $e^+e^-$  collisions [159] and charged sleptons in  $p\bar{p}$  and  $pp$  collisions [160].

**I.9. Extensions beyond the MSSM:** Extensions of the MSSM have been proposed to solve a variety of theoretical problems. One such problem involves the  $\mu$  parameter of the MSSM. Although  $\mu$  is a supersymmetric-*preserving* parameter, it must be of order the supersymmetry-breaking scale to yield a consistent supersymmetric phenomenology. In the MSSM, one must devise a theoretical mechanism to guarantee that the

# Searches Particle Listings

## Supersymmetric Particle Searches

magnitude of  $\mu$  is not larger than the TeV-scale (*e.g.*, in gravity-mediated supersymmetry, the Giudice-Masiero mechanism of Ref. 161 is the most cited explanation).

In extensions of the MSSM, new compelling solutions to the so-called  $\mu$ -problem are possible. For example, one can replace  $\mu$  by the vacuum expectation value of a new  $SU(3) \times SU(2) \times U(1)$  singlet scalar field. In such a model, the Higgs sector of the MSSM is enlarged and the corresponding fermionic higgsino superpartner is added. This is the so-called NMSSM (here, NM stands for non-minimal) [162]. There are some advantages to extending the model further by adding an additional  $U(1)$  broken gauge symmetry [163] (which yields the USSM [72]).

Non-minimal extensions of the MSSM involving additional matter and/or Higgs super-multiplets can also yield a less restrictive bound on the mass of the lightest Higgs boson (as compared to the bound quoted in Section I.5.2). For example, MSSM-extended models consistent with gauge coupling unification can be constructed in which the upper limit on the lightest Higgs boson mass can be as high as 200–300 GeV [164] (a similar relaxation of the Higgs mass bound occurs in split supersymmetry [165] and extra-dimensional scenarios [166]).

Other MSSM extensions considered in the literature include an enlarged electroweak gauge group beyond  $SU(2) \times U(1)$  [167]; and/or the addition of new, possibly exotic, matter super-multiplets (*e.g.*, new  $U(1)$  gauge groups and a vector-like color triplet with electric charge  $\frac{1}{3}e$  that appear as low-energy remnants in  $E_6$  grand unification models [168]). A possible theoretical motivation for such new structures arises from the study of phenomenologically viable string theory ground states [169].

### References

1. R. Haag, J.T. Lopuszanski, and M. Sohnius, Nucl. Phys. **B88**, 257 (1975);  
S.R. Coleman and J. Mandula, Phys. Rev. **159** (1967) 1251.
2. H.P. Nilles, Phys. Reports **110**, 1 (1984).
3. P. Nath, R. Arnowitt, and A.H. Chamseddine, *Applied  $N = 1$  Supergravity* (World Scientific, Singapore, 1984).
4. S.P. Martin, in *Perspectives on Supersymmetry II*, edited by G.L. Kane (World Scientific, Singapore, 2010) pp. 1–153; see <http://zippy.physics.niu.edu/primer.html> for the latest version and errata.
5. S. Weinberg, *The Quantum Theory of Fields, Volume III: Supersymmetry* (Cambridge University Press, Cambridge, UK, 2000);  
P. Binétruy, *Supersymmetry: Theory, Experiment, and Cosmology* (Oxford University Press, Oxford, UK, 2006).
6. L. Maiani, in *Vector bosons and Higgs bosons in the Salam-Weinberg theory of weak and electromagnetic interactions, Proceedings of the 11th GIF Summer School on Particle Physics*, Gif-sur-Yvette, France, 3–7 September, 1979, edited by M. Davier *et al.*, (IN2P3, Paris, 1980) pp. 1–52.
7. E. Witten, Nucl. Phys. **B188**, 513 (1981).
8. S. Dimopoulos and H. Georgi, Nucl. Phys. **B193**, 150 (1981).
9. N. Sakai, Z. Phys. **C11**, 153 (1981);  
R.K. Kaul, Phys. Lett. **109B**, 19 (1982).
10. L. Susskind, Phys. Reports **104**, 181 (1984).
11. L. Girardello and M. Grisaru, Nucl. Phys. **B194**, 65 (1982).
12. L.J. Hall and L. Randall, Phys. Rev. Lett. **65**, 2939 (1990);  
I. Jack and D.R.T. Jones, Phys. Lett. **B457**, 101 (1999).
13. For a review, see N. Polonsky, *Supersymmetry: Structure and phenomena. Extensions of the standard model*, Lect. Notes Phys. **M68**, 1 (2001).
14. G. Bertone, D. Hooper, and J. Silk, Phys. Rept. **405**, 279 (2005).
15. D. Hooper, “TASI 2008 Lectures on Dark Matter,” in *The Dawn of the LHC Era, Proceedings of the 2008 Theoretical and Advanced Study Institute in Elementary Particle Physics*, Boulder, Colorado, 2–27 June 2008, edited by Tao Han (World Scientific, Singapore, 2009).
16. G. Jungman, M. Kamionkowski, and K. Griest, Phys. Reports **267**, 195 (1996);  
K. Griest and M. Kamionkowski, Phys. Reports **333**, 167 (2000).
17. F.D. Steffen, Eur. Phys. J. **C59**, 557 (2009).
18. M. Drees and G. Gerbier, “Dark Matter,” in the section on Reviews, Tables, and Plots in this *Review*.
19. H.E. Haber and G.L. Kane, Phys. Rept. **117**, 75 (1985).
20. M. Drees, R. Godbole, and P. Roy, *Theory and Phenomenology of Sparticles* (World Scientific, Singapore, 2005);  
H. Baer and X. Tata, *Weak Scale Supersymmetry: from Superfields to Scattering Events* (Cambridge University Press, Cambridge, UK, 2006);  
I.J.R. Aitchison, *Supersymmetry in Particle Physics: an elementary introduction* (Cambridge University Press, Cambridge, UK, 2007).
21. P. Fayet, Nucl. Phys. **B78**, 14 (1974); *ibid.*, **B90**, 104 (1975).
22. K. Inoue *et al.*, Prog. Theor. Phys. **67**, 1889 (1982);  
R. Flores and M. Sher, Ann. Phys. (NY) **148**, 95 (1983).
23. J.F. Gunion and H.E. Haber, Nucl. Phys. **B272**, 1 (1986) [erratum: **B402**, 567 (1993)].
24. For an overview of the theory and models of the soft-supersymmetry-breaking Lagrangian, see D.J.H. Chung *et al.*, Phys. Rept. **407**, 1 (2005).
25. P. Fayet, Phys. Lett. **69B**, 489 (1977);  
G. Farrar and P. Fayet, Phys. Lett. **76B**, 575 (1978).
26. J. Ellis *et al.*, Nucl. Phys. **B238**, 453 (1984).
27. S. Raby, Phys. Lett. **B422**, 158 (1998);  
S. Raby and K. Tobe, Nucl. Phys. **B539**, 3 (1999);  
A. Mafi and S. Raby, Phys. Rev. **D62**, 035003 (2000).
28. P. Fayet, Phys. Lett. **84B**, 421 (1979); Phys. Lett. **86B**, 272 (1979).
29. P. van Nieuwenhuizen, Phys. Reports **68**, 189 (1981).
30. S. Deser and B. Zumino, Phys. Rev. Lett. **38**, 1433 (1977);  
E. Cremmer *et al.*, Phys. Lett. **79B**, 231 (1978).
31. R. Casalbuoni *et al.*, Phys. Lett. **B215**, 313 (1988); Phys. Rev. **D39**, 2281 (1989);  
A.L. Maroto and J.R. Pelaez, Phys. Rev. **D62**, 023518 (2000).

32. Z. Komargodski and N. Seiberg, JHEP **0909**, 066 (2009).
33. A.H. Chamseddine, R. Arnowitt, and P. Nath, Phys. Rev. Lett. **49**, 970 (1982); R. Barbieri, S. Ferrara, and C.A. Savoy, Phys. Lett. **119B**, 343 (1982); H.-P. Nilles, M. Srednicki, and D. Wyler, Phys. Lett. **120B**, 346 (1983); **124B**, 337 (1983); E. Cremmer, P. Fayet, and L. Girardello, Phys. Lett. **122B**, 41 (1983); L. Ibáñez, Nucl. Phys. **B218**, 514 (1982); L. Alvarez-Gaumé, J. Polchinski, and M.B. Wise, Nucl. Phys. **B221**, 495 (1983).
34. L.J. Hall, J. Lykken, and S. Weinberg, Phys. Rev. **D27**, 2359 (1983).
35. S.K. Soni and H.A. Weldon, Phys. Lett. **126B**, 215 (1983); Y. Kawamura, H. Murayama, and M. Yamaguchi, Phys. Rev. **D51**, 1337 (1995).
36. A.B. Lahanas and D.V. Nanopoulos, Phys. Reports **145**, 1 (1987).
37. J.L. Feng, A. Rajaraman, and F. Takayama, Phys. Rev. Lett. **91**, 011302 (2003); Phys. Rev. **D68**, 063504 (2003); Gen. Rel. Grav. **36**, 2575 (2004).
38. M. Dine, W. Fischler, and M. Srednicki, Nucl. Phys. **B189**, 575 (1981); S. Dimopoulos and S. Raby, Nucl. Phys. **B192**, 353 (1982); **B219**, 479 (1983); M. Dine and W. Fischler, Phys. Lett. **110B**, 227 (1982); C. Nappi and B. Ovrut, Phys. Lett. **113B**, 175 (1982); L. Alvarez-Gaumé, M. Claudson, and M. Wise, Nucl. Phys. **B207**, 96 (1982).
39. M. Dine and A.E. Nelson, Phys. Rev. **D48**, 1277 (1993); M. Dine, A.E. Nelson, and Y. Shirman, Phys. Rev. **D51**, 1362 (1995); M. Dine *et al.*, Phys. Rev. **D53**, 2658 (1996).
40. G.F. Giudice and R. Rattazzi, Phys. Reports **322**, 419 (1999).
41. E. Poppitz and S.P. Trivedi, Phys. Rev. **D55**, 5508 (1997); H. Murayama, Phys. Rev. Lett. **79**, 18 (1997); M.A. Luty and J. Terning, Phys. Rev. **D57**, 6799 (1998); N. Arkani-Hamed, J. March-Russell, and H. Murayama, Nucl. Phys. **B509**, 3 (1998); K. Agashe, Phys. Lett. **B435**, 83 (1998); C. Csaki, Y. Shirman, and J. Terning, JHEP **0705**, 099 (2007); M. Ibe and R. Kitano, Phys. Rev. **D77**, 075003 (2008).
42. M.J. Strassler and K. M. Zurek, Phys. Lett. **B651**, 374 (2007); T. Han *et al.*, JHEP **0807**, 008 (2008).
43. M.J. Strassler, arXiv:hep-ph/0607160; K.M. Zurek, Phys. Rev. **D79**, 115002 (2009).
44. Pedagogical lectures describing such mechanisms can be found in: M. Quiros, in *Particle Physics and Cosmology: The Quest for Physics Beyond the Standard Model(s), Proceedings of the 2002 Theoretical Advanced Study Institute in Elementary Particle Physics (TASI 2002)*, edited by H.E. Haber and A.E. Nelson (World Scientific, Singapore, 2004) pp. 549–601; C. Csaki, in *ibid.*, pp. 605–698.
45. See, *e.g.*, J. Parsons and A. Pomarol “Extra Dimensions,” in the section on Reviews, Tables, and Plots in this Review.
46. These ideas are reviewed in: V.A. Rubakov, Phys. Usp. **44**, 871 (2001); J. Hewett and M. Spiropulu, Ann. Rev. Nucl. Part. Sci. **52**, 397 (2002).
47. L. Randall and R. Sundrum, Nucl. Phys. **B557**, 79 (1999).
48. Z. Chacko, M.A. Luty, and E. Ponton, JHEP **0007**, 036 (2000); D.E. Kaplan, G.D. Kribs, and M. Schmaltz, Phys. Rev. **D62**, 035010 (2000); Z. Chacko *et al.*, JHEP **0001**, 003 (2000).
49. J. Scherk and J.H. Schwarz, Phys. Lett. **82B**, 60 (1979); Nucl. Phys. **B153**, 61 (1979).
50. See, *e.g.*, R. Barbieri, L.J. Hall, and Y. Nomura, Phys. Rev. **D66**, 045025 (2002); Nucl. Phys. **B624**, 63 (2002).
51. N. Arkani-Hamed and S. Dimopoulos, JHEP **0506**, 073 (2005); G.F. Giudice and A. Romanino, Nucl. Phys. **B699**, 65 (2004) [erratum: **B706**, 487 (2005)].
52. N. Arkani-Hamed *et al.*, Nucl. Phys. **B709**, 3 (2005); W. Kilian *et al.*, Eur. Phys. J. **C39**, 229 (2005).
53. K. Cheung and W. Y. Keung, Phys. Rev. **D71**, 015015 (2005); P. Gambino, G.F. Giudice, and P. Slavich, Nucl. Phys. **B726**, 35 (2005).
54. H.E. Haber, in *Recent Directions in Particle Theory, Proceedings of the 1992 Theoretical Advanced Study Institute in Particle Physics*, edited by J. Harvey and J. Polchinski (World Scientific, Singapore, 1993) pp. 589–686.
55. S. Dimopoulos and D. Sutter, Nucl. Phys. **B452**, 496 (1995); D.W. Sutter, Stanford Ph. D. thesis, hep-ph/9704390.
56. H.E. Haber, Nucl. Phys. B (Proc. Suppl.) **62A-C**, 469 (1998).
57. R.M. Barnett, J.F. Gunion, and H.E. Haber, Phys. Lett. **B315**, 349 (1993); H. Baer, X. Tata, and J. Woodside, Phys. Rev. **D41**, 906 (1990).
58. S.M. Bilenky, E.Kh. Khristova, and N.P. Nedelcheva, Phys. Lett. **B161**, 397 (1985); Bulg. J. Phys. **13**, 283 (1986); G. Moortgat-Pick and H. Fraas, Eur. Phys. J. **C25**, 189 (2002).
59. J. Rosiek, Phys. Rev. **D41**, 3464 (1990) [erratum: hep-ph/9511250]. The most recent corrected version of this manuscript can be found on the author’s webpage, [www.fuw.edu.pl/~rosiek/physics/prd41.html](http://www.fuw.edu.pl/~rosiek/physics/prd41.html).
60. J. Alwall *et al.*, JHEP **0709**, 028 (2007). The MadGraph homepage is located at [madgraph.hep.uiuc.edu/](http://madgraph.hep.uiuc.edu/).
61. T. Hahn, Comput. Phys. Commun. **140**, 418 (2001); T. Hahn and C. Schappacher, Comput. Phys. Commun. **143**, 54 (2002). The FeynArts homepage is located at [www.feynarts.de/](http://www.feynarts.de/).
62. A. Pukhov *et al.*, INP MSU report 98-41/542 (arXiv: hep-ph/9908288); E. Boos *et al.*[CompHEP Collab.], Nucl. Instrum. Meth. **A534**, 250 (2004). The CompHEP homepage is located at <http://comphep.sinp.msu.ru>.
63. For further details, see *e.g.*, Appendix C of Ref. 19 and Appendix A of Ref. 23.
64. J.L. Kneur and G. Moulhaka, Phys. Rev. **D59**, 015005 (1999).

# Searches Particle Listings

## Supersymmetric Particle Searches

65. S.Y. Choi *et al.*, *Eur. Phys. J.* **C14**, 535 (2000).
66. R.A. Horn and C.R. Johnson, *Matrix Analysis*, (Cambridge University Press, Cambridge, UK, 1985).
67. H.K. Dreiner, H.E. Haber, and S.P. Martin, *Phys. Reports* **494**, 1 (2010).
68. L. Pape and D. Treille, *Prog. Part. Nucl. Phys.* **69**, 63 (2006).
69. S.Y. Choi *et al.*, *Eur. Phys. J.* **C22**, 563 (2001); **C23**, 769 (2002).
70. G.J. Gounaris, C. Le Mouel, and P.I. Porfyriadis, *Phys. Rev.* **D65**, 035002 (2002); G.J. Gounaris and C. Le Mouel, *Phys. Rev.* **D66**, 055007 (2002).
71. T. Takagi, *Japan J. Math.* **1**, 83 (1925).
72. S.Y. Choi *et al.*, *Nucl. Phys.* **B778**, 85 (2007).
73. M.M. El Kheishen, A.A. Aboshousha, and A.A. Shafik, *Phys. Rev.* **D45**, 4345 (1992); M. Guchait, *Z. Phys.* **C57**, 157 (1993) [erratum: **C61**, 178 (1994)].
74. T. Hahn, preprint MPP-2006-85, [physics/0607103](http://physics/0607103).
75. K. Hikasa and M. Kobayashi, *Phys. Rev.* **D36**, 724 (1987); F. Gabbiani and A. Masiero, *Nucl. Phys.* **B322**, 235 (1989); Ph. Brax and C.A. Savoy, *Nucl. Phys.* **B447**, 227 (1995).
76. J. Ellis and S. Rudaz, *Phys. Lett.* **128B**, 248 (1983); F. Browning, D. Chang, and W.Y. Keung, *Phys. Rev.* **D64**, 015010 (2001); A. Bartl *et al.*, *Phys. Lett.* **B573**, 153 (2003); *Phys. Rev.* **D70**, 035003 (2004).
77. D.M. Pierce *et al.*, *Nucl. Phys.* **B491**, 3 (1997).
78. P. Skands *et al.*, *JHEP* **07** 036 (2004); B.C. Allanach *et al.*, *Comput. Phys. Commun.* **180**, 8 (2009). The Supersymmetry Les Houches Accord homepage is located at [home.fnal.gov/~skands/slha/](http://home.fnal.gov/~skands/slha/).
79. J.F. Gunion *et al.*, *The Higgs Hunter's Guide* (Perseus Publishing, Cambridge, MA, 1990); M. Carena and H.E. Haber, *Prog. Part. Nucl. Phys.* **50**, 63 (2003); A. Djouadi, *Phys. Reports* **459**, 1 (2008).
80. H.E. Haber and R. Hempfling, *Phys. Rev. Lett.* **66**, 1815 (1991); Y. Okada, M. Yamaguchi, and T. Yanagida, *Prog. Theor. Phys.* **85**, 1 (1991); J. Ellis, G. Ridolfi, and F. Zwirner, *Phys. Lett.* **B257**, 83 (1991).
81. See, *e.g.*, G. Degrassi *et al.*, *Eur. Phys. J.* **C28**, 133 (2003); B.C. Allanach *et al.*, *JHEP* **0409**, 044 (2004); S.P. Martin, *Phys. Rev.* **D75**, 055005 (2007); P. Kant *et al.*, *JHEP* **1008**, 104 (2010).
82. A. Pilaftsis and C.E.M. Wagner, *Nucl. Phys.* **B553**, 3 (1999); D.A. Demir, *Phys. Rev.* **D60**, 055006 (1999); S.Y. Choi, M. Drees, and J.S. Lee, *Phys. Lett.* **B481**, 57 (2000); M. Carena *et al.*, *Nucl. Phys.* **B586**, 92 (2000); *Phys. Lett.* **B495**, 155 (2000); *Nucl. Phys.* **B625**, 345 (2002); M. Frank *et al.*, *JHEP* **0702**, 047 (2007); S. Heinemeyer *et al.*, *Phys. Lett.* **B652**, 300 (2007).
83. The Standard Model and MSSM Higgs mass limits is reviewed in G. Bernardi, M. Carena, and T. Junk, "Higgs Bosons: Theory and Searches," in "Particle Listings—Gauge and Higgs bosons" in this *Review*.
84. S. Khalil, *Int. J. Mod. Phys.* **A18**, 1697 (2003).
85. W. Fischler, S. Paban, and S. Thomas, *Phys. Lett.* **B289**, 373 (1992); S.M. Barr, *Int. J. Mod. Phys.* **A8**, 209 (1993); T. Ibrahim and P. Nath, *Phys. Rev.* **D58**, 111301 (1998) [erratum: **D60**, 099902 (1999)]; M. Brhlik, G.J. Good, and G.L. Kane, *Phys. Rev.* **D59**, 115004 (1999); V.D. Barger *et al.*, *Phys. Rev.* **D64**, 056007 (2001); S. Abel, S. Khalil, and O. Lebedev, *Nucl. Phys.* **B606**, 151 (2001); K.A. Olive *et al.*, *Phys. Rev.* **D72**, 075001 (2005); G.F. Giudice and A. Romanino, *Phys. Lett.* **B634**, 307 (2006).
86. A. Masiero and L. Silvestrini, in *Perspectives on Supersymmetry*, edited by G.L. Kane (World Scientific, Singapore, 1998) pp. 423–441.
87. M. Pospelov and A. Ritz, *Annals Phys.* **318**, 119 (2005).
88. See, *e.g.*, F. Gabbiani *et al.*, *Nucl. Phys.* **B477**, 321 (1996); A. Masiero, and O. Vives, *New J. Phys.* **4**, 1 (2002).
89. For a recent review and references to the original literature, see: M.J. Ramsey-Musolf and S. Su, *Phys. Reports* **456**, 1 (2008).
90. W. Altmannshofer *et al.*, *Nucl. Phys.* **B830**, 17 (2010).
91. M.B. Einhorn and D.R.T. Jones, *Nucl. Phys.* **B196**, 475 (1982).
92. For a review, see R.N. Mohapatra, in *Particle Physics 1999*, ICTP Summer School in Particle Physics, Trieste, Italy, 21 June–9 July, 1999, edited by G. Senjanovic and A.Yu. Smirnov (World Scientific, Singapore, 2000) pp. 336–394; W.J. Marciano and G. Senjanovic, *Phys. Rev.* **D25**, 3092 (1982).
93. L.E. Ibáñez and G.G. Ross, *Phys. Lett.* **B110**, 215 (1982).
94. P. de Jong and O. Buchmüller "Supersymmetry Part II (Experiment)," in the 2012 edition of PDG book. See also *Particle Listings: Other Searches—Supersymmetric Particles*.
95. H.K. Dreiner *et al.*, *Eur. Phys. J.* **C62**, 547 (2009).
96. J.F. Gunion and H.E. Haber, *Phys. Rev.* **D37**, 2515 (1988); S.Y. Choi, M. Drees, and B. Gaissmaier, *Phys. Rev.* **D70**, 014010 (2004).
97. J.L. Feng *et al.*, *Phys. Rev. Lett.* **83**, 1731 (1999); T. Gherghetta, G.F. Giudice, and J.D. Wells, *Nucl. Phys.* **B559**, 27 (1999); J.F. Gunion and S. Mrenna, *Phys. Rev.* **D62**, 015002 (2000).
98. See *e.g.*, I. Jack, D.R.T. Jones, and R. Wild, *Phys. Lett.* **B535**, 193 (2002); B. Murakami and J.D. Wells, *Phys. Rev.* **D68**, 035006 (2003); R. Kitano, G.D. Kribs, and H. Murayama, *Phys. Rev.* **D70**, 035001 (2004); R. Hodgson *et al.*, *Nucl. Phys.* **B728**, 192 (2005); D.R.T. Jones and G.G. Ross, *Phys. Lett.* **B642**, 540 (2006).
99. M. Endo, M. Yamaguchi, and K. Yoshioka, *Phys. Rev.* **D**, 015004 (2005);



See key on page 457

## Searches Particle Listings

### Supersymmetric Particle Searches

- K. Choi, K.S. Jeong, and K.-I. Okumura, JHEP **0509**, 039 (2005).
100. See, *e.g.*, A. Brignole, L.E. Ibanez, and C. Munoz, in *Perspectives on Supersymmetry II*, edited by G.L. Kane (World Scientific, Singapore, 2010) pp. 244–268.
101. M. Drees and S.P. Martin, in *Electroweak Symmetry Breaking and New Physics at the TeV Scale*, edited by T. Barklow *et al.* (World Scientific, Singapore, 1996) pp. 146–215.
102. J.R. Ellis *et al.*, Phys. Lett. **B573**, 162 (2003); Phys. Rev. **D70**, 055005 (2004).
103. L.E. Ibáñez and D. Lüst, Nucl. Phys. **B382**, 305 (1992); B. de Carlos, J.A. Casas, and C. Munoz, Phys. Lett. **B299**, 234 (1993); V. Kaplunovsky and J. Louis, Phys. Lett. **B306**, 269 (1993); A. Brignole, L.E. Ibáñez, and C. Munoz, Nucl. Phys. **B422**, 125 (1994) [erratum: **B436**, 747 (1995)].
104. B.C. Allanach *et al.*, Eur. Phys. J. **C25**, 113 (2002).
105. K. Intriligator, N. Seiberg, and D. Shih, JHEP **0604**, 021 (2006); **0707**, 017 (2007).
106. See, *e.g.*, M. Dine, J.L. Feng, and E. Silverstein, Phys. Rev. **D74**, 095012 (2006); H. Murayama and Y. Nomura, Phys. Rev. Lett. **98**, 151803 (2007); Phys. Rev. **D75**, 095011 (2007); R. Kitano, H. Ooguri, and Y. Ookouchi, Phys. Rev. **D75**, 045022 (2007); A. Delgado, G.F. Giudice, and P. Slavich, Phys. Lett. **B653**, 424 (2007); O. Aharony and N. Seiberg, JHEP **0702**, 054 (2007); C. Csaki, Y. Shirman, and J. Terning, JHEP **0705**, 099 (2007); N. Haba and N. Maru, Phys. Rev. **D76**, 115019 (2007).
107. P. Meade, N. Seiberg, and D. Shih, Prog. Theor. Phys. Suppl. **177**, 143 (2009); M. Buican *et al.*, JHEP **0903**, 016 (2009).
108. A. Rajaraman *et al.*, Phys. Lett. **B678**, 367 (2009); L.M. Carpenter *et al.*, Phys. Rev. **D79**, 035002 (2009).
109. For a review and guide to the literature, see J.F. Gunion and H.E. Haber, in *Perspectives on Supersymmetry II*, edited by G.L. Kane (World Scientific, Singapore, 2010) pp. 420–445.
110. A. Djouadi, J.L. Kneur, and G. Moultaka, Comput. Phys. Commun. **176**, 426–455 (2007); C.F. Berger *et al.*, JHEP **0902**, 023 (2009).
111. J.A. Conley *et al.*, Eur. Phys. J. **C71**, 1697 (2011); B.C. Allanach *et al.*, JHEP **1107**, 104 (2011).
112. B.C. Allanach *et al.*, JHEP **0708**, 023 (2007); R. Lafaye *et al.*, Eur. Phys. J. **C54**, 617 (2008); O. Buchmueller *et al.*, JHEP **0809**, 117 (2008); O. Buchmueller *et al.*, Eur. Phys. J. **C64**, 391 (2009); S.S. AbdusSalam *et al.*, Phys. Rev. **D80**, 035017 (2009); S.S. AbdusSalam *et al.*, Phys. Rev. **D81**, 095012 (2010); P. Bechtle *et al.*, Eur. Phys. J. **C66**, 215 (2010); O. Buchmueller *et al.*, Eur. Phys. J. **C71**, 1583 (2011); O. Buchmueller *et al.*, Eur. Phys. J. **C71**, 1722 (2011).
113. See *e.g.*, O. Buchmueller *et al.*, arXiv:1110.3568 [hep-ph].
114. S. Sekmen *et al.*, JHEP **1202**, 075 (2012).
115. R. Barbieri and G.F. Giudice, Nucl. Phys. **B305**, 63 (1988).
116. G.W. Anderson and D.J. Castano, Phys. Lett. **B347**, 300 (1995); Phys. Rev. **D52**, 1693 (1995); Phys. Rev. **D53**, 2403 (1996); J.L. Feng, K.T. Matchev, and T. Moroi, Phys. Rev. **D61**, 075005 (2000); P. Athron and D.J. Miller, Phys. Rev. **D76**, 075010 (2007); M.E. Cabrera, J.A. Casas, and R.R. de Austri, JHEP **0903**, 075 (2009).
117. G.L. Kane and S.F. King, Phys. Lett. **B451**, 113 (1999); M. Bastero-Gil, G.L. Kane, and S.F. King, Phys. Lett. **B474**, 103 (2000); J.A. Casas, J.R. Espinosa, and I. Hidalgo, JHEP **0401**, 008 (2004); J. Abe, T. Kobayashi, and Y. Omura, Phys. Rev. **D76**, 015002 (2007); R. Essig and J.-F. Fortin, JHEP **0804**, 073 (2008).
118. A. Strumia, JHEP **1104**, 073 (2011); S. Cassel *et al.*, JHEP **1105**, 120 (2011).
119. R. Barbieri and A. Strumia, Talk given at *4th Rencontres du Vietnam: International Conference on Physics at Extreme Energies (Particle Physics and Astrophysics)*, Hanoi, Vietnam, 19–25 July 2000, hep-ph/0007265.
120. J.A. Casas, J.R. Espinosa, and I. Hidalgo, JHEP **0401**, 008 (2004); P. Batra *et al.*, JHEP **0406**, 032 (2004); R. Harnik *et al.*, Phys. Rev. **D70**, 015002 (2004); A. Birkedal, Z. Chacko, and M.K. Gaillard, JHEP **0410**, 036 (2004).
121. L. Giusti, A. Romanino, and A. Strumia, Nucl. Phys. **B550**, 3 (1999); H.C. Cheng and I. Low, JHEP **0309**, 051 (2003); **0408**, 061 (2004).
122. J. Feng, K. Matchev, and T. Moroi, Phys. Rev. Lett. **84**, 2322 (2000); Phys. Rev. **D61**, 075005 (2000); J. Feng and F. Wilczek, Phys. Lett. **B631**, 170 (2005).
123. J.L. Feng, K.T. Matchev and D. Sanford, Phys. Rev. **D85**, 075007 (2012).
124. S. Akula *et al.*, Phys. Lett. **B709**, 192 (2012).
125. M. Drees, Phys. Rev. **D33**, 1468 (1986); S. Dimopoulos and G.F. Giudice, Phys. Lett. **B357**, 573 (1995); A. Pomarol and D. Tommasini, Nucl. Phys. **B466**, 3 (1996).
126. M. Dine, A. Kagan, and S. Samuel, Phys. Lett. **B243**, 250 (1990); A.G. Cohen, D.B. Kaplan, and A.E. Nelson, Phys. Lett. **B388**, 588 (1996).
127. R. Kitano and Y. Nomura, Phys. Rev. **D73**, 095004 (2006); M. Perelstein and C. Spethmann, JHEP **0704**, 070 (2007); H. Abe, T. Kobayashi, and Y. Omura, Phys. Rev. **D76**, 015002 (2007); D. Horton and G.G. Ross, Nucl. Phys. **B830**, 221 (2010); H. Baer *et al.*, JHEP **1010**, 018 (2010); H. Baer, V. Barger, and P. Huang, JHEP **1111**, 031 (2011); C. Brust *et al.*, JHEP **1203**, 103 (2012); M. Papucci, J.T. Ruderman, and A. Weiler, arXiv:1110.6926 [hep-ph].
128. R. Dermisek and J.F. Gunion, Phys. Rev. Lett. **95**, 041801 (2005); Phys. Rev. **D75**, 095019 (2007); Phys.

# Searches Particle Listings

## Supersymmetric Particle Searches

- Rev. **D76**, 095006 (2007);  
 B. Bellazzini *et al.*, Phys. Rev. **D79**, 095003 (2009);  
 G.G. Ross and K.Schmidt-Hoberg, [arXiv:1108.1284](#) [hep-ph];  
 L.J. Hall, D. Pinner, and J.T. Ruderman, JHEP **1204**, 131 (2012).
129. S.P. Martin, Phys. Rev. **D75**, 115005 (2007); Phys. Rev. **D78**, 055019 (2009);  
 T.J. LeCompte and S.P. Martin, Phys. Rev. **D85**, 035023 (2012).
130. J. Fan, M. Reece, J.T. Ruderman, JHEP **1111**, 012 (2011).
131. N. Arkani-Hamed *et al.*, [hep-ph/0703088](#);  
 J. Alwall *et al.*, Phys. Rev. **D79**, 015005 (2009);  
 J. Alwall, P. Schuster, and N. Toro, Phys. Rev. **D79**, 075020 (2009);  
 D.S.M. Alves, E. Izaguirre, and J. G. Wacker, Phys. Lett. **B702**, 64 (2011); JHEP **1110**, 012 (2011);  
 D. Alves *et al.*, [arXiv:1105.2838](#) [hep-ph].
132. For a review, see D. Stockinger, J. Phys. **G34**, R45 (2007).
133. A. Hoecker, Nucl. Phys. Proc. Suppl. **218**, 189 (2011);  
 K. Hagiwara *et al.*, J. Phys. **G38**, 085003 (2011).
134. M. Benayoun *et al.*, Eur. Phys. J. **C72**, 1848 (2012).
135. A. Limosani *et al.* [Belle Collab.], Phys. Rev. Lett. **103**, 241801 (2009).
136. M. Misiak *et al.*, Phys. Rev. Lett. **98**, 022002 (2007);  
 T. Becher and M. Neubert, Phys. Rev. Lett. **98**, 022003 (2007).
137. See, *e.g.*, M. Ciuchini *et al.*, Phys. Rev. **D67**, 075016 (2003);  
 T. Hurth, Rev. Mod. Phys. **75**, 1159 (2003).
138. T. Moroi, Phys. Rev. **D53**, 6565 (1996) [erratum: **D56**, 4424 (1997)];  
 U. Chattopadhyay and P. Nath, Phys. Rev. **D66**, 093001 (2002);  
 S.P. Martin and J.D. Wells, Phys. Rev. **D67**, 015002 (2003).
139. S.R. Choudhury and N. Gaur, Phys. Lett. **B451**, 86 (1999);  
 K.S. Babu and C.F. Kolda, Phys. Rev. Lett. **84**, 228 (2000);  
 G. Isidori and A. Retico, JHEP **0111**, 001 (2001); JHEP **0209**, 063 (2002).
140. S. Chatrchyan *et al.* [CMS Collab.], Phys. Rev. Lett. **107**, 191802 (2011);  
 T. Kuhr *et al.* [CDF Collab.], [arXiv:1111.2428](#) [hep-ex];  
 R. Aaij *et al.* [LHCb Collab.], Phys. Lett. **B708**, 55 (2012).
141. J.R. Ellis *et al.*, Phys. Lett. **B653**, 292 (2007);  
 J.R. Ellis *et al.*, JHEP **0708**, 083 (2007);  
 S. Heinemeyer *et al.*, JHEP **0808**, 087 (2008);  
 A.G. Akeroyd, F. Mahmoudi, and D.M. Santos, JHEP **1112**, 088 (2011).
142. For a review of the current status of neutrino masses and mixing, see: M.C. Gonzalez-Garcia and M. Maltoni, Phys. Reports **460**, 1 (2008);  
 M.C. Gonzalez-Garcia, M. Maltoni, and J. Salvado, JHEP **1004**, 056 (2010);  
 T. Schwetz, M. Tortola, and J.W.F. Valle, New J. Phys. **13**, 063004 (2011); New J. Phys. **13**, 109401 (2011).
143. See the section on neutrinos in “Particle Listings—Leptons” in this *Review*.
144. K. Zuber, Phys. Reports **305**, 295 (1998).
145. For a review of neutrino masses in supersymmetry, see B. Mukhopadhyaya, *Proc. Indian National Science Academy* **A70**, 239 (2004);  
 M. Hirsch and J.W.F. Valle, New J. Phys. **6**, 76 (2004).
146. F. Borzumati and Y. Nomura, Phys. Rev. **D64**, 053005 (2001).
147. P. Minkowski, Phys. Lett. **67B**, 421 (1977);  
 M. Gell-Mann, P. Ramond, and R. Slansky, in *Supergravity*, edited by D. Freedman and P. van Nieuwenhuizen (North Holland, Amsterdam, 1979) p. 315;  
 T. Yanagida, Prog. Theor. Phys. **64**, 1103 (1980);  
 R. Mohapatra and G. Senjanovic, Phys. Rev. Lett. **44**, 912 (1980); Phys. Rev. **D23**, 165 (1981).
148. J. Hisano *et al.*, Phys. Lett. **B357**, 579 (1995);  
 J. Hisano *et al.*, Phys. Rev. **D53**, 2442 (1996);  
 J.A. Casas and A. Ibarra, Nucl. Phys. **B618**, 171 (2001);  
 J. Ellis *et al.*, Phys. Rev. **D66**, 115013 (2002);  
 A. Masiero, S.K. Vempati, and O. Vives, New J. Phys. **6**, 202 (2004);  
 E. Arganda *et al.*, Phys. Rev. **D71**, 035011 (2005);  
 F.R. Joaquim and A. Rossi, Phys. Rev. Lett. **97**, 181801 (2006);  
 J.R. Ellis and O. Lebedev, Phys. Lett. **B653**, 411 (2007).
149. Y. Grossman and H.E. Haber, Phys. Rev. Lett. **78**, 3438 (1997);  
 A. Dedes, H.E. Haber, and J. Rosiek, JHEP **0711**, 059 (2007).
150. M. Hirsch, H.V. Klapdor-Kleingrothaus, and S.G. Kovalenko, Phys. Lett. **B398**, 311 (1997);  
 L.J. Hall, T. Moroi, and H. Murayama, Phys. Lett. **B424**, 305 (1998);  
 K. Choi, K. Hwang, and W.Y. Song, Phys. Rev. Lett. **88**, 141801 (2002);  
 T. Honkavaara, K. Huitu, and S. Roy, Phys. Rev. **D73**, 055011 (2006).
151. A. Dedes, S. Rimmer, and J. Rosiek, JHEP **0608**, 005 (2006);  
 B.C. Allanach and C.H. Kom, JHEP **0804**, 081 (2008);  
 H.K. Dreiner *et al.*, Phys. Rev. **D84**, 113005 (2011).
152. For a review and references to the original literature, see M. Chemtob, Prog. Part. Nucl. Phys. **54**, 71 (2005);  
 R. Barbier *et al.*, Phys. Rept. **420**, 1 (2005).
153. H. Dreiner, in *Perspectives on Supersymmetry II*, edited by G.L. Kane (World Scientific, Singapore, 2010) pp. 565–583.
154. B.C. Allanach, A. Dedes, and H.K. Dreiner, Phys. Rev. **D60**, 075014 (1999).
155. L.E. Ibáñez and G.G. Ross, Nucl. Phys. **B368**, 3 (1992);  
 L.E. Ibáñez, Nucl. Phys. **B398**, 301 (1993).
156. For a review, see J.C. Romao, Nucl. Phys. Proc. Suppl. **81**, 231 (2000).
157. R.N. Mohapatra, Phys. Rev. **D34**, 3457 (1986);  
 K.S. Babu and R.N. Mohapatra, Phys. Rev. Lett. **75**, 2276 (1995);  
 M. Hirsch, H.V. Klapdor-Kleingrothaus, and S.G. Kovalenko, Phys. Rev. Lett. **75**, 17 (1995); Phys. Rev. **D53**, 1329 (1996).
158. Y. Grossman and H.E. Haber, Phys. Rev. **D59**, 093008 (1999).

159. S. Dimopoulos and L.J. Hall, Phys. Lett. **B207**, 210 (1988);  
J. Kalinowski *et al.*, Phys. Lett. **B406**, 314 (1997);  
J. Erler, J.L. Feng, and N. Polonsky, Phys. Rev. Lett. **78**, 3063 (1997).
160. H.K. Dreiner, P. Richardson, and M.H. Seymour, Phys. Rev. **D63**, 055008 (2001).
161. G.F. Giudice and A. Masiero, Phys. Lett. **B206**, 480 (1988).
162. See, *e.g.*, U. Ellwanger, M. Rausch de Traubenberg, and C.A. Savoy, Nucl. Phys. **B492**, 21 (1997);  
U. Ellwanger and C. Hugonie, Eur. J. Phys. **C25**, 297 (2002);  
U. Ellwanger, C. Hugonie, and A.M. Teixeira, Phys. Reports **496**, 1 (2010), and references contained therein.
163. M. Cvetič *et al.*, Phys. Rev. **D56**, 2861 (1997) [erratum: **D58**, 119905 (1998)].
164. J.R. Espinosa and M. Quiros, Phys. Rev. Lett. **81**, 516 (1998);  
P. Batra *et al.*, JHEP **0402**, 043 (2004);  
K.S. Babu, I. Gogoladze, and C. Kolda, hep-ph/0410085;  
R. Barbieri *et al.*, Phys. Rev. **D75**, 035007 (2007).
165. N. Haba and N. Okada, Prog. Theor. Phys. **114**, 1057 (2006).
166. A. Birkedal, Z. Chacko, and Y. Nomura, Phys. Rev. **D71**, 015006 (2005).
167. J.L. Hewett and T.G. Rizzo, Phys. Reports **183**, 193 (1989).
168. S.F. King, S. Moretti, and R. Nevzorov, Phys. Lett. **B634**, 278 (2006); Phys. Rev. **D73**, 035009 (2006).
169. M. Cvetič and P. Langacker, Mod. Phys. Lett. **A11**, 1247 (1996);  
K.R. Dienes, Phys. Reports **287**, 447 (1997).

## SUPERSYMMETRY, PART II (EXPERIMENT)

Written March 2012 by O. Buchmueller (Imperial College London) and P. de Jong (Nikhef).

- II.1. Introduction
- II.2. Experimental search program
- II.3. Interpretation of results
- II.4. Exclusion limits on gluino and squark masses
  - II.4.1 Exclusion limits on the gluino mass
  - II.4.2. Exclusion limits on first and second generation squark masses
  - II.4.3. Exclusion limits on third generation squark masses
- II.5. Exclusion limits on slepton masses
  - II.5.1. Exclusion limits on the masses of charged sleptons
  - II.5.2. Exclusion limits on sneutrino masses
- II.6. Exclusion limits on masses of charginos and neutralinos
  - II.6.1. Exclusion limits on chargino masses
  - II.6.2. Exclusion limits on neutralino masses
- II.7. Global interpretations
- II.8. Summary and Outlook

### II.1. Introduction

Supersymmetry (SUSY) [1–9] is one of the most compelling possible extensions of the Standard Model of particle physics (SM), and a leading contender for a new principle about nature

that could be discovered at high-energy colliders such as the Large Hadron Collider (LHC).

On theoretical grounds SUSY is motivated as a generalization of space-time symmetries. A low-energy realization of SUSY, *i.e.*, SUSY at the TeV scale, is, however, not a necessary consequence. Instead, low-energy SUSY is motivated by the possible cancellation of quadratic divergences in radiative corrections to the Higgs boson mass [10–15]. Furthermore, it is intriguing that a weakly interacting, (meta)stable supersymmetric particle might make up some or all of the dark matter in the universe [16–18]. In addition, SUSY predicts that gauge couplings, as measured experimentally at the electroweak scale, unify at an energy scale  $\mathcal{O}(10^{16})\text{GeV}$  (“GUT scale”) near the Planck scale [19–25].

In the minimal supersymmetric extension to the Standard Model, the so called MSSM [26,27,11], a supersymmetry transformation pairs bosons with fermions and therefore relates every particle in the SM to a supersymmetric partner with half a unit of spin difference, but otherwise with the same properties and quantum numbers. These are the “sfermions”: squarks and sleptons, the “gauginos,” and the partners of the Higgs doublets, the “higgsinos.” The charged weak gauginos and higgsinos mix to “charginos,” and the neutral ones mix to “neutralinos.” The fact that such particles are not yet observed leads to the conclusion that, if supersymmetry is realized, it is a broken symmetry. A description of SUSY in the form of an effective Lagrangian with only “soft” SUSY-breaking terms and SUSY masses at the TeV scale maintains cancellation of quadratic divergences in particle physics models.

The phenomenology of SUSY is to a large extent determined by the SUSY-breaking mechanism and the SUSY-breaking scale. This determines the SUSY particle masses, the mass hierarchy, the field contents of physical particles, and their decay modes. In addition, phenomenology crucially depends on whether the multiplicative quantum number of R-parity [27],  $R = (-1)^{3(B-L)+2S}$ , where  $B$  and  $L$  are baryon and lepton numbers and  $S$  is the spin, is conserved or violated. If R-parity is conserved, SUSY particles, which have odd R-parity, are produced in pairs and the decays of each SUSY particle must involve an odd number of lighter SUSY particles. The lightest SUSY particle (LSP) is then stable and often assumed to be a weakly interacting massive particle (WIMP). If R-parity is violated, new terms  $\lambda_{ijk}$ ,  $\lambda'_{ijk}$  and  $\lambda''_{ijk}$  appear in the superpotential, where  $ijk$  are generation indices;  $\lambda$ -type couplings appear between lepton superfields only,  $\lambda'$ -type are between quark superfields only, and  $\lambda''$ -type couplings connect the two. R-parity violation implies lepton and/or baryon number violation. More details of the theoretical framework of SUSY are discussed elsewhere in this volume [28].

Today low-energy data from flavor physics experiments, high-precision electroweak observables as well as astrophysical data impose strong constraints on the allowed SUSY parameter space. Examples of such data include measurements of precision electroweak observables, of the anomalous magnetic

# Searches Particle Listings

## Supersymmetric Particle Searches

moment of the muon and of the cosmological dark matter relic density, as well as limits on rare B-meson and K-meson decays, on electric dipole moments, on proton decay, and on WIMP-nucleon scattering cross sections. These indirect constraints are often more sensitive to higher SUSY mass scales than experiments searching for direct SUSY particle (sparticle) production at colliders, but the interpretation of these results are often strongly model dependent. In contrast, direct searches for sparticle production at collider experiments are much less subject to interpretation ambiguities and therefore they play a crucial role in the discovery strategy for SUSY.

In the rest of this review we limit ourselves to direct searches, covering data analyses at LEP, HERA, the Tevatron and the LHC. With the advent of the LHC, the experimental situation is changing rapidly. Compared to earlier PDG reviews, more emphasis is given to LHC results; for more details on LEP and Tevatron constraints, see earlier PDG reviews [29]. The SUSY Higgs sector is covered elsewhere in this volume [30].

### II.2. Experimental search program

The electron-positron collider LEP was operational at CERN between 1989 and 2000. In the initial phase, center-of-mass energies around the  $Z$ -peak were probed, but after 1995 the LEP experiments collected a significant amount of luminosity at higher center-of-mass energies, some  $235 \text{ pb}^{-1}$  per experiment at  $\sqrt{s} \geq 204 \text{ GeV}$ , with a maximum  $\sqrt{s}$  of  $209 \text{ GeV}$ .

Searches for new physics at  $e^+e^-$  colliders benefit from the clean experimental environment and the fact that momentum balance can be measured not only in the plane transverse to the beam, but also in the direction along the beam (up to the beam pipe holes), the longitudinal direction. Searches at LEP are dominated by the data samples taken at the highest center-of-mass energies. The LEP limits for electroweak gauginos and sleptons are still competitive.

Significant constraints on SUSY have been set by the CDF and D0 experiments at the Tevatron, a proton-antiproton collider at a center-of-mass energy of up to  $1.96 \text{ TeV}$ . CDF and D0 have collected integrated luminosities between  $10$  and  $11 \text{ fb}^{-1}$  each up to the end of collider operations in 2011.

The electron-proton collider HERA provided collisions to the H1 and ZEUS experiments between 1992 and 2007, at a center-of-mass energy up to  $318 \text{ GeV}$ . A total integrated luminosity of approximately  $0.5 \text{ fb}^{-1}$  has been collected by each experiment. Since in  $ep$  collisions no annihilation process takes place, SUSY searches at HERA typically look for R-parity violating production of single SUSY particles.

The landscape of SUSY searches, however, has significantly changed since the Large Hadron Collider (LHC) at CERN has started proton-proton operation at a center-of-mass energy of  $7 \text{ TeV}$  in 2010. By the end of 2011 the experiments CMS and ATLAS had collected about  $5 \text{ fb}^{-1}$  of integrated luminosity each, and the LHCb experiment had collected approximately  $1 \text{ fb}^{-1}$ .

Proton-(anti)proton colliders produce interactions at higher center-of-mass energies than those available at LEP, and cross

sections of QCD-mediated processes are larger, which is reflected in the higher sensitivity for SUSY particles carrying color charge: squarks and gluinos. Large backgrounds, however, pose challenges to trigger and analysis. Such backgrounds are dominated by multijet production processes, including, particularly at the LHC, those of top quark production, as well as jet production in association with vector bosons. The proton momentum is shared between its parton constituents, and in each collision only a fraction of the total center-of-mass energy is available in the hard parton-parton scattering. Since the parton momenta in the longitudinal direction are not known on an event-by-event basis, momentum conservation is restricted to the transverse plane, leading to the use in the experimental analyses of transverse variables, such as the missing transverse momentum, and the transverse mass. Proton-proton collisions at the LHC differ from proton-antiproton collisions at the Tevatron in the sense that there are no valence anti-quarks in the proton, and that gluon-initiated processes play a more dominant role. The increased center-of-mass energy of the LHC compared to the Tevatron significantly extends the kinematic reach for SUSY searches. This is reflected foremost in the sensitivity for squarks and gluinos, but also for other SUSY particles.

The main production mechanisms of massive colored sparticles at hadron colliders are squark-squark, squark-gluino and gluino-gluino production; when “squark” is used “antisquark” is also implied. The typical SUSY search signature at hadron colliders contains high- $p_T$  jets, which are produced in the decay chains of heavy squarks and gluinos, and significant missing momentum originating from the two lightest supersymmetric particles (LSP) produced at the end of the decay chain. Assuming R-parity conservation, the LSPs are neutral and weakly interacting massive particles which escape detection. Backgrounds to such searches arise from multijet events with real missing momentum, dominated by heavy flavor decays, but also from instrumental effects in multijet events such as non-uniform calorimeter response or jet mismeasurement. Selection variables designed to separate the SUSY signal from the backgrounds include  $H_T$ ,  $E_T^{\text{miss}}$  and  $m_{\text{eff}}$ . The quantities  $H_T$  and  $E_T^{\text{miss}}$  refer to the measured energy and missing transverse momentum in the event, respectively. They are usually defined as the scalar ( $H_T$ ) and negative vector sum  $E_T^{\text{miss}}$  of the transverse jet energies or transverse calorimeter clusters energies measured in the event. The quantity  $m_{\text{eff}}$  is referred to as the effective mass of the event and is defined as  $m_{\text{eff}} = H_T + |E_T^{\text{miss}}|$ . The peak of the  $m_{\text{eff}}$  distribution for SUSY signal events correlates with the SUSY mass scale [31]. Additional reduction of multijet backgrounds can be achieved by demanding isolated leptons, multileptons or photons in the final states.

In the past few years alternative approaches have been developed to increase the sensitivity to pair production of heavy sparticles with masses around  $1 \text{ TeV}$  focusing on the kinematics of their decays, and to further suppress the background from multijet production. Prominent examples of these

See key on page 457

new approaches are searches using the  $\alpha_T$  [32–34], *razor* [35], *stransverse mass* ( $m_{T2}$ ) [36], and *contransverse mass* ( $m_{CT}$ ) [37] variables.

### II.3. Interpretation of results

Since the mechanism by which SUSY is broken is unknown, a general approach to SUSY via the most general soft SUSY breaking Lagrangian adds a significant number of new free parameters. For the minimal supersymmetric standard model, MSSM, *i.e.*, the model with the minimal particle content, these comprise 105 new parameters. A phenomenological analysis of SUSY searches leaving all these parameters free is not feasible. For the practical interpretation of SUSY searches at colliders several approaches are taken to reduce the number of free parameters.

One approach is to assume a SUSY breaking mechanism and lower the number of free parameters through the assumption of additional constraints. In particular, interpretations of experimental results are often done in constrained models of gravity mediated [38,39], gauge mediated [40,41], and anomaly mediated [42,43] SUSY breaking. The most popular model for interpretation of collider based SUSY searches is the constrained MSSM (CMSSM) [38,44,45], which in the literature is also referred to as minimal supergravity, or MSUGRA. The CMSSM is described by five parameters: the common sfermion mass  $m_0$ , the common gaugino mass  $m_{1/2}$ , and the common trilinear coupling parameter  $A_0$ , all expressed at the GUT scale, the ratio of the vacuum expectation values of the Higgs fields for up-type and down-type fermions  $\tan\beta$ , and the sign of the Higgsino mass parameter  $\mu$ . In gauge mediation models, the paradigm of general gauge mediation (GGM) [46] is slowly replacing minimal gauge mediation, denoted traditionally as GMSB (gauge mediated SUSY breaking).

These constrained SUSY models are theoretically well motivated and provide a rich spectrum of experimental signatures. Therefore, they represent a useful framework to benchmark performance, compare limits or reaches and assess the expected sensitivity of different search strategies. However, with universality relations imposed on the soft SUSY-breaking parameters, they do not cover all possible kinematic signatures and mass relations of SUSY. For this reason, an effort has been made in the past years to complement the traditional constrained models with more flexible interpretation approaches.

One answer to study a broader and more comprehensive subset of the MSSM is via the phenomenological-MSSM, or pMSSM [47–49]. It is derived from the MSSM, using experimental data to eliminate parameters that are free in principle but have already been highly constrained by measurements of *e.g.*, flavor mixing and CP-violation. This effective approach reduces the number of free parameters in the MSSM to 19, making it a practical compromise between the full MSSM and highly constrained universality models such as the CMSSM.

Even less dependent on fundamental assumptions are interpretations in terms of so-called simplified models [50–53].

Such models assume a limited set of SUSY particle production and decay modes and leave open the possibility to vary masses and other parameters freely. Therefore, simplified models enable comprehensive studies of individual SUSY topologies without limitations on fundamental kinematic properties such as masses, production cross sections, and decay modes.

The landscape of SUSY searches and corresponding interpretations continues to change rapidly and this review covers results up to March 2012. Since none of the searches performed so far have shown significant excess above the SM background prediction, the interpretation of the presented results are exclusion limits on SUSY parameter space. This review will mainly focus on limits expressed in the context of CMSSM, gauge mediation, pMSSM and various simplified models.

### II.4. Exclusion limits on gluino and squark masses

Gluinos and squarks are the SUSY partners of gluons and quarks, and thus carry color charge. Although limits on squark masses of the order 100 GeV have been set by the LEP experiments, hadron collider experiments are able to set much higher mass limits. The results of the LHC experiments now dominate the search for direct squark and gluino production. Pair production of these massive colored sparticles at hadron colliders generally involve both s-channel and t-channel parton-parton interactions. Since there is a negligible amount of bottom and top quark content in the proton, top- and bottom squark production proceeds through s-channel diagrams only with small cross sections. Experimental analyses of squark and/or gluino production typically assume the first and second generation squarks to be approximately degenerate in mass.

Assuming R-parity conservation, squarks will predominantly decay to a quark and a neutralino or chargino, if kinematically allowed. Other decay modes depend on the masses of the weak gauginos and may involve heavier neutralinos or charginos. For first and second generation squarks, the simplest decay modes involve two jets and missing momentum, with potential extra jets stemming from initial state radiation (ISR) or from decay modes with longer cascades. Similarly, gluino pair production leads to four jets and missing momentum, and possibly additional jets from ISR or cascades. Associated production of a gluino and a (anti)squark is also possible, in particular if squarks and gluinos have similar masses, typically leading to three or more jets in the final state. In cascades, isolated photons or leptons may appear from the decays of sparticles such as neutralinos or charginos. Final states are thus characterized by significant missing transverse momentum, and at least two, and possibly many more high  $p_T$  jets, which can be accompanied by one or more isolated objects like photons or leptons, including  $\tau$  leptons, in the final state. Table 1 shows a schematic overview of characteristic final state signatures of gluino and squark production for different mass hierarchy assumptions.

# Searches Particle Listings

## Supersymmetric Particle Searches

**Table 1:** Typical search signatures at hadron colliders for direct gluino and first- and second-generation squark production assuming different mass hierarchies.

Mass Hierarchy	Main Production	Dominant Decay	Typical Signature
$m_{\tilde{q}} \ll m_{\tilde{g}}$	$\tilde{q}\tilde{q}, \tilde{q}\tilde{\bar{q}}$	$\tilde{q} \rightarrow q\tilde{\chi}_1^0$	$\geq 2$ jets + $E_T^{\text{miss}}$ + X
$m_{\tilde{q}} \approx m_{\tilde{g}}$	$\tilde{q}\tilde{g}, \tilde{q}\tilde{\bar{g}}$	$\tilde{q} \rightarrow q\tilde{\chi}_1^0$ $\tilde{g} \rightarrow q\tilde{q}\tilde{\chi}_1^0$	$\geq 3$ jets + $E_T^{\text{miss}}$ + X
$m_{\tilde{q}} \gg m_{\tilde{g}}$	$\tilde{g}\tilde{g}$	$\tilde{g} \rightarrow q\tilde{q}\tilde{\chi}_1^0$	$\geq 4$ jets + $E_T^{\text{miss}}$ + X

### II.4.1 Exclusion limits on the gluino mass

Limits set by the Tevatron experiments on the gluino mass assume the framework of the CMSSM, with  $\tan\beta = 5$  (CDF) or  $\tan\beta = 3$  (D0),  $A_0 = 0$  and  $\mu < 0$ , and amount to lower limits of about 310 GeV for all squark masses, or 390 GeV for the case  $m_{\tilde{q}} = m_{\tilde{g}}$  [54,55].

At the LHC, limits on the gluino mass have been set using up to approximately  $5 \text{ fb}^{-1}$  of data. As shown in Fig. 1, in the framework of the CMSSM, gluino masses below 800 GeV are excluded by the ATLAS collaboration for all squark masses. For equal squark and gluino masses, the limit is about 1400 GeV [56]. Similar results are reported by the CMS collaboration [57]. These limits are dominated by hadronic searches, which veto any contribution from isolated leptons and, for CMS, isolated photons. Although these results are derived for  $\tan\beta = 10$ ,  $A_0 = 0$ , and  $\mu > 0$ , they are only mildly dependent on the choice of these CMSSM parameters.

In a simplified model, assuming only gluino pair production and a single decay chain of  $\tilde{g} \rightarrow q\tilde{q}\tilde{\chi}_1^0$ , upper limits on gluino production are derived as a function of the gluino and neutralino (LSP) mass. As shown in Fig. 2, using the next to leading order cross section for gluino pair production as reference, the CMS collaboration excludes in this simplified model gluino masses below 900 GeV, for a massless neutralino. In scenarios where neutralinos are not very light, the efficiency of analyses is reduced by the fact that jets are less energetic, and there is less missing transverse momentum in the event. Therefore, limits on gluino masses are strongly affected by the assumption of the neutralino mass. For example, for a gluino mass of around 1 TeV the upper limit on the gluino pair production cross section in this simplified model ranges from a few  $10^{-2}$  pb for a massless neutralino to about 1 pb for a neutralino of  $\approx 800$  GeV. Furthermore, for neutralino masses above 300 – 400 GeV no general limit on the gluino mass can be set. Similar results have been obtained by ATLAS [60].

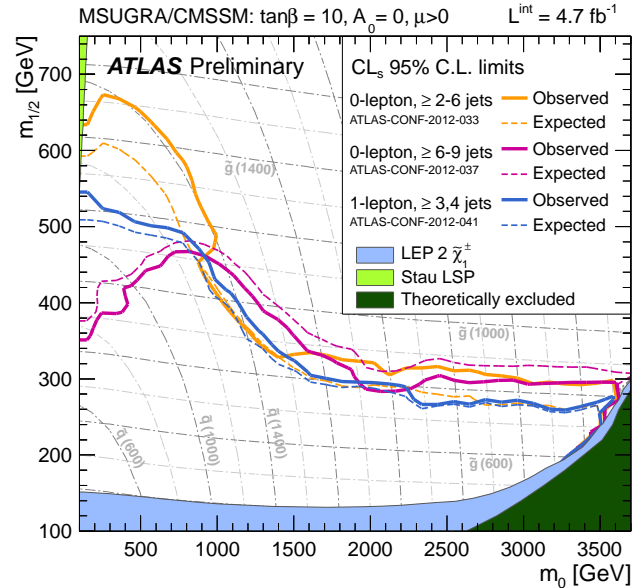


**Figure 1:** Limits, at 95% C.L., on the CMSSM parameters  $m_0$  and  $m_{1/2}$  derived from multi-jet analyses [56,58] and an analysis of jets and one isolated lepton [59] by the ATLAS experiment, for  $\tan\beta = 10$ ,  $A_0 = 0$  and  $\mu > 0$ .

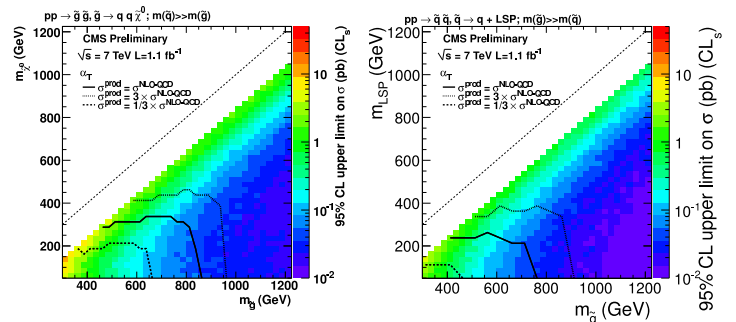


**Figure 2:** Upper limits, at 95% C.L., on the cross section of gluino pair production (left) or first- or second generation squark pair production (right) set by the CMS collaboration defined in the framework of simplified models assuming a single decay chain of  $\tilde{g} \rightarrow q\tilde{q}\tilde{\chi}_1^0$  (left) or  $\tilde{q} \rightarrow q\tilde{\chi}_1^0$  (right). The contours illustrate where the reference cross section, calculated at next to leading order, and the upper limit on the cross section intersect. The reference cross section is scaled by a factor 3 or 1/3 to illustrate the effect of cross section or branching ratio variations. The diagonal part of  $m_{\tilde{g}/\tilde{q}} - m_{\tilde{\chi}_1^0} < 200$  GeV is not kinematically accessible for the analysis and therefore no limit is provided.

If the gluino decay is suppressed, for example if squark masses are high, gluinos may live longer than typical hadronization times. It is expected that such gluinos will hadronize to semi-stable strongly interacting particles known as R-hadrons. Searches for R-hadrons exploit the typical signature of stable charged massive particles in the detector. As shown in Fig. 3, the CMS experiment excludes semi-stable gluino R-hadrons with masses below approximately 1 TeV [61]. The limits depend on the probability for gluinos to form bound states known as gluinoballs, as these are neutral and not observed in the tracking detectors. Similar limits are obtained by the ATLAS experiment [62].

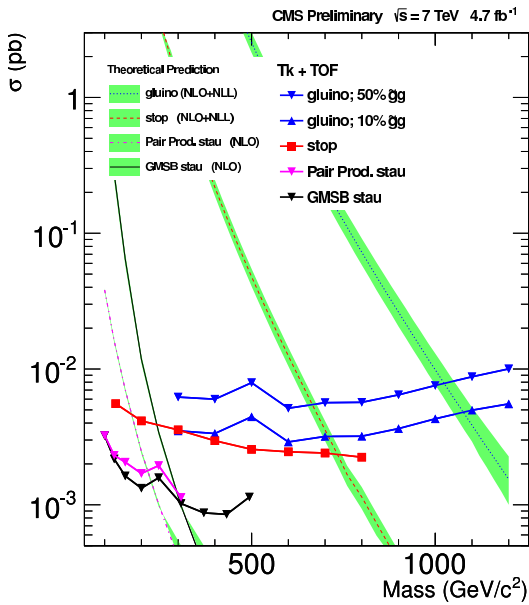


**Figure 3:** Observed 95% C.L. upper limits on the cross section for different combinations of models and scenarios considered: pair production of semi-stable tau sleptons, top squarks or gluinos. For gluinos, different fractions of gluinoball states produced after hadronization scenarios are indicated. The observed limits are compared with the predicted theoretical cross sections where the bands represent the theoretical uncertainties on the cross section values.

Alternatively, since such R-hadrons are strongly interacting, they may be stopped in the calorimeter or in other material, and decay later into energetic jets. These decays are searched for by identifying the jets outside the time window associated with bunch-bunch collisions [63–65]. The CMS analysis sets limits at 95% C.L. on gluino production over 13 orders of magnitude of gluino lifetime. For a mass difference  $m_{\tilde{g}} - m_{\tilde{\chi}_1^0} > 100$  GeV, assuming a 100% branching fraction for gluino decay to gluon + neutralino, gluinos with lifetimes from 10  $\mu\text{s}$  to 1000 s and  $m_{\tilde{g}} < 600$  GeV are excluded.

#### II.4.2. Exclusion limits on first and second generation squark masses

Limits on first and second generation squark masses set by the Tevatron experiments assume the CMSSM model, and amount to lower limits of about 380 GeV for all gluino masses, or 390 GeV for the case  $m_{\tilde{q}} = m_{\tilde{g}}$  [54,55].

At the LHC, limits on squark masses have been set using up to approximately  $5 \text{ fb}^{-1}$  of data. As for limits on the gluino mass, the highest sensitivity on squark production is obtained from fully-hadronic searches. As shown in Fig. 1, the ATLAS collaboration [56] excludes in the framework of the CMSSM squark masses below 1300 GeV for all gluino masses; for equal squark and gluino masses, the limit is about 1400 GeV. The limits obtained by CMS [57] are again very similar.

An interpretation of the CMS analysis using a simplified model characterizing squark pair production with only one decay chain of  $\tilde{q} \rightarrow q\tilde{\chi}_1^0$  yields an exclusion of squark masses below 750 GeV for a massless neutralino (see Fig. 2). The effects of heavy neutralinos on squark limits are similar to those discussed in the gluino case (see section “Exclusion limits on the gluino mass”) and only for neutralino masses below 200 – 300 GeV squark masses can be excluded.

The ATLAS analysis [56] is also interpreted in the framework of a simplified model with only squark and gluino production, for a massless neutralino, and assuming that all other sparticles are very massive. Results are shown in Fig. 4. In this interpretation, squark masses below 1500 GeV are excluded for  $m_{\tilde{g}} \approx m_{\tilde{q}}$ , while for large gluino masses the limit is reduced to about 1400 GeV in squark mass. Increasing the neutralino mass to values above  $\sim 200$  GeV again leads to a degradation of these limits.

An overview of exclusion limits on first and second generation squark and gluino masses from CMS for different simplified models [66] is shown in Fig. 5. Like for the other simplified model limits, the reference cross sections for the different processes are calculated at next to leading order precision. To illustrate the impact of the neutralino mass on the limits, two mass scenarios for  $m_{\tilde{\chi}_1^0} = 0$  GeV (dark blue) and  $m_{\text{mother}} - m_{\tilde{\chi}_1^0} = 200$  GeV (light blue) are presented. As expected, the simplified model exclusion limits vary strongly with the assumption on the mass splitting ( $m_{\text{mother}} - m_{\tilde{\chi}_1^0}$ ) between the mother sparticle and LSP. The exclusion limits are strongest for maximal mass splitting and significantly weakened for more compressed spectra. Depending on the simplified model, the least stringent limits for compressed spectra are in the range of 400 GeV to 550 GeV, while the most stringent ones for maximal splitting are in the range of 650 GeV to 900 GeV. The corresponding results of ATLAS are very similar [67].

A summary of the most important first generation squark and gluino mass limits for different interpretations assuming R-parity conservation is shown in Table 2.



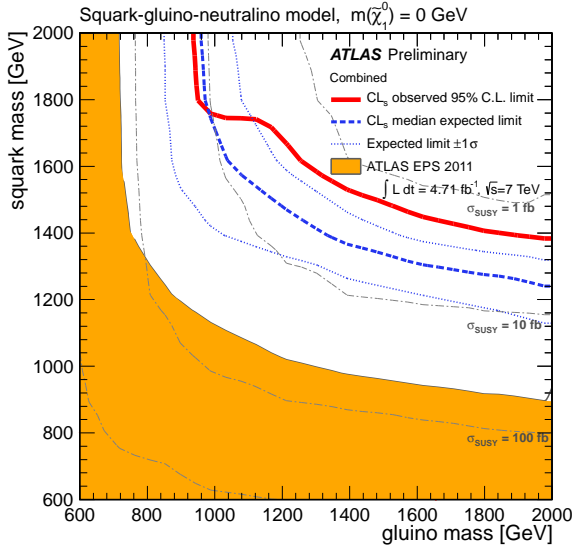


**Figure 4:** Limits on the masses of gluinos and first and second generation squarks, at 95% C.L., derived by ATLAS using simplified models with a massless neutralino, and assuming that the masses of all other SUSY particles are very large.

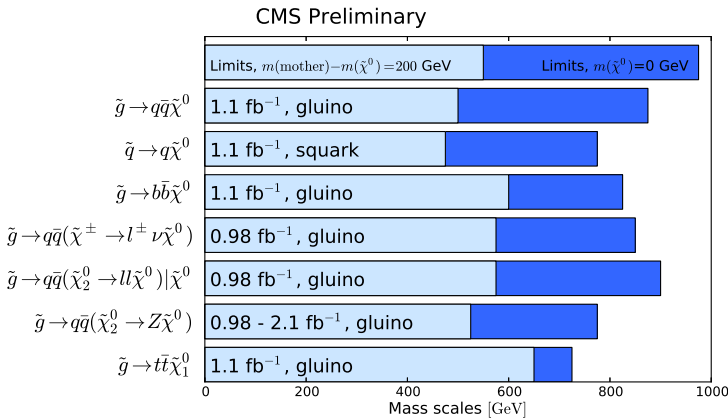


**Figure 5:** Exclusion limits, at 95% C.L., on first- or second generation squark and gluino masses from CMS for different simplified models. The reference cross sections for gluino and squark pair production are calculated at next to leading order precision and the branching fraction of their decays to daughter particles is assumed to be 100%. To show the impact of the neutralino mass on the limits, two mass scenarios are displayed:  $m_{\chi_1^0} = 0$  GeV (dark blue) and  $m_{\text{mother}} - m_{\chi_1^0} = 200$  GeV (light blue).

R-parity violating production of single squarks via a  $\lambda'$ -type coupling has been studied at HERA. In such models, a lower limit on the squark mass of the order of 275 GeV has been set for electromagnetic-strength-like couplings  $\lambda' = 0.3$  [68].

**Table 2:** Summary of first- or second generation squark mass and gluino mass limits using different interpretation approaches assuming R-parity conservation. Masses in this table are provided in GeV.

Model	Assumption	$m_{\tilde{q}}$	$m_{\tilde{g}}$
CMSSM	$m_{\tilde{q}} \approx m_{\tilde{g}}$	1400	1400
	all $m_{\tilde{q}}$	-	800
	all $m_{\tilde{g}}$	1300	-
Simplified model $\tilde{g}\tilde{g}$	$m_{\chi_1^0} = 0$	-	900
	$m_{\chi_1^0} > 300$	-	no limit
Simplified model $\tilde{q}\tilde{q}$	$m_{\chi_1^0} = 0$	750	-
	$m_{\chi_1^0} > 250$	no limit	-
Simplified model $\tilde{g}\tilde{q}, \tilde{g}\tilde{\bar{q}}$	$m_{\chi_1^0} = 0, m_{\tilde{q}} \approx m_{\tilde{g}}$	1500	1500
	$m_{\chi_1^0} = 0, \text{all } m_{\tilde{g}}$	1400	-
	$m_{\chi_1^0} = 0, \text{all } m_{\tilde{q}}$	-	900

### II.4.3. Exclusion limits on third generation squark masses

TeV-scale SUSY is often motivated by naturalness arguments, most notably as a solution to stabilize quadratic divergences in radiative corrections to the Higgs boson mass. In this context, the most relevant terms for SUSY phenomenology arise from the interplay between the masses of the third generation squarks and the (large) Yukawa coupling of the top quark to the Higgs boson. This motivates a potential constraint on the masses of the top squarks and the left-handed bottom squark. Due to the large top quark mass, significant mixing between  $\tilde{t}_L$  and  $\tilde{t}_R$  is expected, leading to a lighter mass state  $\tilde{t}_1$  and a heavier mass state  $\tilde{t}_2$ . In much of MSSM parameter space, the lightest top squark ( $\tilde{t}_1$ ) is also the lightest squark. Top squark masses below the top quark mass are not excluded.

In the absence of a SUSY discovery so far, searches for third generation squark production have become a major focus. Direct- and gluino mediated top and/or bottom squark production processes, leading to experimental signatures that are rich in jets originating from bottom quarks ( $b$ -jets), are either subject of re-interpretation of inclusive analyses or targets for dedicated third generation squark searches. This review contains results up to March 2012, but more results from the LHC experiments on the 2011 data sample are expected.

The top squark decay modes depend on the SUSY mass spectrum. If kinematically allowed,  $\tilde{t} \rightarrow t\tilde{\chi}^0$  and  $\tilde{t} \rightarrow b\tilde{\chi}^\pm$  are expected to dominate. If not,  $\tilde{t} \rightarrow bf\tilde{\nu}\tilde{\chi}^0$  (where  $f$  and  $\tilde{\nu}$  denote a fermion-antifermion pair with appropriate quantum numbers) or the two-body decay  $\tilde{t} \rightarrow c\tilde{\chi}^0$  is open. For light sneutrinos,  $\tilde{t} \rightarrow b\tilde{l}\tilde{\nu}$  needs to be taken into account.

Limits from LEP on the  $\tilde{t}_1$  mass are  $> 96$  GeV in the charm plus neutralino final state, and  $> 93$  GeV in the lepton,  $b$ -quark and sneutrino final state [69].

Direct production of top squark pairs at hadron colliders is suppressed with respect to first generation squarks, due to the



See key on page 457

## Searches Particle Listings Supersymmetric Particle Searches

absence of  $t$ -quarks in the proton. At the LHC, for example, this suppression is typically a factor 100 at  $m_{\tilde{t}} = 600$  GeV. Moreover, at the LHC, there is a very large background of top quark pair production, making experimental analysis of top squark pair production a challenge.

The Tevatron experiments have performed a number of searches for top squarks, often assuming direct pair production. In the  $b\ell\bar{\nu}$  decay channel, and assuming a 100% branching fraction, limits are set as  $m_{\tilde{t}} > 210$  GeV for  $m_{\tilde{\nu}} < 110$  GeV and  $m_{\tilde{t}} - m_{\tilde{\nu}} > 30$  GeV, or  $m_{\tilde{t}} > 235$  GeV for  $m_{\tilde{\nu}} < 50$  GeV [70,71]. In the  $\tilde{t} \rightarrow c\tilde{\chi}^0$  decay mode, a top squark with a mass below 180 GeV is excluded for a neutralino lighter than 95 GeV [72,73]. In both analyses, no limits on the top squark can be set for heavy sneutrinos or neutralinos. In the  $\tilde{t} \rightarrow b\tilde{\chi}_1^\pm$  decay channel, searches for a relatively light top squark have been performed in the dilepton final state [74,75]. CDF sets limits in the  $\tilde{t} - \tilde{\chi}_1^0$  mass plane for various branching fractions of the chargino decay to leptons and for two values of  $m_{\tilde{\chi}_1^\pm}$ . For  $m_{\tilde{\chi}_1^\pm} = 105.8$  GeV and  $m_{\tilde{\chi}_1^0} = 47.6$  GeV, top squarks between 128 and 135 GeV are excluded for  $W$ -like leptonic branching fractions of the chargino.

Top squarks may also be the product of gluino decays, if kinematically allowed:  $\tilde{g} \rightarrow \tilde{t}t$ . This leads to the characteristic “four tops” final state  $tttt\tilde{\chi}_1^0\tilde{\chi}_1^0$ , *i.e.*, a signature with as many as four isolated leptons, four  $b$ -jets, several light quark jets, and significant missing momentum from the neutrinos in the  $W$  decay and the two neutralinos. At the LHC, such final states are searched for in analyses demanding  $b$ -tagged jets and a lepton, or two leptons of the same charge (same-sign leptons), or many jets plus large missing momentum [76–78].

The interpretation of the results is performed in simplified models assuming specific decay modes, and MSSM production cross sections. Assuming the top squark is light enough, a simplified model with the decay chain  $\tilde{g} \rightarrow \tilde{t}t$  and  $\tilde{t} \rightarrow t\tilde{\chi}_1^0$  is used to characterize the reach of the searches, with gluino mass, stop mass and neutralino mass as free parameters. As shown in Fig. 6, a CMS search for same-sign lepton production accompanied with  $b$ -jets excludes gluino masses below some 850 GeV for top squark masses up to 650 GeV [78].

Taking into account top squark decay via  $\tilde{t} \rightarrow t\tilde{\chi}_1^0$ , and thus assuming  $\tilde{g} \rightarrow \tilde{t}t\tilde{\chi}_1^0$ , as shown in Fig. 7, an ATLAS analysis searching for multijet plus  $E_T^{\text{miss}}$  final states excludes gluino masses below 880(830) GeV for  $m_{\tilde{\chi}_1^0} < 100(200)$  GeV [58]. For neutralino masses above 250 GeV, no limit can be placed on the top squark mass for this scenario.

R-parity violating production of single top squarks has been searched for at HERA [79]. Top squarks are assumed to be produced via a  $\lambda'$  coupling and decay either to  $b\tilde{\chi}_1^\pm$  or R-parity-violating to a lepton and a jet. Limits are set on  $\lambda'_{131}$  as a function of the top squark mass in an MSSM framework with gaugino mass unification at the GUT scale. Within a variant of the CMSSM with R-parity violation, and assuming  $\tan\beta = 6$ ,  $A_0 = 0$ ,  $\mu < 0$ , a top squark with mass below 260 GeV is excluded for  $\lambda' = 0.3$ .

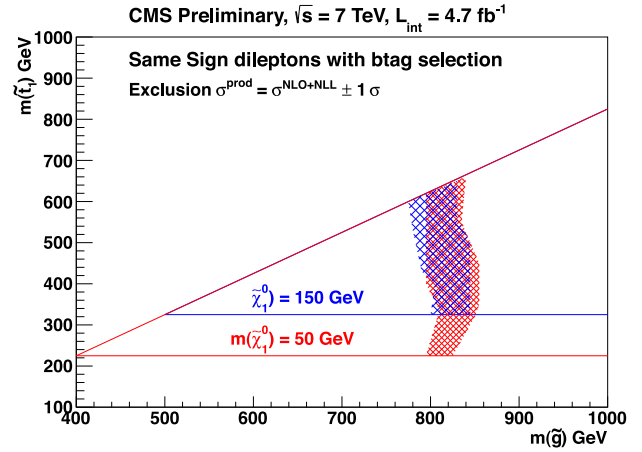


**Figure 6:** 95% C.L. exclusion in the stop-gluino mass plane for different choices of the neutralino mass. The used simplified model assumes the decay chain  $\tilde{g} \rightarrow \tilde{t}t$ ,  $\tilde{t} \rightarrow t\tilde{\chi}_1^0$ . The bands represent the theoretical uncertainty on the gluino pair production cross-section.

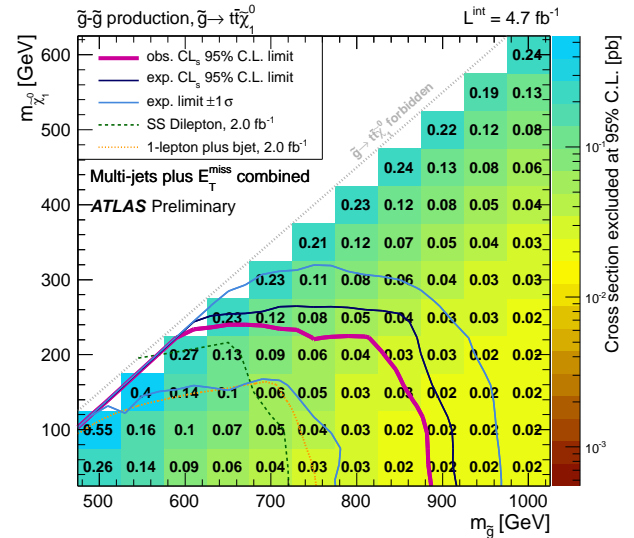


**Figure 7:** 95% C.L. upper limits on the cross section for gluino pair production as a function of gluino and neutralino mass. The used simplified model assumes the decay chain  $\tilde{g} \rightarrow \tilde{t}t\tilde{\chi}_1^0$ . The contours illustrate where the reference cross section and the upper limit on the cross section intersect. Apart from the limit of the multijet analysis, also limits arising from a same-sign dilepton analysis, and a lepton plus  $b$ -jet analysis are shown.

Top squarks can also be long-lived and hadronize to a R-hadron, for example in the scenario where the top squark is the next-to-lightest SUSY particle (NLSP), with a small mass difference to the LSP. Searches for massive stable charged particles are sensitive to such top squarks. As shown in Fig. 3

## Searches Particle Listings

### Supersymmetric Particle Searches

for the CMS analysis [61], the LHC experiments have set limits  $m_{\tilde{\tau}} > 720$  GeV in such scenarios, surpassing the earlier Tevatron limits of about 300 GeV [80,81].

Bottom squarks are expected to decay predominantly to  $b\tilde{\chi}^0$ . Direct production of bottom squark pairs has been studied at the Tevatron and at the LHC. Limits from the Tevatron are  $m_{\tilde{b}} > 247$  GeV for a massless neutralino [82,83]. The LHC experiments now surpass these limits; as shown in Fig. 8, ATLAS has set a limit of  $m_{\tilde{b}} > 392$  GeV for the same scenario, and  $m_{\tilde{b}} > 375$  GeV for  $m_{\tilde{\chi}_1^0} < 100$  GeV [84].

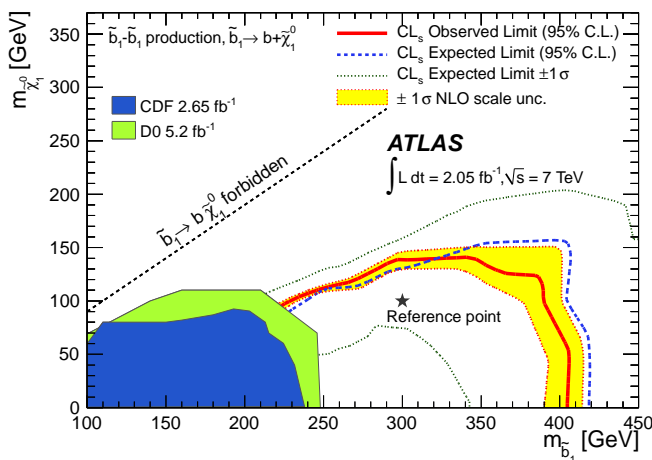


**Figure 8:** 95% C.L. exclusion contours in the sbottom-neutralino mass plane, for direct bottom squark pair production followed by the decay  $\tilde{b} \rightarrow b\tilde{\chi}_1^0$ .

Gluino pair production followed by  $\tilde{g} \rightarrow \tilde{b}b$  has been searched for [85–86], and results exclude a gluino with a mass below 920 GeV for sbottom masses below 750 GeV and a light neutralino. Interpreting this search in a simplified model for gluino pair production and  $\tilde{g} \rightarrow \tilde{b}b\tilde{\chi}_1^0$  excludes a gluino with a mass below 900 GeV for neutralino masses below 300 GeV.

#### II.5. Exclusion limits on slepton masses

In models with slepton and gaugino mass unification at the GUT scale, the right-handed slepton,  $\tilde{\ell}_R$ , is expected to be lighter than the left-handed slepton,  $\tilde{\ell}_L$ . For tau sleptons there may be considerable mixing between the L and R states, leading to a significant mass difference between the lighter  $\tilde{\tau}_1$  and the heavier  $\tilde{\tau}_2$ .

##### II.5.1. Exclusion limits on the masses of charged sleptons

The cleanest searches for selectrons, smuons and staus originate from the LEP experiments [87]. Smuon production only takes place via s-channel  $\gamma^*/Z$  exchange. Search results are often quoted for  $\tilde{\mu}_R$ , since it is typically lighter than  $\tilde{\mu}_L$  and has a weaker coupling to the Z boson; limits are therefore conservative. Decays are expected to be dominated by

$\tilde{\mu}_R \rightarrow \mu\tilde{\chi}_1^0$ , leading to two non-back-to-back muons and missing momentum. Limits are calculated in the MSSM under the assumption of gaugino mass unification at the GUT scale, and depend on the mass difference between the smuon and  $\tilde{\chi}_1^0$ . A  $\tilde{\mu}_R$  with a mass below 94 GeV is excluded for  $m_{\tilde{\mu}_R} - m_{\tilde{\chi}_1^0} > 10$  GeV. The selectron case is similar to the smuon case, except that an additional production mechanism is provided by t-channel neutralino exchange. The  $\tilde{e}_R$  lower mass limit is 100 GeV for  $m_{\tilde{\chi}_1^0} < 85$  GeV. Due to the t-channel neutralino exchange,  $\tilde{e}_R\tilde{e}_L$  pair production was possible at LEP, and a lower limit of 73 GeV was set on the selectron mass regardless of the neutralino mass. The potentially large mixing between  $\tilde{\tau}_1$  and  $\tilde{\tau}_R$  not only makes the  $\tilde{\tau}_1$  light, but also decreases its coupling to the Z boson. LEP limits range between 87 and 93 GeV depending on the  $\tilde{\chi}_1^0$  mass, for  $m_{\tilde{\tau}} - m_{\tilde{\chi}_1^0} > 7$  GeV [87].

In gauge-mediated SUSY breaking models, sleptons can be (co-)NLSPs, *i.e.*, the next-to-lightest SUSY particles and almost degenerate in mass, decaying to a lepton and a gravitino. This decay can either be prompt, or the slepton can have a non-zero lifetime. Combining several analyses, lower mass limits on  $\tilde{\mu}_R$  of 96.3 GeV and on  $\tilde{e}_R$  of 66 GeV are set for all slepton lifetimes at LEP [88]. In a considerable part of parameter space in these models, the  $\tilde{\tau}$  is the NLSP. The LEP experiments have set lower limits on the mass of such a  $\tilde{\tau}$  between 87 and 97 GeV, depending on the  $\tilde{\tau}$  lifetime. ATLAS has searched for final states with  $\tau$ s, jets and missing transverse momentum, and has interpreted the results in GMSB models setting limits on the model parameters [89,90]. CMS has interpreted a multilepton analysis in terms of limits on gauge mediation models with slepton (co-)NLSP [91].

Limits also exist on sleptons in R-parity violating models, both from LEP and the Tevatron experiments. From LEP, lower limits on  $\tilde{\mu}_R$  and  $\tilde{e}_R$  masses in such models are 97 GeV, and the limits on the stau mass are very close: 96 GeV [92].

Charged slepton decays may be kinematically suppressed, for example in the scenario of a NLSP slepton with a very small mass difference to the LSP. Such a slepton may appear to be a stable charged massive particle. Interpretation of searches at LEP for such signatures within GMSB models with stau NLSP or slepton co-NLSP exclude masses up to 99 GeV [93]. Searches of stable charged particles at the Tevatron [80,81] and at the LHC [94,61] are also interpreted in terms of limits on stable charged sleptons. As shown in Fig. 3, CMS excludes stable staus with masses below approximately 300 GeV [61].

##### II.5.2. Exclusion limits on sneutrino masses

The invisible width of the Z boson puts a lower limit on the sneutrino mass of about 45 GeV. Tighter limits are derived from other searches, notably for gauginos and sleptons, under the assumption of gaugino and sfermion mass universality at the GUT scale, and amount to approximately 94 GeV in the MSSM. It is possible that the lightest sneutrino is the LSP; however, a lefthanded sneutrino LSP is ruled out as a cold dark matter candidate [95,96].

Production of pairs of sneutrinos in R-parity violating models has been searched for at LEP [92]. Assuming fully leptonic decays via  $\lambda$ -type couplings, lower mass limits between 85 and 100 GeV are set. At the Tevatron [97,98] and at the LHC [99], searches have focused on scenarios with resonant production of a sneutrino, decaying to  $e\mu$  final states (as well as to  $\mu\tau$ , and  $e\tau$  for CDF). No signal has been seen, and limits have been set on sneutrino masses as a function of the value of relevant RPV couplings. As an example, the ATLAS analysis excludes a resonant tau sneutrino with a mass below 600 GeV for  $\lambda_{312} > 0.01$  and  $\lambda'_{311} > 0.01$  [99].

## II.6. Exclusion limits on the masses of charginos and neutralinos

Charginos and neutralinos result from mixing of the charged wino and higgsino states, and the neutral bino, wino and higgsino states, respectively. The mixing is determined by a limited number of parameters. For charginos these are the wino mass parameter  $M_2$ , the Higgsino mass parameter  $\mu$ , and  $\tan\beta$ , and for neutralinos these are the same parameters plus the bino mass parameter  $M_1$ . The mass states are four charginos  $\tilde{\chi}_1^\pm$  and  $\tilde{\chi}_2^\pm$ , and four neutralinos  $\tilde{\chi}_1^0$ ,  $\tilde{\chi}_2^0$ ,  $\tilde{\chi}_3^0$  and  $\tilde{\chi}_4^0$ , ordered in increasing mass. Depending on the mixing, the chargino and neutralino composition is dominated by specific states, which are referred to as bino-like ( $M_1 \ll M_2, \mu$ ), wino-like ( $M_2 \ll M_1, \mu$ ), or Higgsino-like ( $\mu \ll M_1, M_2$ ). If gaugino mass unification at the GUT scale is assumed, a relation between  $M_1$  and  $M_2$  at the electroweak scale follows:  $M_1 = 5/3 \tan^2 \theta_W M_2 \approx 0.5 M_2$  (with  $\theta_W$  the weak mixing angle), with consequences for the chargino-neutralino mass relation after mixing. Charginos and neutralinos carry no color charge, and only have electroweak couplings (neglecting gravity).

### II.6.1. Exclusion limits on chargino masses

If kinematically allowed, two body decay modes such as  $\tilde{\chi}^\pm \rightarrow \ell^\pm \tilde{\nu}$  are dominant. If not, three body decay  $\tilde{\chi}^\pm \rightarrow f\bar{f}'\tilde{\chi}^0$  are mediated through virtual  $W$  bosons or sfermions. If sfermions are heavy, the  $W$  mediation dominates, and  $f\bar{f}'$  are distributed with branching fractions similar to  $W$  decay products. If, on the other hand, sleptons are light enough to play a significant role in the decay mediation, leptonic final states will be enhanced.

At LEP, charginos have been searched for in fully-hadronic, semi-leptonic and fully leptonic decay modes [100,101]. A general lower limit on the lightest chargino mass of 103.5 GeV is derived, except in corners of phase space with low electron sneutrino mass, where destructive interference in chargino production, or two-body decay modes, play a role. The limit is also affected if the mass difference between  $\tilde{\chi}_1^\pm$  and  $\tilde{\chi}_1^0$  is small; dedicated searches for such scenarios set a lower limit of 92 GeV.

At the Tevatron, charginos are searched for via production of a pair of charginos, or associated production of  $\tilde{\chi}_1^\pm + \tilde{\chi}_2^0$ . Decay modes involving multilepton final states provide the best discrimination against the large multijet background. Analyses

look for at least three charged isolated leptons, or for two leptons with the same charge. Depending on the  $\tilde{\chi}_1^\pm - \tilde{\chi}_1^0$  and/or  $\tilde{\chi}_2^0 - \tilde{\chi}_1^0$  mass differences, leptons may be soft. In a recent CDF analysis, results are interpreted in CMSSM-inspired scenarios, with  $\tan\beta = 3$ ,  $A_0 = 0$  and  $\mu > 0$ , and assuming  $m_{\tilde{\chi}_1^\pm} = m_{\tilde{\chi}_2^0} = 2m_{\tilde{\chi}_1^0}$  [102]. Slepton masses are either assumed to be just above  $m_{\tilde{\chi}^\pm}$ , maximizing leptonic branching ratios in three-body chargino decays, or to be very large. In the first scenario, charginos with a mass below 168 GeV are excluded. D0 excludes a chargino below 130 GeV for the maximized leptonic branching fraction case for all  $\tan\beta < 10$ , and sets limits in the CMSSM  $m_0 - m_{1/2}$  plane for  $\tan\beta = 3$ ,  $A_0 = 0$ , and  $\mu > 0$  [103].

At the LHC, the search strategy is similar to that at the Tevatron. In an ATLAS analysis of the three lepton final state [104], interpretation of the results is performed in the MSSM as well as using simplified models. In the MSSM, a scan over  $M_2$  and  $\mu$  is made for  $M_1 = 100$  GeV and  $\tan\beta = 6$ , and  $M_2$  values below 350 GeV are excluded for  $|\mu| < 190$  GeV. The simplified models assume  $\tilde{\chi}_1^\pm + \tilde{\chi}_2^0$  production, and  $m_{\tilde{\chi}^\pm} = m_{\tilde{\chi}_2^0}$ , leaving  $m_{\tilde{\chi}^\pm}$  and  $m_{\tilde{\chi}_1^0}$  free. In a scenario that favors leptonic decays of  $\tilde{\chi}_1^\pm$  and  $\tilde{\chi}_2^0$ , charginos with masses up to 300 GeV are excluded for massless neutralinos, and charginos up to 250 GeV are excluded for  $m_{\tilde{\chi}_1^0} < 150$  GeV. More LHC results in these channels based on the 2011 data sample are expected.

In both the wino region (a characteristic of anomaly-mediated SUSY-breaking models) and the higgsino region of the MSSM, the mass splitting between  $\tilde{\chi}_1^\pm$  and  $\tilde{\chi}_1^0$  is small. In such scenarios, charginos may be long-lived. Charginos decaying in the detectors away from the primary vertex could lead to signatures such as kinked-tracks, or apparently disappearing tracks, since, for example, the pion in  $\tilde{\chi}_1^\pm \rightarrow \pi^\pm \tilde{\chi}_1^0$  might be too soft to be reconstructed. At the LHC, a search has been performed for such disappearing tracks, and interpreted with anomaly-mediated SUSY breaking models. For specific AMSB parameters, charginos with lifetimes between 0.2 and 90 ns are excluded for chargino masses up to 90 GeV, and limits reach up to 118 GeV for lifetimes around 1 ns [105].

Charginos with a lifetime longer than the time needed to pass through the detector appear as charged stable massive particles. Limits have been derived by the LEP experiments [93] and by D0 at the Tevatron [81]. D0 results exclude higgsino-like stable charginos below 217 GeV, and gaugino-like stable charginos below 267 GeV.

### II.6.2. Exclusion limits on neutralino masses

In a considerable part of the MSSM parameter space, and in particular when demanding that the LSP carries no electric or color charge, the lightest neutralino  $\tilde{\chi}_1^0$  is the LSP. If R-parity is conserved, such a  $\tilde{\chi}_1^0$  is stable. Since it is weakly interacting, it will typically escape detectors unseen. Limits on the invisible width of the  $Z$  boson apply to neutralinos with a mass below 45.5 GeV, but depend on the  $Z$ -neutralino coupling. Such a coupling could be small or even absent; in such a scenario

## Searches Particle Listings

### Supersymmetric Particle Searches

there is no general lower limit on the mass of the lightest neutralino [106]. In models with gaugino mass unification at high energy scales, a neutralino limit is derived from the chargino mass limit, and amounts to 47 GeV. Assuming a constraining model like the CMSSM, this limit increases to 50 GeV at LEP; however the strong constraints now set by the LHC increase such CMSSM-derived  $\tilde{\chi}_1^0$  mass limits to well above 100 GeV.

Even though a LSP neutralino is only weakly interacting, collider experiments are not blind to neutralino pair production. Pair production of neutralinos accompanied by initial state radiation could lead to an observable final state. At LEP, final states with only a single isolated photon were studied, but backgrounds from neutrino pair production were too large. At hadron colliders, monojet final states have been used to set limits on the pair production cross section [107,108].

The lightest neutralino can decay in models with R-parity violation, or in cases where it is not the LSP, as in gauge mediation models. In the latter case, a NLSP neutralino will decay to a gravitino and a SM particle whose nature is determined by the neutralino composition. Final states with two high  $p_T$  photons and missing momentum are searched for, and interpreted in gauge mediation models with bino-like neutralinos [109–113]. Assuming only gluino pair production and a bino-like neutralino produced in gluino decay, limits on gluino masses of about 1 TeV are set for all neutralino masses, as shown in Fig. 9 for the CMS diphoton analysis.

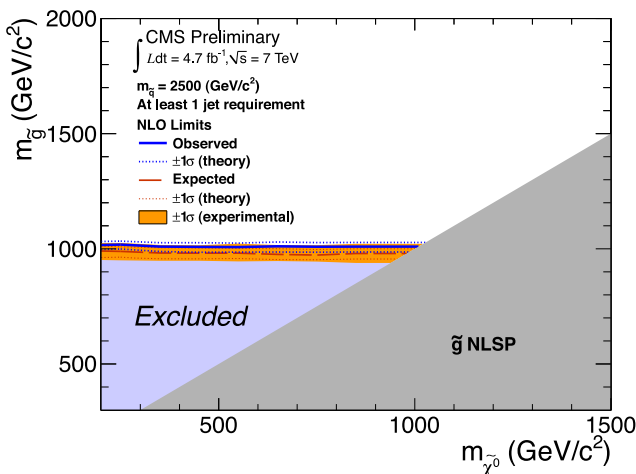


**Figure 9:** Observed 95% C.L. limits on the gluino mass as a function of the neutralino mass, in general gauge mediation models assuming only gluino pair production, with a bino-like neutralino produced in gluino decay, and a neutralino decay to photon plus gravitino.

Assuming the production of at least two neutralinos per event, neutralinos with large non-bino components can also be searched for in  $ZZ$  and  $\gamma Z$  final states. Searches for final states with  $Z$  ( $\rightarrow \ell^+ \ell^-$ ) bosons and missing transverse momentum have been performed at the Tevatron [114] and at the LHC [115], and are interpreted in such models.

In gauge mediation models, NLSP neutralino decay need not be prompt, and experiments have searched for late decays. CDF have searched for delayed  $\tilde{\chi}_1^0 \rightarrow \gamma Z$  decays using the timing of photon signals in the calorimeter [116], and exclude a neutralino with mass below 101 GeV with a lifetime of 5 ns. CMS has used converted photons to search for photon production away from the primary vertex [117]. Results are given as upper limits on the neutralino production cross section of order  $0.12 - 0.24$  pb for  $c\tau$  between 5 and 25 cm. D0 has looked at the direction of showers in the electromagnetic calorimeter with a similar goal [118].

Heavier neutralinos, in particular  $\tilde{\chi}_2^0$ , have been searched for in their decays to the lightest neutralino plus a  $Z$  boson. Analyses include searches for  $Z$  production plus missing energy,  $Z$  plus jets plus missing energy, two  $Z$  bosons plus missing energy, and  $Z$  plus  $W$  production plus missing energy [118,119–122]. In  $\tilde{\chi}_2^0$  decays to  $\tilde{\chi}_1^0$  and a lepton pair, the lepton pair invariant mass distribution may show a structure that can be used to measure the  $\tilde{\chi}_2^0 - \tilde{\chi}_1^0$  mass difference in case of a signal [123], but it can also be used in the search itself, in order to suppress background [124].

#### II.7. Global interpretations

Apart from the interpretation of the direct searches for sparticle production at colliders in terms of limits on masses of individual SUSY particles, model-dependent interpretations of allowed SUSY parameter space are derived from global SUSY fits. Typically these fits combine the results from collider experiments with indirect constraints on SUSY as obtained from low-energy experiments, flavor physics, high-precision electroweak results, and astrophysical data.

In the pre-LHC era these fits were mainly dominated by indirect constraints. Even for very constrained models like the CMSSM, the allowed parameter space, in terms of squark and gluino masses, ranged from several hundreds of GeV to a few TeV. For the theoretically well motivated class of constrained supergravity models like the CMSSM, global fits indicated that squarks and gluino masses in the range of 500 to 1000 GeV were the preferred region of parameter space, although values as high as few TeV were allowed with lower probabilities [125].

With ATLAS and CMS now probing mass scales around 1 TeV and even beyond, the importance of the direct searches for global analyses of allowed SUSY parameter space has significantly increased. For example, imposing the new experimental limits on constrained supergravity models pushes the most likely values of first generation squark and gluino masses beyond 1 TeV, typically resulting in overall values of fit quality

significantly worse than those in the pre-LHC era [126]. Although these constrained models are not yet ruled out, the extended experimental limits impose tight constraints on the allowed parameter space.

For this reason, the emphasis of global SUSY fits has shifted more towards less-constrained SUSY models. Especially interpretations in the pMSSM [48,127,128] and in simplified models have been useful to generalize SUSY searches, for example in order to increase their sensitivity for compressed spectra where the mass of the LSP is much closer to squark and gluino masses than predicted by for example the CMSSM. As shown in Table 2, for neutralino masses above a few hundred GeV the current set of ATLAS and CMS searches cannot exclude the existence of light squarks and gluinos.

## II.8. Summary and Outlook

Although the search for SUSY at the LHC has just begun, results of the ATLAS and CMS experiments are already probing direct production of colored SUSY particles at the 1 TeV mass scale. So far no evidence of new particle production has been observed in the data and therefore limits on allowed parameter space in various models have been set. While typically squark and gluino masses around 1 TeV and below are excluded in constrained models, weaker bounds on SUSY particle masses are obtained in less constrained scenarios demonstrating that SUSY below the 1 TeV scale is certainly not ruled out in general. For non-colored sparticles the impact of the LHC is to a large extent yet to come, and limits from LEP and the Tevatron are still competitive. An overview of the current landscape of SUSY searches and corresponding exclusion limits at the LHC is shown in Fig. 10 from the ATLAS experiment [67]. The corresponding results of the CMS experiment are similar [66].

Furthermore, the LHC experiments have reported significant constraints on the allowed mass range of a SM-like Higgs boson based on an analysis of  $5 \text{ fb}^{-1}$  of data [129,130]. A SM-like Higgs boson is excluded over a large mass range, except in a narrow window around 125 GeV or at a large mass above some 600 GeV. These results impose further tight bounds on the allowed SUSY parameter space, and the first studies of global analyses indicate (see *e.g.*, [131–133]) that the limits on the Higgs boson mass worsen the overall compatibility of the available data with constrained models like the CMSSM. Scenarios of rather light third generation squarks, however, perhaps accompanied with heavy neutralinos as realized in compressed spectra, or first generation squarks and gluinos with masses significantly above 1 TeV are still compatible with the present set of direct and indirect constraints.

Additional searches at the LHC in 2012, at a higher center-of-mass energy of 8 TeV, are expected to make further important steps in the experimental search for SUSY. Once the LHC reaches its full energy after 2013, even higher mass scales will be in reach.

Like the experimental landscape of SUSY searches, the field of global interpretations of allowed SUSY parameters is still rapidly changing. Yet, it seems reasonable to expect that

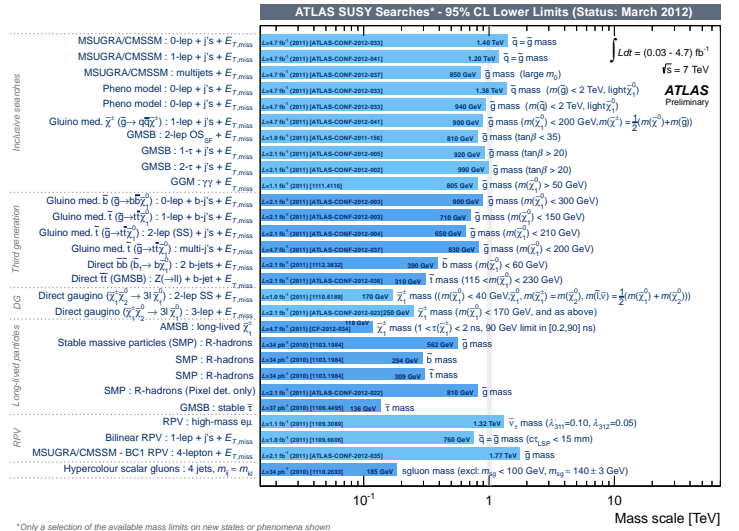


**Figure 10:** Overview of the current landscape of SUSY searches at the LHC. The plot shows exclusion mass limits of ATLAS for different searches and interpretation assumptions. The corresponding results of CMS are comparable.

the emphasis on interpretations in constrained SUSY models is now shifting towards more flexible models, which in turn motivates an even stronger experimental emphasis on searches for direct production of third generation squarks, of electroweak gauginos, or involving compressed  $m_{\text{mother}} - m_{\tilde{\chi}_1^0}$  mass spectra. An increased emphasis on R-parity violating models and on models with long-lived particles can also be expected.

## References

1. H. Miyazawa, Prog. Theor. Phys. **36**, 1266 (1966).
2. Yu. A. Golfand and E.P. Likhthman, Sov. Phys. JETP Lett. **13**, 323 (1971).
3. J.L. Gervais and B. Sakita, Nucl. Phys. **B34**, 632 (1971).
4. D.V. Volkov and V.P. Akulov, Phys. Lett. **B46**, 109 (1973).
5. J. Wess and B. Zumino, Phys. Lett. **B49**, 52 (1974).
6. J. Wess and B. Zumino, Nucl. Phys. **B70**, 39 (1974).
7. A. Salam and J.A. Strathdee, Nucl. Phys. **B76**, 477 (1974).
8. H.P. Nilles, Phys. Reports **110**, 1 (1984).
9. H.E. Haber and G.L. Kane, Phys. Reports **117**, 75 (1987).
10. E. Witten, Nucl. Phys. **B188**, 513 (1981).
11. S. Dimopoulos and H. Georgi, Nucl. Phys. **B193**, 150 (1981).
12. M. Dine, W. Fischler, and M. Srednicki, Nucl. Phys. **B189**, 575 (1981).
13. S. Dimopoulos and S. Raby, Nucl. Phys. **B192**, 353 (1981).
14. N. Sakai, Z. Phys. **C11**, 153 (1981).
15. R.K. Kaul and P. Majumdar, Nucl. Phys. **B199**, 36 (1982).



# Searches Particle Listings

## Supersymmetric Particle Searches

---

16. H. Goldberg, Phys. Rev. Lett. **50**, 1419 (1983).
17. J.R. Ellis *et al.*, Nucl. Phys. **B238**, 453 (1984).
18. G. Jungman and M. Kamionkowski, Phys. Reports **267**, 195 (1996).
19. S. Dimopoulos, S. Raby, and F. Wilczek, Phys. Rev. **D24**, 1681 (1981).
20. W. J. Marciano and G. Senjanović, Phys. Rev. **D25**, 3092 (1982).
21. M.B. Einhorn and D.R.T. Jones, Nucl. Phys. **B196**, 475 (1982).
22. L.E. Ibanez and G.G. Ross, Phys. Lett. **B105**, 439 (1981).
23. N. Sakai, Z. Phys. **C11**, 153 (1981).
24. U. Amaldi, W. de Boer, and H. Furstenau, Phys. Lett. **B260**, 447 (1991).
25. P. Langacker and N. Polonsky, Phys. Rev. **D52**, 3081 (1995).
26. P. Fayet, Phys. Lett. **B64**, 159 (1976).
27. G.R. Farrar and P. Fayet, Phys. Lett. **B76**, 575 (1978).
28. H.E. Haber, *Supersymmetry, Part I (Theory)*, this volume.
29. J.-F. Grivaz, *Supersymmetry, Part II (Experiment)*, in: 2010 Review of Particle Physics, K. Nakamura *et al.*, (Particle Data Group), J. Phys. **G37**, 075021 (2010).
30. G. Bernardi, M. Carena, and T. Junk, *Higgs Bosons: Theory and Searches*, this volume.
31. I. Hinchliffe *et al.*, Phys. Rev. **D55**, 5520 (1997).
32. L. Randall and D. Tucker-Smith, Phys. Rev. Lett. **101**, 221803 (2008).
33. CMS Collab., Phys. Lett. **B698**, 196 (2011).
34. CMS Collab., Phys. Rev. Lett. **107**, 221804 (2011).
35. CMS Collab., Phys. Rev. **D85**, 012004 (2012).
36. C.G. Lester and D.J. Summers, Phys. Lett. **B463**, 99 (1999).
37. D.R. Tovey, JHEP **04**, 034 (2008).
38. A.H. Chamseddine, R. Arnowitt, and P Nath, Phys. Rev. Lett. **49**, 970 (1982).
39. E. Cremmer *et al.*, Nucl. Phys. **B212**, 413 (1983).
40. P. Fayet, Phys. Lett. **B70**, 461 (1977).
41. M. Dine, A.E. Nelson, and Yu. Shirman, Phys. Rev. **D51**, 1362 (1995).
42. G.F. Giudice *et al.*, JHEP **9812**, 027 (1998).
43. L. Randall and R. Sundrum, Nucl. Phys. **B557**, 79 (1999).
44. R. Arnowitt and P Nath, Phys. Rev. Lett. **69**, 725 (1992).
45. G.L. Kane *et al.*, Phys. Rev. **D49**, 6173 (1994).
46. P. Meade, N. Seiberg, and D. Shih, Prog. Theor. Phys. Supp. **177**, 143 (2009).
47. A. Djouadi, J.-L. Kneur, and G. Moultaka, Comp. Phys. Comm. **176**, 426 (2007).
48. C.F. Berger *et al.*, JHEP **02**, 023 (2009).
49. H. Baer *et al.*, hep-ph/9305342, 1993.
50. R.M. Barnett, H.E. Haber, and G.L. Kane, Nucl. Phys. **B267**, 625 (1986).
51. H. Baer, D. Karatas, and X. Tata, Phys. Lett. **B183**, 220 (1987).
52. J. Alwall, Ph.C. Schuster, and N. Toro, Phys. Rev. **D79**, 075020 (2009).
53. J. Alwall *et al.*, Phys. Rev. **D79**, 015005 (2009).
54. CDF Collab., Phys. Rev. Lett. **102**, 121801 (2009).
55. D0 Collab., Phys. Lett. **B660**, 449 (2008).
56. ATLAS Collab., *Search for squarks and gluinos using final states with jets and missing transverse momentum with the ATLAS detector in  $\sqrt{s} = 7$  TeV proton-proton collisions*, ATLAS-CONF-2012-033 (2012).
57. CMS Collab., *Search for supersymmetry with the razor variables*, CMS-PAS-SUS-12-005 (2012).
58. ATLAS Collab., *Hunt for new phenomena using large jet multiplicities and missing transverse momentum at ATLAS, in  $\mathcal{L} = 4.7$  fb<sup>-1</sup> of  $\sqrt{s} = 7$  TeV proton-proton collisions*, ATLAS-CONF-2012-037 (2012).
59. ATLAS Collab., *Further search for supersymmetry at  $\sqrt{s} = 7$  TeV in final states with jets, missing transverse momentum and one isolated lepton*, ATLAS-CONF-2012-041 (2012).
60. ATLAS Collab., *Search for supersymmetry with jets and missing transverse momentum: Additional model interpretations*, ATLAS-CONF-2011-155 (2011).
61. Update to 4.7fb<sup>-1</sup> based on: CMS Collab., *Search for Heavy Stable Charged Particles in pp collisions at  $\sqrt{s} = 7$  TeV*, CMS-PAS-EXO-11-022 (2011).
62. ATLAS Collab., *Search for charged long-lived heavy particles with the ATLAS Experiment at the LHC*, ATLAS-CONF-2012-022 (2012).
63. D0 Collab., Phys. Rev. Lett. **99**, 131801 (2007).
64. ATLAS Collab., arXiv:1201.5595(2012), accepted by Eur. Phys. J. C.
65. CMS Collab., *Search for Stopped Heavy Stable Charged Particles in pp collisions at  $\sqrt{s} = 7$  TeV*, CMS-PAS-EXO-11-020 (2011).
66. Supersymmetry Physics Results, CMS experiment, <http://twiki.cern.ch/twiki/bin/view/CMSPublic/PhysicsResultsSUS>.
67. Physics Summary Plots, ATLAS experiment, <http://twiki.cern.ch/twiki/bin/view/AtlasPublic/CombinedSummaryPlots>.
68. H1 Collab., Eur. Phys. J. **C71**, 1572 (2011).
69. LEP2 SUSY Working Group, ALEPH, DELPHI, L3 and OPAL experiments, note LEPSUSYWG/04-02.1, <http://lepsusy.web.cern.ch/lepsusy>.
70. CDF Collab., Phys. Rev. **D82**, 092001 (2010).
71. D0 Collab., Phys. Lett. **B696**, 321 (2011).
72. CDF Collab., arXiv:1203.4171(2012), submitted to Phys. Rev. Lett.
73. D0 Collab., Phys. Lett. **B665**, 1 (2008).
74. CDF Collab., Phys. Rev. Lett. **104**, 251801 (2010).
75. D0 Collab., Phys. Lett. **B674**, 4 (2009).
76. ATLAS Collab., arXiv:1203.6193(2012), submitted to Phys. Rev. D.
77. ATLAS Collab., arXiv:1203.5763(2012), submitted to Phys. Rev. Lett.
78. CMS Collab., *Search for New Physics in Events with Same-sign Dileptons, b-tagged Jets and Missing Energy*, CMS-PAS-SUS-11-020 (2011).
79. ZEUS Collab., Eur. Phys. J. **C50**, 269 (2007).
80. CDF Collab., Phys. Rev. Lett. **103**, 021802 (2009).
81. D0 Collab., Phys. Rev. Lett. **108**, 121802 (2012).
82. CDF Collab., Phys. Rev. Lett. **105**, 081802 (2010).

83. D0 Collab., Phys. Lett. **B693**, 95 (2010).
84. ATLAS Collab., arXiv:1112.3832(2011), accepted by Phys. Rev. Lett.
85. CDF Collab., Phys. Rev. Lett. **102**, 1801 (2009).
86. CMS Collab., *Search for New Physics in Events with b-quark Jets and Missing Transverse Energy in Proton-Proton Collisions at 7 TeV*, CMS-PAS-SUS-11-006 (2011).
87. LEP2 SUSY Working Group, ALEPH, DELPHI, L3 and OPAL experiments, note LEPSUSYWG/04-01.1, <http://lepsusy.web.cern.ch/lepsusy>.
88. LEP2 SUSY Working Group, ALEPH, DELPHI, L3 and OPAL experiments, note LEPSUSYWG/02-09.2, <http://lepsusy.web.cern.ch/lepsusy>.
89. ATLAS Collab., *Search for Supersymmetry with jets, missing transverse momentum and one or more tau leptons in proton-proton collisions at  $\sqrt{s} = 7$  TeV with the ATLAS detector*, ATLAS-CONF-2012-005 (2012).
90. ATLAS Collab., arXiv:1203.6580(2012), submitted to Phys. Lett. B.
91. CMS Collab., *Searches for Supersymmetry using Multi-lepton Signatures in pp Collisions at 7 TeV*, CMS-PAS-SUS-11-013 (2011).
92. LEP2 SUSY Working Group, ALEPH, DELPHI, L3 and OPAL experiments, note LEPSUSYWG/02-10.1, <http://lepsusy.web.cern.ch/lepsusy>.
93. LEP2 SUSY Working Group, ALEPH, DELPHI, L3 and OPAL experiments, note LEPSUSYWG/02-05.1, <http://lepsusy.web.cern.ch/lepsusy>.
94. ATLAS Collab., Phys. Lett. **B703**, 428 (2011).
95. T. Falk, K.A. Olive, and M. Srednicki, Phys. Lett. **B339**, 248 (1994).
96. C. Arina and N. Fornengo, JHEP **11**, 029 (2007).
97. CDF Collab., Phys. Rev. Lett. **105**, 191801 (2010).
98. D0 Collab., Phys. Rev. Lett. **105**, 191802 (2010).
99. ATLAS Collab., Eur. Phys. J. **C71**, 1809 (2011).
100. LEP2 SUSY Working Group, ALEPH, DELPHI, L3 and OPAL experiments, note LEPSUSYWG/01-03.1, <http://lepsusy.web.cern.ch/lepsusy>.
101. LEP2 SUSY Working Group, ALEPH, DELPHI, L3 and OPAL experiments, note LEPSUSYWG/02-04.1, <http://lepsusy.web.cern.ch/lepsusy>.
102. CDF Collab., *Search for trilepton new physics and chargino-neutralino production at the Collider Detector at Fermilab*, CDF Note 10636 (2011).
103. D0 Collab., Phys. Lett. **B680**, 34 (2009).
104. ATLAS Collab., *Search for supersymmetry in events with three leptons and missing transverse momentum in  $\sqrt{s} = 7$  TeV pp collisions with the ATLAS detector*, ATLAS-CONF-2012-023 (2012).
105. ATLAS Collab., *Search for long-lived charginos in anomaly-mediated supersymmetry breaking scenarios with the ATLAS detector using 4.7 fb<sup>-1</sup> data of pp collisions at  $\sqrt{s} = 7$  TeV*, ATLAS-CONF-2012-034 (2012); ATLAS Collab., arXiv:1202.4847(2012), submitted to Eur. Phys. J. C.
106. H. Dreiner *et al.*, Eur. Phys. J. **C62**, 547 (2009).
107. CDF Collab., arXiv:1203.0742(2012), submitted to Phys. Rev. Lett.
108. CMS Collab., *Search for Dark Matter and Large Extra Dimensions in Monojet Events in pp Collisions at  $\sqrt{s} = 7$  TeV*, CMS-PAS-EXO-11-059 (2011).
109. LEP2 SUSY Working Group, ALEPH, DELPHI, L3 and OPAL experiments, note LEPSUSYWG/04-09.1, <http://lepsusy.web.cern.ch/lepsusy>.
110. CDF Collab., Phys. Rev. Lett. **104**, 011801 (2010).
111. D0 Collab., Phys. Rev. Lett. **105**, 221802 (2010).
112. ATLAS Collab., Phys. Lett. **B710**, 519 (2012).
113. CMS Collab., *Search for Supersymmetry in Events with Photons and Missing Energy*, CMS-PAS-SUS-12-001 (2012).
114. D0 Collab., arXiv:1203.5311(2012), submitted to Phys. Rev. Lett.
115. CMS Collab., *Search for Physics Beyond the Standard Model in Events with a Z Boson, Jets and Missing Transverse Energy*, CMS-PAS-SUS-11-021 (2011).
116. CDF Collab., Phys. Rev. **D78**, 032015 (2008).
117. CMS Collab., *Search for new physics with long-lived particles decaying to photons and missing energy*, CMS-PAS-EXO-11-067 (2011).
118. D0 Collab., Phys. Rev. Lett. **101**, 111802 (2008).
119. CDF Collab., Phys. Rev. **D85**, 011104 (2012).
120. CDF Collab., *Gaugino Search using the Z<sup>0</sup> + W<sup>±</sup> + ME<sub>T</sub> channel*, CDF Note CDF/PUB/EXOTIC/PUBLIC/9791 (2009).
121. CMS Collab., *Search for Physics Beyond the Standard Model in Z + Jets + E<sub>T</sub><sup>miss</sup> events at the LHC*, CMS-PAS-SUS-11-019 (2011).
122. ATLAS Collab., Phys. Lett. **B709**, 137 (2012).
123. ATLAS Collab., *Expected Performance of the ATLAS experiment, Detector, Trigger and Physics*, CERN-OPEN-2008-020 (2008).
124. CMS Collab., *Search for New Physics in Events with Opposite-sign Leptons, Jets and Missing Transverse Energy*, CMS-PAS-SUS-11-011 (2011).
125. For a sampling of pre-LHC global analyses, see: O. Buchmueller *et al.*, Eur. Phys. J. **C71**, 1722 (2011) [arXiv:1106.2529 [hep-ph]]; E.A. Baltz and P. Gondolo, JHEP **0410**, 052 (2004) [arXiv:hep-ph/0407039]; B.C. Allanach and C.G. Lester, Phys. Rev. **D73**, 015013 (2006) [arXiv:hep-ph/0507283]; R.R. de Austri, R. Trotta and L. Roszkowski, JHEP **0605**, 002 (2006) [arXiv:hep-ph/0602028]; R. Lafaye *et al.*, Eur. Phys. J. **C54**, 617 (2008) [arXiv:0709.3985 [hep-ph]]; S. Heinemeyer *et al.*, JHEP **0808**, 08 (2008) [arXiv:0805.2359 [hep-ph]]; R. Trotta *et al.*, JHEP **0812**, 024 (2008) [arXiv:0809.3792 [hep-ph]]; P. Bechtle *et al.*, Eur. Phys. J. **C66**, 215 (2010) [arXiv:0907.2589 [hep-ph]].
126. For a sampling of post-LHC global analyses, see: O. Buchmueller *et al.*, Eur. Phys. J. **C71**, 1722 (2011), [arXiv:1106.2529 [hep-ph]]; D. Feldman *et al.*, arXiv:1102.2548 [hep-ph]; B.C. Allanach, arXiv:1102.3149 [hep-ph]; S. Scopel *et al.*, arXiv:1102.4033 [hep-ph]; P. Bechtle *et al.*, arXiv:1102.4693 [hep-ph]; B.C. Allanach *et al.*, arXiv:1103.0969 [hep-ph]; S. Akula *et al.*, arXiv:1103.1197 [hep-ph]; M.J. Dolan *et al.*, arXiv:1104.0585 [hep-ph]; S. Akula *et al.*, arXiv:1103.5061 [hep-ph] (v2);

# Searches Particle Listings

## Supersymmetric Particle Searches

- M. Farina *et al.*, arXiv:1104.3572 [hep-ph];  
 S. Profumo, arXiv:1105.5162 [hep-ph];  
 T. Li *et al.*, arXiv:1106.1165 [hep-ph];  
 N. Bhattacharyya, A. Choudhury, and A. Datta,  
 arXiv:1107.1997 [hep-ph];  
 G. Bertone *et al.*, arXiv:1107.1715 [hep-ph].
127. S. Sekmen *et al.*, JHEP **1202**, 075 (2012).  
 128. A. Arbey *et al.*, Eur. Phys. J. **C72**, 1847 (2012).  
 129. CMS Collab., Phys. Lett. **B710**, 26 (2012).  
 130. ATLAS Collab., Phys. Lett. **B710**, 49 (2012).  
 131. H. Baer, V. Barger, and A. Mustafayev,  
 arXiv:1112.3017, 2011.  
 132. S. Heinemeyer, O. Stal, and G. Weiglein,  
 arXiv:1112.3026, 2011.  
 133. A. Arbey *et al.*, Phys. Lett. **B708**, 162 (2012).

### SUPERSYMMETRIC MODEL ASSUMPTIONS

The exclusion of particle masses within a mass range ( $m_1, m_2$ ) will be denoted with the notation “none  $m_1$ – $m_2$ ” in the VALUE column of the following Listings. The latest unpublished results are described in the “Supersymmetry: Experiment” review.

Most of the results shown below, unless stated otherwise, are based on the Minimal Supersymmetric Standard Model (MSSM), as described in the Note on Supersymmetry. Unless otherwise indicated, this includes the assumption of common gaugino and scalar masses at the scale of Grand Unification (GUT), and use of the resulting relations in the spectrum and decay branching ratios. It is also assumed that  $R$ -parity ( $R$ ) is conserved. Unless otherwise indicated, the results also assume that:

- 1) The  $\tilde{\chi}_1^0$  is the lightest supersymmetric particle (LSP)
- 2)  $m_{\tilde{f}_L}^c = m_{\tilde{f}_R}^c$ , where  $\tilde{f}_{L,R}$  refer to the scalar partners of left- and right-handed fermions.

Limits involving different assumptions are identified in the Comments or in the Footnotes. We summarize here the notations used in this Chapter to characterize some of the most common deviations from the MSSM (for further details, see the Note on Supersymmetry).

Theories with  $R$ -parity violation ( $\tilde{R}$ ) are characterized by a superpotential of the form:  $\lambda_{ijk} L_i L_j e_k^c + \lambda'_{ijk} L_i Q_j d_k^c + \lambda''_{ijk} u_i^c d_j^c d_k^c$ , where  $i, j, k$  are generation indices. The presence of any of these couplings is often identified in the following by the symbols  $LL\tilde{E}$ ,  $LQ\tilde{D}$ , and  $UDD$ . Mass limits in the presence of  $\tilde{R}$  will often refer to “direct” and “indirect” decays. Direct refers to  $\tilde{R}$  decays of the particle in consideration. Indirect refers to cases where  $\tilde{R}$  appears in the decays of the LSP.

In several models, most notably in theories with so-called Gauge Mediated Supersymmetry Breaking (GMSB), the gravitino ( $\tilde{G}$ ) is the LSP. It is usually much lighter than any other massive particle in the spectrum, and  $m_{\tilde{G}}$  is then neglected in all decay processes involving gravitinos. In these scenarios, particles other than the neutralino are sometimes considered as the next-to-lightest supersymmetric particle (NLSP), and are assumed to decay to their even- $R$  partner plus  $\tilde{G}$ . If the lifetime is short enough for the decay to take place within the detector,

$\tilde{G}$  is assumed to be undetected and to give rise to missing energy ( $\cancel{E}$ ) or missing transverse energy ( $\cancel{E}_T$ ) signatures.

When needed, specific assumptions on the eigenstate content of  $\tilde{\chi}^0$  and  $\tilde{\chi}^\pm$  states are indicated, using the notation  $\tilde{\gamma}$  (photino),  $\tilde{H}$  (higgsino),  $\tilde{W}$  (wino), and  $\tilde{Z}$  (zino) to signal that the limit of pure states was used. The terms gaugino is also used, to generically indicate wino-like charginos and zino-like neutralinos.

### CONTENTS:

- $\tilde{\chi}_1^0$  (Lightest Neutralino) Mass Limit
  - Accelerator limits for stable  $\tilde{\chi}_1^0$
  - Bounds on  $\tilde{\chi}_1^0$  from dark matter searches
  - $\tilde{\chi}_1^0$ – $p$  elastic cross section
    - Spin-dependent interactions
    - Spin-independent interactions
  - Other bounds on  $\tilde{\chi}_1^0$  from astrophysics and cosmology
  - Unstable  $\tilde{\chi}_1^0$  (Lightest Neutralino) Mass Limit
- $\tilde{\chi}_2^0, \tilde{\chi}_3^0, \tilde{\chi}_4^0$  (Neutralinos) Mass Limits
- $\tilde{\chi}_1^\pm, \tilde{\chi}_2^\pm$  (Charginos) Mass Limits
- Long-lived  $\tilde{\chi}^\pm$  (Chargino) Mass Limits
- $\tilde{\nu}$  (Sneutrino) Mass Limit
- Charged Sleptons
  - $\tilde{e}$  (Selectron) Mass Limit
  - $\tilde{\mu}$  (Smuon) Mass Limit
  - $\tilde{\tau}$  (Stau) Mass Limit
  - Degenerate Charged Sleptons
  - Long-lived  $\tilde{\ell}$  (Slepton) Mass Limit
- $\tilde{q}$  (Squark) Mass Limit
- Long-lived  $\tilde{q}$  (Squark) Mass Limit
- $\tilde{b}$  (Sbottom) Mass Limit
- $\tilde{t}$  (Stop) Mass Limit
- Heavy  $\tilde{g}$  (Glucino) Mass Limit
- Long-lived/light  $\tilde{g}$  (Glucino) Mass Limit
- Light  $\tilde{G}$  (Gravitino) Mass Limits from Collider Experiments
- Supersymmetry Miscellaneous Results

### $\tilde{\chi}_1^0$ (Lightest Neutralino) MASS LIMIT

$\tilde{\chi}_1^0$  is often assumed to be the lightest supersymmetric particle (LSP). See also the  $\tilde{\chi}_2^0, \tilde{\chi}_3^0, \tilde{\chi}_4^0$  section below.

We have divided the  $\tilde{\chi}_1^0$  listings below into five sections:

- 1) Accelerator limits for stable  $\tilde{\chi}_1^0$ ,
- 2) Bounds on  $\tilde{\chi}_1^0$  from dark matter searches,
- 3)  $\tilde{\chi}_1^0$ – $p$  elastic cross section (spin-dependent, spin-independent interactions),
- 4) Other bounds on  $\tilde{\chi}_1^0$  from astrophysics and cosmology, and
- 5) Unstable  $\tilde{\chi}_1^0$  (Lightest Neutralino) mass limit.

### Accelerator limits for stable $\tilde{\chi}_1^0$

Unless otherwise stated, results in this section assume spectra, production rates, decay modes, and branching ratios as evaluated in the MSSM, with gaugino and sfermion mass unification at the GUT scale. These papers generally study production of  $\tilde{\chi}_i^0 \tilde{\chi}_j^0$  ( $i \geq 1, j \geq 2$ ),  $\tilde{\chi}_1^+ \tilde{\chi}_1^-$ , and (in the case of hadronic collisions)  $\tilde{\chi}_1^+ \tilde{\chi}_2^0$  pairs. The mass limits on  $\tilde{\chi}_1^0$  are either direct, or follow indirectly from the constraints set by the non-observation of  $\tilde{\chi}_1^\pm$  and  $\tilde{\chi}_2^0$  states on the gaugino and higgsino MSSM parameters  $M_2$  and  $\mu$ . In some cases, information is used from the nonobservation of slepton decays.

Obsolete limits obtained from  $e^+e^-$  collisions up to  $\sqrt{s}=184$  GeV have been removed from this compilation and can be found in the 2000 Edition (The European Physical Journal **C15** 1 (2000)) of this Review.  
 $\Delta m = m_{\tilde{\chi}_2^0} - m_{\tilde{\chi}_1^0}$ .

VALUE (GeV)	CL%	DOCUMENT ID	TECN	COMMENT
>40	95	1 ABBIENDI	04H OPAL	all $\tan\beta$ , $\Delta m > 5$ GeV, $m_0 > 500$ GeV, $A_0 = 0$
>42.4	95	2 HEISTER	04 ALEP	all $\tan\beta$ , all $\Delta m$ , all $m_0$
>39.2	95	3 ABDALLAH	03M DLPH	all $\tan\beta$ , $m_{\tilde{\nu}} > 500$ GeV
>46	95	4 ABDALLAH	03M DLPH	all $\tan\beta$ , all $\Delta m$ , all $m_0$
>32.5	95	5 ACCIARRI	00D L3	$\tan\beta > 0.7$ , $\Delta m > 3$ GeV, all $m_0$
• • • We do not use the following data for averages, fits, limits, etc. • • •				
		6 DREINER	09 THEO	
		7 ABBOTT	98c D0	$p\bar{p} \rightarrow \tilde{\chi}_1^\pm \tilde{\chi}_2^0$
>41	95	8 ABE	98J CDF	$p\bar{p} \rightarrow \tilde{\chi}_1^\pm \tilde{\chi}_2^0$



1 ABBIENDI 04H search for charginos and neutralinos in events with acoplanar leptons+jets and multi-jet final states in the 192–209 GeV data, combined with the results on leptonic final states from ABBIENDI 04. The results hold for a scan over the parameter space covering the region  $0 < M_2 < 5000$  GeV,  $-1000 < \mu < 1000$  GeV and  $\tan\beta$  from 1 to 40. This limit supersedes ABBIENDI 00h.

2 HEISTER 04 data collected up to 209 GeV. Updates earlier analysis of selectrons from HEISTER 02e, includes a new analysis of charginos and neutralinos decaying into stau and uses results on charginos with initial state radiation from HEISTER 02j. The limit is based on the direct search for charginos and neutralinos, the constraints from the slepton search and the Higgs mass limits from HEISTER 02 using a top mass of 175 GeV, interpreted in a framework with universal gaugino and sfermion masses. Assuming the mixing in the stau sector to be negligible, the limit improves to 43.1 GeV. Under the assumption of MSUGRA with unification of the Higgs and sfermion masses, the limit improves to 50 GeV, and reaches 53 GeV for  $A_0 = 0$ . These limits include and update the results of BARATE 01.

3 ABDALLAH 03M uses data from  $\sqrt{s} = 192\text{--}208$  GeV. A limit on the mass of  $\tilde{\chi}_1^0$  is derived from direct searches for neutralinos combined with the chargino search. Neutralinos are searched in the production of  $\tilde{\chi}_1^0\tilde{\chi}_2^0$ ,  $\tilde{\chi}_1^0\tilde{\chi}_3^0$ , as well as  $\tilde{\chi}_2^0\tilde{\chi}_3^0$  and  $\tilde{\chi}_2^0\tilde{\chi}_4^0$  giving rise to cascade decays, and  $\tilde{\chi}_1^0\tilde{\chi}_2^0$  and  $\tilde{\chi}_1^0\tilde{\chi}_3^0$ , followed by the decay  $\tilde{\chi}_2^0 \rightarrow \tilde{\tau}\tau$ . The results hold for the parameter space defined by values of  $M_2 < 1$  TeV,  $|\mu| \leq 2$  TeV with the  $\tilde{\chi}_1^0$  as LSP. The limit is obtained for  $\tan\beta = 1$  and large  $m_0$ , where  $\tilde{\chi}_2^0\tilde{\chi}_3^0$  and chargino pair production are important. If the constraint from Higgs searches is also imposed, the limit improves to 49.0 GeV in the  $M_h^{max}$  scenario with  $m_t = 174.3$  GeV. These limits update the results of ABREU 00l.

4 ABDALLAH 03M uses data from  $\sqrt{s} = 192\text{--}208$  GeV. An indirect limit on the mass of  $\tilde{\chi}_1^0$  is derived by constraining the MSSM parameter space by the results from direct searches for neutralinos (including cascade decays and  $\tilde{\tau}\tau$  final states), for charginos (for all  $\Delta m_{\pm}$ ) and for sleptons, stop and sbottom. The results hold for the full parameter space defined by values of  $M_2 < 1$  TeV,  $|\mu| \leq 2$  TeV with the  $\tilde{\chi}_1^0$  as LSP. Constraints from the Higgs search in the  $M_h^{max}$  scenario assuming  $m_t = 174.3$  GeV are included. The limit is obtained for  $\tan\beta \geq 5$  when stau mixing leads to mass degeneracy between  $\tilde{\tau}_1$  and  $\tilde{\chi}_1^0$  and the limit is based on  $\tilde{\chi}_2^0$  production followed by its decay to  $\tilde{\tau}_1\tau$ . In the pathological scenario where  $m_0$  and  $|\mu|$  are large, so that the  $\tilde{\chi}_2^0$  production cross section is negligible, and where there is mixing in the stau sector but not in stop nor sbottom, the limit is based on charginos with soft decay products and an ISR photon. The limit then degrades to 39 GeV. See Figs 40–42 for the dependence of the limit on  $\tan\beta$  and  $m_{\tilde{\tau}}$ . These limits update the results of ABREU 00w.

5 ACCIARRI 00D data collected at  $\sqrt{s} = 189$  GeV. The results hold over the full parameter space defined by  $0.7 \leq \tan\beta \leq 60$ ,  $0 \leq M_2 \leq 2$  TeV,  $m_0 \leq 500$  GeV,  $|\mu| \leq 2$  TeV. The minimum mass limit is reached for  $\tan\beta = 1$  and large  $m_0$ . The results of slepton searches from ACCIARRI 99w are used to help set constraints in the region of small  $m_0$ . The limit improves to 48 GeV for  $m_0 \geq 200$  GeV and  $\tan\beta \geq 10$ . See their Figs. 6–8 for the  $\tan\beta$  and  $m_0$  dependence of the limits. Updates ACCIARRI 98f.

6 DREINER 09 show that in the general MSSM with non-universal gaugino masses there exists no model-independent laboratory bound on the mass of the lightest neutralino. An essentially massless  $\tilde{\chi}_1^0$  is allowed by the experimental and observational data, imposing some constraints on other MSSM parameters, including  $M_2$ ,  $\mu$  and the slepton and squark masses.

7 ABBOTT 98c searches for trilepton final states ( $\ell = e, \mu$ ). See footnote to ABBOTT 98c in the Chargino Section for details on the assumptions. Assuming a negligible decay rate of  $\tilde{\chi}_1^{\pm}$  and  $\tilde{\chi}_2^0$  to quarks, they obtain  $m_{\tilde{\chi}_1^0} \gtrsim 51$  GeV.

8 ABE 98J searches for trilepton final states ( $\ell = e, \mu$ ). See footnote to ABE 98J in the Chargino Section for details on the assumptions. The quoted result corresponds to the best limit within the selected range of parameters, obtained for  $m_{\tilde{q}} > m_{\tilde{g}}$ ,  $\tan\beta = 2$ , and  $\mu = -600$  GeV.

Bounds on  $\tilde{\chi}_1^0$  from dark matter searches

These papers generally exclude regions in the  $M_2 - \mu$  parameter plane assuming that  $\tilde{\chi}_1^0$  is the dominant form of dark matter in the galactic halo. These limits are based on the lack of detection in laboratory experiments, telescopes, or by the absence of a signal in underground neutrino detectors. The latter signal is expected if  $\tilde{\chi}_1^0$  accumulates in the Sun or the Earth and annihilates into high-energy  $\nu^2$ s.

VALUE	DOCUMENT ID	TECN
• • • We do not use the following data for averages, fits, limits, etc. • • •		
1	ABRAMOWSKI11	HESS
2	ABDO 10	FRMI
3	ACKERMANN 10	FRMI
4	ABBASI 09b	ICCB
5	ACHTERBERG 06	AMND
6	ACKERMANN 06	AMND
7	DEBOER 06	RVUE
8	DESAI 04	SKAM
8	AMBROSIO 99	MCRO
9	LOSECCO 95	RVUE
10	MORI 93	KAMI
11	BOTTINO 92	COSM
12	BOTTINO 91	RVUE
13	GELMINI 91	COSM
14	KAMIONKOWSKI.91	RVUE
15	MORI 91b	KAMI
16	OLIVE 88	COSM
none 4–15 GeV		

1 ABRAMOWSKI 11 place upper limits on the annihilation cross section with  $\gamma\gamma$  final states.

2 ABDO 10 place upper limits on the annihilation cross section with  $\gamma\gamma$  or  $\mu^+\mu^-$  final states.

3 ACKERMANN 10 place upper limits on the annihilation cross section with  $b\bar{b}$  or  $\mu^+\mu^-$  final states.

4 ABBASI 09 is based on data collected during 104.3 effective days with the IceCube 22-string detector. They looked for interactions of  $\nu_{\mu}$ 's from neutralino annihilations in the Sun over a background of atmospheric neutrinos and set 90% CL limits on the moon flux. They also obtain limits on the spin dependent neutralino-proton cross section for neutralino masses in the range 250–5000 GeV.

5 ACHTERBERG 06 is based on data collected during 421.9 effective days with the AMANDA detector. They looked for interactions of  $\nu_{\mu}$ 's from the centre of the Earth over a background of atmospheric neutrinos and set 90% CL limits on the moon flux. Their limit is compared with the moon flux expected from neutralino annihilations into  $W^+W^-$  and  $b\bar{b}$  at the centre of the Earth for MSSM parameters compatible with the relic dark matter density, see their Fig. 7.

6 ACKERMANN 06 is based on data collected during 143.7 days with the AMANDA-II detector. They looked for interactions of  $\nu_{\mu}$ 's from the Sun over a background of atmospheric neutrinos and set 90% CL limits on the moon flux. Their limit is compared with the moon flux expected from neutralino annihilations into  $W^+W^-$  in the Sun for SUSY model parameters compatible with the relic dark matter density, see their Fig. 3.

7 DEBOER 06 interpret an excess of diffuse Galactic gamma rays observed with the EGRET satellite as originating from  $\pi^0$  decays from the annihilation of neutralinos into quark jets. They analyze the corresponding parameter space in a supergravity inspired MSSM model with radiative electroweak symmetry breaking, see their Fig. 3 for the preferred region in the  $(m_0, m_{1/2})$  plane of a scenario with large  $\tan\beta$ .

8 AMBROSIO 99 and DESAI 04 set new neutrino flux limits which can be used to limit the parameter space in supersymmetric models based on neutralino annihilation in the Sun and the Earth.

9 LOSECCO 95 reanalyzed the IMB data and places lower limit on  $m_{\tilde{\chi}_1^0}$  of 18 GeV if the LSP is a photino and 10 GeV if the LSP is a higgsino based on LSP annihilation in the sun producing high-energy neutrinos and the limits on neutrino fluxes from the IMB detector.

10 MORI 93 excludes some region in  $M_2 - \mu$  parameter space depending on  $\tan\beta$  and lightest scalar Higgs mass for neutralino dark matter  $m_{\tilde{\chi}_1^0} > m_{\nu\tau}$ , using limits on ongoing muons produced by energetic neutrinos from neutralino annihilation in the Sun and the Earth.

11 BOTTINO 92 excludes some region  $M_2 - \mu$  parameter space assuming that the lightest neutralino is the dark matter, using ongoing muons at Kamiokande, direct searches by Ge detectors, and by LEP experiments. The analysis includes top radiative corrections on Higgs parameters and employs two different hypotheses for nucleon-Higgs coupling. Effects of rescaling in the local neutralino density according to the neutralino relic abundance are taken into account.

12 BOTTINO 91 excluded a region in  $M_2 - \mu$  plane using ongoing muon data from Kamioka experiment, assuming that the dark matter surrounding us is composed of neutralinos and that the Higgs boson is not too heavy.

13 GELMINI 91 exclude a region in  $M_2 - \mu$  plane using dark matter searches.

14 KAMIONKOWSKI 91 excludes a region in the  $M_2 - \mu$  plane using IMB limit on ongoing muons originated by energetic neutrinos from neutralino annihilation in the sun, assuming that the dark matter is composed of neutralinos and that  $m_{H_1^0} \lesssim 50$  GeV. See Fig. 8 in the paper.

15 MORI 91B exclude a part of the region in the  $M_2 - \mu$  plane with  $m_{\tilde{\chi}_1^0} \lesssim 80$  GeV using a limit on ongoing muons originated by energetic neutrinos from neutralino annihilation in the earth, assuming that the dark matter surrounding us is composed of neutralinos and that  $m_{H_1^0} \lesssim 80$  GeV.

16 OLIVE 88 result assumes that photinos make up the dark matter in the galactic halo. Limit is based on annihilations in the sun and is due to an absence of high energy neutrinos detected in underground experiments. The limit is model dependent.

$\tilde{\chi}_1^0$ -p elastic cross section

Experimental results on the  $\tilde{\chi}_1^0$ -p elastic cross section are evaluated at  $m_{\tilde{\chi}_1^0} = 100$  GeV. The experimental results on the cross section are often mass dependent. Therefore, the mass and cross section results are also given where the limit is strongest, when appropriate. Results are quoted separately for spin-dependent interactions (based on an effective 4-Fermi Lagrangian of the form  $\bar{\chi}\gamma^\mu\gamma^5\chi\bar{q}\gamma_\mu\gamma^5q$ ) and spin-independent interactions ( $\bar{\chi}\chi\bar{q}q$ ). For calculational details see GRIEST 88b, ELLIS 88b, BARBIERI 89c, DREES 93b, ARNOWITT 96, BERGSTROM 96, and BAER 97 in addition to the theory papers listed in the Tables. For a description of the theoretical assumptions and experimental techniques underlying most of the listed papers, see the review on "Dark matter" in this "Review of Particle Physics," and references therein. Most of the following papers use galactic halo and nuclear interaction assumptions from (LEWIN 96).

Spin-dependent interactions

VALUE (pb)	CL%	DOCUMENT ID	TECN	COMMENT
• • • We do not use the following data for averages, fits, limits, etc. • • •				
< 0.07	90	1 BEHNKE 11	COUP	CF <sub>3</sub>
$5 \times 10^{-10}$ to $10^{-5}$	95	2 BUCHMUEL... 11b	THEO	
< 0.3	90	3 ARCHAMBAU.09	PICA	F
< 0.8	90	4 LEBEDENKO 09a	ZEP3	Xe
< 1	90	5 ANGLE 08a	XE10	Xe
< 0.055	90	6 BEDNYAKOV 08	HDMS	Ge
< 0.33	90	7 BUHNKE 08	COUP	CF <sub>3</sub>
< 15	90	8 ALNER 07	ZEP2	Xe
< 0.17	90	9 LEE 07a	KIMS	Csl
< 5	10	10 AKERIB 06	CDMS	Ge
< 2	11	11 SHIMIZU 06a	CNTR	CaF <sub>2</sub>

# Searches Particle Listings

## Supersymmetric Particle Searches

< 0.4	12	ALNER	05	NAIA	Nal Spin Dep.
< 2	13	BARNABE-HE..05		PICA	C
< 1.4	14	GIRARD	05	SMPL	F, Cl
$2 \times 10^{-11}$ to $1 \times 10^{-4}$	15	ELLIS	04	THEO	$\mu > 0$
< 16	16	GIULIANI	04	SIMP	F
< 0.8	17	AHMED	03	NAIA	Nal Spin Dep.
< 40	18	TAKEDA	03	BOLO	NaF Spin Dep.
< 10	19	ANGLOHER	02	CRES	Sapphire
$8 \times 10^{-7}$ to $2 \times 10^{-5}$	20	ELLIS	01c	THEO	$\tan\beta \leq 10$
< 3.8	21	BERNABEI	00d	DAMA	Xe
< 15	22	COLLAR	00	SMPL	F
< 0.8		SPOONER	00	UKDM	Nal
< 4.8	23	BELLI	99c	DAMA	F
< 100	24	OOTANI	99	BOLO	LiF
< 0.6		BERNABEI	98c	DAMA	Xe
< 5	23	BERNABEI	97	DAMA	F

- The strongest limit is 0.05 pb and occurs at  $m_\chi = 55$  GeV.
- Predictions for the spin-dependent elastic cross section based on a frequentist approach to electroweak observables in the framework of  $N = 1$  supergravity models with radiative breaking of the electroweak gauge symmetry.
- The strongest limit is 0.16 pb and occurs at  $m_\chi = 24$  GeV. The strongest limit for the scattering on neutrons is 2.6 pb, also at  $m_\chi = 24$  GeV.
- The strongest upper limit is 0.76 pb and occurs at  $m_\chi \approx 55$  GeV. The strongest limit on the neutron spin-dependent cross section is 0.01 pb, also at  $m_\chi \approx 55$  GeV (the same limit is achieved for  $m_\chi = 100$  GeV).
- The strongest limit is 0.6 pb and occurs at  $m_\chi = 30$  GeV. The limit for scattering on neutrons is 0.01 pb at  $m_\chi = 100$  GeV, and the strongest limit is 0.0045 pb at  $m_\chi = 30$  GeV.
- Limit applies to neutron elastic cross section.
- The strongest upper limit is 0.25 pb and occurs at  $m_\chi \approx 40$  GeV.
- The strongest upper limit is 14 pb and occurs at  $m_\chi \approx 65$  GeV. The limit on the neutron spin-dependent cross section is 0.08 pb at  $m_\chi = 100$  GeV and the strongest limit for scattering on neutrons is 0.07 pb at  $m_\chi = 65$  GeV.
- The limit on the neutron spin-dependent cross section is 6 pb at  $m_\chi = 100$  GeV.
- The strongest upper limit is 4 pb and occurs at  $m_\chi \approx 60$  GeV. The limit on the neutron spin-dependent elastic cross section is 0.07 pb. This latter limit is improved in AHMED 09, where a limit of 0.02 pb is obtained at  $m_\chi = 100$  GeV. The strongest limit in AHMED 09 is 0.018 pb and occurs at  $m_\chi = 60$  GeV.
- The strongest upper limit is 1.2 pb and occurs at  $m_\chi \approx 40$  GeV. The limit on the neutron spin-dependent cross section is 35 pb.
- The strongest upper limit is 0.35 pb and occurs at  $m_\chi \approx 60$  GeV.
- The strongest upper limit is 1.2 pb and occurs  $m_\chi \approx 30$  GeV.
- The strongest upper limit is 1.2 pb and occurs  $m_\chi \approx 40$  GeV.
- ELLIS 04 calculates the  $\chi p$  elastic scattering cross section in the framework of  $N=1$  supergravity models with radiative breaking of the electroweak gauge symmetry, but without universal scalar masses. In the case of universal squark and slepton masses, but non-universal Higgs masses, the limit becomes  $2 \times 10^{-4}$ , see ELLIS 03e.
- The strongest upper limit is 10 pb and occurs at  $m_\chi \approx 30$  GeV.
- The strongest upper limit is 0.75 pb and occurs at  $m_\chi \approx 70$  GeV.
- The strongest upper limit is 30 pb and occurs at  $m_\chi \approx 20$  GeV.
- The strongest upper limit is 8 pb and occurs at  $m_\chi \approx 30$  GeV.
- ELLIS 01c calculates the  $\chi p$  elastic scattering cross section in the framework of  $N=1$  supergravity models with radiative breaking of the electroweak gauge symmetry. In models with nonuniversal Higgs masses, the upper limit to the cross section is  $6 \times 10^{-4}$ .
- The strongest upper limit is 3 pb and occurs at  $m_\chi \approx 60$  GeV. The limits are for inelastic scattering  $\chi^0 + {}^{129}\text{Xe} \rightarrow \chi^0 + {}^{129}\text{Xe}^* (39.58 \text{ keV})$ .
- The strongest upper limit is 9 pb and occurs at  $m_\chi \approx 30$  GeV.
- The strongest upper limit is 4.4 pb and occurs at  $m_\chi \approx 60$  GeV.
- The strongest upper limit is about 35 pb and occurs at  $m_\chi \approx 15$  GeV.

### Spin-independent interactions

VALUE (pb)	CL%	DOCUMENT ID	TECN	COMMENT
••• We do not use the following data for averages, fits, limits, etc. •••				
< $3.3 \times 10^{-8}$	90	1 AHMED	11A	Ge
< $3.1 \times 10^{-8}$	90	2 APRILE	11	X100 Xe
< $1.0 \times 10^{-8}$	90	3 APRILE	11b	X100 Xe
< $4.4 \times 10^{-8}$	90	4 ARMENGAUD 11	EDE2	Ge
$3.5 \times 10^{-11}$ to $8 \times 10^{-8}$	95	5 BUCHMUEL...	11b	THEO
$3.5 \times 10^{-11}$ to $1.4 \times 10^{-8}$	95	6 FARINA	11	THEO
< $4 \times 10^{-8}$	90	7 AHMED	10	CDMS Ge
< $4 \times 10^{-8}$	90	8 APRILE	10	X100 Xe
< $1 \times 10^{-7}$	90	9 ARMENGAUD 10	EDE2	Ge
$1 \times 10^{-10}$ to $1 \times 10^{-7}$		10 CAO	10	THEO
< $5 \times 10^{-8}$	90	11 AHMED	09	CDM2 Ge
< $7 \times 10^{-7}$	90	12 ANGLOHER	09	CRES CaWO <sub>4</sub>
$3 \times 10^{-10}$ to $3 \times 10^{-8}$	95	13 BUCHMUEL...	09	THEO
< $1 \times 10^{-7}$	90	14 LEBEDENKO	09	ZEP3 Xe
< $1 \times 10^{-7}$	90	15 ANGLE	08	XE10 Xe
< $1 \times 10^{-6}$	90	BENETTI	08	WARP Ar
< $7.5 \times 10^{-7}$	90	16 ALNER	07A	ZEP2 Xe
< $22 \times 10^{-7}$	90	17 LEE	07A	KIMS Csl
< $2 \times 10^{-7}$		18 AKERIB	06A	CDMS Ge

$4 \times 10^{-11}$ to $2 \times 10^{-7}$	95	19 DE-AUSTRI	06	THEO
< $90 \times 10^{-7}$		20 LEE	06	KIMS Csl
< $5 \times 10^{-7}$		21 AKERIB	05	CDMS Ge
< $90 \times 10^{-7}$		ALNER	05	NAIA Nal Spin Indep.
< $12 \times 10^{-7}$		22 ALNER	05A	ZEPL
< $20 \times 10^{-7}$		23 ANGLOHER	05	CRES CaWO <sub>4</sub>
< $14 \times 10^{-7}$		SANGLARD	05	EDEL Ge
< $4 \times 10^{-7}$		24 AKERIB	04	CDMS Ge
$2 \times 10^{-11}$ to $1.5 \times 10^{-7}$	95	25 BALTZ	04	THEO
$2 \times 10^{-11}$ to $8 \times 10^{-6}$		26,27 ELLIS	04	THEO $\mu > 0$
< $5 \times 10^{-8}$		28 PIERCE	04A	THEO
< $2 \times 10^{-5}$		29 AHMED	03	NAIA Nal Spin Indep.
< $3 \times 10^{-6}$		30 AKERIB	03	CDMS Ge
$2 \times 10^{-13}$ to $2 \times 10^{-7}$		31 BAER	03A	THEO
< $1.4 \times 10^{-5}$		32 KLAPDOR-K..	03	HDMS Ge
< $6 \times 10^{-6}$		33 ABRAMS	02	CDMS Ge
< $1.4 \times 10^{-6}$		34 BENOIT	02	EDEL Ge
$1 \times 10^{-12}$ to $7 \times 10^{-6}$		26 KIM	02b	THEO
< $3 \times 10^{-5}$		35 MORALES	02b	CSME Ge
< $1 \times 10^{-5}$		36 MORALES	02c	IGEX Ge
< $1 \times 10^{-6}$		BALTZ	01	THEO
< $3 \times 10^{-5}$		37 BAUDIS	01	HDMS Ge
< $4.5 \times 10^{-6}$		BENOIT	01	EDEL Ge
< $7 \times 10^{-6}$		38 BOTTINO	01	THEO
< $1 \times 10^{-8}$		39 CORSETTI	01	THEO $\tan\beta \leq 25$
$5 \times 10^{-10}$ to $1.5 \times 10^{-8}$		40 ELLIS	01c	THEO $\tan\beta \leq 10$
< $4 \times 10^{-6}$		39 GOMEZ	01	THEO
$2 \times 10^{-10}$ to $1 \times 10^{-7}$		39 LAHANAS	01	THEO
< $3 \times 10^{-6}$		ABUSAIDI	00	CDMS Ge, Si
< $6 \times 10^{-7}$		41 ACCOMANDO	00	THEO
		42 BERNABEI	00	DAMA Nal
$2.5 \times 10^{-9}$ to $3.5 \times 10^{-8}$		43 FENG	00	THEO $\tan\beta=10$
< $1.5 \times 10^{-5}$		MORALES	00	IGEX Ge
< $4 \times 10^{-5}$		SPOONER	00	UKDM Nal
< $7 \times 10^{-6}$		BAUDIS	99	HDMS <sup>76</sup> Ge
		44 BERNABEI	99	DAMA Nal
		45 BERNABEI	98	DAMA Nal
		BERNABEI	98c	DAMA Xe

- AHMED 11A gives combined results from CDMS and EDELWEISS. The strongest limit is at  $m_\chi = 90$  GeV.
- APRILE 11 updates the result of APRILE 10. The strongest upper limit is  $2.4 \times 10^{-8}$  pb and occurs at  $m_\chi \approx 50$  GeV. Superseded by APRILE 11b.
- APRILE 11B updates the result of APRILE 10 and APRILE 11. The strongest upper limit is  $7 \times 10^{-9}$  pb and occurs at  $m_\chi \approx 50$  GeV.
- ARMENGAUD 11 updates result of ARMENGAUD 10. Strongest limit at  $m_\chi = 85$  GeV.
- Predictions for the spin-independent elastic cross section based on a frequentist approach to electroweak observables in the framework of  $N = 1$  supergravity models with radiative breaking of the electroweak gauge symmetry.
- Predictions for the spin-independent elastic cross section based on a frequentist approach to electroweak observables in the framework of  $N = 1$  supergravity models with radiative breaking of the electroweak gauge symmetry.
- The strongest upper limit is  $< 3.8 \times 10^{-8}$  pb and occurs at  $m_\chi \approx 70$  GeV. AHMED 10 updates the results of AHMED 09.
- The strongest upper limit is  $< 3.4 \times 10^{-8}$  pb and occurs at  $m_\chi \approx 55$  GeV. Superseded by APRILE 11.
- The strongest limit is at  $m_\chi = 80$  GeV. Superseded ARMENGAUD 11.
- Uses relic density and various collider experiments to set limits on neutralino-nucleon cross section in MSSM models with gaugino mass unification.
- AHMED 09 updates the results of AKERIB 06A. The strongest limit is  $4.6 \times 10^{-8}$  pb and occurs at  $m_\chi = 60$  GeV. Superseded by AHMED 10.
- The strongest upper limit is  $4.8 \times 10^{-7}$  pb and occurs at  $m_\chi = 50$  GeV.
- BUCHMUELLER 09 makes predictions for the spin-independent elastic cross section based on a frequentist approach to electroweak observables in the framework of  $N = 1$  supergravity models with radiative breaking of the electroweak gauge symmetry.
- The strongest upper limit is  $8.1 \times 10^{-8}$  pb and occurs at  $m_\chi = 60$  GeV.
- The strongest upper limit is  $5.1 \times 10^{-8}$  pb and occurs at  $m_\chi \approx 30$  GeV. The values quoted here are based on the analysis performed in ANGLE 08 with the update from SORENSEN 09.
- The strongest upper limit is  $6.6 \times 10^{-7}$  pb and occurs at  $m_\chi \approx 65$  GeV.
- The strongest upper limit is  $1.9 \times 10^{-7}$  pb and occurs at  $m_\chi \approx 65$  GeV. Supersedes LEE 06.
- AKERIB 06A updates the results of AKERIB 05. The strongest upper limit is  $1.6 \times 10^{-7}$  pb and occurs at  $m_\chi \approx 60$  GeV.
- Predictions for the spin-independent elastic cross section based on a Bayesian approach to electroweak observables in the framework of  $N = 1$  supergravity models with radiative breaking of the electroweak gauge symmetry.
- The strongest upper limit is  $8 \times 10^{-6}$  pb and occurs at  $m_\chi \approx 70$  GeV.
- AKERIB 05 is incompatible with the DAMA most likely value. The strongest upper limit is  $4 \times 10^{-7}$  pb and occurs at  $m_\chi \approx 60$  GeV.
- The strongest upper limit is also close to  $1.0 \times 10^{-6}$  pb and occurs at  $m_\chi \approx 70$  GeV. BENOIT 06 claim that the discrimination power of ZEPLIN-I measurement (ALNER 05A) is not reliable enough to obtain a limit better than  $1 \times 10^{-3}$  pb. However, SMITH 06 do not agree with the criticisms of BENOIT 06.
- The strongest upper limit is also close to  $1.4 \times 10^{-6}$  pb and occurs at  $m_\chi \approx 70$  GeV.

See key on page 457

# Searches Particle Listings Supersymmetric Particle Searches

24 AKERIB 04 is incompatible with BERNABEI 00 most likely value, under the assumption of standard WIMP-halo interactions. The strongest upper limit is  $4 \times 10^{-7}$  pb and occurs at  $m_\chi \simeq 60$  GeV.

25 Predictions for the spin-independent elastic cross section in the framework of  $N = 1$  supergravity models with radiative breaking of the electroweak gauge symmetry.

26 KIM 02 and ELLIS 04 calculate the  $\chi p$  elastic scattering cross section in the framework of  $N=1$  supergravity models with radiative breaking of the electroweak gauge symmetry, but without universal scalar masses.

27 In the case of universal squark and slepton masses, but non-universal Higgs masses, the limit becomes  $2 \times 10^{-6}$  ( $2 \times 10^{-11}$  when constraint from the BNL  $g-2$  experiment are included), see ELLIS 03e. ELLIS 05 display the sensitivity of the elastic scattering cross section to the  $\pi$ -Nucleon  $\Sigma$  term.

28 PIERCE 04A calculates the  $\chi p$  elastic scattering cross section in the framework of models with very heavy scalar masses. See Fig. 2 of the paper.

29 The strongest upper limit is  $1.8 \times 10^{-5}$  pb and occurs at  $m_\chi \approx 80$  GeV.

30 Under the assumption of standard WIMP-halo interactions, Akerib 03 is incompatible with BERNABEI 00 most likely value at the 99.98% CL. See Fig. 4.

31 BAER 03A calculates the  $\chi p$  elastic scattering cross section in several models including the framework of  $N=1$  supergravity models with radiative breaking of the electroweak gauge symmetry.

32 The strongest upper limit is  $7 \times 10^{-6}$  pb and occurs at  $m_\chi \simeq 30$  GeV.

33 ABRAMS 02 is incompatible with the DAMA most likely value at the 99.9% CL. The strongest upper limit is  $3 \times 10^{-6}$  pb and occurs at  $m_\chi \simeq 30$  GeV.

34 BENOIT 02 excludes the central result of DAMA at the 99.8% CL.

35 The strongest upper limit is  $2 \times 10^{-5}$  pb and occurs at  $m_\chi \simeq 40$  GeV.

36 The strongest upper limit is  $7 \times 10^{-6}$  pb and occurs at  $m_\chi \simeq 46$  GeV.

37 The strongest upper limit is  $1.8 \times 10^{-5}$  pb and occurs at  $m_\chi \simeq 32$  GeV.

38 BOTTINO 01 calculates the  $\chi-p$  elastic scattering cross section in the framework of the following supersymmetric models:  $N=1$  supergravity with the radiative breaking of the electroweak gauge symmetry,  $N=1$  supergravity with nonuniversal scalar masses and an effective MSSM model at the electroweak scale.

39 Calculates the  $\chi-p$  elastic scattering cross section in the framework of  $N=1$  supergravity models with radiative breaking of the electroweak gauge symmetry.

40 ELLIS 01c calculates the  $\chi-p$  elastic scattering cross section in the framework of  $N=1$  supergravity models with radiative breaking of the electroweak gauge symmetry. ELLIS 02b find a range  $2 \times 10^{-8}$ - $1.5 \times 10^{-7}$  at  $\tan\beta=50$ . In models with nonuniversal Higgs masses, the upper limit to the cross section is  $4 \times 10^{-7}$ .

41 ACCOMANDO 00 calculate the  $\chi-p$  elastic scattering cross section in the framework of minimal  $N=1$  supergravity models with radiative breaking of the electroweak gauge symmetry. The limit is relaxed by at least an order of magnitude when models with nonuniversal scalar masses are considered. A subset of the authors in ARNOWITT 02 updated the limit to  $< 9 \times 10^{-8}$  ( $\tan\beta < 55$ ).

42 BERNABEI 00 search for annual modulation of the WIMP signal. The data favor the hypothesis of annual modulation at  $4\sigma$  and are consistent, for a particular model framework quoted there, with  $m_{\chi^0} = 44^{+12}_{-9}$  GeV and a spin-independent  $X^0$ -proton cross section of  $(5.4 \pm 1.0) \times 10^{-6}$  pb. See also BERNABEI 01 and BERNABEI 00c.

43 FENG 00 calculate the  $\chi-p$  elastic scattering cross section in the framework of  $N=1$  supergravity models with radiative breaking of the electroweak gauge symmetry with a particular emphasis on focus point models. At  $\tan\beta=50$ , the range is  $8 \times 10^{-8}$ - $4 \times 10^{-7}$ .

44 BERNABEI 99 search for annual modulation of the WIMP signal. The data favor the hypothesis of annual modulation at 99.6%CL and are consistent, for the particular model framework considered there, with  $m_{\chi^0} = 59^{+17}_{-14}$  GeV and spin-independent  $X^0$ -proton cross section of  $(7.0^{+0.4}_{-1.2}) \times 10^{-6}$  pb ( $1\sigma$  errors).

45 BERNABEI 98 search for annual modulation of the WIMP signal. The data are consistent, for the particular model framework considered there, with  $m_{\chi^0} = 59^{+36}_{-19}$  GeV and spin-independent  $X^0$ -proton cross section of  $(1.0^{+0.1}_{-0.4}) \times 10^{-5}$  pb ( $1\sigma$  errors).

> 6 GeV

> 6 GeV

> 18 GeV

< 600 GeV

none 100 eV - 15 GeV

none 100 eV-5 GeV

19	BALTZ	04	COSM
20,21	BELANGER	04	THEO
22	ELLIS	04B	COSM
23	PIERCE	04A	COSM
24	BAER	03	COSM
20	BOTTINO	03	COSM
24	CHATTOPAD.	03	COSM
25	ELLIS	03	COSM
9	ELLIS	03B	COSM
24	ELLIS	03C	COSM
20	HOOPER	03	COSM $\Omega_\chi = 0.05-0.3$
24	LAHANAS	03	COSM
26	BAER	02	COSM
27	ELLIS	02	COSM
28	LAHANAS	02	COSM
29	BARGER	01C	COSM
26	DJOUADI	01	COSM
30	ELLIS	01B	COSM
26	ROSKOWSKI	01	COSM
25	BOEHM	00B	COSM
31	FENG	00	COSM
32	LAHANAS	00	COSM
33	ELLIS	98B	COSM
34	EDSJO	97	COSM Co-annihilation
35	BAER	96	COSM
9	BEREZINSKY	95	COSM
36	FALK	95	COSM CP-violating phases
37	DREES	93	COSM Minimal supergravity
38	FALK	93	COSM Sfermion mixing
37	KELLEY	93	COSM Minimal supergravity
39	MIZUTA	93	COSM Co-annihilation
40	LOPEZ	92	COSM Minimal supergravity, $m_0=A=0$
41	MCDONALD	92	COSM
42	GRIEST	91	COSM
43	NOJIRI	91	COSM Minimal supergravity
44	OLIVE	91	COSM
45	ROSKOWSKI	91	COSM
46	GRIEST	90	COSM
44	OLIVE	89	COSM
	SREDNICKI	88	COSM $\tilde{\tau}; m_{\tilde{f}}=100$ GeV
	ELLIS	84	COSM $\tilde{\tau};$ for $m_{\tilde{f}}=100$ GeV
	GOLDBERG	83	COSM $\tilde{\tau}$
47	KRAUSS	83	COSM $\tilde{\tau}$
	VYSOTSKII	83	COSM $\tilde{\tau}$

1 ELLIS 00 updates ELLIS 98. Uses LEP  $e^+e^-$  data at  $\sqrt{s}=202$  and 204 GeV to improve bound on neutralino mass to 51 GeV when scalar mass universality is assumed and 46 GeV when Higgs mass universality is relaxed. Limits on  $\tan\beta$  improve to  $> 2.7$  ( $\mu > 0$ ),  $> 2.2$  ( $\mu < 0$ ) when scalar mass universality is assumed and  $> 1.9$  (both signs of  $\mu$ ) when Higgs mass universality is relaxed.

2 AKULA 11A places constraints on the SUSY parameter space in the framework of  $N = 1$  supergravity models with radiative breaking of the electroweak gauge symmetry using results from 35 pb<sup>-1</sup> of LHC data.

3 ALLANACH 11A updates the results of ALLANACH 11 and places constraints on the SUSY parameter space in the framework of  $N = 1$  supergravity models with radiative breaking of the electroweak gauge symmetry using results from 35 pb<sup>-1</sup> of LHC data.

4 BUCHMUELLER 11 places constraints on the SUSY parameter space in the framework of  $N = 1$  supergravity models with radiative breaking of the electroweak gauge symmetry using indirect experimental searches and including supersymmetry breaking relations between A and B parameters.

5 BUCHMUELLER 11A places constraints on the SUSY parameter space in the framework of  $N = 1$  supergravity models with radiative breaking of the electroweak gauge symmetry using indirect experimental searches and results from 35 pb<sup>-1</sup> of LHC data. Superseded by BUCHMUELLER 11B.

6 BUCHMUELLER 11B places constraints on the SUSY parameter space in the framework of  $N = 1$  supergravity models with radiative breaking of the electroweak gauge symmetry using results from 35 pb<sup>-1</sup> of LHC data and from XENON100 data as well as indirect experimental searches. See also BUCHMUELLER 11A.

7 FARINA 11 places constraints on the SUSY parameter space in the framework of  $N = 1$  supergravity models with radiative breaking of the electroweak gauge symmetry using results from 1.1 fb<sup>-1</sup> of LHC data and from XENON100 data as well as indirect experimental searches.

8 PROFUMO 11 places constraints on the SUSY parameter space in the framework of  $N = 1$  supergravity models with radiative breaking of the electroweak gauge symmetry using results from 35 pb<sup>-1</sup> of LHC data and from XENON100.

9 Places constraints on the SUSY parameter space in the framework of  $N=1$  supergravity models with radiative breaking of the electroweak gauge symmetry but non-Universal Higgs masses.

10 BECHTLE 10 places constraints on the SUSY parameter space in the framework of  $N = 1$  supergravity models with radiative breaking of the electroweak gauge symmetry.

11 ELLIS 10 places constraints on the SUSY parameter space in the framework of  $N = 1$  supergravity models with radiative breaking of the electroweak gauge symmetry with universality above the GUT scale.

12 BUCHMUELLER 09 places constraints on the SUSY parameter space in the framework of  $N = 1$  supergravity models with radiative breaking of the electroweak gauge symmetry using indirect experimental searches.

### Other bounds on $\tilde{\chi}_1^0$ from astrophysics and cosmology

Most of these papers generally exclude regions in the  $M_2 - \mu$  parameter plane by requiring that the  $\tilde{\chi}_1^0$  contribution to the overall cosmological density is less than some maximal value to avoid overclosure of the Universe. Those not based on the cosmological density are indicated. Many of these papers also include LEP and/or other bounds.

VALUE	DOCUMENT ID	TECN	COMMENT
>46 GeV	1 ELLIS 00	RVUE	
•••	We do not use the following data for averages, fits, limits, etc. •••		
2	AKULA 11A	COSM	
3	ALLANACH 11A	COSM	
4	BUCHMUEL... 11	COSM	
5	BUCHMUEL... 11A	COSM	
6	BUCHMUEL... 11B	COSM	
7	FARINA 11	COSM	
8	PROFUMO 11	COSM	
9	ROSKOWSKI 11	COSM	
10	BECHTLE 10	COSM	
11	ELLIS 10	COSM	
12	BUCHMUEL... 09	COSM	
13	DREINER 09	THEO	
14	BUCHMUEL... 08	COSM	
9	ELLIS 08	COSM	
15	CALIBBI 07	COSM	
16	ELLIS 07	COSM	
17	ALLANACH 06	COSM	
18	DE-AUSTRI 06	COSM	
9	BAER 05	COSM	

# Searches Particle Listings

## Supersymmetric Particle Searches

- 13 DREINER 09 show that in the general MSSM with non-universal gaugino masses there exists no model-independent laboratory bound on the mass of the lightest neutralino. An essentially massless  $\tilde{\chi}_1^0$  is allowed by the experimental and observational data, imposing some constraints on other MSSM parameters, including  $M_2$ ,  $\mu$  and the slepton and squark masses.
- 14 BUCHMUELLER 08 places constraints on the SUSY parameter space in the framework of  $N=1$  supergravity models with radiative breaking of the electroweak gauge symmetry using indirect experimental searches.
- 15 CALIBBI 07 places constraints on the SUSY parameter space in the framework of  $N=1$  supergravity models with radiative breaking of the electroweak gauge symmetry with universality above the GUT scale including the effects of right-handed neutrinos.
- 16 ELLIS 07 places constraints on the SUSY parameter space in the framework of  $N=1$  supergravity models with radiative breaking of the electroweak gauge symmetry with universality below the GUT scale.
- 17 ALLANACH 06 places constraints on the SUSY parameter space in the framework of  $N=1$  supergravity models with radiative breaking of the electroweak gauge symmetry.
- 18 DE-AUSTRI 06 places constraints on the SUSY parameter space in the framework of  $N=1$  supergravity models with radiative breaking of the electroweak gauge symmetry.
- 19 BALTZ 04 places constraints on the SUSY parameter space in the framework of  $N=1$  supergravity models with radiative breaking of the electroweak gauge symmetry.
- 20 HOOPER 03, BOTTINO 03 (see also BOTTINO 03A and BOTTINO 04), and BELANGER 04 do not assume gaugino or scalar mass unification.
- 21 Limit assumes a pseudo scalar mass  $< 200$  GeV. For larger pseudo scalar masses,  $m_\chi > 18(29)$  GeV for  $\tan\beta = 50(10)$ . Bounds from WMAP,  $(g-2)_\mu$ ,  $b \rightarrow s\gamma$ , LEP.
- 22 ELLIS 04b places constraints on the SUSY parameter space in the framework of  $N=1$  supergravity models with radiative breaking of the electroweak gauge symmetry including supersymmetry breaking relations between A and B parameters. See also ELLIS 03d.
- 23 PIERCE 04a places constraints on the SUSY parameter space in the framework of models with very heavy scalar masses.
- 24 BAER 03, CHATTOPADHYAY 03, ELLIS 03c and LAHANAS 03 place constraints on the SUSY parameter space in the framework of  $N=1$  supergravity models with radiative breaking of the electroweak gauge symmetry based on WMAP results for the cold dark matter density.
- 25 BOEHM 00b and ELLIS 03 place constraints on the SUSY parameter space in the framework of minimal  $N=1$  supergravity models with radiative breaking of the electroweak gauge symmetry. Includes the effect of  $\chi$ - $\tilde{\tau}$  co-annihilations.
- 26 DJOUADI 01, ROSZKOWSKI 01, and BAER 02 place constraints on the SUSY parameter space in the framework of minimal  $N=1$  supergravity models with radiative breaking of the electroweak gauge symmetry.
- 27 ELLIS 02 places constraints on the soft supersymmetry breaking masses in the framework of minimal  $N=1$  supergravity models with radiative breaking of the electroweak gauge symmetry.
- 28 LAHANAS 02 places constraints on the SUSY parameter space in the framework of minimal  $N=1$  supergravity models with radiative breaking of the electroweak gauge symmetry. Focuses on the role of pseudo-scalar Higgs exchange.
- 29 BARGER 01c use the cosmic relic density inferred from recent CMB measurements to constrain the parameter space in the framework of minimal  $N=1$  supergravity models with radiative breaking of the electroweak gauge symmetry.
- 30 ELLIS 01b places constraints on the SUSY parameter space in the framework of minimal  $N=1$  supergravity models with radiative breaking of the electroweak gauge symmetry. Focuses on models with large  $\tan\beta$ .
- 31 FENG 00 explores cosmologically allowed regions of MSSM parameter space with multi-TeV masses.
- 32 LAHANAS 00 use the new cosmological data which favor a cosmological constant and its implications on the relic density to constrain the parameter space in the framework of minimal  $N=1$  supergravity models with radiative breaking of the electroweak gauge symmetry.
- 33 ELLIS 98b assumes a universal scalar mass and radiative supersymmetry breaking with universal gaugino masses. The upper limit to the LSP mass is increased due to the inclusion of  $\chi$  -  $\tilde{\tau}_R$  coannihilations.
- 34 EDSJO 97 included all coannihilation processes between neutralinos and charginos for any neutralino mass and composition.
- 35 Notes the location of the neutralino Z resonance and h resonance annihilation corridors in minimal supergravity models with radiative electroweak breaking.
- 36 Mass of the bino (=LSP) is limited to  $m_{\tilde{B}} \lesssim 350$  GeV for  $m_t = 174$  GeV.
- 37 DREES 93, KELLEY 93 compute the cosmic relic density of the LSP in the framework of minimal  $N=1$  supergravity models with radiative breaking of the electroweak gauge symmetry.
- 38 FALK 93 relax the upper limit to the LSP mass by considering sfermion mixing in the MSSM.
- 39 MIZUTA 93 include coannihilations to compute the relic density of Higgsino dark matter.
- 40 LOPEZ 92 calculate the relic LSP density in a minimal SUSY GUT model.
- 41 MCDONALD 92 calculate the relic LSP density in the MSSM including exact tree-level annihilation cross sections for all two-body final states.
- 42 GRIEST 91 improve relic density calculations to account for coannihilations, pole effects, and threshold effects.
- 43 NOJRI 91 uses minimal supergravity mass relations between squarks and sleptons to narrow cosmologically allowed parameter space.
- 44 Mass of the bino (=LSP) is limited to  $m_{\tilde{B}} \lesssim 350$  GeV for  $m_t \leq 200$  GeV. Mass of the higgsino (=LSP) is limited to  $m_{\tilde{H}} \lesssim 1$  TeV for  $m_t \leq 200$  GeV.
- 45 ROSZKOWSKI 91 calculates LSP relic density in mixed gaugino/higgsino region.
- 46 Mass of the bino (=LSP) is limited to  $m_{\tilde{B}} \lesssim 550$  GeV. Mass of the higgsino (=LSP) is limited to  $m_{\tilde{H}} \lesssim 3.2$  TeV.
- 47 KRAUSS 83 finds  $m_{\tilde{\gamma}}$  not 30 eV to 2.5 GeV. KRAUSS 83 takes into account the gravitino decay. Find that limits depend strongly on reheated temperature. For example a new allowed region  $m_{\tilde{\gamma}} = 4-20$  MeV exists if  $m_{\text{gravitino}} < 40$  TeV. See figure 2.

other masses. In the following,  $\tilde{G}$  is assumed to be undetected and to give rise to a missing energy ( $\cancel{E}$ ) signature.

VALUE (GeV)	CL%	DOCUMENT ID	TECN	COMMENT
• • • We do not use the following data for averages, fits, limits, etc. • • •				
>149	95	1 CHATRCHYAN11B 2 AALTONEN	CMS 10 CDF	$\tilde{W}^0 \rightarrow \gamma \tilde{G}, \tilde{W}^\pm \rightarrow \ell^\pm \tilde{G}, \text{GMSB}$ $p\bar{p} \rightarrow \tilde{\chi}\tilde{\chi}, \tilde{\chi} = \tilde{\chi}_2^0, \tilde{\chi}_1^\pm, \tilde{\chi}_1^0 \rightarrow \gamma \tilde{G},$ $\text{GMSB}$
>175	95	3 ABAZOV	10P D0	$\tilde{\chi}_1^0 \rightarrow \gamma \tilde{G}, \text{GMSB}$
>125	95	4 AALTONEN 5 ABAZOV	08U CDF 08F D0	$\tilde{\chi}_1^0 \rightarrow \gamma \tilde{G}, \text{GMSB}$ $p\bar{p} \rightarrow \tilde{\chi}\tilde{\chi}, \tilde{\chi} = \tilde{\chi}_2^0, \tilde{\chi}_1^\pm, \tilde{\chi}_1^0 \rightarrow \gamma \tilde{G},$ $\text{GMSB}$
		6 ABAZOV	08x D0	$\tilde{\chi}_1^0 \rightarrow Z^0 \tilde{G}, \text{GMSB}$
		7 ABULENCIA	07H CDF	$R, L\tilde{L}\tilde{E}$
		8 ABAZOV	06D D0	$R, L\tilde{L}\tilde{E}$
		9 ABAZOV	06P D0	$R, \lambda_{122}$
> 96.8	95	10 ABBIENDI	06B OPAL	$e^+e^- \rightarrow \tilde{B}\tilde{B}, (\tilde{B} \rightarrow \tilde{G}\gamma)$
		11 ABDALLAH	05B DLPH	$e^+e^- \rightarrow \tilde{G}\tilde{\chi}_1^0, (\tilde{\chi}_1^0 \rightarrow \tilde{G}\gamma)$
> 96	95	12 ABDALLAH	05B DLPH	$e^+e^- \rightarrow \tilde{B}\tilde{B}, (\tilde{B} \rightarrow \tilde{G}\gamma)$
> 93	95	13 ACOSTA	05E CDF	$p\bar{p} \rightarrow \tilde{\chi}\tilde{\chi}, \tilde{\chi} = \tilde{\chi}_2^0, \tilde{\chi}_1^\pm, \tilde{\chi}_1^0 \rightarrow \gamma \tilde{G},$ $\text{GMSB}$
		14 AKTAS	05 H1	$e^\pm p \rightarrow q\tilde{\chi}_1^0, \tilde{\chi}_1^0 \rightarrow \gamma \tilde{G},$ $\text{GMSB} + R L Q \tilde{D}$
> 66	95	15 ABBIENDI	04N OPAL	$e^+e^- \rightarrow \gamma\gamma\tilde{E}$
> 38.0	95	16,17 ABDALLAH 18,19 ABDALLAH	04H DLPH 04M DLPH	$\text{AMS}\tilde{B}, \mu > 0$ $R(\tilde{U}\tilde{D}\tilde{D})$
		20 ACHARD	04E L3	$e^+e^- \rightarrow \tilde{G}\tilde{\chi}_1^0, \tilde{\chi}_1^0 \rightarrow \tilde{G}\gamma$
> 99.5	95	21 ACHARD	04E L3	$e^+e^- \rightarrow \tilde{B}\tilde{B}, (\tilde{B} \rightarrow \tilde{G}\gamma)$
> 89		22 ABDALLAH	03D DLPH	$e^+e^- \rightarrow \tilde{\chi}_1^0\tilde{\chi}_1^0, \text{GMSB},$ $m(\tilde{G}) < 1\text{eV}$
		23 HEISTER	03c ALEP	$e^+e^- \rightarrow \tilde{B}\tilde{B}, (\tilde{B} \rightarrow \gamma\tilde{G})$
		24 HEISTER	03c ALEP	$e^+e^- \rightarrow \tilde{G}\tilde{\chi}_1^0, (\tilde{\chi}_1^0 \rightarrow \tilde{G}\gamma)$
> 39.9	95	25 ACHARD	02 L3	$R, \text{MSUGRA}$
> 92	95	26 HEISTER	02R ALEP	short lifetime
> 54	95	26 HEISTER	02R ALEP	any lifetime
> 85	95	27 ABBIENDI	01 OPAL	$e^+e^- \rightarrow \tilde{\chi}_1^0\tilde{\chi}_1^0, \text{GMSB}, \tan\beta=2$
> 76	95	27 ABBIENDI	01 OPAL	$e^+e^- \rightarrow \tilde{\chi}_1^0\tilde{\chi}_1^0, \text{GMSB}, \tan\beta=20$
> 32.5	95	28 ACCIARRI	01 L3	$R, \text{all } m_0, 0.7 \leq \tan\beta \leq 40$
		29 ADAMS	01 NTEV	$\tilde{\chi}_1^0 \rightarrow \mu\mu\nu, R, L\tilde{L}\tilde{E}$
> 29	95	30 ABBIENDI	09T OPAL	$e^+e^- \rightarrow \tilde{\chi}_1^0\tilde{\chi}_1^0, R, m_0=500 \text{ GeV},$ $\tan\beta > 1.2$
> 29	95	31 BARATE	99E ALEP	$R, LQ\tilde{D}, \tan\beta=1.41, m_0=500 \text{ GeV}$
		32 ABREU	98 DLPH	$e^+e^- \rightarrow \tilde{\chi}_1^0\tilde{\chi}_1^0, (\tilde{\chi}_1^0 \rightarrow \gamma\tilde{G})$
> 23	95	33 BARATE	98s ALEP	$R, L\tilde{L}\tilde{E}$
		34 ELLIS	97 THEO	$e^+e^- \rightarrow \tilde{\chi}_1^0\tilde{\chi}_1^0, \tilde{\chi}_1^0 \rightarrow \gamma\tilde{G}$
		35 CABIBBO	81 COSM	

- 1 CHATRCHYAN 11B looked in 35 pb<sup>-1</sup> of  $pp$  collisions at  $\sqrt{s}=7$  TeV for events with an isolated lepton ( $e$  or  $\mu$ ), a photon and  $\cancel{E}_T$  which may arise in a generalized gauge mediated model from the decay of Wino-like NLSPs. No evidence for an excess over the expected background is observed. Limits are derived in the plane of squark/gluino mass versus Wino mass (see Fig. 4). Mass degeneracy of the produced squarks and gluinos is assumed.
- 2 AALTONEN 10 searched in 2.6 fb<sup>-1</sup> of  $p\bar{p}$  collisions at  $\sqrt{s} = 1.96$  TeV for diphoton events with large  $\cancel{E}_T$ . They may originate from the production of  $\tilde{\chi}^\pm$  in pairs or associated to a  $\tilde{\chi}_2^0$ , decaying into  $\tilde{\chi}_1^0$  which itself decays in GMSB to  $\gamma\tilde{G}$ . There is no excess of events beyond expectation. An upper limit on the cross section is calculated in the GMSB model as a function of the  $\tilde{\chi}_1^0$  mass and lifetime, see their Fig. 2. A limit is derived on the  $\tilde{\chi}_1^0$  mass of 149 GeV for  $\tau_{\tilde{\chi}_1^0} \ll 1$  ns, which improves the results of previous searches.
- 3 ABAZOV 10P looked in 6.3 fb<sup>-1</sup> of  $p\bar{p}$  collisions at  $\sqrt{s} = 1.96$  TeV for events with at least two isolated  $\gamma$ s and large  $\cancel{E}_T$ . These could be the signature of  $\tilde{\chi}_2^0$  and  $\tilde{\chi}_1^\pm$  production, decaying to  $\tilde{\chi}_1^0$  and finally  $\tilde{\chi}_1^0 \rightarrow \gamma\tilde{G}$  in a GMSB framework. No significant excess over the SM expectation is observed, and a limit at 95% C.L. on the cross section is derived for  $N_{mes} = 1$ ,  $\tan\beta = 15$  and  $\mu > 0$ , see their Fig. 2. This allows them to set a limit on the effective SUSY breaking scale  $\Lambda > 124$  TeV, from which the excluded  $\tilde{\chi}_1^0$  mass range is obtained.
- 4 AALTONEN 08U searched in 570 pb<sup>-1</sup> of  $p\bar{p}$  collisions at  $\sqrt{s} = 1.96$  TeV for events that contain a time-delayed photon, at least one jet, and large  $\cancel{E}_T$ . The time-of-arrival is measured for each electromagnetic tower with a resolution of 0.50 ns. The number of observed events in the signal region is consistent with the background estimation. An upper limit on the cross section is derived as a function of the  $\tilde{\chi}_1^0$  mass and lifetime, shown in their Fig. 24. The comparison with the NLO cross section for GMSB yields an exclusion of the  $\tilde{\chi}_1^0$  mass as a function of its lifetime, see Fig. 25. See ABULENCIA 07P for a previous analysis of the same data set.
- 5 ABAZOV 08F looked in 1.1 fb<sup>-1</sup> of  $p\bar{p}$  collisions at  $\sqrt{s} = 1.96$  TeV for diphoton events with large  $\cancel{E}_T$ . They may originate from the production of  $\tilde{\chi}^\pm$  in pairs or associated to a  $\tilde{\chi}_2^0$ , decaying to a  $\tilde{\chi}_1^0$  which itself decays promptly in GMSB to  $\tilde{\chi}_1^0 \rightarrow \gamma\tilde{G}$ . No significant excess was found compared to the background expectation. A limit is derived on the masses of SUSY particles in the GMSB framework for  $M = 2\Lambda, N = 1, \tan\beta = 15$  and  $\mu > 0$ , see Figure 2. It also excludes  $\Lambda < 91.5$  TeV. Supersedes the results of ABAZOV 05A. Superseded by ABAZOV 10P.
- 6 ABAZOV 08x searched in 1.1 fb<sup>-1</sup> of  $p\bar{p}$  collisions at  $\sqrt{s} = 1.96$  TeV for an excess of events with electron pairs. Their vertex, reconstructed from the directions measured in the segmented electromagnetic calorimeter, is required to be away from the primary interaction point. Such delayed decays might be expected for a Higgsino-like  $\tilde{\chi}_1^0$  in

### Unstable $\tilde{\chi}_1^0$ (Lightest Neutralino) MASS LIMIT

Unless otherwise stated, results in this section assume spectra and production rates as evaluated in the MSSM. Unless otherwise stated, the goldstino or gravitino mass  $m_{\tilde{G}}$  is assumed to be negligible relative to all

- GMSB. No significant excess was found compared to the background expectation. Upper limits on the cross-section times branching ratio are extracted as a function of the lifetime for several ranges of dilepton invariant masses, see their Fig. 3.
- <sup>7</sup> ABULENCIA 07H searched in  $346 \text{ pb}^{-1}$  of  $p\bar{p}$  collisions at  $\sqrt{s} = 1.96 \text{ TeV}$  for events with at least three leptons ( $e$  or  $\mu$ ) from the decay of  $\tilde{\chi}_1^0$  via  $L\bar{L}\bar{E}$  couplings. The results are consistent with the hypothesis of no signal. Upper limits on the cross-section are extracted and a limit is derived in the framework of mSUGRA on the masses of  $\tilde{\chi}_1^0$  and  $\tilde{\chi}_1^\pm$ , see e.g. their Fig. 3 and Tab. II.
- <sup>8</sup> ABAZOV 06D looked in  $360 \text{ pb}^{-1}$  of  $p\bar{p}$  collisions at  $\sqrt{s} = 1.96 \text{ TeV}$  for events with three leptons originating from the pair production of charginos and neutralinos, followed by  $R$  decays mediated by  $L\bar{L}\bar{E}$  couplings. One coupling is assumed to be dominant at a time. No significant excess was found compared to the background expectation in the  $e\ell, \mu\mu\ell$  nor  $e\ell\tau$  ( $\ell = e, \mu$ ) final states. Upper limits on the cross-section are extracted in a specific MSUGRA model and a MSSM model without unification of  $M_1$  and  $M_2$  at the GUT scale. A limit is derived on the masses of charginos and neutralinos for both scenarios assuming  $\lambda_{ijk}$  couplings such that the decay length is less than 1 cm, see their Table III and Fig. 4.
- <sup>9</sup> ABAZOV 06P looked in  $380 \text{ pb}^{-1}$  of  $p\bar{p}$  collisions at  $\sqrt{s} = 1.96 \text{ TeV}$  for events with at least 2 opposite sign isolated muons which might arise from the decays of neutralinos into  $\mu\mu\nu$  via  $R$  couplings  $L\bar{L}\bar{E}$ . No events are observed in the decay region defined by a radius between 5 and 20 cm, in agreement with the SM expectation. Limits are set on the cross-section times branching ratio as a function of lifetime, shown in their Fig. 3. This limit excludes the SUSY interpretation of the NuTeV excess of dimuon events reported in ADAMS 01.
- <sup>10</sup> ABBIENDI 06b use  $600 \text{ pb}^{-1}$  of data from  $\sqrt{s} = 189\text{--}209 \text{ GeV}$ . They look for events with diphotons +  $B$  final states originating from prompt decays of pair-produced neutralinos in a GMSB scenario with  $\tilde{\chi}_1^0$  NLSP. Limits on the cross-section are computed as a function of  $m(\tilde{\chi}_1^0)$ , see their Fig. 14. The limit on the  $\tilde{\chi}_1^0$  mass is for a pure Bino state assuming a prompt decay, with lifetimes up to  $10^{-9}$ s. Supersedes the results of ABBIENDI 04n.
- <sup>11</sup> ABDALLAH 05b use data from  $\sqrt{s} = 180\text{--}209 \text{ GeV}$ . They look for events with single photons +  $B$  final states. Limits are computed in the plane  $(m(\tilde{G}), m(\tilde{\chi}_1^0))$ , shown in their Fig. 9b for a pure Bino state in the GMSB framework and in Fig. 9c for a no-scale supergravity model. Supersedes the results of ABREU 00z.
- <sup>12</sup> ABDALLAH 05b use data from  $\sqrt{s} = 130\text{--}209 \text{ GeV}$ . They look for events with diphotons +  $B$  final states and single photons not pointing to the vertex, expected in GMSB when the  $\tilde{\chi}_1^0$  is the NLSP. Limits are computed in the plane  $(m(\tilde{G}), m(\tilde{\chi}_1^0))$ , see their Fig. 10. The lower limit is derived on the  $\tilde{\chi}_1^0$  mass for a pure Bino state assuming a prompt decay and  $m_{\tilde{e}_R} = m_{\tilde{e}_L} = 2 m_{\tilde{\nu}_\tau}$ . It improves to  $100 \text{ GeV}$  for  $m_{\tilde{e}_R} = m_{\tilde{e}_L} = 1.1 m_{\tilde{\nu}_\tau}$ , and the limit in the plane  $(m(\tilde{\chi}_1^0), m(\tilde{e}_R))$  is shown in Fig. 10b. For long-lived neutralinos, cross-section limits are displayed in their Fig 11. Supersedes the results of ABREU 00z.
- <sup>13</sup> ACOSTA 05e looked in  $202 \text{ pb}^{-1}$  of  $p\bar{p}$  collisions at  $\sqrt{s}=1.96 \text{ TeV}$  for diphoton events with large  $B_T$ . They may originate from the production of  $\tilde{\chi}^\pm$  in pairs or associated to a  $\tilde{\chi}_1^0$ , decaying to a  $\tilde{\chi}_1^0$  which itself decays promptly in GMSB to  $\gamma\tilde{G}$ . No events are selected at large  $B_T$  compared to the background expectation. A limit is derived on the masses of SUSY particles in the GMSB framework for  $M = 2A, N = 1, \tan\beta = 15$  and  $\mu > 0$ , see Figure 2. It also excludes  $A < 69 \text{ TeV}$ . Supersedes the results of ABE 99i.
- <sup>14</sup> AKTAS 05 data collected at  $319 \text{ GeV}$  with  $64.3 \text{ pb}^{-1}$  of  $e^+p$  and  $13.5 \text{ pb}^{-1}$  of  $e^-p$ . They look for  $R$  resonant  $\tilde{\chi}_1^0$  production via  $t$ -channel exchange of a  $\tilde{e}$ , followed by prompt GMSB decay of the  $\tilde{\chi}_1^0$  to  $\gamma\tilde{G}$ . Upper limits at 95% on the cross section are derived, see their Figure 4, and compared to two example scenarios. In Figure 5, they display 95% exclusion limits in the plane of  $M(\tilde{\chi}_1^0)$  versus  $M(\tilde{e}_L) - M(\tilde{\chi}_1^0)$  for the two scenarios and several values of the  $\lambda'$  Yukawa coupling.
- <sup>15</sup> ABBIENDI 04n use data from  $\sqrt{s} = 189\text{--}209 \text{ GeV}$ , setting limits on  $\sigma(e^+e^- \rightarrow X\bar{X}) \times \text{Br}(X \rightarrow Y\gamma)$ , with  $Y$  invisible (see their Fig. 4). Limits on  $\tilde{\chi}_1^0$  masses for a specific model are given. Supersedes the results of ABBIENDI, G 00d.
- <sup>16</sup> ABDALLAH 04H use data from LEP 1 and  $\sqrt{s} = 192\text{--}208 \text{ GeV}$ . They re-use results or re-analyze the data from ABDALLAH 03M to put limits on the parameter space of anomaly-mediated supersymmetry breaking (AMSB), which is scanned in the region  $1 < m_{3/2} < 50 \text{ TeV}, 0 < m_0 < 1000 \text{ GeV}, 1.5 < \tan\beta < 35$ , both signs of  $\mu$ . The constraints are obtained from the searches for mass degenerate chargino and neutralino, for SM-like and invisible Higgs, for leptonically decaying charginos and from the limit on non-SM  $Z$  width of  $3.2 \text{ MeV}$ . The limit is for  $m_t = 174.3 \text{ GeV}$  (see Table 2 for other  $m_t$  values). The limit improves to  $73 \text{ GeV}$  for  $\mu < 0$ .
- <sup>17</sup> ABDALLAH 04M use data from  $\sqrt{s} = 192\text{--}208 \text{ GeV}$  to derive limits on sparticle masses under the assumption of  $R$  with  $L\bar{L}\bar{E}$  or  $\bar{U}\bar{D}\bar{D}$  couplings. The results are valid in the ranges  $90 < m_0 < 500 \text{ GeV}, 0.7 < \tan\beta < 30, -200 < \mu < 200 \text{ GeV}, 0 < M_2 < 400 \text{ GeV}$ . Supersedes the result of ABREU 01D and ABREU 00u.
- <sup>18</sup> The limit improves to  $39.5 \text{ GeV}$  for  $L\bar{L}\bar{E}$  couplings.
- <sup>19</sup> The limit improves to  $39.5 \text{ GeV}$  for  $L\bar{L}\bar{E}$  couplings.
- <sup>20</sup> ACHARD 04E use data from  $\sqrt{s} = 189\text{--}209 \text{ GeV}$ . They look for events with single photons +  $B$  final states. Limits are computed in the plane  $(m(\tilde{G}), m(\tilde{\chi}_1^0))$ , shown in their Fig. 8c for a no-scale supergravity model, excluding, e.g., Gravitino masses below  $10^{-5} \text{ eV}$  for neutralino masses below  $172 \text{ GeV}$ . Supersedes the results of ACCIARRI 99R.
- <sup>21</sup> ACHARD 04E use data from  $\sqrt{s} = 189\text{--}209 \text{ GeV}$ . They look for events with diphotons +  $B$  final states. Limits are computed in the plane  $(m(\tilde{\chi}_1^0), m(\tilde{e}_R))$ , see their Fig. 8d. The limit on the  $\tilde{\chi}_1^0$  mass is for a pure Bino state assuming a prompt decay, with  $m_{\tilde{e}_L} = 1.1 m_{\tilde{\nu}_\tau}$  and  $m_{\tilde{e}_R} = 2.5 m_{\tilde{\nu}_\tau}$ . Supersedes the results of ACCIARRI 99R.
- <sup>22</sup> ABDALLAH 03D use data from  $\sqrt{s} = 161\text{--}208 \text{ GeV}$ . They look for 4-tau +  $B$  final states, expected in GMSB when the  $\tilde{\tau}_1$  is the NLSP, and 4-lepton +  $B$  final states, expected in the co-NLSP scenario, and assuming a short-lived  $\tilde{\chi}_1^0$  ( $m(\tilde{G}) < 1 \text{ eV}$ ). Limits are computed in the plane  $(m(\tilde{\tau}_1), m(\tilde{\chi}_1^0))$  from a scan of the GMSB parameters space, after combining these results with the search for slepton pair production from the same paper to cover prompt decays and for the case of  $\tilde{\chi}_1^0$  NLSP from ABREU 00z. The limit above is reached for a single generation of messengers and when the  $\tilde{\tau}_1$  is the NLSP. Stronger limits are obtained when more messenger generations are assumed or when the other sleptons are co-NLSP, see their Fig. 10. Supersedes the results of ABREU 01G.
- <sup>23</sup> HEISTER 03C use the data from  $\sqrt{s} = 189\text{--}209 \text{ GeV}$  to search for  $\gamma\tilde{E}_T$  final states with non-pointing photons and  $\gamma\tilde{E}_T$  events. Interpreted in the framework of Minimal GMSB, a lower bound on the  $\tilde{\chi}_1^0$  mass is obtained as function of its lifetime. For a laboratory lifetime of less than 3 ns, the limit at 95% CL is  $98.8 \text{ GeV}$ . For other lifetimes, see their Fig. 5. These results are interpreted in a more general GMSB framework in HEISTER 02R.
- <sup>24</sup> HEISTER 03C use the data from  $\sqrt{s} = 189\text{--}209 \text{ GeV}$  to search for  $\gamma\tilde{E}_T$  final states. They obtained an upper bound on the cross section for the process  $e^+e^- \rightarrow \tilde{G}\tilde{\chi}_1^0$ , followed by the prompt decay  $\tilde{\chi}_1^0 \rightarrow \gamma\tilde{G}$ , shown in their Fig. 4. These results supersede BARATE 98H.
- <sup>25</sup> ACHARD 02 searches for the production of sparticles in the case of  $R$  prompt decays with  $L\bar{L}\bar{E}$  or  $\bar{U}\bar{D}\bar{D}$  couplings at  $\sqrt{s}=189\text{--}208 \text{ GeV}$ . The search is performed for direct and indirect decays, assuming one coupling at the time to be nonzero. The MSUGRA limit results from a scan over the MSSM parameter space with the assumption of gaugino and scalar mass unification at the GUT scale, imposing simultaneously the exclusions from neutralino, chargino, sleptons, and squarks analyses. The limit holds for  $\bar{U}\bar{D}\bar{D}$  couplings and increases to  $40.2 \text{ GeV}$  for  $L\bar{L}\bar{E}$  couplings. For L3 limits from  $L\bar{Q}\bar{D}$  couplings, see ACCIARRI 01.
- <sup>26</sup> HEISTER 02R search for signals of GMSB in the  $189\text{--}209 \text{ GeV}$  data. For the  $\tilde{\chi}_1^0$  NLSP scenario, they looked for topologies consisting of  $\gamma\tilde{E}$  or a single  $\gamma$  not pointing to the interaction vertex. For the  $\tilde{e}$  NLSP case, the topologies consist of  $\ell\ell\tilde{E}$  or  $4\ell\tilde{E}$  (from  $\tilde{\chi}_1^0\tilde{\chi}_1^0$  production), including leptons with large impact parameters, kinks, or stable particles. Limits are derived from a scan over the GMSB parameters (see their Table 5 for the ranges). The limits are valid whichever is the NLSP. The absolute mass bound on the  $\tilde{\chi}_1^0$  for any lifetime includes indirect limits from the chargino search, and from the slepton search HEISTER 02E performed within the MSUGRA framework. A bound for any NLSP and any lifetime of  $77 \text{ GeV}$  has also been derived by using the constraints from the neutral Higgs search in HEISTER 02. Limits on the universal SUSY mass scale  $\Lambda$  are also derived in the paper. Supersedes the results from BARATE 00G.
- <sup>27</sup> ABBIENDI 01 looked for final states with  $\gamma\tilde{E}, \ell\ell\tilde{E}$ , with possibly additional activity and four leptons +  $B$  to search for prompt decays of  $\tilde{\chi}_1^0$  or  $\tilde{\tau}_1$  in GMSB. They derive limits in the plane  $(m_{\tilde{\chi}_1^0}, m_{\tilde{\tau}_1})$ , see Fig. 6, allowing either the  $\tilde{\chi}_1^0$  or a  $\tilde{\tau}_1$  to be the NLSP. Two scenarios are considered:  $\tan\beta=2$  with the 3 sleptons degenerate in mass and  $\tan\beta=20$  where the  $\tilde{\tau}_1$  is lighter than the other sleptons. Data taken at  $\sqrt{s}=189 \text{ GeV}$ .
- <sup>28</sup> ACCIARRI 01 searches for multi-lepton and/or multi-jet final states from  $R$  prompt decays with  $L\bar{L}\bar{E}, L\bar{Q}\bar{D}$ , or  $\bar{U}\bar{D}\bar{D}$  couplings at  $\sqrt{s}=189 \text{ GeV}$ . The search is performed for direct and indirect decays of neutralinos, charginos, and scalar leptons, with the  $\tilde{\chi}_1^0$  or a  $\tilde{e}$  as LSP and assuming one coupling to be nonzero at a time. Mass limits are derived using simultaneously the constraints from the neutralino, chargino, and slepton analyses; and the  $Z^0$  width measurements from ACCIARRI 00C in a scan of the parameter space assuming MSUGRA with gaugino and scalar mass universality. Updates and supersedes the results from ACCIARRI 99I.
- <sup>29</sup> ADAMS 01 looked for neutral particles with mass  $> 2.2 \text{ GeV}$ , produced by  $900 \text{ GeV}$  protons incident on a Beryllium oxide target and decaying through weak interactions into  $\mu\mu, \mu e$ , or  $\mu\pi$  final states in the decay channel of the NuTeV detector (E815) at Fermilab. The number of observed events is  $3\mu\mu, 0\mu e$ , and  $0\mu\pi$  with an expected background of  $0.069 \pm 0.010, 0.13 \pm 0.02$ , and  $0.14 \pm 0.02$ , respectively. The  $\mu\mu$  events are consistent with the  $R$  decay of a neutralino with mass around  $5 \text{ GeV}$ . However, they share several aspects with  $\nu$ -interaction backgrounds. An upper limit on the differential production cross section of neutralinos in  $pp$  interactions as function of the decay length is given in Fig. 3.
- <sup>30</sup> ABBIENDI 99T searches for the production of neutralinos in the case of  $R$ -parity violation with  $L\bar{L}\bar{E}, L\bar{Q}\bar{D}$ , or  $\bar{U}\bar{D}\bar{D}$  couplings using data from  $\sqrt{s}=183 \text{ GeV}$ . They investigate topologies with multiple leptons, jets plus leptons, or multiple jets, assuming one coupling at the time to be non-zero and giving rise to direct or indirect decays. Mixed decays (where one particle has a direct, the other an indirect decay) are also considered for the  $\bar{U}\bar{D}\bar{D}$  couplings. Upper limits on the cross section are derived which, combined with the constraint from the  $Z^0$  width, allow to exclude regions in the  $M_2$  versus  $\mu$  plane for any coupling. Limits on the neutralino mass are obtained for non-zero  $L\bar{L}\bar{E}$  couplings  $> 10^{-5}$ . The limit disappears for  $\tan\beta < 1.2$  and it improves to  $50 \text{ GeV}$  for  $\tan\beta > 20$ .
- <sup>31</sup> BARATE 99e looked for the decay of gauginos via  $R$ -violating couplings  $L\bar{Q}\bar{D}$ . The bound is significantly reduced for smaller values of  $m_0$ . Data collected at  $\sqrt{s}=130\text{--}172 \text{ GeV}$ .
- <sup>32</sup> ABREU 98 uses data at  $\sqrt{s}=161$  and  $172 \text{ GeV}$ . Upper bounds on  $\gamma\tilde{E}$  cross section are obtained. Similar limits on  $\gamma\tilde{B}$  are also given, relevant for  $e^+e^- \rightarrow \tilde{\chi}_1^0\tilde{G}$  production.
- <sup>33</sup> BARATE 98s looked for the decay of gauginos via  $R$ -violating coupling  $L\bar{L}\bar{E}$ . The bound improves to  $25 \text{ GeV}$  if the chargino decays into neutralino which further decays into lepton pairs. Data collected at  $\sqrt{s}=130\text{--}172 \text{ GeV}$ .
- <sup>34</sup> ELLIS 97 reanalyzed the LEP2 ( $\sqrt{s}=161 \text{ GeV}$ ) limits of  $\sigma(\gamma\gamma + E_{\text{miss}}) < 0.2 \text{ pb}$  to exclude  $m_{\tilde{\chi}_1^0} < 63 \text{ GeV}$  if  $m_{\tilde{e}_L} = m_{\tilde{e}_R} < 150 \text{ GeV}$  and  $\tilde{\chi}_1^0$  decays to  $\gamma\tilde{G}$  inside detector.
- <sup>35</sup> CABIBBO 81 consider  $\tilde{\gamma} \rightarrow \gamma$  goldstino. Photino must be either light enough ( $< 30 \text{ eV}$ ) to satisfy cosmology bound, or heavy enough ( $> 0.3 \text{ MeV}$ ) to have disappeared at early universe.

### $\tilde{\chi}_2^0, \tilde{\chi}_3^0, \tilde{\chi}_4^0$ (Neutralinos) MASS LIMITS

Neutralinos are unknown mixtures of photinos, z-inos, and neutral higgsinos (the supersymmetric partners of photons and of Z and Higgs bosons). The limits here apply only to  $\tilde{\chi}_2^0, \tilde{\chi}_3^0$ , and  $\tilde{\chi}_4^0$ .  $\tilde{\chi}_1^0$  is the lightest supersymmetric particle (LSP); see  $\tilde{\chi}_1^0$  Mass Limits. It is not possible to quote rigorous mass limits because they are extremely model dependent; i.e. they depend on branching ratios of various  $\tilde{\chi}_i^0$  decay modes, on the masses of decay products ( $\tilde{e}, \tilde{\nu}, \tilde{q}, \tilde{g}$ ), and on the  $\tilde{e}$  mass exchanged in  $e^+e^- \rightarrow \tilde{\chi}_i^0\tilde{\chi}_j^0$ . Limits arise either from direct searches, or from the MSSM constraints set on the gaugino and higgsino mass parameters  $M_2$  and  $\mu$  through searches for lighter charginos and neutralinos. Often limits are given as contour plots in the  $m_{\tilde{\chi}_i^0} - m_{\tilde{e}}$  plane vs other parameters. When specific assumptions are made, e.g. the neutralino is a pure photino ( $\tilde{\gamma}$ ), pure z-ino ( $\tilde{Z}$ ), or pure neutral higgsino ( $\tilde{H}^0$ ), the neutralinos will be labelled as such.

Limits obtained from  $e^+e^-$  collisions at energies up to  $136 \text{ GeV}$ , as well as other limits from different techniques, are now superseded and have not been included in

# Searches Particle Listings

## Supersymmetric Particle Searches

this compilation. They can be found in the 1998 Edition (The European Physical Journal **C3** 1 (1998)) of this Review.  $\Delta m = m_{\tilde{\chi}_2^0} - m_{\tilde{\chi}_1^0}$ .

VALUE (GeV)	CL%	DOCUMENT ID	TECN	COMMENT
> 78	95	1 ABBIENDI	04H OPAL	$\tilde{\chi}_2^0$ , all $\tan\beta$ , $\Delta m > 5$ GeV, $m_0 > 500$ GeV, $A_0 = 0$
> 62.4	95	2 ABREU	00W DLPH	$\tilde{\chi}_2^0$ , $1 \leq \tan\beta \leq 40$ , all $\Delta m$ , all $m_0$
> 99.9	95	2 ABREU	00W DLPH	$\tilde{\chi}_3^0$ , $1 \leq \tan\beta \leq 40$ , all $\Delta m$ , all $m_0$
> 116.0	95	2 ABREU	00W DLPH	$\tilde{\chi}_4^0$ , $1 \leq \tan\beta \leq 40$ , all $\Delta m$ , all $m_0$
• • • We do not use the following data for averages, fits, limits, etc. • • •				
		3 ABULENCIA	07N CDF	$p\bar{p} \rightarrow \tilde{\chi}_1^\pm \tilde{\chi}_2^0$
		4 ABDALLAH	05B DLPH	$e^+e^- \rightarrow \tilde{\chi}_2^0 \tilde{\chi}_2^0, (\tilde{\chi}_2^0 \rightarrow \tilde{\chi}_1^0 \gamma)$
		5 ACHARD	04E L3	$e^+e^- \rightarrow \tilde{\chi}_2^0 \tilde{\chi}_2^0, (\tilde{\chi}_2^0 \rightarrow \tilde{\chi}_1^0 \gamma)$
> 80.0	95	6 ACHARD	02 L3	$\tilde{\chi}_2^0, R$ , MSUGRA
> 107.2	95	6 ACHARD	02 L3	$\tilde{\chi}_3^0, R$ , MSUGRA
		7 ABREU	01B DLPH	$e^+e^- \rightarrow \tilde{\chi}_i^0 \tilde{\chi}_j^0$
> 68.0	95	8 ACCIARRI	01 L3	$\tilde{\chi}_2^0, R$ , all $m_0$ , $0.7 \leq \tan\beta \leq 40$
> 99.0	95	8 ACCIARRI	01 L3	$\tilde{\chi}_3^0, R$ , all $m_0$ , $0.7 \leq \tan\beta \leq 40$
> 50	95	9 ABREU	00U DLPH	$\tilde{\chi}_2^0, R$ ( $LL\bar{E}$ ), all $\Delta m$ , $1 \leq \tan\beta \leq 30$
		10 ABBIENDI	99F OPAL	$e^+e^- \rightarrow \tilde{\chi}_2^0 \tilde{\chi}_1^0$ ( $\tilde{\chi}_2^0 \rightarrow \gamma \tilde{\chi}_1^0$ )
		11 ABBIENDI	99F OPAL	$e^+e^- \rightarrow \tilde{\chi}_2^0 \tilde{\chi}_2^0$ ( $\tilde{\chi}_2^0 \rightarrow \gamma \tilde{\chi}_1^0$ )
		12 ABBOTT	98C D0	$p\bar{p} \rightarrow \tilde{\chi}_1^\pm \tilde{\chi}_2^0$
> 82.2	95	13 ABE	98J CDF	$p\bar{p} \rightarrow \tilde{\chi}_1^\pm \tilde{\chi}_2^0$
> 92	95	14 ACCIARRI	98F L3	$H_2^0, \tan\beta=1.41, M_2 < 500$ GeV
		15 ACCIARRI	98V L3	$e^+e^- \rightarrow \tilde{\chi}_2^0 \tilde{\chi}_{1,2}^0$ ( $\tilde{\chi}_2^0 \rightarrow \gamma \tilde{\chi}_1^0$ )
> 53	95	16 BARATE	98H ALEP	$e^+e^- \rightarrow \tilde{\gamma} \tilde{\gamma} (\tilde{\gamma} \rightarrow \gamma \tilde{H}^0)$
> 74	95	17 BARATE	98J ALEP	$e^+e^- \rightarrow \tilde{\gamma} \tilde{\gamma} (\tilde{\gamma} \rightarrow \gamma \tilde{H}^0)$
		18 ABACHI	96 D0	$p\bar{p} \rightarrow \tilde{\chi}_1^\pm \tilde{\chi}_2^0$
		19 ABE	96K CDF	$p\bar{p} \rightarrow \tilde{\chi}_1^\pm \tilde{\chi}_2^0$

1 ABBIENDI 04H search for charginos and neutralinos in events with acoplanar leptons  $+\bar{j}$  and multi-jet final states in the 192–209 GeV data, combined with the results on leptonic final states from ABBIENDI 04. The results hold for a scan over the parameter space covering the region  $0 < M_2 < 5000$  GeV,  $-1000 < \mu < 1000$  GeV and  $\tan\beta$  from 1 to 40. This limit supersedes ABBIENDI 00H.

2 ABREU 00W combines data collected at  $\sqrt{s}=189$  GeV with results from lower energies. The mass limit is obtained by constraining the MSSM parameter space with gaugino and stfermion mass universality at the GUT scale, using the results of negative direct searches for neutralinos (including cascade decays and  $\tilde{\tau}\tau$  final states) from ABREU 01, for charginos from ABREU 00J and ABREU 00T (for all  $\Delta m_{\pm}$ ), and for charged sleptons from ABREU 01B. The results hold for the full parameter space defined by all values of  $M_2$  and  $|\mu| \leq 2$  TeV with the  $\tilde{\chi}_1^0$  as LSP.

3 ABULENCIA 07N searched in  $1 \text{ fb}^{-1}$  of  $p\bar{p}$  collisions at  $\sqrt{s} = 1.96$  TeV for events with two same sign leptons ( $e$  or  $\mu$ ) from the decay of  $\tilde{\chi}_1^\pm \tilde{\chi}_2^0 X$  and large  $E_T$ . A slight excess of 13 events is observed over a SM background expectation of  $7.8 \pm 1.1$ . However, the kinematic distributions do not show any anomalous deviation from expectations in any particular region of parameter space.

4 ABDALLAH 05B use data from  $\sqrt{s} = 130$ –209 GeV, looking for events with diphotons  $+\bar{E}$ . Limits on the cross-section are computed in the plane  $(m(\tilde{\chi}_2^0), m(\tilde{\chi}_1^0))$ , see Fig. 12. Supersedes the results of ABREU 00Z.

5 ACHARD 04E use data from  $\sqrt{s} = 189$ –209 GeV, looking for events with diphotons  $+\bar{E}$ . Limits are computed in the plane  $(m(\tilde{\chi}_2^0), m(\tilde{\chi}_R))$ , for  $\Delta m > 10$  GeV, see Fig. 7. Supersedes the results of ACCIARRI 99R.

6 ACHARD 02 searches for the production of sparticles in the case of  $R$  prompt decays with  $LL\bar{E}$  or  $UDD$  couplings at  $\sqrt{s}=189$ –208 GeV. The search is performed for direct and indirect decays, assuming one coupling at the time to be nonzero. The MSUGRA limit results from a scan over the MSSM parameter space with the assumption of gaugino and scalar mass unification at the GUT scale, imposing simultaneously the exclusions from neutralino, chargino, sleptons, and squarks analyses. The limit of  $\tilde{\chi}_2^0$  holds for  $UDD$  couplings and increases to 84.0 GeV for  $LL\bar{E}$  couplings. The same  $\tilde{\chi}_3^0$  limit holds for both  $LL\bar{E}$  and  $UDD$  couplings. For L3 limits from  $LQ\bar{D}$  couplings, see ACCIARRI 01.

7 ABREU 01B used data from  $\sqrt{s}=189$  GeV to search for the production of  $\tilde{\chi}_i^0 \tilde{\chi}_j^0$ . They looked for di-jet and di-lepton pairs with  $\bar{E}$  for events from  $\tilde{\chi}_i^0 \tilde{\chi}_j^0$  with the decay  $\tilde{\chi}_j^0 \rightarrow f\bar{f}\tilde{\chi}_1^0$ ; multi-jet and multi-lepton pairs with or without additional photons to cover the cascade decays  $\tilde{\chi}_j^0 \rightarrow f\bar{f}\tilde{\chi}_2^0$ , followed by  $\tilde{\chi}_2^0 \rightarrow f\bar{f}\tilde{\chi}_1^0$  or  $\tilde{\chi}_2^0 \rightarrow \gamma\tilde{\chi}_1^0$ ; multi-tau final states from  $\tilde{\chi}_2^0 \rightarrow \tilde{\tau}\tau$  with  $\tilde{\tau} \rightarrow \tau\tilde{\chi}_1^0$ . See Figs. 9 and 10 for limits on the  $(\mu, M_2)$  plane for  $\tan\beta=1.0$  and different values of  $m_0$ .

8 ACCIARRI 01 searches for multi-lepton and/or multi-jet final states from  $R$  prompt decays with  $LL\bar{E}$ ,  $LQ\bar{D}$ , or  $UDD$  couplings at  $\sqrt{s}=189$  GeV. The search is performed for direct and indirect decays of neutralinos, charginos, and scalar leptons, with the  $\tilde{\chi}_1^0$  or a  $\tilde{\ell}$  as LSP and assuming one coupling to be nonzero at a time. Mass limits are derived using simultaneously the constraints from the neutralino, chargino, and slepton analyses; and the  $Z^0$  width measurements from ACCIARRI 00C in a scan of the parameter space assuming MSUGRA with gaugino and scalar mass universality. Updates and supersedes the results from ACCIARRI 99I.

9 ABREU 00U searches for the production of charginos and neutralinos in the case of  $R$ -parity violation with  $LL\bar{E}$  couplings, using data from  $\sqrt{s}=189$  GeV. They investigate topologies with multiple leptons or jets plus leptons, assuming one coupling to be nonzero

at the time and giving rise to direct or indirect decays. Limits are obtained in the  $M_2$  versus  $\mu$  plane and a limit on the neutralino mass is derived from a scan over the parameters  $m_0$  and  $\tan\beta$ .

10 ABBIENDI 99F looked for  $\gamma\bar{E}$  final states at  $\sqrt{s}=183$  GeV. They obtained an upper bound on the cross section for the production  $e^+e^- \rightarrow \tilde{\chi}_2^0 \tilde{\chi}_1^0$  followed by the prompt decay  $\tilde{\chi}_2^0 \rightarrow \gamma\tilde{\chi}_1^0$  of 0.075–0.80 pb in the region  $m_{\tilde{\chi}_2^0} + m_{\tilde{\chi}_1^0} > m_Z$ ,  $m_{\tilde{\chi}_2^0} = 91$ –183 GeV, and  $\Delta m > 5$  GeV. See Fig. 7 for explicit limits in the  $(m_{\tilde{\chi}_2^0}, m_{\tilde{\chi}_1^0})$  plane.

11 ABBIENDI 99F looked for  $\gamma\gamma\bar{E}$  final states at  $\sqrt{s}=183$  GeV. They obtained an upper bound on the cross section for the production  $e^+e^- \rightarrow \tilde{\chi}_2^0 \tilde{\chi}_2^0$  followed by the prompt decay  $\tilde{\chi}_2^0 \rightarrow \gamma\tilde{\chi}_1^0$  of 0.08–0.37 pb for  $m_{\tilde{\chi}_2^0} = 45$ –81.5 GeV, and  $\Delta m > 5$  GeV. See Fig. 11 for explicit limits in the  $(m_{\tilde{\chi}_2^0}, m_{\tilde{\chi}_1^0})$  plane.

12 ABBOTT 98C searches for trilepton final states ( $\ell=e, \mu$ ). See footnote to ABBOTT 98C in the Chargino Section for details on the assumptions. Assuming a negligible decay rate of  $\tilde{\chi}_1^\pm$  and  $\tilde{\chi}_2^0$  to quarks, they obtain  $m_{\tilde{\chi}_2^0} \gtrsim 103$  GeV.

13 ABE 98J searches for trilepton final states ( $\ell=e, \mu$ ). See footnote to ABE 98J in the Chargino Section for details on the assumptions. The quoted result for  $m_{\tilde{\chi}_2^0}$  corresponds to the best limit within the selected range of parameters, obtained for  $m_{\tilde{q}} > m_{\tilde{g}}$ ,  $\tan\beta=2$ , and  $\mu=-600$  GeV.

14 ACCIARRI 98F is obtained from direct searches in the  $e^+e^- \rightarrow \tilde{\chi}_{1,2}^0 \tilde{\chi}_2^0$  production channels, and indirectly from  $\tilde{\chi}_1^\pm$  and  $\tilde{\chi}_1^0$  searches within the MSSM. See footnote to ACCIARRI 98F in the chargino Section for further details on the assumptions. Data taken at  $\sqrt{s} = 130$ –172 GeV.

15 ACCIARRI 98V looked for  $\gamma(\gamma)\bar{E}$  final states at  $\sqrt{s}=183$  GeV. They obtained an upper bound on the cross section for the production  $e^+e^- \rightarrow \tilde{\chi}_2^0 \tilde{\chi}_{1,2}^0$  followed by the prompt decay  $\tilde{\chi}_2^0 \rightarrow \gamma\tilde{\chi}_1^0$ . See Figs. 4a and 6a for explicit limits in the  $(m_{\tilde{\chi}_2^0}, m_{\tilde{\chi}_1^0})$  plane.

16 BARATE 98H looked for  $\gamma\gamma\bar{E}$  final states at  $\sqrt{s} = 161, 172$  GeV. They obtained an upper bound on the cross section for the production  $e^+e^- \rightarrow \tilde{\chi}_2^0 \tilde{\chi}_2^0$  followed by the prompt decay  $\tilde{\chi}_2^0 \rightarrow \gamma\tilde{\chi}_1^0$  of 0.4–0.8 pb for  $m_{\tilde{\chi}_2^0} = 10$ –80 GeV. The bound above is for the specific case of  $\tilde{\chi}_1^0 = \tilde{H}^0$  and  $\tilde{\chi}_2^0 = \tilde{\gamma}$  and  $m_{\tilde{e}_R} = 100$  GeV. See Fig. 6 and 7 for explicit limits in the  $(\tilde{\chi}_2^0, \tilde{\chi}_1^0)$  plane and in the  $(\tilde{\chi}_2^0, \tilde{e}_R)$  plane.

17 BARATE 98J looked for  $\gamma\gamma\bar{E}$  final states at  $\sqrt{s} = 161$ –183 GeV. They obtained an upper bound on the cross section for the production  $e^+e^- \rightarrow \tilde{\chi}_2^0 \tilde{\chi}_2^0$  followed by the prompt decay  $\tilde{\chi}_2^0 \rightarrow \gamma\tilde{\chi}_1^0$  of 0.08–0.24 pb for  $m_{\tilde{\chi}_2^0} < 91$  GeV. The bound above is for the specific case of  $\tilde{\chi}_1^0 = \tilde{H}^0$  and  $\tilde{\chi}_2^0 = \tilde{\gamma}$  and  $m_{\tilde{e}_R} = 100$  GeV.

18 ABACHI 96 searches for 3-lepton final states. Efficiencies are calculated using mass relations and branching ratios in the Minimal Supergravity scenario. Results are presented as lower bounds on  $\sigma(\tilde{\chi}_1^\pm \tilde{\chi}_2^0) \times B(\tilde{\chi}_1^\pm \rightarrow \ell\nu_R \tilde{\chi}_1^0) \times B(\tilde{\chi}_2^0 \rightarrow \ell^+ \ell^- \tilde{\chi}_1^0)$  as a function of  $m_{\tilde{\chi}_1^0}$ . Limits range from 3.1 pb ( $m_{\tilde{\chi}_2^0} = 45$  GeV) to 0.6 pb ( $m_{\tilde{\chi}_2^0} = 100$  GeV).

19 ABE 96K looked for trilepton events from chargino-neutralino production. They obtained lower bounds on  $m_{\tilde{\chi}_2^0}$  as a function of  $\mu$ . The lower bounds are in the 45–50 GeV range for gaugino-dominant  $\tilde{\chi}_2^0$  with negative  $\mu$ , if  $\tan\beta < 10$ . See paper for more details of the assumptions.

### $\tilde{\chi}_1^\pm, \tilde{\chi}_2^0$ (Charginos) MASS LIMITS

Charginos are unknown mixtures of  $w$ -inos and charged higgsinos (the supersymmetric partners of  $W$  and Higgs bosons). A lower mass limit for the lightest chargino ( $\tilde{\chi}_1^\pm$ ) of approximately 45 GeV, independent of the field composition and of the decay mode, has been obtained by the LEP experiments from the analysis of the  $Z$  width and decays. These results, as well as other now superseded limits from  $e^+e^-$  collisions at energies below 136 GeV, and from hadronic collisions, can be found in the 1998 Edition (The European Physical Journal **C3** 1 (1998)) of this Review.

Unless otherwise stated, results in this section assume spectra, production rates, decay modes and branching ratios as evaluated in the MSSM, with gaugino and stfermion mass unification at the GUT scale. These papers generally study production of  $\tilde{\chi}_1^\pm \tilde{\chi}_2^0$ ,  $\tilde{\chi}_1^\pm \tilde{\chi}_1^\mp$  and (in the case of hadronic collisions)  $\tilde{\chi}_1^\pm \tilde{\chi}_2^0$  pairs, including the effects of cascade decays. The mass limits on  $\tilde{\chi}_1^\pm$  are either direct, or follow indirectly from the constraints set by the non-observation of  $\tilde{\chi}_2^0$  states on the gaugino and higgsino MSSM parameters  $M_2$  and  $\mu$ . For generic values of the MSSM parameters, limits from high-energy  $e^+e^-$  collisions coincide with the highest value of the mass allowed by phase-space, namely  $m_{\tilde{\chi}_1^\pm} \lesssim \sqrt{s}/2$ . The still unpublished combination of the results of the four LEP collaborations from the 2000 run of LEP2 at  $\sqrt{s}$  up to  $\approx 209$  GeV yields a lower mass limit of 103.5 GeV valid for general MSSM models. The limits become however weaker in certain regions of the MSSM parameter space where the detection efficiencies or production cross sections are suppressed. For example, this may happen when: (i) the mass differences  $\Delta m_{\pm} = m_{\tilde{\chi}_1^\pm} - m_{\tilde{\chi}_1^0}$  or  $\Delta m_{\nu} = m_{\tilde{\chi}_1^\pm} - m_{\tilde{\nu}}$  are very small, and the detection efficiency is reduced; (ii) the electron sneutrino mass is small, and the  $\tilde{\chi}_1^\pm$  production rate is suppressed due to a destructive interference between  $s$  and  $t$  channel exchange diagrams. The regions of MSSM parameter space where the following limits are valid are indicated in the comment lines or in the footnotes.

See key on page 457

# Searches Particle Listings

## Supersymmetric Particle Searches

VALUE (GeV)	CL%	DOCUMENT ID	TECN	COMMENT
>101	95	1 ABBIENDI	04H OPAL	all $\tan\beta$ , $\Delta m_{\pm} > 5$ GeV, $m_0 > 500$ GeV, $A_0 = 0$
> 89		2 ABBIENDI	03H OPAL	$0.5 \leq \Delta m_{\pm} \leq 5$ GeV, higgsino-like, $\tan\beta=1.5$
> 97.1	95	3 ABDALLAH	03M DLPH	$\tilde{\chi}_1^{\pm}$ , $\Delta m_{\pm} \geq 3$ GeV, $m_{\tilde{\nu}} > m_{\tilde{\chi}^{\pm}}$
> 75	95	3 ABDALLAH	03M DLPH	$\tilde{\chi}_1^{\pm}$ , higgsino, all $\Delta m_{\pm}, m_{\tilde{\nu}} > m_{\tilde{\chi}^{\pm}}$
> 70	95	3 ABDALLAH	03M DLPH	$\tilde{\chi}_1^{\pm}$ , all $\Delta m_{\pm}$ , $m_{\tilde{\nu}} > 500$ GeV, $M_2 \leq 2M_1 \leq 10M_2$
> 94	95	4 ABDALLAH	03M DLPH	$\tilde{\chi}_1^{\pm}$ , $\tan\beta \leq 40$ , $\Delta m_{\pm} > 3$ GeV, all $m_0$
> 88	95	5 HEISTER	02J ALEP	$\tilde{\chi}_1^{\pm}$ , all $\Delta m_{\pm}$ , large $m_0$
> 67.7	95	6 ACCIARRI	00D L3	$\tan\beta > 0.7$ , all $\Delta m_{\pm}$ , all $m_0$
> 69.4	95	7 ACCIARRI	00K L3	$e^+e^- \rightarrow \tilde{\chi}^{\pm}\tilde{\chi}^{\mp}$ , all $\Delta m_{\pm}$ , heavy scalars
• • • We do not use the following data for averages, fits, limits, etc. • • •				
>163	95	8 CHATRCHYAN 11B	CMS	$\tilde{W}^0 \rightarrow \gamma\tilde{G}, \tilde{W}^{\pm} \rightarrow \ell^{\pm}\tilde{G}, \text{GMSB}$
>129	95	9 CHATRCHYAN 11V	CMS	$\tan\beta=3$ , $m_0=60$ GeV, $A_0=0$ , $\mu > 0$
>138	95	10 AALTONEN	09G CDF	$p\bar{p} \rightarrow \tilde{\chi}_1^{\pm}\tilde{\chi}_2^0$
		11 ABAZOV	09T D0	$p\bar{p} \rightarrow \tilde{\chi}_1^{\pm}\tilde{\chi}_2^0$
		12 AALTONEN	08AE CDF	$p\bar{p} \rightarrow \tilde{\chi}_1^{\pm}\tilde{\chi}_2^0$
		13 AALTONEN	08L CDF	$p\bar{p} \rightarrow \tilde{\chi}_1^{\pm}\tilde{\chi}_2^0$
>229	95	14 ABAZOV	08F D0	$p\bar{p} \rightarrow \tilde{\chi}\tilde{\chi}, \tilde{\chi}=\tilde{\chi}_2^0, \tilde{\chi}_1^{\pm}, \tilde{\chi}_1^0 \rightarrow \gamma\tilde{G}, \text{GMSB}$
		15 AALTONEN	07J CDF	$p\bar{p} \rightarrow \tilde{\chi}_1^{\pm}\tilde{\chi}_2^0$
		16 ABULENCIA	07H CDF	$R, LL\bar{E}$
		17 ABULENCIA	07N CDF	$p\bar{p} \rightarrow \tilde{\chi}_1^{\pm}\tilde{\chi}_2^0$
		18 ABAZOV	06D D0	$R, LL\bar{E}$
>195	95	19 ABAZOV	05A D0	$p\bar{p} \rightarrow \tilde{\chi}\tilde{\chi}, \tilde{\chi}=\tilde{\chi}_2^0, \tilde{\chi}_1^{\pm}, \tilde{\chi}_1^0 \rightarrow \gamma\tilde{G}, \text{GMSB}$
>167	95	20 ACOSTA	05E CDF	$p\bar{p} \rightarrow \tilde{\chi}\tilde{\chi}, \tilde{\chi}=\tilde{\chi}_2^0, \tilde{\chi}_1^{\pm}, \tilde{\chi}_1^0 \rightarrow \gamma\tilde{G}, \text{GMSB}$
> 66	95	21,22 ABDALLAH	04H DLPH	AMSB, $\mu > 0$
>102.5	95	23,24 ABDALLAH	04M DLPH	$R(U\bar{D}\bar{D})$
>100		25 ABDALLAH	03D DLPH	$e^+e^- \rightarrow \tilde{\chi}_1^{\pm}\tilde{\chi}_1^{\mp} (\tilde{\chi}_1^{\pm} \rightarrow \tilde{\tau}_1\nu_{\tau}, \tilde{\tau}_1 \rightarrow \tau\tilde{G})$
>103		26 HEISTER	03G ALEP	$R$ decays, $m_0 > 500$ GeV
>102.7	95	27 ACHARD	02 L3	$R, \text{MSUGRA}$
		28 GHODBANE	02 THEO	
> 94.3	95	29 ABREU	01C DLPH	$\tilde{\chi}^{\pm} \rightarrow \tau J$
> 93.8	95	30 ACCIARRI	01 L3	$R$ , all $m_0$ , $0.7 \leq \tan\beta \leq 40$
>100	95	31 BARATE	01B ALEP	$R$ decays, $m_0 > 500$ GeV
> 91.8	95	32 ABREU	00V DLPH	$e^+e^- \rightarrow \tilde{\chi}_1^{\pm}\tilde{\chi}_1^{\mp} (\tilde{\chi}_1^{\pm} \rightarrow \tilde{\tau}_1\nu_{\tau}, \tilde{\tau}_1 \rightarrow \tau\tilde{G})$
		33 CHO	00B THEO	EW analysis
> 76	95	34 ABBIENDI	99T OPAL	$R$ , $m_0=500$ GeV
> 51	95	35 MALTONI	99B THEO	EW analysis, $\Delta m_{\pm} \sim 1$ GeV
> 81.5	95	36 ABE	98J CDF	$p\bar{p} \rightarrow \tilde{\chi}_1^{\pm}\tilde{\chi}_2^0$
		37 ACKERSTAFF	98K OPAL	$\tilde{\chi}^{\pm} \rightarrow \ell^{\pm}\tilde{E}$
> 65.7	95	38 ACKERSTAFF	98L OPAL	$\Delta m_{\pm} > 3$ GeV, $\Delta m_{\nu} > 2$ GeV
		39 ACKERSTAFF	98V OPAL	light gluino
		40 CARENA	97 THEO	$\tilde{g}_{\mu} = 2$
		41 KALINOWSKI	97 THEO	$W \rightarrow \tilde{\chi}_1^{\pm}\tilde{\chi}_1^0$
		42 ABE	96K CDF	$p\bar{p} \rightarrow \tilde{\chi}_1^{\pm}\tilde{\chi}_2^0$

1 ABBIENDI 04H search for charginos and neutralinos in events with acoplanar leptons+jets and multi-jet final states in the 192–209 GeV data, combined with the results on leptonic final states from ABBIENDI 04. The results hold for a scan over the parameter space covering the region  $0 < M_2 < 5000$  GeV,  $-1000 < \mu < 1000$  GeV and  $\tan\beta$  from 1 to 40. This limit supersedes ABBIENDI 00H.

2 ABBIENDI 03H used  $e^+e^-$  data at  $\sqrt{s} = 188\text{--}209$  GeV to search for chargino pair production in the case of small  $\Delta m_{\pm}$ . They select events with an energetic photon, large  $E$  and little hadronic or leptonic activity. The bound applies to higgsino-like charginos with zero lifetime and a 100% branching ratio  $\tilde{\chi}_1^{\pm} \rightarrow \tilde{\chi}_1^0 W^*$ . The mass limit for gaugino-like charginos, in case of non-universal gaugino masses, is of 92 GeV for  $m_{\tilde{\nu}} = 1000$  GeV and is lowered to 74 GeV for  $m_{\tilde{\nu}} \geq 100$  GeV. Limits in the plane  $(m_{\tilde{\chi}_1^{\pm}}, \Delta m_{\pm})$  are shown in Fig. 7. Exclusion regions are also derived for the AMSB scenario in the  $(m_{3/2}, \tan\beta)$  plane, see their Fig. 9.

3 ABDALLAH 03M searches for the production of charginos using data from  $\sqrt{s} = 192$  to 208 GeV to investigate topologies with multiple leptons, jets plus leptons, multi-jets, or isolated photons. The first limit holds for  $\tan\beta \geq 1$  and is obtained at  $\Delta m_{\pm} = 3$  GeV in the higgsino region. For  $\Delta m_{\pm} \geq 10$  (5) GeV and large  $m_0$ , the limit improves to 102.7 (101.7) GeV. For the region of small  $\Delta m_{\pm}$ , all data from  $\sqrt{s} = 130$  to 208 GeV are used to investigate final states with heavy stable charged particles, decay vertices inside the detector and soft topologies with a photon from initial state radiation. The second limit is obtained in the higgsino region, assuming gaugino mass universality at the GUT scale and  $1 < \tan\beta < 50$ . For the case of non-universality of gaugino masses, the parameter space is scanned in the domain  $1 < \tan\beta < 50$  and, for  $\Delta m_{\pm} < 3$  GeV, for values of  $M_1, M_2$  and  $\mu$  such that  $M_2 \leq 2M_1 \leq 10M_2$  and  $|\mu| \geq M_2$ . The third limit is obtained in the gaugino region. See Fig. 36 for the dependence of the low  $\Delta m_{\pm}$  limits on  $\Delta m_{\pm}$ . These limits include and update the results of ABREU 00J and ABREU 00T.

4 ABDALLAH 03M uses data from  $\sqrt{s} = 192\text{--}208$  GeV to obtain limits in the framework of the MSSM with gaugino and sfermion mass universality at the GUT scale. An indirect limit on the mass of charginos is derived by constraining the MSSM parameter space by the results from direct searches for neutralinos (including cascade decays), for charginos and for sleptons. These limits are valid for values of  $M_2 < 1$  TeV,  $|\mu| \leq 2$  TeV with the  $\tilde{\chi}_1^0$  as LSP. Constraints from the Higgs search in the  $M_{H_u}^{max}$  scenario assuming  $m_t = 174.3$  GeV are included. The quoted limit applies if there is no mixing in the third family or when  $m_{\tilde{\tau}_1} - m_{\tilde{\chi}_1^0} > 6$  GeV. If mixing is included the limit degrades to 90 GeV. See Fig. 43 for the mass limits as a function of  $\tan\beta$ . These limits update the results of ABREU 00W.

5 HEISTER 02J search for chargino production with small  $\Delta m_{\pm}$  in final states with a hard isolated initial state radiation photon and few low-momentum particles, using 189–208 GeV data. This search is sensitive in the intermediate  $\Delta m_{\pm}$  region. Combined with searches for  $E$  topologies and for stable charged particles, the above bound is obtained for  $m_0$  larger than few hundred GeV,  $1 < \tan\beta < 300$  and holds for any chargino field contents. For light scalars, the general limit reduces to the one from the  $Z^0$ , but under the assumption of gaugino and sfermion mass unification the above bound is recovered. See Figs. 4–6 for the more general dependence of the limits on  $\Delta m_{\pm}$ . Updates BARATE 98x.

6 ACCIARRI 00D data collected at  $\sqrt{s}=189$  GeV. The results hold over the full parameter space defined by  $0.7 \leq \tan\beta \leq 60$ ,  $0 \leq M_2 \leq 2$  TeV,  $|\mu| \leq 2$  TeV  $m_0 \leq 500$  GeV. The results of slepton searches from ACCIARRI 99w are used to help set constraints in the region of small  $m_0$ . See their Figs. 5 for the  $\tan\beta$  and  $M_2$  dependence on the limits.

See the text for the impact of a large  $B(\tilde{\chi}^{\pm} \rightarrow \tau\tilde{\nu}_{\tau})$  on the result. The region of small  $\Delta m_{\pm}$  is excluded by the analysis of ACCIARRI 00K. Updates ACCIARRI 98f.

7 ACCIARRI 00k searches for the production of charginos with small  $\Delta m_{\pm}$  using data from  $\sqrt{s}=189$  GeV. They investigate soft final states with a photon from initial state radiation. The results are combined with the limits on prompt decays from ACCIARRI 00D and from heavy stable charged particles from ACCIARRI 99L (see Heavy Charged Lepton Searches). The production and decay branching ratios are evaluated within the MSSM, assuming heavy sfermions. The parameter space is scanned in the domain  $1 < \tan\beta < 50$ ,  $0.3 < M_1/M_2 < 50$ , and  $0 < |\mu| < 2$  TeV. The limit is obtained in the higgsino region and improves to 78.6 GeV for gaugino-like charginos. The limit is unchanged for light scalar quarks. For light  $\tilde{\tau}$  or  $\tilde{\nu}_{\tau}$ , the limit is unchanged in the gaugino-like region and is lowered by 0.8 GeV in the higgsino-like case. For light  $\tilde{\mu}$  or  $\tilde{\nu}_{\mu}$ , the limit is unchanged in the higgsino-like region and is lowered by 0.9 GeV in the gaugino-like region. No direct mass limits are obtained for light  $\tilde{e}$  or  $\tilde{\nu}_{e}$ .

8 CHATRCHYAN 11B looked in  $35 \text{ pb}^{-1}$  of  $pp$  collisions at  $\sqrt{s}=7$  TeV for events with an isolated lepton ( $e$  or  $\mu$ ), a photon and  $E_{T\gamma}$  which may arise in a generalized gauge mediated model from the decay of Wino-like NLSPs. No evidence for an excess over the expected background is observed. Limits are derived in the plane of squark/gluino mass versus Wino mass (see Fig. 4). Mass degeneracy of the produced squarks and gluinos is assumed.

9 CHATRCHYAN 11V looked in  $35 \text{ pb}^{-1}$  of  $pp$  collisions at  $\sqrt{s} = 7$  TeV for events with  $\geq 3$  isolated leptons ( $e, \mu$  or  $\tau$ ), with or without jets and  $E_{T\gamma}$ . No evidence for an excess over the expected background is observed. Limits are derived in the CMSSM  $(m_0, m_{1/2})$  plane for  $\tan\beta = 3$  (see Fig. 5).

10 AALTONEN 09G searched in  $976 \text{ pb}^{-1}$  of  $p\bar{p}$  collisions at  $\sqrt{s} = 1.96$  TeV for events with trileptons ( $\mu\mu\mu$  or  $\mu\mu e$ ) with a low, 5 GeV,  $p_{T\tau}$  threshold, and large  $E_{T\tau}$  from the decay of  $\tilde{\chi}_1^{\pm}\tilde{\chi}_2^0 X$ . The selected number of events is consistent with the SM background expectation. The results are combined with the analysis of AALTONEN 09J to set a limit on the  $\tilde{\chi}_1^{\pm}$  mass for a mSUGRA scenario with no slepton mixing.

11 ABAZOV 09T searched in  $2.3 \text{ fb}^{-1}$  of  $p\bar{p}$  collisions at  $\sqrt{s} = 1.96$  TeV for events with trileptons ( $e, \mu$  or hadronically decaying  $\tau$ ) from the decay of  $\tilde{\chi}_1^{\pm}\tilde{\chi}_2^0 X$  and large  $E_{T\tau}$ . No evidence for a signal is observed. The data are used to constrain the cross section times branching ratio as a function of the  $\tilde{\chi}_1^{\pm}$  mass under the assumption that  $m_{\tilde{\chi}_1^{\pm}} = m_{\tilde{\chi}_2^0} = 2 m_{\tilde{\chi}_1^0}$ ,  $\tan\beta = 3$ ,  $\mu > 0$  and that the sleptons are heavier than the  $\tilde{\chi}_1^{\pm}$ , see their Fig. 8. A chargino lighter than 138 GeV is excluded in the “3l-max” scenario. Exclusion regions in the  $(m_0, m_{1/2})$  plane are shown in their Fig. 9 for a mSUGRA scenario with  $\tan\beta = 3$ ,  $A_0 = 0$  and  $\mu > 0$ . The  $\tan\beta$  dependence of this exclusion is illustrated in Fig. 10. Supersedes the results of ABAZOV 05U.

12 AALTONEN 08AE searched in  $2.0 \text{ fb}^{-1}$  of  $p\bar{p}$  collisions at  $\sqrt{s} = 1.96$  TeV for events with trileptons ( $e, \mu$  or a charged isolated track from  $\tau$ ) from the decay of  $p\bar{p} \rightarrow \tilde{\chi}_1^{\pm}\tilde{\chi}_2^0 X$  and large  $E_{T\tau}$ . The selected number of events is consistent with the SM background expectation. The data are used to constrain the cross section times branching ratio as a function of the  $\tilde{\chi}_1^{\pm}$  mass. Exclusion regions in the  $(m_0, m_{1/2})$  plane are shown in their Fig. 2 for a mSUGRA scenario. When the  $\tilde{\chi}_1^{\pm}$  is nearly mass degenerate with the  $\tilde{\tau}_1$  the leptons are too soft and no limit is obtained. For the case  $m_0 = 60$  GeV a lower limit of 145 GeV on the chargino mass is obtained in this mSUGRA scenario.

13 AALTONEN 08L searched in 0.7 to 1.0  $\text{fb}^{-1}$  of  $p\bar{p}$  collisions at  $\sqrt{s} = 1.96$  TeV for events with one high- $p_{T\tau}$  electron or muon and two additional leptons ( $e$  or  $\mu$ ) from the decay of  $\tilde{\chi}_1^{\pm}\tilde{\chi}_2^0 X$ . The selected number of events is consistent with the SM background expectation. The data are used to constrain the cross section times branching ratio as a function of the  $\tilde{\chi}_1^{\pm}$  mass. The results are compared to three MSSM scenarios. An exclusion on chargino and neutralino production is only obtained in a scenario of no mixing between sleptons, yielding nearly equal branching ratios to all three lepton flavors. It amounts to  $m_{\tilde{\chi}_1^{\pm}} > 151$  GeV, while the analysis is not sensitive to chargino masses below about 110 GeV. The analyses have been combined with the analyses of AALTONEN 07J and ABULENCIA 07N. The observed limits for the combination are less stringent than the one obtained for the high- $p_{T\tau}$  analysis due to slight excesses in the other channels.

14 ABAZOV 08f looked in  $1.1 \text{ fb}^{-1}$  of  $p\bar{p}$  collisions at  $\sqrt{s} = 1.96$  TeV for diphoton events with large  $E_{T\tau}$ . They may originate from the production of  $\tilde{\chi}^{\pm}$  in pairs or associated to a  $\tilde{\chi}_2^0$ , decaying to a  $\tilde{\chi}_1^0$  which itself decays promptly in  $\text{GMSB to } \tilde{\chi}_1^0 \rightarrow \gamma\tilde{G}$ . No significant excess was found compared to the background expectation. A limit is derived on the masses of SUSY particles in the GMSB framework for  $M = 2\Lambda$ ,  $N = 1$ ,  $\tan\beta = 15$  and  $\mu > 0$ , see Figure 2. It also excludes  $\Lambda < 91.5$  TeV. Supersedes the results of ABAZOV 05A.

# Searches Particle Listings

## Supersymmetric Particle Searches

- 15 AALTONEN 07J searched in  $0.7$  to  $1.1 \text{ fb}^{-1}$  of  $p\bar{p}$  collisions at  $\sqrt{s} = 1.96 \text{ TeV}$  for events with either two same sign leptons ( $e$  or  $\mu$ ) or trileptons from the decay of  $\tilde{\chi}_1^\pm \tilde{\chi}_2^0 X$  and large  $\cancel{E}_T$ . The selected number of events is consistent with the SM background expectation. The data are used to constrain the cross section times branching ratio as a function of the  $\tilde{\chi}_1^\pm$  mass. The results, shown in their Fig. 2, are compared to several MSSM scenarios. The strongest exclusion is in the case of no mixing between sleptons, yielding nearly equal branching ratios to all three lepton flavors, and amounting to  $m_{\tilde{\chi}_1^\pm} > 129 \text{ GeV}$ . This analysis includes the same sign dilepton analysis of ABULENCIA 07N.
- 16 ABULENCIA 07H searched in  $346 \text{ pb}^{-1}$  of  $p\bar{p}$  collisions at  $\sqrt{s} = 1.96 \text{ TeV}$  for events with at least three leptons ( $e$  or  $\mu$ ) from the decay of  $\tilde{\chi}_1^0$  via  $LL\bar{E}$  couplings. The results are consistent with the hypothesis of no signal. Upper limits on the cross-section are extracted and a limit is derived in the framework of mSUGRA on the masses of  $\tilde{\chi}_1^0$  and  $\tilde{\chi}_1^\pm$ , see e.g. their Fig. 3 and Tab. II.
- 17 ABULENCIA 07N searched in  $1 \text{ fb}^{-1}$  of  $p\bar{p}$  collisions at  $\sqrt{s} = 1.96 \text{ TeV}$  for events with two same sign leptons ( $e$  or  $\mu$ ) from the decay of  $\tilde{\chi}_1^\pm \tilde{\chi}_2^0 X$  and large  $\cancel{E}_T$ . A slight excess of 13 events is observed over a SM background expectation of  $7.8 \pm 1.1$ . However, the kinematic distributions do not show any anomalous deviation from expectations in any particular region of parameter space.
- 18 ABAZOV 06D looked in  $360 \text{ pb}^{-1}$  of  $p\bar{p}$  collisions at  $\sqrt{s} = 1.96 \text{ TeV}$  for events with three leptons originating from the pair production of charginos and neutralinos, followed by  $\cancel{H}$  decays mediated by  $LL\bar{E}$  couplings. One coupling is assumed to be dominant at a time. No significant excess was found compared to the background expectation in the  $e\bar{e}\ell$ ,  $\mu\bar{\mu}\ell$  nor  $e\bar{e}\tau$  ( $\ell = e, \mu$ ) final states. Upper limits on the cross-section are extracted in a specific MSUGRA model and a MSSM model without unification of  $M_1$  and  $M_2$  at the GUT scale. A limit is derived on the masses of charginos and neutralinos for both scenarios assuming  $\lambda_{ijk}$  couplings such that the decay length is less than 1 cm, see their Table III and Fig. 4.
- 19 ABAZOV 05A looked in  $263 \text{ pb}^{-1}$  of  $p\bar{p}$  collisions at  $\sqrt{s} = 1.96 \text{ TeV}$  for diphoton events with large  $\cancel{E}_T$ . They may originate from the production of  $\tilde{\chi}^\pm$  in pairs or associated to a  $\tilde{\chi}_2^0$ , decaying to a  $\tilde{\chi}_1^0$  which itself decays promptly in GMSB to  $\tilde{\chi}_1^0 \rightarrow \gamma\tilde{G}$ . No significant excess was found at large  $\cancel{E}_T$  compared to the background expectation. A limit is derived on the masses of SUSY particles in the GMSB framework for  $M = 2\Lambda$ ,  $N = 1$ ,  $\tan\beta = 15$  and  $\mu > 0$ , see Figure 2. It also excludes  $\Lambda < 79.6 \text{ TeV}$ . Very similar results are obtained for different choices of parameters, see their Table 2. Supersedes the results of ABBOTT 98.
- 20 ACOSTA 05E looked in  $202 \text{ pb}^{-1}$  of  $p\bar{p}$  collisions at  $\sqrt{s} = 1.96 \text{ TeV}$  for diphoton events with large  $\cancel{E}_T$ . They may originate from the production of  $\tilde{\chi}^\pm$  in pairs or associated to a  $\tilde{\chi}_2^0$ , decaying to a  $\tilde{\chi}_1^0$  which itself decays promptly in GMSB to  $\tilde{\chi}_1^0 \rightarrow \gamma\tilde{G}$ . No events are selected at large  $\cancel{E}_T$  compared to the background expectation. A limit is derived on the masses of SUSY particles in the GMSB framework for  $M = 2\Lambda$ ,  $N = 1$ ,  $\tan\beta = 15$  and  $\mu > 0$ , see Figure 2. It also excludes  $\Lambda < 69 \text{ TeV}$ . Supersedes the results of ABE 99I.
- 21 ABDALLAH 04H use data from LEP 1 and  $\sqrt{s} = 192\text{--}208 \text{ GeV}$ . They re-use results or re-analyze the data from ABDALLAH 03M to put limits on the parameter space of anomaly-mediated supersymmetry breaking (AMSB), which is scanned in the region  $1 < m_{3/2} < 50 \text{ TeV}$ ,  $0 < m_0 < 1000 \text{ GeV}$ ,  $1.5 < \tan\beta < 35$ , both signs of  $\mu$ . The constraints are obtained from the searches for mass degenerate chargino and neutralino, for SM-like and invisible Higgs, for leptonically decaying charginos and from the limit on non-SM Z width of  $3.2 \text{ MeV}$ . The limit is for  $m_t = 174.3 \text{ GeV}$  (see Table 2 for other  $m_t$  values).
- 22 The limit improves to  $73 \text{ GeV}$  for  $\mu < 0$ .
- 23 ABDALLAH 04M use data from  $\sqrt{s} = 192\text{--}208 \text{ GeV}$  to derive limits on sparticle masses under the assumption of  $\cancel{R}$  with  $LL\bar{E}$  or  $UDD$  couplings. The results are valid in the ranges  $90 < m_0 < 500 \text{ GeV}$ ,  $0.7 < \tan\beta < 30$ ,  $-200 < \mu < 200 \text{ GeV}$ ,  $0 < M_2 < 400 \text{ GeV}$ . Supersedes the result of ABREU 01D and ABREU 00U.
- 24 The limit improves to  $103 \text{ GeV}$  for  $LL\bar{E}$  couplings.
- 25 ABDALLAH 03D use data from  $\sqrt{s} = 183\text{--}208 \text{ GeV}$ . They look for final states with two acoplanar leptons, expected in GMSB when the  $\tilde{\tau}_1$  is the NLSP and assuming a short-lived  $\tilde{\chi}_1^\pm$ . Limits are obtained in the plane  $(m(\tilde{\tau}), m(\tilde{\chi}_1^\pm))$  for different domains of  $m(\tilde{G})$ , after combining these results with the search for slepton pair production from the same paper. The limit above is valid if the  $\tilde{\tau}_1$  is the NLSP for all values of  $m(\tilde{G})$  provided  $m(\tilde{\chi}_1^\pm) - m(\tilde{\tau}_1) \geq 0.3 \text{ GeV}$ . For larger  $m(\tilde{G}) > 100 \text{ eV}$  the limit improves to  $102 \text{ GeV}$ , see their Fig. 11. In the co-NLSP scenario, the limits are  $96$  and  $102 \text{ GeV}$  for all  $m(\tilde{G})$  and  $m(\tilde{G}) > 100 \text{ eV}$ , respectively. Supersedes the results of ABREU 01G.
- 26 HEISTER 03G searches for the production of charginos prompt decays. In the case of  $\cancel{R}$  prompt decays with  $LL\bar{E}$ ,  $LQ\bar{D}$  or  $UDD$  couplings at  $\sqrt{s} = 189\text{--}209 \text{ GeV}$ . The search is performed for indirect decays, assuming one coupling at a time to be non-zero. The limit holds for  $\tan\beta = 1.41$ . Excluded regions in the  $(\mu, M_2)$  plane are shown in their Fig. 3.
- 27 ACHARD 02 searches for the production of sparticles in the case of  $\cancel{R}$  prompt decays with  $LL\bar{E}$  or  $UDD$  couplings at  $\sqrt{s} = 189\text{--}208 \text{ GeV}$ . The search is performed for direct and indirect decays, assuming one coupling at a time to be non-zero. The MSUGRA limit results from a scan over the MSSM parameter space with the assumption of gaugino and scalar mass unification at the GUT scale, imposing simultaneously the exclusions from neutralino, chargino, sleptons, and squarks analyses. The limit of  $\tilde{\chi}_1^\pm$  holds for  $UDD$  couplings and increases to  $103.0 \text{ GeV}$  for  $LL\bar{E}$  couplings. For L3 limits from  $LQ\bar{D}$  couplings, see ACCIARRI 01.
- 28 GHODBANE 02 reanalyzes DELPHI data at  $\sqrt{s} = 189 \text{ GeV}$  in the presence of complex phases for the MSSM parameters.
- 29 ABREU 01c looked for  $\tau$  pairs with  $\cancel{E}$  at  $\sqrt{s} = 183\text{--}189 \text{ GeV}$  to search for the associated production of charginos, followed by the decay  $\tilde{\chi}^\pm \rightarrow \tau J$ ,  $J$  being an invisible massless particle. See Fig. 6 for the regions excluded in the  $(\mu, M_2)$  plane.
- 30 ACCIARRI 01 searches for multi-lepton and/or multi-jet final states from  $\cancel{R}$  prompt decays with  $LL\bar{E}$ ,  $LQ\bar{D}$ , or  $UDD$  couplings at  $\sqrt{s} = 189 \text{ GeV}$ . The search is performed for direct and indirect decays of neutralinos, charginos, and scalar leptons, with the  $\tilde{\chi}_1^0$  or a  $\tilde{\ell}$  as LSP and assuming one coupling to be nonzero at a time. Mass limits are derived using simultaneously the constraints from the neutralino, chargino, and slepton analyses; and the  $Z^0$  width measurements from ACCIARRI 00C in a scan of the parameter space assuming MSUGRA with gaugino and scalar mass universality. Updates and supersedes the results from ACCIARRI 99I.
- 31 BARATE 01b searches for the production of charginos in the case of  $\cancel{R}$  prompt decays with  $LL\bar{E}$ ,  $LQ\bar{D}$ , or  $UDD$  couplings at  $\sqrt{s} = 189\text{--}202 \text{ GeV}$ . The search is performed for indirect decays, assuming one coupling at a time to be nonzero. Updates BARATE 00H.
- 32 ABREU 00v use data from  $\sqrt{s} = 183\text{--}189 \text{ GeV}$ . They look for final states with two acoplanar leptons, expected in GMSB when the  $\tilde{\tau}_1$  is the NLSP and assuming a short-lived  $\tilde{\chi}_1^\pm$ . Limits are obtained in the plane  $(m(\tilde{\tau}), m(\tilde{\chi}_1^\pm))$  for different domains of  $m(\tilde{G})$ , after combining these results with the search for slepton pair production in the SUGRA framework from ABREU 01I to cover prompt decays and on stable particle searches from ABREU 00Q. The limit above is valid for all values of  $m(\tilde{G})$ .
- 33 CHO 00b studied constraints on the MSSM spectrum from precision EW observables. Global fits favour charginos with masses at the lower bounds allowed by direct searches. Allowing for variations of the squark and slepton masses does not improve the fits.
- 34 ABBIENDI 99T searches for the production of neutralinos in the case of  $R$ -parity violation with  $LL\bar{E}$ ,  $LQ\bar{D}$ , or  $UDD$  couplings using data from  $\sqrt{s} = 183 \text{ GeV}$ . They investigate topologies with multiple leptons, jets plus leptons, or multiple jets, assuming one coupling at the time to be non-zero and giving rise to direct or indirect decays. Mixed decays (where one particle has a direct, the other an indirect decay) are also considered for the  $UDD$  couplings. Upper limits on the cross section are derived which, combined with the constraint from the  $Z^0$  width, allow to exclude regions in the  $M_2$  versus  $\mu$  plane for any coupling. Limits on the chargino mass are obtained for non-zero  $LL\bar{E}$  couplings  $> 10^{-5}$  and assuming decays via a  $W^*$ .
- 35 MALTONI 99b studied the effect of light chargino-neutralino to the electroweak precision data with a particular focus on the case where they are nearly degenerate ( $\Delta m_{\pm} \sim 1 \text{ GeV}$ ) which is difficult to exclude from direct collider searches. The quoted limit is for higgsino-like case while the bound improves to  $56 \text{ GeV}$  for wino-like case. The values of the limits presented here are obtained in an update to MALTONI 99b, as described in MALTONI 00.
- 36 ABE 98I searches for trilepton final states ( $\ell = e, \mu$ ). Efficiencies are calculated using mass relations in the Minimal Supergravity scenario, exploring the domain of parameter space defined by  $1.1 < \tan\beta < 8$ ,  $-1000 < \mu(\text{GeV}) < -200$ , and  $m_{\tilde{q}}/m_{\tilde{g}} = 1\text{--}2$ . In this region  $m_{\tilde{\chi}_1^\pm} \sim m_{\tilde{\chi}_2^0}$  and  $m_{\tilde{\chi}_1^\pm} \sim 2m_{\tilde{\chi}_1^0}$ . Results are presented in Fig. 1 as upper bounds on  $\sigma(p\bar{p} \rightarrow \tilde{\chi}_1^\pm \tilde{\chi}_2^0) \times \text{B}(3\ell)$ . Limits range from  $0.8 \text{ pb}$  ( $m_{\tilde{\chi}_1^\pm} = 50 \text{ GeV}$ ) to  $0.23 \text{ pb}$  ( $m_{\tilde{\chi}_1^\pm} = 100 \text{ GeV}$ ) at 95%CL. The gaugino mass unification hypothesis and the assumed mass relation between squarks and gluinos define the value of the leptonic branching ratios. The quoted result corresponds to the best limit within the selected range of parameters, obtained for  $m_{\tilde{q}} > m_{\tilde{g}}$ ,  $\tan\beta = 2$ , and  $\mu = -600 \text{ GeV}$ . Mass limits for different values of  $\tan\beta$  and  $\mu$  are given in Fig. 2.
- 37 ACKERSTAFF 98k looked for dilepton+ $\cancel{E}_T$  final states at  $\sqrt{s} = 130\text{--}172 \text{ GeV}$ . Limits on  $\sigma(e^+e^- \rightarrow \tilde{\chi}_1^\pm \tilde{\chi}_1^\mp) \times \text{B}^2(\ell)$ , with  $\text{B}(\ell) = \text{B}(\chi^+ \rightarrow \ell^+ \nu_\ell \chi_1^0)$  ( $\text{B}(\ell) = \text{B}(\chi^+ \rightarrow \ell^+ \tilde{\nu}_\ell)$ ), are given in Fig. 16 (Fig. 17).
- 38 ACKERSTAFF 98l limit is obtained for  $0 < M_2 < 1500$ ,  $|\mu| < 500$  and  $\tan\beta > 1$ , but remains valid outside this domain. The dependence on the trilinear-coupling parameter  $A$  is studied, and found negligible. The limit holds for the smallest value of  $m_0$  consistent with scalar lepton constraints (ACKERSTAFF 97h) and for all values of  $m_0$  where the condition  $\Delta m_{\tilde{\tau}} > 2.0 \text{ GeV}$  is satisfied.  $\Delta m_{\nu} > 10 \text{ GeV}$  if  $\tilde{\chi}^\pm \rightarrow \ell \tilde{\nu}_\ell$ . The limit improves to  $84.5 \text{ GeV}$  for  $m_0 = 1 \text{ TeV}$ . Data taken at  $\sqrt{s} = 130\text{--}172 \text{ GeV}$ .
- 39 ACKERSTAFF 98f excludes the light gluino with universal gaugino mass where chargino, neutralino decay as  $\tilde{\chi}_1^\pm, \tilde{\chi}_2^0 \rightarrow q\bar{q}\tilde{g}$  from total hadronic cross sections at  $\sqrt{s} = 130\text{--}172 \text{ GeV}$ . See paper for the case of nonuniversal gaugino mass.
- 40 CARENA 97 studied the constraints on chargino and sneutrino masses from muon  $g-2$ . The bound can be important for large  $\tan\beta$ .
- 41 KALINOWSKI 97 studies the constraints on the chargino-neutralino parameter space from limits on  $\Gamma(W \rightarrow \tilde{\chi}_1^\pm \tilde{\chi}_1^0)$  achievable at LEP2. This is relevant when  $\tilde{\chi}_1^\pm$  is "invisible", i.e., if  $\tilde{\chi}_1^\pm$  dominantly decays into  $\tilde{\nu}_\ell \ell^\pm$  with little energy for the lepton. Small otherwise allowed regions could be excluded.
- 42 ABE 96k looked for trilepton events from chargino-neutralino production. The bound on  $m_{\tilde{\chi}_1^\pm}$  can reach up to  $47 \text{ GeV}$  for specific choices of parameters. The limits on the combined production cross section times 3-lepton branching ratios range between  $1.4$  and  $0.4 \text{ pb}$ , for  $45 < m_{\tilde{\chi}_1^\pm}(\text{GeV}) < 100$ . See the paper for more details on the parameter dependence of the results.

### Long-lived $\tilde{\chi}^\pm$ (Chargino) MASS LIMITS

Limits on charginos which leave the detector before decaying.

VALUE (GeV)	CL%	DOCUMENT ID	TECN	COMMENT
>171	95	1 ABAZOV	09M D0	$\tilde{H}$
>102	95	2 ABBIENDI	03L OPAL	$m_{\tilde{\tau}} > 500 \text{ GeV}$
none 2-93.0	95	3 ABREU	00T DELPH	$\tilde{H}^\pm$ or $m_{\tilde{\tau}} > m_{\tilde{\chi}^\pm}$
••• We do not use the following data for averages, fits, limits, etc. •••				
> 83	95	4 BARATE	97K ALEP	
> 28.2	95	ADACHI	90C TOPZ	

- 1 ABAZOV 09M searched in  $1.1 \text{ fb}^{-1}$  of  $p\bar{p}$  collisions at  $\sqrt{s} = 1.96 \text{ TeV}$  for events with direct production of a pair of charged massive stable particles identified by their TOF. The number of the observed events is consistent with the predicted background. The data are used to constrain the production cross section as a function of the  $\tilde{\chi}_1^\pm$  mass, see their Fig. 2. The quoted limit improves to  $206 \text{ GeV}$  for gaugino-like charginos.
- 2 ABBIENDI 03L used  $e^+e^-$  data at  $\sqrt{s} = 130\text{--}209 \text{ GeV}$  to select events with two high momentum tracks with anomalous  $dE/dx$ . The excluded cross section is compared to the theoretical expectation as a function of the heavy particle mass in their Fig. 3. The bounds are valid for colorless fermions with lifetime longer than  $10^{-6} \text{ s}$ . Supersedes the results from ACKERSTAFF 98P.
- 3 ABREU 00T searches for the production of heavy stable charged particles, identified by their ionization or Cherenkov radiation, using data from  $\sqrt{s} = 130$  to  $189 \text{ GeV}$ . These limits include and update the results of ABREU 98P.
- 4 BARATE 97k uses  $e^+e^-$  data collected at  $\sqrt{s} = 130\text{--}172 \text{ GeV}$ . Limit valid for  $\tan\beta = \sqrt{2}$  and  $m_{\tilde{\tau}} > 100 \text{ GeV}$ . The limit improves to  $86 \text{ GeV}$  for  $m_{\tilde{\tau}} > 250 \text{ GeV}$ .



See key on page 457

# Searches Particle Listings

## Supersymmetric Particle Searches

### $\tilde{\nu}$ (Sneutrino) MASS LIMIT

The limits may depend on the number,  $N(\tilde{\nu})$ , of sneutrinos assumed to be degenerate in mass. Only  $\tilde{\nu}_L$  (not  $\tilde{\nu}_R$ ) is assumed to exist. It is possible that  $\tilde{\nu}$  could be the lightest supersymmetric particle (LSP).

We report here, but do not include in the Listings, the limits obtained from the fit of the final results obtained by the LEP Collaborations on the invisible width of the Z boson ( $\Delta\Gamma_{\text{inv}} < 2.0$  MeV, LEP-SLC 06):  $m_{\tilde{\nu}} > 43.7$  GeV ( $N(\tilde{\nu})=1$ ) and  $m_{\tilde{\nu}} > 44.7$  GeV ( $N(\tilde{\nu})=3$ ).

VALUE (GeV)	CL%	DOCUMENT ID	TECN	COMMENT
> 94	95	1 ABDALLAH	03M DLPH	$1 \leq \tan\beta \leq 40$ , $m_{\tilde{e}_R} - m_{\tilde{\nu}_0} > 10$ GeV
> 84	95	2 HEISTER	02N ALEP	$\tilde{\nu}_e, \text{ any } \Delta m$
> 37.1	95	3 ADRIANI	93M L3	$\Gamma(Z \rightarrow \text{invisible}); N(\tilde{\nu})=1$
> 41	95	4 DECAMP	92 ALEP	$\Gamma(Z \rightarrow \text{invisible}); N(\tilde{\nu})=3$
> 36	95	5 ABREU	91F DLPH	$\Gamma(Z \rightarrow \text{invisible}); N(\tilde{\nu})=1$
> 31.2	95	5 ALEXANDER	91F OPAL	$\Gamma(Z \rightarrow \text{invisible}); N(\tilde{\nu})=1$
••• We do not use the following data for averages, fits, limits, etc. •••				
		6 AAD	11H ATLS	$\tilde{\nu}_\tau, \tilde{R}, s\text{-channel}$
		7 AAD	11Z ATLS	$\tilde{\nu}_\tau, \tilde{R}, s\text{-channel}$
		8 AALTONEN	10Z CDF	$\tilde{\nu}_\tau, \tilde{R}$
		9 ABAZOV	10M D0	$\tilde{\nu}_\tau, \tilde{R}$
		10 AALTONEN	09V CDF	$p\bar{p} \rightarrow \tilde{\nu} \rightarrow \mu\mu, \tilde{R} L Q\bar{D}$
		11 ABAZOV	08Q D0	$\tilde{\nu}_\tau, \tilde{R}$
		12 SCHAEEL	07A ALEP	$\tilde{\nu}_{\mu,\tau}, \tilde{R}, (s+t)\text{-channel}$
		13 ABAZOV	06I D0	$\tilde{R}, \lambda'_{211}$
		14 ABDALLAH	06C DLPH	$\tilde{\nu}_e, \tilde{R}, (s+t)\text{-channel}$
		15 ABULENCIA	06M CDF	$\tilde{\nu}_\tau, \tilde{R}$
		16 ABULENCIA	05A CDF	$p\bar{p} \rightarrow \tilde{\nu} \rightarrow e e, \mu\mu, \tilde{R} L Q\bar{D}$
		17 ACOSTA	05R CDF	$p\bar{p} \rightarrow \tilde{\nu} \rightarrow \tau\tau, \tilde{R}, L Q\bar{D}$
		18 ABBIENDI	04F OPAL	$\tilde{R}, \tilde{\nu}_{e,\mu,\tau}$
> 95	95	19,20 ABDALLAH	04H DLPH	AMSB, $\mu > 0$
> 98	95	21 ABDALLAH	04M DLPH	$R(LL\bar{E}), \tilde{\nu}_e, \text{indirect}, \Delta m > 5$ GeV
> 85	95	21 ABDALLAH	04M DLPH	$R(LL\bar{E}), \tilde{\nu}_\mu, \text{indirect}, \Delta m > 5$ GeV
> 85	95	21 ABDALLAH	04M DLPH	$R(LL\bar{E}), \tilde{\nu}_\tau, \text{indirect}, \Delta m > 5$ GeV
		22 ABDALLAH	03F DLPH	$\tilde{\nu}_{\mu,\tau}, \tilde{R} LL\bar{E}$ decays
		23 ACOSTA	03E CDF	$\tilde{\nu}, \tilde{R}, L Q\bar{D}$ production and $LL\bar{E}$ decays
> 88	95	24 HEISTER	03G ALEP	$\tilde{\nu}_e, \tilde{R}$ decays, $\mu = -200$ GeV, $\tan\beta=2$
> 65	95	24 HEISTER	03G ALEP	$\tilde{\nu}_{\mu,\tau}, \tilde{R}$ decays
> 95	95	25 ABAZOV	02H D0	$\tilde{R}, \lambda'_{211}$
> 95	95	26 ACHARD	02 L3	$\tilde{\nu}_e, \tilde{R}$ decays, $\mu = -200$ GeV, $\tan\beta=\sqrt{2}$
> 65	95	26 ACHARD	02 L3	$\tilde{\nu}_{\mu,\tau}, \tilde{R}$ decays
> 149	95	26 ACHARD	02 L3	$\tilde{\nu}, \tilde{R}$ decays, MSUGRA
		27 HEISTER	02F ALEP	$e\gamma \rightarrow \tilde{\nu}_{\mu,\tau} \ell_k, \tilde{R} LL\bar{E}$
none 100–264	95	28 ABBIENDI	00R OPAL	$\tilde{\nu}_{\mu,\tau}, \tilde{R}, (s+t)\text{-channel}$
none 100–200	95	29 ABBIENDI	00R OPAL	$\tilde{\nu}_\tau, \tilde{R}, s\text{-channel}$
		30 ABREU	00S DLPH	$\tilde{\nu}_e, \tilde{R}, (s+t)\text{-channel}$
none 50–210	95	31 ACCIARRI	00P L3	$\tilde{\nu}_{\mu,\tau}, \tilde{R}, s\text{-channel}$
none 50–210	95	32 BARATE	00I ALEP	$\tilde{\nu}_{\mu,\tau}, \tilde{R}, (s+t)\text{-channel}$
none 90–210	95	33 BARATE	00I ALEP	$\tilde{\nu}_{\mu,\tau}, \tilde{R}, s\text{-channel}$
none 100–160	95	34 ABBIENDI	99 OPAL	$\tilde{\nu}_e, \tilde{R}, t\text{-channel}$
$\neq m_Z$	95	35 ACCIARRI	97U L3	$\tilde{\nu}_\tau, \tilde{R}, s\text{-channel}$
none 125–180	95	35 ACCIARRI	97U L3	$\tilde{\nu}_\tau, \tilde{R}, s\text{-channel}$
		36 CARENA	97 THEO	$g_{\mu} - 2$
> 46.0	95	37 BUSKULIC	95E ALEP	$N(\tilde{\nu})=1, \tilde{\nu} \rightarrow \nu\nu\ell\bar{\ell}'$
none 20–25000		38 BECK	94 COSM	Stable $\tilde{\nu}$ , dark matter
<600		39 FALK	94 COSM	$\tilde{\nu}$ LSP, cosmic abundance
none 3–90	90	40 SATO	91 KAMI	Stable $\tilde{\nu}_e$ or $\tilde{\nu}_\mu$ , dark matter
none 4–90	90	40 SATO	91 KAMI	Stable $\tilde{\nu}_\tau$ , dark matter

<sup>1</sup> ABDALLAH 03M uses data from  $\sqrt{s} = 192\text{--}208$  GeV to obtain limits in the framework of the MSSM with gaugino and sfermion mass universality at the GUT scale. An indirect limit on the mass is derived by constraining the MSSM parameter space by the results from direct searches for neutralinos (including cascade decays) and for sleptons. These limits are valid for values of  $M_2 < 1$  TeV,  $|\mu| \leq 1$  TeV with the  $\tilde{\chi}_1^0$  as LSP. The quoted limit is obtained when there is no mixing in the third family. See Fig. 43 for the mass limits as a function of  $\tan\beta$ . These limits update the results of ABREU 00W.

<sup>2</sup> HEISTER 02N derives a bound on  $m_{\tilde{\nu}_e}$  by exploiting the mass relation between the  $\tilde{\nu}_e$  and  $\tilde{e}$ , based on the assumption of universal GUT scale gaugino and scalar masses  $m_{1/2}$  and  $m_0$  and the search described in the  $\tilde{e}$  section. In the MSUGRA framework with radiative electroweak symmetry breaking, the limit improves to  $m_{\tilde{\nu}_e} > 130$  GeV, assuming a trilinear coupling  $A_0=0$  at the GUT scale. See Figs. 5 and 7 for the dependence of the limits on  $\tan\beta$ .

<sup>3</sup> ADRIANI 93M limit from  $\Delta\Gamma(Z)(\text{invisible}) < 16.2$  MeV.

<sup>4</sup> DECAMP 92 limit is from  $\Gamma(\text{invisible})/\Gamma(\ell\ell) = 5.91 \pm 0.15$  ( $N_\nu = 2.97 \pm 0.07$ ).

<sup>5</sup> ALEXANDER 91F limit is for one species of  $\tilde{\nu}$  and is derived from  $\Gamma(\text{invisible, new})/\Gamma(\ell\ell) < 0.38$ .

<sup>6</sup> AAD 11H looked in  $35 \text{ pb}^{-1}$  of  $pp$  collisions at  $\sqrt{s} = 7$  TeV for events with one electron and one muon of opposite charge from the production of  $\tilde{\nu}_\tau$  via an  $R \lambda'_{311}$  coupling and followed by a decay via  $\lambda_{312}$  into  $e + \mu$ . No evidence for an excess over the SM expectation is observed, and a limit is derived in the plane of  $\lambda'_{311}$  versus  $m_{\tilde{\nu}}$  for several values of  $\lambda_{312}$ , see their Fig. 2. Superseded by AAD 11Z.

<sup>7</sup> AAD 11Z looked in  $1.07 \text{ fb}^{-1}$  of  $pp$  collisions at  $\sqrt{s} = 7$  TeV for events with one electron and one muon of opposite charge from the production of  $\tilde{\nu}_\tau$  via an  $R \lambda'_{311}$  coupling and followed by a decay via  $\lambda_{312}$  into  $e + \mu$ . No evidence for an  $(e, \mu)$  resonance over the SM expectation is observed, and a limit is derived in the plane of  $\lambda'_{311}$  versus  $m_{\tilde{\nu}}$  for three values of  $\lambda_{312}$ , see their Fig. 2. Masses  $m_{\tilde{\nu}} < 1.32$  (1.45) TeV are excluded for  $\lambda'_{311} = 0.10$  and  $\lambda_{312} = 0.05$  ( $\lambda'_{311} = 0.11$  and  $\lambda_{312} = 0.07$ ).

<sup>8</sup> AALTONEN 10Z searched in  $1 \text{ fb}^{-1}$  of  $p\bar{p}$  collisions at  $\sqrt{s} = 1.96$  TeV for events from the production  $d\bar{d} \rightarrow \tilde{\nu}_\tau$  with the subsequent decays  $\tilde{\nu}_\tau \rightarrow e\mu, \mu\tau, e\tau$  in the MSSM framework with  $R$ . Two isolated leptons of different flavor and opposite charges are required, with  $\tau$ s identified by their hadronic decay. No statistically significant excesses are observed over the SM background. Upper limits on  $\lambda'^2_{311}$  times the branching ratio are listed in their Table III for various  $\tilde{\nu}_\tau$  masses. Limits on the cross section times branching ratio for  $\lambda'_{311} = 0.10$  and  $\lambda_{312} = 0.05$ , displayed in Fig. 2, are used to set limits on the  $\tilde{\nu}_\tau$  mass of 558 GeV for the  $e\mu$ , 441 GeV for the  $\mu\tau$  and 442 GeV for the  $e\tau$  channels.

<sup>9</sup> ABAZOV 10M looked in  $5.3 \text{ fb}^{-1}$  of  $p\bar{p}$  collisions at  $\sqrt{s} = 1.96$  TeV for events with exactly one pair of high  $p_T$  isolated  $e\mu$  and a veto against hard jets. No evidence for an excess over the SM expectation is observed, and a limit at 95% C.L. on the cross section times branching ratio is derived, see their Fig. 3. These limits are translated into limits on couplings as a function of  $m_{\tilde{\nu}_\tau}$  as shown on their Fig. 4. As an example, for  $m_{\tilde{\nu}_\tau} = 100$  GeV and  $\lambda_{312} \leq 0.07$ , couplings  $\lambda'_{311} > 7.7 \times 10^{-4}$  are excluded.

<sup>10</sup> AALTONEN 09v searched in  $2.3 \text{ fb}^{-1}$  of  $p\bar{p}$  collisions at  $\sqrt{s} = 1.96$  TeV for events with an oppositely charged pair originating from the  $R$  production of a sneutrino decaying to dimuons. A limit is derived on the cross section times branching ratio,  $B$ , of  $\tilde{\nu} \rightarrow \mu\mu$  for several values of the coupling  $\lambda'$ , see their Fig. 3. For  $\lambda^2 B = 0.01$ , the range  $100 \text{ GeV} \leq m_{\tilde{\nu}} \leq 810$  GeV is excluded.

<sup>11</sup> ABAZOV 08q searched in  $1.04 \text{ fb}^{-1}$  of  $p\bar{p}$  collisions at  $\sqrt{s} = 1.96$  TeV for an excess of events with oppositely charged  $e\mu$  pairs. They might be expected in a SUSY model with  $R$  where a sneutrino is produced by  $LQ\bar{D}$  couplings and decays via  $LL\bar{E}$  couplings, focusing on  $\tilde{\nu}_\tau$ , hence on the  $\lambda'_{311}$  and  $\lambda_{312}$  constants. No significant excess was found compared to the background expectation. Upper limits on the cross-section times branching ratio are extracted and displayed in their Fig. 2. Exclusion regions are determined for the  $\tilde{\nu}_\tau$  mass as a function of both couplings, see their Fig. 3. As an indication, for  $\tilde{\nu}_\tau$  masses of 100 GeV and  $\lambda_{312} = 0.01$ , values of  $\lambda'_{311} \geq 1.6 \times 10^{-3}$  are excluded at the 95% C.L. Superseded by ABAZOV 10M.

<sup>12</sup> SCHAEEL 07A searches for the  $s$ - or  $t$ -channel exchange of sneutrinos in the case of  $R$  with  $LL\bar{E}$  couplings by studying di-lepton production at  $\sqrt{s} = 189\text{--}209$  GeV. Limits are obtained on the couplings as a function of the  $\tilde{\nu}$  mass, see their Figs. 22–24. The results of this analysis are combined with BARATE 00I.

<sup>13</sup> ABAZOV 06I looked in  $380 \text{ pb}^{-1}$  of  $p\bar{p}$  collisions at  $\sqrt{s} = 1.96$  TeV for events with at least 2 muons and 2 jets for  $s$ -channel production of  $\tilde{\mu}$  or  $\tilde{\nu}$  and subsequent decay via  $R$  couplings  $LQ\bar{D}$ . The data are in agreement with the SM expectation. They set limits on resonant slepton production and derive exclusion contours on  $\lambda'_{211}$  in the mass plane of  $\tilde{e}$  versus  $\tilde{\chi}^0_1$  assuming a MSUGRA model with  $\tan\beta = 5$ ,  $\mu < 0$  and  $A_0 = 0$ , see their Fig. 3. For  $\lambda'_{211} \geq 0.09$  slepton masses up to 358 GeV are excluded. Supersedes the results of ABAZOV 02H.

<sup>14</sup> ABDALLAH 06c searches for anomalies in the production cross sections and forward-backward asymmetries of the  $\ell^+ \ell^- (\gamma)$  final states ( $\ell = e, \mu, \tau$ ) from  $675 \text{ pb}^{-1}$  of  $e^+ e^-$  data at  $\sqrt{s} = 130\text{--}207$  GeV. Limits are set on the  $s$ - and  $t$ -channel exchange of sneutrinos in the presence of  $R$  with  $LL\bar{E}$  couplings. For points between the energies at which data were taken, information is obtained from events in which a photon was radiated. Exclusion limits in the  $(\lambda, m_{\tilde{\nu}})$  plane are given in Fig. 16. These limits include and update the results of ABREU 00s.

<sup>15</sup> ABULENCIA 06M searched in  $344 \text{ pb}^{-1}$  of  $p\bar{p}$  collisions at  $\sqrt{s} = 1.96$  TeV for an excess of events with oppositely charged  $e\mu$  pairs. They might be expected in a SUSY model with  $R$  where a sneutrino is produced by  $LQ\bar{D}$  couplings and decays via  $LL\bar{E}$  couplings, focusing on  $\tilde{\nu}_\tau$ , hence on the  $\lambda'_{311}$  and  $\lambda_{312}$  constants. No significant excess was found compared to the background expectation. Upper limits on the cross-section times branching ratio are extracted and exclusion regions determined for the  $\tilde{\nu}_\tau$  mass as a function of both couplings, see their Fig. 3. As an indication,  $\tilde{\nu}_\tau$  masses are excluded up to 300 GeV for  $\lambda'_{311} \geq 0.01$  and  $\lambda_{312} \geq 0.02$ . Superseded by AALTONEN 10Z.

<sup>16</sup> ABULENCIA 05A looked in  $\sim 200 \text{ pb}^{-1}$  of  $p\bar{p}$  collisions at  $\sqrt{s} = 1.96$  TeV for dimuon and dielectron events. They may originate from the  $R$  production of a sneutrino decaying to dileptons. No significant excess rate was found compared to the background expectation. A limit is derived on the cross section times branching ratio,  $B$ , of  $\tilde{\nu} \rightarrow e e, \mu\mu$  of 25 fb at high mass, see their Figure 2. Sneutrino masses are excluded at 95% CL below 680, 620, 460 GeV ( $e e$  channel) and 665, 590, 450 GeV ( $\mu\mu$  channel) for a  $\lambda'$  coupling and branching ratio such that  $\lambda'^2 B = 0.01, 0.005, 0.001$ , respectively.

<sup>17</sup> ACOSTA 05R looked in  $195 \text{ pb}^{-1}$  of  $p\bar{p}$  collisions at  $\sqrt{s} = 1.96$  TeV for ditau events with one identified hadronic tau decay and one other tau decay. They may originate from the  $R$  production of a sneutrino decaying to  $\tau\tau$ . No significant excess rate was found compared to the background expectation, dominated by Drell-Yan. A limit is derived on the cross section times branching ratio,  $B$ , of  $\tilde{\nu} \rightarrow \tau\tau$ , see their Figure 3. Sneutrino masses below 377 GeV are excluded at 95% CL for a  $\lambda'$  coupling to  $d\bar{d}$  and branching ratio such that  $\lambda'^2 B = 0.01$ .

<sup>18</sup> ABBIENDI 04F use data from  $\sqrt{s} = 189\text{--}209$  GeV. They derive limits on particle masses under the assumption of  $R$  with  $LL\bar{E}$  or  $LQ\bar{D}$  couplings. The results are valid for  $\tan\beta = 1.5$ ,  $\mu = -200$  GeV, and a BR for the decay given by CMSSM, assuming no sensitivity to other decays. Limits are quoted for  $m_{\tilde{\chi}^0_1} = 60$  GeV and degrade for low-mass  $\tilde{\chi}^0_1$ . For  $\tilde{\nu}_e$  the direct (indirect) limits with  $LL\bar{E}$  couplings are 89 (95) GeV and with  $LQ\bar{D}$  they are 89 (88) GeV. For  $\tilde{\nu}_{\mu,\tau}$  the direct (indirect) limits with  $LL\bar{E}$  couplings are 79 (81) GeV and with  $LQ\bar{D}$  they are 74 (no limit) GeV. Supersedes the results of ABBIENDI 00.

<sup>19</sup> ABDALLAH 04H use data from LEP 1 and  $\sqrt{s} = 192\text{--}208$  GeV. They re-use results or re-analyze the data from ABDALLAH 03M to put limits on the parameter space of anomaly-mediated supersymmetry breaking (AMSB), which is scanned in the region  $1 < m_{3/2} < 50$  TeV,  $0 < m_0 < 1000$  GeV,  $1.5 < \tan\beta < 35$ , both signs of  $\mu$ . The constraints are obtained from the searches for mass degenerate chargino and neutralino, for SM-like and invisible Higgs, for leptonically decaying charginos and from the limit on non-SM Z width of 3.2 MeV. The limit is for  $m_t = 174.3$  GeV (see Table 2 for other  $m_t$  values).

<sup>20</sup> The limit improves to 114 GeV for  $\mu < 17.4$ .

# Searches Particle Listings

## Supersymmetric Particle Searches

- 21** ABDALLAH 04M use data from  $\sqrt{s} = 189\text{--}208$  GeV. The results are valid for  $\mu = -200$  GeV,  $\tan\beta = 1.5$ ,  $\Delta m > 5$  GeV and assuming a BR of 1 for the given decay. The limit quoted is for indirect decays using the neutralino constraint of 39.5 GeV, also derived in ABDALLAH 04M. For indirect decays the limit on  $\tilde{\nu}_e$  decreases to 96 GeV if the constraint from the neutralino is not used and for direct decays it remains 96 GeV. For indirect decays the limit on  $\tilde{\nu}_\mu$  decreases to 82 GeV if the constraint from the neutralino is not used and to 83 GeV for direct decays. For indirect decays the limit on  $\tilde{\nu}_\tau$  decreases to 82 GeV if the constraint from the neutralino is not used and improves to 91 GeV for direct decays. Supersedes the results of ABREU 00u.
- 22** ABDALLAH 03F looked for events of the type  $e^+e^- \rightarrow \tilde{\nu} \rightarrow \tilde{\chi}^0 \nu, \tilde{\chi}^\pm e \bar{\nu}$  followed by  $R$  decays of the  $\tilde{\chi}^0$  via  $\lambda_{1j1}$  ( $j = 2, 3$ ) couplings in the data at  $\sqrt{s} = 183\text{--}208$  GeV. From a scan over the SUGRA parameters, they derive upper limits on the  $\lambda_{1j1}$  couplings as a function of the sneutrino mass, see their Figs. 5–8.
- 23** ACOSTA 03E search for  $e\mu, e\tau$  and  $\mu\tau$  final states, and sets limits on the product of production cross-section and decay branching ratio for a  $\tilde{\nu}$  in RPV models (see Fig. 3).
- 24** HEISTER 03G searches for the production of sneutrinos in the case of  $R$  prompt decays with  $L\tilde{L}\tilde{E}$ ,  $LQ\tilde{D}$  or  $U\tilde{D}\tilde{D}$  couplings at  $\sqrt{s} = 189\text{--}209$  GeV. The search is performed for direct and indirect decays, assuming one coupling at a time to be non-zero. The limit holds for indirect  $\tilde{\nu}$  decays via  $U\tilde{D}\tilde{D}$  couplings and  $\Delta m > 10$  GeV. Stronger limits are reached for  $(\tilde{\nu}_e, \tilde{\nu}_{\mu,\tau})$  for  $L\tilde{L}\tilde{E}$  direct (100,90) GeV or indirect (98,89) GeV and for  $LQ\tilde{D}$  direct (–,79) GeV or indirect (91,78) GeV couplings. For  $L\tilde{L}\tilde{E}$  indirect decays, use is made of the bound  $m(\tilde{\chi}_1^0) > 23$  GeV from BARATE 98s. Supersedes the results from BARATE 01b.
- 25** ABAZOV 02H looked in  $94 \text{ pb}^{-1}$  of  $p\bar{p}$  collisions at  $\sqrt{s}=1.8$  TeV for events with at least 2 muons and 2 jets for  $s$ -channel production of  $\tilde{\mu}$  or  $\tilde{\nu}$  and subsequent decay via  $R$  couplings  $LQ\tilde{D}$ . A scan over the MSUGRA parameters is performed to exclude regions of the  $(m_0, m_{1/2})$  plane, examples being shown in Fig. 2.
- 26** ACHARD 02 searches for the associated production of sneutrinos in the case of  $R$  prompt decays with  $L\tilde{L}\tilde{E}$  or  $U\tilde{D}\tilde{D}$  couplings at  $\sqrt{s}=189\text{--}208$  GeV. The search is performed for direct and indirect decays, assuming one coupling at a time to be nonzero. The limit holds for direct decays via  $L\tilde{L}\tilde{E}$  couplings. Stronger limits are reached for  $(\tilde{\nu}_e, \tilde{\nu}_{\mu,\tau})$  for  $L\tilde{L}\tilde{E}$  indirect (99,78) GeV and for  $U\tilde{D}\tilde{D}$  direct or indirect (99,70) GeV decays. The MSUGRA limit results from a scan over the MSSM parameter space with the assumption of gaugino and scalar mass unification at the GUT scale, imposing simultaneously the exclusions from neutralino, chargino, sleptons, and squarks analyses. The limit holds for  $U\tilde{D}\tilde{D}$  couplings and increases to 152.7 GeV for  $L\tilde{L}\tilde{E}$  couplings.
- 27** HEISTER 02F searched for single sneutrino production via  $e\gamma \rightarrow \tilde{\nu}_j \ell_k$  mediated by  $R$   $L\tilde{L}\tilde{E}$  couplings, decaying directly or indirectly via a  $\tilde{\chi}_1^0$  and assuming a single coupling to be nonzero at a time. Final states with three leptons and possible  $B_T$  due to neutrinos were selected in the 189–209 GeV data. Limits on the couplings  $\lambda_{1jk}$  as function of the sneutrino mass are shown in Figs. 10–14. The couplings  $\lambda_{232}$  and  $\lambda_{233}$  are not accessible and  $\lambda_{121}$  and  $\lambda_{131}$  are measured with better accuracy in sneutrino resonant production. For all tested couplings, except  $\lambda_{133}$ , the limits are significantly improved compared to the low-energy limits.
- 28** ABBIENDI 00R studied the effect of  $s$ - and  $t$ -channel  $\tau$  or  $\mu$  sneutrino exchange in  $e^+e^- \rightarrow e^+e^-$  at  $\sqrt{s}=130\text{--}189$  GeV, via the  $R$ -parity violating coupling  $\lambda_{1j1} L_1 L_j e_1^c$  ( $j=2$  or 3). The limits quoted here hold for  $\lambda_{1j1} > 0.13$ , and supersede the results of ABBIENDI 99. See Fig. 11 for limits on  $m_{\tilde{\nu}_j}$  versus coupling.
- 29** ABBIENDI 00R studied the effect of  $s$ -channel  $\tau$  sneutrino exchange in  $e^+e^- \rightarrow \mu^+\mu^-$  at  $\sqrt{s}=130\text{--}189$  GeV, in presence of the  $R$ -parity violating couplings  $\lambda_{1j1} L_1 L_j e_1^c$  ( $j=1$  and 2), with  $\lambda_{131}=\lambda_{232}$ . The limits quoted here hold for  $\lambda_{131} > 0.09$ , and supersede the results of ABBIENDI 99. See Fig. 12 for limits on  $m_{\tilde{\nu}_j}$  versus coupling.
- 30** ABREU 00s searches for anomalies in the production cross sections and forward-backward asymmetries of the  $\ell^+\ell^-(\gamma)$  final states ( $\ell=e,\mu,\tau$ ) from  $e^+e^-$  collisions at  $\sqrt{s}=130\text{--}189$  GeV. Limits are set on the  $s$ - and  $t$ -channel exchange of sneutrinos in the presence of  $R$  with  $L\tilde{L}\tilde{E}$  couplings. For points between the energies at which data were taken, information is obtained from events in which a photon was radiated. Exclusion limits in the  $(\lambda, m_{\tilde{\nu}})$  plane are given in Fig. 5. These limits include and update the results of ABREU 99a.
- 31** ACCIARRI 00p use the dilepton total cross sections and asymmetries at  $\sqrt{s}=m_Z$  and  $\sqrt{s}=130\text{--}189$  GeV data to set limits on the effect of  $R$   $L\tilde{L}\tilde{E}$  couplings giving rise to  $\mu$  or  $\tau$  sneutrino exchange. See their Fig. 5 for limits on the sneutrino mass versus couplings.
- 32** BARATE 00i studied the effect of  $s$ -channel and  $t$ -channel  $\tau$  or  $\mu$  sneutrino exchange in  $e^+e^- \rightarrow e^+e^-$  at  $\sqrt{s}=130\text{--}183$  GeV, via the  $R$ -parity violating coupling  $\lambda_{1j1} L_1 L_j e_1^c$  ( $j=2$  or 3). The limits quoted here hold for  $\lambda_{1j1} > 0.1$ . See their Fig. 15 for limits as a function of the coupling. Superseded by SCHAEL 07A.
- 33** BARATE 00i studied the effect of  $s$ -channel  $\tau$  sneutrino exchange in  $e^+e^- \rightarrow \mu^+\mu^-$  at  $\sqrt{s}=130\text{--}183$  GeV, in presence of the  $R$ -parity violating coupling  $\lambda_{1j1} L_1 L_j e_1^c$  ( $j=1$  and 2). The limits quoted here hold for  $\sqrt{|\lambda_{131} \lambda_{232}|} > 0.2$ . See their Fig. 16 for limits as a function of the coupling. Superseded by SCHAEL 07A.
- 34** ABBIENDI 99 studied the effect of  $t$ -channel electron sneutrino exchange in  $e^+e^- \rightarrow \tau^+\tau^-$  at  $\sqrt{s}=130\text{--}183$  GeV, in presence of the  $R$ -parity violating couplings  $\lambda_{131} L_1 L_3 e_1^c$ . The limits quoted here hold for  $\lambda_{131} > 0.6$ .
- 35** ACCIARRI 97u studied the effect of the  $s$ -channel tau-sneutrino exchange in  $e^+e^- \rightarrow e^+e^-$  at  $\sqrt{s}=m_Z$  and  $\sqrt{s}=130\text{--}172$  GeV, via the  $R$ -parity violating coupling  $\lambda_{131} L_1 L_3 e_1^c$ . The limits quoted here hold for  $\lambda_{131} > 0.05$ . Similar limits were studied in  $e^+e^- \rightarrow \mu^+\mu^-$  together with  $\lambda_{232} L_2 L_3 e_2^c$  coupling.
- 36** CARENA 97 studied the constraints on chargino and sneutrino masses from muon  $g-2$ . The bound can be important for large  $\tan\beta$ .
- 37** BUSKULIC 95e looked for  $Z \rightarrow \tilde{\nu}\tilde{\nu}$ , where  $\tilde{\nu} \rightarrow \nu \chi_1^0$  and  $\chi_1^0$  decays via  $R$ -parity violating interactions into two leptons and a neutrino.
- 38** BECK 94 limit can be inferred from limit on Dirac neutrino using  $\sigma(\tilde{\nu}) = 4\sigma(\nu)$ . Also private communication with H.V. Klapdor-Kleingrothaus.
- 39** FALK 94 puts an upper bound on  $m_{\tilde{\nu}}$  when  $\tilde{\nu}$  is LSP by requiring its relic density does not overclose the Universe.
- 40** SATO 91 search for high-energy neutrinos from the sun produced by annihilation of sneutrinos in the sun. Sneutrinos are assumed to be stable and to constitute dark matter in our galaxy. SATO 91 follow the analysis of NG 87, OLIVE 88, and GAISSER 86.

## CHARGED SLEPTONS

This section contains limits on charged scalar leptons ( $\tilde{\ell}$ , with  $\ell=e,\mu,\tau$ ). Studies of width and decays of the  $Z$  boson (use is made here of  $\Delta\Gamma_{\text{inv}} < 2.0$  MeV, LEP 00) conclusively rule out  $m_{\tilde{\ell}_R} < 40$  GeV (41

GeV for  $\tilde{\ell}_L$ ), independently of decay modes, for each individual slepton. The limits improve to 43 GeV (43.5 GeV for  $\tilde{\ell}_L$ ) assuming all 3 flavors to be degenerate. Limits on higher mass sleptons depend on model assumptions and on the mass splitting  $\Delta m = m_{\tilde{\ell}} - m_{\tilde{\chi}_1^0}$ . The mass and composition

of  $\tilde{\chi}_1^0$  may affect the selectron production rate in  $e^+e^-$  collisions through  $t$ -channel exchange diagrams. Production rates are also affected by the potentially large mixing angle of the lightest mass eigenstate  $\tilde{\ell}_1 = \tilde{\ell}_R \sin\theta_{\tilde{\ell}} + \tilde{\ell}_L \cos\theta_{\tilde{\ell}}$ . It is generally assumed that only  $\tilde{\tau}$  may have significant mixing. The coupling to the  $Z$  vanishes for  $\theta_{\tilde{\ell}}=0.82$ . In the high-energy limit of  $e^+e^-$  collisions the interference between  $\gamma$  and  $Z$  exchange leads to a minimal cross section for  $\theta_{\tilde{\ell}}=0.91$ , a value which is sometimes used in the following entries relative to data taken at LEP2. When limits on  $m_{\tilde{\ell}_R}$  are quoted, it is understood that limits on  $m_{\tilde{\ell}_L}$  are usually at least as strong.

Possibly open decays involving gauginos other than  $\tilde{\chi}_1^0$  will affect the detection efficiencies. Unless otherwise stated, the limits presented here result from the study of  $\tilde{\ell}^+\tilde{\ell}^-$  production, with production rates and decay properties derived from the MSSM. Limits made obsolete by the recent analyses of  $e^+e^-$  collisions at high energies can be found in previous Editions of this Review.

For decays with final state gravitinos ( $\tilde{G}$ ),  $m_{\tilde{G}}$  is assumed to be negligible relative to all other masses.

## $\tilde{e}$ (Selectron) MASS LIMIT

VALUE (GeV)	CL%	DOCUMENT ID	TECN	COMMENT
> 97.5		1 ABBIENDI 04	OPAL	$\tilde{e}_R, \Delta m > 11$ GeV, $ \mu  > 100$ GeV, $\tan\beta=1.5$
> 94.4		2 ACHARD 04	L3	$\tilde{e}_R, \Delta m > 10$ GeV, $ \mu  > 200$ GeV, $\tan\beta \geq 2$
> 71.3		2 ACHARD 04	L3	$\tilde{e}_R$ , all $\Delta m$
none 30–94	95	3 ABDALLAH 03M	DLPH	$\Delta m > 15$ GeV, $\tilde{e}_R^+ \tilde{e}_R^-$
> 94	95	4 ABDALLAH 03M	DLPH	$\tilde{e}_R, 1 \leq \tan\beta \leq 40$ , $\Delta m > 10$ GeV
> 95	95	5 HEISTER 02E	ALEP	$\Delta m > 15$ GeV, $\tilde{e}_R^+ \tilde{e}_R^-$
> 73	95	6 HEISTER 02N	ALEP	$\tilde{e}_R$ , any $\Delta m$
> 107	95	6 HEISTER 02N	ALEP	$\tilde{e}_L$ , any $\Delta m$
••• We do not use the following data for averages, fits, limits, etc. •••				
> 89	95	7 ABBIENDI 04F	OPAL	$\tilde{R}, \tilde{e}_L$
> 92	95	8 ABDALLAH 04M	DLPH	$\tilde{R}, \tilde{e}_R$ , indirect, $\Delta m > 5$ GeV
> 93	95	9 HEISTER 03G	ALEP	$\tilde{e}_R, R$ decays, $\mu = -200$ GeV, $\tan\beta=2$
> 69	95	10 ACHARD 02	L3	$\tilde{e}_R, R$ decays, $\mu = -200$ GeV, $\tan\beta = \sqrt{2}$
> 92	95	11 BARATE 01	ALEP	$\Delta m > 10$ GeV, $\tilde{e}_R^+ \tilde{e}_R^-$
> 77	95	12 ABBIENDI 00J	OPAL	$\Delta m > 5$ GeV, $\tilde{e}_R^+ \tilde{e}_R^-$
> 83	95	13 ABREU 00U	DLPH	$\tilde{e}_R, R$ ( $L\tilde{L}\tilde{E}$ )
> 67	95	14 ABREU 00V	DLPH	$\tilde{e}_R \tilde{e}_R$ ( $\tilde{e}_R \rightarrow e\tilde{G}$ ), $m_{\tilde{G}} > 10$ eV
> 85	95	15 BARATE 00G	ALEP	$\tilde{\ell}_R \rightarrow \ell\tilde{G}$ , any $\tau(\tilde{\ell}_R)$
> 29.5	95	16 ACCIARRI 99I	L3	$\tilde{e}_R, R$ , $\tan\beta \geq 2$
> 56	95	17 ACCIARRI 98F	L3	$\Delta m > 5$ GeV, $\tilde{e}_R^+ \tilde{e}_R^-$ , $\tan\beta \geq 1.41$
> 77	95	18 BARATE 98K	ALEP	Any $\Delta m$ , $\tilde{e}_R^+ \tilde{e}_R^-$ , $\tilde{e}_R \rightarrow e\gamma\tilde{G}$
> 77	95	19 BREITWEG 98	ZEUS	$m_{\tilde{q}}=m_{\tilde{e}}, m(\tilde{\chi}_1^0)=40$ GeV
> 63	95	20 AID 96C	H1	$m_{\tilde{q}}=m_{\tilde{e}}, m_{\tilde{\chi}_1^0}=35$ GeV

1 ABBIENDI 04 search for  $\tilde{e}_R \tilde{e}_R$  production in acoplanar di-electron final states in the 183–208 GeV data. See Fig. 13 for the dependence of the limits on  $m_{\tilde{\chi}_1^0}$  and for the limit at  $\tan\beta=35$ . This limit supersedes ABBIENDI 00G.

2 ACHARD 04 search for  $\tilde{e}_R \tilde{e}_L$  and  $\tilde{e}_R \tilde{e}_R$  production in single- and acoplanar di-electron final states in the 192–209 GeV data. Absolute limits on  $m_{\tilde{e}_R}$  are derived from a scan over the MSSM parameter space with universal GUT scale gaugino and scalar masses  $m_{1/2}$  and  $m_0$ ,  $1 \leq \tan\beta \leq 60$  and  $-2 \leq \mu \leq 2$  TeV. See Fig. 4 for the dependence of the limits on  $m_{\tilde{\chi}_1^0}$ . This limit supersedes ACCIARRI 99W.

3 ABDALLAH 03M looked for acoplanar dielectron +  $\tilde{E}$  final states at  $\sqrt{s} = 189\text{--}208$  GeV. The limit assumes  $\mu = -200$  GeV and  $\tan\beta=1.5$  in the calculation of the production cross section and  $B(\tilde{e} \rightarrow e\tilde{\chi}_1^0)$ . See Fig. 15 for limits in the  $(m_{\tilde{e}_R}, m_{\tilde{\chi}_1^0})$  plane. These limits include and update the results of ABREU 01

4 ABDALLAH 03M uses data from  $\sqrt{s} = 192\text{--}208$  GeV to obtain limits in the framework of the MSSM with gaugino and sfermion mass universality at the GUT scale. An indirect limit on the mass is derived by constraining the MSSM parameter space by the results from direct searches for neutralinos (including cascade decays) and for sleptons. These limits are valid for values of  $M_2 < 1$  TeV,  $|\mu| \leq 1$  TeV with the  $\tilde{\chi}_1^0$  as LSP. The quoted limit is obtained when there is no mixing in the third family. See Fig. 43 for the mass limits as a function of  $\tan\beta$ . These limits update the results of ABREU 00W.

5 HEISTER 02E looked for acoplanar dielectron +  $\tilde{E}$  final states from  $e^+e^-$  interactions between 183 and 209 GeV. The mass limit assumes  $\mu < -200$  GeV and  $\tan\beta=2$  for the production cross section and  $B(\tilde{e} \rightarrow e\tilde{\chi}_1^0)=1$ . See their Fig. 4 for the dependence of the limit on  $\Delta m$ . These limits include and update the results of BARATE 01.

<sup>6</sup> HEISTER 02n search for  $\tilde{e}_L \tilde{e}_L$  and  $\tilde{e}_R \tilde{e}_R$  production in single- and acoplanar di-electron final states in the 183–208 GeV data. Absolute limits on  $m_{\tilde{e}_R}$  are derived from a scan over the MSSM parameter space with universal GUT scale gaugino and scalar masses  $m_{1/2}$  and  $m_0$ ,  $1 \leq \tan\beta \leq 50$  and  $-10 \leq \mu \leq 10$  TeV. The region of small  $|\mu|$ , where cascade decays are important, is covered by a search for  $\tilde{\chi}_1^0 \tilde{\chi}_3^0$  in final states with leptons and possibly photons. Limits on  $m_{\tilde{e}_L}$  are derived by exploiting the mass relation between the  $\tilde{e}_L$  and  $\tilde{e}_R$ , based on universal  $m_0$  and  $m_{1/2}$ . When the constraint from the mass limit of the lightest Higgs from HEISTER 02 is included, the bounds improve to  $m_{\tilde{e}_R} > 77(75)$  GeV and  $m_{\tilde{e}_L} > 115(115)$  GeV for a top mass of 175(180) GeV. In the MSUGRA framework with radiative electroweak symmetry breaking, the limits improve further to  $m_{\tilde{e}_R} > 95$  GeV and  $m_{\tilde{e}_L} > 152$  GeV, assuming a trilinear coupling  $A_0=0$  at the GUT scale. See Figs. 4, 5, 7 for the dependence of the limits on  $\tan\beta$ .

<sup>7</sup> ABBIENDI 04f use data from  $\sqrt{s} = 189$ –209 GeV. They derive limits on sparticle masses under the assumption of  $R$  with  $LL\bar{E}$  or  $LQ\bar{D}$  couplings. The results are valid for  $\tan\beta = 1.5$ ,  $\mu = -200$  GeV, with, in addition,  $\Delta m > 5$  GeV for indirect decays via  $LQ\bar{D}$ . The limit quoted applies to direct decays via  $LL\bar{E}$  or  $LQ\bar{D}$  couplings. For indirect decays, the limits on the  $\tilde{e}_R$  mass are respectively 99 and 92 GeV for  $LL\bar{E}$  and  $LQ\bar{D}$  couplings and  $m_{\tilde{\chi}_1^0} = 10$  GeV and degrade slightly for larger  $\tilde{\chi}_1^0$  mass. Supersedes the results of ABBIENDI 00.

<sup>8</sup> ABDALLAH 04m use data from  $\sqrt{s} = 192$ –208 GeV to derive limits on sparticle masses under the assumption of  $R$  with  $LL\bar{E}$  or  $UDD$  couplings. The results are valid for  $\mu = -200$  GeV,  $\tan\beta = 1.5$ ,  $\Delta m > 5$  GeV and assuming a BR of 1 for the given decay. The limit quoted is for indirect  $UDD$  decays using the neutralino constraint of 39.5 GeV for  $LL\bar{E}$  and of 38.0 GeV for  $UDD$  couplings, also derived in ABDALLAH 04m. For indirect decays via  $LL\bar{E}$  the limit improves to 95 GeV if the constraint from the neutralino is used and to 94 GeV if it is not used. For indirect decays via  $UDD$  couplings it remains unchanged when the neutralino constraint is not used. Supersedes the result of ABREU 00u.

<sup>9</sup> HEISTER 03g searches for the production of selectrons in the case of  $R$  prompt decays with  $LL\bar{E}$ ,  $LQ\bar{D}$  or  $UDD$  couplings at  $\sqrt{s} = 189$ –209 GeV. The search is performed for direct and indirect decays, assuming one coupling at a time to be non-zero. The limit holds for indirect decays mediated by  $LQ\bar{D}$  couplings with  $\Delta m > 10$  GeV. Limits are also given for  $LL\bar{E}$  direct ( $m_{\tilde{e}_R} > 96$  GeV) and indirect decays ( $m_{\tilde{e}_R} > 94$  GeV for  $m(\tilde{\chi}_1^0) > 23$  GeV from BARATE 98s) and for  $UDD$  indirect decays ( $m_{\tilde{e}_R} > 94$  GeV with  $\Delta m > 10$  GeV). Supersedes the results from BARATE 01b.

<sup>10</sup> ACHARD 02 searches for the production of selectrons in the case of  $R$  prompt decays with  $LL\bar{E}$  or  $UDD$  couplings at  $\sqrt{s} = 189$ –208 GeV. The search is performed for direct and indirect decays, assuming one coupling at a time to be non-zero. The limit holds for direct decays via  $LL\bar{E}$  couplings. Stronger limits are reached for  $LL\bar{E}$  indirect (79 GeV) and for  $UDD$  direct or indirect (96 GeV) decays.

<sup>11</sup> BARATE 01 looked for acoplanar dielectron +  $\cancel{E}_T$  final states at 189 to 202 GeV. The limit assumes  $\mu = -200$  GeV and  $\tan\beta = 2$  for the production cross section and 100% branching ratio for  $\tilde{e} \rightarrow e\tilde{\chi}_1^0$ . See their Fig. 1 for the dependence of the limit on  $\Delta m$ . These limits include and update the results of BARATE 99q.

<sup>12</sup> ABBIENDI 00j looked for acoplanar dielectron +  $\cancel{E}_T$  final states at  $\sqrt{s} = 161$ –183 GeV. The limit assumes  $\mu < -100$  GeV and  $\tan\beta = 1.5$  for the production cross section and decay branching ratios, evaluated within the MSSM, and zero efficiency for decays other than  $\tilde{e} \rightarrow e\tilde{\chi}_1^0$ . See their Fig. 12 for the dependence of the limit on  $\Delta m$  and  $\tan\beta$ .

<sup>13</sup> ABREU 00u studies decays induced by  $R$ -parity violating  $LL\bar{E}$  couplings, using data from  $\sqrt{s} = 189$  GeV. They investigate topologies with multiple leptons, assuming one coupling at a time to be non-zero and giving rise to indirect decays. The limits assume a neutralino mass limit of 30 GeV, also derived in ABREU 00u. Updates ABREU 00i. Superseded by ABDALLAH 04m.

<sup>14</sup> ABREU 00v use data from  $\sqrt{s} = 130$ –189 GeV to search for tracks with large impact parameter or visible decay vertices. Limits are obtained as a function of  $m_{\tilde{G}}$ , from a scan of the GMSB parameters space, after combining these results with the search for slepton pair production in the SUGRA framework from ABREU 01 to cover prompt decays and on stable particle searches from ABREU 00q. For limits at different  $m_{\tilde{G}}$ , see their Fig. 12.

<sup>15</sup> BARATE 00g combines the search for acoplanar dileptons, leptons with large impact parameters, kinks, and stable heavy-charged tracks, assuming 3 flavors of degenerate sleptons, produced in the channel. Data collected at  $\sqrt{s} = 189$  GeV.

<sup>16</sup> ACCIARRI 99i establish indirect limits on  $m_{\tilde{e}_R}$  from the regions excluded in the  $M_2$  versus  $m_0$  plane by their chargino and neutralino searches at  $\sqrt{s} = 130$ –183 GeV. The situations where the  $\tilde{\chi}_1^0$  is the LSP (indirect decays) and where a  $\tilde{\ell}$  is the LSP (direct decays) were both considered. The weakest limit, quoted above, comes from direct decays with  $UDD$  couplings;  $LL\bar{E}$  couplings or indirect decays lead to a stronger limit.

<sup>17</sup> ACCIARRI 98f looked for acoplanar dielectron +  $\cancel{E}_T$  final states at  $\sqrt{s} = 130$ –172 GeV. The limit assumes  $\mu = -200$  GeV, and zero efficiency for decays other than  $\tilde{e}_R \rightarrow e\tilde{\chi}_1^0$ . See their Fig. 6 for the dependence of the limit on  $\Delta m$ .

<sup>18</sup> BARATE 98k looked for  $e^+e^- \gamma\gamma + \cancel{E}$  final states at  $\sqrt{s} = 161$ –184 GeV. The limit assumes  $\mu = -200$  GeV and  $\tan\beta = 2$  for the evaluation of the production cross section. See Fig. 4 for limits on the  $(m_{\tilde{e}_R}, m_{\tilde{\chi}_1^0})$  plane and for the effect of cascade decays.

<sup>19</sup> BREITWEG 98 used positron+jet events with missing energy and momentum to look for  $e^+q \rightarrow \tilde{e}q$  via gaugino-like neutralino exchange with decays into  $(e\tilde{\chi}_1^0)(q\tilde{\chi}_1^0)$ . See paper for dependences in  $m(\tilde{q})$ ,  $m(\tilde{\chi}_1^0)$ .

<sup>20</sup> AID 96c used positron+jet events with missing energy and momentum to look for  $e^+q \rightarrow \tilde{e}q$  via neutralino exchange with decays into  $(e\tilde{\chi}_1^0)(q\tilde{\chi}_1^0)$ . See the paper for dependences on  $m_{\tilde{q}}$ ,  $m_{\tilde{\chi}_1^0}$ .

### $\tilde{\mu}$ (Smuon) MASS LIMIT

VALUE (GeV)	CL%	DOCUMENT ID	TECN	COMMENT
>91.0		<sup>1</sup> ABBIENDI 04	OPAL	$\Delta m > 3$ GeV, $\tilde{\mu}_R^+ \tilde{\mu}_R^-$ , $ \mu  > 100$ GeV, $\tan\beta = 1.5$
>86.7		<sup>2</sup> ACHARD 04	L3	$\Delta m > 10$ GeV, $\tilde{\mu}_R^+ \tilde{\mu}_R^-$ , $ \mu  > 200$ GeV, $\tan\beta \geq 2$
none 30–88	95	<sup>3</sup> ABDALLAH 03m	DLPH	$\Delta m > 5$ GeV, $\tilde{\mu}_R^+ \tilde{\mu}_R^-$
>94	95	<sup>4</sup> ABDALLAH 03m	DLPH	$\tilde{\mu}_R, 1 \leq \tan\beta \leq 40$ , $\Delta m > 10$ GeV
>88	95	<sup>5</sup> HEISTER 02e	ALEP	$\Delta m > 15$ GeV, $\tilde{\mu}_R^+ \tilde{\mu}_R^-$

• • • We do not use the following data for averages, fits, limits, etc. • • •

		<sup>6</sup> ABAZOV 06i	D0	$R, \lambda_{211}^{\prime}$
>74	95	<sup>7</sup> ABBIENDI 04f	OPAL	$R, \tilde{\mu}_L$
>87	95	<sup>8</sup> ABDALLAH 04m	DLPH	$R, \tilde{\mu}_R$ , indirect, $\Delta m > 5$ GeV
>81	95	<sup>9</sup> HEISTER 03g	ALEP	$\tilde{\mu}_L, R$ decays
		<sup>10</sup> ABAZOV 02h	D0	$R, \lambda_{211}^{\prime}$
>61	95	<sup>11</sup> ACHARD 02	L3	$\tilde{\mu}_R, R$ decays
>85	95	<sup>12</sup> BARATE 01	ALEP	$\Delta m > 10$ GeV, $\tilde{\mu}_R^+ \tilde{\mu}_R^-$
>65	95	<sup>13</sup> ABBIENDI 00j	OPAL	$\Delta m > 2$ GeV, $\tilde{\mu}_R^+ \tilde{\mu}_R^-$
>80	95	<sup>14</sup> ABREU 00v	DLPH	$\tilde{\mu}_R \tilde{\mu}_R$ ( $\tilde{\mu}_R \rightarrow \mu\tilde{G}$ ), $m_{\tilde{G}} > 8$ eV
>77	95	<sup>15</sup> BARATE 98k	ALEP	Any $\Delta m, \tilde{\mu}_R^+ \tilde{\mu}_R^-, \tilde{\mu}_R \rightarrow \mu\gamma\tilde{G}$

<sup>1</sup> ABBIENDI 04 search for  $\tilde{\mu}_R \tilde{\mu}_R$  production in acoplanar di-muon final states in the 183–208 GeV data. See Fig. 14 for the dependence of the limits on  $m_{\tilde{\chi}_1^0}$  and for the

limit at  $\tan\beta = 35$ . Under the assumption of 100% branching ratio for  $\tilde{\mu}_R \rightarrow \mu\tilde{\chi}_1^0$ , the limit improves to 94.0 GeV for  $\Delta m > 4$  GeV. See Fig. 11 for the dependence of the limits on  $m_{\tilde{\chi}_1^0}$  at several values of the branching ratio. This limit supersedes ABBIENDI 00g.

<sup>2</sup> ACHARD 04 search for  $\tilde{\mu}_R \tilde{\mu}_R$  production in acoplanar di-muon final states in the 192–209 GeV data. Limits on  $m_{\tilde{\mu}_R}$  are derived from a scan over the MSSM parameter space with universal GUT scale gaugino and scalar masses  $m_{1/2}$  and  $m_0$ ,  $1 \leq \tan\beta \leq 60$  and  $-2 \leq \mu \leq 2$  TeV. See Fig. 4 for the dependence of the limits on  $m_{\tilde{\chi}_1^0}$ . This limit supersedes ACCIARRI 99w.

<sup>3</sup> ABDALLAH 03m looked for acoplanar dimuon +  $\cancel{E}$  final states at  $\sqrt{s} = 189$ –208 GeV. The limit assumes  $B(\tilde{\mu} \rightarrow \mu\tilde{\chi}_1^0) = 100\%$ . See Fig. 16 for limits on the  $(m_{\tilde{\mu}_R}, m_{\tilde{\chi}_1^0})$  plane. These limits include and update the results of ABREU 01.

<sup>4</sup> ABDALLAH 03m uses data from  $\sqrt{s} = 192$ –208 GeV to obtain limits in the framework of the MSSM with gaugino and sfermion mass universality at the GUT scale. An indirect limit on the mass is derived by constraining the MSSM parameter space by the results from direct searches for neutralinos (including cascade decays) and for sleptons. These limits are valid for values of  $M_2 < 1$  TeV,  $|\mu| \leq 1$  TeV with the  $\tilde{\chi}_1^0$  as LSP. The quoted limit is obtained when there is no mixing in the third family. See Fig. 43 for the mass limits as a function of  $\tan\beta$ . These limits update the results of ABREU 00w.

<sup>5</sup> HEISTER 02e looked for acoplanar dimuon +  $\cancel{E}_T$  final states from  $e^+e^-$  interactions between 183 and 209 GeV. The mass limit assumes  $B(\tilde{\mu} \rightarrow \mu\tilde{\chi}_1^0) = 1$ . See their Fig. 4 for the dependence of the limit on  $\Delta m$ . These limits include and update the results of BARATE 01.

<sup>6</sup> ABAZOV 06i looked in  $380 \text{ pb}^{-1}$  of  $p\bar{p}$  collisions at  $\sqrt{s} = 1.96$  TeV for events with at least 2 muons and 2 jets for  $s$ -channel production of  $\tilde{\mu}$  or  $\tilde{\nu}$  and subsequent decay via  $R$  couplings  $LQ\bar{D}$ . The data are in agreement with the SM expectation. They set limits on resonant slepton production and derive exclusion contours on  $\lambda_{211}^{\prime}$  in the mass plane of  $\tilde{\ell}$  versus  $\tilde{\chi}_1^0$  assuming a MSUGRA model with  $\tan\beta = 5$ ,  $\mu < 0$  and  $A_0 = 0$ , see their Fig. 3. For  $\lambda_{211}^{\prime} \geq 0.09$  slepton masses up to 358 GeV are excluded. Supersedes the results of ABAZOV 02h.

<sup>7</sup> ABBIENDI 04f use data from  $\sqrt{s} = 189$ –209 GeV. They derive limits on sparticle masses under the assumption of  $R$  with  $LL\bar{E}$  or  $LQ\bar{D}$  couplings. The results are valid for  $\tan\beta = 1.5$ ,  $\mu = -200$  GeV, with, in addition,  $\Delta m > 5$  GeV for indirect decays via  $LQ\bar{D}$ . The limit quoted applies to direct decays with  $LL\bar{E}$  couplings and improves to 75 GeV for  $LQ\bar{D}$  couplings. The limits on the  $\tilde{\mu}_R$  mass for indirect decays are respectively 94 and 87 GeV for  $LL\bar{E}$  and  $LQ\bar{D}$  couplings and  $m_{\tilde{\chi}_1^0} = 10$  GeV. Supersedes the results of ABBIENDI 00.

<sup>8</sup> ABDALLAH 04m use data from  $\sqrt{s} = 192$ –208 GeV to derive limits on sparticle masses under the assumption of  $R$  with  $LL\bar{E}$  or  $UDD$  couplings. The results are valid for  $\mu = -200$  GeV,  $\tan\beta = 1.5$ ,  $\Delta m > 5$  GeV and assuming a BR of 1 for the given decay. The limit quoted is for indirect  $UDD$  decays using the neutralino constraint of 39.5 GeV for  $LL\bar{E}$  and of 38.0 GeV for  $UDD$  couplings, also derived in ABDALLAH 04m. For indirect decays via  $LL\bar{E}$  the limit improves to 90 GeV if the constraint from the neutralino is used and remains at 87 GeV if it is not used. For indirect decays via  $UDD$  couplings it degrades to 85 GeV when the neutralino constraint is not used. Supersedes the result of ABREU 00u.

<sup>9</sup> HEISTER 03g searches for the production of smuons in the case of  $R$  prompt decays with  $LL\bar{E}$ ,  $LQ\bar{D}$  or  $UDD$  couplings at  $\sqrt{s} = 189$ –209 GeV. The search is performed for direct and indirect decays, assuming one coupling at a time to be non-zero. The limit holds for direct decays mediated by  $R$   $LQ\bar{D}$  couplings and improves to 90 GeV for indirect decays (for  $\Delta m > 10$  GeV). Limits are also given for  $LL\bar{E}$  direct ( $m_{\tilde{\mu}_R} > 87$  GeV) and indirect decays ( $m_{\tilde{\mu}_R} > 96$  GeV for  $m(\tilde{\chi}_1^0) > 23$  GeV from BARATE 98s) and for  $UDD$  indirect decays ( $m_{\tilde{\mu}_R} > 85$  GeV for  $\Delta m > 10$  GeV). Supersedes the results from BARATE 01b.

<sup>10</sup> ABAZOV 02h looked in  $94 \text{ pb}^{-1}$  of  $p\bar{p}$  collisions at  $\sqrt{s} = 1.8$  TeV for events with at least 2 muons and 2 jets for  $s$ -channel production of  $\tilde{\mu}$  or  $\tilde{\nu}$  and subsequent decay via  $R$  couplings  $LQ\bar{D}$ . A scan over the MSUGRA parameters is performed to exclude regions of the  $(m_0, m_{1/2})$  plane, examples being shown in Fig. 2.

<sup>11</sup> ACHARD 02 searches for the production of smuons in the case of  $R$  prompt decays with  $LL\bar{E}$  or  $UDD$  couplings at  $\sqrt{s} = 189$ –208 GeV. The search is performed for direct and indirect decays, assuming one coupling at a time to be non-zero. The limit holds for direct decays via  $LL\bar{E}$  couplings. Stronger limits are reached for  $LL\bar{E}$  indirect (87 GeV) and for  $UDD$  direct or indirect (86 GeV) decays.

<sup>12</sup> BARATE 01 looked for acoplanar dimuon +  $\cancel{E}_T$  final states at 189 to 202 GeV. The limit assumes 100% branching ratio for  $\tilde{\mu} \rightarrow \mu\tilde{\chi}_1^0$ . See their Fig. 1 for the dependence of the limit on  $\Delta m$ . These limits include and update the results of BARATE 99q.

<sup>13</sup> ABBIENDI 00j looked for acoplanar dimuon +  $\cancel{E}_T$  final states at  $\sqrt{s} = 161$ –183 GeV. The limit assumes  $B(\tilde{\mu} \rightarrow \mu\tilde{\chi}_1^0) = 1$ . Using decay branching ratios derived from the MSSM, a lower limit of 65 GeV is obtained for  $\mu < -100$  GeV and  $\tan\beta = 1.5$ . See their Figs. 10 and 13 for the dependence of the limit on the branching ratio and on  $\Delta m$ .

<sup>14</sup> ABREU 00v use data from  $\sqrt{s} = 130$ –189 GeV to search for tracks with large impact parameter or visible decay vertices. Limits are obtained as function of  $m_{\tilde{G}}$ , after combining these results with the search for slepton pair production in the SUGRA framework from ABREU 01 to cover prompt decays and on stable particle searches from ABREU 00q. For limits at different  $m_{\tilde{G}}$ , see their Fig. 12.

# Searches Particle Listings

## Supersymmetric Particle Searches

<sup>15</sup> BARATE 98k looked for  $\mu^+ \mu^- \gamma \gamma + \cancel{E}$  final states at  $\sqrt{s}=161\text{--}184$  GeV. See Fig. 4 for limits on the  $(m_{\tilde{\mu}_R}, m_{\tilde{\chi}_1^0})$  plane and for the effect of cascade decays.

### $\tilde{\tau}$ (Stau) MASS LIMIT

VALUE (GeV)	CL%	DOCUMENT ID	TECN	COMMENT
>85.2		<sup>1</sup> ABBIENDI 04	OPAL	$\Delta m > 6$ GeV, $\theta_\tau = \pi/2$ , $ \mu  > 100$ GeV, $\tan\beta = 1.5$
>78.3		<sup>2</sup> ACHARD 04	L3	$\Delta m > 15$ GeV, $\theta_\tau = \pi/2$ , $ \mu  > 200$ GeV, $\tan\beta \geq 2$
<b>&gt;81.9</b>	95	<sup>3</sup> ABDALLAH 03M	DLPH	$\Delta m > 15$ GeV, all $\theta_\tau$
none $m_\tau - 26.3$	95	<sup>3</sup> ABDALLAH 03M	DLPH	$\Delta m > m_\tau$ , all $\theta_\tau$
>79	95	<sup>4</sup> HEISTER 02E	ALEP	$\Delta m > 15$ GeV, $\theta_\tau = \pi/2$
>76	95	<sup>4</sup> HEISTER 02E	ALEP	$\Delta m > 15$ GeV, $\theta_\tau = 0.91$
• • • We do not use the following data for averages, fits, limits, etc. • • •				
>87.4	95	<sup>5</sup> ABBIENDI 06B	OPAL	$\tilde{\tau}_R \rightarrow \tau \tilde{G}$ , all $\tau(\tilde{\tau}_R)$
>74	95	<sup>6</sup> ABBIENDI 04F	OPAL	$\tilde{R}, \tilde{\tau}_1$
>68	95	<sup>7,8</sup> ABDALLAH 04H	DLPH	AMSB, $\mu > 0$
>90	95	<sup>9</sup> ABDALLAH 04M	DLPH	$\tilde{R}, \tilde{\tau}_R$ , indirect, $\Delta m > 5$ GeV
>82.5	95	<sup>10</sup> ABDALLAH 03D	DLPH	$\tilde{\tau}_R \rightarrow \tau \tilde{G}$ , all $\tau(\tilde{\tau}_R)$
>70	95	<sup>11</sup> HEISTER 03G	ALEP	$\tilde{\tau}_R, \tilde{R}$ decay
>61	95	<sup>12</sup> ACHARD 02	L3	$\tilde{\tau}_R, \tilde{R}$ decays
>77	95	<sup>13</sup> HEISTER 02R	ALEP	$\tau_1$ , any lifetime
>70	95	<sup>14</sup> BARATE 01	ALEP	$\Delta m > 10$ GeV, $\theta_\tau = \pi/2$
>68	95	<sup>14</sup> BARATE 01	ALEP	$\Delta m > 10$ GeV, $\theta_\tau = 0.91$
>64	95	<sup>15</sup> ABBIENDI 00J	OPAL	$\Delta m > 10$ GeV, $\tilde{\tau}_R^+ \tilde{\tau}_R^-$
>84	95	<sup>16</sup> ABREU 00V	DLPH	$\tilde{\tau}_R \tilde{\ell}_R$ ( $\tilde{\ell}_R \rightarrow \ell \tilde{G}$ ), $m_{\tilde{G}} > 9$ eV
>73	95	<sup>17</sup> ABREU 00V	DLPH	$\tilde{\tau}_1 \tilde{\tau}_1$ ( $\tilde{\tau}_1 \rightarrow \tau \tilde{G}$ ), all $\tau(\tilde{\tau}_1)$
>52		<sup>18</sup> BARATE 98K	ALEP	Any $\Delta m, \theta_\tau = \pi/2, \tilde{\tau}_R \rightarrow \tau \gamma \tilde{G}$

<sup>1</sup> ABBIENDI 04 search for  $\tilde{\tau}\tilde{\tau}$  production in acoplanar di-tau final states in the 183–208 GeV data. See Fig. 15 for the dependence of the limits on  $m_{\tilde{\chi}_1^0}$  and for the limit

at  $\tan\beta = 35$ . Under the assumption of 100% branching ratio for  $\tilde{\tau}_R \rightarrow \tau \tilde{\chi}_1^0$ , the limit improves to 89.8 GeV for  $\Delta m > 8$  GeV. See Fig. 12 for the dependence of the limits on  $m_{\tilde{\chi}_1^0}$  at several values of the branching ratio and for their dependence on  $\theta_\tau$ . This limit supersedes ABBIENDI 00g.

<sup>2</sup> ACHARD 04 search for  $\tilde{\tau}\tilde{\tau}$  production in acoplanar di-tau final states in the 192–209 GeV data. Limits on  $m_{\tilde{\tau}_R}$  are derived from a scan over the MSSM parameter space with universal GUT scale gaugino and scalar masses  $m_{1/2}$  and  $m_0$ ,  $1 \leq \tan\beta \leq 60$  and  $-2 \leq \mu \leq 2$  TeV. See Fig. 4 for the dependence of the limits on  $m_{\tilde{\chi}_1^0}$ .

<sup>3</sup> ABDALLAH 03M looked for acoplanar ditau +  $\cancel{E}$  final states at  $\sqrt{s} = 130\text{--}208$  GeV. A dedicated search was made for low mass  $\tilde{\tau}$ s decoupling from the  $Z^0$ . The limit assumes  $B(\tilde{\tau} \rightarrow \tau \tilde{\chi}_1^0) = 100\%$ . See Fig. 20 for limits on the  $(m_{\tilde{\tau}}, m_{\tilde{\chi}_1^0})$  plane and as function

of the  $\tilde{\chi}_1^0$  mass and of the branching ratio. The limit in the low-mass region improves to 29.6 and 31.1 GeV for  $\tilde{\tau}_R$  and  $\tilde{\tau}_1$ , respectively, at  $\Delta m > m_\tau$ . The limit in the high-mass region improves to 84.7 GeV for  $\tilde{\tau}_R$  and  $\Delta m > 15$  GeV. These limits include and update the results of ABREU 01.

<sup>4</sup> HEISTER 02E looked for acoplanar ditau +  $\cancel{E}_T$  final states from  $e^+e^-$  interactions between 183 and 209 GeV. The mass limit assumes  $B(\tilde{\tau} \rightarrow \tau \tilde{\chi}_1^0) = 1$ . See their Fig. 4 for the dependence of the limit on  $\Delta m$ . These limits include and update the results of BARATE 01.

<sup>5</sup> ABBIENDI 06B use 600 pb<sup>-1</sup> of data from  $\sqrt{s} = 189\text{--}209$  GeV. They look for events from pair-produced staus in a GMSB scenario with  $\tilde{\tau}$  NLSP including prompt  $\tilde{\tau}$  decays to ditau +  $\cancel{E}$  final states, large impact parameters, kinked tracks and heavy stable charged particles. Limits on the cross-section are computed as a function of  $m(\tilde{\tau})$  and the lifetime, see their Fig. 7. The limit is compared to the  $\sigma \cdot BR^2$  from a scan over the GMSB parameter space.

<sup>6</sup> ABBIENDI 04F use data from  $\sqrt{s} = 189\text{--}209$  GeV. They derive limits on sparticle masses under the assumption of  $\tilde{R}$  with  $LL\tilde{E}$  or  $LQ\tilde{D}$  couplings. The results are valid for  $\tan\beta = 1.5$ ,  $\mu = -200$  GeV, with, in addition,  $\Delta m > 5$  GeV for indirect decays via  $LQ\tilde{D}$ . The limit quoted applies to direct decays with  $LL\tilde{E}$  couplings and improves to 75 GeV for  $LQ\tilde{D}$  couplings. The limit on the  $\tilde{\tau}_R$  mass for indirect decays is 92 GeV for  $LL\tilde{E}$  couplings at  $m_{\tilde{\chi}_1^0} = 10$  GeV and no exclusion is obtained for  $LQ\tilde{D}$  couplings. Supersedes the results of ABBIENDI 00.

<sup>7</sup> ABDALLAH 04H use data from LEP 1 and  $\sqrt{s} = 192\text{--}208$  GeV. They re-use results or re-analyze the data from ABDALLAH 03M to put limits on the parameter space of anomaly-mediated supersymmetry breaking (AMSB), which is scanned in the region  $1 < m_{3/2} < 50$  TeV,  $0 < m_0 < 1000$  GeV,  $1.5 < \tan\beta < 35$ , both signs of  $\mu$ . The constraints are obtained from the searches for mass degenerate chargino and neutralino, for SM-like and invisible Higgs, for leptonically decaying charginos and from the limit on non-SM  $Z$  width of 3.2 MeV. The limit is for  $m_t = 174.3$  GeV (see Table 2 for other  $m_t$  values).

<sup>8</sup> The limit improves to 75 GeV for  $\mu < 0$ .

<sup>9</sup> ABDALLAH 04M use data from  $\sqrt{s} = 192\text{--}208$  GeV to derive limits on sparticle masses under the assumption of  $\tilde{R}$  with  $LL\tilde{E}$  couplings. The results are valid for  $\mu = -200$  GeV,  $\tan\beta = 1.5$ ,  $\Delta m > 5$  GeV and assuming a BR of 1 for the given decay. The limit quoted is for indirect decays using the neutralino constraint of 39.5 GeV, also derived in ABDALLAH 04M. For indirect decays via  $LL\tilde{E}$  the limit decreases to 86 GeV if the constraint from the neutralino is not used. Supersedes the result of ABREU 00u.

<sup>10</sup> ABDALLAH 03D use data from  $\sqrt{s} = 130\text{--}208$  GeV to search for tracks with large impact parameter or visible decay vertices and for heavy charged stable particles. Limits are obtained as function of  $m(\tilde{G})$ , after combining these results with the search for slepton pair production in the SUGRA framework from ABDALLAH 03M to cover prompt decays. The above limit is reached for the stau decaying promptly,  $m(\tilde{G}) < 6$  eV, and is computed for stau mixing yielding the minimal cross section. Stronger limits are obtained for longer lifetimes. See their Fig. 9. Supersedes the results of ABREU 01g.

<sup>11</sup> HEISTER 03G searches for the production of stau in the case of  $\tilde{R}$  prompt decays with  $LL\tilde{E}$ ,  $LQ\tilde{D}$  or  $UDD$  couplings at  $\sqrt{s} = 189\text{--}209$  GeV. The search is performed for direct and indirect decays, assuming one coupling at a time to be non-zero. The limit holds for indirect decays mediated by  $\tilde{R}$   $UDD$  couplings with  $\Delta m > 10$  GeV. Limits are also given

for  $LL\tilde{E}$  direct ( $m_{\tilde{\tau}_R} > 87$  GeV) and indirect decays ( $m_{\tilde{\tau}_R} > 95$  GeV for  $m(\tilde{\chi}_1^0) > 23$  GeV from BARATE 98s) and for  $LQ\tilde{D}$  indirect decays ( $m_{\tilde{\tau}_R} > 76$  GeV). Supersedes the results from BARATE 01b.

<sup>12</sup> ACHARD 02 searches for the production of staus in the case of  $\tilde{R}$  prompt decays with  $LL\tilde{E}$  or  $UDD$  couplings at  $\sqrt{s} = 189\text{--}208$  GeV. The search is performed for direct and indirect decays, assuming one coupling at the time to be nonzero. The limit holds for direct decays via  $LL\tilde{E}$  couplings. Stronger limits are reached for  $LL\tilde{E}$  indirect (86 GeV) and for  $UDD$  direct or indirect (75 GeV) decays.

<sup>13</sup> HEISTER 02R search for signals of GMSB in the 189–209 GeV data. For the  $\tilde{\chi}_1^0$  NLSP scenario, they looked for topologies consisting of  $\gamma\gamma\cancel{E}$  or a single  $\gamma$  not pointing to the interaction vertex. For the  $\tilde{\ell}$  NLSP case, the topologies consist of  $\ell\ell\cancel{E}$ , including leptons with large impact parameters, kinks, or stable particles. Limits are derived from a scan over the GMSB parameters (see their Table 5 for the ranges). The limit remains valid whichever is the NLSP. The absolute mass bound on the  $\tilde{\chi}_1^0$  for any lifetime includes indirect limits from the slepton search HEISTER 02e performed within the MSUGRA framework. A bound for any NLSP and any lifetime of 77 GeV has also been derived by using the constraints from the neutral Higgs search in HEISTER 02. In the co-NLSP scenario, limits  $m_{\tilde{\tau}_R} > 83$  GeV (neglecting t-channel exchange) and  $m_{\tilde{\mu}_R} > 88$  GeV are obtained independent of the lifetime. Supersedes the results from BARATE 00g.

<sup>14</sup> BARATE 01 looked for acoplanar ditau +  $\cancel{E}_T$  final states at 189 to 202 GeV. A slight excess (with 1.2% probability) of events is observed relative to the expected SM background. The limit assumes 100% branching ratio for  $\tilde{\tau} \rightarrow \tau \tilde{\chi}_1^0$ . See their Fig. 1 for the dependence of the limit on  $\Delta m$ . These limits include and update the results of BARATE 99g.

<sup>15</sup> ABBIENDI 00j looked for acoplanar ditau +  $\cancel{E}_T$  final states at  $\sqrt{s} = 161\text{--}183$  GeV. The limit assumes  $B(\tilde{\tau} \rightarrow \tau \tilde{\chi}_1^0) = 1$ . Using decay branching ratios derived from the MSSM, a lower limit of 60 GeV at  $\Delta m > 9$  GeV is obtained for  $\mu < -100$  GeV and  $\tan\beta = 1.5$ . See their Figs. 11 and 14 for the dependence of the limit on the branching ratio and on  $\Delta m$ .

<sup>16</sup> ABREU 00v use data from  $\sqrt{s} = 130\text{--}189$  GeV to search for tracks with large impact parameter or visible decay vertices. Limits are obtained as function of  $m_{\tilde{G}}$ , after combining these results with the search for slepton pair production in the SUGRA framework from ABREU 01 to cover prompt decays and on stable particle searches from ABREU 00q. The above limit assumes the degeneracy of stau and smuon. For limits at different  $m_{\tilde{G}}$ , see their Fig. 12.

<sup>17</sup> ABREU 00v use data from  $\sqrt{s} = 130\text{--}189$  GeV to search for tracks with large impact parameter or visible decay vertices. Limits are obtained as function of  $m_{\tilde{G}}$ , after combining these results with the search for slepton pair production in the SUGRA framework from ABREU 01 to cover prompt decays and on stable particle searches from ABREU 00q. The above limit is reached for the stau mixing yielding the minimal cross section and decaying promptly. Stronger limits are obtained for longer lifetimes or for  $\tilde{\tau}_R$ ; see their Fig. 11. For  $10 \leq m_{\tilde{G}} \leq 310$  eV, the whole range  $2 \leq m_{\tilde{\tau}_1} \leq 80$  GeV is excluded. Supersedes the results of ABREU 99c and ABREU 99f.

<sup>18</sup> BARATE 98k looked for  $\tau^+ \tau^- \gamma \gamma + \cancel{E}$  final states at  $\sqrt{s} = 161\text{--}184$  GeV. See Fig. 4 for limits on the  $(m_{\tilde{\tau}_R}, m_{\tilde{\chi}_1^0})$  plane and for the effect of cascade decays.

### Degenerate Charged Sleptons

Unless stated otherwise in the comment lines or in the footnotes, the following limits assume 3 families of degenerate charged sleptons.

VALUE (GeV)	CL%	DOCUMENT ID	TECN	COMMENT
>93	95	<sup>1</sup> BARATE 01	ALEP	$\Delta m > 10$ GeV, $\tilde{\ell}_R^+ \tilde{\ell}_R^-$
>70	95	<sup>1</sup> BARATE 01	ALEP	all $\Delta m$ , $\tilde{\ell}_R^+ \tilde{\ell}_R^-$
• • • We do not use the following data for averages, fits, limits, etc. • • •				
>91.9	95	<sup>2</sup> ABBIENDI 06B	OPAL	$\tilde{\ell}_R \rightarrow \ell \tilde{G}$ , all $\ell(\tilde{\ell}_R)$
>88	95	<sup>3</sup> ABDALLAH 03D	DLPH	$\tilde{\ell}_R \rightarrow \ell \tilde{G}$ , all $\ell(\tilde{\ell}_R)$
>82.7	95	<sup>4</sup> ACHARD 02	L3	$\tilde{\ell}_R, \tilde{R}$ decays, MSUGRA
>83	95	<sup>5</sup> ABBIENDI 01	OPAL	$e^+e^- \rightarrow \tilde{\ell}_1 \tilde{\ell}_1$ , GMSB, $\tan\beta = 2$
>68.8	95	<sup>6</sup> ABREU 01	DLPH	$\tilde{\ell} \rightarrow \ell \tilde{\chi}_2^0, \tilde{\chi}_2^0 \rightarrow \gamma \tilde{\chi}_1^0$ , $\ell = e, \mu$
>84	95	<sup>7</sup> ACCIARRI 01	L3	$\tilde{\ell}_R, \tilde{R}, 0.7 \leq \tan\beta \leq 40$
>84	95	<sup>8,9</sup> ABREU 00V	DLPH	$\tilde{\ell}_R \tilde{\ell}_R$ ( $\tilde{\ell}_R \rightarrow \ell \tilde{G}$ ), $m_{\tilde{G}} > 9$ eV

<sup>1</sup> BARATE 01 looked for acoplanar dilepton +  $\cancel{E}_T$  and single electron (for  $\tilde{e}_R \tilde{e}_L$ ) final states at 189 to 202 GeV. The limit assumes  $\mu = -200$  GeV and  $\tan\beta = 2$  for the production cross section and decay branching ratios, evaluated within the MSSM, and zero efficiency for decays other than  $\tilde{\ell} \rightarrow \ell \tilde{\chi}_1^0$ . The slepton masses are determined from the GUT relations without stau mixing. See their Fig. 1 for the dependence of the limit on  $\Delta m$ .

<sup>2</sup> ABBIENDI 06B use 600 pb<sup>-1</sup> of data from  $\sqrt{s} = 189\text{--}209$  GeV. They look for events from pair-produced staus in a GMSB scenario with  $\tilde{\ell}$  co-NLSP including prompt  $\tilde{\ell}$  decays to dileptons +  $\cancel{E}$  final states, large impact parameters, kinked tracks and heavy stable charged particles. Limits on the cross-section are computed as a function of  $m(\tilde{\ell})$  and the lifetime, see their Fig. 7. The limit is compared to the  $\sigma \cdot BR^2$  from a scan over the GMSB parameter space. The highest mass limit is reached for  $\tilde{\mu}_R$ , from which the quoted mass limit is derived by subtracting  $m_\tau$ .

<sup>3</sup> ABDALLAH 03D use data from  $\sqrt{s} = 130\text{--}208$  GeV to search for tracks with large impact parameter or visible decay vertices and for heavy charged stable particles. Limits are obtained as function of  $m(\tilde{G})$ , after combining these results with the search for slepton pair production in the SUGRA framework from ABDALLAH 03M to cover prompt decays. The above limit is reached for prompt decays and assumes the degeneracy of the sleptons. For limits at different  $m(\tilde{G})$ , see their Fig. 9. Supersedes the results of ABREU 01g.

<sup>4</sup> ACHARD 02 searches for the production of sparticles in the case of  $\tilde{R}$  prompt decays with  $LL\tilde{E}$  or  $UDD$  couplings at  $\sqrt{s} = 189\text{--}208$  GeV. The search is performed for direct and indirect decays, assuming one coupling at the time to be nonzero. The MSUGRA limit results from a scan over the MSSM parameter space with the assumption of gaugino and scalar mass unification at the GUT scale and no mixing in the slepton sector, imposing simultaneously the exclusions from neutralino, chargino, sleptons, and squarks analyses. The limit holds for  $LL\tilde{E}$  couplings and increases to 88.7 GeV for  $UDD$  couplings. For L3 limits from  $LQ\tilde{D}$  couplings, see ACCIARRI 01.

- 5 ABBIENDI 01 looked for final states with  $\gamma\gamma\mathbb{E}$ ,  $\ell\ell\mathbb{E}$ , with possibly additional activity and four leptons +  $\mathbb{E}$  to search for prompt decays of  $\tilde{\chi}_1^0$  or  $\tilde{\ell}_1$  in GMSB. They derive limits in the plane  $(m_{\tilde{\chi}_1^0}, m_{\tilde{\tau}_1})$ , see Fig. 6, allowing either the  $\tilde{\chi}_1^0$  or a  $\tilde{\ell}_1$  to be the NLSP. Two scenarios are considered:  $\tan\beta=2$  with the 3 sleptons degenerate in mass and  $\tan\beta=20$  where the  $\tilde{\tau}_1$  is lighter than the other sleptons. Data taken at  $\sqrt{s}=189$  GeV. For  $\tan\beta=20$ , the obtained limits are  $m_{\tilde{\tau}_1} > 69$  GeV and  $m_{\tilde{e}_1, \tilde{\mu}_1} > 88$  GeV.
- 6 ABREU 01 looked for acoplanar dilepton + diphoton +  $\mathbb{E}$  final states from  $\tilde{\ell}$  cascade decays at  $\sqrt{s}=130-189$  GeV. See Fig. 9 for limits on the  $(\mu, M_2)$  plane for  $m_{\tilde{\ell}}=80$  GeV,  $\tan\beta=1.0$ , and assuming degeneracy of  $\tilde{\mu}$  and  $\tilde{e}$ .
- 7 ACCIARRI 01 searches for multi-lepton and/or multi-jet final states from  $\mathbb{R}$  prompt decays with  $LLE$ ,  $LQ\bar{D}$ , or  $UDD$  couplings at  $\sqrt{s}=189$  GeV. The search is performed for direct and indirect decays of neutralinos, charginos, and scalar leptons, with the  $\tilde{\chi}_1^0$  or a  $\tilde{\ell}$  as LSP and assuming one coupling to be nonzero at a time. Mass limits are derived using simultaneously the constraints from the neutralino, chargino, and slepton analyses; and the  $Z^0$  width measurements from ACCIARRI 00c in a scan of the parameter space assuming MSUGRA with gaugino and scalar mass universality. Updates and supersedes the results from ACCIARRI 99i.
- 8 ABREU 00v use data from  $\sqrt{s}=130-189$  GeV to search for tracks with large impact parameter or visible decay vertices. Limits are obtained as function of  $m_{\tilde{G}}$ , after combining these results with the search for slepton pair production in the SUGRA framework from ABREU 01 to cover prompt decays and on stable particle searches from ABREU 00q. For limits at different  $m_{\tilde{G}}$ , see their Fig. 12.
- 9 The above limit assumes the degeneracy of stau and smuon.

**Long-lived  $\tilde{\ell}$  (Slepton) MASS LIMIT**

Limits on scalar leptons which leave detector before decaying. Limits from Z decays are independent of lepton flavor. Limits from continuum  $e^+e^-$  annihilation are also independent of flavor for smuons and staus. Selection limits from  $e^+e^-$  collisions in the continuum depend on MSSM parameters because of the additional neutralino exchange contribution.

VALUE (GeV)	CL%	DOCUMENT ID	TECN	COMMENT
> 98	95	1 ABBIENDI	03L OPAL	$\tilde{\mu}_R, \tilde{\tau}_R$
<b>none 2-87.5</b>		2 ABREU	00q DLPH	$\tilde{\mu}_R, \tilde{\tau}_R$
> 81.2	95	3 ACCIARRI	99H L3	$\tilde{\mu}_R, \tilde{\tau}_R$
> 81	95	4 BARATE	98K ALEP	$\tilde{\mu}_R, \tilde{\tau}_R$
> 136	95	5 AAD	11P ATLS	stable $\tilde{\tau}$ , GMSB scenario, $\tan\beta=5$

- 1 ABBIENDI 03L used  $e^+e^-$  data at  $\sqrt{s}=130-209$  GeV to select events with two high momentum tracks with anomalous dE/dx. The excluded cross section is compared to the theoretical expectation as a function of the heavy particle mass in their Fig. 3. The limit improves to 98.5 GeV for  $\tilde{\mu}_L$  and  $\tilde{\tau}_L$ . The bounds are valid for colorless spin 0 particles with lifetimes longer than  $10^{-6}$  s. Supersedes the results from ACKERSTAFF 98P.
- 2 ABREU 00q searches for the production of pairs of heavy, charged stable particles in  $e^+e^-$  annihilation at  $\sqrt{s}=130-189$  GeV. The upper bound improves to 88 GeV for  $\tilde{\mu}_L, \tilde{\tau}_L$ . These limits include and update the results of ABREU 98P.
- 3 ACCIARRI 99H searched for production of pairs of back-to-back heavy charged particles at  $\sqrt{s}=130-183$  GeV. The upper bound improves to 82.2 GeV for  $\tilde{\mu}_L, \tilde{\tau}_L$ .
- 4 The BARATE 98K mass limit improves to 82 GeV for  $\tilde{\mu}_L, \tilde{\tau}_L$ . Data collected at  $\sqrt{s}=161-184$  GeV.
- 5 AAD 11P looked in 37 pb $^{-1}$  of  $pp$  collisions at  $\sqrt{s}=7$  TeV for events with two heavy stable particles, reconstructed in the Inner tracker and the Muon System and identified by their time of flight in the Muon System. No evidence for an excess over the SM expectation is observed. Limits on the mass are derived, see Fig. 3, for  $\tilde{\tau}$  in a GMSB scenario and for sleptons produced by electroweak processes only, in which case the limit degrades to 110 GeV.

**$\tilde{q}$  (Squark) MASS LIMIT**

For  $m_{\tilde{q}} > 60-70$  GeV, it is expected that squarks would undergo a cascade decay via a number of neutralinos and/or charginos rather than undergo a direct decay to photinos as assumed by some papers. Limits obtained when direct decay is assumed are usually higher than limits when cascade decays are included.

Limits from  $e^+e^-$  collisions depend on the mixing angle of the lightest mass eigenstate  $\tilde{q}_1 = \tilde{q}_R \sin\theta + \tilde{q}_L \cos\theta$ . It is usually assumed that only the sbottom and stop squarks have non-trivial mixing angles (see the stop and sbottom sections). Here, unless otherwise noted, squarks are always taken to be either left/right degenerate, or purely of left or right type. Data from Z decays have set squark mass limits above 40 GeV, in the case of  $\tilde{q} \rightarrow q\tilde{\chi}_1^0$  decays if  $\Delta m = m_{\tilde{q}} - m_{\tilde{\chi}_1^0} \gtrsim 5$  GeV. For smaller values of  $\Delta m$ , current constraints on the invisible width of the Z ( $\Delta\Gamma_{inv} < 2.0$  MeV, LEP 00) exclude  $m_{\tilde{u}_{L,R}} < 44$  GeV,  $m_{\tilde{d}_R} < 33$  GeV,  $m_{\tilde{d}_L} < 44$  GeV and, assuming all squarks degenerate,  $m_{\tilde{q}} < 45$  GeV.

Limits made obsolete by the most recent analyses of  $e^+e^-$ ,  $p\bar{p}$ , and  $ep$  collisions can be found in previous Editions of this Review.

VALUE (GeV)	CL%	DOCUMENT ID	TECN	COMMENT
> 690	95	1 AAD	11B ATLS	$\ell^\pm \ell^\pm + \mathbb{E}_T$ , $m_{\tilde{g}}=m_{\tilde{q}}+10\text{GeV}$ , $m_{\tilde{\chi}_1^0}=100\text{GeV}$ , $\tan\beta=4$
> 550	95	1 AAD	11B ATLS	$\ell^+ \ell^- + \mathbb{E}_T$ , $m_{\tilde{g}}=m_{\tilde{q}}+10\text{GeV}$ , $m_{\tilde{\chi}_1^0}=100\text{GeV}$ , $\tan\beta=4$

> 558	95	2 AAD	11c ATLS	$\ell^+ \ell^- + \text{jets} + \mathbb{E}_T$ , $m_{\tilde{g}}=m_{\tilde{q}}+10\text{GeV}$ , $m_{\tilde{\chi}_1^0}=100\text{GeV}$ , $\tan\beta=4$
> 700	95	3 AAD	11G ATLS	$\ell + \text{jets} + \mathbb{E}_T$ , $\tan\beta=3$ , $A_0=0$ , $\mu > 0$ , $m_{\tilde{g}}=m_{\tilde{q}}$
> 870	95	4 AAD	11N ATLS	$\text{jets} + \mathbb{E}_T$ , degenerate $m_{\tilde{q}}$ of first two generations, $m_{\tilde{\chi}_1^0}=0$ , all other supersymmetric particles heavy, $m_{\tilde{q}}=m_{\tilde{g}}$
> 775	95	4 AAD	11N ATLS	$\text{jets} + \mathbb{E}_T$ , CMSSM, $m_{\tilde{q}}=m_{\tilde{g}}$
> 1100	95	5 CHATRCHYAN	11W CMS	$\text{jets} + \mathbb{E}_T$ , CMSSM
> 392	95	6 AALTONEN	09S CDF	$\text{jets} + \mathbb{E}_T$ , $m_{\tilde{q}}=m_{\tilde{g}}$
> 379	95	7 ABAZOV	08G D0	$\text{jets} + \mathbb{E}_T$ , $\tan\beta=3$ , $\mu < 0$ , $A_0=0$ , any $m_{\tilde{g}}$
> 99.5		8 ACHARD	04 L3	$\Delta m > 10$ GeV, $e^+e^- \rightarrow \bar{q}_L, R \bar{q}_L, R$
> 97		8 ACHARD	04 L3	$\Delta m > 10$ GeV, $e^+e^- \rightarrow \bar{q}_R \bar{q}_R$
> 138	95	9 ABBOTT	01D D0	$\ell\ell + \text{jets} + \mathbb{E}_T$ , $\tan\beta < 10$ , $m_0 < 300$ GeV, $\mu < 0$ , $A_0=0$
> 255	95	9 ABBOTT	01D D0	$\tan\beta=2$ , $m_{\tilde{g}}=m_{\tilde{q}}$ , $\mu < 0$ , $A_0=0$ , $\ell\ell + \text{jets} + \mathbb{E}_T$
> 97	95	10 BARATE	01 ALEP	$e^+e^- \rightarrow \bar{q}\bar{q}$ , $\Delta m > 6$ GeV
> 224	95	11 ABE	96D CDF	$m_{\tilde{g}} \leq m_{\tilde{q}}$ ; with cascade decays, $\ell\ell + \text{jets} + \mathbb{E}_T$
••• We do not use the following data for averages, fits, limits, etc. •••				
		12 CHATRCHYAN	12 CMS	$e, \mu$ , jets, razor, CMSSM
		13 AAD	11AE ATLS	$\ell^\pm \ell^\pm$
		14 AAD	11AF ATLS	$\geq 6$ jets + $\mathbb{E}_T$ , CMSSM
	95	15 AARON	11 H1	$e^-p \rightarrow \bar{d}_R, R, L Q\bar{D}$ , $\lambda'=0.3$
	95	15 AARON	11 H1	$e^+p \rightarrow \bar{u}_L, R, L Q\bar{D}$ , $\lambda'=0.3$
	95	16 AARON	11c H1	$\bar{u}, R, L Q\bar{D}$ , $\lambda'=0.3$
		17 CHATRCHYAN	11AC CMS	$\text{jets} + \mathbb{E}_T$ , CMSSM
		18 CHATRCHYAN	11B CMS	$\tilde{q} \rightarrow X\tilde{\chi}_1^0 \rightarrow X\ell^+ \ell^- \tilde{\chi}_1^0$
		19 CHATRCHYAN	11G CMS	$\tilde{\chi}_1^0 \rightarrow \gamma\tilde{G}$
		20 CHATRCHYAN	11Q CMS	$\ell + \text{jets} + \mathbb{E}_T$
	95	21 CHATRCHYAN	11V CMS	GMSB scenario, $\tilde{\ell}$ co-NLSP
		22 CHATRCHYAN	11V CMS	$R$
		23 KHACHATRY...	11I CMS	$\text{jets} + \mathbb{E}_T$
		24 ABAZOV	09S D0	$\text{jets} + \tau + \mathbb{E}_T$ , $\tan\beta=15$ , $\mu < 0$ , $A_0=-2m_0$
	95	25 SCHAEEL	07A ALEP	$\bar{d}_R, R, \lambda=0.3$
	95	25 SCHAEEL	07A ALEP	$\bar{s}_R, R, \lambda=0.3$
	95	26 CHEKANOV	05A ZEUS	$\tilde{q} \rightarrow \mu q, R, L Q\bar{D}$ , $\lambda=0.3$
	95	26 CHEKANOV	05A ZEUS	$\tilde{q} \rightarrow \tau q, R, L Q\bar{D}$ , $\lambda=0.3$
		27 AKTAS	04D H1	$e^\pm p \rightarrow \bar{u}_L, R, L Q\bar{D}$
		27 AKTAS	04D H1	$e^\pm p \rightarrow \bar{D}_R, R, L Q\bar{D}$
		28 ADLOFF	03 H1	$e^\pm p \rightarrow \bar{q}, R, L Q\bar{D}$
	95	29 CHEKANOV	03B ZEUS	$\bar{d} \rightarrow e^- u, \nu d, R, L Q\bar{D}$ , $\lambda > 0.1$
	95	29 CHEKANOV	03B ZEUS	$\bar{u} \rightarrow e^+ d, R, L Q\bar{D}$ , $\lambda > 0.1$
	95	30 HEISTER	03G ALEP	$\bar{u}_R, R$ decay
	95	30 HEISTER	03G ALEP	$\bar{d}_R, R$ decay
	95	31 ABAZOV	02F D0	$\bar{q}, R \lambda'_{2jk}$ indirect decays, $\tan\beta=2$ , any $m_{\tilde{g}}$
	95	31 ABAZOV	02F D0	$\bar{q}, R \lambda'_{2jk}$ indirect decays, $\tan\beta=2$ , $m_{\tilde{q}}=m_{\tilde{g}}$
		32 ABAZOV	02G D0	$p\bar{p} \rightarrow \bar{g}\bar{g}, \bar{g}\bar{q}$
	95	33 ABBIENDI	02 OPAL	$e\gamma \rightarrow \bar{u}_L, R L Q\bar{D}$ , $\lambda=0.3$
	95	33 ABBIENDI	02 OPAL	$e\gamma \rightarrow \bar{d}_R, R L Q\bar{D}$ , $\lambda=0.3$
	95	34 ABBIENDI	02B OPAL	$e\gamma \rightarrow \bar{u}_L, R L Q\bar{D}$ , $\lambda=0.3$
	95	34 ABBIENDI	02B OPAL	$e\gamma \rightarrow \bar{d}_R, R L Q\bar{D}$ , $\lambda=0.3$
	95	35 ACHARD	02 L3	$\bar{u}_R, R$ decays
	95	35 ACHARD	02 L3	$\bar{d}_R, R$ decays
	95	36 CHEKANOV	02 ZEUS	$\bar{u}_L \rightarrow \mu q, R, L Q\bar{D}$ , $\lambda=0.3$
	95	36 CHEKANOV	02 ZEUS	$\bar{u}_L \rightarrow \tau q, R, L Q\bar{D}$ , $\lambda=0.3$
	95	37 BARATE	01B ALEP	$\bar{u}_R, R$ decays
	95	37 BARATE	01B ALEP	$\bar{d}_R, R$ decays
	95	38 BREITWEG	01 ZEUS	$e^+p \rightarrow \bar{d}_R, R L Q\bar{D}$ , $\lambda=0.3$
	95	39 ABBOTT	00C D0	$\bar{u}_L, R, \lambda'_{2jk}$ decays
	95	39 ABBOTT	00C D0	$\bar{d}_R, R, \lambda'_{2jk}$ decays
	95	40 ACCIARRI	00P L3	$e^+e^- \rightarrow q\bar{q}, R, \lambda=0.3$
	95	41 AFFOLDER	00K CDF	$\bar{d}_L, R \lambda'_{1j3}$ decays
	95	42 BARATE	00I ALEP	$e^+e^- \rightarrow q\bar{q}, R, \lambda=0.3$
	95	43 BREITWEG	00E ZEUS	$e^+p \rightarrow \bar{u}_L, R, L Q\bar{D}$ , $\lambda=0.3$
	95	44 ABBOTT	99 D0	$\tilde{q} \rightarrow \tilde{\chi}_2^0 X \rightarrow \tilde{\chi}_1^0 \gamma X$ , $m_{\tilde{\chi}_2^0} - m_{\tilde{\chi}_1^0} > 20$ GeV
	95	44 ABBOTT	99 D0	$\tilde{q} \rightarrow \tilde{\chi}_1^0 X \rightarrow \tilde{G} \gamma X$
	95	45 ABBOTT	99K D0	any $m_{\tilde{g}}, R, \tan\beta=2, \mu < 0$

# Searches Particle Listings

## Supersymmetric Particle Searches

> 250	95	46	ABBOTT	99L	D0	$\tan\beta=2, \mu < 0, A=0, \text{jets} + \cancel{E}_T$
> 200	95	47	ABE	99M	CDF	$p\bar{p} \rightarrow \bar{q}\bar{q}, R$
none 80–134	95	48	ABREU	99G	DLPH	$e\gamma \rightarrow \bar{u}_L, R, LQ\bar{D}, \lambda=0.3$
none 80–161	95	48	ABREU	99G	DLPH	$e\gamma \rightarrow \bar{d}_R, R, LQ\bar{D}, \lambda=0.3$
> 225	95	49	ABBOTT	98E	D0	$\bar{u}_L, R, \lambda'_{ijk}$ decays
> 204	95	49	ABBOTT	98E	D0	$\bar{d}_R, R, \lambda'_{ijk}$ decays
> 79	95	49	ABBOTT	98E	D0	$\bar{d}_L, R, \lambda'_{ijk}$ decays
> 202	95	50	ABE	98S	CDF	$\bar{u}_L, R, \lambda'_{2jk}$ decays
> 160	95	50	ABE	98S	CDF	$\bar{d}_R, R, \lambda'_{2jk}$ decays
> 140	95	51	ACKERSTAFF	98V	OPAL	$e^+e^- \rightarrow q\bar{q}, R, \lambda=0.3$
> 77	95	52	BREITWEG	98	ZEUS	$m_{\tilde{q}} = m_{\tilde{e}}, m(\tilde{\chi}_1^0) = 40 \text{ GeV}$
		53	DATTA	97	THEO	$\tilde{\nu}$ 's lighter than $\tilde{\chi}_1^\pm, \tilde{\chi}_2^0$
> 216	95	54	DERRICK	97	ZEUS	$e\bar{p} \rightarrow \bar{q}, \bar{q} \rightarrow \mu\bar{j}$ or $\tau\bar{j}, R$
none 130–573	95	55	HEWETT	97	THEO	$q\bar{g} \rightarrow \bar{q}, \bar{q} \rightarrow q\bar{g}$ , with a light gluino
none 190–650	95	56	TEREKHOV	97	THEO	$q\bar{g} \rightarrow \bar{q}\bar{g}, \bar{q} \rightarrow q\bar{g}$ , with a light gluino
> 63	95	57	AID	96C	H1	$m_{\tilde{q}} = m_{\tilde{e}}, m_{\tilde{\chi}_1^0} = 35 \text{ GeV}$
none 330–400	95	58	TEREKHOV	96	THEO	$u\bar{g} \rightarrow \bar{u}\bar{g}, \bar{u} \rightarrow u\bar{g}$ with a light gluino
> 176	95	59	ABACHI	95C	D0	Any $m_{\tilde{g}} < 300 \text{ GeV}$ ; with cascade decays
		60	ABE	95T	CDF	$\bar{q} \rightarrow \tilde{\chi}_2^0 \rightarrow \tilde{\chi}_1^0\gamma$
> 90	90	61	ABE	92L	CDF	Any $m_{\tilde{g}} < 410 \text{ GeV}$ ; with cascade decay
> 100		62	ROY	92	RVUE	$p\bar{p} \rightarrow \bar{q}\bar{q}; R$
		63	NOJIRI	91	COSM	

- 1 AAD 11B looked in 35 pb<sup>-1</sup> of  $pp$  collisions at  $\sqrt{s} = 7 \text{ TeV}$  for events with same or opposite charge dileptons ( $e$  or  $\mu$ ) and  $\cancel{E}_T$  from the production of squarks and gluinos with leptonic decays from  $\tilde{\chi}_1^\pm$  or  $\tilde{\chi}_2^0$ . No evidence for an excess over the SM expectation is observed, and limits are derived in the CMSSM ( $m_0, m_{1/2}$ ) plane (see Fig. 2) and in the  $(m_{\tilde{g}}, m_{\tilde{q}})$  plane under the assumptions  $\tan\beta = 4, \mu = 1.5 M, m_{\tilde{\chi}_2^0} = M - 100 \text{ GeV}, m_{\tilde{L}} = M/2, m_{\tilde{\chi}_1^0} = 100 \text{ GeV}$ , where  $M = \min(m_{\tilde{g}}, m_{\tilde{q}})$  (see Fig. 3). The exclusion limit for a compressed spectrum is 590 GeV for the same charge and 450 GeV for the opposite charge events.
- 2 AAD 11C looked in 35 pb<sup>-1</sup> of  $pp$  collisions at  $\sqrt{s} = 7 \text{ TeV}$  for events with jets, same flavor opposite charge dileptons ( $e$  or  $\mu$ ) and  $\cancel{E}_T$  from the production of squarks and gluinos with decays  $\bar{q} \rightarrow q\tilde{\chi}_2^0$  and  $\tilde{\chi}_2^0 \rightarrow \ell^+\ell^-\tilde{\chi}_1^0$ . No evidence for an excess over the SM expectation is observed, and a limit is derived in the  $(m_{\tilde{g}}, m_{\tilde{q}})$  plane under the assumptions  $\tan\beta = 4, \mu = 1.5 M, m_{\tilde{\chi}_2^0} = M - 100 \text{ GeV}, m_{\tilde{L}} = M/2, m_{\tilde{\chi}_1^0} = 100 \text{ GeV}$ , where  $M = \min(m_{\tilde{g}}, m_{\tilde{q}})$ . The excluded mass region is shown in a plane of  $(m_{\tilde{g}}, m_{\tilde{q}})$ , see their Fig. 3. The exclusion limit for a compressed spectrum is 503 GeV.
- 3 AAD 11G looked in 35 pb<sup>-1</sup> of  $pp$  collisions at  $\sqrt{s} = 7 \text{ TeV}$  for events with a single lepton ( $e$  or  $\mu$ ), jets and  $\cancel{E}_T$  from the production of squarks and gluinos. No evidence for an excess over the SM expectation is observed, and a limit is derived in the CMSSM ( $m_0, m_{1/2}$ ) plane for  $\tan\beta = 3$ , see Fig. 2.
- 4 AAD 11N looked in 35 pb<sup>-1</sup> of  $pp$  collisions at  $\sqrt{s} = 7 \text{ TeV}$  for events with  $\geq 2$  jets and  $\cancel{E}_T$ . Four signal regions were defined, and the background model was found to be in good agreement with the data. Limits are derived in the  $(m_{\tilde{g}}, m_{\tilde{q}})$  plane (see Fig. 2) for a simplified model where degenerate masses of the squarks of the first two generations are assumed,  $m_{\tilde{\chi}_1^0} = 0$ , and all other masses including third generation squarks are set to 5 TeV. Limits are also derived in the CMSSM ( $m_0, m_{1/2}$ ) plane (see Fig. 3) for  $\tan\beta = 3$ .
- 5 CHATRCHYAN 11W looked in 1.14 fb<sup>-1</sup> of  $pp$  collisions at  $\sqrt{s} = 7 \text{ TeV}$  for events with  $\geq 2$  jets, large total jet energy, and  $\cancel{E}_T$ . After combining multi-jet events into two pseudo-jets signal events are selected by a cut on  $\alpha_T = E_T^2/M_T$ , the transverse energy of the less energetic jet over the transverse mass. Given the lack of an excess over the SM backgrounds, limits are derived in the CMSSM ( $m_0, m_{1/2}$ ) plane (see Fig. 4) for  $\tan\beta = 10$ . The limits are only weakly dependent on  $\tan\beta$  and  $A_0$ .
- 6 AALTONEN 09s searched in 2 fb<sup>-1</sup> of  $p\bar{p}$  collisions at  $\sqrt{s} = 1.96 \text{ TeV}$  for events with at least 2 jets and  $\cancel{E}_T$ . No evidence for a signal is observed. A limit is derived for a mSUGRA scenario in the  $m_{\tilde{q}}$  versus  $m_{\tilde{g}}$  plane, see their Fig. 2. For  $m_{\tilde{g}} < 340 \text{ GeV}$  the bound increases to 400 GeV.
- 7 ABAZOV 08G looked in 2.1 fb<sup>-1</sup> of  $p\bar{p}$  collisions at  $\sqrt{s} = 1.96 \text{ TeV}$  for events with acoplanar jets or multijets with large  $\cancel{E}_T$ . No significant excess was found compared to the background expectation. A limit is derived on the masses of squarks and gluinos for specific MSUGRA parameter values, see Figure 3. Similar results would be obtained for a large class of parameter sets. Supersedes the results of ABAZOV 06c.
- 8 ACHARD 04 search for the production of  $q\bar{q}$  of the first two generations in acoplanar di-jet final states in the 192–209 GeV data. Degeneracy of the squark masses is assumed either for both left and right squarks or for right squarks only, as well as  $B(\bar{q} \rightarrow q\tilde{\chi}_1^0) = 1$ . See Fig. 7 for the dependence of the limits on  $m_{\tilde{\chi}_1^0}$ . This limit supersedes ACCIARRI 99v.
- 9 ABBOTT 01D looked in  $\sim 108 \text{ pb}^{-1}$  of  $p\bar{p}$  collisions at  $\sqrt{s} = 1.8 \text{ TeV}$  for events with  $e, \mu, \mu, \mu$ , or  $e\mu$  accompanied by at least 2 jets and  $\cancel{E}_T$ . Excluded regions are obtained in the MSUGRA framework from a scan over the parameters  $0 < m_0 < 300 \text{ GeV}, 10 < m_{1/2} < 110 \text{ GeV}$ , and  $1.2 < \tan\beta < 10$ .
- 10 BARATE 01 looked for acoplanar dijets +  $\cancel{E}_T$  final states at 189 to 202 GeV. The limit assumes  $B(\bar{q} \rightarrow q\tilde{\chi}_1^0) = 1$ , with  $\Delta m = m_{\tilde{q}} - m_{\tilde{\chi}_1^0}$ . It applies to  $\tan\beta = 4, \mu = -400 \text{ GeV}$ . See their Fig. 2 for the exclusion in the  $(m_{\tilde{q}}, m_{\tilde{g}})$  plane. These limits include and update the results of BARATE 99Q.
- 11 ABE 96D searched for production of gluinos and five degenerate squarks in final states containing a pair of leptons, two jets, and missing  $\cancel{E}_T$ . The two leptons arise from the semileptonic decays of charginos produced in the cascade decays. The limit is derived for

- fixed  $\tan\beta = 4.0, \mu = -400 \text{ GeV}$ , and  $m_{H^\pm} = 500 \text{ GeV}$ , and with the cascade decays of the squarks and gluinos calculated within the framework of the Minimal Supergravity scenario.
- 12 CHATRCHYAN 12 looked in 35 pb<sup>-1</sup> of  $pp$  collisions at  $\sqrt{s} = 7 \text{ TeV}$  for events with  $e$  and/or  $\mu$  and/or jets, a large total transverse energy, and  $\cancel{E}_T$ . The event selection is based on the dimensionless razor variable  $R$ , related to the  $\cancel{E}_T$  and  $M_R$ , an indicator of the heavy particle mass scale. No evidence for an excess over the expected background is observed. Limits are derived in the CMSSM ( $m_0, m_{1/2}$ ) plane for  $\tan\beta = 3, 10$  and 50 (see Fig. 7 and 8). Limits are also obtained for Simplified Model Spectra.
- 13 AAD 11AE looked in 34 pb<sup>-1</sup> of  $pp$  collisions at  $\sqrt{s} = 7 \text{ TeV}$  for events with  $\geq 2$  same charge isolated leptons ( $e, \mu$ ) and  $\geq 1$  jet. They are assumed to come from  $q\bar{q}$  production, where the  $\bar{q}$  decays to  $\tilde{\chi}_1^\pm$  or  $\tilde{\chi}_2^0$  with equal branching ratios, followed by the decays  $\tilde{\chi}_1^\pm \rightarrow W^\pm\tilde{\chi}_1^0$  and  $\tilde{\chi}_2^0 \rightarrow Z^0\tilde{\chi}_1^0$ . No evidence for an excess over the expected background is observed. Limits are derived on the cross sections as a function of the masses of the  $\bar{q}, \tilde{\chi}_1^\pm/\tilde{\chi}_2^0$  and  $\tilde{\chi}_1^0$  (see Fig. 9 and 10).
- 14 AAD 11AF looked in 1.34 fb<sup>-1</sup> of  $pp$  collisions at  $\sqrt{s} = 7 \text{ TeV}$  for events with 6 up to 8 jets and  $\cancel{E}_T$ . No evidence for an excess over the expected background is observed. Limits are derived in the CMSSM ( $m_0, m_{1/2}$ ) plane for  $\tan\beta = 10$  (see Fig. 5). The limit improves to  $m_{\tilde{g}} > 680 \text{ GeV}$  for  $m_{\tilde{q}} = 2 m_{\tilde{g}}$ .
- 15 AARON 11 looked in 255 pb<sup>-1</sup> of  $e^+p$  and 183 pb<sup>-1</sup> of  $e^-p$  collisions at  $\sqrt{s} = 319 \text{ GeV}$  for events with at least 1 lepton and jets from  $R_p$  violation with  $LQ\bar{D}$  couplings, assuming dominance of a single  $\lambda'_{ijk}$  coupling. No evidence for an excess over the SM expectation is observed, and limits are derived in the  $(\lambda', m_{\tilde{q}})$  plane for the MSSM with  $\tan\beta = 6$ , see their Figs. 7 and 8. Limits are also derived in a CMSSM-type scenario.
- 16 AARON 11C looked in 281 pb<sup>-1</sup> of  $e^+p$  and 165 pb<sup>-1</sup> of  $e^-p$  collisions at  $\sqrt{s} = 319 \text{ GeV}$  and  $\sqrt{s} = 301 \text{ GeV}$  for contact interactions measured from deviations of the  $d\sigma/dQ^2$  of neutral current events. They are interpreted in the framework of R-parity violation with  $LQ\bar{D}$  couplings. No evidence for an excess over the SM expectation is observed, and limits are derived for  $m_{\tilde{q}}/\lambda'$ , see Table 4.
- 17 CHATRCHYAN 11AC looked in 36 pb<sup>-1</sup> of  $pp$  collisions at  $\sqrt{s} = 7 \text{ TeV}$  for events with  $\geq 3$  jets, a large total transverse energy, and  $\cancel{E}_T$ . No evidence for an excess over the expected background is observed. Limits are derived in the CMSSM ( $m_0, m_{1/2}$ ) plane and the  $(m_{\tilde{g}}, m_{\tilde{q}})$  plane for  $\tan\beta = 10$  (see Fig. 10). Limits are also obtained for Simplified Model Spectra.
- 18 CHATRCHYAN 11C looked in 34 pb<sup>-1</sup> of  $pp$  collisions at  $\sqrt{s} = 7 \text{ TeV}$  for events with opposite charge isolated dileptons ( $e$  or  $\mu$ ), jets and  $\cancel{E}_T$  from pair production of  $\tilde{g}$  and  $\tilde{q}$ . No evidence for an excess over the expected background is observed. Limits are derived in the CMSSM ( $m_0, m_{1/2}$ ) plane for  $\tan\beta = 3$  (see Fig. 4).
- 19 CHATRCHYAN 11G looked in 36 pb<sup>-1</sup> of  $pp$  collisions at  $\sqrt{s} = 7 \text{ TeV}$  for events with  $\geq 2$  isolated photons,  $\geq 1$  jet and  $\cancel{E}_T$ , which may arise in a generalized gauge mediated model from the decay of a  $\tilde{\chi}_1^0$  NLSP. No evidence for an excess over the expected background is observed. Limits are derived in the plane of squark versus gluino mass (see Fig. 4) for several values of  $m_{\tilde{\chi}_1^0}$ .
- 20 CHATRCHYAN 11Q looked in 36 pb<sup>-1</sup> of  $pp$  collisions at  $\sqrt{s} = 7 \text{ TeV}$  for events with a single isolated lepton ( $e$  or  $\mu$ ),  $\geq 4$  jets and  $\cancel{E}_T$ . No evidence for an excess over the expected background is observed. Limits are derived in the CMSSM ( $m_0, m_{1/2}$ ) plane for  $\tan\beta = 10$  (see Fig. 7).
- 21 CHATRCHYAN 11V looked in 35 pb<sup>-1</sup> of  $pp$  collisions at  $\sqrt{s} = 7 \text{ TeV}$  for events with  $\geq 3$  isolated leptons ( $e, \mu$  or  $\tau$ ), with or without jets and  $\cancel{E}_T$ . Multi-lepton final states originate from  $\bar{q} \rightarrow \tilde{\chi}_1^0 + X$ , followed by  $\tilde{\chi}_1^0 \rightarrow \tilde{\tau}^\pm\ell^\mp$  and  $\tilde{\ell} \rightarrow \ell\tilde{g}$ . No evidence for an excess over the expected background is observed. Limits are derived (see Fig. 4) for a GMSB-type scenario with mass-degenerate right-handed sleptons (slepton co-NLSP scenario).
- 22 CHATRCHYAN 11V looked in 35 pb<sup>-1</sup> of  $pp$  collisions at  $\sqrt{s} = 7 \text{ TeV}$  for events with  $\geq 3$  isolated leptons ( $e, \mu$  or  $\tau$ ), with or without jets and  $\cancel{E}_T$ . No evidence for an excess over the expected background is observed. Limits are derived in the  $\tilde{R}$  framework (see Fig. 4) in the  $(m_{\tilde{g}}, m_{\tilde{q}})$  plane assuming the dominance of a  $\lambda_{122}$  or  $\lambda_{123}$  coupling,  $m_{\tilde{\chi}_1^0} = 300 \text{ GeV}, m_{\tilde{g}} = 1000 \text{ GeV}$ , and decoupled wino and Higgsino.
- 23 KHACHATRYAN 11I looked in 35 pb<sup>-1</sup> of  $pp$  collisions at  $\sqrt{s} = 7 \text{ TeV}$  for events with  $\geq 2$  jets and  $\cancel{E}_T$ . After combining multi-jet events into two pseudo-jets signal events are selected by a cut on  $\alpha_T = E_T^2/M_T$ , the transverse energy of the less energetic jet over the transverse mass. No evidence for an excess over the expected background is observed. Limits are derived in the CMSSM ( $m_0, m_{1/2}$ ) plane (see Fig. 5) for  $\tan\beta = 3$ . Superseded by CHATRCHYAN 11W.
- 24 ABAZOV 09s looked in 0.96 fb<sup>-1</sup> of  $p\bar{p}$  collisions at  $\sqrt{s} = 1.96 \text{ TeV}$  for events with at least 2 jets, a tau decaying hadronically and  $\cancel{E}_T$  from the production  $q_L\bar{q}_R$ , with the taus originating from the decay of a  $\tilde{\chi}_2^0$  or  $\tilde{\chi}_1^\pm$ . The results were combined with ABAZOV 08G which searched for events with jets and  $\cancel{E}_T$  without requiring taus. No evidence for an excess over the SM expectation is observed. The excluded region is shown for an mSUGRA model in a plane of  $m_{1/2}$  versus  $m_0$  in the "tau corridor," see their Figs. 5 and 6. The largest excluded squark mass in the corridor is 340 GeV for the tau analysis only and 410 GeV for the combined analysis.
- 25 SCHAEEL 07A studied the effect on hadronic cross sections and charge asymmetries of t-channel down-type squark exchange via R-parity violating couplings  $LQ\bar{D}$  at  $\sqrt{s} = 189\text{--}209 \text{ GeV}$ . The limit here refers to the case  $j = 1, 2$  and holds for  $\lambda'_{ijk}$  of electromagnetic strength. The results of this analysis are combined with BARATE 00i.
- 26 CHEKANOV 05A search for lepton flavor violating processes  $e^\pm p \rightarrow \ell X$ , where  $\ell = \mu$  or  $\tau$  with high  $p_T$ , in 130 pb<sup>-1</sup> at 300 and 318 GeV. Such final states may originate from  $LQ\bar{D}$  couplings with simultaneously non-zero  $\lambda'_{ijk}$  and  $\lambda'_{ijk}$  ( $i=2$  or 3). The quoted mass bounds hold for a  $u$ -type squark, assume a  $\lambda'$  of electromagnetic strength and contributions from only direct squark decays. For  $d$ -type squarks the bounds are strengthened to 278 and 275 GeV for the  $\mu$  and  $\tau$  final states, respectively. Supersedes the results of CHEKANOV 02.
- 27 AKTAS 04D looked in 77.8 pb<sup>-1</sup> of  $e^\pm p$  collisions at  $\sqrt{s} = 319 \text{ GeV}$  for resonant production of  $\bar{q}$  by R-parity violating  $LQ\bar{D}$  couplings assuming that one of the  $\lambda'$  couplings

- dominates over all others. They consider final states with or without leptons and/or jets and/or  $p_T$  resulting from direct and indirect decays. They combine the channels to derive limits on  $\lambda'_{1j1}$  and  $\lambda'_{11k}$  as a function of the squark mass, see their Figs. 8 and 9, from a scan over the parameters  $70 < M_2 < 350$  GeV,  $-300 < \mu < 300$  GeV,  $\tan\beta = 6$ , for a fixed mass of 90 GeV for degenerate sleptons and an LSP mass  $> 30$  GeV. The quoted limits refer to  $\lambda' = 0.3$ , with  $U=u,c,t$  and  $D=d,s,b$ . Supersedes the results of ADLOFF 01b. Superseded by AARON 11.
- 28 ADLOFF 03 looked for the s-channel production of squarks via  $R$   $LQ\bar{D}$  couplings in  $117.2 \text{ pb}^{-1}$  of  $e^+p$  data at  $\sqrt{s} = 301$  and  $319$  GeV and of  $e^-p$  data at  $\sqrt{s} = 319$  GeV. The comparison of the data with the SM differential cross section allows limits to be set on couplings for processes mediated through contact interactions. They obtain lower bounds on the value of  $m_{\tilde{q}}/\lambda'$  of 710 GeV for the process  $e^+\bar{u} \rightarrow \tilde{u}^k$  (and charge conjugate), mediated by  $\lambda'_{11k}$ , and of 430 GeV for the process  $e^+d \rightarrow \tilde{u}^j$  (and charge conjugate), mediated by  $\lambda'_{1j1}$ . Superseded by AARON 11c.
- 29 CHEKANOV 03b used  $131.5 \text{ pb}^{-1}$  of  $e^+p$  and  $e^-p$  data taken at 300 and 318 GeV to look for narrow resonances in the  $e\bar{q}$  or  $\nu q$  final states. Such final states may originate from  $LQ\bar{D}$  couplings with non-zero  $\lambda'_{1j1}$  (leading to  $\tilde{u}^j$ ) or  $\lambda'_{11k}$  (leading to  $\tilde{d}^k$ ). See their Fig. 8 and explanations in the text for limits. The quoted mass bound assumes that only direct squark decays contribute.
- 30 HEISTER 03g searches for the production of squarks in the case of  $R$  prompt decays with  $U\bar{D}\bar{D}$  direct couplings at  $\sqrt{s} = 189$ –209 GeV.
- 31 ABAZOV 02f looked in  $77.5 \text{ pb}^{-1}$  of  $pp$  collisions at 1.8 TeV for events with  $\geq 2\mu + \geq 4$  jets, originating from associated production of squarks followed by an indirect  $R$  decay (of the  $\tilde{\chi}_1^0$ ) via  $LQ\bar{D}$  couplings of the type  $\lambda'_{2jk}$  where  $j=1,2$  and  $k=1,2,3$ . Bounds are obtained in the MSUGRA scenario by a scan in the range  $0 \leq M_0 \leq 400$  GeV,  $60 \leq m_{1/2} \leq 120$  GeV for fixed values  $A_0=0$ ,  $\mu < 0$ , and  $\tan\beta=2$  or 6. The bounds are weaker for  $\tan\beta=6$ . See Figs. 2,3 for the exclusion contours in  $m_{1/2}$  versus  $m_0$  for  $\tan\beta=2$  and 6, respectively.
- 32 ABAZOV 02g search for associated production of gluinos and squarks in  $92.7 \text{ pb}^{-1}$  of  $pp$  collisions at  $\sqrt{s}=1.8$  TeV, using events with one electron,  $\geq 4$  jets, and large  $E_T$ . The results are compared to a MSUGRA scenario with  $\mu < 0$ ,  $A_0=0$ , and  $\tan\beta=3$  and allow to exclude a region of the  $(m_0, m_{1/2})$  shown in Fig. 11.
- 33 ABBIENDI 02 looked for events with an electron or neutrino and a jet in  $e^+e^-$  at 189 GeV. Squarks (or leptoquarks) could originate from a  $LQ\bar{D}$  coupling of an electron with a quark from the fluctuation of a virtual photon. Limits on the couplings  $\lambda'_{1jk}$  as a function of the squark mass are shown in Figs. 8–9, assuming that only direct squark decays contribute.
- 34 ABBIENDI 02b looked for events with an electron or neutrino and a jet in  $e^+e^-$  at 189–209 GeV. Squarks (or leptoquarks) could originate from a  $LQ\bar{D}$  coupling of an electron with a quark from the fluctuation of a virtual photon. Limits on the couplings  $\lambda'_{1jk}$  as a function of the squark mass are shown in Fig. 4, assuming that only direct squark decays contribute. The quoted limits are read off from Fig. 4. Supersedes the results of ABBIENDI 02.
- 35 ACHARD 02 searches for the production of squarks in the case of  $R$  prompt decays with  $U\bar{D}\bar{D}$  couplings at  $\sqrt{s}=189$ –208 GeV. The search is performed for direct and indirect decays, assuming one coupling at the time to be nonzero. The limit holds for indirect decays. Stronger limits are reached for  $(\tilde{u}_R, \tilde{d}_R)$  direct (80,56) GeV and  $(\tilde{u}_L, \tilde{d}_L)$  direct or indirect (87,86) GeV decays.
- 36 CHEKANOV 02 search for lepton flavor violating processes  $e^+p \rightarrow \ell X$ , where  $\ell = \mu$  or  $\tau$  with high  $p_T$ , in  $47.7 \text{ pb}^{-1}$  of  $e^+p$  collisions at 300 GeV. Such final states may originate from  $LQ\bar{D}$  couplings with simultaneously nonzero  $\lambda'_{1jk}$  and  $\lambda'_{ijk}$  ( $i=2$  or 3). The quoted mass bound assumes that only direct squark decays contribute.
- 37 BARATE 01b searches for the production of squarks in the case of  $R$  prompt decays with  $LLE$  indirect or  $U\bar{D}\bar{D}$  direct couplings at  $\sqrt{s}=189$ –202 GeV. The limit holds for direct decays mediated by  $R$   $U\bar{D}\bar{D}$  couplings. Limits are also given for  $LLE$  indirect decays ( $m_{\tilde{u}_R} > 90$  GeV and  $m_{\tilde{d}_R} > 89$  GeV). Supersedes the results from BARATE 00h.
- 38 BREITWEG 01 searches for squark production in  $47.7 \text{ pb}^{-1}$  of  $e^+p$  collisions, mediated by  $R$  couplings  $LQ\bar{D}$  and leading to final states with  $\tilde{\nu}$  and  $\geq 1$  jet, complementing the  $e^+X$  final states of BREITWEG 00e. Limits are derived on  $\lambda'\sqrt{\beta}$ , where  $\beta$  is the branching fraction of the squarks into  $e^+q+\bar{q}$ , as function of the squark mass, see their Fig. 15. The quoted mass limit assumes that only direct squark decays contribute.
- 39 ABBOTT 00c searched in  $\sim 94 \text{ pb}^{-1}$  of  $p\bar{p}$  collisions for events with  $\mu\mu$ +jets, originating from associated production of squarks followed by direct  $R$  decay via  $\lambda'_{2jk}L_2Q_jd_k^c$  couplings. Bounds are obtained on the cross section for branching ratios of 1 and of 1/2, see their Fig. 4. The former yields the limit on the  $\tilde{u}_L$ . The latter is combined with the bound of ABBOTT 99j from the  $\mu\nu$ +jets channel and of ABBOTT 98e and ABBOTT 98j from the  $\nu\nu$ +jets channel to yield the limit on  $\tilde{d}_R$ .
- 40 ACCIARRI 00p studied the effect on hadronic cross sections of  $t$ -channel down-type squark exchange via  $R$ -parity violating coupling  $\lambda'_{1jk}L_1Q_jd_k^c$ . The limit here refers to the case  $j=1,2$ , and holds for  $\lambda'_{1jk}=0.3$ . Data collected at  $\sqrt{s}=130$ –189 GeV, superseding the results of ACCIARRI 98j.
- 41 AFFOLDER 00k searched in  $\sim 88 \text{ pb}^{-1}$  of  $p\bar{p}$  collisions for events with 2–3 jets, at least one being  $b$ -tagged, large  $E_T$  and no high  $p_T$  leptons. Such  $\nu\nu$ + $b$ -jets events would originate from associated production of squarks followed by direct  $R$  decay via  $\lambda'_{1j3}L_1Q_jd_3^c$  couplings. Bounds are obtained on the production cross section assuming zero branching ratio to charged leptons.
- 42 BARATE 00i studied the effect on hadronic cross sections and charge asymmetries of  $t$ -channel down-type squark exchange via  $R$ -parity violating coupling  $\lambda'_{1jk}L_1Q_jd_k^c$ . The limit here refers to the case  $j=1,2$ , and holds for  $\lambda'_{1jk}=0.3$ . A 50 GeV limit is found for up-type squarks with  $k=3$ . Data collected at  $\sqrt{s}=130$ –183 GeV. Superseded by SCHAEEL 07a.
- 43 BREITWEG 00e searches for squark exchange in  $e^+p$  collisions, mediated by  $R$  couplings  $LQ\bar{D}$  and leading to final states with an identified  $e^+$  and  $\geq 1$  jet. The limit applies to up-type squarks of all generations, and assumes  $B(\tilde{q} \rightarrow qe)=1$ .
- 44 ABBOTT 99 searched for  $\gamma E_T + \geq 2$  jet final states, and set limits on  $\sigma(p\bar{p} \rightarrow \tilde{q}+X) \cdot B(\tilde{q} \rightarrow \gamma E_T+X)$ . The quoted limits correspond to  $m_{\tilde{g}} \geq m_{\tilde{q}}$ , with  $B(\tilde{\chi}_2^0 \rightarrow \tilde{\chi}_1^0\gamma)=1$  and  $B(\tilde{\chi}_1^0 \rightarrow \tilde{G}\gamma)=1$ , respectively. They improve to 310 GeV (360 GeV in the case of  $\gamma\tilde{G}$  decay) for  $m_{\tilde{g}}=m_{\tilde{q}}$ .
- 45 ABBOTT 99k uses events with an electron pair and four jets to search for the decay of the  $\tilde{\chi}_1^0$  LSP via  $R$   $LQ\bar{D}$  couplings. The particle spectrum and decay branching ratios are taken in the framework of minimal supergravity. An excluded region at 95% CL is obtained in the  $(m_0, m_{1/2})$  plane under the assumption that  $A_0=0$ ,  $\mu < 0$ ,  $\tan\beta=2$  and any one of the couplings  $\lambda'_{1jk} > 10^{-3}$  ( $j=1,2$  and  $k=1,2,3$ ) and from which the above limit is computed. For equal mass squarks and gluinos, the corresponding limit is 277 GeV. The results are essentially independent of  $A_0$ , but the limit deteriorates rapidly with increasing  $\tan\beta$  or  $\mu > 0$ .
- 46 ABBOTT 99l consider events with three or more jets and large  $E_T$ . Spectra and decay rates are evaluated in the framework of minimal Supergravity, assuming five flavors of degenerate squarks, and scanning the space of the universal gaugino ( $m_{1/2}$ ) and scalar ( $m_0$ ) masses. See their Figs. 2–3 for the dependence of the limit on the relative value of  $m_{\tilde{q}}$  and  $m_{\tilde{g}}$ .
- 47 ABE 99m looked in  $107 \text{ pb}^{-1}$  of  $p\bar{p}$  collisions at  $\sqrt{s}=1.8$  TeV for events with like sign dielectrons and two or more jets from the sequential decays  $\tilde{q} \rightarrow q\tilde{\chi}_1^0$  and  $\tilde{\chi}_1^0 \rightarrow e q\bar{q}'$ , assuming  $R$  coupling  $L_1Q_jD_k^c$ , with  $j=2,3$  and  $k=1,2,3$ . They assume five degenerate squark flavors,  $B(\tilde{q} \rightarrow q\tilde{\chi}_1^0)=1$ ,  $B(\tilde{\chi}_1^0 \rightarrow e q\bar{q}')=0.25$  for both  $e^+$  and  $e^-$ , and  $m_{\tilde{g}} \geq 200$  GeV. The limit is obtained for  $m_{\tilde{\chi}_1^0} \geq m_{\tilde{q}}/2$  and improves for heavier gluinos or heavier  $\tilde{\chi}_1^0$ .
- 48 ABREU 99g looked for events with an electron or neutrino and a jet in  $e^+e^-$  at 183 GeV. Squarks (or leptoquarks) could originate from a  $LQ\bar{D}$  coupling of an electron with a quark from the fluctuation of a virtual photon. Limits on the couplings  $\lambda'_{1jk}$  as a function of the squark mass are shown in Fig. 4, assuming that only direct squark decays contribute.
- 49 ABBOTT 98e searched in  $\sim 115 \text{ pb}^{-1}$  of  $p\bar{p}$  collisions for events with  $e\nu$ +jets, originating from associated production of squarks followed by direct  $R$  decay via  $\lambda'_{1jk}L_1Q_jd_k^c$  couplings. Bounds are obtained by combining these results with the previous bound of ABBOTT 97b from the  $e e$ +jets channel and with a reinterpretation of ABACHI 96b  $\nu\nu$ +jets channel.
- 50 ABE 98s looked in  $\sim 110 \text{ pb}^{-1}$  of  $p\bar{p}$  collisions at  $\sqrt{s}=1.8$  TeV for events with  $\mu\mu$ +jets originating from associated production of squarks followed by direct  $R$  decay via  $\lambda'_{2jk}L_2Q_jd_k^c$  couplings. Bounds are obtained on the production cross section times the square of the branching ratio, see Fig. 2. Mass limits result from the comparison with theoretical cross sections and branching ratio equal to 1 for  $\tilde{u}_L$  and 1/2 for  $\tilde{d}_R$ .
- 51 ACKERSTAFF 98v and ACCIARRI 98j studied the interference of  $t$ -channel squark ( $\tilde{d}_R$ ) exchange via  $R$ -parity violating  $\lambda'_{1jk}L_1Q_jd_k^c$  coupling in  $e^+e^- \rightarrow q\bar{q}$ . The limit is for  $\lambda'_{1jk}=0.3$ . See paper for related limits on  $\tilde{u}_L$  exchange. Data collected at  $\sqrt{s}=130$ –172 GeV.
- 52 BREITWEG 98 used positron+jet events with missing energy and momentum to look for  $e^+q \rightarrow \tilde{e}q$  via gaugino-like neutralino exchange with decays into  $(e\tilde{\chi}_1^0)(q\tilde{\chi}_1^0)$ . See paper for dependences in  $m_{\tilde{e}}$ ,  $m_{\tilde{\chi}_1^0}$ .
- 53 DATTA 97 argues that the squark mass bound by ABACHI 95c can be weakened by 10–20 GeV if one relaxes the assumption of the universal scalar mass at the GUT-scale so that the  $\tilde{\chi}_1^\pm\tilde{\chi}_2^0$  in the squark cascade decays have dominant and invisible decays to  $\tilde{\nu}$ .
- 54 DERRICK 97 looked for lepton-number violating final states via  $R$ -parity violating couplings  $\lambda'_{ijk}L_iQ_jd_k$ . When  $\lambda'_{11k}\lambda'_{ijk} \neq 0$ , the process  $e u \rightarrow \tilde{d}_k^+ \rightarrow \ell_i u_j$  is possible. When  $\lambda'_{1j1}\lambda'_{ijk} \neq 0$ , the process  $e\bar{u} \rightarrow \tilde{u}_j^+ \rightarrow \ell_i \bar{d}_k$  is possible. 100% branching fraction  $\tilde{q} \rightarrow \ell j$  is assumed. The limit quoted here corresponds to  $\tilde{t} \rightarrow \tau q$  decay, with  $\lambda'=0.3$ . For different channels, limits are slightly better. See Table 6 in their paper.
- 55 HEWETT 97 reanalyzed the limits on possible resonances in di-jet mode ( $\tilde{q} \rightarrow q\bar{q}$ ) from ALITTI 93 quoted in “Limits for Excited  $q(q^*)$  from Single Production,” ABE 96 in “SCALE LIMITS for Contact Interactions:  $\Lambda(qq^*)$ ,” and unpublished CDF,  $D\bar{0}$  bounds. The bound applies to the gluino mass of 5 GeV, and improves for lighter gluino. The analysis has gluinos in parton distribution function.
- 56 TEREKHOV 97 improved the analysis of TEREKHOV 96 by including di-jet angular distributions in the analysis.
- 57 AID 96c used positron+jet events with missing energy and momentum to look for  $e^+q \rightarrow \tilde{e}q$  via neutralino exchange with decays into  $(e\tilde{\chi}_1^0)(q\tilde{\chi}_1^0)$ . See the paper for dependences on  $m_{\tilde{e}}$ ,  $m_{\tilde{\chi}_1^0}$ .
- 58 TEREKHOV 96 reanalyzed the limits on possible resonances in di-jet mode ( $\tilde{u} \rightarrow u\bar{q}$ ) from ABE 95n quoted in “MASS LIMITS for  $g_A$  (axigluon).” The bound applies only to the case with a light gluino.
- 59 ABACHI 95c assume five degenerate squark flavors with  $m_{\tilde{d}_L} = m_{\tilde{q}_R}$ . Sleptons are assumed to be heavier than squarks. The limits are derived for fixed  $\tan\beta = 2.0$ ,  $\mu = -250$  GeV, and  $m_{H^\pm} = 500$  GeV, and with the cascade decays of the squarks and gluinos calculated within the framework of the Minimal Supergravity scenario. The bounds are weakly sensitive to the three fixed parameters for a large fraction of parameter space. No limit is given for  $m_{\text{gluino}} > 547$  GeV.
- 60 ABE 95t looked for a cascade decay of five degenerate squarks into  $\tilde{\chi}_1^0$  which further decays into  $\tilde{\chi}_1^0$  and a photon. No signal is observed. Limits vary widely depending on the choice of parameters. For  $\mu = -40$  GeV,  $\tan\beta = 1.5$ , and heavy gluinos, the range  $50 < m_{\tilde{q}} \text{ (GeV)} < 110$  is excluded at 90% CL. See the paper for details.
- 61 ABE 92l assume five degenerate squark flavors and  $m_{\tilde{q}_L} = m_{\tilde{q}_R}$ . ABE 92l includes the effect of cascade decay, for a particular choice of parameters,  $\mu = -250$  GeV,  $\tan\beta = 2$ . Results are weakly sensitive to these parameters over much of parameter space. No limit for  $m_{\tilde{q}} \leq 50$  GeV (but other experiments rule out that region). Limits are 10–20 GeV higher if  $B(\tilde{q} \rightarrow q\bar{q}) = 1$ . Limit assumes GUT relations between gaugino masses

# Searches Particle Listings

## Supersymmetric Particle Searches

and the gauge coupling; in particular that for  $|\mu|$  not small,  $m_{\tilde{\chi}_1^0} \approx m_{\tilde{g}}/6$ . This last relation implies that as  $m_{\tilde{g}}$  increases, the mass of  $\tilde{\chi}_1^0$  will eventually exceed  $m_{\tilde{q}}$  so that no decay is possible. Even before that occurs, the signal will disappear; in particular no bounds can be obtained for  $m_{\tilde{g}} > 410$  GeV,  $m_{H^\pm} = 500$  GeV.

<sup>62</sup>ROY 92 reanalyzed CDF limits on di-lepton events to obtain limits on squark production in  $R$ -parity violating models. The 100% decay  $\tilde{q} \rightarrow q\tilde{\chi}$  where  $\tilde{\chi}$  is the LSP, and the LSP decays either into  $\ell q\bar{d}$  or  $\ell\ell\bar{e}$  is assumed.

<sup>63</sup>NOJIRI 91 argues that a heavy squark should be nearly degenerate with the gluino in minimal supergravity not to overclose the universe.

### Long-lived $\tilde{q}$ (Squark) MASS LIMIT

The following are bounds on long-lived scalar quarks, assumed to hadronise into hadrons with lifetime long enough to escape the detector prior to a possible decay. Limits may depend on the mixing angle of mass eigenstates:  $\tilde{q}_1 = \tilde{q}_L \cos\theta_q + \tilde{q}_R \sin\theta_q$ .

The coupling to the  $Z^0$  boson vanishes for up-type squarks when  $\theta_u = 0.98$ , and for down type squarks when  $\theta_d = 1.17$ .

VALUE (GeV)	CL%	DOCUMENT ID	TECN	COMMENT
•••		We do not use the following data for averages, fits, limits, etc. •••		
>249	95	1 AALTONEN	09Z CDF	$\tilde{t}$
> 95	95	2 HEISTER	03H ALEP	$\tilde{u}$
> 92	95	2 HEISTER	03H ALEP	$\tilde{d}$
none 2–85	95	3 ABREU	98P DLPH	$\tilde{u}_L$
none 2–81	95	3 ABREU	98P DLPH	$\tilde{u}_R$
none 2–80	95	3 ABREU	98P DLPH	$\tilde{u}$ , $\theta_u = 0.98$
none 2–83	95	3 ABREU	98P DLPH	$\tilde{d}_L$
none 5–40	95	3 ABREU	98P DLPH	$\tilde{d}_R$
none 5–38	95	3 ABREU	98P DLPH	$\tilde{d}$ , $\theta_d = 1.17$

<sup>1</sup>AALTONEN 09Z searched in  $1 \text{ fb}^{-1}$  of  $p\bar{p}$  collisions at  $\sqrt{s} = 1.96$  TeV for events with direct production of a pair of charged massive stable particles identified by their TOF. No excess of events is observed over the expected background. The data are used to set a bound on the production cross section, and the result is compared with the pair production cross section of stable stops as a function of the  $\tilde{t}$  mass, see their Fig. 2.

<sup>2</sup>HEISTER 03H use  $e^+e^-$  data at and around the  $Z^0$  peak to look for hadronizing stable squarks. Combining their results on searches for charged and neutral R-hadrons with JANOT 03, a lower limit of 15.7 GeV on the mass is obtained. Combining this further with the results of searches for tracks with anomalous ionization in data from 183 to 208 GeV yields the quoted bounds.

<sup>3</sup>ABREU 98P assumes that 40% of the squarks will hadronise into a charged hadron, and 60% into a neutral hadron which deposits most of its energy in hadron calorimeter. Data collected at  $\sqrt{s} = 130\text{--}183$  GeV.

### $\tilde{b}$ (Sbottom) MASS LIMIT

Limits in  $e^+e^-$  depend on the mixing angle of the mass eigenstate  $\tilde{b}_1 = \tilde{b}_L \cos\theta_b + \tilde{b}_R \sin\theta_b$ . Coupling to the  $Z$  vanishes for  $\theta_b \sim 1.17$ . As a consequence, no absolute constraint in the mass region  $\lesssim 40$  GeV is available in the literature at this time from  $e^+e^-$  collisions. In the Listings below, we use  $\Delta m = m_{\tilde{b}_1} - m_{\tilde{\chi}_1^0}$ .

VALUE (GeV)	CL%	DOCUMENT ID	TECN	COMMENT
>230	95	1 AALTONEN	10R CDF	$\tilde{b}_1 \rightarrow b\tilde{\chi}_1^0, m_{\tilde{\chi}_1^0} < 70$ GeV
>247	95	2 ABAZOV	10L D0	$\tilde{b}_1 \rightarrow b\tilde{\chi}_1^0, m_{\tilde{\chi}_1^0} = 0$ GeV
>220	95	3 ABULENCIA	06I CDF	$\tilde{g} \rightarrow \tilde{b}b, \Delta m > 6$ GeV, $\tilde{b}_1 \rightarrow b\tilde{\chi}_1^0, m_{\tilde{g}} < 270$ GeV
> 95		4 ACHARD	04 L3	$\tilde{b} \rightarrow b\tilde{\chi}_1^0, \theta_b = 0, \Delta m > 15\text{--}25$ GeV
> 81		4 ACHARD	04 L3	$\tilde{b} \rightarrow b\tilde{\chi}_1^0$ , all $\theta_b, \Delta m > 15\text{--}25$ GeV
> 7.5	95	5 JANOT	04 THEO	unstable $\tilde{b}_1, e^+e^- \rightarrow$ hadrons
> 93	95	6 ABDALLAH	03M DLPH	$\tilde{b} \rightarrow b\tilde{\chi}_1^0, \theta_b = 0, \Delta m > 7$ GeV
> 76	95	6 ABDALLAH	03M DLPH	$\tilde{b} \rightarrow b\tilde{\chi}_1^0$ , all $\theta_b, \Delta m > 7$ GeV
> 85.1	95	7 ABBIENDI	02H OPAL	$\tilde{b} \rightarrow b\tilde{\chi}_1^0$ , all $\theta_b, \Delta m > 10$ GeV,
> 89	95	8 HEISTER	02K ALEP	$\tilde{b} \rightarrow b\tilde{\chi}_1^0$ , all $\theta_b, \Delta m > 8$ GeV,
none 3.5–4.5	95	9 SAVINOV	01 CLEO	$\tilde{B}$ meson
none 80–145	95	10 AFFOLDER	00D CDF	$\tilde{b} \rightarrow b\tilde{\chi}_1^0, m_{\tilde{\chi}_1^0} < 50$ GeV
•••		We do not use the following data for averages, fits, limits, etc. •••		
>294	95	11 AAD	11K ATLS	stable $\tilde{b}$
		12 AAD	11o ATLS	$\tilde{g} \rightarrow \tilde{b}_1 b, \tilde{b}_1 \rightarrow b\tilde{\chi}_1^0, m_{\tilde{\chi}_1^0} = 60$ GeV
		13 CHATRCHYAN	11D CMS	$\tilde{b}, \tilde{t} \rightarrow b$
		14 AALTONEN	09R CDF	$\tilde{g} \rightarrow \tilde{b}b, \tilde{b} \rightarrow b\tilde{\chi}_1^0$
>193	95	15 AALTONEN	07E CDF	$\tilde{b}_1 \rightarrow b\tilde{\chi}_1^0, m_{\tilde{\chi}_1^0} = 40$ GeV
none 35–222	95	16 ABAZOV	06R D0	$\tilde{b} \rightarrow b\tilde{\chi}_1^0, m_{\tilde{\chi}_1^0} = 50$ GeV
> 78	95	17 ABDALLAH	04M DLPH	$\tilde{R}, \tilde{b}_L$ , indirect, $\Delta m > 5$ GeV
none 50–82	95	18 ABDALLAH	03C DLPH	$\tilde{b} \rightarrow b\tilde{g}$ , stable $\tilde{g}$ , all $\theta_b, \Delta m > 10$ GeV
		19 BERGER	03 THEO	$\tilde{b}_L, \tilde{R}$ decay
> 71.5	95	20 HEISTER	03G ALEP	$\tilde{b}_L, \tilde{R}$ decay
> 27.4	95	21 HEISTER	03H ALEP	$\tilde{b} \rightarrow b\tilde{g}$ , stable $\tilde{g}$ or $\tilde{b}$

> 48	95	22 ACHARD	02 L3	$\tilde{b}_1, \tilde{R}$ decays
		23 BAEK	02 THEO	
		24 BECHER	02 THEO	
		25 CHEUNG	02B THEO	
		26 CHO	02 THEO	
		27 BERGER	01 THEO	$p\bar{p} \rightarrow X + b\text{-quark}$
none 52–115	95	28 ABBOTT	99F D0	$\tilde{b} \rightarrow b\tilde{\chi}_1^0, m_{\tilde{\chi}_1^0} < 20$ GeV

<sup>1</sup>AALTONEN 10R searched in  $2.65 \text{ fb}^{-1}$  of  $p\bar{p}$  collisions at  $\sqrt{s} = 1.96$  TeV for events with  $\mathcal{E}_T$  and exactly two jets, at least one of which is  $b$ -tagged. The results are in agreement with the SM prediction, and a limit on the cross section of  $0.1 \text{ pb}$  is obtained for the range of masses  $80 < m_{\tilde{b}_1} < 280$  GeV assuming that the sbottom decays exclusively to  $b\tilde{\chi}_1^0$ . The excluded mass region in the framework of conserved  $R_p$  is shown in a plane of  $(m_{\tilde{b}_1}, m_{\tilde{\chi}_1^0})$ , see their Fig. 2.

<sup>2</sup>ABAZOV 10L looked in  $5.2 \text{ fb}^{-1}$  of  $p\bar{p}$  collisions at  $\sqrt{s} = 1.96$  TeV for events with at least 2  $b$ -jets and  $\mathcal{E}_T$  from the production of  $\tilde{b}_1\tilde{b}_1$ . No evidence for an excess over the SM expectation is observed, and a limit on the cross section is derived under the assumption of 100% branching ratio. The excluded mass region in the framework of conserved  $R_p$  is shown in a plane of  $(m_{\tilde{b}_1}, m_{\tilde{\chi}_1^0})$ , see their Fig. 3b. The exclusion also extends to  $m_{\tilde{\chi}_1^0} = 110$  GeV for  $160 < m_{\tilde{b}_1} < 200$  GeV.

<sup>3</sup>ABULENCIA 06I searched in  $156 \text{ pb}^{-1}$  of  $p\bar{p}$  collisions at  $\sqrt{s} = 1.96$  TeV for multijet events with large  $\mathcal{E}_T$ . They request at least 2  $b$ -tagged jets and no isolated leptons. They investigate the production of gluinos decaying into  $\tilde{b}_1 b$  followed by  $\tilde{b}_1 \rightarrow b\tilde{\chi}_1^0$ . Both branching fractions are assumed to be 100% and the LSP mass to be 60 GeV. No significant excess was found compared to the background expectation. Upper limits on the cross-section are extracted and a limit is derived on the masses of sbottom and gluinos, see their Fig. 3.

<sup>4</sup>ACHARD 04 search for the production of  $\tilde{b}\tilde{b}$  in acoplanar  $b$ -tagged di-jet final states in the 192–209 GeV data. See Fig. 6 for the dependence of the limits on  $m_{\tilde{\chi}_1^0}$ . This limit supersedes ACCIARRI 99v.

<sup>5</sup>JANOT 04 reanalyzes  $e^+e^- \rightarrow$  hadrons total cross section data with  $\sqrt{s} = 20\text{--}209$  GeV from PEP, PETRA, TRISTAN, SLC, and LEP and constrains the mass of  $\tilde{b}_1$  assuming it decays quickly to hadrons.

<sup>6</sup>ABDALLAH 03M looked for  $\tilde{b}$  pair production in events with acoplanar jets and  $\mathcal{E}$  at  $\sqrt{s} = 189\text{--}208$  GeV. The limit improves to 87 (98) GeV for all  $\theta_b$  ( $\theta_b = 0$ ) for  $\Delta m > 10$  GeV. See Fig. 24 and Table 11 for other choices of  $\Delta m$ . These limits include and update the results of ABREU, P 00D.

<sup>7</sup>ABBIENDI 02H search for events with two acoplanar jets and  $\mathcal{E}_T$  in the 161–209 GeV data. The limit assumes 100% branching ratio and uses the exclusion at large  $\Delta m$  from CDF (AFFOLDER 00D). For  $\theta_b = 0$ , the bound improves to  $> 96.9$  GeV. See Fig. 4 and Table 6 for the more general dependence on the limits on  $\Delta m$ . These results supersede ABBIENDI 99M.

<sup>8</sup>HEISTER 02K search for bottom squarks in final states with acoplanar jets with  $b$  tagging, using 183–209 GeV data. The mass bound uses the CDF results from AFFOLDER 00b. See Fig. 5 for the more general dependence of the limits on  $\Delta m$ . Updates BARATE 01.

<sup>9</sup>SAVINOV 01 use data taken at  $\sqrt{s} = 10.52$  GeV, below the  $B\bar{B}$  threshold. They look for events with a pair of leptons with opposite charge and a fully reconstructed hadronic  $D$  or  $D^*$  decay. These could originate from production of a light-sbottom hadron followed by  $\tilde{B} \rightarrow D^{(*)}\ell\bar{\nu}$ , in case the  $\bar{\nu}$  is the LSP, or  $\tilde{B} \rightarrow D^{(*)}\pi\ell\bar{\nu}$ , in case of  $\tilde{R}$ . The mass range  $3.5 \leq M(\tilde{B}) \leq 4.5$  GeV was explored, assuming 100% branching ratio for either of the decays. In the  $\bar{\nu}$  LSP scenario, the limit holds only for  $M(\bar{\nu})$  less than about 1 GeV and for the  $D^*$  decays it is reduced to the range 3.9–4.5 GeV. For the  $\tilde{R}$  decay, the whole range is excluded.

<sup>10</sup>AFFOLDER 00b search for final states with 2 or 3 jets and  $\mathcal{E}_T$ , one jet with a  $b$  tag. See their Fig. 3 for the mass exclusion in the  $m_{\tilde{t}}, m_{\tilde{\chi}_1^0}$  plane.

<sup>11</sup>AAD 11k looked in  $34 \text{ pb}^{-1}$  of  $p\bar{p}$  collisions at  $\sqrt{s} = 7$  TeV for events with heavy stable particles, identified by their anomalous  $dE/dx$  in the tracker or time of flight in the tile calorimeter, from pair production of  $\tilde{b}$ . No evidence for an excess over the SM expectation is observed and limits on the mass are derived for pair production of sbottom, see Fig. 4.

<sup>12</sup>AAD 11o looked in  $35 \text{ pb}^{-1}$  of  $p\bar{p}$  collisions at  $\sqrt{s} = 7$  TeV for events with jets, of which at least one is a  $b$ -jet, and  $\mathcal{E}_T$ . No excess above the Standard Model was found. Limits are derived in the  $(m_{\tilde{g}}, m_{\tilde{b}_1})$  plane (see Fig. 2) under the assumption of 100% branching ratios and  $\tilde{b}_1$  being the lightest squark. The quoted limit is valid for  $m_{\tilde{b}_1} < 500$  GeV. A similar approach for  $\tilde{t}_1$  as the lightest squark with  $\tilde{g} \rightarrow \tilde{t}_1 t$  and  $\tilde{t}_1 \rightarrow b\tilde{\chi}_1^\pm$  with 100% branching ratios leads to a gluino mass limit of 520 GeV for  $130 < m_{\tilde{t}_1} < 300$  GeV. Limits are also derived in the CMSSM  $(m_0, m_{1/2})$  plane for  $\tan\beta = 40$ , see Fig. 4, and in scenarios based on the gauge group  $SO(10)$ .

<sup>13</sup>CHATRCHYAN 11D looked in  $35 \text{ pb}^{-1}$  of  $p\bar{p}$  collisions at  $\sqrt{s} = 7$  TeV for events with  $\geq 2$  jets, at least one of which is  $b$ -tagged, and  $\mathcal{E}_T$ , where the  $b$ -jets are decay products of  $\tilde{t}$  or  $\tilde{b}$ . No evidence for an excess over the expected background is observed. Limits are derived in the CMSSM  $(m_0, m_{1/2})$  plane for  $\tan\beta = 50$  (see Fig. 2).

<sup>14</sup>AALTONEN 09R searched in  $2.5 \text{ fb}^{-1}$  of  $p\bar{p}$  collisions at  $\sqrt{s} = 1.96$  TeV for events with at least 2  $b$ -tagged jets and  $\mathcal{E}_T$ , originating from the decay  $\tilde{g} \rightarrow \tilde{b}b$  followed by  $\tilde{b} \rightarrow b\tilde{\chi}_1^0$ . Both decays are assumed to have 100% branching ratio. No significant deviation from the SM prediction is observed. An upper limit on the gluino pair production cross section is calculated as a function of the gluino mass, see their Fig. 2. A limit is derived in the  $m_{\tilde{g}} \text{ versus } m_{\tilde{b}_1}$  plane which improves the results of previous searches, see their Fig. 3.

<sup>15</sup>AALTONEN 07E searched in  $295 \text{ pb}^{-1}$  of  $p\bar{p}$  collisions at  $\sqrt{s} = 1.96$  TeV for multijet events with large  $\mathcal{E}_T$ . They request at least one heavy flavor-tagged jet and no identified leptons. The branching ratio  $\tilde{b}_1 \rightarrow b\tilde{\chi}_1^0$  is assumed to be 100%. No significant excess was found compared to the background expectation. Upper limits on the cross-section are extracted and a limit is derived on the masses of sbottom versus  $\tilde{\chi}_1^0$ , see their Fig. 5. Superseded by AALTONEN 10R.



See key on page 457

# Searches Particle Listings

## Supersymmetric Particle Searches

- 16 ABAZOV 06R looked in 310 pb<sup>-1</sup> of p $\bar{p}$  collisions at  $\sqrt{s} = 1.96$  TeV for events with 2 or 3 jets and large  $E_T$  with at least 1 b-tagged jet and a veto against isolated leptons. No excess is observed relative to the SM background expectations. Limits are set on the sbottom pair production cross-section under the assumption that the only decay mode is into  $b\tilde{\chi}_1^0$ . Exclusion contours are derived in the plane of sbottom versus neutralino masses, shown in their Fig. 2. The observed limit is more constraining than the expected one due to a lack of events corresponding to large sbottom masses. Superseded by ABAZOV 10L.
- 17 ABDALLAH 04M use data from  $\sqrt{s} = 192\text{--}208$  GeV to derive limits on sparticle masses under the assumption of  $R$  with  $U\bar{D}\bar{D}$  couplings. The results are valid for  $\mu = -200$  GeV,  $\tan\beta = 1.5$ ,  $\Delta m > 5$  GeV and assuming a BR of 1 for the given decay. The limit quoted is for indirect  $U\bar{D}\bar{D}$  decays using the neutralino constraint of 38.0 GeV, also derived in ABDALLAH 04M, and assumes no mixing. For indirect decays it remains at 78 GeV when the neutralino constraint is not used. Supersedes the result of ABREU 01D.
- 18 ABDALLAH 03c looked for events of the type  $q\bar{q}R^\pm R^\pm$ ,  $q\bar{q}R^\pm R^0$ , or  $q\bar{q}R^0 R^0$  in  $e^+e^-$  interactions at  $\sqrt{s} = 189\text{--}208$  GeV. The  $R^\pm$  bound states are identified by anomalous  $dE/dx$  in the tracking chambers and the  $R^0$  by missing energy due to their reduced energy loss in the calorimeters. Excluded mass regions in the  $(m(\tilde{b}), m(\tilde{g}))$  plane for  $m(\tilde{g}) > 2$  GeV are obtained for several values of the probability for the gluino to fragment into  $R^\pm$  or  $R^0$ , as shown in their Fig. 19. The limit improves to 94 GeV for  $\theta_b = 0$ .
- 19 BERGER 03 studies the constraints on a  $\tilde{b}_1$  with mass in the 2.2–5.5 GeV region coming from radiative decays of  $\Upsilon(nS)$  into sbottomonium. The constraints apply only if  $\tilde{b}_1$  lives long enough to permit formation of the sbottomonium bound state. A small region of mass in the  $m_{\tilde{b}_1} - m_{\tilde{g}}$  plane survives current experimental constraints from CLEO.
- 20 HEISTER 03g searches for the production of  $\tilde{b}$  pairs in the case of  $R$  prompt decays with  $LLE$ ,  $LQD$  or  $U\bar{D}\bar{D}$  couplings at  $\sqrt{s} = 189\text{--}209$  GeV. The limit holds for indirect decays mediated by  $R$   $U\bar{D}\bar{D}$  couplings. It improves to 90 GeV for indirect decays mediated by  $R$   $LLE$  couplings and to 80 GeV for indirect decays mediated by  $R$   $LQD$  couplings. Supersedes the results from BARATE 01b.
- 21 HEISTER 03H use their results on bounds on stable squarks, on stable gluinos and on squarks decaying to a stable gluino from the same paper to derive a mass limit on  $\tilde{b}$ , see their Fig. 13. The limit for a long-lived  $\tilde{b}_1$  is 92 GeV.
- 22 ACHARD 02 searches for the production of squarks in the case of  $R$  prompt decays with  $U\bar{D}\bar{D}$  couplings at  $\sqrt{s} = 189\text{--}208$  GeV. The search is performed for direct and indirect decays, assuming one coupling at the time to be nonzero. The limit is computed for the minimal cross section and holds for indirect decays and reaches 55 GeV for direct decays.
- 23 BAEK 02 studies the constraints on a  $\tilde{b}_1$  with mass in the 2.2–5.5 GeV region coming from precision measurements of  $Z^0$  decays. It is noted that  $CP$ -violating couplings in the MSSM parameters relax the strong constraints otherwise derived from  $CP$  conservation.
- 24 BECHER 02 studies the constraints on a  $\tilde{b}_1$  with mass in the 2.2–5.5 GeV region coming from radiative  $B$  meson decays, and sets limits on the off-diagonal flavor-changing couplings  $q\bar{b}\tilde{g}$  ( $q=d,s$ ).
- 25 CHEUNG 02b studies the constraints on a  $\tilde{b}_1$  with mass in the 2.2–5.5 GeV region and a gluino in the mass range 12–16 GeV, using precision measurements of  $Z^0$  decays and  $e^+e^-$  annihilations at LEP2. Few detectable events are predicted in the LEP2 data for the model proposed by BERGER 01.
- 26 CHO 02 studies the constraints on a  $\tilde{b}_1$  with mass in the 2.2–5.5 GeV region coming from precision measurements of  $Z^0$  decays. Strong constraints are obtained for  $CP$ -conserving MSSM couplings.
- 27 BERGER 01 reanalyzed interpretation of Tevatron data on bottom-quark production. Argues that pair production of light gluinos ( $m \sim 12\text{--}16$  GeV) with subsequent 2-body decay into a light sbottom ( $m \sim 2\text{--}5.5$  GeV) and bottom can reconcile Tevatron data with predictions of perturbative QCD for the bottom production rate. The sbottom must either decay hadronically via a  $R$ -parity- and  $B$ -violating interaction, or be long-lived. Constraints on the mass spectrum are derived from the measurements of time-averaged  $B^0\text{--}\bar{B}^0$  mixing.
- 28 ABBOTT 99F looked for events with two jets, with or without an associated muon from  $b$  decay, and  $E_T$ . See Fig. 2 for the dependence of the limit on  $m_{\tilde{\chi}_1^0}$ . No limit for  $m_{\tilde{\chi}_1^0} > 47$  GeV. Superseded by ABAZOV 06R.

### $\tilde{\tau}$ (Stop) MASS LIMIT

Limits depend on the decay mode. In  $e^+e^-$  collisions they also depend on the mixing angle of the mass eigenstate  $\tilde{t}_1 = \tilde{t}_L \cos\theta_t + \tilde{t}_R \sin\theta_t$ . The coupling to the  $Z$  vanishes when  $\theta_t = 0.98$ . In the Listings below, we use  $\Delta m \equiv m_{\tilde{t}_1} - m_{\tilde{\chi}_1^0}$  or  $\Delta m \equiv m_{\tilde{t}_1} - m_{\tilde{\nu}_\tau}$ , depending on relevant decay mode. See also bounds in “ $\tilde{q}$  (Squark) MASS LIMIT.” Limits made obsolete by the most recent analyses of  $e^+e^-$  and  $p\bar{p}$  collisions can be found in previous Editions of this Review.

VALUE (GeV)	CL%	DOCUMENT ID	TECN	COMMENT
>210	95	1 ABAZOV	11N D0	$\tilde{t}_1 \rightarrow b\ell\bar{\nu}, m_{\tilde{\nu}} < 110$ GeV, $m_{\tilde{t}_1} - m_{\tilde{\nu}} > 30$ GeV
none 60–180	95	2 AALTONEN	10Y CDF	$\tilde{t}_1 \rightarrow b\ell\bar{\nu}, m_{\tilde{\nu}} = 45$ GeV
none 95–150	95	3 ABAZOV	08Z D0	$\tilde{t}_1 \rightarrow c\tilde{\chi}_1^0$ , $m_c < \Delta m < m_{W+m_b}$
none 80–120	95	4 ABAZOV	04 D0	$\tilde{t}_1 \rightarrow b\ell\nu\tilde{\chi}_1^0, m_{\tilde{\chi}_1^0} = 50$ GeV
> 90		5 ACHARD	04 L3	$\tilde{t}_1 \rightarrow c\tilde{\chi}_1^0$ , all $\theta_t$ , $\Delta m > 15\text{--}25$ GeV
> 93		5 ACHARD	04 L3	$\tilde{t}_1 \rightarrow b\ell\bar{\nu}$ , all $\theta_t$ , $\Delta m > 15$ GeV
> 88		5 ACHARD	04 L3	$\tilde{t}_1 \rightarrow b\tau\bar{\nu}$ , all $\theta_t$ , $\Delta m > 15$ GeV
> 75	95	6 ABDALLAH	03M DLPH	$\tilde{t}_1 \rightarrow c\tilde{\chi}_1^0, \theta_t = 0$ , $\Delta m > 2$ GeV
> 71	95	6 ABDALLAH	03M DLPH	$\tilde{t}_1 \rightarrow c\tilde{\chi}_1^0$ , all $\theta_t$ , $\Delta m > 2$ GeV

> 96	95	6 ABDALLAH	03M DLPH	$\tilde{t}_1 \rightarrow c\tilde{\chi}_1^0, \theta_t = 0, \Delta m > 10$ GeV
> 92	95	6 ABDALLAH	03M DLPH	$\tilde{t}_1 \rightarrow c\tilde{\chi}_1^0$ , all $\theta_t, \Delta m > 10$ GeV
> 95.7	95	7 ABBIENDI	02H OPAL	$c\tilde{\chi}_1^0$ , all $\theta_t, \Delta m > 10$ GeV
> 92.6	95	7 ABBIENDI	02H OPAL	$b\ell\bar{\nu}$ , all $\theta_t, \Delta m > 10$ GeV
> 91.5	95	7 ABBIENDI	02H OPAL	$b\tau\bar{\nu}$ , all $\theta_t, \Delta m > 10$ GeV
> 63	95	8 HEISTER	02K ALEP	any decay, any lifetime, all $\theta_t$
> 92	95	8 HEISTER	02K ALEP	$\tilde{t}_1 \rightarrow c\tilde{\chi}_1^0$ , all $\theta_t, \Delta m > 8$ GeV, CDF
> 97	95	8 HEISTER	02K ALEP	$\tilde{t}_1 \rightarrow b\ell\bar{\nu}$ , all $\theta_t, \Delta m > 8$ GeV, DØ
> 78	95	8 HEISTER	02K ALEP	$\tilde{t}_1 \rightarrow b\tilde{\chi}_1^0 W^*$ , all $\theta_t, \Delta m > 8$ GeV
••• We do not use the following data for averages, fits, limits, etc. •••				
>309	95	9 AAD	11K ATLS	stable $\tilde{t}_1$
>202	95	10 KHACHATRY...	11C CMS	stable $\tilde{t}_1$
none 128–135	95	11 AALTONEN	10o CDF	$\tilde{t}_1 \rightarrow b\tilde{\chi}_1^\pm \rightarrow b\ell\tilde{\chi}_1^0\nu, m_{\tilde{\chi}_1^\pm} = 106$ GeV, $m_{\tilde{\chi}_1^0} = 48$ GeV
		12 ABAZOV	09N D0	$\tilde{t}_1 \rightarrow b\tilde{\chi}_1^\pm$
		13 ABAZOV	09o D0	$\tilde{t}_1 \rightarrow b\ell\bar{\nu}$
>153	95	14 AALTONEN	08Z CDF	$R, \tilde{t}_1 \rightarrow b\tau$
>185	95	15 ABAZOV	08 D0	$\tilde{t}_1 \rightarrow b\ell\bar{\nu}, m_{\tilde{\nu}} = 70$ GeV
>132		16 AALTONEN	07E CDF	$\tilde{t}_1 \rightarrow c\tilde{\chi}_1^0, m_{\tilde{\chi}_1^0} = 48$ GeV
none 80–134	95	17 ABAZOV	07B D0	$\tilde{t}_1 \rightarrow c\tilde{\chi}_1^0, m_{\tilde{\chi}_1^0} < 48$ GeV
		18 CHEKANOV	07 ZEUS	$e^+p \rightarrow \tilde{t}_1, R, LQ\bar{D}$
> 77	95	19 ABBIENDI	04F OPAL	$R$ , direct, all $\theta_t$
> 77	95	20 ABDALLAH	04M DLPH	$R$ , indirect, all $\theta_t, \Delta m > 5$ GeV
		21 AKTAS	04B H1	$R, \tilde{t}_1$
> 74.5		22 DAS	04 THEO	$\tilde{t}\tilde{t} \rightarrow b\ell\nu\ell\chi^0\bar{b}q\bar{q}'\chi^0, m_{\tilde{\chi}_1^0} = 15$ GeV, no $\tilde{\tau} \rightarrow c\chi^0$
none 50–87	95	23 ABDALLAH	03C DLPH	$\tilde{t}_1 \rightarrow c\tilde{g}, \text{ stable } \tilde{g}, \text{ all } \theta_t, \Delta m > 10$ GeV
none 80–131	95	24 ACOSTA	03C CDF	$\tilde{t}_1 \rightarrow b\ell\bar{\nu}, m_{\tilde{\nu}} \leq 63$ GeV
		25 CHAKRAB...	03 THEO	$p\bar{p} \rightarrow \tilde{t}\tilde{t}^*$ , RPV
> 71.5	95	26 HEISTER	03G ALEP	$\tilde{t}_1, R$ decay
> 80	95	27 HEISTER	03H ALEP	$\tilde{t}_1 \rightarrow c\tilde{g}, \text{ stable } \tilde{g} \text{ or } \tilde{t}, \text{ all } \theta_t, \text{ all } \Delta m$
>144	95	28 ABAZOV	02C D0	$\tilde{t}_1 \rightarrow b\ell\bar{\nu}, m_{\tilde{\nu}} = 45$ GeV
> 77	95	29 ACHARD	02 L3	$\tilde{t}_1, R$ decays
		30 AFFOLDER	01B CDF	$\tilde{t}_1 \rightarrow \tilde{t}\tilde{\chi}_1^0$
> 61	95	31 ABREU	00i DLPH	$R(LLE), \theta_t = 0.98, \Delta m > 4$ GeV
none 68–119	95	32 AFFOLDER	00D CDF	$\tilde{t}_1 \rightarrow c\tilde{\chi}_1^0, m_{\tilde{\chi}_1^0} < 40$ GeV
none 84–120	95	33 AFFOLDER	00G CDF	$\tilde{t}_1 \rightarrow b\ell\bar{\nu}, m_{\tilde{\nu}} < 45$ GeV
>120	95	34 ABE	99M CDF	$p\bar{p} \rightarrow \tilde{t}_1\tilde{t}_1, R$
none 9–24.4	95	35 AID	96 H1	$e p \rightarrow \tilde{t}\tilde{t}, R$ decays
>138	95	36 AID	96 H1	$e p \rightarrow \tilde{t}, R, \lambda\cos\theta_t > 0.03$
> 45		37 CHO	96 RVUE	$B^0\text{--}\bar{B}^0$ and $e, \theta_t = 0.98, \tan\beta < 2$
none 11–41	95	38 BUSKULIC	95E ALEP	$R(LLE), \theta_t = 0.98$
none 6.0–41.2	95	AKERS	94K OPAL	$\tilde{t}_1 \rightarrow c\tilde{\chi}_1^0, \theta_t = 0, \Delta m > 2$ GeV
none 5.0–46.0	95	AKERS	94K OPAL	$\tilde{t}_1 \rightarrow c\tilde{\chi}_1^0, \theta_t = 0, \Delta m > 5$ GeV
none 11.2–25.5	95	AKERS	94K OPAL	$\tilde{t}_1 \rightarrow c\tilde{\chi}_1^0, \theta_t = 0.98, \Delta m > 2$ GeV
none 7.9–41.2	95	AKERS	94K OPAL	$\tilde{t}_1 \rightarrow c\tilde{\chi}_1^0, \theta_t = 0.98, \Delta m > 5$ GeV
none 7.6–28.0	95	39 SHIRAI	94 VNS	$\tilde{t}_1 \rightarrow c\tilde{\chi}_1^0$ , any $\theta_t, \Delta m > 10$ GeV
none 10–20	95	39 SHIRAI	94 VNS	$\tilde{t}_1 \rightarrow c\tilde{\chi}_1^0$ , any $\theta_t, \Delta m > 2.5$ GeV

- 1 ABAZOV 11N looked in 5.4 fb<sup>-1</sup> of p $\bar{p}$  collisions at  $\sqrt{s} = 1.96$  TeV for events with exactly one  $e$  and  $\mu$  and  $E_T$  from the production of  $\tilde{t}_1\tilde{t}_1$ . No evidence for an excess over the SM expectation is observed, and a limit is derived in a plane of  $(m_{\tilde{t}_1}, m_{\tilde{\nu}_\tau})$ , see their Fig. 4, under the assumption of 100% branching ratio for  $\tilde{t}_1 \rightarrow b\ell\bar{\nu}$ .
- 2 AALTONEN 10Y searched in 1 fb<sup>-1</sup> of p $\bar{p}$  collisions at  $\sqrt{s} = 1.96$  TeV for events with an oppositely charged lepton pair ( $e$  or  $\mu$ ),  $E_T$  and at least one jet. A limit is derived on the cross section assuming 100% branching ratio of  $\tilde{t}_1 \rightarrow b\ell\bar{\nu}$  and an invisible  $\tilde{\nu}$ , see their Fig. 10. In Fig. 11, the exclusion contour is shown in the plane of  $(m_{\tilde{t}_1}, m_{\tilde{\nu}_\tau})$ .
- 3 ABAZOV 08Z looked in 995 pb<sup>-1</sup> of p $\bar{p}$  collisions at  $\sqrt{s} = 1.96$  TeV for events with exactly 2 jets, at least one being tagged as heavy quark, and  $E_T$ , originating from stop pair production. Branching ratios are assumed to be 100% for  $\tilde{t}_1 \rightarrow c\tilde{\chi}_1^0$ . No evidence for an excess over the SM expectation is observed. The excluded region is shown in a plane of  $m_{\tilde{t}_1}$  versus  $m_{\tilde{\chi}_1^0}$ , see their Fig. 5. No limit can be obtained for  $m_{\tilde{\chi}_1^0} > 70$  GeV. Supersedes the results of ABAZOV 07b.
- 4 ABAZOV 04 looked at 108.3 pb<sup>-1</sup> of p $\bar{p}$  collisions at  $\sqrt{s} = 1.8$  TeV for events with  $e+\mu+E_T$  as signature for the 3- and 4-body decays of stop into  $b\ell\nu\tilde{\chi}_1^0$  final states. For the  $b\ell\bar{\nu}$  channel they use the results from ABAZOV 02c. No significant excess is observed compared to the Standard Model expectation and limits are derived on the mass of  $\tilde{t}_1$  for the 3- and 4-body decays in the  $(m_{\tilde{t}_1}, m_{\tilde{\chi}_1^0})$  plane, see their Figure 4.
- 5 ACHARD 04 search in the 192–209 GeV data for the production of  $\tilde{t}\tilde{t}$  in acoplanar di-jet final states and, in case of  $b\ell\bar{\nu}$  ( $b\tau\bar{\nu}$ ) final states, two leptons (taus). The limits for  $\theta_t = 0$  improve to 95, 96 and 93 GeV, respectively. All limits assume 100% branching ratio

# Searches Particle Listings

## Supersymmetric Particle Searches

- for the respective decay modes. See Fig. 6 for the dependence of the limits on  $m_{\tilde{\chi}_1^0}$ . These limits supersede ACCIARRI 99v.
- 6** ABDALLAH 03M looked for  $\tilde{t}$  pair production in events with acoplanar jets and  $\cancel{E}$  at  $\sqrt{s} = 189\text{--}208$  GeV. See Fig. 23 and Table 11 for other choices of  $\Delta m$ . These limits include and update the results of ABREUP 00D.
- 7** ABBIENDI 02H looked for events with two acoplanar jets,  $\cancel{E}_T$ , and, in the case of  $b\bar{t}\bar{\nu}$  final states, two leptons, in the 161–209 GeV data. The bound for  $c\tilde{\chi}_1^0$  applies to the region where  $\Delta m < m_W + m_b$ , else the decay  $\tilde{t}_1 \rightarrow b\tilde{\chi}_1^0 W^+$  becomes dominant. The limit for  $b\bar{t}\bar{\nu}$  assumes equal branching ratios for the three lepton flavors and for  $b\tau\bar{\nu}$  100% for this channel. For  $\theta_t=0$ , the bounds improve to  $> 97.6$  GeV ( $c\tilde{\chi}_1^0$ ),  $> 96.0$  GeV ( $b\bar{t}\bar{\nu}$ ), and  $> 95.5$  ( $b\tau\bar{\nu}$ ). See Figs. 5–6 and Table 5 for the more general dependence of the limits on  $\Delta m$ . These results supersede ABBIENDI 99M.
- 8** HEISTER 02k search for top squarks in final states with jets (with/without  $b$  tagging or leptons) or long-lived hadrons, using 183–209 GeV data. The absolute mass bound is obtained by varying the branching ratio of  $\tilde{t} \rightarrow c\tilde{\chi}_1^0$  and the lepton fraction in  $\tilde{t} \rightarrow b\tilde{\chi}_1^0 \ell\bar{\nu}$  decays. The mass bound for  $\tilde{t} \rightarrow c\tilde{\chi}_1^0$  uses the CDF results from AFFOLDER 00b and for  $\tilde{t} \rightarrow b\bar{t}\bar{\nu}$  the DØ results from ABAZOV 02c. See Figs. 2–5 for the more general dependence of the limits on  $\Delta m$ . Updates BARATE 01 and BARATE 00p.
- 9** AAD 11k looked in 34 pb<sup>-1</sup> of  $pp$  collisions at  $\sqrt{s} = 7$  TeV for events with heavy stable particles, identified by their anomalous dE/dx in the tracker or time of flight in the tile calorimeter, from pair production of  $\tilde{t}$ . No evidence for an excess over the SM expectation is observed and limits on the mass are derived for pair production of stop, see Fig. 4.
- 10** KHACHATRYAN 11c looked in 3.1 pb<sup>-1</sup> of  $pp$  collisions at  $\sqrt{s} = 7$  TeV for events with heavy stable particles, identified by their anomalous dE/dx in the tracker or time of flight in the muon chambers, from pair production of  $\tilde{t}_1$ . No evidence for an excess over the expected background is observed. Limits are derived for pair production of stop as a function of mass, see Fig. 3, and compared to the production cross section in a benchmark scenario.
- 11** AALTONEN 10o searched in 2.7 fb<sup>-1</sup> of  $p\bar{p}$  collisions at  $\sqrt{s} = 1.96$  TeV for events with a charged lepton pair ( $e$  or  $\mu$ ),  $\cancel{E}_T$  and at least two jets. A fit of the data is made to the  $\tilde{t}_1\tilde{t}_1$  hypothesis. Assuming a 100% branching ratio of  $\tilde{t}_1 \rightarrow b\tilde{\chi}_1^\pm$ , the exclusion is independent of the value of the  $\tilde{\chi}_1^\pm \rightarrow \ell\tilde{\chi}_1^0 \nu$  branching ratio.
- 12** ABAZOV 09N looked in 0.9 fb<sup>-1</sup> of  $p\bar{p}$  collisions at  $\sqrt{s} = 1.96$  TeV for events with  $\geq 3$  jets, at least one being  $b$ -tagged, one electron or muon and  $\cancel{E}_T$  originating from associated production  $\tilde{t}\bar{t}$ , with one  $\tilde{t}$  decaying leptonically, the other hadronically. The branching ratios for  $\tilde{t}_1 \rightarrow b\tilde{\chi}_1^\pm$  and  $\tilde{\chi}_1^\pm \rightarrow \tilde{\chi}_1^0 W^\pm$  are assumed to be 100%. The separation from the dominant  $\tilde{t}\bar{t}$  background is based on a multivariate likelihood discriminant analysis. The tested mass range is 130 GeV  $\leq m_{\tilde{t}_1} \leq 190$  GeV, 90 GeV  $\leq m_{\tilde{\chi}_1^\pm} \leq 150$  GeV and  $m_{\tilde{\chi}_1^0} = 50$  GeV fixed. The excluded cross section is a factor 2–13 larger than the theoretical expectation in the considered MSSM scenarios, see their Fig. 3.
- 13** ABAZOV 09o looked in 1 fb<sup>-1</sup> of  $p\bar{p}$  collisions at  $\sqrt{s} = 1.96$  TeV for events with two electrons or one electron and one muon and  $\cancel{E}_T$  originating from associated production  $\tilde{t}\bar{t}$ , followed by the three-body decays  $\tilde{t} \rightarrow b\bar{t}\bar{\nu}$ . No evidence for an excess over the SM expectation is observed. The excluded region is shown in a plane of  $m_{\tilde{\nu}}$  versus  $m_{\tilde{t}}$ , see their Fig. 3. The largest excluded  $\tilde{t}$  mass is 175 GeV for a  $\tilde{\nu}$  mass of 45 GeV, and the largest excluded  $\tilde{\nu}$  mass is 96 GeV for a  $\tilde{t}$  mass of 140 GeV. Superseded by ABAZOV 11N.
- 14** AALTONEN 08z searched in 322 pb<sup>-1</sup> of  $p\bar{p}$  collisions at  $\sqrt{s} = 1.96$  TeV for dijet events with a lepton ( $e$  or  $\mu$ ) and a hadronic  $\tau$  decay produced via  $R$ -parity violating couplings  $LQ\bar{D}$ . No heavy flavour-tagged jets are requested. No significant excess was found compared to the background expectation. Upper limits on the cross-section times the square of the branching ratio  $B(\tilde{t}_1 \rightarrow b\tau)$  are extracted, and a limit is derived on the stop mass assuming  $B(\tilde{t}_1 \rightarrow b\tau) = 1$ , see their Fig. 2. Supersedes the results of ACOSTA 04b.
- 15** ABAZOV 08 looked at approximately 400 pb<sup>-1</sup> of  $p\bar{p}$  collisions at  $\sqrt{s} = 1.96$  TeV for events with  $b\bar{t}\bar{\nu}$  with  $\ell\bar{\nu} = e^\pm\mu^\mp$  or  $\ell\bar{\nu} = \mu^\pm\mu^\mp$ , originating from associated production  $\tilde{t}\bar{t}$ . Branching ratios are assumed to be 100% for both  $\tilde{\chi}_1^\pm \rightarrow \tilde{\nu}\bar{\nu}$  and  $\tilde{\nu} \rightarrow \nu\tilde{\chi}_1^0$ . No evidence for an excess over the SM expectation is observed. The excluded region is shown in a plane of  $m_{\tilde{\nu}}$  versus  $m_{\tilde{t}}$ , see their Fig. 3. Superseded by ABAZOV 09o.
- 16** AALTONEN 07e searched in 295 pb<sup>-1</sup> of  $p\bar{p}$  collisions at  $\sqrt{s} = 1.96$  TeV for multijet events with large  $\cancel{E}_T$ . They request at least one heavy flavor-tagged jet and no identified leptons. The branching ratio  $\tilde{t}_1 \rightarrow c\tilde{\chi}_1^0$  is assumed to be 100%. No significant excess was found compared to the background expectation. Upper limits on the cross-section are extracted and a limit is derived on the masses of stop versus  $\tilde{\chi}_1^0$ , see their Fig. 4.
- 17** ABAZOV 07b looked in 360 pb<sup>-1</sup> of  $p\bar{p}$  collisions at  $\sqrt{s} = 1.96$  TeV for events with a pair of acoplanar heavy-flavor jets with  $\cancel{E}_T$ . No excess is observed relative to the SM background expectations. Limits are set on the production of  $\tilde{t}_1$  under the assumption that the only decay mode is into  $c\tilde{\chi}_1^0$ , see their Fig. 4 for the limit in the  $(m_{\tilde{t}_1}, m_{\tilde{\chi}_1^0})$  plane. No limit can be obtained for  $m_{\tilde{\chi}_1^0} > 54$  GeV. Supersedes the results of ABAZOV 04b.
- 18** CHEKANOV 07 search for the  $LQ\bar{D}$   $R$ -parity violating process  $e^+p \rightarrow \tilde{t}_1$  in 65 pb<sup>-1</sup> at 318 GeV. Final states may originate from  $LQ\bar{D}$  couplings  $\tilde{t} \rightarrow e^+d$  and from the  $R$ -parity conserving decay  $\tilde{t} \rightarrow \tilde{\chi}^+b$ , giving rise to  $e + \text{jet}$ ,  $e + \text{multi-jet}$ , and  $\nu + \text{multi-jet}$ . The excluded region in a MSSM scenario is presented for  $\lambda'_{131}$  as a function of the stop mass in Fig. 6. Other excluded regions in a more restricted mSUGRA model are shown in Fig. 7 and 8.
- 19** ABBIENDI 04f use data from  $\sqrt{s} = 189\text{--}209$  GeV. They derive limits on the stop mass under the assumption of  $R$  with  $LQ\bar{D}$  or  $U\bar{D}\bar{D}$  couplings. The limit quoted applies to direct decays with  $U\bar{D}\bar{D}$  couplings when the stop decouples from the  $Z^0$  and improves to 88 GeV for  $\theta_t = 0$ . For  $LQ\bar{D}$  couplings, the limit improves to 98 (100) GeV for  $\lambda'_{13k}$  or  $\lambda'_{23k}$  couplings and all  $\theta_t$  ( $\theta_t = 0$ ). For  $\lambda'_{33k}$  couplings it is 96 (98) GeV for all  $\theta_t$  ( $\theta_t = 0$ ). Supersedes the results of ABBIENDI 00.
- 20** ABDALLAH 04M use data from  $\sqrt{s} = 192\text{--}208$  GeV to derive limits on sparticle masses under the assumption of  $R$  with  $L\bar{L}\bar{E}$  or  $U\bar{D}\bar{D}$  couplings. The results are valid for  $\mu =$
- 200 GeV,  $\tan\beta = 1.5$ ,  $\Delta m > 5$  GeV and assuming a BR of 1 for the given decay. The limit quoted is for decoupling of the stop from the  $Z^0$  and indirect  $U\bar{D}\bar{D}$  decays using the neutralino constraint of 39.5 GeV for  $L\bar{L}\bar{E}$  and of 38.0 GeV for  $U\bar{D}\bar{D}$  couplings, also derived in ABDALLAH 04M. For no mixing (decoupling) and indirect decays via  $L\bar{L}\bar{E}$  the limit improves to 92 (87) GeV if the constraint from the neutralino is used and to 88 (81) GeV if it is not used. For indirect decays via  $U\bar{D}\bar{D}$  couplings it improves to 87 GeV for no mixing and using the constraint from the neutralino, whereas it becomes 81 GeV (67) GeV for no mixing (decoupling) if the neutralino constraint is not used. Supersedes the result of ABREU 01d.
- 21** AKTAS 04B looked in 106 pb<sup>-1</sup> of  $e^\pm p$  collisions at  $\sqrt{s} = 319$  GeV and 301 GeV for resonant production of  $\tilde{t}_1$  by  $R$ -parity violating  $LQ\bar{D}$  couplings with  $\lambda'_{131}$ , others being zero. They consider the decays  $\tilde{t}_1 \rightarrow e^+d$  and  $\tilde{t}_1 \rightarrow W\bar{b}$  followed by  $\bar{b} \rightarrow \bar{\nu}_e d$  and assume gauginos too heavy to participate in the decays. They combine the channels  $j\cancel{E}_T$ ,  $j\mu\cancel{E}_T$ ,  $j\cancel{E}_T$  to derive limits in the plane  $(m_{\tilde{t}_1}, \lambda'_{131})$ , see their Fig. 5.
- 22** DAS 04 reanalyzes AFFOLDER 00g data and obtains constraints on  $m_{\tilde{t}_1}$  as a function of  $B(\tilde{t} \rightarrow b\bar{t}\bar{\nu}) \times B(\tilde{t} \rightarrow b\bar{q}q'\bar{\chi}_1^0)$ ,  $B(\tilde{t} \rightarrow c\tilde{\chi}_1^0)$  and  $m_{\tilde{\chi}_1^0}$ . Bound weakens for larger  $B(\tilde{t} \rightarrow c\tilde{\chi}_1^0)$  and  $m_{\tilde{\chi}_1^0}$ .
- 23** ABDALLAH 03c looked for events of the type  $q\bar{q}R^\pm R^\pm$ ,  $q\bar{q}R^\pm R^0$  or  $q\bar{q}R^0 R^0$  in  $e^+e^-$  interactions at  $\sqrt{s} = 189\text{--}208$  GeV. The  $R^\pm$  bound states are identified by anomalous dE/dx in the tracking chambers and the  $R^0$  by missing energy, due to their reduced energy loss in the calorimeters. Excluded mass regions in the  $(m(\tilde{t}), m(\tilde{g}))$  plane for  $m(\tilde{g}) > 2$  GeV are obtained for several values of the probability for the gluino to fragment into  $R^\pm$  or  $R^0$ , as shown in their Fig. 18. The limit improves to 90 GeV for  $\theta_t = 0$ .
- 24** ACOSTA 03c searched in 107 pb<sup>-1</sup> of  $p\bar{p}$  collisions at  $\sqrt{s} = 1.8$  TeV for pair production of  $\tilde{t}$  followed by the decay  $\tilde{t} \rightarrow b\bar{t}\bar{\nu}$ . They looked for events with two isolated leptons ( $e$  or  $\mu$ ), at least one jet and  $\cancel{E}_T$ . The excluded mass range is reduced for larger  $m_{\tilde{\nu}}$ , and no limit is set for  $m_{\tilde{\nu}} > 88.4$  GeV (see Fig. 2). Superseded by AALTONEN 10v.
- 25** Theoretical analysis of  $e^+e^- + 2$  jet final states from the RPV decay of  $\tilde{t}\bar{t}^*$  pairs produced in  $p\bar{p}$  collisions at  $\sqrt{s} = 1.8$  TeV. 95%CL limits of 220 (165) GeV are derived for  $B(\tilde{t} \rightarrow e q) = 1$  (0.5).
- 26** HEISTER 03G searches for the production of  $\tilde{t}$  pairs in the case of  $R$  prompt decays with  $L\bar{L}\bar{E}$ ,  $LQ\bar{D}$  or  $U\bar{D}\bar{D}$  couplings at  $\sqrt{s} = 189\text{--}209$  GeV. The limit holds for indirect decays mediated by  $R$   $U\bar{D}\bar{D}$  couplings. It improves to 91 GeV for indirect decays mediated by  $R$   $L\bar{L}\bar{E}$  couplings, to 97 GeV for direct (assuming  $B(\tilde{t}_1 \rightarrow q\tau) = 100\%$ ) and to 85 GeV for indirect decays mediated by  $R$   $LQ\bar{D}$  couplings. Supersedes the results from BARATE 01b.
- 27** HEISTER 03H use  $e^+e^-$  data from 183–208 GeV to look for the production of stop decaying into a  $c$  quark and a stable gluino hadronizing into charged or neutral  $R$ -hadrons. Combining these results with bounds on stable squarks and on a stable gluino LSP from the same paper yields the quoted limit. See their Fig. 13 for the dependence of the mass limit on the gluino mass and on  $\theta_t$ .
- 28** ABAZOV 02c looked in 108.3 pb<sup>-1</sup> of  $p\bar{p}$  collisions at  $\sqrt{s} = 1.8$  TeV for events with  $e\mu\cancel{E}_T$  originating from associated production  $\tilde{t}\bar{t}$ . Branching ratios are assumed to be 100%. The bound for the  $b\bar{t}\bar{\nu}$  decay weakens for large  $\tilde{\nu}$  mass (see Fig. 3), and no limit is set when  $m_{\tilde{\nu}} > 85$  GeV. See Fig. 4 for the limits in case of decays to a real  $\tilde{\chi}_1^\pm$ , followed by  $\tilde{\chi}_1^\pm \rightarrow \ell\bar{\nu}$ , as a function of  $m_{\tilde{\chi}_1^\pm}$ .
- 29** ACHARD 02 searches for the production of squarks in the case of  $R$  prompt decays with  $U\bar{D}\bar{D}$  couplings at  $\sqrt{s} = 189\text{--}208$  GeV. The search is performed for direct and indirect decays, assuming one coupling at the time to be nonzero. The limit is computed for the minimal cross section and holds for both direct and indirect decays.
- 30** AFFOLDER 01B searches for decays of the top quark into stop and LSP, in  $\tilde{t}\bar{t}$  events. Limits on the stop mass as a function of the LSP mass and of the decay branching ratio are shown in Fig. 3. They exclude branching ratios in excess of 45% for SLP masses up to 40 GeV.
- 31** ABREU 00I searches for the production of stop in the case of  $R$ -parity violation with  $L\bar{L}\bar{E}$  couplings, for which only indirect decays are allowed. They investigate topologies with jets plus leptons in data from  $\sqrt{s} = 183$  GeV. The lower bound on the stop mass assumes a neutralino mass limit of 27 GeV, also derived in ABREU 00I.
- 32** AFFOLDER 00b search for final states with 2 or 3 jets and  $\cancel{E}_T$ , one jet with a  $c$  tag. See their Fig. 2 for the mass exclusion in the  $(m_{\tilde{t}_1}, m_{\tilde{\chi}_1^0})$  plane. The maximum excluded  $m_{\tilde{t}_1}$  value is 119 GeV, for  $m_{\tilde{\chi}_1^0} = 40$  GeV.
- 33** AFFOLDER 00g searches for  $\tilde{t}_1\tilde{t}_1^*$  production, with  $\tilde{t}_1 \rightarrow b\bar{t}\bar{\nu}$ , leading to topologies with  $\geq 1$  isolated lepton ( $e$  or  $\mu$ ),  $\cancel{E}_T$ , and  $\geq 2$  jets with  $\geq 1$  tagged as  $b$  quark by a secondary vertex. See Fig. 4 for the excluded mass range as a function of  $m_{\tilde{\nu}}$ . Cross-section limits for  $\tilde{t}_1\tilde{t}_1^*$ , with  $\tilde{t}_1 \rightarrow b\tilde{\chi}_1^\pm$  ( $\tilde{\chi}_1^\pm \rightarrow \ell^\pm\nu\tilde{\chi}_1^0$ ), are given in Fig. 2. Superseded by AALTONEN 10v.
- 34** ABE 99M looked in 107 pb<sup>-1</sup> of  $p\bar{p}$  collisions at  $\sqrt{s} = 1.8$  TeV for events with like sign dielectrons and two or more jets from the sequential decays  $\tilde{q} \rightarrow q\tilde{\chi}_1^0$  and  $\tilde{\chi}_1^0 \rightarrow e q\bar{q}'$ , assuming  $R$  coupling  $L_1 Q_j D_k^c$ , with  $j=2,3$  and  $k=1,2,3$ . They assume  $B(\tilde{t}_1 \rightarrow c\tilde{\chi}_1^0) = 1$ ,  $B(\tilde{\chi}_1^0 \rightarrow e q\bar{q}') = 0.25$  for both  $e^+$  and  $e^-$ , and  $m_{\tilde{\chi}_1^0} \geq m_{\tilde{t}_1}/2$ . The limit improves for heavier  $\tilde{\chi}_1^0$ .
- 35** AID 96 considers photoproduction of  $\tilde{t}\bar{t}$  pairs, with 100%  $R$ -parity violating decays of  $\tilde{t}$  to  $e q$ , with  $q=d, s$ , or  $b$  quarks.
- 36** AID 96 considers production and decay of  $\tilde{t}$  via the  $R$ -parity violating coupling  $\lambda' L_1 Q_3 \tilde{t}_1^*$ .
- 37** CHO 96 studied the consistency among the  $B^0\text{--}\bar{B}^0$  mixing,  $\epsilon$  in  $K^0\text{--}\bar{K}^0$  mixing, and the measurements of  $V_{cb}$ ,  $V_{ub}/V_{cb}$ . For the range 25.5 GeV  $< m_{\tilde{t}_1} < m_Z/2$  left by AKERS 94k for  $\theta_t = 0.98$ , and within the allowed range in  $M_2\text{--}\mu$  parameter space from chargino, neutralino searches by ACCIARRI 95e, they found the scalar top contribution to  $B^0\text{--}\bar{B}^0$  mixing and  $\epsilon$  to be too large if  $\tan\beta < 2$ . For more on their assumptions, see the paper and their reference 10.
- 38** BUSKULIC 95E looked for  $Z \rightarrow \tilde{t}\bar{t}$ , where  $\tilde{t} \rightarrow c\tilde{\chi}_1^0$  and  $\tilde{\chi}_1^0$  decays via  $R$ -parity violating interactions into two leptons and a neutrino.

See key on page 457

# Searches Particle Listings

## Supersymmetric Particle Searches

<sup>39</sup> SHIRAI 94 bound assumes the cross section without the s-channel Z-exchange and the QCD correction, underestimating the cross section up to 20% and 30%, respectively. They assume  $m_c=1.5$  GeV.

### Heavy $\tilde{g}$ (Gluino) MASS LIMIT

For  $m_{\tilde{g}} > 60\text{--}70$  GeV, it is expected that gluinos would undergo a cascade decay via a number of neutralinos and/or charginos rather than undergo a direct decay to photinos as assumed by some papers. Limits obtained when direct decay is assumed are usually higher than limits when cascade decays are included. Limits made obsolete by the most recent analyses of  $p\bar{p}$  collisions can be found in previous Editions of this Review.

VALUE (GeV)	CL%	DOCUMENT ID	TECN	COMMENT
> 520	95	<sup>1</sup> AAD	11AF ATLS	$\geq 6$ jets + $\cancel{E}_T$ , CMSSM
> 700	95	<sup>2</sup> AAD	11G ATLS	$\ell$ +jets+ $\cancel{E}_T$ , $\tan\beta=3$ , $A_0=0$ , $\mu > 0$ , $m_{\tilde{g}}=m_{\tilde{q}}$
> 500	95	<sup>3</sup> AAD	11N ATLS	jets+ $\cancel{E}_T$ , degenerate $m_{\tilde{q}}$ of first two generations, $m_{\tilde{\chi}_1^0}=0$ , all other supersymmetric particles heavy, any $m_{\tilde{q}}$
> 870	95	<sup>3</sup> AAD	11N ATLS	jets+ $\cancel{E}_T$ , degenerate $m_{\tilde{q}}$ of first two generations, $m_{\tilde{\chi}_1^0}=0$ , all other supersymmetric particles heavy, $m_{\tilde{q}}=m_{\tilde{g}}$
> 775	95	<sup>3</sup> AAD	11N ATLS	jets+ $\cancel{E}_T$ , CMSSM, $m_{\tilde{q}}=m_{\tilde{g}}$
> 590	95	<sup>4</sup> AAD	11o ATLS	$\tilde{g} \rightarrow \tilde{b}_1 b$ , $\tilde{b}_1 \rightarrow b\tilde{\chi}_1^0$ , $m_{\tilde{\chi}_1^0}=60$ GeV
> 500	95	<sup>5</sup> CHATRCHYAN 11AC	CMS	jets + $\cancel{E}_T$ , CMSSM, $m_{\tilde{q}} < 1000$ GeV
> 280	95	<sup>6</sup> AALTONEN	09s CDF	jets+ $\cancel{E}_T$ , $\tan\beta=5$ , $\mu < 0$ , $A_0=0$ , any $m_{\tilde{q}}$
> 392	95	<sup>6</sup> AALTONEN	09s CDF	jets+ $\cancel{E}_T$ , $\tan\beta=5$ , $\mu < 0$ , $A_0=0$ , $m_{\tilde{q}}=m_{\tilde{g}}$
> 308	95	<sup>7</sup> ABAZOV	08G D0	jets+ $\cancel{E}_T$ , $\tan\beta=3$ , $\mu < 0$ , $A_0=0$ , any $m_{\tilde{q}}$
> 390	95	<sup>7</sup> ABAZOV	08G D0	jets+ $\cancel{E}_T$ , $\tan\beta=3$ , $\mu < 0$ , $A_0=0$ , $m_{\tilde{q}}=m_{\tilde{g}}$
> 270	95	<sup>8</sup> ABULENCIA	06i CDF	$\tilde{g} \rightarrow \tilde{b}b$ , $\Delta m > 6$ GeV, $\tilde{b}_1 \rightarrow b\tilde{\chi}_1^0$ , $m_{\tilde{b}_1} < 220$ GeV
> 195	95	<sup>9</sup> AFFOLDER	02 CDF	Jets+ $\cancel{E}_T$ , any $m_{\tilde{q}}$
> 300	95	<sup>9</sup> AFFOLDER	02 CDF	Jets+ $\cancel{E}_T$ , $m_{\tilde{q}}=m_{\tilde{g}}$
> 129	95	<sup>10</sup> ABBOTT	01D D0	$\ell\ell$ +jets+ $\cancel{E}_T$ , $\tan\beta < 10$ , $m_0 < 300$ GeV, $\mu < 0$ , $A_0=0$
> 175	95	<sup>10</sup> ABBOTT	01D D0	$\ell\ell$ +jets+ $\cancel{E}_T$ , $\tan\beta=2$ , large $m_0$ , $\mu < 0$ , $A_0=0$
> 255	95	<sup>10</sup> ABBOTT	01D D0	$\ell\ell$ +jets+ $\cancel{E}_T$ , $\tan\beta=2$ , $m_{\tilde{g}}=m_{\tilde{q}}$ , $\mu < 0$ , $A_0=0$
> 168	95	<sup>11</sup> AFFOLDER	01J CDF	$\ell\ell$ +Jets+ $\cancel{E}_T$ , $\tan\beta=2$ , $\mu=-800$ GeV, $m_{\tilde{q}} \gg m_{\tilde{g}}$
> 221	95	<sup>11</sup> AFFOLDER	01J CDF	$\ell\ell$ +Jets+ $\cancel{E}_T$ , $\tan\beta=2$ , $\mu=-800$ GeV, $m_{\tilde{q}}=m_{\tilde{g}}$
> 190	95	<sup>12</sup> ABBOTT	99L D0	Jets+ $\cancel{E}_T$ , $\tan\beta=2$ , $\mu < 0$ , $A=0$
> 260	95	<sup>12</sup> ABBOTT	99L D0	Jets+ $\cancel{E}_T$ , $m_{\tilde{g}}=m_{\tilde{q}}$
••• We do not use the following data for averages, fits, limits, etc. •••				
> 560	95	<sup>13</sup> CHATRCHYAN 12	CMS	$e, \mu$ , jets, razor, CMSSM
> 155	95	<sup>14</sup> AAD	11X ATLS	$\tilde{g} \rightarrow \tilde{\chi}_1^0 X \rightarrow \gamma \tilde{G} X$
> 155	95	<sup>15</sup> AALTONEN	11q CDF	$R, \tilde{U}\tilde{D}\tilde{D}, m_{\tilde{q}}=m_{\tilde{g}} + 10$ GeV
> 1040	95	<sup>16</sup> CHATRCHYAN 11AB	CMS	$\ell \pm \ell \pm$
> 1040	95	<sup>17</sup> CHATRCHYAN 11G	CMS	$\tilde{\chi}_1^0 \rightarrow \gamma \tilde{G}$
> 1040	95	<sup>18</sup> CHATRCHYAN 11Q	CMS	$\ell$ + jets + $\cancel{E}_T$
> 1040	95	<sup>19</sup> CHATRCHYAN 11V	CMS	GMSB scenario, $\tilde{\tau}$ co-NLSP
> 1040	95	<sup>20</sup> CHATRCHYAN 11W	CMS	jets + $\cancel{E}_T$ , CMSSM
> 1040	95	<sup>21</sup> KHACHATRY...11i	CMS	jets + $\cancel{E}_T$
> 224	95	<sup>22</sup> ABAZOV	02F D0	$R \lambda_{2jk}$ indirect decays, $\tan\beta=2$ , any $m_{\tilde{q}}$
> 265	95	<sup>22</sup> ABAZOV	02F D0	$R \lambda'_{2jk}$ indirect decays, $\tan\beta=2$ , $m_{\tilde{q}}=m_{\tilde{g}}$
> 240	95	<sup>23</sup> ABAZOV	02G D0	$p\bar{p} \rightarrow \tilde{g}\tilde{g}, \tilde{g}\tilde{q}$
> 240	95	<sup>24</sup> CHEUNG	02B THEO	
> 240	95	<sup>25</sup> BERGER	01 THEO	$p\bar{p} \rightarrow X+b$ -quark
> 240	95	<sup>26</sup> ABBOTT	99 D0	$\tilde{g} \rightarrow \tilde{\chi}_2^0 X \rightarrow \tilde{\chi}_1^0 \gamma X$ , $m_{\tilde{\chi}_2^0} - m_{\tilde{\chi}_1^0} > 20$ GeV
> 320	95	<sup>26</sup> ABBOTT	99 D0	$\tilde{g} \rightarrow \tilde{\chi}_1^0 X \rightarrow \tilde{G} \gamma X$
> 227	95	<sup>27</sup> ABBOTT	99K D0	any $m_{\tilde{q}}$ , $R$ , $\tan\beta=2$ , $\mu < 0$
> 212	95	<sup>28</sup> ABACHI	95c D0	$m_{\tilde{g}} \geq m_{\tilde{q}}$ ; with cascade decays

> 144	95	<sup>28</sup> ABACHI	95c D0	Any $m_{\tilde{q}}$ ; with cascade decays
		<sup>29</sup> ABE	95T CDF	$\tilde{g} \rightarrow \tilde{\chi}_2^0 \rightarrow \tilde{\chi}_1^0 \gamma$
		<sup>30</sup> HEBBEKER	93 RVUE	$e^+e^-$ jet analyses
> 218	90	<sup>31</sup> ABE	92L CDF	$m_{\tilde{q}} \leq m_{\tilde{g}}$ ; with cascade decay
> 100		<sup>32</sup> ROY	92 RVUE	$p\bar{p} \rightarrow \tilde{g}\tilde{g}; R$
		<sup>33</sup> NOJIRI	91 COSM	
none 4-53	90	<sup>34</sup> ALBAJAR	87D UA1	Any $m_{\tilde{q}} > m_{\tilde{g}}$
none 4-75	90	<sup>34</sup> ALBAJAR	87D UA1	$m_{\tilde{q}} = m_{\tilde{g}}$
none 16-58	90	<sup>35</sup> ANSARI	87D UA2	$m_{\tilde{q}} \lesssim 100$ GeV

- AAD 11AF looked in  $1.34 \text{ fb}^{-1}$  of  $pp$  collisions at  $\sqrt{s} = 7$  TeV for events with 6 up to 8 jets and  $\cancel{E}_T$ . No evidence for an excess over the expected background is observed. Limits are derived in the CMSSM  $(m_0, m_{1/2})$  plane for  $\tan\beta = 10$  (see Fig. 5). The limit improves to  $m_{\tilde{g}} > 680$  GeV for  $m_{\tilde{q}} = 2 m_{\tilde{g}}$ .
- AAD 11G looked in  $35 \text{ pb}^{-1}$  of  $p\bar{p}$  collisions at  $\sqrt{s} = 7$  TeV for events with a single lepton ( $e$  or  $\mu$ ), jets and  $\cancel{E}_T$  from the production of squarks and gluinos. No evidence for an excess over the SM expectation is observed, and a limit is derived in the CMSSM  $(m_0, m_{1/2})$  plane for  $\tan\beta = 3$ , see Fig. 2.
- AAD 11N looked in  $35 \text{ pb}^{-1}$  of  $pp$  collisions at  $\sqrt{s} = 7$  TeV for events with  $\geq 2$  jets and  $\cancel{E}_T$ . Four signal regions were defined, and the background model was found to be in good agreement with the data. Limits are derived in the  $(m_{\tilde{g}}, m_{\tilde{q}})$  plane (see Fig. 2) for a simplified model where degenerate masses of the squarks of the first two generations are assumed,  $m_{\tilde{\chi}_1^0} = 0$ , and all other masses including third generation squarks are set to 5 TeV. Limits are also derived in the CMSSM  $(m_0, m_{1/2})$  plane (see Fig. 3) for  $\tan\beta = 3$ .
- AAD 11o looked in  $35 \text{ pb}^{-1}$  of  $pp$  collisions at  $\sqrt{s} = 7$  TeV for events with jets, of which at least one is a  $b$ -jet, and  $\cancel{E}_T$ . No excess above the Standard Model was found. Limits are derived in the  $(m_{\tilde{g}}, m_{\tilde{b}_1})$  plane (see Fig. 2) under the assumption of 100% branching ratios and  $\tilde{b}_1$  being the lightest squark. The quoted limit is valid for  $m_{\tilde{b}_1} < 500$  GeV. A similar approach for  $\tilde{t}_1$  as the lightest squark with  $\tilde{g} \rightarrow \tilde{t}_1 t$  and  $\tilde{t}_1 \rightarrow b\tilde{\chi}_1^\pm$  with 100% branching ratios leads to a gluino mass limit of 520 GeV for  $130 < m_{\tilde{t}_1} < 300$  GeV. Limits are also derived in the CMSSM  $(m_0, m_{1/2})$  plane for  $\tan\beta = 40$ , see Fig. 4, and in scenarios based on the gauge group  $SO(10)$ .
- CHATRCHYAN 11AC looked in  $36 \text{ pb}^{-1}$  of  $p\bar{p}$  collisions at  $\sqrt{s} = 7$  TeV for events with  $\geq 3$  jets, a large total transverse energy, and  $\cancel{E}_T$ . No evidence for an excess over the expected background is observed. Limits are derived in the CMSSM  $(m_0, m_{1/2})$  plane and the  $(m_{\tilde{g}}, m_{\tilde{q}})$  plane for  $\tan\beta = 10$  (see Fig. 10). Limits are also obtained for Simplified Model Spectra.
- AALTONEN 09s searched in  $2 \text{ fb}^{-1}$  of  $p\bar{p}$  collisions at  $\sqrt{s} = 1.96$  TeV for events with at least 2 jets and  $\cancel{E}_T$ . No evidence for a signal is observed. A limit is derived for a MSUGRA scenario in the  $m_{\tilde{q}}$  versus  $m_{\tilde{g}}$  plane, see their Fig. 2.
- ABAZOV 08G looked in  $2.1 \text{ fb}^{-1}$  of  $p\bar{p}$  collisions at  $\sqrt{s}=1.96$  TeV for events with acoplanar jets or multijets with large  $\cancel{E}_T$ . No significant excess was found compared to the background expectation. A limit is derived on the masses of squarks and gluinos for specific MSUGRA parameter values, see Figure 3. Similar results would be obtained for a large class of parameter sets. Supersedes the results of ABAZOV 06c.
- ABULENCIA 06i searched in  $156 \text{ pb}^{-1}$  of  $p\bar{p}$  collisions at  $\sqrt{s} = 1.96$  TeV for multijet events with large  $\cancel{E}_T$ . They request at least 2  $b$ -tagged jets and no isolated leptons. They investigate the production of gluinos decaying into  $\tilde{b}_1 b$  followed by  $\tilde{b}_1 \rightarrow b\tilde{\chi}_1^0$ . Both branching fractions are assumed to be 100% and the LSP mass to be 60 GeV. No significant excess was found compared to the background expectation. Upper limits on the cross-section are extracted and a limit is derived on the masses of sbottom and gluinos, see their Fig. 3.
- AFFOLDER 02 searched in  $\sim 84 \text{ pb}^{-1}$  of  $p\bar{p}$  collisions for events with  $\geq 3$  jets and  $\cancel{E}_T$ , arising from the production of gluinos and/or squarks. Limits are derived by scanning the parameter space, for  $m_{\tilde{q}} \geq m_{\tilde{g}}$  in the framework of minimal Supergravity, assuming five flavors of degenerate squarks, and for  $m_{\tilde{q}} < m_{\tilde{g}}$  in the framework of constrained MSSM, assuming conservatively four flavors of degenerate squarks. See Fig. 3 for the variation of the limit as function of the squark mass. Supersedes the results of ABE 97k.
- ABBOTT 01b looked in  $\sim 108 \text{ pb}^{-1}$  of  $p\bar{p}$  collisions at  $\sqrt{s}=1.8$  TeV for events with  $e, \mu, \mu, \mu$ , or  $e, \mu$  accompanied by at least 2 jets and  $\cancel{E}_T$ . Excluded regions are obtained in the MSUGRA framework from a scan over the parameters  $0 < m_0 < 300$  GeV,  $10 < m_{1/2} < 110$  GeV, and  $1.2 < \tan\beta < 10$ .
- AFFOLDER 01j searched in  $\sim 106 \text{ pb}^{-1}$  of  $p\bar{p}$  collisions for events with 2like-sign leptons ( $e$  or  $\mu$ ),  $\geq 2$  jets and  $\cancel{E}_T$ , expected to arise from the production of gluinos and/or squarks with cascade decays into  $\tilde{\chi}^\pm$  or  $\tilde{\chi}_2^0$ . Spectra and decay rates are evaluated in the framework of minimal Supergravity, assuming five flavors of degenerate squarks and a pseudoscalar Higgs mass  $m_A=500$  GeV. The limits are derived for  $\tan\beta=2$ ,  $\mu=-800$  GeV, and scanning over  $m_{\tilde{g}}$  and  $m_{\tilde{q}}$ . See Fig. 2 for the variation of the limit as function of the squark mass. These limits supersede the results of ABE 96d.
- ABBOTT 99l consider events with three or more jets and large  $\cancel{E}_T$ . Spectra and decay rates are evaluated in the framework of minimal Supergravity, assuming five flavors of degenerate squarks, and scanning the space of the universal gaugino  $(m_{1/2})$  and scalar  $(m_0)$  masses. See their Figs. 2-3 for the dependence of the limit on the relative value of  $m_{\tilde{q}}$  and  $m_{\tilde{g}}$ .
- CHATRCHYAN 12 looked in  $35 \text{ pb}^{-1}$  of  $pp$  collisions at  $\sqrt{s} = 7$  TeV for events with  $e$  and/or  $\mu$  and/or jets, a large total transverse energy, and  $\cancel{E}_T$ . The event selection is based on the dimensionless razor variable  $R$ , related to the  $\cancel{E}_T$  and  $M_R$ , an indicator of the heavy particle mass scale. No evidence for an excess over the expected background is observed. Limits are derived in the CMSSM  $(m_0, m_{1/2})$  plane for  $\tan\beta = 3, 10$  and 50 (see Fig. 7 and 8). Limits are also obtained for Simplified Model Spectra.

# Searches Particle Listings

## Supersymmetric Particle Searches

- 14 AAD 11x looked in  $36 \text{ pb}^{-1}$  of  $pp$  collisions at  $\sqrt{s} = 7 \text{ TeV}$  for events with  $\geq 2$  photons and  $\cancel{E}_T$  from the pair production of gluinos with cascade decays to  $\tilde{\chi}_1^0$  followed by  $\tilde{\chi}_1^0 \rightarrow \gamma \tilde{G}$  prompt decay. No evidence for an excess over the SM expectation is observed, and a limit on the number of new physics events is set. Limits are derived in a Generalized Gauge Mediated model in the  $(m_{\tilde{g}}, m_{\tilde{\chi}_1^0})$  plane (see Fig. 5) under the assumptions  $\tan\beta = 2$  and all sparticle masses at 1.5 TeV, except the  $\tilde{g}$ ,  $\tilde{\chi}_1^0$ , and  $\tilde{G}$ .
- 15 AALTONEN 11Q searched in  $3.2 \text{ fb}^{-1}$  of  $p\bar{p}$  collisions at  $\sqrt{s} = 1.96 \text{ TeV}$  for events with at least 6 jets from the pair production of gluinos and squarks with the subsequent decays  $\tilde{g} \rightarrow 3$  jets in the MSSM framework with  $R$ . No statistically significant bumps in the 3-jet systems are observed over the SM background. Limits on the cross section times branching ratio are derived as a function of the gluino mass, displayed in Fig. 3. For decoupled squarks in the range  $0.5 < m_{\tilde{q}} < 0.7 \text{ TeV}$  gluinos are excluded below 144 GeV. The quoted limit is for near degeneracy of squark and gluino masses.
- 16 CHATRCHYAN 11AB looked in  $35 \text{ pb}^{-1}$  of  $pp$  collisions at  $\sqrt{s} = 7 \text{ TeV}$  for events with  $\geq 2$  same charge isolated leptons ( $e, \mu$  or  $\tau$ ), jets and  $\cancel{E}_T$ . Such events might be produced from  $\tilde{g}\tilde{g}$  or  $\tilde{g}\tilde{q}$  decaying via charginos into leptons. No evidence for an excess over the expected background is observed. Limits are derived in the CMSSM  $(m_0, m_{1/2})$  plane for  $\tan\beta = 3$  (see Fig. 10).
- 17 CHATRCHYAN 11G looked in  $36 \text{ pb}^{-1}$  of  $pp$  collisions at  $\sqrt{s} = 7 \text{ TeV}$  for events with  $\geq 2$  isolated photons,  $\geq 1$  jet and  $\cancel{E}_T$ , which may arise in a generalized gauge mediated model from the decay of a  $\tilde{\chi}_1^0$  NLSP. No evidence for an excess over the expected background is observed. Limits are derived in the plane of squark versus gluino mass (see Fig. 4) for several values of  $m_{\tilde{\chi}_1^0}$ .
- 18 CHATRCHYAN 11Q looked in  $36 \text{ pb}^{-1}$  of  $pp$  collisions at  $\sqrt{s} = 7 \text{ TeV}$  for events with a single isolated lepton ( $e$  or  $\mu$ ),  $\geq 4$  jets and  $\cancel{E}_T$ . No evidence for an excess over the expected background is observed. Limits are derived in the CMSSM  $(m_0, m_{1/2})$  plane for  $\tan\beta = 10$  (see Fig. 7).
- 19 CHATRCHYAN 11V looked in  $35 \text{ pb}^{-1}$  of  $pp$  collisions at  $\sqrt{s} = 7 \text{ TeV}$  for events with  $\geq 3$  isolated leptons ( $e, \mu$  or  $\tau$ ), with or without jets and  $\cancel{E}_T$ . Multi-lepton final states originate from  $\tilde{q} \rightarrow \tilde{\chi}_1^0 + X$ , followed by  $\tilde{\chi}_1^0 \rightarrow \tilde{\tau}^+ \ell^{\mp}$  and  $\tilde{\ell} \rightarrow \ell \tilde{G}$ . No evidence for an excess over the expected background is observed. Limits are derived (see Fig. 4) for a GMSB-type scenario with mass-degenerate right-handed sleptons (slepton co-NLSP scenario).
- 20 CHATRCHYAN 11W looked in  $1.14 \text{ fb}^{-1}$  of  $pp$  collisions at  $\sqrt{s} = 7 \text{ TeV}$  for events with  $\geq 2$  jets, large total jet energy, and  $\cancel{E}_T$ . After combining multi-jet events into two pseudo-jets signal events are selected by a cut on  $\alpha_T = E_T^2/M_T$ , the transverse energy of the less energetic jet over the transverse mass. Given the lack of an excess over the SM backgrounds, limits are derived in the CMSSM  $(m_0, m_{1/2})$  plane (see Fig. 4) for  $\tan\beta = 10$ . The limits are only weakly dependent on  $\tan\beta$  and  $A_0$ .
- 21 KHACHATRYAN 11I looked in  $35 \text{ pb}^{-1}$  of  $pp$  collisions at  $\sqrt{s} = 7 \text{ TeV}$  for events with  $\geq 2$  jets and  $\cancel{E}_T$ . After combining multi-jet events into two pseudo-jets signal events are selected by a cut on  $\alpha_T = E_T^2/M_T$ , the transverse energy of the less energetic jet over the transverse mass. No evidence for an excess over the expected background is observed. Limits are derived in the CMSSM  $(m_0, m_{1/2})$  plane (see Fig. 5) for  $\tan\beta = 3$ . Superseded by CHATRCHYAN 11W.
- 22 ABAZOV 02F looked in  $77.5 \text{ pb}^{-1}$  of  $p\bar{p}$  collisions at 1.8 TeV for events with  $\geq 2\mu + \geq 4$  jets, originating from associated production of squarks followed by an indirect  $R$  decay (of the  $\tilde{\chi}_1^0$ ) via  $LQD$  couplings of the type  $\lambda_{2jk}^i$  where  $j=1,2$  and  $k=1,2,3$ . Bounds are obtained in the MSUGRA scenario by a scan in the range  $0 \leq M_0 \leq 400 \text{ GeV}$ ,  $60 \leq m_{1/2} \leq 120 \text{ GeV}$  for fixed values  $A_0=0$ ,  $\mu < 0$ , and  $\tan\beta=2$  or  $6$ . The bounds are weaker for  $\tan\beta=6$ . See Figs. 2,3 for the exclusion contours in  $m_{1/2}$  versus  $m_0$  for  $\tan\beta=2$  and  $6$ , respectively.
- 23 ABAZOV 02G search for associated production of gluinos and squarks in  $92.7 \text{ pb}^{-1}$  of  $p\bar{p}$  collisions at  $\sqrt{s}=1.8 \text{ TeV}$ , using events with one electron,  $\geq 4$  jets, and large  $\cancel{E}_T$ . The results are compared to a MSUGRA scenario with  $\mu < 0$ ,  $A_0=0$ , and  $\tan\beta=3$  and allow to exclude a region of the  $(m_0, m_{1/2})$  shown in Fig. 11.
- 24 CHEUNG 02B studies the constraints on a  $\tilde{b}_1$  with mass in the 2.2-5.5 GeV region and a gluino in the mass range 12-16 GeV, using precision measurements of  $Z^0$  decays and  $e^+e^-$  annihilations at LEP2. Few detectable events are predicted in the LEP2 data for the model proposed by BERGER 01.
- 25 BERGER 01 reanalyzed interpretation of Tevatron data on bottom-quark production. Argues that pair production of light gluinos ( $m \sim 12-16 \text{ GeV}$ ) with subsequent 2-body decay into a light sbottom ( $m \sim 2-5.5 \text{ GeV}$ ) and bottom can reconcile Tevatron data with predictions of perturbative QCD for the bottom production rate. The sbottom must either decay hadronically via a  $R$ -parity- and  $B$ -violating interaction, or be long-lived.
- 26 ABBOTT 99 searched for  $\gamma\cancel{E}_T + \geq 2$  jet final states, and set limits on  $\sigma(p\bar{p} \rightarrow \tilde{g} + X) \cdot \text{B}(\tilde{g} \rightarrow \gamma\cancel{E}_T X)$ . The quoted limits correspond to  $m_{\tilde{g}} \geq m_{\tilde{g}}$ , with  $\text{B}(\tilde{\chi}_2^0 \rightarrow \tilde{\chi}_1^0 \gamma) = 1$  and  $\text{B}(\tilde{\chi}_1^0 \rightarrow \tilde{G} \gamma) = 1$ , respectively. They improve to 310 GeV (360 GeV in the case of  $\gamma\tilde{G}$  decay) for  $m_{\tilde{g}} = m_{\tilde{q}}$ .
- 27 ABBOTT 99k uses events with an electron pair and four jets to search for the decay of the  $\tilde{\chi}_1^0$  LSP via  $R LQD$  couplings. The particle spectrum and decay branching ratios are taken in the framework of minimal supergravity. An excluded region at 95% CL is obtained in the  $(m_0, m_{1/2})$  plane under the assumption that  $A_0=0$ ,  $\mu < 0$ ,  $\tan\beta=2$  and any one of the couplings  $\lambda_{1jk}^i > 10^{-3}$  ( $j=1,2$  and  $k=1,2,3$ ) and from which the above limit is computed. For equal mass squarks and gluinos, the corresponding limit is 277 GeV. The results are essentially independent of  $A_0$ , but the limit deteriorates rapidly with increasing  $\tan\beta$  or  $\mu > 0$ .
- 28 ABACHI 95c assume five degenerate squark flavors with  $m_{\tilde{q}_i} = m_{\tilde{q}_R}$ . Sleptons are assumed to be heavier than squarks. The limits are derived for fixed  $\tan\beta = 2.0$ ,  $\mu = -250 \text{ GeV}$ , and  $m_{H^\pm} = 500 \text{ GeV}$ , and with the cascade decays of the squarks and gluinos calculated within the framework of the Minimal Supergravity scenario. The bounds are weakly sensitive to the three fixed parameters for a large fraction of parameter space.
- 29 ABE 95T looked for a cascade decay of gluino into  $\tilde{\chi}_2^0$  which further decays into  $\tilde{\chi}_1^0$  and a photon. No signal is observed. Limits vary widely depending on the choice of parameters. For  $\mu = -40 \text{ GeV}$ ,  $\tan\beta = 1.5$ , and heavy squarks, the range  $50 < m_{\tilde{g}} (\text{GeV}) < 140$  is excluded at 90% CL. See the paper for details.

- 30 HEBBEKER 93 combined jet analyses at various  $e^+e^-$  colliders. The 4-jet analyses at TRISTAN/LEP and the measured  $\alpha_s$  at PEP/PETRA/TRISTAN/LEP are used. A constraint on effective number of quarks  $N=6.3 \pm 1.1$  is obtained, which is compared to that with a light gluino,  $N=8$ .
- 31 ABE 92L bounds are based on similar assumptions as ABACHI 95c. Not sensitive to  $m_{\text{gluino}} < 40 \text{ GeV}$  (but other experiments rule out that region).
- 32 ROY 92 reanalyzed CDF limits on di-lepton events to obtain limits on gluino production in  $R$ -parity violating models. The 100% decay  $\tilde{g} \rightarrow q\bar{q}\tilde{\chi}$  where  $\tilde{\chi}$  is the LSP, and the LSP decays either into  $\ell q\bar{d}$  or  $\ell\ell\bar{e}$  is assumed.
- 33 NOJIRI 91 argues that a heavy gluino should be nearly degenerate with squarks in minimal supergravity not to overclose the universe.
- 34 The limits of ALBAJAR 87D are from  $p\bar{p} \rightarrow \tilde{g}\tilde{g}X$  ( $\tilde{g} \rightarrow q\bar{q}\tilde{\gamma}$ ) and assume  $m_{\tilde{q}} > m_{\tilde{g}}$ . These limits apply for  $m_{\tilde{\gamma}} \lesssim 20 \text{ GeV}$  and  $\tau(\tilde{g}) < 10^{-10} \text{ s}$ .
- 35 The limit of ANSARI 87D assumes  $m_{\tilde{q}} > m_{\tilde{g}}$  and  $m_{\tilde{\gamma}} \approx 0$ .

### Long-lived/light $\tilde{g}$ (Gluino) MASS LIMIT

Limits on light gluinos ( $m_{\tilde{g}} < 5 \text{ GeV}$ ), or gluinos which leave the detector before decaying.

VALUE (GeV)	CL%	DOCUMENT ID	TECN	COMMENT
● ● ● We do not use the following data for averages, fits, limits, etc. ● ● ●				
>586	95	1 AAD	11K ATLS	stable $\tilde{g}$
>544	95	2 AAD	11P ATLS	stable $\tilde{g}$ , GMSB scenario, $\tan\beta=5$
>370	95	3 KHACHATRY..11	CMS	long lived $\tilde{g}$
>398	95	4 KHACHATRY..11c	CMS	stable $\tilde{g}$
> 15	90	5 BERGER	10 THEO	hadron scattering data, $\alpha_s$
> 51	95	6 KAPLAN	08 THEO	event shapes at LEP
> 12		7 ABAZOV	07L D0	long-lived $\tilde{g}$
> 12		8 BERGER	05 THEO	hadron scattering data
none 2-18	95	9 ABDALLAH	03C DLPH	$e^+e^- \rightarrow q\bar{q}\tilde{g}\tilde{g}$ , stable $\tilde{g}$
> 5		10 ABDALLAH	03G DLPH	QCD beta function
> 26.9	95	11 HEISTER	03 ALEP	Color factors
> 6.3		12 HEISTER	03H ALEP	$e^+e^- \rightarrow q\bar{q}\tilde{g}\tilde{g}$
> 6.3		13 JANOT	03 RVUE	$\Delta\Gamma_{had} < 3.9 \text{ MeV}$
		14 MAFI	00 THEO	$p\bar{p} \rightarrow \text{jets} + \cancel{E}_T$
		15 ALAVI-HARATI	99E KTEV	$pN \rightarrow R^0$ , with $R^0 \rightarrow \rho^0\tilde{\gamma}$ and $R^0 \rightarrow \pi^0\tilde{\gamma}$
		16 BAER	99 RVUE	Stable $\tilde{g}$ hadrons
		17 FANTI	99 NA48	$pBe \rightarrow R^0 \rightarrow \eta\tilde{\gamma}$
		18 ACKERSTAFF	98V OPAL	$e^+e^- \rightarrow \tilde{\chi}_1^0\tilde{\chi}_1^0$
		19 ADAMS	97B KTEV	$pN \rightarrow R^0 \rightarrow \rho^0\tilde{\gamma}$
		20 ALBUQUERQ..97	E761	$R^+(uu\tilde{d}\tilde{g}) \rightarrow S^0(uds\tilde{g})\pi^+$ , $X^-(ss\tilde{d}\tilde{g}) \rightarrow S^0\pi^-$
> 6.3	95	21 BARATE	97L ALEP	Color factors
> 5	99	22 CSIKOR	97 RVUE	$\beta$ function, $Z \rightarrow \text{jets}$
> 1.5	90	23 DEGOUVEA	97 THEO	$Z \rightarrow jjjj$
		24 FARRAR	96 RVUE	$R^0 \rightarrow \pi^0\tilde{\gamma}$
none 1.9-13.6	95	25 AKERS	95R OPAL	$Z$ decay into a long-lived $(\tilde{g}q\bar{q})^\pm$
< 0.7		26 CLAVELLI	95 RVUE	quarkonia
none 1.5-3.5		27 CAKIR	94 RVUE	$\Upsilon(1S) \rightarrow \gamma + \text{gluonium}$
not 3-5		28 LOPEZ	93C RVUE	LEP
$\approx 4$		29 CLAVELLI	92 RVUE	$\alpha_s$ running
		30 ANTONIADIS	91 RVUE	$\alpha_s$ running
> 1		31 ANTONIADIS	91 RVUE	$pN \rightarrow \text{missing energy}$
		32 NAKAMURA	89 SPEC	$R-\Delta^{++}$
> 3.8	90	33 ARNOLD	87 EMUL	$\pi^- (350 \text{ GeV})$ . $\sigma \approx A^1$
> 3.2	90	33 ARNOLD	87 EMUL	$\pi^- (350 \text{ GeV})$ . $\sigma \approx A^{0.72}$
none 0.6-2.2	90	34 TUTS	87 CUSB	$\Upsilon(1S) \rightarrow \gamma + \text{gluonium}$
none 1-4.5	90	35 ALBRECHT	86C ARG	$1 \times 10^{-11} \lesssim \tau \lesssim 1 \times 10^{-9} \text{ s}$
none 1-4	90	36 BADIER	86 BDMP	$1 \times 10^{-10} < \tau < 1 \times 10^{-7} \text{ s}$
none 3-5		37 BARNETT	86 RVUE	$p\bar{p} \rightarrow \text{gluino gluino gluon}$
none		38 VOLOSHIN	86 RVUE	If (quasi) stable; $\tilde{g}uud$
none 0.5-2		39 COOPER...	85B BDMP	For $m_{\tilde{q}}=300 \text{ GeV}$
none 0.5-4		39 COOPER...	85B BDMP	For $m_{\tilde{q}} < 65 \text{ GeV}$
none 0.5-3		39 COOPER...	85B BDMP	For $m_{\tilde{q}}=150 \text{ GeV}$
none 2-4		40 DAWSON	85 RVUE	$\tau > 10^{-7} \text{ s}$
none 1-2.5		40 DAWSON	85 RVUE	For $m_{\tilde{q}}=100 \text{ GeV}$
none 0.5-4.1	90	41 FARRAR	85 RVUE	FNAL beam dump
> 1		42 GOLDMAN	85 RVUE	Gluonium
>1-2		43 HABER	85 RVUE	
		44 BALL	84 CALO	
		45 BRICK	84 RVUE	
		46 FARRAR	84 RVUE	
> 2		47 BERGSMASMA	83C RVUE	For $m_{\tilde{q}} < 100 \text{ GeV}$
>2-3		48 CHANOWITZ	83 RVUE	$\tilde{g}u\bar{d}, \tilde{g}uud$
>1.5-2		49 KANE	82 RVUE	Beam dump
		FARRAR	78 RVUE	R-hadron

- 1 AAD 11K looked in  $34 \text{ pb}^{-1}$  of  $pp$  collisions at  $\sqrt{s} = 7 \text{ TeV}$  for events with heavy stable particles, identified by their anomalous  $dE/dx$  in the tracker or time of flight in the tile calorimeter, from pair production of  $\tilde{g}$ . No evidence for an excess over the SM expectation is observed. Limits are derived for pair production of gluinos as a function of mass (see Fig. 4), for a fraction,  $f$ , of formation of  $\tilde{g} \rightarrow g$  (R-gluonball). If instead of a phase space driven approach for the hadronic scattering of the R-hadrons, a triple-Regge model or a bag-model is used, the limit degrades to 566 and 562 GeV, respectively.
- 2 AAD 11P looked in  $37 \text{ pb}^{-1}$  of  $pp$  collisions at  $\sqrt{s} = 7 \text{ TeV}$  for events with heavy stable particles, reconstructed and identified by their time of flight in the Muon System. There is no requirement on their observation in the tracker to increase the sensitivity to cases where gluinos have a large fraction,  $f$ , of formation of neutral  $\tilde{g} \rightarrow g$  (R-gluonball). No evidence for an excess over the SM expectation is observed. Limits are derived as a function of mass (see Fig. 4), for  $f=0.1$ . For fractions  $f = 0.5$  and  $1.0$  the limit degrades to 537 and 530 GeV, respectively.
- 3 KHACHATRYAN 11 looked in  $10 \text{ pb}^{-1}$  of  $pp$  collisions at  $\sqrt{s} = 7 \text{ TeV}$  for events with pair production of long-lived gluinos. The hadronization of the gluinos leads to R-hadrons which may stop inside the detector and later decay via  $\tilde{g} \rightarrow g \tilde{\chi}_1^0$  during gaps between the proton bunches. No significant excess over the expected background is observed. From a counting experiment, a limit at 95% C.L. on the cross section times branching ratio is derived for  $m_{\tilde{g}} - m_{\tilde{\chi}_1^0} > 100 \text{ GeV}$ , see their Fig. 2. Assuming 100% branching ratio, lifetimes between 75 ns and  $3 \times 10^5 \text{ s}$  are excluded for  $m_{\tilde{g}} = 300 \text{ GeV}$ . The  $\tilde{g}$  mass exclusion is obtained with the same assumptions for lifetimes between  $10 \mu\text{s}$  and  $1000 \text{ s}$ , but shows some dependence on the model for R-hadron interactions with matter, illustrated in Fig. 3. From a time-profile analysis, the mass exclusion is 382 GeV for a lifetime of  $10 \mu\text{s}$  under the same assumptions as above.
- 4 KHACHATRYAN 11C looked in  $3.1 \text{ pb}^{-1}$  of  $pp$  collisions at  $\sqrt{s} = 7 \text{ TeV}$  for events with heavy stable particles, identified by their anomalous  $dE/dx$  in the tracker or additionally requiring that it be identified as muon in the muon chambers, from pair production of  $\tilde{g}$ . No evidence for an excess over the expected background is observed. Limits are derived for pair production of gluinos as a function of mass (see Fig. 3), depending on the fraction,  $f$ , of formation of  $\tilde{g} \rightarrow g$  (R-gluonball). The quoted limit is for  $f=0.1$ , while for  $f=0.5$  it degrades to 357 GeV. In the conservative scenario where every hadronic interaction causes it to become neutral, the limit decreases to 311 GeV for  $f=0.1$ .
- 5 BERGER 10 updated the results of BERGER 05. They fit parton distribution functions including the effects of a light gluino as an extra parton. Different data on  $\alpha_s$  is also included. A fit for  $\alpha_s(M_Z)$  is performed as a function of the gluino mass. The bound is determined by comparing the quality of the fit to the CT10 fit, and the CT10 tolerance criterion is used to define the significance. The lower bound is 25 GeV for fixed  $\alpha_s(M_Z) = 0.118$ .
- 6 KAPLAN 08 reanalysed jet event shape data from LEP 1 and LEP 2 using soft collinear effective theory methods. These data are sensitive to the effects of new degrees of freedom, including a relatively light gluino, at different energy scales, roughly between 5 and 50 GeV. The analysis relies on theoretical modeling of and approximations for non-perturbative effects and matching between different scales.
- 7 ABAZOV 07L looked in approximately  $410 \text{ pb}^{-1}$  of  $p\bar{p}$  collisions at  $\sqrt{s} = 1.96 \text{ TeV}$  for events with a long-lived gluino from split supersymmetry, decaying after stopping in the detector into  $g \tilde{\chi}_1^0$  with lifetimes from  $30 \mu\text{s}$  to  $100 \text{ h}$ . The signal signature is a largely empty event with a single large transverse energy deposit in the calorimeter. The main background is due to cosmic muons interacting in the calorimeter. The data agree with the estimated background and allow the authors to estimate a limit on the rate of an out-of-time monojet signal of a given energy. Assuming the branching ratios  $\tilde{g} \rightarrow g \tilde{\chi}_1^0$  to be 100% the results can be translated to limits on the gluino cross section versus the gluino mass for fixed  $\tilde{\chi}_1^0$  mass. After comparing to the expected gluino cross sections, the excluded region of gluino masses can be obtained, see examples in their Fig. 3.
- 8 BERGER 05 include the light gluino in proton PDF and perform global analysis of hadronic data. Effects on the running of  $\alpha_s$  also included. Strong dependency on  $\alpha_s(m_Z)$ . Bound quoted for  $\alpha_s(m_Z) = 0.118$ . Superseded by BERGER 10.
- 9 ABDALLAH 03C looked for events of the type  $q\bar{q}R^\pm R^\pm$ ,  $q\bar{q}R^\pm R^0$  or  $q\bar{q}R^0 R^0$  in  $e^+e^-$  interactions at 91.2 GeV collected in 1994. The  $R^\pm$  bound states are identified by anomalous  $dE/dx$  in the tracking chambers and the  $R^0$  by missing energy, due to their reduced energy loss in the calorimeters. The upper value of the excluded range depends on the probability for the gluino to fragment into  $R^\pm$  or  $R^0$ , see their Fig. 17. It improves to 23 GeV for 100% fragmentation to  $R^\pm$ .
- 10 ABDALLAH 03G used  $e^+e^-$  data at and around the  $Z^0$  peak, above the  $Z^0$  up to  $\sqrt{s} = 202 \text{ GeV}$  and events from radiative return to cover the low energy region. They perform a direct measurement of the QCD beta-function from the means of fully inclusive event observables. Compared to the energy range, gluinos below 5 GeV can be considered massless and are firmly excluded by the measurement.
- 11 HEISTER 03 use  $e^+e^-$  data from 1994 and 1995 at and around the  $Z^0$  peak to measure the 4-jet rate and angular correlations. The comparison with QCD NLO calculations allow  $\alpha_s(M_Z)$  and the color factor ratios to be extracted and the results are in agreement with the expectations from QCD. The inclusion of a massless gluino in the beta functions yields  $T_R / C_F = 0.15 \pm 0.06 \pm 0.06$  (expectation is  $T_R / C_F = 3/8$ ), excluding a massless gluino at more than 95% CL. As no NLO calculations are available for massive gluinos, the earlier LO results from BARATE 97L for massive gluinos remain valid.
- 12 HEISTER 03H use  $e^+e^-$  data at and around the  $Z^0$  peak to look for stable gluinos hadronizing into charged or neutral R-hadrons with arbitrary branching ratios. Combining these results with bounds on the  $Z^0$  hadronic width from electroweak measurements (JANOT 03) to cover the low mass region the quoted lower limit on the mass of a long-lived gluino is obtained.
- 13 JANOT 03 excludes a light gluino from the upper limit on an additional contribution to the Z hadronic width. At higher confidence levels,  $m_{\tilde{g}} > 5.3(4.2) \text{ GeV}$  at  $3\sigma(5\sigma)$  level.
- 14 MAFI 00 reanalyzed CDF data assuming a stable heavy gluino as the LSP, with model for R-hadron-nucleon scattering. Gluino masses between 35 GeV and 115 GeV are excluded based on the CDF Run I data. Combined with the analysis of BAER 99, this allows a LSP gluino mass between 25 and 35 GeV if the probability of fragmentation into charged R-hadron  $P > 1/2$ . The cosmological exclusion of such a gluino LSP are assumed to be avoided as in BAER 99. Gluino could be NLSP with  $\tau_{\tilde{g}} \sim 100 \text{ yrs}$ , and decay to gluon gravitino.
- 15 ALAVI-HARATI 99E looked for  $R^0$  bound states, yielding  $\pi^+\pi^-$  or  $\pi^0$  in the final state. The experiment is sensitive to values of  $\Delta m = m_{R^0} - m_{\tilde{g}}$  larger than 280 MeV and 140 MeV for the two decay modes, respectively, and to  $R^0$  mass and lifetime in the ranges 0.8-5 GeV and  $10^{-10}$ - $10^{-3} \text{ s}$ . The limits obtained depend on  $B(R^0 \rightarrow \pi^+\pi^- \text{ photino})$  and  $B(R^0 \rightarrow \pi^0 \text{ photino})$  on the value of  $m_{R^0}/m_{\tilde{g}}$ , and on the ratio of production rates  $\sigma(R^0)/\sigma(K_L^0)$ . See Figures in the paper for the excluded  $R^0$  production rates as a function of  $\Delta m$ ,  $R^0$  mass and lifetime. Using the production rates expected from perturbative QCD, and assuming dominance of the above decay channels over the suitable phase space,  $R^0$  masses in the range 0.8-5 GeV are excluded at 90%CL for a large fraction of the sensitive lifetime region. ALAVI-HARATI 99E updates and supersedes the results of ADAMS 97B.
- 16 BAER 99 set constraints on the existence of stable  $\tilde{g}$  hadrons, in the mass range  $m_{\tilde{g}} > 3 \text{ GeV}$ . They argue that strong-interaction effects in the low-energy annihilation rates could leave small enough relic densities to evade cosmological constraints up to  $m_{\tilde{g}} < 10 \text{ TeV}$ . They consider jet +  $E_T$  as well as heavy-ionizing charged-particle signatures from production of stable  $\tilde{g}$  hadrons at LEP and Tevatron, developing modes for the energy loss of  $\tilde{g}$  hadrons inside the detectors. Results are obtained as a function of the fragmentation probability  $P$  of the  $\tilde{g}$  into a charged hadron. For  $P < 1/2$ , and for various energy-loss models, OPAL and CDF data exclude gluinos in the  $3 < m_{\tilde{g}}(\text{GeV}) < 130$  mass range. For  $P > 1/2$ , gluinos are excluded in the mass ranges  $3 < m_{\tilde{g}}(\text{GeV}) < 23$  and  $50 < m_{\tilde{g}}(\text{GeV}) < 200$ .
- 17 FANTI 99 looked for  $R^0$  bound states yielding high  $P_T \eta \rightarrow 3\pi^0$  decays. The experiment is sensitive to a region of  $R^0$  mass and lifetime in the ranges of 1-5 GeV and  $10^{-10}$ - $10^{-3} \text{ s}$ . The limits obtained depend on  $B(R^0 \rightarrow \eta\gamma)$ , on the value of  $m_{R^0}/m_{\tilde{g}}$ , and on the ratio of production rates  $\sigma(R^0)/\sigma(K_L^0)$ . See Fig. 6-7 for the excluded production rates as a function of  $R^0$  mass and lifetime.
- 18 ACKERSTAFF 98V excludes the light gluino with universal gaugino mass where charginos, neutralinos decay as  $\tilde{\chi}_1^\pm, \tilde{\chi}_2^0 \rightarrow q\bar{q}\tilde{g}$  from total hadronic cross sections at  $\sqrt{s}=130$ -172 GeV. See paper for the case of nonuniversal gaugino mass.
- 19 ADAMS 97B looked for  $\rho^0 \rightarrow \pi^+\pi^-$  as a signature of  $R^0=(\tilde{g}g)$  bound states. The experiment is sensitive to an  $R^0$  mass range of 1.2-4.5 GeV and to a lifetime range of  $10^{-10}$ - $10^{-3} \text{ sec}$ . Precise limits depend on the assumed value of  $m_{R^0}/m_{\tilde{g}}$ . See Fig. 7 for the excluded mass and lifetime region.
- 20 ALBUQUERQUE 97 looked for weakly decaying baryon-like states which contain a light gluino, following the suggestions in FARRAR 96. See their Table 1 for limits on the production fraction. These limits exclude gluino masses in the range 100-600 MeV for the predicted lifetimes (FARRAR 96) and production rates, which are assumed to be comparable to those of strange or charmed baryons.
- 21 BARATE 97L studied the QCD color factors from four-jet angular correlations and the differential two-jet rate in Z decay. Limit obtained from the determination of  $n_f = 4.24 \pm 0.29 \pm 1.15$ , assuming  $T_F/C_F=3/8$  and  $C_A/C_F=9/4$ .
- 22 CSIKOR 97 combined the  $\alpha_s$  from  $\sigma(e^+e^- \rightarrow \text{hadron})$ ,  $\tau$  decay, and jet analysis in Z decay. They exclude a light gluino below 5 GeV at more than 99.7%CL.
- 23 DEGOUVEA 97 reanalyzed AKERS 95A data on Z decay into four jets to place constraints on a light stable gluino. The mass limit corresponds to the pole mass of 2.8 GeV. The analysis, however, is limited to the leading-order QCD calculation.
- 24 FARRAR 96 studied the possible  $R^0=(\tilde{g}g)$  component in Fermilab E799 experiment and used its bound  $B(K_L^0 \rightarrow \pi^0 \nu\bar{\nu}) \leq 5.8 \times 10^{-5}$  to place constraints on the combination of  $R^0$  production cross section and its lifetime.
- 25 AKERS 95R looked for Z decay into  $q\bar{q}\tilde{g}\tilde{g}$ , by searching for charged particles with  $dE/dx$  consistent with  $\tilde{g}$  fragmentation into a state  $(\tilde{g}q\bar{q})^\pm$  with lifetime  $\tau > 10^{-7} \text{ sec}$ . The fragmentation probability into a charged state is assumed to be 25%.
- 26 CLAVELLI 95 updates the analysis of CLAVELLI 93, based on a comparison of the hadronic widths of charmonium and bottomonium S-wave states. The analysis includes a parametrization of relativistic corrections. Claims that the presence of a light gluino improves agreement with the data by slowing down the running of  $\alpha_s$ .
- 27 CAKIR 94 reanalyzed TUTS 87 and later unpublished data from CUSB to exclude pseudo-scalar gluonium  $\eta_{\tilde{g}}(\tilde{g}\tilde{g})$  of mass below 7 GeV. It was argued, however, that the perturbative QCD calculation of the branching fraction  $T \rightarrow \eta_{\tilde{g}}\gamma$  is unreliable for  $m_{\eta_{\tilde{g}}} < 3 \text{ GeV}$ . The gluino mass is defined by  $m_{\tilde{g}} = (m_{\eta_{\tilde{g}}})/2$ . The limit holds for any gluino lifetime.
- 28 LOPEZ 93C uses combined restraint from the radiative symmetry breaking scenario within the minimal supergravity model, and the LEP bounds on the  $(M_2, \mu)$  plane. Claims that the light gluino window is strongly disfavored.
- 29 CLAVELLI 92 claims that a light gluino mass around 4 GeV should exist to explain the discrepancy between  $\alpha_s$  at LEP and at quarkonia ( $\Upsilon$ ), since a light gluino slows the running of the QCD coupling.
- 30 ANTONIADIS 91 argue that possible light gluinos ( $< 5 \text{ GeV}$ ) contradict the observed running of  $\alpha_s$  between 5 GeV and  $m_Z$ . The significance is less than 2 s.d.
- 31 ANTONIADIS 91 interpret the search for missing energy events in 450 GeV/c  $pN$  collisions, AKESSON 91, in terms of light gluinos.
- 32 NAKAMURA 89 searched for a long-lived ( $\tau \gtrsim 10^{-7} \text{ s}$ ) charge-( $\pm 2$ ) particle with mass  $\lesssim 1.6 \text{ GeV}$  in proton-Pt interactions at 12 GeV and found that the yield is less than  $10^{-8}$  times that of the pion. This excludes  $R-\Delta^{++}$  (a  $\tilde{g}uuu$  state) lighter than 1.6 GeV.
- 33 The limits assume  $m_{\tilde{g}} = 100 \text{ GeV}$ . See their figure 3 for limits vs.  $m_{\tilde{g}}$ .
- 34 The gluino mass is defined by half the bound  $\tilde{g}\tilde{g}$  mass. If zero gluino mass gives a  $\tilde{g}\tilde{g}$  of mass about 1 GeV as suggested by various glueball mass estimates, then the low-mass bound can be replaced by zero. The high-mass bound is obtained by comparing the data with nonrelativistic potential-model estimates.
- 35 ALBRECHT 86C search for secondary decay vertices from  $\chi_{b1}(1P) \rightarrow \tilde{g}\tilde{g}g$  where  $\tilde{g}$ 's make long-lived hadrons. See their figure 4 for excluded region in the  $m_{\tilde{g}} - m_{\tilde{q}}$  and  $m_{\tilde{g}} - m_{\tilde{q}}$  plane. The lower  $m_{\tilde{g}}$  region below  $\sim 2 \text{ GeV}$  may be sensitive to fragmentation effects. Remark that the  $\tilde{g}$ -hadron is expected to be  $\sim 1 \text{ GeV}$  (glueball mass) in the zero  $\tilde{g}$  mass limit.
- 36 BADIER 86 looked for secondary decay vertices from long-lived  $\tilde{g}$ -hadrons produced at 300 GeV  $\pi^-$  beam dump. The quoted bound assumes  $\tilde{g}$ -hadron nucleon total cross section of  $10 \mu\text{b}$ . See their figure 7 for excluded region in the  $m_{\tilde{g}} - m_{\tilde{q}}$  plane for several assumed total cross-section values.
- 37 BARNETT 86 rule out light gluinos ( $m = 3$ -5 GeV) by calculating the monojet rate from gluino gluon events (and from gluino gluino events) and by using UA1 data from  $p\bar{p}$  collisions at CERN.

# Searches Particle Listings

## Supersymmetric Particle Searches

- <sup>38</sup> VOLOSHIN 86 rules out stable gluino based on the cosmological argument that predicts too much hydrogen consisting of the charged stable hadron  $\tilde{g}uud$ . Quasi-stable ( $\tau > 1 \cdot 10^{-7}$ s) light gluino of  $m_{\tilde{g}} < 3$  GeV is also ruled out by nonobservation of the stable charged particles,  $\tilde{g}uud$ , in high energy hadron collisions.
- <sup>39</sup> COOPER-SARKAR 85B is BEBC beam-dump. Gluinos decaying in dump would yield  $\tilde{\gamma}$ 's in the detector giving neutral-current-like interactions. For  $m_{\tilde{q}} > 330$  GeV, no limit is set.
- <sup>40</sup> DAWSON 85 first limit from neutral particle search. Second limit based on FNAL beam dump experiment.
- <sup>41</sup> FARRAR 85 points out that BALL 84 analysis applies only if the  $\tilde{g}$ 's decay before interacting, i.e.  $m_{\tilde{q}} < 80m_{\tilde{g}}^{1.5}$ . FARRAR 85 finds  $m_{\tilde{g}} < 0.5$  not excluded for  $m_{\tilde{q}} = 30-100$  GeV and  $m_{\tilde{g}} < 1.0$  not excluded for  $m_{\tilde{q}} = 100-500$  GeV by BALL 84 experiment.
- <sup>42</sup> GOLDMAN 85 use nonobservation of a pseudoscalar  $\tilde{g}-\tilde{g}$  bound state in radiative  $\psi$  decay.
- <sup>43</sup> HABER 85 is based on survey of all previous searches sensitive to low mass  $\tilde{g}$ 's. Limit makes assumptions regarding the lifetime and electric charge of the lightest supersymmetric particle.
- <sup>44</sup> BALL 84 is FNAL beam dump experiment. Observed no interactions of  $\tilde{\gamma}$  in the calorimeter, where  $\tilde{\gamma}$ 's are expected to come from pair-produced  $\tilde{g}$ 's. Search for long-lived  $\tilde{\gamma}$  interacting in calorimeter 56m from target. Limit is for  $m_{\tilde{q}} = 40$  GeV and production cross section proportional to  $A^{0.72}$ . BALL 84 find no  $\tilde{g}$  allowed below 4.1 GeV at CL = 90%. Their figure 1 shows dependence on  $m_{\tilde{q}}$  and  $A$ . See also KANE 82.
- <sup>45</sup> BRICK 84 reanalyzed FNAL 147 GeV HBC data for  $R-\Delta(1232)^{++}$  with  $\tau > 10^{-9}$  s and  $p_{\text{lab}} > 2$  GeV. Set CL = 90% upper limits 6.1, 4.4, and 29 microbarns in  $pp, \pi^+p, K^+p$  collisions respectively.  $R-\Delta^{++}$  is defined as being  $\tilde{g}$  and 3 up quarks. If mass = 1.2-1.5 GeV, then limits may be lower than theory predictions.
- <sup>46</sup> FARRAR 84 argues that  $m_{\tilde{g}} < 100$  MeV is not ruled out if the lightest R-hadrons are long-lived. A long lifetime would occur if R-hadrons are lighter than  $\tilde{\gamma}$ 's or if  $m_{\tilde{q}} > 100$  GeV.
- <sup>47</sup> BERGSMAN 83c is reanalysis of CERN-SPS beam-dump data. See their figure 1.
- <sup>48</sup> CHANOWITZ 83 find in bag-model that charged s-hadron exists which is stable against strong decay if  $m_{\tilde{g}} < 1$  GeV. This is important since tracks from decay of neutral s-hadron cannot be reconstructed to primary vertex because of missed  $\tilde{\gamma}$ . Charged s-hadron leaves track from vertex.
- <sup>49</sup> KANE 82 inferred above  $\tilde{g}$  mass limit from retroactive analysis of hadronic collision and beam dump experiments. Limits valid if  $\tilde{g}$  decays inside detector.

<sup>3</sup> ABAZOV	10N	D0	$\gamma_D$ , hidden valley
<sup>4</sup> LOVE	08A	CLEO	$R, Y \rightarrow \mu\tau$
<sup>5</sup> ABULENCIA	06P	CDF	$\ell\gamma\cancel{E}_T, \ell\ell\gamma, \text{GMSB}$
<sup>6</sup> ACOSTA	04E	CDF	
<sup>7</sup> TCHIKILEV	04	ISTR	$K^- \rightarrow \pi^- \pi^0 P$
<sup>8</sup> AFFOLDER	02D	CDF	$p\bar{p} \rightarrow \gamma b(\cancel{E}_T)$
<sup>9</sup> AFFOLDER	01H	CDF	$p\bar{p} \rightarrow \gamma\gamma X$
<sup>10</sup> ABBOTT	00G	D0	$p\bar{p} \rightarrow 3\ell + \cancel{E}_T, R, LL\bar{E}$
<sup>11</sup> ABREU,P	00C	DLPH	$e^+e^- \rightarrow \gamma + S/P$
<sup>12</sup> ABACHI	97	D0	$\gamma\gamma X$
<sup>13</sup> BARBER	84B	RVUE	
<sup>14</sup> HOFFMAN	83	CNTR	$\pi p \rightarrow n(e^+e^-)$

- <sup>1</sup> AAD 11AA looked in  $34 \text{ pb}^{-1}$  of  $pp$  collisions at  $\sqrt{s} = 7$  TeV for events with  $\geq 4$  jets originating from pair production of scalar gluons, each decaying to two gluons. No two-jet resonances are observed over the SM background. Limits are derived on the cross section times branching ratio (see Fig. 3). Assuming 100% branching ratio for the decay to two gluons, the quoted exclusion range is obtained, except for a 5 GeV mass window around 140 GeV.
- <sup>2</sup> CHATRCHYAN 11E looked in  $35 \text{ pb}^{-1}$  of  $pp$  collisions at  $\sqrt{s} = 7$  TeV for events with collimated  $\mu$  pairs (leptonic jets) from the decay of hidden sector states. No evidence for new resonance production is found. Limits are derived and compared to various SUSY models (see Fig. 4) where the LSP, either the  $\tilde{\chi}_1^0$  or a  $\tilde{q}$ , decays to dark sector particles.
- <sup>3</sup> ABAZOV 10N looked in  $5.8 \text{ fb}^{-1}$  of  $p\bar{p}$  collisions at  $\sqrt{s} = 1.96$  TeV for events from hidden valley models in which a  $\tilde{\chi}_1^0$  decays into a dark photon,  $\gamma_D$ , and the unobservable lightest SUSY particle of the hidden sector. As the  $\gamma_D$  is expected to be light, it may decay into a tightly collimated lepton pair, called lepton jet. They searched for events with  $\cancel{E}_T$  and two isolated lepton jets observable by an opposite charged lepton pair  $e, e, \mu$  or  $\mu, \mu$ . No significant excess over the SM expectation is observed, and a limit at 95% CL on the cross section times branching ratio is derived, see their Table I. They also examined the invariant mass of the lepton jets for a narrow resonance, see their Fig. 4, but found no evidence for a signal.
- <sup>4</sup> LOVE 08A searched for decays of  $Y(nS)$  with  $n = 1, 2, 3$  into  $\mu\tau$  in 1.1, 1.3, 1.4  $\text{fb}^{-1}$ , respectively, in the CLEO III detector at CESR. The signature is a muon with  $\approx 97\%$  of the beam energy and an electron from the decay of  $\tau$ . No evidence for lepton flavour violation is found and 95% CL limits on the branching ratio are estimated to be 6.0, 14.4 and  $20.3 \times 10^{-6}$  for  $n = 1, 2, 3$ , respectively.
- <sup>5</sup> ABULENCIA 06P searched in  $305 \text{ pb}^{-1}$  of  $p\bar{p}$  collisions at  $\sqrt{s} = 1.96$  TeV for an excess of events with  $\ell\gamma\cancel{E}_T$  and  $\ell\ell\gamma$  ( $\ell = e, \mu$ ). No significant excess was found compared to the background expectation. No events are found such as the  $e\ell\gamma\cancel{E}_T$  event observed in ABE 99I.
- <sup>6</sup> ACOSTA 04E looked in  $107 \text{ pb}^{-1}$  of  $p\bar{p}$  collisions at  $\sqrt{s} = 1.8$  TeV for events with two same sign leptons without selection of other objects nor  $\cancel{E}_T$ . No significant excess is observed compared to the Standard Model expectation and constraints are derived on the parameter space of MSUGRA models, see Figure 4.
- <sup>7</sup> Looked for the scalar partner of a goldstino in decays  $K^- \rightarrow \pi^- \pi^0 P$  from a 25 GeV  $K^-$  beam produced at the IHEP 70 GeV proton synchrotron. The goldstino is assumed to be sufficiently long-lived to be invisible. A 90% CL upper limit on the decay branching ratio is set at  $\sim 9.0 \times 10^{-6}$  for a goldstino mass range from 0 to 200 MeV, excluding the interval near  $m(\pi^0)$ , where the limit is  $\sim 3.5 \times 10^{-5}$ .
- <sup>8</sup> AFFOLDER 02D looked in  $85 \text{ pb}^{-1}$  of  $p\bar{p}$  collisions at  $\sqrt{s} = 1.8$  TeV for events with a high- $E_T$  photon, and a b-tagged jet with or without  $\cancel{E}_T$ . They compared the data with models where the final state could arise from cascade decays of gluinos and/or squarks into  $\tilde{\chi}_1^{\pm}$  and  $\tilde{\chi}_2^0$  or direct associated production of  $\tilde{\chi}_2^0 \tilde{\chi}_2^{\pm}$ , followed by  $\tilde{\chi}_2^0 \rightarrow \gamma\tilde{\chi}_1^0$  or a GMSB model where  $\tilde{\chi}_1^0 \rightarrow \gamma\tilde{G}$ . It is concluded that the experimental sensitivity is insufficient to detect the associated production or the GMSB model, but some sensitivity may exist to the cascade decays. A model independent limit for the above topology is also given in the paper.
- <sup>9</sup> AFFOLDER 01H searches for  $p\bar{p} \rightarrow \gamma\gamma X$  events, where the di-photon system originates from goldstino production, in  $100 \text{ pb}^{-1}$  of data. Upper limits on the cross section times branching ratio are shown as function of the di-photon mass  $> 70$  GeV in Fig. 5. Excluded regions are derived in the plane of the goldstino mass versus the supersymmetry breaking scale for two representative sets of parameter values, as shown in Figs. 6 and 7.
- <sup>10</sup> ABBOTT 00c searches for trilepton final states ( $\ell = e, \mu$ ) with  $\cancel{E}_T$  from the indirect decay of gauginos via  $LL\bar{E}$  couplings. Efficiencies are computed for all possible production and decay modes of SUSY particles in the framework of the Minimal Supergravity scenario. See Figs. 1-4 for excluded regions in the  $m_{1/2}$  versus  $m_0$  plane.
- <sup>11</sup> ABREU,P 00C look for the CP-even (S) and CP-odd (P) scalar partners of the goldstino, expected to be produced in association with a photon. The  $S/P$  decay into two photons or into two gluons and both the tri-photon and the photon + two jets topologies are investigated. Upper limits on the production cross section are shown in Fig. 5 and the excluded regions in Fig. 6. Data collected at  $\sqrt{s} = 189-202$  GeV.
- <sup>12</sup> ABACHI 97 searched for  $p\bar{p} \rightarrow \gamma\gamma\cancel{E}_T + X$  as supersymmetry signature. It can be caused by selectron, sneutrino, or neutralino production with a radiative decay of their decay products. They placed limits on cross sections.
- <sup>13</sup> BARBER 84B consider that  $\tilde{\mu}$  and  $\tilde{e}$  may mix leading to  $\mu \rightarrow e\tilde{\gamma}$ . They discuss mass-mixing limits from decay dist. asym. in LBL-TRIUMF data and  $e^+$  polarization in SIN data.
- <sup>14</sup> HOFFMAN 83 set CL = 90% limit  $d\sigma/dt B(e^+e^-) < 3.5 \times 10^{-32} \text{ cm}^2/\text{GeV}^2$  for spin-1 partner of Goldstone fermions with  $140 < m < 160$  MeV decaying  $\rightarrow e^+e^-$  pair.

### LIGHT $\tilde{G}$ (Gravitino) MASS LIMITS FROM COLLIDER EXPERIMENTS

The following are bounds on light ( $< 1$  eV) gravitino indirectly inferred from its coupling to matter suppressed by the gravitino decay constant.

Unless otherwise stated, all limits assume that other supersymmetric particles besides the gravitino are too heavy to be produced. The gravitino is assumed to be undetected and to give rise to a missing energy ( $\cancel{E}$ ) signature.

VALUE (eV)	CL%	DOCUMENT ID	TECN	COMMENT
• • •				We do not use the following data for averages, fits, limits, etc. • • •
$> 1.09 \times 10^{-5}$	95	<sup>1</sup> ABDALLAH 05B	DLPH	$e^+e^- \rightarrow \tilde{G}\tilde{G}\gamma$
$> 1.35 \times 10^{-5}$	95	<sup>2</sup> ACHARD 04E	L3	$e^+e^- \rightarrow \tilde{G}\tilde{G}\gamma$
$> 1.3 \times 10^{-5}$		<sup>3</sup> HEISTER 03c	ALEP	$e^+e^- \rightarrow \tilde{G}\tilde{G}\gamma$
$> 11.7 \times 10^{-6}$	95	<sup>4</sup> ACOSTA 02H	CDF	$p\bar{p} \rightarrow \tilde{G}\tilde{G}\gamma$
$> 8.7 \times 10^{-6}$	95	<sup>5</sup> ABBIENDI,G 00D	OPAL	$e^+e^- \rightarrow \tilde{G}\tilde{G}\gamma$
$> 10.0 \times 10^{-6}$	95	<sup>6</sup> ABREU 00Z	DLPH	$e^+e^- \rightarrow \tilde{G}\tilde{G}\gamma$
$> 11 \times 10^{-6}$	95	<sup>7</sup> AFFOLDER 00J	CDF	$p\bar{p} \rightarrow \tilde{G}\tilde{G} + \text{jet}$
$> 8.9 \times 10^{-6}$	95	<sup>8</sup> ACCIARRI 99R	L3	$e^+e^- \rightarrow \tilde{G}\tilde{G}\gamma$
$> 7.9 \times 10^{-6}$	95	<sup>9</sup> ACCIARRI 98V	L3	$e^+e^- \rightarrow \tilde{G}\tilde{G}\gamma$
$> 8.3 \times 10^{-6}$	95	<sup>9</sup> BARATE 98J	ALEP	$e^+e^- \rightarrow \tilde{G}\tilde{G}\gamma$

- <sup>1</sup> ABDALLAH 05B use data from  $\sqrt{s} = 180-208$  GeV. They look for events with a single photon +  $\cancel{E}$  final states from which a cross section limit of  $\sigma < 0.18 \text{ pb}$  at 208 GeV is obtained, allowing a limit on the mass to be set. Supersedes the results of ABREU 00Z.
- <sup>2</sup> ACHARD 04E use data from  $\sqrt{s} = 189-209$  GeV. They look for events with a single photon +  $\cancel{E}$  final states from which a limit on the Gravitino mass is set corresponding to  $\sqrt{\tilde{F}} > 238$  GeV. Supersedes the results of ACCIARRI 99R.
- <sup>3</sup> HEISTER 03c use the data from  $\sqrt{s} = 189-209$  GeV to search for  $\gamma\cancel{E}_T$  final states.
- <sup>4</sup> ACOSTA 02H looked in  $87 \text{ pb}^{-1}$  of  $p\bar{p}$  collisions at  $\sqrt{s} = 1.8$  TeV for events with a high- $E_T$  photon and  $\cancel{E}_T$ . They compared the data with a GMSB model where the final state could arise from  $q\bar{q} \rightarrow \tilde{G}\tilde{G}\gamma$ . Since the cross section for this process scales as  $1/|F|^4$ , a limit at 95% CL is derived on  $|F|^{1/2} > 221$  GeV. A model independent limit for the above topology is also given in the paper.
- <sup>5</sup> ABBIENDI,G 00D searches for  $\gamma\cancel{E}$  final states from  $\sqrt{s} = 189$  GeV.
- <sup>6</sup> ABREU 00Z search for  $\gamma\cancel{E}$  final states using data from  $\sqrt{s} = 189$  GeV. Superseded by ABDALLAH 05B.
- <sup>7</sup> AFFOLDER 00J searches for final states with an energetic jet (from quark or gluon) and large  $\cancel{E}_T$  from undetected gravitinos.
- <sup>8</sup> ACCIARRI 99R search for  $\gamma\cancel{E}$  final states using data from  $\sqrt{s} = 189$  GeV. Superseded by ACHARD 04E.
- <sup>9</sup> Searches for  $\gamma\cancel{E}$  final states at  $\sqrt{s} = 183$  GeV.

### Supersymmetry Miscellaneous Results

Results that do not appear under other headings or that make nonminimal assumptions.

VALUE	CL%	DOCUMENT ID	TECN	COMMENT
• • •				We do not use the following data for averages, fits, limits, etc. • • •
none 100-185	95	<sup>1</sup> AAD 11AA	ATLS	scalar gluons
		<sup>2</sup> CHATRCHYAN 11E	CMS	$\mu\mu$ resonances

### REFERENCES FOR Supersymmetric Particle Searches

CHATRCHYAN 12A	PR D85 012004	S. Chatrchyan et al.	(CMS Collab.)
AAD 11AA	EPJ C71 1828	G. Aad et al.	(ATLAS Collab.)
AAD 11AE	JHEP 1110 107	G. Aad et al.	(ATLAS Collab.)
AAD 11AF	JHEP 1111 099	G. Aad et al.	(ATLAS Collab.)
AAD 11B	EPJ C71 1682	G. Aad et al.	(ATLAS Collab.)
AAD 11C	EPJ C71 1647	G. Aad et al.	(ATLAS Collab.)
AAD 11G	PRL 106 131802	G. Aad et al.	(ATLAS Collab.)
AAD 11H	PRL 106 251801	G. Aad et al.	(ATLAS Collab.)
AAD 11K	PL B701 1	G. Aad et al.	(ATLAS Collab.)
AAD 11N	PL B701 186	G. Aad et al.	(ATLAS Collab.)
AAD 11O	PL B701 398	G. Aad et al.	(ATLAS Collab.)







COOPER...	85B	PL 160B 212	A.M. Cooper-Sarkar <i>et al.</i>	(WA66 Collab.)
DAWSON	85	PR D31 1581	S. Dawson, E. Eichten, C. Quigg	(LBL, FNAL)
FARRAR	85	PRL 55 895	G.R. Farrar	(RUTG)
GOLDMAN	85	Physica 15D 181	T. Goldman, H.E. Haber	(LANL, UCSC)
HABER	85	PRPL 117 75	H.E. Haber, G.L. Kane	(UCSC, MICH)
BALL	84	PRL 53 1314	R.C. Ball <i>et al.</i>	(MICH, FIRZ, OSU, FNAL+)
BARBER	84B	PL 139B 427	J.S. Barber, R.E. Shrock	(STON)
BRICK	84	PR D30 1134	D.H. Brick <i>et al.</i>	(BROW, CAVE, IIT+)
ELLIS	84	NP B238 453	J. Ellis <i>et al.</i>	(CERN)
FARRAR	84	PRL 53 1029	G.R. Farrar	(RUTG)
BERGSMA	83C	PL 121B 429	F. Bergsma <i>et al.</i>	(CHARM Collab.)
CHANOWITZ	83	PL 126B 225	M.S. Chanowitz, S. Sharpe	(UCB, LBL)
GOLDBERG	83	PRL 50 1419	H. Goldberg	(NEAS)
HOFFMAN	83	PR D28 660	C.M. Hoffman <i>et al.</i>	(LANL, ARZS)
KRAUSS	83	NP B227 556	L.M. Krauss	(HARV)
VYSOTSKII	83	SJNP 37 948	M.I. Vysotsky	(ITEP)
		Translated from YAF 37 1597		
KANE	82	PL 112B 227	G.L. Kane, J.P. Leveille	(MICH)
CABIBBO	81	PL 105B 155	N. Cabibbo, G.R. Farrar, L. Maiani	(ROMA, RUTG)
FARRAR	78	PL 76B 575	G.R. Farrar, P. Fayet	(CIT)
Also		PL 79B 442	G.R. Farrar, P. Fayet	(CIT)

## Technicolor

### DYNAMICAL ELECTROWEAK SYMMETRY BREAKING

Revised April 2012 by R.S. Chivukula (Michigan State University), M. Narain (Brown University), and J. Womersley (STFC, Rutherford Appleton Laboratory).

In theories of dynamical electroweak symmetry breaking, the electroweak interactions are broken to electromagnetism by the vacuum expectation value of a fermion bilinear. These theories may thereby avoid the introduction of fundamental scalar particles, of which we have no examples in nature. In this note, we review the status of experimental searches for the particles predicted in technicolor, topcolor, and related models. The limits from these searches are summarized in Table 1.

#### I. Technicolor

The earliest models [1,2] of dynamical electroweak symmetry breaking [3] include a new asymptotically free non-abelian gauge theory (“technicolor”) and additional massless fermions (“technifermions” transforming under a vectorial representation of the gauge group) which feel this new force. The global chiral symmetry of the fermions is spontaneously broken by the formation of a technifermion condensate, just as the approximate chiral  $SU(2) \times SU(2)$  symmetry in QCD is broken down to  $SU(2)$  isospin by the formation of a quark condensate. If the quantum numbers of the technifermions are chosen correctly (*e.g.*, by choosing technifermions in the fundamental representation of an  $SU(N)$  technicolor gauge group, with the left-handed technifermions being weak doublets and the right-handed ones weak singlets), this condensate can break the electroweak interactions down to electromagnetism.

The breaking of the global chiral symmetries implies the existence of Goldstone bosons, the “technipions” ( $\pi_T$ ). Through the Higgs mechanism, three of the Goldstone bosons become the longitudinal components of the  $W$  and  $Z$ , and the weak gauge bosons acquire a mass proportional to the technipion decay constant (the analog of  $f_\pi$  in QCD). The quantum numbers and masses of any remaining technipions are model-dependent. There may be technipions which are colored (octets and triplets), as well as those carrying electroweak quantum numbers, and some color-singlet technipions are too light [4,3] unless additional sources of chiral-symmetry breaking are introduced. The next lightest technicolor resonances are expected to

**Table 1:** Summary of the mass limits. Symbols are defined in the text.

Process	Excluded mass range	Decay channels	Ref.
$p\bar{p} \rightarrow \rho_T \rightarrow W\pi_T$	$170 < m_{\rho_T} < 215$ GeV and $80 < m_{\pi_T} < 115$ GeV for $M_V = 500$ GeV	$\rho_T \rightarrow W\pi_T$ $\pi_T^0 \rightarrow b\bar{b}$ $\pi_T^\pm \rightarrow b\bar{c}$	[24]
$pp \rightarrow \omega_T/\rho_T$	$130 < m_{\rho_T/\omega_T} < 180$ GeV for $50 < m_{\pi_T} < 480$ GeV	$\omega_T/\rho_T \rightarrow \ell^+\ell^-$	[36]
$pp \rightarrow \rho_T/a_T$	$m_{\rho_T/a_T} < 382$ GeV for $M(\pi_T) = \frac{3}{4}M(\rho_T) - 25$ GeV $m_{\rho_T/a_T} < 436$ GeV for $M(\rho_T) < M(\pi_T) + M_W$	$\rho_T \rightarrow WZ \rightarrow \ell\ell\nu$	[37]
$p\bar{p} \rightarrow \omega_T \rightarrow \gamma\pi_T$	$140 < m_{\omega_T} < 290$ GeV for $m_{\pi_T} \approx m_{\omega_T}/3$ and $M_T = 100$ GeV	$\omega_T \rightarrow \gamma\pi_T$ $\pi_T^0 \rightarrow b\bar{b}$ $\pi_T^\pm \rightarrow b\bar{c}$	[26]
$p\bar{p} \rightarrow \omega_T/\rho_T$	$m_{\omega_T} = m_{\rho_T} < 203$ GeV for $m_{\omega_T} < m_{\pi_T} + m_W$ or $M_T > 200$ GeV $m_{\omega_T} = m_{\rho_T} < 280$ GeV for $m_{\omega_T} < m_{\pi_T} + m_W$ or $M_T > 500$ GeV	$\omega_T/\rho_T \rightarrow \ell^+\ell^-$	[27]
$e^+e^- \rightarrow \omega_T/\rho_T$	$90 < m_{\rho_T} < 206.7$ GeV $m_{\pi_T} < 79.8$ GeV	$\rho_T \rightarrow WW,$ $W\pi_T, \pi_T\pi_T,$ $\gamma\pi_T, \text{hadrons}$	[29]
$p\bar{p} \rightarrow \rho_{T8}$	$260 < m_{\rho_{T8}} < 480$ GeV	$\rho_{T8} \rightarrow q\bar{q}, gg$	[31]
$p\bar{p} \rightarrow \rho_{T8}$ $\rightarrow \pi_{LQ}\pi_{LQ}$	$m_{\rho_{T8}} < 510$ GeV $m_{\rho_{T8}} < 600$ GeV $m_{\rho_{T8}} < 465$ GeV	$\pi_{LQ} \rightarrow c\nu$ $\pi_{LQ} \rightarrow b\nu$ $\pi_{LQ} \rightarrow \tau q$	[34] [34] [33]
$p\bar{p} \rightarrow g_t$	$0.3 < m_{g_t} < 0.6$ TeV for $0.3m_{g_t} < \Gamma < 0.7m_{g_t}$	$g_t \rightarrow b\bar{b}$	[47]
$p\bar{p} \rightarrow Z'$	$m_{Z'} < 900$ GeV $m_{Z'} < 835$ GeV for $\Gamma = 0.012m_{Z'}$ $m_{Z'} < 940$ GeV for $\Gamma = 0.03m_{Z'}$	$Z' \rightarrow t\bar{t}$ $Z' \rightarrow t\bar{t}$	[48] [49]
$pp \rightarrow Z'$	$m_{Z'} < 500 - 860$ GeV	$Z' \rightarrow t\bar{t}$	[50]
$p\bar{p} \rightarrow \text{Coloron}$	$m_{\text{Coloron}} < 775$ GeV for $\Gamma = 0.12m_{\text{coloron}}$ and $r=0.2$	$\text{Coloron} \rightarrow t\bar{t}$	[49]
$pp \rightarrow \text{Coloron}$	$320 < m_{\text{Coloron}} < 580$ GeV	$\text{Coloron} \rightarrow q\bar{q}$	[63]

be the analogs of the vector mesons in QCD. The technivector mesons can also have color and electroweak quantum numbers and, for a theory with a small number of technifermions, are expected to have a mass in the TeV range [5].

While technicolor chiral symmetry breaking can give mass to the  $W$  and  $Z$  particles, additional interactions must be introduced to produce the masses of the standard model fermions. The most thoroughly studied mechanism for this invokes “extended technicolor” (ETC) gauge interactions [4,6]. In ETC, technicolor and flavor are embedded into a larger gauge group, which is broken at a sequence of mass scales down to the residual, exact technicolor gauge symmetry. The massive gauge bosons associated with this breaking mediate

transitions between quarks/leptons and technifermions, giving rise to the couplings necessary to produce fermion masses. The ETC gauge bosons also mediate transitions among technifermions themselves, leading to interactions which can explicitly break unwanted chiral symmetries and raise the masses of any light technipions. The ETC interactions connecting technifermions to quarks/leptons also mediate technipion decays to ordinary fermion pairs. Since these interactions are responsible for fermion masses, one generally expects technipions to decay to the heaviest fermions kinematically allowed (though this need not hold in all models).

In addition to quark masses, ETC interactions must also give rise to quark mixing. One expects, therefore, that there are ETC interactions coupling quarks of the same charge from different generations. A stringent limit on these flavor-changing neutral current interactions comes from  $K^0-\bar{K}^0$  mixing [4]. These force the scale of ETC breaking and the corresponding ETC gauge boson masses to be in the 100-1000 TeV range (at least insofar as ETC interactions of first two generations are concerned). To obtain quark and technipion masses that are large enough then requires an enhancement of the technifermion condensate over that expected naively by scaling from QCD. Such an enhancement can occur if the technicolor gauge coupling runs very slowly, or “walks” [7]. Some theories of walking technicolor incorporate many technifermions, implying that the technicolor scale and, in particular, the technivector mesons may be much lighter than 1 TeV [3,8].

It should be noted that there are no reliable analytical calculation techniques to analyze the properties of strongly-coupled gauge theories. Recently, however, progress has been made in simulating these theories using lattice gauge theory [9], including preliminary studies of condensate enhancement [10], precision electroweak parameters and parity doubling [11,12,13], and vector-boson scattering [14]. Progress has also been made in constructing a complete theory of fermion masses (including neutrino masses) in the context of extended technicolor [15].

In existing colliders, technivector mesons are dominantly produced when an off-shell standard model gauge boson “resonates” into a technivector meson with the same quantum numbers [16]. The technivector mesons may then decay, in analogy with  $\rho \rightarrow \pi\pi$ , to pairs of technipions. However, in walking technicolor the technipion masses may be increased to the point that the decay of a technirho to pairs of technipions is kinematically forbidden [8]. In this case the decay to a technipion and a longitudinally polarized weak boson (an “eaten” Goldstone boson) may be preferred, and the technivector meson would be very narrow. Alternatively, the technivector may also decay, in analogy with the decay  $\rho \rightarrow \pi\gamma$ , to a technipion plus a photon, gluon, or transversely polarized weak gauge boson. Finally, in analogy with the decay  $\rho \rightarrow e^+e^-$ , the technivector meson may resonate back to an off-shell gluon or electroweak gauge boson, leading to a decay into a pair of leptons, quarks, or gluons.

When comparing the various results presented in this review, one should be aware that the more recent analyses [23,24,27,29] make use of newer calculations [17] of technihadron production and decay, as implemented in PYTHIA [19] version 6.126 and higher [20]. The LHC analyses use the calculations given in reference [18] and PYTHIA [19] version 6.4. The results obtained with older cross section calculations are not generally directly comparable, and have only been listed in Table 1 when newer results are not available.

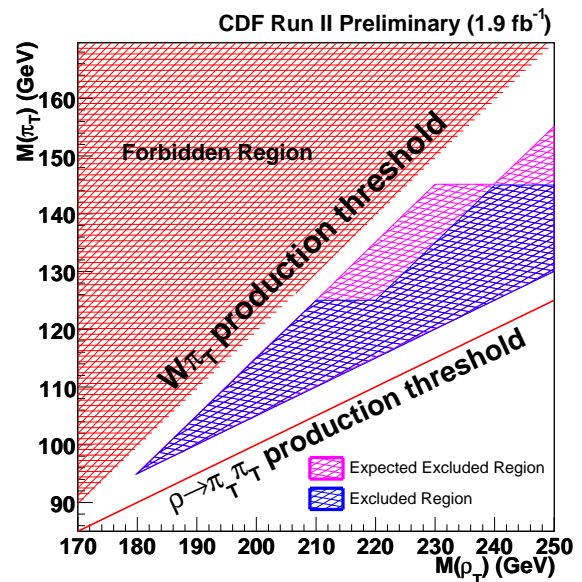


**Figure 1:** Search for a light technirho decaying to  $W^\pm$  and a  $\pi_T$ , and in which the  $\pi_T$  decays to two jets including at least one  $b$  quark [23]. Exclusion region at the 95% C.L. in the  $M(\rho_T)$ ,  $M(\pi_T)$  plane for  $\rho_T \rightarrow W\pi_T \rightarrow e\nu b\bar{b}(\bar{c})$  production. Kinematic thresholds from  $W\pi_T$  and  $\pi_T\pi_T$  are shown on the figure.

If the dominant decay mode of the technirho is  $W_L\pi_T$ , promising signal channels [21] are  $\rho_T^\pm \rightarrow W^\pm\pi_T^0$  and  $\rho_T^0 \rightarrow W^\pm\pi_T^\mp$ . If we assume that the technipions decay to  $b\bar{b}$  (neutral) and  $b\bar{c}$  (charged), then both channels yield a signal of  $W(\ell\nu) + 2$  jets, with one or more heavy flavor tags. The CDF collaboration carried out a search in this final state [22] based on Run I data and using PYTHIA version 6.1 for the signal simulation. Using  $1.9 \text{ fb}^{-1}$  of data from Run II, CDF [23] has published an update of this analysis. A large region of  $M(\rho_T) = 180\text{--}250 \text{ GeV}$  and  $M(\pi_T) = 95\text{--}145 \text{ GeV}$  are excluded at 95% CL, with the exact exclusion region displayed in Fig. 1.

The DØ [24] collaboration published an analysis based on  $388 \text{ pb}^{-1}$  of data from Run II and PYTHIA 6.22. The searches are sensitive to  $\sigma \cdot B \gtrsim 4 \text{ pb}$  and DØ finds mass combinations up to  $m_{\rho_T} = 215 \text{ GeV}$ ,  $m_{\pi_T} = 115 \text{ GeV}$  to be excluded for certain values of the model parameters. The expected sensitivity and the region excluded at 95% C.L. by the DØ analysis for  $M_V = 500 \text{ GeV}$  is shown in Fig. 2. For  $M_V = 100 \text{ GeV}$ , only a

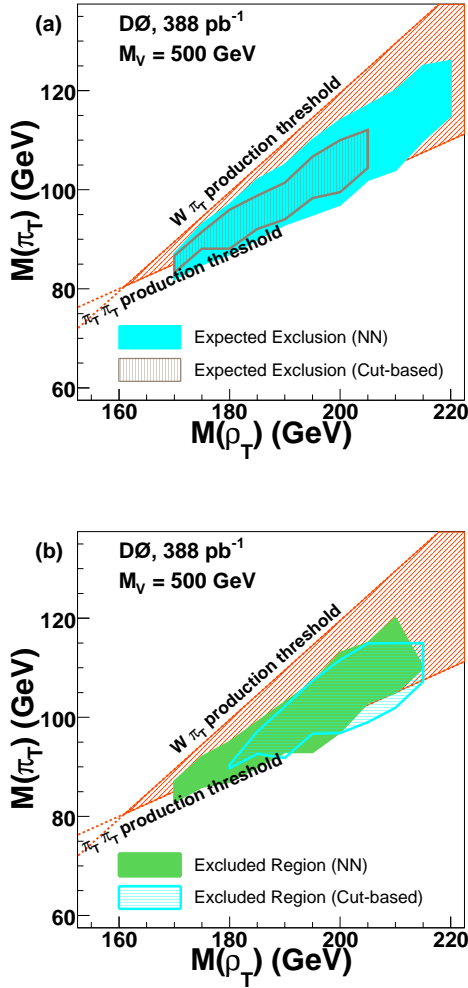


**Figure 2:** Search for a light technirho decaying to  $W^\pm$  and a  $\pi_T$ , and in which the  $\pi_T$  decays to two jets including at least one  $b$  quark [24]. Expected region of exclusion (a) and excluded region (b) at the 95% C.L. in the  $M(\rho_T), M(\pi_T)$  plane for  $\rho_T \rightarrow W\pi_T \rightarrow e\nu b\bar{b}(c)$  production with  $M_V = 500$  GeV. Kinematic thresholds from  $W\pi_T$  and  $\pi_T\pi_T$  are shown on the figures.

small region around  $M(\rho_T) = 190$  GeV and  $M(\pi_T) = 95$  GeV can be excluded. For an integrated luminosity of  $2 \text{ fb}^{-1}$ , the  $5\sigma$  discovery reach is expected to extend to  $m_{\rho_T} = 210$  GeV and  $m_{\pi_T} = 110$  GeV, while the 95% exclusion sensitivity will extend to  $m_{\rho_T} = 250$  GeV and  $m_{\pi_T} = 145$  GeV.

$D\mathcal{O}$  has also performed a search for technihadrons decaying to  $WZ$  [25]. These decays can be searched in the tri-lepton final state, where the  $W$  decays into a lepton and neutrino and the accompanying  $Z$  decays to dileptons. With a dataset corresponding to a  $4.1 \text{ fb}^{-1}$  of integrated luminosity,  $D\mathcal{O}$  excludes  $\rho_T$  with mass between 208 and 408 GeV at 95% C.L. for  $M(\rho_T) < M(\pi_T) + M(W)$  as displayed in Fig. 4.

CDF also searched [26] in Run I for the process  $\omega_T^0 \rightarrow \gamma\pi_T^0$ , yielding a signal of a hard photon plus two jets, with one or

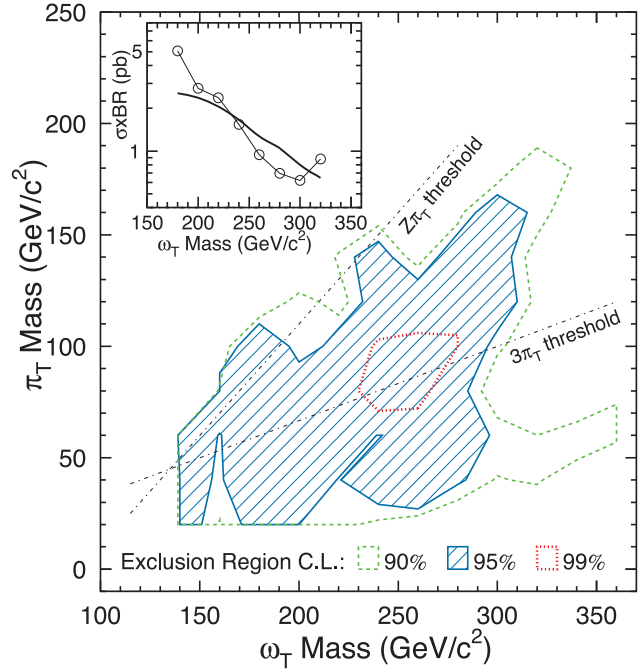


**Figure 3:** 95% CL exclusion region [26] for a light technimega decaying to  $\gamma$  and a  $\pi_T$ , and in which the  $\pi_T$  decays to two jets, including at least one  $b$  quark. (Inset: cross section limit for  $m_{\pi_T} = 120$  GeV.)

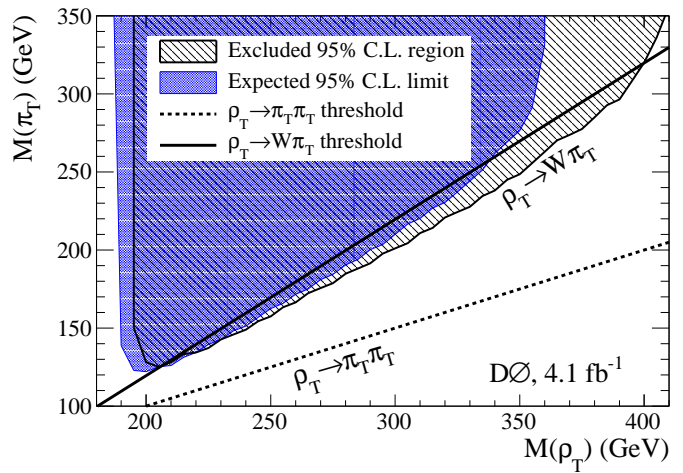


**Figure 4:** 95% CL exclusion region by the  $D\mathcal{O}$  experiment [25] in the  $M(\rho_T), M(\pi_T)$  plane for  $\rho_T \rightarrow WZ \rightarrow lll\nu$  (with  $l = e, \mu$ ) final state.

more heavy flavor tags. The sensitivity to  $\sigma \cdot B$  is of order 1 pb. The excluded region is shown in Fig. 3 and is roughly  $140 < m_{\omega_T} < 290$  GeV at the 95% level, for  $m_{\pi_T} \approx m_{\omega_T}/3$ .

# Searches Particle Listings

## Technicolor

The analysis assumes four technicolors,  $Q_D = Q_U - 1 = \frac{1}{3}$  and  $M_T = 100 \text{ GeV}/c^2$ . Here  $Q_U$  and  $Q_D$  are the charges of the lightest technifermion doublet, and  $M_T$  is a dimensionful parameter, of order  $100 \text{ GeV}/c^2$ , which controls the rate of  $\rho_T, \omega_T \rightarrow \gamma\pi_T$ .

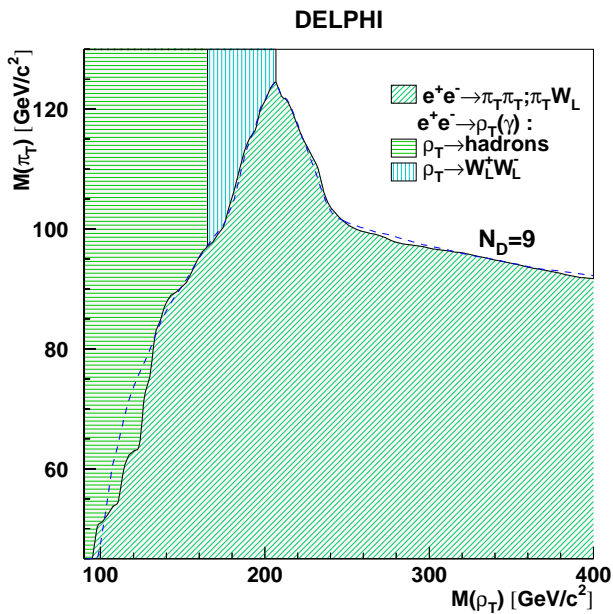


**Figure 5:** 95% CL exclusion region [29] in the technirho-technipion mass plane obtained from searches by the DELPHI collaboration at LEP 2, for nine technifermion doublets. The dashed line shows the expected limit for the 4-jet analysis.

The DØ experiment has searched [27] for low-scale technicolor resonances  $\rho_T$  and  $\omega_T$  decaying to dileptons, using an inclusive  $e^+e^-$  sample from Run I. In the search, the  $\rho_T$  and  $\omega_T$  are assumed to be degenerate in mass. The absence of structure in the dilepton invariant mass distribution is then used to set limits. Masses  $m_{\rho_T} = m_{\omega_T} \lesssim 200 \text{ GeV}$  are excluded, provided either  $m_{\rho_T} < m_{\pi_T} + m_W$ , or  $M_T > 200 \text{ GeV}$ . The CDF experiment also performed a similar search with  $200 \text{ pb}^{-1}$  of Run II data, and excluded equal  $m_{\rho_T} = m_{\omega_T}$  masses below  $280 \text{ GeV}$  for  $M_V = 500 \text{ GeV}$  and  $m_{\rho_T} < m_{\pi_T} + m_W$  at 95% C.L. [28]. With  $2 \text{ fb}^{-1}$  of data, the sensitivity will extend to  $m_{\rho_T} = m_{\omega_T} \approx 500 \text{ GeV}$ .

DELPHI [29] has reported a search for technicolor production in  $452 \text{ pb}^{-1}$  of  $e^+e^-$  data taken between 192 and 208 GeV. The analysis combines searches for  $e^+e^- \rightarrow \rho_T(\gamma)$  with  $\rho_T \rightarrow W_L W_L$ ,  $\rho_T \rightarrow \text{hadrons}$  ( $\pi_T \pi_T$  or  $q\bar{q}$ ),  $\rho_T \rightarrow \pi_T \gamma$ , and  $e^+e^- \rightarrow \rho_T^* \rightarrow W_L \pi_T$  or  $\pi_T \pi_T$ . Technirho masses in the range  $90 < m_{\rho_T} < 206.7 \text{ GeV}$  are excluded, while technipion masses  $m_{\pi_T} < 79.8 \text{ GeV}$  are ruled out independent of the parameters of the technicolor model.

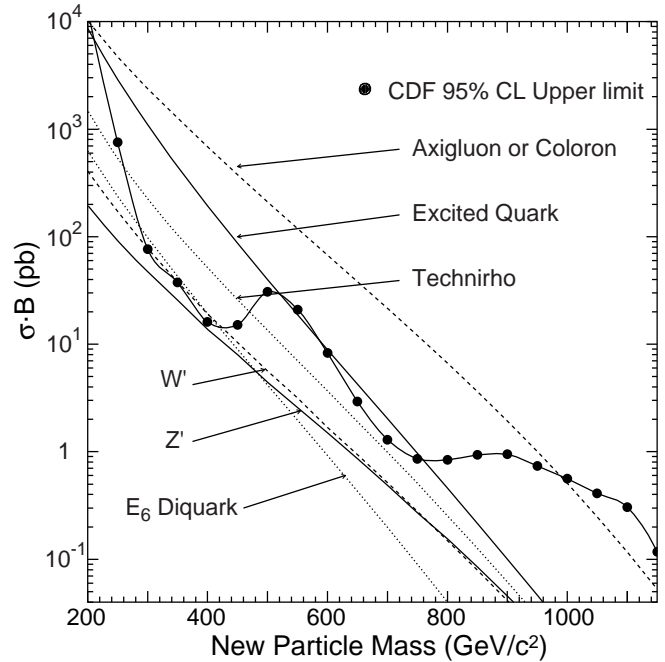


**Figure 6:** 95% CL Cross-section limits [31] for a technirho decaying to two jets at the Tevatron.

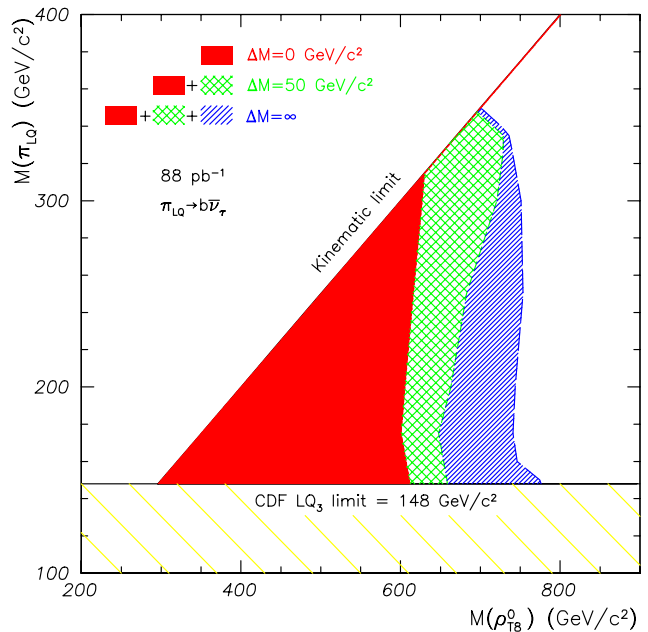


**Figure 7:** 95% CL exclusion region [34] in the technirho-technipion mass plane for pair produced technipions, with leptoquark couplings, decaying to  $b\nu$ .

Searches have also been carried out at the Tevatron for colored technihadron resonances [30,31]. CDF has used a search for structure in the dijet invariant mass spectrum to set limits on a color-octet technirho  $\rho_{T8}$  produced by an off-shell gluon, and decaying to two real quarks or gluons. As shown in Fig. 6, masses  $260 < m_{\rho_{T8}} < 480$  GeV are excluded; in Run II the limits will improve to cover the whole mass range up to about 0.8 TeV [32].

The CDF second- and third-generation leptoquark searches (see Refs. [33,34]) have also been interpreted in terms of the complementary  $\rho_{T8}$  decay mode:  $p\bar{p} \rightarrow \rho_{T8} \rightarrow \pi_{LQ}\pi_{LQ}$ . Here  $\pi_{LQ}$  denotes a color-triplet technipion carrying both color and lepton number, assumed to decay to  $b\nu$  or  $c\nu$  [34], or to a  $\tau$  plus a quark [33]. The searches exclude technirho masses  $m_{\rho_{T8}}$  less than 510 GeV ( $\pi_{LQ} \rightarrow c\nu$ ), 600 GeV ( $\pi_{LQ} \rightarrow b\nu$ ), and 465 GeV ( $\pi_{LQ} \rightarrow \tau q$ ) for technipion masses up to  $m_{\rho_{T8}}/2$ . Figure 7 shows the  $\pi_{LQ} \rightarrow b\nu$  exclusion region. (Leptoquark masses  $m_{\pi_{LQ}}$  less than 123 GeV ( $c\nu$ ), 148 GeV ( $b\nu$ ), and 99 GeV ( $\tau q$ ) are already ruled out by standard continuum-production leptoquark searches).

It has been demonstrated that there is substantial uncertainty in the theoretical estimate of the  $\rho_{T8}$  production cross section at the Tevatron and that the cross section may be as much as an order of magnitude lower than the naive vector meson dominance estimate [35]. To establish the range of allowed masses, these limits will need to be redone with a reduced theoretical cross section.

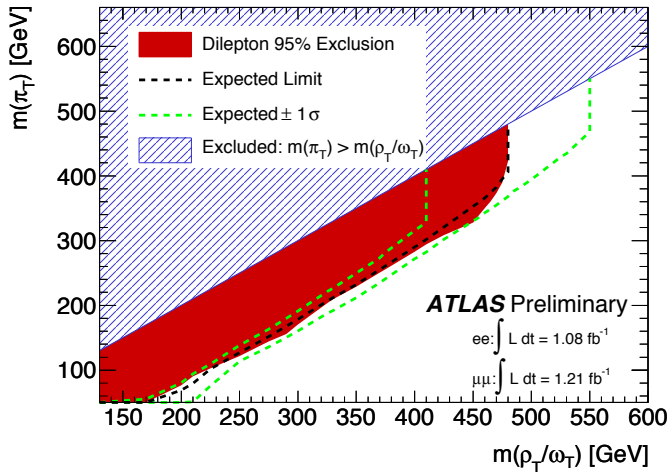


**Figure 8:** 95% CL excluded region by the ATLAS experiment [36] in the  $M(\rho_T), M(\pi_T)$  plane for  $\rho_T/\omega_T \rightarrow ll$  ( $l = e, \mu$ ).

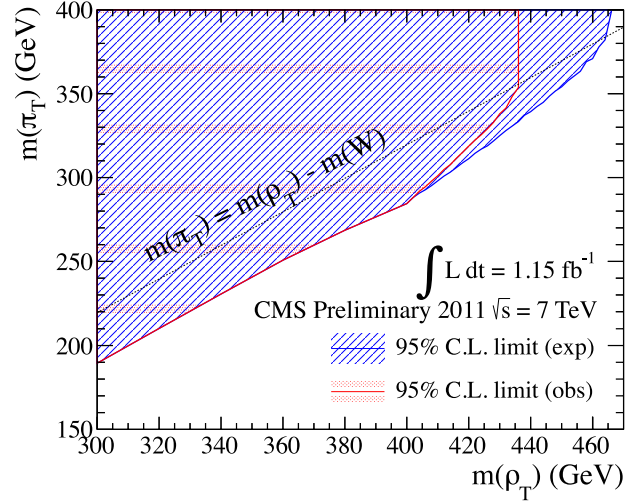


**Figure 9:** 95% CL Exclusion contour in the  $M(\rho_T), M(\pi_T)$  plane for  $\rho_T/a_T \rightarrow WZ \rightarrow ll\nu$  (with  $l = e, \mu$ ) final state by the CMS experiment [37].

Within the context of the model in reference [18], both the ATLAS and CMS experiments have carried out searches for technihadron production in proton-proton collisions at  $\sqrt{s} = 7$  TeV LHC running during 2011. An analysis of the process  $\rho_T$  and  $\omega_T$  decaying to  $\mu^+\mu^-$  and  $e^+e^-$  has been carried out by the ATLAS experiment [36]. This analysis based on  $1.08 \text{ fb}^{-1}$  ( $1.21 \text{ fb}^{-1}$ ) of integrated luminosity, for the  $e^+e^-$  ( $\mu^+\mu^-$ ) channel, as shown in Fig. 8, excludes  $\rho_T$  and  $\omega_T$  with masses in the range 130–480 GeV at 95% CL for  $\pi_T$  masses between 50–480 GeV. The CMS experiment has searched for  $\rho_T$  and its axial-vector partner,  $a_T$  production at  $\sqrt{s} = 7$  TeV using the  $\rho_T/a_T \rightarrow WZ \rightarrow ll\nu$  (with  $l = e, \mu$ ) final state [37]. Using a sample of  $1.15 \text{ fb}^{-1}$  of data, CMS excludes  $\rho_T$  with masses below 382 GeV in the parameter space  $M(\pi_T) = \frac{3}{4}M(\rho_T) - 25$  GeV. If  $M(\rho_T) < M(\pi_T) + M_W$ , then  $\rho_T$  with masses below 436 GeV are excluded. The exclusion contour in the  $\rho_T$  vs.  $\pi_T$  mass plane is shown in Fig. 9.

LHC searches for Higgs Bosons in di-photon [40,41] or di-tau [42] decay modes place strong constraints [43] on the light top-pion state predicted in technicolor models that include colored technifermions. Compared with the standard Higgs Boson, the top-pions have an enhanced production rate (largely because the technipion decay constant is smaller than the weak scale) and also enhanced branching ratios into di-photon and di-tau final states (largely due to the suppression of  $WW$  decays of the technipions). These factors combine to make such technipions more visible in both channels than a standard model Higgs would be, though the precise bounds are model-dependent.



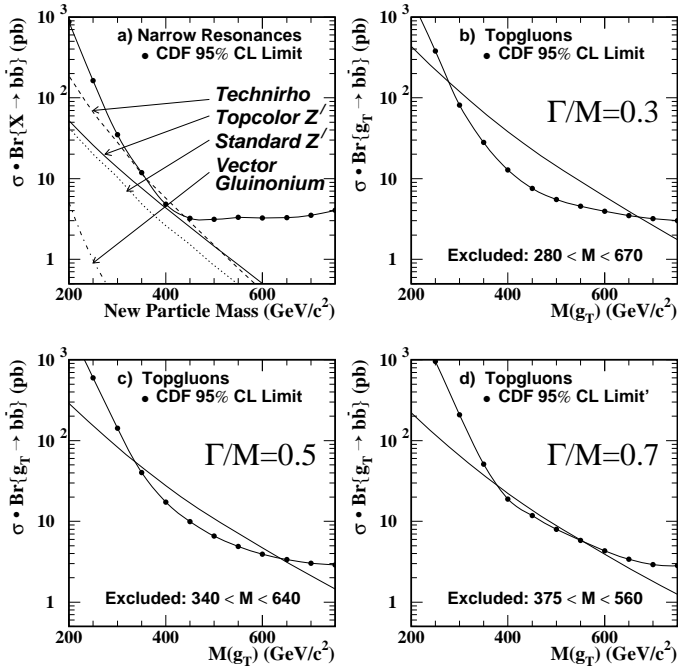


**Figure 10:** Tevatron limits [47] on new particles decaying to  $b\bar{b}$ : narrow resonances and topgluons for various widths.

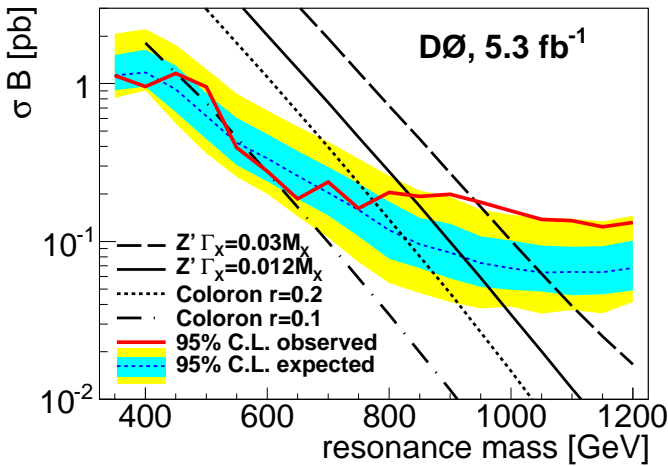


**Figure 11:** 95% CL exclusion limit on a narrow  $t\bar{t}$  resonance as a function of the resonance mass by the  $D\bar{0}$  experiment [49].

## II. Top Condensate, Higgsless, and Related Models

The top quark is much heavier than other fermions and must be more strongly coupled to the symmetry-breaking sector. It is natural to consider whether some or all of electroweak-symmetry breaking is due to a condensate of top quarks [3,44]. Top quark condensation alone, without additional fermions, seems to produce a top quark mass larger [45] than observed experimentally, and is therefore not favored. Topcolor-assisted

technicolor [46] combines technicolor and top condensation. In addition to technicolor, which provides the bulk of electroweak symmetry breaking, top condensation and the top quark mass arise predominantly from “topcolor,” a new QCD-like interaction which couples strongly to the third generation of quarks. An additional, strong, U(1) interaction (giving rise to a topcolor  $Z'$ ) precludes the formation of a  $b$ -quark condensate.

CDF has searched [47] for the “topgluon,” a massive color-octet vector which couples preferentially to the third generation, in the mode  $p\bar{p} \rightarrow g_t \rightarrow b\bar{b}$ . The results are shown in Fig. 10. Topgluon masses from approximately 0.3 to 0.6 TeV are excluded at 95% confidence level, for topgluon widths in the range  $0.3m_{g_t} < \Gamma < 0.7m_{g_t}$ . Results have also been reported by CDF [48] on a search for narrow resonances in the  $t\bar{t}$  invariant mass distribution. Using a data sample corresponding to 4.8  $\text{fb}^{-1}$  integrated luminosity, CDF excludes a leptophobic topcolor  $Z'$  with masses less than 900 GeV, for the case where its width  $\Gamma = 0.012m_{Z'}$ .  $D\bar{0}$  has carried out a similar search, with greater sensitivity [49], and excludes a leptophobic topcolor  $Z'$  bosons at the 95% confidence level for masses below 835 GeV (940 GeV) if its width is 1.2% (3%) of its mass (see Fig. 11). A similar study by ATLAS searches for  $Z' \rightarrow t\bar{t}$  events, excludes leptophobic topcolor  $Z'$  with a width of 1.2% in the mass region 500–860 GeV [50]. The CMS experiment [51] quotes a 95% CL upper limit on the  $\sigma(pp \rightarrow Z') \times Z' \rightarrow t\bar{t}$  as a function of the invariant mass of the resonance. A limit of 2.51 pb is set for  $Z'$  mass of 1 TeV, resonance width 1%, and 0.62 pb or below for  $Z'$  mass above 2 TeV. A broad topgluon could also be detected in the same final state, though no results are yet available. In Run II, the Tevatron [32] should be sensitive to topgluon and topcolor  $Z'$  masses up to of order 1 TeV in  $b\bar{b}$  and  $t\bar{t}$  final states. A detailed theoretical analysis of  $B$ - $\bar{B}$  mixing and light quark mass generation in top-color-assisted technicolor shows that, at least in some models, the topgluon and  $Z'$  boson masses must be greater than about 5 TeV [53].

The top quark seesaw model of electroweak symmetry breaking [54] is a variant of the original top condensate idea which reconciles top condensation with a lighter top quark mass. Such a model can easily be consistent with precision electroweak tests, either because the spectrum includes a light composite Higgs [55], or because additional interactions allow for a heavier Higgs [56]. Such theories may arise naturally from gauge fields propagating in compact extra spatial dimensions [57].

A variant of topcolor-assisted technicolor is flavor-universal, in which the topcolor SU(3) gauge bosons, called colorons, couple equally to all quarks [58]. Flavor-universal versions of the seesaw model [59] incorporating a gauged flavor symmetry are also possible. In these models *all* left-handed quarks (and possibly leptons as well) participate in electroweak-symmetry-breaking condensates with separate (one for each flavor) right-handed weak singlets, and the different fermion masses arise by adjusting the parameters which control the mixing of each fermion with the corresponding condensate.

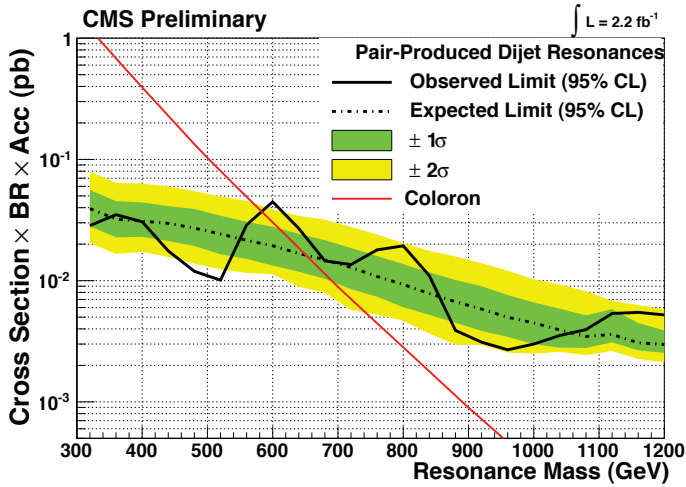


**Figure 12:** 95% CL exclusion limit on pair production cross section of colorons by the CMS experiment [63]. Colorons with mass in the range 320-580 GeV are excluded.

A prediction of these flavor-universal models is the existence of new heavy gauge bosons, coupling to color or flavor, at relatively low mass scales. The absence of an excess of high- $E_T$  jets in  $D\bar{O}$  data [60] has been used to constrain strongly coupled flavor-universal colorons (massive color-octet bosons coupling to all quarks). A mass limit of between 0.8 and 3.5 TeV is set [61] depending on the coloron-gluon mixing angle. Precision electroweak measurements constrain [62] the masses of these new gauge bosons to be greater than 1–3 TeV in a variety of models, for strong couplings. A direct search for colorons has been performed in the proton-proton collisions at  $\sqrt{s} = 7$  TeV, during the 2011 running of the LHC. From analysis of dijet events, the CMS experiment excludes pair production of colorons with mass between 320 and 580 GeV at 95% CL, as shown in Fig. 12 [63]. A recent  $D\bar{O}$  analysis [49] of a resonance decaying to  $t\bar{t}$  can also be interpreted to search for colorons which would decay to  $t\bar{t}$  with a branching fraction of about 1/6 and have a width substantially below 1% of its mass. This study is performed for different values of the coupling to light quarks  $r=0.1$  and  $0.2$  [64]. This  $D\bar{O}$  analysis can exclude such a coloron for  $r=0.2$  with masses below 775 GeV (displayed in Fig. 11).

LHC searches for the standard model Higgs Boson in  $WW$  or  $ZZ$  decay modes [65,66] place strong constraints [67] on the top-Higgs state predicted in top-color models. Such a state couples strongly to top-quarks, and is therefore produced through gluon fusion at a rate enhanced relative to the rate for the standard model Higgs boson. A top-Higgs state with mass less than 300 GeV is excluded at 95% CL if the associated top-pion has a mass of 150 GeV, and the constraint is even stronger if the mass of the top-pion state exceeds the top-quark

mass or if the top-pion decay constant is a substantial fraction of the weak scale.

A class [68] of composite Higgs model [69], dubbed “Little Higgs Theory,” has been developed which gives rise to naturally light Higgs bosons without supersymmetry [70]. Inspired by discretized versions of higher-dimensional gauge theory [71], these models are based on the chiral symmetries of “theory space.” The models involve extended gauge groups and novel gauge symmetry-breaking patterns [72]. The new chiral symmetries prevent large corrections to the Higgs boson mass, and allow the scale ( $\Lambda$ ) of the underlying strong dynamics giving rise to the composite particles to be as large as 10 TeV. These models typically require new gauge bosons and fermions, and possibly additional composite scalars beyond the Higgs, in the TeV mass range [73].

Finally, “Higgsless” models [74] provide electroweak symmetry breaking, including unitarization of the scattering of longitudinal  $W$  and  $Z$  bosons, without employing a scalar Higgs boson. The most extensively studied models [75] are based on a five-dimensional  $SU(2) \times SU(2) \times U(1)$  gauge theory in a slice of Anti-deSitter space, and electroweak symmetry breaking is encoded in the boundary conditions of the gauge fields. Using the AdS/CFT correspondence [76], these theories may be viewed as “dual” descriptions of walking technicolor theories [7]. In addition to a massless photon and near-standard  $W$  and  $Z$  bosons, the spectrum includes an infinite tower of additional massive vector bosons (the higher Kaluza-Klein or  $KK$  excitations), whose exchange is responsible for unitarizing longitudinal  $W$  and  $Z$  boson scattering [77]. Depending on how these  $KK$  bosons couple to fermions, searches for the  $W'$  bosons decaying to  $WZ$  [37] may be used to place bounds in these theories.

Using deconstruction it has been shown [78] that a Higgsless model whose fermions are localized (*i.e.*, derive their electroweak properties from a single site on the deconstructed lattice) cannot simultaneously satisfy unitarity bounds and precision electroweak constraints. The [79] size of corrections to electroweak processes in Higgsless models may be reduced, however, by considering delocalized fermions, *i.e.*, considering the effect of the distribution of the wavefunctions of ordinary fermions in the fifth dimension (corresponding, in the deconstruction language, to allowing the fermions to derive their electroweak properties from several sites on the lattice). It has been shown [80] that, in an arbitrary Higgsless model, if the probability distribution of the delocalized fermions is related to the  $W$  wavefunction (a condition called “ideal” delocalization), then deviations in precision electroweak parameters are minimized. Phenomenological limits on delocalized Higgsless models may be derived [81] from limits on the deviation of the triple-gauge boson ( $WWZ$ ) vertices from the standard model, and current constraints allow for the lightest  $KK$  resonances (which tend to be fermiophobic in the case of ideal fermion delocalization) to have masses of only a few hundred

## Searches Particle Listings

## Technicolor

GeV. Such resonances would have to be studied using  $WW$  scattering [82].

An alternative approach to “Higgsless” models, dubbed “holographic technicolor” [83], incorporates a generalized extra-dimensional framework and allows for arbitrary couplings of the vector mesons to the light fermions, resulting in a wide variety of potential signatures at the LHC [84].

**Acknowledgments**

We thank Tom Appelquist, Bogdan Dobrescu, Emilian Dudas, Robert Harris, Chris Hill, Greg Landsberg, Kenneth Lane, Bob Shrock, Elizabeth Simmons, and John Terning for help in the preparation of this article. *This work was supported in part by the Department of Energy under grant DE-FG02-91ER40688 and by the National Science Foundation under grant PHY-0854889.*

**References**

1. S. Weinberg, Phys. Rev. **D19**, 1277 (1979).
2. L. Susskind, Phys. Rev. **D20**, 2619 (1979).
3. For a recent reviews, see K. Lane, hep-ph/0202255; C.T. Hill, E.H. Simmons, Phys. Rept. **381**, 235 (2003); R. Shrock, hep-ph/0703050.
4. E. Eichten and K. Lane, Phys. Lett. **90B**, 125 (1980).
5. S. Dimopoulos, S. Raby, and G.L. Kane, Nucl. Phys. **B182**, 77 (1981).
6. S. Dimopoulos and L. Susskind, Nucl. Phys. **B155**, 237 (1979).
7. B. Holdom, Phys. Rev. **D24**, 1441 (1981) and Phys. Lett. **150B**, 301 (1985); K. Yamawaki, M. Bando, and K. Matumoto, Phys. Rev. Lett. **56**, 1335 (1986); T.W. Appelquist, D. Karabali, and L.C.R. Wijewardhana, Phys. Rev. Lett. **57**, 957 (1986); T. Appelquist and L.C.R. Wijewardhana, Phys. Rev. **D35**, 774 (1987) and Phys. Rev. **D36**, 568 (1987).
8. E. Eichten and K. Lane, Phys. Lett. **B222**, 274 (1989).
9. L. Del Debbio, arXiv:1102.4066; E. Pallante, arXiv:0912.5188; G. Fleming, arXiv:0812.2035.
10. T. Appelquist *et al.*, Phys. Rev. Lett. **104**, 071601 (2010).
11. J. Erler and P. Langacker, “Electroweak Model and Constraints on New Physics,” in the section on Reviews, Tables, and Plots in this *Review*.
12. T. Appelquist *et al.*, Phys. Rev. Lett. **106**, 231601 (2011).
13. T. Appelquist, P. S. Rodrigues da Silva, and F. Sannino, Phys. Rev. **D60**, 116007 (1999).
14. T. Appelquist *et al.*, arXiv:1201.3977.
15. T.W. Appelquist and R. Shrock, Phys. Lett. **B548**, 204 (2002) and Phys. Rev. Lett. **90**, 201801 (2003); T.W. Appelquist, M. Piai, and R. Shrock, Phys. Rev. **D69**, 015002 (2004); T. Appelquist *et al.*, Phys. Rev. **D70**, 093010 (2004).
16. E. Eichten *et al.*, Rev. Mod. Phys. **56**, 579 (1984) and Phys. Rev. **D34**, 1547 (1986).
17. K. Lane, Phys. Rev. **D60**, 075007 (1999); K. Lane and S. Mrenna, Phys. Rev. **D67**, 115011 (2003); see also K. Lane and A. Martin, arXiv:0907.3737.
18. E. Eichten and K. Lane, Phys. Lett. **B669**, 235 (2008).
19. T. Sjostrand, Comp. Phys. Comm. **82**, 74 (1994).
20. S. Mrenna, Technihadron production and decay at LEP2, Phys. Lett. **B461**, 352 (1999).
21. E. Eichten, K. Lane, and J. Womersley, Phys. Lett. **B405**, 305 (1997).
22. CDF Collab. (T. Affolder *et al.*), Phys. Rev. Lett. **84**, 1110 (2000).
23. CDF Collab., Phys. Rev. Lett. **104**, 111802 (2010).
24. DØ Collab. (V.M. Abazov *et al.*), Phys. Rev. **98**, 221801 (2007).
25. DØ Collab. (V.M. Abazov *et al.*), Phys. Rev. Lett. **104**, 061801 (2010).
26. CDF Collab. (F. Abe *et al.*), Phys. Rev. Lett. **83**, 3124 (1999).
27. DØ Collab. (V.M. Abazov *et al.*), Phys. Rev. Lett. **87**, 061802 (2001).
28. CDF Collab. (A. Abulencia *et al.*), Phys. Rev. Lett. **95**, 252001 (2005).
29. DELPHI Collab. (J. Abdallah *et al.*), Eur. Phys. J. **C22**, 17 (2001).
30. K. Lane and M.V. Ramana, Phys. Rev. **D44**, 2678 (1991).
31. CDF Collab. (F. Abe *et al.*), Phys. Rev. **D55**, R5263 (1997).
32. K. Cheung and R.M. Harris, hep-ph/9610382.
33. CDF Collab. (F. Abe *et al.*), Phys. Rev. Lett. **82**, 3206 (1999).
34. CDF Collab. (T. Affolder *et al.*), Phys. Rev. Lett. **85**, 2056 (2000).
35. A. Zerwekh and R. Rosenfeld, Phys. Lett. **B503**, 325 (2001); R.S. Chivukula, *et al.*, Boston Univ. preprint BUHEP-01-19.
36. ATLAS Collab., ATLAS-CONF-2011-125 (2011).
37. CMS Collab., CMS Physics Analysis Summary EXO-11-041 (2011).
38. ATLAS Collab., CERN-OPEN-2008-020, (2008).
39. CMS Collab., CMS Physics Analysis Summary EXO-08-001 (2008).
40. CMS Collab., arXiv:1202.1487.
41. ATLAS Collab., arXiv:1202.1414.
42. ATLAS Collab., arXiv:1107.5003.
43. R. S. Chivukula *et al.*, Phys. Rev. **D84**, 115025 (2011).
44. V.A. Miransky, M. Tanabashi, and K. Yamawaki, Phys. Lett. **221B**, 177 (1989), and Mod. Phys. Lett. **4**, 1043 (1989); Y. Nambu, EFI-89-08 (1989); W.J. Marciano, Phys. Rev. Lett. **62**, 2793 (1989).
45. W.A. Bardeen, C.T. Hill, and M. Lindner, Phys. Rev. **D41**, 1647 (1990).
46. C.T. Hill, Phys. Lett. **B345**, 483 (1995); see also Phys. Lett. **266B**, 419 (1991).
47. CDF Collab. (F. Abe *et al.*), Phys. Rev. Lett. **82**, 2038 (1999).
48. CDF Collab. (T. Aaltonen *et al.*), Phys. Rev. **D85**, 051101 (2012).
49. D0 Collab. (T. Aaltonen *et al.*), Phys. Rev. **D84**, 072004 (2011).
50. ATLAS Collab., ATLAS-CONF-2012-029 (2012).



51. CMS Collab., CMS Physics Analysis Summary EXO-11-092 (2011).
52. D0 Collab. (V. Abazov *et al.*), Phys. Rev. Lett. **87**, 231801 (2001).
53. G. Burdman *et al.*, Phys. Lett. **B514**, 41 (2001).
54. B.A. Dobrescu and C.T. Hill, Phys. Rev. Lett. **81**, 2634 (1998).
55. R.S. Chivukula *et al.*, Phys. Rev. **D59**, 075003 (1999).
56. H. Collins, A. Grant, and H. Georgi, Phys. Rev. **D61**, 055002 (2000).
57. B.A. Dobrescu, Phys. Lett. **B461**, 99 (1999); H.-C. Cheng, *et al.*, Nucl. Phys. **B589**, 249 (2000).
58. E.H. Simmons, Nucl. Phys. **B324**, 315 (1989).
59. G. Burdman and N. Evans, Phys. Rev. **D59**, 115005 (1999).
60. DØ Collab. (B. Abbott *et al.*), Phys. Rev. Lett. **82**, 2457 (1999).
61. I. Bertram and E.H. Simmons, Phys. Lett. **B443**, 347 (1998).
62. G. Burdman, R.S. Chivukula, and N. Evans, Phys. Rev. **D61**, 035009 (2000).
63. CMS Collab., CMS Physics Analysis Summary EXO-11-016 (2011).
64. B. A. Dobrescu, K. Kong, and R. Mahbubani, JHEP **06**, 001 (2009).
65. CMS Collab., arXiv:1202.1488.
66. ATLAS Collab., arXiv:1202.1408.
67. R. S. Chivukula, *et al.*, Phys. Rev. **D84**, 095022 (2011).
68. N. Arkani-Hamed, A.G. Cohen, and H. Georgi, Phys. Lett. **B513**, 232 (2001).
69. D.B. Kaplan and H. Georgi, Phys. Lett. **B136**, 183 (1984) and Phys. Lett. **B145**, 216 (1984); T. Banks, Nucl. Phys. **B243**, 123 (1984); D.B. Kaplan, H. Georgi, and S. Dimopoulos, Phys. Lett. **B136**, 187 (1984); M.J. Dugan, H. Georgi, and D.B. Kaplan, Nucl. Phys. **B254**, 299 (1985).
70. See also review by P. Igo-Kemenes, "Searches for Higgs Bosons," in the Boson Listings in this *Review*.
71. N. Arkani-Hamed, A. G. Cohen, and H. Georgi, Phys. Rev. **D86**, 4757 (2001); H. C. Cheng, C. T. Hill, and J. Wang, Phys. Rev. **D64**, 095003 (2001).
72. M. Schmaltz and D. Tucker-Smith, Ann. Rev. Nucl. Part. Sci. **55**, 229 (2005).
73. C. Csaki *et al.*, Phys. Rev. **D67**, 115002 (2003); J. Hewett, F. Petriello, and T. Rizzo, JHEP **310**, 062 (2003); T. Han *et al.*, Phys. Rev. **D67**, 095004 (2003); Z. Han and W. Skiba, Phys. Rev. **D72**, 035005 (2005).
74. C. Csaki *et al.*, Phys. Rev. **D69**, 055006 (2003).
75. K. Agashe *et al.*, JHEP **0308**, 050 (2003); C. Csaki *et al.*, Phys. Rev. Lett. **92**, 101802 (2004).
76. J. Maldacena, Adv. Theor. Math. Phys. **2**, 231 (1998).
77. R. S. Chivukula, D. Dicus, and H.-J. He, Phys. Lett. **B525**, 175 (2002).
78. R. S. Chivukula *et al.*, Phys. Rev. **D71**, 035007 (2005).
79. G. Cacciapaglia *et al.*, Phys. Rev. **D71**, 035015 (2005); R. Foadi, S. Gopalkrishna, and C. Schmidt, Phys. Lett.

**B606**, 157 (2005);

G. Cacciapaglia *et al.*, Phys. Rev. **D72**, 095018 (2005).

80. R. S. Chivukula *et al.*, Phys. Rev. **D72**, 015008 (2005).

81. R. S. Chivukula *et al.*, Phys. Rev. **D72**, 075012 (2005).

82. A. Birkedal, K. Matchev, and M. Perelstein, Phys. Rev. Lett. **94**, 191803 (2005); H.-J. He, *et al.*, arXiv:0708.2588.

83. J. Hirn and V. Sanz, Phys. Rev. Lett. **97**, 121803 (2006).

84. J. Hirn, A. Martin, and V. Sanz, JHEP **0805**, 084 (2008) and Phys. Rev. **D78**, 075026 (2008).

The latest unpublished results are described in "Dynamical Electroweak Symmetry Breaking" review.

### MASS LIMITS for Resonances in Models of Dynamical Electroweak Symmetry Breaking

VALUE (GeV)	CL%	DOCUMENT ID	TECN	COMMENT
••• We do not use the following data for averages, fits, limits, etc. •••				
>805	95	1 AALTONEN	11AD CDF	top-color $Z'$
>805	95	1 AALTONEN	11AE CDF	top-color $Z'$
		2 CHIVUKULA	11 RVUE	top-Higgs
		3 CHIVUKULA	11A RVUE	techni- $\pi$
		4 AALTONEN	10I CDF	$\rho\bar{p} \rightarrow \rho_T/\omega_T \rightarrow W\pi_T$
none 208-408	95	5 ABAZOV	10A DØ	$\rho_T \rightarrow WZ$
		6 ABAZOV	07I DØ	$\rho\bar{p} \rightarrow \rho_T/\omega_T \rightarrow W\pi_T$
>280	95	7 ABULENCIA	05A CDF	$\rho_T \rightarrow e^+e^-, \mu^+\mu^-$
		8 CHEKANOV	02B ZEUS	color octet techni- $\pi$
>207	95	9 ABAZOV	01B DØ	$\rho_T \rightarrow e^+e^-$
none 90-206.7	95	10 ABDALLAH	01I DLPH	$e^+e^- \rightarrow \rho_T$
		11 AFFOLDER	00F CDF	color-singlet techni- $\rho$ , $\rho_T \rightarrow W\pi_T, 2\pi_T$
>600	95	12 AFFOLDER	00K CDF	color-octet techni- $\rho$ , $\rho_{T8} \rightarrow 2\pi_{LQ}$
none 350-440	95	13 ABE	99F CDF	color-octet techni- $\rho$ , $\rho_{T8} \rightarrow \bar{b}b$
		14 ABE	99N CDF	techni- $\omega$ , $\omega_T \rightarrow \gamma\bar{b}b$
none 260-480	95	15 ABE	97G CDF	color-octet techni- $\rho$ , $\rho_{T8} \rightarrow 2\text{jets}$

<sup>1</sup>AALTONEN 11AD and AALTONEN 11AE search for top-color  $Z'$  decaying to  $t\bar{t}$ . The quoted limit is for  $Z'_{\text{top}}$  with decay width  $\Gamma = 0.012 M_{Z'}$ .

<sup>2</sup>Using the LHC limit on the Higgs boson production cross section, CHIVUKULA 11 obtain a limit on the top-Higgs mass  $> 300$  GeV at 95% CL assuming 150 GeV top-pion mass.

<sup>3</sup>Using the LHC limit on the Higgs boson production cross section, CHIVUKULA 11A obtain a limit on the technipion mass ruling out the region  $110 \text{ GeV} < m_P < 2m_t$ . Existence of color technifermions, top-color mechanism, and  $N_{TC} \geq 3$  are assumed.

<sup>4</sup>AALTONEN 10I search for the vector techni-resonances ( $\rho_T, \omega_T$ ) decaying into  $W\pi_T$  with  $W \rightarrow \ell\nu$  and  $\pi_T \rightarrow b\bar{b}, b\bar{c}$ , or  $b\bar{u}$ . See their Fig. 3 for the exclusion plot in the  $M_{\pi_T} - M_{\rho_T}$  plane.

<sup>5</sup>ABAZOV 10A search for a vector techni-resonance decaying into  $WZ$ . The limit assumes  $M_{\rho_T} < M_{\pi_T} + M_W$ .

<sup>6</sup>ABAZOV 07I search for the vector techni-resonances ( $\rho_T, \omega_T$ ) decaying into  $W\pi_T$  with  $W \rightarrow e\nu$  and  $\pi_T \rightarrow b\bar{b}$  or  $b\bar{c}$ . See their Fig. 2 for the exclusion plot in the  $M_{\pi_T} - M_{\rho_T}$  plane.

<sup>7</sup>ABULENCIA 05A search for resonances decaying to electron or muon pairs in  $p\bar{p}$  collisions. at  $\sqrt{s} = 1.96$  TeV. The limit assumes Technicolor-scale mass parameters  $M_V = M_A = 500$  GeV.

<sup>8</sup>CHEKANOV 02B search for color octet techni- $\pi$   $P$  decaying into dijets in  $ep$  collisions. See their Fig. 5 for the limit on  $\sigma(ep \rightarrow ePX) \cdot B(P \rightarrow 2j)$ .

<sup>9</sup>ABAZOV 01B searches for vector techni-resonances ( $\rho_T, \omega_T$ ) decaying to  $e^+e^-$ . The limit assumes  $M_{\rho_T} = M_{\omega_T} < M_{\pi_T} + M_W$ .

<sup>10</sup>The limit is independent of the  $\pi_T$  mass. See their Fig. 9 and Fig. 10 for the exclusion plot in the  $M_{\rho_T} - M_{\pi_T}$  plane. ABDALLAH 01 limit on the technipion mass is  $M_{\pi_T} > 79.8$  GeV for  $N_D=2$ , assuming its point-like coupling to gauge bosons.

<sup>11</sup>AFFOLDER 00F search for  $\rho_T$  decaying into  $W\pi_T$  or  $\pi_T\pi_T$  with  $W \rightarrow \ell\nu$  and  $\pi_T \rightarrow \bar{b}b, \bar{b}c$ . See Fig. 1 in the above Note on "Dynamical Electroweak Symmetry Breaking" for the exclusion plot in the  $M_{\rho_T} - M_{\pi_T}$  plane.

<sup>12</sup>AFFOLDER 00K search for the  $\rho_{T8}$  decaying into  $\pi_{LQ}\pi_{LQ}$  with  $\pi_{LQ} \rightarrow b\nu$ . For  $\pi_{LQ} \rightarrow c\nu$ , the limit is  $M_{\rho_{T8}} > 510$  GeV. See their Fig. 2 and Fig. 3 for the exclusion plot in the  $M_{\rho_{T8}} - M_{\pi_{LQ}}$  plane.

<sup>13</sup>ABE 99F search for a new particle  $X$  decaying into  $b\bar{b}$  in  $p\bar{p}$  collisions at  $E_{\text{cm}} = 1.8$  TeV. See Fig. 7 in the above Note on "Dynamical Electroweak Symmetry Breaking" for the upper limit on  $\sigma(p\bar{p} \rightarrow X) \times B(X \rightarrow b\bar{b})$ . ABE 99F also exclude top gluons of width  $\Gamma = 0.3M$  in the mass interval  $280 < M < 670$  GeV, of width  $\Gamma = 0.5M$  in the mass interval  $340 < M < 640$  GeV, and of width  $\Gamma = 0.7M$  in the mass interval  $375 < M < 560$  GeV.

<sup>14</sup>ABE 99N search for the techni- $\omega$  decaying into  $\gamma\pi_T$ . The technipion is assumed to decay  $\pi_T \rightarrow b\bar{b}$ . See Fig. 2 in the above Note on "Dynamical Electroweak Symmetry Breaking" for the exclusion plot in the  $M_{\omega_T} - M_{\pi_T}$  plane.

<sup>15</sup>ABE 97G search for a new particle  $X$  decaying into dijets in  $p\bar{p}$  collisions at  $E_{\text{cm}} = 1.8$  TeV. See Fig. 5 in the above Note on "Dynamical Electroweak Symmetry Breaking" for the upper limit on  $\sigma(p\bar{p} \rightarrow X) \times B(X \rightarrow 2j)$ .

# Searches Particle Listings

## Technicolor, Quark and Lepton Compositeness

### REFERENCES FOR Technicolor

AALTONEN	11AD	PR D84 072003	T. Aaltonen <i>et al.</i>	(CDF Collab.)
AALTONEN	11AE	PR D84 072004	T. Aaltonen <i>et al.</i>	(CDF Collab.)
CHIVUKULA	11	PR D84 095022	R.S. Chivukula <i>et al.</i>	
CHIVUKULA	11A	PR D84 115025	R. S. Chivukula <i>et al.</i>	
AALTONEN	10I	PRL 104 111802	T. Aaltonen <i>et al.</i>	(CDF Collab.)
ABAZOV	10A	PRL 104 061801	V.M. Abazov <i>et al.</i>	(DO Collab.)
ABAZOV	07I	PRL 98 221801	V.M. Abazov <i>et al.</i>	(DO Collab.)
ABULENCIA	05A	PRL 95 252001	A. Abulencia <i>et al.</i>	(CDF Collab.)
CHEKANOV	02B	PL B531 9	S. Chekanov <i>et al.</i>	(ZEUS Collab.)
ABAZOV	01B	PRL 87 061802	V.M. Abazov <i>et al.</i>	(DO Collab.)
ABDALLAH	01	EPJ C22 17	J. Abdallah <i>et al.</i>	(DELPHI Collab.)
AFFOLDER	00F	PRL 84 1110	T. Affolder <i>et al.</i>	(CDF Collab.)
AFFOLDER	00K	PRL 85 2056	T. Affolder <i>et al.</i>	(CDF Collab.)
ABE	99F	PRL 82 2038	F. Abe <i>et al.</i>	(CDF Collab.)
ABE	99N	PRL 83 3124	F. Abe <i>et al.</i>	(CDF Collab.)
ABE	97G	PR D55 R5263	F. Abe <i>et al.</i>	(CDF Collab.)

## Quark and Lepton Compositeness, Searches for

The latest unpublished results are described in the “Quark and Lepton Compositeness” review.

### SEARCHES FOR QUARK AND LEPTON COMPOSITENESS

Revised 2001 by K. Hagiwara (KEK), and K. Hikasa and M. Tanabashi (Tohoku University).

If quarks and leptons are made of constituents, then at the scale of constituent binding energies, there should appear new interactions among quarks and leptons. At energies much below the compositeness scale ( $\Lambda$ ), these interactions are suppressed by inverse powers of  $\Lambda$ . The dominant effect should come from the lowest dimensional interactions with four fermions (contact terms), whose most general chirally invariant form reads [1]

$$L = \frac{g^2}{2\Lambda^2} \left[ \eta_{LL} \bar{\psi}_L \gamma_\mu \psi_L \bar{\psi}_L \gamma^\mu \psi_L + \eta_{RR} \bar{\psi}_R \gamma_\mu \psi_R \bar{\psi}_R \gamma^\mu \psi_R + 2\eta_{LR} \bar{\psi}_L \gamma_\mu \psi_L \bar{\psi}_R \gamma^\mu \psi_R \right]. \quad (1)$$

Chiral invariance provides a natural explanation why quark and lepton masses are much smaller than their inverse size  $\Lambda$ . We may determine the scale  $\Lambda$  unambiguously by using the above form of the effective interactions; the conventional method [1] is to fix its scale by setting  $g^2/4\pi = g^2(\Lambda)/4\pi = 1$  for the new strong interaction coupling and by setting the largest magnitude of the coefficients  $\eta_{\alpha\beta}$  to be unity. In the following, we denote

$$\begin{aligned} \Lambda &= \Lambda_{LL}^\pm \text{ for } (\eta_{LL}, \eta_{RR}, \eta_{LR}) = (\pm 1, 0, 0), \\ \Lambda &= \Lambda_{RR}^\pm \text{ for } (\eta_{LL}, \eta_{RR}, \eta_{LR}) = (0, \pm 1, 0), \\ \Lambda &= \Lambda_{VV}^\pm \text{ for } (\eta_{LL}, \eta_{RR}, \eta_{LR}) = (\pm 1, \pm 1, \pm 1), \\ \Lambda &= \Lambda_{AA}^\pm \text{ for } (\eta_{LL}, \eta_{RR}, \eta_{LR}) = (\pm 1, \pm 1, \mp 1), \end{aligned} \quad (2)$$

as typical examples. Such interactions can arise by constituent interchange (when the fermions have common constituents, *e.g.*, for  $ee \rightarrow ee$ ) and/or by exchange of the binding quanta (when ever binding quanta couple to constituents of both particles).

Another typical consequence of compositeness is the appearance of excited leptons and quarks ( $\ell^*$  and  $q^*$ ). Phenomenologically, an excited lepton is defined to be a heavy lepton which shares leptonic quantum number with one of the existing leptons (an excited quark is defined similarly). For example, an excited electron  $e^*$  is characterized by a nonzero transition-magnetic coupling with electrons. Smallness of the lepton mass

and the success of QED prediction for  $g-2$  suggest chirality conservation, *i.e.*, an excited lepton should not couple to both left- and right-handed components of the corresponding lepton.

Excited leptons may be classified by  $SU(2) \times U(1)$  quantum numbers. Typical examples are:

1. Sequential type

$$\begin{pmatrix} \nu^* \\ \ell^* \end{pmatrix}_L, \quad [\nu_R^*], \quad \ell_R^*.$$

$\nu_R^*$  is necessary unless  $\nu^*$  has a Majorana mass.

2. Mirror type

$$[\nu_L^*], \quad \ell_L^*, \quad \begin{pmatrix} \nu^* \\ \ell^* \end{pmatrix}_R.$$

3. Homodoublet type

$$\begin{pmatrix} \nu^* \\ \ell^* \end{pmatrix}_L, \quad \begin{pmatrix} \nu^* \\ \ell^* \end{pmatrix}_R.$$

Similar classification can be made for excited quarks.

Excited fermions can be pair produced via their gauge couplings. The couplings of excited leptons with  $Z$  are listed in the following table (for notation see Eq. (1) in “Standard Model of Electroweak Interactions”):

	Sequential type	Mirror type	Homodoublet type
$V^{\ell^*}$	$-\frac{1}{2} + 2\sin^2\theta_W$	$-\frac{1}{2} + 2\sin^2\theta_W$	$-1 + 2\sin^2\theta_W$
$A^{\ell^*}$	$-\frac{1}{2}$	$+\frac{1}{2}$	0
$V^{\nu_D^*}$	$+\frac{1}{2}$	$+\frac{1}{2}$	+1
$A^{\nu_D^*}$	$+\frac{1}{2}$	$-\frac{1}{2}$	0
$V^{\nu_M^*}$	0	0	—
$A^{\nu_M^*}$	+1	-1	—

Here  $\nu_D^*$  ( $\nu_M^*$ ) stands for Dirac (Majorana) excited neutrino. The corresponding couplings of excited quarks can be easily obtained. Although form factor effects can be present for the gauge couplings at  $q^2 \neq 0$ , they are usually neglected.

In addition, transition magnetic type couplings with a gauge boson are expected. These couplings can be generally parameterized as follows:

$$\begin{aligned} \mathcal{L} &= \frac{\lambda_\gamma^{(f^*)}}{2m_{f^*}} \bar{f}^* \sigma^{\mu\nu} (\eta_L \frac{1-\gamma_5}{2} + \eta_R \frac{1+\gamma_5}{2}) f F_{\mu\nu} \\ &+ \frac{\lambda_Z^{(f^*)}}{2m_{f^*}} \bar{f}^* \sigma^{\mu\nu} (\eta_L \frac{1-\gamma_5}{2} + \eta_R \frac{1+\gamma_5}{2}) f Z_{\mu\nu} \\ &+ \frac{\lambda_W^{(\ell^*)}}{2m_{\ell^*}} \bar{\ell}^* \sigma^{\mu\nu} \frac{1-\gamma_5}{2} \nu W_{\mu\nu} \\ &+ \frac{\lambda_W^{(\nu^*)}}{2m_{\nu^*}} \bar{\nu}^* \sigma^{\mu\nu} (\eta_L \frac{1-\gamma_5}{2} + \eta_R \frac{1+\gamma_5}{2}) \ell W_{\mu\nu}^\dagger \\ &+ \text{h.c.}, \end{aligned} \quad (3)$$

where  $g = e/\sin\theta_W$ ,  $F_{\mu\nu} = \partial_\mu A_\nu - \partial_\nu A_\mu$  is the photon field strength,  $Z_{\mu\nu} = \partial_\mu Z_\nu - \partial_\nu Z_\mu$ , etc. The normalization of the coupling is chosen such that

$$\max(|\eta_L|, |\eta_R|) = 1.$$

Chirality conservation requires

$$\eta_L \eta_R = 0. \quad (4)$$

Some experimental analyses assume the relation  $\eta_L = \eta_R = 1$ , which violates chiral symmetry. We encode the results of such analyses if the crucial part of the cross section is proportional to the factor  $\eta_L^2 + \eta_R^2$  and the limits can be reinterpreted as those for chirality conserving cases  $(\eta_L, \eta_R) = (1, 0)$  or  $(0, 1)$  after rescaling  $\lambda$ .

These couplings in Eq. (3) can arise from  $SU(2) \times U(1)$ -invariant higher-dimensional interactions. A well-studied model is the interaction of homodoublet type  $\ell^*$  with the Lagrangian [2,3]

$$\mathcal{L} = \frac{1}{2\Lambda} \bar{L}^* \sigma^{\mu\nu} (g f \frac{\tau^a}{2} W_{\mu\nu}^a + g' f' Y B_{\mu\nu}) \frac{1-\gamma_5}{2} L + \text{h.c.}, \quad (5)$$

where  $L$  denotes the lepton doublet  $(\nu, \ell)$ ,  $\Lambda$  is the compositeness scale,  $g, g'$  are  $SU(2)$  and  $U(1)_Y$  gauge couplings, and  $W_{\mu\nu}^a$  and  $B_{\mu\nu}$  are the field strengths for  $SU(2)$  and  $U(1)_Y$  gauge fields. The same interaction occurs for mirror-type excited leptons. For sequential-type excited leptons, the  $\ell^*$  and  $\nu^*$  couplings become unrelated, and the couplings receive the extra suppression of  $(250 \text{ GeV})/\Lambda$  or  $m_{L^*}/\Lambda$ . In any case, these couplings satisfy the relation

$$\lambda_W = -\sqrt{2} \sin^2 \theta_W (\lambda_Z \cot \theta_W + \lambda_\gamma). \quad (6)$$

Additional coupling with gluons is possible for excited quarks:

$$\mathcal{L} = \frac{1}{2\Lambda} \bar{Q}^* \sigma^{\mu\nu} \left( g_s f_s \frac{\lambda^a}{2} G_{\mu\nu}^a + g f \frac{\tau^a}{2} W_{\mu\nu}^a + g' f' Y B_{\mu\nu} \right) \times \frac{1-\gamma_5}{2} Q + \text{h.c.}, \quad (7)$$

where  $Q$  denotes a quark doublet,  $g_s$  is the QCD gauge coupling, and  $G_{\mu\nu}^a$  the gluon field strength.

It should be noted that the electromagnetic radiative decay of  $\ell^*(\nu^*)$  is forbidden if  $f = -f'$  ( $f = f'$ ). These two possibilities ( $f = f'$  and  $f = -f'$ ) are investigated in many analyses of the LEP experiments above the Z pole.

Several different conventions are used by LEP experiments on Z pole to express the transition magnetic couplings. To facilitate comparison, we re-express these in terms of  $\lambda_Z$  and  $\lambda_\gamma$  using the following relations and taking  $\sin^2 \theta_W = 0.23$ . We assume chiral couplings, *i.e.*,  $|c| = |d|$  in the notation of Ref. 2.

1. ALEPH (charged lepton and neutrino)

$$\lambda_Z^{\text{ALEPH}} = \frac{1}{2} \lambda_Z \quad (1990 \text{ papers}) \quad (8a)$$

$$\frac{2c}{\Lambda} = \frac{\lambda_Z}{m_{\ell^*} [\text{or } m_{\nu^*}]} \quad (\text{for } |c| = |d|) \quad (8b)$$

2. ALEPH (quark)

$$\lambda_u^{\text{ALEPH}} = \frac{\sin \theta_W \cos \theta_W}{\sqrt{\frac{1}{4} - \frac{2}{3} \sin^2 \theta_W + \frac{8}{9} \sin^4 \theta_W}} \lambda_Z = 1.11 \lambda_Z \quad (9)$$

3. L3 and DELPHI (charged lepton)

$$\lambda^{\text{L3}} = \lambda_Z^{\text{DELPHI}} = -\frac{\sqrt{2}}{\cot \theta_W - \tan \theta_W} \lambda_Z = -1.10 \lambda_Z \quad (10)$$

4. L3 (neutrino)

$$f^{\text{L3}} = \sqrt{2} \lambda_Z \quad (11)$$

5. OPAL (charged lepton)

$$\frac{f^{\text{OPAL}}}{\Lambda} = -\frac{2}{\cot \theta_W - \tan \theta_W} \frac{\lambda_Z}{m_{\ell^*}} = -1.56 \frac{\lambda_Z}{m_{\ell^*}} \quad (12)$$

6. OPAL (quark)

$$\frac{f^{\text{OPAL}c}}{\Lambda} = \frac{\lambda_Z}{2m_{q^*}} \quad (\text{for } |c| = |d|) \quad (13)$$

7. DELPHI (charged lepton)

$$\lambda_\gamma^{\text{DELPHI}} = -\frac{1}{\sqrt{2}} \lambda_\gamma \quad (14)$$

If leptons are made of color triplet and antitriplet constituents, we may expect their color-octet partners. Transitions between the octet leptons ( $\ell_8$ ) and the ordinary lepton ( $\ell$ ) may take place via the dimension-five interactions

$$\mathcal{L} = \frac{1}{2\Lambda} \sum_\ell \left\{ \bar{\ell}_8^\alpha g_S F_{\mu\nu}^\alpha \sigma^{\mu\nu} (\eta_L \ell_L + \eta_R \ell_R) + \text{h.c.} \right\} \quad (15)$$

where the summation is over charged leptons and neutrinos. The leptonic chiral invariance implies  $\eta_L \eta_R = 0$  as before.

## References

1. E.J. Eichten, K.D. Lane, and M.E. Peskin, Phys. Rev. Lett. **50**, 811 (1983).
2. K. Hagiwara, S. Komamiya, and D. Zeppenfeld, Z. Phys. **C29**, 115 (1985).
3. N. Cabibbo, L. Maiani, and Y. Srivastava, Phys. Lett. **139B**, 459 (1984).

## CONTENTS:

- Scale Limits for Contact Interactions:  $\Lambda(eeee)$
- Scale Limits for Contact Interactions:  $\Lambda(ee\mu\mu)$
- Scale Limits for Contact Interactions:  $\Lambda(ee\tau\tau)$
- Scale Limits for Contact Interactions:  $\Lambda(\ell\ell\ell\ell)$
- Scale Limits for Contact Interactions:  $\Lambda(eeqq)$
- Scale Limits for Contact Interactions:  $\Lambda(\mu\mu qq)$
- Scale Limits for Contact Interactions:  $\Lambda(\ell\nu\ell\nu)$
- Scale Limits for Contact Interactions:  $\Lambda(e\nu qq)$
- Scale Limits for Contact Interactions:  $\Lambda(qqqq)$
- Scale Limits for Contact Interactions:  $\Lambda(\nu\nu qq)$
- Mass Limits for Excited  $e$  ( $e^*$ )
  - Limits for Excited  $e$  ( $e^*$ ) from Pair Production
  - Limits for Excited  $e$  ( $e^*$ ) from Single Production
  - Limits for Excited  $e$  ( $e^*$ ) from  $e^+ e^- \rightarrow \gamma\gamma$
  - Indirect Limits for Excited  $e$  ( $e^*$ )
- Mass Limits for Excited  $\mu$  ( $\mu^*$ )
  - Limits for Excited  $\mu$  ( $\mu^*$ ) from Pair Production
  - Limits for Excited  $\mu$  ( $\mu^*$ ) from Single Production
  - Indirect Limits for Excited  $\mu$  ( $\mu^*$ )
- Mass Limits for Excited  $\tau$  ( $\tau^*$ )
  - Limits for Excited  $\tau$  ( $\tau^*$ ) from Pair Production
  - Limits for Excited  $\tau$  ( $\tau^*$ ) from Single Production
- Mass Limits for Excited Neutrino ( $\nu^*$ )

# Searches Particle Listings

## Quark and Lepton Compositeness

- Limits for Excited  $\nu$  ( $\nu^*$ ) from Pair Production
- Limits for Excited  $\nu$  ( $\nu^*$ ) from Single Production
- Mass Limits for Excited  $q$  ( $q^*$ )
- Limits for Excited  $q$  ( $q^*$ ) from Pair Production
- Limits for Excited  $q$  ( $q^*$ ) from Single Production
- Mass Limits for Color Sextet Quarks ( $q_6$ )
- Mass Limits for Color Octet Charged Leptons ( $\ell_8$ )
- Mass Limits for Color Octet Neutrinos ( $\nu_8$ )
- Mass Limits for  $W_8$  (Color Octet  $W$  Boson)

### SCALE LIMITS for Contact Interactions: $\Lambda(eeee)$

Limits are for  $\Lambda_{LL}^{\pm}$  only. For other cases, see each reference.

$\Lambda_{LL}^+(TeV)$	$\Lambda_{LL}^-(TeV)$	CL%	DOCUMENT ID	TECN	COMMENT
>8.3	>10.3	95	<sup>1</sup> BOURLIKOV 01	RVUE	$E_{cm} = 192\text{--}208$ GeV
>4.5	>7.0	95	<sup>2</sup> SCHAEEL 07A	ALEP	$E_{cm} = 189\text{--}209$ GeV
>5.3	>6.8	95	ABDALLAH 06c	DLPH	$E_{cm} = 130\text{--}207$ GeV
>4.7	>6.1	95	<sup>3</sup> ABBIENDI 04g	OPAL	$E_{cm} = 130\text{--}207$ GeV
>4.4	>5.4	95	ABREU 00s	DLPH	$E_{cm} = 183\text{--}189$ GeV
>4.3	>4.9	95	ACCIARRI 00P	L3	$E_{cm} = 130\text{--}189$ GeV

- • • We do not use the following data for averages, fits, limits, etc. • • •
- <sup>1</sup> A combined analysis of the data from ALEPH, DELPHI, L3, and OPAL.
- <sup>2</sup> SCHAEEL 07A limits are from  $R_{e^+e^-}$ ,  $Q_{FB}^{depl}$ , and hadronic cross section measurements.
- <sup>3</sup> ABBIENDI 04g limits are from  $e^+e^- \rightarrow e^+e^-$  cross section at  $\sqrt{s} = 130\text{--}207$  GeV.

### SCALE LIMITS for Contact Interactions: $\Lambda(ee\mu\mu)$

Limits are for  $\Lambda_{LL}^{\pm}$  only. For other cases, see each reference.

$\Lambda_{LL}^+(TeV)$	$\Lambda_{LL}^-(TeV)$	CL%	DOCUMENT ID	TECN	COMMENT
>6.6	>9.5	95	<sup>4</sup> SCHAEEL 07A	ALEP	$E_{cm} = 189\text{--}209$ GeV
>8.5	>3.8	95	ACCIARRI 00P	L3	$E_{cm} = 130\text{--}189$ GeV
>7.3	>7.6	95	ABDALLAH 06c	DLPH	$E_{cm} = 130\text{--}207$ GeV
>8.1	>7.3	95	<sup>5</sup> ABBIENDI 04g	OPAL	$E_{cm} = 130\text{--}207$ GeV
>6.6	>6.3	95	ABREU 00s	DLPH	$E_{cm} = 183\text{--}189$ GeV

- • • We do not use the following data for averages, fits, limits, etc. • • •
- <sup>4</sup> SCHAEEL 07A limits are from  $R_{e^+e^-}$ ,  $Q_{FB}^{depl}$ , and hadronic cross section measurements.
- <sup>5</sup> ABBIENDI 04g limits are from  $e^+e^- \rightarrow \mu\mu$  cross section at  $\sqrt{s} = 130\text{--}207$  GeV.

### SCALE LIMITS for Contact Interactions: $\Lambda(ee\tau\tau)$

Limits are for  $\Lambda_{LL}^{\pm}$  only. For other cases, see each reference.

$\Lambda_{LL}^+(TeV)$	$\Lambda_{LL}^-(TeV)$	CL%	DOCUMENT ID	TECN	COMMENT
>7.9	>5.8	95	<sup>6</sup> SCHAEEL 07A	ALEP	$E_{cm} = 189\text{--}209$ GeV
>7.9	>4.6	95	ABDALLAH 06c	DLPH	$E_{cm} = 130\text{--}207$ GeV
>4.9	>7.2	95	<sup>7</sup> ABBIENDI 04g	OPAL	$E_{cm} = 130\text{--}207$ GeV
>5.2	>5.4	95	ABREU 00s	DLPH	$E_{cm} = 183\text{--}189$ GeV
>5.4	>4.7	95	ACCIARRI 00P	L3	$E_{cm} = 130\text{--}189$ GeV

- • • We do not use the following data for averages, fits, limits, etc. • • •
- <sup>6</sup> SCHAEEL 07A limits are from  $R_{e^+e^-}$ ,  $Q_{FB}^{depl}$ , and hadronic cross section measurements.
- <sup>7</sup> ABBIENDI 04g limits are from  $e^+e^- \rightarrow \tau\tau$  cross section at  $\sqrt{s} = 130\text{--}207$  GeV.

### SCALE LIMITS for Contact Interactions: $\Lambda(\ell\ell\ell\ell)$

Lepton universality assumed. Limits are for  $\Lambda_{LL}^{\pm}$  only. For other cases, see each reference.

$\Lambda_{LL}^+(TeV)$	$\Lambda_{LL}^-(TeV)$	CL%	DOCUMENT ID	TECN	COMMENT
>7.9	>10.3	95	<sup>8</sup> SCHAEEL 07A	ALEP	$E_{cm} = 189\text{--}209$ GeV
>9.1	>8.2	95	ABDALLAH 06c	DLPH	$E_{cm} = 130\text{--}207$ GeV
>7.7	>9.5	95	<sup>9</sup> ABBIENDI 04g	OPAL	$E_{cm} = 130\text{--}207$ GeV
>9.0	>5.2	95	<sup>10</sup> BABICH 03	RVUE	$E_{cm} = 130\text{--}189$ GeV

- • • We do not use the following data for averages, fits, limits, etc. • • •
- <sup>8</sup> SCHAEEL 07A limits are from  $R_{e^+e^-}$ ,  $Q_{FB}^{depl}$ , and hadronic cross section measurements.
- <sup>9</sup> ABBIENDI 04g limits are from  $e^+e^- \rightarrow \ell^+\ell^-$  cross section at  $\sqrt{s} = 130\text{--}207$  GeV.
- <sup>10</sup> BABICH 03 obtain a bound  $-0.175 \text{ TeV}^{-2} < 1/\Lambda_{LL}^2 < 0.095 \text{ TeV}^{-2}$  (95%CL) in a model independent analysis allowing all of  $\Lambda_{LL}, \Lambda_{LR}, \Lambda_{RL}, \Lambda_{RR}$  to coexist.

### SCALE LIMITS for Contact Interactions: $\Lambda(eeqq)$

Limits are for  $\Lambda_{LL}^{\pm}$  only. For other cases, see each reference.

$\Lambda_{LL}^+(TeV)$	$\Lambda_{LL}^-(TeV)$	CL%	DOCUMENT ID	TECN	COMMENT
>8.4	>10.2	95	<sup>11</sup> ABDALLAH 09	DLPH	( $eebb$ )
>9.4	>5.6	95	<sup>12</sup> SCHAEEL 07A	ALEP	( $eecc$ )
>9.4	>4.9	95	<sup>11</sup> SCHAEEL 07A	ALEP	( $eebb$ )
>23.3	>12.5	95	<sup>13</sup> CHEUNG 01B	RVUE	( $eeuu$ )
>11.1	>26.4	95	<sup>13</sup> CHEUNG 01B	RVUE	( $eedd$ )

- • • We do not use the following data for averages, fits, limits, etc. • • •

>4.2	>4.0	95	<sup>14</sup> AARON 11C	H1	( $eeqq$ )
>3.8	>3.8	95	<sup>15</sup> ABDALLAH 11	DLPH	( $ee\tau c$ )
>12.9	>7.2	95	<sup>16</sup> SCHAEEL 07A	ALEP	( $eeqq$ )
>3.7	>5.9	95	<sup>17</sup> ABULENCIA 06L	CDF	( $eeqq$ )

<sup>11</sup> ABDALLAH 09 and SCHAEEL 07A limits are from  $R_b, A_{FB}^b$ .

<sup>12</sup> SCHAEEL 07A limits are from  $R_c, Q_{FB}^{depl}$ , and hadronic cross section measurements.

<sup>13</sup> CHEUNG 01B is an update of BARGER 98E.

<sup>14</sup> AARON 11C limits are from  $Q^2$  spectrum measurements of  $e^\pm p \rightarrow e^\pm X$ .

<sup>15</sup> ABDALLAH 11 limit is from  $e^+e^- \rightarrow t\bar{c}$  cross section.  $\Lambda_{LL} = \Lambda_{LR} = \Lambda_{RL} = \Lambda_{RR}$  is assumed.

<sup>16</sup> SCHAEEL 07A limit assumes quark flavor universality of the contact interactions.

<sup>17</sup> ABULENCIA 06L limits are from  $p\bar{p}$  collisions at  $\sqrt{s} = 1.96$  TeV.

### SCALE LIMITS for Contact Interactions: $\Lambda(\mu\mu qq)$

$\Lambda_{LL}^+(TeV)$	$\Lambda_{LL}^-(TeV)$	CL%	DOCUMENT ID	TECN	COMMENT
>4.5	>4.9	95	<sup>18</sup> AAD 11E	ATLS	( $\mu\mu qq$ ) (isosinglet)
>2.9	>4.2	95	<sup>19</sup> ABE 97T	CDF	( $\mu\mu qq$ ) (isosinglet)

<sup>18</sup> AAD 11E limits are from  $\mu^+\mu^-$  mass distribution in  $p\bar{p}$  collisions at  $E_{cm} = 7$  TeV.

<sup>19</sup> ABE 97T limits are from  $\mu^+\mu^-$  mass distribution in  $p\bar{p} \rightarrow \mu^+\mu^- X$  at  $E_{cm} = 1.8$  TeV.

### SCALE LIMITS for Contact Interactions: $\Lambda(\ell\nu\ell\nu)$

VALUE (TeV)	CL%	DOCUMENT ID	TECN	COMMENT
>3.10	90	<sup>20</sup> JODIDIO 86	SPEC	$\Lambda_{LR}^{\pm}(\nu_\mu\nu_e\mu e)$
>3.8		<sup>21</sup> DIAZCRUZ 94	RVUE	$\Lambda_{LL}^+(\tau\nu_\tau e\nu_e)$
>8.1		<sup>21</sup> DIAZCRUZ 94	RVUE	$\Lambda_{LL}^-(\tau\nu_\tau e\nu_e)$
>4.1		<sup>22</sup> DIAZCRUZ 94	RVUE	$\Lambda_{LL}^+(\tau\nu_\tau\mu\nu_\mu)$
>6.5		<sup>22</sup> DIAZCRUZ 94	RVUE	$\Lambda_{LL}^-(\tau\nu_\tau\mu\nu_\mu)$

- • • We do not use the following data for averages, fits, limits, etc. • • •
- <sup>20</sup> JODIDIO 86 limit is from  $\mu^+ \rightarrow \bar{\nu}_\mu e^+ \nu_e$ . Chirality invariant interactions  $L = (g^2/\Lambda^2) [\eta_{LL} (\bar{\nu}_\mu L \gamma^\alpha \mu_L) (\bar{e} L \gamma^\alpha \nu_e L) + \eta_{LR} (\bar{\nu}_\mu L \gamma^\alpha \nu_e L) (\bar{e} R \gamma^\alpha \mu_R)]$  with  $g^2/4\pi = 1$  and  $(\eta_{LL}, \eta_{LR}) = (0, \pm 1)$  are taken. No limits are given for  $\Lambda_{LL}^{\pm}$  with  $(\eta_{LL}, \eta_{LR}) = (\pm 1, 0)$ . For more general constraints with right-handed neutrinos and chirality nonconserving contact interactions, see their text.
- <sup>21</sup> DIAZCRUZ 94 limits are from  $\Gamma(\tau \rightarrow e\nu\nu)$  and assume flavor-dependent contact interactions with  $\Lambda(\tau\nu_\tau e\nu_e) \ll \Lambda(\mu\nu_\mu e\nu_e)$ .
- <sup>22</sup> DIAZCRUZ 94 limits are from  $\Gamma(\tau \rightarrow \mu\nu\nu)$  and assume flavor-dependent contact interactions with  $\Lambda(\tau\nu_\tau\mu\nu_\mu) \ll \Lambda(\mu\nu_\mu e\nu_e)$ .

### SCALE LIMITS for Contact Interactions: $\Lambda(e\nu qq)$

VALUE (TeV)	CL%	DOCUMENT ID	TECN	COMMENT
>2.81	95	<sup>23</sup> AFFOLDER 01I	CDF	

<sup>23</sup> AFFOLDER 00I bound is for a scalar interaction  $\bar{q}_R q_L \bar{\nu}_e \ell$ .

### SCALE LIMITS for Contact Interactions: $\Lambda(qqqq)$

Limits are for  $\Lambda_{LL}^{\pm}$  with color-singlet isoscalar exchanges among  $u_L$ 's and  $d_L$ 's only, unless otherwise noted. See EICHTEN 84 for details.

VALUE (TeV)	CL%	DOCUMENT ID	TECN	COMMENT
>5.6	95	<sup>24</sup> KHACHATRYAN 11F	CMS	$p\bar{p} \rightarrow$ dijet angl.; $\Lambda_{LL}^{\pm}$
>3.4	95	<sup>25</sup> AAD 11	ATLS	$p\bar{p} \rightarrow$ dijet; $\Lambda_{LL}^{\pm}$
>4.0	95	<sup>26</sup> KHACHATRYAN 10A	CMS	$p\bar{p}$ ; dijet centrality; $\Lambda_{LL}^{\pm}$
>2.96	95	<sup>27</sup> ABAZOV 09AE	D0	$p\bar{p} \rightarrow$ dijet, angl. $\Lambda_{LL}^{\pm}$

- • • We do not use the following data for averages, fits, limits, etc. • • •
- <sup>24</sup> KHACHATRYAN 11F limit is from dijet angular distribution in  $p\bar{p}$  collisions at  $E_{cm} = 7$  TeV. They also obtain  $\Lambda_{LL}^- > 6.7$  TeV.
- <sup>25</sup> AAD 11 limit is from dijet angular distribution and dijet centrality ratio in  $p\bar{p}$  collisions at  $E_{cm} = 7$  TeV.
- <sup>26</sup> The quoted limit is from dijet centrality ratio measurement in  $p\bar{p}$  collisions at  $\sqrt{s} = 7$  TeV.
- <sup>27</sup> ABAZOV 09AE also obtain  $\Lambda_{LL}^- > 2.96$  TeV.

### SCALE LIMITS for Contact Interactions: $\Lambda(\nu\nu qq)$

Limits are for  $\Lambda_{LL}^{\pm}$  only. For other cases, see each reference.

$\Lambda_{LL}^+(TeV)$	$\Lambda_{LL}^-(TeV)$	CL%	DOCUMENT ID	TECN	COMMENT
>5.0	>5.4	95	<sup>28</sup> MCFARLAND 98	CCFR	$\nu N$ scattering

<sup>28</sup> MCFARLAND 98 assumed a flavor universal interaction. Neutrinos were mostly of muon type.

**MASS LIMITS for Excited  $e$  ( $e^*$ )**

Most  $e^+e^-$  experiments assume one-photon or  $Z$  exchange. The limits from some  $e^+e^-$  experiments which depend on  $\lambda$  have assumed transition couplings which are chirality violating ( $\eta_L = \eta_R$ ). However they can be interpreted as limits for chirality-conserving interactions after multiplying the coupling value  $\lambda$  by  $\sqrt{2}$ ; see Note.

Excited leptons have the same quantum numbers as other ortholeptons. See also the searches for ortholeptons in the "Searches for Heavy Leptons" section.

**Limits for Excited  $e$  ( $e^*$ ) from Pair Production**

These limits are obtained from  $e^+e^- \rightarrow e^*e^*$  and thus rely only on the (electroweak) charge of  $e^*$ . Form factor effects are ignored unless noted. For the case of limits from  $Z$  decay, the  $e^*$  coupling is assumed to be of sequential type. Possible  $t$  channel contribution from transition magnetic coupling is neglected. All limits assume a dominant  $e^* \rightarrow e\gamma$  decay except the limits from  $\Gamma(Z)$ .

For limits prior to 1987, see our 1992 edition (Physical Review **D45** S1 (1992)).

VALUE (GeV)	CL%	DOCUMENT ID	TECN	COMMENT
>103.2	95	29 ABBIENDI	02G OPAL	$e^+e^- \rightarrow e^*e^*$ Homodoublet type
• • • We do not use the following data for averages, fits, limits, etc. • • •				
>102.8	95	30 ACHARD	03B L3	$e^+e^- \rightarrow e^*e^*$ Homodoublet type
29 From $e^+e^-$ collisions at $\sqrt{s} = 183-209$ GeV. $f = f'$ is assumed.				
30 From $e^+e^-$ collisions at $\sqrt{s} = 189-209$ GeV. $f = f'$ is assumed. ACHARD 03B also obtain limit for $f = -f'$ : $m_{e^*} > 96.6$ GeV.				

**Limits for Excited  $e$  ( $e^*$ ) from Single Production**

These limits are from  $e^+e^- \rightarrow e^*e$ ,  $W \rightarrow e^*\nu$ , or  $ep \rightarrow e^*X$  and depend on transition magnetic coupling between  $e$  and  $e^*$ . All limits assume  $e^* \rightarrow e\gamma$  decay except as noted. Limits from LEP, UA2, and H1 are for chiral coupling, whereas all other limits are for nonchiral coupling,  $\eta_L = \eta_R = 1$ . In most papers, the limit is expressed in the form of an excluded region in the  $\lambda-m_{e^*}$  plane. See the original papers.

For limits prior to 1987, see our 1992 edition (Physical Review **D45** S1 (1992)).

VALUE (GeV)	CL%	DOCUMENT ID	TECN	COMMENT
>1070	95	31 CHATRCHYAN11x	CMS	$pp \rightarrow e^*e^*X$
• • • We do not use the following data for averages, fits, limits, etc. • • •				
> 272	95	32 AARON	08A H1	$ep \rightarrow e^*X$
		33 ABAZOV	08H D0	$p\bar{p} \rightarrow e^*e$
> 209	95	34 ACOSTA	05B CDF	$p\bar{p} \rightarrow e^*X$
> 206	95	35 ACHARD	03B L3	$e^+e^- \rightarrow ee^*$
> 208	95	36 ABBIENDI	02G OPAL	$e^+e^- \rightarrow ee^*$
> 228	95	37 CHEKANOV	02D ZEUS	$ep \rightarrow e^*X$
31 CHATRCHYAN 11x search for single $e^*$ production in $pp$ collisions with the decay $e^* \rightarrow e\gamma$ . $f = f' = \Lambda/m_{e^*}$ is assumed. See their Fig. 2 for the exclusion plot in the mass-coupling plane.				
32 AARON 08A search for single $e^*$ production in $ep$ collisions with the decays $e^* \rightarrow e\gamma$ , $eZ$ , $\nu W$ . The quoted limit assumes $f = f' = \Lambda/m_{e^*}$ . See their Fig. 3 and Fig. 4 for the exclusion plots in the mass-coupling plane.				
33 ABAZOV 08H search for single $e^*$ production in $p\bar{p}$ collisions with the decays $e^* \rightarrow e\gamma$ . The $e^*$ production is assumed to be described by an effective four-fermion interaction. See their Fig. 5 for the exclusion plot in the mass-coupling plane.				
34 ACOSTA 05B search for single $e^*$ production in $p\bar{p}$ collisions with the decays $e^* \rightarrow e\gamma$ . $f = f' = \Lambda/m_{e^*}$ is assumed for the $e^*$ coupling. See their Fig.3 for the exclusion limit in the mass-coupling plane.				
35 ACHARD 03B result is from $e^+e^-$ collisions at $\sqrt{s} = 189-209$ GeV. See their Fig. 4 for the exclusion plot in the mass-coupling plane.				
36 ABBIENDI 02G result is from $e^+e^-$ collisions at $\sqrt{s} = 183-209$ GeV. $f = f' = \Lambda/m_{e^*}$ is assumed for $e^*$ coupling. See their Fig. 4c for the exclusion limit in the mass-coupling plane.				
37 CHEKANOV 02D search for single $e^*$ production in $ep$ collisions with the decays $e^* \rightarrow e\gamma$ , $eZ$ , $\nu W$ . $f = f' = \Lambda/m_{e^*}$ is assumed for the $e^*$ coupling. See their Fig. 5a for the exclusion plot in the mass-coupling plane.				

**Limits for Excited  $e$  ( $e^*$ ) from  $e^+e^- \rightarrow \gamma\gamma$**

These limits are derived from indirect effects due to  $e^*$  exchange in the  $t$  channel and depend on transition magnetic coupling between  $e$  and  $e^*$ . All limits are for  $\lambda_\gamma = 1$ . All limits except ABE 89J and ACHARD 02D are for nonchiral coupling with  $\eta_L = \eta_R = 1$ . We choose the chiral coupling limit as the best limit and list it in the Summary Table.

For limits prior to 1987, see our 1992 edition (Physical Review **D45** S1 (1992)).

VALUE (GeV)	CL%	DOCUMENT ID	TECN	COMMENT
>356	95	38 ABDALLAH	04N DLPH	$\sqrt{s} = 161-208$ GeV
• • • We do not use the following data for averages, fits, limits, etc. • • •				
>310	95	ACHARD	02D L3	$\sqrt{s} = 192-209$ GeV
38 ABDALLAH 04N also obtain a limit on the excited electron mass with $ee^*$ chiral coupling, $m_{e^*} > 295$ GeV at 95% CL.				

**Indirect Limits for Excited  $e$  ( $e^*$ )**

These limits make use of loop effects involving  $e^*$  and are therefore subject to theoretical uncertainty.

VALUE (GeV)	DOCUMENT ID	TECN	COMMENT
• • • We do not use the following data for averages, fits, limits, etc. • • •			
	39 DORENBOS...	89 CHR	$\bar{\nu}_\mu e \rightarrow \bar{\nu}_\mu e, \nu_\mu e \rightarrow \nu_\mu e$
	40 GRIFOLS	86 THEO	$\nu_\mu e \rightarrow \nu_\mu e$
	41 RENARD	82 THEO	$g-2$ of electron
39 DORENBOSCH 89 obtain the limit $\lambda_{\text{cut}}^2 \Lambda_{\text{cut}}^2 / m_{e^*}^2 < 2.6$ (95% CL), where $\Lambda_{\text{cut}}$ is the cutoff scale, based on the one-loop calculation by GRIFOLS 86. If one assumes that $\Lambda_{\text{cut}} = 1$ TeV and $\lambda_\gamma = 1$ , one obtains $m_{e^*} > 620$ GeV. However, one generally expects $\lambda_\gamma \approx m_{e^*} / \Lambda_{\text{cut}}$ in composite models.			
40 GRIFOLS 86 uses $\nu_\mu e \rightarrow \nu_\mu e$ and $\bar{\nu}_\mu e \rightarrow \bar{\nu}_\mu e$ data from CHARM Collaboration to derive mass limits which depend on the scale of compositeness.			
41 RENARD 82 derived from $g-2$ data limits on mass and couplings of $e^*$ and $\mu^*$ . See figures 2 and 3 of the paper.			

**MASS LIMITS for Excited  $\mu$  ( $\mu^*$ )**

**Limits for Excited  $\mu$  ( $\mu^*$ ) from Pair Production**

These limits are obtained from  $e^+e^- \rightarrow \mu^*\mu^*$  and thus rely only on the (electroweak) charge of  $\mu^*$ . Form factor effects are ignored unless noted. For the case of limits from  $Z$  decay, the  $\mu^*$  coupling is assumed to be of sequential type. All limits assume a dominant  $\mu^* \rightarrow \mu\gamma$  decay except the limits from  $\Gamma(Z)$ .

For limits prior to 1987, see our 1992 edition (Physical Review **D45** S1 (1992)).

VALUE (GeV)	CL%	DOCUMENT ID	TECN	COMMENT
>103.2	95	42 ABBIENDI	02G OPAL	$e^+e^- \rightarrow \mu^*\mu^*$ Homodoublet type
• • • We do not use the following data for averages, fits, limits, etc. • • •				
>102.8	95	43 ACHARD	03B L3	$e^+e^- \rightarrow \mu^*\mu^*$ Homodoublet type
42 From $e^+e^-$ collisions at $\sqrt{s} = 183-209$ GeV. $f = f'$ is assumed.				
43 From $e^+e^-$ collisions at $\sqrt{s} = 189-209$ GeV. $f = f'$ is assumed. ACHARD 03B also obtain limit for $f = -f'$ : $m_{\mu^*} > 96.6$ GeV.				

**Limits for Excited  $\mu$  ( $\mu^*$ ) from Single Production**

These limits are from  $e^+e^- \rightarrow \mu^*\mu$  and depend on transition magnetic coupling between  $\mu$  and  $\mu^*$ . All limits assume  $\mu^* \rightarrow \mu\gamma$  decay. Limits from LEP are for chiral coupling, whereas all other limits are for nonchiral coupling,  $\eta_L = \eta_R = 1$ . In most papers, the limit is expressed in the form of an excluded region in the  $\lambda-m_{\mu^*}$  plane. See the original papers.

For limits prior to 1987, see our 1992 edition (Physical Review **D45** S1 (1992)).

VALUE (GeV)	CL%	DOCUMENT ID	TECN	COMMENT
>1090	95	44 CHATRCHYAN11x	CMS	$pp \rightarrow \mu\mu^*X$
• • • We do not use the following data for averages, fits, limits, etc. • • •				
> 221	95	45 ABAZOV	06E D0	$p\bar{p} \rightarrow \mu\mu^*$
> 180	95	46 ABULENCIA,A	06B CDF	$p\bar{p} \rightarrow \mu\mu^*, \mu^* \rightarrow \mu\gamma$
> 190	95	47 ACHARD	03B L3	$e^+e^- \rightarrow \mu\mu^*$
	95	48 ABBIENDI	02G OPAL	$e^+e^- \rightarrow \mu\mu^*$
44 CHATRCHYAN 11x search for single $\mu^*$ production in $pp$ collisions with the decay $\mu^* \rightarrow \mu\gamma$ . $f = f' = \Lambda/m_{\mu^*}$ is assumed. See their Fig. 2 for the exclusion plot in the mass-coupling plane.				
45 ABAZOV 06E assume $\mu\mu^*$ production via four-fermion contact interaction $(4\pi/\Lambda^2)(\bar{q}_L \gamma^\mu q_L)(\bar{l}_L \gamma_\mu l)$ . The obtained limit is $m_{\mu^*} > 618$ GeV ( $m_{\mu^*} > 688$ GeV) for $\Lambda = 1$ TeV ( $\Lambda = m_{\mu^*}$ ).				
46 $f = f' = \Lambda/m_{\mu^*}$ is assumed for the $\mu^*$ coupling. See their Fig.4 for the exclusion limit in the mass-coupling plane. ABULENCIA,A 06B also obtain $m_{\mu^*}$ limit in the contact interaction model with $\Lambda = m_{\mu^*}$ , $m_{\mu^*} > 696$ GeV.				
47 ACHARD 03B result is from $e^+e^-$ collisions at $\sqrt{s} = 189-209$ GeV. $f = f' = \Lambda/m_{\mu^*}$ is assumed. See their Fig. 4 for the exclusion plot in the mass-coupling plane.				
48 ABBIENDI 02G result is from $e^+e^-$ collisions at $\sqrt{s} = 183-209$ GeV. $f = f' = \Lambda/m_{\mu^*}$ is assumed for $\mu^*$ coupling. See their Fig. 4c for the exclusion limit in the mass-coupling plane.				

**Indirect Limits for Excited  $\mu$  ( $\mu^*$ )**

These limits make use of loop effects involving  $\mu^*$  and are therefore subject to theoretical uncertainty.

VALUE (GeV)	DOCUMENT ID	TECN	COMMENT
• • • We do not use the following data for averages, fits, limits, etc. • • •			
	49 RENARD	82 THEO	$g-2$ of muon
49 RENARD 82 derived from $g-2$ data limits on mass and couplings of $e^*$ and $\mu^*$ . See figures 2 and 3 of the paper.			

# Searches Particle Listings

## Quark and Lepton Compositeness

### MASS LIMITS for Excited $\tau$ ( $\tau^*$ )

#### Limits for Excited $\tau$ ( $\tau^*$ ) from Pair Production

These limits are obtained from  $e^+e^- \rightarrow \tau^+\tau^-$  and thus rely only on the (electroweak) charge of  $\tau^*$ . Form factor effects are ignored unless noted. For the case of limits from Z decay, the  $\tau^*$  coupling is assumed to be of sequential type. All limits assume a dominant  $\tau^* \rightarrow \tau\gamma$  decay except the limits from  $\Gamma(Z)$ .

For limits prior to 1987, see our 1992 edition (Physical Review **D45** S1 (1992)).

VALUE (GeV)	CL%	DOCUMENT ID	TECN	COMMENT
>103.2	95	50 ABBIENDI	02G OPAL	$e^+e^- \rightarrow \tau^*\tau^*$ Homodoublet type
• • • We do not use the following data for averages, fits, limits, etc. • • •				
>102.8	95	51 ACHARD	03B L3	$e^+e^- \rightarrow \tau^*\tau^*$ Homodoublet type
50 From $e^+e^-$ collisions at $\sqrt{s} = 183\text{--}209$ GeV. $f = f'$ is assumed.				
51 From $e^+e^-$ collisions at $\sqrt{s} = 189\text{--}209$ GeV. $f = f'$ is assumed. ACHARD 03B also obtain limit for $f = -f'$ : $m_{\tau^*} > 96.6$ GeV.				

#### Limits for Excited $\tau$ ( $\tau^*$ ) from Single Production

These limits are from  $e^+e^- \rightarrow \tau^*\tau$  and depend on transition magnetic coupling between  $\tau$  and  $\tau^*$ . All limits assume  $\tau^* \rightarrow \tau\gamma$  decay. Limits from LEP are for chiral coupling, whereas all other limits are for nonchiral coupling,  $\eta_L = \eta_R = 1$ . In most papers, the limit is expressed in the form of an excluded region in the  $\lambda\text{--}m_{\tau^*}$  plane. See the original papers.

VALUE (GeV)	CL%	DOCUMENT ID	TECN	COMMENT
>185	95	52 ABBIENDI	02G OPAL	$e^+e^- \rightarrow \tau^*\tau$
• • • We do not use the following data for averages, fits, limits, etc. • • •				
>180	95	53 ACHARD	03B L3	$e^+e^- \rightarrow \tau^*\tau$
52 ABBIENDI 02G result is from $e^+e^-$ collisions at $\sqrt{s} = 183\text{--}209$ GeV. $f = f' = \Lambda/m_{\tau^*}$ is assumed for $\tau^*$ coupling. See their Fig. 4c for the exclusion limit in the mass-coupling plane.				
53 ACHARD 03B result is from $e^+e^-$ collisions at $\sqrt{s} = 189\text{--}209$ GeV. $f = f' = \Lambda/m_{\tau^*}$ is assumed. See their Fig. 4 for the exclusion plot in the mass-coupling plane.				

### MASS LIMITS for Excited Neutrino ( $\nu^*$ )

#### Limits for Excited $\nu$ ( $\nu^*$ ) from Pair Production

These limits are obtained from  $e^+e^- \rightarrow \nu^*\nu^*$  and thus rely only on the (electroweak) charge of  $\nu^*$ . Form factor effects are ignored unless noted. The  $\nu^*$  coupling is assumed to be of sequential type unless otherwise noted. All limits assume a dominant  $\nu^* \rightarrow \nu\gamma$  decay except the limits from  $\Gamma(Z)$ .

VALUE (GeV)	CL%	DOCUMENT ID	TECN	COMMENT
>102.6	95	54 ACHARD	03B L3	$e^+e^- \rightarrow \nu^*\nu^*$ Homodoublet type
• • • We do not use the following data for averages, fits, limits, etc. • • •				
		55 ABBIENDI	04N OPAL	
54 From $e^+e^-$ collisions at $\sqrt{s} = 189\text{--}209$ GeV. $f = -f'$ is assumed. ACHARD 03B also obtain limit for $f = f'$ : $m_{\nu_e^*} > 101.7$ GeV, $m_{\nu_\mu^*} > 101.8$ GeV, and $m_{\nu_\tau^*} > 92.9$ GeV.				
See their Fig. 4 for the exclusion plot in the mass-coupling plane.				
55 From $e^+e^-$ collisions at $\sqrt{s} = 192\text{--}209$ GeV, ABBIENDI 04N obtain limit on $\sigma(e^+e^- \rightarrow \nu^*\nu^*) B^2(\nu^* \rightarrow \nu\gamma)$ . See their Fig.2. The limit ranges from 20 to 45fb for $m_{\nu_e^*} > 45$ GeV.				

#### Limits for Excited $\nu$ ( $\nu^*$ ) from Single Production

These limits are from  $e^+e^- \rightarrow \nu^*\nu$ ,  $Z \rightarrow \nu^*\nu$ , or  $e\bar{p} \rightarrow \nu^*X$  and depend on transition magnetic coupling between  $\nu$  and  $\nu^*$ . Assumptions about  $\nu^*$  decay mode are given in footnotes.

VALUE (GeV)	CL%	DOCUMENT ID	TECN	COMMENT
>213	95	56 AARON	08 H1	$e\bar{p} \rightarrow \nu^*X$
• • • We do not use the following data for averages, fits, limits, etc. • • •				
>190	95	57 ACHARD	03B L3	$e^+e^- \rightarrow \nu^*\nu$
none 50–150	95	58 ADLOFF	02 H1	$e\bar{p} \rightarrow \nu^*X$
>158	95	59 CHEKANOV	02D ZEUS	$e\bar{p} \rightarrow \nu^*X$
>171	95	60 ACCIARRI	01D L3	$e^+e^- \rightarrow \nu^*\nu$
56 AARON 08 search for single $\nu^*$ production in $e\bar{p}$ collisions with the decays $\nu^* \rightarrow \nu\gamma$ , $\nu Z$ , $eW$ . The quoted limit assumes $f = -f' = \Lambda/m_{\nu^*}$ . See their Fig. 3 and Fig. 4 for the exclusion plots in the mass-coupling plane.				
57 ACHARD 03B result is from $e^+e^-$ collisions at $\sqrt{s} = 189\text{--}209$ GeV. The quoted limit is for $\nu_e^*$ . $f = -f' = \Lambda/m_{\nu^*}$ is assumed. See their Fig.4 for the exclusion plot in the mass-coupling plane.				
58 ADLOFF 02 search for single $\nu^*$ production in $e\bar{p}$ collisions with the decays $\nu^* \rightarrow \nu\gamma$ , $\nu Z$ , $eW$ . The quoted limit assumes $f = -f' = \Lambda/m_{\nu^*}$ . See their Fig. 1 for the exclusion plots in the mass-coupling plane.				
59 CHEKANOV 02D search for single $\nu^*$ production in $e\bar{p}$ collisions with the decays $\nu^* \rightarrow \nu\gamma$ , $\nu Z$ , $eW$ . $f = -f' = \Lambda/m_{\nu^*}$ is assumed for the $e^*$ coupling. CHEKANOV 02D also obtain limit for $f = f' = \Lambda/m_{\nu^*}$ : $m_{\nu_e^*} > 135$ GeV. See their Fig. 5c and Fig. 5d for the exclusion plot in the mass-coupling plane.				
60 ACCIARRI 01D search for $\nu^*\nu$ production in $e^+e^-$ collisions at $\sqrt{s} = 192\text{--}202$ GeV with decays $\nu^* \rightarrow \nu\gamma$ , $\nu^* \rightarrow eW$ . $f = -f' = \Lambda/m_{\nu^*}$ is assumed for the $\nu^*$ coupling. See their Fig. 4 for limits in the mass-coupling plane.				

### MASS LIMITS for Excited $q$ ( $q^*$ )

#### Limits for Excited $q$ ( $q^*$ ) from Pair Production

These limits are mostly obtained from  $e^+e^- \rightarrow q^*\bar{q}^*$  and thus rely only on the (electroweak) charge of the  $q^*$ . Form factor effects are ignored unless noted. Assumptions about the  $q^*$  decay are given in the comments and footnotes.

VALUE (GeV)	CL%	DOCUMENT ID	TECN	COMMENT
>338	95	61 AALTONEN	10H CDF	$q^* \rightarrow tW^-$
• • • We do not use the following data for averages, fits, limits, etc. • • •				
> 45.6	95	62 BARATE	98U ALEP	$Z \rightarrow q^*q^*$
> 41.7	95	63 ADRIANI	93M L3	$u$ or $d$ type, $Z \rightarrow q^*q^*$
> 44.7	95	64 BARDADIN...	92 RVUE	$u$ -type, $\Gamma(Z)$
> 40.6	95	64 BARDADIN...	92 RVUE	$d$ -type, $\Gamma(Z)$
> 44.2	95	65 DECAMP	92 ALEP	$u$ -type, $\Gamma(Z)$
> 45	95	65 DECAMP	92 ALEP	$d$ -type, $\Gamma(Z)$
> 45	95	66 DECAMP	92 ALEP	$u$ or $d$ type, $Z \rightarrow q^*q^*$
> 45	95	65 ABREU	91F DLPH	$u$ -type, $\Gamma(Z)$
> 45	95	65 ABREU	91F DLPH	$d$ -type, $\Gamma(Z)$
61 AALTONEN 10H obtain limits on the $q^*q^*$ production cross section in $p\bar{p}$ collisions. See their Fig. 3.				
62 BARATE 98U obtain limits on the form factor. See their Fig.16 for limits in mass-form factor plane.				
63 ADRIANI 93M limit is valid for $B(q^* \rightarrow qg) > 0.25$ (0.17) for up (down) type.				
64 BARDADIN-OTWINOWSKA 92 limit based on $\Delta\Gamma(Z) < 36$ MeV.				
65 These limits are independent of decay modes.				
66 Limit is for $B(q^* \rightarrow qg) + B(q^* \rightarrow q\gamma) = 1$ .				

#### Limits for Excited $q$ ( $q^*$ ) from Single Production

These limits are from  $e^+e^- \rightarrow q^*\bar{q}$ ,  $p\bar{p} \rightarrow q^*X$ , or  $pp \rightarrow q^*X$  and depend on transition magnetic couplings between  $q$  and  $q^*$ . Assumptions about  $q^*$  decay mode are given in the footnotes and comments.

VALUE (GeV)	CL%	DOCUMENT ID	TECN	COMMENT
>2490	95	67 CHATRCHYAN11Y	CMS	$pp \rightarrow q^*X$ , $q^* \rightarrow qg$
• • • We do not use the following data for averages, fits, limits, etc. • • •				
none 300–1260	95	68 ABAZOV	11F D0	$p\bar{p} \rightarrow q^*X$ , $q^* \rightarrow qZ, qW$
none 500–1580	95	69 AAD	10 ATLS	$pp \rightarrow q^*X$ , $q^* \rightarrow qg$
> 510	95	69 KHACHATRY...	10 CMS	$pp \rightarrow q^*X$ , $q^* \rightarrow qg$
> 775	95	70 ABAZOV	06F D0	$p\bar{p} \rightarrow q^*X$ , $q^* \rightarrow qZ$
		71 ABAZOV	04c D0	$p\bar{p} \rightarrow q^*X$ , $q^* \rightarrow qg$
67 CHATRCHYAN 11Y assume degenerate $q^*$ with $f_5 = \Lambda/m_{q^*}$ .				
68 ABAZOV 11F search for vectorlike quarks decaying to $W$ +jet and $Z$ +jet in $p\bar{p}$ collisions. See their Fig. 3 and Fig. 4 for the limits on $\sigma \cdot B$ .				
69 AAD 10, KHACHATRYAN 10 search for heavy resonance decaying to 2 jets in $pp$ collisions at $\sqrt{s} = 7$ TeV. $f_5 = f = f' = 1$ is assumed.				
70 ABAZOV 06F assume $q^*$ production via $qg$ fusion and via contact interactions. The quoted limit is for $\Lambda = m_{q^*}$ .				
71 ABAZOV 04c assume $f_5 = f = f' = \Lambda/m_{q^*}$ .				

### MASS LIMITS for Color Sextet Quarks ( $q_6$ )

VALUE (GeV)	CL%	DOCUMENT ID	TECN	COMMENT
>84	95	72 ABE	89D CDF	$p\bar{p} \rightarrow q_6\bar{q}_6$
72 ABE 89D look for pair production of unit-charged particles which leave the detector before decaying. In the above limit the color sextet quark is assumed to fragment into a unit-charged or neutral hadron with equal probability and to have long enough lifetime not to decay within the detector. A limit of 121 GeV is obtained for a color decuplet.				

### MASS LIMITS for Color Octet Charged Leptons ( $\ell_8$ )

VALUE (GeV)	CL%	DOCUMENT ID	TECN	COMMENT
>86	95	73 ABE	89D CDF	Stable $\ell_8$ : $p\bar{p} \rightarrow \ell_8\bar{\ell}_8$
• • • We do not use the following data for averages, fits, limits, etc. • • •				
		74 ABT	93 H1	$e\bar{p} \rightarrow e_8X$
73 ABE 89D look for pair production of unit-charged particles which leave the detector before decaying. In the above limit the color octet lepton is assumed to fragment into a unit-charged or neutral hadron with equal probability and to have long enough lifetime not to decay within the detector. The limit improves to 99 GeV if it always fragments into a unit-charged hadron.				
74 ABT 93 search for $e_8$ production via $e$ -gluon fusion in $e\bar{p}$ collisions with $e_8 \rightarrow e\gamma$ . See their Fig. 3 for exclusion plot in the $m_{e_8}\text{--}\Lambda$ plane for $m_{e_8} = 35\text{--}220$ GeV.				

### MASS LIMITS for Color Octet Neutrinos ( $\nu_8$ )

VALUE (GeV)	CL%	DOCUMENT ID	TECN	COMMENT
>110	90	75 BARGER	89 RVUE	$\nu_8$ : $p\bar{p} \rightarrow \nu_8\bar{\nu}_8$
• • • We do not use the following data for averages, fits, limits, etc. • • •				
none 3.8–29.8	95	76 KIM	90 AMY	$\nu_8$ : $e^+e^- \rightarrow$ acoplanar jets
none 9–21.9	95	77 BARTEL	87B JADE	$\nu_8$ : $e^+e^- \rightarrow$ acoplanar jets

- <sup>75</sup> BARGER 89 used ABE 89B limit for events with large missing transverse momentum. Two-body decay  $\nu_g \rightarrow \nu g$  is assumed.
- <sup>76</sup> KIM 90 is at  $E_{cm} = 50\text{--}60.8$  GeV. The same assumptions as in BARTEL 87B are used.
- <sup>77</sup> BARTEL 87B is at  $E_{cm} = 46.3\text{--}46.78$  GeV. The limit assumes the  $\nu_g$  pair production cross section to be eight times larger than that of the corresponding heavy neutrino pair production. This assumption is not valid in general for the weak couplings, and the limit can be sensitive to its  $SU(2)_L \times U(1)_Y$  quantum numbers.

**MASS LIMITS for  $W_8$  (Color Octet  $W$  Boson)**

VALUE (GeV)	DOCUMENT ID	TECN	COMMENT
• • • We do not use the following data for averages, fits, limits, etc. • • •			
	<sup>78</sup> ALBAJAR 89	UA1	$p\bar{p} \rightarrow W_8 X, W_8 \rightarrow Wg$
<sup>78</sup> ALBAJAR 89 give $\sigma(W_8 \rightarrow W + \text{jet})/\sigma(W) < 0.019$ (90% CL) for $m_{W_8} > 220$ GeV.			

**REFERENCES FOR Searches for Quark and Lepton Compositeness**

AAD	11	PL B694 327	G. Aad et al.	(ATLAS Collab.)
AAD	11E	PR D84 011101	G. Aad et al.	(ATLAS Collab.)
AARON	11C	PL B705 52	F. D. Aaron et al.	(H1 Collab.)
ABAZOV	11F	PRL 106 1081801	V. M. Abazov et al.	(D0 Collab.)
ABDALLAH	11	EPJ C71 1555	J. Abdallah et al.	(DELPHI Collab.)
CHATRCHYAN	11X	PL B704 143	S. Chatrchyan et al.	(CMS Collab.)
CHATRCHYAN	11Y	PL B704 123	S. Chatrchyan et al.	(CMS Collab.)
KHACHATRYAN	11F	PRL 106 201804	V. Khachatryan et al.	(CMS Collab.)
AAD	10	PRL 105 161801	G. Aad et al.	(ATLAS Collab.)
AALTONEN	10H	PRL 104 091801	T. Aaltonen et al.	(CDF Collab.)
KHACHATRYAN	10	PRL 105 211801	V. Khachatryan et al.	(CMS Collab.)
Also		PRL 106 029902E	V. Khachatryan et al.	(CMS Collab.)
KHACHATRYAN	10A	PRL 105 262001	V. Khachatryan et al.	(CMS Collab.)
ABAZOV	09AE	PRL 103 191803	V. M. Abazov et al.	(D0 Collab.)
ABDALLAH	09	EPJ C60 1	J. Abdallah et al.	(DELPHI Collab.)
AARON	08	PL B663 382	F. D. Aaron et al.	(H1 Collab.)
AARON	08A	PL B666 131	F. D. Aaron et al.	(H1 Collab.)
ABAZOV	08H	PR D77 091102R	V. M. Abazov et al.	(D0 Collab.)
SCHAEF	07A	EPJ C49 411	S. Schaefer et al.	(ALEPH Collab.)
ABAZOV	06E	PR D73 111102R	V. M. Abazov et al.	(D0 Collab.)
ABAZOV	06F	PR D74 011104R	V. M. Abazov et al.	(D0 Collab.)
ABDALLAH	06C	EPJ C45 589	J. Abdallah et al.	(DELPHI Collab.)
ABULENCIA	06L	PRL 96 211801	A. Abulencia et al.	(CDF Collab.)
ABULENCIA	06B	PRL 97 191802	A. Abulencia et al.	(CDF Collab.)
ACOSTA	05B	PRL 94 101802	D. Acosta et al.	(CDF Collab.)
ABAZOV	04C	PR D69 111101R	V. M. Abazov et al.	(D0 Collab.)
ABBIENDI	04G	EPJ C33 173	G. Abbiendi et al.	(OPAL Collab.)
ABBIENDI	04N	PL B602 167	G. Abbiendi et al.	(OPAL Collab.)
ABDALLAH	04N	EPJ C37 405	J. Abdallah et al.	(DELPHI Collab.)
ACHARD	03B	PL B568 23	P. Achard et al.	(L3 Collab.)
BABICH	03	EPJ C29 103	A. A. Babich et al.	(OPAL Collab.)
ABBIENDI	02G	PL B544 57	G. Abbiendi et al.	(OPAL Collab.)
ACHARD	02D	PL B531 28	P. Achard et al.	(L3 Collab.)
ADLOFF	02	PL B525 9	C. Adloff et al.	(H1 Collab.)
CHEKANOV	02D	PL B549 32	S. Chekanov et al.	(ZEUS Collab.)
ACCIARRI	01D	PL B502 37	M. Acciarri et al.	(L3 Collab.)
AFOLDER	01I	PRL 87 231803	T. Affolder et al.	(CDF Collab.)
BOURILKOV	01	PR D64 071701	D. Bourilkov	(CDF Collab.)
CHEUNG	01B	PL B517 167	K. Cheung	(CDF Collab.)
ABREU	00S	PL B485 45	P. Abreu et al.	(DELPHI Collab.)
ACCIARRI	00P	PL B489 81	M. Acciarri et al.	(L3 Collab.)
AFOLDER	00I	PR D62 012004	T. Affolder et al.	(CDF Collab.)
BARATE	98U	EPJ C4 571	R. Barate et al.	(ALEPH Collab.)
BARGER	98E	PR D57 391	V. Barger et al.	(CCFR/NuTeV Collab.)
MCFARLAND	98	EPJ C1 509	K.S. McFarland et al.	(CDF Collab.)
ABE	97T	PRL 79 2198	F. ABE et al.	(H1 Collab.)
DIACRUZ	94	PR D49 R2149	J.L. Diaz Cruz, O.A. Sampayo	(CINV Collab.)
ABT	93	NP B396 3	I. Abt et al.	(H1 Collab.)
ADRIANI	93M	PRPL 236 1	O. Adriani et al.	(L3 Collab.)
BARADIN...	92	ZPHY C55 163	M. Baradin-Otwinowska	(CLER Collab.)
DECAMP	92	PRPL 216 253	D. Decamp et al.	(ALEPH Collab.)
PDG	92	PR D45 51	K. Hikasa et al.	(KEK, LBL, BOST+)
ABREU	91F	NP B367 511	P. Abreu et al.	(DELPHI Collab.)
KIM	90	PL B240 243	G.N. Kim et al.	(AMY Collab.)
ABE	89B	PRL 62 1825	F. Abe et al.	(CDF Collab.)
ABE	89D	PRL 63 1447	F. Abe et al.	(CDF Collab.)
ABE	89J	ZPHY C45 175	K. Abe et al.	(VENUS Collab.)
ALBAJAR	89	ZPHY C44 15	C. Alajar et al.	(UA1 Collab.)
BARGER	89	PL B220 464	V. Barger et al.	(WIS C, KEK)
DORENBOS...	89	ZPHY C41 567	J. Dorenbosch et al.	(CHARM Collab.)
BARTEL	87B	ZPHY C36 15	W. Bartel et al.	(JADE Collab.)
GRIFOLS	86	PL 168B 264	J.A. Grifols, S. Peris	(BARC)
JODIDIO	86	PR D34 1967	A. Jodidio et al.	(LBL, NWES, TRIU)
Also		PR D37 237 (erratum)	A. Jodidio et al.	(LBL, NWES, TRIU)
EICHTEN	84	RMP 56 579	E. Eichten et al.	(FNAL, LBL, OSU)
RENARD	82	PL 116B 264	F.M. Renard	(CERN)

**Extra Dimensions**

For explanation of terms used and discussion of significant model dependence of following limits, see the "Extra Dimensions" review. Footnotes describe originally quoted limit.  $\delta$  indicates the number of extra dimensions.

Limits not encoded here are summarized in the "Extra Dimensions" review, where the latest unpublished results are also described.

**EXTRA DIMENSIONS**

Updated November 2011 by John Parsons (Columbia University) and Alex Pomarol (Universitat Autònoma de Barcelona).

**I Introduction**

Proposals for a spacetime with more than three spatial dimensions date back to the 1920s, mainly through the work of Kaluza and Klein, in an attempt to unify the forces of nature [1]. Although their initial idea failed, the formalism that they and others developed is still useful nowadays. Around 1980, string theory proposed again to enlarge the number of space dimensions, this time as a requirement for describing a consistent theory of quantum gravity. The extra dimensions were supposed to be compactified at a scale close to the Planck scale, and thus not testable experimentally in the near future.

A different approach was given by Arkani-Hamed, Dimopoulos and Dvali (ADD) in their seminal paper in 1998 [2]. They showed that the weakness of gravity could be explained by postulating two or more extra dimensions in which only gravity could propagate. The size of these extra dimensions should range between roughly a millimeter and  $\sim 1/\text{TeV}$ , leading to possible observable consequences in current and future experiments. A year later, Randall and Sundrum (RS) [3] found a new possibility using a warped geometry. They postulated a five-dimensional Anti-de Sitter (AdS) spacetime with a compactification scale of order TeV. The origin of the smallness of the electroweak scale versus the Planck scale was explained by the gravitational redshift factor present in the warped AdS metric. As in the ADD model, originally only gravity was assumed to propagate in the extra dimensions, although it was soon clear that this was not necessary in the RS model and also the SM gauge fields [4] and SM fermions [5,6] could propagate in the five-dimensional space.

The physics of warped extra-dimensional models have an alternative interpretation by means of the AdS/CFT correspondence [7]. Models with warped extra dimensions are related to four-dimensional strongly-interacting theories, allowing an understanding of the properties of five-dimensional fields as those of four-dimensional (4D) composite states [8]. This has opened new directions for tackling outstanding questions in particle physics, such as the flavor problem, grand unification, and the origin of electroweak symmetry breaking or supersymmetry breaking.

**I.1 Kaluza-Klein Theories**

Theories with compact extra dimensions can be written as theories in ordinary four dimensions by performing a Kaluza-Klein (KK) reduction. As an illustration, consider a simple example, namely a field theory of a complex scalar in flat five-dimensional (5D) spacetime. The action will be given by  $\dagger$

$$S_5 = - \int d^4x dy M_5 [ |\partial_\mu \phi|^2 + |\partial_y \phi|^2 + \lambda_5 |\phi|^4 ], \quad (1)$$

where  $y$  refers to the extra (fifth) dimension. A universal scale  $M_5$  has been extracted in front of the action in order to keep the 5D field with the same mass-dimension as in four dimensions. This theory is perturbative for energies  $E \lesssim \ell_5 M_5 / \lambda_5$  where  $\ell_5 = 24\pi^3$  [9].

$\dagger$  Our convention for the metric is  $\eta_{MN} = \text{Diag}(-1, 1, 1, 1, 1)$ .

# Searches Particle Listings

## Extra Dimensions

Let us now consider that the fifth dimension is compact with the topology of a circle  $S^1$  of radius  $R$ , which corresponds to the identification of  $y$  with  $y + 2\pi R$ . In such a case, the 5D complex scalar field can be expanded in a Fourier series:

$$\phi(x, y) = \frac{1}{\sqrt{2\pi R M_5}} \sum_{n=-\infty}^{\infty} e^{iny/R} \phi^{(n)}(x),$$

that, inserted in Eq. (1) and integrating over  $y$ , gives

$$S_5 = S_4^{(0)} + S_4^{(n)},$$

where

$$S_4^{(0)} = - \int d^4x \left[ |\partial_\mu \phi^{(0)}|^2 + \lambda_4 |\phi^{(0)}|^4 \right], \quad (2)$$

$$S_4^{(n)} = - \int d^4x \sum_{n \neq 0} \left[ |\partial_\mu \phi^{(n)}|^2 + \left(\frac{n}{R}\right)^2 |\phi^{(n)}|^2 \right] + \text{quartic int.}$$

The  $n = 0$  mode self-coupling is given by

$$\lambda_4 = \frac{\lambda_5}{2\pi R M_5}. \quad (3)$$

The above action corresponds to a 4D theory with a massless scalar  $\phi^{(0)}$ , referred to as the zero-mode, and an infinite tower of massive modes  $\phi^{(n)}$ , known as KK modes. The KK reduction thus allows a treatment of 5D theories as 4D field theories with an infinite number of fields. At energies smaller than  $1/R$ , the KK modes can be neglected, leaving the zero-mode action of Eq. (2). The strength of the interaction of the zero-mode, given by Eq. (3), decreases as  $R$  increases. Thus, for a large extra dimension  $R \gg 1/M_5$ , the massless scalar is weakly coupled.

## II Large Extra Dimensions for Gravity

### II.1 The ADD Scenario

The ADD scenario [2,10,11] assumes a  $D = 4 + \delta$  dimensional spacetime, with  $\delta$  compactified spatial dimensions. The weakness of gravity arises since it propagates in the higher-dimensional space. The SM is assumed to be localized in a 4D subspace, a 3-brane, as can be found in certain string constructions [12]. Gravity is described by the Einstein-Hilbert action in  $D = 4 + \delta$  spacetime dimensions

$$S_D = - \frac{\bar{M}_D^{2+\delta}}{2} \int d^4x d^\delta y \sqrt{-g} \mathcal{R} + \int d^4x \sqrt{-g_{\text{ind}}} \mathcal{L}_{\text{SM}}, \quad (4)$$

where  $x$  labels the ordinary four coordinates,  $y$  the  $\delta$  extra coordinates,  $g$  refers to the determinant of the  $D$ -dimensional metric whose Ricci scalar is defined by  $\mathcal{R}$ , and  $\bar{M}_D$  is the reduced Planck scale of the  $D$ -dimensional theory. In the second term of Eq. (4), which gives the gravitational interactions of SM fields, the  $D$ -dimensional metric reduces to the induced metric on the 3-brane where the SM fields propagate. The extra dimensions are assumed to be flat and compactified in a volume  $V_\delta$ . As an example, consider a toroidal compactification of equal radii  $R$  and volume  $V_\delta = (2\pi R)^\delta$ . After a KK reduction, one finds that the fields that couple to the SM are the spin-2 gravitational field  $G_{\mu\nu}(x, y)$  and a tower of spin-1 KK graviscalars [13]. The

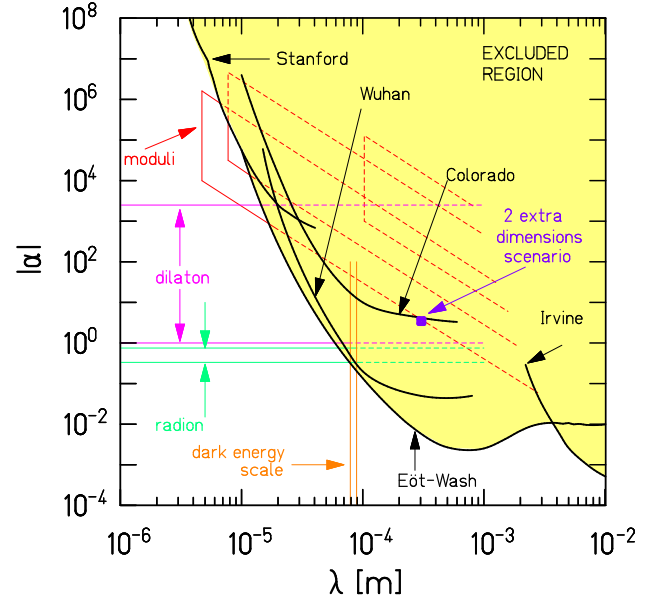


**Figure 1:** Experimental limits (from Ref. [15]) on  $\alpha$  and  $\lambda$  of Eq. (8), which parametrize deviations from Newton's law of gravitation.

graviscalars, however, only couple to SM fields through the trace of the energy-momentum tensor, resulting in weaker couplings to the SM fields. The Fourier expansion of the spin-2 field is given by

$$G_{\mu\nu}(x, y) = G_{\mu\nu}^{(0)}(x) + \frac{1}{\sqrt{V_\delta}} \sum_{\vec{n} \neq 0} e^{i\vec{n}\cdot\vec{y}/R} G_{\mu\nu}^{(\vec{n})}(x), \quad (5)$$

where  $\vec{y} = (y_1, y_2, \dots, y_\delta)$  are the extra-dimensional coordinates and  $\vec{n} = (n_1, n_2, \dots, n_\delta)$ . Eq. (5) contains a massless state, the 4D graviton, and its KK tower with masses  $m_{\vec{n}}^2 = |\vec{n}|^2/R^2$ . At energies below  $1/R$  the action is that of the zero-mode

$$S_4^{(0)} = - \frac{\bar{M}_D^{2+\delta}}{2} \int d^4x V_\delta \sqrt{-g^{(0)}} \mathcal{R}^{(0)} + \int d^4x \sqrt{-g_{\text{ind}}^{(0)}} \mathcal{L}_{\text{SM}},$$

where we can identify the 4D reduced Planck mass,  $M_P \equiv G_N/\sqrt{8\pi} \simeq 2.4 \times 10^{18}$  GeV, as a function of the  $D$ -dimensional parameters:

$$M_P^2 = V^\delta \bar{M}_D^{2+\delta} \equiv R^\delta M_D^{2+\delta}. \quad (6)$$

Fixing  $M_D$  at around the electroweak scale  $M_D \sim \text{TeV}$  to avoid introducing a new mass-scale in the model, Eq. (6) gives a prediction for  $R$ :

$$\delta = 1, 2, \dots, 6 \rightarrow R \sim 10^9 \text{ km}, 0.5 \text{ mm}, \dots, 0.1 \text{ MeV}^{-1}. \quad (7)$$

The option  $\delta = 1$  is clearly ruled out. However this is not the case for  $\delta \geq 2$ , and possible observable consequences can be sought in present and future experiments.

Consistency of the model requires a stabilization mechanism for the radii of the extra dimensions, to the values shown in Eq. (7). The fact that we need  $R \gg 1/M_D$  leads to a new hierarchy problem, the solution of which might require imposing supersymmetry in the extra-dimensional bulk [14].



## II.2 Tests of the Gravitational Force Law at Sub-mm Distances

The KK modes of the graviton give rise to deviations from Newton's law of gravitation for distances  $\lesssim R$ . Such deviations are usually parametrized by a modified Newtonian potential of the form

$$V(r) = -G_N \frac{m_1 m_2}{r} \left[ 1 + \alpha e^{-r/\lambda} \right]. \quad (8)$$

For a 2-torus compactification,  $\alpha = 16/3$  and  $\lambda = R$ . Searches for deviations from Newton's law of gravitation have been performed in several experiments. Fig. 1, taken from Ref. [15], gives the present constraints. We find  $R < 37\mu\text{m}$  at 95% CL for  $\delta = 2$ , corresponding to  $M_D > 3.6$  TeV.

## II.3 Astrophysical and Cosmological Constraints

The light KK gravitons could be copiously produced in stars, carrying away energy. Ensuring that the graviton luminosity is low enough to preserve the agreement of stellar models with observations provides powerful bounds on the scale  $M_D$ . The most stringent arises from supernova SN1987A, giving  $M_D > 27$  (2.4) TeV for  $\delta = 2$  (3) [16]. After a supernova explosion, most of the KK gravitons stay gravitationally trapped in the remnant neutron star. The requirement that neutron stars are not excessively heated by KK decays into photons leads to  $M_D > 1700$  (76) TeV for  $\delta = 2$  (3) [17].

Cosmological constraints are also quite stringent [18]. To avoid overclosure of the universe by relic gravitons one needs  $M_D > 7$  TeV for  $\delta = 2$ . Relic KK gravitons decaying into photons contribute to the cosmic diffuse gamma radiation, from which one can derive the bound  $M_D > 100$  TeV for  $\delta = 2$ .

We must mention however that bounds coming from the decays of KK gravitons into photons can be reduced if we assume that KK gravitons decay mainly into other non-SM states. This could happen, for example, if there are other 3-branes with hidden sectors residing on them [10].

## II.4 Collider Signals

### II.4a Graviton and Other Particle Production

Although each KK graviton has a purely gravitational coupling, suppressed by  $1/M_P$ , inclusive processes in which one sums over the almost continuous spectrum of available gravitons have cross sections suppressed only by powers of  $M_D$ . Processes involving gravitons are therefore detectable in collider experiments if  $M_D \sim \text{TeV}$ . A number of experimental searches for evidence of large extra dimensions have been performed at colliders, and interpreted in the context of the ADD model.

One signature arises from direct graviton emission. By making a derivative expansion of Einstein gravity, one can construct an effective theory, valid for energies much lower than  $M_D$ , and use it to make predictions for graviton-emission processes at colliders [13,19,20]. Gravitons produced in the final state would escape detection, giving rise to missing transverse energy ( $\cancel{E}_T$ ). The results quoted below are 95% CL lower limits on  $M_D$  for a range of values of  $\delta$  between 2 and 6, with more stringent limits corresponding to lower  $\delta$  values.

A combined  $\gamma + \cancel{E}_T$  result from LEP yields limits of  $M_D > 0.66 - 1.60$  TeV [21], and less stringent results also exist from LEP for the  $Z + \cancel{E}_T$  final state. At hadron colliders, experimentally sensitive channels include the  $j + \cancel{E}_T$  and  $\gamma + \cancel{E}_T$  final states. The most stringent limits from the Tevatron include CDF results of  $M_D > 0.94 - 1.94$  TeV [22], using the combined  $j/\gamma + \cancel{E}_T$  final state. DØ results limit  $M_D > 0.80 - 0.88$  TeV [23] from  $\gamma + \cancel{E}_T$ , and  $M_D > 0.63 - 0.89$  TeV [24] from  $j + \cancel{E}_T$ . At the LHC, using a dataset of  $1 \text{ fb}^{-1}$  and assuming leading order (LO) signal cross sections, CMS sets limits of  $M_D > 2.25 - 3.67$  TeV [25] from analyzing the  $j + \cancel{E}_T$  final state, and  $M_D > 1.03 - 1.21$  TeV [26] from  $\gamma + \cancel{E}_T$ . To account for next-to-leading order (NLO) signal enhancements, sizeable k-factors, in the range  $1.3 - 2$  depending on  $\delta$ , would increase these limits by typically  $\approx 10\%$  if applied. ATLAS  $j + \cancel{E}_T$  results with  $1 \text{ fb}^{-1}$  provide limits of  $M_D > 1.68 - 3.16$  TeV [27], using LO cross sections. For the  $j + \cancel{E}_T$  analyses, the LHC experiments handle somewhat differently the issue that the effective theory is only valid for energies much less than  $M_D$ : CMS suppresses the graviton cross section by a factor  $M_D^2/\hat{s}$  for  $\sqrt{\hat{s}} > M_D$ , where  $\sqrt{\hat{s}}$  is the parton-level center-of-mass energy of the hard collision. ATLAS simply truncates the differential cross section to remove the contribution from events where  $\sqrt{\hat{s}} > M_D$ , and points out that the effect of the truncation grows with  $\delta$ , from a negligible impact for  $\delta = 2$  up to a 16% reduction in the limit for  $\delta = 6$ .

In models in which the ADD scenario is embedded in a string theory at the TeV scale [12], we expect the string scale  $M_s$  to be smaller than  $M_D$ , and therefore production at the LHC of string resonances [28]. Analysis of the dijet invariant mass distribution have been interpreted by CMS for a  $1 \text{ fb}^{-1}$  dataset to exclude at 95% CL string excitations of quarks and gluons that decay predominantly to  $q + g$  with masses less than 4 TeV [29].

### II.4b Virtual graviton effects

One can also search for virtual graviton effects, the calculation of which however depends on the ultraviolet cut-off of the theory and is therefore very model dependent. In the literature, several different formulations exist [13,20,30] for the dimension-eight operator for gravity exchange at tree level:

$$\mathcal{L}_8 = \pm \frac{4}{M_{TT}^4} \left( T_{\mu\nu} T^{\mu\nu} - \frac{1}{\delta + 2} T_\mu^\mu T_\nu^\nu \right), \quad (9)$$

where  $T_{\mu\nu}$  is the energy-momentum tensor and  $M_{TT}$  is related to  $M_D$  by some model-dependent coefficient [31]. The relations with the parametrizations of Refs. [30] and [13] are, respectively,  $M_{TT} = M_S$  and  $M_{TT} = (2/\pi)^{1/4} \Lambda_T$ . The experimental results below are given as 95% CL lower limits on  $M_{TT}$ , including in some cases the possibility of both constructive or destructive interference, depending on the sign chosen in Eq. (9). Results from  $e^\pm p \rightarrow e^\pm X$  at HERA limit  $M_{TT} \gtrsim 800$  GeV [32]. The most sensitive limits from LEP arise from the  $e^+e^- \rightarrow ee$  and  $e^+e^- \rightarrow \gamma\gamma$  final states, with limits for the case of constructive (destructive) interference corresponding

# Searches Particle Listings

## Extra Dimensions

to  $M_{TT} > 1.1$  (1.0) TeV [33] and  $M_{TT} > 1.0$  (0.9) TeV [34], respectively. The most stringent results, for constructive (destructive) interference, from the Tevatron include limits of  $M_{TT} > 1.48$  (1.37) TeV [35] from  $p\bar{p} \rightarrow ee/\gamma\gamma + X$ , and  $M_{TT} > 1.48$  (1.34) TeV [36] from an analysis of the angular distributions in dijet events. Results from the LHC extend the sensitivity to higher scales. CMS has reported  $1 \text{ fb}^{-1}$  results in the diphoton and dimuon final states. For constructive interference and using NLO cross sections, the CMS  $\gamma\gamma$  and  $\mu\mu$  results correspond approximately to limits of  $M_{TT} > 2.8$  TeV [37] and 2.4 TeV [38], respectively. A  $2 \text{ fb}^{-1}$  update of the ATLAS  $\gamma\gamma$  analysis in Ref. [39] provides limits of  $M_{TT} > 2.7$  TeV (2.3 TeV) for constructive (destructive) interference.

At the one-loop level, gravitons can also generate dimension-six operators with coefficients that are also model dependent. Experimental bounds on these operators can also give stringent constraints on  $M_D$  [31].

### II.4c Black Hole Production

The physics at energies  $\sqrt{s} \sim M_D$  is sensitive to the details of the quantum theory of gravity. Nevertheless, in the transplanckian regime,  $\sqrt{s} \gg M_D$ , one can rely on a semiclassical description of gravity to obtain predictions. An interesting feature of transplanckian physics is the creation of black holes [40]. A black hole is expected to be formed in a collision in which the impact parameter is smaller than the Schwarzschild radius [41]:

$$R_S = \frac{1}{M_D} \left[ \frac{2^\delta \pi^{(\delta-3)/2}}{\delta+2} \Gamma\left(\frac{\delta+3}{2}\right) \frac{M_{BH}}{M_D} \right]^{1/(\delta+1)}, \quad (10)$$

where  $M_{BH}$  is the mass of the black hole, which would roughly correspond to the total energy in the collision. The cross section for black hole production can be estimated to be of the same order as the geometric area  $\sigma \sim \pi R_S^2$ . For  $M_D \sim \text{TeV}$ , this gives a production of  $\sim 10^7$  black holes at the  $\sqrt{s} = 14$  TeV LHC with an integrated luminosity of  $30 \text{ fb}^{-1}$  [40]. A black hole would provide a striking experimental signature since it is expected to thermally radiate with a Hawking temperature  $T_H = (\delta+1)/(4\pi R_S)$ , and therefore would evaporate democratically into all SM states.

At the LHC, one starts to be able to access a regime where the energies are large compared to (or at least comparable to)  $M_D$  values in the TeV range. However, given the present constraints on  $M_D$ , the LHC will not be able to reach energies much above  $M_D$ . This implies that predictions based on the semiclassical approximation could receive sizeable modifications from model-dependent quantum-gravity effects.

The LHC experiments have performed searches for microscopic black holes by looking for excesses above the SM background in final states with multiple high  $p_T$  objects [42,43], high  $p_T$  jets [44], high  $p_T$  leptons and jets [45], and in same-sign dimuon events [46]. No excesses have been observed. The results are usually quoted as model-independent limits on the cross section for new physics in the final state and kinematic region analyzed. These results can then be used to provide

constraints on models of low-scale gravity and weakly-coupled string theory. In addition, limits are sometimes quoted on particular implementations of models, which are used as benchmarks to illustrate the sensitivity. For example, using  $1 \text{ fb}^{-1}$ , CMS provides limits in the mass range of 4-5 TeV [42] for semiclassical black holes, and ATLAS gets similar results [45]. ATLAS have also searched for black holes via a  $36 \text{ pb}^{-1}$  analysis of the invariant mass and angular distributions in dijet events, excluding  $M_D$  values in the range from 0.75 up to 3.26 (3.69) TeV [47] for the case of 2 (6) extra dimensions.

In weakly-coupled string models the semiclassical description of gravity fails in the energy range between  $M_s$  and  $M_s/g_s^2$  since stringy effects are important. In this regime one expects, instead of black holes, the formation of string balls, made of highly excited long strings, that could be copiously produced at the LHC for  $M_s \sim \text{TeV}$  [48], and would evaporate thermally at the Hagedorn temperature giving rise to high-multiplicity events. CMS has interpreted their  $1 \text{ fb}^{-1}$  multi-object search to exclude the production of string balls with a minimum mass in the range of 4.1-4.5 TeV [42], depending on the details of the model. ATLAS gets similar results [45] for their  $1 \text{ fb}^{-1}$  search for an excess of events with high  $p_T$  leptons and jets.

## III TeV-Scale Extra Dimensions

### III.1 Warped Extra Dimensions

The RS model [3] is the most attractive setup of warped extra dimensions at the TeV scale, since it provides an alternative solution to the hierarchy problem. The RS model is based on a 5D theory with the extra dimension compactified on an orbifold,  $S^1/Z_2$ , a circle  $S^1$  with the extra identification of  $y$  with  $-y$ . This corresponds to the segment  $y \in [0, \pi R]$ , a manifold with boundaries at  $y = 0$  and  $y = \pi R$ . Let us now assume that this 5D theory has a cosmological constant in the bulk  $\Lambda$ , and on the two boundaries  $\Lambda_0$  and  $\Lambda_{\pi R}$ :

$$S_5 = - \int d^4x dy \left\{ \sqrt{-g} \left[ \frac{1}{2} M_5^3 \mathcal{R} + \Lambda \right] + \sqrt{-g_0} \delta(y) \Lambda_0 + \sqrt{-g_{\pi R}} \delta(y - \pi R) \Lambda_{\pi R} \right\}, \quad (11)$$

where  $g_0$  and  $g_{\pi R}$  are the values of the determinant of the induced metric on the two respective boundaries. Einstein's equations can be solved, giving in this case the metric

$$ds^2 = a(y)^2 dx^\mu dx^\nu \eta_{\mu\nu} + dy^2, \quad a(y) = e^{-ky}, \quad (12)$$

where  $k = \sqrt{-\Lambda/(6M_5^3)}$ . Consistency of the solution requires  $\Lambda_0 = -\Lambda_{\pi R} = -\Lambda/k$ . The metric in Eq. (12) corresponds to a 5D AdS space. The factor  $a(y)$  is called the ‘‘warp’’ factor and determines how 4D scales change as a function of the position in the extra dimension. In particular, this implies that energy scales for 4D fields localized at the boundary at  $y = \pi R$  are red-shifted by a factor  $e^{-k\pi R}$  with respect to those localized at  $y = 0$ . For this reason, the boundaries at  $y = 0$  and  $y = \pi R$  are usually referred to as the ultraviolet (UV) and infrared (IR) boundaries, respectively.

As in the ADD case, we can perform a KK reduction and obtain the low-energy effective theory of the 4D massless graviton. In this case we obtain

$$M_P^2 = \int_0^{\pi R} dy e^{-2ky} M_5^3 = \frac{M_5^3}{2k} (1 - e^{-2k\pi R}). \quad (13)$$

Taking  $M_5 \sim k \sim M_P$ , we can generate an IR-boundary scale of order  $ke^{-k\pi R} \sim \text{TeV}$  for an extra dimension of radius  $R \simeq 11/k$ . Mechanisms to stabilize  $R$  to this value have been proposed [49] that, contrary to the ADD case, do not require introducing any new small or large parameter. Therefore a natural solution to the hierarchy problem can be achieved in this framework if the Higgs field, whose vacuum expectation value (VEV) is responsible for electroweak symmetry breaking, is localized at the IR-boundary where the effective mass scales are of order TeV.

In the original RS model [3], all the SM fields were assumed to be localized on the IR-boundary. Nevertheless, for the hierarchy problem, only the Higgs field has to be localized there. SM gauge bosons and fermions can propagate in the 5D bulk [4,5,6,50]. By performing a KK reduction from the 5D action of a gauge boson, we find [4]

$$\frac{1}{g_4^2} = \int_0^{\pi R} dy \frac{1}{g_5^2} = \frac{\pi R}{g_5^2},$$

where  $g_D$  ( $D = 4, 5$ ) is the gauge coupling in  $D$ -dimensions. Therefore the 4D gauge couplings can be of order one, as is the case of the SM, if we demand  $g_5^2 \sim \pi R$ . Using  $kR \sim 10$  and  $g_4 \sim 0.5$ , we obtain the 5D gauge coupling

$$g_5 \sim 4/\sqrt{k}. \quad (14)$$

Boundary kinetic terms for the gauge bosons can modify this relation, allowing for larger values of  $g_5\sqrt{k}$ .

Fermions propagating in the RS extra dimension have 4D massless zero-modes with wavefunctions which vary as  $f_0 \sim \text{Exp}[(1/2 - c_f)ky]$ , where  $c_fk$  is their 5D mass [51,6]. Depending on the free parameter  $c_fk$ , fermions can be localized either towards the UV-boundary ( $c_f > 1/2$ ) or IR-boundary ( $c_f < 1/2$ ). Since the Higgs is localized on the IR-boundary, we can generate exponentially suppressed Yukawa couplings by having the fermion zero-modes localized towards the UV-boundary, generating naturally the light SM fermion spectrum [6]. A large overlap with the wavefunction of the Higgs is needed for the top quark, in order to generate its large mass, thus requiring it to be localized towards the IR-boundary. In conclusion, the large mass hierarchies present in the SM fermion spectrum can be easily obtained in warped models via suitable choices of the order-one parameters  $c_f$  [52]. In these scenarios deviations in flavor physics from the SM predictions are expected to arise from flavor-changing KK gluon couplings [53]. These put certain constraints on the parameters of the models and predicts new physics effects to be observed in  $B$ -physics processes [54].

The masses of the KK states can also be calculated. One finds [6]

$$m_n \simeq \left( n + \frac{\alpha}{2} - \frac{1}{4} \right) \pi k e^{-\pi k R}, \quad (15)$$

where  $n = 1, 2, \dots$  and  $\alpha = \{|c_f - 1/2|, 0, 1\}$  for KK fermions, KK gauge bosons and KK gravitons, respectively. Their masses are of order  $ke^{-\pi k R} \sim \text{TeV}$ ; the first KK state of the gauge bosons would be the lightest, while gravitons are expected to be the heaviest.

### III.1a Models of Electroweak Symmetry Breaking

Theories in warped extra dimensions can be used to implement symmetry breaking at low energies by boundary conditions [55]. For example, for a  $U(1)$  gauge symmetry in the 5D bulk, this can be easily achieved by imposing a Dirichlet boundary condition on the IR-boundary,  $A_\mu|_{y=\pi R} = 0$ . This makes the zero-mode gauge boson get a mass, given by  $m_A = g_4 \sqrt{2k/g_5^2} e^{-\pi k R}$ , that can be smaller than the KK masses for  $g_5^2 \gg 1/k$ . A very different situation occurs if the Dirichlet boundary condition is imposed on the UV-boundary,  $A_\mu|_{y=0} = 0$ . In this case the zero-mode gauge boson disappears from the spectrum. Finally, if a Dirichlet boundary condition is imposed on the two boundaries, we obtain a massless 4D scalar corresponding to the fifth component of the 5D gauge boson,  $A_5$ . Thus, different scenarios can be implemented by appropriately choosing the 5D bulk gauge symmetry,  $\mathcal{G}_5$ , and the symmetries to which it reduces on the UV and IR-boundary,  $\mathcal{H}_{UV}$  and  $\mathcal{H}_{IR}$  respectively. In all cases the KK spectrum comes in representations of the group  $\mathcal{G}_5$ .

**Higgsless models:** One of the most interesting applications of warped extra dimensions is for models of electroweak symmetry breaking. To guarantee the relation  $M_W^2 \simeq M_Z^2 \cos^2 \theta_W$ , a custodial  $SU(2)_V$  symmetry is needed in the bulk and IR-boundary [56]. For this reason the minimal symmetry pattern is [57]

$$\begin{aligned} \mathcal{G}_5 &= SU(3)_c \times SU(2)_L \times SU(2)_R \times U(1)_X \\ \mathcal{H}_{IR} &= SU(3)_c \times SU(2)_V \times U(1)_X \\ \mathcal{H}_{UV} &= G_{SM} \end{aligned}$$

where  $G_{SM} \equiv SU(3)_c \times SU(2)_L \times U(1)_Y$  is the SM gauge group with the identification of hypercharge as  $Y = T_3^R + X$ . In this theory the  $W$  and  $Z$  bosons are massive, there is no Higgs boson, and the first KK mode associated to the  $W$  boson has a mass given by

$$m_{KK} \simeq \frac{3\pi g_5 \sqrt{k}}{4g_4} M_W. \quad (16)$$

Using Eq. (14), one obtains  $m_{KK} \simeq 1.2 \text{ TeV}$ .

**Composite Higgs models:** Alternatively, warped extra dimensions can give rise to scenarios, often called gauge-Higgs unified models, where the Higgs appears as the fifth component of a 5D gauge boson,  $A_5$ . The Higgs mass is protected by the

# Searches Particle Listings

## Extra Dimensions

5D gauge invariance and can only get a nonzero value from non-local one-loop effects [58]. As in the Higgsless case, a custodial symmetry is needed. The simplest realization [59] has

$$\begin{aligned}\mathcal{G}_5 &= SU(3)_c \times SO(5) \times U(1)_X \\ \mathcal{H}_{IR} &= SU(3)_c \times SO(4) \times U(1)_X \\ \mathcal{H}_{UV} &= G_{SM}\end{aligned}$$

The Higgs gets a potential at the one-loop level that triggers a VEV, breaking the electroweak symmetry. In these models there is a light Higgs with mass 100 – 200 GeV that, as will be explained in Sec. III.3, behaves as a composite state. The lightest KK modes of the model are color fermions with charges  $Q = -1/3, 2/3$  and  $5/3$  [60].

### III.1b Constraints from Electroweak Precision Tests

Models in which the SM gauge bosons propagate in 1/TeV-sized extra dimensions give generically large corrections to electroweak observables. When the SM fermions are confined on a boundary these corrections are universal and can be parametrized by four quantities:  $\hat{S}$ ,  $\hat{T}$ ,  $W$  and  $Y$ , as defined in Ref. [61]. For warped models, where the 5D gauge coupling of Eq. (14) is large, the most relevant parameter is  $\hat{T}$ , which gives the bound  $m_{KK} \gtrsim 10$  TeV [50]. When a custodial symmetry is imposed [56], the main constraint comes from the  $\hat{S}$  parameter, requiring  $m_{KK} \gtrsim 3$  TeV independently of the value of  $g_5$ . Notice that this bound, when applied to 5D Higgsless models where Eq. (16) holds, constrains the coupling  $g_5^2 k$  to be close to its nonperturbative value [62]. Also corrections to the  $Zb_L\bar{b}_L$  coupling can be important [50], especially in warped models for electroweak symmetry breaking as the ones described above.

### III.1c Kaluza-Klein Searches

The main prediction of 1/TeV-sized extra dimensions is the presence of a discretized KK spectrum, with masses around the TeV scale, associated with the SM fields that propagate in the extra dimension.

In the original RS model, only gravity propagates in the 5D bulk. Experimental searches have been performed for the lightest RS graviton through its decay to a variety of SM particle-antiparticle pairs. The results are usually interpreted in the plane of the dimensionless coupling  $k/M_P$  versus  $m_1$ , where  $M_P$  is the reduced Planck mass defined previously and  $m_1$  is the mass of the lightest KK excitation of the graviton. Since the AdS curvature  $\sim k$  cannot exceed the cut-off scale of the model, which is estimated to be  $\ell_5^{1/3} M_5$  [31], we must demand  $k \ll \sqrt{2}\ell_5 M_P$ . The results quoted below are 95% CL lower limits on the KK graviton mass for a coupling  $k/M_P = 0.1$ .

Tevatron limits exist for the diphoton, dielectron and dimuon final states, and are typically near the kinematic limit of order 1 TeV. The most stringent results from the Tevatron are the CDF limit of  $m_1 > 1.11$  TeV [64] from combining  $G \rightarrow \gamma\gamma/ee/\mu\mu$ , and the DØ limit of  $m_1 > 1.05$  TeV [65] using  $G \rightarrow \gamma\gamma/ee$ . The LHC experiments can probe higher masses, with recent results available using  $\approx 1 \text{ fb}^{-1}$  of 7 TeV data. No published predictions exist for NLO cross sections for 7 TeV  $pp$

collisions, and CMS and ATLAS adopted different conventions with regard to k-factors, meaning some care is required when comparing their results. CMS used a k-factor value of  $\approx 1.6$  for their combined  $ee/\mu\mu$  result of  $m_1 > 1.78$  TeV [66], and for their preliminary result of  $m_1 > 1.72$  TeV [37] using the  $\gamma\gamma$  final state. The ATLAS limit of  $m_1 > 1.63$  TeV [67] from the  $ee/\mu\mu$  final state combination assumes the signal cross section as obtained with LO\* PDFs; this choice corresponds to an effective k-factor of  $\approx 1.1$  for masses near the obtained limit. A  $2 \text{ fb}^{-1}$  update of the ATLAS  $\gamma\gamma$  analysis in Ref. [39] assumes a k-factor of 1.75 and provides a limit of  $m_1 > 1.95$  TeV when combined with the  $1 \text{ fb}^{-1}$   $ee/\mu\mu$  results.

Less stringent limits on the KK graviton mass come from the  $WW/ZZ$  final states at the Tevatron. By combining searches with one, two, or three charged leptons, DØ sets a limit in the  $WW$  final state of  $m_1 > 754$  GeV [68]. An earlier CDF result in the  $e + \cancel{E}_T + jj$  final state limits  $m_1 > 606$  GeV [69]. A preliminary  $ZZ$  result from CDF [70] reports 4 events compatible with a mass of  $\approx 325$  GeV in the final state with four charged leptons (electrons or muons), and they state that the probability to observe such a distribution of events given the SM background lies in the range  $(2.7 - 10.5) \times 10^{-5}$ . However, CDF analyses with two charged leptons and either a pair of jets or  $\cancel{E}_T$  do not confirm a signal for a new heavy particle decaying to a pair of  $Z$  bosons. The combined result is quoted as a limit of 0.26 pb on the production cross section of a 325 GeV RS Graviton decaying to  $ZZ$ . A DØ measurement of the  $ZZ$  production cross section in the four charged lepton final state [71] also shows no evidence of an enhancement at a  $ZZ$  invariant mass near 325 GeV.

If the SM fields propagate in the 5D bulk, the couplings of the KK graviton to  $ee/\mu\mu/\gamma\gamma$  are suppressed [72], and the above bounds would not apply. In this case the graviton is the heaviest KK state, so experimental searches for KK gauge bosons and fermions are more appropriate discovery channels in these scenarios. For the scenarios discussed above in which only the Higgs and the top quark are localized towards the IR-boundary, the KK gauge bosons mainly decay into top quarks, longitudinal  $W/Z$  bosons, and Higgs bosons. Couplings to light SM fermions are suppressed by a factor  $g_4/\sqrt{g_3^2 k} \sim 0.2$  [6]. Searches have been made for evidence of the lightest KK excitation of the gluon, through its decay to  $t\bar{t}$  pairs. An ATLAS analysis of the lepton-plus-jets final state using  $0.2 \text{ fb}^{-1}$  of data excludes KK gluons with masses below 650 GeV [73], while a  $1 \text{ fb}^{-1}$  analysis of the dilepton final state yields a lower limit of 0.84 TeV [74]. A  $0.9 \text{ fb}^{-1}$  CMS analysis of the fully hadronic final state searches uses “top tagging” techniques to identify events where one or both of the top quarks is highly boosted and reconstructed as a single merged jet; this analysis claims to exclude KK gluons with a mass lying between 1 and 1.5 TeV [75], though the paper states that the large width expected for the KK gluon was not taken into account in determining the result. A gauge KK excitation could be also sought through its decay to longitudinal  $W/Z$  bosons. While, as

reported elsewhere in this volume, searches for  $WZ$  resonances have been used to set limits on sequential SM  $W'$  bosons or other models, as yet no  $WZ$  experimental results have been interpreted in the context of warped extra-dimensions.

The lightest KK states are usually the partners of the top quark. In warped models of electroweak symmetry breaking, these are color states with charges  $Q = -1/3, 2/3$  and  $5/3$ , and masses between 0.5 and 1.5 TeV [60]. They can be either singly- or pair-produced, and mainly decay into a combination of  $W/Z$  with top/bottom. Of particular note, the  $Q = 5/3$  state decays mainly into  $W^+t \rightarrow W^+W^+b$ , giving a pair of same-sign leptons in the final state [76]. DØ searched with  $5.4 \text{ fb}^{-1}$  for single production of heavy vector-like quarks decaying to  $W/Z + j$  [77], and set limits on their production cross sections that could be reinterpreted to provide some exclusion on KK fermions decaying to  $W/Z + b$ , though the sensitivity might be less than optimal since  $b$ -tagging was not used in the analysis. CMS performed a  $1 \text{ fb}^{-1}$  search for pair-production of heavy vector-like quarks  $T$ , which excludes such quarks with masses below 475 GeV [78], assuming a 100% branching ratio for the decay  $T \rightarrow tZ$ .

### III.2 Connection with Strongly-Coupled Models via the AdS/CFT Correspondence

The AdS/CFT correspondence [7] provides a connection between warped extra-dimensional models and strongly-coupled theories in ordinary 4D. Although the exact connection is only known for certain cases, the AdS/CFT techniques have been very useful to obtain, at the qualitative level, a 4D holographic description of the various phenomena in warped extra-dimensional models [8].

The connection goes as follows. The physics of the bulk AdS<sub>5</sub> models can be interpreted as that of a 4D conformal field theory (CFT) which is strongly-coupled. The extra-dimensional coordinate  $y$  plays the role of the renormalization scale  $\mu$  of the CFT by means of the identification  $\mu \equiv ke^{-ky}$ . Therefore the UV-boundary corresponds in the CFT to a UV cut-off scale at  $\Lambda_{UV} = k \sim M_P$ , breaking explicitly conformal invariance, while the IR-boundary can be interpreted as a spontaneous breaking of the conformal symmetry at energies  $ke^{-k\pi R} \sim \text{TeV}$ . Fields localized on the UV-boundary are elementary fields external to the CFT, while fields localized on the IR-boundary and KK states corresponds to composite resonances of the CFT. Furthermore, local gauge symmetries in the 5D models,  $\mathcal{G}_5$ , correspond to global symmetries of the CFT, while the UV-boundary symmetry can be interpreted as a gauging of the subgroup  $\mathcal{H}_{UV}$  of  $\mathcal{G}_5$  in the CFT. Breaking gauge symmetries by IR-boundary conditions corresponds to the spontaneous breaking  $\mathcal{G}_5 \rightarrow \mathcal{H}_{IR}$  in the CFT at energies  $\sim ke^{-k\pi R}$ . Using this correspondence we can easily derive the 4D massless spectrum of the compactified AdS<sub>5</sub> models. We also have the identification  $k^3/M_5^3 \approx 16\pi^2/N^2$  and  $g_5^2k \approx 16\pi^2/N^r$  ( $r = 1$  or  $2$  for CFT fields in the fundamental or adjoint representation of the gauge group, respectively), where  $N$  plays the role of the

number of colors of the CFT. Therefore the weak-coupling limit in AdS<sub>5</sub> corresponds to a large- $N$  expansion in the CFT.

Following the above AdS/CFT dictionary we can understand the RS solution to the hierarchy problem from a 4D viewpoint. The equivalent 4D model is a CFT with a TeV mass-gap and a Higgs emerging as a composite state. The AdS/CFT correspondence also shows that the 5D Higgsless models described above should share similar physics as Technicolor models [79]. Indeed, the lowest KK  $SU(2)_L$ -gauge boson behaves as the Techni-rho  $\rho_T$  with a coupling to longitudinal  $W/Z$  bosons given by  $g_5\sqrt{k} \approx g_{\rho T}$ , while the coupling to elementary fermions is  $g_4^2/\sqrt{g_5^2k} \approx g^2F_{\rho T}/M_{\rho T}$ . Also, models with the Higgs identified as  $A_5$  correspond to models, similar to those proposed in Ref. [80], where the Higgs is a composite pseudo-Goldstone boson arising from the spontaneous breaking  $\mathcal{G}_5 \rightarrow \mathcal{H}_{IR}$  in the CFT.

Fermions in compactified AdS<sub>5</sub> also have a simple 4D holographic interpretation. The 4D massless mode described in sec. III.1 corresponds to an external fermion  $\psi_i$  linearly coupled to a fermionic CFT operator  $\mathcal{O}_i$ :  $\mathcal{L}_{\text{int}} = \lambda_i\psi_i\mathcal{O}_i + h.c.$ . The dimension of the operator  $\mathcal{O}_i$  is related to the 5D fermion mass according to  $\text{Dim}[\mathcal{O}_i] = |c_f + 1/2| - 1$ . Therefore, by varying  $c_f$  we vary  $\text{Dim}[\mathcal{O}_i]$ , making the coupling  $\lambda_i$  irrelevant ( $c_f > 1/2$ ), marginal ( $c_f = 1/2$ ) or relevant ( $c_f < 1/2$ ). When irrelevant, the coupling is exponentially suppressed at low energies, and then the coupling of  $\psi_i$  to the CFT (and eventually to the composite Higgs) is very small. When relevant, it grows towards the IR and become as large as  $g_5$  (in units of  $k$ ), meaning that the fermion is as strongly coupled as the CFT states [59]. In this latter case  $\psi_i$  behaves as a composite fermion.

### III.3 Flat Extra Dimensions

Models with quantum-gravity at the TeV scale, as in the ADD scenario, can have extra (flat) dimensions of  $1/\text{TeV}$  size, as it happens in string scenarios [81]. All SM fields may propagate in these extra dimensions, leading to the possibility of observing their corresponding KK states.

A simple example is to assume that the SM gauge bosons propagate in a flat five-dimensional orbifold  $S^1/Z_2$  of radius  $R$ , with the fermions localized on a 4D boundary. The KK gauge bosons behave as sequential SM gauge bosons with a coupling to fermions enhanced by a factor  $\sqrt{2}$  [81]. The experimental limits on such sequential gauge bosons could therefore be recast as limits on KK gauge bosons. Bounds from LEP2 require  $1/R \gtrsim 6 \text{ TeV}$  [61].

An alternative scenario, known as Universal Extra Dimensions (UED) [82], assumes that all SM fields propagate universally in a flat orbifold  $S^1/Z_2$  with an extra  $Z_2$  parity, called KK-parity, that interchanges the two boundaries. In this case, the lowest KK state is stable becoming a Dark Matter candidate. At colliders, the KK particles would have to be created in pairs, and would then cascade decay to the lightest KK particle (LKP), which would be stable and escape detection. Experimental signatures, such as jets or leptons and

## Searches Particle Listings

## Extra Dimensions

$\cancel{E}_T$ , would be similar to those of typical  $R$ -parity conserving SUSY searches. However, few experimental searches have as yet been interpreted in the UED scenario. DØ and ATLAS have both examined a specific UED model in which the KK parity is violated by gravitational interactions [83]. In this case the LKP can decay via  $\gamma^* \rightarrow \gamma + G$ , where  $G$  represents one of a tower of eV-spaced KK graviton states. Beginning with strong production of a pair of KK quarks and/or gluons [84], the final state would be  $\gamma\gamma + \cancel{E}_T + X$ , where  $\cancel{E}_T$  results from the escaping gravitons and  $X$  represents SM particles emitted during the cascade decays. The experimental analyses treat  $R$ , the UED compactification radius, as a free parameter and follow the theory calculation [85] that sets  $\Lambda$ , the cut-off used in the calculation of radiative corrections to the KK masses, such that  $\Lambda R = 20$ . The gravitational decay widths of the KK particles are set by the values of  $\delta$  and of  $M_D$ , the Planck scale in the  $(4+\delta)$ -dimensional theory. Setting  $\delta = 6$  and  $M_D = 5$  TeV, and provided  $1/R < 2$  TeV, only the LKP has an appreciable gravitational decay, with a sizeable branching ratio for  $\gamma^* \rightarrow \gamma + G$ . In this scenario, DØ set a 95% CL limit that  $1/R > 477$  GeV [86]. The initial ATLAS result used only  $3 \text{ pb}^{-1}$  to increase this limit to  $1/R > 729$  GeV; a recent ATLAS  $1 \text{ fb}^{-1}$  update extends it further to  $1/R > 1.23$  TeV [87].

Finally, realistic models of electroweak symmetry breaking can also be constructed with flat extra spatial dimensions, similarly to those in the warped case, requiring, however, the presence of sizeable boundary kinetic terms [88]. There is also the possibility of breaking supersymmetry by boundary conditions [89]. Models of this type could explain naturally the presence of a Higgs boson lighter than  $M_D$  [90].

## References

- For a comprehensive collection of the original papers see, "Modern Kaluza-Klein Theories", edited by T. Appelquist *et al.*, Addison-Wesley (1987).
- N. Arkani-Hamed *et al.*, Phys. Lett. **B429**, 263 (1998).
- L. Randall and R. Sundrum, Phys. Rev. Lett. **83**, 3370 (1999).
- H. Davoudiasl *et al.*, Phys. Lett. **B473**, 43 (2000); A. Pomarol, Phys. Lett. **B486**, 153 (2000).
- S. Chang *et al.*, Phys. Rev. **D62**, 084025 (2000).
- T. Gherghetta and A. Pomarol, Nucl. Phys. **B586**, 141 (2000).
- J.M. Maldacena, Adv. Theor. Math. Phys. **2**, 231 (1998); E. Witten, Adv. Theor. Math. Phys. **2**, 253 (1998); S.S. Gubser *et al.*, Phys. Lett. **B428**, 105 (1998).
- N. Arkani-Hamed *et al.*, JHEP **0108**, 017 (2001).
- Z. Chacko *et al.*, JHEP **0007**, 036 (2000).
- N. Arkani-Hamed *et al.*, Phys. Rev. **D59**, 086004 (1999).
- For a review see for example, R. Rattazzi, hep-ph/0607055 (2006); I. Antoniadis, Yellow report CERN-2002-002 (2002).
- I. Antoniadis *et al.*, Phys. Lett. **B436**, 257 (1998).
- G.F. Giudice *et al.*, Nucl. Phys. **B544**, 3 (1999).
- For the case of two extra dimensions, see for example, N. Arkani-Hamed *et al.*, Phys. Rev. **D62**, 105002 (2000).
- E.G. Adelberger *et al.*, Prog. Part. Nucl. Phys. **62**, 102 (2009).
- C. Hanhart *et al.*, Phys. Lett. **B509**, 1 (2001).
- S. Hannestad and G.G. Raffelt, Phys. Rev. **D67**, 125008 (2003).
- L.J. Hall and D. Tucker-Smith, Phys. Rev. **D60**, 085008 (1999).
- E.A. Mirabelli *et al.*, Phys. Rev. Lett. **82**, 2236 (1999).
- T. Han *et al.*, Phys. Rev. **D59**, 105006 (1999).
- LEP Exotica WG 2004-03 (2004).
- CDF Collab., Phys. Rev. Lett. **101**, 181602 (2008).
- DØ Collab., Phys. Rev. Lett. **101**, 011601 (2008).
- DØ Collab., Phys. Rev. Lett. **90**, 251802 (2003).
- CMS Collab., CMS Note PAS-EXO-11-059 (2011).
- CMS Collab., CMS Note PAS-EXO-11-058 (2011).
- ATLAS Collab., ATLAS Note CONF-2011-096 (2011).
- See for example S. Cullen *et al.*, Phys. Rev. **D62**, 055012 (2000).
- CMS Collab., Phys. Lett. **B704**, 123 (2011).
- J.L. Hewett, Phys. Rev. Lett. **82**, 4765 (1999).
- G.F. Giudice and A. Strumia, Nucl. Phys. **B663**, 377 (2003).
- H1 Collab., Phys. Lett. **B568**, 35 (2003); ZEUS Collab., Phys. Lett. **B591**, 23 (2004).
- LEP Working Group LEP2FF/03-01 (2003); ALEPH Collab., Eur. Phys. J. **C49**, 411 (2007).
- LEP Working Group LEP2FF/02-02 (2002).
- DØ Collab., Phys. Rev. Lett. **102**, 051601 (2009).
- DØ Collab., Phys. Rev. Lett. **103**, 191803 (2009).
- CMS Collab., CMS Note PAS-11-038 (2011).
- CMS Collab., CMS Note PAS-11-039 (2011).
- ATLAS Collab., ATLAS Note CONF-2011-044 (2011).
- S.B. Giddings and S. Thomas, Phys. Rev. **D65**, 056010 (2002); S. Dimopoulos and G. Landsberg, Phys. Rev. Lett. **87**, 161602 (2001); for a review see for example, P. Kanti, Int. J. Mod. Phys. **A19**, 4899 (2004).
- R.C. Myers and M.J. Perry, Annals Phys. **172**, 304 (1986).
- CMS Collab., CMS Note PAS-EXO-2011-071 (2011).
- ATLAS Collab., ATLAS Note CONF-2010-088 (2010).
- ATLAS Collab., ATLAS Note CONF-2011-068 (2011).
- ATLAS Collab., ATLAS Note CONF-2011-147 (2011).
- ATLAS Collab., ATLAS Note CONF-2010-065 (2010).
- ATLAS Collab., New J. Phys. **13**, 053044 (2011).
- S. Dimopoulos and R. Emparan, Phys. Lett. **B526**, 393 (2002).
- W.D. Goldberger and M.B. Wise, Phys. Rev. Lett. **83**, 4922 (1999); J. Garriga, A. Pomarol, Phys. Lett. **B560**, 91 (2003).
- For a review see for example, H. Davoudiasl *et al.*, New J. Phys. **12**, 075011 (2010); T. Gherghetta, arXiv:1008.2570 [hep-ph].
- Y. Grossman and M. Neubert, Phys. Lett. **B474**, 361 (2000).
- S.J. Huber and Q. Shafi, Phys. Lett. **B498**, 256 (2001).
- A. Delgado *et al.*, JHEP **0001**, 030 (2000).
- K. Agashe *et al.*, Phys. Rev. **D71**, 016002 (2005); for a recent analysis see for example, M. Bauer *et al.*, JHEP **1009**, 017 (2010).

55. For a review see for example, A. Pomarol, *Int. J. Mod. Phys.* **A24**, 61 (2009).
56. K. Agashe *et al.*, *JHEP* **0308**, 050 (2003).
57. C. Csaki *et al.*, *Phys. Rev. Lett.* **92**, 101802 (2004); for a review see for example, C. Csaki *et al.*, [hep-ph/0510275](#).
58. Y. Hosotani, *Phys. Lett.* **B126**, 309 (1983).
59. K. Agashe *et al.*, *Nucl. Phys.* **B719**, 165 (2005); for a review see for example, R. Contino, [arXiv:1005.4269](#).
60. R. Contino *et al.*, *Phys. Rev.* **D75**, 055014 (2007).
61. R. Barbieri *et al.*, *Nucl. Phys.* **B703**, 127 (2004).
62. R. Barbieri *et al.*, *Phys. Lett.* **B591**, 141 (2004).
63. H. Davoudiasl *et al.*, *Phys. Rev. Lett.* **84**, 2080 (2000).
64. CDF Collab., *CDF Note* 10479 (2011).
65. DØ Collab., *Phys. Rev. Lett.* **104**, 241802 (2010).
66. CMS Collab., *CMS Note PAS-EXO-11-019* (2011).
67. ATLAS Collab., [arXiv:1108.1582](#) (2011), accepted by PRL.
68. DØ Collab., *Phys. Rev. Lett.* **107**, 011801 (2011).
69. CDF Collab., *Phys. Rev. Lett.* **104**, 241801 (2010).
70. CDF Collab., *Phys. Rev.* **D78**, 012008 (2008); *CDF note* 9640 (2011).
71. DØ Collab., *Phys. Rev.* **D84**, 011103 (2011).
72. K. Agashe *et al.*, *Phys. Rev.* **D76**, 036006 (2007).
73. ATLAS Collab., *ATLAS Note CONF-2011-087* (2011).
74. ATLAS Collab., *ATLAS Note CONF-2011-123* (2011).
75. CMS Collab., *CMS Note PAS EXO-11-006* (2011).
76. R. Contino and G. Servant, *JHEP* **0806**, 026 (2008); J.A. Aguilar-Saavedra, *JHEP* **0911**, 030 (2009); J. Mrazek and A. Wulzer, *Phys. Rev.* **D81**, 075006 (2010); G. Dissertori *et al.*, *JHEP* **1009**, 019 (2010).
77. DØ Collab., *Phys. Rev. Lett.* **106**, 081801 (2011).
78. CMS Collab., [arXiv:1109.4985](#) (2011), submitted to PRL.
79. R.S. Chivukula *et al.*, “Technicolor”, in this *Review*.
80. H. Georgi *et al.*, *Phys. Lett.* **B143**, 152 (1984); D.B. Kaplan *et al.*, *Phys. Lett.* **B136**, 183 (1984).
81. See for example, I. Antoniadis and K. Benakli, *Int. J. Mod. Phys.* **A15**, 4237 (2000).
82. T. Appelquist *et al.*, *Phys. Rev.* **D64**, 035002 (2001); for a review, see for example, A. Datta *et al.*, *New J. Phys.* **12**, 075017 (2010).
83. C. Macesanu, *Phys. Lett.* **B546**, 253 (2002).
84. C. Macesanu *et al.*, *Phys. Rev.* **D66**, 015009 (2002).
85. H.C. Cheng *et al.*, *Phys. Rev.* **D66**, 036005 (2002).
86. DØ Collab., *Phys. Rev. Lett.* **105**, 221802 (2010).
87. ATLAS Collab., *Eur. Phys. J.* **C71**, 1744 (2011).
88. For a review, see for example, G. Panico *et al.*, *JHEP* **1102**, 103 (2011).
89. J. Scherk and J.H. Schwarz, *Phys. Lett.* **B82**, 60 (1979).
90. See for example, A. Pomarol and M. Quiros, *Phys. Lett.* **B438**, 255 (1998); I. Antoniadis *et al.*, *Nucl. Phys.* **B544**, 503 (1999); R. Barbieri *et al.*, *Phys. Rev.* **D63**, 105007 (2001).

Direct Limits on Gravitational or String Mass Scale  
Limits on  $1/R = M_C$   
Limits on Kaluza-Klein Gravitons in Warped Extra Dimensions  
Limits on Mass of Radion

### Limits on $R$ from Deviations in Gravitational Force Law

This section includes limits on the size of extra dimensions from deviations in the Newtonian ( $1/r^2$ ) gravitational force law at short distances. Deviations are parametrized by a gravitational potential of the form  $V = -(G m m'/r) [1 + \alpha \exp(-r/R)]$ . For  $\delta$  toroidal extra dimensions of equal size,  $\alpha = 8\delta/3$ . Quoted bounds are for  $\delta = 2$  unless otherwise noted.

VALUE ( $\mu\text{m}$ )	CL%	DOCUMENT ID	COMMENT
• • • We do not use the following data for averages, fits, limits, etc. • • •			
		<sup>1</sup> BEZERRA	11 Torsion oscillator
		<sup>2</sup> SUSHKOV	11 Torsion pendulum
		<sup>3</sup> BEZERRA	10 Microcantilever
		<sup>4</sup> MASUDA	09 Torsion pendulum
		<sup>5</sup> GERACI	08 Microcantilever
		<sup>6</sup> TRENKEL	08 Newton's constant
		<sup>7</sup> DECCA	07A Torsion oscillator
< 30	95	<sup>8</sup> KAPNER	07 Torsion pendulum
< 47	95	<sup>9</sup> TU	07 Torsion pendulum
		<sup>10</sup> SMULLIN	05 Microcantilever
<130	95	<sup>11</sup> HOYLE	04 Torsion pendulum
		<sup>12</sup> CHIAVERINI	03 Microcantilever
$\lesssim 200$	95	<sup>13</sup> LONG	03 Microcantilever
<190	95	<sup>14</sup> HOYLE	01 Torsion pendulum
		<sup>15</sup> HOSKINS	85 Torsion pendulum

- <sup>1</sup> BEZERRA 11 obtain constraints on non-Newtonian forces with strengths  $10^{11} \lesssim |\alpha| \lesssim 10^{18}$  and length scales  $R = 30\text{--}1260$  nm. See their Fig. 2 for more details. These constraints do not place limits on the size of extra flat dimensions.
- <sup>2</sup> SUSHKOV 11 obtain improved limits on non-Newtonian forces with strengths  $10^7 \lesssim |\alpha| \lesssim 10^{11}$  and length scales  $0.4 \mu\text{m} < R < 4 \mu\text{m}$  (95% CL). See their Fig. 2. These bounds do not place limits on the size of extra flat dimensions. However, a model dependent bound of  $M_* > 70$  TeV is obtained assuming gauge bosons that couple to baryon number also propagate in  $(4 + \delta)$  dimensions.
- <sup>3</sup> BEZERRA 10 obtain improved constraints on non-Newtonian forces with strengths  $10^{19} \lesssim |\alpha| \lesssim 10^{29}$  and length scales  $R = 1.6\text{--}14$  nm (95% CL). See their Fig. 1. This bound does not place limits on the size of extra flat dimensions.
- <sup>4</sup> MASUDA 09 obtain improved constraints on non-Newtonian forces with strengths  $10^9 \lesssim |\alpha| \lesssim 10^{11}$  and length scales  $R = 1.0\text{--}2.9 \mu\text{m}$  (95% CL). See their Fig. 3. This bound does not place limits on the size of extra flat dimensions.
- <sup>5</sup> GERACI 08 obtain improved constraints on non-Newtonian forces with strengths  $|\alpha| > 14,000$  and length scales  $R = 5\text{--}15 \mu\text{m}$ . See their Fig. 9. This bound does not place limits on the size of extra flat dimensions.
- <sup>6</sup> TRENKEL 08 uses two independent measurements of Newton's constant  $G$  to constrain new forces with strength  $|\alpha| \simeq 10^{-4}$  and length scales  $R = 0.02\text{--}1$  m. See their Fig. 1. This bound does not place limits on the size of extra flat dimensions.
- <sup>7</sup> DECCA 07A search for new forces and obtain bounds in the region with strengths  $|\alpha| \simeq 10^{13}\text{--}10^{18}$  and length scales  $R = 20\text{--}86$  nm. See their Fig. 6. This bound does not place limits on the size of extra flat dimensions.
- <sup>8</sup> KAPNER 07 search for new forces, probing a range of  $\alpha \simeq 10^{-3}\text{--}10^5$  and length scales  $R \simeq 10\text{--}1000 \mu\text{m}$ . For  $\delta = 1$  the bound on  $R$  is  $44 \mu\text{m}$ . For  $\delta = 2$ , the bound is expressed in terms of  $M_*$ , here translated to a bound on the radius. See their Fig. 6 for details on the bound.
- <sup>9</sup> TU 07 search for new forces probing a range of  $|\alpha| \simeq 10^{-1}\text{--}10^5$  and length scales  $R \simeq 20\text{--}1000 \mu\text{m}$ . For  $\delta = 1$  the bound on  $R$  is  $53 \mu\text{m}$ . See their Fig. 3 for details on the bound.
- <sup>10</sup> SMULLIN 05 search for new forces, and obtain bounds in the region with strengths  $\alpha \simeq 10^3\text{--}10^8$  and length scales  $R = 6\text{--}20 \mu\text{m}$ . See their Figs. 1 and 16 for details on the bound. This work does not place limits on the size of extra flat dimensions.
- <sup>11</sup> HOYLE 04 search for new forces, probing  $\alpha$  down to  $10^{-2}$  and distances down to  $10 \mu\text{m}$ . Quoted bound on  $R$  is for  $\delta = 2$ . For  $\delta = 1$ , bound goes to  $160 \mu\text{m}$ . See their Fig. 34 for details on the bound.
- <sup>12</sup> CHIAVERINI 03 search for new forces, probing  $\alpha$  above  $10^4$  and  $\lambda$  down to  $3 \mu\text{m}$ , finding no signal. See their Fig. 4 for details on the bound. This bound does not place limits on the size of extra flat dimensions.
- <sup>13</sup> LONG 03 search for new forces, probing  $\alpha$  down to 3, and distances down to about  $10 \mu\text{m}$ . See their Fig. 4 for details on the bound.
- <sup>14</sup> HOYLE 01 search for new forces, probing  $\alpha$  down to  $10^{-2}$  and distances down to  $20 \mu\text{m}$ . See their Fig. 4 for details on the bound. The quoted bound is for  $\alpha \geq 3$ .
- <sup>15</sup> HOSKINS 85 search for new forces, probing distances down to 4 mm. See their Fig. 13 for details on the bound. This bound does not place limits on the size of extra flat dimensions.

### Limits on $R$ from On-Shell Production of Gravitons: $\delta = 2$

This section includes limits on on-shell production of gravitons in collider and astrophysical processes. Bounds quoted are on  $R$ , the assumed common radius of the flat extra dimensions, for  $\delta = 2$  extra dimensions. Studies often quote bounds in terms of derived parameter; experiments are actually sensitive to the masses of the KK gravitons:  $m_{\vec{n}} = |\vec{n}|/R$ . See the Review on “Extra Dimensions” for details. Bounds are given in  $\mu\text{m}$  for  $\delta=2$ .

VALUE ( $\mu\text{m}$ )	CL%	DOCUMENT ID	TECN	COMMENT
• • • We do not use the following data for averages, fits, limits, etc. • • •				
< 92	95	<sup>16</sup> AAD	11s ATLS	$pp \rightarrow jG$

### CONTENTS:

Limits on  $R$  from Deviations in Gravitational Force Law  
Limits on  $R$  from On-Shell Production of Gravitons:  $\delta = 2$   
Limits on  $R$  from On-Shell Production of Gravitons:  $\delta \geq 3$   
Mass Limits on  $M_{\mathcal{T}\mathcal{T}}$

# Searches Particle Listings

## Extra Dimensions

< 72	95	17	CHATRCHYAN11U	CMS	$pp \rightarrow jG$
< 245	95	18	AALTONEN 08Ac	CDF	$p\bar{p} \rightarrow \gamma G, jG$
< 615	95	19	ABAZOV 08s	D0	$p\bar{p} \rightarrow \gamma G$
< 0.916	95	20	DAS	08	Supernova cooling
< 350	95	21	ABULENCIA,A	06	CDF $p\bar{p} \rightarrow jG$
< 270	95	22	ABDALLAH 05B	DLPH	$e^+e^- \rightarrow \gamma G$
< 210	95	23	ACHARD 04E	L3	$e^+e^- \rightarrow \gamma G$
< 480	95	24	ACOSTA 04C	CDF	$p\bar{p} \rightarrow jG$
< 0.00038	95	25	CASSE 04		Neutron star $\gamma$ sources
< 610	95	26	ABAZOV 03	D0	$p\bar{p} \rightarrow jG$
< 0.96	95	27	HANNESTAD 03		Supernova cooling
< 0.096	95	28	HANNESTAD 03		Diffuse $\gamma$ background
< 0.051	95	29	HANNESTAD 03		Neutron star $\gamma$ sources
< 0.00016	95	30	HANNESTAD 03		Neutron star heating
< 300	95	31	HEISTER 03c	ALEP	$e^+e^- \rightarrow \gamma G$
		32	FAIRBAIRN 01		Cosmology
< 0.66	95	33	HANHART 01		Supernova cooling
		34	CASSISI 00		Red giants
<1300	95	35	ACCIARRI 99s	L3	$e^+e^- \rightarrow ZG$

### Limits on $R$ from On-Shell Production of Gravitons: $\delta \geq 3$

This section includes limits similar to those in the previous section, but for  $\delta = 3$  extra dimensions. Bounds are given in nm for  $\delta = 3$ . Entries are also shown for papers examining models with  $\delta > 3$ .

VALUE (nm)	CL%	DOCUMENT ID	TECN	COMMENT
••• We do not use the following data for averages, fits, limits, etc. •••				
< 1.1	95	16	AAD 11s	ATLS $pp \rightarrow jG$
< 1.05	95	17	CHATRCHYAN11U	CMS $pp \rightarrow jG$
< 2.8	95	18	AALTONEN 08Ac	CDF $p\bar{p} \rightarrow \gamma G, jG$
< 4.56	95	19	ABAZOV 08s	D0 $p\bar{p} \rightarrow \gamma G$
< 2.09	95	20	DAS	08 Supernova cooling
< 3.6	95	21	ABULENCIA,A	06 CDF $p\bar{p} \rightarrow jG$
< 3.5	95	22	ABDALLAH 05B	DLPH $e^+e^- \rightarrow \gamma G$
< 2.9	95	23	ACHARD 04E	L3 $e^+e^- \rightarrow \gamma G$
	95	24	ACOSTA 04C	CDF $p\bar{p} \rightarrow jG$
< 0.0042	95	25	CASSE 04	Neutron star $\gamma$ sources
< 6.1	95	26	ABAZOV 03	D0 $p\bar{p} \rightarrow jG$
< 1.14	95	27	HANNESTAD 03	Supernova cooling
< 0.025	95	28	HANNESTAD 03	Diffuse $\gamma$ background
< 0.11	95	29	HANNESTAD 03	Neutron star $\gamma$ sources
< 0.0026	95	30	HANNESTAD 03	Neutron star heating
< 3.9	95	31	HEISTER 03c	ALEP $e^+e^- \rightarrow \gamma G$
		32	FAIRBAIRN 01	Cosmology
< 0.8	95	33	HANHART 01	Supernova cooling
		34	CASSISI 00	Red giants
<18	95	35	ACCIARRI 99s	L3 $e^+e^- \rightarrow ZG$

- 16 AAD 11s search for  $pp \rightarrow jG$ , using 33 pb<sup>-1</sup> of data at  $\sqrt{s} = 7$  TeV, to place bounds on  $M_D$  for two to four extra dimensions, from which these bounds on  $R$  are derived. See their Table 3 for bounds on all  $\delta \leq 4$ .
- 17 CHATRCHYAN 11U search for  $pp \rightarrow jG$ , using 36 pb<sup>-1</sup> of data at  $\sqrt{s} = 7$  TeV, to place bounds on  $M_D$  for two to six extra dimensions, from which these bounds on  $R$  are derived. See their Table 3 for bounds on all  $\delta \leq 6$ .
- 18 AALTONEN 08Ac search for  $p\bar{p} \rightarrow \gamma G$  and  $p\bar{p} \rightarrow jG$  at  $\sqrt{s} = 1.96$  TeV with 2.0 fb<sup>-1</sup> and 1.1 fb<sup>-1</sup> respectively, in order to place bounds on the fundamental scale and size of the extra dimensions. See their Table III for limits on all  $\delta \leq 6$ .
- 19 ABAZOV 08s search for  $p\bar{p} \rightarrow \gamma G$ , using 1 fb<sup>-1</sup> of data at  $\sqrt{s} = 1.96$  TeV to place bounds on  $M_D$  for two to eight extra dimensions, from which these bounds on  $R$  are derived. See their paper for intermediate values of  $\delta$ .
- 20 DAS 08 obtain a limit on  $R$  from Kaluza-Klein graviton cooling of SN1987A due to plasmon-plasmon annihilation.
- 21 ABULENCIA,A 06 search for  $p\bar{p} \rightarrow jG$  using 368 pb<sup>-1</sup> of data at  $\sqrt{s} = 1.96$  TeV. See their Table II for bounds for all  $\delta \leq 6$ .
- 22 ABDALLAH 05B search for  $e^+e^- \rightarrow \gamma G$  at  $\sqrt{s} = 180$ -209 GeV to place bounds on the size of extra dimensions and the fundamental scale. Limits for all  $\delta \leq 6$  are given in their Table 6. These limits supersede those in ABREU 00z.
- 23 ACHARD 04E search for  $e^+e^- \rightarrow \gamma G$  at  $\sqrt{s} = 189$ -209 GeV to place bounds on the size of extra dimensions and the fundamental scale. See their Table 8 for limits with  $\delta \leq 8$ . These limits supersede those in ACCIARRI 99r.
- 24 ACOSTA 04c search for  $p\bar{p} \rightarrow jG$  at  $\sqrt{s} = 1.8$  TeV to place bounds on the size of extra dimensions and the fundamental scale. See their paper for bounds on  $\delta = 4, 6$ .
- 25 CASSE 04 obtain a limit on  $R$  from the gamma-ray emission of point  $\gamma$  sources that arises from the photon decay of gravitons around newly born neutron stars, applying the technique of HANNESTAD 03 to neutron stars in the galactic bulge. Limits for all  $\delta \leq 7$  are given in their Table I.
- 26 ABAZOV 03 search for  $p\bar{p} \rightarrow jG$  at  $\sqrt{s} = 1.8$  TeV to place bounds on  $M_D$  for 2 to 7 extra dimensions, from which these bounds on  $R$  are derived. See their paper for bounds on intermediate values of  $\delta$ . We quote results without the approximate NLO scaling introduced in the paper.
- 27 HANNESTAD 03 obtain a limit on  $R$  from graviton cooling of supernova SN1987A. Limits for all  $\delta \leq 7$  are given in their Tables V and VI.
- 28 HANNESTAD 03 obtain a limit on  $R$  from gravitons emitted in supernovae and which subsequently decay, contaminating the diffuse cosmic  $\gamma$  background. Limits for all  $\delta \leq 7$  are given in their Tables V and VI. These limits supersede those in HANNESTAD 02.
- 29 HANNESTAD 03 obtain a limit on  $R$  from gravitons emitted in two recent supernovae and which subsequently decay, creating point  $\gamma$  sources. Limits for all  $\delta \leq 7$  are given in their Tables V and VI. These limits are corrected in the published erratum.
- 30 HANNESTAD 03 obtain a limit on  $R$  from the heating of old neutron stars by the surrounding cloud of trapped KK gravitons. Limits for all  $\delta \leq 7$  are given in their Tables V and VI. These limits supersede those in HANNESTAD 02.

- 31 HEISTER 03c use the process  $e^+e^- \rightarrow \gamma G$  at  $\sqrt{s} = 189$ -209 GeV to place bounds on the size of extra dimensions and the scale of gravity. See their Table 4 for limits with  $\delta \leq 6$  for derived limits on  $M_D$ .
- 32 FAIRBAIRN 01 obtains bounds on  $R$  from over production of KK gravitons in the early universe. Bounds are quoted in paper in terms of fundamental scale of gravity. Bounds depend strongly on temperature of QCD phase transition and range from  $R < 0.13 \mu\text{m}$  to 0.001  $\mu\text{m}$  for  $\delta=2$ ; bounds for  $\delta=3,4$  can be derived from Table 1 in the paper.
- 33 HANHART 01 obtain bounds on  $R$  from limits on graviton cooling of supernova SN 1987A using numerical simulations of proto-neutron star neutrino emission.
- 34 CASSISI 00 obtain rough bounds on  $M_D$  (and thus  $R$ ) from red giant cooling for  $\delta=2,3$ . See their paper for details.
- 35 ACCIARRI 99s search for  $e^+e^- \rightarrow ZG$  at  $\sqrt{s}=189$  GeV. Limits on the gravity scale are found in their Table 2, for  $\delta \leq 4$ .

### Mass Limits on $M_{TT}$

This section includes limits on the cut-off mass scale,  $M_{TT}$ , of dimension-8 operators from KK graviton exchange in models of large extra dimensions. Ambiguities in the UV-divergent summation are absorbed into the parameter  $\lambda$ , which is taken to be  $\lambda = \pm 1$  in the following analyses. Bounds for  $\lambda = -1$  are shown in parenthesis after the bound for  $\lambda = +1$ , if appropriate. Different papers use slightly different definitions of the mass scale. The definition used here is related to another popular convention by  $M_{TT}^4 = (2/\pi) \Lambda_{T,4}^4$ , as discussed in the above Review on "Extra Dimensions."

VALUE (TeV)	CL%	DOCUMENT ID	TECN	COMMENT
••• We do not use the following data for averages, fits, limits, etc. •••				
> 0.90 (>0.92)	95	36	AARON 11c	H1 $e^\pm p \rightarrow e^\pm X$
> 1.74 (>1.71)	95	37	CHATRCHYAN11A	CMS $pp \rightarrow \gamma\gamma$
> 1.48	95	38	ABAZOV 09AE	D0 $p\bar{p} \rightarrow$ dijet, angular distrib.
> 1.45	95	39	ABAZOV 09D	D0 $p\bar{p} \rightarrow e^+e^-, \gamma\gamma$
> 1.1 (> 1.0)	95	40	SCHAEF 07A	ALEP $e^+e^- \rightarrow e^+e^-$
> 0.898 (> 0.998)	95	41	ABDALLAH 06C	DLPH $e^+e^- \rightarrow \ell^+\ell^-$
> 0.853 (> 0.939)	95	42	GERDES 06	$p\bar{p} \rightarrow e^+e^-, \gamma\gamma$
> 0.96 (> 0.93)	95	43	ABAZOV 05V	D0 $p\bar{p} \rightarrow \mu^+\mu^-$
> 0.78 (> 0.79)	95	44	CHEKANOV 04B	ZEUS $e^\pm p \rightarrow e^\pm X$
> 0.805 (> 0.956)	95	45	ABBIENDI 03D	OPAL $e^+e^- \rightarrow \gamma\gamma$
> 0.7 (> 0.7)	95	46	ACHARD 03D	L3 $e^+e^- \rightarrow ZZ$
> 0.82 (> 0.78)	95	47	ADLOFF 03	H1 $e^\pm p \rightarrow e^\pm X$
> 1.28 (> 1.25)	95	48	GIUDICE 03	RVUE
>20.6 (> 15.7)	95	49	GIUDICE 03	RVUE Dim-6 operators
> 0.80 (> 0.85)	95	50	HEISTER 03C	ALEP $e^+e^- \rightarrow \gamma\gamma$
> 0.84 (> 0.99)	95	51	ACHARD 02D	L3 $e^+e^- \rightarrow \gamma\gamma$
> 1.2 (> 1.1)	95	52	ABBOTT 01	D0 $p\bar{p} \rightarrow e^+e^-, \gamma\gamma$
> 0.60 (> 0.63)	95	53	ABBIENDI 00R	OPAL $e^+e^- \rightarrow \mu^+\mu^-$
> 0.63 (> 0.50)	95	53	ABBIENDI 00R	OPAL $e^+e^- \rightarrow \tau^+\tau^-$
> 0.68 (> 0.61)	95	53	ABBIENDI 00R	OPAL $e^+e^- \rightarrow \mu^+\mu^-, \tau^+\tau^-$
		54	ABREU 00A	DLPH $e^+e^- \rightarrow \gamma\gamma$
> 0.680 (> 0.542)	95	55	ABREU 00S	DLPH $e^+e^- \rightarrow \mu^+\mu^-, \tau^+\tau^-$
> 15-28	99.7	56	CHANG 00B	RVUE Electroweak
> 0.98	95	57	CHEUNG 00	RVUE $e^+e^- \rightarrow \gamma\gamma$
> 0.29-0.38	95	58	GRAESSER 00	RVUE $(g-2)_\mu$
> 0.50-1.1	95	59	HAN 00	RVUE Electroweak
> 2.0 (> 2.0)	95	60	MATHEWS 00	RVUE $p\bar{p} \rightarrow jj$
> 1.0 (> 1.1)	95	61	MELE 00	RVUE $e^+e^- \rightarrow VV$
		62	ABBIENDI 99P	OPAL
		63	ACCIARRI 99M	L3
		64	ACCIARRI 99S	L3
> 1.412 (> 1.077)	95	65	BOURILKOV 99	$e^+e^- \rightarrow e^+e^-$
36 AARON 11c search for deviations in the differential cross section of $e^\pm p \rightarrow e^\pm X$ in 446 pb <sup>-1</sup> of data taken at $\sqrt{s} = 301$ and 319 GeV to place a bound on $M_{TT}$ .				
37 CHATRCHYAN 11A use 36 pb <sup>-1</sup> of data from $pp$ collisions at $\sqrt{s} = 7$ TeV to place lower limits on $\Lambda_T$ , here converted to $M_{TT}$ .				
38 ABAZOV 09AE use dijet angular distributions in 0.7 fb <sup>-1</sup> of data from $p\bar{p}$ collisions at $\sqrt{s} = 1.96$ TeV to place lower bounds on $\Lambda_T$ (equivalent to their $M_S$ ), here converted to $M_{TT}$ .				
39 ABAZOV 09D use 1.05 fb <sup>-1</sup> of data from $p\bar{p}$ collisions at $\sqrt{s} = 1.96$ TeV to place lower bounds on $\Lambda_T$ (equivalent to their $M_S$ ), here converted to $M_{TT}$ .				
40 SCHAEF 07A use $e^+e^-$ collisions at $\sqrt{s} = 189$ -209 GeV to place lower limits on $\Lambda_T$ , here converted to limits on $M_{TT}$ .				
41 ABDALLAH 06c use $e^+e^-$ collisions at $\sqrt{s} \sim 130$ -207 GeV to place lower limits on $M_{TT}$ , which is equivalent to their definition of $M_S$ . Bound shown includes all possible final state leptons, $\ell = e, \mu, \tau$ . Bounds on individual leptonic final states can be found in their Table 31.				
42 GERDES 06 use 100 to 110 pb <sup>-1</sup> of data from $p\bar{p}$ collisions at $\sqrt{s} = 1.8$ TeV, as recorded by the CDF Collaboration during Run I of the Tevatron. Bound shown includes a $K$ -factor of 1.3. Bounds on individual $e^+e^-$ and $\gamma\gamma$ final states are found in their Table I.				
43 ABAZOV 05V use 246 pb <sup>-1</sup> of data from $p\bar{p}$ collisions at $\sqrt{s} = 1.96$ TeV to search for deviations in the differential cross section to $\mu^+\mu^-$ from graviton exchange.				
44 CHEKANOV 04b search for deviations in the differential cross section of $e^\pm p \rightarrow e^\pm X$ with 130 pb <sup>-1</sup> of combined data and $Q^2$ values up to 40,000 GeV <sup>2</sup> to place a bound on $M_{TT}$ .				
45 ABBIENDI 03D use $e^+e^-$ collisions at $\sqrt{s}=181$ -209 GeV to place bounds on the ultraviolet scale $M_{TT}$ , which is equivalent to their definition of $M_S$ .				
46 ACHARD 03D look for deviations in the cross section for $e^+e^- \rightarrow ZZ$ from $\sqrt{s} = 200$ -209 GeV to place a bound on $M_{TT}$ .				
47 ADLOFF 03 search for deviations in the differential cross section of $e^\pm p \rightarrow e^\pm X$ at $\sqrt{s}=301$ and 319 GeV to place bounds on $M_{TT}$ .				



- 48 GIUDICE 03 review existing experimental bounds on  $M_{TT}$  and derive a combined limit.
- 49 GIUDICE 03 place bounds on  $\Lambda_6$ , the coefficient of the gravitationally-induced dimension-6 operator  $(2\pi\lambda/\Lambda_6^2)(\sum \bar{\tau}\gamma_\mu^5\eta)(\sum \bar{\tau}\gamma^\mu\gamma^5\eta)$ , using data from a variety of experiments. Results are quoted for  $\lambda=\pm 1$  and are independent of  $\delta$ .
- 50 HEISTER 03c use  $e^+e^-$  collisions at  $\sqrt{s}=189-209$  GeV to place bounds on the scale of dim-8 gravitational interactions. Their  $M_S^4$  is equivalent to our  $M_{TT}$  with  $\lambda=\pm 1$ .
- 51 ACHARD 02 search for s-channel graviton exchange effects in  $e^+e^- \rightarrow \gamma\gamma$  at  $E_{cm}=192-209$  GeV.
- 52 ABBOTT 01 search for variations in differential cross sections to  $e^+e^-$  and  $\gamma\gamma$  final states at the Tevatron.
- 53 ABBIENDI 00R uses  $e^+e^-$  collisions at  $\sqrt{s}=189$  GeV.
- 54 ABREU 00A search for s-channel graviton exchange effects in  $e^+e^- \rightarrow \gamma\gamma$  at  $E_{cm}=189-202$  GeV.
- 55 ABREU 00s uses  $e^+e^-$  collisions at  $\sqrt{s}=183$  and 189 GeV. Bounds on  $\mu$  and  $\tau$  individual final states given in paper.
- 56 CHANG 00B derive  $3\sigma$  limit on  $M_{TT}$  of (28,19,15) TeV for  $\delta=(2,4,6)$  respectively assuming the presence of a torsional coupling in the gravitational action. Highly model dependent.
- 57 CHEUNG 00 obtains limits from anomalous diphoton production at OPAL due to graviton exchange. Original limit for  $\delta=4$ . However, unknown UV theory renders  $\delta$  dependence unreliable. Original paper works in HLZ convention.
- 58 GRAESSER 00 obtains a bound from graviton contributions to  $g-2$  of the muon through loops of 0.29 TeV for  $\delta=2$  and 0.38 TeV for  $\delta=4,6$ . Limits scale as  $\lambda^{1/2}$ . However calculational scheme not well-defined without specification of high-scale theory. See the "Extra Dimensions Review."
- 59 HAN 00 calculates corrections to gauge boson self-energies from KK graviton loops and constrain them using  $S$  and  $T$ . Bounds on  $M_{TT}$  range from 0.5 TeV ( $\delta=6$ ) to 1.1 TeV ( $\delta=2$ ); see text. Limits have strong dependence,  $\lambda^{\delta+2}$ , on unknown  $\lambda$  coefficient.
- 60 MATHEWS 00 search for evidence of graviton exchange in CDF and DØ dijet production data. See their Table 2 for slightly stronger  $\delta$ -dependent bounds. Limits expressed in terms of  $M_S^4 = M_{TT}^4/8$ .
- 61 MELE 00 obtains bound from KK graviton contributions to  $e^+e^- \rightarrow VV$  ( $V=\gamma, W, Z$ ) at LEP. Authors use Hewett conventions.
- 62 ABBIENDI 99P search for s-channel graviton exchange effects in  $e^+e^- \rightarrow \gamma\gamma$  at  $E_{cm}=189$  GeV. The limits  $G_{\pm} > 660$  GeV and  $G_{\pm} > 634$  GeV are obtained from combined  $E_{cm}=183$  and 189 GeV data, where  $G_{\pm}$  is a scale related to the fundamental gravity scale.
- 63 ACCIARRI 99M search for the reaction  $e^+e^- \rightarrow \gamma G$  and s-channel graviton exchange effects in  $e^+e^- \rightarrow \gamma\gamma, W^+W^-, ZZ, e^+e^-, \mu^+\mu^-, \tau^+\tau^-, q\bar{q}$  at  $E_{cm}=183$  GeV. Limits on the gravity scale are listed in their Tables 1 and 2.
- 64 ACCIARRI 99S search for the reaction  $e^+e^- \rightarrow ZG$  and s-channel graviton exchange effects in  $e^+e^- \rightarrow \gamma\gamma, W^+W^-, ZZ, e^+e^-, \mu^+\mu^-, \tau^+\tau^-, q\bar{q}$  at  $E_{cm}=189$  GeV. Limits on the gravity scale are listed in their Tables 1 and 2.
- 65 BOURILKOV 99 performs global analysis of LEP data on  $e^+e^-$  collisions at  $\sqrt{s}=183$  and 189 GeV. Bound is on  $\Lambda_T$ .

### Direct Limits on Gravitational or String Mass Scale

This section includes limits on the fundamental gravitational scale and/or the string scale from processes which depend directly on one or the other of these scales.

VALUE (TeV)	DOCUMENT ID	TECN	COMMENT
$\bullet \bullet \bullet$ We do not use the following data for averages, fits, limits, etc. $\bullet \bullet \bullet$			
$> 1-2$	66 ANCHORDOQ.02B	RVUE	Cosmic Rays
$> 0.49$	67 ACCIARRI 00P L3		$e^+e^- \rightarrow e^+e^-$
66 ANCHORDOQ.02B			derive bound on $M_D$ from non-observation of black hole production in high-energy cosmic rays. Bound is stronger for larger $\delta$ , but depends sensitively on threshold for black hole production.
67 ACCIARRI 00P			uses $e^+e^-$ collisions at $\sqrt{s}=183$ and 189 GeV. Bound on string scale $M_S$ from massive string modes. $M_S$ is defined in hep-ph/0001166 by $M_S(1/\pi)^{1/8}\alpha^{-1/4} = M$ where $(4\pi G)^{-1} = M^2 + 2R^n$ .

### Limits on $1/R = M_C$

This section includes limits on  $1/R = M_C$ , the compactification scale in models with TeV extra dimensions, due to exchange of Standard Model KK excitations. Bounds assume fermions are not in the bulk, unless stated otherwise. See the "Extra Dimensions" review for discussion of model dependence.

VALUE (TeV)	CL%	DOCUMENT ID	TECN	COMMENT
$\bullet \bullet \bullet$ We do not use the following data for averages, fits, limits, etc. $\bullet \bullet \bullet$				
$> 0.729$	95	68 AAD	11F ATLS	$pp \rightarrow \gamma\gamma, \delta=6, M_D=5$ TeV
$> 0.961$	95	69 AAD	11X ATLS	$pp \rightarrow \gamma\gamma, \delta=6, M_D=5$ TeV
$> 0.477$	95	70 ABAZOV	10P D0	$p\bar{p} \rightarrow \gamma\gamma, \delta=6, M_D=5$ TeV
$> 1.59$	95	71 ABAZOV	09AE D0	$p\bar{p} \rightarrow$ dijet, angular dist.
$> 0.6$	95	72 HAISCH	07 RVUE	$\bar{B} \rightarrow X_s \gamma$
$> 0.6$	90	73 GOGOLADZE	06 RVUE	Electroweak
$> 3.3$	95	74 CORNET	00 RVUE	Electroweak
$> 3.3-3.8$	95	75 RIZZO	00 RVUE	Electroweak

- 68 AAD 11F use diphoton events with large missing transverse energy in 3.1 pb<sup>-1</sup> of data produced from  $pp$  collisions at  $\sqrt{s}=7$  TeV to place a lower bound on the compactification scale in a universal extra dimension model with gravitational decays. The bound assumes that the cutoff scale  $\Lambda$ , for the radiative corrections to the Kaluza-Klein masses, satisfies  $\Lambda/M_C=20$ . The model parameters are chosen such that the decay  $\gamma^* \rightarrow G\gamma$  occurs with an appreciable branching fraction.
- 69 AAD 11X use diphoton events with large missing transverse energy in 36 pb<sup>-1</sup> of data produced from  $pp$  collisions at  $\sqrt{s}=7$  TeV to place a lower bound on the compactification scale in a universal extra dimension model with gravitational decays. The bound assumes that the cutoff scale  $\Lambda$ , for the radiative corrections to the Kaluza-Klein masses, satisfies  $\Lambda/M_C=20$ . The model parameters are chosen such that the decay  $\gamma^* \rightarrow G\gamma$  occurs with an appreciable branching fraction.

- 70 ABAZOV 10P use diphoton events with large missing transverse energy in 6.3 fb<sup>-1</sup> of data produced from  $p\bar{p}$  collisions at  $\sqrt{s}=1.96$  TeV to place a lower bound on the compactification scale in a universal extra dimension model with gravitational decays. The bound assumes that the cutoff scale  $\Lambda$ , for the radiative corrections to the Kaluza-Klein masses, satisfies  $\Lambda/M_C=20$ . The model parameters are chosen such that the decay  $\gamma^* \rightarrow G\gamma$  occurs with an appreciable branching fraction.
- 71 ABAZOV 09AE use dijet angular distributions in 0.7 fb<sup>-1</sup> of data from  $p\bar{p}$  collisions at  $\sqrt{s}=1.96$  TeV to place a lower bound on the compactification scale.
- 72 HAISCH 07 use inclusive  $\bar{B}$ -meson decays to place a Higgs mass independent bound on the compactification scale  $1/R$  in the minimal universal extra dimension model.
- 73 GOGOLADZE 06 use electroweak precision observables to place a lower bound on the compactification scale in models with universal extra dimensions. Bound assumes a 115 GeV Higgs mass. See their Fig. 3 for the bound as a function of the Higgs mass.
- 74 CORNET 00 translates a bound on the coefficient of the 4-fermion operator  $(\bar{\ell}\gamma_\mu\tau^a\ell)(\bar{\ell}\gamma^\mu\tau^a\ell)$  derived by Hagiwara and Matsumoto into a limit on the mass scale of KK  $W$  bosons.
- 75 RIZZO 00 obtains limits from global electroweak fits in models with a Higgs in the bulk (3.8 TeV) or on the standard brane (3.3 TeV).

### Limits on Kaluza-Klein Gravitons in Warped Extra Dimensions

This section places limits on the mass of the first Kaluza-Klein (KK) excitation of the graviton in the warped extra dimension model of Randall and Sundrum. Experimental bounds depend strongly on the warp parameter,  $k$ . See the "Extra Dimensions" review for a full discussion.

Here we list limits for the value of the warp parameter  $k/\bar{M}_P = 0.1$ .

VALUE (GeV)	CL%	DOCUMENT ID	TECN	COMMENT
$> 1630$	95	76 AAD	11AD ATLS	$p\bar{p} \rightarrow G \rightarrow \ell\bar{\ell}$
$\bullet \bullet \bullet$ We do not use the following data for averages, fits, limits, etc. $\bullet \bullet \bullet$				
$> 1058$	95	77 AALTONEN	11G CDF	$p\bar{p} \rightarrow G \rightarrow ZZ$
$> 754$	95	78 AALTONEN	11R CDF	$p\bar{p} \rightarrow G \rightarrow e^+e^-, \gamma\gamma$
$> 1079$	95	79 ABAZOV	11H D0	$p\bar{p} \rightarrow G \rightarrow WW$
$> 607$		80 CHATRCHYAN 11	CMS	$p\bar{p} \rightarrow G \rightarrow \ell\bar{\ell}$
$> 1050$		81 AALTONEN	10N CDF	$p\bar{p} \rightarrow G \rightarrow WW$
		82 ABAZOV	10F D0	$p\bar{p} \rightarrow G \rightarrow e^+e^-, \gamma\gamma$
		83 AALTONEN	08S CDF	$p\bar{p} \rightarrow G \rightarrow ZZ$
$> 900$		84 ABAZOV	08J D0	$p\bar{p} \rightarrow G \rightarrow e^+e^-, \gamma\gamma$
		85 AALTONEN	07G CDF	$p\bar{p} \rightarrow G \rightarrow \gamma\gamma$
$> 889$		86 AALTONEN	07H CDF	$p\bar{p} \rightarrow G \rightarrow e\bar{e}$
$> 785$		87 ABAZOV	05N D0	$p\bar{p} \rightarrow G \rightarrow \ell\ell, \gamma\gamma$
$> 710$		88 ABULENCIA	05A CDF	$p\bar{p} \rightarrow G \rightarrow \ell\bar{\ell}$

- 76 AAD 11AD use 1.08 and 1.21 fb<sup>-1</sup> of data from  $pp$  collisions at  $\sqrt{s}=7$  TeV in the dielectron and dimuon channels, respectively, to place a lower bound on the mass of the lightest graviton. For warp parameter values  $k/\bar{M}_P$  between 0.01 to 0.1 the lower limit on the mass of the lightest graviton is between 0.71 and 1.63 TeV. See their Table IV for more details.
- 77 AALTONEN 11G use 2.5-2.9 fb<sup>-1</sup> of data from  $p\bar{p}$  collisions at  $\sqrt{s}=1.96$  TeV to search for KK gravitons in a warped extra dimension decaying to  $ZZ$  dibosons via the  $eee, ee\mu\mu, \mu\mu\mu\mu, eejj,$  and  $\mu\mu jj$  channels. See their Fig. 20 for limits on the cross section  $\sigma(G \rightarrow ZZ)$  as a function of the graviton mass.
- 78 AALTONEN 11R uses 5.7 fb<sup>-1</sup> of data from  $p\bar{p}$  collisions at  $\sqrt{s}=1.96$  TeV in the dielectron channel to place a lower bound on the mass of the lightest graviton. It provides combined limits with the diphoton channel analysis of AALTONEN 11U. For warp parameter values  $k/\bar{M}_P$  between 0.01 to 0.1 the lower limit on the mass of the lightest graviton is between 612 and 1058 GeV. See their Table I for more details.
- 79 ABAZOV 11H use 5.4 fb<sup>-1</sup> of data from  $p\bar{p}$  collisions at  $\sqrt{s}=1.96$  TeV to place a lower bound on the mass of the lightest graviton. Their 95% C.L. exclusion limit does not include masses less than 300 GeV.
- 80 CHATRCHYAN 11 use 35 and 40 pb<sup>-1</sup> of data from  $pp$  collisions at  $\sqrt{s}=7$  TeV in the dielectron and dimuon channels, respectively, to place a lower bound on the mass of the lightest graviton. For a warp parameter value  $k/\bar{M}_P = 0.05$ , the lower limit on the mass of the lightest graviton is 0.855 TeV.
- 81 AALTONEN 10N use 2.9 fb<sup>-1</sup> of data from  $p\bar{p}$  collisions at  $\sqrt{s}=1.96$  TeV to place a lower bound on the mass of the lightest graviton.
- 82 ABAZOV 10F use 5.4 fb<sup>-1</sup> of data from  $p\bar{p}$  collisions at  $\sqrt{s}=1.96$  TeV to place a lower bound on the mass of the lightest graviton. For warp parameter values of  $k/\bar{M}_P$  between 0.01 and 0.1 the lower limit on the mass of the lightest graviton is between 560 and 1050 GeV. See their Fig. 3 for more details.
- 83 AALTONEN 08S use  $p\bar{p}$  collisions at  $\sqrt{s}=1.96$  TeV to search for KK gravitons in warped extra dimensions. They search for graviton resonances decaying to four electrons via two  $Z$  bosons using 1.1 fb<sup>-1</sup> of data. See their Fig. 8 for limits on  $\sigma \cdot B(G \rightarrow ZZ)$  versus the graviton mass.
- 84 ABAZOV 08J use  $p\bar{p}$  collisions at  $\sqrt{s}=1.96$  TeV to search for KK gravitons in warped extra dimensions. They search for graviton resonances decaying to electrons and photons using 1 fb<sup>-1</sup> of data. For warp parameter values of  $k/\bar{M}_P$  between 0.01 and 0.1 the lower limit on the mass of the lightest excitation is between 300 and 900 GeV. See their Fig. 4 for more details.
- 85 AALTONEN 07G use  $p\bar{p}$  collisions at  $\sqrt{s}=1.96$  TeV to search for KK gravitons in warped extra dimensions. They search for graviton resonances decaying to photons using 1.2 fb<sup>-1</sup> of data. For warp parameter values of  $k/\bar{M}_P = 0.1, 0.05,$  and  $0.01$  the bounds on the graviton mass are 850, 694, and 230 GeV, respectively. See their Fig. 3 for more details. See also AALTONEN 07H.
- 86 AALTONEN 07H use  $p\bar{p}$  collisions at  $\sqrt{s}=1.96$  TeV to search for KK gravitons in warped extra dimensions. They search for graviton resonances decaying to electrons using 1.3 fb<sup>-1</sup> of data. For a warp parameter value of  $k/\bar{M}_P = 0.1$  the bound on the graviton mass is 807 GeV. See their Fig. 4 for more details. A combined analysis with the diphoton data of AALTONEN 07G yields for  $k/\bar{M}_P = 0.1$  a graviton mass lower bound of 889 GeV.
- 87 ABAZOV 05N use  $p\bar{p}$  collisions at  $\sqrt{s}=1.96$  TeV to search for KK gravitons in warped extra dimensions. They search for graviton resonances decaying to muons, electrons or photons, using 260 pb<sup>-1</sup> of data. For warp parameter values of  $k/\bar{M}_P = 0.1, 0.05,$  and

## Searches Particle Listings

## Extra Dimensions, WIMPs and Other Particle Searches

0.01, the bounds on the graviton mass are 785, 650 and 250 GeV respectively. See their Fig. 3 for more details.

<sup>88</sup> ABULENCIA 05A use  $p\bar{p}$  collisions at  $\sqrt{s} = 1.96$  TeV to search for KK gravitons in warped extra dimensions. They search for graviton resonances decaying to muons or electrons, using  $200 \text{ pb}^{-1}$  of data. For warp parameter values of  $k/\sqrt{M_P} = 0.1, 0.05,$  and  $0.01$ , the bounds on the graviton mass are 710, 510 and 170 GeV respectively.

## Limits on Mass of Radion

This section includes limits on mass of radion, usually in context of Randall-Sundrum models. See the "Extra Dimension Review" for discussion of model dependence.

VALUE (GeV)	DOCUMENT ID	TECN	COMMENT
-------------	-------------	------	---------

• • • We do not use the following data for averages, fits, limits, etc. • • •

$> 35$	<sup>89</sup> ABBIENDI	05	OPAL $e^+e^- \rightarrow Z$ radion
$> 120$	<sup>90</sup> MAHANTA	00	$Z \rightarrow$ radion $\ell\bar{\ell}$
	<sup>91</sup> MAHANTA	00B	$p\bar{p} \rightarrow$ radion $\rightarrow \gamma\gamma$
<sup>89</sup> ABBIENDI 05	use $e^+e^-$ collisions at $\sqrt{s} = 91$ GeV and $\sqrt{s} = 189\text{--}209$ GeV to place bounds on the radion mass in the RS model. See their Fig. 5 for bounds that depend on the radion-Higgs mixing parameter $\xi$ and on $\Lambda_{WV} = \Lambda_\phi/\sqrt{6}$ . No parameter-independent bound is obtained.		
<sup>90</sup> MAHANTA 00	obtain bound on radion mass in the RS model. Bound is from Higgs boson search at LEP I.		
<sup>91</sup> MAHANTA 00B	uses $p\bar{p}$ collisions at $\sqrt{s} = 1.8$ TeV; production via gluon-gluon fusion. Authors assume a radion vacuum expectation value of 1 TeV.		

## REFERENCES FOR Extra Dimensions

AAD	11AD	PRL 107 272002	G. Aad <i>et al.</i>	(ATLAS Collab.)
AAD	11F	PRL 106 121803	G. Aad <i>et al.</i>	(ATLAS Collab.)
AAD	11S	PL B705 294	G. Aad <i>et al.</i>	(ATLAS Collab.)
AAD	11X	EPJ C71 1744	G. Aad <i>et al.</i>	(ATLAS Collab.)
AALTONEN	11G	PR D83 112008	T. Aaltonen <i>et al.</i>	(CDF Collab.)
AALTONEN	11R	PRL 107 051801	T. Aaltonen <i>et al.</i>	(CDF Collab.)
AALTONEN	11U	PR D83 011102	T. Aaltonen <i>et al.</i>	(CDF Collab.)
AARON	11C	PL B705 52	F. D. Aaron <i>et al.</i>	(H1 Collab.)
ABAZOV	11H	PRL 107 011801	V. M. Abazov <i>et al.</i>	(DO Collab.)
BEZERRA	11	PR D83 075004	V.B. Bezerra <i>et al.</i>	
CHATRCHYAN	11	JHEP 1105 093	S. Chatrchyan <i>et al.</i>	(CMS Collab.)
CHATRCHYAN	11A	JHEP 1105 085	S. Chatrchyan <i>et al.</i>	(CMS Collab.)
CHATRCHYAN	11U	PRL 107 201804	S. Chatrchyan <i>et al.</i>	(CMS Collab.)
SUSHKOV	11	PRL 107 171101	A.O. Sushkov <i>et al.</i>	
AALTONEN	10N	PRL 104 241801	T. Aaltonen <i>et al.</i>	(CDF Collab.)
ABAZOV	10F	PRL 104 241802	V.M. Abazov <i>et al.</i>	(DO Collab.)
ABAZOV	10P	PRL 105 221802	V.M. Abazov <i>et al.</i>	(DO Collab.)
BEZERRA	10	PR D81 055003	V.B. Bezerra <i>et al.</i>	
ABAZOV	09AE	PRL 103 191803	V.M. Abazov <i>et al.</i>	(DO Collab.)
ABAZOV	09D	PRL 102 051601	V.M. Abazov <i>et al.</i>	(DO Collab.)
MASUDA	09	PRL 102 171101	M. Masuda, M. Sasaki	(ICRR)
AALTONEN	08AC	PRL 101 181602	T. Aaltonen <i>et al.</i>	(CDF Collab.)
AALTONEN	08S	PR D78 012008	T. Aaltonen <i>et al.</i>	(CDF Collab.)
ABAZOV	08J	PRL 100 091802	V.M. Abazov <i>et al.</i>	(DO Collab.)
ABAZOV	08S	PRL 101 011601	V.M. Abazov <i>et al.</i>	(DO Collab.)
DAS	08	PR D78 063011	P.K. Das, V.H.S. Kumar, P.K. Suresh	
GERACI	08	PR D78 022002	A.A. Geraci <i>et al.</i>	(STAN)
TRENKEL	08	PR D77 122001	C. Trenkel	
AALTONEN	07G	PRL 99 171801	T. Aaltonen <i>et al.</i>	(CDF Collab.)
AALTONEN	07H	PRL 99 171802	T. Aaltonen <i>et al.</i>	(CDF Collab.)
DECCA	07A	EPJ C51 963	R.S. Decca <i>et al.</i>	
HAISCH	07	PR D76 034014	U. Haisch, A. Weiler	
KAPNER	07	PRL 98 021101	D.J. Kapner <i>et al.</i>	
SCHAEF	07A	EPJ C49 411	S. Schaefer <i>et al.</i>	(ALEPH Collab.)
TU	07	PRL 98 201101	L.C. Tu <i>et al.</i>	
ABDALLAH	06C	EPJ C45 589	J. Abdallah <i>et al.</i>	(DELPHI Collab.)
ABULENCIA	06	PRL 97 171802	A. Abulencia <i>et al.</i>	(CDF Collab.)
GERDES	06	PR D73 112008	D. Gerdes <i>et al.</i>	
GOGOLADZE	06	PR D74 093012	I. Gogoladze, C. Macesanu	
ABAZOV	05N	PRL 95 091801	V.M. Abazov <i>et al.</i>	(DO Collab.)
ABAZOV	05V	PRL 95 161602	V.M. Abazov <i>et al.</i>	(DO Collab.)
ABBIENDI	05	PL B609 20	G. Abbiendi <i>et al.</i>	(OPAL Collab.)
ABDALLAH	05B	EPJ C38 395	J. Abdallah <i>et al.</i>	(DELPHI Collab.)
ABULENCIA	05A	PRL 95 252001	A. Abulencia <i>et al.</i>	(CDF Collab.)
SMULLIN	05	PR D72 122001	S.J. Smullin <i>et al.</i>	
ACHARD	04E	PL B587 16	P. Achard <i>et al.</i>	(L3 Collab.)
ACOSTA	04C	PRL 92 121802	D. Acosta <i>et al.</i>	(CDF Collab.)
CASSE	04	PRL 92 111102	M. Casse <i>et al.</i>	
CHEKANOV	04B	PL B591 23	S. Chekanov <i>et al.</i>	(ZEUS Collab.)
HOYLE	04	PR D70 042004	C.D. Hoyle <i>et al.</i>	(WASH)
ABAZOV	03	PRL 90 251802	V.M. Abazov <i>et al.</i>	(DO Collab.)
ABBIENDI	03D	EPJ C26 331	G. Abbiendi <i>et al.</i>	(OPAL Collab.)
ACHARD	03D	PL B572 133	P. Achard <i>et al.</i>	(L3 Collab.)
ADLOFF	03	PL B568 35	C. Adloff <i>et al.</i>	(H1 Collab.)
CHIAVERINI	03	PRL 90 151101	J. Chilverini <i>et al.</i>	
GIUDICE	03	NP B463 377	G.F. Giudice, A. Strumia	
HANNENSTAD	03	PR D67 125008	S. Hannestad, G.G. Raffelt	
Also	PR D69 029901(Erratum)	S. Hannestad, G.G. Raffelt		
HEISTER	03C	EPJ C28 1	A. Heister <i>et al.</i>	(ALEPH Collab.)
LONG	03	Nature 421 922	J.C. Long <i>et al.</i>	
ACHARD	02	PL B524 65	P. Achard <i>et al.</i>	(L3 Collab.)
ACHARD	02D	PL B531 28	P. Achard <i>et al.</i>	(L3 Collab.)
ANCHORDOQUI	02B	PR D66 103002	L. Anchordoqui <i>et al.</i>	
HANNENSTAD	02	PRL 88 071301	S. Hannestad, G. Raffelt	
ABBOTT	01	PRL 86 1156	B. Abbott <i>et al.</i>	(DO Collab.)
FAIRBAIRN	01	PL B508 335	M. Fairbairn	
HANHART	01	PL B509 1	C. Hanhart <i>et al.</i>	
HOYLE	01	PRL 86 1418	C.D. Hoyle <i>et al.</i>	
ABBIENDI	00R	EPJ C13 553	G. Abbiendi <i>et al.</i>	(OPAL Collab.)
ABREU	00A	PL B491 67	P. Abreu <i>et al.</i>	(DELPHI Collab.)
ABREU	00S	PL B485 45	P. Abreu <i>et al.</i>	(DELPHI Collab.)
ABREU	00Z	EPJ C17 53	P. Abreu <i>et al.</i>	(DELPHI Collab.)
ACCIARRI	00P	PL B489 81	M. Acciarri <i>et al.</i>	(L3 Collab.)
CASSISI	00	PL B481 323	S. Cassisi <i>et al.</i>	
CHANG	00B	PRL 85 3765	L.N. Chang <i>et al.</i>	
CHEUNG	00	PR D61 015005	K. Cheung	
CORNET	00	PR D61 037701	F. Cornet, M. Relano, J. Rico	
GRÄSSER	00	PR D61 074019	M.L. Graesser	
HAN	00	PR D62 125018	T. Han, D. Marfatia, R.-J. Zhang	
MAHANTA	00	PL B480 176	U. Mahanta, S. Rakshit	
MAHANTA	00B	PL B483 196	U. Mahanta, A. Datta	
MATHEWS	00	JHEP 0007 008	P. Mathews, S. Raychaudhuri, K. Sridhar	
MELE	00	PR D61 117901	S. Mele, E. Sanchez	

RIZZO	00	PR D61 016007	T.G. Rizzo, J.D. Wells	
ABBIENDI	99P	PL B465 303	G. Abbiendi <i>et al.</i>	(OPAL Collab.)
ACCIARRI	99M	PL B464 135	M. Acciarri <i>et al.</i>	(L3 Collab.)
ACCIARRI	99R	PL B470 268	M. Acciarri <i>et al.</i>	(L3 Collab.)
ACCIARRI	99S	PL B470 281	M. Acciarri <i>et al.</i>	(L3 Collab.)
BOURILKOV	99	JHEP 9908 006	D. Bourilkov	
HOSKINS	85	PR D32 3084	J.K. Hoskins <i>et al.</i>	

## WIMPs and Other Particles Searches for

OMITTED FROM SUMMARY TABLE  
WIMPS AND OTHER PARTICLE SEARCHES

Revised March 2012 by K. Hikasa (Tohoku University).

We collect here those searches which do not appear in any of the above search categories. These are listed in the following order:

1. Galactic WIMP (weakly-interacting massive particle) searches
2. Concentration of stable particles in matter
3. General new physics searches
4. Limits on jet-jet resonance in hadron collisions
5. Limits on neutral particle production at accelerators
6. Limits on charged particles in  $e^+e^-$  collisions
7. Limits on charged particles in hadron reactions
8. Limits on charged particles in cosmic rays

Note that searches appear in separate sections elsewhere for Higgs bosons (and technipions), other heavy bosons (including  $W_R, W', Z'$ , leptoquarks, axiglons), axions (including pseudo-Goldstone bosons, Majorons, familons), heavy leptons, heavy neutrinos, free quarks, monopoles, supersymmetric particles, and compositeness. We include specific WIMP searches in the appropriate sections when they yield limits on hypothetical particles such as supersymmetric particles, axions, massive neutrinos, monopoles, *etc.*

We omit papers on CHAMP's, millicharged particles, and other exotic particles. We no longer list for limits on tachyons and centauros. See our 1994 edition for these limits.

## GALACTIC WIMP SEARCHES

Cross-Section Limits for Dark Matter Particles ( $X^0$ ) on Nuclei

These limits are for weakly-interacting stable particles that may constitute the invisible mass in the galaxy. Unless otherwise noted, a local mass density of  $0.3 \text{ GeV/cm}^3$  is assumed; see each paper for velocity distribution assumptions. In the papers the limit is given as a function of the  $X^0$  mass. Here we list limits only for typical mass values of 20 GeV, 100 GeV, and 1 TeV. Specific limits on supersymmetric dark matter particles may be found in the Supersymmetry section.

For  $m_{X^0} = 20 \text{ GeV}$ 

VALUE (nb)	CL%	DOCUMENT ID	TECN	COMMENT
------------	-----	-------------	------	---------

• • • We do not use the following data for averages, fits, limits, etc. • • •

1	AALSETH	11	CGNT	Ge
2	AALSETH	11A	CGNT	Ge
3	AHLEN	11	DMTP	CF <sub>4</sub>
4	AHMED	11	CDM2	Ge, inelastic
5	AHMED	11A	RVUE	Ge
6	AHMED	11B	CDM2	Ge, low threshold
7	ANGLE	11	XE10	Xe
8	APRILE	11	X100	Xe
9	APRILE	11B	X100	Xe
10	BEHNKE	11	COUP	CF <sub>3</sub> I
11	HORN	11	ZEP3	Xe
12	TANAKA	11	SKAM	H, solar $\nu$
13	AKERIB	10	CDM2	Si, Ge, low threshold
14	APRILE	10	X100	Xe
15	ARMENGAUD	10	EDE2	Ge

		16	FELIZARDO	10	SMPL	C <sub>2</sub> ClF <sub>3</sub>
		17	AHMED	09	CDM2	Ge
		18	ARCHAMBAU..09	PICA	F	
		19	LEBEDENKO	09A	ZEP3	Xe
		20	LIN	09	TEXO	Ge
		21	AALSETH	08	CGNT	Ge
		22	ANGLE	08A	XE10	Xe
		23	ALNER	07	ZEP2	Xe
		24	LEE	07A	KIMS	Csl
		25	AKERIB	06	CDMS	<sup>73</sup> Ge, <sup>29</sup> Si
		26	SHIMIZU	06A	CNTR	F (CaF <sub>2</sub> )
		27	ALNER	05	NAIA	Nal
		28	BARNABE-HE..05	PICA	F (C <sub>4</sub> F <sub>10</sub> )	
		29	BENOIT	05	EDEL	<sup>73</sup> Ge
		30	GIRARD	05	SMPL	F (C <sub>2</sub> ClF <sub>3</sub> )
		31	KLAPDOR-K...05	HDMS	<sup>73</sup> Ge (enriched)	
		32	MIUCHI	03	BOLO	LiF
		33	TAKEDA	03	BOLO	NaF
< 0.08	90	34	ANGLOHER	02	CRES	Al
		35	BENOIT	00	EDEL	Ge
< 0.04	95	36	KLIMENKO	98	CNTR	<sup>73</sup> Ge, inel.
< 0.8			ALESSAND...	96	CNTR	O
< 6			ALESSAND...	96	CNTR	Te
< 0.02	90	37	BELLI	96	CNTR	<sup>129</sup> Xe, inel.
		38	BELLI	96c	CNTR	<sup>129</sup> Xe
< 0.004	90	39	BERNABEI	96	CNTR	Na
< 0.3	90	39	BERNABEI	96	CNTR	I
< 0.2	95	40	SARSA	96	CNTR	Na
< 0.015	90	41	SMITH	96	CNTR	Na
< 0.05	95	42	GARCIA	95	CNTR	Natural Ge
< 0.1	95		QUENBY	95	CNTR	Na
< 90	90	43	SNOWDEN...	95	MICA	<sup>16</sup> O
< 4 × 10 <sup>3</sup>	90	43	SNOWDEN...	95	MICA	<sup>39</sup> K
< 0.7	90		BACCI	92	CNTR	Na
< 0.12	90	44	REUSSER	91	CNTR	Natural Ge
< 0.06	95		CALDWELL	88	CNTR	Natural Ge

- 1 AALSETH 11 give  $\sigma < 5 \times 10^{-5}$  pb (90% CL) for spin-independent  $X^0$ -nucleon cross section. See their Fig. 4 for limits extending to  $m_{X^0} = 3.5$  GeV.
- 2 AALSETH 11A find indications of annual modulation of the data, the energy spectrum being compatible with  $X^0$  mass around 8 GeV.
- 3 AHLEN 11 give  $\sigma < 1 \times 10^5$  pb (90% CL) for spin-dependent  $X^0$ -proton cross section.
- 4 AHMED 11 search for  $X^0$  inelastic scattering. See their Figs. 8-10 for limits.
- 5 AHMED 11A combine CDMS and EDELWEISS data and give  $\sigma < 2.7 \times 10^{-7}$  pb (90% CL) for spin-independent  $X^0$ -nucleon cross section.
- 6 AHMED 11B give limits on spin-independent  $X^0$ -nucleon and spin-dependent  $X^0$ -neutron cross section for  $m_{X^0} = 4-12$  GeV in the range  $10^{-5}-10^{-3}$  pb and  $10-10^3$  pb, respectively. See their Fig. 3.
- 7 ANGLE 11 give  $\sigma < 5 \times 10^{-7}$  pb (90% CL) for spin-independent  $X^0$ -nucleon cross section. See their Fig. 3 for limits down to  $m_{X^0} = 4$  GeV.
- 8 APRILE 11 reanalyze APRILE 10 data and give  $\sigma < 7 \times 10^{-8}$  pb (90% CL) for spin-independent  $X^0$ -nucleon cross section.
- 9 APRILE 11B give  $\sigma < 2 \times 10^{-8}$  pb (90% CL) for spin-independent  $X^0$ -nucleon cross section.
- 10 BEHNKE 11 give  $\sigma < 0.1$  pb (90% CL) for spin-dependent  $X^0$ -proton cross section with a direction sensitive detector.
- 11 HORN 11 perform detector calibration by neutrons. Earlier results are only marginally affected.
- 12 TANAKA 11 search for neutrinos produced by  $X^0$  annihilation in the Sun and give  $\sigma < 1.5 \times 10^{-2}$  pb (90% CL) (for  $m_{X^0} = 10$  GeV) for spin-dependent  $X^0$ -proton cross section, assuming that  $X^0$  pairs annihilate to  $b\bar{b}$ .
- 13 AKERIB 10 give  $\sigma < 1 \times 10^{-5}$  pb (90% CL) for spin-independent  $X^0$ -nucleon cross section. See their Figs. 10 and 12 for limits extending to  $X^0$  mass of 1 GeV.
- 14 APRILE 10 give  $\sigma < 1 \times 10^{-7}$  pb (90% CL) for spin-independent  $X^0$ -nucleon cross section.
- 15 ARMENGAUD 10 give  $\sigma < 2 \times 10^{-6}$  pb (90% CL) for spin-independent  $X^0$ -nucleon cross section.
- 16 FELIZARDO 10 give  $\sigma < 4 \times 10^{-5}$  pb (90% CL) for spin-independent  $X^0$ -nucleon cross section.
- 17 AHMED 09 give  $\sigma < 0.06$  pb (90% CL) for spin-dependent  $X^0$ -neutron cross section.
- 18 ARCHAMBAULT 09 give  $\sigma < 0.2$  pb (90% CL) for spin-dependent  $X^0$ -proton cross section.
- 19 LEBEDENKO 09A give  $\sigma < 4$  (0.04) pb (90% CL) for spin-dependent  $X^0$ -proton (neutron) cross section.
- 20 See their Fig. 6(b) for limits on spin-dependent  $X^0$ -neutron cross section for  $m_{X^0}$  between 2 and 10 GeV.
- 21 See their Fig. 2 for cross section limits for  $m_{X^0}$  between 4 and 10 GeV.
- 22 ANGLE 08A give  $\sigma < 0.6$  (0.007) pb (90% CL) for spin-dependent  $X^0$ -proton (neutron) cross section.
- 23 ALNER 07 give  $\sigma < 100$  (0.5) pb (90% CL) for spin-dependent  $X^0$ -proton (neutron) cross section.
- 24 LEE 07A give  $\sigma < 1$  (25) pb (90% CL) for spin-dependent  $X^0$ -proton (neutron) cross section.
- 25 AKERIB 06 give  $\sigma < 20$  (0.3) pb (90% CL) for spin-dependent  $X^0$ -proton (neutron) cross section. See also AKERIB 05.
- 26 SHIMIZU 06A give  $\sigma < 2$  (30) pb (90% CL) for spin-dependent  $X^0$ -proton (neutron) cross section.
- 27 ALNER 05 give  $\sigma < 0.5$  (60) pb (90% CL) for spin-dependent  $X^0$ -proton (neutron) cross section.

- 28 BARNABE-HEIDER 05 give  $\sigma < 1.5$  (20) pb (90% CL) for spin-dependent  $X^0$ -proton (neutron) cross section.
- 29 BENOIT 05 give  $\sigma < 10$  pb (90% CL) for spin-dependent  $X^0$ -neutron cross section.
- 30 GIRARD 05 give  $\sigma < 1.5$  pb (90% CL) for spin-dependent  $X^0$ -proton cross section.
- 31 KLAPDOR-KLEINGROTHAUS 05 give  $\sigma < 4$  pb (90% CL) for spin-dependent  $X^0$ -neutron cross section.
- 32 MIUCHI 03 give model-independent limit  $\sigma < 35$  pb (90% CL) for spin-dependent  $X^0$ -proton cross section.
- 33 TAKEDA 03 give model-independent limit  $\sigma < 0.03$  (0.6) nb (90% CL) for spin-dependent  $X^0$ -proton (neutron) cross section.
- 34 ANGLOHER 02 limit is for spin-dependent WIMP-Aluminum cross section.
- 35 BENOIT 00 find four event categories in Ge detectors and suggest that low-energy surface nuclear recoils can explain anomalous events reported by UKDMC and Saclay Nal experiments.
- 36 KLIMENKO 98 limit is for inelastic scattering  $X^0 \ ^{73}\text{Ge} \rightarrow X^0 \ ^{73}\text{Ge}^*$  (13.26 keV).
- 37 BELLI 96 limit for inelastic scattering  $X^0 \ ^{129}\text{Xe} \rightarrow X^0 \ ^{129}\text{Xe}^*$  (39.58 keV).
- 38 BELLI 96c use background subtraction and obtain  $\sigma < 150$  pb ( $< 1.5$  fb) (90% CL) for spin-dependent (independent)  $X^0$ -proton cross section. The confidence level is from R. Bernabei, private communication, May 20, 1999.
- 39 BERNABEI 96 use pulse shape discrimination to enhance the possible signal. The limit here is from R. Bernabei, private communication, September 19, 1997.
- 40 SARSA 96 search for annual modulation of WIMP signal. See SARSA 97 for details of the analysis. The limit here is from M.L. Sarsa, private communication, May 26, 1997.
- 41 SMITH 96 use pulse shape discrimination to enhance the possible signal. A dark matter density of  $0.4 \text{ GeV cm}^{-3}$  is assumed.
- 42 GARCIA 95 limit is from the event rate. A weaker limit is obtained from searches for diurnal and annual modulation.
- 43 SNOWDEN-IFFT 95 look for recoil tracks in an ancient mica crystal. Similar limits are also given for <sup>27</sup>Al and <sup>28</sup>Si. See COLLAR 96 and SNOWDEN-IFFT 96 for discussion on potential backgrounds.
- 44 REUSSER 91 limit here is changed from published (0.04) after reanalysis by authors. J.L. Vuilleumier, private communication, March 29, 1996.

For  $m_{X^0} = 100 \text{ GeV}$

VALUE (nb)	CL%	DOCUMENT ID	TECN	COMMENT		
•••				We do not use the following data for averages, fits, limits, etc. •••		
		1	AALSETH	11	CGNT	Ge
		2	AHLEN	11	DMTP	CF <sub>4</sub>
		3	AHMED	11	CDM2	Ge, inelastic
		4	AHMED	11A	RVUE	Ge
		5	AJELLO	11	FLAT	
		6	APRILE	11	X100	Xe
		7	APRILE	11A	X100	Xe, inelastic
		8	APRILE	11B	X100	Xe
		9	ARMENGAUD	11	EDE2	Ge
		10	BEHNKE	11	COUP	CF <sub>3</sub> I
		11	HORN	11	ZEP3	Xe
		12	TANAKA	11	SKAM	H, solar $\nu$
		13	AKERIB	10	CDM2	Si, Ge, low threshold
		14	AKIMOV	10	ZEP3	Xe, inelastic scattering
		15	APRILE	10	X100	Xe
		16	ARMENGAUD	10	EDE2	Ge
		17	FELIZARDO	10	SMPL	C <sub>2</sub> ClF <sub>3</sub>
		18	MIUCHI	10	NAGE	CF <sub>4</sub>
		19	AHMED	09	CDM2	Ge
		20	ANGLE	09	XE10	Xe, inelastic
		21	ARCHAMBAU..09	PICA	F	
		22	LEBEDENKO	09A	ZEP3	Xe
		23	ANGLE	08A	XE10	Xe
		24	BEDNYAKOV	08	RVUE	Ge
		25	ALNER	07	ZEP2	Xe
		26	LEE	07A	KIMS	Csl
		27	MIUCHI	07	CNTR	F (CF <sub>4</sub> )
		28	AKERIB	06	CDMS	<sup>73</sup> Ge, <sup>29</sup> Si
		29	SHIMIZU	06A	CNTR	F (CaF <sub>2</sub> )
		30	ALNER	05	NAIA	Nal
		31	BARNABE-HE..05	PICA	F (C <sub>4</sub> F <sub>10</sub> )	
		32	BENOIT	05	EDEL	<sup>73</sup> Ge
		33	GIRARD	05	SMPL	F (C <sub>2</sub> ClF <sub>3</sub> )
		34	GIULIANI	05	RVUE	
		35	GIULIANI	05A	RVUE	
		36	KLAPDOR-K...05	HDMS	<sup>73</sup> Ge (enriched)	
		37	GIULIANI	04	RVUE	
		38	GIULIANI	04A	RVUE	
		39	MIUCHI	03	BOLO	LiF
		40	MIUCHI	03	BOLO	LiF
		41	TAKEDA	03	BOLO	NaF
< 0.3	90	42	ANGLOHER	02	CRES	Al
		43	BELLI	02	RVUE	
		44	BERNABEI	02c	DAMA	
		45	GREEN	02	RVUE	
		46	ULLIO	01	RVUE	
		47	BENOIT	00	EDEL	Ge
< 0.004	90	48	BERNABEI	00d		<sup>129</sup> Xe, inel.
		49	AMBROSIO	99	MCRO	
		50	BRHLIK	99	RVUE	
< 0.008	95	51	KLIMENKO	98	CNTR	<sup>73</sup> Ge, inel.

# Searches Particle Listings

## WIMPs and Other Particle Searches

< 0.08	95	52	KLIMENKO	98	CNTR	<sup>73</sup> Ge, inel.
< 4			ALESSAND...	96	CNTR	O
< 25			ALESSAND...	96	CNTR	Te
< 0.006	90	53	BELLI	96	CNTR	<sup>129</sup> Xe, inel.
		54	BELLI	96c	CNTR	<sup>129</sup> Xe
< 0.001	90	55	BERNABEI	96	CNTR	Na
< 0.3	90	55	BERNABEI	96	CNTR	I
< 0.7	95	56	SARSA	96	CNTR	Na
< 0.03	90	57	SMITH	96	CNTR	Na
< 0.8	90	57	SMITH	96	CNTR	I
< 0.35	95	58	GARCIA	95	CNTR	Natural Ge
< 0.6	95		QUENBY	95	CNTR	Na
< 3	95		QUENBY	95	CNTR	I
< 1.5 × 10 <sup>2</sup>	90	59	SNOWDEN...	95	MICA	<sup>16</sup> O
< 4 × 10 <sup>2</sup>	90	59	SNOWDEN...	95	MICA	<sup>39</sup> K
< 0.08	90	60	BECK	94	CNTR	<sup>76</sup> Ge
< 2.5	90		BACCI	92	CNTR	Na
< 3	90		BACCI	92	CNTR	I
< 0.9	90	61	REUSSER	91	CNTR	Natural Ge
< 0.7	95		CALDWELL	88	CNTR	Natural Ge

- 1 AALSETH 11 give  $\sigma < 2 \times 10^{-4}$  pb (90% CL) for spin-independent  $X^0$ -nucleon cross section.
- 2 AHLEN 11 give  $\sigma < 2 \times 10^3$  pb (90% CL) for spin-dependent  $X^0$ -proton cross section.
- 3 AHMED 11 search for  $X^0$  inelastic scattering. See their Figs. 8–10 for limits.
- 4 AHMED 11A combine CDMS and EDELWEISS data and give  $\sigma < 3.3 \times 10^{-8}$  pb (90% CL) for spin-independent  $X^0$ -nucleon cross section.
- 5 AJELLO 11 search for  $e^\pm$  flux from  $X^0$  annihilations in the Sun. Models in which  $X^0$  annihilates into an intermediate long-lived weakly interacting particles or  $X^0$  scatters inelastically are constrained. See their Figs. 6–8 for limits.
- 6 APRILE 11 reanalyze APRILE 10 data and give  $\sigma < 3 \times 10^{-8}$  pb (90% CL) for spin-independent  $X^0$ -nucleon cross section.
- 7 APRILE 11A search for  $X^0$  inelastic scattering. See their Figs. 2 and 3 for limits.
- 8 APRILE 11B give  $\sigma < 1 \times 10^{-8}$  pb (90% CL) for spin-independent  $X^0$ -nucleon cross section.
- 9 ARMENGAUD 11 give  $\sigma < 5 \times 10^{-8}$  pb (90% CL) for spin-independent  $X^0$ -nucleon cross section. Supersedes ARMENGAUD 10. A limit on inelastic cross section is also given.
- 10 BEHNKE 11 give  $\sigma < 0.07$  pb (90% CL) for spin-dependent  $X^0$ -proton cross section with a direction sensitive detector.
- 11 HORN 11 perform detector calibration by neutrons. Earlier results are only marginally affected.
- 12 TANAKA 11 search for neutrinos produced by  $X^0$  annihilation in the Sun and give  $\sigma < 2.7 \times 10^{-4}$  ( $4.5 \times 10^{-3}$ ) pb (90% CL) for spin-dependent  $X^0$ -proton cross section, if  $X^0$  pairs annihilate to  $W^+W^-$  ( $b\bar{b}$ ).
- 13 AKERIB 10 give  $\sigma < 9 \times 10^{-6}$  pb (90% CL) for spin-independent  $X^0$ -nucleon cross section.
- 14 AKIMOV 10 give cross section limits for inelastically scattering dark matter. See their Fig. 4.
- 15 APRILE 10 give  $\sigma < 5 \times 10^{-8}$  pb (90% CL) for spin-independent  $X^0$ -nucleon cross section.
- 16 ARMENGAUD 10 give  $\sigma < 1 \times 10^{-7}$  pb (90% CL) for spin-independent  $X^0$ -nucleon cross section.
- 17 FELIZARDO 10 give  $\sigma < 3 \times 10^{-5}$  pb (90% CL) for spin-independent  $X^0$ -nucleon cross section. See their Fig. 3 for limits on spin-dependent proton/neutron couplings for  $X^0$  mass of 50 GeV.
- 18 MIUCHI 10 give  $\sigma < 6 \times 10^3$  pb (90% CL) for spin-dependent  $X^0$ -proton cross section with a direction sensitive detector.
- 19 AHMED 09 give  $\sigma < 0.02$  pb (90% CL) for spin-dependent  $X^0$ -neutron cross section.
- 20 ANGLE 09 search for  $X^0$  inelastic scattering. See their Fig. 4 for limits.
- 21 ARCHAMBAULT 09 give  $\sigma < 0.4$  pb (90% CL) for spin-dependent  $X^0$ -proton cross section.
- 22 LEBEDENKO 09a give  $\sigma < 0.8$  (0.01) pb (90% CL) for spin-dependent  $X^0$ -proton (neutron) cross section.
- 23 ANGLE 08a give  $\sigma < 0.9$  (0.01) pb (90% CL) for spin-dependent  $X^0$ -proton (neutron) cross section.
- 24 BEDNYAKOV 08 reanalyze KLAPDOR-KLEINGROTHAUS 05 and BAUDIS 01 data and give  $\sigma < 0.05$  pb (90% CL) for spin-dependent  $X^0$ -neutron cross section.
- 25 ALNER 07 give  $\sigma < 15$  (0.08) pb (90% CL) for spin-dependent  $X^0$ -proton (neutron) cross section.
- 26 LEE 07a give  $\sigma < 0.2$  (6) pb (90% CL) for spin-dependent  $X^0$ -proton (neutron) cross section.
- 27 MIUCHI 07 give  $\sigma < 1 \times 10^4$  pb (90% CL) for spin-dependent  $X^0$ -proton cross section with a direction-sensitive detector.
- 28 AKERIB 06 give  $\sigma < 5$  (0.07) pb (90% CL) for spin-dependent  $X^0$ -proton (neutron) cross section. See also AKERIB 05.
- 29 SHIMIZU 06a give  $\sigma < 2$  (30) pb (90% CL) for spin-dependent  $X^0$ -proton (neutron) cross section.
- 30 ALNER 05 give  $\sigma < 0.3$  (10) pb (90% CL) for spin-dependent  $X^0$ -proton (neutron) cross section.
- 31 BARNABE-HEIDER 05 give  $\sigma < 2$  (30) pb (90% CL) for spin-dependent  $X^0$ -proton (neutron) cross section.
- 32 BENOIT 05 give  $\sigma < 100$  (0.7) pb (90% CL) for spin-dependent  $X^0$ -proton (neutron) cross section.
- 33 GIRARD 05 give  $\sigma < 1.5$  pb (90% CL) for spin-dependent  $X^0$ -proton cross section.
- 34 GIULIANI 05 analyzes the spin-independent  $X^0$ -nucleon cross section limits with both isoscalar and isovector couplings. See Figs. 3 and 4 for limits on the couplings.
- 35 GIULIANI 05a analyze available data and give combined limits  $\sigma < 0.7$  (0.2) pb for spin-dependent  $X^0$ -proton (neutron) cross section.
- 36 KLAPDOR-KLEINGROTHAUS 05 give  $\sigma < 1.5$  pb (90% CL) for spin-dependent  $X^0$ -neutron cross section.
- 37 GIULIANI 04 reanalyze COLLAR 00 data and give limits for spin-dependent  $X^0$ -proton and neutron couplings.

- 38 GIULIANI 04a gives limits for spin-dependent  $X^0$ -proton and neutron couplings from existing data.
- 39 MIUCHI 03 give model-independent limit for spin-dependent  $X^0$ -proton and neutron cross sections. See their Fig. 5.
- 40 MIUCHI 03 give model-independent limit  $\sigma < 35$  pb (90% CL) for spin-dependent  $X^0$ -proton cross section.
- 41 TAKEDA 03 give model-independent limit  $\sigma < 0.04$  (0.8) nb (90% CL) for spin-dependent  $X^0$ -proton (neutron) cross section.
- 42 ANGLÖHER 02 limit is for spin-dependent WIMP-Aluminum cross section.
- 43 BELLI 02 discuss dependence of the extracted WIMP cross section on the assumptions of the galactic halo structure.
- 44 BERNABEI 02c analyze the DAMA data in the scenario in which  $X^0$  scatters into a slightly heavier state as discussed by SMITH 01.
- 45 GREEN 02 discusses dependence of extracted WIMP cross section limits on the assumptions of the galactic halo structure.
- 46 ULLIO 01 disfavor the possibility that the BERNABEI 99 signal is due to spin-dependent WIMP coupling.
- 47 BENOIT 00 find four event categories in Ge detectors and suggest that low-energy surface nuclear recoils can explain anomalous events reported by UKDMC and Saclay NaI experiments.
- 48 BERNABEI 00b limit is for inelastic scattering  $X^0 129\text{Xe} \rightarrow X^0 129\text{Xe}^*$  (39.58 keV).
- 49 AMBROSIO 99 search for upgoing muon events induced by neutrinos originating from WIMP annihilations in the Sun and Earth.
- 50 BRHLIK 99 discuss the effect of astrophysical uncertainties on the WIMP interpretation of the BERNABEI 99 signal.
- 51 KLIMENKO 98 limit is for inelastic scattering  $X^0 73\text{Ge} \rightarrow X^0 73\text{Ge}^*$  (13.26 keV).
- 52 KLIMENKO 98 limit is for inelastic scattering  $X^0 73\text{Ge} \rightarrow X^0 73\text{Ge}^*$  (66.73 keV).
- 53 BELLI 96 limit for inelastic scattering  $X^0 129\text{Xe} \rightarrow X^0 129\text{Xe}^*$  (39.58 keV).
- 54 BELLI 96c use background subtraction and obtain  $\sigma < 0.35$  pb ( $< 0.15$  fb) (90% CL) for spin-dependent (independent)  $X^0$ -proton cross section. The confidence level is from R. Bernabei, private communication, May 20, 1999.
- 55 BERNABEI 96 use pulse shape discrimination to enhance the possible signal. The limit here is from R. Bernabei, private communication, September 19, 1997.
- 56 SARSA 96 search for annual modulation of WIMP signal. See SARSA 97 for details of the analysis. The limit here is from M.L. Sarsa, private communication, May 26, 1997.
- 57 SMITH 96 use pulse shape discrimination to enhance the possible signal. A dark matter density of  $0.4 \text{ GeV cm}^{-3}$  is assumed.
- 58 GARCIA 95 limit is from the event rate. A weaker limit is obtained from searches for diurnal and annual modulation.
- 59 SNOWDEN-IFFT 95 look for recoil tracks in an ancient mica crystal. Similar limits are also given for <sup>27</sup>Al and <sup>28</sup>Si. See COLLAR 96 and SNOWDEN-IFFT 96 for discussion on potential backgrounds.
- 60 BECK 94 uses enriched <sup>76</sup>Ge (86% purity).
- 61 REUSSER 91 limit here is changed from published (0.3) after reanalysis by authors. J.L. Vuilleumier, private communication, March 29, 1996.

### For $m_{X^0} = 1 \text{ TeV}$

VALUE (nb)	CL%	DOCUMENT ID	TECN	COMMENT
• • •				We do not use the following data for averages, fits, limits, etc. • • •
1		AHLEN 11	DMTP	CF <sub>4</sub>
2		AHMED 11	CDM2	Ge, inelastic
3		AHMED 11A	RVUE	Ge
4		APRILE 11	X100	Xe
5		APRILE 11A	X100	Xe, inelastic
6		APRILE 11B	X100	Xe
7		ARMENGAUD 11	EDE2	Ge
8		BEHNKE 11	COUP	CF <sub>3</sub> I
9		HORN 11	ZEP3	Xe
10		TANAKA 11	SKAM	H, solar $\nu$
11		ABBASI 10	ICCB	KK dark matter
12		APRILE 10	X100	Xe
13		ARMENGAUD 10	EDE2	Ge
14		MIUCHI 10	NAGE	CF <sub>4</sub>
15		ABBASI 09B	ICCB	H, solar $\nu$
16		AHMED 09	CDM2	Ge
17		ARCHAMBAULT 09	PICA	F
18		LEBEDENKO 09A	ZEP3	Xe
19		ANGLE 08A	XE10	Xe
20		BEDNYAKOV 08	RVUE	Ge
21		ALNER 07	ZEP2	Xe
22		LEE 07A	KIMS	Csl
23		MIUCHI 07	CNTR	F (CF <sub>4</sub> )
24		AKERIB 06	CDMS	<sup>73</sup> Ge, <sup>29</sup> Si
25		ALNER 05	NAIA	NaI
26		BARNABE-HEIDER 05	PICA	F (C <sub>4</sub> F <sub>10</sub> )
27		BENOIT 05	EDEL	<sup>73</sup> Ge
28		GIRARD 05	SMP	F (C <sub>2</sub> ClF <sub>5</sub> )
29		KLAPDOR-K...	05	HDM5 <sup>73</sup> Ge (enriched)
30		MIUCHI 03	BOLO	LiF
31		TAKEDA 03	BOLO	NaF
32	< 3	ANGLOHER 02	CRES	Al
33		BENOIT 00	EDEL	Ge
34		BERNABEI 99D	CNTR	SIMP
35		DERBIN 99	CNTR	SIMP
36	< 0.06	KLIMENKO 98	CNTR	<sup>73</sup> Ge, inel.
37	< 0.4	KLIMENKO 98	CNTR	<sup>73</sup> Ge, inel.

See key on page 457

# Searches Particle Listings

## WIMPs and Other Particle Searches

< 40		ALESSAND...	96	CNTR	O
< 700		ALESSAND...	96	CNTR	Te
< 0.05	90	38 BELLI	96	CNTR	$^{129}\text{Xe}$ , inel.
< 1.5	90	39 BELLI	96	CNTR	$^{129}\text{Xe}$ , inel.
		40 BELLI	96c	CNTR	$^{129}\text{Xe}$
< 0.01	90	41 BERNABEI	96	CNTR	Na
< 9	90	41 BERNABEI	96	CNTR	I
< 7	95	42 SARSA	96	CNTR	Na
< 0.3	90	43 SMITH	96	CNTR	Na
< 6	90	43 SMITH	96	CNTR	I
< 6	95	44 GARCIA	95	CNTR	Natural Ge
< 8	95	QUENBY	95	CNTR	Na
< 50	95	QUENBY	95	CNTR	I
< 7 $\times 10^2$	90	45 SNOWDEN...	95	MICA	$^{16}\text{O}$
< 1 $\times 10^3$	90	45 SNOWDEN...	95	MICA	$^{39}\text{K}$
< 0.8	90	46 BECK	94	CNTR	$^{76}\text{Ge}$
< 30	90	BACCI	92	CNTR	Na
< 30	90	BACCI	92	CNTR	I
< 15	90	47 REUSSER	91	CNTR	Natural Ge
< 6	95	CALDWELL	88	CNTR	Natural Ge

- AHLEN 11 give  $\sigma < 8 \times 10^3$  pb (90% CL) for spin-dependent  $X^0$ -proton cross section.
- AHMED 11 search for  $X^0$  inelastic scattering. See their Figs. 8–10 for limits.
- AHMED 11A combine CDMS and EDELWEISS data and give  $\sigma < 1.5 \times 10^{-7}$  pb (90% CL) for spin-independent  $X^0$ -nucleon cross section.
- APRILE 11 reanalyze APRILE 10 data and give  $\sigma < 2 \times 10^{-7}$  pb (90% CL) for spin-independent  $X^0$ -nucleon cross section.
- APRILE 11A search for  $X^0$  inelastic scattering. See their Figs. 2 and 3 for limits.
- APRILE 11B give  $\sigma < 8 \times 10^{-8}$  pb (90% CL) for spin-independent  $X^0$ -nucleon cross section.
- ARMENGAUD 11 give  $\sigma < 2 \times 10^{-7}$  pb (90% CL) for spin-independent  $X^0$ -nucleon cross section. Supersedes ARMENGAUD 10. A limit on inelastic cross section is also given.
- BEHNKE 11 give  $\sigma < 0.4$  pb (90% CL) for spin-dependent  $X^0$ -proton cross section with a direction sensitive detector.
- HORN 11 perform detector calibration by neutrons. Earlier results are only marginally affected.
- TANAKA 11 search for neutrinos produced by  $X^0$  annihilation in the Sun and give  $\sigma < 2 \times 10^{-3}$  ( $2 \times 10^{-2}$ ) pb (90% CL) for spin-dependent  $X^0$ -proton cross section, if  $X^0$  pairs annihilate to  $W^+W^-$  ( $b\bar{b}$ ).
- ABBASI 10 search for  $\nu_\mu$  from annihilations of Kaluza-Klein photon dark matter in the Sun and give  $\sigma < 1 \times 10^{-3}$  pb (90% CL) for spin-dependent  $X^0$ -proton cross section.
- APRILE 10 give  $\sigma < 4 \times 10^{-7}$  pb (90% CL) for spin-independent  $X^0$ -nucleon cross section.
- ARMENGAUD 10 give  $\sigma < 6 \times 10^{-7}$  pb (90% CL) for spin-independent  $X^0$ -nucleon cross section.
- MIUCHI 10 give  $\sigma < 2 \times 10^4$  pb (90% CL) for spin-dependent  $X^0$ -proton cross section with a direction sensitive detector.
- ABBASI 09B search for neutrinos produced by  $X^0$  annihilation in the Sun and give  $\sigma < 8.7 \times 10^{-4}$  ( $2.2 \times 10^{-2}$ ) pb (90% CL) for spin-dependent  $X^0$ -proton cross section, if  $X^0$  pairs annihilate to  $W^+W^-$  ( $b\bar{b}$ ).
- AHMED 09 give  $\sigma < 0.2$  pb (90% CL) for spin-dependent  $X^0$ -neutron cross section. Superseded by AHMED 10.
- ARCHAMBAULT 09 give  $\sigma < 3$  pb (90% CL) for spin-dependent  $X^0$ -proton cross section.
- LEBEDENKO 09A give  $\sigma < 6$  (0.1) pb (90% CL) for spin-dependent  $X^0$ -proton (neutron) cross section.
- ANGLE 08A give  $\sigma < 8$  (0.1) pb (90% CL) for spin-dependent  $X^0$ -proton (neutron) cross section.
- BEDNYAKOV 08 reanalyze KLAPDOR-KLEINGROTHAUS 05 and BAUDIS 01 data and give  $\sigma < 0.25$  pb (90% CL) for spin-dependent  $X^0$ -neutron cross section.
- ALNER 07 give  $\sigma < 100$  (0.6) pb (90% CL) for spin-dependent  $X^0$ -proton (neutron) cross section.
- LEE 07A give  $\sigma < 0.8$  (30) pb (90% CL) for spin-dependent  $X^0$ -proton (neutron) cross section.
- MIUCHI 07 give  $\sigma < 4 \times 10^4$  pb (90% CL) for spin-dependent  $X^0$ -proton cross section with a direction-sensitive detector.
- AKERIB 06 give  $\sigma < 30$  (0.5) pb (90% CL) for spin-dependent  $X^0$ -proton (neutron) cross section. See also AKERIB 05.
- ALNER 05 give  $\sigma < 1.5$  (40) pb (90% CL) for spin-dependent  $X^0$ -proton (neutron) cross section.
- BARNABE-HEIDER 05 give  $\sigma < 15$  (200) pb (90% CL) for spin-dependent  $X^0$ -proton (neutron) cross section.
- BENOIT 05 give  $\sigma < 600$  (4) pb (90% CL) for spin-dependent  $X^0$ -proton (neutron) cross section.
- GIRARD 05 give  $\sigma < 10$  pb (90% CL) for spin-dependent  $X^0$ -proton cross section.
- KLAPDOR-KLEINGROTHAUS 05 give  $\sigma < 10$  pb (90% CL) for spin-dependent  $X^0$ -neutron cross section.
- MIUCHI 03 give model-independent limit  $\sigma < 260$  pb (90% CL) for spin-dependent  $X^0$ -proton cross section.
- TAKEDA 03 give model-independent limit  $\sigma < 0.15$  (4) nb (90% CL) for spin-dependent  $X^0$ -proton (neutron) cross section.
- ANGLOHER 02 limit is for spin-dependent WIMP-Aluminum cross section.
- BENOIT 00 find four event categories in Ge detectors and suggest that low-energy surface nuclear recoils can explain anomalous events reported by UKDMC and Saclay NaI experiments.
- BERNABEI 99b search for SIMPs (Strongly Interacting Massive Particles) in the mass range  $10^3$ – $10^{16}$  GeV. See their Fig. 3 for cross-section limits.
- DERBIN 99 search for SIMPs (Strongly Interacting Massive Particles) in the mass range  $10^2$ – $10^{14}$  GeV. See their Fig. 3 for cross-section limits.
- KLIMENKO 98 limit is for inelastic scattering  $X^0 \ ^{73}\text{Ge} \rightarrow X^0 \ ^{73}\text{Ge}^*$  (13.26 keV).
- KLIMENKO 98 limit is for inelastic scattering  $X^0 \ ^{73}\text{Ge} \rightarrow X^0 \ ^{73}\text{Ge}^*$  (66.73 keV).

- BELLI 96 limit for inelastic scattering  $X^0 \ ^{129}\text{Xe} \rightarrow X^0 \ ^{129}\text{Xe}^*$  (39.58 keV).
- BELLI 96 limit for inelastic scattering  $X^0 \ ^{129}\text{Xe} \rightarrow X^0 \ ^{129}\text{Xe}^*$  (236.14 keV).
- BELLI 96c use background subtraction and obtain  $\sigma < 0.7$  pb ( $< 0.7$  fb) (90% CL) for spin-dependent (independent)  $X^0$ -proton cross section. The confidence level is from R. Bernabei, private communication, May 20, 1999.
- BERNABEI 96 use pulse shape discrimination to enhance the possible signal. The limit here is from R. Bernabei, private communication, September 19, 1997.
- SARSA 96 search for annual modulation of WIMP signal. See SARSA 97 for details of the analysis. The limit here is from M.L. Sarsa, private communication, May 26, 1997.
- SMITH 96 use pulse shape discrimination to enhance the possible signal. A dark matter density of  $0.4 \text{ GeV cm}^{-3}$  is assumed.
- GARCIA 95 limit is from the event rate. A weaker limit is obtained from searches for diurnal and annual modulation.
- SNOWDEN-IFFT 95 look for recoil tracks in an ancient mica crystal. Similar limits are also given for  $^{27}\text{Al}$  and  $^{28}\text{Si}$ . See COLLAR 96 and SNOWDEN-IFFT 96 for discussion on potential backgrounds.
- BECK 94 uses enriched  $^{76}\text{Ge}$  (86% purity).
- REUSSER 91 limit here is changed from published (5) after reanalysis by authors. J.L. Vuilleumier, private communication, March 29, 1996.

### $X^0$ Annihilation Cross Section

Limits are on  $\sigma v$  for  $X^0$  pair annihilation at threshold.

VALUE ( $\text{cm}^3\text{s}^{-1}$ )	CL%	DOCUMENT ID	TECN	COMMENT
$< 10^{-22}$	90	1 ABBASI	11c	ICCB Galactic halo, $m=1$ TeV
$< 3 \times 10^{-25}$	95	2 ABRAMOWSKI11	HESS	Near Galactic center, $m=1$ TeV
$< 10^{-26}$	95	3 ACKERMANN 11	FLAT	Satellite galaxy, $m=10$ GeV
$< 10^{-25}$	95	3 ACKERMANN 11	FLAT	Satellite galaxy, $m=100$ GeV
$< 10^{-24}$	95	3 ACKERMANN 11	FLAT	Satellite galaxy, $m=1$ TeV

- ABBASI 11c search for  $\nu_\mu$  from  $X^0$  annihilation in the outer halo of the Milky Way. The limit assumes annihilation into  $\nu\nu$ . See their Fig. 9 for limits with other annihilation channels.
- ABRAMOWSKI 11 search for  $\gamma$  from  $X^0$  annihilation near the Galactic center. The limit assumes Einasto DM density profile.
- ACKERMANN 11 search for  $\gamma$  from  $X^0$  annihilation in ten dwarf spheroidal satellite galaxies of the Milky Way. The limit for  $m = 10$  GeV assumes annihilation into  $b\bar{b}$ , the others  $W^+W^-$ . See their Fig. 2 for limits with other final states. See also GERINGER-SAMETH 11 for a different analysis of the same data.

### CONCENTRATION OF STABLE PARTICLES IN MATTER

#### Concentration of Heavy (Charge +1) Stable Particles in Matter

VALUE	CL%	DOCUMENT ID	TECN	COMMENT
$< 4 \times 10^{-17}$	95	1 YAMAGATA	93	SPEC Deep sea water, $M=5$ – $1600 m_p$
$< 6 \times 10^{-15}$	95	2 VERKERK	92	SPEC Water, $M=10^5$ to $3 \times 10^7$ GeV
$< 7 \times 10^{-15}$	95	2 VERKERK	92	SPEC Water, $M=10^4$ , $6 \times 10^7$ GeV
$< 9 \times 10^{-15}$	95	2 VERKERK	92	SPEC Water, $M=10^8$ GeV
$< 3 \times 10^{-23}$	90	3 HEMMICK	90	SPEC Water, $M=1000 m_p$
$< 2 \times 10^{-21}$	90	3 HEMMICK	90	SPEC Water, $M=5000 m_p$
$< 3 \times 10^{-20}$	90	3 HEMMICK	90	SPEC Water, $M=10000 m_p$
$< 1. \times 10^{-29}$		SMITH	82B	SPEC Water, $M=30$ – $4000 m_p$
$< 2. \times 10^{-28}$		SMITH	82B	SPEC Water, $M=12$ – $1000 m_p$
$< 1. \times 10^{-14}$		SMITH	82B	SPEC Water, $M > 1000 m_p$
$< (0.2-1.) \times 10^{-21}$		SMITH	79	SPEC Water, $M=6$ – $350 m_p$

- YAMAGATA 93 used deep sea water at 4000 m since the concentration is enhanced in deep sea due to gravity.
- VERKERK 92 looked for heavy isotopes in sea water and put a bound on concentration of stable charged massive particle in sea water. The above bound can be translated into into a bound on charged dark matter particle ( $5 \times 10^6$  GeV), assuming the local density,  $\rho=0.3 \text{ GeV/cm}^3$ , and the mean velocity ( $v$ )=300 km/s.
- See HEMMICK 90 Fig. 7 for other masses 100–10000  $m_p$ .

#### Concentration of Heavy Stable Particles Bound to Nuclei

VALUE	CL%	DOCUMENT ID	TECN	COMMENT
$< 1.2 \times 10^{-11}$	95	1 JAVORSEK	01	SPEC Au, $M=3$ GeV
$< 6.9 \times 10^{-10}$	95	1 JAVORSEK	01	SPEC Au, $M=144$ GeV
$< 1 \times 10^{-11}$	95	2 JAVORSEK	01B	SPEC Au, $M=188$ GeV
$< 1 \times 10^{-8}$	95	2 JAVORSEK	01B	SPEC Au, $M=1669$ GeV
$< 6 \times 10^{-9}$	95	2 JAVORSEK	01B	SPEC Fe, $M=188$ GeV
$< 1 \times 10^{-8}$	95	2 JAVORSEK	01B	SPEC Fe, $M=647$ GeV
$< 4 \times 10^{-20}$	90	3 HEMMICK	90	SPEC C, $M=100 m_p$
$< 8 \times 10^{-20}$	90	3 HEMMICK	90	SPEC C, $M=1000 m_p$
$< 2 \times 10^{-16}$	90	3 HEMMICK	90	SPEC C, $M=10000 m_p$
$< 6 \times 10^{-13}$	90	3 HEMMICK	90	SPEC Li, $M=1000 m_p$
$< 1 \times 10^{-11}$	90	3 HEMMICK	90	SPEC Be, $M=1000 m_p$
$< 6 \times 10^{-14}$	90	3 HEMMICK	90	SPEC B, $M=1000 m_p$
$< 4 \times 10^{-17}$	90	3 HEMMICK	90	SPEC O, $M=1000 m_p$
$< 4 \times 10^{-15}$	90	3 HEMMICK	90	SPEC F, $M=1000 m_p$
$< 1.5 \times 10^{-13}/\text{nucleon}$	68	4 NORMAN	89	SPEC $^{206}\text{Pb}X^-$
$< 1.2 \times 10^{-12}/\text{nucleon}$	68	4 NORMAN	87	SPEC $^{56.58}\text{Fe}X^-$

# Searches Particle Listings

## WIMPs and Other Particle Searches

- <sup>1</sup> JAVORSEK 01 search for (neutral) SIMPs (strongly interacting massive particles) bound to Au nuclei. Here  $M$  is the effective SIMP mass.
- <sup>2</sup> JAVORSEK 01b search for (neutral) SIMPs (strongly interacting massive particles) bound to Au and Fe nuclei from various origins with exposures on the earth's surface, in a satellite, heavy ion collisions, etc. Here  $M$  is the mass of the anomalous nucleus. See also JAVORSEK 02.
- <sup>3</sup> See HEMMICK 90 Fig. 7 for other masses 100–10000  $m_p$ .
- <sup>4</sup> Bound valid up to  $m_{\chi^-} \sim 100 \text{ TeV}$ .

### GENERAL NEW PHYSICS SEARCHES

This subsection lists some of the search experiments which look for general signatures characteristic of new physics, independent of the framework of a specific model.

VALUE	DOCUMENT ID	TECN	COMMENT
• • • We do not use the following data for averages, fits, limits, etc. • • •			
	1 AAD 11s ATLS	jet + $\cancel{E}_T$	
	2 AALTONEN 11AF CDF	$\ell^\pm \ell^\pm$	
	3 CHATRCHYAN 11C CMS	$\ell^+ \ell^- + \text{jets} + \cancel{E}_T$	
	4 CHATRCHYAN 11U CMS	jet + $\cancel{E}_T$	
	5 AALTONEN 10AF CDF	$\gamma\gamma + \ell, \cancel{E}_T$	
	6 AALTONEN 09AF CDF	$\ell\gamma b \cancel{E}_T$	
	7 AALTONEN 09G CDF	$\ell\ell\ell \cancel{E}_T$	

- <sup>1</sup> AAD 11s search for events with one jet and missing  $E_T$  in  $pp$  collisions at  $E_{cm} = 7 \text{ TeV}$  with  $L = 33 \text{ pb}^{-1}$ . The observed events are compatible with Standard Model expectation.
- <sup>2</sup> AALTONEN 11AF search for high- $p_T$  like-sign dileptons in  $p\bar{p}$  collisions at  $E_{cm} = 1.96 \text{ TeV}$  with  $L = 6.1 \text{ fb}^{-1}$ . The observed events are compatible with Standard Model expectation.
- <sup>3</sup> CHATRCHYAN 11C search for events with an opposite-sign lepton pair, jets, and missing  $E_T$  in  $pp$  collisions at  $E_{cm} = 7 \text{ TeV}$  with  $L = 34 \text{ pb}^{-1}$ . The observed events are compatible with Standard Model expectation.
- <sup>4</sup> CHATRCHYAN 11U search for events with one jet and missing  $E_T$  in  $pp$  collisions at  $E_{cm} = 7 \text{ TeV}$  with  $L = 36 \text{ pb}^{-1}$ . The observed events are compatible with Standard Model expectation.
- <sup>5</sup> AALTONEN 10AF search for  $\gamma\gamma$  events with  $e, \mu, \tau$ , or missing  $E_T$  in  $p\bar{p}$  collisions at  $E_{cm} = 1.96 \text{ TeV}$  with  $L = 1.1\text{--}2.0 \text{ fb}^{-1}$ . The observed events are compatible with Standard Model expectation.
- <sup>6</sup> AALTONEN 09AF search for  $\ell\gamma b$  events with missing  $E_T$  in  $p\bar{p}$  collisions at  $E_{cm} = 1.96 \text{ TeV}$  with  $L = 1.9 \text{ fb}^{-1}$ . The observed events are compatible with Standard Model expectation including  $t\bar{t}\gamma$  production.
- <sup>7</sup> AALTONEN 09G search for  $\mu\mu\mu$  and  $\mu\mu e$  events with missing  $E_T$  in  $p\bar{p}$  collisions at  $E_{cm} = 1.96 \text{ TeV}$  with  $L = 976 \text{ pb}^{-1}$ . The observed events are compatible with Standard Model expectation.

### LIMITS ON JET-JET RESONANCES

#### Heavy Particle Production Cross Section

Limits for a particle decaying to two hadronic jets.

Units(pb)	CL%	Mass(GeV)	DOCUMENT ID	TECN	COMMENT
• • • We do not use the following data for averages, fits, limits, etc. • • •					
			1 AAD 11AG ATLS	7 TeV $pp \rightarrow 2$ jets	
			2 AALTONEN 11M CDF	1.96 TeV $p\bar{p} \rightarrow W + 2$ jets	
			3 ABAZOV 11i D0	1.96 TeV $p\bar{p} \rightarrow W + 2$ jets	
			4 AAD 10 ATLS	7 TeV $pp \rightarrow 2$ jets	
			5 KHACHATRYAN 10 CMS	7 TeV $pp \rightarrow 2$ jets	
			6 ABE 99F CDF	1.8 TeV $p\bar{p} \rightarrow b\bar{b} + \text{anything}$	
			7 ABE 97G CDF	1.8 TeV $p\bar{p} \rightarrow 2$ jets	
			8 ABE 93G CDF	1.8 TeV $p\bar{p} \rightarrow 2$ jets	
			8 ABE 93G CDF	1.8 TeV $p\bar{p} \rightarrow 2$ jets	
			8 ABE 93G CDF	1.8 TeV $p\bar{p} \rightarrow 2$ jets	
			8 ABE 93G CDF	1.8 TeV $p\bar{p} \rightarrow 2$ jets	
<2603	95	200			
< 44	95	400			
< 7	95	600			

- <sup>1</sup> AAD 11AG search for dijet resonances in  $pp$  collisions at  $E_{cm} = 7 \text{ TeV}$  with  $L = 36 \text{ pb}^{-1}$ . Limits on number of events for  $m = 0.6\text{--}4 \text{ TeV}$  are given in their Table 3.
- <sup>2</sup> AALTONEN 11M find a peak in two jet invariant mass distribution around 140 GeV in  $W + 2$  jet events in  $p\bar{p}$  collisions at  $E_{cm} = 1.96 \text{ TeV}$  with  $L = 4.3 \text{ fb}^{-1}$ .
- <sup>3</sup> ABAZOV 11i search for two-jet resonances in  $W + 2$  jet events in  $p\bar{p}$  collisions at  $E_{cm} = 1.96 \text{ TeV}$  with  $L = 4.3 \text{ fb}^{-1}$  and give limits  $\sigma < (2.6\text{--}1.3) \text{ pb}$  (95% CL) for  $m = 110\text{--}170 \text{ GeV}$ . The result is incompatible with AALTONEN 11M.
- <sup>4</sup> AAD 10 search for narrow dijet resonances in  $pp$  collisions at  $E_{cm} = 7 \text{ TeV}$  with  $L = 315 \text{ nb}^{-1}$ . Limits on the cross section in the range  $10\text{--}10^3 \text{ pb}$  is given for  $m = 0.3\text{--}1.7 \text{ TeV}$ .
- <sup>5</sup> KHACHATRYAN 10 search for narrow dijet resonances in  $pp$  collisions at  $E_{cm} = 7 \text{ TeV}$  with  $L = 2.9 \text{ pb}^{-1}$ . Limits on the cross section in the range  $1\text{--}300 \text{ pb}$  is given for  $m = 0.5\text{--}2.6 \text{ TeV}$  separately in the final states  $qq, qg, \text{ and } gg$ .
- <sup>6</sup> ABE 99F search for narrow  $b\bar{b}$  resonances in  $p\bar{p}$  collisions at  $E_{cm} = 1.8 \text{ TeV}$ . Limits on  $\sigma(p\bar{p} \rightarrow X + \text{anything}) \times \text{B}(X \rightarrow b\bar{b})$  in the range  $3\text{--}10^3 \text{ pb}$  (95%CL) are given for  $m_{\chi} = 200\text{--}750 \text{ GeV}$ . See their Table I.
- <sup>7</sup> ABE 97G search for narrow dijet resonances in  $p\bar{p}$  collisions with  $106 \text{ pb}^{-1}$  of data at  $E_{cm} = 1.8 \text{ TeV}$ . Limits on  $\sigma(p\bar{p} \rightarrow X + \text{anything}) \times \text{B}(X \rightarrow jj)$  in the range  $10^4\text{--}10^{-1} \text{ pb}$  (95%CL) are given for dijet mass  $m = 200\text{--}1150 \text{ GeV}$  with both jets having  $|\eta| < 2.0$  and the dijet system having  $|\cos\theta^*| < 0.67$ . See their Table I for the list of limits. Supersedes ABE 93G.
- <sup>8</sup> ABE 93G gives cross section times branching ratio into light ( $d, u, s, c, b$ ) quarks for  $\Gamma = 0.02 M$ . Their Table II gives limits for  $M = 200\text{--}900 \text{ GeV}$  and  $\Gamma = (0.02\text{--}0.2) M$ .

### LIMITS ON NEUTRAL PARTICLE PRODUCTION

#### Production Cross Section of Radiatively-Decaying Neutral Particle

VALUE (pb)	CL%	DOCUMENT ID	TECN	COMMENT
• • • We do not use the following data for averages, fits, limits, etc. • • •				
<(0.043–0.17)	95	1 ABBIENDI 00D	OPAL	$e^+e^- \rightarrow \chi^0\gamma^0$ , $\chi^0 \rightarrow \gamma^0\gamma$
<(0.05–0.8)	95	2 ABBIENDI 00D	OPAL	$e^+e^- \rightarrow \chi^0\chi^0$ , $\chi^0 \rightarrow \gamma^0\gamma$
<(2.5–0.5)	95	3 ACKERSTAFF 97B	OPAL	$e^+e^- \rightarrow \chi^0\gamma^0$ , $\chi^0 \rightarrow \gamma^0\gamma$
<(1.6–0.9)	95	4 ACKERSTAFF 97B	OPAL	$e^+e^- \rightarrow \chi^0\chi^0$ , $\chi^0 \rightarrow \gamma^0\gamma$

- <sup>1</sup> ABBIENDI 00D associated production limit is for  $m_{\chi^0} = 90\text{--}188 \text{ GeV}$ ,  $m_{\gamma^0} = 0$  at  $E_{cm} = 189 \text{ GeV}$ . See also their Fig. 9.
- <sup>2</sup> ABBIENDI 00D pair production limit is for  $m_{\chi^0} = 45\text{--}94 \text{ GeV}$ ,  $m_{\gamma^0} = 0$  at  $E_{cm} = 189 \text{ GeV}$ . See also their Fig. 12.
- <sup>3</sup> ACKERSTAFF 97B associated production limit is for  $m_{\chi^0} = 80\text{--}160 \text{ GeV}$ ,  $m_{\gamma^0} = 0$  from  $10.0 \text{ pb}^{-1}$  at  $E_{cm} = 161 \text{ GeV}$ . See their Fig. 3(a).
- <sup>4</sup> ACKERSTAFF 97B pair production limit is for  $m_{\chi^0} = 40\text{--}80 \text{ GeV}$ ,  $m_{\gamma^0} = 0$  from  $10.0 \text{ pb}^{-1}$  at  $E_{cm} = 161 \text{ GeV}$ . See their Fig. 3(b).

#### Heavy Particle Production Cross Section

VALUE (cm <sup>2</sup> /N)	CL%	EVTS	DOCUMENT ID	TECN	COMMENT
• • • We do not use the following data for averages, fits, limits, etc. • • •					
			1 ADAMS 97B	KTEV	$m = 1.2\text{--}5 \text{ GeV}$
			2 GALLAS 95	TOF	$m = 0.5\text{--}20 \text{ GeV}$
			3 AKESSON 91	CNTR	$m = 0\text{--}5 \text{ GeV}$
			4 BADIER 86	BDMP	$\tau = (0.05\text{--}1.) \times 10^{-8} \text{ s}$
			5 GUSTAFSON 76	CNTR	$\tau > 10^{-7} \text{ s}$

- <sup>1</sup> ADAMS 97B search for a hadron-like neutral particle produced in  $pN$  interactions, which decays into a  $p^0$  and a weakly interacting massive particle. Upper limits are given for the ratio to  $K_L$  production for the mass range  $1.2\text{--}5 \text{ GeV}$  and lifetime  $10^{-9}\text{--}10^{-4} \text{ s}$ . See also our Light Gluino Section.
- <sup>2</sup> GALLAS 95 limit is for a weakly interacting neutral particle produced in  $800 \text{ GeV}/c$   $pN$  interactions decaying with a lifetime of  $10^{-4}\text{--}10^{-8} \text{ s}$ . See their Figs. 8 and 9. Similar limits are obtained for a stable particle with interaction cross section  $10^{-29}\text{--}10^{-33} \text{ cm}^2$ . See Fig. 10.
- <sup>3</sup> AKESSON 91 limit is from weakly interacting neutral long-lived particles produced in  $pN$  reaction at  $450 \text{ GeV}/c$  performed at CERN SPS. Bourquin-Gaillard formula is used as the production model. The above limit is for  $\tau > 10^{-7} \text{ s}$ . For  $\tau > 10^{-9} \text{ s}$ ,  $\sigma < 10^{-30} \text{ cm}^2/\text{nucleon}$  is obtained.
- <sup>4</sup> BADIER 86 looked for long-lived particles at  $300 \text{ GeV}$   $\pi^-$  beam dump. The limit applies for nonstrongly interacting neutral or charged particles with mass  $> 2 \text{ GeV}$ . The limit applies for particle modes,  $\mu^+\pi^-, \mu^+\mu^-, \pi^+\pi^-, \pi^+\chi^-, \pi^+\pi^-\pi^\pm$  etc. See their figure 5 for the contours of limits in the mass- $\tau$  plane for each mode.
- <sup>5</sup> GUSTAFSON 76 is a  $300 \text{ GeV}$  FNAL experiment looking for heavy ( $m > 2 \text{ GeV}$ ) long-lived neutral hadrons in the M4 neutral beam. The above typical value is for  $m = 3 \text{ GeV}$  and assumes an interaction cross section of  $1 \text{ mb}$ . Values as a function of mass and interaction cross section are given in figure 2.

#### Production of New Penetrating Non- $\nu$ Like States in Beam Dump

VALUE	DOCUMENT ID	TECN	COMMENT
• • • We do not use the following data for averages, fits, limits, etc. • • •			
	1 LOSECCO 81	CALO	28 GeV protons

<sup>1</sup> No excess neutral-current events leads to  $\sigma(\text{production}) \times \sigma(\text{interaction}) \times \text{acceptance} < 2.26 \times 10^{-71} \text{ cm}^4/\text{nucleon}^2$  (CL = 90%) for light neutrals. Acceptance depends on models ( $0.1$  to  $4. \times 10^{-4}$ ).

### LIMITS ON CHARGED PARTICLES IN $e^+e^-$

#### Heavy Particle Production Cross Section in $e^+e^-$

Ratio to  $\sigma(e^+e^- \rightarrow \mu^+\mu^-)$  unless noted. See also entries in Free Quark Search and Magnetic Monopole Searches.

VALUE	CL%	EVTS	DOCUMENT ID	TECN	COMMENT
• • • We do not use the following data for averages, fits, limits, etc. • • •					
			1 ACKERSTAFF 98P	OPAL	$Q=1, 2/3, m=45\text{--}89.5 \text{ GeV}$
			2 ABREU 97D	DLPH	$Q=1, 2/3, m=45\text{--}84 \text{ GeV}$
			3 BARATE 97K	ALEP	$Q=1, m=45\text{--}85 \text{ GeV}$
			4 AKERS 95R	OPAL	$Q=1, m=5\text{--}45 \text{ GeV}$
			4 AKERS 95R	OPAL	$Q=2, m=5\text{--}45 \text{ GeV}$
			5 BUSKULIC 93C	ALEP	$Q=1, m=32\text{--}72 \text{ GeV}$
			6 ADACHI 90C	TOPZ	$Q=1, m=1\text{--}16, 18\text{--}27 \text{ GeV}$
			7 ADACHI 90E	TOPZ	$Q=1, m=5\text{--}25 \text{ GeV}$
			8 KINOSHITA 82	PLAS	$Q=3\text{--}180, m < 14.5 \text{ GeV}$
			9 BARTEL 80	JADE	$Q=(3, 4, 5)/3, 2\text{--}12 \text{ GeV}$

- 1 ACKERSTAFF 98P search for pair production of long-lived charged particles at  $E_{cm}$  between 130 and 183 GeV and give limits  $\sigma < (0.05-0.2) \text{ pb}$  (95%CL) for spin-0 and spin-1/2 particles with  $m=45-89.5 \text{ GeV}$ , charge 1 and 2/3. The limit is translated to the cross section at  $E_{cm}=183 \text{ GeV}$  with the  $s$  dependence described in the paper. See their Figs. 2-4.
- 2 ABREU 97D search for pair production of long-lived particles and give limits  $\sigma < (0.4-2.3) \text{ pb}$  (95%CL) for various center-of-mass energies  $E_{cm}=130-136, 161,$  and  $172 \text{ GeV}$ , assuming an almost flat production distribution in  $\cos\theta$ .
- 3 BARATE 97K search for pair production of long-lived charged particles at  $E_{cm} = 130, 136, 161,$  and  $172 \text{ GeV}$  and give limits  $\sigma < (0.2-0.4) \text{ pb}$  (95%CL) for spin-0 and spin-1/2 particles with  $m=45-85 \text{ GeV}$ . The limit is translated to the cross section at  $E_{cm}=172 \text{ GeV}$  with the  $E_{cm}$  dependence described in the paper. See their Figs. 2 and 3 for limits on  $J = 1/2$  and  $J = 0$  cases.
- 4 AKERS 95R is a CERN-LEP experiment with  $W_{cm} \sim m_Z$ . The limit is for the production of a stable particle in multihadron events normalized to  $\sigma(e^+e^- \rightarrow \text{hadrons})$ . Constant phase space distribution is assumed. See their Fig. 3 for bounds for  $Q = \pm 2/3, \pm 4/3$ .
- 5 BUSKULIC 93c is a CERN-LEP experiment with  $W_{cm} = m_Z$ . The limit is for a pair or single production of heavy particles with unusual ionization loss in TPC. See their Fig. 5 and Table 1.
- 6 ADACHI 90C is a KEK-TRISTAN experiment with  $W_{cm} = 52-60 \text{ GeV}$ . The limit is for pair production of a scalar or spin-1/2 particle. See Figs. 3 and 4.
- 7 ADACHI 90E is KEK-TRISTAN experiment with  $W_{cm} = 52-61.4 \text{ GeV}$ . The above limit is for inclusive production cross section normalized to  $\sigma(e^+e^- \rightarrow \mu^+\mu^-) \cdot \beta(3-\beta^2)/2$ , where  $\beta = (1 - 4m^2/W_{cm}^2)^{1/2}$ . See the paper for the assumption about the production mechanism.
- 8 KINOSHITA 82 is SLAC PEP experiment at  $W_{cm} = 29 \text{ GeV}$  using lexan and  $^{39}\text{Cr}$  plastic sheets sensitive to highly ionizing particles.
- 9 BARTEL 80 is DESY-PETRA experiment with  $W_{cm} = 27-35 \text{ GeV}$ . Above limit is for inclusive pair production and ranges between  $1. \times 10^{-1}$  and  $1. \times 10^{-2}$  depending on mass and production momentum distributions. (See their figures 9, 10, 11).

**Branching Fraction of  $Z^0$  to a Pair of Stable Charged Heavy Fermions**

VALUE	CL%	DOCUMENT ID	TECN	COMMENT
••• We do not use the following data for averages, fits, limits, etc. •••				
$<5 \times 10^{-6}$	95	1 AKERS	95R OPAL	$m = 40.4-45.6 \text{ GeV}$
$<1 \times 10^{-3}$	95	AKRAWY	90o OPAL	$m = 29-40 \text{ GeV}$

1 AKERS 95R give the 95% CL limit  $\sigma(X\bar{X})/\sigma(\mu\mu) < 1.8 \times 10^{-4}$  for the pair production of singly- or doubly-charged stable particles. The limit applies for the mass range 40.4-45.6 GeV for  $X^\pm$  and  $< 45.6 \text{ GeV}$  for  $X^{\pm\pm}$ . See the paper for bounds for  $Q = \pm 2/3, \pm 4/3$ .

**LIMITS ON CHARGED PARTICLES IN HADRONIC REACTIONS**

**Heavy Particle Production Cross Section**

VALUE (nb)	CL%	DOCUMENT ID	TECN	COMMENT
••• We do not use the following data for averages, fits, limits, etc. •••				
$<1.2 \times 10^{-3}$	95	1 AAD	11I ATLS	$ q =10e, m=0.2-1 \text{ TeV}$
$<1.0 \times 10^{-5}$	95	2,3 AALTONEN	09Z CDF	$m > 100 \text{ GeV}$ , noncolored
$<4.8 \times 10^{-5}$	95	2,4 AALTONEN	09Z CDF	$m > 100 \text{ GeV}$ , colored
$< 0.31-0.04 \times 10^{-3}$	95	5 ABAZOV	09M D0	pair production
$<0.19$	95	6 AKTAS	04c H1	$m=3-10 \text{ GeV}$
$<0.05$	95	7 ABE	92J CDF	$m=50-200 \text{ GeV}$
$<10-130$		8 CARROLL	78 SPEC	$m=2-2.5 \text{ GeV}$
$<100$		9 LEIPUNER	73 CNTR	$m=3-11 \text{ GeV}$

- 1 AAD 11I search for production of highly ionizing massive particles in  $pp$  collisions at  $E_{cm} = 7 \text{ TeV}$  with  $L = 3.1 \text{ pb}^{-1}$ . See their Table 5 for similar limits for  $|q| = 6e$  and  $17e$ , Table 6 for limits on pair production cross section.
- 2 AALTONEN 09Z search for long-lived charged particles in  $p\bar{p}$  collisions at  $E_{cm} = 1.96 \text{ TeV}$  with  $L = 1.0 \text{ fb}^{-1}$ . The limits are on production cross section for a particle of mass above  $100 \text{ GeV}$  in the region  $|\eta| \lesssim 0.7, p_T > 40 \text{ GeV}$ , and  $0.4 < \beta < 1.0$ .
- 3 Limit for weakly interacting charge-1 particle.
- 4 Limit for up-quark like particle.
- 5 ABAZOV 09M search for pair production of long-lived charged particles in  $p\bar{p}$  collisions at  $E_{cm} = 1.96 \text{ TeV}$  with  $L = 1.1 \text{ fb}^{-1}$ . Limit on the cross section of  $(0.31-0.04) \text{ pb}$  (95% CL) is given for the mass range of 60-300 GeV, assuming the kinematics of stau pair production.
- 6 AKTAS 04c look for charged particle photoproduction at HERA with mean c.m. energy of  $200 \text{ GeV}$ .
- 7 ABE 92J look for pair production of unit-charged particles which leave detector before decaying. Limit shown here is for  $m=50 \text{ GeV}$ . See their Fig. 5 for different charges and stronger limits for higher mass.
- 8 CARROLL 78 look for neutral,  $S = -2$  dihyperon resonance in  $pp \rightarrow 2K^+ X$ . Cross section varies within above limits over mass range and  $p_{lab} = 5.1-5.9 \text{ GeV}/c$ .
- 9 LEIPUNER 73 is an NAL 300 GeV  $p$  experiment. Would have detected particles with lifetime greater than 200 ns.

**Heavy Particle Production Differential Cross Section**

VALUE ( $\text{cm}^2\text{sr}^{-1}\text{GeV}^{-1}$ )	CL%	EVTS	DOCUMENT ID	TECN	CHG	COMMENT
••• We do not use the following data for averages, fits, limits, etc. •••						
$<2.6 \times 10^{-36}$	90	0	1 BALDIN	76	CNTR	$Q = 1, m=2.1-9.4 \text{ GeV}$
$<2.2 \times 10^{-33}$	90	0	2 ALBROW	75	SPEC	$Q = \pm 1, m=4-15 \text{ GeV}$
$<1.1 \times 10^{-33}$	90	0	2 ALBROW	75	SPEC	$Q = \pm 2, m=6-27 \text{ GeV}$
$<8. \times 10^{-35}$	90	0	3 JOVANO...	75	CNTR	$Q = \pm 2, m=15-26 \text{ GeV}$
$<1.5 \times 10^{-34}$	90	0	3 JOVANO...	75	CNTR	$Q = \pm 2, m=3-10 \text{ GeV}$
$<6. \times 10^{-35}$	90	0	3 JOVANO...	75	CNTR	$Q = \pm 2, m=10-26 \text{ GeV}$

$<1. \times 10^{-31}$	90	0	4 APPEL	74	CNTR	$\pm, m=3.2-7.2 \text{ GeV}$
$<5.8 \times 10^{-34}$	90	0	5 ALPER	73	SPEC	$\pm, m=1.5-24 \text{ GeV}$
$<1.2 \times 10^{-35}$	90	0	6 ANTIPOV	71B	CNTR	$Q = -, m=2.2-2.8$
$<2.4 \times 10^{-35}$	90	0	7 ANTIPOV	71c	CNTR	$Q = -, m=1.2-1.7, 2.1-4$
$<2.4 \times 10^{-35}$	90	0	BINON	69	CNTR	$Q = -, m=1-1.8 \text{ GeV}$
$<1.5 \times 10^{-36}$	0	8 DORFAN	65	CNTR		Be target $m=3-7 \text{ GeV}$
$<3.0 \times 10^{-36}$	0	8 DORFAN	65	CNTR		Fe target $m=3-7 \text{ GeV}$

- 1 BALDIN 76 is a 70 GeV Serpukhov experiment. Value is per Al nucleus at  $\theta = 0$ . For other charges in range  $-0.5$  to  $-3.0$ , CL = 90% limit is  $(2.6 \times 10^{-36})/|(charge)|$  for mass range  $(2.1-9.4 \text{ GeV}) \times |(charge)|$ . Assumes stable particle interacting with matter as do antiprotons.
- 2 ALBROW 75 is a CERN ISR experiment with  $E_{cm} = 53 \text{ GeV}$ .  $\theta = 40 \text{ mr}$ . See figure 5 for mass ranges up to 35 GeV.
- 3 JOVANOVIH 75 is a CERN ISR 26+26 and 15+15 GeV  $pp$  experiment. Figure 4 covers ranges  $Q = 1/3$  to 2 and  $m = 3$  to 26 GeV. Value is per GeV momentum.
- 4 APPEL 74 is NAL 300 GeV  $pW$  experiment. Studies forward production of heavy (up to 24 GeV) charged particles with momenta 24-200 GeV (-charge) and 40-150 GeV (+charge). Above typical value is for 75 GeV and is per GeV momentum per nucleon.
- 5 ALPER 73 is CERN ISR 26+26 GeV  $pp$  experiment.  $p > 0.9 \text{ GeV}$ ,  $0.2 < \beta < 0.65$ .
- 6 ANTIPOV 71B is from same 70 GeV  $p$  experiment as ANTIPOV 71c and BINON 69.
- 7 ANTIPOV 71c limit inferred from flux ratio. 70 GeV  $p$  experiment.
- 8 DORFAN 65 is a 30 GeV/c  $p$  experiment at BNL. Units are per GeV momentum per nucleus.

**Long-Lived Heavy Particle Invariant Cross Section**

VALUE ( $\text{cm}^2/\text{GeV}^2/N$ )	CL%	DOCUMENT ID	TECN	CHG	COMMENT
••• We do not use the following data for averages, fits, limits, etc. •••					
$< 5-700 \times 10^{-35}$	90	1 BERNSTEIN	88	CNTR	
$< 5-700 \times 10^{-37}$	90	1 BERNSTEIN	88	CNTR	
$< 2.5 \times 10^{-36}$	90	2 THRON	85	CNTR	$Q = 1, m=4-12 \text{ GeV}$
$< 1. \times 10^{-35}$	90	2 THRON	85	CNTR	$Q = 1, m=4-12 \text{ GeV}$
$< 6. \times 10^{-33}$	90	3 ARMITAGE	79	SPEC	$m=1.87 \text{ GeV}$
$< 1.5 \times 10^{-33}$	90	3 ARMITAGE	79	SPEC	$m=1.5-3.0 \text{ GeV}$
		4 BOZZOLI	79	CNTR	$Q = (2/3, 1, 4/3, 2)$
$< 1.1 \times 10^{-37}$	90	5 CUTTS	78	CNTR	$m=4-10 \text{ GeV}$
$< 3.0 \times 10^{-37}$	90	6 VIDAL	78	CNTR	$m=4.5-6 \text{ GeV}$

- 1 BERNSTEIN 88 limits apply at  $x = 0.2$  and  $p_T = 0$ . Mass and lifetime dependence of limits are shown in the regions:  $m = 1.5-7.5 \text{ GeV}$  and  $\tau = 10^{-8}-2 \times 10^{-6} \text{ s}$ . First number is for hadrons; second is for weakly interacting particles.
- 2 THRON 85 is FNAL 400 GeV proton experiment. Mass determined from measured velocity and momentum. Limits are for  $\tau > 3 \times 10^{-9} \text{ s}$ .
- 3 ARMITAGE 79 is CERN-ISR experiment at  $E_{cm} = 53 \text{ GeV}$ . Value is for  $x = 0.1$  and  $p_T = 0.15$ . Observed particles at  $m = 1.87 \text{ GeV}$  are found all consistent with being antideuterons.
- 4 BOZZOLI 79 is CERN-SPS 200 GeV  $pN$  experiment. Looks for particle with  $\tau$  larger than  $10^{-8} \text{ s}$ . See their figure 11-18 for production cross-section upper limits vs mass.
- 5 CUTTS 78 is pBe experiment at FNAL sensitive to particles of  $\tau > 5 \times 10^{-8} \text{ s}$ . Value is for  $-0.3 < x < 0$  and  $p_T = 0.175$ .
- 6 VIDAL 78 is FNAL 400 GeV proton experiment. Value is for  $x = 0$  and  $p_T = 0$ . Puts lifetime limit of  $< 5 \times 10^{-8} \text{ s}$  on particle in this mass range.

**Long-Lived Heavy Particle Production**

**( $\sigma(\text{Heavy Particle}) / \sigma(\pi)$ )**

VALUE	EVTS	DOCUMENT ID	TECN	CHG	COMMENT
••• We do not use the following data for averages, fits, limits, etc. •••					
$< 10^{-8}$	0	1 NAKAMURA	89	SPEC	$Q = (-5/3, \pm 2)$
	0	2 BUSSIERE	80	CNTR	$Q = (2/3, 1, 4/3, 2)$

- 1 NAKAMURA 89 is KEK experiment with 12 GeV protons on Pt target. The limit applies for mass  $\lesssim 1.6 \text{ GeV}$  and lifetime  $\gtrsim 10^{-7} \text{ s}$ .
- 2 BUSSIERE 80 is CERN-SPS experiment with 200-240 GeV protons on Be and Al target. See their figures 6 and 7 for cross-section ratio vs mass.

**Production and Capture of Long-Lived Massive Particles**

VALUE ( $10^{-36} \text{ cm}^2$ )	EVTS	DOCUMENT ID	TECN	COMMENT	
••• We do not use the following data for averages, fits, limits, etc. •••					
$< 20$ to 800	0	1 ALEKSEEV	76	ELEC	$\tau = 5 \text{ ms}$ to 1 day
$< 200$ to 2000	0	1 ALEKSEEV	76B	ELEC	$\tau = 100 \text{ ms}$ to 1 day
$< 1.4$ to 9	0	2 FRANKEL	75	CNTR	$\tau = 50 \text{ ms}$ to 10 hours
$< 0.1$ to 9	0	3 FRANKEL	74	CNTR	$\tau = 1$ to 1000 hours

- 1 ALEKSEEV 76 and ALEKSEEV 76B are 61-70 GeV  $p$  Serpukhov experiment. Cross section is per Pb nucleus.
- 2 FRANKEL 75 is extension of FRANKEL 74.
- 3 FRANKEL 74 looks for particles produced in thick Al targets by 300-400 GeV/c protons.

**Long-Lived Particle Search at Hadron Collisions**

Limits are for cross section times branching ratio.

VALUE (nb/nucleon)	CL%	EVTS	DOCUMENT ID	TECN	COMMENT	
••• We do not use the following data for averages, fits, limits, etc. •••						
$< 2$	90	0	1 BADIER	86	BDMP	$\tau = (0.05-1.) \times 10^{-8} \text{ s}$

1 BADIER 86 looked for long-lived particles at 300 GeV  $\pi^-$  beam dump. The limit applies for nonstrongly interacting neutral or charged particles with mass  $> 2 \text{ GeV}$ . The limit applies for particle modes,  $\mu^+\pi^-, \mu^+\mu^-, \pi^+\pi^-, X, \pi^+\pi^-\pi^\pm$  etc. See their figure 5 for the contours of limits in the mass- $\tau$  plane for each mode.

# Searches Particle Listings

## WIMPs and Other Particle Searches

### Long-Lived Heavy Particle Cross Section

VALUE (pb/sr)	CL%	DOCUMENT ID	TECN	COMMENT
<34	95	1 RAM	94	SPEC 1015 <math>m_{X^{++}} < 1085 \text{ MeV}</math>
<75	95	1 RAM	94	SPEC 920 <math>m_{X^{++}} < 1025 \text{ MeV}</math>

• • • We do not use the following data for averages, fits, limits, etc. • • •

<sup>1</sup> RAM 94 search for a long-lived doubly-charged fermion  $X^{++}$  with mass between  $m_N$  and  $m_N + m_\pi$  and baryon number +1 in the reaction  $pp \rightarrow X^{++} + n$ . No candidate is found. The limit is for the cross section at  $15^\circ$  scattering angle at 460 MeV incident energy and applies for  $\tau(X^{++}) \gg 0.1 \mu\text{s}$ .

### LIMITS ON CHARGED PARTICLES IN COSMIC RAYS

#### Heavy Particle Flux in Cosmic Rays

VALUE (cm <sup>-2</sup> sr <sup>-1</sup> s <sup>-1</sup> )	CL%	EVTs	DOCUMENT ID	TECN	CHG	COMMENT
~ 6 × 10 <sup>-9</sup>		2	1 SAITO	90		$Q \approx 14, m \approx 370 m_p$
< 1.4 × 10 <sup>-12</sup>	90	0	2 MINCER	85	CALO	$m \geq 1 \text{ TeV}$
< 1.7 × 10 <sup>-11</sup>	99	0	3 SAKUYAMA	83B	PLAS	$m \sim 1 \text{ TeV}$
< 1 × 10 <sup>-9</sup>	90	0	4 BHAT	82	CC	
2 × 10 <sup>-9</sup>		3	5 MARINI	82	CNTR ±	$Q = 1, m \sim 4.5 m_p$
		3	6 YOCK	81	SPRK ±	$Q = 1, m \sim 4.5 m_p$
		3	6 YOCK	81	SPRK	Fractionally charged
3.0 × 10 <sup>-9</sup>		3	7 YOCK	80	SPRK	$m \sim 4.5 m_p$
(4 ± 1) × 10 <sup>-11</sup>		3	GOODMAN	79	ELEC	$m \geq 5 \text{ GeV}$
< 1.3 × 10 <sup>-9</sup>	90	0	8 BHAT	78	CNTR ±	$m > 1 \text{ GeV}$
< 1.0 × 10 <sup>-9</sup>	0	0	BRIATORE	76	ELEC	
< 7 × 10 <sup>-10</sup>	90	0	YOCK	75	ELEC ±	$Q > 7e \text{ or } < -7e$
> 6 × 10 <sup>-9</sup>		5	9 YOCK	74	CNTR	$m > 6 \text{ GeV}$
< 3.0 × 10 <sup>-8</sup>	0	0	DARDO	72	CNTR	
< 1.5 × 10 <sup>-9</sup>	0	0	TONWAR	72	CNTR	$m > 10 \text{ GeV}$
< 3.0 × 10 <sup>-10</sup>	0	0	BJORNBOE	68	CNTR	$m > 5 \text{ GeV}$
< 5.0 × 10 <sup>-11</sup>	90	0	JONES	67	ELEC	$m = 5-15 \text{ GeV}$

- <sup>1</sup> SAITO 90 candidates carry about 450 MeV/nucleon. Cannot be accounted for by conventional backgrounds. Consistent with strange quark matter hypothesis.
- <sup>2</sup> MINCER 85 is high statistics study of calorimeter signals delayed by 20–200 ns. Calibration with AGS beam shows they can be accounted for by rare fluctuations in signals from low-energy hadrons in the shower. Claim that previous delayed signals including BJORNBOE 68, DARDO 72, BHAT 82, SAKUYAMA 83b below may be due to this fake effect.
- <sup>3</sup> SAKUYAMA 83b analyzed 6000 extended air shower events. Increase of delayed particles and change of lateral distribution above  $10^{17}$  eV may indicate production of very heavy parent at top of atmosphere.
- <sup>4</sup> BHAT 82 observed 12 events with delay  $> 2 \times 10^{-8}$  s and with more than 40 particles. 1 eV has good hadron shower. However all events are delayed in only one of two detectors in cloud chamber, and could not be due to strongly interacting massive particle.
- <sup>5</sup> MARINI 82 applied PEP-counter for TOF. Above limit is for velocity = 0.54 of light. Limit is inconsistent with YOCK 80 YOCK 81 events if isotropic dependence on zenith angle is assumed.
- <sup>6</sup> YOCK 81 saw another 3 events with  $Q = \pm 1$  and  $m$  about  $4.5 m_p$ , as well as 2 events with  $m > 5.3 m_p$ ,  $Q = \pm 0.75 \pm 0.05$  and  $m > 2.8 m_p$ ,  $Q = \pm 0.70 \pm 0.05$  and 1 event with  $m = (9.3 \pm 3.) m_p$ ,  $Q = \pm 0.89 \pm 0.06$  as possible heavy candidates.
- <sup>7</sup> YOCK 80 events are with charge exactly or approximately equal to unity.
- <sup>8</sup> BHAT 78 is at Kolar gold fields. Limit is for  $\tau > 10^{-6}$  s.
- <sup>9</sup> YOCK 74 events could be tritons.

### Superheavy Particle (Quark Matter) Flux in Cosmic Rays

VALUE (cm <sup>-2</sup> sr <sup>-1</sup> s <sup>-1</sup> )	CL%	EVTs	DOCUMENT ID	TECN	COMMENT
< 5 × 10 <sup>-16</sup>	90	1	1 AMBROSIO	00B	MCRO $m > 5 \times 10^{14} \text{ GeV}$
< 1.8 × 10 <sup>-12</sup>	90	2	2 ASTONE	93	CNTR $m \geq 1.5 \times 10^{-13} \text{ gram}$
< 1.1 × 10 <sup>-14</sup>	90	3	3 AHLEN	92	MCRO $10^{-10} < m < 0.1 \text{ gram}$
< 2.2 × 10 <sup>-14</sup>	90	0	4 NAKAMURA	91	PLAS $m > 10^{11} \text{ GeV}$
< 6.4 × 10 <sup>-16</sup>	90	0	5 ORITO	91	PLAS $m > 10^{12} \text{ GeV}$
< 2.0 × 10 <sup>-11</sup>	90	6	6 LIU	88	BOLO $m > 1.5 \times 10^{-13} \text{ gram}$
< 4.7 × 10 <sup>-12</sup>	90	7	7 BARISH	87	CNTR $1.4 \times 10^8 < m < 10^{12} \text{ GeV}$
< 3.2 × 10 <sup>-11</sup>	90	0	8 NAKAMURA	85	CNTR $m > 1.5 \times 10^{-13} \text{ gram}$
< 3.5 × 10 <sup>-11</sup>	90	0	9 ULLMAN	81	CNTR Planck-mass $10^{19} \text{ GeV}$
< 7 × 10 <sup>-11</sup>	90	0	9 ULLMAN	81	CNTR $m \leq 10^{16} \text{ GeV}$

- <sup>1</sup> AMBROSIO 00B searched for quark matter ("nuclearites") in the velocity range  $(10^{-5}-1)c$ . The listed limit is for  $2 \times 10^{-3} c$ .
- <sup>2</sup> ASTONE 93 searched for quark matter ("nuclearites") in the velocity range  $(10^{-3}-1)c$ . Their Table 1 gives a compilation of searches for nuclearites.
- <sup>3</sup> AHLEN 92 searched for quark matter ("nuclearites"). The bound applies to velocity  $< 2.5 \times 10^{-3} c$ . See their Fig. 3 for other velocity/ $c$  and heavier mass range.
- <sup>4</sup> NAKAMURA 91 searched for quark matter in the velocity range  $(4 \times 10^{-5}-1)c$ .
- <sup>5</sup> ORITO 91 searched for quark matter. The limit is for the velocity range  $(10^{-4}-10^{-3})c$ .
- <sup>6</sup> LIU 88 searched for quark matter ("nuclearites") in the velocity range  $(2.5 \times 10^{-3}-1)c$ . A less stringent limit of  $5.8 \times 10^{-11}$  applies for  $(1-2.5) \times 10^{-3} c$ .

- <sup>7</sup> BARISH 87 searched for quark matter ("nuclearites") in the velocity range  $(2.7 \times 10^{-4}-5 \times 10^{-3})c$ .
- <sup>8</sup> NAKAMURA 85 at KEK searched for quark-matter. These might be lumps of strange quark matter with roughly equal numbers of  $u, d, s$  quarks. These lumps or nuclearites were assumed to have velocity of  $(10^{-4}-10^{-3})c$ .
- <sup>9</sup> ULLMAN 81 is sensitive for heavy slow singly charge particle reaching earth with vertical velocity 100–350 km/s.

### Highly Ionizing Particle Flux

VALUE (m <sup>-2</sup> yr <sup>-1</sup> )	CL%	EVTs	DOCUMENT ID	TECN	COMMENT
< 0.4	95	0	KINOSHITA	81B	PLAS $Z/\beta$ 30–100

• • • We do not use the following data for averages, fits, limits, etc. • • •

### REFERENCES FOR Searches for WIMPs and Other Particles

AAD	11AG	NJP 13 053044	G. Aad <i>et al.</i>	(ATLAS Collab.)
AAD	11L	PL B698 353	G. Aad <i>et al.</i>	(ATLAS Collab.)
AAD	11S	PL B705 294	G. Aad <i>et al.</i>	(ATLAS Collab.)
AALSETH	11	PRL 106 131301	C.E. Aalseth <i>et al.</i>	(CoGeNT Collab.)
AALSETH	11A	PRL 107 141301	C.E. Aalseth <i>et al.</i>	(CoGeNT Collab.)
AALTONEN	11AF	PRL 107 181801	T. Aaltonen <i>et al.</i>	(CDF Collab.)
AALTONEN	11M	PRL 106 171801	T. Aaltonen <i>et al.</i>	(CDF Collab.)
ABAZOV	11I	PRL 107 011804	V. M. Abazov <i>et al.</i>	(D0 Collab.)
ABBASI	11C	PR D84 022004	R. Abbasi <i>et al.</i>	(IceCube Collab.)
ABRAMOWSKI	11	PRL 106 161301	A. Abramowski <i>et al.</i>	(H.E.S.S. Collab.)
ACKERMANN	11	PRL 107 241302	M. Ackermann <i>et al.</i>	(Fermi-LAT Collab.)
AHLEN	11	PL B695 124	S. Ahlen <i>et al.</i>	(DMTPC Collab.)
AHMED	11	PR D83 112002	Z. Ahmed <i>et al.</i>	(CDMS Collab.)
AHMED	11A	PR D84 011102	Z. Ahmed <i>et al.</i>	(CDMS and EDELWEISS Collabs.)
AHMED	11B	PRL 106 131302	Z. Ahmed <i>et al.</i>	(CDMS Collab.)
AJELLO	11	PR D84 032007	M. Ajello <i>et al.</i>	(Fermi-LAT)
ANGLE	11	PRL 107 051301	J. Angle <i>et al.</i>	(XENON10 Collab.)
APRILE	11	PR D84 052003	E. Aprile <i>et al.</i>	(XENON100 Collab.)
APRILE	11A	PR D84 061101	E. Aprile <i>et al.</i>	(XENON100 Collab.)
APRILE	11B	PRL 107 131302	E. Aprile <i>et al.</i>	(XENON100 Collab.)
ARMENGAUD	11	PL B702 329	E. Armengaud <i>et al.</i>	(EDELWEISS II Collab.)
BEHNKE	11	PRL 106 021303	E. Behnke <i>et al.</i>	(COUPP Collab.)
CHATRCHYAN	11C	JHEP 1106 026	S. Chatrchyan <i>et al.</i>	(CMS Collab.)
CHATRCHYAN	11U	PRL 107 201804	S. Chatrchyan <i>et al.</i>	(CMS Collab.)
GERINGER-SA.	11I	PRL 107 241303	A. Gerlinger-Sameth, S.M. Koushiappas	(ZEPLIN-III Collab.)
HORN	11	PL B705 471	M. Horn <i>et al.</i>	(Super-Kamiokande Collab.)
TANAKA	11	APJ 742 78	T. Tanaka <i>et al.</i>	(ATLAS Collab.)
AAD	10	PRL 105 161801	G. Aad <i>et al.</i>	(CDF Collab.)
AALTONEN	10AF	PR D82 052005	T. Aaltonen <i>et al.</i>	(CDF Collab.)
ABBASI	10	PR D81 057101	R. Abbasi <i>et al.</i>	(IceCube Collab.)
AHMED	10	SCI 327 1619	Z. Ahmed <i>et al.</i>	(CDMS II Collab.)
AKERIB	10	PR D82 122004	D.S. Akerib <i>et al.</i>	(CDMS-II Collab.)
AKIMOV	10	PL B692 180	D. Yu. Akimov <i>et al.</i>	(ZEPLIN-III Collab.)
APRILE	10	PRL 105 131302	E. Aprile <i>et al.</i>	(XENON100 Collab.)
ARMENGAUD	10	PL B687 294	E. Armengaud <i>et al.</i>	(EDELWEISS II Collab.)
FELIZARDO	10	PRL 105 211301	M. Felizardo <i>et al.</i>	(THE SIMPLE Collab.)
KHACHATRYAN	10	PRL 105 211801	V. Khachatryan <i>et al.</i>	(CMS Collab.)
Also	10	PRL 106 029902E	V. Khachatryan <i>et al.</i>	(CMS Collab.)
MIUCHI	10	PL B686 11	K. Miuchi <i>et al.</i>	(NEWAGE Collab.)
AALTONEN	09AF	PR D80 011102R	T. Aaltonen <i>et al.</i>	(CDF Collab.)
AALTONEN	09G	PR D79 052004	T. Aaltonen <i>et al.</i>	(CDF Collab.)
AALTONEN	09J	PRL 103 021802	T. Aaltonen <i>et al.</i>	(CDF Collab.)
ABAZOV	09M	PRL 102 161802	V.M. Abazov <i>et al.</i>	(D0 Collab.)
ABBASI	09B	PRL 102 201302	R. Abbasi <i>et al.</i>	(IceCube Collab.)
AHMED	09	PR 102 011301	Z. Ahmed <i>et al.</i>	(CDMS Collab.)
ANGLE	09	PR D80 115005	J. Angle <i>et al.</i>	(XENON10 Collab.)
ARCHAMBAUD	09	PL B682 185	S. Archambault <i>et al.</i>	(PICASSO Collab.)
LEBEDENKO	09A	PRL 103 151302	V.N. Lebedenko <i>et al.</i>	(ZEPLIN-III Collab.)
LIN	09	PR D79 061101R	S.T. Lin <i>et al.</i>	(TEXONO Collab.)
AALSETH	08	PRL 101 251301	C.E. Aalseth <i>et al.</i>	(CoGeNT Collab.)
Also	08	PRL 102 109903 (errata)	C.E. Aalseth <i>et al.</i>	(CoGeNT Collab.)
ANGLE	08A	PRL 101 091301	J. Angle <i>et al.</i>	(XENON10 Collab.)
BEDNYAKOV	08	PAN 71 111	V.A. Bednyakov, H.P. Klapdor-Kleingrothaus, I.V. Krivosheina	(XENON10 Collab.)
ALNER	07	PL B653 161	G.J. Alner <i>et al.</i>	(ZEPLIN-II Collab.)
LEE	07A	PRL 99 091301	H.S. Lee <i>et al.</i>	(KIMS Collab.)
MIUCHI	07	PL B654 58	K. Miuchi <i>et al.</i>	(CDMS Collab.)
AKERIB	06	PR D73 011102R	D.S. Akerib <i>et al.</i>	(CDMS Collab.)
SHIMIZU	06A	PL B633 195	Y. Shimizu <i>et al.</i>	(CDMS Collab.)
AKERIB	05	PR D72 052009	D.S. Akerib <i>et al.</i>	(CDMS Collab.)
ALNER	05	PL B616 17	G.J. Alner <i>et al.</i>	(UK Dark Matter Collab.)
BARNABE-HE.	05	PL B624 186	M. Barnabe-Heider <i>et al.</i>	(PICASSO Collab.)
BENOIT	05	PL B616 28	A. Benoit <i>et al.</i>	(EDELWEISS Collab.)
GIRARD	05	PL B621 233	T.A. Girard <i>et al.</i>	(SIMPLE Collab.)
GIULIANI	05	PRL 95 101301	F. Giuliani	(OPAL Collab.)
GIULIANI	05A	PR D71 123503	F. Giuliani, T.A. Girard	(OPAL Collab.)
KLAPDOR-K.	05	PL B609 226	H.V. Klapdor-Kleingrothaus, I.V. Krivosheina, C. Tomei	(H1 Collab.)
AKTAS	04C	EPJ C36 413	A. Aktas <i>et al.</i>	(H1 Collab.)
GIULIANI	04	PL B588 151	F. Giuliani, T.A. Girard	(H1 Collab.)
GIULIANI	04A	PRL 93 161301	F. Giuliani	(H1 Collab.)
MIUCHI	03	ASP 19 135	K. Miuchi <i>et al.</i>	(OPAL Collab.)
TAKEDA	03	PL B572 145	A. Takeda <i>et al.</i>	(OPAL Collab.)
ANGLOHER	02	ASP 18 43	G. Angloher <i>et al.</i>	(OPAL Collab.)
BELLI	02	PR D66 043503	P. Belli <i>et al.</i>	(CRESST Collab.)
BERNABE	02C	EPJ C23 61	R. Bernabei <i>et al.</i>	(DAMA Collab.)
GREEN	02	PR D66 083003	A.M. Green	(DAMA Collab.)
JAVOREK	02	PR D65 072003	D. Javorek II <i>et al.</i>	(Heidelberg-Moscow Collab.)
BAUDIS	01	PR D63 022001	L. Baudis <i>et al.</i>	(Heidelberg-Moscow Collab.)
JAVOREK	01	PR D64 012005	D. Javorek II <i>et al.</i>	(Heidelberg-Moscow Collab.)
JAVOREK	01B	PRL 87 231804	D. Javorek II <i>et al.</i>	(Heidelberg-Moscow Collab.)
SMITH	01	PR D64 043502	D. Smith, N. Weiner	(Heidelberg-Moscow Collab.)
ULLIO	01	JHEP 0107 044	P. Ullio, M. Kamionkowski, P. Vogel	(Heidelberg-Moscow Collab.)
ABBIENDI	00D	EPJ C13 197	G. Abbiendi <i>et al.</i>	(OPAL Collab.)
AMBROSIO	00B	EPJ C13 453	M. Ambrosio <i>et al.</i>	(OPAL Collab.)
BENOIT	00	PL B479 8	A. Benoit <i>et al.</i>	(EDELWEISS Collab.)
BERNABE	00D	NJP 2 15	R. Bernabei <i>et al.</i>	(DAMA Collab.)
COLLAR	00	PRL 85 3083	J.J. Collar <i>et al.</i>	(SIMPLE Collab.)
ABE	99F	PRL D2 2038	F. Abe <i>et al.</i>	(CDF Collab.)
AMBROSIO	99	PR D60 082002	M. Ambrosio <i>et al.</i>	(CDF Collab.)
BERNABE	99	PL B450 448	R. Bernabei <i>et al.</i>	(DAMA Collab.)
BERNABE	99D	PRL 83 4918	R. Bernabei <i>et al.</i>	(DAMA Collab.)
BRHLIK	99	PL B464 303	M. Brhlik, L. Roszkowski	(DAMA Collab.)
DERBIN	99	PAN 62 1886	A.V. Derbin <i>et al.</i>	(DAMA Collab.)
ACKERSTAFF	98P	Translated from YAF 62 2034.	K. Akerstaff <i>et al.</i>	(OPAL Collab.)
KLIMENKO	98	PL B433 195	A.A. Klimenko <i>et al.</i>	(OPAL Collab.)
		Translated from ZETFP 67 835.		



See key on page 457

Searches Particle Listings  
WIMPs and Other Particle Searches

ABE	97G	PR D55 R5263	F. Abe <i>et al.</i>	(CDF Collab.)	NAKAMURA	85	PL 161B 417	K. Nakamura <i>et al.</i>	(KEK, INUS)
ABREU	97D	PL B396 315	P. Abreu <i>et al.</i>	(DELPHI Collab.)	THRON	85B	PR D31 451	J.L. Thron <i>et al.</i>	(YALE, FNAL, IOWA)
ACKERSTAFF	97B	PL B391 210	K. Akerstaff <i>et al.</i>	(OPAL Collab.)	SAKUYAMA	83B	LNC 37 17	H. Sakuyama, N. Suzuki	(MEIS)
ADAMS	97B	PRL 79 4083	J. Adams <i>et al.</i>	(FNAL KTeV Collab.)	Also	LNC 36 389	H. Sakuyama, K. Watanabe	(MEIS)	
BARATE	97K	PL B405 379	R. Barate <i>et al.</i>	(ALEPH Collab.)	Also	NC 78A 147	H. Sakuyama, K. Watanabe	(MEIS)	
SARSA	97	PR D56 1856	M.L. Sarsa <i>et al.</i>	(ZARA)	Also	NC 6C 371	H. Sakuyama, K. Watanabe	(MEIS)	
ALESSAND...	96	PL B384 316	A. Alessandrello <i>et al.</i>	(MILA, MILAI, SASSO)	BHAT	82	PR D25 2820	P.N. Bhat <i>et al.</i>	(TATA)
BELLI	96	PL B387 222	P. Belli <i>et al.</i>	(DAMA Collab.)	KINOSHITA	82	PRL 48 77	K. Kinoshita, P.B. Price, D. Fryberger	(UCB+)
Also	PL B389 783 (erratum)	P. Belli <i>et al.</i>	(DAMA Collab.)	MARINI	82	PR D26 1777	A. Marini <i>et al.</i>	(FRAS, LBL, NWES, STAN+)	
BELLI	96C	NC 19C 537	P. Belli <i>et al.</i>	(DAMA Collab.)	SMITH	82B	NP B206 333	P.F. Smith <i>et al.</i>	(RAL)
BERNABEI	96	PL B389 757	R. Bernabei <i>et al.</i>	(DAMA Collab.)	KINOSHITA	81B	PR D24 1707	K. Kinoshita, P.B. Price	(UCB)
COLLAR	96	PRL 76 331	J.J. Collar	(SUCU)	LOSECCO	81	PL 102B 209	J.M. LoSecco <i>et al.</i>	(MICH, PENN, BNL)
SARSA	96	PL B386 458	M.L. Sarsa <i>et al.</i>	(ZARA)	ULLMAN	81	PRL 47 289	J.D. Ullman	(LEHM, BNL)
Also	PR D56 1856	M.L. Sarsa <i>et al.</i>	(ZARA)	YOCK	81	PR D23 1207	P.C.M. Yock	(AUCK)	
SMITH	96	PL B379 299	P.F. Smith <i>et al.</i>	(RAL, SHEF, LOIC+)	BARTEL	80	ZPHY C6 295	W. Bartel <i>et al.</i>	(JADE Collab.)
SNOWDEN-...	96	PRL 76 332	D.P. Snowden-Ifft, E.S. Freeman, P.B. Price	(UCB)	BUSSIERE	80	NP B174 1	A. Bussiere <i>et al.</i>	(BGNA, SACL, LAPP)
AKERS	95R	ZPHY C67 203	R. Akers <i>et al.</i>	(OPAL Collab.)	YOCK	80	PR D22 61	P.C.M. Yock	(AUCK)
GALLAS	95	PR D52 6	E. Gallas <i>et al.</i>	(MSU, FNAL, MIT, FLOR)	ARMITAGE	79	NP B150 87	J.C.M. Armitage <i>et al.</i>	(CERN, DARE, FOM+)
GARCIA	95	PR D51 1458	E. Garcia <i>et al.</i>	(ZARA, SCUC, PNL)	BOZZOLI	79	NP B159 363	W. Bozzoli <i>et al.</i>	(BGNA, LAPP, SACL+)
QUENBY	95	PL B351 70	J.J. Quenby <i>et al.</i>	(LOIC, RAL, SHEF+)	GOODMAN	79	PR D19 2572	J.A. Goodman <i>et al.</i>	(UMD)
SNOWDEN-...	95	PRL 74 4133	D.P. Snowden-Ifft, E.S. Freeman, P.B. Price	(UCB)	SMITH	79	NP B149 525	P.F. Smith, J.R.J. Bennett	(RHEL)
Also	PRL 76 331	J.J. Collar	(SUCU)	BHAT	78	PRAM 10 115	P.N. Bhat, P.V. Ramana Murthy	(TATA)	
Also	PRL 76 332	D.P. Snowden-Ifft, E.S. Freeman, P.B. Price	(UCB)	CARROLL	78	PRL 41 777	A.S. Carroll <i>et al.</i>	(BNL, PRIN)	
BECK	94	PL B336 141	M. Beck <i>et al.</i>	(MPIH, KIAE, SASSO)	CUTTS	78	PRL 41 363	D. Cutts <i>et al.</i>	(BROW, FNAL, ILL, BARI+)
RAM	94	PR D49 3120	S. Ram <i>et al.</i>	(TELA, TRIU)	VIDAL	78	PL 77B 344	R.A. Vidal <i>et al.</i>	(COLU, FNAL, STON+)
ABE	93G	PRL 71 2542	F. Abe <i>et al.</i>	(CDF Collab.)	ALEKSEEV	76	SJNP 22 531	G.D. Alekseev <i>et al.</i>	(JINR)
ASTONE	93	PR D47 4770	P. Astone <i>et al.</i>	(ROMA, ROMAI, CATA, FRAS)	ALEKSEEV	76B	SJNP 23 633	Translated from YAF 22 1021.	(JINR)
BUSKULIC	93C	PL B303 198	D. Buskulic <i>et al.</i>	(ALEPH Collab.)	BALDIN	76	SJNP 22 264	Translated from YAF 23 1190.	(JINR)
YAMAGATA	93	PR D47 1231	T. Yamagata, Y. Takamori, H. Utsunomiya	(KONAN)	BRIATORE	76	NC 31A 553	L. Briatore <i>et al.</i>	(LCGT, FRAS, FREIB)
ABE	92J	PR D46 R1889	F. Abe <i>et al.</i>	(CDF Collab.)	GUSTAFSON	76	PRL 37 474	H.R. Gustafson <i>et al.</i>	(MICH)
AHLEN	92	PRL 69 1860	S.P. Ahlen <i>et al.</i>	(MACRO Collab.)	ALBROW	75	NP B97 189	M.G. Albrow <i>et al.</i>	(CERN, DARE, FOM+)
BACCI	92	PL B293 460	C. Bacci <i>et al.</i>	(Beijing-Roma-Saclay Collab.)	FRANKEL	75	PR D12 2561	S. Frankel <i>et al.</i>	(PENN, FNAL)
VERKERK	92	PRL 68 1116	P. Verkerk <i>et al.</i>	(ENSP, SACL, PAST)	JOVANOV...	75	PL 56B 105	J.V. Jovanovich <i>et al.</i>	(MANI, AACH, CERN+)
AKESSON	91	ZPHY C52 219	T. Akesson <i>et al.</i>	(HELIOS Collab.)	YOCK	75	NP B86 216	P.C.M. Yock	(AUCK, SLAC)
NAKAMURA	91	PL B263 529	S. Nakamura <i>et al.</i>	(ICEPP, WASCR, NIHO, ICRR)	APPEL	74	PRL 32 428	J.A. Appel <i>et al.</i>	(COLU, FNAL)
ORITO	91	PRL 66 1951	S. Orito <i>et al.</i>	(NEUC, CIT, PSI)	FRANKEL	74	PR D9 1932	S. Frankel <i>et al.</i>	(PENN, FNAL)
REUSSER	91	PL B255 143	D. Reusser <i>et al.</i>	(TOPAZ Collab.)	YOCK	74	NP B76 175	P.C.M. Yock	(AUCK)
ADACHI	90C	PL B244 352	I. Adachi <i>et al.</i>	(OPAL Collab.)	ALPER	73	PL 46B 265	B. Alper <i>et al.</i>	(CERN, LVP, LUND, BOHR+)
ADACHI	90E	PL B249 336	I. Adachi <i>et al.</i>	(ROCH, MICH, OHIO+)	LEIPUNER	73	PRL 31 1226	L.B. Leipuner <i>et al.</i>	(BNL, YALE)
AKRAWY	90O	PL B252 290	M.Z. Akrawy <i>et al.</i>	(ICRR, KOBE)	DARDO	72	NC 9A 319	M. Dardo <i>et al.</i>	(TORI)
HENMICK	90	PR D41 2074	T.K. Hemmick <i>et al.</i>	(KYOT, TMTCT)	TONWAR	72	JPA 5 569	S.C. Tonwar, S. Naranan, B.V. Sreekantan	(TATA)
SAITO	90	PRL 65 2094	T. Saito <i>et al.</i>	(STAN, WIS C)	ANTIPOV	71B	NP B31 235	Y.M. Antipov <i>et al.</i>	(SERP)
NAKAMURA	89	PR D39 1261	T.T. Nakamura <i>et al.</i>	(UCSB, UCB, LBL)	BINON	69	PL 34B 164	Y.M. Binon <i>et al.</i>	(SERP)
NORMAN	89	PR D39 2499	R.M. Norman <i>et al.</i>	(CIT)	BJORNBOE	68	NC B53 241	F.G. Binon <i>et al.</i>	(SERP)
BERNSTEIN	88	PR D37 3103	E.B. Bernstein <i>et al.</i>	(NA3 Collab.)	JONES	67	PR 164 1584	J. Bjornboe <i>et al.</i>	(BOHR, TATA, BERN+)
CALDWELL	88	PRL 61 510	D.O. Caldwell <i>et al.</i>	(UMD, GMAS, NSF)	DORFAN	65	PRL 14 999	L.W. Jones	(MICH, WISC, LBL, UCLA, MINN+)
LIU	88	PRL 61 271	G. Liu, B. Barish					D.E. Dorfan <i>et al.</i>	(COLU)
BARISH	87	PR D36 2641	B.C. Barish, G. Liu, C. Lane						
NORMAN	87	PRL 58 1403	E.B. Norman, S.B. Gazes, D.A. Bennett						
BADIER	86	ZPHY C31 21	J. Badier <i>et al.</i>						
MINCER	85	PR D32 541	A. Mincer <i>et al.</i>						



## INDEX



- A, a* meson resonances
- $A(1680)$  or [*now called*  $\pi_2(1670)$ ] . . . . . **38**, 781
  - $A(2100)$  [*now called*  $\pi_2(2100)$ ] . . . . . 805
  - $a_0(980)$  [*was*  $\delta(980)$ ] . . . . . **35**, 734
  - $a_0(1450)$  . . . . . 766
  - $a_1(1260)$  [*was*  $A_1(1270)$  or  $A_1$ ] . . . . . **36**, 743
  - $a_1(1640)$  . . . . . 779
  - $a_2(1320)$  [*was*  $A_2(1320)$ ] . . . . . **36**, 752
  - $a_2(1700)$  . . . . . 792
  - $A_3$  [*now called*  $\pi_2(1670)$ ] . . . . . **38**, 781
  - $a_4(2040)$  [*was*  $\delta_4(2040)$ ] . . . . . 803
  - $a_6(2450)$  [*was*  $\delta_6(2450)$ ] . . . . . 813
- Abbreviations used in Particle Listings . . . . . 458
- Accelerator-induced radioactivity . . . . . 383
- Accelerator parameters (colliders) . . . . . 317
- Accelerator physics of colliders . . . . . 313
- Acceptance-rejection method in Monte Carlo . . . . . 402
- Activity, unit of, for radioactivity . . . . . 381
- Age of the universe . . . . . 108, 266
- Air showers (cosmic ray) . . . . . 309
- Algorithms for Monte Carlo . . . . . 403
- Amplitudes, Lorentz invariant . . . . . 422
- Angular-diameter distance,  $d_A$  . . . . . 266
- Anisotropy of cosmic microwave background radiation (CBR) 284, 297
- Anomalous  $W/Z$  Quartic Couplings . . . . . 477
- Anomalous  $ZZ\gamma$ ,  $Z\gamma\gamma$ , and  $ZZV$  couplings . . . . . 498
- Argand diagram, definition . . . . . 425
- Astronomical unit . . . . . 108
- Astrophysics . . . . . 264, 289
- Asymmetries of  $Z$ -boson decay . . . . . 479
- Asymmetry formulae in Standard Model . . . . . 139
- Atmospheric cosmic rays . . . . . 306
- Atmospheric fluorescence . . . . . 368
- Atmospheric pressure . . . . . 107
- Atomic and nuclear properties of materials . . . . . 114
- Atomic mass unit . . . . . 107
- Atomic weights of elements . . . . . 111
- Attenuation length for photons . . . . . 331
- Authors and consultants . . . . . 11
- Average hadron multiplicities in  $e^+e^-$  annihilation events . . . . . 441
- Averaging of data . . . . . 14
- Avogadro number . . . . . 107
- Axial vector couplings,  $g_V$ ,  $g_A$  vector . . . . . 136
- Axions as dark matter . . . . . 264, 290
- Axion searches . . . . . **28**, 562
- Axion searches, note on . . . . . 562
- b*-baryon ADMIXTURE ( $\Lambda_b$ ,  $\Xi_b$ ,  $\Sigma_b$ ,  $\Omega_b$ ) . . . . . **91**, 1409
- b*-flavored hadrons, production and decay of, note on . . . . . 963
- b*-hadron mixing and production fractions, note on . . . . . 1069
- $b_1(1235)$  [*was*  $B(1235)$ ] . . . . . **36**, 742
- b* (quarks) . . . . . **33**, 667
- b*-quark fragmentation . . . . . 254
- b'* quark ( $4^{th}$  generation), searches for, . . . . . **33**, 687
- $b\bar{b}$  mesons . . . . . **71**, 1223
- $B^0-\bar{B}^0$  mixing, note on . . . . . 1066
- B* decay,  $CP$  violation in . . . . . 166
- B* decays, hadronic, note on . . . . . 968
- B* decays, rare, note on . . . . . 968
- B*, bottom mesons
- Bottom mesons, HFAG activities . . . . . 974
  - B* (bottom meson) . . . . . **50**, 963
  - $B^\pm$  (bottom meson) . . . . . **50**, 974
  - $B^0, \bar{B}^0$  (bottom meson) . . . . . **55**, 1020
  - $B^\pm/B^0$  ADMIXTURE . . . . . **60**, 1087
  - $B^\pm/B^0/B_s^0/b$ -baryon ADMIXTURE . . . . . **62**, 1104
  - $B^*$  . . . . . **63**, 1126
  - $B_J^*(5732)$  . . . . . 1126
  - $B_c^\pm$  . . . . . 1139
  - $B_s^0$  . . . . . **63**, 1128
  - $B_s$  mixing studies, note on . . . . . 1068
  - $B_s^*$  . . . . . 1138
  - $B_{s,J}^*(5850)$  . . . . . 1138
  - $b\bar{b}$  mesons . . . . . **71**, 1223
- Baryogenesis . . . . . 269
- Baryon decay parameters, note on . . . . . 1264
- Baryon magnetic moments, note on . . . . . 1327
- Baryon number conservation . . . . . 95
- Baryon resonances, SU(3) classification of . . . . . 202
- Baryonium candidates . . . . . 815
- Baryons . . . . . **79**, 1253
- Bottom (beauty) baryons . . . . . **91**, 1405
  - Cascade baryons ( $\Xi$  baryons) . . . . . **86**, 1367
  - Charmed baryons . . . . . **87**, 1383
  - Dibaryons
    - (see p. VIII.118 in our 1992 edition, Phys. Rev. **D45**, Part II)  - Hyperon baryons ( $\Lambda$  baryons) . . . . . **83**, 1327
  - Hyperon baryons ( $\Sigma$  baryons) . . . . . **84**, 1343
  - Nucleon resonances ( $\Delta$  resonances) . . . . . **82**, 1305
  - Nucleon resonances ( $N$  resonances) . . . . . **80**, 1271
  - Nucleons . . . . . **79**, 1253
  - $\Omega$  baryons . . . . . **87**, 1380
- Baryons in quark model . . . . . 202
- Baryons, stable . . . . . **79**, 1253
- (see entries for  $p$ ,  $n$ ,  $\Lambda$ ,  $\Sigma$ ,  $\Xi$ ,  $\Omega$ ,  $\Lambda_c$ ,  $\Xi_c$ ,  $\Omega_c$ ,  $\Lambda_b$ , and  $\Xi_b$ )
- Bayes' theorem . . . . . 386

- Bayesian statistics . . . . . 396
- Beam momentum, c.m. energy and momentum vs . . . . . 422
- Beauty – see Bottom
- Becquerel, unit of radioactivity . . . . . 381
- BEPC (China) collider parameters . . . . . 317
- BEPC-II (China) collider parameters . . . . . 317
- $\beta$  decay, neutrinoless double, search for . . . . . 631
- $\beta$ -rays, from radioactive sources . . . . . 385
- Bethe-Bloch equation . . . . . 323
- Bias of an estimator . . . . . 390
- Big-bang cosmology . . . . . 264
- Binary pulsars . . . . . 261
- Binomial distribution . . . . . 387
- Binomial distribution, Monte Carlo algorithm for . . . . . 403
- Binomial distribution, table of . . . . . 388
- Birks' law . . . . . 342
- Black holes . . . . . 1489
- Bohr magneton . . . . . 107
- Bohr radius . . . . . 107
- Boiling points of cryogenic gases . . . . . 114
- Boltzmann constant . . . . . 107
- Booklet, Particle Physics, how to get . . . . . 11
- Bosons . . . . . **27**, 469  
(see individual entries for  $\gamma$ ,  $W$ ,  $Z$ ,  $g$ , Axions, graviton, Higgs)
- Bottom baryons ( $\Lambda_b^0, \Xi_b$ ) . . . . . **91**, 1405
- Bottom,  $B^0$ - $\bar{B}^0$  mixing, note on . . . . . 1066
- Bottom-changing neutral currents, tests for . . . . . 95
- Bottom, charmed meson . . . . . **64**, 1139
- Bottom mesons ( $B, B^*, B_s, B_s^*, B_c^\pm$ ) . . . . . **50**, 963  
Bottom mesons, note on HFAG activities . . . . . 974
- Bottom quark ( $b$ ) . . . . . **33**, 667
- Bottom, strange mesons . . . . . **63**, 1128
- Bottomonium system, level diagram . . . . . 1223
- Bragg additivity . . . . . 328
- Branes . . . . . 1489
- Breit-Wigner  
distribution, Monte Carlo algorithm for . . . . . 403  
resonance, definition . . . . . 425  
vs pole parameters of  $N$  and  $\Delta$  Resonances . . . . . 1268
- Bremsstrahlung by electrons . . . . . 330
- $C$  (charge conjugation), tests of conservation . . . . . 95
- $c$  (quark) . . . . . **33**, 666
- $c\bar{c}$  Region in  $e^+e^-$  Collisions, plot of . . . . . 445
- $c$ -quark fragmentation . . . . . 254
- $c\bar{c}$  mesons . . . . . **64**, 1146
- Cabibbo-Kobayashi-Maskawa mixing in  $B$  decay, note on . . . . . 1066
- Calorimetry . . . . . 360
- Cascade baryons ( $\Xi$  baryons) . . . . . **86**, 1367
- CBR—Cosmic background radiation (see CMB) . . . . . 297
- Central limit theorem . . . . . 388
- Cepheid variable stars . . . . . 283
- CESR (Cornell) collider parameters . . . . . 318
- CESR-C (Cornell) collider parameters . . . . . 318
- Change of random variables . . . . . 387
- Characteristic functions . . . . . 387
- Charge conjugation ( $C$ ) conservation . . . . . 95
- Charge conservation . . . . . 95
- Charge conservation and the Pauli exclusion principle, note on  
(see p. VI.10 in our 1992 edition, Phys. Rev. **D45**)
- Chargino searches . . . . . 1456
- Charm-changing neutral currents, tests for . . . . . 95
- Charm Dalitz analyses, note on . . . . . 893
- Charm quark ( $c$ ) . . . . . **33**, 666
- Charmed baryons ( $\Lambda_c^+, \Sigma_c, \Xi_c, \Omega_c^0$ ) . . . . . **87**, 1385
- Charmed, bottom meson ( $B_c^\pm$ ) . . . . . **64**, 1139
- Charmed mesons ( $D, D^*, D_J$ ) . . . . . **43**, 885
- Charmed, strange mesons [ $D_s, D_s^*, D_{sJ}$ ] . . . . . **48**, 941
- Charmonium system, level diagram . . . . . 1146
- Cherenkov detectors  
at accelerators . . . . . 346  
differential . . . . . 347  
ring imaging . . . . . 347  
threshold . . . . . 346  
tracking . . . . . 346  
nonaccelerator  
atmospheric . . . . . 369  
deep underground . . . . . 370
- Cherenkov radiation . . . . . 335
- $\chi^2$  distribution . . . . . 389
- $\chi^2$  distribution, Monte Carlo algorithm for . . . . . 403
- $\chi^2$  distribution, table of . . . . . 388
- $\chi_b$  and  $\chi_c$  mesons  
 $\chi_{b0}(1P)$  . . . . . **72**, 1228  
 $\chi_{b0}(2P)$  . . . . . **73**, 1235  
 $\chi_{b1}(1P)$  . . . . . **72**, 1229  
 $\chi_{b1}(2P)$  . . . . . **73**, 1237  
 $\chi_{b2}(1P)$  . . . . . **72**, 1231  
 $\chi_{b2}(2P)$  . . . . . **73**, 1239  
 $\chi_b(3P)$  . . . . . , 1244  
 $\chi_{c0}(1P)$  . . . . . **66**, 1168  
 $\chi_{c1}(1P)$  . . . . . **66**, 1176  
 $\chi_{c2}(1P)$  . . . . . **67**, 1183
- $\chi_{c0,1,2}$  and  $\psi(2S)$ , branching ratios, note on . . . . . 1168
- CKM mixing elements in  $B$  decay, note on . . . . . 1066
- Clebsch-Gordan coefficients . . . . . 419

- CLIC . . . . . 318
- c.m. energy and momentum vs beam momentum . . . . . 422
- CMB–Cosmic microwave background . . . . . 270, 297, 284
- Collaboration databases . . . . . 19
- Collider parameters . . . . . 317
- Colliders, accelerator physics of . . . . . 313
- Color octet leptons . . . . . **94**, 1488
- Color sextet quarks . . . . . **94**, 1488
- Compensating calorimeters . . . . . 361
- Compositeness, quark and lepton, searches . . . . . **93**, 1484
- Compositeness, quark and lepton, searches, note on . . . . . 1484
- Composition of the Universe . . . . . 275
- Compton wavelength, electron . . . . . 107
- Concordance cosmology . . . . . 281
- Conditional probability density function . . . . . 387
- Confidence intervals . . . . . 396
- Confidence intervals, frequentist . . . . . 396
- Confidence intervals, Poisson . . . . . 399
- Conservation laws . . . . . 95
- Consistency of an estimator . . . . . 390
- Cosmic microwave background . . . . . 284
- Constrained fits, procedures for . . . . . 15
- Consultants . . . . . 12
- Conversion probability for photons to  $e^+e^-$  . . . . . 331
- Correlation coefficient, definition . . . . . 387
- Cosmic background radiation (CBR) temperature . . . . . 108
- Cosmic ray(s) . . . . . 305
- air showers . . . . . 309
- ankle . . . . . 310
- at surface of earth . . . . . 306
- background in counters . . . . . 381
- composition . . . . . 305
- fluxes . . . . . 306
- in atmosphere . . . . . 306, 309
- knee . . . . . 310
- primary spectra . . . . . 305
- secondary neutrinos . . . . . 308
- underground . . . . . 307
- Cosmological constant  $\Lambda$  . . . . . 108, 264, 280
- Cosmological density parameter,  $\Omega$  . . . . . 265
- Cosmological equation of state . . . . . 265
- Cosmological mass density parameter . . . . . 265
- Cosmological mass density parameter of vacuum (dark energy) . 265
- Cosmological parameters . . . . . 280, 281
- Cosmology . . . . . 264, 280, 289
- Coulomb scattering through small angles, multiple . . . . . 328
- Coupling between matter and gravity . . . . . 259
- Coupling unification . . . . . 209
- Couplings, anomalous  $W/Z$  Quartic . . . . . 477
- Couplings, anomalous  $ZZ\gamma$ ,  $Z\gamma\gamma$ , and  $ZZV$  . . . . . 498
- Couplings for photon,  $W$ ,  $Z$  . . . . . 136
- Couplings, note on the extraction of triple-gauge . . . . . 474
- Covariance, definition . . . . . 387
- Coverage . . . . . 396
- $CP$ , tests of conservation . . . . . 95
- $CP$  violation
- in  $B$  decay . . . . . 166
- in  $K_L^0$  decay . . . . . 166
- in  $K_L^0$  decays, note on . . . . . 859
- in  $K_S^0 \rightarrow 3\pi$  decays, note on . . . . . 845
- overview . . . . . 166
- $CPT$  Invariance tests in neutral kaon decay . . . . . 839
- $CPT$ , tests of conservation . . . . . 95
- Critical density in cosmology . . . . . 108, 264
- Critical energy, electrons . . . . . 331
- Critical energy, muons . . . . . 334
- Cross sections and related quantities, plots of . . . . . 439
- $e^+e^-$  annihilation cross section near  $M_Z$  . . . . . 446
- Fragmentation functions . . . . . 249
- gamma production in  $p\bar{p}$  interactions . . . . . 439
- Jet production in  $pp$  and  $\bar{p}p$  interactions . . . . . 439
- Nucleon structure functions . . . . . 241
- Pseudorapidity distributions . . . . . 440
- $W$  and  $Z$  differential cross section . . . . . 440
- Cross sections, neutrino . . . . . 436
- Cross sections, Regge theory fits to total, table . . . . . 447
- Cross sections, relations for . . . . . 424, 427
- Cryogenic gases, boiling points . . . . . 114
- Cumulative distribution function, definition . . . . . 386
- Curie, unit of radioactivity . . . . . 381
- $d$  (quark) . . . . . **33**, 662
- $d$  functions . . . . . 419
- $D^0$ – $\bar{D}^0$  mixing, note on . . . . . 903
- $D$ -meson, Dalitz analyses, note on . . . . . 893
- $D$  mesons
- $D^\pm$  . . . . . **43**, 885
- $D^0, \bar{D}^0$  . . . . . **44**, 903
- $D(2550)^0$  . . . . . , 939
- $D(2600)$  . . . . . , 940
- $D(2750)$  . . . . . , 940
- $D_1(2420)^0$  . . . . . **48**, 936
- $D_1(2420)^\pm$  . . . . . , 937
- $D^*(2007)^0$  . . . . . **47**, 933
- $D^*(2010)^\pm$  . . . . . **48**, 934
- $D^*(2640)^\pm$  . . . . . 940

- $D_2^*(2460)^0$  . . . . . 48, 937  
 $D_2^*(2460)^\pm$  . . . . . 48, 939  
 $D_s^\pm$  [*was*  $F^\pm$ ] . . . . . 48, 941  
 $D_s^{*\pm}$  [*was*  $F^{*\pm}$ ] . . . . . 49, 957  
 $D_{s1}(2536)^\pm$  . . . . . 50, 960  
 $D_{s2}(2573)$  . . . . . 50, 961  
 $D_{sJ}^*(2860)^\pm$  . . . . . , 962  
 $D_{sJ}(3040)^\pm$  . . . . . , 962  
 $D_s^+$  Branching Fractions, note on . . . . . 943  
Dalitz analyses,  $D$ -meson, note on . . . . . 893  
Dalitz plot, relations for . . . . . 423  
DAΦNE (Frascati) collider parameters . . . . . 317  
Dark energy . . . . . 265, 283  
Dark energy equation of state parameter  $w$  . . . . . 283  
Dark energy parameter,  $\Omega_N$  . . . . . 265  
Dark matter . . . . . 272, 289, 281, 282  
Dark matter detectors . . . . . 375  
    sub-Kelvin detectors . . . . . 375  
    table . . . . . 375  
Dark matter limits:  
    Neutralinos mass limits . . . . . 1455  
    Sneutrino mass limits . . . . . 1459  
Dark matter, nonbaryonic . . . . . 289  
Data, averaging and fitting procedures . . . . . 14  
Data, selection and treatment . . . . . 13  
Databases, availability online . . . . . 18  
Databases, high-energy physics . . . . . 18  
Databases, particle physics . . . . . 18  
Day, sidereal . . . . . 108  
 $dE/dx$  . . . . . 323  
Decay amplitudes (for hyperon decays)  
    (see p. 286 in our 1982 edition, Phys. Lett. **111B**)  
Decay constant,  $D_s^+$ , note on . . . . . 943  
Decay constants of charged pseudoscalar mesons, note on . . . . . 946  
Decays, kinematics and phase space for . . . . . 422  
Deceleration parameter,  $q_0$  . . . . . 265  
Definitions for abbreviations used in Particle Listings . . . . . 458  
 $\delta$ -rays . . . . . 326  
 $\delta(980)$  [*now called*  $a_0(980)$ ] . . . . . **35**, 734  
 $\delta_4(2040)$  [*now called*  $a_4(2040)$ ] . . . . . 803  
 $\delta_6(2450)$  [*now called*  $a_6(2450)$ ] . . . . . 813  
 $\Delta$  resonances (see also  $N$  and  $\Delta$  resonances) . . . . . **82**, 1305  
 $\Delta B = 1$ , weak-neutral currents, tests for . . . . . 95  
 $\Delta B = 2$ , tests for . . . . . 95  
 $\Delta C = 1$ , weak-neutral currents, tests for . . . . . 95  
 $\Delta C = 2$ , tests for . . . . . 95  
 $\Delta I = 1/2$  rule for hyperon decays, test of  
    (see p. 286 in our 1982 edition, Phys. Lett. **111B**)  
 $\Delta S = 1$ , weak-neutral currents, tests for . . . . . 95  
 $\Delta S = 2$ , tests for . . . . . 95  
 $\Delta S = \Delta Q$  rule in  $K^0$  decay, note on . . . . . 866  
 $\Delta S = \Delta Q$ , tests of . . . . . 95  
 $\Delta T = 1$ , weak-neutral currents, tests for . . . . . 95  
Density effect in energy loss rate . . . . . 326  
Density of materials, table . . . . . 114  
Density of matter, critical . . . . . 108  
Density of matter, local . . . . . 108  
Density parameter of the universe,  $\Omega_0$  . . . . . 108  
Detector parameters . . . . . 339  
Deuteron mass . . . . . 107  
Deuteron structure function . . . . . 242, 243  
Dibaryons  
    (see p. VIII.118 in our 1992 edition, Phys. Rev. **D45**, Part II)  
Dielectric constant of gaseous elements, table . . . . . 115  
Dielectric suppression of bremsstrahlung . . . . . 332  
DIEHARD . . . . . 402  
Differential Cherenkov detectors . . . . . 347  
Dimensions, extra . . . . . **94**, 1489  
Directories, online, people, and organizations . . . . . 18  
Disk density . . . . . 108  
Distance-redshift relation . . . . . 264, 280  
Dose, radioactivity, unit of absorbed . . . . . 382  
Dose rate from gamma ray sources . . . . . 383  
Double- $\beta$  Decay . . . . . 631  
    Double- $\beta$  Decay, Limits from Neutrinoless, note on . . . . . 631  
Double- $\beta$  decay, neutrinoless, search for . . . . . 631  
Drift Chambers . . . . . 350  
Drift velocities of electrons in liquids . . . . . 363  
Durham databases . . . . . 18  
Dynamical electroweak symmetry breaking . . . . . 1475  
 $e$  (electron) . . . . . **30**, 581  
 $e$  (natural log base) . . . . . 107  
    Charge conservation and the Pauli exclusion principle, note on  
    (see p. VI.10 in our 1992 edition, Phys. Rev. **D45**)  
 $e^+e^-$  average multiplicity, plot of . . . . . 443  
 $E(1420)$  [*now called*  $f_1(1420)$ ] . . . . . **37**, 763  
Earth equatorial radius . . . . . 108  
Earth mass . . . . . 108  
Education databases . . . . . 18  
Efficiency of an estimator . . . . . 390  
Electric charge ( $Q$ ) conservation . . . . . 95  
Electrical resistivity of elements, table . . . . . 115  
Electromagnetic  
    calorimeters . . . . . 360  
    interactions of  $N$  and  $\Delta$  baryons (review) . . . . . 1270



penguin decays, note on . . . . .	969	$\eta(2225)$ . . . . .	810
relations . . . . .	116	$\eta_2(1645)$ . . . . .	780
shower detectors, energy resolution . . . . .	360	$\eta_2(1870)$ . . . . .	798
showers, lateral distribution . . . . .	334	$\eta'(958)$ . . . . .	<b>35</b> , 726
showers, longitudinal distribution . . . . .	333	$\eta_b(1S)$ . . . . .	1224
Electron . . . . .	<b>30</b> , 581	$\eta_c(1S)$ . . . . .	<b>64</b> , 1146
and photon interactions in matter . . . . .	329	$\eta_c(2S)$ . . . . .	1191
charge . . . . .	107	Excitation energy . . . . .	325
critical energy . . . . .	331	Excited lepton searches . . . . .	<b>93</b> , 1487
cyclotron frequency/field . . . . .	107	(see p. VIII.58 in our 1992 edition, Phys. Rev. <b>D45</b> , Part II)	
mass . . . . .	107, <b>30</b>	Expansion of the Universe . . . . .	265
radius, classical . . . . .	107	Expectation value, definition . . . . .	386
volt . . . . .	107	Experiment databases . . . . .	19
Electron drift velocities in liquids . . . . .	363	Experimental issues in $B^0$ - $\bar{B}^0$ mixing, note on . . . . .	1067
Electronic structure of the elements . . . . .	112	Experimental tests of gravitational theory . . . . .	259
Electroweak interactions, Standard Model of . . . . .	136	Extensions to the cosmological standard model . . . . .	282
Elements, electronic structure of . . . . .	112	Extra Dimensions . . . . .	<b>94</b> , 1489
Elements, ionization energies of . . . . .	112	$f_{D^+}, f_{D_s^+}, f_{K^+}, f_{\pi^+}$ decay constants . . . . .	946
Elements, periodic table of . . . . .	111	$F, f$ meson resonances	
Energy and momentum (c.m.) vs beam momentum . . . . .	422	$F^\pm$ [ <i>now called</i> $D_s^\pm$ ] . . . . .	<b>48</b> , 941
Energy density / Boltzmann constant . . . . .	108	$F^{*\pm}$ [ <i>now called</i> $D_s^{*\pm}$ ] . . . . .	<b>49</b> , 957
Energy density of CBR . . . . .	108	$f_0(500)$ [ <i>was</i> $\epsilon(1200)$ ] . . . . .	<b>34</b> , 706
Energy density of relativistic particles . . . . .	108	$f_0(980)$ [ <i>was</i> $S(975)$ or $S^*$ ] . . . . .	<b>35</b> , 731
Energy loss		$f_0(1370)$ . . . . .	<b>37</b> , 755
by electrons . . . . .	330	$f_0(1500)$ . . . . .	<b>37</b> , 770
(fractional) for electrons and positrons in lead . . . . .	329	$f_0(1710)$ [ <i>was</i> $\theta(1690)$ ] . . . . .	<b>38</b> , 793
rate for charged particles . . . . .	324	$f_0(2020)$ . . . . .	802
rate for muons at high energies . . . . .	334	$f_0(2100)$ . . . . .	806
rate, form factor corrections . . . . .	325	$f_0(2200)$ . . . . .	809
rate in compounds . . . . .	328	$f_1(1285)$ . . . . .	<b>36</b> , 748
rate, restricted . . . . .	327	$f_1(1420)$ [ <i>was</i> $E(1420)$ ] . . . . .	<b>37</b> , 763
Entropy density . . . . .	269	$f_1(1420)$ , note on . . . . .	759
Entropy density / Boltzmann constant . . . . .	108	$f_1(1510)$ . . . . .	773
$\epsilon(1200)$ [ <i>now called</i> $f_0(500)$ ] . . . . .	<b>34</b> , 706	$f_1(1510)$ , note on . . . . .	759
$\epsilon(2150)$ [ <i>now called</i> $f_2(2150)$ ] . . . . .	806	$f_2(1270)$ . . . . .	<b>36</b> , 745
$\epsilon(2300)$ [ <i>now called</i> $f_4(2300)$ ] . . . . .	811	$f_2(1430)$ . . . . .	766
$\epsilon$ (permittivity) . . . . .	107, 115, 116	$f_2(1565)$ . . . . .	776
$\epsilon_0$ (permittivity of free space) . . . . .	107, 116	$f_2(1640)$ . . . . .	779
$\hat{\epsilon}_1, \hat{\epsilon}_2, \hat{\epsilon}_3$ electroweak variables . . . . .	149–150	$f_2(1810)$ . . . . .	797
Error function . . . . .	388	$f_2(1910)$ . . . . .	800
Error procedure for masses and widths of meson resonances . . . . .	870	$f_2(1950)$ . . . . .	801
Errors, treatment of . . . . .	14	$f_2(2010)$ [ <i>was</i> $g_T(2010)$ ] . . . . .	<b>39</b> , 802
Estimator . . . . .	390	$f_2(2150)$ [ <i>was</i> $\epsilon(2150)$ ] . . . . .	806
$\eta$ meson . . . . .	<b>34</b> , 701	$f_2(2300)$ [ <i>was</i> $g_T'(2300)$ ] . . . . .	<b>39</b> , 811
$\eta(1295)$ . . . . .	<b>36</b> , 751	$f_2(2340)$ [ <i>was</i> $g_T''(2340)$ ] . . . . .	<b>39</b> , 812
$\eta(1405)$ [ <i>was</i> $\iota(1440)$ ] . . . . .	<b>37</b> , 759	$f_2'(1525)$ [ <i>was</i> $f'(1525)$ ] . . . . .	<b>37</b> , 774
$\eta(1440)$ , note on . . . . .	759	$f_4(2050)$ [ <i>was</i> $h(2030)$ ] . . . . .	<b>39</b> , 804
$\eta(1760)$ . . . . .	795		

$f_4(2300)$ [ <i>was</i> $\epsilon(2300)$ ]	811	Gas-filled detectors	348
$f_6(2510)$ [ <i>was</i> $r(2510)$ ]	814	electron drift velocity	348
$f_7(2220)$ [ <i>was</i> $\xi(2220)$ ]	809	gas properties	348
$F_2$ structure function, plots	241	high rate effects	351
Familon searches	574	mobility of ions	349
Fermi coupling constant	107	Townsend coefficient	349
Fermi plateau	326	Gauge bosons	<b>27</b> , 469
Feynman's $x$ variable	424	(see individual entries for $\gamma$ , $W$ , $Z$ , $g$ , Axions, graviton, Higgs)	
Field equations, electromagnetic	116	Gauge couplings	136
Fine structure constant	107	Gaussian confidence intervals	398
Fit to $Z$ electroweak measurements	478	Gaussian confidence intervals close to physical boundary	400
Fits to data	14	Gaussian distribution, Monte Carlo algorithm for	403
Flatness of Universe	108	Gaussian distribution, Multivariate	389
Flavor-changing neutral currents, tests for	95	Gaussian ellipsoid	389
Fluorescence, atmospheric	368	Glauino searches	<b>93</b> , 1469
Fly's Eye	310, 368	gluon, $g$	<b>27</b> , 469
Forbidden states in quark model	118	Goldstone boson searches	574
Force, Lorentz	116	Grand unified theories	209
Form factors, $K_{\ell 3}$ , note on	833	Gravitational	
Form factors, $\pi \rightarrow \ell\nu\gamma$ and $K \rightarrow \ell\nu\gamma$ , note on	696	acceleration $g$	107
Fourth generation ( $b'$ ) searches	<b>33</b> , 687	constant $G_N$	107, 108
Fractional energy loss for electrons and positrons in lead	329	field in the strong field regime, dynamical tests	260
Fragmentation functions	249	field in the weak field regime, dynamical tests	260
Fragmentation, heavy-quark	254	lensing	271, 286
Fragmentation in $e^+e^-$ annihilation	249	theory, experimental tests of	259
Fragmentation, longitudinal	251	graviton	470
Fragmentation models	252	Gravitons	1489
Free quark searches	<b>33</b> , 688	Gravity in extra dimensions	1489
Frequentist statistics	396	Gray, unit of absorbed dose of radiation	381
Friedmann-Lemaître equations	264	GUTs	209
Further States	815	$h(2030)$ [ <i>now called</i> $f_4(2050)$ ]	<b>39</b> , 804
$g$ (gluon)	<b>27</b> , 469	$h_1(1170)$ [ <i>was</i> $H(1190)$ ]	<b>36</b> , 741
$g(1690)$ [ <i>now called</i> $\rho_3(1690)$ ]	<b>38</b> , 784	$h_1(1380)$	758
$g_T(2010)$ [ <i>now called</i> $f_2(2010)$ ]	<b>39</b> , 802	$h_1(1595)$	778
$g'_T(2300)$ [ <i>now called</i> $f_2(2300)$ ]	<b>39</b> , 811	$h_c(1P)$	1182
$g''_T(2340)$ [ <i>now called</i> $f_2(2340)$ ]	<b>39</b> , 812	$h_b(1P)$	1231
$g_V, g_A$ vector, axial vector couplings	136	$h_b(2P)$	1239
Galaxy clustering	285	Hadron (average) multiplicities in $e^+e^-$ annihilation events	441
Galaxy power spectrum	285	Hadronic	
$\gamma$ (Euler constant)	107	calorimeters	361
$\gamma$ (photon)	<b>27</b> , 469	flavor conservation	95
$\gamma p$ and $\gamma d$ cross sections, plots of	454	shower detectors	361
gamma production in $p\bar{p}$ interactions	439	Half-lives of commonly used radioactive nuclides	385
$\gamma$ -rays, from radioactive sources	385	Halo density	108
Gamma distribution	389	Harrison-Zel'dovich effect	280
Gamma distribution, Monte Carlo algorithm for	403	Heavy boson searches	<b>28</b> , 543
Gamma distribution, table of	388	Heavy lepton searches	<b>32</b> , 621

- Heavy-Neutral Leptons, Searches for . . . . . **32**, 647
- Heavy particle searches . . . . . 1504
- Heavy-quark fragmentation . . . . . 254
- HERA (DESY) collider parameters . . . . . 320
- Hierarchy problem . . . . . **1420**, 1489
- Higgs boson in Standard Model . . . . . 136, 147, 501
- Higgs boson mass in electroweak analyses . . . . . 147–150
- Higgs,  $M_H$ , constraints on . . . . . 147–150
- Higgs production in  $e^+e^-$  annihilation, cross-section formula . . 429
- Higgs searches . . . . . **28**, 501
- Higgs searches, note on . . . . . 501
- History of measurements, discussion . . . . . 16
- Hubble constant (expansion rate) . . . . . 108
- Hubble constant  $H_0$  . . . . . 280
- Hubble expansion . . . . . 265
- Hyperon baryons (see  $\Lambda$  and  $\Sigma$  baryons) . . . . . **83**, 1327
- Hyperon decays, nonleptonic decay amplitudes  
    (see p. 286 in our 1982 edition, Phys. Lett. **111B**)
- Hyperon decays, test of  $\Delta I = 1/2$  rule for  
    (see p. 286 in our 1982 edition, Phys. Lett. **111B**)
- Hyperon radiative decays, note on . . . . . 1368
- ID particle codes for Monte Carlo . . . . . 415
- Ideograms, criteria for presentation . . . . . 15
- Illustrative key to the Particle Listings . . . . . 457
- Imaging Cherenkov detectors . . . . . 346
- Impedance, relations for . . . . . 117
- Importance sampling in Monte Carlo calculations . . . . . 402
- Inclusive hadronic reactions . . . . . 429
- Inclusive reactions, kinematics for . . . . . 424
- Inconsistent data, treatment of . . . . . 15
- Independence of random variables . . . . . 387
- Inflation of early universe . . . . . 269, 280
- Information horizon . . . . . 267
- Inorganic scintillators . . . . . 344
- Inorganic scintillator parameters . . . . . 342
- International System (SI) units . . . . . 110
- INTERNET address for comments . . . . . 11
- Introduction . . . . . 11
- Inverse transform method in Monte Carlo . . . . . 402
- Ionization energies of the elements . . . . . 112
- Ionization energy loss at minimum, table . . . . . 114
- Ionization yields for charged particles . . . . . 328
- $\iota(1440)$  [*now called*  $\eta(1405)$ ] . . . . . **37**, 759
- Jansky . . . . . 108
- Jet production in  $pp$  and  $\bar{p}p$  interactions, plot of . . . . . 439
- $J/\psi(1S)$  or  $\psi(1S)$  . . . . . **64**, 1151
- $K^+p$ ,  $K^+n$ , and  $K^+d$  cross sections, plots of . . . . . 453
- $K^-p$ ,  $K^-n$ , and  $K^-d$  cross sections, plots of . . . . . 452
- $K$  stable mesons (see meson resonances below)
- $K^\pm$  . . . . . **39**, 820
- $K^0, \bar{K}^0$  . . . . . **40**, 839
- $K_L^0$  . . . . . **41**, 846
- $K_S^0$  . . . . . **40**, 842
- $K$  stable mesons, notes therein
- $K_L^0$   $CP$ -violation parameters, fits for, note on . . . . . 859
- $K$  decay,  $CPT$  invariance tests in neutral . . . . . 839
- $K^0$  decay, note on  $\Delta S = \Delta Q$  rule in . . . . . 866
- $K_L^0$  decay,  $CP$  violation in . . . . . 166
- $K_{\ell 3}$  form factors, note on . . . . . 833
- $K^\pm$  mass, note on . . . . . 820
- $K$  rare decay, note on . . . . . 822
- $K \rightarrow \ell\nu\gamma$  form factors, note on . . . . . 696
- $K \rightarrow 3\pi$  Dalitz plot parameters, note on . . . . . 832
- $K_S^0 \rightarrow 3\pi$  decay, note on  $CP$  violation in . . . . . 845
- $K, K^*$  meson resonances
- $K(1460)$  [*was*  $K(1400)$ ] . . . . . 877
- $K(1630)$  . . . . . 878
- $K(1830)$  . . . . . 881
- $K(3100)$  . . . . . 884
- $K^*(892)$  . . . . . **42**, 869
- $K^*(892)$  mass and mass differences, note on . . . . . 870
- $K^*(1410)$  . . . . . **42**, 874
- $K^*(1680)$  [*was*  $K^*(1790)$ ] . . . . . **42**, 878
- $K_0^*(1430)$  [*was*  $\kappa(1350)$ ] . . . . . **42**, 874
- $K_0^*(1950)$  . . . . . 881
- $K_1(1270)$  [*was*  $Q(1280)$  or  $Q_1$ ] . . . . . **42**, 872
- $K_1(1400)$  [*was*  $Q(1400)$  or  $Q_2$ ] . . . . . **42**, 873
- $K_1(1650)$  . . . . . 878
- $K_2(1580)$  [*was*  $L(1580)$ ] . . . . . 878
- $K_2(1770)$  [*was*  $L(1770)$ ] . . . . . **42**, 879
- $K_2(1820)$  . . . . . **43**, 881
- $K_2(2250)$  [*was*  $K(2250)$ ] . . . . . 883
- $K_2^*(1430)$  [*was*  $K^*(1430)$ ] . . . . . **42**, 875
- $K_2^*(1980)$  . . . . . 882
- $K_3(2320)$  [*was*  $K(2320)$ ] . . . . . 883
- $K_3^*(1780)$  [*was*  $K^*(1780)$ ] . . . . . **42**, 880
- $K_4(2500)$  [*was*  $K(2500)$ ] . . . . . 883
- $K_4^*(2045)$  [*was*  $K^*(2060)$ ] . . . . . **43**, 882
- $K_5^*(2380)$  . . . . . 883
- $K_{\ell 3}$  form factors, note on . . . . . 833
- Kaluza-Klein states . . . . . 1489
- Kaon (see also  $K$ ) . . . . . **39**, 820
- Kaon decay,  $CPT$  invariance tests in neutral . . . . . 839
- Kaon rare decay, note on . . . . . 822
- $\kappa(1350)$  [*now called*  $K_0^*(1430)$ ] . . . . . **42**, 874

KEKB collider parameters . . . . .	319	Light year . . . . .	108
Key to the Particle Listings . . . . .	457	Lineshape of $Z$ boson . . . . .	479
Kinematics, decays, and scattering . . . . .	422	Liquid ionization chambers, free electron drift velocity . . . . .	363
Knock-on electrons, energetic . . . . .	326	Listings, Full, keys to reading . . . . .	457
Kobayashi-Maskawa (Cabibbo-) mixing matrix . . . . .	157	Local group velocity relative to CBR . . . . .	108
$L(1580)$ [ <i>now called</i> $K_2(1580)$ ] . . . . .	878	Longitudinal fragmentation . . . . .	251
$L(1770)$ [ <i>now called</i> $K_2(1770)$ ] . . . . .	<b>42</b> , 879	Longitudinal structure function, plots of . . . . .	246
Lagrangian, standard electroweak . . . . .	136	Lorentz force . . . . .	116
$\Lambda$ , cosmological constant . . . . .	108, 264, 280	Lorentz invariant amplitudes . . . . .	422
$\Lambda$ CDM (cold dark matter with dark energy) . . . . .	281	Lorentz transformations of four-vectors . . . . .	422
$\Lambda$ . . . . .	<b>83</b> , 1327	Low-noise electronics . . . . .	357
$\Lambda$ and $\Sigma$ baryons . . . . .	<b>83</b> , 1327	Low-radioactivity background techniques . . . . .	377
Listings, $\Lambda$ baryons . . . . .	1327	cosmic rays . . . . .	379
Listings, $\Sigma$ baryons . . . . .	1343	cosmogenic . . . . .	379
Status of (review) . . . . .	1330	environmental . . . . .	378
$\Lambda p$ cross section, plot of . . . . .	454	neutrons . . . . .	379
$\Lambda_b^0$ . . . . .	1405	radioimpurities . . . . .	378
$\Lambda_c^+$ . . . . .	<b>87</b> , 1385	radon . . . . .	378
$\Lambda_c^+$ branching fractions, note on . . . . .	1386	Luminosity conversion . . . . .	108
$\Lambda_c(2595)^+$ . . . . .	<b>88</b> , 1391	Luminosity distance $d_L$ . . . . .	266
$\Lambda_c(2625)^+$ . . . . .	<b>88</b> , 1392	Ly $\alpha$ forest . . . . .	270
$\Lambda_c(2765)^+$ . . . . .	1393	Magnetic moments, baryon, note on . . . . .	1327
$\Lambda_c(2880)^+$ . . . . .	1393	Magnetic Monopole Searches . . . . .	<b>93</b> , 1413
Lagged-Fibonacci-based random number generator . . . . .	402	Magnetic Monopoles, note on . . . . .	1413
Landau-Pomeranchuk-Migdal (LPM) effect . . . . .	332	Majoron searches . . . . .	574
Large-scale structure of the Universe . . . . .	271	Mandelstam variables . . . . .	424
Least squares . . . . .	391	Marginal probability density function . . . . .	387
Least squares with nonindependent data . . . . .	391	Mass attenuation coefficient for photons . . . . .	331
LEP (CERN) collider parameters . . . . .	318	Mass density parameter, $\Omega_m$ . . . . .	281
Lepton conservation, tests of . . . . .	95	Massive neutrinos and lepton mixing, search for . . . . .	<b>32</b> , 636
Lepton family number conservation . . . . .	95	Materials, atomic and nuclear properties of . . . . .	114
Lepton (heavy) searches . . . . .	<b>32</b> , 621	Matter, passage of particles through . . . . .	323
Lepton mixing, neutrinos (massive) and, search for . . . . .	<b>32</b> , 636	Maximum energy transfer to $e^-$ . . . . .	325
Lepton, quark compositeness searches . . . . .	<b>93</b> , 1484	Maximum likelihood . . . . .	391
Lepton, quark substructure searches . . . . .	<b>93</b> , 1484	Maxwell equations . . . . .	116
Leptons . . . . .	<b>30</b> , 581	Mean energy loss rate in $H_2$ liquid, He gas, C, Al, Fe, Sn, and Pb, plots . . . . .	325
(see individual entries for $e$ , $\mu$ , $\tau$ , and neutrino properties)		Mean excitation energy . . . . .	325
Leptons, weak interactions of quarks and . . . . .	136, 148	Mean range in $H_2$ liquid, He gas, C, Fe, Pb, plots . . . . .	325
Leptoquark quantum numbers, note on . . . . .	555	Median, definition . . . . .	386
Leptoquark searches . . . . .	557	Meson multiplets in quark model . . . . .	199
Lethal dose from penetrating ionizing radiation . . . . .	382	Mesons . . . . .	<b>34</b> , 695
LHC (CERN) collider parameters . . . . .	321	$b\bar{b}$ mesons . . . . .	<b>71</b> , 1223
Lifetimes of $b$ -flavored hadrons, note on . . . . .	963	Bottom, charmed mesons . . . . .	<b>64</b> , 1139
Light boson searches . . . . .	562	Bottom mesons . . . . .	<b>50</b> , 963
Light neutrino types, number of . . . . .	<b>32</b> , 629	Bottom, strange mesons . . . . .	<b>63</b> , 1128
Light neutrino types from collider expts., number of, note on . . . . .	629	$c\bar{c}$ mesons . . . . .	<b>64</b> , 1146
Light, speed of . . . . .	107		

- Charmed, bottom meson . . . . . **64**, 1139
- Charmed mesons . . . . . **64**, 1146
- Charmed, strange mesons . . . . . **48**, 941
- Nonstrange mesons . . . . . **34**, 695
- Strange mesons . . . . . **39**, 820
- Mesons, stable . . . . . **34**, 695  
(see individual entries for  $\pi$ ,  $\eta$ ,  $K$ ,  $D$ ,  $D_s$ ,  $B$ , and  $B_s$ )
- Metric prefixes, commonly used . . . . . 110
- Michel parameter  $\rho$  . . . . . **30**, 618
- Micro-pattern gas detectors (MPDG) . . . . . 351  
  gas electron multiplier (GEM) . . . . . 351  
  micro-mesh gaseous structure (MicroMegas) . . . . . 351  
  micro-strip gas chamber . . . . . 352
- Microwave background . . . . . 270
- Minimum ionization . . . . . 325
- Minimum ionization loss, table . . . . . 114
- MIP (minimum ionizing particle) . . . . . 325
- Mistag probabilities in  $B^0-\bar{B}^0$  mixing, note on . . . . . 1067
- Mixing angle, weak ( $\sin^2\theta_W$ ) . . . . . 107, 136, 146
- Mixing,  $B^0-\bar{B}^0$ , note on . . . . . 1066
- Mixing,  $D^0-\bar{D}^0$ , note on . . . . . 903
- Mixing studies,  $B_s$ , note on . . . . . 1068
- Molar volume . . . . . 107
- Molière radius . . . . . 334
- Momenta, measurement of, in a magnetic field . . . . . 365
- Momentum — c.m. energy and momentum  
  vs beam momentum . . . . . 422
- Momentum transfer, minimum and maximum . . . . . 422
- Monopole searches . . . . . **93**, 1413  
  Monopole searches, note on . . . . . 1413
- Monte Carlo particle numbering scheme . . . . . 415
- Monte Carlo techniques . . . . . 402
- $\overline{\text{MS}}$  renormalization scheme (Standard Model) . . . . . 136
- $\mu$  (muon) . . . . . **30**, 582
- $\mu \rightarrow e$  conversion . . . . . 587
- $\mu_0$  (permeability of free space) . . . . . 107, 116
- Multibody decay kinematics . . . . . 423
- Multiple Coulomb scattering through small angles . . . . . 328
- Multiplets, meson in quark model . . . . . 199
- Multiplets, SU(n) . . . . . 421
- Multiplicities, average in  $e^+e^-$  interactions, table of . . . . . 441
- Multiplicity, average in  $e^+e^-$  interactions, plot of . . . . . 443
- Multiplicity, average in  $pp$  and  $\bar{p}p$  interactions, plot of . . . . . 443
- Multivariate Gaussian distribution . . . . . 389
- Multivariate Gaussian distribution, table of . . . . . 388
- Multi-wire proportional chamber (see also MWPC) . . . . . 350
- Muon . . . . . **30**, 582  
  anomalous magnetic moment, note on . . . . . 583
- critical energy . . . . . 334
- decay parameters, note on . . . . . 587
- energy loss rate at high energies . . . . . 334
- g-2 . . . . . 583
- range/energy in rock . . . . . 307
- MWPC, Multi-wire proportional chamber . . . . . 350  
  drift chambers . . . . . 350  
  maximum wire tension . . . . . 350  
  wire stability . . . . . 350
- $n$  (neutron) . . . . . **79**, 1262
- $n$ -body differential cross sections . . . . . 424
- $n$ -body phase space . . . . . 422
- $n - \bar{n}$  oscillations . . . . . 1264
- $N$  and  $\Delta$  resonances . . . . . **80**, 1268  
  Breit-Wigner vs pole parameters of . . . . . 1268  
  Electromagnetic interactions (review) . . . . . 1270  
  Listings,  $\Delta$  resonances . . . . . 1305  
  Listings,  $N$  resonances . . . . . 1268  
  Status of (review) . . . . . 1268
- $N^*$  resonances (see  $N$  and  $\Delta$  resonances) . . . . . **80**, 1268
- Names, hadrons . . . . . 13, 118
- Neutral-current parameters, values for . . . . . 148
- Neutralino as dark matter . . . . . 264
- Neutralino searches . . . . . 1455
- Neutrino(s) . . . . . **30**, 581  
  from cosmic rays . . . . . 308  
  mass, cosmological limit . . . . . 285  
  mass, mixing, and oscillations, note on . . . . . 177  
  masses . . . . . 209  
  (massive) and lepton mixing, search for . . . . . **32**, 636  
  mixing . . . . . **32**, 636  
  oscillation searches . . . . . **32**, 636  
  properties . . . . . **32**, 622  
  solar, review . . . . . 177  
  types (light), number of . . . . . **32**, 629  
  types (light) from collider experiments, number of, note on . . . . . 629
- Neutrino cross section measurements . . . . . 436
- Neutrino detectors (deep, large, enclosed volume) . . . . . 370  
  heavy water . . . . . 372  
  liquid scintillator . . . . . 371  
  table of detectors . . . . . 370  
  water-filled . . . . . 371
- Neutrinoless double- $\beta$  decay, search for . . . . . 631
- Neutrino mass density parameter,  $\Omega_\nu$  . . . . . 280
- Neutron . . . . . **79**, 1262
- Neutrons at accelerators . . . . . 382
- Neutrons, from radioactive sources . . . . . 385

Newtonian gravitational constant $G_N$ . . . . .	108	Other particle searches, note on . . . . .	1500
Nomenclature for hadrons . . . . .	13, 118	$P$ (parity), tests of conservation . . . . .	95
Nonbaryonic dark matter . . . . .	275	$p$ (proton) . . . . .	<b>79</b> , 1253
Normal distribution . . . . .	388	$pp, \bar{p}p$ average multiplicity, plot of . . . . .	443
Normal distribution, table of . . . . .	388	$pp$ jet production . . . . .	439
Neutrino Mixing . . . . .	<b>32</b> , 636	$pp, pn$ , and $pd$ cross sections, plots of . . . . .	449, 450
Neutrino Properties . . . . .	<b>32</b> , 622	$\bar{p}p$	
$\nu N$ and $\bar{\nu}N$ cross sections, plot of		average multiplicity, plot of . . . . .	443
(see p. III.75 in our 1992 edition, Phys. Rev. <b>D45</b> , Part II)		gamma production . . . . .	439
Nuclear collision length, table . . . . .	114	jet production . . . . .	439
Nuclear interaction length, table . . . . .	114	$\bar{p}n$ , and $\bar{p}d$ cross sections, plots of . . . . .	449, 450
Nuclear magneton . . . . .	107	pseudorapidity . . . . .	440
Nuclear (and atomic) properties of materials . . . . .	114	Parameter estimation . . . . .	390
Nucleon decay . . . . .	209	Parity of $q\bar{q}$ states . . . . .	199
Nucleon resonances (see $N$ and $\Delta$ resonances) . . . . .	<b>80</b> , 1268	Parsec . . . . .	108
Nucleon structure functions, plots of . . . . .	241	Partial-wave expansion of scattering amplitude . . . . .	425
Nuclides, radioactive, commonly used . . . . .	385	Particle detectors . . . . .	339
Number density of baryons . . . . .	108	Particle detectors for non-accelerator physics . . . . .	368
Number density of CBR photons . . . . .	108	Particle ID numbers for Monte Carlos . . . . .	415
Numbering scheme for particles in Monte Carlos . . . . .	415	Particle Listings, key to reading . . . . .	457
Occupational radiation dose, U.S. maximum permissible . . . . .	382	Particle Listings, organization of . . . . .	11
Omega baryons ( $\Omega$ baryons) . . . . .	<b>87</b> , 1380	Particle nomenclature . . . . .	13, 118
$\Omega^-$ resonances . . . . .	1381	Particle Physics Booklet, how to get . . . . .	11
$\Omega^-$ . . . . .	<b>87</b> , 1380	Particle symbol style conventions . . . . .	118
$\Omega_c^0$ . . . . .	1402	Parton distributions . . . . .	237
$\Omega$ , cosmological density parameter . . . . .	265	Passage of particles through matter . . . . .	323
$\Omega_b$ , baryon mass density . . . . .	281	Pauli exclusion principle, charge conservation, note on	
$\Omega_{\text{dm}}$ , dark matter density . . . . .	281, 282	(see p. VI.10 in our 1992 edition, Phys. Rev. <b>D45</b> )	
$\Omega_i$ , density parameter for $i$ th matter constituent . . . . .	280	Pentaquarks (see “Exotic Baryons,” p. 1199 of the 2010 <i>Review</i> , J. Phys. <b>G37</b> , 075021 (2010)).	
$\Omega_\Lambda$ , scaled cosmological constant . . . . .	108, 265	Penguin decays, electromagnetic, note on . . . . .	969
$\Omega_m$ , mass density parameter . . . . .	108, 265, 281	Periodic table of the elements . . . . .	111
$\Omega_\nu$ , neutrino mass density parameter . . . . .	280	Permeability $\mu_0$ of free space . . . . .	107, 116
$\Omega_m + \Omega_\Lambda$ . . . . .	108	Permittivity $\epsilon_0$ of free space . . . . .	107, 116
$\Omega_{\text{tot}}$ , total energy density of Universe . . . . .	108, 287	Phase space, Lorentz invariant . . . . .	422
$\Omega_Q$ , quintessence (dark) energy density . . . . .	283, 284	Phase space, relations for . . . . .	422
$\Omega_v$ , vacuum energy parameter . . . . .	265	$\phi(1020)$ . . . . .	<b>35</b> , 735
$\omega(782)$ . . . . .	<b>35</b> , 721	$\phi(1680)$ . . . . .	<b>38</b> , 783
$\omega(1420)$ . . . . .	<b>37</b> , 765	$\phi_3(1850)$ [ <i>was</i> $X(1850)$ ] . . . . .	<b>39</b> , 798
$\omega(1650)$ . . . . .	<b>38</b> , 780	Photino searches . . . . .	1450
$\omega_3(1670)$ . . . . .	<b>38</b> , 781	Photon . . . . .	<b>27</b> , 469
Opposite-side tag in $B^0-\bar{B}^0$ mixing, note on . . . . .	1068	and electron interactions with matter . . . . .	329
Optical theorem . . . . .	425	attenuation length . . . . .	331
Organic scintillators . . . . .	342	collection efficiency, scintillators . . . . .	342
Organization of Particle Listings and Summary Tables . . . . .	11	coupling . . . . .	136
Oscillation analyses in $B^0-\bar{B}^0$ mixing, note on . . . . .	1067	cross section in carbon and lead, contributions to . . . . .	330
Oscillation parameters, three-flavor, note . . . . .	640	pair production cross section . . . . .	332
Other particle searches . . . . .	1500	to $e^+e^-$ conversion probability . . . . .	331

- total cross sections (C and Pb) . . . . . 330
- Physical constants, table of . . . . . 107
- Physical region, for confidence intervals . . . . . 400
- $\pi$ , value of . . . . . 107
- $\pi^\pm p$  and  $\pi^\pm d$  cross sections, plots of . . . . . 451
- $\pi \rightarrow \ell\nu\gamma$  form factors, note on . . . . . 696
- $\pi$  mesons
- $\pi^\pm$  . . . . . **34**, 695
  - $\pi^0$  . . . . . **34**, 699
  - $\pi(1300)$  . . . . . **36**, 751
  - $\pi(1800)$  . . . . . 795
  - $\pi_1(1400)$  . . . . . 758
  - $\pi_1(1600)$  . . . . . 778
  - $\pi_2(1670)$  [*was*  $A(1680)$  or  $A_3$ ] . . . . . **38**, 781
  - $\pi_2(2100)$  [*was*  $A(2100)$ ] . . . . . 805
- Pion . . . . . **34**, 695
- Planck constant . . . . . 107
- Planck mass . . . . . 108
- Plasma energy . . . . . 323
- Plastic scintillators . . . . . 342
- Poisson distribution . . . . . 388
- Poisson distribution, Monte Carlo algorithm for . . . . . 403
- Poisson distribution, table of . . . . . 388
- Potentials, electromagnetic . . . . . 116
- Prefixes, metric, commonly used . . . . . 110
- Primary spectra, cosmic rays . . . . . 305
- Probability . . . . . 386
- Probability density function, definition . . . . . 386
- Production and spectroscopy of  $b$ -flavored hadrons, note on . . . . . 964
- Propagation of errors . . . . . 393
- Properties (atomic and nuclear) of materials . . . . . 114
- Proton (see  $p$ ) . . . . . **79**, 1253
- Proton cyclotron frequency/field . . . . . 107
- Proton decay . . . . . 209
- Proton mass . . . . . **79**, 107
- Proton structure function . . . . . 234
- Proton structure function, plots . . . . . 241, 244
- Pseudorapidity distribution in  $\bar{p}p$  interactions, plot of . . . . . 440
- Pseudorapidity  $\eta$ , defined . . . . . 424
- Pseudoscalar mesons, decay constants of charged, note on . . . . . 946
- $\psi$  mesons
- $\psi(1S) = J/\psi(1S)$  . . . . . **64**, 1151
  - $\psi(2S)$  . . . . . **68**, 1192
  - $\psi(2S)$  and  $\chi_{c0,1,1}$ , branching ratios, note on . . . . . 1168
  - $\psi(3770)$  . . . . . **69**, 1205
  - $X(3915)$  . . . . . 1212
  - $\psi(4040)$  . . . . . **70**, 1213
  - $\psi(4160)$  . . . . . **70**, 1215
- $\psi(4415)$  . . . . . **71**, 1220
- Pulsars, binary . . . . . 261
- $Q(1280)$  or  $Q_1$  [*now called*  $K_1(1270)$ ] . . . . . **42**, 872
- $Q(1400)$  or  $Q_2$  [*now called*  $K_1(1400)$ ] . . . . . **42**, 873
- and structure functions . . . . . 235
- Quintessence (general dark energy of Universe) . . . . . 283, 284
- Quantum mechanics in  $B^0-\bar{B}^0$  mixing, note on . . . . . 1066
- Quantum numbers in quark model . . . . . 199
- Quarks . . . . . **33**, 655
- and lepton compositeness searches . . . . . **93**, 1484
  - and lepton substructure searches . . . . . **93**, 1484
  - current masses of . . . . . 136, 655
  - fragmentation in  $e^+e^-$  annihilation, heavy . . . . . 254
  - and leptons, weak interactions of . . . . . 136, 148
  - mass, note on . . . . . 655
  - model . . . . . 199
  - model assignments . . . . . 199
  - model, dynamical ingredients . . . . . 205
  - properties of . . . . . 199
- Quark searches, free . . . . . **33**, 688
- Quark searches, note on . . . . . 688
- $R$  function,  $e^+e^-$  collisions, plot of . . . . . 444
- $r(2510)$  [*now called*  $f_6(2510)$ ] . . . . . 814
- Rad, unit of absorbed dose of radiation . . . . . 381
- Radiation
- Cherenkov . . . . . 335
  - damage in Silicon detectors . . . . . 357
  - dominated epoch . . . . . 268
  - length . . . . . 329
  - length of materials, table . . . . . 114
  - lethal dose from . . . . . 382
  - weighting factor . . . . . 381
- Radiative corrections in Standard Model . . . . . 136
- Radiative decays, hyperons, note on . . . . . 1368
- Radiative loss by muons . . . . . 334
- Radioactive sources, commonly used . . . . . 385
- Radioactivity
- and radiation protection . . . . . 381
  - at accelerators . . . . . 383
  - natural annual background . . . . . 381
  - unit of absorbed dose . . . . . 381
  - unit of activity . . . . . 381
- Radioactivity, low-radioactivity background techniques . . . . . 377
- cosmic rays . . . . . 379
  - cosmogenic . . . . . 379
  - environmental . . . . . 378
  - neutrons . . . . . 379

- radioimpurities . . . . . 378
- radon . . . . . 378
- Radon, as component of natural background radioactivity . . . 381
- Random angle, Monte Carlo algorithm for sine and cosine of . . 403
- Random number generators . . . . . 402
- RANLUX . . . . . 402
- Rapidity . . . . . 424
- Rare  $B$  decays, note on . . . . . 968
- Redshift . . . . . 264
- Refractive index of materials, table . . . . . 114
- Regge theory fits to total cross sections, table . . . . . 447
- Re-ionization of the Universe . . . . . 285
- Relativistic kinematics . . . . . 422
- Relativistic rise . . . . . 326
- Relativistic transformation of electromagnetic fields . . . . . 116
- Renormalization in Standard Model . . . . . 136
- Representations,  $SU(n)$  . . . . . 421
- Resistive plate chambers . . . . . 355
- Resistivity, electrical, of elements, table . . . . . 115
- Resistivity of metals . . . . . 117
- Resistivity, relations for . . . . . 117
- Resonance, Breit-Wigner form and Argand plot for . . . . . 425
- Resonances (see Mesons and Baryons)
- Restricted energy loss rate, charged particles . . . . . 327
- RHIC (Brookhaven) collider parameters . . . . . 321
- $\rho$  mesons
- $\rho(770)$  . . . . . **34**, 715
- $\rho(770)$ , note on . . . . . 715
- $\rho(1450)$  . . . . . **37**, 767
- $\rho(1450)$  and  $\rho(1770)$ , note on . . . . . 788
- $\rho(1700)$  . . . . . **38**, 788
- $\rho(1900)$  . . . . . 799
- $\rho(2150)$  . . . . . 807
- $\rho_3(1690)$  [*was*  $g(1690)$ ] . . . . . **38**, 784
- $\rho_3(1990)$  . . . . . 802
- $\rho_3(2250)$  . . . . . 810
- $\rho_5(2350)$  . . . . . 813
- $\rho$  parameter of electroweak interactions . . . . . 148
- $\rho$  parameter in electroweak analyses (Standard Model) . . . . 149
- $\rho_c$ , critical density . . . . . 108
- Ring-Imaging Cherenkov detectors . . . . . 347
- Robertson-Walker metric . . . . . 264
- Robustness of an estimator . . . . . 390
- RPC (Resistive Plate Chambers) . . . . . 355
- Rounding errors, treatment of . . . . . 16
- Rydberg energy . . . . . 107
- $s$  (quark) . . . . . **33**, 662
- $S, T, U$  electroweak variables . . . . . 150, 150  
(see p. VIII.58 in our 1992 edition, Phys. Rev. **D45**, Part II)
- $S(975)$  or  $S^*$  [*now called*  $f_0(980)$ ] . . . . . **35**, 731
- S-matrix approach to  $Z$  lineshape . . . . . 478
- S-matrix for two-body scattering . . . . . 422
- Sachs-Wolfe effect . . . . . 284
- Same-side tag in  $B^0-\bar{B}^0$  mixing, note on . . . . . 1068
- Scalar mesons, note on . . . . . 706
- Scale factor, definition of . . . . . 14
- Scaled cosmological constant,  $\Omega_\Lambda$  . . . . . 108, 265
- Scaled Hubble constant . . . . . 108, 265
- Schwarzschild radius of the Earth . . . . . 108
- Schwarzschild radius of the Sun . . . . . 108
- Scintillator parameters . . . . . 342
- Sea-level cosmic ray fluxes . . . . . 305
- Searches:
- Axion searches . . . . . **28**, 562
- Baryonium candidates . . . . . 815
- Chargino searches . . . . . 1456
- Color octet leptons . . . . . **94**, 1488
- Color sextet quarks . . . . . **94**, 1488
- Compositeness, quark and lepton, searches . . . . . **93**, 1484
- Excited lepton searches . . . . . **93**, 1487
- Familon searches . . . . . 574
- Fourth generation ( $b'$ ) searches . . . . . **33**, 687
- Free quark searches . . . . . **33**, 688
- Gluino searches . . . . . **93**, 1469
- Goldstone boson searches . . . . . 574
- Heavy boson searches . . . . . **28**, 543
- Heavy lepton searches . . . . . **32**, 621
- Heavy particle searches . . . . . 1504
- Higgs searches . . . . . **28**, 501
- Lepton (heavy) searches . . . . . **32**, 621
- Lepton mixing, neutrinos (massive) and, search for . . . **32**, 636
- Lepton, quark compositeness searches . . . . . **93**, 1484
- Lepton, quark substructure searches . . . . . **93**, 1484
- Leptoquark searches . . . . . 557
- Light boson searches . . . . . **28**, 562
- Light neutrino types, number of . . . . . **32**, 629
- Magnetic Monopoles . . . . . **93**, 1413
- Majoron searches . . . . . 574
- Massive neutrinos and lepton mixing, searches . . . . . **32**, 636
- Monopole searches . . . . . **93**, 1413
- Neutralino searches . . . . . 1455
- Neutrino oscillation searches . . . . . **32**, 636
- Neutrino, solar, experiments . . . . . 177
- Neutrino types, number of . . . . . **32**, 629
- Neutrinoless double- $\beta$  decay searches . . . . . 631



Neutrinos (massive) and lepton mixing, search for . . . . .	<b>32</b> , 636	radius in galaxy . . . . .	108
Other particle searches . . . . .	1500	velocity in galaxy . . . . .	108
Photino searches . . . . .	1450	velocity with respect to CBR . . . . .	108
Quark and lepton compositeness searches . . . . .	<b>93</b> , 1484	Solenoidal collider detector magnets . . . . .	363
Quark and lepton substructure searches . . . . .	<b>93</b> , 1484	Sources, radioactive, commonly used . . . . .	385
Quark searches, free . . . . .	<b>33</b> , 688	Specific heats of elements, table . . . . .	115
Slepton searches . . . . .	1459	Spectroscopy of $b$ -flavored hadrons, note on . . . . .	964
Sneutrino searches . . . . .	1459	Speed of light . . . . .	108
Squark searches . . . . .	1463	Spherical harmonics . . . . .	419
Solar $\nu$ experiments . . . . .	177	Spin-dependent structure functions . . . . .	247
Substructure, quark and lepton, searches . . . . .	<b>93</b> , 1484	Squark searches . . . . .	1463
Supersymmetric partner searches . . . . .	<b>93</b> , 1420	Standard cosmological model . . . . .	281
Technicolor, review of . . . . .	1475	Standard Model of electroweak interactions . . . . .	136
Techniparticle searches . . . . .	<b>93</b> , 1475	Standard Model predictions in $B^0-\bar{B}^0$ mixing, note on . . . . .	1066
Technipion searches . . . . .	<b>28</b> , 541	Standard particle numbering for Monte Carlos . . . . .	415
Vector meson candidates . . . . .	815	Statistical procedures . . . . .	14
$W'$ searches, note on . . . . .	543	Statistical significance in $B^0-\bar{B}^0$ mixing, note on . . . . .	1067
Weak gauge boson searches . . . . .	<b>28</b> , 543	Statistics . . . . .	390
$Z'$ searches, note on . . . . .	547	Stefan-Boltzmann constant . . . . .	107
Selection and treatment of data . . . . .	13	Stopping power . . . . .	324
Shower detector energy resolution . . . . .	360	Stopping power for heavy-charged projectiles . . . . .	323
Showers, electromagnetic, lateral distribution of . . . . .	334	Strange baryons . . . . .	<b>83</b> , 1327
Showers, electromagnetic, longitudinal distribution of . . . . .	333	Strange, bottom meson . . . . .	<b>63</b> , 1128
SI units, complete set . . . . .	110	Strange, charmed mesons . . . . .	<b>48</b> , 941
Sidereal day . . . . .	108	Strange mesons . . . . .	<b>39</b> , 820
Sidereal year . . . . .	108	Strange quark ( $s$ ) . . . . .	<b>33</b> , 662
Sievert, unit of radiation dose equivalent . . . . .	381	Strangeness-changing neutral currents, tests for . . . . .	95
$\sigma_R$ function, $e^+e^-$ collisions, plot of . . . . .	444	Structure functions . . . . .	234
$\Sigma$ baryons (see also $\Lambda$ and $\Sigma$ baryons) . . . . .	<b>84</b> , 1343	Student's $t$ distribution . . . . .	389
$\Sigma^+$ . . . . .	<b>84</b> , 1343	Student's $t$ distribution, Monte Carlo algorithm for . . . . .	403
$\Sigma^0$ . . . . .	<b>85</b> , 1345	Student's $t$ distribution, table of . . . . .	388
$\Sigma^-$ . . . . .	<b>85</b> , 1346	SU(2) $\times$ U(1) . . . . .	136
$\Sigma(1670)$ , note on . . . . .	1353	SU(3) classification of baryon resonances . . . . .	202
$\Sigma_c(2455)$ . . . . .	<b>89</b> , 1394	SU(3), generators of transformations . . . . .	420
$\Sigma_c(2520)$ . . . . .	1395	SU(3) isoscalar factors . . . . .	420
Silicon detectors, radiation damage . . . . .	357	SU(3) multiplets (representations) . . . . .	203
Silicon particle detectors . . . . .	356	SU(3) representation matrices . . . . .	420
Silicon photodiodes . . . . .	356	SU(6) multiplets . . . . .	204
Silicon strip detectors . . . . .	356	SU( $n$ ) multiplets . . . . .	421
$\sin^2\theta_W$ , weak-mixing angle . . . . .	107, 136, 146	Substructure, quark and lepton, searches . . . . .	<b>93</b> , 1484
Slepton searches . . . . .	1459	Substructure, quark and lepton, searches, note on . . . . .	1484
Sloan Digital Sky Survey (SDSS) . . . . .	285	Summary Tables, organization of . . . . .	11
Sneutrino searches . . . . .	1459	Sunyaev-Zel'dovich effect . . . . .	280
Solar		Superconducting solenoidal magnet . . . . .	363
equatorial radius . . . . .	108	Supernovae, Type Ia and Type II supernovae . . . . .	283
luminosity . . . . .	108	Supersymmetric partner searches . . . . .	<b>93</b> , 1420
mass . . . . .	108	Supersymmetry, electroweak analyses of . . . . .	150
$\nu$ experiments . . . . .	177	Superweak model of $CP$ violation . . . . .	859

Greek letters are alphabetized by their English-language spelling. Bold page numbers signify entries in the Particle Properties Summary Tables.

Survival probability, relations for . . . . .	422	Two-body differential cross sections . . . . .	422
Symmetry breaking . . . . .	209, 136	Two-body partial decay rate . . . . .	422
Synchrotron radiation . . . . .	117	Two-body scattering kinematics . . . . .	422
Systematic errors, treatment of . . . . .	14	Two-photon processes in $e^+e^-$ annihilation . . . . .	428
$t$ (quark) . . . . .	<b>33</b> , 668	$u$ (quark) . . . . .	<b>33</b> , 662
$T$ (time reversal), tests of conservation . . . . .	95	Ultra-high-energy cosmic rays . . . . .	310
Tags in $B^0-\bar{B}^0$ mixing, note on . . . . .	1068	Underground cosmic rays . . . . .	307
$\tau$ lepton . . . . .	<b>30</b> , 592	Unified atomic mass unit . . . . .	107
$\tau$ branching fractions, note on . . . . .	596	Unified theories, grand . . . . .	209
$\tau$ -decay parameters, note on . . . . .	617	Uniform distribution, table of . . . . .	388
$\tau$ polarization in $Z$ decay . . . . .	479	Units and conversion factors . . . . .	107
Technicolor, electroweak analyses of . . . . .	149	Units, electromagnetic . . . . .	116
Technicolor, review of . . . . .	1475	Units, SI, complete set . . . . .	110
Techniparticle searches . . . . .	<b>93</b> , 1475	Universe	
Technipion searches . . . . .	<b>28</b> , 541	age of . . . . .	108, 264, 266, 287
Temperature of CBR . . . . .	108	baryon density of . . . . .	108, 275
TEVATRON (Fermilab) collider parameters . . . . .	320	composition . . . . .	266, 275
Thermal conductivity of elements, table . . . . .	115	cosmological properties of . . . . .	264
Thermal expansion coefficients of elements, table . . . . .	115	cosmological structure . . . . .	268
Thermal history of the Universe . . . . .	267	critical density of . . . . .	108
$\theta(1690)$ [ <i>now called</i> $f_0(1710)$ ] . . . . .	<b>38</b> , 793	curvature of . . . . .	265
$\theta_W$ , weak-mixing angle . . . . .	107, 136, 147	density fluctuations . . . . .	271
Thomson cross section . . . . .	107	density parameter of . . . . .	108
Three-body decay kinematics . . . . .	422	entropy density . . . . .	269
Three-body phase space . . . . .	422	(Hubble) expansion of . . . . .	264, 280
Threshold Cherenkov detectors . . . . .	346	large-scale structure of . . . . .	266, 271
Time-projection chambers (TPC) . . . . .	353	mass-energy . . . . .	289
Time-projection chambers (TPC) (non-accelerator) . . . . .	373	Universe (cont.)	
Top-changing neutral currents, tests for . . . . .	95	matter-dominated . . . . .	270
Top quark ( $t$ ) . . . . .	<b>33</b> , 668	phase transitions . . . . .	269
Top quark, note on . . . . .	668	radiation content at early times . . . . .	268
Top quark mass from electroweak analyses . . . . .	145	thermodynamic equilibrium . . . . .	268
Toroidal collider detector magnets . . . . .	365	thermal history of . . . . .	267
Total cross sections, table of fit parameters . . . . .	447	$\Upsilon$ states, width determinations of, note on . . . . .	1223
Total cross sections, summary plot . . . . .	448	$\Upsilon(1S)$ . . . . .	<b>71</b> , 1224
Total energy density of Universe, $\Omega_{\text{tot}}$ . . . . .	287	$\Upsilon(2S)$ . . . . .	<b>72</b> , 1232
Total lepton number conservation . . . . .	95	$\Upsilon(3S)$ . . . . .	<b>73</b> , 1241
TPC, Time-projection chambers . . . . .	353	$\Upsilon(4S)$ . . . . .	<b>73</b> , 1244
TPC, Time-projection chambers (non-accelerator) . . . . .	373	$\Upsilon(10860)$ . . . . .	<b>74</b> , 1247
Tracking Cherenkov detectors . . . . .	346	$\Upsilon(11020)$ . . . . .	<b>74</b> , 1249
Transformation of electromagnetic fields, relativistic . . . . .	116	$V_{cb}$ and $V_{ub}$ CKM Matrix Elements . . . . .	1111
Transition radiation . . . . .	335	$V_{cb}$ and $V_{ub}$ determination of, note on . . . . .	1111
Transition radiation detectors (TRD) . . . . .	354	$V_{ud}$ , $V_{us}$ determination of, note on . . . . .	852
Triangles, unitarity, note on . . . . .	157	$V_{ud}$ , $V_{us}$ , $V_{ub}$ , $V_{cd}$ , $V_{cs}$ , $V_{cb}$ , $V_{td}$ , $V_{ts}$ , $V_{tb}$ . . . . .	157
Triple gauge couplings, note on the extraction of . . . . .	474	Vacuum energy parameter, $\Omega_v$ . . . . .	265
Tropical year . . . . .	108	Variance, definition . . . . .	386
Two-body decay kinematics . . . . .	422	Vector meson candidates . . . . .	815

$W$ (gauge boson) . . . . .	<b>27</b> , 470	$X(4360)$ . . . . .	1220
$W$ -boson mass, note on . . . . .	470	$X(4430)^\pm$ . . . . .	1222
$W$ boson, mass, width, branching ratios, and coupling to fermions . . . . .	<b>27</b> , 107, 138, 145, 146	$X(4660)$ . . . . .	1222
$W^\pm$ : Triple gauge couplings, note on the extraction of . . . . .	474	$X(10610)^\pm$ . . . . .	1246
$W$ and $Z$ differential cross section . . . . .	440	$X(10650)^\pm$ . . . . .	1247
$w$ , dark energy equation of state parameter . . . . .	265, 283	$\Xi$ baryons . . . . .	<b>86</b> , 1367
$W'$ searches, note on . . . . .	543	$\Xi$ resonances, note on . . . . .	1372
WMAP, NASA's Wilkinson Microwave Anisotropy Probe . . . . .	285	$\Xi^0$ . . . . .	<b>86</b> , 1367
Weak boson searches . . . . .	<b>28</b> , 543	$\Xi^-$ . . . . .	<b>86</b> , 1369
Weak neutral currents, tests for ( $\Delta B = 1, \Delta C = 1, \Delta S = 1, \Delta T = 1$ )	95	$\Xi_b^0, \Xi_b^-$ . . . . .	1408
Weinberg angle ( $\sin^2 \theta_W$ ) . . . . .	107, 136	$\Xi_c^+$ . . . . .	<b>89</b> , 1396
Width determinations of $\Upsilon$ states, note on . . . . .	1223	$\Xi_c^0$ . . . . .	<b>89</b> , 1398
Width of $W$ and $Z$ bosons . . . . .	145	$\Xi_c^{'+}$ . . . . .	<b>90</b> , 1399
Wien displacement law constant . . . . .	107	$\Xi_c^{'0}$ . . . . .	<b>90</b> , 1399
WIMPs (also see dark matter limits) . . . . .	291	$\Xi_c(2645)$ . . . . .	<b>90</b> , 1399
WIMPs and other particle searches, note on . . . . .	1500	$\Xi_c(2790)$ . . . . .	<b>90</b> , 1400
Wire chambers . . . . .	348	$\Xi_c(2815)$ . . . . .	<b>90</b> , 1400
$xF_3$ structure function, plots of . . . . .	245	$\xi(2220)$ [ <i>now called</i> $f_J(2220)$ ] . . . . .	809
$x$ variable (of Feynman's) . . . . .	424	Year, sidereal . . . . .	108
$X$ mesons		Year, tropical . . . . .	108
$X(1850)$ [ <i>now called</i> $\phi_3(1850)$ ] . . . . .	<b>39</b> , 798	Young diagrams (tableaux) . . . . .	421
$X(3872)$ . . . . .	<b>70</b> , 1210	Young's modulus of solid elements, table . . . . .	115
$X(3940)$ . . . . .	1213	Yukawa coupling unification . . . . .	209
$X(3915)$ . . . . .	1212	$Z$ : Anomalous $ZZ\gamma$ , $Z\gamma\gamma$ , and $ZZV$ couplings . . . . .	498
$X(4050)^\pm$ . . . . .	1215	$Z$ (gauge boson) . . . . .	<b>27</b> , 478
$X(4140)$ . . . . .	1215	$Z$ boson, note on . . . . .	478
$X(4160)$ . . . . .	1217	$Z$ boson, mass, width, branching ratios, and coupling to fermions . . . . .	<b>27</b> , 107, 138, 145, 146, 547
$X(4250)^\pm$ . . . . .	1217	$Z$ decay to heavy flavors . . . . .	482
$X(4260)$ . . . . .	<b>70</b> , 1218	$Z$ width, plot . . . . .	446
$X(4350)$ . . . . .	1220	$Z'$ searches, note on . . . . .	547

